Editor-In-Chief

Andrew P. Schachat

RYAN'S RETINA

SIXTH EDITION

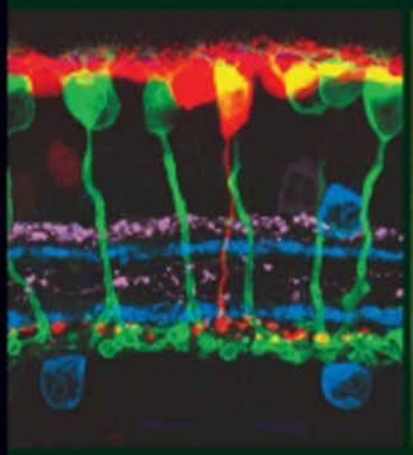
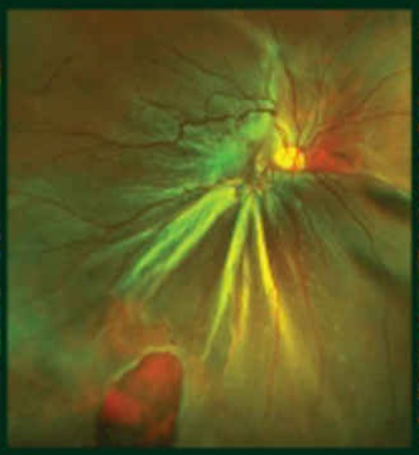
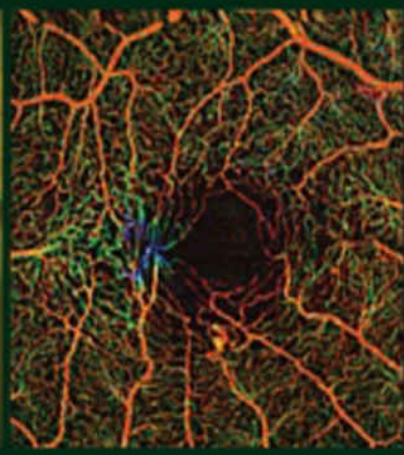

C. P. Wilkinson

David R. Hinton

SriniVas R. Sadda

Peter Wiedemann

ELSEVIER

Ryan's Retina

SIXTH EDITION

Editor-In-Chief

ANDREW P. SCHACHAT MD

Vice Chairman, Cole Eye Institute, Cleveland Clinic Foundation, Cleveland, OH, USA

Volume One

Part 1 Retinal Imaging and Diagnostics

Edited by

SRINIVAS R. SADDA MD

Part 2 Basic Science and Translation to Therapy

Edited by

DAVID R. HINTON MD

Volume Two

Medical Retina

Edited by

ANDREW P. SCHACHAT MD AND SRINIVAS R. SADDA MD

Volume Three

Part 1 Surgical Retina

Edited by

C.P. WILKINSON MD AND PETER WIEDEMANN MD

Part 2 Tumors of the Retina, Choroid, and Vitreous

Edited by

ANDREW P. SCHACHAT MD

Table of Contents

Section 1 Anatomy and Physiology

Section 2 Basic Mechanisms of Injury in the Retina

Volume Two Medical Retina
Section 1 Retinal Degenerations and Dystrophies

Section 3 Choroidal Vascular/Bruch's Membrane Disease

Section 4 Inflammatory Disease/Uveitis

Inflammation

Infections

Section 2 Retinal Reattachment: General Surgical Principles and Techniques

Section 3 Complicated Forms of Retinal Detachment

Section 4 Vitreous Surgery for Macular Disorders

Section 2 Tumors of the Choroid

Section 3 Hematologic and Miscellaneous Tumors

Copyright

First edition 1989
Second edition 1994
Third edition 2001
Fourth edition 2006
Fifth edition 2013
Sixth edition 2018

Notices

Knowledge and best practice in this field are constantly changing. As new research and experience broaden our understanding, changes in research methods, professional practices, or medical treatment may become necessary.

Practitioners and researchers must always rely on their own experience and knowledge in evaluating and using any information, methods, compounds, or experiments described herein. In using such information or methods they should be mindful of their own safety and the safety of others, including parties for whom they have a professional responsibility.

With respect to any drug or pharmaceutical products identified, readers are advised to check the most current information provided (i) on procedures featured or (ii) by the manufacturer of each product to be administered, to verify the recommended dose or formula, the method and duration of administration, and contraindications. It is the responsibility of practitioners, relying on their own experience and knowledge of their patients, to make diagnoses, to determine dosages and the best treatment for each individual patient, and to take all appropriate safety precautions.

To the fullest extent of the law, neither the Publisher nor the authors, contributors, or editors, assume any liability for any injury and/or damage to persons or property as a matter of products liability, negligence or otherwise, or from any use or operation of any methods, products, instructions, or ideas contained in the material herein.

ISBN: 978-0-323-40197-5
eBook: 978-0-323-40198-2
Inkling: 978-0-323-40199-9

Printed in China

Last digit is the print number: 9 8 7 6 5 4 3 2 1

Content Strategist: Russell Gabbedy
Content Development Specialist: Nani Clansey
Content Coordinator: Joshua Mearns
Project Manager: Joanna Souch
Design: Miles Hitchen
Illustration Manager: Karen Giacomucci
Illustrator: Angie MacAllister
Marketing Manager: Melissa Fogarty

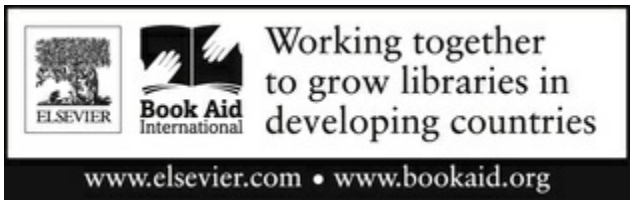

Video Table of Contents

6.4 Real-Time Volumetric Peeling with Diamond-Dusted Membrane Scraper Visualized with a Swept Source Optical Coherence Tomography System

Justis P. Ehlers, Cynthia A. Toth – Chapter 6

6.5 Intraoperative Optical Coherence Tomography Feedback during Macular Hole Surgery

Justis P. Ehlers, Cynthia A. Toth – Chapter 6

VOLUME 1, PART 2 Basic Science and Translation to Therapy

36.1 Perfluouron Placement and Subretinal Injection Procedure

Albert M. Maguire, Jean Bennett – Chapter 36

VOLUME 3, PART 1 Surgical Retina

SECTION 2 **Retinal Reattachment: General Surgical Principles and Techniques**

104.1 Techniques of Scleral Buckling

Paul Sullivan – Chapter 104

106.1 A Case of Primary Vitrectomy for Treating Rhegmatogenous Retinal Detachment

Young Hee Yoon – Chapter 106

SECTION 5 **Vitreous Surgery: Additional Considerations**

131.1 Subluxated Intraocular Lens without Haptics

Renaud Duval – *Chapter 131*

131.2 Posterior Synechiae and Small Pupil during Vitrectomy

Ehab N. El Rayes – *Chapter 131*

131.3 Induction of Posterior Vitreous Detachment in Retinal Detachment

Andre V. Gomes – *Chapter 131*

131.4 Induction of Posterior Vitreous Detachment in High Myopia

Ramin Tadayoni – *Chapter 131*

131.5 Iatrogenic Retinal Breaks During Peeling

Manish Nagpal – *Chapter 131*

131.6 Internal Limiting Membrane Peeling

Sjakon G. Tahija – *Chapter 131*

131.7 Subretinal Injection of Brilliant Blue

Arturo Alezzandrini, Francisco J. Rodriguez – *Chapter 131*

151.1 Surgical Resection of Choroidal Melanoma

Bertil E. Damato – Chapter 151

Contributors

Michael D. Abràmoff MD, PhD
The Robert C. Watzke, MD, Professor of Ophthalmology and Visual Sciences
Department of Ophthalmology and Visual Sciences
University of Iowa Hospital and Clinics
Iowa City, IA, USA

Gary W. Abrams MD
Director, Ligon Research Center of Vision
Professor, Ophthalmology
Kresge Eye Institute
Wayne State University
Detroit, MI, USA

Armin R. Afshar MD, MBA
Assistant Professor of Ophthalmology
University of California, San Francisco
San Francisco, CA, USA

Aniruddha Agarwal MD
Clinical Fellow in Vitreoretina
Advanced Eye Center
Post Graduate Institute of Medical Education and Research (PGIMER)Chandigarh, India

Anita Agarwal MD
West Coast Retina
San Francisco, CA, USA

Adjoint Professor of Ophthalmology
Retina, Vitreous & Uvea
Vanderbilt Eye Institute
Vanderbilt University
School of Medicine
Nashville, TN, USA

Lloyd M. Aiello MD
Clinical Professor of Ophthalmology
Harvard Medical School
Director Emeritus, Beetham Eye Institute
Joslin Diabetes Center
Boston, MA, USA

Lloyd Paul Aiello MD, PhD, FARVO
Director, Beetham Eye Institute
Professor of Ophthalmology
Joslin Diabetes Center and Harvard Medical School
Boston, MA, USA

Daniel M. Albert MD, MS
Professor of Ophthalmology
Oregon Health and Science University
Casey Eye Institute
Portland, OR, USA

Michael T. Andreoli MD
Vitreoretinal Surgery Fellow
Illinois Eye and Ear Infirmary
Department of Ophthalmology and Visual Sciences
University of Illinois, Chicago
Chicago, IL, USA

Karen R. Armbrust MD, PhD
Clinical Fellow
National Eye Institute
National Institutes of Health
Bethesda, MD, USA

Mary E. Aronow MD
Assistant Professor of Ophthalmology
Wilmer Eye Institute
Johns Hopkins University
School of Medicine
Baltimore, MD, USA

Mathew W. Aschbrenner MD
Vitreoretinal Surgeon
Eye Clinic of Wisconsin
Wausau, WI, USA

Marcos Ávila MD, PhD
Head Professor
Department of Ophthalmology
Federal University of Goias
Goiania, GO, Brazil

G.W. Aylward FRCOphth, FRCS, MD
Consultant Ophthalmologist
Department of Vitreoretinal Surgery
Moorfields Eye Hospital
London, UK

Andrew J. Baldwin MD
Ophthalmology Resident
Truhlsen Eye Institute
University of Nebraska Medical Center
Omaha, NE, USA

Angela N. Baldwin MD, MPH
Clinical Research Fellow
University of California, Berkeley
Berkeley, CA, USA

Rubens Belfort Jr., MD, PhD
Head Professor of Ophthalmology
Department of Ophthalmology
Federal University of São Paulo

São Paulo, Brazil

Jean Bennett MD, PhD
Professor
Co-Director of Center for Advanced Retinal and Ocular Therapeutics (CAROT)
Department of Ophthalmology
Scheie Eye Institute
Department of Cell and Developmental Biology
University of Pennsylvania
Perelman School of Medicine
Philadelphia, PA, USA

Chris Bergstrom MD
Retina Consultants of Carolina, PA
Greenville, SC, USA

Cagri G. Besirli MD, PhD
Assistant Professor
Department of Ophthalmology and Visual Sciences
University of Michigan
Ann Arbor, MI, USA

Angela Bessette MD
Assistant Professor
Flaum Eye Institute
University of Rochester
Rochester, NY, USA

Muna Bhende MS
Senior Consultant
Shri Bhagwan Mahavir Vitreoretinal Service
Sankara Nethralaya
Chennai, India

Pramod S. Bhende MS
Senior Consultant
Shri Bhagwan Mahavir Vitreoretinal Services
Sankara Nethralaya

Chennai, India

Susanne Binder MD
Professor
Department of Ophthalmology
Rudolph Foundation Hospital (Rudolfstiftung)
Vienna, Austria

Alan Bird MD
Emeritus Professor
Department of Ophthalmic Genetics
Institute of Ophthalmology
University College London
London, UK

Barbara A. Blodi MD
Professor of Ophthalmology and Visual Sciences
University of Wisconsin
School of Medicine and Public Health
Madison, WI, USA

Mark S. Blumenkranz MD
H.J. Smead Professor of Ophthalmology
Stanford University
School of Medicine
Palo Alto, CA, USA

H. Culver Boldt MD
Marion and Frederick Fureste
Professor of Ophthalmology
Department of Ophthalmology
University of Iowa
College of Medicine
Iowa City, IA, USA

Durga S. Borkar MD
Ophthalmology Resident
Massachusetts Eye and Ear Infirmary
Department of Ophthalmology

Harvard Medical School
Boston, MA, USA

Norbert Bornfeld MD
Zentrum für Augenheilkunde
Universitätsklinikum Essen
Essen, Germany

Ferdinando Bottoni MD
Ophthalmologist
Department of Biomedical and Clinical Sciences "Luigi Sacco"
Eye Clinic – Sacco Hospital
University of Milan
Milan, Italy

Michael E. Boulton PhD
Professor
Department of Ophthalmology
Indiana University School of Medicine
Indianapolis, IN, USA

Sara J. Bowne PhD
Faculty Associate
Human Genetics Center
School of Public Health
The University of Texas Health Science Center
Houston, TX, USA

Christopher J. Brady MD
Assistant Professor of Ophthalmology
Retina Division – Wilmer Eye Institute
Johns Hopkins University
School of Medicine
Baltimore, MD, USA

Milam A. Brantley Jr., MD, PhD
Associate Professor
Ophthalmology and Visual Sciences
Vanderbilt Eye Institute

Vanderbilt University Medical Center
Nashville, TN, USA

Neil M. Bressler MD
The James P. Gills Professor of Ophthalmology
Retina Division – Wilmer Eye Institute
Johns Hopkins University
School of Medicine
Baltimore, MD, USA

Susan B. Bressler MD
The Julia G. Levy Professor of Ophthalmology
Retina Division – Wilmer Eye Institute
Johns Hopkins University
School of Medicine
Baltimore, MD, USA

Andreas Bringmann PhD
Associate Professor
Department of Ophthalmology and Eye Hospital
University of Leipzig
Faculty of Medicine
Leipzig, Germany

Daniel A. Brinton MD
Assistant Clinical Professor
Department of Ophthalmology
University of California, San Francisco
East Bay Retina Consultants
Oakland, CA, USA

Gary C. Brown MD, MBA
Professor of Ophthalmology
Wills Eye Hospital
Jefferson Medical University
Philadelphia, PA, USA

Melissa M. Brown MD, MN, MBA
Professor of Ophthalmology

Wills Eye Hospital
Jefferson Medical University
Philadelphia, PA, USA

Simon Brunner MD
Assistant Medical Director
Vitreoretinal Surgeon
Department of Ophthalmology
Rudolph Foundation Hospital (Rudolfstiftung)
Vienna, Austria

Christopher K.H. Burris MD
Ophthalmic Pathology Fellow
Department of Ophthalmology and Visual Sciences
University of Wisconsin-Madison
School of Medicine and Public Health
Madison, WI, USA

Ronald A. Bush PhD
Staff Scientist
Section on Translational Research on Retinal and Macular Degeneration
National Institute of Deafness and Other Communication Disorders
National Institutes of Health
Bethesda, MD, USA

Dingcai Cao PhD
Associate Professor
Department of Ophthalmology and Visual Sciences
University of Illinois at Chicago
Chicago, IL, USA

Antonio Capone Jr., MD
Associated Retinal Consultants
William Beaumont Hospital
Royal Oak, MI, USA

David Carruthers PhD, FRCP
Consultant Rheumatologist

Sandwell & West Birmingham Hospitals NHS Trust
Birmingham, UK
Honorary Senior Lecturer in Rheumatology
Institute of Inflammation and Ageing
University of Birmingham
Birmingham, UK

Jerry D. Cavallerano OD, PhD
Associate Professor of Ophthalmology
Harvard Medical School
Staff Optometrist
Beetham Eye Institute
Joslin Diabetes Center
Boston, MA, USA

Usha Chakravarthy MD
Professor of Ophthalmology and Vision Science
Queens University of Belfast
Consultant in Ophthalmology
Belfast Health and Social Care Trust
Belfast, Northern Ireland, UK

Helen Chan MBBS (Hons)
Ophthalmology Registrar
Royal Victorian Eye and Ear Hospital
Melbourne, VIC, Australia

Steve Charles MD
Clinical Professor of Ophthalmology
University of Tennessee
College of Medicine
Memphis, TN, USA

David G. Charteris MD
Professor of Ophthalmology
Institute of Ophthalmology
Consultant Vitreoretinal Surgeon
Service Director, Vitreoretinal Unit
Moorfields Eye Hospital

London, UK

Jeannie Chen PhD
Professor
Zilkha Neurogenetic Institute
Departments of Cell & Neurobiology and Ophthalmology
Keck School of Medicine
University of Southern California
Los Angeles, CA, USA

Carol Yim-lui Cheung PhD
Assistant Professor
Department of Ophthalmology and Visual Sciences
The Chinese University of Hong Kong
Hong Kong, China

Emily Y. Chew MD
Deputy Director of Division of Epidemiology and Clinical Applications
Deputy Clinical Director
National Eye Institute
National Institutes of Health
Bethesda, MD, USA

Allen Chiang MD
The Retina Service of Wills Eye Hospital
Mid Atlantic Retina
Assistant Professor of Ophthalmology
Thomas Jefferson University
Philadelphia, PA, USA

Michael F. Chiang MD
Knowles Professor
Departments of Ophthalmology & Medical Informatics and Clinical Epidemiology
Casey Eye Institute
Oregon Health & Science University
Portland, OR, USA

Rao V. Chundury MD, MBA
Oculofacial and Orbital Surgery
Assistant Professor of Ophthalmology
Assistant Residency Program Director
Eugene and Marilyn Glick Eye Institute
Indiana University
Indianapolis, IN, USA

Dennis O. Clegg PhD
Wilcox Family Chair in Biomedicine
Co-Director, Center for Stem Cell Biology and Engineering
Professor, Department of Molecular, Cellular and Developmental Biology
University of California, Santa Barbara
Santa Barbara, CA, USA

Ian J. Constable FRANZCO, FRCSE, DSc(hon)
Professor of Ophthalmology
Lions Eye Institute
University of Western Australia
Perth, Australia

Gabriel Coscas MD
Professor of Ophthalmology
Department of Ophthalmology
University of Paris XII
Créteil, France

Alan F. Cruess MD
Professor
Department of Ophthalmology and Visual Sciences
Dalhousie University
Halifax, Nova Scotia, Canada

Emmett T. Cunningham Jr., MD, PhD, MPH
Director, The Uveitis Service
West Coast Retina
Clinical Professor of Ophthalmology
California Pacific Medical Center

San Francisco, CA, USA
Adjunct Clinical Professor of Ophthalmology
Stanford University School of Medicine
Stanford, CA, USA

Christine A. Curcio PhD, FARVO, Eminent Scholar in Retina
Director, AMD Histopathology Lab
Department of Ophthalmology
The University of Alabama at Birmingham
Birmingham, AL, USA

Stephen P. Daiger PhD
TS Matney Professor
Human Genetics Center
School of Public Health and Ruiz Deptartment of Ophthalmology
The University of Texas Health Science Center
Houston, TX, USA

Bertil E. Damato MD, PhD
Professor of Ophthalmology and Radiation Oncology
University of California, San Francisco
San Francisco, CA, USA

Sudipta Das MS
International Faculty
C-MER (Shenzhen) Dennis Lam Eye Hospital
Shenzhen, China

Janet L. Davis MD
Leach Distinguished Professor of Ophthalmology
Bascom Palmer Eye Institute
University of Miami
Miller School of Medicine
Miami, FL, USA

Matthew D. Davis MD
Emeritus Professor of Ophthalmology and Visual Sciences
University of Wisconsin
School of Medicine and Public Health

Madison, WI, USA

Shelley Day MD
Partner
Austin Retina Associates
Clinical Assistant Professor
Dell Medical School
University of Texas-Austin
Austin, TX, USA

Carlos Alexandre de Amorim Garcia Filho, MD
Retina Specialist
Universidade Federal Do Rio Grande Do Norte
Natal, RN, Brazil

Patrick De Potter MD, PhD
Professor of Ophthalmology
Chairman of Ophthalmology
Ocular Oncology Unit
Saint Luc University Hospital
Catholic University of Leuven
Brussels, Belgium

Marc D. de Smet MDCM, PhD, FRCSC, FRCOphth, FEBOphth
Retina and Uveitis Division, MIOS sa.
Lausanne, Switzerland

Alastair K. Denniston MRCP, FRCOphth, PhD
Consultant Ophthalmologist
University Hospitals Birmingham NHS Foundation Trust
Birmingham, UK
Honorary Reader in Ophthalmology
Institute of Inflammation and Ageing
University of Birmingham
Birmingham, UK

Ranjit S. Dhaliwal MD, FRCSC, FACS
Vitreoretinal Surgeon
Retina Consultants PC

Augusta, GA, USA
Adjunct Faculty
Department of Ophthalmology
Emory University
Atlanta, GA, USA
Adjunct Faculty
Department of Ophthalmology
Queen's University
Kingston, Ontario, Canada

Andrew D. Dick MBBS, MD, FRCOphth, FRSB, FMedSci
Professor of Ophthalmology
Academic Unit of Ophthalmology
University of Bristol
Bristol, UK
Duke Elder Chair of Ophthalmology
Institute of Ophthalmology
University College London
London, UK

Xiaoyan Ding MD,PhD
Professor, Retina Division
Zhongshan Ophthalmic Center
Sun Yat-Sen University
Guangzhou, Guangdong, China

Diana V. Do MD
Professor of Ophthalmology
Byers Eye Institute
Stanford University
School of Medicine
Palo Alto, CA, USA

Jay S. Duker MD
Professor and Chair of Ophthalmology
New England Eye Center
Tufts Medical Center
Tufts University School of Medicine
Boston, MA, USA

Jacque L. Duncan MD
Professor of Ophthalmology
Vice Chair of Medical Student Affairs
Department of Ophthalmology
University of California, San Francisco
San Francisco, CA, USA

Justis P. Ehlers MD
The Norman C. and Donna L. Harbert Endowed Chair for Ophthalmic Research
Cole Eye Institute
Cleveland Clinic
Cleveland, OH, USA

Dean Eliott MD
Associate Director, Retina Service
Massachusetts Eye and Ear
Associate Professor of Ophthalmology
Harvard Medical School
Boston, MA, USA

Lisa J. Faia MD
Partner
Associated Retinal Consultants, PC
Royal Oak, MI, USA
Associate Professor of Ophthalmology
William Beaumont Oakland University
School of Medicine
Rochester, MI, USA

Benedetto Falsini MD
Associate Professor of Ophthalmology
Department of Ophthalmology
Università Cattolica del S. Cuore
Rome, Italy

Sharon Fekrat MD, FACS
Associate Professor of Ophthalmology and Surgery
Duke University Medical Center

Associate Chief of Staff for Surgical Services
Durham VA Medical Center
Durham, NC, USA

Steven E. Feldon MD, MBA
Professor and Chair
Department of Ophthalmology
Flaum Eye Institute
University of Rochester
School of Medicine and Dentistry
Rochester, NY, USA

Henry A. Ferreyra MD
Associate Clinical Professor
Department of Ophthalmology
UC San Diego School of Medicine
La Jolla, CA, USA

Deborah A. Ferrington MD
Associate Professor
Department of Ophthalmology
University of Minnesota
Minneapolis, MN, USA

Frederick L. Ferris III, MD
Director, Division of Epidemiology and Clinical Applications
Clinical Director, National Eye Institute
National Institutes of Health
Bethesda, MD, USA

Paul T. Finger MD
Director, The New York Eye Cancer Center
Clinical Professor of Ophthalmology
New York University
School of Medicine
New York, NY, USA

Steven K. Fisher PhD
Research Professor

Neuroscience Research Institute
Professor Emeritus
Molecular, Cellular and Developmental Biology
University of California, Santa Barbara
Santa Barbara, CA, USA

Gerald A. Fishman MD
Professor Emeritus
Department of Ophthalmology
University of Illinois at Chicago
Chicago, IL, USA
Director, The Pangere Center for Hereditary Retinal Diseases
Chicago, IL, USA

Monika Fleckenstein MD
Consultant
Department of Ophthalmology
University of Bonn
Bonn, Germany

Harry W. Flynn Jr., MD
J. Donald M. Gass Chair in Ophthalmology
Bascom Palmer Eye Institute
University of Miami
Miller School of Medicine
Miami, FL, USA

Wallace S. Foulds CBE, MD, FRCS
Emeritus Professor of Ophthalmology
University of Glasgow
Glasgow UK
Senior Consultant (Research)
Singapore Eye Research Institute
Singapore National Eye Centre
Singapore

Austin R. Fox BS
Research Fellow
Laboratory of Immunology

National Eye Institute
National Institutes of Health
Bethesda, MD, USA

William R. Freeman MD
Distinguished Professor of Ophthalmology
Director of the Jacobs Retina Center
University of California, San Diego
La Jolla, CA, USA

Martin Friedlander MD, PhD
Professor
Department of Cell Biology
The Scripps Research Institute
Division of Ophthalmology
Department of Surgery
Scripps Clinic
La Jolla, CA, USA

Laura J. Frishman PhD
Professor
Department of Basic Vision Science
College of Optometry
University of Houston
Houston, TX, USA

Arthur D. Fu MD
West Coast Retina
Chief of Retina Service
Clinical Professor of Ophthalmology
California Pacific Medical Center
San Francisco, CA, USA

David M. Gamm MD, PhD
Associate Professor
Department of Ophthalmology and Visual Sciences
Emmett A. Humble Distinguished Director
McPherson Eye Research Institute
Sandra Lemke Chair in Eye Research

Waisman Center Stem Cell Research Program
University of Wisconsin
Madison, WI, USA

Enrique Garcia-Valenzuela MD, PhD
Vitreoretinal Surgeon
Midwest Retina Consultants, SC
Des Plaines, IL, USA

Sunir J. Garg MD, FACS
MidAtlantic Retina
The Retina Service of Wills Eye Hospital
Professor of Ophthalmology
Thomas Jefferson University
Philadelphia, PA, USA

Alain Gaudric MD
Emeritus Professor of Ophthalmology
Université Paris Diderot
Sorbonne Paris Cité
AP-HP, Hôpital Lariboisière
Paris, France

Mary Gayed MRes, MRCP
Specialist Registrar in Rheumatology
University Hospitals Birmingham NHS Foundation Trust
Birmingham, UK
Honorary Research Associate
Institute of Inflammation and Ageing
University of Birmingham
Birmingham, UK

Heinrich Gerding MD, FEBO, FMH
Professor of Ophthalmology
Director
Pallas Kliniken
Olten, SO, Switzerland

Andrea Giani MD

Assistant Professor
Department of Biomedical and Clinical Sciences "Luigi Sacco"
Eye Clinic – Sacco Hospital
University of Milan
Milan, Italy

Morton F. Goldberg MD
Joseph Green Professor of Ophthalmology and Director Emeritus
Wilmer Eye Institute
Johns Hopkins University
School of Medicine
Baltimore, MD, USA

Lingam Gopal MS, FRCSEd, DNBE
Consultant
Vitreo-Retinal Services
Sankara Nethralaya
Medical and Vision Research Foundations
Chennai, India

Caroline Gordon MD, FRCP
Professor of Rheumatology
Institute of Inflammation and Ageing
University of Birmingham
Birmingham, UK
Honorary Consultant Rheumatologist
Sandwell & West Birmingham
Hospitals NHS Trust
Birmingham, UK

Hiroshi Goto MD
Chirman/Professor
Department of Ophthalmology
Tokyo Medical University
Tokyo, Japan

Evangelos S. Gragoudas MD
Professor of Ophthalmology
Department of Ophthalmology

Harvard Medical School
Retina Service
Massachusetts Eye and Ear Infirmary
Boston, MA, USA

Maria B. Grant MD
Professor
Department of Pharmacology and Therapeutics
University of Florida, Gainesville
Director of Translational Research
Department of Ophthalmology
Gainesville, FL, USA

Ronald G. Gregg PhD
Professor and Chair
Department of Biochemistry & Molecular Biology
University of Louisville
Louisville, KY, USA

Kevin Gregory-Evans MD, PhD, FRCS, FRCOphth, FRCSC
Professor and Julia Levy BC Leadership Chair in Macular Research
Department of Ophthalmology and Visual Science
University of British Columbia
Vancouver, British Columbia, Canada

Carl Groenewald MD
Consultant Ophthalmologist
Department of Ophthalmology
Royal Liverpool University Hospital
Liverpool, UK

Hans E. Grossniklaus MD
Professor
Department of Ophthalmology
Emory University
School of Medicine
Atlanta, GA, USA

Sandeep Grover MD

Associate Professor, Ophthalmology
Director, Inherited Retinal Diseases & Electrophysiology
University of Florida at Jacksonville
Jacksonville, FL, USA

Vamsi K. Gullapalli MD, PhD
Associate
Central Minnesota Retina Specialists
Sartell, MN, USA

Rudolf F. Guthoff MD
Professor of Ophthalmology
Department of Ophthalmology
University of Rostock
Rostock, Germany

J. Silvio Gutkind PhD
Professor, Department of Pharmacology
Associate Director of Basic Science
Moores Cancer Center
University of California, San Diego
San Diego, CA, USA

Paul Hahn MD, PhD
NJ Retina
Teaneck, NJ, USA

Julia A. Haller MD
Ophthalmologist in Chief
Wills Eye Hospital
Philadelphia, PA, USA

James T. Handa MD
Robert Bond Welch Professor
Wilmer Eye Institute
Johns Hopkins School of Medicine
Baltimore, MD, USA

Christos Haritoglou FEBO

Chief Ophthalmologist
Herzog Carl Theodor Eye Clinic
München, Germany

Sara Haug MD, PhD
West Coast Retina
Clinical Professor of Ophthalmology
California Pacific Medical Center
San Francisco, CA, USA

Barbara S. Hawkins PhD, FSCT
Professor Emeritus of Ophthalmology (School of Medicine)
Professor of Epidemiology (Bloomberg School of Public Health)
The Wilmer Eye Institute
Johns Hopkins University
Baltimore, MD, USA

Shikun He MD
Associate Professor
Departments of Pathology and Ophthalmology
Keck School of Medicine
USC Eye Institute
University of Southern California
Los Angeles, CA, USA

Martina C. Herwig-Carl MD, FEBO
Assistant Professor
University Eye Hospital Bonn
Bonn, Germany

Florian M.A. Heussen MD
Ophthalmology Fellow
St. Paul's Eye Unit
Royal Liverpool University Hospital
Liverpool, UK

David R. Hinton MD
Gavin S. Herbert Professor of Retinal Research
Professor of Pathology and Ophthalmology

USC Roski Eye Institute
Keck School of Medicine
University of Southern California
Los Angeles, CA, USA

Nickisa M. Hodgson MD, MAS
Resident Physician
Department of Ophthalmology
UC San Diego School of Medicine
La Jolla, CA, USA

Frank G. Holz MD, FEBO
Professor, Head of Department
Department of Ophthalmology
University of Bonn
Bonn, Germany

Samuel K. Houston MD
Florida Retina Institute
Orlando, FL, USA

Yan-Nian Hui MD
Professor
Department of Ophthalmology
Xijing Hospital
Fourth Military Medical University
Xi'an, China

Mark S. Humayun MD, PhD
Cornelius J. Pings Chair in Biomedical Sciences
Director, Institute for Biomedical Therapeutics
USC Eye Institute
University of Southern California
Los Angeles, CA, USA

Yasushi Ikuno MD
Invited Professor of Ophthalmology
Osaka University
Graduate School of Medicine

Clinical Professor
Kanazawa University
Graduate School of Medicine
Director and Founder
Ikuno Eye Center
Osaka, Japan

David Isaac MD, PhD
Associate Professor
Department of Ophthalmology
Federal University of Goias
Goiania, GO, Brazil

Tatsuro Ishibashi MD, PhD
Vice Dean
Department of Ophthalmology
Kyushu University
Fukuoka City, Japan

Douglas A. Jabs MD, MBA
Professor of Ophthalmology and Professor of Medicine
Chairman Emeritus
Department of Ophthalmology
Director, Mount Sinai/New York Eye and Ear Eye and Vision Research Institute
Icahn School of Medicine at Mount Sinai
New York, NY, USA
Adjunct Professor of Epidemiology
The Johns Hopkins University
Bloomberg School of Public Health
Baltimore, MD, USA

Glenn J. Jaffe MD
Professor of Ophthalmology
Duke University Eye Center
Durham, NC, USA

Lee M. Jampol MD
Louis Feinberg Professor in Ophthalmology

Department of Ophthalmology
Northwestern University
Feinberg School of Medicine
Chicago, IL, USA

Leonard Joffe MD, MB, BCH, FCS (SA), FRCS
Retina Specialists of Southern Arizona
Tuczon, AZ, USA

Mark Johnson PhD
Professor
Departments of Biomedical Engineering Mechanical Engineering and Ophthalmology
Northwestern University
Evanston, IL, USA

Mark W. Johnson MD
Professor
Department of Ophthalmology and Visual Sciences
University of Michigan
Ann Arbor, MI, USA

Robert N. Johnson MD
West Coast Retina
Clinical Professor of Ophthalmology
California Pacific Medical Center
San Francisco, CA, USA

Antonia M. Joussen MD
Professor and Chair
Department of Ophthalmology
Charité, University Medicine Berlin
Berlin, Germany

Karina Julian MD
Uveitis Specialist
Eye Institute
Cleveland Clinic Abu Dhabi
Abu Dhabi, United Arab Emirates

J. Michael Jumper MD
West Coast Retina
Clinical Professor of Ophthalmology
California Pacific Medical Center
Co-Director, Vitreoretinal Fellowship Program
San Francisco, CA, USA

Peter K. Kaiser MD
Chaney Family Endowed Chair in Ophthalmology Research
Professor of Ophthalmology
Cleveland Clinic Lerner College of Medicine
Cleveland, OH, USA

Maarten Kamermans PhD
Professor
Retinal Signal Processing Lab
Netherlands Institute for Neuroscience
Amsterdam, The Netherlands

Anselm Kampik MD, FEBO, FARVO
Chairman Emeritus
Department of Ophthalmology
Ludwig Maximilians University
Munich, Germany

Rustum Karanjia MD, PhD
Assistant Professor
University of Ottawa Eye Institute
Ottawa Hospital Research Institute
Ottawa, ON, Canada
Researcher
Doheny Eye Institute and
Doheny Eye Centers UCLA
Department of Ophthalmology
David Geffen School of Medicine
University of California, Los Angeles
Los Angeles, CA, USA

Amir H. Kashani MD, PhD

Assistant Professor of Clinical Ophthalmology
USC Eye Institute
Department of Ophthalmology
University of Southern California
Keck School of Medicine
Los Angeles, CA, USA

Pearse A. Keane MD, MSc, FRCOphth, MRCSINIHR
Clinician Scientist and Consultant Ophthalmologist
Moorfields Eye Hospital NHS Foundation Trust and
UCL Institute of Ophthalmology
London, UK

M. Cristina Kenney MD, PhD
Professor
Director of Research
Gavin Herbert Eye Institute
Ophthalmology Research Laboratories
University of California, Irvine
Irvine, CA, USA

S. Khizer R. Khaderi MD, MPH
Adjunct Associate Professor
Moran Eye Center
University of Utah
Salt Lake City, UT, USA

Mohamad A. Khodair PhD
Pharmacology, Physiology and Neuroscience
New Jersey Medical School
Rutgers University
Newark, NJ, USA

Ivana K. Kim MD
Associate Professor of Ophthalmology
Department of Ophthalmology
Harvard Medical School
Retina Service
Massachusetts Eye and Ear Infirmary

Boston, MA, USA

Jonathan W. Kim MD
Director of Retinoblastoma Service
Children's Hospital Los Angeles
Associate Professor of Ophthalmology
USC Keck School of Medicine
Los Angeles, CA, USA

Tae Wan Kim MD, PhD
Associate Professor
Department of Ophthalmology
Seoul National University
Seoul, South Korea

Bernd Kirchhof MD
Department of Vitreo-Retinal Surgery
Center of Ophthalmology
University of Cologne
Cologne, Germany

Szilard Kiss MD
Department of Ophthalmology
Weill Cornell Medical College
New York-Presbyterian Hospital
New York, NY, USA

Barbara E.K. Klein MD, MPH
Professor
Department of Ophthalmology and Visual Sciences
University of Wisconsin
School of Medicine and Public Health
Madison, WI, USA

Ronald Klein MD, MPH
Professor
Department of Ophthalmology and Visual Sciences
University of Wisconsin
School of Medicine and Public Health

Madison, WI, USA

Michael A. Klufas MD
Retina Division
Stein Eye Institute
University of California, Los Angeles
Los Angeles, CA, USA

Anton M. Kolomeyer MD, PhD
Resident
Eye and Ear Institute
University of Pittsburgh Medical Center
Pittsburgh, PA, USA

Lazaros Konstantinidis MD
Hôpital Ophtalmique Jules-Gonin
University of Lausanne
Lausanne, Switzerland

Renu Kowluru PhD, FARVO
Professor
Ophthalmology, Anatomy/Cell Biology & Endocrinology
Wayne State University
Kresge Eye Institute
Detroit, MI, USA

Igor Kozak MD, PhD
Senior Academic Consultant
King Khaled Eye Specialist Hospital
Riyadh, Saudi Arabia

Baruch D. Kuppermann MD
Professor of Ophthalmology and Biomedical Engineering
University of California, Irvine
The Gavin Herbert Eye Institute
University of California, Irvine
Irvine, CA, USA

Ajay E. Kuriyan MD, MSc

Assistant Professor, Ophthalmology
University of Rochester
School of Medicine and Dentistry
Rochester, NY, USA

Leanne T. Labriola MD
Clinical Assistant Professor of Ophthalmology
Medical Retina Service
University of Pittsburgh
School of Medicine
Pittsburgh, PA, USA

Dennis Lam MD
Director
Dennis Lam & Partners Eye Center
Central, Hong Kong
Director
C-MER (Shenzhen) Dennis Lam Eye Hospital
Shenzhen, China
Director
State Key Laboratory (Ophthalmology)
Sun Yat-Sen University
Guangzhou, China

Linda A. Lam MD, MBA
Associate Professor
Vice Chair of Clinical Satellite Affairs
USC Roski Eye Institute
Department of Ophthalmology
USC Keck School of Medicine
Los Angeles, CA, USA

Anne Marie Lane MPH
Instructor in Ophthalmology
Department of Ophthalmology
Harvard Medical School
Retina Service
Massachusetts Eye and Ear Infirmary
Boston, MA, USA

Erin B. Lavik ScD
Professor
Department of Chemical, Biochemical, and Environmental Engineering
University of Maryland
Baltimore, MD, USA

James F. Leary PhD
Professor Emeritus
Purdue University
West Lafayette, IN, USA

Richard W.J. Lee BMedSci (Hons), BMBS, MRCS (Eng), MRCOphth, PhD
Consultant Senior Lecturer
University of Bristol
Bristol, UK
Lead for Experimental Medicine (Inflammation and Immunotherapy)
National Institute for Health Research Biomedical Research Centre at Moorfields Eye Hospital NHS Foundation Trust
UCL Institute of Ophthalmology
London, UK

Sun Young Lee MD, PhD
Vitreoretinal Surgery Fellow
Department of Ophthalmology
University of Iowa
Iowa City, IA, USA

Thomas C. Lee MD
Associate Professor of Ophthalmology
Vision Center, Children's Hospital Los Angeles and USC Eye Institute
Los Angeles, CA, USA

Vincent Lee FRCSEd, FCSHK
Faculty
Dennis Lam & Partners Eye Center

Central
Hong Kong, China

Loh-Shan B. Leung MD
Clinical Assistant Professor of Ophthalmology
Department of Ophthalmology
Stanford University School of Medicine
Palo Alto, CA, USA

Geoffrey P. Lewis PhD
Research Biologist
Neuroscience Research Institute
University of California, Santa Barbara
Santa Barbara, CA, USA

Anita Leys MD, PhD
Professor of Ophthalmology
Department of Medical Retina
Department of Ophthalmology
Catholic University of Leuven
Leuven, Belgium

Xiaoxin Li MD
Professor of Ophthalmology
Xiamen Eye Center of Xiamen University
Xiamen, China

Sandra Liakopoulos MD
Professor of Ophthalmology
Department of Ophthalmology
University of Cologne
Cologne, Germany

Chang-Ping Lin MD
Lecturer
Department of Ophthalmology
National Taiwan University
College of Medicine
National Taiwan University Hospital

Taipei, Taiwan

Phoebe Lin MD, PhD
Assistant Professor of Ophthalmology
Casey Eye Institute
Oregon Health and Science University
Portland, OR, USA

Enchun M. Liu MD
Vitreoretinal Surgeon
Retina Associates of South Texas
San Antonio, TX, USA

Shirley Liu PhD
Resident
C-MER (Shenzhen) Dennis Lam Eye Hospital
Shenzhen, China

Noemi Lois MD, PhD, FRCSEd, FRCOphth
Clinical Professor of Ophthalmology
Queen's University
Honorary Consultant Ophthalmic Surgeon
The Belfast Health and Social Care Trust
Belfast, Northern Ireland, UK

Nikolas J.S. London MD, FACS
Retina Consultants San Diego
Poway, CA, USA

Lin Lu PhD
Professor
Zhongshan Ophthalmic Center
Sun Yat-Sen University
Guangzhou, China

Brandon J. Lujan MD
West Coast Retina
Clinical Professor of Ophthalmology
California Pacific Medical Center

San Francisco, CA, USA
Assistant Clinical Professor
University of California, San Francisco
San Francisco, CA, USA

Yan Luo MD, PhD
Professor, Retina Division
Zhongshan Ophthalmic Center
Sun Yat-Sen University
Guangzhou, Guangdong, China

Gerard A. Lutty PhD
G. Edward and G. Britton Durell Professor of Ophthalmology
Wilmer Eye Institute
Johns Hopkins University
School of Medicine
Baltimore, MD, USA

Robert MacLaren FRCOphth
Professor of Ophthalmology
Nuffield Laboratory of Ophthalmology
Department of Clinical Neurosciences
University of Oxford
Oxford University Eye Hospital
Oxford, UK
Honorary Consultant Vitreoretinal Surgeon
Moorfields Eye Hospital
London, UK

Steven Madreperla MD, PhD
Assistant Clinical Professor
Institute of Ophthalmology and Visual Science
New Jersey Medical School
Rutgers University
Newark, NJ, USA

Albert M. Maguire MD
Professor
Co-Director of Center for Advanced Retinal and Ocular

Therapeutics (CAROT)
Department of Ophthalmology
Scheie Eye Institute
University of Pennsylvania
Perelman School of Medicine
Philadelphia, PA, USA

Martin A. Mainster PhD, MD, FRCOphth
Luther and Ardis Fry Professor Emeritus of Ophthalmology
University of Kansas
School of Medicine
Kansas City, KS, USA

Nancy C. Mansfield (posthumously)
Retinoblastoma service
Children's Hospital Los Angeles
Los Angeles, CA, USA

Arnold M. Markoe MD, ScD
Professor and Chairman Emeritus
Department of Radiation Oncology
University of Miami
Sylvester Comprehensive Cancer Center
Miami, FL, USA

Michael F. Marmor MD
Professor of Ophthalmology
Department of Ophthalmology and Byers Eye Institute
Stanford University School of Medicine
Palo Alto, CA, USA

Daniel F. Martin MD
Professor and Chairman
Cleveland Clinic Cole Eye Institute
Cleveland, OH, USA

Stephen C. Massey PhD
Elizabeth Morford Professor and Research Director
Department of Ophthalmology and Visual Science

University of Texas Medical School
Houston, TX, USA

Maureen A. McCall PhD
Professor
Department of Ophthalmology and Visual Sciences
University of Louisville
Louisville, KY, USA

Tara A. McCannel MD, PhD
Assistant Professor
Director of Ophthalmic Oncology Center
Department of Ophthalmology
The Jules Stein Eye Institute
University of California, Los Angeles
Los Angeles, CA, USA

J. Allen McCutchan MD, MAS
Professor of Medicine
Medical Center
University of California, San Diego
San Diego, CA, USA

H. Richard McDonald MD
West Coast Retina
Clinical Professor of Ophthalmology
California Pacific Medical Center
Co-Director, Vitreoretinal Fellowship Program
San Francisco, CA, USA

Petra Meier MD
Associate Professor
Department of Ophthalmology
University of Leipzig
Leipzig, Germany

Travis A. Meredith MD
Professor and Chair Emeritus
Department of Ophthalmology

University of North Carolina, Chapel Hill
Chapel Hill, NC, USA

Carsten H. Meyer MD, FEBO, FMH
Professor of Ophthalmology
Head of the Department
Department of Ophthalmology
Pallas Clinics
Aarau, AR, Switzerland

William F. Mieler MD
Cless Family Professor and Vice-Chairman
Illinois Eye and Ear Infirmary
Department of Ophthalmology and Visual Sciences
University of Illinois, Chicago
Chicago, IL, USA

Joan W. Miller MD
Henry Willard Williams Professor of Ophthalmology
Chief of Ophthalmology
Mass Eye and Ear and Massachusetts General Hospital
Chair, Department of Ophthalmology
Harvard Medical School
Boston, MA, USA

Rukhsana G. Mirza MD
Associate Professor
Department of Ophthalmology
Northwestern University
Feinberg School of Medicine
Chicago, IL, USA

Sayak K. Mitter PhD
Research Fellow
Department of Ophthalmology
Indiana University School of Medicine
Indianapolis, IN, USA

Robert A. Mittra MD

Assistant Clinical Professor
University of Minnesota
Minneapolis, MN, USA

Yozo Miyake MD, PhD
Chairman of the Board of Directors
Aichi Medical University
Aichi, Japan

Carlo Montemagno PhD
Director, Ingenuity Lab
Professor of Chemical Engineering and Material Science
University of Alberta
Edmonton, Alberta, Canada

Anthony T. Moore MD
Professor of Ophthalmology
Department of Ophthalmology
University of California, San Francisco
San Francisco, CA, USA

Prithvi Mruthyunjaya MD, MHS
Associate Professor of Ophthalmology
Director, Ocular Oncology Service
Byers Eye Institute
Stanford University
Palo Alto, CA, USA

Cristina Muccioli MD, PhD
Associate Professor of Ophthalmology
Department of Ophthalmology
Federal University of São Paulo
São Paulo, Brazil

Robert F. Mullins PhD
Professor
Department of Ophthalmology and Visual Sciences
Wynn Institute for Vision Research
University of Iowa

Iowa City, IA, USA

A. Linn Murphree MD
Professor Emeritus
Children's Hospital Los Angeles
USC Keck School of Medicine
Los Angeles, CA, USA

Robert P. Murphy MD
Retina Group of Washington
Washington, DC, USA

Philip I. Murray PhD, FRCP, FRCS, FRCOphth
Professor of Ophthalmology
Institute of Inflammation and Ageing
University of Birmingham
Birmingham, UK
Honorary Consultant Ophthalmologist
Sandwell & West Birmingham Hospitals NHS Trust
Birmingham, UK

Timothy G. Murray MD, MBA, FACS
Director, Miami Ocular Oncology and Retina
Miami, FL, USA
Professor
Department of Ophthalmology
Bascom Palmer Eye Institute
Miami, FL, USA

Manish Nagpal MS, DO, FRCS(UK)
Vitreoretinal Consultant
Retina Foundation
Shahibag, Ahmedabad, India

Perumalsamy Namperumalsamy MS, FAMS
Chairman Emeritus and Professor of Ophthalmology
Retina-Vitreous Service
Aravind Eye Care System
Madurai, Tamil Nadu, India

Sumit K. Nanda MD
Clinical Associate Professor
Department of Ophthalmology
Integris Baptist Medical Center
Oklahoma City, OK, USA

Hossein Nazari MD
Department of Ophthalmology and Visual Sciences
University of Texas Medical Branch
Galveston, TX, USA

Quan Dong Nguyen MD, MSc
Professor of Ophthalmology
Byers Eye Institute
Stanford University
Palo Alto, CA, USA
Ocular Imaging Research and Reading Center
Menlo Park, CA, USA

Robert B. Nussenblatt MD, MPH (posthumously)
Chief
Laboratory of Immunology
National Eye Institute, NIH
Bethesda, MD, USA

Patrick Oellers MD
Vitreoretinal Surgery Fellow
Harvard Medical School
Department of Ophthalmology
Massachusetts Eye and Ear
Boston, MA, USA

Masahito Ohji MD
Professor and Chairman
Department of Ophthalmology
Shiga University of Medical Science
Otsu, Shiga, Japan

Kyoko Ohno-Matsui MD, PhD

Professor
Department of Ophthalmology and Visual Sciences
Tokyo Medical and Dental University
Tokyo, Japan

Daniel Palanker PhD
Professor
Department of Ophthalmology
Hansen Experimental Physics Laboratory
Stanford University
Stanford, CA, USA

Thanos D. Papakostas MD
Retina Fellow
Massachusetts Eye and Ear
Harvard Medical School
Boston, MA, USA

Avni V. Patel MD, MBA
Massachusetts Eye and Ear Infirmary
Department of Ophthalmology
Harvard Medical School
Boston, MA, USA

Purnima S. Patel MD
Associate Professor of Ophthalmology
Emory Unviersity
School of Medicine
Atlanta Veterans Affairs Medical Center
Atlanta, GA, USA

Anna C. Pavlick MD
Professor of Medicine and Dermatology
Department of Medicine
New York University
School of Medicine
New York, NY, USA

S. Louise Pay BSc

Graduate Student
Department of Ophthalmology
Indiana University
School of Medicine
Indianapolis, IN, USA

David M. Peereboom MD
Professor of Medicine and Director of Clinical Research
The Rose Ella Burkhardt Brain Tumor and Neuro-Oncology Center
Cleveland Clinic
Cleveland, OH, USA

Mark E. Pennesi MD, PhD
Associate Professor
Department of Ophthalmology
Casey Eye Institute
Oregon Health & Science University
Portland, OR, USA

Jay S. Pepose MD, PhD
Medical Director
PeposeVision Institute
Professor of Clinical Ophthalmology
Washington University
School of Medicine
St. Louis, MO, USA

Julian D. Perry MD
Director
Orbital and Oculoplastic Surgery
Cole Eye Institute
Cleveland Clinic Foundation
Cleveland, OH, USA

Polly A. Quiram MD, PhD
Vitreoretinal Surgery, PA
Minneapolis, MN, USA

Rajiv Raman MS, DNB

Consultant
Department of Vitreo-Retinal Services
Sankara Nethralaya
Chennai, India

Rajeev S. Ramchandran MD, MBA
Associate Professor
Department of Ophthalmology
Flaum Eye Institute
University of Rochester
School of Medicine and Dentistry
Rochester, NY, USA

P. Kumar Rao MD
Associate Professor of Ophthalmology and Visual Sciences
Department of Ophthalmology
School of Medicine
Washington University in St Louis
St Louis, MO, USA

Narsing A. Rao MD
Professor of Ophthalmology and Pathology
USC Eye Institute
Keck School of Medicine
University of Southern California
Los Angeles, CA, USA

Sivakumar R. Rathinam FAMS, PhD
Professor of Ophthalmology
Head of Uveitis Service
Uveitis Service
Aravind Eye Hospital & Postgraduate Institute of Ophthalmology
Madurai, India

Franco M. Recchia MD
Vitreoretinal Surgeon
Tennessee Retina, PC
Nashville, TN, USA

Kristin J. Redmond MD, MPH
Assistant Professor
Department of Radiation Oncology and Molecular Radiation Sciences
Johns Hopkins University
School of Medicine
Baltimore, MD, USA

David Reed MD
Attending Physician
Ophthalmic Consultants of Boston
Boston, MA, USA

Thomas A. Reh PhD
Professor
Department of Biological Structure
University of Washington
School of Medicine
Seattle, WA, USA

Andreas Reichenbach MD
Professor
Paul Flechsig Institute of Brain Research
University of Leipzig
Faculty of Medicine
Leipzig, Germany

Kourous A. Rezaei MD
Senior Partner, Illinois Retina Associates
Director of Vitreoretinal Fellowship
Associate Professor of Ophthalmology
Rush University Medical Center
Chicago, IL, USA

William R. Rhoades MD
Associated Retinal Consultants
Grand Rapids, MI, USA

Benjamin Rhodes MD

Consultant Rheumatologist
University Hospitals Birmingham NHS Foundation Trust
Birmingham, UK

Robert Ritch MD
Shelley and Steven Einhorn Distinguished Chair
Professor of Ophthalmology
Surgeon Director Emeritus and Chief, Glaucoma Services
The New York Eye and Ear Infirmary of Mount Sinai
New York, NY, USA

Anthony G. Robson PhD
Consultant Electrophysiologist & Honorary Senior Lecturer
Moorfields Eye Hospital & Institute of Ophthalmology
University College London
London, UK

Philip J. Rosenfeld MD, PhD
Professor of Ophthalmology
Bascom Palmer Eye Institute
Department of Ophthalmology
University of Miami
Miller School of Medicine
Miami, FL, USA

Teisha J. Rowland PhD
Postdoctoral Fellow
Cardiovascular Institute and Adult Medical Genetics Program
University of Colorado
Denver Anschutz Medical Campus
Aurora, CO, USA

Gary S. Rubin PhD
Helen Keller Professor of Ophthalmology
Department of Visual Neuroscience
UCL Institute of Ophthalmology
London, UK

SriniVas R. Sadda MD

President and Chief Scientific Officer
Doheny Eye Institute
Professor of Ophthalmology
David Geffen School of Medicine
University of California, Los Angeles
Los Angeles, CA, USA

Alfredo A. Sadun MD, PhD
Thornton Professor of Vision
Doheny Eye Institute
Professor and Vice-Chair
Department of Ophthalmology
For Doheny Eye Centers
David Geffen School of Medicine
University of California, Los Angeles
Los Angeles, CA, USA

Alapakkam P. Sampath PhD
Associate Professor
Jules Stein Eye Institute
Department of Ophthalmology
David Geffen School of Medicine
University of California, Los Angeles
Los Angeles, CA, USA

Amit A. Sangave MD
PGY-4 Ophthalmology Resident
Department of Ophthalmology
Flaum Eye Institute
University of Rochester
School of Medicine and Dentistry
Rochester, NY, USA

Andrew P. Schachat MD
Vice Chairman
Cole Eye Institute
Cleveland Clinic Foundation
Cleveland, OH, USA

Sid Schechet MD
Department of Ophthalmology and Vision Sciences
University of Maryland
School of Medicine
Baltimore, MD, USA

Steffen Schmitz-Valckenberg MD, FEBO
Professor, Senior Consultant
Department of Ophthalmology
University of Bonn
Bonn, Germany

Stephen G. Schwartz MD, MBA
Associate Professor and Medical Director, Naples
Bascom Palmer Eye Institute
University of Miami
Miller School of Medicine
Naples, FL, USA

Adrienne W. Scott MD
Assistant Professor of Ophthalmology
Retina Division, Wilmer Eye Institute
Johns Hopkins University
School of Medicine
Baltimore, MD, USA

J. Sebag MD, FACS, FRCOphth, FARVO
Founding Director
VMR Institute for Vitreous Macula Retina
Huntington Beach, CA, USA

Johanna M. Seddon MD, ScM
Founding Director, Ophthalmic Epidemiology and Genetics Service
New England Eye Center
Tufts Medical Center
Professor of Ophthalmology
Professor in Department of Medicine
Tufts University School of Medicine
Professor, Tufts Clinical and Translational Science Institute

Tufts University
Boston, MA, USA

Michael I. Seider MD
Ocular Oncology and Vitreoretinal Surgery
The Permanente Medical Group
San Francisco, CA, USA

H. Nida Sen MD, MHS
Director, Uveitis and Ocular Immunology Fellowship Program
National Eye Institute
National Institutes of Health
Bethesda, MD, USA

Yasir Jamal Sepah MBBS
Senior Research Scientist
Byers Eye Institute
Stanford University
Palo Alto, CA, USA
Director
Ocular Imaging Research and Reading Center
Menlo Park, CA, USA

Sanjay Sharma MD, MSc(Epid), MBA
Professor of Ophthalmology and Epidemiology
Queen's Medical College
Kingston, Ontario, Canada

Tarun Sharma MD, FRCSEd, MBA
Professor of Ophthalmology
Director, Shri Bhagwan Mahavir Vitreoretinal Services
Sankara Nethralaya
Medical Research Foundation
Chennai, India

Shwu-Jiuan Sheu MD
Professor
Department of Ophthalmology
Kaohsiung Veterans General Hospital

Kaohsiung
National Yang Ming University
Taipei, Taiwan

Carol L. Shields MD
Co-Director, Ocular Oncology Service
Wills Eye Hospital
Thomas Jefferson University
Philadelphia, PA, USA

Jerry A. Shields MD
Co-Director, Ocular Oncology Service
Wills Eye Hospital
Thomas Jefferson University
Philadelphia, PA, USA

Kei Shinoda MD, PhD
Professor
Department of Ophthalmology
Saitama Medical University
Faculty of Medicine
Saitama, Japan

Dhananjay Shukla MS, MAMS
Senior Consultant and Director
Retina-Vitreous Service
Ratan Jyoti Netralaya
Gwalior, Madhya Pradesh, India

Paul A. Sieving MD, PhD
Director
National Eye Institute
National Institutes of Health
Bethesda, MD, USA

Paolo S. Silva MD
Assistant Professor of Ophthalmology
Harvard Medical School
Staff Ophthalmologist and Assistant Chief of Telemedicine

Beetham Eye Institute
Joslin Diabetes Center
Boston, MA, USA

Claudio Silveira MD, PhD
Department of Ophthalmology
Federal University of São Paulo
São Paulo, Brazil

Joshua Singer PhD
Associate Professor
Department of Biology
University of Maryland
College Park, MD, USA

Arun D. Singh MD
Professor of Ophthalmology and Director of Ophthalmic Oncology
Cole Eye Institute, Cleveland Clinic
Cleveland, OH, USA

Alison Skalet MD, PhD
Assistant Professor of Ophthalmology
Casey Eye Institute
Oregon Health and Science University
Portland, OR, USA

Mario Skugor MD, FACE
Associated Professor of Medicine at CCLCM of CWRU
Endocrinology and Metabolism
Cleveland Clinic
Cleveland, OH, USA

Sylvia B. Smith PhD, FARVO
Regents' Professor and Chair
Department of Cellular Biology/Anatomy
Medical College of Georgia
Professor of Ophthalmology
Co-Director James and Jean Culver Vision Discovery Institute
Augusta University

Augusta, GA, USA

Lucia Sobrin MD, MPH
Associate Professor of Ophthalmology
Massachusetts Eye and Ear Infirmary
Harvard Medical School
Boston, MA, USA

Akrit Sodhi MD, PhD
Assistant Professor
Retina Division
Wilmer Eye Institute
Johns Hopkins School of Medicine
Baltimore, MD, USA

Elliott H. Sohn MD
Associate Professor
Director, Retina Fellowships
Department of Ophthalmology and Visual Sciences
Wynn Institute for Vision Research
University of Iowa
Iowa City, IA, USA

Gisèle Soubrane-Daguet MD, PhD
Professor of Ophthalmology
Department of Ophthalmology
University of Paris V
Paris, France

Leigh Spielberg MD, FEBO
Vitreoretinal Surgeon
Department of Ophthalmology
Ghent University Hospital
Ghent, Belgium

Sunil K. Srivastava MD
Staff Physician
Cole Eye Institute
Cleveland Clinic Foundation

Cleveland, OH, USA

Oliver Stachs PhD
Professor of Experimental Ophthalmology
Department of Ophthalmology
University of Rostock
Rostock, Germany

Giovanni Staurenghi MD, FARVO
Professor of Ophthalmology
Chairman Eye Clinic
Director, Residency Program
Department of Biomedical and Clinical Sciences "Luigi Sacco"
Sacco Hospital
University of Milan
Milan, Italy

Paul Sternberg Jr., MD
G. W. Hale Professor and Chair
Vanderbilt Eye Institute
Chief Medical Officer
Vanderbilt Medical Group
Chief Patient Experience Officer
Associate Dean for Clinical Affairs
Assistant Vice Chancellor for Adult Health Affairs
Nashville, TN, USA

Jay M. Stewart MD
Associate Professor of Ophthalmology
University of California, San Francisco
Chief of Ophthalmology
San Francisco General Hospital
San Francisco, CA, USA

Alan Stitt PhD
Professor and McCauley Chair of Experimental Ophthalmology
Centre for Experimental Medicine
Queen's University Belfast
Belfast, Northern Ireland, UK

Edwin M. Stone MD, PhD
Professor
Director, Wynn Institute for Vision Research
Department of Ophthalmology and Visual Sciences
University of Iowa
Iowa City, IA, USA

Ilene K. Sugino MA
Principal Research Associate
Institute of Ophthalmology and Visual Science
New Jersey Medical School
Rutgers University
Newark, NJ, USA

Lori S. Sullivan PhD
Faculty Associate
Human Genetics Center
School of Public Health
University of Texas Health Science Center
Houston, TX, USA

Paul Sullivan MBBS, MD, FRCOphth
Consultant Ophthalmic Surgeon
Director of Education
Moorfields Eye Hospital
London, UK

Jennifer K. Sun MD, MPH
Associate Professor of Ophthalmology
Harvard Medical School
Staff Ophthalmologist and Chief
Center for Clinical Eye Research and Trials
Beetham Eye Institute
Joslin Diabetes Center
Boston, MA, USA

Janet S. Sunness MD
Medical Director
Richard E. Hoover Low Vision Rehabilitation Services

Greater Baltimore Medical Center
Clinical Professor, Department of Ophthalmology and Vision Sciences
University of Maryland
School of Medicine
Baltimore, MD, USA

R.C. Andrew Symons MBBS, PhD, FRANZCO
Head of Ophthalmology
Royal Melbourne Hospital
Clinical Associate Professor
University of Melbourne
Melbourne, VIC, Australia

Ramin Tadayoni MD, PhD
Professor of Ophthalmology
Université Paris Diderot
Sorbonne Paris Cité
AP-HP, Hôpital Lariboisière
Chairman of the Department of Ophthalmology
Paris, France

Shibo Tang MD, PhD
Professor of Ophthalmology
Dean, Aier School of Ophthalmology
Central South University
Director, Aier Eye Institute
Aier Eye Hospital Group
Changsha, Hunan, China

Hiroko Terasaki MD
Professor and Chair
Department of Ophthalmology
Nagoya University
Graduate School of Medicine
Nagoya, Japan

Aristomenis Thanos MD
Associated Retinal Consultants

William Beaumont Hospital
Royal Oak, MI, USA

Matthew A. Thomas MD
Clinical Professor of Ophthalmology
The Retina Institute
Washington University
St Louis, MO, USA

John T. Thompson MD
Partner, Retina Specialists
Department of Ophthalmology
Greater Baltimore Medical Center
Baltimore, MD, USA

Cynthia A. Toth MD
Joseph A.C. Wadsworth Professor of Ophthalmology
Professor of Biomedical Engineering
Duke University Medical Center
Durham, NC, USA

Brian Toy MD
Department of Ophthalmology
Stanford University School of Medicine
Palo Alto, CA, USA

Michael T. Trese MD
Professor of Ophthalmology
Oakland University
William Beaumont School of Medicine
Associated Retinal Consultants
Royal Oak, MI, USA

Julie H. Tsai MD
Assistant Professor of Clinical Ophthalmology
Albany, NY, USA

Nitin Udar PhD
Gavin Herbert Eye Institute

Ophthalmology Research Laboratories
University of California, Irvine
Irvine, CA, USA

J. Niklas Ulrich MD
Assistant Professor of Ophthalmology
Department of Ophthalmology
University of North Carolina, Chapel Hill
Chapel Hill, NC, USA

Allison C. Umfress MD
Vanderbilt Eye Institute
Vanderbilt University Medical Center
Nashville, TN, USA

Russell N. Van Gelder MD, PhD
Professor and Boyd K. Bucey Memorial Chair
Department of Ophthalmology
Adjunct Professor
Departments of Biological Structure and Pathology
University of Washington
School of Medicine
Seattle, WA, USA

Jan C. van Meurs MD, PhD
The Rotterdam Eye Hospital
Erasmus University
Rotterdam, The Netherlands

Daniel Vítor Vasconcelos-Santos MD, PhD
Adjunct Professor of Ophthalmology
Universidade Federal de Minas Gerais
Hospital São Geraldo / HC-UFMG
Belo Horizonte, MG, Brazil

Demetrios G. Vavvas MD, PhD
Associate Professor of Ophthalmology
Massachusetts Eye & Ear Infirmary
Department of Ophthalmology

Harvard Medical School
Boston, MA, USA

G. Atma Vemulakonda MD
Chief of Vitreoretinal Surgery
Department of Ophthalmology
Palo Alto Medical Foundation
Palo Alto, CA, USA

Nadia K. Waheed MD, MPH
Associate Professor of Ophthalmology
New England Eye Center
Department of Ophthalmology
Tufts University School of Medicine
Boston, MA, USA

James Weiland PhD
Professor
Department of Biomedical Engineering
University of Michigan
Ann Arbor, MI, USA

Richard G. Weleber MD
Department of Ophthalmology
Casey Eye Institute
Oregon Health & Science University
Portland, OR, USA

Adam S. Wenick MD, PhD
Assistant Professor of Ophthalmology
The Wilmer Eye Institute
Johns Hopkins University
Baltimore, MD, USA

Moody D. Wharam Jr., MD
Professor of Radiation Oncology
Department of Radiation Oncology and Molecular Radiation Sciences
The Sidney Kimmel Comprehensive Cancer Center

Johns Hopkins CRB II
Baltimore, MD, USA

Louisa Wickham FRCOphth, MSc, MD
Clinical Director
Consultant Ophthalmologist
Department of Vitreoretinal Surgery
Moorfields Eye Hospital
London, UK

Peter Wiedemann MD
Professor and Chair
Department of Ophthalmology
University of Leipzig
Leipzig, Germany

Henry E. Wiley MD
Staff Clinician
Division of Epidemiology and Clinical Applications
National Eye Institute
National Institutes of Health
Bethesda, MD, USA

C.P. Wilkinson MD
Distinguished Emeritus Chairman
Department of Ophthalmology
Greater Baltimore Medical Center
Professor, Department of Ophthalmology
John Hopkins University
Baltimore, MD, USA

David Wilson MD
Professor and Chair of Ophthalmology
Director, Casey Eye Institute
Oregon Health & Science University
Portland, OR, USA

Sebastian Wolf MD, PhD
Department of Ophthalmology

Inselspital, Bern University Hospital
University of Bern
Bern, Switzerland

Thomas J. Wolfensberger MD, MBA
Hôpital Ophtalmique Jules-Gonin
University of Lausanne
Lausanne, Switzerland

David Wong FRCOphth
Honorary Clinical Professor
Department of Ophthalmology, LKS
Faculty of Medicine
The University of Hong Kong
Hong Kong, China

Ian Y. Wong FRCOphth
Clinical Assistant Professor
Department of Ophthalmology, LKS
Faculty of Medicine
The University of Hong Kong
Hong Kong, China

Tien Y. Wong MD, PhD
Professor & Medical Director, Singapore National Eye Center
Chair of Ophthalmology & Vice-Dean of Clinical Sciences
Duke-NUS Medical School
National University of Singapore

Frances Wu BS
Medical Student
UC San Diego School of Medicine
La Jolla, CA, USA

Yanors Yandiev MD, PhD
Department of Ophthalmology
University of Leipzig
School of Medicine
Leipzig, Germany

Chang-Hao Yang MD, PhD
Professor
Department of Ophthalmology
National Taiwan University
College of Medicine
National Taiwan University Hospital
Taipei, Taiwan

Chung-May Yang MD
Professor
Department of Ophthalmology
National Taiwan University
College of Medicine
National Taiwan University Hospital
Taipei, Taiwan

Lawrence A. Yannuzzi MD
Vitreous-Retina-Macula Consultants of New York
New York Eye and Ear Infirmary
New York, NY, USA

Po-Ting Yeh MD, MMS
Clinical Assistant Professor
Department of Ophthalmology
National Taiwan University
College of Medicine
National Taiwan University Hospital
Taipei, Taiwan

Yoshihiro Yonekawa MD
Massachusetts Eye and Ear Infirmary
Boston Children's Hospital
Harvard Medical School
Boston, MA, USA

Young Hee Yoon MD, PhD
Professor
Department of Ophthalmology
Asan Medical Center

University of Ulsan College of Medicine
Seoul, Korea

Hyeong Gon Yu MD, PhD
Professor
Department of Ophthalmology
Seoul National University
Seoul, South Korea

Marco A. Zarbin MD, PhD
Professor and Chair
Institute of Ophthalmology and Visual Science
New Jersey Medical School
Rutgers University
Newark, NJ, USA

Kang Zhang MD, PhD
Professor of Ophthalmology
Department of Ophthalmology
UC San Diego School of Medicine
La Jolla, CA, USA

Jie Zhu MD, PhD
Department of Ophthalmology
UC San Diego School of Medicine
La Jolla, CA, USA

Martin Zinkernagel MD, PhD
Department of Ophthalmology
Inselspital, Bern University Hospital
University of Bern
Bern, Switzerland

Video Contributors

Arturo Alezzandrini MD, PhD
Chairman of Ophthalmology
Oftalmos Instituto Oftalmologico de Alta Complejidad
Chairman of Ophthalmology
Hospital Luis Federico Leloir
University of Buenos Aires
Buenos Aires, Argentina

J. Fernando Arevalo MD, FACS
Edmund F. and Virginia B. Ball Professor of Ophthalmology
Chairman, Department of Ophthalmology
Johns Hopkins Bayview Medical Center
Retina Division, Wilmer Eye Institute
The Johns Hopkins University
School of Medicine
Baltimore, MD, USA

Jose Garcia Arumi MD
Professor and Chairman of Ophthalmology
Instituto de Microcirugia Ocular IMO
Universidad Autonoma de Barcelona
Hospital Universitario Valle Hebrón
Barcelona, Spain

G.W. Aylward FRCOphth, FRCS, MD
Consultant Ophthalmologist
Department of Vitreoretinal Surgery
Moorfields Eye Hospital

London, UK

Jean Bennett MD, PhD
Professor
Co-Director of Center for Advanced Retinal and Ocular Therapeutics (CAROT)
Department of Ophthalmology
Scheie Eye Institute
Department of Cell and Developmental Biology
University of Pennsylvania
Perelman School of Medicine
Philadelphia, PA, USA

Maria H. Berrocal MD
Director Berrocal & Associates
University of Puerto Rico
San Juan, Puerto Rico

Carl Claes MD
Head of Vitreoretinal Surgery
St Augustinus Hospital
Antwerp, Belgium

Ian J. Constable FRANZCO, FRCSE, DSc(hon)
Professor of Ophthalmology
Lions Eye Institute
University of Western Australia
Perth, Australia

Bertil E. Damato MD, PhD
Professor of Ophthalmology and Radiation Oncology
University of California, San Francisco
San Francisco, CA, USA

Renaud Duval MD, FRCSC
Assistant Professor of Ophthalmology
Department of Ophthalmology
University of Montreal
Montreal, Quebec,

Canada

Justis P. Ehlers MD
The Norman C. and Donna L. Harbert Endowed Chair for Ophthalmic Research
Cole Eye Institute
Cleveland Clinic
Cleveland, OH, USA

Alain Gaudric MD
Emeritus Professor of Ophthalmology
Université Paris Diderot
Sorbonne Paris Cité
Ophthalmology Department
AP-HP, Hopital Lariboisière
Paris, France

Andre V. Gomes MD, PhD
Colaborator Professor
Department of Ophthalmology
University of São Paulo
Director Retina Department
OSC Institute
São Paulo, Brazil

Stratos Gotzaridis MD
Vitreoretinal Consultant
Head of "My Retina Eye Center of Athens"
Director of the Surgical Retina
Department of OMMA Ophthalmic Institute of Athens
Athens, Greece

Albert M. Maguire MD
Professor
Co-Director of Center for Advanced Retinal and Ocular Therapeutics (CAROT)
Department of Ophthalmology
Scheie Eye Institute
University of Pennsylvania

Perelman School of Medicine
Philadelphia, PA, USA

Kazuaki Kadonosono MD
Professor and Chair
Department of Ophthalmology and Micro-technology
Yokohama City University
Medical School
Yokohama, Japan

Manish Nagpal MS, DO, FRCS(UK)
Vitreoretinal Consultant
Retina Foundation
Shahibag, Ahmedabad, India

Yusuke Oshima MD, PhD
Founder and Director
Vitreoretina & Cataract Surgery Center
Oshima Eye Clinic
Osaka, Japan
Managing Partner and Surgeon-in-Chief
Cataract & Refractive Surgery Center
Kawasaki Eye Clinic
Adviser, Consultant Ophthalmologist & Vitreoretinal Surgeon
Nishikasai Inouye Eye Hospital
Tokyo, Japan
Visiting Professor of Ophthalmology
Nankai University
Tianjin, China

Grazia Pertile MD
Head of Ophthalmology Department
Hospital Sacro Cuore
Verona, Italy

Ehab N. El Rayes, MD, PhD
Professor and Chair
Department of Ophthalmology
Institute of Ophthalmology

Vitreoretinal Consultant
The Retina Clinic
Cairo, Egypt

Carl D. Regillo MD, FACS
Director, Retina Service
Wills Eye Hospital
Professor of Ophthalmology
Thomas Jefferson University
Philadelphia, PA, USA

Stanislao Rizzo MD
Chairman Ophthalmology
University of Florence
Florence, Italy

Francisco J. Rodriguez MD
Chairman
Fundacion Oftalmologica Nacional
Department of Ophthalmology
University of Rosario
School of Medicine
Bogota, DC, Colombia

Paul Sullivan MBBS, MD, FRCOphth
Consultant Ophthalmic Surgeon
Director of Education
Moorfields Eye Hospital
London, UK

Homayoun Tabandeh MD
Partner, The Retina-Vitreous Associates Medical Group
Los Angeles, CA, USA

Ramin Tadayoni MD, PhD
Professor of Ophthalmology
Université Paris Diderot
Sorbonne Paris Cité
APHP, Hôpital Lariboisière

Chairman of the Department of Ophthalmology
Paris, France

Sjakon G. Tahija MD
Vitreoretinal Consultant
Klinik Mata Nusantara
Jakarta, Indonesia

Hiroko Terasaki MD
Professor and Chair
Department of Ophthalmology
Nagoya University
Graduate School of Medicine
Nagoya, Japan

Cynthia A. Toth MD
Joseph A.C. Wadsworth Professor of Ophthalmology
Professor of Biomedical Engineering
Duke University
Durham, NC, USA

Louisa Wickham FRCOphth, MSc, MD
Clinical Director
Consultant Ophthalmologist
Department of Vitreoretinal Surgery
Moorfields Eye Hospital
London, UK

Young Hee Yoon MD, PhD
Professor
Department of Ophthalmology
Asan Medical Center
University of Ulsan College of Medicine
Seoul, Korea

Dedication

The original and all subsequent editions of *RETINA* are dedicated to the clinicians and scientists who have contributed to the education in our field of medical students, residents, and fellows, and especially to retina specialists and all ophthalmologists who participate in continuing medical education. We recognize that we are all students and committed to lifelong learning, especially in our field of retina.

The Second Edition included a special dedication to **Ronald G. Michels (1942–1991)**, who was vitally involved in the planning of the original edition and in the recruitment of our initial team of editors and authors. Ron was an enthusiastic and talented leader in vitreoretinal surgery. His teaching and innovations had a major impact on the other editors of RETINA specifically and on the entire field of ophthalmology generally. We are thankful for the privilege of having known and worked with Ron.

For the Third Edition we offered an additional special dedication to **A. Edward Maumenee (1913–1998)**, a true giant who influenced virtually every field and subspecialty in ophthalmology. While most of his later contributions

involved anterior segment surgery, his original observations regarding macular degeneration provided a basis for subsequent clinical and research investigations in this area. As a gifted teacher, relentless investigator, and treasured mentor, Ed inspired the editors and many authors of this textbook, as well as a multitude of academicians and clinicians around the world. He was the Professors' Professor.

For the Fourth Edition we added a special dedication to **Arnall Patz (1920–2010)**, who was an editor of the original edition. Arnall was a pioneer and leader in the establishment of the field of medical retina. He founded the Retinal Vascular Center at the Wilmer Institute and, subsequently, he became the Director of the Wilmer Institute. He trained many of today's leaders in the field and many contributing authors to RETINA. Arnall was an inspiration for the multitude of retinal specialists around the world.

For the Fifth Edition we wished to stress the development of knowledge and the contribution of the international community of retinal specialists. From the time of the First Edition in 1989 we have benefited from the rapid evolution of science – basic and clinical – in all fields related to biology and medicine, and especially in relation to ophthalmology and our chosen specialty of retina. The evolution of knowledge and contributions of colleagues from around the world have shown that there are no borders; the free exchange of information directly benefits our patients in the prevention of the most common forms of blindness caused by retinal diseases. Thus, we felt it was wholly appropriate that the Fifth Edition of RETINA be dedicated to the **international community of retinal**

clinicians and educators.

The Editors dedicate this Sixth Edition to **Stephen J. Ryan**. Steve was born in Honolulu in 1940. A Johns Hopkins University medical graduate, he was recruited to the University of Southern California to become the first fulltime chairman of the Ophthalmology Department. Under his leadership, the department became one of the leading eye departments in the country. In 1991 he became Dean of the medical school at USC, which became the Keck School of Medicine. This book was his idea and we hope the current edition reflects well on his legacy.

Andrew P. Schachat MD

C.P. Wilkinson MD

David R. Hinton MD

SriniVas R. Sadda MD

Peter Wiedemann MD

Stephen J. Ryan MD 1940–2013

Stephen J. Ryan MD, founding Editor-in-Chief of *RETINA* (Editions 1 through 5), received his MD degree from Johns Hopkins University and launched his academic career at the Wilmer Eye Institute of Johns Hopkins. In 1974, he was recruited to the University of Southern California, Los Angeles, as Chairman of the Department of Ophthalmology and President of the Doheny Eye Institute. Throughout the ensuing 39 years, he devoted his talent and energy to building the Doheny Eye Institute as a

center of excellence for ophthalmology education, patient care, and vision research.

Author of nine books and more than 250 peer-reviewed articles, Dr. Ryan received numerous honors, including the American Academy of Ophthalmology Laureate Award, the Association for Research in Vision and Ophthalmology Kupfer Award, and election to the National Academy of Sciences Institute of Medicine. By his many friends, Dr. Ryan is remembered as a brilliant scholar, scientist and visionary.

Bradley R. Straatsma MD, JD

Preface

Ryan's RETINA intends to provide both a roadmap and resource for those who study, diagnose, and treat diseases of the retina. In 1958, Duke-Elder's *System of Ophthalmology* addressed the entire scope of ophthalmology in 14 volumes with a 15th volume for the index; retina was covered in one volume. When Steve Ryan set out to develop the first edition of this retina text in the late 1980s, the book contained three volumes – basic science and tumors, medical retina, and surgical retina. But, with the explosion of medical knowledge in the 20th century, three volumes, while "hitting more than just the highlights," cannot lay claim to covering all that a reader may want to learn or know about the subject. And, as we present the 6th Edition in the second half of the second decade of the 21st century, this is truer than ever. The editors have encouraged the authors to seek out and supply the key references for each of the chapters. We hope that each chapter provides an in-depth resource for each disease or condition, but by no means should each chapter be viewed as complete. For those who want or need more, we anticipate the key words to search on should be there, and searching on those and delving into the references I hope will lead readers to what they hope to learn about the topic being addressed.

We have updated and revised the book at approximately five-year intervals. Medicine generally and ophthalmology specifically change quickly. When the book first came out, laser treatment for retinal vascular disease was the new standard. In Duke-Elder's time, diabetic retinopathy was blinding in perhaps 50% of eyes; shortly before the first edition of *Ryan's RETINA*, laser therapy as demonstrated by the Diabetic Retinopathy Study and Early

Treatment Diabetic Retinopathy Study, if applied in a timely manner, should reduce blindness rates to 1–2%. Now, laser therapy is mainly supplanted by anti-vascular endothelial factor drugs with much greater chances for improvement. Similarly, retinal surgery has moved from open sky vitrectomy to 20-gauge and now 25- or smaller gauge surgery. The "artificial retina" has US Food and Drug Administration approval, gene therapy trials are underway, and advances in our field are remarkable. To bring all this to the reader would require a 15-volume Duke-Elder-like work. I doubt too many of us would buy such a book nowadays. So, as we have added new material with entire new chapters in each section of the book, we have also removed less important or more dated aspects which appeared in earlier editions. A mantra was "the book should not gain weight."

We salute the authors, who are leading experts in specific fields from around the world. In particular, I (A.P.S.) recognize and thank my collaborating editors who have upheld Steve Ryan's vision and standards for the book – David R. Hinton, SriniVas R. Sadda, C.P. Wilkinson, and Peter Wiedemann. We thank the team at Elsevier, led by Russell Gabbedy, Nani Clansey, and Joanna Souch. Importantly, I thank my mentors who helped guide me, A.E. Maumenee, Stuart Fine, Arnall Patz, Morton F. Goldberg, and Alfred Sommer. I also recognize my retina colleagues at the Cole Eye Institute led by Daniel F. Martin. Most thanks go of course to Steve Ryan, who allowed me to participate, and to my wife, Robin.

Andrew P. Schachat MD

C.P. Wilkinson MD

David R. Hinton MD

SriniVas R. Sadda MD

Peter Wiedemann MD

Volume One

OUTLINE

PART 1

Retinal Imaging and Diagnostics

OUTLINE

1

Fluorescein Angiography

Basic Principles and Interpretation

Sara Haug, Arthur D. Fu, Robert N. Johnson, H. Richard McDonald, J. Michael Jumper, Emmett T. Cunningham Jr., Brandon J. Lujan

Since their introduction in the late 1960s, fundus photography and fluorescein angiography have been valuable in expanding our knowledge of the anatomy, pathology, and pathophysiology of the retina and choroid.[1] Initially, fluorescein angiography (FA) was used primarily as a laboratory and clinical research tool; only later was it used for the diagnosis of fundus diseases in the infant stages in the field of medical retina.[1–4] The landmark text *Atlas of Macular Diseases* by Dr. J. Donald Gass set a new standard for the use of stereoscopic FA in fundus diagnosis.[2] An understanding of FA and the ability to interpret fluorescein angiograms are essential to accurately evaluate, diagnose, and treat patients with retinal vascular and macular disease.

This chapter discusses the basic principles of FA and the equipment and techniques needed to produce a high-quality angiogram. Potential side-effects and complications of fluorescein injection are also discussed. Finally, interpretation of FA, including fundus anatomy and histology, the normal fluorescein angiogram, and conditions responsible for abnormal fundus fluorescence are described.

Basic Principles

To understand fluorescein angiography, knowledge of fluorescence is essential. Likewise, to understand fluorescence, one must know the principles of luminescence. Luminescence is the emission of light from any source other than high temperature. Luminescence occurs when energy in the form of electromagnetic radiation is absorbed and then re-emitted at another frequency. When light energy is absorbed into a luminescent material, free electrons are elevated into higher energy states. This energy is then reemitted by spontaneous decay of the electrons into their lower energy states. When this decay occurs in the visible spectrum, it is called luminescence. Luminescence therefore always entails a shift from a shorter wavelength to a longer wavelength. The shorter wavelengths represent higher energy, and the longer wavelengths represent lower energy.

Fluorescence

Fluorescence is luminescence that is maintained only by continuous excitation. In other words, excitation at one wavelength occurs and is emitted immediately through a longer wavelength. Emission stops at once when the excitation stops. Fluorescence thus does not have an afterglow. Sodium fluorescein is a hydrocarbon that responds to light energy between 465 and 490 nm and fluoresces at a wavelength of 520–530 nm. The excitation wavelength, the type that is absorbed and changed, is blue; the resultant fluorescence, or emitted wavelength, is green–yellow. If blue light between 465 and 490 nm is directed to unbound sodium fluorescein, it emits a light that appears green–yellow (520–530 nm).

This is a fundamental principle of FA. A patient, whose eyes have been dilated, is seated behind the fundus camera, on which a blue filter has been placed in front of the flash. Fluorescein is then injected intravenously. Eighty percent of the fluorescein becomes bound to protein and is not available for fluorescence, but 20% remains free in the bloodstream and is available for fluorescence. The blue flash of the fundus camera excites the unbound fluorescein within the blood vessels or the fluorescein that has leaked out of the blood vessels. The blue filter shields out (reflects or absorbs) all other light and allows through only the blue excitation light. The blue light then changes those structures in the eye containing fluorescein to green–yellow light at 520–530 nm. In addition, blue light is reflected off fundus structures that do not contain fluorescein. The blue reflected light and the green–yellow fluorescent light are directed back to the fundus camera. A filter is placed that allows the green–yellow fluorescent light through but keeps out the blue reflected light. Therefore, the only light that penetrates the filter is true fluorescent light (Fig. 1.1).

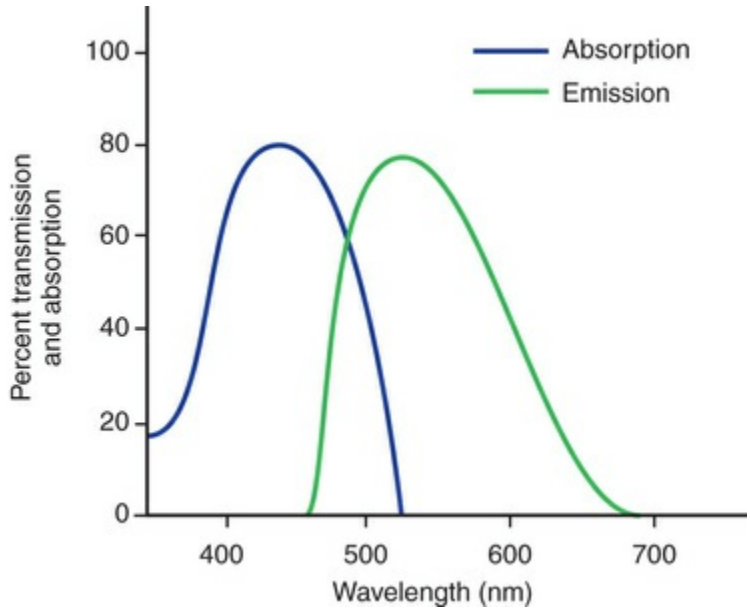

FIG. 1.1 Absorption and emission curves of sodium fluorescein dye. The peak absorption (excitation) is at 465–490 nm (blue light). The peak emission occurs at 520–530 nm (yellow–green light).

Pseudofluorescence

Pseudofluorescence occurs when nonfluorescent light passes through the entire filter system. If green–yellow light penetrates the original blue filter, it will pass through the entire system. If blue light reflected from nonfluorescent fundus structures penetrates the green–yellow filter, pseudofluorescence occurs (Fig. 1.2). Pseudofluorescence can confuse the physician interpreting the fluorescein angiogram and lead him or her to think that certain fundus structures or materials are fluorescing when they are not. Pseudofluorescence also causes decreased contrast, as well as decreased resolution. The background illumination from pseudofluorescence is especially heightened if there are white or yellowish-white areas of the fundus, such as highly reflective hard exudates. Pseudofluorescence must be avoided. Therefore, the excitation (blue) and barrier (green–yellow) filters are carefully matched so that the overlap of light between them is minimal.

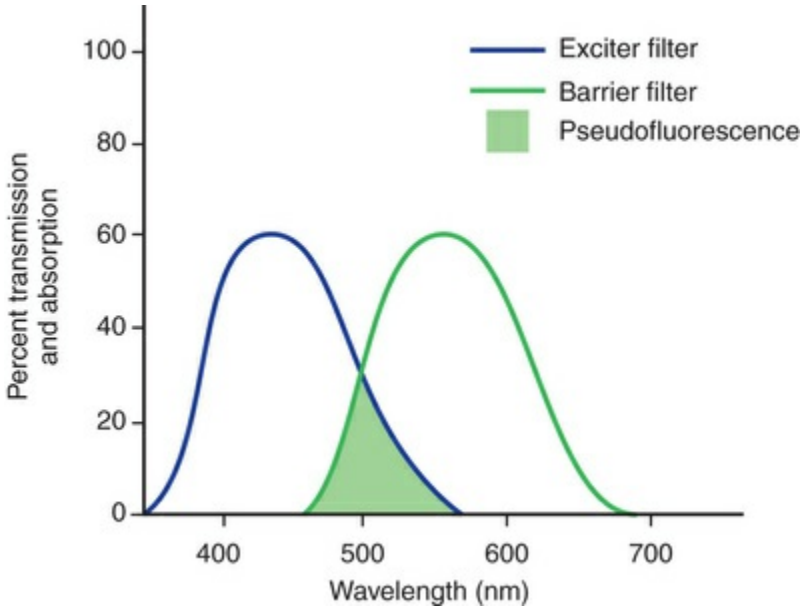

FIG. 1.2 Pseudofluorescence. The blue exciter filter overlaps into the yellow–green zone, and the yellow–green barrier filter overlaps into the blue zone. The combination results in pseudofluorescence.)

Equipment (Box 1.1)

Camera and Auxiliary Equipment

Today's widely used cameras differ in the degree of fundus area included in the photographs. In clinical retinal practice, cameras ranging from 35° to 200° are routinely used. Regardless of range, a camera with the ability to yield high resolutions of the posterior pole is essential for most macular problems, especially when laser treatment is to be done, as with background diabetic retinopathy, branch vein occlusion, or choroidal neovascularization.

Box 1.1

Equipment and Materials Needed for Angiography

Fundus camera and auxiliary equipment

Matched fluorescein filters (barrier and exciter)

Digital photoprocessing unit (computer-based) and software user interface

23-gauge scalp vein needle

5 mL syringe

5 mL of l0% fluorescein solution

20-gauge, 1½-inch needle to draw the dye

Armrest for fluorescein injection

Tourniquet

Alcohol swabs

Bandage

Standard emergency equipment

Wide-angle angiography (Chapter 5, Wide-field imaging) has the

benefit of capturing a single image of the retina in high resolution well beyond the equator. The potential for clinical efficiency and sensitivity in detecting neovascularization in the far periphery as well as acquiring an excellent clinical picture of the degree of capillary retinal nonperfusion is an exciting development in FA (Fig. 1.3).[3] Modern angiography systems also allow for video recording of the entire filling process in real time which combined with wide-field views allows for precise imaging of the exact time that structures fill or leak.[4]

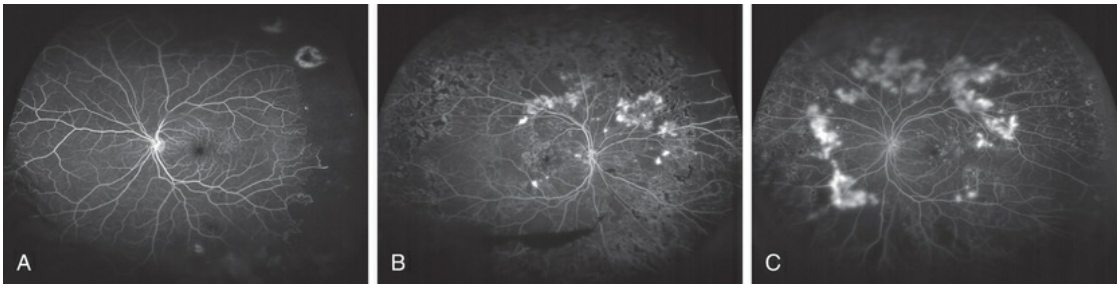

FIG. 1.3 Optos wide-field images. (A) Nonperfusion detected in the left eye with wide-field fluorescein imaging. (B,C) Wide-field angiography of the right and left eyes of a patient with diabetic retinopathy. Note the multiple areas of leakage corresponding to areas of retinal neovascularization associated with capillary nonperfusion. It is often difficult in certain wide-field images to determine the presence of small neovascular complexes versus leakage from capillary nonperfusion, unless areas are magnified further. (Panel A courtesy of Umar Mian, MD. Image taken by Carolina Costa. Panels B and C courtesy of Szilárd Kiss, MD.)

FA can also be performed using the camera application on a smartphone, which is a low-cost portable alternative useful in patients with physical ailments that prevent positioning at a standard camera or in poor resource settings.[5] Finally, the ability to share images for screening purposes for conditions such as diabetic retinopathy and age-related macular degeneration will likely expand. Thus far, teleophthalmology has been limited to color fundus images and optical coherence tomography images, but angiographic images for diseases such as new-onset choroidal neovascularization maybe cost-effective without leading to

significant treatment delays.[6]

Matched Fluorescein Filters

FA uses both exciter and barrier filters, which are typically included in modern camera units. The exciter filter must transmit blue light at 465–490 nm, the absorption peak of fluorescein excitation. The barrier filter transmits light at 525–530 nm, the fluorescent, or emitted, peak of fluorescein. The filters should allow maximal transmission of light in the proper spectral range to achieve a good image without the use of an excessively powerful flash unit.

Fluorescein Solution

Sodium fluorescein, an orange-red crystalline hydrocarbon ($C_{20}H_{12}O_5Na$), has a low molecular weight (376.27 Da) and readily diffuses through most of the body fluids and through the choriocapillaris, but it does not diffuse through the retinal vascular endothelium or the pigment epithelium.

Solutions containing 500 mg fluorescein are available in vials of 10 mL of 5% fluorescein or 5 mL of 10% fluorescein. Also available are 3 mL of 25% fluorescein solution (750 mg). The greater the volume, the longer the injection time will be; the smaller the volume, the more likely a significant percentage of fluorescein will remain in the venous dead space between the arm and the heart. For this reason, we prefer 5 mL of 10% solution (500 mg fluorescein).

Fluorescein is eliminated by the liver and kidneys within 24 hours, although traces may be found in the body for up to a week after injection. Retention may increase if renal function is impaired. The skin has a yellowish tinge for a few hours after injection, and the urine has a characteristic yellow–orange color for most of the first day after injection.

Various side-effects and complications can occur with fluorescein injection (Box 1.2).[7] One complication of the injection is extravasation of the fluorescein under the skin. This can be extremely painful and may result in a number of uncomfortable symptoms. Necrosis and sloughing of the skin may occur, although

this is extremely rare. Superficial phlebitis also has been noted. A subcutaneous granuloma has occurred in a few patients after fluorescein extravasation. In each instance, however, the granuloma has been small, cosmetically invisible, and painless. Toxic neuritis caused by infiltration of extravasated fluorescein along a nerve in the antecubital area can result in considerable pain for up to a few hours.

Box 1.2

Side-Effects and Complications of Fluorescein Injection

Extravasation and local-tissue necrosis

Inadvertent arterial injection

Nausea

Vomiting

Vasovagal reaction (circulatory shock, myocardial infarction)

Allergic reaction, anaphylaxis (hives and itching, respiratory problems, laryngeal edema, bronchospasm)

Nerve palsy

Neurologic problems (tonic–clonic seizures)

Thrombophlebitis

Pyrexia

Death

Nausea is the most frequent side-effect of fluorescein injection, occurring in about 5% of patients. It is most likely to occur in patients under 50 years of age or when fluorescein is injected rapidly. When nausea occurs, it usually begins approximately 30 seconds after injection, lasts for 2–3 minutes, and disappears slowly.

Vomiting occurs infrequently, affecting only 0.3–0.4% of

patients.[7] When it does occur, it usually begins 40–50 seconds after injection. By this time most of the initial-transit photographs of the angiogram will have been taken. Photographs can be taken after the vomiting episode has passed. A slower, more gradual injection may help to prevent vomiting.

Vasovagal attacks occur much less frequently during FA than does nausea and are probably caused more by patient anxiety than by the actual injection of fluorescein. Shock and syncope (more severe vasovagal reaction) consist of bradycardia, hypotension, reduced cardiovascular perfusion, sweating, and the sense of feeling cold. If the photographer and person injecting see that the patient is lightheaded, the patient should be allowed to bend over or lie down with the feet elevated. The patient's blood pressure and pulse should be carefully monitored. It is important to differentiate this from anaphylaxis, in which hypotension, tachycardia, bronchospasm, hives, and itching occur.

Hives and itching are the most frequent allergic reactions, occurring 2–15 minutes after fluorescein injection. Although hives usually disappear within a few hours, an antihistamine, such as diphenhydramine hydrochloride (Benadryl), may be administered intravenously for an immediate response. Bronchospasm and even anaphylaxis are other reactions that have been reported, but these are extremely rare. Epinephrine, systemic steroids, aminophylline, and pressor agents should be available to treat bronchospasm or any other allergic or anaphylactic reactions. Other equipment that should be readily available in the event of a severe vasovagal or anaphylactic reaction includes oxygen, a sphygmomanometer, a stethoscope, and a device to provide an airway. The skilled photographer observes each patient carefully and is alert to any scratching, wheezing, or difficulty in breathing that the patient may have after injection.

There are a few published and unpublished reports of death following intravenous fluorescein injection. The mechanism may be a severe allergic reaction or a hypotensive episode induced by a vasovagal reaction in a patient with preexisting cardiac or cerebral vascular disease. The cause of death in each case may have been coincidental. Acute pulmonary edema following fluorescein injection has also been reported.

There are no known contraindications to fluorescein injections in patients with a history of heart disease, cardiac arrhythmia, or cardiac pacemakers. Although there have been no reports of fetal complications from fluorescein injection during pregnancy, it is current practice to avoid angiography in women who are pregnant, especially those in the first trimester.

Technique

Aligning Camera and Photographing

The camera is equipped with a joystick with which the photographer can adjust the camera laterally and for depth. The camera is also equipped with a knob for vertical adjustment. The photographer finds the red fundus reflex, which is an even, round, sharply defined, pink or red light reflex. Most fundus cameras are equipped with an external fixation arm that has a very small LED bulb on the tip. The photographer begins by instructing the patient to follow this light to the desired position so that the correct field comes into view. The photographer moves the camera from side to side to ascertain the width of the pupil and the focusing peculiarities of the particular cornea and lens. The photographer studies the eye through the camera lens, moving the camera back and forth and up and down, looking for fundus details (e.g., retinal blood vessels). The photographer then determines the single best position from which to photograph (Figs. 1.4 and 1.5). With new wide-field angiography systems, the patient set-up is similar (Fig. 1.6).

FIG. 1.4 The patient's arm rests on an adjustable armrest that is elevated so that the patient's arm is at or above the level of her heart. The armrest also facilitates easy placement of the intravenous needle and injection of fluorescein.

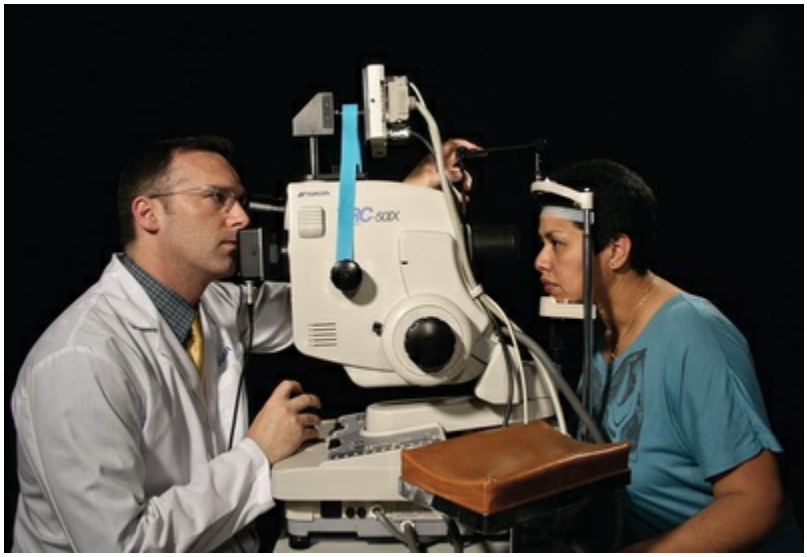

FIG. 1.5 The patient's head is kept steady in the chinrest and headrest of the fundus camera. The photographer aligns the camera and focuses on the patient's right fundus. Each is in a comfortable position, facilitating the stability necessary to achieve a good fluorescein angiogram.

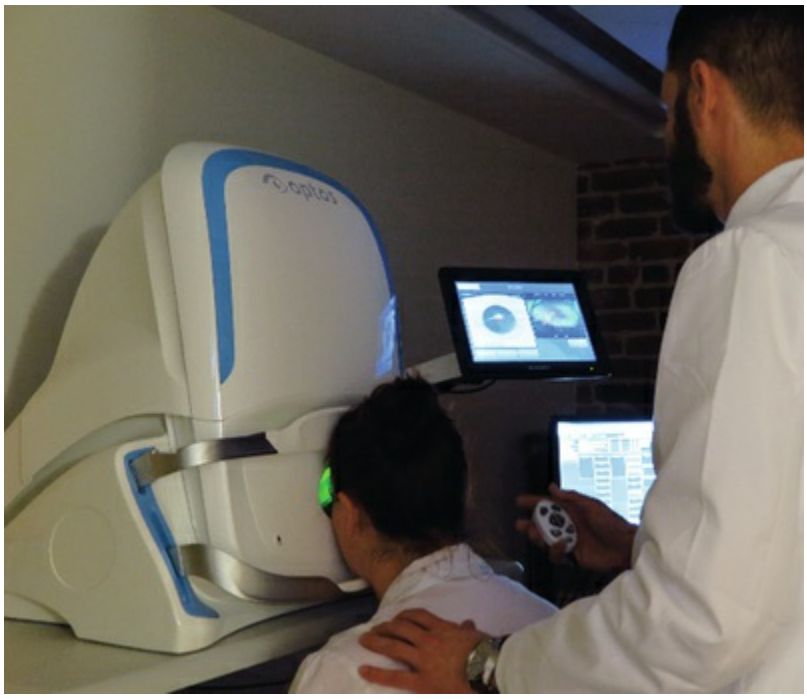

FIG. 1.6 The patient is positioned at an Optos California Ultra Widefield retinal imaging machine with the photographer positioned behind the patient watching the angiogram in real time. The photographer is able to capture images throughout the angiogram without adjusting the camera or the patient's gaze.

Any abnormalities, such as an unusual light reflex or a poorly resolved image the photographer sees through the camera system, will appear on the photograph. If the ophthalmoscopic view seen through the camera is not optimal, the photograph will not be optimal (Fig. 1.7). A helpful concept for the photographer is "what you see is what you get (or worse – never better)."

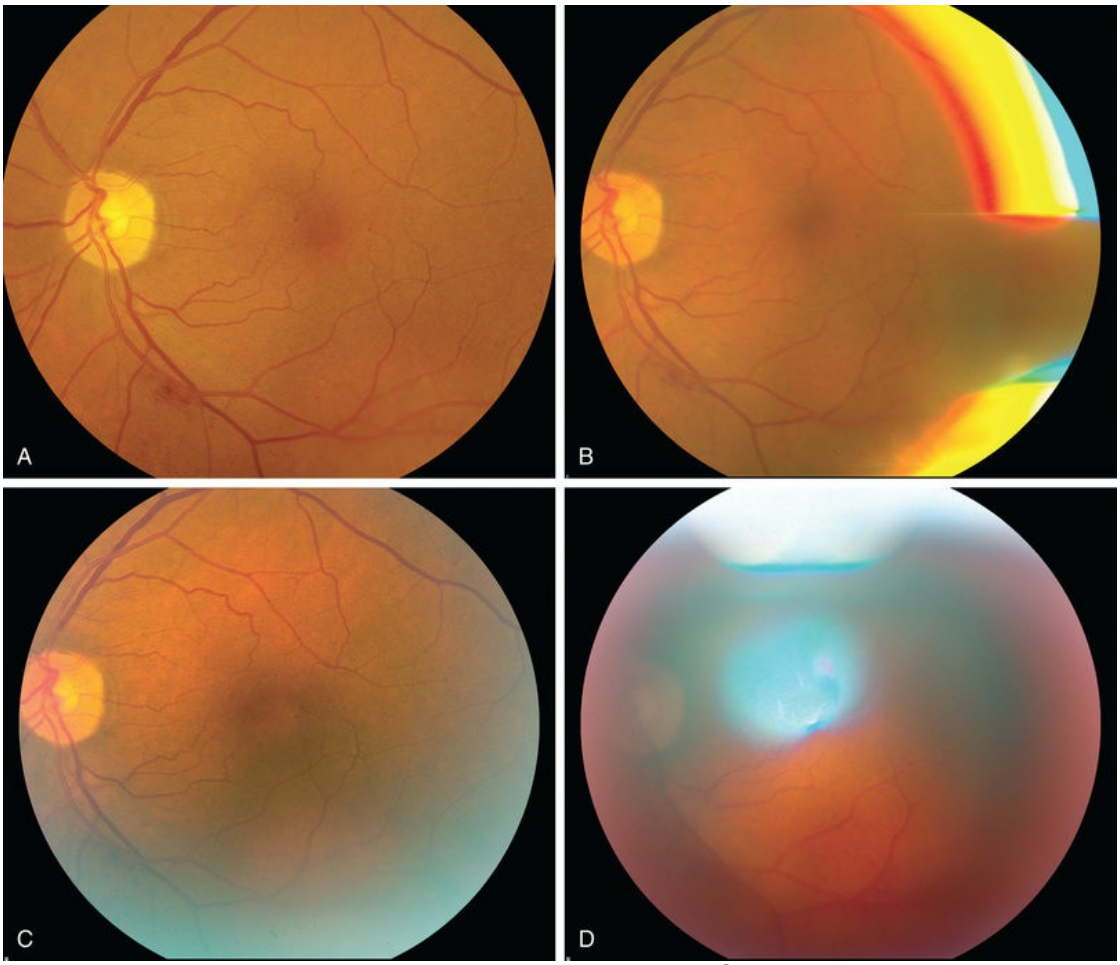

FIG. 1.7 Fundus photograph and reflexes. (A) Photograph of right fundus without reflexes. The camera was properly aligned and focused. (B) Note the bright red, yellow, and blue arc on the right side. The flash is reflecting off the iris. This can be remedied by repositioning the camera slightly to the right or left. (C) In this case the camera was placed at the proper distance from the fundus but was placed too far to one side (down and to the right), which allowed the bright white arc reflex to the lower right. (D) Note white reflex, especially above, in, and below the papillomacular bundle. In this case the camera was in proper alignment but was placed too far away from the patient's eye.

Focusing

Achieving perfect focus is a major factor in the photographic process. Both the eyepiece crosshairs and the fundus details must

be in sharp focus to obtain a well-resolved photograph. The proper position of the eyepiece is determined by the refractive error of the photographer and the degree to which he or she accommodates while focusing the camera.

The photographer first turns the eyepiece counterclockwise (toward the plus, or hyperopic, range) to relax his or her own accommodation; this causes the crosshairs to blur. The photographer then turns the eyepiece slowly clockwise to bring the crosshairs into sharp focus. The eyepiece is focused properly when the crosshairs appear sharp and clear (Fig. 1.8 online). They must remain perfectly clear while the photographer focuses on the fundus with the camera's focusing detail. With experience, the photographer becomes expert in adjusting the eyepiece and in keeping the crosshairs in focus throughout the entire photographic sequence.

FIG. 1.8 The photographer focuses the eyepiece of the camera by initially turning the eyepiece counterclockwise, then clockwise, and stopping when it is in exact focus. The photographer must be sure that the eyepiece crosshairs remain in perfect focus throughout the photographic procedure.

The best position for the eyepiece is the point at which the crosshairs are in focus while the photographer's accommodation is relaxed. Photographers learn to relax accommodation by keeping both eyes open. The photographer focuses the eyepiece with one

eye and, with the other eye, keeps a distant object, such as the eye chart, in sharp focus. This skill may be difficult for technicians without ophthalmic training, but it is seldom impossible to learn.

Keeping the crosshairs in sharp focus, the photographer then turns the focusing dial on the camera to focus the fundus detail. Some photographers focus the crosshairs just once at the beginning of each day and control their accommodation throughout the day. This is not a good idea because the photographer's accommodation may change during a photographic session; the photographer should be aware of this possibility and regularly check and readjust the eyepiece for focus. With the camera properly aligned and focused, the photographer is ready to start the preliminary photographs and angiograms.

Using Stereo Photography

Stereoscopic photography allows the viewer to perceive depth by separating, photographically, the tissues of the eye for the observer. This facilitates the interpretation of stereo FA by visually separating retinal and choroidal circulation.[8] The photographic protocol for some clinical trials requires that FA, as well as fundus photos, be captured in stereo. Though not always necessary, well-resolved stereo images can aid in the interpretation of angiograms with, for instance, choroidal neovascularization associated with age-related macular degeneration.

Adequate stereo photographs can be achieved with a pupillary dilation of 4 mm, although dilation of 6 mm or more is best. The first photograph of any stereo pair is taken with the camera positioned as far to the photographer's right (the patient's left) of the pupil's center as possible (of course, without inducing reflexes). The second photograph of the stereo pair is taken with the camera held as far to the photographer's left (the patient's right) of the pupil's center as possible.

Positioning the Patient

The patient is positioned at the camera with the chin in the chinrest and the forehead against the head bar. Because the most common cause of poor fluorescein photographs is involuntary movement of

the patient's head, the photographer should prepare and make adjustment for this before the fluorescein is injected. If so, the photographer can make some adjustment before injecting the fluorescein dye. Sometimes having an assistant hold the patient's head in the chinrest is helpful (Fig. 1.9 online). The photographer either may lower the entire camera and chinrest or raise the patient's chair. This causes the patient to lean forward in the chinrest and against the forehead bar, making it more difficult for the patient to pull back.

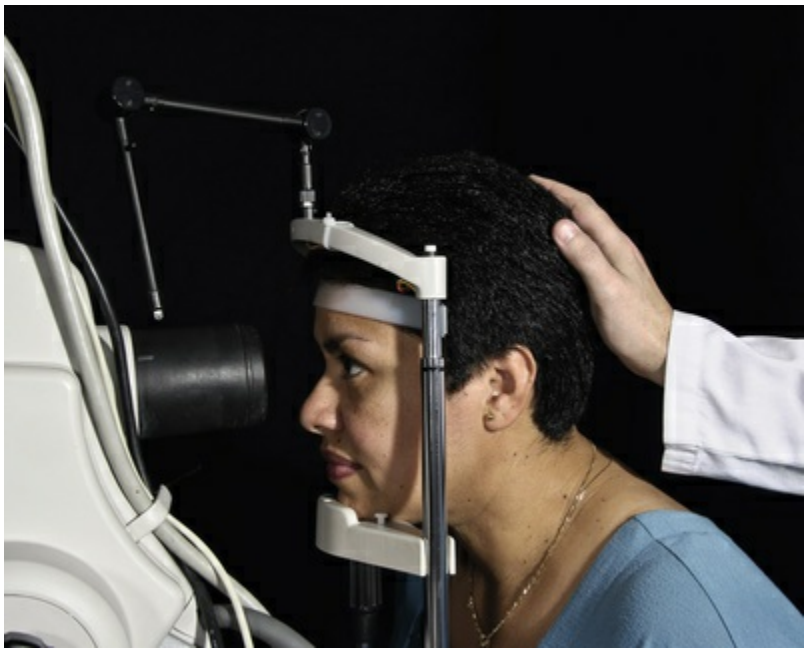

FIG. 1.9 An assistant holds the patient's head as a reminder to the patient to keep the chin in the chinrest and forehead against the bar.

Before photography begins, and between shots, the photographer may ask the patient to blink several times. This usually makes the patient more comfortable and also moistens the cornea and keeps it clear. When the pictures are actually being shot, the patient should be instructed to blink as infrequently as possible.

The photographer should talk to the patient frequently during the procedure, informing the patient of the progress of the testing and assuring him or her that all is going well. Explanation and reinforcement produce better photographs.

Injecting the Fluorescein

Color fundus photographs are taken first, followed by a red-free image of each macula. Once these images have been captured, the fluorescein can be injected. For injection, we recommend a syringe with a 23-gauge winged infusion set, or scalp-vein needle (Fig. 1.10 online). The scalp-vein needle has several advantages: it is small enough to enter most visible veins, and an intravenous opening is then available in the event of an emergency.

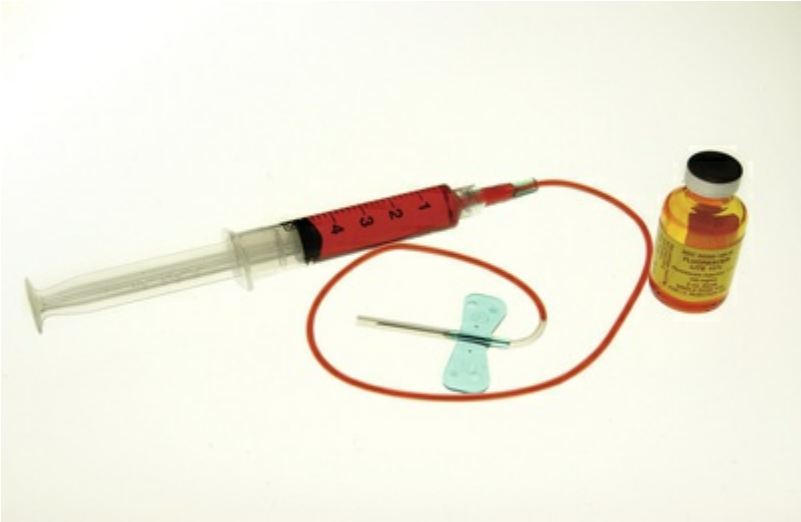

FIG. 1.10 Ten percent fluorescein solution, 5 mL syringe, and 23-gauge scalp-vein needle.

Injection of the fluorescein is coordinated with the photographic process and is done after the first photographs (color fundus and control photographs; see next section) have been taken. When ready, the photographer will signal the physician. After inserting the needle, the physician will say "starting" aloud to indicate that the injection has commenced. The photographer immediately takes a control photograph which automatically starts the timer. This frame will show zero time on the photograph. In this way, the time from the beginning of injection is recorded on each subsequent angiographic photograph. When the injecting clinician has completed infusion, he or she announces "injection complete" and the photographer takes the "end-of-injection" image. A rapid injection of 2 or 3 seconds delivers a high concentration of fluorescein to the bloodstream in a short time and yields somewhat

better photographs than a slower injection. However, the more rapid the injection, the greater the incidence of nausea from a highly concentrated bolus of fluorescein. For this reason a slower injection (4–6 seconds) is preferable; the photographs will still be of good quality. Because some fluorescein dye remains in the tubing, the scalp-vein needle should have short, rather than long, tubing to ensure that more of the dye is injected (Fig. 1.11 online).

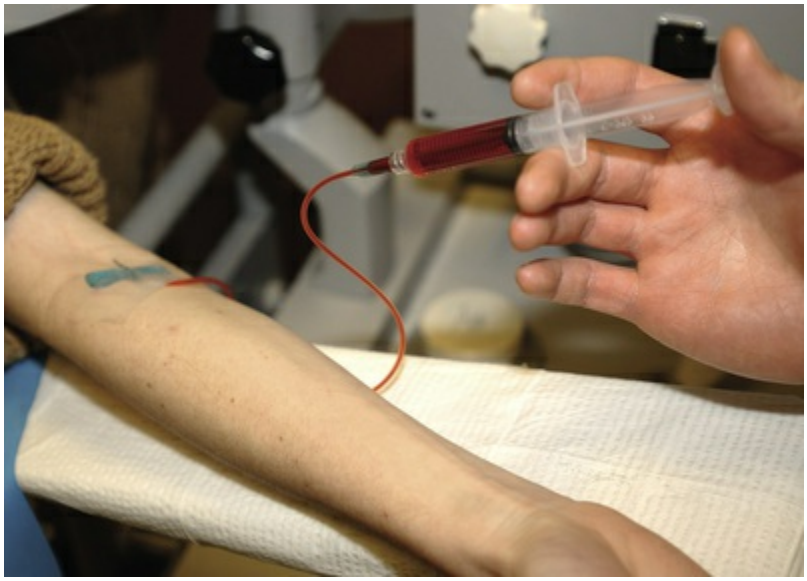

FIG. 1.11 After the needle is placed in the vein, the lights can be turned off so that the photographer can become dark-adapted and see fluorescein flow in the eye. With the use of a hand light, the person injecting can carefully observe the injection site so as to be sure extravasation is not occurring. In this way the fluorescein solution can be injected while the room lights are out.

In angiograms in which videoangiography is not performed, the photographer should begin taking the initial-transit fluorescein photographs 8 seconds after the beginning of the injection of the dye if the patient is young and 12 seconds after injection for older patients. This is done so that these early photographs will not miss the appearance of fluorescein as it enters the fundus. Then, a rapid succession of images should be taken at intervals of 1.5–2 seconds, until all veins and arteries are full. If the photographer does not see fluorescein entering and filling the retinal vessels while the initial

transit photographs are taken, he or she must continue to photograph the fundus until filling takes place. If no dye appears, the photographer should check with the patient to see if they have a burning sensation around the injection site, indicating possible extravasation.

After the initial-transit photographs and approximately 20–30 seconds after injection, with sufficient fluorescein concentration in the eye, the photographer should take a photograph centered on the optic disc, followed by the macula and optic disc of the fellow eye and any other pertinent areas. It is important to photograph both discs and macula and any other areas of abnormal fluorescence and to note any areas that could not be photographed. This ensures that the physician will have adequate information for a complete interpretation of the angiogram.

The entire photographic process lasts 5–10 minutes. Late-stage angiographs are taken of the pertinent areas of each eye when 5 minutes have elapsed. Some pathologies such as central serous retinopathy (CSR) and cystoid macular edema (CME) are better visualized when taken at 7 minutes. In an angiogram of a diabetic patient, peripheral scans may be included at the request of the clinician surveying for neovascularization if wide-angle visualization is not available. In a patient with possible choroidal neovascularization due to age-related macular degeneration, additional photographs of the suspicious lesion may be useful. When inflammatory or postsurgical CME is suspected, late frame images of the optic nerve may be of value to assess for associated disk hyperfluorescence (“hot disk”).

At the end of the session the patient is asked regarding any sensations related to an allergic reaction and reminded that the urine will be discolored for about a day.

In the event of a technical difficulty, such as camera breakdown, repeat fluorescein injection or photography can be carried out with satisfactory results after a waiting period of 30–60 minutes.

The plan we have suggested allows the fluorescein angiogram to yield all the information necessary to make a proper and thorough interpretation.

Box 1.3 provides a checklist of important steps in the FA procedure.

Box 1.3

Checklist for Fluorescein Angiography

- Inform patient about fluorescein angiography. Obtain written informed consent
- Dilate patient's pupil if necessary
- Prepare fluorescein solution, scalp-vein needle, and syringe
- Prepare fundus camera
- Clean front lens
- Focus eyepiece crosshairs
- Input patient identification and demographic data in computer database
- Position patient for alignment, focus, and comfort
- Align and focus camera
- Complete color photography
- Take red-free photos if indicated
- Insert scalp-vein needle
- Simultaneously start timer from zero and inject fluorescein dye
- Take preinjection photograph: these serve as controls in detecting auto- and pseudofluorescence
- Shoot at exact start of injection as timer is turned on and shoot second shot at exact finish of injection (length of time of injection is automatically recorded)
- Start fluorescein photograph 8 seconds after the start of injection in young patients and 12 seconds in older patients
- Follow fluorescein angiography plan

- When photography is done, reassure patient that urine will be discolored for a day or so
- At the discretion of the physician, have patient wait for observation for possible reactions to fluorescein

Developing a Photographic Plan

To photograph a 30–50° fluorescein angiogram, we suggest following a comprehensive plan, designed to yield maximal angiographic information from each fundus and to facilitate a thorough and complete interpretation (Fig. 1.12). The photographic strategy essentially begins when the clinician has identified a condition or finding that requires angiographic study. The pathology dictates whether the photographic approach should image a magnified highly detailed finding versus a wider field of view for more diffuse disease. Narrower field limits with higher magnification yield optimal images for focal pathology in conditions such as maculopathies, optic nerve disorders, and small focal lesions. Wider field of view may sacrifice magnification, but is effective in documenting conditions involving the periphery, such as diabetic retinopathy and vascular occlusive disease. Elevated lesions such as tumors require great care in capturing high-quality stereo images.

	Inject fluorescein, when injection ends, begin angio-photography of primary macula Youth: 10 sec Elderly 12 sec	Preinjection photograph with fluorescein filters secondary macula	Preinjection photograph with fluorescein filters primary macula	Left eye macula	Right eye macula
Stereo pair Secondary macula	1–2 sec later primary macula	1–2 sec later primary macula	1–2 sec later primary macula	1–2 sec later primary macula	1–2 sec later primary macula
Stereo pair Secondary macula	Stereo pair Secondary macula	Stereo pair Primary disc	Stereo pair Primary disc	Stereo pair Primary macula	Stereo pair Primary macula
Patient rest period unless peripheral scans indicated	Angiophotograph other areas of importance in either eye according to fluorescein angioscopy or nature of case	Post venous filling Secondary macula and disc	Post venous filling Primary macula and disc	Stereo pair Secondary disc	Stereo pair Secondary disc
Late angiophotographs of other areas of importance		Late secondary disc	Late secondary macula	Late primary disc	Late primary macula

FIG. 1.12 Photographic plan for fluorescein angiography of macular disease.

The photographer should be directed as to where to start the angiogram and the issues important for each specific angiogram. Wasted data storage and patient inconvenience can be avoided with good technique and a repeatable, accurate algorithm for angiography. Historically, because the roll of 35-mm negative film used for FA has 36 frames, it was convenient to think of the photograph session in terms of six rows of six frames each. With the advent of digital imaging, theoretically an unlimited number of frames can be acquired. However, to maximize efficiency of resources, digital storage of 20 frames per digital proof sheet is typically adequate for most clinical scenarios.

Diabetic Retinopathy

Diabetic retinopathy presents a unique challenge for the photographer, as significant pathology may be located both within the macula and the periphery. A photographic plan must yield information regarding leakage contributing to diabetic macular edema and nonfilling from capillary nonperfusion. At the same time, peripheral scans confirming the presence of neovascularization in preproliferative and proliferative diabetic retinopathy must also be obtained. A similar sequence is then performed on the secondary eye. Wide-field camera systems with high resolution have been especially effective in visualizing peripheral neovascularization and fibrovascular proliferation while also simultaneously delivering excellent images of the optic disc and macula.[9,10]

Interpretation

Fundus Anatomy and Histology

FA graphically demonstrates fundus pathophysiology and we rely on histologic points of reference to interpret a fluorescein angiogram. Therefore, a thorough knowledge of the anatomy of the fundus and its microscopic layers is necessary to interpret fluorescein angiograms correctly. A logical place to begin this study is at the vitreous. In its normal state, and in a normal angiogram, the vitreous is clear and nonfluorescent. However, when it contains opacities that block the view of retinal and choroidal fluorescence, hypofluorescence occurs. The vitreous is also an important point of reference when intraocular inflammation or retinal neovascularization is present. In these cases fluorescein leaks into the vitreous, causing fluffy fluorescence as fluorescein molecules disperse into fluid vitreous and vitreous gel.

For the purpose of fluorescein angiographic interpretation, it is convenient to divide the sensory retina into two layers: the inner vascular half and the outer half, which is avascular. The inner vascular half extends from the internal limiting membrane to the inner nuclear layer. This portion of the retina contains the retinal blood vessels, which are located in two separate planes: the larger

retinal arteries and veins are located in the nerve fiber layer; the retinal capillaries are located in the inner nuclear layer. In a well-focused stereoscopic fluorescein angiogram, these two vascular layers can be seen as distinct planes in the retina. An extremely important fluorescein angiographic concept is that normal retinal blood vessels are impermeable to fluorescein leakage; that is, fluorescein flows through the normal retinal vessels without leakage into the retina.

The outer avascular half of the sensory retina comprises the outer plexiform layer, the outer nuclear layer, and the rods and cones. The outer plexiform layer is the primary interstitial space in the retina. When the retina becomes edematous, it is in this layer that fluid accumulates, causing cystoid spaces. Deep retinal hemorrhages and exudates (lipid deposits) may also be deposited in the outer plexiform layer.

The rods and cones are very loosely attached to the pigment epithelium, especially in the macular region, whereas the pigment epithelium is very firmly attached to Bruch's membrane. In FA interpretation the pigment epithelium is an extremely important tissue because it prevents fluorescein leakage from the choroid and blocks, to a greater or lesser extent, visualization of choroidal fluorescence.

Bruch's membrane separates the pigment epithelium from the choriocapillaris, which is permeable to fluorescein. Fluorescein passes freely from the choriocapillaris and diffuses through Bruch's membrane up to, but not into, the pigment epithelium. Beneath the choriocapillaris are the larger choroidal vessels, which are impermeable to fluorescein. Melanocytes are dispersed throughout the choroid but are most heavily concentrated in the lamina fusca, the thin layer between the choroid and sclera. The sclera lies beneath the choroidal vessels.

The ophthalmic artery gives rise usually to two main posterior ciliary arteries: the lateral and medial. However, three posterior ciliary arteries may be present, in which case the medial artery is the one usually duplicated less frequently. In rare instances there may be a superior posterior ciliary artery.

The posterior ciliary arteries supply the lateral and medial halves of the disc and choroid. During angiography a vertical zone of

slightly delayed filling may be seen passing through the papillomacular region, including the disc. Occasionally, there is an oblique orientation to this supply or even a superoinferior distribution. This border between the main posterior ciliary arteries has been termed the watershed zone, where patchy choroidal filling often can be seen on fluorescein angiograms.

Each main posterior ciliary artery divides into numerous short arteries and one long artery. On the temporal side the short posterior ciliary arteries supply small, variously sized, wedge-shaped choroidal segments, whose apices are centered near the macula. The lateral long posterior ciliary artery passes obliquely through the sclera. It supplies a wedge of choroid that begins temporal to the macular region and participates in the formation of the greater circle of the iris.

The choriocapillaris is made up of discrete units called lobules, thought to be approximately one-fourth to one-half of a disc diameter in size. The center of each lobule is fed by a precapillary arteriole (terminal choroidal arteriole), which comes from a short posterior ciliary artery. Each lobule functions independently in the normal state. It has been assumed that angiographic zones of delayed or patchy choroidal filling gradually fill in a transverse fashion, with one lobule spilling over into another. Careful inspection, however, indicates that these filling defects generally remain the same size, indicating a delayed filling from a posterior origin (its own arteriolar feeder). In the abnormal state, as when a choroidal vascular occlusion occurs, there is a freely connecting "spilling over" of blood flow from well-perfused choroid to the occluded area.

Around the margin of each lobule is a ring of postcapillary venules that drain each lobule. These postcapillary venules drain into the vortex veins, which drain the entire choroid. There are usually four vortex veins, and each functions as a well-defined quadrantic segmental drainage system for the entire uvea. In the case of a posterior ciliary artery obstruction, this occluded portion of the choroid can fill by a retrograde mechanism from an adjacent posterior ciliary artery by way of the choroidal venous system. This mechanism may provide adequate nourishment to prevent extensive ischemic changes until the occluded artery reopens.

Knowledge of each of these layers of the fundus is important in understanding fundus histopathology. The following six areas, however, are more important than others in the interpretation of abnormal fundus fluorescence:

1. Preretinal area, where contraction from an epiretinal membrane may influence the retinal circulation and where hemorrhage may be located

2. Vascular layers of the sensory retina, both superficial and deep

3. Avascular portion of the sensory retina, particularly the outer plexiform layer, the principal site of intraretinal edema and exudate

4. Retinal pigment epithelium, which has the potential for many manifestations, including proliferation, depigmentation, hyperpigmentation, and detachment

5. Choroidal circulation, including the choriocapillaris and the large choroidal vessels

6. Sclera, which lies beneath the choroid.

Throughout this chapter a modified schematic drawing relates various fluorescein angiographic abnormalities to fundus histopathologic changes (Fig. 1.13). The size and proportion of these various layers have been modified to include various pathologic manifestations and to illustrate the effects of these abnormalities on the angiogram. Because of its importance and various pathologic changes, the pigment epithelium is drawn to a larger scale in relation to other fundus structures. Only the inner portion of the sclera is represented because the outer portion of the sclera is usually of little importance to angiographic interpretation. The retinal and choroidal vessels are drawn larger and more numerous than they appear in a normal histopathologic section to emphasize the contribution of circulatory pathophysiologic interpretation.

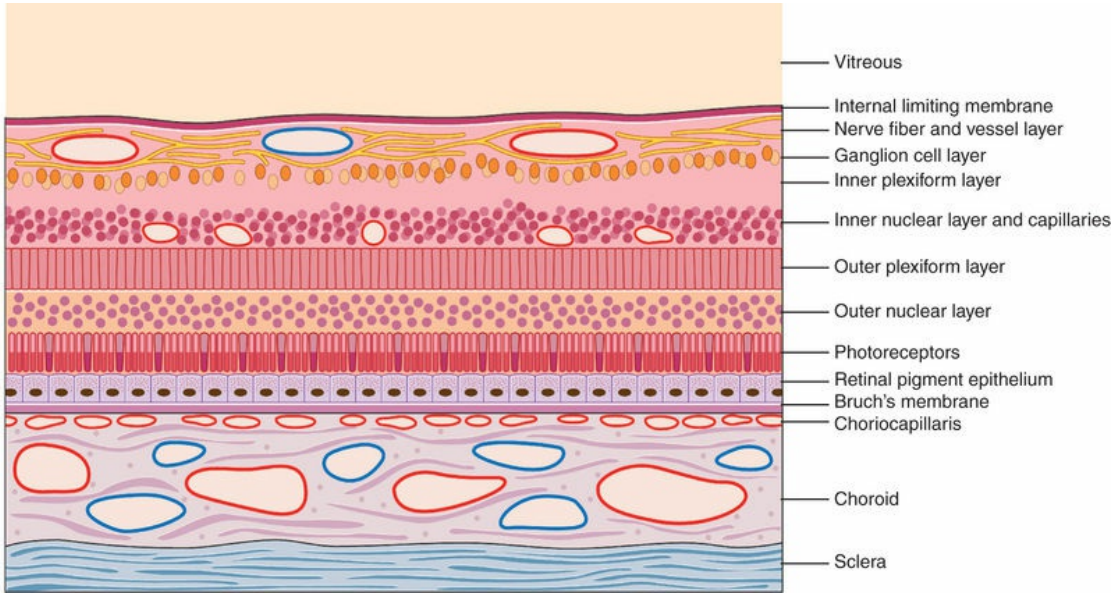

FIG. 1.13 Modified schematic drawing of a microscopic section of retina, pigment epithelium, and choroid.

Two specialized areas of the fundus warrant more detailed discussion: the macula (Fig. 1.14) and the optic nerve head. The fovea is the center of the macula and contains only four layers of the retina: (1) the internal limiting membrane; (2) the outer plexiform layer; (3) the outer nuclear layer; and (4) the rods and cones. No intermediate layers exist between the internal limiting membrane and the outer plexiform layer in the fovea, which in the macula is oblique. This is an important factor in understanding the stellate appearance of cystoid edema in the macula as opposed to the honeycomb appearance of cystoid edema outside the macula. Beyond the macular region the outer plexiform layer is perpendicular rather than oblique.

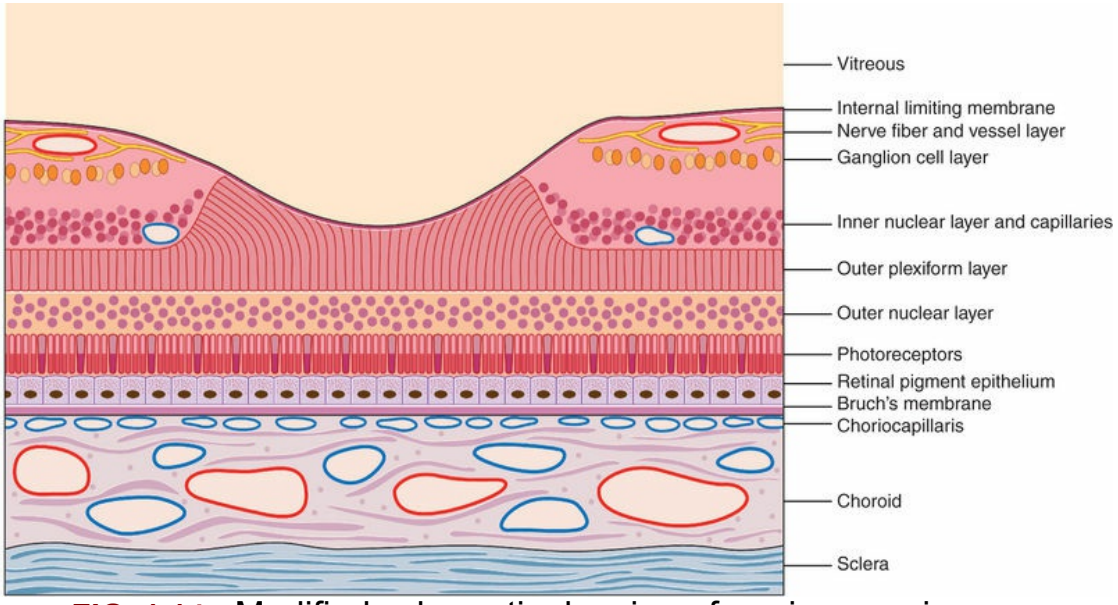

FIG. 1.14 Modified schematic drawing of a microscopic section of the macula.

The pigment epithelial cells in the macula are more columnar and have a greater concentration of melanin and lipofuscin granules than in the remainder of the fundus.

Xanthophyll is present in the fovea, located probably in the outer plexiform layer. These differences in pigmentation are the chief factors responsible for producing the characteristic dark zone in the macular region on normal angiograms. The absence of retinal vessels in the fovea (i.e., the perifoveal capillary-free zone), in most cases approximately 400–500 mm in diameter in the center of the fovea, is another cause of the dark appearance of the macula.

The optic nerve head, or disc, is the other highly specialized tissue of the posterior pole. The disc is fed by two circulatory systems: the retinal vascular system and the posterior ciliary vascular system. Widespread anastomotic channels exist between the posterior ciliary vasculature and the optic nerve and retinal vasculature and become exaggerated in certain pathologic conditions. The disc is made up of many layers of nerve fibers and glial supporting columns that contain the large retinal vessels.

The central retinal artery arises from the ophthalmic artery in close proximity to the main posterior ciliary arteries. In about 45% of the population, the central retinal artery and the medial posterior ciliary artery arise from a common trunk. In 12% of persons the central retinal artery originates from the ciliary artery. Therefore it

is impossible to have a choroidal infarction, anterior ischemic optic neuropathy, and a central retinal artery occlusion all due to a single site of obstruction.

The central retinal artery provides a major source of blood supply to the axial portion of the anterior orbital portion of the optic nerve. In the intraneural or axial course, short centrifugal branches arise but usually end a short distance behind the lamina cribrosa. There are then no further branches from the central retinal artery until it reaches the retina. If a cilioretinal artery is present, it supplies the corresponding segment of the disc.

The peripapillary nerve fiber layer is supplied by small, recurrent branches from the retinal arterioles at the peripapillary region. Emanating from these arterioles at the disc are the radial papillary capillaries. These capillaries are rather straight and long, have few anastomoses, and lie in the superficial portion of the peripapillary nerve fiber layer. The capillaries to the disc are continuous with these retinal peripapillary capillaries.

The short posterior ciliary arteries, or the recurrent branches from the peripapillary choroid, supply the retrolaminar portion of the optic nerve. The laminar cribrosa portion of the nerve is supplied by centripetal branches of the short posterior ciliary arteries. In this region a partial, or, rarely, a complete Zinn's vascular circle is occasionally found. The prelaminar portion is supplied by centripetal branches from the peripapillary choroid.

Because most of the disc is fed by the ciliary system, fluorescein appears simultaneously at the optic nerve head and the choroid and before it is apparent in the retinal arteries.

The main venous drainage of the disc is into the central retinal vein. The prelaminar portion empties into both the central retinal vein and the peripapillary choroid, thus providing potential collateral drainage in the case of obstruction of the central retinal vein behind the lamina cribrosa. Such large dilated collaterals are frequently seen following central retinal vein occlusion and are called retinociliary veins. Some mistakenly call them opticociliary shunts, a misnomer because they are not true shunts (defined as a congenital artery that empties into a vein and that skips the capillary bed, sometimes part of the Wyburn–Mason syndrome), and they are not because they emanate from the retina. They are,

most accurately, retinovenous to ciliovenous collaterals.

In summary, FA provides an in vivo understanding of the histopathologic and pathophysiologic changes of various fundus abnormalities. Therefore, an anatomic and, more specifically, a histologic understanding of important fundus landmarks is essential to fluorescein angiographic interpretation.

Normal Fluorescein Angiogram

The normal fluorescein angiogram is distinguished by certain specific characteristics. Knowledge of these characteristics provides an essential frame of reference for interpreting abnormal fluorescein angiograms.

In the normal fluorescein angiogram (Fig. 1.15), the first true fluorescence begins to show in the choroid approximately 10–12 seconds after injection in young patients (e.g., adolescents) and 12–15 seconds after injection in older patients.

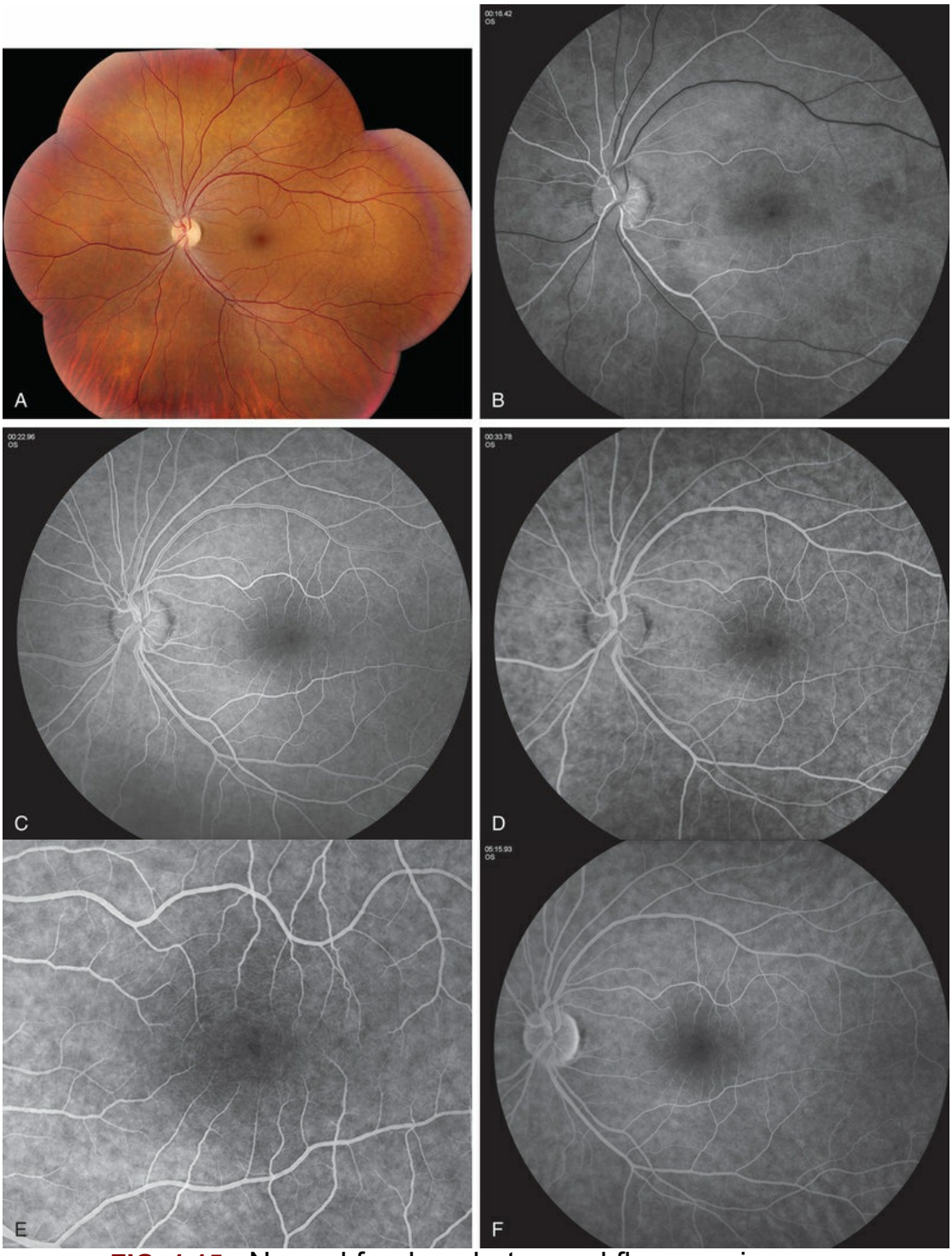

FIG. 1.15 Normal fundus photos and fluorescein angiogram of left disc and macula taken with a 50° camera. (A) Montage photograph of multiple fields shows normal macula, fovea, and retinal vessels. (B) Early arterial phase of the fluorescein angiogram. Note the ground-glass fluorescence of the choriocapillaris. There is very little fluorescence in the retinal veins; just the margins of the veins are fluorescent. This is the earliest portion of the laminar filling phase of the vein.

Note some hyperfluorescence of choriocapillaris. These dark patches of the choroid are areas that have not fully filled, referred to as patchy choroidal filling. (C) The retinal arteries and capillaries have filled and the retinal veins have filled more substantially. Note the laminar flow in the retinal veins; this is indicated by the white line of fluorescence along the walls of the retinal veins. (D) Late venous phase. Laminar filling is no longer detectable and uniform filling is seen in both arterial and venous circulation. (E) Mid to later arteriovenous phase of fluorescein angiogram. Note that the ground-glass fluorescence of the choriocapillaris is complete. The retinal arteries and veins are completely filled. (F) Arteriovenous phase of fluorescein angiogram showing the disc. Again, there is diffuse fluorescence of the choriocapillaris. The arteries and veins have completely filled, and optic nerve fluorescence is normal.

Fluorescence can appear even earlier than 8 seconds in very young patients. The choroid occasionally begins to fluoresce 1 or 2 seconds before the initial filling of the central retinal artery. Early choroidal fluorescence is faint, patchy, and irregularly scattered throughout the posterior fundus. It is interspersed with scattered islands of delayed fluorescein filling. This early phase is referred to as the choroidal flush. When adjacent areas of choroidal filling and nonfilling are quite distinct, the pattern is designated as patchy choroidal filling.

Within the next l0 seconds (approximately 20–25 seconds after injection), the angiogram becomes very bright for about 5 seconds because of the extreme choroidal fluorescence. Choroidal fluorescence, however, is not visible in the macula because of the taller, more pigmented epithelium present in the fovea (retina). Therefore the macula remains dark throughout the angiogram.

If present, a cilioretinal artery usually begins to fluoresce as the choroid fluoresces, rather than as the retina fluoresces. Within 1–3 seconds after choroidal fluorescence is visible, or approximately 10–15 seconds after injection, the central retinal artery begins to fluoresce. The less dense the concentration of pigment in the pigment epithelium, the greater the time between the visibility of the choroidal fluorescence and the filling of the retinal vessels. The

lighter pigment presents less interference to choroidal fluorescence, allowing it to be evident earlier in its filling phase. With a more densely pigmented pigment epithelium, the blockage barrier effect is greater. Therefore choroidal fluorescence appears somewhat later because a greater concentration of fluorescein is required to overcome the increased density of the pigment epithelial barrier.

Because no barrier exists in front of the retinal vessels, the patient's pigmentation has no effect on the visibility of the retinal vessels, although the degree of pigmentation does affect the contrast of the angiophotographs. The darker the pigment epithelium is, the less visible the choroidal fluorescence will be and the greater the contrast of the retinal vascular fluorescence (i.e., the better they stand out). The lighter the pigment epithelium is, the more visible the choroidal fluorescence will be and the less the contrast of the fluorescence from the retinal vessels.

After the central retinal artery begins to fill, the fluorescein flows into the retinal arteries, then into the precapillary arterioles, the capillaries, the postcapillary venules, and finally the retinal veins. Because the fluorescein from the venules enters the veins along their walls, the flow of fluorescein in the veins is laminar. Because vascular flow is faster in the center of a lumen (tube) than on the sides, the fluorescein seems to stick to the sides, creating the laminar pattern of retinal venous flow. The dark (nonfluorescent) central lamina is nonfluorescent blood that comes from the periphery, which takes longer to fluoresce because of its more distant location.

In the next 5–10 seconds, fluorescence of the two parallel laminae along the walls of the retinal veins becomes thicker. At the junction of two veins, the inner lamina of each vein may merge. This creates three laminae: one in the center and one on each side of the vein. As fluorescein filling increases in the veins, the laminae eventually enlarge and meet, resulting in complete fluorescence of the retinal veins.

Fluorescence of the disc emanates from the posterior ciliary vascular system, both from the edge of the disc and from the tissue between the center and the circumference of the disc. Filling also comes from the capillaries of the central retinal artery on the surface of the disc. Because healthy disc tissue contains many capillaries,

the disc becomes fairly hyperfluorescent on the angiogram.

The perifoveal capillary net cannot always be seen on the fluorescein angiogram. It can be seen best in young patients with clear ocular media about 20–25 seconds after a rapid fluorescein injection. This is called the "peak" phase of the fluorescein angiogram. The photographer should be aware of this phase and be sure not to miss it by shooting as rapidly as possible as the fluorescein concentration increases and by continuing to shoot rapidly until the concentration of fluorescein begins to decrease.

Approximately 30 seconds after injection, the first high-concentration flush of fluorescein begins to empty from the choroidal and retinal circulations. Recirculation phases follow, during which fluorescein in a lower concentration continues to pass through the circulation of the fundus.

Generally, 3–5 minutes after injection, the choroidal and retinal vasculatures slowly begin to empty of fluorescein and become gray. Vessels of most normal patients almost completely empty of fluorescein in approximately 10 minutes. The large choroidal vessels and the retinal vessels do not leak fluorescein. However, because of large gaps in its endothelium, the choriocapillaris does leak fluorescein. The extravasated fluorescein diffuses through the choroidal tissue, Bruch's membrane, and sclera. Leakage of fluorescein with retention in tissues is designated as staining. In the later phase of the angiogram, staining of Bruch's membrane, the choroid, and especially the sclera may be visible if the pigment epithelium is lightly pigmented. The disc and adjacent visible sclera remain hyperfluorescent because of staining. When the retinal pigment epithelium is especially lightly pigmented, the large choroidal vessels can be seen in silhouette against the fluorescent (fluorescein-stained) sclera. The lamina cribrosa within the disc also remains hyperfluorescent because of staining. This depends on the cup-to-disc ratio and the presence of any visible sclera, such as occurs within a conus adjacent to the disc. The edge of the disc stains from the adjacent choriocapillaris, which normally leaks.

To summarize, the angiogram is initially dark; choroidal and retinal filling is seen 10–15 seconds after fluorescein injection. The retinal and choroidal vasculatures fill maximally about 20–30 seconds after injection. Late angiophotographs show fluorescence

of the choroid and sclera (if the pigment epithelium is light) and fluorescence of the optic cup and the edge of the disc, but otherwise the fundus is dark (nonfluorescent in the late phase).

Abnormal Fluorescein Angiogram

Interpretation of the fluorescein angiogram follows a simple and logical progression. The first step is to recognize areas of abnormal fluorescence and determine if they are hypofluorescent or hyperfluorescent (Fig. 1.16).

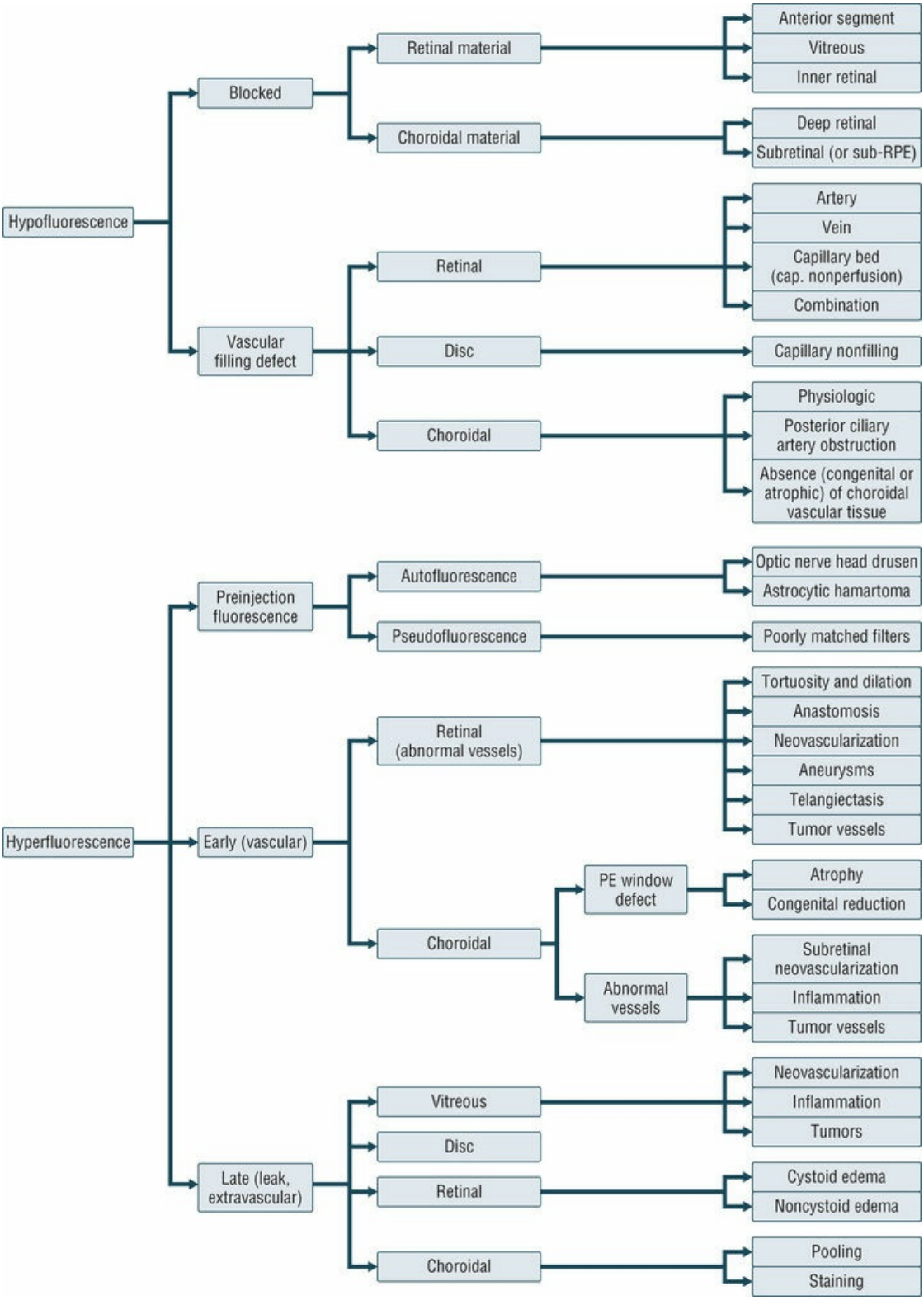

FIG. 1.16 Flow sheet for abnormal fluorescein angiography. PE window, pigment epithelial window; RPE, retinal pigment epithelium.

Hypofluorescence

Hypofluorescence is a reduction or absence of normal fluorescence, whereas hyperfluorescence is abnormally excessive fluorescence. A systematic series of decisions follows this initial differentiation to arrive at a proper diagnosis. These decisions relate to (l) the anatomic location of various abnormalities; (2) the quality and quantity of the abnormal fluorescence; and (3) other unique characteristics, as indicated in Fig. 1.16.

Hypofluorescence is any abnormally dark area on the positive print of an angiogram. There are two possible causes of hypofluorescence: blocked fluorescence or a vascular filling defect.

Blocked fluorescence is sometimes referred to as masked, obscured, or negative fluorescence or transmission decrease. Each of these terms indicates a reduction or absence of normal retinal or choroidal fluorescence because of a tissue or fluid barrier located anterior to the respective retinal or choroidal circulation. For example, blood in the vitreous or a layer of blood in front of the retina obscures the view of the retinal and choroidal circulations and therefore blocks fundus fluorescence from these tissues. Hemorrhage that lies under the retina or retinal pigment epithelium, but in front of the choroidal circulation, does not obstruct visibility of the retinal circulation but does block the view of the choroidal circulation. Therefore the approximate histologic location of blocking material can be determined by the presence or absence of visibility of one or both fundus circulations.

Fluorescein is present but cannot be seen in blocked fluorescence. With vascular filling defects, however, fluorescein cannot be seen because it is not present.

The key to differentiating blocked fluorescence from a vascular filling defect is to correlate the hypofluorescence on the angiogram with the ophthalmoscopic view. If there is material visible ophthalmoscopically that corresponds in size, shape, and location to the hypofluorescence on the angiogram, then blocked fluorescence is present. If there is no corresponding material on the color photograph, then it must be assumed that fluorescein has not perfused the vessels and that the hypofluorescence is caused by a vascular filling defect.

Hypofluorescence resulting from a vascular filling defect occurs

when either of the two fundus circulations is not perfusing normally. This is caused by an absence of the vascular tissue or by a complete or partial obstruction of the particular vessels. In these situations an absence or delay of fluorescence of the involved vessels will occur. This type of hypofluorescence has a pattern that follows the geographic distribution of the vessels involved. Although the ophthalmoscopic picture will demonstrate the material blocking fluorescence, it may show nothing if the hypofluorescence is the result of a vascular filling defect.

To summarize, after an area of hypofluorescence is recognized, one must refer to the ophthalmoscopic photograph to determine the cause. If material is visible ophthalmoscopically and corresponds to the area of hypofluorescence, this is blocked fluorescence. If no corresponding blocking material exists, the hypofluorescence is therefore a vascular filling defect.

Anatomic Location of Hypofluorescence

After determining the cause of the hypofluorescence, the next step is (1) to determine the anatomic location of the material that is blocking fluorescence or (2) to determine which of the two fundus circulations is involved in the filling defect. Blocking material affects the retinal and choroidal circulations if it is located in front of the retina. The material blocks only the choroidal circulation if it is located beneath the retinal circulation and in front of the choroid. Similarly, vascular filling defects occur in either the retinal or the choroidal vasculature or in the vessels of the optic nerve head.

Blocked Retinal Fluorescence

Blocked retinal vascular hypofluorescence is caused by anything that reduces media clarity. An opacification in front of the retinal vessels involving the cornea, anterior chamber, iris, lens, vitreous, or the most anterior portion of the retina or disc produces hypofluorescence.

The further the opacification is in front of the fundus, the less it will block fluorescence and the more it will affect the overall quality of the photographs. The closer the material is to the fundus, the more it will block, causing hypofluorescent images on the angiogram. Any material that blocks retinal vascular fluorescence

will, of course, block choroidal fluorescence as well.

Any anterior-segment material, such as a corneal opacity, anterior-chamber haziness, or lens opacity, obscuring the view of the ocular fundus will result in an angiogram of reduced brilliance, contrast, and resolution. This affects the quality of the angiogram and is, in a sense, a type of blocked fluorescence.

Many conditions of the vitreous produce a hazy medium that prevents visualizing fundus detail. The most common vitreous opacity to cause blockage is hemorrhage. Whether diffusely dispersed in the vitreous gel or more densely accumulated, vitreous hemorrhage reduces or completely blocks fundus fluorescence. In addition to hemorrhage, media haze may be caused by a variety of opacifications, including asteroid hyalosis, vitreous condensation resulting from vitreous degenerative disease, inflammatory debris, vitreous membranes, or opacification secondary to amyloidosis. When anterior-segment and vitreous opacities are present, the angiogram may be of higher resolution and quality than the color photograph because the light scattered from the nonfluorescing opacities is not transmitted through the barrier filter and therefore has no effect on the angiographic photograph.

Any translucent or opacified material in the retina or in the nerve fiber layer blocks fluorescence from both planes of retinal vessels, as well as from the choroidal vessels. The large retinal vessels and precapillary arterioles are located in the nerve fiber layer in the anterior plane of the retina. The capillaries and postcapillary venules are located deeper in the retina, in the inner nuclear layer. If a blocking material lies in front of the nerve fiber layer, it blocks both planes of retinal vessels (Fig. 1.17). However, if the material lies beneath the nerve fiber layer but within or in front of the inner nuclear layer (where the smaller retinal vessels are located), it blocks only the retinal capillaries (and choroidal vessels), leaving the view of the large retinal vessels unobstructed. If a blocking material lies deeper than the retinal vascular structures, deep to the inner nuclear layer, it does not block the vessels but will block the choroidal vascular fluorescence. In other words, deep intraretinal blocking material, such as hemorrhage or exudate, does not obstruct retinal vascular fluorescence, since the retinal vessels are located in the inner half of the retina (Fig. 1.18).

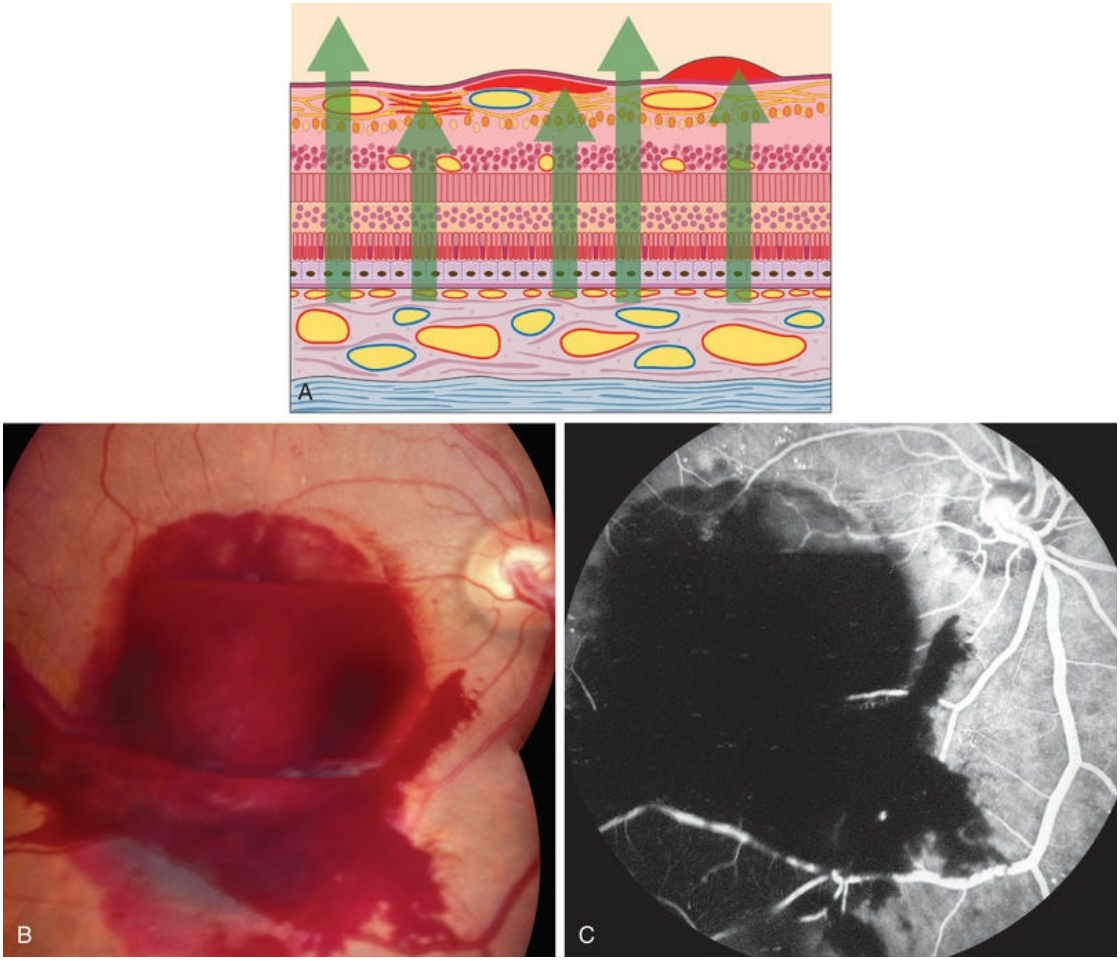

FIG. 1.17 Preretinal hemorrhage causing hypofluorescent blockage of all retinal and choroidal fluorescence. (A) Schematic drawing of subhyaloid (right), subinternal limiting membrane (central), and nerve fiber layer (left) hemorrhages. Each hemorrhage lies in front of the retinal, and therefore choroidal, vasculature, causing hypofluorescence-blocked fluorescence. (B) Color photograph of the right disc showing substantial preretinal hemorrhage. (C) Fluorescein angiogram of the right disc showing hypofluorescence caused by blockage as a result of the preretinal hemorrhage. Comment: All fluorescence of the fundus is blocked because the hemorrhage lies in front of the retinal vasculature.

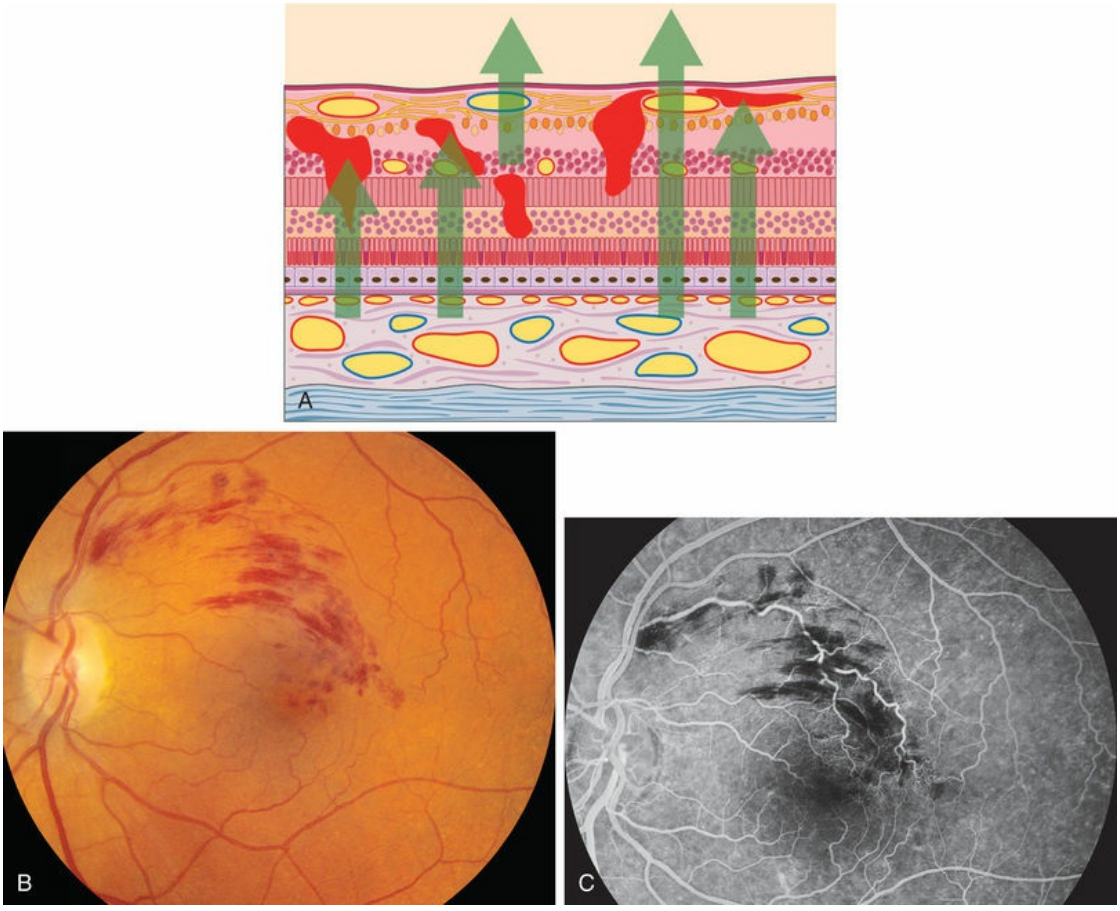

FIG. 1.18 Intraretinal hemorrhages causing hypofluorescent blockage. (A) Schematic of retina showing hemorrhages located in most of the layers of the retina from the internal limiting membrane to the outer nuclear layer. (B) Color photograph of left macula shows dot-and-blot, as well as flame-shaped hemorrhages just above the fovea. This is a case of branch vein occlusion. (C) Fluorescein angiogram of left macula shows that the hemorrhage causes irregular hypofluorescent blockage. The flame-shaped hemorrhage located in the nerve fiber layer blocks all the retinal vasculature. The dot-and-blot hemorrhages do not block the large retinal vessels and therefore can be localized deeper in the retina. The hemorrhages that do not block retinal capillary fluorescence can be located deeper to the capillary layer, which is in the inner nuclear layer. Comment: Once hypofluorescent blockage is determined, an anatomic localization of the blocking material can be made by determining which normally fluorescent structures can be seen and which are being blocked.

Therefore one can determine the location of a retinal abnormality, such as hemorrhage, by the vessels that are blocked by it and by the fluorescence of the vessels that are not blocked.

The most common cause of blocked retinal vascular fluorescence is hemorrhage. Subinternal limiting membrane hemorrhage blocks fluorescence of all underlying retinal vessels and choroidal vasculature. Nerve fiber layer hemorrhage, which usually is flame-shaped, blocks the smaller retinal vessels lying deeper in the retina but only partially blocks the larger retinal vessels in the nerve fiber layer. Blockage from hemorrhage is usually complete, as opposed to the partial blockage caused by the myelinated nerve fibers.

Various retinal vascular (arteriolar) occlusive diseases may cause white ischemic thickening (nerve fiber edema), which results in some opacification of the retina and blockage of the remaining retinal vascular and choroidal fluorescence. Conditions such as arterial occlusion in hypertension or Purtscher retinopathy cause enough intracellular "cloudy" swelling and opacification to block fluorescence. It should be noted that, because there is occlusion in this type of hypofluorescence, the hypofluorescence is caused partly by the vascular filling defect. However, the opacified ischemic retina effectively blocks fluorescence from underlying retinal and choroidal vasculature.

In summary, when the retinal vessels do not fluoresce, the ophthalmoscopic view should be studied to determine if blocking material is located in front of the retinal vessels. If blocking material is present, the next step is to determine its anatomic location.

Blocked Choroidal Fluorescence

Hypofluorescence caused by blocked choroidal vasculature occurs when fluid, exudate, hemorrhage, pigment, scar, inflammatory material, or the like accumulates in front of the choroidal vasculature and deep to the retinal vasculature (Fig. 1.19).

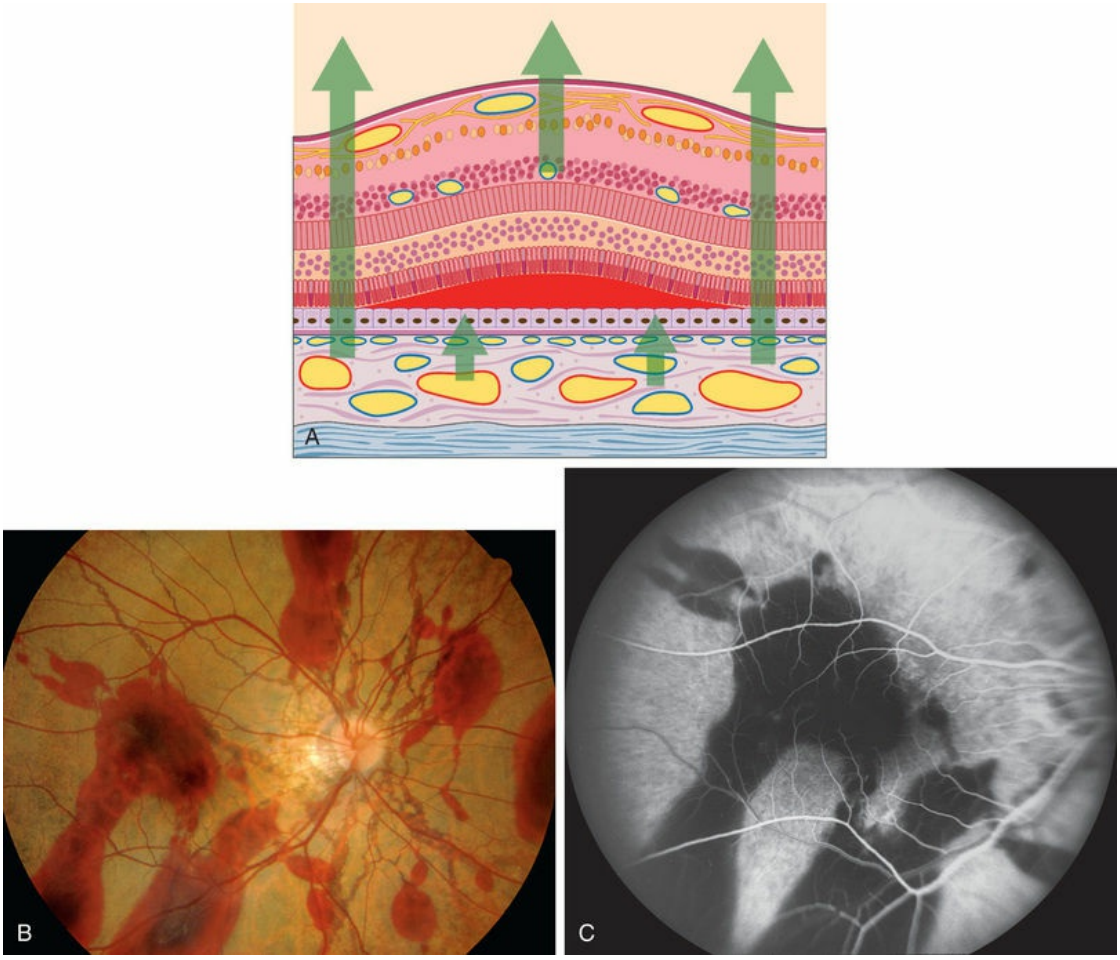

FIG. 1.19 Subretinal hemorrhage causing hypofluorescence, specifically, blockage of choroidal fluorescence. (A) Schematic of retina with subretinal hemorrhage (blood located between photoreceptors and pigment epithelium). (B) Color photograph of right macula of an eye with angioid streaks showing large scattered areas of subretinal hemorrhage. (C) Fluorescein angiogram of right macula shows marked hypofluorescence caused by blocked choroidal fluorescence (the retinal vessels are visible) that is due to the subretinal hemorrhage. Comment: The subretinal hemorrhage completely obscures fluorescence from the choroid. The retinal vessels are clearly seen overlying the subretinal hemorrhage.

Deep Retinal Material.

Materials deposited in the deep retina that cause blockage of choroidal fluorescence are fluid, hard exudate, hemorrhage, and pigment.

Fluid that accumulates in the deep retina has a predilection for the tissue of least resistance, the outer plexiform layer. Deposition of edema fluid, originating from leaking retinal vessels or migrating from subretinal space into the retina, most frequently occurs in the outer plexiform layer. After reaching a certain volume, the fluid tends to form spaces, or pockets, between compressed nerve and Müller fibers, which are pushed aside in the process. This pattern of fluid accumulation in the outer plexiform layer is called cystoid retinal edema. Noncystoid retinal edema occurs when the volume of extracellular fluid is insufficient to produce pockets, or spaces, in the outer plexiform layer or other layers of the retina. A significant amount of retinal edema, whether cystoid or noncystoid, especially if turbid or containing lipid-laden macrophages, partially blocks choroidal fluorescence in the early phase of the fluorescein angiogram. Later in the angiogram, retinal edema fluoresces. Intraretinal hard exudates and lipid-laden macrophages, usually located in the outer plexiform layer, partially block choroidal fluorescence. When retinal vessels bleed, the blood can be deposited anywhere in the retina. When located deep to the retinal vessels beneath the inner nuclear layer, retinal vascular fluorescence is visible, whereas choroidal fluorescence is blocked.

Subretinal Material.

Any opaque or translucent substance located beneath the retina but in front of the choroid blocks fluorescence of the choroidal vasculature but does not block retinal vascular fluorescence (Fig. 1.19). Blood located under the retina causes complete blockage of choroidal fluorescence, with the retinal fluorescence showing through normally. Subretinal hemorrhage appears red, and subpigment epithelial hemorrhage is dark. Subretinal hemorrhage is generally scalloped with somewhat irregular margins, whereas subpigment epithelial hemorrhage is often quite round and well demarcated (Fig. 1.19).

Accumulated pigment (melanin and lipofuscin) from diseased retinal pigment epithelium causes blocked choroidal fluorescence (Fig. 1.20). Any hyperpigmentation of the pigment epithelium causes blocked choroidal fluorescence. Xanthophyll, the pigment present in the outer layers of the fovea, blocks choroidal

fluorescence by selectively absorbing the blue exciting light, which results in less fluorescence. Finally, a choroidal nevus may block much of the choroidal fluorescence (Fig. 1.21) and especially blocks the later hyperfluorescent staining of the sclera. The choriocapillaris may be seen normally over the nevus.

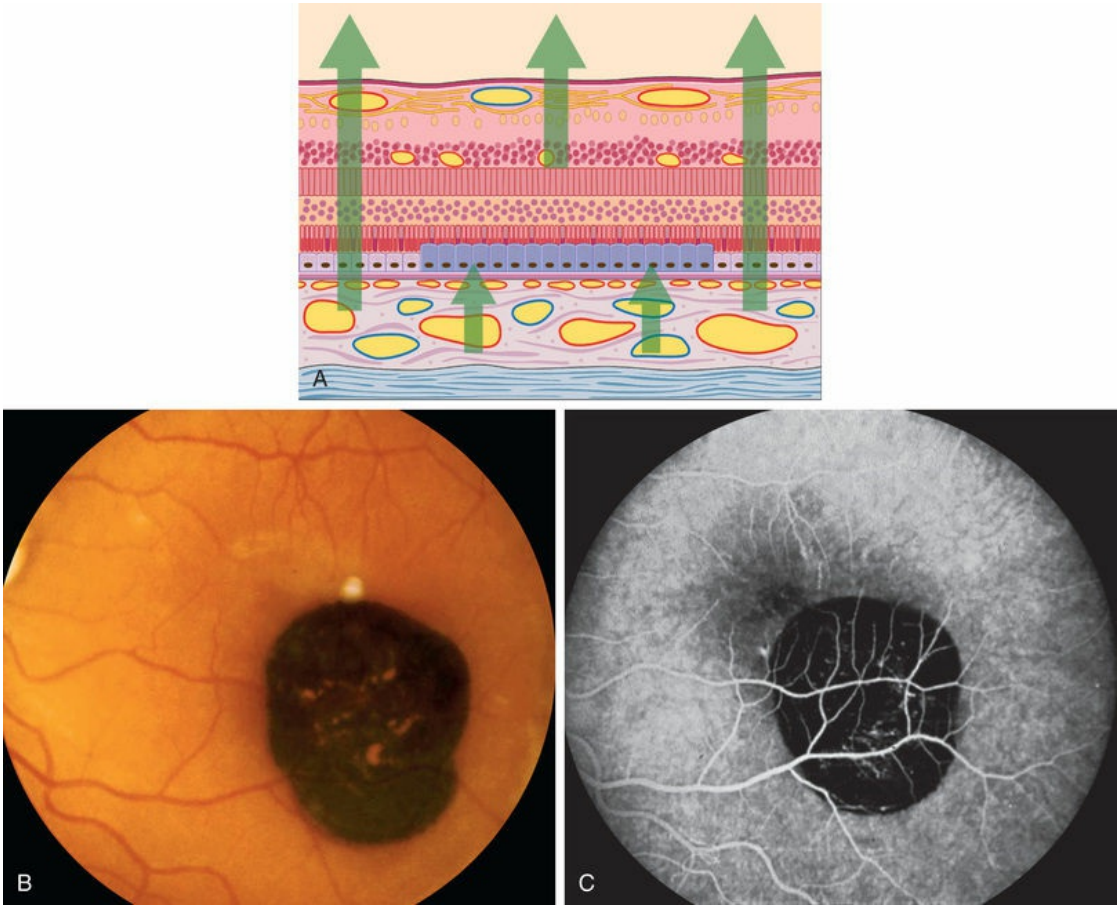

FIG. 1.20 Hypertrophy of the retinal pigment epithelium. (A) Schematic showing hypertrophic pigment epithelial cells. (B) Color photograph of the macula shows a well-demarcated hyperpigmented lesion. (C) Fluorescein angiogram of the same area shows marked hypofluorescence of the choroid resulting from blocked fluorescence. Comment: This patient had marked hypertrophy of the retinal pigment epithelium, which allowed normal retinal fluorescence; it completely blocked choroidal fluorescence.

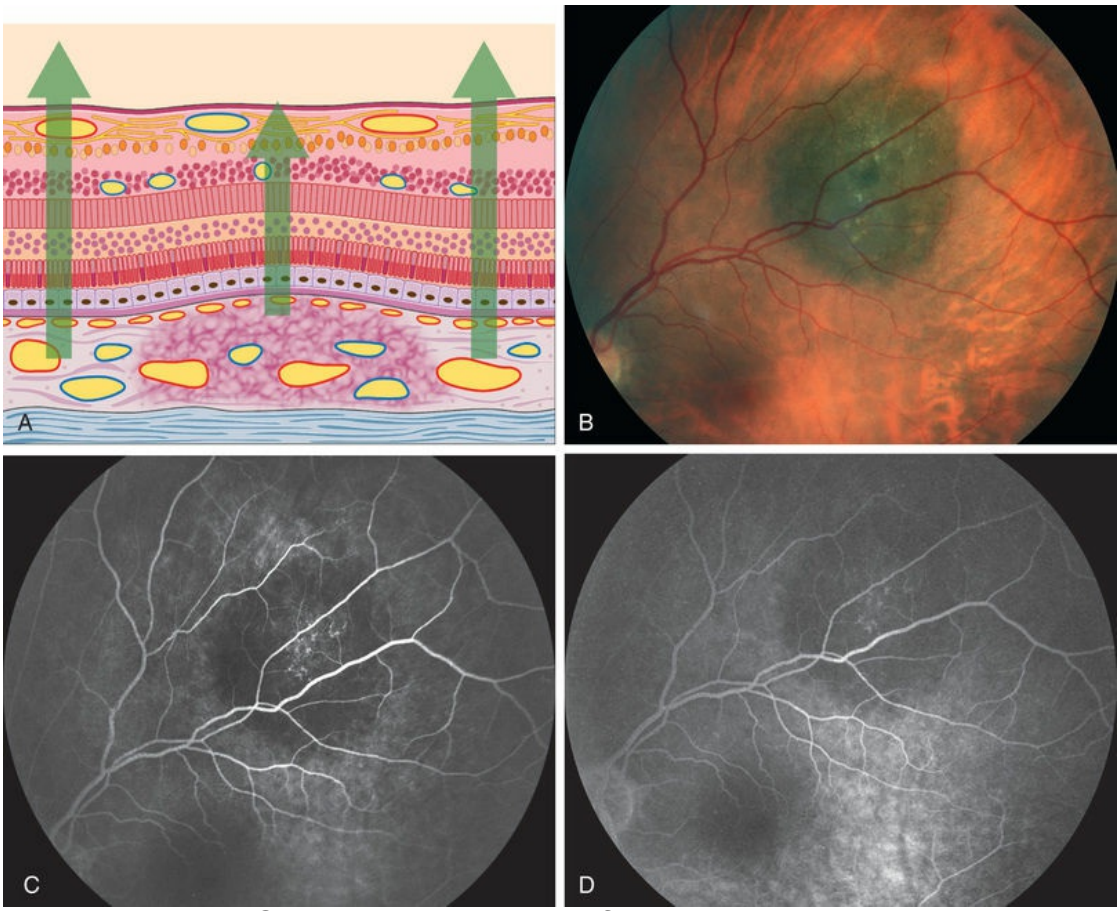

FIG. 1.21 Choroidal nevus hypofluorescent blockage. (A) Schematic drawing of retina showing choroidal nevus. Note that the choriocapillaris is intact. (B) Color photograph of nevus. (C) Arteriovenous phase of fluorescein angiogram shows hypofluorescence corresponding to the area of the nevus. (D) Later arteriovenous phase of fluorescein angiogram shows that the nevus is still hypofluorescent, although the choriocapillaris ground-glass fluorescence can be seen surrounding.

To summarize, various materials located in the deep retinal layers, or beneath the retina, block choroidal fluorescence and are evident ophthalmoscopically. These materials result from a variety of disease processes.

Vascular Filling Defect.

The second cause of abnormal hypofluorescence is vascular filling defect. With blocked fluorescence, the fluorescein is present in the circulations of the fundus but is not visible because a tissue or fluid

barrier conceals it. With vascular filling defect, fluorescein cannot be seen because it is not present. Since fluorescein reaches the retina and choroid by way of vessels, lack of the fluorescein dye in either vascular system indicates an obstructive problem or a lack of vessels (i.e., a vascular filling defect).

As previously indicated, when a hypofluorescent area is seen on an angiogram, the best way to differentiate blocked fluorescence from a vascular filling defect is to compare the angiogram with the ophthalmoscopic picture. When blood, pigment, or exudate can be seen ophthalmoscopically corresponding to the area of hypofluorescence, the material is causing blocked fluorescence. When no material is visible ophthalmoscopically (on the color photograph), one must assume that fluorescein has not perfused the vessels and that the abnormal hypofluorescence is caused by a vascular filling defect. In some instances both forms of hypofluorescent mechanisms play a role simultaneously, as with retinal arteriolar occlusion, when the retina is not only not perfused (vascular filling defect) but is ischemic and therefore white and opaque, causing blocked fluorescence.

Vascular filling defects result from vascular obstruction, atrophy, or absence (congenital or otherwise) of vessels. Any of these conditions can be total or partial. When the obstruction is complete (occlusion) or the vascular tissue is atrophied completely, the hypofluorescence is complete and lasts throughout the angiogram. When the obstruction is only partial or the vascular tissue is not entirely atrophied, the vascular fluorescein filling is delayed or reduced relative to corresponding areas that fill normally. Whatever the cause of a partial vascular filling defect, hypofluorescence will be seen in the early phases of the angiogram but may not persist throughout the entire angiogram. Some vascular filling, although delayed or reduced, will eventually occur.

Once it is determined that a vascular filling defect is the cause of an area of hypofluorescence, the next step is to determine which of the retinal, disc, or choroidal vessels are involved. A vascular filling defect of the disc is easy to discern angiographically. Determining whether a vascular filling defect is retinal or choroidal can be more difficult. Since retinal vessels are normally present, however, the absence of retinal vessels is usually readily apparent. If, on the

other hand, a vascular filling defect is found but the retinal vessels are full and visible, the hypofluorescence must be choroidal in origin.

Retinal Vascular Filling Defect.

If a retinal vascular filling defect is present, the clinician then considers whether the defect results from obstruction of a retinal artery or vein, capillary bed, or any combination of these. Distinguishing the cause of the obstruction is not difficult because the fluorescein angiographic process is dynamic and timed. When nonfilling of a specific retinal vessel occurs, it is easy to differentiate an arterial occlusion from a venous occlusion because the retinal arteries fill first, then the retinal capillary bed, followed by the retinal veins. In addition, retinal vascular filling defects can be localized by tracing the course of a particular vessel; these defects correspond anatomically to the normal distribution of the retinal vasculature (Figs. 1.22 and 1.23). Thus retinal vascular filling defects result from a variety of disease processes, but most are commonly associated with atherosclerosis and diabetes.

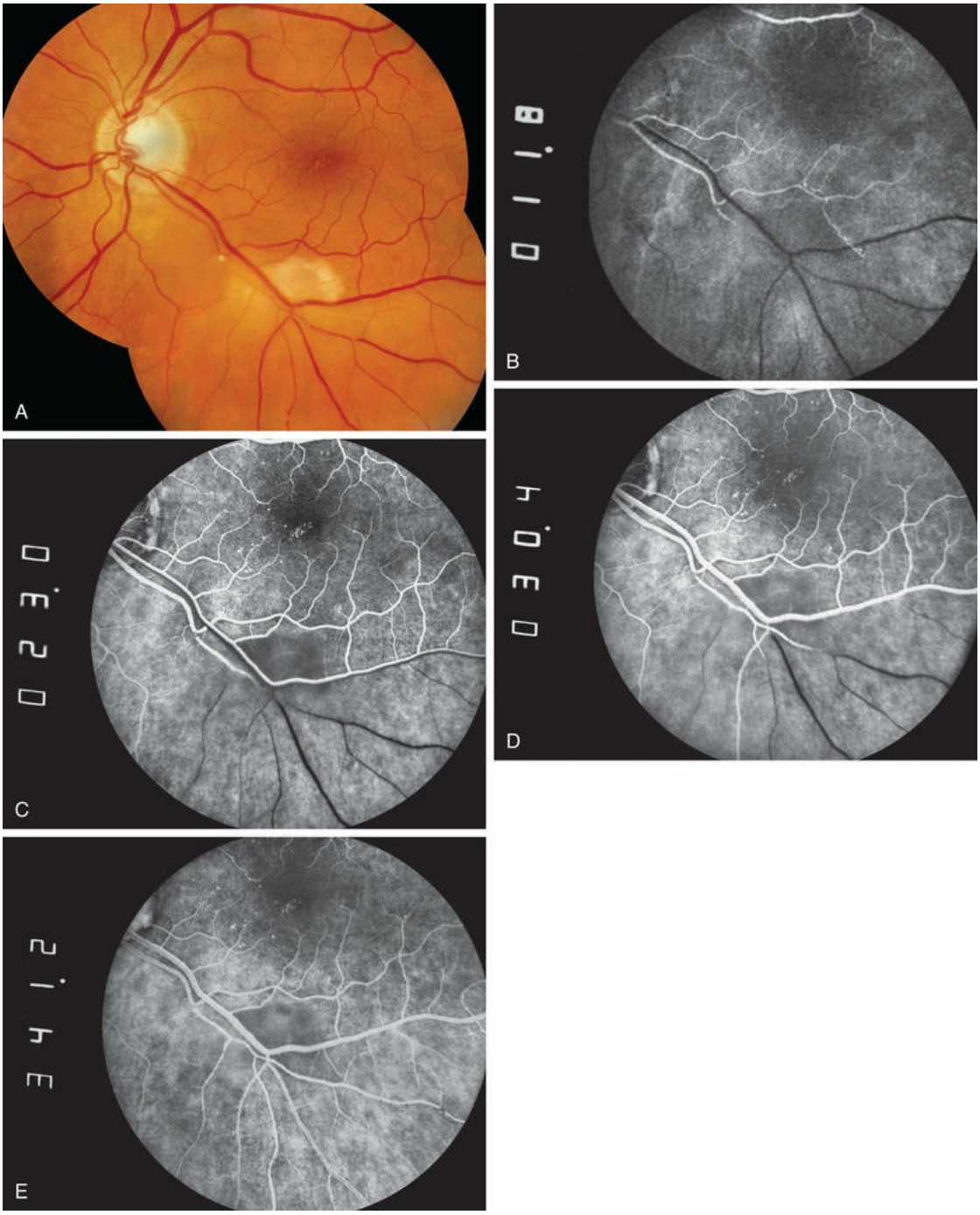

FIG. 1.22 Branch retinal artery occlusion. (A) Color photograph showing areas of retinal whitening inferior to the macula. An intraarterial embolus is seen proximal to the whitened retina. (B) Earliest arterial filling. An area of hypofluorescence is located inferior to the macula. A small retinal artery feeding this area is occluded at the site of the embolus previously identified on panel (A). (C) Midarterial venous filling with a small area of intraarterial hyperfluorescence distal to the site of embolic obstruction. (D) Late

arteriovenous phase of fluorescein angiogram shows that the occluded artery is still mostly hypofluorescent. (E) Portions of the area did fill with fluorescein due to retrograde filling from surrounding areas. There is some mild staining of the occluded retinal artery.

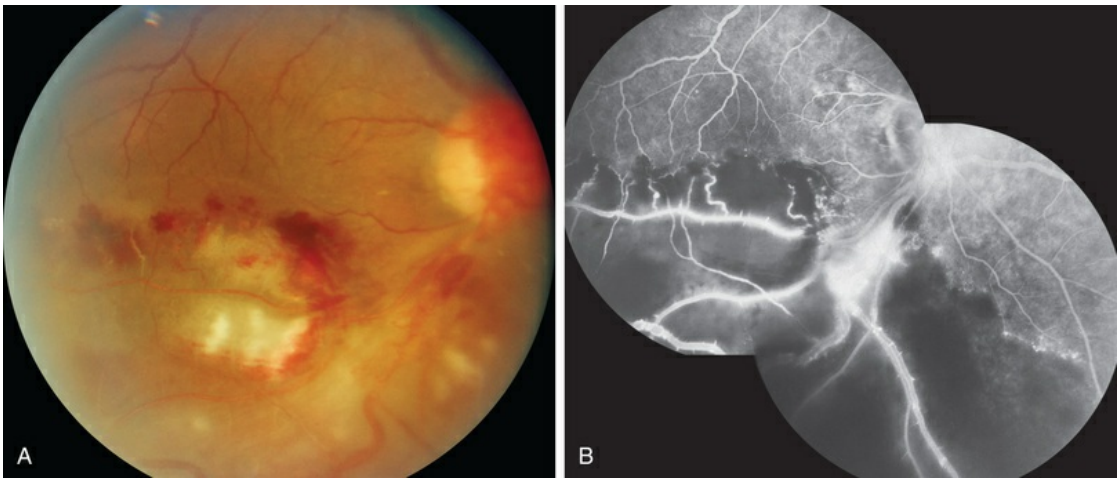

FIG. 1.23 Retinal branch vein occlusion. (A) Color photograph of the right macula and disc. There are areas of retinal hemorrhage, retinal whitening, and cotton-wool spots. (B) The fluorescein angiogram of the right disc and macula shows normal fluorescence of the superior portion of the macula. The inferior portion shows substantial hypofluorescence due to retinal capillary nonperfusion. The very bright hyperfluorescent areas are due to neovascularization. Comment: This patient had a very ischemic inferotemporal branch retinal vein occlusion of the right eye. This was a severe occlusion, as evidenced by closure of large areas of the capillary bed. The hypofluorescence was caused not only by vascular filling defect but also by the nonperfused retina, which becomes partially opaque and caused hypofluorescence of the choroid. (In other words, there was blockage of choroidal fluorescence by the opaque retina, which was caused by the retinal capillary nonperfusion.)

Vascular Filling Defects of the Disc.

Vascular filling defects of the disc occur because of the failure of the capillaries of the optic nerve head to fill. This failure can be caused by (1) congenital absence of disc tissue, as in an optic pit or optic nerve head coloboma (Fig. 1.24); (2) atrophy of the disc tissue and its vasculature, as in optic atrophy; or (3) vascular occlusion, as in an ischemic optic neuropathy. Each condition is characterized by early hypofluorescence caused by nonfilling and late hyperfluorescence resulting from staining of the involved tissue.

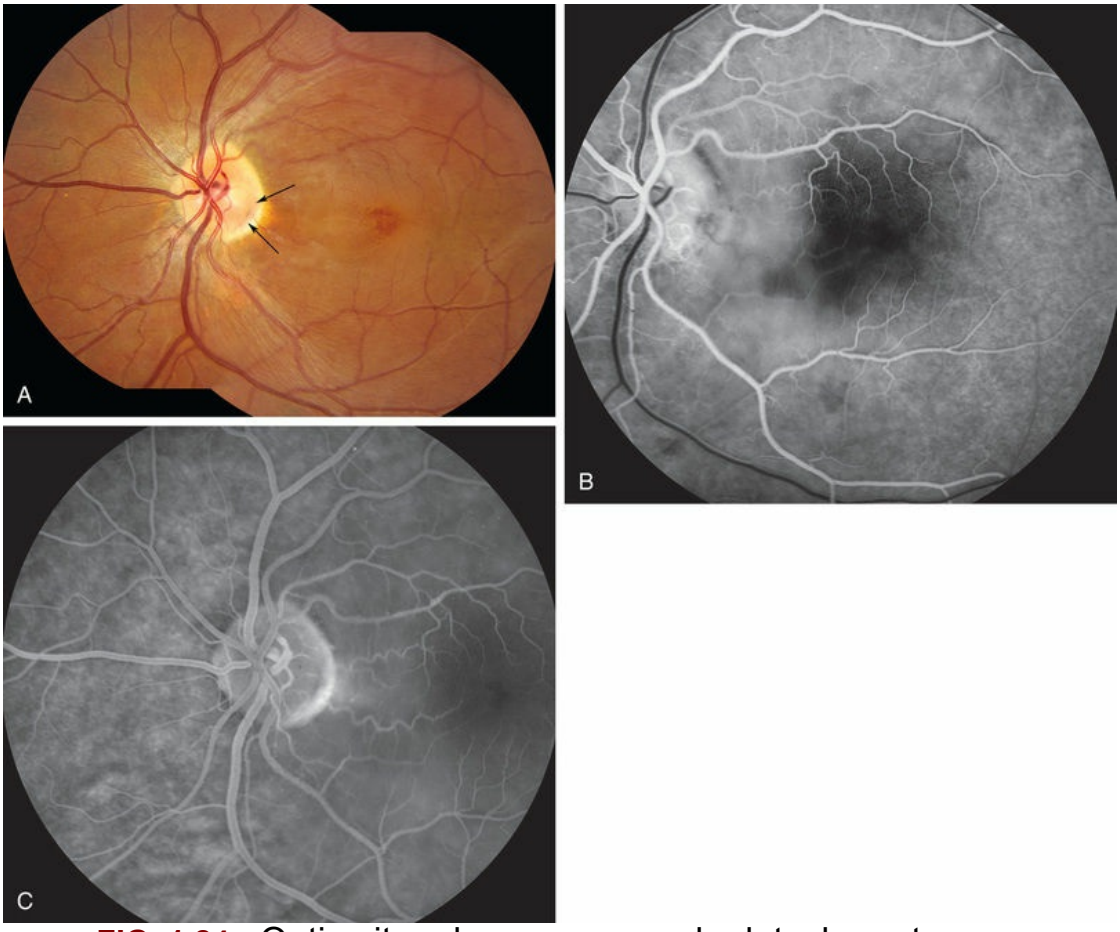

FIG. 1.24 Optic pit and sensory macula detachment. (A) Color photograph of left macula. Note the dark area of the optic pit (*arrows*). Cystic edema is present in the macula secondary to the macular schisis detachment from the optic pit. (B) Early arteriovenous phase of fluorescein angiogram shows hypofluorescence of the disc in the area of the pit due to absence of tissue and vessels. (C) In the late arteriovenous phase fluorescein angiogram, the hypofluorescent area of the pit is evident.

Choroidal Vascular Filling Defect.

The normal choroidal vasculature is usually difficult to document with fluorescein angiography because of the pigment epithelial barrier. If chronic choroidal vascular filling defects exist, the pigment epithelium is often secondarily depigmented or atrophied. In these cases the hypofluorescence caused by a vascular filling abnormality of the choroid and choriocapillaris can be documented angiographically.

When choroidal vessels do not fill, dark patches of hypofluorescence beneath the retina appear early in the angiogram. The distribution and morphology of the hypofluorescence vary according to the disease process. Because the choroidal circulation is completely separate from the retinal circulation, choroidal vascular filling defects do not correlate with the retinal vascular distribution. If the choriocapillaris is absent and the large choroidal vessels are still present, the choroidal and retinal vessels fluoresce, but hypofluorescent gaps appear because of the loss of the diffuse "ground-glass" fluorescence from the choriocapillaris (Fig. 1.25). When the choroidal vasculature does not fill, as in total occlusion or in atrophy, hypofluorescence occurs early in the angiogram. The hypofluorescence remains throughout the late stages of the procedure, although leakage from surrounding areas of normal choriocapillaris extends into the occluded area. When sufficient leakage occurs, the sclera retains fluorescein (stains) late in the angiogram. When the involved area is large and the leakage is minimal, the hypofluorescence remains throughout the later stages.

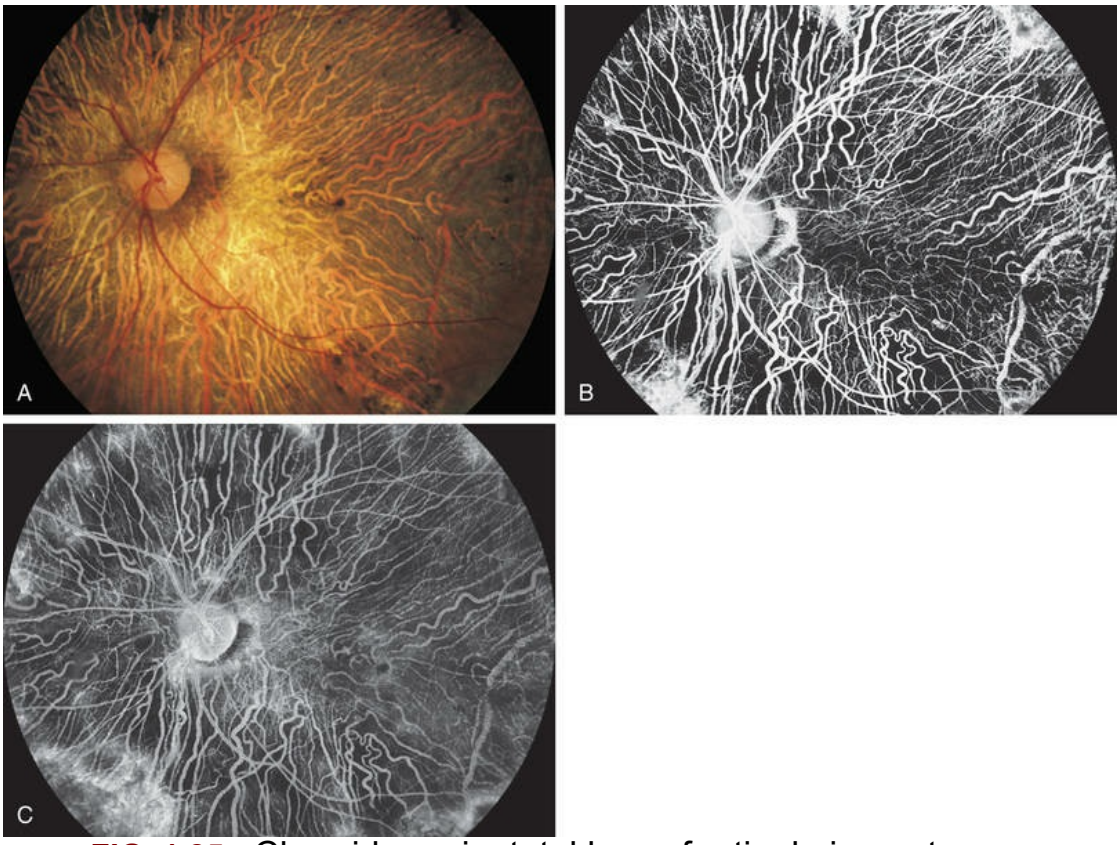

FIG. 1.25 Choroideremia: total loss of retinal pigment epithelium (RPE) and choriocapillaris with much of the large choroidal vasculature remaining. (A) Color photograph of the left disc and macula. The large choroidal vasculature can be seen as pale, irregular lines. Dark patches of pigment are located in the macula and around the disc. (B) Late venous phase of fluorescein angiogram of the left disc and macula. The large choroidal vessels can be seen filling, as can the retinal arteries. The choriocapillaris is not seen. (C) Recirculation phase of fluorescein angiogram. The large choroidal vessels and retinal vessels can be seen, but the choriocapillaris (usually seen as ground-glass fluorescence) is not seen except in the far edges of the view. Comment: This patient had a total loss of RPE and choriocapillaris in most areas of the fundus. The ground-glass choroidal fluorescence was absent from most areas. The large choroidal vessels could be seen. The large choroidal vessels do not leak fluorescein, and therefore the sclera did not stain in these areas. The RPE and choriocapillaris were partially intact in a few areas. These can be seen at the far extremes, where there is some mild ground-glass appearance.

A normal physiologic condition exists in many patients in which the choroid fills in a patchy manner. Areas adjacent to the foci that are filling show early hypofluorescence but eventually fill normally, usually 2–5 seconds later. This has been termed patchy choroidal filling, and it is the most common form of choroidal vascular filling defect. This form of filling follows a pattern in which the short posterior ciliary arteries enter the eye perpendicularly through the sclera. These vessels then feed the choriocapillaris lobules.

The prechoriocapillaris arterioles and lobules are end, or terminal, vessels demonstrating no anastomoses with adjacent choriocapillaris arterioles or lobules. Each choriocapillaris lobule is connected to adjacent lobules on the venous, or emptying, side of the circulation. Fluorescence in each choriocapillaris segment or lobule is in the form of a round, irregular, or hexagonal patch. When some of the channels fill late, a heterogeneous filling pattern results. The choriocapillaris fills most areas, whereas dark hypofluorescent patches are present in other areas. These dark areas are lobules from separate end channels that are not filled simultaneously with adjacent choriocapillaris lobules. They are filled in a delayed fashion by the single feeder choroidal arteriole.

In general, vascular filling defects of the choroid are caused by obstructive disorders or absence of tissue with the following FA characteristics: (1) normal retinal vascular flow; (2) depigmentation of the pigment epithelium; (3) reduction of choroidal blood flow; and (4) hypofluorescence in the early phases of angiography caused by loss of the normal ground-glass choriocapillaris fluorescence. In some conditions the large choroidal vessels are also absent, resulting in total early hypofluorescence in the affected area, with scleral staining only on the circumference of the lesion because of the adjacent patent choriocapillaris. Choroidal vascular defects result from a variety of disease processes (Figs. 1.26 and 1.27).

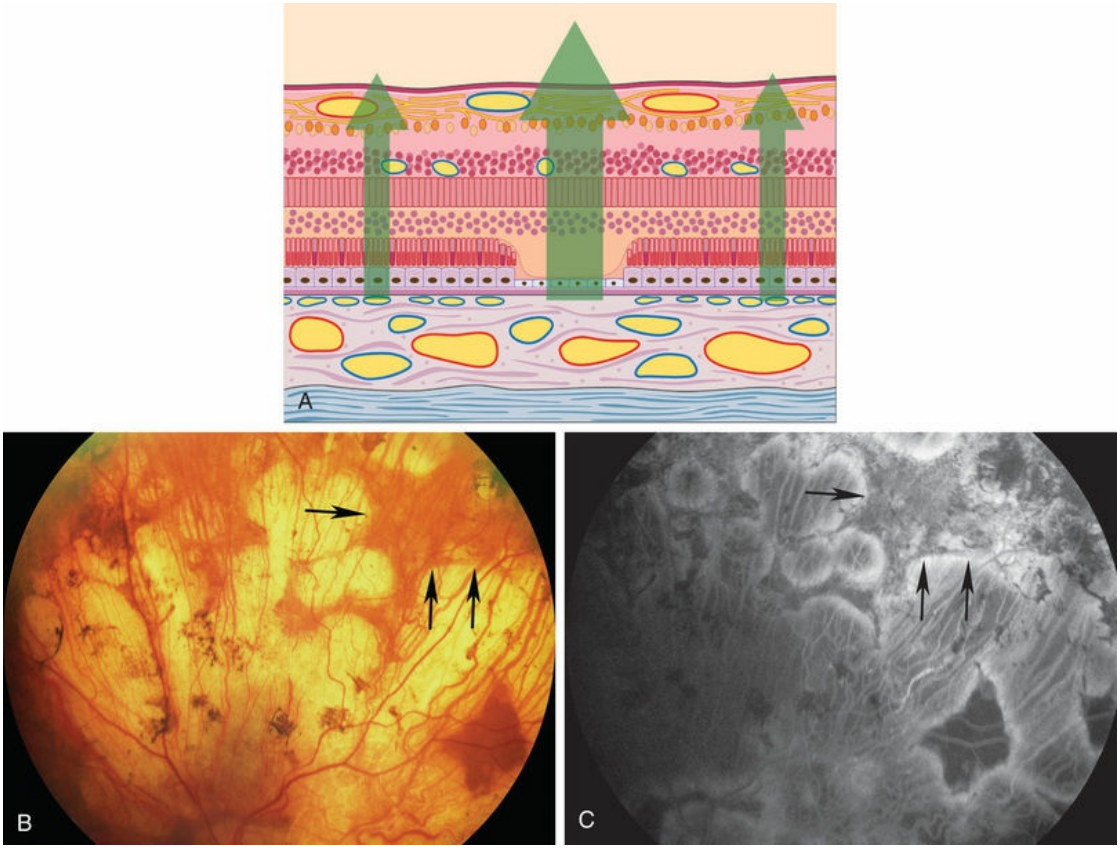

FIG. 1.26 Choroidal atrophy, with some remaining islands of choriocapillaris, due to choroideremia. (A) Schematic of retina shows loss of pigment epithelium and choriocapillaris and some of the outer retina (especially photoreceptors). (B) Color photograph of left superior retina showing areas of severe atrophy and more intact areas of retinal pigment epithelium (RPE) peripherally. Arrows delineate margins between normal RPE and RPE atrophy producing window defect. (C) The arteriovenous phase of fluorescein angiogram shows normal fluorescence of the retinal arteries. The large choroidal vessels can be seen temporally on the right side of the photograph. The ground-glass fluorescence of the choriocapillaris can be seen more peripherally on the left side of the angiogram, where the RPE and choriocapillaris are more intact. Comment: This patient had severe atrophy of the RPE and choriocapillaris. Large choroidal vessels could be seen causing hypofluorescence in relationship to absence of ground-glass choroidal fluorescence. Some areas of choriocapillaris remained and showed normal hyperfluorescence (perhaps increased hyperfluorescence caused by loss of overlying RPE).

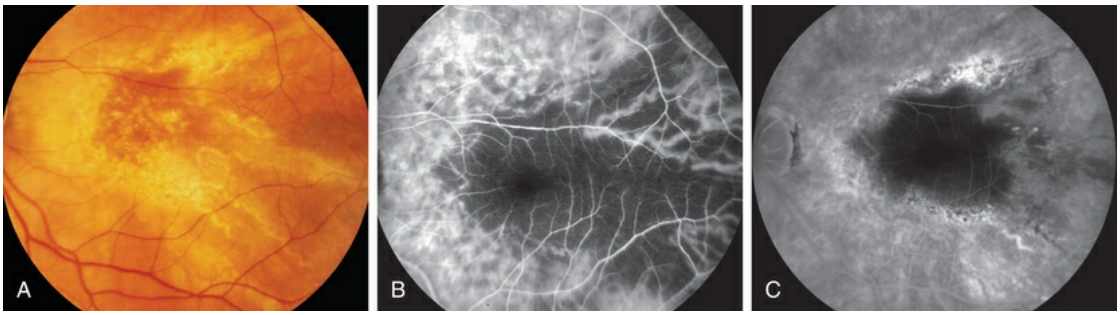

FIG. 1.27 Choroidal hypoperfusion caused by photodynamic therapy with verteporfin. (A) Left macula. Color photograph shows widespread retinal pigment epithelial alterations and drusen secondary to an occult choroidal neovascular membrane secondary to age-related macular degeneration. This treatment was considered standard therapy prior to the advent of intraocular antivascular endothelial growth factor medications. (B) The late arteriovenous phase of the fluorescein angiogram of the left macula shows hypofluorescence of the macula and a large area temporally. Larger choroidal vessels are perfused. The macular hypofluorescence corresponds to the laser treated area. The large area of hypofluorescence temporally represents an area of choroidal nonperfusion caused by selective choriocapillaris occlusion from photodynamic therapy. (C) Later phase of the fluorescein angiogram shows continued hypofluorescence of the area temporal to the macula despite relative restoration of perfusion to choriocapillaris temporal to macula.

Hyperfluorescence

Hyperfluorescence is any abnormally light area on the positive print of an angiogram, that is, an area showing fluorescence in excess of what would be expected on a normal angiogram. There are four possible causes of abnormal hyperfluorescence: (1) preinjection fluorescence; (2) transmitted fluorescence; (3) abnormal vessels; and (4) leakage. The appearance of fluorescence depends in part on the relationship of its appearance to the timing of the

fluorescein injection.

Preinjection fluorescence is hyperfluorescence that can be seen before fluorescein is injected and is caused by structures that naturally fluoresce (autofluorescence) or by poorly matched filters (pseudofluorescence).

Transmitted fluorescence and abnormal vascular fluorescence occur in the early, or vascular, stage of the angiogram, when fluorescein fills patent blood vessels. Transmitted fluorescence appears when fluorescein fills the normal choriocapillaris, but it is more noticeable when there is reduced pigment in the pigment epithelium or loss of retinal pigment epithelium. This is designated pigment epithelial window defect.

When abnormal retinal, disc, or choroidal vessels are present and fill with fluorescein, hyperfluorescence occurs. This type of hyperfluorescence, abnormal vascular fluorescence, is also seen in the early, or vascular, phase of the angiography.

Hyperfluorescence caused by leakage is seen predominantly in the later, or extravascular, phase of angiography. In this phase, fluorescein has emptied from normal and abnormal vessels. Any significant fluorescein that remains in the eye is fluorescein that has escaped or leaked from vascular or tissue barriers and is thus extravascular.

Therefore, to ascertain the type of hyperfluorescence, one must determine the time at which the hyperfluorescence appears in relation to when the fluorescein was injected. Once the hyperfluorescence is determined to be caused by preinjection fluorescence, transmitted fluorescence, the presence of abnormal vessels, or by leakage, the next step is to determine the anatomic location of the hyperfluorescence. Abnormal blood vessels may come from the retina and disc or from the choroid. Leakage can occur in the vitreous, disc, retina, or choroid.

Preinjection Fluorescence

Each angiographic study should include one photograph of the fundus taken with the fluorescein filters in place and before fluorescein is injected. This exposure is called the preinjection, or control, fluorescein photograph. In normal situations this photograph is totally dark; it is completely hypofluorescent. When

the photograph is not dark, autofluorescence or pseudofluorescence is present. The conditions that cause autofluorescence occur infrequently, and the filter problems that produce pseudofluorescence have in recent years been minimized by the development of more precisely matched filter systems.

Autofluorescence

Autofluorescence is the emission of fluorescent light from ocular structures in the absence of sodium fluorescein. Conditions that cause autofluorescence are optic nerve head drusen and astrocytic hamartoma (Fig. 1.28).

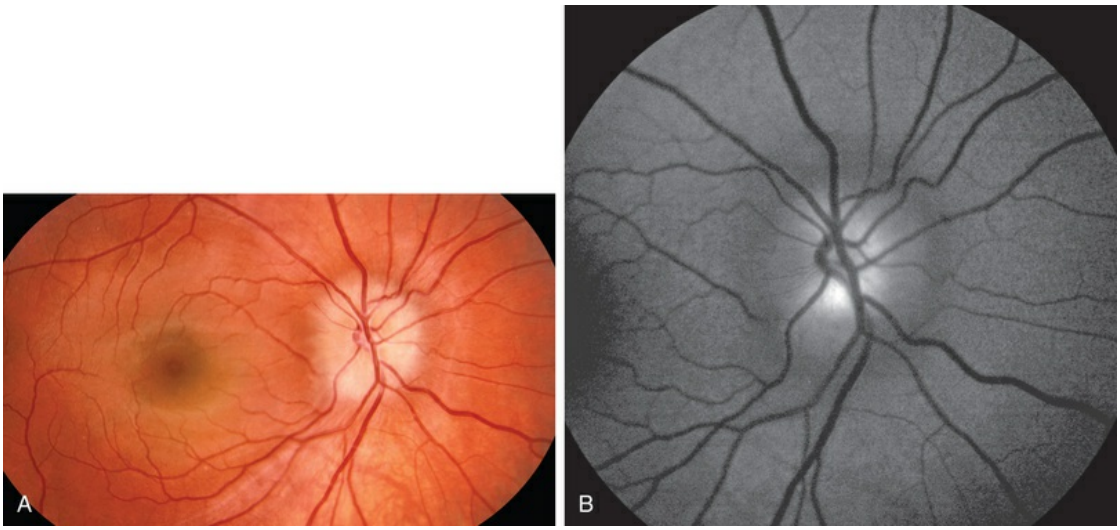

FIG. 1.28 Autofluorescence of optic nerve drusen. (A) Right disc and macula show a blurred disc margin with nonhyperemic vessels. Blurring of the central optic nerve is consistent with disc edema noted on stereophotos. (B) Preinjection or "control" photos are performed with filters in place, prior to any injection of fluorescein. This allowed for the identification of optic nerve drusen, which autofluoresce.

Pseudofluorescence occurs when the blue exciter and green barrier filters overlap. The blue filter overlaps into the green range, allowing the passage of green light, or the green barrier filter overlaps into the blue range, allowing the passage of blue light (Fig. 1.2). The overlapping light passes through the system, reflects off highly reflective surfaces (light-colored or white structures), and

stimulates the film. This reflected nonfluorescent light is called pseudofluorescence.

Conditions that tend to produce pseudofluorescence include any light-colored or white (reflective) fundus change (e.g., sclera, exudate, scar tissue, myelinated nerve fibers, foreign body).

Currently, fluorescein angiographic filters are usually very well matched; overlap is minimal, so pseudofluorescence is faint and rarely a major problem. However, filters do tend to get thin with time. The frequent flashes of light from the fundus camera wear them down, and most filter pairs eventually allow pseudofluorescence. Therefore, depending on frequency of use, fluorescein filters must be changed occasionally. Our experience indicates that change is required approximately every 5 years.

Transmitted Fluorescence (Pigment Epithelial Window Defect)

This fluorescence is an accentuation of the visibility of normal choroidal fluorescence. Transmitted fluorescence occurs when fluorescence from the choroidal vasculature appears to be increased because of the absence of pigment in the pigment epithelium, which normally forms a visual barrier to choroidal fluorescence. The major cause of pigment epithelial window defect is atrophy of the pigment epithelium (Figs. 1.29–1.32).

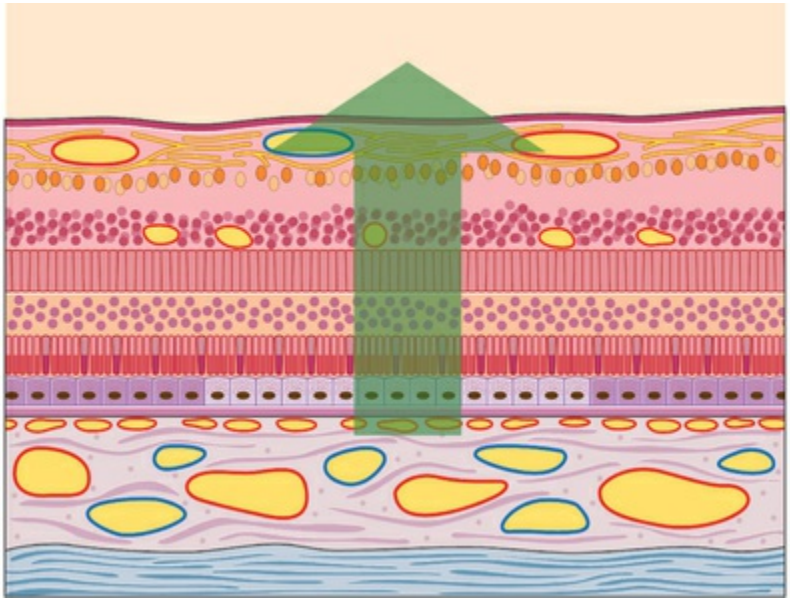

FIG. 1.29 Pigment epithelial window defect. This schematic of the retina shows that the pigment epithelium in the center of the section is less pigmented than the normal pigment epithelium. This allows the normal choroidal and choriocapillaris fluorescence to show through; that is, this pathologic condition would create a typical pigment epithelial window defect.

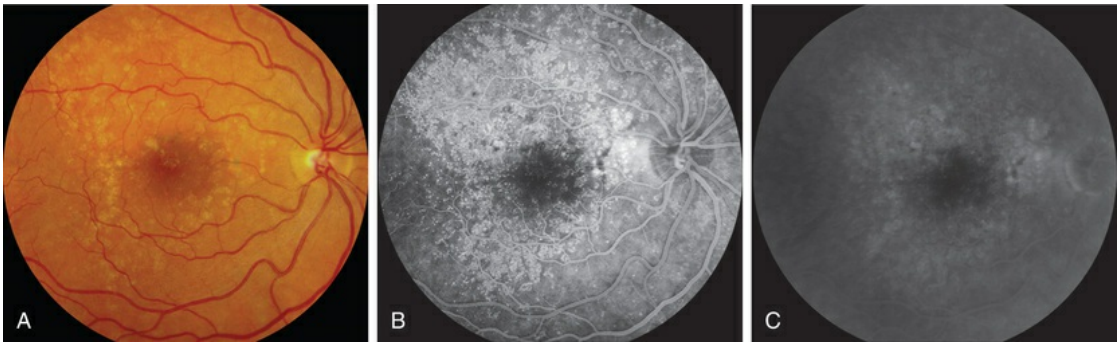

FIG. 1.30 An eye with drusen demonstrating pigment epithelial window defects. (A) Color photograph: right macula shows multiple drusen temporally. (B) Late arteriovenous phase of fluorescein angiogram shows marked hyperfluorescence in the areas of the drusen. (C) Late recirculation phase of fluorescein angiogram shows fading of fluorescence. Comment: Note the degree of fluorescence of the entire fundus vasculature. This is typical of a pigment epithelial window defect, which is a type of vascular fluorescence. The drusen allow a better view to the choriocapillaris because of the thinning of the pigment epithelium overlying them.

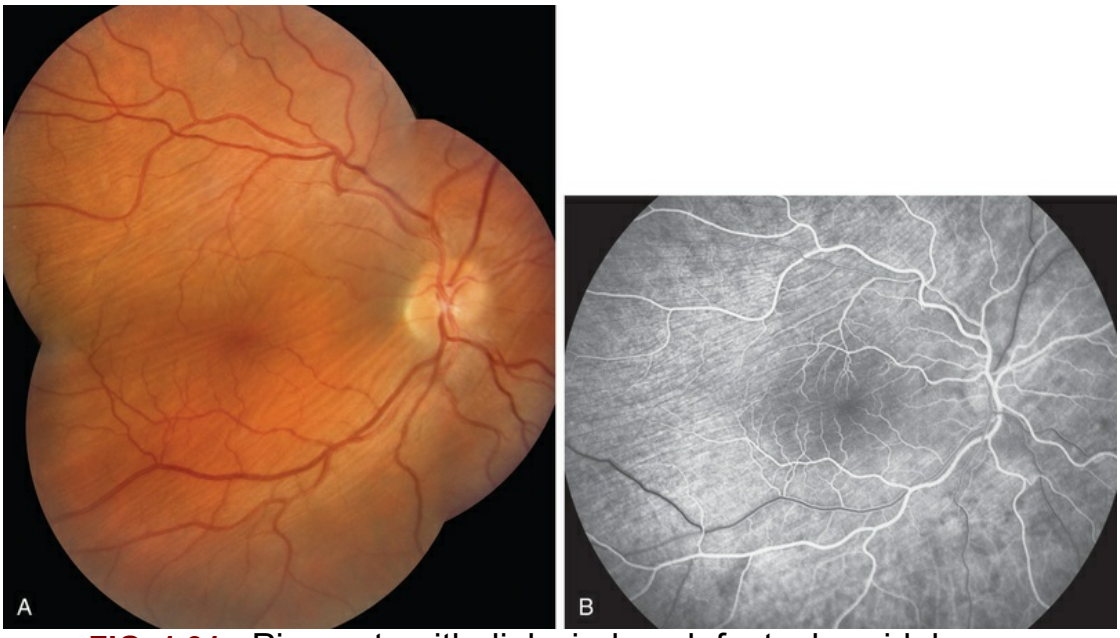

FIG. 1.31 Pigment epithelial window defect: choroidal folds. (A) Montage color photograph of right disc and macula. Note the pale lines (choroidal folds) scattered throughout the posterior pole. (B) Arteriovenous phase of fluorescein angiogram of the disc and macula. Hyperfluorescent lines correspond to the folds, and adjacent hypofluorescent lines are present throughout the macula and surrounding the disc. Comment: This patient had pigment epithelial folds caused by prolonged hypotony from a filtering bleb. The hyperfluorescent lines are thought to be the hills of the folds, in the apices of which the pigment epithelium is thinned, allowing hyperfluorescence in the early phases of the fluorescein angiogram (pigment epithelial window defect). The dark lines are thought to be the valleys of the folds, with an increase in pigmentation causing blockage of choroidal fluorescence. The later phases of fluorescein angiograms often show fading of fluorescence. Choroidal folds represent a type of pigment epithelial window defect with early vascular fluorescence and late fading of fluorescence.

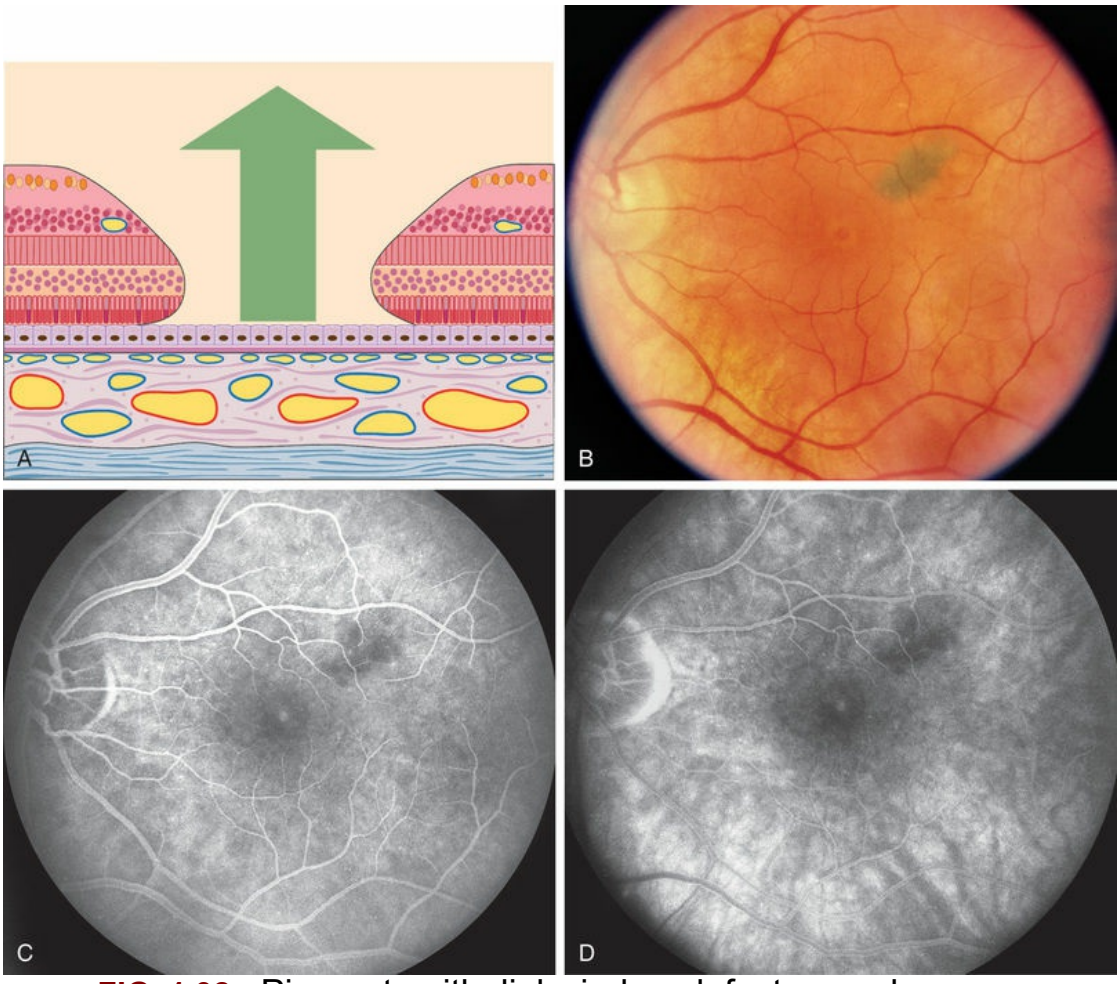

FIG. 1.32 Pigment epithelial window defect: macular hole. (A) Schematic drawing of macula showing loss of entire central foveal tissue. (B) Color photograph of the left macula. This patient has a macular hole. Note a corona of lighter detached, swollen retinal tissue surrounding the foveal center where the hole is located. (C) Late phase of fluorescein angiogram shows hyperfluorescence within the macular hole. (D) Later phase of the fluorescein angiogram shows some fading of the hyperfluorescence within the macular hole. Comment: The choriocapillaris was intact. Therefore the angiogram showed normal fluorescence of the choriocapillaris (early hyperfluorescence within the center of the fovea) and fading in the late phase of the angiogram.

When the pigment epithelium is dense, choroidal fluorescence is not clearly visible because the pigment blocks the view of the choroid and acts as a barrier to fluorescein. The density of the pigment determines the degree to which transmission of the normal

choroidal fluorescence is blocked. The visibility of choroidal fluorescence is inversely proportional to the concentration of pigment in the pigment epithelium. If the pigment epithelium contains less than the normal amount of pigment or is defective, the choriocapillaris appears to fluoresce more brightly. The presence of hyperfluorescence caused by a defect in the pigment epithelium depends on the state of both the pigment epithelium and the choriocapillaris. The choriocapillaris must be intact for a depigmented area of the pigment epithelium to be apparent. If the choriocapillaris does not fill, a depigmented area of the pigment epithelium does not fluoresce.

Transmitted fluorescence has the following four basic characteristics:

1. It appears early in angiography, coincidental with choroidal filling.

2. It increases in intensity as dye concentration increases in the choroid.

3. It does not increase in size or shape during the later phases of angiography.

4. It tends to fade and sometimes disappear as the choroid empties of dye at the end of angiography.

In short, transmitted fluorescence appears, peaks early, and fades late without changing size or shape, as would any normal vascular fluorescence. When pigment epithelial depigmentation is extensive, late fluorescein staining of the choroid and sclera may be visible, although it is less intense than the fluorescence of the window defect.

Abnormal Retinal and Disc Vessels.

Abnormal vascular fluorescence occurs when abnormal vessels are present. Such pathologic vessels may be in the retina, on the disc, or at the level of the choroid. Normal and abnormal retinal and disc vessels are clearly visible on the angiogram because no barrier obscures them from view. Gross abnormalities of the retinal and

disc vasculature and subtle microvascular changes that cannot be appreciated adequately by ophthalmoscopic examination will be well defined and easily distinguished by FA. These changes in the retinal vasculature can be classified into six morphologic categories: (1) tortuosity and dilation (Figs. 1.33 and 1.34); (2) telangiectasis (Figs. 1.35 and 1.36); (3) neovascularization (Fig. 1.37); (4) anastomosis (Fig. 1.34); (5) aneurysms (Figs. 1.34 and 1.35); and (6) tumor vessels (Figs. 1.38 and 1.39).

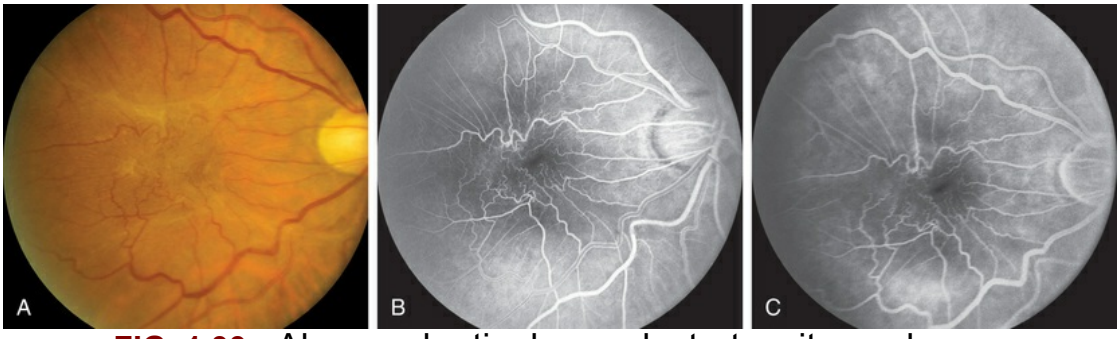

FIG. 1.33 Abnormal retinal vessels, tortuosity, and dilation: internal limiting membrane contraction. (A) Color photograph of right macula shows a pale membrane overlying the right macula, producing contraction of the retina and tortuosity of the retinal vessels. (B) Arteriovenous phase of fluorescein angiogram shows marked irregularity and tortuosity of the retinal vessels in association with the preretinal membrane (macular pucker). (C) Late phase of fluorescein angiogram shows a small amount of vascular leakage due to contraction of the membrane and pulling on the retinal vessels. Comment: This is tortuosity and dilation, a type of abnormal retinal vascular fluorescence. It is caused by the mechanical traction of an epiretinal membrane.

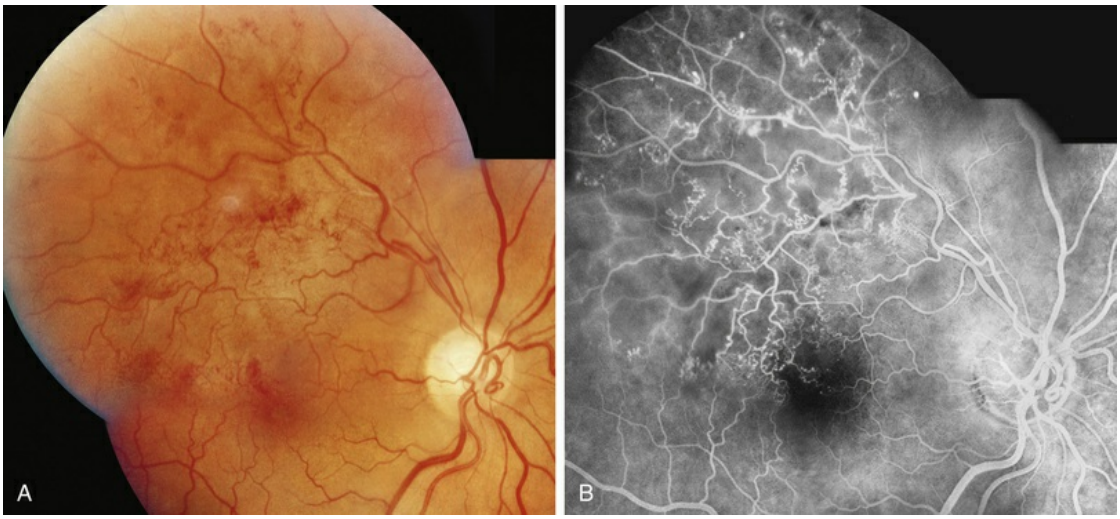

FIG. 1.34 Abnormal retinal vascular fluorescence: retinal vascular microaneurysms, telangiectasis, and anastomoses. (A) Color photography of right eye shows numerous telangiectatic retinal vessels due to a superotemporal branch-vein occlusion. (B) Arteriovenous-phase fluorescein angiogram shows multiple areas of smaller and larger microaneurysms and telangiectasis. Several small venous–venous anastomoses can be seen just temporal to the macula. The venous system of the occluded area has collateralized with patent vessels in uninvolved areas.

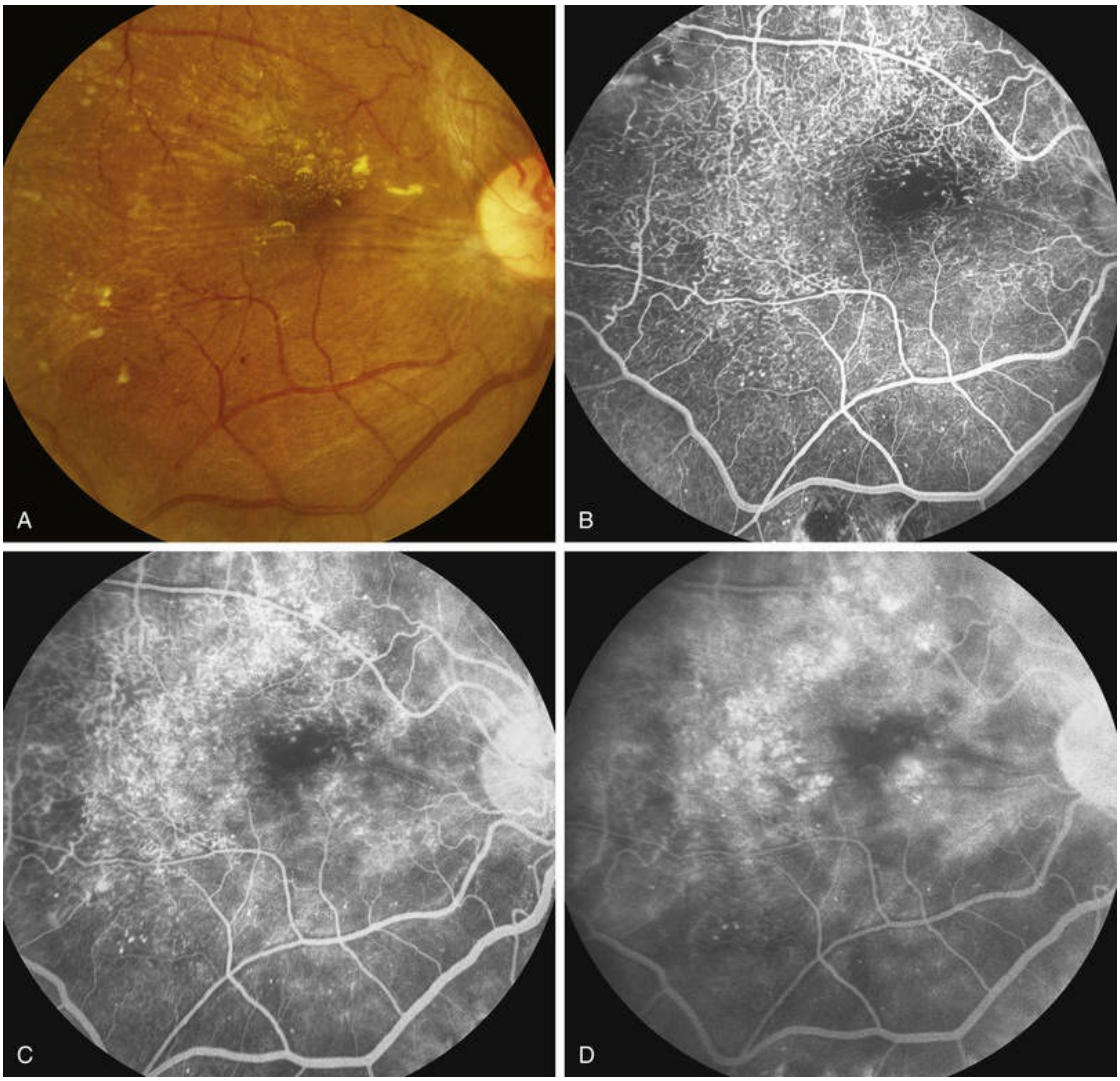

FIG. 1.35 Retinal telangiectasis and microaneurysms secondary to diabetic retinopathy. (A) Color photography of right macula showing retinal exudate, retinal striae, and irregularly dilated retinal vessels (telangiectasis). (B) Arteriovenous-phase fluorescein angiogram shows extensive hyperfluorescence from the numerous microaneurysms, and telangiectatic retinal vessels. (C) Later arteriovenous-phase fluorescein angiogram of right macula showing leakage from many of these vessels. (D) Late-phase fluorescein angiogram of right macula shows multiple circular areas of hyperfluorescence due to accumulation of dye in extensive cystoid spaces. Comment**:** This patient had significant retinal microvascular changes due to diabetic retinopathy.

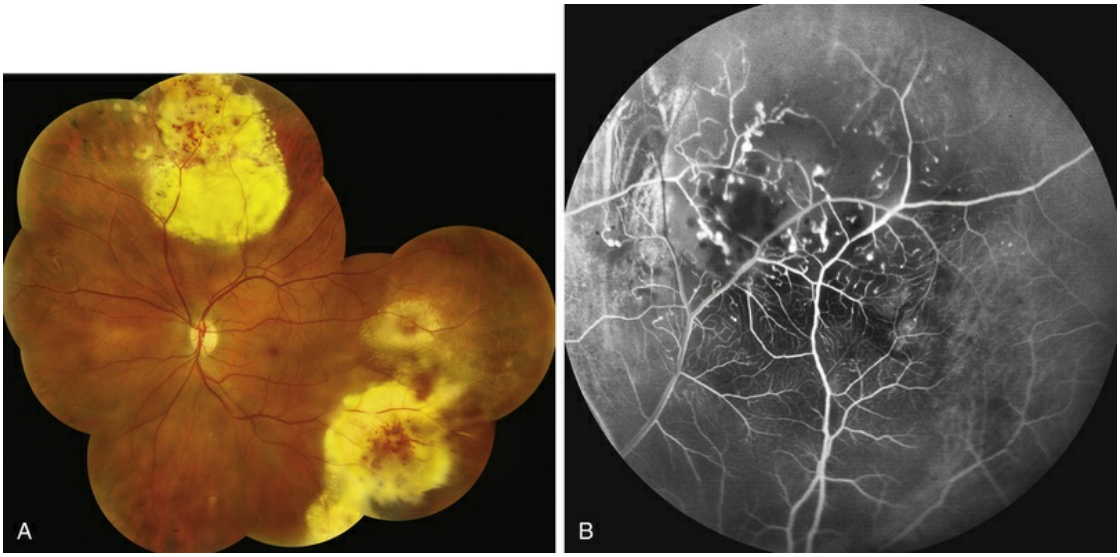

FIG. 1.36 Abnormal retinal vessels: telangiectasis. (A) Color montage photograph demonstrating severe areas of exudation, as well as dilated and telangiectatic vessels. The retina is very edematous. (B) Arteriovenous phase of fluorescein angiogram shows marked irregularity of the retinal vasculature. There are areas of capillary nonperfusion, telangiectasis, and tortuosity. Comment: This patient had Coats disease with a markedly abnormal retinal capillary bed, including telangiectasis and dilated vessels.

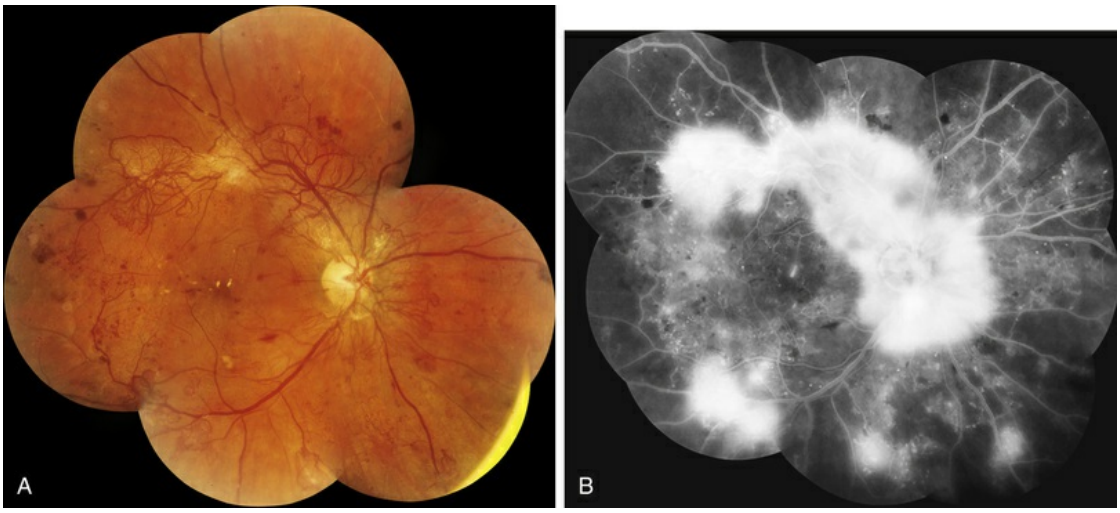

FIG. 1.37 Abnormal retinal vessels: retinal neovascularization due to proliferative diabetic retinopathy. (A) Montage color photograph of the posterior pole of the right eye. Extensive irregular

tortuous vessels extend from the optic nerve along the vascular arcades and nasally. These vessels lie on the surface of the retina. (B) Later arteriovenous phase of fluorescein angiogram montage shows increasing hyperfluorescence of the retinal neovascularization. Comment: This patient had severe proliferative diabetic retinopathy with extensive neovascularization of the right disc. The vessels fluoresced early (vascular fluorescence) and leaked late. This is very typical of retinal or disc neovascularization.

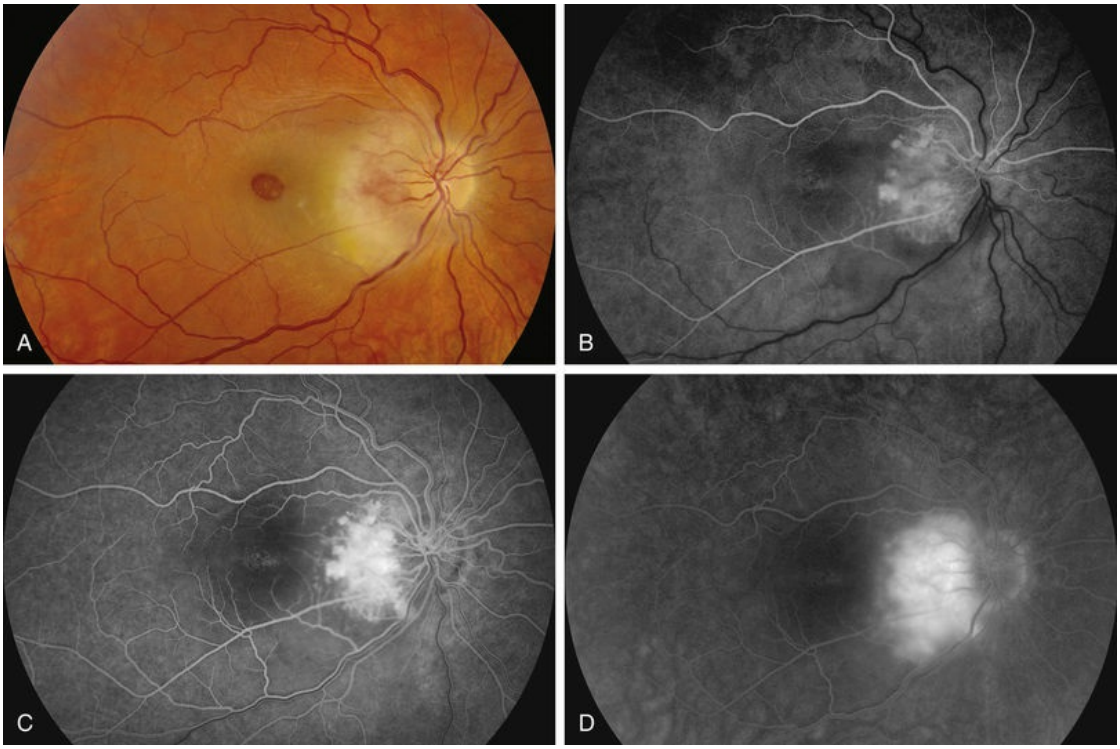

FIG. 1.38 Abnormal retinal vessels: tumor–retinal angioma as part of von Hippel's disease. (A) Color photograph of right macula and disc shows exudate temporal and inferior to the disc. A very vascular, slightly elevated mass was noted on the temporal border of the disc. Ophthalmoscopy showed that it has a reddish appearance. A large full-thickness macular hole is also observed. (B) Early arterial phase of the fluorescein angiogram shows marked fluorescence of the mass. (C) Midarteriovenous phase of the fluorescein angiogram shows an increased fluorescence of the mass. (D) Late phase of the fluorescein angiogram shows leakage of fluorescein

within the mass. Comment: This patient had a peripapillary retinal angioma. It was very vascular and showed early fluorescence and extensive late leakage.

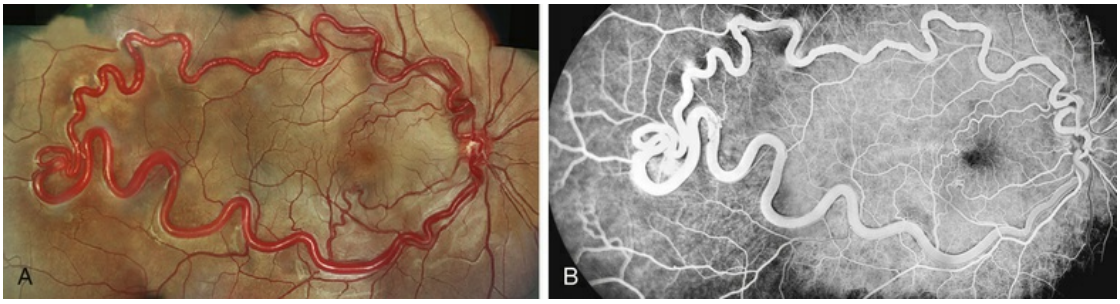

FIG. 1.39 Arteriovenous malformation: Wyburn–Mason type. (A) Color montage photograph of right macula and temporal retina showing enlarged, dilated retinal artery, with direct connection to an engorged draining vein. There is no intervening capillary bed. (B) Fluorescein angiogram showing marked hyperfluorescence of the abnormal, dilated retinal artery and vein. Two smaller arteriovenous malformations appear to be present, one just above the macula, and the other just below.

These aforementioned changes can be viewed in the early (vascular) phases of angiography. Later, as the vessels empty, some of these vascular abnormalities leak fluorescein, whereas others do not.

Vascular abnormalities of the retina and disc are readily apparent on the fluorescein angiogram. The changes are characterized by early vascular-appearing hyperfluorescence. Each of the six morphologic types indicates specific disease processes that aid the clinician in making a diagnosis, determining the degree of the distinct pathologic process, and understanding the pathophysiology of retinal vascular disease.

Abnormal Choroidal Vessels.

Abnormal vessels that may be present under the retina and originate from the choroid are subretinal neovascularization and vessels within a tumor. When subretinal neovascularization is

present, the early angiogram often shows a lacy, irregular, and nodular hyperfluorescence (Figs. 1.40 and 1.41). With a choroidal tumor, the abnormal hyperfluorescence is a similar, early vascular-type fluorescence, although it may be coarser, as seen in choroidal hemangioma (Fig. 1.42) and malignant melanoma (Fig. 1.43).

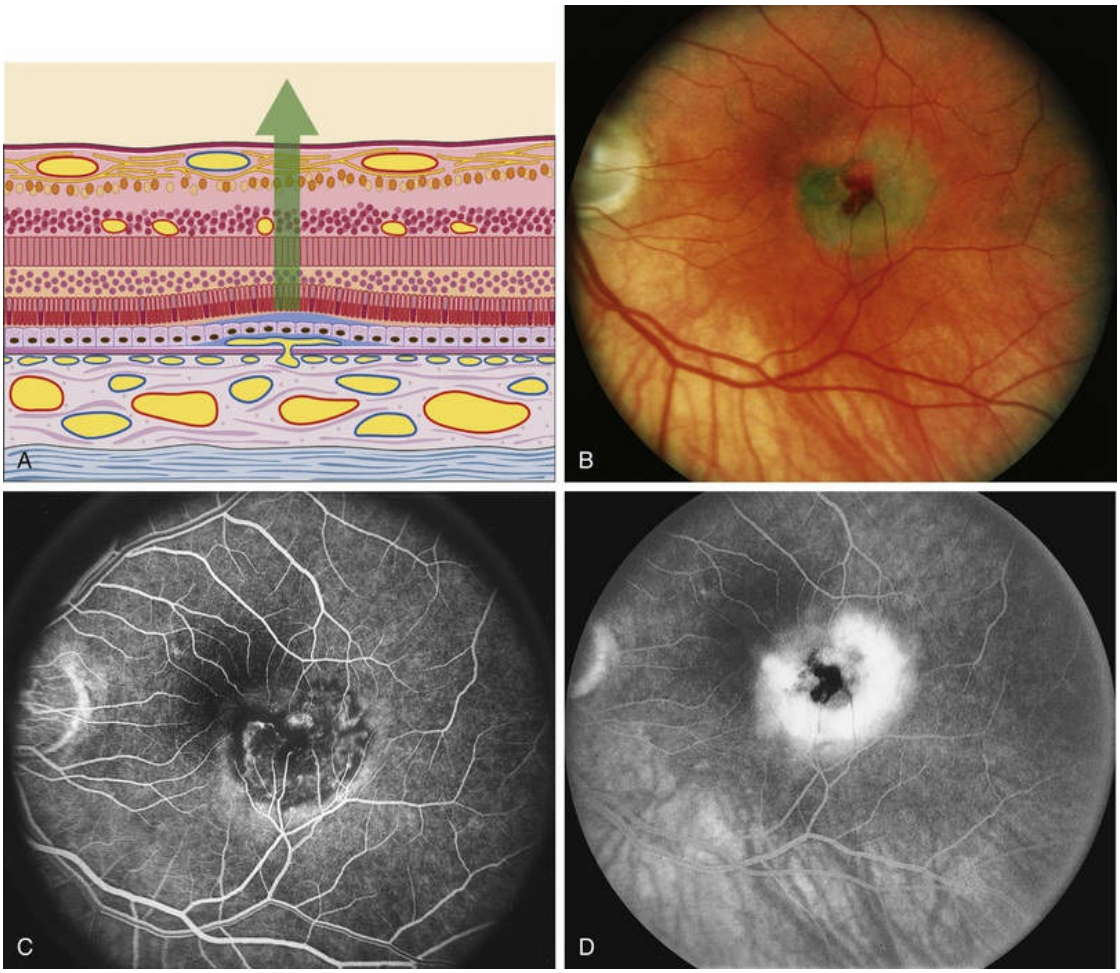

FIG. 1.40 Abnormal choroidal vessels: subretinal neovascularization. (A) Schematic view of the retina shows a small break in Bruch's membrane, with a fine proliferation of capillaries through the break dissecting under and lifting up the pigment epithelium. There is a shallow sensory retinal detachment. (B) Color photograph of the left macula. There is a dirty-gray membrane involving the central macula. Note the small area of subretinal hemorrhage. There is a shallow sensory retinal detachment. (C) The arteriovenous phase of fluorescein angiogram shows fine, lacy, irregular hyperfluorescence corresponding to a small, fine patch of subretinal neovascularization. (D) Late

phase of fluorescein angiogram shows leakage of these vessels into the subpigment epithelial and subretinal spaces. Comment: This patient had a small patch of subretinal neovascularization involving the central fovea. The angiogram shows typical, early vascular fluorescence (in a nodular, irregular, lacelike fashion) and late hyperfluorescent leakage.

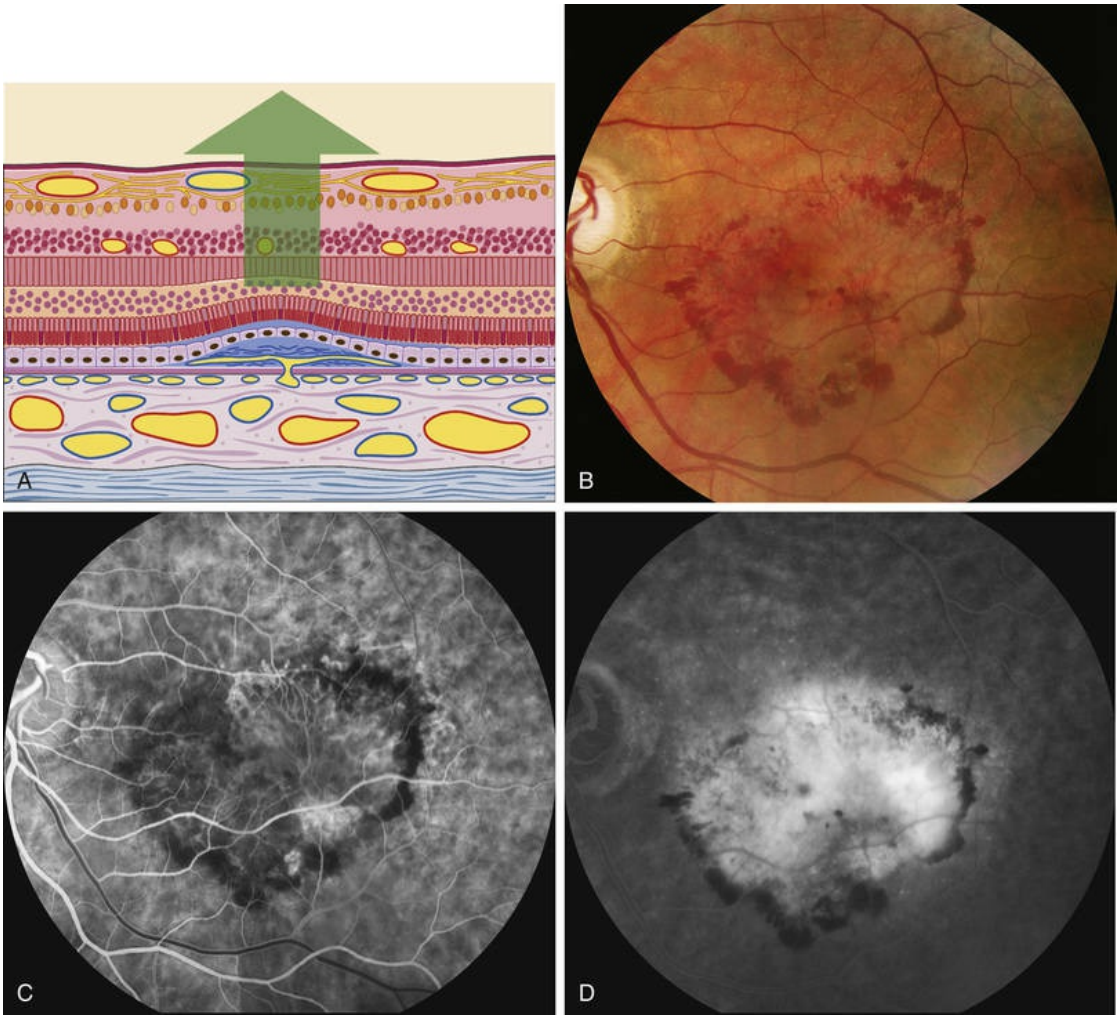

FIG. 1.41 Abnormal choroidal vessels: subretinal neovascularization. (A) Schematic drawing of retina shows vascular proliferation from the choriocapillaris dissecting under the pigment epithelium, with associated fibrous tissue. The pigment epithelium has become thinned and the sensory retina detached. The outer plexiform layer of the sensory retina shows cystic spaces. (B) Red-free photograph of left macula shows some hemorrhage and exudate. On the color

photograph and slit-lamp biomicroscopy, a dirty-gray membrane was noted in the inferotemporal portion of the macula. This is seen as a slightly pale lesion in the inferotemporal macula. (C) Early arteriovenous phase of fluorescein angiogram shows a lacy, irregular, nodular area of hyperfluorescence in the inferotemporal macula. This is a flat patch of vessels that has proliferated from the choriocapillaris under the pigment epithelium. (D) Late phase of the fluorescein angiogram shows leakage from the patch of subretinal neovascularization. Most of the fluorescence is pooling of fluorescein under the sensory retinal detachment, although there is some cystic change in the fovea. Comment: This patient had a patch of subretinal neovascularization that was nearly 4 disc diameters in size. It fluoresced early with the vascular phase of the angiogram (typical for subretinal neovascularization) and leaked late. Actually, “subretinal neovascularization” is a misnomer because the new vessels are initially located in the subpigment epithelial space.

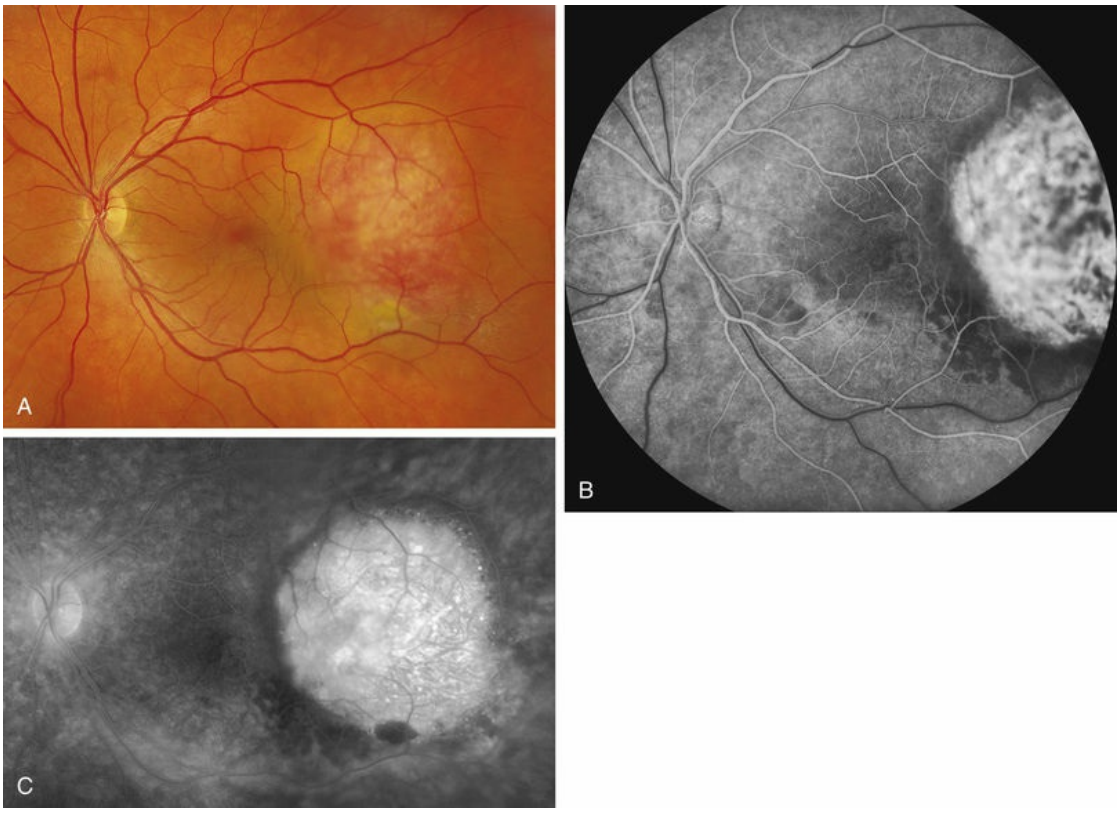

FIG. 1.42 Abnormal choroidal vessels in a patient with choroidal hemangioma. (A) Color photos of left macula and disc with elevated choroidal hemangioma. (B) Arteriovenous phase of the fluorescein angiogram shows prominent hyperfluorescence in this area demonstrating the tumor vessels. (C) Late phase of the fluorescein angiogram shows marked leakage in this area. Comment: This patient had a choroidal hemangioma, which is a very vascularized choroidal mass. The vascularity in this mass causes the marked hyperfluorescence and leakage.

FIG. 1.43 Abnormal choroidal vascular fluorescence due to malignant melanoma. (A) Color photograph of left eye. Note the darkly pigmented mass nasal to the optic nerve. There is some orange lipofuscin pigment overlying the surface of this as well. (B) Arteriovenous phase of fluorescein angiogram of the mass shows hyperfluorescence over the surface of the tumor. This patient also had some macular drusen, which show some early hyperfluorescence in the macula. (C) Late phase of the fluorescein angiogram shows leakage from the mass. There are multiple “hot spots” overlying the tumor. Comment: This patient had a choroidal malignant melanoma. This was a medium-sized tumor that showed the typical early fluorescence that is seen in a medium-sized melanoma.

Leakage.

Fluorescence of the retinal and choroidal vessels begins to diminish about 40–60 seconds after injection. Fluorescein empties almost completely from the retinal and choroidal vasculature about 10–15

minutes after injection. Any fluorescence that remains in the fundus after the retinal and choroidal vessels have emptied of fluorescein is extravascular fluorescence and represents leakage.

Four types of late extravascular hyperfluorescent leakage occur in the normal eye: (1) fluorescence of the disc margins from the surrounding choriocapillaris; (2) fluorescence of the lamina cribrosa; (3) fluorescence of the sclera at the disc margin if the retinal pigment epithelium terminates away from the disc, as in an optic crescent; and (4) fluorescence of the sclera when the pigment epithelium is lightly pigmented. These are the only forms of late hyperfluorescence or leakage that can be considered "normal." Any other hyperfluorescence observed 15 minutes after the fluorescein injection represents extravascular fluorescein and is referred to as leakage.

Either or both of the two vascular systems of the fundus can produce abnormal late hyperfluorescence (leakage) if defects are present in their respective barriers to fluorescein. The barrier to fluorescein leakage from the retinal vessels is the retinal vascular endothelium. The barrier to leakage from the choroidal circulation is the pigment epithelium. An abnormality of the retinal vascular endothelium can result in permeability to fluorescein and leakage of fluorescein into the retinal tissue. Similarly, an abnormality of the pigment epithelium can result in permeability to fluorescein, and fluorescein will leak from the choroidal tissue through the pigment epithelium. Abnormal late hyperfluorescence of the choroid, however, can occur without damage to the pigment epithelium, as in cellular infiltrates of the choroid that occur in choroidal inflammation or tumor.

There are two other types of late abnormal fluorescence: one occurs when fluorescein enters the vitreous, and the other when fluorescein leaks into the optic nerve head.

Vitreous Leakage.

Leakage of fluorescein into the vitreous creates a diffuse, white haze in the late phase of the fluorescein angiogram. In some instances the haze is generalized and evenly dispersed, and in other cases the white haze is localized.

Leakage of fluorescein into the vitreous is due to three major

causes: (l) neovascularization growing from the retinal vessels on to the surface of the retina or disc or into the vitreous cavity; (2) intraocular inflammation; and (3) intraocular tumors.

Vitreous hyperfluorescence secondary to retinal neovascularization is usually localized and appears as a cotton-ball type of fluorescence surrounding the neovascularization (Fig. 1.37B). The vitreous fluorescence secondary to intraocular inflammation is often generalized, giving a diffuse, white haze to the vitreous because of generalized leakage of fluorescein from the iris and ciliary body. The vitreous fluorescence secondary to tumors is most often localized over the tumor.

Disc Leakage.

The optic nerve head normally has some fluorescein leakage (late hyperfluorescence) as a result of staining of the lamina cribrosa and the surrounding margins of the disc (from the normally leaking peripapillary choriocapillaris). The difference between normal and abnormal leakage at the disc may be subtle.

Papilledema and Optic Disc Edema.

Papilledema is swelling of the optic nerve head as a result of increased intracranial pressure. Edema of the optic disc is defined as swelling of the optic nerve head secondary to local or systemic causes (Fig. 1.44). The angiogram is similar in each case, demonstrating leakage associated with swelling of the optic nerve head. In the early phases of the angiogram, dilation of the capillaries on the optic nerve head may be seen; in the late angiogram, the dilated vessels leak, resulting in a fuzzy fluorescence of the disc margin.

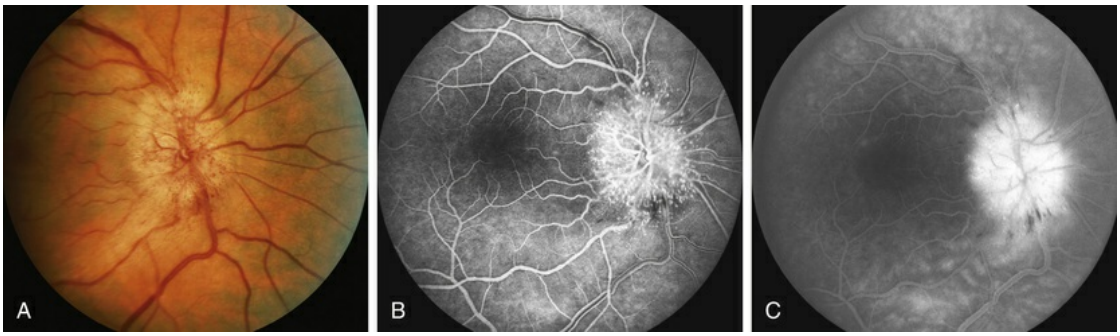

FIG. 1.44 Disc leakage. (A) Color photograph of right optic nerve. Note the dilation of the disc capillaries. (B) The arteriovenous-phase angiogram of the right disc and macula shows the hyperfluorescence due to these dilated disc capillaries. (C) The late phase of the angiogram shows significant leakage from these dilated optic disc capillaries. Comment: This patient had a papillopathy related to diabetes. This produced significant dilation of the disc capillaries. The leakage from this abnormal disc is quite obvious.

Retinal Leakage.

In the late stages of the normal angiogram, the retinal vessels have emptied of fluorescein and the retina is dark. Any late retinal hyperfluorescence is abnormal and indicates leakage of retinal vessels. When the leakage is severe, the extracellular fluid may flow into cystic pockets, and the angiogram shows fluorescence of the cystic spaces. Fluorescein flows out of the patent retinal vessels to lie in pools in the cystoid spaces or stains the edematous (noncystic) retinal tissue. Cystoid retinal edema is apparent as the fluorescein pools in small loculated pockets. In the macula, cystoid edema takes on a stellate or petalloid appearance (Fig. 1.45); elsewhere in the retina, it has a honeycombed appearance (Fig. 1.46). Fluorescent staining of noncystoid edema is diffuse, irregular, and not confined to well-demarcated spaces (Figs. 1.47 and 1.48).

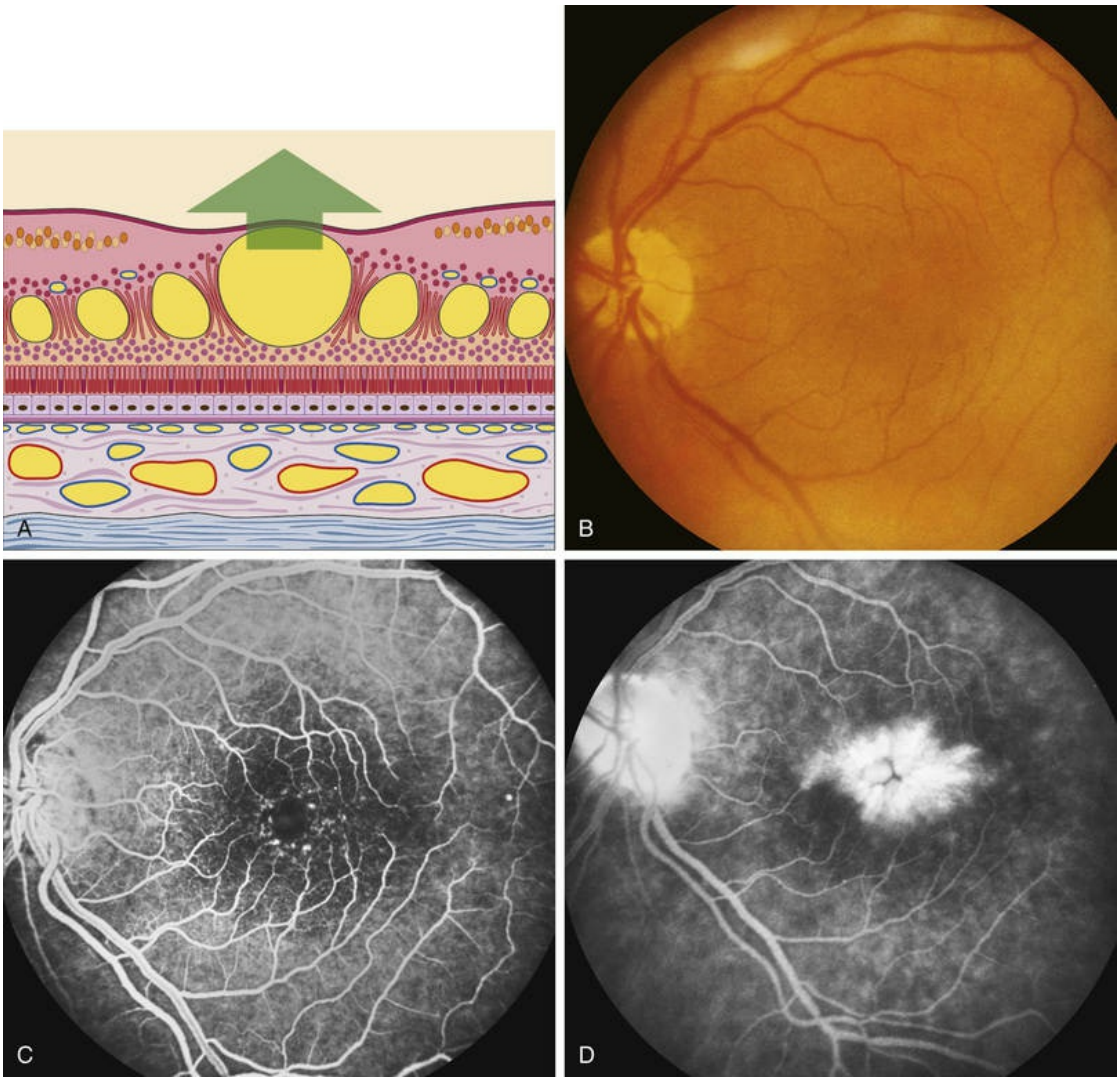

FIG. 1.45 Retinal leak: cystoid macular edema. (A) Schematic drawing of the macula shows large cystic spaces in the outer plexiform layer. There are some cystic spaces in the inner nuclear layer. (B) Color photograph of left macula. Careful inspection of the retina is often necessary on biomicroscopy to detect intraretinal cystoid. (C) Arteriovenous phase of fluorescein angiogram shows some dilation of the fine capillary network around the fovea. (D) Late phase of fluorescein angiogram shows hyperfluorescence from the accumulation of dye filling the cystic spaces. Note the stellate appearance of the cystoid macular edema. Comment: This patient had late hyperfluorescence (i.e., leakage) into the retina that was severe enough to create cystic spaces. This is a typical example of cystoid macular edema.

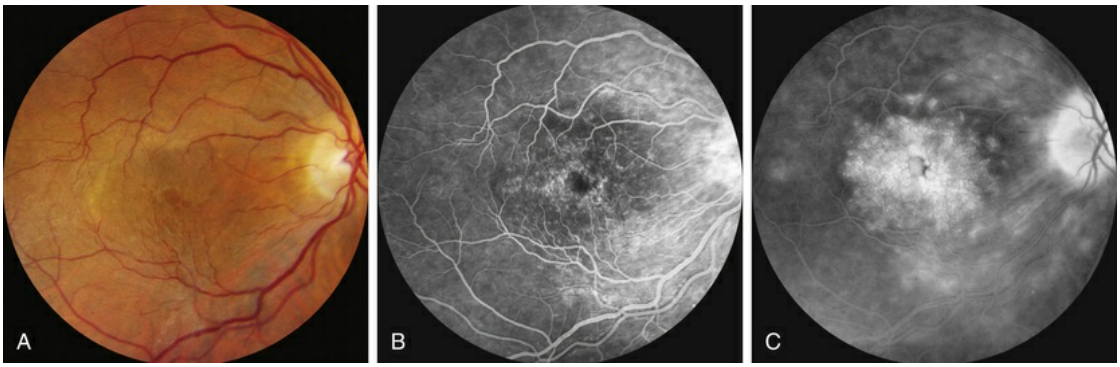

FIG. 1.46 Retinal leakage: cystoid retinal edema. (A) Color photograph of the right macula. Large central cystoid cavity is seen corresponding to fovea. (B) Arteriovenous phase of fluorescein angiogram shows well-defined telangiectatic retinal vessels. (C) Late phase of fluorescein angiogram shows leakage from these vessels. In the center of the macula, the leakage is in stellate cystic pockets, and just outside the macula, temporally, the leakage has taken a honeycomb form. Comment: This patient had leakage of telangiectatic vessels into the retina, and the leakage formed cystoid spaces. Cystoid edema in the center of the macula takes on a stellate form because of the oblique nature of the outer plexiform layer. The cystic spaces take on a honeycomb form in nonmacular areas of the retina because of the perpendicular nature of the fibers of the outer plexiform layer.

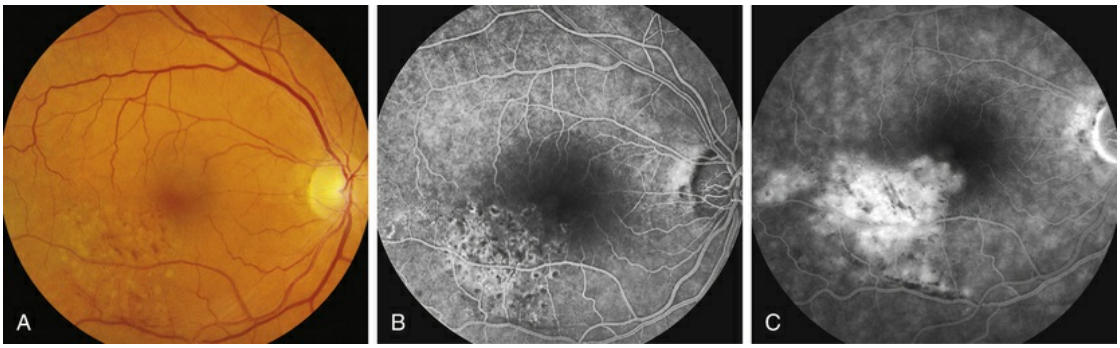

FIG. 1.47 Retinal leakage, severe noncystoid edema. Branch vein occlusion. (A) Color photograph of right macula shows multiple retinal hemorrhages inferotemporally due to a retinal branch vein occlusion. (B) Arteriovenous phase of fluorescein angiogram

shows the vascular abnormalities associated with the branch vein occlusion. Hypofluorescence corresponds to areas previously treated with grid pattern laser photocoagulation. (C) Late phase of fluorescein angiogram shows diffuse leakage of the fluorescein dye. Comment: This patient had generalized leakage of the retinal vascular bed in the distribution of the blocked branch vein. The leakage was not yet severe enough, however, to form clearly defined cystic spaces. Late hyperfluorescence indicates leakage, and this fluorescence is located in the retina; thus this was retinal edema.

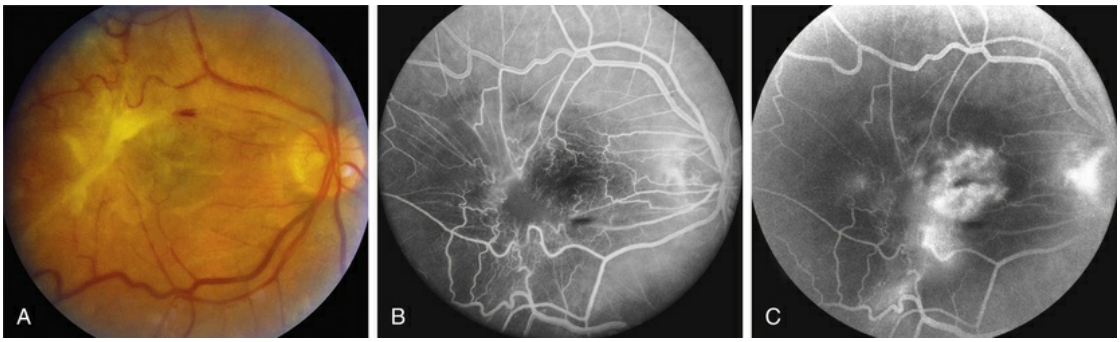

FIG. 1.48 Late hyperfluorescence, retinal leakage: severe epiretinal membrane contraction. (A) Color photograph of right macula showing thick epiretinal membrane overlying the macula and producing severe traction and contraction of the retina and vessels. (B) Arteriovenous phase of fluorescein angiogram shows that the retinal vasculature is tortuous and irregular. (C) Late arteriovenous phase of fluorescein angiogram shows leakage from the retinal vessels. Comment: The marked preretinal membrane caused sufficient traction on the retina, resulting in marked retinal vascular leakage.

The amount of fluorescein leakage depends on the dysfunction of the retinal vascular endothelium (Fig. 1.48). When leakage is not pronounced, the cystoid spaces fill slowly and become visible only late in angiography. When this occurs, the area of cystoid retinal edema may be somewhat hypofluorescent early in the angiogram because the fluid in these spaces acts as a barrier and blocks the

underlying choroidal fluorescence. When there is heavy fluorescein leakage, the cystoid spaces fill rapidly, in some cases within a minute after injection. The large confluent cysts seen with severe cystoid macular edema may fill late in the angiogram. The large retinal vessels can also leak. This is called perivascular staining and is seen in three distinct situations: inflammation (indicating a perivasculitis), traction (severe pulling on a large retinal vessel, Fig. 1.48), and occlusion. When a large retinal vessel leak is partially occluded, or when it traverses an area of occlusion (and capillary nonperfusion), it will leak (Fig. 1.49).

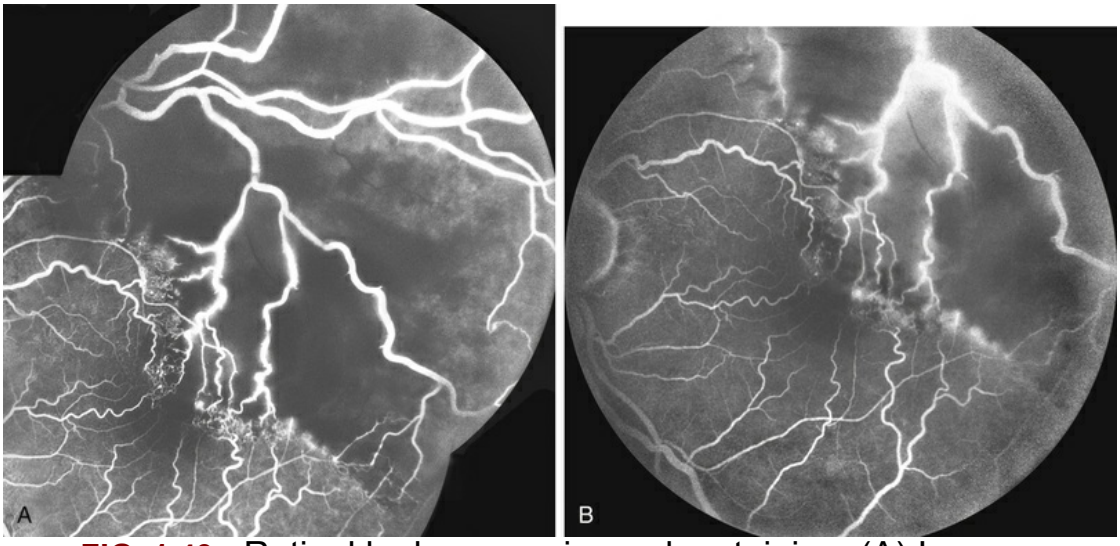

FIG. 1.49 Retinal leakage: perivascular staining. (A) In this late arteriovenous-phase fluorescein angiogram, note the beading of the large retinal veins. There is also associated leakage from these vessels. (B) Later phase of fluorescein angiogram shows perivascular staining (leakage) from the large retinal vessels that are traversing large zones of capillary nonperfusion. Comment: Typically, when a large retinal vessel (artery or vein) is perfused but traverses an area of capillary nonperfusion, ischemic retinal factors will act adversely on the endothelium of the large vessel and cause it to leak. This is called perivascular staining. Perivascular staining also occurs with traction or inflammation.

Choroidal Leakage.

Late hyperfluorescence under the retina can be classified as either pooling or staining (Fig. 1.50). Pooling is defined as leakage of fluorescein into a distinct anatomic space; staining is leakage of fluorescein diffused into tissue.

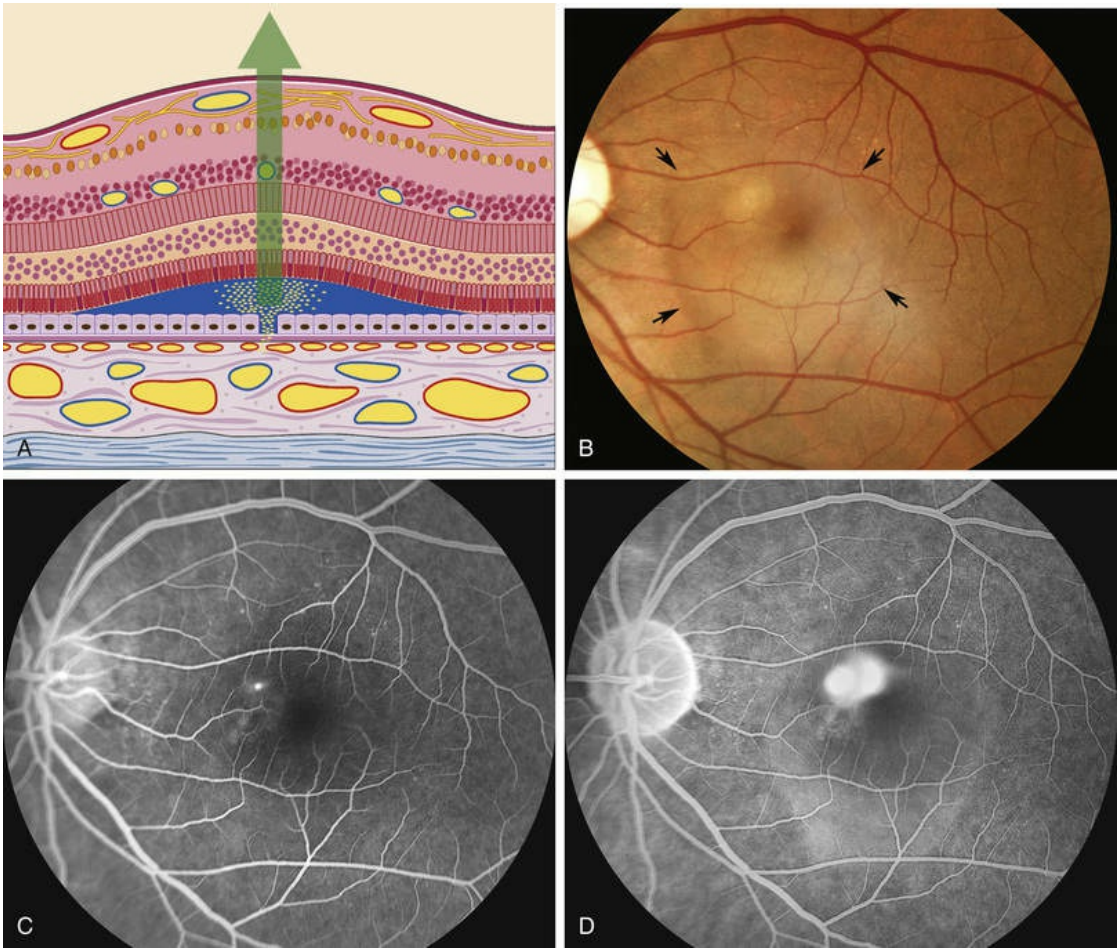

FIG. 1.50 Late hyperfluorescence, subretinal pooling: central serous chorioretinopathy. (A) Schematic drawing of retina shows a sensory retinal detachment. There is a break in the pigment epithelium. Fluorescein flows from the choriocapillaris through Bruch's membrane, through the break in the pigment epithelium, and into the subretinal space, under the detached retina. (B) Color photograph of left macula shows a shallow sensory detachment (*arrows*). Just superonasal to the fovea is a small white area with a gray center. The fluorescein angiogram will reveal that this is the area of the leak. (C) Arteriovenous phase of fluorescein angiogram shows a hyperfluorescent spot that was seen on stereoangiography to be leakage of

fluorescein coming from the pigment epithelium. (D) Late phase of fluorescein angiogram shows that the spot of pigment epithelial leakage has enlarged and become fuzzy. This is the release of fluorescein molecules into the fluid under the detached sensory retina. Comment: This patient had central serous chorioretinopathy. There was a break in the pigment epithelium that allowed leakage of fluorescein through it and into the subretinal space. Late hyperfluorescence means leakage, and in this case, there is pooling of fluorescein under the detached retina.

Fluorescein pools in the spaces created by detachment of the sensory retina from the pigment epithelium or in the space created by detachment of the pigment epithelium from Bruch's membrane. The posterior layer of the sensory retina is made up of rods and cones that are loosely attached to the pigment epithelium. When a sensory retinal detachment occurs, the detached segment separates with little force, forming a very gradual angle at the point of attachment to the pigment epithelium. Because of this narrow angle, the exact limits of a sensory retinal detachment are difficult to locate ophthalmoscopically or by slit-lamp biomicroscopy.

Depending on the specific disease, the late angiogram may or may not portray the full fluorescent filling of the subretinal fluid. For example, in central serous chorioretinopathy the leakage is gradual, and fluorescence of the subsensory retinal fluid will not be complete. In other conditions, such as subretinal neovascularization, fluorescein leakage is profuse, and the subsensory fluid often completely fluoresces (Fig. 1.51).

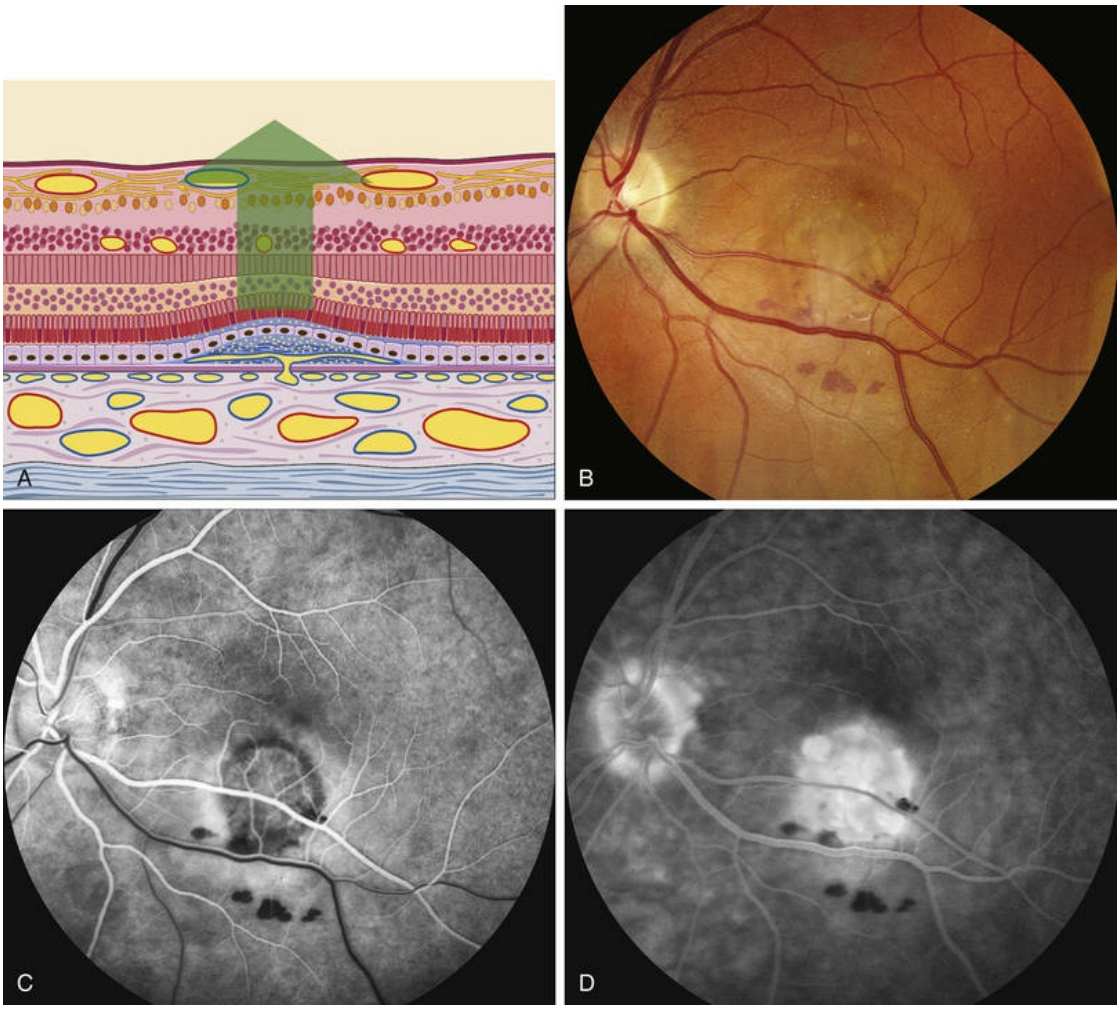

FIG. 1.51 Late hyperfluorescence, leakage, and pooling under the sensory retina caused by subretinal neovascularization, resulting in a sensory retinal detachment. (A) Schematic of the retina showing that it has detached (photoreceptors are separated from pigment epithelium). Vessels have proliferated from the choriocapillaris through Bruch's membrane. There is a fibrovascular scar involving the pigment epithelium. The sensory retina is detached. (B) Color photograph of left macula shows a pale gray lesion in the inferior portion of the macula with some associated hemorrhage. (C) Arteriovenous phase of fluorescein angiogram shows a patch of subretinal neovascularization inferior to the fovea; this is evidenced by the lacy, irregular hyperfluorescence in this area. (D) Late phase of fluorescein angiogram shows fuzzy fluorescence. There is pooling of fluorescein under the detached retina and some staining of the fibrous tissue associated with the subretinal neovascularization. Comment: This patient

had a patch of subretinal neovascularization with a great deal of leakage, causing a sensory detachment. The early-phase angiogram showed the vascular nature of the lesion, and the late-phase angiogram showed the leakage and pooling in the subretinal space.

In contrast to the attachment of the sensory retina, the basement membrane of the pigment epithelium adheres firmly to the collagenous fibers of Bruch's membrane. The firm adhesion and wide angle of detachment make it easy to discern a pigment epithelial detachment ophthalmoscopically. Occasionally a light-orange ring appears around the periphery of a pigment epithelial detachment, further facilitating identification (Fig. 1.52).

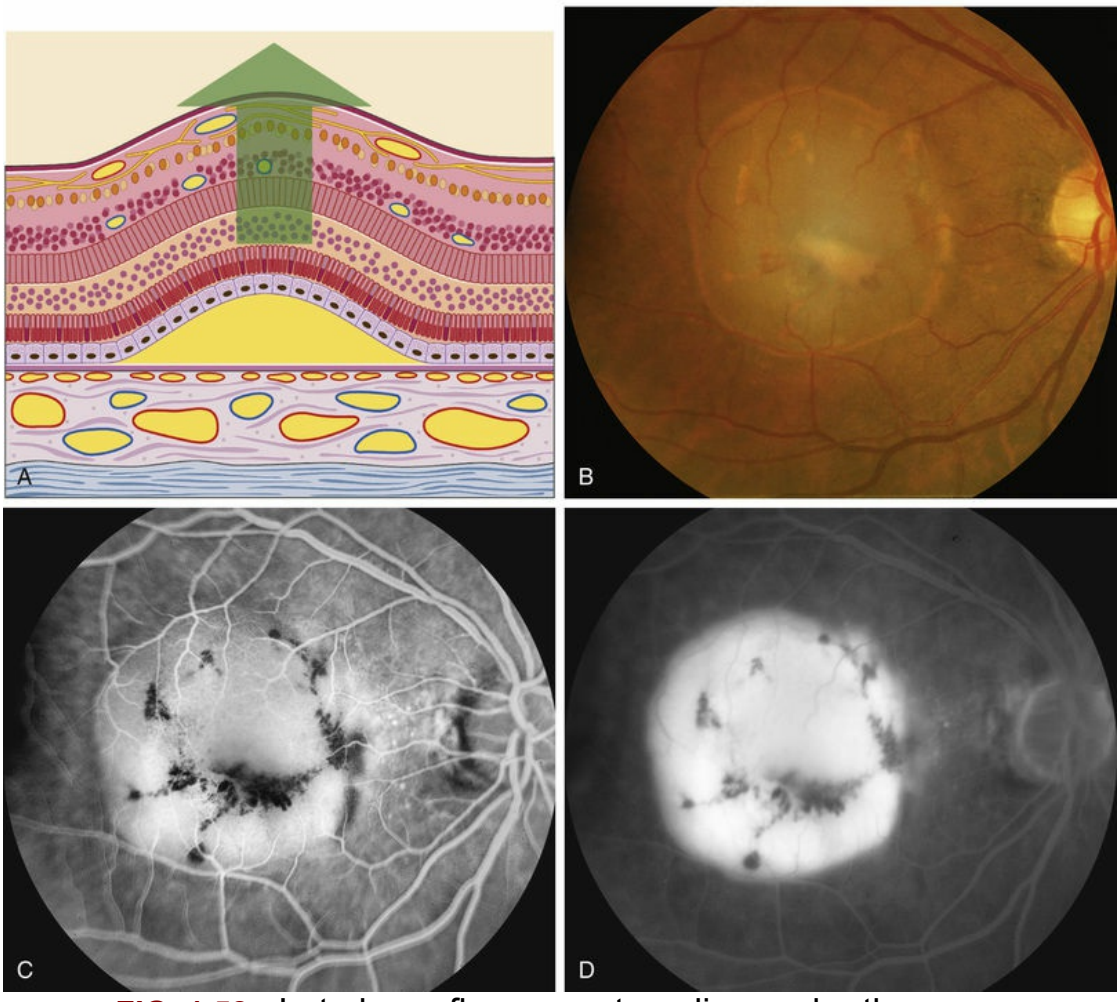

FIG. 1.52 Late hyperfluorescent pooling under the retinal pigment epithelium (pigment epithelial

detachment). (A) Schematic diagram illustrating detachment and elevation of the pigment epithelium; the pigment epithelium is separated from Bruch's membrane. Because the attachment of the pigment epithelium to Bruch's membrane is quite firm, the angle of detachment is quite large. (B) Color photography of right macula shows a round detachment of the pigment epithelium. (C) Early arteriovenous phase of fluorescein angiogram shows early fluorescence from the area of detachment pigment epithelium. (D) Late-phase angiogram of right macula shows well-demarcated hyperfluorescent pooling of fluorescein under the detached pigment epithelium. Comment: Fluorescein flows freely through Bruch's membrane and stops at the pigment epithelium. When the pigment epithelium is detached, the fluorescein flows right through Bruch's membrane into the space made by the detached pigment epithelium. Therefore a pigment epithelial detachment fluoresces evenly and slowly (like a light bulb on a rheostat) and shows intense hyperfluorescent pooling that is well demarcated (indicating its well-defined angle of attachment) late in the angiogram.

The differences in the adherence and the angle of detachment between a sensory retinal detachment and a pigment epithelial detachment result in specific differences in fluorescent pooling patterns. The hyperfluorescent pooling of a sensory retinal detachment tends to fade gradually toward the site where the sensory retina is attached. This makes fluorescein angiographic determination of the extent of a sensory retinal detachment difficult. In contrast, the hyperfluorescent pooling under a pigment epithelial detachment extends to the edges of the detachment, making the entire detachment and its margins hyperfluorescent and clearly discernible.

Pooling of fluorescein under a sensory retinal detachment in central serous retinopathy takes place slowly, since the dye passes through one or more points of leakage in the defective pigment epithelium (Fig. 1.50). When leakage comes from subretinal neovascularization (Fig. 1.51) or a tumor (Fig. 1.43), it is more rapid and complete. When the pigment epithelium is detached from

Bruch's membrane, fluorescein passes freely and rapidly through Bruch's membrane from the choriocapillaris into the subpigment epithelial space (Fig. 1.52).

In some cases of central serous chorioretinopathy, there is an associated pigment epithelial detachment, and pooling under each (sensory retinal detachment and the pigment epithelial detachment) is evident. Occasionally, the edge of a pigment epithelial detachment may tear, or rip, and allow fluorescein dye to pass freely into the subretinal space (Fig. 1.53). Drusen may also show late hyperfluorescence similar to that seen with a pigment epithelial detachment (Fig. 1.54). In some cases of pigment epithelial detachment, especially in older patients, subretinal neovascularization is also present. This combination of subretinal neovascularization and pigment epithelial detachment results in an interesting angiogram that can be challenging to interpret (Fig. 1.55).

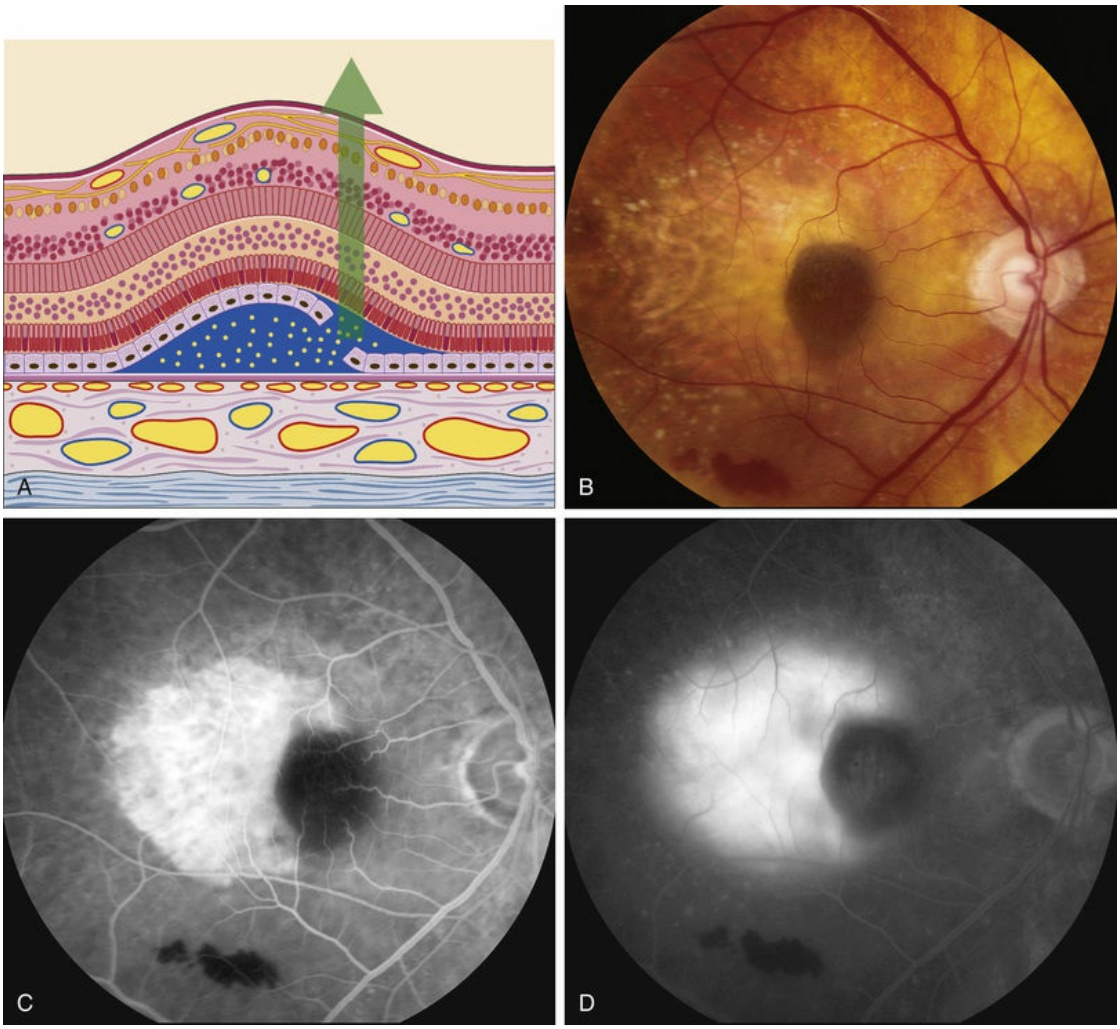

FIG. 1.53 Late hyperfluorescence under the retina – leakage from the choroid due to a retinal pigment epithelial (RPE) rip. (A) Schematic of a pigment epithelial detachment that has developed a tear along one edge. The barrier function of the pigment epithelium is lost and fluorescein dye can diffuse easily and rapidly in the subretinal space. (B) Color photography of right macula showing a round dark area under the fovea, and light (depigmented area) area extending temporally. In the inferior portion of the macula, some subretinal hemorrhage is seen. (C) Early arteriovenous-phase fluorescein angiogram shows bright hyperfluorescence of the depigmented area temporally, and hypofluorescence under the fovea as well as inferiorly in the area of the subretinal blood. (D) Late-phase fluorescein angiogram shows pooling of fluorescein under the retina where the dye has been able to diffuse freely through Bruch's membrane in the sensory retinal detachment.

Comment: This patient developed a tear of the pigment epithelial detachment. The dark area under the fovea is where the pigment epithelium has rolled up after tearing away from the area temporally. The area temporal to the macula appears light due to absence of the RPE in this area. Since the RPE barrier is absent in this area, the dye diffuses readily and rapidly into overlying sensory retinal detachment, producing late pooling of fluorescein.

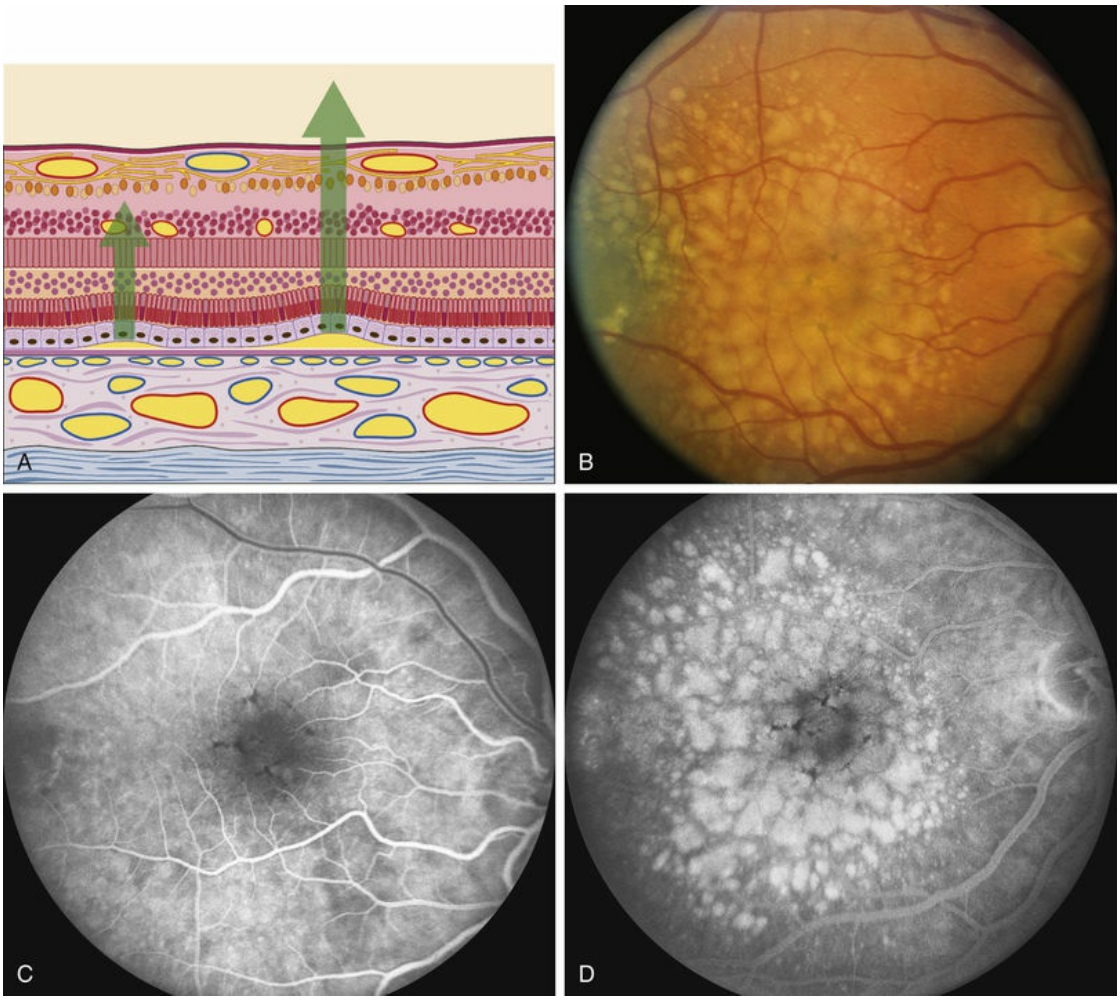

FIG. 1.54 Late hyperfluorescent pooling (or staining) of large drusen. (A) Schematic section of retina shows progressively larger detachments of pigment epithelium. Drusen deposit between the pigment epithelium and Bruch's membrane and lift the pigment epithelium up, forming small or large pigment epithelial detachments, depending on the size of the drusen. (B) Color photograph of right macula shows multiple, pale,

round, and variably sized drusen. (C) Arteriovenous phase of fluorescein angiogram shows some early hyperfluorescence of the areas of the drusen. (D) Late phase of fluorescein angiogram shows marked hyperfluorescence of the drusen. The larger drusen take longer for the hyperfluorescence to develop. Comment: The larger the drusen, the more similar they are to pigment epithelial detachments, and therefore the more likely it is that they will show pooling of fluorescein (or staining of the drusen material).

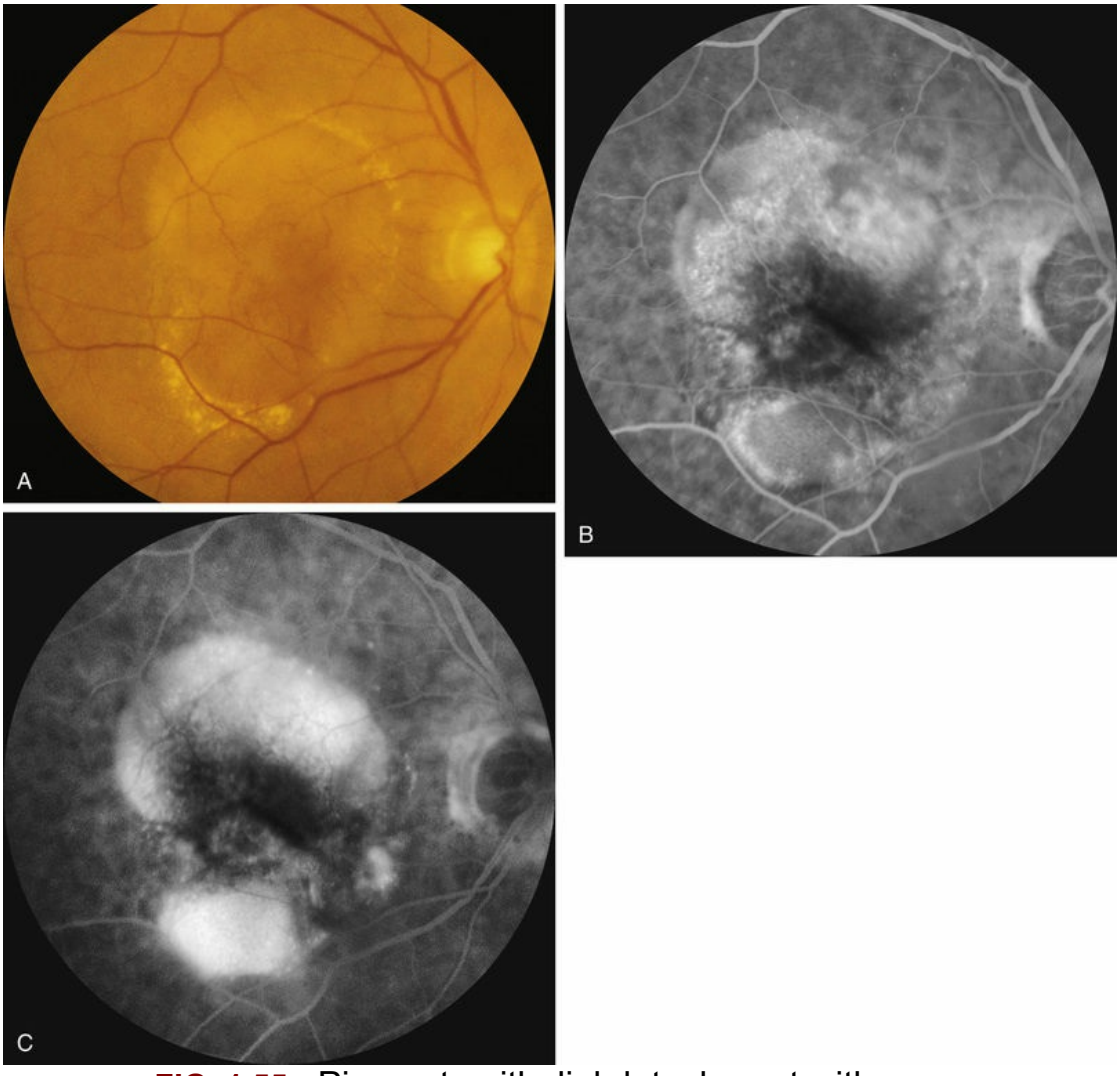

FIG. 1.55 Pigment epithelial detachment with associated (suspicious) subretinal neovascularization. (A) Color photograph of right macula. Note the pigment epithelial detachment temporally and sensory retinal detachment. (B) Arteriovenous-phase fluorescein

angiogram shows early hyperfluorescence of the superotemporal pigment epithelial detachment. (C) Late-phase fluorescein angiogram of left macula shows that the fluorescence of the pigment epithelial detachment temporally has increased significantly. Comment: This patient had an irregularly shaped pigment epithelial detachment, which is a sign of possible choroidal neovascularization. The irregular, fuzzy hyperfluorescence is due to likely occult choroidal neovascularization.

In summary, late hyperfluorescence beneath the retina should first be distinguished as pooling of fluorescein into a space or as tissue staining with fluorescein. When pooling is present, one must determine whether a sensory retinal or a pigment epithelial detachment is present. Similarly, if staining is present, one must find out whether the tissue involved is the retinal pigment epithelium and Bruch's membrane, choroid, or sclera. From this anatomic determination a more specific diagnosis can be determined.

Staining

Staining refers to leakage of fluorescein into tissue or material and is contrasted with pooling of the fluorescein into an anatomic space. Many abnormal subretinal structures and materials can retain fluorescein and demonstrate later hyperfluorescent staining.

Drusen.

The most common form of staining occurs with drusen. Most drusen hyperfluoresce early in the angiogram because choroidal fluorescence is transmitted through defects in the pigment epithelium overlying the drusen (Fig. 1.30). Fluorescence from most small drusen diminishes as the dye leaves the choroidal circulation. However, some larger drusen display later hyperfluorescence or staining (Fig. 1.54). The larger the drusen, the more likely they will retain fluorescein and staining will occur. When drusen are large and have smooth edges, the late staining on the angiogram is similar in appearance to that of pooling of fluorescein under a pigment epithelial detachment. In many cases it is difficult, if not

impossible, to differentiate large drusen from small pigment epithelial detachments: they have a similar ophthalmoscopic, fluorescein angiographic, and even microscopic appearance.

Scar.

Scar tissue retains fluorescein and usually demonstrates well-demarcated hyperfluorescence because little, if any, fluid surrounds the scar. Later in the healing process, when only a few vessels remain, the early angiogram is hypofluorescent because of the paucity of vessels and blockage by the scar tissue. The most commonly seen scar tissue is the disciform scar, which is the endstage of subretinal neovascularization. Scarring is also seen following numerous other insults to the pigment epithelium and choroid, especially inflammation (Fig. 1.56).

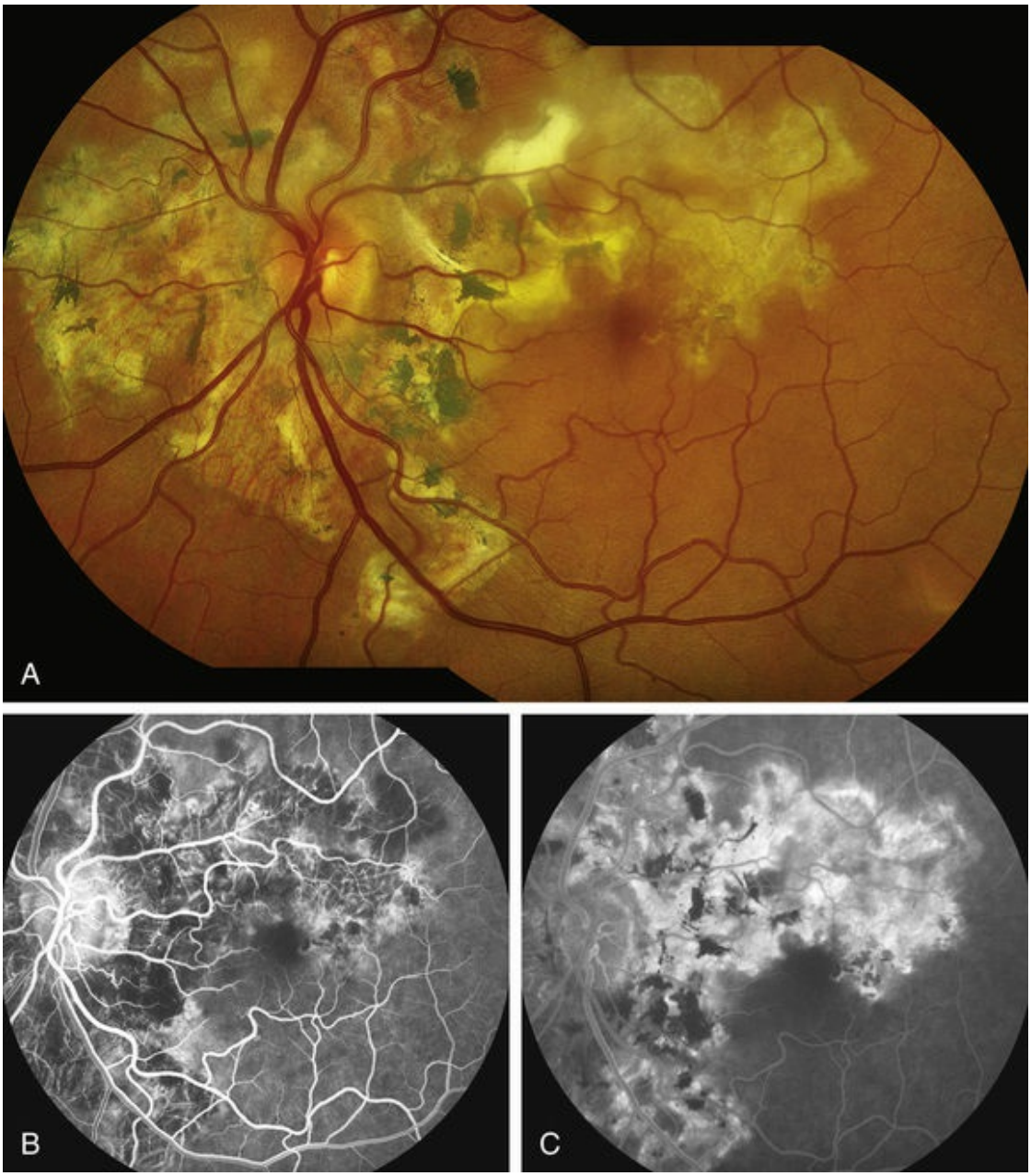

FIG. 1.56 Late hyperfluorescence and leakage – staining in geographic helicoid peripapillary choroidopathy (GHPC). (A) Color montage of left disc and macula shows large geographic areas of atrophy of pigment epithelium and choriocapillaris. There is some hyperplasia of the pigment epithelium noted as hyperpigmentation (especially in the macula and papillomacular bundle). Some fibrous scar tissue is present. (B) Arteriovenous-phase fluorescein angiogram shows that the geographic lesions are mostly hypofluorescent; they are caused by loss of pigment epithelium and choriocapillaris. Note that the large choroidal vessels can be seen within these

lesions, indicating that the pigment epithelium and choriocapillaris are both gone. There is some hyperfluorescence along the edges of the geographic lesions. The pigment epithelial hyperplasia causes blocked fluorescence. (C) Late fluorescein angiogram of left macula shows hyperfluorescent staining along the edges of the geographic lesion. Comment: This patient had GHPC; inflammation of choroid and pigment epithelium resulted in a loss of the pigment epithelium and choriocapillaris and some of the choroid. The angiogram showed that only large choroidal vessels remained within these lesions. The choriocapillaris was intact, however, in the normal tissue adjacent to the geographic atrophic tissue. The normal choriocapillaris leaked into the atrophic area in a horizontal fashion, causing late hyperfluorescence of areas of scar tissue and some scleral staining.

Sclera.

In several situations the sclera is visible ophthalmoscopically and exhibits late hyperfluorescent staining on fluorescein angiography. Scleral staining is best seen when the retinal pigment epithelium is very pale (as in a blonde patient) or when the choriocapillaris is fully intact. When the choriocapillaris is not intact, fluorescein staining of the sclera can occur from the edges of the atrophic area where fluorescein leaks from the intact choriocapillaris inward toward the atrophy (Fig. 1.56).

In conditions such as physiologically light-colored (blonde) fundus or in myopia, the choriocapillaris is usually sufficient to stain the sclera completely. After the choroidal vessels have emptied of fluorescein in the later phases of angiography, the large hypofluorescent choroidal vessels appear as dark lines in silhouette against the stained sclera.

When a loss of choroid and choriocapillaris has occurred, there is a consequent diminution of fluorescein flow in the choroid. When this occurs, the sclera stains with fluorescein only from adjacent normal patent choriocapillaris vasculature. These vessels stain the sclera on the borders of the lesion because the dye tends to diffuse toward the center of the lesion. The entire lesion may not stain if the

distance from the edge of the sclera is more than 1 mm. When the choriocapillaris is intact or the lesion is not expansive, the sclera will stain completely.

In summary, late hyperfluorescence beneath the retina should first be distinguished as pooling of fluorescein into a space or as tissue stained with fluorescein. When pooling is present, it must be determined whether a sensory retinal or a pigment epithelium detachment is present. Similarly, if staining is present, it must be determined whether the tissue involved is the retinal pigment epithelium and Bruch's membrane, choroid, or sclera. From this anatomic differentiation, a more specific diagnosis can be determined.

Acknowledgments

This work was supported by the San Francisco Retina Foundation. The authors would like to thank Ryan Terribilini, head of photography at West Coast Retina Medical Group, for his assistance in acquiring many of the images used in this text.

References

1. Novotny HR, Alvis DL. A method of photographing fluorescence in circulating blood in the human retina. *Circulation*. 1961;24:82–86.
2. Gass JD. *Atlas of macular diseases: Diagnosis and treatment*. Mosby: St. Louis; 1970.
3. Patel RD, Messner LV, Teitelbaum B, et al. Characterization of ischemic index using ultrawide-field fluorescein angiography in patients with focal and diffuse recalcitrant diabetic macular edema. *Am J Ophthalmol*. 2013;155(6):1038–1044.e2.
4. Witmer MT, Parlitsis G, Patel S, Kiss S. Comparison of ultra-widefield fluorescein angiography with the Heidelberg Spectralis(®) noncontact ultra-widefield module versus the Optos(®) Optomap(®). *Clin Ophthalmol*. 2013;7:389–394.
5. Suto S, Hiraoka T, Oshika T. Fluorescein fundus

angiography with smartphone. *Retina*. 2014;34(1):203–205.
6. Li B, Powell AM, Hooper PL, et al. Prospective evaluation of teleophthalmology in screening and recurrence monitoring of neovascular age-related macular degeneration: a randomized clinical trial. *JAMA Ophthalmol*. 2015;133(3):276–282.
7. Lipson BK, Yannuzzi LA. Complications of intravenous fluorescein injections. *Int Ophthalmol Clin*. 1989;29(3):200–205.
8. Olson JA. Stereo atlas of fluorescein and indocyanine green angiography. *Br J Ophthalmol*. 2000;84(7):805C.
9. Sim DA, Keane PA, Rajendram R, et al. Patterns of peripheral retinal and central macula ischemia in diabetic retinopathy as evaluated by ultra-widefield fluorescein angiography. *Am J Ophthalmol*. 2014;158(1):144–153.e1.
10. Rasmussen ML, Broe R, Frydkjaer-Olsen U, et al. Comparison between Early Treatment Diabetic Retinopathy Study 7-field retinal photos and non-mydriatic, mydriatic and mydriatic steered widefield scanning laser ophthalmoscopy for assessment of diabetic retinopathy. *J Diabetes Complications*. 2015;29(1):99–104.

2

Clinical Applications of Diagnostic Indocyanine Green Angiography

Giovanni Staurenghi, Ferdinando Bottoni, Andrea Giani

Introduction

Intravenous fluorescein angiography (FA) provides excellent spatial and temporal resolution of the retinal circulation, with a high degree of fluorescence efficiency and minimal penetration of the retinal pigment epithelium (RPE). Unfortunately, imaging of the choroidal circulation is prevented by secondary poor transmission of fluorescence through ocular media opacities, pathologic manifestations such as serosanguineous fluid or lipid exudation

and fundus pigmentation, including that from the RPE layer.

In medicine a core principle for diagnostic imaging is the selection of a technique that best visualizes the disease undergoing investigation. Indocyanine green (ICG) has several advantages over sodium fluorescein in imaging the choroidal vasculature. Its physical characteristics allow for visualization of the dye through overlying melanin, xanthophyll pigment, serosanguineous fluid, or lipid exudates. The use of high-resolution infrared digital fundus cameras and confocal scanning laser ophthalmoscopes (SLOs), specifically designed for ICG angiography (ICGA), has reflected a growing awareness and interest in choroidal vascular lesions, and has facilitated the rapid diffusion of ICGA in the ophthalmic community.

Even in the era of anti-vascular endothelial growth factor (VEGF) intravitreal injections, a therapy for which accurate localization of the choroidal neovascular membrane is not as critical, ICGA, among other imaging techniques, is still extremely useful in clinical practice.[1]

History

ICG was developed by Kodak Research Laboratories,[2] on request by cardiologists, to be used as an indicator of cardiac output, which was not influenced by variations in blood oxygen saturation.[3,4] Hepatologists subsequently began to use ICGA to evaluate hepatic blood flow[5] and hepatocellular function.[6]

In 1969 Kogure and Choromokos first used ICGA for studying the cerebral circulation in a dog.[7] The following year Kogure et al. reported on intraarterial ICG absorption of the choroid in monkeys.[8] The first human ICG angiogram was of the carotid artery.[9] In 1971 Hochheimer modified the system for ICGA by changing the color film that had been used previously to black-and-white infrared film.[10]

In 1972 Flower and Hochheimer performed the first intravenous ICGA to image the human choroid.[11] In the following years Flower and coworkers evaluated the potential utility of ICGA in the investigation of the normal and pathologic eye.[11,12] The relatively poor fluorescence efficiency of the ICG molecule and its limited

ability to produce high-resolution images on infrared film initially restricted its angiographic application. The resolution of ICGA was improved in the mid-1980s by Hayashi and coworkers, who developed improved filter combinations with sufficient sensitivity for near-infrared wavelengths.[13] They were also instrumental in the transition from still-frame to dynamic imaging by introducing videoangiography.[14,15]

Although the sensitivity of the initial video camera system was a vast improvement over previous techniques, its inability to study individual images and the potential light toxicity using a 300-watt halogen bulb restricted the duration and quality of the technique. In 1989 Destro and Puliafito performed ICGA using a system very similar to that described by Hayashi.[16] In the same year, the use of the SLO for ICG videoangiography was introduced by Scheider and Schroedel.[17] In 1992, Guyer introduced the use of a 1024 × 1024 line digital imaging system to produce high-resolution ICGA.[18] However, this system lacked flash synchronization with the video camera.

Finally, Yannuzzi and coworkers described a 1024-line resolution system, which was synthesized with the appropriate flash synchronization and image storage capability, permitting high-resolution, long-duration ICGA.[19]

Chemical and Pharmacokinetics

ICG is a tricarbocyanine, anionic dye. Its structural formula is 2,2′-indo-6,7,6′,7′-dibenzocarbocyanine sodium salt[20] with a molecular weight of 774.96 D.[2] ICG is soluble in highly distilled water,[21] even though in protein-free buffer it is difficult to obtain stable and simple ICG solutions, because of the formation of reversible dimers/polymers.[2] Binding to albumin or plasma proteins improves the stability of ICG solutions.[2] ICG is supplied with a solvent consisting of sterile water at pH 5.5–6.5. The final product contains 5–9.5% sodium iodine.[22] to prevent recrystallization.[23]

ICG absorbs light in the near-infrared region of the spectrum. The maximum absorption is at 790 nm,[23] while the maximum emission occurs at approximately 835 nm.[24] These optical properties allow the penetration through macular pigment, melanin[25] blood and

pigment.

About 98% of ICG is bound to plasma protein, in particular to globulins, such as A1-lipoproteins.[22] In pig plasma, lipoprotein HDL3 is the major binding protein.[2] ICG is excreted by the liver,[5,26] with negligible extrahepatic removal.[5,27] The presumed mechanism is active[27] and depends both on liver blood flow and hepatocellular function.[28] ICG is excreted into the bile without metabolic process or enters the enteropathic circulation[27] through three steps: uptake over the hepatotocyte sinusoidal (basolateral) membrane (Na^+ mediated); passage through the cell, with some role of the microfilaments and vesicular transport;[2] and excretion over the canalicular (apical) membrane.[2] Rate of ICG disappearance from vascular compartment is 18–24% per minute, and after 20 minutes no more than 4% remains in the plasma.[29] The plasma decay curve is initially exponential, than decelerates.[26] No peripheral uptake has been described in the kidney,[26] lungs, or placenta.[30]

The high molecular weight of ICG, in combination with the high percentage of dye bound to plasma proteins, reduces the amount of dye that exits from fenestrations in choroid vessels. This feature and its optical properties make ICG suitable for choroidal vascular network visualization. Although it has been reported that ICG can diffuse through the choroid and can accumulates in RPE cells, no dye should remain in the late phases (30–40 minutes) of the angiogram.[29]

Toxicity

ICG is considered a safe and well-tolerated dye. Its LD_{50} is 60 mg/kg in mice.[20] Constant infusions over a 3-hour period with dosages as high as 50 mg/kg of body weight were well tolerated.[27] Subcutaneous extravasation also does not produce significant local effects.[26,31] Overall, the side-effect rate is low: 0.15% with mild events (nausea, vomiting, sneezing, pruritus), 0.2% with moderate events (urticaria, syncope, pyrexia, nerve palsy), 0.05% with severe events (bronchospasm, laryngospasm, anaphylaxis).[31]

The mechanism of these various adverse side-effects is uncertain. For some, a dose-dependent pseudoallergic mechanism has been proposed;[32] though there does not appear to be correlation with

iodide or shellfish intolerance, suggesting that the sodium iodide component is of little significance.[22,33] Nevertheless patients with a history of definite iodine allergy should not be given the dye, because of concerns for possible anaphylaxis.[31] Caution should also be observed in patients affected by liver diseases[29] and kidney diseases, since a 9.3% incidence of adverse reactions has been reported in dialysis patients.[22,34]

ICG was extensively used as a chromodiagnostic agent in the evaluation of hemodynamic changes during pregnancy.[35] Nevertheless there are concerns among ophthalmologists, since the FDA has classified ICG as a pregnancy category C drug, meaning that adequate studies of safety have not been conducted.[30]

Instrument Comparison

There are several instruments at present that can be used to perform ICGA. All of them can be divided into two main categories: digital flash fundus cameras and SLOs.

At the time of writing of this chapter, the flash camera group includes the TRC-50DX ICG (Topcon, Tokyo, Japan), the FF 450plus (Carl Zeiss Meditec, Inc., Dublin, CA, United States), and the VX-10i (Kowa, Tokyo, Japan). ICG-capable SLO systems include the Spectralis HRA (Heidelberg Engineering, Heidelberg, Germany), the F10 (Nidek, Gamagori, Japan), and the Optos California (Optos plc, Dunfermline, Scotland).

The differences between these instruments are largely related to the acquisition modality (Fig. 2.1). The light source for a digital camera is a white light with an excitation filter (640–780 nm) and a barrier filter (820–900 nm). In an SLO a laser monochromatic light is used to excite (785–790 nm) with a barrier filter at 805 nm. The laser light for an SLO system is moved on the fundus by two rotating mirrors and the image is acquired point by point. For a typical 30° image, this takes approximately from 60 to 200 msec. The presence of a confocal aperture in SLO systems allows selective acquisition of light from a particular tissue layer (from the focal plane) and blocks the light that is coming from the surrounding tissue.[36,37] Flash systems, in contrast, do not use a confocal aperture, and thus the fluorescent light returning to the camera will emanate from

multiple layers. However, even for clinical confocal SLO ICG systems, the confocal aperture is much larger than one would choose for optimum z-resolution imaging. The reason for this is that fluorescence light from different depth planes (i.e., from the choroid and from the retinal vessel) needs to be imaged simultaneously for many clinical applications.

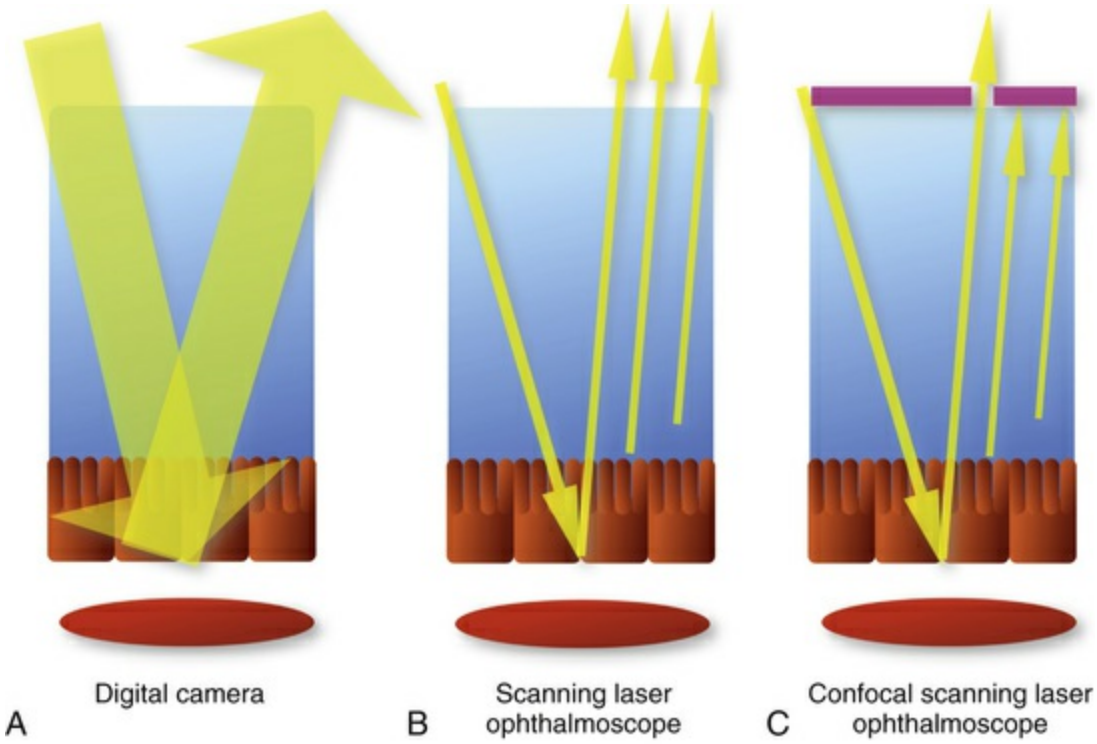

FIG. 2.1 Schematic representation of the differences between digital flash fundus cameras (A), scanning laser ophthalmoscopes (SLOs) (B), and confocal SLO instruments (C). In digital flash fundus cameras, white light (with or without excitation/barrier filters) is used. In SLO systems the light source is a monochromatic laser. In SLO confocal systems a pinhole aperture blocks the reflected or fluorescent light from areas outside the focal plane.

These characteristics are important to recognize to understand the different appearance of ICGA images obtained by different instruments (Fig. 2.2). Another difference is the number of images acquired per second. With SLO systems the frame rate may reach 12 images per second, thus permitting dynamic ICGA (Fig. 2.2). With

digital fundus cameras the maximum rate is one frame per second.

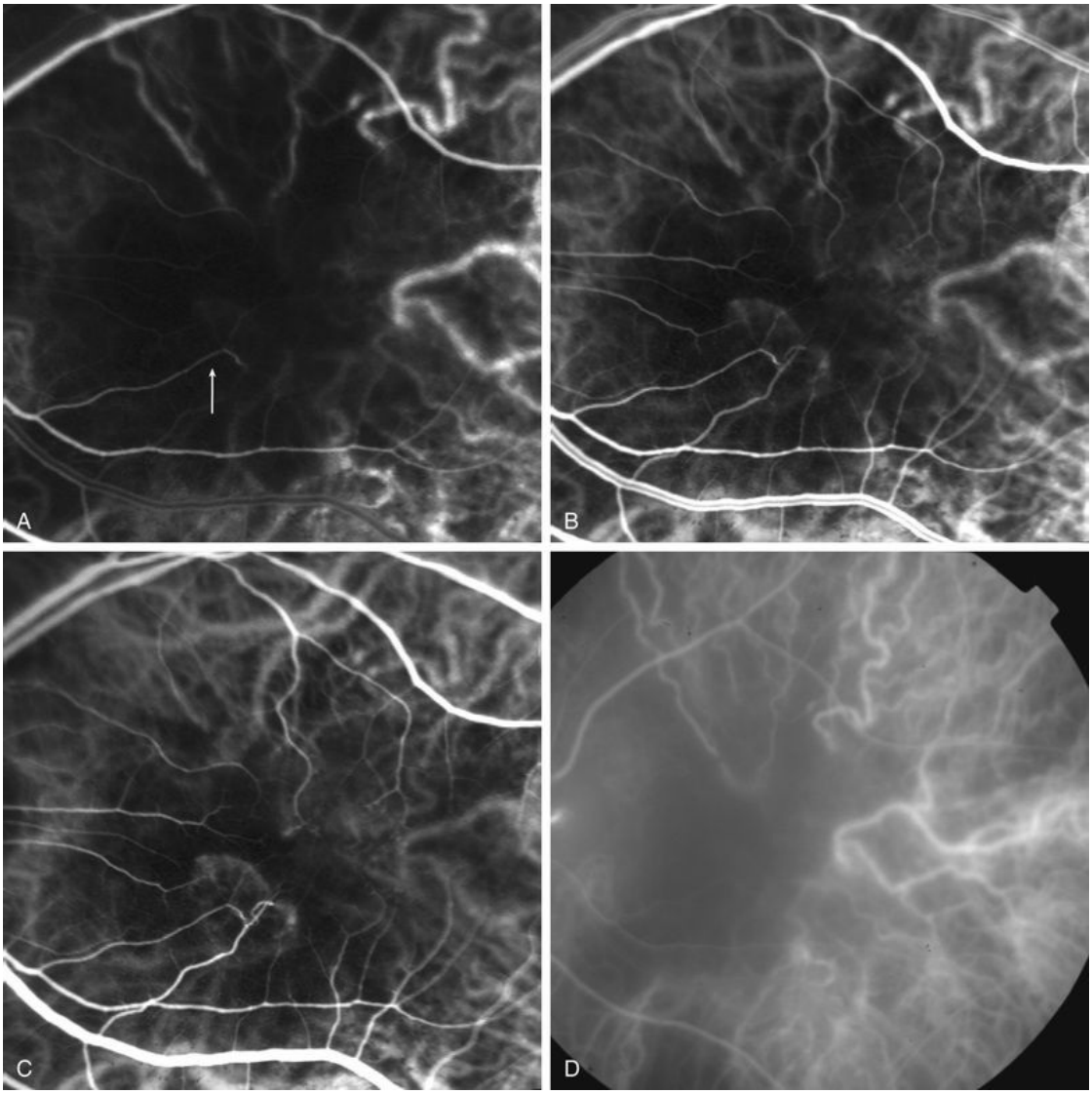

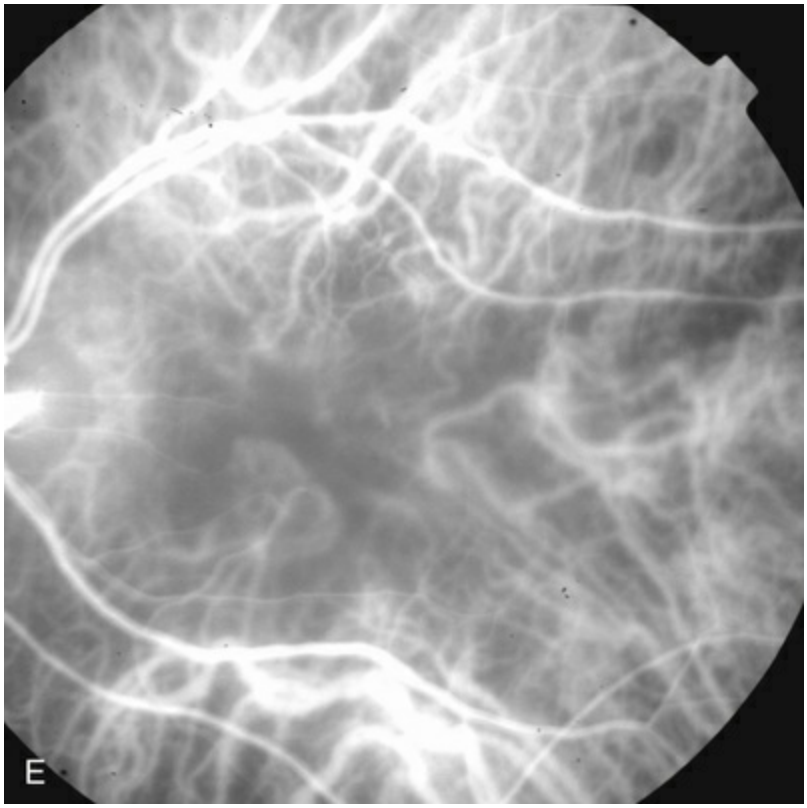

FIG. 2.2 Comparison of dynamic (6 frames per second) and conventional indocyanine green angiography of a stage II retinal angiomatous proliferation lesion. A feeding retinal arteriole (A, *arrow*), filling of the vascular lesion, and a draining retinal vein are all characteristic features visible in the dynamic sequences (A–C). The filling sequence is missed during the first two images captured with a conventional flash fundus camera system (D,E).

Injection Technique

The concentration and preparation for intravenous injection of ICG vary with the instrument used. For fundus cameras the standard concentration is 25 mg of ICG dissolved in 5 mL solvent.[38] The dosage may be increased to 50 mg in patients with poorly dilated pupils and heavy pigmentation.[39] For SLOs the standard dosage is 25 mg of ICG dissolved in 3 mL, and 1 mL of the solution is injected. The solvent may be either saline alone or fluorescein sodium solution at 10–20–25% concentrations, for combined FA and ICGA. Intravenous ICG injection should be rapid and immediately

followed by a 5 mL saline flush.

In patients with iodine allergy, infracyanine green is available, which is the iodine-free formula of indocyanine green. The technique of injection is equivalent, but a glucosate solvent should be used for preparation. As a result, combined fluorescein angiography and infracyanine green angiography is not possible.

Indocyanine Green Angiography Interpretation

Normal Eye

To understand the manifestations of disease on ICGA, a recognition of the normal appearance of ICGA in normal subjects is essential.

Since ICGA is a dynamic examination, the characteristic findings may vary depending on the time after dye injection or the "phase" of the angiogram. It is well known that FA has an arterial retinal phase, an arteriovenous, and a venous phase. Similarly for ICGA, one can recognize an early phase when the retinal artery is not yet filled, a mid phase where both arteries and veins are filled, and a late or recirculation phase after more than 10 minutes after injection.

In ICGA the early filling phase may best be correlated with the filling of different layers of the choroid. The first choroidal vessels to be filled are the ones of the deeper Haller's layer, followed by the intermediate Sattler's layer (Fig. 2.3). The choriocapillaris is the last layer to be filled (therefore the sequence progresses from the biggest and outermost to the smallest and innermost vessels). However, the choriocapillaris is typically quite difficult to visualize, since the resolution of the cameras is insufficient to resolve the size of its small lobular morphology. Therefore the choriocapillaris is visualized as a diffuse indistinct haze, more evident in the posterior pole and less evident in the peripheral retina (Fig. 2.3).

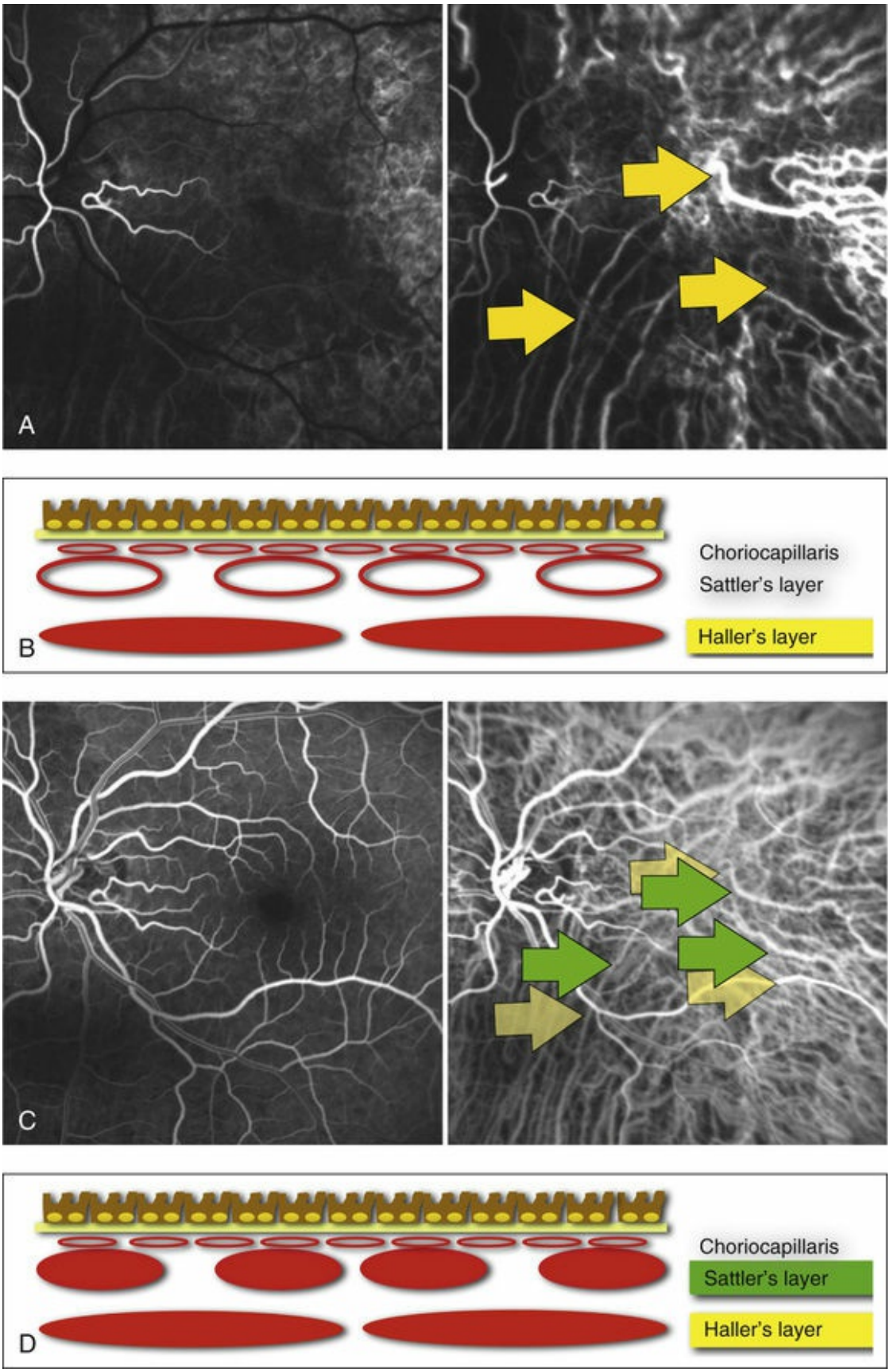
A
Choriocapillaris
Sattler's layer
Haller's layer
B
C
Choriocapillaris
Sattler's layer
Haller's layer
D

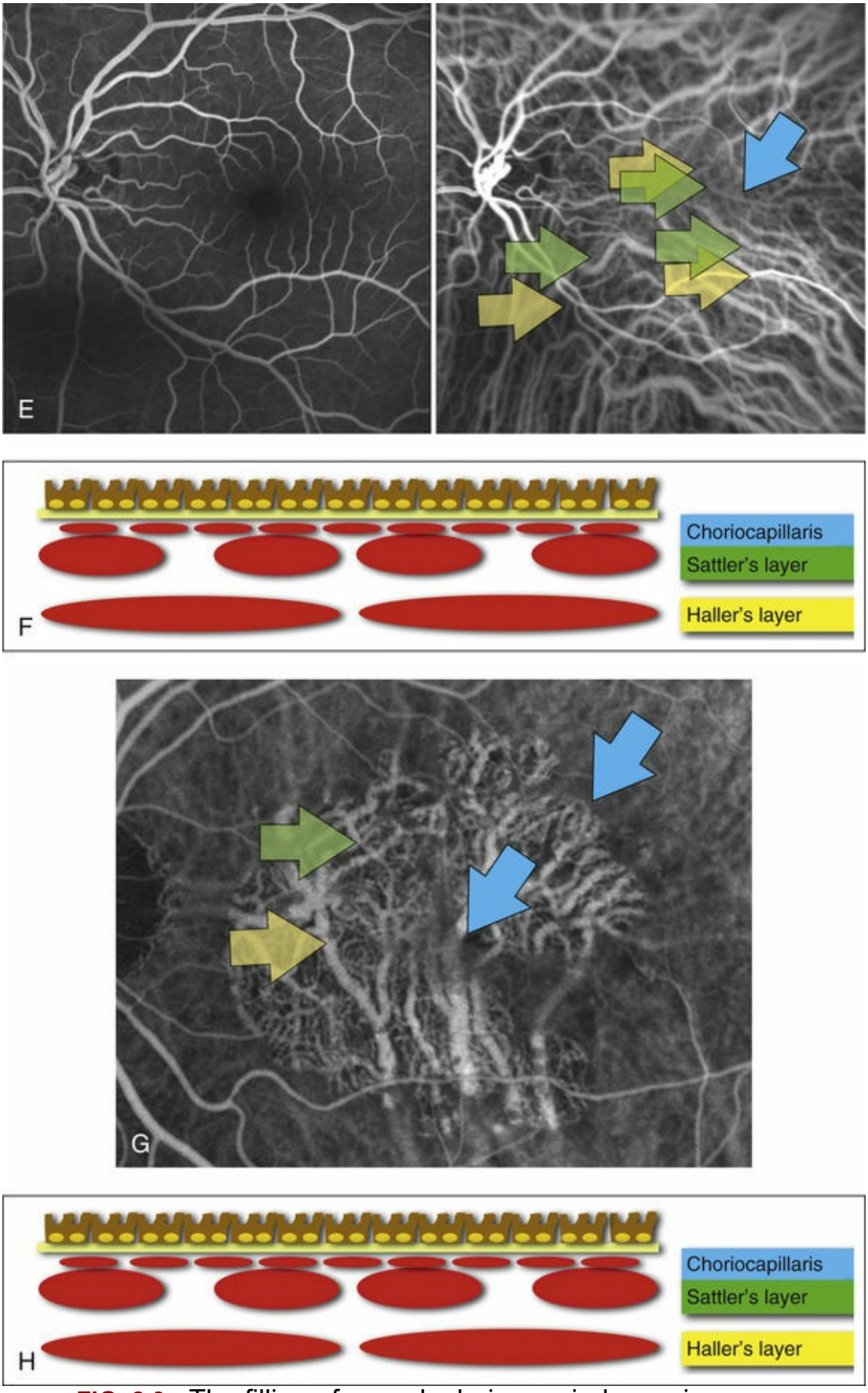

FIG. 2.3 The filling of vessels during an indocyanine

green angiogram follows a precise sequence. The first layer to be filled is Haller's layer (A,B), followed by Sattler's layer (C,D), and then the choriocapillaris (E,F). Simultaneous dynamic fluorescein and indocyanine green angiography (A,C,E) permits the different phases to be resolved. The choriocapillaris may be better appreciated when there are adjacent areas of focal loss, as in this example of geographic atrophy (G,H).

Choroidal vessels are usually first observed emanating from the posterior ciliary arteries. A well-defined watershed zone is present between the medial and lateral posterior ciliary artery (Fig. 2.4).[40] Compared to fluorescein, the watershed zone is more difficult to visualize, since there is less contrast between perfused and nonperfused choroid.

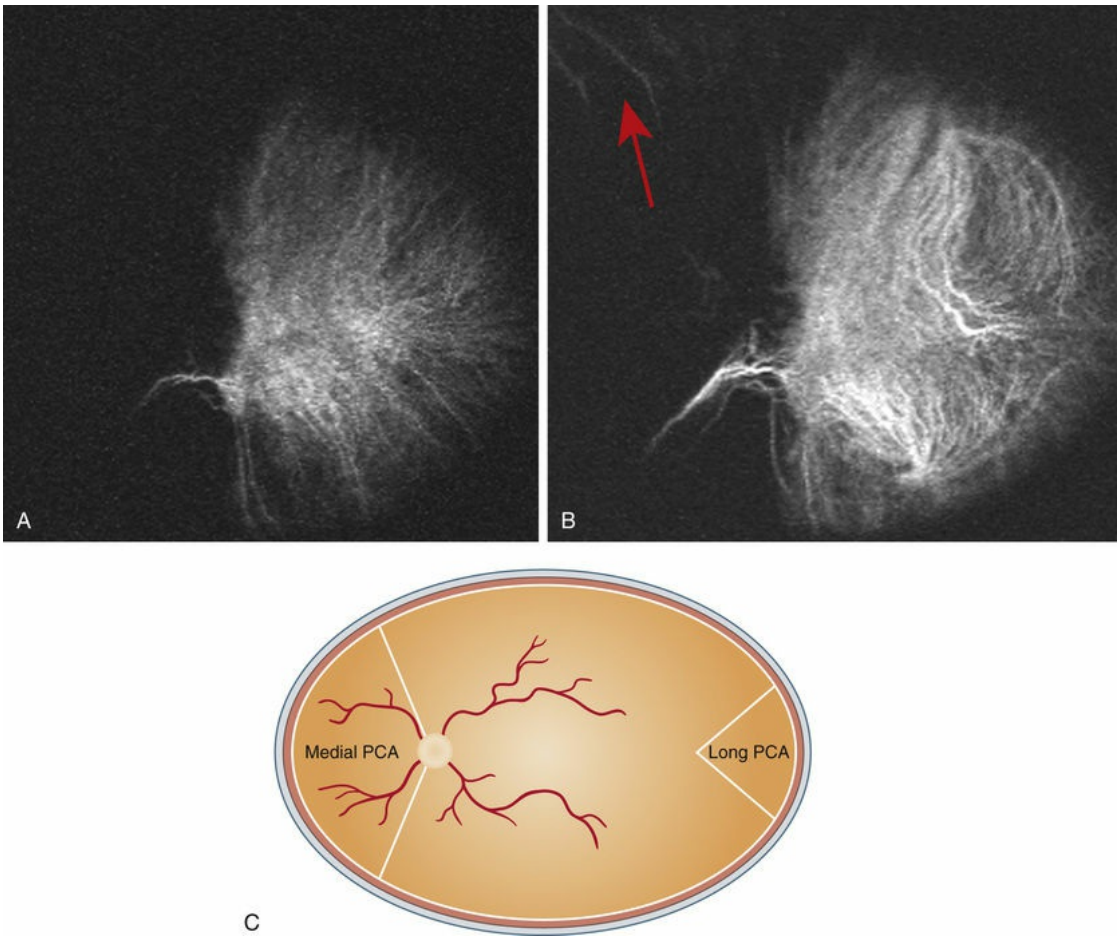

FIG. 2.4 A case of occlusion of the medial long posterior ciliary artery (PCA). Indocyanine green

angiography (ICGA) allows one to appreciate the different territories supplied by this artery and the lateral long PCA (A). Venous phase of ICGA shows the filling of the lateral vortex veins (B). In the upper left area, the vortex vein is partially filled due to drainage from the iris (B, *arrow*). (C) Schematic representation of the different vascular territories of the two arteries.
(Panel C modified from Hayreh SS. Physiological anatomy of the choroidal vascular bed. Int Ophthalmol 1983;6:85–93.)

Choroidal vortex veins are visible in the late phase of ICGA and are usually four in number (Fig. 2.5). They drain the corresponding segment of the iris, ciliary body, and choroid. Sometimes, especially in the myopic eye, a vein may be seen passing from the choroid through the sclera closely adjacent to the optic nerve head and draining into the venous plexus of the pial sheath of the optic nerve (choriovaginal vein) (Fig. 2.5).[40]

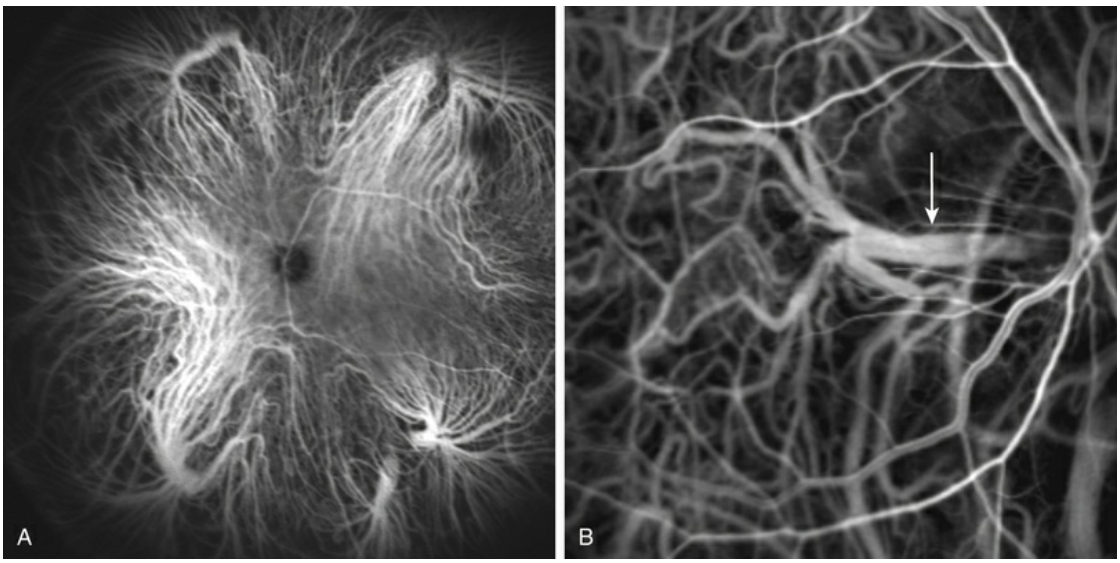

FIG. 2.5 Indocyanine green angiography allows visualization of the four vortex veins (A), and the choriovaginal vessels (B, *arrow*).

In case of a thin sclera, such as in the setting of a choroidal staphyloma, extrabulbar vessels may be visualized. These can be distinguished from normal choroidal vessels because they pulsate in accordance with the heartbeat. Moreover, they change shape and position with eye movements.[41,42]

Exudative Age-Related Macular Degeneration

Exudative age-related macular degeneration is generally classified based upon the axial location of the choroidal neovascularization (CNV). A type 1 CNV is a neovascular membrane that is located under the RPE, whereas a type 2 CNV has passed through the RPE and lies under the neurosensory retina.[43] According to the Macular Photocoagulation Study, type 1 CNV is generally considered to correspond with "occult" CNV on FA (as defined by the Macular Photocoagulation Study), and type 2 CNV generally corresponds with "classic" CNV.[44,45] More recently, type 3 CNV has been defined to be CNV with a definite intraretinal component.[46]

The fact that occult CNV accounts for the vast majority of the exudative complications in age-related macular degeneration (AMD)[47] explains in part why ICGA, with its ability to delineate occult CNV, has become part of standard care in exudative AMD for many clinicians.[19,48,49] Nonetheless, in peer-reviewed journals the number of articles published whose title included the terms "indocyanine green angiography (or videoangiography)" decreased between 1995 and 2010.[1] One likely explanation might be the advent of anti-VEGF therapy which inaugurated a new era in the management of exudative AMD: it was the first therapy to improve the mean visual acuity of eyes treated with monthly injections of ranibizumab, regardless of whether the CNV lesion was predominantly classic[50] or occult.[51] Thus, the management of CNV has changed from the use of therapy for which accurate localization of the membrane was crucial (i.e., laser photocoagulation, photodynamic therapy) to the nonspecific intravitreal delivery of active and highly effective biologic drugs. Nonetheless, we would still argue that the gold-standard diagnostic procedure should be the one that best visualizes the disease (CNV) under investigation.

Type 1 Choroidal Neovascularization

This type of choroidal neovascularization is by definition under the RPE, and corresponds to the occult neovascular network on FA. The Macular Photocoagulation Study recognized two forms of occult CNV: a fibrovascular pigment epithelial detachment (PED)

and a late-phase leakage of an undetermined source (LLUS).[44] As for the fibrovascular PED, its prevalence may vary from 22% to 50%[47–49,52] of occult CNV lesions; dynamic ICGA may delineate the presence of a neovascular network usually located along the edges of the PED[49,53,54] (Fig. 2.6). Moreover, dynamic ICGA may reveal a feeder vessel that can be successfully treated with laser photocoagulation, when it is located outside the foveal region[55,56] (Fig. 2.7). In case of LLUS, which may represent 36–78% of occult CNV,[47,48,52] dynamic ICGA may differentiate an occult form of CNV from retinal angiomatous proliferation[52] (Fig. 2.8). Considering that one-fourth of patients with a LLUS do have a retinal angiomatous proliferation,[52] and that an early diagnosis of these lesions is crucial for the functional prognosis,[57] the importance of an ICG evaluation for these cases becomes readily apparent.

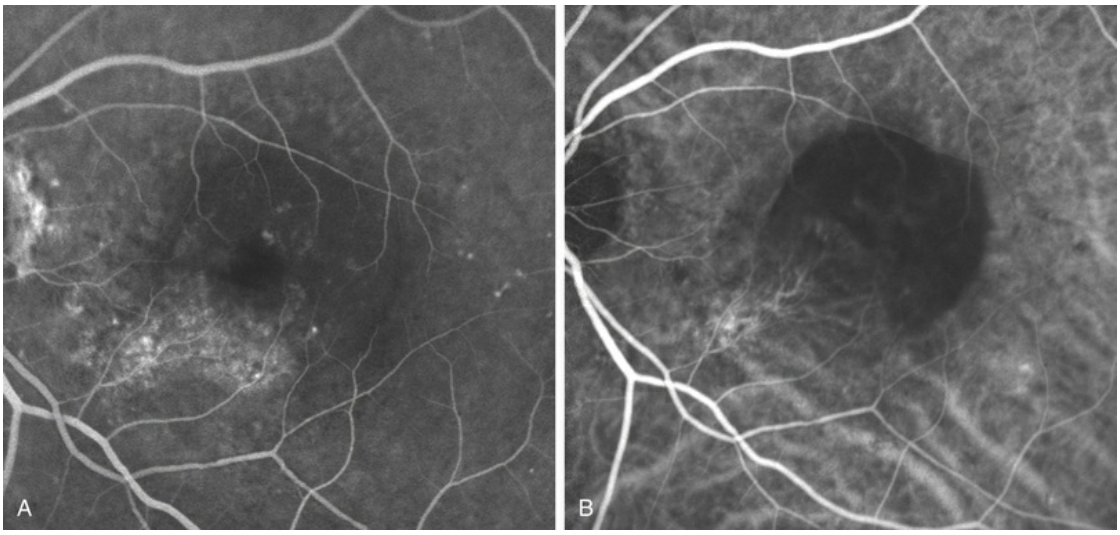

FIG. 2.6 A pigment epithelium detachment (PED) (A, fluorescein angiography) with a well-delineated neovascular network located along the edges of the PED (B, indocyanine green angiography).

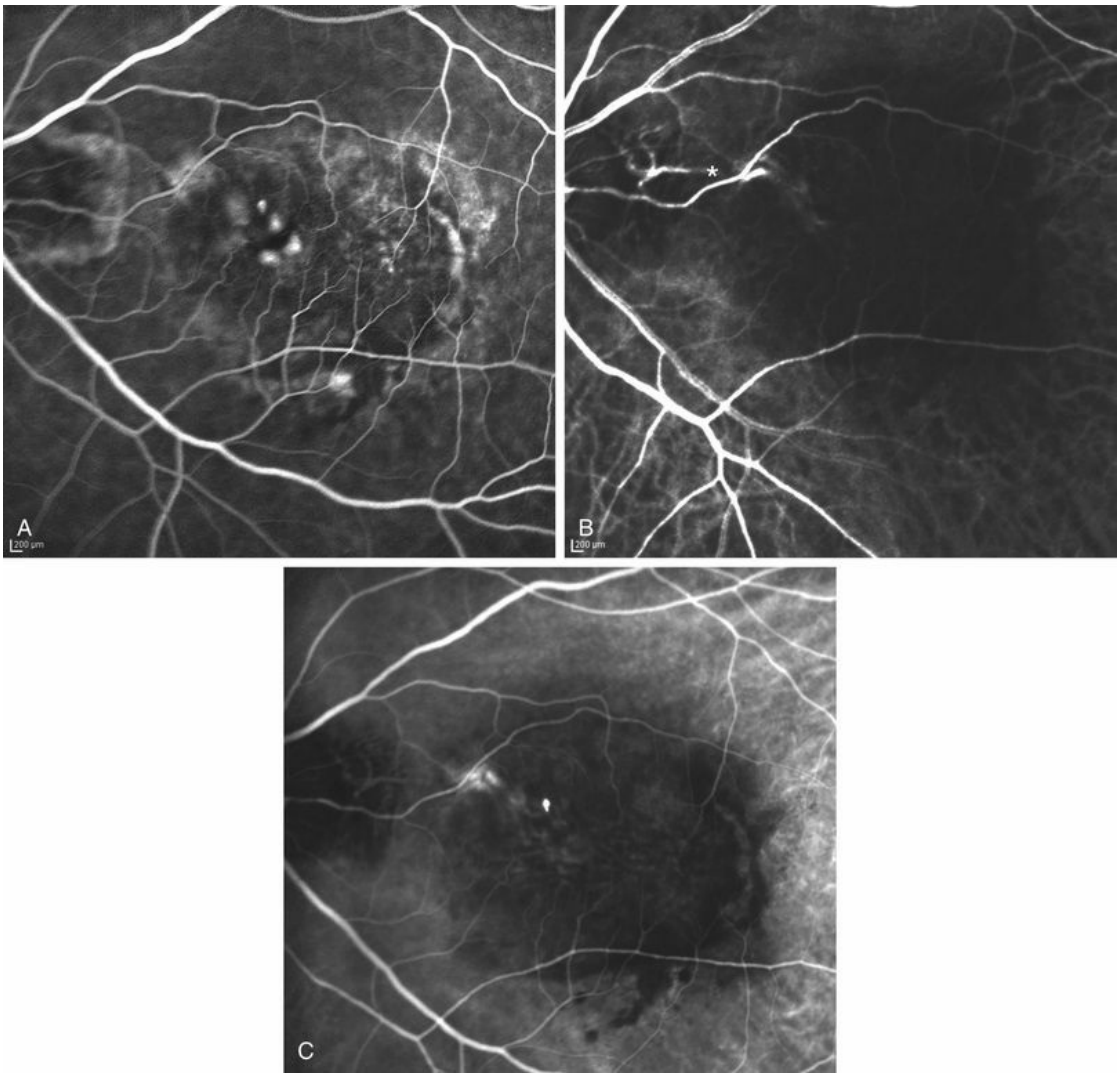

FIG. 2.7 Fibrovascular pigment epithelium detachment (PED). Fluorescein angiography demonstrates occult choroidal neovascularization with PED (A). In the early phases of indocyanine green angiography (ICGA) a feeder vessel originating in the juxtapapillary area is clearly delineated (B, *asterisk*). Feeder vessel and draining vein are indistinguishable in the late phases of ICGA (C).

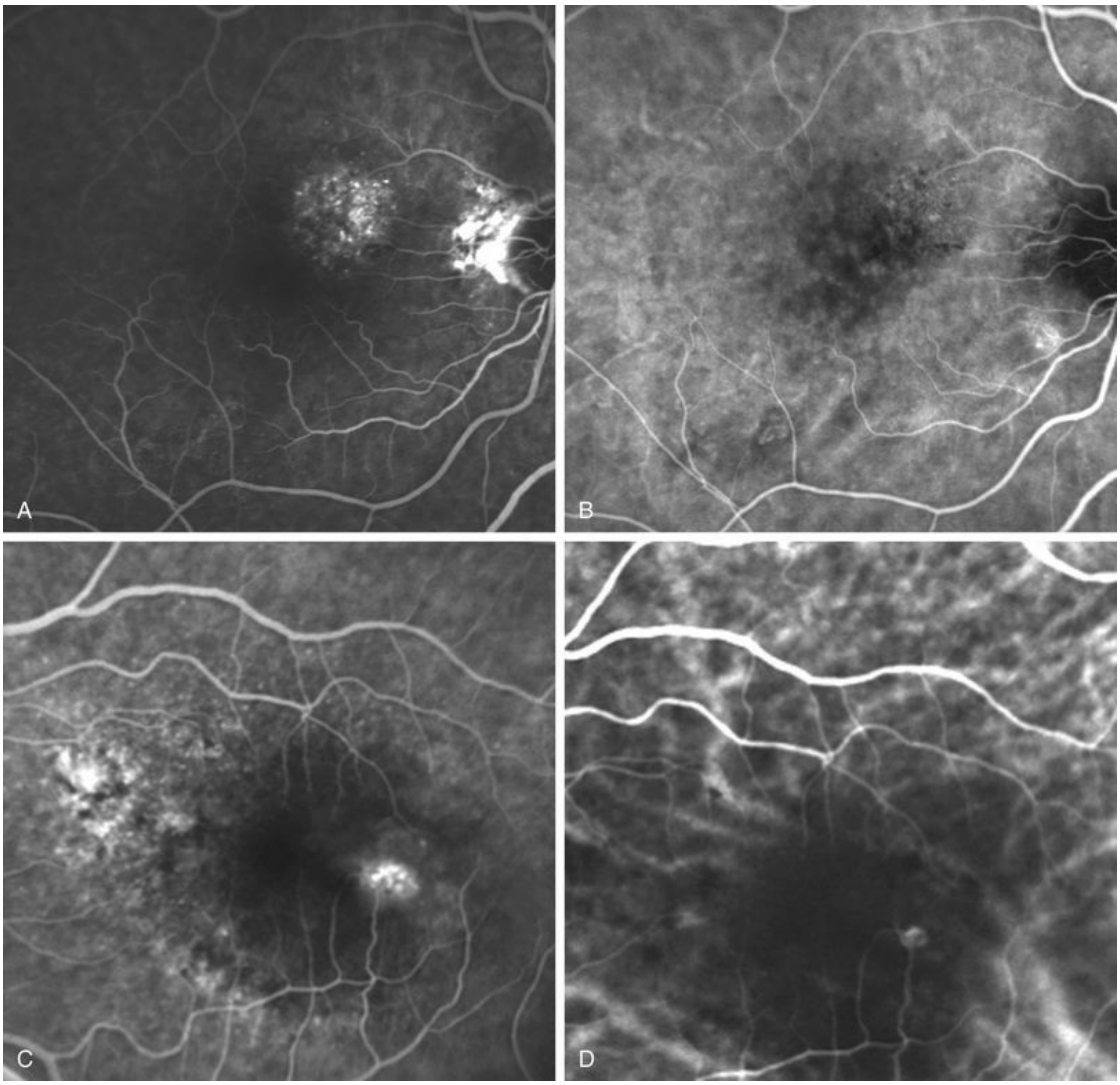

FIG. 2.8 Late leakage of undetermined source (A,C). Indocyanine green angiography may clearly differentiate a subtype of occult choroidal neovascularization (B) from retinal angiomatous proliferation (D).

In conclusion, ICG facilitates a better and more complete classification of occult CNV subtypes, compared to FA. Of note, Yannuzzi[19] found that 39% of lesions classified as poorly demarcated occult lesions by FA were well defined by ICGA.

Type 2 Choroidal Neovascularization

In classic CNV, ICGA improves visualization of the fine structure of the neovascular network[1] (Fig. 2.9), allowing the choroidal and retinal circulation to be distinguished. This high spatial and temporal resolution permits identification of choroidal vessels that

feed into the CNV.[58] In early phases, ICG shows a dark rim which corresponds to a whitish ring on infrared imaging,[59] and a discreet neovascular network surrounded by a hypocyanescent margin which is more visible after 15 minutes.[60] Watzke et al.[54] showed that 87% of eyes with classic choroidal neovascular membranes were hypercyanescent with distinct edges.

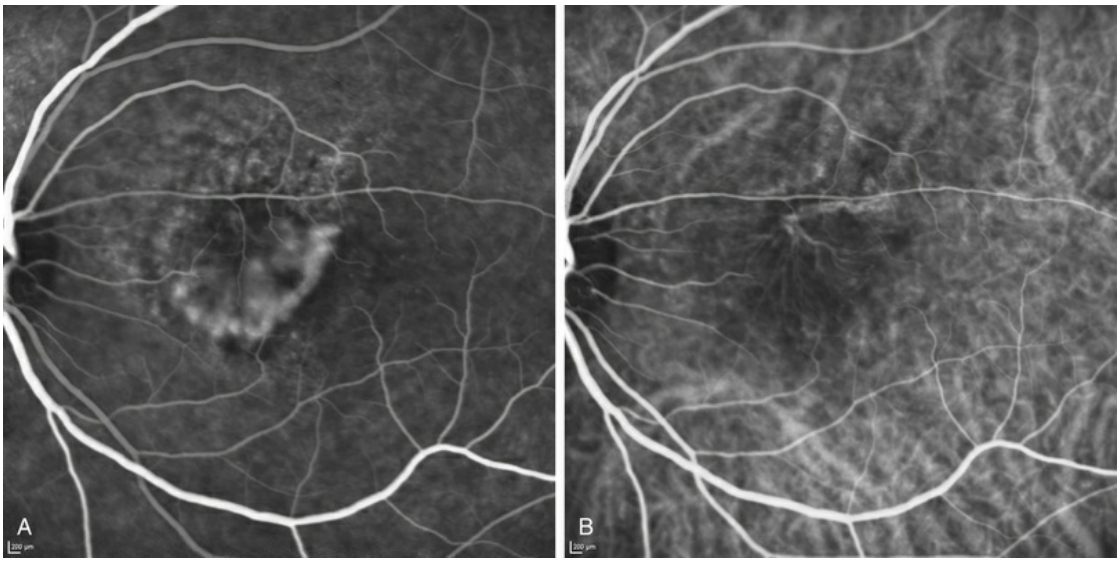

FIG. 2.9 A case of type 2 choroidal neovascularization. In fluorescein angiography images (A), the leakage of the dye from the lesions is evident and obscures the boundaries of the neovascular network. In indocyanine green angiography (ICGA) (B), the limits of the neovascularization are much more visible. Moreover, ICGA allows the visualization of a central feeder vessel, with a surrounding net of smaller neovessels.

This ability to provide a clear delineation of the neovascular network may confer an important advantage in the era of anti-VEGF therapy. It has been reported that VEGF inhibitors were more effective in controlling immature vessels, whereas a VEGF inhibitor along with a platelet-derived growth factor (PDGF) inhibitor appeared to show a synergistic effect for controlling the growth of mature vessels.[61] This is likely because pericyte recruitment is part of the maturation process in blood vessel development. Once the pericyte cell population is well established, the effectiveness of anti-VEGF agents is greatly reduced. PDGF-B is a key requirement for

the recruitment of pericytes to the newly formed vessels. Mature, larger choroidal vessels may be readily differentiated from immature choroidal capillaries on ICGA (Fig. 2.10). Thus, in patients with chronic AMD or those who did not benefit from previous treatments with anti-VEGF, ICGA might better delineate a more mature stage of CNV. This has potential implications for therapeutic decision-making.

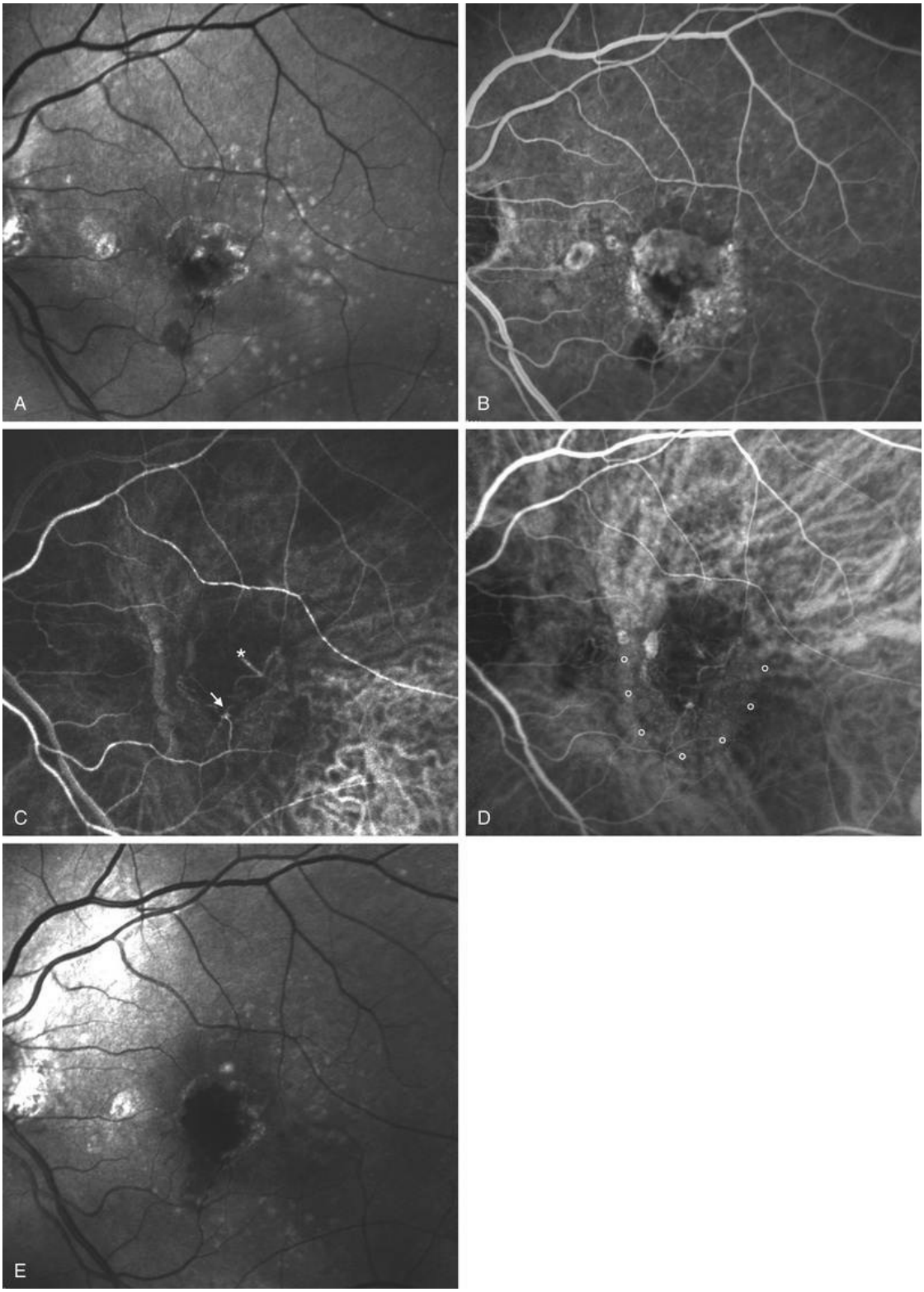

FIG. 2.10 Red-free image showing intraretinal blood within a central atrophic area. A small subretinal hemorrhage is also present inferiorly (A). Corresponding fluorescein angiogram demonstrating late leakage of undetermined source along the inferior

edge of the atrophic area (B). Simultaneous early phase indocyanine green angiography (C) reveals mature, large choroidal vessel (C, *asterisk*) feeding the large net of neovascularization along the inferior edge of central atrophy. A real chorioretinal anastomosis (C, *arrow*) is also present. Four minutes after injection (D), the draining choroidal veins are well visualized as is the neovascular network inferiorly (D, *open circles*). Red-free image after a 3-month-loading-phase with ranibizumab (E) shows an increase in size of the central retinal hemorrhage despite loading phase with anti-VEGF.

Type 3 Choroidal Neovascularization

During the past decade, retinal angiomatous proliferation (RAP) has been labeled with a number of different terms, including "retinal vascular anomalous complex," "retinal choroidal anastomosis," "retinal anastomosis to the lesion," and "chorioretinal anastomosis." In a comprehensive article[62] on this entity, Yannuzzi provided evidence to support the original concept of capillaries arising within the inner half of the retina, or "retinal angiomatous proliferation," thus suggesting the acronym of RAP as the appropriate descriptor for the disease. Subsequently, Gass[63] suggested a possible choroidal origin for these vessels, emanating from occult choroidal neovascularization and developing into an occult chorioretinal anastomosis. The new category, type 3 neovascularization, has been recently proposed[45] to harmonize these conflicting theories. Type 3 lesions would encompass the following disease manifestations: (1) focal neovascular proliferation arising from the deep retinal capillary plexus (the original RAP concept); (2) intraretinal neovascular extension from an underlying occult/type I CNV; and (3) de novo breaks in Bruch's membrane with neovascular infiltration into the retina.

Whatever the origin or initial location might be, our understanding of the importance of RAP as a component of neovascular AMD has been enhanced by ICGA. The fluorescein angiographic study generally shows manifestations of occult CNV, either fibrovascular PED (Fig. 2.11) or LLUS (Fig. 2.12) without a characteristic feature to identify and delineate the angiomatous

process in the retina (indistinct zone of staining within and beyond the retina). By contrast, ICGA may clearly delineate the vascular structure of the lesion. When associated with PED, the RAP is usually well within the area of detachment and not at the edges, as is typically the case with CNV, which vascularizes a serous PED (so called "notched PED" configuration on FA). As previously reported, RAP may be present in up to one-fourth of eyes thought to have occult CNV with LLUS.[52] Dynamic ICGA (d-ICGA) has further expanded our capability for an early diagnosis. By definition, a diagnosis of RAP is based upon the temporal evidence of "dye filling of at least one retinal arteriole descending into the deep retinal space to a vascular communication and at least one draining retinal vein."[64] In conventional angiography, images are usually captured at 1 frame per second. This makes it virtually impossible to visualize the progression of the dye through the vascular complex, even though images are taken at very early phases. By contrast, d-ICGA takes up to 12 frames per second and captures the progressive filling of the lesion, allowing detection of very small and recent onset cases of RAP (Fig. 2.2). The possibility of repeated viewing of the dynamic sequence of progression on ICG may further increase our chances of an early diagnosis of RAP (Fig. 2.13). In a recent series of RAP diagnosed using d-ICGA,[52] the incidence of stage 1 RAP (64.9%) and the mean distance of the lesions from the fovea (682 ± 304 μm) were both consistent with an early-stage disease process, supporting the utility of this imaging procedure.

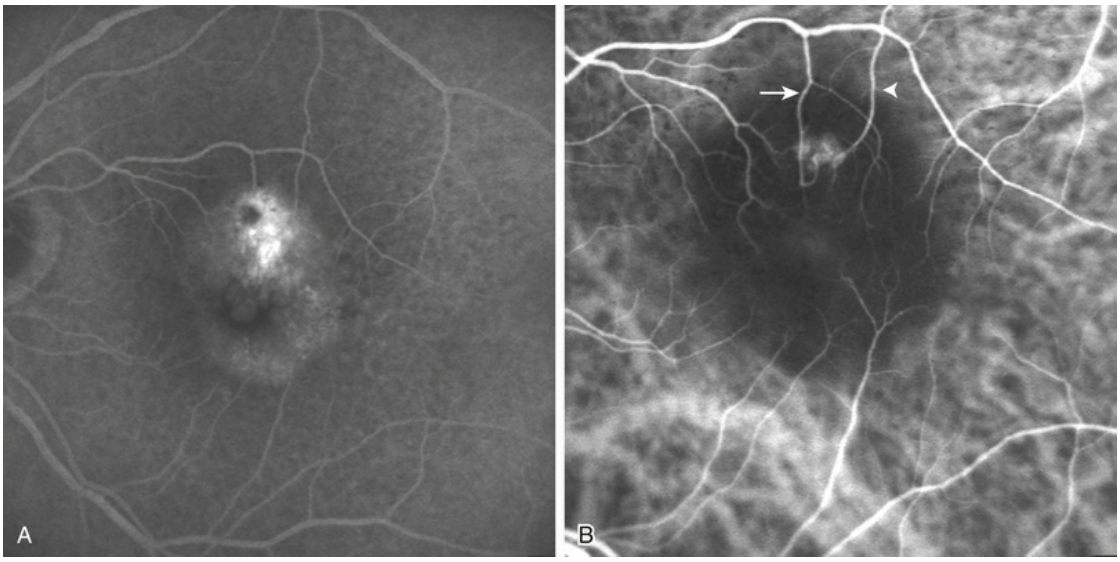

FIG. 2.11 Late-phase fluorescein angiography (A) shows a pigment epithelium detachment (PED) with a "hot spot." Indocyanine green angiography (B) reveals the presence of retinal angiomatous proliferation (RAP) overlying the PED. Feeding retinal arteriole (*arrow*) and draining retinal venule (*arrowhead*) are clearly visualized.

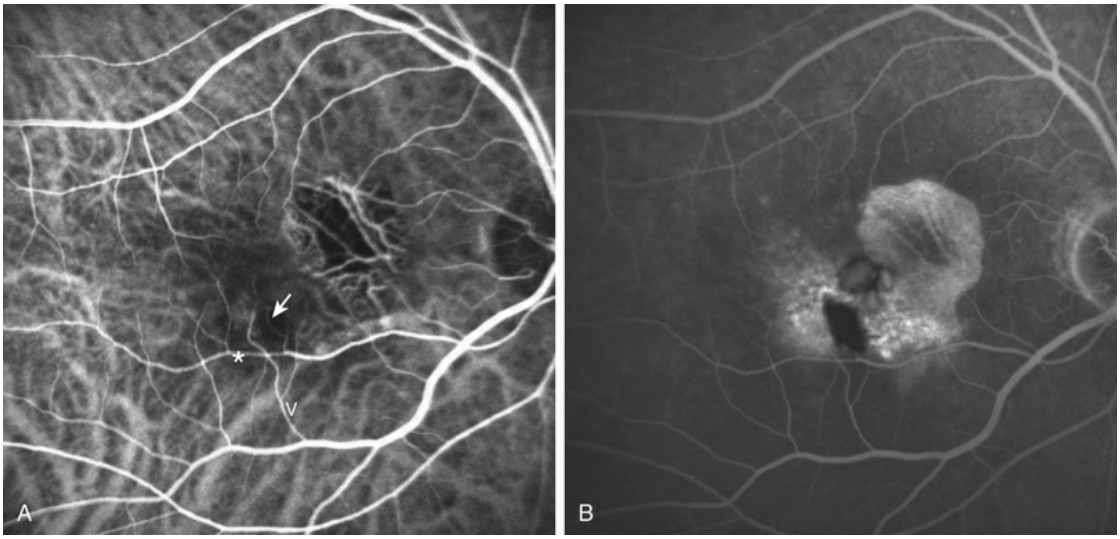

FIG. 2.12 Indocyanine green angiography (A) and fluorescein angiography (B) demonstrating an extrafoveal stage II retinal angiomatous proliferation (RAP). One feeding first-order macular arteriole (A, *arrow*) shunts blood flow from the vascular arcade (A, *asterisk*) to the RAP and to one draining retinal vein (A, *V*). Cystoid macular edema is evident in late

fluorescein phases.

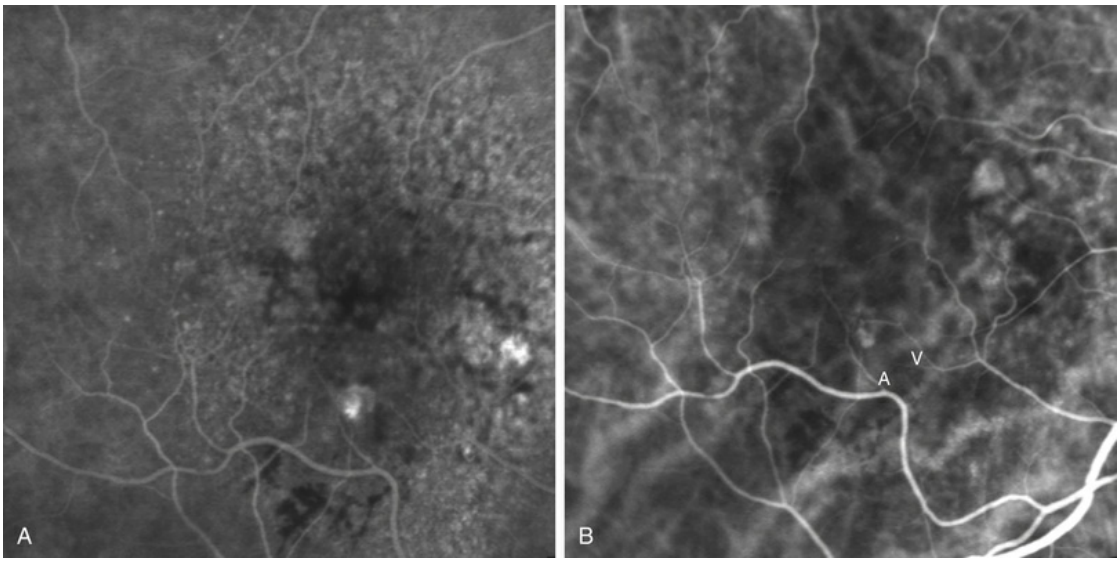

FIG. 2.13 Mid-phase fluorescein angiography (A) showing a small area of progressive extrafoveal staining at 6 o'clock. Dynamic indocyanine green angiography (B) reveals a well-delineated stage I retinal angiomatous proliferation with a feeding retinal arteriole (B, *A*) and a draining retinal vein (B, *V*).

Early and accurate diagnosis of RAP is important for at least two reasons. First, RAP lesions are thought to be more aggressive,[65] with a treatment response that is likely to diminish with more advanced disease stages.[57] Second, recent data from the literature suggest that successful anatomic and functional results with RAP may be achieved more consistently with combined treatments (i.e., intravitreal injection of steroid or anti-VEGF + photodynamic therapy) rather than with intravitreal injection of anti-VEGF therapy alone.[66,67] Dynamic ICGA is also extremely useful for monitoring the therapeutic effect: a complete remodeling of the vascular structure may be achieved after successful closure and it is clearly highlighted in d-ICGA (Fig. 2.14).[68]

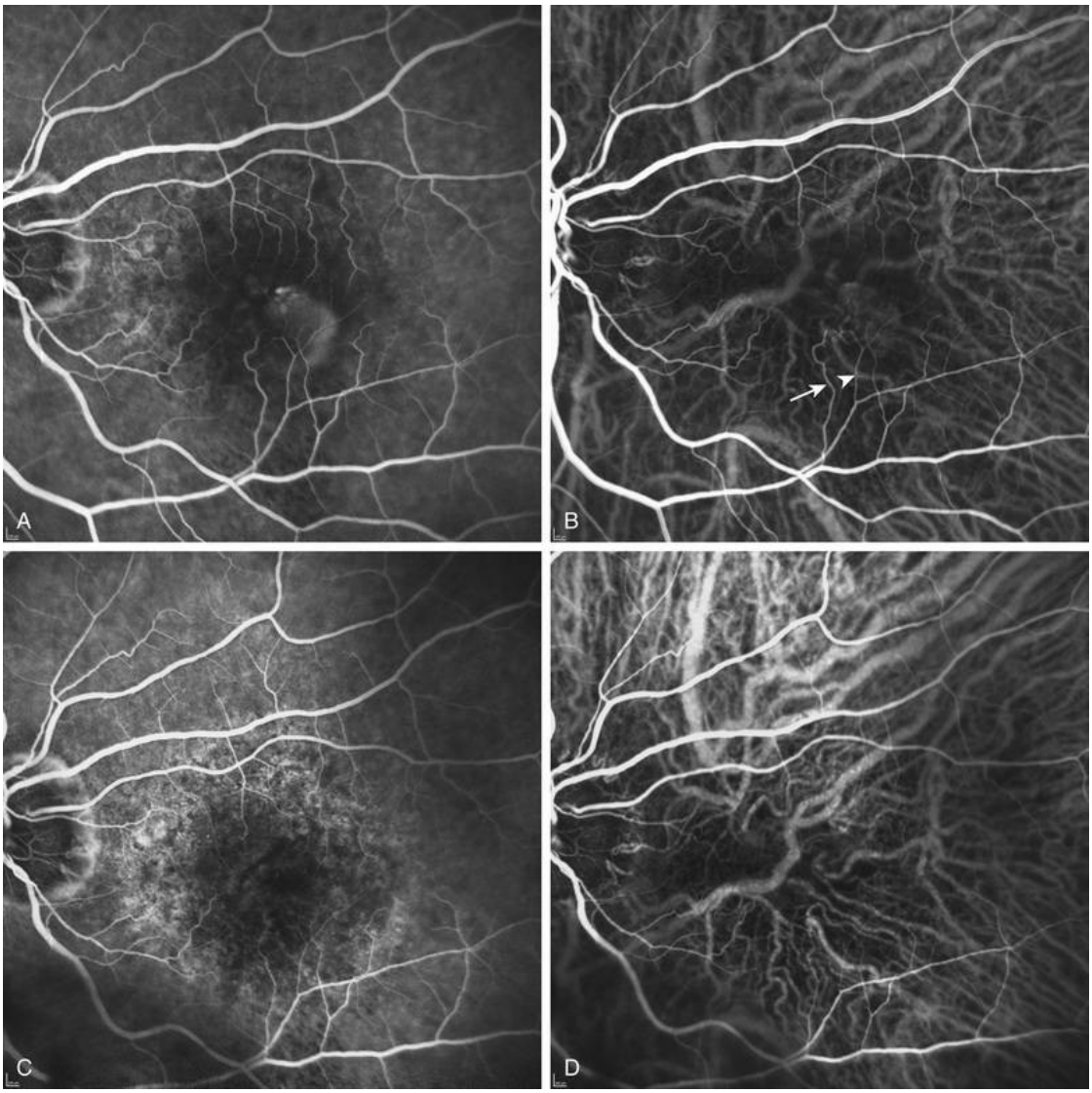

FIG. 2.14 Baseline fluorescein angiography (FA) (A) and dynamic indocyanine green angiography (ICGA) (B) shows a stage II extrafoveal retinal angiomatous proliferation (RAP) located inferotemporal to the fovea. One feeding first-order macular arteriole (B, *arrowhead*) shunts blood flow from the vascular arcade to the RAP and to the draining retinal vein (B, *arrow*). Two months after one combined treatment (intravitreal triamcinolone acetonide + photodynamic therapy), the RAP is no longer detectable by either FA (C) or ICGA (D). There is an evident reduction in size of both the first-order macular arteriole and the draining retinal vein (barely visible) (C,D).

Polypoidal Choroidal Vasculopathy

Polypoidal choroidal vasculopathy (PCV) is a primary abnormality of the choroidal circulation characterized by an inner choroidal vascular network of vessels ending in an aneurysmal bulge or outward projection, visible clinically as a reddish-orange, spheroid, polyp-like structure.[69] It was first described in the peripapillary area[69,70] (Fig. 2.15) but it may affect the macula[71] (Fig. 2.16), and also extramacular areas (Fig. 2.17).

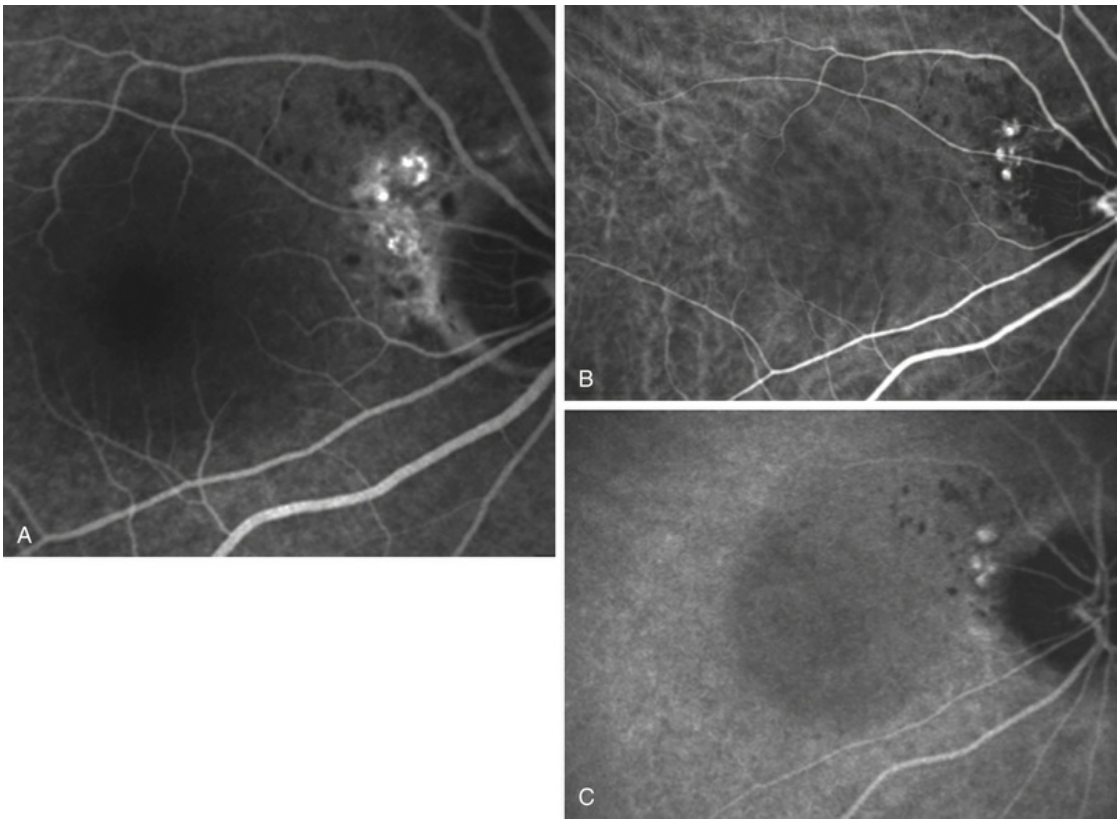

FIG. 2.15 Late phase fluorescein angiography (A) shows a neurosensorial detachment with multiple juxtapapillary "hot spots." Early (B) and late (C) indocyanine green angiography reveals the presence of juxtapapillary polypoidal choroidal vasculopathy.

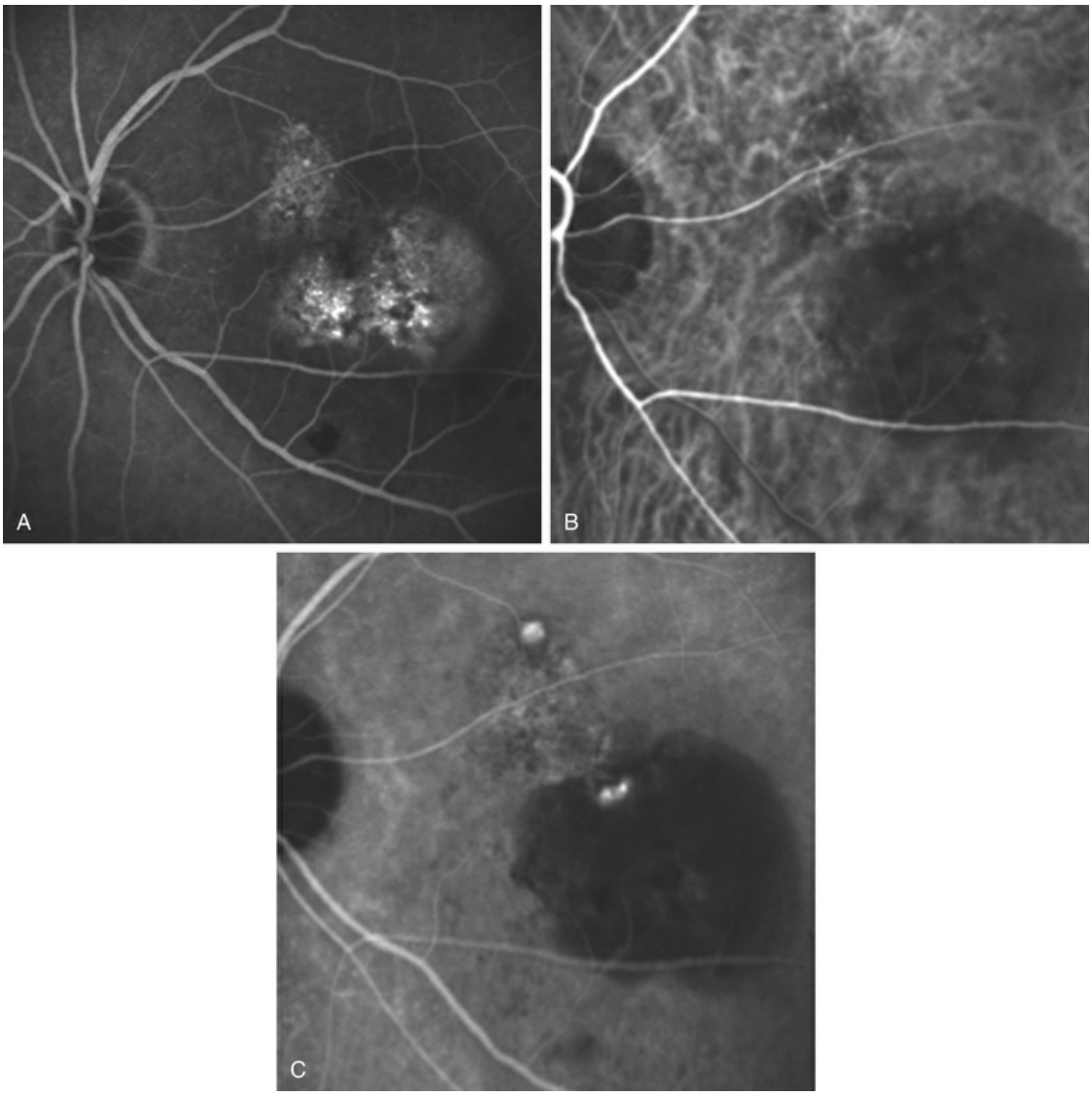

FIG. 2.16 Late phase fluorescein angiographic image revealing type 1 occult choroidal neovascularization with a subfoveal pigment epithelium detachment (PED) (A). Early (B) and late (C) indocyanine green angiography demonstrate a distinct network of vessels within the macular choroid ending with two hyperfluorescent “polyps.” One of the two is located within the PED.

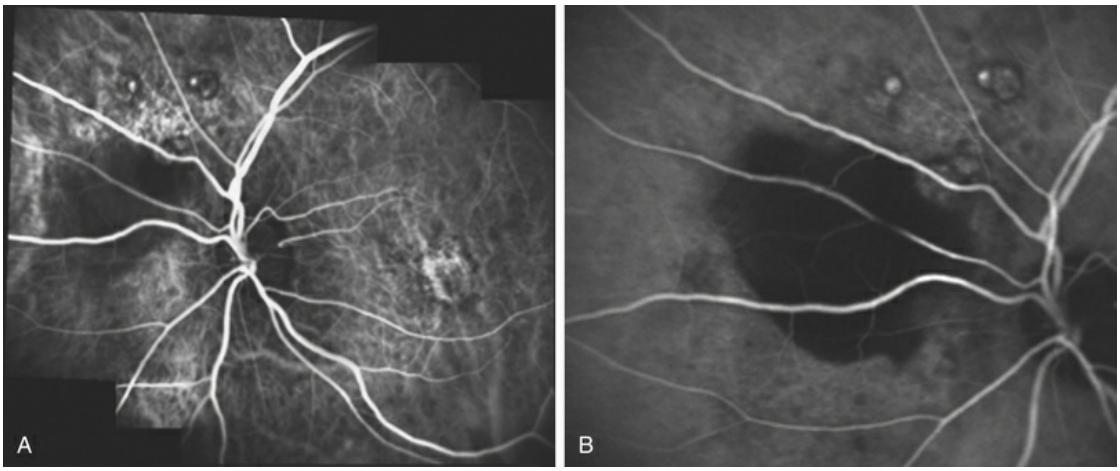

FIG. 2.17 Early (A) and late (B) indocyanine green angiography showing extramacular polypoidal choroidal vasculopathy with a pigment epithelium detachment.

The disorder is associated with multiple, recurrent, serosanguineous detachments of the RPE and neurosensory retina secondary to leakage and bleeding from the peculiar choroidal vascular abnormality. It has been reported that 85% of patients with serosanguineous detachments of the RPE have evidence of PCV.[72] ICGA has been used to detect and characterize the PCV abnormality with enhanced sensitivity and specificity.[1,71] The early phase of the ICG angiogram shows a distinct network of vessels within the choroid (Fig. 2.16B). In patients with juxtapapillary lesions, the vascular channels may follow a radial, arching pattern. In PCV limited to the macula, a vascular network often arises in the macula and follows an oval distribution pattern.[73] Larger choroidal vessels of the PCV network begin to fill before retinal vessels, and the PCV network fills also at a slower rate than retinal vessels. Shortly after the network can be identified by the ICG angiogram, small hyperfluorescent "polyps" become visible (Fig. 2.16C). These polypoidal structures correspond to the reddish-orange choroidal excrescence seen clinically. They appear to leak slowly as the surrounding hypofluorescent area becomes increasingly hyperfluorescent. In the later phase of the angiogram there is uniform disappearance of dye ("washout") from the bulging polypoidal lesions.

PCV is often misdiagnosed or confused with chronic central serous chorioretinopathy[74,75] and with exudative age-related

maculopathy,[71,76] and may represent a transitional condition between the two pathologies.[1] Moreover, the treatment strategies for PCV differ from exudative AMD. The use of anti-VEGF agents is controversial in PCV,[1] while verteporfin photodynamic therapy, alone or in combination with bevacizumab,[77] as well as selective laser photocoagulation have been shown to be effective treatments.[78]

Given the facts that ICGA is the most sensitive and specific tool for PCV identification and the treatment for PCV may differ from other diseases for which it is frequently confused, it would seem apparent that ICGA is an important tool in the evaluation of all cases of exudative lesions suspected of harboring PCV.

Central Serous Chorioretinopathy

Central serous chorioretinopathy (CSC) is characterized by multifocal areas of choroidal hyperpermeability on ICG,[79–81] visible in the mid- and late phases of the angiogram[82] (Fig. 2.18). These areas surround the active retinal pigment epithelial leaks but can also be found in areas apparently unaffected by leakage or abnormal fluorescence on FA, even in the fellow eyes.[79] Zones of choroidal hyperpermeability tend to persist in cases of severe and chronic CSC[83] (Fig. 2.19), and are of value for distinguishing CSC from age-related macular degeneration in older patients with suspected occult neovascularization.[80,84]

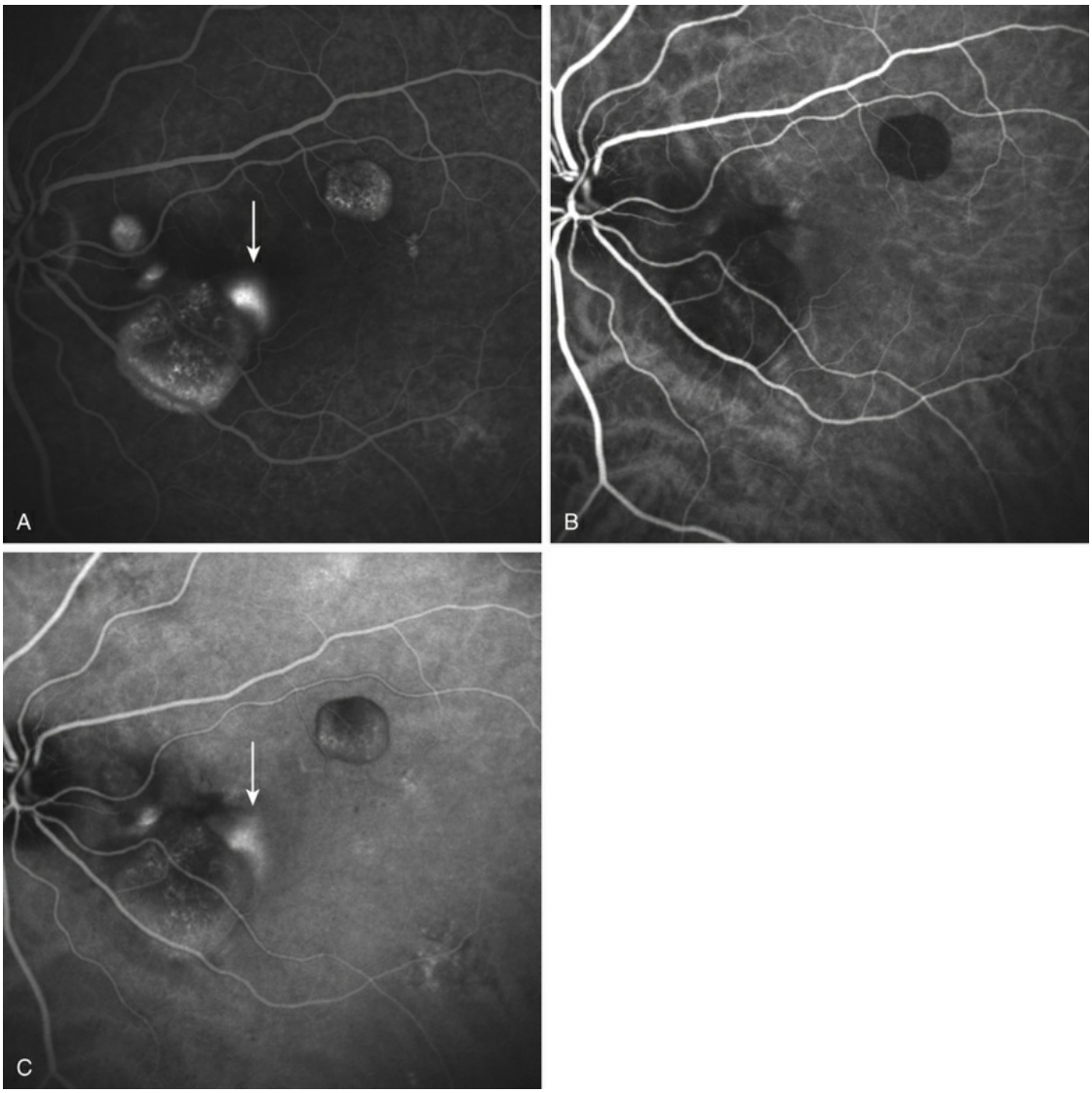

FIG. 2.18 A case of central serous chorioretinopathy. In the fluorescein angiographic image (A) it is possible to visualize three distinct serous detachments of the pigment epithelium, and one point of leakage. Another hyperfluorescent area is visible (A, *arrow*), but it is not clear if it corresponds to another point of leakage or represents an additional detachment. Indocyanine green angiographic images (B,C) allow one to clearly distinguish points of leakage as hyperfluorescent areas, with marked leakage in the late phases (C, *arrow*). The uncertain area noted on fluorescein angiography is another leaky point.

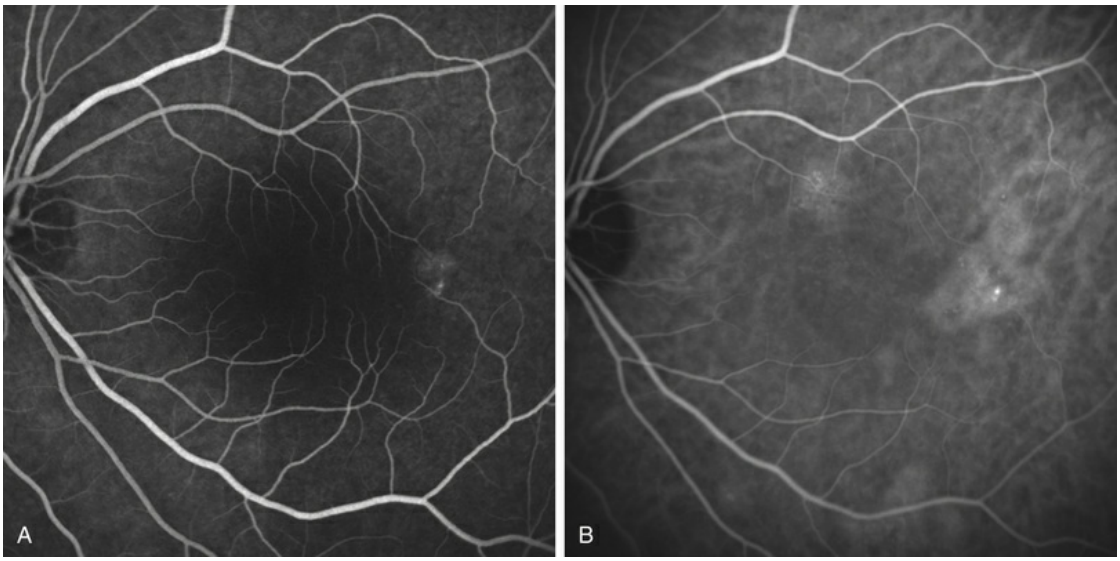

FIG. 2.19 A case of central serous chorioretinopathy. Fluorescein angiographic image (A) shows only an area of pigment epithelium disturbance. Indocyanine green angiographia (B) reveals a more extensive alteration of the choriocapillaris, with multiple areas of hyperfluorescence.

Moreover, ICG assessment of the location of these areas of hyperpermeability may be useful when considering treatment with verteporfin photodynamic therapy (PDT), using normal[80] or half-fluence laser energy.[85] The treatment focused on these areas showed rapid reduction of fluid and improvement in visual acuity,[80] possibly by leading to hypoperfusion of choriocapillaris and vascular remodeling.[86] In these studies, verteporfin PDT success rate seemed to be dependent on the degree of hyperpermeability, as the treatment was less effective or had more frequent recurrence of CSC in eyes without intense hyperfluorescence.[87]

Other findings in CSC using ICGA include multiple "occult" serous PED,[79] punctate hyperfluorescent spots,[88] delays in arterial filling of the choroidal arteries and choriocapillaris,[89,90] and venous congestion.[90] ICG is also useful in differentiating CSC from polypoidal choroidal vasculopathy.[75]

Choroidal Tumors

Choroidal Hemangioma

Unlike diffuse choroidal hemangiomas, which are usually evident

at birth and typically occur as part of neuro-oculocutaneous hemangiomatosis or Sturge–Weber syndrome, circumscribed choroidal hemangioma may be more difficult to diagnose.

Circumscribed choroidal hemangiomas are benign hamartomas that typically present from the second to fourth decades of life.[91] They usually occur sporadically in the absence of systemic disease. Histopathology reveals that the tumor is composed by vascular channels lined with endothelium. It involves the full thickness of the choroid with secondary changes of the overlying RPE and the retina.[92] Although commonly asymptomatic, choroidal hemangiomas can be associated with exudative retinal detachment resulting in reduced visual function, metamorphopsia, and photopsia.

On ophthalmoscopic examination, a circumscribed choroidal hemangioma appears as an orange choroidal mass with indistinct margins that blend with the surrounding choroid. They are frequently located in the macular region of the posterior pole, and are not usually thicker than 6 mm.[93] Surrounding subretinal fluid leading to exudative retinal detachment with macular involvement is common in symptomatic cases. Retinal hard exudates are minimal or absent.

Angiographic studies such as fluorescein and ICG can be helpful in establishing the diagnosis and differentiating these benign lesions from other tumors, namely amelanotic malignant melanoma and choroidal metastases. Fluorescein angiography demonstrates a hyperfluorescent mass with a fine lacy vascular network of intrinsic vessels in the early choroidal filling phase. The hyperfluorescence increases throughout the angiogram, and there is variable leakage in late views[94] (Fig. 2.20A-B). ICGA is the most useful study for demonstrating the intrinsic vascular pattern of circumscribed choroidal hemangioma.[95] The advantage of ICG dye over sodium fluorescein dye is that it diffuses much more slowly out of fenestrated small choroidal vessels than does sodium fluorescein. Within 30 seconds of injection of the ICG dye, the tumor's intrinsic vascular pattern becomes apparent. By 1 minute, choroidal hemangiomas completely fill with the dye showing brilliant hyperfluorescence. This 1-minute stage of intense hyperfluorescence seen with choroidal hemangiomas is brighter

than any other tumor, and it is very suggestive of the diagnosis. In the following phases (6–10 minutes), the hyperfluorescence can persist or begin to wane (Figs. 2.20C–E). In the late phases of the ICG angiogram (30 minutes), a "washout" effect with reduction of the initial hyperfluorescence is observed secondary to the outflow of dye from the hemangioma (Fig. 2.20F).[95] The low-resistance, high-flow properties of the tumor allow rapid flow of the dye into and out of the tumor. The resulting final effect is that the tumor empties sooner than the normal surrounding choroid and thus appears hypofluorescent in comparison. This "washout" sign is very helpful in differentiating choroidal hemangiomas from amelanotic malignant melanoma and choroidal metastases.

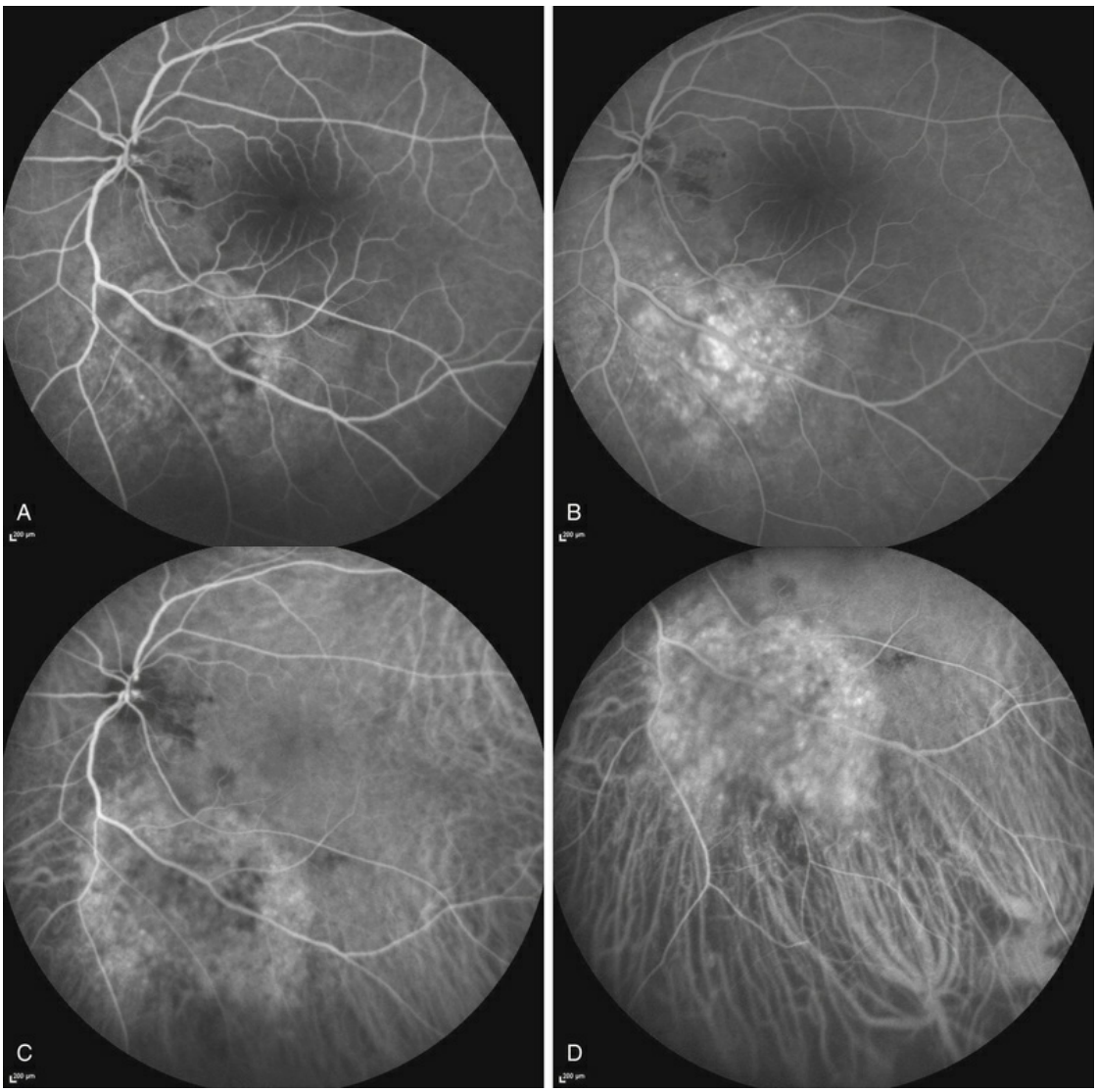

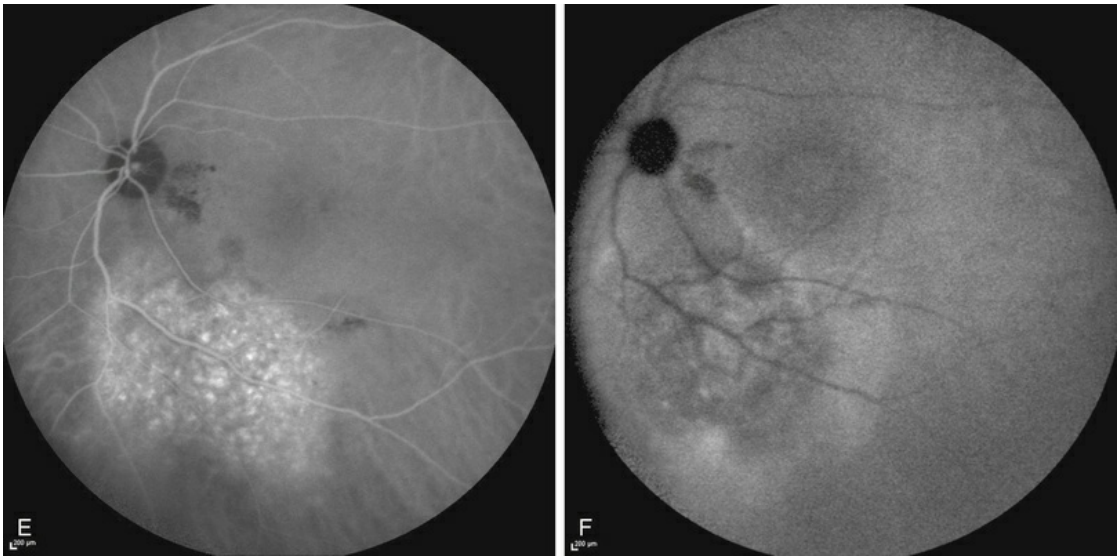

FIG. 2.20 Fluorescein angiography demonstrating a hyperfluorescent mass along the inferior vascular arcade (A). The hyperfluorescence increases progressively throughout the angiogram with variable leakage in late views (B). Early-phase indocyanine green angiography (ICGA) (49 seconds) revealing a fine lacy vascular network of intrinsic vessels (C). Increasing hyperfluorescence is detected at 2 min (D) and 5 minutes (E) after injection. Of note, the margins of the tumor appear scalloped. Late-phase ICGA study demonstrating hypofluorescence within the tumor (washout effect) (F). A halo of minimal hyperfluorescence surrounds the tumor. This may result from staining of the retinal pigment epithelium or leakage of indocyanine green into the subneurosensory retinal space.

Choroidal Melanoma

Indocyanine green angiography findings in uveal melanoma are variable.[96] No study revealed any pathognomonic sign with ICG to identify choroidal melanoma.[23,97]

Nevertheless ICGA was found to be capable of identifying tumor vessels (Fig. 2.21),[98,99] which are usually irregularly tortuous, with anarchic branching,[97] dilated with a parallel cours,[98] and characterized by vasculogenic mimicry patterns.[100] ICGA was demonstrated to be superior to FA in detecting both tumor borders and vasculature.[97,101]

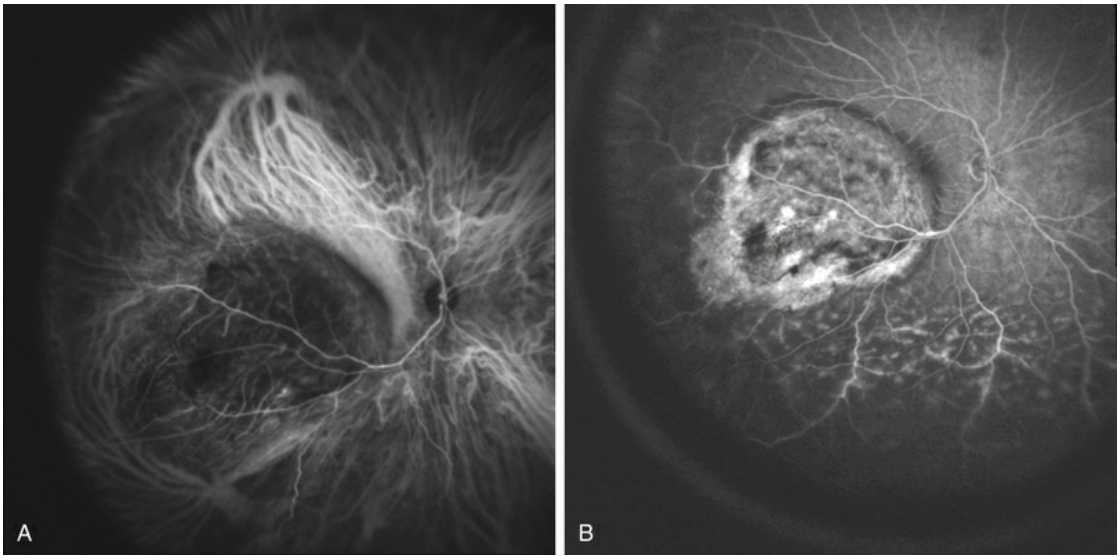

FIG. 2.21 A case of choroidal melanoma. Indocyanine green angiography (A) allows visualization of the tumor's intrinsic vasculature with irregular tortuosity and anarchic branching. Note the strong fluorescence within the large choroidal vessels around the lesion, a possible sign of increased flow due to the presence of the tumor. Melanoma intrinsic vessels are leaky by fluorescein angiography (B), and therefore they cannot be identified with this diagnostic tool. In fluorescein angiographic images (B), in the inferior quadrant it is possible to visualize damage to retinal vessels with associated exudative detachment.

Mueller et al. found that different patterns of the microcirculation within the tumor may be useful in the prognosis of the disease.[101] The evidence of microcirculation patterns characterized by networks and a parallel course with cross-linking may be associated with a higher risk of metastatic disease.[101] Other studies reported the possible role of ICGA in evaluating the outcome of brachytherapy,[102] proton beam irradiation,[103] and transpupillary thermotherapy.[104]

Peripheral Exudative Hemorrhagic Chorioretinopathy

Peripheral exudative hemorrhagic chorioretinopathy (PEHCR) is a bilateral peripheral exudative-hemorrhagic retinal degenerative process of the eye.[105,106] The condition is characterized by blood in the subretinal or subretinal pigment epithelial space. PEHCR is most often found in older Caucasian patients and may simulate a

vitreous hemorrhage with suspicion of underlying retinal detachment or break, intraocular inflammatory process, retinal artery macroaneurysm, or choroidal melanoma.[105] In fact, PEHCR often appears as a visible intraocular elevated mass with a mean basal dimension of 10 mm and a mean thickness of 3 mm, consistent with the size of a small to medium-sized melanoma.[106] The lesion is most often located temporally (77%) between the equator and the ora serrata (89%) and involves 1 (46%) or 2 (46%) quadrants.[106] In comparison, eyes with uveal melanoma show tumor location in the macula (5%), between the macula and the equator (78%), and between the equator and the ora serrata (17%).[106]

Many eyes with PEHCR have features of macular or extramacular (peripheral) degeneration such as drusen, RPE alterations, or choroidal neovascularization.[106] The majority of PEHCR lesions spontaneously resolve, leaving RPE atrophy, hyperplasia, and fibrosis. These features imply a bilateral generalized aging process within the eye and are consistent with the degenerative nature of the disease. Although almost half of patients may be asymptomatic, a decrease in visual acuity related to PEHCR may occur in up to 20% of cases.[106] Both for this reason and for the fact that the acute hemorrhagic form is typically mistaken for melanoma, PEHCR deserves an early and proper clinical diagnosis. Fluorescein angiography is of little help because choroidal neovascular lesions are visible in only 3% of cases.[106] This is due to the blockage of choroidal fluorescence related to subretinal hemorrhage, sub-RPE hemorrhage, or RPE hyperplasia. Diffuse peripheral changes consistent with variable degrees of RPE hyperplasia or atrophy are also common FA features.

By contrast, ICGA may clearly delineate the choroidal neovascular process, which is often located at the edges of the blood pool, even in the far periphery. Photodynamic therapy or laser photocoagulation applied to the choroidal new vessels may further accelerate the reabsorption of subretinal blood with decreased risk of subsequent visual acuity loss (Figs. 2.22 and 2.23).

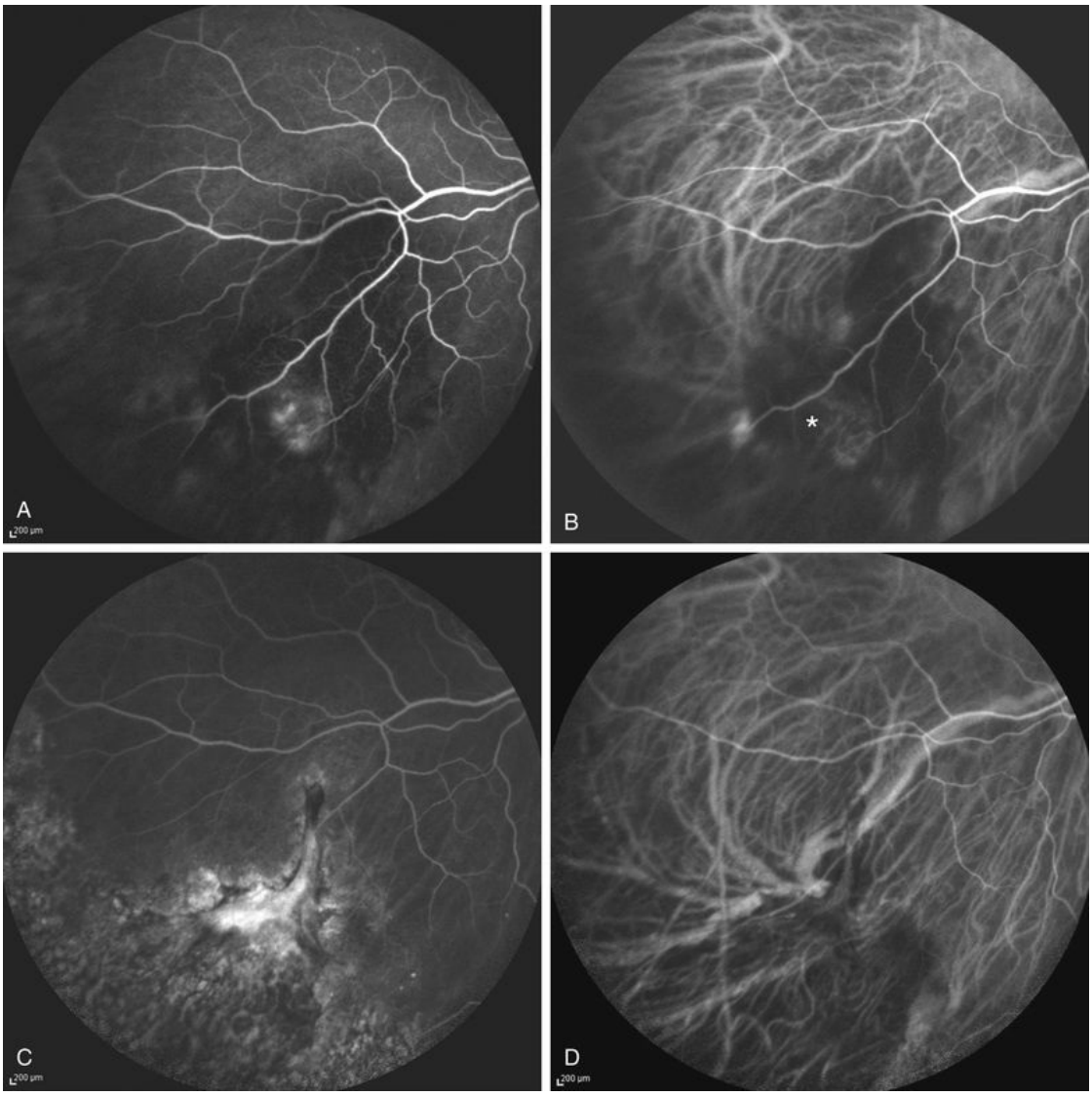

FIG. 2.22 A case of a midperipheral inferotemporal subretinal hemorrhage. Mid-phase fluorescein angiography showing a hyperfluorescent leaking spot within the hemorrhage (A). To be noted are the diffuse peripheral changes consistent with variable degrees of RPE hyperplasia or atrophy. Indocyanine green angiography (ICGA) 31 seconds after injection (B): the choroidal neovascularization (CNV) is clearly outlined (B, *asterisk*). Six months after laser photocoagulation of the CNV: fluorescein (C) and ICGA reveal fibrosis of the CNV with late staining and no leakage.

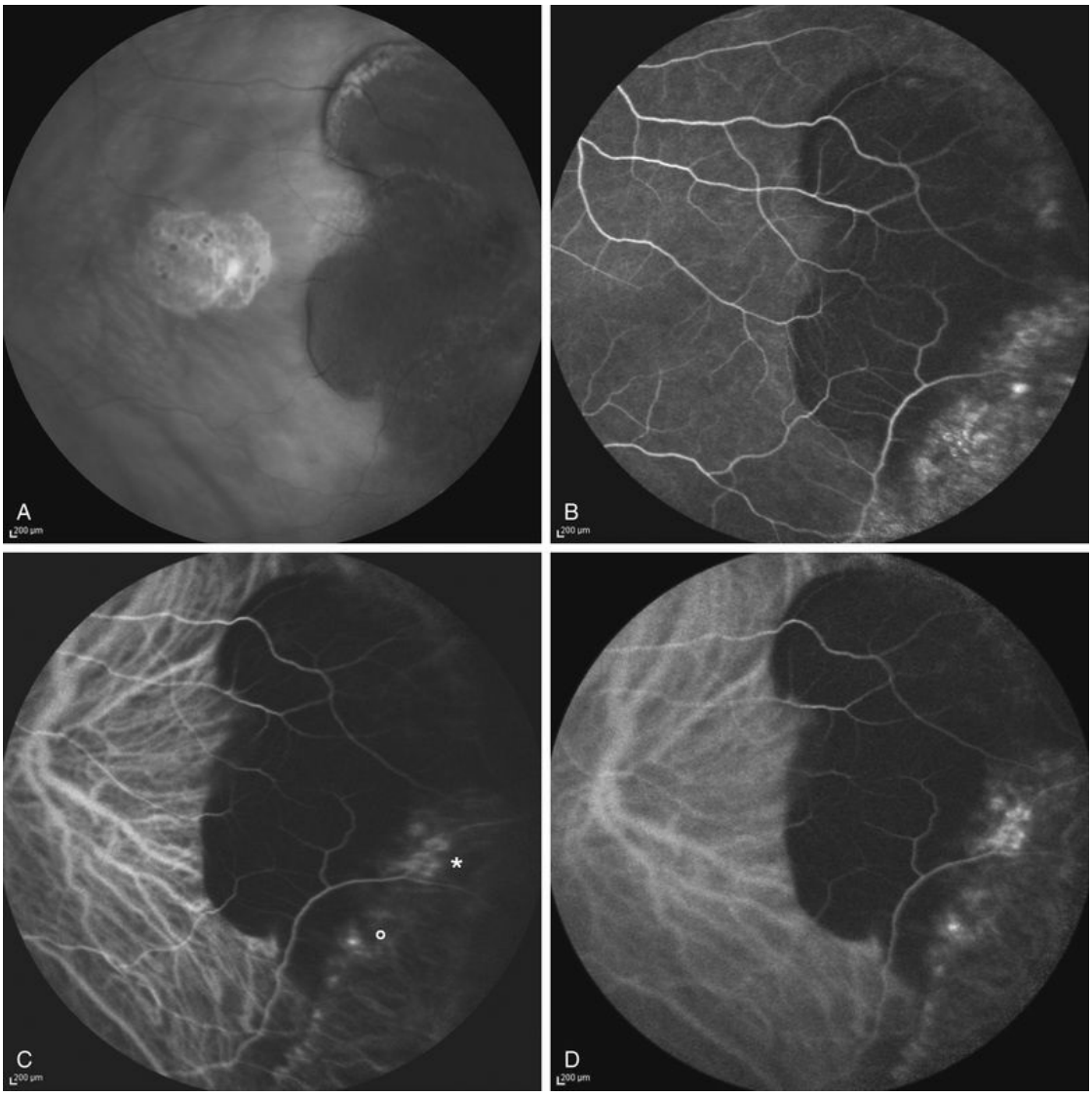
A
200 µm
B
200 µm
*
°
C
200 µm
D
200 µm

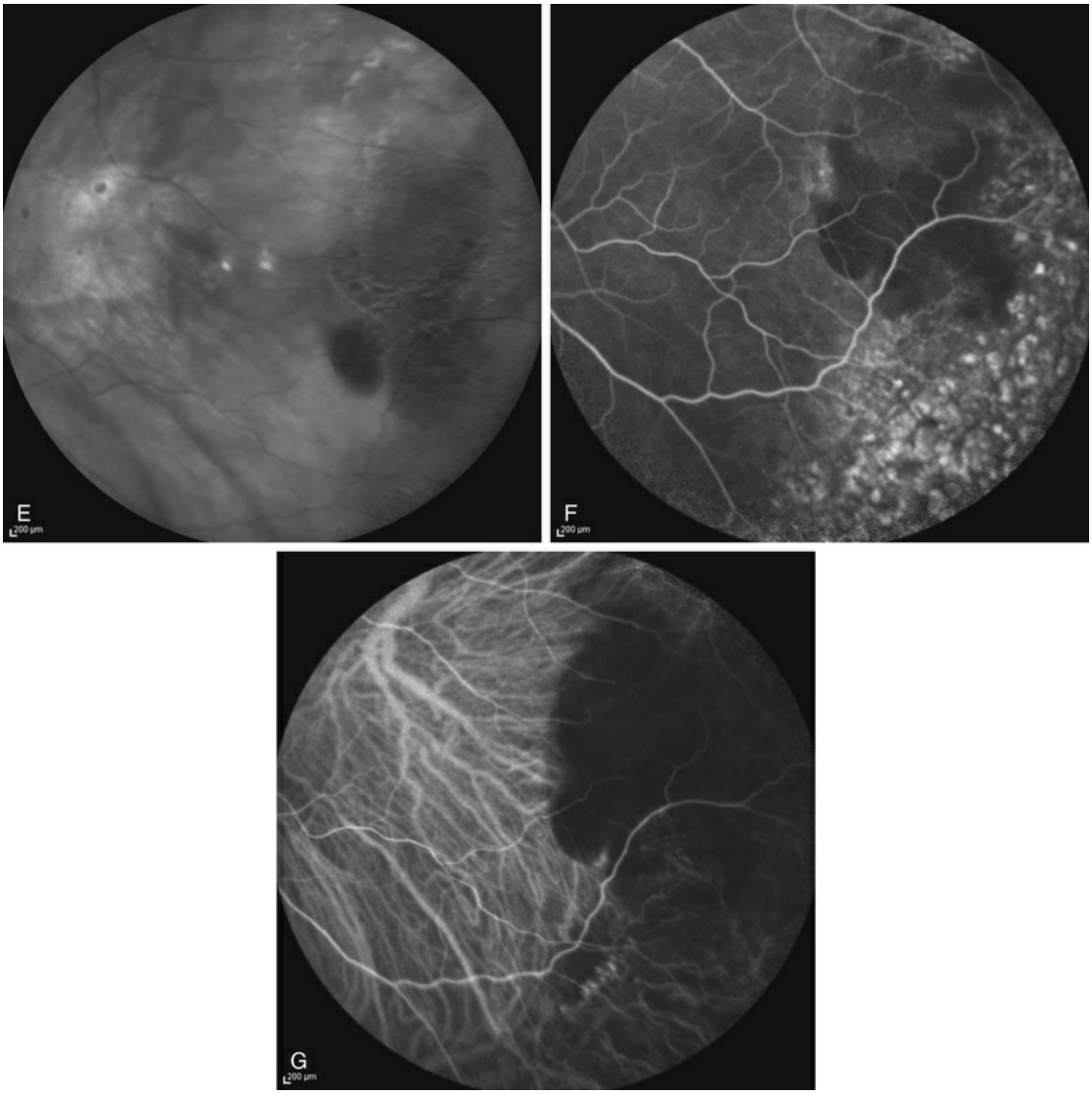

FIG. 2.23 Infrared image of a peripheral temporal subretinal hemorrhage (A). Mid-phase fluorescein angiography showing diffuse peripheral changes consistent with variable degrees of retinal pigment epithelium hyperplasia or atrophy. Typical features of choroidal neovascularization (CNV) are absent (B). Corresponding indocyanine green angiography (ICGA) 2 minutes after injection (C): CNV is clearly visible (*asterisk*) while a second choroidal new vessel is suspected (*circle*). Six minutes after injection, ICGA shows progressive leakage (D). Infrared image 3 months after photodynamic therapy on the two leaking spots: the reabsorption of the subretinal hemorrhage is almost complete (E). Corresponding fluorescein (F) and indocyanine green (G) angiograms reveal persistent obliteration of CNV with no late leakage.

Varix of the Vortex Vein Ampulla

Varix of the vortex vein ampulla is a rare, benign, asymptomatic condition, which may be confused with a choroidal nevus or melanoma.[107] The choroidal veins drain into an average of four vortex veins, which exit the globe through scleral canals.[108] About half of the vortex veins show dilatations of varying sizes and shapes, and are referred to as vortex vein ampullae. The varix of the vortex vein ampulla is an unusually large dilatation of the vortex vein. The cause remains unclear. The gaze-dependent dynamic nature of the lesion suggested gaze-evoked kinking of the extrascleral vortex vein or narrowing of the scleral canal to be considered as the possible cause.[109] The varix may be enlarged also by factors that increase ocular venous pressure, such as the Valsalva maneuver, head-down positioning, and jugular vein compression.[109] Biomicroscopically, the lesion appears as a smooth red-brown elevation in the equatorial region, usually in the nasal quadrants.[107] It is usually a single lesion but may be bilateral.[109] A proper diagnosis may be achieved by pressure on the globe that readily collapses the varix (Fig. 2.24).[109] ICGA[96,97,110] is particularly useful because it demonstrates the relationship of the varix to the choroidal vasculature and also allows visualization of the pressure and gaze-dependent changes. Relatively early maximum fluorescence and a homogeneous filling pattern may further help differentiate the varix from other choroidal masses.[107]

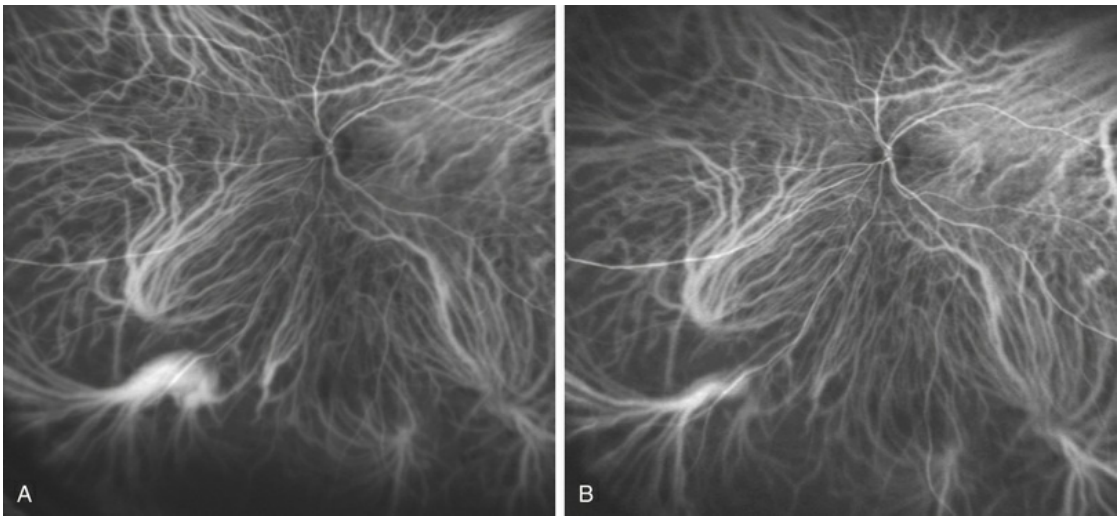

FIG. 2.24 Indocyanine green angiography in a case of

varix of the vortex vein in the nasal equatorial region (A). Application of sufficient pressure on the globe readily collapses the varix (B).

Choroidal Inflammation and White Dot Syndromes

Multiple Evanescent White Dot Syndrome

Multiple evanescent white dot syndrome (MEWDS) is a unilateral acute disease that affects young women, presenting with a transient, self-limiting visual loss. The disease involves the choroid and the outer retina.[111,112] ICGA shows a pattern of multiple hypofluorescent areas at the posterior pole and peripheral retina. These spots become visible in the mid–late phases, range in size between 50 and 1000 μm,[112] and are more apparent in ICGA images than by fundus examination and FA[1,112] (Fig. 2.25). In addition, ICGA may show hypofluorescence surrounding the disc area.[111] The hypofluorescent spots disappear at the recovery stage of the disease, and sometimes are more persistent with ICGA.[113]

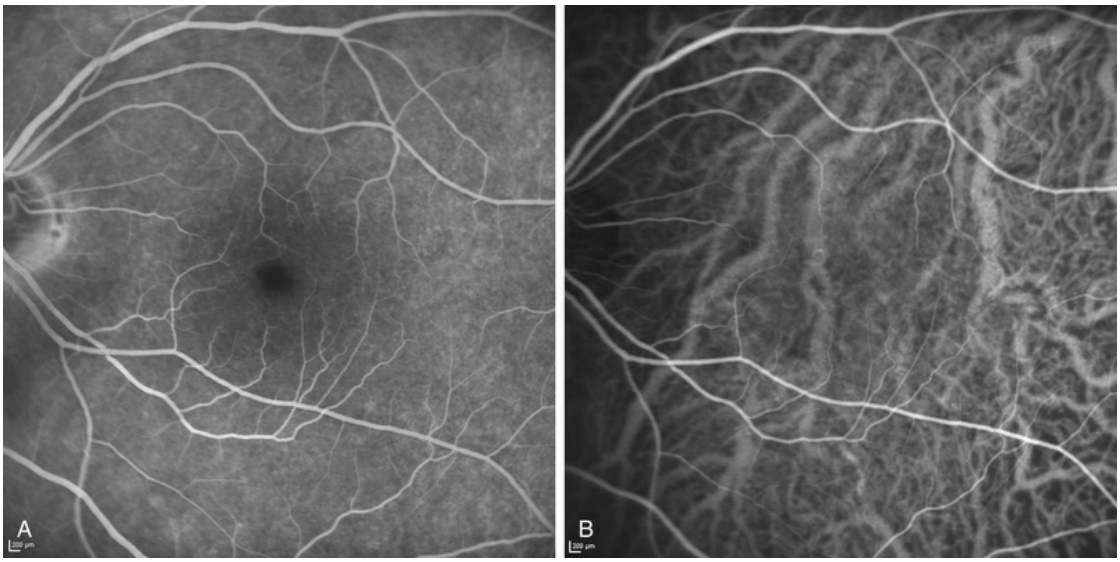

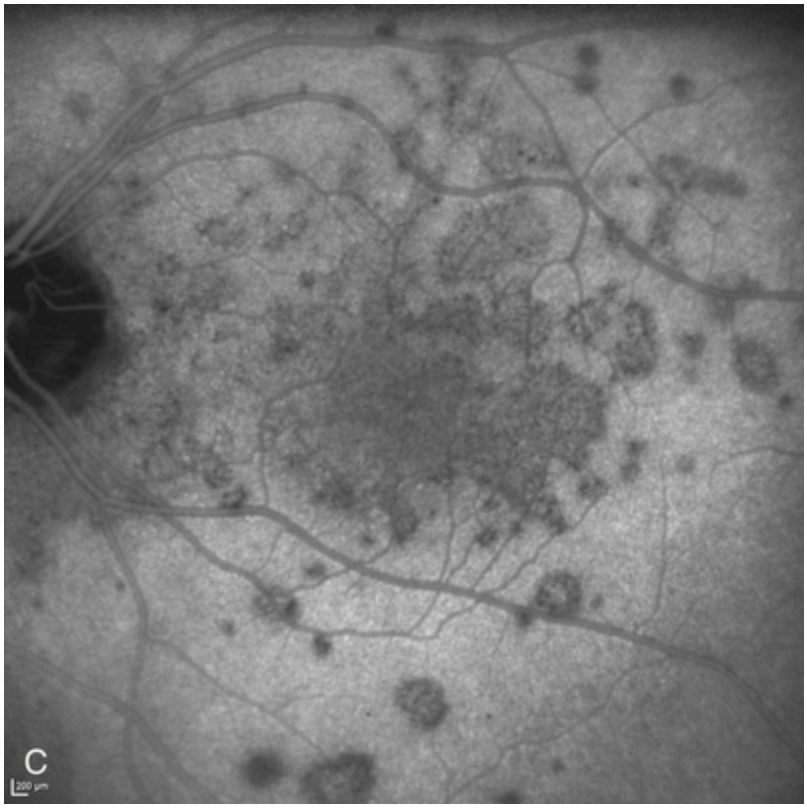

FIG. 2.25 A case of multiple evanescent white dot syndrome. Late phases of the fluorescein angiogram reveal only mild alterations at the level of the outer retina and retinal pigment epithelium (A). Early phases of indocyanine green angiography (B) begin to reveal areas of hypofluorescence, which become much more evident in the mid–late phases of the angiogram (C).

Multifocal Choroiditis

In multifocal choroiditis the white lesions are visualized as hypofluorescent spots in ICGA images. These lesions may be followed up with ICGA both in the natural course of the pathology and in the response to treatment with oral prednisone.[114] A reduction in size and number of hypofluorescent spots is observed after successful treatment. Other findings visible on ICGA are hyperfluorescent spots, which usually do not correspond with the hyperfluorescent foci seen on FA, and a large hypofluorescent area surrounding the optic nerve.

Birdshot Chorioretinopathy

This disease is characterized by deep cream-colored dots scattered

diffusely throughout both fundi. The lesions appear as round–oval, hypofluorescent, symmetric dots on ICGA.[115] These lesions are typically not seen by FA, and therefore ICGA may detect birdshot lesions more rapidly than FA.[116] Other findings on ICGA include diffuse ICG hyperfluorescence, predominantly found in the posterior pole in the late phase of angiography, and an alteration of the vascular pattern of the choroid, with choroidal vessels appearing fuzzy and indistinct in the intermediate phase of angiography.[115] In the chronic phase of the disease the hypofluorescent dots persist in the late phases of the angiogram and correspond to RPE atrophy or choroidal granulomas.[1,117]

Acute Multifocal Placoid Pigment Epitheliopathy

ICGA of acute posterior multifocal placoid pigment epitheliopathy (AMPPE) shows areas of hypofluorescence in both early and late phases that correlate with the placoid lesions. These lesions may be caused by choroidal hypoperfusion, secondary to occlusive vasculitis,[118] and ICGA often shows partial or complete resolution throughout the time-course of the disease.[119] New, active and healed, inactive lesions in AMPPE can both be imaged and differentiated using ICG angiography.[120]

Serpiginous Choroidopathy

ICGA allows better staging and identification of active lesions in serpiginous chorioretinopathy.[121] The active phase of the pathology is characterized by hypofluorescent areas with poorly defined margins (Fig. 2.26). These findings can predict the active lesions observed by FA. The presence of late hyperfluorescence in ICGA images represents a sign of choroidal hyperpermeability and may be associated with a more aggressive evolution of the disease. The healed lesions appear hypofluorescent with well-defined margins. The atrophy of the RPE and choriocapillaris allows better identification of large and medium-size choroidal vessels.

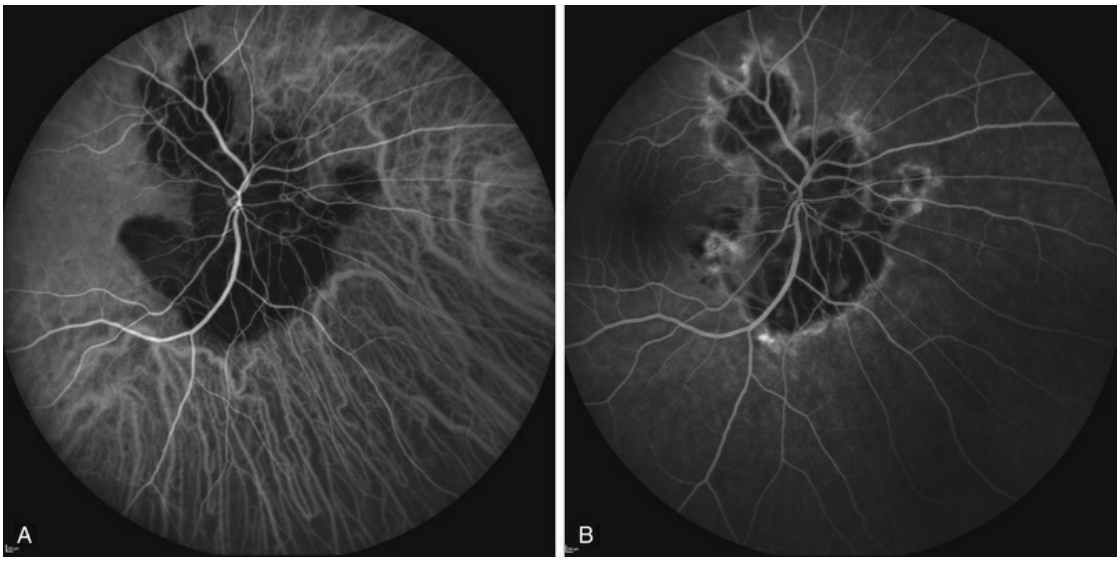

FIG. 2.26 A case of serpiginous chorioretinopathy. The lesion observed by indocyanine green angiography (ICGA) (A) occupies a greater extent than is evident on fluorescein angiography (B). This may indicate a progression of the pathology that can be anticipated or predicted using ICGA.

Punctate Inner Chorioretinopathy

The subretinal lesions observed in punctate inner chorioretinopathy are visualized by ICGA as hypofluorescent areas throughout all the phases of the angiogram.[122] These areas may correspond to localized choroidal hypoperfusion[123] and are greater in number compared to FA.[124] Another finding in ICGA images is the presence of hyperfluorescent points situated close to the vessel wall, representing a possible sign of vasculitis.[123]

Acute Zonal Occult Outer Retinopathy

In acute zonal occult outer retinopathy, ICGA shows a variety of pattern of presentations. Spaide reported that the peripapillary drusenoid material blocks the choroidal fluorescence in ICGA and therefore the involved areas appear hypofluorescent.[125] The secondary atrophy of the choriocapillaris produces hypofluorescence as well, which does not affect the fluorescence from the underlying larger choroidal vessels.[125] In some cases though, ICGA may show an increase of the fluorescence from the affected areas, due to the lack of photoreceptor outer segments and

the minor blocking effect from this layer (Fig. 2.27).

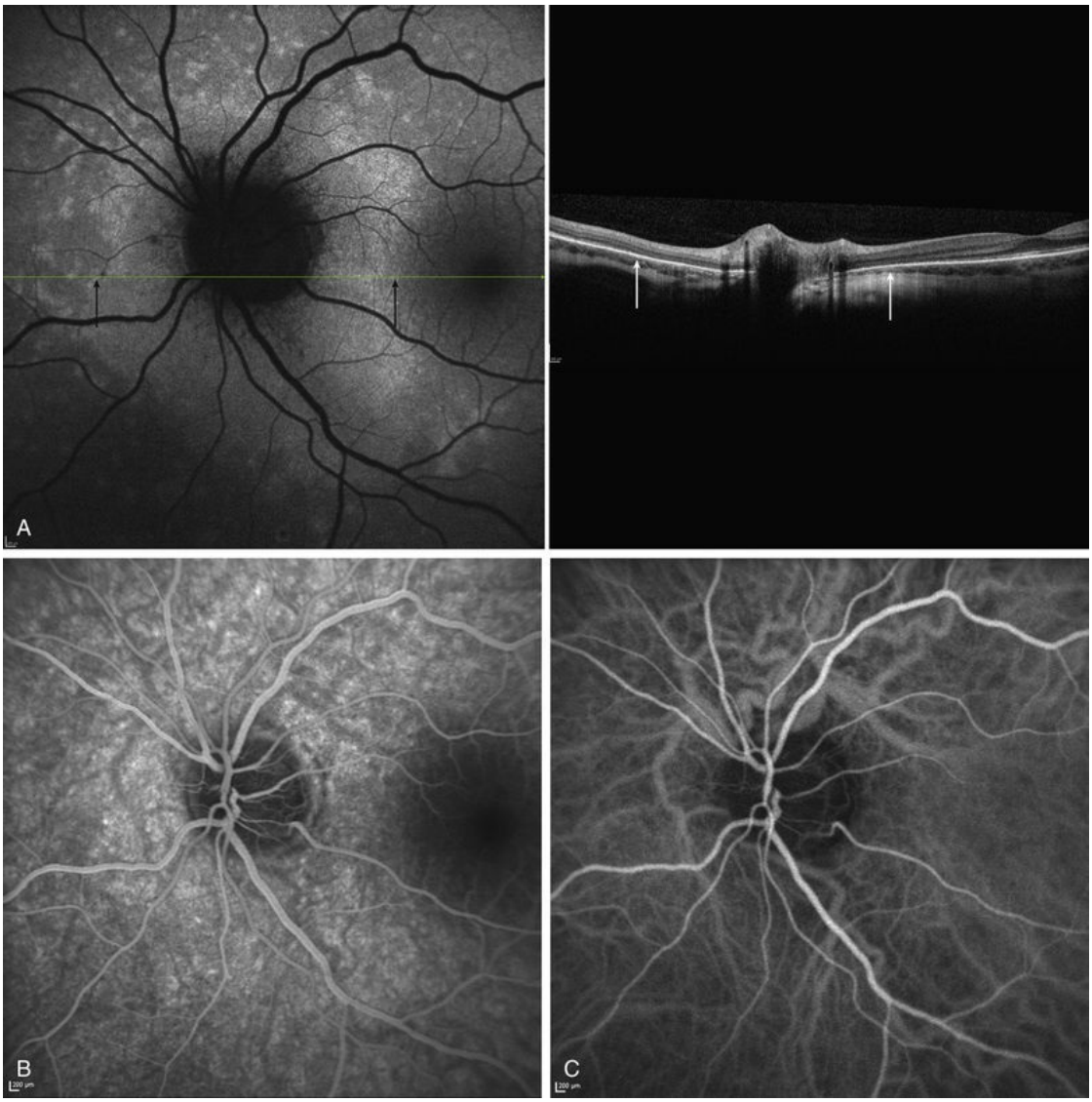

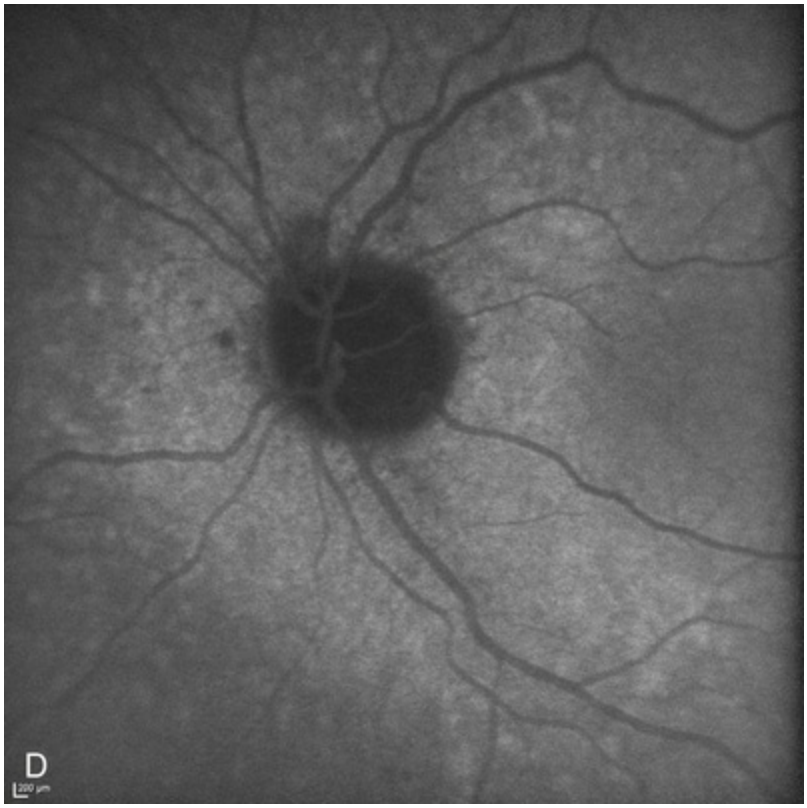

FIG. 2.27 A case of acute zonal occult outer retinopathy. Autofluorescence shows the typical features of this disorder, with hyperautofluorescent areas around the optic disc. Simultaneous spectral domain optical coherence tomography suggests that these areas (A, *black arrows*) correspond to zones with loss of the outer segments of the photoreceptors (A, *white arrows*), thus resulting in less blockage of the autofluorescence originating from the retinal pigment epithelium. Fluorescein angiography shows increased fluorescence corresponding to these areas (B). Early phase of indocyanine green angiography does not reveal alterations (C), while the late phase of the angiogram allows the affected areas to be distinguished by increased fluorescence (D).

Chorioretinal Atrophy

ICGA may be of help in the evaluation of the choriocapillaris in different stages of chorioretinal atrophy. The presence of hypocyanescence in the late phases of the examination suggests a complete absence of choriocapillaris. This condition, also called "dark atrophy," is more frequent in Stargardt disease as compared

with nonexudative AMD (Fig. 2.28).[126] In the former there is a complete loss of the choriocapillaris layer whereas in AMD there may be residual areas of patent choriocapillaris in areas otherwise deemed to be atrophic. The presence of residual choriocapillaris in atrophic AMD has been demonstrated by McLeod et al.[127] and Bhutto and Lutty.[128] Different pathogenetic mechanisms may be responsible for the distinct ICG appearance in the two diseases but the "dark atrophy" sign is of great help in the differential diagnosis between late-onset Stargardt disease and geographic atrophy.

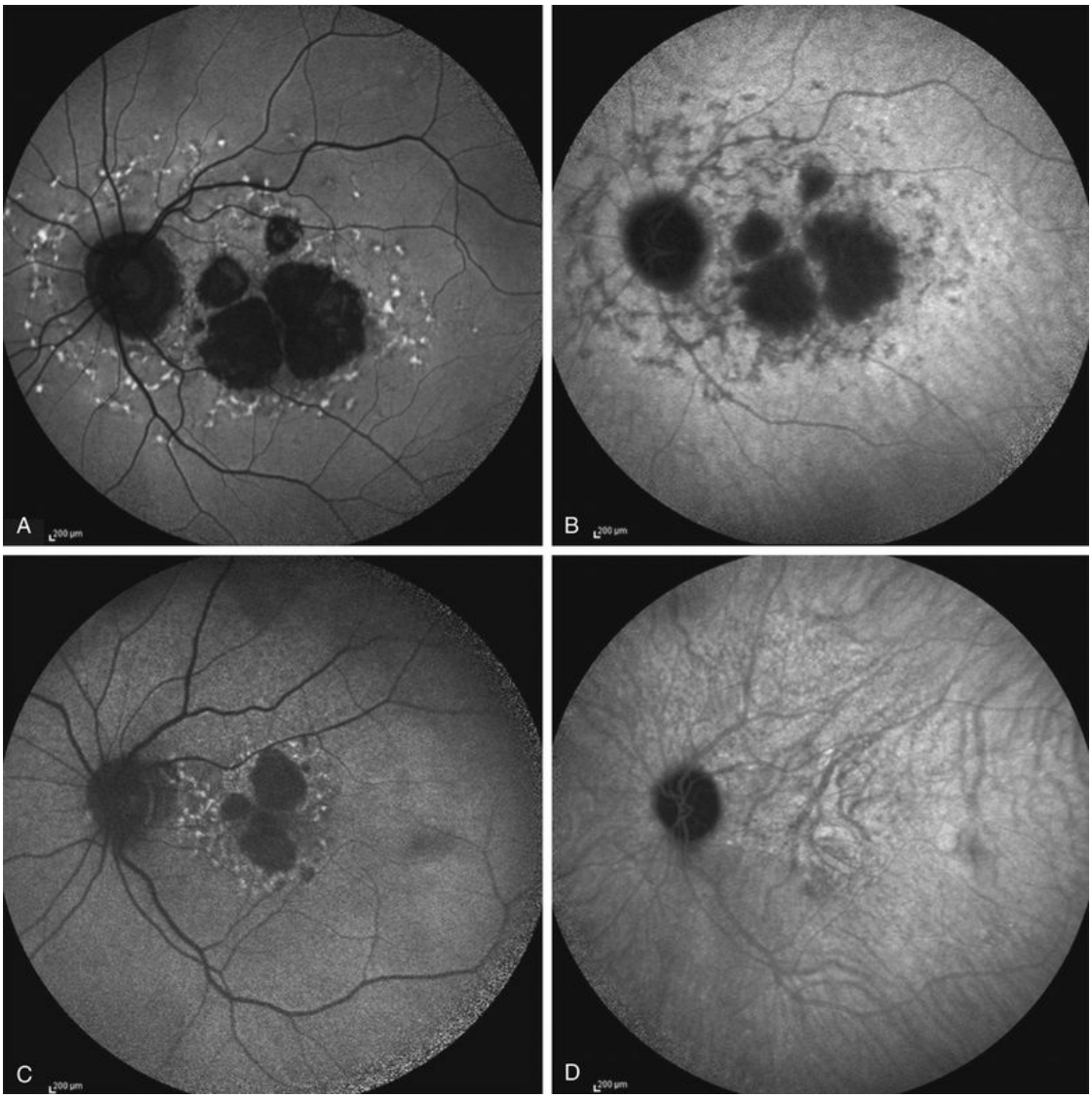

FIG. 2.28 Differences apparent on indocyanine green angiography (ICGA) in two cases of chorioretinal atrophy associated with Stargardt disease (SD) (A,B) and nonexudative age-related macular degeneration

(AMD) (C,D). In SD, areas of atrophy visible by fundus autofluorescence (A) appear hypocyanescent in late phases ICGA (B). In AMD areas of atrophy revealed by fundus autofluorescence (C) appear isocyanescent in late-phase ICGA (D).

In summary, despite the changing landscape of retinal disease therapeutics with an increased emphasis on pharmacotherapies and the rise in prominence of noninvasive diagnostic technologies such as optical coherence tomography, indocyanine green angiography remains an important tool in the diagnosis and management of a variety of retinal disorders.

References

1. Cohen SY, Dubois L, Quentel G, et al. Is indocyanine green angiography still relevant? *Retina*. 2011;31:209–221.
2. Ott P. Hepatic elimination of indocyanine green with special reference to distribution kinetics and the influence of plasma protein binding. *Pharmacol Toxicol*. 1998;83(Suppl. 2):1–48.
3. Fox IJ, Brooker LG, Heseltine DW, et al. A tricarbocyanine dye for continuous recording of dilution curves in whole blood independent of variations in blood oxygen saturation. *Proc Staff Meet Mayo Clin*. 1957;32:478–484.
4. Fox IJ, Wood EH. Applications of dilution curves recorded from the right side of the heart or venous circulation with the aid of a new indicator dye. *Proc Staff Meet Mayo Clin*. 1957;32:541–550.
5. Caesar J, Shaldon S, Chiandussi L, et al. The use of indocyanine green in the measurement of hepatic blood flow and as a test of hepatic function. *Clin Sci*. 1961;21:43–57.
6. Hunton DB, Bollman JL, Hoffman HN. Studies of hepatic function with indocyanine green. *Gastroenterology*. 1960;39:713–724.
7. Kogure K, Choromokos E. Infrared absorption angiography. *J Appl Physiol*. 1969;26:154–157.
8. Kogure K, David NJ, Yamanouchi U, et al. Infrared

absorption angiography of the fundus circulation. *Arch Ophthalmol*. 1970;83:209–214.
9. Choromokos E, Kogure K, David NJ. Infrared absorption angiography. *J Biol Photogr Assoc*. 1969;37:100–104.
10. Hochheimer BF. Angiography of the retina with indocyanine green. *Arch Ophthalmol*. 1971;86:564–565.
11. Flower RW, Hochheimer BF. Clinical infrared absorption angiography of the choroid. *Am J Ophthalmol*. 1972;73:458–459.
12. Hyvarinen L, Flower RW. Indocyanine green fluorescence angiography. *Acta Ophthalmol (Copenh)*. 1980;58:528–538.
13. Hayashi K, de Laey JJ. Indocyanine green angiography of submacular choroidal vessels in the human eye. *Ophthalmologica*. 1985;190:20–29.
14. Hayashi K, Hasegawa Y, Tokoro T. Indocyanine green angiography of central serous chorioretinopathy. *Int Ophthalmol*. 1986;9:37–41.
15. Hasegawa Y, Hayashi K, Tokoro T, et al. Clinical use of indocyanine green angiography in the diagnosis of choroidal neovascular diseases. *Fortschr Ophthalmol*. 1988;85:410–412.
16. Destro M, Puliafito CA. Indocyanine green videoangiography of choroidal neovascularization. *Ophthalmology*. 1989;96:846–853.
17. Scheider A, Schroedel C. High resolution indocyanine green angiography with a scanning laser ophthalmoscope. *Am J Ophthalmol*. 1989;108:458–459.
18. Guyer DR, Puliafito CA, Mones JM, et al. Digital indocyanine-green angiography in chorioretinal disorders. *Ophthalmology*. 1992;99:287–291.
19. Yannuzzi LA, Slakter JS, Sorenson JA, et al. Digital indocyanine green videoangiography and choroidal neovascularization. *Retina*. 1992;12:191–223.
20. Lutty GA. The acute intravenous toxicity of biological stains, dyes, and other fluorescent substances. *Toxicol Appl Pharmacol*. 1978;44:225–249.
21. Tripp MR, Cohen GM, Gerasch DA, et al. Effect of protein and electrolyte on the spectral stabilization of concentrated

solutions of indocyanine green. *Proc Soc Exp Biol Med*. 1973;143:879–883.
22. Benya R, Quintana J, Brundage B. Adverse reactions to indocyanine green: a case report and a review of the literature. *Cathet Cardiovasc Diagn*. 1989;17:231–233.
23. Bischoff PM, Flower RW. Ten years experience with choroidal angiography using indocyanine green dye: a new routine examination or an epilogue? *Doc Ophthalmol*. 1985;60:235–291.
24. Flower RW, Hochheimer BF. Indocyanine green dye fluorescence and infrared absorption choroidal angiography performed simultaneously with fluorescein angiography. *Johns Hopkins Med J*. 1976;138:33–42.
25. Geeraets WJ, Berry ER. Ocular spectral characteristics as related to hazards from lasers and other light sources. *Am J Ophthalmol*. 1968;66:15–20.
26. Cherrick GR, Stein SW, Leevy CM, et al. Indocyanine green: observations on its physical properties, plasma decay, and hepatic extraction. *J Clin Invest*. 1960;39:592–600.
27. Leevy CM, Bender J. Physiology of dye extraction by the liver: comparative studies of sulfobromophtthalein and indocyanine green. *Ann N Y Acad Sci*. 1963;111:161–176.
28. Stehr A, Ploner F, Traeger K, et al. Plasma disappearance of indocyanine green: a marker for excretory liver function? *Intensive Care Med*. 2005;31:1719–1722.
29. Costa DL, Huang SJ, Orlock DA, et al. Retinal-choroidal indocyanine green dye clearance and liver dysfunction. *Retina*. 2003;23:557–561.
30. Fineman MS, Maguire JI, Fineman SW, et al. Safety of indocyanine green angiography during pregnancy: a survey of the retina, macula, and vitreous societies. *Arch Ophthalmol*. 2001;119:353–355.
31. Hope-Ross M, Yannuzzi LA, Gragoudas ES, et al. Adverse reactions due to indocyanine green. *Ophthalmology*. 1994;101:529–533.
32. Speich R, Saesseli B, Hoffmann U, et al. Anaphylactoid reactions after indocyanine-green administration. *Ann Intern Med*. 1988;109:345–346.

33. Michie DD, Wombolt DG, Carretta RF, et al. Adverse reactions associated with the administration of a tricarbocyanine dye (Cardio-Green) to uremic patients. *J Allergy Clin Immunol*. 1971;48:235–239.
34. Iseki K, Onoyama K, Fujimi S, et al. Shock caused by indocyanine green dye in chronic hemodialysis patients. *Clin Nephrol*. 1980;14:210.
35. Robson SC, Mutch E, Boys RJ, et al. Apparent liver blood flow during pregnancy: a serial study using indocyanine green clearance. *Br J Obstet Gynaecol*. 1990;97:720–724.
36. Flower RW, Csaky KG, Murphy RP. Disparity between fundus camera and scanning laser ophthalmoscope indocyanine green imaging of retinal pigment epithelium detachments. *Retina*. 1998;18:260–268.
37. Wolf S, Wald KJ, Elsner AE, et al. Indocyanine green choroidal videoangiography: a comparison of imaging analysis with the scanning laser ophthalmoscope and the fundus camera. *Retina*. 1993;13:266–269.
38. Stanga PE, Lim JI, Hamilton P. Indocyanine green angiography in chorioretinal diseases: indications and interpretation: an evidence-based update. *Ophthalmology*. 2003;110:15–21 [quiz 22–3].
39. Yannuzzi LA, Flower RW, Slakter JS. *Indocyanine green angiography*. Mosby Year Book: St. Louis; 1997:46.
40. Hayreh SS. Physiological anatomy of the choroidal vascular bed. *Int Ophthalmol*. 1983;6:85–93.
41. Mutoh T, Sakurai M, Tamai M. Indocyanine green fundus angiography of retrobulbar vasculature. *Arch Ophthalmol*. 1995;113:631–633.
42. Ohno-Matsui K, Morishima N, Ito M, et al. Indocyanine green angiography of retrobulbar vascular structures in severe myopia. *Am J Ophthalmol*. 1997;123:494–505.
43. Gass JD. Biomicroscopic and histopathologic considerations regarding the feasibility of surgical excision of subfoveal neovascular membranes. *Am J Ophthalmol*. 1994;118:285–298.
44. Macular Photocoagulation Study Group. Subfoveal neovascular lesions in age-related macular degeneration.

Guidelines for evaluation and treatment in the macular photocoagulation study. *Arch Ophthalmol*. 1991;109:1242–1257.
45. Sadda SR, Liakopoulos S, Keane PA, et al. Relationship between angiographic and optical coherence tomographic (OCT) parameters for quantifying choroidal neovascular lesions. *Graefes Arch Clin Exp Ophthalmol*. 2010;248:175–184.
46. Freund KB, Ho IV, Barbazetto IA, et al. Type 3 neovascularization: the expanded spectrum of retinal angiomatous proliferation. *Retina*. 2008;28:201–211.
47. Olsen TW, Feng X, Kasper TJ, et al. Fluorescein angiographic lesion type frequency in neovascular age-related macular degeneration. *Ophthalmology*. 2004;111:250–255.
48. Guyer DR, Yannuzzi LA, Slakter JS, et al. Classification of choroidal neovascularization by digital indocyanine green videoangiography. *Ophthalmology*. 1996;103:2054–2060.
49. Yannuzzi LA, Hope-Ross M, Slakter JS, et al. Analysis of vascularized pigment epithelial detachments using indocyanine green videoangiography. *Retina*. 1994;14:99–113.
50. Brown DM, Kaiser PK, Michels M, et al. Ranibizumab versus verteporfin for neovascular age-related macular degeneration. *N Engl J Med*. 2006;355:1432–1444.
51. Rosenfeld PJ, Brown DM, Heier JS, et al. Ranibizumab for neovascular age-related macular degeneration. *N Engl J Med*. 2006;355:1419–1431.
52. Massacesi AL, Sacchi L, Bergamini F, et al. The prevalence of retinal angiomatous proliferation in age-related macular degeneration with occult choroidal neovascularization. *Graefes Arch Clin Exp Ophthalmol*. 2008;246:89–92.
53. Lim JI, Aaberg TM, Capone AJ, et al. Indocyanine green angiography-guided photocoagulation of choroidal neovascularization associated with retinal pigment epithelial detachment. *Am J Ophthalmol*. 1997;123:524–532.
54. Watzke RC, Klein ML, Hiner CJ, et al. A comparison of stereoscopic fluorescein angiography with indocyanine green videoangiography in age-related macular degeneration. *Ophthalmology*. 2000;107:1601–1606.

55. Shiraga F, Ojima Y, Matsuo T, et al. Feeder vessel photocoagulation of subfoveal choroidal neovascularization secondary to age-related macular degeneration. *Ophthalmology*. 1998;105:662–669.
56. Staurenghi G, Orzalesi N, La Capria A, et al. Laser treatment of feeder vessels in subfoveal choroidal neovascular membranes: a revisitation using dynamic indocyanine green angiography. *Ophthalmology*. 1998;105:2297–2305.
57. Bottoni F, Massacesi A, Cigada M, et al. Treatment of retinal angiomatous proliferation in age-related macular degeneration: a series of 104 cases of retinal angiomatous proliferation. *Arch Ophthalmol*. 2005;123:1644–1650.
58. Flower RW. Optimizing treatment of choroidal neovascularization feeder vessels associated with age-related macular degeneration. *Am J Ophthalmol*. 2002;134:228–239.
59. Semoun O, Guigui B, Tick S, et al. Infrared features of classic choroidal neovascularisation in exudative age-related macular degeneration. *Br J Ophthalmol*. 2009;93:182–185.
60. Schmidt-Erfurth U, Kriechbaum K, Oldag A. Three-dimensional angiography of classic and occult lesion types in choroidal neovascularization. *Invest Ophthalmol Vis Sci*. 2007;48:1751–1760.
61. Hlushchuk R, Baum O, Gruber G, et al. The synergistic action of a VEGF-receptor tyrosine-kinase inhibitor and a sensitizing PDGF-receptor blocker depends upon the stage of vascular maturation. *Microcirculation*. 2007;14:813–825.
62. Yannuzzi LA, Negrao S, Iida T, et al. Retinal angiomatous proliferation in age-related macular degeneration. *Retina*. 2001;21:416–434.
63. Gass JD, Agarwal A, Lavina AM, et al. Focal inner retinal hemorrhages in patients with drusen: an early sign of occult choroidal neovascularization and chorioretinal anastomosis. *Retina*. 2003;23:741–751.
64. Hartnett ME, Weiter JJ, Staurenghi G, et al. Deep retinal vascular anomalous complexes in advanced age-related macular degeneration. *Ophthalmology*. 1996;103:2042–2053.
65. Viola F, Massacesi A, Orzalesi N, et al. Retinal angiomatous

proliferation: natural history and progression of visual loss. *Retina*. 2009;29:732–739.
66. Rouvas AA, Papakostas TD, Vavvas D, et al. Intravitreal ranibizumab, intravitreal ranibizumab with PDT, and intravitreal triamcinolone with PDT for the treatment of retinal angiomatous proliferation: a prospective study. *Retina*. 2009;29:536–544.
67. Saito M, Shiragami C, Shiraga F, et al. Comparison of intravitreal triamcinolone acetonide with photodynamic therapy and intravitreal bevacizumab with photodynamic therapy for retinal angiomatous proliferation. *Am J Ophthalmol*. 2010;149:472–481.e1.
68. Bottoni F, Romano M, Massacesi A, et al. Remodeling of the vascular channels in retinal angiomatous proliferations treated with intravitreal triamcinolone acetonide and photodynamic therapy. *Graefes Arch Clin Exp Ophthalmol*. 2006;244:1528–1533.
69. Yannuzzi LA, Sorenson J, Spaide RF, et al. Idiopathic polypoidal choroidal vasculopathy (IPCV). *Retina*. 1990;10:1–8.
70. Spaide RF, Yannuzzi LA, Slakter JS, et al. Indocyanine green videoangiography of idiopathic polypoidal choroidal vasculopathy. *Retina*. 1995;15:100–110.
71. Yannuzzi LA, Wong DW, Sforzolini BS, et al. Polypoidal choroidal vasculopathy and neovascularized age-related macular degeneration. *Arch Ophthalmol*. 1999;117:1503–1510.
72. Ahuja RM, Stanga PE, Vingerling JR, et al. Polypoidal choroidal vasculopathy in exudative and haemorrhagic pigment epithelial detachments. *Br J Ophthalmol*. 2000;84:479–484.
73. Ciardella AP, Donsoff IM, Huang SJ, et al. Polypoidal choroidal vasculopathy. *Surv Ophthalmol*. 2004;49:25–37.
74. Ahuja RM, Downes SM, Stanga PE, et al. Polypoidal choroidal vasculopathy and central serous chorioretinopathy. *Ophthalmology*. 2001;108:1009–1010.
75. Yannuzzi LA, Freund KB, Goldbaum M, et al. Polypoidal choroidal vasculopathy masquerading as central serous chorioretinopathy. *Ophthalmology*. 2000;107:767–777.

76. Maruko I, Iida T, Saito M, et al. Combined cases of polypoidal choroidal vasculopathy and typical age-related macular degeneration. *Graefes Arch Clin Exp Ophthalmol*. 2010;248:361–368.
77. Lai TY, Chan WM, Liu DT, et al. Intravitreal bevacizumab (Avastin) with or without photodynamic therapy for the treatment of polypoidal choroidal vasculopathy. *Br J Ophthalmol*. 2008;92:661–666.
78. Eandi CM, Ober MD, Freund KB, et al. Selective photodynamic therapy for neovascular age-related macular degeneration with polypoidal choroidal neovascularization. *Retina*. 2007;27:825–831.
79. Guyer DR, Yannuzzi LA, Slakter JS, et al. Digital indocyanine green videoangiography of central serous chorioretinopathy. *Arch Ophthalmol*. 1994;112:1057–1062.
80. Yannuzzi LA, Slakter JS, Gross NE, et al. Indocyanine green angiography-guided photodynamic therapy for treatment of chronic central serous chorioretinopathy: a pilot study. *Retina*. 2003;23:288–298.
81. Piccolino FC, Borgia L. Central serous chorioretinopathy and indocyanine green angiography. *Retina*. 1994;14:231–242.
82. Spaide RF, Hall L, Haas A, et al. Indocyanine green videoangiography of older patients with central serous chorioretinopathy. *Retina*. 1996;16:203–213.
83. Shiraki K, Moriwaki M, Matsumoto M, et al. Long-term follow-up of severe central serous chorioretinopathy using indocyanine green angiography. *Int Ophthalmol*. 1997;21:245–253.
84. Lafaut BA, Salati C, Priem H, et al. Indocyanine green angiography is of value for the diagnosis of chronic central serous chorioretinopathy in elderly patients. *Graefes Arch Clin Exp Ophthalmol*. 1998;236:513–521.
85. Reibaldi M, Cardascia N, Longo A, et al. Standard-fluence versus low-fluence photodynamic therapy in chronic central serous chorioretinopathy: a nonrandomized clinical trial. *Am J Ophthalmol*. 2010;149:307–315.e2.
86. Chan WM, Lam DS, Lai TY, et al. Choroidal vascular remodelling in central serous chorioretinopathy after

indocyanine green guided photodynamic therapy with verteporfin: a novel treatment at the primary disease level. *Br J Ophthalmol*. 2003;87:1453–1458.
87. Inoue R, Sawa M, Tsujikawa M, et al. Association between the efficacy of photodynamic therapy and indocyanine green angiography findings for central serous chorioretinopathy. *Am J Ophthalmol*. 2010;149:441–446.e1–2.
88. Tsujikawa A, Ojima Y, Yamashiro K, et al. Punctate hyperfluorescent spots associated with central serous chorioretinopathy as seen on indocyanine green angiography. *Retina*. 2010;30:801–809.
89. Kitaya N, Nagaoka T, Hikichi T, et al. Features of abnormal choroidal circulation in central serous chorioretinopathy. *Br J Ophthalmol*. 2003;87:709–712.
90. Prunte C, Flammer J. Choroidal capillary and venous congestion in central serous chorioretinopathy. *Am J Ophthalmol*. 1996;121:26–34.
91. Anand R, Augsburger JJ, Shields JA. Circumscribed choroidal hemangiomas. *Arch Ophthalmol*. 1989;107:1338–1342.
92. Shields CL, Honavar SG, Shields JA, et al. Circumscribed choroidal hemangioma: clinical manifestations and factors predictive of visual outcome in 200 consecutive cases. *Ophthalmology*. 2001;108:2237–2248.
93. Witschel H, Font RL. Hemangioma of the choroid: a clinicopathologic study of 71 cases and a review of the literature. *Surv Ophthalmol*. 1976;20:415–431.
94. Singh AD, Kaiser PK, Sears JE. Choroidal hemangioma. *Ophthalmol Clin North Am*. 2005;18:151–161 [ix].
95. Arevalo JF, Shields CL, Shields JA, et al. Circumscribed choroidal hemangioma: characteristic features with indocyanine green videoangiography. *Ophthalmology*. 2000;107:344–350.
96. Shields CL, Shields JA, De Potter P. Patterns of indocyanine green videoangiography of choroidal tumours. *Br J Ophthalmol*. 1995;79:237–245.
97. Sallet G, Amoaku WM, Lafaut BA, et al. Indocyanine green angiography of choroidal tumors. *Graefes Arch Clin Exp*

Ophthalmol. 1995;233:677–689.
98. Andersen MV, Scherfig E, Prause JU. Differential diagnosis of choroidal melanomas and nevi using scanning laser ophthalmoscopical indocyanine green angiography. *Acta Ophthalmol Scand*. 1995;73:453–456.
99. Mueller AJ, Bartsch DU, Folberg R, et al. Imaging the microvasculature of choroidal melanomas with confocal indocyanine green scanning laser ophthalmoscopy. *Arch Ophthalmol*. 1998;116:31–39.
100. Frenkel S, Barzel I, Levy J, et al. Demonstrating circulation in vasculogenic mimicry patterns of uveal melanoma by confocal indocyanine green angiography. *Eye (Lond)*. 2008;22:948–952.
101. Mueller AJ, Freeman WR, Schaller UC, et al. Complex microcirculation patterns detected by confocal indocyanine green angiography predict time to growth of small choroidal melanocytic tumors: MuSIC Report II. *Ophthalmology*. 2002;109:2207–2214.
102. Schaller UC, Mueller AJ, Bartsch DU, et al. Choroidal melanoma microcirculation with confocal indocyanine green angiography before and 1 year after radiation brachytherapy. *Retina*. 2000;20:627–632.
103. Krause L, Bechrakis NE, Heinrich S, et al. Indocyanine green angiography and fluorescein angiography of malignant choroidal melanomas following proton beam irradiation. *Graefes Arch Clin Exp Ophthalmol*. 2005;243:545–550.
104. Midena E, Pilotto E, de Belvis V, et al. Choroidal vascular changes after transpupillary thermotherapy for choroidal melanoma. *Ophthalmology*. 2003;110:2216–2222.
105. Annesley WHJ. Peripheral exudative hemorrhagic chorioretinopathy. *Trans Am Ophthalmol Soc*. 1980;78:321–364.
106. Shields CL, Salazar PF, Mashayekhi A, et al. Peripheral exudative hemorrhagic chorioretinopathy simulating choroidal melanoma in 173 eyes. *Ophthalmology*. 2009;116:529–535.
107. Gunduz K, Shields CL, Shields JA. Varix of the vortex vein

ampulla simulating choroidal melanoma: report of four cases. *Retina*. 1998;18:343–347.
108. Rutnin U. Fundus appearance in normal eyes. I. The choroid. *Am J Ophthalmol*. 1967;64:821–839.
109. Osher RH, Abrams GW, Yarian D, et al. Varix of the vortex ampulla. *Am J Ophthalmol*. 1981;92:653–660.
110. Singh AD, De Potter P, Shields CL, et al. Indocyanine green angiography and ultrasonography of a varix of vortex vein. *Arch Ophthalmol*. 1993;111:1283–1284.
111. Gross NE, Yannuzzi LA, Freund KB, et al. Multiple evanescent white dot syndrome. *Arch Ophthalmol*. 2006;124:493–500.
112. Dell'omo R, Wong R, Marino M, et al. Relationship between different fluorescein and indocyanine green angiography features in multiple evanescent white dot syndrome. *Br J Ophthalmol*. 2010;94:59–63.
113. Tsukamoto E, Yamada T, Kadoi C, et al. Hypofluorescent spots on indocyanine green angiography at the recovery stage in multiple evanescent white dot syndrome. *Ophthalmologica*. 1999;213:336–338.
114. Slakter JS, Giovannini A, Yannuzzi LA, et al. Indocyanine green angiography of multifocal choroiditis. *Ophthalmology*. 1997;104:1813–1819.
115. Fardeau C, Herbort CP, Kullmann N, et al. Indocyanine green angiography in birdshot chorioretinopathy. *Ophthalmology*. 1999;106:1928–1934.
116. Howe LJ, Stanford MR, Graham EM, et al. Choroidal abnormalities in birdshot chorioretinopathy: an indocyanine green angiography study. *Eye (Lond)*. 1997;11:554–559.
117. Trinh L, Bodaghi B, Fardeau C, et al. Clinical features, treatment methods, and evolution of birdshot chorioretinopathy in 5 different families. *Am J Ophthalmol*. 2009;147:1042–1047 [1047.e1].
118. Howe LJ, Woon H, Graham EM, et al. Choroidal hypoperfusion in acute posterior multifocal placoid pigment epitheliopathy: an indocyanine green angiography study. *Ophthalmology*. 1995;102:790–798.

119. Park D, Schatz H, McDonald HR, et al. Indocyanine green angiography of acute multifocal posterior placoid pigment epitheliopathy. *Ophthalmology*. 1995;102:1877–1883.
120. Schneider U, Inhoffen W, Gelisken F. Indocyanine green angiography in a case of unilateral recurrent posterior acute multifocal placoid pigment epitheliopathy. *Acta Ophthalmol Scand*. 2003;81:72–75.
121. Giovannini A, Mariotti C, Ripa E, et al. Indocyanine green angiographic findings in serpiginous choroidopathy. *Br J Ophthalmol*. 1996;80:536–540.
122. Amer R, Lois N. Punctate inner choroidopathy. *Surv Ophthalmol*. 2011;56:36–53.
123. Tiffin PA, Maini R, Roxburgh ST, et al. Indocyanine green angiography in a case of punctate inner choroidopathy. *Br J Ophthalmol*. 1996;80:90–91.
124. Levy J, Shneck M, Klemperer I, et al. Punctate inner choroidopathy: resolution after oral steroid treatment and review of the literature. *Can J Ophthalmol*. 2005;40:605–608.
125. Spaide RF. Collateral damage in acute zonal occult outer retinopathy. *Am J Ophthalmol*. 2004;138:887–889.
126. Giani A, Pellegrini M, Carini E, et al. The dark atrophy with indocyanine green angiography in Stargardt disease. *Invest Ophthalmol Vis Sci*. 2012;53:3999–4004.
127. McLeod DS, Taomoto M, Otsuji T, et al. Quantifying changes in RPE and choroidal vasculature in eyes with age-related macular degeneration. *Invest Ophthalmol Vis Sci*. 2002;43:1986–1993.
128. Bhutto I, Lutty G. Understanding age-related macular degeneration (AMD): relationships between the photoreceptor/retinal pigment epithelium/Bruch's membrane/choriocapillaris complex. *Mol Aspects Med*. 2012;33:295–317.

3

Optical Coherence Tomography

Nadia K. Waheed, Amir H. Kashani, Carlos Alexandre de Amorim, Garcia Filho, Jay S. Duker, Philip J. Rosenfeld

Physical Principles of Optical

Coherence Tomography

During the past two and a half decades, optical coherence tomography (OCT) has evolved to become an essential tool in ophthalmology. Its ability to noninvasively image detailed ocular structures and associated microvasculature in vivo with high resolution has revolutionized patient care.[1,2] OCT technology is based on the principle of low-coherence interferometry, where a low-coherence (high-bandwidth) light beam is directed on to the target tissue and the scattered back-reflected light is combined with a second beam (reference beam), which was split off from the original light beam. The resulting interference patterns are used to reconstruct an axial A-scan, which represents the scattering properties of the tissue along the beam path. Moving the beam of light along the tissue in a line results in a compilation of A-scans with each A-scan having a different incidence point. From all these A-scans, a two-dimensional cross-sectional image of the target tissue can be reconstructed and this is known as a B-scan. If these B-scans are repeated at multiple adjacent positions using a raster scan pattern, then a three-dimensional volume of structural and flow information can be compiled.

Typically, spectral domain OCT instruments use an infrared light source centered at a wavelength of about 840 nm. For a given wavelength, the axial resolution is dictated by the bandwidth of the light source. The latest commercial instruments typically have an axial resolution of approximately 5 μm, while research instruments have been built with a resolution as high as approximately 2 μm.[1] The lateral resolution is limited by the diffraction caused by the pupil and it is normally about 20 μm. For clinical purposes, the image acquisition time is limited by the patient's ability to avoid eye movements, the availability of scanning techniques to adjust for movements, and the availability of tracking software that adjusts for eye movements. The instrument's scanning speed (number of A-scans acquired per second) is then the crucial parameter determining the amount of data available for a single OCT volumetric dataset.

The early OCT instruments, known as time domain OCT (TD-OCT), used a single photon detector, and an A-scan was created by

moving a mirror to change the optical path of the reference beam in order to match different axial depths in the target tissue. This setup limited the scanning speed to a few thousand A-scans per second. Another more recent technique, known as spectral domain OCT (SD-OCT), Fourier domain OCT (FD-OCT), or high-definition OCT (HD-OCT), is able to acquire an entire A-scan by using an array of detectors instead of using multiple reference beams from a moving mirror. Scanning speeds with SD-OCT instruments can exceed 100,000 A-scans per second, about 200 times faster than TD-OCT. Currently available SD-OCT commercial systems operate at a scanning rates of approximately 27,000–70,000 A-scans per second.[1] A newer OCT imaging technique that had been available only for research, but is now commercially available, is known as swept source OCT (SS-OCT).[3] In SS-OCT, the broadband superluminescent diode light source found in the SD-OCT is replaced with a swept source tunable laser with a center wavelength of about 1050 nm, and the spectrometer from the SD-OCT is replaced with a single detector. The advantages of SS-OCT include faster scanning speeds at 100,000–400,000 A-scans per second and the longer wavelength that provides better visualization of structures and flow beneath the retinal pigment epithelium with less sensitivity roll-off.

The scanning pattern used in the commercial TD-OCT instrument (Stratus OCT, Carl Zeiss Meditec, Dublin, CA) incorporated six radial, concentric, 6-mm-long B-scans centered on the fovea. With the development of high-speed SD-OCT systems, several novel and important imaging strategies have been introduced based on acquiring three-dimensional datasets and B-scan averaging (Fig. 3.1). Three-dimensional datasets are obtained using a dense two-dimensional raster array over a defined retinal region. The resulting datasets can be rendered as a volume image in three dimensions and can be analyzed by showing two-dimensional slices (i.e., sequences of parallel B-scans). Three-dimensional datasets give detailed information about the retinal structure over large areas. In addition, it is possible to generate en face fundus-like images directly from the OCT datasets. These OCT fundus images (OFIs) provide an accurate spatial colocalization of retinal features observed on the en face and cross-sectional images. Therefore, exact

correlations can be achieved between the retinal cross-sectional geometry seen on the OCT B-scans and the retinal landmarks seen on en face images, known as the OFI. The potential exists for registration between several SD-OCT datasets of the same eye and images obtained using other imaging modalities, such as color fundus photography, fluorescein angiography, and fundus autofluorescence imaging. This holds the promise for an unprecedented ability to describe and monitor changes in the local geometry of the retina.[4] In addition to the OFI generated by a full OCT dataset, partial OFIs (or slabs) can be generated to produce en face renderings that correspond to particular retinal layers or features.[5,6] These slabs can be very useful to visualize and quantify specific pathologies (Fig. 3.2). In addition to imaging geographic atrophy, en face imaging of the outer retina has been shown to be useful for predicting the progression of geographic atrophy and for diagnosing and following the progression of macular telangiectasia type 2 and subretinal drusenoid deposits.[7–11]

FIG. 3.1 Three-dimensional dataset. (Courtesy of Cirrus HD-OCT, Carl Zeiss Meditec, Dublin, CA.)

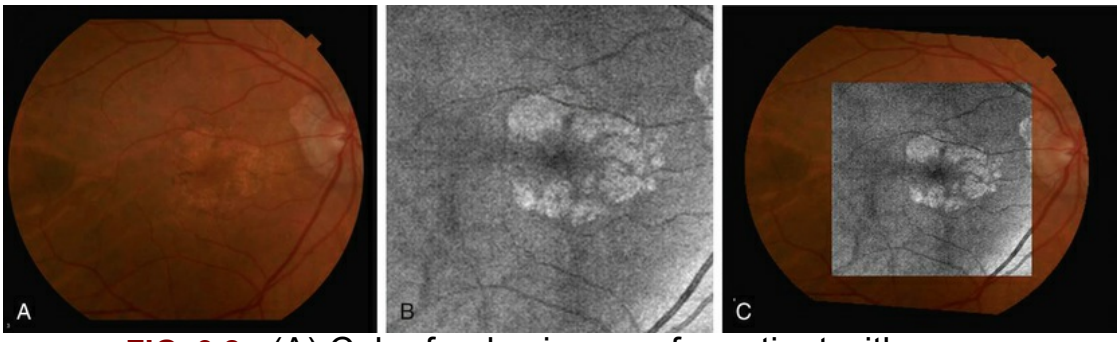

FIG. 3.2 (A) Color fundus image of a patient with geographic atrophy secondary to age-related macular degeneration. (B) Optical coherence tomography (OCT) fundus image, which is the en face image from the reflected light from each A-scan, of the same patient obtained with a scan pattern of 200 × 200 A-scans in the Cirrus high-definition OCT instrument. (C) Registration of the color fundus image with the OCT fundus image. Since the area of the OCT fundus image is known to be 6×6 mm, it is possible to quantify lesion area and calibrate the fundus camera to use this technique.

The scanning speed of SD-OCT can also be used to produce very high-quality individual B-scan images through a combination of high sampling density and image averaging. One of the main factors affecting the perceived quality of OCT images is noise, in particular the speckle noise which is responsible for the characteristic "granular" appearance of OCT. Noise can be reduced through the acquisition, registration, and averaging of a number of B-scans at approximately the same retinal position (Fig. 3.3).

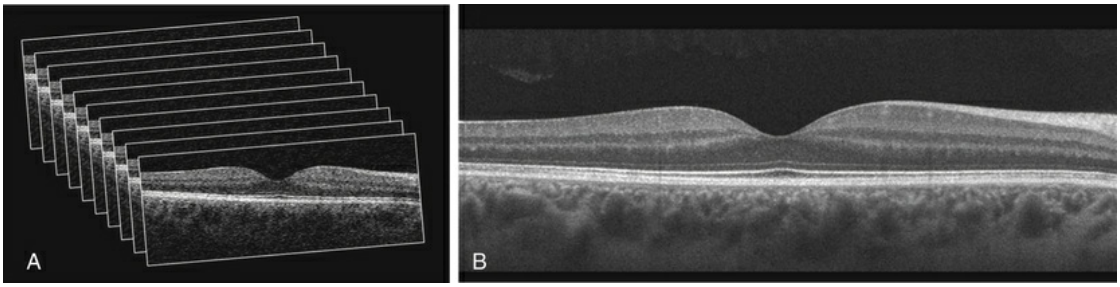

FIG. 3.3 Averaging process. (A) Multiple B-scans acquired through the foveal center of a normal patient. (B) The registration and averaging of these B-scans can reduce the speckled noise and improve the image

quality. In these examples the image was averaged 20 times using the Cirrus high-definition optical coherence tomograph.

Although en face registration and B-scan averaging strategies can be implemented in many ways, a particularly powerful and flexible solution is the use of a separate built-in laser eye-tracking system. The main limitation of this approach is that the necessary acquisition times can become very long and sometimes unmanageable, particularly for large raster scans and for subjects with poor fixation. Newer techniques use the image obtained from the scanning laser ophthalmoscopic image that is obtained as part of the routine scanning technique.

Recently, different companies have invested in research in the field of retinal imaging, especially in the development and improvement of SD-OCT. It is not an objective of this section to discuss the differences between each of the currently available instruments since these instruments are continuously evolving. Table 3.1 lists currently available instruments.

TABLE 3.1

Commercially Available Spectral Domain Optical Coherence Tomography (OCT) Instruments

Device (Manufacturer)	Axial Resolution; Scanning Rate	Special Characteristics
3D-OCT 2000 (Topcon, Tokyo, Japan)	5 μm; 27 kHz	Fundus camera
Bioptigen SD-OCT (Bioptigen, Research Triangle Park, NC)	4 μm; 20 kHz	Designed for research applications, handheld use and intraoperative use
Cirrus HD-OCT (Carl Zeiss Meditec, Dublin, CA)	5 μm; 27 kHz	Automated en face analysis software with drusen volume and area of geographic atrophy; OCT angiography module available with eye tracking
RTVue-100 (Optovue, Fremont, CA)	5 μm; 26 kHz	OCT angiography module available with automated retinal vessel density measurements
SOCT Copernicus (Canon, Tokyo, Japan)	6 μm; 27 kHz	B-scans with color overlay, 3D retinal imaging with anterior segment module
Spectral/Optos OCT SLO	6 μm; 27 kHz	SLO and microperimetry

(Optos, Dunfermline, UK)		
Spectralis OCT (Heidelberg Engineering, Heidelberg, Germany)	8 μm; 40 kHz	Eye-tracking, fluorescein angiography, ICGA, autofluorescence
Nidek SD-OCT (Nidek Co Ltd, Maehama Hiroishi GamagoriJapan)	4 μm; 53 kHz	Eye tracking, SLO

3D, three-dimensional; HD, high-definition; ICGA, indocyanine green angiography; SD, spectral domain; SLO, scanning laser ophthalmoscope; SOCT, spectral optical coherence tomography.

Quantitative Analysis of OCT Datasets

A crucial step towards a clinically useful, quantitative understanding of the retinal anatomy is the development of accurate, robust, reproducible segmentation algorithms that can automatically identify the boundaries between specific retinal layers and/or other retinal features. The currently available SD-OCT instruments have several advantages over the previous generation of TD-OCT instruments. SD-OCT instruments generally have a higher axial resolution and can produce B-scans with better image quality by increasing the A-scan density and through averaging techniques. Much more importantly, the higher scanning speed made possible by the SD-OCT technology reduces the effect of artifacts associated with eye motion and produces images that provide a true picture of the retinal geometry. The large, dense raster scans make it possible to obtain detailed surfaces of individual retina layers over large areas, resulting in segmentation maps. These maps allow for an unprecedented visualization and quantitative evaluation of the corresponding retinal structures.

Several commercially available SD-OCT instruments offer some level of quantitative analysis using different, proprietary segmentation algorithms. The various segmentation algorithms make different design choices and have been shown to have very different performance profiles in terms of accuracy, reproducibility, and robustness.[12–15] Care should be exercised when comparing measurements obtained from different OCT instruments.

The most commonly used quantitative parameter derived from OCT datasets is retinal thickness, obtained by segmenting the internal limiting membrane (ILM) and a boundary representing the retinal pigment epithelium (RPE). This information can be used to generate surface maps of the ILM and the RPE as well as two-dimensional and three-dimensional retinal thickness maps. These maps can be very useful in identifying and describing deviations from the normal anatomy and changes over time. Registering OCT datasets acquired over time can give very precise information about the dynamics of disease progression and response to treatment based on changes in retinal anatomy (Fig. 3.4).

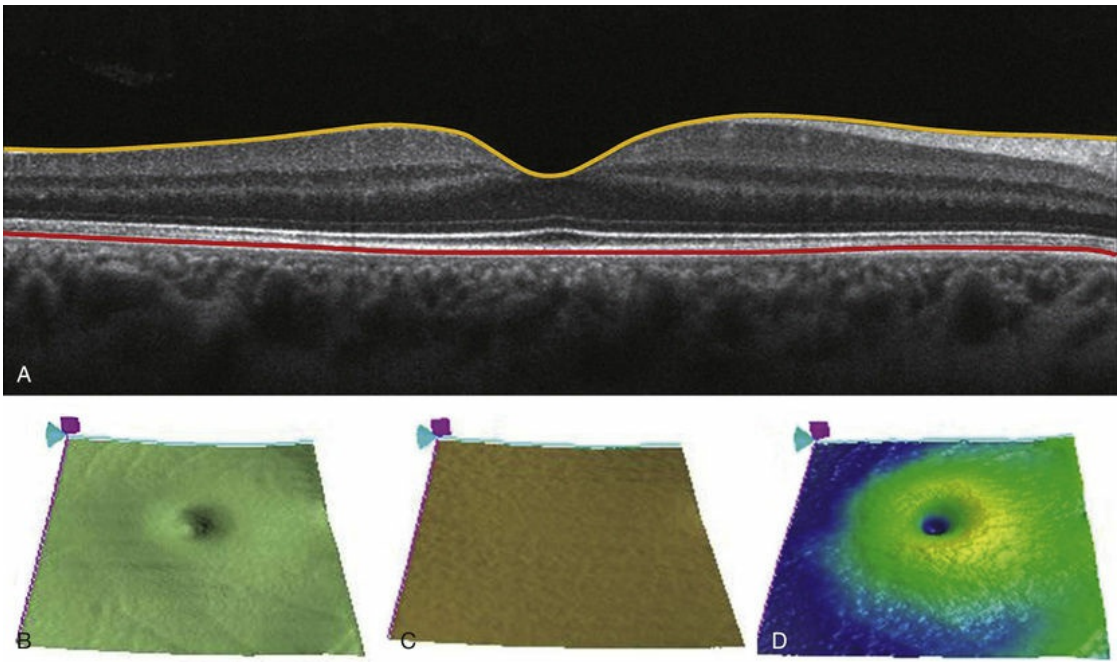

FIG. 3.4 Segmentation process. (A) B-scan through the foveal center of a normal patient with a yellow line identifying the internal limiting membrane (ILM) and a red line corresponding to the retinal pigment epithelium (RPE). Three-dimensional map of the ILM (B), RPE (C), and the retinal thickness map (D) acquired with a 200 × 200 scan pattern with the Cirrus high-definition optical coherence tomography instrument.

It is important to keep in mind that there is some confusion in the definition of the outer retinal boundary. In a normal eye, the bright reflective band at the external aspect of the retina, often referred to

as the RPE complex, can be resolved in ultrahigh-resolution images, and occasionally in images acquired with a commercially available SD-OCT instrument, consisting of three individual layers.[16] Different segmentation algorithms from different instruments tend to follow different borders and therefore result in different measurements. For example, the Spectralis SD-OCT instrument typically follows the posterior surface of the RPE complex, the Stratus TD-OCT instrument typically follows Band #2, also known as the ellipsoid zone or inner segment–outer segment (IS/OS) junction, which is anterior to the RPE complex, and the Cirrus SD-OCT instrument typically follows the anterior edge of the RPE layer (Fig. 3.5). This situation becomes even more complicated and sometimes inconsistent when the normal retinal structure is deformed by the presence of pathology.[17]

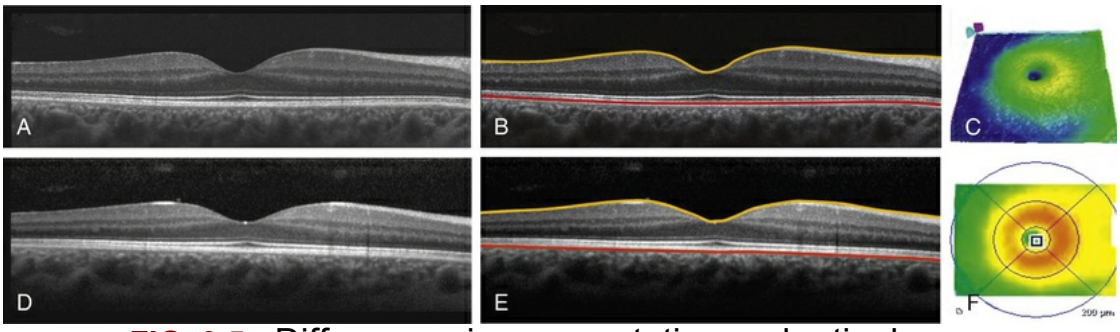

FIG. 3.5 Differences in segmentation and retinal thickness maps between instruments. The B-scan identifying the internal limiting membrane (yellow line), and the retinal pigment epithelium (red line), and the retinal thickness map acquired with the Cirrus high-definition optical coherence tomograph (A–C) and the Spectralis (D–F). Note that, using the Cirrus instrument, the segmentation algorithm identifies the actual retinal pigment epithelium (B) and using the Spectralis the segmentation algorithm identifies Bruch's membrane. This subtle difference in the segmentation algorithm between each instrument can be responsible for different retinal thickness measurements.

In addition to total retinal thickness, a number of other quantitative parameters have been proposed. For example, it is

possible to obtain measurements of particular retinal layers, such as the thickness of the ganglion cell layer or the thickness of the photoreceptors' outer segments, as well as measurements of retinal lesions, like the area of geographic atrophy (GA).[16,18–20]

An area of particular promise is the measurement of RPE deformations associated with drusen.[21–23] These measurements are obtained by comparing the actual RPE geometry with the geometry of a virtual RPE free of deformations. Parameters like drusen area and volume can be generated in a fully automated manner and have been shown to be quite robust and reproducible (Fig. 3.6).

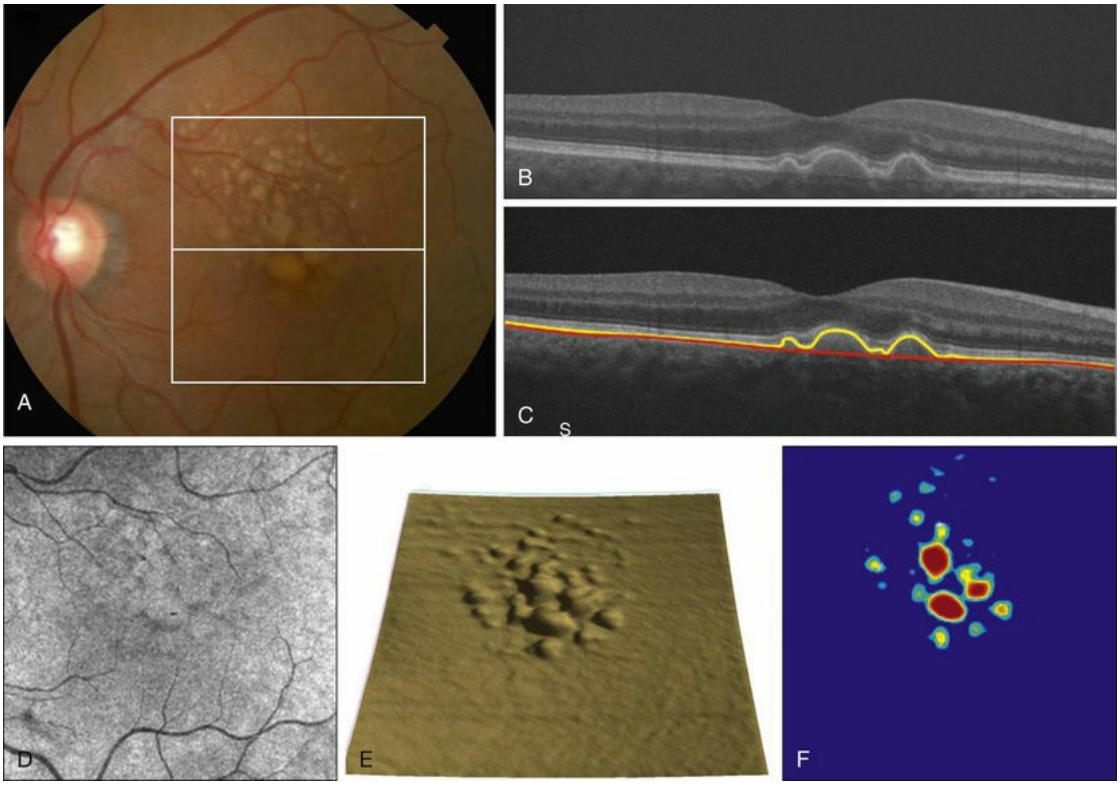

FIG. 3.6 Retinal pigment epithelium (RPE) deformation algorithm. (A) Color fundus image of a patient with drusen. A 6×6-mm white box was superimposed on the image to represent the scan area. (B) B-scan from the spectral domain optical coherence tomography dataset that corresponds to the central line on the color fundus image. (C) B-scan with a yellow line representing the RPE segmentation and a red line showing the RPE floor (virtual map of the RPE free of deformations). (D) En face image of the 6×6-mm scan pattern (optical coherence tomography fundus image). (E) Three-

dimensional RPE map delineating the drusen conformation. (F) RPE elevation map with drusen area (1.41 mm^2) and volume (0.08 mm^3).

The amount of information provided by each dataset, together with the possibility for image registration and longitudinal studies, makes SD-OCT a valuable tool for the quantitative study of retinal pathologies. Despite the advantages of SD-OCT, segmentation algorithms can produce artifacts, particularly in the presence of macular disorders with complex morphology like neovascular age-related macular degeneration (AMD).[24–28] Therefore, it is important to be vigilant and monitor the quality of the segmentation in order to eliminate artifacts arising from flawed segmentation and associated measurements.

Normal Macular Anatomy

The OCT image closely approximates the histologic appearance of the macula and, for this reason, it has been referred to as an in vivo optical biopsy. With the increase in the axial resolution of the new SD-OCT instruments (5–8 μm) and the ultrahigh-resolution OCT (2 μm), it has become possible to correlate OCT images accurately with histologic features of the retina.[29] However, care must be taken when making assumptions about these correlations because histologic sections require fixation and exogenous staining to produce contrast within tissue, and this can introduce artifacts, while OCT relies on intrinsic differences in tissue optical properties to produce image contrast.[30] When light travels through the retinal tissue it can be reflected, scattered, or absorbed, and this creates the multilayered pattern of the retina. The angle of incidence of the light, motion artifacts, speckled noise, and image contrast can affect the axial resolution of the retinal imaging. Therefore, one-to-one correspondence of histology with OCT images cannot be expected.[2,30]

Although the interpretation of features of the retina, which can be defined for our purpose to span from the ILM to the outer segments of the photoreceptors appears to correlate well with histology, the OCT features of the outer retina are less well understood and

remain a topic of discussion (Fig. 3.7)[16,31–34]

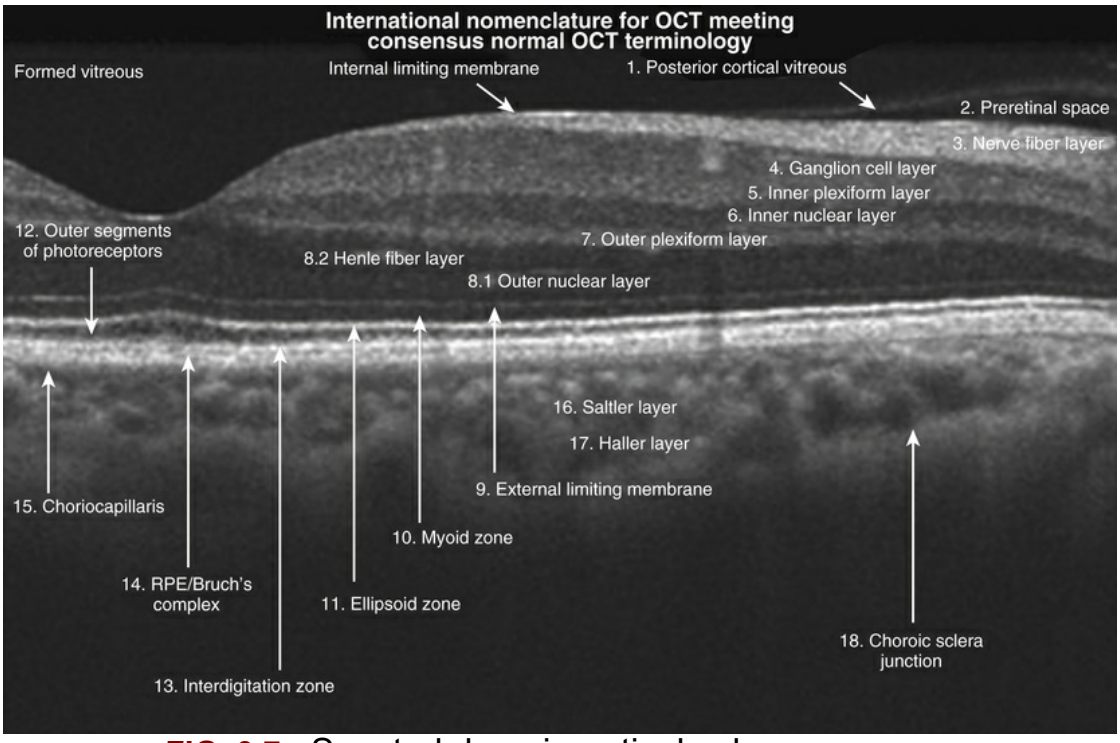

FIG. 3.7 Spectral domain optical coherence tomography (Spectralis, Heidelberg) image of a normal individual. The multilayered retinal architecture can be observed and each retinal layer can be identified.

(Reproduced with permission from Staurenghi G, Sadda S, Chakravarthy U, Spaide RF, International Nomenclature for Optical Coherence Tomography P. Proposed lexicon for anatomic landmarks in normal posterior segment spectral-domain optical coherence tomography: the IN*OCT consensus. Ophthalmology 2014 Aug;121(8):1572-8)

The first detected layer in most OCT scans is the ILM that appears as a hyperreflective layer at the vitreoretinal interface. In some patients, the posterior hyaloid can be seen above the ILM as a hyperreflective layer. Within the retina, the retinal nerve fiber layer and the plexiform layers (both inner and outer) are seen as hyperreflective while the ganglion cell layer and the nuclear layers (both inner and outer) are relatively hyporeflective. A recent study demonstrated that the incidence of the light beam could affect the appearance of Henle fiber layer by OCT, resulting in a thin hyperreflective layer corresponding to the photoreceptor synapses or a thicker hyperreflective layer corresponding to photoreceptor

axonal extensions enveloped by the outer cytoplasm of Müller cells (Fig. 3.8).[35] The retinal vessels may sometimes be seen on OCT images as circular hyperreflective structures located in the inner retina, with a vertical shadow or reduced reflectivity extending into deeper layers.

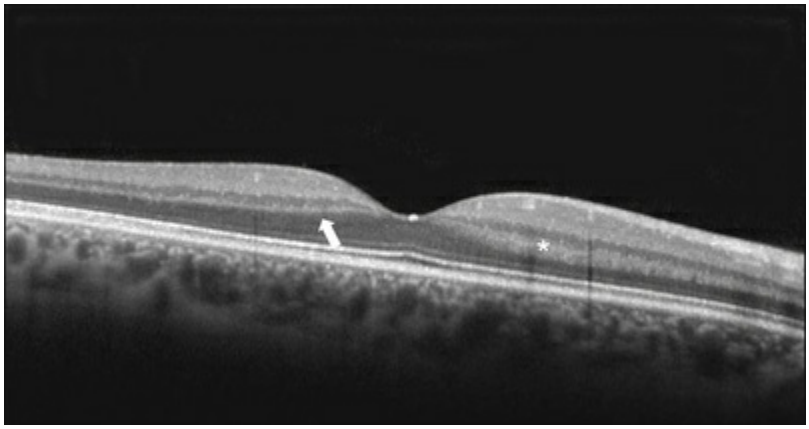

FIG. 3.8 Spectral domain optical coherence tomography of the same patient using a different light incidence. This results in a thin hyperreflective layer that corresponds to the photoreceptor synapses (*white arrow*) or a thicker hyperreflective layer corresponding to photoreceptor axonal extensions enveloped by the outer cytoplasm of Müller cells (*white asterisk*).

Outside the central fovea, commercially available SD-OCT instruments typically resolve four bands in the outer retina. There is discordance between different authors regarding which anatomic structure correlates with each band.[29,30,36] The innermost band has been attributed to the external limiting membrane (ELM). This band is typically thinner and fainter than the others. The nomenclature for the middle two bands has much less supportive evidence. The second of the four bands has been commonly ascribed to the boundary between the IS/OS photoreceptors, but a recent consensus meeting suggested that this band correlates with the inner segment ellipsoid zone (EZ), although this interpretation is not universally accepted.[33,34] The third band is referred to as either the OS tips or as Verhoeff membrane.[16,37] This third band appears to correspond to the contact cylinder between the RPE apical process and the external portion of the cone outer segment, and has been suggested

to be called the interdigitation zone by the recent consensus meeting.[33] This band typically merges with the fourth band in the central fovea, and this is explained by a greater height of the contact cylinder of the cones and RPE outside the fovea.[36] The fourth hyperreflective outer retinal band is attributed to the RPE, with potential contribution from Bruch's membrane and choriocapillaris, with abundant experimental and clinical evidence supporting this designation.[16,31,38]

Although the current SD-OCT uses a short wavelength of approximately 840 nm, which results in light scattering at the level of the RPE and a lower signal from the deep choroidal tissue, it is also possible to image the choroid and extract quantitative information (Fig. 3.9).[39–42] Choroidal thickness may be influenced by age, axial length, and perhaps refractive abnormalities.[43] It also varies in different retinal regions within the same normal subject, being thickest beneath the fovea,[42] or in the superior outer macula (Early Treatment Diabetic Retinopathy Study (ETDRS) subfield), with the thinnest choroid being located in the nasal outer ETDRS subfield.[44] When centering the optic nerve head as a reference point, the choroid appears thin in the peripapillary region and increases in thickness with eccentricity in all directions, up to a certain point, except inferiorly.[44] This is the embryonic location of the optic fissure closure and thus may be responsible for the localized thinning.[44,45] OCT that uses a light source with a wavelength around 1050 nm can better visualize the posterior choroid and sclera than currently available SD-OCT instruments.[41,45,46]

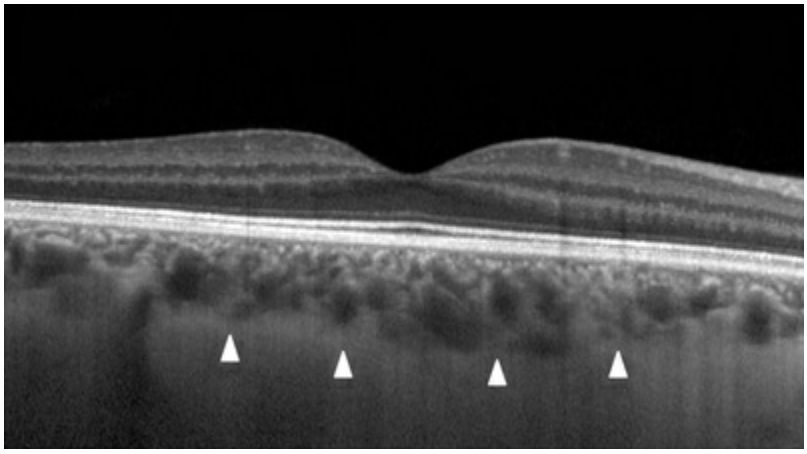

FIG. 3.9 Enhanced-depth spectral domain optical

coherence tomography image (Spectralis, Heidelberg) of a normal subject showing the boundaries of the choroid (*arrowheads*).

The high axial resolution and the different scan patterns offered by SD-OCT provide comprehensive structural information that can be used to map retinal layer thicknesses and perform volumetric analyses. Using different SD-OCT instruments, several authors have reported an approximate central retinal thickness of 265 μm in normal subjects.[47] However, caution is required, as errors in automated measurements may occur and are more often found in macular disorders with complex morphology like neovascular AMD, which alters the ability of segmentation algorithms to detect normal boundaries.[24–28] Therefore, care must be taken that high-quality and artifact-free scans are obtained before running the retinal thickness algorithm.

It is essential to consider the following points when analyzing OCT images: location, shape, and reflectivity of the structure, along with its histologic correlation. It is also important to remember that the alignment of the instrument with the pupil can generate signals that may lead to a misinterpretation of the exam.

Characteristic OCT findings in several common retinal disorders, which are frequently studied using OCT, are discussed below. For OCT findings in other disorders, such as retinal degenerations, the reader is directed to the specific chapters describing these diseases.

SD-OCT in Retinal Disorders

Vitreoretinal Interface Disorders

Abnormalities of the vitreoretinal interface are involved in the pathogenesis of several macular conditions. In idiopathic epiretinal membranes (ERMs), a layer of fibrotic tissue develops on the surface of the retina, usually after a posterior vitreous detachment. Contraction of this membrane can result in retinal distortion, leading to vision loss. In other conditions, such as vitreomacular traction (VMT) syndrome or idiopathic macular hole, there are abnormal attachments between the vitreous and the retina. The resulting traction exerted on the retina causes anatomical alteration

and subsequent visual loss.

Vitreomacular Adhesion

Vitreomacular adhesion (VMA) syndrome results from persistent vitreoretinal attachments in the setting of a partial posterior vitreous detachment.[48] In normal eyes, as the vitreous liquefies due to age, it detaches from the macula. This natural progression has been demonstrated using OCT.[49] In some people, an unusually strong adhesion is present between the vitreous and macula, and as the vitreous detaches peripherally, it continues to pull on areas of the macula. The vitreoretinal adhesions transmit tractional forces to the retina from the vitreous body, having the potential to cause tensile deformation, foveal cavitations, cystoid macular edema (CME), limited macular detachment, or a macular hole.[50,51] Patients can present with visual loss and metamorphopsia.

Diagnosis of VMA by biomicroscopy may be challenging, particularly when the area of vitreoretinal attachment is broad. OCT better defines the vitreoretinal relationships in eyes with VMA and also documents concomitant ERM and macular edema.[52–56] With OCT imaging, the abnormal VMA bands from the prominent posterior hyaloid are well delineated as reflective lines from the perifoveal area into the vitreous cavity, distorting the macular contour with or without accumulation of intraretinal or subretinal fluid (Fig. 3.10).

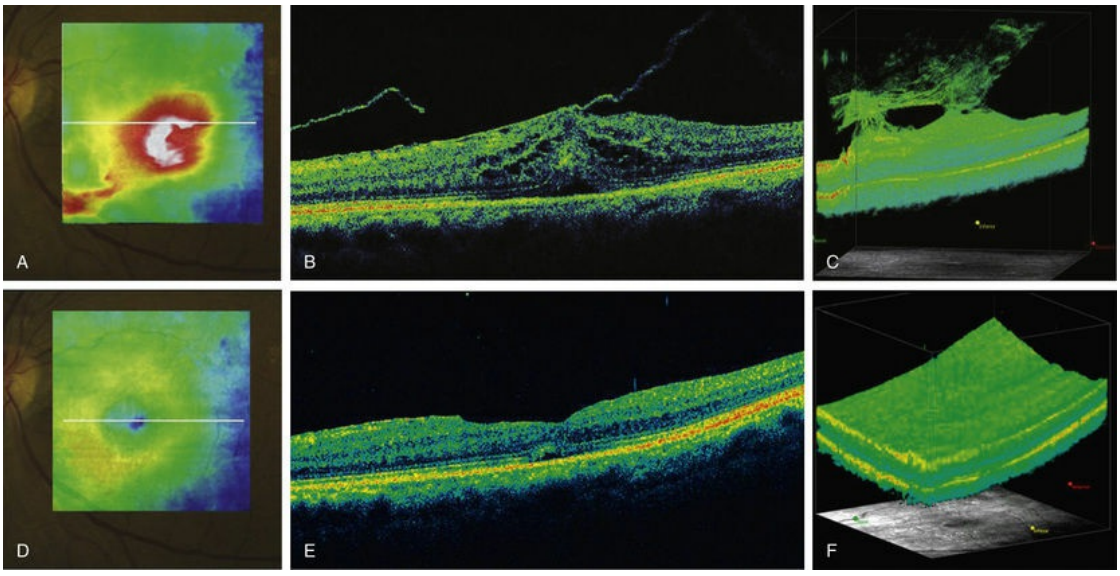

FIG. 3.10 Vitreomacular traction syndrome: color fundus image of the left eye of a 71-year-old woman superimposed with the retinal thickness map (A) showing an increase in the retinal thickness (red areas). The B-scan of the macular region shows an increase in the retinal thickness and the presence of subretinal fluid and intraretinal cysts due to vitreomacular traction and an epiretinal membrane (B). A three-dimensional spectral domain optical coherence tomography is presented in panel (C) (courtesy of Cirrus, Carl Zeiss Meditec). The patient underwent surgery and, 2 months after pars plana vitrectomy, the retinal thickness decreased, with resolution of the intraretinal cysts (D–F).

In recent years, OCT has been most beneficial in diagnosing VMA and subsequently directing treatment of this condition. In fact, vitreomacular abnormalities, including vitreomacular adhesion, traction, and macular holes, have recently been reclassified primarily on the basis of OCT.[57] This current scheme includes OCT-based assessment of vitreous traction, measurement of the size of the hole and whether the hole is primary or secondary, all of which are related to the medical and surgical prognosis. According to this International Classification System, VMA is defined on OCT as "perifoveal vitreous separation with remaining vitreomacular attachment and unperturbed foveal morphologic features." Vitreomacular traction, on the other hand, is defined by "anomalous posterior vitreous detachment *accompanied by anatomic distortion of the fovea.*" Pseudocysts, cystoid macular edema, macular schisis, and subretinal fluid are typical findings of VMT. Both VMA and VMT can be further subclassified as having focal (1500 μm or less) or broad (more than 1500 μm) vitreoretinal attachment. Generally, pharmacologic vitreolysis may be indicated for focal but not broad VMT.

OCT also allows detailed assessment of structural changes in the retina associated with vitreomacular adhesion or traction. This allows for a more accurate visual prognosis, obtained by the tomographic integrity of the photoreceptor layer, specifically the inner/outer photoreceptor cell junction/ellipsoid zone, as well as the integrity of the external limiting membrane.

In some cases, spontaneous resolution can occur with separation of the vitreous from the macula, leading to subsequent resolution of the intraretinal and subretinal fluid and restoration of normal vision.[58,59] However, in most eyes, VMA leading to VMT persists and vitrectomy or ocriplasmin may be effective treatment options for patients with symptomatic VMT.[52,60–62] Consequently, OCT is useful in monitoring subtle changes in the retinal architecture and in assisting with the treatment decision-making process.

Macular Hole

Idiopathic macular holes typically occur in the sixth to seventh decade of life with a 2 : 1 female preponderance. Symptoms include decreased visual acuity, metamorphopsia, and central scotoma. Bilateral involvement occurs in 15–20% of patients.[30]

A full-thickness defect in the neural retina as seen with OCT can differentiate a true macular hole from a pseudohole seen clinically. Pseudoholes are seen in the presence of a dense sheet of ERM with a central defect that overlies the foveal center, giving the ophthalmoscopic appearance of a true macular hole.[30,63]

Gass described the stages of macular hole formation based on biomicroscopic findings, and this traditional staging system is still widely used in clinics and in the literature.[64] A stage 1 impending hole is characterized by a foveal detachment seen as a yellow spot (1A) or ring (1B) in the fovea (Fig. 3.11A). Spontaneous resolution will occur in approximately 50% of these cases. In stages 2–4, there is a full-thickness retinal defect, with a complete absence of neural retinal tissue overlying the foveal center. What differentiates these stages is the size of the retinal defect (<400 μm in stage 2 and >400 μm in stage 3) or the presence of a complete posterior vitreous detachment regardless of the hole size (stage 4) (Fig. 3.11B).

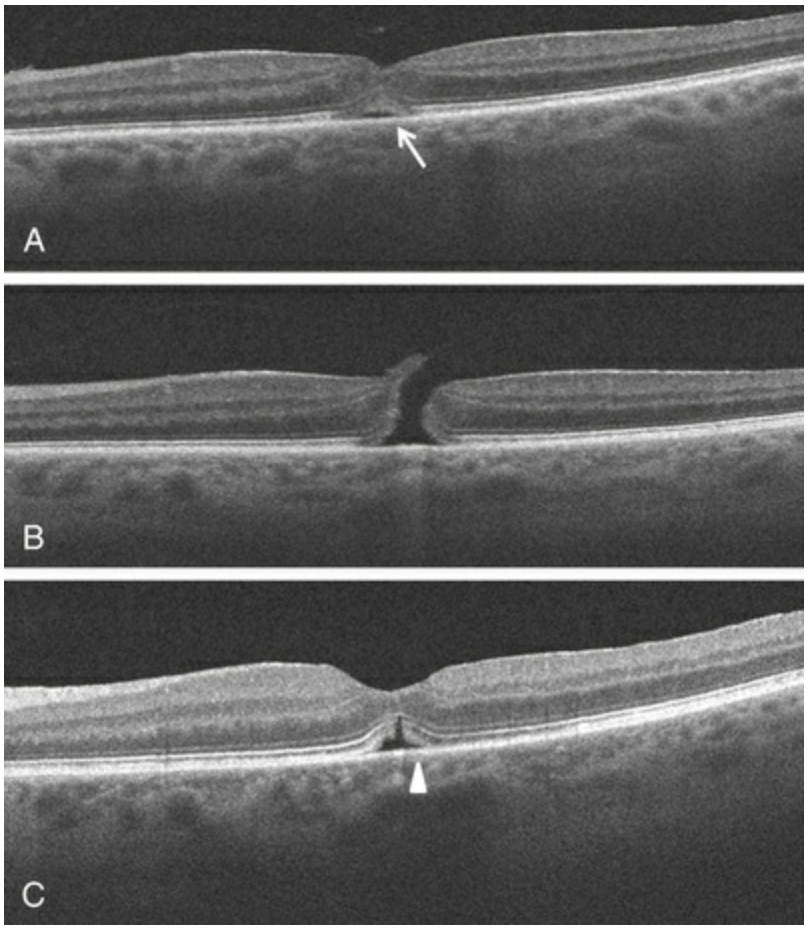

FIG. 3.11 Macular hole. (A) Stage 1 macular hole in a 63-year-old woman with a 3-month history of decreased visual acuity (20/60). An outer retinal defect can be observed in the B-scan (*arrow*). (B) A full-thickness retinal defect developed after 2 months of follow-up with worsening in the visual acuity (20/80). The posterior vitreous remains adhered to the edge of the macular hole. (C) One month after surgery, the macular hole was closed and the visual acuity improved to 20/50, but a persistent foveal outer defect could be observed (*arrowhead*).

OCT has enhanced our understanding of the pathogenesis of macular holes, the healing process after surgical repair, and helped in identifying pre- and postoperative features that are related to visual outcome. The anatomic changes identified on OCT have been correlated with the various stages of macular hole. In stage 1A, patients usually present with a localized foveolar detachment, which can resolve spontaneously after posterior vitreous detachment with resolution of the yellow foveal spot, or it can

progress to stage 1B with a development of a pseudocyst with loss of the outer retinal layers and later develop into a full-thickness macular hole.[65,66] Generally, the retinal defect is accompanied by a variable amount of intraretinal fluid appearing as cysts and a variable amount of subretinal fluid at the edge of the hole. The edge of the hole can appear elevated, as a result of the significant intraretinal fluid accumulation or due to persistent vitreofoveal traction. In a stage 4 macular hole, OCT can demonstrate complete hyaloid separation and occasionally a retinal operculum can be seen floating above the foveal center.

The changes noted on OCT have become the basis for a new classification system of macular holes proposed by the International Vitreomacular Traction Study Group.[57] This classification divides macular holes based on the cause, size of the hole, and the presence or absence of vitreomacular adhesion. Full-thickness macular holes can be either primary (if caused by VMT) or secondary (if caused by other conditions unrelated to abnormal vitreoretinal traction), and can be further subclassified by the size of the hole measured on SD-OCT. Based on the minimum horizontal aperture size (hole width), macular holes are divided as follows: small holes measure 250 μm or less; medium size holes are between 250 μm and 400 μm, and large holes are larger than 400 μm. Holes are also further subclassified by presence or absence of vitreomacular adhesion. This classification is of clinical importance because it determines the management and prognosis of macular holes.

According to the OCT-based classification, Gass Stage 0 macular hole corresponds to vitreomacular adhesion in the setting of a history of full-thickness macular hole in the contralateral eye. A Stage 1 macular hole corresponds to vitreomacular traction, a stage 2 or 3 macular hole corresponds to a small, medium, or large hole on the OCT-based classification with vitreomacular adhesion present, and a stage 4 macular hole corresponds to a small, medium or large-sized macular hole with release of the vitreomacular adhesion.

Vitrectomy has become the standard treatment for macular hole with anatomic success rates of 85–100%.[67,68] OCT can be used to confirm complete macular hole closure and restoration of the normal foveal contour.[69–72] In cases with suboptimal postoperative

visual outcomes, OCT can visualize persistent retinal abnormalities despite anatomically successful macular hole surgery (Fig. 3.11C). Restoration of the ELM and the so-called junction of the inner and outer segment of photoreceptors may reflect the morphologic and functional recovery of the photoreceptors in surgically closed macular holes.[71–74] A residual small defect in the ELM is often still evident in closed holes, particularly in those that are spontaneously healed. The ability to perform OCT imaging in eyes filled with gas or silicone oil has also been useful as an adjunct to determine the extension of the face-down position in patients following vitrectomy for macular hole.[75–77]

Epiretinal Membrane

ERM occurs in approximately 6% of patients over the age of 60, with incidence increasing with age.[78,79] ERMs can be classified as idiopathic or secondary to an initiating event. Most idiopathic ERMs are thought to result from fibroglial proliferation on the inner surface of the retina secondary to a break in ILM occurring during posterior vitreous detachment.[80,81] Secondary ERMs result from an already-existing ocular pathology such as central or branch retinal vein occlusion, diabetic retinopathy, uveitis, and retinal breaks with or without detachment.[82] Glial cells, RPE cells, and myofibroblasts are shown to be mostly involved in ERM formation.[80,81] ERM may lead to loss of normal retinal anatomy, with the patient experiencing metamorphopsia, micropsia, monocular diplopia, and decreased visual acuity. These symptoms vary in severity depending on the location, density, and contraction of the membrane.

On slit-lamp biomicroscopy, a mild ERM appears as a glistening layer on the retinal surface. Denser membranes may be seen as a gray sheet overlying the retina and causing distortion in the macular vascular architecture. Occasionally, ERMs can evolve into macular pseudoholes and ERMs are often seen in conjunction with idiopathic full-thickness macular holes.[50] Fluorescein angiography may demonstrate macular leakage, which can be variable from case to case.

OCT provides qualitative and quantitative information about the retinal anatomy, which can identify factors contributing to vision

loss in patients with ERM. On OCT, ERMs are seen as a highly reflective layer on the inner retinal surface (Fig. 3.12). In most eyes, the membrane is globally adherent to the retina but, in some cases, it can be separated from the inner aspect of the retina, which enhances its visibility by OCT. In this situation, it is usually distinguishable from a detached posterior hyaloid. Secondary effects of the membrane include loss of the normal foveal contour, increased retinal thickness, and the presence of cystoid changes – these features may be observed in more advanced membranes. OCT is useful for monitoring changes in cases that are being observed and for documenting the response to treatment in patients undergoing pars plana vitrectomy with membrane peeling.

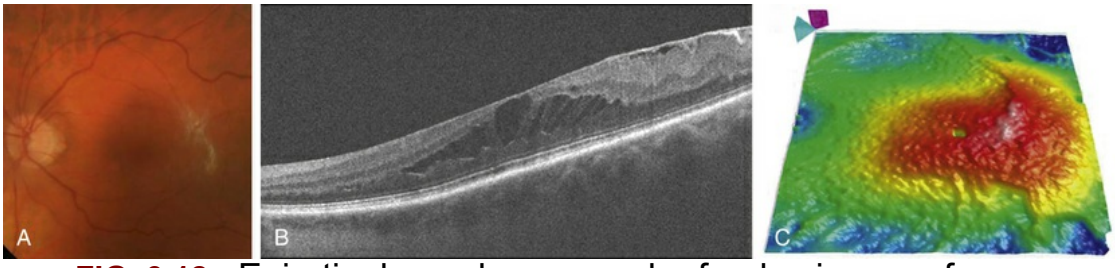

FIG. 3.12 Epiretinal membrane – color fundus image of the left eye of a 65-year-old man with grayish tissue over the retina (A). Cross-sectional optical coherence tomography image showing a hyperreflective tissue overlying the retina, resulting in increased retinal thickness and cysts in the retina (B and C).

Age-Related Macular Degeneration

AMD is a common cause of irreversible vision loss among the elderly worldwide. It is estimated that approximately 30% of adults older than 75 years have some sign of AMD and that approximately 10% of these patients have advanced stages of the disease.[83–86] AMD can be classified in two forms: non-neovascular (dry) and neovascular (wet or exudative). The non-neovascular form accounts for 80–90% of cases while the neovascular form accounts for 10–20% of cases, but was responsible for the majority of severe vision loss (80–90%) prior to the widespread use of vascular endothelial growth factor (VEGF) inhibitors.[85,87]

Non-Neovascular Age-Related Macular Degeneration

Non-neovascular (dry) AMD is characterized by abnormalities of the RPE, Bruch's membrane, and choriocapillaris (see Chapter 68, Age-related macular degeneration: non-neovascular early AMD, intermediate AMD, and geographic atrophy). These abnormalities may be asymptomatic or accompanied by compromised vision, and are considered to be the precursors of GA and choroidal neovascularization (CNV).[88,89]

Early Non-Neovascular AMD: Drusen and Pigmentary Changes.

Drusen appear clinically as focal white–yellow excrescences deep to the retina. They vary in number, size, shape, and distribution. Several strategies have been developed to grade drusen using color fundus imaging.[90,91] Although color fundus imaging is useful for assessing the appearance of drusen, these images only provide two-dimensional area information on the geometry of the drusen and cannot be used to measure quantitative properties such as drusen volume. Until the advent of high-speed spectral domain technology, evaluation of drusen with OCT was often difficult as motion artifacts commonly resulted in apparent undulation of the RPE, mimicking the appearance of drusen.[92,93] SD-OCT can provide a three-dimensional, geometric assessment of drusen.

The high-definition B-scans obtained with SD-OCT are useful to assess the ultrastructure of drusen and to evaluate for evidence of disruption of adjacent retinal layers. Drusen are seen as discrete areas of RPE elevation with variable reflectivity, which is consistent with the variable composition of the underlying material (Fig. 3.13).[94,95] In larger drusen or drusenoid retinal pigment epithelial detachments (PEDs), the RPE has a greater elevation with a dome-shaped configuration.[96] Larger drusen may often become confluent and can sometimes be accompanied by fluid accumulation under the retina in the absence of CNV (Fig. 3.14).[94] Recognition of this feature may avoid unnecessary treatment with anti-VEGF drugs. SD-OCT imaging has the resolution to evaluate the retinal layers overlying drusen. A thinning in the photoreceptor layer can be observed in up to 97% of cases, with average photoreceptor layer thickness reduced by 27% compared to age-matched control eyes.

The inner retinal layers usually remain unchanged. These findings demonstrate a degenerative process, with photoreceptor loss leading to visual impairment.[97]

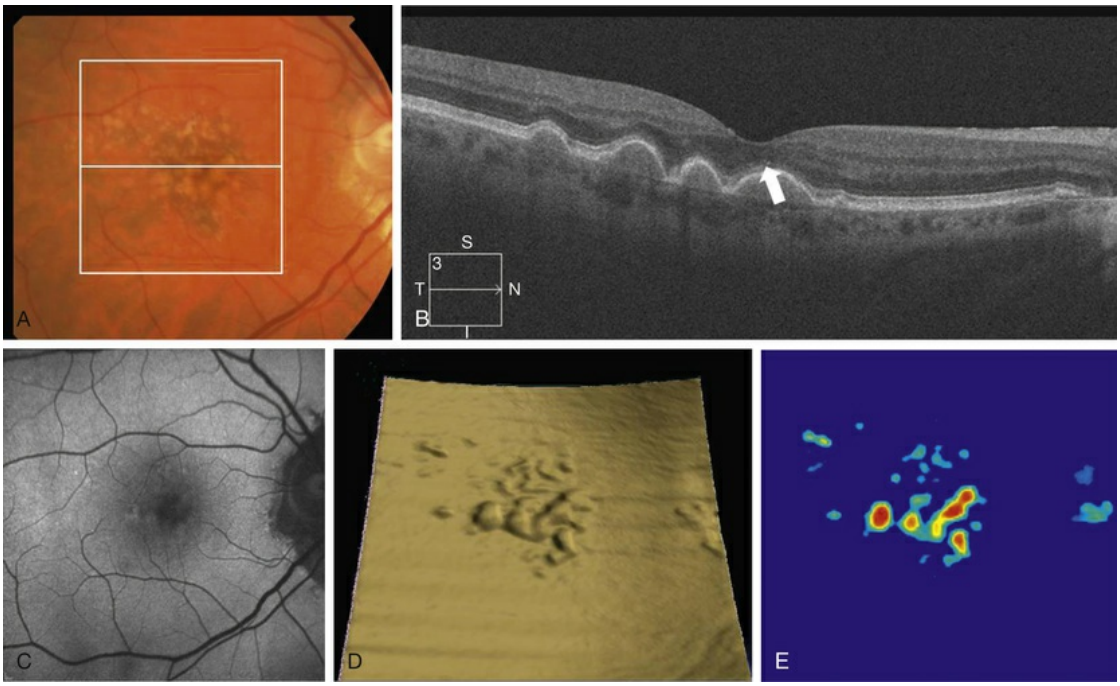

FIG. 3.13 Early non-neovascular age-related macular degeneration. (A) Color fundus image of the right eye of a 61-year-old man with drusen and pigmentary changes in the macula. (B) Foveal B-scan showing the drusen as elevations of the retinal pigment epithelium (RPE). The inner and outer segment junction of the photoreceptors adjacent to the drusen appears disrupted (*arrow*). (C) Fundus autofluorescence illustrating that drusen cannot be reliably identified by this imaging modality. (D) RPE segmentation map showing drusen in a unique three-dimensional perspective. (E) RPE elevation map providing the drusen area (1.37 mm^2) and volume (0.063 mm^3).

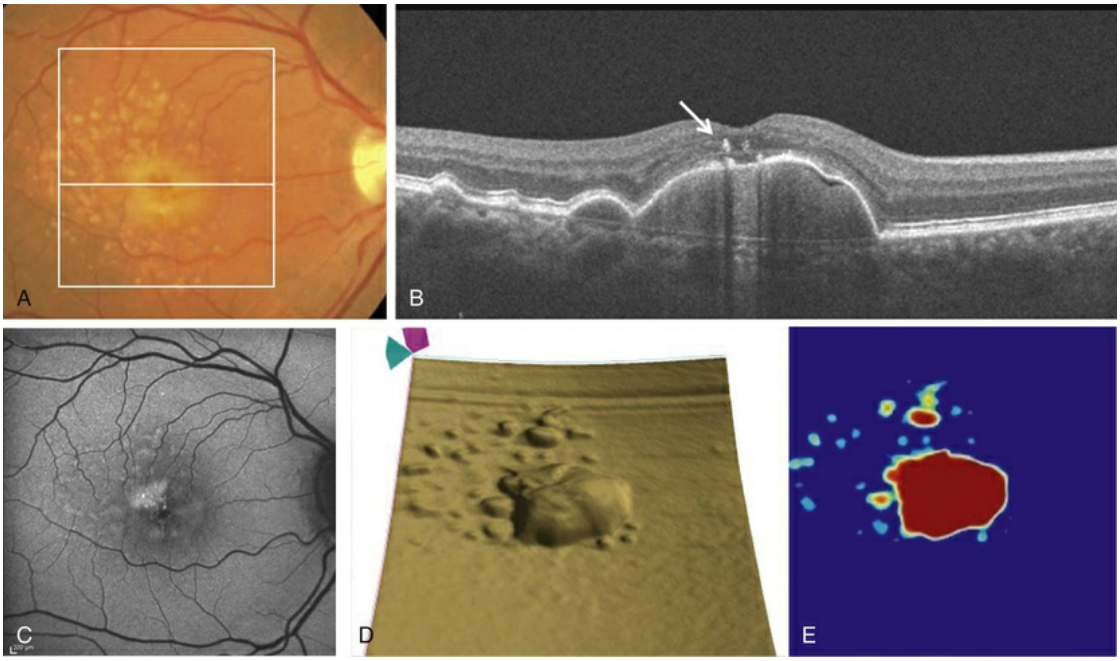

FIG. 3.14 Drusenoid retinal pigment epithelium detachment (DPED). (A) Color fundus image of the right eye of a 66-year-old man with a DPED and pigmentary changes in the macula. (B) Foveal B-scan showing the confluent drusenoid material as a large elevation of the retinal pigment epithelium (RPE). Intraretinal pigment migration can be observed (*arrow*). (C) Fundus autofluorescence image (Heidelberg retina angiograph, Heidelberg). (D) RPE segmentation map showing the DPED in a three-dimensional perspective. (E) RPE elevation map providing the DPED area (3.87 mm^2) and volume (0.508 mm^3).

The acquisition of dense raster scans comprised of a large number of lower-density B-scans combined with the use of segmentation algorithms results in the ability to generate maps of the RPE, which provides information on RPE geometry and therefore a unique perspective of drusen. A novel algorithm developed to identify RPE deformations such as drusen has been shown to be highly reproducible in the measurement of drusen area and volume.[21] The algorithm creates a drusen map from a scan pattern of 40 ,000 uniformly spaced A-scans organized as 200 A-scans in each B-scan and 200 horizontal B-scans, covering an area of 6×6 mm centered in the fovea. The algorithm uses the actual RPE geometry and compares this RPE map to a virtual map of the RPE free of any deformations (RPE floor). The algorithm creates a

difference map from these two maps, which permits reproducible measurements of drusen area and volume (Fig. 3.6). This algorithm was used to study the natural history of drusen in AMD.[22] Drusen were shown to undergo three different growth patterns. In most eyes, drusen were found to increase in volume and area. Drusen could also remain stable or they could dramatically decrease over time. When these drusen decreased, they could evolve into GA or neovascular AMD, or they could decrease with in no apparent residual anatomic defect in the macula.

The RPE cells are capable of hypertrophy and proliferation in response to different stimuli and in many cases an intraretinal pigment migration may occur (Fig. 3.14B). The Age-Related Eye Disease Study research group reported a severity scale defining large drusen (≥125 μm) and pigment abnormality in the macula as being a risk factor for disease progression in patients with intermediate AMD.[98,99] This pigmentary abnormality can be observed on OCT imaging as small discrete hyperreflective lesions within the neurosensory retina, usually within the outer nuclear layer.[100] Recently, these hyperreflective lesions were noted to precede the development of retinal angiomatous proliferation.[101]

Typical drusen in AMD are seen as deposits between the RPE and the inner collagenous layer of Bruch's membrane. OCT imaging is also useful for the assessment of a variety of conditions characterized by variant forms of drusen. These deposits can also be seen on top of the RPE and are known as "subretinal drusenoid deposits."[102,103] They appear on OCT imaging as granular hyperreflective material between the RPE and the IS/OS junction and are also well visualized on blue-light reflectance imaging and autofluorescence imaging (Fig. 3.15).

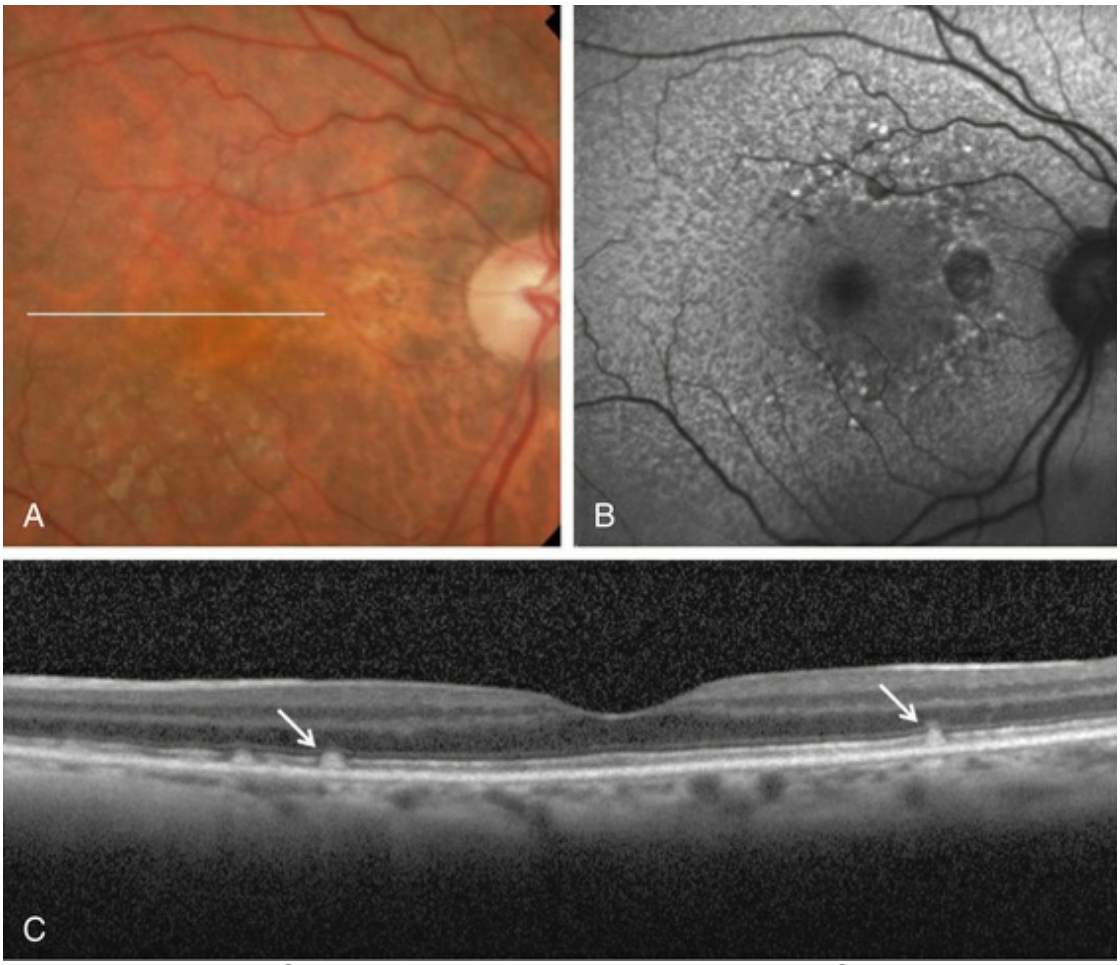

FIG. 3.15 Subretinal drusenoid deposits. (A) Color fundus image of a 76-year-old woman shows multiple yellowish, small, and round lesions. (B) Fundus autofluorescence clearly shows these deposits as small and multiple hyperautofluorescent spots. (C) On optical coherence tomography, these lesions appear as multiple areas of granular hyperreflectivity between the retinal pigment epithelium and the inner/outer-segment junction (*arrows*).

Another form of drusen, known as "cuticular drusen," appears as numerous, uniform, round, yellow–white punctuate accumulations under the RPE. Cuticular drusen are usually seen on OCT imaging as elevations of the RPE with occasional disruption of the overlying IS/OS junction and ELM.[95] Although cuticular drusen, subretinal drusenoid deposits, and soft drusen are composed of common components, they are distinguishable by multimodal imaging because of differences in location, morphology, and the optical properties of the drusenoid material and the RPE.

Late Non-Neovascular AMD: Geographic Atrophy.

The natural history of GA has been described as a progressive condition that evolves through stages with loss of vision occurring over many years.[104–106] Multiple imaging modalities have been used to document and quantify the area of GA. Until recently, color fundus photography was used as the standard method to image GA; however, the use of color photos can be challenging due to the reported difficulty in detecting and accurately delineating GA.[106,107] Other imaging modalities such as fluorescein angiography, fundus autofluorescence, and SD-OCT imaging are now used to evaluate and quantify GA (Fig. 3.16). Although these imaging modalities provide different information, none has been shown to be superior to the other.

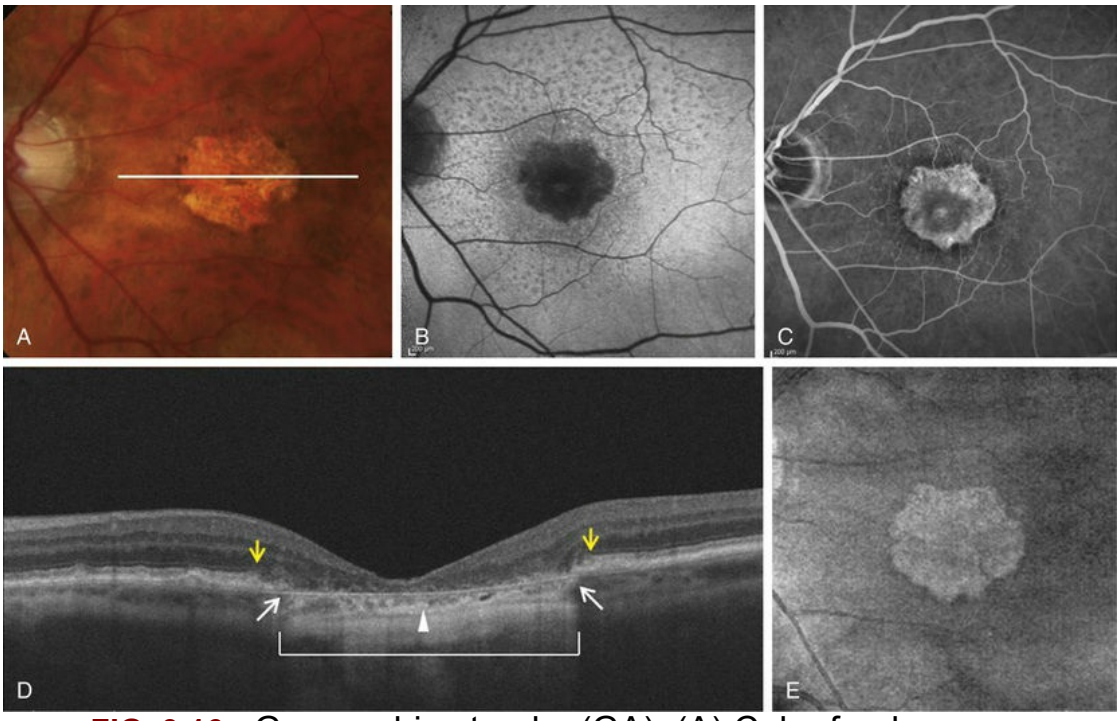

FIG. 3.16 Geographic atrophy (GA). (A) Color fundus image of the left eye of a 74-year-old male with central GA secondary to age-related macular degeneration. (B) Fundus autofluorescence (Spectralis, Heidelberg) showing a central area of hypoautofluorescence corresponding to the GA seen on the color image. (C) Late-phase fluorescein angiography showing a central window defect corresponding to the GA. (D) Horizontal B-scan through the foveal center demonstrating retinal

thinning, loss of the retinal pigment epithelium (RPE), and photoreceptors. The loss of photoreceptors (*yellow arrows*) often extends beyond the margins of the RPE loss (*white arrows*). Observe the increased light penetration in the areas where the RPE is absent (*bracket*) and thin choroid (*arrowhead*). (E) Optical coherence tomography fundus image (courtesy of Cirrus, Carl Zeiss Meditec), showing the GA as a bright area.

GA is seen clinically as one or more well-demarcated areas of hypopigmentation or depigmentation due to the absence or severe attenuation of the underlying RPE. The larger, deeper choroidal vessels are more readily visualized through the atrophic areas, and are accompanied by varying degrees of photoreceptor and choriocapillaris loss. Associated retinal atrophy is seen as thinning or loss of the outer nuclear layer and the absence of ELM and IS/OS junctions.[108,109] The loss of photoreceptors often extends beyond the margins of GA, with the ELM and IS/OS junctions disappearing while bridging across the GA margin.[110] Evaluation of these junctional zones may provide information about the pathogenesis of GA, and the role of RPE, photoreceptor, and choriocapillaris loss in the initiation and propagation of this condition.[110] SD-OCT has been shown to be useful in detecting some of these morphologic alterations (Fig. 3.16D).

With the use of SD-OCT enhanced-depth imaging (EDI) protocols, it is now possible to visualize the structure of the choroid in greater detail.[40] EDI demonstrated that subfoveal choroidal thickness decreases with age and axial length.[42] In a subset of elderly patients complaining of unexplained vision loss, abnormal choroidal thinning was identified, and this condition was named "age-related choroidal atrophy."[111] Future studies are necessary to confirm if this represents a new clinical entity or a subtype of AMD. In contrast, the choroidal thickness appears to be unaffected in early non-neovascular AMD patients.[112]

SD-OCT can also be used to quantify the areas of GA and monitor the progression of the disease. GA is currently imaged with SD-OCT by using the OFI, which represents a virtual fundus image resulting from the en face summation of the reflected light from

each A-scan. This en face OCT fundus image identifies GA as a bright area due to the increased penetration of light into the choroid where atrophy has occurred in the macula. The absence of the RPE and choriocapillaris is responsible for this increased penetration of light associated with GA. The OFI was shown to correlate well with the GA seen on clinical examination, color fundus imaging, and autofluorescence imaging (Fig. 3.16E).[19,113,114] More recently, a newer algorithm provides an enhanced (partial) OFI, which is the summation of the reflected light from beneath the RPE (Fig. 3.17). In addition, this new algorithm is able to quantify the area of GA automatically. The enhanced OFI has advantages over the conventional OFI because the area of GA appears brighter than in the conventional OFI due to a better contrast at the boundaries of the lesions and there is less interference from other macular pathologies such as ERMs.

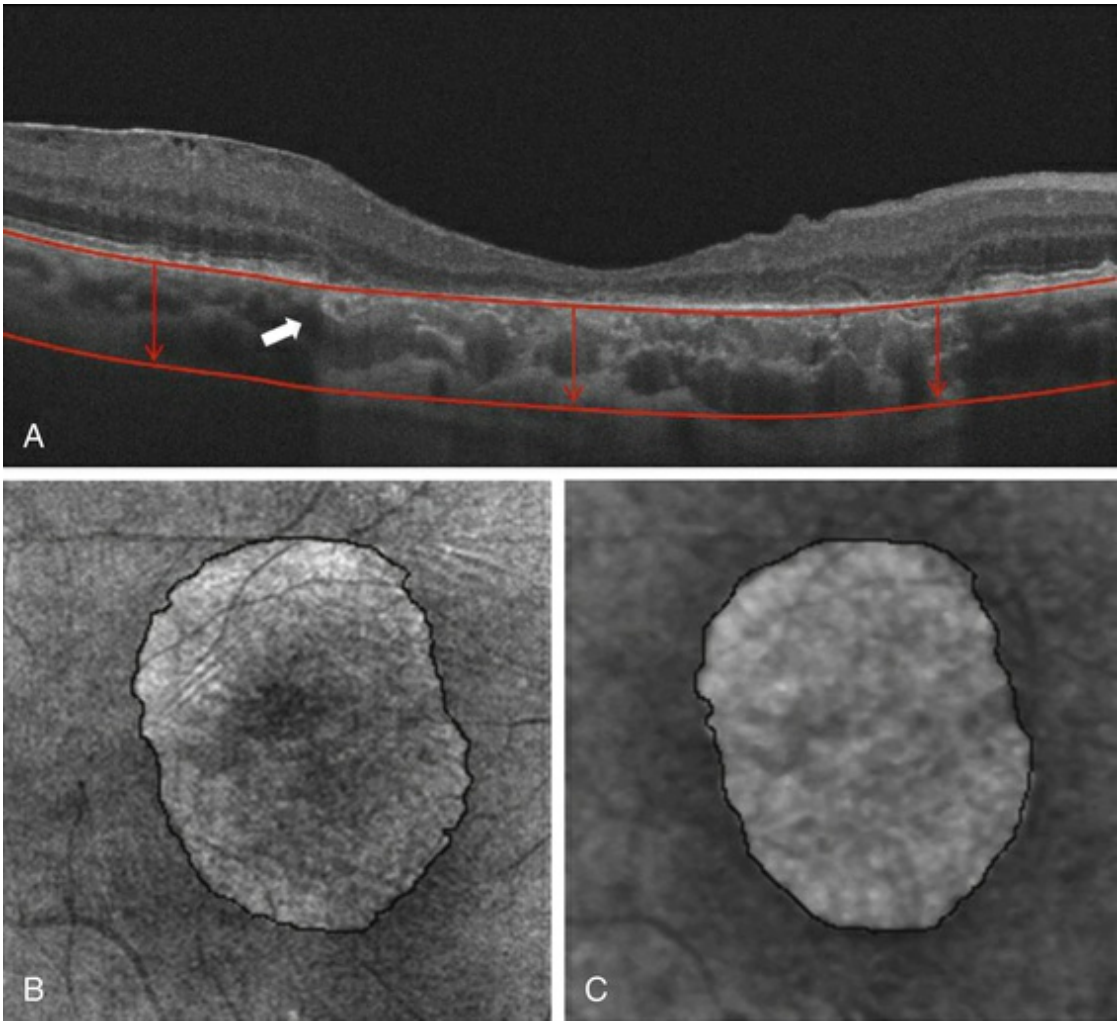

FIG. 3.17 Geographic atrophy (GA). (A) Horizontal B-scan through the foveal center of a 73-year-old man with GA showing increased light penetration in the areas where the retinal pigment epithelium (RPE) is absent. *White arrow* shows the junction where the RPE is present and absent. (B) Optical coherence tomography (OCT) fundus image represents a virtual fundus image resulting from the en face summation of the reflected light from each A-scan. GA lesions are identified as a bright area due to the increased penetration of light into the choroid where atrophy has occurred. (C) Enhanced OCT fundus image (courtesy of Cirrus, Carl Zeiss Meditec), which represents the summation of the reflected light from beneath the RPE (*red lines and arrows* in panel A).

Neovascular AMD

The neovascular (wet) form of AMD is characterized by the overproduction of VEGF and the growth of abnormal vessels in the macular region (see Chapter 69, Neovascular (exudative or "wet") age-related macular degeneration). These vessels may arise from the choroidal circulation and penetrate Bruch's membrane to form a fibrovascular tissue beneath or above the RPE, or these vessels may arise primarily from the retinal circulation. In either case, the presence of VEGF and abnormal vessels leads to structural changes in the retina and choroid with the accumulation of fluid within the retina, in the subretinal space, or under the RPE. Furthermore, this neovascular invasion may lead to significant disorganization and remodeling of the retina, resulting in the loss of the RPE and photoreceptors with the formation of a disciform scar.[115,116]

Intraretinal and Subretinal Fluid

In cases suspicious for exudative changes, OCT imaging can be extremely useful in detecting intraretinal, subretinal, or sub-RPE fluid. In cases with active neovascular AMD, OCT imaging can be used to establish baseline retinal thickness and volume, and determine the extent of neovascularization, fluid involvement, and other lesion components (blood, fluid, pigment, and fibrosis).

The growth of neovascularization is often accompanied by VEGF-

dependent leakage from both the mature vessels and the growing immature vessels. Intraretinal edema can range from mild retinal thickening of the outer nuclear layer to large and diffuse cystoid edema, seen as round or oval hyporeflective areas (Fig. 3.18).[30] Lipid exudation can also be present in patients with profuse intraretinal edema and appear as small hyperreflective dots in the outer retina. The fluid may also accumulate in the space between the RPE and the neurosensory retina. The subretinal fluid appears on OCT imaging as homogeneous hyporeflective spaces when the fluid exudation is serous, or may be separated by fibrinous membranes when profuse proteinaceous exudation is present.[117] Usually, neovascular lesions growing in the subretinal space are associated with a larger volume of subretinal fluid compared with sub-RPE lesions.[118]

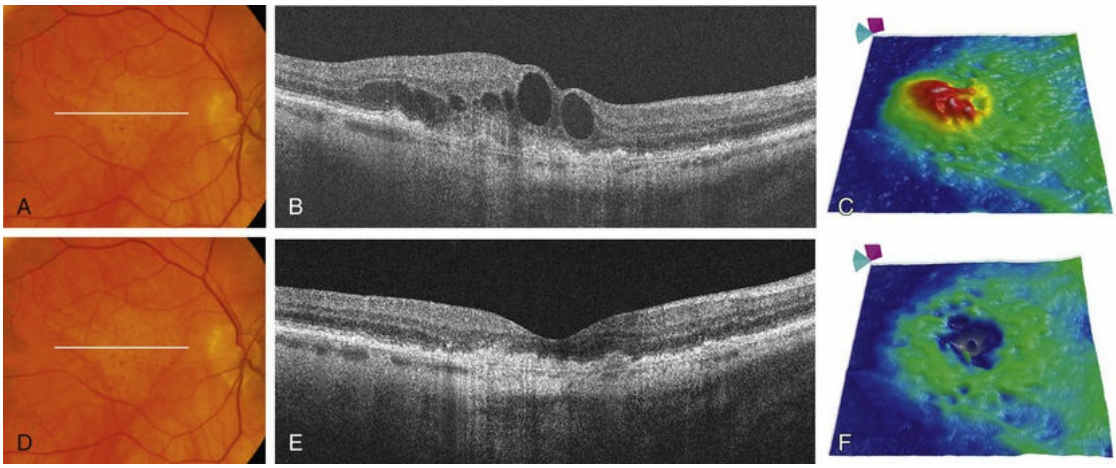

FIG. 3.18 Neovascular age-related macular degeneration. (A) Color fundus image of the right eye of an 81-year-old man with a 1-month history of vision loss. Visual acuity was 20/100. (B) Horizontal B-scan through the foveal center showing retinal thickening and the presence of intraretinal fluid with large cysts. (C) Retinal thickness map (courtesy of Cirrus, Carl Zeiss Meditec) showing the increase in retinal thickness (*red areas*). After three intravitreal injections of antivascular endothelial growth factor, the intraretinal fluid was reabsorbed (D). This is better observed in the B-scan and retinal thickness map (E,F).

Retinal Pigment Epithelium Detachment

In wet AMD, a retinal PED is formed by the separation of the RPE from Bruch's membrane due to the presence of sub-RPE fluid, blood, or fibrovascular tissue. A serous PED is defined as an area of smooth, sharply demarcated dome-shaped elevation of the RPE, often yellow–orange in color with a reddish halo of subretinal fluid. On fluorescein angiography, serous PEDs are associated with early hyperfluorescence with a well-defined border, which increases gradually throughout the study and classically demonstrates a pooling of dye rather than leakage.[119,120] Serous PEDs can be categorized as vascular or avascular.[121] On OCT imaging, serous PEDs appear as a dome-shaped elevation of the RPE typically seen overlying a homogeneously hyporeflective space, bound inferiorly by a visible Bruch's membrane, which is seen as a thin hyperreflective line at the outer aspect of the PED (Fig. 3.19).[122,123] The appearance of vascularized serous PEDs is similar. However, in some cases, the apparent fibrovascular proliferation can be seen adjacent to the PED and even adherent to the outer surface of the RPE.

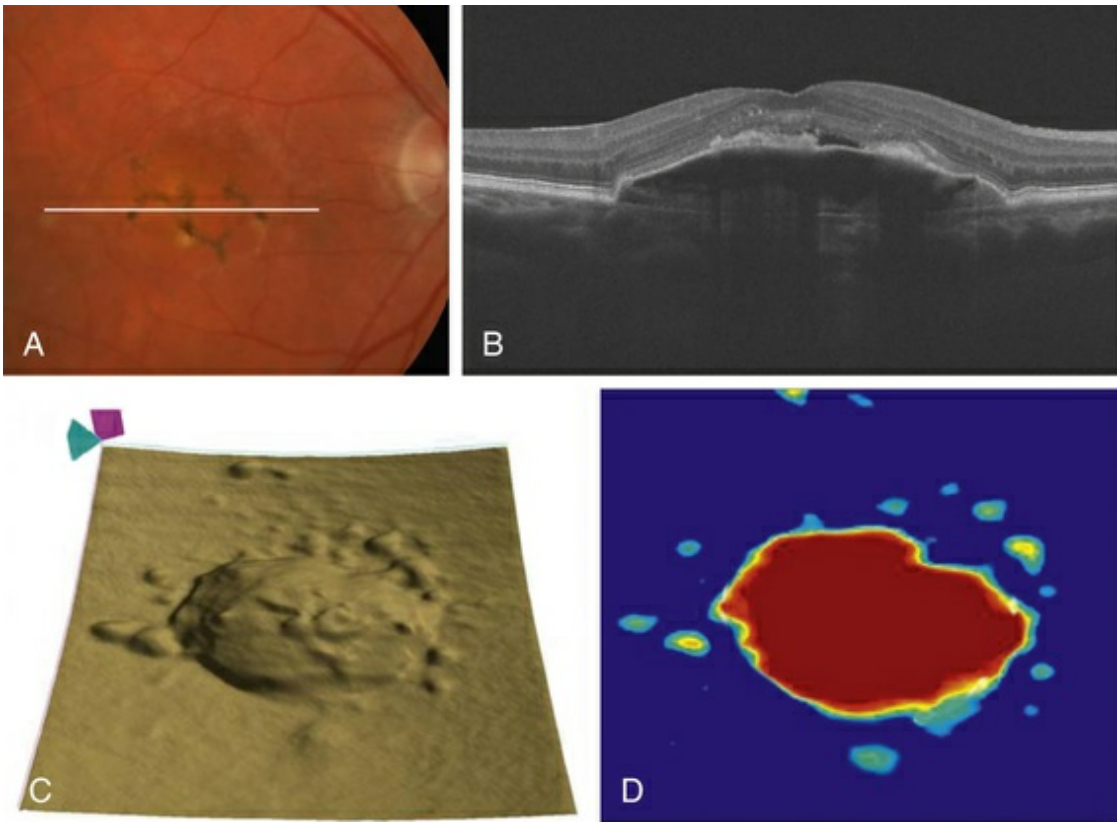

FIG. 3.19 Vascularized serous retinal pigmented epithelium detachment (PED). (A) Color fundus image of the left eye of a 77-year-old woman with pigmentary changes in the macula associated with an elevation of the macula. (B) Horizontal B-scan through the fovea showing a dome-shaped retinal pigment epithelium (RPE) elevation overlying a homogeneous hyporeflective space. Observe the presence of subretinal fluid above the PED. (C) RPE segmentation map showing a three-dimensional perspective of the PED. (D) RPE elevation map showing the area (5.84 mm^2) and volume (0.83 mm^3) measurements of the PED.

The fibrovascular PED usually produces an irregularly elevated lesion visible on clinical examination and can be associated with RPE hyperpigmentation, subretinal hemorrhage, subretinal lipid exudation, and intra- or subretinal fluid collection.[124] The elevation is often low and the borders are ill defined. The detailed structural characteristics and precise mechanism of PED formation have not been completely resolved. Recent studies using SD-OCT imaging revealed that many of the fibrovascular PEDs appear to be filled with solid layers of material of medium reflectivity, separated by hyporeflective clefts (Fig. 3.20).[125]

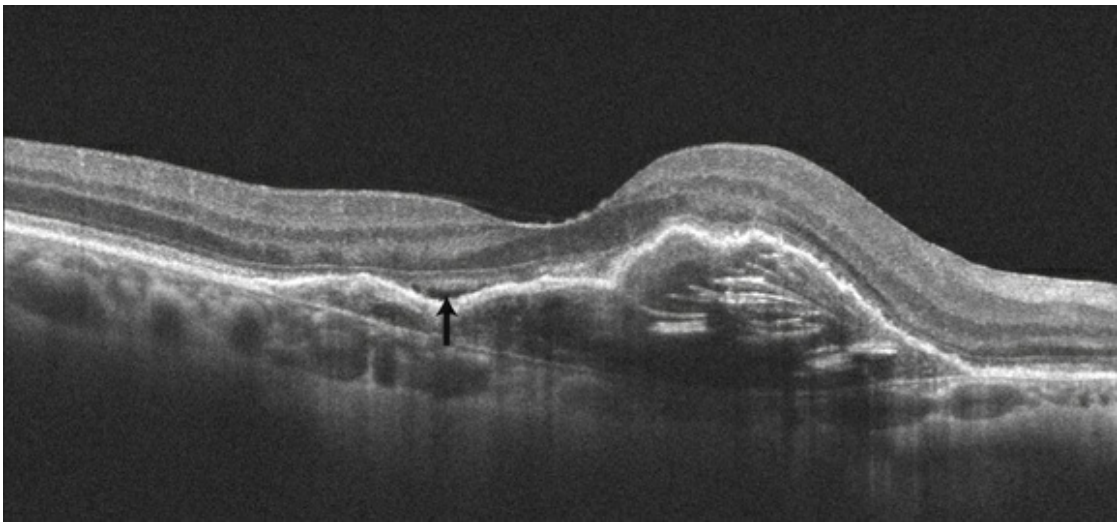

FIG. 3.20 Fibrovascular retinal pigmented epithelium detachment (PED). Cross-sectional B-scan of the right eye of an 87-year-old woman with a fibrovascular PED.

The space below the retinal pigment epithelium is filled with solid layers of medium reflectivity separated by hyporeflective clefts. A small amount of subretinal fluid can be identified over the PED (*arrow*).

Hemorrhagic PEDs occur when a CNV membrane bleeds into the sub-RPE space or as a result of an RPE tear. The hemorrhage can invade the subretinal space, with the sub-RPE blood having a typically darker appearance than subretinal blood. OCT demonstrates a dome-shaped lesion, similar to serous PEDs, although the slope of the elevation is more acute and the blood under the RPE appears hyperreflective, attenuating the signal from deeper structures, with the loss of choroidal detail (Fig. 3.21).[122,124,126]

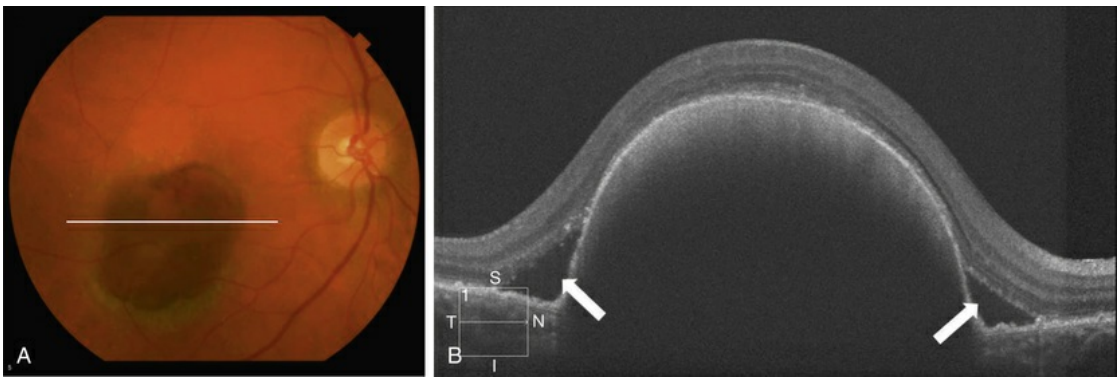

FIG. 3.21 Hemorrhagic retinal pigmented epithelium detachment (PED). (A) Color fundus image of the right eye of a 65-year-old woman with a large subretinal pigment epithelium (RPE) hemorrhage secondary to neovascular age-related macular degeneration. (B) Optical coherence tomography demonstrates a dome-shaped lesion, similar to serous PEDs. The blood under the RPE appears hyperreflective, attenuating the signal from deeper structures. Subretinal fluid can be observed as hyporeflective spaces above the RPE (*arrows*).

In addition, the same algorithm used to measure drusen can be used to measure PEDs, since both involve the deformation of the RPE. This algorithm is able to measure both the area and volume of PEDs (Fig. 3.19D). In addition, algorithms may be developed to characterize the internal architecture of the PEDs automatically.[127]

The qualitative appearance of the B-scans and the qualitative and quantitative changes in the retinal thickness maps and RPE elevation map can be used to appreciate better the natural history of the disease and to monitor the effect of anti-VEGF therapy in patients with PEDs associated with wet AMD.

Tear of the Retinal Pigment Epithelium

RPE tears are most commonly seen in association with CNV secondary to AMD, especially when a PED is present.[128,129] RPE tears may also be associated with central serous chorioretinopathy (CSC), trauma, as well as other causes of CNV.[130,131] Although RPE tears can occur spontaneously in AMD patients, they have also been related temporally to various treatments for AMD, such as verteporfin photodynamic therapy and intravitreal injection of anti-VEGF agents.[132–136] Hemodynamic factors play a role in the pathogenesis of the tear. The RPE layer is put on stretch as a result of accumulating sub-RPE fluid, and this stress leads to a tear in the RPE. A sheet of RPE cells then contracts and scrolls up upon itself in a radial fashion, leaving an area of retina without underlying RPE.[129,137] Subretinal and sub-RPE hemorrhages frequently accompany an RPE tear, which appears ophthalmoscopically as an area of well-demarcated hyperpigmentation immediately adjacent to an area of relative hypopigmentation.

On OCT imaging, an area of discontinuity in a large PED is often seen, with the free edge of the RPE often curled under the PED. Adjacent to the tear, there is increased reflectivity from the choroid vessels, due to the absence of the RPE. The overlying retina is typically intact, but may be separated from the area of atrophy by subretinal fluid.[129] The tear tends to occur at the base of the PED, near or at the intersection of attached and detached retina (Fig. 3.22).[128] During anti-VEGF therapy, the height of the PED and the irregular surface contour may help in predicting the risk for RPE tear, which may also occur without treatment as part of normal disease progression.[138,139] The visual outcome in patients with RPE tears is generally poor when the fovea is involved.

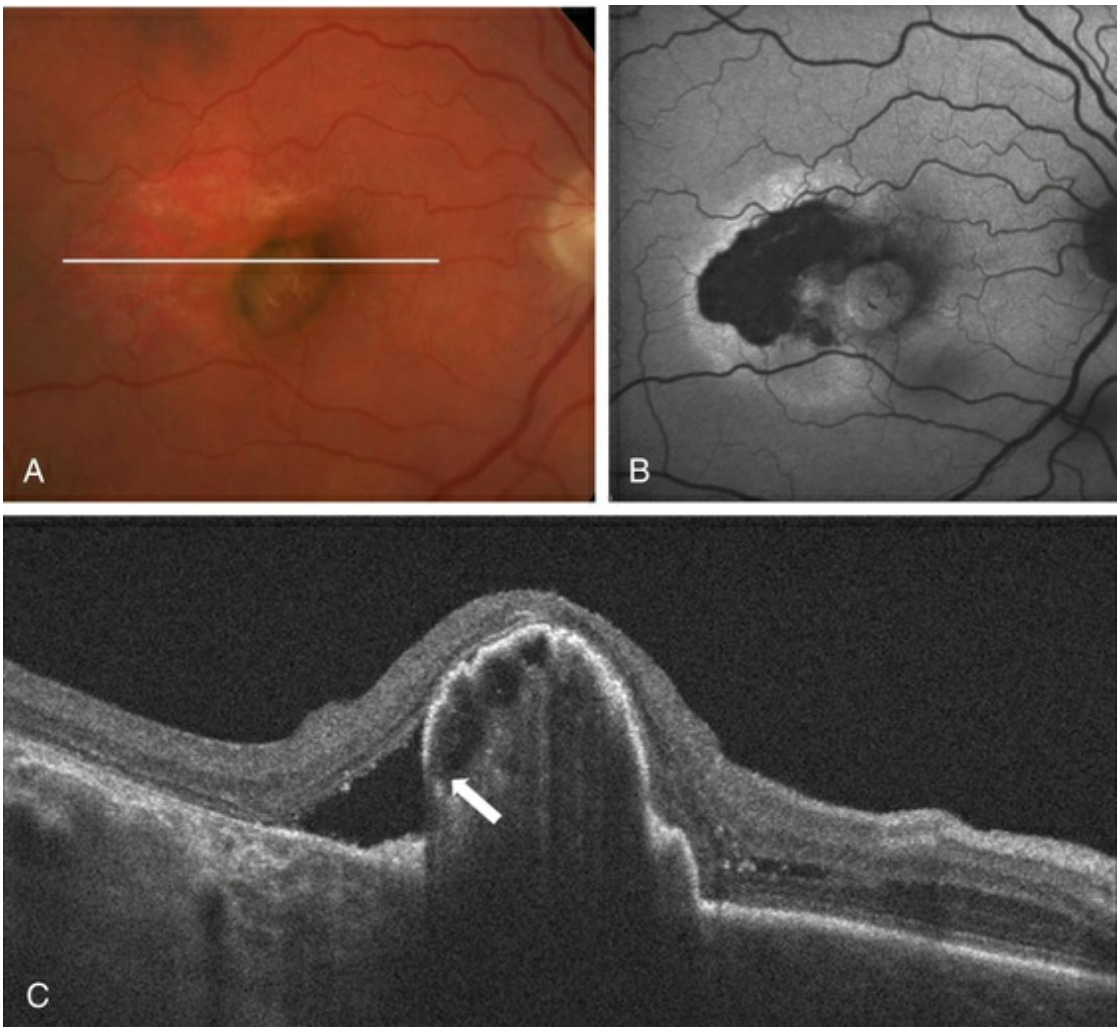

FIG. 3.22 Retinal pigment epithelium (RPE) tear. (A) Color image of the right eye of an 81-year-old man with an area of relative hypopigmentation that corresponds to the RPE tear. (B) Heidelberg fundus autofluorescence showing hypoautofluorescence in the area where the RPE is absent. (C) On the B-scan there is an area of discontinuity of the RPE near the base of the pigmented epithelium detachment with the free edge of the RPE curled under the pigmented epithelium detachment (*arrow*).

Disciform Scarring

Disciform scarring and subretinal fibrosis mark the endstage of CNV. The vascular components of CNV typically regress as the lesion becomes less active, and the fibrous components typically increase, resulting in disciform scar formation. Clinically the scar appears as smooth, elevated white or gray tissue in the subretinal

space, and on OCT imaging the scar corresponds to a highly reflective outer retinal or subretinal lesion (Fig. 3.23).[30] Scar formation may be associated with loss of the overlying photoreceptor layer and irreversible reduction in visual acuity. This may be observed on OCT imaging as a disruption of the IS/OS junction and ELM.[140,141] In this stage of the disease, the OCT is very helpful in identifying the presence of subretinal fluid or intraretinal cysts that are associated with the neovascular activity of the lesion, and may help in making the retreatment decision.

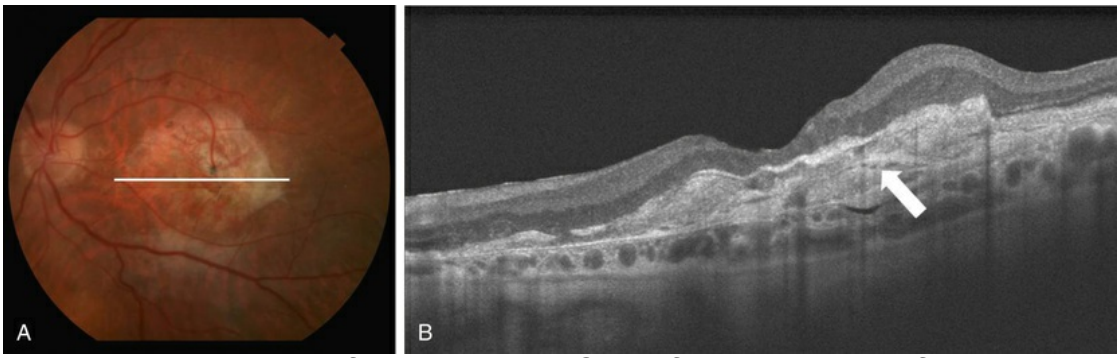

FIG. 3.23 Disciform scar. (A) Color fundus image of the left eye of an 80-year-old woman with a white-grayish tissue involving the macula. (B) Horizontal B-scan with a large hyperreflective lesion under the retina (*arrow*).

Retinal Angiomatous Proliferation

The term "retinal angiomatous proliferation" was introduced by Yannuzzi and coworkers to describe a form of neovascularization in AMD patients, which arises from within the retina with possible formation of a retinochoroidal anastomosis as the disease progresses.[142] Whether the development of the retinochoroidal anastomosis is a result of a primary intraretinal neovascularization or a sub-RPE lesion remains controversial.[142,143] Recently, studies with SD-OCT imaging concluded that the initial neovascular process could originate from either the retinal or choroidal circulation; however, histopathologic studies suggest that all the neovascularization is within the retina.[144,145] On OCT imaging, the most common feature is the presence of a serous PED with CME

overlying the PED (Fig. 3.24).[144,146,147] An intraretinal hyperreflective angiomatous complex consistent with the intraretinal neovascularization and subretinal fluid may also be seen.[142] A recent analysis of the natural evolution of RAP lesions (also termed Type 3 neovascularization), revealed that pigment migration typically precedes the development of RAP, leading to the hypothesis that elaboration of angiogenic factors from migrated RPE may be important in the initiation of these lesions.[101]

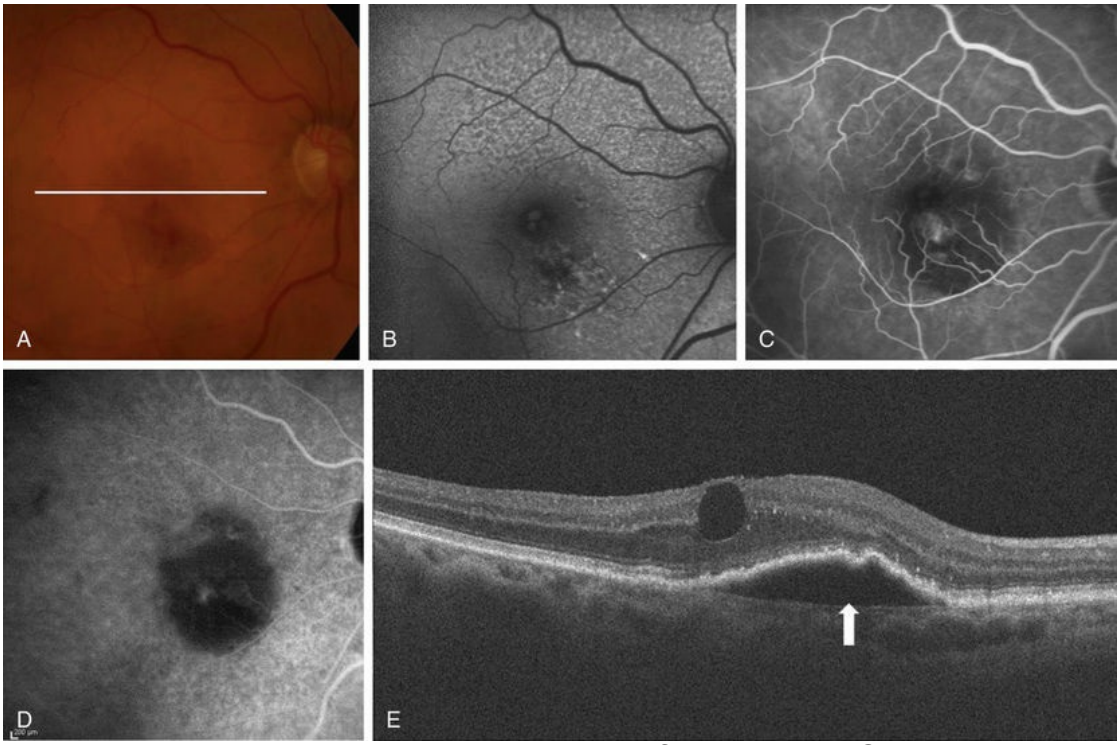

FIG. 3.24 Retinal angiomatous proliferation. (A) Color fundus image of the right eye of a 90-year-old woman with a history of blurred vision and metamorphopsia for 2 weeks. Visual acuity was 20/40. Fundus examination revealed multiple drusen, pigmentary changes, and hemorrhage inferior to the fovea with a subtle elevation of the retina. (B) Fundus autofluorescence demonstrates hypoautofluorescence in the area corresponding to the hemorrhage. (C) Fluorescein angiography demonstrates a focal area of leakage inferior to the fovea. (D) Late-phase indocyanine green angiography reveals a hot spot. (E) B-scan through the lesion reveals a retinal pigment epithelium detachment (*arrow*) with cystoid macular edema overlying the pigmented epithelium detachment.

Polypoidal Choroidal Vasculopathy

Polypoidal choroidal vasculopathy is considered a variant form of CNV characterized by the presence of multiple vascular saccular dilations (polyps) in the choroidal circulation that manifests clinically with variably sized serous and serosanguineous detachments of the neurosensory retina and RPE, usually around the optic nerve or in the central macula.[148] Indocyanine green angiography (ICGA) is particularly useful in imaging the polypoidal abnormalities seen in polypoidal choroidal vasculopathy, with a branching vascular network of vessels ending in polyp-like structures.[149] SD-OCT images can demonstrate the polypoidal structure beneath the RPE, which remains adherent to the RPE, even with increased exudation. It is especially useful to detect the abnormalities surrounding the polypoidal lesions such as intraretinal, subretinal, and sub-RPE fluid.[150,151]

Choroidal Neovascularization: Response to Treatment

The combination of clinical examination, fluorescein angiography, OCT images, and, less frequently, ICGA is usually required to diagnose neovascular AMD and exclude other macular conditions that can mimic the features of neovascular AMD.[152] With the use of anti-VEGF drugs the ideal strategy for following eyes with wet AMD has evolved from monthly injections to OCT imaging to determine whether the treatment is effective in resolving the macular fluid.[153,154] Many alternative treatment regimens have used OCT-guided strategies, with good visual and anatomical results with fewer intravitreal injections compared with monthly dosing.[155–159] The macular fluid can be identified by examining the B-scans and reviewing the retinal thickness maps, which calculate the retinal thickness between the ILM and the RPE segmentation maps. The effect of anti-VEGF therapy can then be assessed based on the qualitative appearance of the B-scans and the qualitative, as well as quantitative, changes in the retinal thickness maps (Figs. 3.18 and 3.25). The presence or recurrence of intraretinal or subretinal fluid has to be differentiated from the appearance of "outer retinal tubulation" since the latter represents a

rearrangement of photoreceptors in response to injury and RPE loss and is usually present in patients with chronic and advanced neovascular AMD (Fig. 3.26). Importantly, this tubulation does not respond to anti-VEGF therapy.[160] In patients with PEDs, the area and volume of the lesion can be assessed and used to monitor the effect of anti-VEGF therapy in patients with wet AMD associated with PEDs, and an increase in the area and volume of PEDs could be used to indicate when retreatment is necessary.

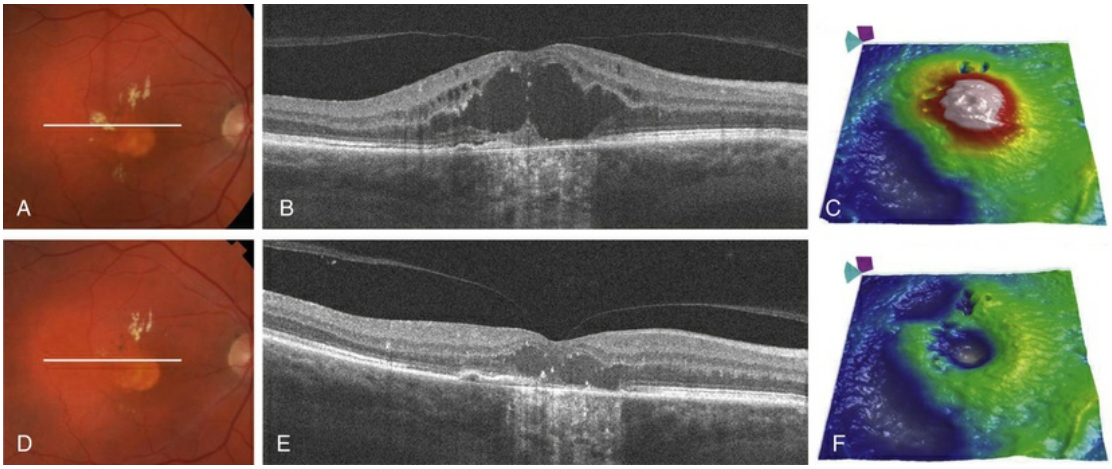

FIG. 3.25 Neovascular age-related macular degeneration (response to treatment). Color fundus image, horizontal B-scan, and retinal thickness map of the right eye of a 65-year-old man with wet age-related macular degeneration before (A–C) and after (D–F) a single treatment with intravitreal anti-vascular endothelial growth factor. Observe the improvement of the intraretinal fluid and cysts in the B-scans (B,E) and the decrease in retinal thickness (C,F).

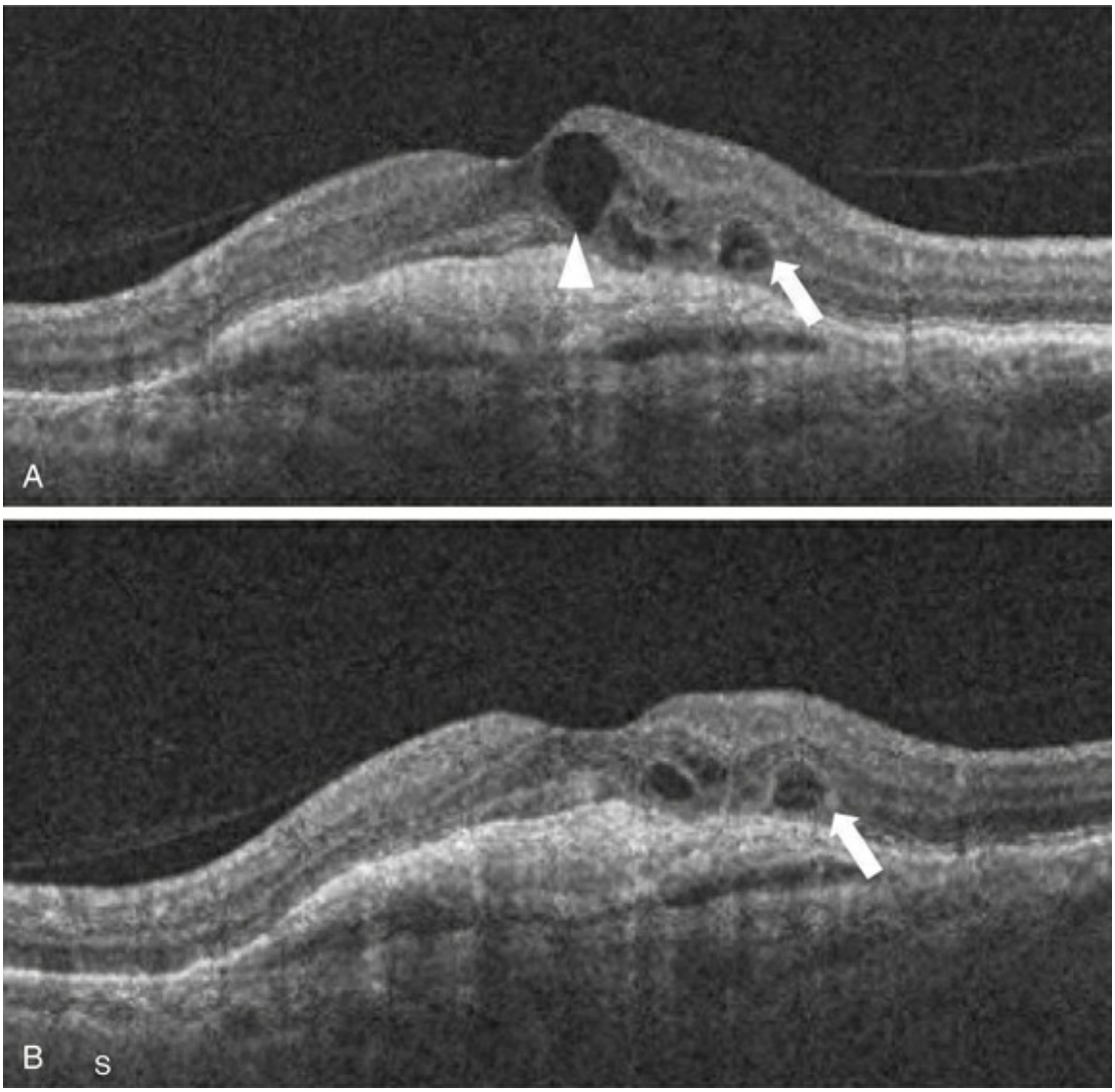

FIG. 3.26 Outer retinal tubulation: a 67-year-old woman with wet age-related macular degeneration who has received 13 intravitreal injections over the last 2 years. The foveal horizontal B-scans before (A) and after the last (B) treatment are presented. The larger intraretinal cyst present in the image before treatment (*arrowhead*) disappeared after treatment. The small cyst (*arrow*) showed no response to the intravitreal injection of anti-vascular endothelial growth factor. This smaller cyst corresponds to an outer retinal tubulation which is frequently present in patients with chronic and advanced neovascular age-related macular degeneration.

Central Serous Chorioretinopathy

CSC is an idiopathic syndrome that typically affects young to middle-aged males and is characterized by serous detachment of the neurosensory retina. Focal and multifocal areas of leakage secondary to increased permeability of the choroidal vessels and a barrier defect at the level of the RPE have been described in the pathogenesis of this disorder.[161–163]

Presenting symptoms include central vision loss, a decrease in vision that can be corrected with an increased hyperopic correction, metamorphopsia, central scotoma, and decreased color saturation. The symptoms are usually self-limited but can recur in the same or the opposite eye. In most cases, CSC resolves spontaneously within 6 months, with a good visual prognosis. However, prolonged and recurrent macular detachment in some cases may cause degenerative changes in the subfoveal RPE and neurosensory retina with poor visual outcome.[164,165]

The primary pathology of acute CSC is thought to begin with disruption of the choroidal circulation. The RPE then decompensates, and exudation from the choroidal vasculature passes into the subretinal space. These hypotheses were based on fluorescein angiography and ICGA findings.[162,166–169] The development of OCT imaging has provided a better understanding of CSC, especially the abnormalities in the RPE layer.[170–174]

There are two forms of the disease, acute and chronic. Acute CSC (Fig. 3.27) is classically unilateral and characterized by one or more focal leaks at the level of the RPE on fluorescein angiography. The chronic form (Fig. 3.28) is believed to be due to diffuse RPE disease and is usually bilateral. It presents with diffuse RPE atrophic changes, varying degree of subretinal fluid, RPE alterations, and RPE tracks. It is characterized by diffuse RPE leakage on fluorescein angiography.

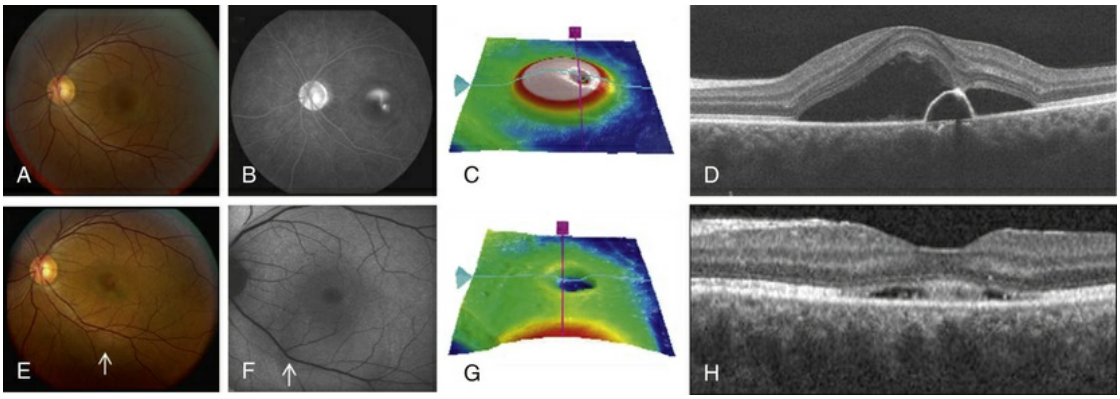

FIG. 3.27 Acute central serous chorioretinopathy. (A) Color photo shows a well-defined, circular area of retinal elevation. (B) Fluorescein angiography shows an area of hyperfluorescence with "smokestack" leakage. (C) Retinal thickness map shows elevation of the retina. (D) Spectral domain optical coherence tomography (OCT), horizontal, acquired through the fovea, shows serous detachment of the neurosensory retina above an optically clear, fluid-filled cavity, associated with a pigment epithelial detachment. The retinal pigment epithelium detachment corresponds to the area of hyperfluorescence seen on the angiogram. (E–H) Follow-up visit 1 month later. (E) Color photo shows resolution of the retinal elevation in the area of the fovea but illustrates a well-defined, circular area of retinal elevation inferior to the fovea (*small arrow*). (F) Fundus autofluorescence shows a well-defined, circular area of retinal elevation inferior to the fovea involving the inferior arcade (*small arrow*). (G) Retinal thickness map shows decrease in the thickness of the retina in the fovea. (H) Spectral domain OCT, horizontal B-scan acquired through the fovea, shows decrease in the amount of subretinal fluid.

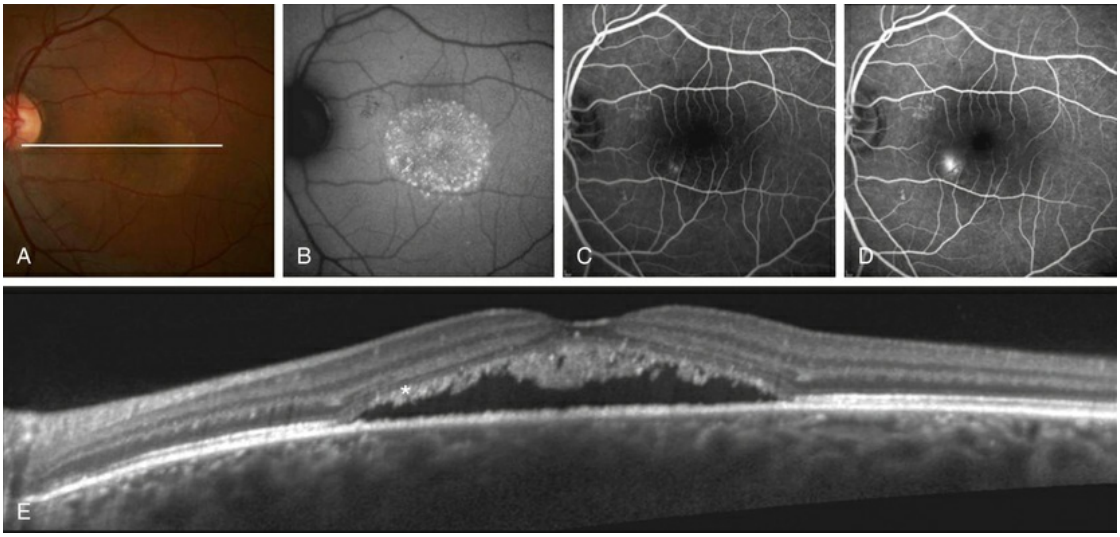

FIG. 3.28 Central serous chorioretinopathy. (A) Color photo shows a well-defined, circular area of retinal elevation: white line represents the location of the B-scan. (B) Fundus autofluorescence shows an area of hyperfluorescence. (C,D) Fluorescein angiography shows an inkblot appearance that leaks later. (E) Spectral domain optical coherence tomography shows serous detachment of the neurosensory retina associated with an irregular, granulated retinal pigment epithelial layer and sagging/dipping of the posterior layer of the neurosensory retina (*asterisk*).

OCT imaging is helpful in diagnosing and managing patients with CSC. OCT imaging can noninvasively identify the presence and extent of subretinal fluid and PEDs. OCT imaging is also useful for assessing the resolution of subretinal fluid and the morphologic retinal changes during normal disease progression. OCT is more sensitive than clinical exam and fluorescein angiography in identifying small amounts of subretinal fluid.[175] OCT is useful in predicting the recovery of visual acuity and explaining poor visual outcomes even after the resolution of the fluid. With SD-OCT imaging, topographic changes in CSC can be visualized with two- and three-dimensional reconstructions. SD-OCT also offers the ability of exact localization of the pathology and accurate volumetric measurements.[176]

OCT features of acute CSC include thickening of the neurosensory retina within the area of retinal detachment, PED, the presence of fibrinous exudates in the subretinal space, and the

shaggy outer segments of the neurosensory retina above the leakage site. OCT features of the chronic form include foveal atrophy, retinal thinning, and cystoid degenerative changes.[171,172,177–181] OCT can also visualize the subretinal yellow deposits as highly reflective material. Precipitates are not only on the posterior surface of the detached retina but also in the detached neurosensory retina. Photoreceptor segment morphologic changes along the detached retina show elongation of the photoreceptor outer segments and decreased thickness of the outer nuclear layer.[182] Accumulation of abnormal outer segments in the neurosensory retina is related to clinical manifestation on OCT as a granulated shaggy profile of the outer surface of the detached retina.[183]

En face OCT imaging has been found to detect alterations of the RPE in the form of a PED or a small defect in the RPE. Most alterations of RPE are associated with choroidal abnormalities.[174] OCT imaging has been found to detect morphologic changes at the point of dye leakage in eyes with CSC. Transverse images (C-scans) have shown serous retinal detachments and irregular lesions of the RPE. These findings, along with other findings on B-scans and segmentation maps, are consistent with location of lesions in areas of fluorescein angiographic leakage.[184,185]

Visual prognosis in patients with CSC can be linked to retinal morphologic changes by OCT.[186,187] Mastsumoto et al. correlated the visual outcome with the preservation of outer nuclear layer thickness and continuity of photoreceptor IS/OS in resolved CSC. The outer nuclear layer thickness was positively correlated with visual acuity. Discontinuity of the IS/OS line was prevalent in eyes with thinner outer nuclear layer and lower visual acuity.[187] Ojima et al.[186] reported that microstructural changes occur in the photoreceptor layer of the detached retina and the visualization of the ELM and the photoreceptor layer correlates with visual function. Foveal thickness can be a predictor of visual outcome in patients with CSC.[178] Both foveal thickness and visual acuity have been observed to be proportional to the duration of symptoms, Foveal attenuation, and atrophy, which may be a consequence of prolonged absence of contact between photoreceptor and RPE cells.[175]

Enhanced-Depth Imaging OCT in CSC

Conventional SD-OCT has a limited ability to image the choroid because of scattering by the pigment granules within the RPE and by the pigment and blood within the choroid, and because of a depth-dependent roll-off in sensitivity of SD-OCT instruments in general.[40] A method to improve imaging of the choroid, known as EDI OCT, showed that eyes with CSC had a much thicker choroid compared with normal eyes (Fig. 3.29).[188] Fellow eyes of patients with CSC were also found to have thicker choroids compared with age-matched normal eyes.[189] Maruko et al. reported a thickened choroid in CSC and the association with choroidal vascular hyperpermeability on ICG angiography.[190]

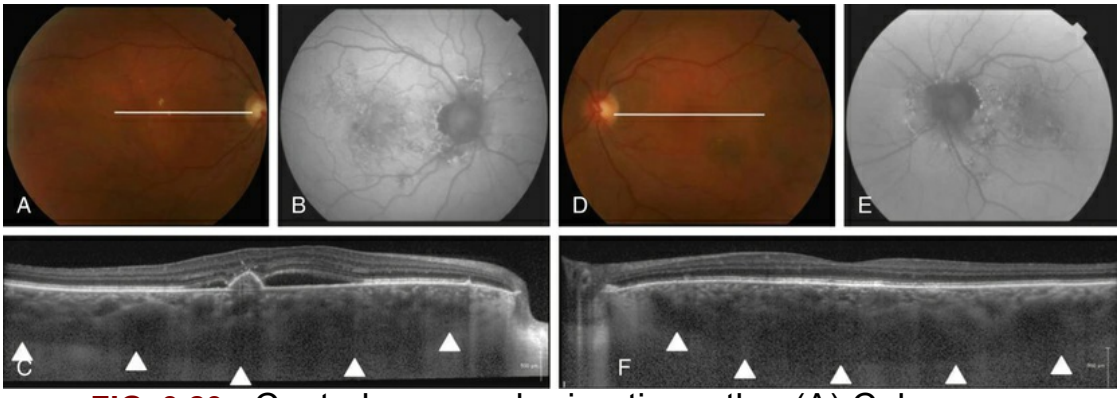

FIG. 3.29 Central serous chorioretinopathy. (A) Color photo of the right eye shows area of retinal elevation with pigmentary changes; white line represents the position of B-scan. (B) Fundus autofluorescence shows an area of hyperfluorescence and hypofluorescence. (C) Spectral domain optical coherence tomography (SD-OCT), enhanced depth imaging, shows serous detachment of the neurosensory retina along with pigmented epithelium detachment, retinal pigment epithelial alterations, granulated posterior detached retina, and thick choroid (*arrowheads* represent the outer boundary of the choroid). (D) Color photo of the left eye shows pigmentary changes without retinal elevation; white line represents location of B-scan. (E) Fundus autofluorescence shows an area of hyperfluorescence and hypofluorescence. (F) SD-OCT, enhanced depth imaging, demonstrates a thick choroid (*arrowheads*

represent the boundary of the choroid) without serous detachment of the neurosensory retina.

Verteporfin photodynamic therapy is one of the therapies used to treat leakage and subretinal fluid in eyes with CSC. Maruko et al.[190] reported that eyes treated with focal laser showed no alteration in choroidal thickness even though there was fluid reabsorption, but eyes treated with verteporfin photodynamic therapy showed a decrease in choroidal thickness by SD-OCT imaging and a decrease in choroidal hyperpermeability seen during ICG angiography. The changes occurring in the choroid after photodynamic therapy may reflect a more normalized choroidal permeability.

Cystoid Macular Edema

CME is an important cause of reduced visual acuity in a wide variety of retinal diseases such as diabetic retinopathy, retinal vein occlusion, CNV, retinal dystrophies, uveitis, and following intraocular surgery. Regardless of the underlying etiology, CME appears as retinal thickening with intraretinal cavities of reduced reflectivity on OCT (Fig. 3.30).

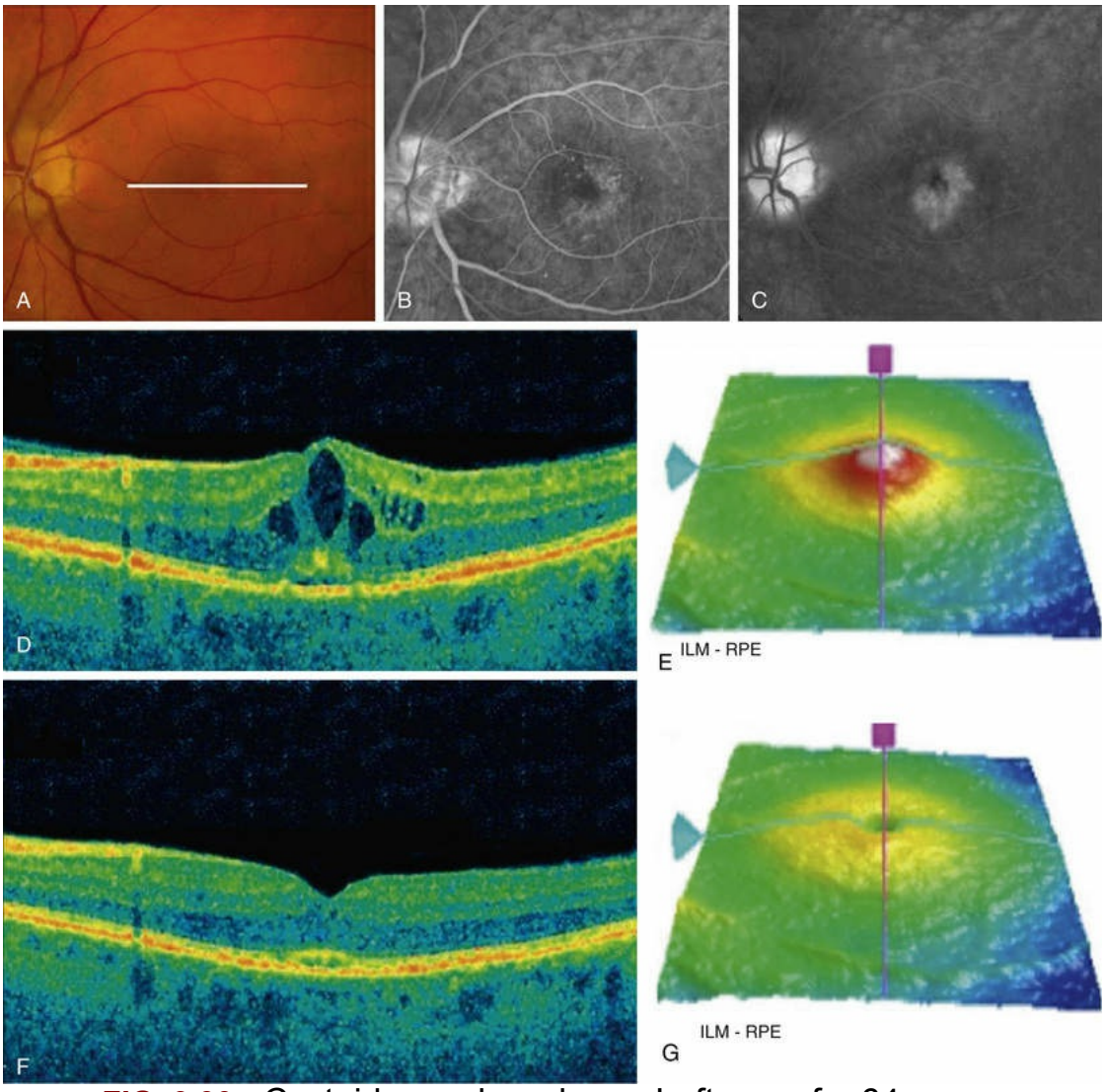

FIG. 3.30 Cystoid macular edema. Left eye of a 64-year-old man 30 days after phacoemulsification. The visual acuity was 20/50. (A) Color fundus image with some cystic changes: white line represents where the B-scan was acquired. (B,C) Fluorescein angiography showing the classic petaloid leakage pattern. (D) B-scan showing the intraretinal cysts as hyporeflective spaces within the retina. (E) Retinal thickness map showing increased retinal thickness due to the presence of cysts. (F,G) Same patient after 45 days of treatment with topical nonsteroid anti-inflammatory medication. The retinal thickness decreased and the intraretinal cysts disappeared. ILM, internal limiting membrane; RPE, retinal pigment epithelium.

Clinically significant pseudophakic CME is estimated to occur in 1–2% of patients undergoing cataract extraction.[191,192] Inflammatory

components induced by surgery along with mechanical forces induced by a modified vitreous are responsible for the macular changes in these patients.[193,194] The diagnosis based only on fundus examination can be challenging, and usually fluorescein angiographic imaging, which shows a classic petaloid pattern of leakage, or OCT imaging is needed for confirmation. OCT has the advantage of being a faster and noninvasive imaging technique, which can also provide quantitative assessment of the macular thickness that can be used to monitor the clinical course and to make therapeutic decisions.

Diabetic Retinopathy

Diabetic retinopathy is the leading cause of blindness in individuals under 65 years of age in the United States, with diabetic macular edema (DME) being the principal cause of vision loss in these patients.[195,196] Diabetic retinopathy can be classified into nonproliferative diabetic retinopathy (NPDR) and proliferative diabetic retinopathy (PDR).

Nonproliferative Diabetic Retinopathy and Diabetic Macular Edema

The important role of OCT in DME management involves the evaluation of retinal pathology, including retinal thickness, CME, intraretinal exudates, vitreomacular interface abnormalities, subretinal fluid, and photoreceptor IS/OS junction abnormalities. OCT is also important in monitoring the response to treatment of DME by laser, intravitreal pharmacotherapies, and vitreoretinal surgery.

Diagnosis of macular edema can be difficult with biomicroscopy or color fundus imaging, especially when the edema is mild.[197–199] It has been suggested that OCT measurements may be a more sensitive and reproducible indicator of true change in retinal thickness than color fundus imaging, supporting the use of OCT as the principal method for documenting retinal thickness. However, OCT is less suitable than fundus imaging for documenting the location and severity of other morphologic features of diabetic retinopathy, such as hard exudates, retinal hemorrhages,

microaneurysms, and vascular abnormalities. Furthermore, OCT cannot provide information on overall retinopathy severity, for which color photographs remain the gold standard.[200–203]

OCT can be used to distinguish patients with normal retinal contour and thickness despite extensive angiopathy from those with early retinal edema. In general, the DME can be classified into several categories: diffuse retinal thickening, CME, serous retinal detachment or subretinal fluid, and vitreomacular interface abnormality.[204–206] Diffuse retinal thickening is usually defined as a sponge-like swelling of the retina with a generalized, heterogeneous, mild hyporeflectivity compared with normal retina. CME is characterized by the presence of intraretinal cystoid areas of low reflectivity, which are typically separated by highly reflective septa (Fig. 3.31). Serous retinal detachment is defined on OCT as a focal elevation of neurosensory retina overlying a hyporeflective, dome-shaped space. The posterior border of the detached retina is usually highly reflective, which helps to differentiate subretinal from intraretinal fluid. Vitreomacular interface abnormalities include the presence of ERMs, VMT, or both. Intraretinal focal hyperreflections that correspond clinically to retinal exudates are a frequent finding in all the patterns described above.

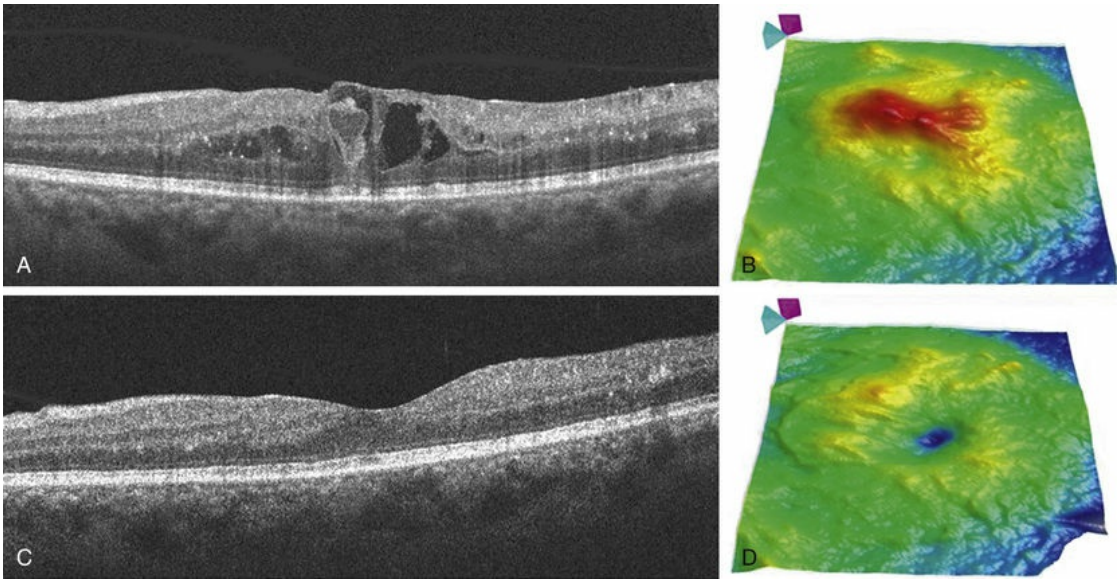

FIG. 3.31 Diabetic macular edema. Right eye of a 43-year-old woman with type 2 diabetes and moderate nonproliferative diabetic retinopathy. (A) B-scan and

(B) retinal thickness map showing diffuse macular edema and the presence of intraretinal cysts with an increased retinal thickness. (C) B-scan and (D) retinal thickness map of the same patient after 3 months of intensive blood sugar control and focal laser therapy. The intraretinal cysts disappeared and the retinal thickness map shows an important decrease in the retinal thickness.

OCT has become widely accepted in monitoring progression and treatment response in patients with DME. Prior to OCT imaging, precision in central retinal thickness monitoring was not possible. The ETDRS provided guidelines for laser management of patients with DME.[207–209] Although OCT was not available for use in this study, quantitative retinal thickness maps can be used to direct laser therapy and may be better than using biomicroscopy alone. In the era of pharmacotherapy, many agents like triamcinolone and anti-VEGF agents (ranibizumab and bevacizumab) have been studied to treat DME. In these studies, OCT played an important role in determining the retinal thickness and the treatment response.[210,211] The treatment response of each OCT pattern of DME has been shown to be different.[212] Patients with diffuse retinal thickening may achieve a greater reduction in retinal thickness and a greater improvement in visual acuity compared with patients exhibiting CME, subretinal fluid, or vitreomacular interface abnormality.[212,213]

Macular traction has become increasingly recognized in patients with DME, especially in eyes with persistent edema after focal laser or pharmacologic treatment. These patients often show the clinical appearance of a thick posterior hyaloid with diffuse fluorescein leakage. Recognition of this condition can be difficult using the clinical exam alone. This is readily recognized on OCT imaging as diffuse cystoid retinal thickening, a flat-appearing foveal contour, and a thickened hyperreflective linear vitreoretinal interface. Focal vitreoretinal adhesions that cannot be identified on clinical exam are also often evident on OCT.[214,215] These findings can direct the decision as to whether to proceed with pars plana vitrectomy and membrane peeling.[216]

Furthermore, the improvement in axial resolution with SD-OCT

has enhanced the ability to evaluate foveal microstructural abnormalities, including the photoreceptor IS/OS junction or EZ, which may reveal damage to macular photoreceptors. Several studies have demonstrated that an intact IS/OS junction or EZ is predictive of a better visual acuity in patients after treatment for DME.[217–219]

Proliferative Diabetic Retinopathy

PDR can be visualized with OCT imaging as highly reflective preretinal bands anterior to the retinal surface consistent with preretinal fibrovascular or fibroglial proliferation. Diffuse retinal thickening, distortion, and irregularity of the retinal contour can also occur as a result of the contraction of these preretinal membranes. An associated traction retinal detachment may be observed as well. OCT imaging is valuable in determining the extent of the tractional component as well as the presence of foveal involvement, assisting in the decision to intervene surgically (Fig. 3.32).[30] The decision for surgery typically hinges on the progressive nature of the traction and the degree to which the macula is affected by the traction.

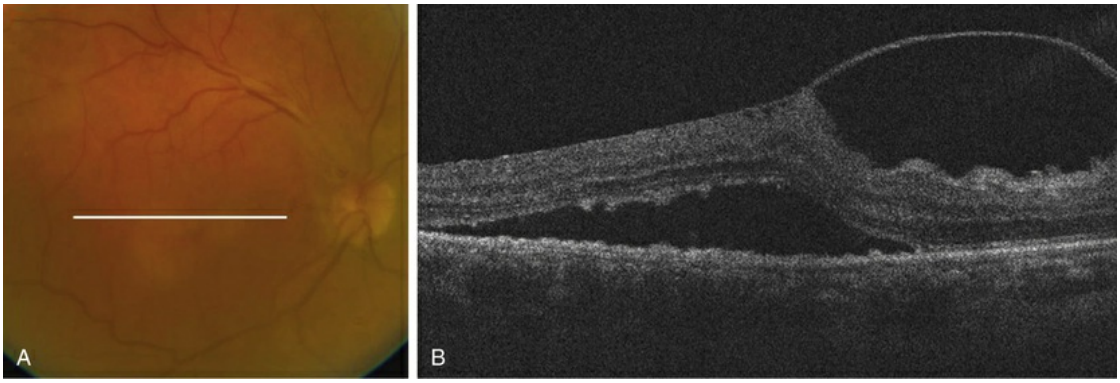

FIG. 3.32 Diabetic retinal tractional detachment. (A) Color fundus image of the right eye of a 72-year-old woman with proliferative diabetic retinopathy. (B) Foveal B-scan of the same patient showing a thick posterior hyaloid distorting the retinal architecture with traction and accumulation of fluid under the retina.

Retinal Vein Occlusion

Retinal vein occlusions have been defined as retinal vascular disorders characterized by engorgement and dilatation of the retinal veins with secondary, mostly intraretinal, hemorrhages and mostly intraretinal (and partially subretinal) fluid, retinal ischemia, including cotton-wool spots, and retinal exudates.[220] Retinal vein occlusions are commonly divided into central retinal vein occlusion and branch retinal vein occlusion, and as soon as the foveal region is involved with macular edema, central visual acuity may be affected.

In retinal vein occlusions, OCT can display intraretinal cysts responsible for the increase in retinal thickness often associated with serous detachment of the neurosensory retina. Retinal cysts can be numerous and confluent, forming large central cystoid spaces. Associated findings can be observed, such as vitreous macular adherence, ERM, and hyperreflectivity of the posterior layer corresponding to atrophy or fibrosis of the RPE, subretinal accumulation of material, subretinal fibrosis, lamellar macular hole formation, intraretinal lipid exudates, and intraretinal hemorrhage (Fig. 3.33).

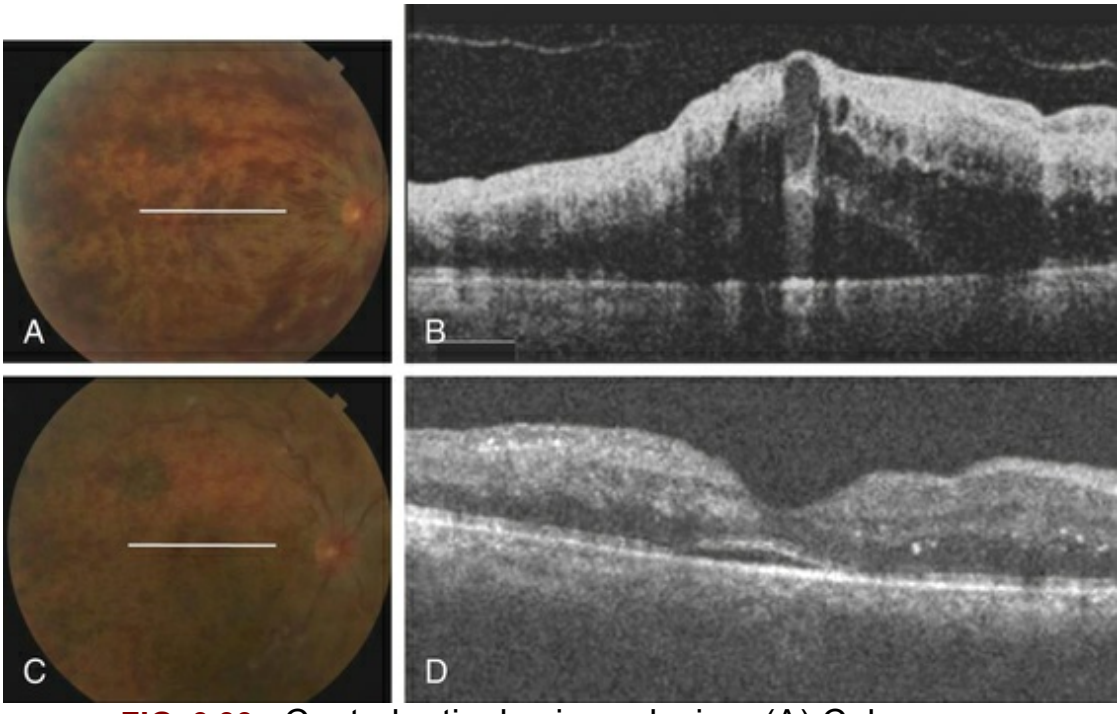

FIG. 3.33 Central retinal vein occlusion. (A) Color

photo of the right eye shows optic nerve head edema, dilated tortuous retinal veins, scattered intraretinal hemorrhages in all quadrants, and macular edema: white line represents the location of the B-scan. (B) Spectral domain optical coherence tomography (SD-OCT) obtained through the fovea illustrates loss of normal foveal contour and marked and diffuse retinal thickening. Large areas of low intraretinal reflectivity consistent with cystic fluid accumulation and edema were seen. A detachment of the neurosensory retina with subretinal fluid was observed below the fovea. (C) Color photo of the right eye 1 month after bevacizumab injection shows dilated tortuous retinal veins and scattered intraretinal hemorrhages in all quadrants: white line represents area of B-scan. (D) SD-OCT, 1 month after bevacizumab injection obtained through the fovea, shows that macular edema almost completely disappeared with a small amount of residual subretinal fluid. Improvement in the normal foveal contour and decrease in the retinal thickening and edema. Areas of high intraretinal reflectivity consistent with the hemorrhages.

Ota et al. reported that, in branch retinal vein occlusion, visual function and recovery of vision are correlated with thickness of the central macula, and that is correlated with the integrity of the inner and outer segments of the photoreceptors in the fovea.[221] SD-OCT imaging helps to quantify the amount of CME. The accumulation of fluid can be located mostly within the retinal layers or additionally in the subretinal space.[222] Anti-VEGF therapy is increasingly used to treat macular edema in patients with retinal vein occlusions. Nevertheless, a significant proportion of eyes retain poor visual acuity despite treatment. Several studies have shown that low visual acuity has been associated with a poor functional outcome after treatment or during the natural course (Fig. 3.34). SD-OCT can help predict visual acuity based on the integrity of the neurosensory retina.

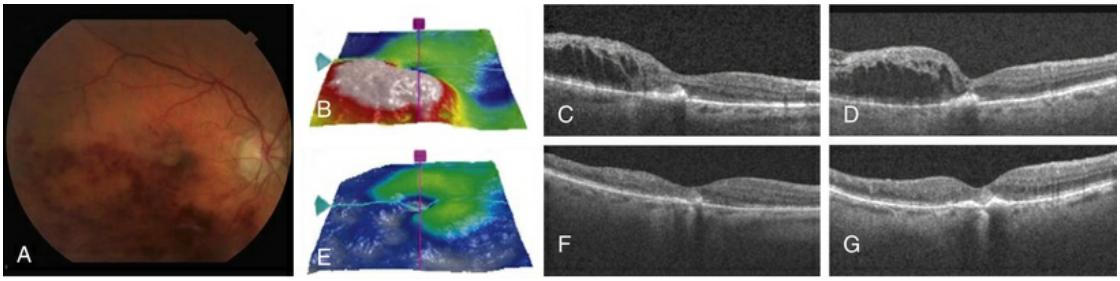

FIG. 3.34 Branch retinal vein occlusion. (A) Color photo of the right eye shows dilated tortuous retinal veins, flame-shaped hemorrhages in an arcuate configuration in the distribution of inferotemporal branch retinal vein occlusion, and macular edema. (B) Retinal thickness map showing increase in retinal thickness. (C,D) Spectral domain optical coherence tomography (SD-OCT) horizontal and vertical scan respectively obtained through the fovea revealed that marked retinal thickening, areas of low intraretinal reflectivity consistent with cystic fluid accumulation, and edema were identified, especially in the outer plexiform layer. High reflectivity is noted in the inner layers from intraretinal hemorrhage. (E) Retinal thickness map 1 month after bevacizumab injection, showing decrease in retinal thickness. (F,G) SD-OCT horizontal and vertical scan respectively, 1 month after bevacizumab injection, obtained through the fovea showed complete resolution of macular edema, improvement in foveal contour, and decrease in retinal thickening.

Central Retinal Artery Occlusion

Central retinal artery occlusion shows a distinct pattern on OCT images. In the acute phase, OCT images demonstrate the increased reflectivity and thickness of the inner retina and a corresponding decrease of reflectivity in the outer layer of the retina and RPE/choriocapillaris layer. Follow-up OCT images demonstrate a decrease in the reflectivity and thickness of the inner retinal layers and a corresponding increase of reflectivity in the outer retina and RPE/choriocapillaris layer compared with the baseline OCT image, suggesting a generalized atrophy of the neurosensory retina as a late finding. Therefore, the use of OCT may help facilitate prompt

recognition of acute and chronic central retinal artery occlusion. In patients with central retinal artery occlusion, OCT images closely correspond with known histopathologic changes. Histology following acute central retinal artery occlusion shows retinal changes limited to the nerve fiber and ganglion cell layers. There are profound losses of ganglion cells and diffuse edema of the inner retinal layers with little change seen in the deeper retinal layers supplied by choroidal vessels. OCT images provide an in vivo view of the retinal structure following central retinal artery occlusion. Increased reflectivity of the inner retina, presumably because of opacification of the ganglion cell and nerve fiber layers, corresponds to previously described histologic findings of "cloudy swelling" of these layers. Attenuation of reflectivity in the outer layer of the retina and the RPE/choriocapillaris layer is due to the ganglion cell and nerve fiber changes allowing less light reflected back from the outer portions of the retina. Further evidence of this phenomenon is at the foveal depression where the ganglion cell layer is absent. As more light is allowed through the fovea, the RPE/choriocapillaris layer directly beneath the fovea shows a relative increase in reflectivity compared with the other regions of the RPE/choriocapillaris. An additional finding on OCT imaging is the thinning and atrophy in the affected area of the retina, which occurs after a period of time (Fig. 3.35).[223]

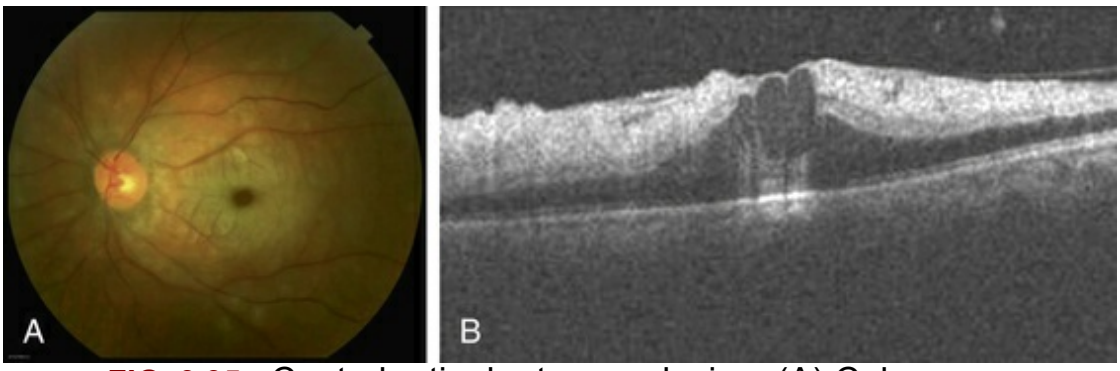

FIG. 3.35 Central retinal artery occlusion. (A) Color photo of the left eye shows cherry-red spot appearance, retinal opacity of posterior fundus, most marked in the parafoveal region, and a small area of normal retina temporal to the optic disc corresponding to the patent cilioretinal retinal artery. (B) Spectral

domain optical coherence tomography horizontal scan through the fovea illustrates increased thickness and hyperreflectivity of the inner retinal layers, denoting the presence of intracellular edema, with decreased reflectivity of photoreceptor and retinal pigment epithelial layers because of the shadowing effect.

Branch Retinal Artery Occlusion

Branch retinal artery occlusions are usually embolic in nature. The embolic source is either a carotid artery atheroma or myocardial thrombus. The embolus usually lodges at the bifurcation of the central retinal artery into the branch retinal artery. Histopathologically, acute branch retinal artery occlusions reveal ischemia in the corresponding retinal quadrant marked by inner retinal edema at the initial stage followed by atrophy in longstanding cases. SD-OCT imaging shows the edematous inner retina, comprising the inner nuclear layer, inner plexiform layer, and ganglion cell layer, as a hyperintense band with increased thickness, which is contrasted by the normal reflectivity and thickness of the corresponding layers of the unaffected macular regions. Prolonged ischemia results in consecutive atrophy of these layers with each layer exhibiting differential sensitivity to the underlying hypoxia. Animal experiments have revealed retinal ganglion cells to be relatively resistant to the ischemia compared to the other retinal neurons.[224] Similar findings in vivo using SD-OCT imaging revealed the relative preservation of ganglion cell layer as opposed to the thinning of the inner plexiform and nuclear layers (Fig. 3.36).[225]

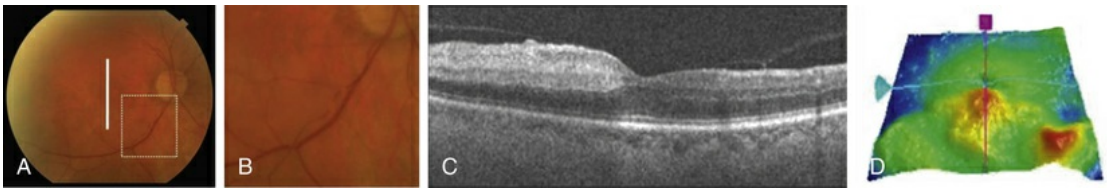

FIG. 3.36 Branch retinal artery occlusion. (A) Color photo of the right eye shows area of whitening in the distribution of an inferotemporal retinal arteriole: white vertical line represents location of B-scan; square

dotted line represents area of embolus in arteriole which is magnified. (B) Embolus was appreciated in the inferior retinal arteriole next to the optic nerve. (C) Spectral domain optical coherence tomography (OCT) vertical scan through the fovea illustrates increased thickness and hyperreflectivity of the inner retinal layers in the inferior perifoveolar area, denoting the presence of intracellular edema, with decreased reflectivity of photoreceptor and retinal pigment epithelial layers. The asymmetry of optical reflectivity in perifoveal region is an important finding; OCT findings in the superior perifoveolar area are normal. (D) Retinal thickness map shows increased thickness in the inferior perifoveal area.

Paracentral Acute Middle Maculopathy

More recently, Sarraf and colleagues described the manifestations of selective ischemia involving the deep retinal plexus capillary, which can lead to a local infarct of the middle retina layers, in particular at the level of the inner nuclear layer.[226] This entity, termed paracentral acute middle maculopathy (PAMM), may be associated with various retinal vascular and systemic diseases, with patients often presenting with an acute scotoma. OCT-imaging in the acute stage reveals a region of increased reflectivity in the inner nuclear layer, with subsequent thinning of this layer over time – much like what is observed in the inner retina with nerve fiber layer infarct or cotton-wool spot.

OCT Angiography

OCT angiography (OCTA) is a method of visualizing the movement of red blood cells by analyzing the changes in the intensity and/or phase signal that arises from repeated B-scans performed in the same location. Other names, which essentially refer to the various approaches to OCTA, include OCT microangiography (OMAG) or split-spectrum amplitude decorrelation angiography (SSADA).[227,228] OCTA does not require dye injection and is noninvasive. In general, OCTA systems can be

divided into spectral domain-based (SD-OCT) and swept-source (SS-OCT) systems. The first SD-OCT system approved by the US Food and Drug Administration is the ZEISS Angioplex™ OCT angiography instrument, while the first system approved for use outside of the United States is the Optovue Angiovue system. However, OCTA instruments will become commercially available from multiple vendors within the next few years. The faster scanning rates and deeper choroidal penetration of the SS-OCT systems should allow larger scan areas and better visualization of the choroidal microvasculature compared with SD-OCT systems.

OCTA discriminates between the scattering signals from stationary and moving tissues to image microvascular blood flow in the retina and choroid. Light scattering from stationary tissues is stable over time, whereas light scattering from moving particles such as erythrocytes will vary randomly over time. OCTA assesses intensity and/or phase changes that result from the movement of these erythrocytes over multiple B-scans performed at the same position.

OCTA can resolve layer-specific microvascular details from within the retina and choroid.[229–231] High-resolution images of normal capillary networks within the retina and choroid are shown in Figs. 3.37 and 3.38. OCTA images demonstrate capillary detail that approaches the resolution of histologic studies. In addition, the variation in normal retinal capillary density between the central macula, temporal macula, and peripapillary retina was described in the living human eye without dye injection for the first time using OCTA. Estimates of retinal vascular density in the superficial and deep capillary plexi using OCTA are also consistent with human cadaver histology studies, demonstrating the high spatial resolution of OCTA. A comparison of the radial peripapillary network using OCTA and fluorescein angiography (FA) in normal human patients showed that the peripapillary capillary network was visualized better in the OCTA images than in FA images. OCTA has also been used to evaluate changes in blood flow upon stimulation of the healthy human retina by flickering light.[232] This may be useful in assessing functional deficits in patients with diabetes and glaucoma, as these conditions have a known abnormal vascular response to flickering light.

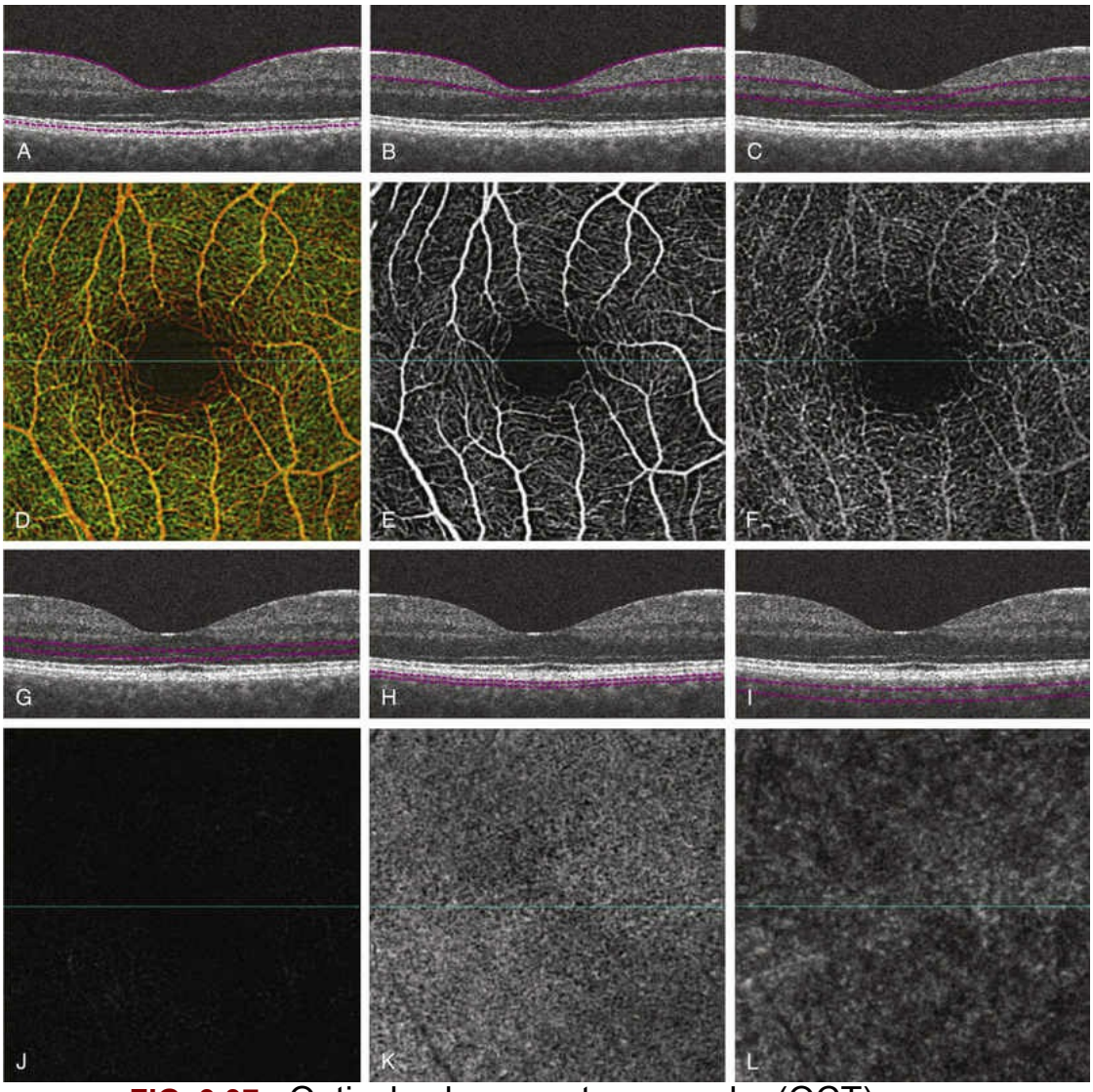

FIG. 3.37 Optical coherence tomography (OCT) angiography of a normal retina with B-scans containing segmentation lines that correspond to 3×3-mm en face flow images from a Zeiss Cirrus HD-OCT Angioplex OCT angiography instrument. (A,B) Total retina B-scan and color-coded depth en face flow image. (C,D) B-scan segmentation with en face superficial retinal flow image. (E,F) B-scan segmentation with en face deep retinal flow image. (G,H) B-scan segmentation with en face avascular retinal flow image. (I,J) B-scan segmentation with en face choriocapillaris flow image. (K,L) B-scan segmentation with en face choroidal flow image.

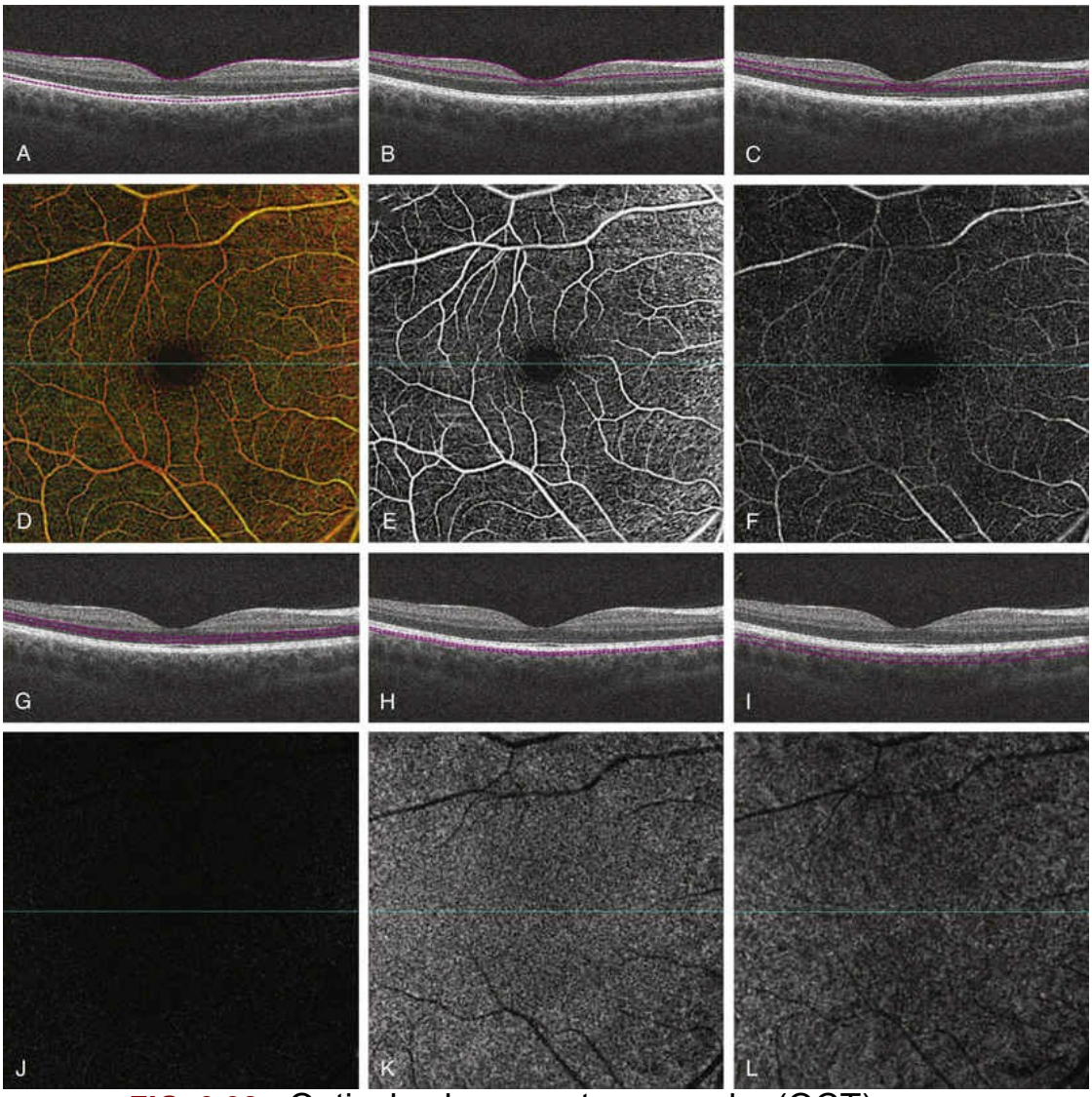

FIG. 3.38 Optical coherence tomography (OCT) angiography of a normal retina with B-scans containing segmentation lines that correspond to 6×6-mm en face flow images from a Zeiss Cirrus HD-OCT Angioplex OCT angiography instrument. (A,B) Total retina B-scan and color-coded depth en face flow image. (C,D) B-scan segmentation with en face superficial retinal flow image. (E,F) B-scan segmentation with en face deep retinal flow image. (G,H) B-scan segmentation with en face avascular retinal flow image. (I,J) B-scan segmentation with en face choriocapillaris flow image. (K,L) B-scan segmentation with en face choroidal flow image.

OCTA in Retinal Vascular Disease

The most common retinal vascular disease for the application of OCTA is to assess the microvascular pathology in diabetic retinopathy (Fig. 3.39).[231,233] It has been shown by epidemiologic studies that the clinically visible signs of diabetic retinopathy take many years to manifest, and this is reviewed in detail in another chapter of this text. However, it is very likely that subclinical changes are occurring long before the well-known clinical manifestations. These microscopic changes are not visible on standard ophthalmoscopy or fundus photography. In the vast majority of cases, fluorescein angiography is not clinically indicated in the assessment of subclinical disease with normal visual acuity. In addition, fluorescein angiography is not adequate for resolution of the deep capillary plexus and significantly underestimates capillary density under the best of circumstances.[234] Therefore, one of the main barriers to detection of early changes in diabetic retinopathy is the lack of appropriate imaging methods. OCTA has excellent spatial resolution, which allows consistent and clear imaging of the finest capillary detail in the retina, often comparable to histology.[233] Due to this excellent spatial resolution, OCTA has the potential to detect novel subclinical microvascular changes in diabetic retinopathy.

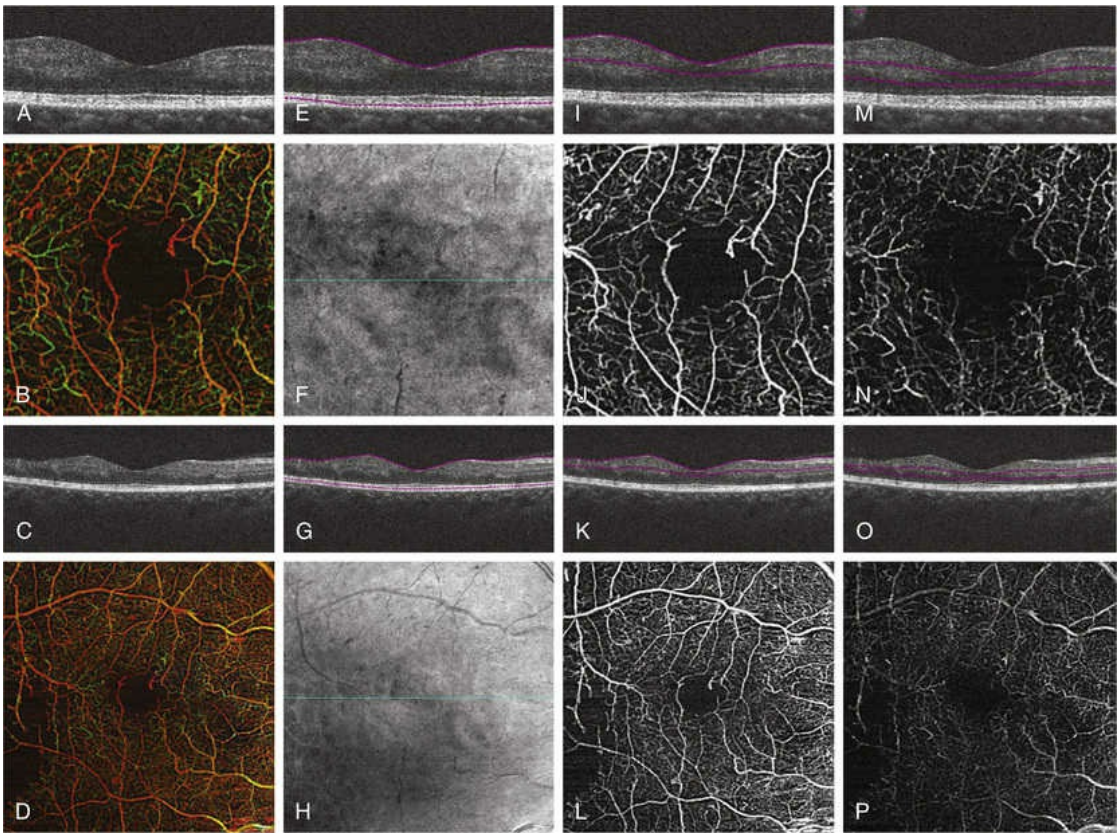

FIG. 3.39 Diabetic retinal en face flow images from a Zeiss Cirrus HD-OCT Angioplex optical coherence tomography (OCT) angiography instrument: 3×3-mm and 6×6-mm en face total retina color-coded depth flow map, total retina intensity map, superficial retinal layer flow images, and deep retinal layer flow images. (A) 3-mm horizontal B-scan through fovea corresponding to B. (B) 3×3-mm total retina color-coded depth flow map. (C) 6-mm horizontal B-scan scan through fovea corresponding to D. (D): 6×6-mm scan total retina color-coded depth flow map. (E) 3-mm horizontal B-scan through fovea with segmentation lines outlining the total retinal intensity layer shown in panel F. (F) 3×3-mm total retinal intensity image. (G) 6-mm horizontal B-scan through fovea with segmentation lines outlining the total retinal intensity layer shown in panel H. (H) 6×6-mm total retinal intensity image. (I) 3-mm horizontal B-scan through fovea with segmentation lines outlining the superficial retinal layer shown in panel J. (J) 3×3-mm superficial retinal layer flow image. (K) 6-mm horizontal B-scan through fovea with segmentation lines outlining the superficial retinal layer shown in panel L. (L) 6×6-mm superficial retinal layer flow image. (M) 3-mm horizontal B-scan through fovea

with segmentation lines outlining the deep retinal layer shown in panel N. (N) 3×3-mm deep retinal layer flow image. (O) 6-mm horizontal B-scan through fovea with segmentation lines outlining the deep retinal layer shown in panel P. (P) 6×6-mm deep retinal layer flow image.

OCTA can be used to characterize typical changes associated with diabetic retinopathy.[231,233,235–238] For example, OCTA can detect many of the key features of diabetic maculopathy, including areas of impaired capillary perfusion, cotton-wool spots, intraretinal microaneurysmal anomalies, and neovascularization. OCTA-based capillary density measurements also correlate closely with clinical staging of diabetic retinopathy and will likely offer a quantitative grading scheme in the near future. Future advances in quantitative OCTA may be used to better characterize the area of impaired capillary perfusion, activity of neovascularization or may be used to detect early findings of diabetic retinopathy such as size of the foveal avascular zone.[235,236] The clinical utility of these findings has yet to be determined but it is likely that OCTA will allow clinicians to detect subtle microvascular changes earlier than conventional clinical examination and fluorescein angiography.

In much the same way that OCTA can help characterize and improve the accuracy of microvascular changes in diabetic retinopathy, it will likely find a role in other retinal vascular diseases such as retinal venous occlusion and retinal arterial occlusion.[239] For example, OCTA can detect many of the key features of retinal venous occlusion, including areas of impaired capillary perfusion, vascular shunting, and some types of intraretinal edema (Fig. 3.40). Quantification of these clinical findings could allow for better clinical assessments of disease progression and may help with disease management, but that remains to be shown. In addition, OCTA images allow detailed localization of findings in a layer specific manner that has not been possible in the past. For example, OCTA images of “twig” retinal venous occlusions demonstrate that the intraretinal hemorrhage occurs largely in the mid-retinal capillary plexus.[239] This finding corroborates earlier histopathologic findings and demonstrates the sensitivity of OCTA as a in vivo optical biopsy.

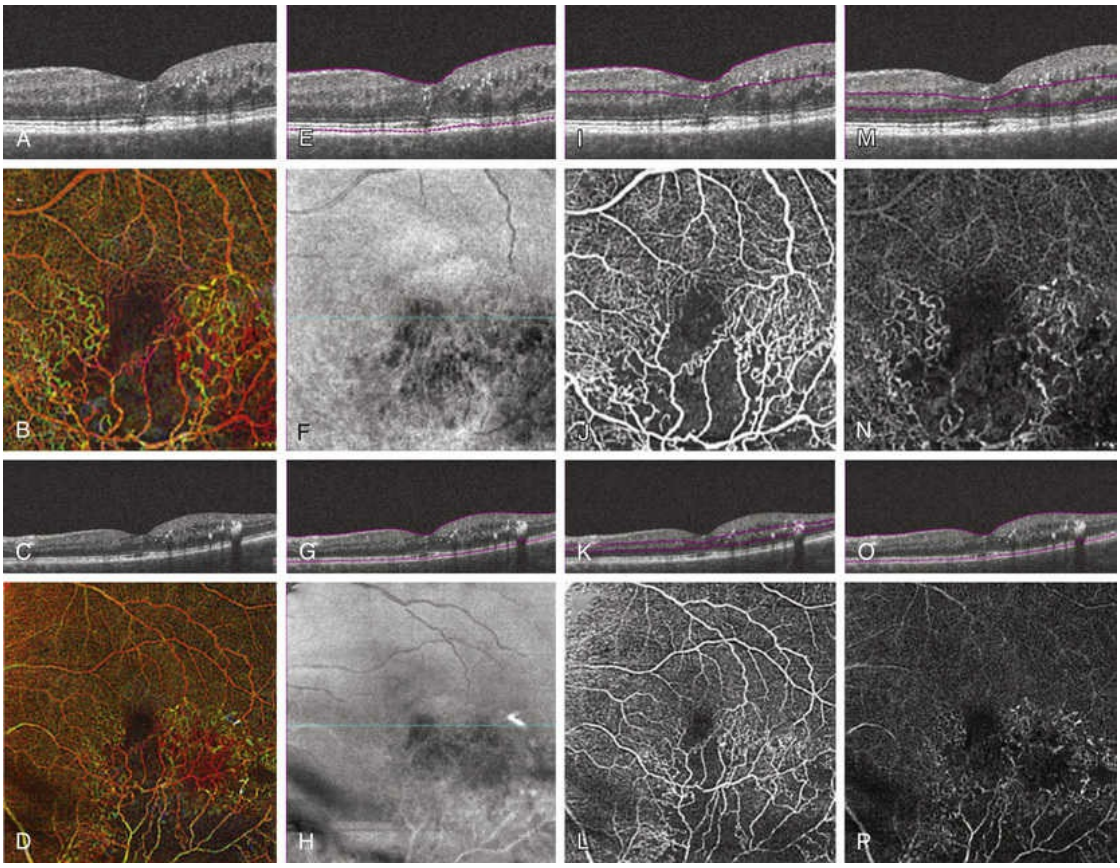

FIG. 3.40 Branch retinal venous occlusion retinal en face flow images from a Zeiss Cirrus HD-OCT Angioplex optical coherence tomography (OCT) angiography instrument: 3×3-mm and 6×6-mm en face total retina color-coded depth flow map, total retina intensity map, superficial retinal layer flow images, and deep retinal layer flow images. (A) 3-mm horizontal B-scan through fovea corresponding to panel B. (B) 3 3-mm total retina color-coded depth flow map. (C) 6-mm horizontal B-scan through fovea corresponding to panel D. (D) 6×6-mm scan total retina color-coded depth flow map. (E) 3-mm horizontal B-scan through fovea with segmentation lines outlining the total retinal intensity layer shown in panel F. (F) 3×3-mm total retinal intensity image. (G) 6-mm horizontal B-scan through fovea with segmentation lines outlining the total retinal intensity layer shown in panel H. (H) 6×6-mm total retinal intensity image. (I) 3-mm horizontal B-scan through fovea with segmentation lines outlining the superficial retinal layer shown in panel J. (J) 3×3-mm superficial retinal layer flow image. (K) 6-mm horizontal B-scan through fovea with segmentation lines outlining the superficial retinal layer shown in

panel L. (L) 6×6-mm superficial retinal layer flow image. (M) 3-mm horizontal B-scan through fovea with segmentation lines outlining the deep retinal layer shown in panel N. (N) 3×3-mm deep retinal layer flow image. (O) 6-mm horizontal B-scan through fovea with segmentation lines outlining the deep retinal layer shown in panel P. (P) 6×6-mm deep retinal layer flow image.

A less common retinal vascular disease, but one that is ideal for OCTA imaging, is macular telangiectasia type 2 (Fig. 3.41)[240,241] This disease is ideal because it is contained within the central 3×3-mm scan area of the macula where the high scanning density allows for the best image quality. Moreover, the disease involves microvascular changes in all the perifoveal retinal layers and progresses to subretinal and choroidal neovascularization late in the late proliferative stages. The first microvascular changes occur in the deep temporal capillary plexus and then spread to the superficial capillary plexus and then circumferentially around the fovea. As abnormal anastomoses form between the retinal capillary layers, the retina undergoes atrophy and the microvasculature becomes prominent in the avascular outer retina. In the late stage of MacTel2, neovascularization arises in the outer retina and communicates with both the retinal and choroidal circulations.

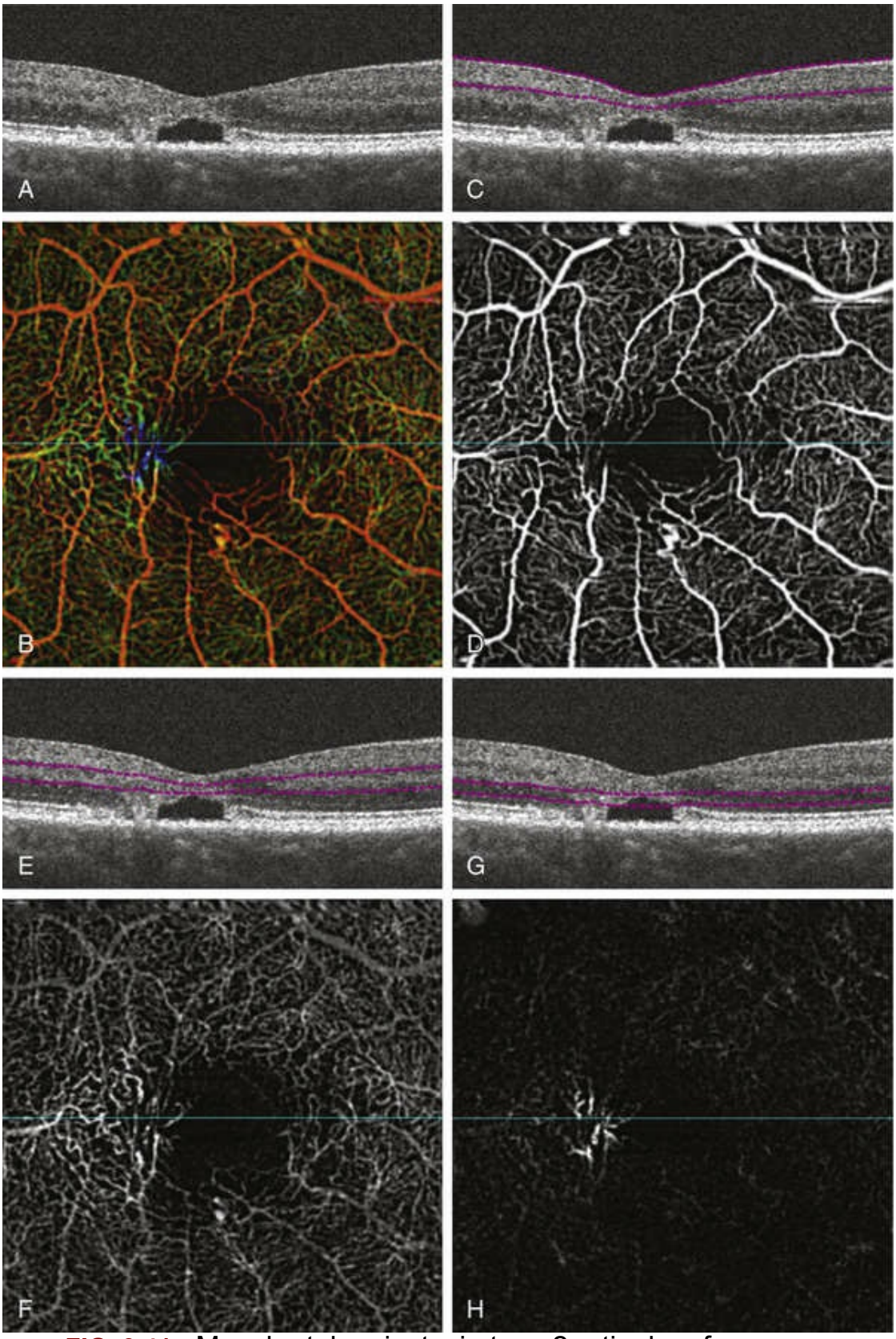

FIG. 3.41 Macular telangiectasia type 2 retinal en face flow images from a Zeiss Cirrus HD-OCT Angioplex optical coherence tomography (OCT) angiography instrument: en face total retina color-coded depth flow

image, superficial retinal layer flow image, deep retinal layer flow image, and avascular retinal layer flow image (3×3-mm scans). (A,C,E,G) B-scans with segmentation lines outlining the layer. (B) En face total retina color-coded depth flow image. (D) Superficial retinal layer flow image. (F) Deep retinal layer flow image. (H) Avascular retinal layer flow map.

One of the drawbacks of OCT is its limited field of view. An increase in the scanning field results in either an unacceptably long scanning time or a lower scan density and resulting lower resolution. However, with the availability of eye-tracking and the ability to montage multiple 3×3-mm or 6×6-mm images, wider fields of view can be obtained that may be especially useful in retinal vascular disease. With the introduction of machines with higher scanning speed, wider fields of view may be available.[242]

Other important limitations of OCTA include motion artifact, segmentation errors, and inconsistencies particularly in the setting of disease, and projection artifact from overlying retinal vascular structures. These artifacts can present significant challenges in the accurate interpretation of OCTA images, though simultaneous viewing of the en face OCTA and the OCT flow B-scan can be of some help. It is hoped that future advances in OCTA processing algorithms can address these limitations.

OCTA in Age-Related Macular Degeneration

OCTA provides us with a unique ability to monitor the vasculature in patients with AMD over time. Traditional intensity-based SD-OCT has provided images of anatomic details of the photoreceptors and RPE, and has shown us the structural changes that precede the formation of GA. However, with increasing focus on the pathogenesis of AMD, one of the fundamental debates is whether AMD is a primary disease of the photoreceptors, the RPE, or the choriocapillaris or whether it is a disease that results from the choreographed dysfunction between all three layers with specific layers playing a more dominant role in different patients depending on their genetics, environment, and overall health. While structural OCT provides us with exquisite detail on the

anatomic features of AMD, it has not provided us with a way to evaluate the choriocapillaris. Thus an incomplete picture of disease progression in AMD results. For example, we do not know if photoreceptor loss is primary, or secondary to RPE dysfunction. Moreover, if RPE dysfunction precedes photoreceptor loss, is it a primary RPE abnormality or secondary to the loss of the choriocapillaris. Up until now, we have been unable to untangle the web of interdependence between these three layers because we can only measure anatomic and functional changes in the photoreceptors and the RPE in vivo, but have been unable to visualize the choriocapillaris changes in vivo and have to rely on extrapolating from in vitro specimens. To help unravel the mystery of disease progression, we need to understand the temporal sequence of anatomic and functional changes in the macula. OCT angiography may bring clarity to the role of the choriocapillaris in disease progression. With the advent of OCT angiography (OCTA), it is now also possible to visualize the vascular changes that occur in dry AMD.[243–245]

OCTA provides a three-dimensional, depth-resolved image of the vasculature in the retina and choroid, which enables us to evaluate independently the vasculature of the inner and outer retina and the choriocapillaris and to correlate the vascular changes with the structural changes noted on cross-registered OCT scans. Moreover, the application of SS-OCT technology allows better visualization of the choriocapillaris as it has a lower sensitivity roll-off with depth and longer wavelength which enables better image penetration below the RPE.[246–250] SS-OCT also can support faster A-scan acquisition rates compared with SD-OCT. The faster acquisition speeds in SS-OCT are especially important because OCTA relies on decorrelation between sequentially acquired OCT B-scans in the eye,[251,252] therefore acquisition speed forces trade-offs between imaging time, retinal coverage, and pixel density in the OCTA data sets. Higher acquisition speeds also support OCTA protocols with multiple repeated B-scan and the use of techniques that can detect flow impairment, such as variable interscan time (VISTA), explained in greater detail below.[253,254]

Early AMD

Early and intermediate AMD are characterized by drusen and pigmentary abnormalities, but it is unknown whether changes in the choriocapillaris occur at these stages. Drusen and RPE changes can be visualized on structural OCT images.[255] With the advent of OCTA, it is now possible to visualize the microvasculature of the retina and choriocapillaris in vivo and to correlate microvascular alterations to structural changes in the retina and RPE.[229,243]

As expected, there are no significant changes noted in the retinal vasculature in early AMD. However, OCTA of the choriocapillaris shows changes beyond what would be expected to be seen due to aging alone. OCTA imaging of the choriocapillaris in normal eyes shows a dense homogenous network, with a fine pattern in the macula, which is near the transverse resolution limit of OCT imaging. More peripheral OCTA images of the choriocapillaris exhibit lobular architecture, consistent with the known morphology from vascular casting studies. These patterns are observed using SD-OCT, centered at 840 nm wavelength as well as SS-OCT, centered at longer 1050 nm wavelength. With age, the density of the choriocapillaris is likely to be reduced, with, however, a homogenous and regular pattern of vasculature still present.

OCTA images of early non-neovascular AMD eyes suggest that there is generalized reduced choriocapillaris density compared to age-matched normal controls, with some focal areas of choriocapillaris loss or flow impairment. The dark patches at the level of the choriocapillaris that correspond to choriocapillaris loss may sometimes be accompanied by displacement of the larger choroidal vessels into the space previously occupied by the choriocapillaris. These changes become more marked in more severe cases. This is in agreement with histopathologic studies which have noted that drusen form over areas devoid of capillary lumens and extend into the intercapillary pillars.[256–258] Increased drusen density in histopathologic studies has been shown to correspond to decreased vascular density of the choriocapillaris.[258] Analysis of en face structural OCT-B images of early AMD has also shown reduced visible choriocapillaris compared with normal eyes, but with a reduction in the OCT signal intensity underlying the drusen, it can be challenging to distinguish between loss of signal and loss of the choriocapillaris.[259]

Although these changes in the choriocapillaris density are visible in both SD-OCT and SS-OCT images, SS-OCT systems have better penetration into the choroid and therefore enable more reliable visualization of the choriocapillaris. In SD-OCT systems, drusen and RPE changes are more likely to cause signal attenuation shadowing. Strong structural OCT signals are required in order to obtain OCTA images, and shadowing causes dark areas on the en face OCTA at the level of the choriocapillaris that are the result of poor signal, rather than lack of blood flow. These areas of shadowing (as opposed to decreased perfusion) can be identified by concurrently looking at an en face OCT intensity image at the level of the choriocapillaris and the OCTA and by examining the cross-sectional OCT image in the area of suspected choriocapillaris pathology. Areas of shadowing will appear dark on both the OCT intensity image as well as the angiographic image, whereas areas of decreased blood flow will appear normal on the intensity image but will appear dark on the en face OCTA image. Because areas of shadowing are so much more prevalent in SD-OCT images than in SS-OCT, it is much easier to assess loss of choriocapillaris flow on the SS-OCTA images than on the SD-OCTA images.

Late Dry AMD

In patients with GA, OCTA shows loss of choriocapillaris flow under the regions of GA. In these areas of choriocapillaris alteration, larger choroidal vessels may be displaced into the area ordinarily occupied by the choriocapillaris and may be seen on the en face OCTA image at the depth level where the choriocapillaris is ordinarily seen. Although the larger choroidal vasculature ordinarily appears dark on SD-OCTA images because of the reduced depth penetration of the SD-OCT signal, in this situation where the larger choroidal vessels are displaced, they may appear as large bright vessels showing flow decorrelation. Fig. 3.42 shows SS-OCTA images from a patient with GA with corresponding red-free (Fig. 3.42A) and fundus autofluorescence images (Fig. 3.42B). In this patient, there were no changes in the retinal vasculature, as visible on OCTA segmented at the level of the retinal vasculature in Fig. 3.41C. In many cases, the areas of choriocapillaris alterations extend beyond the margins of the GA in an asymmetric pattern

(Figs. 3.42D–E). These alterations outside the margins of the GA may be quite extensive, or may be very limited and subtle. In a smaller number of cases, the choriocapillaris alterations may be limited to the area of the GA and not extend beyond that area. The changes underlying the area of GA are usually well visualized on both the spectral domain and the swept source OCTA systems, since the RPE in these areas is missing and therefore does not attenuate the SD-OCT signal. However, especially at the margins of the GA where the RPE is still intact, it may be more difficult to visualize the changes in the choriocapillaris with SD-OCT.

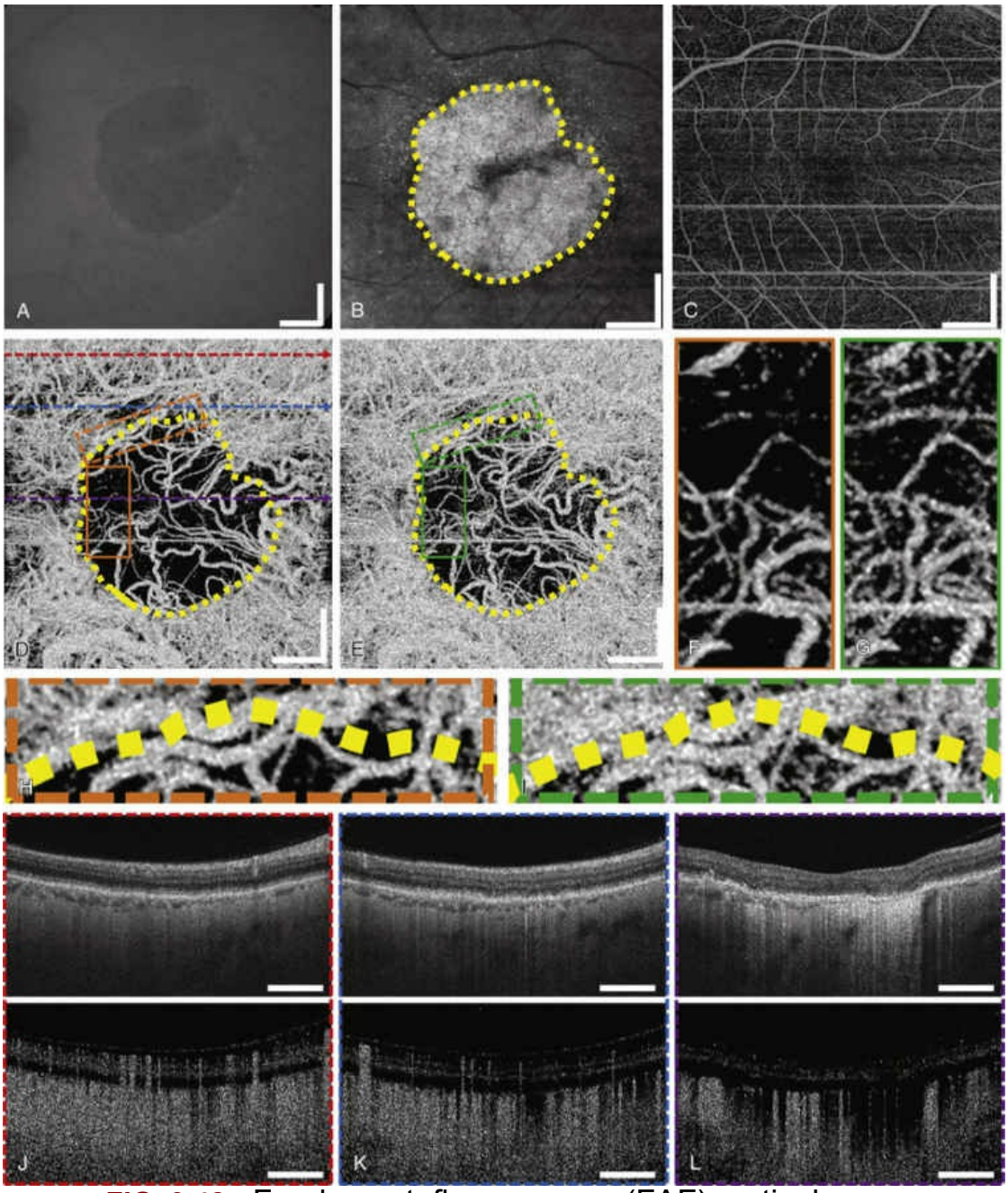

FIG. 3.42 Fundus autofluorescence (FAF), optical coherence tomography (OCT) and optical coherence tomography angiography (OCTA) in a 75-year-old patient with nonexudative age-related macular degeneration (AMD) with geographic atrophy (GA). The FAF (A) and the mean en face projection of the entire OCT volume (B) clearly show the region of GA, outlined by the yellow dashed contour in (B). The GA region appears lighter due to increased light penetration into the choroid caused by RPE atrophy. Panel (C) shows a mean en face projection of the OCTA volume through the depths spanned by the

retinal vasculature; the vasculature appears normal. Panel D shows a 4.4 μm thick en face OCTA choriocapillaris (CC) slab corresponding to a ~1.5 ms interscan time. The yellow dashed contour from (B) is superimposed, and severe CC alteration appears within it. Severe CC alteration is also evident outside the GA margin. Panel E shows the same 4.4-μm thick en face OCTA choriocapillaris (CC) slab as in (D), but corresponding to a ~3.0 ms interscan time. Note how some areas with low decorrelation signal in (D) have increased decorrelation in (E), suggesting flow impairment, not atrophy. Enlarged views of the solid orange and green boxes of (D) and (E) are shown in (F) and (G), respectively. Note that some choroidal vessels that are not visible in (F) become visible in (G). Enlarged views of the dashed orange and green boxes of (D) and (E) are shown in (H) and (I), respectively. Note that some of the regions with low decorrelation signal in (H) have a higher decorrelation signal in (I), suggesting flow impairment along the GA margin. OCT (top) and OCTA (bottom) B-scans through the red, blue, and purple horizontal dashed lines in (D) are shown in (J), (K), and (L), respectively. All scale bars are 1 mm. (Courtesy of Eric M Moult, MIT).

One of the debates in the visualization of choriocapillaris alterations in patients with GA is whether they truly represent absence of flow or merely reduced flow. OCTA creates flow images by comparing the differences between consecutive OCT B-scan images. If the velocity of flow in the vessels is very slow, OCTA may not be able to detect this slow flow. In addition, if flow is fast, then the OCTA image saturates (fast flows appear white) and variations in flow cannot be differentiated.

Thus, OCTA machines have a "slowest detectable flow" or sensitivity threshold below which they cannot detect flow at slow speeds, as well as a "fastest distinguishable flow" or saturation limit above which different flow speeds appear the same. The slowest detectable flow depends on the time between repeated B-scans, with longer interscan times producing a lower slowest detectable flow, because erythrocytes have more time to move between B-scans. In addition, a longer interscan time also reduces

the fastest distinguishable flow. The interscan time of current SD-OCT machines is ~5 ms while the interscan time of the SS-OCTA prototype instrument reported here is ~1.5 ms. The SD-OCT and SS-OCT instruments have acquisition speeds of 70,000 and 400,000 A-scans per second, respectively. The faster scanning speed allows SS-OCT to acquire larger numbers of repeated B-scans for the OCTA scan protocol in the same amount of time as SD-OCT. This allows OCTA data to be generated between B-scans with longer versus shorter interscan times. Looking at the same areas using OCTA from consecutive B-scans scans (Fig. 3.42D) versus every second B-scan scan (Fig. 3.42E) helps us identify areas of flow impairment, which may not be distinguishable using instruments with slower acquisition speeds and OCTA with long interscan times. Using SS-OCTA with variable interscan time analysis (VISTA) in order to vary the slowest detectable flow and fastest discernible flow, we can show that choriocapillaris alterations within the borders of GA tend to have slow flows and may be primarily atrophic, while choriocapillaris alterations beyond the borders of GA have flow impairment. The images in Figs. 3.42F and 3.42G are magnified images that correspond to a region within the borders of the GA when analyzed with varying interscan time OCTA. In Fig. 3.42G, we are better able to visualize slow flow in some vessels in this region of atrophy. However, as is clear when comparing to the surrounding choriocapillaris, there are considerable areas of absent flow or reduced flow underlying this area of geographic atrophy. The images in Figs. 3.42H and 3.42I correspond to a region at the margin of GA when analyzed with varying interscan time. Fig. 3.42H shows an OCTA with 1.5 ms interscan time, while Fig. 3.42I corresponds to a 3.0 ms interscan time. With increased interscan time, we are able to better visualize that most of the areas of choriocapillaris alteration in this region represent slow flow rather than a complete loss of flow. Conversely, if OCTA was performed using only a longer interscan time (which would be typical for SD-OCT instruments) it would not be possible to distinguish areas of flow impairment.

It is still unclear as to why these choriocapillaris flow changes take place in patients with GA. However, these changes in the choriocapillaris clearly seem to precede the obvious detectable

atrophic structural changes in the RPE and retina of these patients when imaged with conventional structural OCT. These results suggest that microstructural changes detectable by OCTA are present before they become detectable using conventional intensity-based OCT. Additional longitudinal studies are needed to better characterize the progression of these choriocapillaris alterations. In response to the debate about whether the primary site of pathogenesis of GA is the choriocapillaris or the RPE, these OCTA findings that choriocapillaris alterations appear to be at least the size of the GA, and often greater, appear to support the hypothesis that choriocapillaris loss may precede RPE changes. However, it has also been reported that there are changes in the RPE and the outer retina lying outside the areas of geographic atrophy and there is not enough information as yet to conclusively determine the site of primary alteration in AMD, and additional studies using high-resolution SD-OCT may be needed to confirm these findings.

In summary, OCTA can be used to visualize alterations in the choriocapillaris of patients with dry age-related macular degeneration. These changes seem to be present in all stages of the disease. The use of high-speed, long wavelength SS-OCT for angiography, with its better penetration into the choroid and high acquisition speeds, enable variable interscan time analysis OCTA. Scaling the slowest detectable flow and fastest distinguishable flow will enable us to better investigate changes in the choriocapillaris of patients with dry AMD. The ability to image choriocapillaris structure and flow impairment may be a useful future tool for detecting and monitoring progression in dry AMD and for monitoring treatment responses in clinical trials for therapies that target disease progression in dry AMD.

Neovascular AMD

Perhaps one of the most interesting applications of OCTA has been in neovascular or wet AMD, since treatment with anti-VEGF agents leads to rapid changes in the vasculature in wet AMD that can be sequentially visualized on OCTA.[260,261] CNV on OCTA can be visualized by both SS and SD-OCTA systems as a network of abnormal, dilated, often tortuous vessels detected in the normally avascular outer retina (type 2 CNV) or lying under the RPE (type 1

CNV)[262] (Figs. 3.43 and 3.44). The CNV may be seen as a medusa-like or seafan-like pattern, often with larger feeder vessel trunks and fine arborizing vessels. Appropriate segmentation of the layer containing the CNV results in improved visualization of the neovascularization (Fig. 3.43). OCT angiography has been shown to have a high sensitivity and specificity in the detection of CNV and has been shown to have a high level of correspondence to traditional multimodal imaging; however, the presence of large amounts of intraretinal or subretinal hemorrhage can interfere with visualization of the CNV.[263,264] Moreover, OCTA can be used in quantitative evaluation of CNV, by measuring the area of the CNV.

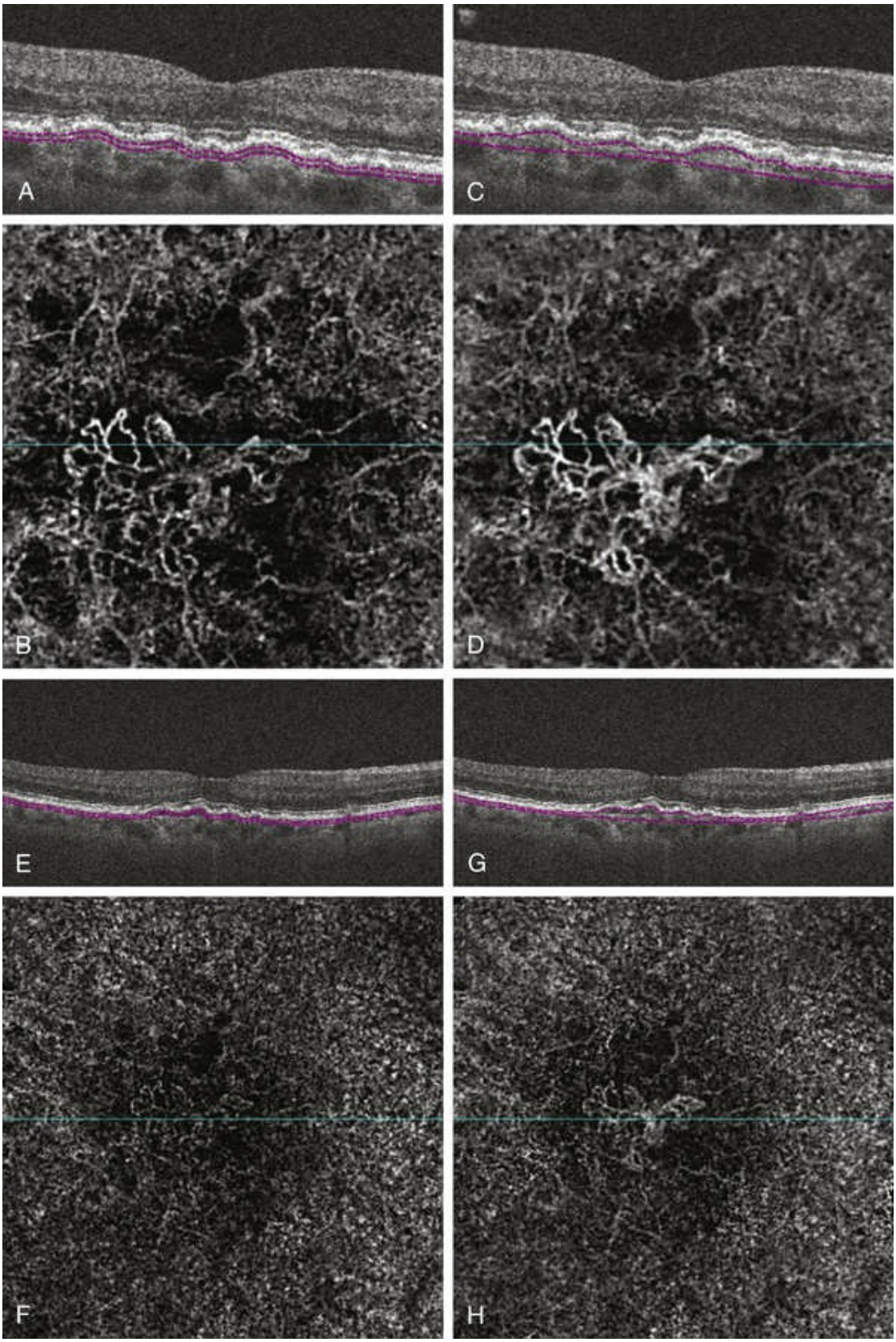

FIG. 3.43 Neovascular age-related macular degeneration: En face choriocapillaris layer flow images and custom map flow image en face flow images from a Zeiss Cirrus HD-OCT Angioplex optical

coherence tomography (OCT) angiography instrument. (A–D) 3×3-mm scans. (E–H) 6×6 mm scans. (A,C,E,G) B-scans with segmentation lines outlining the layer. (B,F) Choriocapillaris layer flow image. (D,H) Custom segmentation flow image with the RPE contour as the inner boundary and the RPE-Fit line (Bruch's membrane) as the contour of the outer boundary.

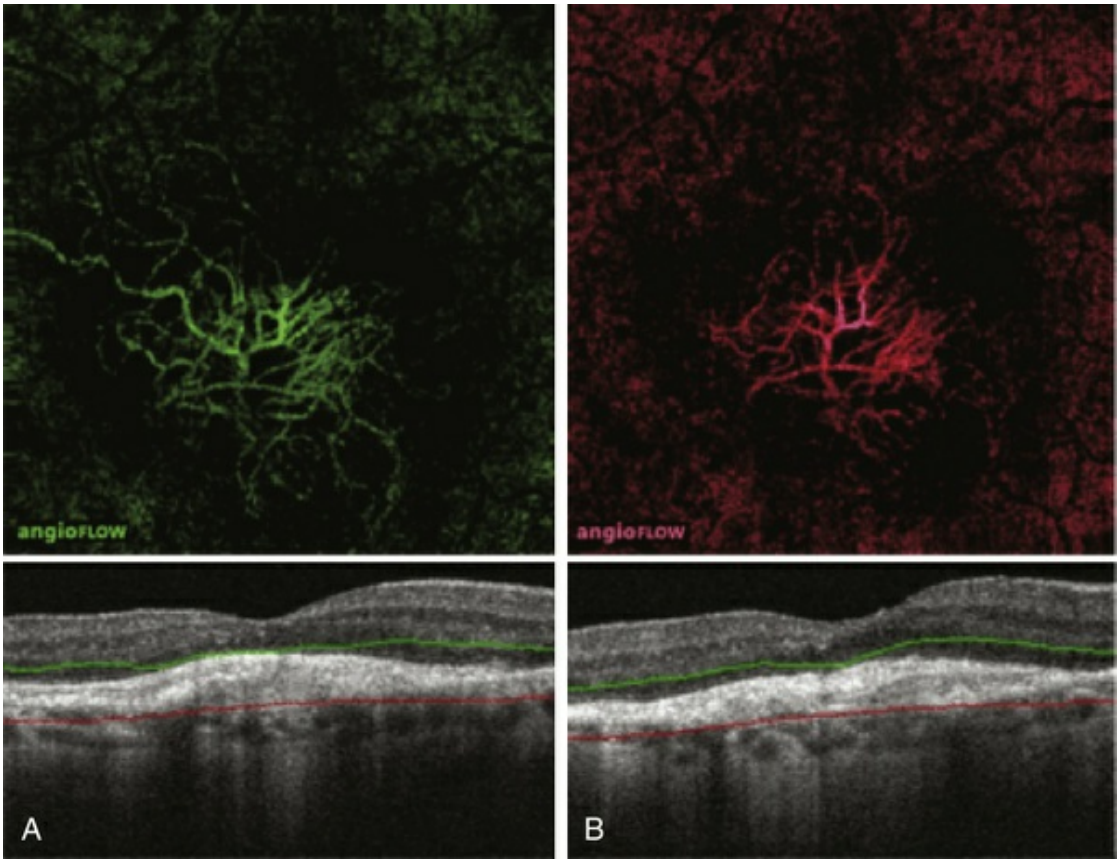

FIG. 3.44 Pre (A) and post (B) treatment with bevacizumab image of choroidal neovascularization. The posttreatment image shows a pruning of the smaller vessels at the margins of the choroidal neovascularization, with a decrease in the overall size of the membrane. Note that the larger trunks at the center of the choroidal neovascularization do not show regression.

OCTA can also be used to follow CNV over time and with treatment. Treatment-naive CNV shows numerous fine, arborizing vessels (Fig. 3.44A). On treatment with anti-VEGF agents, the size

of the CNV can be seen to decrease and regression is seen especially of the fine vessels of the CNV (Fig. 3.44B). Interestingly, follow up of patients with multiple anti-VEGF injections has shown that the vascular diameter of the vessels in the CNV appeared large even in small lesions, with few branch points and many vascular anastomotic connections among larger vessels. In these "chronically treated" CNVs, there was a paucity of capillaries visualized within the lesions. It has therefore been hypothesized that anti-VEGF agents cause regression and pruning of the smaller abnormal vessels in CNV, without causing regression of the larger trunks that have already acquired an endothelial lining.

OCTA may sometimes allow detection of CNV before it is detected as leakage on fluorescein and accumulation of subretinal fluid on structural OCT (Fig. 3.45). Moreover, in patients who have previously been treated with anti-VEGF agents, quiescent, non-leaking CNV may sometimes be visualized as an abnormal pattern of tangled vasculature lying under the RPE. Moreover, it has also been noted that CNV overlies areas of severe choriocapillaris alterations.[265] The significance of these changes in terms of risk of recurrence and frequency of treatment are just beginning to be investigated. However, needless to say, this ushers in an exciting era where in-vivo visualization of vasculature allows us to follow responses to therapy and to better understand the variety of responses observed to treatment in different individuals.

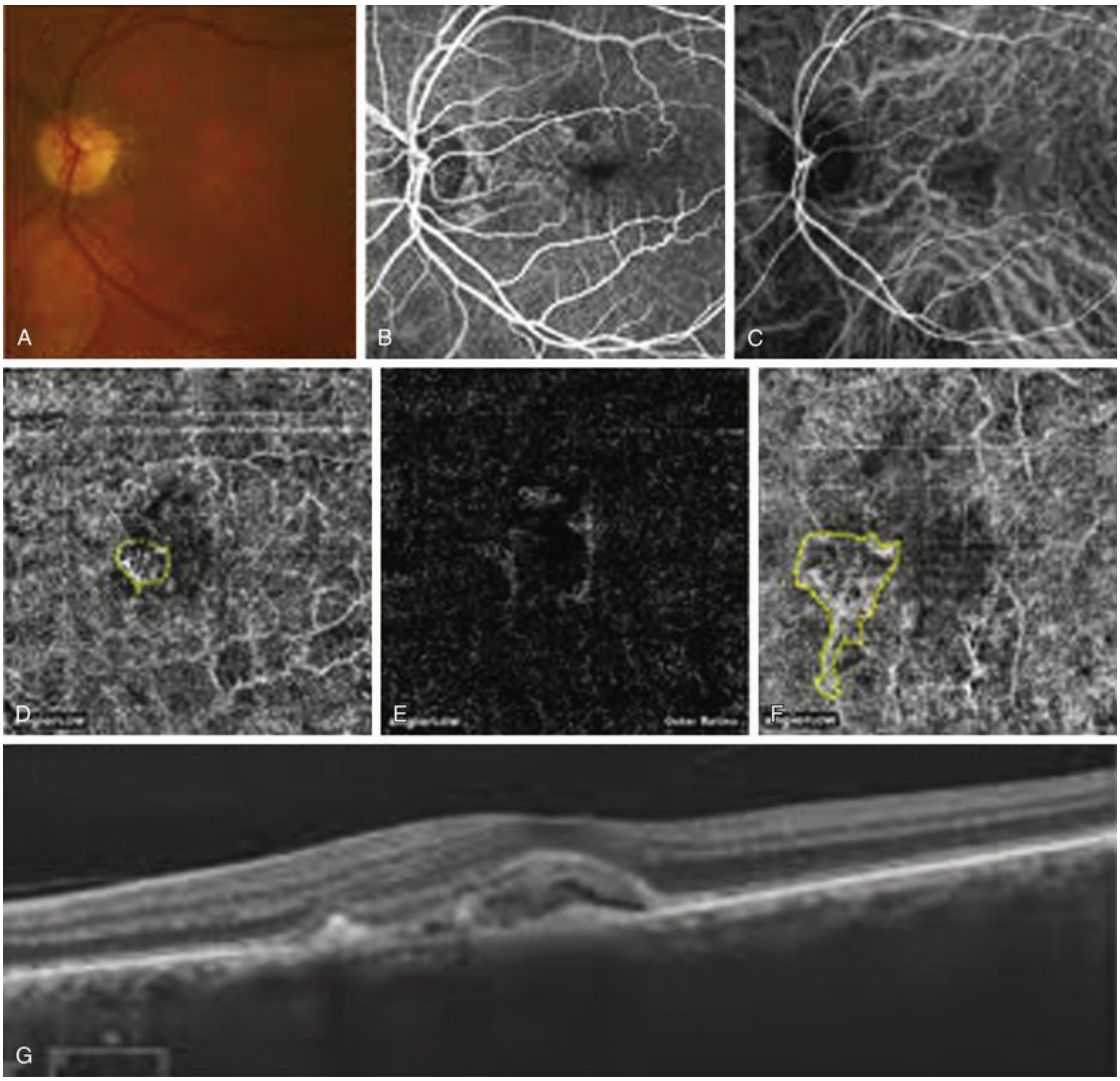

FIG. 3.45 (A) Color fundus photograph, (B) fluorescein angiogram (FA), and (C) indocyanine green angiogram (ICGA) of a patient who was suspected of having choroidal neovascularization (CNV). No clear evidence of CNV is seen on the FA and ICGA, nor on the optical coherence tomography angiogram (OCTA) segmented at the level of the outer retina (E). The 6×6-mm OCTA (D) and the 3×3-mm OCTA (F) segmented at the level of the choriocapillaris show abnormal vascular trunks (outlined in yellow). Panel (G) shows an OCT B-scan acquired through the area of interest.

Future Directions

The recent advances in OCT technology have clearly revolutionized the assessment of patients with retinal disorders. Although SD-OCT

has changed the way we image macular diseases, the future of OCT holds even more promise with the use of longer-wavelength light sources, faster scan times, higher image resolution, and noninvasive angiography.

Current commercially available SD-OCT instruments allow dense scanning of the macula with high axial resolution (approximately 5–8 μm). Ultrahigh-resolution OCT may achieve axial image resolution of 2–3 μm enabling better visualization of retinal structures. However, the price-versus-performance tradeoff remains, limiting the use of this technology to research applications.[2] The use of adaptive optics to correct the ocular aberrations may increase not only the axial resolution, but also the transverse resolution of OCT systems and provide cellular level detail.[266] However, the use of SS-OCT for structural imaging and OCTA should be commercially available in the near future.

SS-OCT systems allow significant increases in imaging sensitivity and speed (100,000–400 000 A-scans per second), through the use of a tunable laser and a photodetector, and faster scan times combined with improved motion-correction strategies should yield larger scan areas that contain few, if any, motion artifacts,. While swept-source OCT can achieve extremely high imaging speeds, the axial image resolution is slightly less than that achieved using SD-OCT.[2,3,267]

Clinically available SD-OCT instruments operate with a light source of approximately 840 nm. This wavelength is highly scattered and absorbed by the melanin in the RPE and choroid, reducing the light penetration into deeper tissues. Imaging the retina with a wavelength of 1050 nm enables greater light penetration and thus a better visualization of choroidal structures.[268,269] The use of this wavelength also has the advantage of less interference by media opacities such as cataract.[270]

In the field of functional OCT, OCT angiography systems are already able to detect retinal and choroidal blood flow, but the role of OCTA in patient management is still being defined. Polarization-sensitive OCT uses tissue birefringence properties to detect the health of different retinal layers.[271] The combination of birefringence and thickness measurements may provide a more sensitive diagnostic tool than either alone.[272–274]

Much has been learned since the development of the first OCT instrument, and OCT holds the promise for continuing advances in fundamental research and improvements in clinical care.

Disclosures

Drs. Garcia Filho and Rosenfeld received research support from Carl Zeiss Meditec. The University of Miami co-owns a patent that is licensed to Carl Zeiss Meditec. Dr. Rosenfeld and Dr. Kashani have received honoraria for lectures from Carl Zeiss Meditec. Dr. Kashani serves as a consultant for Carl Zeiss Meditec. Dr. Waheed has received honoraria for lectures from Carl Zeiss Meditec Nidek and Optovue. Dr. Duker serves as a consultant to Carl Zeiss Meditec and Optovue.

Acknowledgments

We appreciate the contributions by the previous authors of this chapter in the 5th edition of this textbook: Zohar Yehoshua, Giovanni Gregori, and Carmen A. Puliafito. We are also grateful to Karen Schaal, Andrew Miller, Fang Zheng, Gillian Robbins, Eric M. Moult, and Eduardo Novais for their help in assembling the figures.

References

1. Gabriele ML, Wollstein G, Ishikawa H, et al. Optical coherence tomography: history, current status, and laboratory work. *Invest Ophthalmol Vis Sci*. 2011;52:2425–2436.
2. Drexler W, Fujimoto JG. State-of-the-art retinal optical coherence tomography. *Prog Retin Eye Res*. 2008;27:45–88.
3. Potsaid B, Baumann B, Huang D, et al. Ultrahigh speed 1050nm swept source/Fourier domain OCT retinal and anterior segment imaging at 100,000 to 400,000 axial scans per second. *Opt Express*. 2010;18(19):20029–20048.
4. Li Y, Gregori G, Knighton RW, et al. Registration of OCT fundus images with color fundus photographs based on

blood vessel ridges. *Opt Express*. 2011;19:7–16.
5. Jiao S, Knighton R, Huang X, et al. Simultaneous acquisition of sectional and fundus ophthalmic images with spectral-domain optical coherence tomography. *Opt Express*. 2005;13:444–452.
6. Yehoshua Z, Garcia Filho CA, Penha FM, et al. Comparison of geographic atrophy measurements from the OCT fundus image and the sub-RPE slab image. *Ophthalmic Surg Lasers Imaging Retina*. 2013;44(2):127–132.
7. Nunes RP, Gregori G, Yehoshua Z, et al. Predicting the progression of geographic atrophy in age-related macular degeneration with SD-OCT en face imaging of the outer retina. *Ophthalmic Surg Lasers Imaging Retina*. 2013;44(4):344–359.
8. Sallo FB, Peto T, Egan C, et al. "En face" OCT imaging of the IS/OS junction line in type 2 idiopathic macular telangiectasia. *Invest Ophthalmol Vis Sci*. 2012;53(10):6145–6152.
9. Nunes RP, Goldhardt R, de Amorim Garcia Filho CA, et al. Spectral-domain optical coherence tomography measurements of choroidal thickness and outer retinal disruption in macular telangiectasia type 2. *Ophthalmic Surg Lasers Imaging Retina*. 2015;46(2):162–170.
10. Spaide RF. Colocalization of pseudodrusen and subretinal drusenoid deposits using high-density en face spectral domain optical coherence tomography. *Retina*. 2014;34(12):2336–2345.
11. Schaal KB, Legarreta AD, Gregori G, et al. Widefield en face optical coherence tomography imaging of subretinal drusenoid deposits. *Ophthalmic Surg Lasers Imaging Retina*. 2015;46(5):550–559.
12. Han IC, Jaffe GJ. Evaluation of artifacts associated with macular spectral-domain optical coherence tomography. *Ophthalmology*. 2010;117:1177–1189.e4.
13. Ho J, Sull AC, Vuong LN, et al. Assessment of artifacts and reproducibility across spectral- and time-domain optical coherence tomography devices. *Ophthalmology*. 2009;116:1960–1970.

14. Mylonas G, Ahlers C, Malamos P, et al. Comparison of retinal thickness measurements and segmentation performance of four different spectral and time domain OCT devices in neovascular age-related macular degeneration. *Br J Ophthalmol*. 2009;93:1453–1460.
15. Wolf-Schnurrbusch UE, Ceklic L, Brinkmann CK, et al. Macular thickness measurements in healthy eyes using six different optical coherence tomography instruments. *Invest Ophthalmol Vis Sci*. 2009;50:3432–3437.
16. Srinivasan VJ, Monson BK, Wojtkowski M, et al. Characterization of outer retinal morphology with high-speed, ultrahigh-resolution optical coherence tomography. *Invest Ophthalmol Vis Sci*. 2008;49:1571–1579.
17. Krebs I, Smretschnig E, Moussa S, et al. Quality and reproducibility of retinal thickness measurements in two spectral-domain optical coherence tomography machines. *Invest Ophthalmol Vis Sci*. 2011;52:6925–6933.
18. Mwanza JC, Oakley JD, Budenz DL, et al. Macular ganglion cell-inner plexiform layer: automated detection and thickness reproducibility with spectral domain-optical coherence tomography in glaucoma. *Invest Ophthalmol Vis Sci*. 2011;52:8323–8329.
19. Yehoshua Z, Rosenfeld PJ, Gregori G, et al. Progression of geographic atrophy in age-related macular degeneration imaged with spectral domain optical coherence tomography. *Ophthalmology*. 2011;118:679–686.
20. Yehoshua Z, de Amorim Garcia Filho CA, Nunes RP, et al. Comparison of geographic atrophy growth rates using different imaging modalities in the COMPLETE Study. *Ophthalmic Surg Lasers Imaging Retina*. 2015;46(4):413–422.
21. Gregori G, Wang F, Rosenfeld PJ, et al. Spectral domain optical coherence tomography imaging of drusen in nonexudative age-related macular degeneration. *Ophthalmology*. 2011;118:1373–1379.
22. Yehoshua Z, Wang F, Rosenfeld PJ, et al. Natural history of drusen morphology in age-related macular degeneration using spectral domain optical coherence tomography. *Ophthalmology*. 2011;118:2434–2441.

23. Ouyang Y, Heussen FM, Hariri A, et al. Optical coherence tomography-based observation of the natural history of drusenoid lesion in eyes with dry age-related macular degeneration. *Ophthalmology*. 2013;120(12):2656–2665.
24. Malamos P, Ahlers C, Mylonas G, et al. Evaluation of segmentation procedures using spectral domain optical coherence tomography in exudative age-related macular degeneration. *Retina*. 2011;31:453–463.
25. Matt G, Sacu S, Buehl W, et al. Comparison of retinal thickness values and segmentation performance of different OCT devices in acute branch retinal vein occlusion. *Eye (Lond)*. 2011;25:511–518.
26. Krebs I, Haas P, Zeiler F, et al. Optical coherence tomography: limits of the retinal-mapping program in age-related macular degeneration. *Br J Ophthalmol*. 2008;92:933–935.
27. Krebs I, Falkner-Radler C, Hagen S, et al. Quality of the threshold algorithm in age-related macular degeneration: Stratus versus Cirrus OCT. *Invest Ophthalmol Vis Sci*. 2009;50:995–1000.
28. Patel PJ, Chen FK, da Cruz L, et al. Segmentation error in Stratus optical coherence tomography for neovascular age-related macular degeneration. *Invest Ophthalmol Vis Sci*. 2009;50:399–404.
29. Drexler W, Sattmann H, Hermann B, et al. Enhanced visualization of macular pathology with the use of ultrahigh-resolution optical coherence tomography. *Arch Ophthalmol*. 2003;121:695–706.
30. Schuman JS, Pulliafito CA. *Optical coherence tomography of ocular diseases*. Slack: Thorofare, NJ; 2004.
31. Gloesmann M, Hermann B, Schubert C, et al. Histologic correlation of pig retina radial stratification with ultrahigh-resolution optical coherence tomography. *Invest Ophthalmol Vis Sci*. 2003;44:1696–1703.
32. Anger EM, Unterhuber A, Hermann B, et al. Ultrahigh resolution optical coherence tomography of the monkey fovea. Identification of retinal sublayers by correlation with semithin histology sections. *Exp Eye Res*. 2004;78:1117–1125.

33. Staurenghi G, Sadda S, Chakravarthy U, Spaide RF, International Nomenclature for Optical Coherence Tomography P. Proposed lexicon for anatomic landmarks in normal posterior segment spectral-domain optical coherence tomography: the IN*OCT consensus. *Ophthalmology*. 2014;121(8):1572–1578.
34. Jonnal RS, Kocaoglu OP, Zawadzki RJ, Lee SH, Werner JS, Miller DT. The cellular origins of the outer retinal bands in optical coherence tomography images. *Invest Ophthalmol Vis Sci*. 2014;55(12):7904–7918.
35. Lujan BJ, Roorda A, Knighton RW, et al. Revealing Henle's fiber layer using spectral domain optical coherence tomography. *Invest Ophthalmol Vis Sci*. 2010;52:1486–1492.
36. Spaide RF, Curcio CA. Anatomical correlates to the bands seen in the outer retina by optical coherence tomography: literature review and model. *Retina*. 2011;31:1609–1619.
37. Srinivasan VJ, Ko TH, Wojtkowski M, et al. Noninvasive volumetric imaging and morphometry of the rodent retina with high-speed, ultrahigh-resolution optical coherence tomography. *Invest Ophthalmol Vis Sci*. 2006;47:5522–5528.
38. Toth CA, Narayan DG, Boppart SA, et al. A comparison of retinal morphology viewed by optical coherence tomography and by light microscopy. *Arch Ophthalmol*. 1997;115:1425–1428.
39. Manjunath V, Taha M, Fujimoto JG, et al. Choroidal thickness in normal eyes measured using Cirrus HD optical coherence tomography. *Am J Ophthalmol*. 2010;150:325–329.e1.
40. Spaide RF, Koizumi H, Pozzoni MC. Enhanced depth imaging spectral-domain optical coherence tomography. *Am J Ophthalmol*. 2008;146:496–500.
41. Chen Y, Burnes DL, de Bruin M, et al. Three-dimensional pointwise comparison of human retinal optical property at 845 and 1060 nm using optical frequency domain imaging. *J Biomed Opt*. 2009;14:024016.
42. Margolis R, Spaide RF. A pilot study of enhanced depth imaging optical coherence tomography of the choroid in normal eyes. *Am J Ophthalmol*. 2009;147:811–815.

43. Abbey AM, Kuriyan AE, Modi YS, et al. Optical coherence tomography measurements of choroidal thickness in healthy eyes: correlation with age and axial length. *Ophthalmic Surg Lasers Imaging Retina*. 2015;46(1):18–24.
44. Ouyang Y, Heussen FM, Mokwa N, et al. Spatial distribution of posterior pole choroidal thickness by spectral domain optical coherence tomography. *Invest Ophthalmol Vis Sci*. 2011;52:7019–7026.
45. Ikuno Y, Kawaguchi K, Nouchi T, et al. Choroidal thickness in healthy Japanese subjects. *Invest Ophthalmol Vis Sci*. 2009;51:2173–2176.
46. Ikuno Y, Maruko I, Yasuno Y, et al. Reproducibility of retinal and choroidal thickness measurements in enhanced depth imaging and high-penetration optical coherence tomography. *Invest Ophthalmol Vis Sci*. 2011;52:5536–5540.
47. Giammaria D, Ioni A, Bartoli B, et al. Comparison of macular thickness measurements between time-domain and spectral-domain optical coherence tomographies in eyes with and without macular abnormalities. *Retina*. 2011;31:707–716.
48. Gass J. *Stereoscopic atlas of macular diseases: diagnosis and treatment*. Mosby–Year Book: St. Louis; 1997:903–914.
49. Uchino E, Uemura A, Ohba N. Initial stages of posterior vitreous detachment in healthy eyes of older persons evaluated by optical coherence tomography. *Arch Ophthalmol*. 2001;119:1475–1479.
50. Smiddy WE, Michels RG, Green WR. Morphology, pathology, and surgery of idiopathic vitreoretinal macular disorders. A review. *Retina*. 1990;10:288–296.
51. Johnson MW. Perifoveal vitreous detachment and its macular complications. *Trans Am Ophthalmol Soc*. 2005;103:537–567.
52. Witkin AJ, Patron ME, Castro LC, et al. Anatomic and visual outcomes of vitrectomy for vitreomacular traction syndrome. *Ophthalm Surg Lasers Imaging*. 2010;41:425–431.
53. Gallemore RP, Jumper JM, McCuen BW 2nd, et al. Diagnosis of vitreoretinal adhesions in macular disease with optical coherence tomography. *Retina*. 2000;20:115–120.

54. Johnson MW. Tractional cystoid macular edema: a subtle variant of the vitreomacular traction syndrome. *Am J Ophthalmol*. 2005;140:184–192.
55. Do DV, Cho M, et al. Impact of optical coherence tomography on surgical decision making for epiretinal membranes and vitreomacular traction. *Retina*. 2007;27:552–556.
56. Chang LK, Fine HF, Spaide RF, et al. Ultrastructural correlation of spectral-domain optical coherence tomographic findings in vitreomacular traction syndrome. *Am J Ophthalmol*. 2008;146:121–127.
57. Duker JS, Kaiser PK, Binder S, et al. The International Vitreomacular Traction Study Group classification of vitreomacular adhesion, traction, and macular hole. *Ophthalmology*. 2013;120:2611–2619.
58. Hikichi T, Yoshida A, Trempe CL. Course of vitreomacular traction syndrome. *Am J Ophthalmol*. 1995;119:55–61.
59. Sulkes DJ, Ip MS, Baumal CR, et al. Spontaneous resolution of vitreomacular traction documented by optical coherence tomography. *Arch Ophthalmol*. 2000;118:286–287.
60. Yamada N, Kishi S. Tomographic features and surgical outcomes of vitreomacular traction syndrome. *Am J Ophthalmol*. 2005;139:112–117.
61. Sonmez K, Capone A Jr, Trese MT, et al. Vitreomacular traction syndrome: impact of anatomical configuration on anatomical and visual outcomes. *Retina*. 2008;28:1207–1214.
62. Stalmans P, Benz MS, Gandorfer A, et al. Enzymatic vitreolysis with ocriplasmin for vitreomacular traction and macular holes. *N Engl J Med*. 2012;367:606–615.
63. Wilkins JR, Puliafito CA, Hee MR, et al. Characterization of epiretinal membranes using optical coherence tomography. *Ophthalmology*. 1996;103:2142–2151.
64. Gass JD. Reappraisal of biomicroscopic classification of stages of development of a macular hole. *Am J Ophthalmol*. 1995;119:752–759.
65. Takahashi A, Nagaoka T, Yoshida A. Stage 1-A macular hole: a prospective spectral-domain optical coherence tomography study. *Retina*. 2011;31:127–147.

66. Takahashi A, Yoshida A, Nagaoka T, et al. Macular hole formation in fellow eyes with a perifoveal posterior vitreous detachment of patients with a unilateral macular hole. *Am J Ophthalmol*. 2011;151:981–989.e4.
67. Kelly NE, Wendel RT. Vitreous surgery for idiopathic macular holes. Results of a pilot study. *Arch Ophthalmol*. 1991;109:654–659.
68. Brooks HL Jr. Macular hole surgery with and without internal limiting membrane peeling. *Ophthalmology*. 2000;107:1939–1948 [discussion 1948–9].
69. Bottoni F, De Angelis S, Luccarelli S, et al. The dynamic healing process of idiopathic macular holes after surgical repair: a spectral-domain optical coherence tomography study. *Invest Ophthalmol Vis Sci*. 2011;52:4439–4446.
70. Hee MR, Puliafito CA, Wong C, et al. Optical coherence tomography of macular holes. *Ophthalmology*. 1995;102:748–756.
71. Ko TH, Witkin AJ, Fujimoto JG, et al. Ultrahigh-resolution optical coherence tomography of surgically closed macular holes. *Arch Ophthalmol*. 2006;124:827–836.
72. Sano M, Shimoda Y, Hashimoto H, et al. Restored photoreceptor outer segment and visual recovery after macular hole closure. *Am J Ophthalmol*. 2009;147:313–318.e1.
73. Oh J, Smiddy WE, Flynn HW Jr, et al. Photoreceptor inner/outer segment defect imaging by spectral domain OCT and visual prognosis after macular hole surgery. *Invest Ophthalmol Vis Sci*. 2009;51:1651–1658.
74. Ooka E, Mitamura Y, Baba T, et al. Foveal microstructure on spectral-domain optical coherence tomographic images and visual function after macular hole surgery. *Am J Ophthalmol*. 2011;152:283–290.e1.
75. Muqit MM, Akram I, Turner GS, et al. Fourier-domain optical coherence tomography imaging of gas tamponade following macular hole surgery. *Ophthalmic Surg Lasers Imaging*. 2011;41 Online:e1–6.
76. Sano M, Inoue M, Taniuchi S, et al. Ability to determine postoperative status of macular hole in gas-filled eyes by spectral domain-optical coherence tomography. *Clin*

Experiment Ophthalmol. 2011;39:885–892.
77. Eckardt C, Eckert T, Eckardt U, et al. Macular hole surgery with air tamponade and optical coherence tomography-based duration of face-down positioning. *Retina*. 2008;28:1087–1096.
78. Pearlstone AD. The incidence of idiopathic preretinal macular gliosis. *Ann Ophthalmol*. 1985;17:378–380.
79. McCarty DJ, Mukesh BN, Chikani V, et al. Prevalence and associations of epiretinal membranes in the visual impairment project. *Am J Ophthalmol*. 2005;140:288–294.
80. Smiddy WE, Maguire AM, Green WR, et al. Idiopathic epiretinal membranes. Ultrastructural characteristics and clinicopathologic correlation. *Ophthalmology*. 1989;96:811–820 [discussion 821].
81. Vinores SA, Campochiaro PA, Conway BP. Ultrastructural and electron-immunocytochemical characterization of cells in epiretinal membranes. *Invest Ophthalmol Vis Sci*. 1990;31:14–28.
82. Appiah AP, Hirose T. Secondary causes of premacular fibrosis. *Ophthalmology*. 1989;96:389–392.
83. Bressler NM, Bressler SB, Congdon NG, et al. Potential public health impact of Age-Related Eye Disease Study results: AREDS report no. 11. *Arch Ophthalmol*. 2003;121:1621–1624.
84. Congdon N, O'Colmain B, Klaver CC, et al. Causes and prevalence of visual impairment among adults in the United States. *Arch Ophthalmol*. 2004;122:477–485.
85. Friedman DS, O'Colmain BJ, Munoz B, et al. Prevalence of age-related macular degeneration in the United States. *Arch Ophthalmol*. 2004;122:564–572.
86. Klein R, Peto T, Bird A, et al. The epidemiology of age-related macular degeneration. *Am J Ophthalmol*. 2004;137:486–495.
87. Bird AC, Bressler NM, Bressler SB, et al. An international classification and grading system for age-related maculopathy and age-related macular degeneration. The International ARM Epidemiological Study Group. *Surv Ophthalmol*. 1995;39:367–374.

88. Hirvela H, Luukinen H, Laara E, et al. Risk factors of age-related maculopathy in a population 70 years of age or older. *Ophthalmology*. 1996;103:871–877.
89. Vingerling JR, Hofman A, Grobbee DE, et al. Age-related macular degeneration and smoking. The Rotterdam Study. *Arch Ophthalmol*. 1996;114:1193–1196.
90. Seddon JM, Sharma S, Adelman RA. Evaluation of the clinical age-related maculopathy staging system. *Ophthalmology*. 2006;113:260–266.
91. Bartlett H, Eperjesi F. Use of fundus imaging in quantification of age-related macular change. *Surv Ophthalmol*. 2007;52:655–671.
92. Seddon JM, Sharma S, Adelman RA, et al. Optical coherence tomography of age-related macular degeneration and choroidal neovascularization. *Ophthalmology*. 1996;103:1260–1270.
93. Pieroni CG, Witkin AJ, Ko TH, et al. Ultrahigh resolution optical coherence tomography in non-exudative age related macular degeneration. *Br J Ophthalmol*. 2006;90:191–197.
94. Sikorski BL, Bukowska D, Kaluzny JJ, et al. Drusen with accompanying fluid underneath the sensory retina. *Ophthalmology*. 2010;118:82–92.
95. Spaide RF, Curcio CA. Drusen characterization with multimodal imaging. *Retina*. 2010;30:1441–1454.
96. Roquet W, Roudot-Thoraval F, Coscas G, et al. Clinical features of drusenoid pigment epithelial detachment in age related macular degeneration. *Br J Ophthalmol*. 2004;88:638–642.
97. Schuman SG, Koreishi AF, Farsiu S, et al. Photoreceptor layer thinning over drusen in eyes with age-related macular degeneration imaged in vivo with spectral-domain optical coherence tomography. *Ophthalmology*. 2009;116:488–496.e2.
98. Davis MD, Gangnon RE, Lee LY, et al. The Age-Related Eye Disease Study severity scale for age-related macular degeneration: AREDS report no. 17. *Arch Ophthalmol*. 2005;123:1484–1498.
99. Ferris FL, Davis MD, Clemons TE, et al. A simplified severity scale for age-related macular degeneration: AREDS

report no. 18. *Arch Ophthalmol*. 2005;123:1570–1574.
100. Ho J, Witkin AJ, Liu J, et al. Documentation of intraretinal retinal pigment epithelium migration via high-speed ultrahigh-resolution optical coherence tomography. *Ophthalmology*. 2010;118:687–693.
101. Nagiel A, Sarraf D, Sadda SR, et al. Type 3 neovascularization evolution, association with pigment epithelial detachment, and treatment response as revealed by spectral domain optical coherence tomography. *Retina*. 2015;35:638–647.
102. Zweifel SA, Imamura Y, Spaide TC, et al. Prevalence and significance of subretinal drusenoid deposits (reticular pseudodrusen) in age-related macular degeneration. *Ophthalmology*. 2010;117:1775–1781.
103. Zweifel SA, Spaide RF, Curcio CA, et al. Reticular pseudodrusen are subretinal drusenoid deposits. *Ophthalmology*. 2009;117:303–312.e1.
104. Sarks JP, Sarks SH, Killingsworth MC. Evolution of geographic atrophy of the retinal pigment epithelium. *Eye (Lond)*. 1988;2:552–577.
105. Sunness JS. The natural history of geographic atrophy, the advanced atrophic form of age-related macular degeneration. *Mol Vis*. 1999;5:25.
106. Sunness JS, Bressler NM, Tian Y, et al. Measuring geographic atrophy in advanced age-related macular degeneration. *Invest Ophthalmol Vis Sci*. 1999;40:1761–1769.
107. Sunness JS, Margalit E, Srikumaran D, et al. The long-term natural history of geographic atrophy from age-related macular degeneration: enlargement of atrophy and implications for interventional clinical trials. *Ophthalmology*. 2007;114:271–277.
108. Schmitz-Valckenberg S, Fleckenstein M, Gobel AP, et al. Optical coherence tomography and autofluorescence findings in areas with geographic atrophy due to age-related macular degeneration. *Invest Ophthalmol Vis Sci*. 2010;52:1–6.
109. Fleckenstein M, Charbel Issa P, Helb HM, et al. High-resolution spectral domain-OCT imaging in geographic

atrophy associated with age-related macular degeneration. *Invest Ophthalmol Vis Sci*. 2008;49:4137–4144.
110. Bearelly S, Chau FY, Koreishi A, et al. Spectral domain optical coherence tomography imaging of geographic atrophy margins. *Ophthalmology*. 2009;116:1762–1769.
111. Spaide RF. Age-related choroidal atrophy. *Am J Ophthalmol*. 2009;147:801–810.
112. Wood A, Binns A, Margrain T, et al. Retinal and choroidal thickness in early age-related macular degeneration. *Am J Ophthalmol*. 2011;152:1030–1038.
113. Lujan BJ, Wang F, Gregori G, et al. Calibration of fundus images using spectral domain optical coherence tomography. *Ophthalmic Surg Lasers Imaging*. 2008;39(Suppl.):S15–20.
114. Lujan BJ, Rosenfeld PJ, Gregori G, et al. Spectral domain optical coherence tomographic imaging of geographic atrophy. *Ophthalmic Surg Lasers Imaging*. 2009;40:96–101.
115. Green WR. Clinicopathologic studies of treated choroidal neovascular membranes: a review and report of two cases. *Retina*. 1991;11:328–356.
116. Green WR. Histopathology of age-related macular degeneration. *Mol Vis*. 1999;5:27.
117. Keane PA, Aghaian E, Ouyang Y, et al. Acute severe visual decrease after photodynamic therapy with verteporfin: spectral-domain OCT features. *Ophthalmic Surg Lasers Imaging*. 2010;41(Suppl.):S85–8.
118. Keane PA, Liakopoulos S, Chang KT, et al. Relationship between optical coherence tomography retinal parameters and visual acuity in neovascular age-related macular degeneration. *Ophthalmology*. 2008;115:2206–2214.
119. Yannuzzi LA, Hope-Ross M, Slakter JS, et al. Analysis of vascularized pigment epithelial detachments using indocyanine green videoangiography. *Retina*. 1994;14:99–113.
120. Jager RD, Mieler WF, Miller JW. Age-related macular degeneration. *N Engl J Med*. 2008;358:2606–2617.
121. Zayit-Soudry S, Moroz I, Loewenstein A. Retinal pigment epithelial detachment. *Surv Ophthalmol*. 2007;52:227–243.

122. Bloom SM, Singal IP. The outer Bruch membrane layer: a previously undescribed spectral-domain optical coherence tomography finding. *Retina*. 2010;31:316–323.
123. Coscas G, Coscas F, Zourdani A, et al. Optical coherence tomography and ARMD. *J Fr Ophtalmol*. 2004;27:3S7–30.
124. Pepple K, Mruthyunjaya P. Retinal pigment epithelial detachments in age-related macular degeneration: classification and therapeutic options. *Semin Ophthalmol*. 2011;26:198–208.
125. Spaide RF. Enhanced depth imaging optical coherence tomography of retinal pigment epithelial detachment in age-related macular degeneration. *Am J Ophthalmol*. 2009;147:644–652.
126. Joeres S, Tsong JW, Updike PG, et al. Reproducibility of quantitative optical coherence tomography subanalysis in neovascular age-related macular degeneration. *Invest Ophthalmol Vis Sci*. 2007;48:4300–4307.
127. Lee SY, Stetson PF, Ruiz-Garcia H, et al. Automated characterization of pigment epithelial detachment using optical coherence tomography. *Invest Ophthalmol Vis Sci*. 2012;53:164–170.
128. Hoskin A, Bird AC, Sehmi K. Tears of detached retinal pigment epithelium. *Br J Ophthalmol*. 1981;65:417–422.
129. Chang LK, Sarraf D. Tears of the retinal pigment epithelium: an old problem in a new era. *Retina*. 2007;27:523–534.
130. Levin LA, Seddon JM, Topping T. Retinal pigment epithelial tears associated with trauma. *Am J Ophthalmol*. 1991;112:396–400.
131. Ishida Y, Kato T, Minamoto A, et al. Retinal pigment epithelial tear in a patient with central serous chorioretinopathy treated with corticosteroids. *Retina*. 2004;24:633–636.
132. Gelisken F, Inhoffen W, Partsch M, et al. Retinal pigment epithelial tear after photodynamic therapy for choroidal neovascularization. *Am J Ophthalmol*. 2001;131:518–520.
133. Pece A, Introini U, Bottoni F, et al. Acute retinal pigment epithelial tear after photodynamic therapy. *Retina*.

2001;21:661–665.
134. Meyer CH, Mennel S, Schmidt JC, et al. Acute retinal pigment epithelial tear following intravitreal bevacizumab (Avastin) injection for occult choroidal neovascularisation secondary to age related macular degeneration. *Br J Ophthalmol*. 2006;90:1207–1208.
135. Carvounis PE, Kopel AC, Benz MS. Retinal pigment epithelium tears following ranibizumab for exudative age-related macular degeneration. *Am J Ophthalmol*. 2007;143:504–505.
136. Gelisken F, Ziemssen F, Voelker M, et al. Retinal pigment epithelial tears after single administration of intravitreal bevacizumab for neovascular age-related macular degeneration. *Eye (Lond)*. 2009;23:694–702.
137. Gass JD. Pathogenesis of tears of the retinal pigment epithelium. *Br J Ophthalmol*. 1984;68:513–519.
138. Chan CK, Abraham P, Meyer CH, et al. Optical coherence tomography-measured pigment epithelial detachment height as a predictor for retinal pigment epithelial tears associated with intravitreal bevacizumab injections. *Retina*. 2009;30:203–211.
139. Chiang A, Chang LK, Yu F, et al. Predictors of anti-VEGF-associated retinal pigment epithelial tear using FA and OCT analysis. *Retina*. 2008;28:1265–1269.
140. Landa G, Su E, Garcia PM, et al. Inner segment–outer segment junctional layer integrity and corresponding retinal sensitivity in dry and wet forms of age-related macular degeneration. *Retina*. 2011;31:364–370.
141. Oishi A, Hata M, Shimozono M, et al. The significance of external limiting membrane status for visual acuity in age-related macular degeneration. *Am J Ophthalmol*. 2010;150:27–32.e1.
142. Yannuzzi LA, Negrao S, Iida T, et al. Retinal angiomatous proliferation in age-related macular degeneration. *Retina*. 2001;21:416–434.
143. Gass JD, Agarwal A, Lavina AM, et al. Focal inner retinal hemorrhages in patients with drusen: an early sign of occult choroidal neovascularization and chorioretinal

anastomosis. *Retina*. 2003;23:741–751.
144. Truong SN, Alam S, Zawadzki RJ, et al. High resolution Fourier-domain optical coherence tomography of retinal angiomatous proliferation. *Retina*. 2007;27:915–925.
145. Freund KB, Ho IV, Barbazetto IA, et al. Type 3 neovascularization: the expanded spectrum of retinal angiomatous proliferation. *Retina*. 2008;28:201–211.
146. Querques G, Atmani K, Berboucha E, et al. Angiographic analysis of retinal-choroidal anastomosis by confocal scanning laser ophthalmoscopy technology and corresponding (eye-tracked) spectral-domain optical coherence tomography. *Retina*. 2009;30:222–234.
147. Krebs I, Glittenberg C, Hagen S, et al. Retinal angiomatous proliferation: morphological changes assessed by Stratus and Cirrus OCT. *Ophthalmic Surg Lasers Imaging*. 2009;40:285–289.
148. Yannuzzi LA, Sorenson J, Spaide RF, et al. Idiopathic polypoidal choroidal vasculopathy (IPCV). *Retina*. 1990;10:1–8.
149. Costa RA, Navajas EV, Farah ME, et al. Polypoidal choroidal vasculopathy: angiographic characterization of the network vascular elements and a new treatment paradigm. *Prog Retin Eye Res*. 2005;24:560–586.
150. Saito M, Iida T, Nagayama D. Cross-sectional and en face optical coherence tomographic features of polypoidal choroidal vasculopathy. *Retina*. 2008;28:459–464.
151. Ojima Y, Hangai M, Sakamoto A, et al. Improved visualization of polypoidal choroidal vasculopathy lesions using spectral-domain optical coherence tomography. *Retina*. 2009;29:52–59.
152. Harding SP. Neovascular age-related macular degeneration: decision making and optimal management. *Eye (Lond)*. 2010;24:497–505.
153. Brown DM, Kaiser PK, Michels M, et al. Ranibizumab versus verteporfin for neovascular age-related macular degeneration. *N Engl J Med*. 2006;355:1432–1444.
154. Rosenfeld PJ, Brown DM, Heier JS, et al. Ranibizumab for neovascular age-related macular degeneration. *N Engl J*

Med. 2006;355:1419–1431.
155. Engelbert M, Zweifel SA, Freund KB. Long-term follow-up for type 1 (subretinal pigment epithelium) neovascularization using a modified "treat and extend" dosing regimen of intravitreal antivascular endothelial growth factor therapy. *Retina*. 2010;30:1368–1375.
156. Martin DF, Maguire MG, Ying GS, et al. Ranibizumab and bevacizumab for neovascular age-related macular degeneration. *N Engl J Med*. 2011;364:1897–1908.
157. Fung AE, Lalwani GA, Rosenfeld PJ, et al. An optical coherence tomography-guided, variable dosing regimen with intravitreal ranibizumab (Lucentis) for neovascular age-related macular degeneration. *Am J Ophthalmol*. 2007;143:566–583.
158. Engelbert M, Zweifel SA, Freund KB. "Treat and extend" dosing of intravitreal antivascular endothelial growth factor therapy for type 3 neovascularization/retinal angiomatous proliferation. *Retina*. 2009;29:1424–1431.
159. Lalwani GA, Rosenfeld PJ, Fung AE, et al. A variable-dosing regimen with intravitreal ranibizumab for neovascular age-related macular degeneration: year 2 of the PrONTO Study. *Am J Ophthalmol*. 2009;148:43–58.e1.
160. Zweifel SA, Engelbert M, Laud K, et al. Outer retinal tubulation: a novel optical coherence tomography finding. *Arch Ophthalmol*. 2009;127:1596–1602.
161. Gass JD. Pathogenesis of disciform detachment of the neuroepithelium. *Am J Ophthalmol*. 1967;63(Suppl.):1–139.
162. Spaide RF, Campeas L, Haas A, et al. Central serous chorioretinopathy in younger and older adults. *Ophthalmology*. 1996;103:2070–2079 [discussion 2079–80].
163. Kitaya N, Nagaoka T, Hikichi T, et al. Features of abnormal choroidal circulation in central serous chorioretinopathy. *Br J Ophthalmol*. 2003;87:709–712.
164. Jalkh AE, Jabbour N, Avila MP, et al. Retinal pigment epithelium decompensation. I. Clinical features and natural course. *Ophthalmology*. 1984;91:1544–1548.
165. Yannuzzi LA, Shakin JL, Fisher YL, et al. Peripheral retinal detachments and retinal pigment epithelial atrophic tracts

secondary to central serous pigment epitheliopathy. *Ophthalmology*. 1984;91:1554–1572.
166. Scheider A, Nasemann JE, Lund OE. Fluorescein and indocyanine green angiographies of central serous choroidopathy by scanning laser ophthalmoscopy. *Am J Ophthalmol*. 1993;115:50–56.
167. Guyer DR, Yannuzzi LA, Slakter JS, et al. Digital indocyanine green videoangiography of central serous chorioretinopathy. *Arch Ophthalmol*. 1994;112:1057–1062.
168. Piccolino FC, Borgia L. Central serous chorioretinopathy and indocyanine green angiography. *Retina*. 1994;14:231–242.
169. Prunte C, Flammer J. Choroidal capillary and venous congestion in central serous chorioretinopathy. *Am J Ophthalmol*. 1996;121:26–34.
170. Kamppeter B, Jonas JB. Central serous chorioretinopathy imaged by optical coherence tomography. *Arch Ophthalmol*. 2003;121:742–743.
171. Montero JA, Ruiz-Moreno JM. Optical coherence tomography characterisation of idiopathic central serous chorioretinopathy. *Br J Ophthalmol*. 2005;89:562–564.
172. van Velthoven ME, Verbraak FD, Garcia PM, et al. Evaluation of central serous retinopathy with en face optical coherence tomography. *Br J Ophthalmol*. 2005;89:1483–1488.
173. Hussain N, Baskar A, Ram LM, et al. Optical coherence tomographic pattern of fluorescein angiographic leakage site in acute central serous chorioretinopathy. *Clin Experiment Ophthalmol*. 2006;34:137–140.
174. Hirami Y, Tsujikawa A, Sasahara M, et al. Alterations of retinal pigment epithelium in central serous chorioretinopathy. *Clin Experiment Ophthalmol*. 2007;35:225–230.
175. Wang MS, Sander B, Larsen M. Retinal atrophy in idiopathic central serous chorioretinopathy. *Am J Ophthalmol*. 2002;133:787–793.
176. Stock G, Ahlers C, Sayegh R, et al. [Three-dimensional imaging in central serous chorioretinopathy.]. *Ophthalmologe*. 2008;105:1127–1134.

177. Eandi CM, Chung JE, Cardillo-Piccolino F, et al. Optical coherence tomography in unilateral resolved central serous chorioretinopathy. *Retina*. 2005;25:417–421.
178. Furuta M, Iida T, Kishi S. Foveal thickness can predict visual outcome in patients with persistent central serous chorioretinopathy. *Ophthalmologica*. 2009;223:28–31.
179. Maruko I, Iida T, Sekiryu T, et al. Morphologic changes in the outer layer of the detached retina in rhegmatogenous retinal detachment and central serous chorioretinopathy. *Am J Ophthalmol*. 2009;147:489–494.e1.
180. Fujimoto H, Gomi F, Wakabayashi T, et al. Morphologic changes in acute central serous chorioretinopathy evaluated by Fourier-domain optical coherence tomography. *Ophthalmology*. 2008;115:1494–1500 [1500.e1–2].
181. Matsumoto H, Kishi S, Otani T, et al. Elongation of photoreceptor outer segment in central serous chorioretinopathy. *Am J Ophthalmol*. 2008;145:162–168.
182. Hee MR, Puliafito CA, Wong C, et al. Optical coherence tomography of central serous chorioretinopathy. *Am J Ophthalmol*. 1995;120:65–74.
183. Kon Y, Iida T, Maruko I, et al. The optical coherence tomography-ophthalmoscope for examination of central serous chorioretinopathy with precipitates. *Retina*. 2008;28:864–869.
184. Mitarai K, Gomi F, Tano Y. Three-dimensional optical coherence tomographic findings in central serous chorioretinopathy. *Graefes Arch Clin Exp Ophthalmol*. 2006;244:1415–1420.
185. Gupta P, Gupta V, Dogra MR, et al. Morphological changes in the retinal pigment epithelium on spectral-domain OCT in the unaffected eyes with idiopathic central serous chorioretinopathy. *Int Ophthalmol*. 2009;30:175–181.
186. Ojima Y, Hangai M, Sasahara M, et al. Three-dimensional imaging of the foveal photoreceptor layer in central serous chorioretinopathy using high-speed optical coherence tomography. *Ophthalmology*. 2007;114:2197–2207.
187. Matsumoto H, Sato T, Kishi S. Outer nuclear layer thickness at the fovea determines visual outcomes in resolved central

serous chorioretinopathy. *Am J Ophthalmol*. 2009;148:105–110.e1.
188. Imamura Y, Fujiwara T, Margolis R, et al. Enhanced depth imaging optical coherence tomography of the choroid in central serous chorioretinopathy. *Retina*. 2009;29:1469–1473.
189. Maruko I, Iida T, Sugano Y, et al. Subfoveal choroidal thickness in fellow eyes of patients with central serous chorioretinopathy. *Retina*. 2011;31:1603–1608.
190. Maruko I, Iida T, Sugano Y, et al. One-year choroidal thickness results after photodynamic therapy for central serous chorioretinopathy. *Retina*. 2011;31:1921–1927.
191. Henderson BA, Kim JY, Ament CS, et al. Clinical pseudophakic cystoid macular edema. Risk factors for development and duration after treatment. *J Cataract Refract Surg*. 2007;33:1550–1558.
192. Wolf EJ, Braunstein A, Shih C, et al. Incidence of visually significant pseudophakic macular edema after uneventful phacoemulsification in patients treated with nepafenac. *J Cataract Refract Surg*. 2007;33:1546–1549.
193. Irvine SR. A newly defined vitreous syndrome following cataract surgery. *Am J Ophthalmol*. 1953;36:499–619.
194. Schepens CL, Avila MP, Jalkh AE, et al. Role of the vitreous in cystoid macular edema. *Surv Ophthalmol*. 1984;28(Suppl.):499–504.
195. Moss SE, Klein R, Klein BE. Ten-year incidence of visual loss in a diabetic population. *Ophthalmology*. 1994;101:1061–1070.
196. Moss SE, Klein R, Klein BE. The 14-year incidence of visual loss in a diabetic population. *Ophthalmology*. 1998;105:998–1003.
197. Strom C, Sander B, Larsen N, et al. Diabetic macular edema assessed with optical coherence tomography and stereo fundus photography. *Invest Ophthalmol Vis Sci*. 2002;43:241–245.
198. Brown JC, Solomon SD, Bressler SB, et al. Detection of diabetic foveal edema: contact lens biomicroscopy compared with optical coherence tomography. *Arch Ophthalmol*. 2004;122:330–335.

199. Browning DJ, Apte RS, Bressler SB, et al. Association of the extent of diabetic macular edema as assessed by optical coherence tomography with visual acuity and retinal outcome variables. *Retina*. 2009;29:300–305.
200. Al-latayfeh MM, Sun JK, Aiello LP. Ocular coherence tomography and diabetic eye disease. *Semin Ophthalmol*. 2010;25:192–197.
201. Browning DJ, McOwen MD, Bowen RM Jr, et al. Comparison of the clinical diagnosis of diabetic macular edema with diagnosis by optical coherence tomography. *Ophthalmology*. 2004;111:712–715.
202. Virgili G, Menchini F, Dimastrogiovanni AF, et al. Optical coherence tomography versus stereoscopic fundus photography or biomicroscopy for diagnosing diabetic macular edema: a systematic review. *Invest Ophthalmol Vis Sci*. 2007;48:4963–4973.
203. Davis MD, Bressler SB, Aiello LP, et al. Comparison of time-domain OCT and fundus photographic assessments of retinal thickening in eyes with diabetic macular edema. *Invest Ophthalmol Vis Sci*. 2008;49:1745–1752.
204. Otani T, Kishi S, Maruyama Y. Patterns of diabetic macular edema with optical coherence tomography. *Am J Ophthalmol*. 1999;127:688–693.
205. Kim BY, Smith SD, Kaiser PK. Optical coherence tomographic patterns of diabetic macular edema. *Am J Ophthalmol*. 2006;142:405–412.
206. Soliman W, Sander B, Hasler PW, et al. Correlation between intraretinal changes in diabetic macular oedema seen in fluorescein angiography and optical coherence tomography. *Acta Ophthalmol*. 2008;86:34–39.
207. Early Treatment Diabetic Retinopathy Study research group. Photocoagulation for diabetic macular edema. Early Treatment Diabetic Retinopathy Study report number 1. *Arch Ophthalmol*. 1985;103:1796–1806.
208. Early Treatment Diabetic Retinopathy Study Research Group. Photocoagulation for diabetic macular edema: Early Treatment Diabetic Retinopathy Study report no. 4. *Int Ophthalmol Clin*. 1987;27:265–272.

209. Early Treatment Diabetic Retinopathy Study Research Group. Treatment techniques and clinical guidelines for photocoagulation of diabetic macular edema. Early Treatment Diabetic Retinopathy Study report no. 2. *Ophthalmology*. 1987;94:761–774.
210. Elman MJ, Bressler NM, Qin H, et al. Expanded 2-year follow-up of ranibizumab plus prompt or deferred laser or triamcinolone plus prompt laser for diabetic macular edema. *Ophthalmology*. 2011;118:609–614.
211. Michaelides M, Kaines A, Hamilton RD, et al. A prospective randomized trial of intravitreal bevacizumab or laser therapy in the management of diabetic macular edema (BOLT study) 12-month data: report 2. *Ophthalmology*. 2010;117:1078–1086.e2.
212. Kim NR, Kim YJ, Chin HS, et al. Optical coherence tomographic patterns in diabetic macular oedema: prediction of visual outcome after focal laser photocoagulation. *Br J Ophthalmol*. 2009;93:901–905.
213. Soliman W, Sander B, Soliman KA, et al. The predictive value of optical coherence tomography after grid laser photocoagulation for diffuse diabetic macular oedema. *Acta Ophthalmol*. 2008;86:284–291.
214. Kaiser PK, Riemann CD, Sears JE, et al. Macular traction detachment and diabetic macular edema associated with posterior hyaloidal traction. *Am J Ophthalmol*. 2001;131:44–49.
215. Ghazi NG, Ciralsky JB, Shah SM, et al. Optical coherence tomography findings in persistent diabetic macular edema: the vitreomacular interface. *Am J Ophthalmol*. 2007;144:747–754.
216. Haller JA, Qin H, Apte RS, et al. Vitrectomy outcomes in eyes with diabetic macular edema and vitreomacular traction. *Ophthalmology*. 2010;117:1087–1093.e3.
217. Maheshwary AS, Oster SF, Yuson RM, et al. The association between percent disruption of the photoreceptor inner segment–outer segment junction and visual acuity in diabetic macular edema. *Am J Ophthalmol*. 2010;150:63–67.e1.

218. Otani T, Yamaguchi Y, Kishi S. Correlation between visual acuity and foveal microstructural changes in diabetic macular edema. *Retina*. 2010;30:774–780.
219. Sakamoto A, Nishijima K, Kita M, et al. Association between foveal photoreceptor status and visual acuity after resolution of diabetic macular edema by pars plana vitrectomy. *Graefes Arch Clin Exp Ophthalmol*. 2009;247:1325–1330.
220. Hayreh SS. Classification of central retinal vein occlusion. *Ophthalmology*. 1983;90:458–474.
221. Ota M, Tsujikawa A, Murakami T, et al. Foveal photoreceptor layer in eyes with persistent cystoid macular edema associated with branch retinal vein occlusion. *Am J Ophthalmol*. 2008;145:273–280.
222. Shroff D, Mehta DK, Arora R, et al. Natural history of macular status in recent-onset branch retinal vein occlusion: an optical coherence tomography study. *Int Ophthalmol*. 2008;28:261–268.
223. Falkenberry SM, Ip MS, Blodi BA, et al. Optical coherence tomography findings in central retinal artery occlusion. *Ophthalmic Surg Lasers Imaging*. 2006;37:502–505.
224. Goldenberg-Cohen N, Dadon S, Avraham BC, et al. Molecular and histological changes following central retinal artery occlusion in a mouse model. *Exp Eye Res*. 2008;87:327–333.
225. Murthy RK, Grover S, Chalam KV. Sequential spectral domain OCT documentation of retinal changes after branch retinal artery occlusion. *Clin Ophthalmol*. 2010;4:327–329.
226. Chen X, Rahimy E, Sergott RC, et al. Spectrum of retinal vascular diseases associated with paracentral acute middle maculopathy. *Am J Ophthalmol*. 2015;160(1):26–34.
227. Wang RK, An L, Francis P, Wilson DJ. Depth-resolved imaging of capillary networks in retina and choroid using ultrahigh sensitive optical microangiography. *Opt Lett*. 2010;35(9):1467–1469.
228. Jia Y, Tan O, Tokayer J, et al. Split-spectrum amplitude-decorrelation angiography with optical coherence tomography. *Opt Express*. 2012;20(4):4710–4725.

229. Matsunaga D, Yi J, Puliafito CA, Kashani AH. OCT angiography in healthy human subjects. *Ophthalmic Surg Lasers Imaging Retina*. 2014;45:510–515.
230. Huang Y, Zhang Q, Thorell MR, et al. Swept-source OCT angiography of the retinal vasculature using intensity differentiation-based optical microangiography algorithms. *Ophthalmic Surg Lasers Imaging Retina*. 2014;45(5):382–389.
231. Agemy SA, Scripsema NK, Shah CM, et al. Retinal vascular perfusion density mapping using optical coherence tomography angiography in normals and diabetic retinopathy patients. *Retina*. 2015;35(11):2353–2363.
232. Wei E, Jia Y, Tan O, et al. Parafoveal retinal vascular response to pattern visual stimulation assessed with OCT angiography. *PLoS ONE*. 2013;8(12):e81343.
233. Matsunaga DR, Yi JJ, De Koo LO, Ameri H, Puliafito CA, Kashani AH. Optical coherence tomography angiography of diabetic retinopathy in human subjects. *Ophthalmic Surg Lasers Imaging Retina*. 2015;46(8):796–805.
234. Mendis KR, Balaratnasingam C, Yu P, et al. Correlation of histologic and clinical images to determine the diagnostic value of fluorescein angiography for studying retinal capillary detail. *Invest Ophthalmol Vis Sci*. 2010;51:5864–5869.
235. Ishibazawa A, Nagaoka T, Takahashi A, et al. Optical coherence tomography angiography in diabetic retinopathy: a prospective pilot study. *Am J Ophthalmol*. 2015;160:35–44.e1.
236. de Carlo TE, Chin AT, Bonini Filho MA, et al. Detection of microvascular changes in eyes of patients with diabetes but not clinical diabetic retinopathy using optical coherence tomography angiography. *Retina*. 2015;35(11):2364–2370.
237. de Carlo TE, Chin AT, Bonini Filho MA, et al. Detection of microvascular changes in eyes of patients with diabetes but not clinical diabetic retinopathy using optical coherence tomography angiography. *Retina*. 2015;35(11):2364–2370.
238. Takase N, Nozaki M, Kato A, Ozeki H, Yoshida M, Ogura Y. Enlargement of foveal avascular zone in diabetic eyes evaluated by en face optical coherence tomography angiography. *Retina*. 2015;35(11):2377–2383.

239. Kashani AH, Lee SY, Moshfeghi A, Durbin MK, Puliafito CA. Optical coherence tomography angiography of retinal venous occlusion. *Retina*. 2015;35(11):2323–2331.
240. Thorell MR, Zhang Q, Huang Y, et al. Swept-source OCT angiography of macular telangiectasia type 2. *Ophthalmic Surg Lasers Imaging Retina*. 2014;45(5):369–380.
241. Zhang Q, Wang RK, Chen CL, et al. Swept source optical coherence tomography angiography of neovascular macular telangiectasia type 2. *Retina*. 2015;35(11):2285–2299.
242. de Carlo TE, Salz DA, Waheed NK, et al. Visualization of the retinal vasculature using wide-field montage optical coherence tomography angiography. *Ophthalmic Surg Lasers Imaging Retina*. 2015;46(6):611–616.
243. de Carlo TE, Romano A, Waheed N, et al. A review of optical coherence tomography angiography (OCTA). *Int J Retina Vitreous*. 2015;1:5.
244. Matsunaga D, Yi J, Puliafito CA, et al. OCT angiography in healthy human subjects. *Ophthalmic Surg Lasers Imaging Retina*. 2014;45(6):510–515.
245. Jia Y, Bailey ST, Hwang TS, et al. Quantitative optical coherence tomography angiography of vascular abnormalities in the living human eye. *Proc Natl Acad Sci USA*. 2015;112(18):E2395–402.
246. Moult E, Choi W, Waheed NK, et al. Ultrahigh-speed swept-source OCT angiography in exudative AMD. *Ophthalmic Surg Lasers Imaging Retina*. 2014;45(6):496–505.
247. Choi W, Mohler KJ, Potsaid B, et al. Choriocapillaris and choroidal microvasculature imaging with ultrahigh speed OCT angiography. *PLoS ONE*. 2013;8(12):e81499.
248. Unterhuber A, Povazay B, Hermann B, et al. In vivo retinal optical coherence tomography at 1040 nm – enhanced penetration into the choroid. *Opt Express*. 2005;13(9):3252–3258.
249. Povazay B, Hermann B, Unterhuber A, et al. Three-dimensional optical coherence tomography at 1050 nm versus 800 nm in retinal pathologies: enhanced performance and choroidal penetration in cataract patients. *J Biomed Opt*. 2007;12(4):041211.

250. Adhi M, Liu JJ, Qavi AH, et al. Choroidal analysis in healthy eyes using swept-source optical coherence tomography compared to spectral domain optical coherence tomography. *Am J Ophthalmol*. 2014;157(6):1272–1281.e1.
251. Jia Y, Tan O, Tokayer J, et al. Split-spectrum amplitude-decorrelation angiography with optical coherence tomography. *Opt Express*. 2012;20(4):4710–4725.
252. Tokayer J, Jia Y, Dhalla AH, et al. Blood flow velocity quantification using split-spectrum amplitude-decorrelation angiography with optical coherence tomography. *Biomed Opt Express*. 2013;4(10):1909–1924.
253. Kraus MF, Potsaid B, Mayer MA, et al. Motion correction in optical coherence tomography volumes on a per A-scan basis using orthogonal scan patterns. *Biomed Opt Express*. 2012;3(6):1182–1199.
254. Choi W, Moult EM, Waheed NK, et al. Ultrahigh-speed, swept-source optical coherence tomography angiography in nonexudative age-related macular degeneration with geographic atrophy. *Ophthalmology*. 2015;122(12):2532–2544.
255. Bhutto I, Lutty G. Understanding age-related macular degeneration (AMD): relationships between the photoreceptor/retinal pigment epithelium/Bruch's membrane/choriocapillaris complex. *Mol Aspects Med*. 2012;33(4):295–317.
256. Lengyel I, Tufail A, Hosaini HA, Luthert P, Bird AC, Jeffery G. Association of drusen deposition with choroidal intercapillary pillars in the aging human eye. *Invest Ophthalmol Vis Sci*. 2004;45(9):2886–2892.
257. Sarks SH, Arnold JJ, Killingsworth MC, Sarks JP. Early drusen formation in the normal and aging eye and their relation to age related maculopathy: a clinicopathological study. *Br J Ophthalmol*. 1999;83(3):358–368.
258. Mullins RF, Johnson MN, Faidley EA, Skeie JM, Huang J. Choriocapillaris vascular dropout related to density of drusen in human eyes with early age-related macular degeneration. *Invest Ophthalmol Vis Sci*. 2011;52(3):1606–1612.
259. Sohrab M, Wu K, Fawzi AA. A pilot study of morphometric

analysis of choroidal vasculature in vivo, using en face optical coherence tomography. *PLoS ONE*. 2012;7(11):e48631.
260. Huang D, Jia Y, Rispoli M, Tan O, Lumbroso B. Optical coherence tomography angiography of time course of choroidal neovascularization in response to anti-angiogenic treatment. *Retina*. 2015;35(11):2260–2264.
261. Muakkassa NW, Chin AT, de Carlo T, et al. Characterizing the effect of anti-vascular endothelial growth factor therapy on treatment-naive choroidal neovascularization using optical coherence tomography angiography. *Retina*. 2015;35(11):2252–2259.
262. de Carlo TE, Bonini Filho MA, Chin AT, et al. Spectral-domain optical coherence tomography angiography of choroidal neovascularization. *Ophthalmology*. 2015;122(6):1228–1238.
263. Coscas GJ, Lupidi M, Coscas F, Cagini C, Souied EH. Optical coherence tomography angiography versus traditional multimodal imaging in assessing the activity of exudative age-related macular degeneration: a new diagnostic challenge. *Retina*. 2015;35(11):2219–2228.
264. Coscas G, Lupidi M, Coscas F, Français C, Cagini C, Souied EH. Optical coherence tomography angiography during follow-up: qualitative and quantitative analysis of mixed type I and II choroidal neovascularization after vascular endothelial growth factor trap therapy. *Ophthalmic Res*. 2015;54(2):57–63.
265. Moult E, Choi W, Waheed NK, et al. Ultrahigh-speed swept-source OCT angiography in exudative AMD. *Ophthalmic Surg Lasers Imaging Retina*. 2014;45(6):496–505.
266. Fernandez EJ, Hermann B, Povazay B, et al. Ultrahigh resolution optical coherence tomography and pancorrection for cellular imaging of the living human retina. *Opt Express*. 2008;16:11083–11094.
267. Huber R, Adler DC, Srinivasan VJ, et al. Fourier domain mode locking at 1050nm for ultra-high-speed optical coherence tomography of the human retina at 236,000 axial scans per second. *Opt Lett*. 2007;32:2049–2051.

268. Unterhuber A, Povazay B, Hermann B, et al. In vivo retinal optical coherence tomography at 1040nm – enhanced penetration into the choroid. *Opt Express*. 2005;13:3252–3258.
269. Povazay B, Hermann B, Hofer B, et al. Wide-field optical coherence tomography of the choroid in vivo. *Invest Ophthalmol Vis Sci*. 2009;50:1856–1863.
270. Povazay B, Hermann B, Unterhuber A, et al. Three-dimensional optical coherence tomography at 1050nm versus 800nm in retinal pathologies: enhanced performance and choroidal penetration in cataract patients. *J Biomed Opt*. 2007;12:041211.
271. Wang Y, Lu A, Gil-Flamer J, et al. Measurement of total blood flow in the normal human retina using Doppler Fourier-domain optical coherence tomography. *Br J Ophthalmol*. 2009;93:634–637.
272. Ahlers C, Gotzinger E, Pircher M, et al. Imaging of the retinal pigment epithelium in age-related macular degeneration using polarization-sensitive optical coherence tomography. *Invest Ophthalmol Vis Sci*. 2010;51:2149–2157.
273. Cense B, Chen TC, Park BH, et al. Thickness and birefringence of healthy retinal nerve fiber layer tissue measured with polarization-sensitive optical coherence tomography. *Invest Ophthalmol Vis Sci*. 2004;45:2606–2612.
274. Sayegh RG, Zotter S, Roberts PK, et al. Polarization-sensitive optical coherence tomography and conventional retinal imaging strategies in assessing foveal integrity in geographic atrophy. *Invest Ophthalmol Vis Sci*. 2015;56(9):5246–5255.

4

Autofluorescence Imaging

Monika Fleckenstein, Steffen Schmitz-Valckenberg, Frank G. Holz

Basic Principles

Fundus Autofluorescence

Fundus autofluorescence (FAF) imaging is a noninvasive imaging method for in vivo mapping of naturally or pathologically occurring fluorophores of the ocular fundus (Fig. 4.1 and Fig. 4.5B). The dominant sources are fluorophores accumulating in lipofuscin (LF) granules in postmitotic retinal pigment epithelium (RPE) cells.[1] In the absence of RPE cells, minor fluorophores including collagen and elastin, e.g., in choroidal blood vessel walls, may also become visible. Bleaching phenomena and loss of photopigment may result in increased FAF by reduced absorbance anterior to the RPE level.

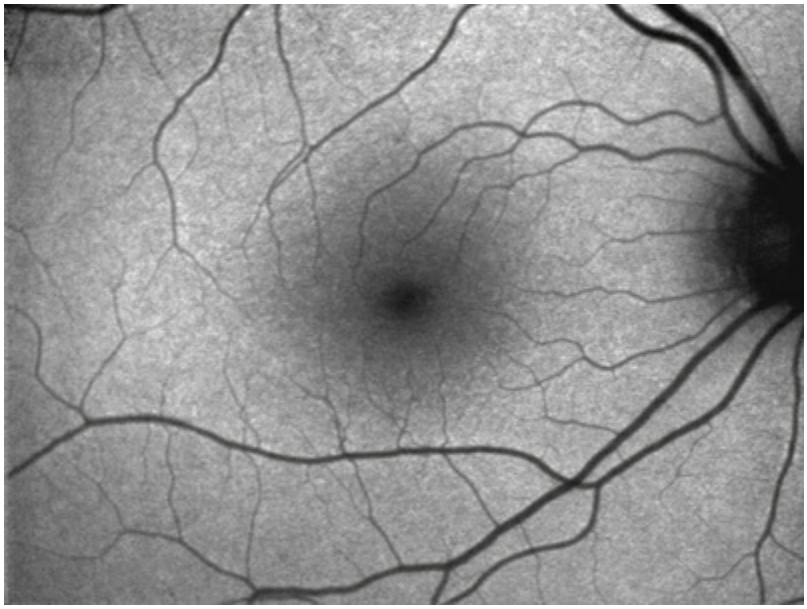

FIG. 4.1 Normal fundus autofluorescence image obtained with a Nidek F-10 scanning laser ophthalmoscope.

Retinal Pigment Epithelium and Lipofuscin

The RPE constitutes a polygonal monolayer between the neurosensory retina and the choroid. Given multiple essential physiologic functions of the RPE, it is not surprising that RPE dysfunction has been implicated in a variety of retinal diseases (reviewed by Schmitz-Valckenberg et al.[2]).

A hallmark of aging is the gradual accumulation of LF granules in the cytoplasm of RPE cells. It is thought that progressive LF accumulation is mainly a byproduct of the constant phagocytosis of shed photoreceptor outer-segment discs.[3–5] Several lines of evidence indicate that adverse effects of excessive LF accumulation represent a common downstream pathogenetic mechanism in various monogenic macular and retinal dystrophies, as well as in multifactorial complex retinal disease entities, including age-related macular degeneration (AMD).[3,4,6–8]

Apparently, once formed, the RPE cell has no means of either degrading or transporting LF material and granules into the extracellular space via exocytosis. Subsequently, these granules are trapped in the cytoplasmic space of the postmitotic RPE cells. Previous studies have shown that various LF components such as

A2-E (*N*-retinylidene-*N*-retinylethanol-amine), a dominant fluorophore, possess toxic properties that may interfere with normal cell function via various molecular mechanisms, including impairment of lysosomal degradation due to inhibition of the lysosomal adenosine triphosphate-dependent proton pump.[9–12] Other components of LF include precursors of A2-E, molecules formed by the mixture of oxygen-containing moieties within photo-oxidized A2-E, reactions between retinoids and other constituents other than ethanolamine, and peroxidation products of proteins and lipids.[13,14] The molecular composition of LF may possibly be dependent on specific underlying molecular mechanisms. Zhou and associates demonstrated with an in vitro assay a link between inflammation, activation of the complement system, oxidative damage, drusen, and RPE LF.[15] They suggested that products of the photo-oxidation of RPE LF components could serve as a trigger for the complement system which could predispose the macular area to a chronic, low-grade inflammatory process over time. A recent study demonstrated that accumulation of lipofuscin-like material in vitro renders RPE cells susceptible to phototoxic destabilization of lysosomes, resulting in inflammasome activation and secretion of inflammatory cytokines. This new mechanism of inflammasome activation links photo-oxidative damage and innate immune activation in RPE pathology.[16]

Detection of LF and its constituents is facilitated by its autofluorescent properties. When stimulated with light in the blue range, LF granules typically emit a green–yellow fluorescence.[17,18] The distribution of LF in postmitotic human RPE cells and its accumulation with age have been extensively studied in vitro, applying fluorescence microscopic techniques.[5,6,8]

Near-Infrared Autofluorescence

Near-infrared autofluorescence (NIR-AF) images can also be obtained in vivo, most commonly and easily by using the indocyanine green angiography (ICGA) mode of the scanning laser ophthalmoscope (SLO), i.e., without dye injection (Fig. 4.2).[19,20] Due to the excitation and emission in the red end of the spectrum, the topographic distribution of fluorophores other than LF may be

studied by this technique. It has been suggested that the NIR-AF signal is largely melanin-derived.[19–21] As such, Keilhauer and Delori[19] further speculated that, to varying degrees, choroidal sources contributed to this signal. Gibbs et al.[22] investigated NIR-AF in humans and mice and suggested that melanosomes in the RPE and choroid were likely the dominant origin of the signal. Except for measurements in cell cultures at low magnification, their analyses were limited to excitation at 633 nm, in contrast to in vivo NIR-AF, which is generated at 795 nm. Using a customized magnification lens attached to the front of the confocal SLO (cSLO), Schmitz-Valckenberg and coworkers studied the distribution of the NIR-AF signal in retinal cross-sections of a human donor eye and correlated ex vivo autofluorescence measurements to in vivo findings in a rat animal model.[23] They observed that the NIR-AF signal was spatially confined to the RPE monolayer and melanin in the choroid.

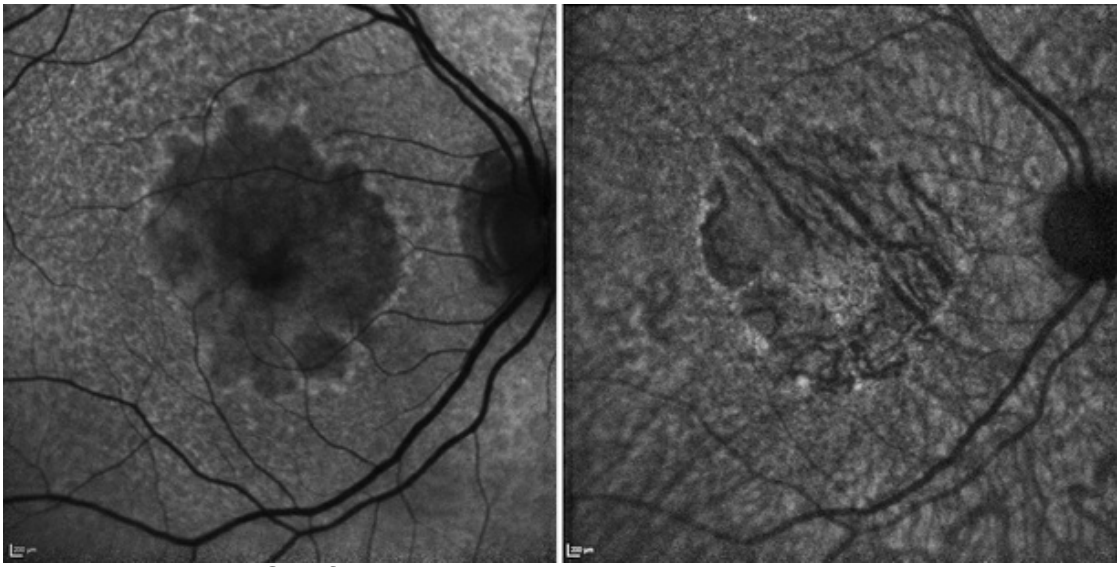

FIG. 4.2 Confocal scanning laser ophthalmoscopy fundus autofluorescence imaging with an excitation of 488 nm (left image) and near-infrared autofluorescence obtained by using the indocyanine green angiography mode (right image) of the scanning laser ophthalmoscope in an eye with geographic atrophy with 'foveal sparing'.

Macular Pigment Imaging

Macular pigment, consisting of lutein and zeaxanthin, extensively accumulates along the axons of the cone photoreceptors in the central retina.[24–26] As has been reported, a number of functions have been proposed for macular pigment,[25,26] including filtration of blue light which may reduce photo damage and glare, minimization of the effects of chromatic aberration on visual acuity, improvement in fine-detail discrimination, and enhancement of contrast sensitivity. Neutralization of reactive oxygen species by macular pigment may have a protective effect on the neurosensory retina. Although there may be a large variation with regard to the concentration of macular pigment, the pattern of distribution is relatively uniform in the normal population. It generally shows a peak concentration at the foveal center and rapidly decreases with eccentricity, with very little present at about 8° of eccentricity.

Peak absorption of luteal pigment is at 460 nm. These absorption properties can be readily recorded in vivo by blue-light autofluorescence imaging.[27] Therefore, blue FAF imaging can also be used to determine the topographic distribution of macular pigment. Compared to other methods, including heterochromatic flicker photometry, the advantage of FAF imaging is its objective acquisition technique which is not dependent on psychophysical cooperation by the examined individual.

Techniques of Fundus Autofluorescence Imaging

Recording of autofluorescence images is noninvasive and requires relatively little time.

The intensity of naturally occurring fluorescence of the ocular fundus is about two orders of magnitude lower than the background of a fluorescein angiogram at the most intense part of the dye transit.[1] Absorption of light with reduction of the fluorescence signal, or excitation and emission of light with an increase in the fluorescence signal by anatomical structures anterior to the retina, may further complicate or interfere with the detection of the FAF signal. In the eye, the principal barrier is the crystalline

lens, which has highly fluorescent properties in the short-wavelength range (excitation between 400 and 600 nm results in peak emission at c. 520 nm). With increasing age and particularly the development of nuclear lens opacities, the fluorescence of the lens becomes even more prominent.

Pioneering work on the spectral analysis of the origin of the autofluorescence signal was performed by Delori and coworkers[1] using a fundus spectrometer. In parallel, von Rückmann et al., in their landmark paper, described the use of cSLO for FAF imaging.[28]

Fundus Spectrophotometer

The fundus spectrophotometer by Delori and coworkers[1] was designed to systematically analyze the excitation and emission spectra of the autofluorescence signals originating from small retinal areas (2° diameter) of the fundus. By incorporating an image intensifier diode array as a detector, a beam separation in the pupil, and confocal detection to minimize contribution of autofluorescence from the crystalline lens, this device allowed the absolute measurements of autofluorescence. These authors showed that fundus fluorescence is emitted across a broad band from 500 to 800 nm. Both at the center of the fovea and at 7° temporally, optimal excitation occurred at 510 nm, with peak emission at approximately 630 nm, indicating the predominance of a fluorophore at these excitation and emission spectra. There was a significant increase with age and the recording along a horizontal line through the fovea showed a minimum fluorescence at the fovea, a maximum intensity at 7–15° from the fovea, and a decrease toward the periphery, most likely reflecting the concomitant distribution of macular pigment and melanin interfering with the emission of the dominant fluorophore. The optic disc was characterized by a less intense signal. The relationship with age and the topographic distribution of the dominant fundus fluorophore were consistent with those of RPE LF as measured in the RPE of human donor eyes.[3,5]

Along with autofluorescence recordings in patients with several pathologic conditions, the initial work by Delori et al.[1] demonstrated that LF is the dominant source of intrinsic

fluorescence of the ocular fundus. However, the small area sampled by the fundus spectrometer as well as the customized relatively complex instrumentation and techniques were not practical for recording FAF from patients in a clinical setting.

Scanning Laser Ophthalmoscopy

Confocal SLO acquisition optimally addresses the limitations of the low intensity of the autofluorescence signal and the interference of the crystalline lens. It was used initially by von Rückmann and coworkers in a clinical imaging system.[28] The cSLO projects a low-power laser beam on the retina which is swept across the fundus in a raster pattern.[29] The intensity of the reflected light at each point, after passing through the confocal pinhole, is registered by means of a detector, and a two-dimensional image is subsequently generated. Confocal optics ensure that out-of-focus light (i.e., light originating outside the adjusted focal plane, but within the light beam) is suppressed and, thus, the image contrast is enhanced. This suppression increases with the distance from the focal plane and signals from sources anterior to the retina, i.e., the lens or the cornea, are effectively reduced.

In contrast to the 2° retinal field of the fundus spectrophotometer, the cSLO allows imaging over larger retinal areas. To reduce background noise and to enhance image contrast, a series of several single images is usually recorded (reviewed by Schmitz-Valckenberg et al.[2]). For the final FAF image, a number of these frames (usually out of 4–32) are averaged and pixel values are normalized. Given the high sensitivity of the cSLO and the high frame rate of up to 16 frames per second, FAF imaging can be performed within seconds and at low excitation energies which are well below the maximum retinal irradiance limits of lasers established by the American National Standards Institute and other international standards.

With cSLO FAF imaging, excitation is usually induced in the blue range (λ = 488 nm), and an emission filter between 500 and 700 nm is used to detect emission of the autofluorescence signal.

At this excitation wavelength – compared to an excitation in the green range – there is reduced FAF intensity in the central retina

due to absorption by macular pigment.

The most widely used cSLO system for FAF imaging is the Heidelberg retina angiograph/Heidelberg Spectralis. One key advantage of the Spectralis system is the simultaneous acquisition of optical coherence tomography (OCT) recordings that allows for both averaging of several OCT B-scans in order to enhance the signal-to-noise ratio and the synchronous topographic alignment of FAF features with OCT findings. Other previous systems, such as the Rodenstock cSLO and the Zeiss prototype SM 30 4024 for FAF imaging, are no longer commercially available. Nidek has introduced the F-10 cSLO platform that also allows for FAF imaging with a variety of confocal pinholes (see Fig. 4.1).

Fundus Camera

The relatively weak FAF signal, absorption effects of the crystalline lens, nonconfocality, and light-scattering effects are important limitations of fundus camera-based systems for FAF recordings. Delori and coworkers described a modified fundus camera for FAF imaging.[30] Their design included the insertion of an aperture in the illumination optics of the camera in order to minimize the loss of contrast caused by light scattering and fluorescence from the crystalline lens. However, the modification also resulted in the restriction of the field of view to a 13° diameter circle; this, together with the complex design, is the likely reason why this configuration has not been further pursued. In 2003, Spaide[31] reported the modification of a commercially available fundus camera system by shifting the excitation and emission wavelengths for FAF imaging towards the red end of the spectrum in order to suppress the fluorescence originating from the lens (Fig. 4.3). The relatively inexpensive purchase of an additional filter set, together with the broad availability of the flash fundus camera, may make this an attractive alternative. These operate with excitation in the green spectrum and emission is recorded in the yellow–orange spectrum.[32]

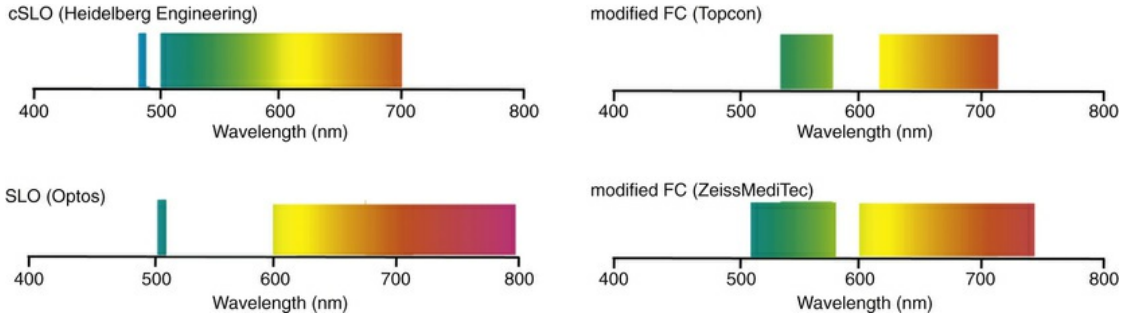

FIG. 4.3 Range of excitation and emission for different camera systems. *cSLO*, confocal scanning laser ophthalmoscopy; *FC*, fundus camera.

In addition to the different excitation light (green versus blue) for FAF recording, other major technical differences between fundus camera systems and the cSLO setup must be considered (Table 4.1). In particular, the absence of confocal optics makes the fundus camera prone to light scattering and generation of secondary reflectance light that interferes with the FAF detection. The visualization of subtle FAF alterations is challenging with the modified fundus camera, as shown in one study of patients with geographic atrophy (GA) secondary to AMD.[33]

TABLE 4.1

Summary of Technical Differences Between the Confocal Scanning Laser Ophthalmoscope (cSLO) and the Modified Fundus Camera for Fundus Autofluorescence Imaging

cSLO	Modified Fundus Camera
One excitation wavelength (laser source) Large emission spectrum (cutoff filter)	Bandwidth filters for excitation and emission
Continuous scanning at low light intensities in a raster pattern	One single flash at maximum intensities
Confocal system	Entire cone of light
Laser power fixed by manufacturer, detector sensitivity adjustable	Flash light intensity, gain and gamma of detector adjustable
Imaging processing with averaging of single frames and pixel normalization	Manual contrast and brightness

Aside from qualitative differences, discrepancies in quantitative assessment between different FAF imaging systems must be accounted for. It has recently been demonstrated that inherent image-scaling differences are not restricted to simple pixel-to-millimeter calibration variances, but appear to vary depending on measurement orientation.[34] These factors should be considered

when comparing measurements obtained using different imaging systems, particularly in the context of clinical trials.[34]

Wide-Field Imaging

The standard image field of the typical cSLO encompasses a retinal field of 30° × 30°. Additional lenses allow for imaging of a 55° field or, using the composite mode, imaging over even larger retinal areas. Using the fundus camera, so-called montage images can be manually generated using image analysis software on the basis of a seven-field panorama survey.

Peripheral FAF images can also be recorded with a wide-field scanning laser ophthalmoscope (P200Tx, Optos). This system allows for FAF acquisition in less than 2 seconds by using green light excitation (532 nm). FAF imaging beyond the vascular arcades is helpful for assessment of the peripheral extension of retinal diseases.[35–37] Therefore, wide-field FAF scanning laser ophthalmoscopy is also useful to evaluate longitudinal variations of diseases affecting the peripheral retina (Fig. 4.4).[38]

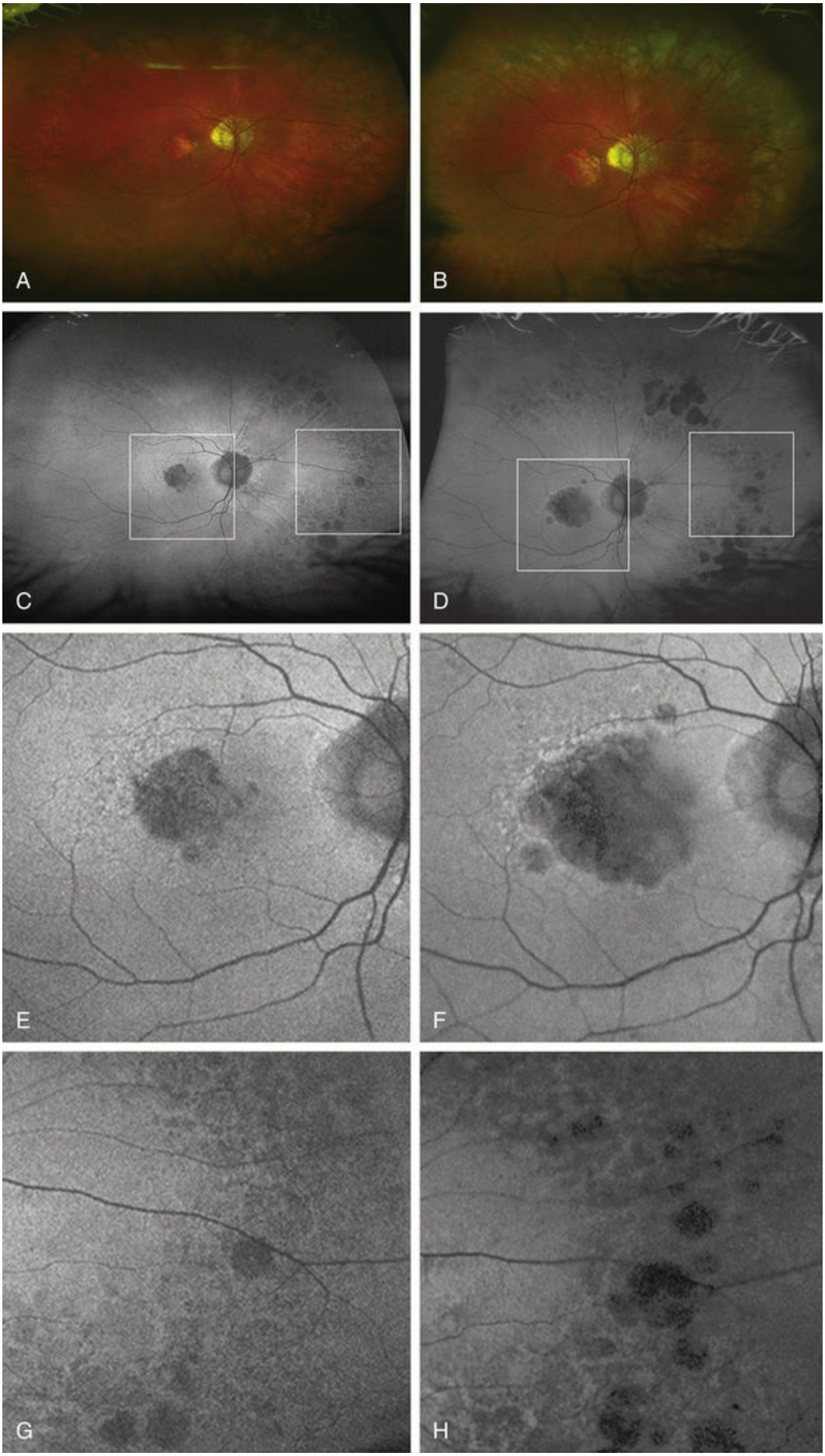
A
B
C
D
E
F
G
H

FIG. 4.4 Patient with geographic atrophy due to age-related macular degeneration. The image was recorded by a wide-field scanning laser ophthalmoscope (P200Tx, Optos). This system allows for fundus autofluorescence acquisition in less than 2 seconds by using green light excitation (532 nm). Marked atrophic areas are already present at baseline in peripheral retinal areas that show progression – in addition to the typical findings within the central atrophic lesions – over time. (Reproduced from Duisdieker V, Fleckenstein M, Zilkens KM, et al. Long-term follow-up of fundus autofluorescence imaging using wide-field scanning laser ophthalmoscopy. Ophthalmologica 2015;234:218-2. Copyright Karger Publishers.)

Interpretation of Fundus Autofluorescence Images

The FAF image shows the spatial distribution of the intensity of the FAF signal for each pixel in gray values (arbitrary values from 0 to 255). Per definition, low pixel values (dark) illustrate low intensities and high pixel values (bright) denote high intensities. The topographical distribution of FAF in normal eyes demonstrates a consistent pattern, as illustrated in Fig. 4.5.[28] A diffuse FAF signal over the posterior pole can be seen, while retinal vessels (due to an absorption phenomenon by blood contents, i.e., hemoglobin) and the optic nerve head (absence of autofluorescent material) are characterized by a very low signal and appear dark. Showing a high degree of interindividual variability, decreased FAF intensities at the macular area with a minimum in the fovea are observed; these are caused by absorption of short-wavelength light due to luteal pigment (lutein and zeaxanthin). Other contributing factors may be an increased accumulation of melanin and a reduced deposition of lipofuscin granules.[1]

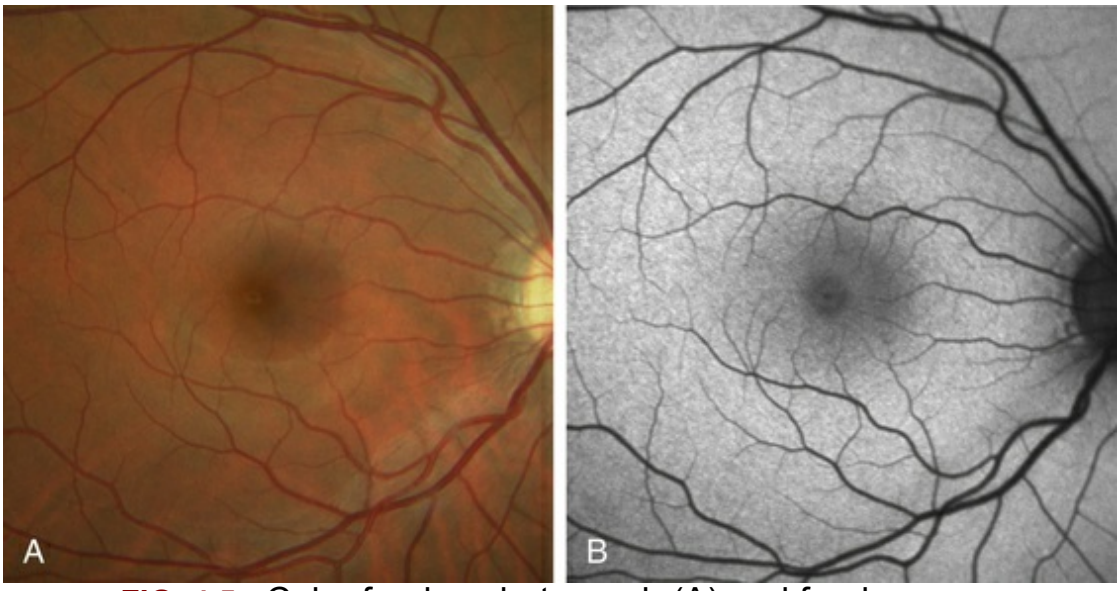

FIG. 4.5 Color fundus photograph (A) and fundus autofluorescence image (B) of the right eye of a normal subject imaged with the confocal scanning laser ophthalmoscope (Heidelberg retina angiograph, HRA 2, Heidelberg Engineering, Heidelberg, Germany). Topographical distribution of fundus autofluorescence intensity shows typical background signal with a dark optic disc (absence of autofluorescent material) and retinal vessels (absorption). Further, intensity is markedly decreased over the fovea due to the absorption of the blue light by yellow macular pigment.
(Reproduced with permission from Schmitz-Valckenberg S, Fleckenstein M, Scholl HP, et al. Fundus autofluorescence and progression of age-related macular degeneration. Surv Ophthalmol 2009;54:96–117.)

Using pixel gray values, typical ratios between the intensity of the fovea and perifoveal macula have been established in normal subjects (reviewed by Schmitz-Valckenberg et al.[2]). Based on these findings, qualitative descriptions of localized FAF changes are widely used. Usually, the FAF signal over a certain retinal location is categorized in decreased, normal, or increased intensities in comparison to the background signal of the same image.

In contrast, the quantification of absolute intensities and their comparison between subjects or within longitudinal observation in the same subject are more complicated and remain a challenge in FAF imaging. Of note, as the pixel histogram in the usual available cSLO images is normalized in order to visualize better the topographic distribution of the FAF intensity (see above), the pixel

values are not absolute and these images must not be used for absolute intensity analyses from the outset. Furthermore, when interpreting FAF images, one should take into account that the digital resolution of the detector in current imaging devices exceeds the maximum spatial resolution of ocular media and the optics of the system, mainly due to high-order aberrations. Therefore, single pixel values of a standard FAF image do not reflect the actual anatomical resolution of the image and should not be used to compare intensities between different locations. This also explains why increasing the digital resolution of the detector usually does not improve the resolution of the actual image, but rather results in an artificially high-resolution, posterized image.

When analyzing absolute intensities on averaged but unnormalized FAF images (after ensuring that the normalization of the pixel histogram is turned off), a great variability of the mean gray value for a certain retinal location is usually noted when FAF images are subsequently acquired from the same subject directly one after the other using the same imaging device. A systematic analysis by Lois and coworkers[39] reported good intraobserver and moderate interobserver reproducibility when comparing the absolute mean pixel value of a 16 × 16 pixel square on the retina. In this report, the image resolution is not provided. When assuming an image resolution of 256 × 256 pixels and a 40° × 30° field (as these settings were published in previous studies using the same cSLO by the same group), the 16 × 16 pixel box would encompass a retinal area of c. 2° × 1.9°. Hence, moderate interobserver reproducibility would just have been achieved over a rather large retinal area, but was not shown for the anatomical resolution of the imaging system.

Several confounding factors have to be taken into account when comparing absolute FAF intensities between different examinations and different individuals. This not only includes standardization of settings (laser power, detector sensitivity, correction of refractive errors, and image-processing steps, including the number of averaged images), but also eye movements, position of the patient in the chin rest, orientation of the camera, distance between the camera and the cornea, subtle variations in the illumination of the frame, fluctuations of laser power, and short-term dynamic changes in FAF intensities caused by prolonged exposure to the excitation

light or previous dark adaptation (reviewed by Schmitz-Valckenberg et al.[2]).

Quantitative Autofluorescence Imaging

Delori and coworkers introduced a method for quantitative autofluorescence (qAF) imaging by insertion of an internal FAF reference to account for variable laser power and detector sensitivity.[40] Autofluorescence intensity is calculated by the use of a calibrated reference in the optical pathway. Attaining reliable qAF measurements is critically dependent upon good image quality.[40] The operator must be experienced and skilled and must follow established protocols. Key requirements for images suitable for qAF measurement are uniform and maximal signal intensity, fine-tuned focus, central alignment of the camera with the eye to avoid obstruction by the iris, and exposure within the range of linearity of the detector.[41] Lens and vitreous opacities still represent a challenge, as absorption confounds measured FAF intensity levels originating from the retina/RPE.

Quantitative autofluorescence levels exhibit a significant increase with age (Fig. 4.6). In healthy eyes, qAF increases with increasing eccentricity up to 10–15° from the fovea with highest values superotemporally.[41] Furthermore, qAF values have been shown to be higher in females. Finally, there may be ethnic differences: compared with Hispanics, qAF is significantly higher in whites and lower in blacks and Asians.[41]

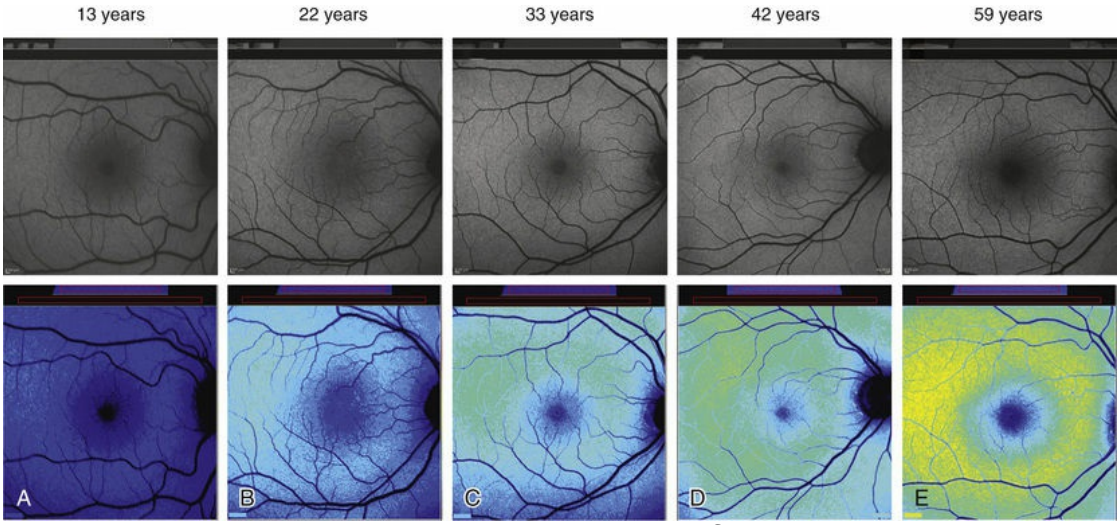

FIG. 4.6 Age-related increase in autofluroescence intensities determined by quantitative autofluorescence imaging. (Courtesy Peter Charbel-Issa, Martin-Gliem.)

Recent studies have demonstrated the potential of qAF to guide clinical diagnosis and genetic testing (see below, "Macular and Diffuse Retinal Dystrophies"). Furthermore, this approach enhances the understanding of disease processes and may serve as a diagnostic aid, as a more sensitive marker of natural disease progression, and as a tool to monitor the effects of therapeutic interventions targeting LF accumulation.[40]

Clinical Applications

Age-Related Macular Degeneration (AMD)

Early and Intermediate AMD

Early manifestations of AMD include focal hypo- and hyperpigmentation at the level of the RPE as well as drusen with extracellular material accumulating in the inner aspects of Bruch's membrane.[42] Increased FAF signal adjacent to drusen, which corresponds to focal hyperpigmentation and pigment figures on biomicroscopy, has been attributed to the presence of melanolipofuscin or changes in the metabolic activity of the RPE. Areas of hypopigmentation on color photographs tend to be associated with a corresponding decreased FAF signal, suggesting the absence of RPE cells or degenerating RPE cells with reduced LF

granule content (reviewed by Schmitz-Valckenberg et al.[2]). Drusen by themselves are not necessarily correlated with notable FAF changes.[43] Overall, larger drusen are more frequently associated with significant FAF abnormalities than smaller ones, with the exception of basal laminar drusen. Crystalline drusen typically demonstrate a corresponding decreased FAF signal. The variability of the FAF phenotype of drusen in AMD contrasts with young patients with monogenic disorders in whom the drusen typically autofluoresce brightly, presumably reflecting a distinctly different composition of the accumulating material from age-related drusen.

Delori and coworkers described a pattern of FAF distribution associated with drusen in AMD which consists of decreased FAF in the center of the druse with a surrounding annulus of increased FAF.[30] It has been speculated that this appearance is caused by attenuated RPE at the center and tangential orientation of RPE cells at the edges of the druse. Several authors have consistently reported that confluent drusen and large foveal soft drusen (drusenoid RPE detachments) topographically correspond well with mildly increased FAF using cSLO (reviewed by Schmitz-Valckenberg et al.[2]). With a fundus camera-based system, large soft drusen have a slightly decreased FAF signal at their centers and are surrounded by a faint ring of increased signal.

Applying a multimodal imaging approach including spectral domain optical coherence tomography (SD-OCT) and FAF revealed that focal hyperreflectivity overlying drusen was most frequently spatially confined to increased FAF while outer nuclear layer thinning and choroidal hyperreflectivity were associated with decreased FAF.[44]

Reticular Pseudodrusen

Several lines of evidence indicate that, in addition to drusen and pigmentary changes, reticular pseudodrusen (RPD) seem to confer a high risk for the development of late-stage AMD. This specific phenotypic pattern, which is best recognizable by SD-OCT, cSLO infrared reflectance, and cSLO FAF imaging, can be detected in over 60% of eyes with GA and in 42% of eyes with intermediate AMD.[45,46] Morphologic variations of RPD have been described, with the characteristic reticular pattern[47] further subdivided into “dot,”

"target," and "ribbon" configurations (Fig. 4.7).[48,49]

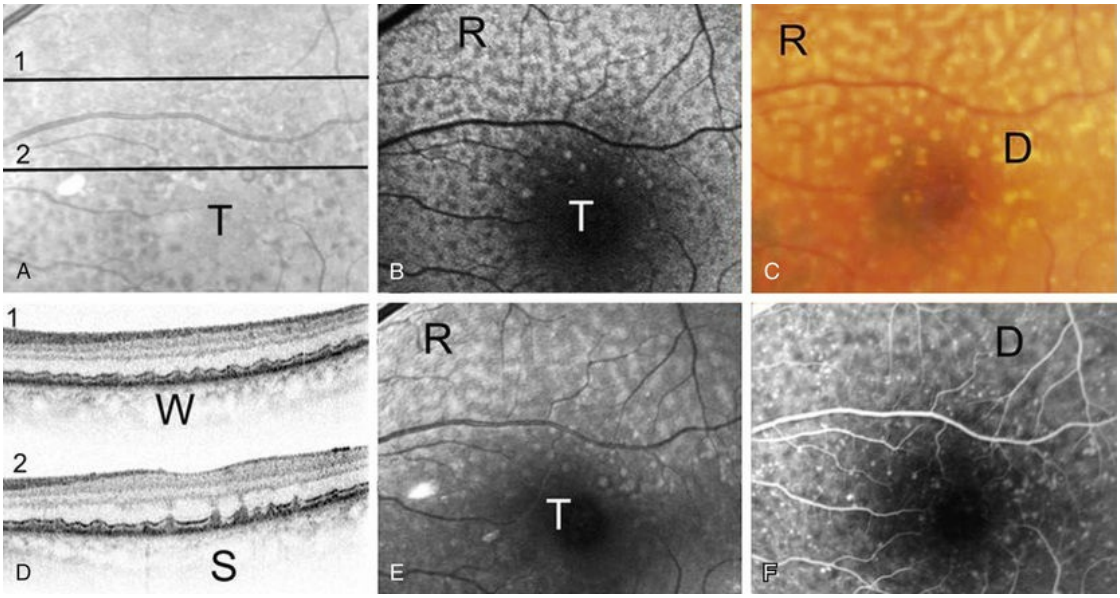

FIG. 4.7 Multimodal imaging of reticular pseudodrusen. The example demonstrates the "ribbon" pattern (*R*), clearly visible in fundus autofluorescence (FAF) (upper middle), color fundus (upper right) and blue reflectance (BR) (lower middle) images. "Targets" (*T*) are well detectable in FAF (upper middle), BR (lower middle) and near-infrared reflectance (IR) (upper left) images. The black line indicates the position of the two corresponding spectral domain optical coherence tomography (SD-OCT) scans (*1* and *2*, lower left). In the IR image, no ribbon pattern but rather coalescence lesions are visible that correspond to waves (*W*) in SD-OCT. Targets are clearly visible in the IR image and correspond to spikes (*S*) in the SD-OCT scan. In the fluorescein angiography image (lower right), "dots" (*D*) are detectable. (Reproduced from Steinberg JS, Göbel AP, Fleckenstein M, et al. Reticular drusen in eyes with high-risk characteristics for progression to late-stage age-related macular degeneration. Br J Ophthalmol 2015;99:1289–94. Copyright BMJ Publishing Group.)

The morphologic substrate of RPD is now assumed to be located anterior to the RPE cell monolayer in contrast to the sub-RPE location of "regular" drusen.

Interestingly, RPD are not specific for AMD and have recently been reported to also frequently occur in other retinal diseases,

including Sorsby fundus dystrophy and pseudoxanthoma elasticum (PXE).[50,51] As the latter diseases are characterized by a primary Bruch's membrane pathology, changes in this anatomic layer may play an important role in the pathophysiology of RPD.[51]

Geographic Atrophy

Areas of GA are associated with RPE cell death as well as with loss or attenuation of adjacent layers, in particular the outer neurosensory retina and the choriocapillaris.[52] With disappearance of the RPE, LF is also lost, resulting in a corresponding marked decrease in FAF intensity (Figs. 4.8 and 4.9).[28] Compared to drusen, which may also exhibit a decreased FAF signal, atrophic areas typically show an even more profound reduction of FAF.[30] The high-contrast difference between atrophic and nonatrophic regions of retina allows more easy and reliable delineation of the area of atrophy than from conventional fundus photographs. These advantages of documenting and studying GA by FAF imaging have been used in natural history studies[53,54,59] (Figs. 4.8 and 4.9).

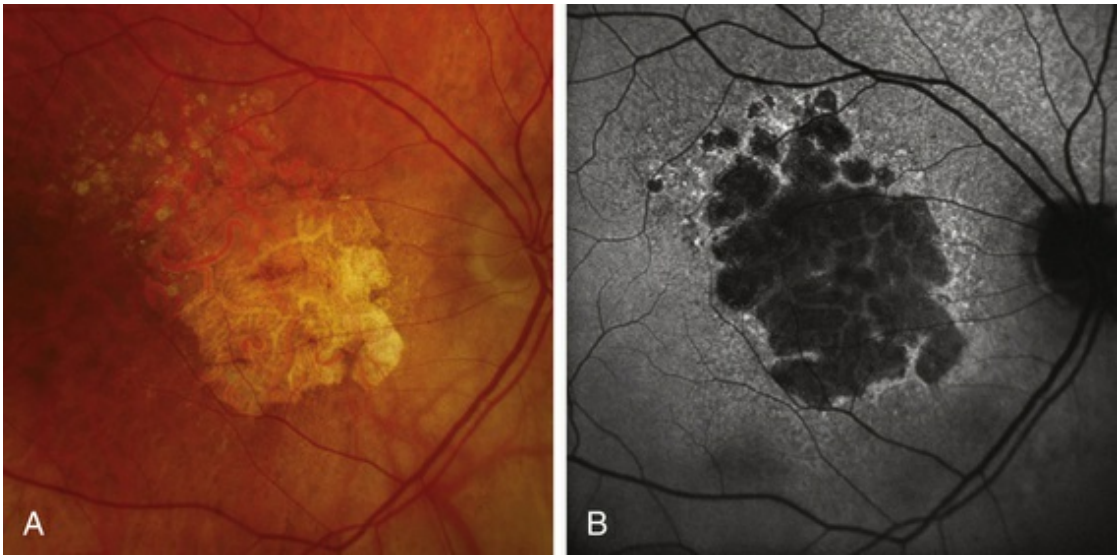

FIG. 4.8 In atrophic age-related macular degeneration, geographic atrophy appears as a sharply demarcated area with depigmentation and enhanced visualization of deep choroidal vessels on the color fundus photograph (A). On the corresponding fundus autofluorescence (FAF) image (B), atrophic patches are clearly delineated by decreased intensity and high-

contrast to adjacent nonatrophic retina. Surrounding the atrophy, in the junctional zone, foci and areas of increased FAF intensity are observed which are invisible on fundus photography. These abnormalities tend to precede atrophy over time and may serve as disease markers. (Reproduced with permission from Holz FG, Spaide RF. Essentials in ophthalmology: Medical retina. Berlin: Springer; 2007, Fig. 5.3.)

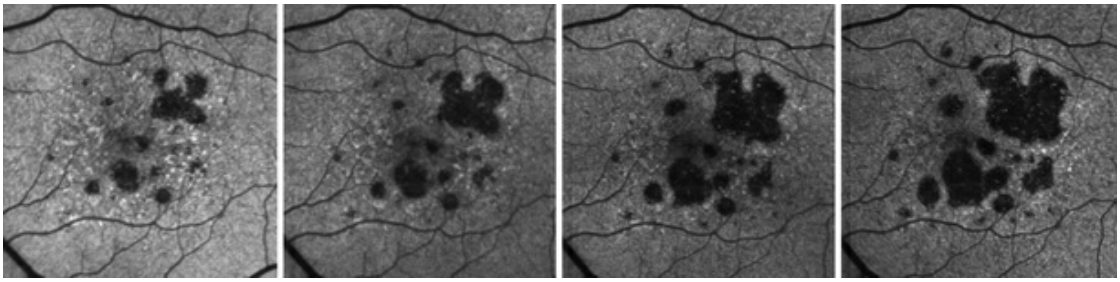

FIG. 4.9 Monitoring of atrophic progression over time with fundus autofluorescence imaging, showing the natural course of the disease over two years in a 73-year-old male patient.

An even more striking finding of FAF imaging in GA patients is the frequent presence of areas of hyperautofluorescence in the junctional zone surrounding the patch of atrophy.[55] Distinct patterns of abnormal FAF in the junctional zone of atrophy and a high degree of intraindividual symmetry between fellow eyes have been described (reviewed by Schmitz-Valckenberg et al.[2]).

A classification system of FAF patterns in the junctional zone of atrophy in GA patients has been proposed (Fig. 4.10).[56] Studies of retinal sensitivity have underscored the importance of increased FAF surrounding areas of GA and, thus, the pathophysiologic role of increased RPE LF accumulation in such patients. Scholl and coworkers have demonstrated that rod photoreceptor function is more severely affected than cone function over areas with increased FAF using fine matrix mapping.[57] Combining SLO microperimetry and FAF imaging in another study, impaired photopic sensitivity has been observed in areas of abnormal FAF in the junctional zone.[58]

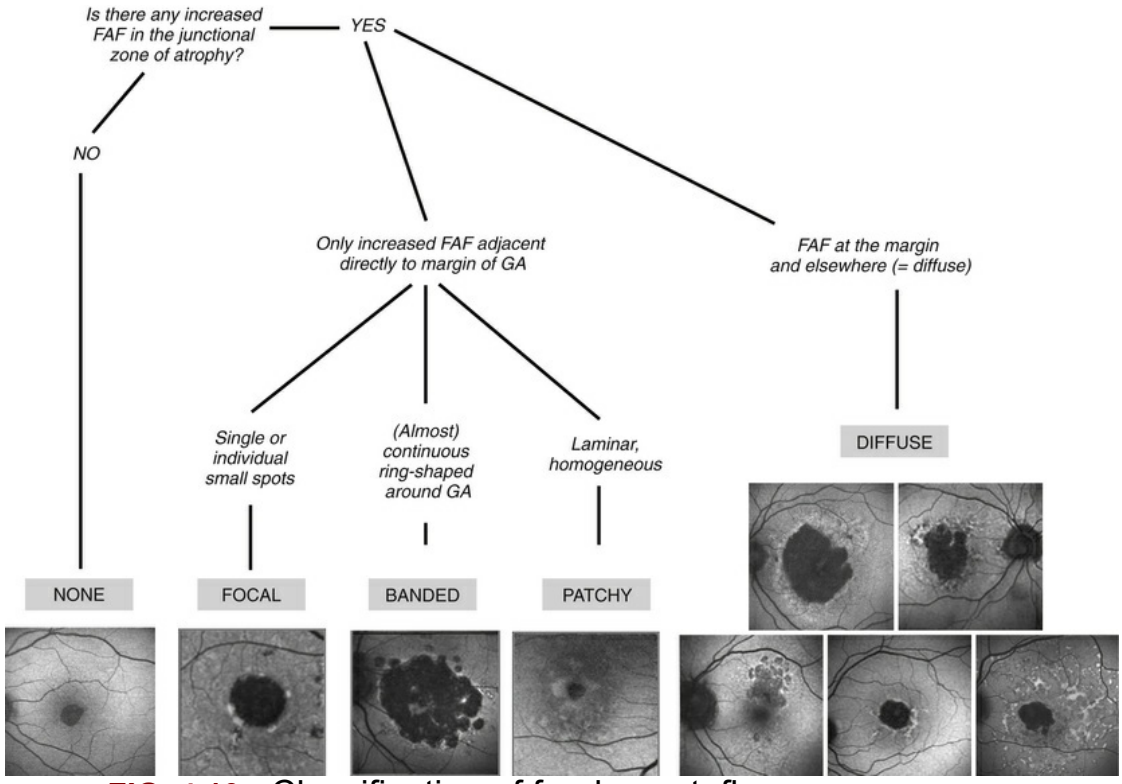

FIG. 4.10 Classification of fundus autofluorescence (FAF) patterns in the junctional zone in patients with geographic atrophy (GA) due to age-related macular degeneration. Eyes with no apparent increased FAF intensity are graded as "none" (slow progressor). The eyes with increased FAF are divided into two groups depending on the configuration of increased FAF surrounding atrophy. Eyes showing areas with increased FAF directly adjacent to the margin of the atrophic patch(es) and elsewhere are called "diffuse" (rapid progressors) and are subdivided into five groups. From left to right: (top row) fine granular, branching, (bottom row) trickling, reticular, and fine granular with punctuated spots. Eyes with increased FAF only at the margin of GA are divided into three subtypes: focal (slow progressor), banded (rapid progressor), and patchy (no data, occurs rarely) according to their typical FAF pattern around atrophy.

(Reproduced with permission from Schmitz-Valckenberg S, Fleckenstein M, Scholl HP, et al. Fundus autofluorescence and progression of age-related macular degeneration. Surv Ophthalmol 2009;54:96–117.)

Outer retinal atrophy in the context of AMD is a dynamic process with gradual enlargement of atrophic areas over time. Initial natural history studies on atrophy progression in GA patients using

FAF imaging demonstrated the occurrence of new atrophic patches and the spread of preexisting atrophy in areas with abnormally high levels of FAF at baseline.[55] Looking at larger patient groups with longer review periods, the significance of increased junctional FAF for foreshadowing atrophy enlargement has been highlighted.[53,54] In accordance with other natural history studies, the FAM (Fundus Autofluorescence Imaging in Age-related Macular Degeneration) study identified a large variability in the rate of atrophy enlargement between patients, which was neither explained by the extent of baseline atrophy nor by any other comorbid factor such as smoking, lens status, or family history. Interestingly, the initial studies using FAF imaging on patients with GA have already reported various patterns of changes in FAF in the junctional zone of GA (reviewed by Schmitz-Valckenberg et al.[2]). These investigators speculated that their observations might reflect heterogeneity of the underlying disease process.

A more detailed analysis of the FAM study of 195 eyes of 129 patients shows that variable rates of progression of GA are dependent on the specific phenotype of abnormal FAF pattern at baseline.[54] Atrophy enlargement was the slowest in eyes with no abnormal FAF pattern (median 0.38 mm^2/year), followed by eyes with the focal FAF pattern (median 0.81 mm^2/year), then by eyes with the diffuse FAF pattern (median 1.77 mm^2/year), and finally, by eyes with the banded FAF pattern (1.81 mm^2/year). The difference in atrophy progression between the groups of no abnormal and focal FAF patterns and the groups of the diffuse and banded FAF patterns was statistically significant ($p<.0001$). These results have subsequently been confirmed in another large-scale study (the Natural History of Geographic Atrophy Progression (GAP) study).[59] These findings underscore the importance of abnormal FAF intensities around atrophy and the pathophysiologic role of increased RPE LF accumulation in patients with GA due to AMD.

In eyes with GA, the fovea may remain uninvolved by the atrophic process until late in the course of the disease, a phenomenon referred to as “foveal sparing.” Detection of “foveal sparing” in eyes with GA using FAF imaging with an excitation wavelength of 488 nm is challenging due to signal absorption by

macular pigment.[60] Evaluation of the integrity of the "spared" fovea is facilitated by combined analysis of SD-OCT or infrared reflectance with FAF images (Fig. 4.11). The approach combining infrared reflectance with FAF images for quantification of "foveal sparing" in eyes with GA has recently been shown to be feasible.[61] In this study, it has been demonstrated that the atrophic area in eyes with "foveal sparing" progresses 2.8-fold faster towards the periphery than towards the central retina. These findings would seem to support the hypothesis of the presence of local factors that protect the fovea, at least for some time, from degeneration.

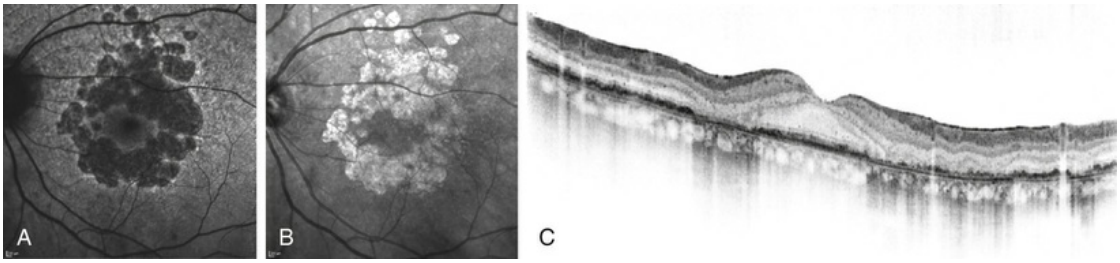

FIG. 4.11 Foveal sparing in geographic atrophy visualized by different imaging modalities. (A) Fundus autofluorescence imaging (excitation wavelength 488 nm); (B) near-infrared reflectance imaging; (C) spectral domain optical coherence tomography (vertical scan).

(Reproduced with permission from Lindner M, Böker A, Mauschitz MM, et al. Fundus Autofluorescence in Age-Related Macular Degeneration Study Group. Directional kinetics of geographic atrophy progression in age-related macular degeneration with foveal sparing. Ophthalmology 2015;122:1356-65. Copyright Elsevier.)

Pigment Epithelium Detachment

FAF imaging in eyes with pigment epithelium detachment (PED) secondary to AMD show variable FAF phenotypes which are not always detectable using conventional imaging techniques such as fundus photography, fluorescein, or ICGA (Fig. 4.12).

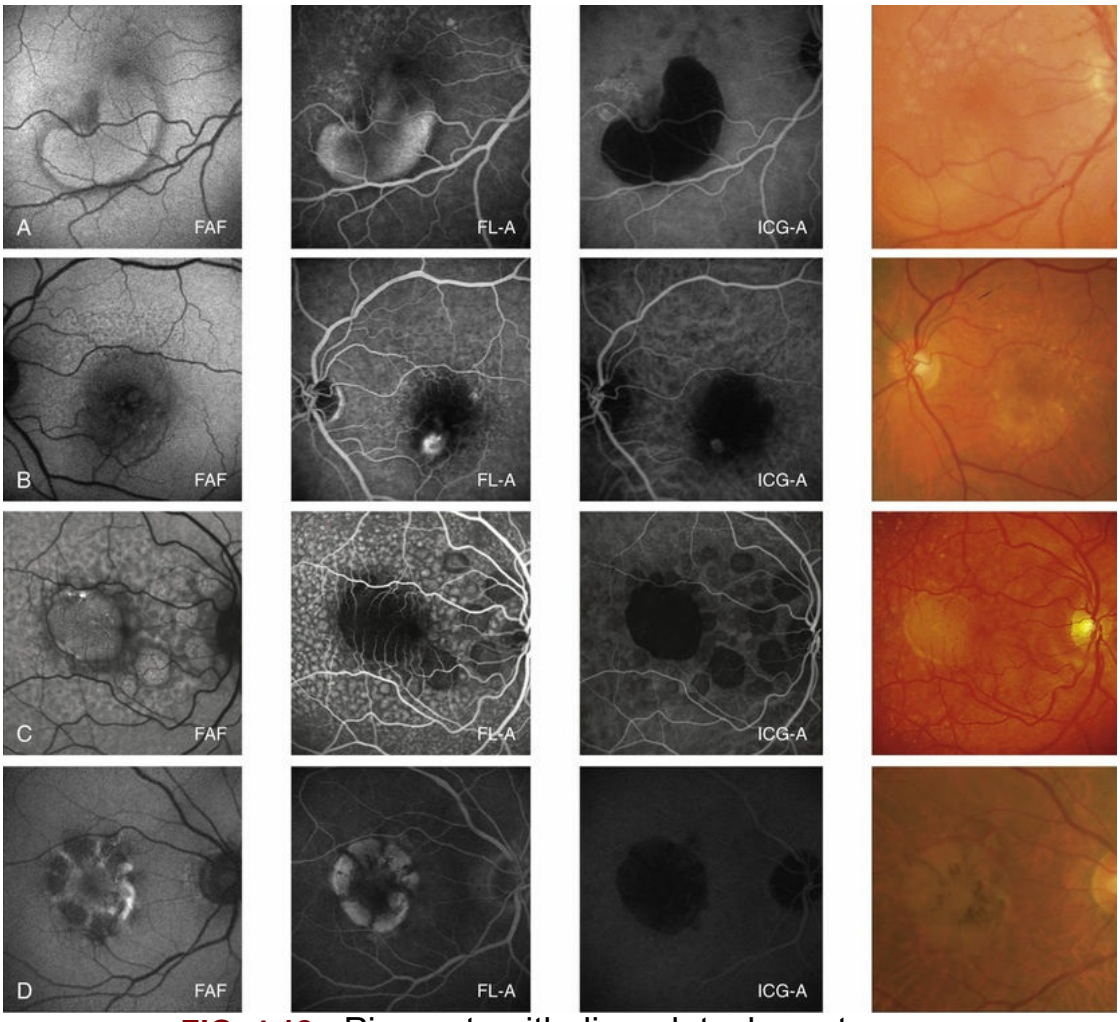

FIG. 4.12 Pigment epithelium detachment classification based on fundus autofluorescence (FAF) characteristics. (A) Increased FAF; (B) decreased FAF; (C) FAF; and (D) cartwheel FAF. *FL-A*, fluorescein angiography; *ICG-A*, indocyanine green angiography.
(Reproduced with permission from Roth F, et al. Fundus autofluorescence imaging of pigment epithelial detachments. ARVO Meet Abstracts 2004;45:2962.)

However, a systematic analysis of these FAF alterations with correlation to the underlying causes of PED such as choroidal neovascularization (CNV), retinal angiomatous proliferation, polypoidal vasculopathy, or serous, nonexudative PED is lacking to date. These changes are probably not only caused by increased or decreased amounts of LF, but may derive from other dominant fluorophores with similar excitation and emission spectra, such as extracellular fluid or degraded photoreceptors (Fig. 4.12).

Choroidal Neovascularization

Theoretical considerations would suggest that FAF imaging may provide important clues to our understanding of CNV secondary to AMD. For example, it may be helpful to assess the integrity of the RPE which may influence the development and behavior of new vascular complexes as well as photoreceptor viability and potential therapeutic success.

Patients with early CNV secondary to AMD tend to have patches of "continuous" or "normal" autofluorescence corresponding with areas of hyperfluorescence on the corresponding fluorescein angiograms, implying that RPE viability is preserved at least initially in CNV development (Fig. 4.13).[62] By contrast, eyes with longstanding CNV typically exhibit more areas of decreased FAF signal, which could be explained by photoreceptor loss and scar formation with increased melanin deposition (Fig. 4.13).

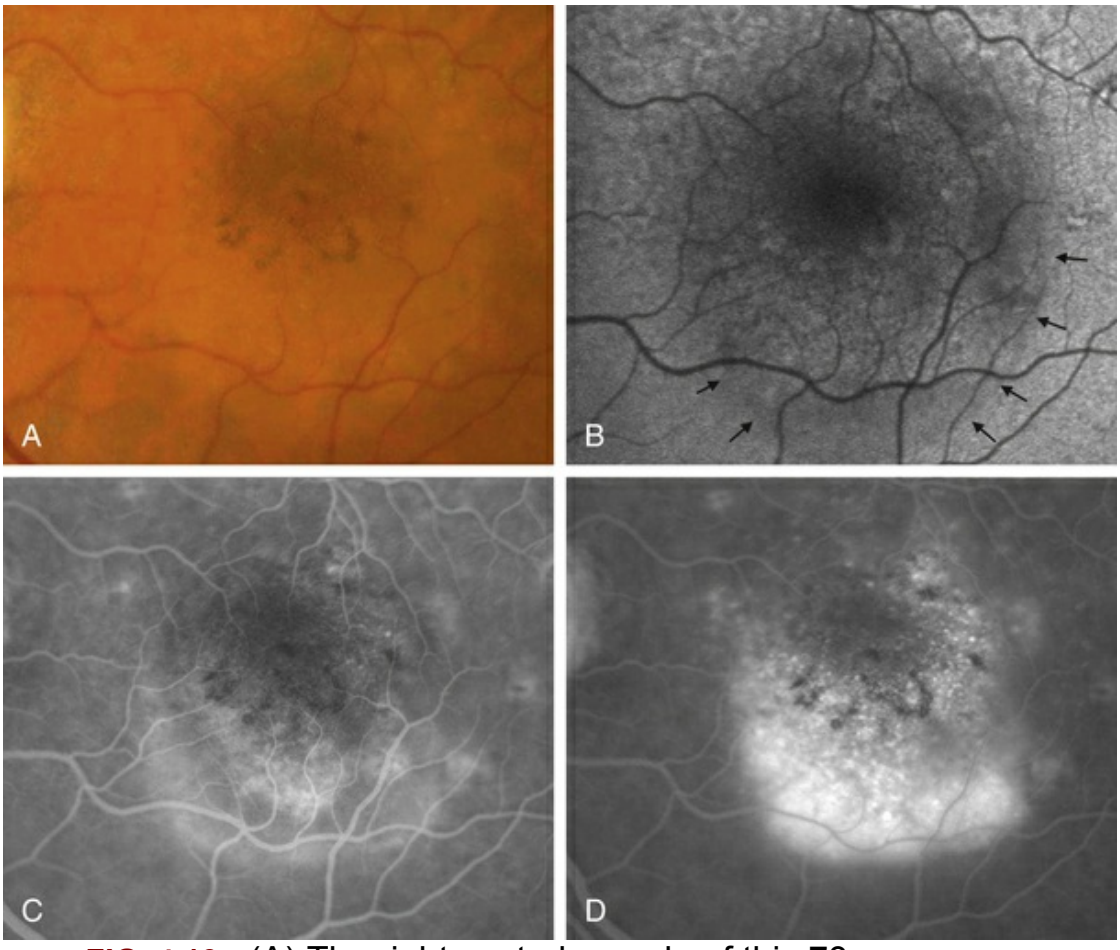

FIG. 4.13 (A) The right central macula of this 73-year-old woman with a history of blurred vision for 2 weeks (central visual acuity 20/30) showed fresh

hemorrhages, subretinal fluid, and a pigment epithelium detachment. (C,D) Fluorescein angiography reveals an active choroidal neovascular membrane with leakage in the inferior part of the lesion. (B) On the autofluorescence image, the borders (*arrows*) of the subretinal fluid can be seen. Of note, the autofluorescence signal appears to be normal at the site of the active neovascularization, suggesting that the retinal pigment epithelium is still viable. (Reproduced with permission from Schmitz-Valckenberg S, Holz FG, Bird AC, et al. Fundus autofluorescence imaging: review and perspectives. Retina 2008;28:385–409.)

Heimes and coworkers analyzed the prognostic value of RPE autofluorescence with respect to the therapeutic outcome of anti-vascular endothelial growth factor therapy in exudative AMD.[63] The analysis of 95 eyes showed a significant difference in visual acuity outcomes in eyes with changes in FAF within the central 500 and 1000 μm.

One other important finding in eyes with CNV is that abnormal FAF intensities typically extend beyond the edge of the angiographically defined lesion, indicating a more widespread involvement than is apparent from conventional imaging studies. Increased FAF signal has also been described around the edge of lesions. It has been speculated that this observation may reflect the proliferation of RPE cells around the CNV.[64] As in other exudative retinal disease, such as central serous chorioretinopathy, areas with increased FAF are commonly found inferior to the leakage on fluorescein angiography, most likely representing gravitational effects of fluid tracking or partial loss of photoreceptor segments resulting in less photopigments. In contrast to fluid, hemorrhages and intraretinal exudates typically show a decreased FAF signal because of light absorption obscuring the underlying retinal details. When retinal hemorrhages undergo organization and evolve into an ocher color on fundoscopy, they may become intensely autofluorescent. Later, with disappearance of the yellowish material seen on biomicroscopy, a large RPE scar and atrophy with decreased autofluorescence may be visible.[65]

Detection of atrophy in eyes with exudative AMD is becoming more important since there is increasing evidence that atrophy development in eyes treated with anti-VEGF is the main cause for

severe visual loss in the long term.[66]

FAF imaging herein represents an important tool,[67] although, delineation of "pure" atrophy by FAF imaging is challenging, since retinal changes associated with exudation also exhibit a decreased FAF signal. Hence, a multimodal imaging approach appears to be most appropriate to detect, evaluate, and quantify atrophy in eyes with exudative AMD.

Macular and Diffuse Retinal Dystrophies

In macular and diffuse retinal dystrophies, various associated abnormalities in FAF have been described (reviewed by von Rückmann et al.[68]).

The extent and pattern of abnormal FAF may show characteristic abnormal distributions in retinal dystrophy disease entities and therefore aids in the differential diagnosis. In particular, in late-onset macular dystrophies (e.g., late-onset Stargardt disease and central areolar choroidal dystrophy), FAF imaging is an important technique to differentiate such masquerading disease entities from AMD.[69]

It is well established that autofluorescent material excessively accumulates in the RPE in association with various genetically determined retinal diseases. Increased FAF due to excessive LF accumulation in RPE cells may result from abnormally high turnover of photoreceptor outer segments or impaired RPE lysosomal degradation of normal or altered phagocytosed molecular substrates.

The fundoscopically visible pale/yellowish lesions at the level of RPE/Bruch's membrane in Best macular dystrophy (Fig. 4.14), adult vitelliform macular dystrophy, and other pattern dystrophies, as well as Stargardt macular dystrophy/fundus flavimaculatus (Fig. 4.15), are associated with an intense focally increased FAF signal.

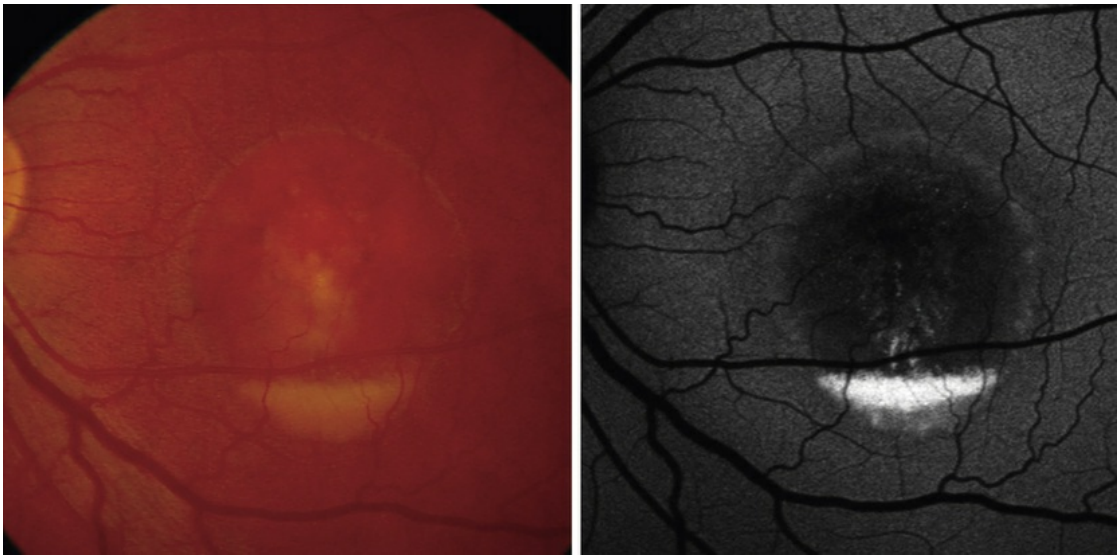

FIG. 4.14 Best macular dystrophy. Vitelliruptive stage. There is prominent increased fundus autofluorescence (FAF) in the lower part of the original vitelliform lesion that is still demarcated by a faint ring of increased FAF.

(Reproduced with permission from De Laey J, Puech B. Color atlas of retinal dystrophy: Springer; 2014.)

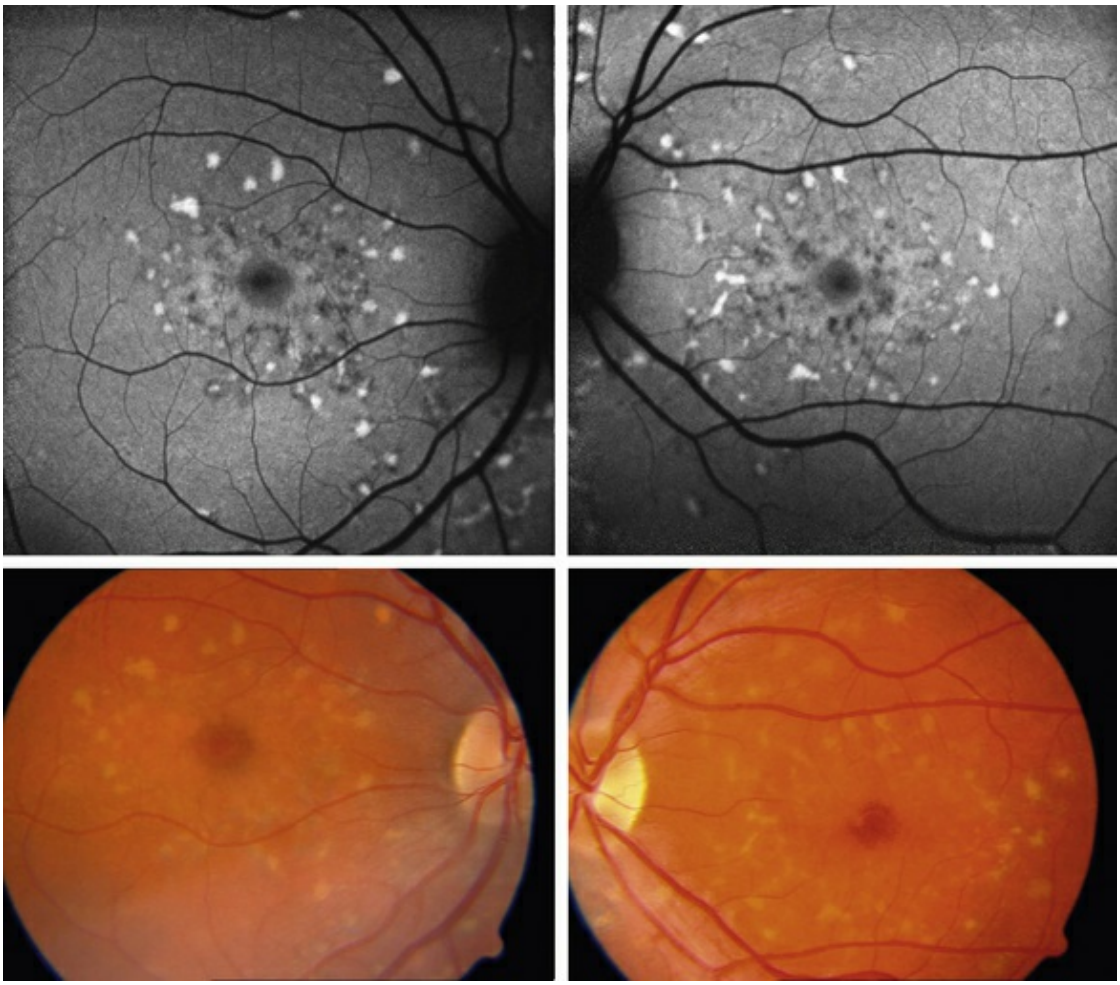

FIG. 4.15 Stargardt macular dystrophy/fundus flavimaculatus. Fundoscopically visible focal flecks show a bright, increased fundus autofluorescence (FAF) signal. Focal areas of decreased FAF seem to correspond with retinal pigment epithelial atrophy.

(Reproduced with permission from Ho AC, Brown GC, McNamara JA, et al. Color atlas and synopsis of clinical ophthalmology: Retina. New York: McGraw Hill; 2003.)

The flecks with increased FAF signal in Stargardt macular dystrophy and fundus flavimaculatus may fade over time, with subsequent atrophy development. This finding is in accordance with histopathologic data which have shown that these flecks represent aggregates of enlarged RPE cells engorged to 10 times their normal size with LF. Interestingly, flecks in recessive Stargardt disease can exhibit increased FAF, while NIR-AF is usually reduced or absent at fleck positions. Sparrow and coworkers further evaluated this incongruous observation, and in 2015 reported that in NIR-AF, flecks are predominantly hypofluorescent and larger,

and that NIR-AF darkening occurs prior to development of a heightened FAF signal. They concluded that these observations indicate that RPE cells associated with flecks in recessive Stargardt disease are considerably changed or lost, and that the bright FAF signal of flecks likely originates from augmented LF formation in degenerating photoreceptor cells impaired by the failure of RPE.[70]

Lorenz and coworkers[71] described absent or minimal FAF intensities in patients with early-onset severe retinal dystrophy associated with mutations on both alleles of *RPE65*. The lack or severe decrease of FAF signal would be consistent with the biochemical defect and could be used as a clinical marker of this genotype. Another study demonstrated that patients with Leber congenital amaurosis having vision reduced to light perception and undetectable electroretinograms (ERGs) may still exhibit normal or minimally decreased FAF intensities.[72] The authors concluded that the RPE–photoreceptor complex is, at least in part, functionally and anatomically intact. This finding would have implications for future treatment, suggesting that photoreceptor function may still be rescuable in such patients.

Discrete, well-defined lines of increased FAF may occur in various forms of retinal dystrophies (Fig. 4.16).[68,73,66] These lines have no prominent correlate on fundus biomicroscopy, although there is evidence that these lines precisely reflect the border of the regions of retinal dysfunction (Figs. 4.17 and 4.18).[73–75] Despite the variable orientation of this line in different entities, e.g., orientation along the retinal veins in pigmented paravenous chorioretinal atrophy (PPCRA) or as a ring-like structure in retinitis pigmentosa (RP) or macular dystrophies (Fig. 4.16), the similar appearance on FAF images and the concordance of functional findings indicate that these lines in heterogeneous diseases share a common underlying pathophysiologic mechanism.[74]

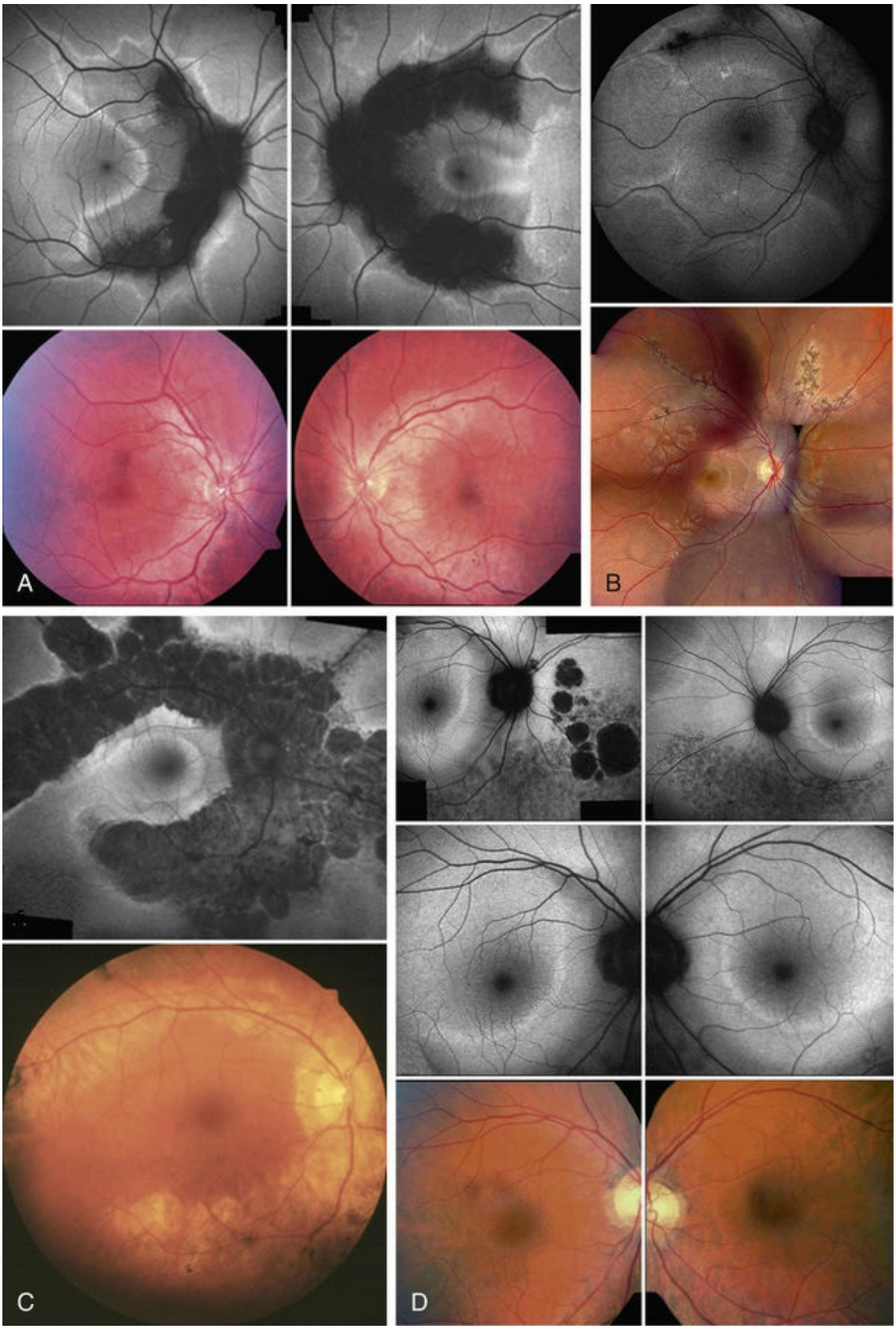
A
B
C
D

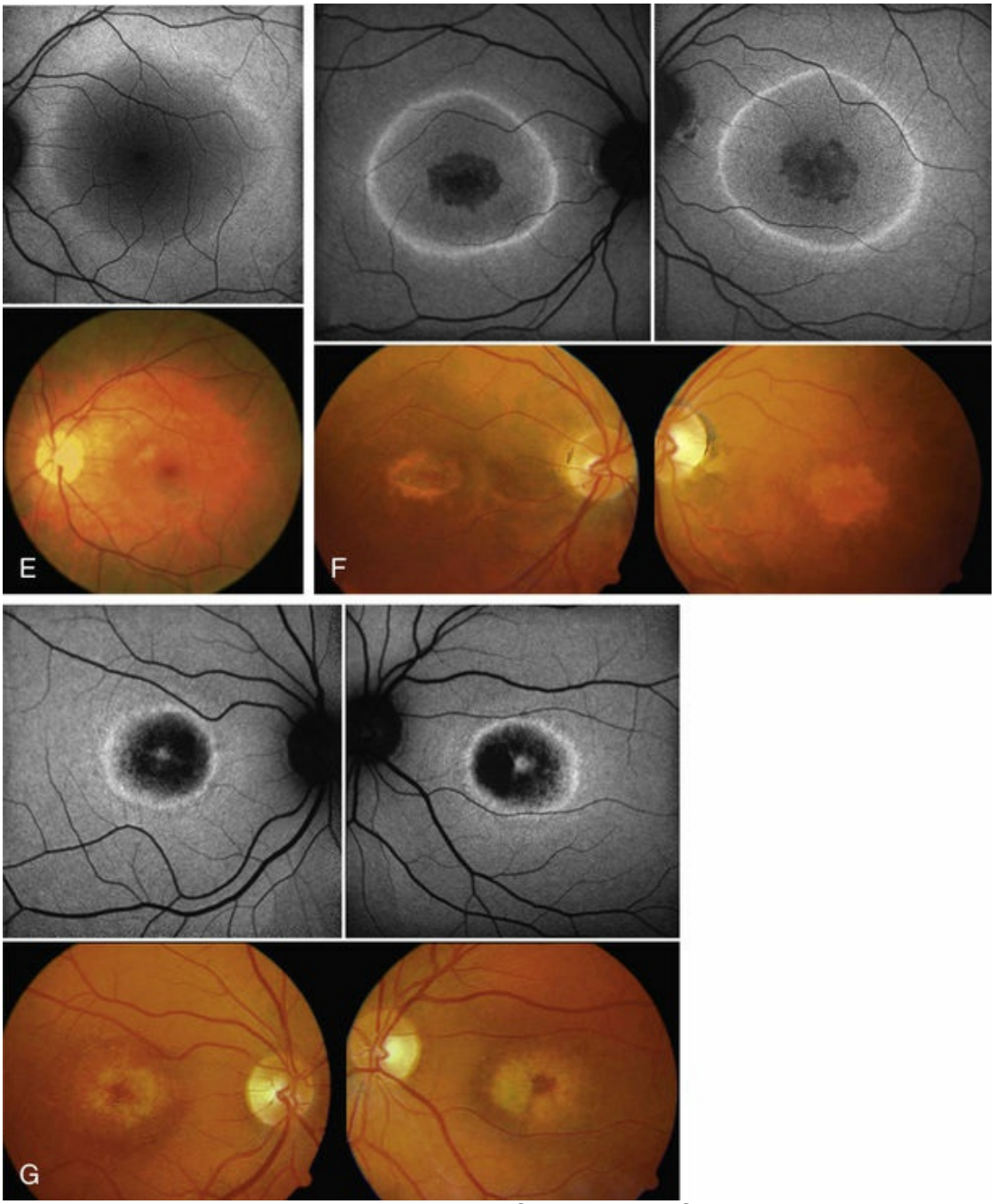

FIG. 4.16 Arcs and rings of increased fundus autofluorescence (FAF) in patients with various forms of retinal dystrophies. Patients 1–3 (A–C), diagnosed with pigmented paravenous chorioretinal atrophy, demonstrate an arc of increased FAF orienting along the retinal veins. There is a normal FAF signal between this arc and the atrophic areas (i.e., decreased FAF) and in the area that is not circumscribed by the line. In the left eye of patient 1 (A) and the right eye of patient 3 (C), the arc of increased FAF almost merges to a parafoveal ring with a temporal opening. In patient 4 (D) with sector retinitis

pigmentosa, there is an arc with a semicircular configuration in the parafoveal region. In typical retinitis pigmentosa (patient 5, E), there is a ring of increased FAF. Within and outside the ring, there is a normal FAF signal. In patient 6 (F), who is diagnosed with macular dystrophy, there is a parafoveal ring of increased FAF. Centrally, there is reduced FAF corresponding to the fundoscopically visible lesion. On both sides of the ring, there is a normal FAF signal. In patient 7 (G) with another bull's-eye macular dystrophy, a ring of increased FAF directly borders the central lesion. In the very center, there is a spot of preserved FAF. Note that there is no significant correlate of the arc of increased FAF in the conventional color fundus photograph. (Reproduced with permission from Fleckenstein M, Charbel Issa P, Fuchs HA, et al. Discrete arcs of increased fundus autofluorescence in retinal dystrophies and functional correlate on microperimetry. Eye (Lond) 2009;23:567–75.)

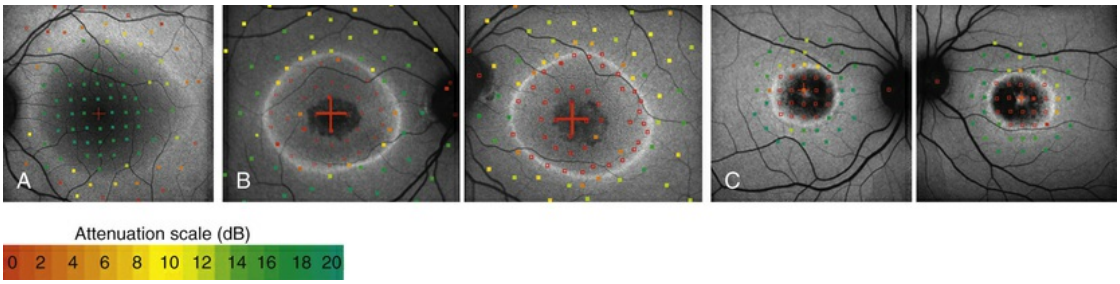

FIG. 4.17 Fundus-controlled microperimetric assessment of rings of increased fundus autofluorescence (FAF). The sensitivity map is superimposed on the FAF image. Light increment sensitivity (LIS) varies from 0 to 20 dB (attenuation scale). Hollow red squares indicate testing points where the brightest stimulus was not seen. (A) In the patient with autosomal dominant retinitis pigmentosa, LIS is preserved within the ring; outside, there is severely impaired LIS despite a normal FAF signal. In patients with macular dystrophy exhibiting a ring of increased FAF (B,C), LIS is significantly impaired within the ring independently of a normal or decreased FAF signal; outside, LIS is preserved. These findings are the inverse of the findings in patients diagnosed

with retinitis pigmentosa (A). (Reproduced with permission from Fleckenstein M, Charbel Issa P, Fuchs HA, et al. Discrete arcs of increased fundus autofluorescence in retinal dystrophies and functional correlate on microperimetry. Eye (Lond) 2009;23:567–75.)

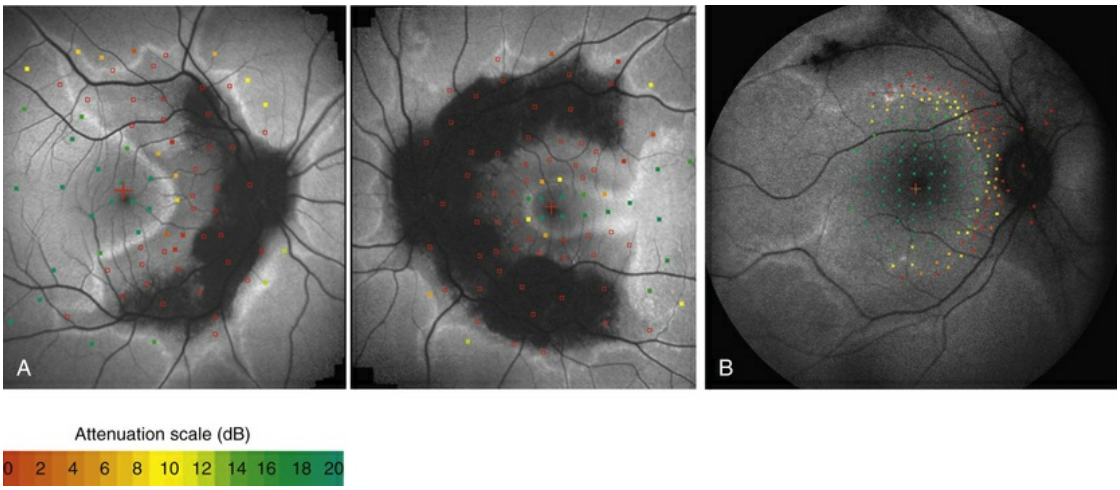

FIG. 4.18 Fundus-controlled microperimetric assessment in pigmented paravenous chorioretinal atrophy. The sensitivity map is superimposed on the fundus autofluorescence (FAF) image. Light increment sensitivity (LIS) varies from 0 to 20 dB (attenuation scale). Hollow red squares indicate testing points where the brightest stimulus was not seen. In the area that is framed by the arc of increased FAF, LIS is severely impaired independently of a normal or abnormal FAF signal. The arc of increased FAF demarcates the area of preserved LIS. (Reproduced with permission from Fleckenstein M, Charbel Issa P, Fuchs HA, et al. Discrete arcs of increased fundus autofluorescence in retinal dystrophies and functional correlate on microperimetry. Eye (Lond) 2009;23:567–75.)

Fleckenstein and coworkers[76] first described the SD-OCT correlate of these lines of increased FAF. Specifically, these corresponded with a discrete junctional zone between an area with preserved OCT layers and an area where the outer aspects of the retina are lost and the external limiting membrane band appeared to rest directly on the RPE (Figs. 4.19 and 4.20).

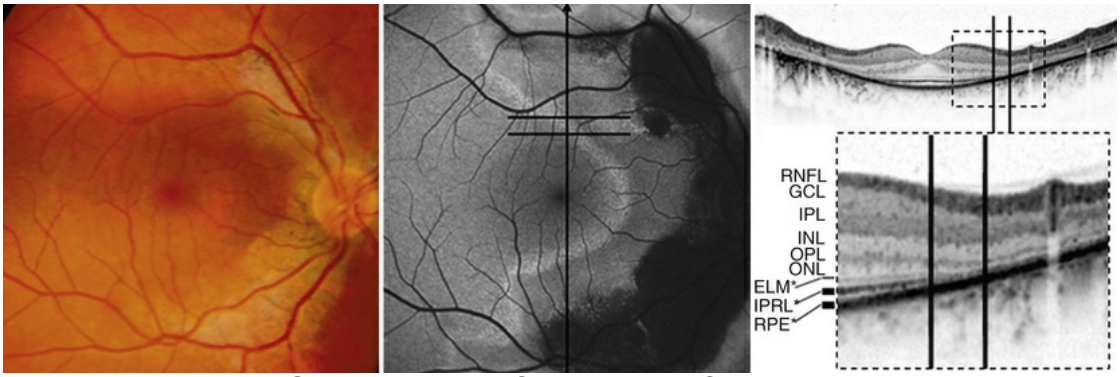

FIG. 4.19 Simultaneous fundus autofluorescence (FAF) and spectral domain optical coherence tomography imaging. The line of increased FAF corresponds to a junctional zone (within black lines) between involved and preserved retina. *RNFL*, retinal nerve fiber layer; *GCL*, ganglion cell layer; *IPL*, inner plexiform layer; *INL*, inner nuclear layer; *OPL*, outer plexiform layer; *ONL*, outer nuclear layer; *ELM**, presumed correspondence of the external limiting membrane; *IPRL**, presumed correspondence of the interface of the inner/outer segments of photoreceptors; *RPE**, presumed correspondence of the retinal pigment epithelium. (Reproduced with permission from Fleckenstein M, Charbel Issa P, Helb HM, et al. Correlation of lines of increased autofluorescence in macular dystrophy and pigmented paravenous retinochoroidal atrophy by optical coherence tomography. Arch Ophthalmol 2008;126:1461–3.)

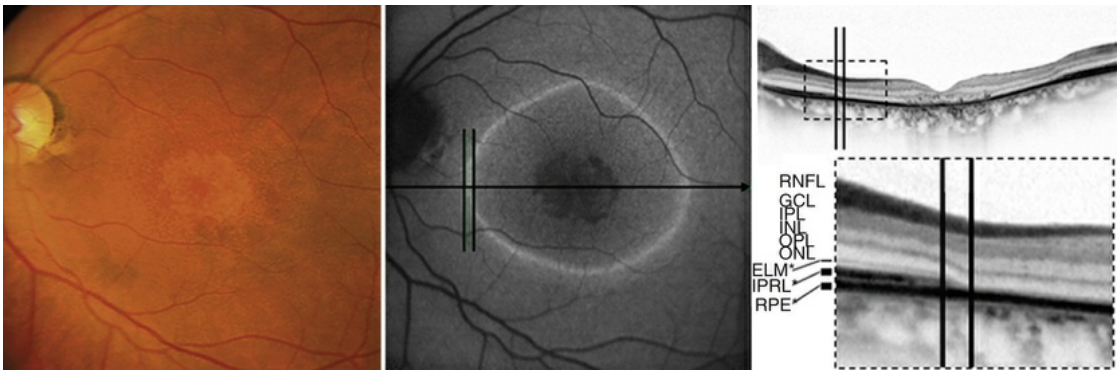

FIG. 4.20 Simultaneous fundus autofluorescence (FAF) and spectral domain optical coherence tomography imaging. The line of increased FAF corresponds to a junctional zone (within black lines) between preserved and involved retina. *RNFL*, retinal nerve fiber layer; *GCL*, ganglion cell layer; *IPL*, inner

plexiform layer; *INL*, inner nuclear layer; *OPL*, outer plexiform layer; *ONL*, outer nuclear layer; *ELM*,* presumed correspondence of the external limiting membrane; *IPRL**, presumed correspondence of the interface of the inner/outer segments of photoreceptors; *RPE**, presumed correspondence of the retinal pigment epithelium. (Reproduced with permission from Fleckenstein M, Charbel Issa P, Helb HM, et al. Correlation of lines of increased autofluorescence in macular dystrophy and pigmented paravenous retinochoroidal atrophy by optical coherence tomography. Arch Ophthalmol 2008;126:1461–3.)

The same SD-OCT correlate has been demonstrated in patients with RP.[77] This junction might be characterized by progressively altered photoreceptor outer and inner segments. While the pathophysiologic mechanism is unknown, it may be hypothesized that the increased FAF signal observed in various retinal dystrophies might result from an increased metabolic burden of corresponding RPE cells and subsequent excessive accumulation of fluorophores in the lysosomal compartment due to phagocytosis of components of severely altered photoreceptors in such junctional zones. Changes in absorption of the FAF signal due to loss of photoreceptor outer segments may also contribute to this phenomenon. In the zone with a normal FAF signal but impaired retinal sensitivity, the structure of the photoreceptors seems to be severely distorted. A normal FAF signal, therefore, does not necessarily reflect an intact photoreceptor–RPE complex, but may rather correspond to a structurally intact-appearing RPE cell monolayer with or without the presence of intact photoreceptors.

Quantitative autofluorescence imaging has been shown to be useful for differential diagnosis in retinal dystrophies, e.g., qAF allows for differentiation between *ABCA4*-associated and non-*ABCA4*-associated retinal disease. Moreover, *PRPH2*/*RDS*- and *ABCA4*-associated disease exhibiting phenotypic overlap can be discriminated when qAF values are corrected for age and race. In general, *ABCA4* patients have been shown to exhibit higher qAF values than *PRPH2*/*RDS* patients, while most patients without mutations in *PRPH2*/*RDS* or *ABCA4* have qAF levels within the normal range.[78]

While high qAF levels represent a hallmark of *ABCA4*-related

disease[78] in the absence of atrophy (Fig. 4.21), patients with mutations in *BEST1* exhibit mean nonlesion qAF values that are within normal limits for age.[79] Therefore, it has been concluded that, based on qAF, mutations in *BEST1* do not cause increased lipofuscin levels outside the yellowish, focal lesions.

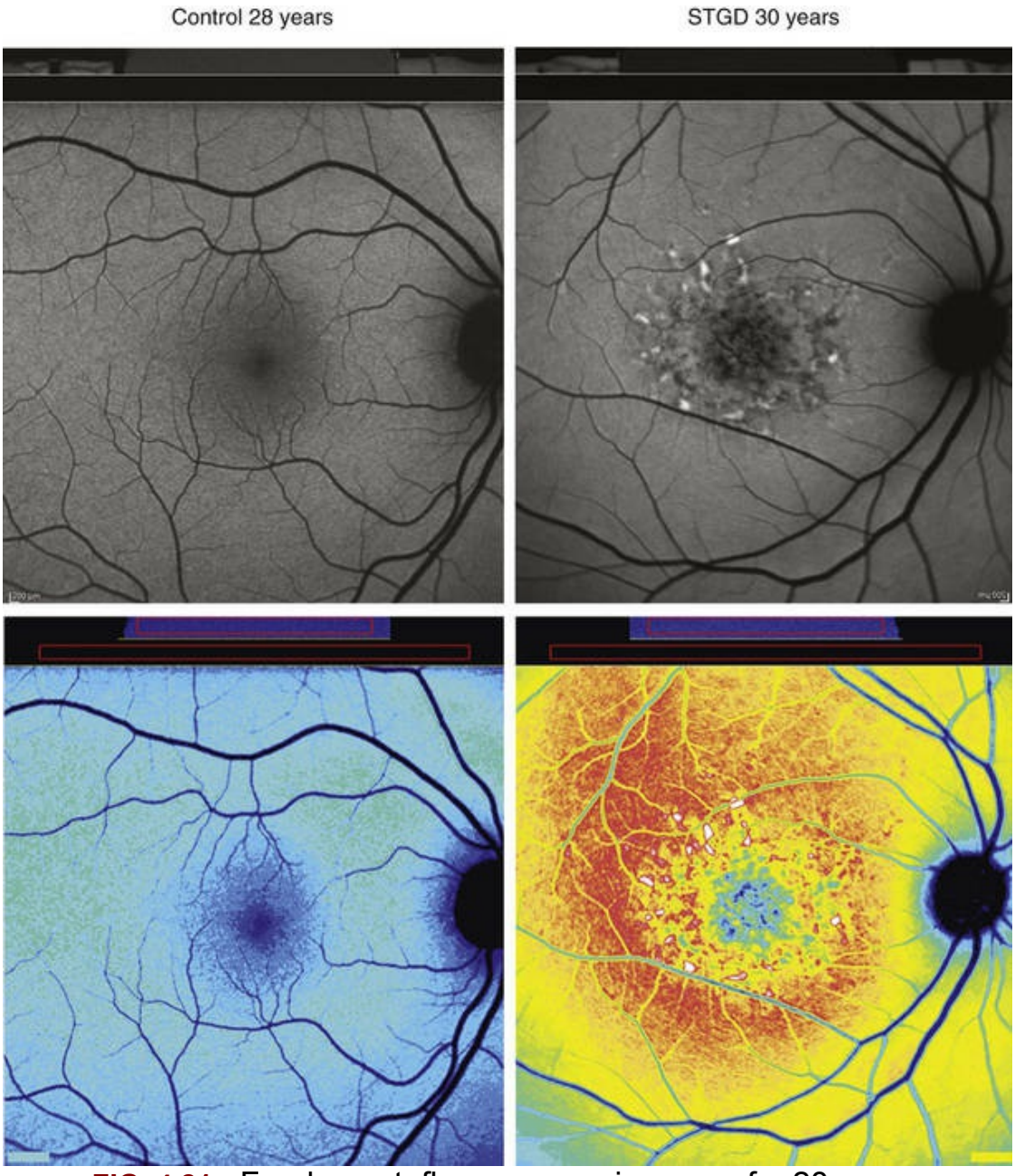

FIG. 4.21 Fundus autofluorescence images of a 28-year-old healthy young female (upper left) and a 30-year-old patient with Stargardt disease (upper right). Quantitative autofluorescence imaging analyses with color-coding (lower panel) showing higher intensities in

the eye affected by Stargardt disease. (Courtesy Peter Charbel-Issa, Martin-Gliem.)

Macular Telangiectasia

Macular telangiectasia (MacTel) type 2 is a bilateral disease of unknown cause with characteristic alterations of the macular capillary network and progressive retinal cell death (see Chapter 58, Macular telangiectasia).[80–82] The disease typically manifests temporal to the fovea, and may later encompass an oval-shaped area centered on the foveola.

As outlined above, normal eyes show masking of the foveal 488-nm blue-light FAF due to the accumulation of luteal pigment. Reduced macular pigment density in MacTel type 2 affects this masking. Eyes with MacTel type 2 show an abnormally increased signal in the macular area to a variable degree with blue-light FAF imaging (Figs. 4.22 and 4.23).[83] A loss of luteal pigment may initially occur in the area temporal to the foveal center.[83,84] Quantitative analysis confirmed that the loss of luteal pigment was more pronounced in the temporal compared with the nasal parafoveolar area and suggested that zeaxanthin would be more reduced than lutein.[84]

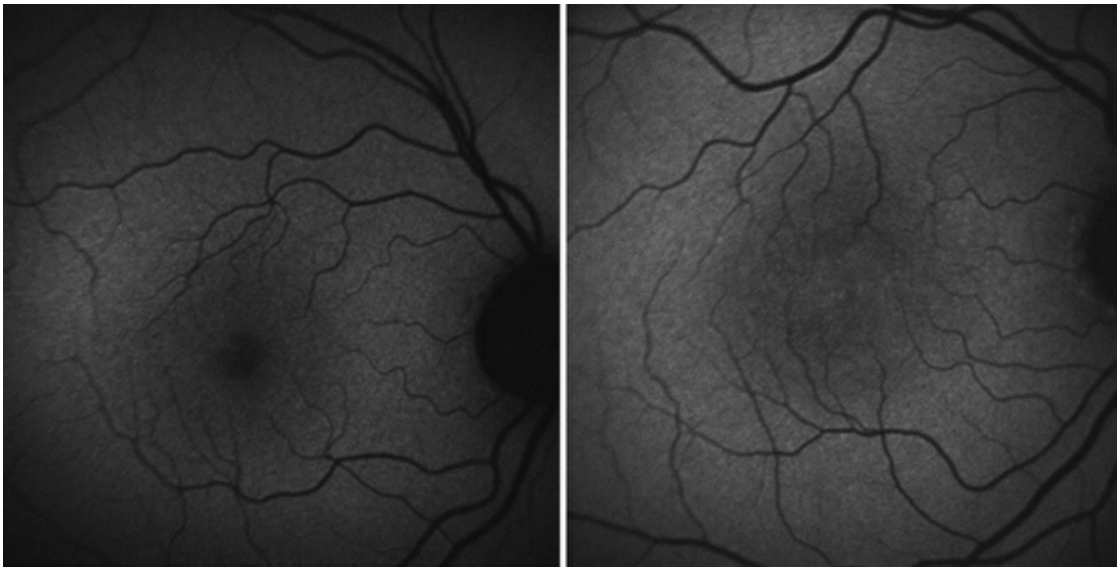

FIG. 4.22 Fundus autofluorescence image obtained at 488 nm (excitation) of a normal eye (*left*) and of a 59-

year-old woman with type 2 idiopathic macular telangiectasis (right). (Reproduced with permission from Helb HM, Charbel Issa P, van der Veen RLP, et al. Macular pigment density and distribution in patients with type II macular telangiectasia. Retina 2008;28:808–16.)

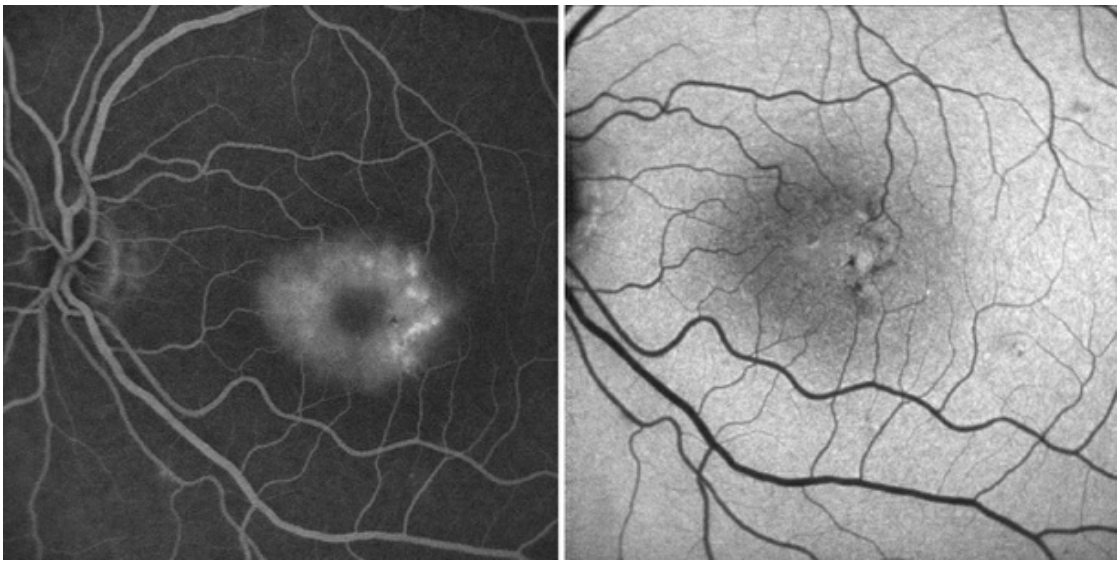

FIG. 4.23 Fluorescein angiogram frame (left) and fundus autofluorescence (FAF) image obtained at 488 nm (right) of a patient with type 2 idiopathic macular telangiectasia showing an abnormal FAF distribution in the macular area due to depletion of luteal pigment. (Reproduced with permission from Helb HM, Charbel Issa P, van der Veen RLP, et al. Macular pigment density and distribution in patients with type II macular telangiectasia. Retina 2008;28:808–16.)

Further proof for the depletion in macular pigment derived from a postmortem analysis of an eye with MacTel type 2. Macroscopic examination disclosed the absence of the central yellowish spot.[85] A yellow ring of residual macular pigment was present eccentrically in accordance with the in vivo imaging observations. The loss of macular pigment was subsequently divided into three classes based on a cross-sectional analysis of two-wavelength (blue-light and green-light) FAF images:[86] class 1 shows a wedge-shaped loss of macular pigment restricted to an area temporal to the foveal center. In class 2, the area is larger and also involves the foveal center. Class 3 is characterized by loss of luteal pigment within an oval-shaped area centered on the foveola. There was a significant

association of these three classes of macular pigment loss with the consecutive disease stages of MacTel type 2 described by Gass and Blodi.[80] Correlation studies with microperimetric data revealed a trend towards worse retinal function with increasing class of macular pigment changes.

A recent study succeeded in visualizing even earlier pathologic changes in fellow eyes which otherwise did not meet diagnostic standards for mac tel type 2.[87] While no functional deficits were detected, eyes consistently showed a severely reduced directional cone reflectance (Stiles–Crawford effect). An additional consistent minimal disease manifestation was an asymmetric configuration of the foveal pit with focal temporal thinning, which was most pronounced at 1° eccentricity. Topographically related, macular pigment optical density was reduced in a small wedge-shaped temporal paracentral sector, resulting in an increased signal on fluorescein angiography and FAF imaging. These described alterations may be helpful for early identification of patients and affected family members.

Pseudoxanthoma Elasticum

Pseudoxanthoma elasticum (PXE) is caused by a mutation in the *ABCC6* gene. More than 300 distinct loss-of-function mutations representative of over 1000 mutant alleles in *ABCC6* have been found. Many of the missense mutations occur at locations in the protein involving domain–domain interactions in the *ABCC6* transporter. Even heterozygotes can show manifestations of disease. FAF abnormalities are common in eyes affected by PXE. Typical phenotypic alterations, including angioid streak and drusen of the optic nerve, have autofluorescence correlates. Peau d'orange is hardly detectable on FAF, whereas comet-tail lesions are typically apparent. RPE atrophy can be widespread and heterogeneous, located mostly adjacent to angioid streaks or CNV.[88]

Furthermore, irregular patterns of increased FAF at the posterior pole with an appearance similar to that of pattern dystrophies can be found in eyes with PXE. In these eyes, areas of yellowish deposits and hyperpigmentation on color photography corresponded to areas of increased FAF (Fig. 4.24). Agarwal et al.[89]

suggested the following classification: a fundus appearance similar to a pattern dystrophy of the fundus flavimaculatus, the reticular, the vitelliform and the fundus pulverulentus types, respectively. The pattern dystrophy-like changes in PXE may occur unilaterally or bilaterally.

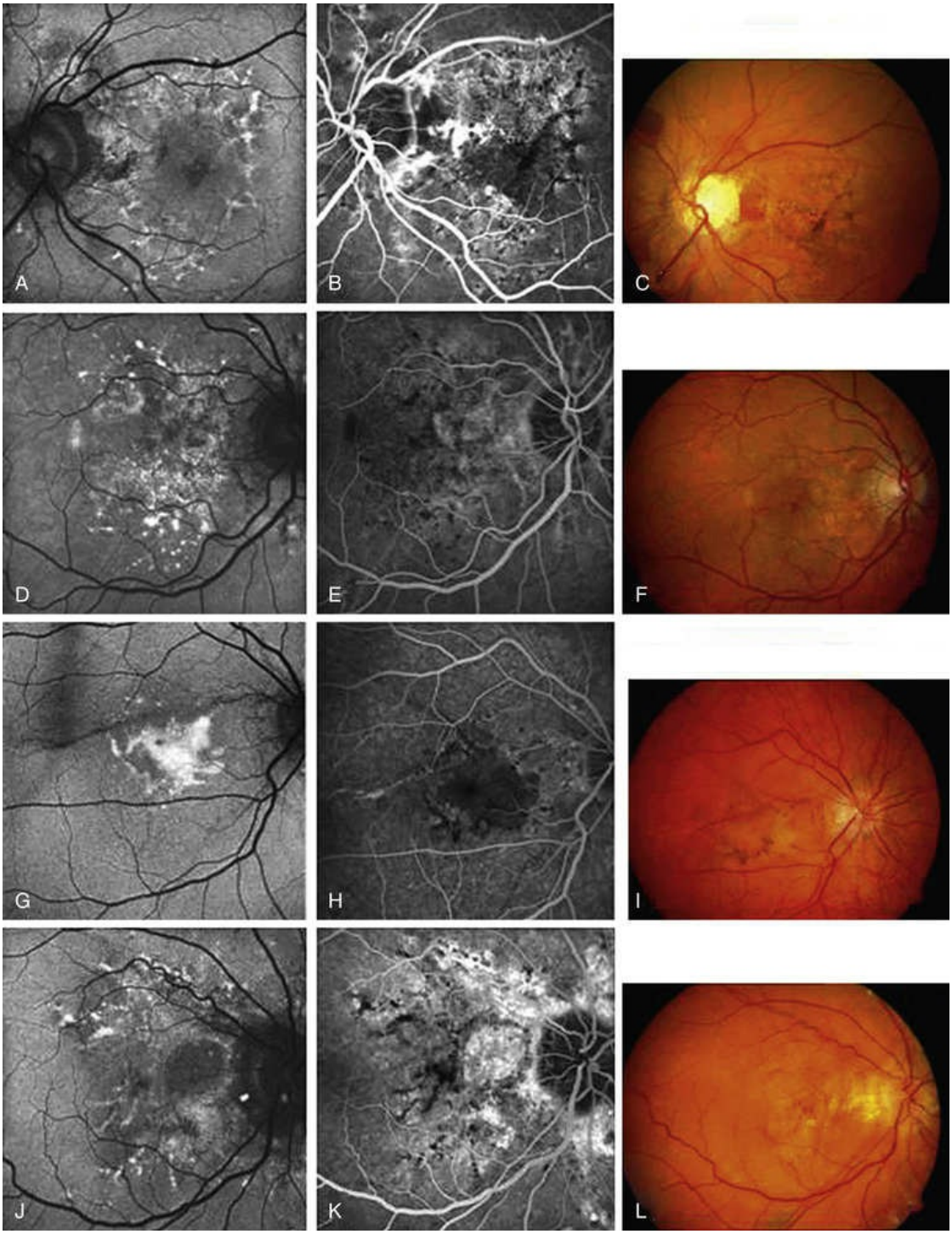

FIG. 4.24 Various types of retinal pigment epithelium degenerative patterns of the macula observed in pseudoxanthoma elasticum (first column: fundus autofluorescence; second column: fluorescein angiography; third column: color fundus photograph). (A–C) Fundus changes resembling reticular dystrophy; (D–F) fundus changes resembling fundus flavimaculatus; (G–I) fundus changes resembling

vitelliform dystrophy; (J–L) fundus changes resembling fundus pulverulentus. (Reproduced with permission from Finger RP, Charbel Issa P, Ladewig M, et al. Fundus autofluorescence in pseudoxanthoma elasticum. Retina 2009;29:1496–505.)

Abnormalities of the RPE–photoreceptor complex detected by FAF imaging are more diverse and widespread than expected from conventional fundus imaging. Such extensive alteration of the RPE suggests an important role of pathologic RPE changes in the evolution of visual loss in PXE.

Ocular alterations related to PXE typically begin at the central fundus and then spread centrifugally, resulting in the most pronounced phenotype in the papillomacular area with the least abnormalities in the periphery.[90] This process also allows the observation of different disease stages from the periphery to the central fundus. It has recently been shown that peau d'orange, which marks the transition from calcified to uncalcified Bruch's membrane, is localized peripheral to areas of RPD. A similar topographic relationship was identified for the transition zone between normal and centrally reduced late-phase ICGA fluorescence, the latter being a result from reduced indocyanine green staining of altered Bruch's membrane and/or RPE.[90] Thus, specific PXE-related fundus changes appear to be localized eccentric to the RPD and precede their development.[51]

Central Serous Chorioretinopathy

Central serous chorioretinopathy (CSC) is a condition characterized by idiopathic leaks at the level of the RPE leading to serous pigment epithelial and neurosensory retinal detachments. In the early phases of the disease, the visual acuity may be good despite the presence of the macular detachment, and after resolution the acuity often shows improvement. More chronic forms of CSC are associated with atrophic and degenerative changes of the retina and RPE and consequently with visual acuity decline.[91]

Accordingly, FAF findings in CSC are dependent on the extent of involvement of the RPE and the stage of the disease.[91] Patients with acute leaks imaged within the first month have minimal abnormalities other than a slight increase in autofluorescence in the

area of the serous retinal detachment. Over time, the area of the detachment increasingly exhibits more irregular increased autofluorescence. In some patients, discrete granules with increased intensity within the detachment are observed which correspond with the pinpoint subretinal precipitates seen on fundoscopy. It has been suggested that these dots may represent macrophages engorged with phagocytosed outer segments. Patients with chronic disease have irregular levels of autofluorescence with markedly decreased intensity over areas of atrophy. A typical finding also includes the visualization of fluid tracks in the inferior retina (Fig. 4.25).

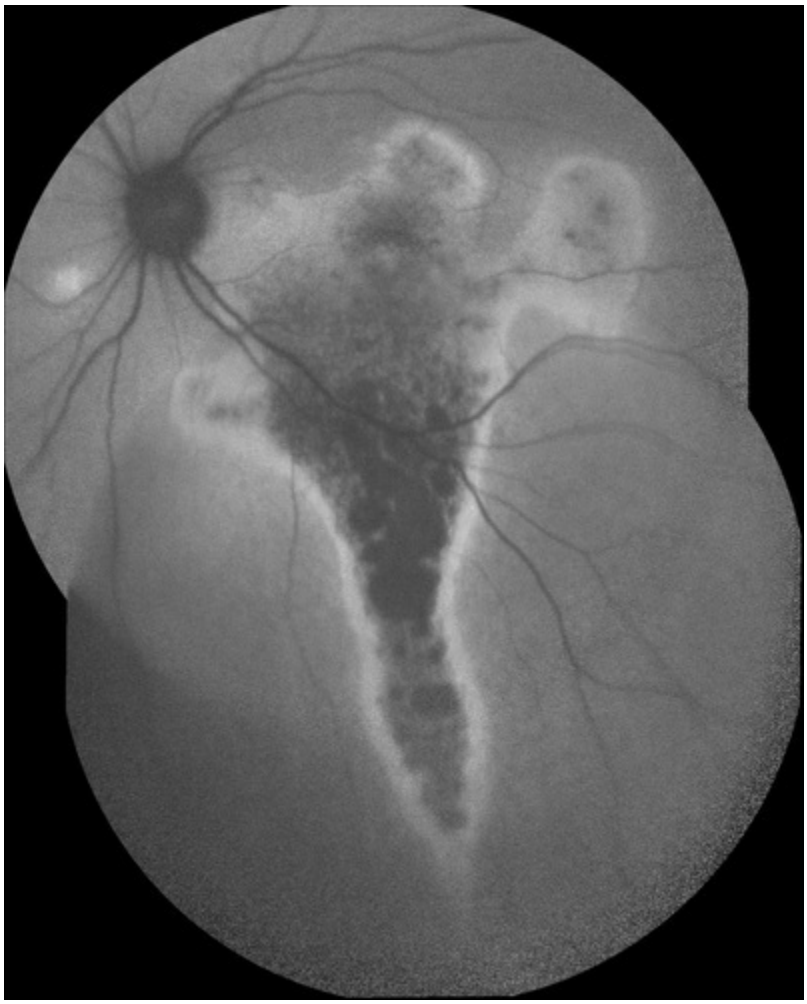

FIG. 4.25 Chronic central serous retinopathy as imaged by confocal scanning laser ophthalmoscopy shows decreased fundus autofluorescence (FAF) in the macula due to atrophy with surrounding increased FAF. Additional FAF abnormalities outside the central

macula, including prominent descending tracts or gutters, are also observed.

The area of the leak also undergoes change in autofluorescence over time. Soon after the development of CSC, little or no change in the autofluorescence pattern in the area around the leak is seen, although the leak site may be somewhat hypoautofluorescent. Patients with more chronic leaks can have decreased autofluorescence surrounding the known leaks. This area of hypoautofluorescence appears to expand in size with increasing chronicity of the leak. Altered FAF in chronic CSC patients has recently been shown to have a functional correlation quantified by microperimetry. This study underlines the impact of FAF changes on retinal sensitivity and their value to reflect the functional impairment in chronic CSC.[92]

Chloroquine and Hydroxychloroquine Retinopathy

FAF imaging may show distinct alterations due to toxic retinal effects of long-term chloroquine and hydroxychloroquine therapy. Various methods have been proposed to detect early stages of chloroquine retinopathy. Early on, a pericentral ring of increased FAF intensity may occur associated with pericentral reduction in multifocal ERG amplitudes and pericentral interruption of the photoreceptor inner/outer-segment junction on SD-OCT imaging.[93] More advanced stages are associated with a more mottled appearance with increased and decreased FAF intensity in the pericentral macula (Fig. 4.26). While electrophysiologic examination has been thought to represent an adequate tool to diagnose early chloroquine maculopathy, FAF imaging can be used as a highly sensitive tool. However, the current recommendation is to apply a multimodal approach as multifocal ERG, FAF, and SD-OCT can all show damage at a relatively early stage, but it is not possible to predict which test will be most definitive for any given individual.[94]

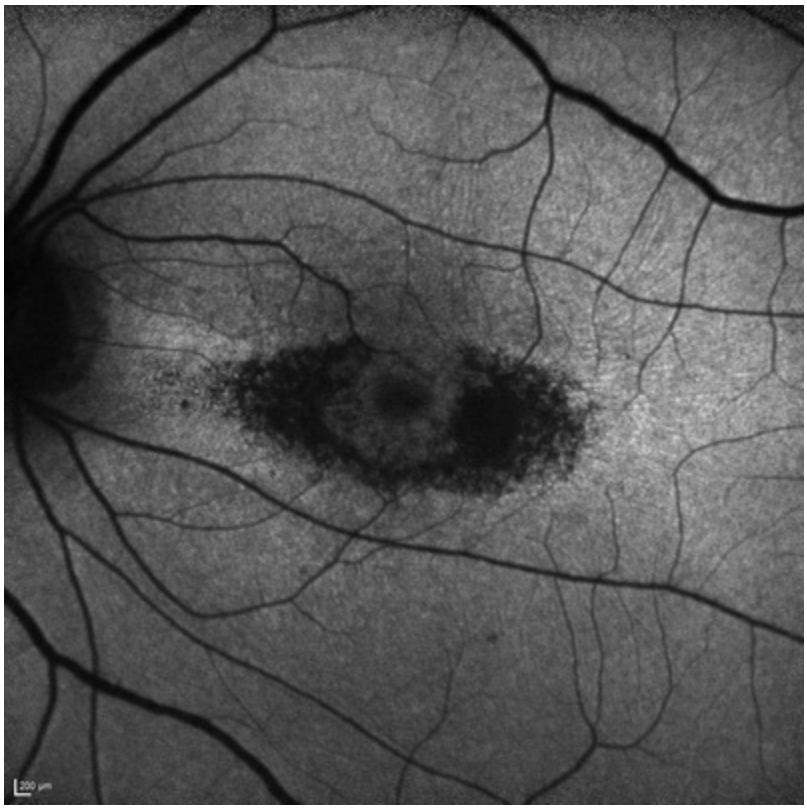

FIG. 4.26 Advanced stage of chloroquine retinopathy. There is a mottled appearance with increased and decreased fundus autofluorescence intensity in the pericentral macula.

Functional Correlates of Fundus Autofluorescence Abnormalities

The relevance of alterations in FAF images can further be addressed by assessing corresponding retinal sensitivity. Severe damage to the RPE such as atrophy, melanin pigment migration, or fibrosis leading to compromised photoreceptor function is confirmed by microperimetry to correspond topographically to areas of decreased autofluorescence.[57,58] In patients with GA secondary to AMD, it has been shown that, in addition to absence of retinal sensitivity over atrophic areas, retinal function is relatively and significantly reduced over areas with increased FAF intensities compared to areas with normal background signal.[58] Localized functional impairment over areas with increased FAF has also been recently confirmed in patients with early AMD. Using fine matrix mapping,

it has been demonstrated that, interestingly, rod function is more severely affected than cone function over areas with increased FAF in patients with AMD.[57] These studies are in accordance with the observation of increased accumulation of autofluorescent material at the level of the RPE prior to the occurrence of cell death. As normal photoreceptor function is dependent on normal RPE function, in particular with regard to the constant phagocytosis of shed distal outer-segment stacks for photoreceptor cell renewal, a negative-feedback mechanism has been proposed, whereby cells with LF-loaded secondary lysosomes would less efficiently phagocytose newly shed photoreceptor outer segments, subsequently leading to impaired retinal sensitivity. This would also be in line with experimental data showing that compounds of LF such as A2-E possess toxic properties and may interfere with normal RPE cell function.[10]

In patients with different retinal dystrophies, lines and rings of increased FAF have been noted (see above).[73] Interestingly, functional testing by microperimetry and electrophysiology indicates that these rings circumscribe areas of preserved photoreceptor function (see Fig. 4.17A).[73–75]

References

1. Delori FC, Dorey CK, Staurenghi G, et al. In vivo fluorescence of the ocular fundus exhibits retinal pigment epithelium lipofuscin characteristics. *Invest Ophthalmol Vis Sci*. 1995;36:718–729.
2. Schmitz-Valckenberg S, Fleckenstein M, Scholl HP, et al. Fundus autofluorescence and progression of age-related macular degeneration. *Surv Ophthalmol*. 2009;54:96–117.
3. Weiter JJ, Delori FC, Wing GL, et al. Retinal pigment epithelial lipofuscin and melanin and choroidal melanin in human eyes. *Invest Ophthalmol Vis Sci*. 1986;27:145–152.
4. Feeney-Burns L, Berman ER, Rothmann H. Lipofuscin of human retinal pigment epithelium. *Am J Ophthalmol*. 1980;90:783–791.
5. Wing GL, Blanchard GC, Weiter JJ. The topography and age relationship of lipofuscin concentration in the retinal

pigment epithelium. *Invest Ophthalmol Vis Sci*. 1978;17:601–607.
6. Sparrow JR, Boulton M. RPE lipofuscin and its role in retinal pathobiology. *Exp Eye Res*. 2005;80:595–606.
7. Eldred GE, Lasky MR. Retinal age-pigments generated by self-assembling lysosomotrophic detergents. *Nature*. 1993;361:724–726.
8. Dorey CK, Wu G, Ebenstein D, et al. Cell loss in the aging retina: relationship to lipofuscin accumulation and macular degeneration. *Invest Ophthalmol Vis Sci*. 1989;30:1691–1699.
9. Schütt F, Davies S, Kopitz J, et al. Photodamage to human RPE cells by A2-E, a retinoid component of lipofuscin. *Invest Ophthalmol Vis Sci*. 2000;41:2303–2308.
10. Bergmann M, Schutt F, Holz FG, et al. Inhibition of the ATP-driven proton pump in RPE lysosomes by the major lipofuscin fluorophore A2-E may contribute to the pathogenesis of age-related macular degeneration. *FASEB J*. 2004;18:562–564.
11. Brunk UT, Wihlmark U, Wrigstad A, et al. Accumulation of lipofuscin within retinal pigment epithelial cells results in enhanced sensitivity to photo-oxidation. *Gerontology*. 1995;41(Suppl. 2):201–212.
12. Hammer M, Richter S, Guehrs KH, et al. Retinal pigment epithelium cell damage by A2-E and its photo-derivatives. *Mol Vis*. 2006;12:1348–1354.
13. Liu J, Itagaki Y, Ben-Shabat S, et al. The biosynthesis of A2E, a fluorophore of aging retina, involves the formation of the precursor, A2-PE, in the photoreceptor outer segment membrane. *J Biol Chem*. 2000;275:29354–29360.
14. Eldred GE, Katz ML. Fluorophores of the human retinal pigment epithelium: separation and spectral characterization. *Exp Eye Res*. 1988;47:71–86.
15. Zhou J, Jang YP, Kim SR, et al. Complement activation by photooxidation products of A2E, a lipofuscin constituent of the retinal pigment epithelium. *Proc Natl Acad Sci USA*. 2006;103:16182–16187.
16. Brandstetter C, Mohr LK, Latz E, et al. Light induces NLRP3 inflammasome activation in retinal pigment epithelial cells

via lipofuscin-mediated photooxidative damage. *J Mol Med*. 2015;93:905–916.
17. Lamb LE, Simon JD. A2E: a component of ocular lipofuscin. *Photochem Photobiol*. 2004;79:127–136.
18. Marmorstein AD, Marmorstein LY, Sakaguchi H, et al. Spectral profiling of autofluorescence associated with lipofuscin, Bruch's membrane, and sub-RPE deposits in normal and AMD eyes. *Invest Ophthalmol Vis Sci*. 2002;43:2435–2441.
19. Keilhauer CN, Delori FC. Near-infrared autofluorescence imaging of the fundus: visualization of ocular melanin. *Invest Ophthalmol Vis Sci*. 2006;47:3556–3564.
20. Weinberger AW, Lappas A, Kirschkamp T, et al. Fundus near infrared fluorescence correlates with fundus near infrared reflectance. *Invest Ophthalmol Vis Sci*. 2006;47:3098–3108.
21. Kellner U, Kellner S, Weinitz S. Fundus autofluorescence (488 nm) and near-infrared autofluorescence (787 nm) visualize different retinal pigment epithelium alterations in patients with age-related macular degeneration. *Retina*. 2010;30:6–15.
22. Gibbs D, Cideciyan AV, Jacobson SG, et al. Retinal pigment epithelium defects in humans and mice with mutations in MYO7A: imaging melanosome-specific autofluorescence. *Invest Ophthalmol Vis Sci*. 2009;50:4386–4393.
23. Schmitz-Valckenberg S, Lara D, Nizari S, et al. Localisation and significance of in vivo near-infrared autofluorescent signal in retinal imaging. *Br J Ophthalmol*. 2011;95:1134–1139.
24. Snodderly DM, Brown PK, Delori FC, et al. The macular pigment. I. Absorbance spectra, localization, and discrimination from other yellow pigments in primate retinas. *Invest Ophthalmol Vis Sci*. 1984;25:660–673.
25. Whitehead AJ, Mares JA, Danis RP. Macular pigment: a review of current knowledge. *Arch Ophthalmol*. 2006;124:1038–1045.
26. Davies NP, Morland AB. Macular pigments: their characteristics and putative role. *Prog Retin Eye Res*.

2004;23:533–559.
27. Wolf S, Wolf-Schnurrbusch U. Macular pigment measurement – theoretical background. Holz FG, Schmitz-Valckenberg S, Spaide RF, et al. *Atlas of autofluorescence imaging*. Springer: Berlin; 2007.
28. von Rückmann A, Fitzke FW, Bird AC. Distribution of fundus autofluorescence with a scanning laser ophthalmoscope. *Br J Ophthalmol*. 1995;79:407–412.
29. Webb RH, Hughes GW, Delori FC. Confocal scanning laser ophthalmoscope. *Appl Opt*. 1987;26:1492–1499.
30. Delori FC, Fleckner MR, Goger DG, et al. Autofluorescence distribution associated with drusen in age-related macular degeneration. *Invest Ophthalmol Vis Sci*. 2000;41:496–504.
31. Spaide RF. Fundus autofluorescence and age-related macular degeneration. *Ophthalmology*. 2003;110:392–399.
32. Spaide RF. Autofluorescence imaging with the fundus camera. Holz FG, Schmitz-Valckenberg S, Spaide RF, et al. *Atlas of autofluorescence imaging*. Springer: Berlin; 2007:49–53.
33. Schmitz-Valckenberg S, Fleckenstein M, Gobel AP, et al. Evaluation of autofluorescence imaging with the scanning laser ophthalmoscope and the fundus camera in age-related geographic atrophy. *Am J Ophthalmol*. 2008;146:183–192.
34. Nittala MG, Hariri A, Wong WT, et al. Image scaling difference between a confocal scanning laser ophthalmoscope and a flash fundus camera. *Ophthalmic Surg Lasers Imaging Retina*. 2015;46:872–879.
35. Oishi M, Oishi A, Ogino K, et al. Widefield fundus autofluorescence abnormalities and visual function in patients with cone and cone–rod dystrophies. *Invest Ophthalmol Vis Sci*. 2014;55:3572–3577.
36. Witmer MT, Kozbial A, Daniel S, et al. Peripheral autofluorescence findings in age-related macular degeneration. *Acta Ophthalmol*. 2012;90:e428–33.
37. Tan CS, Heussen F, Sadda SR. Peripheral autofluorescence and clinical findings in neovascular and non-neovascular age-related macular degeneration. *Ophthalmology*. 2013;120:1271–1277.
38. Duisdieker V, Fleckenstein M, Zilkens KM, et al. Long-term

follow-up of fundus autofluorescence imaging using wide-field scanning laser ophthalmoscopy. *Ophthalmologica*. 2015;234(4):218–226.
39. Lois N, Halfyard AS, Bunce C, et al. Reproducibility of fundus autofluorescence measurements obtained using a confocal scanning laser ophthalmoscope. *Br J Ophthalmol*. 1999;83:276–279.
40. Delori F, Greenberg JP, Woods RL, et al. Quantitative measurements of autofluorescence with the scanning laser ophthalmoscope. *Invest Ophthalmol Vis Sci*. 2011;52:9379–9390.
41. Greenberg JP, Duncker T, Woods RL, et al. Quantitative fundus autofluorescence in healthy eyes. *Invest Ophthalmol Vis Sci*. 2013;54:5684–5693.
42. Bird A. Age-related macular disease. *Br J Ophthalmol*. 1996;80:2–3.
43. Bindewald A, Bird AC, Dandekar SS, et al. Classification of fundus autofluorescence patterns in early age-related macular disease. *Invest Ophthalmol Vis Sci*. 2005;46:3309–3314.
44. Göbel AP, Fleckenstein M, Heeren TF, et al. In-vivo mapping of drusen by fundus autofluorescence and spectral-domain optical coherence tomography imaging. *Graefes Arch Clin Exp Ophthalmol*. 2016;254(1):59–67.
45. Schmitz-Valckenberg S, Alten F, Steinberg JS, et al. Reticular drusen associated with geographic atrophy in age-related macular degeneration. *Invest Ophthalmol Vis Sci*. 2011;52:5009–5015.
46. Steinberg JS, Göbel AP, Fleckenstein M, et al. Reticular drusen in eyes with high-risk characteristics for progression to late-stage age-related macular degeneration. *Br J Ophthalmol*. 2015;99:1289–1294.
47. Arnold JJ, Sarks SH, Killingsworth MC, et al. Reticular pseudodrusen: a risk factor in age-related maculopathy. *Retina*. 1995;15:183–191.
48. Alten F, Clemens CR, Heiduschka P, et al. N. Characterisation of reticular pseudodrusen and their central target aspect in multi-spectral, confocal scanning laser

ophthalmoscopy. *Graefes Arch Clin Exp Ophthalmol*. 2014;252:715–721.
49. Suzuki M, Sato T, Spaide RF. Pseudodrusen subtypes as delineated by multimodal imaging of the fundus. *Am J Ophthalmol*. 2014;157:1005–1012.
50. Gliem M, Müller PL, Mangold E, et al. Reticular pseudodrusen in Sorsby fundus dystrophy. *Ophthalmology*. 2015;122:1555–1562.
51. Gliem M, Hendig D, Finger RP, et al. Reticular pseudodrusen associated with a diseased Bruch membrane in pseudoxanthoma elasticum. *JAMA Ophthalmol*. 2015;133:581–588.
52. Sarks SH. Ageing and degeneration in the macular region: a clinico-pathological study. *Br J Ophthalmol*. 1976;60:324–341.
53. Schmitz-Valckenberg S, Bindewald-Wittich A, Dolar-Szczasny J, et al. Correlation between the area of increased autofluorescence surrounding geographic atrophy and disease progression in patients with AMD. *Invest Ophthalmol Vis Sci*. 2006;47:2648–2654.
54. Holz FG, Bindewald-Wittich A, Fleckenstein M, et al. Progression of geographic atrophy and impact of fundus autofluorescence patterns in age-related macular degeneration. *Am J Ophthalmol*. 2007;143:463–472.
55. Holz FG, Bellman C, Staudt S, et al. Fundus autofluorescence and development of geographic atrophy in age-related macular degeneration. *Invest Ophthalmol Vis Sci*. 2001;42:1051–1056.
56. Bindewald A, Schmitz-Valckenberg S, Jorzik JJ, et al. Classification of abnormal fundus autofluorescence patterns in the junctional zone of geographic atrophy in patients with age related macular degeneration. *Br J Ophthalmol*. 2005;89:874–878.
57. Scholl HP, Bellmann C, Dandekar SS, et al. Photopic and scotopic fine matrix mapping of retinal areas of increased fundus autofluorescence in patients with age-related maculopathy. *Invest Ophthalmol Vis Sci*. 2004;45:574–583.
58. Schmitz-Valckenberg S, Bultmann S, Dreyhaupt J, et al. Fundus autofluorescence and fundus perimetry in the

junctional zone of geographic atrophy in patients with age-related macular degeneration. *Invest Ophthalmol Vis Sci*. 2004;45:4470–4476.
59. Schmitz-Valckenberg S, Sahel J-A, Danis R, et al. Natural History of Geographic Atrophy Progression Secondary to Age-Related Macular Degeneration (GAP-Study). *Ophthalmology*. 2016;123:361–368.
60. Wolf-Schnurrbusch UE, Wittwer VV, Ghanem R, et al. Blue-light versus green-light autofluorescence: lesion size of areas of geographic atrophy. *Invest Ophthalmol Vis Sci*. 2011;52:9497–9502.
61. Lindner M, Böker A, Mauschitz MM, et al. Fundus Autofluorescence in Age-Related Macular Degeneration Study Group. Directional kinetics of geographic atrophy progression in age-related macular degeneration with foveal sparing. *Ophthalmology*. 2015;122:1356–1365.
62. Vaclavik V, Vujosevic S, Dandekar SS, et al. Autofluorescence imaging in age-related macular degeneration complicated by choroidal neovascularization: a prospective study. *Ophthalmology*. 2008;115:342–346.
63. McBain VA, Townend J, Lois N. Fundus autofluorescence in exudative age-related macular degeneration. *Br J Ophthalmol*. 2007;91:491–496.
64. Sawa M, Ober MD, Spaide RF. Autofluorescence and retinal pigment epithelial atrophy after subretinal hemorrhage. *Retina*. 2006;26:119–120.
65. Heimes B, Lommatzsch A, Zeimer M, et al. Foveal RPE autofluorescence as a prognostic factor for anti-VEGF therapy in exudative AMD. *Graefes Arch Clin Exp Ophthalmol*. 2008;246:1229–1234.
66. Bhisitkul RB, Mendes TS, Rofagha S, et al. Macular atrophy progression and 7-year vision outcomes in subjects from the ANCHOR, MARINA, and HORIZON studies: the SEVEN-UP study. *Am J Ophthalmol*. 2015;159:915–924.
67. Kumar N, Mrejen S, Fung AT, et al. Retinal pigment epithelial cell loss assessed by fundus autofluorescence imaging in neovascular age-related macular degeneration. *Ophthalmology*. 2013;120:334–341.

68. von Rückmann A, Fitzke F, Schmitz-Valckenberg S, et al. Macular and retinal dystrophies. Holz FG, Schmitz-Valckenberg S, Spaide R, et al. *Atlas of fundus and fluorescence imaging*. Springer: Berlin; 2007.
69. Saksens NT, Fleckenstein M, Schmitz-Valckenberg S, et al. Macular dystrophies mimicking age-related macular degeneration. *Prog Retin Eye Res*. 2014;39:23–57.
70. Sparrow JR, Marsiglia M, Allikmets R, et al. Flecks in recessive Stargardt disease: short-wavelength autofluorescence, near-infrared autofluorescence, and optical coherence tomography. *Invest Ophthalmol Vis Sci*. 2015;56:5029–5039.
71. Lorenz B, Wabbels B, Wegscheider E, et al. Lack of fundus autofluorescence to 488 nanometers from childhood on in patients with early-onset severe retinal dystrophy associated with mutations in RPE65. *Ophthalmology*. 2004;111:1585–1594.
72. Scholl HP, Chong NH, Robson AG, et al. Fundus autofluorescence in patients with Leber congenital amaurosis. *Invest Ophthalmol Vis Sci*. 2004;45:2747–2752.
73. Robson AG, Michaelides M, Saihan Z, et al. Functional characteristics of patients with retinal dystrophy that manifest abnormal parafoveal annuli of high density fundus autofluorescence; a review and update. *Doc Ophthalmol*. 2008;116:79–89.
74. Fleckenstein M, Charbel Issa P, Fuchs HA, et al. Discrete arcs of increased fundus autofluorescence in retinal dystrophies and functional correlate on microperimetry. *Eye (Lond)*. 2009;23:567–575.
75. Popovic P, Jarc-Vidmar M, Hawlina M. Abnormal fundus autofluorescence in relation to retinal function in patients with retinitis pigmentosa. *Graefes Arch Clin Exp Ophthalmol*. 2005;243:1018–1027.
76. Fleckenstein M, Charbel Issa P, Helb HM, et al. Correlation of lines of increased autofluorescence in macular dystrophy and pigmented paravenous retinochoroidal atrophy by optical coherence tomography. *Arch Ophthalmol*. 2008;126:1461–1463.

77. Lima LH, Cella W, Greenstein VC, et al. Structural assessment of hyperautofluorescent ring in patients with retinitis pigmentosa. *Retina*. 2009;29:1025–1031.
78. Duncker T, Tsang SH, Woods RL, et al. Quantitative fundus autofluorescence and optical coherence tomography in PRPH2/RDS- and ABCA4-associated disease exhibiting phenotypic overlap. *Invest Ophthalmol Vis Sci*. 2015;56:3159–3170.
79. Duncker T, Greenberg JP, Ramachandran R, et al. Quantitative fundus autofluorescence and optical coherence tomography in best vitelliform macular dystrophy. *Invest Ophthalmol Vis Sci*. 2014;55:1471–1482.
80. Gass JD, Blodi BA. Idiopathic juxtafoveolar retinal telangiectasis. Update of classification and follow-up study. *Ophthalmology*. 1993;100:1536–1546.
81. Hutton WL, Snyder WB, Fuller D, et al. Focal parafoveal retinal telangiectasis. *Arch Ophthalmol*. 1978;96:1362–1367.
82. Gass JDM. *Stereoscopic atlas of macular diseases: diagnosis and treatment*. 2nd ed. Mosby: St. Louis; 1977.
83. Helb HM, Charbel Issa P, van der Veen RL, et al. Abnormal macular pigment distribution in type 2 idiopathic macular telangiectasia. *Retina*. 2008;28:808–816.
84. Charbel Issa P, van der Veen RL, Stijfs A, et al. Quantification of reduced macular pigment optical density in the central retina in macular telangiectasia type 2. *Exp Eye Res*. 2009;89:25–31.
85. Powner MB, Gillies MC, Tretiach M, et al. Perifoveal Müller cell depletion in a case of macular telangiectasia type 2. *Ophthalmology*. 2010;117:2407–2416.
86. Zeimer MB, Padge B, Heimes B, et al. Idiopathic macular telangiectasia type 2: distribution of macular pigment and functional investigations. *Retina*. 2010;30:586–595.
87. Charbel Issa P, Heeren TFC, Kupitz E, et al. Very early disease manifestations of macular telangiectasia type 2. *Retina*. 2016;36:524–534.
88. Finger RP, Charbel Issa P, Ladewig M, et al. Fundus autofluorescence in pseudoxanthoma elasticum. *Retina*. 2009;29:1496–1505.

89. Agarwal A, Patel P, Adkins T, et al. Spectrum of pattern dystrophy in pseudoxanthoma elasticum. *Arch Ophthalmol*. 2005;123:923–928.
90. Charbel Issa P, Finger RP, Gotting C, et al. Centrifugal fundus abnormalities in pseudoxanthoma elasticum. *Ophthalmology*. 2010;117:1406–1414.
91. Spaide RF, Klancnik JM Jr. Fundus autofluorescence and central serous chorioretinopathy. *Ophthalmology*. 2005;112:825–833.
92. Eandi CM, Piccolino FC, Alovisi C, et al. Correlation between fundus autofluorescence and central visual function in chronic central serous chorioretinopathy. *Am J Ophthalmol*. 2015;159:652–658.
93. Kellner S, Weinitz S, Kellner U. Spectral domain optical coherence tomography detects early stages of chloroquine retinopathy similar to multifocal electroretinography, fundus autofluorescence and near-infrared autofluorescence. *Br J Ophthalmol*. 2009;93:1444–1447.
94. Marmor MF. Comparison of screening procedures in hydroxychloroquine toxicity. *Arch Ophthalmol*. 2012;130:461–469.

5

Wide-Field Imaging

Michael A. Klufas, Szilard Kiss

Introduction

Retinal imaging continues to undergo significant advances and innovations. One posterior segment imaging modality that continues to evolve is wide-field imaging. Traditional fundus cameras image 30–60° of the ocular fundus. Newer devices are capable of providing up to a 200° view of the posterior pole. The role and clinical utility of wide-field imaging continues to evolve as this imaging modality becomes more widely available and utilized in clinical research, including large clinical trials. This chapter will provide a comprehensive overview of wide-field retinal imaging.

Historical Perspective and Terms

Early clinical examination of the fundus prior to the development of the ophthalmoscope relied either on postmortem histologic analysis of eyes or rudimentary examination of the gross red reflex observed through the pupil.[1] Development of the ophthalmoscope by Helmholtz in 1851 permitted detailed clinical examination of the fundus, but with a narrow field of view.[2] Luminaries such as Gonin

depended on a modified indirect ophthalmoscope based on Reute's "inverted image instrument,"[3] which offered a superior and more illuminated view, permitting Gonin and Dufour a distinct advantage over their contemporaries to definitively describe the pathogenesis of retinal detachments. Further developments in instrumentation and technology led to the development of the modern binocular indirect ophthalmoscope by Schepens which allowed a wider field of view, transforming examination of the peripheral fundus and operative repair of retinal detachments with scleral buckling. Similarly, modern wide-field imaging is now allowing enhanced examination of the retina beyond the posterior pole.

The Carl Zeiss Company produced the first fundus camera in 1926 capable of providing a 20° field of view,[4] which later increased to the "normal" 30° field of view which is the current "standard" field of view for fundus cameras. Any device with a larger field of view was then variably referred to as "wide-field" or "wide-angle." The actual definition of wide-field imaging in terms of number of degrees of the fundus images was historically not well established.

However, the Diabetic Retinopathy Clinical Research Network (DRCR.net) has recently defined ultrawide-field (UWF) images to have at least a 100° view of the fundus, and protocol AA[5] from this research network is a large ongoing prospective study specifically investigating the role of UWF imaging with results expected in approximately 2020. More recently with results from DRCR.net protocol S supporting the noninferiority of primary intravitreal ranibizumab to panretinal photocoagulation for the treatment of proliferative diabetic retinopathy (PDR),[6] the potential role of wide-field imaging to asses the peripheral retina for pathology including neovascularization is potentially of greater interest.

Historical Wide-Field Imaging Systems

Montage With Traditional Fundus Camera

Wide-field imaging may have been first described in 1977 by Lotmar who utilized a traditional fundus camera with a small field

of view, and with the assistance of a fixation lamp and rotatable mirror, was able to acquire up to 19 images to create a 96° montage. This technique is limited by patient and photographer cooperation and requires a large pupil[7] **(**Fig. 5.1**)**. Furthermore, this method is unable to acquire simultaneous images, which may limit its use for time-dependent or dynamic studies such as fluorescein angiography (FA).

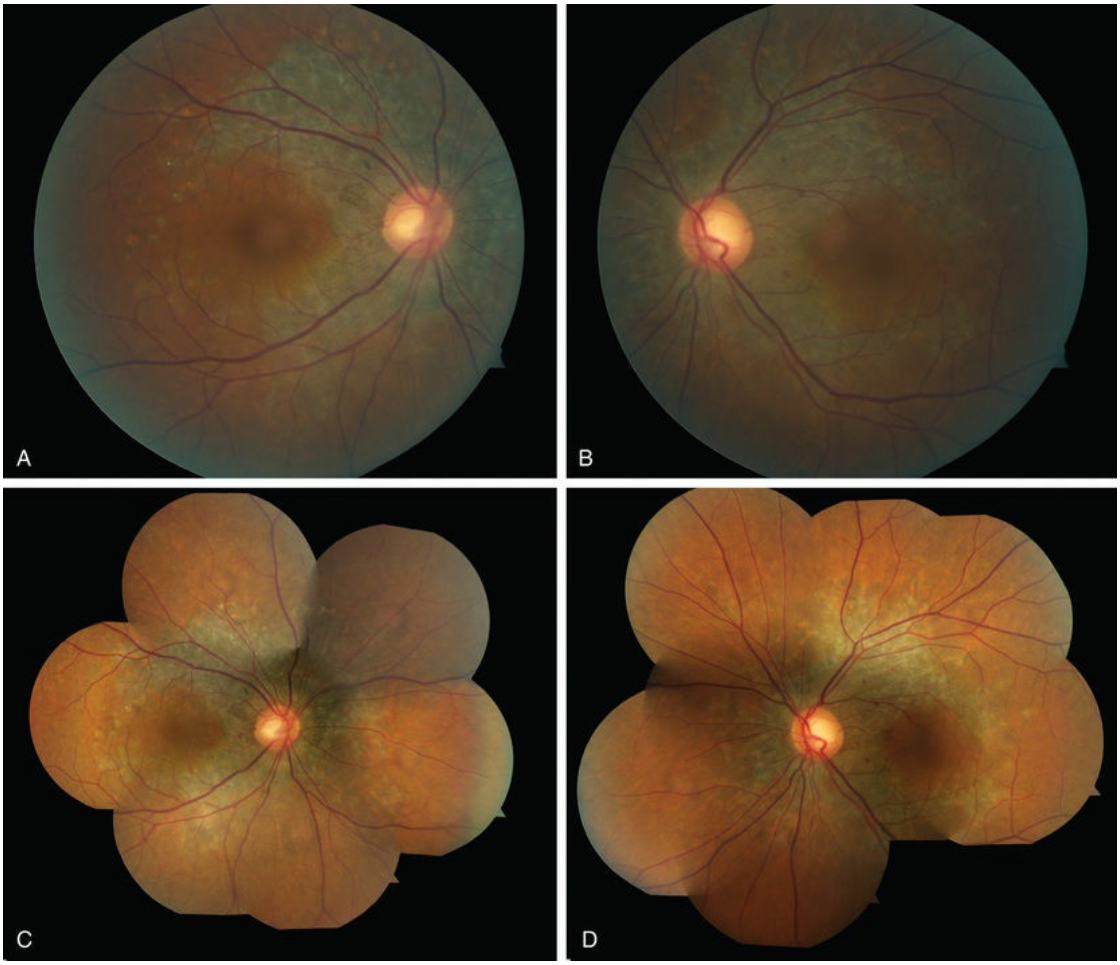

FIG. 5.1 Posterior polar choroidal annular dystrophy: Zeiss color photographs (A,B) and corresponding color photo montage (C,D).

Pomerantzeff Camera

In 1975, Pomerantzeff reported on the Equator-plus fundus camera which is a contact lens-based system requiring pupillary dilation and employed fiberoptic transpupillary illumination and scleral

transillumination to obtain images up to 148° degrees of the retina.[8,9] Major limitations of this technique included limited resolution secondary to the location and intensity of the light source.[10]

Panoret

The Panoret-1000 (Medibell Medical Vision Technologies, Haifa, Israel) is based on the concept used in Pomerantzeff's camera utilizing transscleral illumination, but was handheld, capable of digital image acquisition, and provided a 100° view through an undilated pupil using a contact lens.[11,12] This system allowed image acquisition through miotic pupils and lenticular opacity (i.e., cataract) with limited glare given the transscleral light source. It is unwieldy to obtain images, requiring one hand to hold the camera, the other hand to hold the light and the use of a foot or assistant to capture the image by activating a foot switch. Nevertheless, with a skilled photographer, image acquisition is possible in approximately 3 minutes. One series reported reliable and high-quality imaging in 1500 patients with only six instances of an inability to acquire images due to poor patient cooperation.[12]

Modern Wide-Field Imaging Systems

RetCam

The RetCam (Clarity Medical Systems, Inc., Pleasanton, CA), first introduced in 1997, is a contact-based digital imaging system with an external fiberoptic light source that is primarily used to image neonatal and pediatric patients[13–16] (Fig. 5.2). Given that the illumination is performed through the cornea and crystalline lens, even small lenticular opacities may produce poor image quality, limiting its use in the adult population with cataract. The handpiece portion of the system has five interchangeable lenses capable of providing varying degrees of view, the wide-angle lens being able to image 130° degrees of the retina. This imaging system may be outfitted with a commercially available FA module at additional cost, an imaging modality that is becoming increasingly important

in many pediatric vitreoretinal conditions.[17–21] The RetCam is commonly used in telescreening applications for retinopathy of prematurity (ROP) – see Chapter 65, Telescreening for retinopathy of prematurity.

FIG. 5.2 Crystalline retinopathy in pediatric patient status post renal transplant. Comparison of Zeiss non-wide-angle color fundus photograph, wide-angle RetCam color fundus photographs with 80° and 130° lens along with corresponding 130°-angle fluorescein angiogram and Optos fundus photograph.

Staurenghi Lens System and Precursors

In 2005, Staurenghi and colleagues reported on the use of a wide-angle contact lens system with a confocal scanning laser ophthalmoscopy (SLO)-based imaging platform (Ocular Staurenghi 230 SLO Retina Lens; Ocular Instruments Inc, Bellevue, WA).[22–24] The integrated, multielement, wide-field system consists of two biconvex aspheric lenses and a two-element convex–concave lens, which is able to image up to 150° degrees of the ocular fundus. Disadvantages of this system include that it requires topical anesthesia given a contact lens must be placed, image quality may be limited by lenticular opacities, and it requires a skilled

photographer to stabilize the lens while simultaneously acquiring the images.

Prior to the development of the Staurenghi lens system, investigators in Japan become interested in wide-angle (up to 70°) indocyanine green angiography (ICGA) to examine the peripheral choroidal circulation and watershed zones.[25] In 1996, this team performed ICGA using a SLO and a handheld 30-diopter lens. Soon after in 1998, Spaide and colleagues reported on the use of a wide-angle contact lens (Volk SuperQuad 160, Volk Optical Inc., Mentor, OH) in combination with a fundus camera to provide a greater view of the peripheral fundus circulation.[26] These systems, like the Staurenghi lens system, have the disadvantage of autofluorescence from the crystalline lens, which degrades image quality.

Mobile Phone Imaging With Indirect Lenses

In an era of smartphone mobile technology, reports have been published on utilizing the camera light of a smartphone with a conventional indirect condensing lens to acquire digital images of the fundus.[27,28] Low cost software applications may be needed to facilitate image acquisition. Modifications of the technique, including placement of a Koeppe lens on the cornea, can be used to improve image quality and prevent corneal desiccation when imaging is done during exams under anesthesia. Globally, this may prove to be a cost-effective alternative to more expensive systems such as the RetCam, but at the expense of decreased resolution and challenging image acquisition.

Heidelberg Spectralis Non-Contact Ultrawide-Field Module

Recently, a non-contact lens has been developed that may be attached to the existing Heidelberg Spectralis or HRA2 cSLO (Heidelberg Engineering, Inc., Heidelberg, Germany) to expand the existing 55° maximum field of view available with this system to 105°.[29] Although this adapted system images less area than the other commercially available non-contact UWF system from Optos, it may have the advantage of less lash artifact, resulting in

improved imaging of the superior and inferior periphery in some patients. In a single view, this system is capable of providing real-time, UWF multimodal imaging including simultaneous FA and ICGA.

Optos

The Optos cSLO UWF imaging system (Optos PLC, Dunfermline, United Kingdom) utilizes an ellipsoid mirror to image up to 200° or approximately 80% of the ocular fundus [30] (Fig. 5.3). It first became commercially available in 2000. It does not require the use of a contact lens and is capable of imaging through a nondilated pupil or other conditions where there is a small optical aperture to the posterior segment such as a permanent keratoprosthesis[31] or implanted telescope in patients with advanced macular degeneration. The image acquisition time is rapid at approximately 0.25 seconds by using two galvanometer mirrors to provide quick two-dimensional scanning. This technical aspect can be particularly useful to acquire images of the posterior pole in patients with nystagmus and photographphobia and in children. The ellipsoid mirror of the device has two focal points with the laser of the Optos being directed to one of the focal points and the patient positioned in front of the machine such that the second focal point is within the eye near the pupillary plane thereby creating large scan angles, allowing imaging out to the ora serrata in patients with good compliance and wide pupillary dilation.[30] The Optos platform is capable of pseudocolor fundus photography, green-light fundus autofluorescence (FAF), FA, and ICGA.

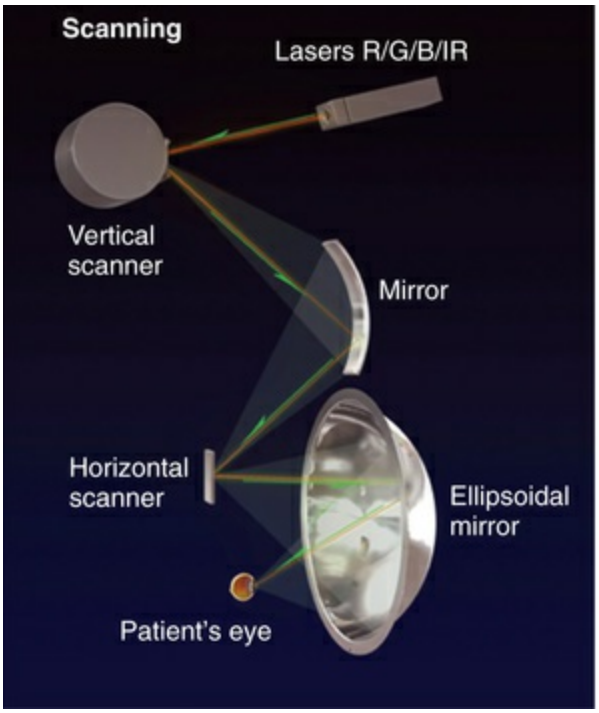

FIG. 5.3 Optics of Optos scanning laser ophthalmoscope with ellipsoidal mirror.

Although this platform currently provides the largest single frame view of the posterior pole, there are some disadvantages or limitations. Currently, the SLO only employs a red and green channel SLO that are combined to create a pseudocolor image. The manufacturer may add a blue channel in the future to better simulate the true colors of the posterior segment that are seen with traditional flash fundus photography. Additionally, mapping a three-dimensional structure onto a two-dimensional surface creates a map distortion. Peripheral areas of the ocular fundus are disproportionately imaged by nearly twice that of the posterior pole with the horizontal axis being warped and stretched more so than the vertical axis.[32] These distortions may be mitigated by a stereographic projection/correction that has recently been developed.[33] This stereographic projection maintains the same angular magnification at all eccentricities, allowing reliable measurements to be made. Lastly, UWF images captured with the device provide a lower resolution image of the posterior pole compared with other SLO systems such as the Heidelberg Spectralis. This shortcoming is partially reduced when utilizing the

ResMax™ feature which allows a smaller area to be imaged (i.e., posterior pole) on the same sensor that would be used to image a much larger area of the retina, thereby resulting in a higher resolution image. Additionally, the large depth of focus in this system is useful to maintain the entire ocular fundus in focus despite different anterior and posterior locations and for imaging elevated lesions such as choroidal tumors or depressed areas such as a posterior staphyloma. However, this large depth of field also commonly allows the patient's eyelashes and nose to appear in the image. The eyelash artifact can be diminished by placement of a speculum.[34]

Overview of Imaging Capabilities and Optical Principles

Traditional fundus cameras produce color fundus photographs by using white light as an illumination source and capturing the image on traditional film or via digital methods. Among UWF devices, this type of imaging or acquisition strategy is employed by the RetCam platform. However, both the Heidelberg and Optos UWF platforms utilize SLO optics. For instance, the Heidelberg Spectralis in a non-wide-field platform is able to produce a multicolor image from infrared (820 nm), green (518 nm), and blue (488 nm) reflectance channels. Similarly, the Optos platform produces color images of the retina by confocal scanning with green (red-free) laser light at 532 nm and also red-light at 633 nm. The images may be viewed together which provides a colored image of the fundus, and a “white-balance” mode may be employed to more closely approximate the true colors of posterior segment pathology. Furthermore, the separate SLO channels may be viewed separately. Green (red-free) highlights the retinal vasculature and anterior retinal structures, and the red channel accentuates deeper retinal structures and the choroidal vasculature. It is important for the clinician to be aware that the SLO derived images are acquired differently than traditional fundus cameras, which employ a full spectrum of white light, therefore the coloration between the two types of systems will be distinct. This has implications for the

assessment of many lesions for which coloration is of significant importance such as with intraocular tumors or areas of retinitis.

For FA, the Optos employs a 488 nm excitation signal through its dichroic beam-splitters and confocal aperture and a 500 nm filter when detecting the fluorescence from the fundus.[35,36] For ICGA with the Optos platform, a 805 nm excitation beam is emitted and the cyanescence returns through a 835 nm filter.[37] Identical excitation and barrier filter wavelengths are used for FA in the Heidelberg Wide-Field Non-Contact System. However, for indocyanine green angiography a diode laser at 790 nm is used together with a barrier filter at 830 nm to separate excitation and cyanescence.

With regard to the spectrums used for wide-field FAF, the Optos system employed the green 532 nm for excitation and a 570–780 nm filter (yellow–orange–red range) to detect fundus autofluorescence. In comparison, the Heidelberg platform most commonly uses a 488 nm to produce short-wavelength autofluorescence images, though the capability for green autofluorescence has also been added to some systems. The Heidelberg system is also capable of producing near-infrared autofluorescence using a 787 nm wavelength. The most striking difference with the near-infrared images of the posterior pole is that there is an area of increased hyperautofluorescence centered on the fovea which likely corresponds to the area with higher retinal pigment epithelial melanin seen in color photographs.[38] Comparing the short-wavelength of the Optos versus Heidelberg SLO systems for fundus autofluorescence (532 nm vs. 488 nm), the slightly longer wavelength of the Optos system may be less affected by absorbance from cataract,[39] but both systems utilize a confocal pinhole which greatly reduces out of focus autofluorescence signal from the lens to limit image quality degradation.[40]

Clinical Utility of Wide-Field Imaging

Wide-field and more recently ultrawide-field imaging continues to have an evolving role in the diagnosis and management of retinal diseases. Though the majority of published reports utilizing UWF imaging are predominately descriptive and retrospective in nature,

they have led to important observations which have prompted more detailed prospective studies that are in progress.

Diabetic Retinopathy

The importance of the periphery in diabetes was apparent in early prospective trials such as the Early Treatment of Diabetic Retinopathy Study (ETDRS) where seven standard field 30° images could be combined to create a 75° montage. This 75° assessment became the early standard for diabetic clinical trials.[41] The use of UWF imaging has revealed potentially important clinical findings in the periphery of diabetic eyes beyond the seven standard ETDRS field, and the clinical significance of these findings are continuing to be investigated.

Initial studies utilizing nonmydriatic UWF imaging for screening of diabetic retinopathy found that there was a 94% sensitivity compared to the clinical exam, and follow-up recommendations corresponded to clinical recommendations at a rate of 82%.[30] Subsequent studies have found moderate agreement between slit-lamp examination and review of Optos UWF imaging for the detection of diabetic retinopathy in a real-life setting.[42] Another study comparing nonmydriatic Optos UWF images with dilated ophthalmoscopy reported a sensitivity of 94% and specificity of 100% for detection of diabetic retinopathy worse than mild nonproliferative disease, with moderate to substantial intergrader agreement for retinopathy severity grading using an unweighted kappa statistic.[43] Another study found similar sensitivity and specificity of nonmydriatic UWF imaging compared to single-field and dual-field mydriatic digital retina photography, with sensitivity of 83.6% and specificity of 89.5% for UWF, albeit with a slightly higher technical failure rate with wide-field imaging.[44] More recently, studies have compared the seven standard field ETDRS photographs to UWF imaging and have found substantial agreement in determining disease severity, with UWF also identifying peripheral lesions suggesting more severe disease than observed within the ETDRS fields in 10% of eyes.[45] Telemedicine screening paradigms are now being reported using real-time, point-of-care UWF image acquisition and interpretation by nonphysician

imagers in which <0.1% of referable diabetic retinopathy would be missed.[46–48]

Early reports also noted the benefit of UWF–FA for the diagnosis of PDR[49] (Fig. 5.4) and that this type of wide-field imaging could be particularly useful in the setting of vitreous media opacity such as asteroid hyalosis.[50] A study from Weill Cornell found that UWF–FA compared to the seven standard fields (7SF) FA imaged 3.9 times more nonperfusion, 1.9 times more neovascularization, and prompted 3.8 times more panretinal photocoagulation.[51] This study, in addition to others, also found that in 10% of eyes, UWF–FA demonstrated peripheral nonperfusion and neovascularization not evident on 7SF imaging.

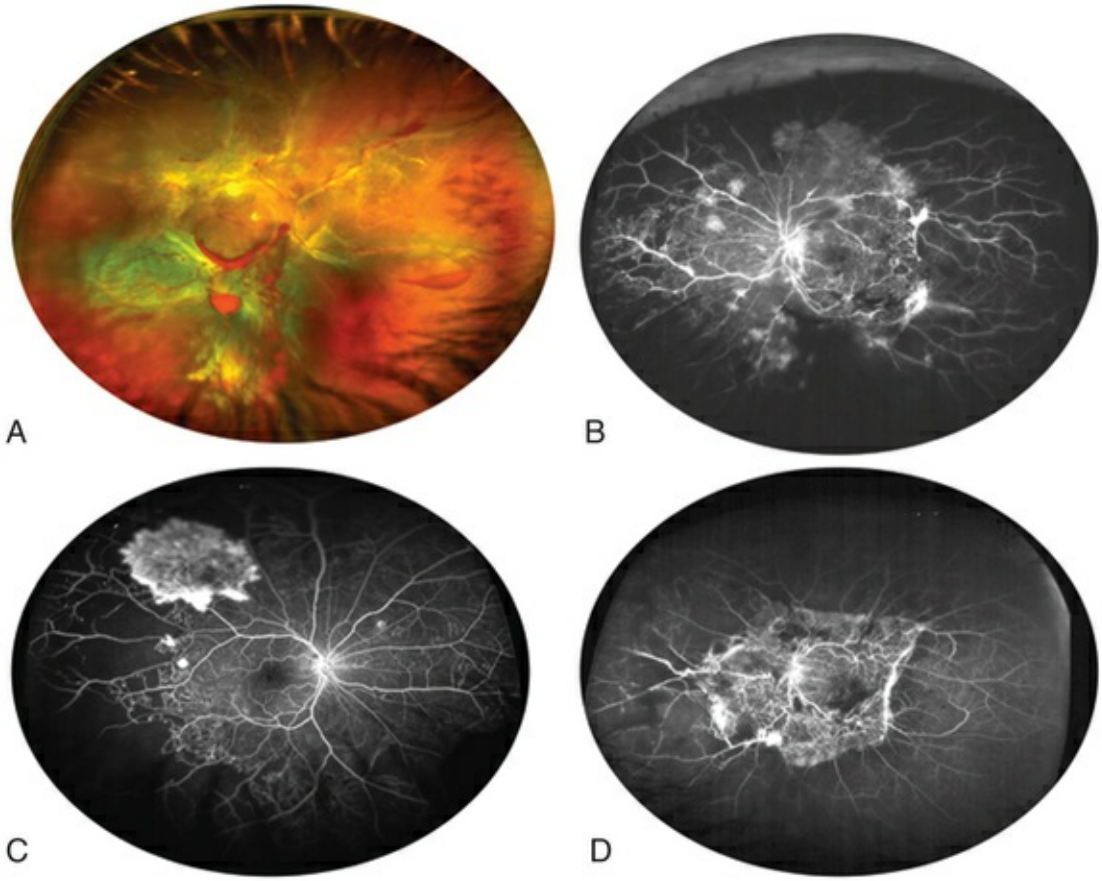

FIG. 5.4 Optos photograph of proliferative diabetic retinopathy (PDR) (A) and additional cases of PDR on Optos ultrawide-field–fluorescein angiography (UWF–FA).

UWF imaging has also been used to specifically investigate

peripheral nonperfusion and neovascularization and the relationship to macular ischemia and diabetic macular edema.[52] A study of 264 eyes with diabetic retinopathy found that peripheral vascular leakage (PVL) was present in 41% of eyes as frequently as neovascularization, but less commonly than peripheral nonperfusion (54%) or focal or diffuse angiographic macular edema (57%).[53] This study found an association between PVL and peripheral nonperfusion and posterior neovascularization, but not with macular edema. An additional retrospective study found a moderate association between the peripheral ischemic index and increased foveal avascular zone (FAZ).[52] Other studies have found a direct correlation between peripheral retinal ischemia in diabetic retinopathy and diabetic macular edema, reporting a 3.75 increased odds of DME in association with peripheral retinal nonperfusion.[54] Another report investigated the correlation of the ischemic index (ratio of nonperfused fundus area to total fundus area) in patients with recalcitrant DME.[55] Eyes with a greater ischemic index and more severe diabetic retinopathy were found to have more severe DME as measured by number of focal macular laser treatments and less reduction in central macular thickness on SD-OCT. Previous studies utilizing "ischemic index" with Optos imaging should be interpreted with caution given that they did not employ standardized technique for quantification, nor did they account for the distortion and overrepresentation of the peripheral fundus in these UWF images, or the differing metabolic requirements and types of cells present in peripheral areas of the fundus.[56,57]

Naturally, clinicians utilizing UWF imaging including angiography for the evaluation of diabetic retinopathy have investigated its use for delivering angiographic guided therapy including targeted laser photocoagulation (TRP).[58] In contrast to panretinal photocoagulation (PRP), TRP implies viewing the UWF–FA and specifically treating area of retinal nonperfusion along with the intermediate, transition zones between perfused and nonperfused retina. A prospective study of treatment-naïve PDR with a single session 20 msec, 1500-spot pattern scan laser (PASCAL) retinal photocoagulation found that 76% of patients exhibited regression of PDR at 12 weeks.[59] If these results can be replicated, potential benefits of TRP over PRP include decreased

incidence of post-laser macular edema, nyctalopia, and peripheral visual field loss. Future prospective, randomized clinical trials are needed to assess the safety and efficacy of this modified treatment paradigm.

Retinal Venous Occlusions

Retinal vein occlusion is the most common retinal vascular occlusion and may lead to peripheral retinal ischemia, neovascularization, and macular edema. UWF–FA has been shown to be important for diagnosing central retinal vein occlusion (CRVO) with peripheral nonperfusion and is reliable at detecting macular leakage and ischemia[60] (Fig. 5.5). UWF–FA has been reported in branch and hemiretinal vein occlusion, and it has been shown that untreated peripheral nonperfusion was significantly associated with macular edema and neovascularization[61] (Fig. 5.6).

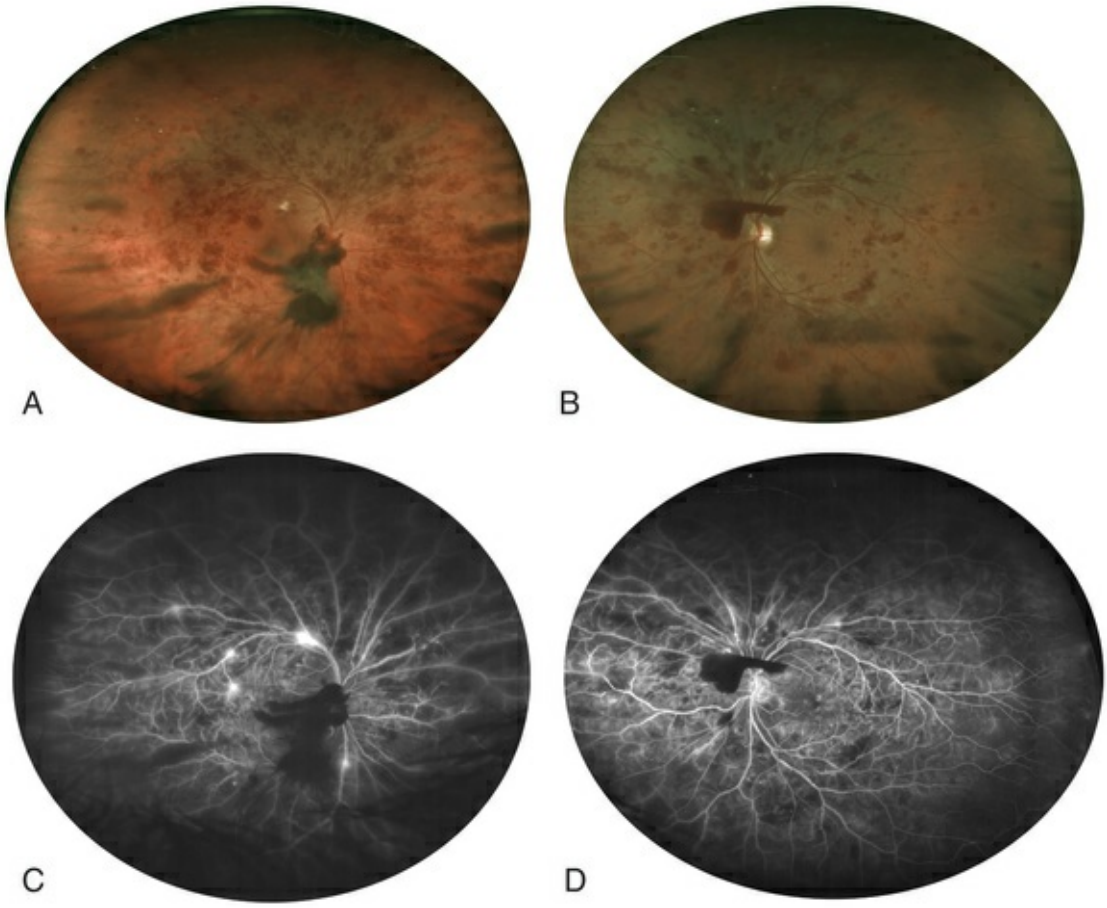

FIG. 5.5 Bilateral central retinal vein occlusion in

patient with leukemia: Optos photographs (A,B), fluorescein angiography (C,D).

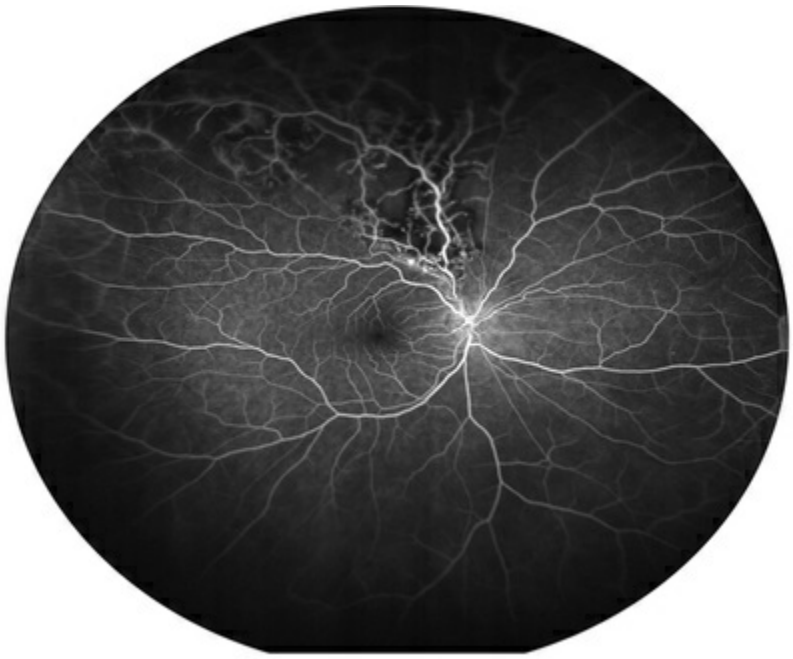

FIG. 5.6 Optos fluorescein angiogram of superior retinal vein occlusion.

Tsui and colleagues found that treatment-naïve eyes with CRVO and neovascularization on presentation were found to have a significantly larger ischemic index than eyes not presenting with neovascularization (mean 75% vs. 25%), however, the study was not prospective and the time of onset of CRVO to presentation could not be precisely ascertained.[62] Spaide evaluated peripheral nonperfusion on UWF–FA in eyes with CRVO undergoing anti-VEGF therapy and found no correlation between the number of intravitreal injections and peripheral nonperfusion. He did, however, observe an inverse statistically significant correlation between the area of peripheral nonperfusion and visual acuity.[63] In a study of retinal vein occlusions, patients with ischemic index >10% had increased subfoveal macular thickness on SD-OCT and worse visual acuity.[64] Similar to diabetic retinopathy treatment, TRP has been reported in a patient with CRVO and rebound macular edema which resulted in regression of rubeosis and rebound edema.[65] Further studies are needed to better correlate peripheral

nonperfusion on UWF–FA with actual retinal ischemia to better characterize and subgroup retinal vein occlusion phenotypes, which may have important diagnostic, prognostic, and treatment implications (Figs. 5.7 and 5.8). The ongoing SCORE-2 trial, comparing aflibercept and bevacizumab for the treatment of macular edema associated with retinal vein occlusion, is employing Optos wide-field angiography, and should yield additional information in this regard. UWF imaging may also be of clinical benefit in other retinal occlusive disease such as retina arterial occlusion, but few studies have been reported.

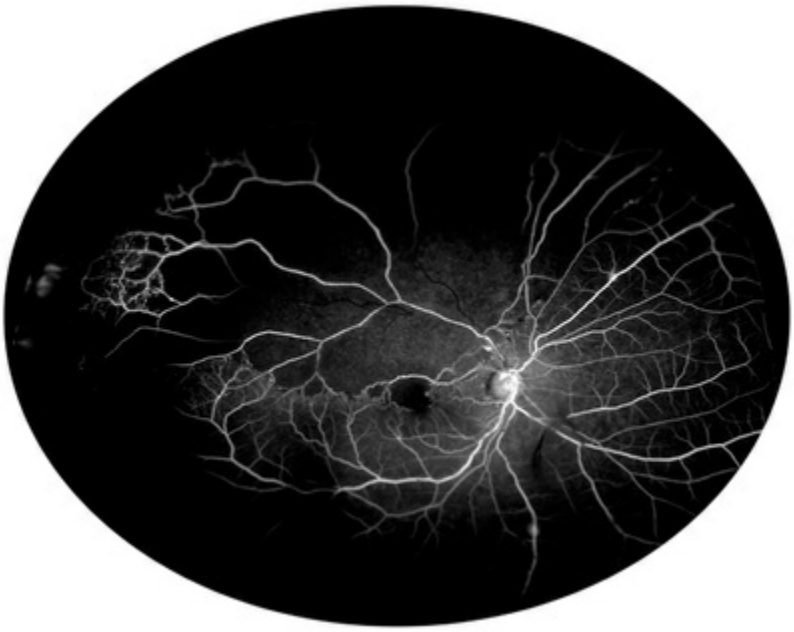

FIG. 5.7 Optos fluorescein angiogram of retinal artery occlusion.

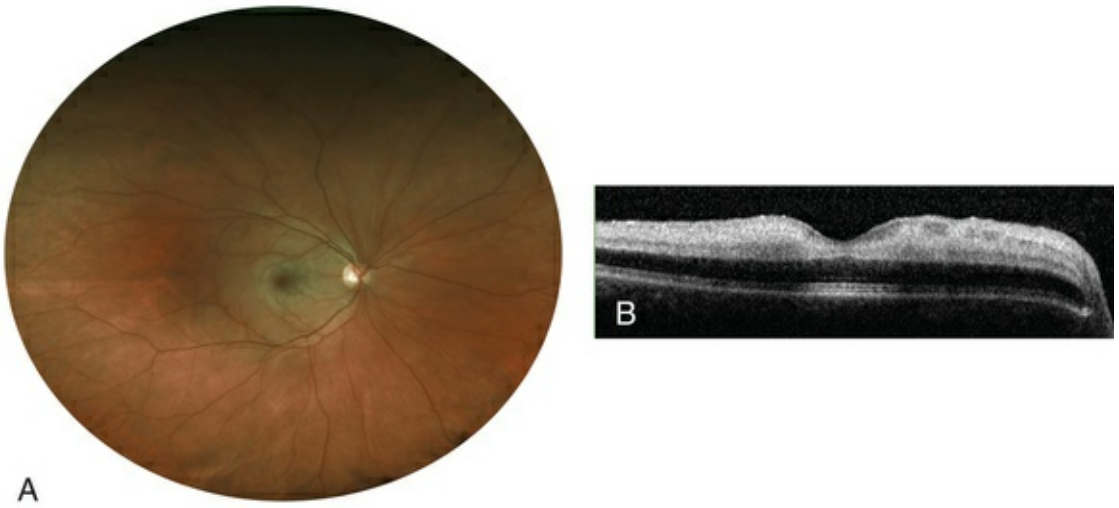

FIG. 5.8 Nonmydriatic Optos color photograph (A) in a pregnant patient demonstrates cherry-red spot consistent with central retinal artery occlusion and corresponding optical coherence tomography (B) demonstrated inner retinal edema.

Other Retinal Vascular Conditions

UWF imaging has been utilized in other conditions with posterior segment pathology including sickle cell disease[66] (Fig. 5.9), beta-thalassemia,[67] antiphospholipid antibody syndrome,[68] Takayasu arteritis,[69,70] retinopathy associated with facioscapulohumeral muscular dystrophy,[71] Duchenne muscular dystrophy,[72] Susac syndrome,[73] preeclampsia with HELLP syndrome,[74] and Valsalva retinopathy (Fig. 5.10).

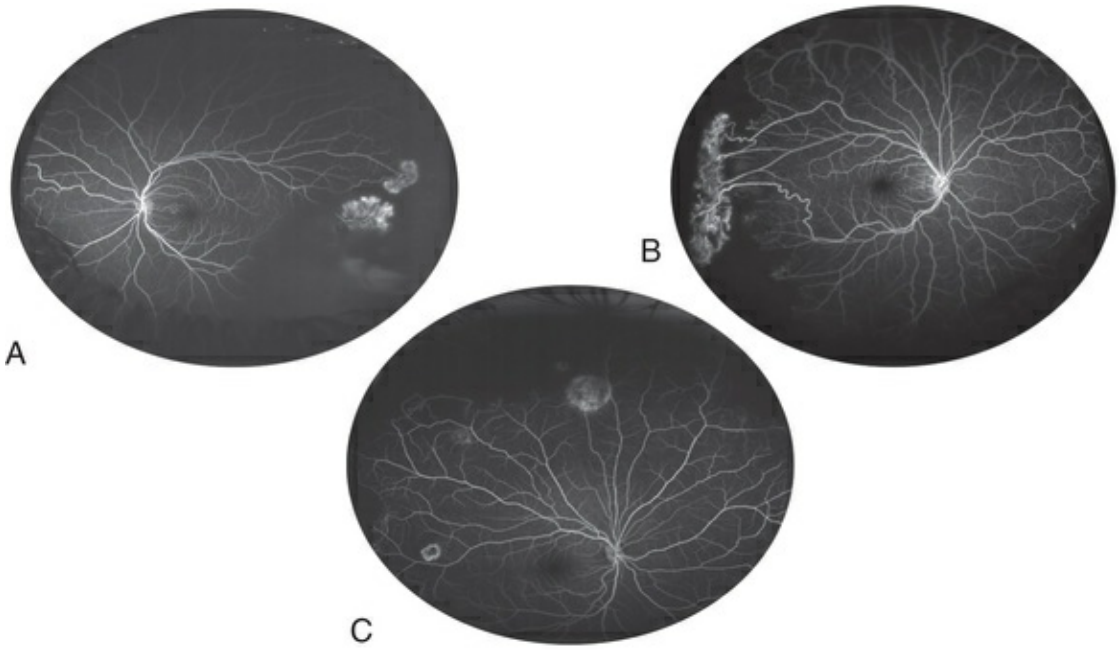

FIG. 5.9 Sickle cell retinopathy: Optos fluorescein angiography in three distinct cases reveals peripheral nonperfusion and neovascularization in two cases (A,B).

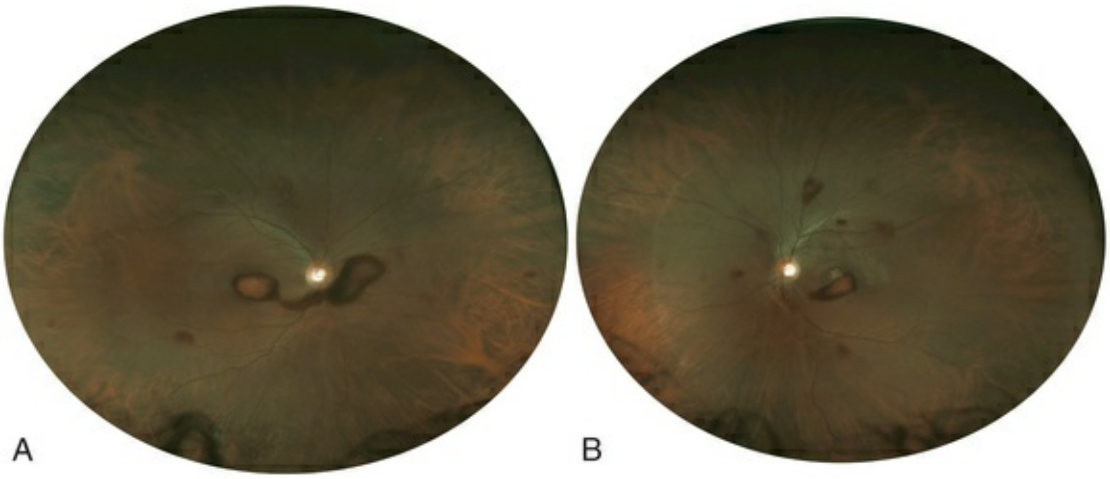

FIG. 5.10 Optos color photograph of Valsalva retinopathy.

Uveitis

The use of UWF in various types of intraocular inflammation has provided additional information about the retinal periphery in

these diverse disease entities (Figs. 5.11–5.14). However, the optimal use, clinical impact and utility in dictating therapeutic interventions, and monitoring response to treatment remain controversial among uveitis specialists. Early reports have shown the utility of UWF–FA to assess the extent and severity of retinal disease and progression and response to treatment in intermediate[75] and posterior uveitis (Fig. 5.15) including systemic lupus erythematous, cytomegalovirus (CMV) retinitis (Figs. 5.16–5.18), idiopathic and acute posterior multifocal placoid pigment epitheliopathy.[76] A study with 12 eyes with CMV retinitis demonstrated that UWF imaged 48.3% greater retinal area and 40.0% more active retinitis area compared to conventional nine-field photography.[77] Importantly, standard field photography missed CMV lesions in two eyes. A patient satisfaction survey indicated a preference for UWF imaging due to increased comfort and decreased image acquisition times. Subsequently a study of 52 eyes of 31 patients, compared Optos UWF imaging to standard nine-field montage and found that Optos UWF–FA captured more retinal vascular pathology in the periphery and posterior pole, but noted the clinical implications of these findings remains to be determined.[78] Another study utilized the Staurenghi lens system in 26 patients with posterior uveitis.[24] The study found UWF imaging assisted in the diagnosis, quantifying the extent of vasculitis and planning treatment (photocoagulation or immunosuppression titration) in 62% and enhanced disease monitoring in 35%. The UWF imaging in this study detected vasculitis that was not clinically evident in 31% of patients.[24] Collectively, these studies support the concept that UWF–FA in uveitis may aid in planning targeted laser photocoagulation to areas with significant nonperfusion with or without neovascularization (Figs. 5.19 and 5.20).

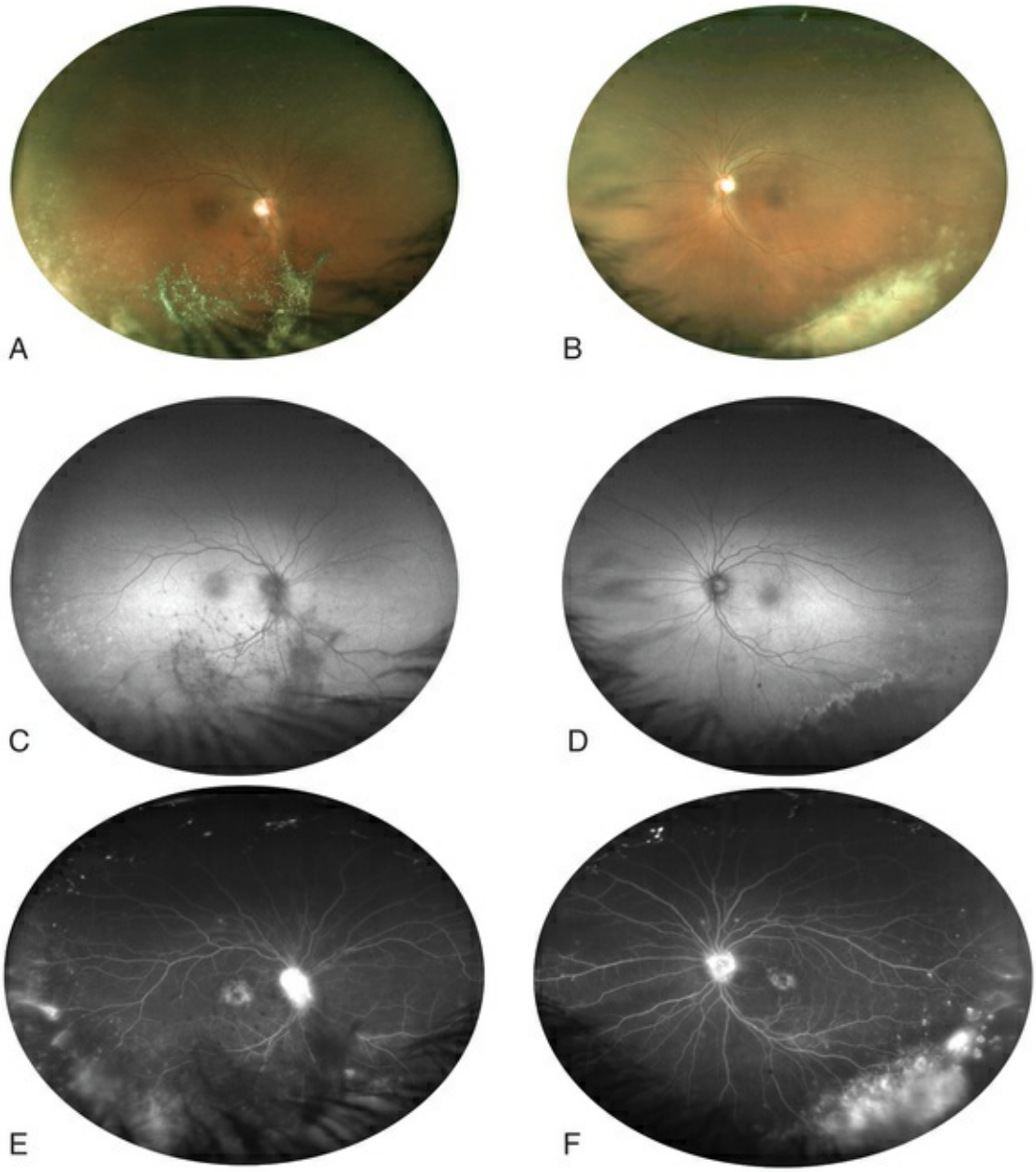

FIG. 5.11 Ocular syphilis: Optos color photographs (A,B), autofluorescence (C,D), late fluorescein angiogram (E,F).

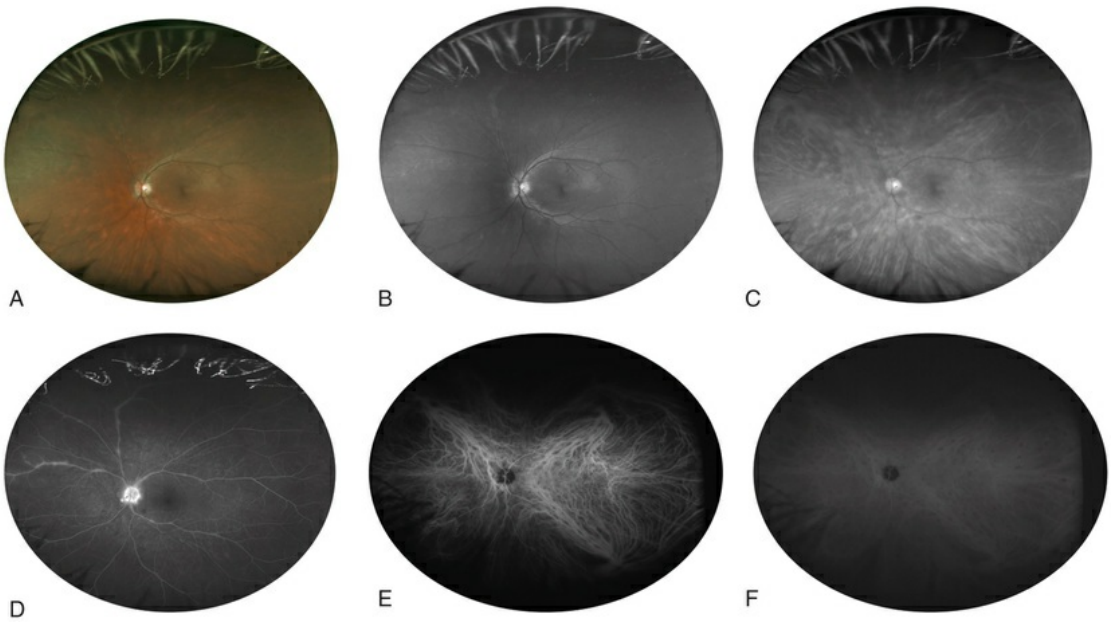

FIG. 5.12 Birdshot chorioretinopathy: Optos color photograph (A), green channel (B), red channel (C), fluorescein angiography (D), early indocyanine green angiography (ICGA) (E), late ICGA (F).

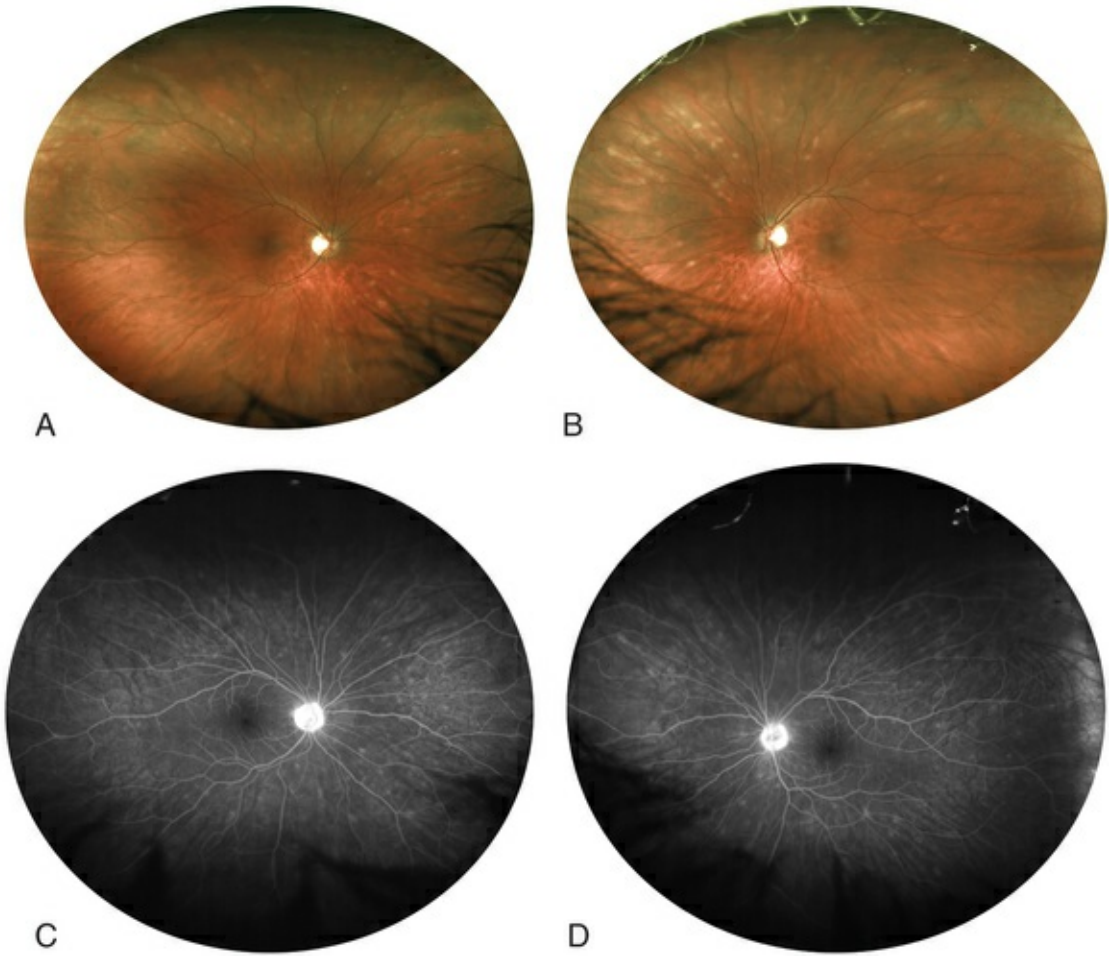

FIG. 5.13 Ocular sarcoidosis: Optos color photograph (A,B) and fluorescein angiography (C,D) demonstrating staining of diffuse choroidal lesions.

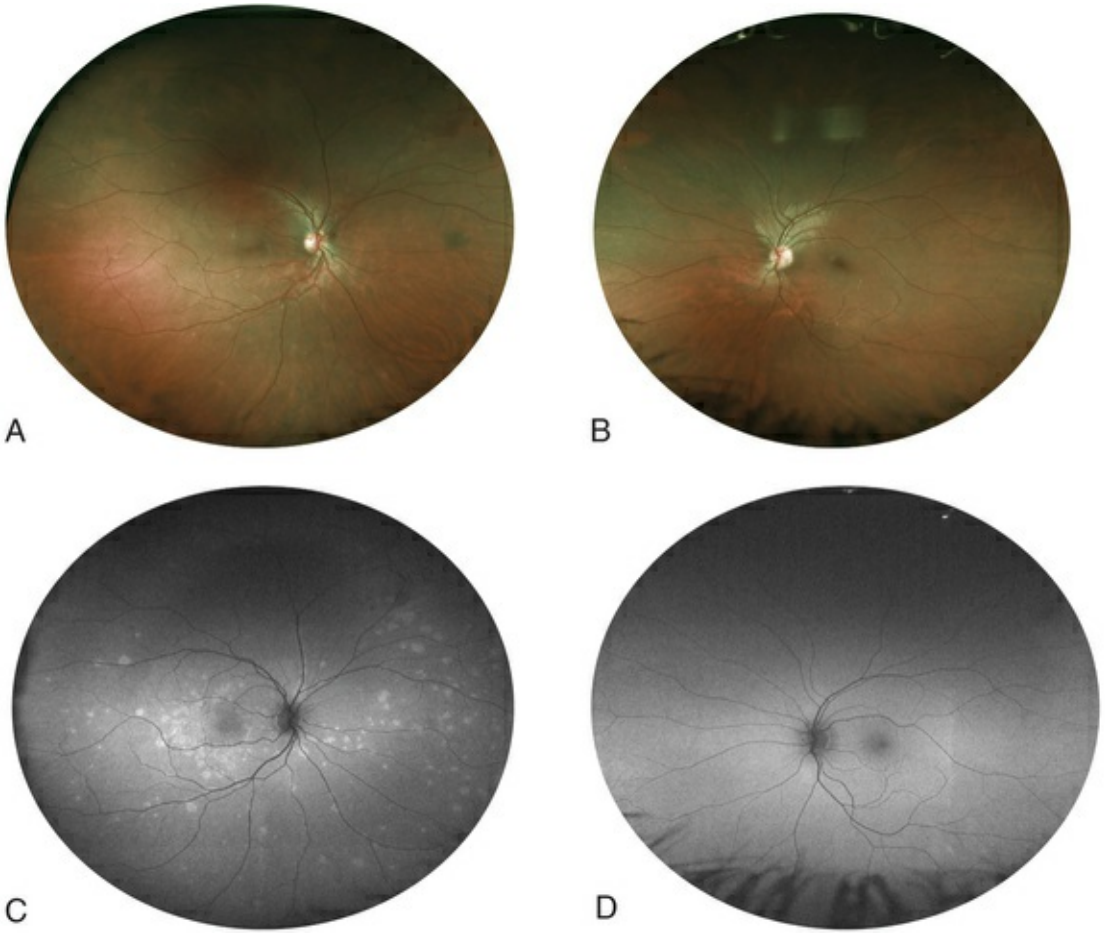

FIG. 5.14 Multiple evanescent white dot syndrome (MEWDS): Optos color photograph (A,B) and fundus autofluorescence (C,D) demonstrating multiple prominent punctate areas of increased hyperautofluorescence in the right eye which are not readily apparent on fundus photography.

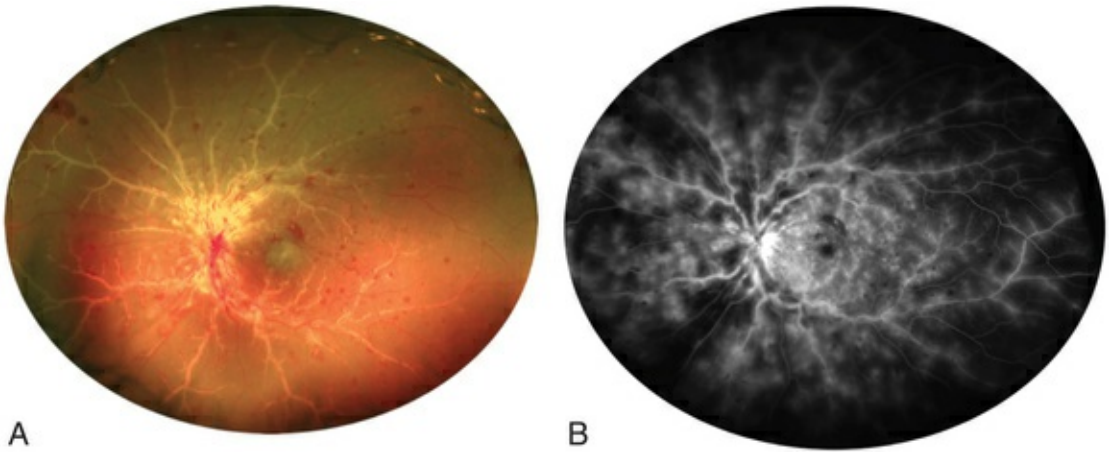

FIG. 5.15 Idiopathic unilateral posterior uveitis on

Optos color photograph (A) and corresponding fluorescein angiogram (B) demonstrating diffuse vasculitis and papillitis.

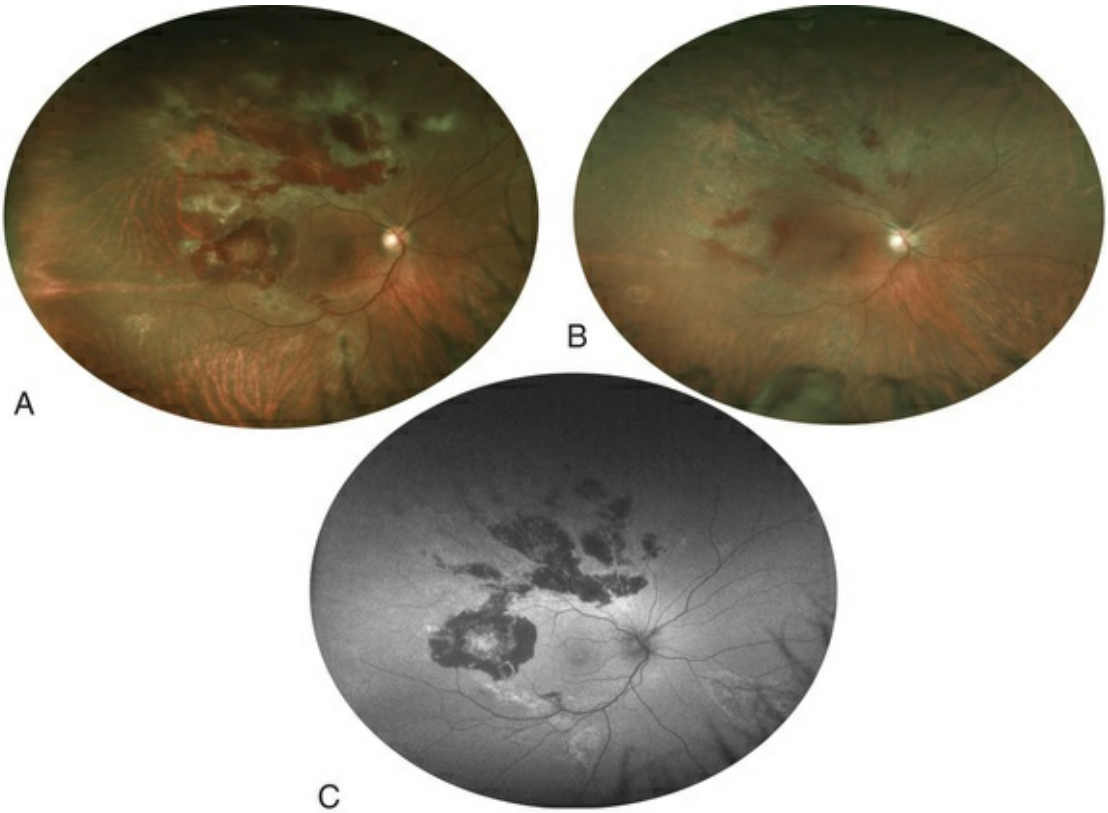

FIG. 5.16 Cytomegalovirus retinitis pre (A) and post (B) treatment, with corresponding initial Optos fundus autofluorescence (C).

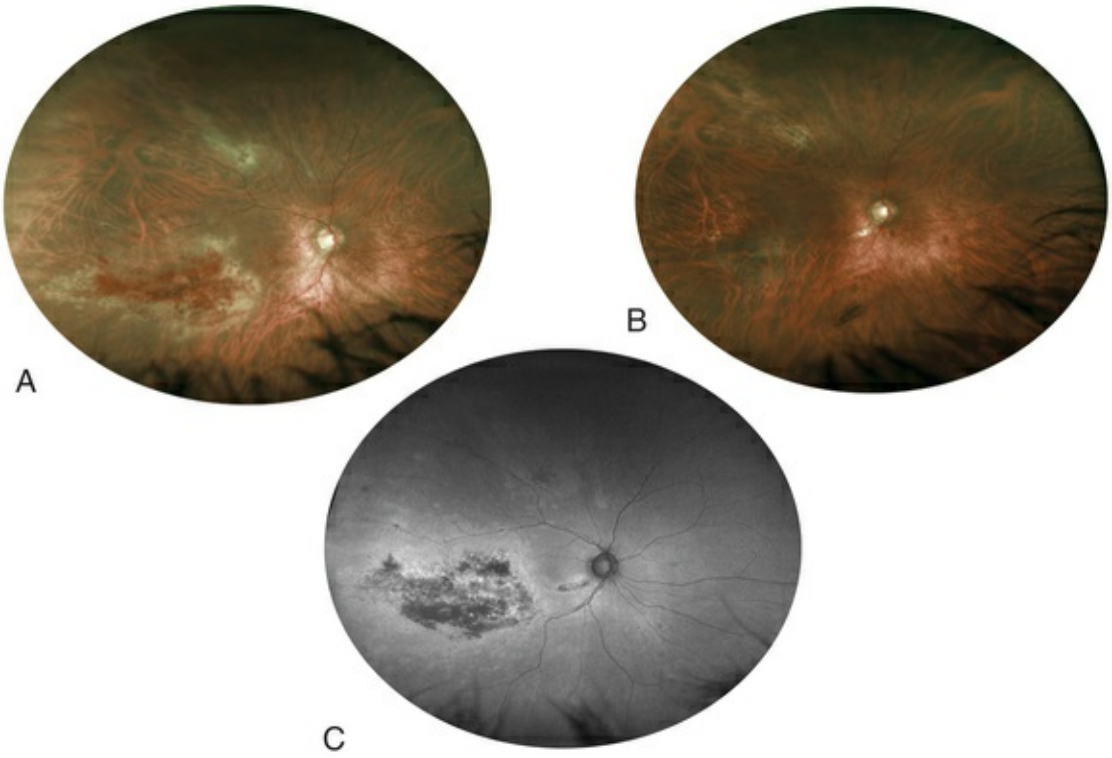

FIG. 5.17 Cytomegalovirus retinitis pre (A) and post (B) treatment, with corresponding Optos fundus autofluorescence (C).

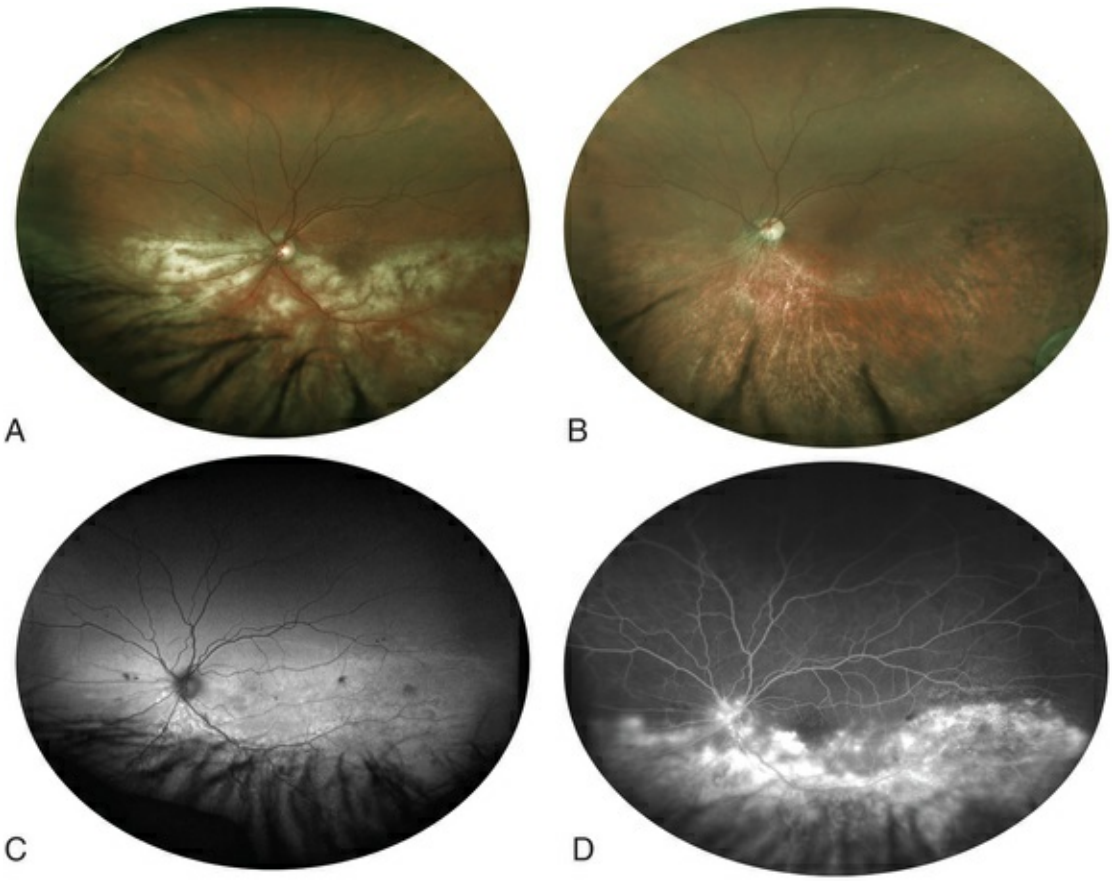

FIG. 5.18 Cytomegalovirus retinitis pre (A) and post (B) treatment, with corresponding Optos fundus autofluorescence (C) and Optos fluorescein angiogram (D).

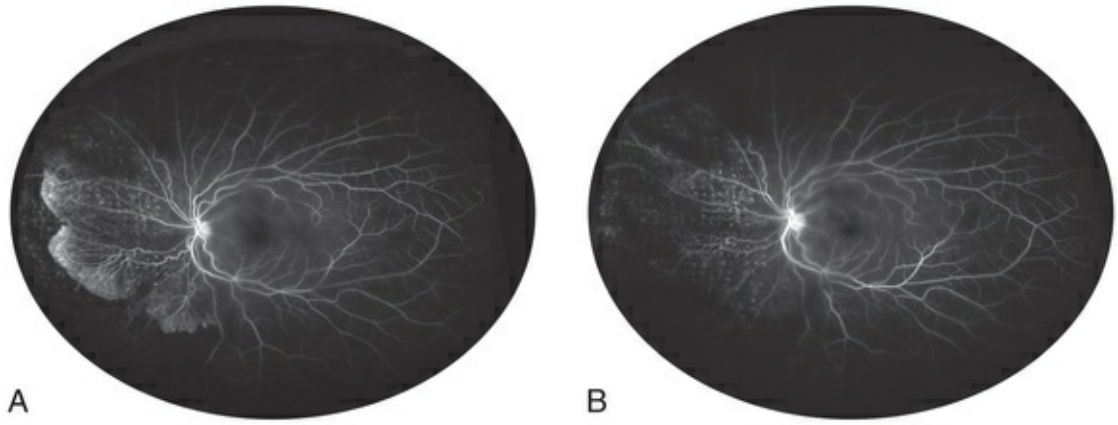

FIG. 5.19 Peripheral neovascularization in a patient with uveitis (A) status post treatment and regression of neovascularization after a single intravitreal dose of bevacizumab (B).

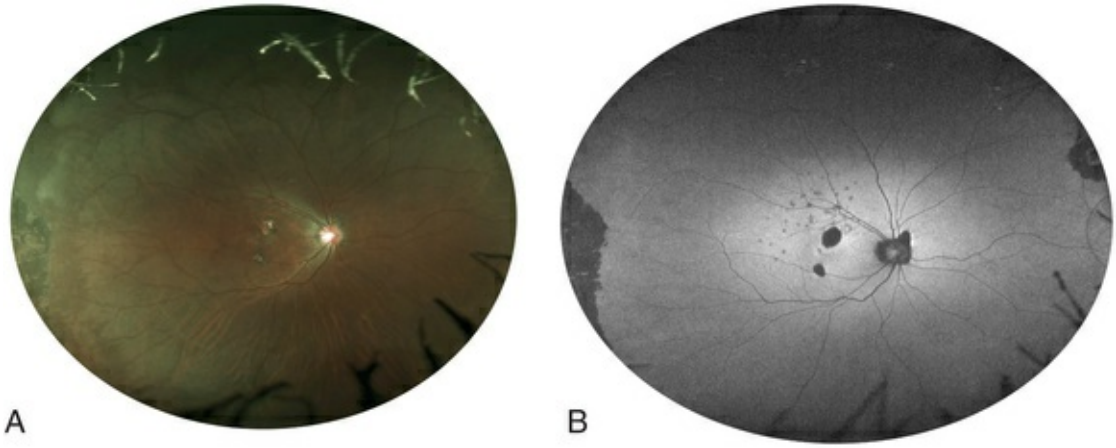

FIG. 5.20 Multifocal choroiditis with choroidal neovascular membrane: Optos color photograph (A) and autofluorescence (B).

Although initial studies were primarily descriptive in nature, prospective studies have also been conducted to evaluate the relevance of UWF imaging on management decisions. In a study of 43 eyes with noninfectious posterior uveitis, only 16% had a change in management based on findings evident on a standard posterior pole FA, but this increased to a change in management in 48% of cases when an UWF–FA with visualization of the periphery was available.[79] A similar study from the same group examining the role of UWF in retinal vasculitis found that management was altered in 4% of eyes with the addition of simulated non-wide-field color images, in 14% with the addition of Optos pseudocolor images, and in 51% of eyes with the addition of Optos UWF–FA.[80] A study of wide-field imaging in Beçhet disease associated with retinal vasculitis found that Optos UWF imaging assisted in diagnosis and quantification of the degree of retinal vasculitis in 80% which led to enhanced diseased monitoring in 55% and medical treatment or laser photocoagulation in 65%.[81] These studies support the evolving clinical role of UWF imaging in the diagnosis, therapeutic decision-making, and monitoring of disease activity in the setting of uveitis.

Pediatric Retina

Wide-field imaging in the pediatric population has several unique considerations including potential challenges related to patient cooperation. Many pediatric vitreoretinal disorders can manifest

with significant peripheral pathology, and some, in particular retinopathy of prematurity (ROP), have lent themselves to telescreening programs. Although binocular indirect ophthalmoscopy remains the gold standard for the diagnosis of conditions such as ROP,[82] it requires a skilled examiner and may result in cardiac or respiratory distress in neonates,[83] which may be lessened with wide-field imaging.[84] The two imaging platforms primarily utilized in the pediatric population include the RetCam and Optos. The main disadvantage of the RetCam system is it requires a cooperative patient or examination under anesthesia given it is a contact-based system. Optos is an alternative, non-contact system that is increasingly being used to diagnose and monitor a variety of pediatric retinal conditions including uveitis, Coats disease, hereditary dystrophies, congenital anomalies such as coloboma (Fig. 5.21), and familial exudative vitreoretinopathy (FEVR) (Fig. 5.22) in the outpatient setting without the need for examination under anesthesia.[85,86] Optos UWF imaging and FA has also led to improved classification and new insights into the pathophysiology and varying phenotypes of disorders such as FEVR.[87,88] Wide-field FA has also provided insights into the normal retinal vascular periphery in children which may include areas of nonperfusion.[89]

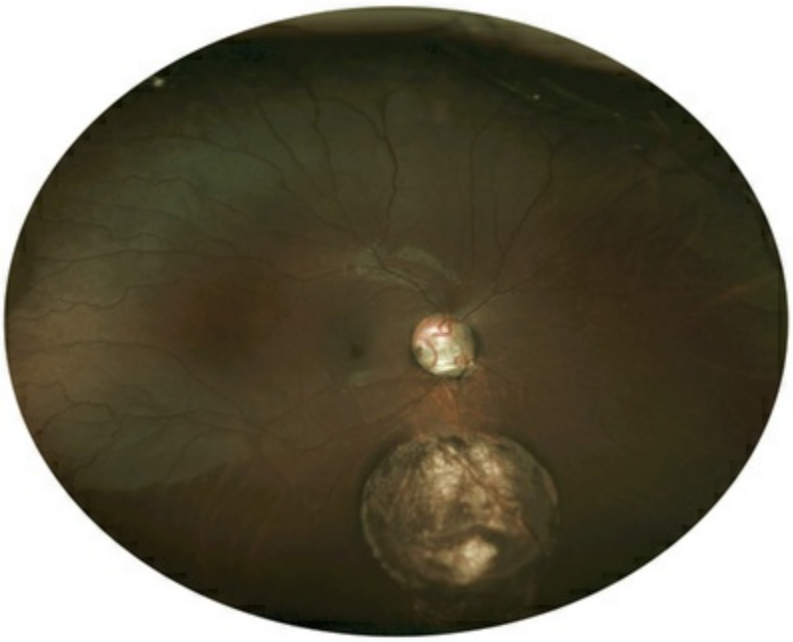

FIG. 5.21 Optos color photograph of inferior coloboma.

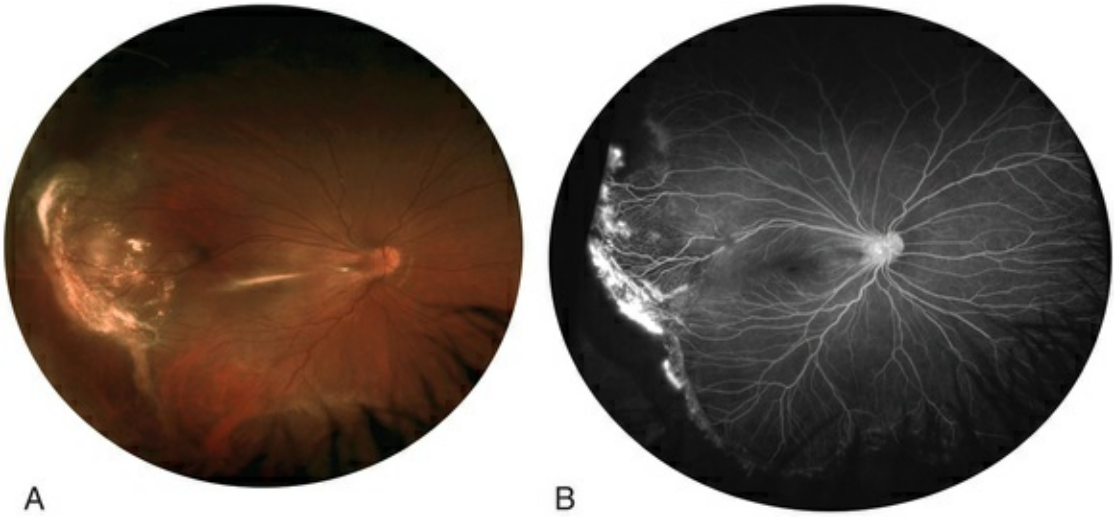

FIG. 5.22 Familial exudative vitreoretinopathy: Optos color photograph demonstrated macular dragging and temporal traction (A) with corresponding fluorescein angiogram showing peripheral nonperfusion (B).

Wide-field imaging has been extensively studied in retinopathy of prematurity, in part related to the growth of telemedicine screening programs.[14,16,20,90–102] This is discussed at length in Chapter 65, Telescreening for retinopathy of prematurity. Multiple studies have evaluated the sensitivity and specificity for detecting ROP compared to the clinical exam,[14,93,94] with generally favorable results, including one study reporting RetCam photography having 82% sensitivity and 94% specificity for detecting any stage of ROP.[14] More recently, several studies have investigated the role of fluorescein angiography for the diagnosis and management of ROP, as FA may improve the ability to detect certain subtypes of ROP, including disease requiring treatment.[20,21] Although the RetCam is the wide-field imaging system most commonly used in neonatal screening for ROP, reports have also been published using the Optos system with a special "flying baby" position to obtain high-resolution UWF images in ROP babies.[103,104]

Retinal Detachment and Myopia

Wide-field imaging is increasingly being used to preoperatively

document retinal detachments, assist in preoperative planning, and postoperatively monitor the status of the retina. The peripheral documentation capability of UWF imaging is especially important in the era of co-management and the primary retina surgeon practicing at multiple sites[105–107] (Figs. 5.23–5.26). It may be also used to document less common entities such as choroidal detachment.[74,108] Nevertheless, binocular indirect ophthalmoscopy remains the gold standard for the diagnosis of retinal detachments and visualization of pathology in the far periphery.[105,109] One study noted that in patients with acute posterior vitreous detachment, the Staurenghi lens system detected all (100%) peripheral retinal tears.[110] This is in contrast to the Optos system which has satisfactory sensitivity and specificity for the detection of retinal detachments and retinal tears or holes,[109,111] but may not perform as well in the superior and inferior periphery.[105,112] This limitation can be overcome to some extent by good dilation and obtaining additional steered images, where the photographer instructs the patient to gaze toward the desired quadrant prior to image capture.[113]

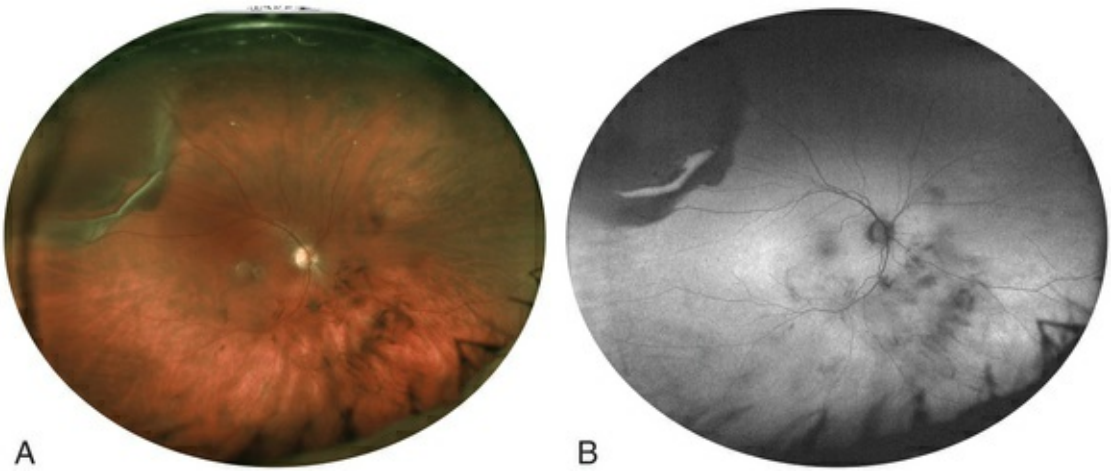

FIG. 5.23 Optos color photograph (A) and autofluorescence (B) of retina detachment with areas of patchy hyper- and hypoautofluorescence.

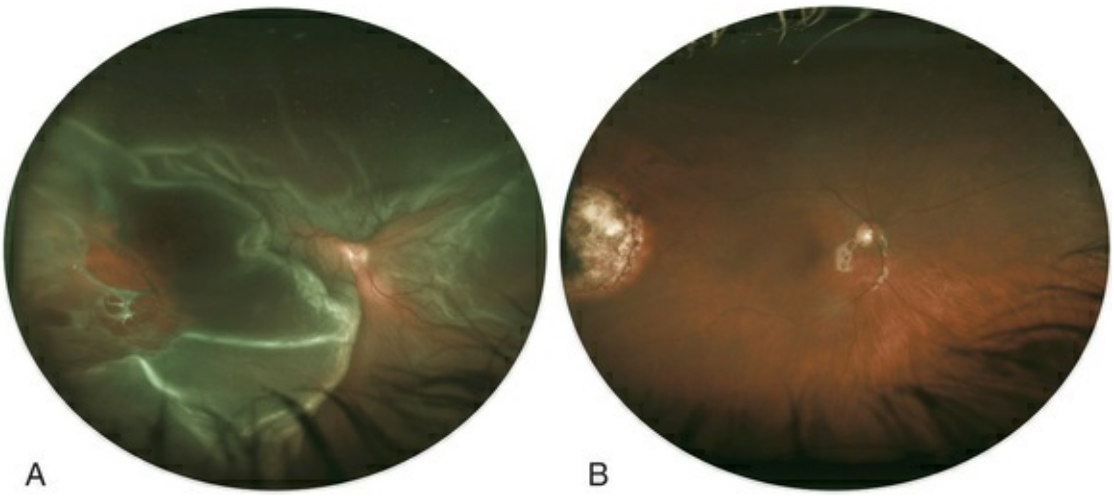

FIG. 5.24 Optos photograph of subtotal retinal detachment with temporal retinal tear (A) and status post repair with pars plana vitrectomy (B).

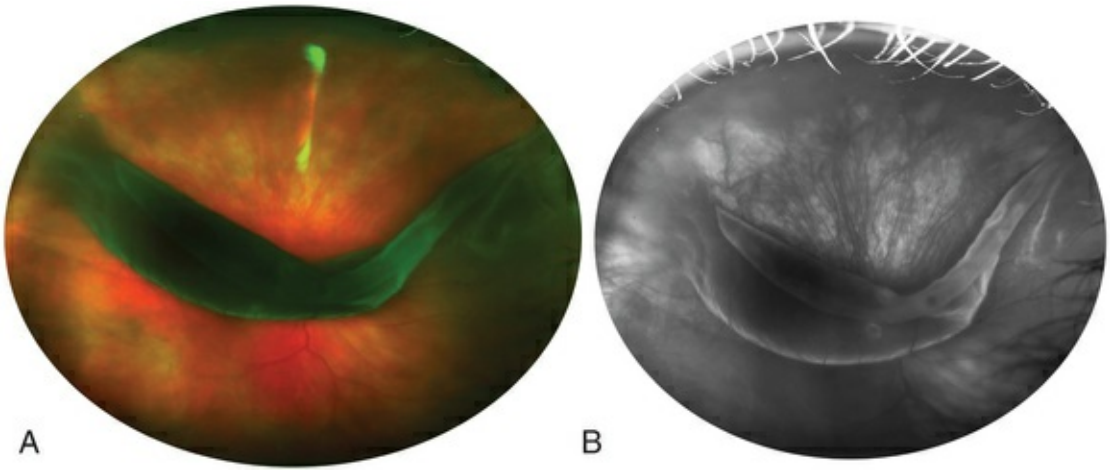

FIG. 5.25 Optos photograph of superior giant retinal tear extending from 10 to 2 o'clock (A) with corresponding red-free channel image (B).

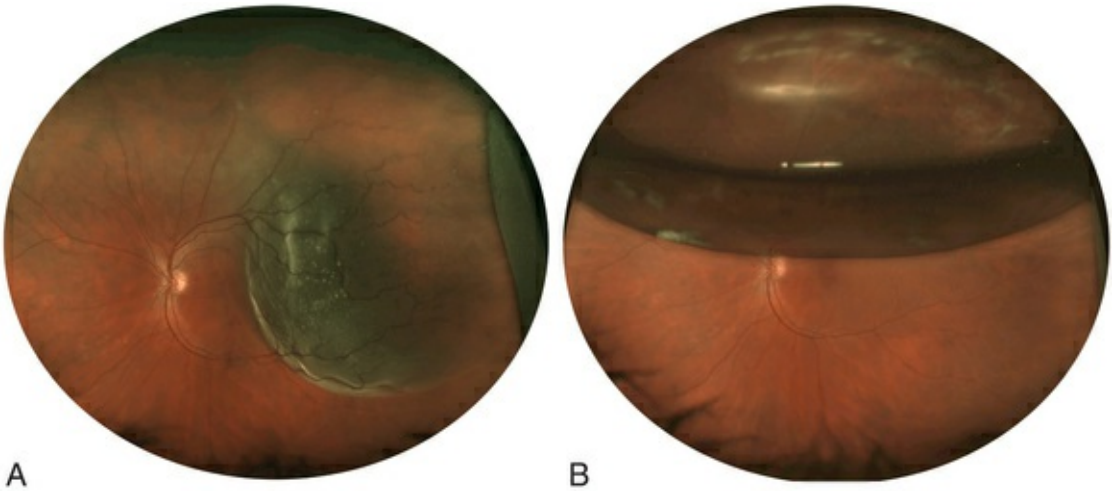

FIG. 5.26 Optos photograph of retinal detachment (A) and status post pneumatic retinopexy (B) with C_3F_8 gas, note early chorioretinal scarring to retinal breaks superiorly.

Multimodal wide-field imaging including fundus autofluorescence (FAF) has been evaluated in the setting of retinal detachment by Witmer and colleagues.[114] This study found that UWF–FAF is useful for determining the complete extent of the retinal detachment by areas of increased hypoautofluorescence. Additionally, in all but one case they observed a hyperfluorescent leading edge (HLE) preoperatively which resolved in all eyes postoperatively. The study also noted that granular autofluorescent changes were associated with worse preoperative and postoperative visual acuities.[114]

Although UWF imaging is not a substitute for clinical examination, its role currently appears to be as a useful adjunct to binocular indirect ophthalmoscopy, colored fundus drawings, and electronic medical records. For instance, one group has investigated UWF imaging to assess the adequacy of cryotherapy and determining buckle height based upon autofluorescence changes. The study found the ideal amount of cryotherapy was associated with central increased hypoautofluorescence and a ring of increased hyperautofluorescence. Additionally, a higher buckle height was associated with an increase in hyperautofluorescent streaks in the area of imbrication.[115] A study on proliferative vitreoretinopathy-associated detachments revealed that early Optos imaging could document the extent of fibrotic epiretinal and subretinal tissue as

well as anatomic reattachment with inferior retinectomy.[107] A case report has also described the use of UWF to monitor for postoperative complications such as neovascularization and macrocyst associated with chronic rhegmatogenous retinal detachment.[116] A study from our group has also suggested that though Optos UWF was not as good as the clinical exam for evaluating superior and inferior pathology, it was better for documenting the actual, precise clock hours and extent of retinal detachments.[105]

Degenerative high myopia is a risk factor for retinal detachment and is associated with other complications including myopic choroidal neovascularization (CNV). One study reported a sensitivity of 43.8% for detecting retinal breaks and 66.7% for retinal detachments with an overall 90.9% sensitivity for detecting other peripheral lesions, including lattice degeneration and white without pressure.[113] The Optos UWF system can be advantageous for documenting posterior staphyloma, which may extend outside of the traditional 30–50° view and can be well imaged due to the device's large depth of field. One study proposed a new classification for posterior staphyloma and found that multimodal Optos UWF imaging compared to three-dimensional magnetic resonance imaging had a sensitivity of 85% and specificity of 85.7% for detecting the borders and extent of the staphyloma.[117] Another group from Japan has also found that UWF–FAF documents radial tracts emanating from the staphyloma edge in pathologic myopia.[118] UWF–FA has also provided new insights into peripheral retinal circulation of eyes with high myopia, showing that compared with emmetropic eyes which had significant peripheral nonperfusion present in only 4.8%, eyes with high myopia exhibited similar changes at a rate of 82.6%.[119]

Retinal and Choroidal Dystrophies

UWF imaging, particularly fundus autofluorescence (FAF), can be a useful imaging modality in these disorders for not only aiding in detection and diagnosis, but also in facilitating phenotype–genotype correlations, in conjunction with other definitive testing such as electroretinogram (ERG) or genetic analysis (Figs.

5.27–5.30). Gyrate atrophy and choroidemia were the first dystrophies reported to have UWF fundus photography and fluorescein angiography performed and compared to non-wide-angle imaging.[120]

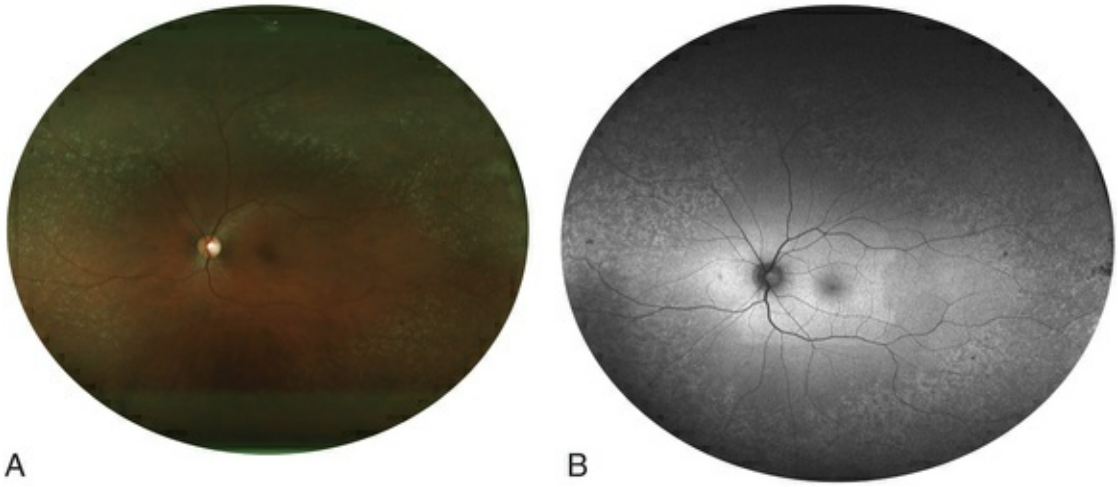

FIG. 5.27 Familial dominant drusen: Optos color photograph (A) and corresponding autofluorescence (B).

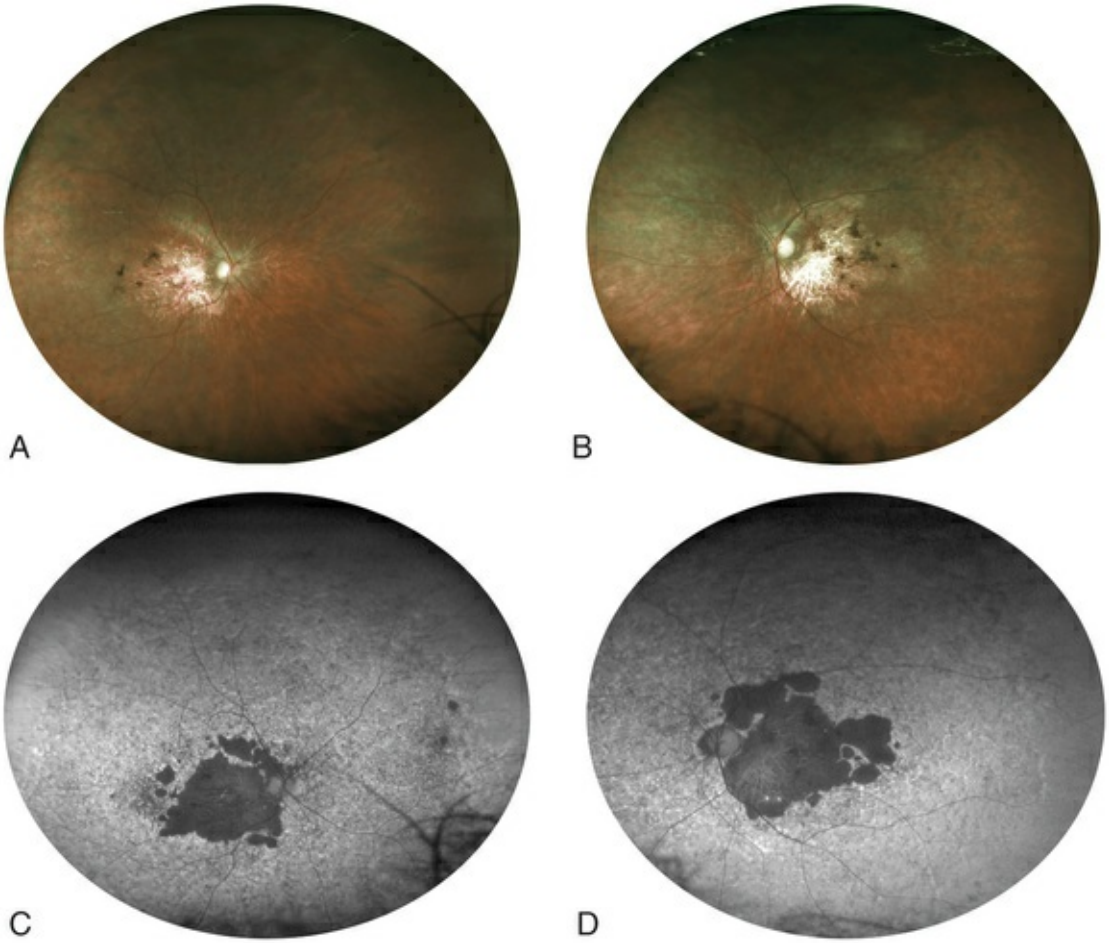

FIG. 5.28 Autosomal dominant retinal degeneration: Optos color photograph (A,B) and fundus autofluorescence (C,D).

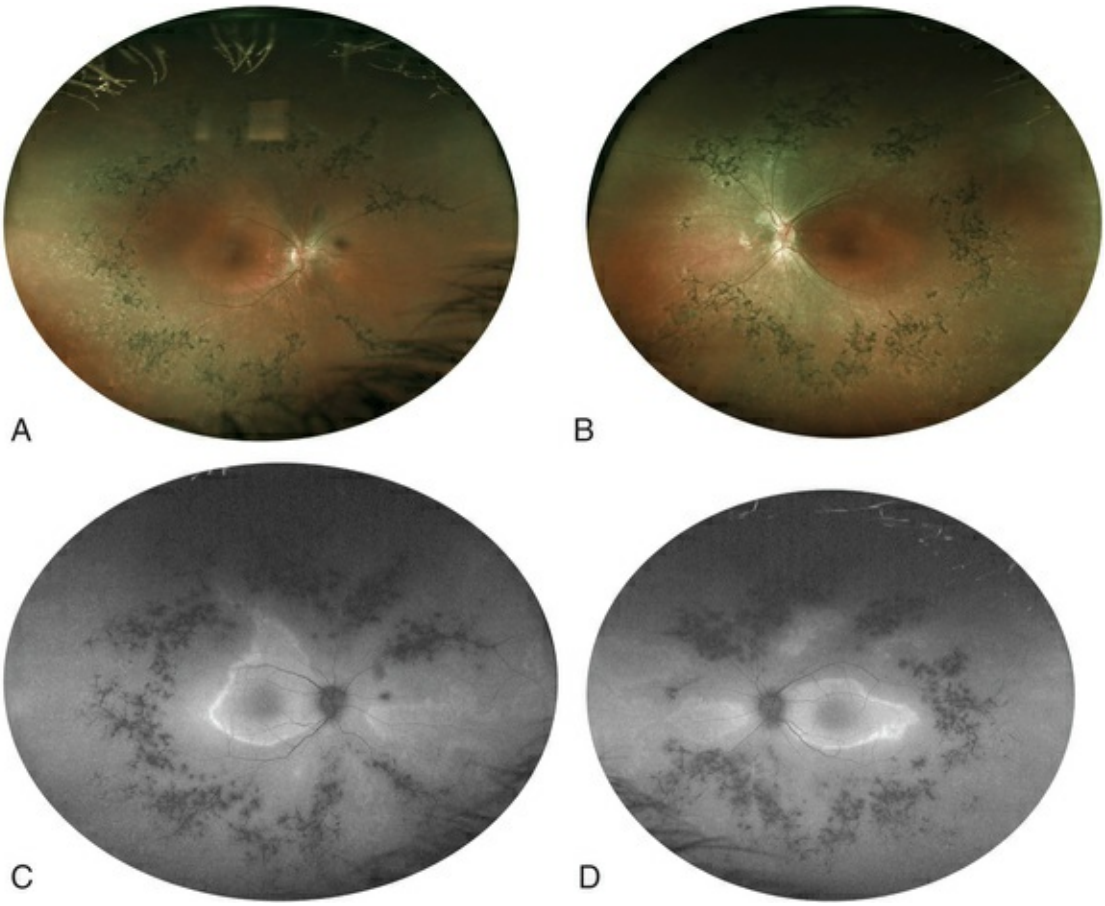

FIG. 5.29 Retinitis pigmentosa: Optos color photograph (A,B) and fundus autofluorescence (C,D).

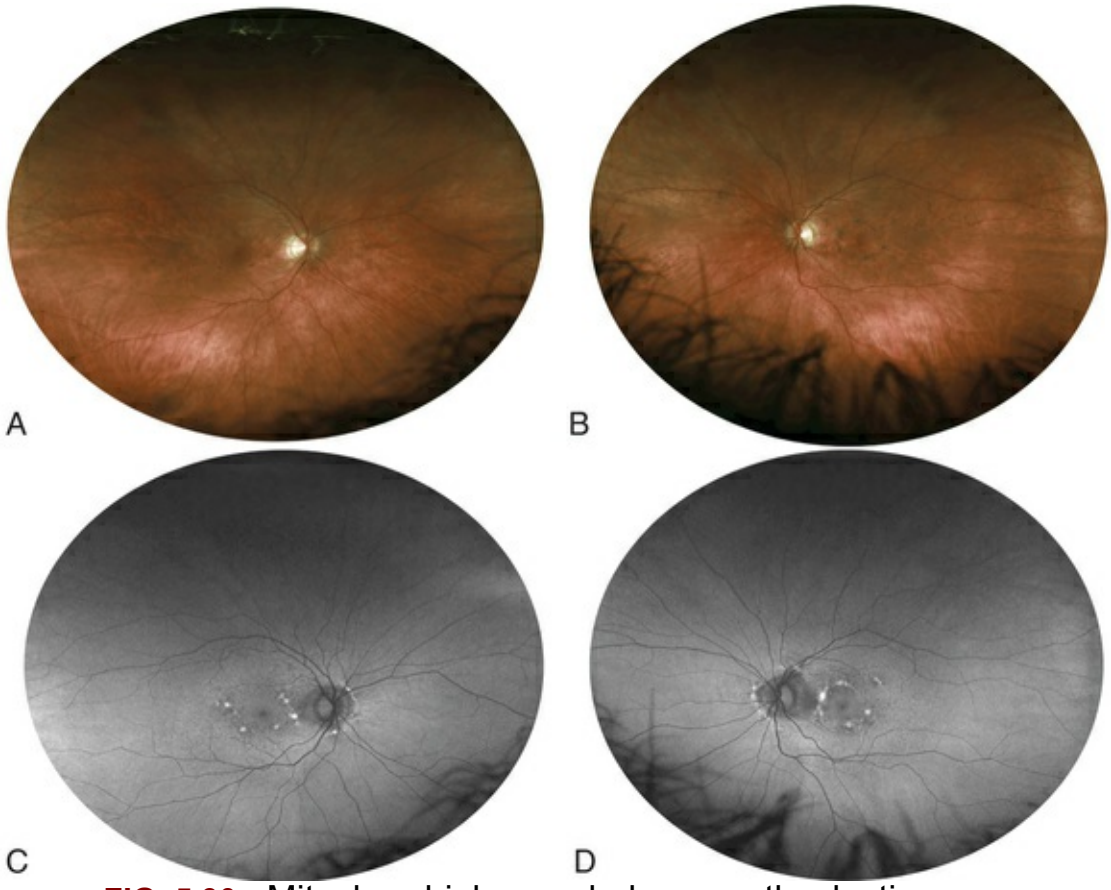

FIG. 5.30 Mitochondrial encephalomyopathy, lactic acidosis, and stroke-like episodes (MELAS): Optos color photograph (A,B) and fundus autofluorescence (C,D).

A study reported on multimodal UWF imaging in a large family with a novel *CHM* mutation resulting in X-linked choroidemia.[121] All males displayed characteristic peripheral chorioretinal atrophy with islands of macular sparing, however, female carriers exhibited a wide range of variability on FAF with more severe changes observed with increasing age. Additionally, studies have been published on retinitis pigmentosa[122] and cone–rod dystrophies.[123] In retinitis pigmentosa, investigators found that the total area of abnormal FAF on UWF imaging correlated with the visual field area measured by Goldmann visual field (GVF) testing.[122] These results in retinitis pigmentosa were also supported by similar results from another group, who also report that UWF–FAF can be important for monitoring disease progression as FAF changes precede loss of retinal function.[124] A similar study conducted by this group found that in cone–rod dystrophies the area of abnormal FAF

on UWF imaging correlated with scotoma measured by GVF I4e isopter testing, amplitude of rod ERG, combined ERG a-wave and b-wave, cone ERG and flicker ERG.[123]

Ophthalmic Oncology

Many peripheral fundus lesions including choroidal nevi, uveal melanoma (Figs. 5.31 and 5.32), retinoblastoma, choroidal metastases (Fig. 5.33), tumors of the retinal pigment epithelium, retinal hemangioblastomas (Fig. 5.34), choroidal hemangiomas, and vasoproliferative tumors may occur or have secondary effects in the retinal periphery such as exudation and inferior serous retinal detachments. Initial reports utilized the Panoret-1000 imaging platform to image peripheral tumors.[11,12] More recent reports have utilized the Optos UWF imaging system.[125–131] UWF–FAF, available with Optos SLO, may have particular value in lesions with orange pigment, a surrogate for lipofuscin, which is a risk factor for growth and mestastasis of melanocytic lesions.[132]

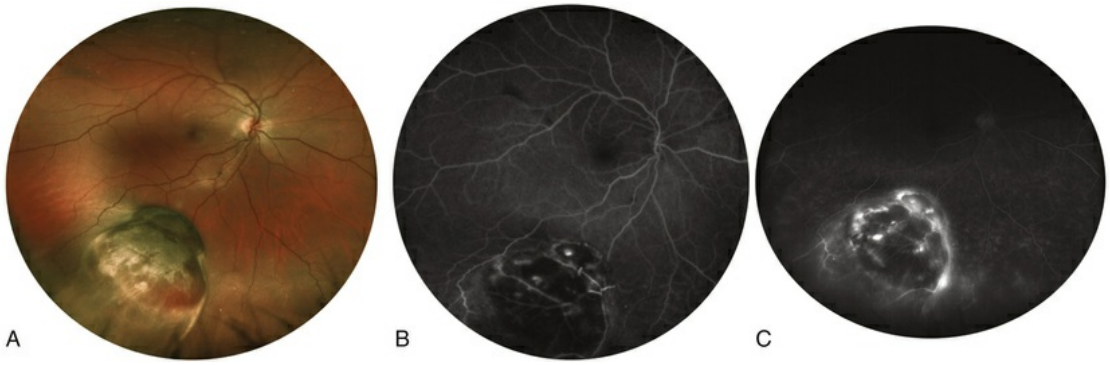

FIG. 5.31 Optos photograph of choroidal melanoma (A) and early (B) and late (C) fluorescein angiogram.

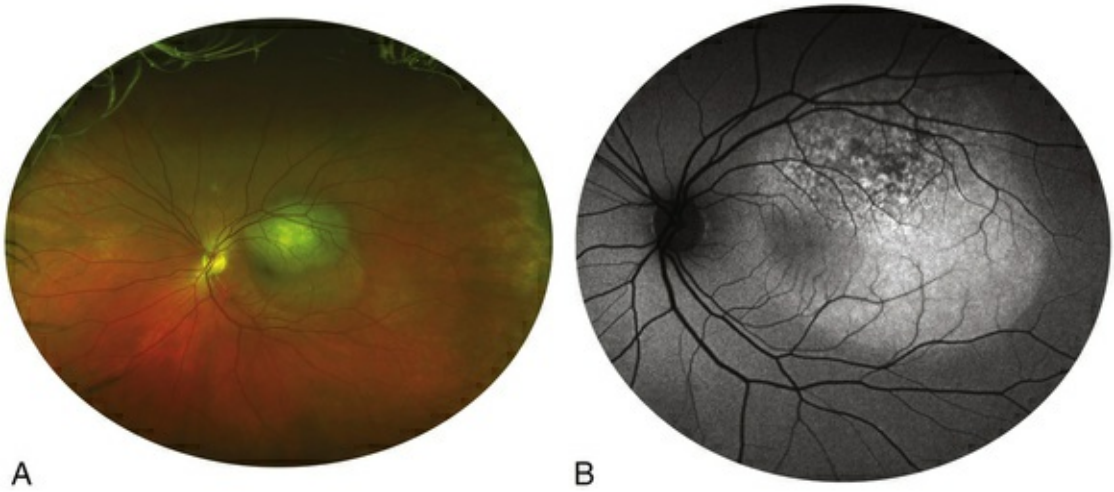

FIG. 5.32 Optos photograph of choroidal melanoma with subretinal fluid (A) and Heidelberg autofluorescence (B) illustrating mottled areas of increased hyperautofluorescence corresponding to lesion and increased hyperautofluorescence corresponding to areas of subretinal fluid.

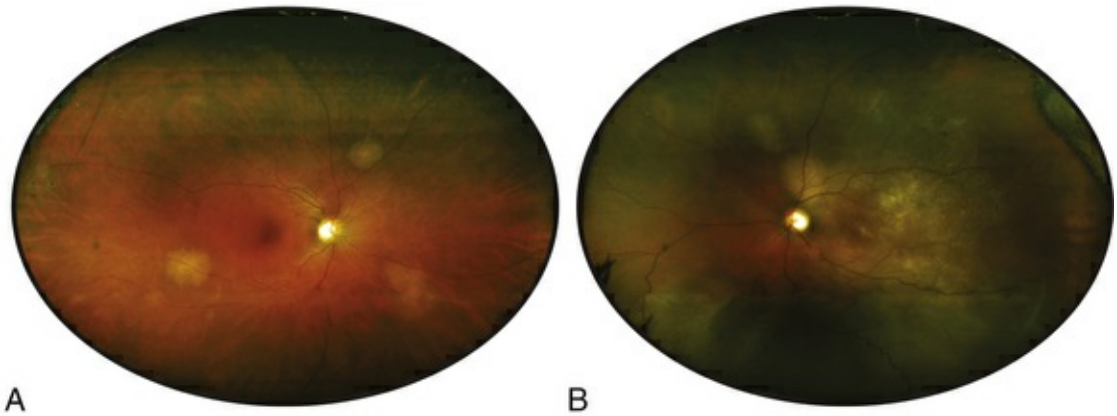

FIG. 5.33 Choroidal metastasis from metastatic breast cancer: Optos photograph right eye (A) demonstrated multifocal choroidal lesions and left eye (B) shows choroidal lesions with inferior serous retinal detachment.

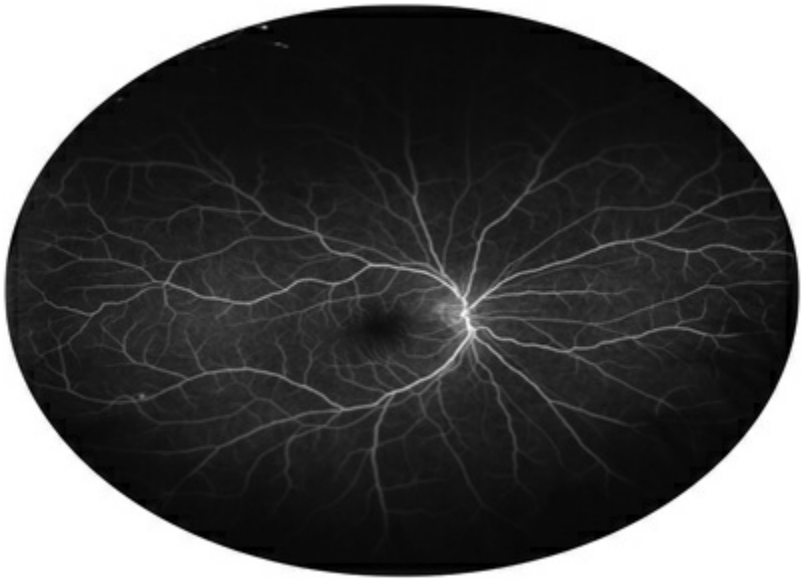

FIG. 5.34 Von Hippel–Lindau syndrome: Optos fluorescein angiogram shows small retinal capillary hemangioblastoma along inferotemporal arcade.

Consequently, clinicians have begun to investigate the clinical utility of wide-field imaging for the diagnosis, monitoring, and progression of melanocytic lesions. Studies have also suggested that UWF imaging may be more accurate at determining the true prevalence of choroidal nevi in a healthy population.[133] Basal diameters of tumors determined with Panoret-1000 imaging were found to be larger when compared with measurements obtained by B-scan ultrasonography (US).[11] This discrepancy may be attributable to photography documenting the extent of pigmentation or pigment alteration which extend beyond the area of elevation detectable on the B-scan. A more recent study found good concordance between B-scan US dimensions and Optos UWF but with a slightly greater correlation for transverse versus longitudinal scans.[128] Reports have also assessed the red and green SLO channels on the Optos system independently,[128,129] with one study suggesting on the "green channel separation," a trend towards a more mixed FAF appearance of melanomas compared to nevi.[129] Another study suggested that melanomas appeared dark on the red channel and bright on the green channel, with this binary characteristic providing relatively high sensitivity and specificity for the correct classification of lesions.[128]

Given the widespread and increasing use of UWF imaging,

particularly UWF–FA, in retinal diseases such as diabetic retinopathy and retinal venous occlusive disease, a similar future area of applicability for wide-field imaging is in the diagnosis, evaluation and management of radiation retinopathy. Radiation retinopathy shares many similarities to diabetic retinopathy, including microvascular angiopathy with peripheral nonperfusion, possible retinal neovascularization, and macular edema.[134–136] UWF imaging may also be important to determine the effects of therapies aimed to reduced radiation retinopathy such as pars plana vitrectomy with placement of silicone oil at the time of plaque brachytherapy.[137]

Central Serous Chorioretinopathy

With UWF–FAF and the recent addition of UWF indocyanine green angiography (ICGA),[37] new insights into the extent of choroidal vessel hyperpermeability, extent of serous retinal detachments, and pigment epithelial detachments have been appreciated in the periphery of the fundus in central serous chorioretinopathy (CSCR)[138] (Fig. 5.35). A multicenter retrospective study found that dilated choroidal vessels and hyperpermeability on UWF–ICGA corresponded with areas of altered FAF, with 57% of eyes displaying pathology outside the standard 50° field of view. Additionally, in 83.3% of eyes, dilated vessels were associated with one or more congested vortex vein ampullas, suggesting impeded ocular outflow as a novel pathophysiologic contributing factor to CSCR.[138] Another study including 24 eyes with CSCR found peripheral abnormalities on UWF–ICGA in 64.6% of eyes.[37] A report compared the non-wide-field Heidelberg FAF to Optos UWF–FAF and found differences in lesion intensity before and after resolution but similar lesion composite patterns.[139] Future studies are needed to ascertain the ability of UWF imaging to provide further phenotypic differentiation in this disorder, direct treatments such as photodynamic therapy, and better monitor disease activity including recurrence.

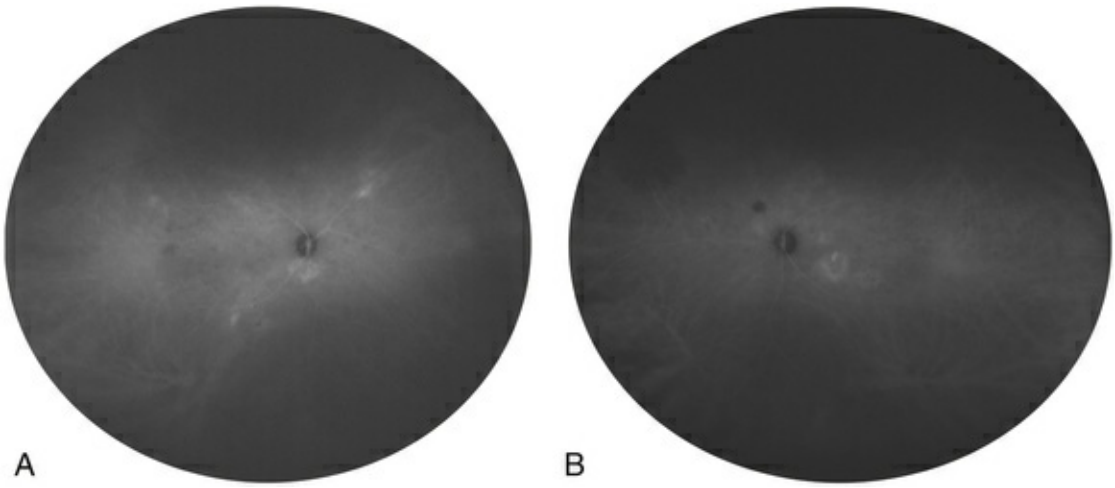

FIG. 5.35 Central serous chorioretinopathy (CSCR): Optos fluorescein angiography demonstrated diffuse multifocal late leakage.

Age-Related Macular Degeneration

Although the clinical management of macular degeneration hinges upon macular imaging including OCT and FA, wide-field imaging has allowed for monitoring of concurrent peripheral findings in both neovascular and non-neovascular age-related macular degeneration (AMD).[37] The benefits of wide-field imaging apply to related neovascular disorders such as polypoidal choroidal vasculopathy (PCV). Initial reports highlighted the ability of UWF imaging to detect peripheral CNV[140,141] (Fig. 5.36). A study of participants in the Reykjavik Eye Study found that Optos pseudocolor SLO images compared to Zeiss fundus camera 45° images had overall agreement of 96.43% with excellent intergrader agreement (kappa = 0.93).[142] Importantly, a large, multicenter study of multiple disease conditions including AMD and PCV found that Optos UWF imaging was able to provide excellent quality images of the macula as well as the fundus periphery for the detection and diagnosis of vascular changes on ICGA.[37]

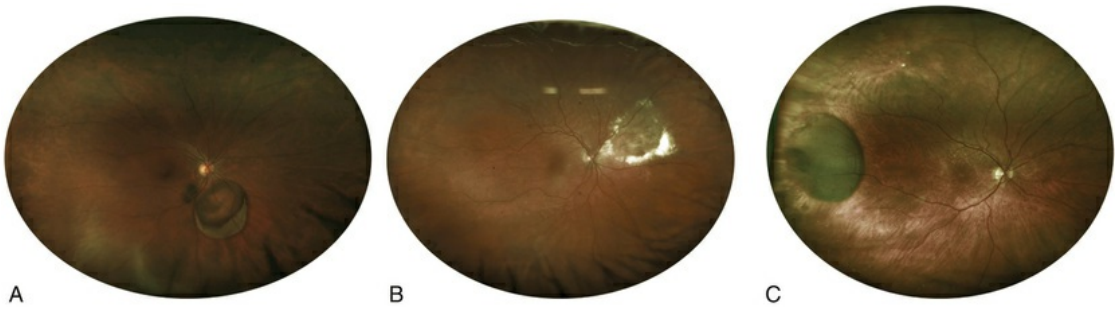

FIG. 5.36 Optos color photographs of several cases of extrafoveal choroidal neovascular membranes which would be incompletely detected by non-wide-field imaging.

Other studies have focused on peripheral FAF findings in AMD.[143–145] A retrospective study of UWF–FAF and UWF pseudcolor images found that among 135 eyes with AMD, 73.9% had peripheral FAF changes and 79.3% of pseudocolor images had peripheral findings outside the central field of view (standard ETDRS Field 2 and Field 1M photographs used in AREDS study).[143] A prospective study of 119 patients (100 with AMD and 19 without AMD) reported peripheral FAF abnormalities in 68.9% of eyes with significant risk factors for peripheral abnormalities including neovascular AMD (OR 12.7, compared to normals), non-neovascular AMD (OR 6.2), older age (OR 6.5), and female sex (OR 4.1).[145] A study found increased peripheral FAF changes with age, but found that age-corrected peripheral FAF irregularity was greater in both treated (anti-VEGF) and untreated eyes with AMD compared to normal controls.[144] More recent studies are proposing new classifications and phenotypes for AMD-like changes in the far periphery even in those without macula-threatening disease[146] (Fig. 5.37).

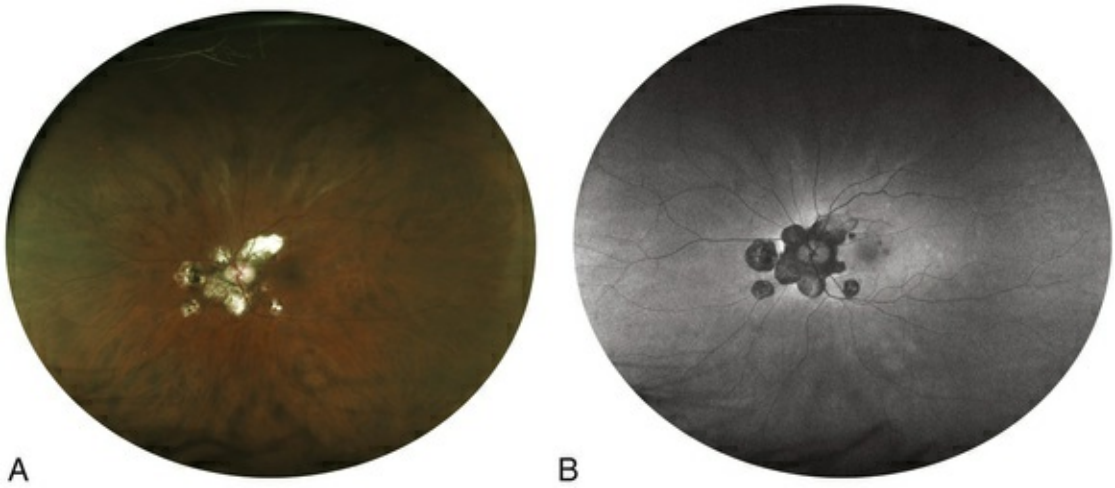

FIG. 5.37 Presumed ocular histoplasmosis syndrome (POHS): Optos color photograph (A) and fundus autofluorescence (B).

Limitations

The most important limitation of wide-field imaging or UWF imaging systems is the inability to image the entire retina ora-to-ora with a single acquisition in most patients.

Traditional fundus cameras image approximately 5–15% of the total retinal surface area, where as the Optos manufacturer states their system is capable of imaging 82% of the retinal surface based on several assumptions, including a standardized radius of the eye of 11 mm.[106] Likewise, the representation of a three-dimensional image on a two-dimensional surface overrepresents areas of the periphery compared to their true anatomic proportions, which may limit quantitative assessment of UWF images.[63] The optics of the device, combined with the large depth of field (Fig. 5.38), also tend to provide poorer imaging of the superior and inferior quadrants of the retina,[105,112] which may also be limited by lash artifact and other structures anterior to the retina.[147] Reports also suggest that image acquisition with devices such as the Optos have a learning curve, given that it is a SLO acquisition, there is no preview of the image to be acquired such as with traditional fundus photography or the Heidelberg system, which provides an infrared image for the photographer to focus prior to acquisition of OCT or FAF.[148] Finally, many of these systems, including the Optos and RetCam, may be

costly and present a challenge in a era of rising healthcare costs and a desire to keep these costs contained.

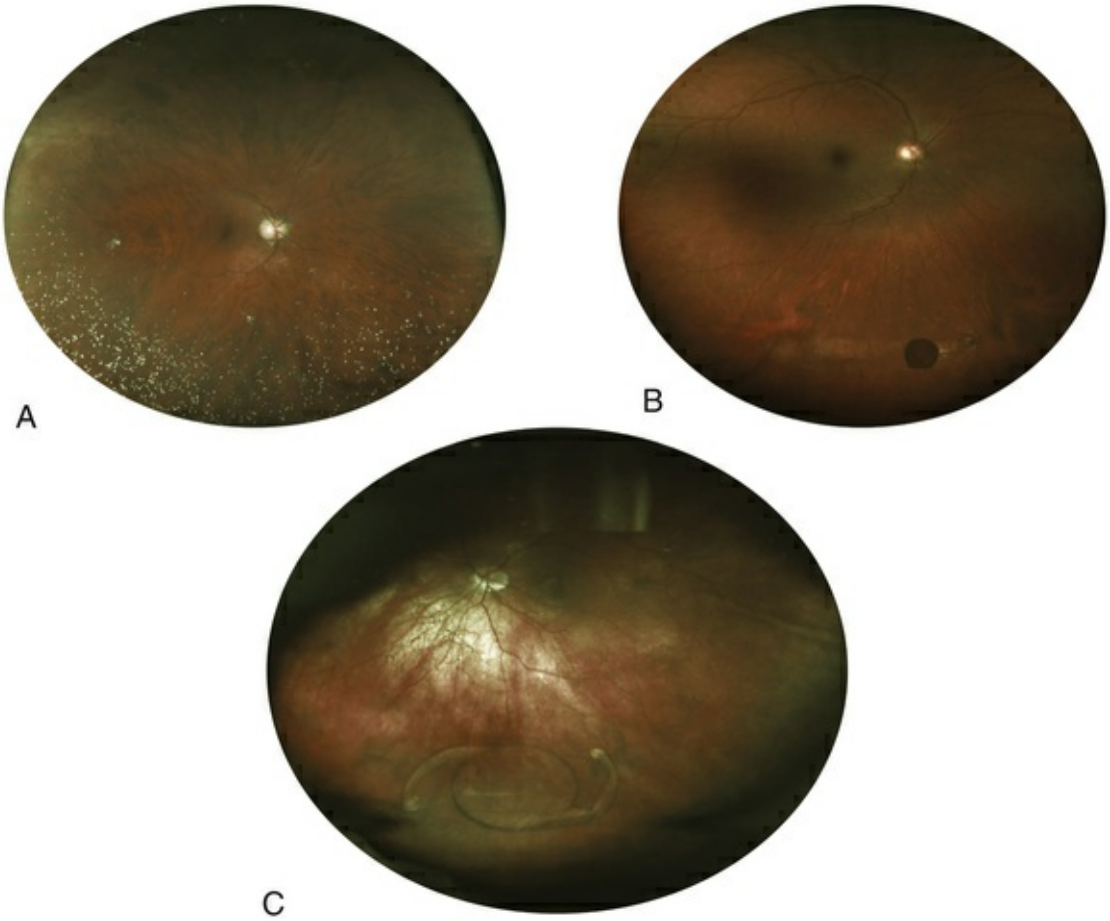

FIG. 5.38 Optos vitreous imaging: Asteroid hyalosis (A), free-floating vitreous cyst (B), dislocated intraocular lens in a patient with pseudoexfoliation (C). The large depth of field of the Optos platform allows relatively focused simultaneous imaging of both the fundus and vitreous cavity.

Future Directions

The role of wide-field imaging continues to evolve, with an increasing number of initial case reports, followed by retrospective series and now prospective trials incorporating this imaging technology. In an era of increasing numbers of patients with a limited pool of healthcare providers, wide-field imaging will

continue to have a role in screening and telemedicine applications for diseases such as diabetic retinopathy and retinopathy of prematurity.

The Optos platform initially became available as a SLO with pseudocolor imaging capability, and has now evolved into a multimodal imaging device capable of FAF, FA, and ICGA. Newer platforms such as the PanoCam LT (Visunex Medical Systems, Fremont, CA) have recently been approved by the Food and Drug Administration in the United States and provide another option for wide-field imaging (Figs. 5.39 and 5.40). Additional imaging technologies, such as swept source OCT, may be incorporated in the future with advances in optics that may allow for noninvasive wide-field OCT angiography. As UWF imaging continues to allow us to further study the retinal periphery with multimodal imaging, the pathophysiology of different retinal diseases will continue to be studied noninvasively, which may translate into improved disease diagnosis, staging, and treatment.

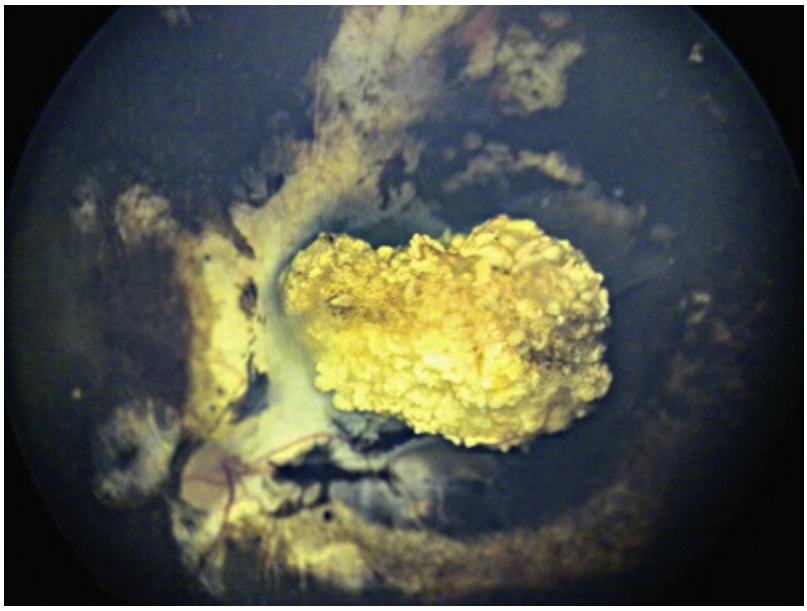

FIG. 5.39 PanoCam LT photograph of retinoblastoma.

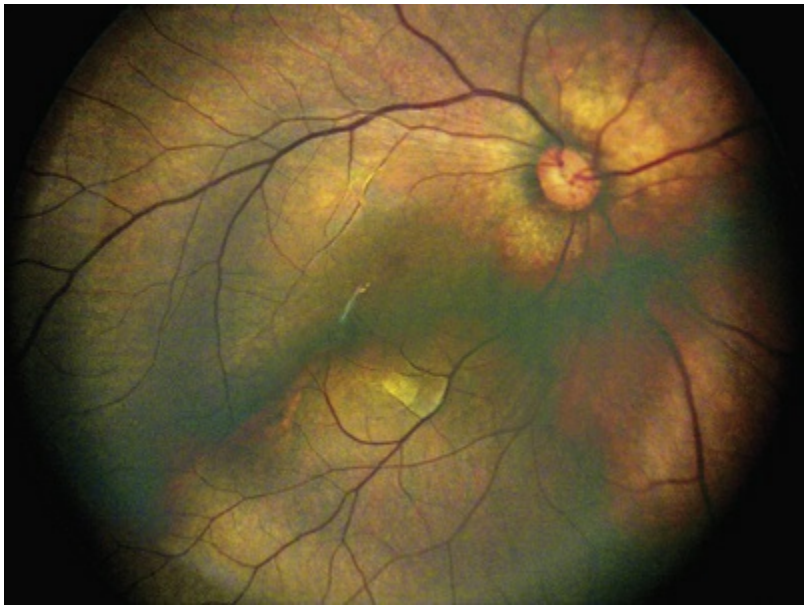

FIG. 5.40 PanoCam LT photograph of retinopathy of prematurity.

Additionally, in an era of electronic medical records (EMR), traditional color fundus drawings are becoming a lost art. Cumbersome digital interfaces on EMR, which focus on efficiency and prioritize billing criteria, result in inferior fundus drawings. Wide-field imaging may become a useful adjunct or replacement for documentation of the appearance of the fundus at office visits, which may have numerous positive implications for the physician and patient alike.

Conclusion

Technologic innovations and the realization that the periphery of the ocular fundus is a key site of primary vitreoretinal pathology and secondary changes has led to the continued use and improvement in wide-field imaging. Current studies with this imaging modality have suggested important clinical applications for numerous retinal diseases, including diabetic retinopathy, retinal vein occlusions, ophthalmic oncology, uveitis, pediatric vitreoretinal disorders, and hereditary retinal degenerations. Ongoing prospective trials will serve to refine and optimize the use of this technology. (Fig. 5.41 online).

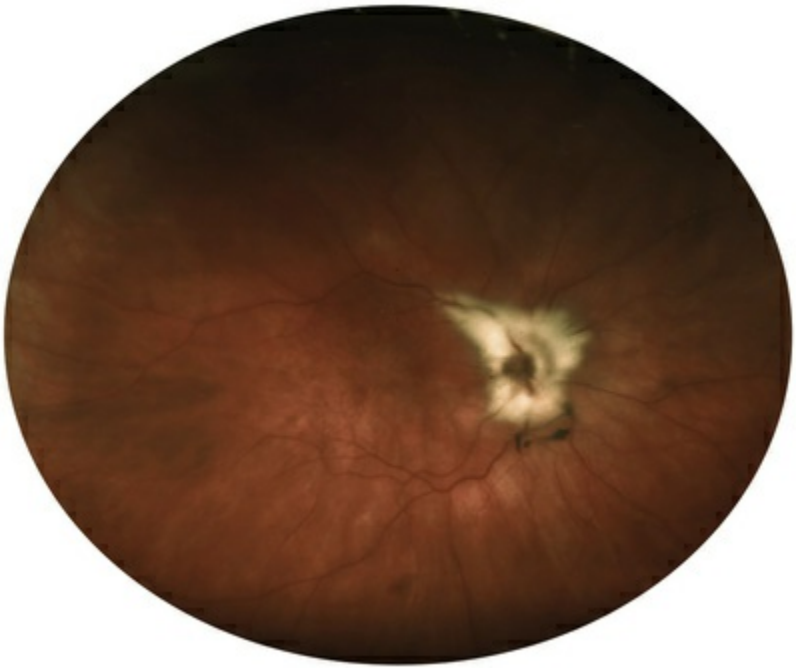

FIG. 5.41 Optos color photograph of myelinated nerve fiber layer.

References

1. Rucker C. *A history of the ophthalmoscope*. Whiting Printers: Rochester, MN; 1971.
2. Helmholtz H. *Beschreibung eines Augen-spiegels zur Untersuchung der Netzhaut im Lebenden Auge. Forstner'sche Verlagsbuchhandlung*. [Berlin, A] 1851.
3. Albert DM, Gloor BP, McPherson AR. Why Jules Gonin achieved his "audacious goal initiative" and why he is a model for the present day. *Ophthalmology*. 2015;122(10):1955–1957.
4. Ciardella A, Brown D. *Wide field imaging*. Slack Incorporated: New York; 2007.
5. Diabetic Retinopathy Clinical Research Network. *Peripheral diabetic retinopathy (DR) lesions on ultrawide-field fundus images and risk of DR worsening over time. DRCRnet*. http://drcrnet.jaeb.org/Studies.aspx?RecID=239.
6. Gross JG, Glassman AR, Jampol LM, et al. Panretinal photocoagulation vs intravitreous ranibizumab for proliferative diabetic retinopathy: a randomized clinical

trial. *JAMA*. 2015;314(20):2137–2146.
7. Lotmar W. A fixation lamp for panoramic fundus pictures. *Klin Monatsbl Augenheilkd*. 1977;170(5):767–774.
8. Pomerantzeff O. Equator-Plus camera. *Invest Ophthalmol*. 1975;14(5):401–406.
9. Pomerantzeff O, Webb RH, Delori FC. Image formation in fundus cameras. *Invest Ophthalmol Vis Sci*. 1979;18(6):630–637.
10. Ducrey N, Pomerantzeff O, Schepens CL, et al. Clinical trials with the Equator-Plus camera. *Am J Ophthalmol*. 1977;84(6):840–846.
11. Pe'er J, Sancho C, Cantu J, et al. Measurement of choroidal melanoma basal diameter by wide-angle digital fundus camera: a comparison with ultrasound measurement. *Ophthalmologica*. 2006;220(3):194–197.
12. Shields CL, Materin M, Shields JA. Panoramic imaging of the ocular fundus. *Arch Ophthalmol*. 2003;121(11):1603–1607.
13. Nakagawa TA, Skrinska R. Improved documentation of retinal hemorrhages using a wide-field digital ophthalmic camera in patients who experienced abusive head trauma. *Arch Pediatr Adolesc Med*. 2001;155(10):1149–1152.
14. Roth DB, Morales D, Feuer WJ, et al. Screening for retinopathy of prematurity employing the retcam 120: sensitivity and specificity. *Arch Ophthalmol*. 2001;119(2):268–272.
15. Adams GG, Clark BJ, Fang S, et al. Retinal haemorrhages in an infant following RetCam screening for retinopathy of prematurity. *Eye (Lond)*. 2004;18(6):652–653.
16. Schwartz SD, Harrison SA, Ferrone PJ, et al. Telemedical evaluation and management of retinopathy of prematurity using a fiberoptic digital fundus camera. *Ophthalmology*. 2000;107(1):25–28.
17. Kim JW, Ngai LK, Sadda S, et al. Retcam fluorescein angiography findings in eyes with advanced retinoblastoma. *Br J Ophthalmol*. 2014;98(12):1666–1671.
18. Lepore D, Quinn GE, Molle F, et al. Intravitreal bevacizumab versus laser treatment in type 1 retinopathy of prematurity: report on fluorescein angiographic findings.

Ophthalmology. 2014;121(11):2212–2219.
19. Suzani M, Moore AT. Intraoperative fluorescein angiography-guided treatment in children with early Coats' disease. *Ophthalmology*. 2015;122(6):1195–1202.
20. Klufas MA, Patel SN, Ryan MC, et al. Influence of fluorescein angiography on the diagnosis and management of retinopathy of prematurity. *Ophthalmology*. 2015;122(8):1601–1608.
21. Patel SN, Klufas MA, Ryan MC, et al. Color fundus photography versus fluorescein angiography in identification of the macular center and zone in retinopathy of prematurity. *Am J Ophthalmol*. 2015;159(5):950–957.e2.
22. Staurenghi G, Viola F, Mainster MA, et al. Scanning laser ophthalmoscopy and angiography with a wide-field contact lens system. *Arch Ophthalmol*. 2005;123(2):244–252.
23. Mantel I, Schalenbourg A, Zografos L. Peripheral exudative hemorrhagic chorioretinopathy: polypoidal choroidal vasculopathy and hemodynamic modifications. *Am J Ophthalmol*. 2012;153(5):910–922.e2.
24. Reeves GM, Kumar N, Beare NA, et al. Use of Staurenghi lens angiography in the management of posterior uveitis. *Acta Ophthalmol*. 2013;91(1):48–51.
25. Takahashi K, Muraoka K, Kishi S, et al. Watershed zone in the human peripheral choroid. *Ophthalmology*. 1996;103(2):336–342.
26. Spaide RF, Orlock DA, Herrmann-Delemazure B, et al. Wide-angle indocyanine green angiography. *Retina*. 1998;18(1):44–49.
27. Haddock LJ, Kim DY, Mukai S. Simple, inexpensive technique for high-quality smartphone fundus photography in human and animal eyes. *J Ophthalmol*. 2013;2013:518479.
28. Kim DY, Delori F, Mukai S. Smartphone photography safety. *Ophthalmology*. 2012;119(10):2200–2201 [author reply 2201].
29. Witmer MT, Parlitsis G, Patel S, Kiss S. Comparison of ultra-widefield fluorescein angiography with the Heidelberg Spectralis® noncontact ultra-widefield module versus the Optos® Optomap®. *Clin Ophthalmol*. 2013;7:389–394.

30. Friberg TR, Pandya A, Eller AW. Non-mydriatic panoramic fundus imaging using a non-contact scanning laser-based system. *Ophthalmic Surg Lasers Imaging*. 2003;34(6):488–497.
31. Klufas MA, Yannuzzi NA, D'Amico DJ, Kiss S. Vitreoretinal aspects of permanent keratoprosthesis. *Surv Ophthalmol*. 2015;60(3):216–228.
32. Piffer AL, Boissonnot M, Gobert F, et al. Relevance of wide-field autofluorescence imaging in Birdshot retinochoroidopathy: descriptive analysis of 76 eyes. *Acta Ophthalmol*. 2014;92(6):e463–9.
33. Sagong M, van Hemert J, Olmos de Koo LC, et al. Assessment of accuracy and precision of quantification of ultra-widefield images. *Ophthalmology*. 2015;122(4):864–866.
34. Inoue M, Yanagawa A, Yamane S, et al. Wide-field fundus imaging using the Optos Optomap and a disposable eyelid speculum. *JAMA Ophthalmol*. 2013;131(2):226.
35. Friberg TR, Gupta A, Yu J, et al. Ultrawide angle fluorescein angiographic imaging: a comparison to conventional digital acquisition systems. *Ophthalmic Surg Lasers Imaging*. 2008;39(4):304–311.
36. Manivannan A, Plskova J, Farrow A, McKay S, Sharp PF, Forrester JV. Ultra-wide-field fluorescein angiography of the ocular fundus. *Am J Ophthalmol*. 2005;140(3):525–527.
37. Klufas MA, Yannuzzi NA, Pang CE, et al. Feasibility and clinical utility of ultra-widefield indocyanine green angiography. *Retina*. 2015;35(3):508–520.
38. Keilhauer CN, Delori FC. Near-infrared autofluorescence imaging of the fundus: visualization of ocular melanin. *Invest Ophthalmol Vis Sci*. 2006;47(8):3556–3564.
39. Spaide RF. Fundus autofluorescence and age-related macular degeneration. *Ophthalmology*. 2003;110(2):392–399.
40. Schmitz-Valckenberg S, Holz FG, Bird AC, Spaide RF. Fundus autofluorescence imaging: review and perspectives. *Retina*. 2008;28(3):385–409.
41. Early Treatment Diabetic Retinopathy Study design and baseline patient characteristics. ETDRS report number 7. *Ophthalmology*. 1991;98(5 Suppl.):741–756.
42. Purbrick RM, Izadi S, Gupta A, Chong NV. Comparison of

Optomap ultrawide-field imaging versus slit-lamp biomicroscopy for assessment of diabetic retinopathy in a real-life clinic. *Clin Ophthalmol*. 2014;8:1413–1417.
43. Neubauer AS, Kernt M, Haritoglou C, Priglinger SG, Kampik A, Ulbig MW. Nonmydriatic screening for diabetic retinopathy by ultra-widefield scanning laser ophthalmoscopy (Optomap). *Graefes Arch Clin Exp Ophthalmol*. 2008;246(2):229–235.
44. Wilson PJ, Ellis JD, MacEwen CJ, Ellingford A, Talbot J, Leese GP. Screening for diabetic retinopathy: a comparative trial of photography and scanning laser ophthalmoscopy. *Ophthalmologica*. 2010;224(4):251–257.
45. Silva PS, Cavallerano JD, Sun JK, Soliman AZ, Aiello LM, Aiello LP. Peripheral lesions identified by mydriatic ultrawide field imaging: distribution and potential impact on diabetic retinopathy severity. *Ophthalmology*. 2013;120(12):2587–2595.
46. Silva PS, Aiello LP. Telemedicine and eye examinations for diabetic retinopathy: a time to maximize real-world outcomes. *JAMA Ophthalmol*. 2015;133(5):525–526.
47. Silva PS, Cavallerano JD, Tolls D, et al. Potential efficiency benefits of nonmydriatic ultrawide field retinal imaging in an ocular telehealth diabetic retinopathy program. *Diabetes Care*. 2014;37(1):50–55.
48. Silva PS, Cavallerano JD, Tolson AM, et al. Real-time ultrawide field image evaluation of retinopathy in a diabetes telemedicine program. *Diabetes Care*. 2015;38(9):1643–1649.
49. Kaines A, Oliver S, Reddy S, Schwartz SD. Ultrawide angle angiography for the detection and management of diabetic retinopathy. *Int Ophthalmol Clin*. 2009;49(2):53–59.
50. Win PH, Young TA. Optos Panoramic200A fluorescein angiography for proliferative diabetic retinopathy with asteroid hyalosis. *Semin Ophthalmol*. 2007;22(2):67–69.
51. Wessel MM, Aaker GD, Parlitsis G, Cho M, D'Amico DJ, Kiss S. Ultra-wide-field angiography improves the detection and classification of diabetic retinopathy. *Retina*. 2012;32(4):785–791.

52. Sim DA, Keane PA, Rajendram R, et al. Patterns of peripheral retinal and central macula ischemia in diabetic retinopathy as evaluated by ultra-widefield fluorescein angiography. *Am J Ophthalmol*. 2014;158(1):144–153.e1.
53. Oliver SC, Schwartz SD. Peripheral vessel leakage (PVL): a new angiographic finding in diabetic retinopathy identified with ultra wide-field fluorescein angiography. *Semin Ophthalmol*. 2010;25(1–2):27–33.
54. Wessel MM, Nair N, Aaker GD, Ehrlich JR, D'Amico DJ, Kiss S. Peripheral retinal ischaemia, as evaluated by ultra-widefield fluorescein angiography, is associated with diabetic macular oedema. *Br J Ophthalmol*. 2012;96(5):694–698.
55. Patel RD, Messner LV, Teitelbaum B, Michel KA, Hariprasad SM. Characterization of ischemic index using ultra-widefield fluorescein angiography in patients with focal and diffuse recalcitrant diabetic macular edema. *Am J Ophthalmol*. 2013;155(6):1038–1044.e2.
56. Croft DE, van Hemert J, Wykoff CC, et al. Precise montaging and metric quantification of retinal surface area from ultra-widefield fundus photography and fluorescein angiography. *Ophthalmic Surg Lasers Imaging Retina*. 2014;45(4):312–317.
57. Croft DE, Wykoff CC, van Hemert J, Verhoek M, Brown DM. Not all retina is created equal: metabolic quantification of ultra-widefield images. *Ophthalmology*. 2015;122(12):2580–2582.
58. Reddy S, Hu A, Schwartz SD. Ultra wide field fluorescein angiography guided targeted retinal photocoagulation (TRP). *Semin Ophthalmol*. 2009;24(1):9–14.
59. Muqit MM, Marcellino GR, Henson DB, et al. Optos-guided pattern scan laser (Pascal)-targeted retinal photocoagulation in proliferative diabetic retinopathy. *Acta Ophthalmol*. 2013;91(3):251–258.
60. Tsui I, Franco-Cardenas V, Hubschman JP, Yu F, Schwartz SD. Ultra wide field fluorescein angiography can detect macular pathology in central retinal vein occlusion. *Ophthalmic Surg Lasers Imaging*. 2012;43(3):257–262.

61. Prasad PS, Oliver SC, Coffee RE, Hubschman JP, Schwartz SD. Ultra wide-field angiographic characteristics of branch retinal and hemicentral retinal vein occlusion. *Ophthalmology*. 2010;117(4):780–784.
62. Tsui I, Kaines A, Havunjian MA, et al. Ischemic index and neovascularization in central retinal vein occlusion. *Retina*. 2011;31(1):105–110.
63. Spaide RF. Peripheral areas of nonperfusion in treated central retinal vein occlusion as imaged by wide-field fluorescein angiography. *Retina*. 2011;31(5):829–837.
64. Singer M, Tan CS, Bell D, Sadda SR. Area of peripheral retinal nonperfusion and treatment response in branch and central retinal vein occlusion. *Retina*. 2014;34(9):1736–1742.
65. Singer MA, Tan CS, Surapaneni KR, Sadda SR. Targeted photocoagulation of peripheral ischemia to treat rebound edema. *Clin Ophthalmol*. 2015;9:337–341.
66. Cho M, Kiss S. Detection and monitoring of sickle cell retinopathy using ultra wide-field color photography and fluorescein angiography. *Retina*. 2011;31(4):738–747.
67. Cho M, Aaker G, D'Amico DJ, Kiss S. Peripheral vascular abnormalities in beta-thalassemia major detected by ultra wide-field fundus imaging. *Retin Cases Brief Rep*. 2011;5(4):339–342.
68. Lyles GW, Moyer S, Chavala SH. Clinical images: peripheral retinal neovascularization in the antiphospholipid antibody syndrome. *Arthritis Rheum*. 2012;64(4):1144.
69. Lee JC, Wang MY, Damodar D, Sadun AA, Sadda S. Headache and whiteout vision as the presenting symptoms in a case of Takayasu retinopathy. *Retin Cases Brief Rep*. 2014;8(4):273–275.
70. Goldman DR, Prasad PS, Schwartz SD. Dramatic resolution of extreme ocular ischemia in a case of Takayasu's arteritis. *Ophthalmic Surg Lasers Imaging Retina*. 2013;44(2):198–200.
71. Bass SJ, Sherman J, Giovinazzo V. Bilateral Coats' response in a female patient leads to diagnosis of facioscapulohumeral muscular dystrophy. *Optometry*. 2011;82(2):72–76.
72. Hahn P, Lin P, Fekrat S. Ultra-widefield imaging of

Duchenne muscular dystrophy-associated proliferative retinal vasculopathy improved with panretinal laser photocoagulation alone. *Ophthalmic Surg Lasers Imaging Retina*. 2013;44(3):293–295.
73. Klufas MA, Dinkin MJ, Bhaleeya SD, Chapman KO, Riley CS, Kiss S. Ultra-widefield fluorescein angiography reveals retinal phlebitis in Susac's syndrome. *Ophthalmic Surg Lasers Imaging Retina*. 2014;45(4):335–337.
74. Mayer WJ, Hakim I, Ulbig MW, Kernt M, Haritoglou C. Non-mydriatic wide field fundus photography in bilateral serous retinal detachment due to HELLP syndrome. *Arch Gynecol Obstet*. 2012;286(3):819–820.
75. Tsui I, Kaines A, Schwartz S. Patterns of periphlebitis in intermediate uveitis using ultra wide field fluorescein angiography. *Semin Ophthalmol*. 2009;24(1):29–33.
76. Kaines A, Tsui I, Sarraf D, Schwartz S. The use of ultra wide field fluorescein angiography in evaluation and management of uveitis. *Semin Ophthalmol*. 2009;24(1):19–24.
77. Mudvari SS, Virasch VV, Singa RM, MacCumber MW. Ultra-wide-field imaging for cytomegalovirus retinitis. *Ophthalmic Surg Lasers Imaging*. 2010;41(3):311–315.
78. Nicholson BP, Nigam D, Miller D, et al. Comparison of wide-field fluorescein angiography and 9-field montage angiography in uveitis. *Am J Ophthalmol*. 2014;157(3):673–677.
79. Campbell JP, Leder HA, Sepah YJ, et al. Wide-field retinal imaging in the management of noninfectious posterior uveitis. *Am J Ophthalmol*. 2012;154(5):908–911.e2.
80. Leder HA, Campbell JP, Sepah YJ, et al. Ultra-wide-field retinal imaging in the management of non-infectious retinal vasculitis. *J Ophthalmic Inflamm Infect*. 2013;3(1):30.
81. Mesquida M, Llorenc V, Fontenla JR, Navarro MJ, Adan A. Use of ultra-wide-field retinal imaging in the management of active Behçet retinal vasculitis. *Retina*. 2014;34(10):2121–2127.
82. Good WV. Final results of the Early Treatment for Retinopathy of Prematurity (ETROP) randomized trial. *Trans Am Ophthalmol Soc*. 2004;102:233–248 [discussion 248–

50].
83. Laws DE, Morton C, Weindling M, Clark D. Systemic effects of screening for retinopathy of prematurity. *Br J Ophthalmol*. 1996;80(5):425–428.
84. Mukherjee AN, Watts P, Al-Madfai H, Manoj B, Roberts D. Impact of retinopathy of prematurity screening examination on cardiorespiratory indices: a comparison of indirect ophthalmoscopy and retcam imaging. *Ophthalmology*. 2006;113(9):1547–1552.
85. Kang KB, Wessel MM, Tong J, D'Amico DJ, Chan RV. Ultra-widefield imaging for the management of pediatric retinal diseases. *J Pediatr Ophthalmol Strabismus*. 2013;50(5):282–288.
86. Tsui I, Franco-Cardenas V, Hubschman JP, Schwartz SD. Pediatric retinal conditions imaged by ultra wide field fluorescein angiography. *Ophthalmic Surg Lasers Imaging Retina*. 2013;44(1):59–67.
87. Kashani AH, Brown KT, Chang E, Drenser KA, Capone A, Trese MT. Diversity of retinal vascular anomalies in patients with familial exudative vitreoretinopathy. *Ophthalmology*. 2014;121(11):2220–2227.
88. Kashani AH, Learned D, Nudleman E, Drenser KA, Capone A, Trese MT. High prevalence of peripheral retinal vascular anomalies in family members of patients with familial exudative vitreoretinopathy. *Ophthalmology*. 2014;121(1):262–268.
89. Blair MP, Shapiro MJ, Hartnett ME. Fluorescein angiography to estimate normal peripheral retinal nonperfusion in children. *J AAPOS*. 2012;16(3):234–237.
90. The Photographic Screening for Retinopathy of Prematurity Study (photo-ROP). Primary outcomes. *Retina*. 2008;28(3 Suppl.):S47–54.
91. Chiang MF, Wang L, Busuioc M, et al. Telemedical retinopathy of prematurity diagnosis: accuracy, reliability, and image quality. *Arch Ophthalmol*. 2007;125(11):1531–1538.
92. Coste V, Paya C, Korobelnik JF. Retinopathy of prematurity evolution after laser treatment: Retcam findings. *JAMA Ophthalmol*. 2015;133(1):e141808.
93. Dai S, Chow K, Vincent A. Efficacy of wide-field digital

retinal imaging for retinopathy of prematurity screening. *Clin Experiment Ophthalmol*. 2011;39(1):23–29.
94. Dhaliwal C, Wright E, Graham C, McIntosh N, Fleck BW. Wide-field digital retinal imaging versus binocular indirect ophthalmoscopy for retinopathy of prematurity screening: a two-observer prospective, randomised comparison. *Br J Ophthalmol*. 2009;93(3):355–359.
95. Ells AL, Holmes JM, Astle WF, et al. Telemedicine approach to screening for severe retinopathy of prematurity: a pilot study. *Ophthalmology*. 2003;110(11):2113–2117.
96. Fleck BW. Where is the junction of zone 2 and zone 3 temporal retina in RetCam images of acute retinopathy of prematurity? *Eye (Lond)*. 2015;29(7):981.
97. Murakami Y, Jain A, Silva RA, Lad EM, Gandhi J, Moshfeghi DM. Stanford University Network for Diagnosis of Retinopathy of Prematurity (SUNDROP): 12-month experience with telemedicine screening. *Br J Ophthalmol*. 2008;92(11):1456–1460.
98. Tejada-Palacios P, Zarratea L, Moral M, de la Cruz-Bertolo J. Comparative study of RetCamRetCam II vs. binocular ophthalmoscopy in a screening program for retinopathy of prematurity. *Arch Soc Esp Oftalmol*. 2015;90(8):373–378.
99. Wang SK, Callaway NF, Wallenstein MB, Henderson MT, Leng T, Moshfeghi DM. SUNDROP: six years of screening for retinopathy of prematurity with telemedicine. *Can J Ophthalmol*. 2015;50(2):101–106.
100. Weaver DT, Murdock TJ. Telemedicine detection of type 1 ROP in a distant neonatal intensive care unit. *J AAPOS*. 2012;16(3):229–233.
101. Williams SL, Wang L, Kane SA, et al. Telemedical diagnosis of retinopathy of prematurity: accuracy of expert versus non-expert graders. *Br J Ophthalmol*. 2010;94(3):351–356.
102. Wu C, Petersen RA, VanderVeen DK. RetCam imaging for retinopathy of prematurity screening. *J AAPOS*. 2006;10(2):107–111.
103. Fung TH, Muqit MM, Mordant DJ, Smith LM, Patel CK. Noncontact high-resolution ultra-wide-field oral fluorescein angiography in premature infants with retinopathy of

prematurity. *JAMA Ophthalmol*. 2014;132(1):108–110.
104. Fung TH, Yusuf IH, Smith LM, Brett J, Weston L, Patel CK. Outpatient ultra wide-field intravenous fundus fluorescein angiography in infants using the Optos P200MA scanning laser ophthalmoscope. *Br J Ophthalmol*. 2014;98(3):302–304.
105. Kornberg DL, Klufas MA, Yannuzzi NA, Orlin A, D'Amico DJ, Kiss S. Clinical utility of ultra-widefield imaging with the Optos optomap compared with indirect ophthalmoscopy in the setting of non-traumatic rhegmatogenous retinal detachment. *Semin Ophthalmol*. 2014;17:1–8.
106. Witmer MT, Kiss S. Wide-field imaging of the retina. *Surv Ophthalmol*. 2013;58(2):143–154.
107. Quiram PA, Gonzales CR, Hu W, et al. Outcomes of vitrectomy with inferior retinectomy in patients with recurrent rhegmatogenous retinal detachments and proliferative vitreoretinopathy. *Ophthalmology*. 2006;113(11):2041–2047.
108. Shah SP, Jain A, Tsui I, McCannel TA. Optos Optomap Panoramic 200MA imaging of a serous choroidal detachment responsive to furosemide. *Semin Ophthalmol*. 2009;24(1):40–42.
109. Mackenzie PJ, Russell M, Ma PE, Isbister CM, Maberley DA. Sensitivity and specificity of the optos optomap for detecting peripheral retinal lesions. *Retina*. 2007;27(8):1119–1124.
110. Lara-Medina J, Ispa-Callen MC, Gonzalez-Del-Valle F, Nunez A, Dominguez MJ, Arias-Palomero A. Peripheral vitreoretinal traction exploration by Staurenghi 230 lens and HRA-II. *Arch Soc Esp Oftalmol*. 2009;84(12):625–630.
111. Khandhadia S, Madhusudhana KC, Kostakou A, Forrester JV, Newsom RS. Use of Optomap for retinal screening within an eye casualty setting. *Br J Ophthalmol*. 2009;93(1):52–55.
112. Bonnay G, Nguyen F, Meunier I, Ducasse A, Hamel C, Arndt C. Screening for retinal detachment using wide-field retinal imaging. *J Fr Ophtalmol*. 2011;34(7):482–485.
113. Lee DH, Kim SS, Kim M, Koh HJ. Identifiable Peripheral

retinal lesions using ultra-widefield scanning laser ophthalmoscope and its usefulness in myopic patients. *J Korean Ophthalmol Soc*. 2014;55(12):1814.
114. Witmer MT, Cho M, Favarone G, Chan RV, D'Amico DJ, Kiss S. Ultra-wide-field autofluorescence imaging in non-traumatic rhegmatogenous retinal detachment. *Eye (Lond)*. 2012;26(9):1209–1216.
115. Salvanos P, Navaratnam J, Ma J, Bragadottir R, Moe MC. Ultra-widefield autofluorescence imaging in the evaluation of scleral buckling surgery for retinal detachment. *Retina*. 2013;33(7):1421–1427.
116. Labriola LT, Brant AM, Eller AW. Chronic retinal detachment with secondary retinal macrocyst and peripheral neovascularization. *Semin Ophthalmol*. 2009;24(1):2–4.
117. Ohno-Matsui K. Proposed classification of posterior staphylomas based on analyses of eye shape by three-dimensional magnetic resonance imaging and wide-field fundus imaging. *Ophthalmology*. 2014;121(9):1798–1809.
118. Ishida T, Moriyama M, Tanaka Y, et al. Radial tracts emanating from staphyloma edge in eyes with pathologic myopia. *Ophthalmology*. 2015;122(1):215–216.
119. Kaneko Y, Moriyama M, Hirahara S, Ogura Y, Ohno-Matsui K. Areas of nonperfusion in peripheral retina of eyes with pathologic myopia detected by ultra-widefield fluorescein angiography. *Invest Ophthalmol Vis Sci*. 2014;55(3):1432–1439.
120. Yuan A, Kaines A, Jain A, Reddy S, Schwartz SD, Sarraf D. Ultra-wide-field and autofluorescence imaging of choroidal dystrophies. *Ophthalmic Surg Lasers Imaging*. 2010;41 Online:e1–5.
121. Huang AS, Kim LA, Fawzi AA. Clinical characteristics of a large choroideremia pedigree carrying a novel CHM mutation. *Arch Ophthalmol*. 2012;130(9):1184–1189.
122. Oishi A, Ogino K, Makiyama Y, Nakagawa S, Kurimoto M, Yoshimura N. Wide-field fundus autofluorescence imaging of retinitis pigmentosa. *Ophthalmology*. 2013;120(9):1827–1834.

123. Oishi M, Oishi A, Ogino K, et al. Wide-field fundus autofluorescence abnormalities and visual function in patients with cone and cone–rod dystrophies. *Invest Ophthalmol Vis Sci*. 2014;55(6):3572–3577.
124. Ogura S, Yasukawa T, Kato A, et al. Wide-field fundus autofluorescence imaging to evaluate retinal function in patients with retinitis pigmentosa. *Am J Ophthalmol*. 2014;158(5):1093–1098.
125. Jain A, Shah SP, Tsui I, McCannel TA. The value of Optos Panoramic 200MA imaging for the monitoring of large suspicious choroidal lesions. *Semin Ophthalmol*. 2009;24(1):43–44.
126. Shah SP, Jain A, Coffee RE, McCannel TA. Optos Panoramic 200MA ultrawide-field imaging of peripheral RPE adenoma. *Semin Ophthalmol*. 2009;24(1):37–39.
127. Coffee RE, Jain A, McCannel TA. Ultra wide-field imaging of choroidal metastasis secondary to primary breast cancer. *Semin Ophthalmol*. 2009;24(1):34–36.
128. Kernt M, Schaller UC, Stumpf C, Ulbig MW, Kampik A, Neubauer AS. Choroidal pigmented lesions imaged by ultra-wide-field scanning laser ophthalmoscopy with two laser wavelengths (Optomap). *Clin Ophthalmol*. 2010;4:829–836.
129. Reznicek L, Stumpf C, Seidensticker F, Kampik A, Neubauer AS, Kernt M. Role of wide-field autofluorescence imaging and scanning laser ophthalmoscopy in differentiation of choroidal pigmented lesions. *Int J Ophthalmol*. 2014;7(4):697–703.
130. Miller KV, Eller AW. Sclerochoroidal calcifications: wide-field imaging. *Semin Ophthalmol*. 2009;24(1):5–8.
131. Heimann H, Jmor F, Damato B. Imaging of retinal and choroidal vascular tumours. *Eye (Lond)*. 2013;27(2):208–216.
132. Shields CL, Shields JA, Kiratli H, De Potter P, Cater JR. Risk factors for growth and metastasis of small choroidal melanocytic lesions. *Ophthalmology*. 1995;102(9):1351–1361.
133. Gordon-Shaag A, Barnard S, Millodot M, et al. Prevalence of choroidal naevi using scanning laser ophthalmoscope. *Ophthalmic Physiol Opt*. 2014;34(1):94–101.

134. Groenewald C, Konstantinidis L, Damato B. Effects of radiotherapy on uveal melanomas and adjacent tissues. *Eye (Lond)*. 2013;27(2):163–171.
135. Reichstein D. Current treatments and preventive strategies for radiation retinopathy. *Curr Opin Ophthalmol*. 2015;26(3):157–166.
136. Seregard S, Pelayes DE, Singh AD. Radiation therapy: posterior segment complications. *Dev Ophthalmol*. 2013;52:114–123.
137. McCannel TA, McCannel CA. Iodine 125 brachytherapy with vitrectomy and silicone oil in the treatment of uveal melanoma: 1-to-1 matched case-control series. *Int J Radiat Oncol Biol Phys*. 2014;89(2):347–352.
138. Pang CE, Shah VP, Sarraf D, Freund KB. Ultra-widefield imaging with autofluorescence and indocyanine green angiography in central serous chorioretinopathy. *Am J Ophthalmol*. 2014;158(2):362–371.e2.
139. Nam KT, Yun CM, Kim JT, et al. Central serous chorioretinopathy fundus autofluorescence comparison with two different confocal scanning laser ophthalmoscopes. *Graefes Arch Clin Exp Ophthalmol*. 2015;253(12):2121–2127.
140. Goldman DR, Freund KB, McCannel CA, Sarraf D. Peripheral polypoidal choroidal vasculopathy as a cause of peripheral exudative hemorrhagic chorioretinopathy: a report of 10 eyes. *Retina*. 2013;33(1):48–55.
141. Tsui I, Jain A, Shah S, Schwartz SD, McCannel TA. Ultra widefield imaging of peripheral exudative hemorrhagic chorioretinopathy. *Semin Ophthalmol*. 2009;24(1):25–28.
142. Csutak A, Lengyel I, Jonasson F, et al. Agreement between image grading of conventional (45 degrees) and ultra wide-angle (200 degrees) digital images in the macula in the Reykjavik eye study. *Eye (Lond)*. 2010;24(10):1568–1575.
143. Heussen FM, Tan CS, Sadda SR. Prevalence of peripheral abnormalities on ultra-widefield greenlight (532 nm) autofluorescence imaging at a tertiary care center. *Invest Ophthalmol Vis Sci*. 2012;53(10):6526–6531.
144. Reznicek L, Wasfy T, Stumpf C, et al. Peripheral fundus

autofluorescence is increased in age-related macular degeneration. *Invest Ophthalmol Vis Sci*. 2012;53(4):2193–2198.
145. Tan CS, Heussen F, Sadda SR. Peripheral autofluorescence and clinical findings in neovascular and non-neovascular age-related macular degeneration. *Ophthalmology*. 2013;120(6):1271–1277.
146. Lengyel I, Csutak A, Florea D, et al. A Population-based ultra-widefield digital image grading study for age-related macular degeneration-like lesions at the peripheral retina. *Ophthalmology*. 2015;122(7):1340–1347.
147. Dunphy RW, Wentzolf JN, Subramanian M, Conlin PR, Pasquale LR. Structural features anterior to the retina represented in Panoramic Scanning Laser fundus images. *Ophthalmic Surg Lasers Imaging*. 2008;39(2):160–163.
148. Chou B. Limitations of the Panoramic 200 Optomap. *Optom Vis Sci*. 2003;80(10):671–672.

6

Intraoperative Optical Coherence Tomography Imaging

Justis P. Ehlers, Cynthia A. Toth

Background and Historical

Prospective

The development of pars plana vitreoretinal surgery in the 1970s required a sea change in surgical tools, shifting from operating with loupes, which had been sufficient for open-sky techniques, to the use of an operating microscope as a stable platform to view the vitreous and retina.[1] In the early years of vitreoretinal surgery, the development of novel illumination methods, lens systems, and positioning techniques allowed surgeons to view the target tissues and determine achievement of surgical endpoints. The retinal surgeon in the 21st century has continued to use this conventional optical microscope system to view the illuminated surgical site.

Over the past two decades, optical coherence tomography (OCT) emerged from a bench-top research instrument to a disruptive diagnostic technology, which provided novel information useful for the management of a vast number of vitreoretinal disorders.[2–5] Accompanying this transition in technology was the emergence of new pharmacologic therapeutics that changed our treatment paradigms and management approach to various retinal conditions.[6–8] OCT provided the detailed, morphologic insight into the disease process and disease state that allowed clinicians to make critical judgments on diagnosis, management, and prognosis. During that time, OCT emerged as one of the most commonly ordered diagnostic tests in medicine.

Although the interpretation of OCT images transformed our clinical assessment of the microanatomy before and after surgery in diseases such as macular hole, vitreomacular traction, epiretinal membrane, myopic schisis, and retinal detachment, the application of this technology to real-time surgical management lagged behind. Numerous barriers existed, hindering the adoption of intraoperative OCT. Integrative solutions, high-speed imaging, OCT-compatible surgical instrumentation, novel software analysis systems, and optimal surgeon feedback systems were all lacking. This chapter will review the current state-of-the-art of intraoperative OCT, a technology that continues to evolve at a rapid rate.

OCT in the Operating Room: Integrative Advances

The initial transition from imaging in the clinic to imaging in the operating room was based on modifications to available tabletop OCT systems. In an early attempt to utilize perioperative OCT imaging, infants with retinopathy of prematurity were positioned on their side while under general anesthesia, for tabletop time domain OCT system (with the headrest removed) imaging prior to vitreoretinal surgery.[9] Another approach modified the clinical system to reposition the tabletop component which then allowed for imaging of supine patients. This was used to examine infants with retinopathy of prematurity outside of the surgical suite.[10] However, this approach had significant limitations for portability and practical use in a sterile operating room field. One of the first major breakthroughs in intraoperative imaging technology was the development of a compact, light, handheld OCT scan head and the introduction of this technology to the surgical suite (Fig. 6.1).[11–14] This smaller scan head no longer rested on a tabletop over the OCT engine and computer system, creating significantly improved flexibility for intraoperative imaging of the supine patient. The two most common systems for intraoperative use featuring a portable scan head are the handheld Bioptigen SDOIS/Envisu portable system (Bioptigen, Research Triangle Park, NC) and the stand-mounted Optovue IVue (Optovue, Fremont, CA) system.[12,13,15–22]

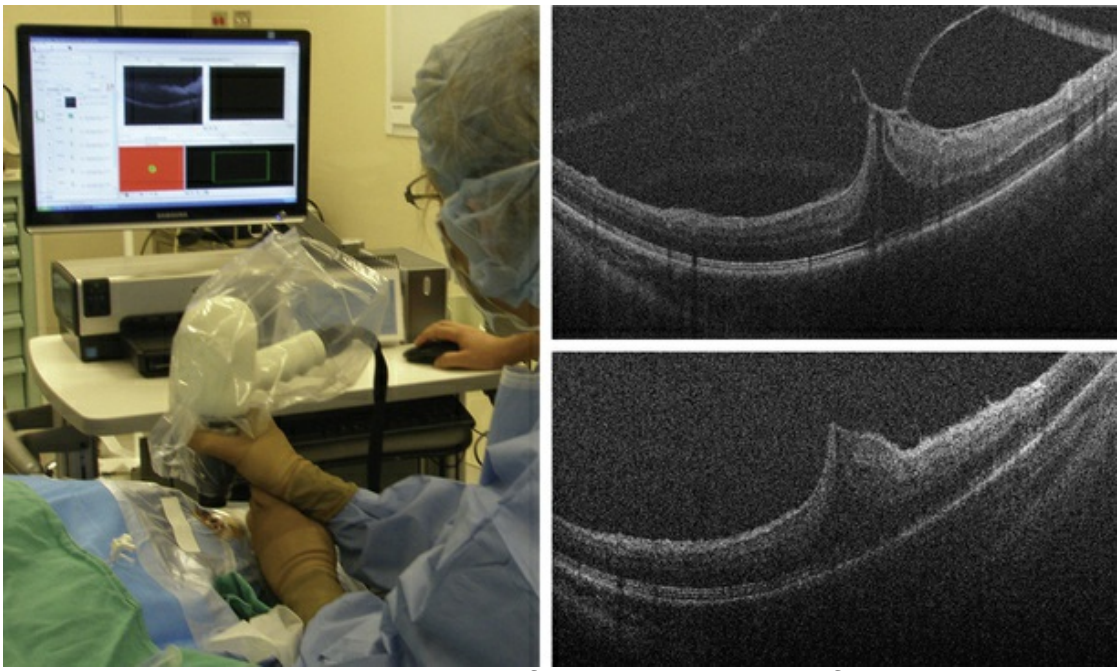

FIG. 6.1 Research use of an early version of the Bioptigen handheld portable spectral domain optical coherence tomography system in surgery. (Left) At a pause in surgery, the surgeon captures and views the macular B-scan. (Right upper) A scan prior to release of vitreomacular traction and removal of epiretinal membrane. (Right lower) Imaging in the same region after completion of the surgical maneuvers. The epiretinal membrane is absent and inner retinal surface irregularity is present, while on the left side of the scan the interdigitation zone (presumed outer border of photoreceptors) is now separated from the retinal pigment epithelium by a thin hyporeflective band. (See Video 6.1.)

Initial approaches to acquiring images with these systems utilized either handheld imaging or external mounting systems. Handheld imaging has both advantages and limitations. There is tremendous flexibility of scanhead orientation and the ability to dynamically alter the position of the scan during acquisition (Fig. 6.1, Video 6.1 online). However, there may be significant challenges with surgeon learning curves, reproducibility of scan location, and optimal targeting to the area of interest. To address some of the challenges of handheld imaging, microscope-mounting systems have been developed to tether the portable scanhead to the microscope (Fig. 6.2, Video 6.1 online).[15–18,22,23] This allows the user

to control lateral and vertical translation of the system utilizing the joystick and focus control of the microscope foot pedal. Microscope-mounting portable systems provides increased stability and precision, while potentially improving learning curves for users and increasing scan efficiency. The microscope mount maintains the OCT scan head on the side of the microscope and the system remains nearby throughout the case, while the handheld system offers the convenience of being able to introduce or remove the system from the surgical area as needed. An alternate OCT system, IVue, utilizes a supporting armature on a stand to provide similar stability and precision for a larger scan head not connected to the operating microscope.

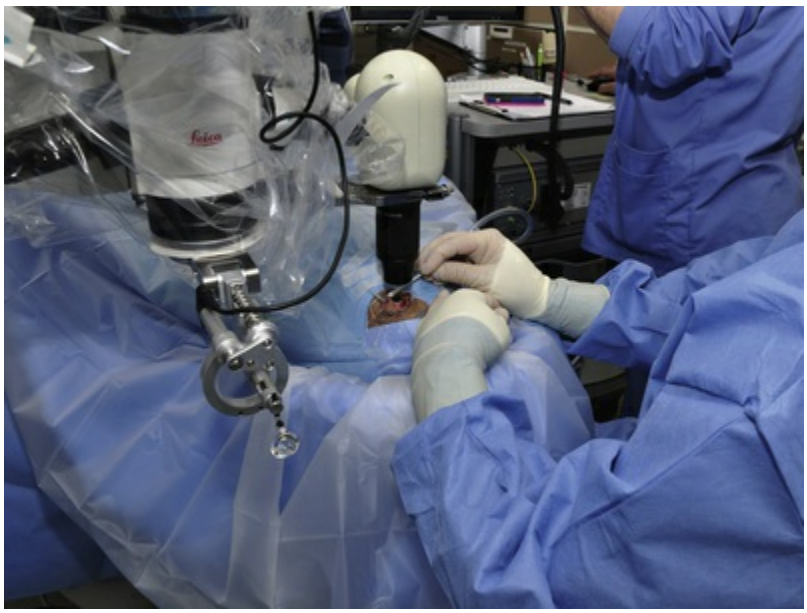

FIG. 6.2 Microscope-mounted portable spectral domain optical coherence tomography system. Scan head is tethered to a microscope that allows foot-pedal control of X–Y–Z translation utilizing a combination of the joystick and focus controls. (See Video 6.1.)

Though a major step forward, these systems still lacked true microscope-integration, and this results in multiple limitations, including the need to halt the surgical procedure to perform imaging, lack of "real-time" video-rate imaging, the need for additional space in the operating room to position the system, and limited opportunities for integrated surgeon feedback. These

systems did, however, provide the surgeon with rapid feedback on the impact of surgical maneuvers on the tissues, often with excellent visualization of tissue details and subclinical alterations.[13,15,19,21,22] However, given the need to stop surgery to perform the scan, none of these systems allow for the actual OCT-based visualization of tissue-instrument interaction.

To address many of these limitations, researchers and engineers began to develop microscope-integrated OCT systems. Early iterations on these systems included novel OCT scan heads that were adapted to the various microscopes and then utilized a commercial OCT engine. One example was the research adaptation of the Bioptigen portable spectral domain optical coherence tomography (SD-OCT) system into a novel scanner head that was integrated into a Leica operating microscope (Fig. 6.3).[24,25] Another example was the adaptation of the Zeiss SD-OCT system into a Zeiss surgical microscope (Carl Zeiss Meditec, Oberkochen, Germany)(Fig. 6.3).[26] The development of these systems represented a major advance in intraoperative OCT and for the first time allowed true "real-time" intraoperative OCT with visualization of surgical motion.[26–30] Utilizing a combined optical pathway, in each case, the OCT would be able to be parfocal with the surgeon view.[24] System enhancements to these early generation platforms allowed for targeting and tracking the OCT scan beam, tunable focus, optimized visualization of surgical motion, and heads-up display of the OCT data stream, all of which improved the interface with the surgeon (Fig. 6.3).[27,30–32] Building on this momentum, commercial integrated systems are now available worldwide, including from Haag–Streit (Haag–Streit, Koeniz, Switzerland) Leica, and Zeiss.[33–36] Leica, which recently acquired Bioptigen, has developed the EnFocus system which is a microscope-integrated OCT platform. Microscope-integrated OCT system that can be introduced as an add-on for a standard surgical microscope.[36] The Haag–Streit system, the *i*OCT, is powered by an OPMedT (OPMedT, Lubeck, Germany) OCT engine and utilizes a microscope side-port for integration.[35] The Rescan 700 is built on the Lumera 700 microscope platform allowing the form factor of the microscope head to remain undisturbed (Fig. 6.3).[33,34]

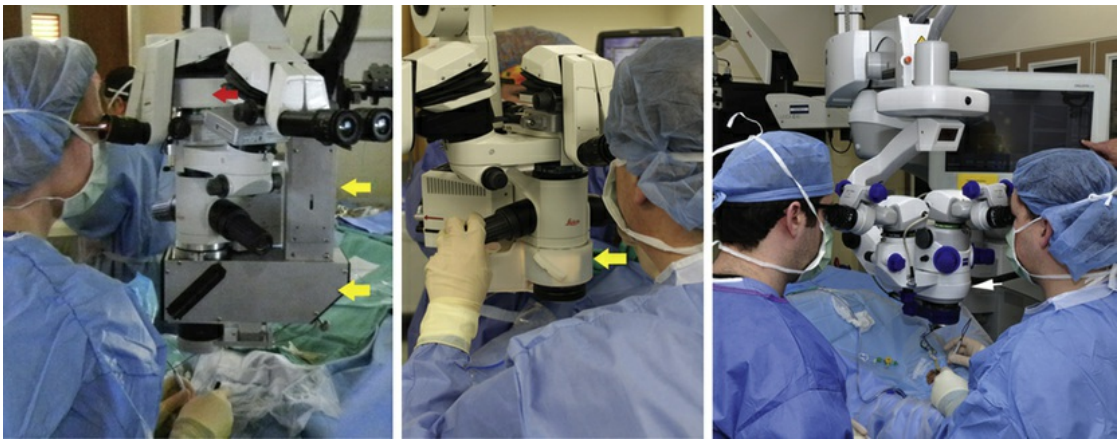

FIG. 6.3 Microscope-integrated optical coherence tomography systems. (Left) The research prototype system (*yellow arrows*) developed at Duke University by Dr. Joseph Izatt and Dr. Yuankai Tao and used for either spectral domain (SD) or swept source (SS) OCT imaging with heads-up three-dimensional stereo display (*red arrow*) to both oculars of the surgeon. (Center) A more recent microscope-integrated research scanner (*yellow arrow*) developed at the Cleveland Clinic for use with SD-OCT or SS-OCT. (Right) The Zeiss Rescan system with integrated SD-OCT scanner (*white arrow*) and heads-up display projected into one ocular of the surgeon.

Research and active development is underway for the next generation of intraoperative OCT systems. Key areas of need include enhanced image quality, faster acquisition speed, automated tracking, and advanced software analysis. Emerging OCT technology may provide unique opportunities for intrasurgical solutions.[37,38] Spectrometers that provide enhanced range may increase the flexibility of visualization of pathology.[36] Swept source OCT acquisition represents a potential opportunity to further enhance the capabilities of intraoperative OCT (Fig. 6.4, Video 6.2 online).[39] Swept source microscope-integrated intraoperative OCT systems have demonstrated the ability to not only capture instrument–tissue interaction, but to also capture the three-dimensional motion and interaction that occurs during surgery (Fig. 6.5, Video 6.3 online).[39] The tremendous increased speed provides the opportunity to perform real-time volumetric scanning at near video rates.[39] High-speed image processing methods have been integral to the intraoperative visualization of

instrument-tissue interaction (Figs. 6.4 and 6.5) and will continue to evolve.[40]

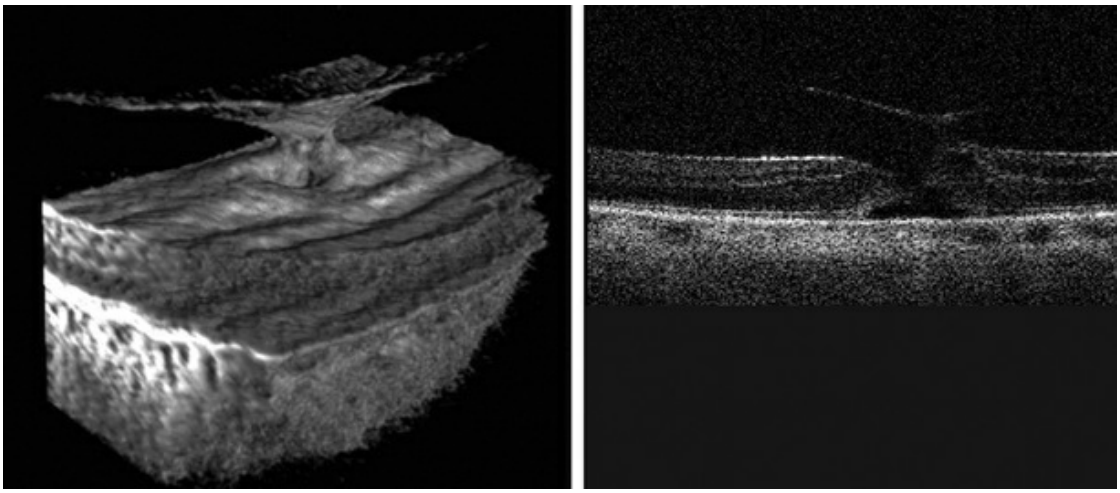

FIG. 6.4 Three-dimensional view which is possible in real time because of the high speed of the research microscope integrated swept source optical coherence tomography system. (See Video 6.2.)

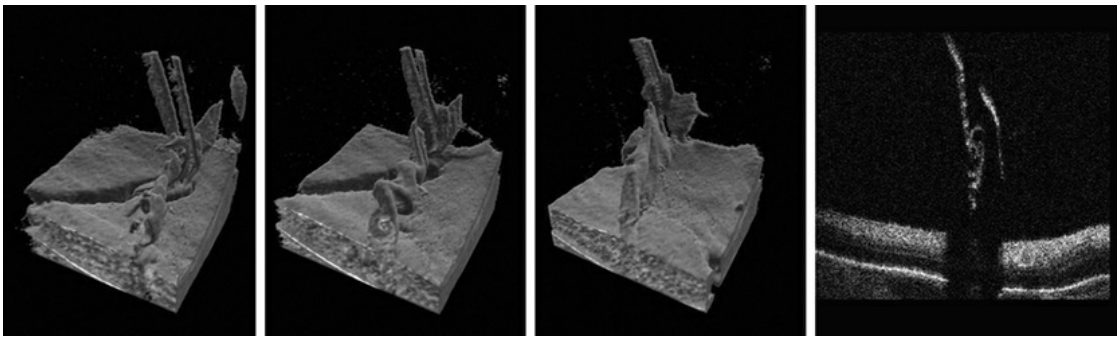

FIG. 6.5 Three frames of microscope integrated swept source optical coherence tomography three-dimensional images taken from the streaming video visible to the surgeon in a stereo heads-up display, and a B-scan across the middle frame of the series. The surgeon is peeling the scrolled internal limiting membrane from right to left and the tips of the 25-gauge forceps are visible grasping the center of the scrolled edge and pulling to the left. Note the shadow in the retina in the first two frames and on the B-scan from the metallic forceps. (See Video 6.3.)

Surgeon Feedback Platform Enhancements

Bringing OCT technology to the operating room requires unique features to maximize integration, including automated aiming, OCT-compatible instrumentation, heads-up display systems, and software analysis. Current systems utilize surgeon or assistant-directed control of the aiming beam of the OCT to the area of interest.[30,31,33,34,36] Control systems include mouse-based, manual control screen operation, and foot-pedal control. Although these control capabilities are significant improvements over external systems, they are still limited by the need for surgeon input and lack of automation. Integrated automated aiming or region-of-interest tracking could enhance visualization of surgical maneuvers and improving imaging workflow.[38] There are numerous potential approaches to improved aiming to the area of interest. One option is to augment the surgical instrument to allow it to provide feedback regarding location or position to the OCT scanner.[38] An additional option is to utilize an image processing approach to analyze dynamic changes to the image that result from surgical motion and direct the OCT to that area of interest.[41,42] An additional option is to place the OCT scanner within the instrument so that the OCT is always directed to the tissue immediately proximal to the instrument being used.[43]

The information to the surgeon related to the OCT can be presented in numerous ways, including as an external display screen or ocular-injected heads-up display.[31,33,34,39,44] Multiple research systems and commercial systems have featured heads-up display systems (Fig. 6.6).[31,33,34,39] Optimizing the surgeon's heads-up visualization is an area of active development and a variety of novel approaches are being explored.[45] Providing surgeon-critical information in an optimal format is vital to maximizing the effectiveness of these system. Customized visualization with ocular selection, data type display, and data formatting will all be important to maximizing surgeon comfort.

FIG. 6.6 (Left) Heads-up display of the horizontal and vertical spectral domain optical coherence tomography (OCT) B-scans viewed through the right eyepiece in the Zeiss Rescan microscope (image courtesy Zeiss). The location of scanning is changeable and the display can be turned on and off during surgery. (Right) In a model eye in the research lab, the surgeon turns off the fiberoptic light and peels membranes using either (a) real-time stereoscopic three-dimensional (3D) OCT volumes projected into the oculars via the heads-up display (*red arrow*) or (b) as shown here, displayed on a 3D video screen and viewed by the surgeon wearing 3D glasses while she operates. (See Videos 6.3 and 6.4.)

Current generation metallic surgical instruments and other surgical materials result in absolute shadowing on OCT imaging and limit visualization of the tissue–instrument interaction (Figs. 6.5 and 6.7, Videos 6.3 and 6.4 online).[24] To maximize real-time visualization of surgical maneuvers, compensatory techniques will need to be introduced to minimize the disruption to visualization caused by shadowing. One potential approach relies on advances in image processing. Utilizing a variety of methods, such as spatial compounding, the impact of shadowing can be minimized and surgical visualization can be enhanced.[27] An alternate approach is to change the material composition of the surgical instruments.[31] Identifying materials that provide both the optical properties needed for OCT visualization and material properties needed for surgical precision and reliability is critical for the success of this approach. Prototypes of OCT-compatible instrumentation have been developed and appear to enhance visualization of both the surgical instrument and the tissue–instrument interaction.[31,44]

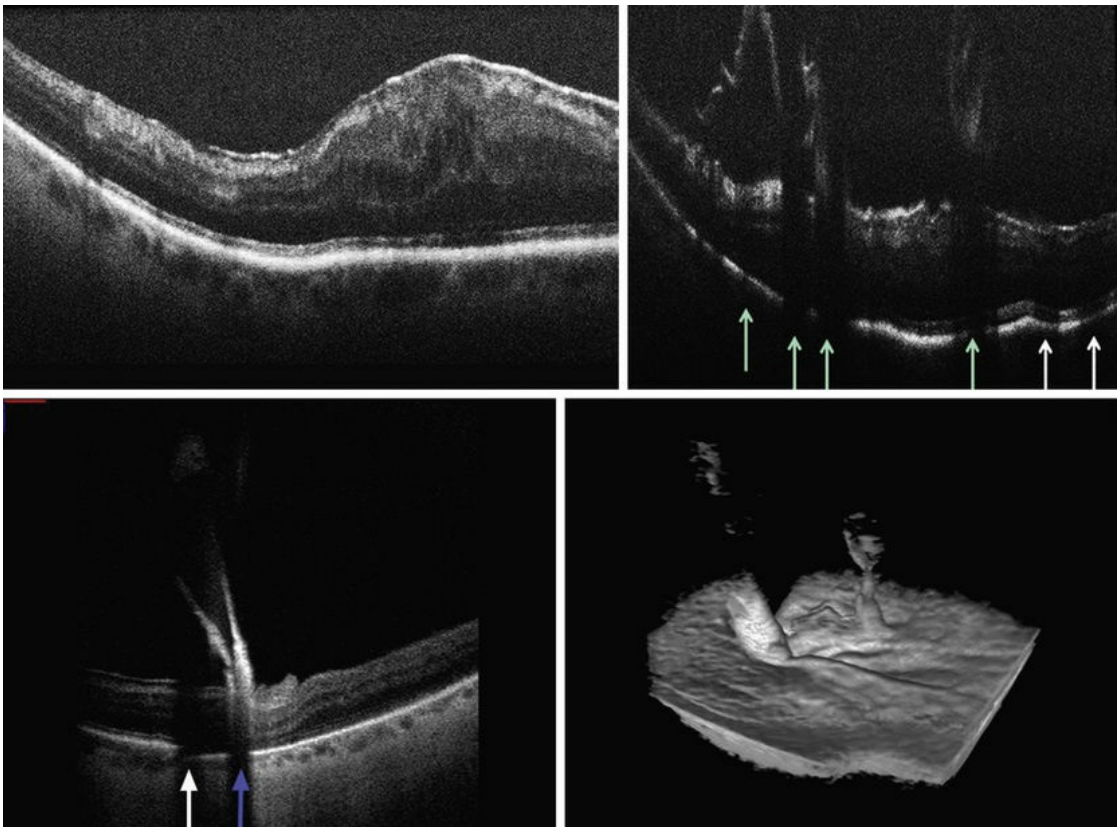

FIG. 6.7 Research microscope integrated spectral domain optical coherence tomography imaging (upper frames) of an epiretinal membrane before (left) and during (right) removal of an epiretinal membrane and internal limiting membrane stained with indocyanine green. During surgery, there are shadows from both the forceps (*white arrows*) and scrolled indocyanine green-stained membrane (*green arrows*). In the research microscope integrated swept source optical coherence tomography (SS-OCT) B-scan (lower left) from the three-dimensional (3D) real-time volume (lower right), the reflective diamond-dusted instrument tip casts a shadow (*blue arrow*), as does the suspended debris (*white arrow*), but not the silicone tube between these. The diamond-dusted tip similarly shows up well dragging the membrane across the retinal surface, however the silicone behind the tip is nearly invisible on the SS-OCT 3D volume. (See Videos 6.3 and 6.4.)

Lastly, alterations to the tissue conformation change rapidly and potentially dramatically during surgery (Figs. 6.5 and 6.7).[13,17,18,22,46,47] New software packages will be needed to help facilitate surgeon

decision-making and provide immediate assessment of clinically relevant alterations in tissue architecture. Automated assessment of changes in inner and outer retinal features, macular hole geometry, and fluid interfaces may all have potential impact on anatomic and visual outcomes following surgery.[18,47–50] Optimally integrating this information into new systems will be a key element in the next evolution of OCT-guided surgery.

Surgical Findings With Intraoperative OCT in Vitreoretinal Conditions

Membrane Peeling in Vitreoretinal Interface Disorders

Disorders of the vitreoretinal interface (e.g., macular hole [MH], epiretinal membrane [ERM], and vitreomacular traction [VMT]) may be one of the optimal applications of intraoperative OCT. Numerous studies have described the ability of intraoperative OCT to visualize residual membranes and potentially alter surgical decision-making.[13,15,17,18,22,33,47,51] Visualizing tissue alterations with OCT is a common application, and it is clear that surgical manipulations impact tissue conformation and relationships.[17,18,47,52]

Intraoperative OCT may be particularly helpful during surgical procedures for membrane peeling. Multiple subclinical alterations have been reported with intraoperative OCT following membrane peeling, including residual membranes, perturbations to the inner retinal architecture, and full-thickness retinal elevations (Fig. 6.8).[11,13,17,18,22,26,47,52] Intraoperative OCT appears to impact surgical decision-making in membrane peeling procedures in 15–30% of cases, including the identification of membranes that need additional peeling or alternatively confirming successful attainment of surgical objectives prior to surgeon realization through conventional visualization.[13,15,33] Additional changes have been described at the macro (e.g., full-thickness retinal elevation) and micro (e.g., diffuse subtle alterations in retinal layer thickness) level of the retinal architecture.[52] Common microarchitectural alterations after membrane peeling include the expansion of the distance

between the ellipsoid zone and the retinal pigment epithelium, and alterations to the inner retinal surface (Fig. 6.1, lower right).[15,22,47,52] In one report, for example, inner retinal projections (e.g., connecting strands) to the internal limiting membrane (ILM) were visible on the inner retinal surface immediately following ILM peeling, and subsequently resolved postoperatively without significant nerve fiber layer alterations.[47] The macroarchitectural alterations appear to be frequently related to direct tissue–instrument interaction.[52] One report identified with video/intraoperative OCT correlation that the alterations appeared to be more common with forceps application compared with the diamond-dusted membrane scraper.[52] The overall clinical significance of these retinal alterations remains unknown. Intraoperative OCT may also impact our utilization of vital dyes and stains. Indocyanine green and triamcinolone and other steroid suspensions have significant impact on intraoperative OCT-based visualization of tissues (Fig. 6.7).[53–55] Additionally, OCT-guided membrane peeling has the potential to reduce the need for utilization of these stains, which may reduce surgical time and minimize potential pharmacotoxicity to the retina.[56]

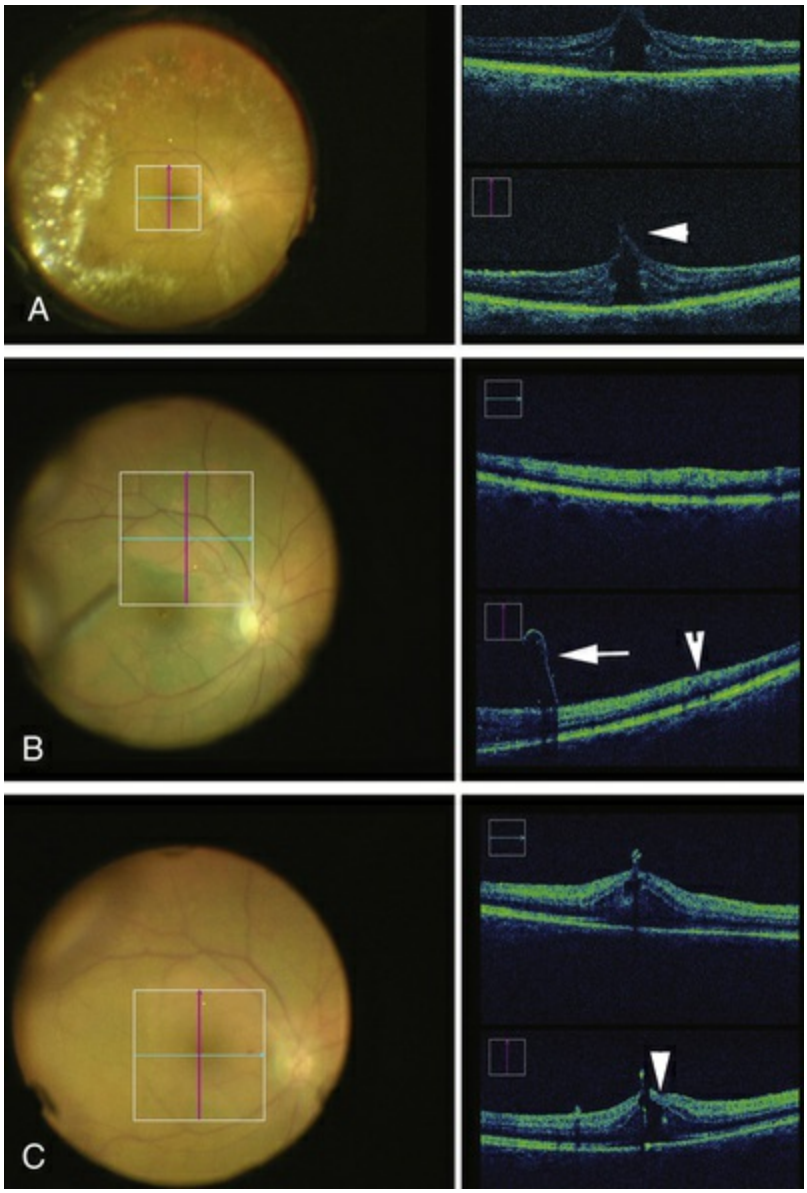

FIG. 6.8 Intraoperative optical coherence tomography (OCT) during macular hole repair. (A) Preincision scan reveals full-thickness macular hole with associated vitreomacular traction (*arrowhead*). (B) Partial peel scan revealing residual membrane (*arrow*) and area of retina where peel has been completed (*arrowhead*). (C) Following completed peel, OCT identifies changes in macular hole architecture. (See Video 6.5.)

In MH cases, peeling of the ILM results in variable changes in MH configuration (Fig. 6.8, Video 6.5 online).[13,18,19,22] These configuration changes include alterations in MH volume, base area, and height. Focal areas of inner retinal elevation or full-thickness retinal elevation have also been described following surgical

manipulation. Similar to ERM peeling, more diffuse changes in the outer retina have also been identified.[15,18,22,46,52] In particular, an increase in the ellipsoid zone to retinal pigment epithelium distance appears to occur following ILM peeling. These changes have been associated with the rate of visual recovery following MH surgery and architectural normalization rate.[46]

Vitreomacular traction syndrome is an additional condition that may benefit from image-guided feedback with intraoperative OCT (Figs. 6.1 and 6.4).[13,15,17,33] Intraoperative OCT can identify subclinical full-thickness macular holes or unroofed cysts following hyaloid elevation. These findings can directly impact surgical decision-making, such as choice of gas tamponade or peeling of the ILM.[15,17,33]

Retinal Detachment and Other Vitreoretinal Conditions

Although membrane peeling procedures are an intuitive use for intraoperative OCT, the potential benefit of intraoperative OCT feedback for retinal detachment repair may not be immediately apparent. However, multiple reports have identified potentially important novel OCT-identified features evident during the course of retinal detachment repair.[15,23,33] In fact, the foveal microarchitecture visualized under perfluorocarbon liquid tamponade has been linked to visual acuity outcomes.[23] Additionally, nearly all eyes under perfluorocarbon liquid have some degree of subretinal fluid.[15,23,33] In other reports, intraoperative OCT has been used to confirm the absence of fluid in peripheral areas of white without pressure and to identify optimal locations for drainage of subretinal fluid.[33]

Other conditions that have been impacted by intraoperative OCT include optic pit-associated maculopathy and proliferative diabetic retinopathy.[33,57,58] In one publication, intraoperative OCT was able to confirm collapse of the nasal schisis in the macula following aspiration over the area of the pit. This potentially confirmed a direct connection between the vitreous cavity and the area of schisis.[58] In complex vitreoretinal pathology, such as proliferative diabetic retinopathy, intraoperative OCT may facilitate

identification of tractional membranes, candidate dissection planes, and areas of retinal detachment. This can provide rapid feedback to the surgeon and help inform appropriate surgical maneuvers.[33]

The delivery of subretinal therapeutics, such as tissue plasminogen activator, may also be facilitated by intraoperative OCT technology. Visualization of subretinal injections and retinal perturbations following injection has been successfully documented with intraoperative OCT.[16] The objective assessment of volumetric delivery may prove critical to an emerging field of novel therapeutics, such as with gene therapy and stem cells.

Additional immediate surgeon feedback and guidance has been described during the removal of subretinal perfluorocarbon liquid.[59] In these challenging cases, optimally and completely removing the subretinal perfluorocarbon liquid can be quite difficult. Intraoperative OCT provides immediate feedback to the surgeon regarding the successful completion of these objectives.[59]

Pediatric Vitreoretinal Surgery

Because infants and children may not readily cooperate for OCT imaging in the clinical setting, OCT imaging may be useful in the preoperative setting during examination under anesthesia. OCT imaging under anesthesia has revealed the extent of retinal detachment and retinoschisis in retinopathy of prematurity, macular holes or pseudoholes in the setting of shaken baby, and the configuration of epiretinal membranes and the underlying retina in a wide range of pediatric vitreoretinal diseases (Figs. 6.1 and 6.9).[11,12,51,60] In other vitreoretinal conditions such as childhood tumors, imaging under anesthesia has been useful in monitoring response to treatment.[61] As with adult surgery, and perhaps more so since postoperative evaluation may again be hampered by an inability to cooperate, intraoperative imaging after surgical maneuvers may be especially useful in determining the anatomical results (Figs. 6.1 and 6.9).[11,51] As the technology evolves and is applied in pediatric vitreoretinal surgeries, intraoperative OCT imaging is likely to inform the pediatric surgeon and be applicable to a wide range of pediatric retinal diseases.

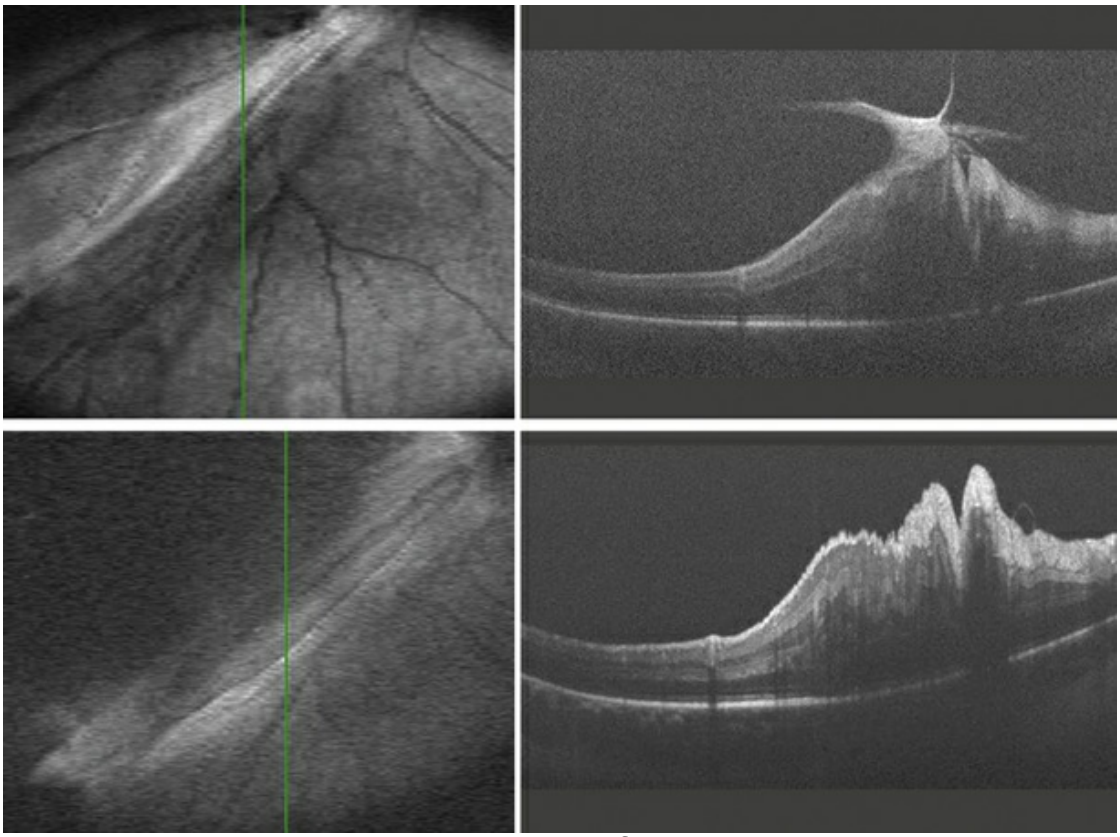

FIG. 6.9 In a young child with familial exudative vitreoretinopathy and tractional membranes across the macula, the preoperative and postoperative assessment in clinic may be limited. Intraoperative handheld spectral domain optical coherence tomography imaging before surgery (upper frames) demonstrates the deep retinal folds and thickness of preretinal membranes. After membrane removal (lower frames), a scroll of inner limiting membrane is visible above the folded inner retinal surface, the pronounced distortion and thickening of retinal layers is evident, and the presence of the ellipsoid zone across the area of peel points to an absence of subretinal fluid at this location.

Conclusion

Though still an emerging field, research in intraoperative OCT has made tremendous progress over the last several years and is likely to enable new procedures not achievable with conventional retinal visualization. Numerous clinical studies and reports emphasize the

potential role for intraoperative OCT in image-guided surgery as well as the potential impact on patient outcomes and surgical decision-making. Technologic advances in integrated OCT systems, surgical instruments, and software have made these initial steps possible. However, hurdles remain in maximizing these integrative approaches, enhancing surgeon feedback systems, and improving our ability to seamlessly incorporate this technology into our surgical procedures. As capabilities improve, establishing specific parameters or procedures where intraoperative OCT adds value and enhances outcomes will also be critical to facilitate its widespread adoption.

References

1. Parel JM, Machemer R, Aumayr W. A new concept for vitreous surgery. 5. An automated operating microscope. *Am J Ophthalmol*. 1974;77(2):161–168.
2. Hee MR, Izatt JA, Swanson EA, et al. Optical coherence tomography of the human retina. *Arch Ophthalmol*. 1995;113(3):325–332.
3. Swanson EA, Izatt JA, Hee MR, et al. In vivo retinal imaging by optical coherence tomography. *Opt Lett*. 1993;18(21):1864–1866.
4. Puliafito CA, Hee MR, Lin CP, et al. Imaging of macular diseases with optical coherence tomography. *Ophthalmology*. 1995;102(2):217–229.
5. Chen TC, Cense B, Pierce MC, et al. Spectral domain optical coherence tomography: ultra-high speed, ultra-high resolution ophthalmic imaging. *Arch Ophthalmol*. 2005;123(12):1715–1720.
6. Brown DM, Kaiser PK, Michels M, et al. Ranibizumab versus verteporfin for neovascular age-related macular degeneration. *N Engl J Med*. 2006;355(14):1432–1444.
7. Heier JS, Brown DM, Chong V, et al. Intravitreal aflibercept (VEGF trap-eye) in wet age-related macular degeneration. *Ophthalmology*. 2012;119(12):2537–2548.
8. Martin DF, Maguire MG, Ying GS, et al. Ranibizumab and bevacizumab for neovascular age-related macular

degeneration. *N Engl J Med*. 2011;364(20):1897–1908.
9. Joshi MM, Trese MT Jr. CA. Optical coherence tomography findings in stage 4A retinopathy of prematurity: a theory for visual variability. *Ophthalmology*. 2006;113(4):657–660.
10. Vinekar A, Sivakumar M, Shetty R, et al. A novel technique using spectral-domain optical coherence tomography (Spectralis, SD-OCT+HRA) to image supine non-anesthetized infants: utility demonstrated in aggressive posterior retinopathy of prematurity. *Eye (Lond)*. 2010;24(2):379–382.
11. Scott AW, Farsiu S, Enyedi LB, et al. Imaging the infant retina with a hand-held spectral-domain optical coherence tomography device. *Am J Ophthalmol*. 2009;147(2):364–373.e2.
12. Chavala SH, Farsiu S, Maldonado R, et al. Insights into advanced retinopathy of prematurity using handheld spectral domain optical coherence tomography imaging. *Ophthalmology*. 2009;116(12):2448–2456.
13. Dayani PN, Maldonado R, Farsiu S, Toth CA. Intraoperative use of handheld spectral domain optical coherence tomography imaging in macular surgery. *Retina*. 2009;29(10):1457–1468.
14. Radhakrishnan S, Rollins AM, Roth JE, et al. Real-time optical coherence tomography of the anterior segment at 1310 nm. *Arch Ophthalmol*. 2001;119(8):1179–1185.
15. Ehlers JP, Dupps WJ, Kaiser PK, et al. The Prospective Intraoperative and Perioperative Ophthalmic ImagiNg With Optical CoherEncE TomogRaphy (PIONEER) Study: 2-year results. *Am J Ophthalmol*. 2014;158(5):999–1007.e1.
16. Ehlers JP, Petkovsek DS, Yuan A, et al. Intrasurgical assessment of subretinal tPA injection for submacular hemorrhage in the PIONEER study utilizing intraoperative OCT. *Ophthalmic Surg Lasers Imaging Retina*. 2015;46(3):327–332.
17. Ehlers JP, Tam T, Kaiser PK, et al. Utility of intraoperative optical coherence tomography during vitrectomy surgery for vitreomacular traction syndrome. *Retina*. 2014;34(7):1341–1346.

18. Ehlers JP, Xu D, Kaiser PK, et al. Intrasurgical dynamics of macular hole surgery: an assessment of surgery-induced ultrastructural alterations with intraoperative optical coherence tomography. *Retina*. 2014;34(2):213–221.
19. Hayashi A, Yagou T, Nakamura T, et al. Intraoperative changes in idiopathic macular holes by spectral-domain optical coherence tomography. *Case Rep Ophthalmol*. 2011;2(2):149–154.
20. Lee LB, Srivastava SK. Intraoperative spectral-domain optical coherence tomography during complex retinal detachment repair. *Ophthalmic Surg Lasers Imaging*. 2011;42 [Online:e71–4].
21. Pichi F, Alkabes M, Nucci P, et al. Intraoperative SD-OCT in macular surgery. *Ophthalmic Surg Lasers Imaging*. 2012;43(6 Suppl.):S54–60.
22. Ray R, Baranano DE, Fortun JA, et al. Intraoperative microscope-mounted spectral domain optical coherence tomography for evaluation of retinal anatomy during macular surgery. *Ophthalmology*. 2011;118(11):2212–2217.
23. Ehlers JP, Ohr MP, Kaiser PK, et al. Novel microarchitectural dynamics in rhegmatogenous retinal detachments identified with intraoperative optical coherence tomography. *Retina*. 2013;33(7):1428–1434.
24. Ehlers JP, Tao YK, Farsiu S, et al. Integration of a spectral domain optical coherence tomography system into a surgical microscope for intraoperative imaging. *Invest Ophthalmol Vis Sci*. 2011;52(6):3153–3159.
25. Tao YK, Ehlers JP, Toth CA, et al. Intraoperative spectral domain optical coherence tomography for vitreoretinal surgery. *Opt Lett*. 2010;35(20):3315–3317.
26. Binder S, Falkner-Radler CI, Hauger C, et al. Feasibility of intrasurgical spectral-domain optical coherence tomography. *Retina*. 2011;31(7):1332–1336.
27. Ehlers JP, Tao YK, Farsiu S, et al. Visualization of real-time intraoperative maneuvers with a microscope-mounted spectral domain optical coherence tomography system. *Retina*. 2013;33(1):232–236.
28. Hahn P, Migacz J, O'Connell R, et al. Unprocessed real-time

imaging of vitreoretinal surgical maneuvers using a microscope-integrated spectral-domain optical coherence tomography system. *Graefes Arch Clin Exp Ophthalmol*. 2013;251(1):213–220.
29. Hahn P, Migacz J, O'Donnell R, et al. Preclinical evaluation and intraoperative human retinal imaging with a high-resolution microscope-integrated spectral domain optical coherence tomography device. *Retina*. 2013;33(7):1328–1337.
30. Hahn P, Carrasco-Zevallos O, Cunefare D, et al. Intrasurgical human retinal imaging with manual instrument tracking using a microscope-integrated spectral-domain optical coherence tomography device. *Transl Vis Sci Technol*. 2015;4(4):1.
31. Ehlers JP, Srivastava SK, Feiler D, et al. Integrative advances for OCT-guided ophthalmic surgery and intraoperative OCT: microscope integration, surgical instrumentation, and heads-up display surgeon feedback. *PLoS ONE*. 2014;9(8):e105224.
32. Tao YK, Srivastava SK, Ehlers JP. Microscope-integrated intraoperative OCT with electrically tunable focus and heads-up display for imaging of ophthalmic surgical maneuvers. *Biomed Opt Express*. 2014;5(6):1877–1885.
33. Ehlers JP, Goshe J, Dupps WJ, et al. Determination of feasibility and utility of microscope-integrated optical coherence tomography during ophthalmic surgery: the DISCOVER study RESCAN results. *JAMA Ophthalmol*. 2015;133(10):1124–1132.
34. Ehlers JP, Kaiser PK, Srivastava SK. Intraoperative optical coherence tomography using the RESCAN 700: preliminary results from the DISCOVER study. *Br J Ophthalmol*. 2014;98(10):1329–1332.
35. Steven P, Le Blanc C, Velten K, et al. Optimizing Descemet membrane endothelial keratoplasty using intraoperative optical coherence tomography. *JAMA Ophthalmol*. 2013;131(9):1135–1142.
36. Ehlers JP, Kaiser PK, Singh RP, et al. *Feasibility and utility of microscope-integrated intraoperative oct for vitreoretinal surgery: the DISCOVER study 1-year results*. American Society of

Retina Specialists: Vienna, Austria; 2015.
37. Carrasco-Zevallos O, Nankivil D, Keller B, et al. Pupil tracking optical coherence tomography for precise control of pupil entry position. *Biomed Opt Express*. 2015;6(9):3405–3419.
38. El-Haddad MT, Tao YK. Automated stereo vision instrument tracking for intraoperative OCT guided anterior segment ophthalmic surgical maneuvers. *Biomed Opt Express*. 2015;6(8):3014–3031.
39. Toth CA, Izatt JA. *Surgically Integrated 4-dimensional, swept-source optical coherence tomography (SSOCT) with heads up display to guide vitreoretinal surgery*. American Society of Retina Specialists: Vienna, Austria; 2015.
40. Viehland C, Carrasco-Zevallos O, Keller B, et al. *Lighting, edge, and depth enhanced ray casting for real-time volumetric visualization of intraoperative ophthalmic OCT*. SPIE: San Francisco, CA; 2015.
41. Yang S, Balicki M, Wells TS, et al. Improvement of optical coherence tomography using active handheld micromanipulator in vitreoretinal surgery. *Conf Proc IEEE Engl Med Biol Sci*. 2013;5674–5677.
42. Song C, Gehlbach PL, Kang JU. Active tremor cancellation by a "smart" handheld vitreoretinal microsurgical tool using swept source optical coherence tomography. *Opt Express*. 2012;20(21):23414–23421.
43. Balicki M, Han JH, Iordachita I, et al. Single fiber optical coherence tomography microsurgical instruments for computer and robot-assisted retinal surgery. *Med Image Comput Comput Assist Interv*. 2009;12(Pt 1):108–115.
44. Ehlers JP, Tao YK, Srivastava SK. The value of intraoperative optical coherence tomography imaging in vitreoretinal surgery. *Curr Opin Ophthalmol*. 2014;25(3):221–227.
45. Shen L, Carrasco-Zevallos O, Keller B, et al. *Novel microscope-integrated stereoscopic display for intrasurgical optical coherence tomography*. SPIE: San Francisco, CA; 2015.
46. Ehlers JP, Itoh Y, Xu L, et al. Factors associated with persistent subfoveal fluid and complete macular hole closure in the PIONEER study. *Invest Ophthalmol Vis Sci*.

2014;56(2):1141–1146.
47. Nam DH, Desouza PJ, Hahn P, et al. Intraoperative spectral domain optical coherence tomography imaging after internal limiting membrane peeling in idiopathic epiretinal membrane with connecting strands. *Retina*. 2015;35(8):1622–1630.
48. Itoh Y, Vasanji A, Ehlers JP. Volumetric ellipsoid zone mapping for enhanced visualisation of outer retinal integrity with optical coherence tomography. *Br J Ophthalmol*. 2016;100(3):295–299.
49. Xu D, Dupps WJ, Srivastava S, et al. Automated volumetric analysis of interface fluid in descemet stripping automated endothelial keratoplasty utilizing intraoperative optical coherence tomography. *Invest Ophthalmol Vis Sci*. 2014;55(9):5610–5615.
50. Xu D, Yuan A, Kaiser PK, et al. A novel segmentation algorithm for volumetric analysis of macular hole boundaries identified with optical coherence tomography. *Invest Ophthalmol Vis Sci*. 2013;54(1):163–169.
51. Rothman AL, Folgar FA, Tong AY, et al. Spectral domain optical coherence tomography characterization of pediatric epiretinal membranes. *Retina*. 2014;34(7):1323–1334.
52. Ehlers JP, Han J, Petkovsek D, et al. Membrane peeling-induced retinal alterations on intraoperative OCT in vitreomacular interface disorders from the PIONEER Study. *Invest Ophthalmol Vis Sci*. 2015;56(12):7324–7330.
53. Ehlers JP, McNutt S, Dar S, et al. Visualisation of contrast-enhanced intraoperative optical coherence tomography with indocyanine green. *Br J Ophthalmol*. 2014;98(11):1588–1591.
54. Ehlers JP, McNutt SA, Kaiser PK, et al. Contrast-enhanced intraoperative optical coherence tomography. *Br J Ophthalmol*. 2013;97(11):1384–1386.
55. Ehlers JP, Gupta PK, Farsiu S, et al. Evaluation of contrast agents for enhanced visualization in optical coherence tomography. *Invest Ophthalmol Vis Sci*. 2010;51(12):6614–6619.
56. Falkner-Radler CI, Glittenberg C, Gabriel M, et al.

Intrasurgical microscope-integrated spectral domain optical coherence tomography-assisted membrane peeling. *Retina*. 2015;35(10):2100–2106.
57. Ehlers JP, Griffith JF, Srivastava SK. Intraoperative optical coherence tomography during vitreoretinal surgery for dense vitreous hemorrhage in the pioneer study. *Retina*. 2015;35(12):2537–2542.
58. Ehlers JP, Kernstine K, Farsiu S, et al. Analysis of pars plana vitrectomy for optic pit-related maculopathy with intraoperative optical coherence tomography: a possible connection with the vitreous cavity. *Arch Ophthalmol*. 2011;129(11):1483–1486.
59. Smith AG, Cost BM, Ehlers JP. Intraoperative OCT-assisted subretinal perfluorocarbon liquid removal in the DISCOVER study. *Ophthalmic Surg Lasers Imaging Retina*. 2015;46(9):964–966.
60. Seider MI, Toth CA. Macular pseudo-hole in shaken baby syndrome: underscoring the importance of optical coherence tomography under anesthesia. *Retin Cases Brief Rep*. 2016;10(3):283–285.
61. Cao C, Markovitz M, Ferenczy S, et al. Hand-held spectral domain optical coherence tomography of small macular retinoblastoma in infants before and after chemotherapy. *J Pediatr Ophthalmol Strabismus*. 2014;51(4):230–234.

7

Advanced Imaging Technologies

Pearse A. Keane, SriniVas R. Sadda

Introduction: Retinal Imaging to Date

Assessment of chorioretinal disease is dependent on the ability to visualize pathologic changes occurring in the posterior segment of the eye using optical instruments, termed ophthalmoscopy (Fig. 7.1A).[1] Ophthalmoscopy, in turn, has been greatly enhanced by the development of techniques that allow recording of these changes.[2]

By the end of the 19th century the first images of the living human retina had been obtained (Fig. 7.1B) and, by the 1950s, with the advent of electronic flashes and 35 mm cameras, the field of modern retinal/fundal imaging had been born.[3]

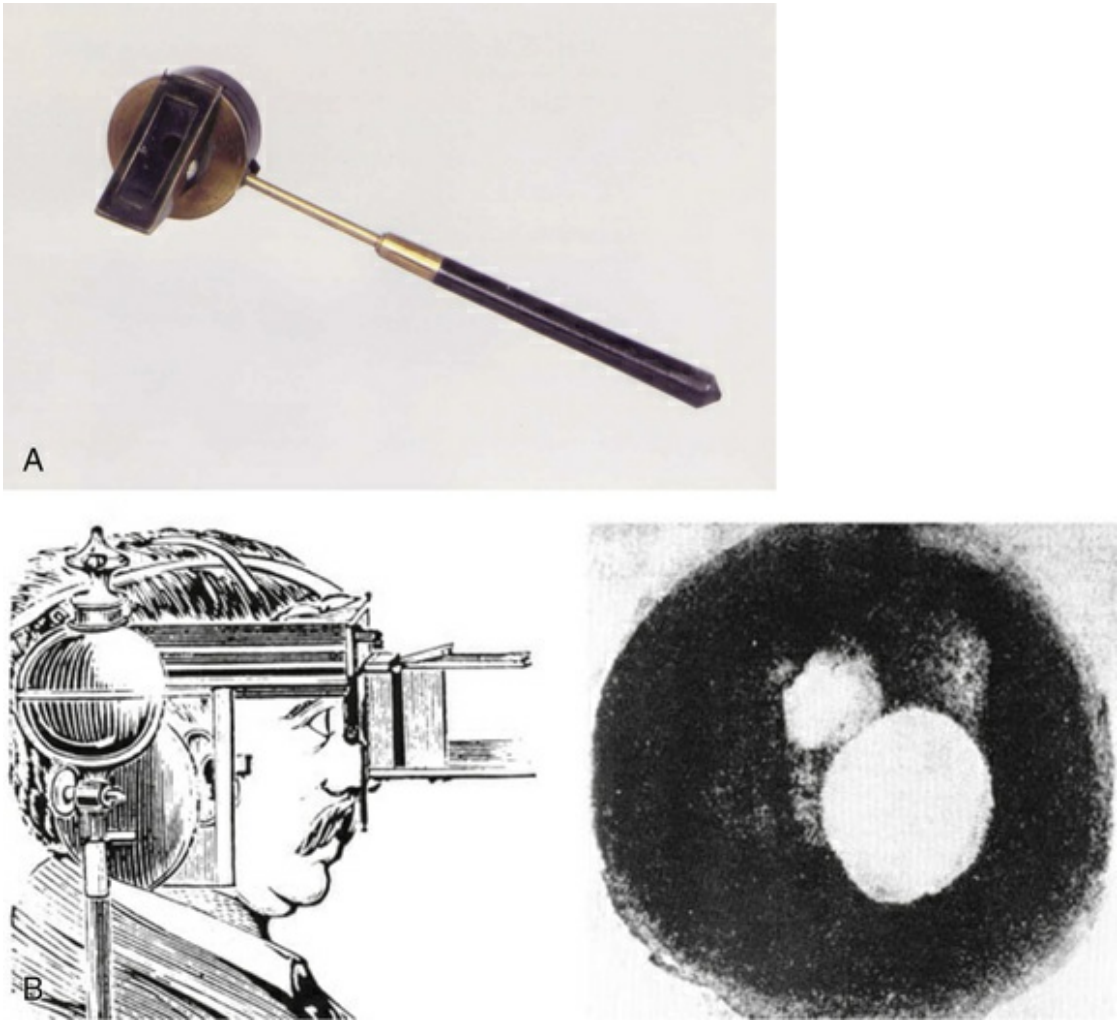

FIG. 7.1 Early attempts at retinal visualization and image capture. (A) Early model of the Helmholtz ophthalmoscope, 1851. (B) The first published human fundus photograph involved this apparatus, an albocarbon burner, and a $2\frac{1}{2}$-minute exposure. Blood vessels cannot be defined, but the optic disc can be seen as a white area superiorly, while inferiorly, the larger light area is an artifact (Panel A reproduced with permission from Alcon Laboratories Museum of Ophthalmology, The Sherman Collection, Fort Worth, TX, USA. Historical image: Helmholtz ophthalmoscope, 1851. Ophthalmology. 2002; 109(4):729. Panel B reproduced with permission from Same PJ. Landmarks in the historical development of fluorescein angiography. J

As well as documenting pathology, fundal imaging facilitates the identification of morphologic features not visible to the clinician on biomicroscopy. For example, from an early stage in its development, fundus photography has incorporated angiographic methodologies for the visualization of blood vessels.[1,4] In the 1960s, the assessment of retinal disease was revolutionized by the introduction of fluorescein angiography (Fig. 7.2A). In the 1970s, evaluation of the choroidal circulation was also improved through the use of indocyanine green dye. The development of these angiographic techniques has also led, at least in part, to the discovery that certain fundal structures fluoresce in the absence of contrast – the subsequent evolution of fundus autofluorescence imaging has greatly extended our ability to evaluate retinal degenerative and other disorders.[2]

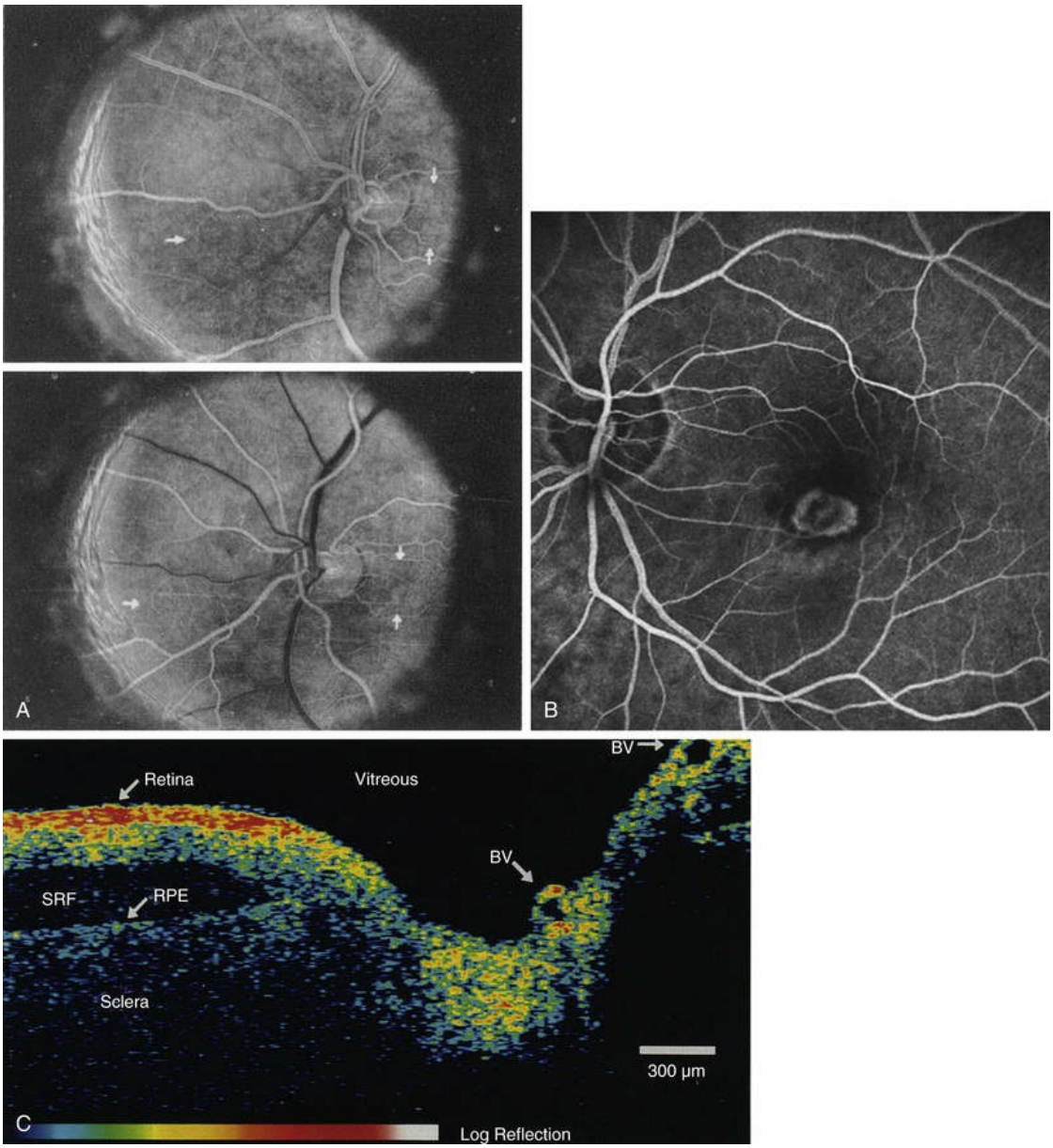

FIG. 7.2 Fluorescein angiography, scanning laser ophthalmoscopy, and optical coherence tomography (OCT). (A) Early attempt at fundus fluorescein angiography in a normal subject. (B) A single frame from a fluorescein angiogram taken with a confocal scanning laser ophthalmoscope (cSLO) showing a choroidal neovascular membrane. (C) Early attempt at OCT imaging of the human retina and optic nerve, obtained in vitro. *BV*, blood vessel; *RPE*, retinal pigment epithelium; *SRF*, subretinal fluid. (Panel A reproduce with permission from Novotny HR, Alvis DL. A method of photographing fluorescence in circulating blood in the human retina. Circulation 1961; 24:82-86. Panel B reproduced with permission from Bennett PJ, Barry CJ. Ophthalmic imaging today: an ophthalmic photographer's viewpoint – a review. Clin Exp Ophthalmol 2009;37(1):2-13. Panel C reproduced with permission from Huang D,

Swanson EA, Lin CP, et al. Optical coherence tomography. 1991;254(5035):1178–1181.)

Since the 1990s, fundus photographic systems have also made the transition from "analog" image capture using film, to digital image capture using charge-coupled devices (CCDs), allowing for improved image processing and analysis.[2] In parallel with this, new image capture technologies have emerged, such as scanning laser ophthalmoscopy (SLO) and optical coherence tomography (OCT) (Fig. 7.2B–C). In particular, the widespread adoption of OCT in recent years has greatly extended our knowledge of chorioretinal disease pathophysiology, and proven important for the provision of new pharmacotherapeutics.[1]

Despite the unprecedented advances of recent years, considerable deficiencies exist in our retinal imaging capability. While angiographic techniques provide exquisite detail of vascular structures, our ability to quantify chorioretinal blood flow and subsequent oxygen saturations – in a noninvasive manner – remains inadequate. While OCT provides cross-sectional images of the neurosensory retina (and more recently the choroid) with high axial resolution, its transverse resolution is limited, and our ability to assess many retinal cell types remains poor (e.g., Müller cells, microglia, astrocytes, and individual neuronal elements). Furthermore, many advances in microscopic techniques that permit "molecular" imaging in basic science research have yet to make the transition to human clinical studies.

In this chapter we discuss the attempts that are underway to address the shortcomings of current retinal imaging technologies. We begin by describing the recent introduction of smartphone ophthalmoscopy, an advance that may usher in the demise of the direct ophthalmoscope and, in turn, change the way in which ocular examination is performed by nonophthalmologists. We next describe the use of adaptive optics to provide cellular-level image resolution, before moving on to describe Doppler and spectral imaging techniques for the assessment of retinal blood flow and oxygenation. We then describe a number of technologies with the potential for assessment of novel functional parameters, such as photoacoustic and magnetic resonance imaging. We conclude by introducing the emerging field of "molecular imaging," an area

where the continued discovery of retinal molecular biomarkers is combined with advances in ocular imaging technologies. Throughout the chapter, we focus on emerging imaging techniques that, for the most part, are not yet commercially available, or are not yet in widespread clinical use (detailed descriptions of fundus angiography, autofluorescence, ultrasonography, and OCT, are provided elsewhere in the text).

Smartphone Ophthalmoscopy – Replacing the Direct Ophthalmoscope?

Basic Principles

Since its widespread introduction in the 1960s, ophthalmic fundus photography has relied on expensive and bulky tabletop devices, operated by skilled medical photographers in a hospital or eye clinic setting. In 2007 the introduction of the iPhone (Apple Inc., California) heralded a new era of "smartphone" technology. As most clinicians now carry a smartphone, and as these smartphones typically incorporate sophisticated cameras, the opportunity has arisen to make fundus cameras cheaper, more robust, and easier to use. Due to their portability, wireless connectivity, and data storage capability, smartphone ophthalmoscopy has the potential to enter widespread clinical usage.

Technology

A number of smartphone fundus cameras are now available.[5] Welch Allyn (Skaneateles Falls, New York) has developed a PanOptic™ Ophthalmoscope that uses a halogen lamp for illumination and provides ×5 zoom image acquisition through an undilated pupil. The Welch Allyn "iExaminer" turns this ophthalmoscope into a mobile imaging device by aligning its optical axis to the visual axis of a smartphone. An associated iExaminer application allows storage and printing of images.

"Ocular Cellscope" is another form of smartphone fundus

camera currently under development.[6] It comprises a mobile phone, a housing that contains the illuminating and collecting optics, and an integrated smartphone holder that ensures alignment with the smartphone camera. Both the optical components and the smartphone are integrated within a polymer casing, and a single 54 D ophthalmic lens is used for focusing and capturing reflected light.

A number of cheaper and potentially more portable devices have more recently been developed. The D-EYE system (D-EYE, Pasadena, California) works on the principles of direct ophthalmoscopy and exploits the autofocus capabilities of smartphone cameras to account for a patient's refractive error (this allows for compensation of refractive error from −12.00 to +6.00 diopters).[7] The D-EYE system consists of a small optical device, which is attached magnetically to the back of a smartphone. The light emitted by the "flash" of the smartphone camera is conveyed into the eye by a mirror and a beamsplitter, in the same manner as a direct ophthalmoscope. Image acquisition with this device is similar to direct ophthalmoscopy with the device being held at a distance of ~10 mm from the patient's eye. Unlike direct ophthalmoscopy, the device is targeted using the screen of the smartphone so that the examiner has no need to lean towards the patient's face and can work from a comfortable position. For a patient with a dilated pupil, the system captures a field-of-view of ~20°, for a single fundus image at a distance of ~10 mm from the patient's eye. This field-of-view is much wider than that obtained with conventional direct ophthalmoscopes (typically 5–8°) and is comparable to that of the iExaminer. In 2015 the D-EYE system was evaluated in patients with diabetic retinopathy in a hospital eye clinic – grading of diabetic retinopathy using the system was found to be comparable to that of dilated slit-lamp biomicroscopy.[8] The D-EYE system is now commercially available for approximately $400 (www.d-eyecare.com).

"PEEK (Portable Eye Examination Kit)" is a smartphone-based system for comprehensive eye examinations (www.peekvision.org).[9,10] PEEK consists of a plastic clip that covers the smartphone camera and flash with a prism assembly. The prism deflects light from the flash to match the illumination path with the field of view of the camera. This allows acquisition of fundus

images. Similar to D-EYE, PEEK allows the smartphone to be held in front of and close to the patient's eye for image capture. PEEK also allows other ophthalmic testing to be performed, for example visual acuity measurements. PEEK is undergoing extensive clinical validation studies as part of the Nakuru Eye Disease Project in Kenya. These studies have demonstrated that PEEK provides accurate and repeatable measurements of visual acuity,[10] and that images of the optic nerve head can be obtained comparable with those from digital retinal cameras.[9] Of note, in both cases, PEEK testing was performed by nonhealthcare personnel.

Conclusion

The development of smartphone ophthalmoscopy is likely to have profound benefits for general ophthalmic examination in the developing world, as well as greatly improving eye examination in pediatric settings and by nonophthalmic-trained physicians in the developed world. In 2016 the widespread availability of devices like PEEK and D-EYE may signal the end of conventional direct ophthalmoscopy for many nonophthalmologists.

Adaptive Optics: Imaging of Single Cells in the Retina

Basic Principles

Our ability to obtain high-resolution images of the human retina is limited by the presence of defects, or aberrations, in the optical system of the eye (i.e., the cornea and lens).[11] In addition to exhibiting lower-order monochromatic aberrations such as defocus and astigmatism, normal eyes also exhibit higher-order monochromatic aberrations such as coma, trefoil, and spherical aberration. The combined effects of these aberrations limit the quality of images obtainable for the diagnosis and management of retinal disease. Until the early 1990s there existed no effective way to obtain rapid, precise measurements of the human eye's optical aberrations. However, wavefront sensors based on the Hartmann–Shack principle, originally developed for astronomical purposes,

have now been adapted for use in the human eye. These sensors consist of an array of lenses, each having the same focal length, which can be used to approximate the whole wavelength of incident light. Once measured, the detected aberrations can then be corrected (i.e., rendered flat) using one or more deformable mirrors (mirrors have large numbers of small electronically controlled actuators on their rear surface that can push and pull the mirror within a range of ±2 μm, allowing it to adopt any desired configuration) (Fig. 7.3). By incorporating wavefront sensing and correction into existing optical imaging platforms – "adaptive optics" – it is now possible to acquire images of the retina with cellular-level resolution, and in a noninvasive fashion.[11,12]

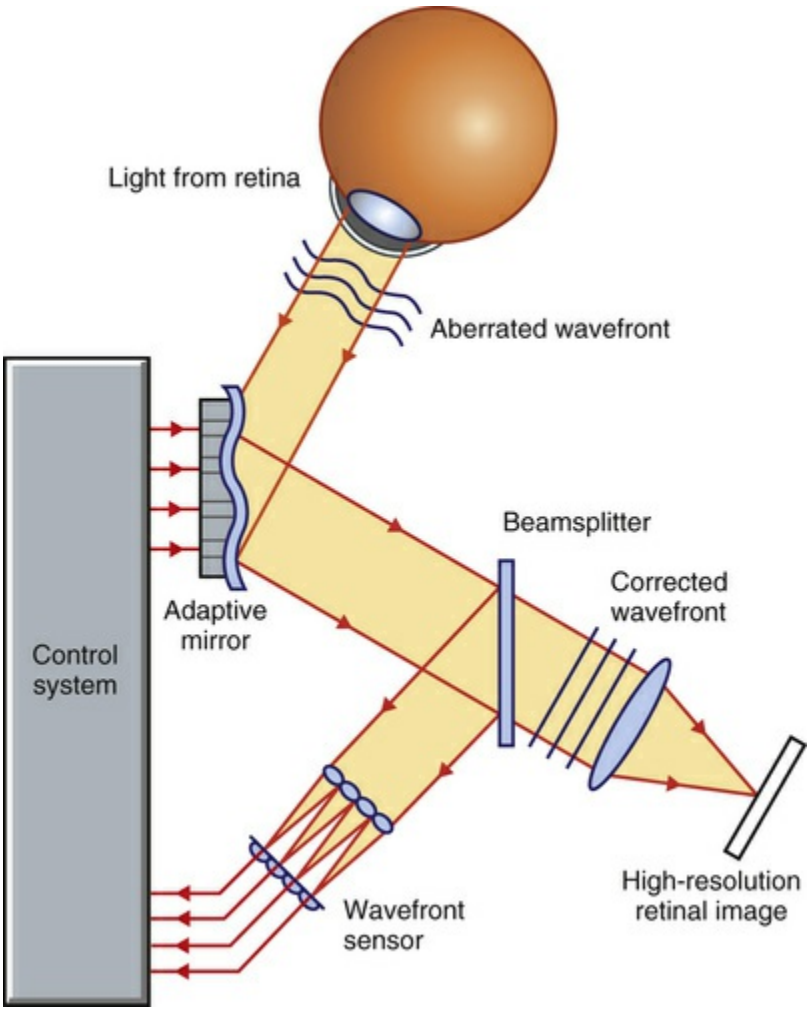

FIG. 7.3 Schematic representation of a typical adaptive optics system. (Courtesy of Joseph Carroll, Williams Laboratory, University of Rochester).

Technology

The adaptive optics devices first developed for ophthalmic use were conventional fundus cameras modified to incorporate wavefront sensing and correction.[13,14] These systems typically focus a laser beam on the retina at a location of interest. The light reflected from the retina is then distorted by the optical system of the eye before returning to the wavefront sensor. Information obtained from the wavefront sensor is then used to alter the shape of the deformable mirrors and compensate for the aberration. This process continues in a closed loop until the ocular aberrations have been reduced to near diffraction-limited levels; at this point, a flash from a separate incoherent light source is triggered by the wavefront sensor, illuminating the retina as an image is captured by the digital fundus camera. Adaptive optics "flood-illuminated" fundus cameras are now commercially available and approved for use in clinical settings (e.g., "rtx1 Adaptive Optics Retinal Camera", Imagine Eyes, France). The rtx1 system uses a light source with a wavelength of 840 nm to provide a near-infrared reflectance image that is particularly well suited to deep retinal structures (see above). While these devices offer greatly improved transverse resolution, their field of view is still limited (e.g., 4° × 4°).

Adaptive optics components have also been incorporated into confocal SLO systems, offering the advantage of increased contrast, cross-sectional imaging, and the measurement of dynamic changes such as blood flow.[11,15] In an adaptive optics SLO, light returning from the retina is split into a light detection path and a wavefront-sensing path. Again, deformable mirrors are used to provide closed-loop dynamic compensation for ocular aberrations. In contrast to flood-illuminated adaptive optics devices, the adaptive optics SLO uses the same source of light for the wavefront sensor as for the retinal illumination – as a result, the wavefront sensor is able to measure aberrations from the entire scanned area of the retina. When imaging the retina, SLO devices provide a transverse resolution of approximately 15 μm but are limited to an axial resolution of approximately 300 μm. With the addition of adaptive optics correction to an SLO, the transverse resolution may be

increased to less than 3 μm while the axial resolution may be improved to 40 μm. Adaptive optics SLO systems are not yet commercially available, although a prototype system has recently been developed by Canon Medical Imaging.

Adaptive optics devices have also been incorporated into prototype OCT systems.[16,17] The axial resolution achievable using OCT is many orders of magnitude greater than that achievable using an SLO device, with commercially available devices commonly achieving axial resolutions of approximately 5 μm. However, the transverse resolution of OCT systems is determined by the size of the laser spot that can be focused on the retina – a factor limited by ocular aberrations. A successful combination of OCT and adaptive optics could potentially demonstrate, therefore, the narrowest point-spread function of all in vivo retinal imaging techniques (Fig. 7.4). However, a number of technical challenges remain, in particular, the reductions in image quality that occur as a result of chromatic aberrations when large bandwidth light sources are used.[18,19] Nevertheless, recent use of a prototype adaptive optics OCT device has reopened the debate about the identity of the outer retinal hyperreflective lines on OCT, in particular whether the 2nd hyperreflective band constitutes the photoreceptor inner segment ellipsoid zone or inner/outer-segment junction.[20]

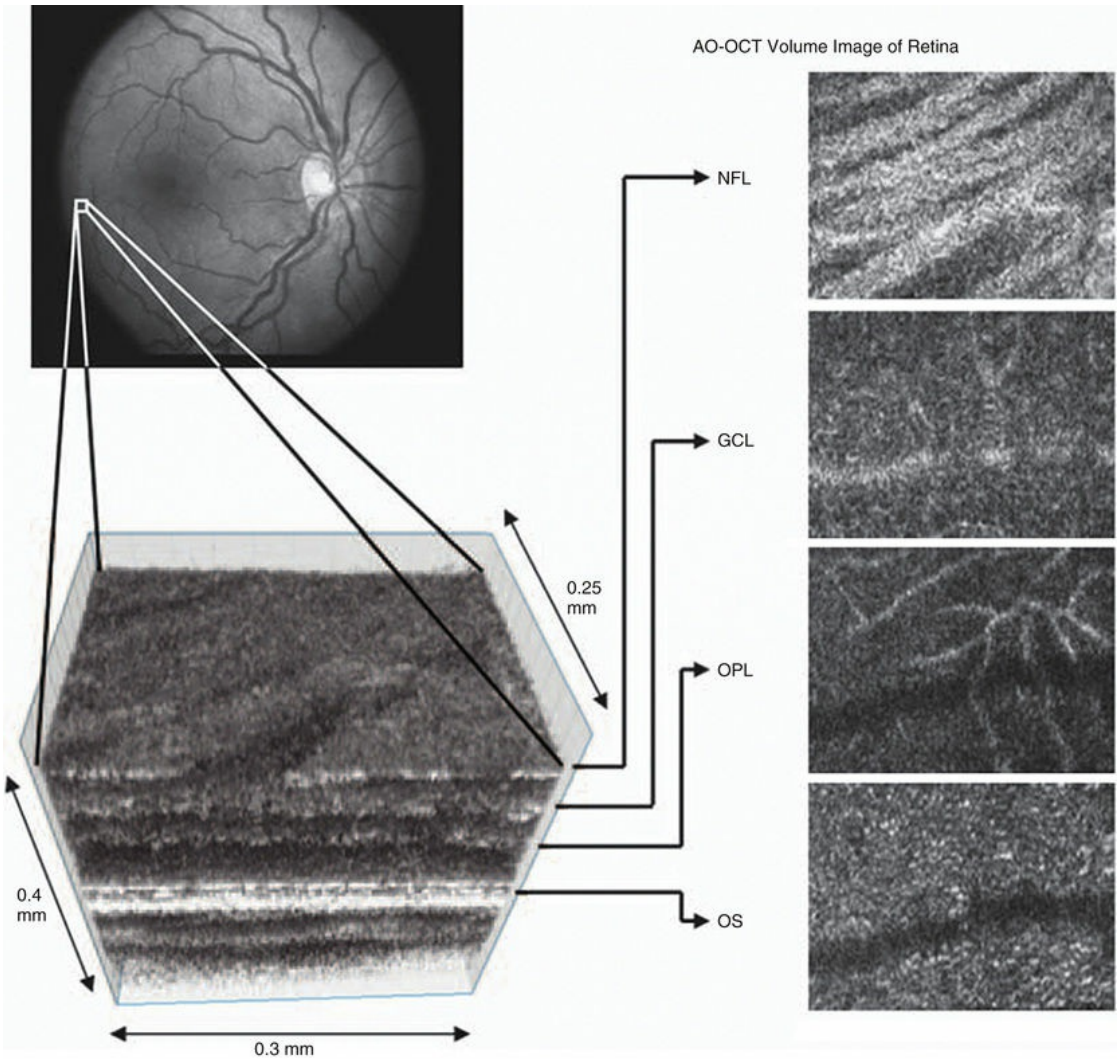

FIG. 7.4 Adaptive optics optical coherence tomography (AO-OCT) volume acquired over a 1° retinal region located temporal of the fovea, as illustrated by the rectangle in the fundus photograph. The images on the right are en face views of particular retinal layers extracted from the AO–OCT volume. Retinal layers from top to bottom are nerve fiber layer (*NFL*), ganglion cell layer (*GCL*), outer plexiform layer (*OPL*), and outer segment layer of photoreceptors (*OS*) (Reproduced with permission from Miller DT, Kocaoglu OP, Wang Q, Lee S. Adaptive optics and the eye (super resolution OCT). Eye 2011; 25(3):321–330.)

Finally, adaptive optics may be useful for the performance of fundus perimetry ("microperimetry") in the study of macular disease.[1] In current microperimetry systems, macular light sensitivity is measured using a stimulus size that covers an area containing in excess of 150 cones at the foveal center. As with the

imaging modalities described above, further reductions in stimulus size are hindered by aberrations of the optical systems in the human eye, a shortcoming that may be overcome through the incorporation of adaptive optics.[21] In addition, by analyzing the warping that occurs both within individual SLO frames, and between frames, adaptive optics can be used to resolve the effects of eye movements at a fine spatial scale. As a consequence, in adaptive optics microperimetry, real-time stabilization of the retinal image is possible, allowing for targeted delivery of the small visual stimulus to the retina.[22,23]

Visualization of Retinal Structures

Cone photoreceptors are the dominant feature seen with both flood-illuminated and SLO devices (Fig. 7.5A).[12,24] Light projected into the eye from these devices passes through the cone outer segment and is reflected by the retinal pigment epithelium (RPE), the most highly reflective surface in the retina. As light is reflected out of the eye, it is guided toward a small area of the pupil by the cone inner segments (in this respect cones act as "optical fibers," rejecting stray light in the retina and maximizing efficiency in light collection). As a result, the cones appear as hyperreflective dots (recently referred to as a "positive" mosaic). However, when adaptive optics is used to examine the peripheral retina of healthy eyes, cones often appear as hyporeflective dots (a "negative" mosaic). This finding has only recently been recognized and it is likely to represent a physiologic manifestation of the optical Stiles–Crawford effect.[25] Numerous studies have evaluated the reproducibility of both manual and automated approaches to cone density quantification using adaptive optics.[26,27] Recent studies have correlated these measures of cone density with outer retinal reflectivities as measured using OCT.[28] Adaptive optics has also supplied the first data regarding the proportion, and arrangement, of each cone photoreceptor class (blue [S], green [M], or red [L]) in the human eye.[29] Regional variabilities in cone topography have also been explored,[30] as well as the effects of refractive status. Cone packing appears to be less dense in highly myopic eyes versus emmetropic eyes – a finding consistent with the reduced visual

acuity and contrast sensitivity observed in the eyes of axial myopes.[31]

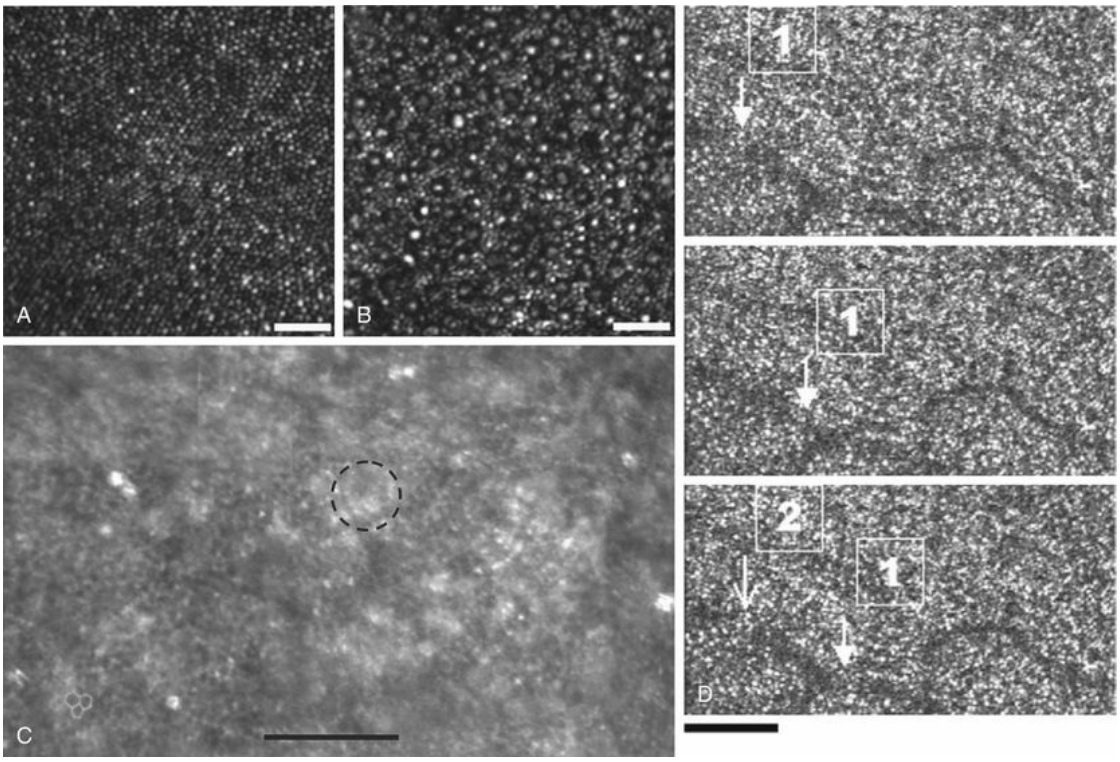

FIG. 7.5 Visualization of photoreceptors, retinal pigment epithelium (RPE) and retinal vasculature using adaptive optics. (A)The complete foveal cone mosaic and (B) the complete peripheral photoreceptor mosaic showing both rods and cones, imaged at 10° temporal and 1° inferior. Scale bars: 20 μm. (C) Adaptive optics scanning laser ophthalmoscopy image revealing a patchy foveal cone mosaic with increased cone spacing, and resulting visualization of the RPE cells (three RPE cells in the bottom left corner have been outlined, and the preferred retinal locus is also indicated by the dashed circle in the image). (D) Three successive frames demonstrate a single leukocyte's (*1*) change in position from left to right in each frame. A second leukocyte (*2*) has just come into view in the last frame. Scale bar: 100 μm. (Panels A and B are reproduced with permission from Rossi EA, Chung M, Dubra A, et al. Imaging retinal mosaics in the living eye. Eye 2011; 25(3):301–308. Panel C reproduced with permission from Roorda A, Zhang Y, Duncan JL. High-resolution in vivo imaging of the RPE mosaic in eyes with retinal disease. Invest Ophthalmol Vis Sci 2007;48(5):2297–2303. Panel D reproduced with permission from Martin JA, Roorda A. Direct and

noninvasive assessment of parafoveal capillary leukocyte velocity. Ophthalmology 2005;112(12):2219–2224.)

Rod photoreceptors are abundant in the peripheral retina but are also seen in the macular region of human eyes. Rods are not as easily visualized in the normal retina, even in areas of the retina where they outnumber cones approximately 10-fold.[12] The difficulty in imaging rods is consistent with their smaller size (approximately 2 μm in diameter), and their broad angular tuning, which reflects less light back through the pupil where it can be collected for imaging. However, recent advances, including the use of smaller confocal pinholes and improvements in registration algorithms, have allowed clear images of single rods to be obtained in the living human eye (as well as aiding visualization of the smallest cones at the foveal center) (Fig. 7.5A).[32]

Rod and cone photoreceptors rest on a monolayer of RPE cells. Each RPE cell in the monolayer has an approximate diameter of 10 μm, dimensions well within the resolution limits of adaptive optics systems; however, direct in vivo visualization of single RPE cells remains challenging. Unlike cone photoreceptors, the intrinsic contrast of RPE cells is poor. In addition, much of the light scattered by the RPE is masked by the overlying photoreceptors, which are also highly scattering. As a result, direct imaging of the RPE was initially only possible in human subjects with retinal disease where absence of cone photoreceptors allowed visualization of the underlying RPE (Fig. 7.5B).[33] More recently, use of a "dark-field" imaging technique has achieved moderate success in noninvasive visualization of the hexagonal RPE mosaic in healthy human volunteers.[34] In this approach, the traditional small confocal aperture is replaced by a larger aperture with a central filament. The central filament attenuates the light back scattered from the photoreceptors (the direct signal), while the larger aperture collects light multiply scattered by the RPE cells (the indirect, or so-called dark-field signal).

Adaptive optics may also be used to allow high-resolution, noninvasive visualization of the retinal nerve fiber layer (RNFL). Using adaptive optics, it is possible to identify individual retinal nerve fiber layer bundles, their direction of travel and width, and other features such as fiber "bridges" among bundles. The

separation of bundles by hyperreflective Müller cell septae may also be seen.[35] Adaptive optics OCT has been used to investigate the microarchitecture of the lamina cribrosa.[36]

Finally, adaptive optics-based imaging allows high-resolution visualization of the retinal vascular parenchyma and the assessment of retinal blood constituents and flow. Although conventional fundus photography/angiography allows mapping of the retinal vasculature, this is mainly achieved through visualization of the retinal vessel contents as opposed to direct visualization of the vessel walls or their substructure (retinal vessel mural cells are of relatively low contrast). However, using dark-field adaptive optics, visualization of distinct mural cells lying along the lumen of retinal arteries and arterioles (precapillary retinal arterioles and larger) has recently been described.[37] By contrast, with "standard" adaptive optics, the retinal vascular map appears as a dark outline only. Adaptive optics SLO systems allow video image acquisition and, using this approach, bright particles can be seen to flow within parafoveal capillaries. These bright particles may represent direct visualization of circulating leukocytes, or may be reflections from the underlying photoreceptors passing through the transparent leukocytes (i.e., indirect leukocyte visualization). These bright particles are followed by "dark tails" – black "tadpole-like" regions darker than the normal vessel shadow, which are thought to represent aggregates of erythrocytes.[38] Retinal imaging with adaptive optics may also be useful for detection of structural changes in the retinal vasculature not visible with other imaging modalities, such as microaneurysms and hard exudates in diabetic retinopathy.[39]

Adaptive optics SLO imaging can also be performed after injection of sodium fluorescein as a contrast agent (akin to a very high resolution fluorescein angiogram).[40] In the "unaffected" fellow eyes of patients with central retinal vein occlusion (CRVO), adaptive optics SLO fluorescein angiography has been used to show nonperfused capillaries and reductions in microvascular density – a hitherto unseen finding.[40]

Clinical Applications

The cellular-level resolution provided by adaptive optics retinal imaging allows direct measurement of photoreceptor density and diameter and is, therefore, an ideal tool for the examination of patients with inherited retinal degenerations (Fig. 7.6). On examination with adaptive optics, diseased cones do not show the same reflectance pattern as healthy photoreceptors, resulting in dark gaps or areas of "drop-out" within the cone photoreceptor mosaic.[41] With gene therapy trials ongoing, or about to start, adaptive optics imaging of patients with choroideremia and achromatopsia are of particular interest.[42,43] This is particularly the case as significant correlations have been found between parafoveal cone density and a number of functional parameters, including best corrected visual acuity, contrast sensitivity and detection sensitivities for visual stimuli recorded using multifocal electroretinography.[44–46]

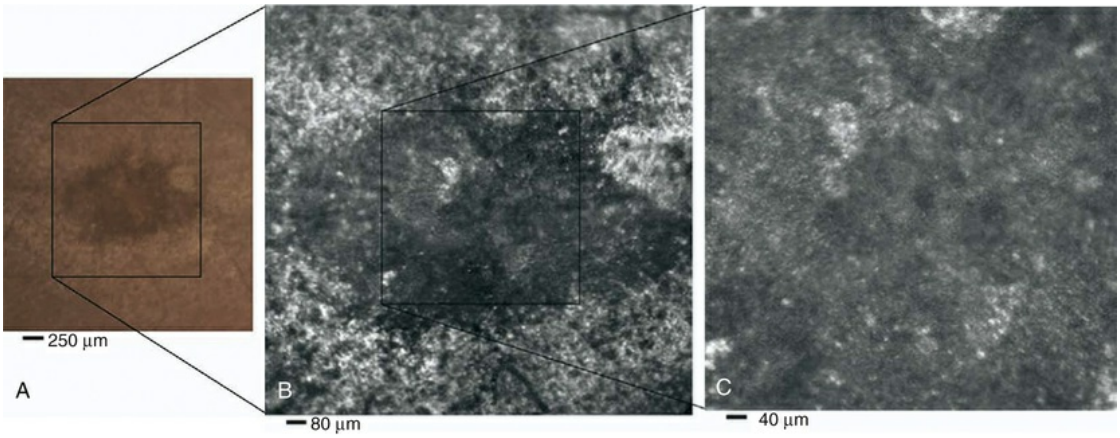

FIG. 7.6 Adaptive optics scanning laser ophthalmoscope (AO-SLO) images at different magnifications with corresponding features on the fundus photograph (A). (B) Six-degree montage from 3° adaptive optics images of the central macula of the cone–rod dystrophy patient's right eye. In addition to the features detected in the fundus photograph, detailed structures in the granular pattern of the retinal pigment epithelium in the atrophic bull's-eye lesion are observed. Within the central relatively spared region (box), photoreceptors are seen as gray dots. (C) Three-degree montage from 1.5° images. The photoreceptors are visible in the central relatively spared area of the retina. (Reproduced with permission from Wolfing

JI, Chung M, Carroll J, et al. High-resolution retinal imaging of cone–rod dystrophy. Ophthalmology 2006;113(6):1019.)

High-resolution adaptive optics imaging has been used to demonstrate evidence of photoreceptor loss or perturbation in a range of conditions, including subretinal drusenoid deposits,[47] white dot syndromes,[48] macular telangiectasia type 2,[49] screening for hydroxychloroquine toxicity,[50] and following retinal detachment repair.[51] In patients with uveitis, adaptive optics has been used to show paravascular opacification in retinal vasculitis – findings consistent with a putative ocular "glymphatic" system.[52, 53] In patients with glaucoma and other optic neuropathies, adaptive optics has revealed evidence of structural changes, both the peripapillary RNFL bundles,[54] and their associated cone photoreceptors.[55]

Conclusions

It is clear that the addition of adaptive optics to existing retinal imaging platforms is an important step for clinical ophthalmology, providing extremely high-resolution images of the retina. While commercial adaptive optics devices are now available, image acquisition needs to become quicker and easier, for both the patient and the clinician. Adaptive optics devices are also limited by a small field of view and difficulties in acquiring good quality images in patients with poor fixation, poor compliance, or with significant disruption of their retinal anatomy.

Doppler Imaging: Assessment of Blood Flow

Basic Principles

The Doppler effect, first described in the 19th century by the Austrian physicist Christian Doppler, is the change in frequency of a wave as it is reflected off a moving object; if the reflecting object is moving away from the observer/transducer, the frequency of the reflected waves is lower than that of the waves emitted, and vice

versa. As the frequency shift is dependent on the velocity of the moving object, this effect can be used to measure the velocity of blood flowing in the eye.[56] Importantly, the Doppler effect is also dependent on the angle between the axis of the wave and the axis of movement of the object. Therefore, if the observer/transducer is not parallel to the axis of the moving object, calculations must be performed using a Doppler angle correction formula.

Accurate measurement of this Doppler angle is a significant obstacle to the noninvasive assessment of ocular blood flow. Furthermore, as the Doppler angle increases between 60° and 90°, velocity calculations are subject to significant errors.

Utilization of the Doppler effect in ocular imaging systems allows calculation of ocular blood flow velocities.[56] Reductions in blood flow velocity may occur as a result of vascular degenerative changes in diseases such as diabetic retinopathy, or as a result of vascular occlusion in diseases such as CRVO. However, changes in retinal blood flow velocity may also occur as a result of either constriction or dilation of vessels during normal physiologic autoregulation (according to Bernoulli's principle, constriction of a blood vessel increases the velocity of the blood but decreases its pressure). Therefore, measurements of the absolute quantities of "blood flow" may represent a more clinically relevant parameter.

Blood flow (Q) is the volume of blood passing through a vessel in a given time, and is determined by the velocity of the blood (V) multiplied by the cross-sectional area of the blood vessel through which it passes (πr^2).[57] Consequently, if blood flow velocity can be measured using the Doppler effect, and the diameter of the blood vessel can also be measured, then absolute values for blood flow may be determined. Measurements of retinal vascular diameter can be acquired from fundus images obtained with standard optical imaging techniques (e.g., fundus photography).[58,59] However, in order to measure retinal vascular diameters in real units of length, the magnification of the image induced by the eye, as well as the magnification of the camera, must be known (failure to account for such magnification will result in significant errors).

Non-Doppler Assessment of Retinal Blood

Flow

Measurement of retinal blood flow is possible using quantitative angiography, based on use of dye-dilution techniques.[56,58,59] In this method, the concentration of fluorescent dye within the blood at a specific observation point is graphed over time, producing a dye-dilution curve. The enhanced contrast provided by SLO systems is particularly suited to this approach, and it can be used to evaluate vascular parameters such as retinal arteriovenous passage (AVP) time and mean dye velocity. The increased contrast provided by SLO images also allows measurement of blood velocities in the small vessels surrounding the fovea and the optic nerve head (in the future, this technique is likely to be enhanced through the incorporation of adaptive optics).[59] Indocyanine green angiography (ICGA) may also be used to evaluate the choroidal circulatory flow, as the infrared light sources employed penetrate the RPE more efficiently than the shorter wavelengths used in fluorescein angiography. In one analysis method, the choroid is divided into six regions, and dye dilution curves are created for each region (Fig. 7.7A). Parameters such as 10% filling time and maximum brightness can then be calculated.[59] SLO-based fluorescein and ICGA provides significant information regarding retinal and choroidal blood velocities. However, without measurement of corresponding vascular diameters, it is not possible to measure blood flow. In addition, the invasive nature of the dye injections required for these approaches precludes their routine use in many clinical scenarios.

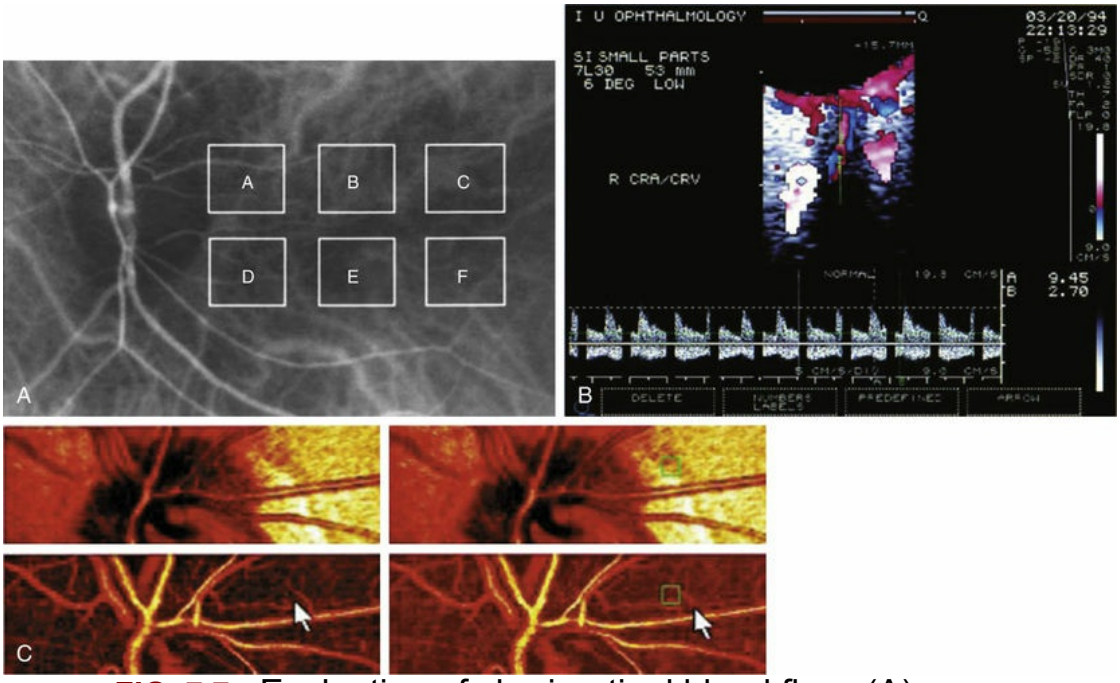

FIG. 7.7 Evaluation of chorioretinal blood flow. (A) Quantification of choroidal blood flow using indocyanine green angiography. Six locations, each a 6° square, are identified on the image for dye dilution analysis. (B) Color Doppler image (CDI) of the central retinal artery and vein. The Doppler shifted spectrum (time velocity curve) is displayed at the bottom of the image. Red and blue pixels represent blood movement toward and away from the transducer, respectively. (C) Confocal scanning laser Doppler flowmetry (Heidelberg Retinal Flowmeter) of optic nerve head and peripapillary retina. The left arrow indicates a 1×1 pixel measurement window, which collects flow values from the entire retina except for large vessels, for new pixel-by pixel analysis. The right arrow indicates a 10×10 pixel measurement window used for conventional analysis. (Reproduced with permission from Harris A, Chung HS, Ciulla TA, et al. Progress in measurement of ocular blood flow and relevance to our understanding of glaucoma and age-related macular degeneration. Prog Retin Eye Res 1999; 18(5):673–677.)

Doppler Ultrasound

Color Doppler imaging (CDI) is an ultrasound technique that combines B-scan grayscale imaging of tissue structure, color representation of blood flow based on Doppler shifted frequencies,

and pulsed-Doppler measurement of blood flow velocities (Fig. 7.7B).[56,59] As in other Doppler-based methods, blood flow velocity is determined by the shift in the frequency of sound waves reflected from the moving blood column. Color is then added to the B-scan grayscale image of the eye to represent the motion of blood through the vessels. The color varies in proportion to the flow velocity and is typically coded red–white for motion toward the probe, and blue–white for motion away from the probe. Using the color Doppler image, the operator can then identify the vessel of interest and place the sampling window for pulsed Doppler measurements (this window is generally situated in the centre of the vessel). At this point, the general flow axis of the blood flow is detected simply by observation to determine the Doppler flow angle for the appropriate calculation of velocity. Flow-velocity data is then graphed against time, and the computer identifies the peak and trough of the waves.

Current CDI analysis focuses primarily on the arteries located behind the globe: ophthalmic artery, central retinal artery, and posterior ciliary arteries. CDI can be used to describe blood flow to the eye in terms of a set of well-defined parameters including (1) peak systolic velocity (PSV), (2) end-diastolic velocity (EDV), and (3) resistance index.[56,59] It does not provide absolute measurements of blood flow (no quantitative information on vessel diameter is obtained). With a 7.5-MHz probe, CDI is able to resolve structures 0.2 mm (200 μm) or larger, but can also be used to measure Doppler shifts in smaller vessels such as the posterior ciliary arteries (diameter of approximately 40 μm). CDI may be of particular use for the primary evaluation and follow-up of orbital vascular lesions, such as varices, arteriovenous malformations, and carotid-cavernous sinus fistulas. It has also been used for the semiquantitative assessment of perfusion in retinal and choroidal vascular disease. Specifically, in patients with CRVO, the central retinal artery PSV and EDV have been found to be much lower than in unaffected fellow eyes and in healthy control subjects.[60] Patients with ocular ischemic syndromes also present reduced PSVs in the central retinal and posterior ciliary arteries, as well as increased resistance.[61]

Laser Doppler Velocimetry

Bidirectional laser Doppler velocimetry (LDV) is a technique used to quantify maximum blood velocity in large retinal vessels.[56,62] Instruments based on this principle typically consist of a modified fundus camera where the body of the camera has been replaced by a fiberoptic unit. A low-powered laser light source casts a beam onto the ocular fundus, which is positioned by the operator on the retinal vessel of interest. The Doppler shifted frequency spectra of the returning light can then be measured. These spectra exhibit large fluctuations up to a clearly measurable maximum shift – this maximum shift arises from scattered light from red blood cells flowing at the maximum speed at the center of the vessel. If the Doppler angles are then known, the maximum frequency shift can be used to calculate the maximum vessel velocity; however, these angles are difficult to measure reproducibly. Therefore, a bidirectional technique was developed to expand the capability of LDV to provide absolute measurements of maximum velocity.[62] In the bidirectional technique, one incident beam is used to illuminate a sight along a retinal vessel. The light scattered by the blood cells at the illuminated site is then detected simultaneously in two distinct directions separated by a known, fixed angle. Two Doppler shifted frequency spectra are measured and the difference between their maximum shifts is then used to calculate the maximum velocity in units of speed.

By combining an eye-tracking system with a retinal laser instrument based on bidirectional LDV, Canon have developed a commercially available instrument (Canon Laser Blood Flowmeter (CLBF)-100, Tokyo, Japan).[63] This device allows concomitant measurement of blood vessel diameter; as a result, total retinal blood flow in a single vessel can be calculated in absolute units. Thus far, the smallest vessels in which the blood flow rate has been measured were approximately 40 μm in diameter.[44] It has been used to investigate retinal blood flow in diabetic patients with kidney disease,[64] and both with and without diabetic retinopathy.[65]

Laser Doppler Flowmetry

Laser Doppler flowmetry (LDF) is a technique where laser light is

not directed at a retinal vessel, but on an area of vascularized retinal tissue with no large vessels visible.[56,58] LDF instruments are based on the theories of Bonner and Nossal, which describe the characteristics of laser light injected at one point into capillary tissue and collected at an adjacent point.[62] This theory relates the Doppler shift of the light to the total number of blood cells moving in the illuminated tissue volume, and to the flow rate of the moving cells. By using this theory, relative measurements of the mean velocity of the red blood cells, and the blood volume, can be obtained. Relative values of blood flow can then be calculated as the product of velocity and volume. However, such measurements are not absolute, and variations in vascular density and vessel orientation, even within relatively small volumes of tissue, can lead to considerable differences in the scattering properties between subjects.

Scanning laser Doppler flowmetry combines the principles of scanning laser tomography and LDF with the commercially available Heidelberg Retina Flowmeter (HRF), providing two-dimensional flow maps of the retina and optic nerve head (Fig. 7.7C).[66] In this system, the HRF images a 2880 μm × 720 μm area of the retina or optic nerve, at a resolution of approximately 10 μm/pixel. After the scan is performed, the HRF computer performs a fast Fourier transform to extract the Doppler shift spectrum from each measured pixel of reflected light. The HRF device is simple to use and sensitive to small changes over time in the same eye. However, the flow measurements are displayed in arbitrary units and there is a lack of accuracy when dealing with very high and very low blood speeds. Furthermore, contributions to blood flow measurements from the underlying choriocapillaris cannot be excluded and previous experimental tests of the instrumentation have demonstrated that large flow readings can be obtained from sample volumes even when they contain no moving cells.[62] The HRF device has, perhaps, most commonly been used in the investigation of patients with glaucoma. A number of such studies have investigated the correlation between optic nerve head morphology (as assessed using scanning laser tomography) and peripapillary retinal blood flow (as assessed using laser Doppler flowmetry). These studies suggest that decreased retinal blood flow

is associated with glaucomatous structural damage.[67]

Doppler Optical Coherence Tomography

OCT, first described by Huang et al. in 1991, uses interferometry to generate high resolution cross-sectional images of the neurosensory retina.[68] Since the mid-1990s, Doppler measurements have been incorporated into prototype OCT imaging systems (Fig. 7.8).[16] In the original time-domain OCT systems, the blood velocity can be determined by measurement of the Doppler shift of the interference fringe frequency after Fourier transformation of the data, whereas, in newer spectral domain OCT systems, direct recording of the interference fringe frequency is possible. However, in this approach, blood velocity sensitivity and image spatial resolution are coupled and inversely related (increasing the velocity sensitivity decreases the spatial resolution). In order to overcome this limitation, a number of Doppler OCT prototypes utilize the phase change between sequential A-scans in order to generate information regarding the Doppler shift.[16]

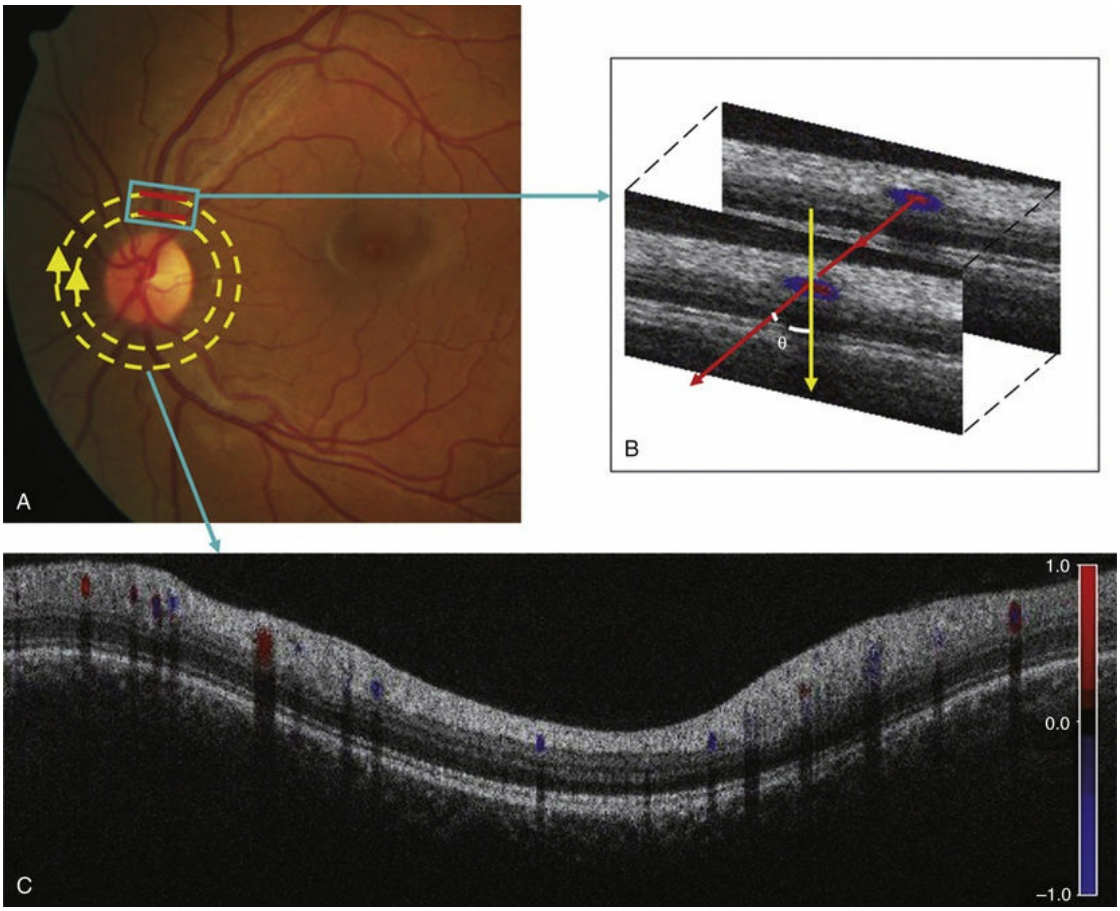

FIG. 7.8 Doppler optical coherence tomography (OCT). (A) Fundus photograph showing the double circular pattern of the OCT beam scanning retinal blood vessels emerging from the optic disc. (B) The relative position of a blood vessel in the two OCT cross-sections is used to calculate the Doppler angle θ between the beam and the blood vessel. (C) Color Doppler OCT image showing the unfolded cross-section from a circular scan. Arteries and veins can be distinguished by the direction of flow as determined by the signs (blue or red) of the Doppler shift and the angle θ. (Reproduced with permission from Wang Y, Fawzi AA, Varma R, et al. Pilot study of optical coherence tomography measurement of retinal blood flow in retinal and optic nerve diseases. Invest Ophthalmol Vis Sci 2011; 52(2):841.)

Although Doppler OCT can generate cross-sectional images of retinal blood flow (so-called "OCT angiography"), accurate quantification of this flow remains challenging: to achieve this it is necessary to measure the geometry of the vessel and, in particular, the Doppler angle. Furthermore, current Doppler OCT systems are limited in terms of the maximal velocities measurable, and in terms

of the smallest vessel diameters measurable (capillary flow involves single erythrocyte movement rather than continuous fluid flow). In a recent study, measurements of total retinal blood flow from Doppler OCT were combined with measurements of oxygen saturation using a spectral approach (see below). This combination allowed calculation of oxygen extraction and thus has considerable promise for investigation of oxygen metabolism within the retina.[69]

Conclusions

The prospects for quantification of retinal blood flow with Doppler OCT appear good, yet it is still at an early stage in its development pathway. Furthermore, due to the complexity of retinal hemodynamics, extensive validation and reproducibility studies are required before acceptance of any new measurement approach.

Spectral Imaging: Assessment of Retinal Oxygenation

Basic Principles

Spectroscopy is the study of the interaction between any form of matter and radiated energy (e.g., visible light). By measuring radiation intensity as a function of wavelength, and through the identification of characteristic signatures, it is possible to determine the constituents of a material. For example, in astronomy, spectral analysis can be used to derive many properties of distant stars and galaxies. As well as its uses in remote sensing, spectroscopy has also been adapted for a number of laboratory-based applications. In biologic systems, the combination of spectroscopy with conventional imaging techniques – "spectral imaging" – allows determination of the spatial distribution of spectroscopic data.[70] In clinical settings, the application of spectroscopic principles has been of particular use for oximetry – the measurement of oxygen saturation in a patient's blood. From as early as 1935, transillumination of the ear has been used as a method of continuously measuring oxygen saturation in human blood. The subsequent incorporation of plethysmography (the analysis of

pulsatile components of the arterial cycle) has facilitated development of pulse oximeters capable of measuring arterial oxygen saturation in isolation.

The use of spectral imaging to perform blood oximetry is dependent on assumptions about the relationship between light transmittance through the blood and its oxygen saturation.[70] According to the Lambert–Beer law, for any given wavelength of light, its transmittance through blood is dependent on the extinction coefficient of the blood (ε), the concentration of blood (c), and the path length (d) through which the light travels. The extinction coefficient of blood (ε) is dependent on its main absorbing component – hemoglobin, which, in turn, is dependent on its oxygen concentration. As the extinction coefficient of blood varies with wavelength, analyzing the optical density of blood at multiple wavelengths compensates for variables such as the concentration and path length and ultimately allows estimation of oxygen levels in the blood (the exact details of these calculations are beyond the scope of this chapter, but have been reviewed in detail by Harris et al.).[71] However, in retinal oximetry, it is impractical to determine optical densities (and thus oxygen concentrations) through the measurement of light transmittance. Instead, measurements of light reflected from the retina are typically used. Although the principles described above require a number of assumptions that may not hold true in the real world, measurement of light reflected from the retina at multiple wavelengths, in this manner, forms the basis for a number of noninvasive retinal oximetry technologies.

Technology

Spectral imaging devices typically employ one of three different approaches: (1) multispectral imaging; (2) hyperspectral imaging; (3) imaging spectroscopy.[70,71] Initial efforts by Hickam et al. in the 1950s employed film-based fundus cameras; more recently, digital fundus cameras and confocal scanning laser ophthalmoscopes have also been employed. Early attempts have also been made at the utilization of OCT in association with spectral analysis techniques.[72]

Multispectral imaging involves the measurement of reflected

light from images obtained at discrete and somewhat narrow spectral bands. Adopting a similar approach to that first described by Beach et al.,[73] Stefansson and coworkers have recently developed "Oxymap," a commercially available device approved for investigational usage.[74] This device consists of a fundus camera, which is coupled with a beamsplitter and a digital camera. The beamsplitter separates the original image into four optical channels, each of which contains a different narrow band-pass filter (each band-pass filter only allows light of specific wavelengths to pass). This simultaneously yields four fundus images, each with a specific wavelength of light. Specialized software automatically selects measurement points on these images and calculates the optical density of retinal vessels at two wavelengths, 605 nm and 586 nm (optical density is sensitive to oxygen saturation at 605 nm but not at 586 nm). The ratio of these optical densities is approximately linearly related to the hemoglobin oxygen concentration. The oximeter is then calibrated to yield relative oxygen saturation values. This approach has been shown to be sensitive to changes in oxygen concentration and to yield reproducible results. In recent years, efforts have also been made to generate normative databases for retinal oxygenation measurements across different ethnic groups.[75,76] In lightly pigmented individuals, it has even been possible to use this device to measure choroidal oxygenation.[77] Finally, using Oxymap software, it has been possible to adapt an ultrawide-field SLO system (Optomap 200Tx, Optos Inc., Scotland) to perform retinal oximetry (this device uses two lasers for image acquisition, 532 and 633 nm, and thus can be used for multispectral imaging).[78]

Hyperspectral imaging involves the measurement of light from images obtained at narrow spectral bands over a contiguous spectral range. Mordant et al. have recently described the validation of a hyperspectral fundus camera for noninvasive retinal oximetry (Fig. 7.9).[79] In their system, a commercial fundus camera is linked to a liquid crystal tunable filter in the optical path of the camera's light source; this enables the electronic selection of a combination of desired wavelengths between 400 and 700 nm. A CCD camera is then used to record a sequence of spectral images between 500 and 650 nm in 2-nm increments (this process takes approximately 10–15

minutes in healthy volunteers). Further image processing and analysis then takes place: the images are registered, the retinal vessel profiles extracted, and their optical densities estimated. Oxygen saturations can then be calculated. Use of hyperspectral imaging in this manner may provide more accurate measurements of oxygen saturation than two-wavelength multispectral approaches (such approaches have been reported to overestimate oxygen saturation). However, such an approach requires the use of sensitive detectors and powerful computers to enable fast and accurate processing of images. In 2014, Kashani et al. described human studies of another form of hyperspectral imaging device, using computed tomography (CT) algorithms to extract spectral data patterns.[80]

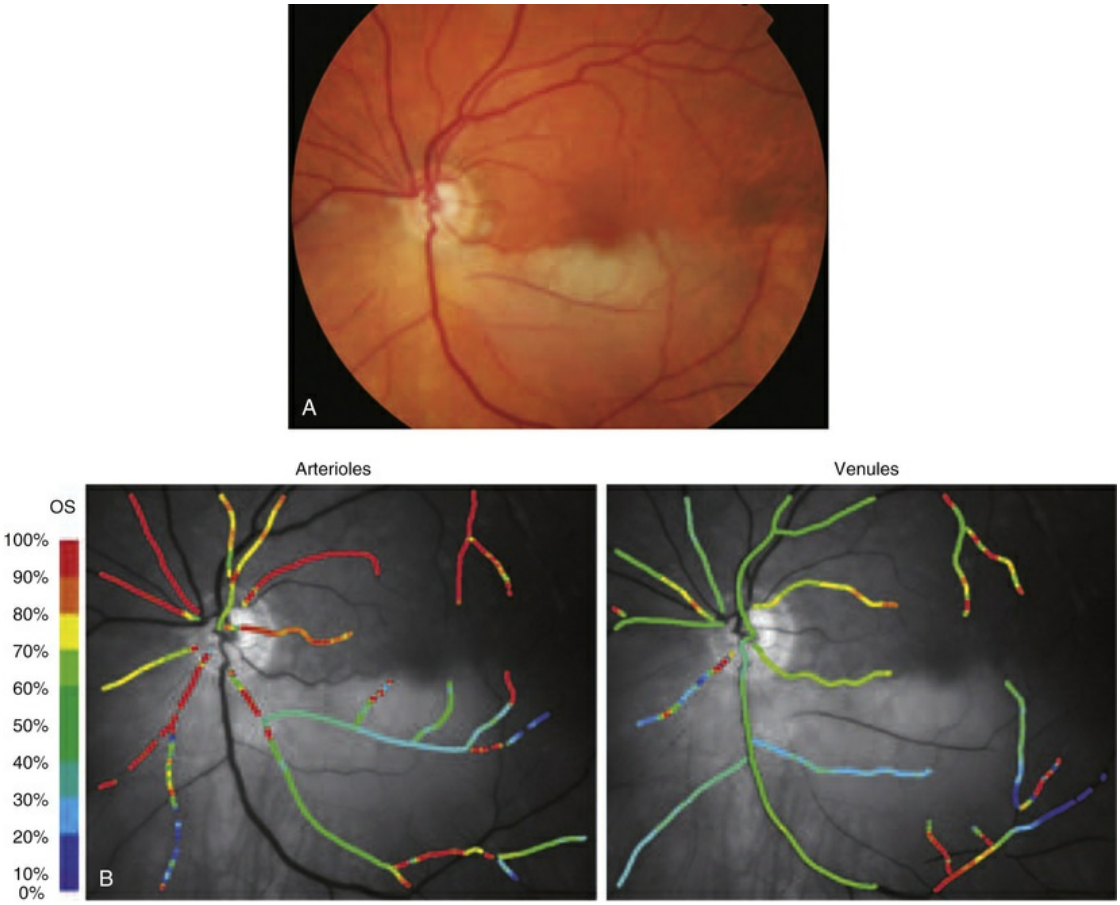

FIG. 7.9 Spectral imaging of the retina. (A) Color fundus photograph demonstrating a left inferotemporal branch retinal arteriole occlusion. (B) Pseudocolor oximetry map showing abnormally low oxygen saturation within the affected inferotemporal retinal

arteriole in contrast to the normal OS levels in the unaffected superotemporal arteriole. The corresponding inferotemporal retinal venule has a normal level of oxygen saturation. (Reproduced with permission from Mordant DJ, Al-Abboud I, Muyo G, et al. Spectral imaging of the retina. Eye 2011; 25(3):317.)

A third method utilized for the noninvasive measurement of retinal oxygen saturation involves imaging spectroscopy. Schweitzer et al. have described an imaging ophthalmospectrometer, which consists of a modified fundus camera and an attached spectrograph.[81] The instrument illuminates the retina with a small slit of light and then simultaneous measurements are made at 76 different wavelengths – in this discrete area – using a spectrometer. This approach may be the most accurate, however a major limitation is that measurements are made at one single cross-section of one or two retinal vessels. By contrast, a complete two-dimensional mapping of oxygen saturation in the retinal vascular tree is needed for clinical diagnostics.

Clinical Applications

Using the Oxymap system, Hardarson et al. have evaluated retinal vasculature oxygen saturations in patients following central retinal vein and branch retinal vein occlusion (CRVO/BRVO).[82,83] In patients with CRVO, they demonstrated that retinal venular oxygen saturation is lower than in fellow eyes. However, they also demonstrated considerable variability within and between CRVO eyes. Similarly, in patients with BRVO, they found considerable variability in oxygen saturation between patients. They found evidence of hypoxia in some patients but not others and speculated that this reflected variable disease severity in terms of degree of occlusion, recanalization, collateral circulation, and coexistent tissue atrophy. Traustason et al. used the Oxymap system to examine retinal oxygenation in patients receiving intravitreal ranibizumab for CRVO. They showed that retinal venous oxygen saturation was markedly reduced in untreated CRVO, but was “halfway” normalized during the course of this intravitreal therapy.[84]

A growing body of work has begun to evaluate Oxymap measurements in patients with diabetic retinopathy.[85] This work suggests that retinal vessel oxygen saturation is higher in patients with diabetic retinopathy than in healthy controls. Possible explanations for this include shunting of blood through preferential channels, bypassing nonperfused capillaries in the capillary network. Thus parts of the retina may be hypoxic while blood in larger blood vessels has higher oxygen saturation. Oxymap measurements are now also being incorporated into clinical trials of diabetic retinopathy, e.g., the CLEOPATRA trial looking at the role of light masks in the treatment of early diabetic macular edema.[86]

Hardarson et al., have also used this system to examine the effects of glaucoma filtration surgery, and topical anti-glaucoma medications, on retinal vascular oxygen concentrations.[87] A wide variety of other conditions have now been examined also, including age-related macular degeneration (AMD), retinitis pigmentosa, high myopia, and following pars plana vitrectomy and/or long-term silicone oil tamponade. Perhaps most interestingly, use of the Oxymap system has demonstrated abnormalities in retinal oxygen metabolism in Alzheimer's disease.[88]

Using the Imedos system, Hammer et al. found that, in patients with diabetes, increasing severity of retinopathy was associated with increased retinal venous oxygen saturations (from 63 ± 5 % for mild nonproliferative retinopathy, to 75 ± 8% for proliferative retinopathy).[89] Conversely, earlier work by Tiedeman et al. demonstrated evidence of increased oxygen consumption (i.e., decreased retinal venous oxygen saturation) in diabetic patients with acute hyperglycemia.[90] The Imedos system has shown changes in retinal vascular oxygen saturation in patients with inherited retinal dystrophies (especially rod–cone dystrophies) and glaucoma. Interestingly, it has also been used to show reduced oxygen metabolism in patients with giant cell arteritis but without ocular symptoms,[91] and in patients with chronic obstructive pulmonary disease (COPD).[92]

Spectral Imaging – Other Applications

Spectral imaging approaches may also be used to estimate the

optical density of other absorbers in the eye, including lens optical density, macular pigments (lutein and zeaxanthin), melanin, lipofuscin, and visual pigments. A triple wavelength, multispectral reflectometer has recently been described which has the potential to allow rhodopsin density and regeneration mapping.[93]

Conclusions

Although major progress has been made in recent years, there is currently no consensus on the optimal method for measurement of oxygen saturation in the retinal vasculature. A number of spectral imaging devices provide relative, rather than absolute, measurements of oxygen saturation. Furthermore, all devices rely, to a certain extent, on biophotonic assumptions that may not hold true for in vivo imaging. Therefore, it is vital that detailed validation and reproducibility assessments be performed on all new retinal oximeters before such devices can be widely adopted for clinical or research purposes.

Photoacoustic Imaging: Assessment of Retinal Absorption

Basic Principles

In large part, contemporary retinal imaging modalities are based on the measurement of light reflected from the retina, e.g., fundus photography, SLO, OCT systems.[2] In contrast, no ophthalmic imaging modality exists that can directly measure the absorption of light by retinal tissues. Hemoglobin and melanin are particularly strong absorbers of light, so this information is potentially of great clinical interest. For example, light absorption by hemoglobin may provide contrast for generation of enhanced retinal angiographic maps, while light absorption by melanin could aid visualization of the highly pigmented RPE cell mosaic. Assessment of optical absorption profiles at multiple wavelengths may also improve the accuracy of retinal vascular oxygen saturation measurements (current "spectral imaging" determines optical density ratios indirectly, through the measurement of reflected light). Fortunately,

through recent advances in microscopy, utilizing the photoacoustic effect, it has become possible to acquire optical absorption profiles in the context of noninvasive ophthalmic imaging – photoacoustic ophthalmoscopy (PAOM).[94,95]

The photoacoustic effect was first recognized by Alexander Graham Bell in the 1880s when he discovered that thin discs of Selenium emit sound when exposed to a rapidly interrupted beam of sunlight. This phenomenon occurs as energy absorbed from the incident light is converted into kinetic energy, which results in local heating and, thus, generation of a pressure wave or sound. In the recently described photoacoustic microscopy (PAM),[96] a laser is used to irradiate a target tissue and thus induce ultrasonic pressure waves as a result of specific optical absorption. These pressure waves can then be recorded using a high-resolution ultrasonic transducer, and images generated. As PAOM is the only existing optical-absorption-based ophthalmic imaging modality, it can be readily integrated with other reflectance-based imaging modalities – fundus cameras, SLO devices, fluorescein angiography, fundus autofluorescence, and OCT – for "true" multimodal imaging.[97]

Technology

Through the integration of OCT technology with a laser-scanning, optical resolution PAM, Jiao et al. have recently reported the use of PAOM in small animals.[94,95] In this system, the illumination source is a frequency doubled, Q-switched, Nd:YAG laser producing nanosecond laser pulses, combined with the output laser beam of a fiber-based spectral domain OCT system.[94] The photoacoustic waves induced from the retina are then detected by a stationary, unfocused ultrasonic transducer placed in contact with the eyelid (coupled by ultrasound gel). The resulting photoacoustic images can then be registered with the images generated from the integrated OCT system (Fig. 7.10). As with conventional OCT image sets, maximum amplitude "projection" images can be generated from photoacoustic datasets allowing two-dimensional visualization of the retinal vasculature. Volumetric images can also be generated following automated segmentation of the RPE and retinal vessels. The same group has tested the acquisition of

photoacoustic images in association with fundus autofluorescence signals (apart from generating heat, the absorbed photons may undergo other physical processes, such as stimulating autofluorescence when fluorophores are present). Multimodal imaging in this manner may thus provide spatial information on the distribution of both melanin and lipofuscin via photoacoustic and autofluorescent signals respectively.[98] More recently, Doppler OCT has been integrated with PAM, allowing for quantification of retinal oxygen metabolic rates,[99] and for quantification of RPE melanin in vivo.[100]

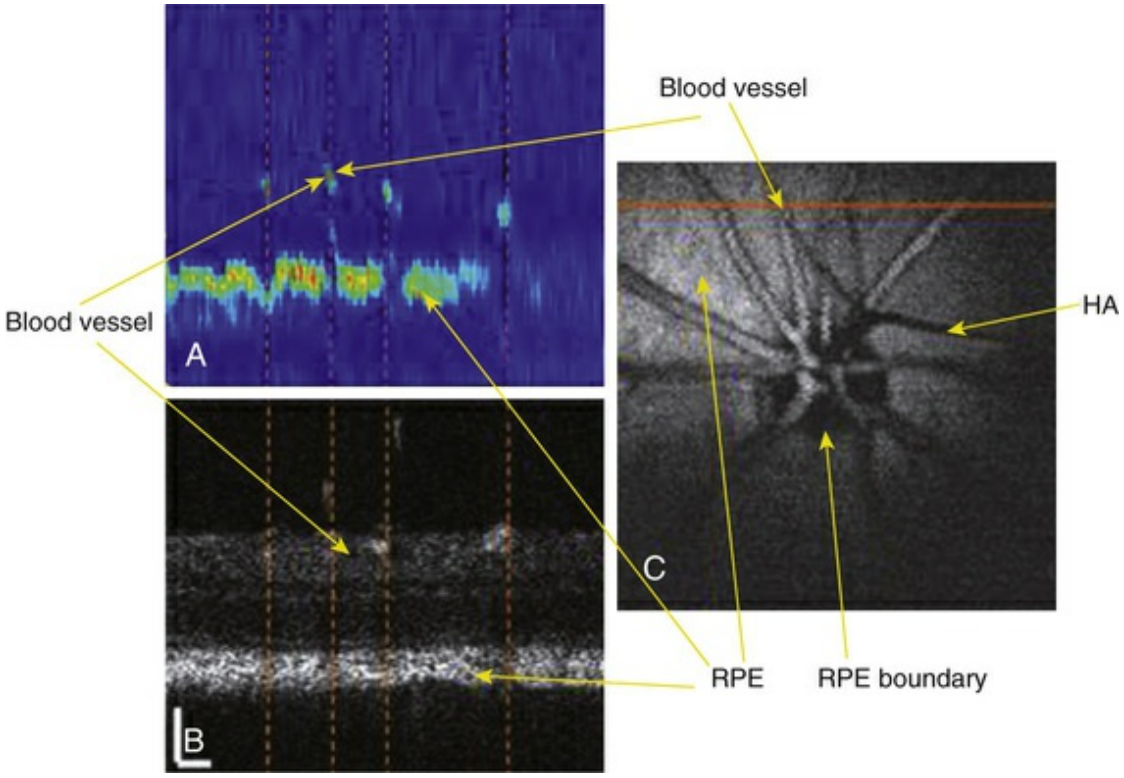

FIG. 7.10 Comparison of optical coherence tomography (OCT) and photoacoustic ophthalmoscopy (PAOM) images acquired simultaneously in vivo. (A) PAOM B-scan image in pseudocolor. (B) OCT B-scan image. (C) Projection image of the PAOM data set. Scale bar: 100 μm. *HA*, hyaloid artery; *RPE*, retinal pigment epithelium. (Reproduced with permission from Jiao S, Jiang M, Hu J, et al. Photoacoustic ophthalmoscopy for in vivo retinal imaging. Optics Express 2010;18(4):3971.)

The combination of OCT imaging with PAM requires two

separate light sources – OCT needs a broadband light source to achieve depth resolution, while PAM requires a pulsed laser. Using a single light source to achieve simultaneous OCT and PAM imaging was first reported in 2012.[101] The technique was termed optical coherence photoacoustic microscopy (OC-PAM). In vivo retinal imaging using an OC-PAM system with center wavelength 830 nm has recently been described. Since the optical absorption of hemoglobin in the near-infrared (NIR) spectrum is much smaller than that in the visible spectrum, this system would not be expected to provide good contrast for imaging the retinal vasculature. However, it may be ideally suited to imaging of melanin distributions in the RPE and choroid.[102]

Conclusions

The development of photoacoustic imaging techniques may greatly extend the scope of future retinal imaging; however, at present, the technology remains at an early stage in the development process. Virtually all the work to date, on photoacoustic imaging in the eye, has been performed in tissue samples or in animals. A number of technical hurdles remain before images can be obtained from living human subjects, or commercial, clinical devices can be introduced.

Magnetic Resonance Imaging

The acquisition of retinal images is largely dependent on optical techniques such as fundus photography. However, many such techniques are constrained by a relatively small field of view, and are often limited when there is disease-induced opacification of the ocular media, such as lens opacity or vitreous hemorrhage. In the clinical setting, these limitations are addressed, at least in part, by acoustic imaging techniques such as ultrasonography. More recently, however, advances in magnetic resonance imaging (MRI) offer the prospect of retinal application in humans.[103,104] In addition to a wide field of view, and the ability to acquire images despite media opacification, retinal MRI may also aid in evaluation of novel functional parameters.

Basic Principles

In MRI systems, a powerful magnetic field is applied to the body leading to alignment of the magnetization of its hydrogen nuclei or protons (the human body is largely made up of water molecules, which contain two hydrogen atoms). Radiofrequency fields are then used to systematically alter this alignment, causing the protons to spin and producing a rotating magnetic field detectable by the scanner. Detectors in the MRI system then evaluate a number of parameters (e.g., spin density, spin–lattice relaxation time [T_1], spin–spin relaxation times [T_2]), which vary depending on the local tissue environment. As a result, soft tissue images can be generated. Image contrast may be further enhanced through the use of exogenous paramagnetic contrast agents such as gadolinium. In this manner, clinical MRI scanners can produce high-resolution images of the entire body, both noninvasively and in a single setting.[103]

As well as its anatomical imaging capability, MRI scanning can also be used to measure blood flow.[103] MRI-derived quantification of blood flow may be performed by the use of exogenous intravenous contrast agents, e.g., with the use of fluorescent microspheres. However, it may also be performed noninvasively by magnetically labeling blood as a means of providing endogenous contrast, so-called continuous arterial spin labeling (CASL). These techniques have been widely used to quantify blood flow to the brain and have been cross-validated using positron emission tomography (PET).

Relative blood oxygen saturations can also be measured using the BOLD (blood oxygenation level dependent) technique. This technique detects differences in magnetic resonance signal intensity that arise from changes in the oxygen saturation of hemoglobin during brain activation – a local decrease in concentration of deoxygenated hemoglobin will increase the BOLD signal (while an increase will decrease the BOLD signal). In the brain, when a specific region is activated in response to stimulation, local blood flow increases in response to the increased metabolic demand; such increases in blood flow will provide a boost in oxygen delivery and thus decrease the concentration of deoxygenated hemoglobin.

Techniques that measure blood flow and oxygenation can thus be used to noninvasively image brain function – fMRI (functional MRI).[103]

Retinal and Choroidal Imaging

To date, most work on retinal imaging using magnetic resonance has been reported in animal studies (Fig. 7.11).[103] As the spatial resolution of MRI is limited compared to that of OCT and other optical imaging modalities, current magnetic resonance-derived retinal imaging only allows delineation of three to four distinct retinal layers. Using gadolinium for contrast provides increased signal from the retinal and choroidal vasculature and thus aids in correlation of MRI retinal scans with histologic sections (the avascular photoreceptor layers do not show any enhancements using this method). Manganese has also been used as a contrast agent to improve the anatomic contrast between layers; using this approach, it has been possible to reveal seven distinct retinal bands of alternating hypo- and hyperintensity.[103]

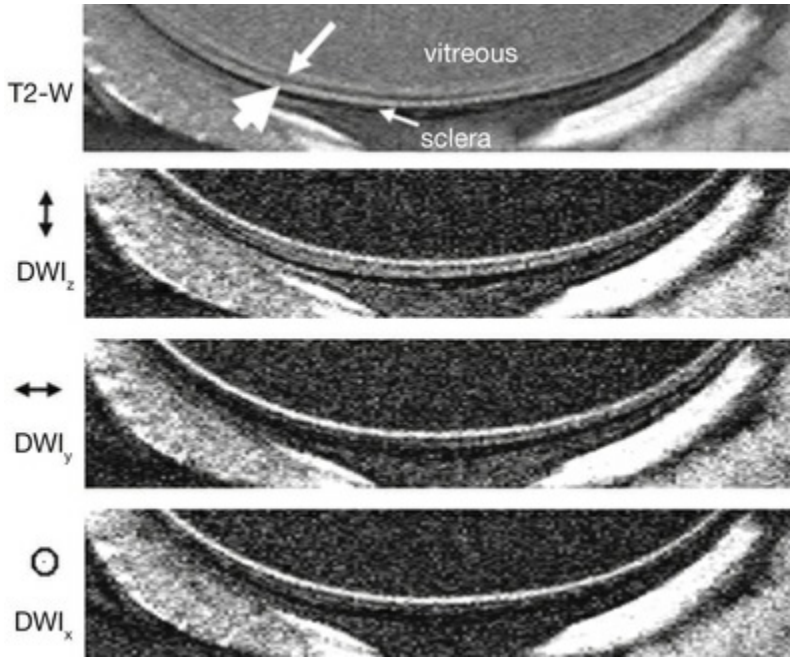

FIG. 7.11 Magnetic resonance imaging (MRI) of the retina in vivo. Higher-resolution T_2-weighted (TE = 40 msec) and diffusion-weighted (b = 504 seconds/mm^2) images (*TWI*, *DWI*) at 50×100 μm resolution. Diffusion-

sensitizing gradients were placed along the *x*, *y*, or *z* axis separately. The small and large white arrows indicate the "inner" and "outer" strips, respectively.
(Reproduced with permission from Shen Q, Cheng H, Pardue MT, et al. Magnetic resonance imaging of tissue and vascular layers in the cat retina. J Magn Reson Imaging 2006;23(4): 470.)

In 2008, the first report of retinal blood flow assessment, using MRI in rats, was published.[105] In this study, a CASL technique was used to quantify basal blood flow levels and their responses to physiologic stimulation. With the improvements in spatial resolution afforded by new MRI devices, visualization of separate retinal and choroidal blood flow has become possible in human subjects. In 2014, an MRI study in human subjects demonstrated reductions in choroidal blood flow with age.[106]

In animals, using BOLD fMRI techniques, differential responses of the retinal and choroidal circulations to physiologic stimuli (e.g., hyperoxia versus hypercapnia), have been demonstrated.[103] BOLD fMRI studies have also suggested that the retinal vasculature is very responsive to visual stimulation, but that the choroidal vasculature only showed small percentage changes.

Conclusions

Translation of retinal MRI from animal studies to human research and clinical practice faces a number of obstacles. The MRI scanners available in clinical environments currently have limited spatial resolutions and low signal to noise ratios. In addition, the issue of eye movements in awake humans is a major limiting factor. As a first step in addressing these issues, the feasibility of multimodal MRI has recently been tested on anesthetized large, nonhuman, primates (baboons) using a standard clinical scanner.[107] Studies of this nature allow optimization of MRI scanning parameters and represent a first step towards magnetic resonance-derived retinal imaging in humans. Zhang et al. have recently demonstrated, for the first time, the use of BOLD fMRI to examine the changes associated with oxygen and carbogen challenges in the unanesthetized human retina.[108] Although much work has still to be done, such imaging may prove a useful adjunct to more established

optical imaging methods, particularly when assessing the differential regulation of the retinal and choroidal circulations. Also of note, MRI scanning has lately been used to image the partial pressures of oxygen within the vitreous of human subjects.[109] The spatially heterogenous PO_2 maps generated may be of particular interest for the assessment of retinal vascular diseases.

Molecular Imaging

Even the potential combination of adaptive optics with OCT will fail to visualize the earliest cellular and biochemical processes that occur in many retinal diseases. In molecular imaging, exogenous contrast agents with targeting ligands are used to enhance the capabilities of conventional imaging platforms, and thus to allow selective visualization of cell types or biochemical processes.[110]

Contrast Agents

Fluorescent dyes are typically employed as contrast agents for use with fundus photographic and SLO imaging techniques. Sodium fluorescein and indocyanine green have a long history of use in humans, with derivatives such as fluorescein isothiocyanate (FITC) commonly used in animal studies. In recent years, however, the use of more novel nanoparticles has increasingly been explored.[111] For example, "quantum dots" are fluorescent nanocrystals consisting of a metalloid crystalline core (e.g., cadmium selenide) surrounded by a shell (e.g., zinc sulfide). The fluorescent properties of quantum dots offer a number of advantages for their use in optical imaging. The brightness of quantum dots is 10–100 times greater than most organic dyes or proteins. Quantum dots also show broad absorption characteristics with narrow emission spectra that are continuous and tunable due to quantum size effects. Quantum dots also possess a long fluorescence lifetime and undergo negligible photobleaching. Most importantly perhaps, quantum dots can be labeled to allow precise targeting of cellular structures. As a result of these features, quantum dots are increasingly being used for *in vivo* imaging in animal studies (Fig. 7.12), although concerns about cytotoxicity must be addressed before they will be suitable for use

in humans.

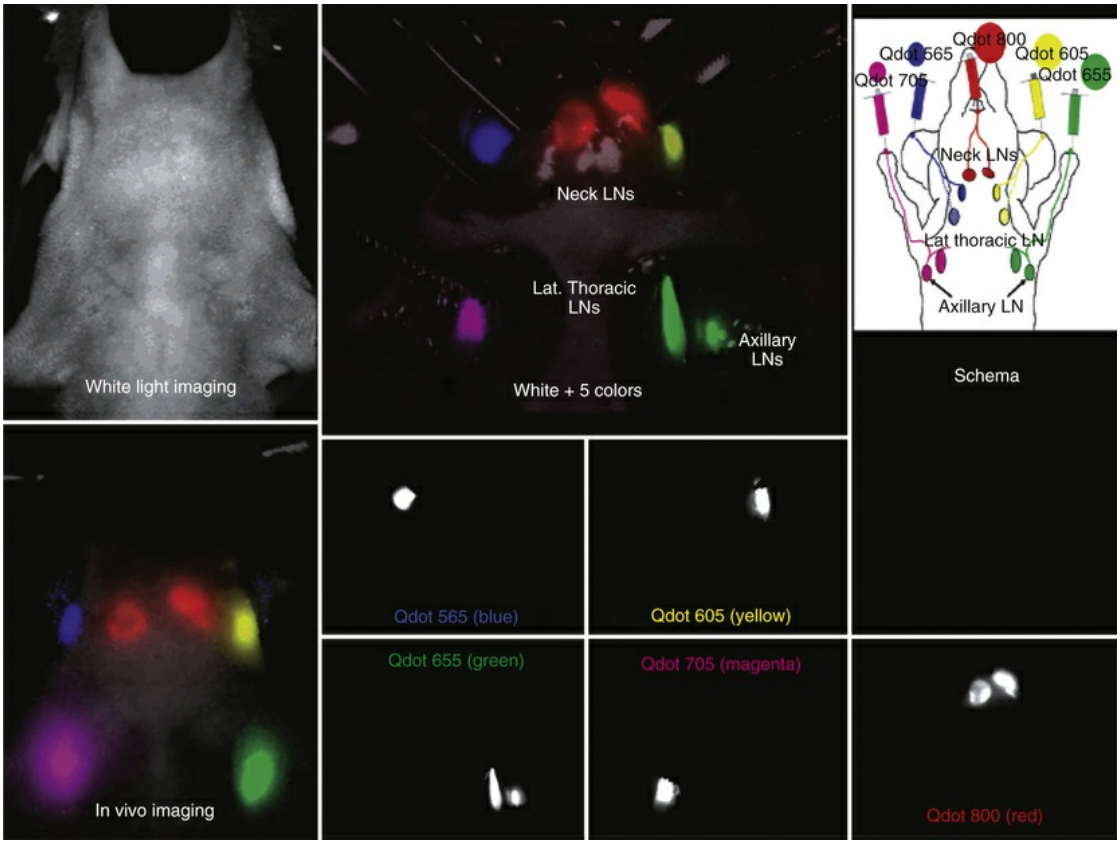

FIG. 7.12 In vivo and intrasurgical spectral fluorescence imaging of a mouse injected with five-carboxyl quantum dots (565, blue; 605, green; 655, yellow; 705, magenta; 800, red), intracutaneously into the middle digits of the bilateral upper extremities, the bilateral ears, and at the median chin, as shown in the schema. Five primary draining lymph nodes (*LNs*) were simultaneously visualized with different colors through the skin in the in vivo image and are more clearly seen in the image taken at the surgery.

(Reproduced with permission from Kobayashi H, Hama Y, Koyama Y, et al. Simultaneous multicolor imaging of five different lymphatic basins using quantum dots. Nano Letters 2007;7(6):1714.)

The use of contrast agents for enhancement of OCT imaging has been less well explored, in large part because, as OCT is "coherence gated," it is inherently blind to fluorescent probes. However, for a number of reasons, gold nanoparticles have potential for use as contrast agents with OCT.[112] Firstly, gold nanoparticles have the

property of localized surface plasmon resonance (LSPR) – this results in light scattering properties up to 40× greater than other identically sized particles that are not plasmonic. Secondly, they can be fabricated so that their light scattering properties attain a peak at the near-infrared wavelengths typically utilized by OCT systems. Thirdly, they can be readily conjugated with targeting ligands. Finally, they are water-soluble and potentially biocompatible – colloidal gold (suspensions of gold nanoparticles in fluid) has a long history of human use for treatment of conditions such as rheumatoid arthritis, while a number of newer gold nanoparticles are being evaluated in early phase clinical studies.[111,113,114]

Targeting Ligands

Targeting ligands are commonly based on macromolecules, such as peptides, antibodies, or proteins, and aimed at molecular imaging of (1) retinal ganglion cells (RGC); (2) RPE; (3) endothelial cells; and (4) leukocytes.[110] Perhaps the most advanced of these areas is the molecular imaging of retinal ganglion cells. This work is driven in large part by the role of retinal ganglion cell dysfunction and apoptosis in glaucomatous optic neuropathy (using conventional imaging techniques and visual field measurements, early recognition of retinal ganglion cell dysfunction is not possible). Using a technique called "detection of apoptosing retinal cells" (DARC), single-cell detection of retinal ganglion cell apoptosis has recently been demonstrated in animal models.[115] In this approach, fluorescently labeled Annexin V is administered via intraocular or intravenous injection and binds specifically to phosphatidylserine on apoptosing retinal ganglion cells (during apoptosis, this molecule is translocated from the inner to the outer plasma membrane, rendering it accessible to extracellular targeting ligands). These apoptosing cells can then be visualized using conventional ophthalmic imaging devices such as a confocal SLO. Significant regulatory hurdles must be overcome before any such testing can be performed in humans. Considerable safety and toxicology testing has already been performed, however, and early phase clinical trials are expected to commence in the near future.[116]

Conclusions

A large number of other nanoparticle groups are currently being investigated for their biomedical potential, with examples including carbon nanotubes, dendrimers, perfluorocarbons, and lipid-based nanoparticles.[117] The unique and tunable optical properties of many nanoparticles, along with their small size and capacity for cellular targeting, make them strong candidates for use as contrast agents in retinal imaging. Using these agents in combination with techniques such as OCT may ultimately allow visualization of many retinal structures (e.g., Müller cells), and cellular processes (e.g., apoptosis), in clinical practice. While such usage has yet to be demonstrated in humans, the previous commercialization of magnetic nanoparticles for MRI, and the early clinical trials of gold nanoparticle therapy in humans, provide grounds for optimism in this regard.

Conclusions and Future Directions

In the past 25 years, advances in retinal imaging have revolutionized the diagnosis and management of retinal disease. As recently as 1990, the conventional wisdom held that axial image resolution was fundamentally constrained by geometric optics and the depth of focus.[12] However, with the advent of OCT, axial resolution has now been improved 1000-fold over that previously thought possible. In the short to medium term, continued advances in OCT will be coupled with advances in adaptive optics technology to provide unprecedented, noninvasive, cellular imaging. In parallel with this, functional extensions of these, and other, imaging modalities will provide greatly enhanced information regarding parameters such as retinal blood flow and oxygenation. Increasing use of nanotechnology may provide "molecular" imaging capabilities, and allow evaluation of biochemical processes such as apoptosis. In the longer term, a number of fundamental limits will need to be overcome, including (1) constraints imposed by maximum light exposure that can be delivered safely to the eye; (2) windows of spectral transmittance imposed by the cornea and lens; and (3) diffraction limits imposed

by the wave nature of light.[12] While many of these barriers seem impenetrable, some early breakthroughs have already taken place in each area. In particular, the diffraction limit has already been surpassed in the field of microscopy,[118] and the use of such techniques may allow a leap forward to much smaller spatial scales in future retinal imaging.

Disclosure

Dr Keane has received a proportion of his funding from the Department of Health's NIHR Biomedical Research Centre for Ophthalmology at Moorfields Eye Hospital and UCL Institute of Ophthalmology. The views expressed in the publication are those of the authors and not necessarily those of the Department of Health.

Dr Keane has received travel grants from Allergan as part of the Allergan European Retina Panel. He has also given educational presentations for Topcon, Heidelberg, Bayer, Novartis, and Allergan.

Dr Sadda is a consultant for Optos and Carl Zeiss Meditec, and has received research instruments from Optos, Carl Zeiss Meditec, Topcon, and Nidek.

References

1. Keane PA, Sadda SR. Imaging chorioretinal vascular disease. *Eye (Lond)*. 2010;24(3):422–427.
2. Yannuzzi LA, Ober MD, Slakter JS, et al. Ophthalmic fundus imaging: today and beyond. *Am J Ophthalmol*. 2004;137(3):511–524.
3. Bennett T, Barry C. Ophthalmic imaging today: an ophthalmic photographer's viewpoint – a review. *Clin Experiment Ophthalmol*. 2009;37:2–13.
4. Yannuzzi LA. Indocyanine green angiography: a perspective on use in the clinical setting. *Am J Ophthalmol*. 2011;151(5):745–751.e1.
5. Panwar N, Huang P, Lee J, et al. Fundus photography in the 21st century – a review of recent technological advances

and their implications for worldwide healthcare. *Telemed J E Health*. 2016;22(3):198–208.
6. Maamari RN, Keenan JD, Fletcher DA, et al. A mobile phone-based retinal camera for portable wide field imaging. *Br J Ophthalmol*. 2014;98(4):438–441.
7. Russo A, Morescalchi F, Costagliola C, et al. A novel device to exploit the smartphone camera for fundus photography. *J Ophthalmol*. 2015;2015:823139.
8. Russo A, Morescalchi F, Costagliola C, et al. Comparison of smartphone ophthalmoscopy with slit-lamp biomicroscopy for grading diabetic retinopathy. *Am J Ophthalmol*. 2015;159(2):360–364.e1.
9. Bastawrous A, Giardini ME, Bolster NM, et al. Clinical validation of a smartphone-based adapter for optic disc imaging in Kenya. *JAMA Ophthalmol*. 2016;134(2):151–158.
10. Bastawrous A, Rono HK, Livingstone IA, et al. Development and validation of a smartphone-based visual acuity test (peek acuity) for clinical practice and community-based fieldwork. *JAMA Ophthalmol*. 2015;133(8):930–937.
11. Roorda A. Adaptive optics ophthalmoscopy. *J Refract Surg*. 2000;16(5):S602–7.
12. Williams DR. Imaging single cells in the living retina. *Vision Res*. 2011;51(13):1379–1396.
13. Liang J, Williams DR, Miller DT. Supernormal vision and high-resolution retinal imaging through adaptive optics. *J Opt Soc Am A Opt Image Sci Vis*. 1997;14(11):2884–2892.
14. Kitaguchi Y, Fujikado T, Bessho K, et al. Adaptive optics fundus camera to examine localized changes in the photoreceptor layer of the fovea. *Ophthalmology*. 2008;115(10):1771–1777.
15. Roorda A, Romero-Borja F, Donnelly W III. Adaptive optics scanning laser ophthalmoscopy. *Opt Express*. 2002;10(9):405–412.
16. Drexler W, Fujimoto JG. State-of-the-art retinal optical coherence tomography. *Prog Retin Eye Res*. 2008;27(1):45–88.
17. Miller DT, Kocaoglu OP, Wang Q, et al. Adaptive optics and the eye (super resolution OCT). *Eye (Lond)*. 2011;25(3):321–330.

18. Fernández EJ, Hermann B, Povazay B, et al. Ultrahigh resolution optical coherence tomography and pancorrection for cellular imaging of the living human retina. *Opt Express*. 2008;16(15):11083–11094.
19. Zawadzki RJ, Cense B, Zhang Y, et al. Ultrahigh-resolution optical coherence tomography with monochromatic and chromatic aberration correction. *Opt Express*. 2008;16(11):8126–8143.
20. Jonnal RS, Kocaoglu OP, Zawadzki RJ, et al. The cellular origins of the outer retinal bands in optical coherence tomography images. *Invest Ophthalmol Vis Sci*. 2014;55(12):7904–7918.
21. Poonja S, Patel S, Henry L, et al. Dynamic visual stimulus presentation in an adaptive optics scanning laser ophthalmoscope. *J Refract Surg*. 2005;21(5):S575–80.
22. Vogel CR, Arathorn DW, Roorda A, et al. Retinal motion estimation in adaptive optics scanning laser ophthalmoscopy. *Opt Express*. 2006;14(2):487–497.
23. Arathorn DW, Yang Q, Vogel CR, et al. Retinally stabilized cone-targeted stimulus delivery. *Opt Express*. 2007;15(21):13731–13744.
24. Miller DT, Williams DR, Morris GM, et al. Images of cone photoreceptors in the living human eye. *Vision Res*. 1996;36(8):1067–1079.
25. Miloudi C, Rossant F, Bloch I, et al. The negative cone mosaic: a new manifestation of the optical Stiles–Crawford effect in normal eyes. *Invest Ophthalmol Vis Sci*. 2015;56(12):7043–7050.
26. Liu BS, Tarima S, Visotcky A, et al. The reliability of parafoveal cone density measurements. *Br J Ophthalmol*. 2014;98(8):1126–1131.
27. Bidaut Garnier M, Flores M, Debellemaniere G, et al. Reliability of cone counts using an adaptive optics retinal camera. *Clin Experiment Ophthalmol*. 2014;42(9):833–840.
28. Flores M, Debellemaniere G, Bully A, et al. Reflectivity of the outer retina on spectral-domain optical coherence tomography as a predictor of photoreceptor cone density. *Am J Ophthalmol*. 2015;160(3):588–595.e2.

29. Roorda A, Williams DR. The arrangement of the three cone classes in the living human eye. *Nature*. 1999;397(6719):520–522.
30. Zhang T, Godara P, Blanco ER, et al. Variability in human cone topography assessed by adaptive optics scanning laser ophthalmoscopy. *Am J Ophthalmol*. 2015;160(2):290–300.e1.
31. Chui TY, Song H, Burns SA. Individual variations in human cone photoreceptor packing density: variations with refractive error. *Invest Ophthalmol Vis Sci*. 2008;49(10):4679–4687.
32. Doble N, Choi SS, Codona JL, et al. In vivo imaging of the human rod photoreceptor mosaic. *Opt Lett*. 2011;36(1):31–33.
33. Roorda A, Zhang Y, Duncan JL. High-resolution in vivo imaging of the RPE mosaic in eyes with retinal disease. *Invest Ophthalmol Vis Sci*. 2007;48(5):2297–2303.
34. Scoles D, Sulai YN, Dubra A. In vivo dark-field imaging of the retinal pigment epithelium cell mosaic. *Biomed Opt Express*. 2013;4(9):1710–1723.
35. Takayama K, Ooto S, Hangai M, et al. High-resolution imaging of the retinal nerve fiber layer in normal eyes using adaptive optics scanning laser ophthalmoscopy. *PLoS ONE*. 2012;7(3):e33158.
36. Nadler Z, Wang B, Schuman JS, et al. In vivo three-dimensional characterization of the healthy human lamina cribrosa with adaptive optics spectral-domain optical coherence tomography. *Invest Ophthalmol Vis Sci*. 2014;55(10):6459–6466.
37. Chui TY, Gast TJ, Burns SA. Imaging of vascular wall fine structure in the human retina using adaptive optics scanning laser ophthalmoscopy. *Invest Ophthalmol Vis Sci*. 2013;54(10):7115–7124.
38. Arichika S, Uji A, Hangai M, et al. Noninvasive and direct monitoring of erythrocyte aggregates in human retinal microvasculature using adaptive optics scanning laser ophthalmoscopy. *Invest Ophthalmol Vis Sci*. 2013;54(6):4394–4402.
39. Doble N. High-resolution, in vivo retinal imaging using

adaptive optics and its future role in ophthalmology. *Expert Rev Med Devices*. 2005;2(2):205–216.
40. Pinhas A, Razeen M, Dubow M, et al. Assessment of perfused foveal microvascular density and identification of nonperfused capillaries in healthy and vasculopathic eyes. *Invest Ophthalmol Vis Sci*. 2014;55(12):8056–8066.
41. Wolfing JI, Chung M, Carroll J, et al. High-resolution retinal imaging of cone–rod dystrophy. *Ophthalmology*. 2006;113(6):1019.e1.
42. Abozaid MA, Langlo CS, Dubis AM, et al. Reliability and repeatability of cone density measurements in patients with congenital achromatopsia. *Adv Exp Med Biol*. 2016;854:277–283.
43. Morgan JI, Han G, Klinman E, et al. High-resolution adaptive optics retinal imaging of cellular structure in choroideremia. *Invest Ophthalmol Vis Sci*. 2014;55(10):6381–6397.
44. Duncan JL, Talcott KE, Ratnam K, et al. Cone structure in retinal degeneration associated with mutations in the peripherin/RDS gene. *Invest Ophthalmol Vis Sci*. 2011;52(3):1557–1566.
45. Duncan JL, Zhang Y, Gandhi J, et al. High-resolution imaging with adaptive optics in patients with inherited retinal degeneration. *Invest Ophthalmol Vis Sci*. 2007;48(7):3283–3291.
46. Carroll J. Adaptive optics retinal imaging: applications for studying retinal degeneration. *Arch Ophthalmol*. 2008;126(6):857–858.
47. Zhang Y, Wang X, Rivero EB, et al. Photoreceptor perturbation around subretinal drusenoid deposits as revealed by adaptive optics scanning laser ophthalmoscopy. *Am J Ophthalmol*. 2014;158(3):584–596.e1.
48. Agarwal A, Soliman MK, Hanout M, et al. Adaptive optics imaging of retinal photoreceptors overlying lesions in white dot syndrome and its functional correlation. *Am J Ophthalmol*. 2015;160(4):806–816.e2.
49. Jacob J, Krivosic V, Paques M, et al. Cone density loss on adaptive optics in early macular telangiectasia type 2.

Retina. 2016;36(3):545–551.
50. Debellemaniere G, Flores M, Tumahai P, et al. Assessment of parafoveal cone density in patients taking hydroxychloroquine in the absence of clinically documented retinal toxicity. *Acta Ophthalmol*. 2015;93(7):e534–40.
51. Saleh M, Debellemaniere G, Meillat M, et al. Quantification of cone loss after surgery for retinal detachment involving the macula using adaptive optics. *Br J Ophthalmol*. 2014;98(10):1343–1348.
52. Errera MH, Coisy S, Fardeau C, et al. Retinal vasculitis imaging by adaptive optics. *Ophthalmology*. 2014;121(6):1311–1312.e2.
53. Denniston AK, Keane PA. Paravascular pathways in the eye: is there an 'ocular glymphatic system'? *Invest Ophthalmol Vis Sci*. 2015;56(6):3955–3956.
54. Hood DC, Chen MF, Lee D, et al. Confocal adaptive optics imaging of peripapillary nerve fiber bundles: implications for glaucomatous damage seen on circumpapillary OCT scans. *Transl Vis Sci Technol*. 2015;4(2):12.
55. Choi SS, Zawadzki RJ, Keltner JL, et al. Changes in cellular structures revealed by ultra-high resolution retinal imaging in optic neuropathies. *Invest Ophthalmol Vis Sci*. 2008;49(5):2103–2119.
56. Ciulla TA, Regillo CD, Harris A. *Retina and optic nerve imaging*. Lippincott Williams & Wilkins: Philadelphia; 2003.
57. Williamson TH, Harris A. Ocular blood flow measurement. *Br J Ophthalmol*. 1994;78(12):939–945.
58. Schmetterer L, Garhofer G. How can blood flow be measured? *Surv Ophthalmol*. 2007;52(Suppl. 2):S134–8.
59. Harris A, Chung H, Ciulla T, et al. Progress in measurement of ocular blood flow and relevance to our understanding of glaucoma and age-related macular degeneration. *Prog Retin Eye Res*. 1999;18(5):669–687.
60. Keyser BJ, Flaharty PM, Sergott RC, et al. Color Doppler imaging of arterial blood flow in central retinal vein occlusion. *Ophthalmology*. 1994;101(8):1357–1361.
61. Ho AC, Lieb WE, Flaharty PM, et al. Color Doppler imaging

of the ocular ischemic syndrome. *Ophthalmology*. 1992;99(9):1453–1462.
62. Feke G, Yoshida A. Laser based instruments for ocular blood flow assessment. *J Biomed Opt*. 1998;3:415–422.
63. Yoshida A, Feke GT, Mori F, et al. Reproducibility and clinical application of a newly developed stabilized retinal laser Doppler instrument. *Am J Ophthalmol*. 2003;135(3):356–361.
64. Nagaoka T, Yoshida A. Relationship between retinal blood flow and renal function in patients with type 2 diabetes and chronic kidney disease. *Diabetes Care*. 2013;36(4):957–961.
65. Omae T, Nagaoka T, Yoshida A. Relationship between retinal blood flow and serum adiponectin concentrations in patients with type 2 diabetes mellitus. *Invest Ophthalmol Vis Sci*. 2015;56(6):4143–4149.
66. Sehi M. Basic technique and anatomically imposed limitations of confocal scanning laser Doppler flowmetry at the optic nerve head level. *Acta Ophthalmol*. 2011;89(1):e1–11.
67. Kanakamedala P, Harris A, Siesky B, et al. Optic nerve head morphology in glaucoma patients of African descent is strongly correlated to retinal blood flow. *Br J Ophthalmol*. 2014;98(11):1551–1554.
68. Huang D, Swanson E, Lin C, et al. Optical coherence tomography. *Science*. 1991;254(5035):1178–1181.
69. Werkmeister RM, Schmidl D, Aschinger G, et al. Retinal oxygen extraction in humans. *Sci Rep*. 2015;5:15763.
70. Mordant DJ, Al-Abboud I, Muyo G, et al. Spectral imaging of the retina. *Eye (Lond)*. 2011;25(3):309–320.
71. Harris A, Dinn RB, Kagemann L, et al. A review of methods for human retinal oximetry. *Ophthalmic Surg Lasers Imaging*. 2003;34(2):152–164.
72. Jaedicke V, Agcaer S, Robles FE, et al. Comparison of different metrics for analysis and visualization in spectroscopic optical coherence tomography. *Biomed Opt Express*. 2013;4(12):2945–2961.
73. Beach JM, Schwenzer KJ, Srinivas S, et al. Oximetry of retinal vessels by dual-wavelength imaging: calibration and

influence of pigmentation. *J Appl Physiol*. 1999;86(2):748–758.
74. Hardarson SH, Harris A, Karlsson RA, et al. Automatic retinal oximetry. *Invest Ophthalmol Vis Sci*. 2006;47(11):5011–5016.
75. Jani PD, Mwanza JC, Billow KB, et al. Normative values and predictors of retinal oxygen saturation. *Retina*. 2014;34(2):394–401.
76. Mohan A, Dabir S, Yadav NK, et al. Normative database of retinal oximetry in Asian Indian eyes. *PLoS ONE*. 2015;10(4):e0126179.
77. Kristjansdottir JV, Hardarson SH, Harvey AR, et al. Choroidal oximetry with a noninvasive spectrophotometric oximeter. *Invest Ophthalmol Vis Sci*. 2013;54(5):3234–3239.
78. Kristjansdottir JV, Hardarson SH, Halldorsson GH, et al. Retinal oximetry with a scanning laser ophthalmoscope. *Invest Ophthalmol Vis Sci*. 2014;55(5):3120–3126.
79. Mordant DJ, Al-Abboud I, Muyo G, et al. Validation of human whole blood oximetry, using a hyperspectral fundus camera with a model eye. *Invest Ophthalmol Vis Sci*. 2011;52(5):2851–2859.
80. Kashani AH, Lopez Jaime GR, Saati S, et al. Noninvasive assessment of retinal vascular oxygen content among normal and diabetic human subjects: a study using hyperspectral computed tomographic imaging spectroscopy. *Retina*. 2014;34(9):1854–1860.
81. Schweitzer D, Hammer M, Kraft J, et al. In vivo measurement of the oxygen saturation of retinal vessels in healthy volunteers. *IEEE Trans Biomed Eng*. 1999;46(12):1454–1465.
82. Hardarson SH, Stefánsson E. Oxygen saturation in central retinal vein occlusion. *Am J Ophthalmol*. 2010;150(6):871–875.
83. Hardarson SH, Stefánsson E. Oxygen saturation in branch retinal vein occlusion. *Acta Ophthalmol*. 2012;90(5):466–470.
84. Traustason S, la Cour M, Larsen M. Retinal vascular oximetry during ranibizumab treatment of central retinal vein occlusion. *Br J Ophthalmol*. 2014;98(9):1208–1211.
85. Hardarson SH, Stefansson E. Retinal oxygen saturation is

altered in diabetic retinopathy. *Br J Ophthalmol*. 2012;96(4):560–563.
86. Sivaprasad S, Arden G, Prevost AT, et al. A multicentre phase III randomised controlled single-masked clinical trial evaluating the clinical efficacy and safety of light-masks at preventing dark-adaptation in the treatment of early diabetic macular oedema (CLEOPATRA): study protocol for a randomised controlled trial. *Trials*. 2014;15:458.
87. Hardarson SH, Gottfredsdottir MS, Halldorsson GH, et al. Glaucoma filtration surgery and retinal oxygen saturation. *Invest Ophthalmol Vis Sci*. 2009;50(11):5247–5250.
88. Einarsdottir AB, Hardarson SH, Kristjansdottir JV, et al. Retinal oximetry imaging in Alzheimer's disease. *J Alzheimers Dis*. 2015;49(1):79–83.
89. Hammer M, Vilser W, Riemer T, et al. Diabetic patients with retinopathy show increased retinal venous oxygen saturation. *Graefes Arch Clin Exp Ophthalmol*. 2009;247(8):1025–1030.
90. Tiedeman JS, Kirk SE, Srinivas S, et al. Retinal oxygen consumption during hyperglycemia in patients with diabetes without retinopathy. *Ophthalmology*. 1998;105(1):31–36.
91. Turksever C, Daikeler T, Konieczka K, et al. Retinal vessel oxygen saturation in giant cell arteritis patients without ocular symptoms. *Klin Monatsbl Augenheilkd*. 2014;231(4):442–446.
92. Palkovits S, Lasta M, Boltz A, et al. Measurement of retinal oxygen saturation in patients with chronic obstructive pulmonary disease. *Invest Ophthalmol Vis Sci*. 2013;54(2):1008–1013.
93. Cui X, Fraser S. Assess the function and health of retina in vivo with triple wavelengths imaging multispectral reflectometry. *Invest Ophthalmol Vis Sci*. 2012;53:2160.
94. Jiao S, Jiang M, Hu J, et al. Photoacoustic ophthalmoscopy for in vivo retinal imaging. *Opt Express*. 2010;18(4):3967–3972.
95. Jiao S, Xie Z, Zhang HF, et al. Simultaneous multimodal imaging with integrated photoacoustic microscopy and

optical coherence tomography. *Opt Lett*. 2009;34(19):2961–2963.
96. Zhang HF, Maslov K, Stoica G, et al. Functional photoacoustic microscopy for high-resolution and noninvasive in vivo imaging. *Nat Biotechnol*. 2006;24(7):848–851.
97. Song W, Wei Q, Liu T, et al. Integrating photoacoustic ophthalmoscopy with scanning laser ophthalmoscopy, optical coherence tomography, and fluorescein angiography for a multimodal retinal imaging platform. *J Biomed Opt*. 2012;17(6):061206.
98. Zhang X, Jiang M, Fawzi AA, et al. Simultaneous dual molecular contrasts provided by the absorbed photons in photoacoustic microscopy. *Opt Lett*. 2010;35(23):4018–4020.
99. Liu W, Zhang HF. Noninvasive in vivo imaging of oxygen metabolic rate in the retina. *Conf Proc IEEE Eng Med Biol Soc*. 2014;2014:3865–3868.
100. Shu X, Liu W, Zhang HF. Monte Carlo investigation on quantifying the retinal pigment epithelium melanin concentration by photoacoustic ophthalmoscopy. *J Biomed Opt*. 2015;20(10):106005.
101. Zhang X, Zhang HF, Jiao S. Optical coherence photoacoustic microscopy: accomplishing optical coherence tomography and photoacoustic microscopy with a single light source. *J Biomed Opt*. 2012;17(3):030502.
102. Liu X, Liu T, Wen R, et al. Optical coherence photoacoustic microscopy for in vivo multimodal retinal imaging. *Opt Lett*. 2015;40(7):1370–1373.
103. Duong TQ. Magnetic resonance imaging of the retina: a brief historical and future perspective. *Saudi J Ophthalmol*. 2011;25(2):137–143.
104. Duong TQ, Muir ER. Magnetic resonance imaging of the retina. *Jpn J Ophthalmol*. 2009;53(4):352–367.
105. Li Y, Cheng H, Duong TQ. Blood-flow magnetic resonance imaging of the retina. *Neuroimage*. 2008;39(4):1744–1751.
106. Emeterio Nateras OS, Harrison JM, Muir ER, et al. Choroidal blood flow decreases with age: an MRI study. *Curr Eye Res*. 2014;39(10):1059–1067.

107. Zhang Y, Wey HY, Nateras OS, et al. Anatomical, blood oxygenation level-dependent, and blood flow MRI of nonhuman primate (baboon) retina. *Magn Reson Med*. 2011;66:546–554.
108. Zhang Y, Peng Q, Kiel JW, et al. Magnetic resonance imaging of vascular oxygenation changes during hyperoxia and carbogen challenges in the human retina. *Invest Ophthalmol Vis Sci*. 2011;52(1):286–291.
109. Muir ER, Zhang Y, San Emeterio Nateras O, et al. Human vitreous: MR imaging of oxygen partial pressure. *Radiology*. 2013;266(3):905–911.
110. Capozzi ME, Gordon AY, Penn JS, et al. Molecular imaging of retinal disease. *J Ocul Pharmacol Ther*. 2013;29(2):275–286.
111. Zarbin MA, Montemagno C, Leary JF, et al. Nanomedicine in ophthalmology: the new frontier. *Am J Ophthalmol*. 2010;150(2):144–162.e2.
112. Arvizo R, Bhattacharya R, Mukherjee P. Gold nanoparticles: opportunities and challenges in nanomedicine. *Expert Opin Drug Deliv*. 2010;7(6):753–763.
113. Morton JG, Day ES, Halas NJ, et al. Nanoshells for photothermal cancer therapy. *Methods Mol Biol*. 2010;624:101–117.
114. Gobin AM, Lee MH, Halas NJ, et al. Near-infrared resonant nanoshells for combined optical imaging and photothermal cancer therapy. *Nano Lett*. 2007;7(7):1929–1934.
115. Cordeiro MF, Migdal C, Bloom P, et al. Imaging apoptosis in the eye. *Eye (Lond)*. 2011;25(5):545–553.
116. Normando EM, Turner LA, Cordeiro MF. The potential of annexin-labelling for the diagnosis and follow-up of glaucoma. *Cell Tissue Res*. 2013;353(2):279–285.
117. Nune SK, Gunda P, Thallapally PK, et al. Nanoparticles for biomedical imaging. *Expert Opin Drug Deliv*. 2009;6(11):1175–1194.
118. Betzig E, Patterson GH, Sougrat R, et al. Imaging intracellular fluorescent proteins at nanometer resolution. *Science*. 2006;313(5793):1642–1645.

8

Image Processing

Michael D. Abràmoff

Introduction

This chapter introduces quantitative approaches to retinal image analysis. Special emphasis is placed on familiarizing the reader with basic concepts in imaging and image analysis, and machine learning and deep learning, the main approaches to retinal image

analysis. Fundus and optical coherence tomography (OCT) image analysis are reviewed, as well as the use of these modalities in providing comprehensive descriptions of retinal morphology and function. Relevant translational clinical applications are discussed, including automated early detection of diabetic retinopathy and image analysis-assisted management of choroidal neovascularization. This chapter allows the reader to understand concepts in retinal image analysis, and critically review the clinical and translational impact of the research in this field.

History of Retinal Imaging

The optical properties of the eye that allow image formation prevent direct inspection of the retina. Though existence of the red reflex has been known for centuries, special techniques are needed to obtain a focused image of the retina. The first attempt to image the retina, in a cat, was completed by the French physician Jean Mery, who showed that if a live cat is immersed in water, its retinal vessels are visible from the outside.[1] The impracticality of such an approach for humans led to the invention of the principles of the ophthalmoscope in 1823 by Jan Evangelista Purkyňe and its reinvention in 1845 by Charles Babbage.[2,3] Finally, the ophthalmoscope was reinvented yet again and reported by von Helmholtz in 1851.[4] Thus, inspection and evaluation of the retina became routine for ophthalmologists, and the first images of the retina (Fig. 8.1) were published by the Dutch ophthalmologist van Trigt in 1853.[5] Earlier sketches by Purkyňe provided drawings of his own retinal vasculature.[6]

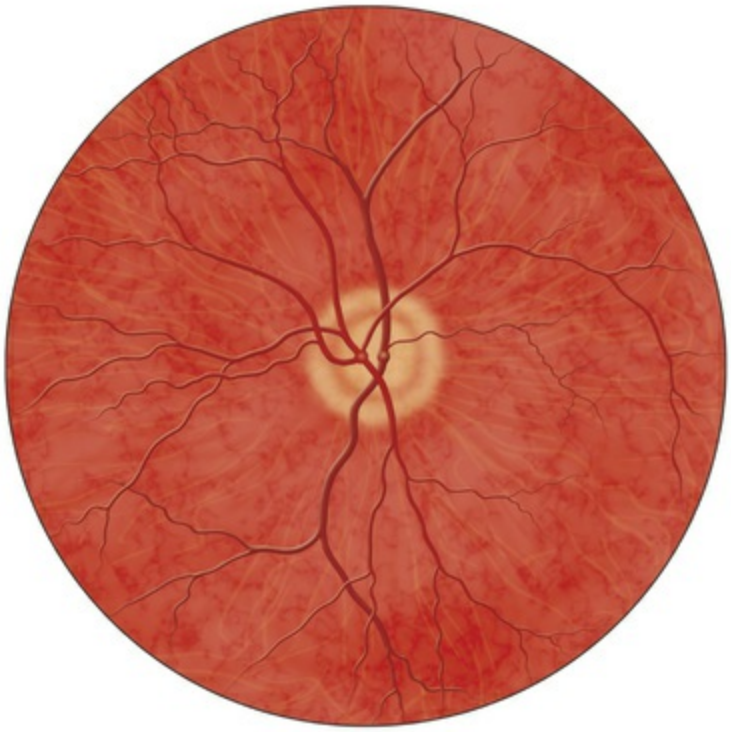

FIG. 8.1 First known image of human retina as drawn by Van Trigt in 1853. (Reproduced from Trigt AC. Dissertatio ophthalmologica inauguralis de speculo oculi. 1853.)

The first useful photographic images of the retina, showing blood vessels, were obtained in 1891 by the German ophthalmologist Gerloff.[7] In 1910, Gullstrand developed the fundus camera, a concept still used to image the retina today;[8] he later received the Nobel Prize for this invention. Because of its safety and cost-effectiveness at documenting retinal abnormalities, fundus imaging has remained the primary method of retinal imaging.

In 1961, Novotny and Alvis published their findings on fluorescein angiographic imaging.[9] In this imaging modality, a fundus camera with additional narrow band filters is used to image a fluorescent dye injected into the bloodstream that binds to leukocytes. It remains widely used, because it allows an understanding of the functional state of the retinal circulation.

The initial approach to depict the three-dimensional shape of the retina was stereo fundus photography, as first described by Allen in 1964, where multiangle images of the retina are combined by the human observer into a three-dimensional shape.[10] Subsequently, confocal scanning laser ophthalmoscopy was developed, using the

confocal aperture to obtain multiple images of the retina at different confocal depths, yielding estimates of three-dimensional shape. However, the optics of the eye limit the depth resolution of confocal imaging to approximately 100 μm, which is poor when compared with the typical 300–500 μm thickness of the whole retina.[11]

Optical coherence, based on Michelson's description of interferometry in 1872,[12] was first used as a method for time of flight measurement of the depth of mechanical structures.[13,14] It was then extended to a tissue imaging technique to determine the position of structures in tissue described by Huang et al. in 1991,[15] termed optical coherence tomography (OCT). In 1993, in vivo retinal OCT was accomplished for the first time.[16] Today, OCT has become a prominent biomedical tissue-imaging technique, especially in the eye, because it is particularly suited to semi-transparent tissues, but also for any tissue imaging requiring micrometer resolution.

History of Retinal Image Processing

Matsui et al. were the first to publish a method for retinal image analysis, primarily focused on vessel segmentation.[17] Their approach was based on mathematical morphology and they used digitized slides of fluorescein angiograms of the retina. In the following years, there were several attempts to segment other anatomical structures in the normal eye, all based on digitized slides. The first method to detect and segment abnormal structures was reported in 1984, when Baudoin et al. described an image analysis method for detecting microaneurysms, a characteristic lesion of diabetic retinopathy.[18] Their approach was also based on digitized angiographic images. They detected microaneurysms using a “top-hat” transform, a step-type digital image filter.[19] This method employs a mathematical morphology technique that eliminates the vasculature from a fundus image yet leaves possible microaneurysm candidates untouched. The field dramatically changed in the 1990s with the development of digital retinal imaging and the expansion of digital filter-based image analysis techniques. These developments resulted in an exponential rise in the number of publications, which continues today. Most recently,

so-called deep-learning techniques, a form of machine learning consisting of multilayer neural networks, and specifically convolutional neural networks, have been gaining attention for retinal imaging tasks.[20–22c]

Current Status of Retinal Imaging

Retinal imaging has developed rapidly during the last 160 years and is a now a mainstay of the clinical care and management of patients with retinal as well as systemic diseases. Fundus photography is widely used for population-based, large-scale detection of diabetic retinopathy, glaucoma, and age-related macular degeneration (AMD). OCT and fluorescein angiography are widely used in the daily management of patients in a retina clinic setting. OCT has also become an increasingly helpful adjunct in preoperative planning and postoperative evaluation of vitreoretinal surgical patients.[23] The overview below is partially based on an earlier review paper.[24]

Fundus Imaging

Fundus imaging is the process whereby reflected light is used to obtain a two-dimensional (2D) representation of the three-dimensional, semi-transparent, retinal tissues projected onto the imaging plane. Thus, any process that results in a 2D image where the image intensities represent the amount of a reflected quantity of light, is fundus imaging. Consequently, OCT imaging is not fundus imaging, while the following modalities/techniques all belong to the broad category of fundus imaging:

1. **Fundus photography** (including so-called red-free photography) – image intensities represent the amount of reflected light of a specific waveband.

2. **Color fundus photography** – image intensities represent the amount of reflected R (red), G (green), and B (blue) wavebands, as determined by the spectral sensitivity of the sensor.

3. **Stereo fundus photography** – image intensities represent the amount of reflected light from two or more different view angles for depth resolution.

4. **Scanning laser ophthalmoscopy (SLO)** – image intensities represent the amount of reflected single wavelength laser light obtained in a time sequence.

5. **Adaptive optics SLO** – image intensities represent the amount of reflected laser light optically corrected by modeling the aberrations in its wavefront.

6. **Fluorescein angiography and indocyanine angiography** – image intensities represent the amounts of emitted photons from the fluorescein or indocyanine green fluorophore that was injected into the subject's circulation.

There are several technical challenges in fundus imaging. Since the retina is normally not illuminated internally, both external illumination projected into the eye as well as the retinal image projected out of the eye must traverse the pupillary plane. Thus the size of the pupil, usually between 2 and 8 mm in diameter, has been the primary technical challenge in fundus imaging.[8] Fundus imaging is complicated by the fact that the illumination and imaging beams cannot overlap because such overlap results in corneal and lenticular reflections diminishing or eliminating image contrast. Consequently, separate paths are used in the pupillary plane, resulting in optical apertures on the order of only a few millimeters. Because the resulting imaging setup is technically challenging, fundus imaging historically involved relatively expensive equipment and highly trained ophthalmic photographers. Over the last ten years or so, there has been a concerted effort and several important developments that have made fundus imaging more accessible, resulting in less dependence on such experience and expertise. There has been a shift from film-based to digital image acquisition, and as a consequence the importance of Picture Archiving and Communication Systems (PACS) has substantially increased in clinical ophthalmology, also allowing integration with electronic medical records. Requirements

for population-based early detection of retinal diseases using fundus imaging have provided the incentive for effective and user-friendly imaging equipment. Operation of fundus cameras by nonophthalmic photographers has become possible due to nonmydriatic imaging, digital imaging with near-infrared focusing, and standardized imaging protocols to increase reproducibility.

Though standard fundus imaging is widely used, it is not suitable for retinal tomography, because of the mixed backscatter caused by the semitransparent retinal layers.

Optical Coherence Tomography Imaging

OCT is a noninvasive optical medical diagnostic imaging modality that enables in vivo cross-sectional tomographic visualization of the internal microstructure in biologic systems. OCT is analogous to ultrasound B mode imaging except that it measures the echo time delay and magnitude of light rather than sound, therefore achieving unprecedented image resolutions (1–10 μm).[25] Optical coherence tomography is an interferometric technique, typically employing near-infrared light. The use of relatively long wavelength light with a very wide-spectrum range allows OCT to penetrate into the scattering medium and achieve micrometer resolution.

The principle of OCT is based upon low coherence interferometry,[26a] where the backscatter from more outer, retinal tissues can be differentiated from that of more inner tissues, because it takes longer for the light to reach the sensor. Because the differences between the most superficial and the deepest layers in the retina are around 300–400 μm, the difference in time of arrival is very small and requires interferometry to measure.[26a]

In OCT, the central wavelength is usually in the near infrared. The principle of low coherence, or low correlation, means that the light coming from the light source is only correlating over a short amount of time. In other words, the autocorrelation function of the light wave is only large for a short duration, and at all other times it is essentially zero. If the light is fully coherent, the autocorrelation

is high forever, and it becomes impossible to create an interference pattern and determine when the light was emitted. If the light is entirely incoherent, there can be no interference at all. Thus, the low coherence nature of the light allows each infinitesimal short duration of light to be "labeled"; the label is its unique wave-pattern over that short duration. This unique wave-pattern sent out at a specific timepoint can be differentiated from the light sent out a little bit later as this has a different wave-pattern. Though wave-pattern is used, it is important to understand that the light wave is actually continuous, not pulsed. A lower coherence means that the wave-pattern is unique over a shorter duration, and this allows a better depth resolution.

The label can uniquely indicate when reflected light was emitted, and thus we can measure differences between arrival times of light. To be able to measure differences, the low coherent light is optically split into two bundles, called arms, before being sent into the eye. One arm, the reference arm, is aimed at a mirror at a known distance, and from there reflected to the interferometer; the other, the sample arm, is sent into the eye and reflects back from the different tissues, primarily the retina, at yet unknown depth, so that light at inner retinal layers is reflected back earlier than that at more outer layers. If the distance to the mirror is exactly the same as the distance to a retinal structure, and thus the timepoint when they were emitted is the same, the two arms, optically combined at the interferometer, will show maximum correlation (they have the same "label"), which results in a high intensity called interference. The more difference in emission time, the less correlation, and the less interference. This is because the more the two light waves resemble each other at a moment in time, the higher the interference; remember that after splitting, each carried the same low coherence "label." Because the optical properties of the eye add noise and thus slightly change the reflected reference arm light wave, the interference will never be perfect, even if the distance to the mirror exactly matches the distance to the retinal structure. Though the coherence pattern or label changes continuously over time, once they are split, they have the same label (but changing rapidly over time), so that the interference will be high as long as the reference and sample distances are the same, and only if light

from both arms has travelled the "same" optical distance ("same" meaning a difference of less than a coherence length). The energy or envelope of the interference is then measured as intensity using a photo sensor. This is then displayed as the familiar grayscale values of the OCT signal intensity. By changing the position of the reference arm mirror, we can "interrogate" the amount of interference at different sample tissue depths. By changing the position of the sample arm on the retina, we can scan the retina, resulting in the familiar B-scans and volumes. Snapshot OCT, where all A-scans are obtained simultaneously, using a lenslet array, has also been described.[26b]

The importance of the choice of a good low-coherence source is clear – with either an incoherent or fully coherent source, interferometry is impossible. Such light can be generated by using superluminescent diodes (superbright light-emitting diodes) or lasers with extremely short pulses, femtosecond lasers. The optical setup typically consists of a Michelson interferometer with a low-coherence, broad-bandwidth light source (Fig. 8.2). By scanning the mirror in the reference arm, as in time domain OCT, modulating the light source, as in swept source OCT, or decomposing the signal from a broadband source into spectral components, as in spectral domain OCT (SD-OCT), a reflectivity profile of the retina can be obtained, as measured by the interferogram. The reflectivity profile, called an A-scan, contains information about the spatial dimensions and location of structures within the retina. A cross-sectional tomograph (B-scan) may be achieved by laterally combining a series of these axial depth scans (A-scan). En face imaging (C-scan) at an acquired depth is possible depending on the imaging engine used.

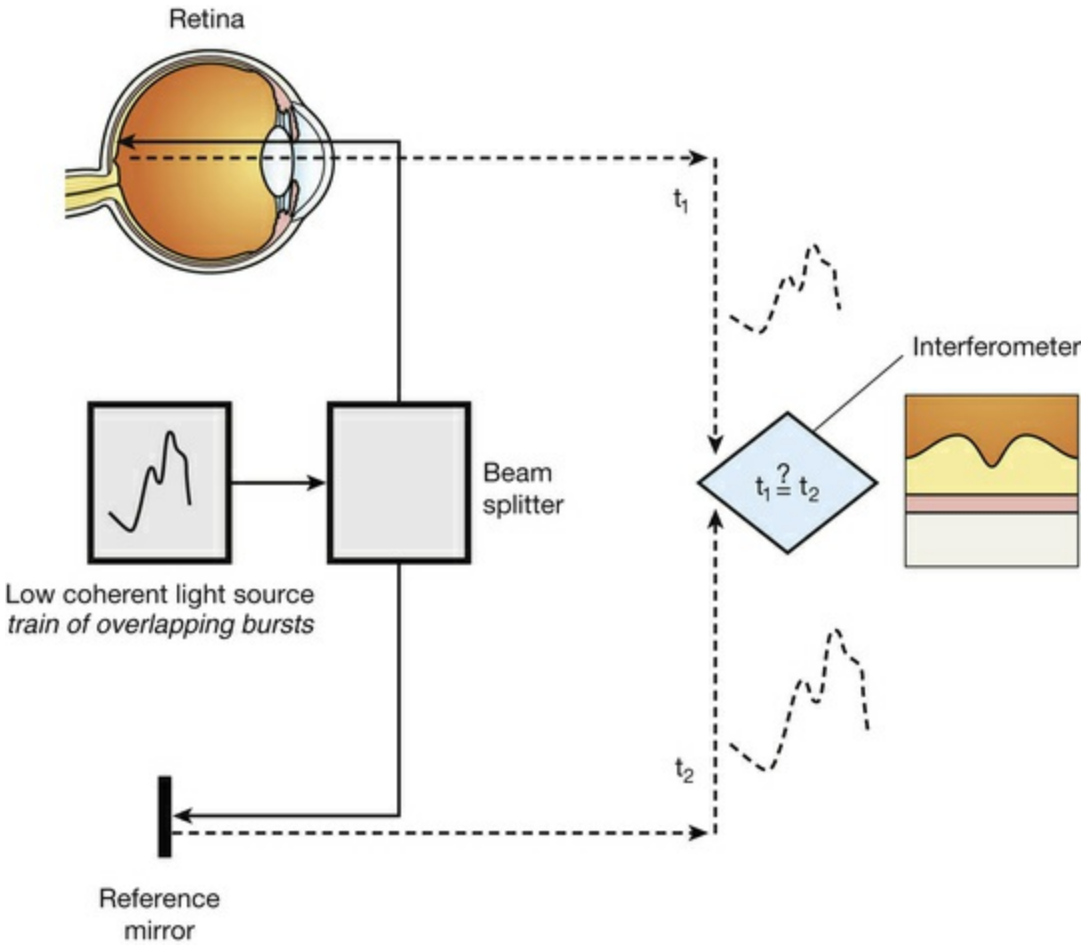

FIG. 8.2 Schematic diagram of operation of optical coherence tomography, emphasizing splitting of the light in two arms, train of overlapping bursts "labeled" based on their autocorrelogram, and their interference after being reflected from retinal tissue as well as from the reference mirror (assuming the time delays of both paths are equal).

In conventional interferometry with long coherence length (laser interferometry), interference of light occurs over a distance of meters. In OCT, this interference is shortened to a distance of micrometers, possible due to the use of broadband light sources, i.e., sources that can emit light over a broad range of wavelengths. Light with broad bandwidths can be generated by using superluminescent diodes (superbright LEDs) or lasers with extremely short pulses, femtosecond lasers. White light is also a broadband source with lower power.

The transverse resolution of OCT scans (x; y) depends on the speed and quality of the galvanic scanning mirrors and the optics of

the eye, and is typically 20–40 μm. The resolution of the A-scans along the z direction depends on the coherence of the light source and is currently 4–8 μm in commercially available scanners. Isotropic (or isometric) means that the size of each imaged element, or voxel, is the same in all three dimensions. Current commercially available OCT devices routinely offer voxel sizes of 30×30×2 μm, achieving isometricity in the x–y plane only. Available spectral domain OCT scanners are never truly isotropic, because the retinal tissue in each A-scan is sampled at much smaller intervals in depth than are the distances between A- and/or B-scans. The resolution in depth, also known as the z-dimension, is currently always higher than the resolution in the x–y plane. The primary advantage of x–y isotropic imaging when quantifying properties of the retina is that fewer assumptions have to be made about the tissue in-between the measured samples, thus potentially leading to more accurate indices of retinal morphology.

Time Domain OCT

With time domain OCT, a reference mirror is moved mechanically to different positions, resulting in different flight time delays for the reference arm light. Because the speed at which the mirror can be moved is mechanically limited, only thousands of A-scans can be obtained per second. The envelope of the interferogram determines the intensity at each depth.[15] The ability to image the retina two-dimensionally and three-dimensionally depends on the number of A-scans that can be acquired over time. Because of motion artifacts such as saccades, safety requirements limiting the amount of light that can be projected onto the retina, and patient comfort, 1–3 seconds per image or volume is essentially the limit. Thus, the commercially available time domain OCT, which allowed collecting of up to 400 A-scans per second, has not yet been suitable for 3D imaging.

Frequency Domain OCT

In frequency domain OCT, the broadband interference is acquired with spectrally separated detectors, either by encoding the optical frequency in time with a spectrally scanning source or with a

dispersive detector, like a grating and a linear detector array. The depth scan can be immediately calculated by a Fourier-transform from the acquired spectra, without movement of the reference arm. This feature improves imaging speed dramatically, while the reduced losses during a single scan improve the signal to noise proportional to the number of detection elements. The parallel detection at multiple wavelength ranges limits the scanning range, while the full spectral bandwidth sets the axial resolution.

Spectral Domain OCT

A broadband light source is used, broader than in time domain OCT, and the interferogram is decomposed spectrally using a diffraction grating and a complementary metal oxide semiconductor (CMOS) or charged-couple device (CCD) linear sensor. The Fourier transform is again applied to the spectral correlogram intensities to determine the depth of each scatter signal.[27] With spectral domain OCT, tens of thousands of A-scans can be acquired each second, and thus true 3D imaging is routinely possible. Consequently, 3D OCT is now in wide clinical use, and has become the standard of care.

Swept Source OCT

Instead of moving the reference arm as with time domain OCT imaging, in swept source OCT the light source is rapidly modulated over its center wavelength, essentially attaching a second label to the light, its wavelength. A photo sensor is used to measure the correlogram for each center wavelength over time. A Fourier transform on the multiwavelength or spectral interferogram is performed to determine the depth of all tissue scatters at the imaged location.[27] With swept-source OCT, hundreds of thousands of A-scans can be obtained every second, promising additional increase in scanning density when acquiring 3D image volumes.

Areas of Active Research in Retinal Imaging

Retinal imaging is rapidly evolving and newly completed research findings are quickly translated into clinical use.

Portable, Cost-Effective Fundus Imaging

For early detection and screening, the optimal place for positioning fundus cameras is at the point of care: primary care clinics, public venues (e.g., drug stores, shopping malls), etc. Though the transition from film-based to digital fundus imaging has revolutionized the art of fundus imaging and made telemedicine applications feasible, the current cameras are still too bulky, expensive, and may be difficult to use for nontrained staff in places lacking ophthalmic imaging expertise. Several groups are attempting to create more cost-effective and easier-to-use handheld fundus cameras, employing a variety of technical approaches.[28,29]

Functional Imaging

For the patient as well as for the clinician, the outcome of disease management is mainly concerned with the resulting organ function, not its structure. In ophthalmology, current functional testing is mostly subjective and patient-dependent, such as assessing visual acuity and utilizing perimetry, which are all psychophysical metrics. Among more recently developed "objective" techniques, oxymetry is a hyperspectral imaging technique, in which multispectral reflectance is used to estimate the concentration of oxygenated and deoxygenated hemoglobin in the retinal tissue.[30] The principle allowing the detection of such differences is simple: deoxygenated hemoglobin reflects longer wavelengths better than does oxygenated hemoglobin. Nevertheless, measuring absolute oxygenation levels with reflected light is difficult because of the large variety in retinal reflection across individuals and the variability caused by the imaging process. The retinal reflectance can be modeled by a system of equations, and this system is typically underconstrained if this variability is not accounted for adequately. Increasingly sophisticated reflectance models have been developed to correct for the underlying variability, with some reported success.[31] Near-infrared fundus reflectance in response to visual stimuli is another way to determine the retinal function in

vivo and has been successful in cats. Initial progress has also been demonstrated in humans.[32]

Adaptive Optics

The optical properties of the normal eye result in a point spread function width approximately the size of a photoreceptor. It is therefore impossible to image individual cells or cell structure using standard fundus cameras because of aberrations in the human optical system. Adaptive optics uses mechanically activated mirrors to correct the wavefront aberrations of the light reflected from the retina, and thus has allowed individual photoreceptors to be imaged in vivo.[33] Imaging other cells, especially the clinically highly important ganglion cells, has thus far been unsuccessful in humans. (See also Chapter 7, Advanced imaging technologies.)

Longer Wavelength OCT Imaging

Three-dimensional OCT imaging is now the clinical standard of care for several eye diseases. The wavelengths around 840 μm used in currently available devices are optimized for imaging of the retina. Deeper structures, such as the choroidal vessels, which are important in AMD and uveitis, and the lamina cribrosa – a deep structure in the optic nerve relevant for glaucomatous damage – are not as well depicted. Low-coherence swept source lasers with center wavelengths of 1000–1300 μm are now available in commercially available clinical devices, allowing resolution of detail in the choroid and lamina cribrosa.[34]

Angiographic OCT

Except for the changes caused by blood particles flowing through the retinal and choroid blood vessels, most retinal tissue changes only slowly over time, on the scale of hours to years. The difference in the timescale of changes allows those voxels where blood flows to be visualized, by displaying brightly voxels that change reflectance rapidly, i.e., between two rapid (on a timescale of ms) sequence sweeps of A-scans. In other words, the rapid *change* in optical properties of blood caused by lymphocytes and erythrocytes

moving through the location of the A-scan is displayed as an intensity, and the faster the blood is flowing, the greater the change in A-scan reflectance, and the brighter it is displayed. This recent important innovation allows, for example, the capillaries in the foveal avascular zone to be imaged with high precision. Because angiographic OCT will only image those blood vessels with relatively rapid flow, slower phenomena such as (fluorescein angiographic) *leakage* from damaged capillaries in diabetic macular edema, cystoid macular edema, and choroidal neovascularization cannot be displayed.

Clinical Applications of Retinal Imaging

The most obvious example of a retinal screening application is retinal disease detection, in which the patient's retinas are imaged in a remote telemedicine approach. This scenario typically utilizes easy-to-use, relatively low-cost fundus cameras, automated analyses of the images, and focused reporting of the results. This screening application has spread rapidly over the last few years, and with the exception of the automated analysis functionality, is one of the most successful examples of telemedicine.[35] While screening programs exist for detection of glaucoma, AMD, and retinopathy of prematurity, the most important screening application focuses on early detection of diabetic retinopathy (DR). (See Chapter 53, Telescreening for diabetic retinopathy; Chapter 65, Telescreening for retinopathy of prematurity.)

Early Detection of Diabetic Retinopathy

Early detection of DR via population screening associated with timely treatment has been shown to prevent visual loss and blindness in patients with retinal complications of diabetes.[36,37] Almost 50% of people with diabetes in the United States currently do not undergo any form of regular documented dilated eye examination, in spite of guidelines published by the American Diabetes Association, the American Academy of Ophthalmology,

and the American Optometric Association.[38] In the United Kingdom, a smaller proportion or approximately 20% of diabetics are not regularly evaluated, as a result of an aggressive effort to increase screening for people with diabetes. Blindness and visual loss can be prevented through early detection and timely management. There is widespread consensus that regular early detection of DR via screening is necessary and cost-effective in patients with diabetes.[39–42] Remote digital imaging and ophthalmologist expert reading have been shown to be comparable or superior to an office visit for assessing DR and have been suggested as an approach to make the dilated eye examination available to unserved and underserved populations that do not receive regular examinations by eye care providers.[43,44] If all of these underserved populations were to be provided with digital imaging, the annual number of retinal images requiring evaluation would exceed 32 million in the United States alone (approximately 40% of people with diabetes with at least two photographs per eye).[44,45] In the next decade, projections for the United States are that the average age will increase, the number of people with diabetes in each age category will increase, and there will be an undersupply of qualified eye care providers, at least in the near term. Several European countries have successfully instigated in their healthcare systems early detection programs for DR using digital photography with reading of the images by human experts. In the United Kingdom, 1.7 million people with diabetes were screened for DR in 2007–2008. In the Netherlands, over 30,000 people with diabetes were screened since 2001 in the same period, through an early detection project called EyeCheck.[46] The United States Department of Veterans Affairs (VA) has deployed a successful photo screening program through which more than 120,000 veterans were screened in 2008. While the remote imaging followed by human expert diagnosis approach was shown to be successful for a limited number of participants, the current challenge is to make the early detection more accessible by reducing the cost and manpower required, while maintaining or improving DR detection performance. This challenge can be met by utilizing computer-assisted or fully automated methods for detection of DR in retinal images.[47–49]

Early Detection of Systemic Disease From Fundus Photography

In addition to detecting DR and AMD, it also deserves mention that fundus photography allows cardiovascular risk factors to be determined. Such metrics are primarily based on measurement of retinal vessel properties, such as the arterial to venous diameter ratio, or A–V ratio, and indicate the risk for stroke, hypertension or myocardial infarct.[50,51]

Image-Guided Therapy for Retinal Diseases With Three-Dimensional OCT

With the introduction of 3D OCT imaging, the wealth of new information about the retinal morphology has enabled its usage for close monitoring of retinal disease status and guidance of retinal therapies. The most obvious example of successful image-guided management in ophthalmology is its use in diabetic macular edema (DME). Currently, OCT imaging is widely used to determine the extent and amount of retinal thickening. Detailed analyses of retinal layer morphology and texture from OCT has the potential to allow direct image-based treatment to be guided by computer-supported or automated quantitative analysis. This can be subsequently optimized allowing personalized approach to retinal disease treatment to become a reality.

Another highly relevant example of a disease that will benefit from image-guided therapy is exudative AMD. With the advent of the anti-VEGF agents ranibizumab and bevacizumab, it has become clear that outer retinal and subretinal fluid is the main indicator of a need for anti-VEGF retreatment.[52–56] Several studies are underway to determine whether OCT-based quantification of fluid parameters and affected retinal tissue can help improve the management of patients with anti-VEGF agents.

Image Analysis Concepts for Clinicians

Image analysis is a field that relies heavily on mathematics and physics. The goal of this section is to explain the major, clinically relevant concepts and challenges in image analysis, with limited use of mathematics or equations. For a detailed explanation of the underlying mathematics, the reader is referred to the appropriate textbooks.[57]

The Retinal Image

Definition of a Retinal Image

As interpreted by a computer, an image is a set of elements with values that are organized. The elements, called pixels, each have a single value, the intensity, when the image is a monochrome or an OCT image; and multiple values, when the image is a color image. For example, in an angiogram or OCT image, the intensity value of each pixel is the amount of reflected light that was measured at that pixel position. In a color image, there are usually three intensity values (for red, blue, and green) assigned to a pixel, which combine make up the color of that pixel.

Retinal Image Quantities

Because computers use a binary system (1s and 0s) to store and process information, and do not use the decimal system, image intensities typically have values ranging between 0–255, 0–65536, or −32767 to +32767, instead of the 0–1000 or 100,000 that one might expect if computers used the decimal system. This can be explained by the fact that, typically, 1, 2, or 3 bytes are used to store the intensity values for a pixel, as combinations of 1s and 0s. Though more bytes take up more space, the precision of the intensity values becomes greater. Psychophysical research has shown that the human visual system can differentiate at most 500 different levels of gray, and at most 10 million different colors, so that increasing the precision of the intensity values beyond these levels will not increase the visual perception of quality of an image. However, there may be some value in increasing the precision despite this fact since image analysis algorithms can discern a higher number of levels than humans can.

Retinal Image Compression

Image compression is useful because it decreases the amount of memory required to store images digitally or communicate these images over a network such as the Internet. Image compression can be "loss-less" or "lossy," and makes use of the fact that images are always somewhat repetitive. If the intensity value of a pixel has a certain value, the values of the pixels in its surround usually have similar values.

In order to explain the concept of an image compression algorithm, let us proceed with an example. We start with an image in which an area of 50 pixels all have the same intensity value. We will pick the value 128. Instead of storing 50 memory elements, all having the value 50 (typically requiring 50 bytes total), the simple image compression algorithm counts the number of repetitions of an intensity value, reducing this number to two memory elements: the first one, the repeat value 50, and the second one, the repeated intensity 128 (requiring only two bytes of storage). To restore the original image area, an uncompression algorithm takes the two elements and reconstitutes the 50 pixels each having 128 as intensity.

Because no image information is lost, and the uncompression algorithm can reconstitute the image perfectly, this is loss-less compression.

Lossy Image Compression

To improve image compression rates even more, lossy compression algorithms make use of the fact that the human visual system does not notice small intensity changes in the image. A lossy compression algorithm would compress the image in the example above in exactly the same manner. However, if we take an image where the 50 pixels in the area did not have exactly the same value, but varied slightly around the value 128, the image compression algorithm would compress the image differently. For the human visual system, this area would be hard to differentiate from the same area where all 50 pixels had intensity values of 128. The simple loss-less algorithm above would not be able to compress this area, because the pixels in the area have different intensities, and would store the 50 pixels as 50 elements. The lossy algorithm is

"smarter" and "knows" the limits of human visual perception, and will assign all pixels varying only a "little" from 128 the intensity value of 128, and store the repeat value, and the repeated intensity. The uncompression algorithm would assign all 50 pixels the same 128 as intensity. Thus the original information in the image is lost, though typically this is not noticeable to the human visual system.

Legal Issues With Lossy Image Compression

Lossy compression is widely used in ophthalmic imaging, especially for storing acquired images in image databases (see PACS section below). In theory, but so far not in practice, a medicolegal situation could arise as a result of lossy compression artifact. In a hypothetical case where the diagnosis of a clinician is disputed, that clinician may have seen an abnormality on an image immediately after acquisition, which subsequently underwent lossy compression, was stored and thus became part of the medical record. Because lossy compression causes irreversible loss of information, that abnormality may not be visible anymore on the archived image after uncompression, making it impossible to view the same image that the clinician originally saw and upon which his/her diagnosis was based. One can certainly envision the legal implications and liability of this scenario.

Examples of loss-less compression image formats are compressed TIFF, GIF, and PNG file formats, as well as the "raw" formats that are generated directly by the imaging device. Common lossy compression-based image formats are JPEG and MPEG.

Storing and Accessing Retinal Images: Ophthalmology Picture Archiving Systems

After an image is acquired on a fundus camera or OCT device, it becomes part of the medical record. It therefore should be stored in some form, so that it can be communicated to other clinicians and providers, or consulted at a later date.

Images can be stored directly on the imaging device, but so-called Picture Archiving Systems (PACS) are available that make image storage more practical, allowing images from a variety of imaging devices to be stored and reviewed. PACS may be standalone, or

may be integrated into an electronic health record. PACS do not need to be separate, and some are an integral part of an Electronic Medical Record System. Most PACS offer manufacturer independence: the images are stored in such a manner that they can still be viewed even if the device they were recorded on is no longer available, and are not lost when the "old" device is retired.

With the advent of SD-OCT technology and dense OCT scanning which can result in image sizes of a gigabyte per examination, deciding how clinical images are stored, and whether all data acquired is stored or just the clinically relevant images, is becoming more and more important for the practitioner, as is choosing the level and type of image compression.

For small practices, keeping images stored on the device can still be a cost-effective solution. For larger practices, storage in a PACS accessible over the clinic computer network allows a patient's images to be accessible in the patient area during clinic. Typically, PACS takes care of compression and uncompression calculations behind the scenes" (Box 8.1).

Box 8.1

Different Strategies for Storing Ophthalmic Images

Slides and computer printouts stored in the paper chart or photo archive

Slides and paper printouts scanned and stored in a PACS

Clinically relevant views stored in a PACS

All raw data and clinically relevant views stored in a PACS

Standards for Storage and Communication of Ophthalmology Images

Digital Exchange of Retinal Images and DICOM

DICOM stands for Digital Imaging and Communications in Medicine and is an organization founded in 1983 to create a standard method for the transmission of medical images and their

associated information across all fields of medicine. For ophthalmology, Working Group 9 (WG-9) of DICOM is a formal part of the American Academy of Ophthalmology (AAO). Until recently, the work of WG-9 has focused on creating standards for fundus, anterior segment, and external ophthalmic photography, resulting in DICOM Supplement 91 Ophthalmic Photography Image SOP Classes, and on OCT imaging in DICOM Supplement 110: Ophthalmic Tomography Image Storage SOP.[58] Later WG-9 went to work on OCT imaging, resulting in DICOM Supplement 110: Ophthalmic Tomography Image Storage SOP.[58]

DICOM standards build as much as possible upon other standards. For example, DICOM does not prescribe an image compression standard, and thus images stored as DICOM images can contain the actual image data. A typical example of this is a JPEG image. DICOM 91 and 110 standardize how metadata for an image, such as patient and visit data, acquisition modes and camera settings, compression settings and data formats, and clinical interpretation, is stored as an integral part of the image, using so-called DICOM "tags," Because the continuous development of new retinal imaging techniques and analysis tools, such as OCT angiography, requires new tags to be added, Supplements 110 and 91 are regularly revised.

Retinal Image Analysis

Image analysis is a process by which meaningful information or measurements can be extracted from digital images, typically by computer algorithms. In ophthalmology, image analysis is primarily used to extract clinically relevant measurements from images of the eye, but also to estimate retinal biomarkers, most commonly from fundus color images and from OCT images. The purpose of this section is to familiarize the reader with the main concepts used in the ophthalmic image analysis literature. Image analysis is best understood as a process consisting of a combination of steps. Not all steps are performed in all image analysis algorithms, and some steps may be explicit as multiple steps in one algorithm and form a combined step in another, different algorithm, but the following steps are typical:

Preprocessing remove variability without losing essential information

Detection locate specific structures of interest, or features

Segmentation determine precise boundaries of objects

Registration find similar regions in two or more images

Interpretation integration of previous steps, and output clinically relevant information.

Though these processing steps are typically explicitly created by the image analysis developers, so called *deep-learning* approaches do not have these explicit steps, instead having learnt these implicitly, as will be clarified further below.

Preprocessing

The purpose of preprocessing is to remove as much variability as possible from the image, without losing essential information. There are many sources of variation during image acquisition. Image device manufacturer and type, different sizes of field of view, variations in flash illumination, exposure duration, patient movement, variability in retinal pigmentation or in cornea/lens/vitreous opacities are all examples of variation between images taken for the same purpose. These variations do not contribute to the understanding of the image, but they may alter further image analysis steps.

Preprocessing attempts to eliminate some or all of these sources of variation, as much as possible. A simple example is field of view: by scaling the image, and subtracting unexposed areas of the image, images from different cameras are normalized to a "standard fundus image". Another example is illumination correction, where the pixel intensity values of underexposed areas are increased, and those of overexposed intensities reduced, so that the pixel intensities fall into a more narrow and more predictable range.

There are many parallels between image preprocessing using computers and human retinal image processing in ganglion cells.[59]

Detection

The purpose of detection is to locate, typically in a preprocessed image, the specific structures of interest, or features, without yet determining their exact boundaries. Examples of such features can be edges, dark or bright spots, oriented lines, and dark–bright transitions in OCT images. Other terms in use for the concept "structure of interest" are wavelets, textures, or filters. Typically, each individual pixel in the image is examined for the presence of one or more features, and usually the surrounding area, or context, of each pixel is included in this examination. The examination itself usually involves a mathematical computation of the similarity between prototypes of the feature and each pixel and its surround. Conceptually similar terms used in the image analysis literature resembling similarity computation are "correlation," "convolution," "lifting," "matching," and "comparison." Usually a nonlinearity is utilized to convert the similarity estimate into a discrete value, for example, "present" versus "nonpresent."

The output of the matching process indicates if and where the features were detected in the image. In some image analysis system, this output is interpreted directly, while in others, a segmentation step (see below) is used to determine the exact boundaries of the object represented by the features.

There are many parallels between the features and the convolution process in digital image analysis, and the filters in the human visual cortex.[28]

Segmentation

The purpose of segmentation is to determine the precise boundaries of objects in the image, when the presence of specific object features has been determined in the detection step. For example, if the ganglion cell layer in an OCT image is detected but still has separate edges and dark–bright transitions, the segmentation step connects these disjointed features into a connected boundary. Commonly used segmentation techniques are graph search and dynamic programming, both of which try to find the mathematically best-fitting boundary, given the specific detection output(s). The output of the segmentation step can be used directly for assessment, for example when showing the different layers on

an macular OCT scan, or can be the input for an interpretation step.

Registration

The purpose of registration is to find similar regions in two or more images so they can be colocalized. Registration is often used to overlay an angiogram on an OCT image, compare images from the same patient from two different visits, to detect improvement of worsening of the patient's condition between visits, or mosaicking, where several fundus images are stitched together into one image covering a larger area of the retina. The registration step often utilizes similar functions as the detection step.

Interpretation

Usually when the preceding steps have been completed, an interpretation step is used to output clinically relevant information from the combined input of the previous steps. If the boundaries of the macular retinal layers have been segmented, interpretation involves calculating the distance between the boundaries, so the user can see the thickness of the different layers at specific locations. These thicknesses can even be compared to a database of normal thicknesses at that same location, so that the output represents how likely it is that the retina is thickened at a specific location. Or, after microaneurysms and exudates have been detected and segmented in multiple images from the same patient, these outputs are combined into the clinically relevant information determining whether the patient has more than minimal diabetic retinopathy or not.[60]

Machine Learning and Image Analysis

The design and development of a retinal image analysis system involves the combination of some of the processing steps as explained above, with specific sizes of features and specific operations used to map the input image into the desired interpretation output. Instead of being programmed, the steps can also be learnt, through *machine learning*, so that for example the features used for detection[61] as in pixel classification (below), or how to combine the output of feature detectors into an output can

be learned.[62]

This term, machine learning, is used when an algorithm is improved incrementally by changing parameters so that it is slightly improved every step. During training, the correct interpretation, or reference standard, also called ground truth, is required, which is typically created by retinal specialists or ophthalmologists.[63] A theoretical disadvantage of using a supervised system with a training set is that the provenance of the different settings is implicit and may not be clear – resulting in a black box. However, because all retinal image analysis algorithms undergo some optimization of parameters based on their initial performance, this is only a relative, not absolute difference.

As mentioned, two distinct stages are required for a supervised learning/classification algorithm to function: A training stage, in which the algorithm "statistically learns" to correctly classify images, regions of images, or even pixels from the reference standard, and a deployment, testing or classification stage in which the algorithm classifies previously unseen images keeping the algorithm settings constant as established during learning. For proper assessment of supervised classification method functionality, training data and performance testing data sets must be completely separately.[57]

Until recently, retinal image analysis used machine learning in modular fashion, i.e., one or more of the processing steps are implemented using machine learning. Recent studies are showing remarkable performance improvements using convolutional neural networks, a machine learning approach where all steps are learnt, as will be explained below.

Pixel Feature Classification

Pixel feature classification is a machine learning technique that assigns one or more classes to the pixels in an image for the detection step. Pixel classification uses multiple pixel features including numeric properties of a pixel and the surroundings of a pixel. Originally, pixel intensity was used as a single feature. More recently, n-dimensional multifeature vectors are utilized, including pixel contrast with the surrounding region and information regarding the pixel's proximity to an edge. The image is

transformed into an n-dimensional feature space and pixels are classified according to their position in space. The resulting hard (categorical) or soft (probabilistic) classification is then used to either assign labels to each pixel (for example "vessel" or "nonvessel" in the case of hard classification), or to construct class-specific likelihood maps (e.g., a vesselness map for soft classification). The number of potential features in the multifeature vector that can be associated with each pixel is essentially infinite. One or more subsets of this infinite set can be considered optimal for classifying the image according to some reference standard. Hundreds of features for a pixel can be calculated in the training stage to cast as wide a net as possible, with algorithmic feature selection steps used to determine the most distinguishing set of features. Extensions of this approach include different approaches to subsequently classify groups of neighboring pixels by utilizing group properties in some manner, for example cluster feature classification, where the size, shape, and average intensity of the cluster may be used.

Deep Learning and Convolutional Neural Networks

As explained above, in classical retinal image analysis, the steps are explicit and their sequence is completely under control of the developers of the image analysis system. Within these steps, forms of machine learning, such as learning the characteristic features,[64] or the fusion of feature detectors,[62] have previously been incorporated.

Deep learning, where all transformation levels are learnt from training data, instead of being designed by experts,[65] has been highly successful in a large number of computer vision and image analysis tasks, substantially outperforming all classical image analysis techniques, and typically implemented as Convolutional Neural Networks (CNNs).[66] Indeed, the highest performing algorithms in the recent Kaggle competition, to identify signs of DR in retinal images, all used CNNs.[67a] As of this writing, the two highest performing algorithms for automated screening of DR, both employ CNNs, though in different ways – see below.[67b,67c]

In these CNNs, the processing steps are learnt and implemented implicitly. The only design work for the developer of such systems is the number of layers and their interconnectedness in the CNN,

and the appropriate choice of training images.

The history of CNNs stretches back far, and because of their complexity, for a long time they were used on extremely simple image analysis tasks, where training on the fastest computers could still take months. In 1980, Fukushima published a study of the pattern recognition performance of one of the first multilayer neural networks, called Neocognitron.[65] This multilayer neural network was directly inspired by the mammalian visual system, with the different *layers* representing the retina, the lateral geniculate nucleus, and the first synaptic layer in the visual cortex (V1). Each layer in the network consists of neurons (with a state, a number between [0,1]), with each neuron in a specific layer connected to all neurons in the previous and next layer, and the strength of these connections represented by a *weight*, typically a number between [0–1] or [−1,1] – though many weights can be zero. The neurons in a layer combine the inputs from the previous layer, consisting of the neuron's state multiplied by the connections' weight, aggregate these in a specified mathematical way, and output to the neurons in the next layer. Convolutional neural networks are a special form of multilayer neural network where the weights are copied among neurons within a layer so that that layer performs the same operation over the entire previous layer, an operation called convolution, whence their name. These multilayer neural networks are strictly forward networks, i.e., information flowed from the input layer through the layers to the output layers, and no feedback to earlier layers was possible.

When faster computers became available, and especially with the more recent development of Graphics Processor Units (GPUs), LeCun and others revised and simplified the architecture and learning rules for CNN. In 2011, a first GPU-implementation of CNNs was described. To be clear, GPUs did not influence any of the fundamental underpinnings, rather, allowed faster training on bigger training datasets so that convergence became practical rather than theoretical.[22a]

Training of CNNs consists of changing all weights in a subtle manner using retinal image examples and the reference standard, for example whether that retinal image contains diabetic retinopathy. Proper learning involves changing the weights only

slightly with each example, according to specific mathematical rules, and then slowly converging to the optimal output for all retinal image in the training set. Because all the processing has to be learnt by the CNN, large amounts of examples are required (typically in the tens of thousands) for the neural network learning phase to converge to a meaningful output for a previously unseen image.

Interestingly, but maybe not surprisingly, the second layer weights of CNNs trained on retinal images typically resemble those originally and painstakingly implemented in the classic systems such as Gabor wavelets.[68a] Integration of CNNs into retinal image analysis is thus proceeding rapidly. An interesting discussion, from a retinal image analysis perspective, has been evolving around how to integrate CNNs into algorithms for the automated detection and diagnosis of retinal diseases, especially DR. Some advocate the use of image-based CNNs: a single CNN is trained to associate a whole set of retinal images with a diagnostic output, such as the presence of DR.[68b] Advantages of this approach are its generalizability, because the same CNN, can be used to detect a wide variety of retinal diseases, if it is trained with different training datasets, making optimization easier, as well as the minimal importance of clinical experts being involved in the design, as these systems learn to associate the image input directly with a diagnostic output, without intervening biomarker or lesion detection. This black-box nature is also a major disadvantage: there are currently no analysis methods to determine how such an image-based CNN works, and it is well known that image-based CNNs are highly sensitive to catastrophic failure, because of small changes in the input image – so called adversarial images.[68c,68d] Others advocate a hybrid or clinically based DR detection system, where multiple CNNs are used that each are trained to detect specific biomarkers or lesions such as hemorrhages, and the outputs of these individual moderately redundant CNNs are combined using standard approaches.[68e] The advantages are that each of these detector CNNS can be individually validated at the lesion level. There is some evidence to suggest that, because it mimics how clinical experts evaluate retinal images, this hybrid approach is more robust and less sensitive to catastrophic failure. Additional studies are

obviously needed to shed more light on this discussion.

In summary, CNNs are making rapid inroads in retinal image analysis, and rapidly increasing computing powers are likely to add to their impact.

Measuring Performance of Image Analysis Algorithms

Crucial for the acceptance of image analysis algorithms are evaluations of its performance. Most often performance is compared to human experts, though this raises its own set of issues as explained below. The agreement between an automatic system and an expert reader may be affected by many influences – system performance may become impaired due to the algorithmic limitations, the imaging protocol, properties of the camera used to acquire the fundus images, and a number of other causes. For example, an imaging protocol that does not allow small lesions to be depicted and thus detected will lead to an artificially overestimated system performance if such small lesions might have been detected with an improved camera or better imaging protocol. Such a system then appears to be performing better than it truly is if human experts and the algorithm both overlook true lesions.

Sensitivity and Specificity

The performance of a lesion detection system can be measured by its *sensitivity*, which is the number of true positives divided by the sum of the total number of (incorrectly missed) false negatives plus the number of (correctly identified) true positives.[57] System *specificity* is determined as the number of true negatives divided by the sum of the total number of false positives (incorrectly identified as disease) and true negatives. Sensitivity and specificity assessment both require ground truth, which is represented by location-specific discrete values (0 or 1) of disease presence or absence for each subject in the evaluation set. The location-specific output of an algorithm can also be represented by a discrete number (0 or 1). However, the output of the assessment algorithm is often a continuous value determining the likelihood p of local disease presence, with an associated probability value between 0

and 1. Consequently, the algorithm can be made more specific or more sensitive by setting an operating threshold on this probability value *p*.

Receiver Operator Characteristics

If an algorithm outputs a continuous value, as explained above, multiple sensitivity/specificity pairs for different operating thresholds can be calculated. These can be plotted in a graph, which yields a curve, the so-called Receiver Operator Characteristics or ROC curve.[57,69a] The area under this ROC curve (AUC, represented by its value Az) is determined by setting a number of different thresholds for the likelihood *p*. Sensitivity and specificity pairs of the algorithm are then obtained at each of these thresholds. The ground truth is kept constant. The maximum AUC is 1, denoting a perfect diagnostic procedure, with some threshold at which both sensitivity and specificity are 1 (100%).

Repeatability and Variability

In addition to the above measures, the performance of an algorithm is also measured by its test–retest variability. With all other variables such as disease state, patient factors, imaging device, and operator held constant while obtaining multiple images, this measure determines how much the algorithm's output remains constant on the "same" input. For an algorithm, test–retest variability is not comparable to intraobserver variability. Almost all image analysis algorithms are deterministic, and if the input image is exactly the same, the output will also be exactly the same.

The Reference Standard or Gold Standard

Typically these performance measurements are made by comparing the output of the image analysis system to some standard, usually called the reference standard or gold standard. Because the performance of some image analysis systems, for example for detection of diabetic retinopathy, is starting to exceed that of individual clinicians or groups of clinicians, creating the reference standard is an area of active research.[47]

The problem is that the true disease state of the patient is *difficult*

and in fact, impossible, to measure. For example, at the limit of retinal specialists' detection performance, one of them may see a microaneurysm in the macula on clinical exam of a patient suspected of having diabetic retinopathy, while another sees only some pigmentary variation. In most cases it is impossible to state that one of these clinicians is right and the other is wrong.

Given that determining the true state of disease necessary to create the reference standard is so challenging, the following options have been developed and are in wide use.[47]

(a) Using the modality under study. The images are read and adjudicated by multiple trained readers according to a standardized protocol. This is less biased and a better estimate than a single clinician, but has higher cost. This method is often used, but the true disease is not known this way.

(b) Using a different modality. In the case of a microaneurysm, an angiogram would be a suitable modality. It requires expert interpretation, and preferably multiple experts. It is less biased towards the imaging modality and may therefore be a better estimate. Because of the added procedure it less patient-friendly, and has higher cost associated with it.

(c) Doing a biopsy. Often this may be ethically unacceptable. It also displaces the problem, because the biopsy would necessarily be interpreted by human expert(s), for example a pathologist, with their intra- and interobserver variability. It is more unequivocal, but also more invasive and has higher cost.

(d) Outcome based. If the clinically relevant question is not so much whether a microaneurysm is present or absent, but instead whether the patient is at risk of going blind from proliferative disease, we can wait for that outcome to occur. However, the true state of disease at this moment would still not be known, only the true state at some time in the past. Clinical outcome is maximally unequivocal and minimally subjective.

(e) True state of disease, which is an unknowable quantity as explained above.

As we have seen, in practice the reference standard therefore almost never represents the true state of the disease of a patient. In addition, there is the problem of what we call “diagnostic drift.”

Research studies in radiology and cardiology have shown that, over time, clinicians increasingly deviate from image reading protocols as these were defined in the original standards[69b,69c] that often led to management and treatment standards. For example, determining whether a red lesion is a microaneurysm or a hemorrhage, which can make the difference between a mild versus moderate level of DR – levels that were used by the reading center in the primary outcome studies that to a great degree still determine the management of diabetic retinopathy: DRS,[70] ETDRS,[71] and EDIC/DCCT.[72] It is thus important to employ image reading protocols.

Clinical Safety Relevant Performance Measurement

Performance of a system that has been developed for screening should not be evaluated based solely on its sensitivity and specificity for detection of that disease. Such metrics do not accurately reflect the complete performance in a screening setup. Rare, irregular, or atypical lesions often do not occur frequently enough in standard datasets to affect sensitivity and specificity but can have dramatic health and safety implications. To maximize screening relevance, the system must therefore include a mechanism to detect rare, atypical, or irregular abnormalities, for example in DR detection algorithms.[48] For proper performance assessment, the types of potential false negatives – lesions that can be expected or shown to be incorrectly missed by the automated system – must be determined. While detection of red lesions and bright lesions is widely covered in the literature, detection of rare or irregular lesions, such as hemorrhages, neovascularization, geographic atrophy, scars, and ocular neoplasms has received much less attention, despite the fact that they all can occur in combination with diabetic retinopathy and other retinal diseases, as well as in isolation. For example, presence of such lesions in isolated forms and without any cooccurrence of small red lesions are rare in DR and thus missing these does not affect standard metrics of performance to a measurable degree.[46] One suitable approach for detecting such lesions is to use a retinal atlas, where the image is routinely compared to a generic normal retina. After building a retinal atlas by registering the fundus images according to a disc,

fovea, and a vessel-based coordinate system, image properties at each atlas location from a previously unseen image can be compared to the atlas-based image properties. Consequently, locations can be identified as abnormal if groups of pixels have values outside the normal atlas range.

Fundus Image Analysis

Planar fundus imaging is the most established method of retinal imaging. Until recently, fundus image analysis was the only source of quantitative indices reflecting retinal morphology. Retinal structures that lend themselves for fundus image analysis include retinal vessels, hemorrhages, microaneurysms, pigment epithelial abnormalities (scars, laser spots), drusen, hyper- or hypopigmentation, choroid related abnormalities or lesions, segmentation of retinal layers. In this section we will discuss retinal vessel detection, retinal lesion detection, construction of fundus-imaging-based retinal atlases, and assessment of image analysis algorithms. The previous section on image analysis concepts for clinicians will be helpful in understanding the concepts in this overview. The next section will explain image analysis of OCT images.

Detection of Retinal Vessels

Automated segmentation of retinal vessels has been highly successful in the detection of large and medium vessels[73–75] (Fig. 8.3). Because retinal vessel diameter and especially the relative diameters of arteries and veins are known to signal the risk of systemic diseases including stroke, accurate determination of retinal vessel diameters, as well as the ability to differentiate veins from arteries, have become more important. Several semiautomated and automated approaches to determining vessel diameter have now been published.[76–78] Other active areas of research include separation of arteries and veins, detection of small vessels with diameters of less than a pixel, and analysis of complete vessel trees using graphs.

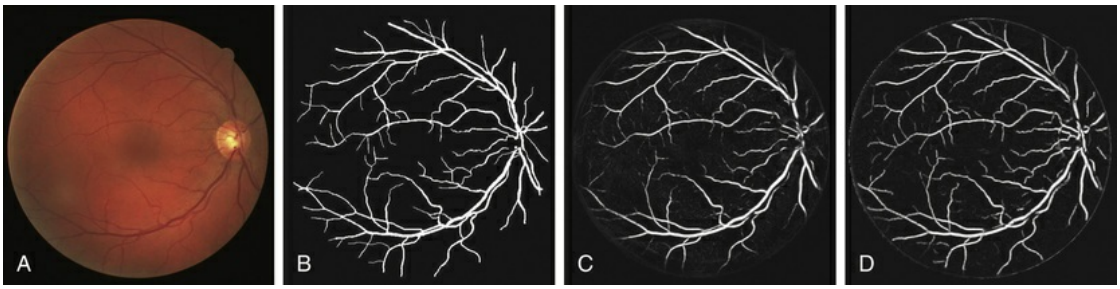

FIG. 8.3 Automated vessel analysis. From left to right: fundus image; retinal specialist annotation; vesselness map from Staal algorithm;[75] vesselness map from direct pixel classification. (Reproduced from Niemeijer M, van Ginneken B, Staal J, Suttorp-Schulten MS, Abràmoff MD. Automatic detection of red lesions in digital color fundus photographs. IEEE Trans Med Imaging 2005;24:584-92.)

Vessel detection approaches can be divided into region-based and edge-based approaches. Region-based segmentation methods label each pixel as either inside or outside a blood vessel. Niemeijer et al. proposed a pixel-based retinal vessel detection method using a Gaussian derivative filter bank and k-nearest-neighbor (k-NN) classification.[73,75] Staal et al. proposed a pixel feature-based method that additionally analyzed the vessels as elongated structures.[75] Edge-based methods can be further classified into two categories: window-based methods and tracking-based methods. Window-based methods estimate a match at each pixel against the pixel's surrounding window. The tracking approach exploits local image properties to trace the vessels from an initial point. A tracking approach can better maintain the connectivity of vessel structure. Lalonde et al.[79] proposed a vessel tracking method by following an edge line while monitoring the connectivity of its twin border on a vessel map computed using a Canny edge operator. Breaks in the connectivity will trigger the creation of seeds that serve as extra starting points for further tracking. Gang et al. proposed a retinal vessel detection using a second-order Gaussian filter with adaptive filter width and adaptive threshold.[80]

Detection of Fovea and Optic Disc

Location of the optic disc and fovea benefits retinal image analysis (Fig. 8.4). It is often necessary to mask out the normal anatomy

before finding abnormal structures. For instance, the optic disc might be mistaken for a bright lesion if not detected. Secondly, the distribution of the abnormalities is not uniform on fundus photographs. Specific abnormalities occur more often in specific areas on the retina. Most optic disc detection methods are based on the fact that the optic disc is the convergence point of blood vessels and it is normally the brightest structure on a fundus image. Most fovea detection methods depend partially on the result of the optic disc detection.

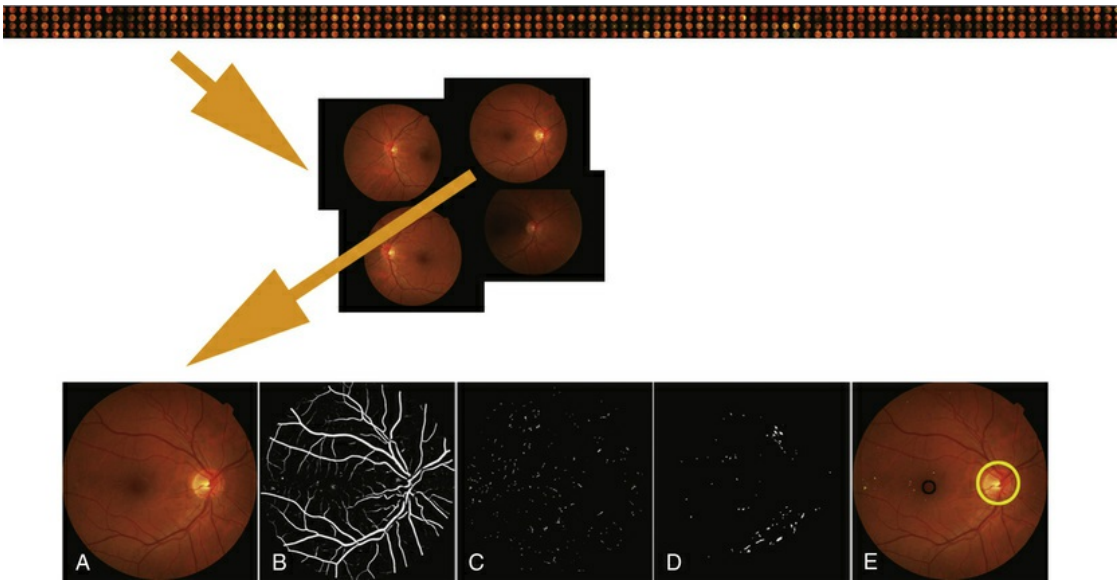

FIG. 8.4 Typical steps necessary for analysis of fundus images, in this case for early diabetic retinopathy. Top row: large sequence of images sets from multiple patients; second row: image set of four retinal images for a single patient; third row: (A) original image; (B) vesselness map; (C) automatically detected red lesions in white; (D) automatically detected bright lesions in white; (E) detection of fovea (black) and optic disc (yellow) as well as automatically detected red lesions indicated in shades of green, bright lesions in shades of blue superimposed on original image.

Hoover et al. proposed a method for optic disc detection based on the combination of vessel structure and pixel brightness.[81] If a strong vessel convergence point is found in the image, it is regarded

as the optic disc. Otherwise the brightest region is detected. Foracchia et al. proposed an optic disc detection method based on vessel directions.[82] A parabolic model of the main vascular arches is established and the model parameters are the directions associated with different locations on the parabolic model. The point with a minimum sum of square error is reported as the optic disc location. Lowell et al., by matching an optic disc model using the Pearson correlation, determined an initial optic disc location, and then traced the optic disc boundary using a deformable contour model.[83]

Most fovea detection methods use the fact that the fovea is a dark region in the image and that it normally lies in a fixed orientation and location relative to the optic disc and the main vascular arch. In Fleming, approximate locations of the optic disc and fovea are obtained using the elliptical form of the main vascular arch.[84] Then, the locations are refined based on the circular edge of the optic disc and the local darkness at the fovea. Li and Chutatape also proposed a method to select the brightest 1% pixels in a gray level image.[85] The pixels are clustered and principal component analysis based on a trained system is applied to extract a single point as the estimated location of optic disc. A fovea candidate region is then selected based on the optic disc location and the main vascular arch shape. Within the candidate region, the centroid of the cluster with the lowest mean intensity and pixel number greater than one-sixth disc area is regarded as the foveal location. In Sinthanayothin's paper, the optic disc was located as the area with the highest variation in intensity of adjacent pixels, while the fovea was extracted using intensity information and a relative distance to the optic disc.[86] Tobin et al. proposed a method to detect the optic disc based on blood vessel features, such as density, average thickness, and orientation.[87] Then the fovea location was determined based on the location of optic disc and a geometry model of the main blood vessel. Niemeijer et al. proposed a method to automatically localize both the optic disc and fovea in 2008.[88,89]. For the optic disc detection, a set of features are extracted from the color fundus image. A k-NN classification is used to give a soft label to each pixel on the test image. The probability image is blurred and the pixel with the highest probability is detected as optic disc. Relative position information between the optic disc and the fovea is used to

limit the search of fovea into a certain region. For each possible location of the optic disc, a possible location of the fovea is given. The possible locations for the fovea are stored in a separate image and the highest probability location is detected as the fovea location.

Detection of Retinal Lesions

In this section, we will primarily focus on detection of lesions in DR. DR has the longest history as a research subject in retinal image analysis. Fig. 8.4 shows examples of a fundus photograph with the typical lesions automatically detected. After preprocessing, most approaches detect candidate lesions after which a mathematical morphology template is utilized to segment and characterize the candidates (Fig. 8.5). This approach or a modification thereof is in use in many algorithms for detecting DR and AMD.[90] Additional enhancements include the contributions of Spencer, Cree, Frame, and coworkers.[91,92] They added additional preprocessing steps, such as shade-correction and matched filter postprocessing, to this basic framework, to improve algorithm performance. Algorithms of this kind function by detecting candidate microaneurysms of various shapes, based on their response to specific image filters. A supervised classifier is typically developed to separate the valid microaneurysms from spurious or false responses. However, these algorithms were originally developed to detect the high-contrast signatures of microaneurysms in fluorescein angiogram images. An important development was the addition of a more sophisticated filter, a modified version of the top-hat filter, so-called because of its cross-section, to red-free fundus photographs rather than angiogram images, as was first described by Hipwell et al.[93] They tested their algorithm on a large set of >3500 images and found a sensitivity/specificity operating point of 0.85/0.76. Once this filter-based approach had been established, development accelerated. The next step was broadening the candidate detection step, originally developed by Baudoin to detect candidate pixels, to a multifilter filter-bank approach.[73,94] The responses of the filters are used to identify pixel candidates using a classification scheme. Mathematical morphology and additional classification steps are

applied to these candidates to decide whether they indeed represent microaneurysms and hemorrhages (Fig. 8.6). A similar approach was also successful in detecting other types of DR lesions, including exudates and cotton-wool spots, as well as drusen in AMD.[95]

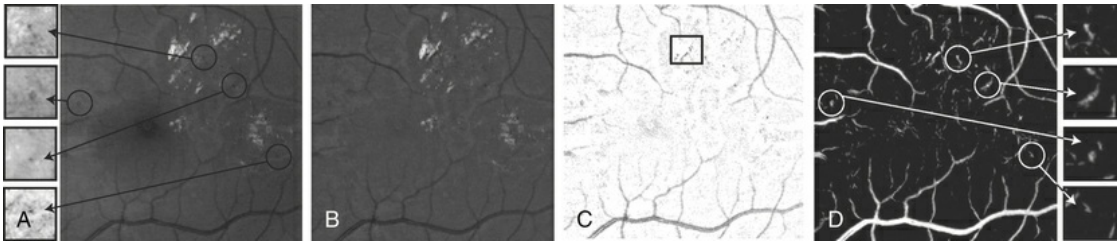

FIG. 8.5 Red lesion pixel feature classification. (A) Part of green color plane of a fundus image. Shown are pieces of vasculature and several red lesions. Circles mark location of some of the red lesions in the image. (B) After subtracting median filtered version of the green plane large background gradients are removed. (C) All pixels with a positive value are set to zero to eliminate bright lesions in the image. Note that exudates often partially occlude red lesions. Nonoccluded parts of red lesions show up clearly in this image. An example of this is marked with a rectangle. (D) Pixel classification result produced by contrast enhancement step. Nonoccluded parts of hemorrhages are visible together with the vasculature and a number of red lesions. (Reproduced from Niemeijer M, van Ginneken B, Staal J, et al. Automatic detection of red lesions in digital color fundus photographs. IEEE Trans Med Imaging 2005;24:584-92.)

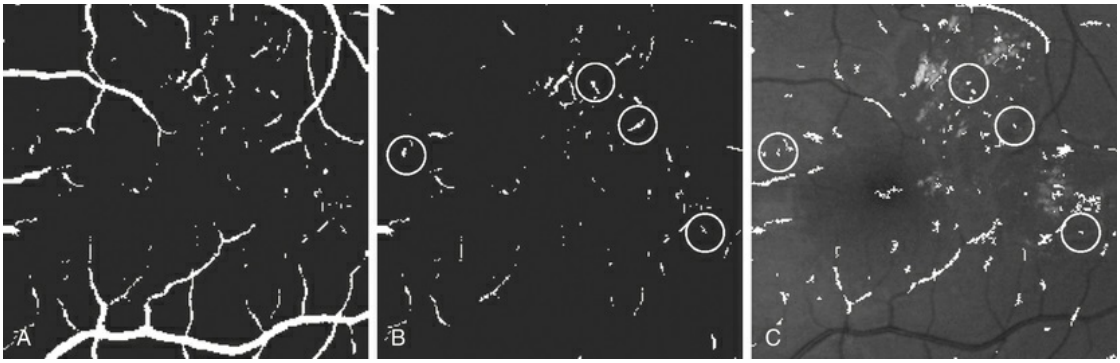

FIG. 8.6 Red lesion detection. (A) Thresholded

probability map. (B) Remaining objects after connected component analysis and removal of large vasculature. (C) Shape and size of extracted objects in panel (B) does not correspond well with actual shape and size of objects in original image. Final region growing procedure is used to grow back actual objects in original image which are shown here. In (B) and (C), the same red lesions as in Fig. 8.8(A) are indicated with a circle. (Reproduced from Niemeijer M, van Ginneken B, Staal J, et al. Automatic detection of red lesions in digital color fundus photographs. IEEE Trans Med Imaging 2005;24:584-92.)

Small red retinal lesions, namely microaneurysms and small retinal hemorrhages, are typical for multiple retinal disorders including diabetic retinopathy, hypertensive retinopathy, venous occlusive disease, and other less common retinal disorders such as idiopathic juxtafoveal telangiectasia. The primary importance of small red lesions is that they are the leading indicators of diabetic retinopathy. Because they are difficult to differentiate for clinicians on standard fundus images from nonmydriatic cameras, hemorrhages and microaneurysms are usually detected together and associated with a single combined label. Historically, red lesion detection algorithms focused on detection of normal anatomical objects, especially the vessels, because they can locally mimic red lesions. Subsequently, a combination of one or more filtering operations combined with mathematical morphology is employed to detect red lesion suspects. In some cases, suspect red lesions are further classified in individual lesion types and refined algorithms are capable of detecting specific retinal structures and abnormalities.

Initially, red lesions were detected in fluorescein angiograms because their contrast against the background is much higher than that of microaneurysms in color fundus photography images.[91,92,96] Hemorrhages mask out fluorescence and present as dark spots in the angiograms. These methods employed a mathematical morphology technique that eliminated the vasculature from a fundus image but left possible microaneurysm candidates untouched, as first described in 1984.[18] Later, this method was extended to high-resolution red-free fundus photographs by Hipwell et al.[93] Instead of using morphology operations, a neural

network was used, as demonstrated by Gardner et al.[97] In their work, images are divided into 20 × 20 pixel grids and the grids are individually classified. Sinthanayothin et al. used a detection step to find blood-like regions and to segment both vessels and red lesions in a fundus image.[98] A neural network was used to detect the vessels exclusively, and the remaining objects were labeled as microaneurysms. Niemeijer et al. presented a hybrid scheme that used a supervised pixel classification-based method to detect and segment the microaneurysm candidates in color fundus photographs.[94] This method allowed for the detection of larger red lesions (i.e., hemorrhages) in addition to the microaneurysms using the same system. A large set of additional features, including color, was added to those that had been previously described.[92,96] Using the features in a supervised classifier distinguished between real and spurious candidate lesions. These algorithms can usually distinguish between overlapping microaneurysms because they give multiple candidate responses.

Other recent algorithms only detect microaneurysms and forego a phase of detecting normal retinal structures like the optic disc, fovea, and retinal vessels, which can act as confounders for abnormal lesions. Instead, the recent approaches find the microaneurysms directly using template matching in wavelet-subbands.[99] In this approach, the optimal adapted wavelet transform is found using a lifting scheme framework. By applying a threshold on the matching result of the wavelet template, the microaneurysms are labeled. This approach has meanwhile been extended to explicitly account for false negatives and false positives.[47] Because it avoids detection of the normal structures, such algorithms can be very fast, on the order of less than a second per image.

Bright lesions, defined as lesions brighter than the retinal background, can be found in the presence of retinal and systemic disease. Some examples of such bright lesions of clinical interest include drusen, cotton-wool spots, and lipoprotein exudates. To complicate the analysis, flash artifacts can be present as false positives for bright lesions. If the lipoprotein exudates would only appear in combination with red lesions, they would only be useful for grading diabetic retinopathy. The exudates can, however, in

some cases appear as isolated signs of diabetic retinopathy in the absence of any other lesion. Several computer-based systems to detect exudates have been proposed (Fig. 8.7).[90,95,97,98,100]

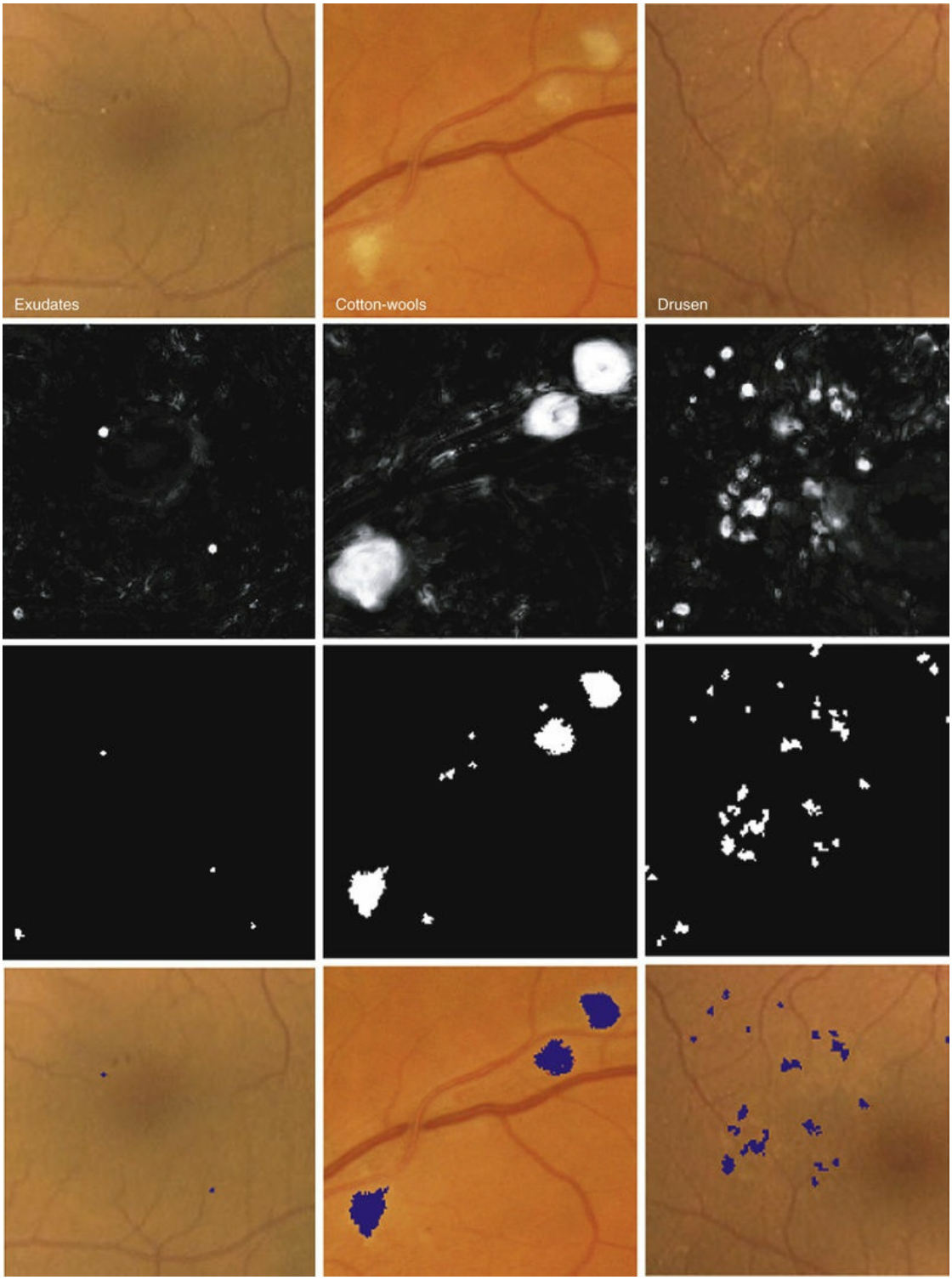

FIG. 8.7 Bright lesion detection algorithm steps performed to detect and differentiate "bright lesions." From left to right: exudates, cotton-wool spots, and drusen. From top to bottom: relevant regions in the retinal color image (all at same scale); a posteriori probability maps after first classification step; pixel clusters labeled as probable bright lesions (potential

lesions); bottom row shows final labeling of objects as true bright lesions, overlaid on original image. (Reproduced from Niemeijer M, van Ginneken B, Russell SR, et al. Automated detection and differentiation of drusen, exudates, and cotton-wool spots in digital color fundus photographs for diabetic retinopathy diagnosis. Invest Ophthalmol Vis Sci 2007;48:2260-7.)

Because the different types of bright lesions have different diagnostic importance, algorithms should be capable not only to detect bright lesions, but also be able to differentiate among the bright lesion types. One example algorithm capable of detection and differentiation of bright lesions was reported by Niemeijer et al. in 2007.[95] This algorithm is based on an earlier red lesion algorithm presented by Hipwell et al. in 2000[93] and includes the following traditional steps, which are illustrated in Fig. 8.6.

These classification steps include:

1. Lesion candidate cluster detection where pixels are clustered into highly probable lesion regions.

2. True bright lesion detection where each candidate cluster is classified as a true lesion based on cluster features including surface area, elongatedness, pixel intensity gradient, standard deviation of pixel values, pixel contrast, and local "vesselness" (as derived from a vessel segmentation map).

3. Differentiation of lesions into drusen, exudates, and cotton-wool spots where a third classifier determines the likelihood for the true bright lesion to represent specific lesion types.

Vessel Analysis

Vessel measures, such as the average width of arterioles and venules, the ratio of arteriolar to venular widths, and the branching ratio, have been established to be predictive of systemic diseases, especially hypertension, and also have potential value in degenerative retinal diseases such as retinitis pigmentosa. The methods described in the section "Detection of retinal vessels" above locate the vessels, but cannot determine vessel width. Additional techniques are needed to accurately measure the vessel

width. Al-Diri et al. proposed an algorithm for segmentation and measurement of retinal blood vessels by growing a "Ribbon of Twins" active contour model. Their approach uses an extraction of segment profiles (ESP) algorithm, which uses two pairs of contours to capture each vessel edge.[101] The half-height full-width (HHFW) algorithm defines the width as the distance between the points on the intensity curve at which the function reaches half its maximum value to either side of the estimated center point.[102–104] The Gregson algorithm fits a rectangle to the profile, setting the width so that the area under the rectangle is equal to the area under the profile.[101] Xu et al. recently published a method based on graph search showing less variability than human experts (Fig. 8.8).[105]

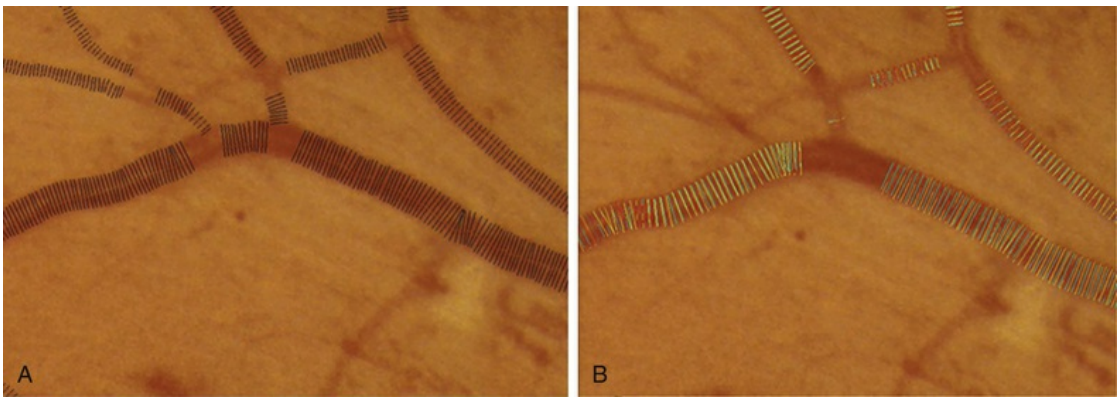

FIG. 8.8 Automated vessel width measurement. (A) Automated measurement of vessel width (black lines). (B) Three human experts marking the widths of the vessel manually (in green, blue and yellow).

A fully automated method from the Abràmoff group to measure the arteriovenous ratio (AVR) in disc center retinal images was published in 2011.[106] This method detects the location of the optic disc, determines an appropriate region of interest (ROI), classifies vessels as arteries or veins, estimates vessel widths, and calculates the AVR. The system eliminates all vessels outside the AVR measurement ROI. A skeletonization operation is then applied to the remaining vessels after which vessel crossings and bifurcation points are removed, leaving a set of vessel segments consisting of only vessel centerline pixels. Features are extracted from each centerline pixel in order to assign these a soft label indicating the

likelihood that the pixel is part of a vein. As all centerline pixels in a connected vessel segment should be the same type, the median soft label is assigned to each centerline pixel in the segment. Next, artery–vein pairs are matched using an iterative algorithm, and finally, the widths of the vessels are used to calculate the average AVR. Recently the required identification of arterial and venous vessel trees has been improved by analyzing the topography of all vessel trees in retinal images.[107]

Retinal Atlas

The retina has a relatively small number of key anatomic structures (landmarks) visible using planar fundus camera imaging. Additionally, the expected shape, size, and color variations across a population are expected to be high. While there have been a few reports on estimating retinal anatomic structure using a single retinal image,[87] we are not aware of any published work demonstrating the construction of a statistical retinal atlas using data from a large number of subjects. The choice of atlas landmarks in retinal images may vary depending on the view of interest. Regardless, the atlas should represent most retinal image properties in a concise and intuitive way. Three landmarks can be used as the retinal atlas key features; the optic disc center, the fovea, and the main vessel arch defined as the location of the largest vein/artery pairs. The disc and fovea provide landmark points, while the arch is a more complicated two-part curved structure that can be represented by its central axis. The atlas coordinate system then defines an intrinsic, anatomically meaningful framework within which anatomic size, shape, color, and other characteristics can be objectively measured and compared. Choosing either the disc center or fovea alone to define the atlas coordinate system would allow each image from the population to be translated so pin-point alignment can be achieved. Choosing both disc and fovea allows corrections for translation, scale, and rotational differences across the population. However, nonlinear shape variations across the population would not be considered – which can be accomplished when the vascular arch information is utilized. The end of the arches can be defined as the first major bifurcations of the arch

branches. The arch shape and orientation vary from individual to individual and influence the structure of the remaining vessel network. Establishing an atlas coordinate system that incorporates the disc, fovea, and arches allows for translation, rotation, scaling, and nonlinear shape variations to be accommodated across a population.

An isotropic coordinate system is a system in which the size of each imaged element is the same in all three dimensions. This is desirable for a retinal atlas so images can refer to the atlas independent of spatial pixel location by a linear one-to-one mapping. The radial-distortion correction (RADIC) model attempts to register images in a distortion-free coordinate system using a planar-to-spherical transformation, so the registered image is isotropic under a perfect registration and places the registered image in an isotropic coordinate system (Fig. 8.9).[108] An isotropic atlas makes it independent of spatial location to map correspondences between the atlas and test image. The intensities in overlapping area are determined by a distance weighted blending scheme.[109]

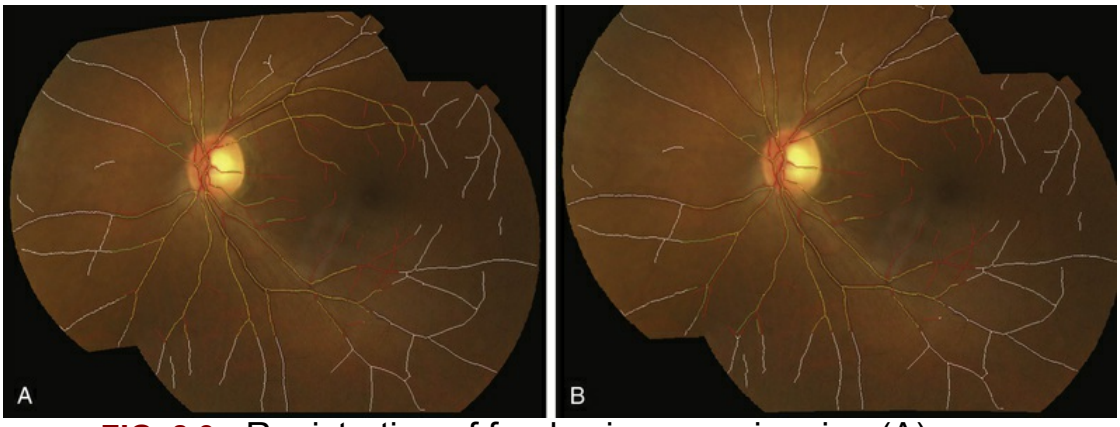

FIG. 8.9 Registration of fundus image pair using (A) quadratic model and (B) RADIC model. Vessel center lines are overlaid for visual assessment of registration accuracy. This registration is performed to disk-centered and macula-centered images to provide an increased anatomic field of view. (Reproduced from Lee S, Abràmoff MD, Reinhardt JM. Retinal image mosaicking using the radial distortion correction model. In: Joseph MR, Josien PWP, editors.; 2008: SPIE; 2008. p. 691435.)

Retinal images in clinical practice are acquired under diverse fundus camera settings subjected to saccadic eye movement, and with variable properties including focal center, zoom, and tilt. Thus, atlas landmarks from training data need to be aligned to derive any meaningful statistical properties from the atlas. Since the projective distortion within an image is corrected in registration, the interimage variations in the registered images appear as the difference in the rigid coordinate transformation parameters of translation, scale, and rotation.

The atlas landmarks serve as the reference set so each color fundus image can be mapped to the coordinate system defined by the landmarks. As the last step of atlas generation, color fundus images are warped to the atlas coordinate system so that the arch of each image is aligned to the atlas vascular arch[110] (Fig. 8.10). Rigid coordinate alignment is done for each fundus image to register the disc center and the fovea. The control points are determined by sampling points from equidistant locations in radial directions from the disc center. Usually, the sampling uses smoothed trace lines utilizing third-order polynomial curve fitting to eliminate locally high tortuosity of vascular tracings which may cause large geometric distortions (Fig. 8.11).

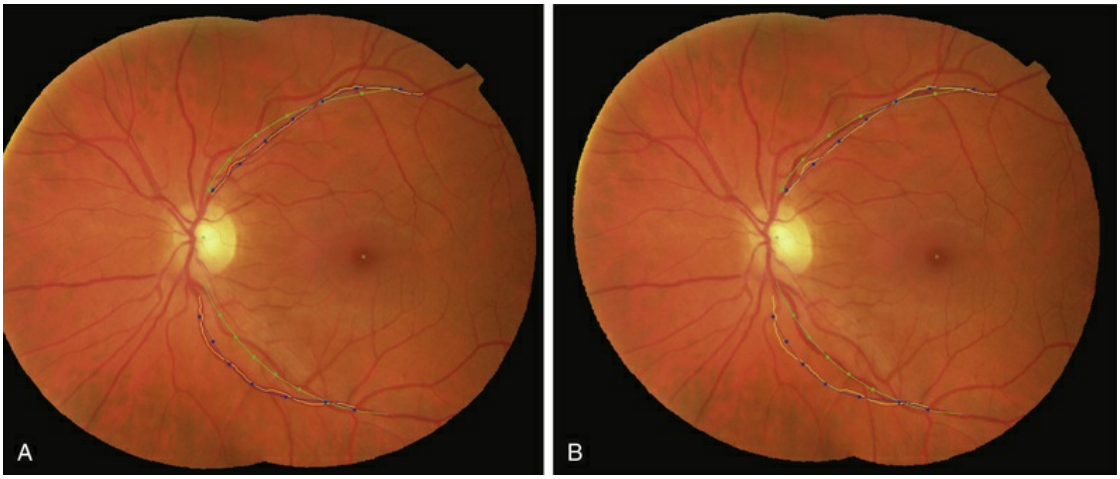

FIG. 8.10 Atlas coordinate mapping by thin plate spline (A) before and (B) after mapping. Naive main arch traces obtained by Dijkstra's line-detection algorithm are drawn as yellow lines that undergo polynomial curve fitting to result in blue lines. Atlas landmarks (disc center, fovea, and vascular arch) are drawn in

green, and equidistant radial sampling points marked with dots. (Reproduced from Abràmoff MD, Garvin M, Sonka M. Retinal Imaging and Image Analysis. IEEE Reviews in Biomedical Engineering 2010:169-208.)

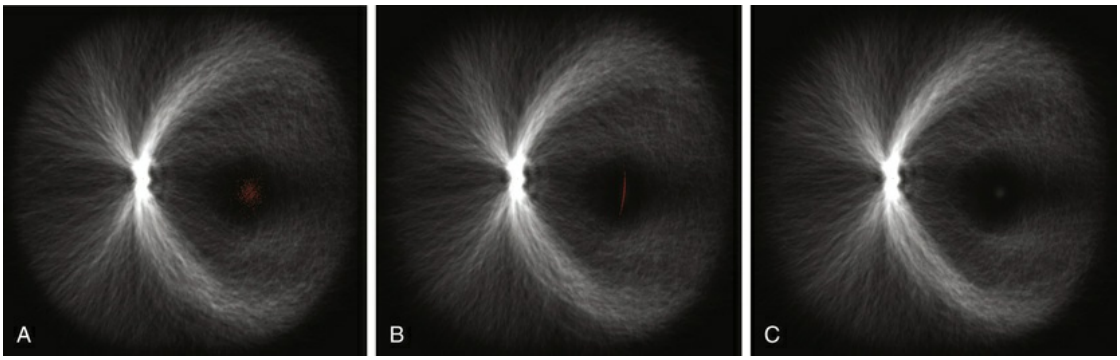

FIG. 8.11 Registration of anatomic structures according to increasing complexity of registration transform 500 retinal vessel images are overlaid and marked with one foveal point landmark each (red spots). Rigid coordinate alignment by (A) translation, (B) translation and scale, and (C) translation, scale, and rotation. (Reproduced from Abràmoff MD, Garvin M, Sonka M. Retinal imaging and image analysis. IEEE Reviews in Biomedical Engineering 2010:169-208.)

A retinal atlas can be used as a reference to quantitatively assess the level of deviation from normality. An analyzed image can be compared with the retinal atlas directly in the atlas coordinate space. The normality can thus be defined in several ways depending on the application purpose – using local or global chromatic distribution, degree of vessel tortuosity, presence of pathologic features, or presence of artifacts (Fig. 8.12). Other uses for a retinal atlas include image quality detection and disease severity assessment. Retinal atlases can also be employed in content-based image retrieval leading to abnormality detection in retinal images.[111]

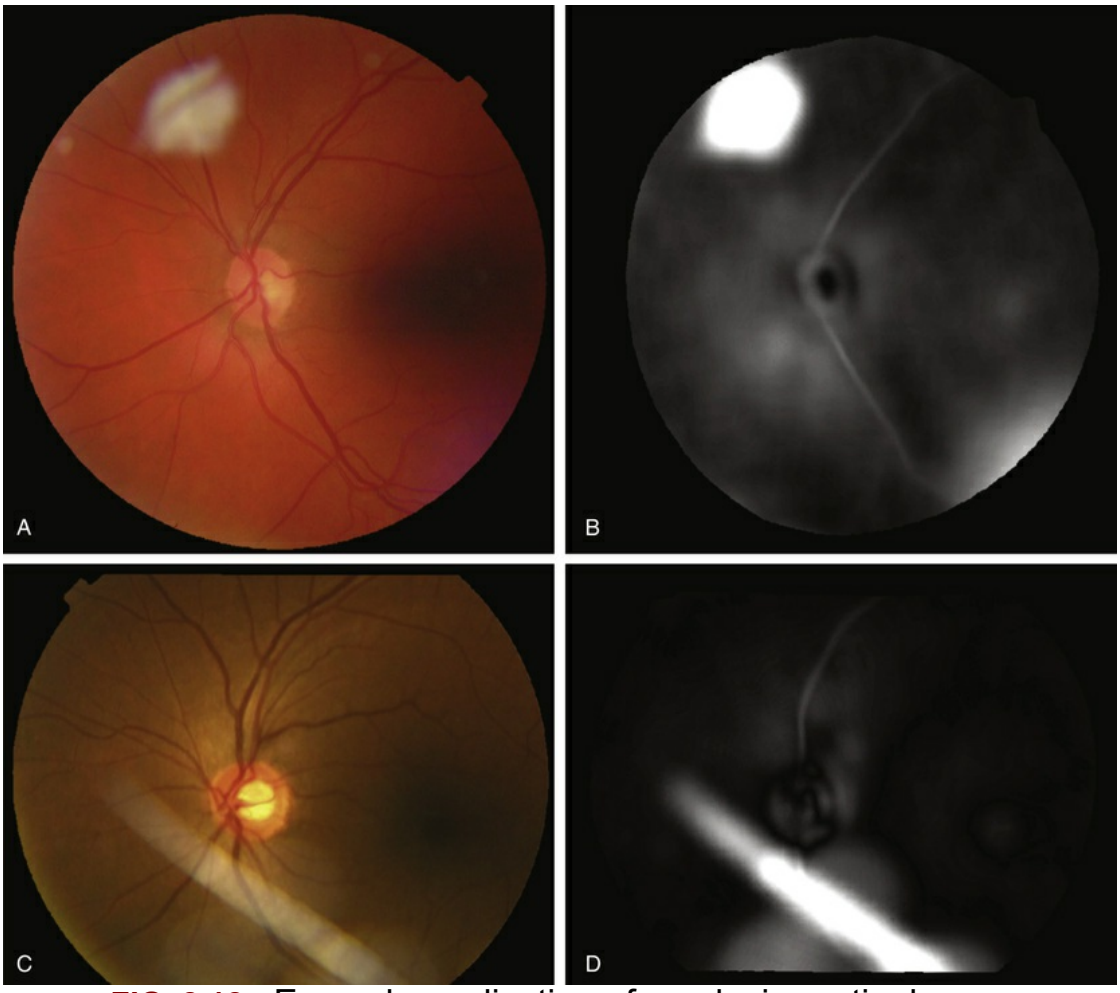

FIG. 8.12 Example application of employing retinal atlas to detect imaging artifacts. (A,C) Color fundus images with artifacts. (B,D) Euclidean distance maps in atlas space using atlas coordinate system. Note that distances are evaluated within atlas image. Consequently, field of view of distance map is not identical to that of fundus image. (Reproduced from Abràmoff MD, Garvin M, Sonka M. Retinal imaging and image analysis. IEEE Reviews in Biomedical Engineering 2010:169-208.)

Performance of Diabetic Retinopathy Detection Algorithms

Several groups have studied the performance of detection algorithms in a real-world setting. The main goal of such a system is to decide whether the patient should be evaluated by a human expert or can return for routine follow-up, based solely on automated analysis of retinal images.[48,49]

DR detection algorithms appear to be mature and competitive algorithms have now reached the human intrareader variability limit.[46,47] Additional validation studies on larger, well-defined, but more diverse populations of patients with diabetes are urgently needed, anticipating cost-effective early detection of DR in millions of people with diabetes to triage those patients who need further care at a time when they have early rather than advanced DR. Validation trials are currently underway in the United States, United Kingdom and the Netherlands.

To drive the development of progressively better fundus image analysis methods, research groups have established publicly available, annotated image databases in various fields. Fundus imaging examples are represented by the STARE,[112] DRIVE,[73] REVIEW[113] and MESSIDOR databases,[114] with large numbers of annotated retinal fundus images, with expert annotations for vessel segmentation, vessel width measurements, and diabetic retinopathy detection. Image analysis competitions, such as the Retinopathy Online Challenge,[115] have also been initiated.

The DRIVE database (Digital Retinal Images for Vessel Evaluation) was established to enable comparative studies on segmentation of retinal blood vessels in retinal fundus images. It contains 40 fundus images from subjects with diabetes, both with and without retinopathy, as well as retinal vessel segmentations performed by two human observers. Starting in 2005, researchers have been invited to test their algorithms on this database and share their results with other researchers through the DRIVE website.[105] At the same web location, results of various methods can be found and compared. Currently, retinal vessel segmentation research is primarily focusing on improved segmentation of small vessels, as well as on segmenting vessels in images with substantial abnormalities.

The DRIVE database was a great success, allowing comparisons of algorithms on a common dataset. In retinal image analysis, it represented a substantial improvement over method evaluations on unknown datasets. However, different groups of researchers tend to use different metrics to compare the algorithm performance, making truly meaningful comparisons difficult or impossible. Additionally, even when using the same evaluation measures,

implementation specifics of the performance metrics may influence final results. Consequently, until the advent of the Retinopathy Online Challenge ROC competition in 2009, comparing the performance of retinal image analysis algorithms was difficult.[115] This competition focused on detection of microaneurysms. Twenty-six groups participated in the competition out of which six groups submitted their results on time.

A logical next step was to provide publically available annotated datasets for use in the context of online, standardized asynchronous competitions. In an asynchronous competition, a subset of images is made available with annotations, while the remainder of the images are available with annotations withheld. This allows researchers to optimize their algorithm performance on the population from which the images were drawn (assuming the subset with annotated images is representative of the entire population), but they are unable to test–retest on the evaluation images, because those annotations are withheld. All results are subsequently evaluated using the same evaluation software, and research groups are allowed to submit results continuously over time.

Areas of Active Research in Fundus Image Analysis

Major progress has been accomplished in fundus image analysis. Current challenges, on which multiple research groups worldwide are actively working, include the following areas: differentiating arteries from veins, assessing accurate vessel diameter (particularly in vessels only a few pixels in diameter) and vessel tortuosity, vessel tree analysis including tree branching patterns, detection of irregularly shaped hemorrhages, detection of lesion distribution patterns (i.e., drusen), and segmentation of atrophy. Finally, integration of fundus image-based quantification with other metrics of disease risk, such as serum glucose level or patient history, is an area of active research with immediate clinical application.

Optical Coherence Tomography

Image Analysis

Because of OCT's relatively recent presence in ophthalmic care compared to fundus photography, the use of image analysis techniques for processing OCT images has a shorter history. Nevertheless, it is a rapidly growing and important area, especially as spectral domain.

OCT (SD-OCT) technology has enabled true three-dimensional volumetric scans of the retina to be acquired. With this ever-increasing wealth of image information, the importance of developing advanced image analysis techniques to maximize the extraction of clinically relevant information is especially important. Nevertheless, the development of such advanced techniques can be challenging as OCT images are inherently noisy, thus often requiring the utilization of 3D contextual information (Fig. 8.13). Furthermore, the structure of the retina can drastically change during disease. Here are some of the important image analysis steps for processing OCT images. We start with the segmentation of retinal layers, one of the earliest, yet still extremely important, OCT image analysis areas. We then discuss techniques for flattening OCT images in order to correct scanning artifacts. Building upon the ability to extract layers, we discuss use of thickness information and use of texture information. This is followed by the segmentation of retinal vessels, which currently has its technical basis in many of the techniques used for segmenting vessels in fundus photography, but is beginning to take advantage of the 3D information available only in SD-OCT. Utilizing both layer-based and texture-based properties to detect the locations of retinal lesions is then described. A 3D-based approach for segmenting the boundaries of such lesions is described in the section "Detection of retinal lesions." The ability to segment layers in the presence of lesions is described in the section "Intraretinal layer segmentation in the presence of SEADs." This section is partially based on a review paper.[59]

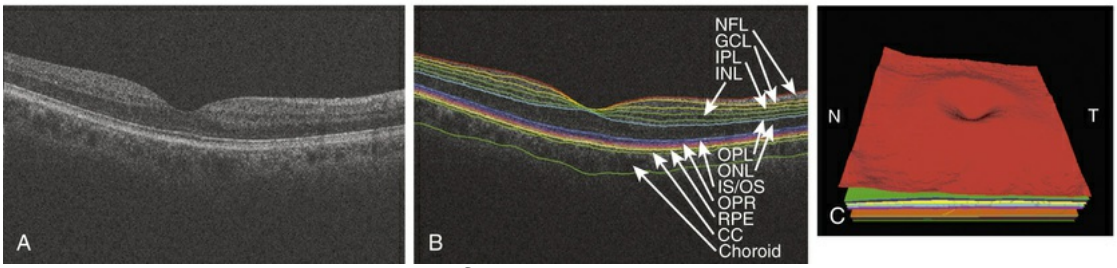

FIG. 8.13 Fourteen-surface segmentation results. (A) X–Z image of optical coherence tomography (OCT) volume. (B) Segmentation results: nerve fiber layer (*NFL*), ganglion cell layer (*GCL*), inner plexiform layer (*IPL*), inner nuclear layer (*INL*), outer plexiform layer (*OPL*), outer nuclear layer (*ONL*), inner/outer-segments junction (*IS/OS*), outer segments–RPE interdigitation complex (*OPR*), retinal pigment epithelium (*RPE*), choriocapillaris (*CC*), choroid (*Ch*). Stated anatomical labeling is based on observed relationships with histology although no general agreement exists about the precise correspondence of some outer retinal layers.[116] (C) Three-dimensional rendering of segmented surfaces (*N*, nasal; *T*, temporal). (Panel C reproduced from Abramoff MD, Garvin M, Sonka M. Retinal imaging and image analysis. IEEE Reviews in Biomedical Engineering 2010:169-208.)

Retinal Layer Analysis From Three-Dimensional OCT

Retinal Layer Detection

The segmentation of retinal layers in OCT scans has been an important goal, because thickness changes in the layers are one indication of disease status. Previous generation time domain scanning systems (such as the Stratus OCT by Carl Zeiss Meditec, Inc.) offered the ability to segment and provide thickness measurements for a single layer of the retina. In particular, the retinal nerve fiber layer (RNFL) thickness measurements of peripapillary circular scans and total retinal thickness measurements were available and used clinically. It can be assumed that commercialized methods utilized an inherently two-dimensional approach (i.e., if multiple 2D slices are available in a

particular scanning sequence they are segmented independently). Indeed, most of the early approaches that have been reported in the literature[117–122] for the segmentation of time domain scans are also 2D in nature.

While variations to each of the early 2D approaches exist for the segmentation of retinal boundaries, a typical 2D approach proceeds as follows: preprocess the image,[117–119,121] perform a 1D peak detection (detection) on each A-scan of the processed image to find points of interest, and (in some methods) correct for possible discontinuities in the 1D border detection.[117] Other 2D time domain approaches include the use of 2D dynamic programming by Baroni et al.[123] and manually initialized deformable models for the segmentation of fluid-filled regions, as well as the Cabrera Ferńandez group which found seven retinal layer boundaries by segmentation analysis.[124,125]

Haeker, Garvin and others reported the first true 3D segmentation approach for the segmentation of retinal layers on OCT scans, taking advantage of 3D contextual information.[126–129] Their approach was unique in that the layers were segmented simultaneously.[130] For time domain macular scans, they segmented 6–7 surfaces (5–6 layers), obtaining an accuracy and reproducibility similar to that of retinal specialists. By extending the approach to spectral domain OCT volumes,[131] utilization of 3D contextual information had more of an advantage (Fig. 8.14). By employing a multiscale approach, the processing time was subsequently decreased from hours to a few minutes while enabling segmenting additional layers.[132] A similar approach for segmenting the intraretinal layers in optic nerve head (ONH)-centered SD-OCT volumes was reported with an accuracy similar to that of the interobserver variability of two human experts.[120] A preliminary layer thickness atlas was built from a small set of normal subjects. Thickness loss of the macular ganglion cell layer in people with diabetes without retinopathy was thus demonstrated, showing that diabetes also leads to retinal neuropathy.[133,134]

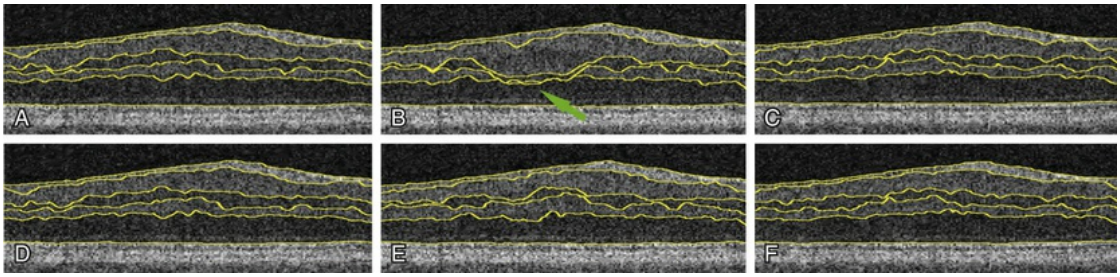

FIG. 8.14 Why using the complete three-dimensional contextual information in intraretinal layer segmentation process is superior. (A–C) Sequence of two-dimensional result on three adjacent slices within spectral-domain volume obtained using a slice-by-slice 2D graph-based approach. Note the "jump" in segmentation result for third and fourth surfaces in middle slice. (D–F) Sequence of 3D results on same three adjacent slices using same graph-based approach, but with addition of 3D contextual information. Three-dimensional contextual information prevented third and fourth surface segmentation from failing.

OCT Image Flattening

SD-OCT volumes frequently demonstrate motion artifacts, and other artifacts may also be present, such as the tilting due to an off-axis placement of the pupil. Approaches for reducing these artifacts include 1D and 2D methods that use cross-correlation of either A-scans[118] or B-scans.[98,135] In some cases, a complete flattening of the volume is desired based on a surface segmentation to ensure a consistent shape for segmentation and visualization. Flattening the volumes makes it possible to truncate the image substantially in the axial direction (z-direction), thereby reducing the memory and time-requirements of an intraretinal layer segmentation approach. Flattening an image involves first segmenting the retinal pigment epithelial surface in a lower resolution, fitting a thin-plate spline to this surface, and then vertically realigning the columns of the volume to make this surface completely flat.[131]

Retinal Layer Thickness Analysis

After flattening and segmentation, the properties of the macular tissues in each layer can be extracted and analyzed. In addition to

layer thickness, textural properties can also be quantified, as explained in the next paragraph. Measuring the thickening of specific layers is crucial in the management of diabetic macular edema and other retinal disorders.[136] Typically, it is useful to compare the obtained thickness values to a normative database or atlas, as is available in commercial machines for the total macular thickness and the retinal nerve fiber layer. However, a normative atlas for all the layers in 3D currently only exists within individual research groups.[137] Nevertheless, work has been done to demonstrate previously unknown changes in the ganglion cell layer in patients with diabetes.[133,134]

Retinal Texture Analysis

Texture, defined as measures of the spatial distribution of image intensities, can be used to characterize tissue properties and tissue differences. Textural properties may be important for assessing changes in the structural or tissue composition of layers that cannot be measured by changes in thickness alone. Texture can be determined in each of the identified layers three-dimensionally.[138–140] 3D formulations of texture descriptors were developed for pulmonary parenchymal analysis[141] and have been directly employed for OCT texture analysis.[142] The wavelet transform, a form of feature detection, has been used in OCT analysis for de-noising and de-speckling[143–145] as well as for texture analysis.[146] Early work on 3D wavelet analysis of OCT images was based on a computationally efficient yet flexible nonseparable lifting scheme in arbitrary dimensions.[142,147]

Texture characteristics can be computed for each segmented layer, several adjacent layers, or in layer combinations (Fig. 8.12).

Detection of Retinal Vessels From Three-Dimensional OCT

Segmenting the retinal vasculature in 3D SD-OCT volumes[148,149] allows OCT-to-fundus and OCT-to-OCT image registration (see Optical coherence tomography imaging, above). The absorption of light by the blood vessel walls causes vessel silhouettes to appear below the position of vessels, which thus causes the projected vessel

positions to appear dark on either a full projection image of the entire volume[149] or a projection image from a segmented layer for which the contrast between the vascular silhouettes and background is highest as proposed by Niemeijer and others.[150,151] In particular, the work by Niemeijer et al. used the layer near the retinal pigment epithelium to create the projection image. Vessels were segmented using feature detection with Gaussian filter banks and a k-NN pixel classification approach. The performance of the automated method was evaluated for both ONH-centered as well as macula-centered scans. The retinal vessels were successfully identified in a set of 16 3D OCT volumes (8 optic nerve head and 8 macula-centered) with high sensitivity and specificity as determined using ROC analysis, AUC = 0:96. Xu et al.[152] reported an approach for segmenting the projected locations of the vasculature by utilizing pixel classification of A-scans. The features used in the pixel classification were based on a projection image of the entire volume in combination with features of the individual A-scans. Both of these reported prior approaches focused on segmenting the vessels in the region outside the optic disc region because of difficulties in the segmentation inside this region. The neural canal opening (NCO) shares similar features with vessels, thus causing false positives. Hu et al.[146] proposed a modified 2D pixel classification algorithm to segment the blood vessels in SD-OCT volumes centered at the ONH, with a special focus on better identifying vessels near the NCO. Given an initial 2D segmentation of the projected vasculature, Lee et al. presented an approach for segmenting the 3D vasculature in the volumetric scans[153] by utilizing a graph-theoretic approach (Fig. 8.15). One of the current limitations of that approach is the inability to properly resolve the depth information of crossing vessels.

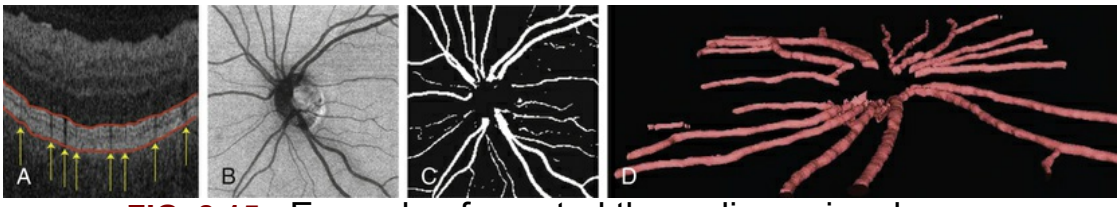

FIG. 8.15 Example of spectral three-dimensional optical coherence tomography (3D OCT) vessel

segmentation. (A) Vessel silhouettes indicate position of vasculature. Also indicated in red are slice intersections of two surfaces that delineate subvolume in which vessels are segmented (superficial retinal layers toward vitreous are at the bottom). (B) Two-dimensional projection image extracted from projected subvolume of spectral 3D OCT volume. (C) Automatic vessel segmentation. (D) Three-dimensional rendering of vessel around the optic nerve head. (Reproduced from Lee K, Abràmoff M, Niemeijer MK, et al. 3D segmentation of retinal blood vessels in spectral-domain OCT volumes of the optic nerve head. Proc. SPIE Medical Imaging 2010:Biomedical Applications Molecular, Structural, Functional Imaging, Feb. 2010, vol. 7626, p. 76260V.)

Detection of Retinal Lesions

Calculated texture and layer-based properties can be used to detect retinal lesions as a 2D footprint[142] or in 3D. Out of many kinds of possible retinal lesions, symptomatic exudate-associated derangements (or SEADs), a general term for fluid-related abnormalities in the retina, are of great interest in assessing severity of AMD, diabetic macular edema, and other diseases. Detection of drusen, cotton-wool spots, areas of pigment epithelial atrophy, or pockets of fluid under epiretinal membranes may be attempted in a similar fashion.

The deviation of local retinal tissue from normal can be computed by determining the local deviations from the normal appearance at each location (x; y) in each layer and selecting the areas where the absolute deviation is greater than a predefined cutoff. More generally, in order to build an abnormality-specific detector, a classifier can be trained, the inputs of which may be the z-scores computed for relevant features. Comprehensive z-scores are appropriate since an abnormality may affect several layers in the neighborhood of a given location (x; y). The classifier-determined label associated with each column may be selected on relevant features by one of the many available cross-validation and/or feature selection methods,[154–156] thus forming a SEAD-ness or probabilistic abnormality map.

Fluid Detection and Segmentation

In AMD, diabetic macular edema, and other retinal diseases, intraretinal or subretinal fluid is reflective of disease status and changes in fluid are an indicator of disease progression or regression. With the availability of anti-VEGF (vascular endothelial growth factor) therapy, assessment of the extent and morphology of fluid is expected to contribute to patient-specific therapy. While regions of fluid are inherently three-dimensional, determining their 2D retinal footprint is highly relevant. Following the above-described analysis, fluid detection employs generalization of properties derived from expert-defined examples. Utilizing the differences between normal regional appearance of retinal layers as described by texture descriptors and other morphologic indices, a classifier can be trained to identify abnormal retinal appearance. The fluid detection starts with 3D OCT layer segmentation resulting in 10 intraretinal layers plus an additional artificial layer below the deepest intraretinal layer so that subretinal abnormalities can also be detected.[142] Texture-based and morphologic descriptors are calculated regionally in rectangular subvolumes, the most discriminative descriptors are identified, and these descriptors are used for training a probabilistic classifier. The performance of a (set of) feature(s) is assessed by calculating the area under the receiver-operating characteristic curve of the fluid classifier. Once the probabilistic classifier is trained, fluid-related probability is determined for each retinal location. In order to obtain a binary footprint for fluid in an image input to the system, the probabilities are thresholded and the footprint of the fluid region in this image is defined as the set of all pixels with a probability greater than a threshold. Useful 3D textural information can be extracted from SD-OCT scans and – together with an anatomical atlas of normal retinas – can be used for clinically important applications.

Fluid Segmentation in Three-Dimensional OCT

Complete volumetric segmentation of fluid from 3D OCT is the subject of active research. A promising approach is based on identification of a seed point in the OCT dataset that is “inside” and “outside” of a fluid region. These points can be identified automatically using a 3D variant of the probabilistic classification

approach outlined in the previous paragraphs. Once these two points are identified, an automated segmentation procedure that is based on regional graph-cut method[157,158] may be employed to detect the fluid volumetric region. The cost function utilized in a preliminary study was designed to identify dark 3D regions with somewhat homogeneous appearance. The desired properties of the fluid region are automatically learned from the vicinity of the identified fluid-region seed point. This adaptive behavior allows the same graph-cut segmentation method driven by the same cost function to reliably segment fluid of different appearance. Fig. 8.16 gives an example of 3D fluid region segmentations obtained using this approach. Note that the figure depicts the same locations in the 3D data sets imaged several times during the course of anti-VEGF treatment. The surfaces of the segmented fluid regions are represented by a 3D mesh, which can be interactively edited to maximize fluid region segmentation accuracy in difficult or ambiguous cases.

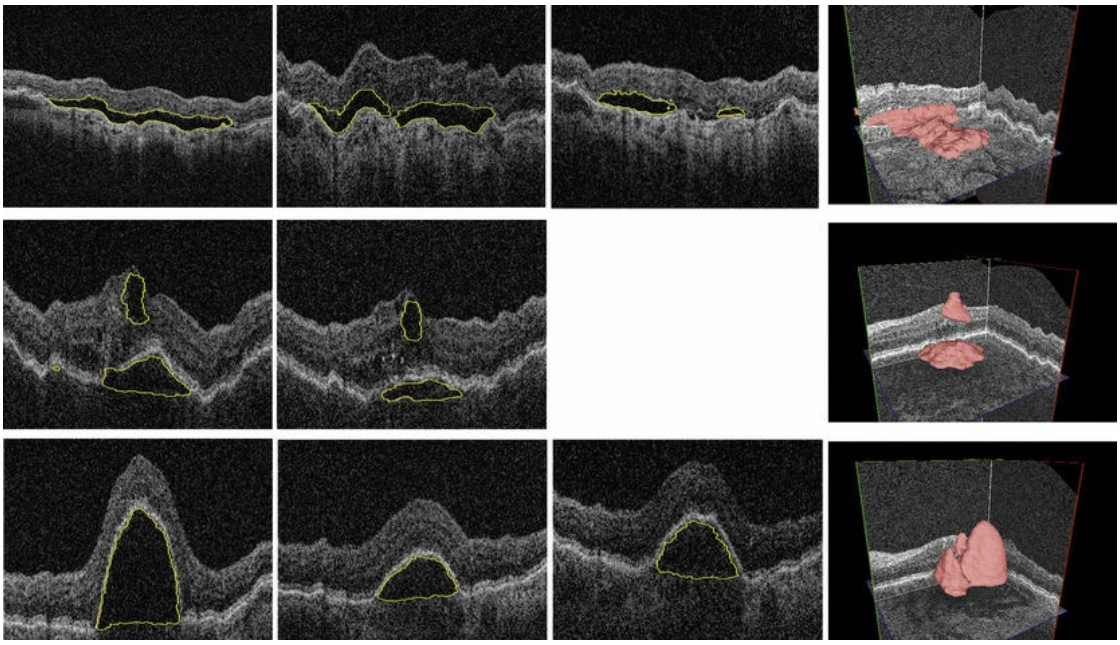

FIG. 8.16 Symptomatic exudate-associated derangements (SEAD) segmentation from three-dimensional optical coherence tomography and SEAD development over time. Top row: 0, 28, and 77 days after first imaging visit; middle row: 0 and 42 days after first imaging visit; bottom row: 0, 14, and 28 days after first imaging visit. Three-dimensional visualization in

right column shows data from week 0. Each imaging session was associated with anti-vascular endothelial growth factor reinjection.

Intraretinal Layer Segmentation in the Presence of SEADs

Another area of active research is layer segmentation in retina that contains SEADs. Most likely a two-step approach is necessary in which layers are initially segmented disregarding the SEAD presence, then SEADs are segmented, and used to constrain the second stage of layer segmentation. This process yields well-segmented retinal layers when fluid occupies a single intraretinal layer as well as in situations when the fluid resides in several adjacent retinal layers.

Multimodality Retinal Imaging

Multimodality imaging, defined as images from the same organ, using different physical techniques, is becoming increasingly common in ophthalmology. For image information from multiple modalities to be usable in mutual context, images must be registered so that the independent information that was acquired by different methods can be concatenated and form a multimodality description vector. Thus, because of its importance in enabling multimodal analysis, retinal image registration reflects another active area of research. The several clinically used methods to image the retina were introduced above and include fundus photography, scanning laser ophthalmoscopy, fluorescence imaging, and OCT. Additional retinal imaging techniques such as hyperspectral imaging, oxymetry, and adaptive optics SLO will bring higher resolution and additional image information. To achieve a comprehensive description of retinal morphology and eventually function, diverse retinal images acquired by different or the same modalities at different time instants must be mutually registered to spatially combine all available local information. The following sections provide a brief overview of fundus photography and OCT registration approaches in both 2D and 3D. A more

detailed review is available.[59] Registration of retinal images from other existing and future imaging devices can be performed in a similar or generally identical manner.

Registration of Fundus Retinal Photographs

Registration of fundus photographs taken either at different regions of the retina, or of the same area of the retina but at different times, are useful to expand the effective field of view of a retinal image, determine what part of the retina is being viewed, or aid in analyzing changes over time.[159] We have previously discussed some other uses for fundus–fundus registration in regard to retinal atlases. To register 2D or planar fundus images, most existing registration approaches utilize identification and extraction of features derived from retinal vasculature segmented separately from the individual fundus images. The choice of a specific image registration algorithm to align retinal images into a montage depends on the image characteristics and the application. Images acquired with only a small overlap may be optimally aligned using feature-based registration approaches, while images acquired with larger overlaps, may be satisfactorily aligned using intensity-based approaches. Examples of feature-based registration are global-to-local matching,[160] hierarchical model refinement,[161] and dual-bootstrap.[162] Local intensity features[163] are particularly useful when an insufficient number of vascular features are available. Following a step of vascular skeletonization, vascular branching points can be easily used as stable landmarks for determining image-to-image correspondence. As an example, the RADIC model[164] parameters are estimated during an optimization step that uses Powell's method[165] and is driven by the vessel centerline distance. The approach presented by Lee et al. in 2010 reported registration accuracy of 1.72 pixels (25–30 μm, depending on resolution) when tested in 462 pairs of green channel fundus images.[108] The registration accuracy was assessed as the vessel line error. The method only needed two correspondence points to be reliably identified and was therefore applicable even to cases when only a very small overlap between the retinal image pairs existed. Based on the identified vascular features, the general approach can be

applied to any retinal imaging modality for which a 2D vessel segmentation is available. In registering poor quality multimodal fundus image pairs, which may not have sufficient vessel-based features available, Chen et al. proposed the detection of corner points using a Harris detector followed by use of a partial intensity invariant feature descriptor.[166,167] They reported obtaining 89.9% "acceptable" registrations (defined as registrations with a median error of 1.5 pixels and a maximum error of 10 pixels when compared with ground truth correspondences) when tested on 168 pairs of multimodal retinal images.

Registration of OCT With Fundus Retinal Photographs

Registration of 2D fundus images with inherently 3D OCT images requires that the dimensionality of OCT be reduced to 2D via z-axis projection. Building on the ability to obtain vascular segmentation from 3D OCT projection images, the problem of fundus–OCT registration becomes virtually identical to that of fundus–fundus registration that was described in the previous section. Using the same general method, high-quality OCT-fundus registration can be achieved. Fig. 8.17 presents the main steps of the registration process and shows the achieved registration performance.

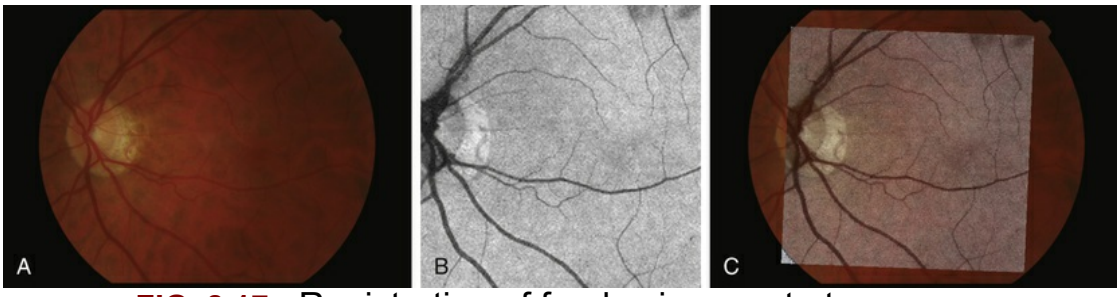

FIG. 8.17 Registration of fundus images to two-dimensional optical coherence tomography (OCT) projection data. (A) Fundus camera image. (B) Two-dimensional projection (through depth dimension) of three-dimensional OCT data. (C) Registered and blended fundus–OCT images via application of affine transformation model with three identified vascular landmarks.

Mutual Registration of Three-Dimensional OCT Images

Temporal changes of retinal layers leading to assessment of disease progression or regression can be accessed from longitudinal OCT images. Comparison of morphology or function over time requires that the respective OCT image data sets be registered. Since OCT is a three-dimensional imaging modality, such registration needs to be performed in 3D. For follow-up studies, image registration is a vital tool to enable more precise, quantitative comparison of disease status. Another important aspect of OCT to OCT registration is the ability to enlarge retinal coverage by registering OCT data resulting from imaging different portions of the retina. A fully three-dimensional SIFT-based (Scale-Invariant Feature Transform) approach was introduced by Niemeijer et al. in 2009.[168] In their work, the SIFT feature extractor locates minima and maxima in the difference of Gaussian scale space to identify salient feature points. Using calculated histograms of local gradient directions around each found extremum in 3D, the matching points are found by comparing the distances between feature vectors. An application of this approach to rigid registration of peripapillary (ONH-centered) and macula-centered 3D OCT scans of the same patient for which the macular and peripapillary OCT scans had only a limited overlap has been reported.[168] The work built on a number of analysis steps introduced earlier, including segmentation of the retinal layers and flattening of each of the two volumes to be registered and then determining 3D SIFT feature points.[169,170] Using the terminology usual for image registration when one of the registered images is called the "source" (say the macular image) and the other the "target" (say the peripapillary image), the feature point detection is performed in both the source and target images. After feature point extraction, those that are in corresponding positions in both images are identified. In a typical pair of two OCT scans, about 70 matching pairs can be found with a high level of certainty. Considering the already flattened 3D OCT image pair, the major remaining deformations that need to be resolved are translation and limited rotation. Consequently, simple rigid or

affine transform is appropriate to achieve the desired image registration. The transform parameters are estimated from the identified correspondence points. OCT–OCT registration of macular and peripapillary OCT scans, achieved 3D accuracy of 2:0 to 3:3 voxels, assessed as an average voxel distance error in 1572 matched locations.[167] Qualitative evaluation of performance demonstrated the utility of this approach to clinical-quality images. Temporal registration of longitudinally acquired OCT images from the same subjects can be obtained in an identical manner.

Future of Retinal Imaging and Image Analysis

Translation of research in imaging and image analysis into the clinic has been relatively rapid in the past, and is likely to accelerate in the future. This is partially explained by the lower capital expenditure for ophthalmic imaging devices compared to radiologic imaging devices – the latter can often be 10 to 100 times more expensive – and partially because we as retinal specialists manage patients directly and are directly involved in the ordering and interpreting of images, while radiologists typically do not directly manage patients. This subtle difference in physician–patient relationship leads to a more direct coupling between imaging innovation and clinical impact that is so well visible in retinal image analysis. Thus, it can be expected that translation of fundamental research findings in retinal imaging will remain rapid in the future. The need to automate image interpretation is correspondingly high.[171] A global push toward cost-effective imaging and image analysis for wide scale retinal and/or systemic disease detection in a population screening setting will mandate continued efforts in perfecting automated image analysis.[59]

Likely, retinal image analysis and interpretation will be coupled to genetic and other assessment indices allowing truly personalized approaches to complex analyses of broad sets of patient-specific data. On the technologic side, this requires development and wide utilization of highly automated techniques for combined analysis of retinal image data in 2D, 3D, and 4D (3D+time), quantification of

temporal changes, including the assessment of local and/or systemic severity of the findings. On the patient management side, it will lead to broad utilization of semiautomated, clinician supervised management of retinal diseases, especially diabetic retinopathy, and choroidal neovascularization. Overall, we envision that in the next decade the utilization of retinal imaging will go far beyond the direct needs of retinal disease management, and that the quantified retinal examination will become broadly used in systemic disease assessment both for patient-specific care and for population studies.

Retinal imaging and image analysis have developed rapidly over the past 10 years, and image analysis plays a crucial role in the care of patients with retinal diseases, and other diseases that manifest in the retina. So far, image analysis has mostly operated reactively, i.e., waiting for what the newest imaging devices have as output, and then trying to find approaches to analyze and quantify the image data. Moving forward, we expect that imaging device development and image analysis research will start to operate more in concert and become closely integrated, so that retinal image analysis successes and difficulties can directly influence device developers to focus on details that will help reliably analyze the images and vice versa. Ultimately, retinal image analysis and the research and development behind it is driven by the overarching goal of preventing visual loss and suffering from retinal and systemic disease.

References

1. Zhang X, Saaddine JB, Chou CF, et al. Prevalence of diabetic retinopathy in the United States, 2005-2008. *JAMA*. 2010;304:649–656.
2. Flick CS. Centenary of Babbage's ophthalmoscope. *Optician*. 1947;113:246.
3. Keeler CR. 150 years since Babbage's ophthalmoscope. *Arch Ophthalmol*. 1997;115:1456–1457.
4. von Helmholtz H. *Beschreibung eines Augens-Spiegels zur Untersuchung der Netzhaut im lebenden Auge*. Foerstner: Berlin; 1851.

5. Trigt AC. *Dissertatio ophthalmologica inauguralis de speculo oculi*. 1853.
6. Rathmann W, Giani G. Global prevalence of diabetes: estimates for the year 2000 and projections for 2030. *Diabetes Care*. 2004;27:2568–2569 [author reply 9].
7. Gerloff O. Uber die Photographie des Augenhintergrundes. *Klin Monatsbl Augenheilkd*. 1891;29:397ff.
8. Gullstrand A. *Neue methoden de reflexlosen Ophthalmoskopie. Berichte Deutsche Ophthalmologische Gesellschaft*. 1910:36.
9. Novotny HR, Alvis DL. A method of photographing fluorescence in circulating blood in the human retina. *Circulation*. 1961;24:82–86.
10. Allen L. Ocular fundus photography: suggestions for achieving consistently good pictures and instructions for stereoscopic photography. *Am J Ophthalmol*. 1964;57:13–28.
11. Webb RH, Hughes GW. Scanning laser ophthalmoscope. *IEEE Trans Biomed Eng*. 1981;28:488–492.
12. Michelson A, Morley E. On the relative motion of the earth and the luminiferous ether. *Am J Sci*. 1872;333–345.
13. Youngquist RC, Carr S, Davies DE. Optical coherence-domain reflectometry: a new optical evaluation technique. *Opt Lett*. 1987;12:158–160.
14. Youngquist RC, Wentworth RH, Fesler KA. Selective interferometric sensing by the use of coherence synthesis. *Opt Lett*. 1987;12:944–946.
15. Huang D, Swanson EA, Lin CP, et al. Optical coherence tomography. *Science*. 1991;254:1178–1181.
16. Swanson EA, Izatt JA, Hee MR, et al. In vivo retinal imaging by optical coherence tomography. *Opt Lett*. 1993;18:1864–1866.
17. Matsui M, Tashiro T, Matsumoto K. A study on automatic and quantitative diagnosis of fundus photographs. I. Detection of contour line of retinal blood vessel images on color fundus photographs (author's transl).*Nippon Ganka Gakkai Zasshi*. 1973;77:907–918.
18. Baudoin CE, Lay BJ, Klein JC. Automatic detection of microaneurysms in diabetic fluorescein angiography. *Rev Epidemiol Sante Publique*. 1984;32:254–261.

19. Wild S, Roglic G, Green A, et al. Global prevalence of diabetes: estimates for the year 2000 and projections for 2030. *Diabetes Care*. 2004;27:1047–1053.
20. Lawrence S, Giles CL, Tsoi AC, et al. Face recognition: a convolutional neural-network approach. *IEEE Trans Neural Netw*. 1997;8:98–113.
21. Schlegl T, Waldstein SM, Vogl WD, et al. Predicting semantic descriptions from medical images with convolutional neural networks. *Inf Process Med Imaging*. 2015;24:437–448.
22a. Ciresan DC, Giusti A, Gambardella LM, et al. Mitosis detection in breast cancer histology images with deep neural networks. *Med Image Comput Comput Assist Interv*. 2013;16:411–418.
22b. Abramoff MD, Lou Y, Erginay A, et al. Improved automated detection of diabetic retinopathy on a publicly available dataset through integration of deep learning. *Invest Ophthalmol Vis Sci*. 2016;57(13):5200–5206.
22c. Gulshan V, Peng L, Coram M, et al. Development and validation of a deep learning algorithm for detection of diabetic retinopathy in retinal fundus photographs. *JAMA*. 2016;316(22):2402–2410.
23. Germain N, Galusca B, Deb-Joardar N, et al. No loss of chance of diabetic retinopathy screening by endocrinologists with a digital fundus camera. *Diabetes Care*. 2011;34:580–585.
24. Abramoff MD, Folk JC, Han DP, et al. Automated analysis of retinal images for detection of referable diabetic retinopathy. *JAMA Ophthalmol*. 2013;131:351–357.
25. Fujimoto JG. Optical coherence tomography for ultrahigh resolution in vivo imaging. *Nat Biotechnol*. 2003;21:1361–1367.
26a. Fercher AF, Mengedoht K, Werner W. Eye-length measurement by interferometry with partially coherent light. *Opt Lett*. 1988;13:186–188.
26b. Michael D. *Abramoff, USPTO US Patent 9155465, Snapshot spectral domain optical coherence tomographer*. Oct 13, 2015.
27. Choma M, Sarunic M, Yang C, et al. Sensitivity advantage of

swept source and Fourier domain optical coherence tomography. *Opt Express*. 2003;11:2183–2189.
28. Abramoff MD, Alward WL, Greenlee EC, et al. Automated segmentation of the optic disc from stereo color photographs using physiologically plausible features. *Invest Ophthalmol Vis Sci*. 2007;48:1665–1673.
29. Hammer DX, Ferguson RD, Ustun TE, et al. Line-scanning laser ophthalmoscope. *J Biomed Opt*. 2006;11:041126.
30. Suansilpong A, Rawdaree P. Accuracy of single-field nonmydriatic digital fundus image in screening for diabetic retinopathy. *J Med Assoc Thai*. 2008;91:1397–1403.
31. Delori FC, Pflibsen KP. Spectral reflectance of the human ocular fundus. *Appl Opt*. 1989;28:1061–1077.
32. Abramoff MD, Kwon YH, Ts'o D, et al. Visual stimulus-induced changes in human near-infrared fundus reflectance. *Invest Ophthalmol Vis Sci*. 2006;47:715–721.
33. Whited JD. Accuracy and reliability of teleophthalmology for diagnosing diabetic retinopathy and macular edema: a review of the literature. *Diabetes Technol Ther*. 2006;8:102–111.
34. Lin DY, Blumenkranz MS, Brothers R. The role of digital fundus photography in diabetic retinopathy screening. Digital Diabetic Screening Group (DDSG). *Diabetes Technol Ther*. 1999;1:477–487.
35. American Telemedicine Association OTSIG. *Telehealth Practice Recommendations for Diabetic Retinopathy*. [February] 2011.
36. Bresnick GH, Mukamel DB, Dickinson JC, et al. A screening approach to the surveillance of patients with diabetes for the presence of vision-threatening retinopathy. *Ophthalmology*. 2000;107:19–24.
37. Kinyoun JL, Martin DC, Fujimoto WY, et al. Ophthalmoscopy versus fundus photographs for detecting and grading diabetic retinopathy. *Invest Ophthalmol Vis Sci*. 1992;33:1888–1893.
38. Panel AAoOR. Preferred practice patterns: Diabetic retinopathy. Panel AAoOR. American Academy of Ophthalmology: San Francisco, CA; 2012 [2008 4th

printing].
39. Fong DS, Aiello L, Gardner TW, et al. Diabetic retinopathy. *Diabetes Care*. 2003;26:226–229.
40. Fong DS, Sharza M, Chen W, et al. Vision loss among diabetics in a group model. Health Maintenance Organization (HMO). *Am J Ophthalmol*. 2002;133:236–241.
41. Wilson C, Horton M, Cavallerano J, et al. Addition of primary care-based retinal imaging technology to an existing eye care professional referral program increased the rate of surveillance and treatment of diabetic retinopathy. *Diabetes Care*. 2005;28:318–322.
42. Klonoff DC, Schwartz DM. An economic analysis of interventions for diabetes. *Diabetes Care*. 2000;23:390–404.
43. Lin DY, Blumenkranz MS, Brothers RJ, et al. The sensitivity and specificity of single-field nonmydriatic monochromatic digital fundus photography with remote image interpretation for diabetic retinopathy screening: a comparison with ophthalmoscopy and standardized mydriatic color photography. *Am J Ophthalmol*. 2002;134:204–213.
44. Williams GA, Scott IU, Haller JA, et al. Single-field fundus photography for diabetic retinopathy screening: a report by the American Academy of Ophthalmology. *Ophthalmology*. 2004;111:1055–1062.
45. Lawrence MG. The accuracy of digital-video retinal imaging to screen for diabetic retinopathy: an analysis of two digital-video retinal imaging systems using standard stereoscopic seven-field photography and dilated clinical examination as reference standards. *Trans Am Ophthalmol Soc*. 2004;102:321–340.
46. Abramoff MD, Suttorp-Schulten MS. Web-based screening for diabetic retinopathy in a primary care population: the EyeCheck project. *Telemed J E Health*. 2005;11:668–674.
47. Abramoff MD, Reinhardt JM, Russell SR, et al. Automated early detection of diabetic retinopathy. *Ophthalmology*. 2010;117:1147–1154.
48. Abramoff MD, Niemeijer M, Suttorp-Schulten MS, et al. Evaluation of a system for automatic detection of diabetic

retinopathy from color fundus photographs in a large population of patients with diabetes. *Diabetes Care*. 2008;31:193–198.
49. Philip S, Fleming AD, Goatman KA, et al. The efficacy of automated "disease/no disease" grading for diabetic retinopathy in a systematic screening programme. *Br J Ophthalmol*. 2007;91:1512–1517.
50. Cheung N, Rogers S, Couper DJ, et al. Is diabetic retinopathy an independent risk factor for ischemic stroke? *Stroke*. 2007;38:398–401.
51. Photocoagulation treatment of proliferative diabetic retinopathy: the second report of Diabetic Retinopathy Study findings. *Ophthalmology*. 1978;85:82–106.
52. Rosenfeld PJ. Optical coherence tomography findings after an intravitreal injection of bevacizumab (Avastin) for neovascular age-related macular degeneration. *Ophthalmic Surg Lasers Imaging*. 2005;36(4):331–335.
53. Heier JS. Ranibizumab for treatment of neovascular age-related macular degeneration: a phase I/II multicenter, controlled, multidose study. *Ophthalmology*. 2006;113(4):633.e1–633.e4.
54. The Diabetic Retinopathy Study Research Group. Preliminary report on effects of photocoagulation therapy. *Am J Ophthalmol*. 1976;81:383–396.
55. Early Treatment Diabetic Retinopathy Study Research Group. Grading diabetic retinopathy from stereoscopic color fundus photographs – extension of the modified Airlie House classification. ETDRS report number 10. *Ophthalmology*. 1991;98:786–806.
56. Harvey JN, Craney L, Nagendran S, et al. Towards comprehensive population-based screening for diabetic retinopathy: operation of the North Wales diabetic retinopathy screening programme using a central patient register and various screening methods. *J Med Screen*. 2006;13:87–92.
57. Sonka M, Fitzpatrick JM. *Handbook of medical imaging – Volume 2, Medical Image processing and analysis*. The International Society for Optical Engineering Press:

Wellingham, WA; 2000.
58. Digital Imaging and Communications in Medicine (DICOM). Supplement 91: Ophthalmic Photography Image SOP Classes. DICOM Standards Committee.
59. Abramoff MD, Garvin M, Sonka M. Retinal imaging and image analysis. *IEEE Rev Biomed Eng*. 2010;169–208.
60. Niemeijer M, Abramoff MD, van Ginneken B. Information fusion for diabetic retinopathy CAD in digital color fundus photographs. *IEEE Trans Med Imaging*. 2009;28:775–785.
61. Quellec G, Russell S, Abramoff MD. Optimal filter framework for automated, instantaneous detection of lesions in retinal images. *IEEE Trans Med Imaging*. 2011;30(2):523–533.
62. Niemeijer M, Abramoff M, van Ginneken B. Information fusion for diabetic retinopathy cad in digital color fundus photographs. *IEEE Trans Med Imaging*. 2009;28:13.
63. Quellec G, Abramoff MD. Estimating maximal measurable performance for automated decision systems from the characteristics of the reference standard. Application to diabetic retinopathy screening. *Conf Proc IEEE Eng Med Biol Soc*. 2014;2014:154–157.
64. Quellec G, Russell SR, Abramoff MD. Optimal filter framework for automated, instantaneous detection of lesions in retinal images. *IEEE Trans Med Imaging*. 2011;30:523–533.
65. Fukushima K. Neocognitron: a self organizing neural network model for a mechanism of pattern recognition unaffected by shift in position. *Biol Cybern*. 1980;36:193–202.
66. Krizhevsky A, Sutskever I, Hinton GE. Imagenet classification with deep convolutional neural networks. *Adv Neural Inform Processing Systems*. 2012;1097–1105.
67a. Kaggle. *Identify signs of diabetic retinopathy in retinal images*. https://www.kaggle.com/c/diabetic-retinopathy-detection; 2015 [February 17 – July 27].
67b. Abramoff MD, Lou Y, Erginay A, et al. Improved automated detection of diabetic retinopathy on a publicly available dataset through integration of deep learning. *Invest Ophthalmol Vis Sci*. 2016;57(13):5200–5206.

67c. Gulshan V, Peng L, Coram M, et al. Development and validation of a deep learning algorithm for detection of diabetic retinopathy in retinal fundus photographs. *JAMA*. 2016;316(22):2402–2410.
68a. Yosinski J, Clune J, Bengio Y, et al. How transferable are features in deep neural networks? *Adv Neural Inform Processing Systems*. 2014;3320–3328.
68b. Gulshan V, Peng L, Coram M, et al. Development and validation of a deep learning algorithm for detection of diabetic retinopathy in retinal fundus photographs. *JAMA*. 2016;316(22):2402–2410.
68c. Nguyen A, Yosinski J, Clune J. *Deep Neural Networks are Easily Fooled: High Confidence Predictions for Unrecognizable Images, CVPR*. https://arxiv.org/abs/1412.1897; 2015.
68d. Goodfellow IJ, Shlens J, Szeged C. *Explaining and Harnessing Adversarial Examples, ARXIV*. https://arxiv.org/abs/1412.6572; 2014.
68e. Abramoff MD, Lou Y, Erginay A, et al. Improved automated detection of diabetic retinopathy on a publicly available dataset through integration of deep learning. *Invest Ophthalmol Vis Sci*. 2016;57(13):5200–5206.
69a. Tobin KW, Abramoff MD, Chaum E, et al. Using a patient image archive to diagnose retinopathy. *Conf Proc IEEE Eng Med Biol Soc*. 2008;2008:5441–5444.
69b. Chen JH, Goldstein MK, Asch SM, Altman RB. Dynamically evolving clinical practices and implications for predicting medical decisions. *Pac Symp Biocomput*. 2016;21:195–206.
69c. Arbel Y, Qiu F, Bennell MC, et al. Association between publication of appropriate use criteria and the temporal trends in diagnostic angiography in stable coronary artery disease: a population-based study. *Am Heart J*. 2016;175:153–159.
70. No authors listed. Photocoagulation treatment of proliferative diabetic retinopathy: second report of Diabetic Retinopathy Study findings. *Ophthalmology*. 1978;85(1):82–106.
71. Early Treatment Diabetic Retinopathy Study Research

Group. Fundus photographic risk factors for progression of diabetic retinopathy. ETDRS report number 12. *Ophthalmology*. 1991;98(5 Suppl):823–833.
72. American Diabetes Association. Executive summary: Standards of medical care in diabetes – 2014. *Diabetes Care*. 2014;37(Suppl. 1):S5–13.
73. Niemeijer M, Staal JS, van Ginneken B, et al. *Comparative study of retinal vessel segmentation on a new publicly available database*. [Proc SPIE] 2004:5370–5379.
74. Soares JV, Leandro JJ, Cesar Junior RM, et al. Retinal vessel segmentation using the 2-D Gabor wavelet and supervised classification. *IEEE Trans Med Imaging*. 2006;25:1214–1222.
75. Staal J, Abramoff MD, Niemeijer M, et al. Ridge-based vessel segmentation in color images of the retina. *IEEE Trans Med Imaging*. 2004;23:501–509.
76. Hubbard LD, Brothers RJ, King WN, et al. Methods for evaluation of retinal microvascular abnormalities associated with hypertension/sclerosis in the Atherosclerosis Risk in Communities Study. *Ophthalmology*. 1999;106:2269–2280.
77. Owens DR, Gibbins RL, Lewis PA, et al. Screening for diabetic retinopathy by general practitioners: ophthalmoscopy or retinal photography as 35 mm colour transparencies? *Diabet Med*. 1998;15:170–175.
78. Niemeijer M, Ginneken BV, Abramoff MD. Automatic determination of the artery vein ratio in retinal images. Nico K, Ronald MS. *Medical imaging 2010: Computer-aided diagnosis*. 2010 [Proc SPIE; 7624].
79. Lalonde M, Gagnon L, Boucher M-C. *Non-recursive paired tracking for vessel extraction from retinal images*. [Proc Conf Vis Interface] 2000:61–68.
80. Gang L, Chutatape O, Krishnan SM. Detection and measurement of retinal vessels in fundus images using amplitude modified second-order Gaussian filter. *IEEE Trans Biomed Eng*. 2002;49:168–172.
81. Hoover A, Goldbaum M. Locating the optic nerve in a retinal image using the fuzzy convergence of the blood vessels. *IEEE Trans Med Imaging*. 2003;22:951–958.
82. Foracchia M, Grisan E, Ruggeri A. Detection of optic disc in

retinal images by means of a geometrical model of vessel structure. *IEEE Trans Med Imaging*. 2004;23:1189–1195.
83. Lowell J, Hunter A, Steel D, et al. Optic nerve head segmentation. *IEEE Trans Med Imaging*. 2004;23:256–264.
84. Fleming AD, Goatman KA, Philip S, et al. Automatic detection of retinal anatomy to assist diabetic retinopathy screening. *Phys Med Biol*. 2007;52:331–345.
85. Li H, Chutatape O. Automated feature extraction in color retinal images by a model based approach. *IEEE Trans Biomed Eng*. 2004;51:246–254.
86. Sinthanayothin C, Boyce JF, Cook HL, et al. Automated localisation of the optic disc, fovea, and retinal blood vessels from digital colour fundus images. *Br J Ophthalmol*. 1999;83:902–910.
87. Tobin KW, Chaum E, Govindasamy VP, et al. Detection of anatomic structures in human retinal imagery. *IEEE Trans Med Imaging*. 2007;26:1729–1739.
88. Abramoff MD, Niemeijer M. The automatic detection of the optic disc location in retinal images using optic disc location regression. *Conf Proc IEEE Eng Med Biol Soc*. 2006;1:4432–4435.
89. Niemeijer M, Abramoff MD, van Ginneken B. Segmentation of the optic disc, macula and vascular arch in fundus photographs. *IEEE Trans Med Imaging*. 2007;26:116–127.
90. Walter T, Klein JC, Massin P, et al. A contribution of image processing to the diagnosis of diabetic retinopathy – detection of exudates in color fundus images of the human retina. *IEEE Trans Med Imaging*. 2002;21:1236–1243.
91. Spencer T, Olson JA, McHardy KC, et al. An image-processing strategy for the segmentation and quantification of microaneurysms in fluorescein angiograms of the ocular fundus. *Comput Biomed Res*. 1996;29:284–302.
92. Frame AJ, Undrill PE, Cree MJ, et al. A comparison of computer based classification methods applied to the detection of microaneurysms in ophthalmic fluorescein angiograms. *Comput Biol Med*. 1998;28:225–238.
93. Hipwell JH, Strachan F, Olson JA, et al. Automated detection of microaneurysms in digital red-free

photographs: a diabetic retinopathy screening tool. *Diabet Med*. 2000;17:588–594.
94. Niemeijer M, van Ginneken B, Staal J, et al. Automatic detection of red lesions in digital color fundus photographs. *IEEE Trans Med Imaging*. 2005;24:584–592.
95. Niemeijer M, van Ginneken B, Russell SR, et al. Automated detection and differentiation of drusen, exudates, and cotton-wool spots in digital color fundus photographs for diabetic retinopathy diagnosis. *Invest Ophthalmol Vis Sci*. 2007;48:2260–2267.
96. Cree MJ, Olson JA, McHardy KC, et al. A fully automated comparative microaneurysm digital detection system. *Eye (Lond)*. 1997;11(Pt 5):622–628.
97. Gardner GG, Keating D, Williamson TH, et al. Automatic detection of diabetic retinopathy using an artificial neural network: a screening tool [see comments]. *Br J Ophthalmol*. 1996;80:940–944.
98. Sinthanayothin C, Boyce JF, Williamson TH, et al. Automated detection of diabetic retinopathy on digital fundus images. *Diabet Med*. 2002;19:105–112.
99. Quellec G, Lamard M, Cazuguel G, et al. Multimodal information retrieval to assist diabetic retinopathy diagnosis. *ARVO Meeting Abstracts*. 2009;50:1363.
100. Osareh A, Mirmehdi M, Thomas B, et al. Automated identification of diabetic retinal exudates in digital colour images. *Br J Ophthalmol*. 2003;87:1220–1223.
101. Al-Diri B, Hunter A, Steel D. An active contour model for segmenting and measuring retinal vessels. *IEEE Trans Med Imaging*. 2009;28:1488–1497.
102. Brinchmann-Hansen O. The light reflex on retinal arteries and veins: a theoretical study and a new technique for measuring width and intensity profiles across retinal vessels. *Acta Ophthalmol Suppl*. 1986;179:1–53.
103. Brinchmann-Hansen O, Sandvik L. The intensity of the light reflex on retinal arteries and veins. *Acta Ophthalmol*. 1986;64:547–552.
104. Brinchmann-Hansen O, Sandvik L. The width of the light reflex on retinal arteries and veins. *Acta Ophthalmol*.

1986;64:433–438.
105. Xu X, Niemeijer M, Song Q, et al. Vessel boundary delineation on fundus images using graph-based approach. *IEEE Trans Med Imaging*. 2011;30(6):1184–1191.
106. Niemeijer M, Xu X, Dumitrescu A, et al. Automated measurement of the arteriolar-to-venular width ratio in digital color fundus photographs. *IEEE Trans Med Imaging*. 2011;30(11):1941–1950.
107. Hu Q, Abramoff MD, Garvin MK. Automated separation of binary overlapping trees in low-contrast color retinal images. *Med Image Comput Comput Assist Interv*. 2013;16:436–443.
108. Lee S, Reinhardt JM, Cattin PC, et al. Objective and expert-independent validation of retinal image registration algorithms by a projective imaging distortion model. *Med Image Anal*. 2010;14:539–549.
109. Lee S, Reinhardt JM, Niemeijer M, et al. Comparing the performance of retinal image registration algorithms using the centerline error measurement metric. *Invest Ophthalm Vis Sci*. 2008;47 [ARVO Abstract 1833].
110. Karnowski TP, Aykac D, Chaum E, et al. Practical considerations for optic nerve location in telemedicine. *Conf Proc IEEE Eng Med Biol Soc*. 2009;2009:6205–6209.
111. Lamard M, Cazuguel G, Quellec G, et al. Content based image retrieval based on wavelet transform coefficients distribution. *Conf Proc IEEE Eng Med Biol Soc*. 2007;2007:4532–4535.
112. Hoover A, Kouznetsova V, Goldbaum M. Locating blood vessels in retinal images by piecewise threshold probing of a matched filter response. *IEEE Trans Med Imaging*. 2000;19:203–210.
113. Giancardo L, Abramoff MD, Chaum E, et al. Elliptical local vessel density: a fast and robust quality metric for retinal images. *Conf Proc IEEE Eng Med Biol Soc*. 2008;2008:3534–3537.
114. *Laboratoire de Traitement de l'Information Médicale (LaTIM - INSERM U650). Messidor-2 dataset (Méthodes d'Evaluation de Systèmes de Segmentation et d'Indexation Dédiées à*

l'Ophtalmologie Rétinienne). http://latim.univ-brest.fr/index.php?option=com_content&view=article&id=61&Itemid=100034&l 2011.
115. Niemeijer M, van Ginneken B, Cree MJ, et al. Retinopathy online challenge: automatic detection of microaneurysms in digital color fundus photographs. *IEEE Trans Med Imaging*. 2010;29:185–195.
116. Jonnal RS, Kocaoglu OP, Zawadzki RJ, et al. The cellular origins of the outer retinal bands in optical coherence tomography images. *Invest Ophthalmol Vis Sci*. 2014;55(12):7904–7918.
117. Tang L, Garvin MK, Lee K, et al. Robust multiscale stereo matching from fundus images with radiometric differences. *IEEE Trans Pattern Anal Mach Intell*. 2011;33:2245–2258.
118. Lee K, Garvin MK, Russell S, et al. Automated intraretinal layer segmentation of 3-D macular OCT scans using a multiscale graph search. *ARVO Meeting Abstracts*. 2010;51:1767.
119. Tang L, Kwon YH, Alward WLM, et al. Automated measurement of optic nerve head shape from stereo color photographs of the optic disc: validation with SD-OCT. *ARVO Meeting Abstracts*. 2010;51:1774.
120. Antony BJ, Tang L, Abramoff M, et al. Automated method for the flattening of optical coherence tomography images. *ARVO Meeting Abstracts*. 2010;51:1781.
121. Mahajan VB, Folk JC, Russell SR, et al. Iowa membrane maps: SD OCT guided therapy for epiretinal membrane. *ARVO Meeting Abstracts*. 2010;51:3604.
122. Verbraak FD, Van Dijk HW, Kok PH, et al. Reduced retinal thickness in patients with type 2 diabetes mellitus. *ARVO Meeting Abstracts*. 2010;51:4671.
123. Baroni M, Fortunato P, La Torre A. Towards quantitative analysis of retinal features in optical coherence tomography. *Med Eng Phys*. 2007;29(4):432–441.
124. Cabrera Fernandez DC. Delineating fluid-filled region boundaries in optical coherence tomography images of the retina. *IEEE Trans Med Imaging*. 2005;24(8):929–945.

125. Cabrera Fernandez DC, Salinas HM, Puliafito CA. Automated detection of retinal layer structures on optical coherence tomography images. *Opt Express*. 2005;13(25):10 200–16.
126. Haeker M, Abramoff MD, Kardon R, et al. Segmentation of the surfaces of the retinal layer from OCT images. *Lecture Notes Comp Sci*. 2006;4190:800–807.
127. Haeker M, Abramoff MD, Wu X, et al. Use of varying constraints in optimal 3-D graph search for segmentation of macular optical coherence tomography images. *Med Image Comput Comput Assist Interv*. 2007;10:244–251.
128. Haeker M, Wu X, Abramoff M, et al. Incorporation of regional information in optimal 3-D graph search with application for intraretinal layer segmentation of optical coherence tomography images. *Inf Process Med Imaging*. 2007;20:607–618.
129. Garvin MK, Abramoff MD, Kardon R, et al. Intraretinal layer segmentation of macular optical coherence tomography images using optimal 3-D graph search. *IEEE Trans Med Imaging*. 2008;27:1495–1505.
130. Galler KE, Folk JC, Russell SR, et al. Patient preference and safety of bilateral intravitreal injection of anti-VEGF therapy. *ARVO Meeting Abstracts*. 2009;50:247.
131. Garvin MK, Abramoff MD, Wu X, et al. Automated 3-D intraretinal layer segmentation of macular spectral-domain optical coherence tomography images. *IEEE Trans Med Imaging*. 2009;28:1436–1447.
132. Reinhardt JM, Lee S, Xu X, et al. Retina atlas mapping from color fundus images. *ARVO Meeting Abstracts*. 2009;50:3811.
133. van Dijk HW, Kok PH, Garvin M, et al. Selective loss of inner retinal layer thickness in type 1 diabetic patients with minimal diabetic retinopathy. *Invest Ophthalmol Vis Sci*. 2009;50:3404–3409.
134. van Dijk HW, Verbraak FD, Kok PH, et al. Decreased retinal ganglion cell layer thickness in patients with type 1 diabetes. *Invest Ophthalmol Vis Sci*. 2010;51:3660–3665.
135. Longmuir SQ, Longmuir R, Matthews K, et al. Retinal arterial but not venous tortuosity correlates with

facioscapulohumeral muscular dystrophy (FSHD) severity. *ARVO Meeting Abstracts*. 2009;50:5419.
136. Agurto Rios C, Pattichis MS, Murillo S, et al. Detection of structures in the retina using AM-FM for diabetic retinopathy classification. *ARVO Meeting Abstracts*. 2009;50:313.
137. Tso DY, Schallek JB, Kardon R, et al. Hemodynamic components contribute to intrinsic signals of the retina and optic disc. *ARVO Meeting Abstracts*. 2009;50:4322.
138. Garvin MK, Niemeijer M, Kardon RH, et al. Automatically correcting for the presence of retinal vessels on spectral-domain optical coherence tomography images decreases variability of the segmented retinal layers. *ARVO Meeting Abstracts*. 2009;50:1099.
139. Quellec G, Lamard M, Cazuguel G, et al. Adaptive non-separable wavelet transform via lifting and its application to content-based image retrieval. *IEEE Trans Image Processing*. 2010;19(1):25–35.
140. Lee K, Niemeijer M, Garvin MK, et al. Automated optic disc segmentation from 3D SD-OCT of the optic nerve head (ONH). *ARVO Meeting Abstracts*. 2009;50:1102.
141. Xu Y, Sonka M, McLennan G, et al. MDCT-based 3-D texture classification of emphysema and early smoking related lung pathologies. *IEEE Trans Med Imaging*. 2006;25:464–475.
142. Quellec G, Lee K, Dolejsi M, et al. Three-dimensional analysis of retinal layer texture: identification of fluid-filled regions in SD-OCT of the macula. *IEEE Trans Med Imaging*. 2010;29:1321–1330.
143. Van Dijk HW, Kok PHB, Garvin M, et al. Selective loss of inner retinal layer thickness in type 1 diabetic patients with minimal diabetic retinopathy. *ARVO Meeting Abstracts*. 2009;50:3244.
144. Abramoff MD, Russell SR, Mahajan V, et al. Performance of automated detection of diabetic retinopathy does not improve by using the distance of each lesion to the fovea. *ARVO Meeting Abstracts*. 2009;50:3268.
145. Barriga ES, Russell SR, Pattichis MS, et al. Relationship

between visual features and analytically derived features in non-exudated AMD phenotypes: closing the semantic gap. *ARVO Meeting Abstracts*. 2009;50:3274.
146. Hu Z, Niemeijer M, Lee K, et al. Automated segmentation of the optic canal in 3d spectral-domain oct of the optic nerve head (ONH) using retinal vessel suppression. *ARVO Meeting Abstracts*. 2009;50:3334.
147. Niemeijer M, Garvin MK, Lee K, et al. Automated segmentation of the retinal vasculature silhouettes in isotropic 3D optical coherence tomography scans. *ARVO Meeting Abstracts*. 2009;50:1103.
148. Niemeijer M, Garvin MK, van Ginneken B, Vessel segmentation in 3D spectral OCT scans of the retina. Medical Imaging 2008: Image Processing 2008;6914:69141R-8.
149. Niemeijer M, Sonka M, Garvin MK, et al. Automated segmentation of the retinal vasculature in 3D optical coherence tomography images. *ARVO Meeting Abstracts*. 2008;49:1832.
150. Zhang L, Lee K, Niemeijer M, et al. Automated segmentation of the choroid from clinical SD-OCT. *Invest Ophthalmol Vis Sci*. 2012;53(12):7510–7519.
151. Yousefi S, Liu T, Wang RK. Segmentation and quantification of blood vessels for OCT-based micro-angiograms using hybrid shape/intensity compounding. *Microvasc Res*. 2015;97:37–46.
152. Xu DA, Tolliver H, Ishikawa G, et al. 3D OCT retinal vessel segmentation based on boosting learning. Springer: Berlin; 2009:179–182. Dössel O, Schlegel WC. *World Congress on Medical Physics and Biomedical Engineering*. vol. 25/4 [Sep 7–12; Munich, Germany; IFMBE Proceedings].
153. Lee K, Niemeijer M, Garvin MK, et al. Segmentation of the optic disc in 3-D OCT scans of the optic nerve head. *IEEE Trans Med Imaging*. 2010;29:159–168.
154. Duda RA, Hart PE, Stork DG. *Pattern classification*. Wiley-Interscience: New York; 2001.
155. Lee S, Reinhardt JM, Niemeijer M, et al. Comparing the performance of retinal image registration algorithms using

the centerline error measurement metric. *ARVO Meeting Abstracts*. 2008;49:1833.
156. Garvin MK, Sonka M, Kardon RH, et al. Three-dimensional analysis of SD OCT: thickness assessment of six macular layers in normal subjects. *ARVO Meeting Abstracts*. 2008;49:1879.
157. Boykov Y, Kolmogorov V. An experimental comparison of min-cut/max-flow algorithms for energy minimization in vision. *IEEE Trans Pattern Anal Mach Intell*. 2004;26:1124–1137.
158. Yang EB, Jin Jones Y, Alward WLM, et al. Comparing resident and fellow performance on evaluation of stereoscopic optic disc images. *ARVO Meeting Abstracts*. 2008;49:3626.
159. Tobin KW, Chaum E, Abramoff MD, et al. Automated diagnosis of retinal disease in a large diabetic population. *ARVO Meeting Abstracts*. 2008;49:3225.
160. Graff JM, Abramoff MD, Russell SR. Stereo video indirect ophthalmoscopy: a novel educational and research tool. *ARVO Meeting Abstracts*. 2008;49:3228.
161. Abramoff MD, Kardon RH, Vermeer KA, et al. Portable, patient friendly scanning laser ophthalmoscope for diabetic retinopathy imaging: exudates and hemorrhages. *ARVO Meeting Abstracts*. 2007;48:2592.
162. Russell SR, Abramoff MD, Radosevich MD, et al. Quantitative assessment of retinal image quality compared to subjective determination. *ARVO Meeting Abstracts*. 2007;48:2607.
163. Piette SD, Adix ML, Abramoff MD, et al. Comparison of computer aided planimetry between simultaneous and non-simultaneous stereo optic disc photographs. *ARVO Meeting Abstracts*. 2007;48:1184.
164. Lee S, Abramoff MD, Reinhardt J. *Feature-based pairwise retinal image registration by radial distortion correction*. [Medical Imaging: Image Analysis Proceedings of SPIE Medical Imaging] 2007:6512.
165. Tso DY, Schallek J, Kwon Y, et al. Blood flow dynamics contribute to functional intrinsic optical signals in the cat

retina in vivo. *ARVO Meeting Abstracts*. 2007;48:1951.
166. Chen J, Tian J, Lee N, et al. A partial intensity invariant feature descriptor for multimodal retinal image registration. *IEEE Trans Biomed Eng*. 2010;57(7):1707–1718.
167. Vermeer KA, Mensink MH, Kardon RH, et al. Super resolution in retinal imaging. *ARVO Meeting Abstracts*. 2007;48:2766.
168. Niemeijer M, Garvin MK, Lee K, et al. *Registration of 3D spectral OCT volumes using 3D SIFT feature point matching*. [Medical Imaging 2009: Image Processing] 2009 [7259:72591I-8].
169. Lowe DG. Distinctive image features from scale-invariant keypoints. *Int J Comput Vision*. 2004;60:91–110.
170. Klein R, Chou CF, Klein BE, et al. Prevalence of age-related macular degeneration in the US population. *Arch Ophthalmol*. 2011;129:75–80.
171. Helmchen LA, Lehmann HP, Abramoff MD. Automated detection of retinal disease. *Am J Manag Care*. 2014;20(11 Spec No. 17):eSP48–52.

9

Electrogenesis of the Electroretinogram

Laura J. Frishman

Introduction

The electroretinogram (ERG) is an electrical potential generated by the retina in response to a change in illumination. It is an excellent tool for evaluating retinal function in both the clinic and the

laboratory because it can be recorded noninvasively from the corneal surface in vivo under physiologic or nearly physiologic (anesthetized) conditions. However, the ERG response to a flash of light is complex. It is the summed activity of all retinal cells, and consists of overlapping positive and negative component potentials that originate from different stages of retinal processing. For the ERG to be an effective tool in assessing normal and pathologic retinal activity, it is important that the contributions of the various retinal cell types be distinguished and characterized.

This chapter will review current knowledge of the cellular origins and mechanisms of generation of the various ERG component waves, progressing from distal retina to proximal retina. As will be described, the ERG is generated by radial currents arising either directly from retinal neurons, or as a result of the effect on retinal glia of changes in extracellular potassium concentration ($[K^+]_o$) brought about by retinal neuronal activity. Our understanding of the electrogenesis of the ERG was initially based on studies in a variety of cold-blooded vertebrates as well as some mammalian species, described in more detail in previous reviews.[1,2] Studies in a nonhuman primate model (macaque monkey) whose retina and ERG are very similar to that of humans (Fig. 9.1),[3] and particularly those over the past two decades, have improved our understanding of the electrogenesis of the ERG in humans. This work will be highlighted wherever possible in this chapter. Clinical applications of the ERG will be described in the Chapter 10 (Clinical electrophysiology). Another recent review has examined the electrogenesis of a common animal model for retinal disease, the mouse.[3]

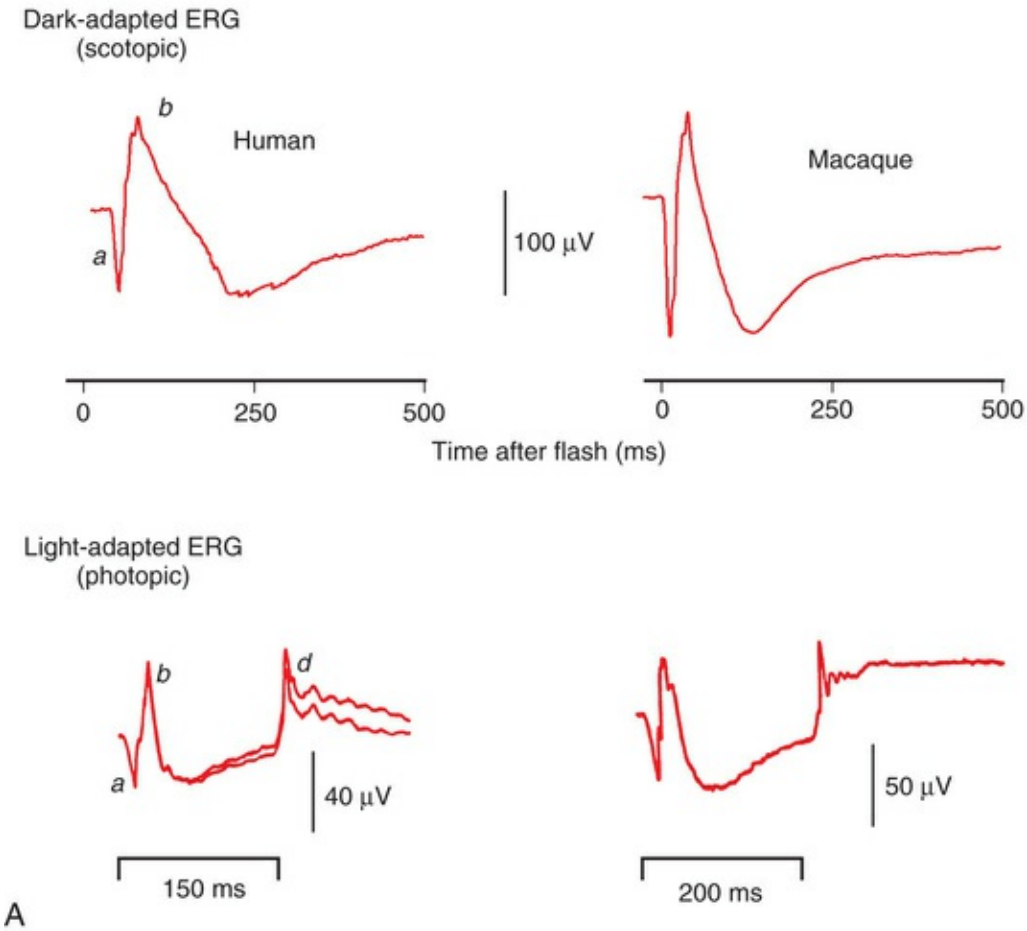

A

Dark- and light-adapted full-field flash electroretinograms (ERGs) of human subjects and macaque monkeys. (A) Top: Dark-adapted (scotopic) ERGs in response to brief high-energy flashes from darkness occurring at time zero for a normal human subject (left) and an anesthetized macaque monkey (right). The stimulus energy was ~400 sc td/s. Bottom: Light-adapted (photopic) flash ERGs in response to longer-duration flashes on a rod-saturating background for a normal human subject (left) and a macaque monkey (right). For the human subject the stimulus was a 150-ms white full-field flash of 4.0 log ph td presented on a steady background of 3.3 log sc td. For the macaque, the same stimulus was used, but the flashes were

200 ms in duration (Adapted from Sieving PA, Murayama K, Naarendorp F. Push–pull model of the primate photopic electroretinogram: a role for hyperpolarizing neurons in shaping the b-wave. Vis Neurosci 1994;11:519–32.)

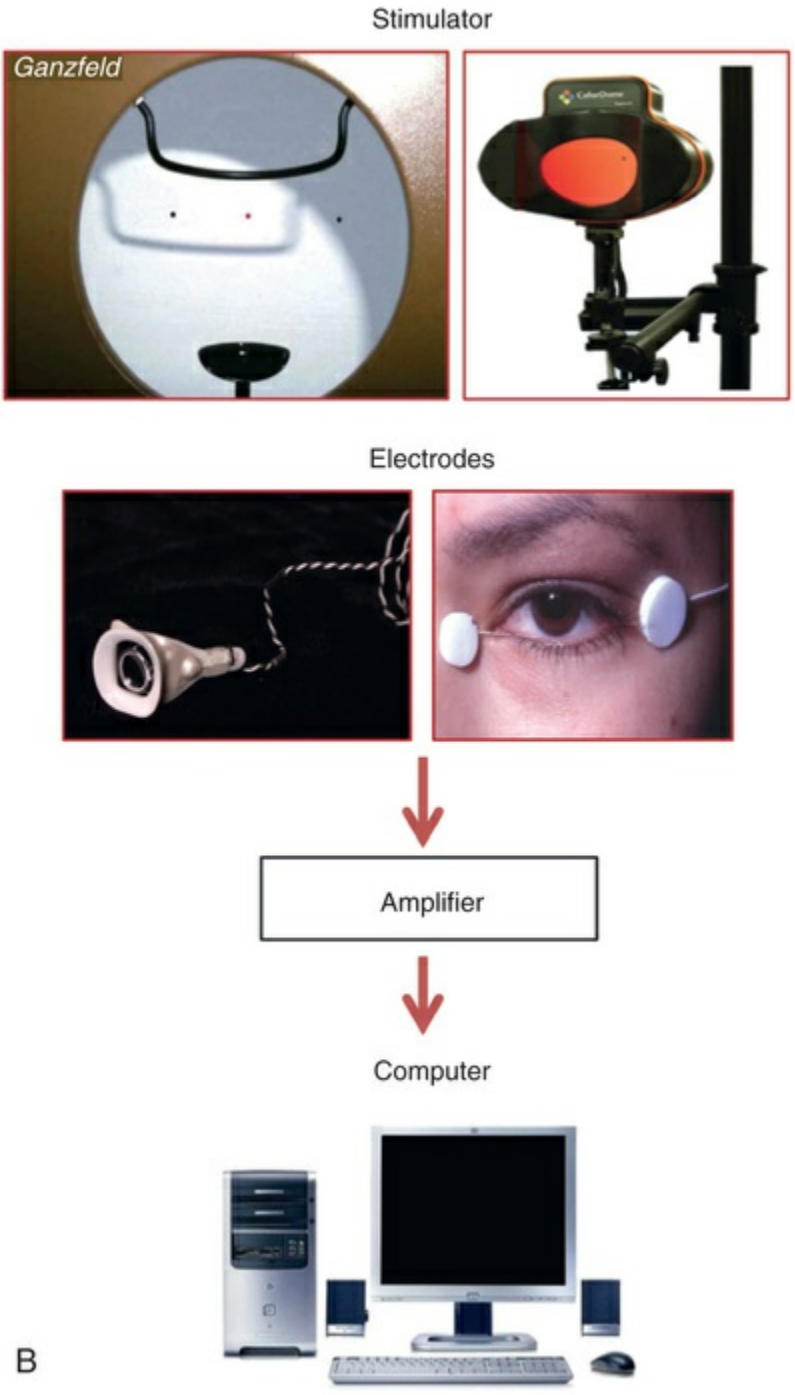

(B) ERG recording setup: recordings are made using a traditional ganzfeld bowl (left) or more modern light-emitting diode-based

full-field stimulator. Burian–Allen and DTL fiber electrodes[4] are illustrated. ERG recordings are amplified and sent to a computer for averaging, display, and analysis.

FIG. 9.1

Generation of Extracellular Potentials: General Concepts

Extracellular potentials that can be recorded noninvasively, such as the ERG (and visual evoked potential of the cortex), are the result of localized conductance changes in the membranes of activated cells that give rise to inward or outward currents. These currents also flow in the extracellular space (ECS) and create extracellular potentials. The current flowing through the conductive fluid surrounding a cell whose activation has given rise to a local current is directed mainly toward the relatively less activated parts of the cell. Thus, when neurons are arranged so that the extracellular currents of many synchronously activated cells all flow in the same direction, the resulting extracellular potential change, called a "field potential," may be large enough to be recorded at a distance, e.g., at the cornea in the case of the ERG. In the retina, because all neurons generate light-evoked currents, in principle they should all contribute to the retinal field potentials. However, depending upon various factors, considered below, the contribution from any particular cell type could be quite large, or not discernible in the response.

An important factor affecting a given cell's contribution to the ERG is its orientation in the retina. Radially oriented neurons in the retina (photoreceptors and bipolar cells) and glial cells (Müller cells and retinal pigment epithelial [RPE] cells) make larger contributions to the ERG than cells that are oriented more irregularly or laterally (e.g., horizontal and amacrine cells) (Fig. 9.2). The currents around cells that underlie the ERG enter the ECS at

one retinal depth (the current source), and return into the cell at another depth (the current sink), creating a current dipole. Although most of the extracellular current flowing from source to sink traverses the ECS within the retina, some travels extraretinally – through the vitreous humor, extraocular tissues, sclera, choroid, the high resistance of the RPE (R-membrane), and back into the neural retina.

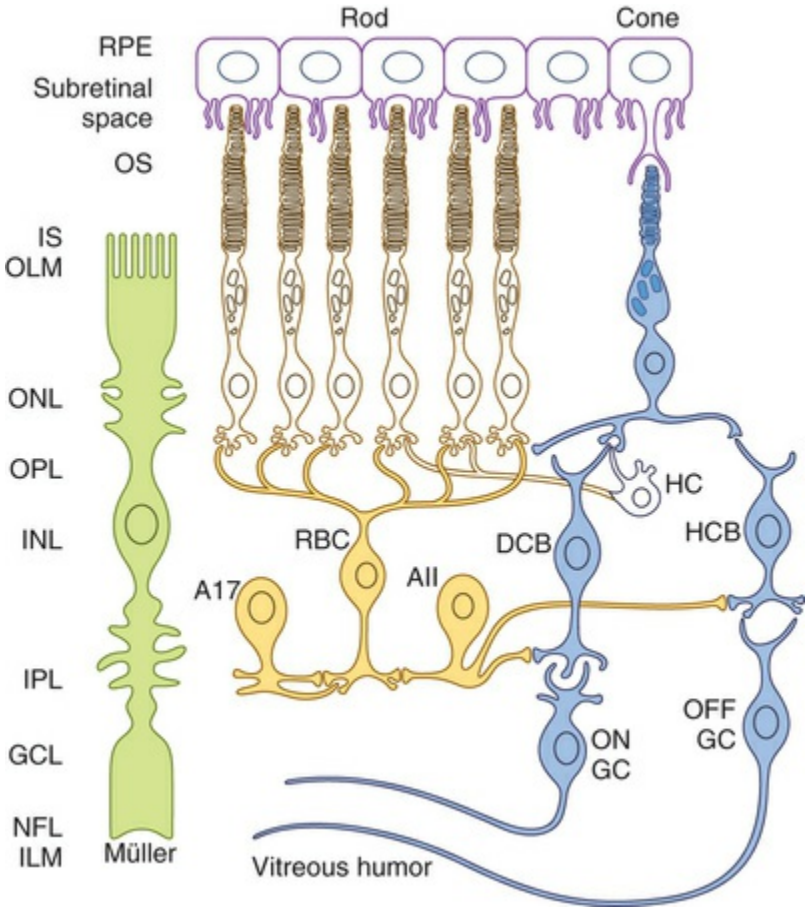

FIG. 9.2 Schematic of rod and cone pathways of the mammalian retina. The blue-filled cells indicate the cone pathways; the yellow-filled cells indicate the primary rod pathway. The green-filled cell is a Müller glia cell. *A*, amacrine cell; *DCB*, depolarizing (ON) cone bipolar cell; *GC*, ganglion cell; *GCL*, ganglion cell layer; *HC*, horizontal cell; *HCB*, hyperpolarizing (OFF) bipolar cell; *ILM*, inner limiting membrane; *INL*, inner nuclear layer; *IPL*, inner plexiform layer; *IS*, inner segment; *NFL*, nerve fiber layer; *OLM*, outer limiting membrane; *ONL*, outer nuclear layer; *OPL*, outer plexiform layer; *OS*, outer segment; *RBC*, rod bipolar

cell; *RPE*, retinal pigment epithelium. Scale bar: 20 μm.

The polarity and amplitude of the recorded ERG will depend upon the location of the active and reference electrodes. In noninvasive studies, a common location for the active electrode is on the cornea via a contact lens electrode, e.g., as illustrated in Fig. 9.1B, a Burian–Allen electrode, or jet electrode, or another type of surface conductive electrode (e.g., a DTL fiber electrode,[4] H–K loop,[5] or gold foil electrode). For comfort, skin electrodes, which yield smaller signals, are sometimes used instead. In invasive studies of ERG components in animals, the active electrode may be positioned anywhere in the current path, including at different retinal depths, near particular cell types. The reference electrode also can be positioned anywhere in the path, but is often placed behind the RPE in studies of isolated retina, or retrobulbar in intact eyes. In noninvasive and clinical applications, the reference is positioned either under the eyelids, such as the speculum of the Burian–Allen electrode for bipolar recording between the contact lens electrode and the reference on the same eye, or remote from the eye (e.g., on the temple) for monopolar recording. The exact position of the remote reference is of minor consequence except for possible contamination of the retinal signal by other sources.

Other factors that influence the magnitude of the contribution to the ERG of a particular cell type include stimulus conditions, such as the strength of the stimulus and its wavelength (spectrum), the background illumination (that determines adaptation level of the retina), the duration and spatial extent of the stimulus, and the location of the stimulus within the visual field, as these stimulus parameters have different effects on the responses of the different cells. For example, the relative contributions of various cell types are different under dark-adapted (scotopic) and light-adapted (photopic) conditions when rod and cone pathways, respectively, are involved in generating responses. Spatially extended diffuse stimuli, i.e., full-field (ganzfeld) flashes that fill the retina evenly, using stimulators such as those illustrated in Fig. 9.1B, are commonly used to elicit the major ERG waves (a-, b-, and d-waves) from photoreceptors and bipolar cells. Contributions from these cells generally increase with the area of the retina stimulated as the

number of cells, and hence the total extracellular current, is increased. In contrast, contributions of retinal ganglion cells (and other cells with antagonistic regions within their receptive fields) to the full-field flash ERG will be limited by the strength of surround antagonism. For photopic ERGs, particularly from subjects with trichromatic color vision, such as the macaque and human, stimulus wavelength also affects contributions from cells whose responses are dependent upon spectral antagonism.[6,7]

Spatial Buffering by Glial Cells

Spatial buffering of $[K^+]_o$ by radially oriented Müller cells, RPE cells, and perhaps astrocytes in the optic nerve head is an important mechanism for generating the currents underlying several ERG components, to be described later in this chapter, e.g., c-wave, slow PIII, tail of the b-wave, scotopic threshold response (STR), M-wave, and photopic negative response (PhNR). Due to its importance in generating ERGs, an overview of $[K^+]_o$ spatial buffering in Müller cells will be presented here.

$[K^+]_o$ spatial buffering is important for maintaining the electrochemical gradients across cell membranes necessary for normal neuronal activity and for minimizing the changes in local $[K^+]_o$ that occur as a consequence of neuronal activation. Membrane depolarization leads to the leak of K^+ from neurons, causing $[K^+]_o$ to be elevated, particularly in synaptic layers of the retina (Fig. 9.3); membrane hyperpolarization leads to reduced $[K^+]_o$ as the leak conductance is reduced, but the Na^+-K^+ ATPase in the membranes continues to pump K^+ into (and Na^+ out of) cells. K^+ from the ECS enters the Müller cells via inwardly rectifying K^+ channels and is carried radially as an intracellular (spatial buffer) current to regions of lower $[K^+]_o$. Thus a current loop is set up: the current inside the Müller cell is carried by K^+ and, to complete the circuit, the dominant extracellular ions, Na^+ and Cl^-, carry the extracellular return current. Because the magnitude of the $[K^+]_o$ changes depends upon the integral of K^+ flow rate into the ECS, ERG components that reflect this glial current will be slower than components that reflect the currents around neurons. This "slowing" would be

equivalent to low-pass filtering of the neuronal signal.

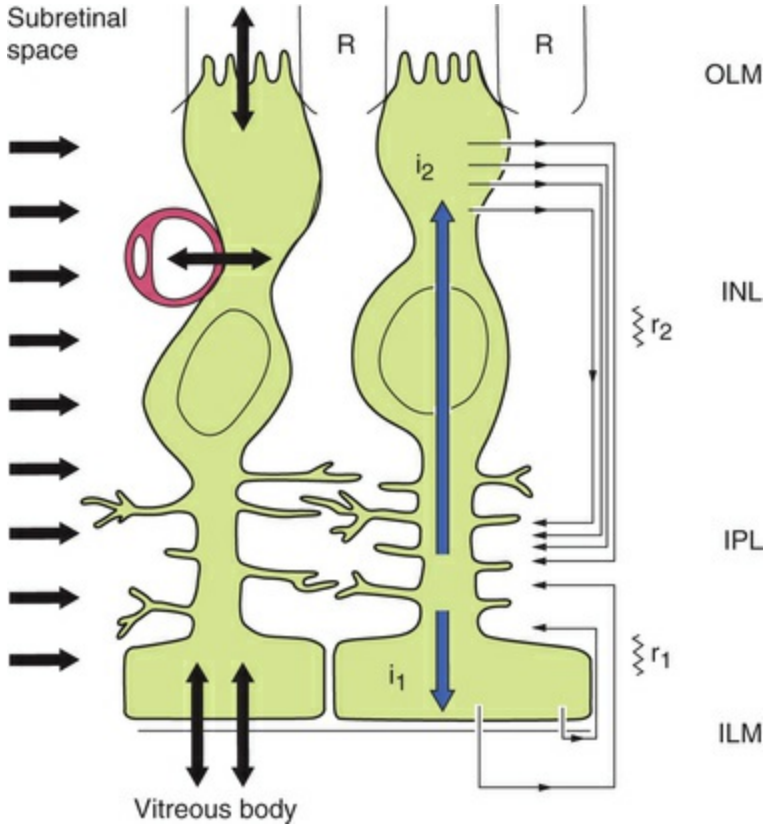

FIG. 9.3 Model of K^+-induced flow of current through Müller cells and extracellular space. The Müller cell K^+ currents (*grey arrows*) are induced by $[K^+]_o$ increases in the inner plexiform layer or $[K^+]_o$ decreases in the subretinal space; the return currents in the extracellular space are carried by Na^+ and Cl^- ions. K^+ enters the Müller cell via strongly rectifying Kir channels (perhaps Kir2.1) in and around the synaptic layers (*short arrows on left*) and leave the cell via weakly rectifying Kir4.1 channels near the vitreous body, blood vessels, and subretinal space (*bidirectional arrows on bottom*). The I_2 current generates slow PIII. Abbreviations as Fig. 9.2. (Adapted from Frishman LJ, Steinberg RH. Light-evoked increases in $[K^+]_o$ in proximal portion of the dark-adapted cat retina. J Neurophysiol 1989;61:1233–43 and Kofuji P, Biedermann B, Siddharthan V, et al. Kir potassium channel subunit expression in retinal glial cells: implications for spatial potassium buffering. Glia 2002;39:292–3.)

The electrical properties of the Müller cell membrane are

important for the creation of spatial buffer currents. The membrane is selectively permeable to K^+,[8,9] but the K^+ conductance is not distributed evenly over the cell surface. Instead, it is concentrated in the vicinity of extracellular sinks (i.e., the vitreous body, subretinal space, and blood vessels). This regional distribution facilitates "K^+ siphoning" from synaptic areas where $[K^+]_o$ is high, to those regions of high K^+ conductance where $[K^+]_o$ is lower.[10,11] In mouse retina, as indicated in Fig. 9.3, strongly inward rectifying Kir channels (perhaps Kir2.1) channels have been localized to synaptic layers (indicated in the figure by short arrows on the left) where K^+ moves from the ECS into Müller cells, whereas less strongly rectifying Kir4.1 channels at the extracellular sinks allow K^+ to leave the Müller cell.[12]

Approaches for Determining the Origins of the Electroretinogram

Historically, several different approaches have been used to determine the neuronal origins and cellular mechanisms of generation of the ERG.

Intraretinal Depth Recordings

A microelectrode positioned at some locus in the retinal ECS records a field potential called the "local" or "intraretinal" ERG.[13] The recorded potential reflects electrical activity of the cells located near the microelectrode tip, and when a local stimulus, such as a small spot of light, is used, the local activity will be the entire signal. However, when full-field diffuse flashes are used, currents can be sufficiently large to produce a corneal ERG simultaneously with the local ERG. Local potentials with a similar timecourse to that of the corneal ERG components can be helpful in locating the cells of origin. However, this type of analysis has some complications:

1. Field potentials that spread over long distances will superimpose in space and time, making it difficult to locate the cells of origin

with certainty.

2. Retinal resistivity varies between and within retinal layers,[14,15] which causes currents passing through layers of different resistance to set up complex voltages.

Both of these problems occur in the intact eye when a scleral reference is used, and the local signal recorded with a microelectrode is contaminated by the diffuse ERG, due to the high resistance of the RPE and sclera. Some of this contamination can be eliminated by using a vitreal reference.[16]

Current source density (CSD) or "source-sink" analysis can provide a solution to these problems. Local field potentials are measured and analyzed, but in addition, radial resistance is taken into account to obtain direct estimates of radial current.[17] The result is a spatiotemporal profile of relatively well-localized current sources and sinks that can be compared with the retinal structure (layers) and physiology. CSD analysis has elucidated the origins of particular ERG components (e.g., for the bipolar cell origin of the b-wave).[18,19]

For ERG components believed to depend specifically on glial K^+ spatial buffer currents, intraretinal depth recordings with ion-selective microelectrodes have been used to locate the retinal layer(s) where neurally induced changes of $[K^+]_o$ were largest and most similar in timecourse to a particular component.[20–25] Application of barium (Ba^{2+}) to block Kir channels in glial cell membranes,[26,27] and the ERG components dependent upon the spatial buffer currents, or genetic inactivation of Kir4.1 channels in mice,[28] have been used to provide evidence for the role of Müller cells in generating certain slow waves of the ERG.

Correlation of ERG With Single-Cell Recordings

Correlations of the ERG with single-cell electrophysiology are most useful when the light-evoked currents from a particular cell type are the primary determinant of an ERG component, as is the case for rod photoreceptors and the currents around the photoreceptor

that generate the scotopic a-wave,[29] or rod bipolar cells and the scotopic b-wave in mammals.[30,31] Correlation also may be useful for identifying the origin of a response property, such as oscillatory potentials (OPs) in the ERG, and the light-evoked oscillatory behavior in amacrine cells as a possible source for the potentials. However, if currents from several cell types contribute to a local field potential, the relationship between field potential and local cellular responses may be difficult to determine without using other tools, such as pharmacologic agents.

Pharmacologic Dissection

The use of pharmacologic agents that have specific effects on cellular functions has been very helpful in determining origins of ERG components. In Granit's classical pharmacologic study of the dark-adapted ERG of the cat, he observed that components disappeared sequentially during induction of ether anesthesia.[32] He called the components "processes" and numbered them in the order of disappearance: PI, the positive c-wave, was first to leave, then PII, the positive b-wave, disappeared, and finally, PIII, the negative a-wave. We now know that these processes correspond roughly to RPE, bipolar, and photoreceptor cell contributions to the ERG respectively. The terms PII and PIII are still used.

In recent years, much has been learned about retinal microcircuitry and biophysics, including information at cellular and molecular levels about retinal neurotransmitters (their identity, release mechanisms, and receptors), signal transduction cascades, ion channels, and other cellular proteins. This knowledge has allowed better use of pharmacologic tools in isolating ERG components and in interpreting experimental observations. For example, specific knowledge about glutamatergic neurotransmission in the retina and appropriate agonists and antagonists for specific receptors has improved our understanding of the major waves of the ERG, including the ERG in primates.[33–35] Use of the voltage-gated Na^+-channel blocker tetrodotoxin (TTX) has made it possible to identify ERG components resulting from the Na^+-dependent spiking activity of inner retinal cells.

Site-Specific Lesions/Pathology or Targeted Mutations

Removal of a cell type or types or circuits allows assessment of their role in the electrogenesis of the ERG. A specific cell type can be lesioned selectively (e.g., retinal ganglion cells as a consequence of optic nerve section) or lost due to pathologic changes (e.g., ganglion cells in glaucoma), or inherited degenerations (e.g., rod and/or cone dystrophy). Cellular functions, such as light responses or synaptic transmission, can be abnormal or eliminated due to inherited or acquired conditions, or targeted genetic manipulation, most commonly done in mice.

Modeling of Cellular Responses and ERG Components

As our understanding of the function of retinal cell types has improved, it has been possible to develop quantitative models that predict the light responses of those cells, and to apply the models to analysis of the ERG. Models based on suction electrode recordings from single photoreceptor outer segments have been used to predict the leading edge of the a-wave,[36–38] although currents around more proximal portions of the photoreceptor cell will also participate in its generation.[39] The models have been extended to predict the leading edge of the scotopic b-wave.[30] Models of stimulus–response relations of specific retinal cells can be used to analyze amplitude versus energy curves obtained from ERG measurements into the components related to the different cell types.[40,41]

Standard ERG Tests in the Clinic

Standard and more specialized tests for use in the clinic that examine key aspects of light- and dark-adapted retinal (and more central visual) function have been described in various publications by the International Society for the Clinical Electrophysiology of Vision (ISCEV), with the most recent update for the flash and flicker ERG in 2015.[42] The “standard” tests advocated by ISCEV for

basic ERG testing are listed in Box 9.1, and typical responses to these tests are illustrated in Fig. 9.4. The standards were developed so that ERGs recorded in clinics around the world would be comparable. The ISCEV publications, which now cover several other ERG tests as well, i.e., the ones with an asterisk in Box 9.1, become the basic technology and clinical protocols.

Box 9.1

Standard and More Specialized Electroretinogram (ERG) Tests

Standard ERG Tests Described by ISCEV Standard for Full-Field Clinical Electroretinography (2015 Update)[42,a]

Dark-adapted 0.01 ERG ("a rod-driven response of ON bipolar cells")

Dark-adapted 3.0 ERG ("combined responses arising from photoreceptors and bipolar cells of rod and cone systems, rod dominated")

Dark-adapted 10.0 ERG ("combined responses with enhanced a-wave reflecting photoreceptor function")

Dark-adapted 3.0 oscillatory potentials ("responses primarily from amacrine cells")

Light-adapted 3.0 ERG ("responses of the cone system; a-wave arises from cones and OFF bipolar cells, b-wave arises from ON and OFF cone bipolar cells")

Light-adapted 3.0 flicker ERG ("a sensitive cone system response")

Recommended additional response: flashes stronger than dark-adapted 10.0 ERG

Specialized Types of ERG and Recording Procedures

Macular or focal ERG

Multifocal ERG[b]

Pattern ERG[b]

Early receptor potential (ERP)

Scotopic threshold response (STR), negative and positive

Photopic negative response (PhNR)

Direct-current (dc) ERG

Electro-oculogram[b]

Long-duration light-adapted ERG (ON–OFF responses)

Paired-flash ERG

Chromatic stimulus ERG (including S-cone ERG)

Dark and light adaptation of the ERG

Dark-adapted and light-adapted luminance response analyses

Saturated a-wave slope analysis

Specialized procedures for young and premature infants[b]

[a]All numbers are stimulus calibrations in cd s/m^2.

[b]See relevant standard or guideline published by International Society for the

Clinical Electrophysiology of Vision (ISCEV).

Data from McCulloch DL, Marmor MF, Brigell MG, et al. ISCEV standard for full-field clinical electroretinography (2015 update). Doc Ophthalmol 2015;130:1-12.

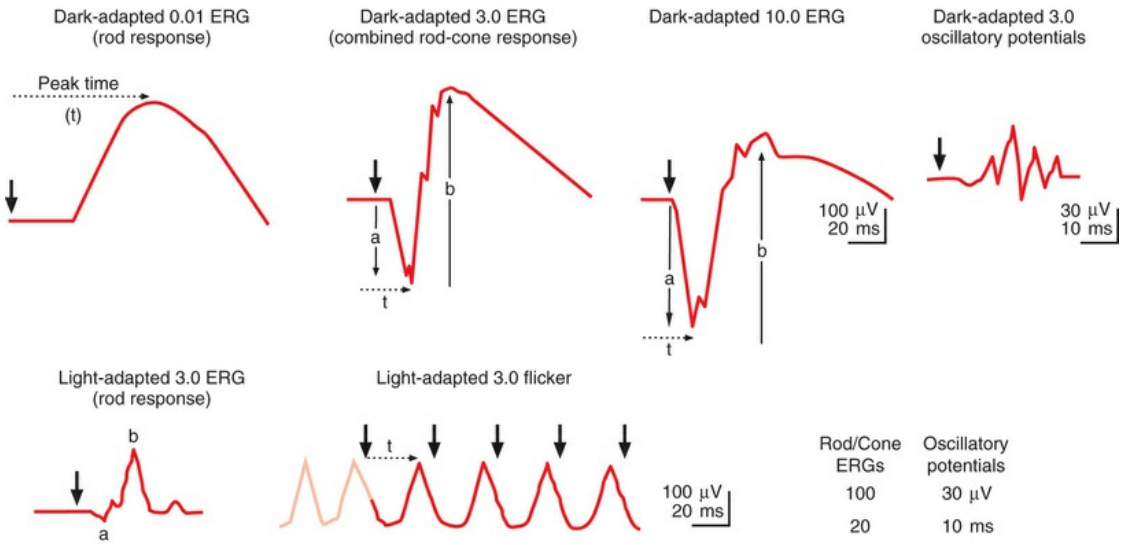

FIG. 9.4 Six standard electroretinogram (ERG) tests with full-field stimulation recommended by the International Society for the Clinical Electrophysiology of Vision (ISCEV) for use worldwide in clinical electrodiagnostic facilities. This figure shows examples, but not norms, of ERG responses to the recommended test stimuli in normal human subjects. Light calibrations in candela seconds per meter squared (cd s/m^2) for each test are indicated above the ERGs. *Large vertical arrowheads* indicate the time at which the stimulus flash occurred; *horizontal arrows* show common ways to measure the time-to-peak (*t*, implicit time); *small vertical arrows* mark a- and b-wave peak amplitude. (Reproduced with permission from McCulloch DL, Marmor MF, Brigell MG, et al. ISCEV standard for full-field clinical electroretinography (2015 update). Doc Ophthalmol 2015;130:1-12.)

Distal Retinal Components: Slow PIII, c-Wave, Fast Oscillation Trough, and Light Peak

After the onset of a step of light, the early waves of the dark-

adapted ERG, the a- and b-waves, are followed by the c-wave and then by a succession of slower responses that include the fast oscillation trough (FOT), which is a negative deflection, and the light peak, which is a large slow positive deflection (Fig. 9.5A). Because these responses are so slow, lasting seconds to minutes, patients cannot keep their eyes steady long enough for them to develop. Therefore, in the clinic, these slower responses are generally recorded by using electro-oculography.

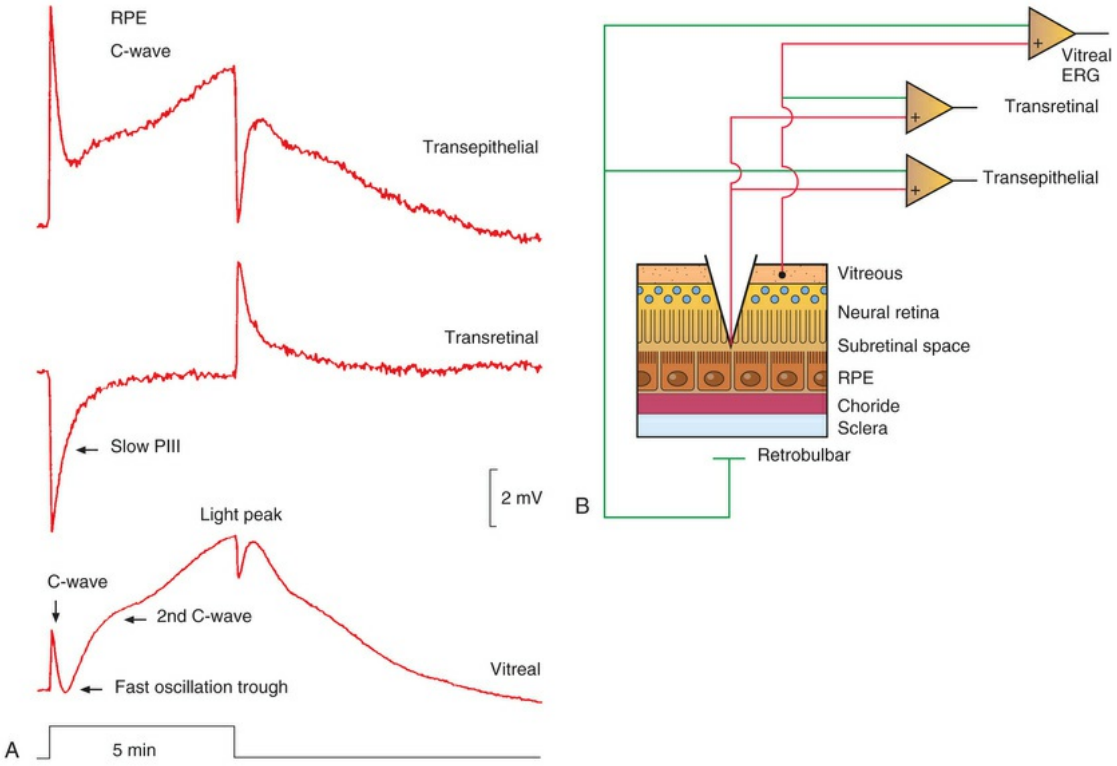

FIG. 9.5 Subretinal recordings from the intact cat eye. (A) The vitreal, transretinal, and transepithelial potentials were recorded simultaneously in response to a 5-minute period of illumination. The a- and b-waves cannot be seen using this compressed timescale. In the vitreal electroretinogram (ERG), the c-wave is followed by the fast oscillation trough (FOT) and then the light peak. The intraretinal recordings show that the c-wave is composed of two (sub)components: the larger cornea-positive retinal pigment epithelial (RPE) transepithelial response, and the slightly smaller cornea-negative transretinal component, the Müller cell-generated slow PIII response. For the light peak,

only an RPE component is present. (B) Schematic showing the recording arrangement for transretinal and transepithelial recordings in the intact eye. The transretinal ERG is recorded between a vitreal reference and a retrobulbar reference. The microelectrode is referenced to the vitreal reference for the transretinal recording and to the retrobulbar reference for the transepithelial recording. Double-barreled microelectrodes were used to measure field potentials and changes in $[K^+]_o$. (Panel A reproduced with permission from Steinberg RH, Linsenmeier RA, Griff ER. Retinal pigment epithelial cell contributions to the electroretinogram and electrooculogram. Prog Retin Res 1985;4:33–66. Panel B reproduced with permission from Frishman LJ, Steinberg RH. Light-evoked increases in $[K^+]_o$ in proximal portion of the dark-adapted cat retina. J Neurophysiol 1989;61:1233–43.)

The electro-oculogram (EOG) is an eye movement-dependent voltage recorded between electrodes placed near the eye at the inner and outer canthus. The patient is asked to look back and forth between a pair of fixation lights separated by 30° of visual angle, situated in a ganzfeld bowl. The source of the voltage is a corneofundal potential, also called the "standing potential" that renders the cornea positive with respect to the back of the eye. Light-evoked changes in the EOG reflect changes in the transepithelial potential (TEP) of the RPE. These changes have been studied experimentally in human and animal preparations using direct current electroretinography (dc-ERG[43]), and these studies will be reviewed briefly here.

Electrogenesis of the c-wave, FOT, and light peak of the dc-ERG involves ion concentration changes in the subretinal space between photoreceptors and the RPE that in turn produce slow membrane responses in the Müller and RPE cells that face the space. Müller and/or RPE component voltages overlap in time and sum to produce the recorded dc-ERG components. The (sub)component voltages from Müller cells and RPE have been recorded in anesthetized animals by placing a microelectrode in the subretinal space, and simultaneously recording the potentials across neural retina and the RPE, as illustrated in the schematic in Fig. 9.5B. Such experiments have provided a good understanding of the origins and mechanisms of generation of the c-wave and other slow

potentials from distal retina.

c-Wave

The cornea-positive c-wave that follows the b-wave is the sum of two major (sub)component voltages: a cornea-negative voltage, generated by the neural retina, and a cornea-positive voltage of similar latency and timecourse, generated by the RPE (Figs. 9.5 and 9.6). The c-wave is cornea-positive when the RPE component is larger than the neural retinal component. If the two components are equal in amplitude, the c-wave will be absent, as observed in some monkeys.[44]

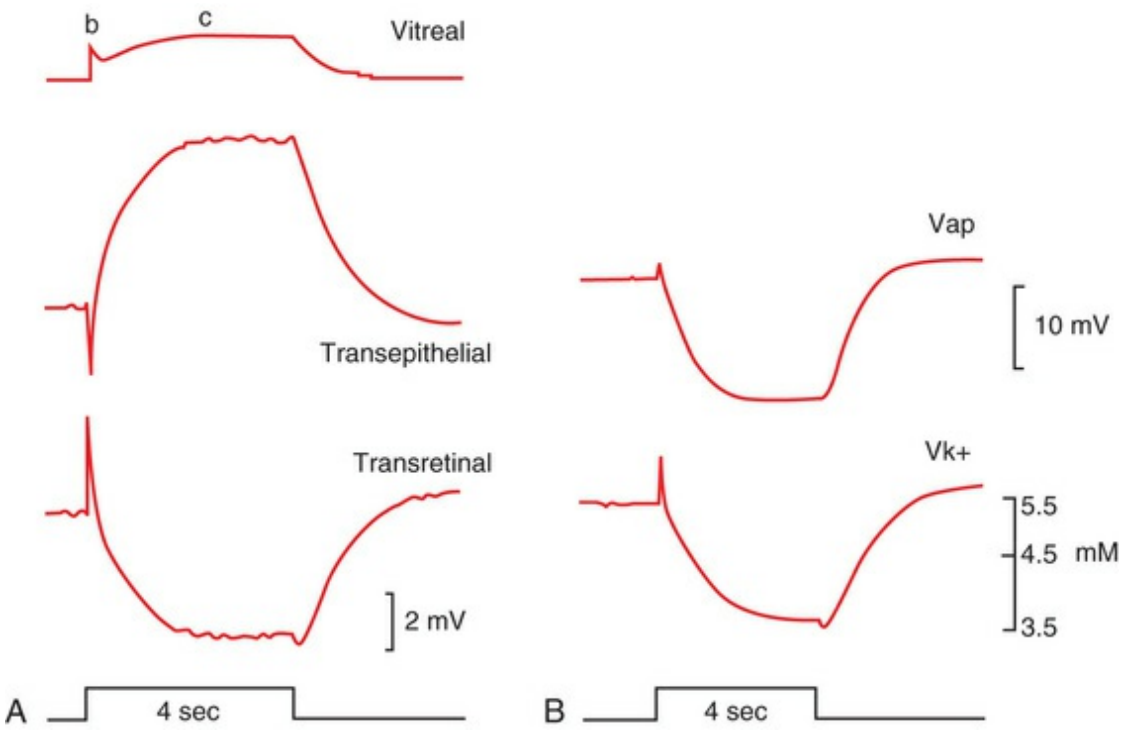

FIG. 9.6 The components of c-wave of the dark-adapted cat (DC) electroretinogram (ERG): the (sub)components, and correlation of recorded $[K^+]_o$ and the retinal pigment epithelial (RPE) apical membrane hyperpolarization. Stimuli were 4-second flashes at 8.3 log q deg^2/s^2. (A) The vitreal c-wave consists of a transepithelial component (TEP c-wave) and a transretinal component (slow PIII). B-wave deflections can be seen in both recordings; the b-wave current generated in neural retina creates a passive voltage drop across the large resistance of the RPE and

sclera. (B) RPE apical membrane and subretinal $[K^+]_o$ in response to the same stimulus as in part A, recorded in a separate experiment. The apical membrane potential was derived by subtracting an intracellular recording of the basal membrane potential from the transepithelial potential. (Reproduced with permission from Steinberg RH, Linsenmeier RA, Griff ER. Retinal pigment epithelial cell contributions to the electroretinogram and electrooculogram. Prog Retin Res 1985;4:33–66.)

There is longstanding evidence that two components of opposite polarity form the ERG c-wave. For example, intravenous injection of sodium iodate in rabbit, which poisons primarily the RPE, abolishes the cornea-positive c-wave and leaves a cornea-negative potential,[45] as occurs in vitro when recording from an isolated neural retina preparation.[46] Microelectrode recordings in retinas of several species,[43] including monkey,[47] have confirmed the presence of the two components. An example of such recordings in intact cat eye is shown in Fig. 9.6. The component from the neural retina is commonly termed slow PIII, to distinguish it from fast PIII, the photoreceptor current. The component from the RPE is the RPE c-wave.

Both slow PIII and the RPE c-wave are responses to the light-evoked decrease in $[K^+]_o$ in the subretinal space that occurs in response to intense light stimulation of the dark-adapted retina. When measurements of $[K^+]_o$ were made with ion-selective microelectrodes, either in intact eyes or in vitro preparations, the timecourse of the $[K^+]_o$ decrease was found to predict that of the ERG c-wave and its component parts (Fig. 9.6). Blocking K^+ conductance (via Kir channels) with various agents eliminated both the slow PIII[48] and the RPE c-wave.[49]

Müller Cell Contribution (Slow PIII)

Intraretinal recording at various depths[50] have shown that slow PIII is generated by a radially oriented current across the neural retina. A Müller cell generator, rather than a neuronal generator, was suggested because slow PIII persisted after treatment with aspartate, a nonselective glutamate agonist, to suppress all

responses of postreceptoral neurons.[51]

Studies in amphibians and mammals have shown that slow PIII is initiated when the distal ends of the Müller cells are passively hyperpolarized by a photoreceptor-dependent decrease in subretinal $[K^+]_o$. This sets up a transretinal "K^+ spatial buffer" current,[25] and the current drop across the extracellular resistance produces the slow PIII voltage.[50,52,53] The slow hyperpolarization recorded in Müller cells was observed to be similar in timecourse to both the subretinal $[K^+]_o$ decrease and to slow PIII.[20,21,53] Further, when Ba^{2+} was used to block Müller cell Kir channel conductance, slow PIII was suppressed but there was little effect on the light-evoked subretinal K^+ decrease.[22,27,54] Finally, slow PIII was not present in ERGs of mice with the dominant Kir channels (Kir4.1) in Müller cells, genetically inactivated.[28]

Distal Versus Proximal PIII

Intraretinal depth recordings in isolated rabbit retina have identified a component of similar timecourse and polarity to slow PIII that is eliminated by aspartate, and therefore, unlike slow PIII, is generated by cells proximal to the photoreceptors.[55] Proximal PIII is now thought to originate from Müller cell K^+ currents that flow in the same direction in the retina as slow PIII currents. However, the proximal PIII currents are initiated by an increase in $[K^+]_o$ due to neuronal activation in proximal retina, rather than the decrease in $[K^+]_o$ in the subretinal space. The term "proximal PIII" is not commonly used now that responses have been identified that are Müller cell, or perhaps astrocyte-mediated, responses to $[K^+]_o$ changes in proximal retina, e.g., STR and PhNR (described in later sections).

Retinal Pigment Epithelial Component

The RPE c-wave is a cornea-positive potential that reflects an increase in the TEP of the RPE, a major component of the standing potential of the eye. The TEP exists because the apical and basal membranes of RPE cells are electrically separated by high-resistance tight junctions that encircle the monolayer of cells (the "R

membrane"). The TEP is equal to the difference between the apical (V_{ap}) and basal (V_{ba}) membrane potentials.[43] V_{ap} is generally more hyperpolarized than V_{ba}, making the TEP cornea-positive. During c-wave generation in response to an increase in light, the TEP increases (becomes even more positive). This is initiated by a hyperpolarization of the apical membrane, and passive shunting of current to the basal membrane, resulting in a (smaller) hyperpolarization of basal membrane, and a greater difference in potential between the two membranes.[43]

As was observed for Müller cells, the slow hyperpolarization of the apical membrane, with its large K^+ conductance,[56] and the RPE c-wave have a timecourse that is very similar to the subretinal $[K^+]_o$ decrease, as illustrated in Fig. 9.6. In an isolated RPE preparation (where only the apical bath $[K^+]$ was altered), Oakley et al.[57] demonstrated that the RPE c-wave was due solely to the $[K^+]_o$ decrease.

The Fast Oscillation Trough

The FOT (usually measured by EOG) is a change in the corneoretinal potential – it decreases and increases in synchrony with an alternating light/dark stimulus. The response in the dc-ERG that corresponds to the EOG decrease (trough) also is termed the FOT. The FOT response to maintained illumination follows the c-wave peak, and, when a light peak occurs, it appears as a dip between the c-wave and the light peak (Fig. 9.5A).

The FOT originates from both neural retina and RPE. It involves recovery of Müller and RPE cells from their peak polarizations as subretinal K^+ reaccumulates following the reduction in concentration caused by light. This recovery may be greater than predicted by the reaccumulation, particularly for the RPE component. Light initially elicits a hyperpolarization of the apical membrane that increases the TEP and then produces a delayed basal hyperpolarization that decreases the TEP. This extra decrease in TEP underlies most of the cornea-negative potential of the FOT.[43]

The ionic mechanisms of the basal membrane hyperpolarization involve Cl^- conductances.[58] In intact sheets of RPE/choroid from human fetal eyes, the Miller lab distinguished two types of basal

membrane Cl^- channels: a 4,4′-diisothiocyanostilbene-2, 2′-disulfonate (DIDS)-inhibitable Ca^{2+}-sensitive Cl^- channel, and a cyclic AMP-dependent channel that is inhibited by DIDS as well as by 5-nitro-2-(3phenylpropylamino) benzoate (NPPB), which identifies it as a cystic fibrosis transmembrane regulator (CFTR) channel.[59] In CF patients, the FOT, but not the light peak (see below), is reduced, implicating CFTR in generation of the FOT.

The Light Peak

Maintained illumination causes a slow increase in the standing potential in the dc-ERG called the light peak that can be recorded as a slow oscillation of the EOG (Fig. 9.6). Intraretinal recordings in several species,[43,58] including monkey,[47] have shown that this cornea-positive potential originates solely from an increase in the TEP (Fig. 9.5A). Intracellular RPE recordings localized the origin of the increase to a slow depolarization of the basal membrane caused by an increase in basal Cl^- conductance. In both chick RPE and human RPE cell sheets the Cl^- conductance increase was suppressed by DIDS.[58,59] In mouse, the light peak is also dependent on a Cl^- conductance, and it is regulated by voltage-dependent Ca^{2+} channel CaV1.3 subunits.[60]

Although the light peak voltage originates from the RPE basal membrane, it is initiated in neural retina via the photoreceptors.[61] Light stimulation leads to a change in concentration of a "light peak substance" which then affects the basal membrane via a second-messenger system. The identities of the "light peak substance" and the second messenger(s) involved in producing the light peak are unresolved. Although dopamine affected the light peak in the perfused cat eye,[62] studies in chick did not support its being the "light peak substance."[61] Epinephrine also has been proposed as a candidate, and a role for ligands binding to adrenergic alpha-1 receptors on the apical membrane is likely.[59] Cyclic AMP has been investigated as a second messenger in light peak generation but, as described above, it may be involved in generation of the FOT, rather than the light peak.[59]

Origin of the a-Wave

Fig. 9.7 shows the dark- and light-adapted flash ERG of macaque monkey, a good animal model for studying the origins of the human response, as illustrated in Fig. 9.1. The a-wave in the dark-adapted ERG is the initial negative wave that occurs in response to strong stimuli from darkness (Fig. 9.7, top left column) and it is primarily rod-driven (scotopic), but contains a cone contribution when flashes are very strong. When the background is rod-saturating the a-wave is cone-driven (photopic; right column). Under both dark- and light-adapted conditions, the a-wave is followed by the rise of the positive-going b-wave that originates primarily from ON bipolar cells,[30] as reviewed below. The slow negative wave in the dark-adapted ERG in response to the weakest stimuli, called the STR, is not the a-wave, but instead is initiated by amacrine and/or ganglion cell activity. This is known because STR is eliminated when postreceptoral activity is blocked pharmacologically.[63,64]

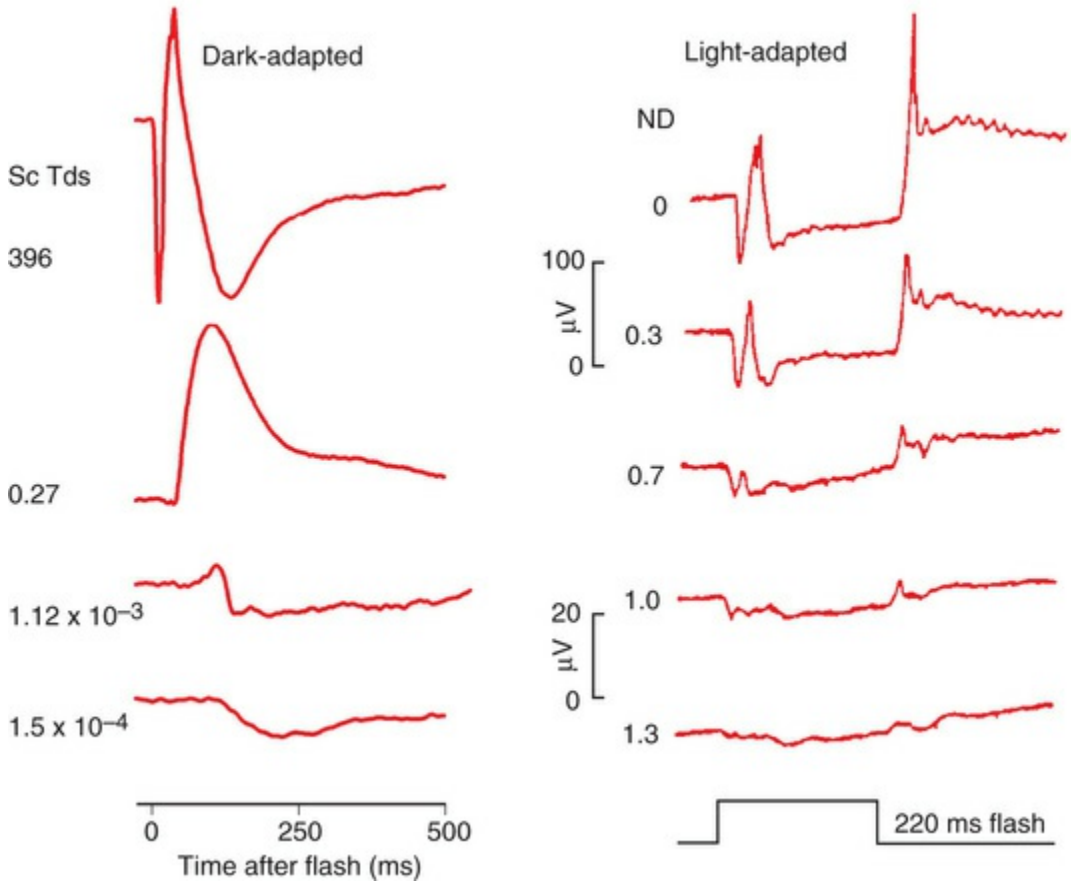

FIG. 9.7 Dark- and light-adapted electroretinograms (ERGs) of the macaque retina. (Left) Dark-adapted full-field ERGs of anesthetized macaque monkeys were measured in response to brief (<5 ms) flashes from darkness generated by computer-controlled light-emitting diodes (LEDs). Responses were recorded differentially between DTL fibers on the two eyes. Flash strength was increased over a 6-log-unit range. Responses to the weakest stimuli were rod-driven (scotopic), whereas for the strongest stimuli there were mixed rod–cone responses. (Right) Light-adapted full-field ERGs of anesthetized macaques were measured using Burian–Allen electrodes. Stimulus strength was controlled with neutral-density (ND) filters. Stimulus strength increased over a 1.3-log-unit range to a maximum at 0 ND of 4.0 log ph td for 220-ms flashes. Stimuli were presented on a steady rod-saturating background of 3.3 log sc td. The 20 μV calibration bar applies both to the dark-adapted ERG responses to weak stimuli and to the light-adapted ERGs. (Left panel reproduced with permission from Robson JG, Frishman LJ. Dissecting the dark-adapted electroretinogram. Doc Ophthalmol 1998;95:187–215. Right panel reproduced with permission from Sieving PA, Murayama K, Naarendorp F. Push–pull mode of the primate photopic electroretinogram: a role for hyperpolarizing neurons in shaping the b-wave. Vis Neurosci 1994;11:519–32.)

The a-Wave as a Reflection of Rod and Cone Receptor Currents

Early intraretinal depth studies in intact cat eyes[13,65] found that the signal at the timecourse of the a-wave was largest in the vicinity of the photoreceptors. The case for a receptoral origin for PIII was strengthened by microelectrode recordings in macaque monkey retina, with the inner retinal circulation clamped to suppress retinal activity proximal to the photoreceptors.[66]

Penn and Hagins[67] in CSD analyses of the isolated rat retina demonstrated that light suppressed the circulating (dark) current of the photoreceptors, and proposed that this suppression was seen in the ERG as the a-wave. Fig. 9.8 provides a schematic of the photoreceptor layer current from a review by Pugh et al.[68] The

figure shows that, in the dark, cation channels (Na^+, Ca^{2+}, and Mg^{2+}) in the receptor outer segment (ROS) are open, current flows into the ROS (a current sink with respect to the ECS), and K^+ leaks out of the inner segment (a current source), creating dipole current. This dipole current produces a corneal (and vitreal) potential that is positive with respect to the scleral side of the retina. Suppression of the dark current reduces the cornea-positive potential, creating the negative-going a-wave. Consistent with this view, as illustrated in Fig. 9.9, intraretinal recordings and CSD analyses in the intact macaque retina have localized current sources and sinks for a local potential, corresponding to the a-wave, to the distal third of the retina.[18]

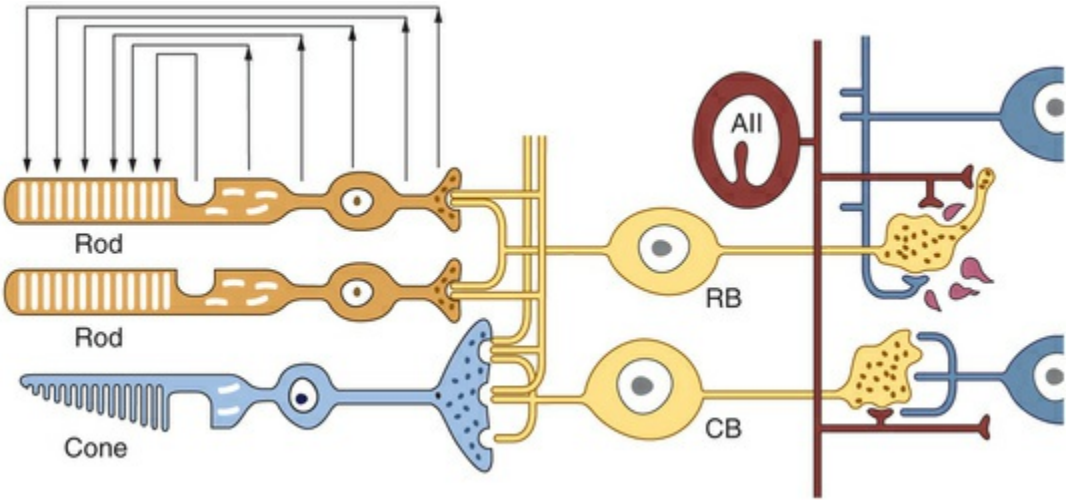

FIG. 9.8 Schematic of a longitudinal section of the mammalian retina illustrating how circulating currents in the photoreceptor layer create an extracellular field potential, in which the vitreal side of the retina has a more positive potential than the scleral side. A very bright flash will suppress the circulating current around the photoreceptor, leading to a vitreal or corneal response which is negative relative to the resting preflash baseline. (Reproduced with permission from Pugh EN Jr., Falsini B, Lyubarsky A. The origin of the major rod- and cone-driven components of the rodent electroretinogram and the effects of age and light-rearing history on the magnitude of these components. Photostasis and related phenomena. New York: Plenum Press; 1998. p 93–128.)

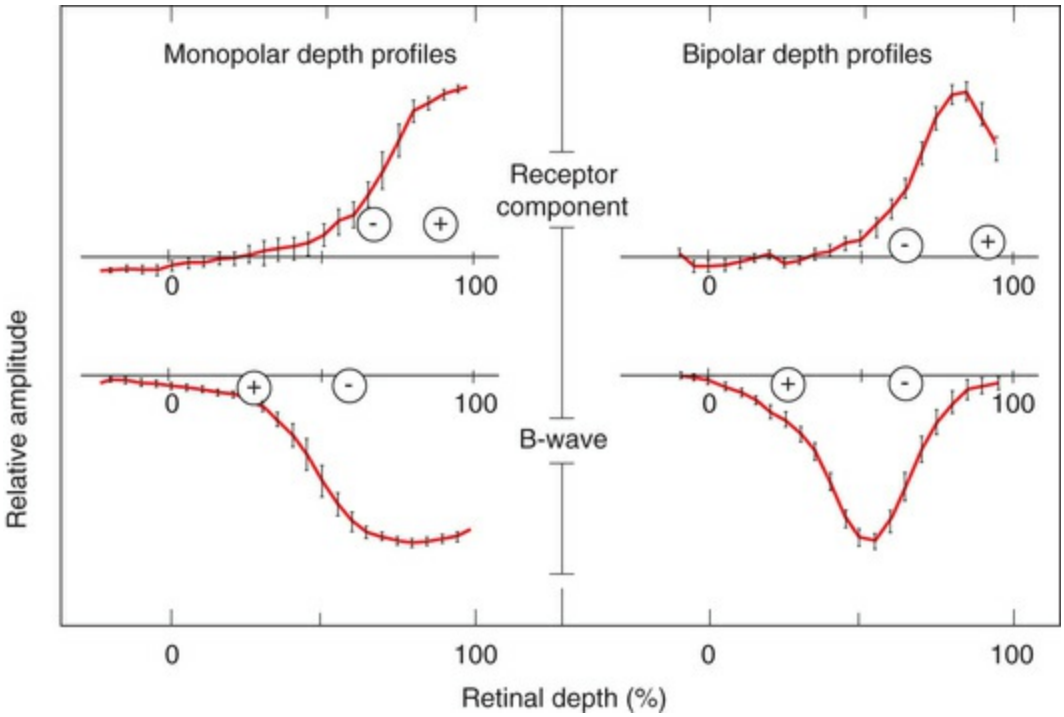

FIG. 9.9 Depth profiles and current source density results in anesthetized macaque monkey retina for the a-wave and the b-wave. (Left) Monopolar depth profiles using an intraretinal microelectrode referenced to the forehead. (Right) Bipolar depth profiles using a coaxial electrode with a distance of 25 μm between the tips to measure field potential amplitudes at the peak time of the receptor component, the b-wave and the dc component of the macaque light-adapted electroretinogram. The pluses and minuses indicate the current sources (+) and sinks (–) for the components, as calculated from current source density analyses based on the coaxial electrode recordings and resistance measurements. The a-wave source and sink are in the distal quarter of the retina. The b-wave has a large sink near the outer nuclear layer and a distributed source extending to the vitreal surface of the retina. Plots represent means of 26 penetrations.

(Adapted from Heynen H, van Norren D. Origin of the electroretinogram in the intact macaque eye – II. Current source-density analysis. Vision Res 1985;25:709–15.)

Hood and Birch[38] sought to relate the timecourse of the leading edge of the ERG a-wave directly to the leading edge of the photoreceptor outer-segment response to light. They demonstrated that both the linear and the nonlinear (i.e., saturating) behavior of

the leading edge of the a-wave in the human ERG was reasonably well predicted by a model of photoreceptor function derived from in vitro suction electrode recordings of currents around the outer segments of primate rod photoreceptors.[69] Subsequently a simplified kinetic model of the leading edge of the photoreceptor response (in vitro current recordings) that took into account the stages of the biochemical phototransduction cascade was developed by Lamb and Pugh.[70] This model could be fit to the leading edge of the human a-wave generated by strong stimuli and it has been used in noninvasive studies of human rod[36,71] and cone photoreceptor[72] function. More recent analyses suggest that the a-wave generated in response to strong stimuli reflects additional currents associated with more proximal regions of the photoreceptor cell, including capacitive currents in the outer nuclear layer, that form a transient "nose" on the leading edge of the response that quickly relaxes to the level of the photocurrent.[39]

Postreceptoral Contributions to the a-Wave

The receptoral origins of the a-wave (Granit's PIII),[32] as well as postreceptoral contributions of similar timecourse, have been clarified in pharmacologic studies. In early in vitro studies of the isolated retina (amphibian and human), the nonspecific glutamate agonist aspartate in the perfusate suppressed all postreceptoral responses, and isolated the a-wave, revealing its presence under the b-wave.[51,73] Our understanding of the receptoral and postreceptoral contributions to the light-adapted a-wave, as well as other waves of the macaque monkey photopic ERG, was greatly advanced by studies of Sieving and colleagues in which they utilized more specific glutamate analogs than aspartate to dissect retinal circuits, and particularly ON versus OFF circuits set up by depolarizing and hyperpolarizing bipolar cells, respectively (Fig. 9.2).[33,35] They made intravitreal injections in anesthetized macaques of an mGluR6 receptor agonist, 2-amino-4-phosphonobutyric acid (APB, L isomer, also called L-AP4) to block metabotropic glutamatergic neurotransmission to depolarizing (ON) bipolar cells. This eliminated light-evoked responses of ON bipolar cells as well as contributions from more proximal cells of the retinal ON pathway.

Alternatively, they injected *cis*-2,3-piperidine dicarboxylic acid (PDA) (or kynurenic acid) to block major ionotropic glutamate receptors in the retina (α-amino-3-hydroxy-5-methyl-4-isoxazolepropionic acid (AMPA) and kainate receptors).[74] These ionotropic receptors, blocked by PDA, mediate signal transmission to hyperpolarizing (OFF) bipolar cells and horizontal (Hz) cells, as well as to amacrine and ganglion cells of both OFF and ON pathways. Results of such experiments are illustrated in Fig. 9.10A for responses to fairly weak stimuli presented on a rod-suppressing background; functions relating a-wave amplitude and stimulus strength over a wider range of stimuli in the same study are shown in Fig. 9.10B. The a-wave was reduced in amplitude by PDA (or kynurenic acid, not shown), but not by APB. Fig. 9.10 also shows that PDA had a similar effect to that of aspartate, or to cobalt (Co^{2+}), which was used to block the voltage-gated Ca^{2+} channels which are essential for vesicular release of glutamate.

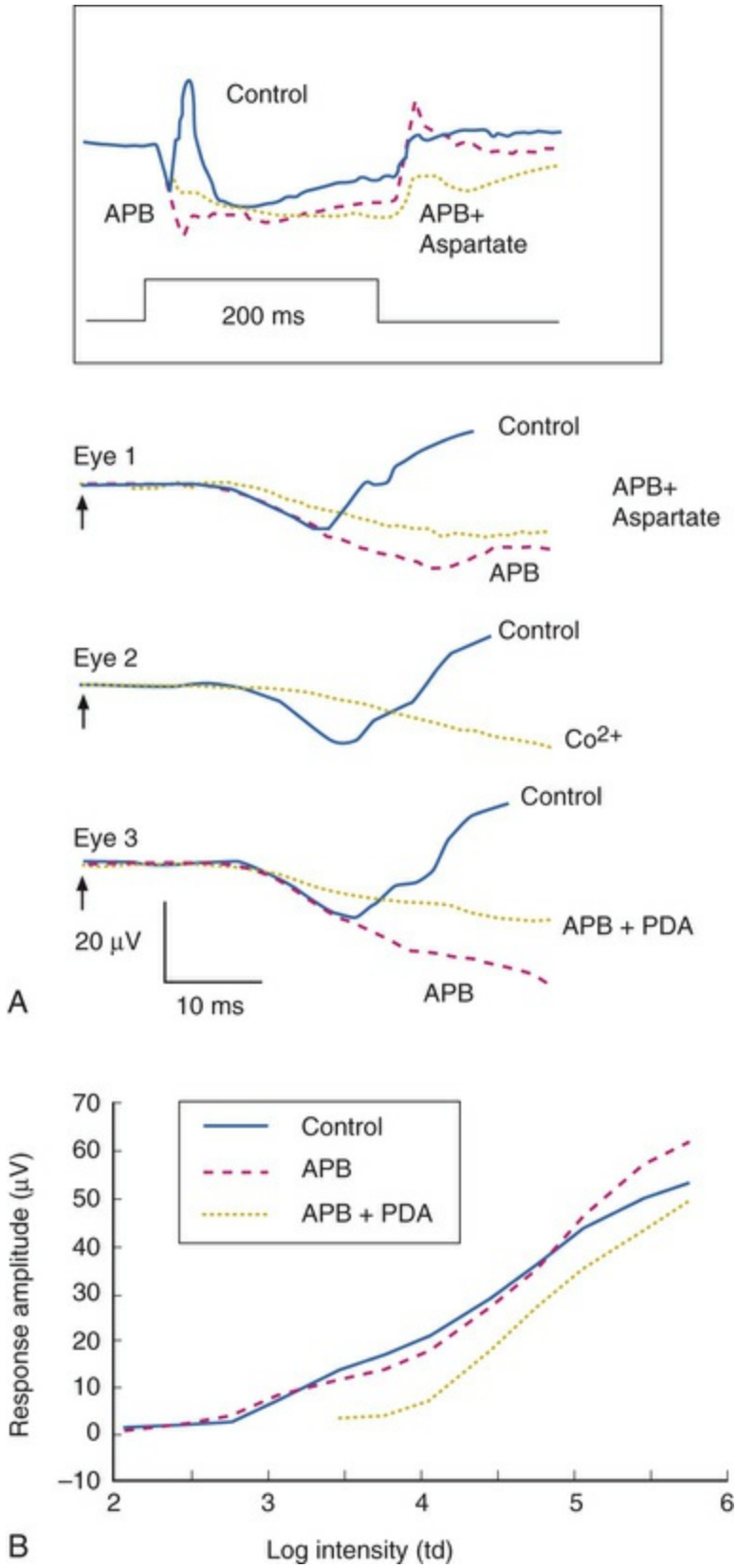

FIG. 9.10 Postreceptoral contributions to the a-wave of the macaque electroretinogram (ERG). (A) Comparison of the effects of 2-amino-4-phosphonobutyric acid (APB:1 mM vitreal

concentration) and APB + *cis*-2,3-piperidine dicarboxylic acid (PDA: 5 mM) with those of aspartate (50 mM) and cobalt (10 mm, CO^{2+}) on the photopic ERG a-wave of three different eyes of two anesthetized monkeys. The inset at the top shows the response of eye number 1 to the 200-ms stimulus of 3.76 log td (2.01 log cd/m^2) on a steady background of 3.3 log td (1.55 cd/m^2). The a-waves for eyes 1, 2, and 3 were all in response to the same stimulus. For this stimulus, most of the small a-wave (10 μV) that was elicited was postreceptoral in origin. In the clinic the a-wave elicited by brief flashes often is larger, 20 μV or more, and therefore also will include several microvolts of photoreceptor contribution, as shown in part B. (B) Stimulus response function (V log I plot) of the photopic a-wave of the macaque measured at times corresponding to the a-wave peak in the control responses (*filled circles*). Amplitudes after APB (*open circles*) and after APB + PDA (*triangles*) were measured at the same latency as the trough of the control a-waves measured at the same stimulus intensity. The points are connected by solid lines. In this figure, as in part A, APB had no effect on the a-wave amplitude. In contrast, PDA reduced the amplitude, and the postreceptoral contribution was maximally between 10 and 15 μV, about 50% of a 20 μV a-wave, but less than 25% of a saturated a-wave of about 65 μV. (Reproduced with permission from Bush RA, Sieving PA. A proximal retinal component in the primate photopic ERG a-wave. Invest Ophthalmol Vis Sci 1994;35:635–45.)

When the effects of PDA versus APB on the photopic a-wave amplitude were evaluated over a wider range of stimuli, PDA-sensitive postreceptoral neurons, rather than photoreceptors, or APB-sensitive contributions from ON pathway, were found to generate the leading edge for the first 1.5 log units of flash strengths that elicited a measurable a-wave (Fig. 9.10B). Postreceptoral cells in the OFF pathway and inner retina continued to contribute 10–15 μV to the total a-wave amplitude when photoreceptoral contributions also were present. Postreceptoral contributions to the a-wave in alert humans have also been demonstrated, by analysis of ERGs.[75]

Postreceptoral contributions to the dark-adapted a-wave have

been observed as well in the monkey.[34,76] For weak to moderate stimuli from darkness, a-waves are dominated by rod signals, but a strong flash elicits a mixed rod–cone ERG like the macaque ERG illustrated in Fig. 9.11. To study purely rod-driven responses it is therefore necessary to separate the rod- and cone-driven responses to strong stimuli when investigating their relative contributions to the ERG.

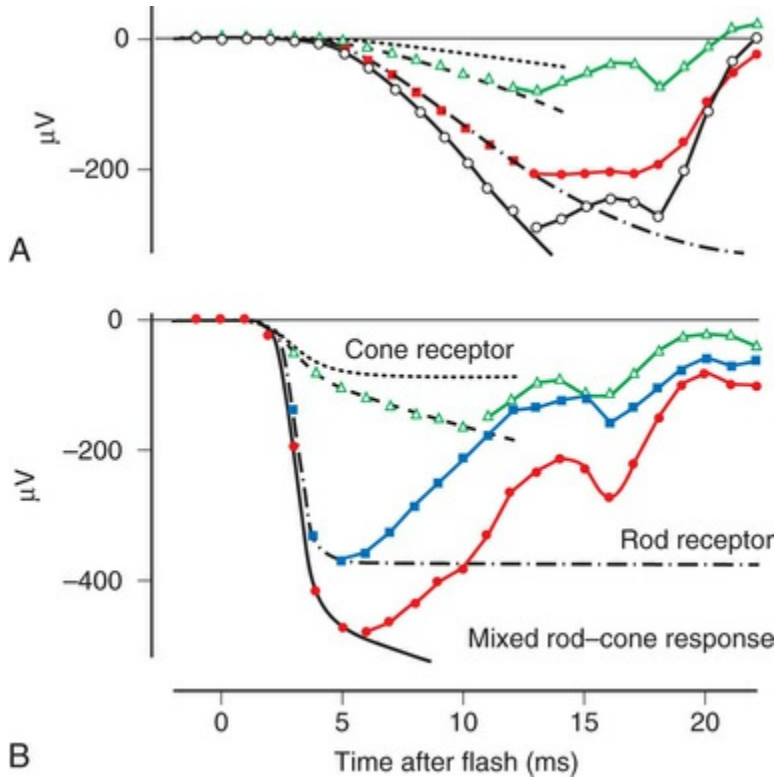

FIG. 9.11 Dark-adapted electroretinogram (ERG) of a macaque showing the mixed rod–cone a-wave and separate components measured (symbols) and modeled (solid lines fit to the leading edge of the a-wave) for two stimulus strengths. (A) Responses of an anesthetized macaque to a brief blue light-emitting diode (LED) flash of 188 sc td/s (57 ph td/s) and (B) responses to a xenon white flash of 59, 000 sc td/s (34, 000 ph td/s). In both parts, the largest response (*open circles* panel A, *solid red circles* panel B) is the entire mixed rod–cone a-wave; the black solid line restricted to the leading edge shows the modeled mixed rod–cone response. The second largest response is the (isolated) rod-driven response (*red filled symbols* panel A, *blue symbols* panel B); the

black dot–-dash line through the leading edge is the modeled rod photoreceptor contribution. The second to smallest response (*green symbols*) is the (isolated) cone-driven response, including the postreceptoral contribution; the black dashed line through the leading edge shows the modeled cone-driven response. The smallest response (*black dotted line*) is the modeled cone photoreceptor contribution, based on post *cis*-2,3-piperidine dicarboxylic acid (PDA) findings for the cone-driven response. Given the animal's 8.5-mm pupil, the stimulus for part A was about 1 cd s/m^2, i.e., about three times less intense (for cones) than International Society for the Clinical Electrophysiology of Vision (ISCEV) standard flash of 3 cd s/m^2, whereas the stimulus for part B is about 2000 times stronger. ISCEV also suggests flashes of 10 and 30 cd s/m^2 for mixed rod–cone ERG. (Adapted from Robson JG, Saszik SM, Ahmed J, et al. Rod and cone contributions to the a-wave of the electroretinogram of the macaque. J Physiol 2003;547:509–30.)

The rod-driven response can be extracted by subtracting the isolated cone-driven response to the same stimulus from the mixed rod–cone response. Isolated cone-driven responses in Fig. 9.11 (*green triangles*) were obtained by briefly suppressing the rod response with an adapting flash, and then measuring the response to the original test stimulus presented a few hundred milliseconds (300 ms) after offset of the adapting flash. Cone-driven responses in primates recover to full amplitude within about 300 ms whereas rod-driven responses take at least a second, making it possible to isolate the cone-driven response.[34]

The effect of PDA on the rod-isolated a-wave of the macaque is shown in Fig. 9.12 for a range of stimulus strengths.[34] Most of the leading edge of the a-wave in response to the weakest stimulus was eliminated (Fig. 9.12A), and much of the leading edge that occurred later than 15 ms after the flash was removed in response to stronger stimuli (Fig. 9.12B), and even for stimuli that saturated the response (not shown). When APB was injected along with PDA, to eliminate remaining ON bipolar cell contributions as well (Fig. 9.13B), the shape of the early portion of PIII could be seen to form a nose, generally obscured by negative-going signals removed by PDA,

and the b-wave removed by APB (Fig. 9.12C).

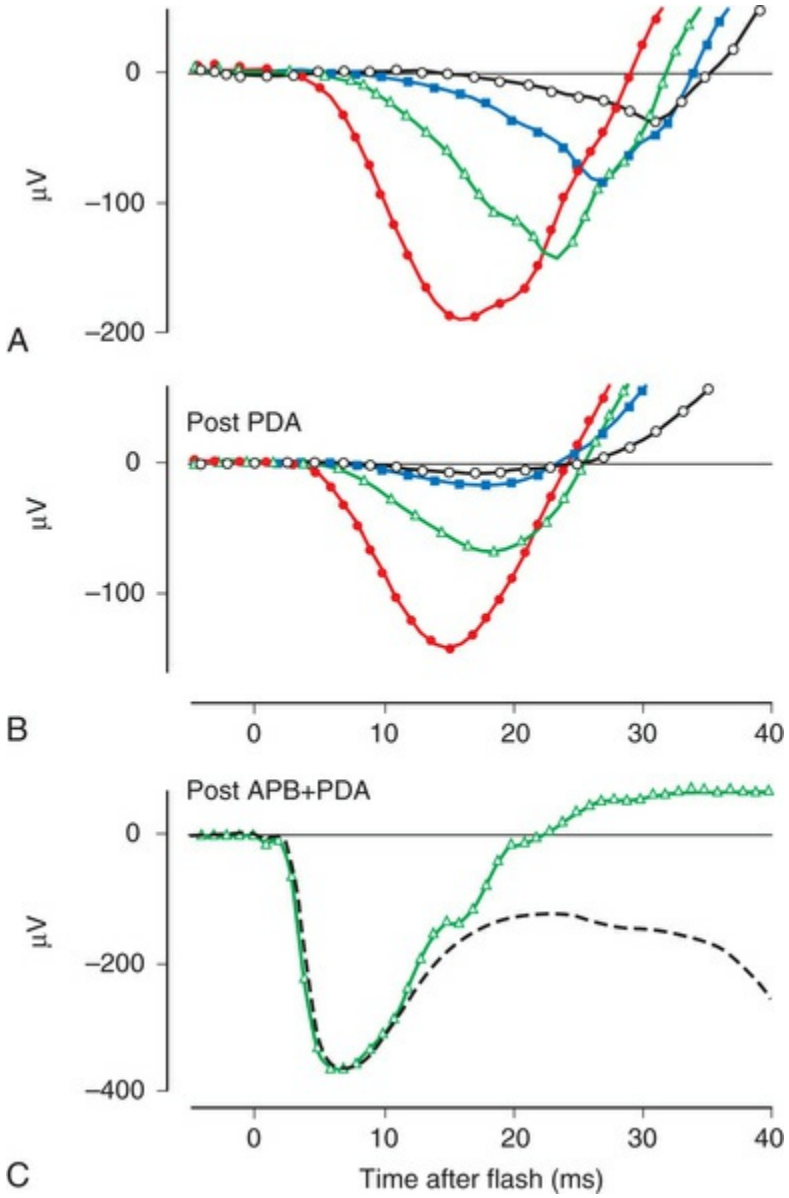

FIG. 9.12 Postreceptoral contribution to rod-driven dark-adapted macaque electroretinogram (ERG). Rod-driven responses from an anesthetized macaque were obtained after subtracting isolated cone-driven response from the mixed rod–cone ERG. Rod-driven responses are shown to a range of stimulus energies (15.8–509 sc td/s) before (A) and after (B) intravitreal injection of *cis*-2,3-piperidine dicarboxylic acid (PDA) (4 mM). For comparison, the ERG remaining after adding PDA and 2-amino-4-phosphonobutyric acid (APB) is shown in part C. The stimulus was a xenon white flash of 59 000 sc td/s, and cone signals were

not removed in this recording. The control response in part C is shown by the *green line*, the post PDA+APB by the *dashed black line*. (Panels A and B, adapted from Robson JG, Saszik SM, Ahmed J, et al. Rod and cone contributions to the a-wave of the electroretinogram of the macaque. J Physiol 2003;547:509–30; C, from unpublished data.)

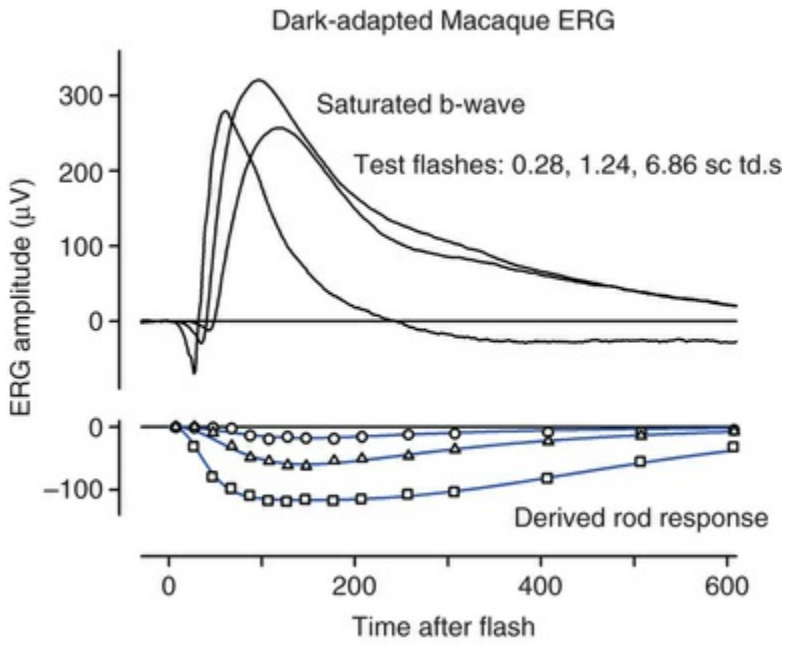

FIG. 9.13 Dark-adapted electroretinogram response of the anesthetized macaque monkey to three different test stimulus strengths (0.28, 1.24, and 6.86 sc td/s) and the derived rod photoreceptor response for each test stimulus. The photoreceptor response was derived using the paired-flash approach of Pepperberg et al.,[78] in which a rod-saturating probe flash follows a test flash at fixed intervals after its onset, and the residual response of the probe is subtracted from the probe alone to derive the rod receptor response at each time point (data points). The model lines used modifications of equations from Robson et al.[34] (From Frishman LJ, Robson JG, unpublished observations.)

PDA blocks signal transmission not only to hyperpolarizing bipolar and horizontal cells, but also to amacrine and ganglion cells of the inner retina. In order to test whether the effect of PDA on the a-wave was due to OFF bipolar cells or more proximal cells, it was

necessary selectively to suppress amacrine and ganglion cell activity. This was done using *N*-methyl-D-aspartate (NMDA), as only the proximal retinal neurons have functional NMDA (ionotropic glutamate) receptors. Results (not shown) were similar in the dark-adapted ERG to those after PDA alone, indicating a proximal retinal origin for most of the rod-driven postreceptoral contributions to the dark-adapted a-wave, rather than a contribution from OFF bipolar cells.[77]

The Timecourse of the Photoreceptor Response

The leading edge of the a-wave is the only visible portion of the photoreceptor response in the normal ERG. In order to see the entire timecourse of the photoreceptor response it is necessary to remove postreceptoral contributions, as was done pharmacologically for the ERGs in Figs. 9.11 and 9.12. However, such a manipulation is invasive, and does not eliminate slow PIII and the c-wave, should they be present. Another approach is to use the paired-flash technique developed by Pepperberg and colleagues[78] to derive, in vivo, the photoreceptor response. The derived photoreceptor response (underneath) and the full ERG responses to three stimuli of the same strength are shown for a macaque monkey in Fig. 9.13. The timecourse of the derived response is similar to that of current recordings in vitro from individual rod photoreceptor outer segments in the macaque, although it reaches its peak a little earlier in vivo in the ERG than in vitro. However, the amplitude of the derived response is rather large, perhaps twice that expected for the photocurrent. The large amplitude of the derived response may occur because the method for deriving responses uses measurements in the "nose" portion of saturated a-wave (Fig. 9.12C), which reflects currents from more proximal regions of the photoreceptor in addition to outer-segment currents.[39]

Origin of the b-Wave

The cornea-positive b-wave, Granit's PII, is the largest component

of the dark-adapted diffuse-flash ERG. There is general consensus that the neuronal generator of the b-wave is primarily the depolarizing (ON) bipolar cells.[30,31,79,80] APB (L-AP4), which binds to mGluR6 receptors of ON bipolar cells and removed the cone b-wave in experiments of Sieving et al., also removed the dark-adapted b-wave in several species, including primates.[30,80] The b-wave is also absent, causing a negative ERG (Fig. 9.12C). Negative ERGs also occur in patients and murine models with complete congenital stationary night blindness (cCSNB) who have mutations that cause a breakdown of the signal transduction cascade in ON bipolar cells.[81,82] However, experimental support also exists for a Müller cell contribution, likely due to K^+ currents as a consequence of bipolar cell depolarization, particularly at times past the leading edge of the response, as described below.

Resolving the role of bipolar cells and Müller cells in generating the b-wave has been difficult. Early intraretinal depth recordings demonstrated a negative-going intraretinal b-wave with a (negative) peak amplitude in distal retina, near the outer plexiform layer (OPL), and the largest change in amplitude across the inner nuclear layer (INL).[13,65] These results suggested that the b-wave was generated by current flowing through a radially oriented cell that acted as a dipole. Bipolar cells, the only radially oriented neurons that span the INL, and Müller cells, the radially oriented glial cells, were implicated.

Müller Cell Hypothesis

CSD profiles for the b-wave from intraretinal recordings in frog retina[83] showed an OPL current sink and a current source extending from the OPL almost all the way to the vitreal surface, and this also was found in monkey retina (Fig. 9.9).[18] Due to the extensive radial spread of sinks and sources, it was hypothesized that Müller cells generate b-wave currents, and supporting this, Miller and Dowling[84] found that intracellular recordings of Müller cell responses in amphibian resembled b-wave responses to the same stimuli. However, studies of local changes in $[K^+]_o$ and Müller K^+ conductances were not fully consistent with the Müller cell hypothesis.

Measurements using intraretinal K^+-selective microelectrodes of local changes in light-evoked $[K^+]_o$ skate,[85] amphibian,[20,86] and rabbit[21] retinas demonstrated only small transient $[K^+]_o$ increases in the OPL at light onset, presumably from dendrites of ON bipolar cells. The Müller cell hypothesis required a large sink activity in the OPL. In contrast, a large sustained inner plexiform layer (IPL) $[K^+]_o$ increase was recorded in the proximal retina of several species at the onset, or at onset and offset of a light stimulus.[87] The large proximal $[K^+]_o$ increase reflected activation of amacrine and ganglion cells as well, and is now understood to contribute strongly to Müller cell or astrocyte-mediated ERG components of proximal retinal origin, e.g., M-wave, STR, or PhNR.

As described in the section on spatial buffering above, the selective permeability of the Müller cell membrane to K^+ and the nonuniform distribution of K^+ conductances (Fig. 9.3) provide the opportunity for K^+ siphoning from synaptic layers where $[K^+]_o$ is high to regions of lower $[K^+]_o$. In species with avascular retinas, e.g., amphibian and rabbit, the Müller cell endfoot adjacent to the vitreous has more than 90% of the K^+ conductance in the cell, as shown in the Newman lab study of enzymatically isolated Müller cells subjected to puffs of K^+ (Fig. 9.14). K^+ entering the Müller cell via strongly inward rectifying Kir channels in synaptic regions will exit predominantly from the vitreal endfoot where the K^+ conductance is only weakly rectifying (Fig. 9.3).[28] The OPL $[K^+]_o$ increase could establish a current loop that extends all the way to the vitreal surface. The IPL $[K^+]_o$ increase would contribute to the same current loop, creating a vitreal positive proximally generated potential in addition to the bipolar cell-dependent b-wave. However, as noted above, the OPL increases in $[K^+]_o$ were small, and because of this, did not predict the large b-wave recorded in the ERG.

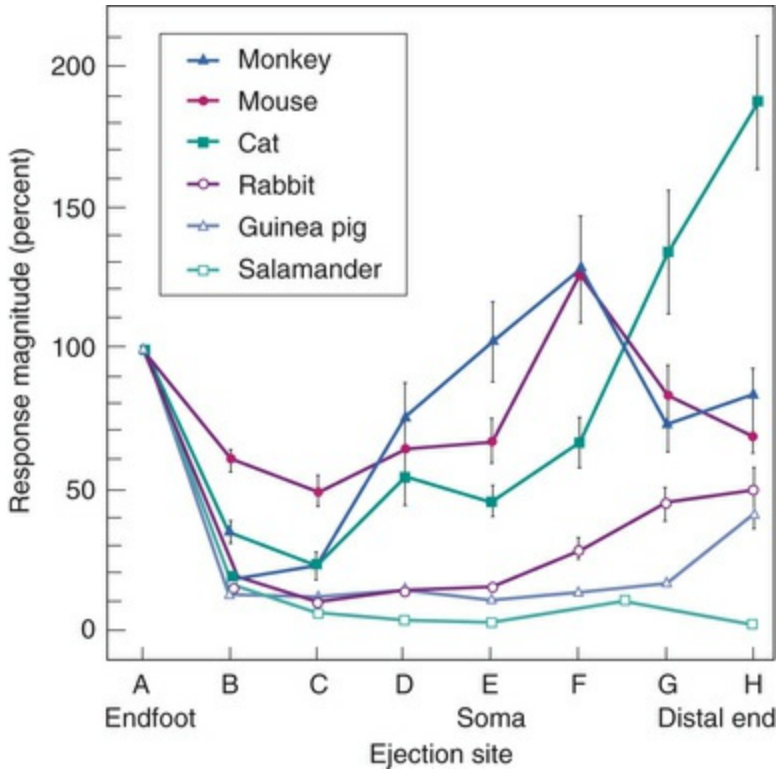

FIG. 9.14 Distribution of K^+ conductance over the surface of enzymatically dissociated Müller glia cells. The magnitude of depolarizations in response to focal K^+ ejections is plotted as a function of ejection location along the Müller cell surface. Responses are normalized to response magnitude at the endfoot. In species with avascular retinas (salamander, rabbit, guinea pig), K^+ conductance is largest at the endfoot. In vascularized species, conductance is largest nearer the cell soma and retinal capillaries (mouse, monkey) or at the distal end of the cell (cat). (Reproduced with permission from Newman EA. Distribution of potassium conductance in mammalian Müller (glial) cells: a comparative study. J Neurosci 1987;7:2423–32.)

In contrast, in species with vascularized retinas such as mouse and monkey, K^+ conductance, although high at the endfoot, is greatest in the INL, near capillaries. In cat, K^+ conductance is greatest near the subretinal space (Fig. 9.14). In these species with vascularized retinas the Müller cell current that arises as a consequence of the proximal $[K^+]_o$ increase contributes to a distally directed current loop (like slow PIII), thereby producing a cornea-negative potential (e.g., m-wave or negative STR), rather than positive b-wave.

ON Bipolar Cells as the Generator of the b-Wave

Experiments using Ba^{2+} to block Kir channels have not supported the Müller cell hypothesis for generation of the b-wave. Although Ba^{2+} blocks slow PIII[48] as well other responses associated with Müller cell K^+ currents, it is far less effective in blocking the b-wave.[23,54,88,89] In CSD studies in frog[88] and rabbit,[89] only the proximal sink source activity associated with the inner retinal M-wave was removed by Ba^{2+}. At least two-thirds of the OPL sink was retained, and the IPL source involved in generating the b-wave was enhanced. These results indicated that the major b-wave generator is the bipolar cell itself.

Scotopic b-Wave (PII) in Mammals

In the mammalian retina, the scotopic ERG response to weak stimuli reflects activity of the sensitive primary rod circuit, including rods, the main interneuron, rod bipolar cells, AII amacrine cells, cone bipolar cell terminals, and ganglion cells (Fig. 9.2). Given the simplicity of the circuit, with contributions from amacrine and ganglion cells pharmacologically suppressed, the isolated b-wave (Granit's PII) should reflect the rod bipolar cell response, either directly as the bipolar cell current, or via Müller cell K^+ currents resulting from K^+ outflow from bipolar cells. Only for strong stimuli would the underlying photoreceptor PIII be a significant factor in the ERG. Fig. 9.15A shows pharmacologically isolated PII from ERGs, recorded in vivo, of four normal C57BL/6 mice, in response to a weak stimulus. An intravitreal injection of the inhibitory neurotransmitter γ-aminobutyric acid (GABA) was used to suppress inner retinal activity.[31,90] Also included in the figure is PII isolated from human ERG using weak adapting backgrounds to suppress the very sensitive STRs.[91] The isolated PII responses have been superimposed on an average of several patch electrode current recordings in a mouse retinal slice preparation of rod bipolar cell responses to a stimulus of similar effect on the rods. The timecourse of the ERG and the single cell currents is very similar, supporting the view that isolated PII reflects rod bipolar cell activity. If Müller cell currents had generated PII, the signal would have been delayed

relative to the bipolar cell responses recorded in the slice, due to the time necessary for accumulation of K^+ ions in the ECS.

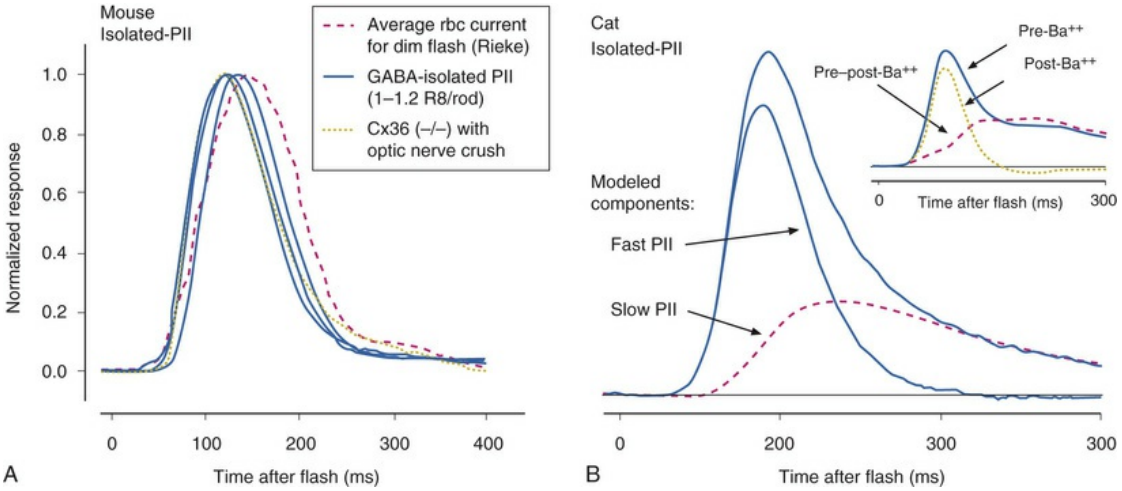

FIG. 9.15 Rod bipolar cell component (PII) of the dark-adapted electroretinogram (ERG) of mouse, cat, and human. (A) Comparison of rod bipolar cell current from patch recordings in mouse retinal slice (courtesy of F. Rieke) with isolated PII (by weak light adaptation) from humans, isolated PII from ERGs of six C57BL/6 mice by intravitreal injection of γ-aminobutyric acid (GABA: 32–46 mM) and additionally from a $Cx36^{(-/-)}$ mouse lacking ganglion cells and the scotopic threshold responses. (B) Pharmacologically isolated cat PII (by inner retinal blockade). The response has been analyzed into a fast component, proposed to be a direct reflection of the postsynaptic current, and a slow component, that is a low-pass filtered version of the faster component, believed to be the Müller cell response, contributing mainly to the tail of the response. Identification of the Müller cell component is supported by the observation (shown in the inset) that intravitreal injection of Ba^{2+}, used to block Kir channels in Müller cells removed a similar portion of the total PII response. For stronger stimuli, in order to isolate the bipolar cell response, it would be necessary also to remove the underlying negative (photoreceptor) PIII signal. (Panel A reproduced with permission from Cameron AM, Mahroo OA, Lamb TD. Dark adaptation of human rod bipolar cells measured from the b-wave of the scotopic electroretinogram. J Physiol 2006;575:507–26. Panel B reproduced with permission from Robson JG, Frishman LJ. Dissecting the dark-adapted

electroretinogram. Doc Ophthalmol 1998;95:187–215, and from LJ Frishman, JG Robson, unpublished observations.)

Pharmacologically isolated PII of cat (Fig. 9.15B) revealed a response similar to that in mouse in its rising phase, but recovered more slowly to baseline. The cat PII response to a brief flash can be analyzed into a fast component and a slow component that is a low-pass filtered version of the fast component, as indicated by the lines in Fig. 9.15B. The inset to Fig. 9.15B shows that intravitreal Ba^{2+} eliminated a slow portion of the response that was very similar in timecourse to the modeled slow component, but did not alter the fast component, suggesting that bipolar cell current provides the leading edge of PII in the cat, and the Müller cell current contributes at later times. Although the slow component (in response to a brief flash) was lower in amplitude than the fast component, the area under the two curves was similar. With longer stimulus durations such as those used in early studies of the b-wave origins, the contribution to the ERG of the two sources would be about equal.[85] Pharmacologic isolation of macaque PII showed a similar waveform to that in cat.[3]

Cone-Driven b-Wave

The photopic ERG is commonly measured in the presence of a rod-suppressing background. Depth profiles of the rod b-wave measured under dark-adapted conditions and the cone b-wave, under light-adapted conditions, are similar in cat[92,93] and monkey retinas, suggesting a similar origin for the two responses, but in the case of the photopic ERG, depolarizing cone rather than rod bipolar cells are involved.

Sieving and colleagues[33,35] studied the origins of the photopic b-wave in monkeys using glutamate analogs in the same series of experiments as those in which the a-wave was studied. Fig. 9.16 shows the macaque photopic ERG response to long-duration flashes, before and after APB was injected into the vitreal cavity (eye 1, left panel). APB removed the transient b-wave supporting ON bipolar cells as the generators (although the possibility of glial mediation was not eliminated in these studies). However, when PDA was injected first in another eye (eye 2, right panel), to remove

the OFF pathway (and horizontal cell inhibitory feedback), a much larger and more sustained b-wave was revealed. These findings indicate that the normally transient nature of the cone b-wave is due to truncation of a more prolonged depolarizing bipolar cell response. This truncation is due to some combination of (PDA-sensitive) OFF pathway response of opposite polarity to the ON bipolar cell contribution to the ERG (a push–pull effect[28]), and inhibition via (PDA-sensitive) horizontal cells of ON bipolar cell signals. The isolated photoreceptor response remaining after all postreceptoral activity was eliminated either by APB followed by PDA, or PDA followed by APB, was similar.

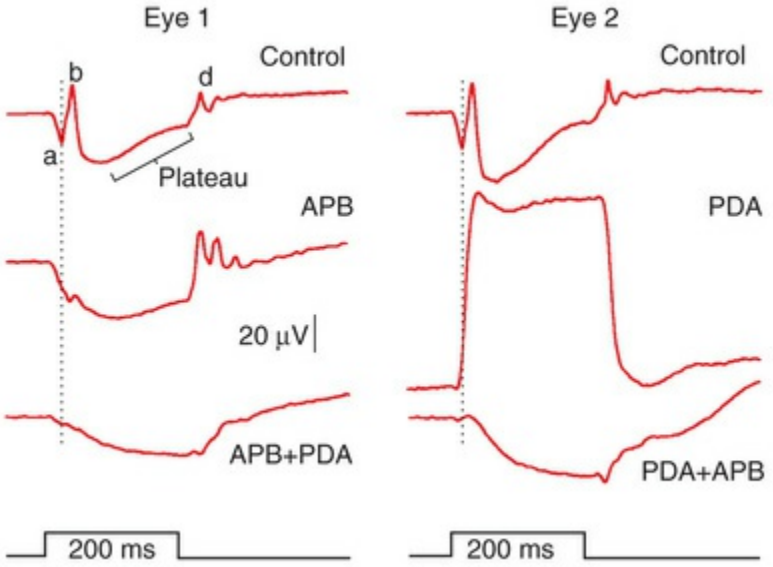

FIG. 9.16 Effects of 2-amino-4-phosphonobutyric acid (APB) and *cis*-2,3-piperidine dicarboxylic acid (PDA) on the light-adapted photopic electroretinogram of a monkey's two eyes. Drugs were given sequentially, APB followed by PDA for eye 1, and PDA followed by APB for eye 2. The vertical line shows the time of the a-wave trough in the control response. The 200-ms stimulus was 3.76 log td (2.01 log cd/m^2) on a steady rod-saturating background of 3.3 log td (1.55 cd/m^2).

(Reproduced with permission from Bush RA, Sieving PA. A proximal retinal component in the primate photopic ERG a-wave. Invest. Ophthalmol Vis Sci 1994;35:635–45.)

Origin of the d-Wave

The d-wave is a positive-going deflection at light offset that occurs in the photopic ERG. It is best seen when the light step is prolonged. In mammals, the d-wave is very prominent in the all-cone retina of the ground squirrel, as seen in the response to a long-duration stimulus in Fig. 9.17, and in the monkey retina, with its mixture of rods and cones, the d-wave, although less prominent, is easily identified when stimulus duration is extended, e.g., Figs. 9.1 and 9.9. Although d-waves have been described in scotopic ERG of mammals, they are probably not "true" d-waves that, as described below, include a strong contribution from the offset of the cone photoreceptor, and the depolarization at light offset of OFF cone bipolar cells. In the predominantly rod-driven cat ERG, the small positive deflection that Granit[32] called a "d-wave" occurred only in response to offset of very intense and long-duration stimuli for which the decay of the rod receptor potential appeared as a small positive deflection that followed, at light offset, the negative-going offset of PII.

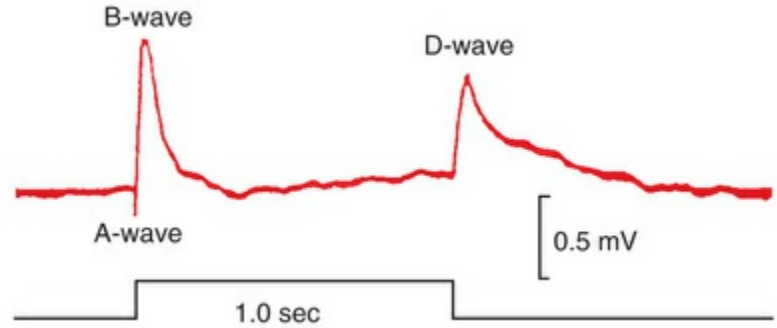

FIG. 9.17 Electroretinogram from the all-cone retina of the ground squirrel in response to a 1-second light step. Recordings were made under light-adapted conditions between a contact lens electrode on the cornea and an electrode on the forehead. (Reproduced with permission from Arden GB, Tansley K. The spectral sensitivity of the pure-cone retina of the grey squirrel (*Sciurus carolinensis leucotis*). J Physiol 1955;127:592–602.)

Intraretinal analysis in monkey retina indicated that the corneal

d-wave represents a combination of the rapid positive-going offset of the cone receptor potential followed by the negative-going offset of the b-wave.[16,66] Although the early work on primate ERG cited above did not identify OFF bipolar cells as major contributors to the d-wave, more recent studies using intravitreal injection of glutamate analogs have demonstrated that these cells provide a significant portion of the response.[35,94] Figs. 9.10 and 9.16 both show that PDA, which blocks OFF bipolar cell responses, reduced the d-wave, eliminating it entirely when a large b-wave was present. The effect of PDA was not replicated by NMDA blockade of inner retinal cells, that also would have been affected by PDA, confirming a role of the OFF bipolar cells themselves. PDA, but not the blockade of inner retinal cells, also eliminated a small positive wave that occurs in the falling phase of the b-wave, or just after it, in the brief flash ERG in monkeys and humans, called the "i-wave."[95]

Photopic Hill

The stimulus response function acquired by measuring b-wave peak amplitudes in response to brief flashes over a range of increasing stimulus strengths has a characteristic inverted "U" shape. More specifically, Peachey et al.[96] observed that the b-wave amplitude increased with increasing stimulus strength until it reached a peak and then decreased for stronger stimuli. This function was later named the "photopic hill" by Wali and Leguire.[97] A model of the stimulus response function has indicated that the positive peak of the function is formed by addition of a saturating b-wave from ON pathway,[98] and an early d-wave from OFF pathway, and this has been confirmed in experiments using glutamate analogs in macaques.[99]

Origin of the Photopic Fast-Flicker ERG

The fast-flicker ERG (nominally 30 Hz flicker) is used to examine cone-driven responses in humans because rod-driven responses generally do not respond to fast flicker. For many years the human

(or macaque) photopic ERG response to fast-flickering stimuli was believed to reflect primarily the response of cone photoreceptors. However pharmacologic dissection studies have shown that most of the fast-flicker response seen clinically with a full-field stimulus (or focal stimulus) is generated postreceptorally.

Bush and Sieving[100] used glutamate analogs to remove selectively postreceptoral ON and OFF pathway responses, as was done in studies of a-, b-, and d-waves. Intravitreal injection of APB to remove the b-wave left a delayed flicker response, reflecting OFF bipolar contribution. When both APB and PDA were used, the flicker response was practically eliminated. From experiments of this type they concluded that postreceptoral cells that normally produce the b- and d-waves are strong contributors to the fast-flicker response. Further experiments in macaques have more thoroughly investigated the interaction of the ON and OFF pathways over a wide range of temporal frequencies and stimulus conditions.[101] The amplitude in both humans and macaques dips around 12 Hz, as ON and OFF inputs cancel, and it reaches a peak around 50 Hz. Other studies have demonstrated a small inner retinal contribution to the flicker response, and particularly to the second harmonic component of the response, which has a strong input from TTX-sensitive sodium-dependent spiking activity of ganglion and perhaps amacrine cells.[102]

Origin of the Multifocal ERG

Multifocal electroretinography (mfERG) was developed by Sutter and Tran[103] as a means of recording many focal retinal responses simultaneously in a brief time period (e.g., 7 minutes) to achieve a topographical array of little ERGs. Recording ERGs from many different focal regions of the retina otherwise would be impractical, due to the time involved in averaging of the small signals. The common mfERG stimulus is an array of hexagons (e.g., 64 or 103 hexagons over 30–40° of central visual field). In the standard mode for stimulation each hexagon reverses in contrast, according to a predetermined random "m-sequence," at the frame rate of the visual display monitor, often 75 Hz for CRTs and 60 Hz for LCD displays. At any given time, each hexagon has a 50% chance of

being light or dark. The m-sequence for all hexagons is the same, except for a specific and unique lag (number of frames) in initiation of the sequence for each hexagon, to allow extraction of the locally generated response by a correlation approach. The resulting "first-order" focal ERGs to the rapidly changing stimulation look similar but not identical to full-field flash ERGs that integrate responses over a longer period of time. The mfERG is generally recorded under photopic conditions, for which the foveal response is large, and is useful for detecting local changes in function that may not be detected in a full-field ERG, such as those that occur in macular dystrophies.

Experiments using intravitreal injections of glutamate analogs, APB, and PDA in macaques showed that, despite differences in the mfERG and full-field flash ERG, the cellular origins of the major negative and positive waves are essentially the same in two types of ERG.[104] The outcome of such experiments is shown in Fig. 9.18, where the findings from the experiments on macaque mfERG were applied to the human response. When blank frames were interposed so that flashes occurred every 100 or 200 ms, a complete ERG including OPs could form before the next m-frame. For this slow-sequence ERG, experiments in macaques again yielded origins similar to full-field flash ERG, and provided some evidence for spike-dependent oscillatory activity related to the optic nerve head component in the mfERG, proposed by Sutter and Bearse.[105–107]

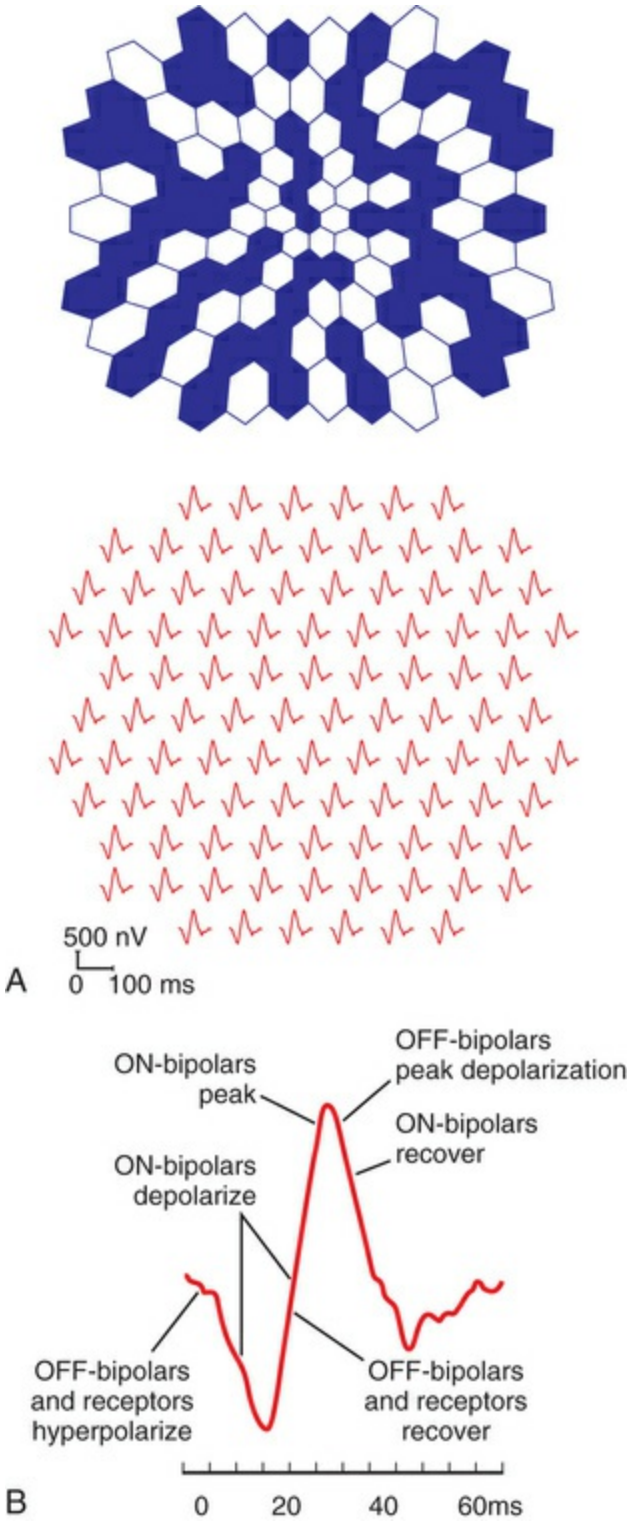

FIG. 9.18 Major components of the multifocal electroretinogram (mfERG). (A) mfERG trace array (field view) using 103 hexagons scaled with eccentricity and covering about 35° of visual angle, as illustrated above the traces. (B) Model for the retinal contributions to the human mfERG based on results from the macular region of a macaque after

pharmacologic separation of components. (Reproduced with permission from Hood DC, Frishman LJ, Saszik S, et al. Retinal origins of the primate multifocal ERG: implications for the human response. Invest Ophthalmol Vis Sci 2002;43:1673–85.)

ERG Waves From Proximal Retina

Origin of the Proximal Negative Response and the M-Wave

The proximal negative response (PNR) is a light-evoked field potential recorded intraretinally in proximal retina, named and most fully described by Burkhardt.[108] The PNR consists of a sharp, negative-going transient at onset and again at offset of a small light spot centered on the microelectrode tip placed in the IPL. It can be recorded in a range of vertebrate retinas, including the cat[109] and primate.[110] A PNR contribution to the transretinal ERG is necessarily small because the intraretinal response, which is largest in response to small spots, will be shunted through adjacent low-resistance retinal regions that are not activated by the light.

The M-wave, like the PNR, is a light-evoked field potential, recorded in proximal retina with microelectrodes in response to the onset and offset of a small well-centered spot, but it has a slower timecourse than the PNR. The M-wave was initially described in studies of amphibians,[87] but also has been identified in the cat,[23,92] as illustrated in Fig. 9.19.

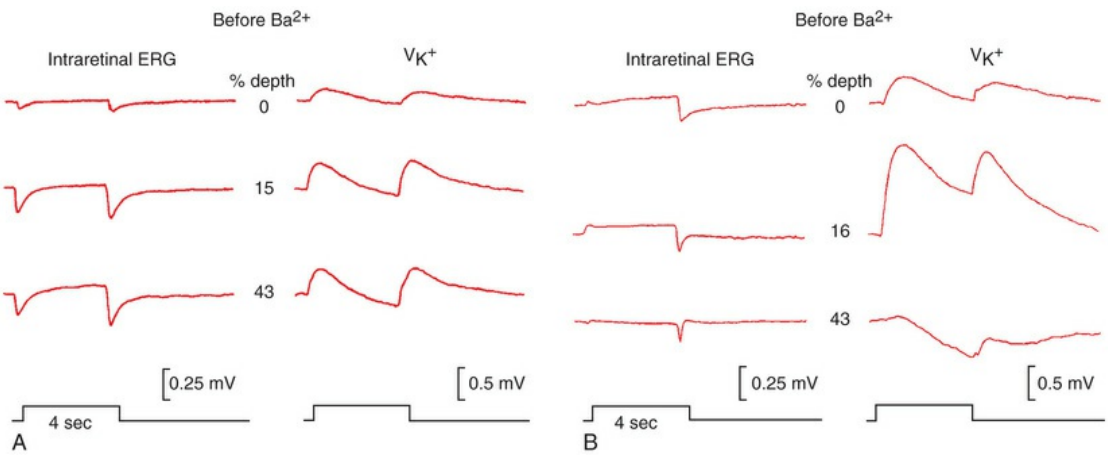

FIG. 9.19 Effect of Ba^{2+} on the M-wave of the light-adapted cat retina. Effect of intravitreal barium chloride ($BaCl^{2+}$, 3 mM vitreal concentration) on the depth distribution of field potentials and $[K^+]_o$ changes in light-adapted retina. Recordings were made before (A) and 30–60 minutes after (B) $BaCl^{2+}$ was injected. The stimulus was a small spot (0.8° in diameter); steady background illumination was 10.5 log q deg^2/s; flash illumination was 11.6 log q deg^2/s. (Adapted from Frishman LJ, Yamamoto F, Bogucka J, et al. Light-evoked changes in $[K^+]o$ in proximal portion of light-adapted cat retina. J Neurophysiol 1992;67:1201–12.)

In retinas in which both an M-wave and a PNR can be recorded (amphibia and cats), the PNR is thought to be the transient neuronally generated portion of the proximal retinal response, while the slower M-wave reflects spatial buffer currents in Müller cells, generated as a consequence of K^+ release from the same proximal neurons.[23,87] As illustrated in Fig. 9.19, for cat, changes in $[K^+]_o$ recorded in proximal retina show a similar timecourse to the simultaneously recorded field potentials. In isolated amphibian retina it was shown that the Kir channel blocker Ba^{2+} had only minor effects on light-evoked neural activity (PNR) and the proximal retinal $[K^+]_o$ increase, but it blocked the M-wave and K^+ spatial buffer currents.[25] Similar findings in intact cat retina are illustrated in Fig. 9.19. Note that after intravitreal Ba^{2+} injection, the proximal $[K^+]_o$ increase was larger, but the more distal increase seen in control records was absent. This is consistent with blockade by Ba^{2+} of spatial buffer currents that normally would carry the K^+ away from proximal retina to the distal extracellular sinks where $[K^+]_o$ was lower.

The local M-wave's contribution to the transretinal ERG would be small. The contribution of the M-wave may be greater when periodic stimuli such as grating patterns that stimulate large regions of retina are used. Sieving and Steinberg[111] showed that the M-wave is tuned to a spot diameter similar to the bar width of the optimal spatial frequency for the intraretinal pattern ERG (PERG) in the cat. The contribution of the proximal retina to the ERG can also be enhanced by using full-field stimulation.

Origin of the Photopic Negative Response

In contrast to the PNR and M-wave, which provide small contributions at most to the transretinal ERG, negative-going responses from proximal retina to full-field stimulation are present in the corneal ERGs of several species, including cats, monkeys, and humans.[40,63,92,93,112–114] These responses, called the PhNR and STR, are generated by mechanisms similar to those documented above for the M-wave.

The PhNR is a negative-going wave in the photopic ERG that occurs after the b-wave in response to a brief flash, and again after the d-wave in response to a long flash. It is more prominent in primates than in rodents. In humans and monkeys, the PhNR is thought to reflect spiking activity of retinal ganglion cells.[113,114] As shown in Fig. 9.20, the PhNR is reduced in macaque eyes with experimental glaucoma (also after TTX injection)[113] and in humans with primary open angle glaucoma. It is reduced in several other disorders affecting inner retina and optic nerve head as well. The slow timecourse of the PhNR suggests glial involvement, perhaps via K^+ currents in Müller cells or astrocytes in the optic nerve head set up by increased $[K^+]_o$ due to spiking of ganglion cells. In intraretinal microelectrode recordings in cats, local signals of the same timecourse as the PhNR were largest in and around the optic nerve head and the PhNR was disrupted in cats by Ba^{2+}, indicating glial involvement in generation of the response (Viswanathan and Frishman, unpublished observations).

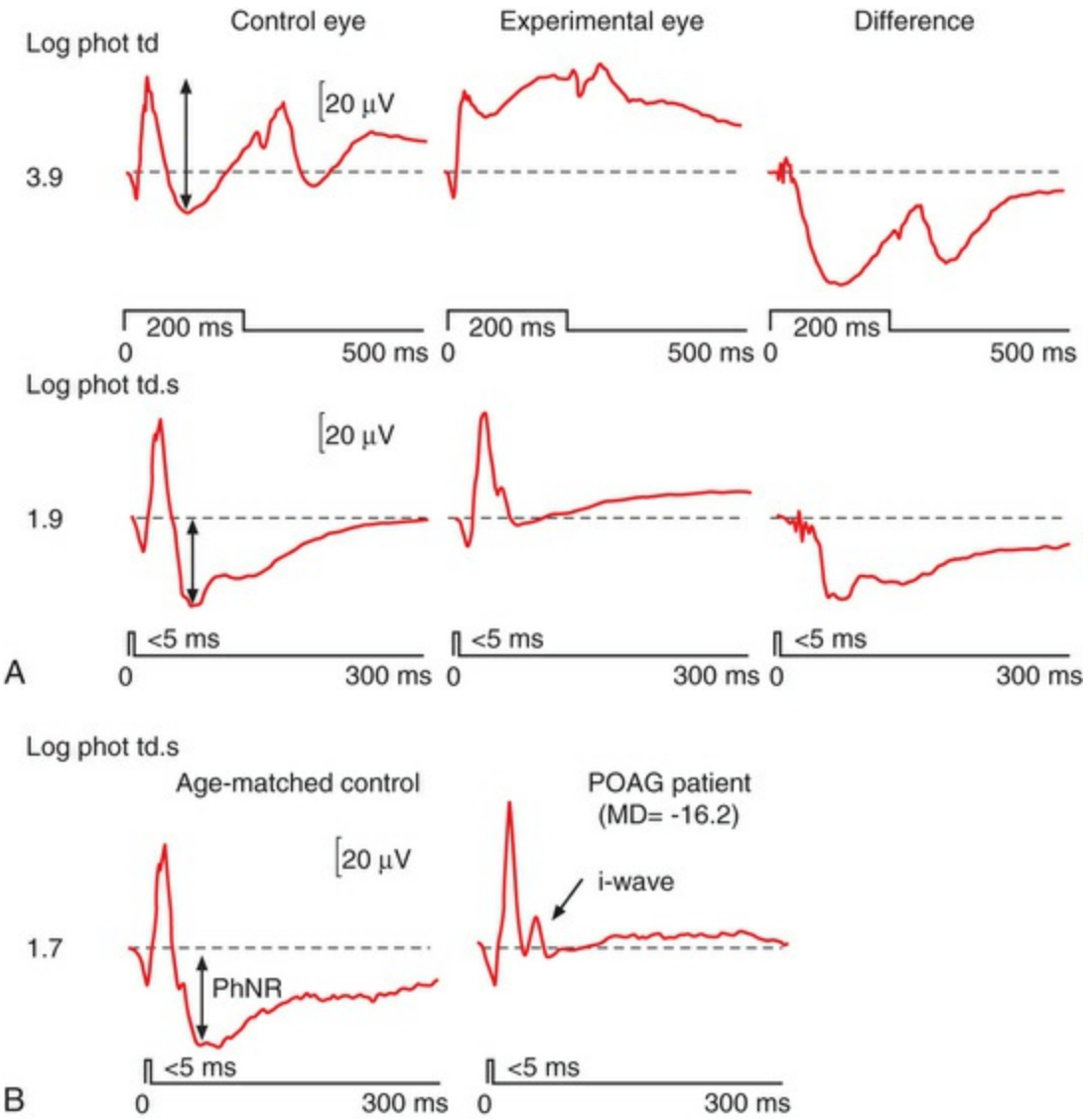

FIG. 9.20 Photopic negative response (PhNR) in macaque monkey and human in normal and glaucomatous eyes. (A) Full-field flash electroretinogram (ERG) showing the PhNR of a macaque in response to long (top) and brief (middle) red light-emitting diode (LED) flashes on a rod-saturating blue background (3.7 log sc td) from the control (left) and "experimental" (middle) fellow eye with laser-induced glaucoma, and the difference between control and experimental records (right). *Arrows* mark the amplitude of the PhNR. The mean deviation (MD, static perimetry, C24–2 full threshold program) for the experimental eye was −2.65 dB. (B) Full-field flash ERGs of an age-matched 63-year-old normal human subject and a patient with primary open angle glaucoma (POAG) under similar stimulus conditions to those used above for monkeys. The MD

(static perimetry, C24–2 full threshold program) for the patient's eye was −16.2 dB. (Panel A adapted from Viswanathan S, Frishman LJ, Robson JG, et al. The photopic negative response of the macaque electroretinogram: reduction by experimental glaucoma. Invest Ophthalmol Vis Sci 1999;40:1124-36, with permission. Panel B adapted from Viswanathan S, Frishman LJ, Robson JG, et al. The photopic negative response of the flash electroretinogram in primary open angle glaucoma. Invest Ophthalmol Vis Sci 2001;42:514–22.)

PhNRs can be evoked using white flashes on a white background, if the flash is strong enough. However a red LED flash on a blue background, as was used for ERGs shown in Fig. 9.20, elicits PhNRs over a wider range of stimulus strengths. The red flash may minimize spectral opponency that would reduce ganglion cell responses, and use of a blue background suppresses rods while minimizing light adaptation of L-cone signals.[7] Blue stimuli on a yellow background which minimize spectral antagonism are good stimuli as well. The PhNR can be enhanced relative to other major ERG components, and can dominate the ERG when using focal stimuli in the region of the macula.[115–117]

Relation to the Pattern ERG

The PERG has been the most commonly used noninvasive retinal measure of ganglion cell activity. It is a small response of a few microvolts elicited by contrast reversal of a bar grating or checkerboard pattern that shows some spatial tuning, consistent with a ganglion cell origin. In response to pattern stimulus, in which mean luminance does not change, the linear signals that produce a- and b-waves cancel, leaving only the nonlinear (mainly second harmonic) signals in the ERG. The PERG is eliminated by loss of ganglion cells as a consequence of optic nerve section.[118] It has been used widely in clinical studies assessing ganglion cell function in eyes with glaucoma and other diseases of inner retina (see reviews by Holder[117] and by Bach and Hoffmann[116]).

PERGs can be recorded as a transient response to low reversal frequencies (1–2 Hz) or as a steady-state response to higher frequencies, i.e., 8 Hz. For 1–2-Hz reversals of the pattern stimulus, a positive wave occurs within about 50 ms of each reversal (P_{50}) and

a negative wave, N_{95}, is maximal at about 95 ms. The N_{95} is often reduced in glaucomatous eyes (the effects on the smaller P_{50} response are less consistent). Because the PhNR has a similar implicit time to the N_{95}, Viswanathan et al.[119] compared effects of experimental glaucoma and of TTX on the two responses in macaques, and found similar effects on both, indicating common retinal origins. Furthermore, the PERG waveform for a given stimulation frequency (2 or 8 Hz) could be simulated by adding together the ERGs at onset and offset of a uniform field, with strong contributions of PhNRs in generation of $N_{95.}$ More recent work using glutamate analogs and simulations has found that both ON and OFF pathways contribute equally to the transient PERG, but the ON pathway dominates the 8 Hz PERG.[120]

Given the similar origins of PhNR and PERG, the PhNR may have some advantages over PERG as a clinical indicator of proximal retinal dysfunction. With appropriate stimulus conditions, the PhNR is a much larger response, it does not require refractive correction, and will be less affected by opacities in the ocular media than the PERG.

Origin of the Scotopic Threshold Response

For very weak flashes from darkness, near psychophysical threshold in humans,[33,90] small negative (n) and positive (p) STR dominate the ERG of most mammals that have been studied. This response, which is more sensitive than the b-wave (or a-wave) and saturates at a lower light level than either component, was thus named because of its sensitivity.[63] As shown in Fig. 9.7, for the monkey and human, the nSTR at stimulus onset dominates the dark-adapted diffuse flash ERG in response to the weakest stimuli. The nSTR is distinct from the scotopic a-wave, although it can appear as a "pseudo a-wave" at light levels where it can be removed by suppressing inner retinal activity pharmacologically.[121,122] The STRs occur in response to stimuli much weaker than those that elicit more distally generated waves of the ERG because convergence of the rod signal in the retinal circuitry increases the gain of responses generated by inner retinal neurons.

The nSTR was initially observed to be generated more proximally

(IPL) than PII (INL) in intraretinal depth analysis studies in cats.[63] As shown in Fig. 9.21, the field potential recorded in proximal retina in response to a weak diffuse stimulus was negative-going for the duration of the stimulus, and returned slowly to baseline after light offset. For stimuli too weak to elicit PII, the nSTR reversed polarity in midretina and became a positive-going signal in the mid- and distal retina. This reversal suggests a source proximal to, and a sink distal to, the reversal point (see description of the Müller cell mechanism, below). For stronger stimuli, the reversed nSTR in mid- and distal retina was replaced by PII, which then dominated the ERG. The similarity of the onset times and timecourse of the proximal retinal STR and the negative STR in the cat vitreal ERG can be seen in Fig. 9.21.

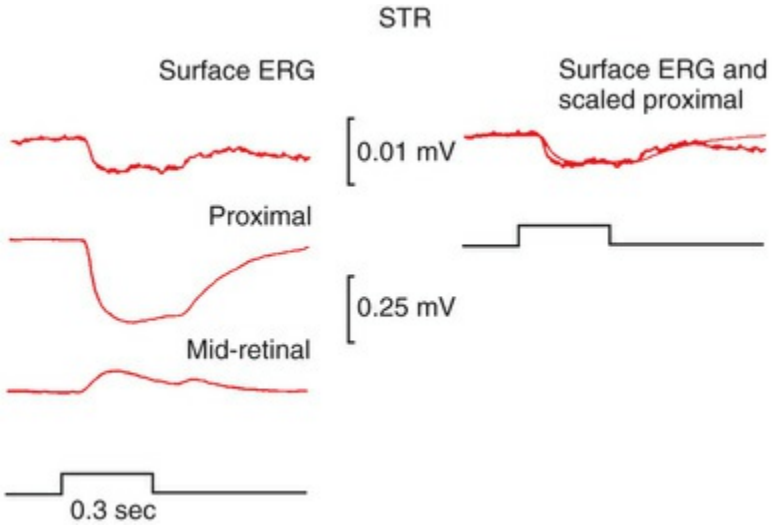

FIG. 9.21 The scotopic threshold response (STR) dominates intraretinal recordings and the electroretinogram (ERG) at low stimulus intensities below the threshold for the b-wave (PII). On the left, the top trace is the surface ERG recorded about 25 μm from the retinal surface, and the bottom two traces are recordings of the STR in the proximal retina (about 6% retinal depth) and the inverted STR around 50% retinal depth. On the right, the scaled STR recorded in the proximal retina is superimposed on the surface ERG to show the similarity of the responses. For the surface ERG, a microelectrode was referenced to a wire in the vitreous in order to reduce the effects of stray light. This minimized contributions to the ERG of retinal

regions distant from the recording site of the intraretinal signals (spot diameter, 9.9°; spot illumination, 4.8 log q deg^2/s). (Adapted from Sieving PA, Frishman LJ, Steinberg RH. Scotopic threshold response of proximal retina in cat. J Neurophysiol 1986;56:1049–61.)

The nSTR also can be separated from PII using pharmacologic agents (GABA, glycine, or NMDA[30,90,121]) to suppress responses of the amacrine and ganglion cells proximal to bipolar cells. These agents remove the STR, but not PII (Fig. 9.15). In contrast, APB eliminates both the scotopic b-wave (PII) and STR, indicating that the STR will not be generated if the primary rod circuit is no longer mediated by rod bipolar cells (Fig. 9.2).

There is a similarly sensitive positive STR in the scotopic ERG of animals that have a negative STR.[40,90] Because the pSTR is small and of opposite polarity to the nSTR, it can easily be cancelled out in the ERG. An instance of this can be seen in the dark-adapted macaque ERG in Fig. 9.7. The delayed onset of nSTR for the weakest stimulus is due to the presence of a pSTR that is slightly larger than the nSTR at early times. In response to a stimulus about 1 log unit higher (just above), the pSTR rides on the emerging PII as an early positive potential. Most pharmacologic agents that eliminate the nSTR also eliminate the pSTR.[40,90] For example, NMDA eliminated both the nSTR and pSTR in the macaque ERG for responses such as those seen for the two weakest stimuli in Fig. 9.7 (Frishman, unpublished observations).

A linear model of the contributions of pSTR, nSTR, and PII to the dark-adapted cat ERG is shown in Fig. 9.22. The model assumes that each ERG component initially rises in proportion to stimulus strength, and then saturates in a characteristic manner, as has been demonstrated in single-cell recordings in mammalian retinas, as well as for ERG a- and b-waves in numerous studies. Only with the inclusion of a small pSTR does the model accurately predict the whole ERG at a given "fixed" time in response to a weak stimulus. The model was fit in Fig. 9.22 to responses measured at 140 ms after a brief full-field flash (<5 ms), which was the peak of the nSTR in the cat scotopic ERG. Similar models have been applied to mouse[90] and human ERG.[40]

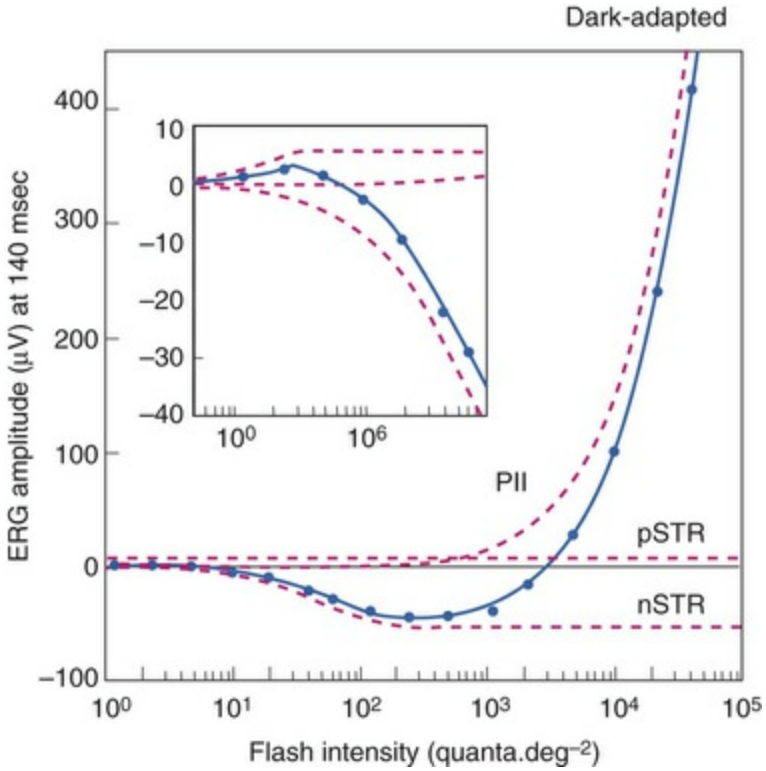

FIG. 9.22 Amplitude of cat dark-adapted electroretinogram responses measured 140 ms after a brief flash at the maximum negativity of the negative scotopic threshold response (nSTR). *Dashed lines* show model curves for the positive scotopic threshold response (pSTR), nSTR, and PII. Explicitly, the pSTR rises as a linear function that saturates abruptly at V_{max}, while the exponential saturation of the nSTR is defined by:

$$V = V_{max}(1 - \exp(-I/I_o))$$

where V_{max} is the maximum saturated amplitude, and I_o is the intensity for an amplitude of $(1 - 1/e)V_{max}$, while the hyperbolic relation used for PII is defined by:

$$V = V_{max} I/(I + I_o)$$

where V_{max} has the same meaning but I_o is the intensity at which the amplitude is $V_{max}/2$. The inset shows the pSTR and nSTR at the lowest light levels that were used. (1 q deg^2 is equivalent to ~–7.5 log sc cd m^2/s).

(Adapted from Frishman LJ, Robson JG. Processing, adaptation to environmental light. In: Archer SN, Djamgoz MBA, Loew ER, et al., editors. Adaptive mechanisms

in the ecology of vision. Dordrecht: Kluwer Academic.; 1999. p. 383–412, with permission.)

K^+ Müller Cell Mechanism for Generation of the STR

The STR, like the M-wave, is associated with Müller cell responses to $[K^+]_o$ released by proximal retinal neurons. In intraretinal studies in cat, a proximal increase in $[K^+]_o$ was observed that had clear similarities to the local STR that was simultaneously recorded: the dynamic range from "threshold" to saturation of the light-evoked proximal $[K^+]_o$ increase was similar to that of the field potentials, and the retinal depth maxima for the two responses were the same.[22,54] A causative role for the $[K^+]_o$ increase in generating the nSTR (and a slow negative response in the vitreal ERG following the initial STR) was supported by the finding (Fig. 9.23) that Ba^{2+} removed the proximal retinal field potential and the nSTR in the ERG but did not, initially, eliminate the light-evoked increase in $[K^+]_o$. The cornea-negative polarity of the nSTR suggests a distally directed Müller cell K^+ current (similar to M-wave and PIII currents in the vascularized cat retina). As noted above for the light-adapted M-wave, in the dark-adapted retina Ba^{2+} also appears to block K^+ siphoning by the Müller cells. Whereas the proximal $[K^+]_o$ increase remained intact when related field potentials were abolished, the distal $[K^+]_o$ increase was eliminated by Ba^{2+}.

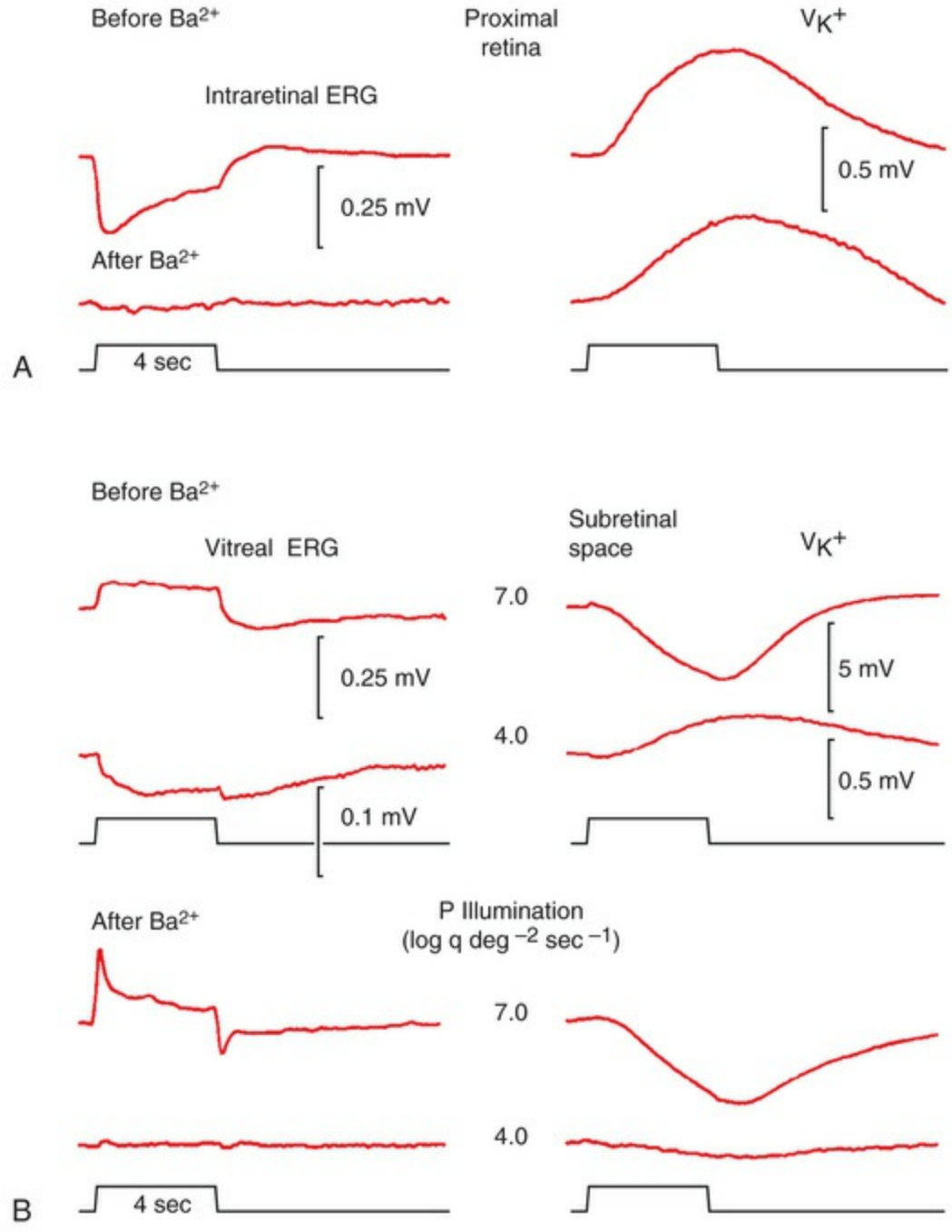

FIG. 9.23 Effect of Ba^{2+} on the scotopic threshold response (STR) and b-wave (PII) in scotopic electroretinogram (ERG) of the cat. (A) Effect of intravitreal Ba^{2+} ($BaCl_2$, 3.9 mM vitreal concentration) on the intraretinal STR and slower K^+-related negative response in response to a 4-second stimulus and the simultaneously recorded light-evoked decrease in $[K^+]_o$ (V_{K+}) in the proximal retina measured at 10% retinal depth, proximal to the peak K^+ change at 17% depth. Top response was measured before Ba^{2+} and the

bottom response 56 minutes after Ba^{2+} injection. (B) Effect of intravitreal $BaCl_2$ (3.9 mM vitreal concentration) on the STR and slow negative response in the vitreal ERG (left) and the simultaneously recorded change in $[K^+]_o$ in the subretinal space. Measurements of the amplitude of dark-adapted responses in the proximal retina and the light-evoked increase in $[K^+]_o$ in proximal and distal retina before and after intravitreal injection of Ba^{2+} were made with double-barreled K^+-sensitive microelectrodes. (Reproduced with permission from Frishman LJ, Steinberg RH. Light-evoked increases in $[K^+]_o$ in proximal portion of the dark-adapted cat retina. J Neurophysiol 1989;61:1233–43.)

Neuronal Origins of the STR

Whether the neurons involved in the genesis of the nSTR and pSTR are amacrine or ganglion cells is species-dependent. In monkeys it is likely that the nSTR arises predominantly from ganglion cells. It was absent in eyes in which the ganglion cells were eliminated as a consequence of experimental glaucoma[112] and by intravitreal injection of TTX to block Na^+-dependent spiking activity of those neurons; the pSTR remained intact. In contrast, in cats and humans[122] as well as in rodents,[3] the nSTR is not eliminated by ganglion cell loss, and thus may be more amacrine cell-based. In rodents the pSTR relies upon the integrity of ganglion cells. A characteristic of Müller/glial cell-mediated ERG components is their slow timecourse. Glial cell mediation of the nSTR was demonstrated most directly in cat, but the timecourse of the nSTR is slow in all species. Glial mediation may explain the similarity in timecourse of nSTR across species regardless of the particular type of neuron producing the local changes in proximal $[K^+]_o$ that generate the response.

Origin of Oscillatory Potentials

The OPs of the ERG consist of a series of high-frequency, low-amplitude wavelets, mainly superimposed on the b-wave, that occur in response to strong stimulation. OPs are present under

light- and dark-adapted conditions, with contributions from both rod- and cone-driven signals.[123] The mixed rod–cone ERG in humans in the ISCEV standards in Fig. 9.4 shows at least four OPs that can be extracted with a filter with a low-frequency cutoff of 75 Hz. OPs are of postreceptoral origin, and occur in isolated retinas in the absence of the RPE.[73] The number of OPs induced by a flash of light varies between about 4 and 10 depending upon species and stimulus conditions; the temporal frequency of the OPs varies as well. Fig. 9.24 shows the photopic flash ERG of a macaque monkey (top); at least five OPs at frequency of about 150 Hz can be seen by filtering the response to extract the high-frequency signals.

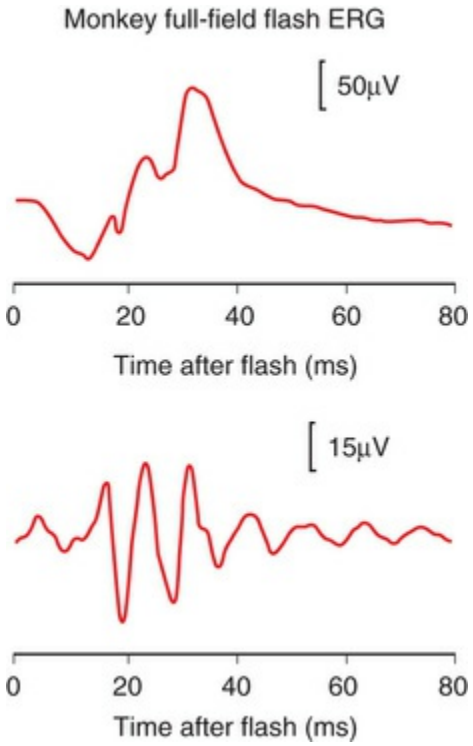

FIG. 9.24 Full-field flash photopic electroretinogram of a macaque monkey (top) and the oscillatory potentials (OPs) extracted from these records. Filtering was between 90 and 300 Hz for OPs that occurred between 100 and 200 Hz. The stimulus was a xenon flash presented on a rod-saturating blue background. (Adapted from Rangaswamy NV, Hood DC, Frishman LJ. Regional variations in local contributions to the primate photopic flash ERG: revealed using the slow-sequence mfERG. Invest Ophthalmol Vis Sci 2003;44:3233–47).

There is consensus that OPs are generated in proximal retina.

Three important and unresolved questions regarding their origins follow: (1) Do all the OPs have the same origin? (2) Which cells generate the OPs? (3) What mechanisms are involved in generating OPs?

Do All the OPs Have the Same Origin?

In amphibians, where early studies were done, the various OPs do not all have the same origin. Depth profiles from isolated frog retina showed that the earliest OPs in the response arose near the IPL whereas the later OPs arose more distally, perhaps in the INL. Studies of Wachmeister[124] in amphibian retina also found that earlier OPs were depressed by GABA antagonists, the dopamine antagonist haloperidol, β-alanine, and substance P; whereas later OPs were depressed by the glycine antagonist strychnine and by ethanol.

In primates, intraretinal studies using stimuli that would elicit responses from both rod and cone systems did not find differences in the depth profiles of the different OPs.[44,125] Considering the complexity of inner retinal circuitry, the similarity in depth profiles does not necessarily mean that the same neurons were involved in all cases. For example, in the photopic flash ERG response to brief stimuli, the major OPs are APB-sensitive in primates and other mammals, indicating an origin in the ON pathways, but later OPs and at light offset originate in the OFF pathway.[105,126] Such a difference could lead to differences in the depth distribution in the IPL which is stratified in outer OFF sublamina and inner ON sublamina.

Pharmacologic agents that block inner retinal activity, such as glycine and GABA, remove OPs in mammals, as does PDA,[105] but the effects were not reported to be specific for given OPs. On the other hand, genetic deletion of a major GABA receptor in the IPL, the $GABA_C$ receptor, enhances the OPs.[127]

Which Cells Generate the OPs?

The observations described above indicate that amacrine or perhaps, in some instances, retinal ganglion cells are involved in generating OPs. A study of rabbit ERG indicates a distal to

proximal progression in origin, with the late but not early OPs having input from spiking cells.[126] The role of ganglion cells in the generation of OPs has been controversial, with inconsistent reports on the effects of ganglion cell loss on OPs. In Ogden's studies in primates, optic nerve section resulted in ganglion cell degeneration and disappearance of the OPs, and antidromic stimulation of the optic nerve reduced OP amplitudes.[125] Further, in the primate photopic ERG elicited using a multifocal paradigm with a slow sequence to allow formation of OPs, both TTX and experimental glaucoma removed or reduced a high-frequency band of OPs, while affecting a lower-frequency band less.[105,106] It is possible in primates that high-frequency OPs (centered around 150 Hz, compared to >100 Hz for the lower-frequency band) under fully photopic conditions reflect activity in ganglion cell axons, and the manifestation of an optic nerve head component of the ERG. Under conditions where rod signals are also involved, the ganglion cell contribution may be less prominent. In other mammals, TTX-sensitive OPs may be among the late ones.

What Mechanisms Are Involved in Generating OPs?

Neuronal Interaction: Iinhibitory Feedback Circuits.

Two mechanisms are commonly proposed for generating OPs: neuronal interactions/feedback circuits, and the intrinsic membrane properties of cells, both of which implicate amacrine cells. The case for an inhibitory feedback mechanism is supported by involvement of receptors for GABA and glycine, which are prominent in feedback circuits in the inner retina. Gap junctions between inner retinal neurons can also be involved in feedforward mechanism.

OPs in Intracellular Responses From Neurons.

In retinal intracellular recordings from many different species, high-frequency oscillations have rarely been observed in responses of photoreceptors, horizontal, or bipolar cells. In contrast, membrane oscillations have been observed in recordings from amacrine cells, especially in turtle and fish retina. For example, GABAergic wide-field ACs isolated from white bass retina generated oscillatory membrane potentials in response to extrinsic

depolarization, as illustrated in Fig. 9.25, that reached more than 100 Hz for strong depolarization. Analysis of the mechanism of generation of the oscillatory membrane potentials in these isolated cells indicated that they arose from "a complex interplay between voltage-dependent Ca^{2+} currents and voltage- and Ca^{2+}-dependent K^+ currents."[128]

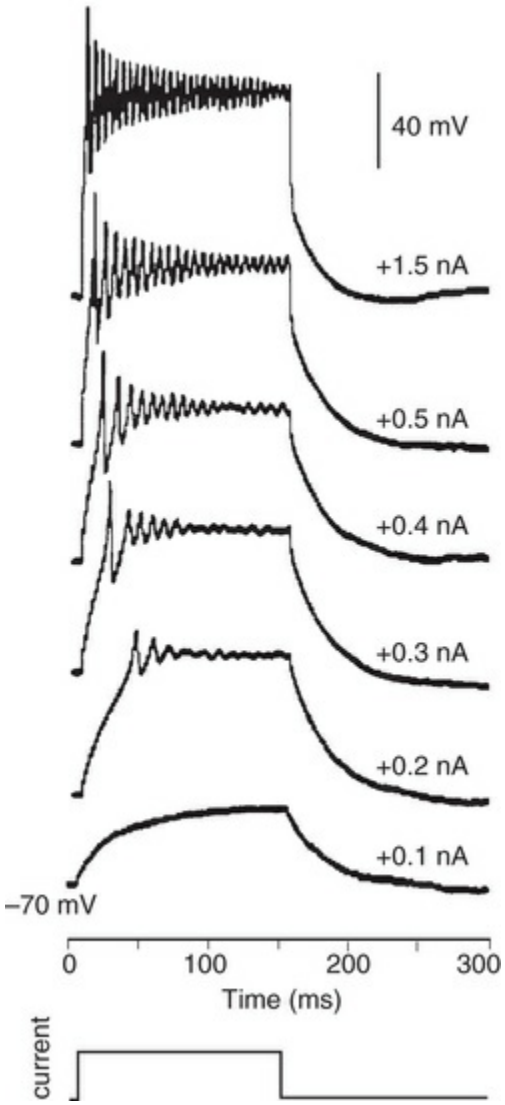

FIG. 9.25 Oscillatory potentials of isolated wide-field amacrine cells in the white perch retina. Oscillatory membrane potentials (OMPs) were elicited by depolarizing current steps of increasing amplitude obtained in whole-cell recordings from isolated amacrine cells that were maintained in culture. The duration and frequency of the OMPs increased with depolarization. Voltage traces are shifted vertically for

visibility. Bottom: application of depolarizing pulse. The magnitude of depolarizing current is indicated with each trace. Holding potential was –70 mV. (Reproduced with permission from Vigh J, Solessio E, Morgans CW, et al. Ionic mechanisms mediating oscillatory membrane potentials in wide-field retinal amacrine cells. J Neurophysiol 2003;90:431–43.)

In summary, there is consensus that high-frequency OPs originate from the inner retina. The exact cellular origins may depend upon species and stimulus conditions. The mechanisms by which they are generated are unresolved, with evidence for both involvement of feedback circuitry, and for intrinsic membrane mechanisms in amacrine cells.

Closing Remarks

This chapter has reviewed the increasingly specific information about the electrogenesis of the ERG that has become available as our understanding of retinal microcircuitry and cellular and synaptic mechanisms has increased. Due to the extensive research on ERG, it has become feasible to use it to assess retinal function at every level, from the RPE to the optic nerve head; also see other recent reviews on this subject.[3,129–131] Tables 9.1 and 9.2 summarize our current understanding of the origins of ERGs recorded in standard and specialized tests. Continued refinement of stimuli, protocols, and analysis will further enhance the power of this noninvasive tool in the laboratory and the clinic.

TABLE 9.1

Retinal Cells Contributing to the Flash and Flicker Electroretinogram in Standard Clinical Testing

a-wave	Photoreceptors Dark-adapted a-wave: rods Light-adapted: cones Late postreceptoral contributions from OFF cone (hyperpolarizing) bipolar cells (HCB) and more proximal cells in the OFF pathway
b-wave	Bipolar cells Dark-adapted b-wave, rod bipolar cells (RBC) Light-adapted b-wave, ON cone (depolarizing bipolar cells: DCB), OFF cone bipolar cells, and horizontal (Hz) cell feedback via the cones
d-wave	Bipolar cells Mainly a light-adapted response: OFF cone bipolar cells, offset of cone

	photoreceptors, and offset of ON cone bipolar cells The d-wave is not present in mice and rats
Oscillatory potentials (OPs)	Amacrine and ganglion cells, bipolar cell terminals?
"30 Hz" fast flicker	Bipolar cells ON and OFF cone bipolar cells, and a small cone photoreceptor contribution

TABLE 9.2

Retinal Cells Contributing to the Electroretinogram (ERG) in Specialized Testing

Scotopic Threshold Response	Inner Retinal Neurons
pSTR	Amacrine cells (monkey) Retinal ganglion cells (rodents)
nSTR	Retinal ganglion cells (monkey) Partially retinal ganglion cells (rats, human?) Amacrine cells (AII) (mice) Partially amacrine cells (rats, human) Glial currents
Photopic negative response (PhNR)	Retinal ganglion cells (human, monkey) Amacrine cells and perhaps ganglion cells (rodents) Glial currents
Pattern ERG (PERG)	Retinal ganglion cells (human, monkey, rodent) Glial currents (transient PERG: N95, N2?)
Multifocal ERG	Initial negative and positive waves have similar origins to a- and b-waves in photopic ERG (monkey, and presumably human)

References

1. Frishman LJ. Origins of the ERG. Heckenlively J, Arden GB. *Principles and practice of clinical electrophysiology of vision*. 2nd ed. MIT Press: Cambridge, MA; 2006:139–183.
2. Frishman LJ. Electrogenesis of the ERG. Ryan SJ. *Retina*. 4th ed. Elsevier/Mosby: St. Louis, MO; 2005:103–135.
3. Frishman LJ, Wang MH. Electroretinogram of human, monkey and mouse. Kaufman PL, Alm A. *Adler's physiology of the eye*. 11th ed. Elsevier: Edinburgh; 2011:480–501.
4. Dawson WW, Trick GL, Litzkow CA. Improved electrode for electroretinography. *Invest Ophthalmol Vis Sci*. 1979;18:988–991.
5. Hawlina M, Konec B. New noncorneal HK-loop electrode for clinical electroretinography. *Doc Ophthalmol*.

1992;81:253–259.
6. Evers HU, Gouras P. Three cone mechanisms in the primate electroretinogram: two with, one without off-center bipolar responses. *Vision Res*. 1986;26:245–254.
7. Rangaswamy NV, Shirato S, Kaneko M, et al. Effects of spectral characteristics of Ganzfeld stimuli on the photopic negative response (PhNR) of the ERG. *Invest Ophthalmol Vis Sci*. 2007;48:4818–4828.
8. Newman EA. Membrane physiology of retinal glial (Müller) cells. *J Neurosci*. 1985;5:2225–2239.
9. Connors NC, Kofuji P. Potassium channel Kir4.1 macromolecular complex in retinal glial cells. *Glia*. 2006;53:124–131.
10. Newman EA, Frambach DA, Odette LL. Control of extracellular potassium levels by retinal glial cell K^+ siphoning. *Science*. 1984;225:1174–1175.
11. Newman E, Reichenbach A. The Müller cell: a functional element of the retina. *Trends Neurosci*. 1996;19:307–312.
12. Kofuji P, Biedermann B, Siddharthan V, et al. Kir potassium channel subunit expression in retinal glial cells: implications for spatial potassium buffering. *Glia*. 2002;39:292–303.
13. Brown KT, Wiesel TN. Localization of origins of electroretinogram components by intraretinal recording in the intact cat eye. *J Physiol*. 1961;158:257–280.
14. Ogden TE, Ito H. Avian retina. II. An evaluation of retinal electrical anisotropy. *J Neurophysiol*. 1971;34:367–373.
15. Karwoski CJ, Frambach DA, Proenza LM. Laminar profile of resistivity in frog retina. *J Neurophysiol*. 1985;54:1607–1619.
16. Brown KT. The electroretinogram: its components and their origins. *Vision Res*. 1968;8:633–677.
17. Freeman JA, Nicholson C. Experimental optimization of current source-density technique for anuran cerebellum. *J Neurophysiol*. 1975;38:369–382.
18. Heynen H, van Norren D. Origin of the electroretinogram in the intact macaque eye–II. Current source-density analysis. *Vision Res*. 1985;25:709–715.
19. Xu X, Karwoski CJ. Current source density (CSD) analysis of

retinal field potentials. I. Methodological considerations and depth profiles. *J Neurophysiol*. 1994;72:84–95.
20. Dick E, Miller RF. Extracellular K^+ activity changes related to electroretinogram components. I. Amphibian (I-type) retinas. *J Gen Physiol*. 1985;85:885–909.
21. Dick E, Miller RF, Bloomfield S. Extracellular K^+ activity changes related to electroretinogram components. II. Rabbit (E-type) retinas. *J Gen Physiol*. 1985;85:911–931.
22. Frishman LJ, Steinberg RH. Light-evoked increases in $[K^+]o$ in proximal portion of the dark-adapted cat retina. *J Neurophysiol*. 1989;61:1233–1243.
23. Frishman LJ, Yamamoto F, Bogucka J, et al. Light-evoked changes in $[K^+]o$ in proximal portion of light-adapted cat retina. *J Neurophysiol*. 1992;67:1201–1212.
24. Oakley B 2nd, Green DG. Correlation of light-induced changes in retinal extracellular potassium concentration with c-wave of the electroretinogram. *J Neurophysiol*. 1976;39:1117–1133.
25. Karwoski CJ, Lu HK, Newman EA. Spatial buffering of light-evoked potassium increases by retinal Müller (glial) cells. *Science*. 1989;244:578–580.
26. Halgrimson CG, Wilson CB, Dixon FJ, et al. Goodpasture's syndrome: treatment with nephrectomy and renal transplantation. *Arch Surg*. 1971;103:283–289.
27. Newman EA. Potassium conductance block by barium in amphibian Müller cells. *Brain Res*. 1989;498:308–314.
28. Kofuji P, Ceelen P, Zahs KR, et al. Genetic inactivation of an inwardly rectifying potassium channel (Kir4.1 subunit) in mice: phenotypic impact in retina. *J Neurosci*. 2000;20:5733–5740.
29. Penn RD, Hagins WA. Signal transmission along retinal rods and the origin of the electroretinographic a-wave. *Nature*. 1969;223:201–204.
30. Robson JG, Frishman LJ. Response linearity and kinetics of the cat retina: the bipolar cell component of the dark-adapted electroretinogram. *Vis Neurosci*. 1995;12:837–850.
31. Robson JG, Maeda H, Saszik SM, et al. In vivo studies of signaling in rod pathways of the mouse using the

electroretinogram. *Vision Res*. 2004;44:3253–3268.
32. Granit R. The components of the retinal action potential in mammals and their relation to the discharge in the optic nerve. *J Physiol*. 1933;77:207–239.
33. Bush RA, Sieving PA. A proximal retinal component in the primate photopic ERG a-wave. *Invest Ophthalmol Vis Sci*. 1994;35:635–645.
34. Robson JG, Saszik SM, Ahmed J, et al. Rod and cone contributions to the a-wave of the electroretinogram of the macaque. *J Physiol*. 2003;547:509–530.
35. Sieving PA, Murayama K, Naarendorp F. Push–pull model of the primate photopic electroretinogram: a role for hyperpolarizing neurons in shaping the b-wave. *Vis Neurosci*. 1994;11:519–532.
36. Breton ME, Schueller AW, Lamb TD, et al. Analysis of ERG a-wave amplification and kinetics in terms of the G-protein cascade of phototransduction. *Invest Ophthalmol Vis Sci*. 1994;35:295–309.
37. Hood DC, Birch DG. A quantitative measure of the electrical activity of human rod photoreceptors using electroretinography. *Vis Neurosci*. 1990;5:379–387.
38. Hood DC, Birch DG. The A-wave of the human electroretinogram and rod receptor function. *Invest Ophthalmol Vis Sci*. 1990;31:2070–2081.
39. Robson JG, Frishman LJ. The rod-driven a-wave of the dark-adapted mammalian electroretinogram. *Prog Retin Eye Res*. 2014;39C:1–22.
40. Frishman LJ, Reddy MG, Robson JG. Effects of background light on the human dark-adapted electroretinogram and psychophysical threshold. *J Opt Soc Am A Opt Image Sci Vis*. 1996;13:601–612.
41. Saszik S, Alexander A, Lawrence T, et al. APB differentially affects the cone contributions to the zebrafish ERG. *Vis Neurosci*. 2002;19:521–529.
42. McCulloch DL, Marmor MF, Brigell MG, et al. ISCEV standard for full-field clinical electroretinography (2015 update). *Doc Ophthalmol*. 2015;130:1–12.
43. Steinberg RH, Linsenmeier RA, Griff ER. Retinal pigment

epithelial cell contributions to the electroretinogram and electrooculogram. *Prog Retin Res*. 1985;4:33–66.
44. Heynen H, Wachtmeister L, van Norren D. Origin of the oscillatory potentials in the primate retina. *Vision Res*. 1985;25:1365–1373.
45. Noell W. *Studies on the electrophysiology and the metabolism of the retina. USAF SAM project no 21-2101-004*. United States Airforce: Randolph Field, TX; 1953:1–122.
46. Sillman AJ, Ito H, Tomita T. Studies on the mass receptor potential of the isolated frog retina. I. General properties of the response. *Vision Res*. 1969;9:1435–1442.
47. Valeton JM, van Norren D. Intraretinal recordings of slow electrical responses to steady illumination in monkey: isolation of receptor responses and the origin of the light peak. *Vision Res*. 1982;22:393–399.
48. Bolnick DA, Walter AE, Sillman AJ. Barium suppresses slow PIII in perfused bullfrog retina. *Vision Res*. 1979;19:1117–1119.
49. Hu KG, Marmor MF. Selective actions of barium on the c-wave and slow negative potential of the rabbit eye. *Vision Res*. 1984;24:1153–1156.
50. Witkovsky P, Dudek FE, Ripps H. Slow PIII component of the carp electroretinogram. *J Gen Physiol*. 1975;65:119–134.
51. Sillman AJ, Ito H, Tomita T. Studies on the mass receptor potential of the isolated frog retina. II. On the basis of the ionic mechanism. *Vision Res*. 1969;9:1443–1451.
52. Faber D. *Analysis of slow transretinal potentials in response to light*. [PhD thesis] University of New York: Buffalo; 1969.
53. Karwoski CJ, Proenza LM. Relationship between Müller cell responses, a local transretinal potential, and potassium flux. *J Neurophysiol*. 1977;40:244–259.
54. Frishman LJ, Steinberg RH. Intraretinal analysis of the threshold dark-adapted ERG of cat retina. *J Neurophysiol*. 1989;61:1221–1232.
55. Hanitzsch R. Intraretinal isolation of P3 subcomponents in the isolated rabbit retina after treatment with sodium aspartate. *Vision Res*. 1973;13:2093–2102.
56. Miller SS, Steinberg RH. Passive ionic properties of frog

retinal pigment epithelium. *J Membr Biol*. 1977;36:337–372.
57. Oakley B 2nd, Steinberg RH, Miller SS, et al. The in vitro frog pigment epithelial cell hyperpolarization in response to light. *Invest Ophthalmol Vis Sci*. 1977;16:771–774.
58. Gallemore RP, Steinberg RH. Light-evoked modulation of basolateral membrane Cl^- conductance in chick retinal pigment epithelium: the light peak and fast oscillation. *J Neurophysiol*. 1993;70:1669–1680.
59. Quinn RH, Quong JN, Miller SS. Adrenergic receptor activated ion transport in human fetal retinal pigment epithelium. *Invest Ophthalmol Vis Sci*. 2001;42:255–264.
60. Wu J, Marmorstein AD, Striessnig J, et al. Voltage-dependent calcium channel CaV1.3 subunits regulate the light peak of the electroretinogram. *J Neurophysiol*. 2007;97:3731–3735.
61. Gallemore RP, Hughes BA, Miller SS. *Light-induced responses of the retinal pigment epithelium*. Oxford University Press: New York; 1998.
62. Dawis SM, Niemeyer G. Dopamine influences the light peak in the perfused mammalian eye. *Invest Ophthalmol Vis Sci*. 1986;27:330–335.
63. Sieving PA, Frishman LJ, Steinberg RH. Scotopic threshold response of proximal retina in cat. *J Neurophysiol*. 1986;56:1049–1061.
64. Wakabayashi K, Gieser J, Sieving PA. Aspartate separation of the scotopic threshold response (STR) from the photoreceptor a-wave of the cat and monkey ERG. *Invest Ophthalmol Vis Sci*. 1988;29:1615–1622.
65. Brown KT, Wiesel TN. Analysis of the intraretinal electroretinogram in the intact cat eye. *J Physiol*. 1961;158:229–256.
66. Brown KT, Watanabe K, Murakami M. The early and late receptor potentials of monkey cones and rods. *Cold Spring Harb Symp Quant Biol*. 1965;30:457–482.
67. Penn RD, Hagins WA. Kinetics of the photocurrent of retinal rods. *Biophys J*. 1972;12:1073–1094.
68. Pugh EN Jr, Falsini B, Lyubarsky A. The origin of the major rod- and cone-driven components of the rodent

electroretinogram and the effects of age and light-rearing history on the magnitude of these components. *Photostasis and related phenomena*. Plenum Press: New York; 1998:93–128.
69. Baylor DA, Nunn BJ, Schnapf JL. The photocurrent, noise and spectral sensitivity of rods of the monkey *Macaca fascicularis*. *J Physiol*. 1984;357:575–607.
70. Lamb TD, Pugh EN Jr. A quantitative account of the activation steps involved in phototransduction in amphibian photoreceptors. *J Physiol*. 1992;449:719–758.
71. Hood DC, Birch DG. Light adaptation of human rod receptors: the leading edge of the human a-wave and models of rod receptor activity. *Vision Res*. 1993;33:1605–1618.
72. Hood DC, Birch DG. Human cone receptor activity: the leading edge of the a-wave and models of receptor activity. *Vis Neurosci*. 1993;10:857–871.
73. Yonemura D, Kawasaki K, Shibata N. The electroretinographic PIII component of the human excised retina. *Jpn J Ophthalmol*. 1974;18:322–333.
74. Slaughter MM, Miller RF. An excitatory amino acid antagonist blocks cone input to sign-conserving second-order retinal neurons. *Science*. 1983;219:1230–1232.
75. Friedburg C, Allen CP, Mason PJ, et al. Contribution of cone photoreceptors and post-receptoral mechanisms to the human photopic electroretinogram. *J Physiol*. 2004;556:819–834.
76. Jamison JA, Bush RA, Lei B, et al. Characterization of the rod photoresponse isolated from the dark-adapted primate ERG. *Vis Neurosci*. 2001;18:445–455.
77. Robson JG, Frishman LJ. Dissecting the dark-adapted electroretinogram. *Doc Ophthalmol*. 1998;95:187–215.
78. Pepperberg DR, Birch DG, Hood DC. Photoresponses of human rods in vivo derived from paired-flash electroretinograms. *Vis Neurosci*. 1997;14:73–82.
79. Stockton RA, Slaughter MM. B-wave of the electroretinogram. A reflection of ON bipolar cell activity. *J Gen Physiol*. 1989;93:101–122.

80. Knapp AG, Schiller PH. The contribution of on-bipolar cells to the electroretinogram of rabbits and monkeys: a study using 2-amino-4-phosphonobutyrate (APB). *Vision Res*. 1984;24:1841–1846.
81. Bech-Hansen NT, Naylor MJ, Maybaum TA, et al. Mutations in NYX, encoding the leucine-rich proteoglycan nyctalopin, cause X-linked complete congenital stationary night blindness. *Nat Genet*. 2000;26:319–323.
82. McCall MA, Gregg RG. Comparisons of structural and functional abnormalities in mouse b-wave mutants. *J Physiol*. 2008;586:4385–4392.
83. Newman EA, Odette LL. Model of electroretinogram b-wave generation: a test of the K^+ hypothesis. *J Neurophysiol*. 1984;51:164–182.
84. Miller RF, Dowling JE. Intracellular responses of the Müller (glial) cells of mudpuppy retina: their relation to b-wave of the electroretinogram. *J Neurophysiol*. 1970;33:323–341.
85. Kline RP, Ripps H, Dowling JE. Light-induced potassium fluxes in the skate retina. *Neuroscience*. 1985;14:225–235.
86. Wen R, Oakley B 2nd. K(+)-evoked Müller cell depolarization generates b-wave of electroretinogram in toad retina. *Proc Natl Acad Sci USA*. 1990;87:2117–2121.
87. Karwoski CJ, Proenza LM. Neurons, potassium, and glia in proximal retina of *Necturus*. *J Gen Physiol*. 1980;75:141–162.
88. Xu X, Karwoski CJ. Current source density analysis of retinal field potentials. II. Pharmacological analysis of the b-wave and M-wave. *J Neurophysiol*. 1994;72:96–105.
89. Karwoski CJ, Xu X. Current source-density analysis of light-evoked field potentials in rabbit retina. *Vis Neurosci*. 1999;16:369–377.
90. Saszik SM, Robson JG, Frishman LJ. The scotopic threshold response of the dark-adapted electroretinogram of the mouse. *J Physiol*. 2002;543:899–916.
91. Cameron AM, Mahroo OA, Lamb TD. Dark adaptation of human rod bipolar cells measured from the b-wave of the scotopic electroretinogram. *J Physiol*. 2006;575:507–526.
92. Sieving PA, Frishman LJ, Steinberg RH. M-wave of proximal retina in cat. *J Neurophysiol*. 1986;56:1039–1048.

93. Sieving PA, Nino C. Scotopic threshold response (STR) of the human electroretinogram. *Invest Ophthalmol Vis Sci*. 1988;29:1608–1614.
94. Ueno S, Kondo M, Ueno M, et al. Contribution of retinal neurons to d-wave of primate photopic electroretinograms. *Vision Res*. 2006;46:658–664.
95. Rangaswamy NV, Frishman LJ, Dorotheo EU, et al. Photopic ERGs in patients with optic neuropathies: comparison with primate ERGs after pharmacologic blockade of inner retina. *Invest Ophthalmol Vis Sci*. 2004;45:3827–3837.
96. Peachey NS, Alexander KR, Fishman GA, et al. Properties of the human cone system electroretinogram during light adaptation. *Appl Opt*. 1989;28:1145–1150.
97. Wali N, Leguire LE. The photopic hill: a new phenomenon of the light adapted electroretinogram. *Doc Ophthalmol*. 1992;80:335–345.
98. Hamilton R, Bees MA, Chaplin CA, et al. The luminance-response function of the human photopic electroretinogram: a mathematical model. *Vision Res*. 2007;47:2968–2972.
99. Ueno S, Kondo M, Niwa Y, et al. Luminance dependence of neural components that underlies the primate photopic electroretinogram. *Invest Ophthalmol Vis Sci*. 2004;45:1033–1040.
100. Bush RA, Sieving PA. Inner retinal contributions to the primate photopic fast flicker electroretinogram. *J Opt Soc Am A Opt Image Sci Vis*. 1996;13:557–565.
101. Kondo M, Sieving PA. Primate photopic sine-wave flicker ERG: vector modeling analysis of component origins using glutamate analogs. *Invest Ophthalmol Vis Sci*. 2001;42:305–312.
102. Viswanathan S, Frishman LJ, Robson JG. Inner-retinal contributions to the photopic sinusoidal flicker electroretinogram of macaques. Macaque photopic sinusoidal flicker ERG. *Doc Ophthalmol*. 2002;105:223–242.
103. Sutter EE, Tran D. The field topography of ERG components in man–I. The photopic luminance response. *Vision Res*. 1992;32:433–446.

104. Hood DC, Frishman LJ, Saszik S, et al. Retinal origins of the primate multifocal ERG: implications for the human response. *Invest Ophthalmol Vis Sci*. 2002;43:1673–1685.
105. Rangaswamy NV, Hood DC, Frishman LJ. Regional variations in local contributions to the primate photopic flash ERG: revealed using the slow-sequence mfERG. *Invest Ophthalmol Vis Sci*. 2003;44:3233–3247.
106. Rangaswamy NV, Zhou W, Harwerth RS, et al. Effect of experimental glaucoma in primates on oscillatory potentials of the slow-sequence mfERG. *Invest Ophthalmol Vis Sci*. 2006;47:753–767.
107. Sutter EE, Bearse MA Jr. The optic nerve head component of the human ERG. *Vision Res*. 1999;39:419–436.
108. Burkhardt DA. Proximal negative response of frog retina. *J Neurophysiol*. 1970;33:405–420.
109. Frishman LJ, Steinberg RH. Origin of negative potentials in the light-adapted ERG of cat retina. *J Neurophysiol*. 1990;63:1333–1346.
110. Ogden TE. The proximal negative response of the primate retina. *Vision Res*. 1973;13:797–807.
111. Sieving PA, Steinberg RH. Proximal retinal contribution to the intraretinal 8-Hz pattern ERG of cat. *J Neurophysiol*. 1987;57:104–120.
112. Frishman LJ, Shen FF, Du L, et al. The scotopic electroretinogram of macaque after retinal ganglion cell loss from experimental glaucoma. *Invest Ophthalmol Vis Sci*. 1996;37:125–141.
113. Viswanathan S, Frishman LJ, Robson JG, et al. The photopic negative response of the macaque electroretinogram: reduction by experimental glaucoma. *Invest Ophthalmol Vis Sci*. 1999;40:1124–1136.
114. Viswanathan S, Frishman LJ, Robson JG, et al. The photopic negative response of the flash electroretinogram in primary open angle glaucoma. *Invest Ophthalmol Vis Sci*. 2001;42:514–522.
115. Kondo M, Kurimoto Y, Sakai T, et al. Recording focal macular photopic negative response (PhNR) from monkeys. *Invest Ophthalmol Vis Sci*. 2008;49:3544–3550.

116. Bach M, Hoffmann MB. Update on the pattern electroretinogram in glaucoma. *Optom Vis Sci*. 2008;85:386–395.
117. Holder GE. Pattern electroretinography (PERG) and an integrated approach to visual pathway diagnosis. *Prog Retin Eye Res*. 2001;20:531–561.
118. Maffei L, Fiorentini A, Bisti S, et al. Pattern ERG in the monkey after section of the optic nerve. *Exp Brain Res*. 1985;59:423–425.
119. Viswanathan S, Frishman LJ, Robson JG. The uniform field and pattern ERG in macaques with experimental glaucoma: removal of spiking activity. *Invest Ophthalmol Vis Sci*. 2000;41:2797–2810.
120. Luo X, Frishman LJ. Retinal pathway origins of the pattern electroretinogram (PERG). *Invest Ophthalmol Vis Sci*. 2011;52:8571–8584.
121. Naarendorp F, Sieving PA. The scotopic threshold response of the cat ERG is suppressed selectively by GABA and glycine. *Vision Res*. 1991;31:1–15.
122. Sieving PA. Retinal ganglion cell loss does not abolish the scotopic threshold response (STR) of the cat and human ERG. *Clin Vis Sci*. 1991;2:149–158.
123. Peachey NS, Alexander KR, Fishman GA. Rod and cone system contributions to oscillatory potentials: an explanation for the conditioning flash effect. *Vision Res*. 1987;27:859–866.
124. Wachtmeister L. Oscillatory potentials in the retina: what do they reveal. *Prog Retin Eye Res*. 1998;17:485–521.
125. Ogden TE. The oscillatory waves of the primate electroretinogram. *Vision Res*. 1973;13:1059–1074.
126. Dong CJ, Agey P, Hare WA. Origins of the electroretinogram oscillatory potentials in the rabbit retina. *Vis Neurosci*. 2004;21:533–543.
127. McCall MA, Lukasiewicz PD, Gregg RG, et al. Elimination of the rho1 subunit abolishes GABA(C) receptor expression and alters visual processing in the mouse retina. *J Neurosci*. 2002;22:4163–4174.
128. Vigh J, Solessio E, Morgans CW, et al. Ionic mechanisms

mediating oscillatory membrane potentials in wide-field retinal amacrine cells. *J Neurophysiol*. 2003;90:431–443.
129. Heckenlively J, Arden GB. *Principles and practice of clinical electrophysiology of vision*. 2nd ed. MIT Press: Cambridge, MA; 2006.
130. Fishman GA, Birch DG, Holder GE, et al. *Electrophysiological testing in disorders of the retina, optic nerve, and visual pathways*. 2nd ed. American Academy of Ophthalmology: Singapore; 2001.
131. Lam BL. *Electrophysiology of vision; clinical testing and applications*. Taylor and Francis Group: Boca Raton, FL; 2005.

10

Clinical Electrophysiology

Yozo Miyake, Kei Shinoda

In this chapter we describe the method and value of various clinical electrophysiologic tests and how they play a role in the diagnosis, analysis of pathogenesis, prognostic evaluation, and understanding of the underlying genetics of retinal disorders, using several examples of clinical cases. We also demonstrate the role of the focal macular electroretinogram (ERG) and multifocal ERG (mfERG) for particular diseases where the affected region is limited to a certain area of the retina. During the recent history of clinical electrophysiology, several new clinical entities have been defined by analyzing electrophysiologic results. These new entities will also be discussed in this chapter.

Standard Full-Field ERG

Stimulus and Recording Devices

The human ERG recorded at the cornea and elicited by a full-field stimulus is a mass response generated by cells across the entire retina. To obtain reproducible amplitudes and implicit times in the response, the stimulus and background light should be homogeneous and cover the entire retina, so all of the receptors are stimulated or adapted in a relatively homogeneous manner. The full-field, or Ganzfeld, stimulator represents such a stimulus. It consists of a large-diameter (40-cm) hemispheric dome (see Chapter 9, Electrogenesis of the electroretinogram) with a xenon stroboscopic light bulb placed at the top of the dome. This stimulus system has been recommended by the International Society of Clinical Electrophysiology for Vision (ISCEV) Standards Committee[1] for use when obtaining clinical ERG recordings internationally.

The ERG is recorded using corneal electrodes, usually referred to surface reference electrodes at the ipsilateral outer canthi or zygomatic fossae. Electrodes in common use[2] include the Burian–Allen and the ERG jet, both of which are contact lens electrodes, the gold foil, Dawson–Trick–Litzkow (DTL), and H–K loop electrodes, which are noncontact approaches. The representative electrodes are shown in Fig. 10.1.

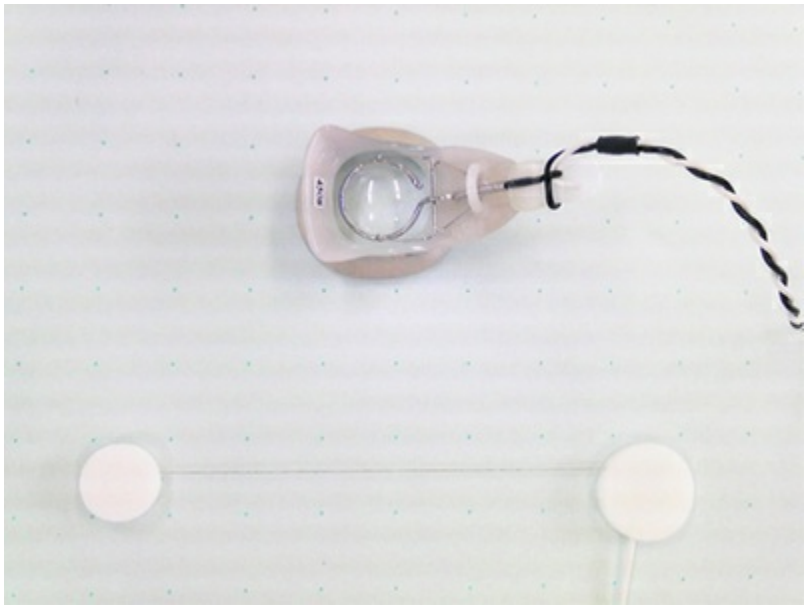

FIG. 10.1 Representative electroretinogram recording

electrodes. (Top) Burian–Allen electrode. A contact lens-type electrode with a lid speculum to minimize the effect of blinking and eyelid closure. (Bottom) Dawson–Trick–Litzkow (DTL) electrode – a conductive Mylar thread usually placed in the lower fornix, it contacts the inferior bulbar conjunctiva or the corneal limbus. Dots show 10-mm distance.

Stimulus Intensity Versus ERG Responses and Components

Scotopic Condition

Fig. 10.2 shows the full-field ERGs elicited by increasing stimulus intensities from a normal subject after 1 hour of dark adaptation. The ERGs elicited by relatively weak stimulus intensities are shown at the left and those by stronger stimulus are shown at the right. The calibrations for the amplitude and time are different for the weak- and strong-stimulus ERGs. The maximum stimulus luminance (0 log unit) is 44.2 cd m^{-2} s^{-1}.

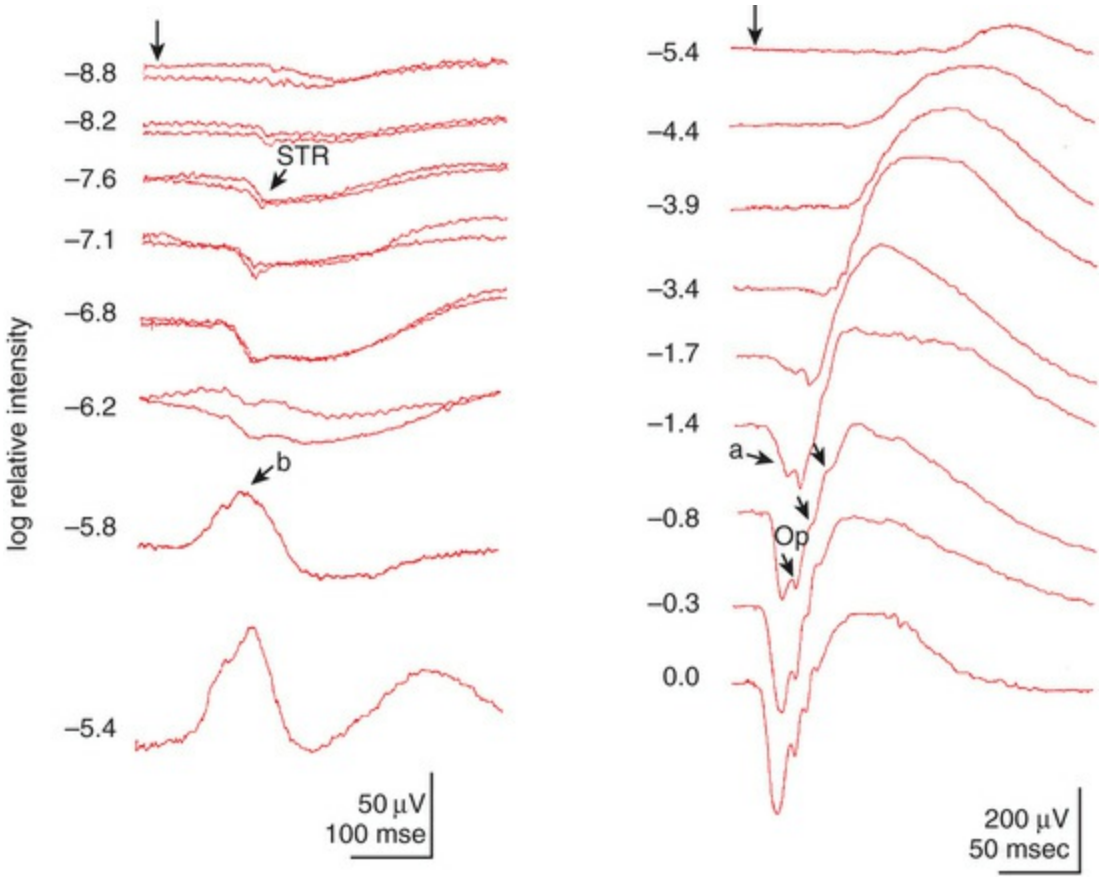

FIG. 10.2 The full-field electroretinogram (ERG) elicited by increasing stimulus intensities recorded from a normal subject after 1 hour of dark adaptation. The left column shows responses elicited by relative low intensity and the right by relative high intensity. Note that the calibration differs for the ERGs in the two columns. Arrowheads indicate the stimulus onset. *STR*, scotopic threshold response; *b*, b-wave; *a*, a-wave; *Op*, oscillatory potentials. (Reproduced with permission from Miyake Y, Horiguchi M, Terasaki H, et al. Invest Ophthalmol Vis Sci 1994;35:3770–5.)

At the left, the scotopic threshold response (STR),[3] a cornea-negative wave, is first recorded at –8.2 log units, approximately 0.6 log units higher than psychophysical threshold. The maximum amplitude of STR is approximately 20 µV before it is masked by the developing b-wave. The implicit time of the STR near threshold is approximately 160 ms, and the implicit time decreases as the stimulus intensity increases. The STR originates from retinal neurons that are postsynaptic to the photoreceptors (see Chapter 9, Electrogenesis of the electroretinogram).

The b-wave is first seen at an intensity of –5.8 log units; the amplitude increases and the implicit time shortens as the stimulus intensity increases. The amplitude of b-wave essentially saturates at –3.4 log units; and at intensities higher than –0.8 log unit, the oscillatory potentials (OPs) become clearly visible on the ascending limb of the b-wave. The a-wave is first seen at –1.7 log units and increases progressively as the stimulus intensity increases.

As described in Chapter 9 (Electrogenesis of the electroretinogram), many studies have shown that the a-wave of the full-field ERGs recorded in the dark is the leading edge of the photoreceptor potential.[4] The b-wave originates indirectly from bipolar and Müller cells in the middle layers of the retina.[5] The OPs are seen as a series of three or four rhythmic wavelets having almost equal intervals of about 6.5 ms in humans.[6] The best experimental evidence indicates that the OPs reflect the activity of feedback synaptic circuits within the retina and represent an inhibitory or modulating effect of amacrine cells on the b-wave.[7]

Photopic Condition

The photopic, short-flash ERGs elicited by increasing stimulus intensities in a normal subject are shown in Fig. 10.3.[8] At lower stimulus intensities, the amplitude of the b-wave increases with increasing stimulus until it reaches a maximum at a stimulus intensity of 3.0 log cd m^{-2}. Further increases in the stimulus intensity result in a progressive decrease in the amplitude of the b-wave. Because a plot of the b-wave amplitude as a function of the stimulus intensity has an inverted U shape, this phenomenon has been termed the photopic hill phenomenon.[9]

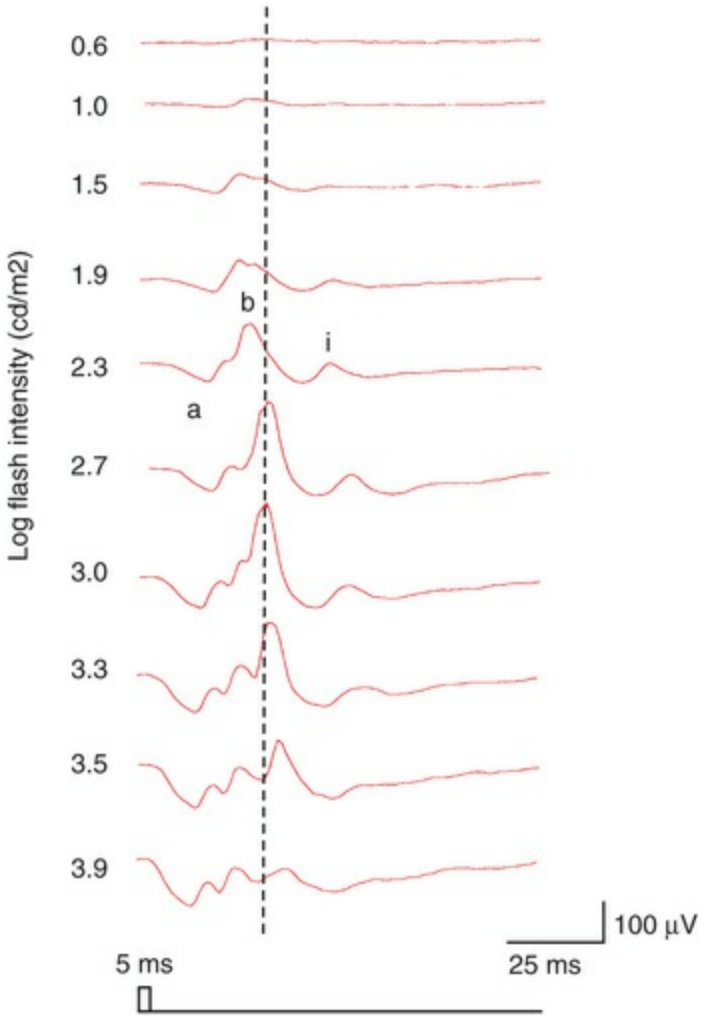

FIG. 10.3 Photopic short-flash electroretinograms elicited by various stimulus intensities from a normal subject. Stimulus duration is 5 ms and the constant background illumination is 40 cd m^{-2}. The vertical dashed line indicates 30 ms. The b-wave amplitude increases with increasing stimulus intensity until 3.0 cd m^{-2}. It decreases with further increases in stimulus intensity. When the b-wave amplitude is plotted against stimulus intensity, it shows an inverted U shape; this phenomenon has been termed the photopic hill phenomenon. (Reproduced with permission from Kondo M, Piao CH, Tanikawa A, et al. Japn J Ophthalmol 2000;44:20–8.)

Bright Flash Mixed Rod–Cone ERG

ERG recorded with a bright flash of light after dark adaptation for 30 minutes or longer (0 log unit in Fig. 10.2) shows mixed rod–cone

response, which can provide variable information about retinal pathology and is of significant diagnostic value. We have an impression that about 70% of ERG information can be obtained by the evaluation of only the mixed rod–cone ERG. The five different types of mixed rod–cone ERG are shown in Fig. 10.4.

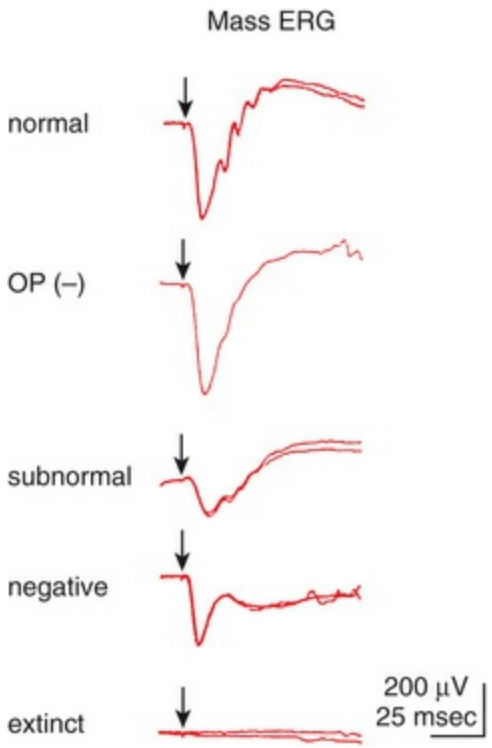

FIG. 10.4 The five different types of mixed rod–cone electroretinogram (ERG). *OP(–),* selective reduction of oscillatory potentials; *subnormal*, both a- and b-waves are attenuated approximately to the same degree; *negative*, the amplitude of the b-wave is smaller than that of the a-wave; *extinct*, no discernible a- or b-wave.

Normal

The normal type shows a-wave, b-wave, and OPs. The amplitude of b-wave is always larger than that of a-wave in the regular stimulus intensity range. The normal ERG can be seen in patients with localized macular dysfunction, optic nerve diseases, and central nervous system disease such as amblyopia. Even when the entire retina is ophthalmoscopically abnormal, such as in rubella retinopathy or in a female carrier of ocular albinism or

choroideremia (Fig. 10.5), the ERG can be essentially normal.

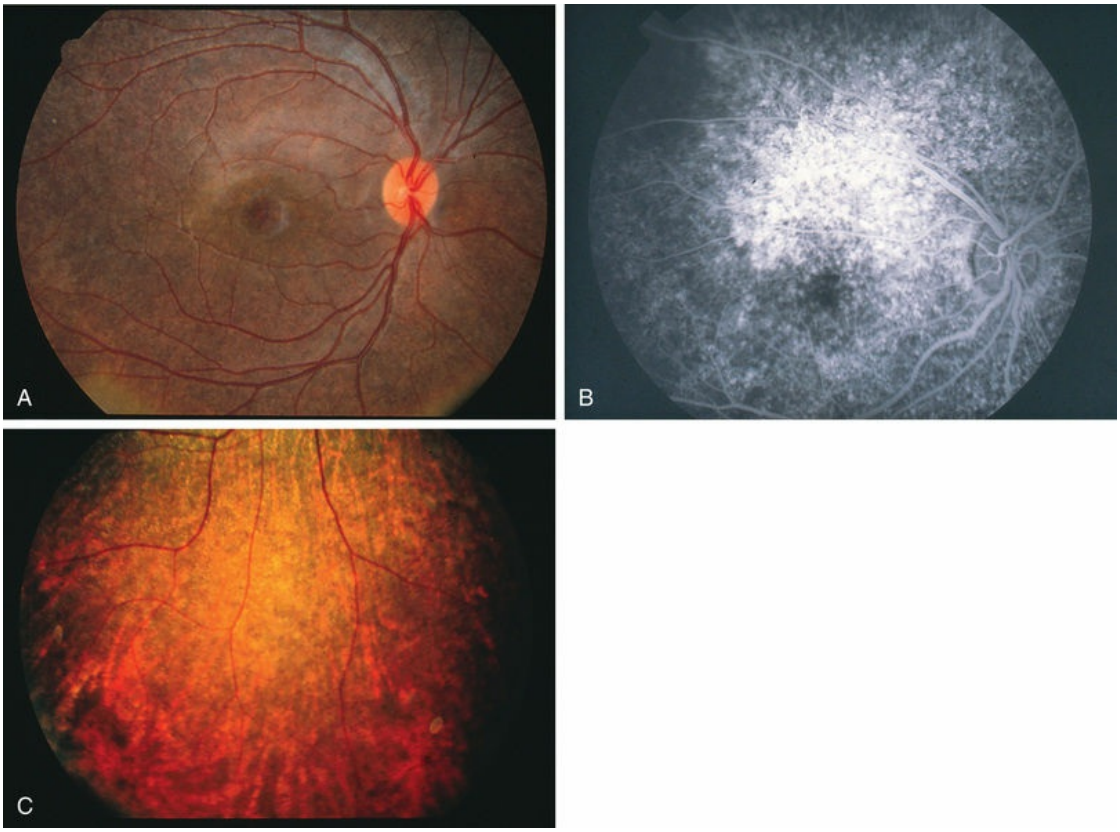

FIG. 10.5 Fundus photograph (A) and fluorescein angiogram (B) obtained from a 20-year-old man with rubella retinitis. Fundus photograph from a 60-year-old female carrier of choroideremia (C). The electroretinograms in these two patients were normal.
(Reproduced with permission from Miyake Y. Electrodiagnosis of retinal diseases. Tokyo: Springer-Verlag; 2006.)

Selectively Abnormal Oscillatory Potentials

An OP abnormality means either reduction of amplitude or delay of implicit time, or both. A selective OP abnormality is observed in the early stage of diabetic retinopathy[10,11] (Fig. 10.6) or mild circulatory disturbance of retina such as central retinal vein occlusion.

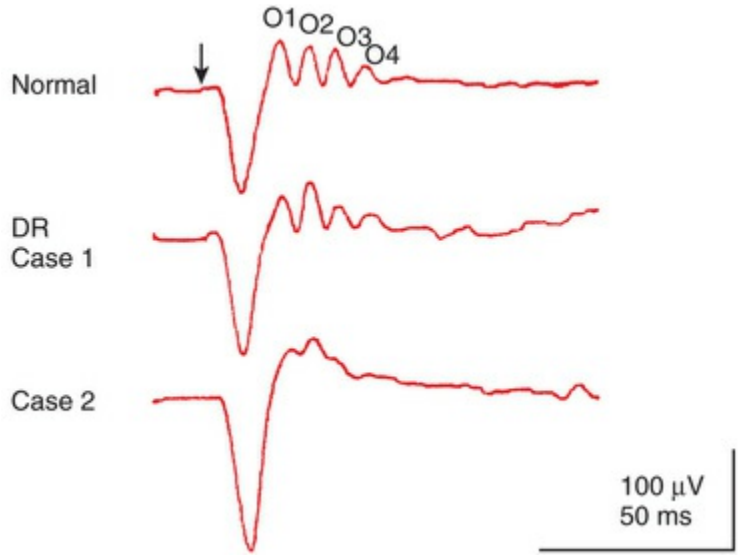

FIG. 10.6 Oscillatory potentials (OPs) of full-field electroretinograms recorded from a normal subject (top) and two patients with diabetic retinopathy (*DR*). The oscillatory potentials were found to have delayed implicit time (Case 1) or reduced amplitude (Case 2).

(Reproduced with permission from Miyake Y. Electrodiagnosis of retinal diseases. Tokyo: Springer-Verlag; 2006.)

Subnormal

The amplitudes of all components are reduced approximately to the same degree. A reduced a-wave indicates abnormal photoreceptor function. Relatively early stages of rod–cone dystrophy may show subnormal ERGa. This pattern is also seen in patients with localized damage of the photoreceptors, such as partial retinal detachment or sectoral retinal degeneration. The amplitude of the full-field ERG is proportional to the area of functioning retina. This principle is evident when the extent of retinal detachment is compared with the ERG (Fig. 10.7).

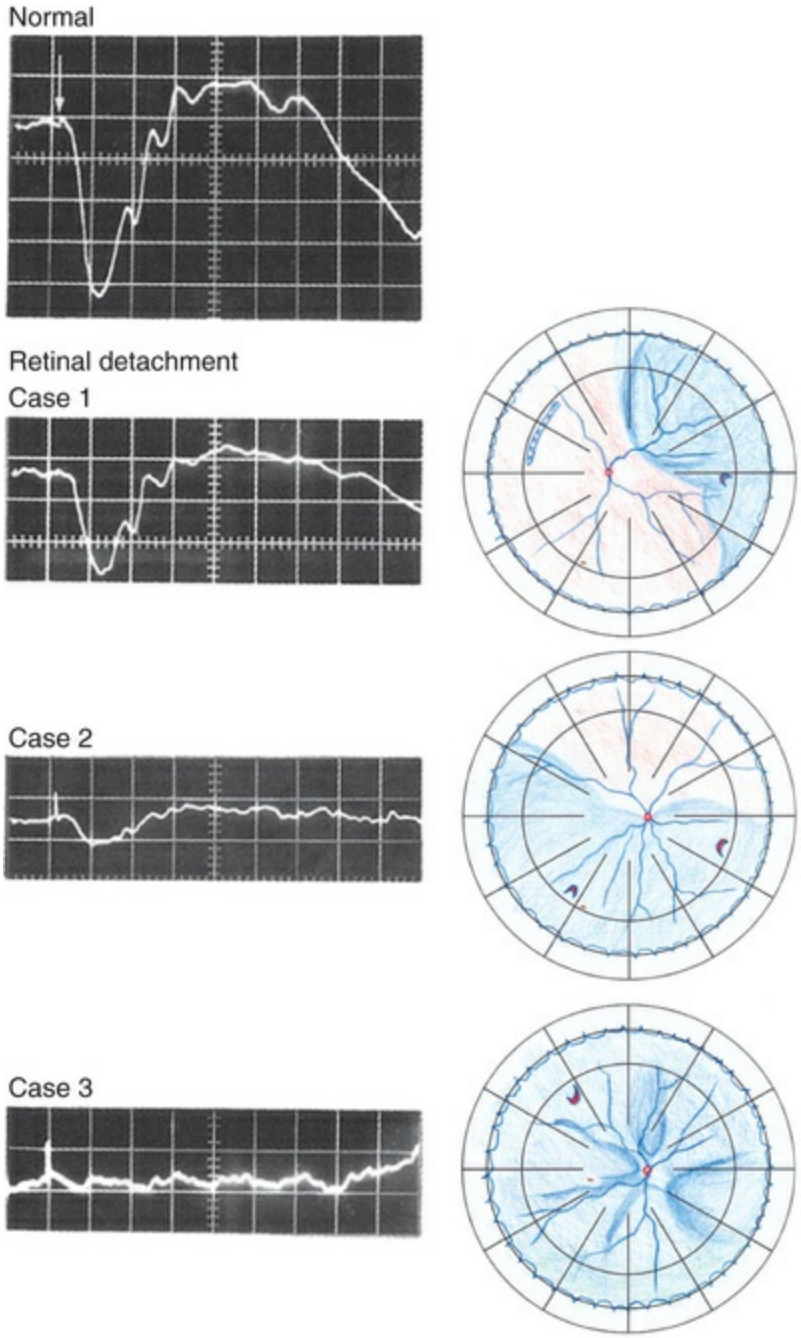

FIG. 10.7 Mixed rod–cone (bright flash) electroretinograms (left) and fundus drawings of three patients with rhegmatogenous retinal detachment (right). The reduction of the electroretinogram amplitude corresponds proportionally to the extent of retinal detachment.

This principle is also demonstrated in eyes receiving panretinal photocoagulation (PRP) for diabetic retinopathy. Following PRP, the amplitudes of ERG components are reduced by 40–45%, but the b-wave : a-wave (b/a) ratio is not changed significantly.[11] When the

media is hazy due to vitreous hemorrhage and the fundus is invisible, the presence or absence of retinal detachment is an important evaluation preoperatively. By combining ERG and ultrasonography, the differentiation between a totally detached retina and dense vitreous membranes may be possible, as shown in Fig. 10.8. When the ERG is recordable, even if the amplitude is small, the thick membrane in the vitreous cavity is not totally detached retina, but vitreous membrane.

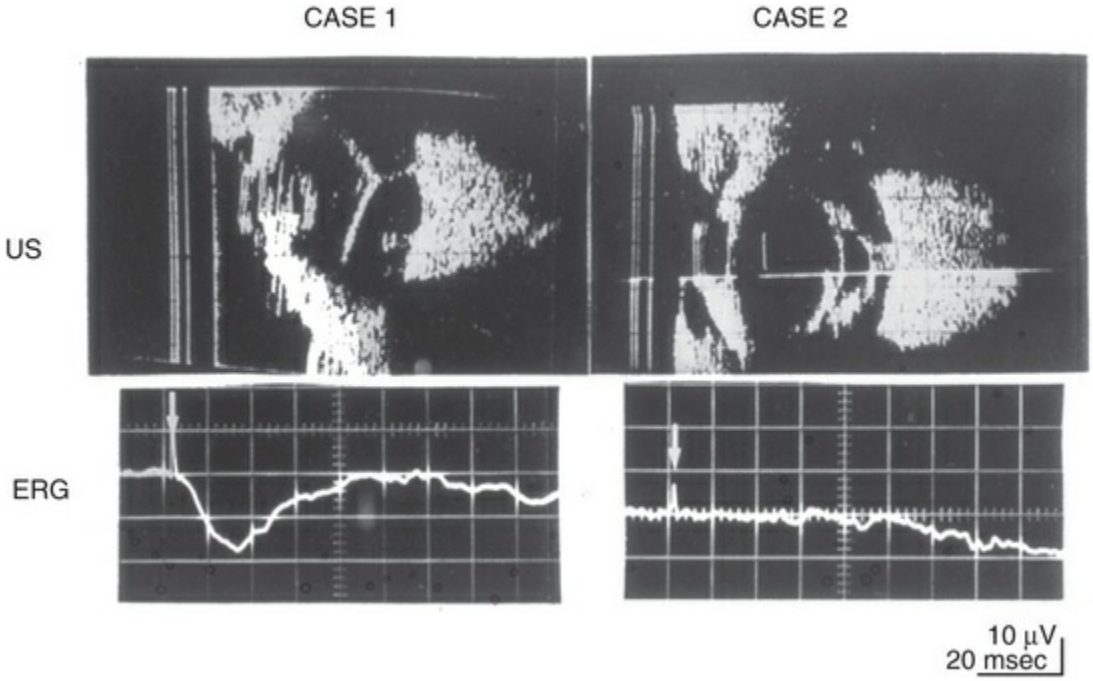

FIG. 10.8 Ultrasonographic (US) image (top) and mixed rod–cone electroretinogram (ERG) (bottom) from eyes with vitreous hemorrhage. Ultrasonography shows thick membrane-like reflex in the vitreous cavity in both eyes. When the ERG is recordable, even if the amplitude is small, the thick membrane in the vitreous cavity is not totally detached retina, but vitreous membrane (Case 1). In contrast, when the ERG is unrecordable, the thick membrane is most likely totally detached retina (Case 2).

Negative

The negative ERG indicates that the amplitude of the b-wave is smaller than that of the a-wave (b/a ratio <1.0). As mentioned

above, the amplitude of the b-wave is always larger than that of the a-wave in normal subjects. A normal a-wave with a reduced b-wave localizes the defect to postphototransduction processes. The negative ERG can be of useful prognostic or diagnostic value in retinal diseases.

Prognostic Value.

Among the acquired retinal diseases, the negative ERG may be seen in severe retinal circulatory disturbances such as central retinal arterial occlusion or proliferative diabetic retinopathy. In central retinal vein occlusion, the ischemic type shows a negative ERG more frequently than the nonischemic type, indicating that the b/a ratio can be an important index for evaluating the prognosis of central retinal vein occlusion.[12,13] Fig. 10.9 shows a patient with an initially normal, but later lower, b/a ratio which resulted in negative configuration in ERG.[11] The fluorescein angiogram evolved from a nonischemic pattern to an ischemic pattern, demonstrating an extensive area of nonperfusion.

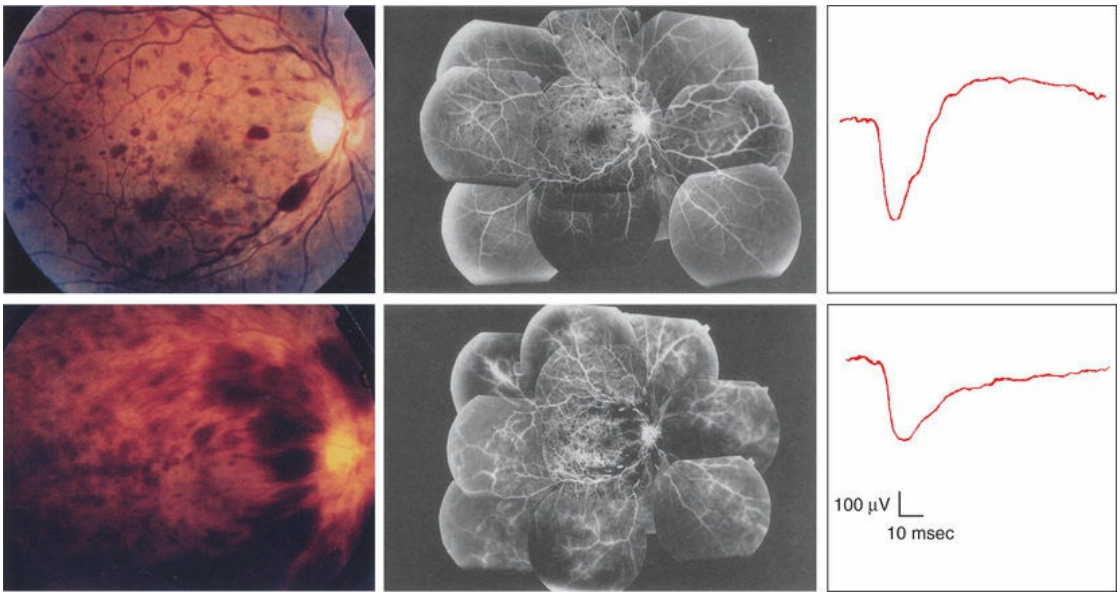

FIG. 10.9 (Top panel) A 39-year-old woman had a central retinal vein occlusion in the right eye (top left). Fluorescein angiogram (top center) and electroretinogram (ERG) (top right) showed nonischemic pattern at her initial visit. (Bottom panel) One month later, the retinal hemorrhage increased

(bottom left), the fluorescein angiogram showed extensive areas of nonperfusion (bottom center), and the waveform of the ERG became negative (right).
(Reproduced with permission from Miyake Y. Electrodiagnosis of retinal diseases. Tokyo: Springer-Verlag; 2006.)

When massive vitreous hemorrhage prevents ophthalmoscopic examination of the fundus in patients with proliferative diabetic retinopathy, it makes it difficult to predict the surgical and visual outcome after vitrectomy. In these eyes, the amplitudes of the ERGs may be markedly reduced by various factors: pathologic changes induced by the diabetic retinopathy, earlier PRP, and vitreous hemorrhage. As mentioned above, PRP reduces the ERG amplitude without changing the b/a ratio.[11] Because most diabetic patients with vitreous hemorrhage have undergone PRP, it is difficult to arrive at a prognosis of the outcome after vitrectomy using only the amplitudes. The b/a ratio provides more useful information about the visual prognosis after vitrectomy.[14] The preoperative mixed rod–cone ERGs were classified into three groups in patients with diabetic retinopathy associated with significant vitreous hemorrhage (Fig. 10.10, left). Group A indicates those with a b/a ratio>1.0 and the OPs are clearly recordable. Group B includes those with a b/a ratio >1.0 but the OPs are absent. Group C comprises those with a b/a ratio <1.0 with absent OPs. Thick proliferative tissues were found at the disc (Fig. 10.11) intraoperatively in 36% of the eyes in group A, 67% in group B, and 90% in group C.[14] It was suggested that the fibrous proliferation at the disc may restrict the retinal circulation by compressing the central retinal artery.

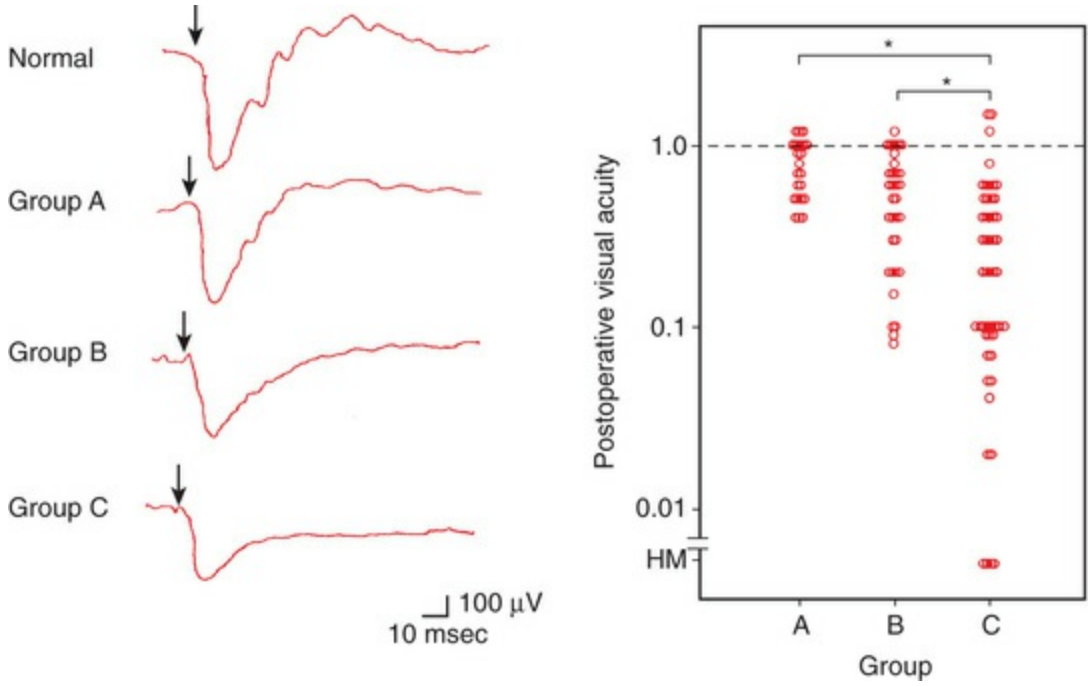

FIG. 10.10 Preoperative full-field electroretinograms (ERGs) recorded from a normal control and three diabetic patients with vitreous hemorrhage (*HM*) who were classified into three groups (left). Postoperative visual acuity in the three groups classified according to the ERG waveform (right), showing that the postoperative visual acuity for group C was significantly worse than that for group A or group B.

(Reproduced with permission from Hiraiwa T, Horio N, Terasaki H et al. Japn J Ophthalmol 2003;47:307-11.)

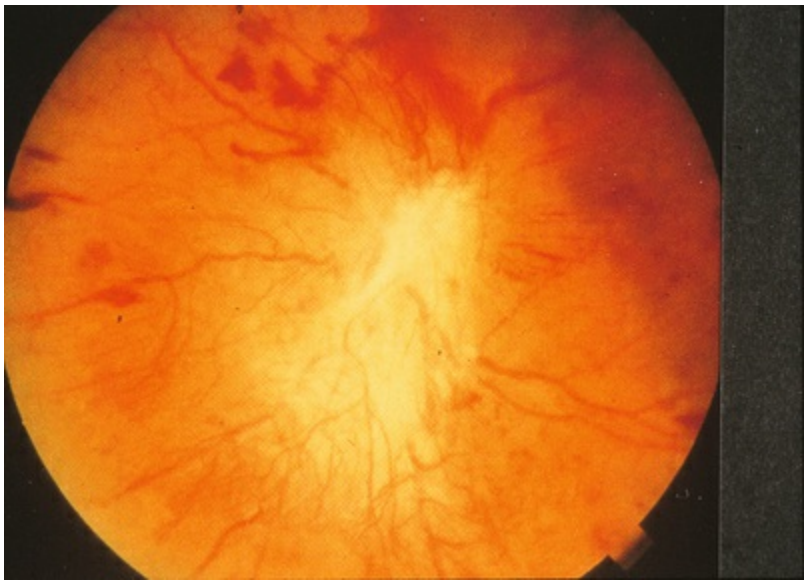

FIG. 10.11 Proliferative tissue on the optic disc in a patient with diabetic retinopathy. (Reproduced with permission from Miyake Y. Electrodiagnosis of retinal diseases. Tokyo: Springer-Verlag; 2006.)

The distribution of the postoperative visual acuity for each group is shown in Fig. 10.10 (right).[14] The postoperative visual acuity for group C was significantly worse than for group A or group B. The low b/a ratio may indicate more severe ischemic retina, which in turn may account for the relatively good correlation with visual acuity. However, among the patients in group C, there were some whose postoperative visual acuity was good, indicating that a b/a ratio <1.0 is not necessarily a contraindication for vitrectomy. Another important finding is that most patients who have distinct OPs preoperatively have favorable visual acuity after vitrectomy. This observation is important when we discuss the visual prognosis with patients before surgery. The light-filtering effect of a dense vitreous hemorrhage should also be considered when evaluating the preoperative ERG in diabetic patients. Severe vitreous hemorrhage reduces the intensity of the stimulus light reaching the retina, which can increase the b/a ratio (see Fig. 10.2). When the vitreous hemorrhage is extremely dense, the intensity of stimulus light may be decreased and the effective stimulus light to evoke ERG may not reach the retina. In such situations, we need a much brighter stimulus than the standard maximum stimulus to evoke the ERG. Such an example is shown in Fig. 10.12. In such cases, we have an impression that the ERG often has a negative configuration, as shown in this patient.

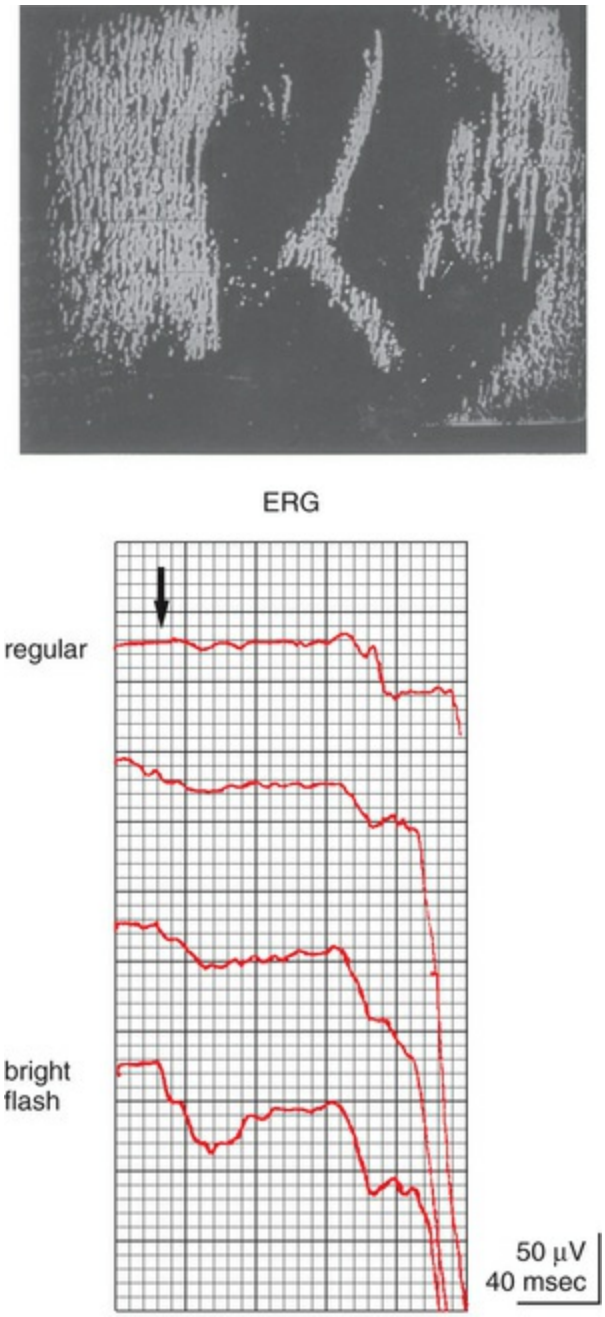

FIG. 10.12 Ultrasonographic image (top) and mixed rod–cone electroretinograms (ERGs) (bottom) with various stimulus intensities from eyes with extremely dense vitreous hemorrhage. As the intensity of the stimulus light is decreased, a sufficiently bright stimulus to evoke the ERG may not reach the retina. In this situation, a much brighter stimulus than the regular maximum stimulus may evoke the ERG response. In such cases, it appears that the ERG frequently shows negative configuration.

In the prognostic evaluation of eyes that develop

endophthalmitis after intraocular lens implantation, the b/a ratio is also valuable.[15] Eyes with early (within 1 week) endophthalmitis associated with a b/a ratio of <1.0 have a worse postoperative prognosis than eyes with late-onset endophthalmitis and/or a b/a ratio of >1.0. These observations are quite important when deciding on the appropriate time to perform vitrectomy for treatment. For example, a patient with endophthalmitis that was detected within 1 week of intraocular lens implantation and with an ERG b/a ratio of <1.0 should undergo vitrectomy urgently. On the other hand, when endophthalmitis develops a relatively long time after surgery and the ERG b/a ratio is >1.0, the timing of the vitrectomy may not be as critical. Representative examples[15] are shown in Fig. 10.13.

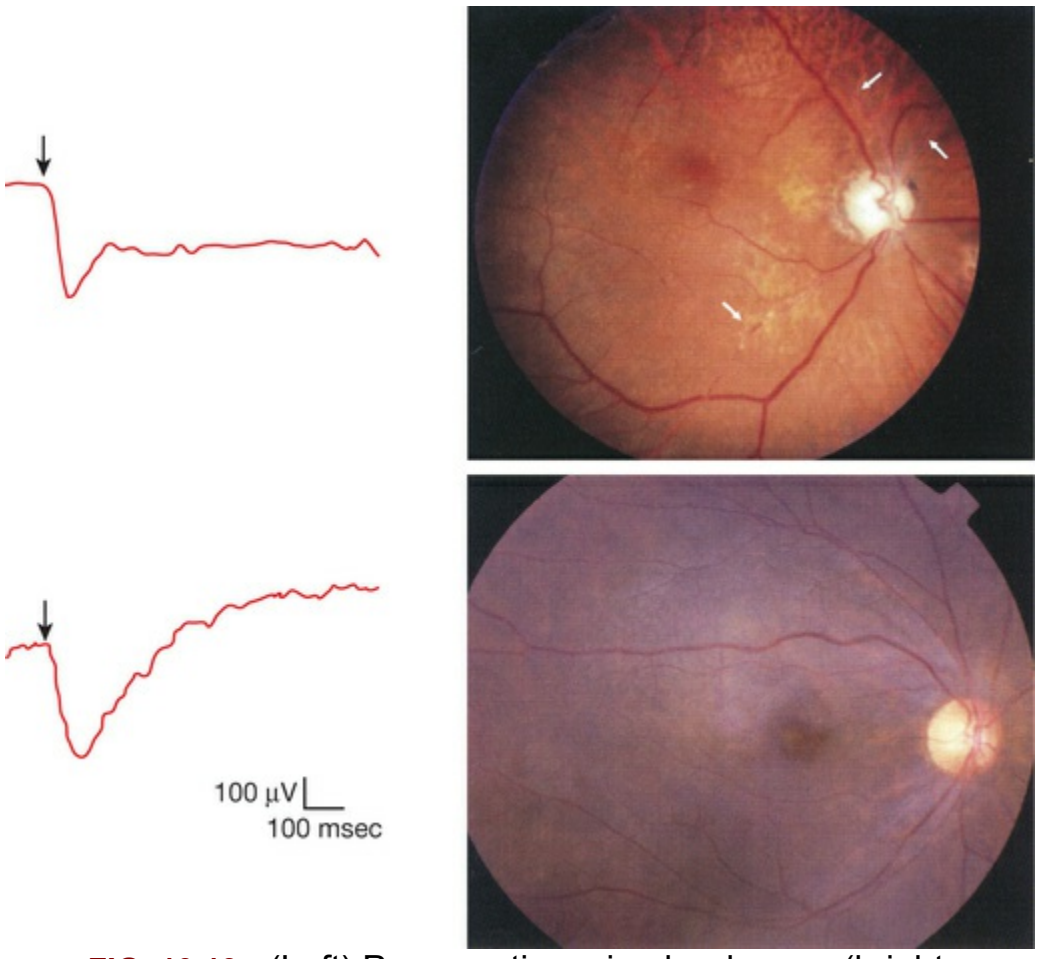

FIG. 10.13 (Left) Preoperative mixed rod–cone (bright flash) electroretinograms (ERGs) recorded from two patients with endophthalmitis after intraocular lens implantation. The negative configuration of the ERG (Case 1) suggests poorer visual prognosis after

vitrectomy than for the patient with normal-shaped ERGs (Case 2). (Right) Postoperative fundus. Case 1 showed extensive retinal vascular occlusions (*arrows*), with poor postoperative visual function, as expected. Case 2 showed an essentially normal fundus with good postoperative visual function. (Reproduced with permission from Horio N, Terasaki H, Yamamoto E, et al. Am J Ophthalmol 2001;132:258–9.)

Diagnostic Value.

The negative ERG is seen in some hereditary retinal diseases, which provides diagnostic information, particularly when the a-wave amplitude is normal. The representative diseases, where the negative ERG is of diagnostic value, include complete-type congenital stationary night blindness[16] (CSNB: see Fig. 10.20), incomplete-type CSNB[16] (see Fig. 10.20), X-linked juvenile retinoschisis[11] (XLRS: see Fig. 10.20), juvenile-onset neuronal ceroid lipofuscinosis,[17] and infantile Refsum disease. Since both complete and incomplete CSNB show essentially normal fundi and most patients with CSNB have moderately low visual acuity,[16] the negative ERG finding is extremely important to identify these disorders, differentiating them from other diseases with normal fundi, low visual acuity, and normal ERG, such as psychologic eye problems, amblyopia, optic nerve disease, central nervous system disease, or occult macular dystrophy (OMD). The detailed findings separating rod and cone components will be described in subsequent sections.

When the a-wave amplitude is normal and the b/a ratio is <1.0, a selective abnormality of the second-order neuron is indicated. On the other hand, when the amplitude of the a-wave is smaller than normal with the b/a ratio <1.0, there are two potential interpretations. One is the combined dysfunction of photoreceptor and middle retinal layer. This situation is often observed in patients with retinitis pigmentosa. The other possibility is the ERG showing the photopic hill phenomenon[8,9] (see above). When the rod function is completely absent and the cone function is well preserved, the ERG shows a cone ERG waveform even in the dark. In this condition, when the stimulus light intensity is strong, the ERG reveals the photopic hill phenomenon (see Fig. 10.3), showing a

negative configuration with a small a-wave. Examples are seen when obtaining a bright flash mixed rod–cone ERG in the dark in Oguchi disease or fundus albipunctatus (see Fig. 10.16).

In acquired diseases, negative ERG may be seen in melanoma-associated retinopathy,[18,19] birdshot choroidopathy,[20] ocular siderosis, quinine retinopathy, and methanol toxicity. The negative configuration of the ERG provides important diagnostic value in these disorders (see Chapter 79, White spot syndromes and related diseases; Chapter 80, Autoimmune retinopathies; Chapter 92, Drug toxicity of the posterior segment; and Chapter 138, Remote effects of cancer of the retina).

Extinct

The extinct ERG is often seen in the advanced stage of rod–cone dystrophy, including retinitis pigmentosa, gyrate atrophy or choroideremia, and total retinal detachment. In retinitis pigmentosa, gyrate atrophy, or choroideremia, even when the macular area is preserved, ERG may become undetectable. Cancer-associated retinopathy,[19] an autoimmune retinopathy, may also show an extinct ERG and should be differentiated from retinitis pigmentosa.

Isolation of Rod and Cone Components in Standardized ERG

Although the rods outnumber the cones 13 to 1 in the normal human retina, the cone ERG response accounts for 20–25% of the ERG response amplitude. For the purposes of diagnosis, it often becomes necessary for the examiner to evaluate rod and cone activity separately. The full-field ERGs using the ISCEV Standard (see Chapter 9, Electrogenesis of the electroretinogram) in a normal subject are shown in Fig. 10.14.

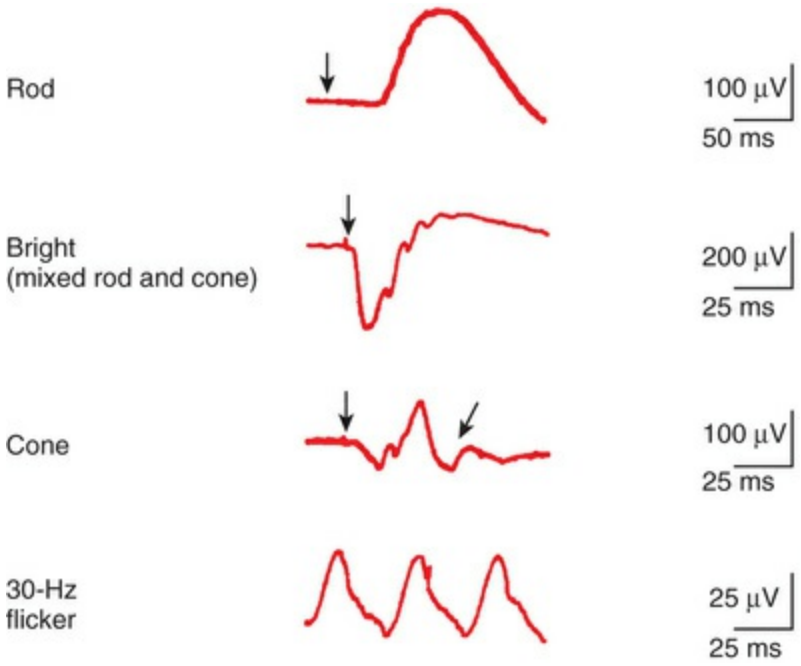

FIG. 10.14 Standard full-field electroretinograms with isolation of the rod and cone components. *Arrowheads* indicate the stimulus onset; *arrow* indicates photopic negative response.

After 30 minutes of dark adaptation, a rod (scotopic) ERG is recorded with a dim flash of light at approximately –3.9 log units in Fig. 10.2. A bright flash (mixed rod–cone) ERG is elicited by a single flash of white light at a maximum intensity of log 0 units in Fig. 10.2. Cone and 30-Hz flicker ERG are recorded with a stimulus intensity of 3.3 log units in Fig. 10.3 under the background illumination of 40 cd m^{-2}, which is sufficient to suppress all rod activity. The photopic recordings (cone and 30-Hz flicker ERG) are made after 10 minutes of light adaptation to 40 cd m^{-2}, because the maximum photopic ERG can be obtained when recorded after light adaptation.[11] In addition to the conventional ERG components, the photopic negative response (PhNR) was introduced:[21] this originates from retinal ganglion cells and is described in more detail in subsequent sections.

The representative patients diagnosed by the isolation of rod and cone components of full-field ERG are shown below in relation to the abnormal cells of the retina.

Cone Photoreceptor Dysfunction

The congenital stationary disorder of cone dysfunction is represented by rod monochromacy which is inherited in an autosomal recessive mode. This disorder is characterized in the complete form by complete absence or severe depression of color vision, reduced visual acuity, nystagmus, and photophobia[11] (see Chapter 46, Abnormalities of cone and rod function). There is also an incomplete form of this disorder, where color vision and/or visual acuity is not severely affected[11] (see Chapter 46, Abnormalities of cone and rod function). In both forms, the fundus and fluorescein angiograms are normal, and the most characteristic feature in terms of the diagnosis is selective reduction or absence of the photopic components with preservation of the normal scotopic components of the full-field ERG, even in incomplete forms (Fig. 10.15). Molecular genetic studies have shown that mutations in the *CNGB3* gene encoding the beta-subunit of the cone photoreceptor cGMP-gated channel are responsible for rod monochromacy.[22]

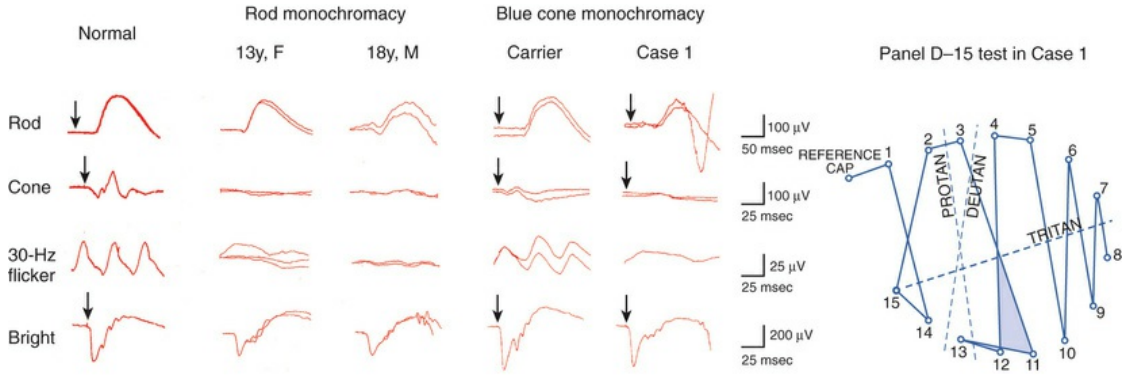

FIG. 10.15 Full-field electroretinograms (ERGs) and Farnsworth dischromous panel D-15 test from patients with cone photoreceptor dysfunction. Second and third columns (from left), full-field ERGs recorded from two siblings with rod monochromacy showing selective absence of the photopic components. During 10-year follow-up, their visual function remained stable and their fundi remained normal. Visual acuity was 0.1/0.4 in a 13-year-old sister and 1.0/1.0 in an 18-year-old brother. The sister showed mild acquired red–green deficiency and the brother had normal color vision due to functional cones preserved only in the fovea. Fourth and fifth (columns from left), full-field ERGs recorded from a family with blue cone monochromacy (carrier

mother and son) showing normal rod components and nearly absent cone components. Although the blue cone ERG is normally present, the amplitude of the normal blue cone ERG is too small to be detected in the regular full-field cone ERG, and the implicit time is too long to follow 30-Hz flicker ERG stimuli. Rightmost column, Farnsworth dischromous panel D-15 test from Case 1 showing that several crossing lines were perpendicular to the tritan axis. (Revised and reproduced with permission from Terasaki H, Miyake Y. Japn J Ophthalmol 1992; 36:132-41.)

Blue cone monochromacy shares many characteristics with rod monochromacy, except that the hereditary mode is X-linked recessive[11] (see Chapter 46, Abnormalities of cone and rod function). The visual acuity is approximately 0.2–0.3, which is slightly better than that of the complete form of rod monochromacy. Unlike rod monochromacy, the blue cone function is selectively preserved. Panel D-15 test shows several crossing lines perpendicular to the tritan axis (Fig. 10.15). The fundus is essentially normal, although in the late stage some atrophic changes may develop in the macula. Molecular genetic studies indicate that mutations exist in the red and green opsin in the blue cone monochromacy. The full-field ERGs are similar to those of rod monochromacy, showing nearly normal rod ERGs with absence of the photopic ERG (Fig. 10.15).[23] Although the blue cone ERG is normally present, the amplitude of the normal blue cone ERG is too small to be detected in the regular full-field cone ERG, and the implicit time is too long to follow 30-Hz flicker ERG stimuli[23] (see section on S-cone ERG, below).

Rod Photoreceptor Dysfunction

The model diseases with congenital rod photoreceptor dysfunction include Oguchi disease and fundus albipunctatus (FA), both of which are categorized as CSNB.

Oguchi disease, first reported by Oguchi[24] in 1907, is an unusual form of CSNB with autosomal recessive inheritance. It is characterized by a peculiar grayish-white discoloration of the fundus. This unusual fundus coloration disappears after a long period of dark adaptation, which is called the Mizuo–Nakamura

phenomenon[25] (see Chapter 46, Abnormalities of cone and rod function). Only the rod function is abnormal and is absent after 30 minutes of dark adaptation, but the subjective and electroretinographic rod function may increase after 2–3 hours of dark adaptation.[26] Mutations in the genes for arrestin[27] or rhodopsin kinase,[28] both of which are important in rod phototransduction, are known to cause the recessive form of Oguchi disease.

Full-field ERGs (Fig. 10.16)[26] recorded after 30 minutes of dark adaptation show absent rod ERG and essentially normal cone-mediated ERG. The mixed rod–cone ERG has a negative configuration with relatively well-preserved OPs. The a-wave amplitude in Oguchi disease is reduced compared to that of normal controls. As mentioned above, this ERG reflects the cone ERG in spite of the fact that the ERG is recorded in the dark and after 30 minutes of dark adaptation, because rod function is absent even under this condition. When the cone ERG is recorded with a bright flash of light, it shows the photopic hill phenomenon, and the ERG configuration is negative with a small a-wave. After 3 hours of dark adaptation, the amplitudes of the a-wave and b-wave of the mixed rod–cone ERGs are larger, but they are still negative in configuration. As the mutated genes indicate, the pathogenesis that only the rod itself is impaired in Oguchi disease is comparable to the normal photopic ERG and negative configuration with a small a-wave in mixed rod–cone ERG, but the negative configuration with a normal a-wave after a long period of dark adaptation may implicate additional abnormalities of bipolar cell function. Electro-oculogram (EOG) is abnormal with low light-to-dark ratio in most patients with Oguchi disease.[26]

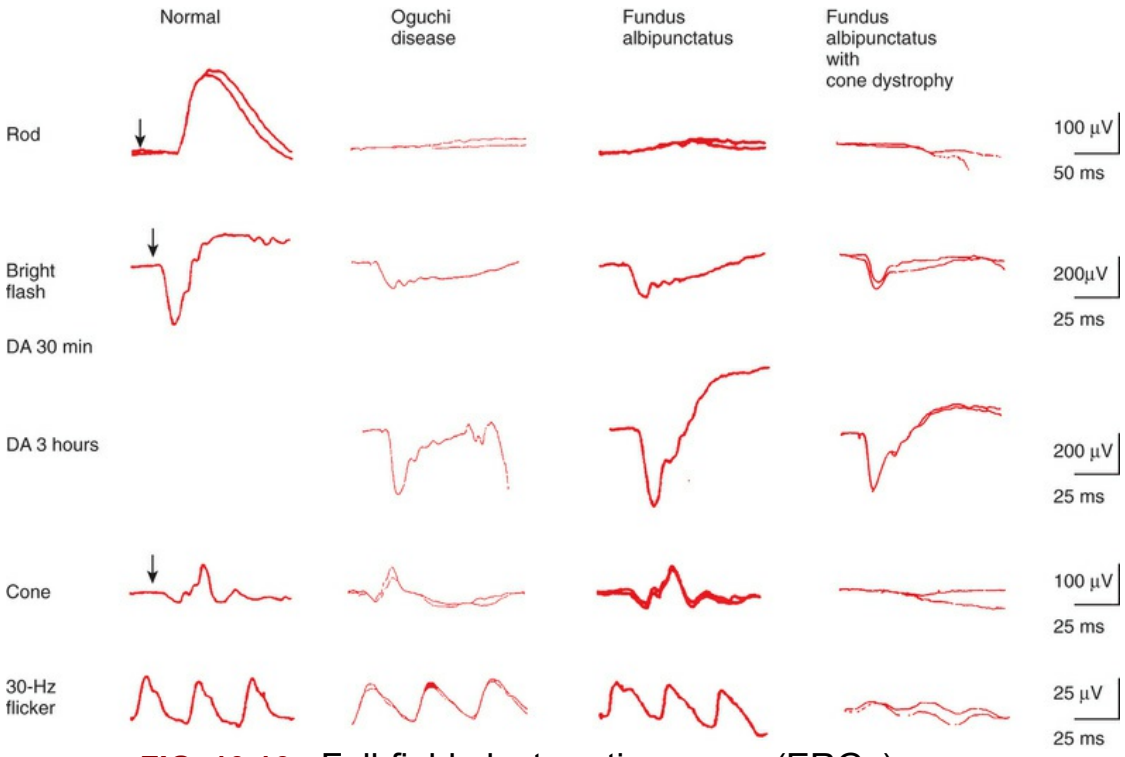

FIG. 10.16 Full-field electroretinograms (ERGs) recorded from normal control, patients with Oguchi disease, fundus albipunctatus (FA), and FA with cone dystrophy. Bright flash ERGs were recorded after 30 minutes and after 3 hours' dark adaptation (*DA*). In Oguchi disease, full-field ERGs recorded after 30 minutes of dark adaptation show absent rod ERG and essentially normal cone-mediated ERG. The mixed rod–cone ERG has a negative configuration with relatively well-preserved oscillatory potentials. Because the rod function is absent, it shows photopic hill phenomenon, and the ERG configuration is negative with a small a-wave. But the negative configuration with normal a-wave after 3 hours' dark adaptation may suggest some additional abnormalities of the bipolar cell function. In FA, the rod ERG is absent after 30 minutes of dark adaptation but becomes normal after 3 hours of dark adaptation. The mixed rod–cone ERG after 30 minutes of dark adaptation shows a negative configuration with a small a-wave, just as is seen in the photopic phenomenon of Oguchi disease. However, unlike Oguchi disease, it becomes normal after 3 hours of dark adaptation. About one-third of patients with FA have associated cone dystrophy, often showing bull's-eye maculopathy (see Fig. 10.17). Such patients show extremely

abnormal photopic ERGs in addition to the characteristic ERG findings of FA.

The pathogenesis of Oguchi disease has long been attributed to defects in rod bipolar function, as seen in complete CSNB, because reports published many years ago[29] indicated a normal a-wave with reduced b-wave (negative ERG) as well as a normal EOG. In addition, normal rhodopsin kinetics were shown by rhodopsin densitometry.[30] We demonstrated, however, that many patients with Oguchi disease show a smaller a-wave than normal as well as an abnormal EOG, suggesting that there is in fact a dysfunction of phototransduction.[26] Our hypothesis, derived from electrophysiologic results, seems to have been confirmed as the relevant mutations in Oguchi disease have been identified.[27,28]

FA has been considered to be a type of CSNB with autosomal recessive inheritance. The fundus has a characteristic appearance of a large number of discrete, small, round or elliptical yellowish-white regions at the level of the retinal pigment epithelium (see Chapter 46, Abnormalities of cone and rod function). The most characteristic property of their visual function is a delay in dark adaptation, which can be detected by the psychologically determined dark adaptation curve, ERGs and EOGs. It requires 2–3 hours to attain the final dark adaptation threshold, the maximum scotopic ERG response, and the normal EOG light rise.[11,30–32] Examples of full-field ERGs after 30 minutes of dark adaptation and after 3 hours of dark adaptation in a typical patient with FA are shown in Fig. 10.16. The scotopic (rod) ERG is absent after 30 minutes of dark adaptation but becomes normal after 3 hours of dark adaptation. The mixed rod–cone ERG after 30 minutes of dark adaptation shows a negative configuration with a small a-wave, just as is seen in Oguchi disease. However, unlike Oguchi disease, it becomes normal after 3 hours of dark adaptation. EOG is abnormal when measured using the regular method of 15 minutes of dark adaptation; however it becomes normal when the dark adaptation is prolonged.[31] Mutations in the gene encoding 11-*cis* retinol dehydrogenase (*RDH5*) cause delayed dark adaptation and FA.[32]

Although FA has been believed to be a stationary condition, our study indicated that about one-third of patients with FA are progressive, and associated with cone dystrophy.[33] Such patients

often have bull's-eye maculopathy (Fig. 10.17). In addition to the characteristic ERG findings of FA, the photopic ERGs are extremely abnormal (see Fig. 10.16). All of these patients also showed *RDH5* gene mutations.[34] The ERG results have changed the disease concept of FA, which previously had been believed to be a subtype of CSNB.

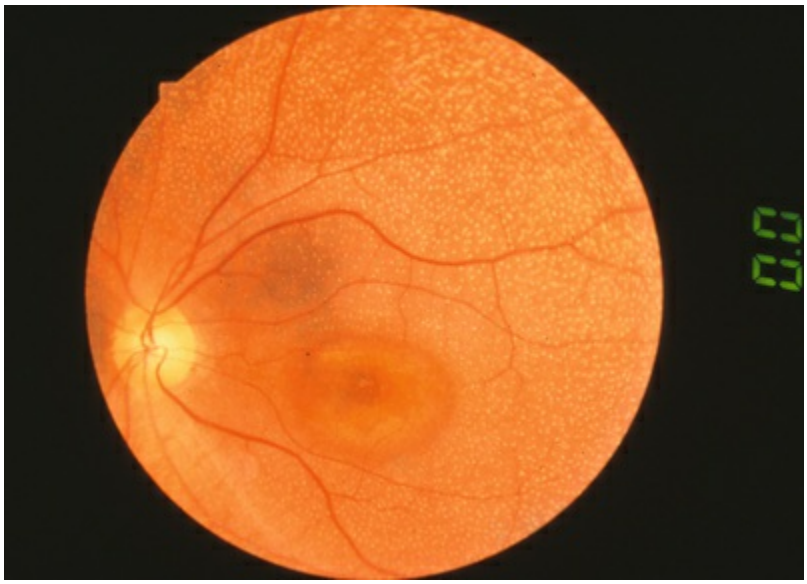

FIG. 10.17 Fundus of a patient with fundus albipunctatus associated with bull's-eye maculopathy.
(Reproduced with permission from Miyake Y, Shiroyama N, Sugita S, et al. Fundus albipunctatus associated with cone dystrophy. Br J Ophthalmol 1992;76:375–9, with permission from BMJ Publishing Group.)

Rod–Cone or Cone–Rod Photoreceptor Dystrophy

Patients with cone–rod or rod–cone dystrophy belong clinically and genetically to a heterogeneous group of patients with inherited retinal dystrophies featuring a progressive disease process. They are characterized by widespread degeneration of predominantly the cone (cone dystrophy) or the rod (rod dystrophy) photoreceptors in the early stage and, at the advanced stage, patients also have remaining rod (cone–rod dystrophy) or cone (rod–cone dystrophy) degeneration. The fundus in patients with cone or cone–rod dystrophy may be within normal limits or may have subtle changes in the early stage. In such cases, patients may

be misdiagnosed as having optic nerve disease, central nervous system disease, amblyopia, or OMD (see below). These changes may progress to bull's-eye maculopathy and diffuse atrophy of the RPE in the far-advanced stage. Patients with rod–cone dystrophy show abnormal scotopic vision first, followed by abnormal photopic vision. The diseases include retinitis pigmentosa, choroideremia, gyrate atrophy, and others. Full-field ERG is important to differentiate between cone–rod and rod–cone dystrophy, particularly in their early stages.

Full-field ERGs in a typical patient with cone dystrophy and rod–cone dystrophy are shown in Fig. 10.18. Selective abnormalities of the photopic components (cone and 30-Hz flicker ERG) are seen in cone dystrophy and a more severe abnormality in rod than cone function is shown in retinitis pigmentosa as a representative example of rod–cone dystrophy. At the advanced stage, most patients with cone dystrophy also have abnormal scotopic vision (cone–rod dystrophy) and may sometimes be difficult to differentiate from rod–cone dystrophies, such as retinitis pigmentosa.

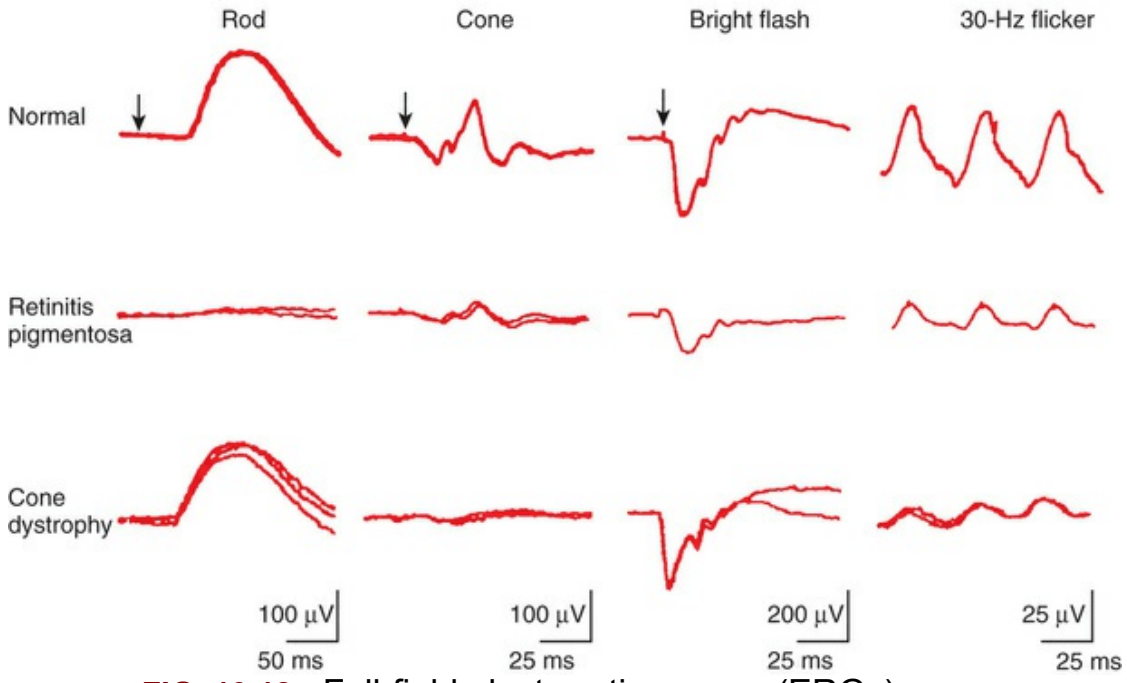

FIG. 10.18 Full-field electroretinograms (ERGs) recorded from a normal control (top) and a patient with retinitis pigmentosa at an early stage (middle) and a

patient with cone dystrophy (bottom). The more severe abnormality in rod than cone function is shown in retinitis pigmentosa as a representative disease of rod–cone dystrophy and selective abnormalities of the photopic components (cone and 30-Hz flicker ERG) are seen in cone dystrophy. At the advanced stage, most patients with cone dystrophy also have abnormal scotopic vision (cone–rod dystrophy) and may sometimes be difficult to differentiate from a rod–cone dystrophy, such as retinitis pigmentosa. (Reproduced with permission from Miyake Y. Electrodiagnosis of retinal diseases. Tokyo: Springer-Verlag; 2006.)

Second-Order Neuron Dysfunction

The fundamental differences between rod and cone connections to the bipolar cells are shown in Fig. 10.19.[35] The photoreceptors transmit visual information to the bipolar cells, which are the second-order neurons. Rods contact only depolarizing (ON) bipolar cells (DBCs), creating ON visual pathways. On the other hand, cones have more extensive postsynaptic connections. They synapse onto both depolarizing DBCs and hyperpolarizing OFF bipolar cells.

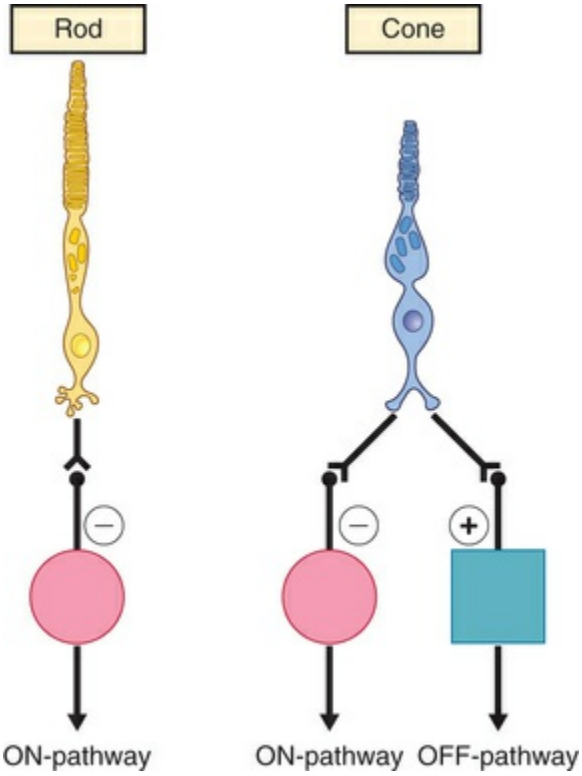

FIG. 10.19 Simplified schema showing retinal wiring of the rod and cone pathway. The photoreceptors transmit visual information to the bipolar cells, which are the second-order neurons. Rods contact only depolarizing bipolar cells (DBCs: ●), creating ON visual pathways. On the other hand, cones have more extensive postsynaptic connections. They synapse on to depolarizing DBCs and hyperpolarizing OFF bipolar cells (HBCs: ■).

Complete and incomplete CSNB were classified as independent clinical entities based mainly on the analysis of full-field ERGs.[36] Unlike Oguchi disease and FA, where the responsible pathology lies mainly in the rod itself, complete and incomplete CSNB are caused by the dysfunction of ON or ON–OFF bipolar cells, respectively.[35,37] They are the model disorders of bipolar cell dysfunction. EOGs in both diseases are normal.[36] It should be noted that all of this new information in terms of the classification and pathology of both complete and incomplete CSNB was obtained from detailed analysis of ERG,[36,37] and molecular genetics subsequently confirmed these ERG-derived observations.

The hereditary mode of complete CSNB is X-linked recessive or autosomal recessive.[36] X-linked complete CSNB has a mutation of

the leucine-rich repeat proteoglycan (*NYX*) gene,[38] and autosomal recessive complete CSNB has a mutation in the *GRM6* gene[39] encoding the metabotropic glutamate receptor mGluR6 and transient receptor potential cation channel subfamily member 1 (*TRPM1*).[40] All these proteins are distributed on the postsynaptic ON bipolar cells and are required for the depolarization of the cell. The visual functions and ERGs are essentially the same in patients with these three different gene mutations, which have an almost complete block of ON synaptic transmission from the photoreceptors to the bipolar cells in both rod and cone visual pathways, preserving the OFF pathway intact.[11]

X-linked incomplete CSNB has a mutation of the calcium channel (*CACNA1F*) gene.[41] Loss of the functional channel impairs the calcium influx into rods and cones that is needed to sustain the tonic release of neurotransmitters from the presynaptic terminals. Therefore it is conceivable that patients with incomplete CSNB have an incomplete defect of the synapses in the ON and OFF bipolar cells in both rod and cone visual pathways.[11]

The comparison of full-field ERGs between complete and incomplete CSNB is shown in Fig. 10.20. The mixed rod–cone ERG shows a negative configuration with a normal a-wave in both types, but OPs can be better recorded in the incomplete type than the complete type. The normal a-wave with reduced b-wave suggests that both types of CSNB have a defect not in the rod photoreceptors but in the second-order neurons or their synapses in the rod visual pathway. These findings are comparable to molecular genetics.[36–41] Rod ERG is absent in the complete type but present with subnormal amplitude in the incomplete type. Absent rod ERG in complete CSNB and subnormal rod ERG in incomplete CSNB are comparable to the pathology of complete defect (complete CSNB) and incomplete defect (incomplete CSNB) of rod bipolar cell transmission. On the other hand, cone and 30-Hz flicker ERGs appear nearly normal in the complete type except that the a-wave of the cone ERG has a plateau-like bottom (Fig. 10.20). In contrast, the cone and 30-Hz flicker ERGs are extremely reduced in incomplete CSNB, which is highly characteristic and extremely important for the differential diagnosis.

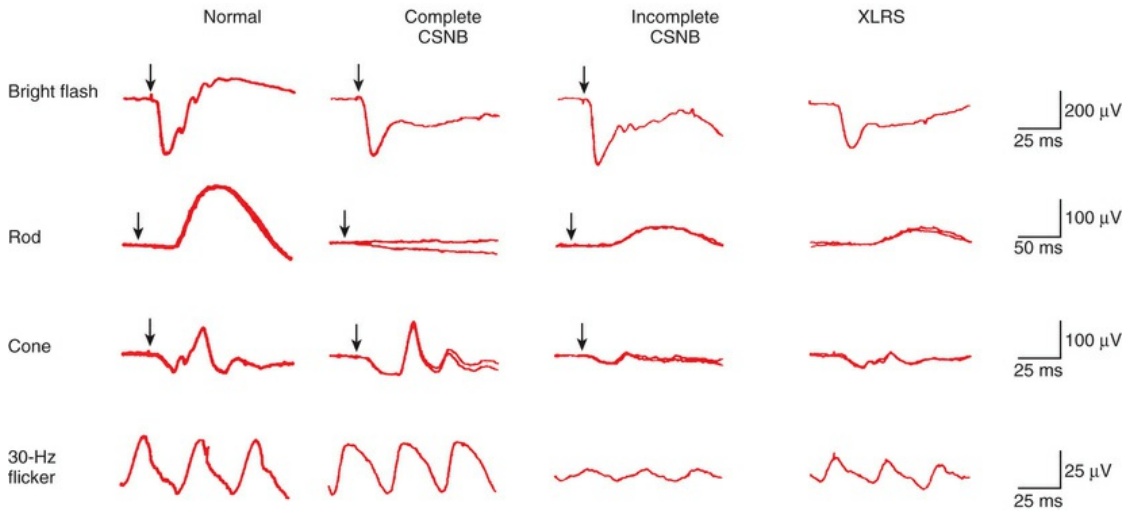

FIG. 10.20 Full-field electroretinograms (ERGs) recorded from a normal control, patient with complete or incomplete congenital stationary night blindness (CSNB), and patient with X-linked retinoschisis (XLRS). In CSNB, the mixed rod–cone ERG shows negative configuration with a normal a-wave in both types, suggesting a defect not in the rod photoreceptors but in the second-order neurons or their synapses in the rod visual pathway. However, oscillatory potentials can be recorded better in the incomplete type than the complete type. Rod ERG is absent in the complete type but present with subnormal amplitude in the incomplete type. On the other hand, cone and 30-Hz flicker ERGs appear nearly normal in the complete type except that the a-wave of the cone ERG has a plateau-like bottom. In contrast, the cone and 30-Hz flicker ERGs are extremely reduced in incomplete CSNB, which is highly characteristic and extremely important for the differential diagnosis. In XLRS, the mixed rod–cone ERG shows a negative configuration, which is observed even when the retinoschisis is confined to the fovea ophthalmoscopically. The full-field ERG findings similar to those of incomplete CSNB suggest that both ON and OFF bipolar cell function is mainly impaired in the rod and cone visual pathways. (Reproduced with permission from Miyake Y. Electrodiagnosis of retinal diseases. Tokyo: Springer-Verlag; 2006.)

In spite of the complete defect of the ON visual pathway, cone and 30-Hz flicker ERG responses in complete CSNB appear nearly

normal. This mechanism can be explained by the analysis of photopic long-flash ERG,[35,37] as shown in Fig. 10.21. Using photopic ERGs elicited by long-duration square-wave stimuli, the cone ON response generated by depolarizing ON bipolar cells is selectively and severely depressed in patients with complete CSNB; moreover, the waveform is similar to that of monkeys after 2-amino-4-phosphonobutyric acid (APB) is injected into the vitreous to block the synapse between photoreceptors and ON bipolar cells.[35] The OFF response, on the other hand, which is generated by hyperpolarizing bipolar cells, is intact in patients with complete CSNB, leading us to hypothesize that the ON function of both the rod and cone visual pathway is completely blocked in eyes with complete CSNB.[35,37] The mechanism as to why normal-looking brief-flash cone ERG can be obtained under this condition is shown in Fig. 10.22. With long-duration stimuli, the a-waves, b-waves, and d-waves are clearly separated. As the stimulus duration is shortened (brief-flash stimuli), the positive component of the photopic ERG consists mainly of the d-wave. Therefore even when the b-wave, a component of the ON response, is absent (as in complete CSNB), the d-wave replaces the b-wave, and a positive wave is recorded with brief-flash stimuli.[11] With incomplete CSNB, on the other hand, the ON and OFF response are both subnormal, suggesting that the ON and OFF systems are incompletely disturbed at the level of the bipolar cells.[11,37]

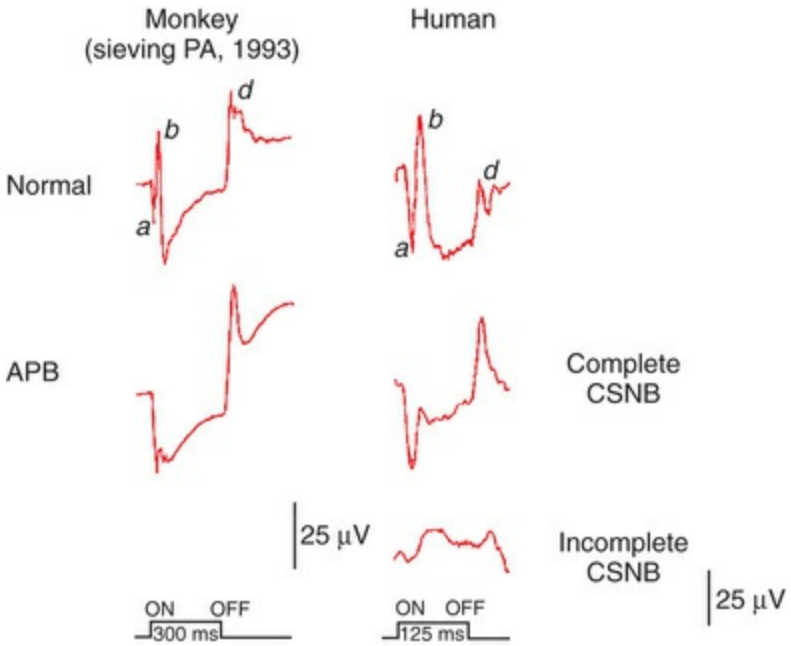

FIG. 10.21 Comparison of photopic long-duration electroretinograms (ERGs) recorded from a monkey and a human. (Left) Normal control ERG for the monkey eye and after being treated by 2-amino-4-phosphonobutyric acid (APB). (Right) ERGs recorded from a normal human control, from a patient with complete congenital stationary night blindness (CSNB), and from a patient with incomplete CSNB. The cone ON response generated by depolarizing ON bipolar cells is selectively depressed whereas the OFF response, which is generated by hyperpolarizing bipolar cells, is intact in patients with complete CSNB; moreover, the waveform is similar to that of monkeys treated with APB. (Reproduced with permission from Kondo M, Piao CH, Tanikawa A, et al. Japn J Ophthalmol 2000;44:20–8, with permission.)

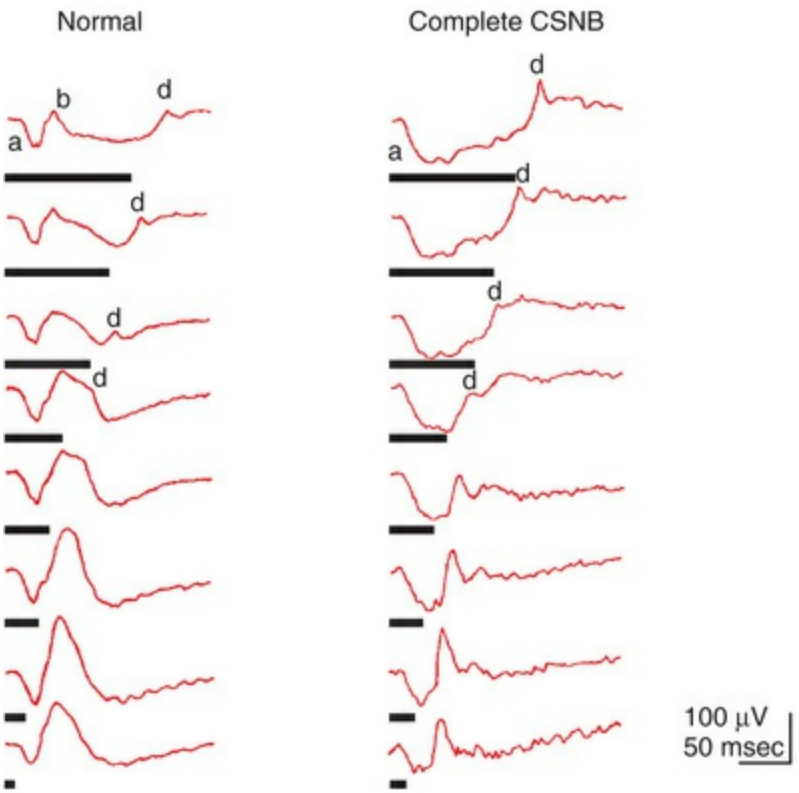

FIG. 10.22 Photopic electroretinograms (ERGs) elicited by square-wave stimuli of various durations from a normal control and a patient with complete congenital stationary night blindness (CSNB), explaining why complete CSNB shows normal-looking brief-flash cone ERG. With long-duration stimuli, the a-waves, b-waves, and d-waves are clearly separated. As the stimulus duration is shortened (brief-flash stimuli), the positive component of the photopic ERG consists mainly of the d-wave. Therefore even when the b-wave, a component of the ON response, is absent (as in complete CSNB), the d-wave replaces the b-wave, and a positive wave is recorded with brief-flash stimuli. Thick lines underneath the responses represent the stimulus duration. (Reproduced with permission from Miyake Y. Nippon Ganka Gakkai Zasshi 2002;106:737–56.)

XLRS is a vitreoretinal dystrophy that manifests early in life. XLRS is one of the more common causes of juvenile macular degeneration in males. Intraretinal cysts form in the macula and splitting of the retinal layers occurs in the peripheral retina (see Chapter 43, Hereditary vitreoretinal degenerations). Most patients, including young individuals show moderately poor visual acuity that gradually decreases with increasing age. Hypermetropia has

been shown to be a frequent accompaniment of this disorder.[42] In fact many patients with XLRS are first diagnosed with hypermetropic amblyopia or heterotropia during infancy.

As mentioned above, mixed rod–cone ERG is of significant diagnostic value because of the negative configuration. The negative ERG is observed even when the retinoschisis is confined to the fovea ophthalmoscopically. The full-field ERG findings (see Fig. 10.20) are similar to those of incomplete CSNB, suggesting that both ON and OFF bipolar cell function is mainly impaired in the rod and cone visual pathways. The EOG in XLRS is normal.

The schisis occurs in the plane of the nerve fiber and ganglion cell layers of the retina. It has long been suggested that degenerating Müller cells or inner retinal cells may be the primary cause of the pathologic changes in XLRS. The XLRS gene was cloned in 1997 and was designated *RS1*.[43] However, the RS1 protein is heavily expressed in inner segments of both rod and cone photoreceptors and is also seen in cells of the inner nuclear layer. There is some discrepancy between the results of full-field ERG and genetic findings. Although the expression of RS1 protein is heavily concentrated in the inner segments of both rods and cones, ERG studies suggest that it does not inherently affect the photoreceptor function of either cell type. And from the above ERG and EOG results, it currently is reasonable to propose that both ON and OFF pathways are defective, although precise subcellular localization has not yet determined whether both depolarizing and hyperpolarizing bipolar cells are involved.[44]

Focal ERG

In order to record the ERG responses with focal stimuli, there are two methods that have been previously described. The conventional focal macular ERG can show a similar waveform as a conventional photopic ERG from the limited area of the macula.[45] The advantage of this method is that the analysis of ERG components can be done using the same concept as that of full-field photopic ERG. By analyzing several components, layer-by-layer macular function can be evaluated.

Another method is the mfERG technique, which was developed

in 1992.[46] With this method, focal ERGs can be recorded simultaneously from multiple retinal locations during a single recording session using cross-correlation techniques. Unlike conventional focal macular ERGs, there are still questions about how this method works and what it measures because the technique is relatively new. We have an impression that the layer-by-layer analysis of the macula can be done more precisely using focal macular ERG than with mfERG.

Principle, Method, and Characteristics

The focal macular ERG is primarily used to evaluate macular function. The full-field ERG is unable to detect small focal lesions or pathologies in the retina, and may be normal in the presence of macular diseases. In contrast, the full-field ERG may be undetectable when only macular function is preserved, such as in patients with retinitis pigmentosa.[11]

The principle of recording of the focal macular ERG includes presenting a small stimulus to the macula and recording the response from the stimulated area by summating the responses using a computer. To eliminate contaminating stray light responses, background illumination must be used to depress the sensitivity of the area surrounding the stimulus. By combining the focal stimulus with background illumination properly, focal responses can be recorded. It is also essential to monitor the location of the stimulus on the fundus during the recordings, particularly in eyes with a central scotoma, to be certain that only the fovea is stimulated. An example of a recording system of focal macular ERG is shown in Fig. 10.23. The examiner records the ERGs while monitoring the fundus by the infrared television fundus camera. The optical system of an adequate combination of stimulus light and background illumination for focal stimulus is installed in the fundus camera, and the focal macular ERGs can be recorded under the fundus monitor by summating the responses with a computer. Focal macular ERGs recorded from a normal subject demonstrating the various components are shown in Fig. 10.24. All components of photopic ERG can be recorded: they are a-waves, b-waves, OPs, PhNR, ON and OFF components, and 30-Hz flicker responses.[11]

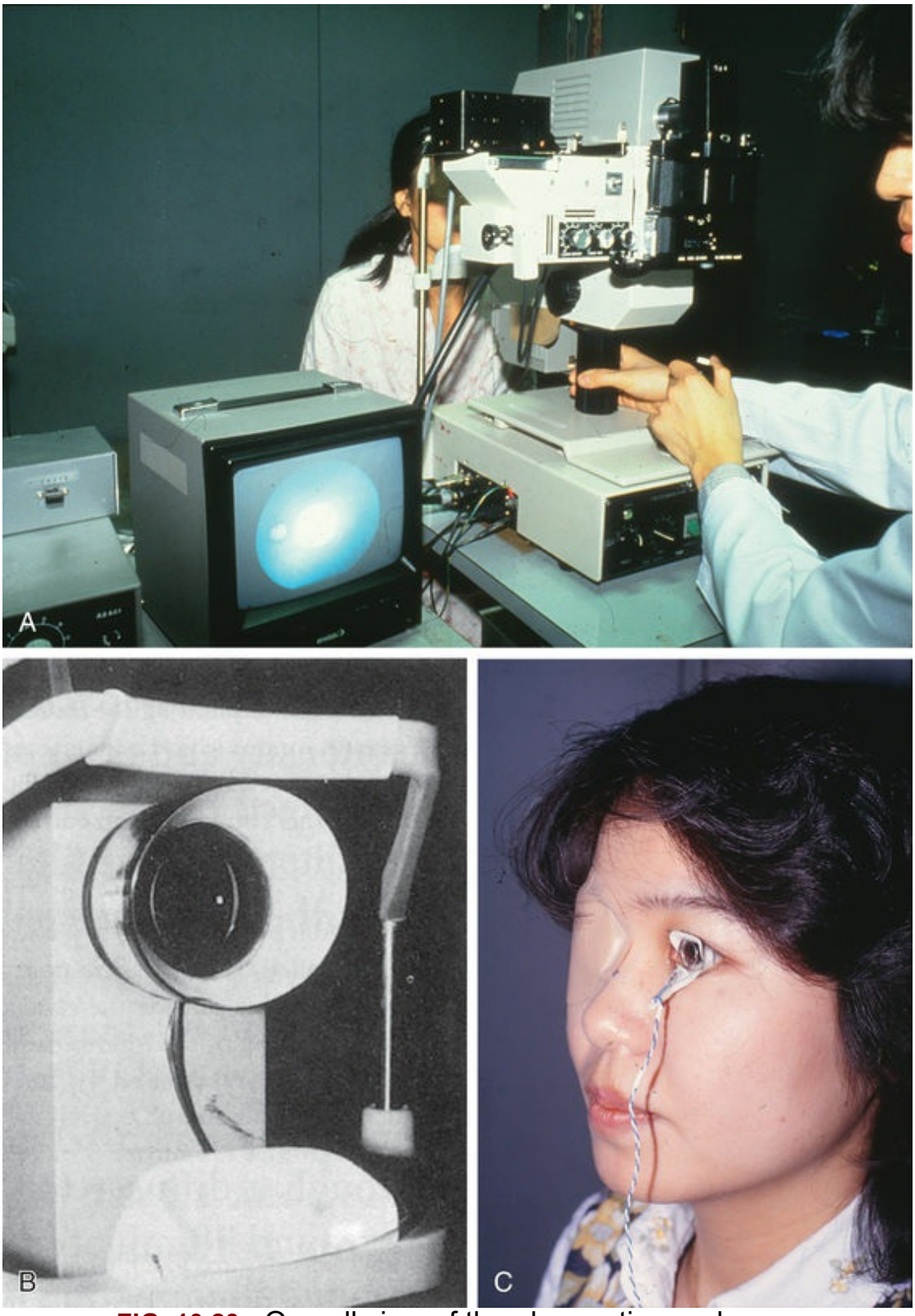

FIG. 10.23 Overall view of the observation and stimulation systems for focal macular electroretinogram (ERG) and visually evoked response (VER) recordings. The examiner records the ERGs while monitoring the stimulus on the fundus by the infrared television fundus camera (A). A plastic

hemisphere with miniature lamps is attached to the top of the camera to obtain background illumination for the peripheral retina (B). A Burian–Allen bipolar contact lens is used to record the ERGs (C). (Revised with permission from Miyake Y, Yanagida K, Kondo T, et al. Nippon Ganka Gakkai Zasshi 1981;85:1521–33.)

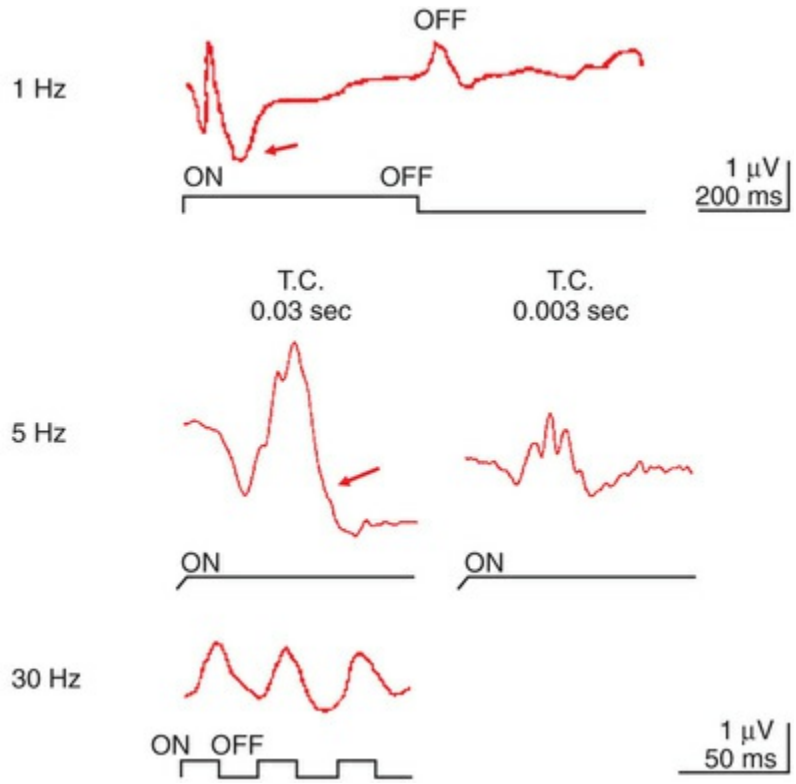

FIG. 10.24 Components of the focal macular electroretinogram recorded from a normal subject. ON and OFF responses recorded with 1-Hz stimulus frequency (top); a-wave, b-wave, and oscillatory potentials recorded with 5-Hz stimulus frequency (middle); and 30-Hz flicker responses (bottom) are shown. Arrows indicate photopic negative response. T.C., time constant. (Reproduced with permission from Miyake Y. Electrodiagnosis of retinal diseases. Tokyo: Springer-Verlag; 2006.)

Several important characteristics of focal macular ERG in humans were detected, particularly in macular OPs.[45] An example is shown in Fig. 10.25, demonstrating nasotemporal asymmetry.[47] Semicircular stimuli were used to compare the ERGs elicited by stimulating the temporal and nasal macula. The amplitudes and

implicit times of the a-waves and b-waves in the nasal retina are almost identical to those from the temporal retina, whereas the amplitudes of the OPs are much larger in the temporal retina than in the nasal retina. The amplitude of the focal ERGs recorded with circular stimulus is approximately the same sum as the amplitudes of the temporal and nasal ERGs.

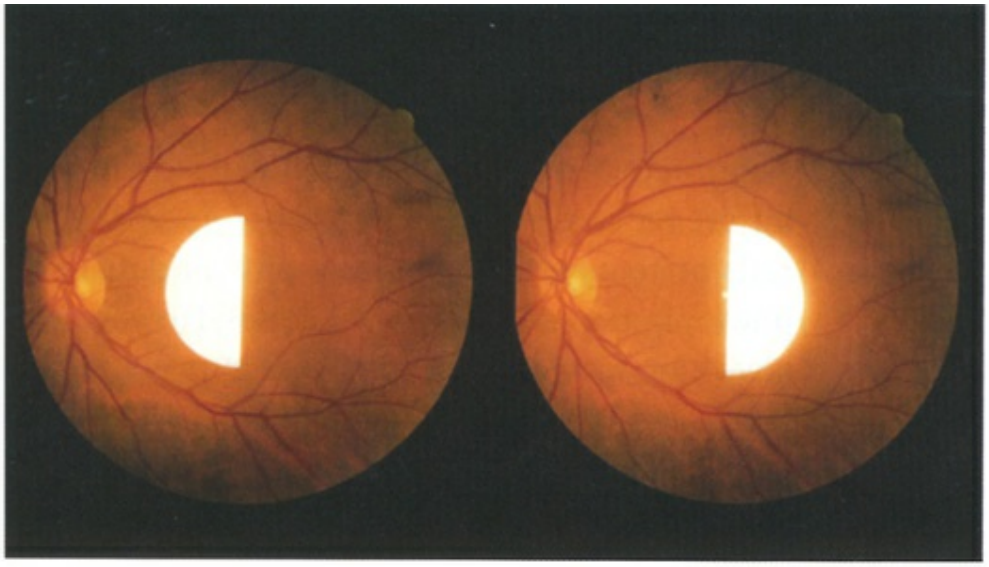

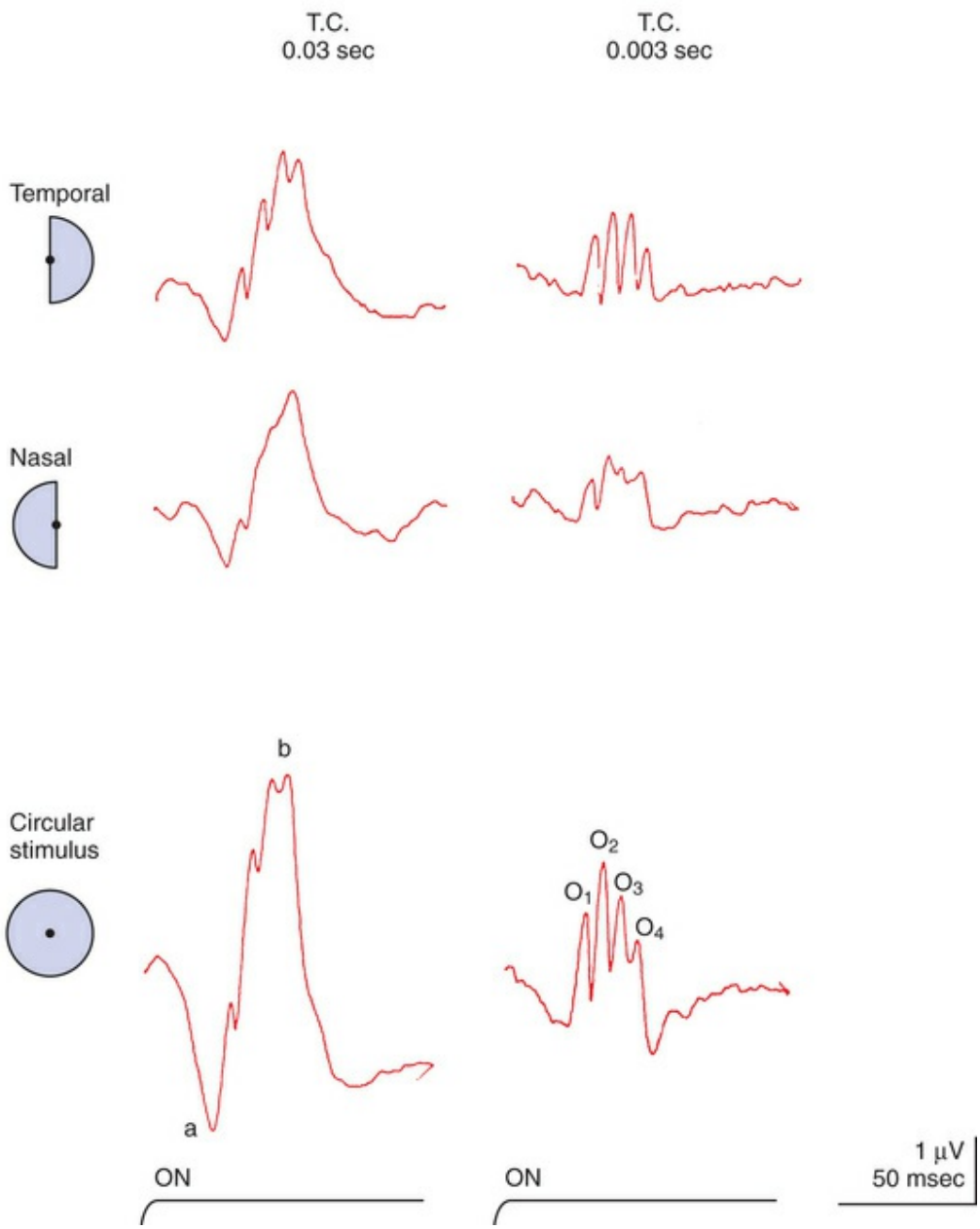
T.C.
0.03 sec
T.C.
0.003 sec
Temporal
Nasal
Circular
stimulus
b
a
O2
O1
O3
O4
ON
ON
1 μV
50 msec

FIG. 10.25 Comparison of focal electroretinograms using semicircular stimuli with the edge of the semicircle passing through the vertical axis (top) on the nasal and temporal macular areas and a circular stimulus (15°). The oscillatory potentials in the temporal macula are significantly larger than those in the nasal macula, and only the oscillatory potentials show this significant asymmetry. T.C., time constant.
(Reproduced with permission from Miyake Y. Electrodiagnosis of retinal diseases. Tokyo: Springer-Verlag; 2006, and Miyake Y, Shiroyama N, Hiroguchi M, et al. Invest Ophthalmol Vis Sci 1989;30:1743–9.)

The principle, recording method, and clinical applications of mfERG are described in an ISCEV guideline.[48] Readers are also referred to Chapter 9 (Electrogenesis of the electroretinogram), where the origin of the mfERG is described in detail.

Clinical Applications

The examples of value of focal ERG are shown here. In focal macular ERG, the macular OPs are the most sensitive indicator in variable macular diseases. The selective reduction of macular OP amplitude is observed in the early stage of macular edema,[49] epimacular membrane,[50] and the convalescent stage of central serous chorioretinopathy.[51] The fluorescein angiograms and focal macular ERGs in an eye with pseudophakic cystoid macular edema (CME) and after resolution of CME are illustrated in Fig. 10.26. The OPs of the focal macular ERGs are selectively reduced compared with that of a normal fellow eye. The visual acuity of this eye with CME was 0.6. Six months later, the CME resolved spontaneously, and fluorescein angiography disclosed a normal pattern; the visual acuity improved to 1.2. The focal macular ERGs returned to normal levels, with the amplitude of the OPs comparable to those from the normal fellow eye.[51]

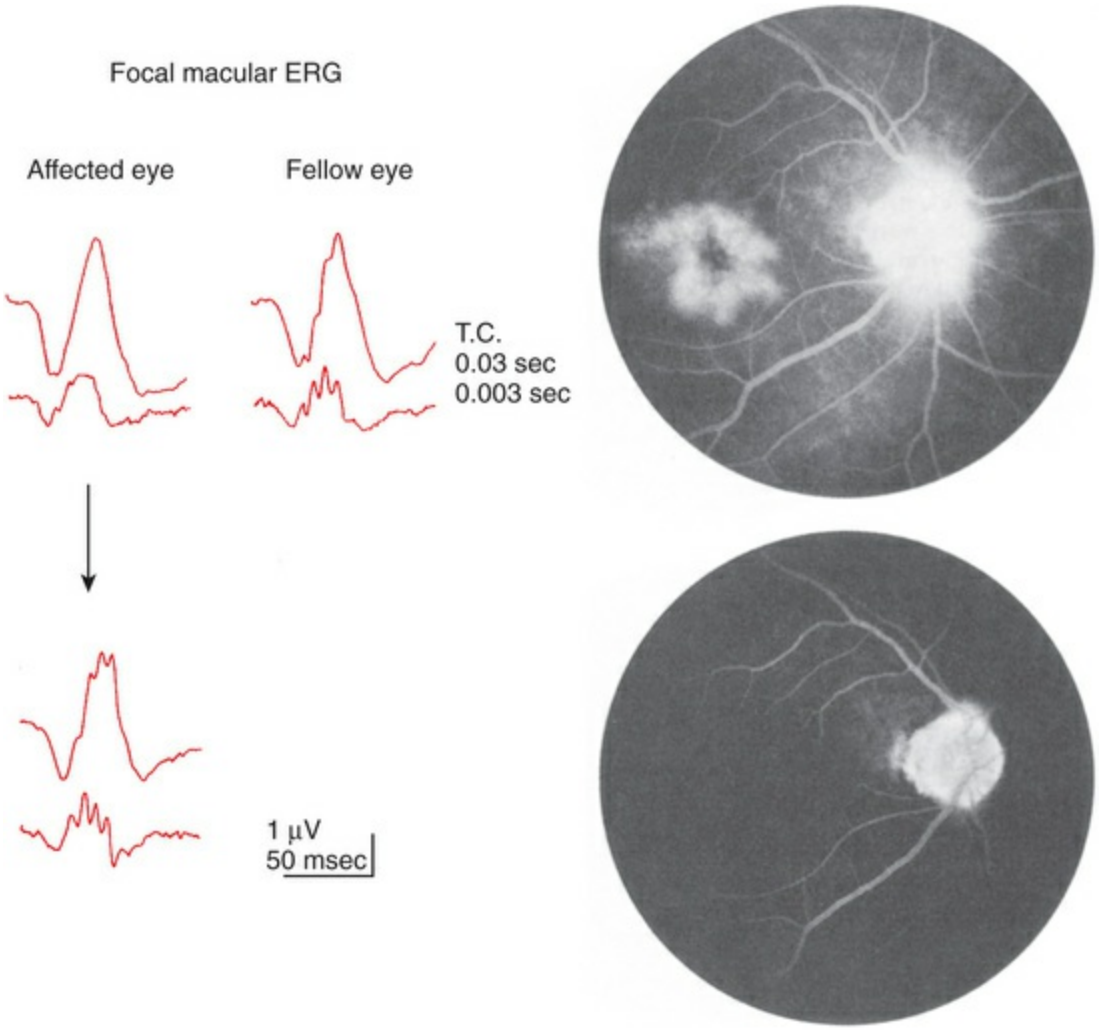

FIG. 10.26 Focal macular electroretinograms (ERGs) (left) and fluorescein angiograms (right) in a 51-year-old man with pseudophakic cystoid macular edema (CME: top) and after the resolution of CME (bottom). The oscillatory potentials of the focal macular ERGs are selectively reduced compared with that of a normal fellow eye. The visual acuity of the eye with CME was 0.6 (20/30). After spontaneous resolution of the CME, the focal macular ERGs returned to normal levels, with the amplitude of the oscillatory potentials comparable to those from the normal fellow eye. The visual acuity improved to 1.2. T.C., time constant. (Reproduced with permission from Miyake Y, Miyake K, Shiroyama N, et al. Am J Ophthalmol 1993;116:576–83.)

Occult macular dystrophy (OMD) is one of the most representative disorders where the focal macular ERG or multifocal ERG is a key for diagnosis. OMD was discovered by focal macular

ERG in 1989.[52] The clinical findings of OMD are progressive decrease of visual acuity, normal fundus and fluorescein angiograms, normal full-field ERGs, but abnormal focal macular ERG and multifocal ERG (Fig. 10.27). Although the fundus appearance and fluorescein angiogram show normal findings in OMD, optical coherence tomography (OCT) may reveal some mild photoreceptor abnormalities even in its early stage. Whether focal macular ERG or OCT is more sensitive to detect early abnormality is an interesting topic of debate. The key point, though, is that OMD may not be a rare disorder and many patients with OMD may be misdiagnosed as having several other diseases, such as a psychologic eye problems, optic nerve disorders, central nervous system disease, or amblyopia.[53]

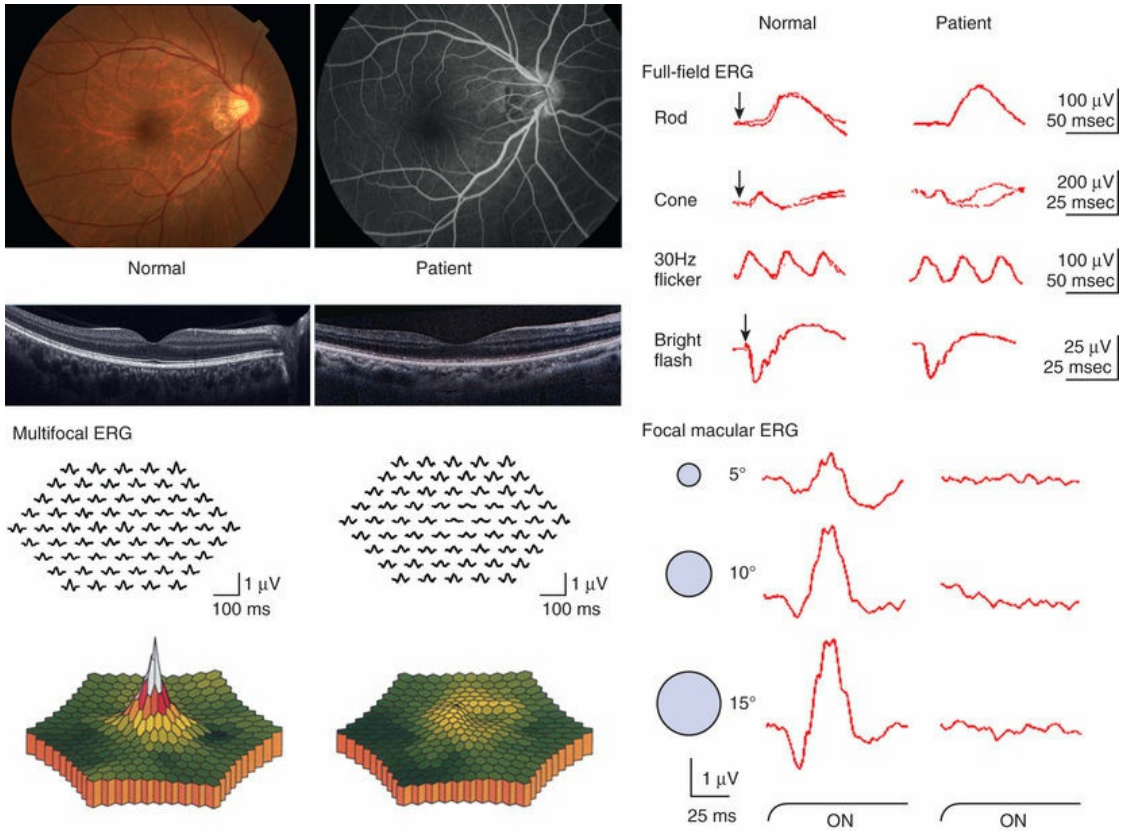

FIG. 10.27 The clinical findings of occult macular dystrophy. (Left top) Normal fundus and fluorescein angiograms;. (left middle) optical coherence tomography images from a normal person and a patient with occult macular dystrophy. The horizontal section through the foveal center demonstrates an abnormality, especially in the outer retinal bands at the

fovea in the patient. (Left bottom) Wave three-dimensional topography and multifocal electroretinogram (ERG) trace array from a normal person and a patient, showing markedly reduced response density in the central 7° of the retina. (Right top) Full-field ERGs showing normal responses; (right bottom) focal macular ERG showing abnormal responses in the patient.

The hereditary mode of OMD is autosomal dominant, although some patients show a sporadic mode.[52,53] Our genetic studies have detected mutations in retinitis pigmentosa 1-like 1 (*RP1L1*) gene in autosomal dominant OMD.[54] It was demonstrated that *RP1L1* plays an essential role in cone function in humans and that disruption of *RP1L1* function leads to OMD.

Acute zonal occult outer retinopathy is characterized by an acute zonal loss of one or more large zones of central retinal function in one or both eyes, predominantly in young women.[55] Other ocular findings include initially minimum ophthalmoscopic changes, photophobia, and permanent visual field loss, often associated with late development of retinal pigmentary changes and narrowing of the retinal vessels in the affected zones (see Chapter 79, White spot syndromes and related diseases). Since the full-field ERG may be normal or only slightly abnormal, it is not informative. The responses of mfERG become abnormal in the limited area where visual field loss is present[11] (Fig. 10.28).

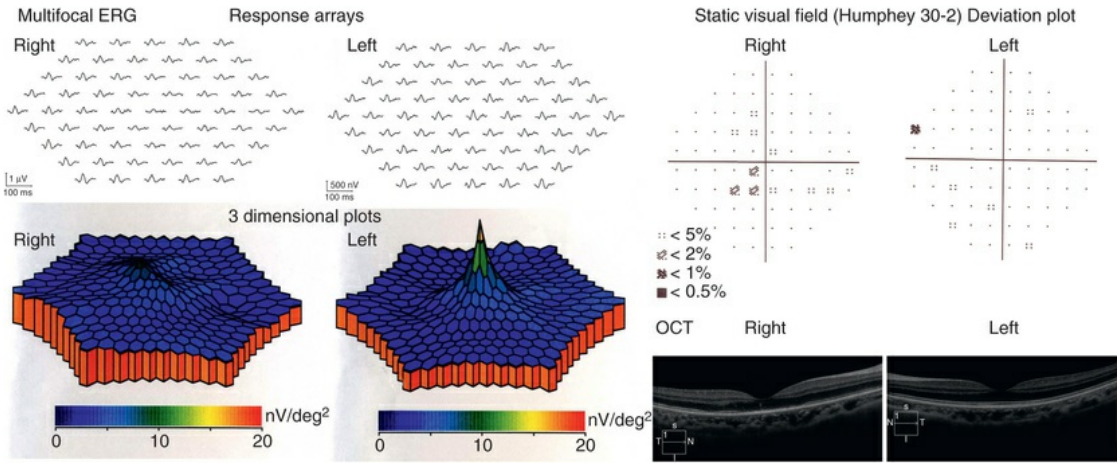

FIG. 10.28 Clinical findings of a patient with acute zonal occult outer retinopathy. A 22-year-old female

developed acute central visual loss in the right eye. Visual acuity was 0.5 (20/40) in the right eye and 1.2 (25/20) in the left eye. The top and bottom left panels are 61 response arrays and three-dimensional plots of the multifocal electroretinograms, respectively, showing abnormal responses in the limited area, where visual field loss is present in the right eye. The top right panels are the deviation plot of the static visual field, showing reduced sensitivity in the central area in the right eye. The bottom right panels are Fourier-domain optical coherence tomographic (FD-OCT) images from the affected right eye and intact left eye, respectively, showing that both the border of the photoreceptor inner- and outer-segment line (IS/OS line, also called ellipsoid zone, EZ) and the cone outer-segment tip (COST, also called interdigitation zone, IZ) line between the EZ and the retinal pigment epithelium (RPE) are absent in the macular area of the right eye. The EZ, IZ, and RPE/Bruch membrane are intact in the left eye.

Other Special Responses or Techniques in ERG

Photopic Negative Response

Photopic negative response (PhNR) has already been described and is a negative wave in the photopic ERG that is evoked following the b-wave (see Figs. 10.14 and 10.24). The origin of the PhNR is the retinal ganglion cells,[21] and this is fully described in Chapter 9 (Electrogenesis of the electroretinogram). Significant reduction in PhNR was reported in patients with open angle glaucoma and several other optic neuropathies.[21] Moreover, recent analysis of PhNR recorded in focal macular ERG (see Fig. 10.24) and mfERG has enabled objective assessment of retinal ganglion cell damage in glaucoma, optic nerve disease, and retinal vascular diseases.[56,57] Other studies showed that PhNR can be correlated with retinal sensitivity as well as retinal microstructure such as nerve fiber layer thickness.[58]

ERG Recordings by Light-Emitting Diodes

Light-emitting diodes (LEDs) (Fig. 10.29) have been a topic of great interest recently, as light sources to elicit and record full-field ERG.[59] The LEDs are small and inexpensive, and they require low currents to drive them. They can be controlled by a simple electronic circuit to provide either a continuous light output or extremely brief flashes over a large range of intensities. The stimulus and recording system using LED can be used not only for routine full-field ERG but also for some other special applications of clinical ERG described below.

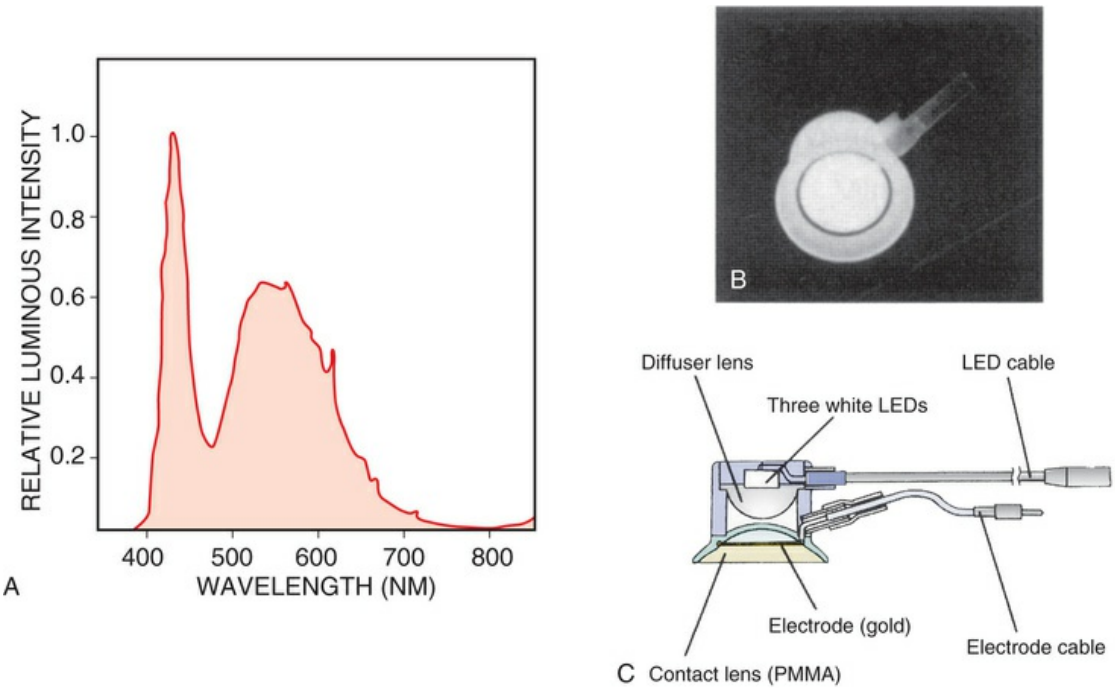

FIG.10.29 Structure of the white light-emitting diode (LED) contact lens electrode. (A) Relative spectral emission of the LED. (B) Output that appears as visible white. (C) Structure of the contact lens electrode with three built-in white LEDs. *PMMA*, polymethylmethacrylate. (Reproduced with permission from Kondo M, Piao CH, Tanikawa A, et al. Doc Ophthalmol 2001;102:1–9.)

ERG Recording Under General Anesthesia[11]

ERG recordings with LED are useful for recording standard ERGs from pediatric patients under general anesthesia. The equipment

needed to obtain recordings that correspond to ISCEV standard ERGs is compact and easily portable.[60] The ERGs recorded using an LED system on a 3-month-old baby under general anesthesia and a normal adult are compared in Fig. 10.30.

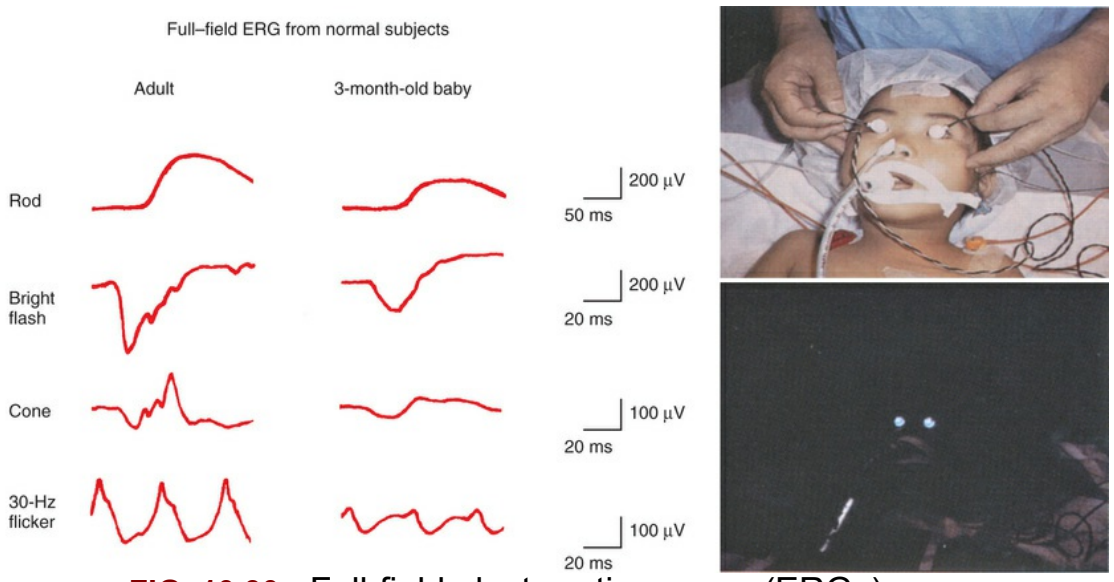

FIG. 10.30 Full-field electroretinograms (ERGs) recorded with white light-emitting diode (LED) contact lens electrodes from a normal adult subject (left) and a normal 3-month-old baby (right). The pictures show standard full-field ERG recording from a baby using this system. (Top) LED contact lenses are placed in both eyes under general anesthesia. (Bottom) Background illumination from the contact lens is used during the recording of the photopic ERGs in the dark.
(Reproduced with permission from Miyake Y. Electrodiagnosis of retinal diseases. Tokyo: Springer-Verlag; 2006.)

ERG Monitoring During Eye Surgery

As vitreoretinal surgery continues to advance, close monitoring of retinal function during these procedures has become important. Although ERGs directly reflect retinal function, monitoring during surgery has proven difficult. Each recording must be made quickly under aseptic conditions, and the instruments and electrodes must be such that they do not cause interference for the retinal surgeon. Furthermore, the eye undergoing surgery is intensively light-

adapted.

The LED contact lens electrode has been found to be highly suitable for this purpose.[61] It is easily sterilized and is used as both a stimulus source and a recording electrode for 30-Hz flicker ERGs during vitreoretinal surgery (Fig. 10.31). An example of ERG monitoring during vitrectomy from a patient with epimacular membrane is shown in Fig. 10.31. The ERGs recorded after local anesthesia (*Start*), and after the introduction of the infusion needle into the vitreous cavity (*Infusion*) were not significantly different in regard to amplitude and peak time. However, after vitrectomy, which required 10 minutes, the peak time was delayed and the amplitude decreased (*Vitrectomy*). Additional studies have demonstrated that lowering the intravitreal temperature by applying an infusion solution kept at room temperature can alter the ERG during vitrectomy. Filling the whole vitreous cavity with air after the epimacular membrane was peeled off resulted in a markedly reduced amplitude and delayed peak time (fluid–air exchange). This extreme reduction of ERG following fluid–air or fluid–silicon oil exchange in the vitreous cavity results from reduced electrical conductivity in the vitreous cavity. Five days after surgery, when the air was resolved from the vitreous cavity, the ERG recovered to the postoperative amplitude and peak time.

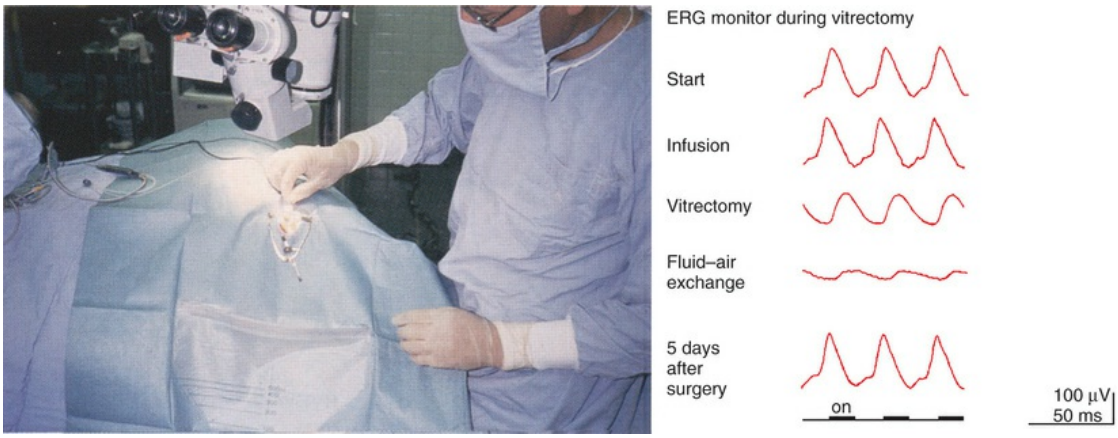

FIG. 10.31 Full-field electroretinogram (ERG) recording during vitrectomy. (Left) A light-emitting diode (LED) electrode is sterilized and placed on the cornea undergoing surgery. (Right) 30-Hz flicker ERGs recorded during vitrectomy in a patient with epimacular membrane. *Start* indicates the time when local

anesthesia was completed and *Infusion* denotes the time the infusion needle was introduced into the vitreous cavity. (Reproduced with permission from Miyake Y. Electrodiagnosis of retinal diseases. Tokyo: Springer-Verlag; 2006, and Horiguchi M, Miyake Y. Arch Ophthalmol 1991;109:1127–9.)

S-Cone ERG

Recording short-wavelength cone (S-cone) ERGs is valuable clinically because it allows us to evaluate the S-cone visual system. S-cone ERGs have been recorded using stimulation with strong blue stimuli on a bright yellow background, which suppresses the middle- and long-wavelength (LM) cone system.[62] LEDs emitting blue light can be used in the LED built-in contact lens electrode[63] (Fig. 10.32). By using bright yellow background illumination, the S-cone ERGs are recordable and are compared with LM cone ERGs (Fig. 10.32). The amplitude is much smaller and the implicit time is longer than those of the LM cone ERG. The components that reflect the OFF visual system (a-waves and d-waves) are essentially absent in S-cone ERGs because, unlike the LM cone system, the S-cone is mainly connected to the ON visual system.[64]

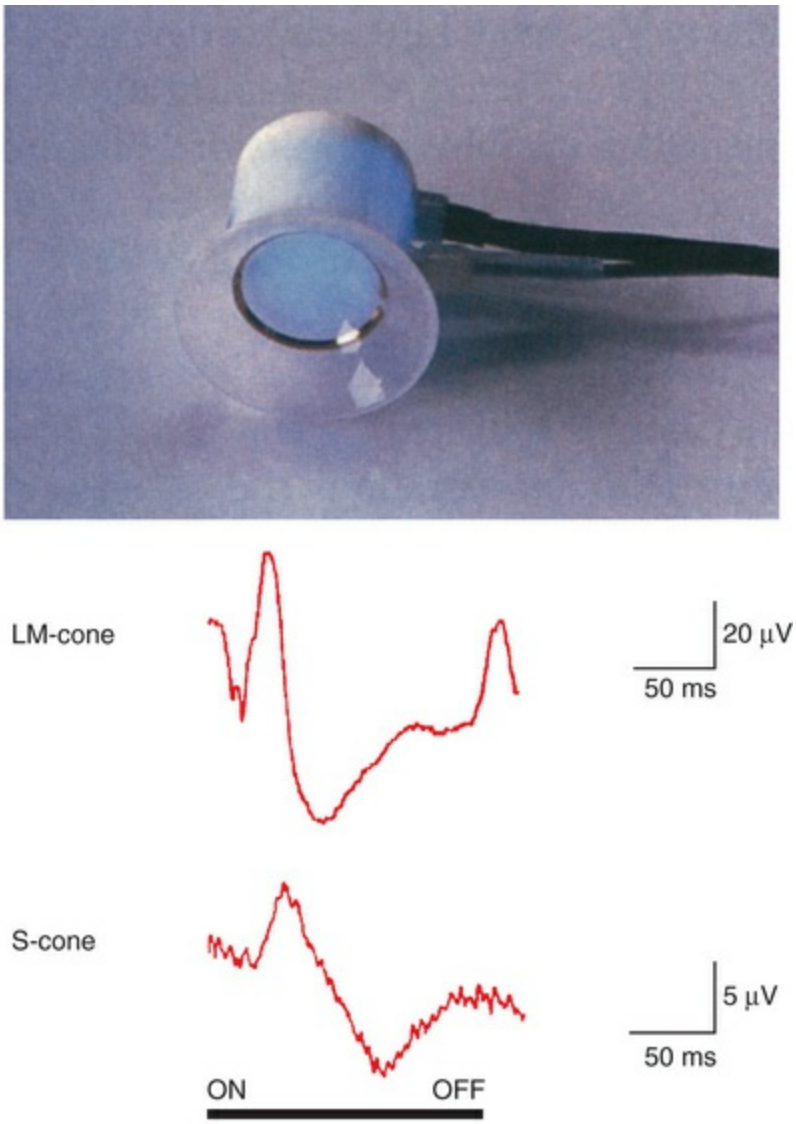

FIG. 10.32 S-cone electroretinogram (ERG) recording with blue-emitting light-emitting diode (LED) built-in contact lens electrode. (Top) LED built-in contact lens electrode with blue-emitting LEDs. (Bottom) Comparison of long-wavelength (LM) cone and S-cone ERGs with long-duration stimuli in a normal subject. The a-wave and d-wave that reflect the OFF visual system are essentially absent in the S-cone ERGs, because, unlike the LM cone system, the S-cone is mainly connected to the ON visual system. (Reproduced with permission from Miyake Y. Electrodiagnosis of retinal diseases. Tokyo: Springer-Verlag; 2006, and Horiguchi M, Miyake Y, Kondo M, et al. Invest Ophthalmol Vis Sci 1995;36:1730–2.)

Electro-Oculogram

In 1849, Du Bois Reymond[65] reported that in the normal eye there is a flow of electrical current, because the cornea is positive with respect to the back of the eye. The source of the voltage is the corneofundal potential. This potential difference is referred to as the standing potential or resting potential of the eye. The EOG is an indirect measure of the amplitude of the standing potential, which changes during dark and light adaptation. To obtain an EOG in humans, electrodes are placed at the inner and outer canthi of the eyes and the patient is asked to look back and forth between a pair of fixation lights. When the cornea moves closer to one of the electrodes, it becomes more positive and the other electrode becomes more negative. The opposite happens when the eyes move to the other side.

The principle and practical use of EOG are described in the ISCEV standard.[66] The changes in the amplitude of the EOG in the dark-adapted and light-adapted state of a normal subject are shown in Fig. 10.33. The smaller amplitudes are recorded when the eyes make the saccadic eye movements in the dark (dark trough); the peak amplitude is recorded against a steady light background (light peak). The light peak/dark trough (L/D) ratio is an index (Arden index)[67] used to assess retinal function. Generally, a ratio of 1.80 is the lower limit of normal.

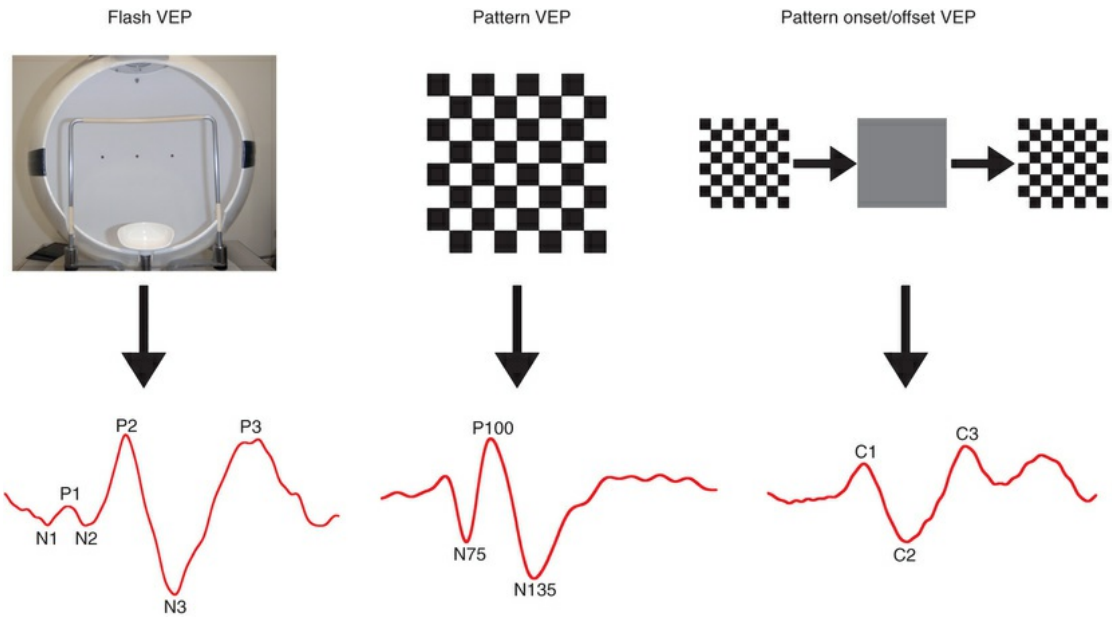

FIG. 10.33 Electro-oculogram (EOG) recordings. (Top) Diagram illustrating the EOG test and the determination of the light peak/dark trough (L/D) ratio (Arden ratio), which is 2.0 in this case. The smaller amplitudes are recorded when the eyes make saccadic eye movements in the dark (dark trough); the peak amplitude is recorded against a steady light background (light peak). (Bottom) Plottings of the amplitude of EOG in a normal subject and a patient with Best disease. The Arden ratio is 2.0 for the normal subject and 1.3 for the patient.

The origin of the retinal standing potential is thought to be in the retinal pigment epithelium. However, the light rise is generated by light stimulation of the photoreceptor–retinal pigment epithelium complex; and it is not detected when certain structures of the middle retinal layers are affected, such as in central retinal arterial occlusion.[68]

The EOG is generally abnormal in any condition in which the flash ERG is abnormal, except complete or incomplete CSNB.[36] The reverse, however, is not true. An abnormal EOG with a normal ERG may be seen in Best disease, pattern dystrophy of the RPE, and dominant drusen. The clinical relevance of EOG in each of these disorders is described in more detail in Chapter 44 (Macular dystrophies).

Visual Evoked Potential

The visual evoked potential (VEP) is the signal of the brain evoked by the visual stimulus. It is recorded, like the electroencephalogram (EEG), at the scalp in the occipital region by surface electrodes. The principle and practical use of clinical VEP are shown in the ISCEV standard.[69]

The cellular sources of the VEP are poorly understood. VEPs can be recorded under either transient or steady-state stimulus conditions. The transient VEP includes flash VEP, pattern reversal VEP, and pattern onset/offset VEP (Fig. 10.34).

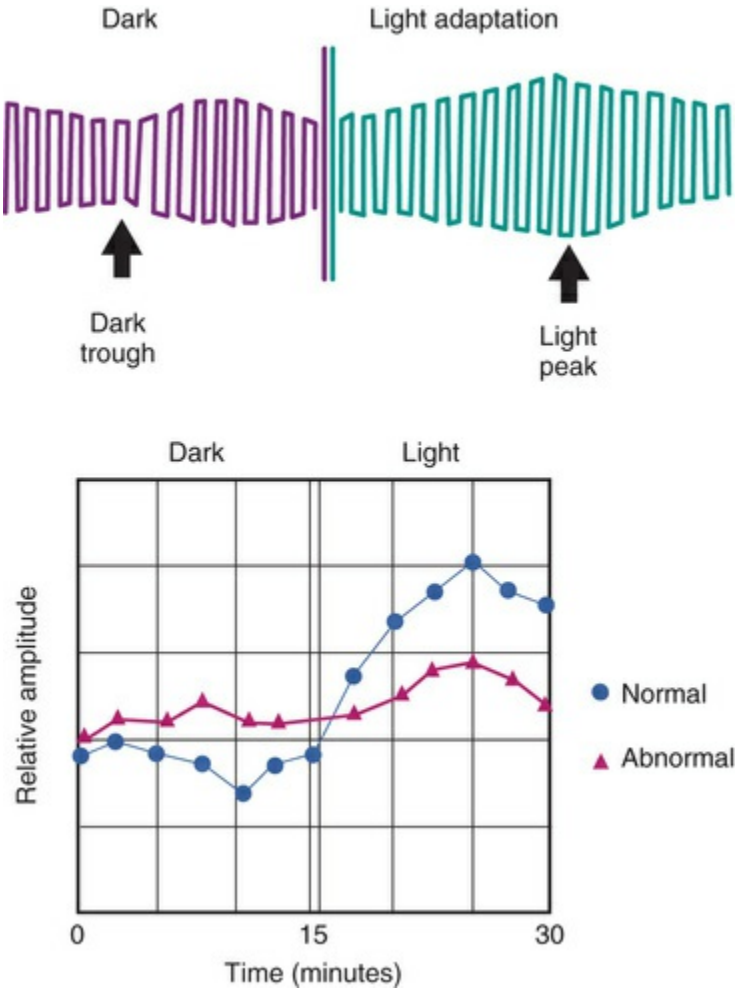

FIG. 10.34 Three standard responses in a clinical visual evoked potential (VEP) test. (Top) VEP stimulation. (Left) Flash stimulus is delivered with monitor or full-field dome. Such a dome is used for recording full-field electroretinogram as well and a pair

of fixation lights in the dome is used for an electro-oculogram test. (Middle) Reversing black-and-white checkerboard stimulus provided using cathode ray tube or light-emitting diode (LED) monitor. (Right) Reversing black-and-white checkerboard stimulus with diffuse blank screen at regular intervals is presented.

Several important features of the VEP can be stated:

1. The VEP is dominated by the central 20° of retina owing to "cortical magnification."

2. The VEP is highly variable among individuals, but varies less than 10% bilaterally when responses from the two eyes of a single person are compared.

3. VEP abnormality can result from abnormality in the retina, optic nerve, optic tracts, optic radiations, or visual cortex.

The flash VEP is easy to record, so it is performed for evaluation of gross visual function in infants, small children, or in individuals who are unable to perform PERG because of poor fixation due to poor visual function, nystagmus, or poor cooperation. Since flash VEP may still be recordable in patients with undetectable ERGs, such as in retinitis pigmentosa or dense vitreous hemorrhage, simultaneous recordings of flash VEP and ERG may provide useful information.[70]

Simultaneous Recording of Focal Macular ERG and VEP

Another useful evaluation featuring a layer-by-layer analysis of the visual pathway is simultaneous recording of focal macular ERG (fERG) and focal macular VEP (fVEP) with special reference to PhNR. The origin of PhNR is considered to be in the ganglion cells (see Fig. 9.20 in Chapter 9) and this component can also be recorded in fERG (see Fig. 10.24). Results of three patients are shown to illustrate how the simultaneous recording can work for layer-by-layer diagnosis in the visual pathway.[71]

Fig. 10.35A (left panel) shows the simultaneous recording of fERG and fVEP recorded (with stimuli 15° in diameter) from a 32-year-old man with longstanding central serous chorioretinopathy in his right eye. The onset was approximately10 years ago and there still remained shallow retinal detachment in the macula with a few precipitates underneath the sensory retina, consistent with the history of central serous chorioretinopathy. His left eye was normal. In our initial examination, his visual acuity was 0.06 (right eye) and 1.5 (left eye). A relative central scotoma, approximately 15° in diameter, was detected in his right eye. fERG of the affected eye shows a definitely smaller amplitude than that of the normal fellow eye in all components, including PhNR. The amplitude of the fVEP, however, did not diminish significantly and the implicit time was slightly delayed as compared with the normal fellow eye. This finding can be a model of photoreceptor dysfunction in the macula.

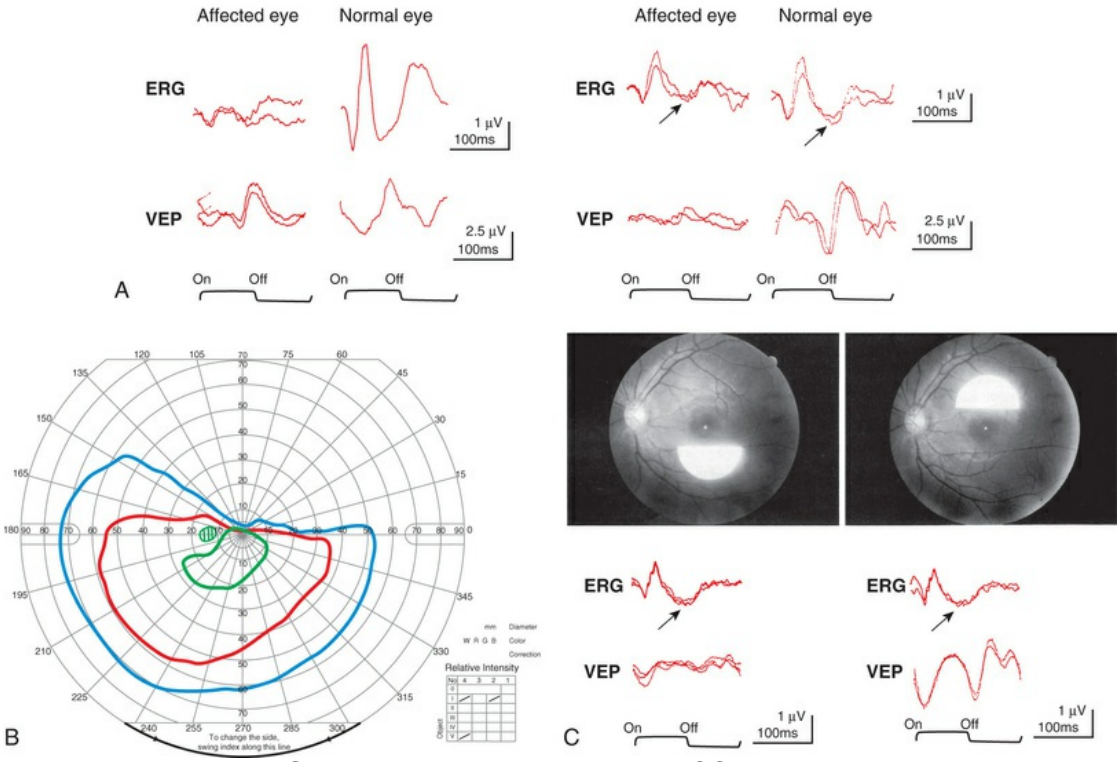

FIG. 10.35 Simultaneous recording of focal macular ERG (fERG) and focal macular VEP (fVEP). (A, left) Comparison of fERG and fVEP between affected eye and normal fellow eye in a 32-year-old man with longstanding central serous chorioretinopathy. (A, right) Comparison of fERG and fVEP between affected

eye and normal fellow eye in a 65-year-old man with unilateral optic atrophy. Bottom tracings indicate responses from photocell. In panels A and C, positivity at inion electrode results in upward deflection in fVEP. (B) Visual field of left eye in a 56-year-old man with posterior cerebral arterial occlusion resulting in bilateral upper hemianopsia. (C) Location of hemicircular stimuli (top) and simultaneously recorded fERG and fVEP with these stimuli (bottom) of left eye of the patient in panel B. (Reproduced with permission from Miyake Y. Japn J Ophthalmol 1990;34:225-2389, with permission.)

Fig. 10.35A (right panel) shows the results of a 65-year-old man with unilateral optic atrophy in his right eye. The fundus of the left eye was normal. His visual acuity was 0.08 (right eye) and 1.0 (left eye). The a-wave and b-wave of the fERG recorded with a 10° spot stimulation were almost identical in both eyes but the PhNR (*arrows*) of the affected eye was smaller than that of the normal fellow eye. fVEP was very abnormal in the affected eye. These results indicate that the abnormal PhNR and fVEP were caused by the dysfunction of the retinal ganglion cells.

A 56-year-old man had posterior cerebral arterial occlusion resulting in bilateral superior hemianopsia (Fig. 10.35B). Because of sparing of the fovea, visual acuity was 1.2 in both eyes. fERG and fVEP were simultaneously recorded in the left eye, with hemicircular stimuli (15° in diameter) projected onto the visual field defect (lower retina) and onto the opposite superior fundus with no visual field defect (Fig. 10.35C). The fovea (small fixating target) was not targeted with either stimulus, and the distance from the fovea of each stimulus was approximately the same. fVEP was very small in the area of the visual field defect, while it was normal in the area of normal visual field. fERG, however, did not show any difference between these two areas, including PhNR (*arrows*). This result indicates that the visual field defect is not caused by the ganglion cell dysfunction, but by an abnormality at the level of the visual cortex.

References

1. McCulloch DL, Marmor MF, Brigell MG, et al. For the International Society for Clinical Electrophysiology of Vision. ISCEV Standard for full-field clinical electroretinography (2015 update). *Doc Ophthalmol*. 2015;130:1–12.
2. Gjötterberg M. Electrodes for electroretinography: a comparison of four different types. *Arch Ophthalmol*. 1986;104:569–570.
3. Sieving PA, Frishman LJ, Steinberg RH. Scotopic threshold response of proximal retina in cat. *J Neurophysiol*. 1986;56:1049–1061.
4. Brown KT. The electroretinogram: its components and their origins. *Vision Res*. 1968;8:633–677.
5. Newman EA, Odette LL. Model of electroretinogram b-wave generation: a test of the K+ hypothesis. *J Neurophysiol*. 1984;51:164–182.
6. Cobb WA, Morton HB. A new component of the human electroretinogram. *J Physiol*. 1954;123:36–37.
7. Wachtmeister L, Dowling JE. The oscillatory potentials of the mudpuppy retina. *Invest Ophthalmol Vis Sci*. 1978;17:1176–1188.
8. Kondo M, Piao CH, Tanikawa A, et al. Amplitude decrease of photopic ERG b-wave at higher stimulus intensities in humans. *Jpn J Ophthalmol*. 2000;44:20–28.
9. Peachey NS, Alexander KR, Fishman GA, et al. Properties of the human cone system electroretinogram during light adaptation. *Appl Opt*. 1989;28:1145–1150.
10. Yonemura D, Aoki T, Tsuzuki K. Electroretinogram in diabetic retinopathy. *Arch Ophthalmol*. 1962;68:19–24.
11. Miyake Y. *Electrodiagnosis of retinal diseases*. Springer: Tokyo; 2006.
12. Karpe G. Uchermann A. The clinical electroretinogram. VII. The electroretinogram in circulatory disturbances of the retina. *Acta Ophthalmol*. 1955;33:493–516.
13. Sabates R, Hirose T, McMeel JW. Electroretinography in the prognosis and classification of central retinal vein occlusion. *Arch Ophthalmol*. 1983;101:232–235.
14. Hiraiwa T, Horio N, Terasaki H, et al. Preoperative

electroretinogram and postoperative visual outcome in patients with diabetic vitreous hemorrhage. *Jpn J Ophthalmol*. 2003;47:307–311.
15. Horio N, Terasaki H, Yamamoto E, et al. Electroretinogram in the diagnosis of endophthalmitis after intraocular lens implantation. *Am J Ophthalmol*. 2001;132:258–259.
16. Miyake Y, Yagasaki K, Horiguchi M, et al. Congenital stationary night blindness with negative electroretinogram: a new classification. *Arch Ophthalmol*. 1986;104:1013–1020.
17. Horiguchi M, Miyake Y. Batten disease: deteriorating course of ocular findings. *Jpn J Ophthalmol*. 1992;36:91–96.
18. Berson EL, Lessell S. Paraneoplastic night blindness with malignant melanoma. *Am J Ophthalmol*. 1988;106:307–311.
19. Heckenlively JR, Aptsiauri N, Holder GE. Autoimmune retinopathy, CAR and MAR syndromes. Heckenlively JR, Arden GB. *Principles and practice of clinical electrophysiology of vision*. 2nd ed. MIT Press: Cambridge, MA; 2006:691–698.
20. Hirose T, Katsumi O, Pruett RC, et al. Retinal function in birdshot retinochoroidopathy. *Acta Ophthalmol*. 1991;69:327–337.
21. Viswanathan S, Frishiman LJ, Robson JG, et al. The photopic negative response of the macaque electroretinogram: reduction by experimental glaucoma. *Invest Ophthalmol Vis Sci*. 1999;40:1124–1136.
22. Kohl S, Baumann B, Broghammer M, et al. Mutatons in the CNGB3 gene encoding the beta-subunit of the cone photoreceptor cGMP-gated channel are responsible for achromatopsia (ACHM3) linked to chromosome 8q21. *Hum Mol Genet*. 2000;9:2107–2116.
23. Terasaki H, Miyake Y. Japanese family with blue cone monochromatism. *Jpn J Ophthalmol*. 1992;36:132–141.
24. Oguchi C. Über die eigenartige Hemeralopie mit diffuser weissgr ä ulicher Verfärbung des Augenhintergrundes. *Graefes Arch Ophthalmol*. 1912;81:109.
25. Mizuo A. On a new discovery in the dark adaptation in Oguchi's disease. *Acta Soc Ophthalmol Jpn*. 1913;17:1854–1859.
26. Miyake Y, Horiguchi M, Suzuki S, et al. Electrophysiological

findings in patients with Oguchi's disease. *Jpn J Ophthalmol*. 1996;40:511–519.
27. Fucks S, Nakazawa M, Maw M, et al. A homozygous 1-base pair deletion in the arrestin gene is a frequent cause of Oguchi disease in Japanese. *Nat Genet*. 1995;10:360–362.
28. Yamamoto S, Sipple KC, Berson EL, et al. Defects in the rhodopsin kinase gene in the Oguchi form of stationary night blindness. *Nat Genet*. 1997;15:175–178.
29. Carr RE, Gouras P. Oguchi's disease. *Arch Ophthalmol*. 1965;73:646–656.
30. Carr RE. Congenital stationary night blindness. *Trans Am Ophthalmol Soc*. 1974;72:448–487.
31. Miyake Y, Watabnabe I, Asano T, et al. Further studies on EOG in retinitis punctate albescens: effect of change of dark adaptation time on EOG. *Folia Ophthalmol Jpn*. 1974;25:518–527.
32. Yamamoto H, Simon A, Eriksson U, et al. Mutations in the gene encoding *11-cis* retinol dehydrogenase cause delayed dark adaptation and fundus albipunctatus. *Nat Genet*. 1999;22:188–191.
33. Miyake Y, Shiroyama N, Sugita S, et al. Fundus albipunctatus associated with cone dystrophy. *Br J Ophthalmol*. 1992;76:375–379.
34. Nakamura M, Hotta Y, Tanikawa A, et al. A high association with cone dystrophy in fundus albipunctatus caused by mutations of the RDH5 gene. *Invest Ophthalmol Vis Sci*. 2000;41:3925–3932.
35. Sieving PA. Photopic ON- and OFF-pathway abnormalities in retinal dytrophies. *Trans Am Ophthalmol Soc*. 1993;91:701–773.
36. Miyake Y, Yagasaki K, Horiguchi M, et al. Congenital stationary night blindness with negative electroretinogram: a new classification. *Arch Ophthalmol*. 1986;104:1013–1020.
37. Miyake Y, Yagasaki K, Horiguchi M, et al. On- and off-responses in photopic electroretinogram in complete and incomplete types of congenital stationary night blindness. *Jpn J Ophthalmol*. 1987;31:81–87.
38. Bech-Hansen NT, Naylor MJ, Maybaum TA, et al. Mutation

in NYX, encoding the leucine-rich proteoglycan nyctalopin, cause X-linked complete congenital stationary night blindness. *Nat Genet*. 2000;26:319–323.
39. Dryja TP, McGee TL, Berson EL, et al. Night blindness and abnormal cone electroretinogram ON responses in patients with mutations in the GRM6 gene encoding mGluR6. *Proc Natl Acad Sci USA*. 2005;102:4884–4889.
40. Audo I, Kohl S, Leroy BP, et al. TRPM1 is mutated in patients with autosomal-recessive complete congenital stationary night blindness. *Am J Hum Genet*. 2009;85:720–729.
41. Strom TM, Nyakatura G, Apfelstedt-Sylla E, et al. An L-type calcium-channel gene mutated in incomplete X-linked congenital stationary night blindness. *Nat Genet*. 1998;19:260–263.
42. Kato K, Miyake Y, Kachi S, et al. Axial length and refractive error in X-linked retinoschisis. *Am J Ophthalmol*. 2001;131:812–814.
43. Sauer CG, Gehrig A, Warneke-Wittstock R, et al. Positional cloning of the gene associated with X-linked juvenile retinoschisis. *Nat Genet*. 1997;17:164–170.
44. Sieving PA, Juvenile X. linked retinoschisis. Heckenlively JR, Arden GB. *Principles and practice of clinical electrophysiology of vision*. 2nd ed. MIT Press: Cambridge, MA; 2006:823–827.
45. Miyake Y, Shiroyama N, Ota I, et al. Oscillatory potentials in electroretinograms of the human macular region. *Invest Ophthalmol Vis Sci*. 1988;29:1631–1635.
46. Sutter EE, Tan D. The field topography of ERG components in man-I: the photopic luminance response. *Vision Res*. 1992;32:433–446.
47. Miyake Y, Shiroyama N, Horiguchi M, et al. Asymmetry of focal ERG in human macular region. *Invest Ophthalmol Vis Sci*. 1989;30:1743–1749.
48. Hood DC, Bach M, Brigell M, et al. ISCEV Standard for clinical multifocal electroretinography (2011 edition). *Doc Ophthalmol*. 2012;124:1–13.
49. Miyake Y, Miyake K, Shiroyama N. Classification of aphakic cystoid macular edema with focal macular

electroretinograms. *Am J Ophthalmol*. 1993;116:576–583.
50. Tanikawa A, Horiguchi M, Kondo M, et al. Abnormal focal macular electroretinograms in eyes with idiopathic epimacular membrane. *Am J Ophthalmol*. 1999;127:559–564.
51. Miyake Y, Shiroyama N, Ota I, et al. Local macular electroretinographic responses in idiopathic central serous chorioretinopathy. *Am J Ophthalmol*. 1988;106:546–550.
52. Miyake Y, Ichikawa K, Shiose Y, et al. Hereditary macular dystrophy without visible fundus abnormality. *Am J Ophthalmol*. 1989;292–299.
53. Miyake Y, Horiguchi M, Tomita N, et al. Occult macular dystrophy. *Am J Ophthalmol*. 1996;122:644–653.
54. Akahori M, Tsunoda K, Miyake Y, et al. Dominant mutations in RP1L1 are responsible for occult macular dystrophy. *Am J Hum Genet*. 2010;87:424–429.
55. Gass JD. Acute zonal occult outer retinopathy. *J Clin Neurol Ophthalmol*. 1993;13:79–97.
56. Ogino K, Tsujikawa A, Nakamura H, et al. Focal macular electroretinogram in macular edema secondary to central retinal vein occlusion. *Invest Ophthalmol Vis Sci*. 2011;52:3514–3520.
57. Nakamura H, Miyamoto K, Yokota S, et al. Focal macular photopic negative response in patients with optic neuritis. *Eye (Lond)*. 2011;25:358–364.
58. Machida S, Gotoh Y, Toba Y, et al. Correlation between photopic negative response and retinal nerve fiber layer thickness and optic disc topography in glaucomatous eyes. *Invest Ophthalmol Vis Sci*. 2008;49:2201–2207.
59. Kooijman AC. Damhof A. ERG lens with built-in ganzfeld light source for stimulation and adaptation. *Invest Ophthalmol Vis Sci*. 1980;19:315–318.
60. Kondo M, Piao CH, Tanikawa A, et al. A contact lens electrode with built-in high intensity white light-emitting diodes: a contact lens electrode with built-in white LEDs. *Doc Ophthalmol*. 2001;102:1–9.
61. Miyake Y, Yagasaki K, Horiguchi M, et al. Electroretinographic monitoring of retinal function during eye surgery. *Arch Ophthalmol*. 1991;109:1123–1126.

62. Miyake Y, Yagasaki K, Ichikawa H. Differential diagnosis of congenital tritanopia and dominantly inherited juvenile optic atrophy. *Arch Ophthalmol*. 1985;103:1496–1501.
63. Horiguchi M, Miyake Y, Kondo M, et al. Blue light-emitting diode built-in contact lens electrode can record human S-cone electroretinogram. *Invest Ophthalmol Vis Sci*. 1995;36:1730–1732.
64. Kolb H. Lipets LE. The anatomical basis for color vision in the vertebrate retina. Gouras P. *The perception of colour*. Macmillan: London; 1991:128–145.
65. Du Bois Reymond EH. G Reimer: Berlin; 1849:251–288. *Chapter 3. Von dem ruhen Nervenstrome. Untersuchungen Über Thierische Electricität*. vol. 2.
66. Marmor MF, Brigell MG, McCulloch DL, et al. For the International Society for Clinical Electrophysiology of Vision. ISCEV standard for clinical electro-oculography (2010 update). *Doc Ophthalmol*. 2011;122:1–7.
67. Arden GB, Barrada A, Kelsey JH. New clinical test of retinal function based upon the standing potential of the eye. *Br J Ophthalmol*. 1962;46:449–467.
68. Arden GB. Origin and significance of the electro-oculogram. Heckenlively JR, Arden GB. *Principles and practice of clinical electrophysiology of vision*. 2nd ed. MIT Press: Cambridge, MA; 2006:123–138.
69. Odom JV, Bach M, Brigell M, et al. ISCEV standard for clinical visual evoked potentials – (2016 update). *Doc Ophthalmol*. 2016;133:1–9.
70. Miyake Y, Hirose T, Hara A. Electrophysiologic testing of visual functions for vitrectomy candidates. I. Results in eyes with known fundus diseases. *Retina*. 1983;3:86–94.
71. Miyake Y. Layer-by-layer analysis of macular diseases with objectively measured visual functions. *Jpn J Ophthalmol*. 1990;34:225–238.

11

Diagnostic Ophthalmic Ultrasound

Rudolf F. Guthoff, Leanne T. Labriola, Oliver Stachs

Introduction

Ultrasonography is a pervasive diagnostic tool within medicine. It is used to obtain noninvasive images that can aid in the management of patients in almost all fields of medicine. Ultrasound technology has a unique role in ophthalmology since it can provide quantitative and qualitative assessments of the globe and orbit. Ultrasound images are formed by capturing the reflected acoustic signal from different tissues. These images can provide important details of almost every part of the eye from the anterior cornea and ciliary body to the posterior retina and choroid. This chapter will explain the principles involved in ophthalmic ultrasound as well as provide examples of its use within ophthalmology.

Ultrasound – Past and Present

In 1880 the Curie brothers first demonstrated that a difference in electric potential could be created by mechanically pressing opposing surfaces of a tourmaline crystal.[1–7] This phenomenon is called the piezoelectric effect. This effect is the basis for ultrasound technology and was first applied in underwater sonar systems during World War II.[8] During that same era the medical community also adopted the use of ultrasound technology. Scientists realized the diagnostic potential of this technology when they were able to use acoustic wavelengths to study the consistency of a material without damaging the material itself.

In 1949 Ludwig used ultrasound to detect gallstones in patients. The first publication on the use of ophthalmologic ultrasound appeared in the medical literature in 1956.[9] By the mid-1970s, ophthalmologists were using ultrasound to determine axial length in a clinical setting. These measurements facilitated calculations of intraocular lens power which led to a revolution in cataract surgery.[10] Further innovations came when Baum and Greenwood introduced their two-dimensional B-mode image to ophthalmology.[11] Soon afterwards, Bronson et al.[12] developed a handheld contact transducer for this type of image acquisition which led to the rapid dissemination of ultrasound devices within ophthalmology clinics. The B-mode images could be used to accurately delineate retinal detachments, vitreous membranes, and choroidal tumors. In the early 1990s new technology made it possible to image the anterior segment of the eye with devices that captured images at higher frequencies of 35–50 MHz. This improved image resolution four- to fivefold and is still the gold standard for analysis of certain anterior-segment disease such as ciliary body effusions, infiltrates, and tumors.

Examination Techniques

The ultrasound examination is performed with the patient in a reclined position. The frequency of the ultrasound cannot pass through air; therefore, a coupling medium is needed to transmit the sound waves from the transducer to the ocular tissues. A common coupling agent is methylcellulose (Fig. 11.1). The coupling agent is applied to the tip of the transducer probe, which is then placed on the patient's anesthetized cornea.

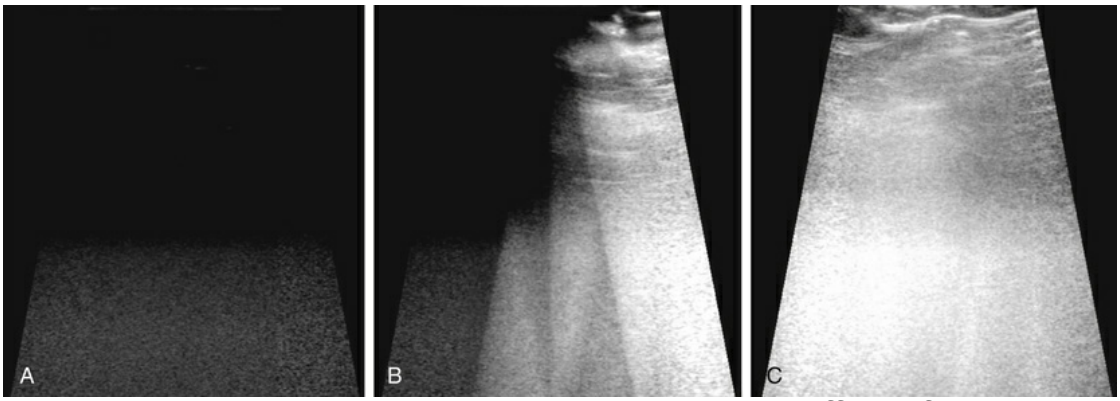

FIG. 11.1 Ultrasound images simulating the effect of transducer (A) without tissue-coupling agent, (B) with partial tissue-coupling agent, and (C) with a complete coupling agent, such as a gel-like contact substance.

A-Mode Technique

The A-scan is a linear representation of echo amplitude that is acquired along a single line of sight. Measurements of the ocular tissue can be achieved using the time interval between emission of the acoustic pulse and echo return to calculate the distance of the tissue being imaged. A-scan images should be obtained only through open lids since the eyelid tissue can attenuate the sound waves and decrease the resolution. The pressure applied by the examiner to the transducer tip is especially important when obtaining A-scan measurements. Excessive pressure can deform the cornea, and lead to inaccurate measurements.

B-Mode Technique

The B-scan is a two-dimensional cross-section image formed by mechanically sweeping the transducer over an angle of 50–60 degrees with the probe oriented in a specific axis. A systematic approach should be used to acquire all images. One method is first to obtain axial scans of the globe by placing the probe in the center of the cornea with the transducer tip oriented toward 12 o'clock in order to image the posterior pole and optic nerve. Next, the transducer can be turned temporally 90 degrees to obtain images through the macula. Finally, radial and transverse images of the globe can be obtained by placing the probe at each clock-hour

around the limbus. Radial scans are acquired when the probe is placed perpendicular to the limbus and the transducer tip is oriented toward the cornea. Transverse scans are obtained by turning the probe 90 degrees, orienting the transducer tip parallel to the limbus. The images obtained are the acoustic reflections from the opposing inner surface of the globe.

The reflected sound waves are recorded by the device and can be viewed as a two-dimensional image on the screen (Fig. 11.2). The ocular structures can be examined individually. The cornea is characterized ultrasonographically by two separate acoustic interfaces. The anterior chamber appears planoconvex in cross-section. The iris diaphragm cannot be satisfactorily imaged because of the limited lateral resolution power of the normal B-mode. A clear lens is acoustically empty and appears as an ellipsoid structure in axial sections. Similarly, normal vitreous does not give an acoustic signal; however, the presence of a detached posterior vitreous membrane presents an interface that can be imaged by increasing the amplification of the echo signal. The sclera is the most strongly reflecting structure on ocular ultrasonography.

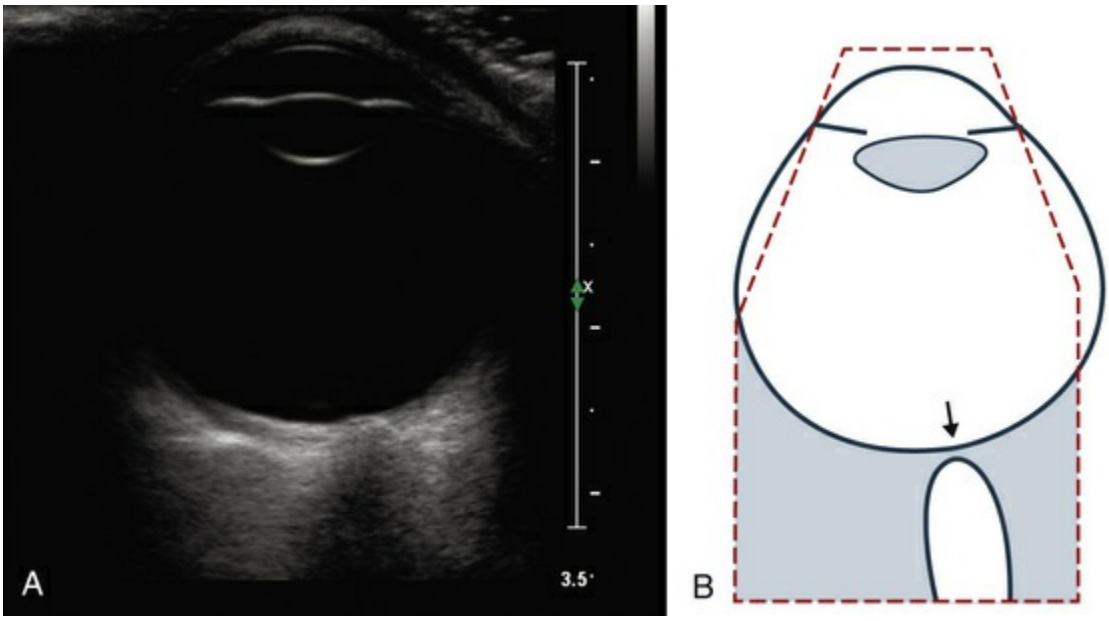

FIG. 11.2 (A) Cross-sectional echogram through a normal globe. (B) Schematic drawing of the eye: the arrow marks the entrance of the optic nerve.

High-Frequency Ultrasound Technique

High-frequency echograms can be used for ultrasound biomicroscopy (UBM). The shorter wavelengths provide better resolution of the anterior structures of the eye, including the cornea, lens, aqueous (Fig. 11.3), and ciliary body (Fig. 11.4).[13] High-frequency probes range from 50 to 100 MHz.[14–16] The 50-MHz probe provides the best balance between depth and resolution for UBM technique. One limitation of this technique is that the shorter wavelengths, from the higher frequency, have poor depth of penetration. UBM cannot visualize structures deeper than 4 mm from the surface.

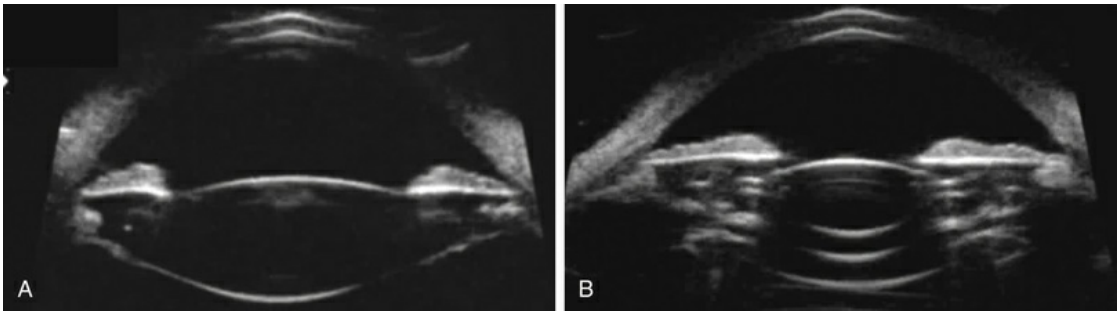

FIG. 11.3 The ultrasound biomicroscopy images of the anterior segment in (A) a phakic and (B) a pseudophakic eye with multiple echo of implant surface.

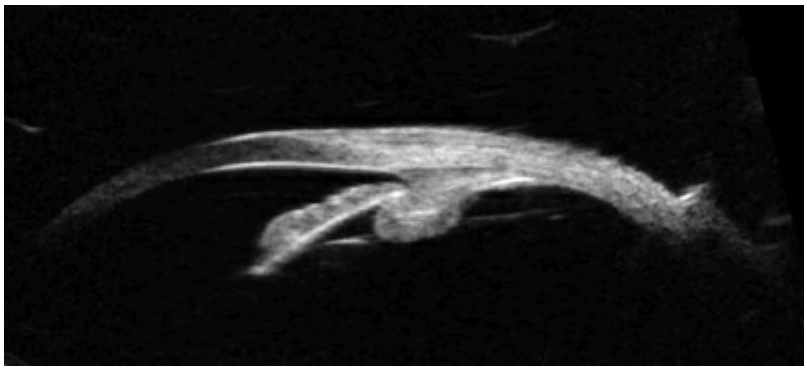

FIG. 11.4 Ultrasound biomicroscopy of the ciliary body. The shorter wavelengths are able to obtain high-resolution images of the anterior structures.

UBM requires immersion of the transducer in a medium to transmit the higher-frequency wavelengths. Saline or methylcellulose can be used as the coupling agent and is held in place over the eye with the use of a custom cup during the examination. UBM is performed through open eyelids in order to obtain a good reflection signal. Images produced by UBM have a resolution of 30–40 μm, which is similar to that seen with a low-power microscope.[17]

The cornea is the first structure seen on UBM. The anterior-chamber depth can be measured from the posterior surface of the cornea to the anterior lens pole. The posterior lens pole cannot be imaged by UBM due to its distance from the anterior surface. The iris is seen as a flat uniform echogenic area. The iris and ciliary body converge in the iris recess and insert into the scleral spur. The area under the peripheral iris and above the ciliary processes is defined as the ciliary sulcus. The angle of the eye can be studied in cross-section by orienting the probe in a radial fashion at the limbus. The scleral spur is the most important landmark in the angle on UBM.

Doppler Ultrasound

Doppler images are obtained by using frequency shifts from acoustic reflections to measure movements within a tissue and flow conditions within vessels. These frequency shifts can be observed in tissue volumes of less than 0.01 mL. False color can be added to the images based on ultrasound frequency to distinguish between higher and lower flow states, which aids in the interpretation of the final result (Fig. 11.5).

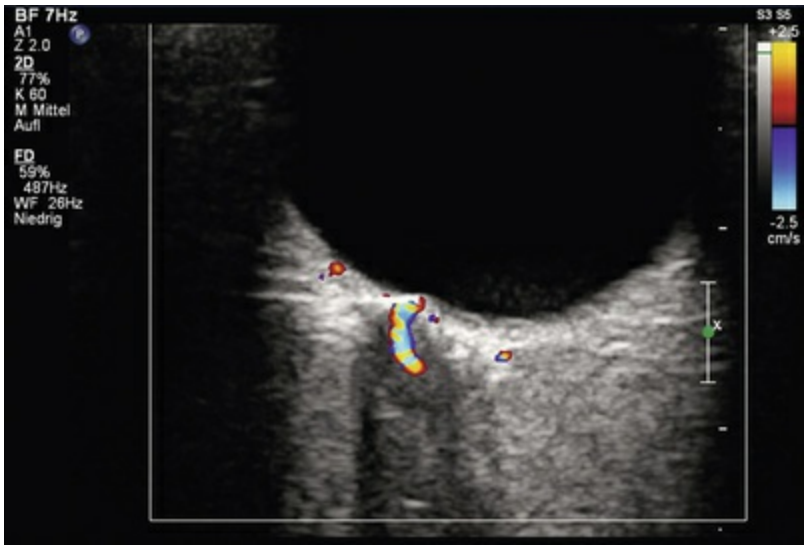

FIG. 11.5 Cross-sectional ultrasonogram through the posterior pole of the eye: color-coded signals from the central retinal artery (red) and the central retinal vein (blue) are displayed inside the optic nerve.

Ultrasound Biometry

Basic physics formulae can be used to calculate the speed of sound as it passes through various ocular tissues. This number can then be used to calculate distance measurements within the eye (Fig. 11.6). In order to obtain accurate measurements, the specific speed of sound of the different intraocular media, such as the lens, aqueous, and vitreous, must be known.[18] These formulae provide precise measurements that can be used to measure intraocular tumors or to deduce the axial length of the globe for intraocular lens power calculations.

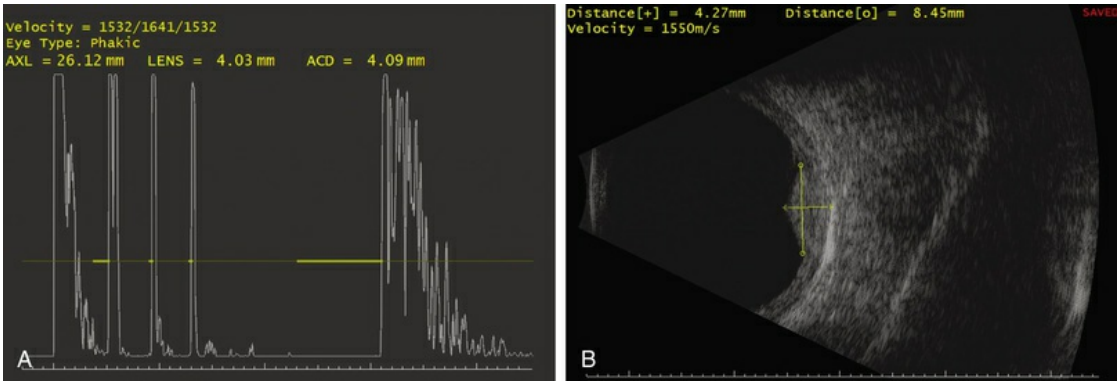

FIG. 11.6 (A) Immersion A-scan biometry showing

peak amplitudes of the signal reflection. (B) B-scan image with distance measurement captured on a frozen scan. Measurements are obtained by placing the cursor marks on the image and reading the distance between points.

Three-Dimensional Reconstructions

Real-time three-dimensional (3D) and four-dimensional (4D) images are currently used in some medical specialties, including gynecology, obstetrics, and cardiology, but their use in ophthalmology is limited. 3D ultrasonic images can be produced from a series of scan planes.[19–22] Silverman et al.[23] characterized the ciliary bodies in rabbits and human subjects using 3D high-resolution ultrasound. In the authors' laboratory, they developed a simple extension of the Ultrasound Biomicroscope Model 840 (Humphrey Instruments, Carl Zeiss Group) and VuMax UBM 35/50 (Sonomed) into a user-friendly 3D ultrasonic imaging system (Figs. 11.7 and 11.8).[24–28]

FIG. 11.7 Prototype of a handpiece for three-dimensional high-frequency scanning using the VuMax UBM 35/50 (Sonomed).

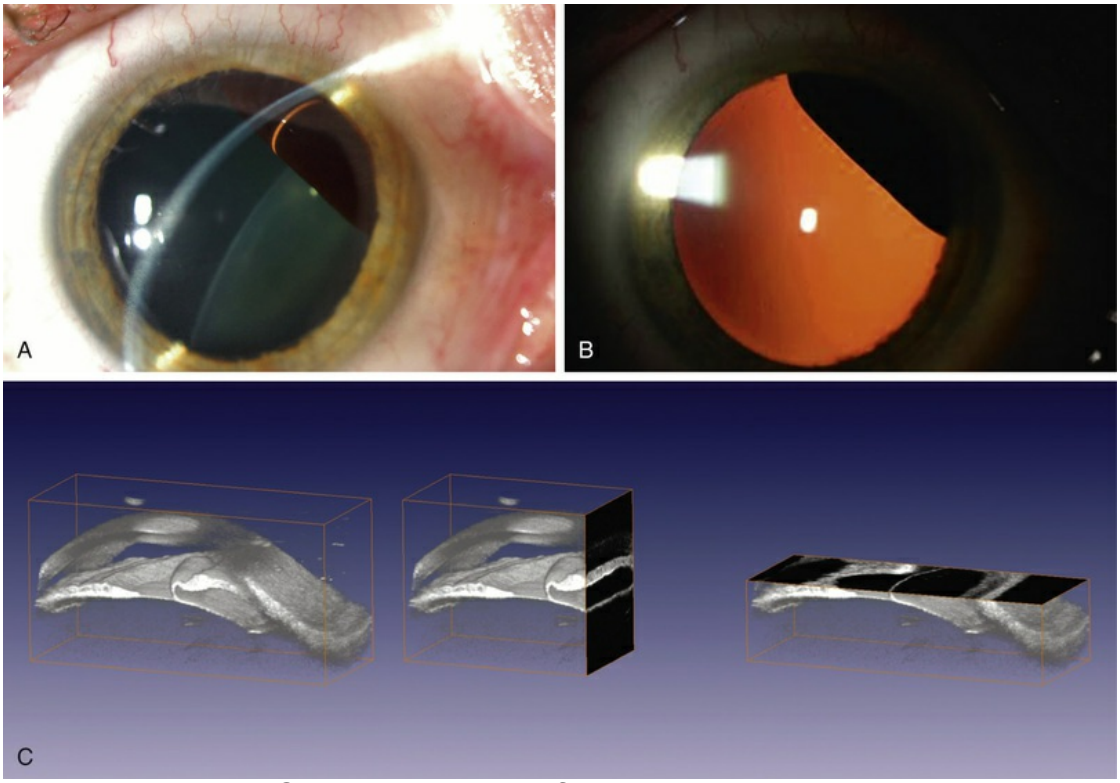

FIG. 11.8 Clinical pictures of the ciliary body with a pigment cyst (A) through a dilated pupil and (B) with retroillumination. (C) The same eye shown with three-dimensional reconstructed volume with oblique sections.

Ultrasound in Intraocular Pathology

Changes in the Shape of the Globe

Staphyloma

A staphyloma is an abnormal ectasia of the globe that involves uveal tissue. The ectasia typically has a smaller radius of curvature then the normal sclera of the globe. It can be identified on ultrasound by taking axial cross-sectional scans with the transducer probe (Fig. 11.9).

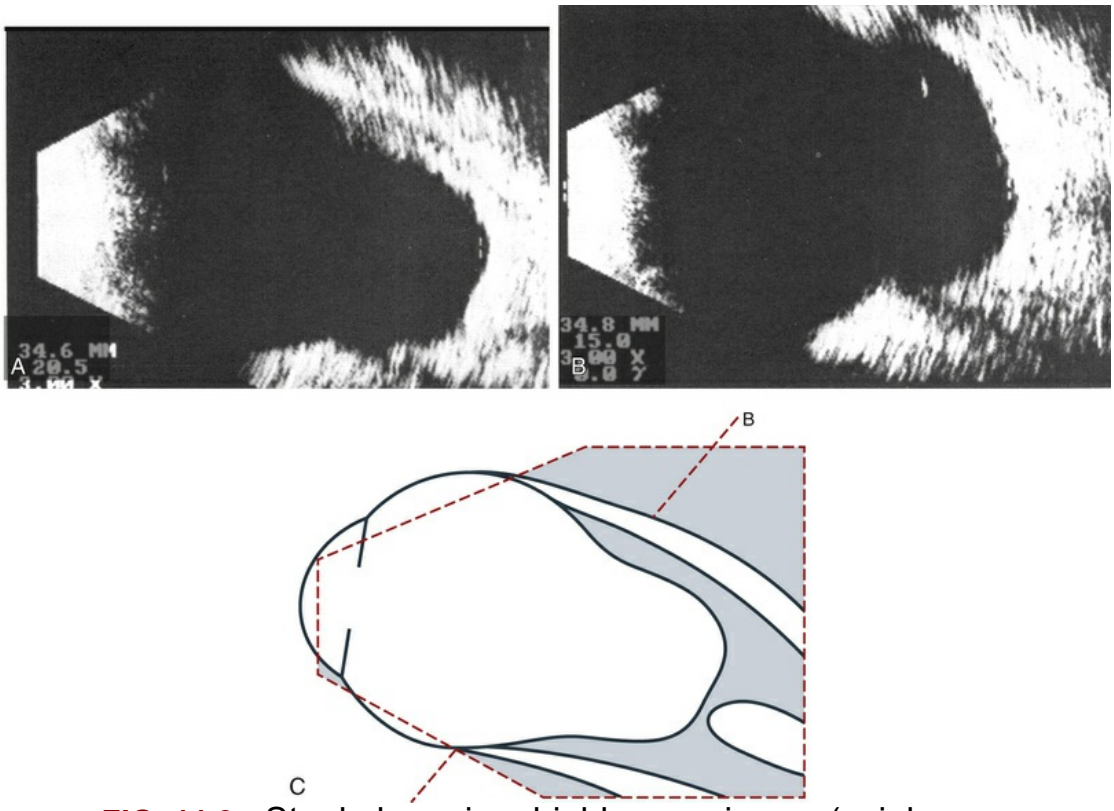

FIG. 11.9 Staphyloma in a highly myopic eye (axial length 34.8 mm). (A) An axial section of the eccentric entrance of the optic nerve can be seen. (B) The misshapen globe is especially well demonstrated on a sectional plane which lies outside the optical axis. (C) Schematic drawing.

Scleral Buckle.

A scleral buckle can create a posterior scleral deformity that looks similar to a staphyloma. It can be distinguished from a true staphyloma by a careful history or identification of the encircling band around the anterior sclera. Also, if silicone oil was used for repair, the higher index of refraction within the silicone oil can alter the reflectance of the ultrasound wavelengths, which might provide a false impression of globe deformation (Fig. 11.10).

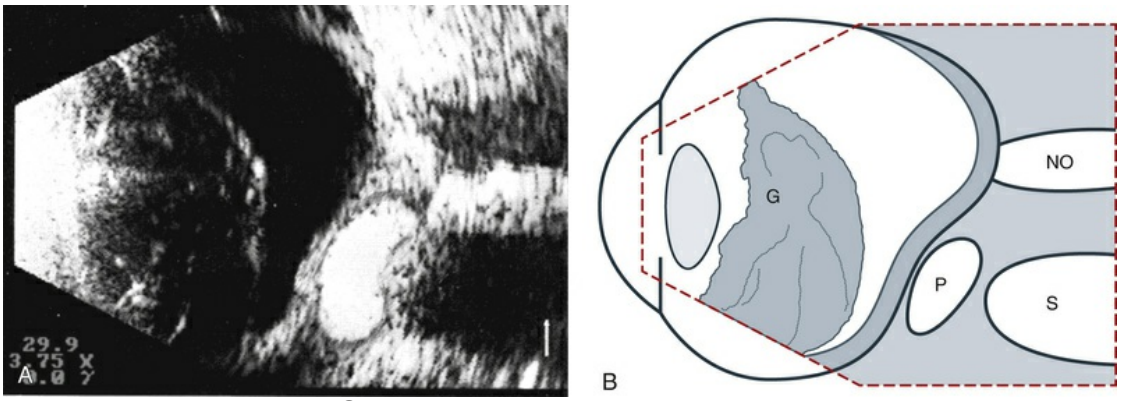

FIG. 11.10 (A) Scleral buckle produced by a silicone sponge explant. After placement of a scleral buckle, the deformity of the globe can be seen in an acoustic cross-section. Silicone explants almost completely reflect the ultrasound. They also cast an acoustic shadow. (B) Schematic drawing. *NO*, optic nerve; *P*, explant; *S*, sound shadow; *G*, syneretic, densified vitreous.

Microphthalmos

Congenital microphthalmos is an abnormally small eye that can be associated with other ocular abnormalities. The main finding in microphthalmos is axial shortening. This can be identified with A-scan measurements. The B-scan mode can be used to obtain radial and transverse scans to identify abnormalities in the vitreous and posterior segment of the eye, which can also be associated features of microphthalmos. These features include the presence of a coloboma of the retina or optic nerve head, orbital cysts (Fig. 11.11), or persistent hyperplastic vitreous.

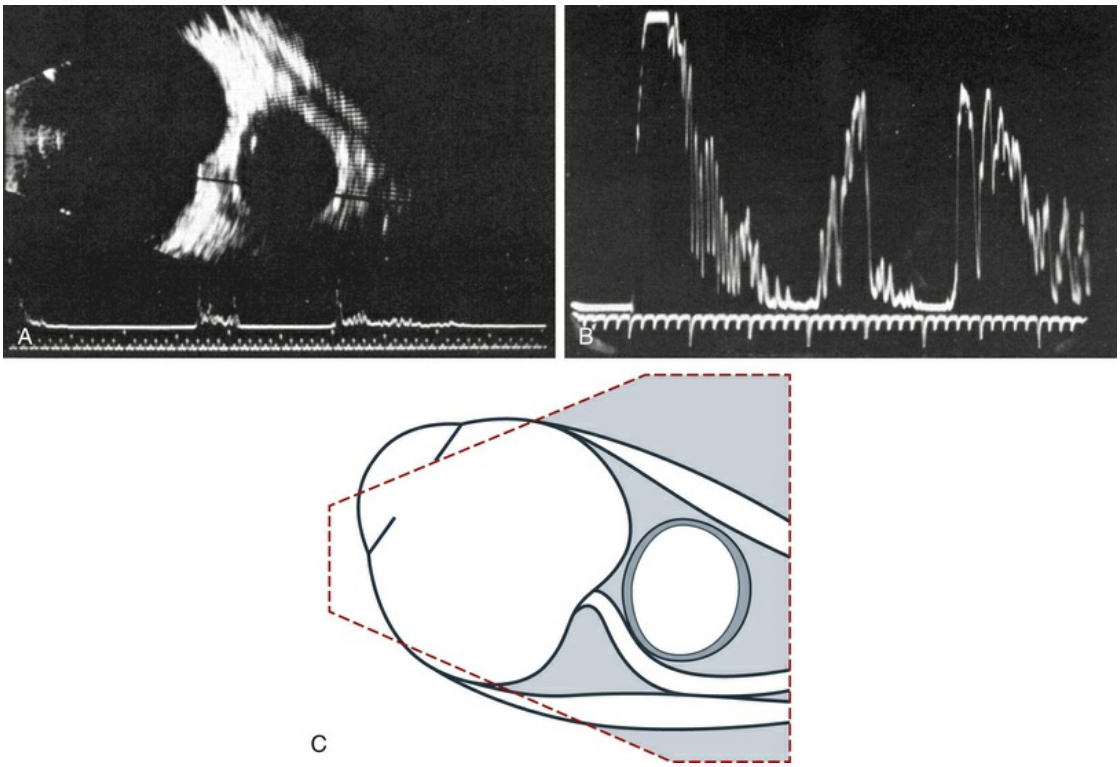

FIG. 11.11 Microphthalmos with orbital cyst. (A) Cystoid space is seen on the B-scan within the muscle cone, which is interpreted as a "completely separated coloboma." (B) A-scan image. (C) Schematic drawing.

Phthisis

Phthisis is defined as severe atrophy of the globe associated with hypotony. Phthisis is characterized ultrasonographically by a thickened outer scleral wall. Occasionally, calcification or ossification may be observed (Fig. 11.12). This may be due to degenerative processes and from metaplasia of the retinal pigment epithelium (RPE). In advanced cases of phthisis, the sclera and choroid can represent up to 70% of the total volume of the globe. The degree of thickening of the globe in chronic hypotony can be an indication of impending phthisis, but the precise thickness threshold for phthisis formation is unknown.

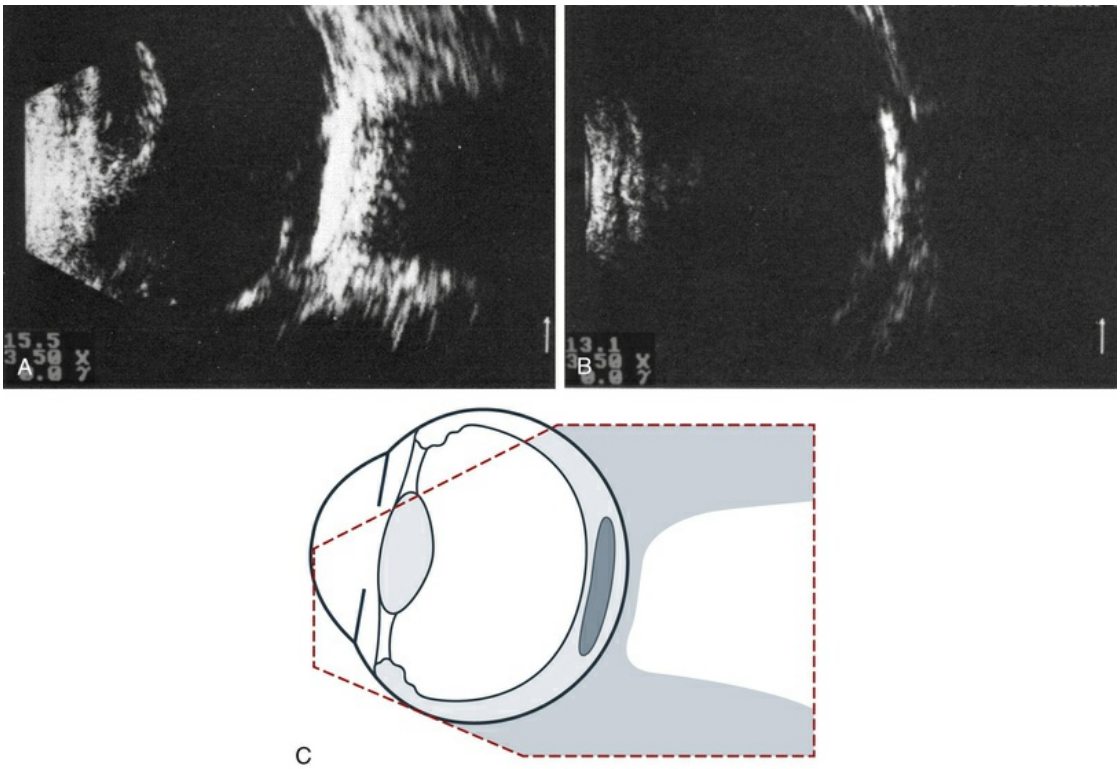

FIG. 11.12 Circumscribed calcification in the ocular wall in advanced phthisis bulbi. (A) Echographically we find highly reflective changes in the ocular wall from calcification or ossification of the choroid which casts a shadow on the soft tissue located posteriorly. (B) These strong echoes can be selectively imaged by reducing the amplification. (C) Schematic drawing.

Vitreous

Echographic examination can provide information on vitreous structure, which is particularly useful when visualization of the posterior pole is poor due to anterior media opacities. Ultrasonographic findings allow the examiner to differentiate dot-, strand-, and membrane-like reflections (Fig. 11.13). Box 11.1 summarizes the most frequent conditions associated with pathologic changes in the vitreous.

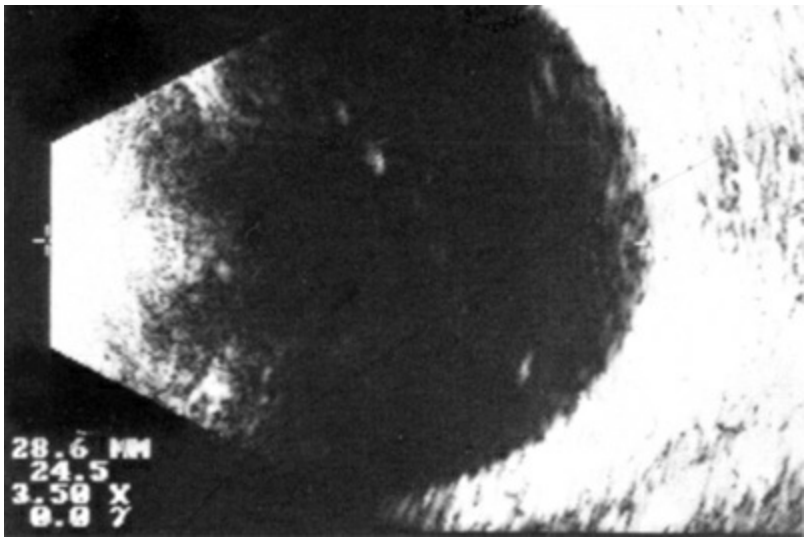

FIG. 11.13 Vitreous opacities. In maximal amplification, small heterogeneous spots can be seen echographically, even though the vitreous appears optically clear (left). They act as dot-like reflectors.

Box 11.1

Clinical Conditions With Ultrasonographically Demonstrable Vitreous Changes

- Changes in the shape of the globe
- Vitreous opacities
- Asteroid hyalosis
- Synchysis scintillans
- Acute posterior vitreous detachment
- Vitreous hemorrhage
- Uveitis (idiopathic)
- Uveitis (infectious)
- Intraocular foreign body
- Persistence and hyperplasia of the primary vitreous

Vitreous Degeneration

Vitreous syneresis can appear as dot-like reflections which can be more pronounced in myopia or senile vitreous. During a symptomatic posterior vitreous detachment, the B-mode echo may demonstrate various stages of vitreous syneresis and may reveal the remaining adhesions of the hyaloid membrane to the retinal surface (Fig. 11.14).

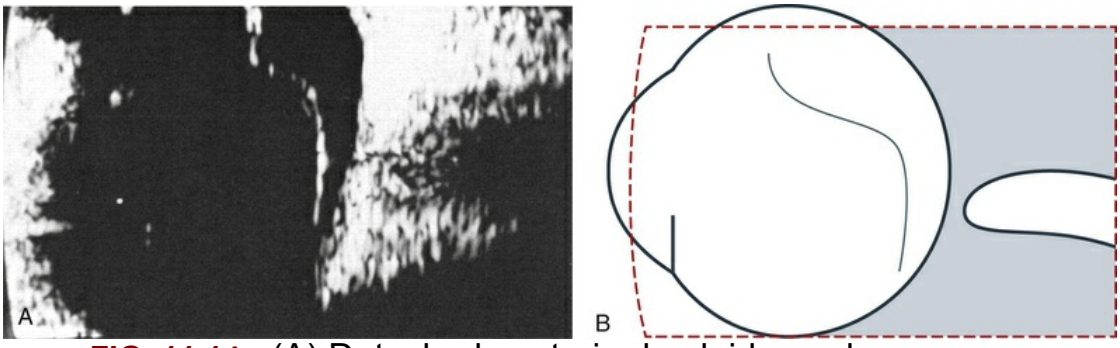

FIG. 11.14 (A) Detached posterior hyaloid membrane imaged as a floating structure of low reflectivity. (B) Schematic drawing.

Asteroid Hyalosis

The calcium-containing lipids of asteroid hyalosis are suspended in the vitreous framework and act as distinctive sound reflectors (Fig. 11.15). They can demonstrate the dynamics of vitreous movements.

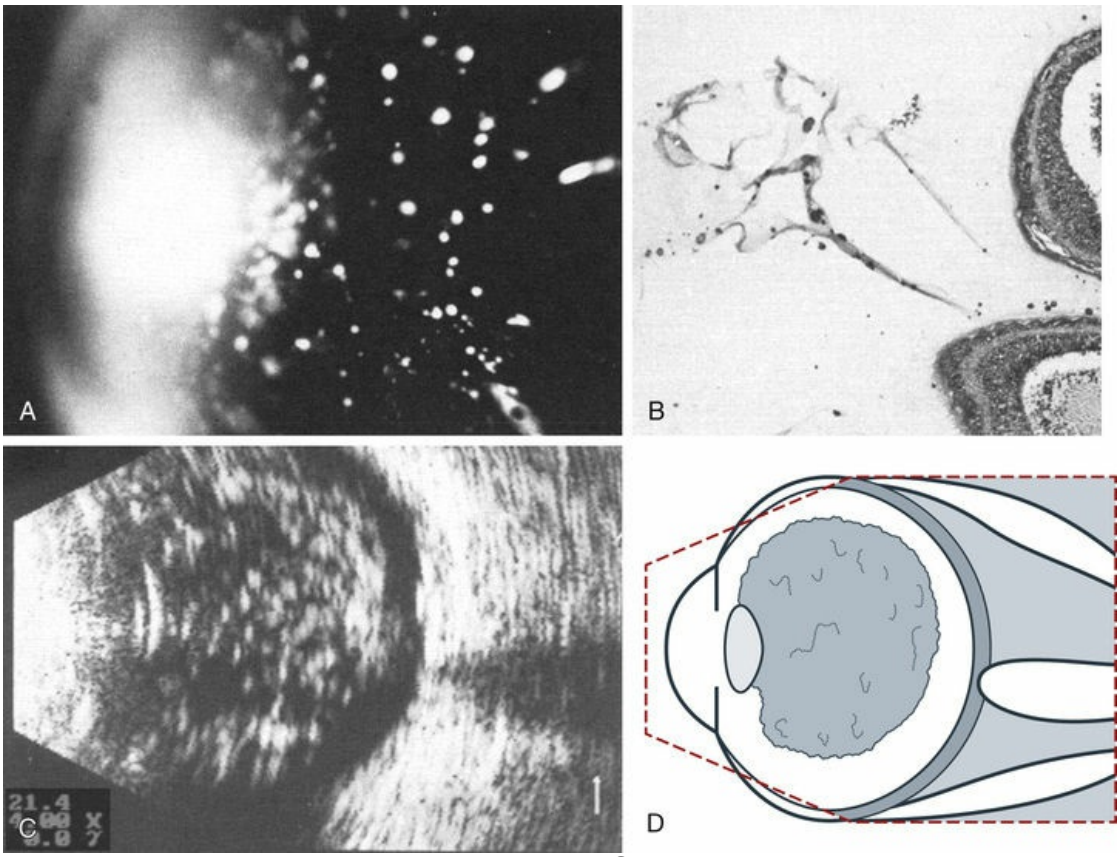

FIG. 11.15 Asteroid hyalosis. (A) Slit-lamp microscopic photograph of the anterior vitreous space. (B) Histologic image of asteroid hyalosis shows the calcium crystals adherent to the vitreous scaffold. (C) B-scan cross-section of the crystals, which represent good reflectors for the ultrasound. There is always an echo-free retrovitreal space seen near the ocular walls. (D) Schematic drawing.

Synchysis Scintillans.

In synchysis scintillans the vitreous is filled with cholesterol crystals. Unlike asteroid hyalosis, these crystals are not suspended within the vitreous but instead float freely in the vitreous space. When the globe moves, the crystals appear in the center of the vitreous body. This clinical picture may resemble asteroid hyalosis, but after a few seconds the cholesterol crystals will sink toward the bottom of the cavity. A-mode images display characteristic flickering spikes from the reflections of these crystals.

Persistent and Hyperplastic Primary Vitreous

The primary vitreous contains the tunica vasculosa lentis, which is part of the fetal vasculature system. During development, the tunica vasculosa lentis emanates from the optic nerve head and supplies the posterior lens. This structure should involute prior to birth. Failure of the primary vitreous to regress fully is termed persistent hyperplastic primary vitreous. As mentioned earlier, this can be associated with microphthalmos and cataract formation in the newborn. The condition persistent hyperplastic primary vitreous can be ultrasonographically characterized by two features. The first is a strand of membrane that extends between the posterior surface of the lens and the area of the optic nerve head. The second is the reduced axial length of the globe from microphthalmos on ultrasound biometry (Fig. 11.16). If the anomaly is only mild, the lens may be clear at birth but may become cataractous when the posterior lens capsule ruptures.

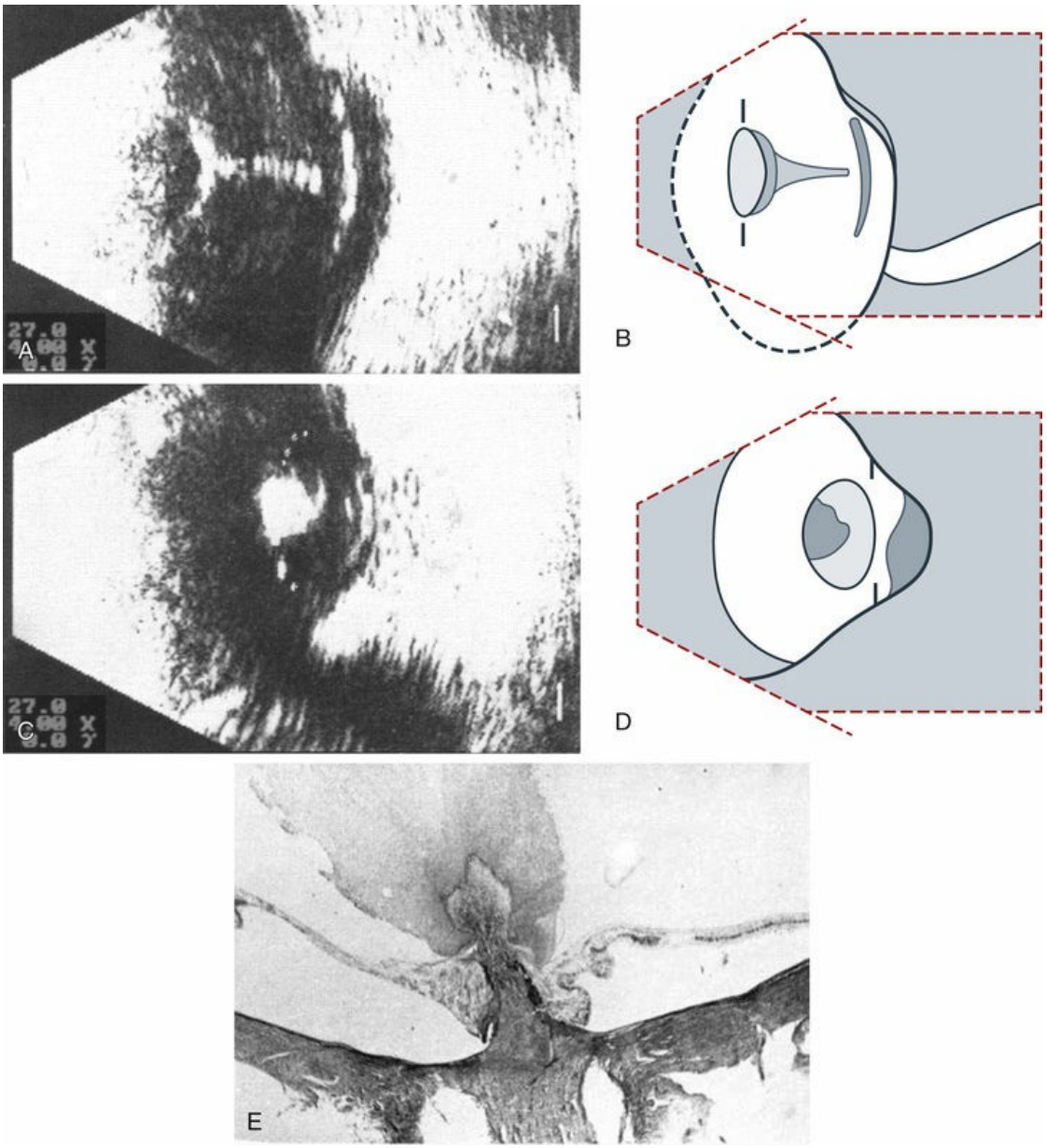

FIG. 11.16 (A–D) Posterior polar cataract in persistent hyperplastic primary vitreous (PHPV). An ultrasonographically demonstrable strand attached to the posterior lens pole points is suspicious for PHPV (A). Frontal plane taken temporally with maximal adduction of the globe (C). (B,D) Schematic drawings. The dark, hatched parts correspond to the opaque area of the posterior cortex and posterior capsule in a child with severe PHPV. (E) Histologic section of PHPV as seen at optic nerve head with loupe magnification.

Vitreous Hemorrhages

An acute vitreous hemorrhage is an important indication for ultrasonography. Acute hemorrhages can fill the vitreous cavity with small opacities from the particles of the red blood cells. These opacities usually accumulate after a few hours in the lower circumference of the vitreous base (Fig. 11.17).

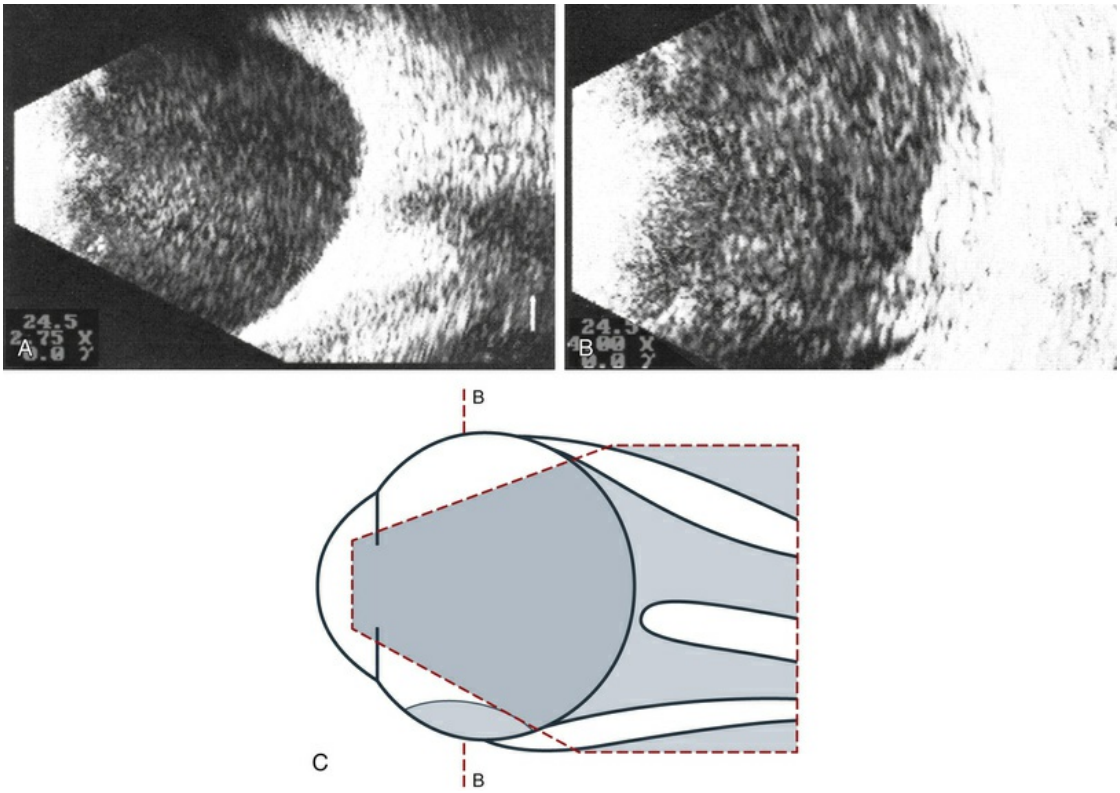

FIG. 11.17 (A) Conspicuous bleeding into syneretic vitreous; erythrocytes within the vitreous create reflective opacities. A static picture may give the impression of a solid lesion. (B) After a few hours the opacities usually accumulate in the lower aspect of the vitreous cavity. (C) Schematic drawing.

If a detachment of the posterior hyaloid membrane precedes a vitreous hemorrhage, the erythrocytes frequently precipitate on to a vitreous strand (Fig. 11.18). This strand may be responsible for the development of a retinal tear, and its traction can be demonstrated directly in acoustic sectioning (Fig. 11.19). A circumscribed thickening of the ocular wall in cross-section may indicate the presence of a retinal operculum (Fig. 11.20). This area should be localized echographically and then carefully scrutinized with

ophthalmoscopy if possible.

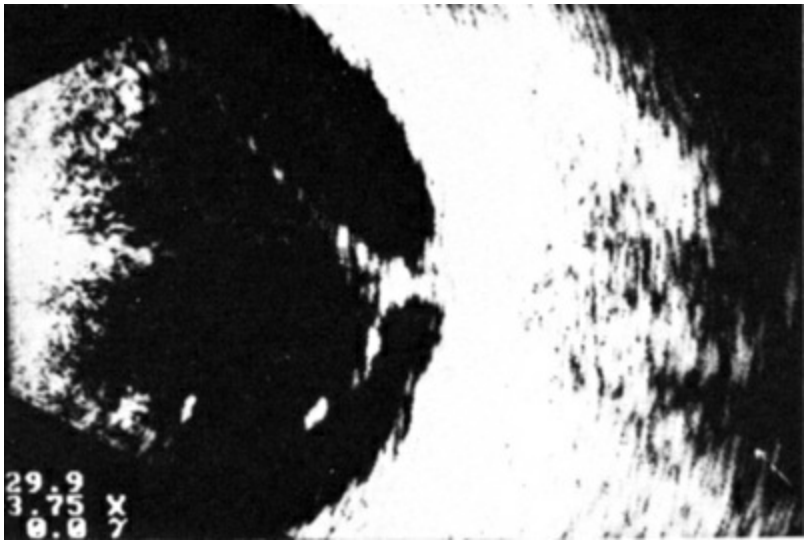

FIG. 11.18 Fresh vitreous hemorrhage. In a cross-sectional echogram the vitreous framework converges towards the ocular wall. Blood precipitates increase the acoustic reflectivity of the vitreous. Traction has to be assumed where the vitreous is in contact with the ocular wall.

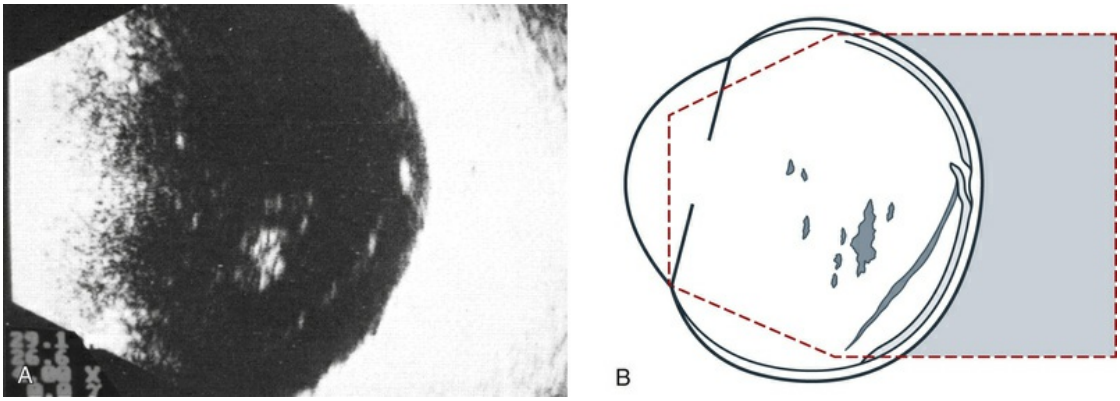

FIG. 11.19 (A) Recent vitreous hemorrhage. The low reflecting membranes float freely with ocular movement. A newly formed horseshoe tear may be present at their connection point to the wall. (B) Schematic drawing.

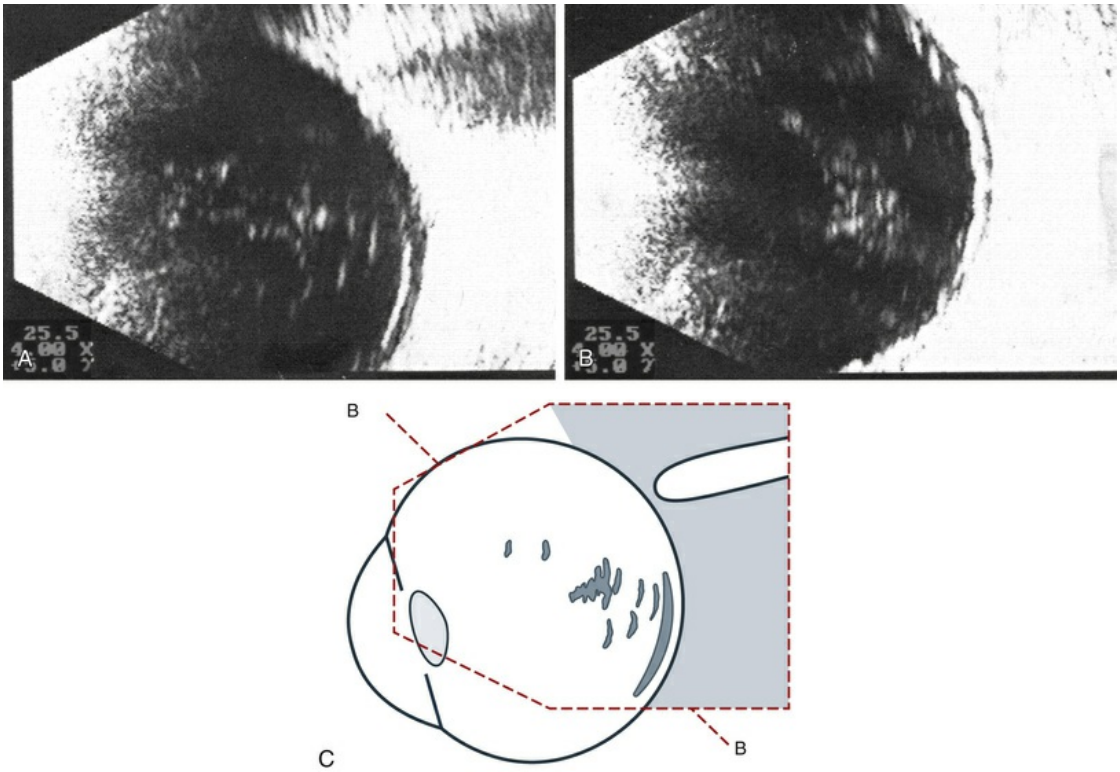

FIG. 11.20 (A,B) Recent vitreous hemorrhage. Erythrocytes have precipitated on to the partly detached posterior hyaloid membrane, increasing its acoustic reflectivity. (C) Schematic drawing.

In larger hemorrhages, the blood can also disseminate into multiple preexisting vitreous compartments. In the early phase of this process, the erythrocytes will collect in the retrovitreal space (Fig. 11.21). The retrovitreal space may completely clear after a few days or weeks due to its high fluid exchange rate; however, blood on the vitreous framework absorbs much more slowly (Fig. 11.22).

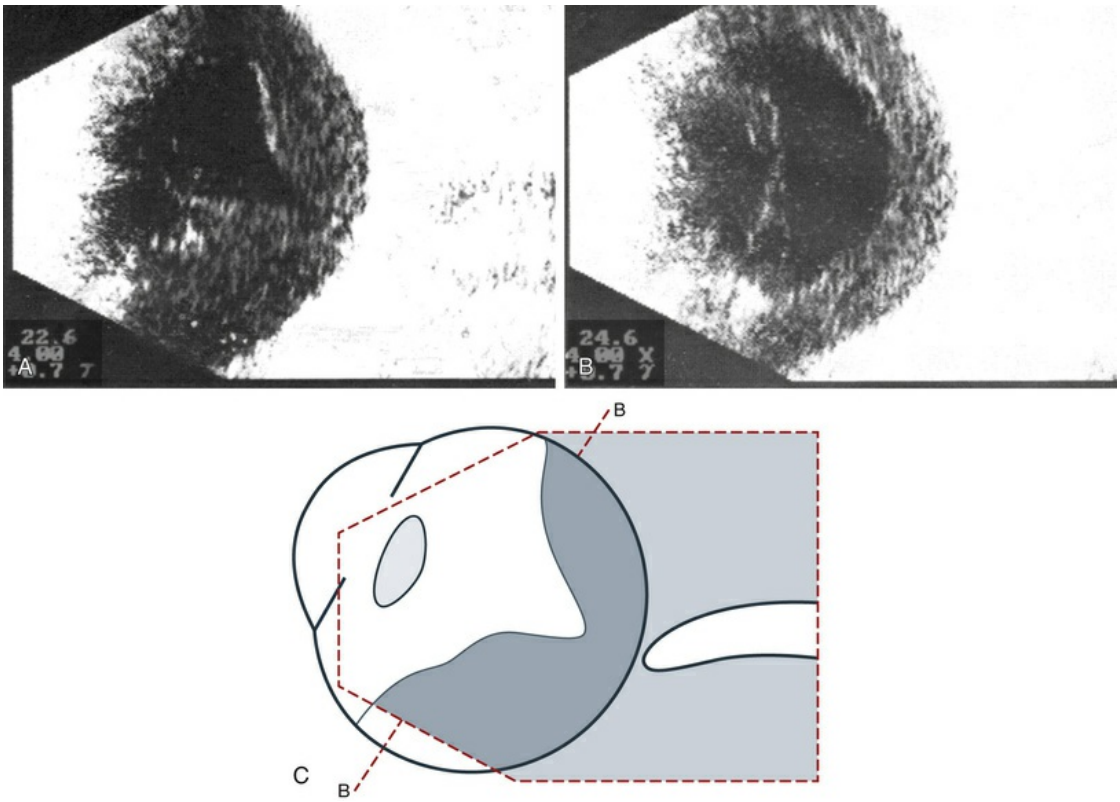

FIG. 11.21 (A) Vitreous hemorrhage with posterior vitreous detachment emphasizing the retrovitreal space. (B) In the early stage after the hemorrhage, erythrocytes accumulate in the retrovitreal space. They may ensheath the part of the vitreous that was free of blood and had a normal structure. (C) Schematic drawing.

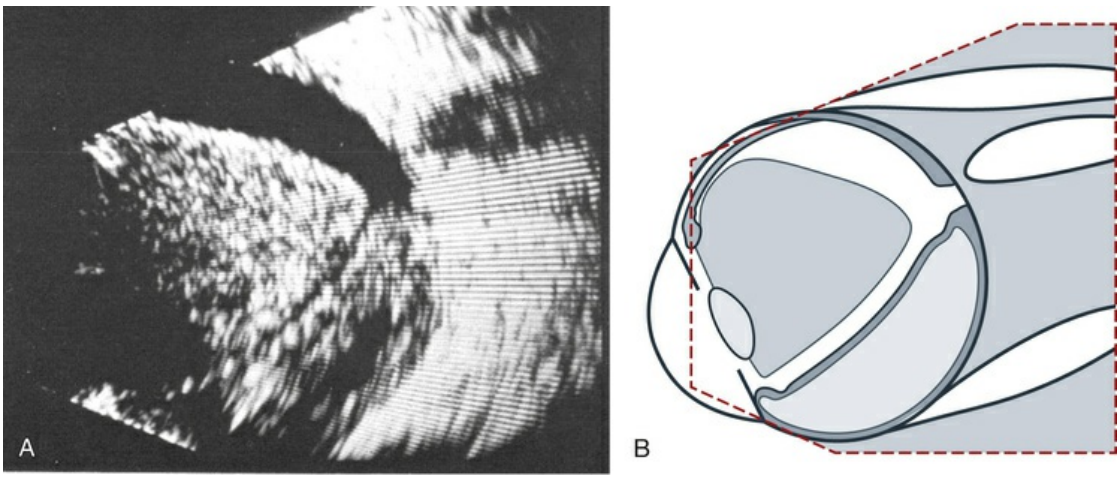

FIG. 11.22 The retrovitreal space may completely clear after a few days or weeks due to its high fluid exchange rate; however, blood on the vitreous

framework or located subretinally absorbs much more slowly (A). (B) Schematic drawing.

Vitreous Hemorrhage From Neovascularization.

Hemorrhages that develop from proliferative changes in patients with diabetic retinopathy and retinal neovascularization will always be accompanied by pathologic changes in the vitreous. Vitreous membranes tent rectilinearly between the adhesions to the retina. The normal aftermovements that should occur in the vitreous after eye movements are extinguished in the presence of peripheral neovascular tufts. The vitreous tufts create adhesions that encircle the posterior pole. This is an ominous sign, which is indicative of early traction retinal detachment from these circular adhesions (Fig. 11.23). Choroidal neovascularization from age-related macular degeneration will have hemorrhage in multiple layers of the eye (Fig. 11.24).

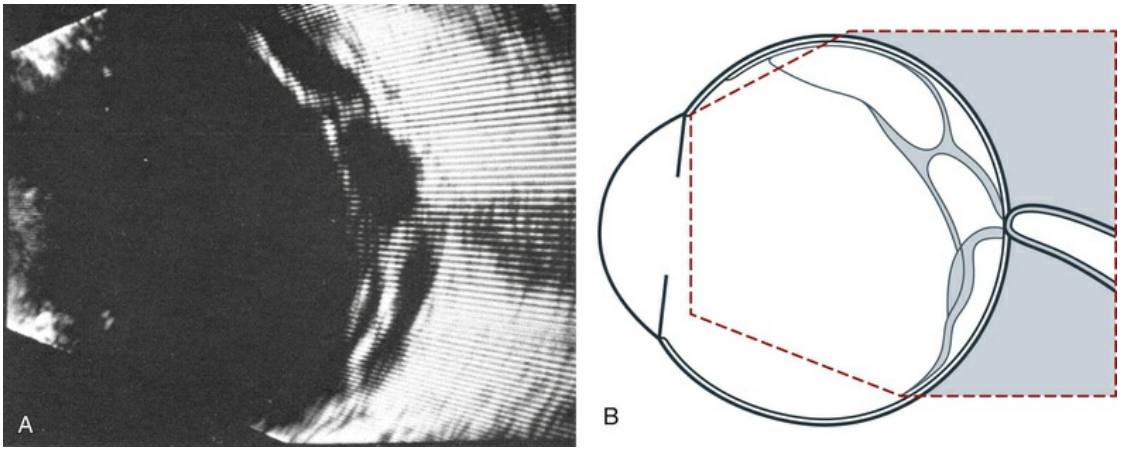

FIG. 11.23 (A) Beginning traction detachment at the posterior pole with vitreous contraction and proliferative diabetic retinopathy, which is hidden behind a diffuse vitreous hemorrhage. A springboard-like, taut, detached hyaloid membrane is still adherent to the retina at the posterior pole and has led to a traction detachment in several places. (B) Schematic drawing.

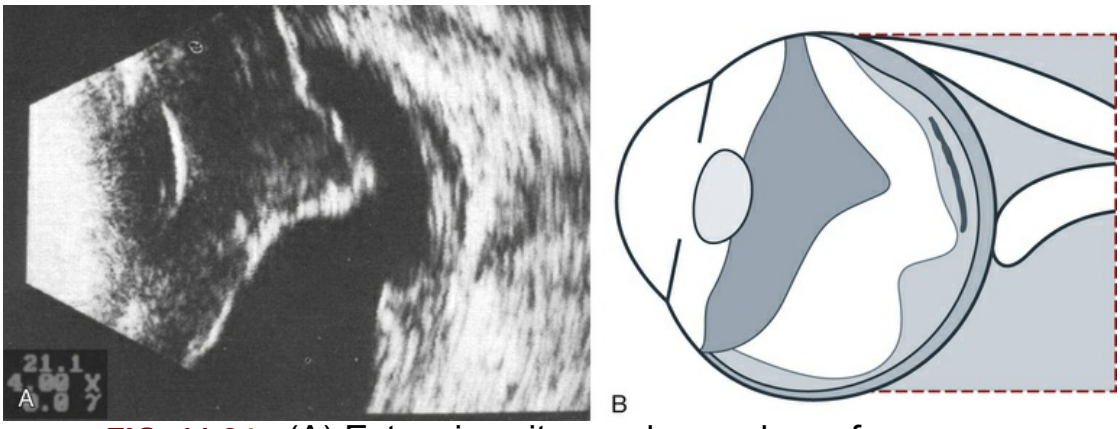

FIG. 11.24 (A) Extensive vitreous hemorrhage from disciform macular degeneration. The blood dissipates into the preretinal or intrachoroidal space, into the area of the macular lesion and into the detached vitreous. The retrovitreal space is echo-free because of its high fluid exchange. (B) Schematic drawing.

Terson Syndrome

Terson's sign is a multilayered, intraocular hemorrhage at the posterior pole that typically occurs after blunt trauma to the head. This is usually accompanied by a subarachnoid hemorrhage. If the posterior hyaloid membrane is still attached, the preretinal bleeding will slowly diffuse into the formed vitreous (Fig. 11.25). This can damage the underlying retina and may be an indication for an early vitrectomy.

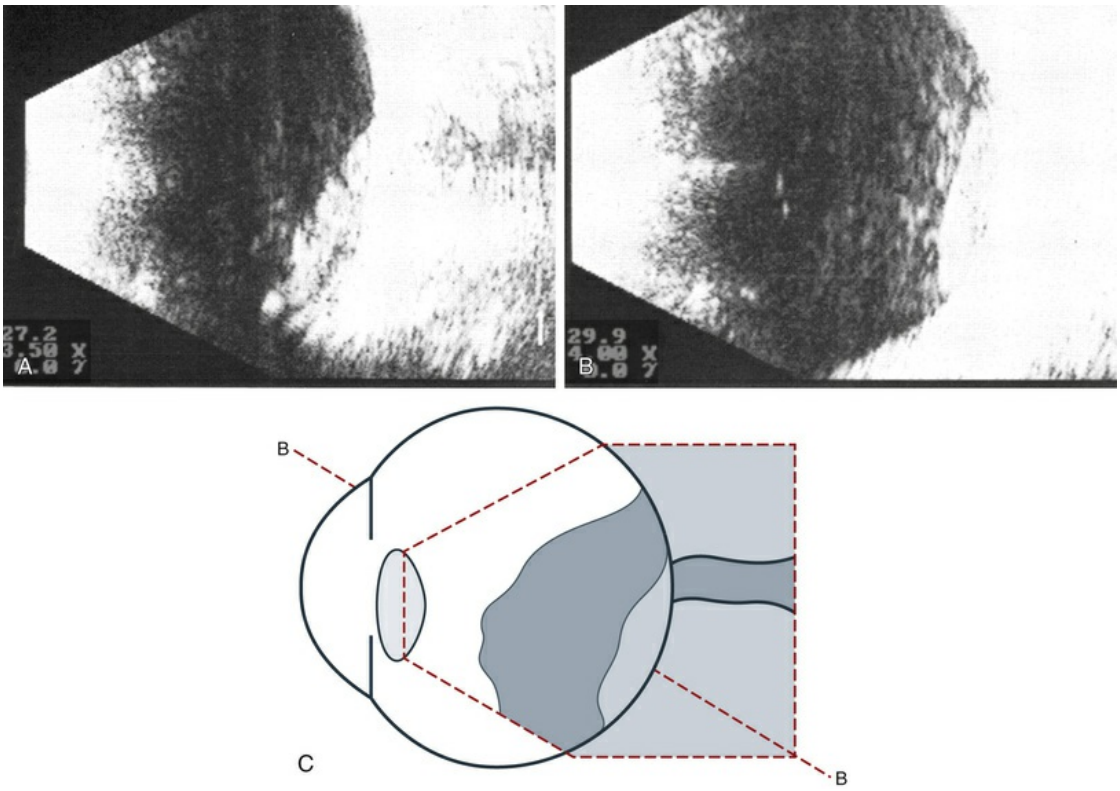

FIG. 11.25 (A,B) Retrovitreal bleeding associated with a subarachnoid hemorrhage (Terson syndrome). The bleeding originates from the area of the optic nerve head. (C) Schematic drawing.

Intraocular Infections

Ocular infection that extends toward the anterior segment or results in a hypopyon formation will have changes within the anterior vitreous space that are demonstrable on ultrasound. A thickening of the retina or choroid can be seen if the inflammation penetrates to the outer layers of the globe (Fig. 11.26). After only a few hours, these changes may involve the entire vitreous body (Fig. 11.27). If panophthalmitis follows a perforating injury, ultrasound evaluation can detect a local reaction at the entrance point of the infection (Figs. 11.28 and 11.29).

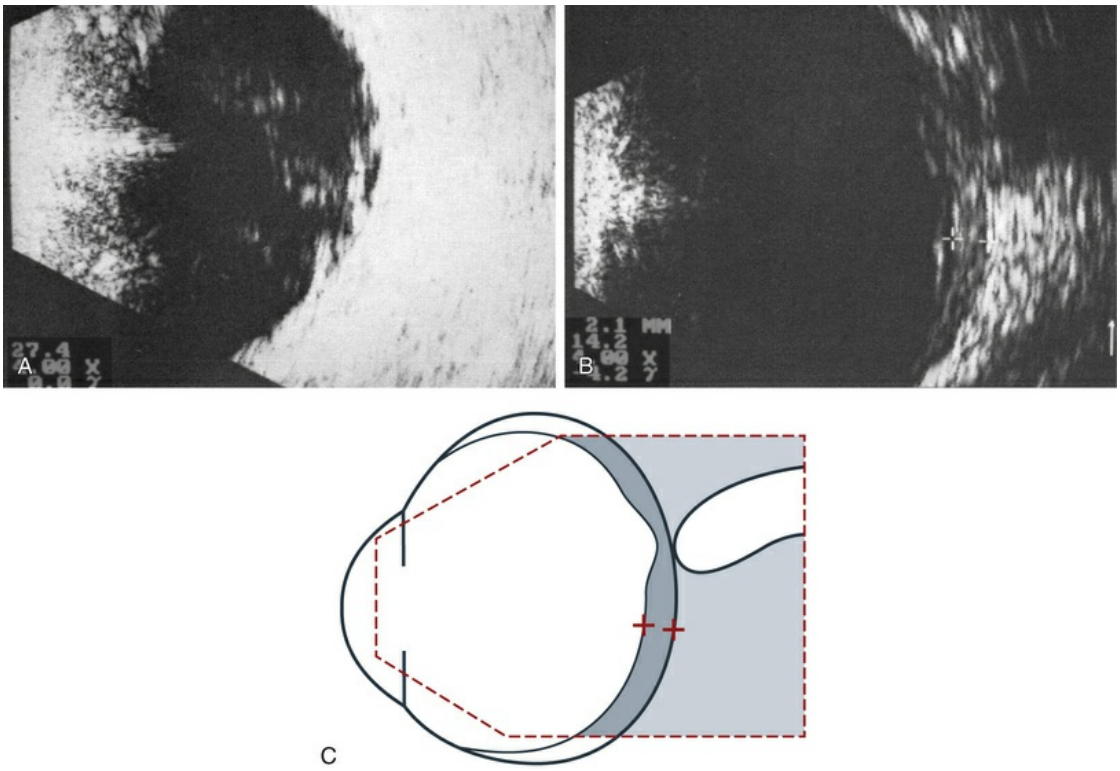

FIG. 11.26 (A,B) Panophthalmitis after an intraocular operation. Widening of the ocular wall to about 2.1 mm indicates inflammatory choroidal infiltrates. (C) Schematic drawing.

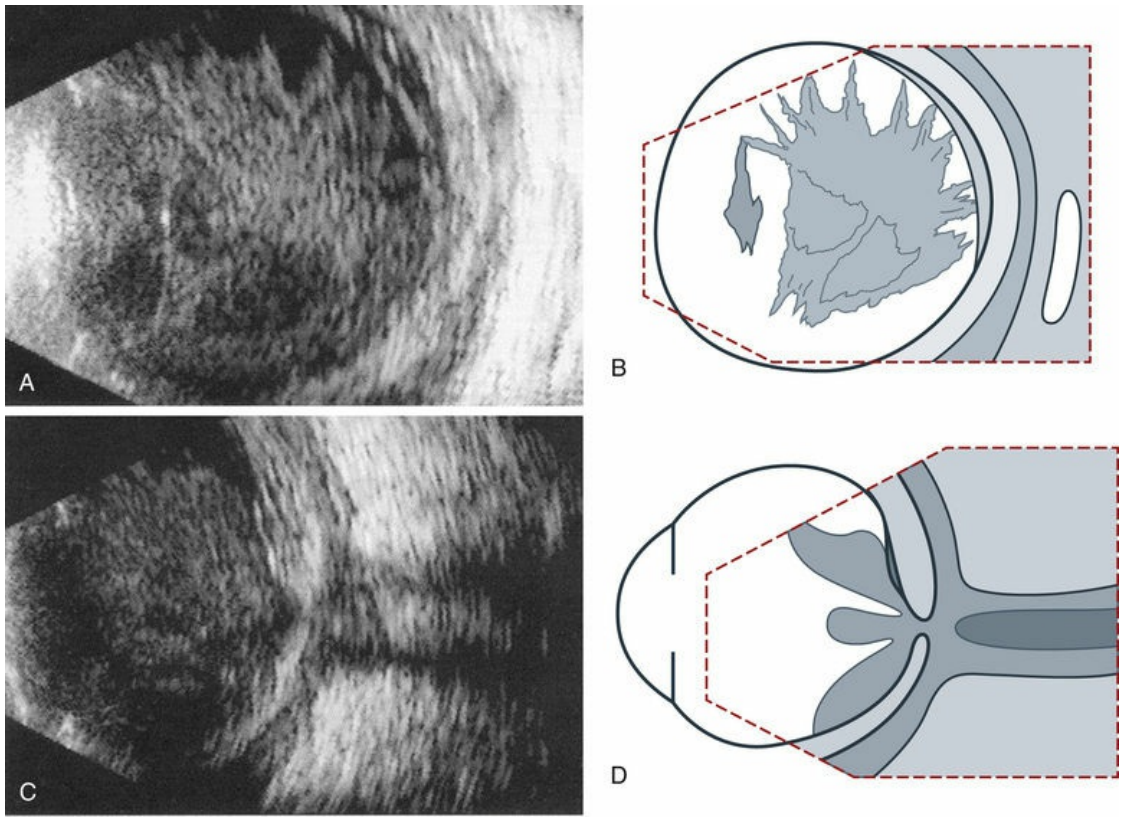

FIG. 11.27 Vitreous abscess that caused a bacterial orbital inflammation. (A) B-scan ultrasonography demonstrates a highly reflective vitreous body which is partly detached from the retina. (B) Schematic drawing of this image. (C) Posterior pole shows infiltration of Tenon's space and widening of the optic nerve sheath. (D) Schematic drawing.

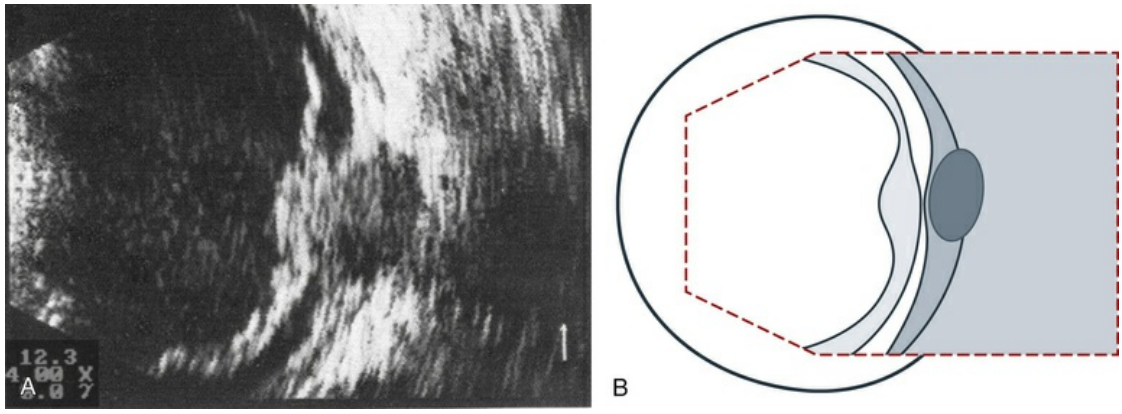

FIG. 11.28 Posttraumatic intraocular infection starting from the side of perforation. (A) B-scan ultrasonography demonstrates localized thickening of the ocular wall indicating the side of the perforation.

The vitreous is filled with inflammatory cells, the posterior hyaloid is thickened, and there is a localized retinal detachment. (B) Schematic drawing.

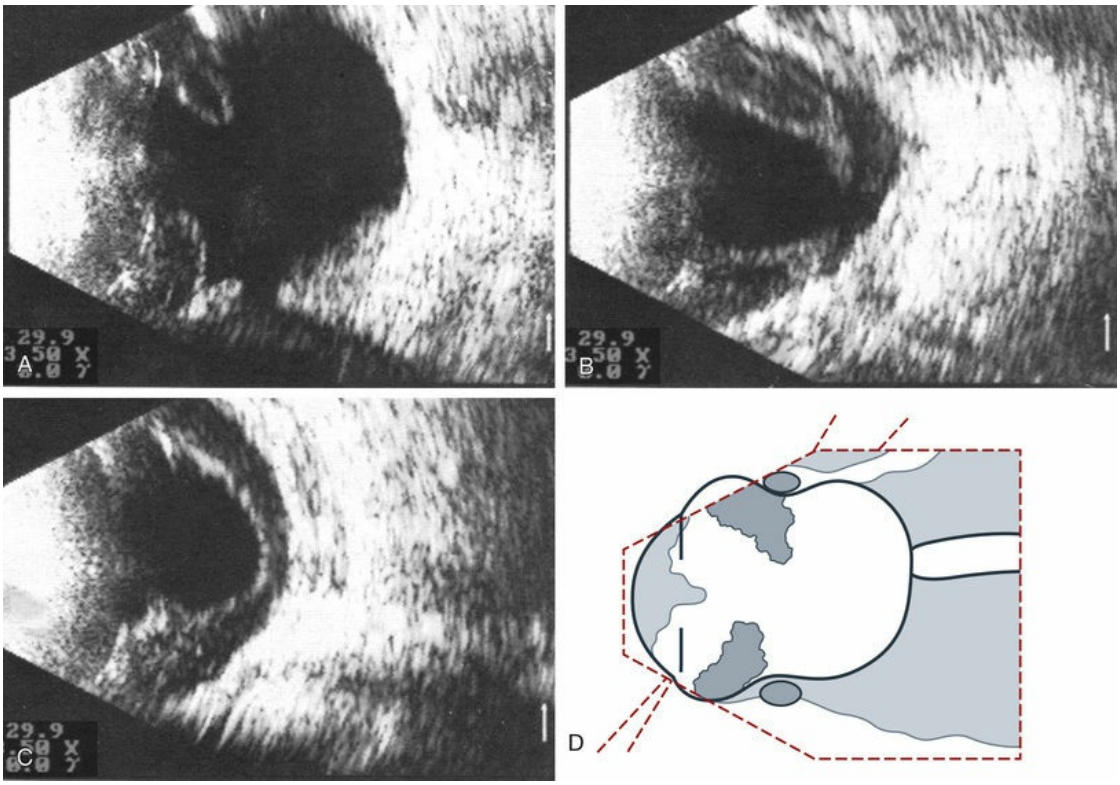

FIG. 11.29 Chronic inflammation with massive vitreous infiltration after pars plana vitrectomy and scleral buckle. (A) Remnants of the infiltrated vitreous can be seen at the vitreous base anterior to the scleral buckle. (B,C) Cross-sections through the vitreous base. (D) Schematic drawing.

Vitreous Inflammation

Inflammatory and hemorrhagic vitreous changes cannot be differentiated on the basis of ultrasonographic findings alone. Both conditions may cause densification of preexisting vitreous structures with subsequent shrinkage of the vitreous; tractional detachment of the retina can occur, especially if there are postinflammatory adhesions between the vitreous and retina. In chronic uveitis, an early and complete posterior vitreous detachment can occur and cause the formed vitreous to shrink and

form a frontal membrane that extends across the vitreous base (Fig. 11.30). If this membrane adheres to the ciliary body, it may detach the ciliary body and produce subsequent ocular hypotony.[29]

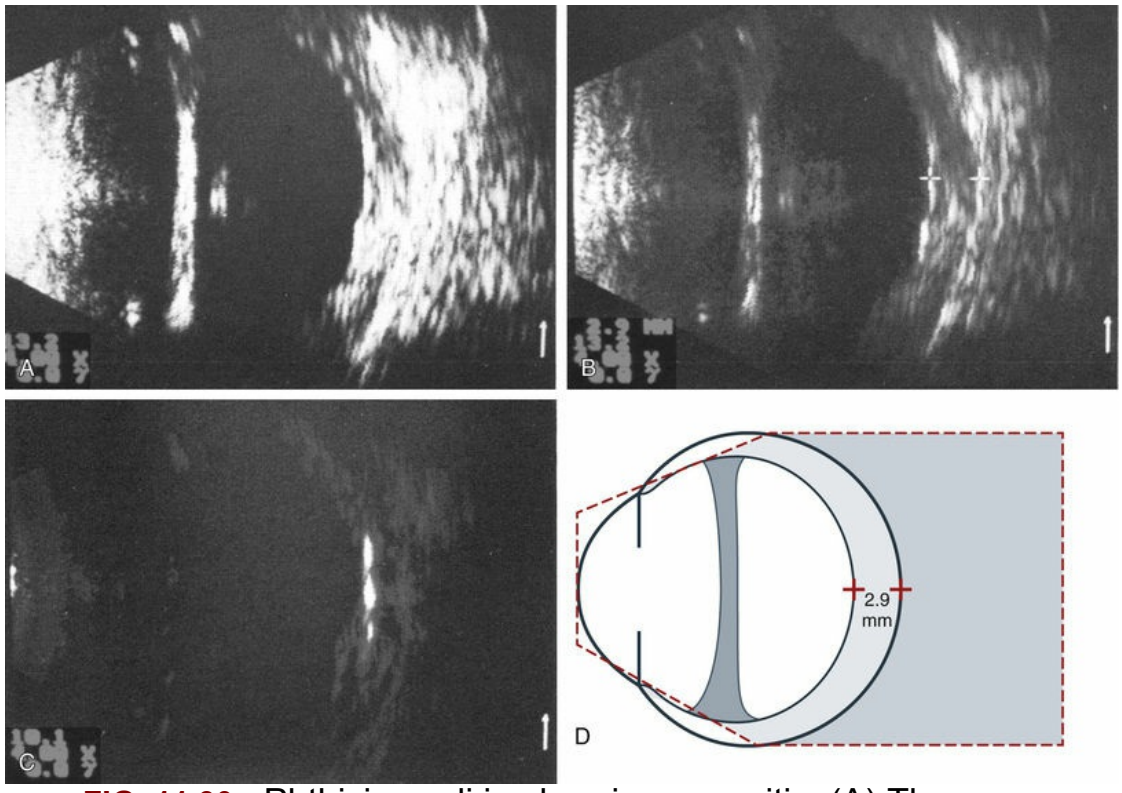

FIG. 11.30 Phthisis oculi in chronic panuveitis. (A) The vitreous has shrunk to form a frontal membrane of high acoustic reflectivity. The ocular wall is widened to 2.9 mm. (B) Using linear amplification, the various layers of the ocular wall have become clearly outlined. (C) Isolated areas of the ocular wall show high acoustic reflectivity, which indicates calcification of the choroid or in the sclera. (D) Schematic drawing highlighting wall thickness.

Intraocular Foreign Bodies

Intraocular foreign bodies induce a change in echo reflectivity which is based on the composition of the material (Figs. 11.31–11.33). The change in the reflectivity on the image should be a helpful clue in the localization of the foreign body within the globe; however, this is not always the case since the foreign bodies can also create signal artifact on echograms that can make identifying

their exact location difficult. For example, large metallic foreign bodies have significant artifacts from strong reflected signals that can distort their true location. In addition, foreign bodies from trauma can be associated with air bubbles within the vitreous that can mask the presence of the nearby foreign body within the acoustic shadow (Fig. 11.34).

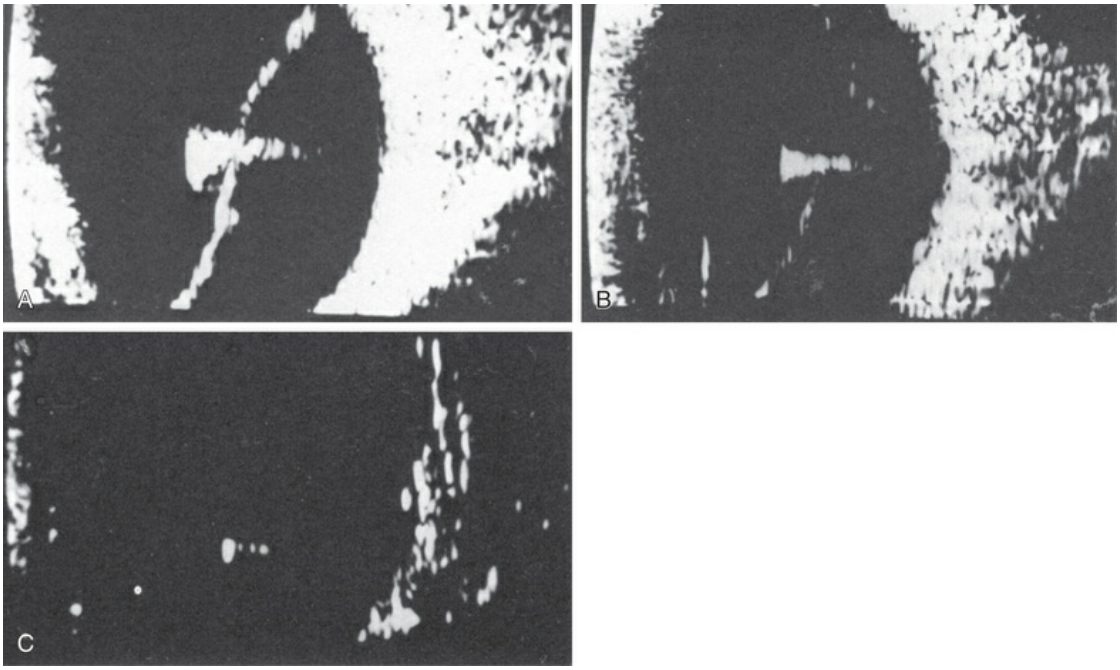

FIG. 11.31 (A) Metallic foreign body in the vitreous with total retinal detachment. (B) The foreign-body spike is characterized by its high amplitude and repetitive echoes. (C) With reduced sensitivity the foreign body can almost be imaged as an isolated echo.

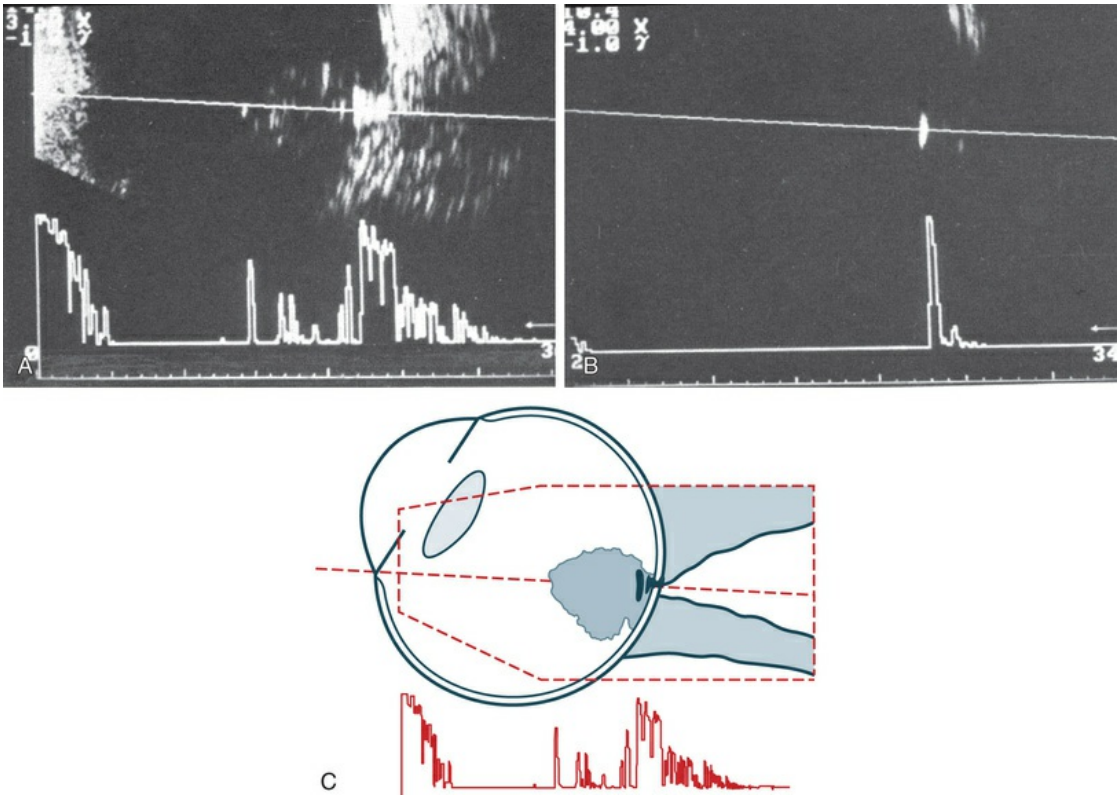

FIG. 11.32 Acute perforating injury with intraocular metallic foreign body. (A) Ultrasonographically, there is a typical foreign-body echo with repetitive spikes in the vitreous about 2 mm in front of the ocular wall. (B) Decreasing the amplification displays the foreign-body echo as the only intraocular structure remaining visible on ultrasonography. (C) Schematic drawing.

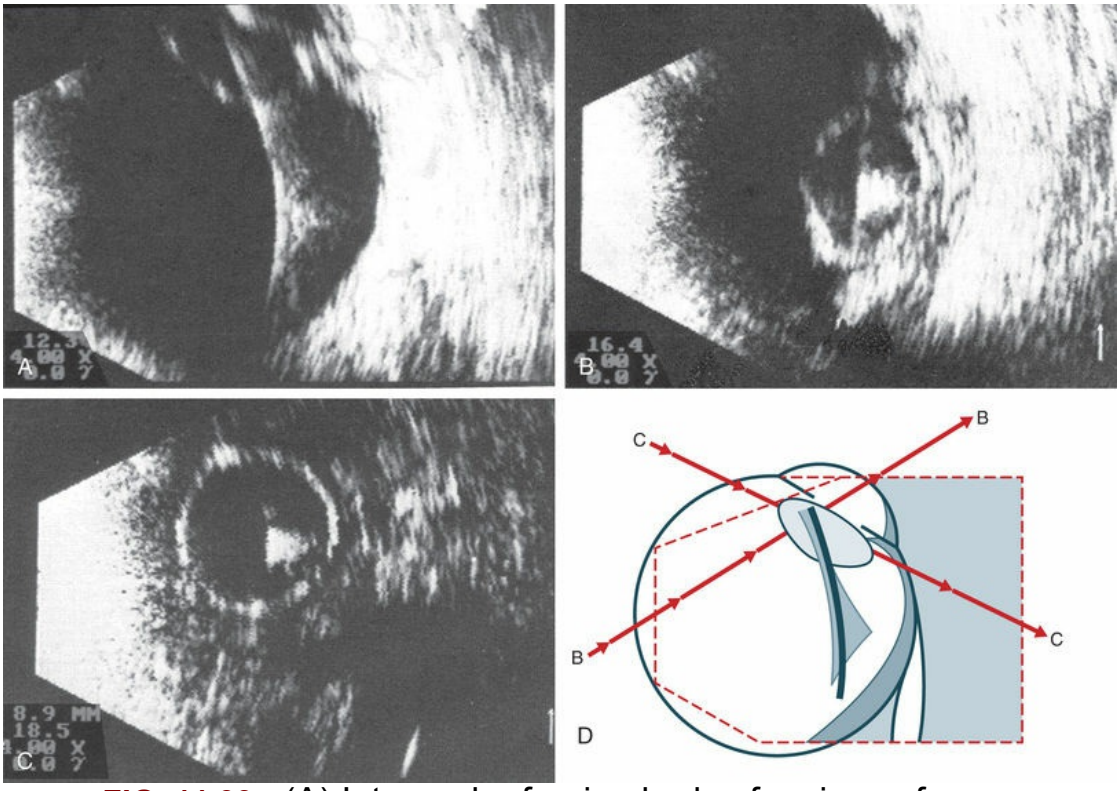

FIG. 11.33 (A) Intraocular foreign body of a piece of wire. (B) The anterior end of the wire remained visible in the lens. Cross-sectional image taken temporally with maximal adduction of the globe. (C) Frontal section through iris and lens. (D) Schematic drawing.

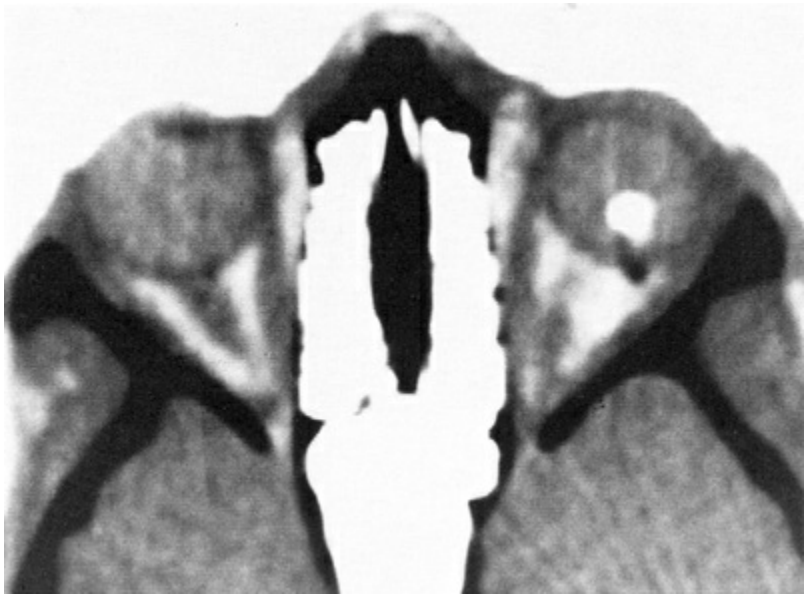

FIG. 11.34 Computed tomography image of a metallic foreign body wedged into the ocular wall with an air

bubble adjacent to it.

Retina

Ultrasound can be used to assess the structure of the retina in order to discern anatomic changes such as retinal tears and detachments. It can also be used to identify changes in retinal thickness from infiltrative or exudative ocular diseases. The sound reflections in ultrasound images can delineate these pathologic retinal changes even in eyes with opaque anterior media. This is a particularly useful tool since many diseases that affect the retina can also lead to vitreous changes that limit direct visualization. It is important to have a strong fundamental knowledge of ocular anatomy as well as a good technical approach for acquiring ultrasound images in order to make accurate assessments of retinal disease on ultrasound. This section will review the anatomic features of common retinal conditions as well as the special techniques needed to examine the retina with ultrasound.

Acute Retinal Detachment

In a retinal detachment, the neurosensory retina separates from the RPE layer. This development allows fluid to collect in the potential space between these two layers. The detached neurosensory retina appears as a membrane in the vitreous space on ultrasound. Partial retinal detachments may still maintain connections to the optic nerve or ora serrata since these areas have the strongest connections to the retina. Identification of these connections on ultrasound can distinguish a partial retinal detachment from a vitreous or choroidal detachment, which would have different anatomic connections (Fig. 11.35). A complete retinal detachment can form a funnel shape due to the retina folding in the center of the globe.

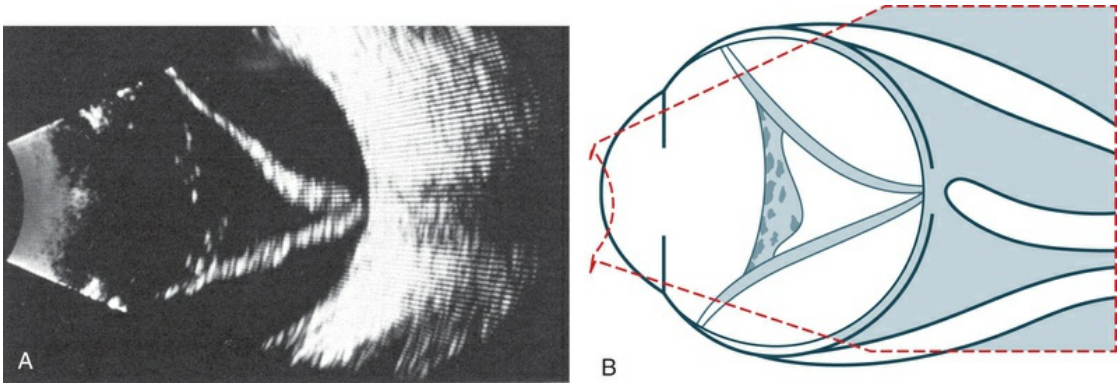

FIG. 11.35 (A) Complete retinal detachment extending between the optic nerve head and the ora serrata. Heterogeneous material in the anterior vitreous is a sign of vitreous reaction. (B) Schematic drawing.

Complicated retinal detachments with severe pathology can make it difficult to identify all the structures on ultrasound (Fig. 11.36). For example, in severe trauma cases that are associated with proliferative vitreoretinopathy or in advanced diabetic disease associated with proliferative retinopathy, the membranes formed within the vitreous can appear similar to a true retinal detachment. The following questions can guide the ultrasound examination of the retina in order to differentiate these common causes of vitreous membranes:

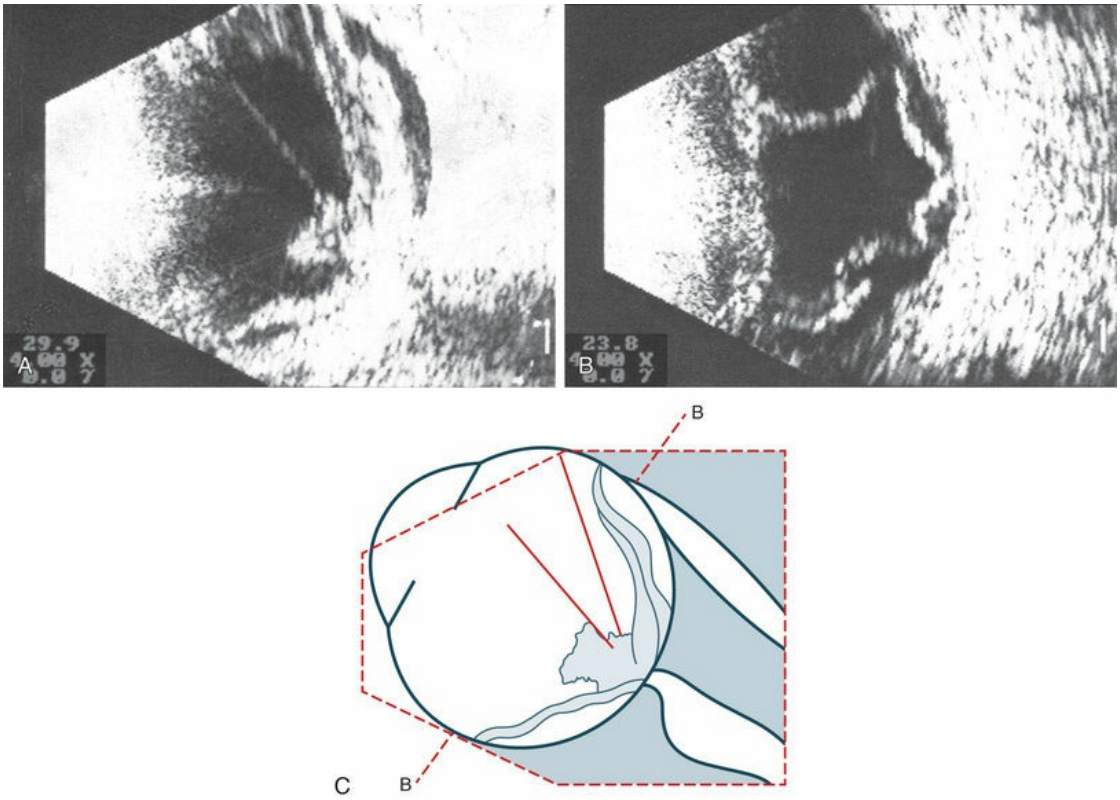

FIG. 11.36 Development of a traction detachment with massive vitreous retraction. (A) Flat subtotal retinal detachment with folds; rigid vitreous strands. (B) In a frontal section, multiple contacts of the retina to the ocular wall can be demonstrated. (C) Schematic drawing.

- What is the spatial extent of the membrane? At which point is there contact with the ocular wall?
- What is the shape of a cross-section of the membrane, especially in the optic nerve head area?
- Which aftermovements occur?
- How great is the difference of the spike from the membrane in question to the scleral standard or to the echo from a standard reflector?

These questions should be clarified in the following way:

1. What is the spatial extent of the membrane? At which point is there contact with the ocular wall? A recent rhegmatogenous retinal detachment can be characterized in cross-section by a membranous structure of high reflectivity that converges in an acute angle

toward the ocular wall. If the imaged acoustic section is centered on the optic nerve head, then the border of the detached retina will be captured as it connects to the nerve head (Fig. 11.37). If the membrane passes over the optic nerve head instead of connecting to the optic nerve in the echo image, it is not a retinal detachment (Fig. 11.38). This feature can help identify retinal membranes from vitreous membranes.

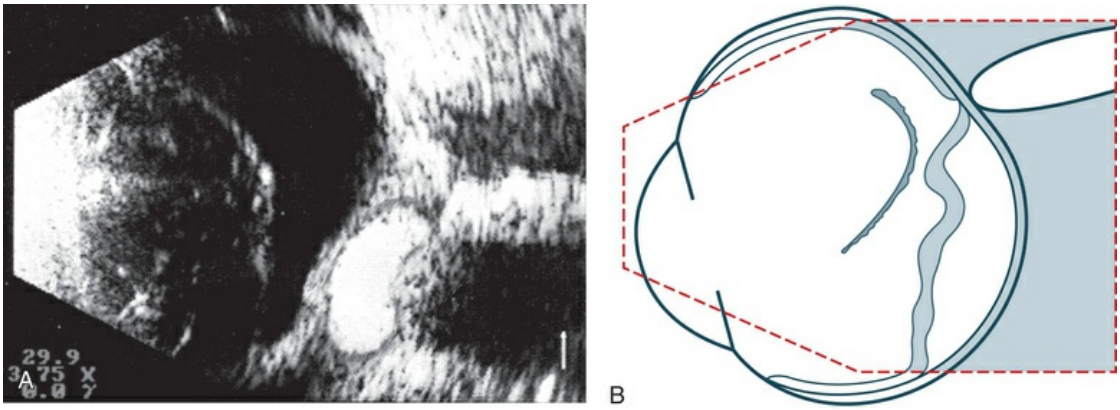

FIG. 11.37 (A) Sectoral retinal detachment. In acute retinal detachment, short aftermovements appear when the globe moves. These aftermovements extend like a whiplash from the area of the contact to the ocular wall. (B) Schematic drawing.

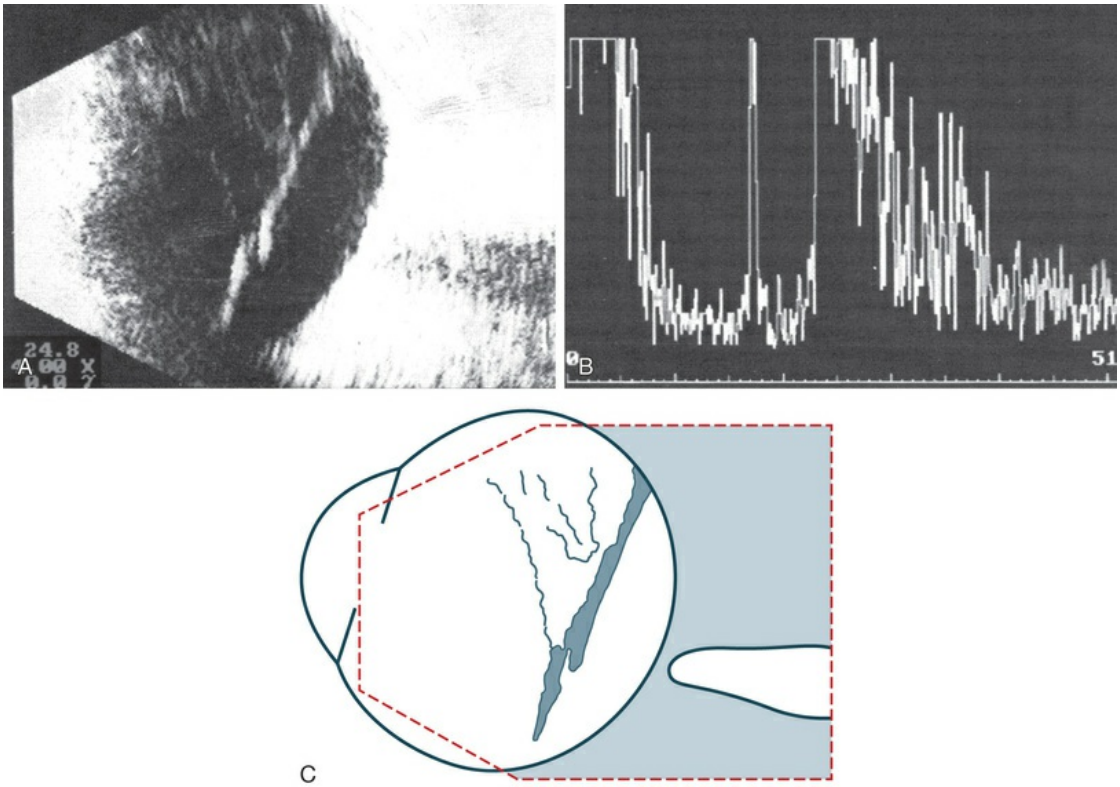

FIG. 11.38 (A,B) Detached posterior hyaloid membrane. Vitreous membranes may reach an acoustic reflectivity similar to that of the retina seen on A-scan. A retinal detachment can be excluded if the membrane tents over the posterior pole without reaching the optic nerve head. (C) Schematic drawing.

2. What is the shape of a cross-section of the membrane, especially at the optic nerve head? In order to appreciate the shape of a retinal detachment, the performance of sonographic examinations in various planes is indicated. First, in a sagittal section, a total detachment looks like an isosceles triangle that is open toward the anterior segment (the sides of which may be unevenly tented: Fig. 11.35). Next, frontal-plane sections should be examined with the disc centered in the image. These sectional plans are obtained at a right-angle to the sagittal. The frontal planes can be examined best with the transducer probe placed in the temporal part of the lid fissure when the globe is maximally adducted. In these images, the conical shape of the detachment will appear oval to nearly circular in the various sections (Fig. 11.39).

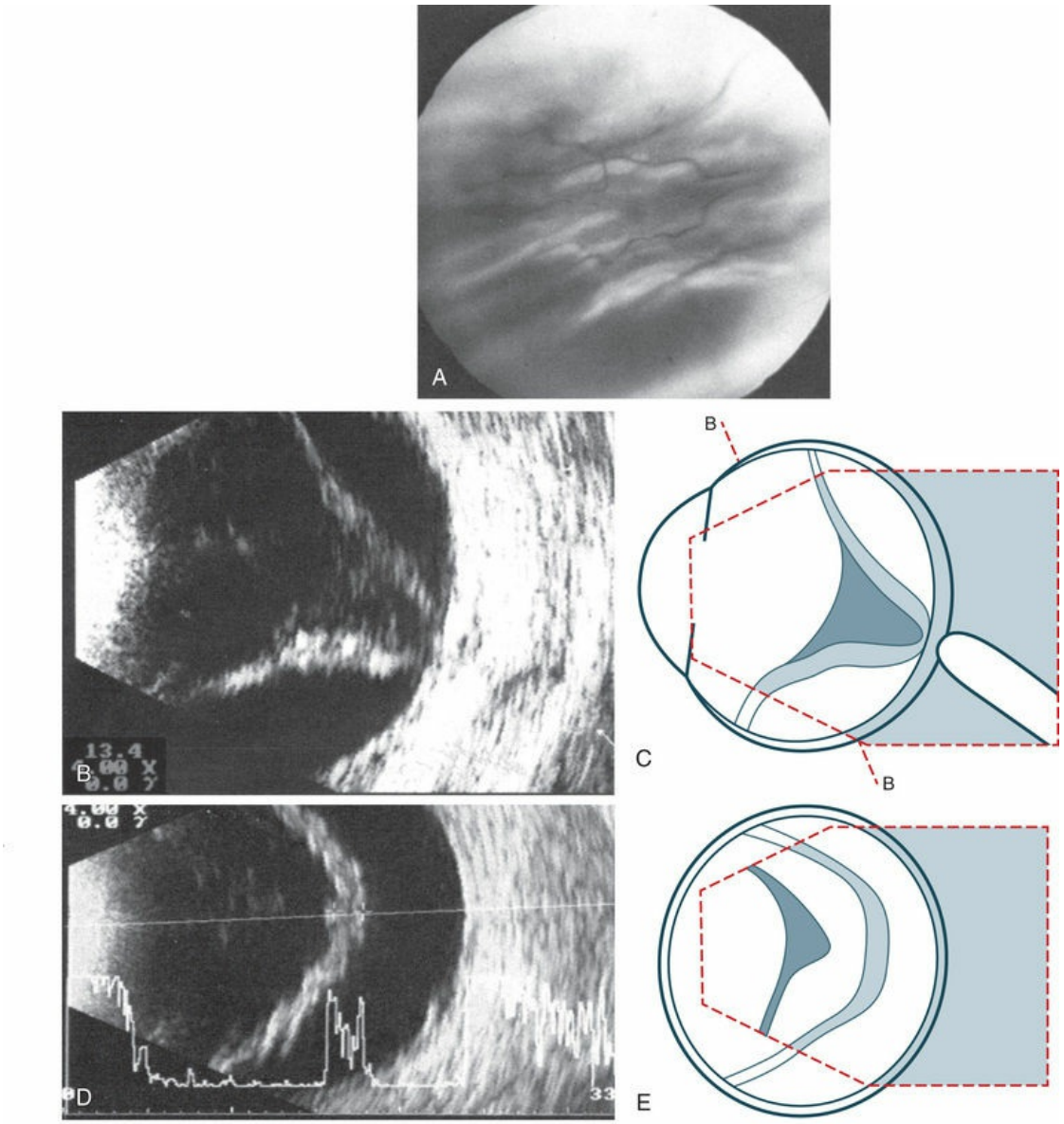

FIG. 11.39 (A) Clinical fundus photography of recurrent retinal detachment. (B–E) Recurrent retinal detachment with massive vitreous retraction. (B) Axial cross-sectional echogram. The amplitudes of the aftermovements decrease. High-frequency flicker of the taut membrane appears after the eye changes position. (D) Frontal section toward 6 o'clock. An epiretinal membrane of the retinal surface appears echographically as an apparent widening of the retina. (C,E) Schematic drawings.

3. Which aftermovements occur? Dynamic ultrasound can be obtained with patient participation. The quality of tissue movement at the end of the ocular saccade, or the aftermovement of the tissue,

can be used to distinguish vitreous tissue from retina tissue. An acute rhegmatogenous retinal detachment shows aftermovements of short duration that extend with a whiplash effect from the area where the retina is still attached, which is usually the optic nerve head. The amplitudes of these aftermovements are smaller and less extensive than those seen in the sinusoidal movements of a vitreous hemorrhage or in asteroid hyalosis.[30]

4. How great is the difference of the spike from the membrane in question to the scleral standard or to the echo from a standard reflector? Quantitative ultrasonography can detect a difference in the echo of the retina compared to that of the sclera, with a range extending from 8 to 15 db.[31] Unfortunately, these measurements provide only guidelines. Well-developed connective tissue membranes may show reflection properties quite similar to those of a detached retina. In complicated cases it may be difficult to correlate an isolated A-spike to the multiple membrane structures as they appear on B-mode.

Chronic Retinal Detachment

The duration of a retinal detachment can affect the thickness and mobility of the retina, the shape and mechanical properties of the vitreous base, and the contents of the subretinal space. Identifying and understanding these changes can help with the management of these conditions.

A few weeks after a retinal detachment develops, changes in the proliferation of Müller cells and astrocytes will lead to alterations in the mechanical properties of the detached retina. The massive periretinal proliferation of these cells creates a decrease in the aftermovement amplitude of the retina (Fig. 11.40). The large excursions are replaced by a high-frequency flicker and the retina may appear thickened. After a longstanding retinal detachment, cyst-like cavities within the detached retina can be seen on ultrasound (Fig. 11.41). A longstanding detachment can also result in a funnel-shaped retinal detachment. The first step in this process is the proliferation of the epiretinal connective tissue that causes the vitreous to contract. This stage can be identified on ultrasound by the presence of new acoustic interfaces, which are seen as increased

vitreous signals that surround the detached retina (Fig. 11.42). The vitreous shrinks, which creates a narrowing of the retinal cavity, which typically begins to narrow anterior to the optic nerve head and continues to the posterior lens. Frontal "cyclitic membranes" can often be seen early, extending from the vitreous base (Fig. 11.43). Next, the peripheral retina is pulled closer to this membrane until the retinal detachment does not show any recognizable cavity of the original funnel. In frontal sections the shrunken retina appears as a strand, only a few millimeters in diameter (Fig. 11.44). Occasionally, a few retinal folds can be observed.

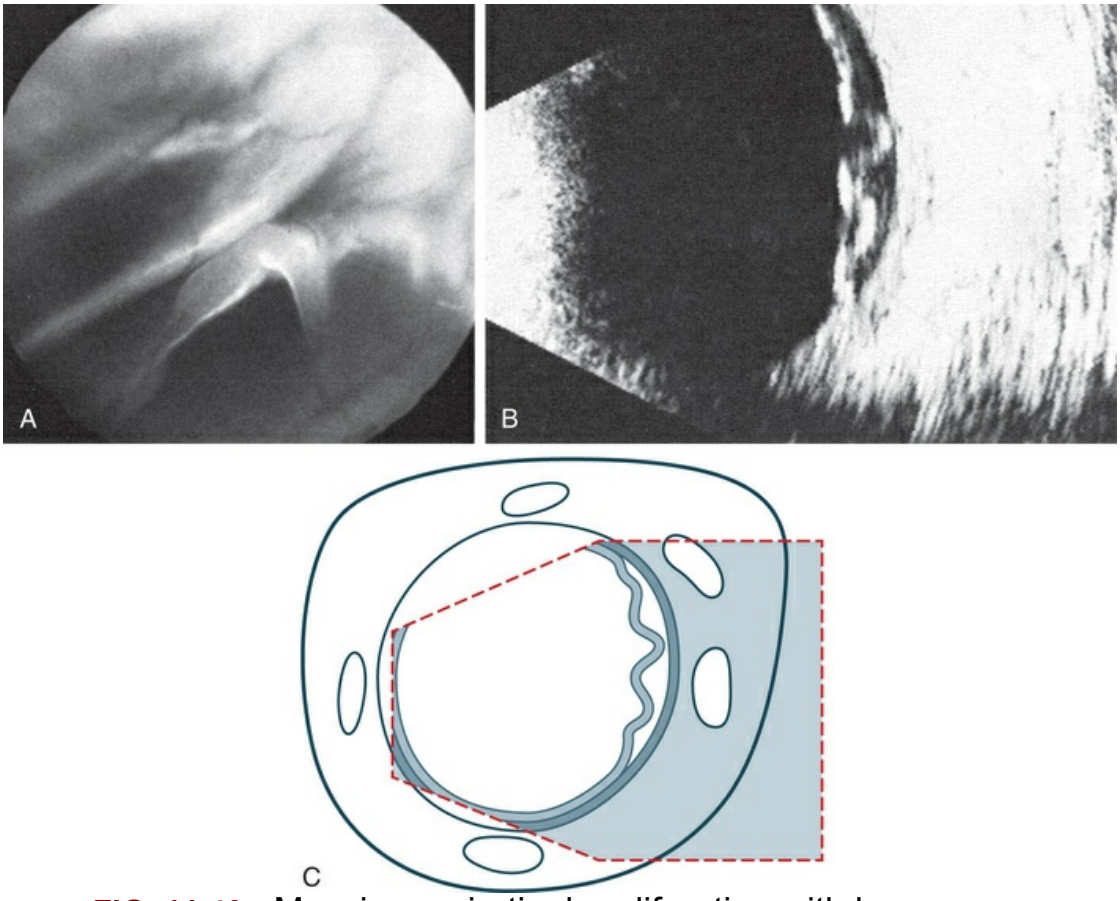

FIG. 11.40 Massive periretinal proliferation with large retinal folds. (A) Ophthalmoscopic picture of large horseshoe tear. (B) The rigid, fixed retinal folds are echographically demonstrable. (C) Schematic drawing.

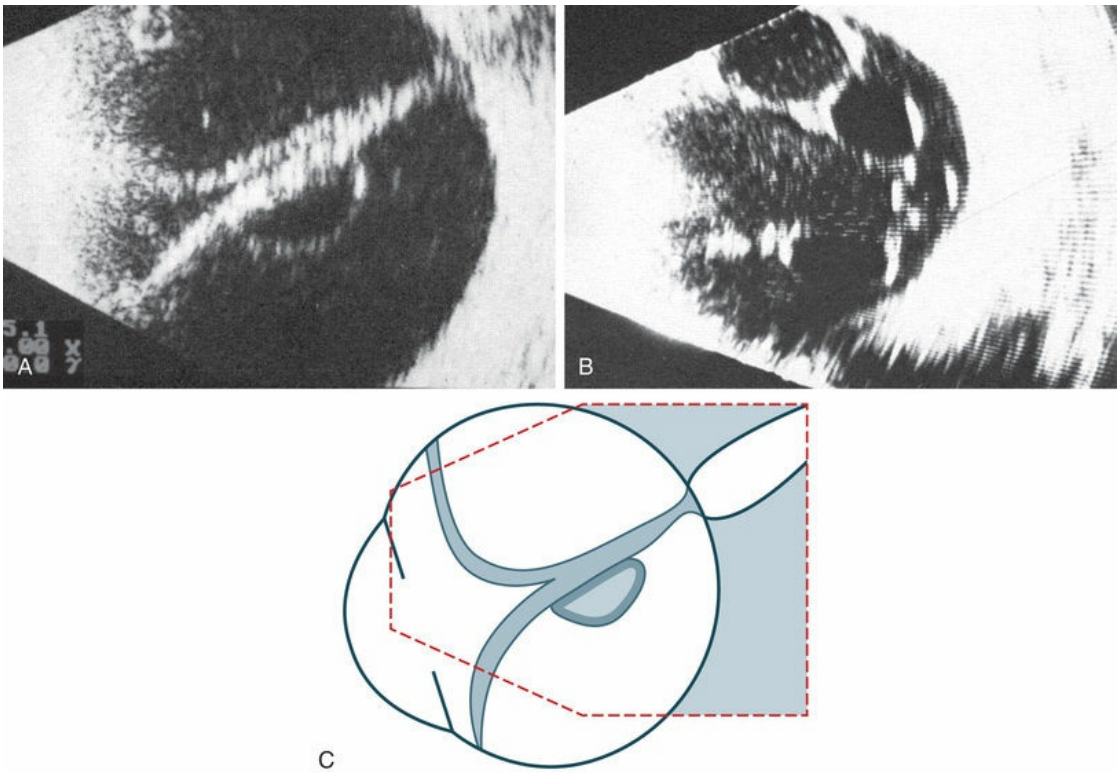

FIG. 11.41 Longstanding total retinal detachment with macrocyst. Intraretinal cyst in the axial area seen on cross-sectional ultrasound (A) and frontal plan (B). The cysts form from coalescing microcystoid degeneration of the retina in chronic detachments. These cavities will not be involved in secondary vitreous changes, such as vitreous hemorrhages or cholesterol deposits. (C) Schematic drawing.

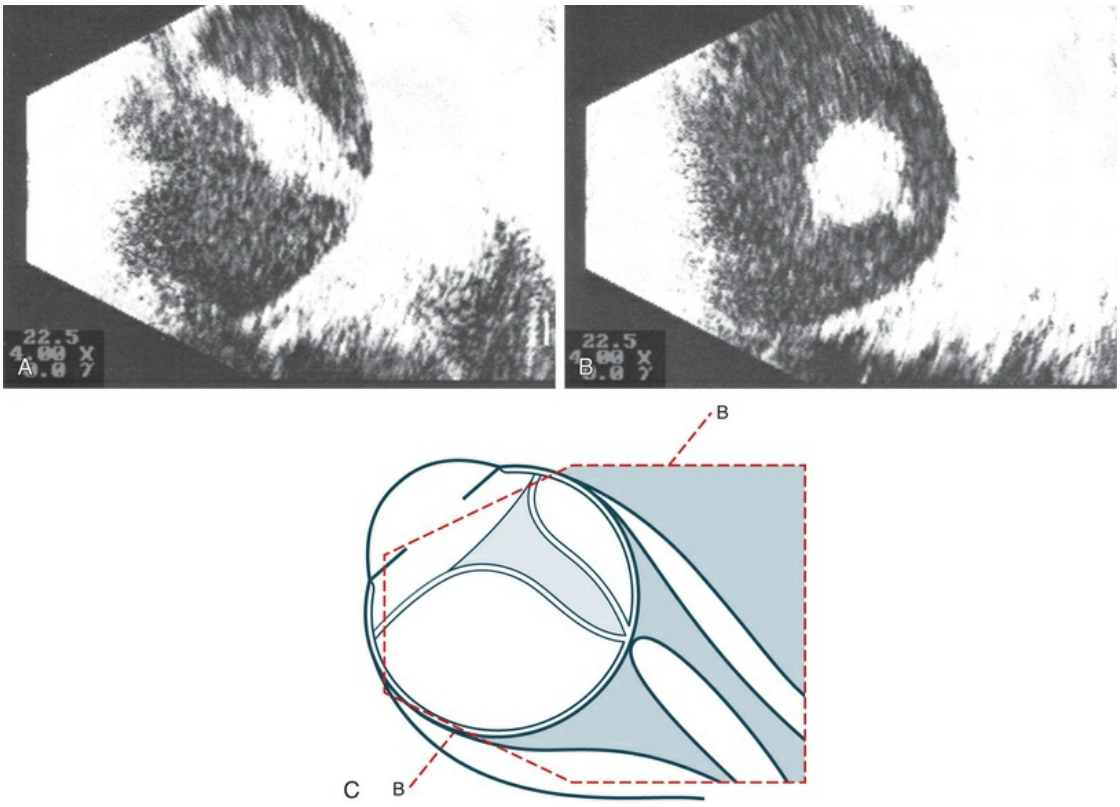

FIG. 11.42 (A,B) Longstanding retinal detachment with increased connective tissue in the vitreous tunnel. Free-floating opacities accumulate in the subretinal space (possibly representing hemorrhage or cholesterol crystals). (C) Schematic drawing.

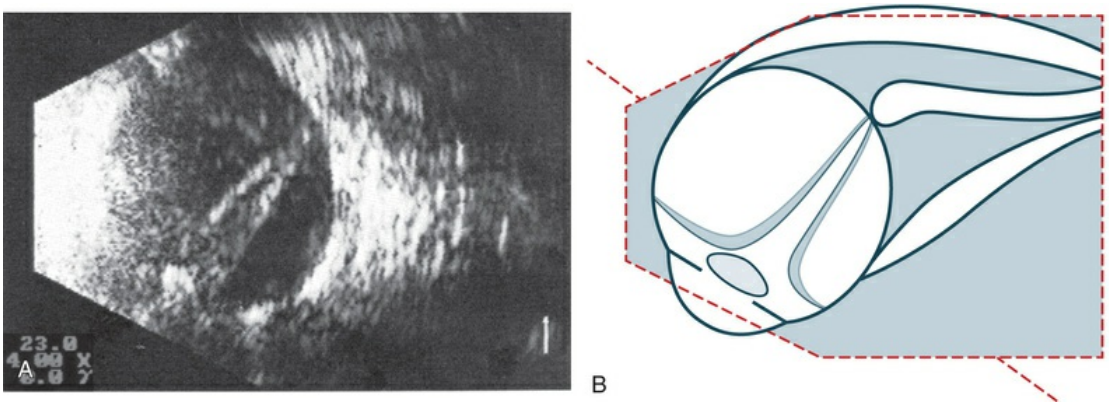

FIG. 11.43 (A) Longstanding total retinal detachment. A tube-like remnant of the vitreous within the shrunken retinal tunnel can be seen. (B) Schematic drawing.

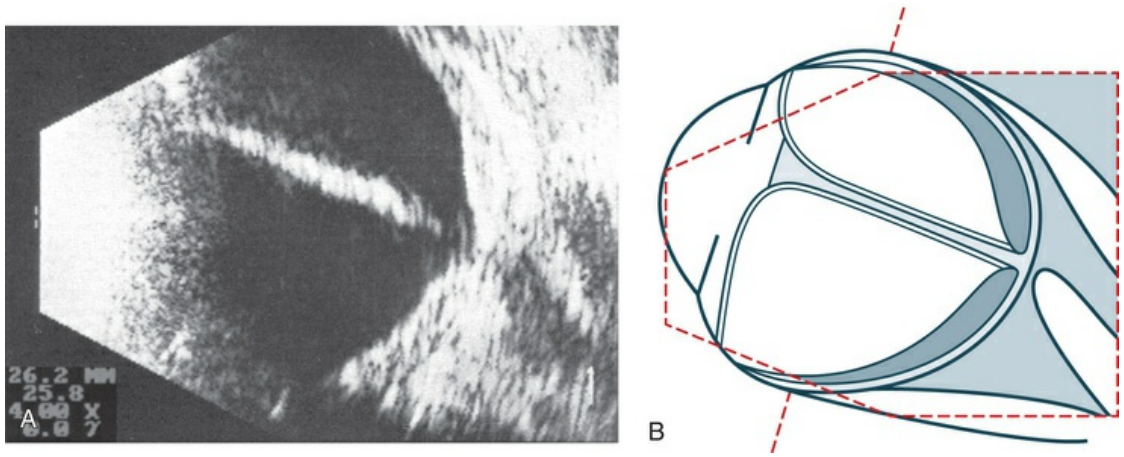

FIG. 11.44 (A) Longstanding retinal detachment with completely obliterated vitreous space. In sagittal sections the extensive adhesions of the retinal leaves produce various acoustic sections. (B) Schematic drawing.

In addition to the above findings, the consistency of the subretinal space can change with increased duration of the detachment. The protein content will increase and may precipitate out of the subretinal fluid. This can be seen as free-floating opacities on ultrasound (Fig. 11.45). If these opacities appear as static particles and not free-floating, then intraocular tumor has to be excluded. Under these circumstances, ultrasonography provides a vital role in obtaining a diagnosis by distinguishing the freely moving protein precipitation in longstanding detachments from the fixed hyperechoic particles of malignant tumors.

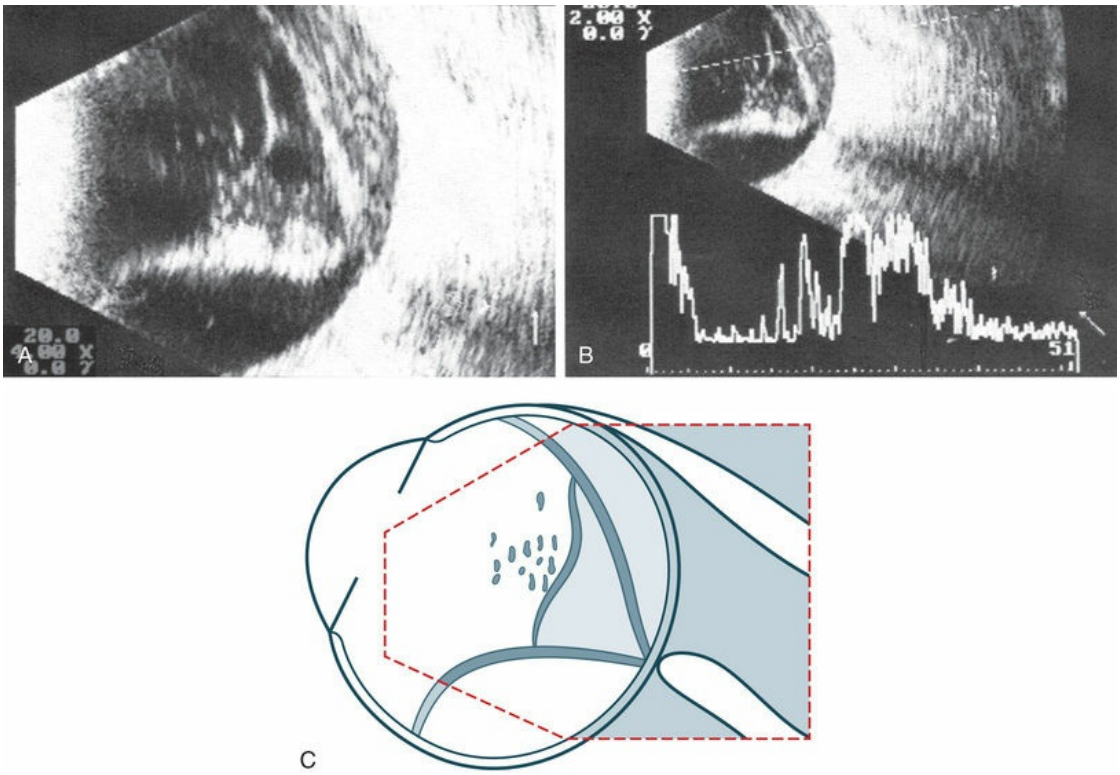

FIG. 11.45 (A,B) Longstanding retinal detachment with floating opacities in the subretinal space. The densifications in the vitreous space indicate a tendency for shrinkage. (C) Schematic drawing.

Retinoschisis.

Retinoschisis is a splitting within the neurosensory layer of the retina. This condition frequently occurs in the inferotemporal quadrant. A cross-section echogram can display a membranous structure in the far periphery that has a convex border facing the vitreous (Fig. 11.46). In this situation, clinical correlation is important in order to distinguish the retinoschisis from a retinal detachment since these two entities can appear identical on static ultrasound. However, use of dynamic ultrasound and evaluation of the aftermovements can show that the aftermovements in retinoschisis are less conspicuous than in a retinal detachment. This is because in retinoschisis the retina is attached and there are no vitreous adhesions.

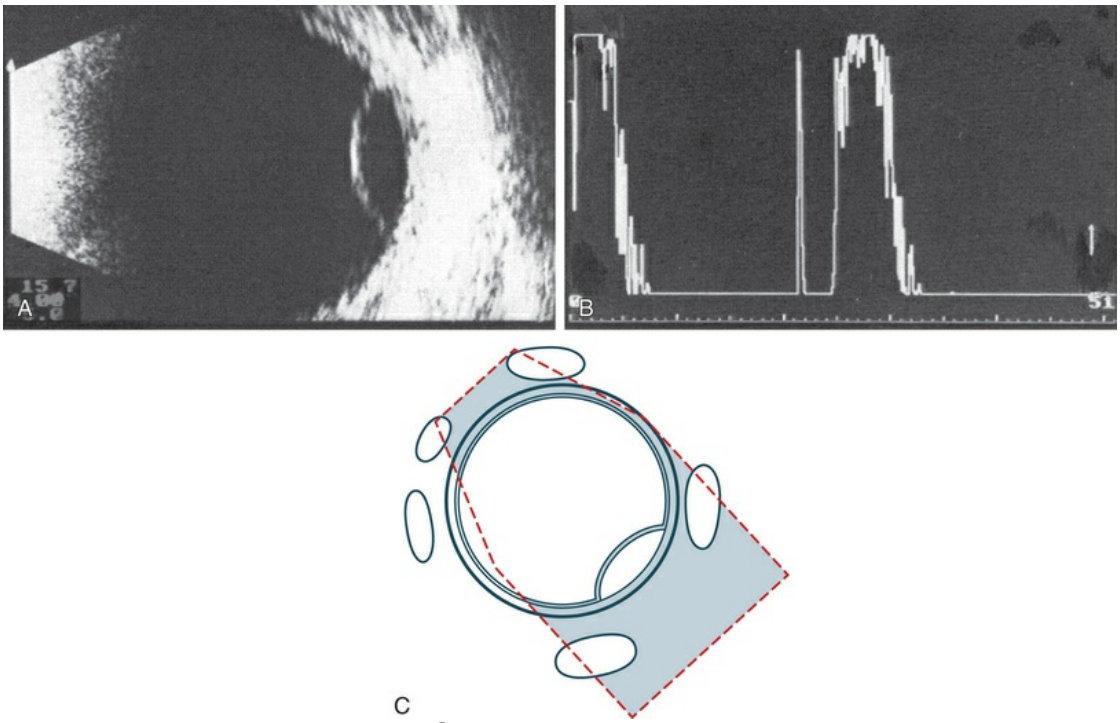

FIG. 11.46 (A) Senile retinoschisis in the inferotemporal quadrant. The typical biconvex cross-sectional image in association with slight aftermovements supports a tentative diagnosis of retinoschisis. (B) The acoustic reflectivity corresponds to that of a detached retina. (C) Schematic drawing.

Coats Disease.

Coats disease is an exudative retinopathy most commonly seen unilaterally. It mainly affects males in the first decade of life. A clinical diagnosis can be made if aneurysmal malformations of retinal vessels and yellowish subretinal plaques are associated with an exudative detachment. Coats disease should be differentiated from retinoblastoma, which can have a similar clinical appearance in this patient group. Ultrasound can differentiate these conditions with careful evaluation of the subretinal space. Retinoblastoma typically shows calcifications with high reflectivity. The exudative detachment that is seen in Coats disease has a different echo quality due to the subretinal cholesterol deposits (Fig. 11.47). In Coats disease, the crystals floating in the subretinal space are seen as floating opacities similar to the appearance of crystals in synchysis scintillans. They appear in an A-mode echogram as flickering spikes.[32] On B-mode images these high-frequency motions of the

echo spikes produce a blurred pattern in the subretinal space.

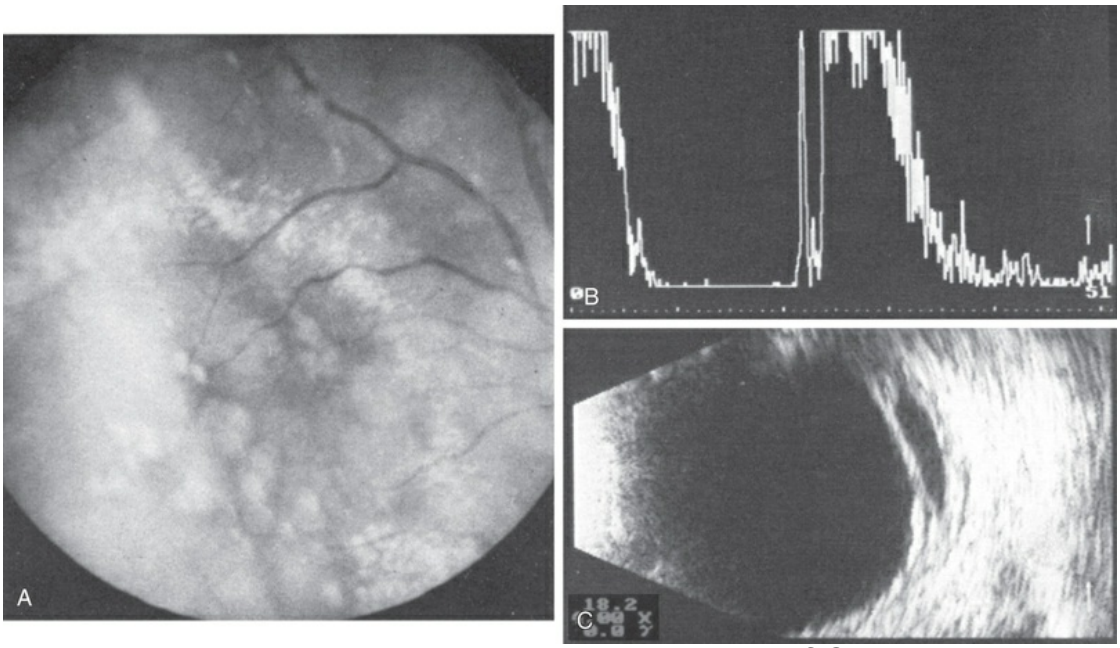

FIG. 11.47 (A) Fundoscopic clinical photo of Coats disease. Circumscribed, strongly reflecting retinal detachment in Coats disease. (B) The A-scan shows the high-intensity signal from the strongly reflecting membrane of the retinal detachment depicted in the image. (C) The B-scan shows the retinal detachment in association with floating opacities in the subretinal space that corroborate the diagnosis of Coats disease.

Retinoblastoma

Retinoblastoma is a life-threatening tumor that can present in children as isolated leukocoria or with a constellation of other ocular findings. Some findings can mimic benign ocular conditions. Since treatment of retinoblastoma can include ocular enucleation, making the appropriate diagnosis is critical. Ophthalmoscopy should be performed but sometimes is limited if there is cataract, hypopyon, vitreous seeding, or opacity. Ultrasound plays a critical role in these patients, especially since certain features on echography can be pathognomonic for retinoblastoma. The presence of calcium deposits in retinoblastoma lesions produces a high sound reflection that creates an acoustic shadow on more

distant structures such as the sclera (Fig. 11.48). The calcium deposits can be selectively demonstrated on the image by decreasing the amplification in the cross-section echogram until they are the only remaining tissue structure visible on the screen (Fig. 11.49). In some retinoblastomas the calcium appears only in a few areas, but any calcification is indicative of tumor burden and is an important feature for the diagnosis. In some cases, ultrasound can also define extraocular tumor extension in retinoblastoma and is of great prognostic and therapeutic importance. Additional imaging to supplement ultrasonography is important in retinoblastoma. Computed tomography can show calcification and magnetic resonance imaging can show tumor extension outside the orbit, optic nerve invasion, or pinealoma (Fig. 11.50).

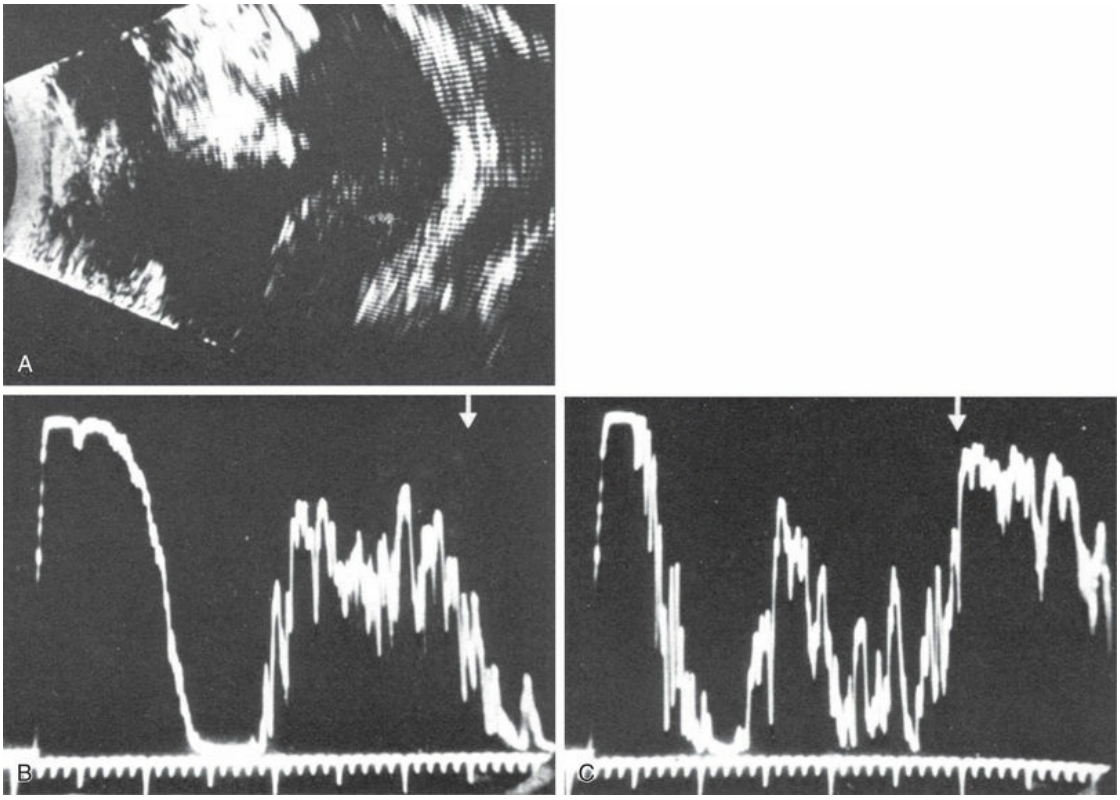

FIG. 11.48 Extensive retinoblastoma with varying appearance. As demonstrated in the cross-sectional echogram (A), the upper tumor portions show high acoustic reflectivity due to massive calcifications. The lower part of the tumor has less acoustic reflectivity than the adjacent sclera. A-scans of the eye (the scleral spikes in the acoustic scans (B,C) are marked

by *arrows*).

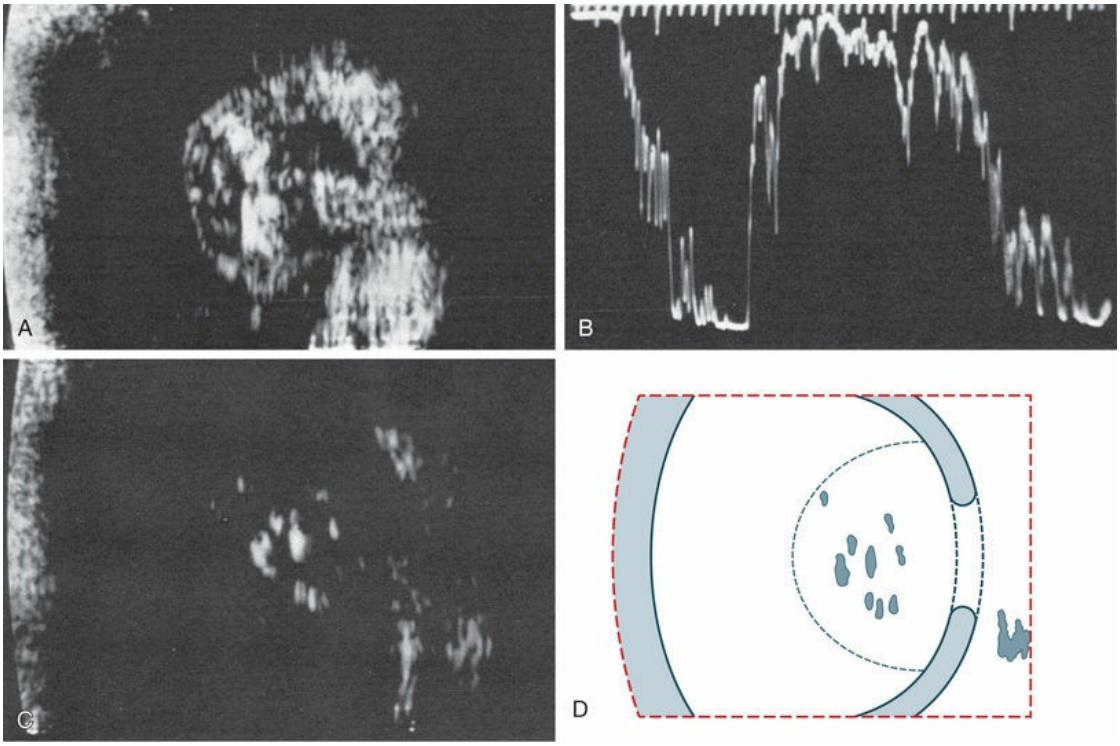

FIG. 11.49 Large retinoblastoma with calcifications and acoustic shadow cast on the adjacent sclera and orbit. (A) The calcifications light up in cross-sectional echograms. (B) In A-mode echograms, they can be quantified as the strongest reflecting structures in the examined area. (C) With reduced amplification, the calcified areas are the only visible signals. (D) Schematic drawing.

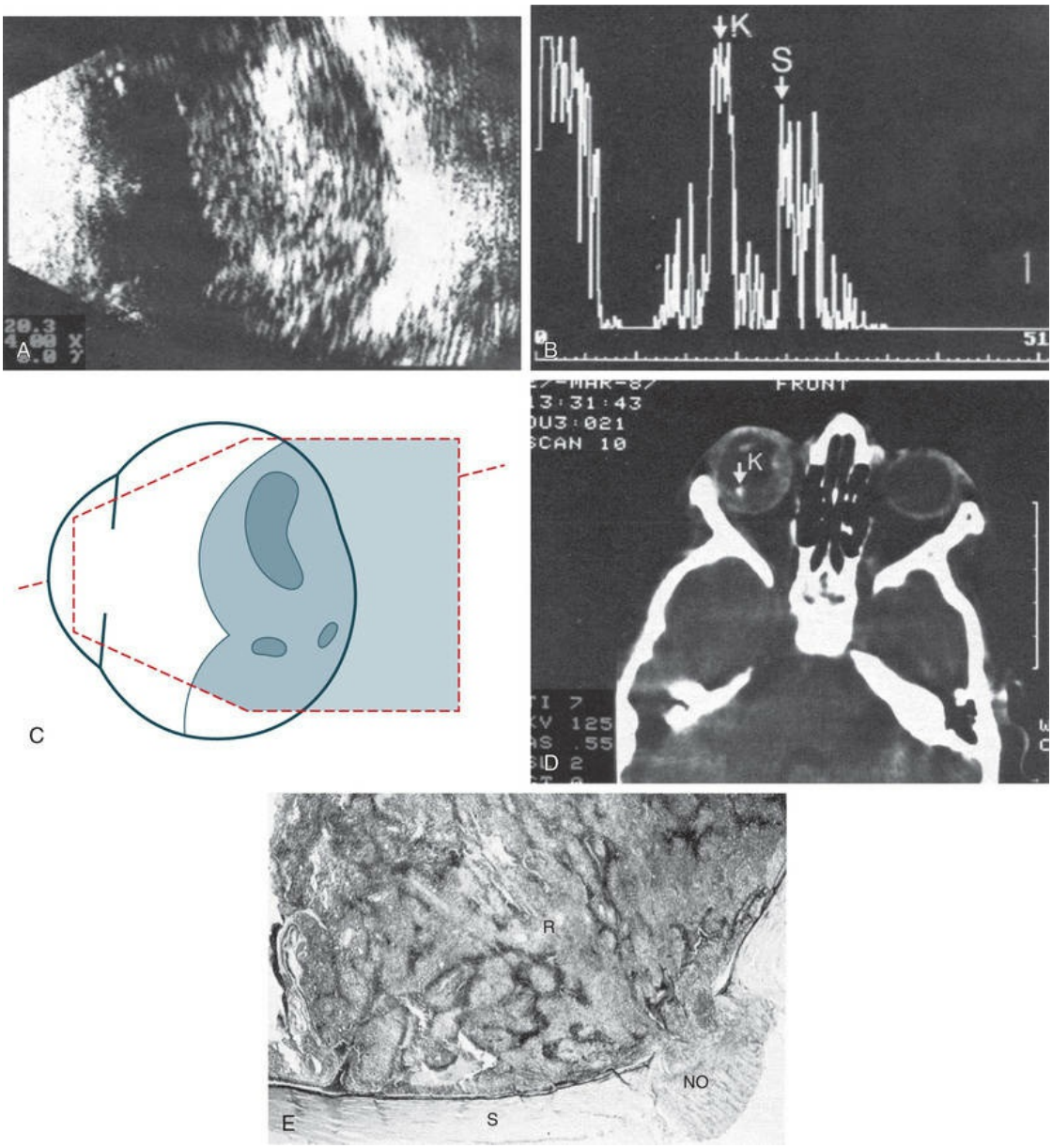

FIG. 11.50 Extensive retinoblastoma. (A) A cross-sectional echographic image. The tumor is characterized by areas of high acoustic reflectivity alternating with areas of low reflectivity. (B) The differences in reflection can be quantified on A-mode echography: calcified parts of the tumor have markedly higher amplitudes as seen at point K as compared to the sclera reflection as seen at point S. (C) Schematic drawing of the ultrasonographical image in (A). (D) Computed tomography scan displays the calcified parts of the retinoblastoma that can be identified with greater certainty than in a plain X-ray picture. (E) A histologic sample of the infiltration into the optic nerve. *NO*, optic nerve; *R*, retinoblastoma. The calcium deposits explain the nearly pathognomonic echogram.

Retinopathy of Prematurity

Early stages of retinopathy of prematurity can be diagnosed by indirect ophthalmoscopy. However, later stages with partial or complete traction retinal detachments from extensive fibrovascular tissue require ultrasonography for diagnosis and surgical planning. Machemer and Aalberg[33] emphasized the importance of information obtained by cross-section ultrasonography in these stages, such as the diameter of the retinal funnel in the retrolental space (Fig. 11.51).

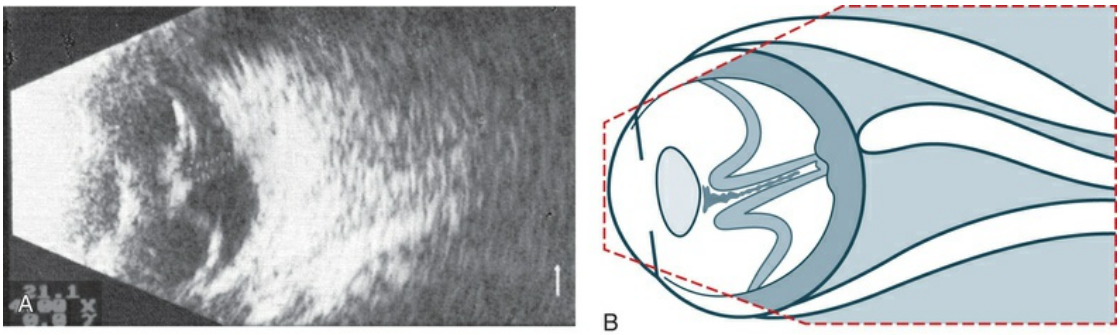

FIG. 11.51 Stage V of retinopathy of prematurity. (A) In cross-sectional images we see a complete retinal detachment with a widening of the avascular peripheral retina toward the subretinal space. (B) Schematic drawing.

Optic Nerve

Acute Optic Neuritis and Papilledema

In patients with acute optic neuritis and papilledema transorbital sonography may reveal a thickening of the retrobulbar portion of the optic nerve. Transorbital sonography is a sensitive, highly accessible technique for the detection of significant optic nerve thickening on the side affected by acute optic neuritis and represents an adjunctive tool for the diagnosis of papilledema.

Coloboma of the Ocular Fundus

Colobomas can occur in the iris, lens, retina, and optic nerve. Some are spontaneous and some occur in association with systemic syndromes. Colobomas are also in the differential diagnosis of retinoblastoma.[34] Colobomas can be seen clearly by ultrasonography even if the fundus cannot be visualized optically (Fig. 11.52).

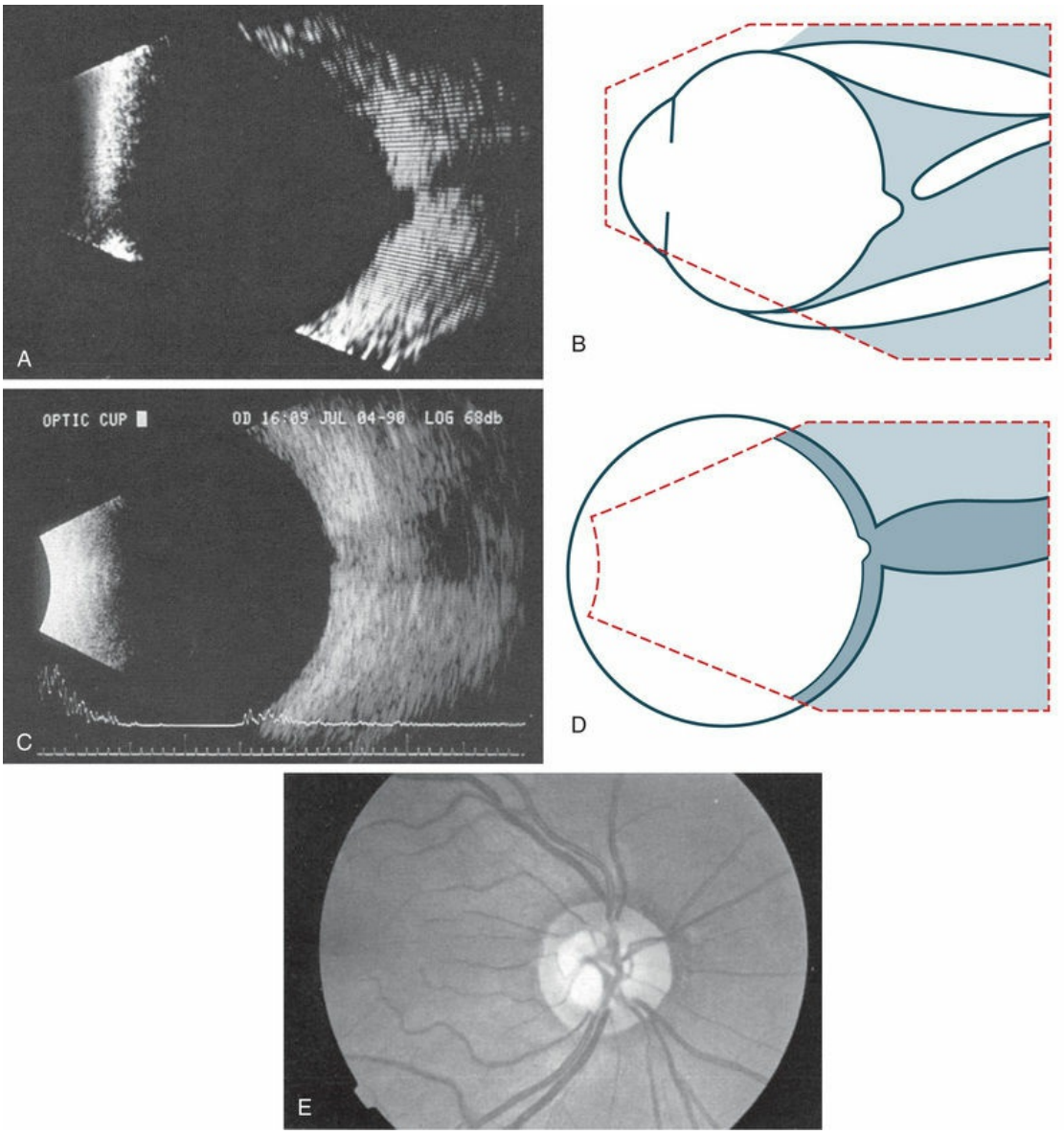

FIG. 11.52 (A) Echogram of the small optic nerve coloboma depicted in (E). In comparison, B-scan section showing normal physiologic cupping of an optic nerve head (C). To obtain this vertical section a probe is placed temporal to the limbus, thereby avoiding any artifacts, caused by the lens. (B,D) Schematic

drawings. (E) Small coloboma of the optic nerve with a diameter of about 2.5 mm. Fundus photograph showing excavation within the nerve.

Assessment of Optic Nerve Cupping

Evaluation of optic nerve cupping is important for treatment of glaucomatous changes. This is difficult with anterior media opacity. Recently, with improvement of the lateral resolution of B-scan images, optic nerve head cupping can be reliably measured and reproduced on ultrasound images.[35]

Choroid

Changes in the Ocular Layers Due to Hypotony

In acute hypotony, exudation into the suprachoroidal space creates an increase in the choroidal vascular pressure. This can lead to a choroidal detachment which will then exacerbate the globe hypotony (Fig. 11.53). This situation is ultrasonographically characterized by a convex border on a cross-section image that denotes the location of the choroidal detachment. This convex shape is formed between the pars plana and location of the vortex veins, both of which have strong choroidal attachments. Knowledge of the choroidal anatomic structure and its attachments can aid in ultrasound diagnosis. In addition to the pars plana and vortex veins, the choroid is firmly attached to the optic nerve. The choroid inserts at the optic nerve at a blunt angle, as compared to the retina, which has a steeper insertion. This feature can be used to help differentiate choroidal and retinal detachments of the posterior pole on ultrasound images. In addition, a choroidal detachment would begin at the ciliary body and not the ora serrata, as in a retinal detachment (Fig. 11.54). Occasionally, the detached ciliary body can compress the lens. In severe cases, choroidal detachments may meet in the center of the globe. This feature has been termed “kissing choroidals” and is typically an indication for surgical management (Fig. 11.55). In typical cases of serous choroidal detachments the subchoroidal space is acoustically silent. In contrast, an expulsive choroidal hemorrhage can be identified by the hyperechoic signal

on ultrasound that the blood clots create within the detachment (Fig. 11.56).

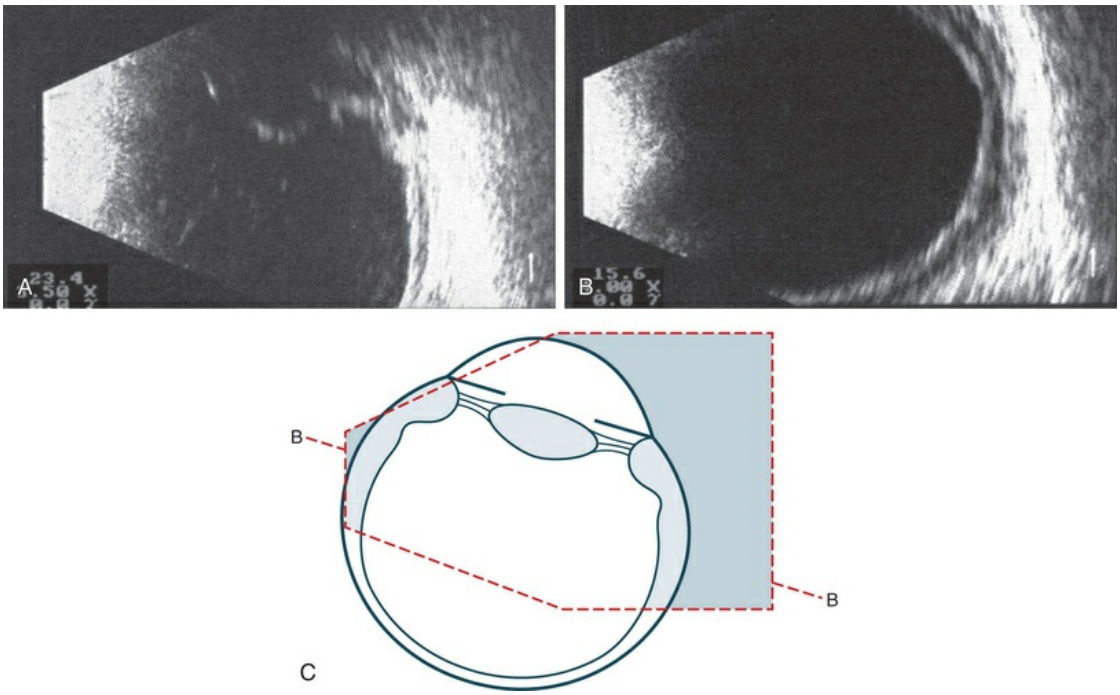

FIG. 11.53 (A) Detachment of the ciliary body and the peripheral choroid due to hypotony. (B) The thickening of the ocular walls begins in the area of the ciliary body and extends to the equator, as seen on the B-scan. (C) Schematic drawing.

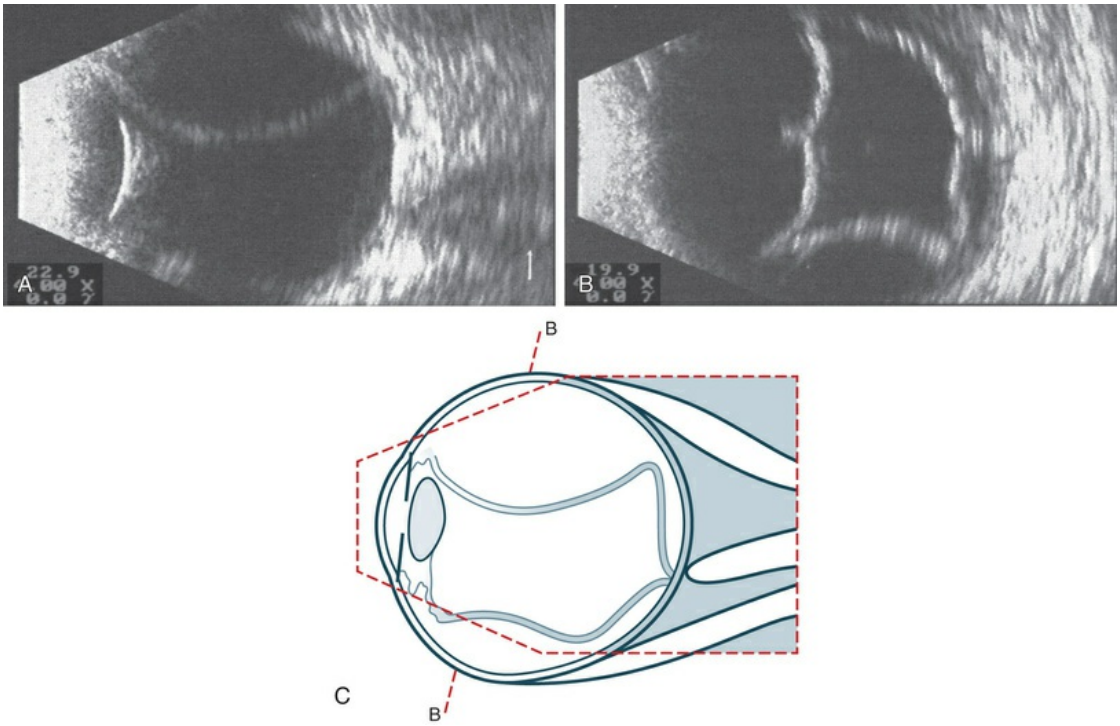

FIG. 11.54 Subtotal exudative choroidal detachment. (A) In contrast to a retinal detachment, the choroidal detachment extends beyond the ora serrata; the detachment extends from the iris diaphragm to the posterior pole without reaching the optic nerve head. (B) The frontal sections depict indentations which are caused by large vessels. (C) Schematic drawing.

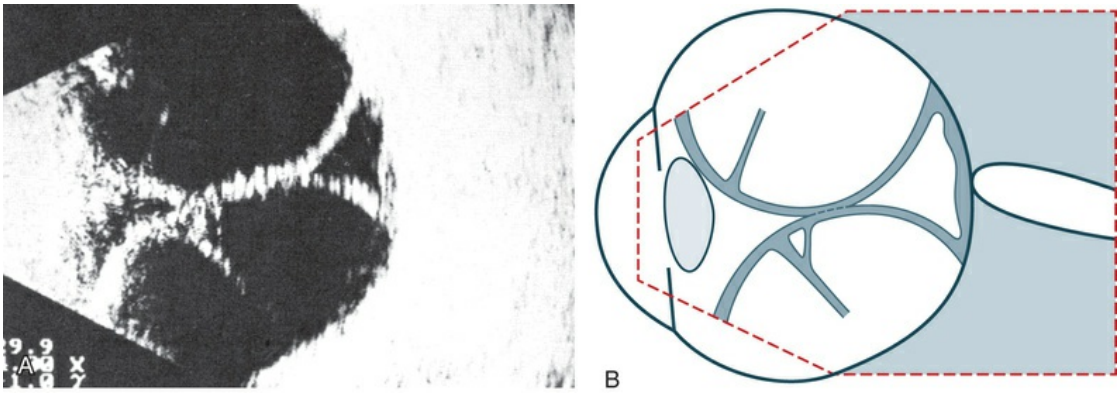

FIG. 11.55 Total exudative choroidal detachment in persistent hypotony after penetrating glaucoma surgery with external fistulation. (A) The apices of the choroidal detachment touch each other in the vitreous and are seen on the echogram. This finding is commonly termed “kissing choroidals.” Strand-like structures (possibly taut vortex veins) course through

the intrachoroidal space. (B) Schematic drawing.

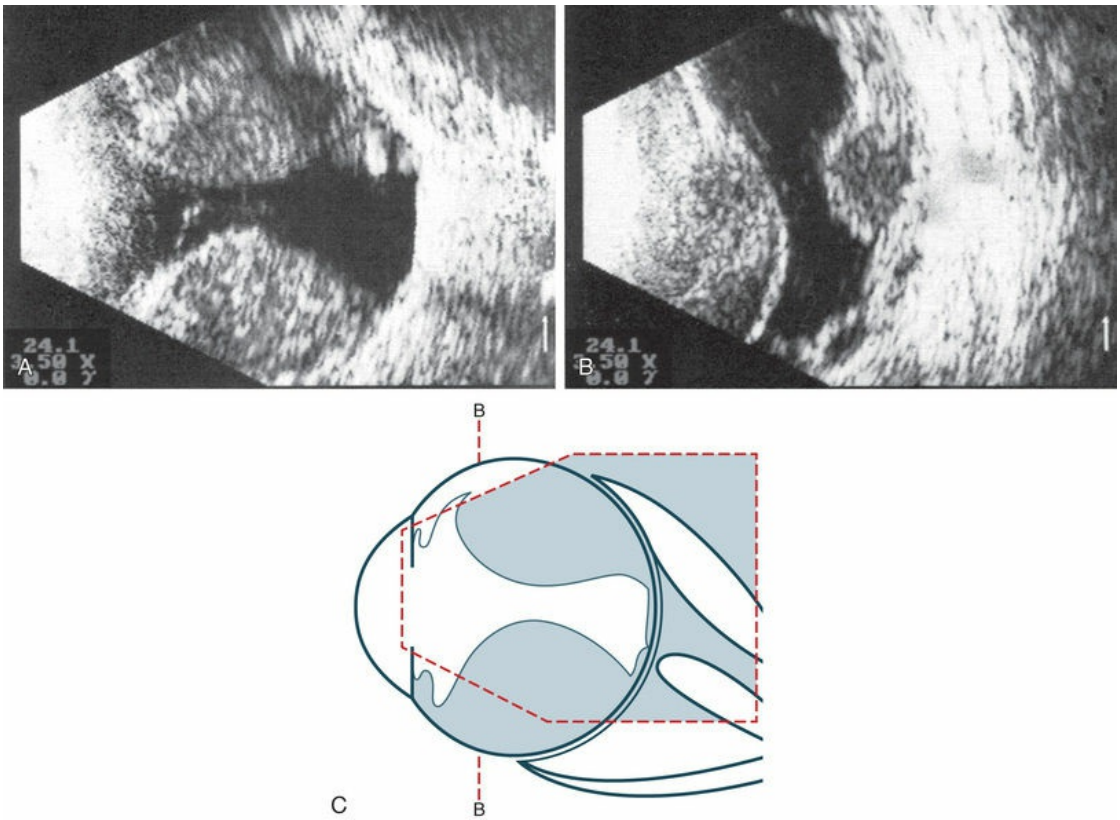

FIG. 11.56 Extensive choroidal detachment in an eye with expulsive hemorrhage. (A) The intrachoroidal space has acquired acoustic reflectivity due to the accumulation of blood. There may be anatomical healing after the absorption of the blood, but we cannot expect visual function to improve. (B) Frontal image of the hemorrhagic choroidal detachments. (C) Schematic drawing.

In chronic hypotony with longstanding choroidal detachments, the outer layer of the globe can appear concentrically widened on ultrasound. In advanced stages, the appearance on ultrasound changes, the outer walls appear thickened, and the vitreous cavity becomes substantially reduced. In these eyes, metaplasia of the pigment epithelium can result in calcification and ossification of ocular tissue that is easily identified on ultrasound because of the total reflection of all sound waves noted on the acoustic image.

Choroidal Neovascularization

Choroidal neovascularization is a complication seen in many eye diseases, most commonly in macular degeneration. The histologic findings include a vascularized collection of connective tissue that extends from the choriocapillaris through defects in Bruch's membrane and then into the subretinal pigment epithelial or subretinal space. This heterogeneous structure produces mixed ultrasound features, including the strong acoustic reflections from the fibrovascular membranes and dense connective tissue septa and the acoustically silent areas of exudate and subretinal fluid (Figs. 11.24 and 11.57). Peripheral choroidal neovascularization membranes can appear similar to choroidal melanomas; therefore, familiarity with the ultrasonographic features of these lesions is important, especially if vitreous hemorrhage prevents direct visualization.

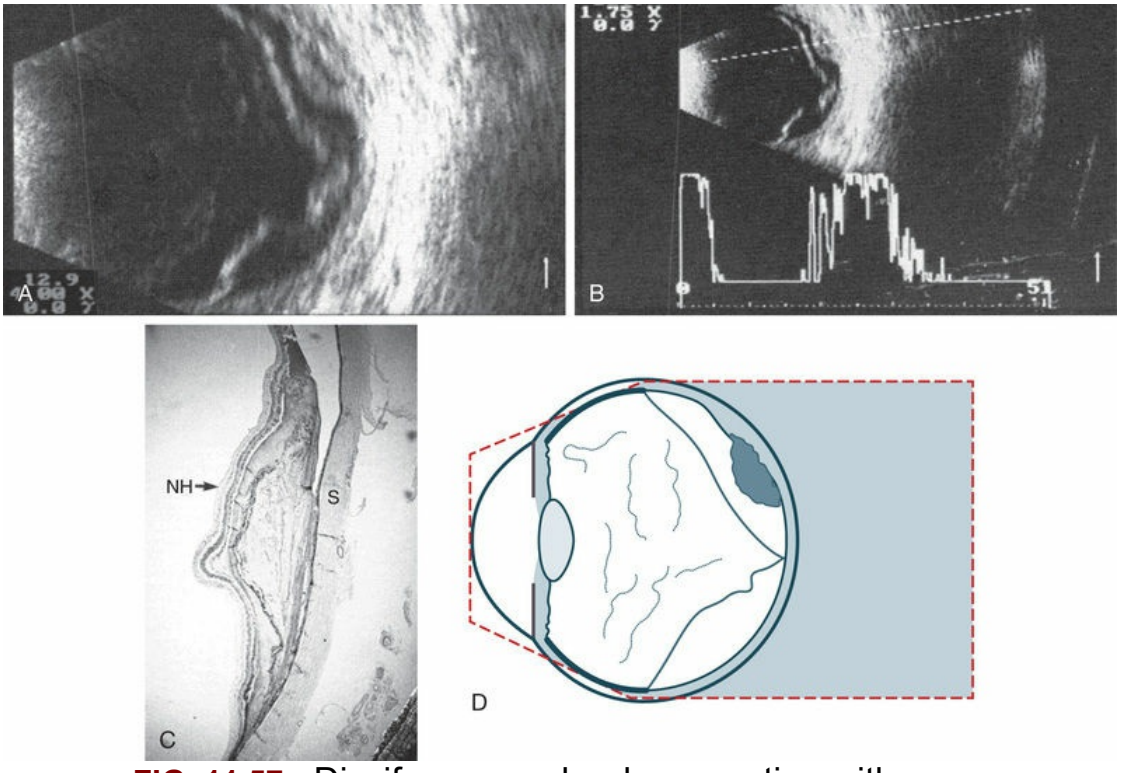

FIG. 11.57 Disciform macular degeneration with exudative retinal detachment. (A) In the cross-sectional echogram, the thickened ocular walls in the macular area appear as a strongly reflecting, layered structure. (B) The acoustic interfaces of the macular degeneration produce high signals. (C) Histologic

section of an eye with disciform macular degeneration under loupe magnification. Vascularized connective tissue scars with exudation without acoustic interfaces produce the substrate for the heterogeneous nature of the echogram. *NH*, retina; *S*, sclera. (D) Schematic drawing.

Choroidal Melanoma

Evaluation of choroidal melanomas includes a comprehensive examination with ophthalmoscopy combined with ultrasound imaging. In choroidal melanomas, the signals produced within the tumor are complicated by overlapping and attenuation of echo signal with depth. Connective tissue septa and vessels vary in their prominence and interfere with the signals from the tumor tissue. Furthermore, the resolution of the image is limited because the densely packed tumor cells are separated by a considerably shorter distance than the ultrasound wavelength. A thorough understanding of the principles of ultrasonography and a strong knowledge base of the tissue complexity in metastatic processes combined with an extensive case reference aids in the image interpretation of choroidal melanomas. The interpretation of echograms in A- and B-mode is based on reports on this topic which were published by Oksala,[36] Baum,[37] Buschmann and Trier,[38] Till and Ossoinig,[32] Trier,[39] Coleman et al.,[40] and Silverman et al.,[41] which include data from the original scans of ocular tissues. The next section will review the principles used to image choroidal tumors and the features of a choroidal melanoma on B-mode and A-mode imaging.

The Characteristics of a Choroidal Melanoma on B-Mode Echography.

In B-mode echograms, a melanoma appears as a biconvex lesion. The internal structure is relatively homogeneous so produces markedly fewer signals than the tumor surface or the sclera (Fig. 11.58). If the tumor has broken through Bruch's membrane, then a mushroom-shaped lesion, or a collar-button, can be demonstrated in cross-section and serves as a pathognomonic sign (Fig. 11.59). If present, this perforation does not necessarily occur at the peak of

the tumor; careful ultrasound examination of the entire lesion is needed (Fig. 11.60). In some sections, the collar-button of a tumor may even simulate a tumor mass lying free in the vitreous (Fig. 11.59). In addition, the collar-button portion of the lesion has unique ultrasound features due to the presence of the mass above Bruch's membrane in some places and below Bruch's membrane in other places. Previously this feature was attributed to sound attenuation, which is the continuous decay of spike altitudes in the A-mode and was called the angle kappa. However, the change in signal is most likely due to more than just an attenuation phenomenon. The features of the collar-button can be explained on the basis of echographic–histopathologic correlations (Fig. 11.61). Usually, a tumor lying immediately beneath the sensory retina reflects ultrasound more than the portion of the tumor beneath Bruch's membrane. In a collar-button, the part of the tumor growing in front of Bruch's membrane will be drained less well, leading to a dilation of the vessels in this part of the tumor.[31,42] This creates new acoustic interfaces with higher signal intensity, resulting in brighter dots in B-mode and higher spikes in A-mode. In the area of the tumor base, a "choroidal excavation" can be seen (Figs. 11.62 and 11.63). This excavation in the acoustic section develops at the edge of the tumor where melanoma tissue intersects the adjacent strongly reflecting intact choroid.[37,43]

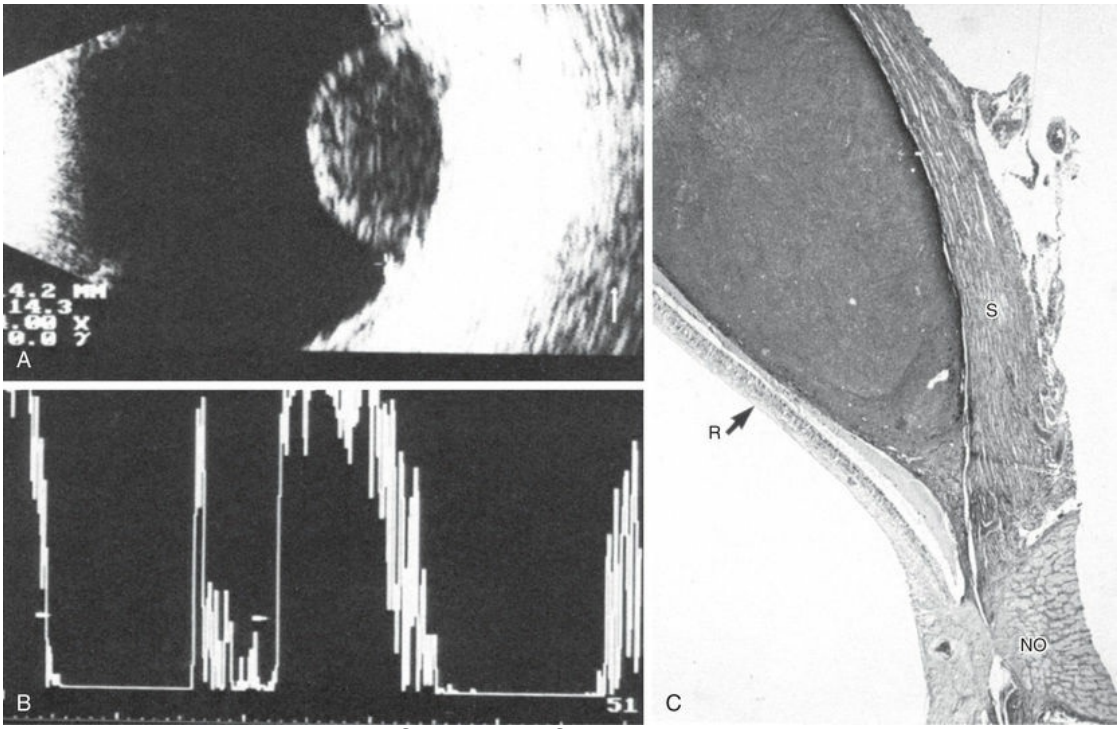

FIG. 11.58 Typical findings of a choroidal melanoma. (A) In cross-section the tumor is biconvex. The diameter of the base is 14 × 14 mm; elevation, 8.5 mm; calculated tumor volume, 0.75 mL. (B) With standardized A-mode, the spike amplitude within the tumor amounts to about 20% of the scleral spike. (C) Histologic section visualized under loupe magnification of a peripapillary choroidal melanoma. The reason for the low homogeneous acoustic reflectivity of a choroidal melanoma is the densely packed tumor cells, the margins of which are separated by a distance much smaller than the wavelength of ultrasound. *R*, retina; *S*, sclera; *NO*, optic nerve.

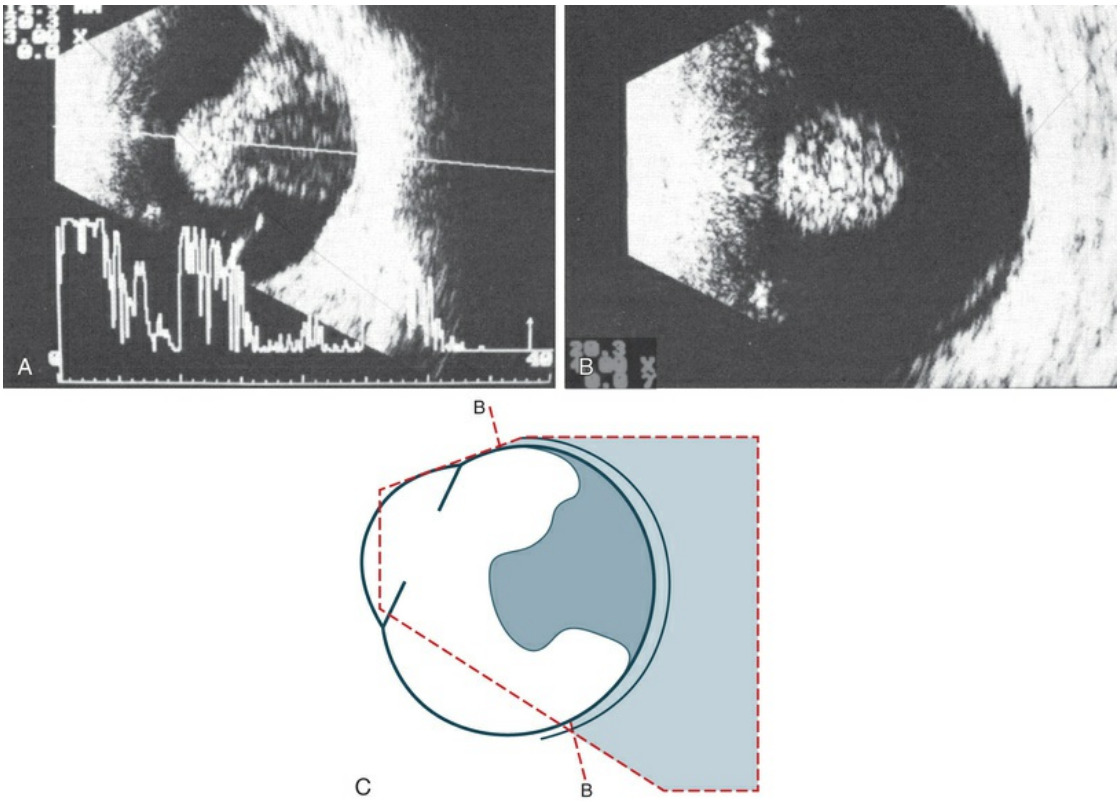

FIG. 11.59 Large choroidal melanoma, mushroom-shaped after perforating Bruch's membrane. (A) Sagittal section. (B) In the frontal plane, one part of the tumor does not seem to have contact with the ocular outer walls, which demonstrates the principle of the necessity to image tumors in multiple planes to define the full extent of invasion. (C) Schematic drawing.

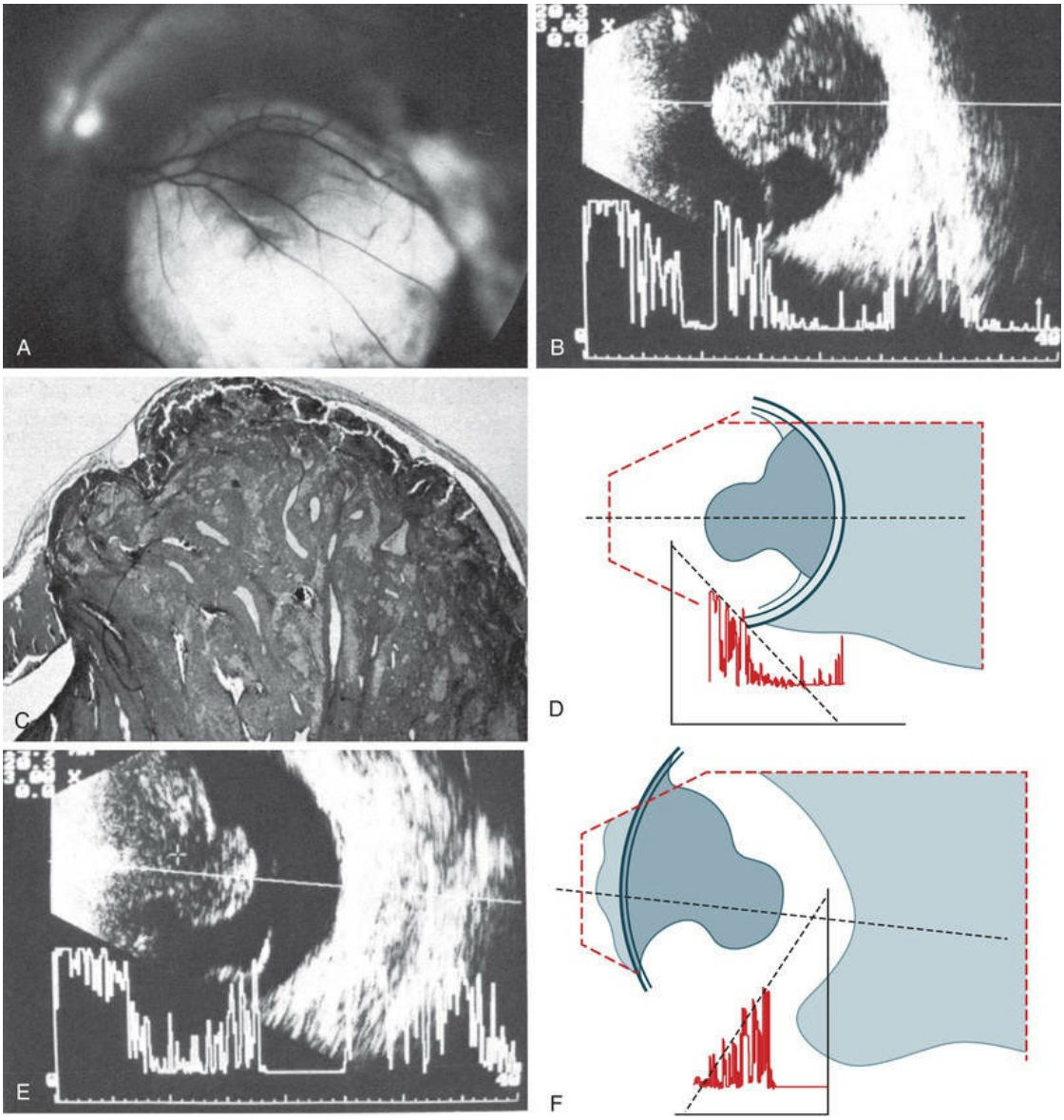

FIG. 11.60 (A) Large mushroom-shaped choroidal melanoma with collar-button seen on fundus photography. (B) Sagittal echogram cross-section with A-mode echogram. There is markedly increased reflection in the area of the tumor peak. The part of the tumor in front of Bruch's membrane often shows dilated vessels, which act as interfaces to increase the acoustic reflectivity. (C) Histologic section through the tumor. (D) Schematic drawing. (E) Echogram from the tumor base. This image was obtained with maximal adduction of the globe, and made possible because of the far temporal location of the tumor base. Also in this direction of examination, the part of the tumor anterior to Bruch's membrane demonstrates high reflectivity. (F) Schematic drawing.

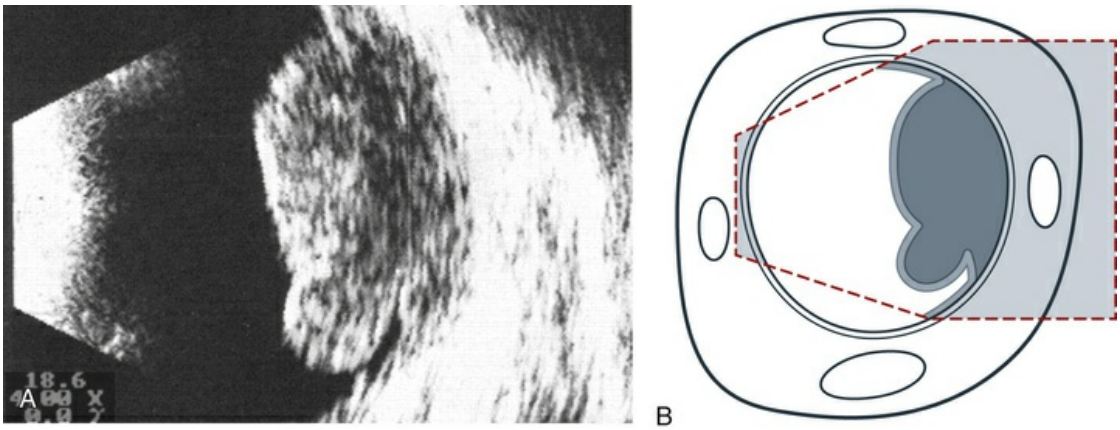

FIG. 11.61 (A) Choroidal melanoma with eccentric perforation of Bruch's membrane. Echogram shows a mushroom-like shape of the lesion, which is nearly pathognomonic for a melanoma and therefore of great differential diagnostic value. (B) Schematic drawing.

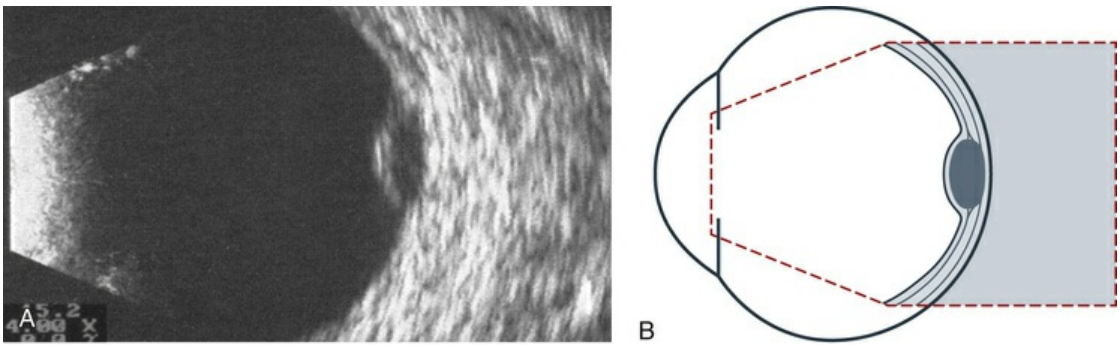

FIG. 11.62 (A) Small choroidal melanoma. Elevation, 2.5 mm; base, 8 × 8 mm; calculated tumor volume: 0.066 mL. The choroid at the tumor base has been replaced by tumor, which has less acoustic reflectivity and provokes a choroidal excavation echographically. (B) Schematic drawing.

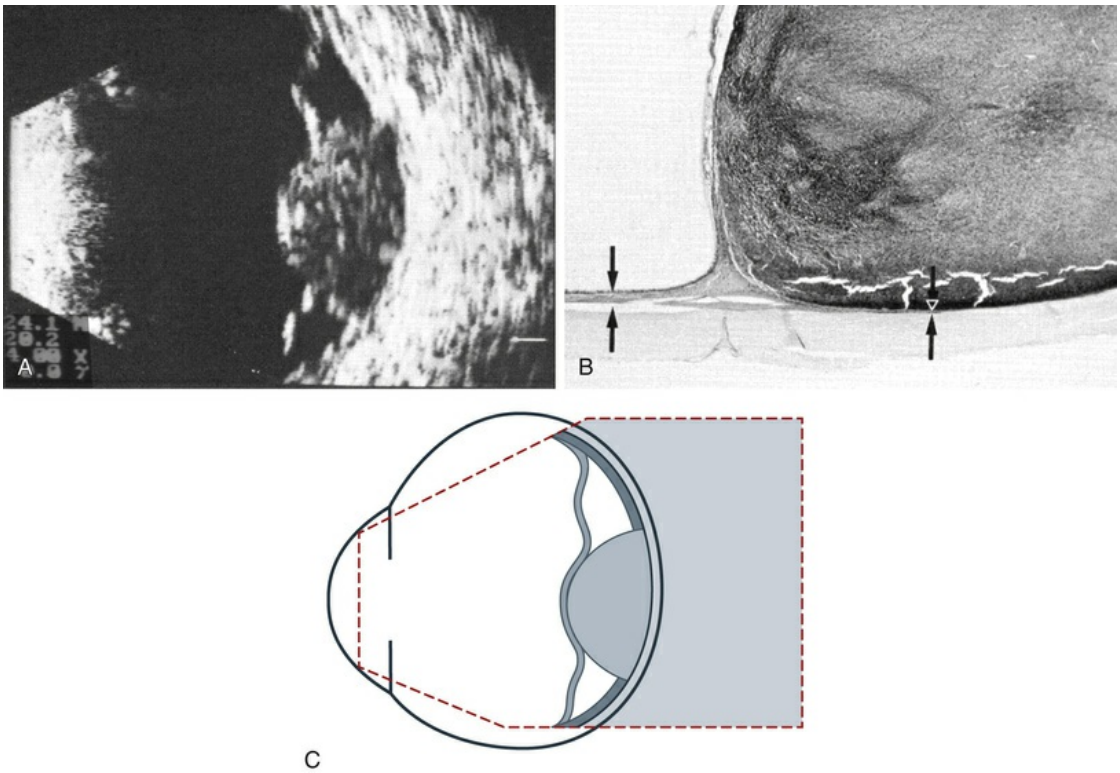

FIG. 11.63 Choroidal melanoma. (A) Elevation, 6 mm; diameter at the base, 11 × 12 mm; calculated tumor volume, 0.33 mL. The highly reflecting choroid has been replaced by the poorly reflecting melanoma, producing a choroidal excavation in the cross-section. (B) Histologic section through the margin of a choroidal melanoma. At the base, normal choroid is replaced by tumor. (C) Schematic drawing.

The Characteristics of a Choroidal Melanoma on A-Mode Ultrasonography.

The ultrasonographic internal structure of a tumor is quantitatively best described in the echogram. An unfocused A-mode transducer can obtain a summation signal from the large tissue area,[31] which typically demonstrates spikes of relatively uniform amplitudes within the large biconvex tumor if the lesion has not extensively broken through Bruch's membrane (Fig. 11.58). This corresponds to the uniform histologic structure of a melanoma (Fig. 11.58). Exceptions occur when features of hemorrhage or necrosis within the tumor develop.[44,45]

Most melanomas consist of solid tissue; therefore, no aftermovements occur as might be expected with a large subretinal

or choroidal hemorrhage. In addition, flickering spike complexes may be seen on the A-mode echogram within the tumor itself. Various authors interpret them differently. It is assumed that they are due to blood circulating in large tumor vessels. Although the features of the ultrasound combined with a thorough clinical examination can establish the diagnosis of choroidal melanoma with enough certainty to recommend treatment, a preoperative correlation between the sonographic pattern and the histopathologic findings is currently still in debate.[40,41]

B-mode Doppler devices can obtain signals from the interior of the tumor by using a high-resolution power and a frequency between 7 and 20 MHz. This method is more sensitive than the visual evaluation of a time amplitude echogram[46] (Fig. 11.64). In some patients it was possible to determine the blood flow within the tumor using Doppler color-coding technology. In a series of 50 eyes with melanoma, Doppler shifts could be detected in all patients except one. The tumor size varied between 0.8 and 1.5 mL. Doppler imaging has also been used to study an eye with secondary glaucoma and significantly increased intraocular pressure. In this patient the tumor perforated the sclera and invaded the muscle cone (Fig. 11.65). An intraocular pressure of 45 mmHg compressed the intraocular tumor, which influenced the maximal flow velocities measured by Doppler sonography (Fig. 11.65).

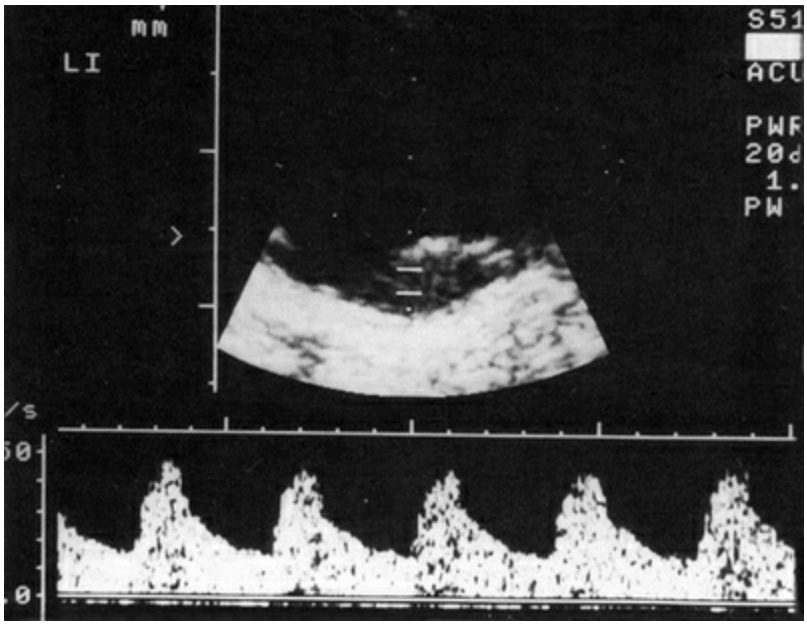

FIG. 11.64 B-mode Doppler sonography (duplex technique) of a choroidal melanoma of average size. In A-mode the occasionally observed flickering amplitudes are produced by the blood flow. They can be quantified when using a B-mode Doppler instrument of high resolution.

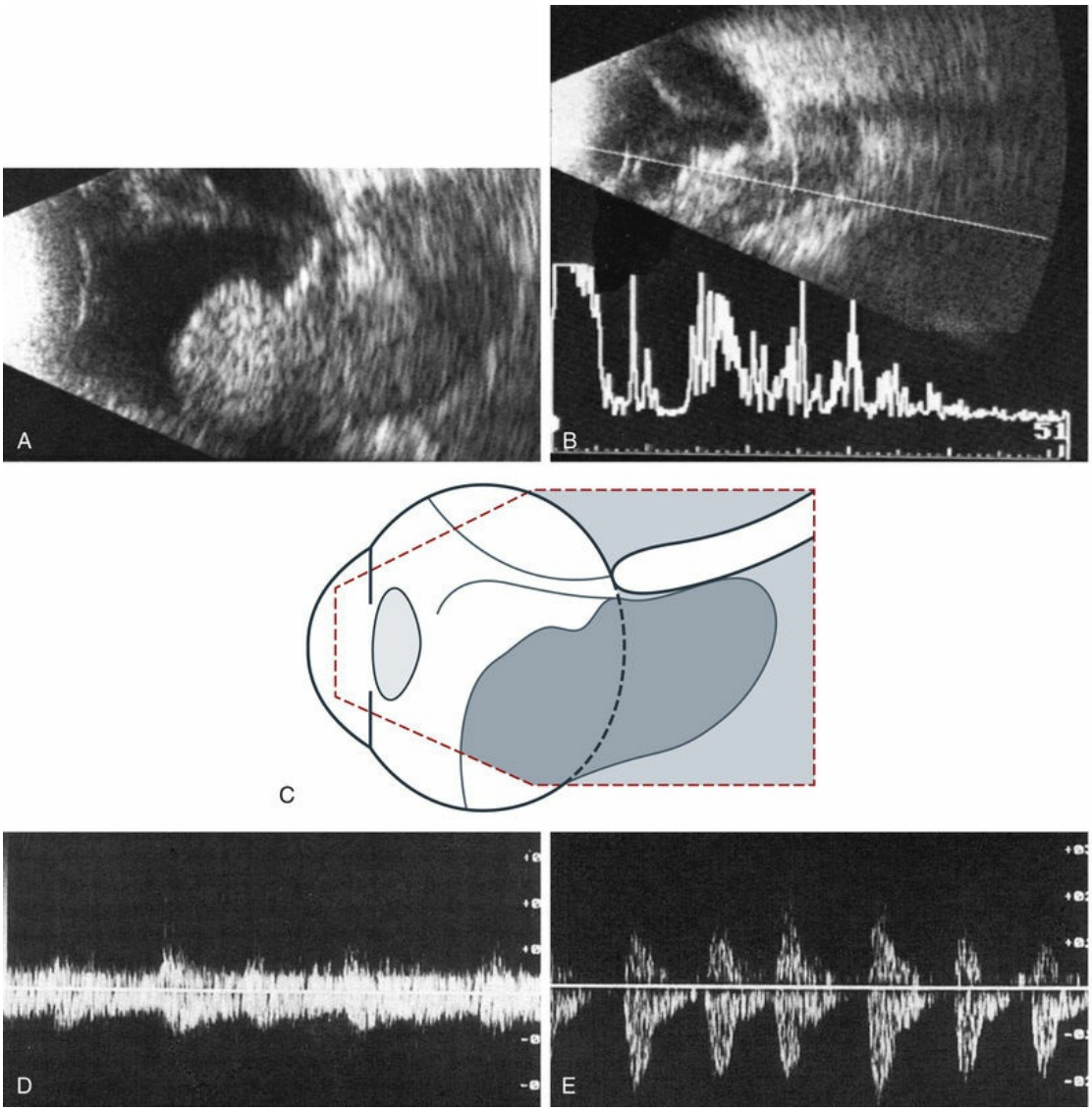

FIG. 11.65 Choroidal melanoma with orbital invasion in a 65-year-old woman. Referral diagnosis was orbital cellulitis. Echographic findings include a large intraocular tumor with wide invasion of the orbital tissues (A). Remnants of the sclera can be demonstrated within the tumor in both A- and B-mode echograms because of their strong acoustic reflectivity (B). Additional findings include a total retinal detachment as seen in both images. (C) Schematic drawing of the echogram. (D,E) Doppler signal of the choroidal tumor. (D) Frequency shift from the intraocular tumor, maximum velocity: 10 cm/s. (E) Frequency shift from the extraocular tumor, maximum velocity: 2 cm/s. With Doppler technique the intraocular part of the tumor shows reduced blood flow compared to the extraocular part.

The use of Doppler ultrasonography in studying ocular blood flow in disease states is increasing; however, at the present time this method does not allow exact measurements of maximal flow velocities.

Determining the Volume of a Choroidal Melanoma by Ultrasonography.

Ultrasonography produces spikes in the recorded signal when interfaces with different media are encountered. In a normal eye, the first acoustic interface after the signal passes through the vitreous is the retina. In the case of a choroidal tumor the apex is adjacent to the retina spike and the base is anterior to the scleral spike. Identifying these positions, however, can be challenging in some settings. For example, if the retina is attached to the tumor surface, no separate discrimination of the two interfaces is possible (Fig. 11.58). On the other hand, if the accompanying retinal detachment is also present over the peak of the tumor, then the retina will be imaged as a separate membranous structure lying in front of the lesion (Fig. 11.66). Then the transition between tumor and scleral must be identified. In most cases, the scleral spike is still the strongest signal even in the presence of a choroidal tumor. If the tumor breaks through the scleral barrier, the continuity of this strong signal is interrupted at the site of perforation. An exact measurement of the volume of the tumor is important when measuring the lesion height, planning a treatment, or analyzing the effect of therapy.

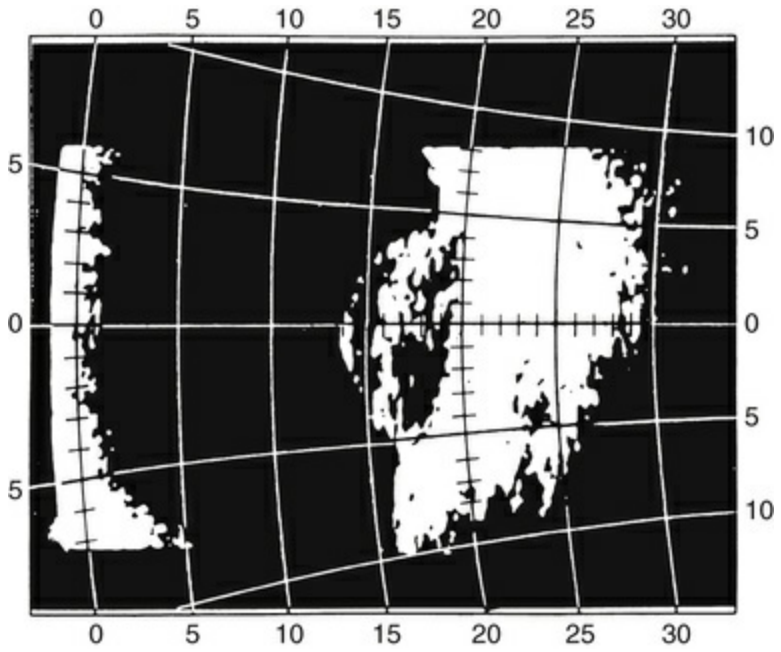

FIG. 11.66 Choroidal melanoma with associated retinal detachment over the peak of the tumor. Tumor size: base, 9 × 9 mm; elevation, 3.5 mm. The detached retina lies about 2 mm in front of the tumor. The calculated tumor volume is about 150 mL. If the retinal detachment were erroneously included, the volume would be about 230 mL.

Ultrasonography is capable of providing precise measurements of tumor size. Ultrasound devices have measurement tools that can be applied in the window of the image. The examiner can use this feature to measure the height of the largest and smallest diameter of the tumor. In biconvex tumors, volume data for the tumor can be calculated from these linear measurements or it can be evaluated using special equipment designed for 3D evaluation (Fig. 11.67).

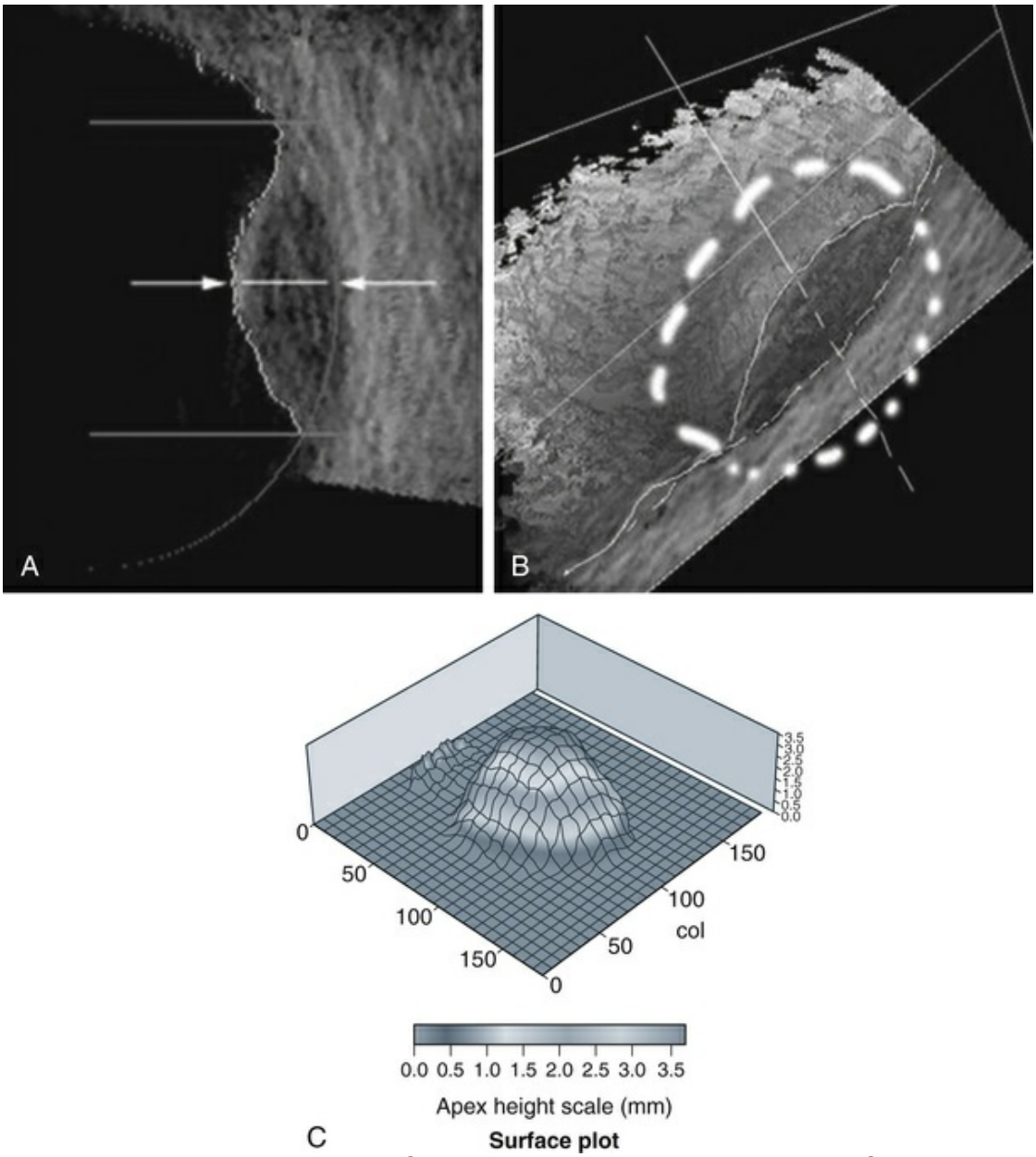

FIG. 11.67 Example of three-dimensional rendering of the posterior segment tumor. (A) Area of interest marked. (B) Contour-finding procedure with outlining of the space-occupying lesion. (C) Surface plot for volume determination.

The Role of Ultrasonography for Planning the Treatment of Choroidal Melanomas.

After a choroidal melanoma is diagnosed by careful clinical examination and ultrasound interpretation, the next step for the physician is to formulate a treatment plan. Radiation therapy is successfully used for the treatment of medium or small ocular

melanomas. Scleral contact radiotherapy using ruthenium-l06, cobalt-90, or iodine-125 applicators shows a relatively steep decay of radiation dosage. At a distance of 8 mm from the radiation surface, only 10% of the energy is still available. In order to achieve complete tumor necrosis in this area, an application of 10 times the duration of radiation is needed. Fig. 11.68 shows the isodose curves for ruthenium-106 applicators. The aim of any radiation therapy is to destroy the tumor tissue and to spare the adjacent normal ocular tissues as much as possible. The radiation pellets are placed on custom scleral plaques that are designed to cover the full extent of the tumor. It is therefore important to have an exact measurement of the size of the tumor and have precise placement of the scleral plaque over the tumor (Figs. 11.69 and 11.70). Ultrasonography provides the most accurate measurements for this purpose. Dynamic imaging using the ultrasound B-mode can also provide information on adjacent pathology such as overlying retinal detachments, which may overestimate the total height of the tumor if not properly identified.

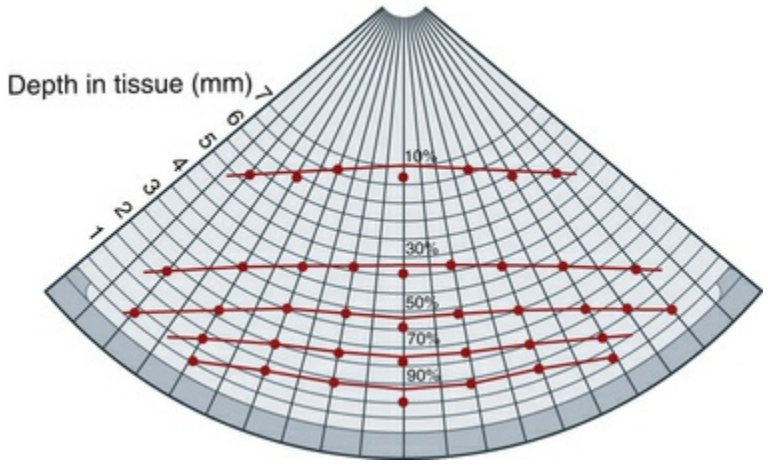

FIG. 11.68 Measuring protocol for a ruthenium applicator type CCC; diameter of the emitting plane, 21 mm. At 5 mm from the applicator surface, only 25% of the scleral contact dose is still available. Because of this steep decay of effective radiation, it is critical to plan the treatment exactly.

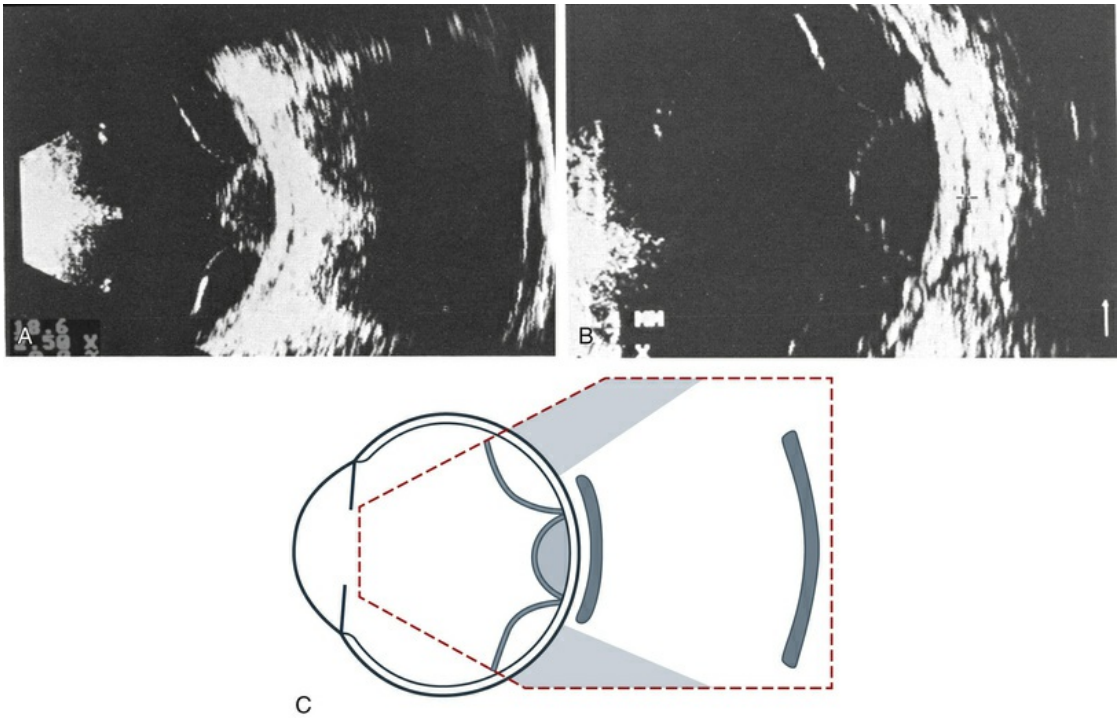

FIG. 11.69 (A,B) Echogram of an eye with the ruthenium-beta applicator in place. The slit between the posterior scleral surface and the applicator is filled with fluid and is less than 0.5 mm wide. The lateral extent of the applicator is marked by the sound shadow. (C) Schematic drawing.

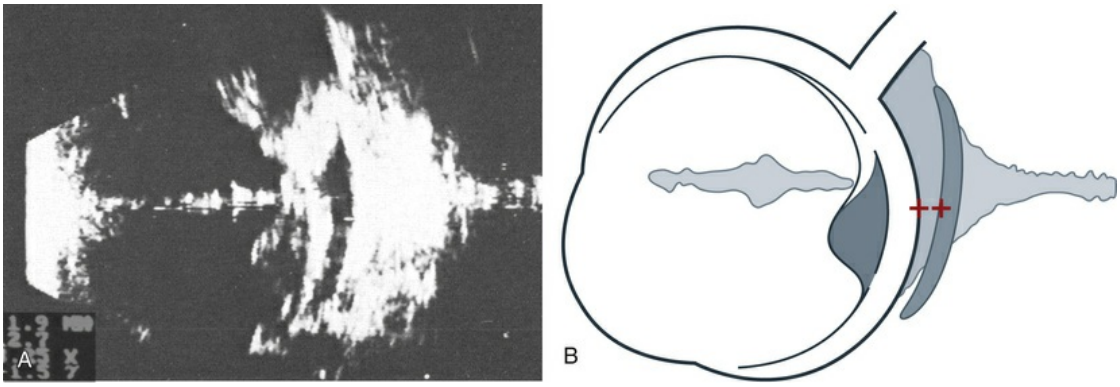

FIG. 11.70 (A) Ruthenium-beta applicator in place with a wide slit between the sclera and the applicator surface. On the basis of this echographic finding, the position of the applicator should be changed or the duration of the treatment has to be prolonged. Distance of the measuring marks: 1.9 mm. (B) Schematic drawing.

Serial examination with ultrasonography following treatment can be used to monitor the effect of the radiation plaque by measuring the tumor elevation, tumor base, and reflectivity of the internal tumor structure as well as by identifying the presence of tumor vessels. Fig. 11.71 illustrates the successful treatment of a choroidal melanoma that was documented echographically. In this case, after 4 months there was a marked increase in reflectivity in the internal tumor structures. Within 10 months the volume was reduced from 0.38 to 0 mL.

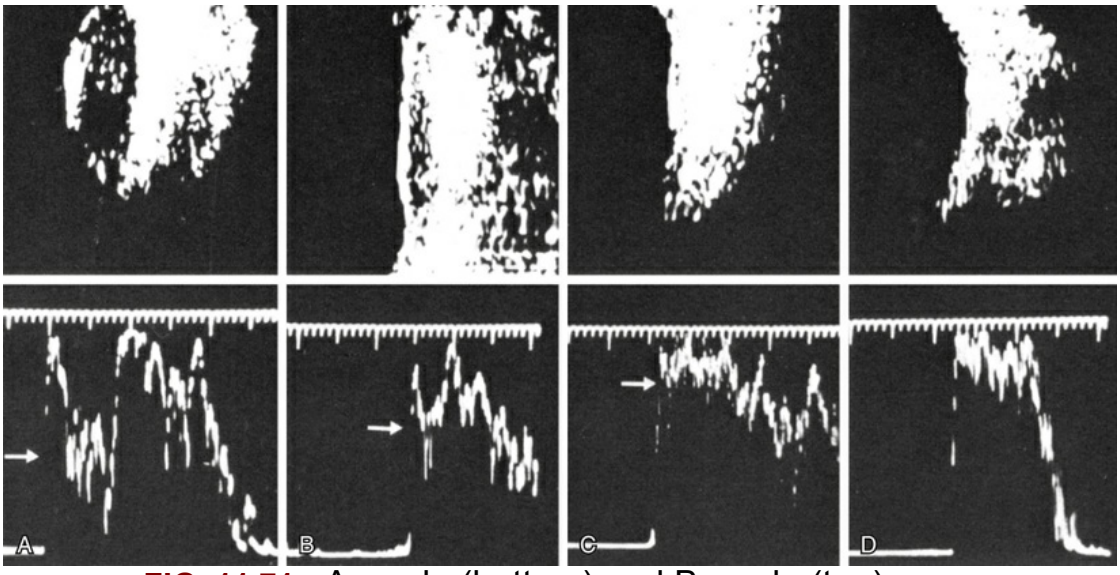

FIG. 11.71 A-mode (bottom) and B-mode (top) echograms during follow-up assessments of a successfully treated choroidal melanoma. The tumor volume was reduced from 0.38 to 0 mL within 10 months. After 8 months the spikes within the tumor increased from about 40% of the scleral spike to about 90% (*white arrows*). (A) Before radiation, 380 mL, reflection 40%; (B) after 4 months, 230 mL, reflection 80%; (C) after 8 months, 100 mL, reflection 90%; (D) after 10 months, 0 mL, no reflection.

In some cases of successfully treated tumors, the increased reflectivity within the tumor is the only ultrasonographic parameter that changes after radiotherapy (Fig. 11.72). Increased reflectivity may demonstrate tumor necrosis; however, this may not always be the case, as some tumors remain viable even with the increase in reflectivity noted on ultrasound.

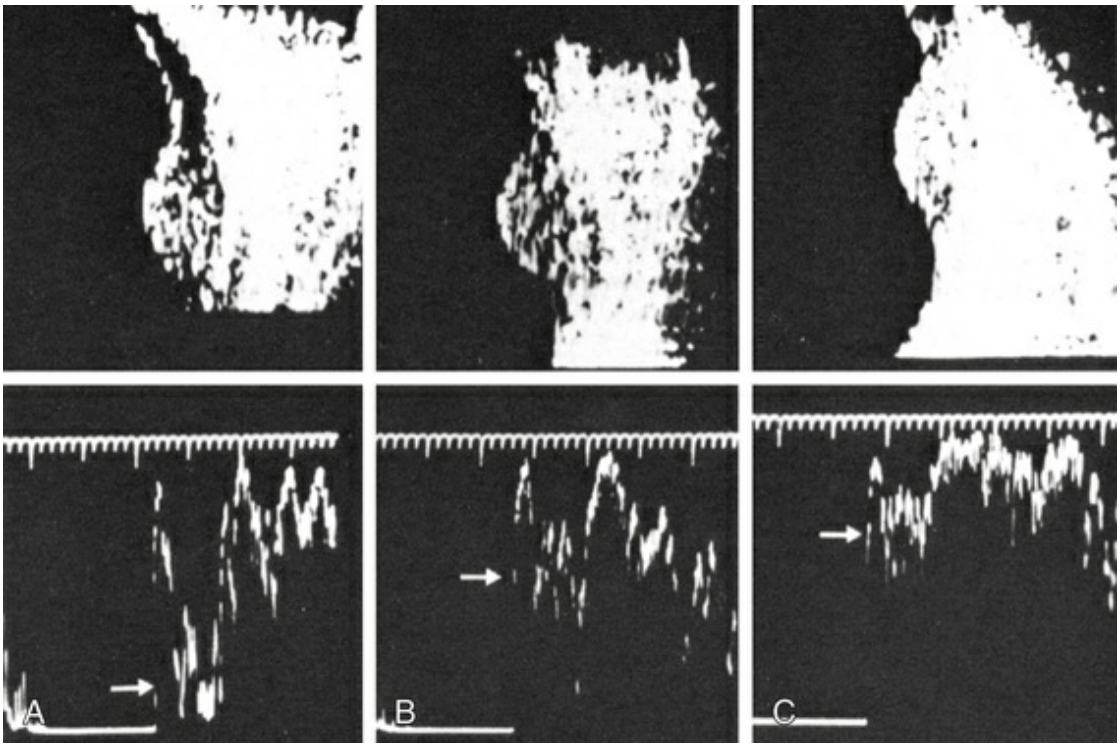

FIG. 11.72 A-mode (bottom) and B-mode (top) echograms demonstrating the effect of brachytherapy on a choroidal melanoma. The external shape of the tumor also remains unchanged after a second series of radiation; the reflectivity of the tumor increases from about 20% of the scleral spike before radiation to about 80% after radiation (*white arrows*). (A) Before radiation, volume 250 mL, reflection 20%; (B) after 8 months, 250 mL, reflection 70%; (C) after 36 months and 22 months after second radiation, volume 250 mL, reflection 80%.

Determining blood flow by B-mode Doppler sonography is an additional parameter that could be used to monitor the treatment response in highly vascularized choroidal tumors, such as choroidal melanomas. Doppler can detect a decrease in blood flow in the necrotic mass that is left after radiation therapy. The necrotic tissue from treated tumors can be absorbed by the adjacent blood vessels, but radiation may damage these vessels and prevent the clearing of these products, which explains the residual mass on ultrasound seen after treatment with radiation: this mass is called tumefaction. This may explain the increased reflectivity of treated tumors. Fig. 11.73 shows an elevated tumor before radiation.

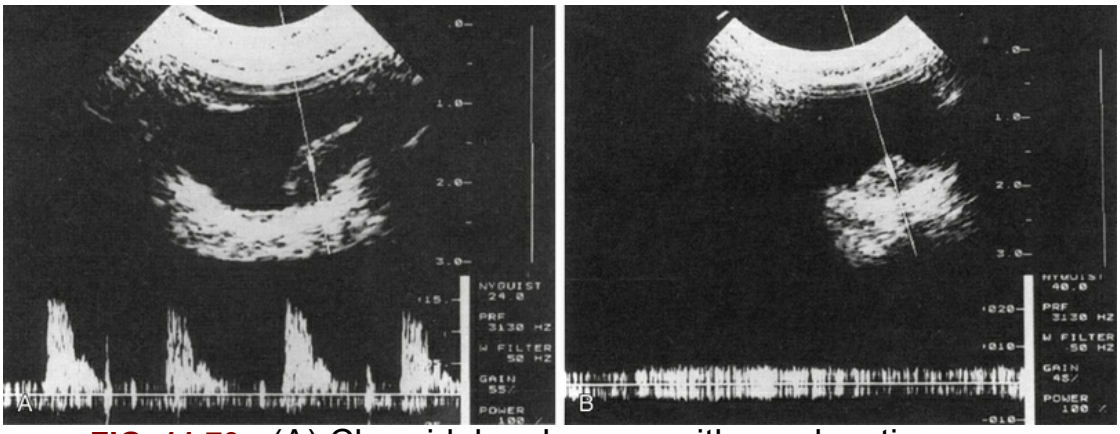

FIG. 11.73 (A) Choroidal melanoma with an elevation of 5 mm. Cross-sectional echogram obtained with the duplex instrument ATL mark 8. The sample volume is identified by the marks on the aiming beam. In this area Doppler spectra are obtained, indicating a high blood flow velocity (represented in the lower part of the illustration). (B) Same patient as in panel A, 4 months after radiation treatment of the choroidal melanoma with ruthenium. There is still a considerable volume of tumor remaining (maximal elevation, about 3.5 mL). No frequency shift can be obtained from the interior of the tumor when using duplex examination. The tissue lying in the guiding beam produces only a biphasic noise (illustrated in the lower part of the image).

Metastatic Choroidal Tumors

Choroidal metastasis is a known complication of several cancers, including all types of carcinomas and sarcomas. The most frequent primary tumors are breast (40%) and lungs (29%). One study examined 230 eyes from deceased patients with known systemic carcinoma and showed that 12% of the eyes had choroidal metastasis on pathologic specimens.[47] Many of these tumors remained undetected at the time of death. The detection of such lesions can be a poor prognostic factor. The average survival time after treatment for choroidal metastasis is 7.4 months.[48] Therefore, many of these patients are not followed for extended periods of time by their ophthalmologist.

Typically carcinoma metastasis presents as a large, highly reflective thickening of the ocular outer layers. The internal acoustic properties can resemble disciform macular degeneration or a

choroidal hemangioma. A metastatic adenocarcinoma typically presents with high reflectivity from the strong acoustic interfaces from its adenoid-like histologic structure (Fig. 11.74).

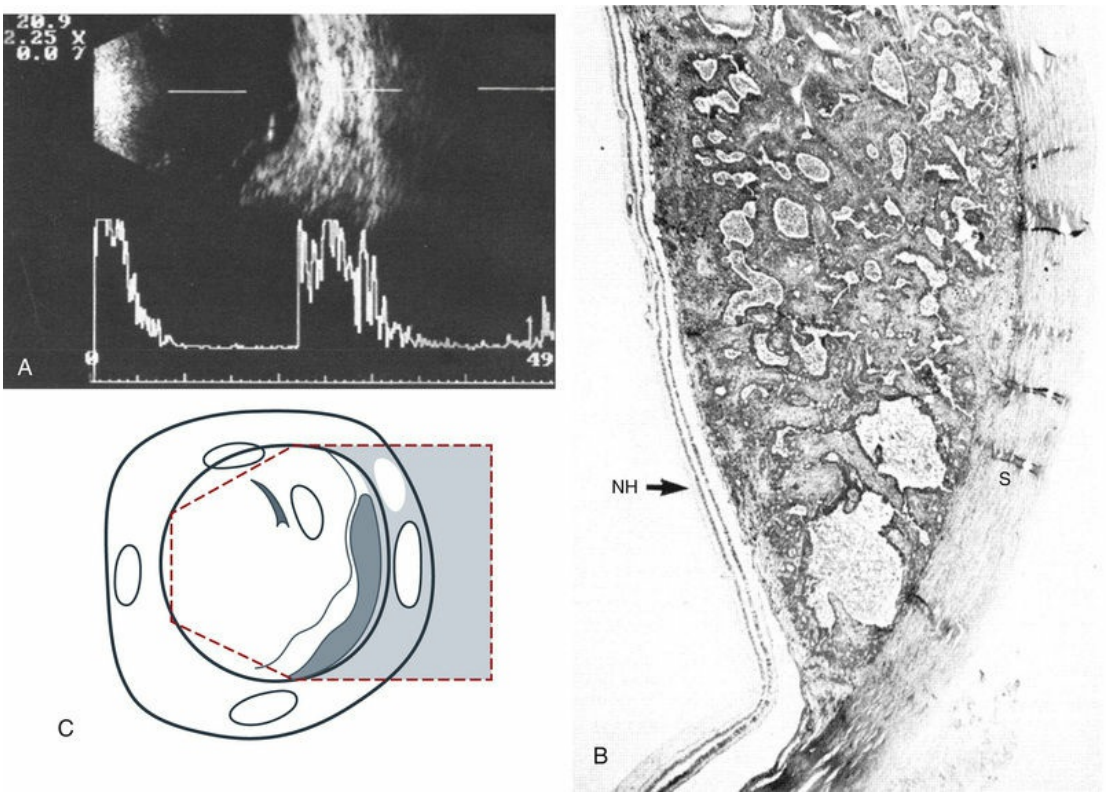

FIG. 11.74 Extensive choroidal metastatic tumor in the lower nasal quadrant. (A) On the echogram the choroid is widened to about 2.5 mm; the retina is partly detached by an exudate. The tissue inside the metastatic tumor shows high acoustic reflectivity. (B) Histologic section of a metastatic adenocarcinoma in the choroid. The gland-like structure provides good acoustic interfaces. *NH*, retina; *S*, sclera. (C) Schematic drawing.

In contrast, there are several atypical presentations of choroidal metastasis that have also been reported.[49,50] Pathologic examination of an eye that was enucleated because of suspicion for choroidal melanoma from ultrasound examination revealed a choroidal metastasis from small-cell bronchial carcinoma (Fig. 11.75).[49]

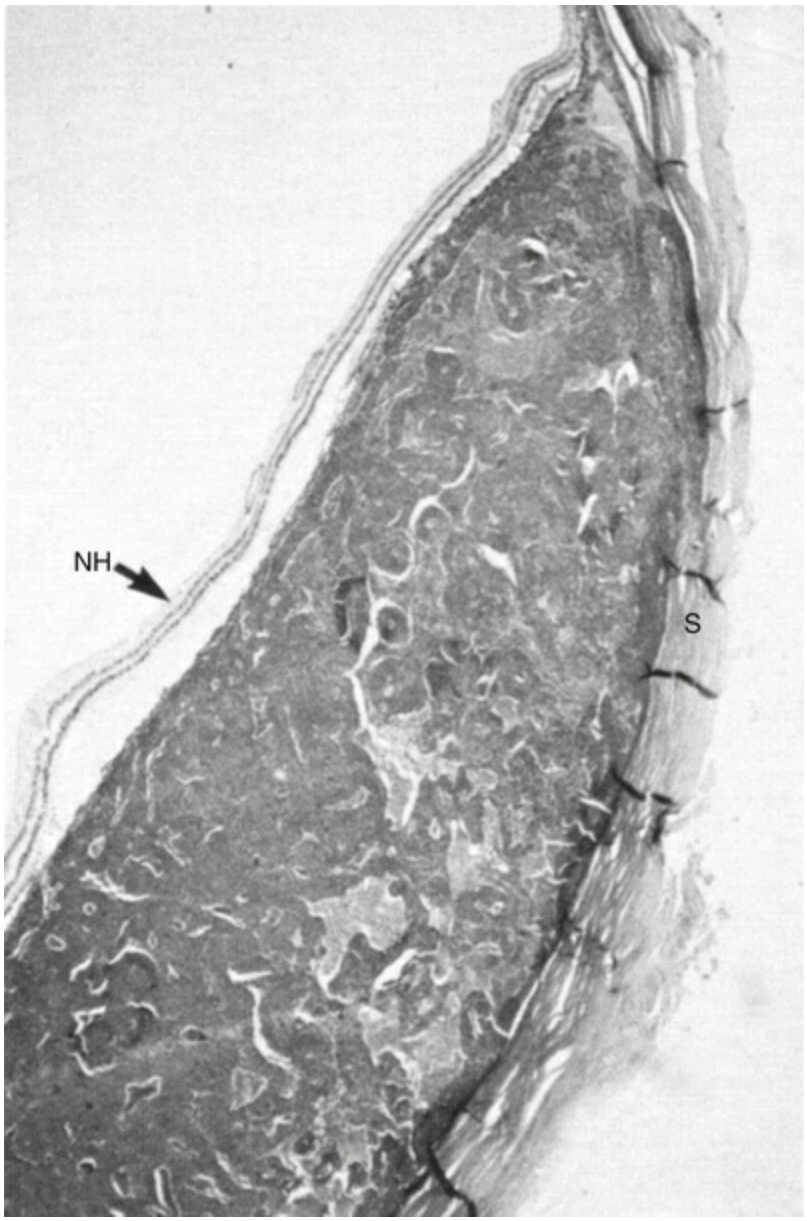

FIG. 11.75 Histologic metastatic tumor from a small-cell bronchial carcinoma. The echogram (not shown) resembled that of a typical choroidal melanoma. Similar findings have been seen in choroidal metastases from cutaneous melanoma. *NH*, retina; *S*, sclera.

Choroidal Hemangioma

Choroidal hemangioma may be an isolated lesion or may be associated with Sturge–Weber syndrome. Isolated hemangiomas, described as circumscribed choroidal hemangiomas, usually occur at the posterior pole. The lesions are typically diffuse, slightly

elevated, and may have indistinct margins. These features make ophthalmic interpretation of the lesion difficult and often they can be missed. However, associated features of these circumscribed lesions can include retinal detachment and secondary changes of the RPE, which makes their presence more conspicuous on exam. Ultrasonographically, choroidal hemangiomas appear as a strongly reflecting, nearly concentric widening of the outer layers of the eye (Fig. 11.76). In spite of the abundant vascularization, ultrasound images of choroidal hemangiomas do not show the circulating blood as in choroidal melanomas. Instead, the echogram of a choroidal hemangioma is similar to that of metastatic adenocarcinoma or disciform macular degeneration, which may be indicative of a slower circulation more consistent with laminar flow in the cavities of dilated blood vessels shown by Doppler ultrasonography (Fig. 11.77). In longstanding cases the epichoroidal layer may ossify and produce sound shadows. In this stage, a hemangioma may appear identical to an osteoma or a metastatic calcification of the choroid.[51,52]

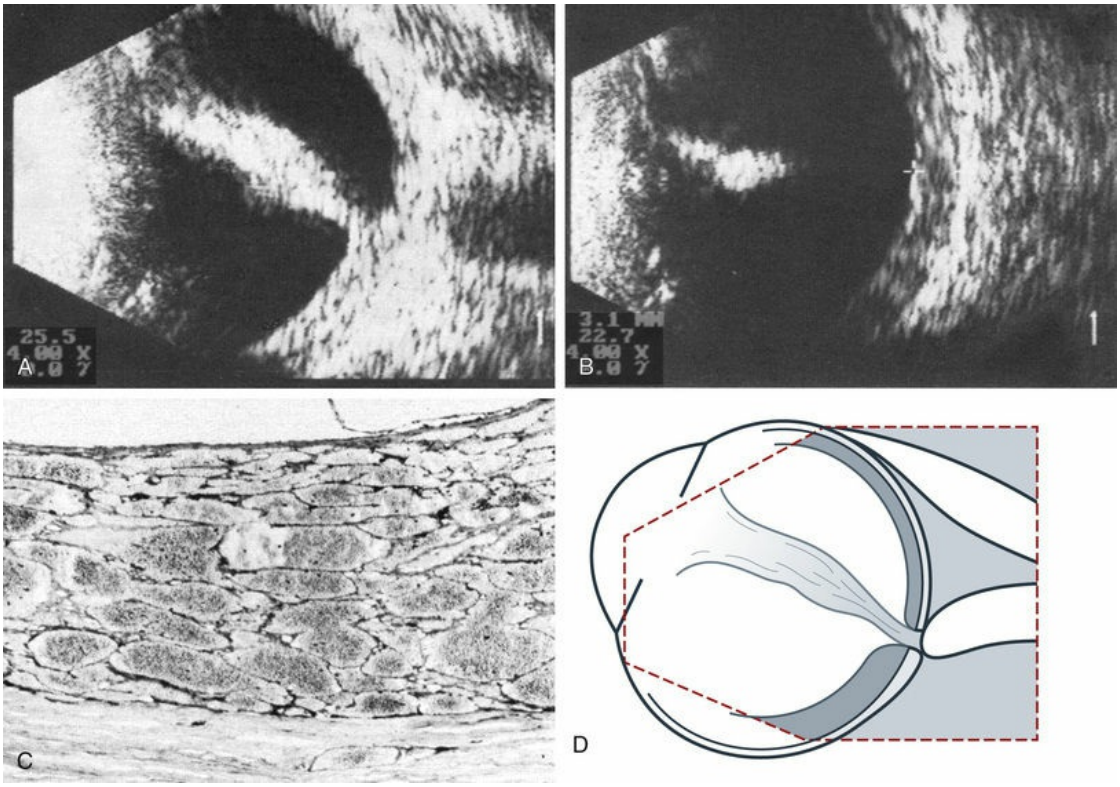

FIG. 11.76 Extensive choroidal hemangioma in Sturge–Weber syndrome (additional finding: total

retinal detachment). (A) Cross-sectional echogram through the area of the optic nerve head. In the lower quadrant, the ocular walls are markedly thickened. (In spite of the associated retinal detachment, the intraocular pressure was 50 mmHg by applanation.) (B) With reduced sensitivity, the scleral surface can be delineated in spite of the high acoustic reflectivity within the tumor (distance of the measuring marks, 3.1 mm). (C) Histologic section through the tumor illustrated in (A) and (B): the septa of the cavities are thin and lined with endothelium. They produce strong reflectivity within the lesion. (D) Schematic drawing.

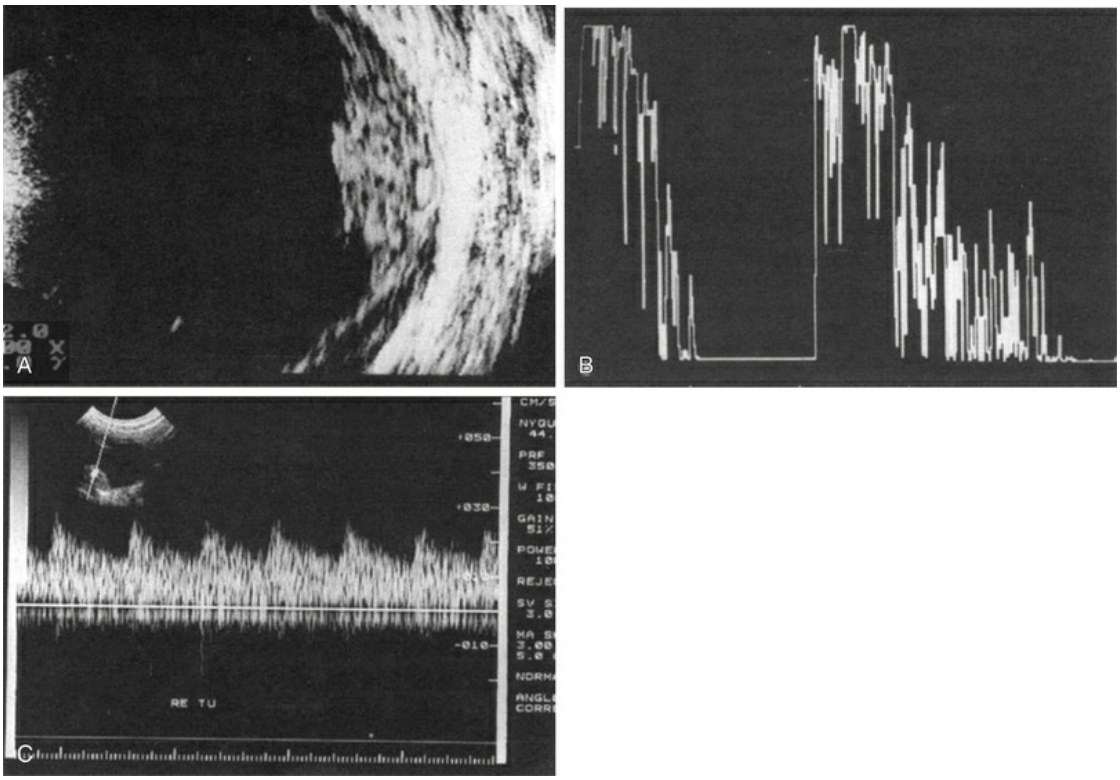

FIG. 11.77 (A) Cross-sectional echogram of a circumscribed choroidal hemangioma in a 12-year-old boy. The tumor has an elevation of 4 mm. (B) In an A-mode echogram with S-shaped amplification the cross-sectional picture corroborates the high reflectivity of the tumor. (C) On Doppler sonography, we see blood circulating within the tumor, synchronous with the pulse. The illustrated velocity profile speaks for a relatively low resistance by the blood vessels.

Choroidal Osteoma – Metastatic Calcifications

Choroidal osteoma is a rare condition that is characterized ultrasonographically by a localized area of high reflectivity at the outer wall (Fig. 11.78). Several conditions can mimic the appearance of a choroidal osteoma. As mentioned above, a chronic circumscribed hemangioma can ossify and resemble a choroidal osteoma.[53–55] In addition, several choroidal lesions can contain calcium, including ocular metastases of the choroid and the sclera[51] or metabolic disorders of calcium metabolism that create a localized calcium deposition within the choroid known as an osseous choristoma (Fig. 11.79).[54]

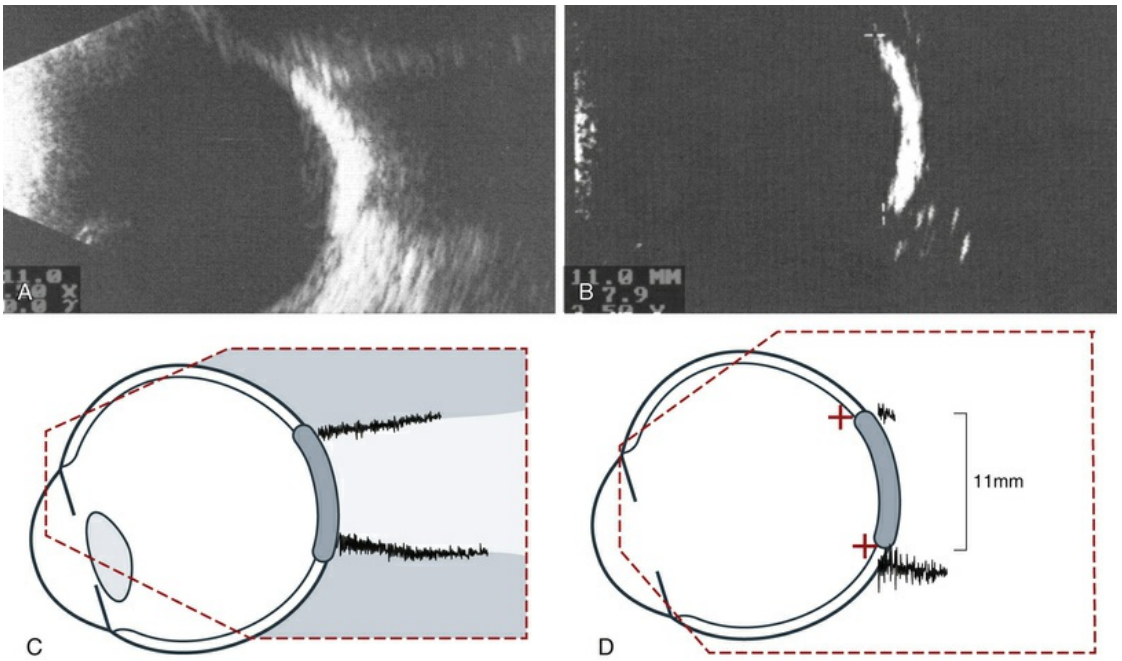

FIG. 11.78 Cross-sectional echogram of the choroidal osteoma. (A) The echogram of the lesion is characterized by total reflection of the ultrasound, and shadow formation. An elevation cannot be unequivocally documented. (B) With reduced amplification it is possible to image the ossification as an isolated signal. The horizontal diameter is 11.0 mm. (C,D) Schematic drawings.

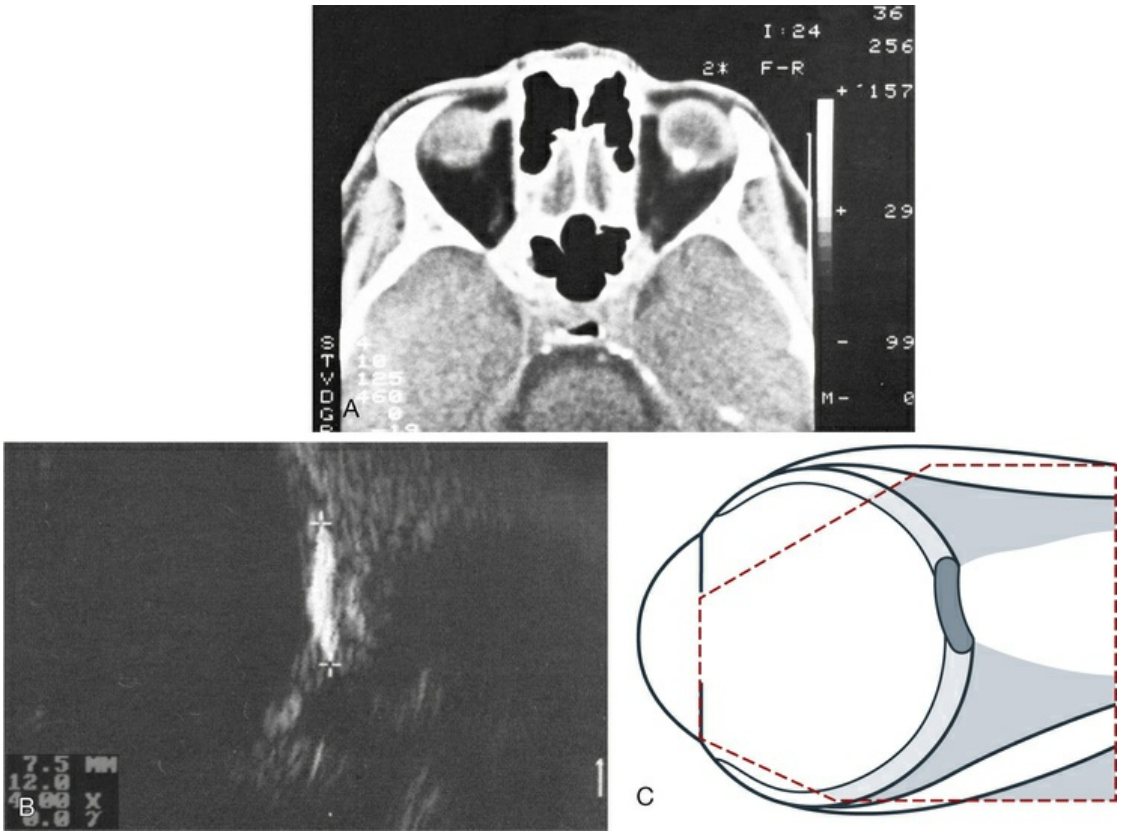

FIG. 11.79 Metastatic calcification of the ocular walls of unknown etiology. Differential diagnosis includes choroidal osteoma. (A) A computed tomography scan was obtained because of nonophthalmologic problems. A circumscribed calcified structure within the ocular walls was found incidentally. (B) In cross-sectional echograms, a lesion of the ocular walls above the optic nerve head showed total reflection of the ultrasound signal. The lateral extension was about 7.5 mm. There was no corresponding lesion seen on fundus examination that would be typical of an osteoma. The etiology of this lesion is unknown. (C) Schematic drawing.

Choroidal Tuberculoma

Choroidal tuberculomas are another extremely rare choroidal lesion (Fig. 11.80).[56] Tuberculomas can also appear similar to choroid melanoma (Figs 11.81). Images that are suggestive of choroidal tuberculomas exemplify the importance of placing the ultrasound image in context with the rest of examination of the patient in order to make the proper diagnosis. Tuberculomas are found in patients

with disseminated tuberculosis and a complete examination can identify other tuberculomas to confirm the diagnosis. Laboratory confirmation of mycobacterium by blood or sputum sampling is also helpful. In addition, these lesions should respond to antituberculous treatment.

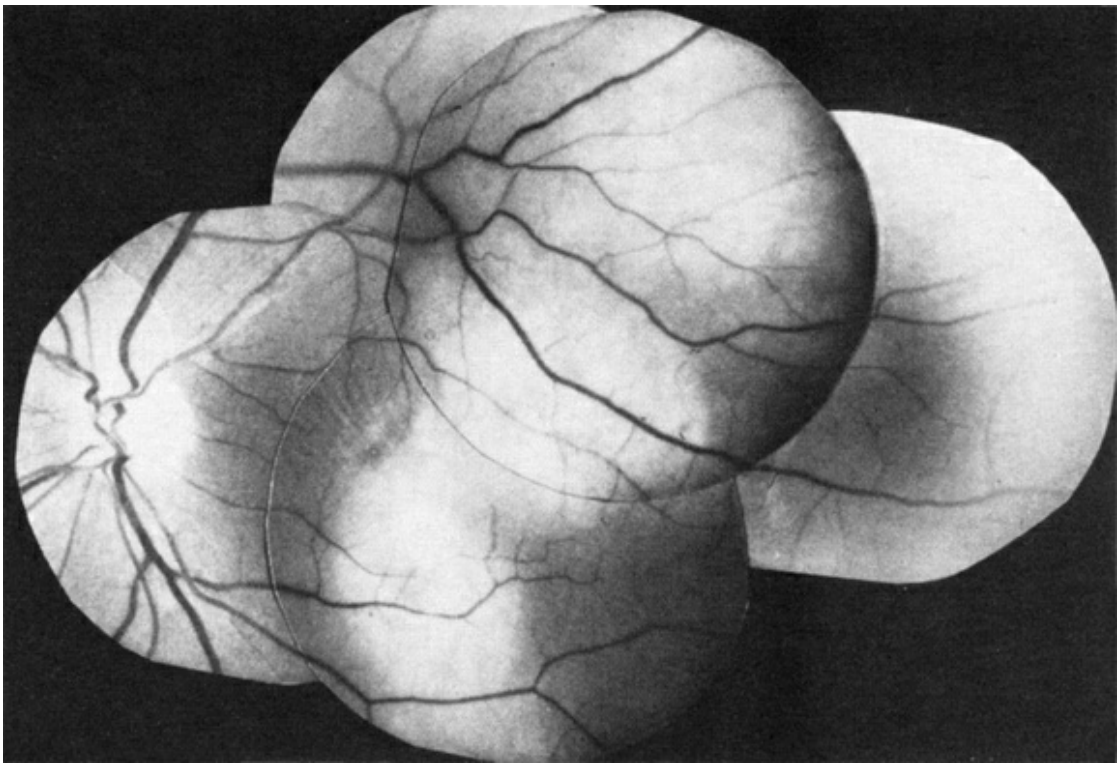

FIG. 11.80 Fundus picture of a 52-year-old woman with active pulmonary tuberculosis. This lesion resolved with antituberculosis treatment.

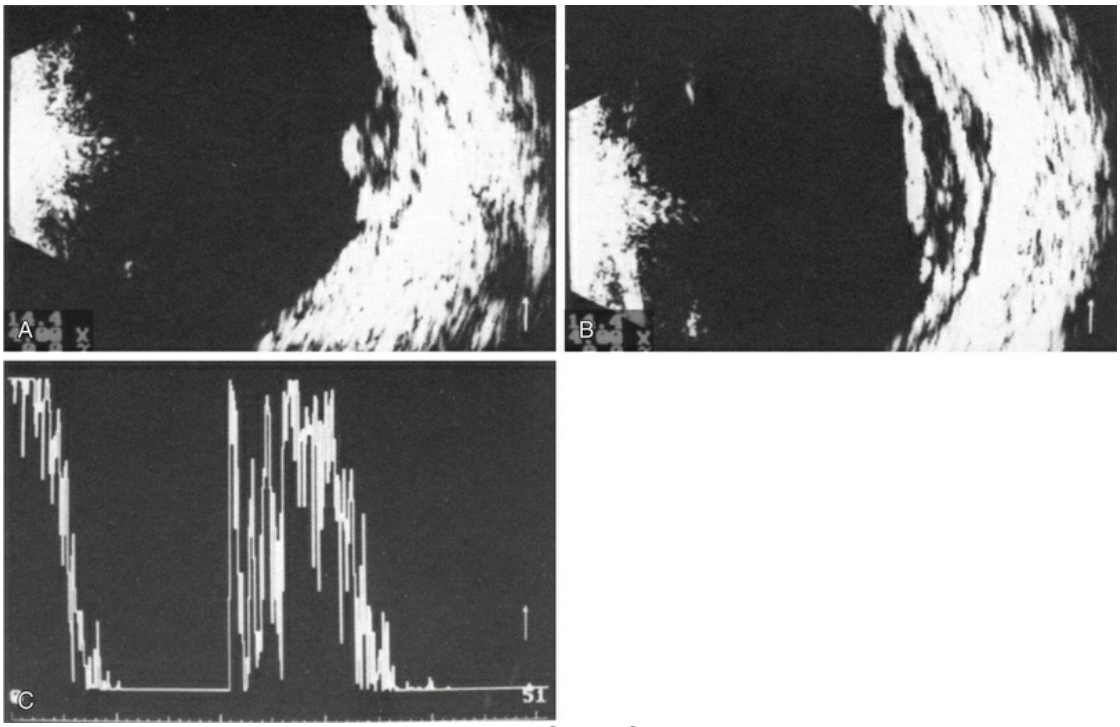

FIG. 11.81 (A,B) Echogram of the fundus lesion shown in Fig. 11.80. (C) The lesion is characterized by low acoustic reflectivity. Tenon's space can be well demonstrated. The reflectivity corresponds to that of a choroidal melanoma. The infiltration of Tenon's space points toward inflammatory etiology.

The Uveal Effusion Syndrome

Patients with uveal effusion syndrome can have partial or circular choroidal detachment combined with an exudative retinal detachment (Fig. 11.82). Ultrasonography is very important in this condition. It can reveal fluid in the suprachoroidal space or differentiate choroidal hemorrhage or tumor from the serous fluid seen on imaging from choroidal effusion syndrome.[49,57]

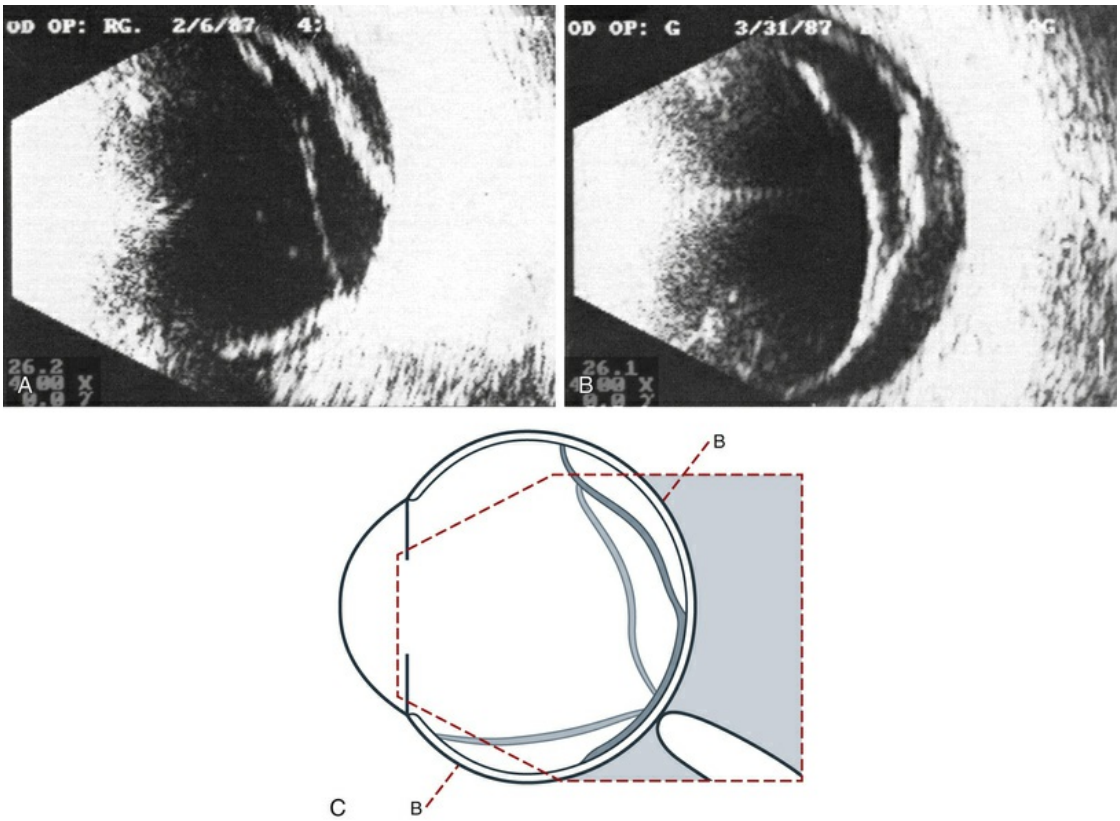

FIG. 11.82 Uveal effusion syndrome in a 55-year-old woman. (A) In the axial cross-section, the retina is attached to the optic nerve head. There is an associated, strongly reflecting choroidal detachment. (B) Cross-section of image in (A). (C) Schematic drawing.

Sclera

Posterior Scleritis

Ultrasonography is the diagnostic method of choice for posterior scleritis.[52,58,59] The clinical picture is characterized by an acute loss of vision associated with folds at the posterior pole. The normal high reflectivity of the sclera will be decreased by changes in the tissue from inflammatory swelling. The result is a low reflective signal from a thickened choroid, which is suggestive of posterior scleritis. Choroid and vitreous may appear normal. Occasionally, there is a slight exudation into the subretinal space with accompanying disc edema. In 50% of the patients, fluid accumulates in Tenon's space.[60] This signal can be similar to a diffuse choroidal melanoma. There is one case report of an eye that was enucleated because of suspicion

of an ocular melanoma based on the finding of brawny scleral thickening (Figs. 11.83 and 11.84). This case highlights the importance of proper ultrasound interpretation in the clinical context of each patient.[61]

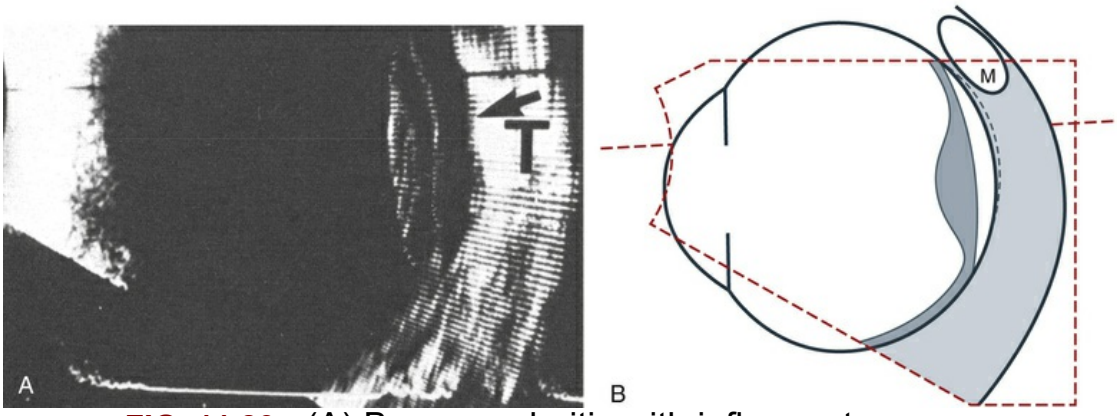

FIG. 11.83 (A) Brawny scleritis with inflammatory infiltration of Tenon's space. This disease entity can be clinically and ultrasonographically identical to a choroidal melanoma. *T*, Tenon's space. (B) Schematic drawing. *M*, muscle.

FIG. 11.84 Macroscopic photo of a brawny scleritis. On the basis of the ultrasonographic findings and a positive P32 test, the eye was enucleated because a melanoma was suspected.

Ultrasound Imaging Used to Differentiate Ocular Disease

Ultrasonography is invaluable in the diagnosis of certain ocular and orbital conditions. Proper imaging with ultrasound can narrow the differential diagnosis in certain conditions and guide further workup and management. These conditions include choroidal folds (Tables 11.1–11.3 and see Fig. 11.85), leukocoria (Table 11.4 and see Fig. 11.86), and vitreous hemorrhage (Table 11.5 and see Fig. 11.87). First, choroidal folds can be from orbital masses, ocular inflammation, disc edema in an atypical presentation, or from idiopathic causes.[49] Next, leukocoria is a condition of a white pupil that blocks ophthalmic examination, typically diagnosed in infancy. This finding can be from retinoblastoma. Differentiating this disease from other benign causes of leukocoria is critical for providing appropriate treatment of the patient. Finally, vitreous hemorrhage may manifest from a variety of changes in the posterior globe; the urgency of treatment is dependent on the diagnosis of a retinal detachment. All of these conditions require ultrasound technology to establish the proper diagnosis. The tables listed above provide information on the differential diagnosis of each condition and ultrasound features that will help guide image interpretation.

TABLE 11.1

Orbital Causes of Orbital Folds

Diagnosis	Number of Patients
Graves orbitopathy	11
Sinusitis	5
Mucocele	2
Hemangioma	6
Orbital pseudotumor	5
Various orbital tumors	8
Unexplained	6
Total	43

Data from Verbeek A. Echographic findings in 36 patients with choroidal folds. Doc Ophthalmol Proc Ser 1981;29.

TABLE 11.2

Ocular Causes of Choroidal Folds

Diagnosis	Number of Patients
Hyperopic eye	17
Macular degeneration	12
Ocular hypotony	12
Posterior scleritis	9
Buckling operation	9
Trauma	6
Intraocular tumor	3
Miscellaneous	10
Total	78

TABLE 11.3

Choroidal Folds: Ultrasonographic Findings Helpful for Differential Diagnosis

Diagnosis		Ultrasonographic Findings
Myositis Graves orbitopathy	1	Thickened extraocular muscles
Periorbital space-occupying lesions	2	Change in the relief of the orbital wall, sound propagation into perinasal sinuses
Orbital neoplasm	3	Directly evident (it may be difficult to demonstrate a small cavernous hemangioma because of its high acoustic reflectivity)
Inflammatory orbital pseudotumor	4	Widening of normal orbital structures, low acoustic reflectivity, Tenon's space may be demonstrated
Disc edema	5	Widened dural diameter of the optic nerve
Axial hyperopia	6	Axial length below 22 mm, ocular walls concentrically thickened
Ocular hypotony	7	Ocular walls concentrically thickened
Macular degeneration		Thickening of the ocular walls in the area of the macula, high acoustic reflectivity
Scleritis	8	Circumscribed widening of the ocular walls Tenon's space apparent

For companion schematic drawing, see Fig. 11.85.

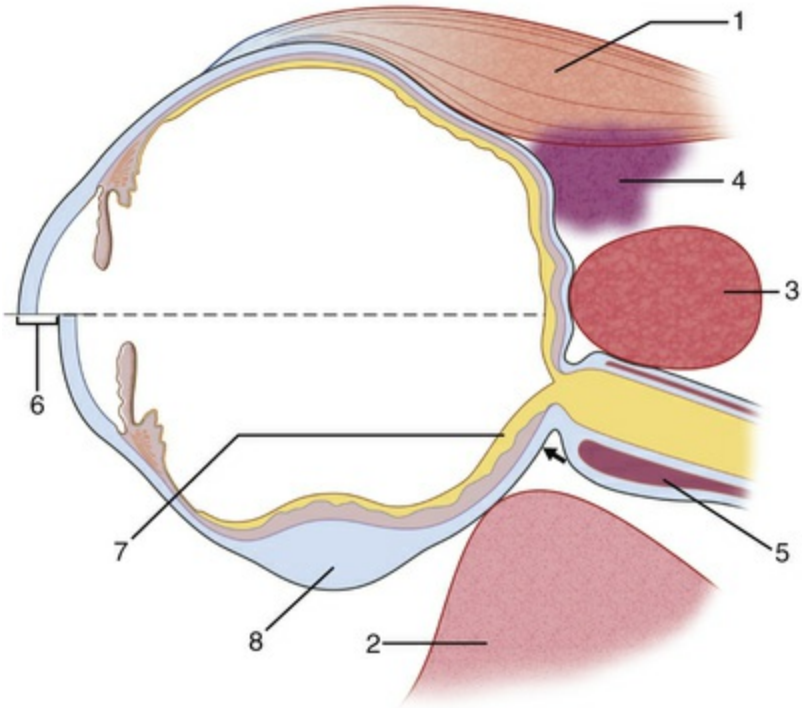

FIG. 11.85 Choroidal folds: ultrasonographic contribution to the differential diagnosis (for detail, see Table 11.3).

TABLE 11.4

Leukocoria: Ultrasonographic Findings Helpful for Differential Diagnosis

Diagnosis		Ultrasonographic Findings
Normal axial length for the patient's age		
Retinoblastoma	1	Widening of the ocular walls, extremely high acoustic reflectivity, shadowing effect, atypical findings possible
Congenital cataract	2	Increased reflectivity from the posterior lens surface, vitreous space empty, ocular walls normal
Shortened axial length		
Retinopathy of prematurity	3	In stages IV and V, beginning or complete traction detachment (normal findings in stages I–III)
Persistent hyperplastic primary vitreous (PHPV)	4	Dense strand of tissue between optic nerve head and posterior lens pole; formes frustes may occur (posterior or anterior PHPV)
Retinal anomalies		Membranes in the vitreous, atypical detachment, which in part appears solid (no typical echogram)
Fundus coloboma	5	Directly demonstrable protrusion of ocular wall, sometimes with orbital cyst (microphthalmos with cyst)
Coats disease	6	Floating crystals in the vitreous and subretinal space (fast-flickering spikes on A-mode)

For companion schematic drawing, see Fig. 11.86.

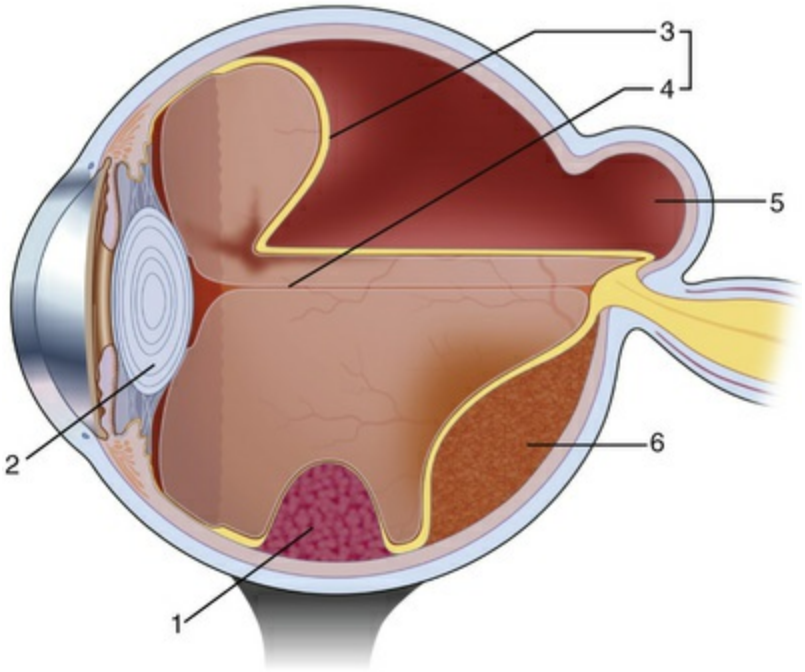

FIG. 11.86 Leukocoria: echographic contribution to the differential diagnosis (for detail, see Table 11.4).

TABLE 11.5

Vitreous Hemorrhage: Ultrasonographic Findings Helpful for Establishing the Etiology

Diagnosis		Ultrasonographic Findings
Symptomatic posterior vitreous detachment	1	Thickened detached posterior hyaloid membrane, occasionally early retinal detachment
Recently formed retinal break with torn vessel	2	Blood-covered vitreous strands converge toward the retinal break; occasionally a high-floating operculum may be detected
Proliferative retinopathy	3	Strands or membranes extending from the optic nerve head or the posterior pole, high acoustic reflectivity
Terson syndrome (vitreous hemorrhage after subchoroidal bleeding	4	Vitreous opacities in front of the optic nerve head or behind the detached vitreous
Disciform macular degeneration	5	Widening of the ocular walls in the macular area, high acoustic reflectivity, vitreous strands extending from the macula
Choroidal melanoma	6	Biconvex thickening of the ocular wall, low acoustic reflectivity, sometimes mushroom-shaped; accompanying retinal detachment distant from the tumor

For companion schematic drawing, see Fig. 11.87.

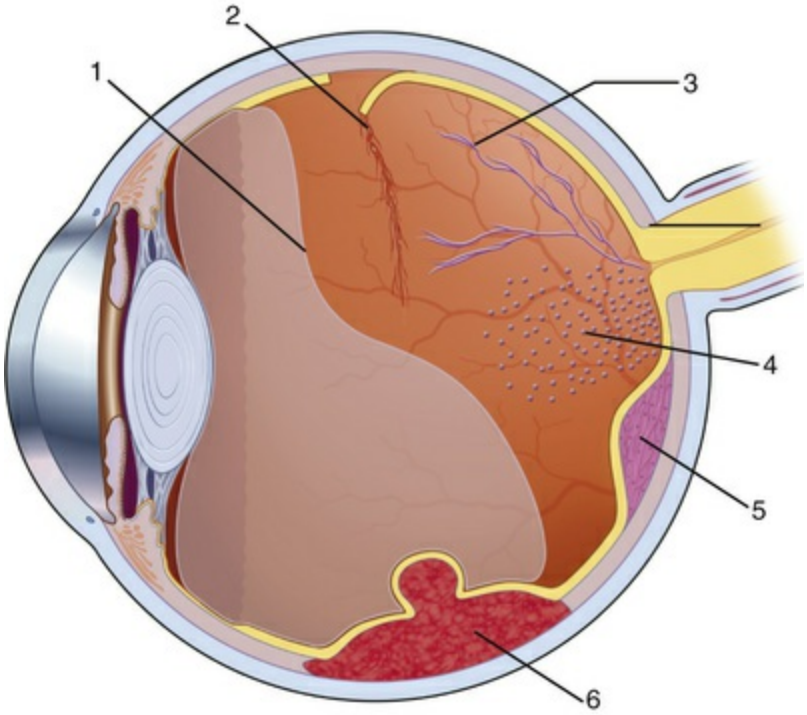

FIG. 11.87 Vitreous hemorrhage: echographic contribution to determine the pathogenesis (for detail, see Table 11.5).

Furthermore, ultrasonography can aid in the preoperative planning and patient counselling for surgery. Table 11.6 lists some of the possible ultrasonographic information and subsequent conclusions that can be obtained for operative planning (Table 11.6 and see Fig. 11.88).

TABLE 11.6

Examination Before a Vitrectomy: Ultrasonographic Findings Helpful for Planning the Operation

Questions on the ultrasonographic examination		Consequences for planning the operation
Is the choroidal detachment including the pars plana?	1	Avoiding this area when inserting the ports
Is the posttraumatic vitreous hemorrhage associated with a detached retina?		If retina is detached, strong indication for vitrectomy
Is an intraocular foreign body demonstrable? If so, where is it in regard to ocular outer wall?	2	Choice of surgical approach, magnet extraction possible?
		Estimating the prognosis
Is there a choroidal detachment caused by blood?	3	Extremely poor prognosis that may not benefit from surgical intervention
Is there a free-floating retinal detachment?	4	Reattachment probable, can be achieved without tamponade from

		the inside
Is there a rigid retinal detachment? Is there a thickened retina?	5	Removal of preretinal membranes necessary
Are there vitreous strands with traction effect demonstrable?	6	Consider intraoperatively cutting the strands
Is there retinal detachment that is displaced anteriorly to be near the lens?	7	Special care indicated when entering the vitreous space
Are there thickened ocular walls in the macula that may indicate a disciform lesion from macular degeneration?	8	Poor prognosis for central vision
Are there indications of a secondary, e.g., solid retinal detachment?	9	Additional diagnostic examinations; enucleation may be necessary
Is there attached retina with minimal remaining vision?		Reconsider indication for operation, prognosis for vision extremely poor

For companion schematic drawing, see Fig. 11.88.

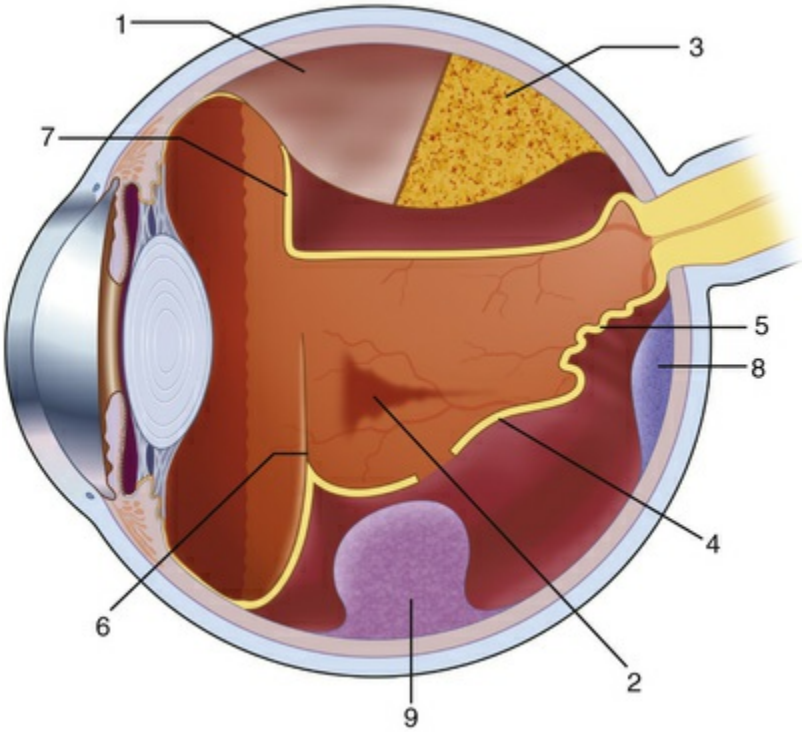

FIG. 11.88 Examination before a vitrectomy: echographic contribution to the planning of the operation (for detail, see Table 11.6).

Future Developments

Many medical fields are using advances in technology to improve ultrasound images. These improvements involve the use of new

piezoelectric materials and broadband transducers.[62] Current and future developments can be focused on the following trends:

- Advances in the signal transmission process
- Advances in the signal reception process
- Compounding, equalization, and extended-field acquisitions
- 3D and 4D imaging[63,64]
- Elastographic imaging
- Fusion imaging[65]
- Miniaturization of units and probes, transfer, and archiving ultrasonic data.

In the field of ophthalmology new Doppler modes for analyzing retinal blood flow are currently being utilized in research initiatives. A new technique is elastographic imaging. Recently, this technique has been used to image ocular tissues in high myopia.[66] Patterns of elastic imaging in the vitreous cavity could be attributed to posterior vitreous detachment, whereas that of medial and lateral rectus muscles may be related to the level of muscle fiber strain. With improved resolution, higher frequencies, and spatial images on ultrasound, new frontiers in ophthalmic imaging are being reached and further research in multimodal imaging is still under way.[67] These advancements as well as the safety in image acquisition maintain the utility of ultrasound imaging within all fields of medicine.

Acknowledgments

A special thank you to a number of colleagues who have been of great assistance in creating this chapter: Sönke Langner, Kirsten Franke, Beate Stroteich, Angrit Stachs, and Enrique Pfeiffer.

References

1. Mundt G, Hughes W. Ultrasonics in ocular diagnosis. *Am J Ophthalmol*. 1956;41:488.
2. Baum G, Greenwood J. The application of ultrasonic locating techniques to ophthalmology, part 1. *Am J*

Ophthalmol. 1958;46:319.
3. Oksala A, Lehtinen A. Diagnostic of detachment of the retina by means of ultrasound. *Acta Ophthalmol*. 1957;35:461–467.
4. Oksala A, Lehtinen A. Diagnostic value of ultrasonics in ophthalmology. *Ophthalmologica*. 1957;134:387–395.
5. Oksala A, Lehtinen A. Diagnostic of rupture of the sclera by means of ultrasound. *Acta Ophthalmol*. 1958;36:37–42.
6. Oksala A, Lehtinen A. Measurement of the velocity of sound in some parts of the eye. *Acta Ophthalmol*. 1958;36:633–639.
7. Ossoinig K. Standardized echography: basic principles, clinical applications and results. *Int Ophthalmol Clin*. 1979;19:127.
8. Buschmann W, Haigis W. Influence of equipment parameters on results in ophthalmic ultrasonography. *Doc Ophthalmol Proc Ser*. 1981;29:487.
9. Ossoinig K, Till P. 10 years' study on clinical echography in orbital disease. *Bibl Ophthalmol*. 1975;83:200.
10. Gernet H. Ultrasonic biometry of the eye. *Klin Monatsbl Augenheilkd*. 1967;151:853–871.
11. Baum G, Greenwood J. Ultrasound in ophthalmology. *Am J Ophthalmol*. 1960;49:249–261.
12. Bronson N, Fisher Y, Pickering N, et al. *Ophthalmic contact B-scan ultrasonography*. Intercontinental: Westport, CT; 1976.
13. Pavlin C, Foster F. *Ultrasound biomicroscopy of the eye*. Springer: New York; 1995.
14. Sherar M, Starkowski B, Taylor W, et al. A 100 Mhz B-scan ultrasound backscatter microscope. *Ultrasound Imaging*. 1989;11:95–105.
15. Pavlin C, Harasiwicz K, Sherar M, et al. Clinical use of ultrasound biomicroscopy. *Ophthalmology*. 1991;98:287–295.
16. Sherar M, Foster F. The design and fabrication of high frequency transducer. *Ultrasound Imaging*. 1989;11:75–94.
17. Pavlin C, Harasiwicz K, Foster F. Ultrasound biomicroscopy of anterior segment structures in normal and glaucomatous eyes. *Am J Ophthalmol*. 1992;113:381–389.
18. Atta HR. New applications in ultrasound technology. *Br J*

Ophthalmol. 1999;83:1246–1249.
19. Iezzi R, Rosen R, Tello C, et al. Personal computer-based 3-dimensional ultrasound biomicroscopy of the anterior segment. *Arch Ophthalmol*. 1996;114:520–524.
20. Cusumano A, Coleman D, Silverman R, et al. Three dimensional ultrasound imaging – clinical applications. *Ophthalmology*. 1998;105:300–306.
21. Coleman D, Silverman R, Daly S. Advances in ophthalmic ultrasound. *Radiol Clin North Am*. 1998;36:1073–1082.
22. Reinstein D, Raevsky T, Coleman D. Improved system for ultrasonic imaging and biometry. *J Ultrasound Med*. 1997;16:117–124.
23. Silverman R, Lizzi F, Ursea B, et al. High-resolution ultrasonic imaging and characterization of the ciliary body. *Invest Ophthalmol Vis Sci*. 2001;42:885–894.
24. Stachs O, Martin H, Behrend D, et al. Three-dimensional ultrasound biomicroscopy, environmental and conventional scanning electron microscopy investigations of the human zonula ciliaris for numerical modelling of accommodation. *Graefes Arch Clin Exp Ophthalmol*. 2006;244:836–844.
25. Stachs O, Martin H, Kirchhoff A, et al. Monitoring accommodative ciliary muscle function using three-dimensional ultrasound. *Graefes Arch Clin Exp Ophthalmol*. 2002;240:906–912.
26. Kirchhoff A, Stachs O, Guthoff R. Three-dimensional ultrasound findings of the posterior iris region. *Graefes Arch Clin Exp Ophthalmol*. 2001;239:968–971.
27. Stachs O, Schneider H, Stave J, et al. Potentially accommodating intraocular lenses – an in vitro and in vivo study using three-dimensional high-frequency ultrasound. *J Refract Surg*. 2005;21:37–45.
28. Schneider H, Stachs O, Göbel K, et al. Changes of the accommodative amplitude and the anterior chamber depth after implantation of an accommodative intraocular lens. *Graefes Arch Clin Exp Ophthalmol*. 2006;244:322–329.
29. Jaffe NS. Complications of acute posterior vitreous detachment. *Arch Ophthalmol*. 1968;79:568–571.
30. McLeod D. (chair) Round table discussion on vitreous

pathology. *Doc Ophthalmol Proc*. 1981;547 [Ser].
31. Ossoinig KC. Advances in diagnostic ultrasound. *Acta 14th Int Congr Ophthalmol*. 1983;89.
32. Till P, Ossoinig KC. 10 years' study on clinical echography in intraocular disease. *Bibl Ophthalmol*. 1975;83:49.
33. Machemer R, Aalberg TM. *Glaskörperchirurgie, Vitrektomie. Indikationen und Technik*. Huber Verlag: Berne; 1981.
34. Shapiro DR, Stone RD. Ultrasonic characteristics of retinopathy of prematurity presenting with leucokoria. *Arch Ophthalmol*. 1885;103:1690.
35. Darnley-Fisch DD, Frazier-Byrne S, Hughes JR, et al. Contact B-scan echography in the assessment of optic nerve cupping. *Am J Ophthalmol*. 1990;109:55.
36. Oksala A. Echogram in melanoma of the choroid. *Br J Ophthalmol*. 1959;43:408.
37. Baum G. Use of ultrasonography in the differential diagnosis of ocular tumors. Boniuk M. *Ocular and adnexal tumors*. Mosby: St. Louis; 1964:308.
38. Buschmann W, Trier H. *Ophthalmologische Ultraschalldiagnostik, mit Atlas, Standardisierung und Einordnung in den ophthalmologischen Untersuchungsbefund*. Springer: Berlin; 1989.
39. Trier H. Gewebsdifferenzierung mit Ultraschall. *Bibl Ophthalmol*. 1977;86:92.
40. Coleman DJ, Silverman R, Rondeau MJ, et al. Explaining the current role of high frequency ultrasound in ophthalmic diagnosis (ophthalmic ultrasound). *Expert Rev Ophthalmol*. 2006;1:63–76.
41. Silverman R, Kong F, Chen Y, et al. High-resolution photoacoustic imaging of ocular tissues. *Ultrasound Med Biol*. 2010;36:733–742.
42. Guthoff R. Ultraschall in der ophthalmologischen Diagnostik. Naumann GOH, Hollwich F, Gloor B. *Ein Leitfaden für die Praxis*. Enke-Verlag: Stuttgart; 1988.
43. Wolter J. Parallel horizontal choroidal folds secondary to an orbital tumor. *Am J Ophthalmol*. 1974;77:669.
44. Coleman D, Lizzi S, Jack R. *Ultrasonography of the eye and orbit*. Lea and Febiger: Philadelphia; 1977.

45. Bujara K, von Domarus D, Guthoff R. Necrotic malignant melanoma of the choroid with unusual clinical, echographical and histological case study. *Ophthalmologica*. 1980;180:222–227.
46. Guthoff R, Berger R, Helmke K, et al. Doppersonographische Befunde bei intraokulären Tumoren. *Forstschr Ophthalmol*. 1989;86:239.
47. Bloch RS, Gartner S. The incidence of ocular metastatic carcinoma. *Arch Ophthalmol*. 1971;85:673.
48. Ferry AP, Font RI. Carcinoma metastatic to the eye and the orbit: a clinical pathological study of 227 cases. *Arch Ophthalmol*. 1974;92:276.
49. Verbeek A. Echographic findings in 36 patients with choroidal folds. *Doc Ophthalmol Proc Ser*. 1981;29.
50. Manschot WA. The relation between histopathological and ultrasonographyin intraocular tumors. *Doc Ophthalmol Proc Ser*. 1981;29:71.
51. Shields CL, Shields JA, Augsburger JJ. *Update on choroidal osteomas*. [Proceedings of the 2nd international meeting on the diagnosis and treatment of intraocular tumors; Lyons] 1987.
52. Wende S, Aulich A, Nover A, et al. Computer tomography of orbital lesions: a cooperative study of 210 cases. *Neuroradiology*. 1978;13:123.
53. Gass JDM, Guerry RK, Jack RI, et al. Choroidal osteoma. *Arch Ophthalmol*. 1978;96:428.
54. Gass JDM. New observations concerning choroidal osteomas. *Int Ophthalmol*. 1979;71.
55. Wing GI, Schepenz CL, Trempe CL, et al. Serous choroidal detachment and the thickened choroidal sign detected by ultrasonography. *Am J Ophthalmol*. 1982;94:499.
56. Blodi FC. Ein Tuberkulom der Aderhaut, ein melanom vortäuschend. *Klin Monatsbl Augenheilkd*. 1977;170:845.
57. Wirold J, Orlowski-Szczypinski J. Ultrasonography of the subretinal space in rhegmatogeneous retinal detachment. *Z Mod Probl Ophthalmol*. 1976;18:40.
58. Cappaert W, Purnell E, Frank K. Use of B-scan ultrasound in the diagnosis of benign choroidal folds. *Am J Ophthalmol*.

1977;84:375.
59. Singh G, Guthoff RF, Foster S. Observations on long-term follow-up of posterior scleritis. *Am J Ophthalmol*. 1986;101:570.
60. Guthoff RF. Die differentialdiagnostische Bedeutung des Tenon'schen Raumes. *Fortschr Ophthalmol*. 1974;81:388.
61. Feldon S, Sigelman J, Albert D, et al. Clinical manifestations of brawny scleritis. *Am J Ophthalmol*. 1978;85:781.
62. Claudon M, Tranquart F, Evans DH, et al. Advances in ultrasound. *Eur Radiol*. 2002;12:7–18.
63. Liu XH, Tao H, Li M, et al. Preliminary study on features of three-dimensional ultrasound reconstruction of the lacrimal sac of normal adults]. *Zhonghua Yan Ke Za Zhi*. 2013;49(11):993–996.
64. Schlosser J, Kirmizibayrak C, Shamdasani V, et al. Automatic 3D ultrasound calibration for image guided therapy using intramodality image registration. *Phys Med Biol*. 2013;58(21):7481–7496.
65. Walter U, Niendorf T, Graessl A, et al. Ultrahigh field magnetic resonance and colour Doppler real-time fusion imaging of the orbit–a hybrid tool for assessment of choroidal melanoma. *Eur Radiol*. 2014;24(5):1112–1117.
66. Pekel G, Ağladoğlu K, Acer S, et al. Evaluation of ocular elasticity in high myopia. *Optom Vis Sci*. 2015;92(5):573–578.
67. Lindner T, Langner S, Falke K, et al. Anatomic and pathological characterization of choroidal melanoma using multimodal imaging: what is practical, what is needed? *Melanoma Res*. 2015;25(3):252–258.

12

Color Vision and Night Vision

Dingcai Cao

Overview

Day vision and night vision are two separate modes of visual perception and the visual system shifts from one mode to the other based on ambient light levels. Each mode is primarily mediated by one of two photoreceptor classes in the retina, i.e., cones and rods. In day vision, visual perception is primarily cone-mediated and

perceptions are chromatic. In night vision, visual perception is rod-mediated and perceptions are principally achromatic. Historically, color vision has been studied as the salient feature of day vision and there has been emphasis on analysis of cone activities in color vision. Night vision has been studied in terms of rod activity and considerations of the shift from day vision to night vision. This chapter will review basic aspects of cone-mediated color vision and rod-mediated night vision and discuss clinical assessments of rod and cone sensitivities and color vision.

Rod and Cone Functions

Differences in the anatomy and physiology (see Chapter 4, Autofluorescence imaging, and Chapter 11, Diagnostic ophthalmic ultrasound) of the rod and cone systems underlie different visual functions and modes of visual perception. The rod photoreceptors are responsible for our exquisite sensitivity to light, operating over a 10^8 (100 millionfold) range of illumination from near-total darkness to daylight. Cones operate over a 10^{11} range of illumination, from moonlit night light levels to light levels that are so high they bleach virtually all photopigments in the cones. Together the rods and cones function over a 10^{14} range of illumination. Depending on the relative activity of rods and cones, a light level can be characterized as photopic (cones alone mediate vision), mesopic (both rods and cones are active), or scotopic (rods alone mediate vision).[1] In the literature, the terms photopic vision and scotopic vision are used to reflect cone and rod vision, respectively. Table 12.1 shows this overlapping range of rod and cone activities.

TABLE 12.1

The Dynamic Range of the Human Visual System

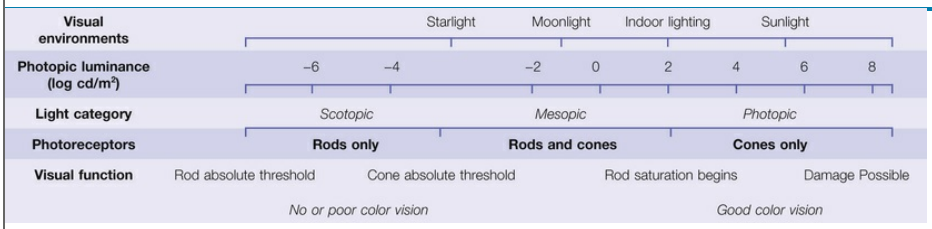

Modified from Hood DC, Finkelstein MA. Sensitivity to light. In: Boff KR, Kaufman L, Thomas JP, editors. The handbook of perception and human

performance, vol. 1. Sensory processes and perception. New York: John Wiley; 1986.

The distribution of rods and cones in the retina (see Chapter 4, Autofluorescence imaging) is also reflected in visual function. The greatest sensitivity to light occurs in the midperiphery of the visual field, which has a predominance of rods, while high-acuity and good color vision are mediated by the fovea, which has a predominance of cones. Nonetheless, the entire retina, with the exception of a very small area within the fovea, is capable of mediating night vision, and color vision is present throughout the visual field with daylight stimulation of the entire retina. The following sections will introduce rod and cone differences in light adaptation, spectral sensitivity, and spatial/temporal sensitivity.

Light Adaptation

Photoreceptors, whether they are rods or cones, respond well to only a small range of variations in illumination within a steady adapting background.[2] However, adaptation mechanisms adjust photoreceptor sensitivity so that this small range of responses is always centered near the current adaptation level, even though adaptation levels can vary over a wide range. This behavior forms the basis for the large operating range of the visual system.

It is possible to assess light adaptation behavior by measuring a threshold for the perception of an increment in light on a large, steady background field. As the background light level is increased, the increment threshold starts to increase. Rods and cones behave differently in this regard. For the rod system, as shown in Fig. 12.1A, the increment threshold increases steadily over almost a thousandfold range. With further increases in background adaptation levels, an increment is not detected, no matter how much additional test light is presented as an increment, due to rod saturation. In comparison, the cone system, as shown in Fig. 12.1B, shows a continuous steady increase in the increment threshold with increases in background illumination, even at light levels that

bleach almost the entire amount of available photopigment. The portion of the curve that rises linearly with illumination levels is called the Weber region (Fig. 12.1). In the Weber region, an incremental light can be detected when it is a constant proportion (i.e., the Weber fraction) of the background light level. Different photoreceptor systems have a characteristic Weber fraction. Cones have lower Weber fractions than rods. Under optimal conditions, the cone system can detect a light level difference of 1%, while rods need a light change of 20%.

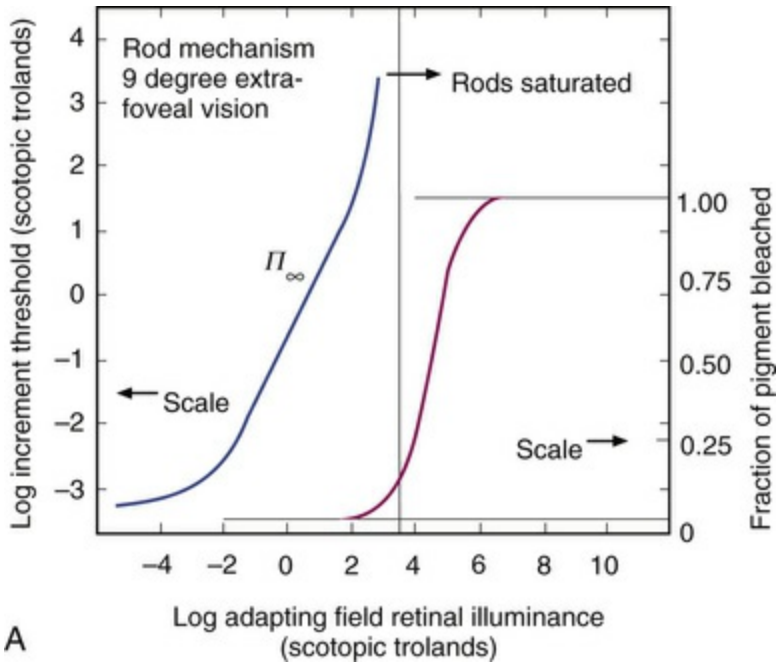

A

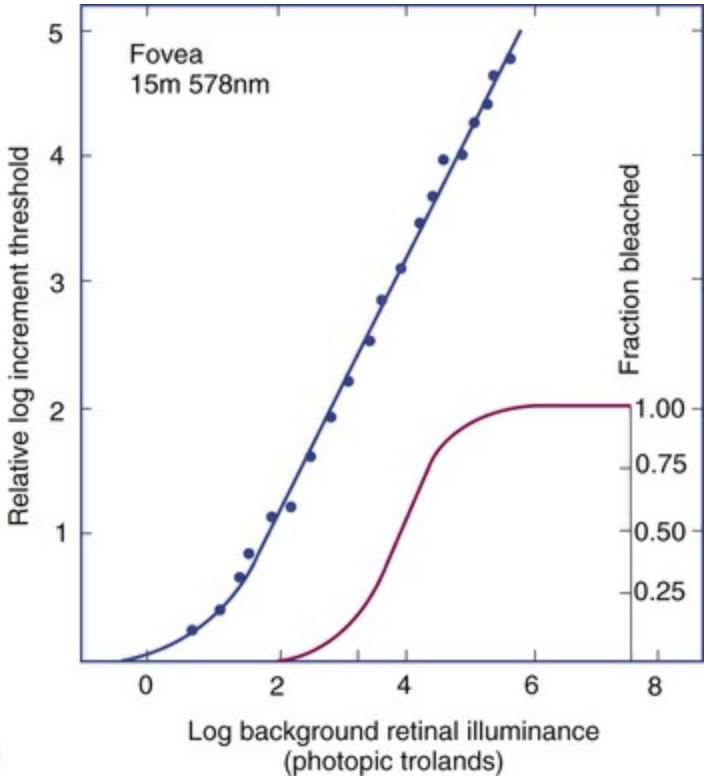

FIG. 12.1 The increment threshold functions for scotopic (rod) and photopic (cone) vision as a function of background illuminance. (A) Rod increment thresholds measured at 9° in the parafovea. The dashed line has a slope of 1. The portion where the curve has unit slope (in parallel to the dashed line) is the Weber region, followed at higher levels by the region of rod saturation. To the right is shown the fraction of rod photopigment bleached. The rods are saturated before there is substantial photopigment bleaching. (B) Cone increment thresholds measured at the fovea. To the right is shown the fraction of photopigment bleached. The Weber region extends to luminances (6 million trolands) that bleach virtually all the cone photopigment. (Reproduced with permission from Enoch JM. The two-color threshold technique of Stiles and derived component color mechanisms. In: Jameson D, Hurvich L, editors. Visual psychophysics: handbook of sensory physiology, vol. VII/4. Berlin: Springer-Verlag; 1972.)

In addition to photoreceptor adaptational properties, other factors, including pupil size, the temporal and spatial summation characteristics, and photopigment depletion, can also contribute to extend the operating range of the visual system over a large luminance range. While some adaptation operates within the

photoreceptors themselves, other properties of adaptation may reflect the effects of the complex neural circuitry of the retina.[2]

Spectral Sensitivity

Day vision is primarily mediated by three types of cone photoreceptors with different but overlapping spectral sensitivities. Each is identified by the relative position of the peak in spectral sensitivity. The three cone types are called the long-, middle-, and short-wavelength-sensitive (L, M, and S) cones. When overall sensitivity to light is measured at the light-adapted fovea, a broad sensitivity spectrum peaking near 555 nm is found. This sensitivity spectrum represents the combined activity of the L and M cones and is called the $V(\lambda)$ function. When sensitivity to light is measured in the dark-adapted peripheral retina, where rods dominate, a broad-sensitivity spectrum is found with a peak sensitivity at 507 nm. This rod spectral sensitivity function is called $V'(\lambda)$ (Fig. 12.2A). Both $V(\lambda)$ and $V'(\lambda)$ functions have practical significance and have been accepted by the Commission Internationale d'Eclairage (CIE) as representative of human vision relative luminous efficiency at photopic and scotopic levels. They are used to relate luminous (perceived energy of light) to radiant (emitted light) energy.

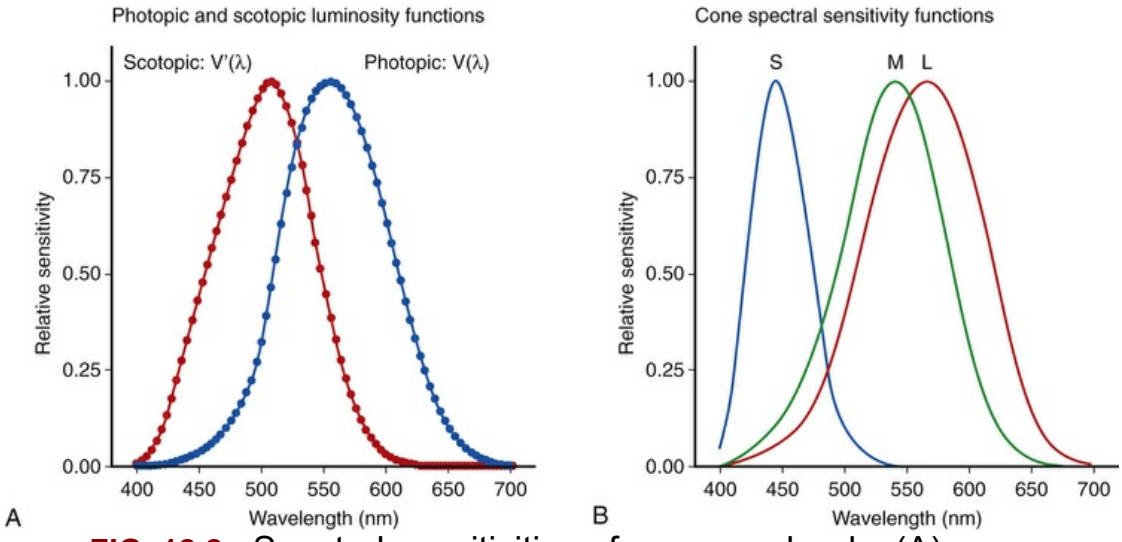

FIG. 12.2 Spectral sensitivities of cones and rods. (A) The relative spectral luminous efficiency functions for scotopic and photopic vision adopted by the

Commission International d'Eclairage (CIE), $V'(\lambda)$ and $V(\lambda)$ respectively. (B) Spectral sensitivities of the S, M, and L cones derived from color-matching function.[14]
(Data in panel A from Wyszecki G, Stiles WS. Color science – concepts and methods, quantitative data, and formulae, 2nd ed. New York: John Wiley; 1982.)

Fig. 12.2B shows the relative spectral sensitivities of the three cone types. The S cones are most sensitive to light near 445 nm, with sensitivity declining rapidly at longer wavelengths. At 555 nm and longer wavelengths, the S cones are virtually unresponsive to light. The M and L cones have overlapping spectral sensitivities that span the entire visible spectrum. The M cones peak in sensitivity near 543 nm, while the L cones peak near 566 nm. The differential spectral sensitivity functions of the L, M, and S cones provide the foundation of early spectral processing.

Spatial and Temporal Resolution

Compared with the cone system, the rod system has poorer spatial resolution (acuity). For an observer with 20/20 photopic acuity, scotopic acuity would be about 20/200 (10 times worse than photopic acuity). The rod system also has poorer temporal resolution, which refers to the ability to perceive a physically alternating light as steady or flickering in time. The transitional temporal frequency at which the light appears from flickering to steady is called the critical fusion frequency (CFF). CFFs increase with light adaptation level, reaching a maximum of ~20 Hz for rods and 55–60 Hz for cones. This means that flickering lights can be perceived at higher frequencies in brighter light conditions. Interestingly, dark-adapted rods can suppress cone-mediated flicker detection.[3,4]

Visual Pathways for Rod and Cone Functions

Retinal Pathways

Rod signals are conveyed by two primary retinal pathways that are

dependent on the illumination level.[5] One pathway is via ON rod bipolars, AII amacrine cells, and ON and OFF cone bipolars. This is a temporally sluggish pathway that mediates rod vision at low scotopic light levels. The second pathway transmits rod information via rod–cone gap junctions and ON and OFF cone bipolar cells in the retina. This is a fast pathway that mediates vision at higher scotopic and mesopic light levels. A third insensitive rod pathway between rods and OFF cone bipolars has been identified in rodents but, thus far, not in primates. The significant point here is that rods and cones share neural pathways and have joint inputs to retinal ganglion cells.

Retinogeniculate Pathways

There are three major neural retinogeniculate pathways in primates that convey retinal information to the visual cortex.[6,7] The pathways are named after the layers of the lateral geniculate nucleus (LGN) that receive input from distinct types of ganglion cells and project to different areas of the primary visual cortex. The magnocellular (MC) layer of the LGN receives inputs from parasol ganglion cells. The MC pathway processes the summed output of the L and M cones to signal luminance information. The parvocellular (PC) layer of the LGN receives input from midget ganglion cells. The PC pathway mediates spectral opponency of L and M cones (discussed later) to signal chromatic information. The koniocellular (KC) layer of the LGN, which receives input from small bistratified as well as other ganglion cells, detects changes in S-cone signals compared to the sum of the L- and M-cone signals. These three pathways mediate different aspects of vision, with the MC pathway mainly carrying out luminance and motion processing, the PC pathway mainly processing red–green color, acuity, and shape information, and the KC pathway mainly handling blue–yellow color processing.

The sharing of neural pathways between rods and cones implies that rods should have input to the MC, PC, and KC pathways. Indeed, physiologic studies have shown that there is strong rod input to the MC pathway, but weak input to the PC pathway.[8] Demonstration of rod input to the KC pathways is less clear. An

earlier study[8] did not find rod input to the bistratified ganglion cells in the parafovea, while two recent studies demonstrated strong rod input in the peripheral retina.[9,10] Fig. 12.3 shows a schematic diagram of the visual pathways conveying rod and cone inputs to the MC, PC, and KC ganglion cells, which would then produce signals that are projected into the cortex to mediate different aspects of visual perception.

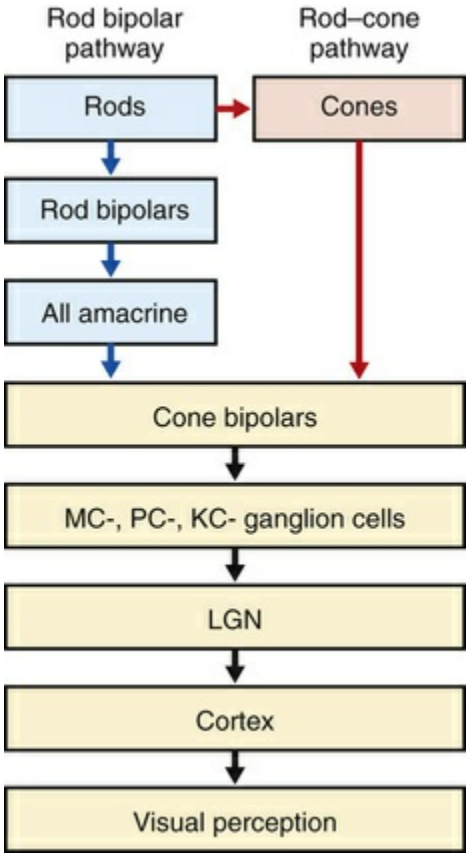

FIG. 12.3 The schematic diagram of visual pathways carrying rod and cone inputs for visual perception. *MC*, magnocellular; *PC*, parvocellular; *KC*, koniocellular; *LGN*, lateral geniculate nucleus.

Dark Adaptation Functions: Assessment of the Shift From Day Vision to Night Vision

Measurements of detection thresholds during adaptation to darkness have produced a characteristic biphasic function with an initial segment that is attributed to cone responses and a subsequent segment attributed to rod responses. Fig. 12.4 shows a characteristic dark adaptation function measured in the peripheral retina. Thresholds decrease quickly initially and this rapid recovery is attributed to cones. Thresholds then reach a plateau in about 5 minutes and remain invariant for another 5 minutes (cone plateau, reflecting cone absolute thresholds). Then, there is a second rapid decrease in thresholds due to sensitivity recovery of the rods, referred to as the rod–cone break, to a new plateau that is reached in 40–50 minutes (rod plateau, reflecting rod absolute thresholds).

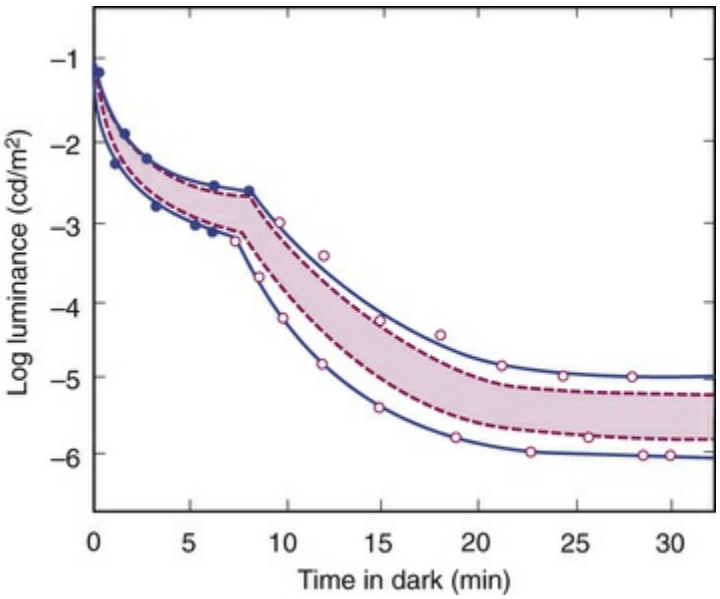

FIG. 12.4 The time course of dark adaptation. The range of threshold sensitivities of 110 normal observers is shown. The circular points represent data of the most and least sensitive individuals. The area enclosed by the dashed lines represents 80% of this population. The cone absolute thresholds are obtained during the cone and rod plateaus, respectively. (Data from Hecht S, Mandlebaum J. The relationship between vitamin A and dark adaptation. JAMA 1939;112:1910–6.)

The shape of the dark adaptation function depends on testing parameters, including retinal location, wavelength, and temporal and spatial characteristics.[1,11] The effects of these parameters on

dark adaptation curves can be understood by the differences between rods and cones in terms of their distributions, spectral sensitivity, and spatial/temporal resolution characteristics. For instance, because there are only cones in the fovea, dark adaptation measured at the fovea using a small test light reveals a rapid monophasic branch attributable to the cones. On the other hand, because the rod and cone systems have similar absolute sensitivities at long wavelengths, dark adaptation measured with long-wavelength lights is monophasic, resembling the cone function. As the test wavelength is changed to shorter wavelengths, a biphasic curve emerges because the rods show greater absolute sensitivity than cones at shorter wavelengths.[12]

Clinical Evaluation Using Dark Adaptation Functions

It is known that certain retinal disorders may selectively affect rods (e.g., retinitis pigmentosa) or cones (e.g., cone dystrophies). Clinically, rod and cone functions can be evaluated electrophysiologically by measuring rod and cone electroretinograms (ERG: see Chapter 9, Electrogenesis of the electroretinogram) or, psychophysically, by measuring dark adaptation functions. Dark adaptation functions quantify the ability of the rod and cone systems to recover sensitivity (i.e., regenerate photopigment) after exposure to a bright light. The recovery is faster for cones, but the absolute level of sensitivity is greatest for rods. Variations in sensitivity and sensitivity recovery times can be used to characterize retinal disorders.

Clinical evaluation using dark adaptation functions involves a measure of the cone and rod absolute thresholds and the time of the rod–cone break. Specifically, rod absolute thresholds have been used as a psychophysical supplement to ERG measurement for night-blindness evaluation. The instrument for dark adaptation rod absolute threshold measurement is called a dark adaptometer and the most widely used is a Goldmann–Weekers dark adaptometer (Haag–Streit). This instrument is old, however, and finding replacement lamps is difficult. Recently, new light-emitting diode (LED)-based, computer-controlled, dark adaptometers have become

commercially available.

Color Vision

Color vision refers to our ability to perceive colors based on spectral variations in light absorbed by the photoreceptors. Color vision includes both chromatic discrimination and color appearance appreciation. Color-matching and color-discrimination experimental tasks are two fundamental psychophysical procedures that have provided theoretical insights into the nature of color vision and have also been developed for clinical diagnosis of color vision. Color-matching and color-discrimination results, however, do not address questions of color appearance – for example, why an object appears red. Color appearance is far more complex because it depends on not only the chromatic properties of an object but also the spatial, temporal, and spectral characteristics of the neighboring objects.[13] Neural processing beyond the retina is required for color appearance appreciation.

Color Matching

Color Matching as the Foundation for the Theory of Trichromacy

The psychophysical procedure in which an observer sets a mixture of three primary lights to match the color of a test stimulus is called color matching. It has been known since the 19th century that different colors perceived by humans can be specified by a three-variable (trichromatic) system. In the 1800s, Thomas Young and Hermann von Helmholtz proposed that there must be three kinds of physiologic entities in the eye accounting for this trichromacy and their theory is called the Young–Helmholtz trichromatic theory of color vision. We now know the basis for trichromacy is the existence of three cone types in the retina. Color matching was one of the methods to uncover the spectral sensitivity functions of the three different cone types (Fig. 12.1B).[14]

Color-Matching Experimental Techniques and Data

Theoretically, a color match occurs when the photoreceptor quantal catch for the test stimulus and the quantal catch for the stimulus that is a combination of the three primary lights are the same. Color matches are unperturbed by changes in luminance levels, as long as no significant photopigment bleaching occurs, which means that the basic nature of trichromacy exists under wide variations in light levels. In a classical color-matching experiment, three spectral lights are chosen as the three primaries and the precise setting of the relative percentages of the three primaries to match a test light is the data for that match. When all three primaries are added together, they can be set to match a neutral white.

Procedurally, due to the mechanics of testing optical equipment, the spectral test color and one primary are made to appear in one field and the other two primaries appear in a second field with the two fields usually appearing as two halves of a circle. The observer's task in a color-matching experiment is to make the two fields appear identical in color. Color-matching data are usually represented in one of two ways. In the first, the amounts of energy of each primary can be plotted as a function of the test wavelength. These are called color-matching or color mixture functions. In such plots, the primary that is added to the test color is given a negative value, and the other two primaries are given positive values. The second plotting method is to normalize the value of each matching primary relative to the sum of the three primaries, leading to the sum of the normalized primaries being equal to 1. Therefore, a plot of one primary value against a second primary value is sufficient to display all the information in the color-matching data. This kind of plot is called a chromaticity diagram, which shows the relative contributions of each spectral primary needed to match any spectral light.

The CIE Colorimetric System

This spectral primary-based chromaticity diagram has proven to be very useful as a generalized color specification system. However, linear transformation is needed to compare data collected with different choices of primaries. In 1931, the CIE standardized the spectral-primary-based chromaticity system by adopting three imaginary primaries (X, Y, Z primaries) that are out of the spectral

locus and therefore do not exist physically. The choices of the imaginary primaries were based on two important considerations: first, to ensure that the chromaticities of all physical lights have positive values and, second, to relate colorimetric functions to the previously adopted luminosity function, $V(\lambda)$. In the system, the color-matching function for the Y primary is identical to $V(\lambda)$ of the photometric system as designed.

Fig. 12.5A shows the 1931 CIE chromaticity chart, in which the coordinates of the normalized Y primary [$y = Y/(X + Y + Z)$] are plotted against those of the normalized X primary [$x = X/(X + Y + Z)$]. The spectrum loci (their wavelengths are indicated on the graph) form a horseshoe-shaped curve. Equal-energy-spectrum (EES) light is plotted in the center, with the coordinates of $x = 0.3333$ and $y = 0.3333$. A straight line connects 400 nm to 700 nm for purples, which result from mixtures of short- and long-wavelength light. All possible lights occur within the boundaries of the spectrum locus and the purple line. Highly saturated colors occur near the spectral loci and desaturated (pale) colors occur near the white point.

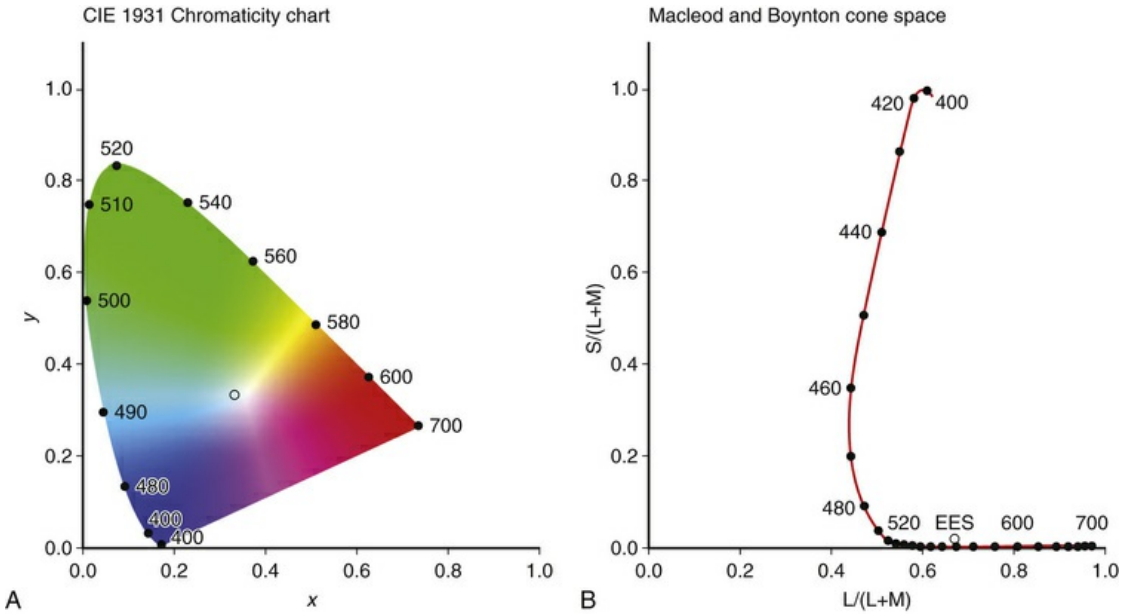

FIG. 12.5 Chromaticity spaces. (A) The Commission International d'Eclairage (CIE) 1931 *x*, *y* chromaticity diagram. An equal-energy-spectrum (EES) light has a coordinate of $x = 0.3333$ and $y = 0.3333$. Spectral wavelengths are represented on the horseshoe-

shaped spectrum locus. All lights can be represented in this diagram. (B) The MacLeod and Boynton cone space, which plots S-cone excitation versus relative L-/M-cone excitations. In this space, the S/(L + M) chromaticity of 400 nm spectral light is normalized to be 1. In such a normalization, an EES light has a chromaticity of L/(L + M) = 0.665 and S/(L + M) = 0.016. In a relative cone troland space, the S/(L + M) for an EES light is normalized to be 1. The chromaticities of the spectral loci form an "L" shape in this space. (Data in panel A from Wyszecki G, Stiles WS. Color science – concepts and methods, quantitative data, and formulae, 2nd ed. New York: John Wiley; 1982.)

The 1931 CIE system was based on the 2° field color-matching functions that were derived from color matches of many observers. The averaged color-matching function from these observers was treated as the standard. Therefore, an observer with the standard color-matching function is referred to as the standard observer. Since the color-matching data are affected by the size of the stimulus field presented to the observer, in 1964, the CIE also adopted a large-field *XYZ* system that was based on the 10° field standard observer color-matching functions. For large stimuli, such as those generated by Ganzfeld for ERG measurements, it is recommended to use the 1964 CIE chromaticities to reflect more accurately the large field color-matching functions.

Cone Chromaticity Space

The CIE colorimetric system is valuable for light specifications; however, psychophysical experiments using the CIE system cannot yield results that allow easy interpretation of the underlying physiologic mechanisms. When the physiologic mechanisms of color vision are of interest, a cone chromaticity space that can represent cone stimulations, as well as the postreceptoral pathways, is preferred.

The concept of cone chromaticity space appeared in the early 20th century. It was not until 1979 that MacLeod and Boynton[15] published a cone chromaticity space based on modern estimates of the cone spectral sensitivities.[14] In the MacLeod and Boynton cone chromaticity space (Fig. 12.5B), the horizontal axis [L/(L + M)]

represents the variation of relative L- versus M-cone stimulation at equiluminance, while the vertical axis [S/(L + M)] represents the variation of S-cone stimulation. The space normalizes S/(L + M) = 1 for spectral light of 400 nm. Later, a relative cone troland space that normalizes S/(L + M) for EES light to be 1 was proposed to link cone excitations with retinal illuminance, which is measured in trolands.[16] Another spectral opponency space, called the DKL space, normalizes the cone chromaticity based at the EES-white to reflect both cone contrasts and postreceptoral opponency signals.[17] These cone chromaticity spaces are a major breakthrough for vision research because neurons in the PC and KC pathways show preferred responses to stimuli along the two axes of the cone chromaticity spaces.[17,18] Therefore, psychophysical experiments can be designed to infer the functions of the postreceptoral pathways by generating stimuli along the two theoretical axes.

Chromatic Discrimination

Chromatic discrimination refers to the ability of an observer to discriminate two colors. Chromatic discrimination has been investigated using three approaches: wavelength discrimination, purity discrimination, and chromaticity discrimination (reviewed by Pokorny and Smith[19]). Chromatic discrimination is usually measured at a constant luminance level to avoid potential interactions between the luminance pathway (MC pathway) and the chromatic pathway (PC or KC pathway).

Wavelength Discrimination

In a typical wavelength discrimination experiment, the stimulus consists of two equiluminant semicircular fields, one filled with a narrow band of spectral light to serve as the standard field and the other as the comparison field. The observer is instructed to change the wavelength of the comparison field to achieve a just noticeable difference (JND) from the standard wavelength. Typical wavelength discrimination thresholds, as a function of standard wavelengths, form a skewed "W" shape with two minima, one at 490 nm and the other at 580 nm.[20]

Purity Discrimination

There are two ways to measure purity discrimination. The first method measures the minimum amount of spectral light the observer adds into a white field to achieve a JND from the same white in another juxtaposed field. Discrimination thresholds measured in this way are the largest at 570 nm and the smallest at 400 nm. The second method measures the minimum amount of white light added into a spectral light to achieve a JND from the spectral light. Purity discrimination thresholds measured in this way do not vary much with variations in the wavelength of the spectral light.

Chromaticity Discrimination

Early attempts to measure chromaticity discrimination included measurement of the minimum variation needed in chromaticity to achieve a JND from any point in the CIE diagram.[21] Another measure of chromatic discrimination involved derived discrimination ellipses using the standard deviations of repeated color matches at a set of chromaticities in the CIE diagram.[22]

In modern chromaticity discrimination experiments, discrimination thresholds are obtained for test field chromaticities varied along the two cardinal axes of a cone chromaticity space in a steady adaptation field. A cone chromaticity space allows that discrimination can be mediated by the L/M cones only (L-/M-cone discrimination) or by the S cones only (S-cone discrimination).[23] Chromatic discrimination was found to be the best at the adaptation chromaticity and then deteriorated with increasing chromatic contrast between the test and adapting fields. Chromatic discrimination data can be explained adequately by a model based on primate ganglion cell responses in the PC and KC pathways.[24]

Color Appearance

In color-matching and color-discrimination experiments, observers determine whether two colors appear the same or different but they do not determine which color is perceived. Color appearance has three perceptual dimensions: hue, saturation, and brightness. Hue is the perceptual dimension that differs from white, such as red,

orange, green, blue, yellow, purple, and pink. Saturation indicates how different the hue is from white. For instance, colors on the spectral locus are highly saturated compared with desaturated colors near white (Fig. 12.5A). Brightness is the perceptual dimension related to luminance variance.

An important feature of color appearance is that colors do not simultaneously appear red and green, nor do they simultaneously appear blue and yellow. However, colors do appear as mixtures of red and yellow or red and blue and they also appear as mixtures of green and yellow or green and blue. Further, human observers can separately abstract the qualities of redness–greenness or blueness–yellowness in an arbitrary test color. These facts have led to the concept that color appearance can be represented in a double-opponent system, with red and green placed in opposite directions on one dimension and blue and yellow placed in opposite directions in the other dimension (Fig. 12.6). Red and green are said to be opponent sensations, as are blue and yellow. This observation triggered Ewald Hering, a German physiologist, to propose the "opponent-color" theory in the late 19th century.

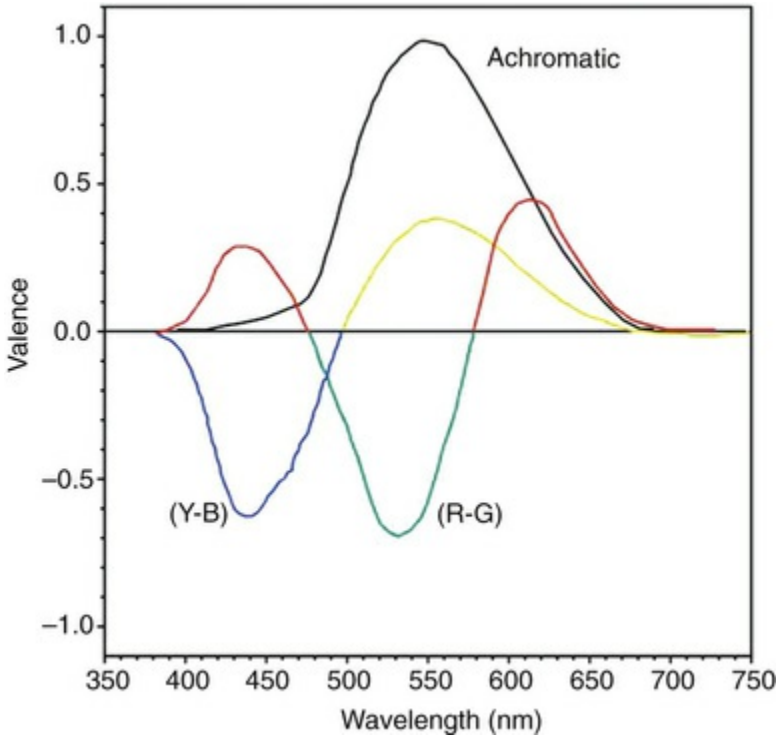

FIG. 12.6 Color opponency. Theoretical curves for the first stage of opponent coding for normal 2° foveal

color vision. The (all-positive) achromatic function represents the whiteness response. Two (opponent) chromatic functions, (*R*–*G*) and (*Y*–*B*), represent redness–greenness and blueness–yellowness, respectively. (Reproduced with permission from Hurvich LM, Jameson D. Some quantitative aspects of an opponent-colors theory. II. Brightness, saturation and hue in normal and dichromatic vision. J Opt Soc Am 1955;45:602–16.)

The theories of opponency and trichromacy were two competing theories in the history of color vision research; however, the two theories have been reconciled in that chromatic processing starts with three types of cones, supporting trichromacy, and spectral responses from the cones are transmitted in bipolar and ganglion cells that have antagonistic receptive field structures, consistent with opponency. This interpretation of color vision, first proposed by von Kries in 1905,[25] is referred to as the two-stage or two-process model of color vision.

In a complex visual scene, the perceived color of a light (emitted from a source or reflected from an object) cannot be predicted from its spectral power distribution because the context of other nearby light affects color appearance. For instance, chromatic induction occurs when perception changes because of the presence of other lights nearby in space or time. Chromatic induction includes both chromatic contrast and chromatic assimilation. Chromatic contrast occurs when the color appearance of a test light shifts away (in terms of color opponency) from the color appearance of a nearby light. Chromatic assimilation occurs when the color appearance of a test light shifts toward the color appearance of inducing nearby light. Therefore, the color of a light seen in isolation (surrounded by darkness) is called an unrelated color while the color perceived in the presence of a complex context is called a related color; that is, its percept is related to the surrounding colors. Cortical mechanisms are likely involved in color perception in a complex scene.[26]

Variations in Human Color Vision

Abnormal color vision that is either inherited or acquired is present in about 4.5% of the population. Congenital color vision defects are stationary over the lifespan and do not result from other visual

problems. These color vision defects have been studied extensively and their classification is well established based on psychophysical and genetic works. The most common are the congenital X-chromosome-linked red–green color vision defects, which have been associated with alterations in the gene sequences encoding the opsins on the X chromosome.[27,28] Acquired color vision defects refer to abnormalities that accompany eye diseases or drug toxicity. Acquired color vision defects are more variable and their classification is more difficult and less satisfactory. Color vision is often tested clinically with screening tests that allow identification of abnormalities and most screening tests are based on color-discrimination and color-matching abilities.[29]

Color Vision Classifications

Color vision classifications are based on both the number of functioning cone types and the presence of abnormal cones. An observer with three functioning cone types is called a trichromat, an observer with two functioning cone types is a dichromat, and an observer with one functioning cone type is a monochromat (monochromacy sometimes is also termed achromatopsia in the literature since it is believed that vision based on a single cone type cannot produce color perception, assuming rods are not involved). An observer with normal color vision has three normal cone types, in terms of spectral sensitivity, and is called a normal trichromat. Observers who are said to have defective color vision have at least one abnormal cone type or are missing at least a cone type with conventional color-matching techniques. An observer with rods only (lack of any cones) is called a rod monochromat, also termed complete achromatopsia.[30]

X-linked color vision defects have been recognized since the 18th century and were subdivided into two qualitatively different types: protan (“red-blind”) and deutan (“green-blind”). The term “protanope” is used for a dichromat who is thought to be missing L cones and the term “deuteranope” is used for a dichromat who is thought to be missing M cones, based on color-matching characteristics using a 2° visual field in the fovea. Anomalous trichromacy is a variation in color vision that is attributed to the

presence of a cone type that is shifted in spectral sensitivity. A protanomalous observer has trichromatic color vision but the L cones have spectral sensitivity that is shifted to shorter wavelengths compared to normal L cones. A deuteranomalous observer also has trichromatic color vision but the M cones have spectral sensitivity that is shifted to longer wavelengths compared to normal M cones. A third qualitatively different type of color vision is tritan ("blue-blind"). Tritan color vision defects are thought to arise from variations in S cones.

The Genes Encoding the Human Photopigments

It has been known for many years that the spectral sensitivities of rods and cones reflect the absorption spectra of the visual photopigments. In a major advance, the genes encoding the opsins of the human visual photopigments were cloned and mapped in the human genome in 1983.[27,31] The gene for rhodopsin was found on chromosome 3 and the human rhodopsin gene showed high homology (93.4%) to that of bovine rhodopsin.[31] A visual photopigment gene for the opsin of S cones (*OPN1SW* gene) was found on chromosome 7. A tandem array of visual photopigment genes for the opsins of the M and L cones (*OPN1MW* and *OPN1LW* genes) was found on the X chromosome. The human opsin genes show about 45% homology between rhodopsin and any of the three cone photopigment genes and between the chromosome 7 and the X-chromosome pigment genes. This similarity among the photopigment genes suggests a common ancestor. The genes on the X chromosome have a high homology to each other (about 96%), suggesting a more recent evolutionary appearance. An unexpected finding was that of multiple genes in a tandem array on the X chromosome, which has been proposed to range from 2 to 6. Nathans et al.[28] postulated that the multiple genes in the tandem array on the X chromosome arose as a result of unequal homologous recombination. Subsequent study has suggested there are polymorphisms among these genes in color-normal and color-defective individuals.[27]

The initial study of the opsin genes on the X chromosome was

based on the longstanding conventional ideas about X-linked congenital color vision defects;[28] that is, protanopes are missing L cones and deuteranopes are missing M cones, and that the genetics of these types of defective color vision may be based on missing genes for either L or M cones. Specifically, protanopes were thought to be dichromats who lacked an L-cone gene and deuteranopes were dichromats who lacked an M-cone gene.

The initial work with the X-chromosome opsin genes, in attempting to link color vision defects with these genes, was carried out using restriction fragment length polymorphisms (RFLPs), an early molecular genetic technique that simplified the study of DNA sequences. The initial RFLP analysis of the X-chromosome genes was done on DNA from one observer with normal color vision and a few protanopes and deuteranopes. Comparisons were carried out to determine which of the fragments found in the normal observer's RFLPs were missing in the protanopes and deuteranopes. A fragment found in the normal observer that was missing in the protanope was said to be part of the assumed missing L-cone gene. Similarly, a fragment found in the normal observer that was missing in the deuteranope was said to be part of the assumed missing M-cone gene. In the initial study, observers with dichromatic as well as anomalous trichromatic color vision defects showed the presence of hybrid genes (genes comprising the head of one type of gene and the tail of the other type of gene). The hybrid genes were said to be the basis for the altered spectral sensitivity of anomalous L or M cones associated with X-linked anomalous trichromacy (discussed previously).

Subsequent studies that have been carried out on both normal and X-linked defective color vision have their roots in the initial RFLP analysis based on the conventional idea of missing cone types and missing genes using one normal observer and a few color-defectives. The variations that have been found in subsequent studies on the visual pigment genes have correlated largely, but not absolutely, with phenotypes established by color vision testing. The current view is that the X-chromosome tandem array consists of one or more opsin genes encoding L-cone photopigment, followed by one or more opsin genes encoding the M-cone photopigment. The expression of the genes in the tandem array is believed to be

governed by a stochastic process.[27]

There have been advances in molecular genetic technology and in the understanding of the human genome since the initial RFLP studies of the opsin genes. Knowledge derived from the Human Genome Project, which has spurred an understanding of the scarcity of genes in the human genome, and the developing knowledge of epigenetics, such as the editing processes of microRNAs, may contribute to future studies and understanding of the genetics of color vision variations.

Clinical Evaluation of Color Vision

Screening Tests

Screening tests are rapid tests (requiring 2–3 minutes) and color-defective observers are identified due to their inability to see the difference between certain colors that are easily discriminated by normal observers. Screening tests can be administered to both children and adults.

Pseudoisochromatic Plate Tests

The most commonly used screening tests are the pseudoisochromatic plate tests. First introduced by Stilling, a pseudoisochromatic plate presents a figure composed of colored dots in a background of differently colored dots. Usually, the colors are chosen so that an X-linked color-defective observer does not see the figure that is easily seen by normal observers. The cleverest designs use four sets of colors, chosen such that the normal observer sees one figure and the defective observer sees a different figure.

The majority of pseudoisochromatic plate tests (such as the Ishihara) were designed to identify observers with X-linked congenital color defects (i.e., protan or deutan color anomalies). The choice of colors was optimized to take advantage of the particular discrimination losses found in X-linked color vision defects and the tests are successful in detecting 90–95% of color-defective observers. Pseudoisochromatic plate tests cannot be used to identify acquired color vision defects, which are most likely to affect blue/yellow

color vision. More recently developed pseudoisochromatic plates (such as the HRR and SPP2 plates) have been designed specifically for acquired color vision deficiencies, including tritan (blue/yellow) anomalies.

Other Rapid Tests of Color Vision

Other rapid tests of color vision involve sorting colored pieces. In principle, this approach can be used successfully with acquired color vision abnormalities since it does not involve the choice of a particular pair of colors that has a prediction based on common X-linked color vision defects.

Chromatic Discrimination Ability Tests

Clinical assessment of color discrimination ability involves arrangement tests that require the observer to arrange a set of colored samples according to their similarity in color. If the samples are closely spaced in chromaticity (e.g., the Farnsworth–Munsell 100-hue test: Fig. 12.7), the task becomes one of fine chromatic discrimination. Tests involving fine chromatic discrimination are usually relatively time-consuming. If the samples are widely spaced in chromaticity (e.g., the Farnsworth panel D-15), the test evaluates color confusions that occur with defective color vision that would not be perceived by a normal observer. Tests with widely spaced colors are conducted rapidly and can even be used for screening. An arrangement test may use samples that differ only in chromaticity to test hue discrimination (e.g., the Farnsworth–Munsell 100-hue test, Farnsworth panel D-15, Farnsworth desaturated panel D-15, and Lanthony new color test), may vary in luminance only to test lightness discrimination (Verriest's lightness discrimination test), or may vary only in grayness to test saturation discrimination (Sahlgren's saturation test, Lanthony new color test). Arrangement tests are easy to administer but require the concept of abstract ordering, manual dexterity, and patience. As a result, they are rarely suitable for children under 10 years of age.

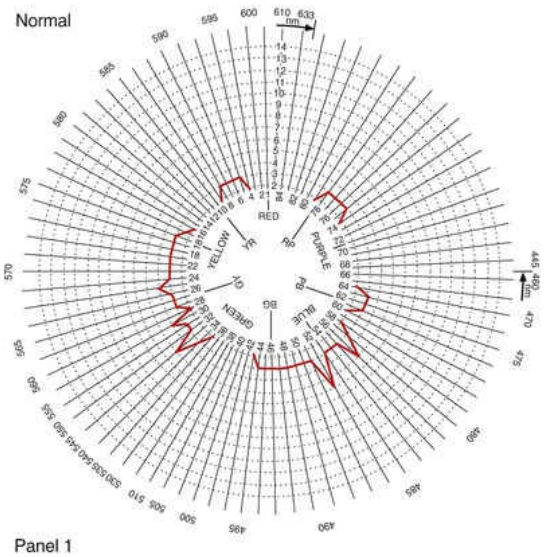

Panel 1

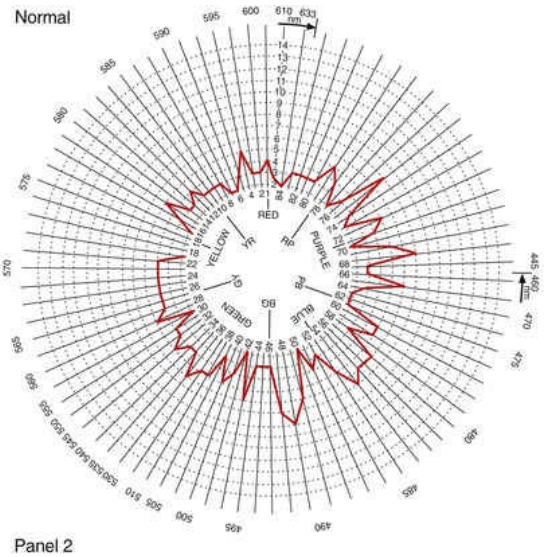

Panel 2

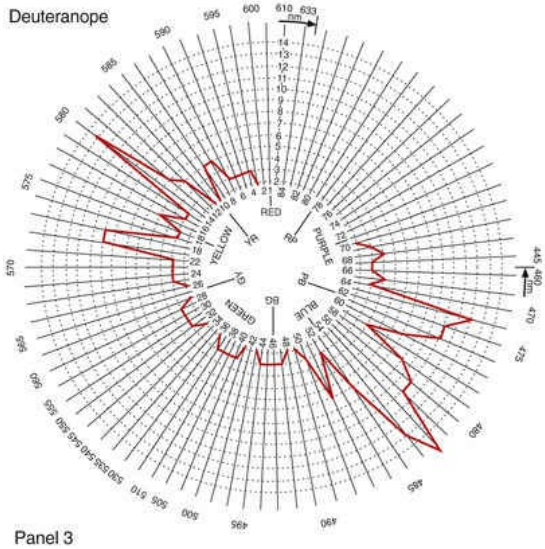

Panel 3

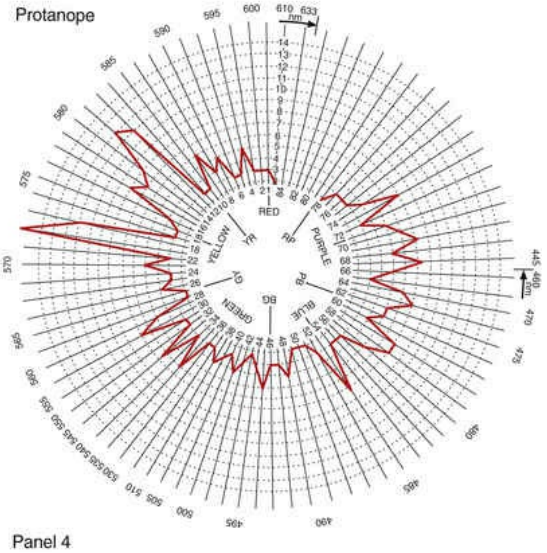

Panel 4

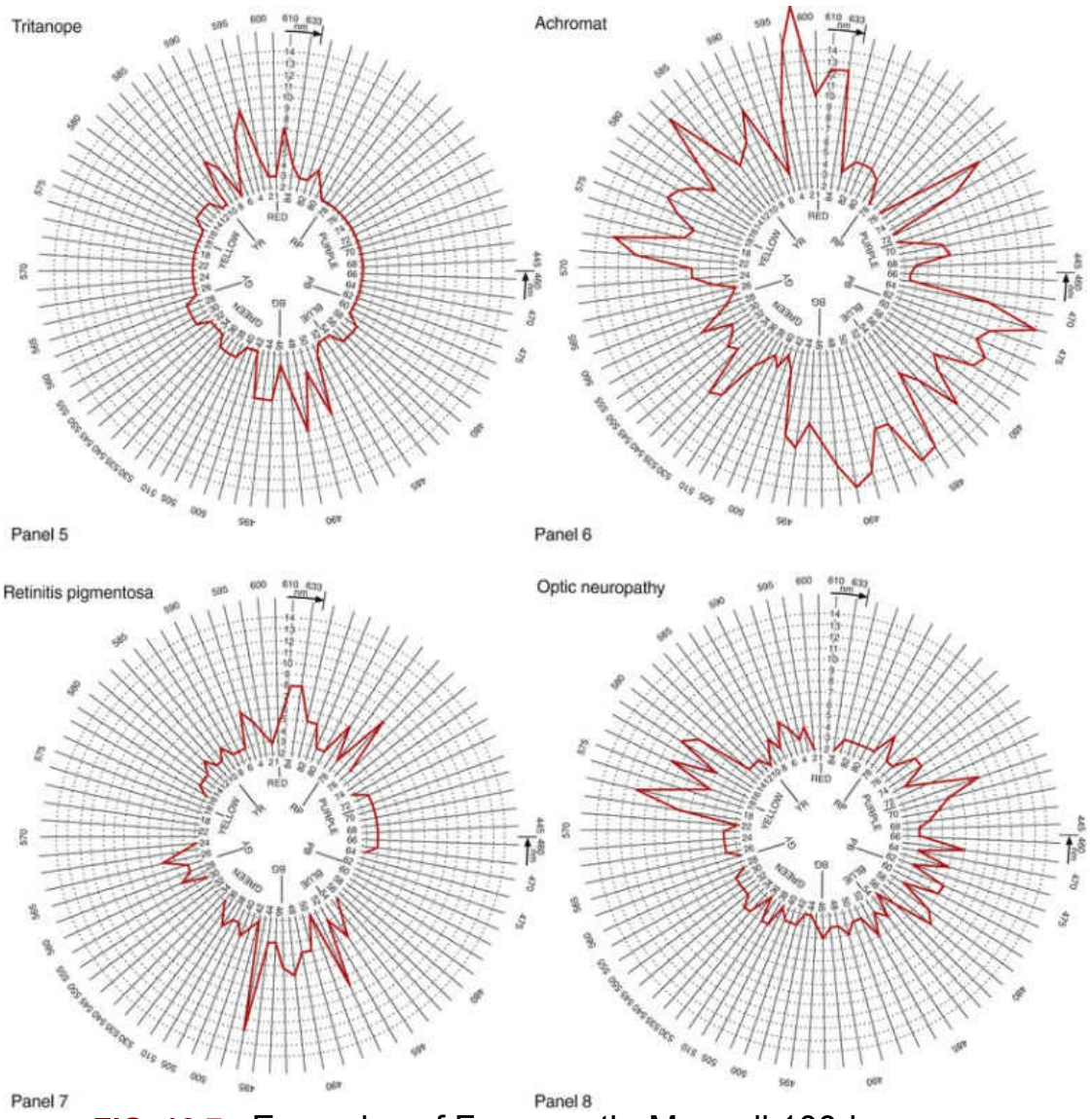

FIG. 12.7 Examples of Farnsworth–Munsell 100-hue test error patterns in normal subjects (panels 1 and 2) and in observers with congenital (panels 3–6) and later onset or acquired (panels 7 and 8) color vision defects. Panel 1, normal with good discrimination. Panel 2, normal with poor discrimination. Panel 3, deuteranope. Panel 4, protanope.Panel 5, tritanope. Panel 6, achromat. Panel 7, retinitis pigmentosa with an acquired violet–yellow defect. Panel 8, optic neuropathy with an acquired red–green defect.

The best known of the arrangement tests is the Farnsworth–Munsell 100-hue test. The test includes 85 black plastic caps with inserted papers that vary in hue but have constant lightness and saturation. The caps are divided into four boxes with each box covering one-quarter of the color circle. Observers being tested

arrange the caps in a natural color order according to their unique perception. An error occurs if the caps are misplaced from the ideal color order. A numeric score can be calculated and displayed on a polar graph. Age norms have been prepared giving the range of the expected total error scores for an unselected population as well as the expected inter-eye variability.

Observers with congenital color vision deficiencies make characteristic errors on arrangement tests because their chromatic discrimination ability is weakened or lost on particular axes in chromaticity space. Discrimination loss in acquired color vision defects is more variable. However, following the idea that discrimination of blueness content is, to a first order, independent of discrimination of redness–greenness, it is possible to partition the caps into those where correct ordering depends on normal function of the S-cone system (caps 1 through 12, 34 through 54, and 76 through 84) and those where correct ordering depends on normal function of the M- and L-cone opponent system (caps 13 through 33 and 55 through 75). The partitioned scores can be examined to determine whether an acquired color vision defect causes a particular type of discrimination loss; i.e., the S or L/M systems.[32]

Importance of the Test Illuminant for Plate and Discrimination Color Vision Tests

The plate and discrimination tests described above use reflective materials as colored test objects and the perceived color presented to an observer depends on the illuminating light as well as the reflective properties of the test materials. The original pseudoisochromatic plate tests were designed to be viewed under afternoon daylight in the northern hemisphere, and more recent tests have followed this design convention. Standardized illuminants (called illuminant C or illuminant D65) that closely simulate the spectra of afternoon daylight are more preferable to natural daylight, which may vary substantially in both spectrum and radiance with time of day and weather. Light sources that approximate these standard illuminants are commercially available and are suitable for use in illuminating clinical color vision tests. Most fluorescent light sources, however, do not accurately mimic

the colors produced in natural light and, therefore, they are not appropriate illuminants for color vision tests.

Color-Matching Tests

Adjusting three primaries to match a test color is not intuitive for many observers and research experimental methods are therefore not appropriate for clinical purposes. To adapt color-matching procedures for clinical evaluation, simplified methods have been developed by using two-variable matches and rapid, less complicated tasks. The instruments that allow these matches to be carried out are called anomaloscopes and the color-matching paradigms are called equations. The equations are named after the researchers who first proposed or used them.

Anomaloscope Color-Matching Test Using the Rayleigh Equation

In a Rayleigh match, a spectral "yellow" test field (589 nm) is presented in one-half of a circular field with an adjustable brightness. In the half field, a mixture of two "green" and "red" spectral primaries (545 and 670 nm) is presented. The mixture field can appear green (545 nm), green–yellow, yellow, orange, or red (670 nm) as the ratio of the primaries is varied. The task of the observer is to adjust the primary red–green ratio and brightness of the yellow to make the two fields appear identical. Observers with normal color vision accept a narrow range of ratios near the middle of the red–green range, but color-deficient observers will pick ratios shifted away from this range, depending on the specific deficiency. Matching abnormalities accompanying ophthalmic disease or X-linked color vision variations may include a widened matching range or acceptance of an abnormal match.[33]

The Rayleigh equation assesses the normality of M- and L-cone functions, since S cones are not contributing to the match because they are unresponsive to the primary wavelengths. A graphic display of the cone photopigment excitations allows the tester to evaluate which photopigments participated in an observer's match. Fig. 12.8A shows the expected yellow setting, based on the L- and M- photopigments, as a function of the red–green primary ratios.

For each photopigment, the quantal catch in cones may be characterized by a straight line in a chromaticity diagram as the red–green primary ratio is changed. Two lines show the predicted responses of the L cones alone (dashed and labeled L) and the M cones alone (dotted and labeled M). The rod photopigment is responsive at these wavelengths as well and the predicted rod response (solid and labeled Rod) is also shown. The normal match occurs at or near the intersection of the L- and M-cone settings and the matching range is narrow.

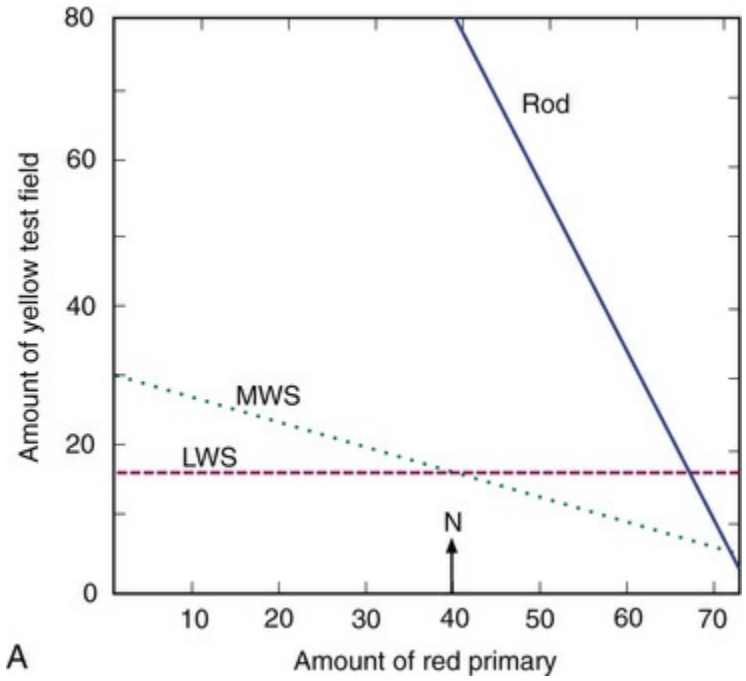

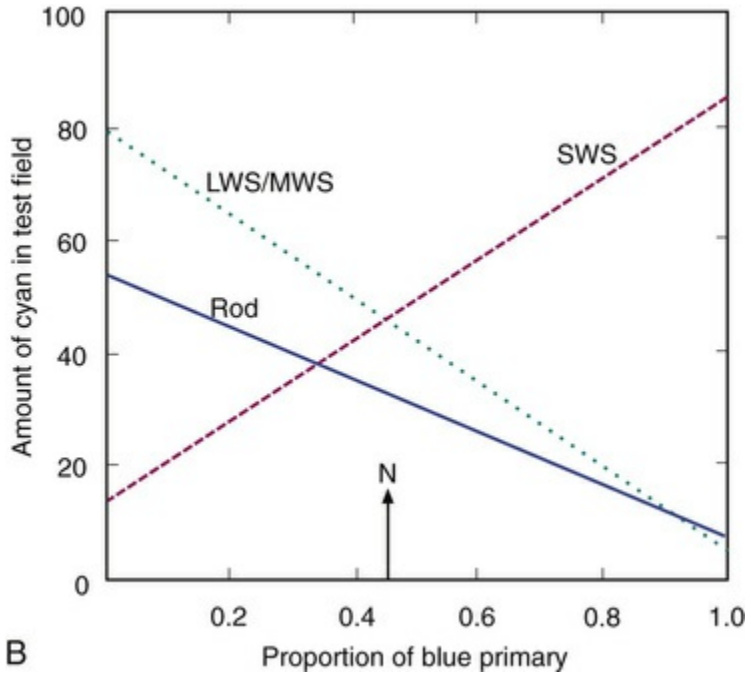

FIG. 12.8 Graphic analysis of the Rayleigh equation and Moreland equation. (A) The Rayleigh equation. The relative light in the "yellow" (589 nm) test is plotted as a function of the proportion of the "red" (670 nm) primary. The lines are calculated from the cone and rod photopigment excitations. The line marked *LWS* represents the L-cone response of Fig. 12.2B and predicts the matching behavior of deuteranopes. The line marked *MWS* represents the middle-wavelength cone response of Fig. 12.2B and predicts the matching behavior of protanopes. The normal match (*N*) occurs at the intersection of the L and M lines. The line marked *Rod* represents the rod response of Fig. 12.2A and predicts the matching behavior of achromats. (B) The Moreland equation. The relative light in the bicolor (480 nm + 580 nm) test is shown as a function of the proportion of the 440-nm primary. The lines are calculated from the cone and rod photopigment excitations. The line marked *LWS/MWS* represents the L- and M-cone response and predicts the matching behavior of tritanopes. The line marked *SWS* represents the short-wavelength cone response. The normal match (*N*) occurs at the intersection of the L/M line with the S line. The line marked *Rod* represents the rod response and predicts the matching behavior of achromats.

Deuteranopes can make satisfactory matches throughout the L

line. A deuteranope is thought to lack functional M cones in the retinal area responding to the stimuli. Studies on the X-chromosome opsin genes in deuteranopes show that many of these observers have only a single gene that is thought to encode the L photopigment. Protanopes can make matches throughout the extent of the M line. It has been speculated that the protanope lacks functional L cones in the retinal area responding to the stimuli and genetic studies have suggested that these observers usually have only a single gene on the X chromosome that has been described as a hybrid gene composed of a piece of the normal L- and a piece of the normal M-opsin genes.

Other X-linked color-defective observers, called anomalous trichromats, have a wider range of acceptable matches that are displaced from the normal match. Such observers are trichromatic but have one cone photopigment with an abnormal spectral sensitivity. Deuteranomalous matches occur along the L line (indicating a normal L-cone photopigment) but are shifted to low red–green primary ratios. The psychophysical interpretation is that the deuteranomalous trichromat has an abnormal M-cone photopigment that is shifted so that its spectral sensitivity closely overlaps that of the normal L-cone photopigment. Protanomalous matches occur along the M line (indicating a normal M-cone photopigment) but are shifted to high red–green primary ratios. The interpretation of these psychophysical studies is that the protanomalous trichromat has an abnormal L-cone photopigment, shifted so that its spectral sensitivity closely overlaps that of the normal M-cone photopigment. Anomaloscope color matching using the Rayleigh equation is recognized as the only clinical method that allows definitive classification of the X-linked color vision defects.

Anomaloscope analysis is important in ophthalmic disease assessment since it can be used to recognize a number of clinical entities, such as rod-dominated vision characteristic of cone degenerations and incomplete and complete achromatopsias. These diseases are characterized by Rayleigh matches extending along the rod line (solid line in Fig. 12.7A). Matching abnormalities that are characteristic of choroidal disorders affecting the fovea lead to Rayleigh matches that extend along or just below the L line but are shifted to higher red primary ratios (pseudoprotanomaly). The

discrimination loss characteristic of optic nerve disorders leads to matches that widen around the normal match on the L line.

Anomaloscope Color-Matching Test Using the Moreland Equation

The Moreland equation[34] is a match of a bicolor test field (480 and 580 nm) to a mixture of two primaries (440 and 500 nm). The test field appears blue–green to a normal observer, while appearance of the mixture field appearance ranges from violet, to blue, to blue–green, to green–blue, to green as the primary ratio is changed from mostly 440 nm to mostly 500 nm. The primary ratio is expressed in terms of the amount of the 440 nm ("violet") primary required for the match. As with the Rayleigh equation, an observer with normal color vision can find a primary ratio and test field luminance at which both fields appear identical.

The Moreland equation assesses the normality of S-cone function. Fig. 12.8B shows the predicted function for a single photopigment to the bicolor test field as a function of the violet–green primary ratio. The L and M cones share the same line (dotted and labeled as L/M). The S-cone response crosses this on the diagonal (dashed and labeled as S). The predicted rod (solid line labeled as Rod) line has the same direction as the L- and M-cone lines. The normal match occurs at the intersection of the S-cone line with the L/M line. Both congenital and acquired color vision defects can be recognized using the Moreland equation.[35] The tritanope (an observer lacking S-cone function) has matches extending along the L/M line, as do observers with acquired defects that affect S-cone function. Point mutations in the S-cone opsin gene on chromosome 7 have been reported in affected individuals in tritan pedigrees.[36]

Patients with X-linked achromatopsia (i.e., S-cone monochromacy) have matches that extend along the S-cone line. The majority of X-linked achromat pedigrees show major deletions of the region just preceding the cone opsin tandem gene array on the X chromosome in affected individuals.[37] This region is thought to be a regulatory area controlling expression of the L- and M-cone opsin genes. Additionally, some X-linked achromat pedigrees show only a single abnormal gene instead of the normal tandem array. Patients with complete achromatopsia have matches extending

along the rod line.

Considerations in the Use of Anomaloscopes

Even though the color-matching task on an anomaloscope is simplified compared with usual research color-matching procedures, anomaloscope testing procedures are not easily explained and an observer may require some practice before being able to complete a match. Correct use of an anomaloscope requires extensive operator training and these instruments are therefore usually found only in research centers. However, if properly used, the anomaloscope is a diagnostic instrument of great power.

Computerized Color Vision Tests

Computer-controlled color vision tests have been developed using a similar principle as that used for pseudoisochromatic plate tests or discrimination ability tests (such as the FM-100 hue test). Computerized tests are automated and therefore easy to use. Further, computerized tests can avoid the illuminating light issue that exists for reflective materials. However, the sensitivity and specificity of the computerized tests largely rely on the accurate presentation of color on computer monitors, such as cathodes ray tubes (CRTs) or liquid crystal displays (LCDs). A CRT is typically preferred over a LCD because CRTs have reliable temporal characteristics. To present color accurately, the displays have to be calibrated, including spectral distribution measurements and linearization. Caution must be taken when using a computerized color vision test that does not incorporate specific display calibration.

Color Assessment and Diagnosis (CAD) Test

The CAD test was developed by Dr Barbur and coworkers at City University, London.[38] The web-based CAD uses a color square that moves against a flickering luminance contrast noise. The color of the square changes along different chromaticity directions. Color-defective observers have difficulty seeing the square moving, whereas normal observers easily see the square move. The web-based CAD test requires a monitor to be balanced at around 9000 K

and the ambient illumination must be kept at a minimum. It is reported that this web-based test has good sensitivity and specificity for red–green color deficiencies.[39]

Cambridge Color Test (CCT)

The CCT is a computer-controlled, easy-to-use color vision test. The CCT was developed by Drs Mollon, Reffin, and Regan at the University of Cambridge, England.[40] The CCT system provides 14-bit color and luminance control on a calibrated CRT display. The stimulus is a Landolt C on an achromatic background. The chromaticity of the target C is varied along the protan, deutan, and tritan lines of a chromaticity diagram. The task is to indicate the position of the gap in the target C. A staircase procedure is used to measure discrimination thresholds along any of the three lines. The results are plotted as discrimination ellipses in a CIE space. Individuals with color vision deficiencies will have elongated discrimination ellipses along a protan, deutan, or tritan line and, therefore, this test can be used for all color vision deficiencies.

The Cone Contrast Test

The cone contrast test is a rapid (about 6 min) computer-based color vision test. The test was developed by Dr Rabin and colleagues based on L, M, and S cone contrast sensitivity.[41] The test presents a randomized series of colored letters that are visible to a single cone type (L, M, or S) in decreasing cone contrast, and subjects are required to read the letter aloud. The letters are selected from the British Standards Institution letters that have equal legibility. The letter cone contrasts range from a clear visible contrast to a threshold level. A technician records the letters read correctly and those missed, and the number of errors (out of 20 letters) is entered into the program to determine the L, M, S cone scores. The test is able to identify the type and severity of the hereditary color vision deficiency.

The Portal Color Sort Test (PCST)

The PCST is based on the FM-100 hue test but uses only 36 colored "chips," which significantly reduces the testing time. The chips are

representative of the original 85 chips in the FM-100 hue test. The observer arranges the order of the chips according to color similarities and the computer provides automatic scores. The correlation between the PCST and FM-100 hue test is high for testing congenital color vision defects but is unknown for testing acquired defects.[42]

Smartphone/Tablet Applications for Color Vision Screening

With the popularity of mobile communication devices (e.g., smartphones or tablets) increasing in medical settings, numerous applications have developed for these devices as tools for clinical testing/screening, patient education, or physician education and reference. Several applications use the pseudoisochromatic plate principle for color vision screening. These applications might be useful for a quick screening of color vision; however, these tools have not been validated and their sensitivity and specificity for color vision defect screening are not known. Further, there are many factors that can affect the test results. The most important is the display characteristics of the mobile device. These displays are not calibrated and they may not be homogeneous; therefore the tests for color vision screening are not necessarily "pseudoisochromatic." Finally, the illumination in the office may impair the test reliability. Therefore, these applications need to be confirmed by comparison with other established tools for color vision screening. Recently, several studies have attempted to assess the efficacy of smartphone/tablet-based color vision tests. For example, Dain and colleagues assessed the color representation in smart phones[43] and evaluated the colorimetric characteristics of iPhone apps for color vision tests based on the Ishihara.[44] In addition, it has been shown that a tablet-based cone contrast color vision test achieved the same sensitivity and specificity as a computer-based cone contrast sensitivity test.[45]

Which Test to Use in a Clinical Setting?

Many clinicians want to have some means of testing color vision without necessarily acquiring expensive instruments and expertise

needed for professional evaluation and diagnosis. Tests using colored papers (pigment tests) and the proper illuminant offer office clinicians the possibility of some color vision evaluation.

A screening plate test with the proper illuminant would be minimal equipment for testing color vision. Approximately 8–10% of American males have one of the X-linked color vision defects. Identification of color vision defects in children before they enter grade school allows the clinician to provide counseling to the parents. Many children with color vision defects have memories of being teased or ridiculed in the early grades and early testing allows appropriate counseling. Also, many males with color vision defects may inadvertently choose careers, for example, as pilots or firefighters, from which they will be barred due to their color vision status. It should be noted, however, that the screening plate tests that may be very useful for the common genetic color vision defects are less successful at identifying acquired color vision defects.

A more ambitious plan to test color vision in an office would be to combine a screening plate test with a test of color discrimination. A discrimination test (e.g., the Farnsworth–Munsell 100-hue test) allows the clinician to follow changes in color vision over time, such as might occur with optic neuritis. Occasionally, a clinician will see a patient who has an extremely rare form of color defect and color vision testing may be informative. For example, cerebral achromatopsia is a fascinating case that likely arises from damage to higher-order visual processes. In these cases, a more complete color vision testing (such as spectral sensitivity and saturation discrimination evaluation) should be considered and case reports would be of wide interest in the medical community. Patients should be referred to a psychophysics laboratory for more visual function testing, such as contrast discrimination evaluation.

New Developments in Color Vision Research

Color vision has been studied considering genetics, evolution, physiology, and psychophysics. A few newer research areas related to color vision are provided here.

Gene Therapy for Color Vision Defects

Drs Jay and Maureen Neitz and coworkers have carried out pioneering studies on "curing" red–green color deficiency in dichromatic adult squirrel monkeys that were missing the L-cone opsin gene at birth.[46,47] As gene therapy, the human L-cone opsin gene was delivered into the photoreceptor layers of the retinas of the monkeys. A few months after the introduction of the new opsin gene, these monkeys exhibited trichromatic color vision behavior with spectral sensitivity shifted, chromatic discrimination improved, and color perception enriched. A clinical trial involving gene therapy in humans would require approval from the National Institutes of Health Office of Recombinant DNA Activities (ORDA)/Recombinant DNA Advisory Committee (RAC) and the Food and Drug Administration and this would not be granted easily without a long and thorough approval process. However, the fundamental question of whether it is necessary to "cure" color deficiencies is currently the point of debate since the majority of congenital dichromats live a normal life and their quality of life is not significantly affected by having the color vision deficiency.

Adaptive Optics (AO) Retinal Imaging System

AO was initially used in astronomy to remove the effects of atmospheric distortion to improve the performance of telescopes and laser communication systems.[48] An AO system has three components: (1) a wavefront sensor for ocular aberration measurement; (2) a deformable mirror for aberration correction; and (3) a control system that compares the sensor output and adjusts the deforming mirrors to achieve optimal resolution. This technology was first adopted for retinal imaging in the 1990s by Dr David Williams to reduce ocular aberrations in the eyes.[49] After its initial introduction, the AO imaging system was considered to have great scientific and clinical application potential because it had the capability of imaging photoreceptors, the retinal pigment epithelium, retinal blood vessels and, potentially, ganglion cells at a high magnification. For instance, AO made it possible to measure

color perception[50] or cell responses in the postreceptoral pathways[51] associated with tiny flashes of light stimulating a single cone in the eye. For color vision screening, in particular, the AO system can provide high resolution of the cone mosaic and it can show whether a particular type of cone (e.g., L cones) is missing in the retina. Combining this information with genetic studies is potentially informative because AO imaging can provide insights about cone distributions that can be related to the cone opsin genes.[52] (See Chapter 7, Advanced imaging technologies, for more details about this topic.)

Rod and Cone Interactions in Color Vision

Duplex theory states that rods and cones independently contribute to different aspect of visual perception. However, rods and cones share common neural pathways from the retina to the brain and this provides a neural basis for rod–cone interactions in visual function, including color vision.[53] Conventionally, rod vision has been considered to be achromatic. However, numerous psychophysical studies have indicated that rods contribute to color vision at either mesopic[54] or even scotopic light levels.[55] Psychophysical evidence for rod contributions to color vision comes from measurements of scotopic color contrast,[56] photochromatic intervals during the course of dark adaptation following a light bleach,[57] chromatic discrimination,[58] and color-matching or color-appearance methods using unique hue measurement or hue-scaling methods.[59,60]

Recently, rod contributions to color vision were studied using a four-primary Maxwellian-view photostimulator[61] that allowed independent control of rod and cone excitations at the same chromaticity, retinal locus, and light level. This new method has yielded new insights into rod contributions to color vision. Specifically, rods contribute to color percepts in a manner analogous to M-cone signals at all mesopic light levels and analogous to S-cone signals only at low mesopic light levels near cone thresholds.[54] Also, the strength of rod contributions is linearly related to rod contrasts.[62]

References

1. Hood DC, Finkelstein MA. Sensitivity to light. Boff KR, Kaufman L, Thomas JP. *Handbook of perception and human performance*. John Wiley: New York; 1986:5-1–66. *Sensory processes and perception*. vol. I.
2. Smith VC, Pokorny J, Lee BB, et al. Sequential processing in vision: the interaction of sensitivity regulation and temporal dynamics. *Vision Res*. 2008;48:2649–2656.
3. Goldberg SH, Frumkes TE, Nygaard RW. Inhibitory influence of unstimulated rods in the human retina: evidence provided by examining cone flicker. *Science*. 1983;221:180–182.
4. Cao D, Zele AJ, Pokorny J. Dark-adapted rod suppression of cone flicker detection: evaluation of receptoral and postreceptoral interactions. *Vis Neurosci*. 2006;23:531–537.
5. Sharpe LT, Stockman A. Rod pathways: the importance of seeing nothing. *Trends Neurosci*. 1999;22:497–504.
6. Dacey DM. Parallel pathways for spectral coding in primate retina. *Annu Rev Neurosci*. 2000;23:743–775.
7. Lee BB. Visual pathways and psychophysical channels in the primate. *J Physiol*. 2011;589(1):41–47.
8. Lee BB, Smith VC, Pokorny J, et al. Rod inputs to macaque ganglion cells. *Vision Res*. 1997;37:2813–2828.
9. Crook JD, Davenport CM, Peterson BB, et al. Parallel ON and OFF cone bipolar inputs establish spatially coextensive receptive field structure of blue–yellow ganglion cells in primate retina. *J Neurosci*. 2009;29:8372–8387.
10. Field GD, Greschner M, Gauthier JL, et al. High-sensitivity rod photoreceptor input to the blue–yellow color opponent pathway in macaque retina. *Nat Neurosci*. 2009;12:1159–1164.
11. Bartlett NR. Dark adaptation and light adaptation. Graham CH. *Vision and visual perception*. John Wiley: New York; 1965:185–207.
12. Graham CH. *Vision and visual perception*. John Wiley: New York; 1965.
13. Shevell SK, Kingdom FA. Color in complex scenes. *Annu Rev*

Psychol. 2008;59:143–166.
14. Smith VC, Pokorny J. Spectral sensitivity of the foveal cone photopigments between 400 and 500 nm. *Vision Res*. 1975;15:161–171.
15. MacLeod DIA, Boynton RM. Chromaticity diagram showing cone excitation by stimuli of equal luminance. *J Opt Soc Am*. 1979;69:1183–1185.
16. Boynton RM, Kambe N. Chromatic difference steps of moderate size measured along theoretically critical axes. *Color Res Appl*. 1980;5:13–23.
17. Derrington AM, Krauskopf J, Lennie P. Chromatic mechanisms in lateral geniculate nucleus of macaque. *J Physiol (Lond)*. 1984;357:241–265.
18. Lee BB, Martin PR, Valberg A. Sensitivity of macaque retinal ganglion cells to chromatic and luminance flicker. *J Physiol (Lond)*. 1989;414:223–243.
19. Pokorny J, Smith VC. Chromatic discrimination. Chalupa LM, Werner JS. *The visual neuroscience*. MIT Press: Cambridge, MA; 2004:908–923.
20. Pokorny J, Smith VC. Wavelength discrimination in the presence of added chromatic fields. *J Opt Soc Am*. 1970;69:562–569.
21. Wright WD. The sensitivity of the eye to small colour differences. *Proc Phys Soc Lond*. 1941;53:93–112.
22. MacAdam DL. Visual sensitivities to color differences in daylight. *J Opt Soc Am*. 1942;32:247–274.
23. Cao D, Zele AJ, Smith VC, et al. S-cone discrimination for stimuli with spatial and temporal chromatic contrast. *Vis Neurosci*. 2008;25:349–354.
24. Krauskopf J, Gegenfurtner K. Color discrimination and adaptation. *Vision Res*. 1992;32:2165–2175.
25. von Kries J. Influence of adaptation on the effects produced by luminous stimuli. MacAdam DL. *Sources of color science*. MIT Press: Cambridge, MA; 1905.
26. Shevell SK, Cao D. *Chromatic assimilation: evidence for a neural mechanism*. Oxford University Press: Oxford; 2003.
27. Neitz J, Neitz M. The genetics of normal and defective color vision. *Vision Res*. 2011;51:633–651.

28. Nathans J, Piantanida TP, Eddy RL, et al. Molecular genetics of inherited variation in human color vision. *Science*. 1986;232:203–210.
29. Working-Group-41. *Procedures for testing color vision, NAS-NRC Committee on Vision*. National Academy Press: Washington, DC; 1981.
30. Pokorny J, Smith VC, Pinckers AJLG, et al. Classification of complete and incomplete autosomal recessive achromatopsia. *Graefes Arch Clin Exp Ophthalmol*. 1982;219:121–130.
31. Nathans J, Hogness DS. Isolation and nucleotide sequence of the gene encoding human rhodopsin. *Proc Natl Acad Sci USA*. 1984;81:4851–4855.
32. Smith VC, Pokorny J, Pass AS. Color-axis determination on the Farnsworth–Munsell 100-hue Test. *Am J Ophthalmol*. 1985;100:176–182.
33. Pokorny J, Smith VC, Verriest G, et al. *Congenital and acquired color vision defects*. Grune and Stratton: New York; 1979.
34. Moreland JD, Kerr J. Optimization of stimuli for trit-anomaloscopy. *Mod Probl Ophthalmol*. 1978;19:162–166.
35. Pokorny J, Smith VC, Went LN. Color matching in autosomal dominant tritan defect. *J Opt Soc Am*. 1981;71:1327–1334.
36. Weitz CJ, Miyake Y, Shinzato K, et al. Human tritanopia associated with two amino acid substitutions in the blue-sensitive opsin. *Am J Hum Genet*. 1992;50:156.
37. Nathans J, Davenport CM, Maumenee IH, et al. Molecular genetics of human blue cone monochromacy. *Science*. 1989;245:831–838.
38. Barbur J, Harlow A, Plant G. Insights into the different exploits of colour in the visual cortex. *Proc Biol Sci*. 1994;258:327–334.
39. Seshadri J, Christensen J, Lakshminarayanan V, et al. Evaluation of the new web-based "Colour Assessment and Diagnosis" test. *Optom Vision Sci*. 2005;82:882–885.
40. Regan BC, Reffin J, Mollon JD. Luminance noise and the rapid determination of discrimination ellipses in colour deficiency. *Vision Res*. 1994;34:1279–1299.

41. Rabin J, Gooch J, Ivan D. Rapid quantification of color vision: the cone contrast test. *Invest Ophthalmol Vis Sci*. 2011;52:816–820.
42. Melamud A, Simpson E, Traboulsi EI. Introducing a new computer-based test for the clinical evaluation of color discrimination. *Am J Ophthalmol*. 2006;142:953–960.
43. Dain SJ, Kwan B, Wong L. *Consistency of colour representation in smart phones*. [International Colour Vision Society, 23rd Symposium, Sendai, Japan] 2015.
44. Dain SJ, Aimerdef A. Colorimetric evaluation of iPhone apps for colour vision tests based on the Ishihara test. *Clin Exp Optom*. 2016;99:264–273.
45. Chacon A, Rabin J, Yu D, et al. Quantification of color vision using a tablet display. *Aerosp Med Hum Perform*. 2015;86:56–58.
46. Mancuso K, Mauck MC, Kuchenbecker JA, et al. A multi-stage color model revisited: implications for a gene therapy cure for red–green colorblindness. *Adv Exp Med Biol*. 2010;664:631–638.
47. Mancuso K, Hauswirth WW, Li Q, et al. Gene therapy for red–green colour blindness in adult primates. *Nature*. 2009;461:784–787.
48. Tyson RK. *Principles of adaptive optics*. Academic Press: San Diego, CA; 1991.
49. Liang J, Williams DR, Miller DT. Supernormal vision and high-resolution retinal imaging through adaptive optics. *J Opt Soc A*. 1997;14:2884–2892.
50. Hofer H, Singer B, Williams DR. Different sensations from cones with the same photopigment. *J Vis*. 2005;5:444–454.
51. Sincich LC, Zhang Y, Tiruveedhula P, et al. Resolving single cone inputs to visual receptive fields. *Nat Neurosci*. 2009;12:967–969.
52. Williams DR. Imaging single cells in the living retina. *Vision Res*. 2011;51:1379–1396.
53. Buck SL. Rod–cone interaction in human vision. Chalupa LM, Werner JS. *The visual neuroscience*. MIT Press: Cambridge, MA; 2004:863–878.
54. Cao D, Pokorny J, Smith VC. Matching rod percepts with

cone stimuli. *Vision Res*. 2005;45:2119–2128.
55. Pokorny J, Lutze M, Cao D, et al. The color of night: surface color perception under dim illuminations. *Vis Neurosci*. 2006;23:525–530.
56. Willmer EN. Low threshold rods and the perception of blue. *J Physiol (Lond)*. 1949;111:17P.
57. Lie I. Dark adaptation and the photochromatic interval. *Doc Ophthalmol*. 1963;17:411–510.
58. Stabell U, Stabell B. Wavelength discrimination of peripheral cones and its change with rod intrusion. *Vision Res*. 1977;17:423–426.
59. Buck SL, Knight RF, Bechtold J. Opponent-color models and the influence of rod signals on the loci of unique hues. *Vision Res*. 2000;40:3333–3344.
60. Volbrecht VJ, Nerger JL, Imhoff SM, et al. Effect of the short-wavelength-sensitive-cone mosaic and rods on the locus of unique green. *J Opt Soc Am A*. 2000;17:628–634.
61. Pokorny J, Smithson H, Quinlan J. Photostimulator allowing independent control of rods and the three cone types. *Vis Neurosci*. 2004;21:263–267.
62. Cao D, Pokorny J, Smith VC, et al. Rod contributions to color perception: linear with rod contrast. *Vision Res*. 2008;48:2586–2592.

13

Visual Acuity and Contrast Sensitivity

Gary S. Rubin

Visual Acuity Tests

Introduction

Visual acuity is the most widely used measure of visual function. In fact, visual function is often equated with visual acuity, thereby ignoring other important dimensions of visual stimuli, such as color and contrast. Visual acuity tests have proven to be useful for assessment of refractive error, screening for ocular health, following the course of eye disease, evaluating the effectiveness of medical and surgical treatment, prescribing aids for the visually impaired, and setting vision standards for employment and driving.

Given the variety of its applications, it is not surprising that many different types of visual acuity tests have evolved. Generally, these tests were developed with little concern for standardization. Since the 1980s several attempts have been made to formulate standards for test design and administration. The Committee on Vision of the National Academy of Sciences–National Research Council (NAS–NRC)[1] has published standards for clinical testing of visual acuity that are widely adopted in the United States, and the British Standards Institution[2] has published similar standards for the United Kingdom. The NAS–NRC standards are used as the basis of this chapter.

Chart Design

Optotypes

Most familiar acuity tests require the subject to identify letters arrayed in rows of decreasing size. The so-called Snellen acuity test is the prime example, although Snellen acuity now usually refers to a way of reporting test results rather than to any particular type of chart. To facilitate testing of young children and people unfamiliar with the Latin alphabet, other optotype tests based on the tumbling E, Landolt C, numerals, or simple pictures of familiar objects are also used. Visual acuity can also be assessed with grating patterns, but grating acuity often overestimates Snellen acuity in patients with age-related maculopathy,[3] typically by a factor of 2 or more.

The NAS–NRC recommends that the Landolt C test be used as the standard by which other acuity tests are compared. The Landolt C is a broken circle in which the width of the break and the stroke width are both equal to one-fifth the height of the C. The ring is shown with the break at one of four locations, and the subject responds by saying "right," "down," "up," or "left," or by pointing in the appropriate direction.

There are several advantages to the Landolt C test, including equal difficulty of all targets (unlike letters that vary in degree of difficulty), sensitivity to astigmatic refractive error, and suitability for use with illiterate subjects. However, the Landolt C test is not widely used because it has a guessing rate of 25%, so an alternative is to standardize another optotype set by comparing acuities obtained with it to Landolt C test acuities. The Sloan letters,[4] a set of 10 upper-case sans serif letters, are the most popular substitute. An acuity chart based on Sloan letters was developed for the Early Treatment Diabetic Retinopathy Study (ETDRS)[5] and is illustrated in Fig. 13.1. The original ETDRS chart has been replaced by the 2000 series revised ETDRS chart that more accurately equates the difficulty of letters on all lines. The ETDRS charts are the most widely used acuity charts for clinical research.

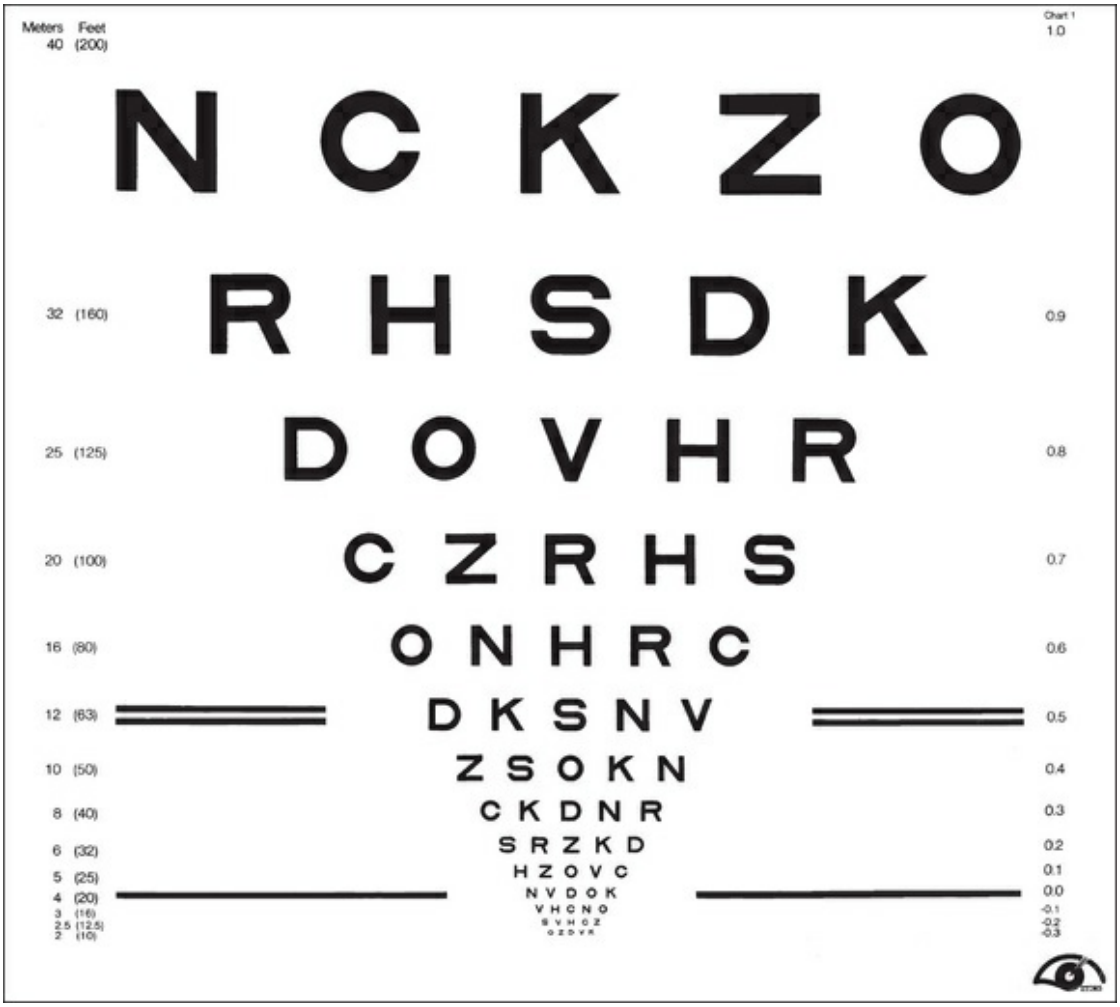

FIG. 13.1 The Early Treatment Diabetic Retinopathy Study (ETDRS) acuity chart. (Reproduced with permission from Ferris FL III, Kassof PA, Bresnick GH, et al. New visual acuity charts for clinical research. Am J Ophthalmol 1982;94:91–96.)

Chart Layout

Careful attention must be paid to the layout of the acuity chart. The chart should follow a uniform progression of letter sizes, typically a 0.1 log unit (or 26%) reduction in size from line to line. The uniform progression ensures that a one-line loss will have the same meaning at any point on the chart and at any viewing distance. The same number of letters should appear on each line, and the spacing should be uniform, both within and between lines. The spacing requirement results in a large chart, with the letters forming an inverted triangle. The NAS–NRC recommends 8–10 letters per line, but studies[6] suggest that as few as three letters are required for an

accurate estimate of visual function. The ETDRS chart uses five letters per line.

Concern about uncontrolled "crowding" effects has led to further modifications of the ETDRS chart. Crowding refers to the reduced visibility of letters when they are surrounded by other letters. Crowding has a larger effect in some types of visual dysfunction, notably amblyopia[7] and macular degeneration.[8] For most acuity charts, letters at either the end of a line or at the top or bottom of the chart are less subject to crowding than are internal letters. To equalize crowding effects, contour interaction bars may be added around the perimeter of the chart.[9]

Testing Procedure

Test Distance

ETDRS charts are available for a range of test distances from 4 meters (13 feet) to 2 meters (6.5 feet) and when used at the designated distance can measure acuities from 20/10 to 20/200. However, given the logarithmic progression of letter sizes, they can be used at any distance with an appropriate correction of the reported results. For patients with very poor acuity, the clinician may resort to finger counting or hand motion. This strategy is strongly discouraged by low-vision practitioners because it can be demeaning and depressing for the patient to be left with the impression that their vision is so poor it cannot even be measured with an eye chart. Instead, it is recommended that the patient be moved closer to the chart. Using a test distance of 50 cm and appropriate refractive correction it is possible to reliably measure "counting fingers" acuity with an ETDRS chart (approximately 20/1460 ± 10%).[10] "Hand motions" can be measured with some electronic acuity tests (see below). Distance itself should have little effect on visual acuity, provided that the subject's accommodative state and pupil size are controlled. However, one study[11] found that acuity changed by as much as seven letters (more than one ETDRS line) when the test distance was reduced to less than 2 meters. The reason for this discrepancy remains unexplained.

Luminance and Contrast

Whatever the test distance, the chart must be adequately illuminated and of high contrast. Illumination standards vary from 100 cd/m^2 in the Unites States to 300 cd/m^2 in Germany. Increasing chart luminance improves visual acuity in normal subjects, but reaches a plateau at about 200 cd/m^2.[12] Various types of visual dysfunction can change the effects of luminance on acuity. For example, patients with retinitis pigmentosa may show a decrease in acuity at higher luminance, whereas patients with age-related macular degeneration often continue to improve at luminances well above the normal plateau.[13] A luminance standard of 100 cd/m^2 can be justified because it represents good room illumination for ordinary reading material. Furthermore, most of the currently proposed standards would yield the same acuity scores, plus or minus one letter (assuming five letters per line and a 0.1 log unit size progression) in normal subjects.

The relationship of visual acuity to letter contrast follows a square-root law.[14] For example, decreasing contrast by a factor of 2 would decrease acuity by roughly a factor of 1.4. The NAS–NRC recommends that letter contrast be at least 0.85. Transilluminated, projection, and reflective charts (wall charts) can all meet these standards, but some transilluminated charts are deficient in luminance, and some projection systems lack sufficient luminance and contrast. Accurate calibration requires a spot photometer, for which procedures are described in the NAS–NRC document.[1]

Test Administration

Administration of visual acuity tests is simple and straightforward. However, one detail often overlooked in clinical testing is that the test must be administered in a "forced-choice" manner. Rather than allowing the patient to decide when the letters become indistinguishable, the patient should be required to guess the identity of each letter until a sufficient number of errors are made to justify terminating the test. People differ in their willingness to respond to questions when they are not confident about the answers. A person with a conservative criterion answers only when absolutely certain about the identity of the letter, whereas a person with a liberal criterion ventures a guess for any letter that is even barely discernible. These two people may receive different acuity

scores because of differences in their criteria rather than because of variations in visual function. This is not merely a theoretical concern. Several studies[15,16] have shown that criterion-dependent test procedures lead to inaccurate and unreliable test results. Forced-choice procedures are criterion-free because the examiner, rather than the observer, determines whether the letter is correctly identified.

Scoring

Until recently, visual acuity tests were usually scored line by line with the patient being given credit for a line when a criterion number of letters were identified correctly. The NAS–NRC recommends that at least two-thirds of the letters on a line be correctly identified to qualify for passing. Allowing a small proportion of errors improves test reliability.[17] For tests that follow the recommended format of an equal number of letters on each line and a constant progression of letter sizes, it is preferable to give partial credit for each letter correctly identified. This is commonly done by counting the number of letters read correctly on the entire chart and converting this to an acuity score by means of a simple formula that values each letter as L/N, where L = difference in acuity between adjacent lines and N = number of letters per line. So for a chart with five letters per line and a 0.1 LogMAR (see below) progression from line to line (such as the standard ETDRS chart) each correct letter is worth 0.1/5 = 0.02 LogMAR. Although differences between scoring methods are usually small, it has been shown[2,6,18] that letter-by-letter scoring is more reproducible than line-by-line scoring.

The most familiar method for reporting visual acuities is the Snellen fraction. The numerator of the Snellen fraction indicates the test distance, and the denominator indicates the relative size of the letter, usually in terms of the distance at which the stroke width would subtend a visual angle of 1 minute. Thus “20/40” indicates that the actual test distance was 20 feet and that the strokes of the letters would subtend 1 minute of arc at 40 feet.

To simplify comparison of acuities measured at different distances, the minimum angle of resolution (MAR) should be used. The MAR is the visual angle corresponding to stroke width in

minutes of arc and is equal to the reciprocal of the Snellen fraction. Visual acuities are frequently converted to log10 and reported as "LogMAR." For example, 20/20 acuity corresponds to a MAR of 1 minute of arc, or a LogMAR of 0, and 20/100 acuity corresponds to a MAR of 5 minutes of arc, or a LogMAR of 0.7 (as does an acuity of 2/10 or 6/30). The MAR and LogMAR scales increase with worsening acuity. One often sees visual acuities reported as the decimal equivalent of the Snellen fraction. However acuities are more normally distributed when converted to LogMAR rather than decimal values. Moreover, decimals give the false impression that acuity scores can be equated with overall loss of visual function. For example, acuity of 0.1 (the decimal equivalent of 20/200) may misleadingly suggest that the patient has retained 10% of residual visual function.

Near and Reading Acuity Tests

Near acuity is usually tested to evaluate reading vision. These tests are particularly important for prescribing visual aids for persons with low vision. Near acuity has been shown to be a better predictor of the optimal magnification needed by visually impaired readers than traditional distance acuity.[19]

Although some near acuity tests are simply reduced versions of distance acuity charts, most tests consist of printed text, either unrelated words or complete sentences or paragraphs, covering a range of sizes. Near acuity tests are even less standardized than distance acuity tests.

Specifying Letter Size

As with all acuity tests, the most critical parameter is the visual angle subtended by the optotype. Many systems have been devised for specification of print size. One of the most common is the Jaeger J notation. Jaeger notation is based on a numeric scale (J1, J2, and so on) that follows no logical progression except that larger numbers correspond to larger print sizes. Furthermore, print with the same J specification can vary by as much as 90% from one test manufacturer to another.[20]

Alternatives to the Jaeger notation are the typesetter's point

system, the British N system, and the M notation introduced by Sloan. The typesetter's point is commonly used to specify letter size for printed text and is equal to 0.32 mm (1/72 inch). However, the measurement refers to the size of the metal slug that contains the letter and varies from one font to another. A study[21] of the effect of font on reading speed showed that the nominal sizes of printed text could be very misleading. Of four fonts, all labeled as 12 point, one was much more legible than the other three. But it turned out that the more legible font was actually larger than the others and when equated for real size there was no difference in legibility.

The British N system standardized the point size specification by adopting the Times Roman font. Sloan's M notation,[4] widely used in the United States, is standardized according to the height of a lower-case "x." A lower-case 1M letter subtends 5 minutes of arc at a 1-meter viewing distance and corresponds roughly to the size of ordinary newsprint. None of the print size specifications can be used for quantitative comparisons unless viewing distance is also specified. For example, 1M print read at a distance of 40 cm would be recorded as 0.40/1.00M.

Words Versus Continuous Text

One issue that remains unresolved is whether near acuity tests should be based on unrelated words or meaningful text. An argument in favor of unrelated words is that contextual information promotes guessing and may lead to an overestimate of near acuity.[22] In addition, the presence of semantic context introduces variability because of cognitive intellectual factors that may mask the visual factors of primary concern.[23] On the other side it is argued that the main reason for measuring near acuity is to gain information about reading performance. Since context is normally available to the reader, a reading test that includes meaningful text will be a better indicator of everyday performance. Fortunately, reading speed for meaningful text is highly correlated with reading speed for unrelated words.[24]

The MNREAD test[25] uses meaningful text to evaluate near acuity. The test is composed of 19 standardized sentences in a logarithmic progression of sizes. Each sentence is 55 characters and the words are drawn from a controlled vocabulary. The test can be used to

measure reading acuity (the smallest print size that can be read), maximum reading speed, and critical print size (the smallest print size for maximum reading speed). The test–retest variability for the MNREAD test has been assessed in patients with macular disease[26] and the coefficient of repeatability was found to be greater than 65 words/minute. The high level of variability may be due, in part, to the short sentences. The International Reading Speed Test (IReST)[27] uses 150-word paragraphs of continuous text to measure reading speed, which should yield more reproducible measures. The IReST is available in 17 languages.

Electronic Acuity Tests

Video-based acuity tests have been available since the 1980s, but did not become popular until the introduction of inexpensive LCD monitors in recent years. These electronic tests include computer software that can be used with the experimenter's own computer hardware (such as the Freiburg Acuity and Contrast Test (FrACT)), devices that display optotypes under operator control (such as the Test Chart 2000) and systems that administer, score, and store the results of the acuity measurement (such as the E-ETDRS and COMPlog systems).

Electronic tests offer several potential advantages over paper-based tests:

1. multiple types of test, such as acuity, contrast sensitivity, and stereoacuity, with one instrument;

2. better randomization of optotypes – each test administration can use a different arrangement of letters instead of being constrained to two or three printed charts;

3. easier standardization of luminance and contrast, although if calibration instructions are ignored, luminance and contrast errors can be greater than for paper tests;

4. the promise of advanced testing algorithms that reduce testing time and/or increase measurement accuracy and precision. Until recently, the electronic systems had not lived up to this promise,

with test times as long as or longer, and measurement accuracy and precision no better than conventional chart tests.[28] One test, the E-ETDRS system used in clinical trials for treatment of central retinal vein occlusion,[29] is reported to take longer without any increase in reliability.[28] But the introduction of new smartphone and tablet display technology has dramatically changed the field.

Modern high-end touchscreen displays have sufficient spatial resolution to test near the acuity limit, but the displays are susceptible to glare, require adequate warm-up time for luminance to stabilize, and must be viewed straight on.[30]

All of these cautions are shared by LCD computer monitors, however many of the smartphone and tablet apps are intended to be self-administered, and the user may not have the same concern for standardization as in researcher-administered testing. However, results of smartphone and tablet acuity tests do not appear to compare well to gold standard ETDRS acuity tests. Two studies looked at validity and reliability of smartphone acuity tests: the PEEK study and the Eye Phone study.[31,32] Both studies show that the smartphone measurements are not biased. On average, the smartphone scores differ from ETDRS or Snellen scores by 2 letters or less. But more importantly, they show, but do not comment on, the very large limits of agreement, which run to ± 0.3 LogMAR or ± 3 ETDRS lines. That is equivalent to a factor of ±2x so the limit of agreement for someone with 6/12 acuity would extend from 6/6 to 6/24, which is three times higher than what is generally observed with ETDRS charts. The reasons for this poor repeatability are not discussed.

Contrast Sensitivity Tests

Introduction

Contrast sensitivity testing has been widely promoted as an important adjunct or even replacement for visual acuity testing. Acuity measures the eye's ability to resolve fine detail but may not adequately describe a person's ability to see large low-contrast objects such as faces. Contrast sensitivity testing was originally

developed as a research tool by engineers and vision scientists interested in characterizing normal visual function. For theoretical reasons, most investigators have used sine-wave grating stimuli, patterns consisting of alternating light and dark bars, which have a sinusoidal luminance profile. Sine-wave gratings vary in spatial frequency (bar width) and contrast. A contrast sensitivity function (CSF) is derived by measuring the lowest detectable contrast across a range of spatial frequencies.

Utility of Contrast Sensitivity Tests

For people with normal vision, contrast sensitivity and visual acuity are correlated. However, various types of visual dysfunction, including cerebral lesions,[33] optic neuritis related to multiple sclerosis,[34] glaucoma,[35] diabetic retinopathy,[36] and cataract,[37] may cause a reduction in contrast sensitivity despite near-normal visual acuity. This led to the suggestion that contrast sensitivity might serve as a tool for differential diagnosis and screening. However, there is no pattern of CSF loss that is unique to any particular vision disorder. The types of CSF measured in patients with macular disease or glaucoma can be similar to the CSFs measured in cataract patients, although detailed analyses with targets of different size or at different retinal eccentricities may help distinguish between various causes of the loss. It is argued that contrast sensitivity tests are more sensitive to early eye disease than visual acuity. While this may be true, much of the apparent difference in sensitivity is due to careless measurement of visual acuity (poorly designed charts and test procedures). Even if the test were more sensitive, its lack of specificity for distinguishing between ocular and retinal/neural disorders limits its usefulness as a screening test.[38]

The real value of clinical contrast sensitivity testing is to gain a better understanding of the impact of visual impairment on functional ability. Several studies have demonstrated that contrast sensitivity is useful for understanding the difficulties in performing everyday visual tasks faced by older people with essentially normal vision[39] and by patients with retinal disease.[40,41] Studies have shown that contrast sensitivity loss leads to mobility problems and difficulty recognizing signs or faces,[42] even when adjusted for loss

of acuity.[43]

The association of contrast sensitivity with functional ability argues in favor of including contrast sensitivity measurements in clinical trials. Although visual acuity is the most common primary visual outcome measure, several studies have included contrast sensitivity as a secondary outcome. Considering both visual acuity and contrast sensitivity when assessing the outcomes of clinical trials may provide a more complete picture of the effects of treatment on vision than either measure alone. Examples where contrast sensitivity has been used as a secondary outcome include the Optic Neuritis Treatment Trial,[44] the TAP study of photodynamic therapy for age-related macular degeneration (AMD),[45] and the ABC trial of bevacizumab for AMD.[46]

Methods

Common Contrast Sensitivity Tests

Traditional methods for measuring contrast sensitivity require relatively expensive and sophisticated equipment – typically a computer-controlled video monitor – and employ time-consuming psychophysical procedures. However, several simpler contrast sensitivity tests have been developed primarily for clinical use. These include the Functional Acuity Contrast Test[47] (FACT, replacement for the popular Vistech VCTS chart) and the CSV-1000,[48] sine-wave grating tests in chart form, and various low-contrast optotype tests such as the Lea test,[49] the Pelli–Robson letter chart,[17] the Melbourne Edge Test[50] and the Mars Letter Contrast Sensitivity Test.[51] Examples of three of the most commonly used clinical contrast sensitivity tests are illustrated in Fig. 13.2.

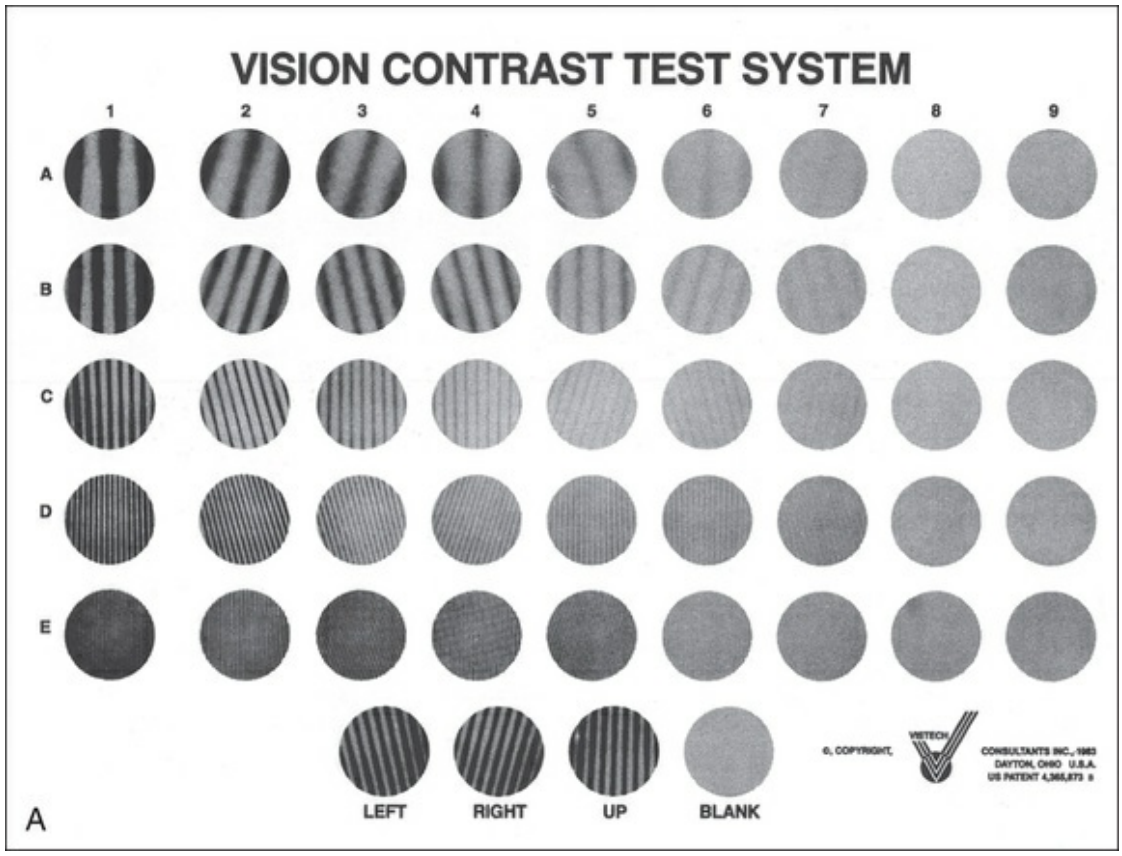
VISION CONTRAST TEST SYSTEM
1
2
3
4
5
6
7
8
9
A
B
C
D
E
LEFT
RIGHT
UP
BLANK
A

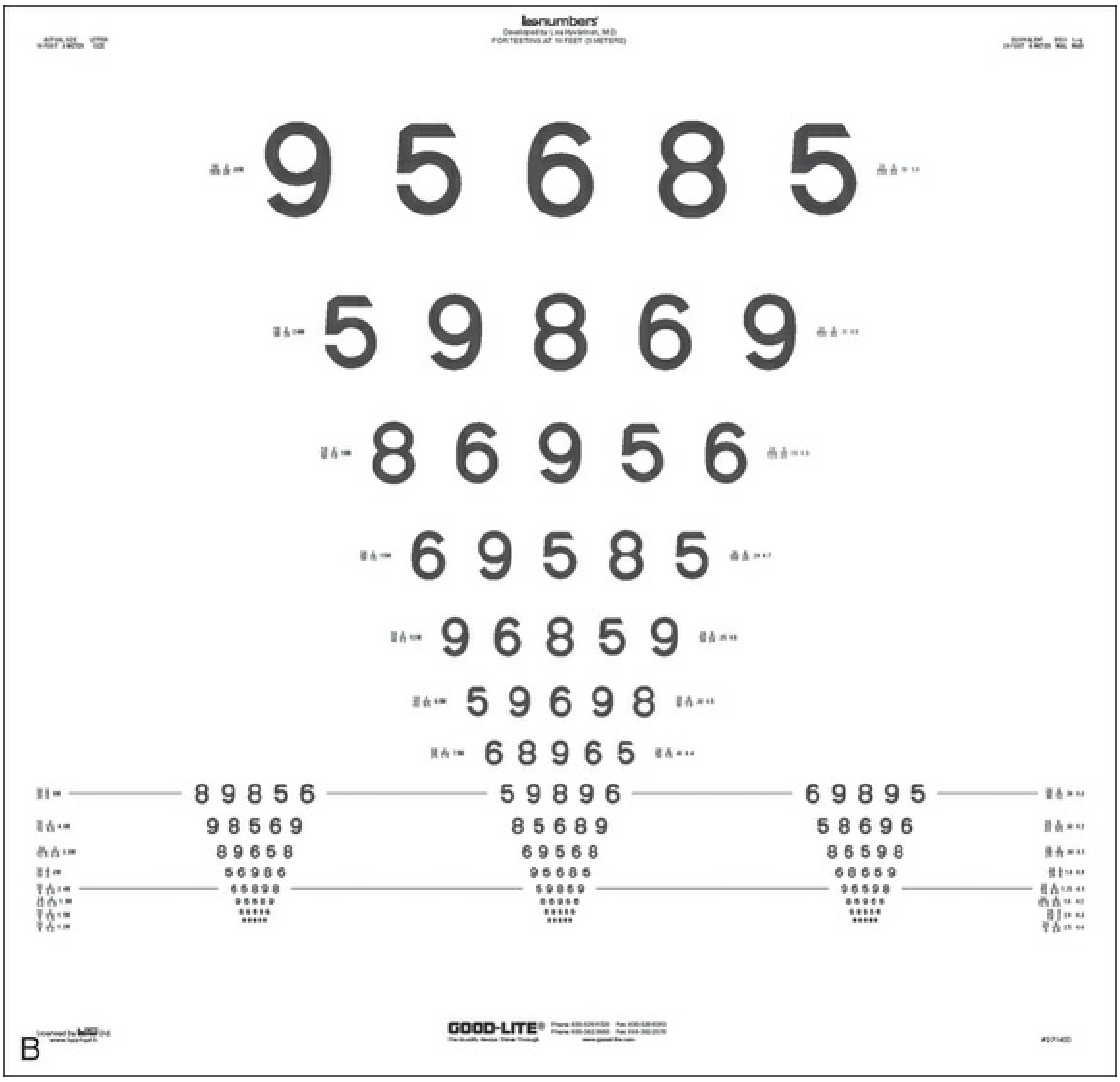
Developed by Lea Hyvärinen, M.D.
FOR TESTING AT 10 FEET (3 METERS)
9 5 6 8 5
5 9 8 6 9
8 6 9 5 6
6 9 5 8 5
9 6 8 5 9
5 9 6 9 8
6 8 9 6 5
8 9 8 5 6
5 9 8 9 6
6 9 8 9 5
9 8 5 6 9
8 5 6 8 9
5 8 6 9 6
8 9 6 5 8
6 9 5 6 8
8 6 5 9 8
5 6 9 8 6
9 5 6 8 5
6 8 6 5 9
GOOD-LITE
B

FIG. 13.2 Commonly used clinical contrast sensitivity tests. (A) Vistech VCTS 6500. (B) Lea numbers low-contrast acuity test. (C) Pelli–Robson letter sensitivity chart. (Panel A courtesy of Vistech Consultants, Dayton, OH. Panel B courtesy of Good-Lite, Streamwood, IL. Panel C reproduced with permission from Pelli DG, Robson JG, Wilkins AJ. The design of a new letter chart for measuring contrast sensitivity. Clin Vis Sci 1988;2:187–200.)

With the advent of smartphone and tablet-based vision testing, there has been a re-kindling of interest in clinical contrast sensitivity testing. High-end tablets have the spatial resolution to test contrast sensitivity but many of these new displays have too small a range of contrasts to cover both normal and impaired vision. Typically the tablet displays are only capable of reproducing contrasts of 1.5 log CS units (3%) or higher, whereas the normal contrast threshold is close to 2.0 log CS.[52]

Gratings Versus Optotypes

A thorough discussion of the relative merits of the various tests is beyond the scope of this chapter; however, a few salient points are worth noting. Various investigators disagree about whether measurement of an entire CSF is necessary or whether a single measure of contrast sensitivity is adequate for clinical purposes. Proponents of the sine-wave grating tests argue that visual dysfunction can cause reductions in contrast sensitivity over a limited range of spatial frequencies, which would be missed by more global measures of contrast sensitivity. On the other hand, advocates of global measures note that contrast sensitivities at specific spatial frequencies tend to be highly correlated with one another, and they maintain that overall changes in contrast sensitivity are clinically more important than subtle bumps and wiggles in the CSF. Data from large-scale studies of vision impairment indicate that global measures of contrast sensitivity are valuable predictors of difficulty in everyday life.[42]

Test Design and Procedure

In order to be useful, contrast sensitivity must be measured accurately and reliably. Many of the same principles of test design previously discussed for visual acuity tests apply to contrast sensitivity tests. Most important, the test should employ a criterion-free procedure, a uniform progression of contrasts, and an adequate number of trials at each contrast to make a reliable estimate of sensitivity. Most of the optotype tests conform to good design principles and produce reliable results, with the Mars test outperforming the very popular Pelli–Robson test.[53] Sine-wave grating charts tend to be less reliable because they have a limited number of trials to make measurements at several spatial frequencies.[54]

Some of the electronic acuity testing systems can also measure contrast sensitivity, including the Vision Test 2000 and FrACT. However, it is difficult to display a wide-enough range of contrasts to measure normal thresholds, and accurate calibration of the display monitor is critical. One study found that the computer-based test was less reliable than paper charts,[53] presumably due to problems generating low-contrast patterns with LCD displays.

Traditionally, accurate measurement of the CSF required many hundreds of trials and an hour or more of the patient's time. However, new adaptive test procedures have reduced the number of trials to 50–100 and the testing time to 5 minutes. The dramatic reduction in number of trials is accomplished by the introduction of a sophisticated Bayesian adaptive test procedure[55] that fits the patient's CSF data to a model with a restricted number of free parameters (four, in this case) and uses Bayesian statistics to select the optimum spatial frequencies and contrasts to fit those free parameters. The method works well if the underlying assumptions are met – that the CSF conforms to the model and the slope of psychometric functions is constant for patients and normal controls. Limited data collected to date supports these assumptions.[56]

It is still to be determined, however, whether the entire CSF provides more useful information about visual function than a single measurement of peak contrast sensitivity such as the Pelli–Robson letter chart.

Interpretation of Clinical Versus Statistical Significance: An Example From the Literature

One of the vexing problems with contrast sensitivity testing is how to interpret the clinical significance of test scores. After many decades of acuity testing, we have arrived at a consensus that a doubling of the MAR (increase of 0.3 LogMAR or 15 ETDRS letters) represents a meaningful change in acuity. Recent data from large population-based studies suggest that a doubling of contrast threshold (reducing sensitivity by 0.3 logCS units or six letters on the Pelli–Robson chart) has a comparable impact on task performance and quality of life.[39,42]

After several decades of laboratory investigation, contrast sensitivity testing is taking its place alongside visual acuity in clinical vision research. While early claims that contrast sensitivity would replace visual acuity proved to be exaggerated, this additional test does have an important role to play. Contrast sensitivity may not be particularly useful for differential diagnosis and screening, but its close association with everyday task difficulty has made it an important outcome measure for assessing treatment safety and efficacy.

References

1. NAS–NRC. Recommended standard procedures for the clinical measurement and specification of visual acuity. Report of Working Group 39. *Adv Ophthalmol*. 1980;41:103–148.
2. British Standards Institution. Specification for test charts determining distance visual acuity. London: British Standards House.
3. White JM, Loshin DS. Grating acuity overestimates Snellen acuity in patients with age-related maculopathy. *Optom Vis Sci*. 1989;66:751–755.
4. Sloan LL, Rowland WM, Altman A. Comparison of three types of test target for the measurement of visual acuity. *Q Rev Opthalmol*. 1952;8:4–16.
5. Ferris FL, Kassoff A, Bresnick GH, et al. New visual acuity charts for clinical research. *Am J Ophthalmol*. 1982;94:91–96.
6. Raasch T, Bailey I, Bullimore M. Repeatability of visual acuity measurement. *Optom Vis Sci*. 1998;75:342–348.
7. Flom MC, Bedell HE. Identifying amblyopia using associated conditions, acuity, and nonacuity features. *Am J Optom Physiol Opt*. 1985;62:153–160.
8. Kitchin JE, Bailey I. Task complexity and visual acuity in senile macular degeneration. *Aust J Optom*. 1981;64:235–242.
9. Strong G, Woo GC. A distance visual acuity chart incorporating some new design features. *Arch Ophthalmol*. 1985;102:44.
10. Schulze-Bonsel K, Feltgen N, Burau H, et al. Visual acuities "hand motion" and "counting fingers" can be quantified with the Freiburg visual acuity test. *Invest Ophthalmol Vis Sci*. 2006;47:1236–1240.
11. Dong LM, Hawkins BS, Marsh MJ. Consistency between visual acuity scores obtained at different test distances: theory vs observations in multiple studies. *Arch Ophthalmol*. 2002;120:1523–1533.
12. Sheedy JE, Bailey IL, Raasch TW. Visual acuity and chart luminance. *Am J Optom Physiol Opt*. 1984;61:595–600.
13. Sloan LL, Habel A, Feiock K. High illumination as an

auxiliary reading aid in diseases of the macula. *Am J Ophthalmol*. 1973;76:745–757.
14. Legge GE, Rubin GS, Luebker A. Psychophysics of reading. V. The role of contrast in normal vision. *Vision Res*. 1987;27:1165–1177.
15. Higgins KE, Jaffe MJ, Coletta NJ, et al. Spatial contrast sensitivity. Importance of controlling the patient's visibility criterion. *Arch Ophthalmol*. 1984;102:1035–1041.
16. Rubin GS. Reliability and sensitivity of clinical contrast sensitivity tests. *Clin Vis Sci*. 1988;2:169–177.
17. Pelli DG, Robson JG, Wilkins AJ. The design of a new letter chart for measuring contrast sensitivity. *Clin Vis Sci*. 1988;2:187–199.
18. Arditi A, Cagenello R. On the statistical reliability of letter-chart visual acuity measurements. *Invest Ophthalmol Vis Sci*. 1993;34:120–129.
19. Lovie-Kitchin JE, Whittaker SG. Prescribing near magnification for low vision patients. *Clin Exp Optom*. 1999;82:214–224.
20. Jose RT, Atcherson RM. Type-size variability for near-point acuity tests. *Am J Optom Physiol Opt*. 1977;54:634–638.
21. Rubin GS, Feely M, Perera S, et al. The effect of font and line width on reading speed in people with mild to moderate vision loss. *Ophthalmic Physiol Opt*. 2006;26:545–554.
22. Sloan LL, Brown DJ. Reading cards for selection of optical aids for the partially sighted. *Am J Ophthalmol*. 1963;55:1187–1199.
23. Baldasare J, Watson GR, Whittaker SG, et al. The development and evaluation of a reading test for low vision individuals with macular loss. *J Vis Impair Blind*. 1986;1986:785–789.
24. Legge GE, Ross JA, Luebker A, et al. Psychophysics of reading. VIII. The Minnesota Low-Vision Reading Test. *Optom Vis Sci*. 1989;66:843–853.
25. Mansfield JS, Legge GE, Bane MC. Psychophysics of reading. XV: Font effects in normal and low vision. *Invest Ophthalmol Vis Sci*. 1996;37:1492–1501.
26. Patel PJ, Chen FK, Da Cruz L, et al. Test–retest variability of

reading performance metrics using MNREAD in patients with age-related macular degeneration. *Invest Ophthalmol Vis Sci*. 2011;52:3854–3859.
27. Hahn GA, Penka D, Gehrlich C, et al. New standardised texts for assessing reading performance in four European languages. *Br J Ophthalmol*. 2006;90:480–484.
28. Laidlaw DA, Tailor V, Shah N, et al. Validation of a computerised LogMAR visual acuity measurement system (COMPlog): comparison with ETDRS and the electronic ETDRS testing algorithm in adults and amblyopic children. *Br J Ophthalmol*. 2008;92:241–244.
29. Scott IU, Ip MS, VanVeldhuisen PC, et al. A randomized trial comparing the efficacy and safety of intravitreal triamcinolone with standard care to treat vision loss associated with macular edema secondary to branch retinal vein occlusion: the Standard care vs Corticosteroid for Retinal Vein Occlusion (SCORE) study report 6. *Arch Ophthalmol*. 2009;127:1115–1128.
30. Aslam TM, Murray IJ, Lai MY, et al. An assessment of a modern touch-screen tablet computer with reference to core physical characteristics necessary for clinical vision testing. *J R Soc Interface*. 2013;10(84):20130239.
31. Bastawrous A, Rono HK, Livingstone IA, et al. Development and validation of a smartphone-based visual acuity test (Peek Acuity) for clinical practice and community-based fieldwork. *JAMA Ophthalmol*. 2015;133(8):930–937.
32. Perera C, Chakrabarti R, Islam FM, et al. The Eye Phone Study: reliability and accuracy of assessing Snellen visual acuity using smartphone technology. *Eye (Lond)*. 2015;29(7):888–894.
33. Bodis-Wollner I. Visual acuity and contrast sensitivity in patients with cerebral lesions. *Science*. 1972;178:769–771.
34. Regan D, Silver R, Murray TJ. Visual acuity and contrast sensitivity in multiple sclerosis-hidden visual loss: an auxiliary diagnostic test. *Brain*. 1977;100:563–579.
35. Bron AJ. Contrast sensitivity changes in ocular hypertension and early glaucoma. *Surv Ophthalmol*. 1989;33(Suppl.):405–406 [discussion 9–11].

36. Howes SC, Caelli T, Mitchell P. Contrast sensitivity in diabetics with retinopathy and cataract. *Aust J Ophthalmol*. 1982;10:173–178.
37. Rubin GS, Adamsons IA, Stark WJ. Comparison of acuity, contrast sensitivity, and disability glare before and after cataract surgery. *Arch Ophthalmol*. 1993;111:56–61.
38. Legge GE, Rubin GS. The contrast sensitivity function as a screening test: A critique. *Am J Optom Physiol Opt*. 1986;63:265–270.
39. West SK, Rubin GS, Broman AT, et al. How does visual impairment affect performance on tasks of everyday life? The SEE project. Salisbury Eye Evaluation. *Arch Ophthalmol*. 2002;120:774–780.
40. Lennerstrand G, Ahlström CO. Contrast sensitivity in macular degeneration and the relation to subjective visual impairment. *Acta Ophthalmol (Copenh)*. 1989;67:225–233.
41. Rubin GS, Legge GE. Psychophysics of reading. VI. The role of contrast in low vision. *Vision Res*. 1989;29:79–91.
42. Rubin GS, Bandeen-Roche K, Huang GH, et al. The association of multiple visual impairments with self-reported visual disability: SEE project. *Invest Ophthalmol Vis Sci*. 2001;42:64–72.
43. Rubin GS, Bandeen-Roche K, Prasada-Rao P, et al. Visual impairment and disability in older adults. *Optom Vis Sci*. 1994;71:750–760.
44. Beck RW, Cleary PA, Anderson MM Jr, et al. A randomized, controlled trial of corticosteroids in the treatment of acute optic neuritis. *N Engl J Med*. 1992;326:581–588.
45. Rubin GS, Bressler NM. Effects of verteporfin therapy on contrast on sensitivity: results from the Treatment of Age-related macular degeneration with Photodynamic therapy (TAP) investigation – TAP report no 4. *Retina*. 2002;22:536–544.
46. Patel PJ, Chen FK, Da Cruz L, et al. Contrast sensitivity outcomes in the ABC trial: a randomized trial of bevacizumab for neovascular age-related macular degeneration. *Invest Ophthalmol Vis Sci*. 2011;52:3089–3093.
47. Ginsburg A. Next generation contrast sensitivity testing.

Rosenthal BP, Cole R. *Functional assessment of low vision*. Mosby Year Book: St Louis; 1996:77–88.
48. Pomerance GN, Evans DW. Test–retest reliability of the CSV-1000 contrast test and its relationship to glaucoma therapy. *Invest Ophthalmol Vis Sci*. 1994;35:3357–3361.
49. Jarvinen P, Hyvarinen L. Contrast sensitivity measurement in evaluations of visual symptoms caused by exposure to triethylamine. *Occup Environ Med*. 1997;54:483–486.
50. Verbaken JH, Johnston AW. Population norms for edge contrast sensitivity. *Am J Optom Physiol Opt*. 1986;63:724–732.
51. Arditi A. Improving the design of the letter contrast sensitivity test. *Invest Ophthalmol Vis Sci*. 2005;46:2225–2229.
52. Kollbaum PS, Jansen ME, Kollbaum E, et al. Validation of an iPad test of letter contrast sensitivity. *Optom Vis Sci*. 2014;91(3):291–296.
53. Thayaparan K, Crossland MD, Rubin GS. Clinical assessment of two new contrast sensitivity charts. *Br J Ophthalmol*. 2007;91:749–752.
54. Pesudovs K, Hazel CA, Doran RM, et al. The usefulness of Vistech and FACT contrast sensitivity charts for cataract and refractive surgery outcomes research. *Br J Ophthalmol*. 2004;88:11–16.
55. Lesmes LA, Lu ZL, Baek J, et al. Bayesian adaptive estimation of the contrast sensitivity function: the quick CSF method. *J Vis*. 2010;10(3):17.1–21.
56. Dorr M, Lesmes LA, Lu ZL, et al. Rapid and reliable assessment of the contrast sensitivity function on an iPad. *Invest Ophthalmol Vis Sci*. 2013;54(12):7266–7273.

14

Visual Fields in Retinal Disease

Rajeev S. Ramchandran, Amit A. Sangave, Steven E. Feldon

Introduction

Visual field testing helps correlate structural changes in the retina or elsewhere in the visual pathway with deficits in function. For example, AM was a 70-year-old woman diagnosed as having an old central retinal vein occlusion (CRVO) in the left eye and an epiretinal membrane in both eyes. She also had been treated for elevated intraocular pressure. Fluorescein angiography of the left eye showed shunting vessels around the optic nerve head, thought to be consistent with the old vein occlusion. However, progressive bilateral visual field loss (Fig. 14.1) over 2 years suggested the need for further investigation. A computed tomography (CT) scan

demonstrated a large subfrontal meningioma compressing both optic nerves (Fig. 14.2).

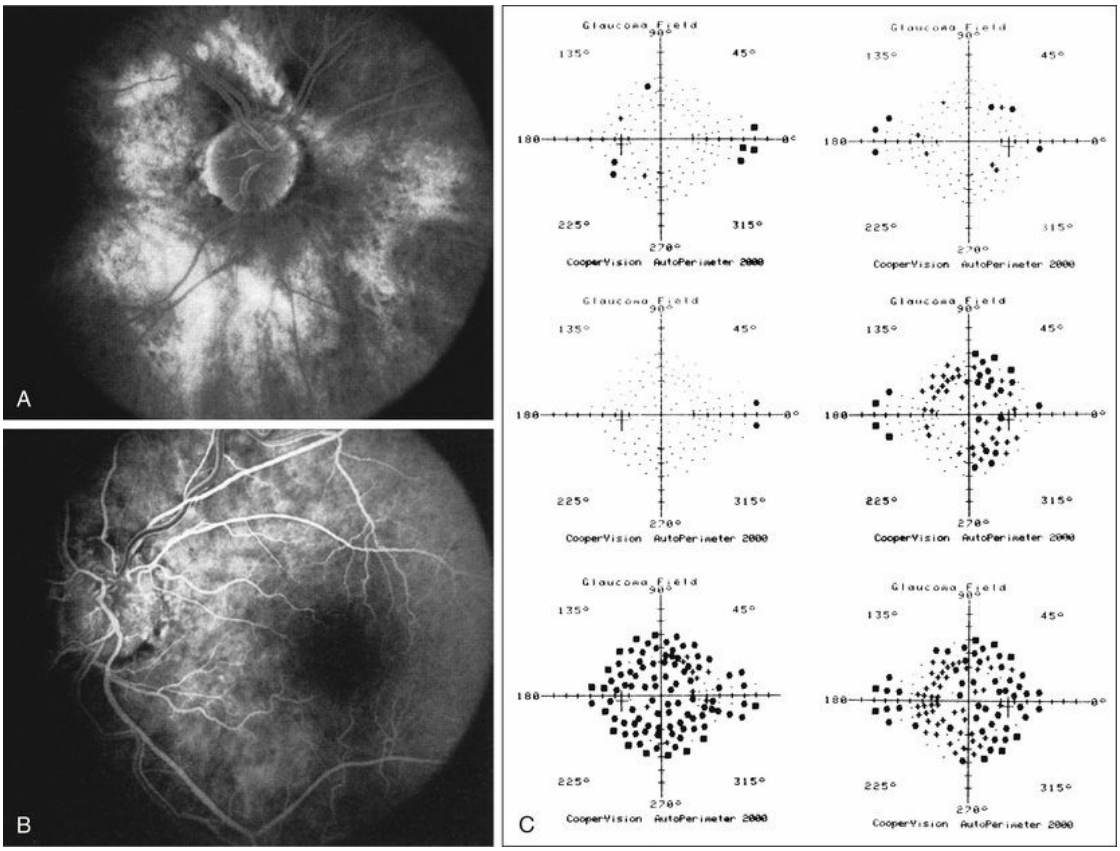

FIG. 14.1 (A,B) Fluorescein angiograms of a 70-year-old woman who has had progressive loss of vision in both eyes over 2 years. She has controlled ocular hypertension and surface-wrinkling retinopathy. The history of an old central retinal vein occlusion in the left eye is supported by the slightly dilated and tortuous retinal veins and the multiple shunting capillaries on the surface of the disc (B). (C) Progressive field loss, documented in both eyes over 3 years, is inconsistent with the ophthalmoscopic appearance. A computed tomographic scan was ordered, the results of which are shown in Fig. 14.2.

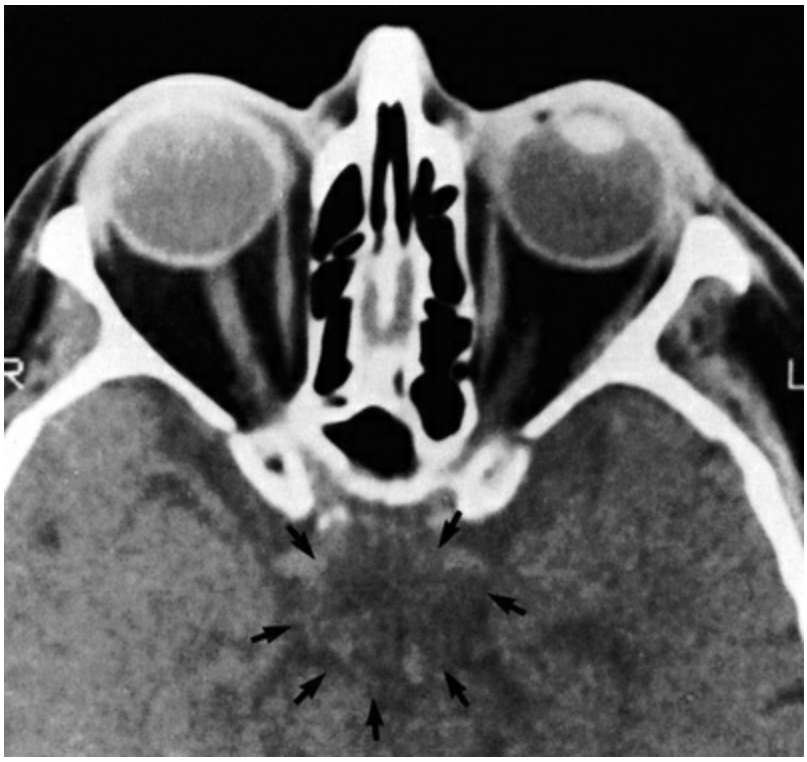

FIG. 14.2 Computed tomographic scan from the patient described in Fig. 14.1 demonstrates a large subfrontal meningioma (arrows) with bilateral optic nerve compression. Surgical resection improved sensorium but not vision.

Visual field tests can be qualitative or quantitative. They span multiple formats, from the simplest confrontation field or Amsler grid to the most advanced quantitative kinetic, static, and microperimetry. For all visual field tests, reliability and reproducibility are important. There are currently three main uses for visual field tests in patients with retinal pathology: (1) to determine the current level of visual field loss and monitor progression; (2) to evaluate the effects of treating retinal pathology on visual function; and (3) to correlate functional and structural changes in the retina.

This chapter reviews the use of visual fields and the principles of perimetry relevant to retinal disease. Visual field defects corresponding to common retinal diseases are described, with an emphasis on clinical situations for which perimetry is useful diagnostically. The value of specialized visual field testing in clinical research is also reviewed.

Principles of Perimetry

The Island of Traquair

The single most important concept in understanding the visual field is depicted by the island of Traquair, which is defined as a "hill of vision" surrounded by a "sea of blindness."[1] The shape of the normal visual field is oval. There is decreasing sensitivity with increasing eccentricity in the field, as the elevation corresponds to the sensitivity of the field, and the flat plane corresponds to location within the field (Fig. 14.3). From the point of fixation, the field extends 60° superiorly, 60° nasally, 70–75° inferiorly, and 100–110° temporally. The blind spot is represented by a hole in the "hill" about 15° temporal to the foveal "peak."

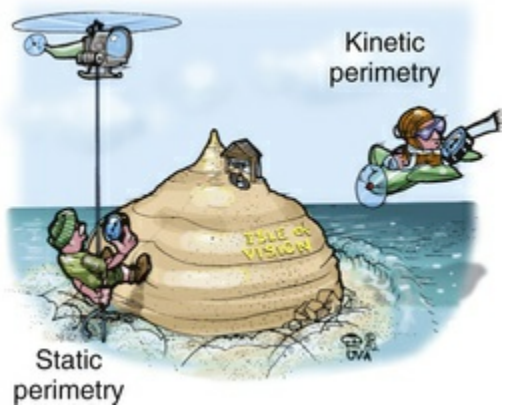

FIG. 14.3 The "island," or "hill of vision," proposed by Traquair is surrounded by a "sea of blindness." The height of the island represents increasing sensitivity. Using kinetic perimetry, the island is intercepted by a moving target of fixed size. Using static perimetry, a target's visibility is increased in size or luminosity until it descends on to the island. The blind spot located 15° temporal to fixation is absolute, creating a small "well" in the sensitivity contour. (Courtesy of Steven Newman, MD.)

Perimetric tests have been developed that systematically measure the level of light sensitivity in the visual field. Two basic types exist: kinetic perimetry and static perimetry. In kinetic perimetry a target is moved from outside the potentially seeing area toward the seeing area until it is detected. In static perimetry a target located within a

potentially seeing area can be increased in size or intensity until it is detected. With either method a region of vision can be defined in relation to a test stimulus of given size, hue, brightness, and uniform level of background illumination. For instance, under standardized conditions, the central visual field of about 30° can be mapped with a moving white target of 3 mm at a distance of 2 meters.[2]

Methods of Visual Field Testing

There is no single best test for the evaluation of visual fields in retinal disease. Depending on the location and extent of the disease, the examiner must choose from an ever-increasing selection of sensitive qualitative and quantitative perimetric techniques.

Qualitative Techniques

Vision may be extremely poor in many patients with widespread visual dysfunction resulting from retinal disease. In such instances visual fields may be obtained only by confrontation testing. However, this technique also may be used to detect even subtle relative field defects and scotomas. Confrontation testing is performed with the examiner facing the patient, usually at about arm's length. The peripheral vision of the patient is evaluated in relation to that of the examiner. To test the patient's right eye, the examiner occludes the right eye and aligns the left eye so that both patient and examiner share a common visual axis. The examiner then moves the hand or test object from outside the visual field toward fixation. Relative preservation of peripheral vision can be established if the examiner places both hands or two test objects in different seeing quadrants of the patient and asking the patient to identify the clearer object. Central visual function is estimated by having the patient look toward the examiner's nose or, if vision is very poor, toward the direction of the examiner's voice. The patient describes which parts of the examiner's face are missing or most clearly seen. Results are recorded either descriptively or with a simple drawing.

Although the tangent screen can be used quantitatively, it is most

effective as a qualitative tool for estimation of visual loss in the central field. A 1-meter screen can be used to evaluate suspected midperipheral field loss, but a 2-meter screen is essential if the intent is to map central scotomas or the physiologic blind spot. The sensitivity of the test can be increased with the use of smaller test objects and by seeking subjective responses about the quality (e.g., blurry, dim, flickering, faded) of seen targets. Most important, conical visual field constriction of retinal origin can be readily distinguished from tubular fields of nonorganic visual loss by using large test objects at varying distances. With a doubling of the distance to the screen, there must be a doubling in size of the test object used. Although not routinely available or performed in a retinal specialist's office, no other form of perimetric evaluation is as effective in discriminating real from fictitious visual field constriction (Fig. 14.4).

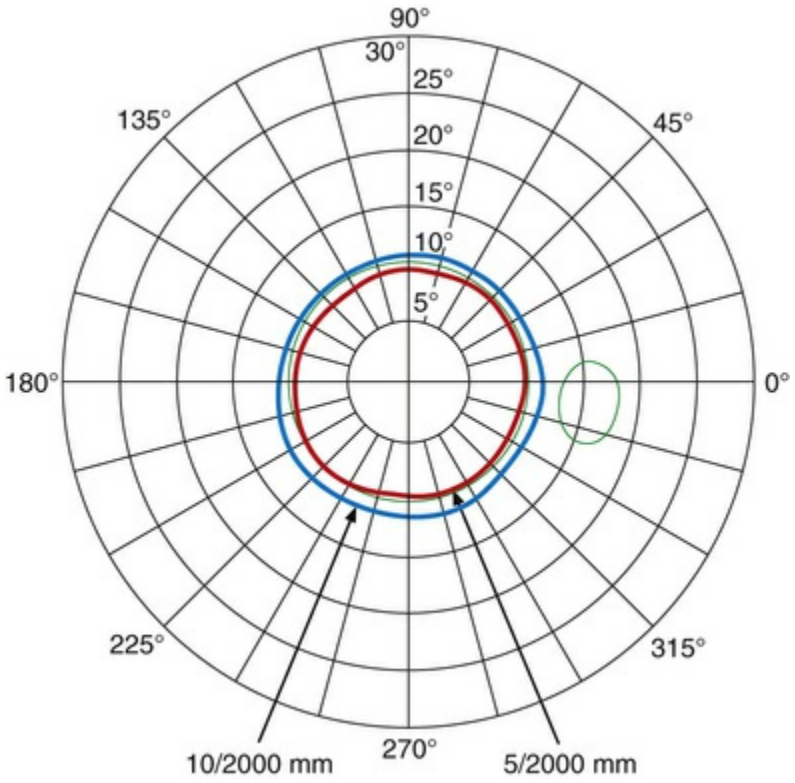

FIG. 14.4 A tangent screen field from a hysterical or malingering patient fails to show expansion of the visual field with doubling of both test object size and distance.

The Amsler grid is another extremely important qualitative tool for the evaluation of central vision. It is routinely used in regular self-monitoring of vision between eye exams by patients with macular degeneration or other progressive macular pathology to detect early signs of disease progression. In its original form, the patient fixates on the center dot of a white grid on a black background from a distance of 35.5 cm (14 inches) (Fig. 14.5). The patient describes the appearance of the grid pattern, especially in regard to missing areas (scotomas) and distortion (metamorphopsia). The sensitivity for detection of macular lesions can be increased with the use of red grids with or without the use of crossed polarizing lenses (Fig. 14.6) to decrease the light entering the patient's eye.[3]

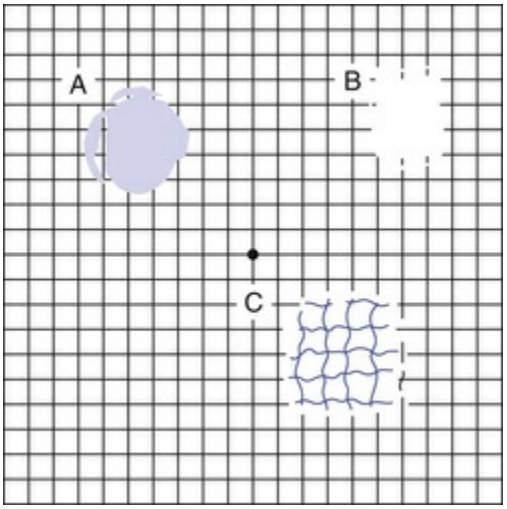

FIG. 14.5 The Amsler grid is viewed at 35.5 cm (14 inches), using the central dot for fixation. Regions of metamorphopsia (C), scotoma (B), and blur (A) are noted.

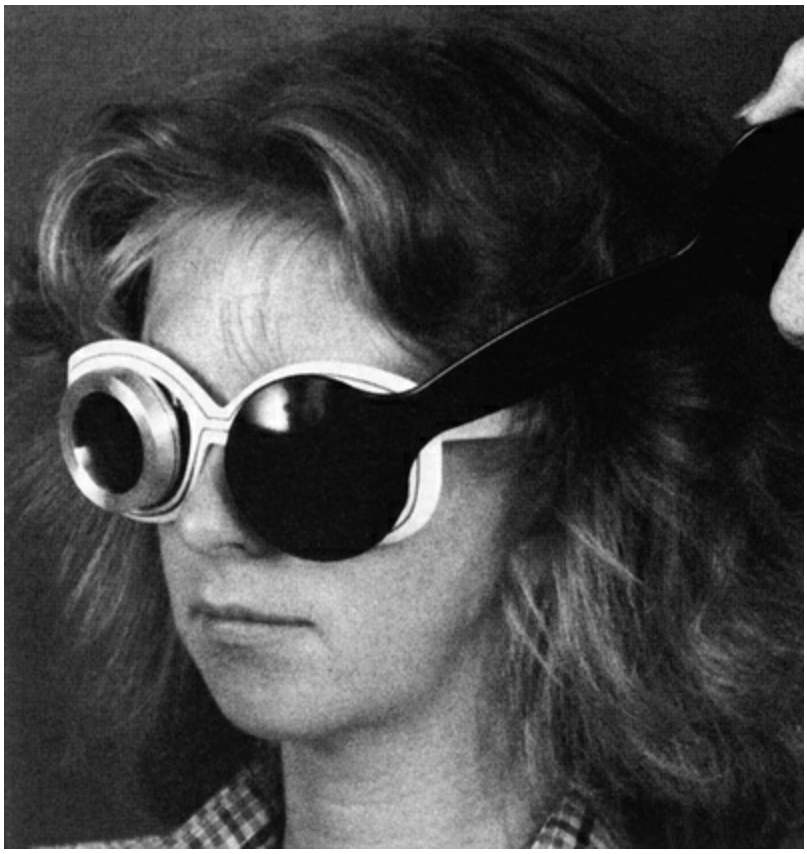

FIG. 14.6 The sensitivity of the Amsler grid test can be increased by using red lines on a black background rather than black or white lines on contrasting backgrounds. Further sensitivity may be achieved by using crossed-polarizing glasses that decrease the amount of light entering the eye. (Courtesy of Alfredo Sadun, MD.)

Quantitative Techniques

Quantitative techniques of perimetry are utilized for both diagnosis of disease and following the course of disease. Documentation of visual recovery in eyes with retinal pathology after treatment, such as retinal detachment surgery, laser therapy, antiinflammatory and anti-vascular endothelial growth factor drug therapy is becoming an important aspect of patient care. Also, quantitative records are invaluable for achieving new insights into the types of visual disturbances found in various retinal diseases.

Both Goldmann and Tübinger perimetry require examiners with a high degree of training. The Goldmann visual field (GVF) perimeter uses a kinetic strategy, although static perimetry is

possible (Fig. 14.7). It is especially useful for monitoring peripheral visual field loss and large scotomas. It has limited capabilities for the evaluation of small central scotomas. The Tübinger perimeter uses a static strategy. It is a sensitive but time-consuming less used technique for identifying small or large relative field defects once the approximate region of the field loss has been determined. Laborious Tübinger profiles are usually made only across a single meridian of the visual field, limiting its screening capabilities (Fig. 14.8).

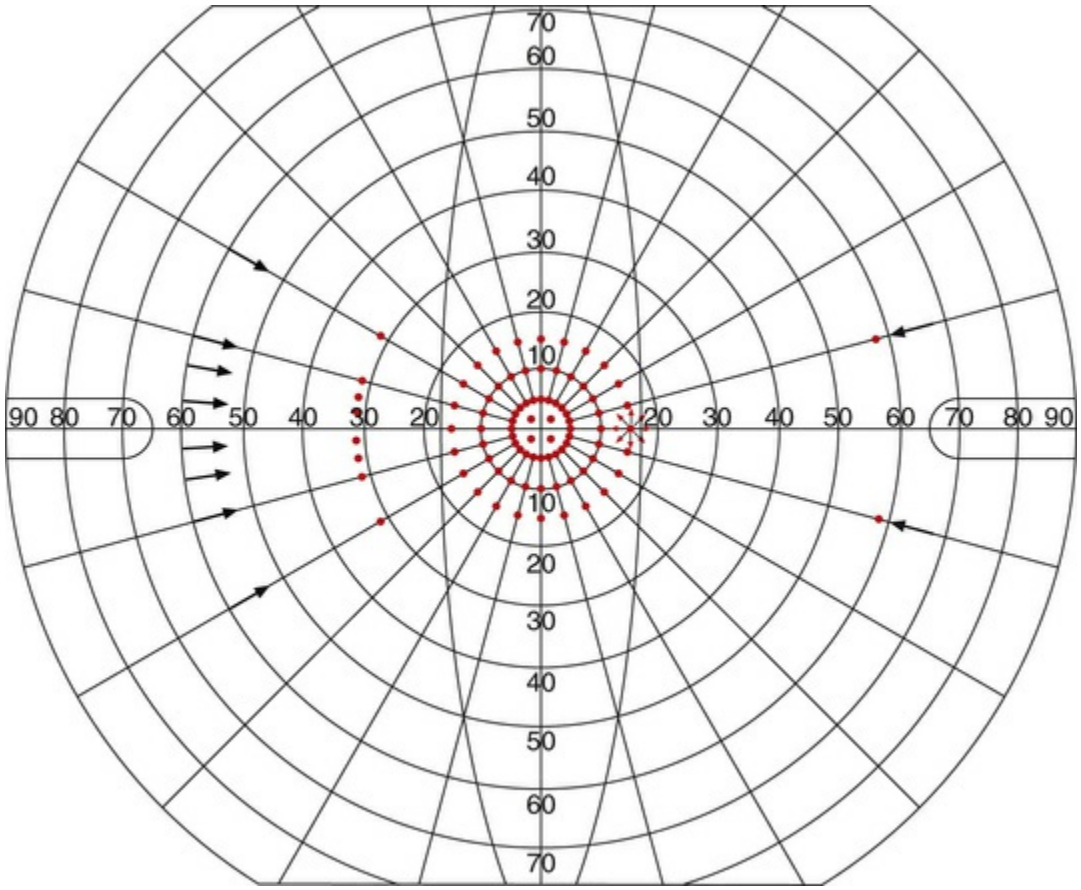

FIG. 14.7 The Goldmann visual field strategy developed by Armaly and Drance uses kinetic targets (*arrows*) to map the peripheral isopters and suprathreshold static targets (*dots*) to check central visual field function. (Reproduced with permission from Rock WJ, Drance SM, Morgan RW. Visual field screening in glaucoma: an evaluation of the Armaly technique for screening glaucomatous visual fields. Arch Ophthalmol 1973;89:287–90.)

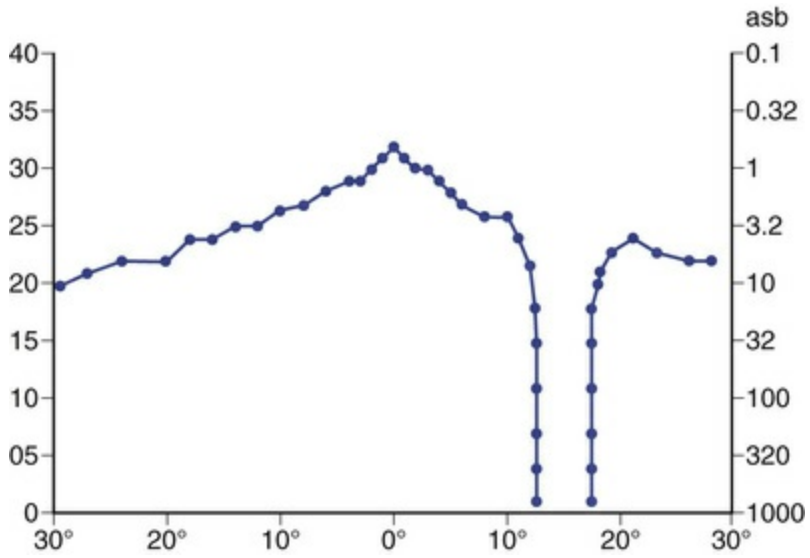

FIG. 14.8 The Tübinger perimeter produces a static profile of visual sensitivity through any chosen meridian. (Reproduced with permission from Harrington DO. The visual fields: a textbook and atlas of clinical perimetry. St. Louis: Mosby, 1981.)

Quantitative perimetry received a tremendous boost with the advent of automated, computerized methodology. Suprathreshold automated visual screeners, such as the Fieldmaster 101 and the Dicon units, did much to popularize visual field testing in the ophthalmic community. Pseudothreshold algorithms were developed for these machines to enhance their quantitative capabilities.[4] However, threshold perimeters, such as the Octopus and the Humphrey visual field (HVF) analyzer, surpassed the capabilities of even the Tübinger instrument. Automated, quantitative threshold perimetry is ideal for the evaluation of retinal disease. Randomized sequences for stimulus presentation within the visual field enhance the possibility of detecting small or irregular field defects. Density of points can be varied to characterize fully field losses that are either focal or diffuse. Although the HVF has the ability to test 60° of visual field, this protocol is very time-consuming. The standard protocols used are the 30-2, 24-2, and 10-2, which measure the central 30°, 24°, and 10° respectively. The choice of field is based on the region of pathology in the visual field. The dash 2 (-2) refers to protocol 2, the analysis of points on either side of the vertical and horizontal meridians rather than just on the vertical and horizontal axis as performed in protocol 1. Thus, both the 24-2 and 30-2 protocols test points 3°

from the horizontal and vertical axis as well as points at 6° intervals beyond this region in the central 24° or 30° respectively. A 10-2 protocol tests points 1° from the horizontal and vertical meridian as well as points at 2° beyond this region in the central 10° and thus is more sensitive for detecting subtle field losses in the macular region.[5]

Algorithms such as the Swedish interactive threshold algorithm (SITA) were developed to increase efficiency and decrease variability in the standard Humphrey strategy. SITA uses normative and real-time data from patients during the test to update estimates of thresholds and adjust presentation times of stimuli continually. Short-wavelength automated perimetry (SWAP) is a variant on the usual white light stimulus used in standard threshold testing. SWAP isolates the S-cone system (blue–yellow pathway), using a blue stimulus on a yellow background. The presence of normal, age-corrected retinal sensitivity values increase the utility in clinical testing.[6,7] Care must be taken when using this technique to correct for chromatic filtering effects from the crystalline lenses.[8] Longer test duration, increased variability, and learning effects make SWAP most applicable to conditions for which early detection has important therapeutic implications and requires careful supervision of the patient by the tester during visual field testing.[9] In each case, the ability to map statically determined threshold retinal sensitivity directly on to the retina with automated quantitative threshold perimetry with a high degree of accuracy is important in the evaluation of retinal disease.[10] This ability has further been refined by techniques such as microperimetry.

Microperimetry

Macular diseases may be degenerative, hereditary, traumatic, toxic, or inflammatory. All are characterized by central visual field defects or distortion, which may be small enough to be undetected without detailed perimetry or Amsler grid testing. Ancillary psychophysical tests of visual acuity, contrast sensitivity, and color vision may be helpful in determining visual function.

Microperimetry is especially helpful for evaluating and following

macular disease. It is used to correlate anatomic pathology with function of the visual system by integrating fundus imaging and computerized threshold perimetry at specific locations in the fundus. One technique of microperimetry uses a scanning laser ophthalmoscope (SLO) (e.g., Rodenstock, Ottobrunn, Germany) to plot field defects within geographically defined regions of the retina. A modulated helium–neon laser beam of variable intensity (0–21 dB) at 633 nm projects stimuli on to the retina during ophthalmoscopy performed with an infrared diode laser at 780 nm.[6,11] Another type of microperimetry is Micro Perimeter 1 (MP 1, Nidek Instruments, Padua, Italy) which uses an infrared fundus camera that provides a 45° view and performs perimetry using a liquid crystal display with special software. The MP-1 allows for eye tracking and real-color fundus image acquisition. Images from other tests, such as fluorescein angiogram, can be overlaid onto the microperimetry, which is not possible in SLO microperimetry. Moreover, as SLO microperimetry is also restricted to red laser light, comparison with standard perimetry or MP-1 is difficult.[11]

Both the SLO and MP-1 microperimetry devices allow for kinetic and static perimetric testing of the macula and permit simultaneous observation of the retina during perimetric testing. Similar to conventional perimetry, stimulus sizes range from Goldmann size I to V and the central 15–20° of visual field can be tested in both devices. However, the MP-1 allows for a slightly larger field for testing. Rohrschneider and colleagues determined that for patients with retinal disease both the SLO and MP-1 microperimetry devices delivered comparable results, with the SLO devices providing better-resolution fundus images and the MP-1 providing better fixation analysis with more accurate real-time image alignment.[12] As efforts to correlate better anatomic and functional changes in the retina have advanced, more refined devices are being developed that combine techniques of visualizing the ultrastructure of the retina, such as three-dimensional spectral optical coherence tomography (OCT) and adaptive optics, with corresponding perimetric functional assessment.[13,14] Next generation microperimetric devices (e.g., Nidek MP-3) also feature increased automation, which should further reduce operator-related variability.

Other Methodologies of Visual Field Testing in Retinal Disease

Perimetric tests are being developed to screen for early changes in retinal diseases affecting the macula. Rarebit testing, or the matching of test targets to receptive field sizes, has been used in select studies to assess central functional vision in a variety of retinal diseases. A compact rarebit screening test has been developed and tested in patients with age-related macular degeneration (AMD).[15] Preferential hyperacuity perimetry (PHP) is another screening device for detecting early visual field changes in retinal disease. PHP uses the phenomenon of hyperacuity (Vernier acuity), the ability to discern differences in the spatial location of two or more stimuli, to test one's ability to identify local distortion of a series of dotted vertical or horizontal signals. The responses are correlated to a normative database and scored to generate a probability of deviation from normal. PHP has been found to be more sensitive than Amsler grid testing for the early detection of exudative AMD in patients with intermediate AMD. Home monitoring devices using PHP have been developed and evaluated for more widespread clinical use, which allow for convenient and timely early detection of progression of AMD.[16] However, as with any repeated test used to follow changes over time, consistency in choice of testing method is important to accurately characterize and follow the progression of retinal diseases.

Reliability and Reproducibility of Visual Field Tests

Anatomic, physiologic, and psychologic factors unrelated to the pathology in question can significantly affect measurement of the visual field. The nose, brow, and lid may constrict the nasal and superior fields artifactually. Numerous variables pertaining to both the patient and the environment must be controlled during testing if meaningful results are to be obtained. Even so, considerable short-term variability must be taken into account. Box 14.1 outlines a list of factors that must be controlled for optimal determination of the visual field. Perimetric testing has a degree of subjectivity and

therefore ultimate reliability and repeatability of the testing rely on the patient and the test-giver.[17] Patients with retinal disease may be more prone to variability in testing over time, which can influence the validity of test results. Seiple and colleagues[18] demonstrated that for patients with retinitis pigmentosa (RP) the results of repeated HVF testing performed at different time points were two times more variable when compared to similar fields performed in normal controls despite controlling for disease progression. Microperimetry has the added advantage of real-time retinal surface monitoring with eye tracking to correct for eye movements during testing. Weingessel and colleagues demonstrated good interexaminer and intraexaminer reliability of microperimetry using the MP-1 device in eyes with and without retinal disease.[19]

Box 14.1

Variables Affecting Measurement of the Visual Field

- Environmental
- Illumination
- Equipment
- Examiner
- Technique
- Ocular
- Retinal adaptation
- Refractive state
- Media
- Pupil size
- Global
- Age

- Fixation
- Reaction time
- Fatigue

Perimetry in Specific Retinal Diseases

The visual fields tests described are used in patients with retinal disease to assess and catalog progression of functional visual field loss, to determine the outcomes of treatment on visual function, and to correlate functional and structural changes in the retina.

Retinal Dystrophies

Retinitis Pigmentosa

Visual fields have traditionally been used to characterize and monitor the progression of visual field loss in retinitis pigmentosa (RP). However, some caution should be exercised when interpreting fields in ill RP patients. A recent study by Bittner[20] suggested that episodic decline in general health was correlated with simultaneous decline in visual field (VF) that was not representative of the true area of visual field loss. The earliest field defect in RP is reported to be a group of isolated scotomas 20–25° from fixation.[2] Eventually these isolated defects coalesce into a "ring scotoma" affecting the midperiphery of the visual field. Usually the peripheral field loss progresses and leaves a small, central island of vision. Eventually, complete visual loss may occur (Fig. 14.9).

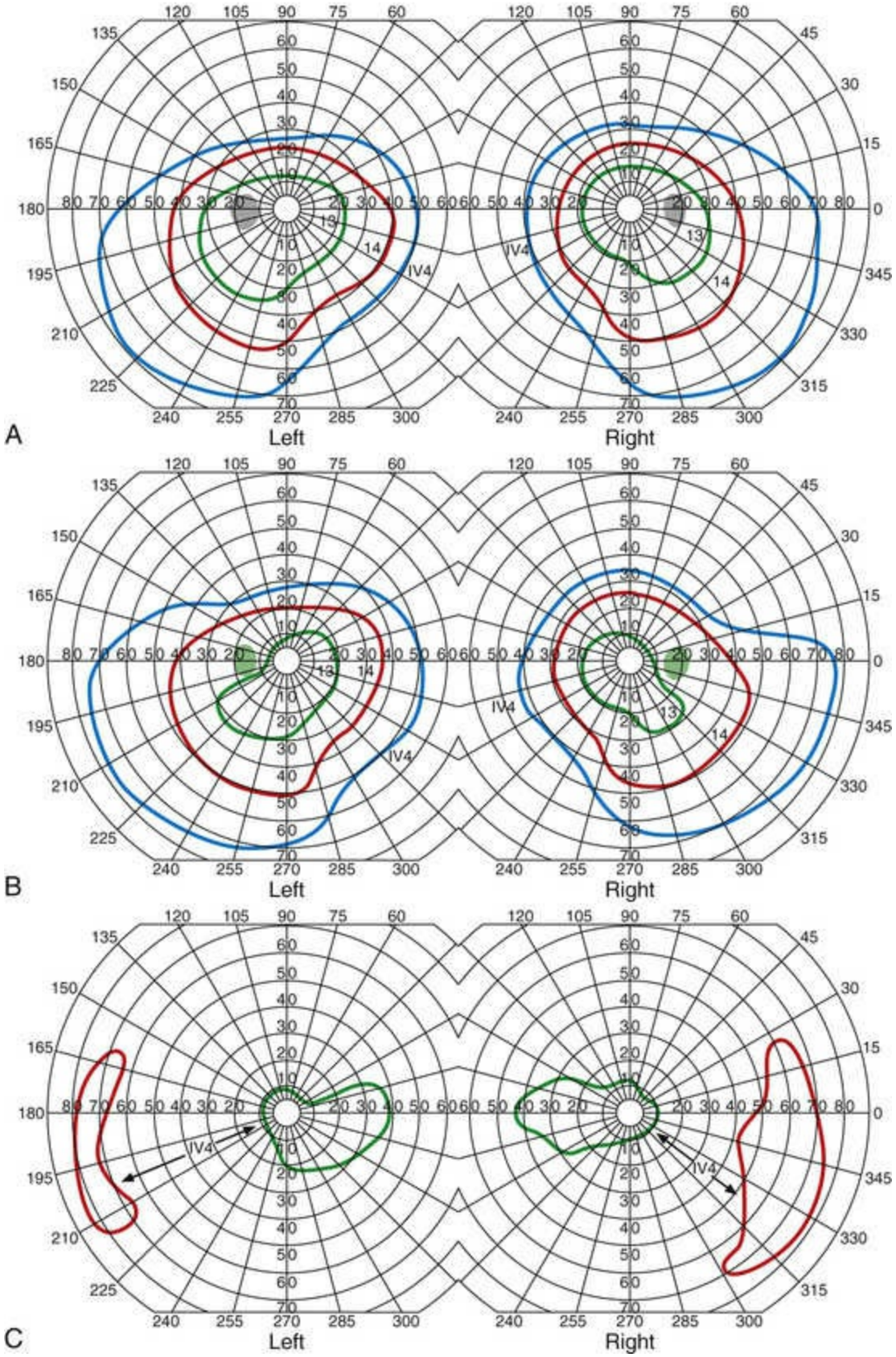

FIG. 14.9 Classic development of a ring scotoma with focal sparing of a peripheral temporal island seen in retinitis pigmentosa and cone–rod dystrophies. (A)

Progressive depression of peripheral visual field in a patient with cone–rod degeneration at presentation. (B) Same patient after 1 year. (C) Same patient during fourth year of follow-up. (Reproduced with permission from Krauss HR, Heckenlively JR. Visual field changes in cone–rod degenerations. Arch Ophthalmol 1982;100:1784–90.)

Characterization and comparison of specific patterns of visual field loss in genotypically and phenotypically different forms of RP such as X-linked, dominant, pericentral, and Usher syndrome, using GVF perimetry have been attempted.[21–24] Association of the degree of visual field loss with different genotypes in syndromic associations of RP, including Bardet–Biedl syndrome 1, has also been studied.[25]

HVF measurements have been correlated with contrast sensitivity in RP and were found to be a sensitive predictor for central visual function in advanced RP.[26,27] Perimetry has been used to test outcomes of treatments for varieties of RP, including fundus albipunctatus.[28] Visual fields have also been used in correlating photoreceptor anatomy and visual function in RP. Decreased retinal sensitivity on electroretinogram has been linked to visual field loss demonstrated by perimetry in RP.[29] Changes in GVF, HVF, and microperimetry have been correlated with anatomical changes at the cellular level using OCT and autofluorescence to identify abnormal photoreceptor morphology and damage to retinal pigment epithelial (RPE) cells.[30–38]

Other Retinal Dystrophies

Perimetric changes occur in a variety of retinal dystrophies. Cone dystrophy produces progressive symmetric to slightly asymmetric central visual loss. Autofluorescence has been shown to correlate with GVF in cone and cone–rod dystrophies.[39] The visual fields demonstrate central scotomas with relative sparing of the fovea. A central or paracentral scotoma can also be seen in Stargardt disease (Fig. 14.10). However, microperimetry identifies two types of scotoma in patients with Stargardt disease. In one type there is a dense ring scotoma associated with stable fixation. In the second type there is a dense central scotoma associated with fixation shift. The second type is also correlated with poorer acuity.[40] Another

recently described microperimetric phenomenon in Stargardt disease is longitudinal decline in retinal sensitivity observed over a 2-year follow-up period.[41] Such microperimetric monitoring could be important in short-term follow-up as a quantitative indicator of the rate of disease progression.

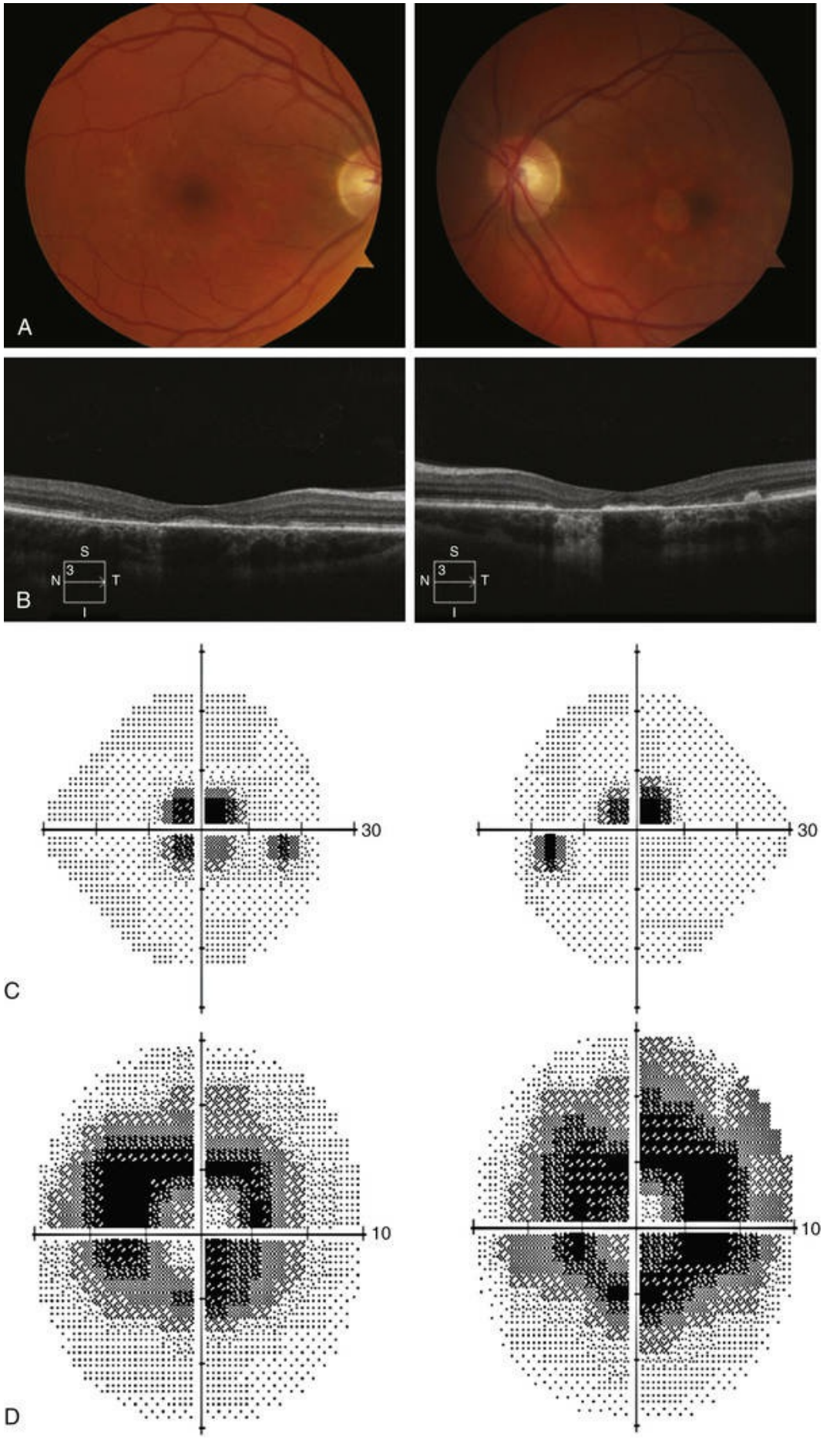
A
B
S
N
3
T
I
S
N
3
T
I
C
30
30
D
10
10

FIG. 14.10 (A) Fundus photos of a 34-year-old female patient with Stargardt disease and visual acuity of 20/30 OD and 20/40 OS. (B) OCT with disruption of the IS–OS junction (ellipsoid zone) in the same patient and (C) corresponding 24-2 HVF and (D) 10-2 HVF with paracentral scotomas corresponding to structural changes seen on imaging.

In gyrate atrophy of the retina and choroid, a rare tapetoretinal degeneration caused by an inborn error of ornithine aminotransferase activity, there is constriction of the visual field corresponding to the progressive peripheral retinal degeneration with scalloped margins (Figs. 14.11 and 14.12). Constricted GVF tests are also seen in Bietti crystalline dystrophy.[42] Correlations between HVF sensitivity and multifocal electroretinogram (mERG) have been documented for eyes with central areolar choroidal dystrophy and North Carolina macular dystrophy.[43,44] Functional changes as evidenced by perimetry and mERG have also been correlated with morphologic changes documented by fundus autofluorescence (FAF) in adult vitelliform macular dystrophy.[45]

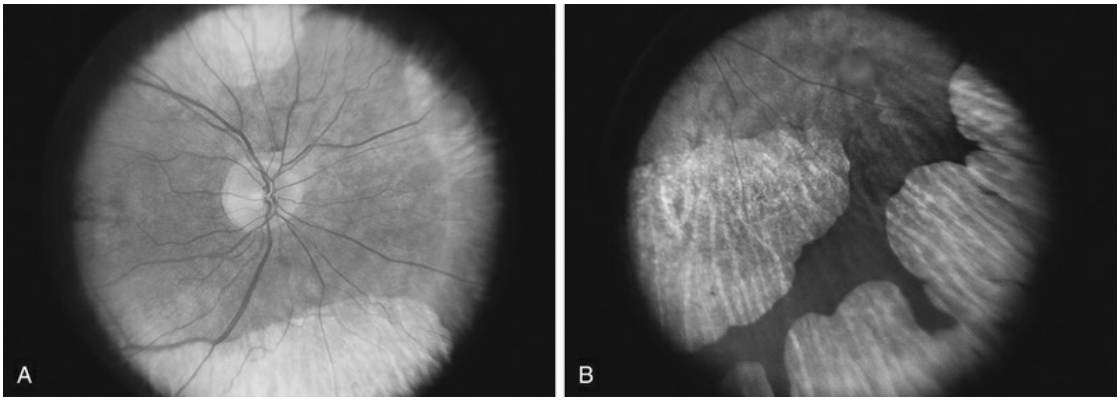

FIG. 14.11 Central (A) and peripheral (B) fundus appearance of a patient with gyrate atrophy of the retina. The visual field of this patient is shown in Fig. 14.12.

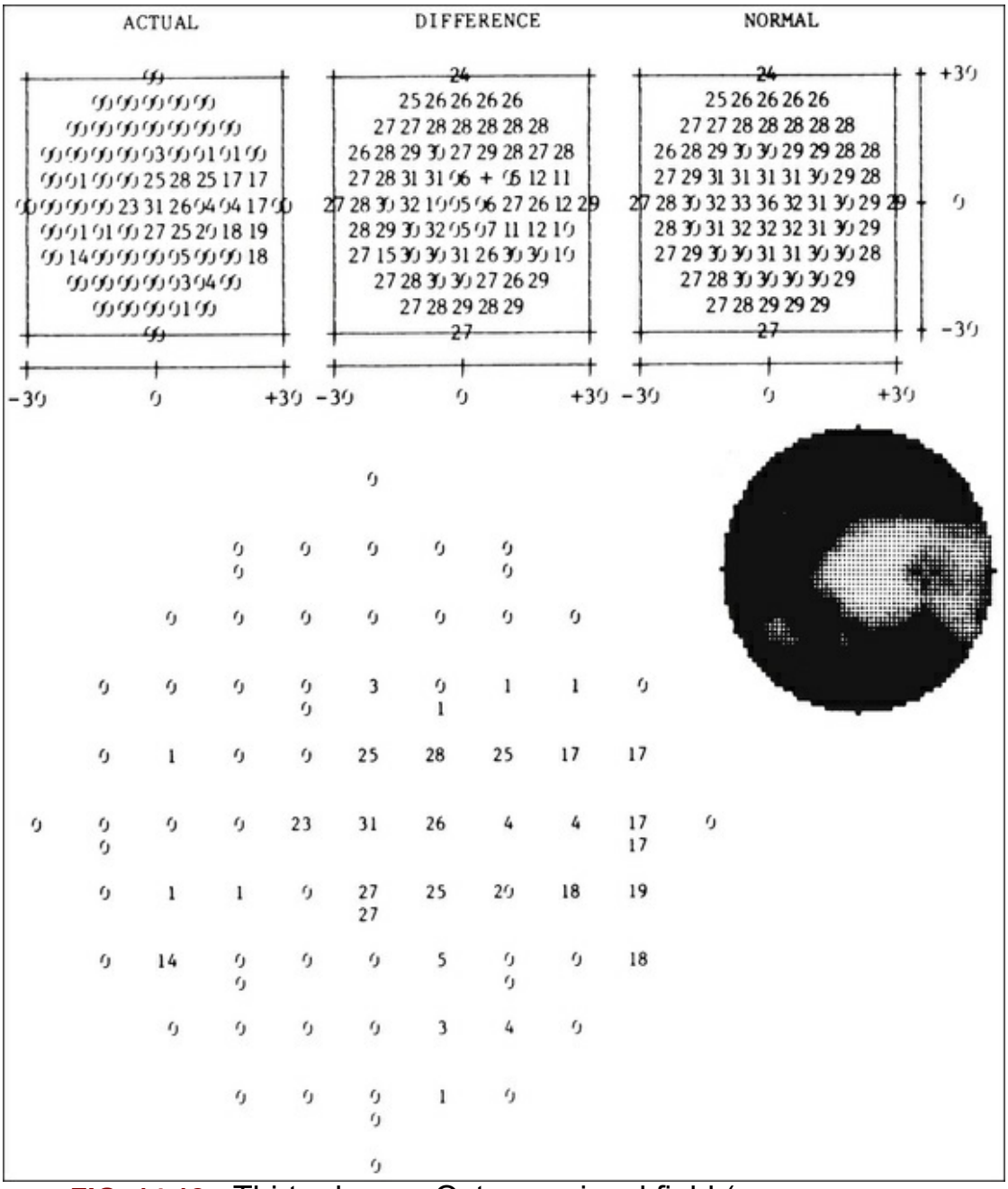

FIG. 14.12 Thirty-degree Octopus visual field (program 31) demonstrates marked peripheral constriction, with relative sparing in the centrocecal region. In addition, there are a few more peripheral islands of reduced sensitivity. (Reproduced with permission from Feldon SE. Computerized perimetry in selected disorders of the retina. In: Whalen WR, Spaeth GL, editors. Computerized visual fields: what they are and how to use them. Thorofare, NJ: Slack; 1985.)

Diabetic Retinopathy

The diffuse retinal ischemia associated with diabetic retinopathy would seem to make visual field assessment an ideal method for follow-up of the disease, but progressive field deterioration in diabetics does not necessarily correlate with changes in retinopathy.[46] Visual fields are not routinely used to evaluate this retinal disease, even though field defects may exist in the absence of observable retinopathy. Roth[47] found central field defects in about 40% of eyes without visible retinopathy and in all diabetic patients with retinopathy. Using frequency-doubling perimetry, Parravano[48] confirmed retinal impairment in type I diabetics that correlated with glycemic control, without evidence of visible retinopathy. SWAP studies on patients with early diabetic maculopathy demonstrated a correlation between the decrease in mean thresholds and the increase in size of the foveal avascular zone and the perifoveal intercapillary area. These changes were not observed with standard white-on-white perimetry.[49]

Microperimetric studies indicate decreased sensitivity in diabetics with retinal thickening despite the absence of frank macular edema.[50] In a group of patients with clinically significant diabetic macular edema, Hudson and colleagues[51] found that one-third had abnormal standard perimetric fields, but all patients had abnormal SWAP 10-2 fields. Further, the area of abnormal sensitivities was greater than that expected by clinical assessment. Using microperimetry, macular scotomas were also found in 74% of 19 patients with clinically significant macular edema.[52] SWAP sensitivity in the central 10° of visual field in diabetic patients without macular edema was significantly reduced compared to standard white-on-white perimetry.[53] A study of visual field defects in diabetic children without retinopathy by Mastropasqua and colleagues[54] suggested that retinal sensitivity was impaired in the midperiphery of the visual field proportional to the degree of microalbuminuria. Inner/outer-segment (IS–OS) junction (now termed the ellipsoid zone, EZ) disruption on OCT has also been correlated with decreased sensitivity on microperimetry in those with diabetic macular edema.[55]

Once diabetic retinopathy is present, visual field loss is readily documented. Gandolfo and colleagues[56] studied 85 eyes with nonproliferative diabetic retinopathy using the Goldmann

perimeter. They were able to identify retinal hemorrhages and exudates of at least 3–4° in diameter as localized depressions in the visual field. Macular exudation and edema caused an irregular depression and flattening of static profiles of the central field. Wisznia and colleagues[57] tried to correlate the degree of retinopathy with the amount of visual field loss. They hypothesized that a correlation might exist between retinal capillary perfusion and field loss. Bell and Feldon[10] used Octopus static perimetry to show that visual sensitivity is quantitatively correlated with retinal perfusion in nonproliferative diabetic retinopathy (Figs. 14.13 and 14.14). Utilizing standard perimetry, Federman and Lloyd[58] found the degree of perfusion to be more important in predicting field loss than the amount of proliferative retinopathy. This relationship between nonperfusion and regional field loss has been confirmed in other studies as well.[56,59]

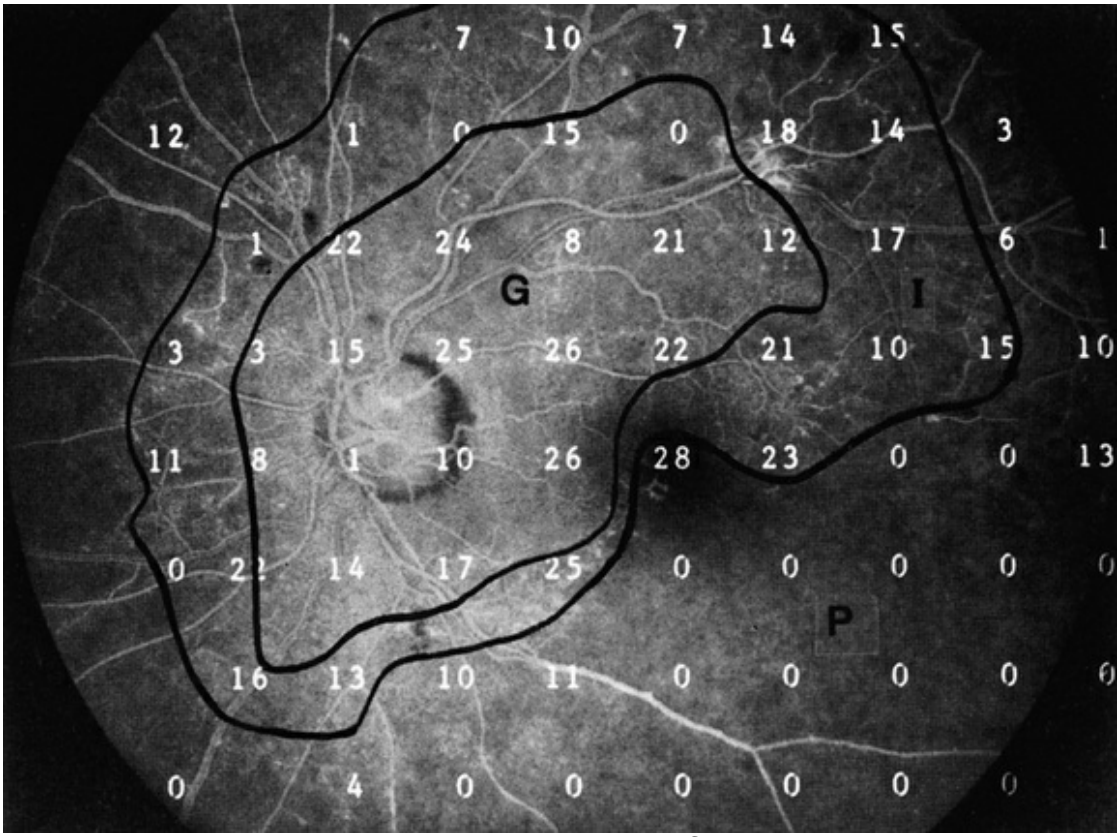

FIG. 14.13 Fluorescein angiogram of a patient with preproliferative diabetic retinopathy. Static sensitivities from Octopus perimetry are superimposed. Areas of good perfusion (*G*) have normal visual function. Areas

of intermediate perfusion (*I*) have a moderate decrease of visual function, and nonperfused areas (*P*) have complete loss of visual function. (Reproduced with permission from Bell JA, Feldon SE. Retinal microangiopathy: correlation of Octopus perimetry with fluorescein angiography. Arch Ophthalmol 1984;102:1294–8.)

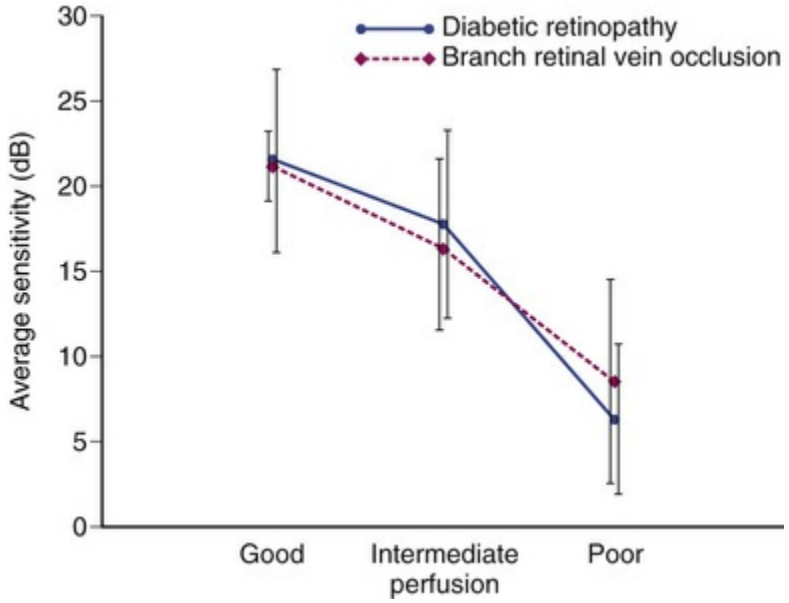

FIG. 14.14 Average sensitivity of the retina decreases with decreasing perfusion, both for diabetic retinopathy (*dots*) and for branch retinal vein occlusion (*diamonds*). (Reproduced with permission from Bell JA, Feldon SE. Retinal microangiopathy: correlation of Octopus perimetry with fluorescein angiography. Arch Ophthalmol 1984;102:1294–8.)

Lutze and Bresnick[60] demonstrated a correlation between the degree of retinopathy in type I diabetic patients and visual field loss using SWAP. These findings were consistent with those of Zwas and coworkers and have been confirmed in more recent studies.[8,53] In addition, automated perimetry was found to correlate better with severity of diabetic retinopathy than visual acuity.[61] A study by Agardh and colleagues demonstrated that SWAP sensitivity of visual field loss was correlated to ischemic changes in areas of macular edema, rather than to the severity of macular edema.[62] SWAP analysis also demonstrated a greater decrease in mean sensitivity in menstruating diabetic women who were in the luteal phase, which was not seen in menstruating control patients.[63] In a

study by Stavrou and Wood,[64] flicker perimetry appeared to be more sensitive than static perimetry in documenting early visual field changes in diabetic retinopathy, especially in a region of clinically significant diabetic macular edema.

In instances of vitreous hemorrhage and tractional retinal detachment due to high-risk proliferative diabetic retinopathy, visual acuity is often dramatically improved by vitrectomy; however, severely impaired visual fields due to extensive retinal ischemia may still preclude driving.[65] Moreover, the treatment of diabetic retinopathy with either panretinal or focal photocoagulation may produce visual field defects, a fact that should be considered in overall patient management.[66,67] In a study by Zingirian and colleagues,[68] isolated photocoagulation of diabetic retinopathy results in small scotomas that are difficult to isolate by kinetic perimetry. Confluent lesions measuring one to two disc diameters cause correspondingly sized scotomas with sloping margins.

Panretinal photocoagulation produces a marked concentric contraction of the visual field. Yoon et al.[69] demonstrate preservation of retinal sensitivity in central visual field after panretinal photocoagulation in diabetic patients. At 1 week after treatment there is significant depression, but recovery of up to 95% occurred within the ensuing 3 months. They attribute these encouraging findings to the use of burn sizes of 200 μm or less, as recommended by Hulbert and Vernon.[70]

Using automated perimetry, an initial loss of sensitivity after grid laser for diabetic macular edema was seen followed by improvement.[71] Hudson and colleagues[71] followed 24 diabetic patients with macular edema before grid laser treatment and up to 12 weeks following treatment with microperimetry. They found correlation between the amount of edema and visual function in some, but not all, patients. In another study of 30 patients, 8 eyes remained stable, 15 had improved mean deviation on HVF after treatment, and laser scars corresponded to marked loss of function.[72]

Retinal sensitivity tested by microperimetry appears to increase after micropulse diode laser, but to decrease after modified Early Treatment Diabetic Retinopathy Study focal laser in eyes with

clinically significant diabetic macular edema. These perimetric changes are observed even though there is no difference in visual acuity or retinal thickness after either treatment.[73] Recent studies highlight associations between morphologic and functional alterations in diabetic macular edema using microperimetry. Microperimetry sensitivities are reduced in eyes with diabetic macular edema, and direct correlations have been made between decreased microperimetry sensitivity and increased cystoid edema, as evidenced by OCT and increased FAF.[74–77] Microperimetry sensitivities are increased in patients receiving intravitreal injections of ranibizumab[78] and triamcinolone[79] for diabetic macular edema when such edema is reduced.

Other Vascular Diseases and Nondiabetic Macular Edema

Many other vascular abnormalities of the choroid and retina have been evaluated with perimetry. For example, visual field defects correspond to retinal vascular occlusions in sickle-cell disease.[80] Microperimetric sensitivity is decreased in sickle-cell retinopathy in areas of retinal thinning.[81] GVF perimetry showed a slight constriction of peripheral visual fields, though visually insignificant, a decade after diode laser retinal ablative therapy for retinopathy of prematurity (ROP) in one series. This field construction is similar to peripheral field changes observed years after cryotherapy for ROP.[82] Laser ablative treatment at the earlier stage of ROP results in a slight preservation of the field when compared with eyes treated at threshold (type I ROP).[83]

Microperimetry has been used to document functional improvement with resolution of absolute scotomas and improvement in vision to baseline in the setting of Purtscher's retinopathy after treatment with oral steroids.[84] However, permanent paracentral scotoma on HVF has been reported in Purtscher's retinopathy secondary to pancreatitis.[85] Perimetric improvement was noted following carotid endarterectomy for clinically significant carotid stenosis.[86,87] Recovery of visual field loss was also seen over time using HVF and microperimetry after central and branch artery occlusions.[88,89] In addition, greater

decrease in scotopic macular sensitivity was shown with microperimetry fine matrix mapping of the macula in eyes with type 2 idiopathic macular telangiectasia. In similar eyes, Wong and colleagues[90] demonstrated correlations between microperimetry sensitivities, OCT retinal morphology, and FAF.

In branch vein occlusions, Bell and Feldon[10] have shown good correlation between residual capillary perfusion and threshold retinal sensitivity (Figs. 14.14 and 14.15). According to the Branch Vein Occlusion Study guidelines, microperimetry is useful in assessing the benefit of laser treatment. Regression of the scotoma from the foveal avascular zone was observed in one-third of patients, but in one-half of treated patients an increase in total scotoma size occurred.[91]

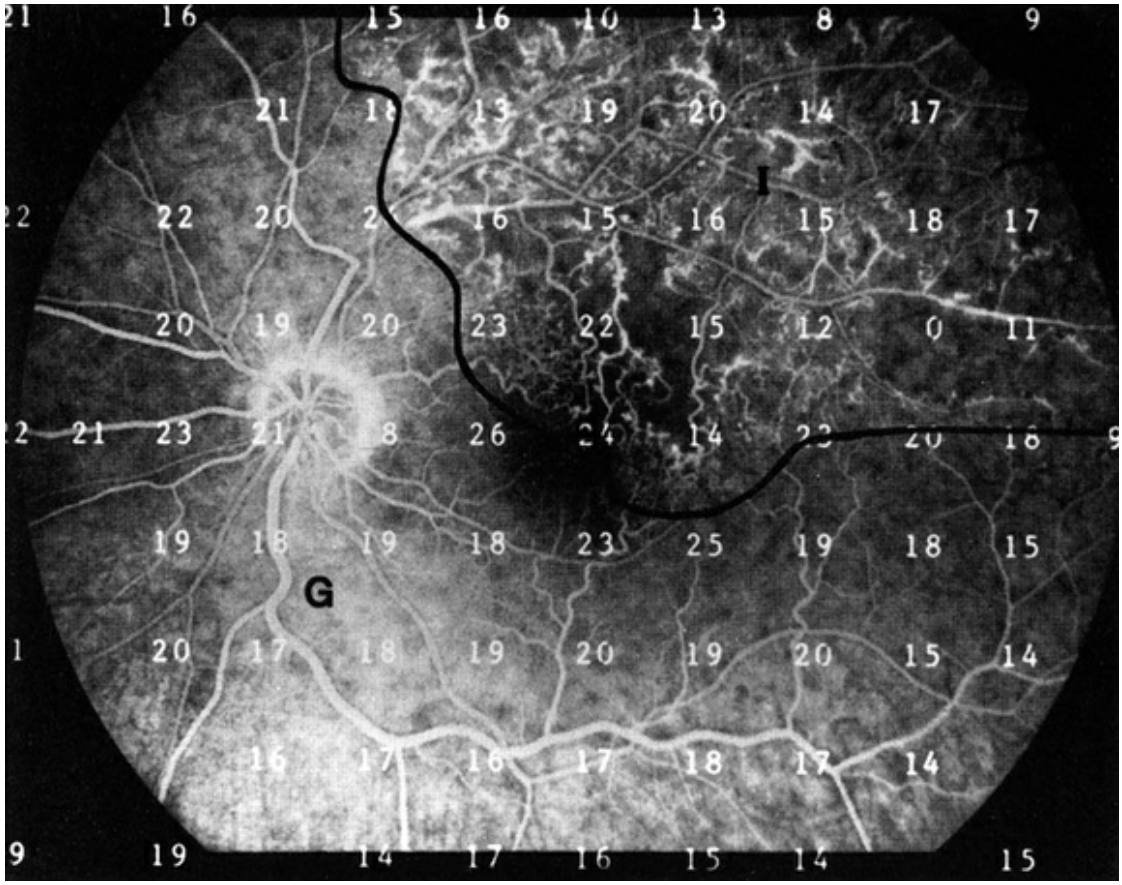

FIG. 14.15 Fluorescein angiogram from a patient with a superior branch retinal vein occlusion. Retinal sensitivities from Octopus perimetry are superimposed to show depressed function in the area of intermediate retinal perfusion (*I*). *G*, Area of good perfusion.

(Reproduced with permission from Bell JA, Feldon SE. Retinal microangiopathy: correlation of Octopus perimetry with fluorescein angiography. Arch Ophthalmol 1984;102:1294–8.)

After injection of intravitreal triamcinolone for treatment of branch retinal vein occlusion, improvement in macular sensitivity by microperimetry correlated with improvement in macular edema.[92] Visual fields may also effectively document the effects of treatments for CRVO.[93] For instance, microperimetry demonstrated improved central fixation and retinal sensitivity following resolution of macular edema due to CRVO after treatment with intravitreal triamcinolone acetonide. An increase in retinal sensitivity is also seen after Ozurdex intravitreal implant for macular edema after CRVO and BRVO.[94] Though microperimetry showed a benefit in macular function and field after radial optic neurotomy for CRVO, according to Tsujikawa and colleagues,[95] persistent peripheral field defects were documented by full-field perimetry corresponding to the incision site on the optic nerve head in similar eyes with CRVO that underwent the same treatment.[96]

Central serous retinopathy is another entity affecting the macula that can present as metamorphopsia on Amsler grid testing. There is also an accompanying mild central depression which varies in size from 2 to 5° (Fig. 14.16). The scotoma is usually substantially larger using SWAP relative to that detected with white-on-white perimetry.[97] HVF and microperimetry central retinal sensitivity is reduced as subretinal fluid in central serous retinopathy increases on OCT.[98,99] Even after resolution of edema, the majority of patients have residual Amsler and perimetric defects[100–102] (Fig. 14.17). Similar changes may result from other causes of fluid accumulation in the macula, such as diabetic retinopathy, Irvine–Gass syndrome, trauma (Berlin's edema), and retinal vasculitis.[2,103]

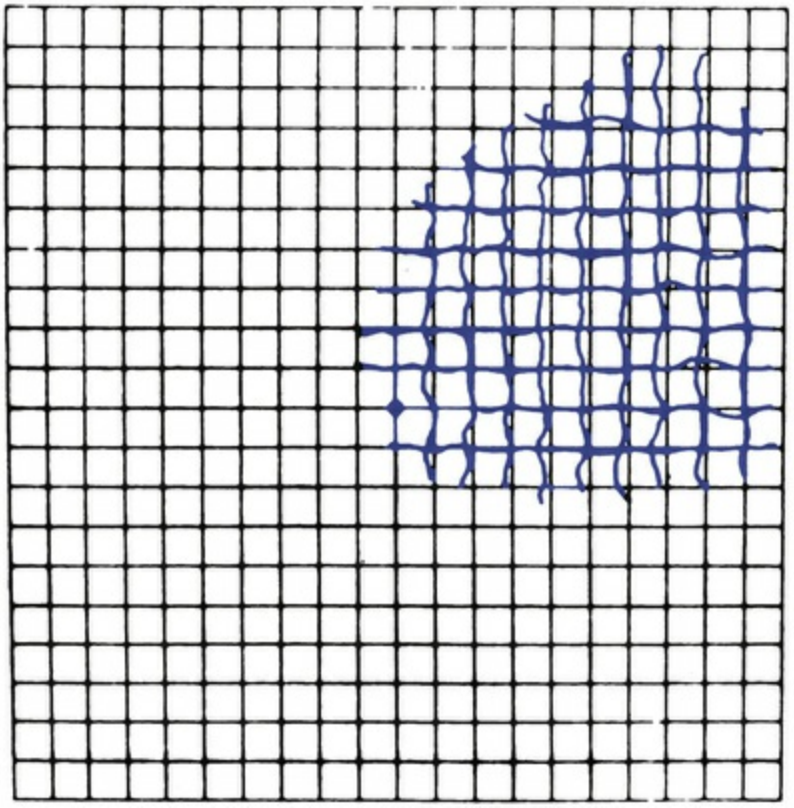

FIG. 14.16 An Amsler grid from a patient with longstanding metamorphopsia caused by central serous retinopathy. (Reproduced with permission from Natsikos VE, Hart JCD. Static perimetric and Amsler chart changes in patients with idiopathic central serous retinopathy. Acta Ophthalmol 1980;58:908–17.)

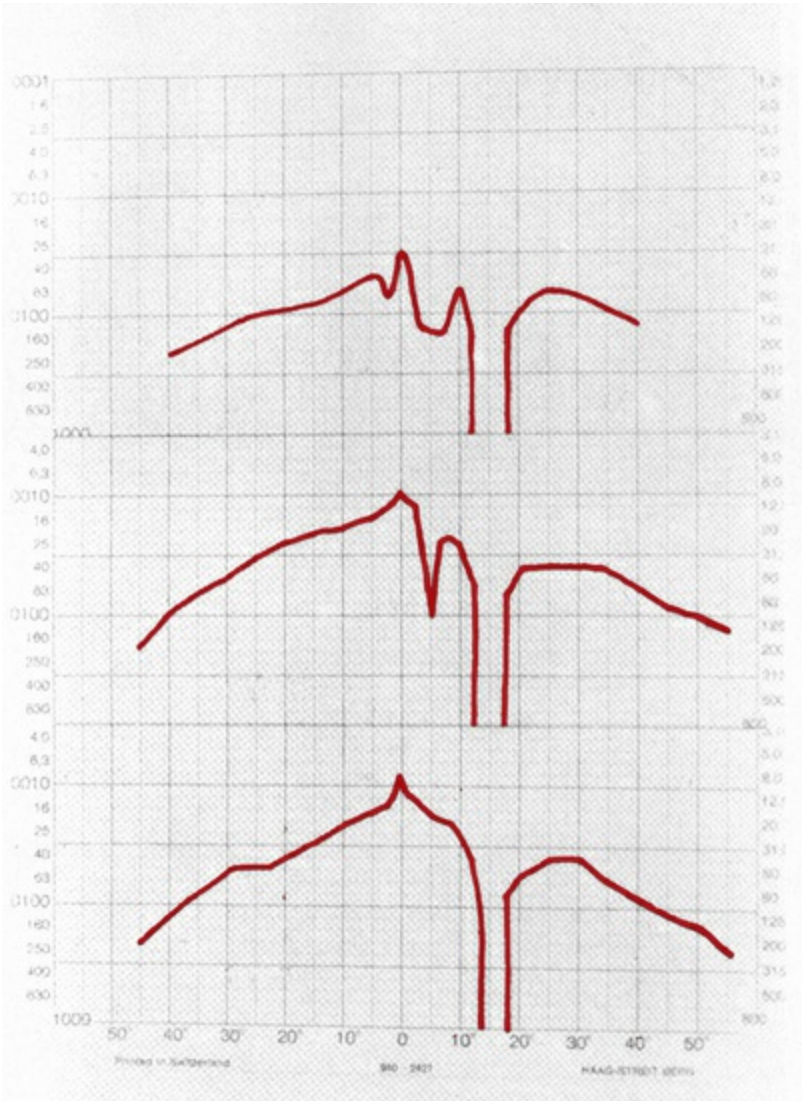

FIG. 14.17 A set of Tübinger static perimetric profiles showing pattern of recovery over 7 months in a patient with central serous retinopathy. (Reproduced with permission from Natsikos VE, Hart JCD. Static perimetric and Amsler chart changes in patients with idiopathic central serous retinopathy. Acta Ophthalmol 1980;58:908–17.)

Age-Related Macular Degeneration and Other Maculopathies

Macular drusen are not usually associated with any reduction of retinal sensitivity using standard techniques. However, in a prospective study using SWAP, the mean sensitivity of patients with soft drusen and early AMD is significantly lower compared to patients without drusen.[104,105] In this study the presence or absence of focal hyperpigmentation did not affect mean sensitivity.

Microperimetry of macular drusen demonstrated decreased overlying sensitivity in some, but not all, studies.[106,107] Microperimetry is used to assess retinal sensitivities for a variety of other diseases affecting retinal function in the macula, including X-linked retinoschisis, S-cone syndrome, retinopathy of membranoproliferative glomerulonephritis type II, and atrophic maculopathy associated with spinocerebellar ataxia type 7.[108–111]

The relationship between microperimetric retinal sensitivity and OCT characteristics in AMD has been the subject of several studies as microperimetry is becoming more popular as a reliable functional outcome measure.[112] In one study[113] the integrity of the IS–OS junction (EZ) and drusen-associated RPE elevation correlated with retinal sensitivity, implicating these criteria as markers of retinal function in early AMD. Both nonexudative[114] and exudative AMD have been associated with reduced microperimetry sensitivity that correlated with a disrupted IS–OS interface.[115] Studies on microperimetry and OCT correlation for exudative AMD have shown similar findings.[116–118] In contrast, one study measured a functional deficit with microperimetry, but found a lack of correlation with the multifocal electroretinogram (greater in microperimetry) in eyes with intermediate nonexudative AMD.[119]

Microperimetry retinal sensitivity correlates with alterations in FAF even in early stages of AMD.[120] Perimetry is also used to evaluate macular retinal sensitivity after novel treatments for nonexudative AMD[121–123] and is more sensitive than low luminance and best corrected visual acuity in early and intermediate nonexudative AMD.[112,124]

Disciform subfoveal scarring from subretinal neovascularization, hemorrhage, and gliosis due to exudative AMD causes a dense central scotoma,[2] as shown in Fig. 14.18. Detailed studies of subfoveal choroidal neovascularization in exudative AMD have been performed by microperimetry (Fig. 14.19). Of 179 eyes evaluated by Fujii and colleagues, 135 (75%) had central fixation, 42% had stable fixation, and in 28%, there was a dense central scotoma. The authors found that both central and stable fixation deteriorated over time. These fixational patterns were felt to be important in the selection of patients for macular translocation surgery.[125] Microperimetry has also been used to assess retinal

sensitivity after autologous RPE and choroid grafting for exudative AMD.[126] When microperimetry was utilized to evaluate the anatomic abnormalities associated with an absolute scotoma in subfoveal choroidal neovascularization, Tezel and associates found that the relative risk (RR) was highest in areas of chorioretinal scar (RR = 107.61) compared to areas of RPE atrophy (RR = 9.97), subretinal hemorrhage (RR = 2.88), and neovascular membrane (RR = 1.86).[127] The majority of patients with stable fixation preferred an area of RPE hyperplasia.

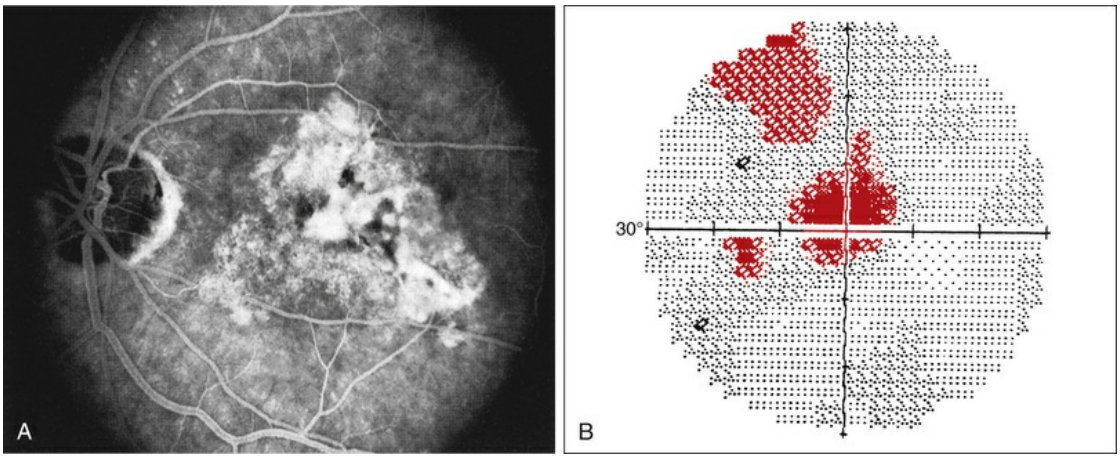

FIG. 14.18 (A) Fluorescein angiogram of a 60-year-old patient referred for evaluation of transient right homonymous hemianopia documents disciform macular degeneration of the left eye. (B) Dense central scotoma corresponding to the fundus lesion is shown by grayscale printout from Humphrey perimeter (program 30–2).

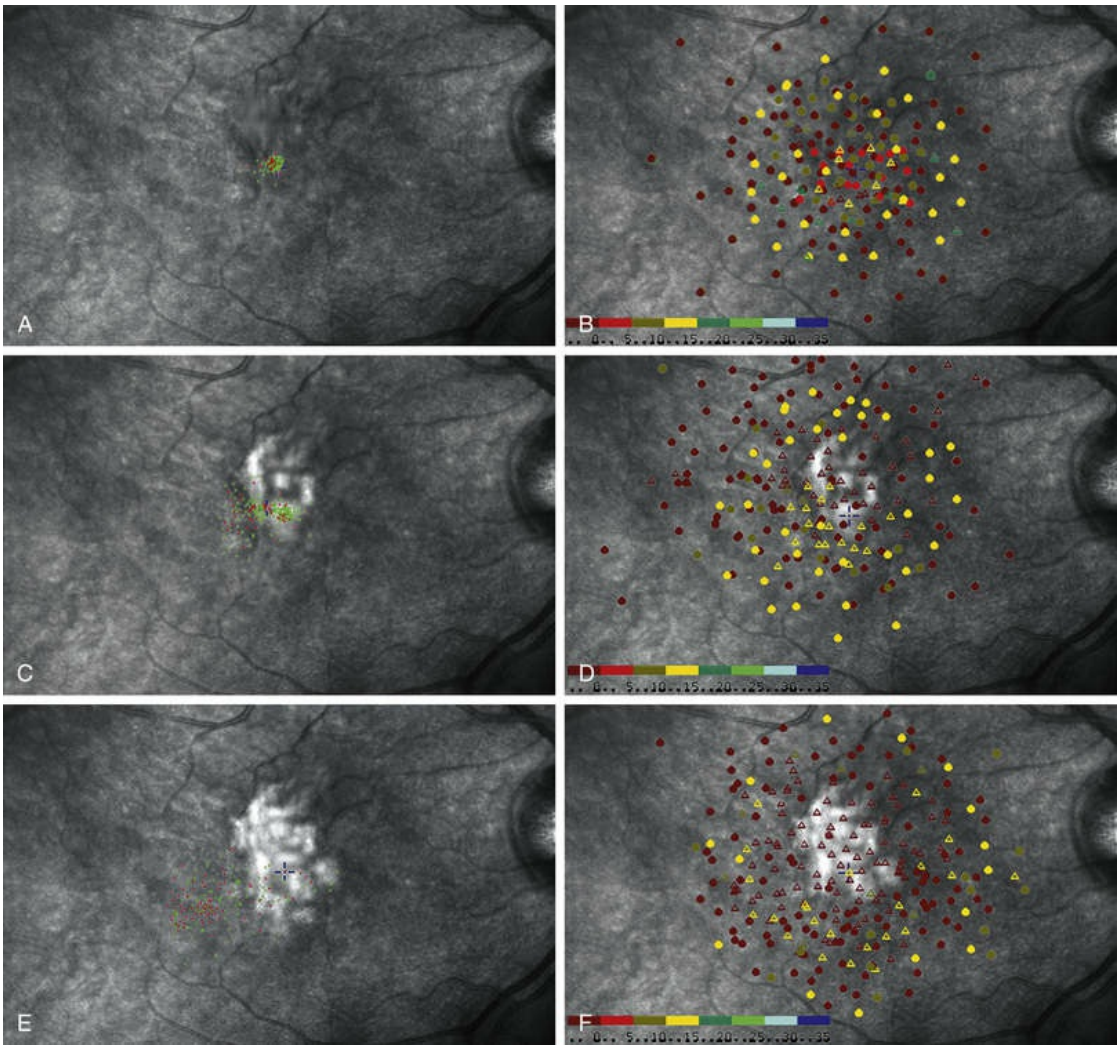

FIG. 14.19 A sequence of scanning laser ophthalmoscope (SLO) microperimetry shows the progressive functional deterioration in one eye with subfoveal choroidal neovascularization (CNV) secondary to age-related macular degeneration (AMD). The SLO testing demonstrated that eyes with subfoveal CNV secondary to AMD experienced a predictable and progressive loss of fixation stability, decreased central retinal sensitivity, and loss of central fixation location. A 65-year-old man presented with 20/150 vision and a 1-month history of decreased vision due to a predominantly classic subfoveal CNV secondary to AMD. (A) The SLO testing performed at presentation disclosed a pattern of predominantly central and stable fixation. (B) The balls indicate the areas where the patient could perceive the stimulus; the triangles indicate the areas where the patient could not perceive the stimulus. Each ball and triangle is color-coded to indicate the intensity of the stimulus.

The SLO microperimetry also showed a mild decrease in central retinal sensitivity. The patient elected not to receive any treatment and had a follow-up visit 4 months after initial visual symptoms. (C) An SLO test was performed and demonstrated that the fixation pattern became poor central and relatively unstable. (D) The microperimetry also showed that retinal sensitivity was markedly affected with some central areas of dense scotoma. Best corrected visual acuity at this visit was 20/200. Twelve months after onset of initial visual symptoms and no treatment, SLO microperimetry was performed and disclosed further functional deterioration. (E) The fixation became predominantly eccentric and unstable. (F) Retinal sensitivity testing demonstrated a large central area of dense central scotoma. (Reproduced with permission from Wong WT, Kam W, Cunnigham D, et al. Treatment of geographic atrophy by the topical administration of OT-551: results of a phase II clinical trial. Invest Ophthalmol Vis Sci 2010;51:6131–9.)

Visual field sensitivity as demonstrated by HVF 10-2 and microperimetry improved after photodynamic therapy for exudative AMD and subfoveal polypoidal choroidal vasculopathy.[128–130] Using the HVF macular threshold protocol, improvement in macular visual field sensitivity occurred after treatment with intravitreal bevacizumab for exudative AMD, even in cases where visual acuity had not improved.[131] Microperimetry in patients with exudative AMD has shown similar improvement in central retinal sensitivity after intravitreal ranibizumab,[132,133] bevacizmab,[101] and aflibercept.[117] However, supplementation of the micronutrient lutein did not improve microperimetric retinal sensitivity or visual acuity in AMD.[134]

Patients with AMD or other macular pathology are routinely instructed to monitor their visual field in each eye with an Amsler grid regularly. The higher contrast of the original white lines on a black background Amsler grid proved to be superior at detecting metamorphopsia and central vision changes compared to the modified grid, which displays black lines on a white background.[135] However, due to ease in photocopying, the grid with black lines on a white background is most commonly used in the office setting and provided to patients for home use.

With the increasing prevalence of AMD and the ability to treat early exudative AMD effectively, new perimetric tests that allow for patient self-monitoring of visual fields are being devised to detect early deficits. Nazemi and colleagues[136] developed a three-dimensional automated computer-based threshold Amsler grid test that maps the visual field and records steep slopes in areas of nonexudative AMD and shallow slopes in regions corresponding to exudative AMD. As discussed at the beginning of this chapter, the psychophysical property of hyperacuity has been used to develop a device that detects progressive maculopathy and the early onset of exudative disease in AMD.[137,138] The device, PreView PHP (Carl Zeiss Meditec, Dublin, CA), was evaluated as a home-based device in a multicenter trial and found to have a sensitivity and specificity of 85% to detect alterations in hyperacuity corresponding to exudative and intermediate nonexudative AMD.[138] Other home-based perimetric devices for patients to monitor their vision routinely are expected in the near future. With the development of better algorithms to detect early disease progression, these home devices will hopefully ensure timely sight-saving treatment.

Epiretinal Membrane and Macular Holes

Perimetry has been used to evaluate visual fields in eyes with epiretinal membrane (ERM). Binocular correspondence perimetry, a method akin to PHP, but which uses the principle of retinal correspondence and requires binocular testing, was used to quantify metamorphopsia in eyes with ERM.[139] This study demonstrated focal areas of abnormal retinal correspondence in eyes with ERM compared to the normal fellow eye. Surprisingly, microperimetry revealed unimpaired central fixation in eyes with idiopathic ERM despite lower visual acuity.[140]

Cysts may develop in the macula without producing appreciable scotomas. In eyes with lamellar macular holes, both mean total and central microperimetric retinal sensitivity were lower than controls and were more pronounced in eyes with outer retinal layer abnormalities.[141] Foveal photoreceptor layer integrity was correlated with central retinal sensitivity in these eyes.[142]

Macular holes, however, result in dense scotomas with steep

margins (Figs. 14.20 and 14.21). Microperimetry may be helpful in predicting the outcome of macular hole surgery. In a study by Amari and associates, visual outcome correlated with the maximum sensitivity adjacent to the hole.[143] In another study, absolute scotomas disappeared completely in 18 of 28 eyes that achieved complete closure, became relative in five of six eyes with partial closure, and remained absolute in four eyes with atrophic closure.[144] Ozedemir and colleagues[145] suggested that MP-1 microperimetry may be more sensitive than visual acuity in measuring retinal function following closure of a macular hole with pars plana vitrectomy and internal limiting membrane (ILM) peeling. Increases in retinal sensitivity by microperimetry have also been correlated with the degree of FAF after macular hole closure.[146] Preoperative extent of the IS–OS junction (EZ) disruption on OCT in macular holes predicted postoperative microperimetric macular sensitivity[147] but final best corrected visual acuity was multifactorial. Similarly, mean retinal sensitivity before surgery also predicted prognosis after macular hole surgery.[148] OCT studies have shown that outer retinal layer integrity was associated with better final microperimetric sensitivity after macular hole surgery.[149] However, ILM peeling may reduce retinal sensitivity and significantly increase the incidence of microscotomas.[150]

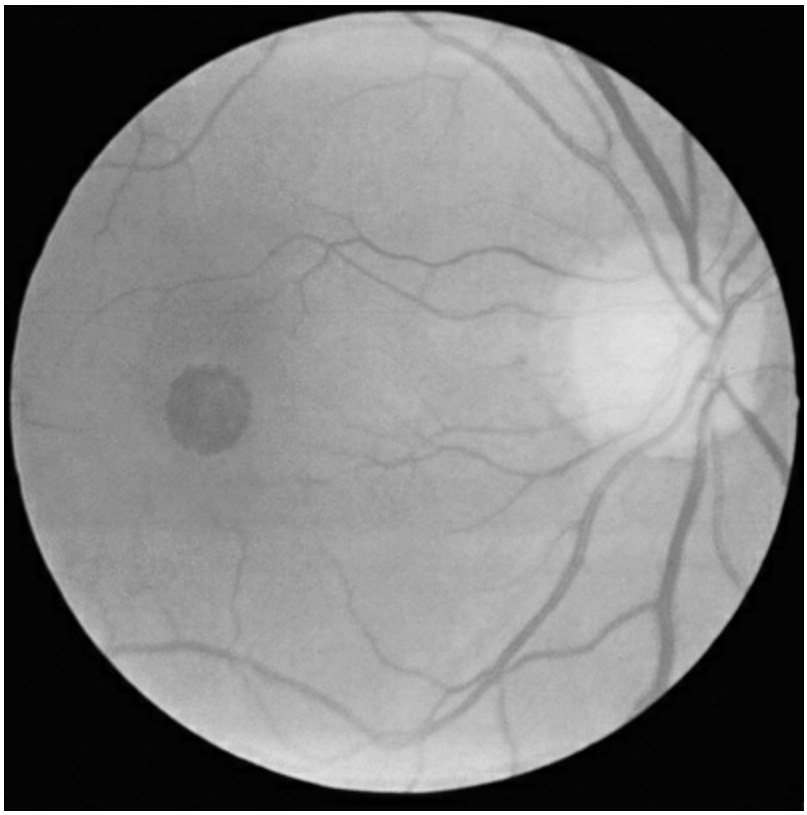

FIG. 14.20 Fundus photograph of an eye with a full-thickness macular hole. The visual field defect is shown in Fig. 14.21.

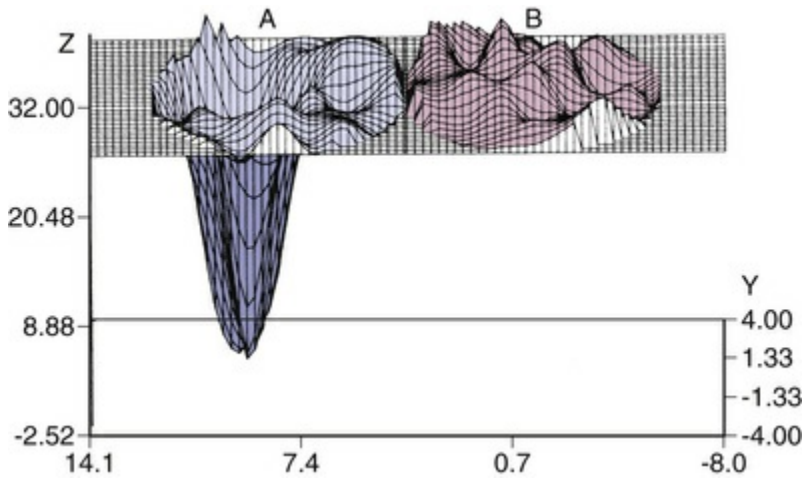

FIG. 14.21 Three-dimensional reconstruction of high-density macular grid (1° spacing) documenting steep absolute central scotoma of the left eye (A) and unaffected right eye (B). Retinal sensitivity is noted on the vertical axis and position is noted on the horizontal axis.

Laboratories, Inc. Courtesy of Dr Herman.)

Richter-Mueksch and colleagues[151] reported increased microperimetry retinal sensitivity without change in metamorphopsia following vitreoretinal surgery for ERM and macular hole using PHP. However, after uncomplicated repair of macular holes and ERM and using pars plana vitrectomy and ILM peeling, several investigators reported a high incidence of peripheral field defects infringing on the central visual field[152–158] (Fig. 14.22). A majority of studies documented postoperative field defects only after patients complained of perceived field loss. Tsuiki and colleagues[159] specifically compared pre- and postoperative GVF tests and found new peripheral field defects in 17 of 140 eyes postoperatively after macular hole repair. In the majority of eyes, indocyanine green (ICG) was used to enhance visualization of the ILM during peeling. In vitro studies demonstrated the toxicity of ICG exposure to human retinal cell lines.[160] The postsurgical visual defects are probably due to (1) toxic effects of ICG; (2) alterations in the retina, such as damage to the peripapillary nerve fibers, during the pars plana vitrectomy (PPV); or (3) mechanical damage incurred with peeling of the ILM. Damage to the nerve fiber layer from intraocular gas tamponade in cases of macular hole repair must also be considered.[151]

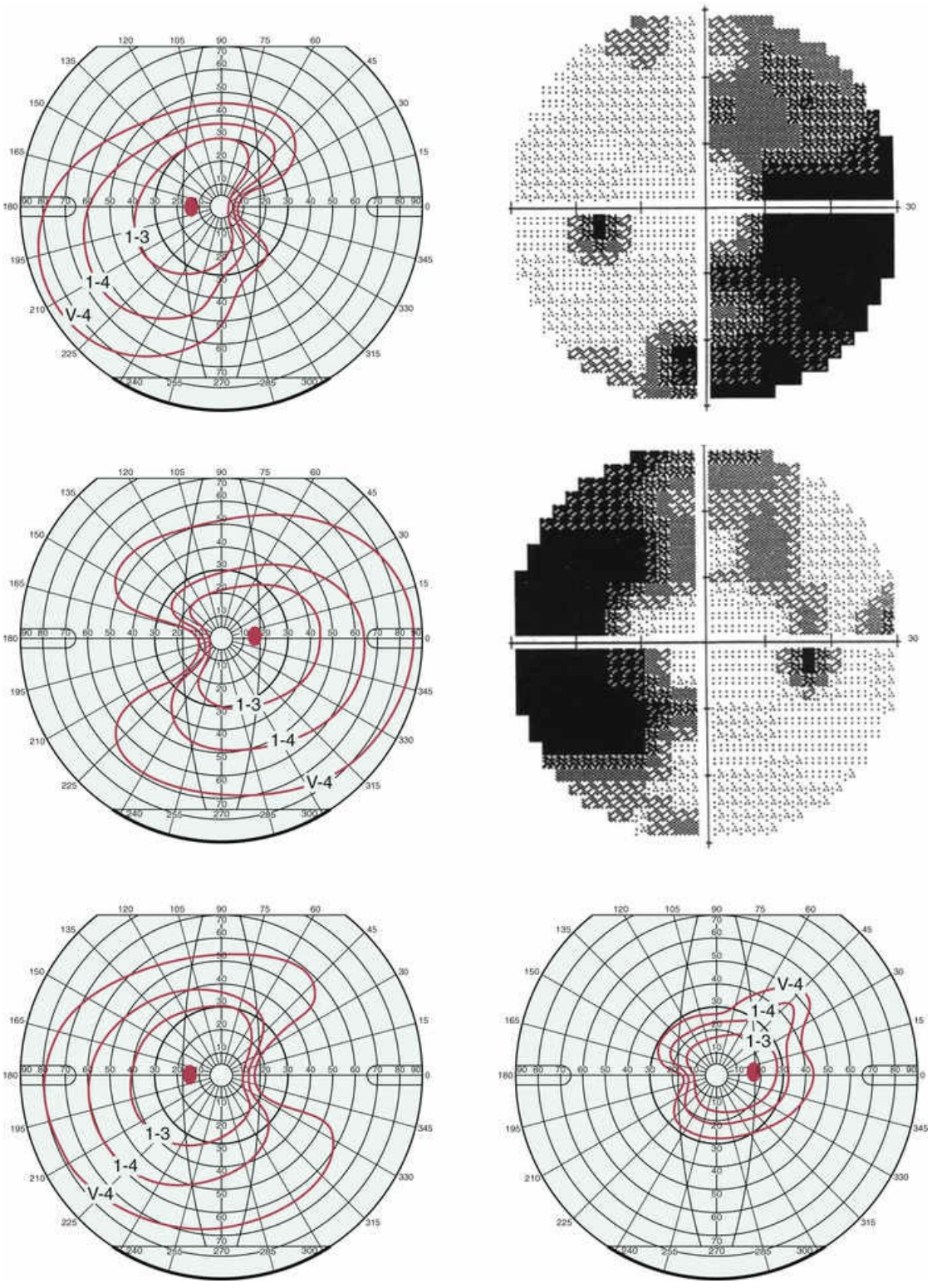

FIG. 14.22 Goldmann and Humphrey 30-2 visual field perimetry depicting peripheral wedge-like visual field loss encroaching on the central visual field in the eyes of three patients after pars plana vitrectomy, internal limiting membrane (ILM) peeling assisted by indocyanine green staining of the ILM for external

limiting membrane. (Reproduced with permission from von Jagow B, Hoing A, Gandorfer A, et al. Functional outcome of indocyanine green-assisted macular surgery: 7-year follow-up. Retina 2009;29:1249–56.)

Recently, brilliant blue G dye was studied for ILM peeling,[161,162] and it provided improved central retinal sensitivity and quicker IS–OS junction (EZ) restoration than ICG dye.[163] Further studies that systematically and more accurately compare pre- and postoperative visual fields in eyes undergoing retinal surgery are needed to understand better the effects of the procedure and the adjuvant dyes or agents used to assist in the procedure on visual function.

Toxic Retinopathies

Toxic maculopathy is epitomized by chloroquine and hydroxychloroquine retinopathy. The most characteristic field defect caused by macular involvement is a ring-like central scotoma with a small island of slightly less visual loss in its center, commonly referred to as a "bull's eye" (Fig. 14.23).[164] GVF and HVF perimetry document visual field changes that can persist and worsen for decades even after stopping the medications[10,165–167] (Fig. 14.24). 10-2 HVFs usually show paracentral changes while 24-2 fields often display central changes.[168] Threshold Amsler grid testing, which varies light transmission through two cross-polarizing filters, and PHP hyperacuity may be useful in screening for early functional changes due to chloroquine and hydroxychloroquine use.[169,170] Microperimetry also detects early macular hyposensitivity.[171] Lower sensitivity is often found in elderly and short statured individuals, likely due to increased toxicity of lower doses of the two drugs.[172]

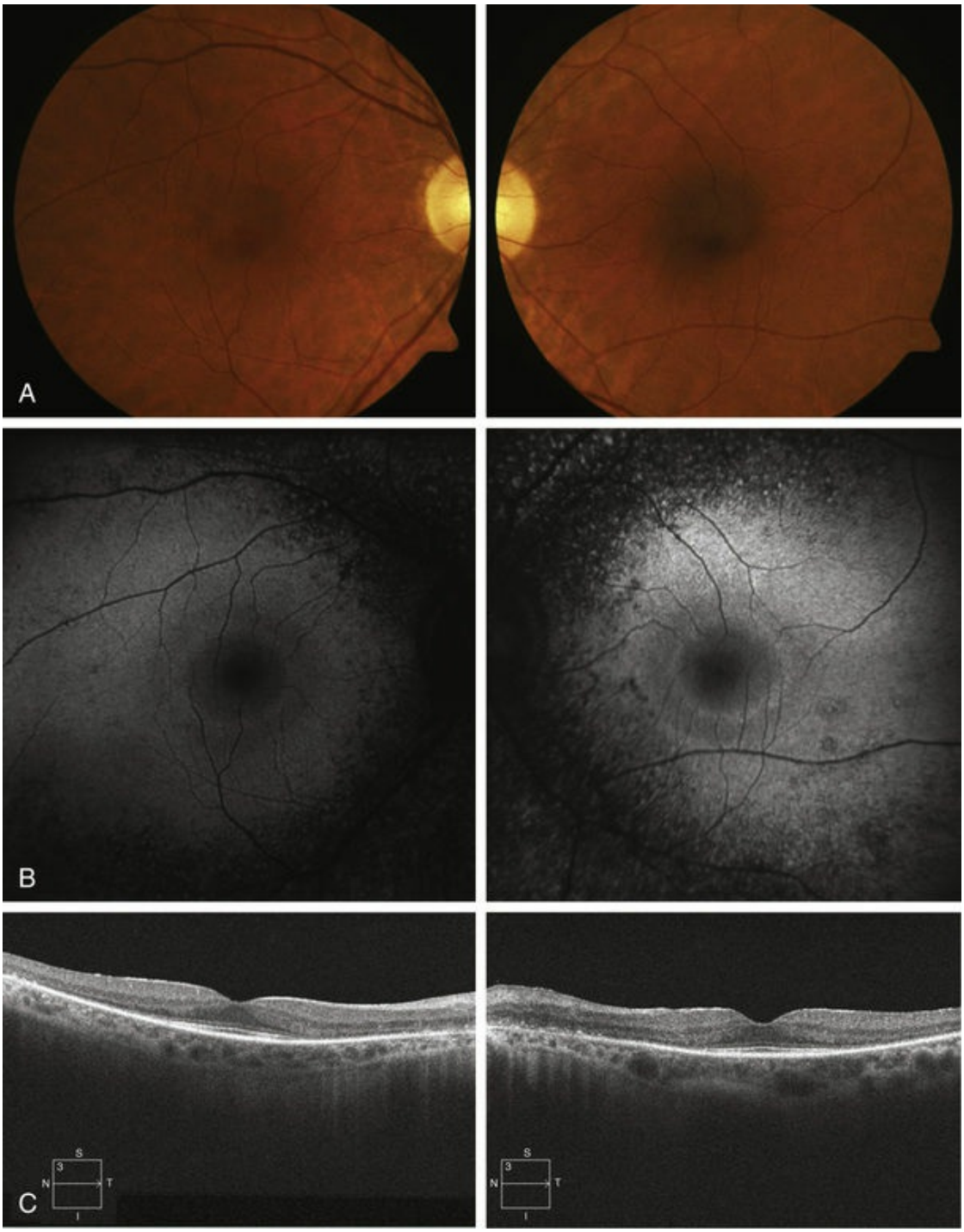

FIG. 14.23 (A) Fundus photos of a 65-year-old female with lupus on hydroxychloroquine (Plaquenil) 400 mg daily) for 8 years displaying perifoveal atrophy of the retinal pigment epithelium (RPE) corresponding to bull's-eye maculopathy. (B) Fundus autofluorescence in the same patient showing RPE changes as concentric rings of hypo- and hyperautofluorescence in a bull's-eye pattern. (C) Macular OCT of the patient with extrafoveal loss of RPE and the IS–OS junction (ellipsoid zone) corresponding to the bull's-eye pattern

seen clinically and to the paracentral scotoma demonstrated by the 10-2 Humphrey visual field in Fig. 14.24C.

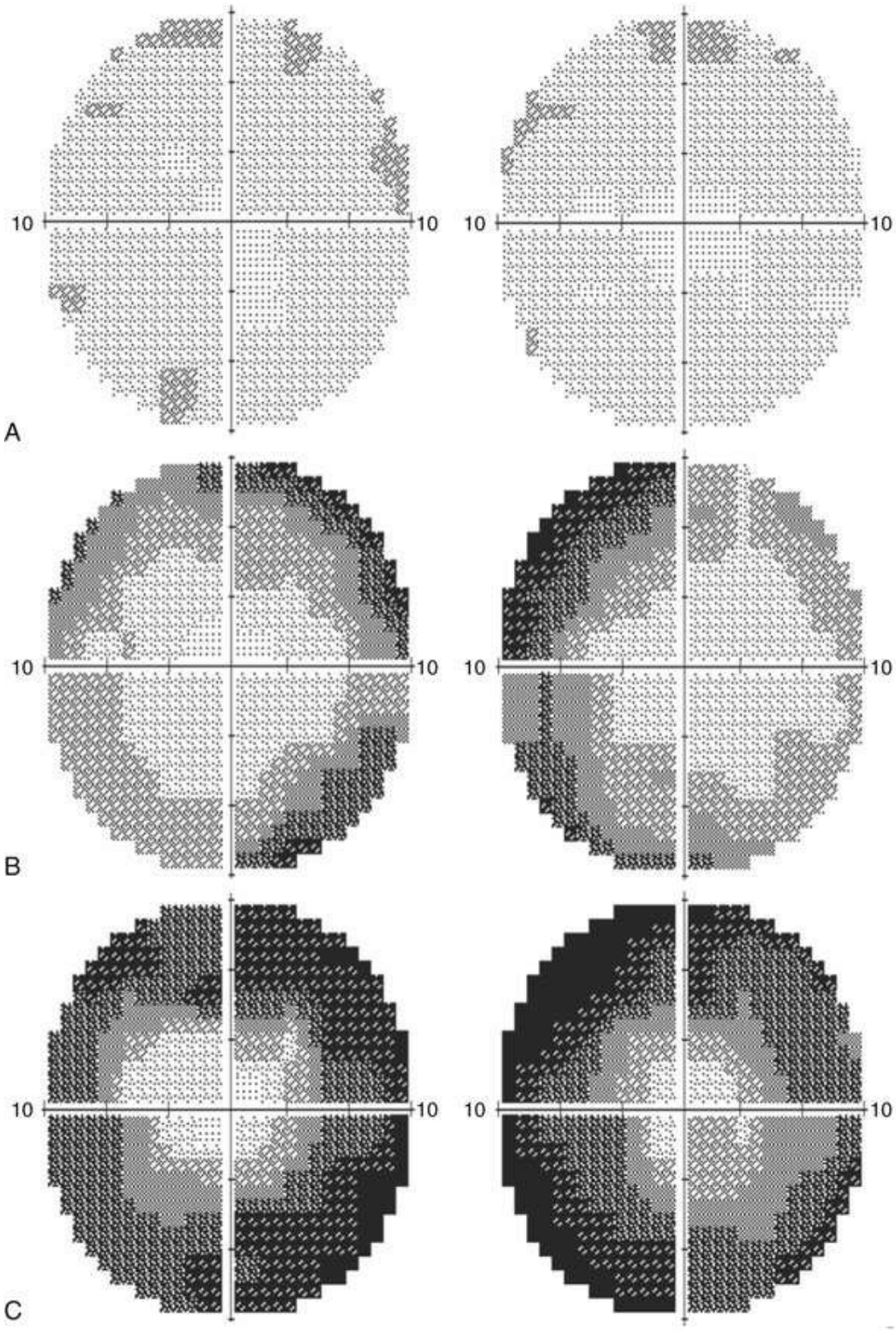

FIG 14.24 (A) 10-2 Humphrey visual fields (HVF) at 2° spacing showing early onset of perifoveal visual field depression in both eyes in the same patient as Fig. 14.23 (1999). (B) 10-2 HVF taken eight years (2007)

later displays increased concentric paracentral visual field loss at which time the patient stopped hydroxychloroquine. (C) Six years later (2013) the patient continued visual field progression with denser paracentral defects encircling the foveal region. Despite the paracentral visual field progression, best corrected visual acuity remained at 20/20 in both eyes.

To screen for chloroquine and hydroxychloroquine toxicity HVF, 10-2 white-on-white protocol is recommended. mERG is a helpful adjunct when early perimetric changes are seen, but may not be readily available in all retina practices. Recent screening guidelines advocate the addition of high-resolution imaging, such as spectral domain OCT and FAF, to correlate functional changes with structural alterations in the photoreceptor and RPE layers.[172,173] Defects seen on standard automated perimetry may precede ultrastructural changes on OCT.[174] In one study 10% of patients had significant ring scotomas without obvious changes on OCT.[175] In concert with other testing modalities, early perimetric changes that may be nonspecific for macular toxicity can be validated to allow for timely changes in medication with ultimate preservation of vision.[175]

A number of medications are associated with retinal toxicity resulting in visual field loss. Thioridazine, a phenothiazine derivative, is a cause of pigmented maculopathy with associated central scotoma. Even in the absence of clinical tamoxifen retinopathy, SWAP fields show depressed mean deviations which correlated with duration of therapy.[176] Peripheral visual field loss is detected in about 30% of patients using the antiepileptic drug vigabatrin.[177–180] Sildenafil (Viagra) has been associated with nonarteritic ischemic optic neuropathy in individuals with preexisting cardiovascular disease.[181] Although visual field defects can occur in these cases, sildenafil has not been proven to cause retinal toxicity.[182,183]

Infectious and Inflammatory Retinopathies

Infectious and inflammatory retinopathies exhibit visual field defects corresponding to the area of pathology. Toxoplasmosis

commonly produces focal chorioretinal destruction that causes corresponding dense, irregular, steep-margined, isolated scotomas.[184] More disseminated types of inflammation, such as syphilitic choroiditis, produce a more diffuse depression of visual field function. In a patient with idiopathic retinal vasculitis, the inferior arcuate field defect corresponded to leakage from the superior temporal branch vein (Fig. 14.25). A review of patients with Behcet uveitis revealed retinal nerve fiber layer defects and corresponding field defects with standard automated perimetry.[185] One unusual case report described the use of microperimetry to determine the focal visual loss associated with nematode-induced unilateral subacute neuroretinitis.[186]

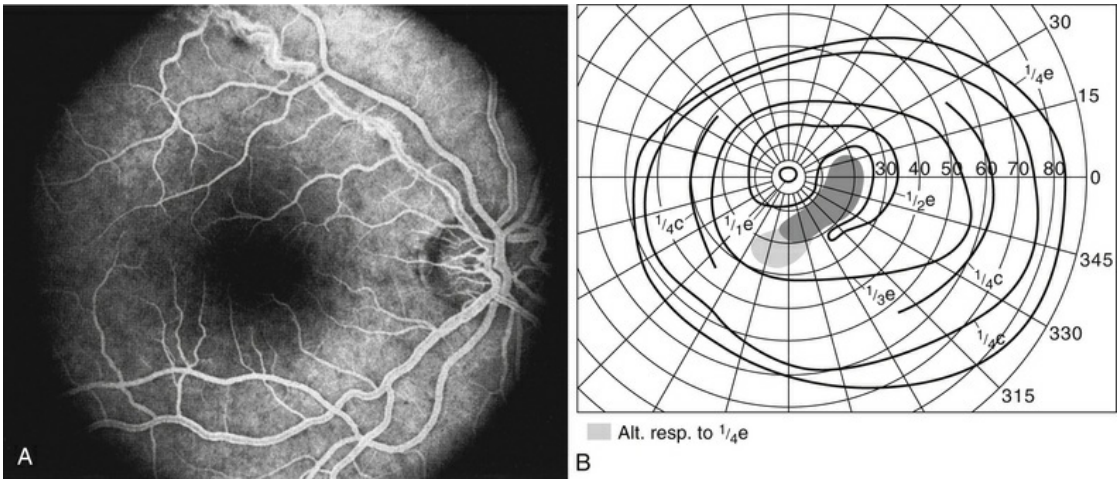

FIG. 14.25 (A) Fluorescein angiogram from a patient with idiopathic retinal vasculitis demonstrates leakage from the superotemporal retinal branch vein of the right eye. (B) Goldmann perimetry shows an inferior arcuate field defect that corresponds to the affected region of the retina.

Even without clinically evident infectious retinopathy, human immunodeficiency virus (HIV)-positive patients had significant localized as well as mean defects. These defects were more apparent in SWAP than in white-on-white automated perimetry.[187] Correlation of HVF perimetry with mERG in similar eyes demonstrated involvement of the inner retina and sparing of the outer retina.[188] Perimetric changes may also be related to HIV-related brain dysfunction.[189] More marked changes in retinal

sensitivity have been found in HIV-positive patients with low CD4 counts.[189]

In a small case series of patients with multiple evanescent white-dot syndrome, areas of decreased microperimetric sensitivity were shown to correlate with focal regions of inner and outer photoreceptor segment disruption documented by spectral domain OCT. Both the microperimetry and OCT findings changed location in keeping with the resolution and presence of new lesions during the disease course, and returned to normal by the end of clinical recovery.[190,191] Similar correlation between function and structure was seen in eyes with acute posterior multifocal placoid pigment epitheliopathy (APMPPE).[192] Field defects on static perimetry may remain after APMPPE.[193] Microperimetry retinal sensitivity was also found to correlate with visual acuity in both serpiginous choroiditis and birdshot chorioretinopathy. HVF in one study revealed multifocal defects (most commonly para/central scotoma coexisting with isolated defects in the nasal or temporal fields) that stabilized after 6 months of treatment in serpiginous choroiditis.[194] Gordon and colleagues[195] documented and analyzed HVF in patients with birdshot chorioretinopathy, in an attempt to determine characteristic patterns of field loss. The visual fields of this small series of patients exhibited diffuse loss, central sparing, and blind-spot enlargement. Long-term immunosuppression appeared to better maintain peripheral visual fields when compared to short-term treatment.[196] A study using microperimetry suggested sustained diminished retinal sensitivity even after the disease became inactive.[197] In addition, assessment of outcomes after valaciclovir treatment for acute zonal occult outer retinopathy using GVF demonstrated improved peripheral visual function.[198]

Retinal Detachment

Typically, rhegmatogenous retinal detachments have sloping isopters on kinetic perimetry. Occasionally, this feature helps to differentiate a retinal detachment from a retinoschisis, which is characterized by dense defects with steep margins, usually located supranasally. However, longstanding retinal detachments may develop steep isopters. In the case of a shallow detachment,

assessment of the visual field may be more accurate than ophthalmoscopy in identifying the border of detached retina.[2]

If the detachment is longstanding, recovery of visual field sensitivity is incomplete.[199] Performing visual fields under conditions of both light and dark adaptation, Alexandridis and Janzarik[200] report that cone function returns before rod function after successful surgical reattachment of the retina. Assessment of visual fields using SWAP is a sensitive measure of functional visual improvement in the macula following surgical repair for macula-involving retinal detachment.[201] One study suggested that central visual field defects occur following a high percentage of retinal detachment surgeries, especially if retinotomy for drainage of subretinal fluid (12 of 14, 86%) is performed. In this study, risk of visual field loss was more frequent if the retinotomy is relatively posterior (less than 5 disc diameters from fixation).[202] Although visual field loss may recover initially after retinal detachment repair, GVF perimetry has shown persistent decreased visual field following scleral buckle repair of retinal detachment despite continued improvement in visual acuity.[203] In a recent report, microperimetry used in conjunction with spectral domain OCT and FAF demonstrated good correlation of visual function with retinal morphology after rhegmatogenous retinal detachment repair.[204] Another study of six eyes with metamorphopsia after macula-involving retinal detachment repair found retinal sensitivity correlated with postoperative best corrected visual acuity.[205]

Tumors

Retinoblastoma and choroidal melanoma are the most common malignant intraocular tumors in children and adults, respectively. Long-term visual field defects that correspond to tumor size, location, and treatment modality have been documented in eyes with retinoblastoma.[206] Anterior melanomas produce localized constriction of the visual field, whereas posterior melanomas produce dense scotomas with steep borders. Only a subtle field defect, if any, is associated with choroidal nevus. Thus, fields may be important in distinguishing between these entities.

Fig. 14.26 shows the Octopus visual field superimposed on the

fundus photograph of a patient with a small melanoma of the posterior pole. In this instance, loss of sensitivity is present only in the center of the mass. Use of a finer grid pattern would have facilitated a better correlation between the pathologic process and the degree of visual loss.

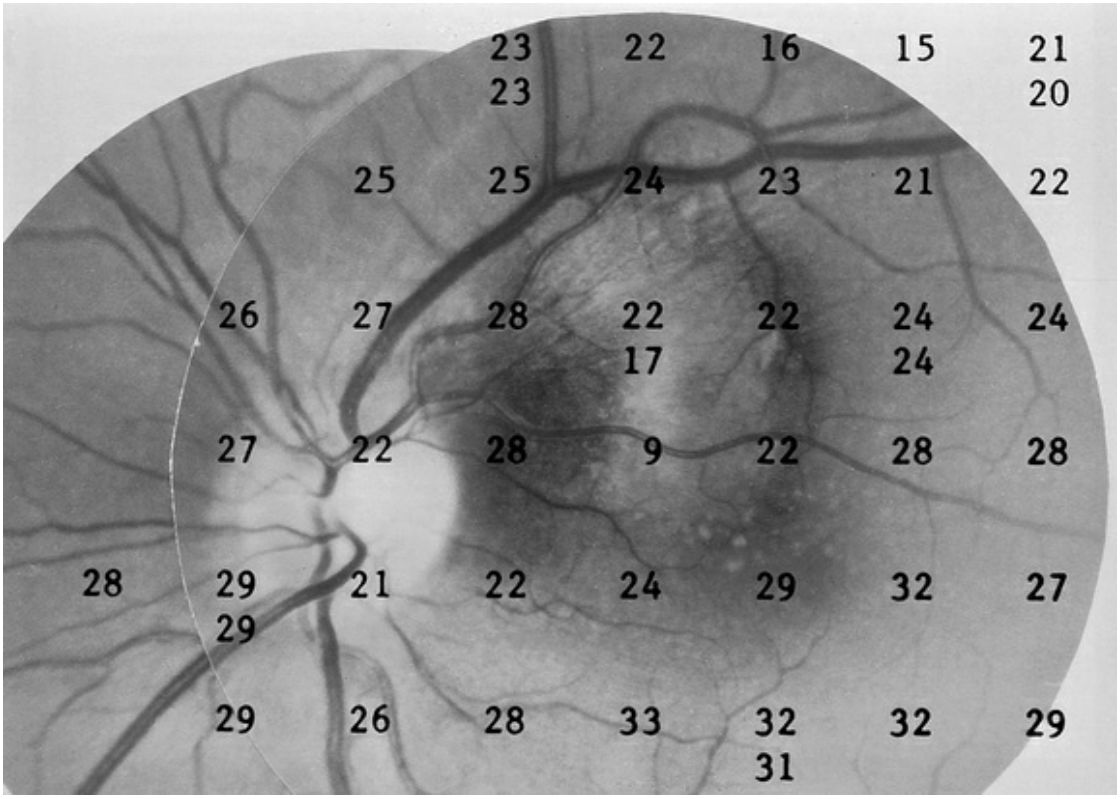

FIG. 14.26 A fundus photograph of a patient with a small malignant melanoma of the posterior pole has been superimposed on the visual field obtained by Octopus perimetry. Because of the relatively coarse (6°) grid pattern of the perimeter, sensitivity is markedly reduced only at the center of the lesion.
(Reproduced with permission from Feldon SE. Computerized perimetry in selected disorders of the retina. In: Whalen WR, Spaeth GL, editors. Computerized visual fields: what they are and how to use them. Thorofare, NJ: Slack, 1985.)

Like melanomas, choroidal metastases also produce dense scotomas with steep borders. However, in a study by Rahhal and colleagues,[207] HVF depression does not consistently correspond with tumor size or location. The visual fields shown in Fig. 14.27 were obtained from a patient with breast carcinoma whose fundus photograph is shown in Fig. 14.28. This patient demonstrated not

only a dense inferonasal field defect corresponding to the choroidal metastasis, but also a bitemporal field defect. Subsequent CT scan demonstrated a suprasellar mass consistent with either a pituitary adenoma or metastasis (Fig. 14.29).

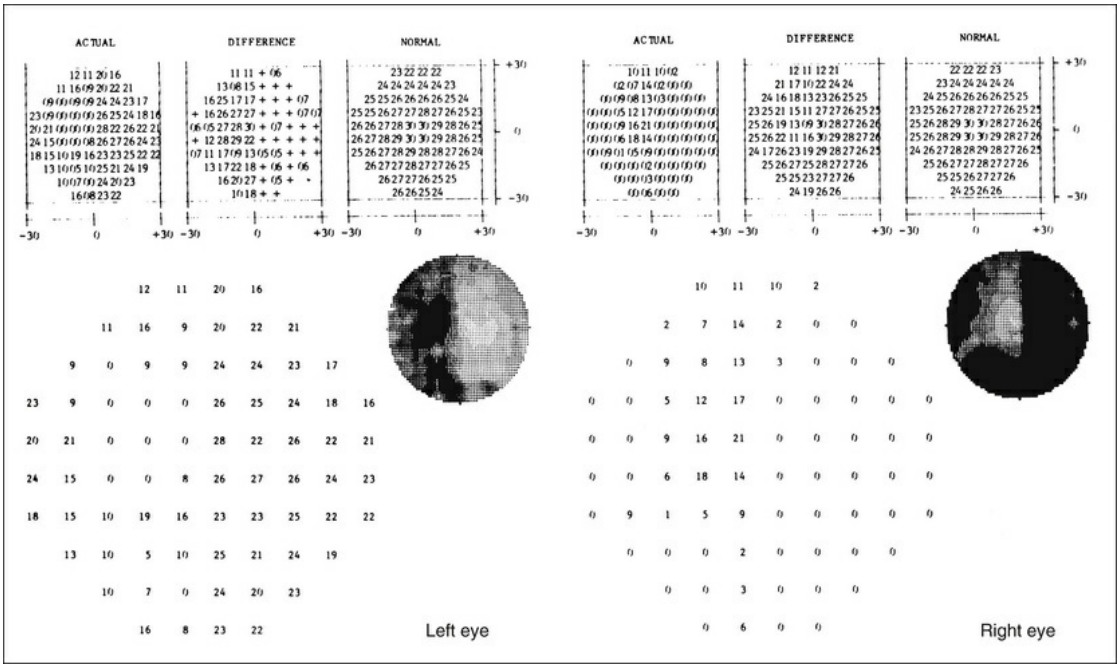

FIG. 14.27 Octopus perimetry (program 32) on the same patient as in Fig. 14.28. An inferonasal field defect in the right eye corresponds to the choroidal metastasis. There is also an unexpected dense bitemporal hemianopsia. A computed tomographic scan was requested for further evaluation. (Reproduced with permission from Feldon SE. Computerized perimetry in selected disorders of the retina. In: Whalen WR, Spaeth GL, editors. Computerized visual fields: what they are and how to use them. Thorofare, NJ: Slack, 1985.)

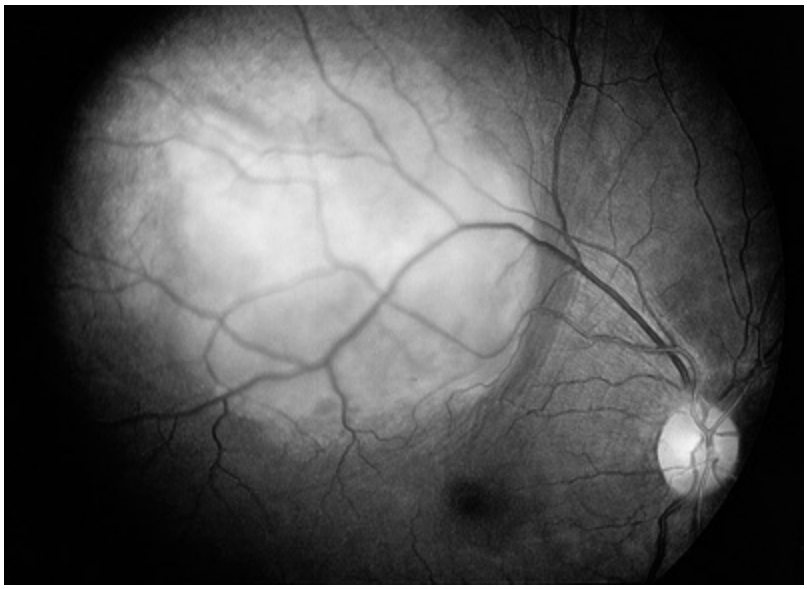

FIG. 14.28 A 50-year-old patient with known breast carcinoma is referred for evaluation of a mass in the posterior pole of the right eye. The visual fields are shown in Fig. 14.27. (Reproduced with permission from Feldon SE. Computerized perimetry in selected disorders of the retina. In: Whalen WR, Spaeth GL, editors. Computerized visual fields: what they are and how to use them. Thorofare, NJ: Slack, 1985.)

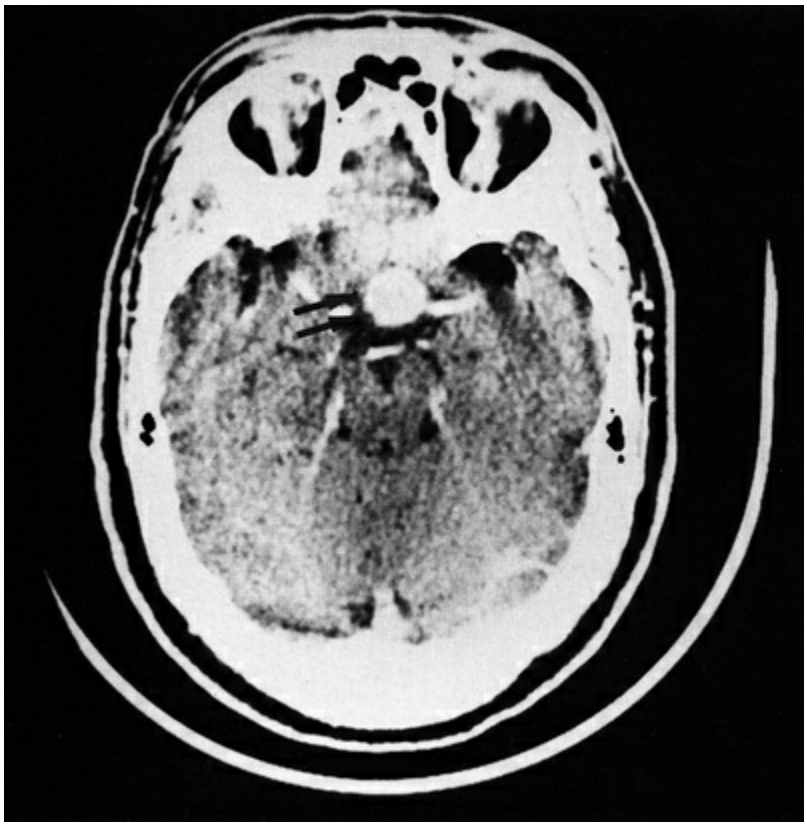

FIG. 14.29 Computed tomographic scan from the patient whose visual field and fundus photograph are shown in Figs 14.27 and 14.28. A suprasellar mass is shown that is consistent with either pituitary tumor or metastasis. (Reproduced with permission from Feldon SE. Computerized perimetry in selected disorders of the retina. In: Whalen WR, Spaeth GL, editors. Computerized visual fields: what they are and how to use them. Thorofare, NJ: Slack, 1985.)

Future of Perimetry in Retinal Disease

Layer-by-Layer Perimetry

Enoch, along with his collaborators Lawrence, Fitzgerald, and Campos,[208–210] developed a clinical perimetric technique emphasizing the detection of a small luminous spot in a stationary (sustained) or flashing (transient) surround, based on analogies with the neural processing of the inner versus outer retinal layers. Graded or "sustained-like" electrical responses are obtained from the retinal receptor, bipolar, and horizontal cells. Transient or "spike" impulses are recorded from amacrine and ganglion cells. Enoch and colleagues investigated layer-by-layer perimetry in diabetic retinopathy, macular drusen, macular degeneration, and angioid streaks. However, layer-by-layer perimetry has not gained clinical acceptance. The relationship between retinal function and the testing parameters of this modality remains unconfirmed.

Color Perimetry

Assessment of color vision may be helpful in screening for retinal disease and in separating neural from retinal causes of visual loss. Acquired diseases of the retina and choroid typically produce a tritan-like pattern of color confusion, and neural diseases typically produce a protan or deutan-like pattern of color confusion on Farnsworth–Munsell 100-hue discrimination testing.[211] Thus color perimetry might be used to advantage in the identification and quantitative description of certain retinal and choroidal diseases. Although color contrast might be more sensitive in finding visual

field defects, Hart and Burde[212] demonstrate that colored test objects used in standard techniques of perimetry may be of little clinical value over small or low-contrast white test objects for detecting scotomas in a number of optic nerve and retinal disorders. Currently there are no commercially available, standardized color perimeters.

High-Resolution OCT and Adaptive Optics With Microperimetry

Although innovative, both layer-by-layer and color perimetry do not appear to add new scientific or clinical information relevant to the etiology, localization, or treatment of retinal diseases beyond already available more standard clinical tests such as electroretinography, electrooculography, contrast sensitivity, and fluorescein angiography. Anatomical imaging of the retina at the ultrastructural level has advanced to a high degree of sophistication, allowing correlations of structure and function at the microscopic level. Hopefully, these new research strategies will result in clinical applications that will allow earlier detection and treatment of potentially debilitating and widely prevalent retinal diseases such as AMD.

The combined spectral domain OCT and SLO, introduced in 2006 (Spectral OCT/SLO; OPKO/OTI, Miami, FL, USA) is a significant achievement in advancing retinal imaging. The enhancement in accurate and real-time image capture with this system allows for integration with microperimetry. Thus, a functional spectral OCT/SLO allows assessment of retinal morphology and function at specific retinal loci. Landa and colleagues[13] demonstrated the effectiveness of a three-dimensional spectral OCT/SLO topography and microperimetry in assessing functional and structural changes of the macula in a variety of retinal disease, including AMD and cystoid macular edema. Continued refinement of this functional imaging modality is expected to allow for better detection and monitoring of retinal disease.

Adaptive optics imaging of cones and other ultrastructural elements of the retina combined with ultrafine microperimetry shows promise in pinpointing finite areas of decreased retinal

sensitivity. The ability to resolve cones and rods through adaptive optics allows for the reduction in the size of retinal image and, hence, the number of photoreceptors stimulated by adaptive optics microperimetry. Using microflashes in a patient with a genetic mutation for a cone photopigment and no clinical visual deficits, Williams and colleagues at the University of Rochester detected retinal microscotomas representing early cone photoreceptor loss.[213] In addition, Roorda and colleagues[14] demonstrated correlations between healthy and unhealthy RPE and microperimetry retinal sensitivity in patients with maculopathy and normal visual acuity. The precision of testing cellular function in the retina with this modality highlights its ability to detect early loss of function of a few photoreceptors. As this focal loss of retinal function is clinically compensated by the redundancy in the visual system, it is not noticed by patients or captured by standard perimetry and visual acuity tests. Detecting very early functional and structural pathology at the photoreceptor level before its clinical manifestation would allow for a better understanding of early pathophysiology and disease course. With this knowledge, refined screening algorithms and timely interventions for vision-threatening retinal disease might be developed.

Tele-Perimetry

Ophthalmology has not been excluded from the widespread use of smartphones and tablets over the last decade. A recent poll[214] indicated that 83% of ophthalmologists utilize smartphones for work. Various applications on handheld devices allow for easily accessed qualitative and quantitative visual field assessment, such as Amsler grid, tangent screen, and perimetric testing. Rigorous testing of the quality and validationof the accuracy of these digital tests is needed. A recent study[215] of tablet-based perimetry utilized a free peripheral vision assessment software (Visual Fields Easy) in an underserved Nepali population. Results of the study suggest that such screening could be a viable method of detecting visual field loss in places without access to healthcare or computers. Concordance between tablet-perimetry and Humphrey SITA Standard 24-2 HVF occurred 51–79% of the time. Agreement was

highest in patients having moderate to severe visual field loss. Such a screening tool could be useful in high-risk groups like African Americans and the elderly.

Conclusions

Achromatic and static SWAP provides a cost-efficient, standardized, and reliable way to evaluate and follow visual fields in patients with retinal disease. Microperimetry seems to be a valuable tool that has been used more frequently to quantify macular function in a variety of retinal diseases. As both simple and complex visual field testing applications become available for handheld computing devices, there will be a need for these formats to be carefully assessed and validated against the gold standards. The availability of new qualitative and quantitative visual field tests will continue to inform how retinal pathology and morphology impact functional vision, which is crucial in developing and delivering effective treatments for retinal disease to preserve and restore eyesight.

References

1. Traquair H. *Introduction to clinical perimetry*. Kimpton: London; 1927.
2. Harrington DO. *The visual fields: a textbook and atlas of clinical perimetry*. 5th ed. Mosby: St. Louis; 1981.
3. Wall M, Sadun AA. Threshold Amsler grid testing: cross-polarizing lenses enhance yield. *Arch Ophthalmol*. 1986;104(4):520–523.
4. Keltner JL, Johnson CA, Balestrery FG. Suprathreshold static perimetry: initial clinical trials with the Fieldmaster automated perimeter. *Arch Ophthalmol*. 1979;97(2):260–272.
5. Wiggins M, Dersu I. Understanding visual fields, part III: Which field should be performed? *J Ophthalmic Med Tech*. 2007;3.
6. Rohrschneider K, Becker M, Schumacher N, et al. Normal values for fundus perimetry with the scanning laser ophthalmoscope. *Am J Ophthalmol*. 1998;126(1):52–58.

7. Mojon DS, Zulauf M. Normal values of short-wavelength automated perimetry. *Ophthalmologica*. 2003;217(4):260–264.
8. Zwas F, Weiss H, McKinnon P. Spectral sensitivity measurements in early diabetic retinopathy. *Ophthalmic Res*. 1980;12:87–96.
9. Wild JM, Cubbidge RP, Pacey IE, et al. Statistical aspects of the normal visual field in short-wavelength automated perimetry. *Invest Ophthalmol Vis Sci*. 1998;39(1):54–63.
10. Bell JA, Feldon SE. Retinal microangiopathy. Correlation of OCTOPUS perimetry with fluorescein angiography. *Arch Ophthalmol*. 1984;102(9):1294–1298.
11. Rohrschneider K, Bultmann S, Springer C. Use of fundus perimetry (microperimetry) to quantify macular sensitivity. *Prog Retin Eye Res*. 2008;27(5):536–548.
12. Rohrschneider K, Springer C, Bultmann S, Volcker HE. Microperimetry – comparison between the micro perimeter 1 and scanning laser ophthalmoscope–fundus perimetry. *Am J Ophthalmol*. 2005;139(1):125–134.
13. Landa G, Rosen RB, Garcia PM, et al. Combined three-dimensional spectral OCT/SLO topography and Microperimetry: steps toward achieving functional spectral OCT/SLO. *Ophthalmic Res*. 2010;43(2):92–98.
14. Roorda A, Zhang Y, Duncan JL. High-resolution in vivo imaging of the RPE mosaic in eyes with retinal disease. *Invest Ophthalmol Vis Sci*. 2007;48(5):2297–2303.
15. Winther C, Frisen L. A compact rarebit test for macular diseases. *Br J Ophthalmol*. 2010;94(3):324–327.
16. Lowenstein A, Ferencz J, Lang Y. Toward earlier detection of choroidal neovascularization secondary to age-related macular degeneration. *Retina*. 2010;30:1058.
17. Norden LC. Reliability in perimetry. *J Am Optom Assoc*. 1989;60(12):880–890.
18. Seiple W, Clemens CJ, Greenstein VC, et al. Test–retest reliability of the multifocal electroretinogram and humphrey visual fields in patients with retinitis pigmentosa. *Doc Ophthalmol*. 2004;109(3):255–272.
19. Weingessel B, Sacu S, Vecsei-Marlovits PV, et al. Interexaminer and intraexaminer reliability of the

microperimeter MP-1. *Eye (Lond)*. 2009;23(5):1052–1058.
20. Bittner AK, Haythornthwaite JA, Diener-West M, et al. Worse-than-usual visual fields measured in retinitis pigmentosa related to episodically decreased general health. *Br J Ophthalmol*. 2013;97(2):145–148.
21. Sandberg MA, Gaudio AR, Berson EL. Disease course of patients with pericentral retinitis pigmentosa. *Am J Ophthalmol*. 2005;140(1):100–106.
22. Sandberg MA, Rosner B, Weigel-DiFranco C, et al. Disease course of patients with X-linked retinitis pigmentosa due to RPGR gene mutations. *Invest Ophthalmol Vis Sci*. 2007;48(3):1298–1304.
23. Schwartz SB, Aleman TS, Cideciyan AV, et al. Disease expression in Usher syndrome caused by VLGR1 gene mutation (USH2C) and comparison with USH2A phenotype. *Invest Ophthalmol Vis Sci*. 2005;46(2):734–743.
24. Comander J, Weigel-DiFranco C, Sandberg MA, et al. Visual function in carriers of X-linked retinitis pigmentosa. *Ophthalmology*. 2015;122(9):1899–1906.
25. Azari AA, Aleman TS, Cideciyan AV, et al. Retinal disease expression in Bardet–Biedl syndrome-1 (BBS1) is a spectrum from maculopathy to retina-wide degeneration. *Invest Ophthalmol Vis Sci*. 2006;47(11):5004–5010.
26. Gerth C, Wright T, Heon E, et al. Assessment of central retinal function in patients with advanced retinitis pigmentosa. *Invest Ophthalmol Vis Sci*. 2007;48(3):1312–1318.
27. Lodha N, Westall CA, Brent M, et al. A modified protocol for the assessment of visual function in patients with retinitis pigmentosa. *Adv Exp Med Biol*. 2003;533:49–57.
28. Rotenstreich Y, Harats D, Shaish A, et al. Treatment of a retinal dystrophy, fundus albipunctatus, with oral 9-cis-{beta}-carotene. *Br J Ophthalmol*. 2010;94(5):616–621.
29. Iarossi G, Falsini B, Piccardi M. Regional cone dysfunction in retinitis pigmentosa evaluated by flicker ERGs: relationship with perimetric sensitivity losses. *Invest Ophthalmol Vis Sci*. 2003;44(2):866–874.
30. Fischer M, Fleischhauer J, Gillies M. A new method to monitor visual field defects caused by photoreceptor

degeneration by quantitative optical coherence tomography. *Invest Ophthalmol Vis Sci*. 2008;49:3617.
31. Rangaswamy NV, Patel HM, Locke KG, et al. A comparison of visual field sensitivity to photoreceptor thickness in retinitis pigmentosa. *Invest Ophthalmol Vis Sci*. 2010;51(8):4213–4219.
32. Jacobson SG, Roman AJ, Aleman TS, et al. Normal central retinal function and structure preserved in retinitis pigmentosa. *Invest Ophthalmol Vis Sci*. 2010;51(2):1079–1085.
33. Aizawa S, Mitamura Y, Hagiwara A, et al. Changes of fundus autofluorescence, photoreceptor inner and outer segment junction line, and visual function in patients with retinitis pigmentosa. *Clin Experiment Ophthalmol*. 2010;38(6):597–604.
34. Genead MA, Fishman GA, Stone EM, et al. The natural history of Stargardt disease with specific sequence mutation in the ABCA4 gene. *Invest Ophthalmol Vis Sci*. 2009;50(12):5867–5871.
35. Wakabayashi T, Sawa M, Gomi F, et al. Correlation of fundus autofluorescence with photoreceptor morphology and functional changes in eyes with retinitis pigmentosa. *Acta Ophthalmol*. 2010;88(5):e177–83.
36. Popovic P, Jarc-Vidmar M, Hawlina M. Abnormal fundus autofluorescence in relation to retinal function in patients with retinitis pigmentosa. *Graefes Arch Clin Exp Ophthalmol*. 2005;243(10):1018–1027.
37. Birch DG, Locke KG, Felius J, et al. Rates of decline in regions of the visual field defined by frequency-domain optical coherence tomography in patients with RPGR-mediated X-linked retinitis pigmentosa. *Ophthalmology*. 2015;122(4):833–839.
38. Lupo S, Grenga PL, Vingolo EM. Fourier-domain optical coherence tomography and microperimetry findings in retinitis pigmentosa. *Am J Ophthalmol*. 2011;151(1):106–111.
39. Oishi M, Oishi A, Ogino K, et al. Wide-field fundus autofluorescence abnormalities and visual function in patients with cone and cone–rod dystrophies. *Invest Ophthalmol Vis Sci*. 2014;55(6):3572–3577.

40. Mori F, Ishiko S, Kitaya N, et al. Scotoma and fixation patterns using scanning laser ophthalmoscope microperimetry in patients with macular dystrophy. *Am J Ophthalmol*. 2001;132(6):897–902.
41. Testa F, Melillo P, Di Iorio V, et al. Macular function and morphologic features in juvenile Stargardt disease: longitudinal study. *Ophthalmology*. 2014;121(12):2399–2405.
42. Gaucher D, Saleh M, Sauer A, et al. Spectral OCT analysis in Bietti crystalline dystrophy. *Eur J Ophthalmol*. 2010;20(3):612–614.
43. Gundogan FC, Dinc UA, Erdem U, et al. Multifocal electroretinogram and central visual field testing in central areolar choroidal dystrophy. *Eur J Ophthalmol*. 2010;20(5):919–924.
44. Szlyk JP, Paliga J, Seiple W, et al. Comprehensive functional vision assessment of patients with North Carolina macular dystrophy (MCDR1). *Retina*. 2005;25(4):489–497.
45. Renner AB, Tillack H, Kraus H, et al. Morphology and functional characteristics in adult vitelliform macular dystrophy. *Retina*. 2004;24(6):929–939.
46. Hellgren KJ, Agardh E, Bengtsson B. Progression of early retinal dysfunction in diabetes over time: results of a long-term prospective clinical study. *Diabetes*. 2014;63(9):3104–3111.
47. Roth J. Central visual field in diabetes. *Br J Ophthalmol*. 1969;53:16.
48. Parravano M, Oddone F, Boccassini B, et al. Functional retinal impairment in type 1 diabetic patients without any signs of retinopathy. *Ophthalmic Res*. 2013;50(2):108–112.
49. Remky A, Arend O, Hendricks S. Short-wavelength automated perimetry and capillary density in early diabetic maculopathy. *Invest Ophthalmol Vis Sci*. 2000;41(1):274–281.
50. De Benedetto U, Querques G, Lattanzio R, et al. Macular dysfunction is common in both type 1 and type 2 diabetic patients without macular edema. *Retina*. 2014;34(11):2171–2177.
51. Hudson C, Flanagan JG, Turner GS, et al. Short-wavelength sensitive visual field loss in patients with clinically

significant diabetic macular oedema. *Diabetologia*. 1998;41(8):918–928.
52. Mori F, Ishiko S, Kitaya N, et al. Use of scanning laser ophthalmoscope microperimetry in clinically significant macular edema in type 2 diabetes mellitus. *Jpn J Ophthalmol*. 2002;46(6):650–655.
53. Remky A, Weber A, Hendricks S, et al. Short-wavelength automated perimetry in patients with diabetes mellitus without macular edema. *Graefes Arch Clin Exp Ophthalmol*. 2003;241(6):468–471.
54. Mastropasqua L, Verrotti A, Lobefalo L, et al. Visual field defects in diabetic children without retinopathy: relation between visual function and microalbuminuria. *Acta Ophthalmol Scand*. 1995;73(2):125–128.
55. Yohannan J, Bittencourt M, Sepah YJ, et al. Association of retinal sensitivity to integrity of photoreceptor inner/outer segment junction in patients with diabetic macular edema. *Ophthalmology*. 2013;120(6):1254–1261.
56. Gandalfo E, Zingirian M, Corrallo G, et al. Diabetic retinopathy: perimetric findings. Greve EL, Heijl A. *Fifth International Visual Field Symposium*. Dr W Junk: The Hague; 1983.
57. Wisznia KI, Lieberman TW, Leopold IH. Visual fields in diabetic retinopathy. *Br J Ophthalmol*. 1971;55(3):183–188.
58. Federman JL, Lloyd J. Automated static perimetry to evaluate diabetic retinopathy. *Trans Am Ophthalmol Soc*. 1984;82:358–370.
59. Pahor D. Automated static perimetry as a screening method for evaluation of retinal perfusion in diabetic retinopathy. *Int Ophthalmol*. 1997–1998;21(6):305–309.
60. Lutze M, Bresnick GH. Lens-corrected visual field sensitivity and diabetes. *Invest Ophthalmol Vis Sci*. 1994;35(2):649–655.
61. Bengtsson B, Heijl A, Agardh E. Visual fields correlate better than visual acuity to severity of diabetic retinopathy. *Diabetologia*. 2005;48(12):2494–2500.
62. Agardh E, Stjernquist H, Heijl A, et al. Visual acuity and perimetry as measures of visual function in diabetic macular oedema. *Diabetologia*. 2006;49(1):200–206.

63. Apaydin KC, Akar Y, Akar ME, et al. Menstrual cycle-dependent changes in blue-on-yellow visual field analysis of young diabetic women with severe non-proliferative diabetic retinopathy. *Clin Experiment Ophthalmol*. 2004;32(3):265–269.
64. Stavrou EP, Wood JM. Central visual field changes using flicker perimetry in type 2 diabetes mellitus. *Acta Ophthalmol Scand*. 2005;83(5):574–580.
65. Barsam A, Laidlaw A. Visual fields in patients who have undergone vitrectomy for complications of diabetic retinopathy: a prospective study. *BMC Ophthalmol*. 2006;26(6):5.
66. Frank RN. Visual fields and electroretinography following extensive photocoagulation. *Arch Ophthalmol*. 1975;93(8):591–598.
67. Wessing A, Meyer-Schwickerath G. Treatment of diabetic retinopathy by light-coagulation. *Diabetologia*. 1969;5(5):312–317.
68. Zingirian M, Pisano E. Gandalfo E. Visual field damage after photocoagulative treatment for diabetic retinopathy. Greve EL. *Second International Visual Field Symposium*. Dr W Junk: The Hague; 1977.
69. Yoon YH, Lee J, Kim YJ. Preservation of retinal sensitivity in central visual field after panretinal photocoagulation in diabetics. *Korean J Ophthalmol*. 1996;10(1):48–54.
70. Hulbert M, Vernon S. Passing the DVLC field regulations following bilateral panretinal photocoagulation in diabetics. *Eye (Lond)*. 1992;6:456–460.
71. Hudson C, Flanagan JG, Turner GS, et al. Correlation of a scanning laser derived oedema index and visual function following grid laser treatment for diabetic macular oedema. *Br J Ophthalmol*. 2003;87(4):455–461.
72. Rohrschneider K, Bultmann S, Gluck R, et al. Scanning laser ophthalmoscope fundus perimetry before and after laser photocoagulation for clinically significant diabetic macular edema. *Am J Ophthalmol*. 2000;129(1):27–32.
73. Vujosevic S, Bottega E, Casciano M, et al. Microperimetry and fundus autofluorescence in diabetic macular edema:

subthreshold micropulse diode laser versus modified early treatment diabetic retinopathy study laser photocoagulation. *Retina*. 2010;30(6):908–916.
74. Deak GG, Bolz M, Ritter M, et al. A systematic correlation between morphology and functional alterations in diabetic macular edema. *Invest Ophthalmol Vis Sci*. 2010;51(12):6710–6714.
75. Okada K, Yamamoto S, Mizunoya S, et al. Correlation of retinal sensitivity measured with fundus-related microperimetry to visual acuity and retinal thickness in eyes with diabetic macular edema. *Eye (Lond)*. 2006;20(7):805–809.
76. Vujosevic S, Midena E, Pilotto E, et al. Diabetic macular edema: correlation between microperimetry and optical coherence tomography findings. *Invest Ophthalmol Vis Sci*. 2006;47(7):3044–3051.
77. Vujosevic S, Casciano M, Pilotto E, et al. Diabetic macular edema: fundus autofluorescence and functional correlations. *Invest Ophthalmol Vis Sci*. 2011;52(1):442–448.
78. Querques G, Bux AV, Martinelli D, et al. Short-term fluctuation of diabetic macular edema after intravitreal ranibizumab injection. *Retina*. 2009;29(9):1274–1281.
79. Kameda T, Nishijima K, Unoki N, et al. Geographic pattern of central retinal sensitivity after intravitreal triamcinolone for diabetic macular edema. *Graefes Arch Clin Exp Ophthalmol*. 2011;249(1):3–9.
80. Cusick M, Toma HS, Hwang TS, et al. Binasal visual field defects from simultaneous bilateral retinal infarctions in sickle cell disease. *Am J Ophthalmol*. 2007;143(5):893–896.
81. Lim JI. Ophthalmic manifestations of sickle cell disease: update of the latest findings. *Curr Opin Ophthalmol*. 2012;23(6):533–536.
82. McLoone E, O'Keefe M, McLoone S, et al. Effect of diode laser retinal ablative therapy for threshold retinopathy of prematurity on the visual field: results of Goldmann perimetry at a mean age of 11 years. *J Pediatr Ophthalmol Strabismus*. 2007;44(3):170–173.
83. Quinn GE, Dobson V, Hardy RJ, et al. Visual field extent at 6

years of age in children who had high-risk prethreshold retinopathy of prematurity. *Arch Ophthalmol*. 2011;129(2):127–132.
84. Meyer CH, Callizo J, Schmidt JC, et al. Functional and anatomical findings in acute Purtscher's retinopathy. *Ophthalmologica*. 2006;220(5):343–346.
85. Hamp AM, Chu E, Slagle WS, et al. Purtscher's retinopathy associated with acute pancreatitis. *Optom Vis Sci*. 2014;91(2):e43–51.
86. Kozobolis VP, Detorakis ET, Georgiadis GS, et al. Perimetric and retrobulbar blood flow changes following carotid endarterectomy. *Graefes Arch Clin Exp Ophthalmol*. 2007;245(11):1639–1645.
87. Qu L, Feng J, Zou S, et al. Improved visual, acoustic, and neurocognitive functions after carotid endarterectomy in patients with minor stroke from severe carotid stenosis. *J Vasc Surg*. 2015;62(3):635–644.
88. Imasawa M, Tsumura T, Kikuchi T, et al. Humphrey perimetry as a predictor of visual improvement after photodynamic therapy. *Jpn J Ophthalmol*. 2009;53(3):281–282.
89. Chalam KV, Agarwal S, Gupta SK, et al. Recovery of retinal sensitivity after transient branch retinal artery occlusion. *Ophthalmic Surg Lasers Imaging*. 2007;38(4):328–329.
90. Wong WT, Forooghian F, Majumdar Z, et al. Fundus autofluorescence in type 2 idiopathic macular telangiectasia: correlation with optical coherence tomography and microperimetry. *Am J Ophthalmol*. 2009;148(4):573–583.
91. Barbazetto IA, Schmidt-Erfurth UM. Evaluation of functional defects in branch retinal vein occlusion before and after laser treatment with scanning laser perimetry. *Ophthalmology*. 2000;107(6):1089–1098.
92. Yamaike N, Kita M, Tsujikawa A, et al. Perimetric sensitivity with the micro perimeter 1 and retinal thickness in patients with branch retinal vein occlusion. *Am J Ophthalmol*. 2007;143(2):342–344.
93. Ageno W, Cattaneo R, Manfredi E, et al. Parnaparin versus

aspirin in the treatment of retinal vein occlusion: a randomized, double blind, controlled study. *Thromb Res*. 2010;125(2):137–141.
94. Parravano M, Oddone F, Boccassini B, et al. Exploring the morphological and functional retinal changes after dexamethasone intravitreal implant (Ozurdex(R) in macular edema due to retinal vein occlusion. *Ophthalmic Res*. 2014;51(3):153–160.
95. Tsujikawa A, Hangai M, Kikuchi M, et al. Visual field defect after radial optic neurotomy for central retinal vein occlusion. *Jpn J Ophthalmol*. 2006;50(2):158–160.
96. Barak A, Kesler A, Gold D, Loewenstein A. Visual field defects after radial optic neurotomy for central retinal vein occlusion. *Retina*. 2006;26(5):549–554.
97. Afrashi F, Erakgun T, Uzunel D. Comparison of achromatic and blue-on-yellow perimetry in patients with resolved central serous chorioretinopathy. *Ophthalmologica*. 2005;219:202–205.
98. Sekine A, Imasawa M, Iijima H. Retinal thickness and perimetric sensitivity in central serous chorioretinopathy. *Jpn J Ophthalmol*. 2010;54(6):578–583.
99. Dinc UA, Yenerel M, Tatlipinar S, et al. Correlation of retinal sensitivity and retinal thickness in central serous chorioretinopathy. *Ophthalmologica*. 2010;224(1):2–9.
100. Baran NV, Gurlu VP, Esgin H. Long-term macular function in eyes with central serous chorioretinopathy. *Clin Experiment Ophthalmol*. 2005;33(4):369–372.
101. Ozdemir H, Karacorlu SA, Senturk F, et al. Assessment of macular function by microperimetry in unilateral resolved central serous chorioretinopathy. *Eye (Lond)*. 2008;22:204–208.
102. Natsikos VE, Hart JC. Static perimetric and Amsler chart changes in patients with idiopathic central serous retinopathy. *Acta Ophthalmol (Copenh)*. 1980;58(6):908–917.
103. Kiss CG, Barisani-Asenbauer T, Simader C, et al. Central visual field impairment during and following cystoid macular oedema. *Br J Ophthalmol*. 2008;92(1):84–88.
104. Remky A, Lichtenberg K, Elsner AE, et al. Short wavelength

automated perimetry in age related maculopathy. *Br J Ophthalmol*. 2001;85(12):1432–1436.
105. Remky A, Elsner AE. Blue on yellow perimetry with scanning laser ophthalmoscopy in patients with age related macular disease. *Br J Ophthalmol*. 2005;89(4):464–469.
106. Takamine Y, Shiraki K, Moriwaki M. Retinal sensitivity measurement over drusen using scanning laser ophthalmoscope microperimetry. *Grafes Arch Kini Exp Ophthalmol*. 1998;236:285–290.
107. Iwama D, Tsujikawa A, Ojima Y, et al. Relationship between retinal sensitivity and morphologic changes in eyes with confluent soft drusen. *Clin Exp Ophthalmol*. 2010;38(5):483–488.
108. Sohn EH, Chen FK, Rubin GS, et al. Macular function assessed by microperimetry in patients with enhanced S-cone syndrome. *Ophthalmology*. 2010;117(6):1199–1206.e1.
109. Biswas S, Funnell CL, Gray J, et al. Nidek MP-1 microperimetry and Fourier domain optical coherence tomography (FD-OCT. in X linked retinoschisis. *Br J Ophthalmol*. 2010;94(7):949–950.
110. Shenoy R, McCilvenny S. Microperimetric evaluation of macula in retinopathy of membranoproliferative glomerulonephritis type II: a case report. *Eur J Ophthalmol*. 2006;16(4):634–636.
111. Ahn JK, Seo JM, Chung H, et al. Anatomical and functional characteristics in atrophic maculopathy associated with spinocerebellar ataxia type 7. *Am J Ophthalmol*. 2005;139(5):923–925.
112. Wu Z, Ayton LN, Luu CD, et al. Longitudinal changes in microperimetry and low luminance visual acuity in age-related macular degeneration. *JAMA Ophthalmol*. 2015;133(4):442–448.
113. Wu Z, Ayton LN, Luu CD, et al. Relationship between retinal microstructures on optical coherence tomography and microperimetry in age-related macular degeneration. *Ophthalmology*. 2014;121(7):1445–1452.
114. Querques L, Querques G, Forte R. Microperimetric correlations of autofluorescence and optical coherence

tomography imaging in dry age-related macular degeneration. *Am J Ophthalmol*. 2012;153(6):1110–1115.
115. Landa G, Su E, Garcia PM, et al. Inner segment–outer segment junctional layer integrity and corresponding retinal sensitivity in dry and wet forms of age-related macular degeneration. *Retina*. 2011;31(2):364–370.
116. Acton JH, Smith RT, Hood DC, et al. Relationship between retinal layer thickness and the visual field in early age-related macular degeneration. *Invest Ophthalmol Vis Sci*. 2012;53(12):7618–7624.
117. Sulzbacher F, Roberts P, Munk MR, et al. Relationship of retinal morphology and retinal sensitivity in the treatment of neovascular age-related macular degeneration using aflibercept. *Invest Ophthalmol Vis Sci*. 2014;56(2):1158–1167.
118. Hautamaki A, Oikkonen J, Onkamo P, et al. Correlation between components of newly diagnosed exudative age-related macular degeneration lesion and focal retinal sensitivity. *Acta Ophthalmol*. 2014;92(1):51–58.
119. Wu Z, Ayton LN, Guymer RH, et al. Comparison between multifocal electroretinography and microperimetry in age-related macular degeneration. *Invest Ophthalmol Vis Sci*. 2014;55(10):6431–6439.
120. Midena E, Vujosevic S, Convento E, et al. Microperimetry and fundus autofluorescence in patients with early age-related macular degeneration. *Br J Ophthalmol*. 2007;91(11):1499–1503.
121. Remky A, Weber A, Arend O, et al. Topical dorzolamide increases pericentral visual function in age-related maculopathy: pilot study findings with short-wavelength automated perimetry. *Acta Ophthalmol Scand*. 2005;83(2):154–160.
122. Feher J, Kovacs B, Kovacs I, et al. Improvement of visual functions and fundus alterations in early age-related macular degeneration treated with a combination of acetyl-L-carnitine, n-3 fatty acids, and coenzyme Q10. *Ophthalmologica*. 2005;219(3):154–166.
123. Wong WT, Kam W, Cunningham D, et al. Treatment of geographic atrophy by the topical administration of OT-551:

results of a phase II clinical trial. *Invest Ophthalmol Vis Sci*. 2010;51(12):6131–6139.
124. Wu Z, Ayton L, Guymer R. Low-luminance visual acuity and microperimetry in age-related macular degeneration. *Ophthalmology*. 2014;121(8):1612–1619.
125. Fujii GY, de Juan E Jr, Sunness J, et al. Patient selection for macular translocation surgery using the scanning laser ophthalmoscope. *Ophthalmology*. 2002;109(9):1737–1744.
126. Chen FK, Uppal GS, MacLaren RE, et al. Long-term visual and microperimetry outcomes following autologous retinal pigment epithelium choroid graft for neovascular age-related macular degeneration. *Clin Expriment Ophthalmol*. 2009;37(3):275–285.
127. Tezel TH, Del Priore LV, Flowers BE, et al. Correlation between scanning laser ophthalmoscope microperimetry and anatomic abnormalities in patients with subfoveal neovascularization. *Ophthalmology*. 1996;103(11):1829–1836.
128. Schmidt-Erfurth UM, Elsner H, Terai N, et al. Effects of verteporfin therapy on central visual field function. *Ophthalmology*. 2004;111(5):931–939.
129. Yodoi Y, Tsujikawa A, Kameda T, et al. Central retinal sensitivity measured with the micro perimeter 1 after photodynamic therapy for polypoidal choroidal vasculopathy. *Am J Ophthalmol*. 2007;143(6):984–994.
130. Imasawa M, Tsumura T, Kikuchi T, et al. Humphrey perimetry as a predictor of visual improvement after photodynamic therapy. *Jpn J Ophthalmol*. 2009;53(3):281–282.
131. Lavinsky F, Tolentino MJ, Lavinsky J. The macular threshold protocol of the Humphrey visual field analyzer: a superior functional outcome of intravitreal bevacizumab for the treatment of neovascular age-related macular degeneration. *Arq Bras Oftalmol*. 2010;73(2):111–115.
132. Squirrell DM, Mawer NP, Mody CH, et al. Visual outcome after intravitreal ranibizumab for wet age-related macular degeneration: a comparison between best-corrected visual acuity and microperimetry. *Retina*. 2010;30(3):436–442.
133. Parravano M, Oddone F, Tedeschi M, et al. Retinal

functional changes measured by microperimetry in neovascular age-related macular degeneration treated with ranibizumab: 24-month results. *Retina*. 2010;30(7):1017–1024.
134. Weigert G, Kaya S, Pemp B, et al. Effects of lutein supplementation on macular pigment optical density and visual acuity in patients with age-related macular degeneration. *Invest Ophthalmol Vis Sci*. 2011;52(11):8174–8178.
135. Augustin AJ, Offermann I, Lutz J, et al. Comparison of the original Amsler grid with the modified Amsler grid: result for patients with age-related macular degeneration. *Retina*. 2005;25(4):443–445.
136. Nazemi PP, Fink W, Lim JI, et al. Scotomas of age-related macular degeneration detected and characterized by means of a novel three-dimensional computer-automated visual field test. *Retina*. 2005;25(4):446–453.
137. Lowenstein A, Malac R, Goldstein M. Replacing the Amsler grid: a new method for monitoring patients with age-related macular degeneration. *Ophthalmology*. 2003;110:966–970.
138. Preferential Hyperacuity Perimetry Research Group. Preferential hyperacuity perimeter (PreView PHP) for detecting choroidal neovascularization study. *Ophthalmology*. 2005;112:1758–1765.
139. Kroyer K, Jensen OM, Larsen M. Objective signs of photoreceptor displacement by binocular correspondence perimetry: a study of epiretinal membranes. *Invest Ophthalmol Vis Sci*. 2005;46(3):1017–1022.
140. Tarita-Nistor L, Mandelcorn MS, Steinbach MJ, et al. Fixation stability and location in patients with unilateral idiopathic epiretinal membrane. *Ophthalmic Surg Lasers Imaging Retina*. 2013;44(1):46–49.
141. Parravano M, Oddone F, Boccassini B, et al. Functional and structural assessment of lamellar macular holes. *Br J Ophthalmol*. 2013;97(3):291–296.
142. Reibaldi M, Parravano M, Varano M, et al. Foveal microstructure and functional parameters in lamellar

macular hole. *Am J Ophthalmol*. 2012;154(6):974–980.e1.
143. Amari F, Ohta K, Kojima H, et al. Predicting visual outcome after macular hole surgery using scanning laser ophthalmoscope microperimetry. *Br J Ophthalmol*. 2001;85(1):96–98.
144. Hikichi T, Ishiko S, Takamiya A, et al. Scanning laser ophthalmoscope correlations with biomicroscopic findings and foveal function after macular hole closure. *Arch Ophthalmol*. 2000;118(2):193–197.
145. Ozdemir H, Karacorlu M, Senturk F, et al. Retinal sensitivity and fixation changes 1 year after triamcinolone acetonide assisted internal limiting membrane peeling for macular hole surgery – a MP-1 microperimetric study. *Acta Ophthalmol*. 2010;88(6):e222–7.
146. Chung H, Shin CJ, Kim JG, et al. Correlation of microperimetry with fundus autofluorescence and spectral-domain optical coherence tomography in repaired macular holes. *Am J Ophthalmol*. 2011;151(1):128–136.e3.
147. Chen WC, Wang Y, Li XX. Morphologic and functional evaluation before and after successful macular hole surgery using spectral-domain optical coherence tomography combined with microperimetry. *Retina*. 2012;32(9):1733–1742.
148. Sun Z, Gan D, Jiang C, et al. Effect of preoperative retinal sensitivity and fixation on long-term prognosis for idiopathic macular holes. *Graefes Arch Clin Exp Ophthalmol*. 2012;250(11):1587–1596.
149. Bonnabel A, Bron AM, Isaico R, et al. Long-term anatomical and functional outcomes of idiopathic macular hole surgery: the yield of spectral-domain OCT combined with microperimetry. *Graefes Arch Clin Exp Ophthalmol*. 2013;251(11):2505–2511.
150. Tadayoni R, Svorenova I, Erginay A, et al. Decreased retinal sensitivity after internal limiting membrane peeling for macular hole surgery. *Br J Ophthalmol*. 2012;96(12):1513–1516.
151. Richter-Mueksch S, Vecsei-Marlovits PV, Sacu SG, et al. Functional macular mapping in patients with vitreomacular

pathologic features before and after surgery. *Am J Ophthalmol*. 2007;144(1):23–31.
152. Ezra E, Arden GB, Riordan-Eva P, et al. Visual field loss following vitrectomy for stage 2 and 3 macular holes. *Br J Ophthalmol*. 1996;80(6):519–525.
153. Hutton WL, Fuller DG, Snyder WB, et al. Visual field defects after macular hole surgery: a new finding. *Ophthalmology*. 1996;103(12):2152–2158 [discussion 2158–9].
154. Melberg NS, Thomas MA. Visual field loss after pars plana vitrectomy with air/fluid exchange. *Am J Ophthalmol*. 1995;120(3):386–388.
155. Hillenkamp J, Saikia P, Gora F, et al. Macular function and morphology after peeling of idiopathic epiretinal membrane with and without the assistance of indocyanine green. *Br J Ophthalmol*. 2005;89(4):437–443.
156. von Jagow B, Hoing A, Gandorfer A, et al. Functional outcome of indocyanine green-assisted macular surgery: 7-year follow-up. *Retina*. 2009;29(9):1249–1256.
157. Uemura A, Kanda S, Sakamoto Y, et al. Visual field defects after uneventful vitrectomy for epiretinal membrane with indocyanine green-assisted internal limiting membrane peeling. *Am J Ophthalmol*. 2003;136(2):252–257.
158. Tari S, Vidne-Hay O, Greenstein V. Functional and structural measurement for the assessment of internal limiting membrane peeling in idiopathic macular pucker. *Am J Ophthalmol*. 2003;136:252–257.
159. Tsuiki E, Fujikawa A, Miyamura N, et al. Visual field defects after macular hole surgery with indocyanine green-assisted internal limiting membrane peeling. *Am J Ophthalmol*. 2007;143(4):704–705.
160. Balaiya S, Brar VS, Murthy RK, et al. Comparative in vitro safety analysis of dyes for chromovitrectomy: indocyanine green, brilliant blue green, bromophenol blue, and infracyanine green. *Retina*. 2011;31(6):1128–1136.
161. Totan Y, Guler E, Guragac FB, et al. Brilliant blue G assisted macular surgery: the effect of air infusion on contrast recognisability in internal limiting membrane peeling. *Br J Ophthalmol*. 2015;99(1):75–80.

162. Machida S, Toba Y, Nishimura T, et al. Comparisons of cone electroretinograms after indocyanine green-, brilliant blue G-, or triamcinolone acetonide-assisted macular hole surgery. *Graefes Arch Clin Exp Ophthalmol*. 2014;252(9):1423–1433.
163. Baba T, Hagiwara A, Sato E, et al. Comparison of vitrectomy with brilliant blue G or indocyanine green on retinal microstructure and function of eyes with macular hole. *Ophthalmology*. 2012;119(12):2609–2615.
164. Hart WM Jr, Burde RM, Johnston GP, et al. Static perimetry in chloroquine retinopathy: perifoveal patterns of visual field depression. *Arch Ophthalmol*. 1984;102(3):377–380.
165. Michaelides M, Stover N, Francis P. Retinal toxicity associated with hydroxychloroquine and chloroquine: risk factors, screening, and progression despite cessation of therapy. *Arch Ophthalmol*. 2011;129:30–39.
166. Salu P, Uvijls A, van den Brande P. Normalization of generalized retinal function and progression of maculopathy after cessation of therapy in a case of severe hydroxychloroquine retinopathy with 19 years follow-up. *Doc Ophthalmol*. 2010;120:251–264.
167. Xiaoyun MA, Dongyi HE, Linping HE. Assessing chloroquine toxicity in RA patients using retinal nerve fibre layer thickness, multifocal electroretinography and visual field test. *Br J Ophthalmol*. 2010;94(12):1632–1636.
168. Anderson C, Blaha GR, Marx JL. Humphrey visual field findings in hydroxychloroquine toxicity. *Eye (Lond)*. 2011;25(12):1535–1545.
169. Almony A, Garg S, Peters RK, et al. Threshold Amsler grid as a screening tool for asymptomatic patients on hydroxychloroquine therapy. *Br J Ophthalmol*. 2005;89(5):569–574.
170. Anderson C, Pahk P, Blaha GR, et al. Preferential hyperacuity perimetry to detect hydroxychloroquine retinal toxicity. *Retina*. 2009;29(8):1188–1192.
171. Jivrajka RV, Genead MA, McAnany JJ, et al. Microperimetric sensitivity in patients on hydroxychloroquine (Plaquenil) therapy. *Eye (Lond)*.

2013;27(9):1044–1052.
172. Martinez-Costa L, Victoria Ibanez M, Murcia-Bello C, et al. Use of microperimetry to evaluate hydroxychloroquine and chloroquine retinal toxicity. *Can J Ophthalmol*. 2013;48(5):400–405.
173. Cukras C, Huynh N, Vitale S, et al. Subjective and objective screening tests for hydroxychloroquine toxicity. *Ophthalmology*. 2015;122(2):356–366.
174. Greenstein VC, Amaro-Quireza L, Abraham ES, et al. A comparison of structural and functional changes in patients screened for hydroxychloroquine retinopathy. *Doc Ophthalmol*. 2015;130(1):13–23.
175. Marmor MF, Melles RB. Disparity between visual fields and optical coherence tomography in hydroxychloroquine retinopathy. *Ophthalmology*. 2014;121(6):1257–1262.
176. Eisner A, Austin DF, Samples JR. Short wavelength automated perimetry and tamoxifen use. *Br J Ophthalmol*. 2004;88(1):125–130.
177. Toggweiler S, Wieser HG. Concentric visual field restriction under vigabatrin therapy: extent depends on the duration of drug intake. *Seizure*. 2001;10(6):420–423.
178. Jensen H, Sjo O, Uldall P. Vigabatrin and retinal changes. *Doc Ophthalmol*. 2002;104(2):171–180.
179. Hosking SL, Hilton EJ. Neurotoxic effects of GABA-transaminase inhibitors in the treatment of epilepsy: ocular perfusion and visual performance. *Ophthalmic Physiol Opt*. 2002;22(5):440–447.
180. Riikonen R, Rener-Primec Z, Carmant L. Does vigabatrin treatment for infantile spasms cause visual field defects? An international multicentre study. *Dev Med Child Neurol*. 2015;57(1):60–67.
181. McGwin G Jr, Vaphiades MS, Hall TA, et al. Non-arteritic anterior ischaemic optic neuropathy and the treatment of erectile dysfunction. *Br J Ophthalmol*. 2006;90(2):154–157.
182. Jagle H, Jagle C, Serey L, et al. Visual short-term effects of Viagra: double-blind study in healthy young subjects. *Am J Ophthalmol*. 2004;137(5):842–849.
183. Izadi S, De Silva SR, Sculfor D, et al. Persistant bilateral

relative central scotomas induced by taking an excessive dose of sildenafil. *Acta Ophthalmol*. 2012;90(6):e496–8.
184. Stanford MR, Tomlin EA, Comyn O, et al. The visual field in toxoplasmic retinochoroiditis. *Br J Ophthalmol*. 2005;89(7):812–814.
185. Oray M, Onal S, Bayraktar S, et al. Nonglaucomatous localized retinal nerve fiber layer defects in Behçet uveitis. *Am J Ophthalmol*. 2015;159(3):475–481.e1.
186. Moraes LR, Cialdini AP, Avila MP, et al. Identifying live nematodes in diffuse unilateral subacute neuroretinitis by using the scanning laser ophthalmoscope. *Arch Ophthalmol*. 2002;120(2):135–138.
187. Plummer DJ, Sample PA, Arevalo JF, et al. Visual field loss in HIV-positive patients without infectious retinopathy. *Am J Ophthalmol*. 1996;122(4):542–549.
188. Falkenstein I, Kozak I, Kayikcioglu O, et al. Assessment of retinal function in patients with HIV without infectious retinitis by multifocal electroretinogram and automated perimetry. *Retina*. 2006;26(8):928–934.
189. Plummer DJ, Marcotte TD, Sample PA, et al. Neuropsychological impairment-associated visual field deficits in HIV infection. HNRC Group. HIV Neurobehavioral Research Center. *Invest Ophthalmol Vis Sci*. 1999;40(2):435–442.
190. Hangai M, Fujimoto M, Yoshimura N. Features and function of multiple evanescent white dot syndrome. *Arch Ophthalmol*. 2009;127(10):1307–1313.
191. Forooghian F, Stetson PF, Gross NE, et al. Quantitative assessment of photoreceptor recovery in atypical multiple evanescent white dot syndrome. *Ophthalmic Surg Lasers Imaging*. 2010;41(Suppl.):S77–80.
192. Souka AA, Hillenkamp J, Gora F, et al. Correlation between optical coherence tomography and autofluorescence in acute posterior multifocal placoid pigment epitheliopathy. *Graefes Arch Clin Exp Ophthalmol*. 2006;244(10):1219–1223.
193. Thomas BC, Jacobi C, Korporal M, et al. Ocular outcome and frequency of neurological manifestations in patients with acute posterior multifocal placoid pigment

epitheliopathy (APMPPE). *J Ophthalmic Inflamm Infect*. 2012;2(3):125–131.
194. Balarabe AH, Biswas J. Serpiginous choroiditis in a referral clinic in India: visual field changes and clinical correlates. *Ocul Immunol Inflamm*. 2014;22(5):379–383.
195. Gordon LK, Goldhardt R, Holland GN, et al. Standardized visual field assessment for patients with birdshot chorioretinopathy. *Ocul Immunol Inflamm*. 2006;14(6):325–332.
196. Tomkins-Netzer O, Taylor SR, Lightman S. Long-term clinical and anatomic outcome of birdshot chorioretinopathy. *JAMA Ophthalmol*. 2014;132(1):57–62.
197. Giuliari GP, Pujari S, Shaikh M, et al. Microperimetry findings in patients with birdshot chorioretinopathy. *Can J Ophthalmol*. 2010;45(4):399–403.
198. Mahajan VB, Stone EM. Patients with an acute zonal occult outer retinopathy-like illness rapidly improve with valacyclovir treatment. *Am J Ophthalmol*. 2010;150(4):511–518.
199. Ozgur S, Esgin H. Macular function of successfully repaired macula-off retinal detachments. *Retina*. 2007;27(3):358–364.
200. Alexandridis E, Janzarik BI. Restitution of the retinal sensitivity after cured retinal detachment. Greve EL. *Second International Visual Field Symposium*. Dr. W Junk: The Hague; 1977.
201. Sakai T, Iida K, Tanaka Y, et al. Evaluation of S-cone sensitivity in reattached macula following macula-off retinal detachment surgery. *Jpn J Ophthalmol*. 2005;49(4):301–305.
202. Bourke RD, Dowler JG, Milliken AB, et al. Perimetric and angiographic effects of retinotomy. *Aust N Z J Ophthalmol*. 1996;24(3):245–249.
203. Sasoh M, Ito Y, Wakitani Y, et al. 10-year follow-up of visual functions in patients who underwent scleral buckling. *Retina*. 2005;25(8):965–971.
204. Lai WW, Leung GY, Chan CW, et al. Simultaneous spectral domain OCT and fundus autofluorescence imaging of the macula and microperimetric correspondence after

successful repair of rhegmatogenous retinal detachment. *Br J Ophthalmol*. 2010;94(3):311–318.
205. Rossetti A, Doro D, Manfre A, et al. Long-term follow-up with optical coherence tomography and microperimetry in eyes with metamorphopsia after macula-off retinal detachment repair. *Eye (Lond)*. 2010;24(12):1808–1813.
206. Abramson DH, Melson MR, Servodidio C. Visual fields in retinoblastoma survivors. *Arch Ophthalmol*. 2004;122(9):1324–1330.
207. Rahhal FM, Abramson DH, Servodidio CA, et al. Automated perimetry in patients with choroidal metastases. *Br J Ophthalmol*. 1996;80(4):309–313.
208. Enoch JM. Quantitative layer-by-layer perimetry. *Invest Ophthalmol Vis Sci*. 1978;17(3):208–257.
209. Enoch J, Fitzgerald C, Campos EC. *Quantitative layer-by-layer perimetry: an extended analysis*. Grune & Stratton: New York; 1980.
210. Enoch JM, Lawrence B. A perimetric technique believed to test receptive field properties: sequential evaluation glaucoma and other conditions. *Am J Ophthalmol*. 1975;80(4):734–758.
211. Dubois P. Acquired dyschromatopsias. *Mod Prob Ophthalmol*. 1972;11:84–93.
212. Hart WM Jr, Burde RM. Color contrast perimetry: the spatial distribution of color defects in optic nerve and retinal diseases. *Ophthalmology*. 1985;92(6):768–776.
213. Makous W, Carroll J, Wolfing JI, et al. Retinal microscotomas revealed with adaptive-optics microflashes. *Invest Ophthalmol Vis Sci*. 2006;47(9):4160–4167.
214. Chhablani J, Kaja S, Shah V. Smartphones in ophthalmology. *Indian J Ophthalmol*. 2012;60(2):127–131.
215. Johnson C, Thapa S, Robin A. *Use of an iPad tablet to perform visual field screening in Nepal*. [Poster presented at: 118th Annual Conference of the American Academy of Ophthalmology] 2014 [Chicago, IL].

PART 2

Basic Science and Translation to Therapy

OUTLINE

SECTION 1

Anatomy and Physiology

OUTLINE

15

The Development of the Retina

Thomas A. Reh

Introduction

Our understanding of the mechanisms by which the complex cellular assemblies of the retina develop has increased tremendously in the past 20 years. The growth of information in this field has been stimulated by the increasing use of molecular

genetic methods and the identification of the genes that control eye development in a variety of species. This chapter provides an overview of the basic principles of retinal development that have been known for some time and then highlights recent data that have significantly extended these principles. It is impossible to present a comprehensive review of this dramatically expanding field in this short a space, but I hope the reader will come to appreciate the complexity of the cellular and molecular interactions that generate this spectacular tissue.

Embryology of the Eye

The development of the eye is an extremely complex process, each step of which requires exquisite coordination among the various tissues that contribute to it. As a result, examples of inductive interactions at precise times during ocular development are numerous. Thus it is not surprising that many teratogens disrupt these processes and lead to developmental abnormalities in eye formation. In addition, there are many congenital defects in eye formation that are caused by mutations in genes critical for different stages in the process.

The retina is first recognized as the optic pit in the anterior neuroectoderm at day 23 of gestation;[1] a few days later (day 25) the optic vesicle can be recognized as an evagination from the diencephalon of the neural tube (Fig. 15.1). The optic vesicles initially lie immediately adjacent to the ectoderm (Fig. 15.1), but then a layer of mesenchymal cells, derived from the neural crest, becomes interposed between the ectoderm and the vesicles. The neural crest cells that surround the developing optic cup, along with the periocular mesenchyme, contribute to many ocular tissues: the corneal endothelium, the choroid, the ciliary body and the retinal vasculature (including the hyaloid artery).[2] During the next stage of ocular development, the optic vesicle folds in on itself, becoming the optic cup, and the lens ectoderm invaginates into the vesicle (Fig. 15.1). The resulting two tissue layers of the optic cup are the outer presumptive retinal pigment epithelium (RPE) and the inner presumptive neural retina, with the lens vesicle filling much of the interior of the cup. In humans, these dramatic morphologic

changes occur at approximately 25–35 days of gestation. The optic stalk, connecting the developing retina with the diencephalon, will form the scaffold for the growing axons of the optic nerve. The developing optic cup grows around the stalk from the dorsal sides, fusing to form the ventral (or embryonic) fissure. This fissure "closes" at day 33 in the human embryo, and incomplete closure of the fissure occurs from mutations in several different genes leading to colobomas (Table 15.1). The hyaloid artery, the major source of blood for the embryonic retina and lens, enters the eye through the ventral fissure. The hyaloid artery regresses by birth, but the central retinal artery remains. Incomplete or delayed regression of the hyaloid artery can lead to vitreal hemorrhage, and studies in mice have implicated the gene *Norrin* in this process.[3]

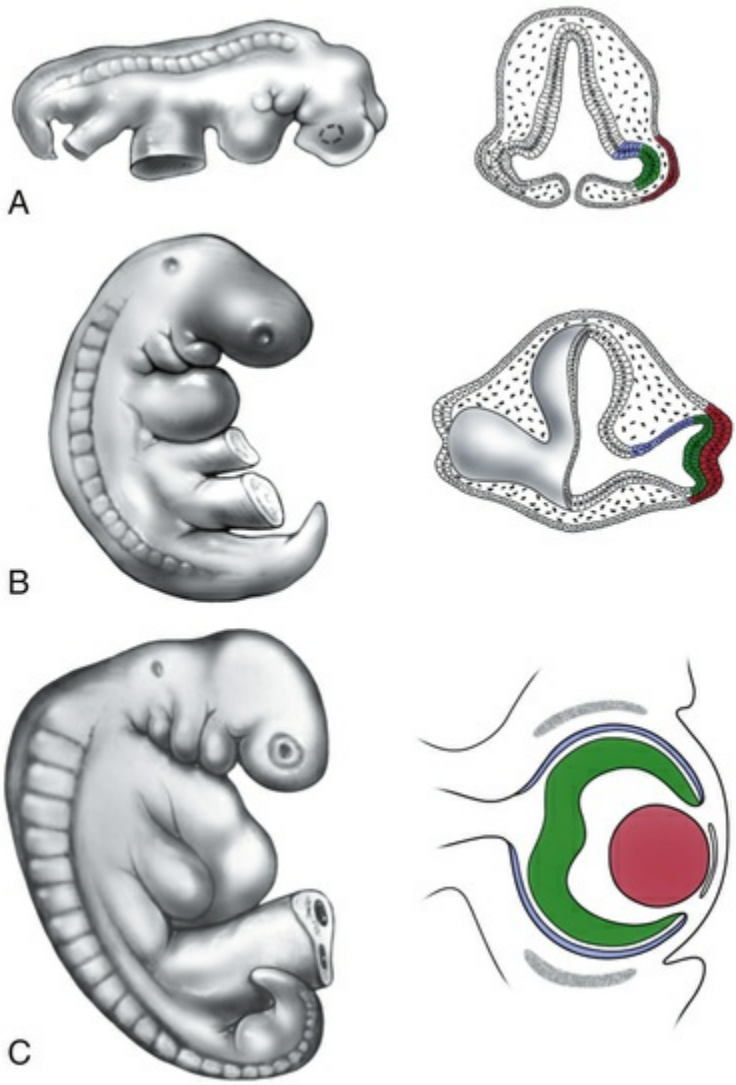

FIG. 15.1 The retinas develop as paired evaginations from the anterior central nervous system. (A) At stage 11 (13–20 somites in humans), the optic vesicles are continuous with the ectoderm near the point of closure of the anterior neuropore. (B) By postovulatory day 26, stage 12, the neuropore has closed and continued rostral growth of the prosencephalon now results in a relative caudal displacement of the vesicles. At this time the presumptive neural retina (*green*) is in close contact with the lens ectoderm (*red*), the ventral part of the optic vesicle contributes to the optic stalk, and the dorsal region of the optic vesicle gives rise to the pigmented epithelium (*blue*). (C) By stage 15, 34 postovulatory days, the lens vesicle has completely formed, and the neural retina and pigment epithelial layers are distinct.

TABLE 15.1

Key Stages of Retinal Development, Genes Associated With Those Stages, and Clinical Conditions Resulting From Their Mutations

Age	Stage	Genes	Phenotype
3–4 weeks	Optic pit; vesicle	*Pax6, Sox2, Rax, Shh, Six3, Bmp7*	Anophthalmia
5 weeks	Optic cup patterned into RPE and neural retina	*Vsx2, Bcor, Maf, Pax2, Bmp4*	Microphthalmia
5.5–6 weeks	Neurogenesis Choroidal fissure closure	*Zfhx1b, Vsx2, Bcor, Maf, Pax2, Vax2*	Microphthalmia, coloboma
8–30 weeks	Neural retina histogenesis	*Aipl1, Crx, Crb1, RPE65, Gucy2d, Rpgrip*	Leber congenital amaurosis

RPE, retinal pigment epithelium.

The Eye Field

Although the eye is first apparent as it evaginates from the diencephalon, this region of the embryo is already specified to give rise to the eye some time earlier.[4] Since much of the experimental embryology of the developing eye has been carried out in frog and chick embryos, most of the information on this process is derived from these species; however, it is likely that the process of eye development has been largely conserved throughout vertebrate

evolution, and most of what has been learned from other species is likely to be true of human eye development as well. During gastrulation, the process known as neural induction transforms a region of ectoderm into the precursors of the central nervous system (CNS), called the neural plate. Even at these early times in development, the anterior region of the neural plate is specified to give rise to the retina. This region is called the eye field. Indelibly labeling the cells in the eye field of the neural plate with vital dyes allowed embryologists of the 1920s to track the cells as they developed into the neural retina and pigmented epithelium. Additional evidence that the eye field cells were specified to produce eye tissue came from transplantation studies of these cells to ectopic locations, such as the trunk or tail of other embryos; ectopic eyes formed from the transplanted cells. In situ hybridization studies to localize these genes have shown that genes that are critical to eye development are expressed in the eye-forming regions of the neural plate before any clear morphologic differentiation into retinal structures (see below).

What makes the eye field cells capable of generating retina? In part, the eye-forming character of these cells comes from their expression of a group of proteins, called the eye field transcription factors (EFTFs), which bind to DNA and selectively activate genes important for eye development.[5] Among the first of these transcription factor genes to be expressed in eye development is *Pax6*. *Pax6* codes for a transcription factor that is a member of the paired class of homeodomain proteins. Transcription factors of this class are expressed very early in the development of many tissues and appear to be involved in controlling the identity of the various regions of the embryo. *Pax6* is expressed in the eye field, and continues to be expressed by both the optic vesicle and the developing lens. Mutations in this gene cause a phenotype in mice characterized by small eyes and aniridia in humans.[6] The homologous gene in *Drosophila*, called *eyeless*, is necessary for eye development in these animals as well.[7] Remarkably, misexpression of the *eyeless* gene in the larval tissue that normally gives rise to the leg causes ectopic eyes to form on the leg in the adult fly.[8] This result has led to the proposal that *Pax6*/*eyeless* is a master control gene, responsible for activating the other genes necessary for eye

development.[9]

More recent data have shown that *Pax6* is only one of many homeodomain proteins that are important for normal eye development in both vertebrates and invertebrates. The coordinated actions of these genes together contribute to the formation of the cells of the neural retina. These can act both as multimeric complexes and/or as part of a hierarchical pathway (Fig. 15.2). One of the key transcription factors, *Rx* (*RAX* in humans), for example, is necessary for the very earliest stages of eye formation, and targeted deletion of this gene in mice blocks eye development almost completely.[10] *Rx*, then, is close to the beginning of the cascade of the EFTFs. When *Rx* is expressed in retinal precursors, it then activates the transcription of *Pax6*, which then turns on many of the other EFTFs. Experimental misexpression of each of the different EFTFs can produce some ectopic eye-like structure, but coordinated misexpression of the EFTFs together (*Pax6*, *Rx1*, *Six3*, *Six6*, *Lhx2*, *Nr2e1*, and *Tbx3*), along with the anterior patterning gene *Otx2*, is sufficient to induce ectopic eye fields and eyes in amphibia at a high frequency even in nonneural regions of the animal like the belly. These experiments in frog embryos, along with others in mice, have led to the current model that EFTFs cross-regulate one another in a feedforward manner.[5] The fact that similar genes are critical for eye development in both *Drosophila* and vertebrates, and that mutations in these genes lead to ocular malformations, has had a major influence on the understanding of the evolution of the eye.[9] Although the cellular components of eyes in the various phyla are quite different, the genes that may ultimately control the expression of the phototransduction machinery may have been shared by a common ancestor.

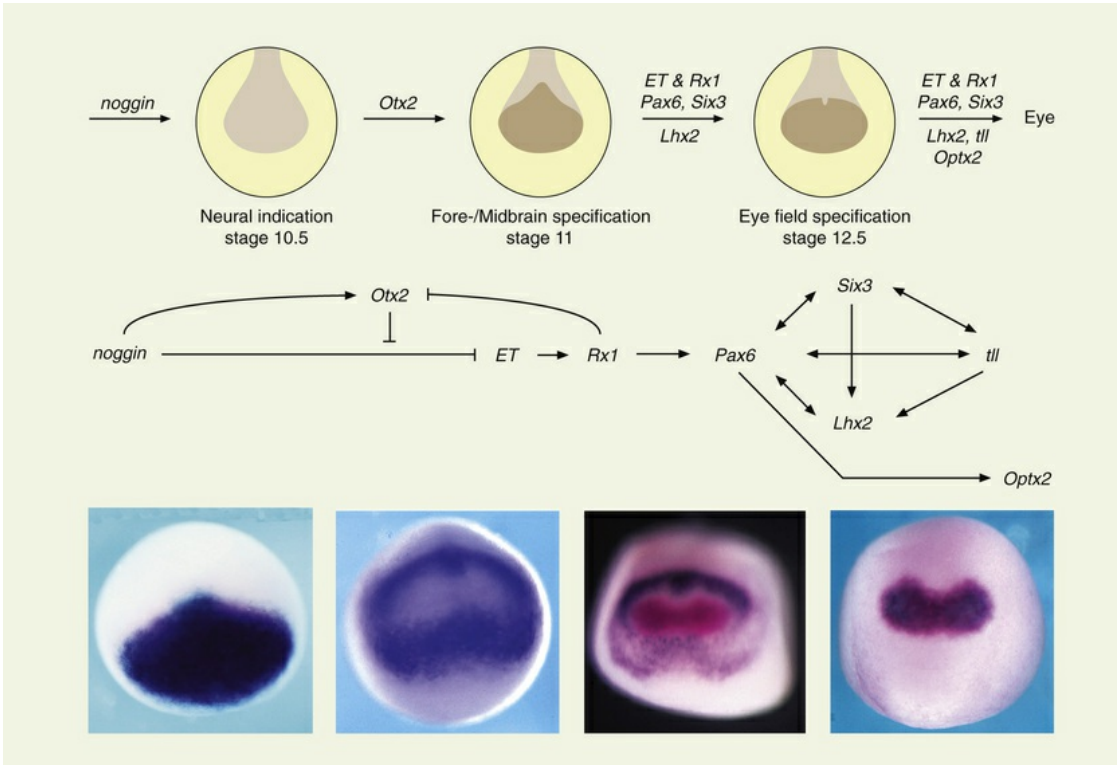

FIG. 15.2 A network of transcription factors, in addition to *Pax6*, regulates the formation of the eye. Upper series of drawings show the neural plate stages of the *Xenopus* frog and the stages in eye field specification. Drawings in the middle panel show the complex genetic regulatory network activated at the corresponding stages. See text for detailed descriptions of these genes. Lower panels show representative in situ hybridization for several of the eye transcription factors at the same stages as drawn above to show their localization in *Xenopus* embryos. From left to right, the panels show Otx2, Stage 12; Otx2, Stage 13; Otx2 (*purple*) and Rx1 (*red*), Stage 13; and *Rx1* alone, Stage 13. (Modified with permission from Zuber ME, Gestri G, Viczian AS, et al. Specification of the vertebrate eye by a network of eye field transcription factors. Development 2003;130:5155–67.)

The eye field is originally continuous across the neural plate at its anterior end; however, this single field is soon split in two by a factor from the underlying prechordal mesoderm that lies immediately adjacent to the ventral midline of the neural plate. Deletion of the prechordal mesoderm results in the development of a single fused eye (cyclopia) at the ventral part of the diencephalon. The factor released by the prechordal mesoderm that suppresses

eye development in the middle of the field is thought to be a molecule called *Sonic hedgehog* (*Shh*), an extracellular glycoprotein important in several other inductive events throughout the embryo. *Shh* is released initially by the prechordal mesoderm and induces cells in the ventral diencephalon (Fig. 15.3) to produce the same factor.[11] This factor then acts on the neighboring cells of the ventral diencephalon to suppress eye development. Mice lacking the *Shh* gene die as embryos; nevertheless, these embryos develop to a stage where the paired optic vesicles would normally form. However, in animals lacking *Shh*, the eye field is not split at the midline and a single optic vesicle forms, resulting in cyclopia.[12] The conservation of these inductive signals in human development has been confirmed by the report that congenital holoprosencephaly, a condition that frequently displays varying ocular defects, including cyclopia, is caused by mutations in the *Shh* gene.[12–14]

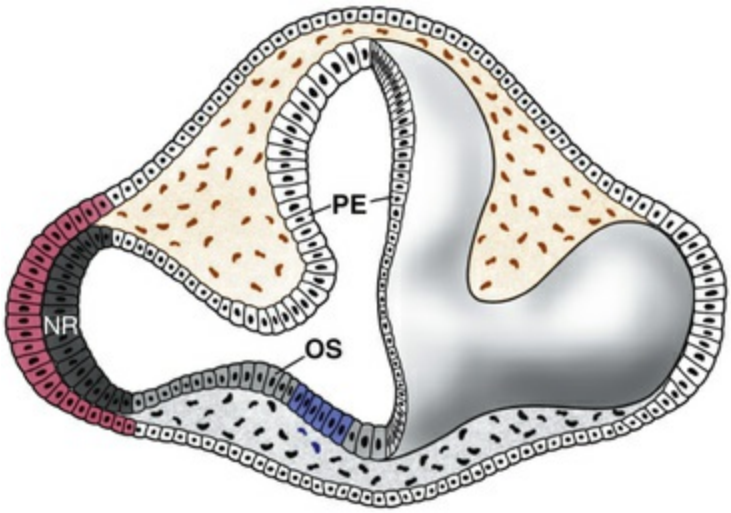

FIG. 15.3 Factors that pattern the embryonic diencephalon. *Shh* (*blue*) inhibits eye development in the ventral diencephalon, and fibroblast growth factor (*red*), in the ectoderm overlying the optic vesicle, promotes neural retinal development. *PE*, pigment epithelium; *NR*, neural retinal differentiation; *OS*, optic stalk.

Patterning the Retinal, RPE, and

Anterior Domains of the Optic Cup

The next stages of eye development in vertebrates also require a number of inductive interactions to coordinate the various tissues that ultimately contribute to the structure. Both the neural retina and the pigmented epithelium arise from the optic vesicle region of the neural tube. Although both are derived from the optic vesicle, these two tissues are quite distinct; the neural retina is a multilayered structure containing millions of neurons and photoreceptors, whereas the pigment epithelium is a single layer of nonneural, pigmented, cuboidal cells. The appropriate development of both of these two very different parts of the retina requires interactions with the adjacent tissues. If the optic vesicle is isolated from the surrounding epidermis and mesenchyme, differentiation is arrested at the optic vesicle stage and the eye does not form. Transplantation experiments in many species have shown that the developmental decision to develop as either a neural retinal progenitor or alternatively as a pigmented epithelial cell is regulated by factors in the microenvironment surrounding the eye. For example, if an optic vesicle is transplanted to a position in an embryo adjacent to the developing hindbrain, near the otic vesicle, a second neural retina is formed from the presumptive pigmented epithelial layer.

The distinction between the RPE and the neural retina comes about as a result of their expression of different transcription factors. The transcription factor *Vsx2*/*Chx10* specifies the neural retinal domain, while the basic helix–loop–helix (bHLH) transcription factor *Mitf* defines the RPE. Loss of *Mitf* leads to conversion of the RPE into a second layer of neural retina, whereas loss of function mutations in *Vsx2*/*Chx10* leads to a conversion of the neural retina into RPE (for review, see Fuhrmann[15]). *Otx2* is also required for RPE development, and expression of *Otx2*, along with the signaling molecule Wnt, can convert neural retina to RPE.[16] Along with these transcription factors, the specification of RPE is also controlled in part by soluble signaling molecules, which induce the outer region of the optic vesicle to adopt the pigmented cell fate instead of becoming retina. In particular, this mesenchymal tissue upregulates RPE-specific genes like *Mitf*, while downregulating

retina-specific genes. The transforming growth factor-β (TGF-β) family member activin was able to mimic the effects of the extraocular tissue on the optic vesicle, which suggests an activin-like signal is required for normal RPE development.[17] Experiments in developing chick embryos have also implicated another TGF-β-like signaling molecule, bone morphogenetic protein (BMP), in the process of RPE specification[18] and deletion of the *Bmp7* gene in mice leads to disruptions in ocular development. Another signaling molecule, *Shh*, introduced earlier in this review in the context of the eye field, is also involved in the induction of RPE cell fate in the ventral region of the optic vesicle, since inhibition of *Shh* signaling with cyclopamine in frog embryos disrupts ventral RPE development, and two strains of mice with altered *Shh* signaling do not develop ventral RPE.[19]

Signaling factors are also important in the specification of the neural retinal domain of the optic cup. Several lines of evidence support a critical role for fibroblast growth factor (FGF) in the development of the neural retinal part of the eye. First, FGFs are expressed in the lens ectoderm and the developing neural retinal domain.[20,21] Second, experimental treatment of the developing chick optic vesicle with exogenous FGFs or antibodies that block FGFs causes perturbations in the development of the retina. The optic vesicle of the chick embryo develops into an optic cup when isolated from the embryo and maintained overnight in culture. The addition of exogenous FGF to these optic vesicle cultures causes the presumptive pigmented epithelial layer to develop instead into a neural retina.[21] Antibodies raised against FGF cause the opposite effect and block neural retinal formation in similar optic vesicle cultures. Although it is not clear which FGFs are necessary in mammals for neural retinal specification, interruption of all FGF signaling by conditional deletion of a downstream factor in the FGF signal transduction pathway, *Shp2*, causes a loss in *Vsx2* expression and a transition of the affected region of the optic cup from neural retina to RPE.[22] These results are consistent with a model in which FGF promotes neural retinal specification in the optic cup, by promoting *Vsx2* expression, which represses expression or activity of *Mitf*. The outer part of the optic cup, the presumptive RPE, is then specified by *Shh*, Wnt and activin/BMP signaling, which

promotes *Mitf* expression to repress *Vsx2*[15] (Fig. 15.3).

Histogenesis of the Retinal Cell Types

In the next phase of retinal development, the various classes of neurons are generated by cells that undergo repeated mitotic cell divisions. The mitotic progenitors have a relatively short cell cycle and are able to produce the hundreds of millions of cells in the human retina in a few months, from the 7th to the 24th week of gestation in humans. At the same time that many of the progenitors undergo symmetric cell divisions to enable the nearly exponential increases in cell numbers, some of the cell divisions of the progenitors result in postmitotic neurons throughout this period of histogenesis. The different types of retinal cells are not produced by the progenitor cells all at the same time. Rather they are generated in a sequence that has been conserved in all vertebrates. The sequence was first described using the ^{3}H-thymidine "birthdating" technique. Following an injection of ^{3}H-thymidine, the nucleotide is incorporated into the DNA of the retinal progenitor cells during the S phase of their cell cycle. Those cells that withdraw from the cycle after their next mitosis, and become postmitotic neurons/photoreceptors, retain a high level of label in their nucleus. Since the ^{3}H-thymidine is available for only a short period, those cells that remain in the cycle for additional cell divisions become progressively less heavily labeled. If the animal is allowed to survive to adulthood and the retina processed for autoradiography to reveal the label in the various retinal cells, those retinal cells that were generated on the day of the thymidine injection are easily identified by the large number of silver grains over their nuclei. In a typical thymidine birthdating study, injections of the nucleotide are made in pregnant animals on each day of gestation, and the number of labeled cells of the various retinal cell classes is calculated to produce a graph like the one shown in Fig. 15.4.[23]

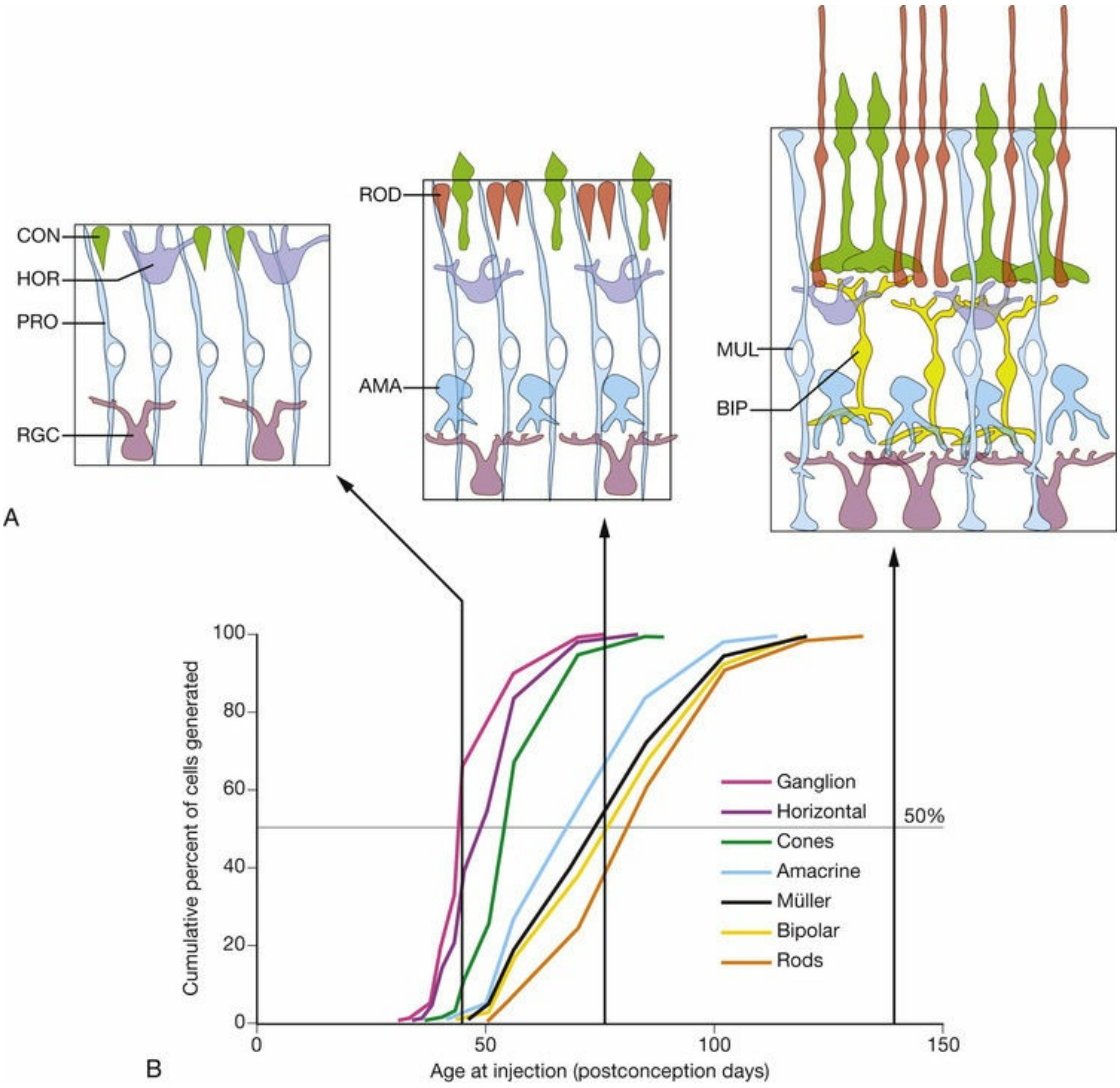

FIG. 15.4 (A,B) Each retinal cell type is generated over a slightly different time course during retinal histogenesis. Addition and integration of new cells during the histogenesis of the retina at three different ages, corresponding to the chart of thymidine birthdating of retinal cells in the monkey. *CON*, cones; *HOR*, horizontal; *PRO*, progenitor cells; *RGC*, retinal ganglion cell; *AMA*, amacrine; *MUL*, Müller; *BIP*, bipolar. (Panel B modified with permission from La Vail MM, Rapaport DH, Rakic P. Cytogenesis in the monkey retina. J Comp Neurol 1991;309:86–114.)

This type of thymidine birthdating analysis has been carried out in the retina in many different animals, and the sequence of cell generation is remarkably conserved among the various vertebrates. Fig. 15.4 shows the sequence of generation of the retinal cell classes in the monkey,[23] but a very similar graph can be produced in other vertebrates. Overall, the cell classes can be divided into two phases

of generation. In the first phase, the ganglion cells, the cones, and the horizontal cells are generated. In the second phase of histogenesis, the rod photoreceptors, the bipolar cells, and the Müller glial cells are produced by the progenitor cells.[24,25] Amacrine cells are primarily generated in the later phase, but many amacrine cells become postmitotic at the same time as ganglion cells are generated, so these cells do not fall as neatly into one or the other phase. Despite this seeming regularity in histogenesis, it should be noted that there are distinct central-to-peripheral gradients of histogenesis, and that peripheral retina may still be in the first "phase" at the time central retina is generating later cell types.

Even though the retinal cell types are generated in a defined sequence, multiple different types of neurons are produced at any given time in development; this has led to the current model in which the progenitors are multipotential, and can generate many different types of retinal neurons up to and including their final mitotic cell division.[26,27] Several methods have been developed for tracing the lineage of individual retinal progenitor cells: (1) retroviral infection of progenitors with a virus containing a reporter gene;[26,27] (2) direct injection of progenitors with a cell-impermeant dye;[28,29] (3) genetically inducing a lineage marker into specific types of progenitors based on their gene expression.[30,31] These methods all show that many of the mitotic progenitor cells can produce various, somewhat random mixtures of the different retinal cell classes; however, they also show that in some cases progenitors can generate only a subset of the different types of retinal cell types; for example, the progenitors that express the transcription factor *Ascl1* can produce all the different types of retinal cells except ganglion cells.[30]

The sequential development of the different retinal cell types has led several investigators to propose that the production of one cell class induces the progenitor cells to make the next cell type in the sequence. For example, the retinal ganglion cells, being generated first by the progenitor cells, might secrete a substance that prevents additional cells from differentiating into this fate, and at the same time instructs the progenitor cells to begin making the next cell type, the horizontal cells; the horizontal cells would then secrete a factor that instructs the progenitor cells to make cones, and so on

until all the retinal cell types have been generated. Cell culture studies have provided some support for this model: when progenitor cells from the retina are isolated from early stages of retina, they predominantly differentiate into retinal ganglion cells.[32] However, if these same early progenitor cells are mixed with retinal cells from later stages of development, presumably containing factors derived from the cell types generated later, the early progenitor cells will be biased to adopt later cell identities.[33–35] Thus the type of cell that the progenitor will produce at any particular time in development can be influenced by factors produced by the neighboring cells. There is also in vivo evidence in mice that cell-type specific feedback mechanisms control the relative ratios of retinal cells: the signaling factor *Shh*, mentioned earlier in the development of the eye field, is also expressed in the retinal ganglion cells, and this factor alters the rate of proliferation of the progenitors and their cell cycle exit, thereby controlling the addition of new ganglion cells.[36] However, while there appear to be feedback mechanisms within cell types for controlling their numbers, elimination of ganglion cells does not appear to affect the development of the other retinal cells drastically,[37] and so the evidence to date supports regulation within cell types rather than between cell types.

There is also considerable evidence that the production of the different retinal cell types from a common precursor is due to a progressive change in the progenitor cell competence, like a clock ticking through the different cell fates.[38,39] In this model the retinal progenitor cells change over development in the cell types they are competent to give rise to. First, the default state, as discussed above, is the retinal ganglion cell. Next, the progenitor cells shift their competence so that they are more likely to produce horizontal cells, then cone photoreceptors, and so on. A cascade of transcription factors might be responsible, with the first one setting in motion the mechanism for the production of the second, which acts to produce a third transcription factor, and so on. Recent data have shown that miRNAs are necessary in this process. Deletion of the gene that codes for the enzyme Dicer, needed to produce mature miRNAs, causes the progenitors to be "stuck" in the early state, and only generate early cell fates, like ganglion cells, cones, and horizontal

cells.[40,41] Three miRNAs, let7, miR-125 and miR-9 are particularly important in controlling the changing competence of the retinal progenitors.[41]

As the different types of retinal neurons begin their differentiation, several transcription factors are critical for the various cell fates. One transcription factor expressed by progenitors that controls the types of cells that are generated is *Pax6*. Although mutations of the *Pax6* gene cause early defects in eye development (see above), it has been possible to delete the gene specifically from the retinal progenitors at later stages of development. This leads to a loss of competence in the progenitor cells to generate anything except amacrine cells.[42] Deletion of a different transcription factor, *FoxN4*, produces the complementary result: all cell types develop normally, except amacrine cells.[43] The combination of *FoxN4* and *Pax6* is therefore able to confer progenitors with competence for all retinal cell fates. Other transcription factors that are expressed in progenitors or newly produced neurons play important roles in the production of cell diversity and/or the maintenance of this diversity as the neurons acquire their differentiated fates. For example deletion of the proneural gene *Atoh7* (*Math5*) leads to a dramatic failure in ganglion cell production;[44] the gene *Otx2* is expressed in the newly developing photoreceptors and genetic deletion of this gene specifically in the retina prevents the progenitors from producing photoreceptors, and instead they produce more amacrine cells;[45–47] the transcription factors *Ptf1a*, *NeuroD1*, and *Math3* are expressed in amacrine cells, and loss of one or more of these genes causes a loss in amacrine cells in the developing retina;[48] deletion of the *Nrl* transcription factor causes all the rods to develop as short-wavelength sensitive cones instead;[49] mutation in the paired-homeodomain gene *Chx10*/*Vsx2* leads to an absence of most bipolar cells;[50] elimination of the transcription factor *Prdm1*/*Blimp* causes the photoreceptors to become bipolar cells instead;[51] deletion in the *Ascl1* gene, another bHLH transcription factor, leads to an increase in the production of Müller glia at the expense of late-generated retinal neurons, like bipolar cells and rods.[52–54] Putting all these molecular interactions into a coherent network model has yet to be accomplished; moreover, integration of these transcriptional regulators with the miRNAs and signaling

factors remains a challenge.

Several cell classes that are resident in the retina are not derived from the progenitor cells in the ventricular zone, including the microglia, vascular endothelial cells, and retinal astrocytes. Microglia in the retina, like microglia elsewhere in the CNS, are derived from the blood; monocytes enter the retina through the vascular endothelial cells and become "ameboid" in morphology.[55,56] These highly motile, phagocytic cells digest those retinal cells that undergo apoptotic cell death (see below) during the course of retinal development. When they are first observed in development, they are concentrated in the ganglion cell layer (GCL), presumably as a result of the large number of degenerating cells in that layer. Later in development, when other types of retinal cells undergo apoptosis, microglia are found in the inner nuclear layer (INL) and outer nuclear layer (ONL). A second type of glial cell that is present in the mature retina is the astrocyte. These cells form from ventricular zone cells in other areas of the CNS, but they are not generated by the retinal progenitors; instead, the retinal astrocytes migrate along the developing optic nerve and enter the retina at the optic nerve head. The vascular endothelial cells emerge from the same point, and both the astrocytes and the endothelial cells migrate across the retinal surface, eventually covering it completely.[57,58]

Inner Retinal Development

The further development of the inner retina follows a sequence similar to that described in other areas of the developing CNS. Immediately after their final mitotic division at the ventricular (scleral) surface, retinal cells migrate to their appropriate lamina. As they migrate, the different types of neurons begin to take on some morphologic features of their characteristic cell type. For example, ganglion cells begin to elongate an axon from their basal/vitreal process before their soma reaches the GCL.[59,60] The next phase in the differentiation of retinal neurons is the growth of dendritic processes. In the last stages of differentiation the retinal neurons make functionally active synapses with one another and express their transmitters and receptors. Although the time course of these

events overlaps considerably, this sequence is typical of most classes of retinal cells.

The development of the inner retina is led by the differentiation of the retinal ganglion cells. The morphologic development of retinal ganglion cells has been well characterized in several species, including primates, and is known to proceed through a characteristic sequence.[61,62] The first phase of ganglion cell morphogenesis begins as soon as the cells complete their final mitotic division at the ventricular surface of the developing retina. The vitreal process begins to resemble an axon, which extends toward the optic disc even before the migration of the cell soma from the ventricular surface. The cell soma then migrates to the vitreal surface of the retina. The molecular mechanisms that underlie ganglion cell migration are not understood; nevertheless, the laminar structure of the retina is likely the result of the selective migration and specific adhesions among the different types of retinal cell. Selective adhesive interactions are mediated by cell adhesion molecules (CAMs). It has been known for some time that interfering with CAM function, particularly the molecule known as N-cadherin, causes a disruption of the normal lamination pattern in the retina.[63] Although interfering with CAM function leads to a disruption in the lamination of the retina, it is still not well understood how these relatively nonselective molecules direct the particular retinal cell types to their appropriate laminae. In the developing cerebral cortex, newly generated neurons migrate to their destinations along radially arranged glial cells that span the expanding neural tube from the ventricular surface at the core of the brain to the external surface. Several different molecules have been identified that are critical in this migration, including adhesion molecules that mediate the selective attachment of the migrating neurons to the glial scaffold.[64] Although similar molecules may be expected to mediate the migration of ganglion cells in the retina, there is little evidence for the presence of radial glial cells in the developing retina. Müller cells could provide such a scaffold; however, these cells have not yet been generated at the time of ganglion cell migration (see above). Although some reports using ultrastructural criteria have claimed that Müller cells are present in the developing retina before they have been birthdated by

thymidine, extensive serial section reconstructions by Hinds and Hinds[59] failed to find any evidence for radial glial cells during the period of ganglion cell genesis. Therefore it is likely that the newly generated ganglion cells use the other retinal progenitor cells as their scaffold for migration. In fact, more recent evidence in the cerebral cortex indicates that the radial glial cells are in fact progenitor cells, consistent with the possibility that migrating neurons in the retina use the progenitors to guide their migration.

In the next phase of ganglion cell development, the cells extend dendrites to form the inner plexiform layer (IPL). These first dendrites are very simple, no more than a single primary large filopodial process, with growth cones at their ends. Ganglion cells next elaborate their dendritic arbors. The complex arbor emerges rather quickly. For many ganglion cells, the dendritic arbors initially span the entire width of the IPL, with numerous secondary and higher-order branches; however, in at least one type of ganglion cell, the cells have laminar subspecificity from the outset.[65] In fact, the arbors have more higher-order branches than adult ganglion cells. As the ganglion cells mature, the dendritic arbor is remodeled; the dendritic processes become restricted to a single sublamina of the IPL, depending on whether the ganglion cell will become an ON or OFF type, and the numerous tertiary processes regress. After the active phase of ganglion cell dendritic growth, the total extent of the dendritic field continues to expand, most likely as the result of the passive stretching of the retina with the continued growth of the eye.

What factors determine the extent and shape of the ganglion cell dendritic arbors? As the ganglion cells begin to send out dendrites, the amacrine cells are migrating to the inner nuclear layer; the processes of these two cell types grow on one another to begin the IPL. The dendritic arbors of ganglion cells are in part regulated by the same CAMs that mediate the lamination of the cells themselves. Kljavin et al.[66] cultured retinal ganglion cells on substrates of purified CAMs and found that cells grown on NCAM, L1, or N-cadherin developed distinctly different morphologies from one another. Those cells grown on N-cadherin developed a highly branched morphology most similar to that observed in vivo, whereas the cells grown on L1 developed simpler, axon-like

processes. However, these generic CAMs cannot provide the degree of specificity characteristic of the retina. To generate the sublaminar specificity, for example, at least two other types of molecule are required. Several members of the immunoglobulin superfamily of adhesion molecules (Dscam [Down syndrome CAM], Dscaml, Sidekick-1 and Sidekick-2) are required in chick retina to define the sublaminae in the IPL[67]; however, in the mouse retina, loss of Dscam does not interfere with sublaminar specificity. Instead, in the mouse retina, molecules known to be critical for axonal pathfinding in the CNS (Sema6A and PlexinA4) are required for sublaminar dendritic stratification of at least some types of ganglion cell and amacrine cell.[68] Sema6A and PlexinA4 have complementary expression patterns in the sublaminae of the IPL (Fig. 15.5B), and mice with PlexA4 knocked out have a defect in the correct sublaminar specificity of the dendrites of some types of retinal neurons; Fig. 15.5 shows the effects of loss in PlexA4 on the dendrites of the tyrosine hydroxylase-expressing dopaminergic amacrine cells. In chick retina laminar specificity of dendrites also depends on contactins, and at least five different members of this family of adhesion molecules are differentially expressed by subsets of amacrine cells. Altogether, these data indicate a growing list of candidate adhesion molecules that for an Ig-superfamily code for laminar-specific connectivity in the IPL.[69]

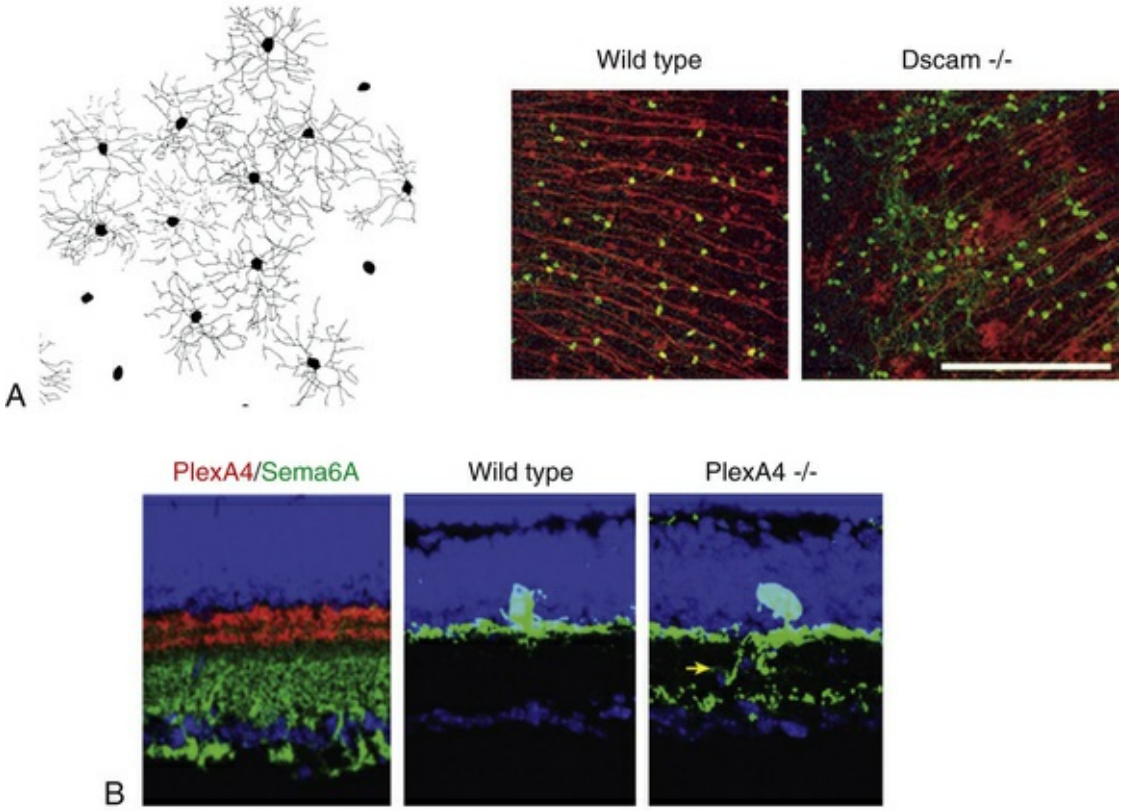

FIG. 15.5 The tiling and lamination of dendrites are regulated by specific cell adhesion molecules. (A, left) Midget ganglion cell mosaic of human retina shows a highly regular distribution, and their dendritic arbors show no overlap. (A, right) In Dscam knockout mice the ganglion cells no longer tile evenly, but have fasciculated dendrites, and their cell bodies (*green*) form large clumps. (B, left) Sema6A (*green*) and PlexinA4 (*red*) have complementary expression patterns in the sublaminae of the inner plexiform layer. (B, right) Tyrosine hydroxylase (TH)-expressing dopaminergic amacrine cells (*green*) in PlexA4 knockout mice send dendrites into the wrong sublamina. (Panel A left, modified with permission from Dacey DM. The mosaic of midget ganglion cells in the human retina. J Neurosci 1993;13:5334. Panel A right, modified with permission from Fuerst PG, Bruce F, Tian M, et al. DSCAM and DSCAML1 function in self-avoidance in multiple cell types in the developing mouse retina. Neuron 2009;64:484–97. Panel B, modified with permission from Matsuoka RL, Nguyen-Ba-Charvet KT, Parray A, et al. Transmembrane semaphorin signaling controls laminar stratification in the mammalian retina. Nature 2011;470:259–63.)

In addition to their laminar specificity, a number of studies in many different species have shown that the dendritic arbor of each

subclass of ganglion cells "tiles" the retinal surface.[70] Interactions among the ganglion cells control the extent of coverage of the dendrites of the various ganglion cell classes. When a region of the retina is experimentally depleted of ganglion cells, the neighboring cells will sprout dendrites into the depleted areas and thereby expand the size of their arbors considerably. In addition, when the density of ganglion cells is increased by monocular enucleation before the period of normal cell death (see below), the ganglion cells have smaller dendritic fields.[71] Although these data demonstrate that size of the dendritic arbor of a ganglion cell is determined by cell–cell interactions, the nature of the interactions is not clear. The ganglion cells could be competing for some dendrite-promoting factor derived from the amacrine cells, so when fewer ganglion cells are present, they can get more of the factor. Alternatively, the ganglion cells may intrinsically extend exuberant dendrites, but their growth may be limited by a phenomenon known as contact inhibition, in which a direct contact between two cells leads to the cessation of process extension because of the collapse of their growth cones. Some evidence for this latter mechanism has been provided from an analysis of the Dscam and Dscaml mouse mutants. As noted above, although these molecules are not required in mouse for sublaminar specificity, they do appear to be critical for the phenomenon of tiling of the dendrites and cell bodies via "self-avoidance." In Dscam knockout mice (Fig. 15.5) the ganglion cells had fasciculated dendrites, and their cell bodies formed large clumps, instead of being spread out evenly across the retinal surface.[72]

The further development of the plexiform layers is a reflection of the dendritic growth and the synapse formation of the various types of retinal cell. As they mature, the bipolar cells begin to produce dendritic arborizations that can form synaptic connections with the ganglion cells. As noted above, the IPL develops before the outer plexiform layer in all species that have been studied. In most mammals, conventional synapses, between amacrine cells and ganglion cells, develop before the ribbon synapses between bipolar cells and ganglion cells. This sequence parallels the sequence of generation of these cell types, since the amacrine cells are born before the bipolar cells in vertebrate retinas. In addition, these first

synapses apparently mediate horizontal interactions among the cells of the inner retina that are important for the development of the appropriate pattern of connections between ganglion cells and their targets. Studies by Wong and collaborators in the ferret have shown that waves of activity are spread among the retinal ganglion cells through synapses in the inner retina before most of the bipolar cells have even been generated.[73] Thus the flow of information in the developing retina is initially horizontal and only later develops the predominantly vertical flow of information characteristic of the mature retina.

An exception to this pattern is found in the primate fovea, where there are virtually no rods at any time in development. In the fovea the first synapses observed in the IPL are the ribbon synapses between bipolar cells and ganglion cells.[74] In the monkey fovea, ganglion cells are born as early as 30 days of gestation, but bipolar and amacrine cells are not generated until approximately 1 week later, at E38. As described above, ganglion cells have primitive dendrites at E55, and the first synapses in the foveal IPL can be morphologically identified at this same time, approximately 2 weeks after the bipolar cells were generated. Thus in the primate fovea the vertical flow of information appears to be in place before the conventional synapses among ganglion cells and amacrine cells. This is not true of peripheral retina in the primate, where the typical mammalian pattern characteristic of rod-dominated retinas is observed. Since the connections among the ganglion cells and amacrine cells in immature retina are thought to contribute to the coordinated bursts of ganglion cell activity required for appropriate retinogeniculate connections, there may be differences in the mechanisms by which the connections from foveal ganglion cells are specified.

The development of functional circuits among the retinal cells requires synaptic transmitters and their receptors to be expressed in the appropriate cells (for review of synaptic development in the retina, see Bleckert and Wong[75] and Yoshimatsu et al.[76]). In fact, the major neurotransmitters of the retina – glutamate, gamma-aminobutyric acid, and glycine – are all localized to specific retinal neurons before development of morphologically identifiable synapses. In addition, both ligand-gated and voltage-gated

channels are present in retinal cells soon after they have been generated by the progenitor cell. For example, ganglion cells in the mouse have Na^+, K^+, and Ca^{2+} channels as early as E15, only a few days after birth. The fact that these very immature neurons have both neurotransmitters and receptors allows for these molecules to act as signals to shape the development of the circuit. Although genetic suppression of bipolar cell transmitter release in mice does not affect the gross dendritic morphology of the ganglion cell dendrites,[77] neurotransmitters may be more important in shaping the dendrites in the outer retina (see below).

Photoreceptor Development

When photoreceptors are first recognizable by their opsin immunoreactivity or mRNA expression, they have a very simple morphology and no outer-segment formation. Fig. 15.6 shows the simple morphology of the early differentiating cones in the monkey retina. In all vertebrates the cone photoreceptors are generated before the rod photoreceptors (see above); however, the rod photoreceptors express their specific opsin before the cones do.[78,79] Thus at least this aspect of rod differentiation proceeds more rapidly than that of cones. The monkey has been a particularly favorable species to study the normal pattern of photoreceptor differentiation, owing to the relatively long time course of retinal development in this species and the fact that the rod-dominated retinas of most other mammals have relatively few cones. The foveal cones of the rhesus monkey are born between gestational days E38 and E50 and first make synapses in the outer plexiform layer by E55. Thymidine birthdating studies indicate that the first foveal cones are generated on fetal day 38 (see above) but do not express their specific opsin until several weeks later at fetal day 75, well after the cones have differentiated to the point of making synaptic connections with bipolar cells (E55). This delay is a general feature of photoreceptor development in vertebrates and suggests that the factors that control opsin expression act at a later time than the factors that direct the retinal progenitor cells to the photoreceptor cell fate.

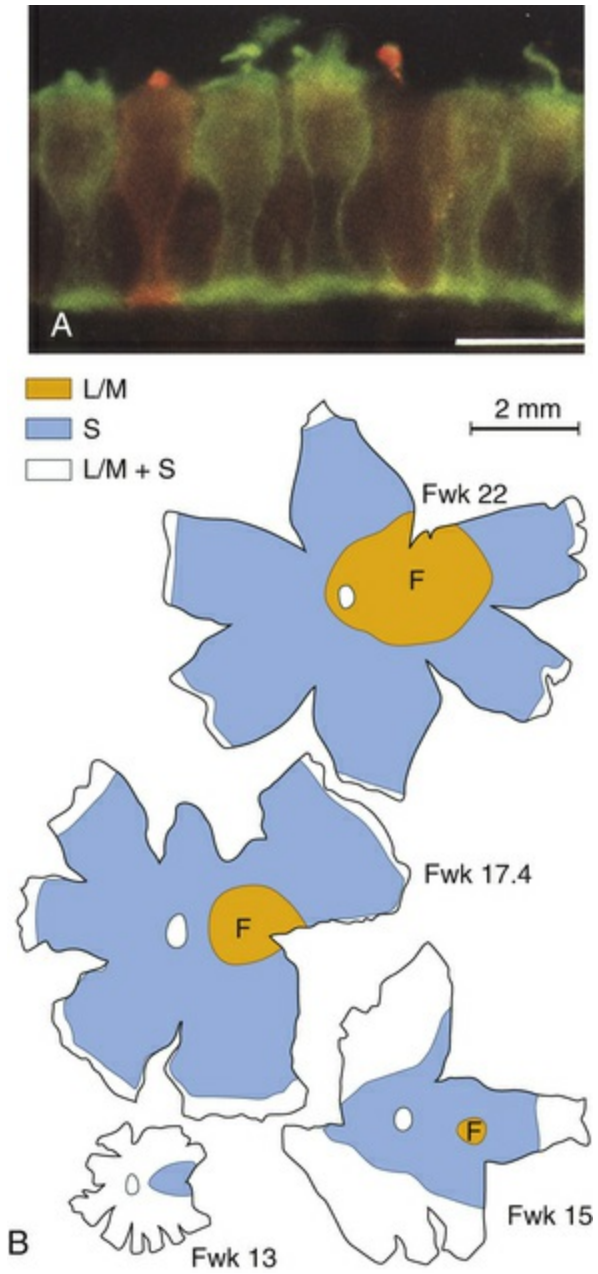

FIG. 15.6 L/M and S cones in the fetal monkey retina. (A) Double-labeled immunohistochemical staining of a fetal day 108 parafoveal retinal section; L/M cones appear green and S cones appear red. (B) The distribution of the different types of cones across the retinal surface as a function of age. *F*, fovea; *Fwk*, fetal week. (Panel A, reproduced with permission from Burnsted K, Jasoni C, Szel, et al. J Comp Neurol 1997;378:117–34. Panel B redrawn with permission from Xiao M, Hendrickson A. Spatial and temporal expression of cone opsins during monkey retinal development. J Comp Neurol 2000;425:545–59.)

The factors that control the mosaics of cell differentiation alluded to above must also be at work in the development of the cone

mosaics. In the primate fovea the cones expressing the S (short-wavelength) opsin and those expressing the long- and middle-wavelength opsins (L/M) both are distributed in regular mosaics. In both primates and mice, the S-opsin-expressing cone photoreceptors emerge first in development.[78] Fig. 15.6 shows the progression of S-opsin expression from the central to peripheral retina in monkey retina. Once the S opsin cones have covered a relatively large fraction of the retinal surface, the L/M opsin cones begin their development in central retina.[80] The L/M opsin cone wave of development then follows that of the S opsin cones from the central retina to the periphery.[81,82]

Emerging evidence suggests that photoreceptor differentiation is controlled by transcription factors that promote a progenitor cell to become a photoreceptor progenitor, then either a protocone or protorod, and then further to a specific type of cone. At each stage, a different transcription factor seems to control the competence of the protophotoreceptor in its fate choices. The homeodomain transcription factor *Otx2* is the earliest factor biasing progenitor cells to become photoreceptor.[45,46] Conditional knockout studies show that photoreceptors do not develop in *Otx2*$^{-/-}$ retinas, and retroviral gene transfer of *Otx2* into retinal progenitors biases cells to become photoreceptors. *Otx2* also activates transcription of cone–rod homeobox gene (*Crx*), which is also required for expression of many photoreceptor-specific genes, including the opsins.[83] *Otx2*-positive *Crx*-positive protophotoreceptors then must choose to become rods or cones, and this decision is made by expression of neural retina leucine (*Nrl*) zipper transcription factor. *Nrl* expression promotes rod cell fate and inhibits cone cell fate. *Nrl*$^{-/-}$ retinas do not develop rods, but have many more cones than normal.[49] Photoreceptor progenitors not expressing Nrl become cones. Interestingly, the choice of cone subtype is determined by yet another transcription factor, *thyroid hormone receptor-ß2* (*TRß2*) and *RXR-gamma*,[84,85] which promote M-opsin expression while inhibiting the expression of S opsin. Mice deficient in the *TRß2* gene have no M-opsin-expressing cones, but rather have only S opsin cones.[86]

A number of studies have used in vitro techniques to identify the factors that control photoreceptor differentiation during retinal

development. Since many of these studies have been carried out in rodents, and since rodent retinas have relatively few cones, most of the in vitro studies have concentrated on rod photoreceptor differentiation. The finding that rod photoreceptors do not differentiate in low-density cell cultures, but do so readily in high-density cultures or retinal explants, led to the development of several in vitro assays for rod differentiation factors and the identification of several signaling molecules that promote rod photoreceptor differentiation in vitro.[87] These factors are now being used to promote photoreceptor development in cultures of embryonic stem cells.[88–91]

The development of the outer plexiform layer and synapses between the photoreceptors, horizontal cells, and bipolar cells lags behind that of the IPL. There is good evidence that the dendrites of the cells are regulated through interactions with one another. For example, the dendritic branching of horizontal cells depends on the ratio of rods to cones. In mice, reducing cone number during development causes an increase in horizontal cell dendritic branching. The formation of ribbon synapses, specialized synaptic structures between rod and cone pedicles and horizontal cell and bipolar cell dendrites, is also dependent on the activity of the cells: inhibition of phototransduction in cones forces the cone bipolar cells instead to make synapses with rods.[92] Blocking transmitter release in rods causes rod bipolar cells and horizontal cells to send aberrant processes into the ONL[93,94] and synapse with cones. Although the specific molecular interactions that regulate OPL formation are not well understood, loss of DSCAM leads to malformation of the dendrites of some types of bipolar cells, indicating a role for this adhesion molecule in OPL formation as well as IPL development. [95] Recent studies show that in both mice and primates, several additional adhesion molecules are localized to cone synapses, including gamma-protocadherin, cadherin-8, MAGI2, and CASK, and these may prove to be important in the formation of these synapses.[96]

Ganglion Cell Death

It has long been recognized that a considerable number of neurons

die during the development of the vertebrate CNS. The death of "excess" neurons is thought to be the result of their inability to compete effectively for a limited supply of trophic support, usually from their postsynaptic targets. Such a mechanism could ensure that presynaptic and postsynaptic populations of neurons are numerically matched during development. In the retina the phenomenon of cell death has been most thoroughly studied in the retinal ganglion cell population,[97] although cell death has been documented in other cell types.[98] A considerable fraction of the ganglion cells that are initially produced are subsequently lost during the phase of cell death. The loss of ganglion cells occurs as the axons of the cells reach the lateral geniculate nucleus and superior colliculus. The neurons in these targets presumably produce only enough trophic factor to keep less than half of the ganglion cells alive in most vertebrates and in humans. In addition to numerically matching ganglion cells and their targets, it is possible that different trophic factors are produced by the different targets, and this ensures that only those ganglion cells survive that have extended their axon to the right place.[99]

The trophic factors supplied by the targets are likely to be among the same molecules identified as survival factors for other cells in the nervous system. The major family of trophic molecules shown to be important for ganglion cell survival is the neurotrophins, including nerve growth factor (NGF), brain-derived neurotrophic factor (BDNF), neurotrophin 3 (NT3), and NT4/5. Of the neurotrophins, the best evidence indicates that BDNF and NT3 are the most important for ganglion cell survival. Both BDNF and NT3 are expressed by cells in the targets of the ganglion cells[100] Both of these neurotrophins promote the survival of ganglion cells when added to cell cultures of retinal cells or when injected in excess into the target during the normal period of cell death. Ganglion cells express receptors for BDNF and NT3, receptor tyrosine kinases known as trkB and trkC, respectively. These data taken together are consistent with the following model. Over twice as many ganglion cells are generated by the retinal progenitor cells than are actually needed in the adult.[101] These cells extend axons to the lateral geniculate nucleus and the superior colliculus and other targets. At the time the axons reach the targets, the ganglion cells express trkB

and trkC, and they now require activation of these receptors for their continued survival. Since the supply of BDNF and NT3 is limited, many of the ganglion cells will have an insufficient activation of their trk receptors, so they then initiate a program of apoptosis. Although this scheme is intellectually attractive and complies with much of the available data, evidence suggests that additional growth factors are also important in controlling the number of ganglion cells in the retina.[102,103]

There is evidence that transcription factors of the *Brn3* class are important for ganglion cell survival. The *Brn3* transcription factors are among a class of molecules called the *POU domain transcriptional regulators.* In the retina, the *Brn3* genes are expressed exclusively in the retinal ganglion cells. Their expression has been characterized in mouse, cat, and monkey retina, but there does not seem to be a simple relationship between the particular *Brn* gene expressed and one of the major morphologic subtypes of ganglion cells. Targeted disruption of the *Brn* genes in mice causes the loss of nearly all of the retinal ganglion cells.[104–106] These experiments lend support to the idea that *Brn* genes may be important for the expression of the neurotrophins or their receptors, as well as other genes critical for their survival.[104,107]

Retinal Maturation

As the retina matures, nearly all of the events continue to proceed in a central to peripheral direction. Once the process of retinal histogenesis and death is complete, considerable remodeling continues, primarily in the form of retinal stretch, owing to the steadily increasing intraocular pressure. The pigmented epithelium and the scleral tissue also participate actively in the growth of the eye, as these tissues proliferate in response to increases in intraocular pressure. Because the retina matures later in the periphery, a disproportionate amount of expansion occurs in the peripheral retina. As a result, the ganglion cell density is lower in the peripheral retina than in the central retina, and the dendritic arbor size of most types of retina cells increases in extent with eccentricity because of the disproportionate retinal stretch.

The development of the fovea in primates is another important

aspect of later retinal development. The fovea is a small, avascular depression that is devoid of all cells except cone photoreceptors and Müller glia in the central part of the retina of Old World primates. Foveal development has been extensively characterized by Hendrickson and her colleagues.[108–111] This region is initially one of the thickest parts of the retina, and by a process of cell migration is transformed into a depression or pit. The GCL begins to thin between the 24th and 26th fetal week in humans, and the number of amacrine and bipolar cells begins to decline soon after. The loss of these cells from the fovea is not due to their death, but rather to their migration from the fovea to the surrounding retina. Since these cells already have formed synaptic connections by this time in development, the synaptic pedicles of the cones remain in contact with horizontal and bipolar cells as they migrate, which causes a dramatic elongation of the fiber of Henle. At birth, the GCL and INL are only a single cell layer thick; after birth, the GCL and INL continue to thin, but now the ONL begins to increase in thickness; by age 4, the ONL has six to seven layers of cone photoreceptor nuclei. Although the development of the fovea has been well described, little is known of the mechanisms by which the cells migrate.

Conclusion

The past 20 years have witnessed an explosive growth in our knowledge of retinal development. The remarkable conservation of molecular mechanisms for eye development throughout evolution has allowed the use of the powerful molecular genetics of *Drosophila* to identify many of the key molecular components required for retinal differentiation. However, many aspects of retinal development remain mysterious. A better understanding, for example, of the mechanisms that control cell fate will allow better derivation of specific retinal cell types from human embryonic stem and induced pluripotent stem cells for cell replacement therapies and disease modeling. Discovery of the mechanisms that control specific synaptic connections will have implications for developmental disorders in the eye and the rest of the CNS. Elucidation of the processes of eye development will

continue to inform the way we look at retinal disease and pathology and potentially lead us to methods to recapitulate developmental processes and provide regenerative treatments of retinal disease.

References

1. O'Rahilly R, Müller F. Neurulation in the normal human embryo. *Ciba Found Symp*. 1994;181:70–82 [discussion 82–9].
2. Gage PJ, et al. Fate maps of neural crest and mesoderm in the mammalian eye. *Invest Ophthalmol Vis Sci*. 2005;46:4200–4208.
3. Luhmann UF, et al. Role of the *Norrie* disease pseudoglioma gene in sprouting angiogenesis during development of the retinal vasculature. *Invest Ophthalmol Vis Sci*. 2005;46:3372–3382.
4. Zuber ME. Eye field specification in *Xenopus laevis*. *Curr Top Dev Biol*. 2010;93:29–60.
5. Zuber ME, et al. Specification of the vertebrate eye by a network of eye field transcription factors. *Development*. 2003;130:5155–5167.
6. Glaser T, et al. PAX6 gene dosage effect in a family with congenital cataracts, aniridia, anophthalmia and central nervous system defects. *Nat Genet*. 1994;7:463–471.
7. Quiring R, et al. Homology of the eyeless gene of *Drosophila* to the *Small* eye gene in mice and aniridia in humans. *Science*. 1994;265:785–789.
8. Halder G, Callaerts P, Gehring WJ. Induction of ectopic eyes by targeted expression of the eyeless gene in *Drosophila*. *Science*. 1995;267:1788–1792.
9. Gehring WJ. The master control gene for morphogenesis and evolution of the eye. *Genes Cells*. 1996;1:11–15.
10. Mathers PH, et al. The Rx homeobox gene is essential for vertebrate eye development. *Nature*. 1997;387:603–607.
11. Pera EM, Kessel M. Patterning of the chick forebrain anlage by the prechordal plate. *Development*. 1997;124:4153–4162.
12. Chiang C, et al. Cyclopia and defective axial patterning in mice lacking Sonic hedgehog gene function. *Nature*.

1996;383:407–413.
13. Belloni E, et al. Identification of Sonic hedgehog as a candidate gene responsible for holoprosencephaly. *Nat Genet*. 1996;14:353–356.
14. Roessler E, et al. Mutations in the human Sonic hedgehog gene cause holoprosencephaly. *Nat Genet*. 1996;14:357–360.
15. Fuhrmann S. Eye morphogenesis and patterning of the optic vesicle. *Curr Top Dev Biol*. 2010;93:61–84.
16. Westenskow P, Piccolo S, Fuhrmann S. Beta-catenin controls differentiation of the retinal pigment epithelium in the mouse optic cup by regulating Mitf and Otx2 expression. *Development*. 2009;136:2505–2510.
17. Fuhrmann S, Levine EM, Reh TA. Extraocular mesenchyme patterns the optic vesicle during early eye development in the embryonic chick. *Development*. 2000;127:4599–4609.
18. Müller F, Rohrer H, Vogel-Hopker A. Bone morphogenetic proteins specify the retinal pigment epithelium in the chick embryo. *Development*. 2007;134:3483–3493.
19. Dakubo GD, et al. Indian hedgehog signaling from endothelial cells is required for sclera and retinal pigment epithelium development in the mouse eye. *Dev Biol*. 2008;320:242–255.
20. Vogel-Hopker A, et al. Multiple functions of fibroblast growth factor-8 (FGF-8) in chick eye development. *Mech Dev*. 2000;94:25–36.
21. Pittack C, Grunwald GB, Reh TA. Fibroblast growth factors are necessary for neural retina but not pigmented epithelium differentiation in chick embryos. *Development*. 1997;124:805–816.
22. Cai Z, Feng GS, Zhang X. Temporal requirement of the protein tyrosine phosphatase Shp2 in establishing the neuronal fate in early retinal development. *J Neurosci*. 2010;30:4110–4119.
23. Rapaport DH, Rakic P, LaVail MM. Spatiotemporal gradients of cell genesis in the primate retina. *Perspect Dev Neurobiol*. 1996;3:147–159.
24. Carter-Dawson LD, LaVail MM. Rods and cones in the mouse retina. II. Autoradiographic analysis of cell

generation using tritiated thymidine. *J Comp Neurol*. 1979;188:263–272.
25. Rapaport DH, et al. Timing and topography of cell genesis in the rat retina. *J Comp Neurol*. 2004;474:304–324.
26. Turner DL, Snyder EY, Cepko CL. Lineage-independent determination of cell type in the embryonic mouse retina. *Neuron*. 1990;4:833–845.
27. Turner DL, Cepko CL. A common progenitor for neurons and glia persists in rat retina late in development. *Nature*. 1987;328:131–136.
28. Wetts R, Fraser SE. Multipotent precursors can give rise to all major cell types of the frog retina. *Science*. 1988;239:1142–1145.
29. Holt CE, et al. Cellular determination in the *Xenopus* retina is independent of lineage and birth date. *Neuron*. 1988;1:15–26.
30. Brzezinski J, et al. Ascl1 expression defines a subpopulation of lineage-restricted progenitors in the mammalian retina. *Development*. 2011;138:3519–3531.
31. Godinho L, et al. Nonapical symmetric divisions underlie horizontal cell layer formation in the developing retina in vivo. *Neuron*. 2007;56:597–603.
32. Reh TA, Kljavin IJ. Age of differentiation determines rat retinal germinal cell phenotype: induction of differentiation by dissociation. *J Neurosci*. 1989;9:4179–4189.
33. Reh TA. Cellular interactions determine neuronal phenotypes in rodent retinal cultures. *J Neurobiol*. 1992;23:1067–1083.
34. Watanabe T, Raff MC. Diffusible rod-promoting signals in the developing rat retina. *Development*. 1992;114:899–906.
35. Watanabe T, Raff MC. Rod photoreceptor development in vitro: intrinsic properties of proliferating neuroepithelial cells change as development proceeds in the rat retina. *Neuron*. 1990;4:461–467.
36. Dakubo GD, et al. Retinal ganglion cell-derived Sonic hedgehog signaling is required for optic disc and stalk neuroepithelial cell development. *Development*. 2003;130:2967–2980.
37. Brown NL, et al. Math5 encodes a murine basic helix-loop-

helix transcription factor expressed during early stages of retinal neurogenesis. *Development*. 1998;125:4821–4833.
38. Reh TA, Cagan RL. Intrinsic and extrinsic signals in the developing vertebrate and fly eyes: viewing vertebrate and invertebrate eyes in the same light. *Perspect Dev Neurobiol*. 1994;2:183–190.
39. Cepko CL, et al. Cell fate determination in the vertebrate retina. *Proc Natl Acad Sci USA*. 1996;93:589–595.
40. Georgi SA, Reh TA. Dicer is required for the transition from early to late progenitor state in the developing mouse retina. *J Neurosci*. 2010;30:4048–4061.
41. La Torre A, Georgi SA, Reh TA. Conserved microRNA pathway regulates developmental timing of retinal neurogenesis. *Proc Natl Acad Sci USA*. 2013;110(26):E2362–70.
42. Marquardt T, et al. Pax6 is required for the multipotent state of retinal progenitor cells. *Cell*. 2001;105:43–55.
43. Li S, et al. Foxn4 controls the genesis of amacrine and horizontal cells by retinal progenitors. *Neuron*. 2004;43:795–807.
44. Brown NL, et al. Math5 is required for retinal ganglion cell and optic nerve formation. *Development*. 2001;128:2497–2508.
45. Koike C, et al. Functional roles of Otx2 transcription factor in postnatal mouse retinal development. *Mol Cell Biol*. 2007;27:8318–8329.
46. Nishida A, et al. Otx2 homeobox gene controls retinal photoreceptor cell fate and pineal gland development. *Nat Neurosci*. 2003;6:1255–1263.
47. Omori Y, et al. Analysis of transcriptional regulatory pathways of photoreceptor genes by expression profiling of the *Otx2*-deficient retina. *PLoS ONE*. 2011;6:e19685.
48. Akagi T, et al. Requirement of multiple basic helix–loop–helix genes for retinal neuronal subtype specification. *J Biol Chem*. 2004;279:28492–28498.
49. Mears AJ, et al. Nrl is required for rod photoreceptor development. *Nat Genet*. 2001;29:447–452.
50. Burmeister M, et al. Ocular retardation mouse caused by

Chx10 homeobox null allele: impaired retinal progenitor proliferation and bipolar cell differentiation. *Nat Genet*. 1996;12:376–384.
51. Brzezinski JAT, Lamba DA, Reh TA. Blimp1 controls photoreceptor versus bipolar cell fate choice during retinal development. *Development*. 2010;137:619–629.
52. Jasoni CL, et al. A chicken achaete-scute homolog (CASH-1) is expressed in a temporally and spatially discrete manner in the developing nervous system. *Development*. 1994;120:769–783.
53. Tomita K, et al. Mash1 promotes neuronal differentiation in the retina. *Genes Cells*. 1996;1:765–774.
54. Nelson BR, et al. Acheate-scute like 1 (Ascl1) is required for normal delta-like (Dll) gene expression and notch signaling during retinal development. *Dev Dyn*. 2009;238:2163–2178.
55. Ashwell KW, et al. The appearance and distribution of microglia in the developing retina of the rat. *Vis Neurosci*. 1989;2:437–448.
56. Schnitzer J, Scherer J. Microglial cell responses in the rabbit retina following transection of the optic nerve. *J Comp Neurol*. 1990;302:779–791.
57. Schnitzer J. The development of astrocytes and blood vessels in the postnatal rabbit retina. *J Neurocytol*. 1988;17:433–449.
58. Watanabe T, Raff MC. Retinal astrocytes are immigrants from the optic nerve. *Nature*. 1988;332:834–837.
59. Hinds JW, Hinds PL. Early ganglion cell differentiation in the mouse retina: an electron microscopic analysis utilizing serial sections. *Dev Biol*. 1974;37:381–416.
60. Snow RL, Robson JA. Ganglion cell neurogenesis, migration and early differentiation in the chick retina. *Neuroscience*. 1994;58:399–409.
61. Kirby MA, Steineke TC. Morphogenesis of retinal ganglion cells: a model of dendritic, mosaic, and foveal development. *Perspect Dev Neurobiol*. 1996;3:177–194.
62. Kirby MA, Steineke TC. Early dendritic outgrowth of primate retinal ganglion cells. *Vis Neurosci*. 1991;7:513–530.
63. Masai I, et al. N-cadherin mediates retinal lamination, maintenance of forebrain compartments and patterning of

retinal neurites. *Development*. 2003;130:2479–2494.
64. Rakic P. Neuronal migration and contact guidance in the primate telencephalon. *Postgrad Med J*. 1978;54(Suppl. 1):25–40.
65. Kim IJ, et al. Laminar restriction of retinal ganglion cell dendrites and axons: subtype-specific developmental patterns revealed with transgenic markers. *J Neurosci*. 2010;30:1452–1462.
66. Kljavin IJ, et al. Cell adhesion molecules regulating neurite growth from amacrine and rod photoreceptor cells. *J Neurosci*. 1994;14:5035–5049.
67. Yamagata M, Sanes JR. Dscam and Sidekick proteins direct lamina-specific synaptic connections in vertebrate retina. *Nature*. 2008;451:465–469.
68. Matsuoka RL, et al. Transmembrane semaphorin signalling controls laminar stratification in the mammalian retina. *Nature*. 2011;470:259–263.
69. Yamagata M, Sanes JR. Expanding the Ig superfamily code for laminar specificity in retina: expression and role of contactins. *J Neurosci*. 2012;32(41):14402–14414.
70. Dacey DM. The mosaic of midget ganglion cells in the human retina. *J Neurosci*. 1993;13:5334–5355.
71. Perry VH, Linden R. Evidence for dendritic competition in the developing retina. *Nature*. 1982;297:683–685.
72. Fuerst PG, et al. DSCAM and DSCAML1 function in self-avoidance in multiple cell types in the developing mouse retina. *Neuron*. 2009;64:484–497.
73. Wong RO, et al. Early functional neural networks in the developing retina. *Nature*. 1995;374:716–718.
74. Hendrickson AE. Synaptic development in macaque monkey retina and its implications for other developmental sequences. *Perspect Dev Neurobiol*. 1996;3:195–201.
75. Bleckert A, Wong RO. Identifying roles for neurotransmission in circuit assembly: insights gained from multiple model systems and experimental approaches. *Bioessays*. 2011;33:61–72.
76. Yoshimatsu T, Suzuki S, Wong ROL. Synapse formation in the developing retina. Rakic P, Rubenstein JL.

Comprehensive developmental neuroscience. Elsevier: Oxford; 2011.
77. Kerschensteiner D, et al. Neurotransmission selectively regulates synapse formation in parallel circuits in vivo. *Nature*. 2009;460:1016–1020.
78. Bumsted K, et al. Spatial and temporal expression of cone opsins during monkey retinal development. *J Comp Neurol*. 1997;378:117–134.
79. Hendrickson A, et al. Rod photoreceptor differentiation in fetal and infant human retina. *Exp Eye Res*. 2008;87:415–426.
80. Packer O, Hendrickson AE, Curcio CA. Development redistribution of photoreceptors across the *Macaca nemestrina* (pigtail macaque) retina. *J Comp Neurol*. 1990;298:472–493.
81. Cornish EE, et al. The role of opsin expression and apoptosis in determination of cone types in human retina. *Exp Eye Res*. 2004;78:1143–1154.
82. Cornish EE, Hendrickson AE, Provis JM. Distribution of short-wavelength-sensitive cones in human fetal and postnatal retina: early development of spatial order and density profiles. *Vision Res*. 2004;44:2019–2026.
83. Furukawa T, Morrow EM, Cepko CL. Crx, a novel Otx-like homeobox gene, shows photoreceptor-specific expression and regulates photoreceptor differentiation. *Cell*. 1997;91:531–541.
84. Roberts MR, et al. Retinoid X receptor (gamma) is necessary to establish the S-opsin gradient in cone photoreceptors of the developing mouse retina. *Invest Ophthalmol Vis Sci*. 2005;46:2897–2904.
85. Roberts MR, et al. Making the gradient: thyroid hormone regulates cone opsin expression in the developing mouse retina. *Proc Natl Acad Sci USA*. 2006;103:6218–6223.
86. Ng L, et al. A thyroid hormone receptor that is required for the development of green cone photoreceptors. *Nat Genet*. 2001;27:94–98.
87. Levine EM, Fuhrmann S, Reh TA. Soluble factors and the development of rod photoreceptors. *Cell Mol Life Sci*. 2000;57:224–234.

88. Lamba DA, Gust J, Reh TA. Transplantation of human embryonic stem cell-derived photoreceptors restores some visual function in Crx-deficient mice. *Cell Stem Cell*. 2009;4:73–79.
89. Lamba DA, Karl MO, Reh TA. Strategies for retinal repair: cell replacement and regeneration. *Prog Brain Res*. 2009;175:23–31.
90. Lamba DA, et al. Efficient generation of retinal progenitor cells from human embryonic stem cells. *Proc Natl Acad Sci USA*. 2006;103:12769–12774.
91. Lamba DA, et al. Generation, purification and transplantation of photoreceptors derived from human induced pluripotent stem cells. *PLoS ONE*. 2010;5:e8763.
92. Haverkamp S, et al. Synaptic plasticity in CNGA3($^{-/-}$) mice: cone bipolar cells react on the missing cone input and form ectopic synapses with rods. *J Neurosci*. 2006;26:5248–5255.
93. Mansergh F, et al. Mutation of the calcium channel gene Cacna1f disrupts calcium signaling, synaptic transmission and cellular organization in mouse retina. *Hum Mol Genet*. 2005;14:3035–3046.
94. Dick O, et al. The presynaptic active zone protein bassoon is essential for photoreceptor ribbon synapse formation in the retina. *Neuron*. 2003;37:775–786.
95. Li S, Sukeena JM, Simmons AB, et al. DSCAM promotes refinement in the mouse retina through cell death and restriction of exploring dendrites. *J Neurosci*. 2015;35(14):5640–5654.
96. Nuhn JS, Fuerst PG. Developmental localization of adhesion and scaffolding proteins at the cone synapse. *Gene Expr Patterns*. 2014;16(1):36–50.
97. Wong RO, Hughes A. Role of cell death in the topogenesis of neuronal distributions in the developing cat retinal ganglion cell layer. *J Comp Neurol*. 1987;262:496–511.
98. Valenciano AI, Boya P, de la Rosa EJ. Early neural cell death: numbers and cues from the developing neuroretina. *Int J Dev Biol*. 2009;53:1515–1528.
99. Shen S, et al. Retinal ganglion cells lose trophic responsiveness after axotomy. *Neuron*. 1999;23:285–295.

100. Frade JM, et al. Control of early cell death by BDNF in the chick retina. *Development*. 1997;124:3313–3320.
101. Farah MH. Neurogenesis and cell death in the ganglion cell layer of vertebrate retina. *Brain Res Rev*. 2006;52:264–274.
102. Isenmann S, Kretz A, Cellerino A. Molecular determinants of retinal ganglion cell development, survival, and regeneration. *Prog Retin Eye Res*. 2003;22:483–543.
103. Pollock GS, et al. TrkB receptor signaling regulates developmental death dynamics, but not final number, of retinal ganglion cells. *J Neurosci*. 2003;23:10137–10145.
104. Mao CA, et al. Eomesodermin, a target gene of Pou4f2, is required for retinal ganglion cell and optic nerve development in the mouse. *Development*. 2008;135:271–280.
105. Wang SW, et al. Abnormal polarization and axon outgrowth in retinal ganglion cells lacking the POU-domain transcription factor Brn-3b. *Mol Cell Neurosci*. 2000;16:141–156.
106. Xiang M, et al. Targeted deletion of the mouse POU domain gene Brn-3a causes selective loss of neurons in the brainstem and trigeminal ganglion, uncoordinated limb movement, and impaired suckling. *Proc Natl Acad Sci USA*. 1996;93:11950–11955.
107. Weishaupt JH, Klocker N, Bahr M. Axotomy-induced early down-regulation of POU-IV class transcription factors Brn-3a and Brn-3b in retinal ganglion cells. *J Mol Neurosci*. 2005;26:17–25.
108. Hendrickson A. A morphological comparison of foveal development in man and monkey. *Eye (Lond)*. 1992;6:136–144.
109. Hendrickson A, Kupfer C. The histogenesis of the fovea in the macaque monkey. *Invest Ophthalmol Vis Sci*. 1976;15:746–756.
110. Hendrickson AE. Primate foveal development: a microcosm of current questions in neurobiology. *Invest Ophthalmol Vis Sci*. 1994;35:3129–3133.
111. Hendrickson AE, Yuodelis C. The morphological development of the human fovea. *Ophthalmology*. 1984;91:603–612.

16

Structure and Function of Rod and Cone Photoreceptors

Jeannie Chen, Alapakkam P. Sampath

Introduction

Our visual experience is initiated by rod and cone photoreceptors in the retina. The human eye contains over 100 million rods and about 6 million cones, which are located within the outer nuclear layer of the retina and allow our visual experience to extend over 12 orders of magnitude in light intensity by splitting this range. Rod photoreceptors mediate vision under conditions of dim illumination, and allow our visual system to reach the limit imposed by the absorption of single photons.[1,2] Cones are less sensitive by ~100-fold, but their tremendous capacity for adaptation allows them to encode light intensities on the brightest of days.[3,4] Over the last two decades, our understanding of structure and function of these cells has increased dramatically. Over 150 genes have been cloned or linked to retinal diseases, and, surprisingly, as many as half of these genes are specifically expressed or highly enriched in the photoreceptor cells. Discovery of the molecular constituents of the rods and cones is progressing at an increasing rate, particularly enhanced by the availability of "complete" genomic sequences for both human and mouse. While photoreceptor genes can be identified through association with a retinal disease (linkage), information about their function does not accompany their identification.[5] Basic science research must then be undertaken to explain their role in both the normal, healthy photoreceptor, as well as in photoreceptor diseases.

Though much of what we know about the structure and function of photoreceptor cells has come from studying animal models of inherited blindness,[6,7] more recently, transgenic and knockout animal technologies have established themselves as powerful tools for understanding function and studying disease. After new photoreceptor genes are identified from patients, mutant animals can be engineered to emulate human photoreceptor pathologies. Before these molecular technologies were available, most data

about retinal disease was gleaned from the rare "informative" patient or donor retina that had surviving photoreceptors to examine.[8] Other major sources of information were studies of animal models that occurred through inbreeding or random inheritance of mutations in photoreceptor genes. Examples of these are the Irish setter dog,[9] the Briard dog,[10] the Abyssinian cat,[11] the RCS rat,[12] and the rd1[13,14] and rds[15,16] mouse models. Now, the ability to engineer transgenic animals has made the search for "informative" patients and naturally occurring animal models less acute – since any single gene of interest can be introduced[17–19] or removed[20–24] from the photoreceptor. However, the most instructive examples of structure–function relationships occur when there are patients and animal models with analogous mutation(s) and/or disease phenotype. Only recently has it become possible to incorporate the insights from numerous studies into biochemical pathways and mechanisms of photoreceptor function. Here, we review the principal proteins and pathways involved in rod photoreceptor structure and function, and highlight the parallelisms in cone photoreceptors.

Photoreceptor Fundamentals

The rod and cone photoreceptors are specialized sensory neurons that contain the protein machinery necessary to convert incident light into a signal that can be interpreted by the nervous system. Rod photoreceptors are more numerous than cones in most mammalian retina, and are highly sensitive. In the fully dark-adapted state, rods can reliably report the absorption of single photons to the retinal output, and they permit our scotopic, or night, vision. Cone photoreceptors are morphologically and functionally distinct from rods and express several types of visual pigments, or opsins, whose spectral sensitivity varies based on the cones subtype. In humans, three classes of cones confer robust color vision: S-cones, M-cones, and L-cones (see Chapter 12, Color vision and night vision). Cones are also less sensitive than rods and generate light responses that are temporally briefer. This allows cones to mediate our photopic, or day, vision with improved temporal resolution. The concerted action of these two types of

photoreceptors, and the retinal circuitry that carries their signals to the retinal output, ultimately underlie our rich visual experience.

Both rod and cone photoreceptors are highly polarized elongated cells that can be described as having four subcellular compartments: the outer segment (OS), the inner segment (IS), the nucleus, and the synaptic terminal (Figs. 16.1 and 16.2). The OS is where photons are captured and activation of the phototransduction cascade begins. The IS lies immediately proximal to the OS, and contains the cell's protein synthesis (Golgi apparatus and endoplasmic reticulum) and metabolic (mitochondria) machinery. Light-evoked signals are relayed passively down the photoreceptor axon (up to 75 μm long) to the synaptic terminals in the outer plexiform layer. The structure of photoreceptor terminals is unique in the nervous system, as they contain a specialized structure called a ribbon that facilitates the release of the excitatory neurotransmitter glutamate onto second-order retinal neurons (bipolar and horizontal cells). Thus, the photoreceptor cells transduce the sensory stimulus, light, and pass on a signal to retinal circuits that carry this information to higher visual centers.

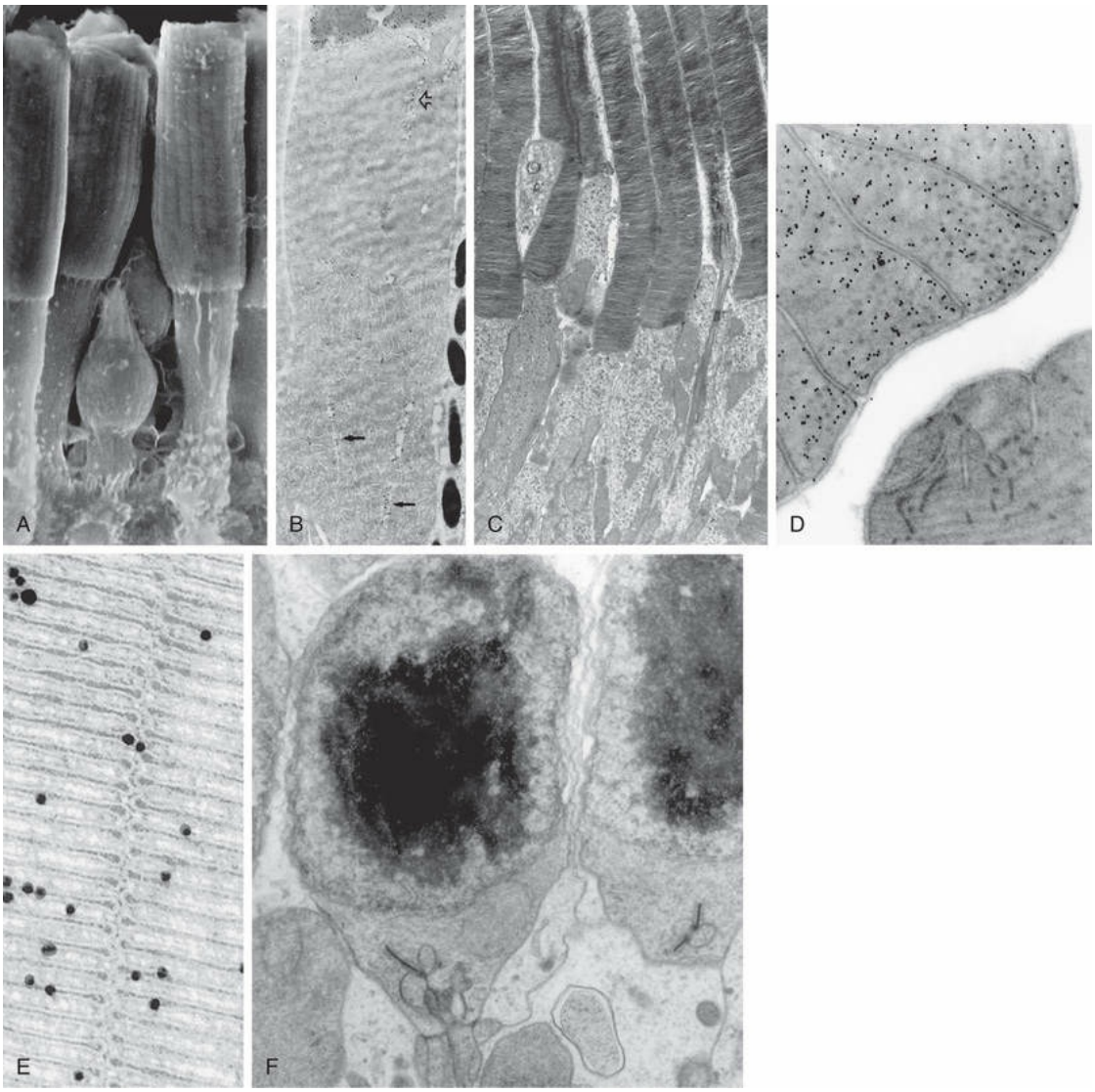

FIG. 16.1 (A) Scanning electron micrograph of rods and cones from the African clawed frog, *Xenopus laevis*. The basic shape of the rod photoreceptor inner and outer segments can be appreciated by this surface view. The cones in this species are exceptionally short and "cone"-shaped, unlike the cylindrical appearance of cone outer segment (OS) in the mammalian retina. (B) Immunolocalization of opsin in the inner segment (IS) of the frog retina. Arrows show location of newly synthesized opsin in the Golgi apparatus (*solid arrows*) and a track of labeled vesicles (*open arrows*) from the myoid to the cilium. (C) Transmission electron micrograph of photoreceptors from the mouse retina. Note the connecting cilium between the inner and outer segments and that a large number of mitochondria are visible in this orientation. (D) High-magnification view of frog photoreceptor OSs as

viewed from the top of the disc stack. Upper left shows a single disc labeled with an anti-rod opsin antibody. The plasma membrane surrounding the disc can be observed in this section. Lower left is a cone photoreceptor OS that is not labeled by the antibody. (E) High-magnification view of frog photoreceptor OSs as viewed from the side of the disc stack. Discs are labeled with an anti-rod opsin antibody. The rim region of the disc can be observed, as well as the close packing of the individual discs within the OS. (F) Synaptic terminal of the rod photoreceptor. Directly below the nucleus is the photoreceptor spherule. Synaptic ribbons are visible in this section. (Panels D and E courtesy of Robert Molday, University of British Columbia.)

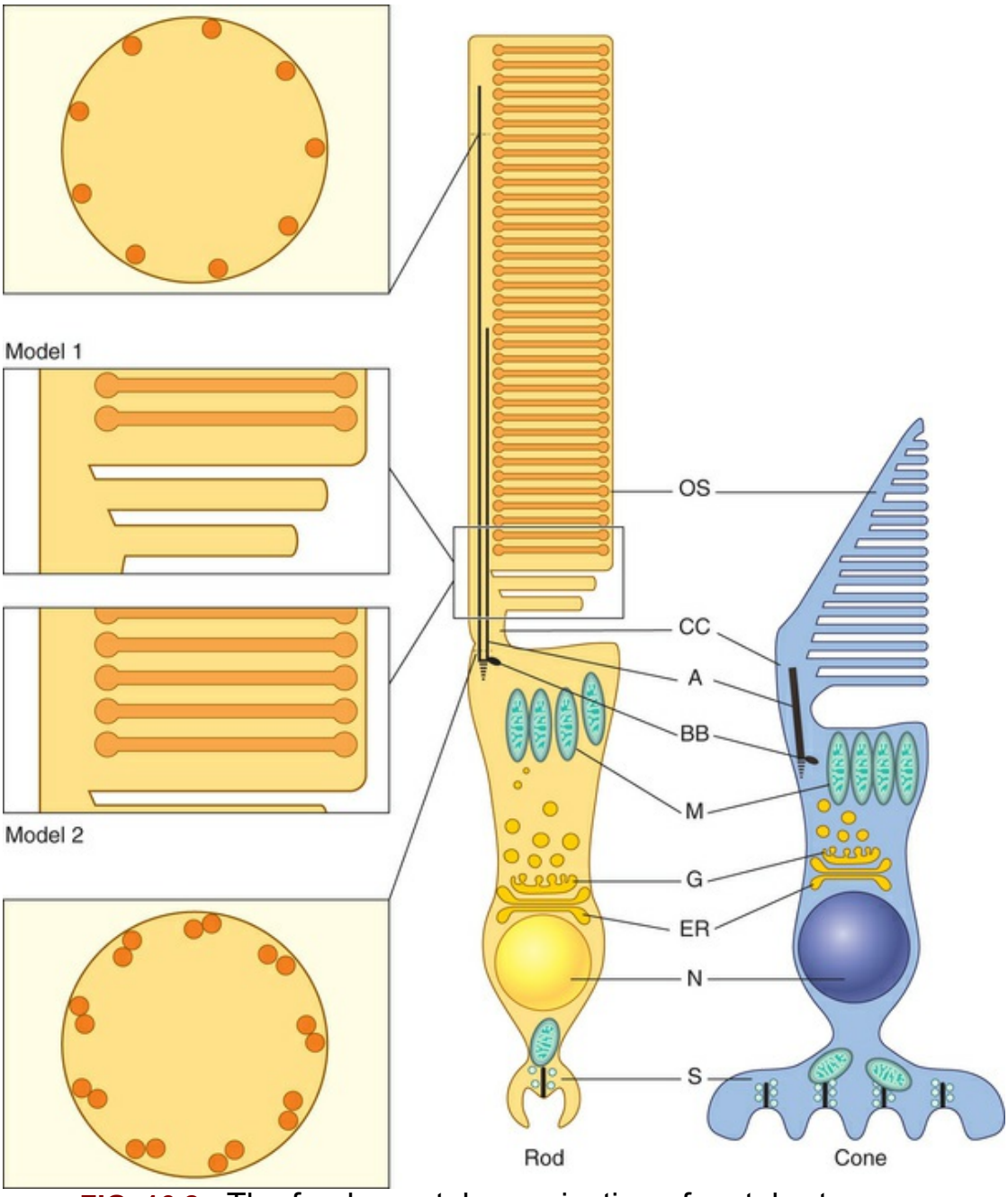

FIG. 16.2 The fundamental organization of vertebrate rod and cone photoreceptors. Parts of the cell include: *OS*, outer segment; *A*, axoneme; *CC*, connecting cilium; *BB*, basal body; *R*, ciliary rootlet; *M*, mitochondria; *G*, Golgi apparatus; *ER*, endoplasmic reticulum; *N*, nucleus; *S*, synaptic terminal. *Insets* depict the structure of the axoneme at the level of the outer segment where microtubule structure is 9 × 1 + 0 (top), and where the inner and outer segment join the microtubule structure is 9 × 2 + 0 (bottom). Middle panels depict two models for outer segment (OS) disc formation. In Model 1, OS discs originate from

evaginations of the plasma membrane but become closed off and separate from the plasma membrane.[56,57] In Model 2, newly generated OS discs are already closed and separate from the plasma membrane.[58] (Modified with permission from Anderson DH, Fisher SK, Steinberg RH. Mammalian cones: disc shedding, phagocytosis, and renewal. Invest Ophthalmol Vis Sci 1978;17(2):117-33; Steinberg RH, Fisher SK, Anderson DH. Disc morphogenesis in vertebrate photoreceptors. J Comp Neurol 1980;190(3):501-8; Chuang JZ, Zhao Y, Sung CH. SARA-regulated vesicular targeting underlies formation of the light-sensing organelle in mammalian rods. Cell 2007;130(3):535-47.)

Photoreceptor Outer-Segment Structure

The OS compartment contains all components necessary for phototransduction, which is a set of biochemical reactions that convert photon capture to a change in a cationic current at the plasma membrane. Rods have a cylindrical OS about 1.3 μm in diameter; the OS length ranges from 25 to 45 μm,[25–28] that depends on numerous factors including the time of day, the light intensity, their location in the retina, and the animal species. The cone OS is shorter, typically half the length as rods, with a larger diameter at the base that gradually tapers towards the tip (Fig. 16.2). Mouse rod OS contains an average of 810 membranous discs, which occupy two-thirds of the volume of the OS.[29] The majority of the protein on these discs is rod opsin (or rhodopsin when the opsin is bound to its chromophore, 11-*cis* retinal). The density of rhodopsin on the disc membrane has been measured to be about 24,000 molecules/μm^2.[30] Despite this dense packing, rhodopsin freely diffuses in the membrane,[31] which facilitates its encounter with, and activation of, transducin molecules to amplify the light signal. Many G-protein-coupled receptors are known to form dimers and higher-order oligomers. Rhodopsin has been observed to form a paracrystalline array of dimers when native disc membrane is viewed under atomic force microscopy[32] and more recently by cryoelectron microscopy.[33] Whether it exists as dimers in vivo is still an area of controversy. However, it is known that rhodopsin is functional as

monomers.[34]

Other integral membrane proteins of the phototransduction pathway that are embedded in the discs are two isoforms of the guanylyl cyclases, RetGC1 and RetGC2, which are single-pass transmembrane proteins. Other transduction proteins, such as the G protein transducin (Tα), phosphodiesterase 6 (PDE6), recoverin, and guanylyl cyclase activating proteins (GCAPs), are peripheral membrane proteins (see below).

Proteins That Stabilize the Structure of Outer-Segment Discs

Rhodopsin is not only integral to the phototransduction cascade, it is also required for the formation and maintenance of OS discs; in the absence of rhodopsin, the OS structure is not formed.[22] Peripherin and Rom-1[15,35,36] are two other disc membrane components that contribute to maintaining the flattened structure of the disc. Both of these proteins belong to the tetraspanin family of integral membrane proteins that form large multiprotein complexes known as the tetraspanin web or tetraspanin-enriched microdomains.[37] Peripherin/rds is normally found within the edge or "rim" of the disc. It self-associates to form higher-order complexes and also interacts with Rom-1.[38] Peripherin/rds and Rom-1 likely function as adhesion molecules that assist in keeping the discs vertically aligned, and may stabilize the disc stack with bridges to the overlying plasma membrane. Peripherin/rds is also thought to function in forming the curvature of the disc rim.[39]

Deletion or disruption of peripherin/rds results in malformation of discs at the OS base. The naturally occurring retinal degeneration in the mouse named "retinal degeneration, slow" (rds) has been shown to be due to a defect in peripherin/rds. The absence of peripherin/rds in the *rds/rds* mouse prevents normal development of the photoreceptor OS and leads to photoreceptor cell death.[15,40] Transgenic mice that lack peripherin/rds fail to form an OS. When the level is reduced, as in the heterozygous mice, large whorls of disc membrane are formed instead of an organized stack of uniform discs.[15,40] Mutations that affect the quaternary structure of peripherin/rds also lead to malformed discs. These observations

underscore the importance of peripherin/rds in the formation and maintenance of disc structure in the OS.

Although Rom-1 is analogous to peripherin in structure and function, its absence in rods shows a less severe phenotype than peripherin/rds knockout mice, suggesting that peripherin/rds is more critical for disc formation. Although the discs grow larger than normal sizes, photoreceptor function appears to be retained to a much higher level than when peripherin/rds is absent. Nevertheless, abnormal Rom-1 does lead to slow and progressive photoreceptor degeneration both in mice and in humans.[41]

Functional differences of peripherin/rds and Rom-1 have been noted in rods and cones. Cones appear to have a lower ratio of Rom-1/peripherin,[37] and different peripherin/rds mutations appear to differentially affect rods and cones. For example, the C214S and N244K mutations have a greater effect on rods whereas R172W and N244H tend to cause cone-dominant diseases such as macular dystrophy.[37]

Transmission electron microscopy has revealed structural elements between the lamellar discs as well as between the discs and the plasma membrane that are mainly localized to the rim region and incisures of discs.[42–45] A recent study of OS structure using cryoelectron tomography of vitrified outer segments showed previously unobserved spacers distributed throughout the discs.[30] These structural elements likely maintain the proper distance between adjacent discs and between discs and the plasma membrane. The protein identities of these spacers are not known, but peripherin/rds and Rom-1 may be candidates.

Another component of the rod disc is ABCR (photoreceptor cell-specific ATP-binding cassette transporter).[46,47] Mutations in *ABCR* are responsible for a large variety of retinal degenerations, including Stargardt macular dystrophy, fundus flavimaculatus, some forms of cone–rod degeneration, and retinitis pigmentosa. Other ABCR mutations are thought to increase the risk of developing age-related macular degeneration (AMD). ABCR is a member of the ATP-binding cassette (ABC) superfamily. This is a large family of transmembrane proteins involved in energy-dependent transport of many different substrates across membrane "barriers." The localization of ABCR at the disc rim suggests that it

is involved in the movement of molecules from the disc lumen into the cytosol. This hypothesis was supported by studies in ABCR knockout mice, which show delayed dark adaptation, increased all-*trans* retinal following light exposure, and elevated phosphatidylethanolamine (PE) in the rod OS.[48] Biochemical analysis of retinas from ABCR knockout mice revealed accumulation of a novel complex of all-*trans* retinal and PE, termed (N-retinylidene-PE), which is not found in normal retina. Once in the cytosol, the all-*trans* retinol moves to the RPE for recycling and chromophore (11-*cis* retinal) regeneration (see Chapter 18, Cell biology of the retinal pigment epithelium). The primary pathologic defect in Stargardt disease, and also in ABCR knockout mice, is accumulation of toxic lipofuscin pigments, such as A2E, in RPE cells. Thus the phenotype is remarkably similar between mice and that observed in the fundus of Stargardt patients. The animal model and further biochemical investigations[41] suggest that ABCR functions as an outwardly directed flippase for N-retinylidene-PE. Delayed dark adaptation is likely due to accumulation (in discs) of the non-covalent complex between opsin and all-*trans* retinal. ABCR-mediated retinal degeneration in patients may result from "poisoning" of the RPE due to A2E accumulation, with secondary photoreceptor degeneration due to loss of the ABCR support role.

Though ABCR most definitely plays a role in the structure of discs, no mutations have been conclusively associated with abnormal structural features, *per se*. In other words, it appears that mutations do not directly affect folding at the disc rim, and more likely affect the biochemical function of the transporter. In corroboration of these data, Radu and colleagues tested the effects of isotretinoin on lipofuscin accumulation in ABCR knockout mice,[49] a model of recessive Stargardt disease. They observed by electron microscopy that isotretinoin blocked both the formation of A2E biochemically, and the accumulation of lipofuscin pigments. Further, no significant visual loss was observed in ABCR null mice by electroretinography (when treated), and isotretinoin also blocked the slower, age-dependent accumulation of lipofuscin in wild-type mice. The results suggest that treatment with isotretinoin may inhibit lipofuscin accumulation and delay the onset of visual loss in patients with Stargardt disease and may be an effective

treatment for other forms of retinal or macular degeneration associated with lipofuscin accumulation, though "normal" visual function may be somewhat compromised by such treatment.

The presence of an OS is clearly not optional, as there are many examples of retinal disease in which the photoreceptor cell dies shortly after loss of the OS.[50–52] Why loss of the OS triggers rod cell death is not obvious, since all of the required cellular organelles inhabit the IS and cell body; the OS appears devoid of organelles. The necessity to maintain an OS is further surprising since photoreceptors continually replace all the OS components. In fact, the renewal of rod cell OS components is perhaps more readily seen in the photoreceptor than in any other cell in the body. The disc and plasma membrane components of the OS are completely replaced within two weeks.[53,54] To support this turnover there is an influx of newly synthesized proteins and lipids from the IS. These components are transported to the base of the OS, and from there discs gradually migrate towards the RPE for phagocytosis and recycling. One idea is that the high oxygen tension coming from the choroidal vasculature may interfere with the cellular machinery in the IS and nucleus of the photoreceptor, and the presence of the OS puts a protective distance between the choroid and the photoreceptor nuclei.[55]

Disc Morphogenesis

Although it is known that new discs are formed at the base of the OS, the process by which these discs are formed is not fully resolved (see Fig. 16.2). One model was described in the work of Anderson, Steinberg, and Fisher (Model 1).[56,57] Based on morphologic studies of adult monkey rods, it was observed that the folded membrane stacks at the base of the OS are continuous with the plasma membrane of the connecting cilium, whereas the older discs are closed off and separated from the plasma membrane. From this appearance a model was proposed that the newly arrived rhodopsin-bearing vesicles fuse with the plasma membrane, and the growing membrane evaginates to form open discs. Eventually these discs pinch off and form the mature closed discs. Another model (Model 2), the "vesicular targeting model," has been

proposed by Chuang and colleagues.[58] They provide molecular evidence that rhodopsin's carboxyl terminus interacts with a protein called SARA (smad anchor for receptor activation), as well as PI3P (phosphatidylinositol 3-phosphate) and syntaxin 3. In their model, the new discs are already closed and enveloped by the OS plasma membrane. Their evidence suggests that the protein–protein and protein–lipid interactions organized by SARA regulate the vesicular targeting of axonemal rhodopsin-bearing vesicles to the newly formed discs. Thus the discs grow by fusing with the rhodopsin-bearing vesicles and not from the evaginated plasma membrane. This model is more consistent with the morphology of their experimental model system, the mouse rods, which do not display open discs at the base of the OS.

The degree of translational and posttranslational control in the processes of disc formation remains an open question. The processes necessary to manage and partition the correct ratio of rhodopsin to the other proteins of the phototransduction cascade (transducin: PDE: GC: GCAP: cGMP-gated channel) in the discs are unknown. Additionally, the insertion of the structural proteins peripherin, Rom-1, and ABCR into the forming disc rim is likely to require precise instruction. How these processes combine to generate a functional OS will require extensive new investigation and methodology. It is unlikely that these complex morphogenic processes will be elucidated using static two-dimensional microscopy methods with fixed materials, the method that has yielded most of information to date. These problems may require the application of three-dimensional microscopy, in conjunction with immunocytochemical tags and fluorescent labels such as GFP, to follow the assembling proteins in preparations of living photoreceptors.

Outer-Segment Plasma Membrane

The plasma membrane of the rod OS encloses the majority of the discs and creates a physical barrier between the discs and the cell's exterior, except perhaps for the newly formed basal discs (see Fig. 16.2, Model 1). In the mammalian cone OS at least several discs are continuous with the outer plasma membrane along the OS.[59] This

open configuration creates additional surface area, which allows for more rapid exchange of retinoids and ions. It is clear that, in addition to its obvious role in phototransduction, the OS plasma membrane contains a rich array of specialized proteins, many of which regulate the movement of ions into and out of the OS. The best-characterized proteins of this type are the retinal cGMP-gated (CNG) cation channels. In the dark-adapted rods and cones, Na^+ and Ca^{2+} flow into the OS through these channels in the plasma membrane. Calcium comprises about 10% of the dark current carried by these channels in rods,[60] and perhaps 20% or more in cones.[61,62] In both rods and cones Na^+ is extruded from the IS through the Na^+/K^+ pump. This flow of ions sets up the circulating dark current, of which the vast majority is carried by the Na^+. The probability of the opening of the CNG channel, which in turn determines the size of the circulating current, depends on the amount of free [cGMP], which in the dark is estimated to be 3–4 μM.[63] At this concentration, the probability of channel opening is estimated to be only 0.1–0.2.[64,65] This underscores the impact that elevated [cGMP] can have on the number of open channels in the diseased state. The influx of Ca^{2+} through the channel is balanced by an efflux of Ca^{2+} by the Na^+/Ca^{2+}-K^+ exchanger in the rod OS plasma membrane, thereby maintaining the intracellular level of Ca^{2+} at a relatively constant level.[66] Kaupp and colleagues[67] cloned the cGMP channel from bovine retina, while Pittler and colleagues[68] determined the primary structures of the human and mouse retinal rod cGMP-gated cation channel. These studies found that the sequence of the cGMP channel has significant similarity (59%) to the olfactory cAMP-gated channel. The retinal rod CNG channel is a hetero-oligomer composed of three alpha- (α) (CNGA1) and one beta- (β) (CNGB1) subunits,[69,70] each with cytoplasmic amino(N)- and carboxyl(C)-termini, six putative transmembrane domains, and a pore region.[15,71] Mutations in *CNGA1* and *CNGB1* have been linked to disease. A point mutation in *CNGB1*[72] and several mutations in *CNGA1*[73] have been identified and linked to recessive RP in humans. The CNG channel instead of cones consists of two CNGA3 and two CNGB3 subunits.[74] Together, mutations in either of these genes account for ~75% of complete acromatopsia.[75,76]

In addition to the CNG channel, there are several other channels

and transporters in the plasma membrane that serve to regulate the intracellular contents of the OS. The best studied of these is the $Na^+/Ca^{2+}–K^+$ exchanger (NCKX), which is the only known route for Ca^{2+} extrusion from the OS. Rods express NCKX1 whereas cones express NCKX2.[77] However, the lack of a clear phenotype in the cone electroretinogram in the *NCKX2* knockout mice[78] raises possibilities for additional *NCKX* expression in cones or yet to be discovered NCKX-independent Ca^{2+} extrusion mechanisms. The exchanger moves with every cycle 4 Na^+ into the OS, and in exchange, moves 1 Ca^{2+} and 1 K^+ into the subretinal space; exchange is thus electrogenic. A mutation in *NCKX1* is associated with autosomal recessive congenital stationary night blindness in humans,[79] and deletion of *NCKX1* in mice resulted in malformed rod OS discs and suppressed expression and function of rod CNG channels. The rods slowly degenerated while cone function was maintained.[80] Other transmembrane proteins, such as the GLUT-1 glucose transporter, have been shown to be present on both rod and cone OS.[81]

Outer-Segment Lipids

Docosahexaenoic acid (DHA, 22:6n-6) is the major fatty acid found in the retinal rod OS, and rod photoreceptors have higher levels of DHA than in any other membrane system examined.[82] Numerous studies have established that the high level of DHA in rod OS membranes provides an optimal microenvironment for rhodopsin. DHA belongs to the n-3 family of essential polyunsaturated fatty acids. These fatty acids cannot be synthesized by vertebrates and they, or their shorter chain precursors, must therefore be obtained in the diet.[83]

Humans with RP and dogs with progressive rod–cone degeneration (prcd) have lower than normal blood levels of long-chain polyunsaturated fatty acids, including DHA. In addition, prcd-affected dogs have lower levels of DHA in their rod OS than control animals.[84] The reason for the reduced level of DHA in rod outer segments of animals with inherited retinal degeneration is not known. However, the fatty acid composition of the rod OS of these animals suggests that the synthesis of DHA containing

glycerolipids is downregulated in retinas of animals with inherited retinal degenerations.

Phototransduction

Visual transduction is initiated by the phototransduction cascade, which is perhaps the best characterized of all G-protein-coupled receptor signaling pathways. Our knowledge about phototransduction is relatively advanced because the components of this pathway are located selectively in the photoreceptor OS and can be isolated in quantities suitable for biochemical analysis. Photoreceptors can also be isolated easily for electrophysiologic measurements, either as single cells using suction electrodes (Fig. 16.3), or en masse using field potentials called electroretinograms (ERG; see Chapter 9, Electrogenesis of the electroretinogram). The phototransduction cascade within rods is so robust such that single photon absorption by rhodopsin gives rise to a change in current that can be monitored by suction electrode recordings. Similarly, the remarkable ability of cone phototransduction to adapt to increases in background light intensity can also be monitored with suction electrodes. The combination of transgenic technology and electrophysiologic analysis has enhanced greatly our understanding of signal transduction within these photoreceptor cells. In particular, transgenic technologies have allowed the introduction of targeted changes into specific components of the signaling pathway. These genetically altered intact photoreceptor cells can then be subjected to electrophysiologic measurements, and their tissues can subsequently be used in biochemical or immunocytochemical assays to pinpoint the molecular mechanism behind the physiologic phenotype. Below, we summarize the current state of our understanding of phototransduction in retinal photoreceptors.

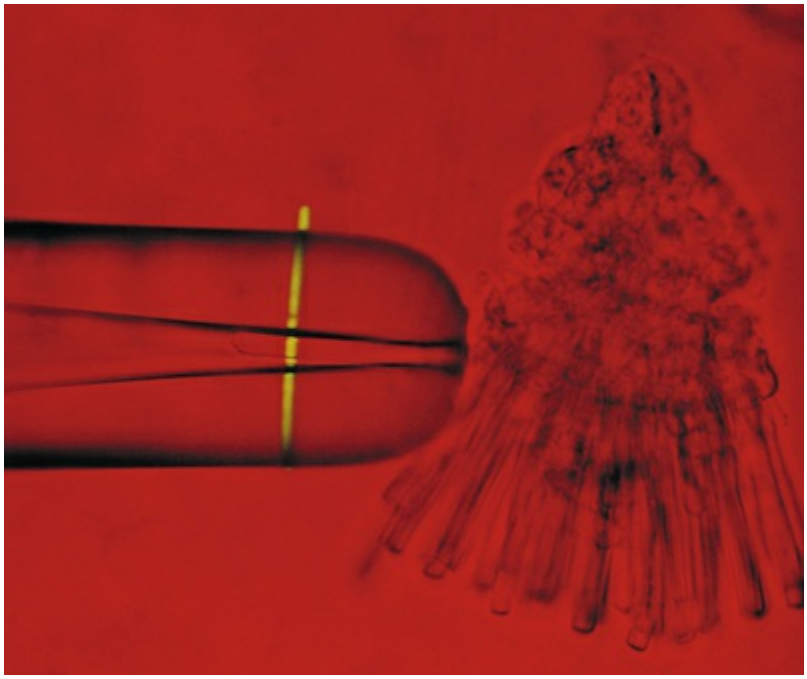

FIG. 16.3 Suction electrode used in recording the outer-segment current. The cells in this clump of toad retina are being superfused with bicarbonate-buffered Ringer solution equilibrated with 5% carbon dioxide. A rod outer segment is carefully drawn into the glass electrode, which makes a high-resistance seal against the cell. Responses are recorded during the presentation of a stimulus, in this case a slit of focused green light.[1] (Modified with permission from Baylor DA, Lamb TD, Yau KW. Responses of retinal rods to single photons. J Physiol 1979;288:613-34.)

Signal Activation and Amplification

A hallmark of rod phototransduction is its high sensitivity. Fully dark-adapted rods achieve sensitivity that reaches the theoretical maximum, the ability to detect individual quanta of light.[1,2] This high sensitivity is generated through several stages of amplification, resulting in a tremendous increase in the signal gain (Fig. 16.4). This cascade of amplification begins at the light-activated G-protein-coupled receptor rhodopsin (R). Absorption of a photon by R leads to a conformation change (R*), allowing it to interact with the heterotrimeric G protein transducin (T alpha (α), beta (β), and gamma (γ)), thereby promoting the exchange of bound GDP for GTP. The complex then dissociates into Tα-GTP and T$\beta\gamma$,

and R* is free to activate many other transducin molecules during its catalytic lifetime.[85] In the subsequent step, Tα-GTP binds and removes the inhibitory gamma- (γ) subunit of the cGMP-phosphodiesterase (PDE) so that it can now hydrolyze cGMP to 5′-GMP; the enzymatic activity of PDE (PDE*) in turn degrades thousands of cGMP molecules. The decrease in cytoplasmic cGMP concentration then leads to closure of the cGMP-gated cation conductance channel in the rod plasma membrane, resulting in a reduction in the influx of ~1,000,000 Na^+ ions.[86] This is a graded effect: a slight lowering in the cGMP concentration leads to closure of some channels, while a large decrease will eventually lead to closure of all channels. In this instance, the rod cell is said to be ″saturated.″

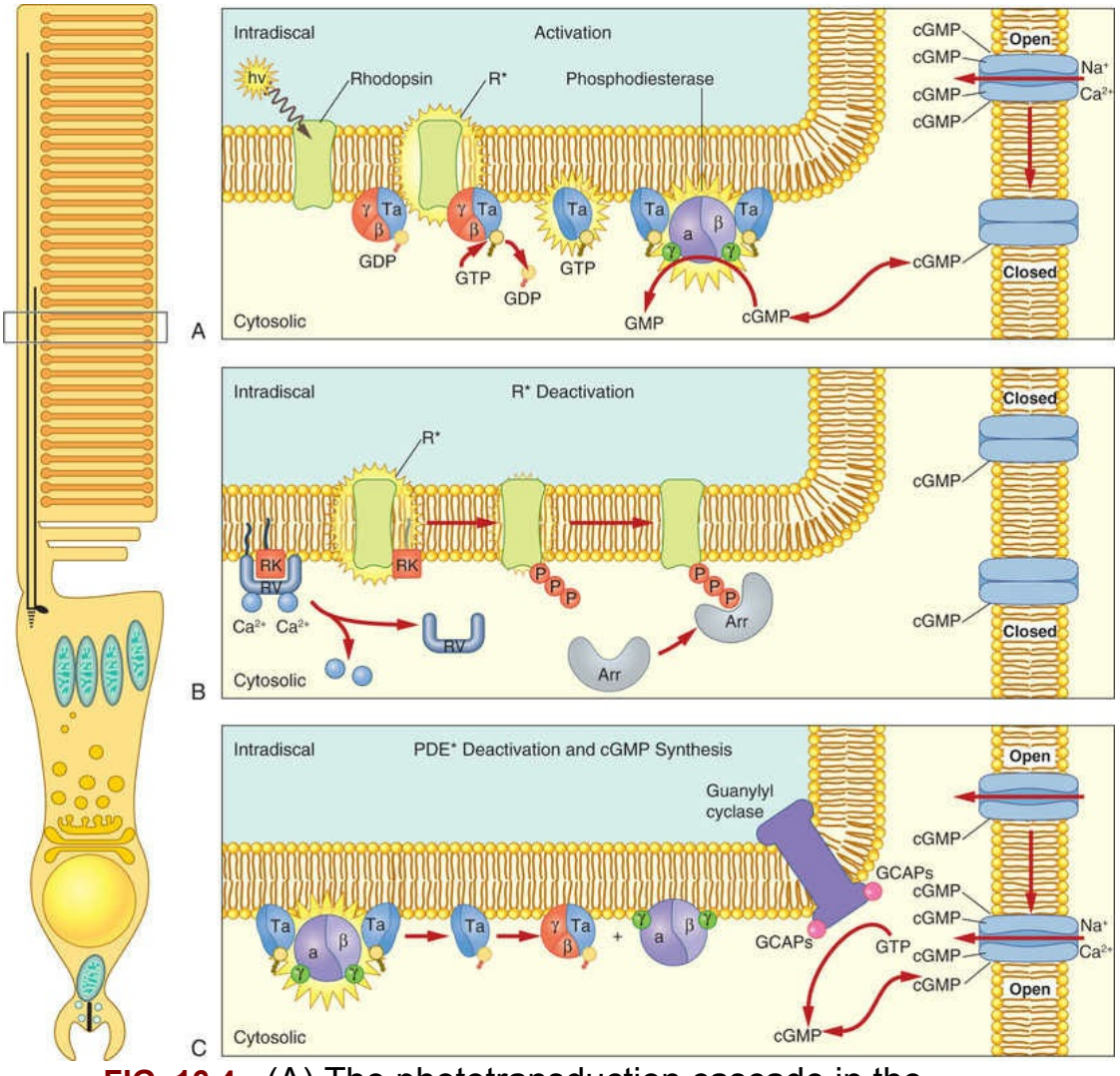

FIG. 16.4 (A) The phototransduction cascade in the

rod and cone outer segment is initiated when a photon (*hv*) strikes the visual pigment, rhodopsin in rods, and promotes it to an active state (R*). R* interacts with a heterotrimeric G-protein and promotes the exchange of GTP for GDP on the alpha-subunit (Tα). Tα in turn disinhibits a cGMP phosphodiesterase (PDE) thereby allowing the hydrolysis of cGMP and the closure of cyclic nucleotide gated (CNG) channels. The closure of CNG channels interrupts the flow of Na^+ and Ca^{2+} into the photoreceptor and hyperpolarizes the membrane potential. (B) Deactivation of R* is required to quench the phototransduction cascade. R* deactivation is initiated by the phosphorylation Ser and Thr residues at its C-terminus by rhodopsin kinase (RK). RK is inhibited by recoverin (Rv), a process which is controlled by Ca^{2+}. Ca^{2+} concentration falls as CNG channels close during the activation of phototransduction, allowing the disassociation of RK from Rv, and subsequently the phosphorylation of R*. The R* catalytic activity is further quenched by the binding of visual arrestin (Arr) to phosphorylated R*. (C) Deactivation of activated PDE (PDE*) requires the hydrolysis of GTP to GDP on Tα. To reopen CNG channels, guanylyl cyclase synthesizes cGMP from GTP, a process that is regulated by the Ca^{2+}-binding protein, guanylyl cyclase activating protein 1 and 2 (GCAPs).

In darkness, glutamate, the transmitter used by both rods and cones, is released at a steady rate because the photoreceptor's membrane potential is in a relatively depolarized state. The closure of CNG channels results in a graded hyperpolarization of the cell, leading to a decrease in glutamate release at the synapse. In this manner, the first sensation of light perception is transmitted from the photoreceptor cell to second-order cells of the retina, where signals are further processed and ultimately conveyed to the retinal ganglion cells (see Chapter 17, Function and anatomy of the mammalian retina).

Signal Deactivation

A reversal of the activation steps is required ultimately for the

photoreceptor to return to its resting state. First, the catalytically active components of the phototransduction cascade, R* and PDE*, must be quenched, then cGMP needs to be resynthesized (see Fig. 16.4). These events must be rapid and reproducible for the photoreceptor to maintain its high sensitivity and respond to subsequent stimuli. Our current understanding of these processes is detailed below.

Quenching R*: Rhodopsin Phosphorylation

Since the early 1980s, phosphorylation was recognized to play an important role in deactivation of R*.[87,88] To determine how receptor deactivation occurs in vivo, transgenic mouse models were developed to assess the contribution of receptor phosphorylation to R* shut-off. It is clear that rhodopsin kinase, or GRK1, is solely responsible for phosphorylating R*, since phosphorylation of R* does not occur in mice lacking rhodopsin kinase.[89] In early experiments, a rhodopsin truncation mutation, S334ter, was expressed in the photoreceptors of transgenic mice[17] that removed the terminal 15 amino acid residues and thus all putative Ser and Thr phosphorylation sites. Single-photon responses produced by S334ter R* failed to shut off in a timely and stereotyped manner, indicating that this domain is important for R* quenching. In the 1990s numerous biochemical experiments suggested that specific Ser residues on the C-terminus are crucial in R* shut-off.[90–92] However, single cell recordings from transgenic mice rods expressing rhodopsin lacking native Ser or Thr residues showed that Ser-only rhodopsin generated abnormally prolonged responses whereas Thr-only rhodopsin generated responses that were only modestly slower than normal rhodopsin.[93–95]

Quenching R*: Arrestin Binding

Subsequent to C-terminus phosphorylation, the catalytic activity of R* is quenched fully through by binding of visual arrestin. Arrestins are soluble cytoplasmic proteins that bind to G-protein-coupled receptors, thus switching off activation of the G-protein and terminating the signaling pathway that triggers the cellular response; the most commonly studied arrestin is β-arrestin. Visual arrestin exhibits exquisite specificity for binding phosphorylated

R*. Our understanding of how this specificity is conferred emerges from extensive mutagenesis studies, and the crystal structure of visual arrestin.[96–99] These studies reveal that arrestin is constrained into a latent, inactive structure by a network of intramolecular interactions.[96] According to the current model of arrestin activation, these intramolecular constraints are released by (1) interaction with multiple phosphates on rhodopsin's C-terminus, and (2) interaction with the cytoplasmic loops of R*. The physiologic role of visual arrestin in controlling the rod single-photon response was studied by Xu and colleagues,[24] who created transgenic mice lacking visual arrestin. Suction electrode recordings of photoresponses from the OS of these transgenic rods displayed a rapid, partial recovery, followed by a prolonged final recovery phase. The timing of the slow phase of shutoff is consistent with the spontaneous decay of the R*. Thus, while R* phosphorylation is required to terminate rapidly its catalytic activity, the full quenching of R* activity requires visual arrestin binding. Together, these extensive studies of light responses arising from rhodopsin phosphorylation site mutants show that coordination of phosphorylation of the cluster of Ser and Thr sites, together with arrestin binding, play a pivotal role in controlling the catalytic lifetime of rhodopsin and in ensuring the reproducibility of the single photon response in rods.

Deactivating PDE: Control of Transducin's GTPase Activity

Quenching of the phototransduction cascade also requires the shutoff of PDE*, which occurs through the deactivation of Tα. The GTPase activity of Tα allows the reassociation of the inhibitory gamma-subunit to the catalytic PDE subunits,[100] a process that is speeded through the participation of a photoreceptor-specific RGS protein, RGS-9, and its binding partner, Gβ5.[101] These proteins act sequentially on Tα to facilitate the hydrolysis of bound GTP. The physiologic role of all these proteins in the shutoff of the rod photoresponse was evaluated with transgenic mice that had alterations in each of these components. Rod photoresponses from transgenic mice expressing a PDE-γ with an impaired ability to stimulate GTP hydrolysis[102] showed abnormally slowed recovery,

demonstrating the necessary role of PDE-γ in Tα deactivation.[103] Similarly, mice lacking RGS-9 showed profoundly slowed response recovery,[104] as do mice lacking Gβ5.[105] RGS-9 is anchored to photoreceptor membranes by the adaptor protein, R9AP.[106–108] Interestingly, human patients with mutations in *R9AP* have difficulties adapting to sudden changes in light levels that are mediated by cones,[109] consistent with the higher concentration of RGS-9 complex in cones compared to rods.[110] Together, the current data support an important role of PDE-γ, RGS-9/Gβ5, and R9AP in Tα deactivation, and consequently, response recovery, in both rods and cones.

Resynthesis of cGMP: Ca^{2+} Dependence of Guanylyl Cyclase

Recovery of the dark current also requires that cGMP is resynthesized to allow CNG channels to open. cGMP is synthesized in photoreceptor outer segments by a retinal guanylyl cyclase (RetGC), which is regulated by the protein GCAPs (guanylyl cyclase activating protein 1 and 2).[111] GCAPs is an EF hand Ca^{2+}-binding protein that confers on RetGC a highly cooperative Ca^{2+}-dependence for cGMP synthesis.[112] Near the dark resting Ca^{2+} concentration RetGC's activity is inhibited, but as OS Ca^{2+} falls in response to illumination as CNG channels close, RetGC's activity accelerates to restore the resting cGMP and reopen CNG channels. The physiologic actions of GCAPs have been evaluated in physiologic recordings. For instance, when GCAP1 is dialyzed into Gecko rods, the recovery phase of the light response is accelerated.[113] In addition, suction electrode recordings from rods of GCAPs knockout mice show that the Ca^{2+}-dependence of cGMP synthesis is required to set the time course of the rod's photoresponse, and to suppress noise within the phototransduction cascade.[114]

Light Adaptation

In a normal cycle of day and night, the illumination at the earth's surface varies over 12 orders of magnitude, making photoreceptor adaptation fundamentally important to the normal functioning of

the vertebrate visual system. Rod cells are able to adjust their sensitivity over 2 to 3 log units of light intensities, while cone cells exhibit no response saturation over 6 to 7 log units.[3,4] The switch between rod and cone function from night to bright daylight covers a large portion of vision's functional range; and downstream circuitry accounts for the remainder of the range extension. While the molecular events underlying the amplification cascade following photon capture by rhodopsin are well delineated, the mechanisms underlying photoreceptor adaptation are less well understood; however, Ca^{2+} is known to play a feedback role in the adaptation process.[105,115]

The Role of Ca^{2+} Feedback

In darkness, Na^+ ions enter the OS through the CNG channels and are extruded in the IS through Na^+/K^+ ATPase pumps. This steady-state influx and efflux of Na^+ is largely the basis for the circulating dark current in photoreceptor cells. Similarly, Ca^{2+} enters through CNG channels in the OS, but is extruded locally by Na^+/Ca^{2+}, K^+ (NCKX) exchangers. In mouse rods the steady-state influx and efflux of Ca^{2+} holds its concentration near 250 nM,[116] but as light closes CNG channels Ca^{2+} entry is blocked, Ca^{2+} efflux continues, and $[Ca^{2+}]_i$ falls. This change in $[Ca^{2+}]_i$ is graded just like the dark current: the degree of lowered $[Ca^{2+}]_i$ is proportional to the intensity of background light in both rods and cones.[117,118] This decrease in $[Ca^{2+}]_i$ triggers a feedback signal that is necessary for light adaptation, since, when the $[Ca^{2+}]_i$ decrease is blocked, adaptation to background illumination is greatly compromised.[60,119] Existing evidence suggests that this feedback is rather complex, as it orchestrates several pathways directed toward different components of the transduction machinery.[120–122] Here we review the role of Ca^{2+} on each of these components.

Adaptation Mediated by Ca^{2+}-Feedback to Retinal Guanylyl Cyclase (RetGC)

It has long been recognized that feedback controlling accelerated recovery contributes to light adaptation.[112] Recovery of the light response requires the resynthesis of cGMP, which is needed to

reopen the CNG channels and reestablish the circulating current. The control of cGMP synthesis by RetGC/GCAPs is central to this process. The contribution of accelerated cGMP synthesis to adaptation in rod photoreceptors was investigated in GCAPs knockout mice.[23,114] This work showed that the presence of GCAPs extends the sensitivity to background light in rod photoreceptors ~10-fold (Fig. 16.5), and can account for about half of the rod's capacity to adapt to background light. Recordings from cones in GCAPs knockout mice also show that GCAPs contributes to background adaptation, but to a lesser extent than it does in mouse rods.[123]

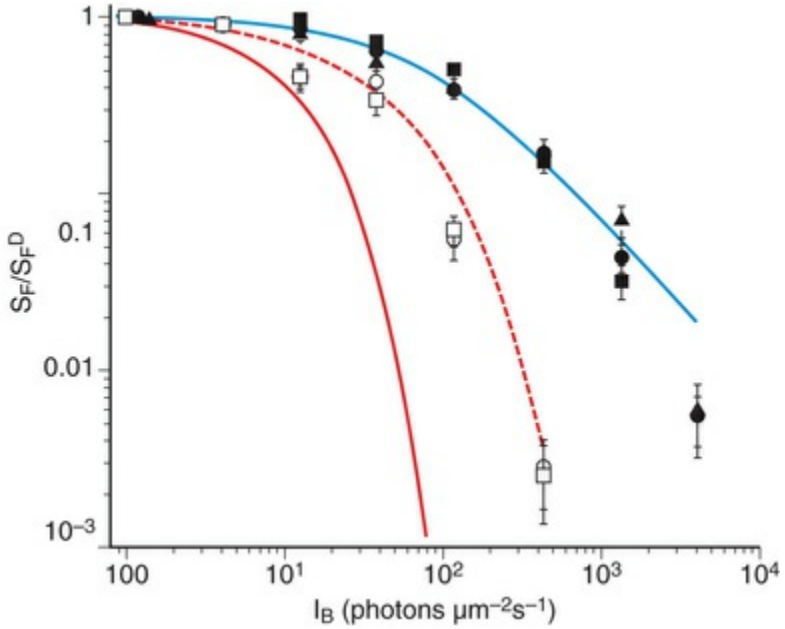

FIG. 16.5 Sensitivity as a function of background light was measured from mouse rod photoreceptors using suction electrodes (see Fig. 16.3). Sensitivity was calculated from dim flash responses as the peak response amplitude divided by the flash strength. Flash sensitivity (S_F) in the presence of increasing background light (I_B) was normalized against the flash sensitivity in darkness (S_F^D) and is plotted for the rods of several transgenic mice with particular elements of the phototransduction cascade altered. These mice include wild-type (●), mice lacking recoverin (■), mice where the calmodulin binding site on the CNG channels has been eliminated (▲), mice lacking

guanylyl cyclase activating proteins 1 and 2 (○), and mice where both the calmodulin binding site on the CNG channel and guanylyl cyclase activating proteins 1 and 2 have been eliminated (□). The dashed line shows the predicted decline in sensitivity as a function of background light intensity if rods displayed no light adaptation. The solid line is best-fitting Weber–Fechner function for wild-type rods, and shows that light adaptation extends the sensitivity of rod photoreceptors to 100-fold higher background light levels. Rods from mice lacking recoverin, or the calmodulin-binding site on the CNG channels, show little deviation from wild-type rods, indicating that these proteins do not play a significant role in light adaptation. However, in mice lacking guanylyl cyclase activating protein 1 and 2, light adaptation is impaired, but not absent, even when the calmodulin-binding site on the CNG channel is also eliminated (red dashed line). The remaining mechanisms that control light adaptation in rod photoreceptors remain unidentified.

(Data replotted from Chen CK, Woodruff ML, Chen FS, Chen D, Fain GL. Background light produces a recoverin-dependent modulation of activated-rhodopsin lifetime in mouse rods. J Neurosci 2010;30(4):1213-20.)

Recoverin and Control of Rhodopsin Kinase

The accelerated response recovery that mediates light adaptation is also achieved through the speeded deactivation of R*. The first step in the quenching of R* activity is the phosphorylation of its C-terminus by rhodopsin kinase, a process that is believed to be regulated in a Ca^{2+}-dependent manner by the protein recoverin. Recoverin is a highly conserved Ca^{2+}-binding protein found in both rod and cone photoreceptors. In vitro, recoverin binds and inhibits rhodopsin kinase when it is Ca^{2+}-bound, and accelerates rhodopsin kinase activity as Ca^{2+} is removed.[124,125] Since $[Ca^{2+}]_i$ is high in darkness, it has been suggested that, under dark-adapted conditions, recoverin prolongs the catalytic activity of R* by inhibiting rhodopsin phosphorylation. Early evidence in experiments that introduce recombinant recoverin into Gecko and salamander rods indicated that recoverin prolongs the light

response.[126,127] However, recoverin's effect was most prominent at Ca^{2+} concentrations outside the rod's physiologic range (>1 μM). The Ca^{2+} requirement for rhodopsin kinase inhibition by recoverin in reconstituted biochemical assays was similarly high.[124] These results placed into doubt the role of recoverin in mediating light adaptation. Suction electrode recordings from the rods of transgenic mice lacking recoverin, however, reveal a response speeding.[128] This speeding effect is exacerbated in rods that lack recoverin, but also have a reduced expression of rhodopsin kinase.[129] Thus, in the physiologic range of Ca^{2+} concentrations recoverin can influence R* lifetime. Despite this effect on R* lifetime, recoverin appears to play a relatively minor role in rod light adaptation (Fig. 16.5).[128] In cone photoreceptors, however, recoverin appears to contribute to sensitivity over a wider range of light intensities,[130] a fact perhaps not totally surprising given experiments from salamander L cones show that R* lifetime dominates the light response.[131]

Feedback Regulation of the cGMP-Gated (CNG) Channel

Another target of the Ca^{2+} feedback is the CNG channel itself. In vitro data have shown that the presence of Ca^{2+}-calmodulin causes a decrease in the apparent affinity of the CNG channels for cGMP.[132] This effect is reversed in light when $[Ca^{2+}]_i$ is low, such that more channels tend to open despite the lowering of cGMP levels. However, the role of CNG channel modulation in intact rods remains controversial, because based upon the measured effect of Ca^{2+} on the apparent affinity of the channel for cGMP and the intracellular range of cGMP concentration, it has been predicted theoretically that the channel contributes little to the overall adaptive behavior of the rod photoreceptor.[121] The site that confers Ca^{2+}-calmodulin sensitivity has been identified in the beta-subunit of the CNG channel.[133,134] Transgenic mice with this Ca^{2+}-binding site disrupted show little influence on the light response or in the adaptive features of rod phototransduction,[129] consistent with previous conjecture (see Fig. 16.5). The role of CNG channel modulation in cones, however, may be more profound than for rods. For instance, the cones of the ground squirrel demonstrate

strong Ca^{2+}-dependent modulation of the CNG gated-current in the normal range of Ca^{2+} concentrations, while the rods of the same species do not.[135] In addition, Ca^{2+} concentration varies over a larger dynamic range in cones than rods[118] allowing the recently identified protein, CNG-modulin, to regulate cone sensitivity more profoundly.[136,137]

Other (Ca^{2+}-Independent) Adaptation Mechanisms: Protein Translocation

A mechanism operating at a longer timescale (minutes rather than seconds) that may contribute to regulating photoreceptor cell performance is the light-driven redistribution of specific signal transduction proteins between the compartments of the photoreceptor cell. The immunoreactivity of both Tα and visual arrestin is known to redistribute in rods in response to light.[138–141] Visual arrestin immunostaining predominates at rod ISs, as well as at the outer nuclear layer and outer plexiform layers of dark-adapted retinas, and shifts to rod OSs upon light exposure. Tα immunoreactivity shifts in the opposite direction in response to light.[140–142] Quantitative measurements show that bright light exposure is required to trigger translocation: for visual arrestin the threshold is 1000 rhodopsin excitations per rod per second, a light intensity at the upper limits of rod vision; for Tα at least 10,000 rhodopsin excitations is required.[143] Sokolov and colleagues confirmed the physiologic movement of Tα by combining serial tangential cryosectioning of the retina with Western blot analysis, and demonstrated that such movement may help to extend the range of light intensities in which the rods are able to operate.[144] More recent evidence indicates that movement of Tα to synaptic terminal enhances synaptic transmission in the light-adapted state.[145] Similarly, visual arrestin movement may regulate rod performance under varying light environments.

Our current understanding of protein translocation is that it occurs by diffusion. In the case of Tα, the lipid modifications on the alpha- and gamma-subunits act synergistically to anchor Tα-GDP on the membrane. Upon activation, the subunits dissociate and become solubilized.[146] In an elegant set of experiments, Lobanova

and colleagues showed that light threshold can be shifted to either a lower or higher light intensity using mutant mice whose GTPase-activating (GAP) complex is enhanced or decreased.[147] Their data suggests that when the GAP complex is saturated, Tα-GTP can escape the OS compartment and diffuse to the IS. Whether such a mechanism also governs cone translocation is uncertain. It has been observed that cones contain a higher concentration of GAP proteins,[110,148] a reason that could explain a much higher threshold for cone Tα translocation.[149] However, others have observed that cone Tα readily translocates.[150] In the case of rod arrestin, its interaction with microtubules restricts its location to the IS in the dark. Light exposure creates its high-affinity binding partner, R*, which drives its movement towards the OS.[151]

It has become increasingly clear that Ca^{2+}-dependent light adaptation results from the sum of multiple mechanisms that act at different sites in the phototransduction cascade. While biochemical experiments have identified the Ca^{2+} sensitive steps in the phototransduction cascade, a full understanding of how these steps contributes to visual adaptation requires a method that critically evaluates the timing, as well as the strength, of feedback modulation under physiologic conditions. Given the complexity of Ca^{2+} feedback, coupled with the possibility that other adaptation mechanisms may overlay on this feedback regulation, visual adaptation, particularly in cones, remains one of the least understood areas in phototransduction. This complexity is being unraveled by the systematic removal of Ca^{2+} feedback pathways in vivo using mouse genetics, and by measuring the resultant change in adaptation with electrophysiologic measurements. The molecular mechanism behind the observed phenotype can then be confirmed by biochemical experiments. Using this approach, the Ca^{2+} feedback loops can be evaluated independently, as well as in sum, since the mice can be bred to combine the individual components (see Fig. 16.5). Eventually, as each and every Ca^{2+}-dependent pathway is peeled away, the remaining (perhaps Ca^{2+}-independent) pathways will be revealed.

Dark Adaptation

The process of *light adaptation* described above represents the mechanisms that desensitize phototransduction during steady background light. Despite the push toward desensitization by these mechanisms, several of which depend on the ROS Ca^{2+} concentration, there is a simultaneous pull toward sensitization. Adaptive mechanisms that pull the system toward the "dark" state (collectively coined "*dark adaptation*") play a crucial role in sensitivity maintenance. Dark adaptation has been classically studied by exposing dark-adapted subjects, or animal retinas, to bright light that bleaches (i.e., causes a *cis* to *trans* isomerization of retinal) the visual pigment and depresses sensitivity, and then observing the recovery with time. While cones recover sensitivity within seconds to minutes, rods take tens of minutes to recover to levels comparable to the dark-adapted state.[152] This slow recovery is attributable to many biochemical processes within rods that quench phototransduction activity fully and reestablish the dark-adapted condition. Among these is the rapid and continuous turnover of the visual pigment, which in rods requires tight apposition with the RPE. Additionally, mechanisms that reset the distribution and state of phototransduction proteins are critical to establish sensitivity. These mechanisms include the decay of long-lasting visual pigment intermediates, such as MetaIII rhodopsin (reviewed in reference 153), and reversing the light-dependent movement of proteins such as Tα, recoverin, and arrestin back to their respective compartments (reviewed in reference 143). The clinical importance of dark adaptation is manifest in pathologic perturbations of this process that lead to a number of blinding eye diseases, including retinal degeneration and diseases of retinoid deficiency.

Differences Between Rod and Cone Phototransduction

What factors underlie the specialized functions of rods and cones? This remains a very important problem in phototransduction. Investigation of rod phototransduction has benefited from rod-dominated species where biochemical and physiologic assays are robust. The relatively low number of cones in most mammalian species has made a biochemical analysis of cone phototransduction

less fruitful, although use of carp[154–156] and the Nrl knockout mouse (that generates a cone-dominant retina) have proven useful.[157] As described above, some quantitative differences may arise for differential modulation of components of the phototransduction cascade. In addition, differences in their characteristic morphology may play a role in setting the response properties. For example, the discontinuous and invaginating OS plasma membrane in cones provides greater surface area for ion exchange and chromophore recycling. To facilitate pigment regeneration in cones, two sources of 11-*cis* chromophore are available: the classic visual cycle within the retinal pigmented epithelium that also supplies the rods, and a newly discovered source within the Müller cells that supplies chromophore only to cones.[158] Also important may be their signal transduction cascades: molecular cloning has revealed that phototransduction in the vertebrate rods and cones are regulated by structurally homologous but distinct groups of signaling proteins. Therefore, it is reasonable to assume that the phototransduction in rods and cones is qualitatively similar, and that quantitative differences in the transduction steps underlie the characteristic rod and cone behavior. For example, R* may activate more rod Tα molecules than cone opsin R* in activating cone Tα (see reference 155), resulting in a higher gain and a larger response amplitude.

To determine the roles of rod and cone phototransduction proteins in setting the response properties of the photoreceptor cells, transgenic technology has recently been used to express rod components in cones, and vice versa. For example, Kefalov and colleagues[159] expressed an L-cone opsin in *Xenopus* rods, and rhodopsin in *Xenopus* cones. They surprisingly found that the activation of rhodopsin and L-cone opsin within the same cell yielded nearly identical photoresponses. In addition, similar photoresponses were observed in mouse rods transgenically expressing an S-cone pigment.[147] These results collectively rule out the visual pigment from being a major contributor to rod-cone functional differences. Similar experiments have also addressed the role of Tα. Mao and colleagues showed no functional differences in mouse rods wherein rod Tα was substituted by cone Tα. They found that rod and cone Tα generated similar photoresponses initiated by either rhodopsin or the short-wave cone opsin.[160]

Finally, the expression of cone PDE in rod PDE null mice (*rd1*/*rd1*) shows a modestly light-adapted phenotype consistent with a higher measured basal PDE activity and faster PDE deactivation.[161] All these studies demonstrate that the difference between the photoresponses of rods and cones is unlikely to be determined by the strong modulation of a few factors, but likely requires more modest changes in many components of the phototransduction cascade.

Inner Segment and Connecting Cilia

Inner Segment

The functional role of the inner segment (IS) can be appreciated by examination of its unique anatomy, which is highly specialized to fuel the high energy and protein synthesis requirements of the photoreceptor. The metabolic functions of the IS are constantly and highly active, generating most of the rod cell's energy as well as being the primary site for synthesizing new proteins. The proximal portion of the IS, termed the myoid, contains the endoplasmic reticulum and Golgi apparatus, while the distal portion, termed the ellipsoid, is densely packed with elongated mitochondria that are aligned circumferentially along the axis of the rod cell (see Fig. 16.2). This unique arrangement of mitochondria may enhance the wave-guiding properties of the photoreceptor.[162] Cones have a larger IS and more mitochondria, perhaps reflecting their higher metabolic needs. In addition, the distribution of mitochondria may optimize the optical properties of cones.[162] This photoreceptor cell compartment is structured for high O_2 consumption, as well as for glycolysis at very high rates.[163] One major metabolic demand comes from the extrusion of Na^+ from the cytoplasm by the Na^+/K^+ pump at the IS plasma membrane, which balances the influx of Na^+ through the cGMP-gated channels at the OS. In darkness, these pumps operate at a very high rate to accommodate the high fluxes generated by many open channels in the OS, setting up the “dark” circulating current.[164] The rate that these pumps can operate at is related to the supply of ATP[165] generated by the mitochondria in the ellipsoid. This ATP synthesis rate is coupled with the O_2 delivery to

the IS, which is completely supplied by the choroidal circulation. Paradoxically, due to the energy consumption required for establishing the dark circulating current, as well for tonic neurotransmitter release at the synapse in darkness (see below), the rod photoreceptor cell consumes more energy in darkness than in light.[163,164] Another major metabolic need is a high rate of protein synthesis that occurs in the myoid region of the IS to meet the demand of high levels of phototransduction proteins at the OS. In particular, each rod contains ~5×10^7 rhodopsin molecules, of which 10% at the tip of the OS is phagocytosed by the RPE before light onset each day. To maintain homeostasis, ~5×10^6 molecules are synthesized daily and added to the base of the OS. Similar events occur in cones, although they express about half the amount of visual pigment as rods. As with other cells, the soluble and peripheral membrane proteins are made in the cytosol, while the transmembrane proteins are made in the endoplasmic reticulum. To facilitate the speed of molecular collisions, many of the phototransduction proteins are associated with the membrane through lipid modifications and protein–protein interactions. These interactions are dynamic, with functional complexes forming and dissociating on the membrane surface on a rapid timescale. For example, the rod Tα is heterogeneously acylated at the amino-terminal glycine residue while the gamma-subunit is carboxyl-methylated and prenylated at the cysteine residue. PDE6α and rhodopsin kinase are farnesylated, while PDE6β is geranylgeranylated.[166,167] In some instances, the lipid modification is exposed as a consequence of a change in protein structure. An example is recoverin that, upon binding calcium, exposes its amino-terminal myristoyl group.[168] GCAP1 and GCAP2 are also calcium-binding proteins that are myristoylated, but exposure of their lipid group is not regulated by calcium binding. These proteins are complexed with RetGCs and regulate their activity in a calcium-dependent manner.

Targeting of Phototransduction Proteins From the Inner Segment to the Outer Segment

How phototransduction proteins traffic from the IS, the site of synthesis, to the OS, the site of phototransduction, is an area of

active research. This question is made more important by the fact that defective trafficking can cause photoreceptor cell death. For example, a cluster of naturally occurring mutations on rhodopsin's carboxyl-terminus causes autosomal dominant retinitis pigmentosa in human patients.[169] These mutations do not affect the biochemical properties of rhodopsin with respect to its ability to bind 11-*cis* retinal and form a visual pigment, nor its ability to activate Tα following photon absorption in reconstituted systems.[170–172] The underlying defect remained a mystery until these mutants were expressed in transgenic mice, whereupon it was observed that they were mis-localized throughout the cell and caused retinal degeneration.[173–175] It is now known that the VxPx motif at the rhodopsin's carboxyl terminus is important for sorting of rhodopsin into transport carriers from the trans-Golgi network towards the connecting cilium en route to the OS.[176] This is a recognition site for transport proteins that include the small GTPase Arf4, ASAP1, Rab11, and FIP3.[177] The VxPx motif is also present in cone opsins. Other integral membrane proteins contain their own trafficking motif. These motifs have been identified in peripherin/rds[178] and the cGMP-gated channel in rods.[179] Often a defect in transport of one transmembrane protein does not affect transport of others, suggesting that transport occurs independently.

Trafficking of membrane-associated proteins to the OS may occur through their interaction with transmembrane proteins as they are delivered out of the trans-Golgi network. It was also recently discovered that membrane-associated phototransduction proteins are transported by prenyl- or acyl-chain binding proteins. For example, rhodopsin kinase and cone PDE6α' require PrBP/δ, which contains a binding site for the prenyl group, for transport to the OS,[180] while the alpha-subunit of rod transducin requires UNC119, which binds acyl chains.[181] Thus diverse mechanisms are responsible for correct targeting of phototransduction proteins from the IS to the OS compartment.

The Connecting Cilium

A slender nonmotile connecting cilium that is 0.3 μm in diameter connects the IS to the OS. The microtubule-based axoneme of the

connecting cilium lacks the central microtubule pair of the motile cilium. The arrangement is a 9 × 2 + 0 microtubule structure towards the base of the cilia, where the doublet microtubules are attached to the plasma membrane via Y-shaped linkers,[182] extending proximally from the vertically arranged basal body is the ciliary rootlet (Fig. 16.2). The doublet microtubules transition to a 9 × 1 + 0 singlet microtubule arrangement more distally from the basal body and continue through much of the OS (Fig. 16.2). The axoneme arises from basal bodies which, together with the centrioles, act as microtubule organizing centers of the photoreceptor cell. The connecting cilium is the site of tremendous vectorial flow of lipids and proteins from their site of synthesis in the IS to the OS. It has been estimated that 2000 opsin molecules are transported every minute from the IS to the OS.[183] As post-Golgi carrier vesicles are delivered to the connecting cilium, proteins destined for the OS need to be sorted between the disk lamellar region, the disk rim region, and the plasma membrane in the OS. How the protein cargo is sorted at this point is not understood fully, but is thought to involve recognition of the specific trafficking motif displayed on the protein cargo by their cognate transport complex that also include the intraflagellar transport (IFT) particles.[183] The IFT particles associate with the post-Golgi carrier vesicles at the base of the cilium and transport them along the connecting cilium to the OS. IFTs are large protein complexes that move along the axoneme by motor proteins and may be viewed as conveyer belts that deliver different cargos to their respective destination.

Ciliary proteins are receiving increased attention because of their association with human retinal disease. They belong to a wide spectrum of diseases associated with defective ciliary function, collectively called ciliopathies.

Actin and myosin are two proteins common to many cells in the body. Both myosin and actin filaments are localized to the photoreceptor connecting cilium and IS. Disruption of either of these proteins causes retinal degeneration.[184] Actin depolymerization promotes disc overgrowth and photoreceptor death,[185] and myosin mutants appear to have defects in the transport of molecules from the IS to the OS. Myosin defects cause

numerous diseases, including Usher syndromes that affect both hearing and vision.[186,187]

RP1 (retinitis pigmentosa-1) is responsible for 5–10% of all retinitis pigmentosa (RP) cases.[188] RP1 is a large protein localized to the connecting cilium in both rods and cones and is especially concentrated at the site of nascent OS disks. RP1 has recently been shown to bind microtubules suggesting that this interaction may stabilize microtubules in the axoneme.[189–191] An RP1 knockout mouse model shows that discs are misshapen, overgrown, and fail to align properly.[189] This phenotype correlates well with ERG abnormalities in RP1 patients.

Mutations in the retinitis pigmentosa GTPase regulator gene (*RPGR*)[192] cause X-linked retinitis pigmentosa-3 (RP3), a severe and progressive retinal dystrophy. Antibodies localize RPGR and a related protein RPGRIP (RPGR interacting protein) in connecting cilia of rods and cones and in the cilia of airway epithelia.[193] An RPGR knockout mouse (an animal model of RP3)[194] demonstrated mislocalization of opsin in cones, and reduced quantities of rhodopsin in rods prior to photoreceptor degeneration. These data suggest a role for RPGR in maintaining the polarized distribution of proteins between the IS and the OS through the connecting cilium.

Centrins are calcium-binding proteins associated with centrosome-related structures. The mammalian rods and cones express four centrin isoforms; three of these (Cen1p-3p) are in the connecting cilium and three (Cen2p-4p) are in the basal body.[195] These centrins may participate in the alignment of the photoreceptor OS. Inasmuch as centrins were shown to interact with transducin in a calcium-dependent manner, they have been proposed to regulate the light-dependent translocation of Tα from the OS to the IS.[195]

The ciliary rootlet, first recognized over a century ago, is a prominent structure originating from the basal body at the proximal end of a cilium. Rootlets appear to be particularly robust in retinal photoreceptors, extending from the basal bodies to the synaptic terminals, anchoring ER membranes along their length. Recent studies indicate that rootlets are composed of a structural protein, aptly named rootletin. Rootletin protofilaments are bundled into variably shaped thick filaments within the cilium.[196]

Additional proteins, such as TULP1,[197,198] cadherin,[199] and myocilin,[200] are associated with the connecting cilium, several of which are known to be associated with rod photoreceptor disease. Collectively, genes that affect ciliary trafficking account for a large portion (~25%) of all genetic loci that influence photoreceptor degeneration.[201,202] This suggests, not surprisingly, that the highly specialized connecting cilium is a complicated structure connecting the IS to OS, and that there will undoubtedly be additional proteins associated with this unique subcellular structure.

Nucleus

The nucleus contains the primary genome of the photoreceptor and is responsible for the initiation of genetic programs in the cell. As a result, the nucleus is the target for gene therapy protocols designed to correct genetic defects in the photoreceptor. Rods and cones differ in their nuclear features. The nucleus of the rod photoreceptor is more round and is stained darker by nucleophilic stains due to the presence of a large clump of heterochromatin. Nuclei of cones are larger and oval in shape, with one to several clumps of heterochromatin and a larger amount of lightly staining euchromatin. Like most cells, photoreceptors also contain a second, non-nuclear genome in the mitochondria. Biochemical pathways linking photoreceptor cell death, the nucleus, and the mitochondria of the IS are beginning to come into focus.

Photoreceptor Synaptic Terminal

The light response generated by the phototransduction cascade in the OS is passively relayed to the synaptic terminal, called a spherule for rods and a pedicle for cones, where it modulates the rate of glutamate release onto second-order retinal neurons (see Fig. 16.6). Since open CNG channels leave the membrane potential of photoreceptors relatively depolarized in darkness, these synapses support a high level of Ca^{2+} influx and thus a high level of glutamate release. Light activates the phototransduction cascade leading to the closure of CNG channels, the hyperpolarization of the membrane potential, and a reduction in Ca^{2+} influx, which in

turn reduces glutamate release. This reduction in glutamate release constitutes the "light response" that is passed to the retinal circuitry.

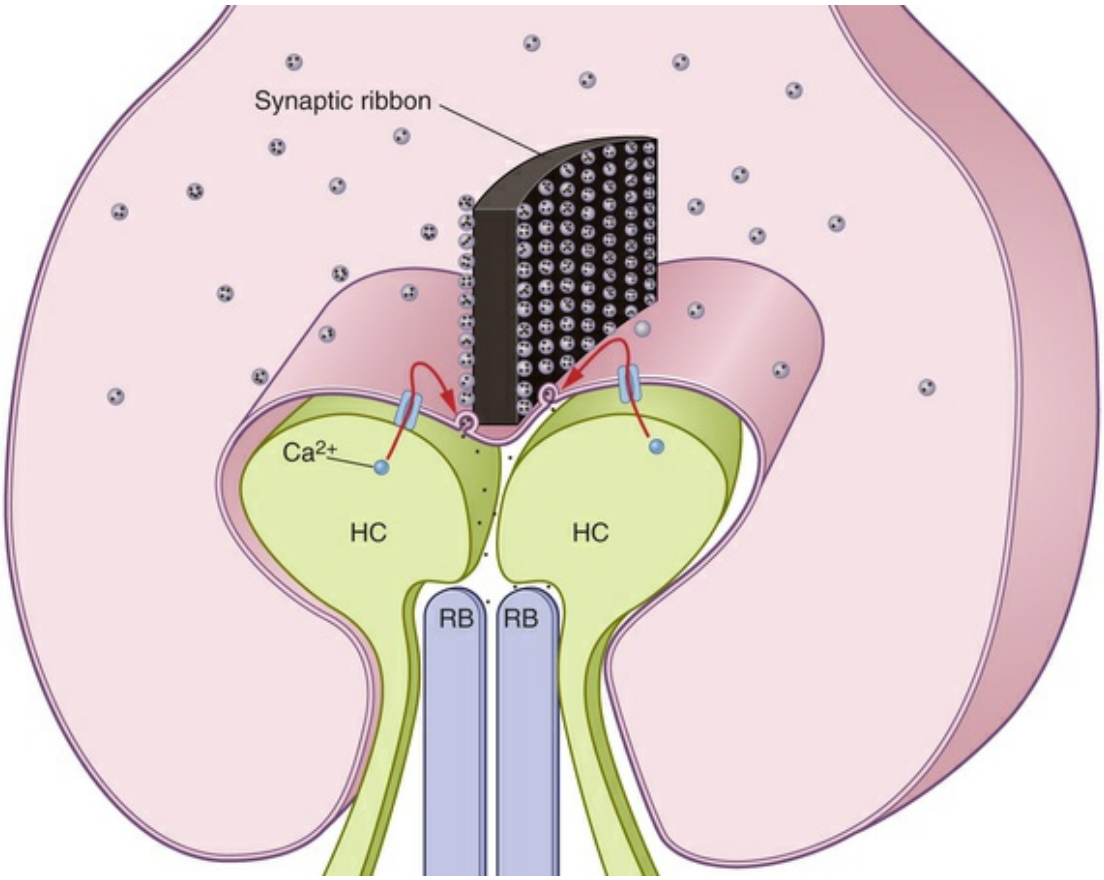

FIG. 16.6 Glutamate release from photoreceptor cells occurs at a specialized synaptic terminal, called a spherule for rods, and a pedicle for cones. Depicted is a slice through a rod spherule. Glutamate release is facilitated by a specialized structure called a synaptic ribbon, which binds glutamatergic vesicles and brings them to the plasma membrane. Vesicle fusion then occurs as L-type calcium channels near the release site allow the influx of Ca^{2+}, allowing glutamate (black dots) to be released into the synaptic cleft where it can be sensed by rod bipolar cells (*RB*) and horizontal cells (*HC*). Both rod bipolar cells and horizontal cells make an invaginating synapse with the photoreceptor cells.

To allow high levels of glutamate release, the photoreceptor synaptic terminals house a specialized synaptic structure, called a

ribbon, which is composed of the protein ribeye.[203] While the exact function of the ribbon has not been fully identified, studies where the ribbon has been photoablated show that the initial release of vesicles is not affected but subsequent release is greatly reduced.[204,205] These results support the prevailing view that the ribbon is required to tether glutamatergic vesicles and acts like a conveyor belt to bring these vesicles to the active zone, where they promote vesicle priming and fusion with the plasma membrane to release glutamate into the synaptic cleft[204,206] (Fig. 16.6). While the spherules of rods contain only one ribbon (i.e., one release site) in mammalian species,[207] the cone pedicles contain many ribbons whose numbers vary by species. In mice, for instance, cone pedicles contain ~10 ribbons,[208] while pedicles in other species like ground squirrels may contain ~15 or more ribbons.[209] Primate cone pedicles may also contain in excess of 25 ribbons.[210,211] Multiple ribbons in each cone pedicle allow the output of the cone to be relayed to many classes of cone bipolar cells (see Chapter 17, Function and anatomy of the mammalian retina).

Compared to conventional central synapses, photoreceptor cells release glutamate in the absence of the stimulus. Such a configuration places fundamental constraints on the mechanisms that regulate glutamate release. For instance, the persistent depolarization of photoreceptors in darkness would cause many types of ion channels to desensitize. To allow robust control of glutamate release with changes in membrane potential, a $Ca_v1.4$ channel located close to the active zone in the rod spherule and cone pedicle allows the Ca^{2+} influx that regulates release. These L-type Ca^{2+} channels display little voltage or Ca^{2+}-dependent desensitization,[212,213] and thus are ideal to support continuous glutamate release in darkness. In addition, in rod spherules these channels associate with the modulatory Ca^{2+}-binding protein, CABP4.[214] The association of $Ca_v1.4$ with CABP4 shifts the voltage sensitivity of $Ca_v1.4$ to more hyperpolarized membrane potentials.[214,215] This allows the gating of $Ca_v1.4$ channels to be modulated robustly over the rod photoreceptor's the physiologic voltage range.

Additional control of glutamate release may also involve the interaction of other proteins with the synaptic machinery. For

instance, visual arrestin serves to quench fully phosphorylated rhodopsin in the rod OS, but has been shown to interact with N-ethylmaleimide-sensitive factor (NSF) at the rod spherule to increase the turnover rate of SNARE complexes.[34] Similarly, the protein recoverin, which serves as a modulator of rhodopsin phosphorylation in the rod OS, has a separate action in the rod spherule that increases the magnitude of the reduction in glutamate release onto rod bipolar cells.[216] Lastly, the translocation of transducin to rod spherules appears to sensitize glutamate release to rod bipolar cells.[145] Overall these forms of modulation may be controlled by the light-dependent translocation of these components,[139,216] or in the activity of signaling cascades initiated by metabotropic glutamate receptors in the photoreceptor terminal.[217,218] Finally, the control of Ca^{2+} homeostasis in photoreceptor terminals can also modulate glutamate release.[219–221]

It should be noted that a majority of our understanding of the structure and function of ribbon synapses has emerged from the study of rod photoreceptors in the amphibian retina, particularly the salamander. However, the characteristics of glutamate release in cones can also be studied in this same species and reveal characteristics that are tuned for the faster kinetics of the light response in cones (reviewed in reference 222). Furthermore, since the cone photocurrent is difficult to saturate, increased vesicle turnover and recruitment is required to maintain the high level of glutamate release.[223,224] Ultimately, the mechanisms that produce these functional distinctions between rod spherules and cone pedicles remain largely unidentified and are currently under investigation.

Photoreceptor Dysfunction and Disease

As of August 2016, a total of 316 genes and loci have been identified to cause retinal diseases (RetNet, http://www.sph.uth.tmc.edu/RetNet/). The majority of these genes affect rod and cone function that includes ciliary trafficking, visual cycle, lipid metabolism, among others.[201] Here we emphasize the

relationship between defective phototransduction components and retinal degeneration.

Rhodopsin Mutations

More than 100 different mutations of rhodopsin have been associated with autosomal dominant and recessive retinitis pigmentosa (adRP and arRP) and autosomal dominant congenital stationary night blindness (CSNB).[225] This phenotypic heterogeneity points to diverse disease mechanisms arising from the same gene product. In the case of adRP, it has been proposed that some mutations lead to misfolding of the opsin protein, which then accumulates in the endoplasmic reticulum and elicits the unfolded protein response.[226] The accumulation of misfolded opsin may also interfere with the sorting and trafficking of normal proteins destined for the OS or other parts of the cell.[227] This may result in a pathologic mechanism where the cell cannot replenish other required proteins that do not harbor mutations.

Other rhodopsin mutations appear to affect trafficking of rhodopsin from the IS to the OS. As mentioned previously, mutations involving the last five carboxyl amino acids, such as P347A, P347S, or S344ter, allow rhodopsin to appear to fold normally and to function normally in terms of Tα activation and deactivation by phosphorylation and visual arrestin binding. Yet, mutations in these residues cause adRP. Several lines of evidence suggest that the C-terminus of opsin contains a signal for vectorial transport of newly synthesized opsin toward the OS. In a retinal cell-free system, it was demonstrated that a monoclonal antibody to the C-terminal domain of rhodopsin inhibited post-Golgi vesicle formation and arrested newly synthesized rhodopsin in the trans-Golgi network.[228] A wild-type C-terminal peptide, but not a mutant peptide bearing the mutation at the P347 position, can also block this process.[229] Another line of evidence comes from an in vivo model where a truncation mutant, S344ter, was expressed in the photoreceptors of transgenic mice. Antibodies that specifically recognize the truncated opsin showed strong immunoreactivity in the IS, indicating a block in the transport to the OS.[175] However, some truncated opsins are also cotransported with the full-length

protein to the OS. The role of the rhodopsin C-terminal domain in vectorial transport was also investigated in MDCK cells.[230] This cell line exhibits polarized structure when it is grown on a porous support. When transfected into this cell line, wild-type opsin was transported to the apical membrane surface, whereas an opsin mutant lacking the terminal 32 amino acids was not.

Constitutive Phototransduction and Retinal Disease

It is thought that constitutive phototransduction causes some forms of retinal disorders. Unabated signal flow can arise from different steps in the visual cascade. For example, certain mutations in rhodopsin, particularly those that affect the salt bridge between Lys-296 and Glu-113 (such as A292E and G90D), can lead to constitutive activity.[231] The interaction between Lys-296 and Glu-113 constrains the chromophore-free opsin to an inactive conformation.[232] Disruption of this bond leads to an opsin conformation that can support Tα activation. This activity is suppressed when the mutant opsin is regenerated with the chromophore 11-*cis* retinal. In the case of G90D and A292E mutations, light exposure leads to formation of opsin that can still activate the visual cascade. This can lead to impairment of visual function because the transduction machinery is overwhelmed by this constitutive activity. Patients carrying these mutations suffer from night blindness because phototransduction in rods cannot be fully quenched.[233,234] However, in the instance of the rhodopsin K296E mutation, no evidence of constitutive activity was observed when it was expressed in rod photoreceptors of transgenic mice; instead, it was found bound to arrestin.[235] It was found subsequently that stable rhodopsin/arrestin complex is toxic, and rod photoreceptor survival can be prolonged if such a complex is prevented in transgenic mice that lack visual arrestin and Tα.[236] Toxicity of the rhodopsin/arrestin complex appears to arise from its ability to recruit endocytic proteins, since preventing this interaction had a long-term rescuing effect on K296E-induced retinal degeneration.[237]

Defective shut-off can also be caused by the lack of visual arrestin

or rhodopsin kinase. These genes are mutated in patients diagnosed with the recessive genetic disorder Oguchi disease,[238,239] a non-progressive disorder characterized by early onset and stationary night blindness. These mutations are thought to cause a loss of function in the visual arrestin or rhodopsin kinase gene. Because of the inability to shut off signal flow, the rod photoreceptor becomes saturated even at very low light levels, leading to night blindness. Interestingly, some patients with the visual arrestin gene mutation also suffer from RP, pointing to a potential causal role between constitutive signal flow and photoreceptor cell death. Using the visual arrestin knockout mouse model, Chen and coworkers demonstrated that the absence of visual arrestin in the rod photoreceptor does lower the threshold for light damage.[240] The pathway leading to cell death is initiated by endoplasmic reticulum stress and induction of the unfolded protein response.[241] Therefore, protection from light exposure is an important preventive measure to prolong photoreceptor cell survival in those instances where constitutive signal flow is the disease mechanism.

Transducin Defects and Retinal Disease

Transducin is composed of three subunits: alpha (α), beta (β), and gamma (γ). Extensive genetic screening has revealed mutations only in the rod Tα.[242] The associated disease is autosomal dominant congenital stationary night blindness. The mutation is in the position homologous to that affected by the oncogenic mutation in p21ras, a small G-protein. It is therefore hypothesized that this mutation may affect Tα deactivation, leading to the night blindness phenotype. Interestingly, mice that lack rod Tα have normal retinal structure, indicating that this abundant visual G-protein has no structural function in the photoreceptor, and that signal flow is not a prerequisite for rod photoreceptor cell survival.[20]

cGMP and Photoreceptor Cell Physiology

Cyclic-GMP gates the open probability of CNG channels with a high cooperativity. The probability of open channels is only 0.1 in the dark-adapted rod, which carries the dark circulating current composing of ~85% Na^+ and 15% Ca^{2+} that enters the rod outer

segment. Therefore a small increase in the level of free cGMP can profoundly affect the open probability of CNG channels. This will in turn influence the ion influx, including Ca^{2+}, which may directly and/or indirectly trigger photoreceptor cell death.

One of the first characterized mutations affecting components in the phototransduction cascade is the null mutation in the beta-subunit of *PDE6,* leading to the rapid retinal degeneration phenotype in the *rd1* mouse.[13,14] The complete PDE6 enzyme is made up of two catalytic chains (α and β), each associated with an inhibitory chain (γ). Since both alpha- and beta-subunits are necessary for the formation of a functional phosphodiesterase holoenzyme, the mutation in either subunit renders the holoenzyme inactive. The gamma-subunit is important for inhibition of the catalytic subunits and is also necessary for structural stability of the holoenzyme.[243] Farber and Lolley[244] showed that photoreceptor cell death is preceded by an accumulation of cGMP in the retina, which is consistent with the role of this enzyme in degrading cGMP. Mutations in genes encoding all three PDE subunits (*PDE6A, PDE6B, PDE6G*) have been found to be associated with autosomal recessive retinitis pigmentosa in humans. RetGCs are responsible for synthesizing the cGMP that is necessary for reopening of the CNG channel leading to recovery of the dark current. Two membrane forms of RetGCs are expressed specifically in the retina of several mammalian species, including humans.[245–248] Whereas other membrane cyclases are activated by the binding of peptide ligands to their extracellular domains, the activity of RetGCs is controlled by interaction with GCAPs through their intracellular domain.[249,250] Because the extracellular domain of RetGCs is situated in the enclosed and seemingly inaccessible intradiscal space, it is questionable whether the extracellular domain serves as a receptor. The retinal cyclases are therefore termed “orphan” receptors because no ligands have yet been identified. Although two forms of RetGCs are expressed in the photoreceptor layer, there is evidence that they are not functionally redundant. First, they appear to be expressed at different levels in different photoreceptors. For example, it was observed that RetGC1 immunoreactivity is stronger in cone OS than in rod OS;[251] RetGC2, on the other hand, is expressed in the rod

OS,[252] but evidence for cone expression is lacking. Second, RetGC1 and RetGC2 behave differently biochemically in terms of their regulation by GCAPs: RetGC1 is regulated by both GCAP1 and GCAP2, whereas RetGC2 is regulated by GCAP2 but not by GCAP1.[116.246,249–251] In humans mutations in RetGC1 are linked to autosomal recessive Leber congenital amaurosis[253] and dominant cone–rod dystrophy.[254] No mutation in *RetGC2* has been associated with human blindness.

Another naturally occurring mutation that is expected to increase intracellular cGMP concentration is the Y99C mutation in *GCAP1*, a mutation that causes cone dystrophy in an autosomal dominant manner.[255] This mutation renders GCAP1 capable of stimulating RetGC, independent of Ca^{2+} concentration.[113,256] Constitutive activity of RetGC may therefore lead to an accumulation of intracellular cGMP. In addition to the Y99C mutation, nine other heterozygous mutations in the gene encoding *GCAP1* (GUCA1A) have been linked to autosomal dominant cone dystrophy, cone–rod dystrophy, or macular degeneration.[257–261] Many of these mutations are found in the Ca^{2+} binding domain. Mutations involving *GCAP2* have also been linked to autosomal dominant retinitis pigmentosa[262] and macular dystrophy.[263]

This hypothesis of cell death pathway through excessive number of open channels by elevated cGMP has been strengthened in a mouse model wherein the absence of CNG channels delayed retinal degeneration associated with elevated cGMP.[264] In support of this idea, survival of rd1 photoreceptors, whose mutation in *PDE6* beta leads to buildup of cGMP, was enhanced when the mutation was put into a *CNG* channel knockout mouse background.[264] This observation motivates effort to synthesize small molecules that specifically block the CNG channel as a means to prolong photoreceptor cell survival.[265] A loss of RetGC1, on the other hand, is expected to lead to lowered cGMP levels. This might be functionally equivalent to constant light and may lead to cell death. However, further experiments will be needed to evaluate rigorously the relationship between cGMP concentration and retinal degeneration.

References

1. Baylor DA, Lamb TD, Yau KW. Responses of retinal rods to single photons. *J Physiol*. 1979;288:613–634.
2. Hecht S, Schlaer S, Pirenne MH. Energy, quanta, and vision. *J Gen Physiol*. 1942;25:819–840.
3. Burkhardt DA. Light adaptation and photopigment bleaching in cone photoreceptors in situ in the retina of the turtle. *J Neurosci*. 1994;14(3 Pt 1):1091–1105.
4. Normann RA, Perlman I. The effects of background illumination on the photoresponses of red and green cones. *J Physiol*. 1979;286:491–507.
5. Morimura H, Fishman GA, Grover SA, et al. Mutations in the RPE65 gene in patients with autosomal recessive retinitis pigmentosa or Leber congenital amaurosis. *Proc Natl Acad Sci USA*. 1998;95(6):3088–3093.
6. Daiger SP. Identifying retinal disease genes: how far have we come, how far do we have to go? *Novartis Found Symp*. 2004;255:17–27 [discussion 27–36, 177–8].
7. Sheffield VC, Fishman GA, Beck JS, et al. Identification of novel rhodopsin mutations associated with retinitis pigmentosa by GC-clamped denaturing gradient gel electrophoresis. *Am J Hum Genet*. 1991;49(4):699–706.
8. Flannery JG, Farber DB, Bird AC, et al. Degenerative changes in a retina affected with autosomal dominant retinitis pigmentosa. *Invest Ophthalmol Vis Sci*. 1989;30(2):191–211.
9. Suber ML, Pittler SJ, Qin N, et al. Irish Setter dogs affected with rod/cone dysplasia contain a nonsense mutation in the rod cGMP phosphodiesterase beta-subunit gene. *Proc Natl Acad Sci USA*. 1993;90(9):3968–3972.
10. Wrigstad A, Narfstrom K, Nilsson SE. Slowly progressive changes of the retina and retinal pigment epithelium in Briard dogs with hereditary retinal dystrophy: a morphological study. *Doc Ophthalmol*. 1994;87(4):337–354.
11. Narfstrom K. Hereditary progressive retinal atrophy in the Abyssinian cat. *J Hered*. 1983;74(4):273–276.
12. Edwards RB, Szamier RB. Defective phagocytosis of isolated

rod outer segments by RCS rat retinal pigment epithelium in culture. *Science*. 1977;197(4307):1001–1003.
13. Bowes C, Li T, Danciger M, et al. Retinal degeneration in the rd mouse is caused by a defect in the beta subunit of rod cGMP-phosphodiesterase. *Nature*. 1990;347(6294):677–680.
14. Pittler SJ, Baehr W. Identification of a nonsense mutation in the rod photoreceptor cGMP phosphodiesterase beta-subunit gene of the rd mouse. *Proc Natl Acad Sci USA*. 1991;88(19):8322–8326.
15. Connell G, Bascom R, Molday L, et al. Photoreceptor peripherin is the normal product of the gene responsible for retinal degeneration in the rds mouse. *Proc Natl Acad Sci USA*. 1991;88(3):723–726.
16. Travis GH, Brennan MB, Danielson PE, et al. Identification of a photoreceptor-specific mRNA encoded by the gene responsible for retinal degeneration slow (rds). *Nature*. 1989;338(6210):70–73.
17. Chen J, Makino CL, Peachey NS, et al. Mechanisms of rhodopsin inactivation in vivo as revealed by a COOH-terminal truncation mutant. *Science*. 1995;267:374–377.
18. Lem J, Flannery JG, Li T, et al. Retinal degeneration is rescued in transgenic rd mice by expression of the cGMP phosphodiesterase beta subunit. *Proc Natl Acad Sci USA*. 1992;89(10):4422–4426.
19. Travis GH, Groshan KR, Lloyd M, et al. Complete rescue of photoreceptor dysplasia and degeneration in transgenic retinal degeneration slow (rds) mice. *Neuron*. 1992;9(1):113–119.
20. Calvert PD, Krasnoperova NV, Lyubarsky AL, et al. Phototransduction in transgenic mice after targeted deletion of the rod transducin alpha-subunit. *Proc Natl Acad Sci USA*. 2000;97(25):13913–13918.
21. Humphries MM, Rancourt D, Farrar GJ, et al. Retinopathy induced in mice by targeted disruption of the rhodopsin gene. *Nat Genet*. 1997;15(2):216–219.
22. Lem J, Krasnoperova NV, Calvert PD, et al. Morphological, physiological, and biochemical changes in rhodopsin knockout mice. *Proc Natl Acad Sci USA*. 1999;96(2):736–741.

23. Mendez A, Burns ME, Sokal I, et al. Role of guanylate cyclase-activating proteins (GCAPs) in setting the flash sensitivity of rod photoreceptors. *Proc Natl Acad Sci USA*. 2001;98(17):9948–9953.
24. Xu J, Dodd RL, Makino CL, et al. Prolonged photoresponses in transgenic mouse rods lacking arrestin. *Nature*. 1997;389:505–509.
25. von Greeff R. Mikroskopische Anatomie des Sehnerven und der Netzhaut. *Graefe umd Saemisch Handbuch der gesamten Augenheilkunde, 2. Aufl., 1, Teil, bd 1, Kap. V*. 1900.
26. von Greeff R. *A guide to the microscopic examination of the eye*. Blackiston: Philadelphia; 1902.
27. Hendrickson A, Drucker D. The development of parafoveal and mid-peripheral human retina. *Behav Brain Res*. 1992;49(1):21–31.
28. Detwiler SR. *Vertebrate photoreceptors*. Macmillan: New York; 1943.
29. Liang Y, Fotiadis D, Maeda T, et al. Rhodopsin signaling and organization in heterozygote rhodopsin knockout mice. *J Biol Chem*. 2004;279(46):48189–48196.
30. Nickell S, Park PS, Baumeister W, et al. Three-dimensional architecture of murine rod outer segments determined by cryoelectron tomography. *J Cell Biol*. 2007;177(5):917–925.
31. Poo M, Cone RA. Lateral diffusion of rhodopsin in the photoreceptor membrane. *Nature*. 1974;247(441):438–441.
32. Liang Y, Fotiadis D, Filipek S, et al. Organization of the G protein-coupled receptors rhodopsin and opsin in native membranes. *J Biol Chem*. 2003;278(24):21655–21662.
33. Gunkel M, Schoneberg J, Alkhaldi W, et al. Higher-order architecture of rhodopsin in intact photoreceptors and its implication for phototransduction kinetics. *Structure*. 2015;23(4):628–638.
34. Bayburt TH, Vishnivetskiy SA, McLean MA, et al. Monomeric rhodopsin is sufficient for normal rhodopsin kinase (GRK1) phosphorylation and arrestin-1 binding. *J Biol Chem*. 2011;286(2):1420–1428.
35. Arikawa K, Molday LL, Molday RS, et al. Localization of peripherin/rds in the disk membranes of cone and rod

photoreceptors: relationship to disk membrane morphogenesis and retinal degeneration. *J Cell Biol*. 1992;116(3):659–667.
36. Travis GH, Sutcliffe JG, Bok D. The retinal degeneration slow (rds) gene product is a photoreceptor disc membrane-associated glycoprotein. *Neuron*. 1991;6(1):61–70.
37. Conley SM, Stuck MW, Naash MI. Structural and functional relationships between photoreceptor tetraspanins and other superfamily members. *Cell Mol Life Sci*. 2012;69(7):1035–1047.
38. Bascom RA, Manara S, Collins L, et al. Cloning of the cDNA for a novel photoreceptor membrane protein (rom-1) identifies a disk rim protein family implicated in human retinopathies. *Neuron*. 1992;8(6):1171–1184.
39. Molday RS, Warren R, Loewen C, et al. Cyclic GMP-gated channel and peripherin/rds-rom-1 complex of rod cells. *Novartis Found Symp*. 1999;224:249–261 [discussion 61–4].
40. McNally N, Kenna PF, Rancourt D, et al. Murine model of autosomal dominant retinitis pigmentosa generated by targeted deletion at codon 307 of the rds-peripherin gene. *Hum Mol Genet*. 2002;11(9):1005–1016.
41. Clarke G, Goldberg AF, Vidgen D, et al. Rom-1 is required for rod photoreceptor viability and the regulation of disk morphogenesis. *Nat Genet*. 2000;25(1):67–73.
42. Corless JM, Schneider TG. Patterns of interdisk connections within the lamellar domains of retinal rod outer segment disks: observations relevant to the axial propagation of incisures. *Exp Eye Res*. 1987;45(6):883–905.
43. Kajimura N, Harada Y, Usukura J. High-resolution freeze-etching replica images of the disk and the plasma membrane surfaces in purified bovine rod outer segments. *J Electron Microsc (Tokyo)*. 2000;49(5):691–697.
44. Miyaguchi K, Kuo CH, Miki N, et al. Topography of opsin within disk and plasma membranes revealed by a rapid-freeze deep-etch technique. *J Neurocytol*. 1992;21(11):807–819.
45. Roof DJ, Korenbrot JI, Heuser JE. Surfaces of rod photoreceptor disk membranes: light-activated enzymes. *J*

Cell Biol. 1982;95(2 Pt 1):501–509.
46. Allikmets R, Gerrard B, Hutchinson A, et al. Characterization of the human ABC superfamily: isolation and mapping of 21 new genes using the expressed sequence tags database. *Hum Mol Genet*. 1996;5(10):1649–1655.
47. Allikmets R, Shroyer NF, Singh N, et al. Mutation of the Stargardt disease gene (ABCR) in age-related macular degeneration. *Science*. 1997;277(5333):1805–1807.
48. Weng J, Mata NL, Azarian SM, et al. Insights into the function of Rim protein in photoreceptors and etiology of Stargardt's disease from the phenotype in abcr knockout mice. *Cell*. 1999;98(1):13–23.
49. Radu RA, Mata NL, Nusinowitz S, et al. Treatment with isotretinoin inhibits lipofuscin accumulation in a mouse model of recessive Stargardt's macular degeneration. *Proc Natl Acad Sci USA*. 2003;100(8):4742–4747.
50. Sanyal S, De Ruiter A, Hawkins RK. Development and degeneration of retina in rds mutant mice: light microscopy. *J Comp Neurol*. 1980;194(1):193–207.
51. Sanyal S, Jansen HG. Absence of receptor outer segments in the retina of rds mutant mice. *Neurosci Lett*. 1981;21(1):23–26.
52. van Nie R, Ivanyi D, Demant P. A new H-2-linked mutation, rds, causing retinal degeneration in the mouse. *Tissue Antigens*. 1978;12(2):106–108.
53. Young RW. The renewal of rod and cone outer segments in the rhesus monkey. *J Cell Biol*. 1971;49(2):303–318.
54. Young RW. Visual cells and the concept of renewal. *Invest Ophthalmol Vis Sci*. 1976;15(9):700–725.
55. Travis GH. Mechanisms of cell death in the inherited retinal degenerations. *Am J Hum Genet*. 1998;62(3):503–508.
56. Anderson DH, Fisher SK, Steinberg RH. Mammalian cones: disc shedding, phagocytosis, and renewal. *Invest Ophthalmol Vis Sci*. 1978;17(2):117–133.
57. Steinberg RH, Fisher SK, Anderson DH. Disc morphogenesis in vertebrate photoreceptors. *J Comp Neurol*. 1980;190(3):501–508.
58. Chuang JZ, Zhao Y, Sung CH. SARA-regulated vesicular

targeting underlies formation of the light-sensing organelle in mammalian rods. *Cell*. 2007;130(3):535–547.
59. Carter-Dawson LD, LaVail MM. Rods and cones in the mouse retina. I. Structural analysis using light and electron microscopy. *J Comp Neurol*. 1979;188(2):245–262.
60. Nakatani K, Yau K-W. Calcium and light adaptation in retinal rods and cones. *Nature*. 1988;334:69–71.
61. Perry RJ, McNaughton PA. Response properties of cones from the retina of the tiger salamander. *J Physiol*. 1991;433:561–587.
62. Picones A, Korenbrot JI. Permeability and interaction of Ca^{2+} with cGMP-gated ion channels differ in retinal rod and cone photoreceptors. *Biophys J*. 1995;69(1):120–127.
63. Pugh EN Jr, Lamb TD. Amplification and kinetics of the activation steps in phototransduction. *Biochim Biophys Acta*. 1993;1141(2–3):111–149.
64. Nakatani K, Yau KW. Guanosine 3',5'-cyclic monophosphate-activated conductance studied in a truncated rod outer segment of the toad. *J Physiol*. 1988;395:731–753.
65. Ruiz ML, Karpen JW. Single cyclic nucleotide-gated channels locked in different ligand-bound states. *Nature*. 1997;389(6649):389–392.
66. Yau KW, Nakatani K. Electrogenic Na–Ca exchange in retinal rod outer segment. *Nature*. 1984;311(5987):661–663.
67. Kaupp UB, Niidome T, Tanabe T, et al. Primary structure and functional expression from complementary DNA of the rod photoreceptor cyclic GMP-gated channel. *Nature*. 1989;342(6251):762–766.
68. Pittler SJ, Lee AK, Altherr MR, et al. Primary structure and chromosomal localization of human and mouse rod photoreceptor cGMP-gated cation channel. *J Biol Chem*. 1992;267(9):6257–6262.
69. Zheng J, Trudeau MC, Zagotta WN. Rod cyclic nucleotide-gated channels have a stoichiometry of three CNGA1 subunits and one CNGB1 subunit. *Neuron*. 2002;36(5):891–896.
70. Zhong H, Molday LL, Molday RS, et al. The heteromeric

cyclic nucleotide-gated channel adopts a 3A:1B stoichiometry. *Nature*. 2002;420(6912):193–198.
71. Molday LL, Cook NJ, Kaupp UB, et al. The cGMP-gated cation channel of bovine rod photoreceptor cells is associated with a 240-kDa protein exhibiting immunochemical cross-reactivity with spectrin. *J Biol Chem*. 1990;265(30):18690–18695.
72. Bareil C, Hamel CP, Delague V, et al. Segregation of a mutation in CNGB1 encoding the beta-subunit of the rod cGMP-gated channel in a family with autosomal recessive retinitis pigmentosa. *Hum Genet*. 2001;108(4):328–334.
73. Dryja TP, Finn JT, Peng YW, et al. Mutations in the gene encoding the alpha subunit of the rod cGMP-gated channel in autosomal recessive retinitis pigmentosa. *Proc Natl Acad Sci USA*. 1995;92(22):10177–10181.
74. Peng C, Rich ED, Varnum MD. Subunit configuration of heteromeric cone cyclic nucleotide-gated channels. *Neuron*. 2004;42(3):401–410.
75. Kohl S, Marx T, Giddings I, et al. Total colourblindness is caused by mutations in the gene encoding the alpha-subunit of the cone photoreceptor cGMP-gated cation channel. *Nat Genet*. 1998;19(3):257–259.
76. Kohl S, Varsanyi B, Antunes GA, et al. CNGB3 mutations account for 50% of all cases with autosomal recessive achromatopsia. *Eur J Hum Genet*. 2005;13(3):302–308.
77. Lytton J. Na^+/Ca^{2+} exchangers: three mammalian gene families control Ca^{2+} transport. *Biochem J*. 2007;406(3):365–382.
78. Li XF, Kiedrowski L, Tremblay F, et al. Importance of K^+-dependent Na^+/Ca^{2+}-exchanger 2, NCKX2, in motor learning and memory. *J Biol Chem*. 2006;281(10):6273–6282.
79. Riazuddin SA, Shahzadi A, Zeitz C, et al. A mutation in SLC24A1 implicated in autosomal-recessive congenital stationary night blindness. *Am J Hum Genet*. 2010;87(4):523–531.
80. Vinberg F, Wang T, Molday RS, et al. A new mouse model for stationary night blindness with mutant Slc24a1 explains the pathophysiology of the associated human disease. *Hum*

Mol Genet. 2015;24(20):5915–5929.
81. Hsu SC, Molday RS. Glycolytic enzymes and a GLUT-1 glucose transporter in the outer segments of rod and cone photoreceptor cells. *J Biol Chem*. 1991;266(32):21745–21752.
82. Fliesler SJ, Anderson RE. Chemistry and metabolism of lipids in the vertebrate retina. *Prog Lipid Res*. 1983;22(2):79–131.
83. Tinoco J. Dietary requirements and functions of alpha-linolenic acid in animals. *Prog Lipid Res*. 1982;21(1):1–45.
84. Anderson RE, Maude MB, Bok D. Low docosahexaenoic acid levels in rod outer segment membranes of mice with rds/peripherin and P216L peripherin mutations. *Invest Ophthalmol Vis Sci*. 2001;42(8):1715–1720.
85. Fung BK, Hurley JB, Stryer L. Flow of information in the light-triggered cyclic nucleotide cascade of vision. *Proc Natl Acad Sci USA*. 1981;78(1):152–156.
86. Yee R, Liebman PA. Light-activated phosphodiesterase of the rod outer segment: kinetics and parameters of activation and deactivation. *J Biol Chem*. 1978;253(24):8902–8909.
87. Wilden U, Hall SW, Kühn H. Phosphodiesterase activation by photoexcited rhodopsin is quenched when rhodopsin is phosphorylated and binds the intrinsic 48-kDa protein of rod outer segments. *Proc Natl Acad Sci USA*. 1986;83:1174–1178.
88. Wilden U, Kuhn H. Light-dependent phosphorylation of rhodopsin: number of phosphorylation sites. *Biochemistry*. 1982;21:3014–3022.
89. Chen CK, Burns ME, Spencer M, et al. Abnormal photoresponses and light-induced apoptosis in rods lacking rhodopsin kinase. *Proc Natl Acad Sci USA*. 1999;96(7):3718–3722.
90. Ohguro H, Johnson RS, Ericsson LH, et al. Control of rhodopsin multiple phosphorylation. *Biochemistry*. 1994;33(4):1023–1028.
91. Ohguro H, Palczewski K, Ericsson LH, et al. Sequential phosphorylation of rhodopsin at multiple sites. *Biochemistry*. 1993;32(21):5718–5724.
92. Ohguro H, Van Hooser JP, Milam AH, et al. Rhodopsin

phosphorylation and dephosphorylation in vivo. *J Biol Chem*. 1995;(24):14259–14262.
93. Mendez A, Burns ME, Roca A, et al. Rapid and reproducible deactivation of rhodopsin requires multiple phosphorylation sites. *Neuron*. 2000;28(1):153–164.
94. Doan T, Mendez A, Detwiler PB, et al. Multiple phosphorylation sites confer reproducibility of the rod's single-photon responses. *Science*. 2006;313(5786):530–533.
95. Azevedo AW, Doan T, Moaven H, et al. C-terminal threonines and serines play distinct roles in the desensitization of rhodopsin, a G protein-coupled receptor. *Elife*. 2015;4.
96. Gurevich VV, Gurevich EV. The molecular acrobatics of arrestin activation. *Trends Pharmacol Sci*. 2004;25(2):105–111.
97. Hirsch JA, Schubert C, Gurevich VV, et al. The 2.8 A crystal structure of visual arrestin: a model for arrestin's regulation. *Cell*. 1999;97(2):257–269.
98. Vishnivetskiy SA, Hosey MM, Benovic JL, et al. Mapping the arrestin-receptor interface: structural elements responsible for receptor specificity of arrestin proteins. *J Biol Chem*. 2004;279(2):1262–1268.
99. Vishnivetskiy SA, Paz CL, Schubert C, et al. How does arrestin respond to the phosphorylated state of rhodopsin? *J Biol Chem*. 1999;274(17):11451–11454.
100. Heck M, Hofmann K. G-protein effector coupling – a real time light-scattering assay for transducin phosphodiesterase interaction. *Biochemistry*. 1993;32:8220–8227.
101. He W, Cowan CW, Wensel TG. RGS9, a GTPase accelerator for phototransduction. *Neuron*. 1998;20:95–102.
102. Slepak VZ, Artemyev NO, Zhu Y, et al. An effector site that stimulates G-protein GTPase in photoreceptors. *J Biol Chem*. 1995;270(24):14319–14324.
103. Tsang SH, Burns ME, Calvert PD, et al. Role for the target enzyme in deactivation of photoreceptor G protein in vivo. *Science*. 1998;282:117–121.
104. Chen CK, Burns ME, He W, et al. Slowed recovery of rod photoresponse in mice lacking the GTPase accelerating

protein RGS9-1. *Nature*. 2000;403(6769):557–560.
105. Krispel CM, Chen CK, Simon MI, et al. Novel form of adaptation in mouse retinal rods speeds recovery of phototransduction. *J Gen Physiol*. 2003;122(6):703–712.
106. Hu G, Wensel TG. R9AP, a membrane anchor for the photoreceptor GTPase accelerating protein, RGS9-1. *Proc Natl Acad Sci USA*. 2002;99(15):9755–9760.
107. Hu G, Zhang Z, Wensel TG. Activation of RGS9-1GTPase acceleration by its membrane anchor, R9AP. *J Biol Chem*. 2003;278(16):14550–14554.
108. Lishko PV, Martemyanov KA, Hopp JA, et al. Specific binding of RGS9-Gbeta 5L to protein anchor in photoreceptor membranes greatly enhances its catalytic activity. *J Biol Chem*. 2002;277(27):24376–24381.
109. Nishiguchi KM, Sandberg MA, Kooijman AC, et al. Defects in RGS9 or its anchor protein R9AP in patients with slow photoreceptor deactivation. *Nature*. 2004;427(6969):75–78.
110. Cowan CW, Fariss RN, Sokal I, et al. High expression levels in cones of RGS9, the predominant GTPase accelerating protein of rods. *Proc Natl Acad Sci USA*. 1998;95(9):5351–5356.
111. Gorczyca WA, Gray-Keller MP, Detwiler PB, et al. Purification and physiological evaluation of a guanylate-cyclase activating protein from retinal rods. *Proc Natl Acad Sci USA*. 1994;91:4014–4018.
112. Koch KW, Stryer L. Highly cooperative feedback-control of retinal rod guanylate-cyclase by calcium-ions. *Nature*. 1988;334:64–66.
113. Gorczyca WA, Polans AS, Surgucheva IG, et al. Guanylyl cyclase-activating protein – a calcium-sensitive regulator of phototransduction. *J Biol Chem*. 1995;270:22029–22036.
114. Burns ME, Mendez A, Chen J, et al. Dynamics of cyclic GMP synthesis in retinal rods. *Neuron*. 2002;36(1):81–91.
115. Detwiler PB, Gray-Keller MP. The mechanisms of vertebrate light adaptation: speeded recovery versus slowed activation. *Curr Opin Neurobiol*. 1996;6(4):440–444.
116. Woodruff ML, Sampath AP, Matthews HR, et al. Measurement of cytoplasmic calcium concentration in the

rods of wild-type and transducin knock-out mice. *J Physiol*. 2002;542(Pt 3):843–854.
117. Younger JP, McCarthy ST, Owen WG. Light-dependent control of calcium in intact rods of the bullfrog *Rana catesbeiana*. *J Neurophysiol*. 1996;75(1):354–366.
118. Sampath AP, Matthews HR, Cornwall MC, et al. Light-dependent changes in outer segment free-Ca^{2+} concentration in salamander cone photoreceptors. *J Gen Physiol*. 1999;113(2):267–277.
119. Matthews HR, Murphy RLW, Fain GL, et al. Photoreceptor light adaptation is mediated by cytoplasmic calcium concentration. *Nature*. 1988;334:67–69.
120. Fain GL, Matthews HR, Cornwall MC, et al. Adaptation in vertebrate photoreceptors. *Physiol Rev*. 2001;81(1):117–151.
121. Koutalos Y, Yau K-W. Regulation of sensitivity in vertebrate rod photoreceptors by calcium. *Trends Neurosci*. 1996;19:73–81.
122. Pugh EN Jr, Nikonov S, Lamb TD. Molecular mechanisms of vertebrate photoreceptor light adaptation. *Curr Opin Neurobiol*. 1999;9(4):410–418.
123. Sakurai K, Chen J, Kefalov VJ. Role of guanylyl cyclase modulation in mouse cone phototransduction. *J Neurosci*. 2011;31(22):7991–8000.
124. Chen CK, Inglese J, Lefkowitz RJ, et al. Ca(2+)-dependent interaction of recoverin with rhodopsin kinase. *J Biol Chem*. 1995;270(30):18060–18066.
125. Kawamura S. Rhodopsin phosphorylation as a mechanism of cyclic GMP phosphodiesterase regulation by S-modulin. *Nature*. 1993;362(6423):855–857.
126. Erickson MA, Lagnado L, Zozulya S, et al. The effect of recombinant recoverin on the photoresponse of truncated rod photoreceptors. *Proc Natl Acad Sci USA*. 1998;95(11):6474–6479.
127. Gray-Keller MP, Polans AS, Palczewski K, et al. The effect of recoverin-like calcium-binding proteins on the photoresponse of retinal rods. *Neuron*. 1993;10(3):523–531.
128. Makino CL, Dodd RL, Chen J, et al. Recoverin regulates light-dependent phosphodiesterase activity in retinal rods. *J*

Gen Physiol. 2004;123(6):729–741.
129. Chen CK, Woodruff ML, Chen FS, et al. Background light produces a recoverin-dependent modulation of activated-rhodopsin lifetime in mouse rods. *J Neurosci*. 2010;30(4):1213–1220.
130. Sakurai K, Chen J, Khani SC, et al. Regulation of mammalian cone phototransduction by recoverin and rhodopsin kinase. *J Biol Chem*. 2015;290(14):9239–9250.
131. Matthews HR, Sampath AP. Photopigment quenching is Ca^{2+} dependent and controls response duration in salamander L-cone photoreceptors. *J Gen Physiol*. 2010;135(4):355–366.
132. Hsu Y-T, Molday RS. Modulation of the cGMP-gated channel of rod photoreceptor cells by calmodulin. *Nature*. 1993;361:76–79.
133. Grunwald ME, Yu W-P, Yu H-H, et al. Identification of a domain on the ß-subunit of the rod cGMP-gated cation channel that mediates inhibition by calcium-calmodulin. *J Biol Chem*. 1998;273:9148–9157.
134. Weitz D, Zoche M, Müller F, et al. Calmodulin controls the rod photoreceptor CNG channel through an unconventional binding site in the N-terminus of the β-subunit. *EMBO J*. 1998;17:2273–2284.
135. Rebrik TI, Korenbrot JI. In intact mammalian photoreceptors, Ca^{2+}-dependent modulation of cGMP-gated ion channels is detectable in cones but not in rods. *J Gen Physiol*. 2004;123(1):63–75.
136. Korenbrot JI, Mehta M, Tserentsoodol N, et al. EML1 (CNG-modulin) controls light sensitivity in darkness and under continuous illumination in zebrafish retinal cone photoreceptors. *J Neurosci*. 2013;33(45):17763–17776.
137. Rebrik TI, Botchkina I, Arshavsky VY, et al. CNG-modulin: a novel Ca-dependent modulator of ligand sensitivity in cone photoreceptor cGMP-gated ion channels. *J Neurosci*. 2012;32(9):3142–3153.
138. Broekhuyse RM, Janssen AP, Tolhuizen EF. Effect of light-adaptation on the binding of 48-kDa protein (S-antigen) to photoreceptor cell membranes. *Curr Eye Res*. 1987;6(4):607–

610.
139. Broekhuyse RM, Tolhuizen EF, Janssen AP, et al. Light induced shift and binding of S-antigen in retinal rods. *Curr Eye Res*. 1985;4(5):613–618.
140. Philp NJ, Chang W, Long K. Light-stimulated protein movement in rod photoreceptor cells of the rat retina. *FEBS Lett*. 1987;225(1–2):127–132.
141. Whelan JP, McGinnis JF. Light-dependent subcellular movement of photoreceptor proteins. *J Neurosci Res*. 1988;20(2):263–270.
142. McGinnis JF, Whelan JP, Donoso LA. Transient, cyclic changes in mouse visual cell gene products during the light-dark cycle. *J Neurosci Res*. 1992;31(3):584–590.
143. Calvert PD, Strissel KJ, Schiesser WE, et al. Light-driven translocation of signaling proteins in vertebrate photoreceptors. *Trends Cell Biol*. 2006;16(11):560–568.
144. Sokolov M, Lyubarsky AL, Strissel KJ, et al. Massive light-driven translocation of transducin between the two major compartments of rod cells: a novel mechanism of light adaptation. *Neuron*. 2002;34(1):95–106.
145. Majumder A, Pahlberg J, Boyd KK, et al. Transducin translocation contributes to rod survival and enhances synaptic transmission from rods to rod bipolar cells. *Proc Natl Acad Sci USA*. 2013;110(30):12468–12473.
146. Rosenzweig DH, Nair KS, Wei J, et al. Subunit dissociation and diffusion determine the subcellular localization of rod and cone transducins. *J Neurosci*. 2007;27(20):5484–5494.
147. Lobanova ES, Finkelstein S, Song H, et al. Transducin translocation in rods is triggered by saturation of the GTPase-activating complex. *J Neurosci*. 2007;27(5):1151–1160.
148. Zhang X, Wensel TG, Kraft TW. GTPase regulators and photoresponses in cones of the eastern chipmunk. *J Neurosci*. 2003;23(4):1287–1297.
149. Lobanova ES, Herrmann R, Finkelstein S, et al. Mechanistic basis for the failure of cone transducin to translocate: why cones are never blinded by light. *J Neurosci*. 2010;30(20):6815–6824.

150. Chen J, Wu M, Sezate SA, et al. Light threshold-controlled cone alpha-transducin translocation. *Invest Ophthalmol Vis Sci*. 2007;48(7):3350–3355.
151. Nair KS, Hanson SM, Mendez A, et al. Light-dependent redistribution of arrestin in vertebrate rods is an energy-independent process governed by protein–protein interactions. *Neuron*. 2005;46(4):555–567.
152. Lamb TD, Pugh EN Jr. Dark adaptation and the retinoid cycle of vision. *Prog Retin Eye Res*. 2004;23(3):307–380.
153. Reuter T. Fifty years of dark adaptation, 1961–2011. [Historical Article Review]. *Vision Res*. 2011;51(21–22):2243–2262.
154. Takemoto N, Tachibanaki S, Kawamura S. High cGMP synthetic activity in carp cones. *Proc Natl Acad Sci USA*. 2009;106(28):11788–11793.
155. Tachibanaki S, Yonetsu S, Fukaya S, et al. Low activation and fast inactivation of transducin in carp cones. *J Biol Chem*. 2012;287(49):41186–41194.
156. Kawakami N, Kawamura S. Difference in the gain in the phototransduction cascade between rods and cones in carp. *J Neurosci*. 2014;34(44):14682–14686.
157. Mears AJ, Kondo M, Swain PK, et al. Nrl is required for rod photoreceptor development. *Nat Genet*. 2001;29(4):447–452.
158. Wang JS, Kefalov VJ. The cone-specific visual cycle. *Prog Retinal Eye Res*. 2011;30(2):115–128.
159. Kefalov V, Fu Y, Marsh-Armstrong N, et al. Role of visual pigment properties in rod and cone phototransduction. *Nature*. 2003;425(6957):526–531.
160. Mao W, Miyagishima KJ, Yao Y, et al. Functional comparison of rod and cone Galpha(t) on the regulation of light sensitivity. *J Biol Chem*. 2013;288(8):5257–5267.
161. Majumder A, Pahlberg J, Muradov H, et al. Exchange of cone for rod phosphodiesterase 6 catalytic subunits in rod photoreceptors mimics in part features of light adaptation. *J Neurosci Res*. 2015;35(24):9225–9235.
162. Hoang QV, Linsenmeier RA, Chung CK, et al. Photoreceptor inner segments in monkey and human retina: mitochondrial density, optics, and regional variation.

Vis Neurosci. 2002;19(4):395–407.
163. Hurley JB, Lindsay KJ, Du J. Glucose, lactate, and shuttling of metabolites in vertebrate retinas. *J Neurosci Res*. 2015;93(7):1079–1092.
164. Okawa H, Sampath AP, Laughlin SB, et al. ATP consumption by mammalian rod photoreceptors in darkness and in light. *Curr Biol*. 2008;18(24):1917–1921.
165. Trachtenberg MC, Packey DJ, Sweeney T. In vivo functioning of the Na+, K+-activated ATPase. *Curr Top Cell Regul*. 1981;19:159–217.
166. Karan S, Zhang H, Li S, et al. A model for transport of membrane-associated phototransduction polypeptides in rod and cone photoreceptor inner segments. *Vision Res*. 2008;48(3):442–452.
167. Wensel TG. Signal transducing membrane complexes of photoreceptor outer segments. *Vision Res*. 2008;48(20):2052–2061.
168. Ames JB, Ishima R, Tanaka T, et al. Molecular mechanics of calcium-myristoyl switches. *Nature*. 1997;389(6647):198–202.
169. Malanson KM, Lem J. Rhodopsin-mediated retinitis pigmentosa. *Prog Mol Biol Transl Sci*. 2009;88:1–31.
170. Kaushal S, Khorana HG. Structure and function in rhodopsin. 7. Point mutations associated with autosomal dominant retinitis pigmentosa. *Biochemistry*. 1994;33(20):6121–6128.
171. Mendes HF, van der Spuy J, Chapple JP, et al. Mechanisms of cell death in rhodopsin retinitis pigmentosa: implications for therapy. *Trends Mol Med*. 2005;11(4):177–185.
172. Sung CH, Davenport CM, Nathans J. Rhodopsin mutations responsible for autosomal dominant retinitis pigmentosa: clustering of functional classes along the polypeptide chain. *J Biol Chem*. 1993;268(35):26645–26649.
173. Concepcion F, Mendez A, Chen J. The carboxyl-terminal domain is essential for rhodopsin transport in rod photoreceptors. *Vision Res*. 2002;42(4):417–426.
174. Li T, Snyder WK, Olsson JE, et al. Transgenic mice carrying the dominant rhodopsin mutation P347S: evidence for defective vectorial transport of rhodopsin to the outer

segments. *Proc Natl Acad Sci USA*. 1996;93(24):14176–14181.
175. Sung CH, Makino C, Baylor D, et al. A rhodopsin gene mutation responsible for autosomal dominant retinitis pigmentosa results in a protein that is defective in localization to the photoreceptor outer segment. *J Neurosci*. 1994;14(10):5818–5833.
176. Deretic D. A role for rhodopsin in a signal transduction cascade that regulates membrane trafficking and photoreceptor polarity. *Vision Res*. 2006;46(27):4427–4433.
177. Deretic D, Williams AH, Ransom N, et al. Rhodopsin C terminus, the site of mutations causing retinal disease, regulates trafficking by binding to ADP-ribosylation factor 4 (ARF4). *Proc Natl Acad Sci USA*. 2005;102(9):3301–3306.
178. Tam BM, Moritz OL, Papermaster DS. The C terminus of peripherin/rds participates in rod outer segment targeting and alignment of disk incisures. *Mol Biol Cell*. 2004;15(4):2027–2037.
179. Huttl S, Michalakis S, Seeliger M, et al. Impaired channel targeting and retinal degeneration in mice lacking the cyclic nucleotide-gated channel subunit CNGB1. *J Neurosci*. 2005;25(1):130–138.
180. Zhang H, Li S, Doan T, et al. Deletion of PrBP/delta impedes transport of GRK1 and PDE6 catalytic subunits to photoreceptor outer segments. *Proc Natl Acad Sci USA*. 2007;104(21):8857–8862.
181. Zhang H, Constantine R, Vorobiev S, et al. UNC119 is required for G protein trafficking in sensory neurons. *Nat Neurosci*. 2011;14(7):874–880.
182. Horst CJ, Forestner DM, Besharse JC. Cytoskeletal-membrane interactions: a stable interaction between cell surface glycoconjugates and doublet microtubules of the photoreceptor connecting cilium. *J Cell Biol*. 1987;105(6 Pt 2):2973–2987.
183. Insinna C, Besharse JC. Intraflagellar transport and the sensory outer segment of vertebrate photoreceptors. *Dev Dyn*. 2008;237(8):1982–1992.
184. Williams DS. Transport to the photoreceptor outer segment by myosin VIIa and kinesin II. *Vision Res*. 2002;42(4):455–

462.
185. Williams DS, Linberg KA, Vaughan DK, et al. Disruption of microfilament organization and deregulation of disk membrane morphogenesis by cytochalasin D in rod and cone photoreceptors. *J Comp Neurol*. 1988;272(2):161–176.
186. Adato A, Weil D, Kalinski H, et al. Mutation profile of all 49 exons of the human myosin VIIA gene, and haplotype analysis, in Usher 1B families from diverse origins. *Am J Hum Genet*. 1997;61(4):813–821.
187. Weil D, Blanchard S, Kaplan J, et al. Defective myosin VIIA gene responsible for Usher syndrome type 1B. *Nature*. 1995;374(6517):60–61.
188. Pierce EA, Quinn T, Meehan T, et al. Mutations in a gene encoding a new oxygen-regulated photoreceptor protein cause dominant retinitis pigmentosa. *Nat Genet*. 1999;22(3):248–254.
189. Gao J, Cheon K, Nusinowitz S, et al. Progressive photoreceptor degeneration, outer segment dysplasia, and rhodopsin mislocalization in mice with targeted disruption of the retinitis pigmentosa-1 (Rp1) gene. *Proc Natl Acad Sci USA*. 2002;99(8):5698–5703.
190. Liu Q, Lyubarsky A, Skalet JH, et al. RP1 is required for the correct stacking of outer segment discs. *Invest Ophthalmol Vis Sci*. 2003;44(10):4171–4183.
191. Liu Q, Zuo J, Pierce EA. The retinitis pigmentosa 1 protein is a photoreceptor microtubule-associated protein. *J Neurosci*. 2004;24(29):6427–6436.
192. Meindl A, Dry K, Herrmann K, et al. A gene (RPGR) with homology to the RCC1 guanine nucleotide exchange factor is mutated in X-linked retinitis pigmentosa (RP3). *Nat Genet*. 1996;13(1):35–42.
193. Hong DH, Pawlyk B, Sokolov M, et al. RPGR isoforms in photoreceptor connecting cilia and the transitional zone of motile cilia. *Invest Ophthalmol Vis Sci*. 2003;44(6):2413–2421.
194. Hong DH, Pawlyk BS, Shang J, et al. A retinitis pigmentosa GTPase regulator (RPGR)-deficient mouse model for X-linked retinitis pigmentosa (RP3). *Proc Natl Acad Sci USA*. 2000;97(7):3649–3654.

195. Trojan P, Krauss N, Choe HW, et al. Centrins in retinal photoreceptor cells: regulators in the connecting cilium. *Prog Retin Eye Res*. 2008;27(3):237–259.
196. Yang J, Liu X, Yue G, et al. Rootletin, a novel coiled-coil protein, is a structural component of the ciliary rootlet. *J Cell Biol*. 2002;159(3):431–440.
197. Hagstrom SA, Adamian M, Scimeca M, et al. A role for the Tubby-like protein 1 in rhodopsin transport. *Invest Ophthalmol Vis Sci*. 2001;42(9):1955–1962.
198. Lewis CA, Batlle IR, Batlle KG, et al. Tubby-like protein 1 homozygous splice-site mutation causes early-onset severe retinal degeneration. *Invest Ophthalmol Vis Sci*. 1999;40(9):2106–2114.
199. Rattner A, Chen J, Nathans J. Proteolytic shedding of the extracellular domain of photoreceptor cadherin: implications for outer segment assembly. *J Biol Chem*. 2004;279(40):42202–42210.
200. Kubota R, Noda S, Wang Y, et al. A novel myosin-like protein (myocilin) expressed in the connecting cilium of the photoreceptor: molecular cloning, tissue expression, and chromosomal mapping. *Genomics*. 1997;41(3):360–369.
201. Wright AF, Chakarova CF, Abd El-Aziz MM, et al. Photoreceptor degeneration: genetic and mechanistic dissection of a complex trait. *Nat Rev Genet*. 2010;11(4):273–284.
202. Rachel RA, Li T, Swaroop A. Photoreceptor sensory cilia and ciliopathies: focus on CEP290, RPGR and their interacting proteins. *Cilia*. 2012;1(1):22.
203. Schmitz F, Konigstorfer A, Sudhof TC. RIBEYE, a component of synaptic ribbons: a protein's journey through evolution provides insight into synaptic ribbon function. *Neuron*. 2000;28(3):857–872.
204. Snellman J, Mehta B, Babai N, et al. Acute destruction of the synaptic ribbon reveals a role for the ribbon in vesicle priming. *Nat Neurosci*. 2011;14(9):1135–1141.
205. Mehta B, Snellman J, Chen S, et al. Synaptic ribbons influence the size and frequency of miniature-like evoked postsynaptic currents. *Neuron*. 2013;77(3):516–527.

206. Jackman SL, Choi SY, Thoreson WB, et al. Role of the synaptic ribbon in transmitting the cone light response. *Nat Neurosci*. 2009;12(3):303–310.
207. Carter-Dawson LD, LaVail MM. Rods and cones in the mouse retina. II. Autoradiographic analysis of cell generation using tritiated thymidine. *J Comp Neurol*. 1979;188(2):263–272.
208. Tsukamoto Y, Morigiwa K, Ueda M, et al. Microcircuits for night vision in mouse retina. *J Neurosci*. 2001;21(21):8616–8623.
209. West RW, Dowling JE. Anatomical evidence for cone and rod-like receptors in the gray squirrel, ground squirrel, and prairie dog retinas. *J Comp Neurol*. 1975;159(4):439–460.
210. Chun MH, Grunert U, Martin PR, et al. The synaptic complex of cones in the fovea and in the periphery of the macaque monkey retina. *Vision Res*. 1996;36(21):3383–3395.
211. Hopkins JM, Boycott BB. The cone synapses of cone bipolar cells of primate retina. *J Neurocytol*. 1997;26(5):313–325.
212. Koschak A, Reimer D, Walter D, et al. Cav1.4alpha1 subunits can form slowly inactivating dihydropyridine-sensitive L-type Ca^{2+} channels lacking Ca^{2+}-dependent inactivation. *J Neurosci*. 2003;23(14):6041–6049.
213. Wahl-Schott C, Baumann L, Cuny H, et al. Switching off calcium-dependent inactivation in L-type calcium channels by an autoinhibitory domain. *Proc Natl Acad Sci USA*. 2006;103(42):15657–15662.
214. Haeseleer F, Imanishi Y, Maeda T, et al. Essential role of Ca^{2+}-binding protein 4, a Cav1.4 channel regulator, in photoreceptor synaptic function. *Nat Neurosci*. 2004;7(10):1079–1087.
215. Morgans CW, Bayley PR, Oesch NW, et al. Photoreceptor calcium channels: insight from night blindness. *Vis Neurosci*. 2005;22(5):561–568.
216. Sampath AP, Strissel KJ, Elias R, et al. Recoverin improves rod-mediated vision by enhancing signal transmission in the mouse retina. *Neuron*. 2005;46(3):413–420.
217. Higgs MH, Lukasiewicz PD. Activation of group II metabotropic glutamate receptors inhibits glutamate release

from salamander retinal photoreceptors. *Vis Neurosci*. 2002;19(3):275–281.
218. Koulen P, Kuhn R, Wassle H, et al. Modulation of the intracellular calcium concentration in photoreceptor terminals by a presynaptic metabotropic glutamate receptor. *Proc Natl Acad Sci USA*. 1999;96(17):9909–9914.
219. Duncan JL, Yang H, Doan T, et al. Scotopic visual signaling in the mouse retina is modulated by high-affinity plasma membrane calcium extrusion. *J Neurosci*. 2006;26(27):7201–7211.
220. Szikra T, Barabas P, Bartoletti TM, et al. Calcium homeostasis and cone signaling are regulated by interactions between calcium stores and plasma membrane ion channels. *PLoS ONE*. 2009;4(8):e6723.
221. Szikra T, Cusato K, Thoreson WB, et al. Depletion of calcium stores regulates calcium influx and signal transmission in rod photoreceptors. *J Physiol*. 2008;586(Pt 20):4859–4875.
222. Thoreson WB. Kinetics of synaptic transmission at ribbon synapses of rods and cones. *Mol Neurobiol*. 2007;36(3):205–223.
223. Choi SY, Jackman S, Thoreson WB, et al. Light regulation of Ca^{2+} in the cone photoreceptor synaptic terminal. *Vis Neurosci*. 2008;25(5–6):693–700.
224. Sheng Z, Choi SY, Dharia A, et al. Synaptic Ca^{2+} in darkness is lower in rods than cones, causing slower tonic release of vesicles. *J Neurosci*. 2007;27(19):5033–5042.
225. Gal A, Apfelstedt-Sylla E, Janecke AR, et al. Rhodopsin mutations in inherited retinal dystrophies and dysfunctions. *Prog Retin Eye Res*. 1997;16(1):51–79.
226. Lin JH, Li H, Yasumura D, et al. IRE1 signaling affects cell fate during the unfolded protein response. *Science*. 2007;318(5852):944–949.
227. Colley NJ, Cassill JA, Baker EK, et al. Defective intracellular transport is the molecular basis of rhodopsin-dependent dominant retinal degeneration. *Proc Natl Acad Sci USA*. 1995;92(7):3070–3074.
228. Deretic D, Puleo-Scheppke B, Trippe C. Cytoplasmic

domain of rhodopsin is essential for post-Golgi vesicle formation in a retinal cell-free system. *J Biol Chem*. 1996;271(4):2279–2286.
229. Deretic D, Schmerl S, Hargrave PA, et al. Regulation of sorting and post-Golgi trafficking of rhodopsin by its C-terminal sequence QVS(A)PA. *Proc Natl Acad Sci USA*. 1998;95(18):10620–10625.
230. Chuang JZ, Sung CH. The cytoplasmic tail of rhodopsin acts as a novel apical sorting signal in polarized MDCK cells. *J Cell Biol*. 1998;142(5):1245–1256.
231. Rao VR, Oprian DD. Activating mutations of rhodopsin and other G protein-coupled receptors. *Annu Rev Biophys Biomol Struct*. 1996;25:287–314.
232. Robinson PR, Cohen GB, Zhukovsky EA, et al. Constitutively active mutants of rhodopsin. *Neuron*. 1992;9(4):719–725.
233. Rao VR, Cohen GB, Oprian DD. Rhodopsin mutation G90D and a molecular mechanism for congenital night blindness. *Nature*. 1994;367(6464):639–642.
234. Sieving PA, Richards JE, Naarendorp F, et al. Dark–light: model for nightblindness from the human rhodopsin Gly-90–>Asp mutation. *Proc Natl Acad Sci USA*. 1995;92(3):880–884.
235. Li T, Franson WK, Gordon JW, et al. Constitutive activation of phototransduction by K296E opsin is not a cause of photoreceptor degeneration. *Proc Natl Acad Sci USA*. 1995;92(8):3551–3555.
236. Chen J, Shi G, Concepcion FA, et al. Stable rhodopsin/arrestin complex leads to retinal degeneration in a transgenic mouse model of autosomal dominant retinitis pigmentosa. *J Neurosci*. 2006;26(46):11929–11937.
237. Moaven H, Koike Y, Jao CC, et al. Visual arrestin interaction with clathrin adaptor AP-2 regulates photoreceptor survival in the vertebrate retina. *Proc Natl Acad Sci USA*. 2013;110(23):9463–9468.
238. Fuchs S, Nakazawa M, Maw M, et al. A homozygous 1-base pair deletion in the arrestin gene is a frequent cause of Oguchi disease in Japanese. *Nat Genet*. 1995;10(3):360–362.

239. Yamamoto S, Sippel KC, Berson EL, et al. Defects in the rhodopsin kinase gene in the Oguchi form of stationary night blindness. *Nat Genet*. 1997;15(2):175–178.
240. Chen J, Simon MI, Matthes MT, et al. Increased susceptibility to light damage in an arrestin knockout mouse model of Oguchi disease (stationary night blindness). *Invest Ophthalmol Vis Sci*. 1999;40(12):2978–2982.
241. Wang T, Chen J. Induction of the unfolded protein response by constitutive G-protein signaling in rod photoreceptor cells. *J Biol Chem*. 2014;289(42):29310–29321.
242. Dryja TP, Hahn LB, Reboul T, et al. Missense mutation in the gene encoding the alpha subunit of rod transducin in the Nougaret form of congenital stationary night blindness. *Nat Genet*. 1996;13(3):358–360.
243. Tsang SH, Gouras P, Yamashita CK, et al. Retinal degeneration in mice lacking the gamma subunit of the rod cGMP phosphodiesterase. *Science*. 1996;272(5264):1026–1029.
244. Farber DB, Lolley RN. Cyclic guanosine monophosphate: elevation in degenerating photoreceptor cells of the C3H mouse retina. *Science*. 1974;186(4162):449–451.
245. Yang RB, Foster DC, Garbers DL, et al. Two membrane forms of guanylyl cyclase found in the eye. *Proc Natl Acad Sci USA*. 1995;92(2):602–606.
246. Lowe DG, Dizhoor AM, Liu K, et al. Cloning and expression of a second photoreceptor-specific membrane retina guanylyl cyclase (RetGC), RetGC-2. *Proc Natl Acad Sci USA*. 1995;92(12):5535–5539.
247. Shyjan AW, de Sauvage FJ, Gillett NA, et al. Molecular cloning of a retina-specific membrane guanylyl cyclase. *Neuron*. 1992;9(4):727–737.
248. Goraczniak RM, Duda T, Sitaramayya A, et al. Structural and functional characterization of the rod outer segment membrane guanylate cyclase. *Biochem J*. 1994;302(Pt 2):455–461.
249. Duda T, Goraczniak R, Surgucheva I, et al. Calcium modulation of bovine photoreceptor guanylate cyclase. *Biochemistry*. 1996;35(26):8478–8482.

250. Laura RP, Dizhoor AM, Hurley JB. The membrane guanylyl cyclase, retinal guanylyl cyclase-1, is activated through its intracellular domain. *J Biol Chem*. 1996;271(20):11646–11651.
251. Dizhoor AM, Lowe DG, Olshevskaya EV, et al. The human photoreceptor membrane guanylyl cyclase, retGC, is present in outer segments and is regulated by calcium and a soluble activator. *Neuron*. 1994;12:1345–1352.
252. Yang RB, Garbers DL. Two eye guanylyl cyclases are expressed in the same photoreceptor cells and form homomers in preference to heteromers. *J Biol Chem*. 1997;272(21):13738–13742.
253. Lotery AJ, Namperumalsamy P, Jacobson SG, et al. Mutation analysis of 3 genes in patients with Leber congenital amaurosis. *Arch Ophthalmol*. 2000;118(4):538–543.
254. Perrault I, Rozet JM, Gerber S, et al. A retGC-1 mutation in autosomal dominant cone-rod dystrophy. *Am J Hum Genet*. 1998;63(2):651–654.
255. Payne AM, Downes SM, Bessant DA, et al. A mutation in guanylate cyclase activator 1A (GUCA1A) in an autosomal dominant cone dystrophy pedigree mapping to a new locus on chromosome 6p21.1. *Hum Mol Genet*. 1998;7(2):273–277.
256. Dizhoor AM, Boikov SG, Olshevskaya EV. Constitutive activation of photoreceptor guanylate cyclase by Y99C mutant of GCAP-1. Possible role in causing human autosomal dominant cone degeneration. *J Biol Chem*. 1998;273(28):17311–17314.
257. Jiang L, Wheaton D, Bereta G, et al. A novel GCAP1(N104K) mutation in EF-hand 3 (EF3) linked to autosomal dominant cone dystrophy. *Vision Res*. 2008;48(23–24):2425–2432.
258. Downes SM, Holder GE, Fitzke FW, et al. Autosomal dominant cone and cone–rod dystrophy with mutations in the guanylate cyclase activator 1A gene-encoding guanylate cyclase activating protein-1. *Arch Ophthalmol*. 2001;119(1):96–105.
259. Kitiratschky VB, Behnen P, Kellner U, et al. Mutations in the GUCA1A gene involved in hereditary cone dystrophies impair calcium-mediated regulation of guanylate cyclase. *Hum Mutat*. 2009;30(8):E782–96.

260. Michaelides M, Wilkie SE, Jenkins S, et al. Mutation in the gene GUCA1A, encoding guanylate cyclase-activating protein 1, causes cone, cone-rod, and macular dystrophy. *Ophthalmology*. 2005;112(8):1442–1447.
261. Nishiguchi KM, Sokal I, Yang L, et al. A novel mutation (I143NT) in guanylate cyclase-activating protein 1 (GCAP1) associated with autosomal dominant cone degeneration. *Invest Ophthalmol Vis Sci*. 2004;45(11):3863–3870.
262. Payne AM, Downes SM, Bessant DA, et al. Genetic analysis of the guanylate cyclase activator 1B (GUCA1B) gene in patients with autosomal dominant retinal dystrophies. *J Med Genet*. 1999;36(9):691–693.
263. Sato M, Nakazawa M, Usui T, et al. Mutations in the gene coding for guanylate cyclase-activating protein 2 (GUCA1B gene) in patients with autosomal dominant retinal dystrophies. *Graefes Arch Clin Exp Ophthalmol*. 2005;243(3):235–242.
264. Paquet-Durand F, Beck S, Michalakis S, et al. A key role for cyclic nucleotide gated (CNG) channels in cGMP-related retinitis pigmentosa. *Hum Mol Genet*. 2011;20(5):941–947.
265. Andrade AL, Melich K, Whatley GG, et al. Cyclic nucleotide-gated channel block by hydrolysis-resistant tetracaine derivatives. *J Med Chem*. 2011;54(13):4904–4912.

17

Function and Anatomy of the Mammalian Retina

Ronald G. Gregg, Joshua Singer, Maarten Kamermans, Maureen A. McCall, Stephen C. Massey

The vertebrate retina forms a thin sheet of neural tissue at the back of the eye that converts light to an electrical signal. The neural retina is approximately 100–200 μm thick, depending on the species, and represents a triumph of miniaturization.[1] The retina is a spatial information processor built upon a mosaic of rod and cone photoreceptors, which are the light-responsive elements that initiate

signaling using graded electrical signals.[2] The spatial information content is preserved through the lateral geniculate nucleus, retinotopically mapped on to area V1 (area 17) of the primary visual cortex and from there on to a number of higher visual processing areas. There is considerable processing both within the retina as well as in higher brain structures and we interpret these electrical signals as vision. While vision is an analog system, a rough approximation to a digital system would result in a resolution in excess of 500 megapixels. Although initially conceived to be a simple model for the brain, more probably, the retina approaches limits imposed by metabolism, blood flow, and diffusion. This pressure to pack more function into a small volume of neural tissue leads to increased complexity.

Visual Illusions and Multiple Channels

Vision appears to be deceptively simple only because we are very good at it: with few exceptions, a large portion of the mammalian brain is devoted to vision. A moment's thought reveals that vision must dovetail neatly with such high-order processes as image storage and retrieval, forms of learning and memory essential to comparison and recognition. However, even in the retina, it is easy to demonstrate the presence of multiple processes using well-known visual illusions.

At first glance, Fig. 17.1 looks like a random array of large pixels with three bright areas. Now, screw up your eyes, glance aside or look at it from the other side of the room, and suddenly you may recognize da Vinci's Mona Lisa. The bright areas are the face, chest, and hands. But why does the image seem to be more recognizable when visual input is distorted? The high-spatial-frequency components have been removed by greatly reducing the pixel number. What detail does remain is a confusing array of boxes. However, this detailed view can be blurred by squinting, which removes the high-frequency components, leaving an easily recognized low-acuity version. So this is a direct demonstration that the visual system operates on at least two channels of information at different spatial scales simultaneously. In fact, there is empirical evidence that vision is composed of at least 15 parallel channels or

streams of information that are transmitted simultaneously throughout the visual system. It is the purpose of this chapter to describe the functional anatomy of the retina that leads to the formation of some of these independent channels of visual information.

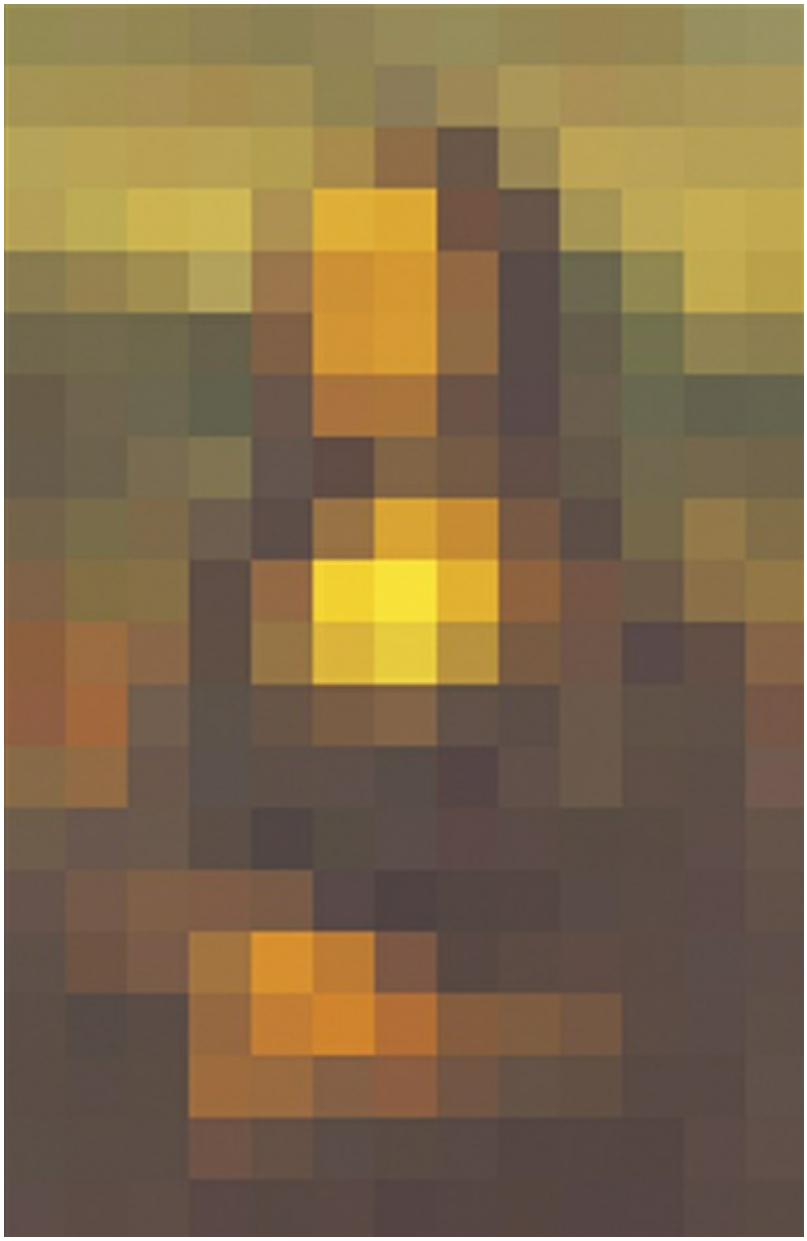

FIG. 17.1 Parallel pathways. A highly filtered image, 13 × 20 pixels, of a well-known icon containing mostly low-spatial-frequency information. At first, it may be hard to recognize because it is natural to focus on the pixel edges. However, if you squint to blur the image, the true identity of the picture may suddenly become

more obvious. This is a direct demonstration that the visual system carries several parallel streams of visual information with different spatial properties. For more details, see the text.

The Retina Is a Piece of Brain

Like the rest of the central nervous system (CNS), the retina is embryologically derived from the neural tube. It is formed from the same components as the rest of the CNS and like all other sensory systems has specialized structures, photoreceptors that transduce environmental energy into electrical potentials. As such, one can divide the retina in two parts:[3] (1) the sensory retina, concerned with phototransduction of light by rod and cone photoreceptors; and (2) the neural retina, consisting of more typical interneurons (bipolar, horizontal, and amacrine cells) and projection neurons (ganglion cells) that carry out the first steps in processing visual information.

The retina has been characterized by Dowling as an approachable part of the brain,[4] because it is a ready-made brain slice with few barriers to the penetration of drugs or antibodies. In addition, its natural stimulus, light, is easily controlled and the same stimuli can be presented either to the intact animal or to the retina removed from the eye and placed in vitro. This chapter focuses on processing in the mammalian retina. However, many of the pioneering studies in retinal function were initially performed in fish and amphibian retina. In particular, the salamander retina has been a longstanding model because its large cells enhance the ease of electrophysiologic recording.

Neuronal Communication: Chemical and Electrical

In the retina, as in the rest of the CNS, the dominant form of communication between neurons uses chemical neurotransmission. Pulses of neurotransmitter (commonly the amino acids glutamate, gamma-aminobutyric acid (GABA) and glycine plus acetylcholine

(ACh), dopamine, and serotonin) are released from a presynaptic neuron and diffuse across the narrow synaptic cleft to bind to one of a variety of postsynaptic receptors. Receptors can be ion channels themselves or can be linked via intracellular mechanisms to ion channels. Depending on the ion selectivity (anion or cation), the opening or closing of the channels produces a hyperpolarization or a depolarization of the postsynaptic cell.

Many neurons also are directly connected via electrical synapses known as gap junctions.[5–9] Gap junctions are named after the narrow gap formed by docked hemichannels, or connexons aligned on either side of two cell membranes. Each hemichannel is built from six connexins that surround a central pore, forming an intercellular channel, which passes ions and small molecules (≤1 kDa). Gap junctions are not static pores; they are modulated by light and contribute to neural processing.

The Retina Is a Layered Structure

The retina is a beautifully layered structure in which three layers of neurons can be visualized without staining (Fig. 17.2). The outer nuclear layer (ONL) contains the cell bodies of photoreceptors, both rods and cones. The inner nuclear layer (INL) contains the cell bodies of horizontal, bipolar, amacrine, and radial glial (or Müller) cells. The ganglion cell layer (GCL) contains displaced amacrine and ganglion cells. Ganglion cells are the projection neurons of the retina: their axons form the optic nerve and project to a variety of subcortical nuclei. The three nuclear layers are separated by two synaptic (plexiform) layers that contain the dendrites and synapses. The outer plexiform layer (OPL) lies between the ONL and the INL. This is where the photoreceptors, horizontal, and bipolar cell dendrites interact. The inner plexiform layer (IPL) separates the INL and the GCL and this is where the bipolar cell axons, amacrine, and ganglion cells interact. When we speak of the retina, outer or distal refers to the scleral side of the retina and inner or proximal refers to the vitreal side of the retina.

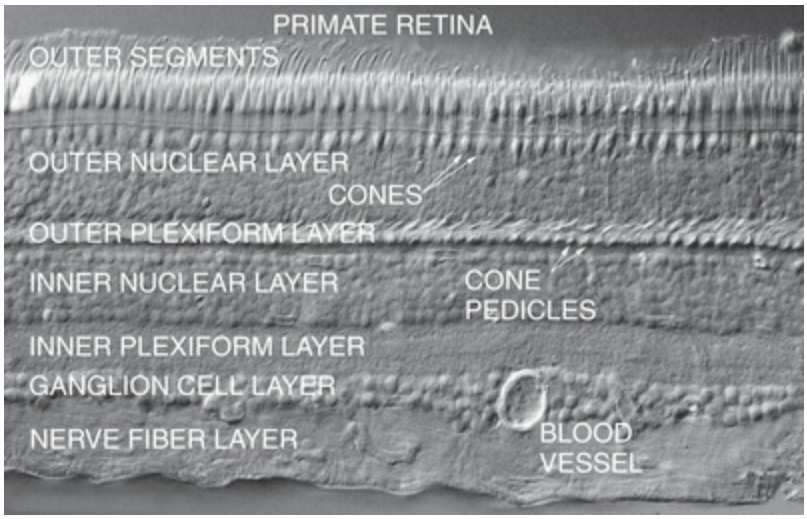

FIG. 17.2 Primate retina. A vertical section through the macaque retina taken with differential interference contrast optics. The retina is a layered structure with two synaptic or plexiform layers sandwiched by three nuclear layers: the outer nuclear layer, inner nuclear layer, and ganglion cell layer. Although many fine details, such as cone pedicles, are visible, individual neurons must be stained to see their dendritic fields and specific connections. *Longer arrows*: cones; *smaller arrows*: cone pedicles. (Courtesy of S.C. Massey.)

The functional stratification of the retina extends to the IPL, which is organized according to the polarity of bipolar cell inputs.[10] Since the time of Cajal, the IPL has been divided into five layers: 1 and 2 for sublamina a and layers 3–5 for sublamina b. In mammalian species, there are 9–11 morphologic types of bipolar cell, plus the rod bipolar cell, which terminate at different depths in the IPL.[11–13] The polarity of a bipolar cell response is determined by the differential expression of postsynaptic glutamate receptors on their dendrites. The dendrites of OFF cone bipolar cells carry α-amino-3-hydroxy-5-methyl-4-isoxazolepropionic acid (AMPA)/kainate receptors and they ramify in sublamina a of the IPL.[14] In contrast, ON cone bipolar cells and rod bipolar cells express mGluR6 receptors and their axons ramify in sublamina b.[15–17] The separation of ON and OFF pathways appears to be a fundamental principle of retinal organization, which is reflected throughout the visual system.[18,19]

There is a wealth of evidence to support the functional division of the IPL into ON and OFF sublaminae. For example, cholinergic

amacrine cells (ChACs), also known as starburst amacrine cells on account of their unique morphology, are present as mirror-image pairs.[20] The conventionally placed ChACs have somas in the innermost layer of the INL. They have OFF responses to light stimulation and ramify in sublamina a. In contrast, the displaced ChACs reside in the GCL, produce ON responses, and ramify in sublamina b. Likewise, alpha ganglion cells are present as paramorphic pairs such that the dendritic trees of OFF alpha ganglion cells are stratified in sublamina a to receive input from OFF bipolar cells while ON alpha ganglion cells ramify in sublamina b to make contact with ON bipolar cells.[21,22] In primate retina, both midget and parasol ganglion cells are present as paramorphic pairs, which conform to the stratification rules of the IPL. ON/OFF directionally selective (DS) ganglion cells produce both ON and OFF responses of short latency, indicating direct input, and they are bistratified with dendrites in sublaminae 2 and 4, coincident with the cholinergic bands.

The ON and OFF stratification of the IPL is a fundamental tenet of retinal organization which applies to many, if not most, cell types. However, several exceptions to this rule have now been identified. For example, the dopaminergic amacrine cells (DACs) stratify predominantly in sublamina a, the OFF layer, yet they apparently produce ON responses to light.[23,24] Likewise, the intrinsically photosensitive retinal ganglion cells (ipRGCs), which stratify in sublamina a of the primate retina, were all ON cells.[25] These cell types, among others, receive input from ON bipolar axons as they traverse sublamina a of the IPL. These axonal ribbons provide a set of inputs that break the stratification rules of the IPL. Thus, there is an additional accessory ON sublayer in the outer portion of the IPL[26,27] (see sections on DACs and ipRGCs) (Table 17.1).

TABLE 17.1

Cellular and Synaptic Layers of the Retina

Layer	Contains:
Outer nuclear layer (ONL)	Photoreceptors, rods, and cones
Inner nuclear layer (INL)	Horizontal cells, bipolar cells, amacrine cells, Müller cells
Ganglion cell layer (GCL)	Ganglion cells, displaced amacrine cells

Outer plexiform layer (OPL)	Photoreceptors talk to horizontal cells and bipolar cells
Inner plexiform layer (IPL)	Bipolar cells talk to amacrine cells and ganglion cells

GCL, ganglion cell layer; INL, inner nuclear layer; IPL, inner plexiform layer; ONL, outer nuclear layer; OPL, outer plexiform layer.

Gross Retinal Morphology

The Fovea

When a peripheral visual stimulus gets our attention, we automatically focus the retinal image in the center of our gaze. In the primate retina this central region of highest visual acuity is known as the fovea. Here there is a depression in the retina, known as the foveal pit, where cone photoreceptor density is highest and there are no rods. The pit results from the lack of overlying neurons (Fig. 17.3). Instead, cone axons, Henle fibers, run obliquely to cone pedicles away from the fovea where the bipolar and ganglion cells connected to the central cones are "piled up" in an annular zone with the GCL 6–8 cells thick. The foveal structure is thought to maximize sensitivity because light cannot be scattered by passing through other retinal layers. It also optimizes acuity by packing the maximum number of cones and reducing their size. In human retina, the peak cone density approaches 200,000/mm^2 and the ONL is slightly thicker to accommodate these extra cells.[28] There are no blood vessels in the fovea, and in the central fovea there are no blue cones. The low density of blue cones lowers their acuity,[29] to match the blurring caused by chromatic aberration in the lens.[30] Other mammals have an area centralis (cat) or a visual streak (rabbit, swine) with similar high cell density but these structures lack the central depression. A consequence of the exclusion of rods from the fovea is that in dark-adapted conditions, say looking for a dim star, it is necessary to look slightly off the visual axis to focus the image in the region of high rod density.

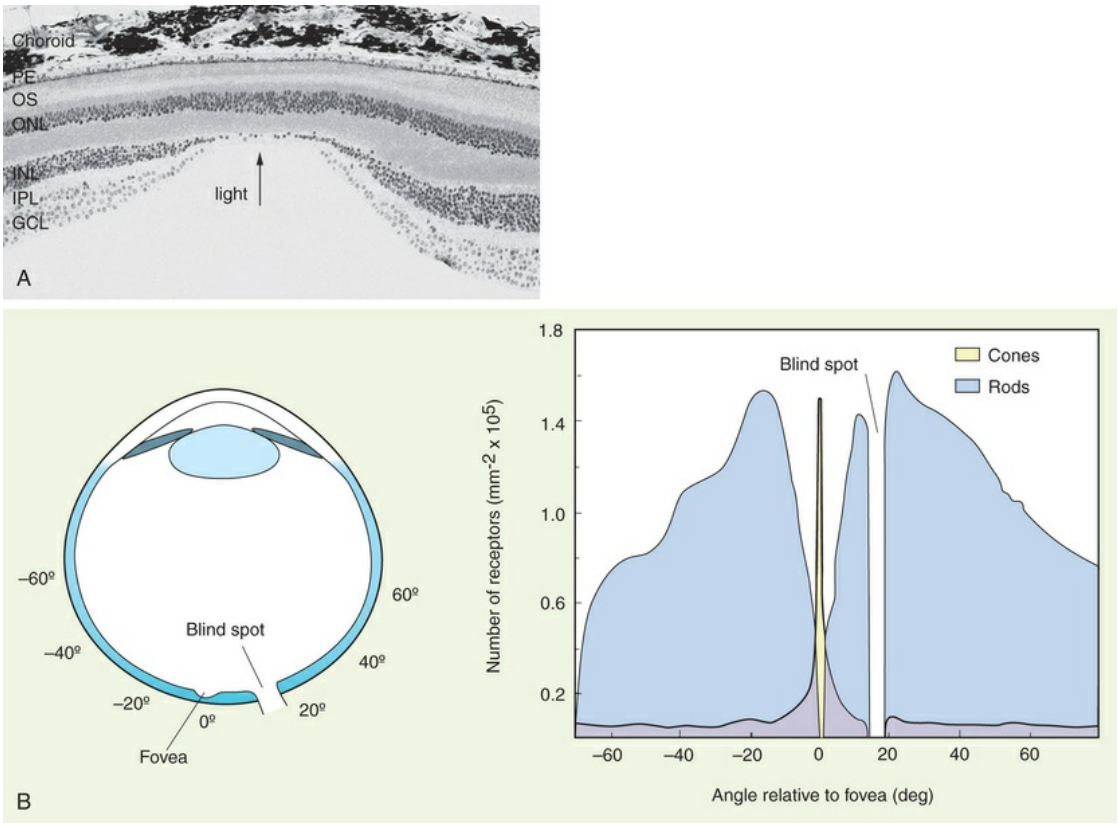

FIG. 17.3 The fovea and distribution of rods and cones in the human eye. (A) This cross-section of the macaque retina shows the foveal pit, a specialization of the primate retina. In this region, the cones are smallest and their packing density reaches a maximum. There are no rods. At the fovea, ganglion cells and other retinal layers are reduced for maximum sensitivity and acuity. *PE*, pigment epithelium; *OS*, outer segments; *ONL*, outer nuclear layer; *INL*, inner nuclear layer; *IPL*, inner plexiform layer; *GCL*, ganglion cell layer. (B) Rod and cone density across the retina. Note how the cones peak at the fovea. Rod density falls to zero at the fovea but reaches a maximum around 5 mm outside the fovea. There are no photoreceptors at the point where the optic nerve leaves the eye, also known as the blind spot. (Panel A, courtesy of Louvenia Carter-Dawson. Panel B, modified with permission from Wandell BA. Foundations of vision. Sunderland, MA: Sinauer Associates, 1995.)

The Blind Spot and How to Find It

There are no photoreceptors where the optic nerve exits the eye and

so any image that falls on this region cannot be processed by the retina. Curiously, we do not perceive a hole in the visual scene because the visual system fills in. To demonstrate the blind spot, hold the page level at normal reading distance. Look at the O in Fig. 17.4, and then close your right eye. The X on the left should disappear because the image of the cross falls on the optic nerve head. You can reverse this demonstration: look at the X, then close the left eye to make the O disappear. Remember, the blind spot is nasal to the fovea. The light rays cross over at the lens so the blind spot is lateral to the point of focus.

FIG. 17.4 How to find the blind spot. To demonstrate the blind spot, hold the page level at normal reading distance. Look at the O in the figure, then close your right eye. The X on the left should disappear because the image of the cross falls on the optic nerve head. You can reverse this demonstration: look at the X, then close the left eye to make the O disappear. Remember, the blind spot is nasal to the fovea. The light rays cross over at the lens so the blind spot is lateral to the point of focus.

Painting the Retina – Techniques to Label and Visualize Retinal Neurons

The major landmarks of the retina, two synaptic layers sandwiched between three nuclear layers, are obvious even in the unstained section of macaque retina shown in Fig. 17.2. In fact, there is an immense amount of detail present in this image. For example, individual cones can be seen with their descending axons terminating in a row of cone pedicles in the OPL. However, the somas of all the other retinal neurons are indistinguishable and the

details of their structures cannot be visualized. One goal of vision scientists is to have a complete map of all the interconnections between the retinal neurons so that the functional outputs can be fully understood. To uncover the hidden pathways and circuits through the retina, we need to stain specific cell types selectively (Fig. 17.5), so that we can differentiate between rod and cone pathways, for example. Furthermore, it is very useful to visualize several cell types at once so that the number and position of one cell type relative to another can be determined. This can be achieved by confocal microscopy, which permits the simultaneous acquisition of three or more different labels in addition to providing improved resolution and three-dimensional visualization (Fig. 17.5). With care, confocal microscopy can be used to visualize both chemical and electrical synapses in the retina.[31] It has been used to measure changes in intracellular calcium concentration of single neurons or dendrites in response to stimulation with visible light.[32,33] One disadvantage of these methods is that individual synapses cannot easily be visualized because of the inherent resolution limits of confocal microscopy. However, high-throughput electron microscopy methods have been developed that allow three-dimensional reconstruction of blocks of retina, albeit in fixed tissue. By careful analysis and multiple staining approaches it is possible to identify all the synapses and cells to which an individual neuron makes connections.[34]

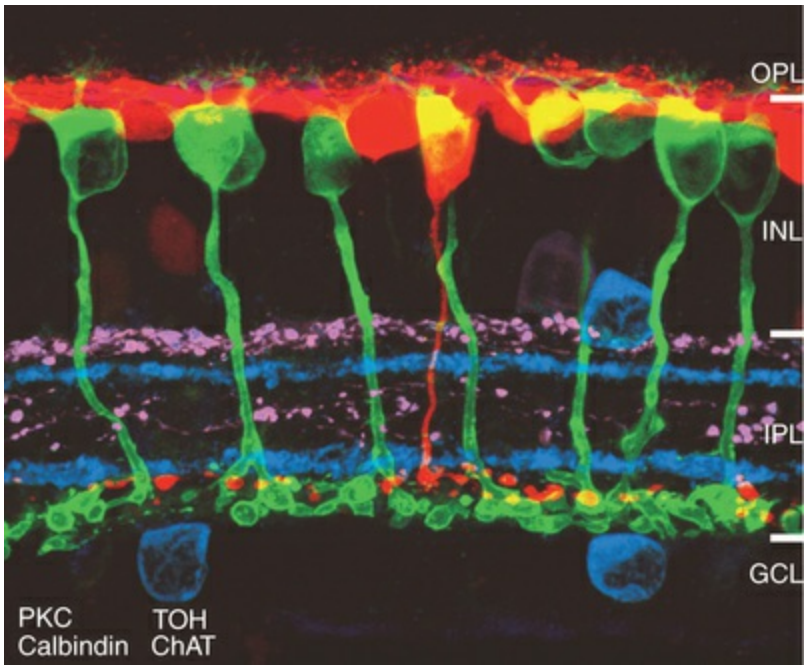

FIG. 17.5 Quad labeling of the rabbit retina. In this vertical section, multiple antibodies were used to label different cell types. Red, calbindin, shows horizontal cells, large somas high in the inner nuclear layer (*INL*) adjacent to the outer plexiform layer (*OPL*). Also in red, an ON cone bipolar cell with a single axon descending to sublamina 4 of the inner plexiform layer (*IPL*). Green, protein kinase C (*PKC*), shows multiple rod bipolar cells descending to sublamina 5 of the IPL where they have prominent terminals. Blue, choline acetyltransferase (*ChAT*), labels starburst amacrine cells, one in the INL and two in the ganglion cell layer. These cells make two dense bands in the IPL. Pink, tyrosine hydroxylase (*TOH*), shows the plexus of dopaminergic processes, mostly in sublamina a, adjacent to the amacrine cell layer. There are also a few processes in the middle of the IPL. As well as staining multiple neurons, this figure demonstrates that the IPL is highly stratified with each cell type at a distinct depth. Ten to 12 distinct layers can be found in the IPL. (Courtesy of W. Li and S.C. Massey.)

The mainstay of structure, function, and morphology studies is immunocytochemistry, which can be used to stain structural components, enzymes, neurotransmitters, synaptic proteins, and postsynaptic receptors (Fig. 17.5). Primary antibodies are currently available for many of these components. Secondary antibodies

conjugated to an ever-increasing variety of fluorochromes are readily available as standard reagents and allow for multiple staining. Single neurons can also be filled with fluorescent dyes via glass microelectrodes. Diffusible tracers such as Neurobiotin can be used to label a network of coupled cells.[5] The optic nerve can be back-filled with fluorescent dyes, which in one useful variant are concentrated in vacuoles that explode when excited to release dye, which diffuses throughout the dendritic structure of individual ganglion cells.[35] Certain ganglion cell types can be selectively labeled by stereotactically injecting a central target with retrograde tracers.[36] Individual neurons of all types can be randomly labeled with ballistic particles coated with fluorescent dyes or DNA to synthesize a specific marker.[37] Finally, there is increasing use of transgenic animals such as mice engineered to express green fluorescent protein (GFP) variants under the control of a specific promoter.[38]

Six Major Neuronal Cell Classes

The retina contains six major neuronal classes. Photoreceptors are located in the ONL and can be subdivided into rods and cones. Bipolar cells take the signals from photoreceptors and transmit them to the inner retina. Horizontal cells and amacrine cells are laterally extensive interneurons in the outer and inner retina, respectively. Ganglion cells receive input from bipolar and amacrine cells and form the output from the retina. In addition, interplexiform cells share many properties with amacrine cells but project back to the outer retina. Finally, the radially oriented Müller cells are the predominant glial cells (Table 17.2).

TABLE 17.2

Major Cell Types in the Retina

Neuronal Types	Role	Types
Photoreceptors	Rod and cones	2
Horizontal cells	Lateral interneurons, OPL	2
Bipolar cells	Vertical connection	10–12
Amacrine cells	Lateral interneurons, IPL	~30
Ganglion cells	Output neurons	~40
Interplexiform cells	Feedback, IPL to OPL	?

Total		~80

IPL, inner plexiform layer; OPL, outer plexiform layer.

Classification of Retinal Cells

Although the retina contains six major neuronal cell classes, these may be further divided into many distinct subtypes for a total of about 80 different neurons. Cells of a given type form nonrandom mosaics across the retina.[39] A single type shares essential morphologic features and uses the same neurotransmitter(s). Furthermore, they ramify at a characteristic depth in the retina and make stereotyped synaptic connections, including the same type and number of postsynaptic cells, and even the same number of synapses.[40,41] As we learn more about neuronal circuits and the functional anatomy, we see repeated patterns across the retina, and we are reminded that it is a two-dimensional array of recurring circuits.

The classification of retinal neurons, which dates back to the work of Cajal more than a century ago, is not a simple matter.[42] However, it is important that we are at least aware of all the major cell types in the retina. Even a basic understanding of a circuit cannot be achieved if critical parts are missing. Classification is complicated by the large number of different cell types, the low probability of obtaining rare types, variation in size with eccentricity, and the normal morphologic variation within a cell type. While the staining and sampling issues have largely been resolved by modern methods, the question of what constitutes a separate cell type, as opposed to subtle differences between examples from the same type, is still a problem. The resolution lies partly in understanding the significance of some morphologic features and partly in considering more variables, i.e., independent criteria to classify a specific cell type. Finally, as a kind of parity check, it is necessary to consider the properties of a whole population for a given cell type to see if it is consistent.

Neurons may be classified into unique cell types on the basis of several properties: (1) their morphology, meaning the size, shape, and complexity of their dendritic arbores; (2) the depth within the IPL that their dendrites ramify; (3) their electrophysiology,

particularly their excitatory and inhibitory inputs; (4) their biochemistry, particularly with regard to the different neurotransmitters used to communicate between neurons and structural proteins or receptors; (5) the pattern of connections with other neurons, which should be consistent for a unique cell type; and (6) the properties of the whole population for a specific cell type.

Photoreceptors

Cones

The mammalian retina contains two types of photoreceptor: rods and cones.[43] Rods account for 95% of all photoreceptors. They are numerous, with slender outer segments, densely packed and specialized for high sensitivity under dark or starlight conditions. Cones are larger, with tapering outer segments, and they are found in the top row of the ONL (Figs. 17.2 and 17.3). Cones make up only ~5% of photoreceptors[28,43] but they provide high-acuity color vision in daylight conditions when photons are abundant. This versatile combination of rods and cones and their associated circuits covers an intensity range of around 10 log units from the darkest night to bright sunlight.[44] While the average visual scene has a range of intensities covering 2–3 log units, the continual adaptation of retinal sensitivity slides this operating range through the entire range of light intensities. This is a critical function of the retina because outside the normal operating range we are functionally blind. Common examples include the inability to see momentarily when entering a dark cinema or driving into the setting sun. Much of the adaptation takes place in photoreceptors but, as we shall see below, this is accompanied by major changes in the neural pathways through the retina. This is arguably the most important function of the retina, after light detection itself.

There are approximately 5 million cones in the human retina and 190,000 in the mouse retina.[45,46] Cones make up approximately 5% of the total photoreceptors in humans, compared to 2.8% in the mouse,[47] so we are all rod-dominated in terms of absolute numbers. One exception is the ground squirrel, which is truly cone-dominated. Importantly, cones are not evenly distributed. In

human retina, there is a massive peak at the fovea (Fig. 17.3) where the density reaches around 200,000/mm^2, approximately 100 times the density in the periphery.[28,45] This is the region of maximum acuity, although the peak density slightly exceeds experimentally measured visual acuity due to blurring by the optics of the eye.[48–50] Where the ganglion cell axons gather to form the optic nerve there are no photoreceptors and their absence from this location is the cause of the blind spot (Fig. 17.3).

Cones support color vision and, in Old World primates and humans, there are three classes: blue, green, and red. They are maximally sensitive to 430, 530, and 561 nm light, respectively.[51–53] Other mammals, including cats, rabbits, and rodents, have an evolutionary ancient form of color vision based on green and blue cones only. The presence of red and green cone opsins in a tandem array on the X chromosome is thought to be due to a recent gene duplication and underlies the preponderance of color blindness among males.[54] Using adaptive optics to correct for blurring in the lens and cornea, the distribution of red, green, and blue cones can be mapped in the living human eye.[55] Surprisingly, the distribution of cones was random and clumpy (Fig. 17.6). In addition, there appears to be enormous variation in the red/green cone ratio among individuals with normal color vision.

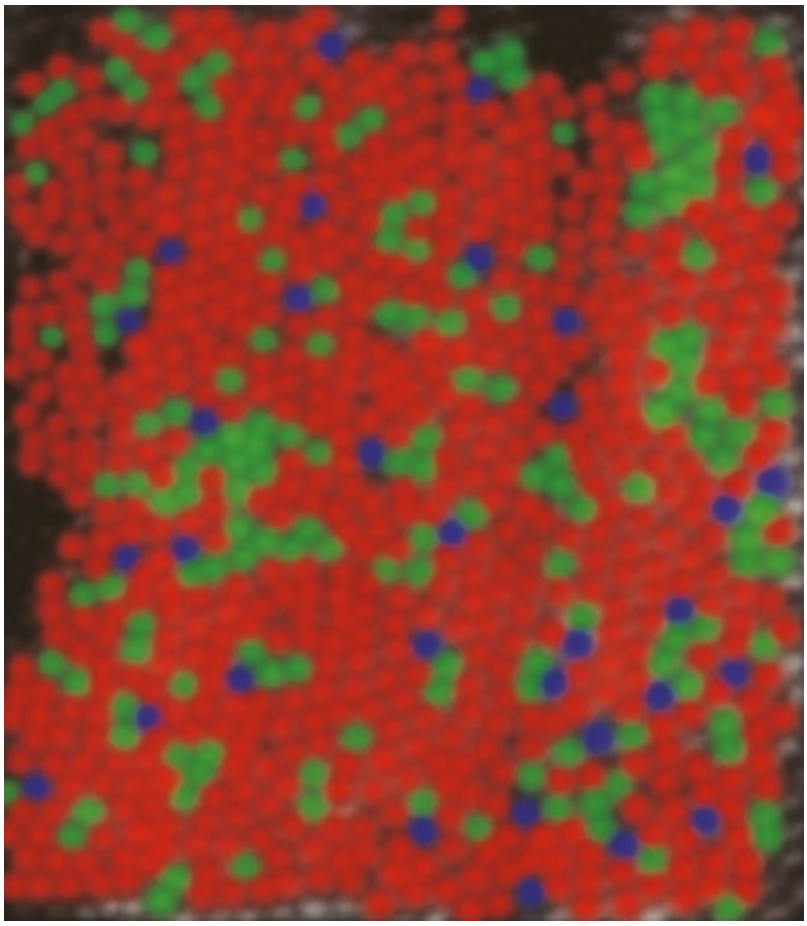

FIG. 17.6 The mosaic of red, green, and blue cones in the human retina. This image, taken from a human subject using adaptive optics, shows the distribution of the three cone classes. Blue cones make up a small fraction, <10%, but make a regular mosaic. Red and green cones have a clumpy, random distribution. In this subject, the red cones outnumber the green cones but this ratio is highly variable, even in subjects who have normal color vision. (Courtesy of Austin Roorda; after Roorda A, Williams DR. The arrangement of the three cone classes in the living human eye. Nature 1999;397:520–2.)

Blue cones are present as a minority: they make up approximately 10% of the cone population (Fig. 17.6). This is not enough to support high acuity but calculations show that the blue cone density is sufficient to support the reduced resolution caused by visual aberration at the blue end of the spectrum.[30] At the very center of the fovea, blue cones are absent.[28,56] The fact that this is not readily apparent is due to the relatively poor spatial acuity of color vision compared to the luminance-driven pathways.

Red and green cones cannot be differentiated morphologically and the red and green cone opsins are so closely related that they are also indistinguishable. However, blue cones can be mapped with a selective antibody against blue cone opsin[29,57] or by their selective accumulation of certain dyes.[56]

Rods

The ONL contains photoreceptor cell bodies, both rods and cones.[43] Even in the cone-dominated human retina, rods far outnumber cones, by a factor of 20 : 1, so they account for most of the ONL except at the fovea. The human retina contains approximately 100 million rods, and they pool signals to provide high sensitivity for dark-adapted vision, say starlight, which appears monochromatic. A lack of color vision is the hallmark of rod-mediated vision. Rods are absent within 350 μm of the fovea but reach a peak density in an annular region at about 20° eccentricity (Fig. 17.3). This does not match the area of maximum scotopic acuity, which occurs around 5°,[58] so it has been suggested that another component of the rod pathway, such as the AII amacrine cells, present at a much lower density, forms a bottleneck to limit acuity[59,60] (see below).

Cone Pedicles and Rod Spherules

Cones and rods make contact with bipolar and horizontal cells in the OPL. Cone axons descend through the massed ranks of rod somas in the ONL to terminate in a two-dimensional array of cone pedicles at the OPL (Fig. 17.7). Near the fovea in primate retinas, the cone axons are splayed out radially so that the pedicles form an annular array around the center (Fig. 17.7B). Cones form two specialized contacts, ribbon synapses and flat contacts, with postsynaptic neurons. Ribbon synapses are so named because of electron-dense structures at invaginations where they contact depolarizing (or ON) bipolar and horizontal cells (Fig. 17.8). Cone pedicles also make flat contacts along the base of the pedicle with hyperpolarizing (or OFF) bipolar cells. Rod axons also descend to form synapses with a single type of depolarizing bipolar cell as well as horizontal cells. The terminals of rods are called spherules, and, similar to cones, they use a ribbon synapse. In contrast to cones, there is only a single invagination in each, containing two rod

bipolar and two horizontal cell dendrites.

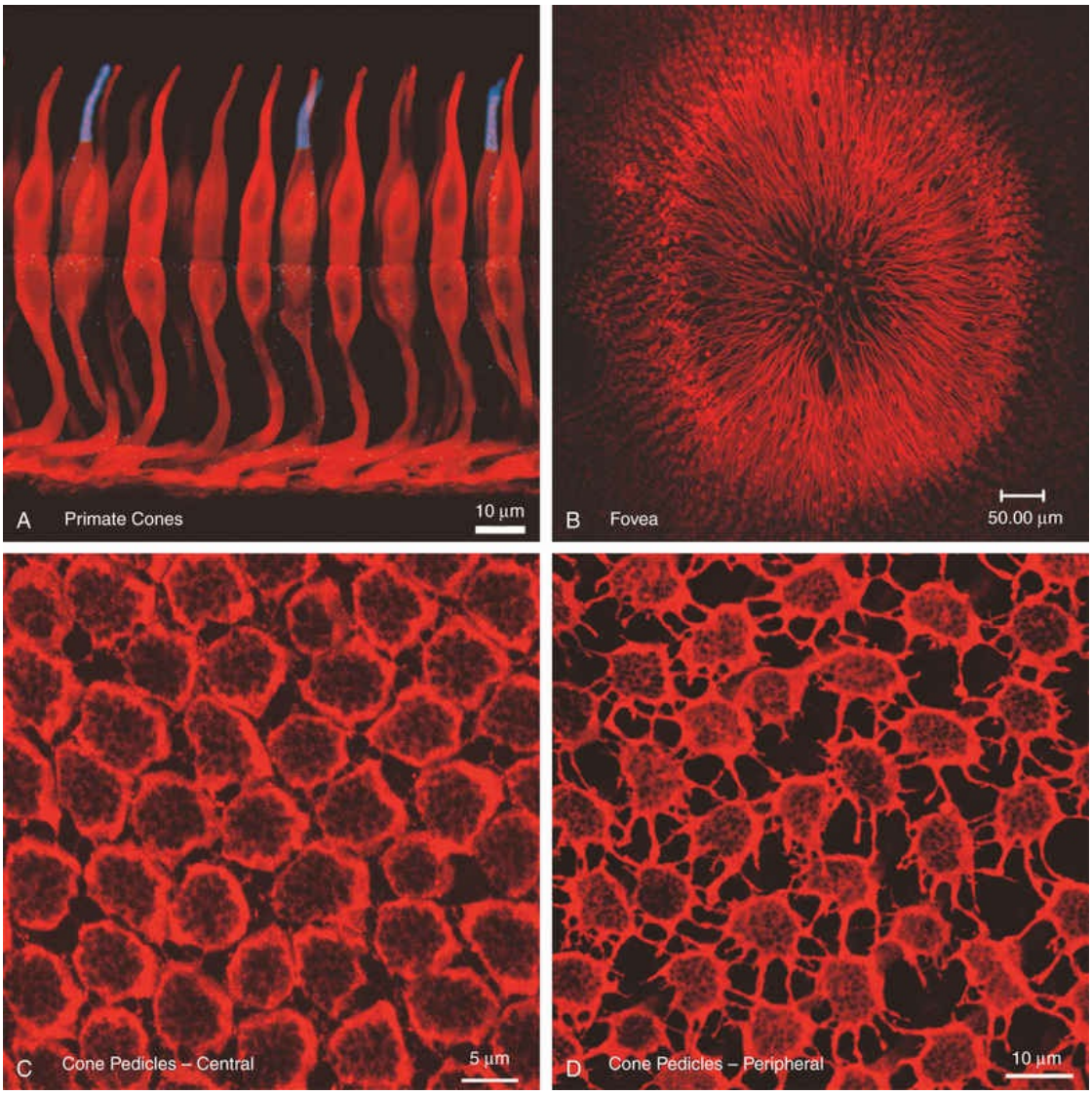

FIG. 17.7 Primate cones. (A) Vertical section of macaque retina shows cones stained with an antibody against cone arrestin. The outer segments of a few cones, <10%, have been double-labeled with an antibody against blue cone opsin. From each cone, an axon descends to the cone terminal or pedicle. (B) Whole-mount view shows how the axons run obliquely away from the fovea to terminate in an annulus of cone pedicles. (C) Close to the fovea, the cone pedicles form a tightly packed array connected by very fine telodendria. The dark regions within each pedicle are the invaginations penetrating from beneath. (D) More peripherally, the cone pedicles are widely spaced and connected by longer telodendria which are the sites of

cone-to-cone coupling. (Antibody donated by Peter MacLeish, images courtesy of J. O'Brien and S.C. Massey.)

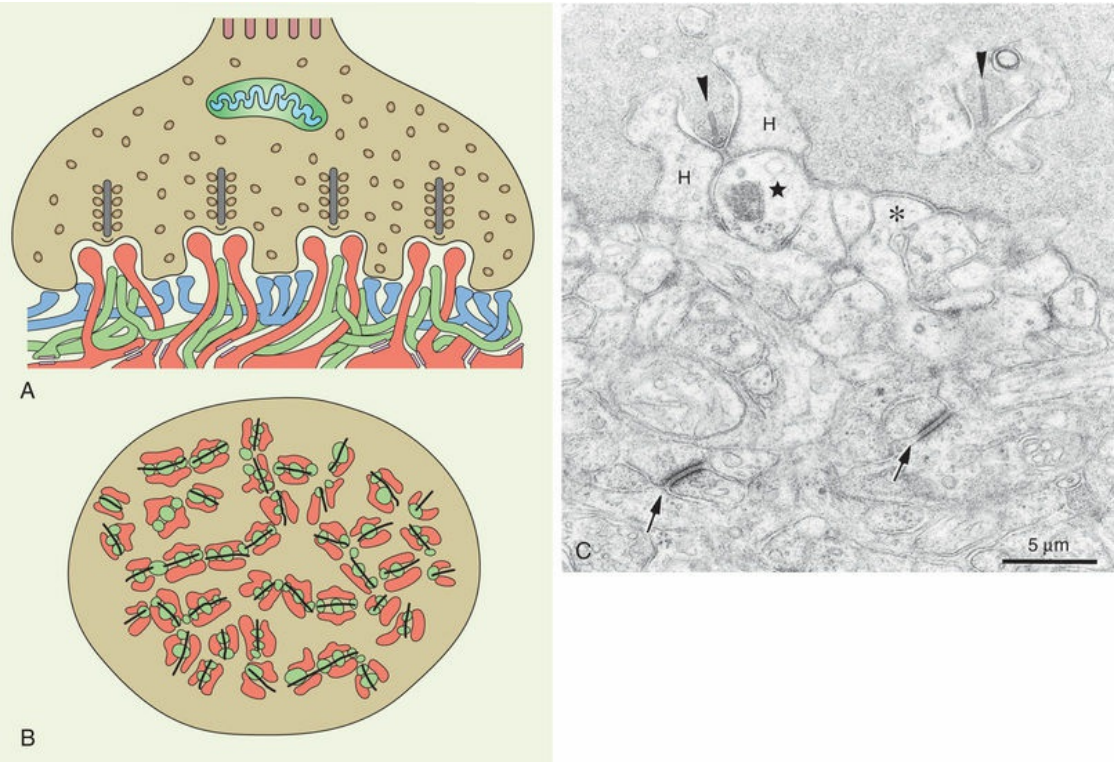

FIG. 17.8 Laminated postsynaptic structure of the cone pedicle. (A) Cross-section of a single cone pedicle contains synaptic ribbons and synaptic vesicles. Horizontal cell dendrites (red) invaginate the cone pedicle deeply and laterally. ON cone bipolar dendrites (green) assume a central position beneath the ribbon. (B) Whole-mount view, in the plane just below the multiple synaptic ribbons, shows the relative positions of horizontal and ON bipolar processes. The OFF bipolar contacts are beneath this plane of focus. (C) Electron microscopic view of a cone pedicle. *Arrowheads* mark synaptic ribbons. Horizontal cell processes (*H*) are lateral, ON bipolar dendrites (*star*) central. OFF bipolar cells (*asterisk*) form basal synapses away from the synaptic ribbon. Beneath each cone pedicle lies a snake's nest of postsynaptic processes. There are also specialized desmosome-like contacts of unknown function between horizontal cell processes (*small arrows*). (Reproduced with permission from Haverkamp S, Grunert V, Wassle H. The cone pedicle, a complex synapse in the

retina. Neuron 2000;27:85–95.)

Each cone pedicle is 6–8 μm in diameter and, near the fovea, contains 20 synaptic ribbons and, in the periphery, around 40.[61] Cones release glutamate constantly in the dark, and the synaptic ribbons are thought to support this high rate of release. As we will describe further below, the multiple ribbon and flat synapses on each cone pedicle form connections with many different types of bipolar cell.

A sense of the complexity of these synapses can be obtained by labeling some of the individual components. Antibodies reactive against a vesicle protein such as synaptophysin provide a way to label photoreceptor terminals in the OPL, because photoreceptor axon terminals are filled with vesicles. To visualize the synaptic ribbons, antibodies to kinesin II can be used. Finally, antibodies to the mGluR6 receptor, which is located on the dendritic tip of the depolarizing bipolar cells, mark one of the postsynaptic processes. When visualizing just the cone pedicle, there are a number of indentations or invaginations (Fig. 17.8). Within each invagination, horizontal cell dendrites are lateral and high, approaching the synaptic ribbons. ON cone bipolar cell processes are central but slightly lower at the synaptic ribbon. In contrast, OFF bipolar dendrites form basal synapses with the cone pedicle at a distinctly lower level. Staining a piece of retina for synaptophysin, kinesin II, and mGluR6 begins to show the complexity of the structures (Fig. 17.9). Rod spherules contain a single large horseshoe-shaped ribbon with two bipolar cell dendrites nestled within. The cones have numerous and slightly smaller ribbons with each also nestled against an mGluR6-labeled dendrite. What is not visible are the horizontal cell dendrites that also invaginate, but are slightly lower than the bipolar cells.

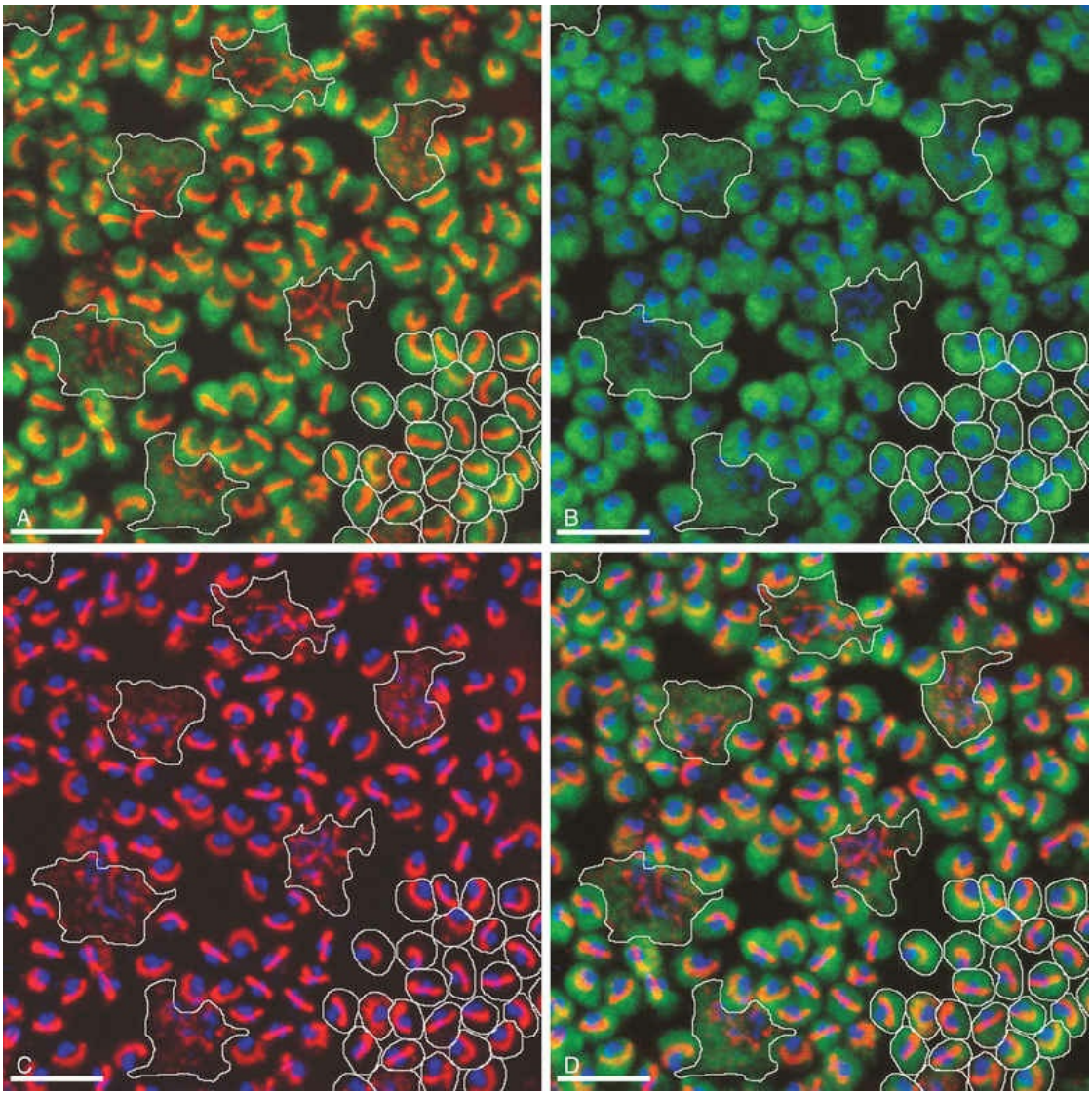

FIG. 17.9 Synaptic structure of rod spherules and cone pedicles. (A) The terminals of rods and cones are packed with synaptic vesicles and contain synaptic ribbons. An antibody against synaptophysin (green), a synaptic vesicle protein, labels rod spherules which appear round (some are outlined to the lower right) and cone pedicles which are polygonal (larger outlines). Each rod spherule contains a single large synaptic ribbon which is curved like a horseshoe, stained with an antibody against kinesin II (red). The cone pedicles contain a complex of smaller synaptic ribbons (also red). (B) The dendritic tips of rod bipolar and ON cone bipolar cells can be marked with an antibody against the glutamate receptor, mGluR6 (blue). The central invagination of each rod spherule contains a pair of mGluR6-positive rod bipolar dendrites. At each cone pedicle, there are a number of

finer ON bipolar dendrites. (C) The rod bipolar dendrites (blue) are nestled within the horseshoe formed by the synaptic ribbon (red) at each rod spherule. At the cone pedicles, the ON bipolar dendrites also approach closely to the cone synaptic ribbons. (D) A triple-label image showing rod spherules and cone pedicles (green, some outlined), synaptic ribbons (red) and the postsynaptic bipolar dendrites tagged for the glutamate receptor mGluR6 (blue). Scale bars = 10 μm. (Courtesy of W. Li and S.C. Massey.)

Around 10–12 cone bipolar cells plus multiple horizontal cell dendrites contact each cone, so under the pedicle there may be as many as 200 postsynaptic processes.[62] In fact, the cone pedicle may be the most complex synaptic structure in the brain. The distribution of postsynaptic processes under the cone pedicle is laminated in a stereotyped fashion (Fig. 17.8).[61,62]

The fundamental problem for rods is to detect a small brief hyperpolarization due to a single photon against a noisy background of thermal noise and the stochastic nature of transmitter release.[63,64] One strategy is to minimize background variation by maintaining a high sustained-release rate in the dark. The synaptic terminal of a rod, or rod spherule, is about 2 μm in diameter and contains a very large synaptic ribbon (Fig. 17.9), a specialization thought to be associated with a high rate of transmitter release. The spherule is packed with synaptic vesicles, containing the neurotransmitter glutamate, to support sustained transmitter release. There is a single invagination (imagine a closed fist and insert a finger between thumb and forefinger to make a pocket) containing a tetrad of processes, two from horizontal cells and two rod bipolar dendrites.[65] This structure brings the postsynaptic processes close to the release site and may prevent spillover to adjacent rods. These anatomic specializations appear to reduce variation in rod signaling so that small single-photon responses can be detected with high reliability.

Photoreceptor Coupling

While the synapses between photoreceptors and second-order neurons are extremely complex, there are still additional

connections between photoreceptors. These take the form of electrical coupling, mediated by gap junctions. Close to the fovea, the cone pedicles are densely packed, almost touching, and connected by very fine processes known as telodendria (Fig. 17.7C).[43] Rod terminals are either absent or displaced slightly higher, towards the outer segments, in this region. More peripherally, the cone pedicles are widely spaced and the telodendria are much more prominent (Fig. 17.7D). The contact points between telodendria of neighboring cones are the sites of connexin (Cx)36 gap junctions, which mediate electrical coupling between cones.[66,67] Recordings between neighboring cones also show that they are coupled.[66,68] This may seem puzzling at first because it should lead to a loss of acuity and blurring. However, the cone array actually oversamples the signal so this leads to little or no loss. Instead, the coupling is thought to reduce noise, which is random, while the light-driven signals, which are correlated between close neighbors, will be reinforcing. It has been calculated that this may improve the signal-to-noise ratio by 77% – a large gain for little loss.[69] Coupling between red/green cones is indiscriminate, which may reflect the close absorption curves of red and green cones.[68] Morphologically, blue cone pedicles are slightly smaller than those of red/green cones and they have only a few withered dendrites, which rarely touch neighboring cones.[70] Hence, blue cones are not coupled into the red/green network.[66,68] This may serve to preserve spectral information in the color pathways.

There are also gap junctions between cone pedicles and rods.[71] These allow rod signals to enter cones, and rod-mediated signals can be detected in second-order neurons that are thought to be connected exclusively to cones.[72] Responses with the signature of rod origin have also been recorded in primate cones.[73] Because rods far outnumber cones, the influence of many rods on a single cone may be substantial. It is now thought that rod–cone coupling forms an alternative rod-driven pathway that may be important at intermediate light intensities, in the mesopic range.[74,75] This influence may relate to the enhancement of cone electroretinogram (ERG) amplitudes in humans and mice by light adaptation, where the cone ERG gradually increases in amplitude following the onset of a steady adapting field.[76–79] Blocking gap junctions inhibits this

effect in the mouse retina. In the human, however, the adaptation dependence of these changes has a photopic (cone) signature. Rod–cone coupling also is very dynamic and influenced by circadian rhythms, increasing at night and decreasing during the day, due to the influence of dopamine.[80–82]

Photoreceptors Release Glutamate in the Dark

The first intracellular recordings from cones were surprising because they showed that photoreceptors hyperpolarize in response to light.[4] This means they are relatively depolarized and release their neurotransmitter, glutamate, in the dark. From the viewpoint of signal information, the sign of the photoreceptor response makes no logical difference; photoreceptors produce graded responses modulated around the mean light level. When a photon is absorbed, the visual pigment is activated and then a cascade of other biochemical events is triggered.[83] This is known as phototransduction and it leads to the closure of a cGMP-gated cation channel in the cell membrane to produce hyperpolarization and a reduction in the release of glutamate.[84] The postsynaptic responses to light are in fact due to a decrease of glutamate release. Thus, glutamate uptake also plays a key role in retinal neurotransmission because the clearance of glutamate must be rapid to provide a fast postsynaptic response to light.[85] The hyperpolarizing light response of photoreceptors is now well established and it is supported by studies of vesicle turnover, which is much higher in the dark.[86] Furthermore, synaptic blocking studies produce the appropriate responses in the different second-order neurons and there is a stereotyped array of distinct glutamate receptors associated with specific cell types. Glutamate, with its library of postsynaptic receptors, seems particularly suitable to orchestrate the large variety of postsynaptic responses at the cone pedicle.

Rods operate in a manner essentially similar to cones: they hyperpolarize in response to light increases, albeit there are many molecular differences. However, everything about the rod pathway in the retina is designed for maximum sensitivity. This is reflected in the anatomic details and synaptic connections of rods.[64] Rods can respond to single photons, obviously the design limit, with a binary

(all or nothing) signal, but visual threshold requires a signal in 5–10 rods. Depending on the species, about 20–100 rods converge on to a single rod bipolar cell[87,88] and this high convergence also contributes to the high sensitivity of the rod pathway. If 100 rods converge to a single rod bipolar cell and 100 rod bipolar cells converge to a ganglion cell, then the absolute threshold for vision is determined by the product, approximately 1 photoisomerization per 10,000 rods.

Second-Order Neurons: Horizontal and Bipolar Cells

Rods and cones make synaptic connections with bipolar and horizontal cells. Horizontal cells are laterally extensive interneurons located in the outer row of the INL, adjacent to the OPL. They respond to diffuse light with a large hyperpolarization. This is the same as cones so we say that the input is sign-conserving. It appears to be mediated by excitatory glutamate receptors of the AMPA subtype, which have been located on horizontal cell dendrites.[89,90] In most mammals there are two morphologic types of horizontal cell, but only one in rodents.[91–93] In all species, horizontal cells are extensively coupled, which dramatically increases the size of the receptive field. In Fig. 17.10 the entire A-type horizontal cell network in the rabbit retina has been labeled by injecting several cells with a diffusible tracer, Neurobiotin, which readily passes through gap junctions.[94] A-type horizontal cells are axonless and have a large irregular shape, giving rise to many fine terminals that contact every cone pedicle within the dendritic field. A high-resolution image shows how fine horizontal cell dendrites converge at cone terminals while ignoring the numerous rod spherules (Fig. 17.10). The cone terminals were marked by the labeling of two different glutamate receptors, GluR5, which marks the basal contacts of certain OFF bipolar cells,[95] and mGluR6, which is expressed by ON cone bipolar cells[17,96] (see below). It should be noted that the three labels are nonoverlapping at the cone terminal, consistent with the presence of three separate neurons, horizontal cells, ON cone bipolar cells, and OFF cone bipolar cells, which all converge independently at the cone pedicles (Fig. 17.10).[62]

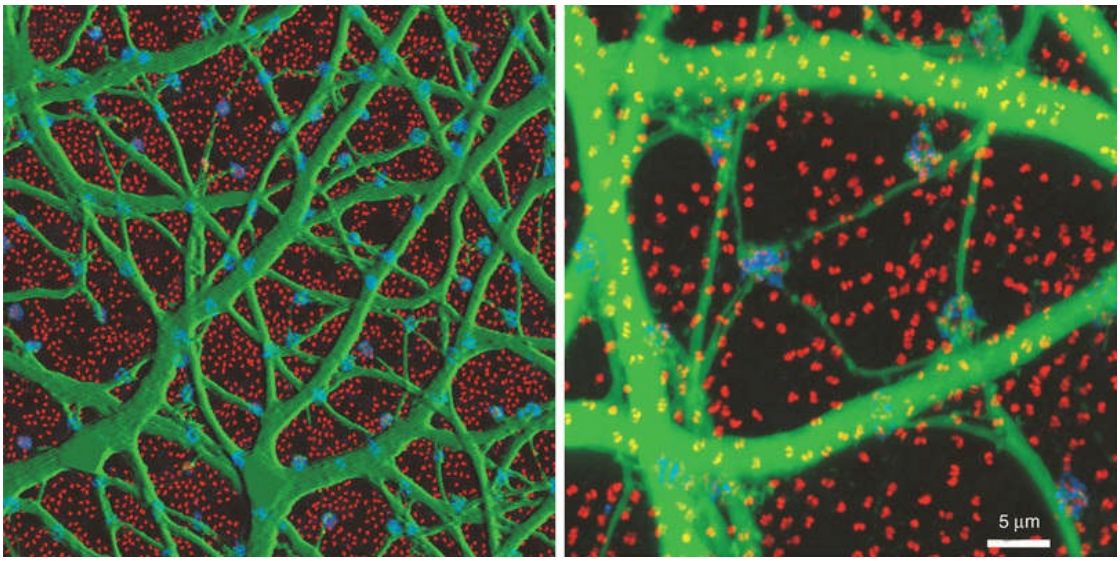

FIG. 17.10 A-type horizontal cells in the rabbit retina. The coupled matrix of A-type horizontal cells following the intracellular injection of Neurobiotin (green) in the rabbit retina and the rod/cone mosaic is shown by labeling postsynaptic glutamate receptors, GluR5 (blue) and mGluR6 (red). The A-type horizontal cells contact every cone in the frame. The high-resolution images (right) show that the fine horizontal cell dendrites (green) converge at individual cone pedicles. The green, red, and blue labels are not colocalized. They label independent neuronal structures: horizontal cells, ON bipolar cells, and OFF bipolar cells, respectively. (Courtesy of F. Pan and S.C. Massey.)

B-type horizontal cells in the rabbit retina are smaller and radially symmetrical (Fig. 17.11). While the somatic dendrites of the B-type horizontal cell also contact cones, each cell gives rise to a long axon that meanders randomly before branching into an elaborate terminal structure (Fig. 17.11C).[94] The electrotonic length of the axon was thought to isolate the somatic region from the axon terminal whose branches contact rods instead of cones,[97] but there is now evidence that at high light levels rods may play a role by acting as relays to transmit horizontal cell surround information to cones.[98] B-type horizontal cells are also coupled by gap junctions and so are the axon terminals (Fig. 17.11B).[94,99–101] For both types of horizontal cell, as the cell density falls with eccentricity, the dendritic field size increases so that an even coverage of 6–8 is maintained across the retina. B-type horizontal cells are always

smaller and more numerous – two to three times the A-type density.[94]

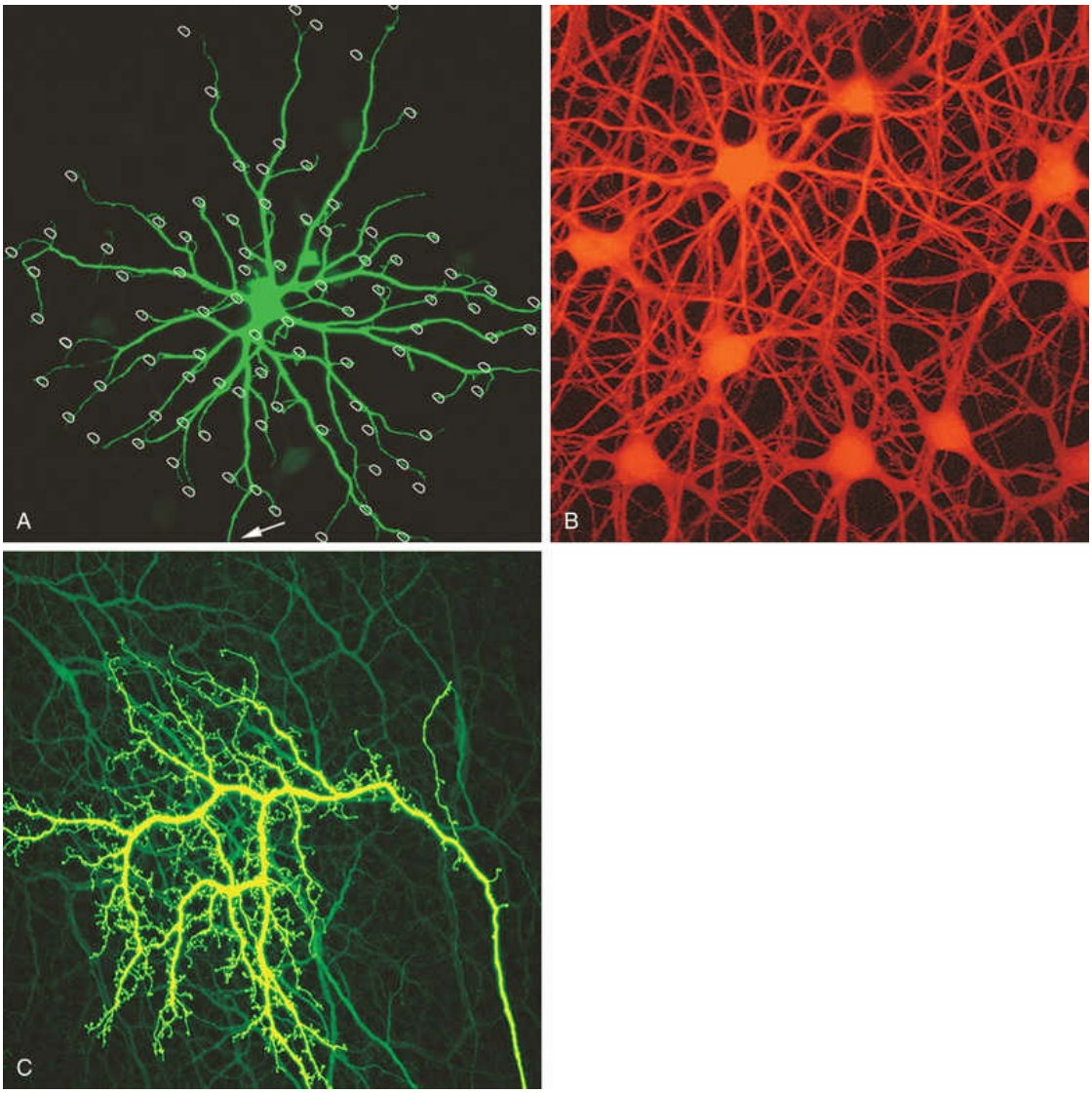

FIG. 17.11 B-type horizontal cells in the rabbit retina. (A) A single B-type horizontal cell filled with Lucifer Yellow contacts all the cone pedicles (white outlines) within its dendritic field. *Arrow* shows the axon leaving the frame. (B) When B-type horizontal cells are filled with Neurobiotin, the coupled network is revealed. (C) Fine details of the elaborate axon terminal of a B-type horizontal cell. Each terminal varicosity contacts a rod spherule. (Panel A, courtesy of W. Li and S.C. Massey; panels B and C, reproduced with permission from Mills SL, Massey SC. A series of biotinylated tracers distinguishes three types of gap junction in retina. J Neurosci 2000;20:8629–36.)

In primates, there are also two kinds of horizontal cell, both axon-bearing, but the H2 only contacts cones and the axon is not well developed.[102] H1 is a large, well-coupled cell that contacts all red/green cones but not blue cones.[103] H2 has a smaller soma and finer dendrites that make sparse contacts with red/green cones but densely innervate blue cone pedicles.[103] Recording from both horizontal cell types shows that they receive sign-conserving inputs from both red and green cones (plus blue for H2).[103] The wiring of the H2 horizontal cell suggests it plays a role in blue/yellow (red+green) processing.

In central retina, there are four times as many H1s as H2s, decreasing to twice as many in peripheral retina.[104] Increasing size with eccentricity compensates for decreasing density so coverage for both types is 3–5 evenly across most of the retina. The peak density for H1 horizontal cells reaches about 18,000/mm^2 near the fovea. This is an order of magnitude higher than rabbit retina. Packer and Dacey[105] have recorded from many primate H1 cells and they make the interesting observation that central cells are not only smaller but less coupled, perhaps because they overlap less. Thus, the H1 receptive field in the fovea may be small enough, 20–30 μm, to match the receptive field surround of midget ganglion cells.

Horizontal cells are extensively coupled by gap junctions and their molecular identity has been determined for many species. In the rabbit retina, the gap junctions between A-type horizontal cells are labeled with an antibody against Cx50 at many contact points in the matrix (Fig. 17.12).[106] Some of the gap junction plaques are very large and the unitary conductance of Cx50 channels is also high. This explains why A-type horizontal cells form an electrical syncytium. B-type horizontal cells are not labeled for Cx50. These gap junctions have different properties so they are likely to be assembled from different connexins. In rodents, there is only one type of axon-bearing horizontal cell.[107] In a Cx57 knockout mouse, these cells are no longer coupled.[108] This suggests that multiple neuronal connexins are present in the retina and that Cx57 gap junctions may be responsible for coupling in axon-bearing horizontal cells. The situation in the primate retina is still unknown but future progress should make it possible to test theories concerning horizontal cell coupling.

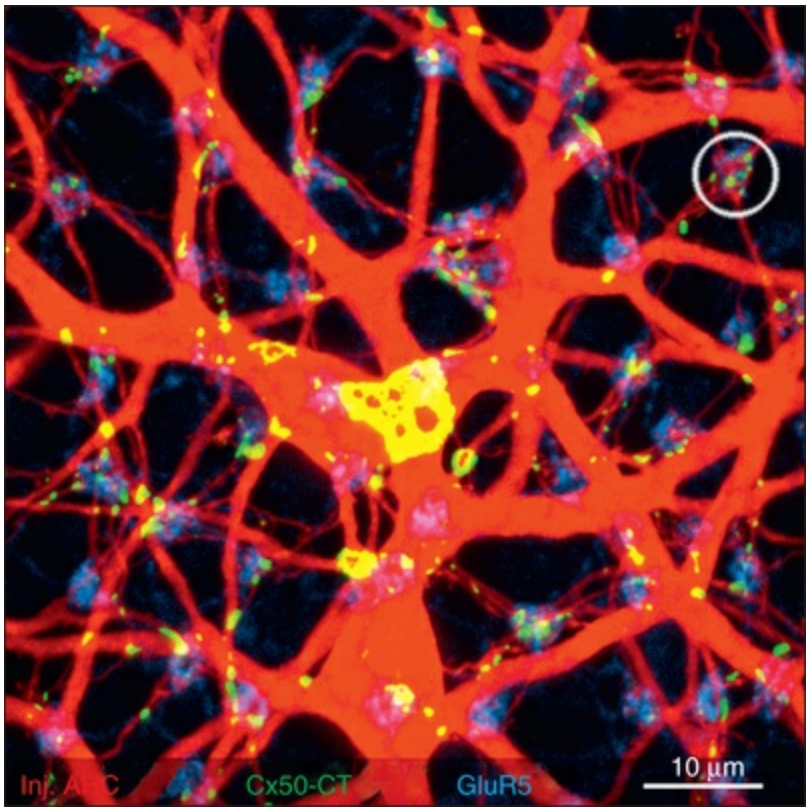

FIG. 17.12 Gap junctions between A-type horizontal cells. A-type horizontal cells are extensively coupled, as observed following Neurobiotin injection (red). An antibody against connexin 50 (green) labels gap junctions in the matrix of A-type horizontal cells. Some large plaques are located at the crossing of two major dendrites (yellow). The background mosaic of cone pedicles is marked by GluR5 labeling (blue). (Reproduced with permission from O'Brien JJ, Li W, Pan F, et al. Coupling between A-type horizontal cells is mediated by connexin 50 gap junctions in the rabbit retina. J Neurosci 2006;26:11624–36.)

Horizontal Cell Function

There is general consensus that horizontal cells provide negative-feedback signals to cones and rods. This can be seen when a full field light flash, which hyperpolarizes photoreceptors and reduces their glutamate release. This causes a sustained hyperpolarization in the horizontal cells, which rest at a relative depolarized membrane potential in the dark. Upon hyperpolarization, horizontal cells send a feedback signal to the photoreceptors that shifts the activation function of their calcium channels to more

negative potentials increasing their calcium current and their glutamate release.[109] This is a sign-inverting signal and forms the basis for the antagonistic center/surround receptive field of bipolar cells.

The Feedback Mechanism

The mechanism responsible for horizontal cell feedback to cones has been hotly debated for the past two decades. Initially it was proposed that horizontal cell feedback to photoreceptors utilized a GABAergic mechanism.[110–112] This hypothesis was based on the observations that horizontal cells synthesize and release GABA[89,113–116] and that photoreceptors express $GABA_A$ receptors.[111,117–120] More recently, results indicate that mammalian horizontal cells release GABA via a vesicular mechanism,[121–123] although pharmacologic manipulation of GABA input has yielded conflicting results.[109,124–127] It may be that GABA modulates the strength of the negative feedback signal by acting on cones and horizontal cell GABA receptors, but is not the basic feedback signal.[128,129]

Both an ephaptic[125,130] and a pH-based mechanism[126] for this feedback pathway have been proposed. The ephaptic feedback mechanism is a purely electrical signal, mediated via connexin hemichannels found at the tips of the horizontal cell dendrites that invaginate at the cone synaptic terminal (Fig. 17.13). The connexin hemichannels act as large nonselective ion-channels and current flows through them into the resting (~ −40 mV) horizontal cell in the dark. Through the feedback pathway photoreceptors sense this as a local depolarization. Horizontal cell hyperpolarization to light increases the current through the hemichannels and the extracellular space, producing an even larger local depolarization in the photoreceptor near their calcium channels. As described above, this leads to an increase in calcium current and glutamate release. A role for hemichannels in this process is supported by pharmacologic and genetic manipulations.[131,132]

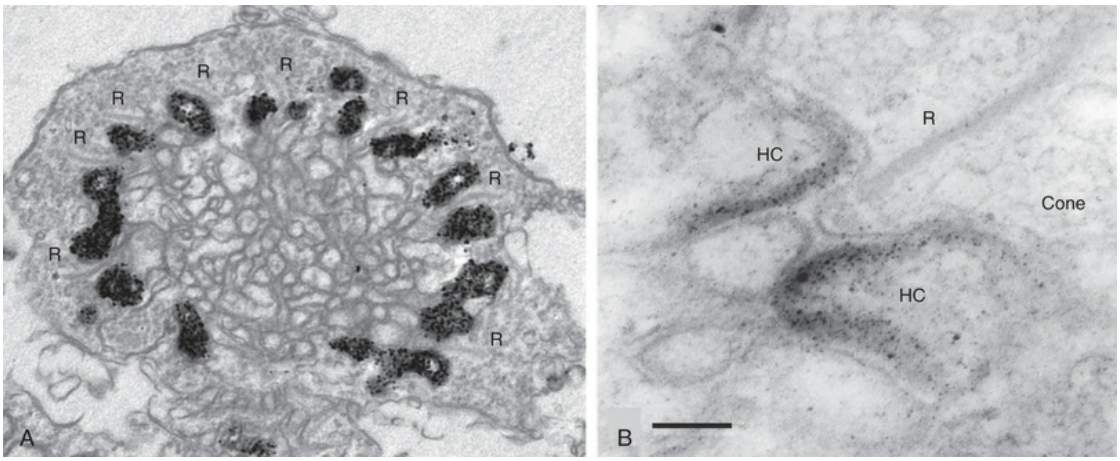

FIG. 17.13 General organization of the cone synaptic terminal. (A) Electron microscopic image of the zebrafish cone synaptic complex, with characteristic synaptic ribbons (*R*) and deep invaginations. The black staining is present in horizontal cell dendrites which terminate close to the synaptic ribbons. Labeling was performed with a GFP antibody in a transgenic zebrafish expressing GFP via the Cx55.5 promoter in horizontal cells. (B) Electron microscopic image of synaptic triad in goldfish showing the location of connexin hemichannels. The membrane of the tips of horizontal cell (*HC*) dendrites, close to the synaptic ribbon (*R*), are stained with an antibody against Cx26.
(Modified from Kamermans et al. Science 2001:292:1178-1180.)

The pH-based feedback mechanism also has considerable experimental support. Here acidification of the extracellular space inhibits photoreceptor calcium channels[133] and feedback is modulated by altering the pH in the synaptic cleft, which modulates the calcium current.[126,134] The mechanism for the pH modulation was highly unexpected and involves release of ATP into the synaptic cleft via pannexin-1 channels located close to the connexin hemichannels at the tips of the horizontal cell dendrites. The ATP is hydrolyzed by the ecto-ATPase NTPDase1 and ADA into inosine, which generates protons and phosphate groups. This forms a pH buffer with a pKa of 7.2, which acidifies the synaptic cleft,[134] and has been directly measured.[135] Light-induced hyperpolarization of horizontal cells leads to a closure of pannexin channels at the tips of the horizontal cell dendrites, reduction of ATP release, leading to a reduction of the pH buffer and producing

a slow alkalization in the synaptic cleft. This disinhibits the photoreceptor calcium current and increases glutamate release from cones.

Recent evidence indicates that both ephaptic and pH mechanisms may function in parallel[134] and that the feedback signal consists of these two components with differing kinetics: a superfast component provided by the ephaptic mechanism and a slow component provided that is ATP/pH mechanism.[134] Layered on this is modulation by GABA, which acts to suppress feedback in the dark-adapted retina.[128,136–138] Because both horizontal and bipolar cells express GABA receptors,[139–141] horizontal cells may use feedforward GABAergic signaling to bipolar cells as well.[142]

Horizontal Cell Function

An important question is why horizontal cell feedback to cones requires two different mechanisms? To answer this question, we have to consider how horizontal cells contribute to visual signaling. As pointed out by Sterling, reading high-contrast images in bright artificial light is one thing,[143] but in the natural scenes in the outside world visual objects often have very low contrast compared to their background. Here what is needed is a way to subtract the common background (which has little information) and amplify the remaining signal to enhance the visibility of small, low-contrast details.

At least in part, this role is accomplished by horizontal cells in the outer retina. Horizontal cells have large receptive fields and are well suited to estimate mean luminance of a scene. This information is fed back to photoreceptors in the negative feedback described above so that the photoreceptor output can signal local deviations in light intensity. Because our eyes are always moving we need to consider how to extract small, low-contrast details moving against the background. When horizontal cell feedback is slow, the receptive field surround it creates should lag temporally behind the center response in bipolar cells. This will create blur. However, with an added superfast ephaptic feedback this should not happen. What about the function of the slow pH mechanism? Responses of neurons become more and more transient when going from the

outer retina to the inner retina. This transience represents temporal redundancy reduction. The essence of a mechanism that reduces temporal redundancy is that it is slow. The ATP/pH system fulfills those requirements.

Horizontal cells also have an impact on color vision, because they are connected to more than one cone type. This means that the feedback signal cones receive will have a different spectral sensitivity than the spectral sensitivity of the cones themselves.[144] The consequence is far reaching. It means that the brain never has access to pure cone signals. The signals will always be modified by horizontal cell action and thus by the other spectral cone types. The output of a cone will depend on the spectral composition of the global illumination. Why would this be an advantage? It has been proposed that these chromatic interactions at the photoreceptor/horizontal cell level lead to phenomena like "color constancy" and "color induction."[145,146]

Bipolar Cell Function

Bipolar cells receive input from photoreceptors and then conduct the visual signal to the inner retina. They are excitatory interneurons, using glutamate as a neurotransmitter, specialized for sustained transmitter release, with terminals containing synaptic ribbons, similar to those of photoreceptors, only smaller. There are approximately 9–12 kinds of cone bipolar cell in the mammalian species that have been studied thoroughly, i.e., primates, rabbits, cats, rats, and mice (Fig. 17.14).[12,147–153] In contrast to the cone bipolar cells, there is only one type of rod bipolar cell, which is morphologically and physiologically distinct from the cone bipolar cells. Rod bipolar cells are numerous – three times the density of any diffuse cone bipolar type. However, there are around 10 types of cone bipolar cell so, in total, they outnumber the rod bipolar cells by a factor of three to four.

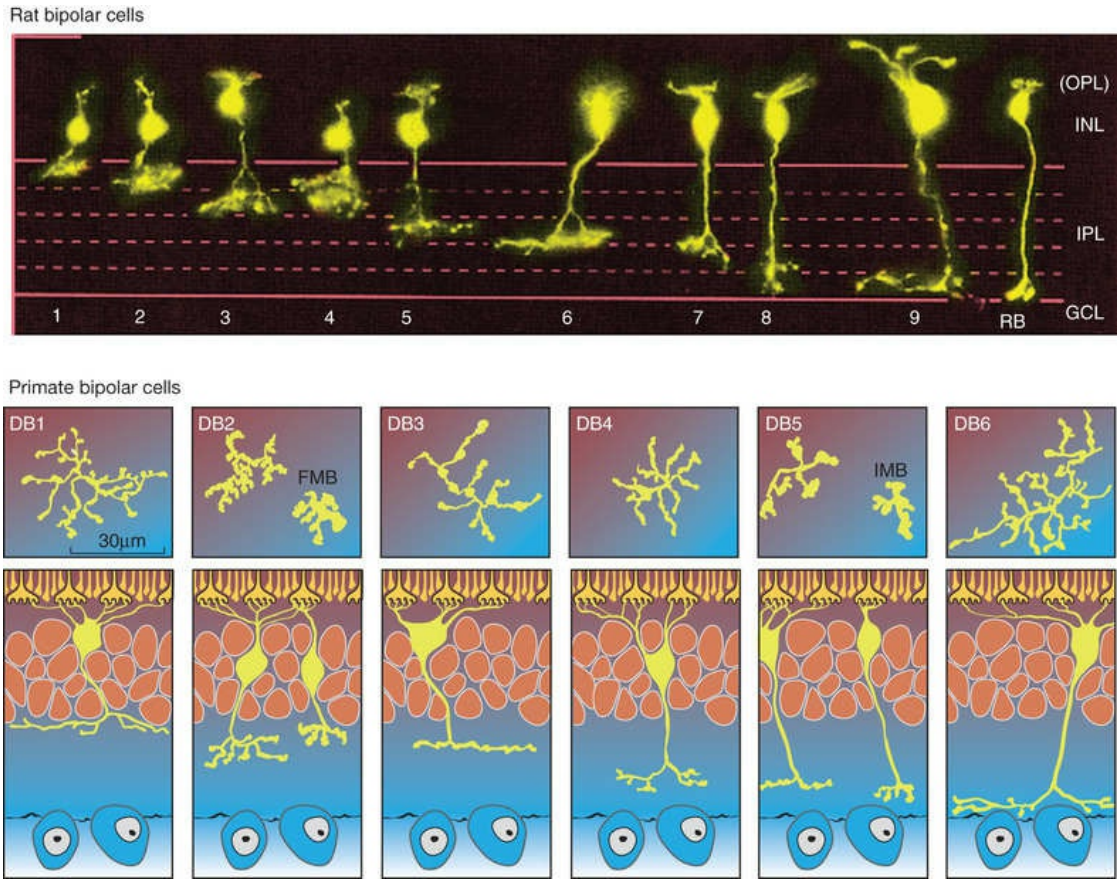

FIG. 17.14 Bipolar cells. Top: Lucifer Yellow-filled examples of bipolar cell types in the rat retina. Bottom: Drawings of Golgi-impregnated bipolar cells from the primate retina. Note the presence of midget bipolar cells in the primate retina. In both species, it may be observed that the main difference between cell types is the depth of stratification in the inner plexiform layer. OFF bipolar cells terminate in sublamina a and ON bipolar cells stratify at a deeper level, in sublamina b. *OPL*, outer plexiform layer; *INL*, inner nuclear layer; *IPL*, inner plexiform layer; *GCL*, ganglion cell layer; *RB*, rod bipolar cells; *FMB*, flat midget bipolar; *IMB*, invaginating midget bipolar. (Top panel, reproduced with permission from Harveit E. Functional organization of cone bipolar cells in the rat retina. J Neurophysiol 1997;77:1716–30, with permission from the authors and the American Physiological Society. Bottom panel, reproduced with permission from Boycott BB, Wassle H. Morphological classification of bipolar cells of the primate retina. Eur J Neurosci 1991;3:1069–88.)

Cone bipolar cells are difficult to identify in a retinal slice preparation. Once filled with a tracer they can be distinguished by the locations of their somas in the INL, by the morphology of their

dendritic and axon terminals, and by the depth of termination in the IPL. An increasing number of selective antibodies are now available to aid in the identification of specific cone bipolar cells.[133–136] In addition, several transgenic reporter mouse lines that mark specific types of bipolar cells have been created.[154–156]

There is a major functional division in the cone pathway that arises at the first synapse and is preserved in all higher visual centers. The retina is divided into ON and OFF channels served by ON and OFF cone bipolar cells (Fig. 17.14). The ON pathway is optimized to detect increases in intensity and the OFF pathway decreases in intensity. Reflecting the importance of depth in the retina, these two types of bipolar cells terminate at different levels in the IPL. OFF bipolar cells ramify in the top half, sublamina a, where they synapse with OFF ganglion cells. ON bipolar cells descend further in the IPL to sublamina b, where they synapse with ON ganglion cells. ON and OFF bipolar cells produce opposite signals in response to changes in light intensity. But how is this achieved if both bipolar types contact the same cones? The short answer is via different postsynaptic receptors and, indeed, glutamate produces opposing responses in ON and OFF bipolar cells.[15,157,158] This simple trick, dividing the cone signal into ON and OFF components, is thought to double the dynamic range of the retina. Half the bipolar cells carry signals greater than the local mean and the other half dimmer than the average.

OFF Cone Bipolar Cells

The dendrites of OFF bipolar cells branch in the OPL and contact every cone within the dendritic field at basal synapses (Fig. 17.15). OFF bipolar cells, like cones themselves, are hyperpolarized by light. So these are sign-conserving excitatory synapses, shown by a + in Fig. 17.15A, served by ionotropic glutamate receptors, i.e., conventional glutamate receptors of the AMPA/kainate type.[159–161] Thus, the dark release of glutamate from cones holds OFF bipolar cells at a relatively depolarized potential and the reduction of glutamate release in response to light produces a hyperpolarization in OFF bipolar cells. In this regard, the photoreceptor/OFF bipolar cell synapse is similar to the photoreceptor/horizontal cell synapse.

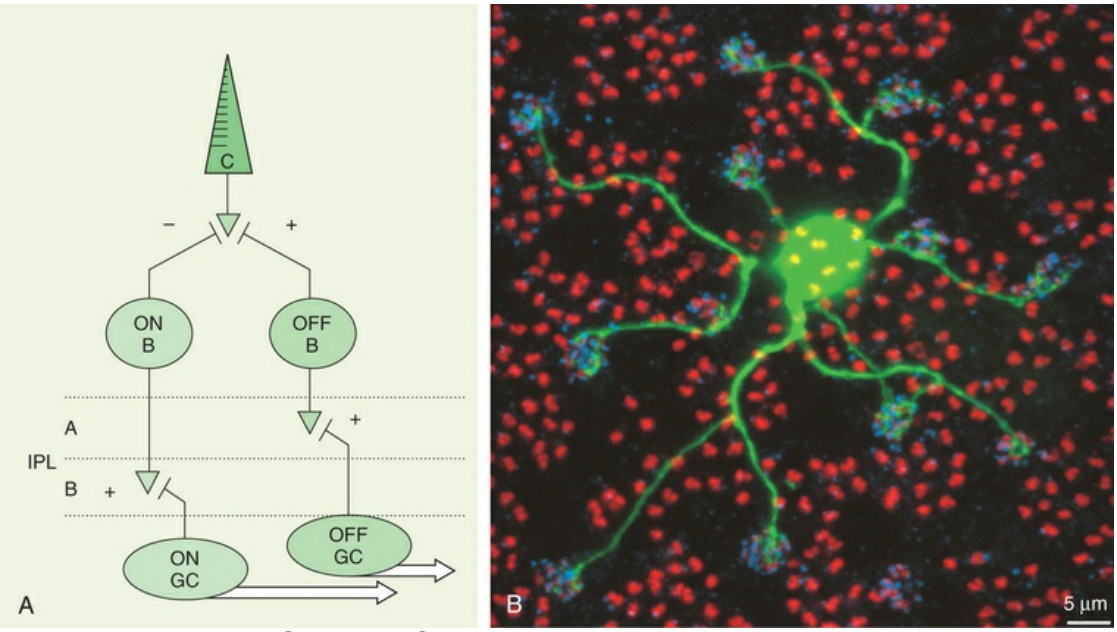

FIG. 17.15 ON and OFF pathways. (A) The opposite responses of ON and OFF cone bipolar cells are generated by the expression of different glutamate receptors. OFF bipolar cells are depolarized by glutamate, the photoreceptor transmitter, hence the + for a sign-conserving synapse. ON bipolar cells are hyperpolarized by glutamate, hence the − for a sign-inverting synapse. This unusual receptor is called the mGluR6 receptor. It is selectively activated by the glutamate analog 2-amino-4-phosphonobutyrate, and it is responsible for the separation of ON and OFF signals through the visual system. Furthermore, the inner retina is functionally stratified. OFF bipolar cells ramify in sublamina a and ON bipolar cells descend to sublamina b. Both bipolar cell types use glutamate and they make excitatory synapses with amacrine and ganglion cells. *IPL*, inner plexiform layer; *GC*, ganglion cell. (B) The image shows an OFF bipolar cell that was filled with Lucifer Yellow (green). In whole mount, with the focus at the outer plexiform layer, fine dendrites extend to contact every cone within the dendritic field. The positions of rod and cone terminals are marked with a combination of glutamate receptor antibodies mGluR6 (red) and GluR5 (blue). (Panel B reproduced with permission from Li W, Keung JW, Massey SC. Direct synaptic connections between rods and OFF cone bipolar cells in the rabbit retina. J Comp Neurol 2004;474:1–12, with permission of the authors and Wiley-Liss, a subsidiary of John Wiley.)

Recordings from cone and OFF bipolar cell pairs in the ground squirrel, which has very large cones particularly suitable for recordings, has shown that three different OFF bipolar cells use three different glutamate receptors – one AMPA receptor and two kainate receptors (Fig. 17.16).[159] These receptors have different affinities for glutamate and kinetics of activation, desensitization, and deactivation and therefore generate synaptic conductances that vary in time course: fast AMPA receptors are well suited to convey transient signals, while the slower kainate receptors may transmit sustained responses.[159] In ground squirrel retina, OFF cone bipolar cell response properties dovetail very well with the differential distribution of glutamate receptors at the cone pedicle complex, and therefore, ionotropic glutamate receptor expression has been suggested to contribute to the separation of cone signals into different temporal processing channels that encode different bandwidths of the cone signal.[90,95,162] All three OFF bipolar types terminate in sublamina a, as expected, but each one branches at a different depth within the OFF sublamina (Fig. 17.16). Thus, the division of the visual signal into different channels, for delivery to different addresses in the IPL, begins at the first synapse in the retina.

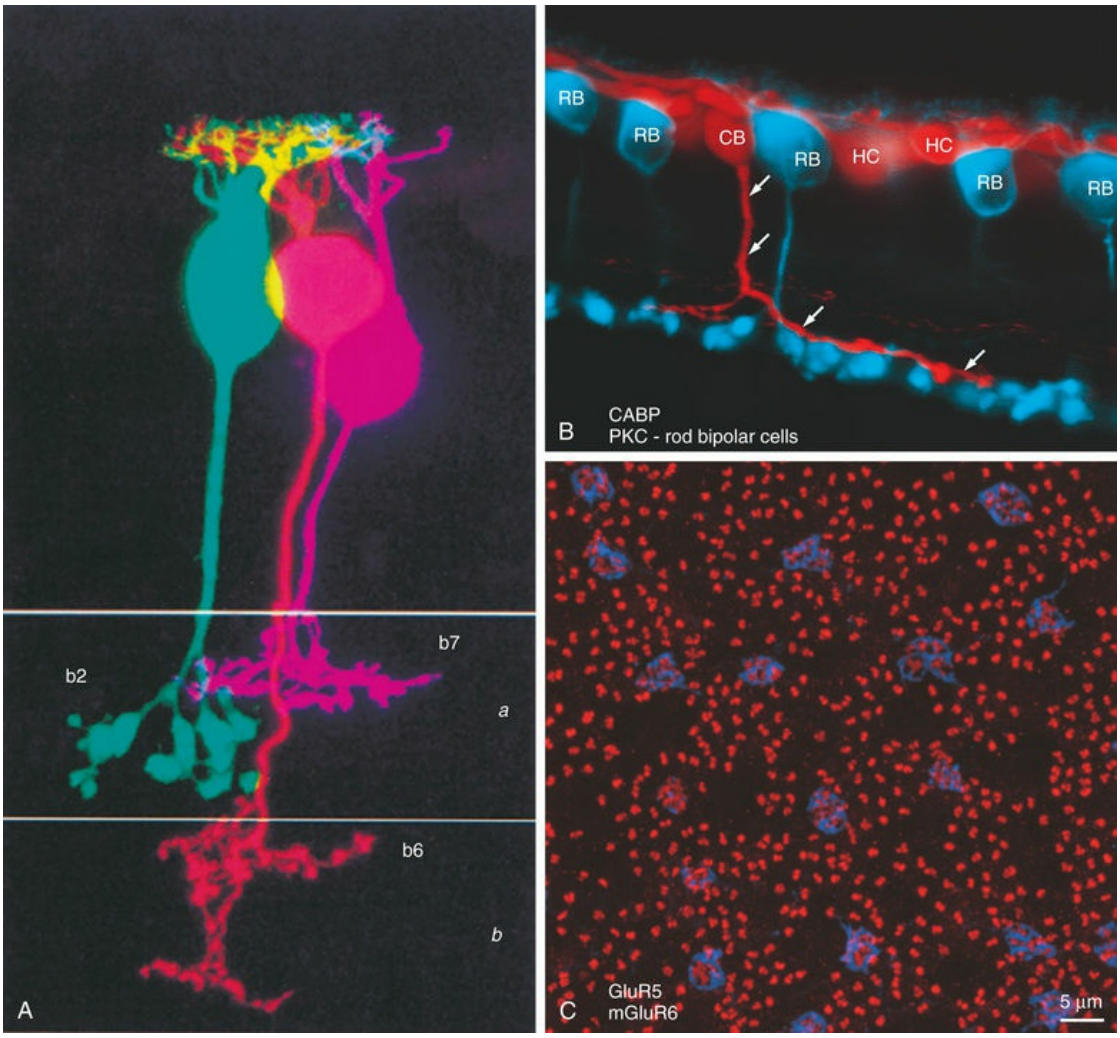

FIG. 17.16 Different OFF bipolar cells and rod/cone mosaic. (A) Three bipolar cells from the ground squirrel filled with different-colored dyes. The two OFF bipolar cells have responses mediated by different classes of glutamate receptor and they stratify at different levels, or addresses, in the inner plexiform layer. (B) A single ON bipolar cell type in the rabbit retina stained for the calcium-binding protein (CABP) calbindin (red). For comparison, the more numerous rod bipolar cells are stained for protein kinase C (PKC) (blue). The calbindin bipolar cell (*CB*) has an axon that descends to sublamina b where it is narrowly stratified just above the rod bipolar terminals (*RB*). This is a different address in the inner plexiform layer. In the outer plexiform layer, horizontal cells (*HC*) are also stained for calbindin. (C) Staining for mGluR6 receptors (red) mark the tips of rod bipolar cells where they enter the rod spherule. A small cluster of ON cone bipolar dendrites is also lightly marked at each cone pedicle.

GluR5 receptors (blue) mark OFF bipolar cell basal contacts at each cone pedicle. (Panel A, reproduced with permission from DeVries Sh. Bipolar cells use kainite and AMPA receptors to filter visual information into separate channels. Neuron 2000;28:847–56. Panel B, reproduced with permission from Massey SC, Mills SL. A calbindin-immunoreactions cone bipolar cell type in the rabbit retina. J Comp Neurol 1996;366:15–33, with permission of the authors and Wiley-Liss, a subsidiary of John Wiley. Panel C, courtesy of F Pan and SC Massey.)

Differences in the temporal features of bipolar cell responses have been observed in a number of species,[160,163–165] but recent studies of OFF bipolar cells in mouse and primate, however, indicate that transmission at cone→OFF bipolar cell synapses is mediated exclusively by kainate receptors.[160,161] Therefore, the different temporal kinetics of different OFF bipolar cells in these two species, unlike the ground squirrel, must be generated via circuit mechanisms.

ON Cone Bipolar Cells

The dendrites of ON bipolar cells invaginate into the cone pedicle and approach the synaptic ribbons in a central position. ON bipolar cells are depolarized by light. This is opposite to the cone signal so we refer to this as a sign-inverting synapse, hence the minus sign at the cone/ON bipolar cell synapse in Fig. 17.15. The dark release of glutamate from the photoreceptors holds ON bipolar cells relatively hyperpolarized. Light turns off the cone transmitter, and the decrease of glutamate release produces a depolarization in ON bipolar cells. Bipolar cells obey the division of the IPL and so ON bipolar cells are stratified in sublamina b (Fig. 17.14).

A hyperpolarizing response to glutamate is unusual and this is an unusual receptor, which is only expressed in the retina. It has now been identified as mGluR6, one in a series of eight metabotropic glutamate receptors, so called because activation of these receptors turns on an intracellular signaling cascade.[166,167] The mGluR6 receptor is selectively activated by glutamate or the glutamate analog 2-amino-4-phosphonobutyrate (APB).[15] Activation of the mGluR6 receptor leads to the closure of a cation channel, producing a hyperpolarization in ON bipolar cells. Light

decreases glutamate release from photoreceptors and produces the opposite response. The cation channel is now known to be the transient receptor melastatin 1 (TRPM1) channel.[168–170] The exact mechanism by which mGluR6 activation closes TRPM1 is not known, but it does not seem to use a cyclic nucleotide-mediated mechanism.[171,172] While the details of the mechanisms remain uncertain, the signal inversion that occurs at the ON bipolar mGluR6 receptor underlies the separation between ON and OFF channels throughout the visual system.

Labeling the retina with an antibody against the mGluR6 receptor stains a narrow band at the level of bipolar dendrites in the OPL.[17,96] In whole mount, the distribution of mGluR6 labeling shows a distinct pattern with two types of terminals (Fig. 17.16C). There are lightly labeled mGluR6-positive clusters of fine ON cone bipolar terminals at each cone pedicle and bright mGluR6-positive terminals, which insert into each rod spherule. These are the terminal dendrites of rod bipolar cells. This mGluR6 pattern also provides a simple way to map the location of rod and cone terminals in the outer retina. All ON bipolar cells, which include ON cone bipolar cells, blue cone bipolar cells, and rod bipolar cells, express mGluR6 at the tips of their dendrites.[17]

A variety of responses may be produced by the different types of ON cone bipolar cell due to modulation of the mGluR6 cascade or to the action of calcium channels or amacrine cells at the bipolar cell terminal,[173] and it is clear that different temporal processing channels exist in the ON as well as in the OFF pathway.[160,163–165,174,175] These differences might arise from diversity in intrinsic conductances (e.g., some bipolar cells express voltage-gated channels that generate transient conductances), the dynamics of neurotransmitter release from bipolar cell synapses, and lateral inhibitory (i.e., circuit-level) interactions that modulate bipolar cell responses.[176–183]

Midget Bipolar Cells

The primate retina is unusual in that the central retina is dominated by midget bipolar cells. Within the central 10 mm, there is one OFF midget bipolar cell and one ON midget bipolar cell for each cone. In this area, they account for more than 80% of all cone bipolar

cells.[149,184] Midget bipolar cells have very small dendritic fields and receive input from single cones and make output to single midget ganglion cells. This is the so-called private line, one cone to one midget bipolar cell to one midget ganglion cell. The ON midget bipolar cells invaginate the cone pedicle, ramify in sublamina b of the IPL, and contact ON midget ganglion cells. OFF midget bipolar cells make flat or basal contacts with cones and terminate in sublamina a where they contact OFF midget ganglion cells. Most investigators think this specialization of the primate retina was designed to achieve maximum acuity at high cone density. It may also, by virtue of the single cone connections, which are automatically color-coded, serve red/green color vision.

Blue Cone Bipolar Cells

In general, diffuse cone bipolar cells contact every cone within the dendritic field and this gives them a characteristic appearance. However, in the primate retina, one bipolar cell type is distinctly different in that it has long dendrites that bypass many cones to seek out only blue cones.[185,186] The dendrites are labeled for mGluR6 and the axon descends deep into sublamina b so the blue cone bipolar cells are ON cells.[17,153]

Rod Bipolar Cells

In contrast to the cone bipolar cells, there is only one morphologic type of rod bipolar cell. They are numerous, with a mop-head of fine dendrites that may receive input from as many as 80–120 rods in the rabbit retina (Fig. 17.17A).[88] This very high convergence contributes to the sensitivity of the primary rod pathway. A single dye-injected rod bipolar cell is shown in Fig. 17.17B. The dendrites branch profusely but avoid the cone pedicles within the dendritic field. Instead, all the terminal dendrites invaginate a rod spherule and they are double-labeled for mGluR6. Only one terminal at each rod spherule comes from this rod bipolar cell. The other half of each mGluR6 doublet is claimed by another unlabeled rod bipolar dendrite. Thus, each rod contacts two different rod bipolar cells.[96] Each rod bipolar cell gives rise to a long slender axon that descends to sublamina 5 of the IPL (Fig. 17.17). Physiologically, rod bipolar cells give ON responses to light stimulation and this is consistent

with the labeling for mGluR6 and the depth of stratification.[13,187] Rod bipolar cells do not usually contact ganglion cells directly. Instead, the primary output of rod bipolar cells is to AII amacrine cells, which pass on the rod signal, or to S1 and S2 amacrine cells[40,187] that provide a powerful negative-feedback signal to rod bipolar terminals (Fig. 17.18; see below). More than 90% of the rod bipolar output is on to these amacrine cells.

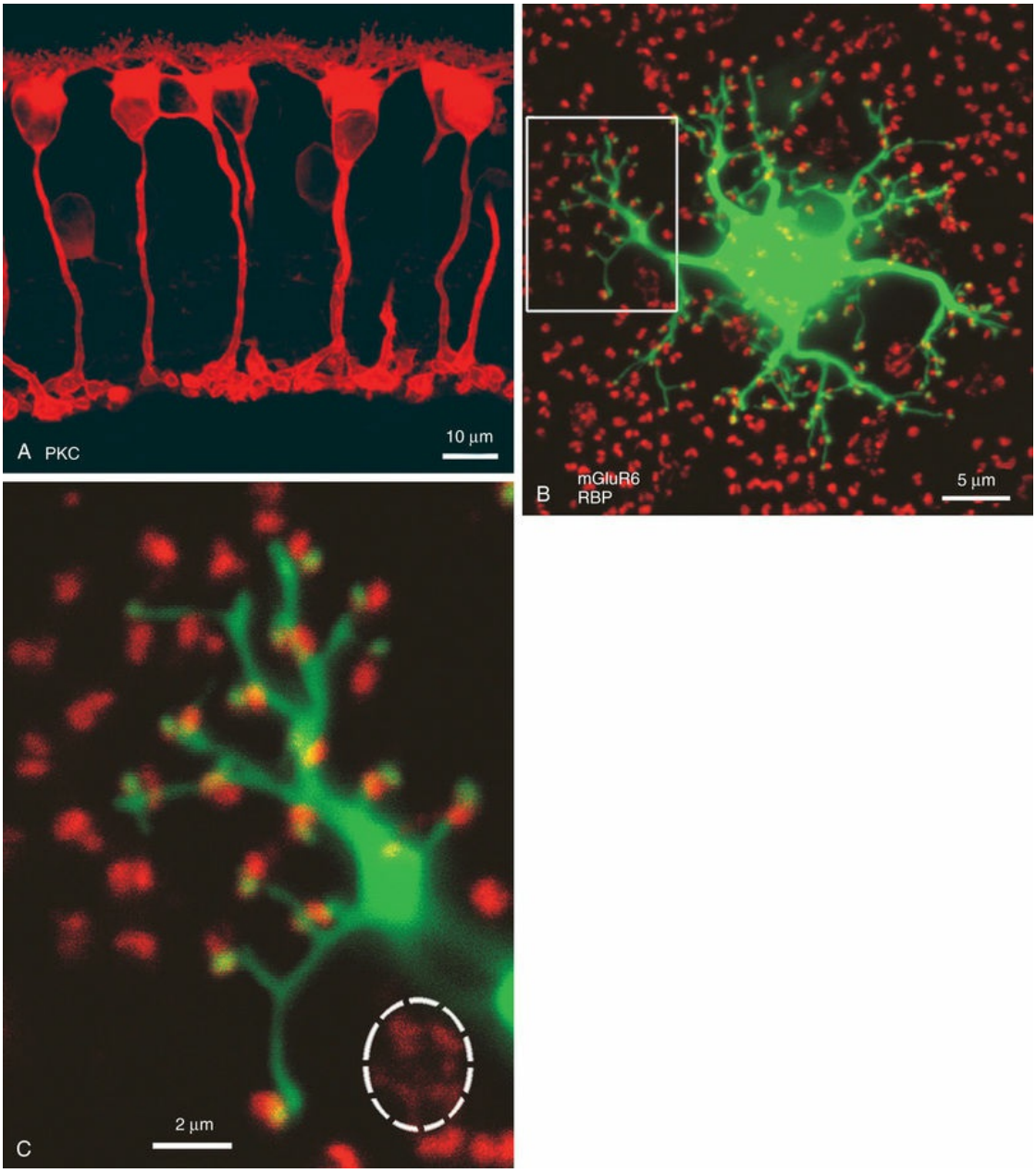

FIG. 17.17 Rod bipolar cells and contacts in the rabbit retina. (A) There is a single morphologic type of rod bipolar cell that can be stained with antibodies against

protein kinase C (PKC). (B) A single rod bipolar cell (RBC) from the rabbit retina, filled with Lucifer Yellow (green), focus at the outer plexiform layer, has a spray of fine dendrites that contact many rod spherules (red puncta). (C) At higher resolution, mGluR6 receptors, which stain the dendritic tips of the rod bipolar cells (red), are doublets where they enter into the rod spherule invagination. The general rule is that each pair of rod bipolar dendrites at a rod spherule originates from different rod bipolar cells. A cone pedicle, marked by a cluster of dimmer, finer ON cone bipolar dendrites, is also outlined (*dashed line*). (Panel A, courtesy of W. Li and S.C. Massey. Panels B and C, reproduced from Li W, Keung JW, Massey SC. Direct synaptic connections between rods and OFF cone bipolar cells in the rabbit retina. J Comp Neurol 2004;474:1–12, with permission from the authors and Wiley-Liss, a subsidiary of John Wiley.)

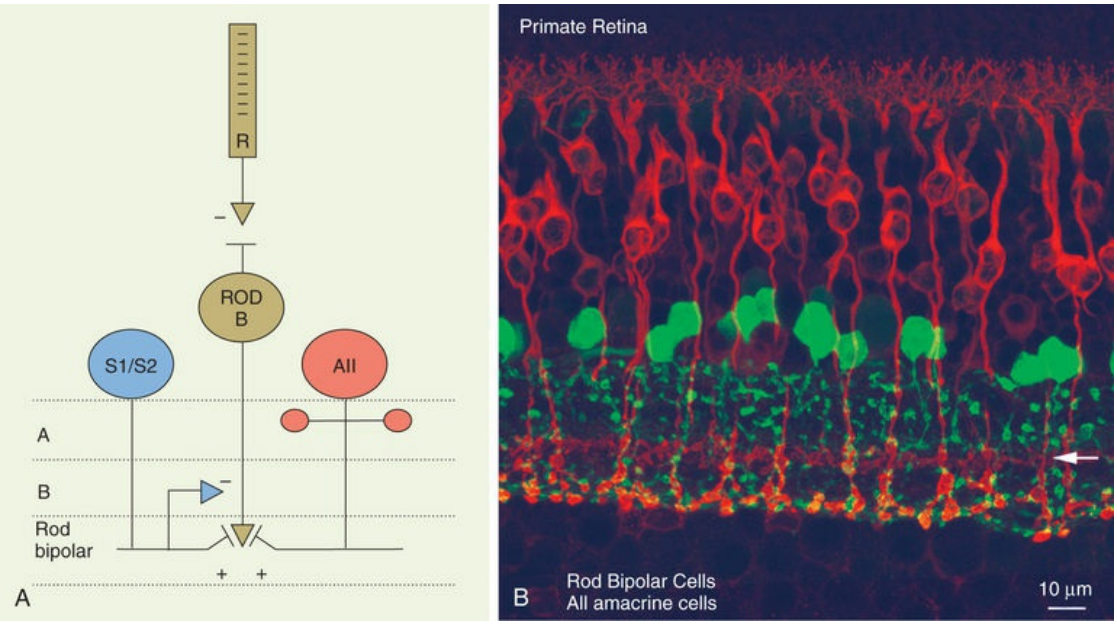

FIG. 17.18 The primary rod pathway. (A) There is only one type of rod bipolar cell (rod B), which produces ON responses to light and terminates at the bottom of the inner plexiform layer (IPL) in sublamina 5. Rod bipolar cells express mGluR6 receptors and are hyperpolarized by glutamate released from rods at a sign-inverting synapse, marked with a minus sign. Rod bipolar cells release glutamate and are connected to AII amacrine cells and S1/S2 amacrine cells via

excitatory receptors, marked by a plus sign. In turn, S1/S2 amacrine cells make inhibitory reciprocal synapses mediated by γ-aminobutyric acid, back on to the rod bipolar terminal. (B) Vertical section of macaque retina: the AII amacrine cells, stained for calretinin (green) descend around the rod bipolar cell axons (protein kinase C, red) as they descend through the IPL. *Arrow* marks fainter staining of cone bipolar cell DB4 at a different level in the IPL. (Panel B reproduced with permission from Massey SC, Mills SL. Antibody to calretinin stains AII amacrine cells in the rabbit retina: double-label and confocal analyses. J Comp Neurol 1999;411:3–18.)

The high convergence allows the rod bipolar cell to collect signals from many rods but is also potentially noisy. However, the rod-to-rod bipolar synapse has a nonlinearity by which small signals are thresholded.[188] The price for this is that many small signals are rejected but the reduction in noise is worth it. Some near-threshold signals may be lost but when a photon signal is captured it has a high signal-to-noise ratio and is transmitted very reliably.[189]

Multiple Rod Pathways

Rods are utilized under low light conditions and provide information over 5 log units. It is now clear that there are at least three pathways, referred to as primary, secondary, and tertiary, by which rod signals reach ganglion cells (Fig. 17.19). They are thought to process signals under slightly different conditions, the primary being the most sensitive and the tertiary being the least sensitive.

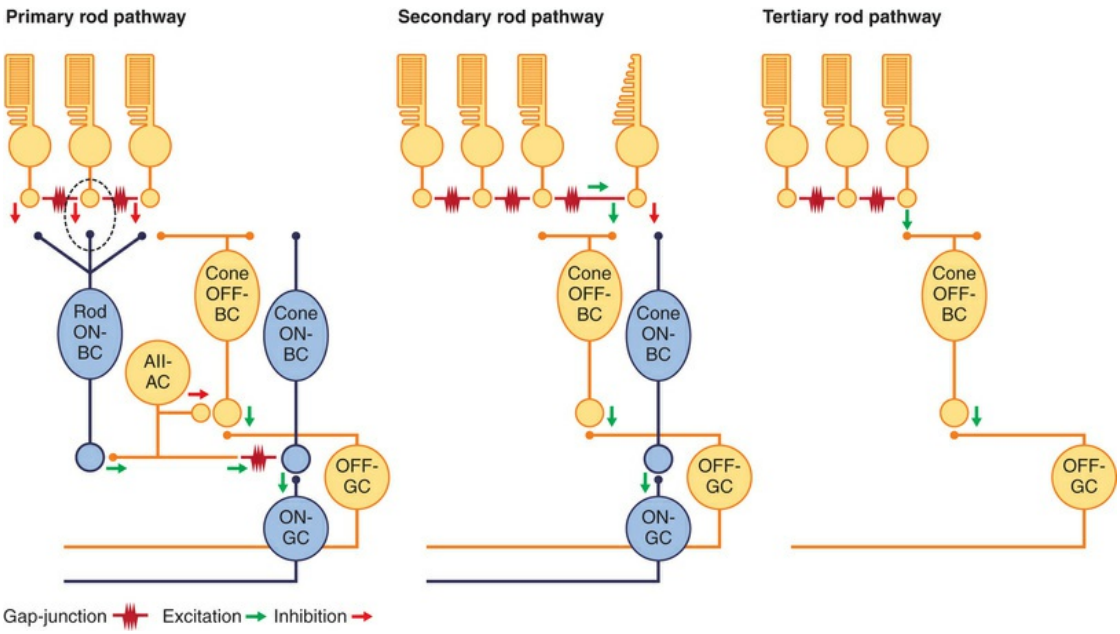

FIG. 17.19 Rod and cone pathways. The primary rod pathway (rod → ON bipolar cell → AII amacrine cell) provides an excitatory input to AII amacrine cells, which are electrically coupled to cone ON bipolar cells and inhibit cone OFF bipolar cells. The secondary rod pathway (rod → cone → bipolar cell) arises from electrical coupling between rods and cones and allows the flow of rod signals into the cones and glutamate release into the cone ON and OFF bipolar cells. The tertiary rod pathway (rod → OFF bipolar cell) is a direct glutamatergic input from rods to cone OFF bipolar cells. Note that the secondary and tertiary pathways are in principle independent of the primary pathway. Red arrows indicate sign-inverting synapses, and green arrows indicate sign-preserving synapses.

(Modified with permission from van Genderen MM, Bijveld MM, Claassen YB, et al. Mutations in TRPM1 are a common cause of complete congenital stationary night blindness. Am J Hum Genet 2009;85:730–6.)

The primary rod pathway utilizes rod bipolar cells, which make ribbon synapses with two postsynaptic amacrine cells in sublamina 5 of the IPL (Fig. 17.18). One of these postsynaptic neurons is the AII amacrine cell, and the other is either an S1 (A17 in the cat) or S2 amacrine cell (Fig. 17.18).[40,187] These two wide-field GABA amacrine cells both make reciprocal synapses with rod bipolar terminals and thus provide another stage of negative feedback. The conspicuous terminals of rod bipolar cells literally plug into holes in the

meshwork of dendrites provided by these amacrine cell types. Rod bipolar cells, like other bipolar cells, release glutamate, and the contact points with the AII matrix are covered with glutamate receptors of the AMPA subtype (Fig. 17.20).[190,191] The glutamate receptors of S1/S2 amacrine cells have not been completely clarified, but the A17 (probably the S1 equivalent in the rodent) uses a Ca^{2+}-permeable AMPA glutamate receptor via L-type Ca^{2+} and Ca^{2+}-activated potassium (BK) channels[192] to modulate feedback inhibition on to the rod bipolar cell and control glutamate release at this synapse. On the rod bipolar cell the postsynaptic targets are the $GABA_A$ and $GABA_C$ receptors.[193–195]

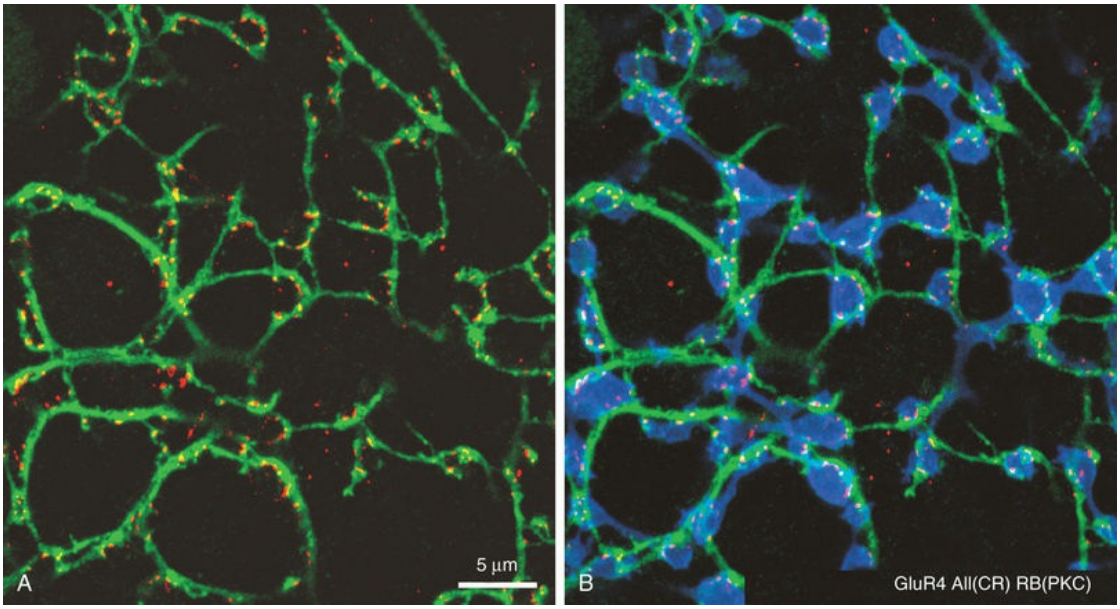

FIG. 17.20 Rod bipolar input to AII is mediated by glutamate receptors. (A) The matrix of AII amacrine cells in the rabbit retina, stained for the calcium-binding protein calretinin (green), is decorated with punctate glutamate receptors (red) of the α-amino-3-hydroxy-5-methyl-4-isoxazolepropionic acid (AMPA) subtype. (B) The AII dendrites carefully wrap around the rod bipolar terminals (blue) at this level. Critically, the glutamate receptors only occur at the contact sites between rod bipolar cells and AII amacrine cells (red + green + blue = white). Intervening sections of AII dendrite, between rod bipolar terminals, have no glutamate receptors. This indicates that AMPA receptors are located at synaptic contacts between rod bipolar cells and AII

amacrine cells. (Reproduced from Li W, Trexler EB, Massey SC. Glutamate receptors at rod bipolar ribbon synapses in the rabbit retina. J Comp Neurol 2002;448:230–48, with permission from the authors and Wiley-Liss, a subsidiary of John Wiley.)

So, there are two obvious questions: how do rod signals reach ganglion cells and, if there is only one type of rod bipolar cell, how are both ON and OFF signals generated in dark-adapted conditions? The answer lies in the way the rod pathway is integrated into the cone pathways via the AII amacrine cell (Fig. 17.19). AII amacrine cells are glycinergic neurons and they also make conventional inhibitory glycinergic synapses with the axon terminals of OFF cone bipolar cells in sublamina a via alpha 1 glycine receptors.[196] In turn, the AII itself is modulated by a glycinergic input at synapses expressing alpha 3 glycine receptors.[197] Their distal processes make electrical synapses or gap junctions with ON cone bipolar cells in sublamina b and provide a direct, presumably sign-conserving, input signal to the ON cone bipolar cells.[41,198,199] Thus, while the cone pathways split via different postsynaptic glutamate receptors in the outer retina, the rod pathway bifurcates at the level of the AII amacrine cell. It is often said that the rod signals piggyback on the cone pathways.

The rod bipolar → AII amacrine cell synapse also plays a fundamental role in rod-mediated vision.[187,200–202] It acts as a high-pass filter, accelerating the time courses of slow rod responses to increase the reliability of their encoding by postsynaptic circuits.[200,203] Therefore, the timing of transmission shapes ganglion cell responses and retinal circuit output.[204] The RB → AII synapse also is the primary site of neural gain control during rod-mediated vision: when light is scarce and few rods are activated, the synapse amplifies small rod inputs so that they are transmitted reliably; as background light intensity increases, the gain of transmission is lowered by a use-dependent reduction in the size of the readily releasable vesicle pool so that the circuit avoids saturation.[202,204-209]

AII amacrine cells themselves are well coupled by gap junctions, as can be demonstrated by injecting a single AII amacrine cell with the diffusible tracer Neurobiotin, which passes through gap junctions to label all the coupled cells.[199,210] Fig. 17.21 shows that many AII amacrine cells are coupled as well as an overlying group,

consisting of four or five different types, of ON cone bipolar cells. The AII-to-AII gap junctions occur preferentially at dendritic crossings (Fig. 17.22) and AII coupling is absent in a Cx36 knockout mouse.[211] Coupling in this complex heterocellular network is modulated by dopamine and, perhaps more importantly, by light.[212] The underlying mechanism is by phosphorylation of Cx36, and this regulation can be achieved on a cell-by-cell basis.[213]

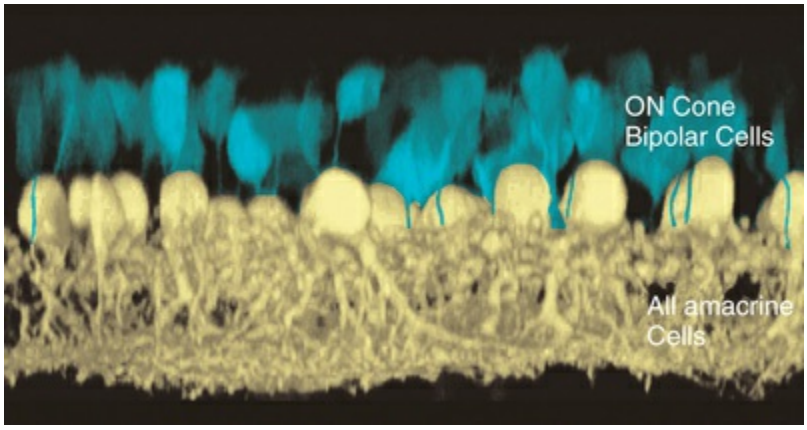

FIG. 17.21 Coupling between AII amacrine cells and ON cone bipolar cells. This three-dimensional reconstruction from a series of confocal images shows the result of injecting a diffusible tracer, such as Neurobiotin, into an AII amacrine cell in the rabbit retina. A matrix of coupled AII amacrine cells (khaki), all with the characteristic morphology, is labeled. In addition, the tracer also spreads into a complex of ON cone bipolar cells (blue) which consists of 3–5 types.
(Courtesy of E.B. Trexler and S.C. Massey.)

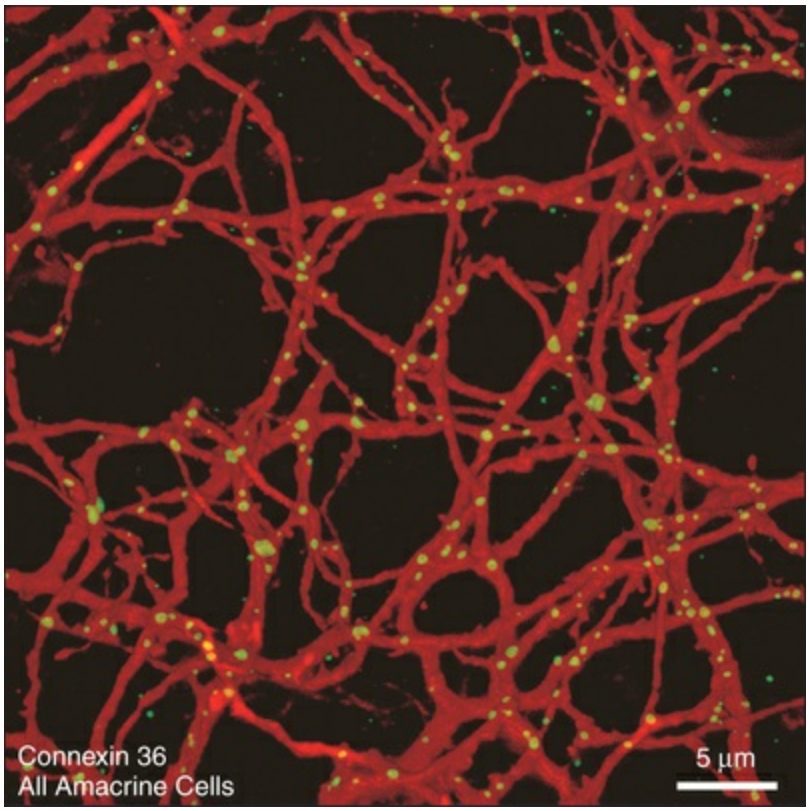

FIG. 17.22 AII/AII gap junctions contain connexin (Cx)36. A confocal image of the AII dendrites (red) in sublamina b of the inner plexiform layer. Staining for Cx36 (green) shows that Cx36 plaques are abundant in the AII matrix. Image analysis indicates that there is a high probability of a Cx36 plaque when two AII dendrites cross. (Reproduced from Mills SL, O'Brien JJ, Li W, et al. Rod pathways in the mammalian retina use connexin 36. J Comp Neurol 2001;436:336–50, with permission from the authors and Wiley-Liss, a subsidiary of John Wiley.)

Gap junctions are bidirectional, meaning that electrical signals and tracers can pass through them in either direction.[214,215] One consequence is that glycine from the AII amacrine cell can enter ON cone bipolar cells and indeed most ON bipolar cells contain glycine, even though they use glutamate as a neurotransmitter. The source of the bipolar cell glycine was definitively established by blocking gap junctions with carbenoxolone. This changed the labeling pattern for glycine, which was subsequently diminished in bipolar cells.[167] Another more relevant consequence of bidirectional coupling is that not only do rod signals pass into the cone pathways but, in fact, cone signals can pass from ON bipolar cells into the AII network. The implication is that the AII network can also influence

cone signals. This has been demonstrated in a number of studies that reveal AIIs act as inhibitory interneurons during cone-mediated vision.[216–218] In addition, transmission at the rod bipolar → AII amacrine cell synapse, by resetting the membrane potential of postsynaptic AIIs, can alter the membrane potential of coupled ON bipolar cells and thereby regulate transmission at their synapses.[207]

The importance of these gap junction pathways has been elegantly demonstrated by the development of a Cx36 knockout mouse.[211] In these animals, filling an AII amacrine cell with Neurobiotin yielded only one cell: there was no coupling without the expression of Cx36. In contrast to the wild type, in the knockout animals no rod signals are detectable in recordings from ON ganglion cells. In the absence of Cx36 gap junctions, rod level signals do not pass into the ON cone pathways. Of course, the OFF pathways are not dependent on transmission via gap junctions and so rod-driven OFF signals are maintained. One obvious explanation is the absence of AII/ON bipolar gap junctions, described above. However, the Cx36 knockout may also interfere with rod/cone coupling in the outer retina. In fact, both these pathways must be missing to eliminate the transmission of rod signals to ON pathways. In either case, this is the first time that a gap junction connection has been shown to be essential for the function of a neuronal pathway in the mammalian CNS.

In the rabbit retina, the gap junctions between one type of ON cone bipolar cell that is selectively labeled by antibodies against the calcium-binding protein calbindin also involve Cx36.[219] However, the properties of AII/bipolar gap junctions are different from AII/AII gap junctions,[199] suggesting that the bipolar side of the gap junction is different in some way, perhaps due to phosphorylation or even the expression of a different connexin by bipolar cells. There is some evidence that bipolar cells express Cx36.[211] However, there is convincing evidence that in some ON bipolar cells the coupling is mediated by Cx36 (AII)/Cx45 (BC) heterotypic gap junctions.[220]

Secondary and Tertiary Rod Pathways

The primary rod pathway is used under threshold conditions such

as starlight[143,187] and it is absolutely dependent on synaptic transmission between rods and rod bipolar cells via mGluR6 receptors. However, when these synapses are blocked with APB it was still possible to record rod level signals in OFF ganglion cells.[221] This alternative pathway was attributed to rod/cone coupling, for which there is both anatomic and physiologic evidence. This second rod pathway runs from rods via gap junctions to cones and then into cone bipolar cells and ganglion cells in the usual way (Fig. 17.19). It has been suggested that this pathway operates in mesopic conditions of intermediate light intensity, though the primary rod pathway utilizing rod bipolar cells likely continues to function throughout the operating range of rod vision.[74,204]

This pathway has also been reported for the mouse retina. However, the rod-driven responses persisted even in a transgenic mouse line in which cones were eliminated.[222] The absence of cones would seem to rule out rod/cone coupling as a pathway. Therefore, a third rod pathway was proposed involving direct connections between rods and OFF cone bipolar cells and subsequently these connections were found.[223,224] This pathway was first thought to be a specialization of the rodent retina but it has now been identified in cats and rabbits.[96,225] It also is present in the ground squirrel, where a specific type of OFF bipolar cell, the b2, was shown to contact rods and provide a means for rods to provide fast photoreceptor signaling.[226] Thus, this third rod pathway may be a general feature of the mammalian retina.

It has been suggested that the rod→OFF bipolar pathway operates at high mesopic/low photopic conditions, around the transition from rod to cone vision. In general, the different rod pathways may be designed to cover different intensity ranges and perhaps they are selectively connected to specific ganglion cell types but, as yet, there are no data on this point. There is physiologic evidence from the mouse retina that different ganglion cell types have different intensity response functions but the ganglion cell types have not been identified and the contributing pathways are unknown.[211] The function of these novel retinal pathways under different light intensities is an important and active area of current research.

Amacrine Cells

Amacrine cells form a morphologically and physiologically diverse group of mostly inhibitory interneurons. Approximately 30 types of amacrine cell have been identified morphologically in mammalian retina (Fig. 17.23).[227–229] The cell bodies of the amacrine cells are primarily located in the innermost portion of the INL, unofficially known as the amacrine cell layer. Amacrine cells are also found in the GCL, where they are known as displaced amacrine cells. Most are GABAergic medium- to wide-field cells[47,230] and many recognized classes of amacrine cells are found in both layers. In fact, in the mouse retina, more than half the cells in the GCL are amacrine cells. In general, the three major connections made by amacrine cells are feedback inhibition to bipolar cell terminals, feedforward inhibition to ganglion cells and serial inhibitory connections where amacrine cells are the postsynaptic targets of other amacrine cells.[231]

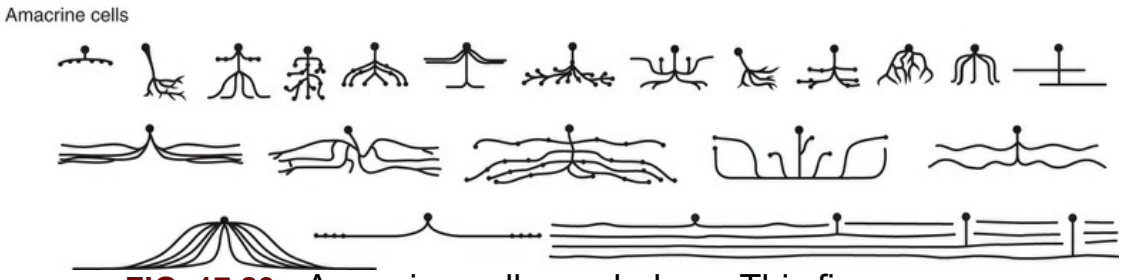

FIG. 17.23 Amacrine cell morphology. This figure shows the comparative morphology of 24 distinct amacrine cell types from the rabbit retina. (Reproduced with permission from Masland D. Neuronal diversity in the retina. Curr Opin Neurobiol 2001;11:431–6.)

Amacrine cells can be divided by their dendritic arbor size into narrow- (<200 μM) and wide-field. The narrow-field amacrine cells are generally glycinergic and frequently provide inputs across the ON/OFF strata in the IPL.[232] Wide-field amacrine cells are mostly GABAergic.[229,230,233–235] Some provide lateral inhibition within a substratum[232] and others provide reciprocal feedback.[195] They are involved in surround inhibition[236] or contrast adaptation.[237] Several of the wide-field cells also release catecholamines or other

neuropeptides.[238] The best characterized in this group are the dopaminergic wide-field amacrine cells that are involved in light adaptation, and those releasing ACh.

In a large population of rabbit amacrine cells, acquired randomly using modern imaging methods, 24 different morphologic types were identified (Fig. 17.23).[227,228] Similar studies have been extended to the mouse, where several groups have identified large numbers of narrow-, medium-, and wide-field amacrine cells.[229,230,233–235]

The most numerous amacrine cell type is the AII amacrine cell, approximately 11%, while other relatively common types, such as the ChACs, make up 3–5% of the total population. Half of the amacrine cells are narrow-field, with coverage factors around 1. Many of these are broadly stratified, which suggests they may interconnect the ON and OFF substrata. Approximately a quarter of the amacrine cells are wide-field and narrowly stratified with very high coverage – as high as 100–500. A cell with an overlap this high forms an extremely dense plexus of fine dendrites that blankets the entire retina. Examples are S1 amacrine cells, DACs, and starburst amacrine cells (see below). Thus, in the rabbit retina, the identification of all the amacrine cell types, started so long ago by Cajal and his contemporaries, is now almost complete. The mouse is probably the next best characterized because of the array of genetic tools that can be used for their analyses.

The reasons for such a variety of amacrine cells are unknown. However, two functions seem to be commonly repeated. First, all bipolar cell terminals seem to receive GABA-mediated negative feedback. In the case of the rod bipolar cell, feedback is mediated by two amacrine cell types, S1 and S2.[239] Bipolar cells (approximately 10 types) are narrowly stratified and if different amacrine cells mediate feedback to each one, this could account for 10–20 different cell types. Secondly, about half the ganglion cells (approximately eight types) are coupled to one or two amacrine cell types by gap junctions.[240–242] Again, if different amacrine cells are coupled to each ganglion cell type, this could account for 10–15 types. These two groups need not be mutually exclusive and doubtless amacrine cells have many functions. In another calculation, we estimate there are 15 ganglion cell types forming independent circuits or channels. If each channel required two amacrine cells, that would produce a

total of 30 amacrine cell types. While necessarily vague, these simple estimates indicate the variety of amacrine cell types may not be extravagant.

General functions attributed to amacrine cells include feedback inhibition, surround inhibition, some forms of adaptation, signal averaging, and noise reduction.[243,244] In a rapid eye movement or saccade, the visual image does not blur. This is because a wave of inhibition sweeps the inner retina, like a vertical blank on a television screen. In one study, the inhibitory wave associated with saccades was attributed to wide-field amacrine cells.[245] However, in terms of specific connections and neuronal circuits, the functional anatomy of amacrine cells, it has only been possible to study a few types, four of which are selected below. We know almost nothing except the shape of 75% of the amacrine cells, not their connections, physiology, or circuit functions – in other words, little more than Cajal knew 100 years ago. As the means of targeting, imaging, and recording from visually identified cell types improves, we can expect further progress in this area.

An example of these new approaches was demonstrated by Knop and colleagues,[246] who used a GFP transgenic mouse line that marked a type 2 wide-field amacrine cell. They characterized the inputs, stratification, and physiology of the cell, showing it was ON-OFF and GABAergic and that its function was maintained over a wide range of light adaptation conditions. A major goal of visual neuroscientists is to characterize fully all the amacrine cells and integrate their function into the retinal circuitry. Several amacrine cells have been studied extensively, and their characteristics are described below.

AII Amacrine Cells

The AII amacrine cell, also known as the rod amacrine cell, is the most numerous of the amacrine cells, accounting for 11% of the total. It is correctly written with a Roman numeral, which is retained from an early classification scheme, while other numbered amacrine cells use Arabic numerals. AII amacrine cells have a distinctive bistratified morphology, which makes them easy to identify, even in retinal slices.[246] The soma protrudes into the IPL and turns into a thick axon that descends to sublamina b of the IPL

and branches into an overlapping matrix.[247] This is the site of glutamate input from rod bipolar cells (Fig. 17.21) and output, via gap junctions to ON cone bipolar cells. There are also fine dendrites, which terminate in lobules in sublamina a. At this level, AII amacrine cells make glycinergic inhibitory contacts with OFF cone bipolar cells, although input from AII ACs appears not to modulate OFF bipolar cell membrane potential during rod bipolar pathway mediated visual signaling.[248] AII ACs also receive input from OFF cone bipolar cells at this level, the function of which is unclear.[187]

Primate AII amacrine cells are similar in morphology to those of other mammalian species.[59,60] The density of rods reaches a maximum at about 20° from the fovea but psychophysical measurements in humans indicate that, in dark-adapted conditions, the maximum acuity occurs at approximately 5° from the fovea, a substantial mismatch. The rod pathway for maximum acuity is thought to be rods → rod bipolar cells → AII → midget bipolar cells → midget ganglion cells (Fig. 17.19). There is good evidence that AII amacrine cells contact midget bipolar cells and other ganglion cell types are too sparse to support the maximum resolution. Now, rods and rod bipolar cells far outnumber AII amacrine cells so they will not present a limit to scotopic acuity. In addition, both ON and OFF midget bipolar cells and ON and OFF midget ganglion cells have a 1 : 1 : 1 correspondence with the tightly packed cones of the central retina. That leaves the AII amacrine cell as the lowest density, the bottleneck, in the pathway. In macaque retina, the peak density of AII amacrine cells is about 5000 cells/mm^2 around 5°, which matches the peak of dark-adapted acuity. If we consider the mosaic of AII amacrine cells and, from sampling theory, calculate the maximum resolution for such an array, we find that it closely matches the peak acuity from psychophysical experiments. Together, these results indicate that the density of AII amacrine cells sets the limit of dark-adapted resolution in central retina.

The AII amacrine cell network seems to be very important since it is found in all mammalian retinas. In general terms, the AII amacrine cell network is thought to reduce noise by canceling out random events that are not correlated and by reinforcing light-driven events that are synchronized.[249,250] Coupling is also strongly

modulated by dopamine,[212] and processes from the DACs make a ring around the neck of each AII where it protrudes into the IPL (Fig. 17.24). Of course, we think that dopamine is the general signal for light adaptation and, in fact, light itself seems to modulate the strength of coupling in the AII network.[251] Disrupting the AII network interrupts the rod-driven ON pathways, as described above. However, even in the rod-driven OFF pathways, which are not routed via AII amacrine cell gap junctions, the sensitivity is reduced by approximately 1 log unit in the Cx36 knockout mouse.[251] This indicates that coupling in the AII amacrine cell network adapts to ambient lighting conditions to optimize rod signaling over a large dynamic range.

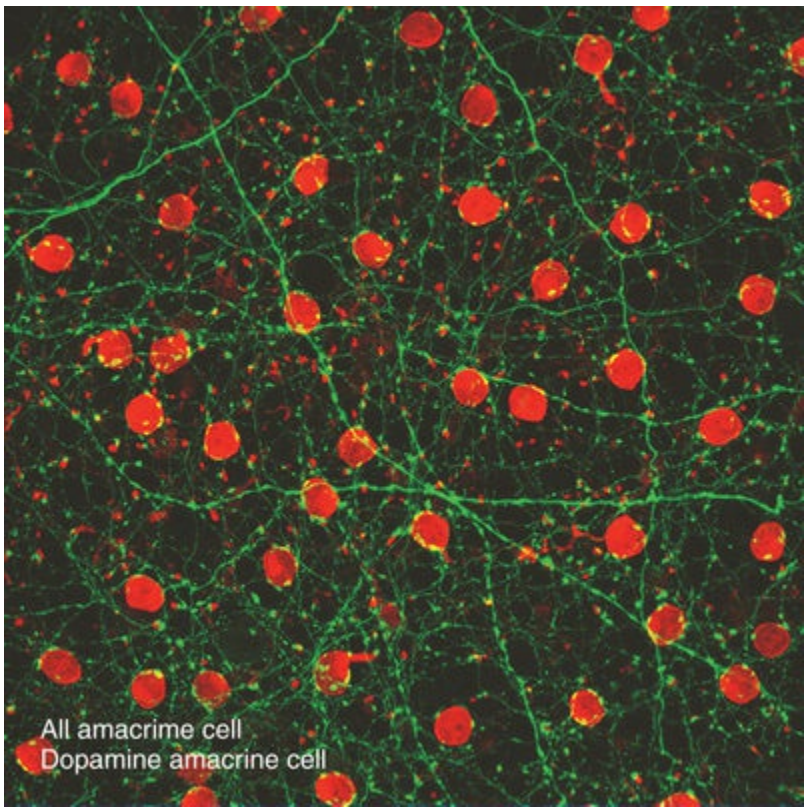

FIG. 17.24 Dopaminergic amacrine cells form a dense matrix. The matrix of dopaminergic dendrites, stained for tyrosine hydroxylase (green), blankets the retina. There are many small varicosities surrounding AII amacrine somas, stained for calretinin (red). (Courtesy of S.C. Massey.)

The AII amacrine cells also appear to have a day job.[216,217,252]

During the day, dark objects that approach the viewer activate a particular class of ganglion cells. An important component of the circuit is the AII amacrine cell. However, unlike in the dark, the information flow is effectively reversed. Depolarization of cone ON bipolar cells results in depolarization of the AII through gap junctions, which increases inhibition by the AII amacrine cell on to OFF bipolar cells. This is a crossover inhibition pathway by which ON channels inhibit OFF pathways.[182] The dual use of the AII amacrine cell depending on lighting condition maximizes circuit efficiency.

S1 and S2 Amacrine Cells

The S1 amacrine cell of the rabbit retina (A17 in the cat) is a wide-field GABA amacrine cell with straight radiating dendrites decorated with prominent varicosities (Fig. 17.25A). The S2 GABA amacrine cell is smaller, the dendrites are more tangled, and the varicosities are smaller but more numerous (Fig. 17.25B).[253,254] Both cell types contribute to a dense overlapping meshwork at the level of the rod bipolar terminals (Fig. 17.26). These large cells are relatively numerous so the dendritic overlap is huge with coverage factors as high as 500. Although the rabbit retina contains little endogenous serotonin, for some unknown reason these cells take up serotonin. Therefore, they are sometimes known as indoleamine-accumulating amacrine cells and this provides a simple way to label the entire population. Electron microscopy shows that S1/S2 amacrine cells make reciprocal synapses with rod bipolar terminals, i.e., they receive input at a rod bipolar ribbon synapse and nearby they synapse back on to the rod bipolar terminal.[40]

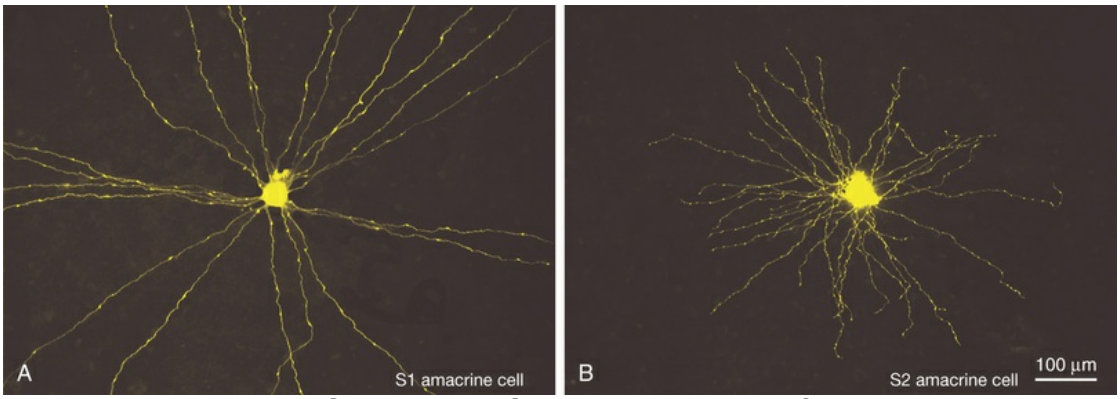

FIG. 17.25 (A) S1 and (B) S2 amacrine cells filled with Lucifer Yellow, from the rabbit retina. These amacrine cells have prominent varicosities, which are synaptic structures, along slender dendrites. (Reproduced with permission from Zhang J, Li W, Trexler EB, et al. Confocal analysis of reciprocal feedback at rod bipolar terminals in the rabbit retina. J Neurosci 2002;22:10871–82.)

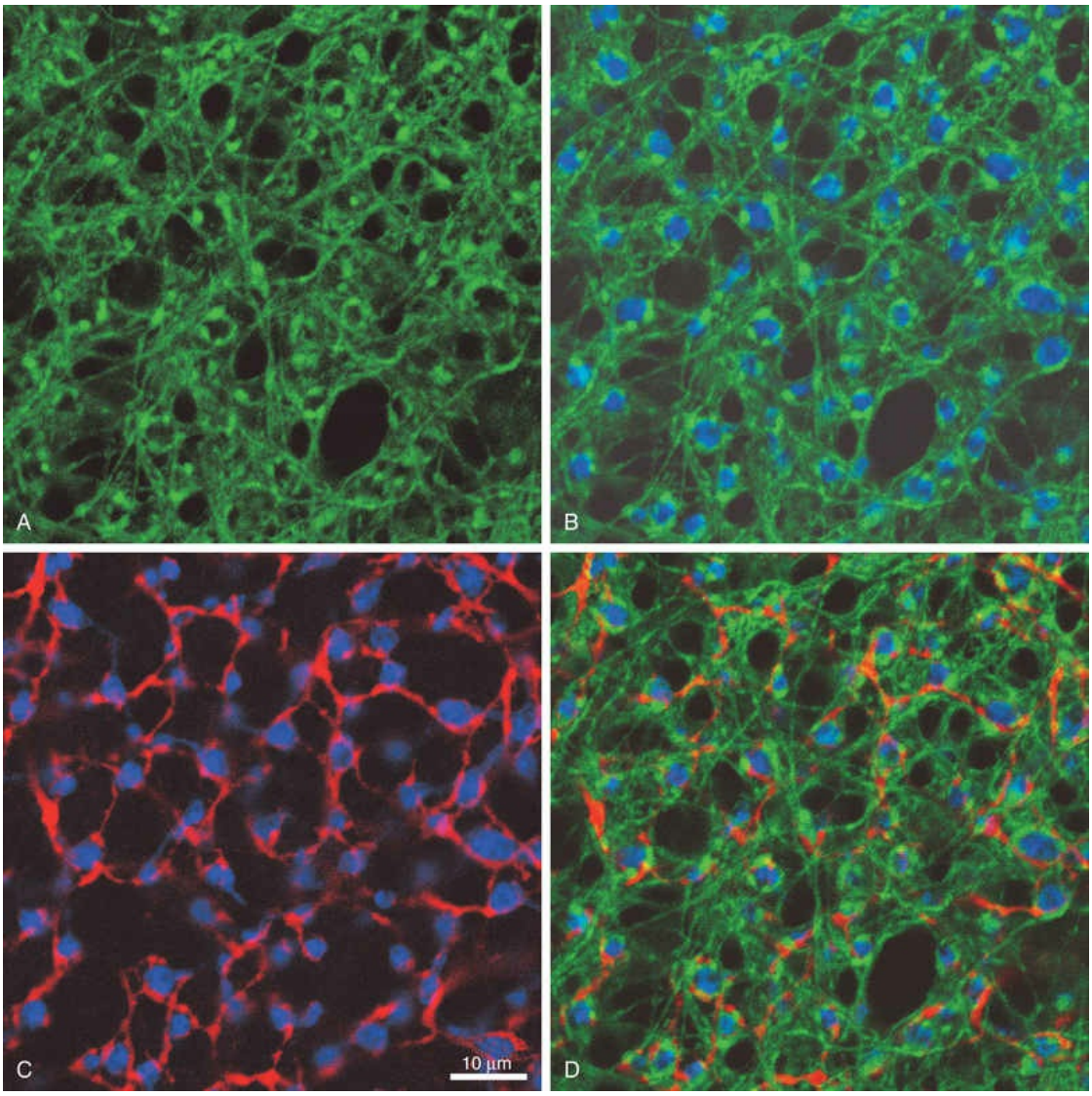

FIG. 17.26 S1/S2 matrix. (A) The S1/S2 matrix (green), stained by serotonin uptake, from whole-mount rabbit retina. (B) Rod bipolar terminals (blue) fill holes in the S1/S2 matrix. (C) AII dendrites (red) also contact the same rod bipolar terminals. (D) Merged triple-label image shows S1/S2 processes and AII dendrites surrounding every rod bipolar terminal. (Reproduced with permission from Zhang J, Li W, Massey SC. Confocal analysis of reciprocal feedback at rod bipolar terminals in the rabbit retina. J Neurosci 2002;22:10871–82.)

The varicosities contain presynaptic markers; they are wrapped around rod bipolar terminals (alternating with AII dendrites) and opposed by synaptic ribbons and GABA receptors (Fig. 17.27). In fact, the varicosities are synaptic sites. Confocal analysis of double-label material shows that every varicosity is in synaptic contact

with a rod bipolar terminal.[254] This means that the functional role of the S1/S2 amacrine cells is to provide a level of GABA-mediated negative feedback to rod bipolar terminals. This is their job and they do nothing else; they have no output to any other cell besides the rod bipolar cell.

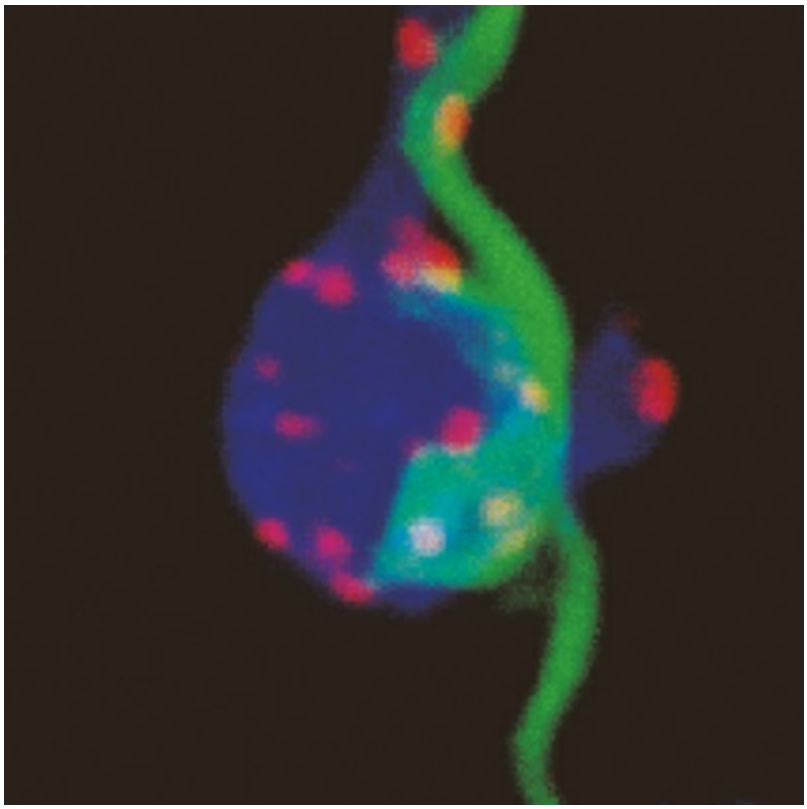

FIG. 17.27 S1 synapse on a rod bipolar terminal. This three-dimensional reconstruction shows a single varicosity from an S1 amacrine cell (green) wrapped around a rod bipolar terminal (blue). The transparency has been adjusted so we can see through these structures. $GABA_C$ (red) receptors are found on the surface of the rod bipolar terminal, including at the interface with the S1 (red + green + blue = white). This is an example of locating a synaptic structure by confocal microscopy. (Courtesy of W. Li and S.C. Massey.)

S1/S2 amacrine cells carry about 300 and 500 varicosities, respectively, and the density of varicosities has been calculated as 330,000/mm^2. Each rod bipolar terminal receives input from about 25 S1 and 50 S2 varicosities. They are both apposed by $GABA_A$ and

$GABA_C$ receptors.[255] Thus, the inhibitory input to bipolar terminals will have two components: a large sustained component from $GABA_C$ receptors, which are only expressed by bipolar terminals, and rapid initial transient input from $GABA_A$ receptors, which are more widespread.[155,193,236,256–258] The S1 and S2 amacrine cells clearly have different spatial and coupling properties.[239] Hence, the S2 input dominates within 200 μm and provides an inhibitory signal that matches the size of the surround recorded from AII amacrine cells. The larger, well-coupled S1 amacrine cell may provide a more distant network or global signal. This analysis suggests that the presence of both S1 and S2 amacrine cells is not redundant: each cell contributes different components of lateral inhibition in the rod pathway. Together, these components will summate to modulate the spatial and temporal properties of rod bipolar output. Further, each of the synaptic sites of S1 (A17) amacrine cells may operate independently of the whole. This is possible because each varicosity appears electrically isolated from its neighbor.[195] In conjunction with the cable properties of the A17 neurites the outputs are compartmentalized, keeping individual reciprocal synaptic dyads independent.[192,195,259] Such local processing has an important consequence: it allows a single A17 to process upwards of 500 signals independently of each other. This represents a large increase in processing power based on what amounts to parallel circuits in a single cell.[195]

It should be emphasized that the reciprocal feedback described at the rod bipolar terminal is, in fact, a general case. It is likely that the terminals of all bipolar cells make reciprocal synapses with GABA amacrine cells and bipolar terminals are literally surrounded by GABA-positive profiles. In the mouse retina, as well as other species, $GABA_C$ receptors, a postsynaptic target of feedback inhibition, are expressed on cone ON and OFF bipolar cells. The current mediated by this receptor is slow and sustained, making it a likely target of feedback control on the cone bipolar cells, as it does in rod ON bipolar cells. The absence (in $GABA_C$ receptors knockout mice) or pharmacologic block of this receptor increases both the spontaneous activity and gain of ON-center ganglion cells relative to wild-type.[256,260,261]

There seem to be $GABA_C$ receptors on all bipolar cell terminals, although the density for each cell type varies.[256–258] If each bipolar cell type, with its unique address, had one GABA amacrine cell type, that would account for 10–12 of the amacrine cell types. The "sharing" of some broadly stratified amacrine cells would tend to reduce this number while those cases, like the rod bipolar cell, which receive feedback inhibition from two amacrine cell types, will inflate it. In either case, negative feedback provides greater stability, increased frequency response, and a wider bandwidth at the level of bipolar cell terminals. A major role for at least some of the multiple types of GABA amacrine cells is to provide negative feedback for all bipolar cells.

Dopaminergic Amacrine Cells

A small number of amacrine cells, less than 0.1%, contain dopamine. To make up for their low density, these cells have very long axon-like processes that can run for millimeters across the retina.[262] The net result is a dense high-coverage plexus of dopaminergic dendrites, which covers the entire retina. Most of the plexus is in sublamina 1, adjacent to the INL, but there are minor bands in sublaminas 3 and 5 of the IPL. In some species, particularly fish, the dopamine neurons project to the OPL. In other words, they are interplexiform cells. In the rabbit retina, a few stunted processes run towards the OPL but they do not form a plexus. In the macaque retina, some dopaminergic dendrites run into the INL where they surround the somas of AII amacrine cells (Fig. 17.24).[60]

Electron microscopy shows that the dendrites in layer 1 receive direct bipolar input at ribbon synapses, many of which appear to be monads, as opposed to the usual dyadic arrangement with two postsynaptic processes.[263] Yet, recordings from GFP-labeled cells in the mouse retina have shown that DACs produce a variety of light responses: ON transient, ON sustained, and light independent.[23,24] But how do these ON responses arise if most dopaminergic processes are stratified in the OFF sublamina? If DACs are ON cells, then they break the rules of stratification for the IPL.

Several different mechanisms have been proposed to overcome this difficulty. For example, it has been shown that ON bipolar

inputs to the DACs occur on the minor bands in layer 3.[264] However, it is also clear that there are bipolar ribbon inputs to the DAC in sublamina 1.[263] Most recently, it has been suggested that the melanopsin-containing ipRGCs may provide an input to the DACs, because the sustained features of the DAC response and the spectral signature match those of the melanopsin ganglion cells. Furthermore, the light-evoked DAC response is maintained when photoreceptors degenerate, although transient light responses are blocked by APB, suggesting they arise from the ON bipolar pathway. In addition, melanopsin ganglion cell dendrites that ramify in sublamina a also have ON responses, thus breaking the stratification rules themselves. Most recent evidence suggests that many ON cone bipolar cells make axonal ribbon or ectopic synapses as their axons descend through stratum 1 (Fig. 17.28). These axonal ribbons provide ON excitatory input via AMPA-type glutamate receptors to DACs (and to ipRGCs) in the OFF layer of the IPL. Thus, axonal ribbons break the stratification rules of the IPL and provide an additional accessory ON sublayer in the outer IPL.[26,27]

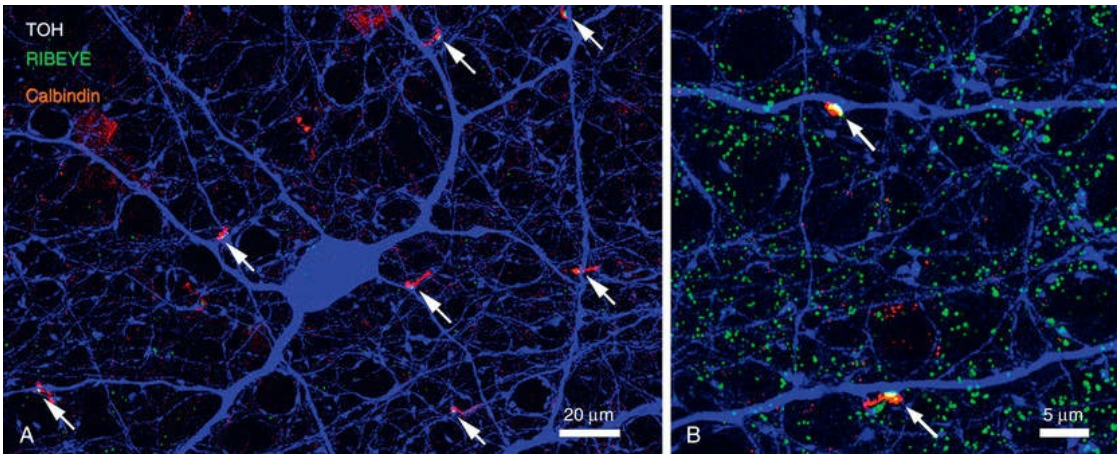

FIG. 17.28 Dopaminergic amacrine cells, stained with an antibody against tyrosine hydroxylase (TOH: blue), receive ectopic, axonal ribbon synaptic input. (A) The dopaminergic dendrites run in sublamina a. At this level, ON cone bipolar cells, labeled with an antibody against calbindin (red), are passing through so the descending axons appear as dots. However, they are nearly all immediately adjacent to the dopaminergic dendrites (*arrows*). (B) At higher magnification, it can

be seen that synaptic ribbons (green) also occur at these contact points. Thus, the arrows show ON synaptic input, via axonal ribbons, in sublamina a, the OFF layer of the inner plexiform layer. (Reproduced with permission from Hoshi H, Liu WL, Massey SC, et al. ON inputs to the OFF layer: bipolar cells that break the stratification rules of the retina. J Neurosci 2009;29:8875–83.)

In the mouse retina, DACs also contain GABA[265] but DACs from the rabbit retina do not display a GABA signature.[34] Dissociated DACs are spontaneously active[266] and, in contrast to GABA, dopamine seems to be steadily released in a paracrine fashion to diffuse throughout the retina.[267] Dopamine levels are higher in the daytime and seem to be under circadian control. The most recent work indicates that the DACs themselves express clock genes.[268–271] This is appropriate because dopamine is intimately involved in the diurnal rhythms associated with the processes of light and dark adaptation. Dopamine acts at a variety of sites in the retina, many of which seem obviously linked to light or dark adaptation.[272] For example, it dramatically reduces coupling in the AII amacrine cell network[212,213] and, in the outer retina, it promotes cone input to second-order neurons. Conversely, in the dark, when dopamine is absent, photoreceptor coupling is increased via a D2 receptor mechanism.[81,82] By controlling rod/cone coupling, it seems that dopamine in the light, or its absence in the night, presets rod and cone pathways as appropriate for the lighting conditions.[80,273]

A role for D1 receptors has recently been shown to be critical in the GABAergic control of the rod ON bipolar cell circuit that enhances light sensitivity and increases the dynamic range of their responses at dim-light levels.[274] The location of this control remains to be discovered and could occur via a novel dopaminergic to GABAergic amacrine serial synapse in the IPL or a horizontal cell-mediated input modulated by dopamine in the outer retina. The retina is like a self-optimizing network controlled, at least in part, by the circadian release of dopamine.

Starburst Amacrine Cells

The ChACs, also known as starburst amacrine cells (SACs) on account of their unique morphology, form two mirror-symmetric

populations on either side of the IPL in all mammals.[20] They are the only source of ACh in the retina. In whole-mount view, they are radially symmetric with dendrites radiating from the soma in all directions (Fig. 17.29). The bipolar cell inputs, via AMPA-type glutamate receptors, occur all along the branches, but the outputs seem to be restricted to the varicosities in the terminal third of each dendrite. The cells in the INL produce OFF responses and stratify in sublamina a while the displaced SACs are ON cells branching in sublamina b. They are relatively numerous wide-field amacrine cells. Consequently, they have a very high coverage factor and in cross-section their dendrites form two continuous bands in the IPL that look like train tracks in cross-section (Fig. 17.29). This is a very dense, narrowly stratified matrix of overlapping dendrites that are cofasciculated with the direction selective (DS) ganglion cell types.[275,276]

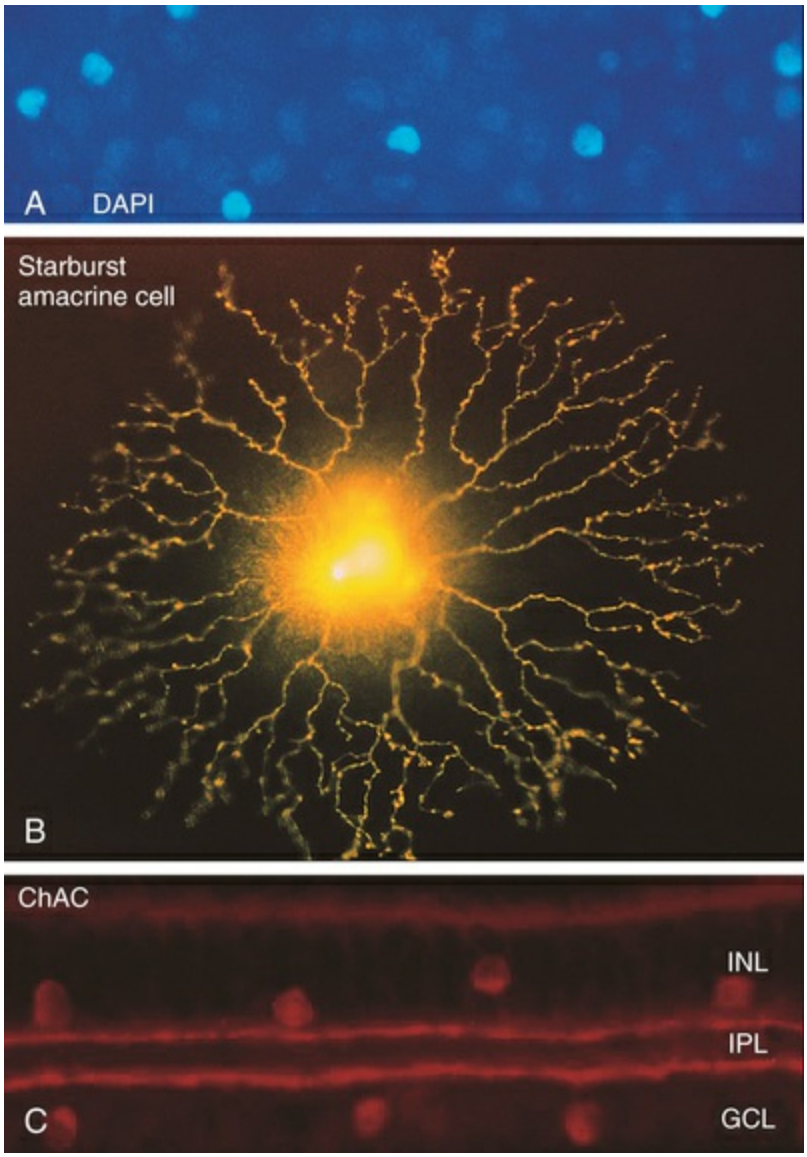

FIG. 17.29 Starburst amacrine cells. (A) The somas of displaced starburst amacrine cells stained with 4',6-diamidino-2-phenylindole (DAPI). This method is used to target this cell type. (B) A single starburst amacrine cell, filled with Lucifer Yelllow. (C) A section of retina stained for choline acetyltransferase (red) showing conventional and displaced somas and two bands in the inner plexiform layer. *INL*, inner nuclear layer; *IPL*, inner plexiform layer; *GCL*, ganglion cell layer. (Courtesy of S.C. Massey.)

SACs also contain GABA.[277] In fact, we should probably think of these cells as wide-field GABA amacrine cells, which also contain ACh. The presence of two classical neurotransmitters in the same cell is unusual and it has aroused a great deal of interest. The

release of both transmitters seems to be dependent on calcium, which indicates a conventional mechanism using synaptic vesicles. But GABA and ACh release have a differential sensitivity to calcium. This implies that the two transmitters may be released from different populations of vesicles, but whether cotransmission occurs at the same sites is unknown.[278]

The SACs have been a focus of attention because they seem to be directly involved in neuronal circuits that produce DS responses in certain ganglion cells. DS ganglion cells were discovered nearly 50 years ago and, although the mechanism has been under intense investigation, the details have still not been fully resolved. However, SACs are in the middle of the puzzle. Ablating them, in a mouse line engineered to respond to an immunotoxin, blocked DS responses in ganglion cells.[279] Furthermore, optokinetic nystagmus, a type of reflex eye movement elicited by a moving stimulus, was also blocked. This combination of physiologic and behavioral data provides convincing evidence that SACs are required for directional selectivity and optokinetic eye movements.

SACs also are found at the same depth as the bistratified ON/OFF DS ganglion cells, which are the most sensitive of all ganglion cells to ACh. But cholinergic input alone is not sufficient to produce DS responses.[280] Rather, the mechanism seems to depend on asymmetrical GABA inhibition that comes from the SACs. In dual recordings, stimulating a starburst amacrine cell on the null side produced an inhibitory GABA input to DS ganglion cells.[278,281]

Furthermore, calcium imaging by two-photon microscopy showed that individual dendrites of SACs can themselves produce directional responses, even though recordings from the soma do not.[33] The dendrites respond better to a centrifugal stimulus, moving away from the soma, than a centripetal stimulus, towards the soma. The directional signals are due to the intrinsic morphologic properties of SACs and a voltage gradient generated by the asymmetric distribution of voltage-dependent channels.[282,283] Most recently, crowd sourced 3D reconstruction (Eyewire) has shown that the OFF layer of starburst dendrites receive input from two bipolar cell types, one sustained and one transient, and this may contribute to the directional asymmetry.[284] In addition, there is GABA-mediated starburst-to-starburst inhibition, which may

enhance or fine-tune the DS responses.[278] These important results confirm a long-held suspicion that there is a great deal of local processing among amacrine cell dendrites and it suggests that SACs are the source of directional signals in the retina.

Given that SACs generate directional signals, they release GABA, and they synapse directly with ON/OFF DS ganglion cells, then the final requirement for specific wiring is that individual starburst dendrites with the appropriate directional asymmetry are connected to ON/OFF DS ganglion cells with the same orientation of the null/preferred axis. (Remember, there are four subsets of ON/OFF DS ganglion cells with different axes, roughly aligned with the four main compass points.) By a combination of calcium imaging to identify the directional preferences combined with serial block-face electron microscopic imaging to reconstruct the underlying retinal circuits, the specific synaptic connections have now been identified.[285] Starburst dendrites with a specific orientation make synaptic connections, identified by varicosities containing presynaptic machinery, with ON/OFF DS ganglion cells with an antiparallel null axis. Thus, preferred excitation in starburst dendrites can provide the GABA input for null inhibition to ON/OFF DS ganglion cells. Often, the starburst dendrites and the ON/OFF DS ganglion cell dendrites are oriented nearly parallel and it is well known that these two cell types are cofasciculated at the level of the two cholinergic bands. Once a local DS response is generated in the ganglion cell, dendritic spikes propagate to the soma with a high probability of generating somatic spikes.[286] After 50 years, the neuronal circuitry underlying directional selectivity has finally been revealed. How this arises developmentally and what the role is for cholinergic input are further important questions that remain.

Finally, the network of SACs appears to play a key role in retinal development.[287] Imaging of neonatal retina shows the presence of calcium waves, which propagate across the retina and elicit bursts of firing in all ganglion cells. These waves apparently are not required to establish directional selectivity, which arises independently of both waves and visual experience.[288] However, in one model, wave activity is thought to promote the development of ganglion cell connections in a retinotopic manner. The cholinergic

plexus is present surprisingly early in development and, in the early stages, the calcium waves are blocked by cholinergic antagonists.[289–291] This suggests that spontaneous activity in the ChACs may initiate the calcium waves. This was thought to be light-independent; however, it now appears that light input via ipRGCs (light-sensitive ganglion cells: see below) is required for aspects of the spiking that are important for retinogeniculate segregation.[292]

Ganglion Cells

Ganglion cells are the output neurons of the retina, and they receive input from bipolar cells, at ribbon synapses, via AMPA-type glutamate receptors.[293] In addition, there are even more amacrine cell inputs, through conventional synapses and via gap junctions, which are thought to tune ganglion cell properties in a complex way that is not well understood. Ganglion cells mostly obey the stratification rules governing the inner retina. Thus OFF ganglion cells receive input from OFF bipolar cells in sublamina a and ON ganglion cells receive input from ON bipolar cells in sublamina b. There are a few ON/OFF types of ganglion cell, such as the famous DS type, and they are bistratified.

Ganglion cell axons run across the vitreal surface of the retina and unite to form the optic nerve. Unlike many other retinal neurons, ganglion cells produce conventional action potentials suitable for transmission over the relatively long distance to the brain. The vast majority of ganglion cells use the excitatory neurotransmitter glutamate to communicate with higher visual centers. Everything you see about the visual world comes to you through the responses of ganglion cells. If they don't signal it, you don't see it! If there are about 30–40 ganglion cell types (see below) and the coverage factors range from one to three, then the total coverage of the retina by the whole ganglion cell population is about 50–100. In other words, each point on the retina is covered by at least 50 ganglion cells. The number of ganglion cells in each human retina is approximately 1.5 million, equal to the number of axons in each optic nerve. In macaque, there are 1.8 million,[143] in rabbit, 380,000,[294] and in mouse retina approximately 60,000

ganglion cells.[47] The actual number of cells has a large genetic component, which produces up to threefold variation in numbers, as demonstrated by quantitative analyses of a large number of mouse strains.[295]

Ganglion cells are physiologically and morphologically diverse. They can be classified by many physiologic and anatomic criteria, including size, response, receptive field, color, bandwidth, ON or OFF, conduction velocity, morphology, branch pattern, stratification, coupling, coverage, and central projections. Earlier estimates are in the range of 15–20 different ganglion cell types. However, the most recent report suggests there are as many as 40 ganglion cell types in the mouse retina.[296] Importantly, this is based on an unbiased sample of 11,000 ganglion cells, obtained by calcium imaging of electroporated retina. Specific ganglion cell types were extracted mathematically by cluster analysis and verified by complementary genetic and anatomical methods. This analysis suggests that the number of ganglion cell types, and therefore the number of channels via which the mouse eye talks to the mouse brain, is substantially greater than previously realized using purely anatomical methods.[296] We think the number of distinct types is extremely important because each ganglion cell type is thought to represent an independent visual channel, perhaps with a specific central target. An important goal now is to characterize fully each RGC type with respect to physiology and synaptic connections. An understanding of the central projections of each ganglion cell type will be necessary before we have a true understanding of the visual process.

New tools by way of transgenic mouse lines that express a marker protein such as GFP in a single type of cell are becoming available.[38,297–301] A particularly striking example of the power of this approach was the ability of Michal Rivlin-Etzion and colleagues to show that two ON/OFF DS RGCs with similar direction selectivity had different projection patterns to the brain. These data suggest there are at least eight ON/OFF DS RGCs with indistinguishable dendritic arbors. If a similar situation arises with other classes of RGCs then the number of independent cell types may increase dramatically, also increasing the number of visual channels leaving the retina. In fact, the total number of ganglion cell types has not yet

been determined for any species. Seemingly rare cell types that account for a small fraction of the total, e.g., ipRGCs, make up less than 1%, but may be split into five subtypes with different morphology and different central projections, further adding to the types of RGCs. There seems to be general agreement that the number of ganglion cell types will be more than 20 and as high as 40.[296] Genetic methods will be increasingly important and they have been used to identify several new ganglion cell types, increasing the anatomical cell count to 30.[302]

The importance of depth in the IPL was emphasized when Roska and Werblin showed that at least 10 ganglion cell types, most narrowly stratified at different depths, received distinct physiologic inputs in the rabbit retina.[303,304] Apparently, the IPL contains a stack of parallel versions of the visual scene coded by depth. Each layer receives a different combination of excitatory and inhibitory inputs to produce at least 10 spatiotemporal channels. Ganglion cells with transient or sustained responses were located at different levels of the IPL. Some ganglion cells received inhibitory inputs that originated in another layer. This type of vertical inhibition could be carried by narrow-field amacrine cells, many of which are broadly stratified.[228] The functional anatomy of the IPL is very precise. In the rabbit retina, OFF and ON alpha ganglion cells are stratified just below the two cholinergic bands (Fig. 17.30).[10,218] They are separated by as little as 1–3 μm but they are clearly different addresses serving different ganglion cells with distinct morphologic and physiologic properties. If a single stratum can be as narrow as this, there is certainly room for a dozen or more different layers within the IPL, each serving one or more different ganglion cell types.

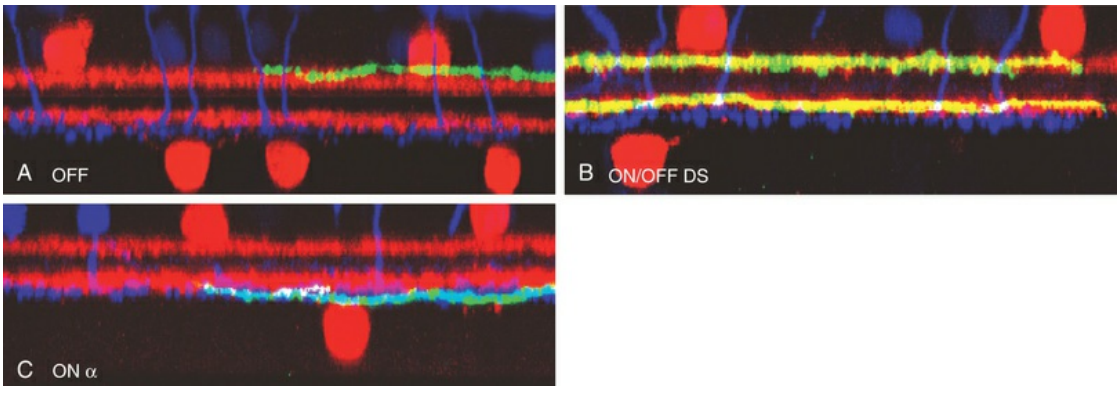

FIG. 17.30 Stratification of the inner plexiform layer. (A) The dendrites of an OFF alpha ganglion cell (green) lie above the cholinergic a band (red). (B) The dendrites of an ON/OFF directionally selective ganglion cell are bistratified and lie within the two cholinergic bands (green + red + yellow). (C) The dendrites of an ON alpha ganglion cell lie immediately below the lower cholinergic b band. This is at the same depth as the terminals of calbindin bipolar cells (blue), so green + blue = cyan. Thus, the inner plexiform layer can be very finely divided into different layers which are actually different addresses for synaptic interactions. (Courtesy of W. Li and S.C. Massey.)

Does Each Ganglion Cell Type Represent a Visual Channel?

The simple answer to this question is yes, we think so. However, we still do not have a definitive value for the number of channels and, for those ganglion cell types that have been classified morphologically, it is not always clear which physiologic class they belong to. The correspondence between functional anatomy and physiologic type is only partially complete.[305] But, it is increasingly apparent that the characteristic responses of the different ganglion cell types represent the diversity of parallel bipolar cell pathway outputs modified by lateral inhibitory interactions; the interplay between vertical excitatory and lateral inhibitory pathways generates the ~20 distinct computations represented by the ganglion cell classes.[4,152,306]

Several recent studies have revealed unexpected complexity within ganglion cells' receptive fields by identifying interactions between excitatory bipolar cell and inhibitory amacrine cell circuits that expand the signaling capacity of ganglion cells. For example, strong, local synaptic inhibition can act to make some ganglion cells sensitive primarily to spatially homogeneous stimuli.[307] Local inhibition also is responsible for a phenomenon termed "sensitization," in which a ganglion cell responds more strongly to a low contrast stimulus following exposure to a high contrast one. A subset of ganglion cells in both the salamander and mouse retinas

exhibit sensitization, which is thought to arise from activity-dependent changes in the balance of local excitation and inhibition.[308,309] Presumably, such spatially tuned synaptic drive permits ganglion cells to encode visual stimuli more precisely.[310] Recent work also has yielded the surprising findings that retinal circuit function is not static, but rather can change with ambient light intensity. For example, some inhibitory circuits are not activated well by rod stimulation, and this makes some ganglion cells' receptive field structure intensity-dependent.[311]

A problem that has yet to be adequately resolved is what features of the functional responses of the ganglion cells are the ones that set individual classes apart. In fact, function alone is probably not sufficient and projection pattern, axon diameter, and terminal morphology may also be important. Regardless, it is widely believed that the retina, with the ganglion cells as the output, produces a large set of neural codes, most of which have not been deciphered, that are transmitted to the brain in parallel both on a temporal scale and to a variety of central structures. These are the visual channels, some of which carry different versions of Mona Lisa (see Fig. 17.1), where we began. The extent to which visual perception represents retinal processing is uncertain, but increasing insight into both retinal and cortical neural computation will permit this issue to be clarified in the future.[312] Below are some examples of different ganglion cells/visual channels that we are beginning to understand.

In a few cases, a particular ganglion cell type seems to have a specific role. Midget ganglion cells in the primate retina are a good example. There are two types, ON and OFF, which are broadly stratified towards the middle of the IPL. Midget ganglion cells are numerically dominant in central retina, where they may account for as many as 95% of all ganglion cells.[184] Importantly, we know that in central retina there is a 1 : 1 : 1 correspondence from cones → midget bipolar cells → midget ganglion cells. Beyond 2 mm or 10°, the midget ganglion cells form separate dendritic clusters that receive input from multiple midget bipolar cells. Sampling theory, based on the density of midget ganglion cells, closely predicts the curve describing a psychophysical measure of human acuity, except close to the fovea where the cone pedicles are laterally displaced.[313]

Thus, it seems clear that midget ganglion cells transmit a high-acuity version of the visual scene from the center of your gaze, the central retina. The 1 : 1 : 1 ratio also means that individual midget ganglion cells will be color-coded according to the type of cone at the beginning of the chain. Midget ganglion cells project to the parvocellular layers of the lateral geniculate nucleus which also carry color signals. Midget ganglion cells are a specialization of the primate retina, perhaps the final point in the relentless survival-driven goal of maximum acuity. There is no exact match in other mammalian species but an equivalent role could be played by beta ganglion cells in the cat retina. In the rabbit retina, there are neither midget nor beta ganglion cells but an ON and OFF pair of relatively small ganglion cells, G4, which are rather broadly stratified toward the middle of the IPL.[314] These are at least morphologically similar. Consistent with the idea that the midget/beta cells are a specialization of animals with a fovea or foveal-like specialization, the rodent retina lacks these types of ganglion cells.

Some of the most convincing evidence that ganglion cells carry specific channels of visual information comes from comparative anatomy, where it can be seen that certain ganglion cell types recur frequently across species. Perhaps the best example is the alpha ganglion cell, which has been reported in many mammalian retinas.[315] Alpha ganglion cells have large somas, come in paramorphic ON and OFF pairs, make up less than 5% of all ganglion cells, and have a large dendritic field with a characteristic radiate branching pattern (Fig. 17.31). In the rabbit retina, alpha ganglion cells are narrowly stratified just below the cholinergic bands. Physiologically, they have transient nonlinear (Y-like) properties, they respond to stimuli of high temporal frequency and project to the magnocellular layers of the lateral geniculate nucleus. Their responses are not color-coded. Alpha ganglion cells seem well suited for detection of low luminance contrast over large areas of the visual field, such as a blurred copy of the Mona Lisa. Their occurrence over such a wide range of species suggests they play a fundamental role common to the visual needs of many animals, e.g., detection of motion. Parasol ganglion cells in the primate retina and A-type cells of rodents have similar properties, although whether they correspond exactly to alpha cells is an open question.

There appear to be wide-field ganglion cells in the primate retina that are morphologically closer to alpha ganglion cells in other species.[316]

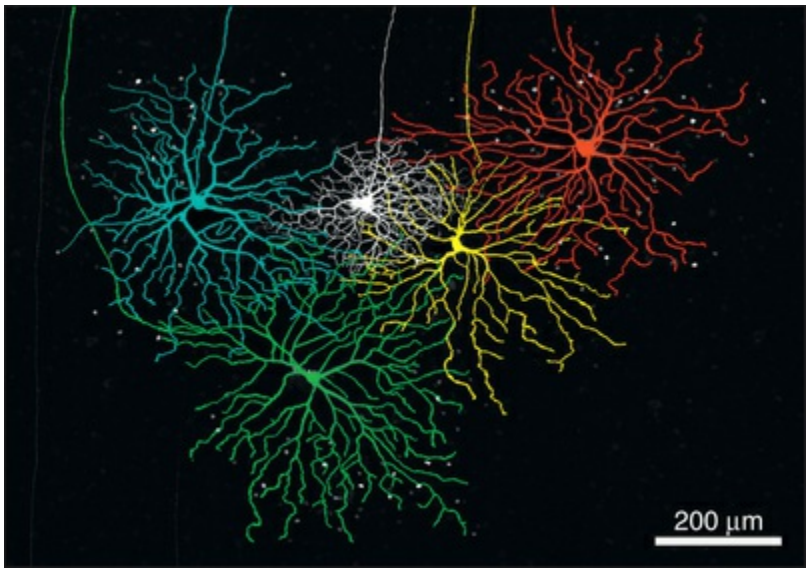

FIG. 17.31 Dye-injected ganglion cells in the rabbit retina. The white cell is an ON/OFF directionally selective ganglion cell surrounded by four much larger transient ON DS ganglion cells. These two ganglion cell types have obviously different dendritic morphology. In addition, the transient ON DS ganglion cells form a nonrandom mosaic. There are also some dye-coupled amacrine cells in the background.
(Reproduced with permission from Hoshi H, Tian LM, Massey SC, et al. Two distinct types of ON directionally selective ganglion cells in the rabbit retina. J Comp Neurol 2011;519:2509–21.)

The ON/OFF DS ganglion cells of the rabbit retina, reported by Barlow and Levick nearly 50 years ago,[317] are one of the best characterized of the retinal ganglion cells. In these ganglion cells, a bar moving in the preferred direction through their receptive field produces a strong burst of spikes, but the same stimulus moving in the opposite direction produces little or no response. As first shown by Amthor and colleagues,[318] bistratified cells fasciculate extensively within the two bands of starburst amacrine cell processes and they have a distinct retroflexive branching pattern (Fig. 17.32). DS ganglion cells are exquisitely sensitive to nicotinic cholinergic agonists but, surprisingly, directional selectivity is not

dependent on this cholinergic input.[280]

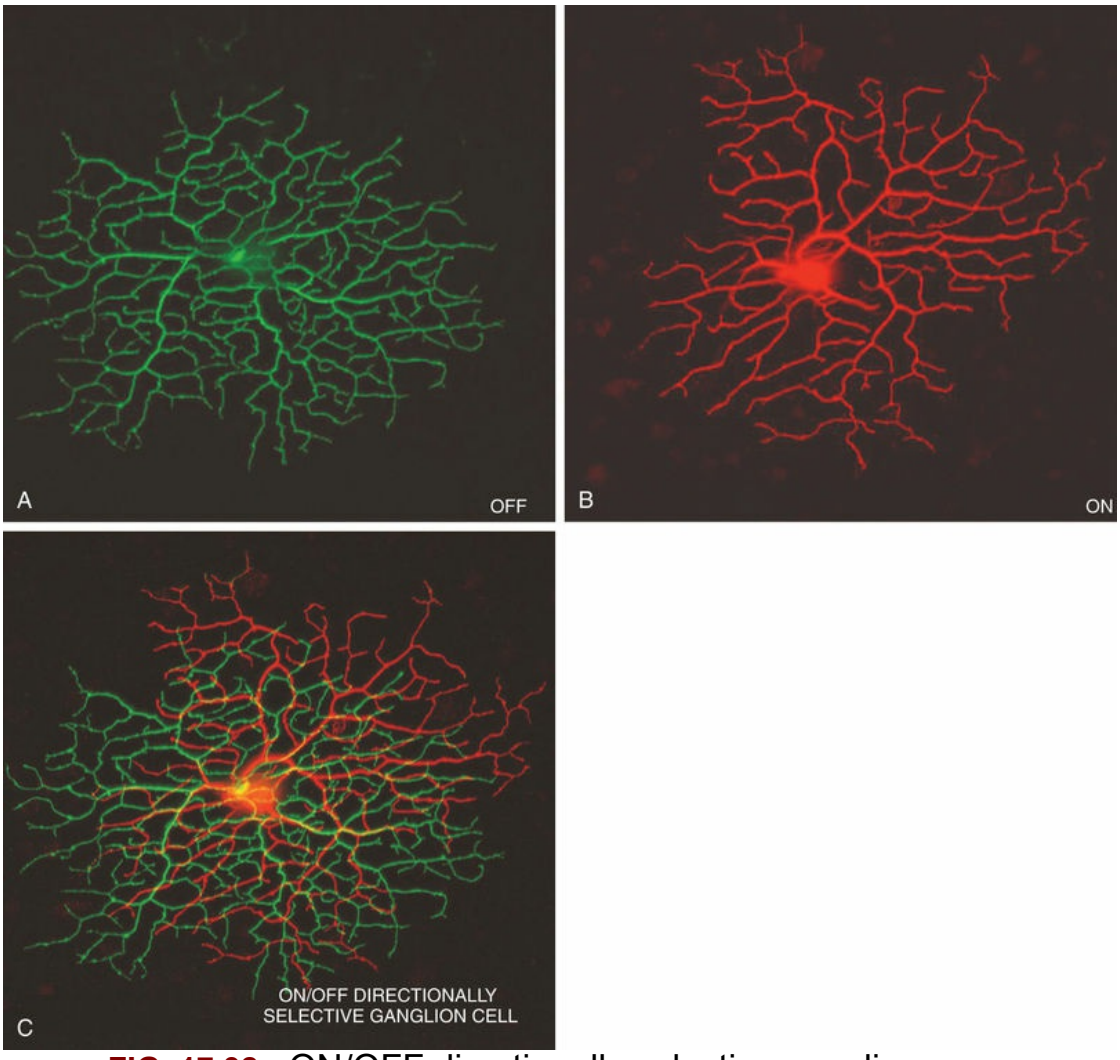

FIG. 17.32 ON/OFF directionally selective ganglion cell. A single ON/OFF directionally selective ganglion cell was dye-injected with Neurobiotin and then, using the confocal microscope, the two dendritic fields were imaged and color-coded. Note the retroflexive branching pattern which fills most of the available space, in contrast to the branch pattern of the alpha ganglion cell above. (Reproduced with permission from Kittila CA, Massey SC. Pharmacology of directionally selective ganglion cells in the rabbit retina. J Neurophysiol 1997;77:675–89.)

Paired recordings showed that SACs on the null side of the DS ganglion cells provide asymmetric GABA inhibition to DS ganglion cells.[281,319] The source of the GABAergic input is from SACs, which

contain GABA as well as ACh.[277] Individual dendrites of the SACs generate directional responses due to their intrinsic properties and this is the origin of directional signals in several other types of DS ganglion cells.[33] This difference is consistent with recent morphologic results using an extensive three-dimensional reconstruction of functionally identified DS ganglion cells by serial block-face electron microscopy that showed specific inhibitory inputs from starburst dendrites with the appropriate orientation.[285]

At present, four ganglion cell types with different null/preferred axes have been described, one of which is dye-coupled and shows a precise dendrite-to-dendrite tiling pattern with a coverage close to 1.[320] DS cells with the other preferred axes are thought to tile the retina independently so that if the dendrites of two DS ganglion cells overlap, they must have different preferred directions. They can also be differentiated by molecular markers and have slightly different central projections.[321] The four null/preferred axes are aligned with the extraocular muscles[322] so it is often suggested that the ON/OFF DS cells play a role in the control of eye movements. Cells with a similar morphology have been noted in mouse and rat,[323,324] cat (the iota cell),[325]and even primate retina.[316] In the mouse two posteriorly tuned, essentially morphologically identical DS cells have been defined that have subtle receptive field differences, and different central projection patterns.[301] If each compass point is duplicated in the same manner, this would predict there should be a total of eight ON/OFF DS ganglion cells. It is not unreasonable to assume a similar situation will exist in most other mammals.

There is another DS cell in the rabbit retina that has interesting properties. Its dendrites are monostratified in the ON starburst band and have a similar retroflexive branch pattern. They also receive specific null-side inhibition from SACs.[326] However, these ON DS cells respond to much slower movements and its three variants have different null/preferred axes, which are aligned with the semicircular canals.[327] Consistent with the hypothesis that DS ganglion cells are critical to eye movement control, the ON DS ganglion cells project to the medial terminal nucleus of the accessory optic system.[327,328] Ganglion cells with a strikingly similar morphology have been reported in mouse, rat, and primate retina.[316] The value of this comparative anatomy becomes clear

when we consider an experiment in the mouse retina. When SACs are ablated, DS responses in ganglion cells are abolished and the optokinetic nystagmus is also blocked.[279] This is a type of reflex eye movement involved with tracking moving objects with the same velocity range as the ON DS ganglion cell. It suggests that ON DS cells provide the input to a system for tracking or stabilizing the retinal image. At least one gene associated with an eye movement disorder is exclusively expressed in SACs, which provide the directional input to the ON DS ganglion cell.[300]

A second type of ON DS ganglion cell has recently been identified in the rabbit retina.[328–330] This cell type, originally reported by Ackert and colleagues,[331] is distinct from the cell described above in terms of morphology and dendritic stratification, just above the lower band of ChAC processes. If the SACs are the source of directional signals in the retina, it is not clear how DS signals are generated in this cell type. Finally, in a stunning example of a cell type-specific molecular marker, a whole population of ganglion cells from the mouse retina was stained using a junctional adhesion molecule B (JAM-B)-driven GFP mouse line.[299] This procedure identified a uniform population of ganglion cells with asymmetrical dendritic trees aligned dorsal to ventral. A similar OFF cell type, G3 in the Masland catalog, has been reported for the rabbit retina.[314,332] In the mouse, this cell type has been characterized as OFF DS, although in the rabbit retina it was identified as orientation-selective.[333] If it is truly DS, then the mechanism may be unusual because it does not stratify with the SACs. Together, these observations suggest that there may be multiple circuits to generate directional signals.[334]

A Ganglion Cell for the Control of Pupil Diameter and Circadian Rhythm

It has long been known that certain visually driven activities persist in mice where rods and cones have completely degenerated. These apparently blind mice retain pupillary light reflexes as well as circadian rhythms and a similar profile has been reported in totally blind humans.[335] It was concluded that these reflexes are driven by connections separate from the usual image-forming pathways. This issue was resolved when a set of ganglion cells were found to

express an additional visual pigment called melanopsin. They form a relatively sparse mosaic (only 2000 per mouse retina) with loopy dendrites (Fig. 17.33) in sublamina a and b and they respond with a slow sustained discharge dependent on the light intensity.[36] Even when these cells are isolated, they still produce light responses.[336] In other words, the melanopsin-containing ganglion cells are intrinsically photosensitive and they are referred to as ipRGCs.

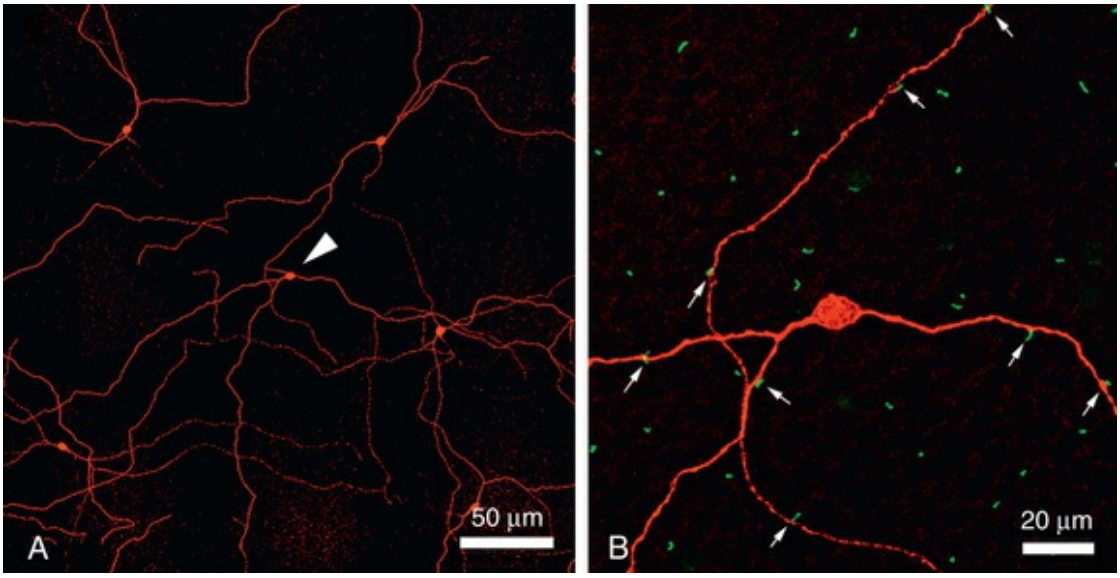

FIG. 17.33 Melanopsin ganglion cell ectopic inputs. (A) Low-resolution picture shows melanopsin ganglion cells in the rabbit retina have sparse randomly arranged dendrites. (B) Staining certain ON cone bipolar cells with an antibody against calbindin showed that the descending axons were frequently adjacent to the melanopsin-positive ganglion cells. These are the sites of axonal ribbon inputs which provide ON input to melanopsin ganglion cells that stratify in sublamina a of the inner plexiform layer. (Reproduced with permission from Hoshi H, Liu WL, Massey SC, et al. ON inputs to the OFF layer: bipolar cells that break the stratification rules of the retina. J Neurosci 2009;29:8875–83.)

The melanopsin-containing ganglion cells project to the suprachiasmatic nucleus (SCN), the brain's circadian pacemaker.[36,336] Labeled axons were also found in the olivary pretectal nucleus (OPN), which is involved with the circuit controlling pupil diameter. These are referred to as nonimage-forming pathways. In mice lacking melanopsin, photoentrainment

of the circadian rhythm and the control of the pupillary light reflex were attenuated at high light intensities.[337]

However, melanopsin ganglion cells also receive the usual rod and cone inputs, which can drive these circuits at low light intensities. The M1 subtype is stratified in sublamina a but it still has ON-driven light responses due to the presence of ectopic or axonal ribbon synapses from ON cone bipolar cells as they traverse sublamina a (Fig. 17.33).[27,28,338] In crossbred mice with photoreceptor degeneration as well as no melanopsin, the pupillary light reflex and the photoentrainment of the circadian clock were completely eliminated.[339] The conclusion is that, at low irradiance, the normal rod/cone inputs drive these circuits but at higher light levels the intrinsic melanopsin system drives these accessory visual functions. These experiments provide anatomic, physiologic, and behavioral evidence that the ganglion cell type defined by the expression of melanopsin forms a specific channel in the mammalian visual system that is connected to the SCN and the OPN among other targets. This is a prime example that different ganglion cell types provide parallel channels in the visual system that serves specific functions.

Based on a combination of morphology and physiology, five subtypes of melanopsin-containing ganglion cells, M1–M5, have been identified in the mouse retina.[340,341] The M1 subtype is the only one stratified in sublamina a; it contains the most melanopsin and has strong intrinsic photoresponses and relatively weak rod/cone input. M2 cells have dendrites in sublamina b but less melanopsin and weaker intrinsic responses. M3 cells are bistratified and do not form a uniform population.[342] M4 and M5 cells have very low levels of melanopsin and correspondingly weak intrinsic responses.[340] Using combinations of markers, the M1-class ipRGCs can be further divided into two types, one projecting to the shell of the OPN, which is required for the pupillary light reflex, and one targeting the SCN, required for circadian photo entrainment.[301] This Brn-3b-negative group of M1 ipRGCs comprises approximately only 10% of all melanopsin ganglion cells. Thus, the specific nonimage-forming visual pathway that resets the circadian clock every morning consists of only 200 ganglion cells.[343] It is very surprising that a distinct visual pathway can be formed by such a small

number of cells.

The roles of non-M1 types are still unclear, but they may contribute to light avoidance in mouse pups, sleep regulation, and, in humans, the light sensitivity of migraine and seasonal affective disorder.[340] The activity of ipRGCs is also important for retinogeniculate segregation, which is now known to involve light sensitivity prior to function of the photoreceptors.[292]

Color Vision and Ganglion Cells

Humans are trichromatic, with red, green, and blue cones. Color vision provides an additional variable to improve visual discrimination. It is organized into two opponent systems, red–green and blue–yellow (where yellow = red + green).[344] Hence, there are no red/green hues and no mixtures of blue and yellow; they are said to be color-opponent. The blue–yellow system is found widely in mammals and is thought to be older on an evolutionary timescale.[54] In primates, once the midget system had reached maximum resolution in the 1 : 1 : 1 pathway, a comparatively recent gene duplication produced red and green pigments. By reason of the connection with a single cone, midget ganglion cells are automatically color-coded.

Midget ganglion cells are concentrically organized as red–green or green–red. The center input is spectrally pure because of the 1 : 1 : 1 connection with single cones. There has been some controversy concerning the origin of the color-opponent surround, whether it is spectrally pure, and whether it arises from the outer or inner retina. Recent recordings from midget ganglion cells in the primate retina indicate that the surround is chromatically mixed. In other words, it is the average of the surrounding cones. On average, the ratio of red to green in the surround was approximately 50%.[345] Furthermore, both center and surround inputs modulated an excitatory conductance with a reversal potential around 0 mV. This means that the surround signal does not arise from amacrine cell inhibition in the inner retina. Rather, the color opponency must be generated in the outer retina by horizontal cell feedback.[345] Horizontal cells are suitably wired to provide the spectrally mixed surround signal because they contact both red and green cones indiscriminately.[346] Enhanced buffering to block pH-dependent horizontal cell feedback

eliminated both the spatial and chromatic surround of midget ganglion cells. Although the exact mechanism of horizontal cell feedback is controversial, this strongly indicates that color opponency is produced by horizontal cell feedback in the outer retina.[131,345] Finally, neither GABA nor glycine antagonists blocked the surround inputs. Thus inhibition in either the outer or inner retina is not required. Nor does horizontal cell feedback in the primate retina depend on GABA or glycine.[345]

Large-scale multielectrode array recording has also been used to analyze the color inputs to primate ganglion cells.[347] Hundreds of ganglion cells may be recorded simultaneously and then sorted by spike size and shape to identify individual ganglion cells. Types of ganglion cells may be identified by their receptive field sizes, center/surround organization, and the mosaic properties by which they tile the retina. Using a fine-grained textual stimulus, local hot spots were found within each receptive field that matched the distribution of the underlying cone array. The spectral characteristics of each hot spot, recorded in several nearby ganglion cells, were used to identify each cone locus as red, green, or blue, and then the contributions of each individual cone were mapped to the overlying array of ganglion cells. Parasol ganglion cells sampled uniformly from red and green cones but not blue cones. In contrast, many midget ganglion cells showed color-opponent responses. As above, the surrounds were spectrally mixed but the center inputs to both ON and OFF midget ganglion cells had a small nonrandom tendency to sample from more red or green cones.[347] Obviously, in central retina, where midget bipolar cells may contact a single cone, this would provide a spectrally pure center with a mixed color-opponent surround. Intellectually, we understand that tracing back from ganglion cells through the retinal circuitry must lead to cones. However, the direct demonstration of ganglion cell sampling from the complete array of identified cones is an experimental triumph. These experiments indicate that parasol ganglion cells are not color-coded while color signals are carried by the midget ganglion cells.

In contrast to the red–green system, the circuits underlying blue–yellow opponency have been relatively well described. Some of this success is due to the morphologic details that make cells in the blue pathway more recognizable. This begins with blue cones

themselves, which can be labeled with antibodies against blue cone opsin.[57] Red and green cone opsins are so close they cannot be discriminated by current antibodies. In addition, blue cone pedicles are noticeably smaller, with fewer telodendria.[70] The blue cone bipolar cells can also be recognized because of their long dendrites, which bypass many cones in search of the blue ones.[186,348,349] Blue ON cone bipolar cells have direct input to a small bistratified ganglion cell that gives blue ON/yellow OFF responses.[350] Blue–yellow small bistratified ganglion cells have also been identified in multielectrode array recordings from primate retina. These experiments suggested that most of the color opponency arose in the outer retina.[351,352] Further physiologic evidence suggests that blue–yellow color opponency originates in the outer retina.[353] Indeed, blue cones themselves are blue–yellow color-opponent, indicating that the yellow-opponent signal is generated by horizontal cell feedback.[354]

In nonprimate mammalian retina, blue-driven ganglion cells were reported as monostratified ON cells.[355] This is quite different from the small bistratified blue–yellow ganglion cell of the primate retina. The color opponency of this monostratified ganglion cell could arise in the outer retina, as suggested for primate retina.[352,354]

Gene Therapy to Cure Color Blindness

Mice are dichromats, expressing a short-wavelength photopigment and a single medium-wavelength pigment on the X chromosome. Jacobs and colleagues[356] showed that adding a human long-wavelength photopigment allowed mice to have a form of color vision. This idea has been extended to primates and could potentially be used in humans. About 5–8% of the population has red–green color blindness, because they lack either the long- or middle-wavelength visual pigments. Some squirrel monkeys also are dichromats and recently Mancuso and colleagues[357] showed that adding a third photopigment, using gene therapy approaches could restore color discrimination, even though the monkeys had been dichromats since birth.

New Tools to Identify Ganglion Cell Types

The lack of genetic markers for individual ganglion cell types is a major handicap. As shown above, classification schemes that rely on morphology are very difficult to implement and there is a less-than-perfect mesh with physiology and biochemistry. This is not a minor issue: the comparatively recent flood of information about ipRGCs depends in large part on the identification of this cell type(s) due to the expression of melanopsin. Mouse lines with GFP-labeled melanopsin ganglion cells, knockout mouse strains, and melanopsin antibodies have all been developed. This one simple attribute allows the identification of melanopsin-containing ganglion cells for recording, filling, manipulating, or deleting. Thus, the connections, subtypes, physiology, light responses, and central projections of the ipRGCs have been uncovered, obtaining essentially a full description of this nonimage-forming pathway and its functions in the pupillary light reflex and circadian entrainment.

However, new molecular techniques are starting to provide a way to mark certain ganglion cell types as a complete population. Thus, it is becoming possible to study a specific ganglion cell type as opposed to a spectrum of mixed cell types with variable properties. One research group has screened a library of bacterial artificial chromosome (BAC) transgenic mice with GFP expressed under the control of different promoters. In particular, they looked for GFP expression in a nonrandom mosaic. This is one of the known properties of specific ganglion cell types, which tile the retina in a uniform manner.[39] In calretinin-enhanced GFP (EGFP) mice, a mosaic of large ganglion cells, stratified in sublamina a, with OFF transient responses to light was found. Collectively, these properties identify the GFP-labeled cells as OFF α ganglion cells.[298] Centrally, this specific ganglion cell type projects to both the superior colliculus, an area integrating sensory input and guiding visual attention, and the dorsal lateral geniculate nucleus, a relay station on the way to the visual cortex. Furthermore, the axonal projections in both areas are precisely organized in columns at a specific laminar depth. Importantly, disrupting cholinergic retinal waves during development prevented the columnar organization of

OFF α ganglion cell axons.[298] This suggests that spontaneous activity during retinal development controls the development of a retinotopic map. It is worth repeating that these experiments were made possible because a genetic marker for a single ganglion cell type, the OFF α ganglion cell, was identified.

In a cadherin-3 GFP mouse line, a small percentage of ganglion cells was labeled, some of which also expressed melanopsin. They also contained cadherin-6 and projected to nonimage-forming visual nuclei such as the ventral lateral geniculate nucleus, the intergeniculate leaflet, and the OPN. These nuclei, known targets of ipRGCs. Importantly, in cadherin-6-deficient mice (cadherin-3/GFP crossed with a cadherin-6 knockout), the cadherin-3-labeled ganglion cells failed to innervate the appropriate visual nuclei. Instead, the GFP-labeled axons projected through and past their usual targets. These experiments, utilizing genetically labeled mouse lines, indicate that cadherin-6 is necessary for certain ganglion cell types to recognize their synaptic targets and form functional circuits.[358]

As mouse lines in which different cell types are labeled by molecular methods become widely available, the methods to differentiate among retinal cell types will continue to expand. One group has published a "genetic address book" of retinal cell types.[38] Moreover, several groups have used GFP-labeled cell types to develop single-cell expression libraries for specific cell types.[321,359] This advance in technique is likely to be a game-changer. It will enable a molecular fingerprint to be developed for each cell type, as well as identifying the transcription factors and signaling molecules which govern development and circuit connections.[360] In particular, a transcription factor-based code was used to sort the cells into relevant groups. Perhaps this methodology will provide the definitive answer to how many ganglion cell types are present in the mammalian retina. Finally, by correlating these single-cell libraries against a database of gene mutations associated with visual system disorders, it may be possible to identify defects arising in specific cell types or circuits. For example, an eye movement disorder was correlated with SACs, which may be the source of DS signals required to control reflex eye movements.[317]

Clinical Relevance of Functional Anatomy

As we have seen, the retina is fundamentally organized as a layered structure. This applies not only to the major cellular and synaptic layers but particularly within the IPL, where the level of stratification is an address. It appears that stratification at the appropriate depth in the IPL allows a ganglion cell to receive input from a certain set of bipolar and amacrine cell processes. The sum of these inputs to a particular type of ganglion cell forms a single channel in the visual system. The overall complexity appears daunting but it may be broken down into a repeated set of stereotyped local circuits, which are strictly governed by a set of rules concerning position and appropriate synaptic partners. Below we discuss briefly some obvious examples where the basic layering and organization of the retina are disrupted, with important clinical consequences.

In glaucoma, the basic defect is in the GCL. Increased intraocular pressure apparently induces programmed cell death in retinal ganglion cells. Factors involved may include anoxia, reduced axonal transport, and excess glutamate, leading to excitatory damage known as excitotoxicity. Ganglion cells appear to be particularly sensitive while other retinal neurons such as amacrine cells are unaffected. Fig. 17.34 shows a retinal section from the same eccentricity of a control macaque eye compared to the operated eye with experimentally induced high intraocular pressure. All retinal layers appear normal, with the exception of the GCL, which is severely depleted compared to the control eye. The absence of retinal ganglion cells may be correlated with dramatically reduced visual acuity, especially in the peripheral retina.[360]

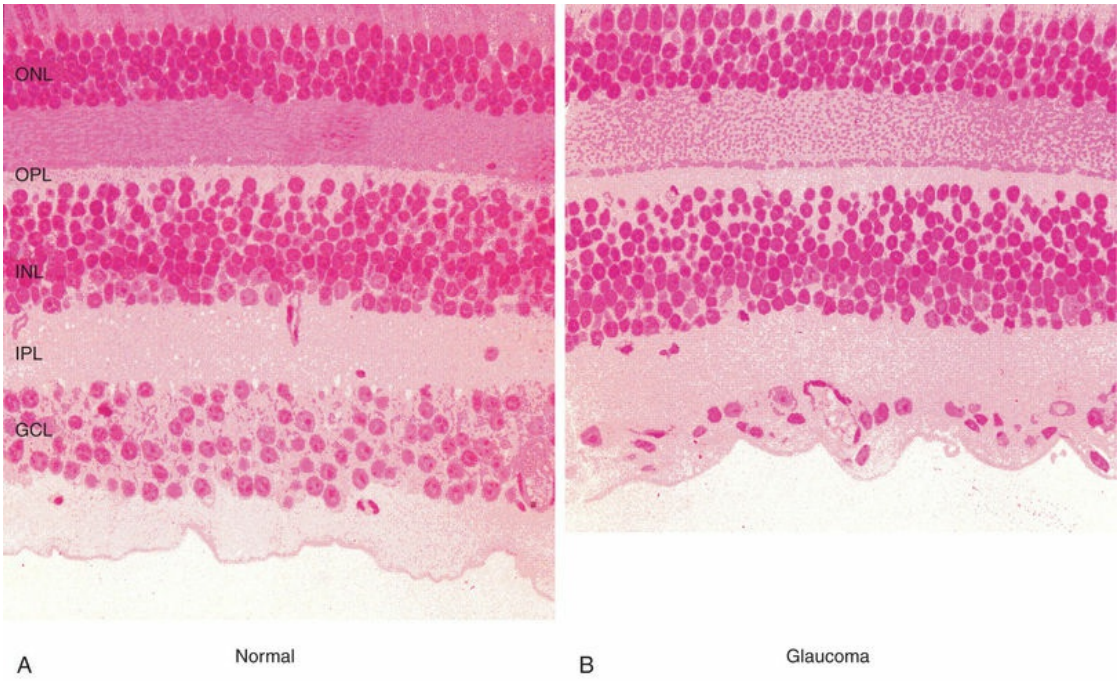

FIG. 17.34 Depletion of ganglion cells in glaucoma. (A) Control retina, near central, as shown by the depth of ganglion cell somas. (B) While the rest of the retina is normal, the ganglion cell layer has been severely depleted by experimental glaucoma. *GCL*, ganglion cell layer; *INL*, inner nuclear layer; *IPL*, inner plexiform layer; *ONL*, outer nuclear layer; *OPL*, outer plexiform layer. (Courtesy of Louvenia Carter-Dawson.)

A large number of photoreceptor mutations, often in the phototransduction cascade, lead to photoreceptor degeneration in conditions such as retinitis pigmentosa (RP). The defect often arises in rods but eventually both rods and cones degenerate. Whether this occurs because rods secrete a maintenance factor for cones, or via rod/cone coupling, known as the bystander effect, or due to the accumulation of cellular debris is a matter of debate beyond the scope of this chapter. However, photoreceptor degeneration has severe consequences for the organization of the remaining retina. The neural retina apparently requires input from the sensory retina to maintain its well-organized structure. When the neural retina has been deafferented, the second-order neurons, such as rod bipolar cells, produce new dendrites and sprout profusely, making many inappropriate contacts.[3,361] Many neurons develop novel processes that invade other layers where they proliferate to produce tangled microneuromas. Glial cells are extensively remodeled; there is mass

neuronal migration and almost total disruption of the layered structure of the retina. Fig. 17.35 shows examples from two rodent lines and a human RP case. In each case, the resulting tangle of misplaced cells and inappropriate contacts is essentially unrecognizable as a section of retina. The basic layered organization of the retina has been destroyed. One consequence of this neural reorganization is that the remaining retina is unlikely to retain sufficient organization to operate in any kind of coherent manner. Thus, in the absence of photoreceptors, strategies aimed at stimulating the remaining neural retina by means of a retinal implant seem unlikely to succeed, unless the process of retinal remodeling can be controlled.

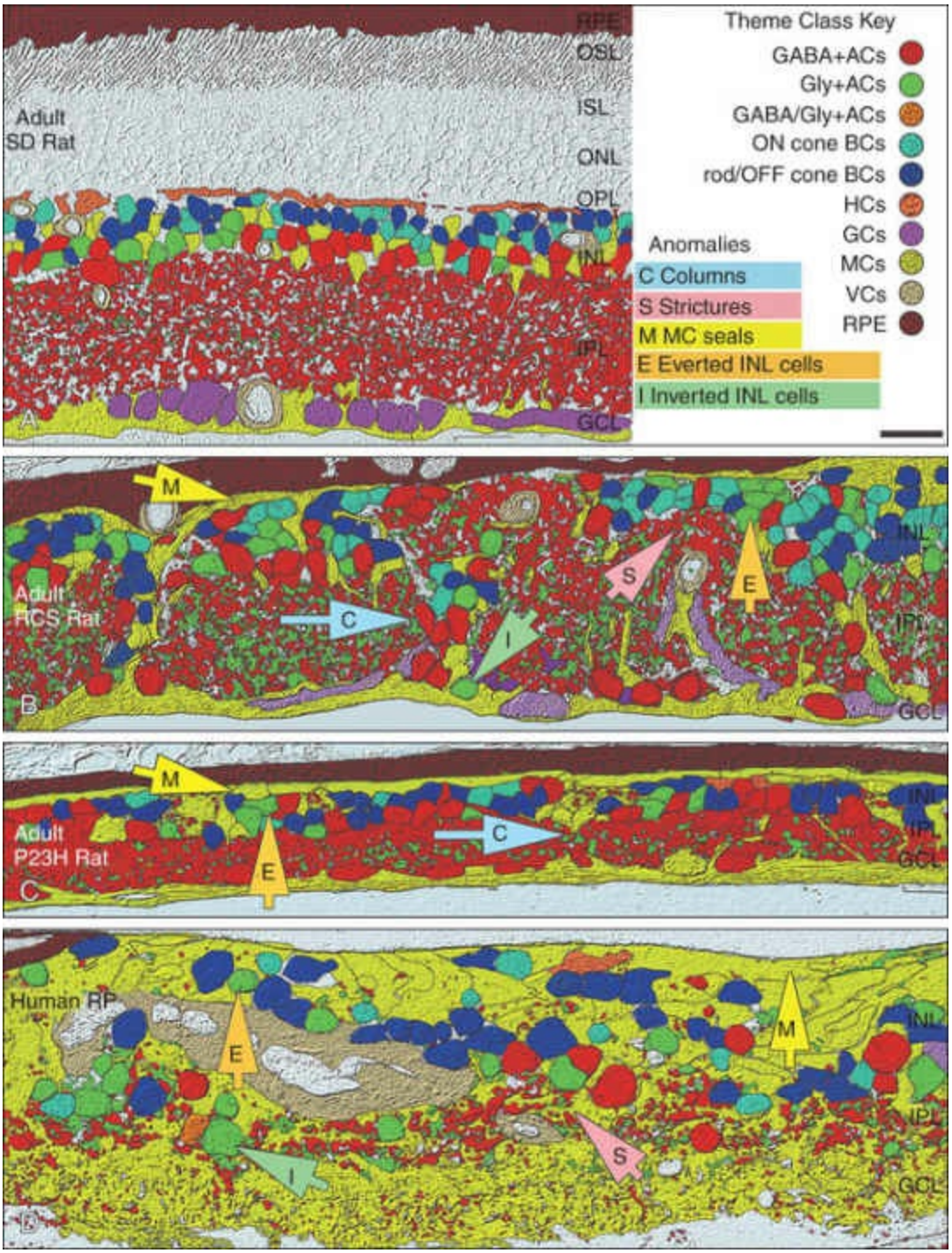

FIG. 17.35 Disruption of retinal organization following photoreceptor degeneration. (A) Control retina: a theme map shows the well-organized, layered structure of the normal retina. (B,C) Rodent retina following photoreceptor degeneration shows severe disruption of the normal layered structure. Many cells have migrated to inappropriate locations. (D) A human retinitis pigmentosa case where the organization of the neural retina has been severely disrupted. *RCS,* Royal College of Surgeons; *SD,* Sprague–Dawley. *ACs,*

amacrine cells; *BCs,* bipolar cells; *GABA,* gamma-aminobutyric acid; *GCs,* ganglion cells; *GCL,* ganglion cell layer; *Gly,* glycine; *HCs,* horizontal cells; *INL,* inner nuclear layer; *IPL,* inner plexiform layer; *ISL,* inner segment layer; *MCs,* Müller cells; *ONL,* outer nuclear layer; *OPL,* outer plexiform layer; *OSL,* outer segment layer; *RPE,* retinal pigment epithelium; *VCs*, vascular cells. (Reproduced with permission from Jones BW, Watt CB, Frederick JM, et al. Retinal remodeling triggered by photoreceptor degenerations. J Comp Neurol 2003;464:1–16.)

Of course, one major advance in the last few years is our ability to identify mutations that cause RP by whole-genome sequencing. In the near future we will no doubt be able to sequence each person's entire genome, and this could be done at birth. Identifying individuals who will get RP, well before the retina undergoes extensive degeneration, might allow curative strategies to be implemented at times that avoid some of the problems associated with remodeling.

In addition to the above diseases that disrupt the gross morphology of the retina, there also are diseases with less severe effects. One group results in night blindness, without any degeneration of retinal cell types. These are called congenital stationary night blindness (CSNB). The result is a greatly diminished amplitude of the electroretinogram b-wave, indicating lack of or poor signal transmission between photoreceptors and bipolar cells. Careful analyses of the electroretinogram indicate that there are two forms, incomplete and complete.[362] The genetic defects that give rise to these defects are now known to be caused by mutations in genes that are involved in release of glutamate from photoreceptors (incomplete, iCSNB) or absence of signaling in depolarizing bipolar cells (complete, cCSNB). Mouse models for iCSNB reveal that the dendritic arbors of ON bipolar and horizontal cells are abnormal. They extend across the OPL into the ONL and often reach the outer limiting membrane.[363] By contrast, models of cCSNB have no morphologic abnormalities, although in some there appears to be some abnormal expression of synaptic proteins, resulting in ribbon synapses being present in dendrites of depolarizing bipolar cells.[364]

Conclusions

In one sense, our understanding of the mammalian retina is very advanced in that most of the cell types have been described and numerically accounted for, more so than in any other part of the CNS. While the rabbit was the preferred model for a long time, our ability to manipulate the mouse genetically means it is increasingly becoming the main model organism. Of course it has major drawbacks with respect to human retina, the most obvious of which are a lack of a fovea and red–green color vision.

Similar data, though less complete, are available for other mammals, particularly rodent and primate. In fact, experimental reasons often govern the choice of species for investigation and, in this regard, fish and salamander still have much to contribute to the understanding of visual processing.

Rods are specialized for high sensitivity at night, while cones provide high acuity and color vision in daylight. Adaptation in the phototransduction cascade plays a crucial role in adjusting sensitivity. Now, we know there are dedicated pathways for rod and cone vision throughout the retina. Horizontal cells provide feedback to photoreceptors and probably subtract a large version of the average background. Visual pathways diverge dramatically into multiple bipolar cell types with outputs at different levels or addresses in the IPL. One role of amacrine cells is to provide another level of negative feedback at bipolar cell terminals, but amacrine cells are extremely diverse and probably serve many other functions, including feature extraction, lateral inhibition, and various types of adaptation to the image parameters. Ganglion cells are the output neurons of the retina. In central primate retina, the midget system dominates with one cone to one midget bipolar cell to one midget ganglion cell. This system may also carry color signals. There are at least 30-40 different types of ganglion cell, each of which is thought to carry a different channel of visual information. Some of these parallel channels represent spatial vision at several bandwidths, but others are involved with eye movements, image tracking, pupil control, and resetting the circadian clock.

While an outline and the gross cell count may have been

completed, much work remains to describe specific circuits and cellular connections, which we refer to as the functional anatomy of the retina. Several obvious problems challenge our current understanding: the role of horizontal cells and the mechanism of horizontal cell feedback, the reason for the presence of two horizontal cell types, the circuitry underlying color vision, the connections of the diffuse cone bipolar cells, a full description of the mGluR6 cascade, the switch from rod to cone pathways, the mechanism of directional selectivity, the reasons for the extensive electrical coupling of neurons in the retina, the circuits that control sensitivity and adaptation, the specific visual function of the many ganglion cell types – in other words, the role of each channel. We could go on. Our ability to combine new imaging modes with electrophysiology will provide a major contribution to many of these problems, and rapid progress may be anticipated in the next few years. The requirement of functional anatomy is to describe the exact neuronal connections that underlie specific pathways and circuits in the retina. These are the building blocks of the visual system.

Acknowledgments

This work was supported by National Eye Institute grants EY 12354 (RGG), EY 014701 (MMC), EY 06515 (SCM), National Eye Institute core grant EY 10608 (SCM), and unrestricted grants from Research to Prevent Blindness to the Departments of Ophthalmology and Visual Science (University of Texas and University of Louisville). SCM is the Elizabeth Morford Professor of Ophthalmology and the grateful recipient of fellowships from the Hanse-Wissenschaftskolleg, Delmenhorst, Germany, and Research to Prevent Blindness.

Thanks to past and present members of our laboratories who contributed figures: Chris Kittila, Brady Trexler, Steve Mills, Wei Li, Jennifer O'Brien, Feng Pan, and John Koomen. Special thanks to Jennifer O'Brien, who prepared many of the figures, and David Marshak, Steve Mills, and John O'Brien for many discussions. And finally, thanks to all those investigators who contributed figures. The authors regret that due to space limitations the outstanding

work of many investigators could not be included or referenced in this brief review.

References

1. Masland RH. The functional architecture of the retina. *Sci Am*. 1986;255(6):102–111.
2. Rodieck R. *The first steps in seeing*. Sinauer Associates: Sunderland, MA; 1998.
3. Marc RE, Jones BW, Watt CB, et al. Neural remodeling in retinal degeneration. *Prog Retin Eye Res*. 2003;22(5):607–655.
4. Dowling JE. *The retina: an approachable part of the brain*. Belknap Press of Harvard University Press: Cambridge. MA; 1987.
5. Vaney DI. Patterns of neuronal coupling in the retina. *Prog Retin Eye Res*. 1994;13:301–355.
6. Vaney DI, Weiler R. Gap junctions in the eye: evidence for heteromeric, heterotypic and mixed-homotypic interactions. *Brain Res Brain Res Rev*. 2000;32(1):115–120.
7. Galarreta M, Hestrin S. Electrical synapses between GABA-releasing interneurons. *Nat Rev Neurosci*. 2001;2(6):425–433.
8. Harris AL. Emerging issues of connexin channels: biophysics fills the gap. *Q Rev Biophys*. 2001;34:325–472.
9. Goodenough DA, Paul DL. Beyond the gap: functions of unpaired connexon channels. *Nat Rev Mol Cell Biol*. 2003;4(4):285–294.
10. Zhang J, Yang Z, Wu SM. Development of cholinergic amacrine cells is visual activity-dependent in the postnatal mouse retina. *J Comp Neurol*. 2005;484(3):331–343.
11. Wassle H. Parallel processing in the mammalian retina. *Nat Rev Neurosci*. 2004;5(10):747–757.
12. Hartveit E. Functional organization of cone bipolar cells in the rat retina. *J Neurophysiol*. 1997;77(4):1716–1730.
13. Dacheux RF, Raviola E. The rod pathway in the rabbit retina: a depolarizing bipolar and amacrine cell. *J Neurosci*. 1986;6(2):331–345.
14. DeVries SH, Schwartz EA. Kainate receptors mediate synaptic transmission between cones and 'Off' bipolar cells

in a mammalian retina. *Nature*. 1999;397(6715):157–160.
15. Slaughter MM, Miller RF. 2-amino-4-phosphonobutyric acid: a new pharmacological tool for retina research. *Science*. 1981;211(4478):182–185.
16. Nakanishi S, Masu M, Bessho Y, et al. Molecular diversity of glutamate receptors and their physiological functions. *Science*. 1994;71:71–80.
17. Vardi N, Duvoisin R, Wu G, et al. Localization of mGluR6 to dendrites of ON bipolar cells in primate retina. *J Comp Neurol*. 2000;423(3):402–412.
18. Nelson R, Famiglietti EV Jr, Kolb H. Intracellular staining reveals different levels of stratification for on- and off-center ganglion cells in cat retina. *J Neurophysiol*. 1978;41(2):472–483.
19. Schiller PH, Sandell JH, Maunsell JH. Functions of the ON and OFF channels of the visual system. *Nature*. 1986;322(6082):824–825.
20. Tauchi M, Masland RH. The shape and arrangement of the cholinergic neurons in the rabbit retina. *Proc R Soc Lond B Biol Sci*. 1984;223(1230):101–119.
21. Peichl L, Buhl EH, Boycott BB. Alpha ganglion cells in the rabbit retina. *J Comp Neurol*. 1987;263(1):25–41.
22. Peichl L, Ott H, Boycott BB. Alpha ganglion cells in mammalian retinae. *Proc R Soc Lond B Biol Sci*. 1987;231(1263):169–197.
23. Zhang DQ, Zhou TR, McMahon DG. Functional heterogeneity of retinal dopaminergic neurons underlying their multiple roles in vision. *J Neurosci*. 2007;27(3):692–699.
24. Zhang DQ, Wong KY, Sollars PJ, et al. Intraretinal signaling by ganglion cell photoreceptors to dopaminergic amacrine neurons. *Proc Natl Acad Sci USA*. 2008;105(37):14181–14186.
25. Dacey DM, Liao HW, Peterson BB, et al. Melanopsin-expressing ganglion cells in primate retina signal colour and irradiance and project to the LGN. *Nature*. 2005;433(7027):749–754.
26. Hoshi H, Liu WL, Massey SC, et al. ON inputs to the OFF layer: bipolar cells that break the stratification rules of the retina. *J Neurosci*. 2009;29(28):8875–8883.

27. Dumitrescu ON, Pucci FG, Wong KY, et al. Ectopic retinal ON bipolar cell synapses in the OFF inner plexiform layer: contacts with dopaminergic amacrine cells and melanopsin ganglion cells. *J Comp Neurol*. 2009;517(2):226–244.
28. Curcio CA, Sloan KR, Kalina RE, et al. Human photoreceptor topography. *J Comp Neurol*. 1990;292(4):497–523.
29. Curcio CA, Allen KA, Sloan KR, et al. Distribution and morphology of human cone photoreceptors stained with anti-blue opsin. *J Comp Neurol*. 1991;312(4):610–624.
30. Wandell B. *Foundations of vision*. Sinauer Associates, Inc.: Sunderland, MA; 1995.
31. Masland RH, Raviola E. Confronting complexity: strategies for understanding the microcircuitry of the retina. *Annu Rev Neurosci*. 2000;23:249–284.
32. Denk W, Detwiler PB. Optical recording of light-evoked calcium signals in the functionally intact retina. *Proc Natl Acad Sci USA*. 1999;96(12):7035–7040.
33. Euler T, Detwiler PB, Denk W. Directionally selective calcium signals in dendrites of starburst amacrine cells. *Nature*. 2002;418(6900):845–852.
34. Anderson JR, Jones BW, Watt CB, et al. Exploring the retinal connectome. *Mol Vis*. 2011;17:355–379.
35. Dacey DM, Peterson BB, Robinson FR, et al. Fireworks in the primate retina: in vitro photodynamics reveals diverse LGN-projecting ganglion cell types. *Neuron*. 2003;37(1):15–27.
36. Hattar S, Liao HW, Takao M, et al. Melanopsin-containing retinal ganglion cells: architecture, projections, and intrinsic photosensitivity. *Science*. 2002;295(5557):1065–1070.
37. Gan WB, Grutzendler J, Wong WT, et al. Multicolor "DiOlistic" labeling of the nervous system using lipophilic dye combinations. *Neuron*. 2000;27(2):219–225.
38. Siegert S, Scherf BG, Del Punta K, et al. Genetic address book for retinal cell types. *Nat Neurosci*. 2009;12(9):1197–1204.
39. Wassle H, Riemann HJ. The mosaic of nerve cells in the mammalian retina. *Proc R Soc Lond B Biol Sci*.

1978;200(1141):441–461.

40. Strettoi E, Dacheux RF, Raviola E. Synaptic connections of rod bipolar cells in the inner plexiform layer of the rabbit retina. *J Comp Neurol*. 1990;295(3):449–466.
41. Strettoi E, Raviola E, Dacheux RF. Synaptic connections of the narrow-field, bistratified rod amacrine cell (AII) in the rabbit retina. *J Comp Neurol*. 1992;325(2):152–168.
42. Masland RH. Neuronal cell types. *Curr Biol*. 2004;14(13):R497–500.
43. Ahnelt PK, Kolb H. The mammalian photoreceptor mosaic-adaptive design. *Prog Retin Eye Res*. 2000;19(6):711–777.
44. Sterling P, Demb JB. Retina. Shepard GM. *The synaptic organization of the brain*. Oxford University Press: New York; 2004:217–293.
45. Curcio CA, Sloan KR Jr, Packer O, et al. Distribution of cones in human and monkey retina: individual variability and radial asymmetry. *Science*. 1987;236(4801):579–582.
46. Whitney IE, Raven MA, Lu L, et al. A QTL on chromosome 10 modulates cone photoreceptor number in the mouse retina. *Invest Ophthalmol Vis Sci*. 2011;52(6):3228–3236.
47. Jeon CJ, Strettoi E, Masland RH. The major cell populations of the mouse retina. *J Neurosci*. 1998;18(21):8936–8946.
48. Williams DR. Visibility of interference fringes near the resolution limit. *J Opt Soc Am A*. 1985;2(7):1087–1093.
49. Hirsch J, Curcio CA. The spatial resolution capacity of human foveal retina. *Vision Res*. 1989;29(9):1095–1101.
50. Williams DR. Aliasing in human foveal vision. *Vision Res*. 1985;25(2):195–205.
51. Baylor DA, Nunn BJ, Schnapf JL. Spectral sensitivity of cones of the monkey Macaca fascicularis. *J Physiol*. 1987;390:145–160.
52. Schnapf JL, Kraft TW, Baylor DA. Spectral sensitivity of human cone photoreceptors. *Nature*. 1987;325(6103):439–441.
53. Schnapf JL, Kraft TW, Nunn BJ, et al. Spectral sensitivity of primate photoreceptors. *Vis Neurosci*. 1988;1(3):255–261.
54. Nathans J. The evolution and physiology of human color vision: insights from molecular genetic studies of visual pigments. *Neuron*. 1999;24(2):299–312.

55. Roorda A, Williams DR. The arrangement of the three cone classes in the living human eye. *Nature*. 1999;397(6719):520–522.
56. DeMonasterio FM, Schein SJ, McCrane EP. Staining of blue-sensitive cones of the macaque retina by a fluorescent dye. *Science*. 1981;213(4513):1278–1281.
57. Szel A, Diamantstein T, Rohlich P. Identification of the blue-sensitive cones in the mammalian retina by anti-visual pigment antibody. *J Comp Neurol*. 1988;273(4):593–602.
58. Lennie P, Fairchild MD. Ganglion cell pathways for rod vision. *Vision Res*. 1994;34(4):477–482.
59. Wassle H, Grunert U, Chun MH, et al. The rod pathway of the macaque monkey retina: identification of AII-amacrine cells with antibodies against calretinin. *J Comp Neurol*. 1995;361(3):537–551.
60. Mills SL, Massey SC. AII amacrine cells limit scotopic acuity in central macaque retina: A confocal analysis of calretinin labeling. *J Comp Neurol*. 1999;411(1):19–34.
61. Chun MH, Grunert U, Martin PR, et al. The synaptic complex of cones in the fovea and in the periphery of the macaque monkey retina. *Vision Res*. 1996;36(21):3383–3395.
62. Haverkamp S, Grunert U, Wassle H. The cone pedicle, a complex synapse in the retina. *Neuron*. 2000;27(1):85–95.
63. Sterling P. Needle from a haystack. Optimal signaling by a nonlinear synapse. *Neuron*. 2002;34(5):670–672.
64. Sterling P, Smith RG. Design for a binary synapse. *Neuron*. 2004;41(3):313–315.
65. Rao-Mirotznik R, Harkins AB, Buchsbaum G, Sterling P. Mammalian rod terminal: architecture of a binary synapse. *Neuron*. 1995;14(3):561–569.
66. Li W, DeVries SH. Separate blue and green cone networks in the mammalian retina. *Nat Neurosci*. 2004;7(7):751–756.
67. O'Brien J, Nguyen HB, Mills SL. Cone photoreceptors in bass retina use two connexins to mediate electrical coupling. *J Neurosci*. 2004;24(24):5632–5642.
68. Hornstein EP, Verweij J, Schnapf JL. Electrical coupling between red and green cones in primate retina. *Nat Neurosci*. 2004;7(7):745–750.

69. DeVries SH, Qi X, Smith R, et al. Electrical coupling between mammalian cones. *Curr Biol*. 2002;12(22):1900–1907.
70. Ahnelt P, Keri C, Kolb H. Identification of pedicles of putative blue-sensitive cones in the human retina. *J Comp Neurol*. 1990;293(1):39–53.
71. Raviola E, Gilula NB. Gap junctions between photoreceptor cells in the vertebrate retina. *Proc Natl Acad Sci USA*. 1973;70(6):1677–1681.
72. Nelson R. Cat cones have rod input: a comparison of the response properties of cones and horizontal cell bodies in the retina of the cat. *J Comp Neurol*. 1977;172(1):109–135.
73. Schneeweis DM, Schnapf JL. The photovoltage of macaque cone photoreceptors: adaptation, noise, and kinetics. *J Neurosci*. 1999;19(4):1203–1216.
74. Smith RG, Freed MA, Sterling P. Microcircuitry of the dark-adapted cat retina: functional architecture of the rod-cone network. *J Neurosci*. 1986;6(12):3505–3517.
75. Hornstein EP, Verweij J, Li PH, Schnapf JL. Gap-junctional coupling and absolute sensitivity of photoreceptors in macaque retina. *J Neurosci*. 2005;25(48):11201–11209.
76. Peachey NS, Alexander KR, Fishman GA. Visual adaptation and the cone flicker electroretinogram. *Invest Ophthalmol Vis Sci*. 1991;32(5):1517–1522.
77. Peachey NS, Arakawa K, Alexander KR, et al. Rapid and slow changes in the human cone electroretinogram during light and dark adaptation. *Vision Res*. 1992;32(11):2049–2053.
78. Peachey NS, Ball SL. Electrophysiological analysis of visual function in mutant mice. *Doc Ophthalmol*. 2003;107(1):13–36.
79. Heikkinen H, Vinberg F, Nymark S, et al. Mesopic background lights enhance dark-adapted cone ERG flash responses in the intact mouse retina: a possible role for gap junctional decoupling. *J Neurophysiol*. 2011;105(5):2309–2318.
80. Ribelayga C, Cao Y, Mangel SC. The circadian clock in the retina controls rod-cone coupling. *Neuron*. 2008;59(5):790–801.
81. Jin NG, Chuang AZ, Masson PJ, et al. Rod electrical coupling is controlled by a circadian clock and dopamine in mouse retina. *J Physiol*. 2015;593(7):1597–1631.

82. Jin NG, Ribelayga CP. Direct evidence for daily plasticity of electrical coupling between rod photoreceptors in the mammalian retina. *J Neurosci*. 2016;36(1):178–184.
83. Arshavsky VY, Lamb TD, Pugh EN Jr. G proteins and phototransduction. *Annu Rev Physiol*. 2002;64:153–187.
84. Copenhagen DR, Jahr CE. Release of endogenous excitatory amino acids from turtle photoreceptors. *Nature*. 1989;341(6242):536–539.
85. Sarantis M, Mobbs P. The spatial relationship between Muller cell processes and the photoreceptor output synapse. *Brain Res*. 1992;584(1–2):299–304.
86. Schaeffer SF, Raviola E. Membrane recycling in the cone cell endings of the turtle retina. *J Cell Biol*. 1978;79(3):802–825.
87. Grunert U, Martin PR. Rod bipolar cells in the macaque monkey retina: immunoreactivity and connectivity. *J Neurosci*. 1991;11(9):2742–2758.
88. Young HM, Vaney DI. Rod-signal interneurons in the rabbit retina: 1. Rod bipolar cells. *J Comp Neurol*. 1991;310(2):139–153.
89. Vardi N, Morigiwa K, Wang TL, et al. Neurochemistry of the mammalian cone "synaptic complex". *Vision Res*. 1998;38(10):1359–1369.
90. Haverkamp S, Grunert U, Wassle H. The synaptic architecture of AMPA receptors at the cone pedicle of the primate retina. *J Neurosci*. 2001;21(7):2488–2500.
91. Kolb H. The connections between horizontal cells and photoreceptors in the retina of the cat: electron microscopy of Golgi preparations. *J Comp Neurol*. 1974;155(1):1–14.
92. Boycott BB, Peichl L, Wassle H. Morphological types of horizontal cell in the retina of the domestic cat. *Proc R Soc Lond B Biol Sci*. 1978;203(1152):229–245.
93. Dacheux RF, Raviola E. Horizontal cells in the retina of the rabbit. *J Neurosci*. 1982;2(10):1486–1493.
94. Mills SL, Massey SC. Distribution and coverage of A- and B-type horizontal cells stained with Neurobiotin in the rabbit retina. *Vis Neurosci*. 1994;11(3):549–560.
95. Haverkamp S, Grunert U, Wassle H. Localization of kainate receptors at the cone pedicles of the primate retina. *J Comp*

Neurol. 2001;436(4):471–486.
96. Li W, Keung JW, Massey SC. Direct synaptic connections between rods and OFF cone bipolar cells in the rabbit retina. *J Comp Neurol*. 2004;474(1):1–12.
97. Nelson R, von Litzow A, Kolb H, et al. Horizontal cells in cat retina with independent dendritic systems. *Science*. 1975;189(4197):137–139.
98. Szikra T, Trenholm S, Drinnenberg A, et al. Rods in daylight act as relay cells for cone-driven horizontal cell-mediated surround inhibition. *Nat Neurosci*. 2014;17(12):1728–1735.
99. Vaney DI. Many diverse types of retinal neurons show tracer coupling when injected with biocytin or Neurobiotin. *Neurosci Lett*. 1991;125(2):187–190.
100. Vaney DI. The coupling pattern of axon-bearing horizontal cells in the mammalian retina. *Proc Biol Sci*. 1993;252(1334):93–101.
101. Mills SL, Massey SC. The kinetics of tracer movement through homologous gap junctions in the rabbit retina. *Vis Neurosci*. 1998;15(4):765–777.
102. Boycott BB, Hopkins JM, Sperling HG. Cone connections of the horizontal cells of the rhesus monkey's retina. *Proc R Soc Lond B Biol Sci*. 1987;229(1257):345–379.
103. Dacey DM, Lee BB, Stafford DK, et al. Horizontal cells of the primate retina: cone specificity without spectral opponency. *Science*. 1996;271(5249):656–659.
104. Wassle H, Dacey DM, Haun T, et al. The mosaic of horizontal cells in the macaque monkey retina: with a comment on biplexiform ganglion cells. *Vis Neurosci*. 2000;17(4):591–608.
105. Packer OS, Dacey DM. Receptive field structure of H1 horizontal cells in macaque monkey retina. *J Vis*. 2002;2(4):272–292.
106. Massey SC, O'Brien JJ, Trexler EB, et al. Multiple neuronal connexins in the mammalian retina. *Cell Commun Adhes*. 2003;10(4–6):425–430.
107. Peichl L, Gonzalez-Soriano J. Morphological types of horizontal cell in rodent retinae: a comparison of rat, mouse, gerbil, and guinea pig. *Vis Neurosci*. 1994;11(3):501–

517.
108. Hombach S, Janssen-Bienhold U, Sohl G, et al. Functional expression of connexin57 in horizontal cells of the mouse retina. *Eur J Neurosci*. 2004;19(10):2633–2640.
109. Verweij J, Kamermans M, Spekreijse H. Horizontal cells feed back to cones by shifting the cone calcium-current activation range. *Vision Res*. 1996;36(24):3943–3953.
110. Wu SM, Dowling JE. Effects of GABA and glycine on the distal cells of the cyprinid retina. *Brain Res*. 1980;199(2):401–414.
111. Tachibana M, Kaneko A. gamma-Aminobutyric acid acts at axon terminals of turtle photoreceptors: difference in sensitivity among cell types. *Proc Natl Acad Sci USA*. 1984;81(24):7961–7964.
112. Tatsukawa T, Hirasawa H, Kaneko A, et al. GABA-mediated component in the feedback response of turtle retinal cones. *Vis Neurosci*. 2005;22(3):317–324.
113. Lam DM, Lasater EM, Naka KI. gamma-Aminobutyric acid: a neurotransmitter candidate for cone horizontal cells of the catfish retina. *Proc Natl Acad Sci USA*. 1978;75(12):6310–6313.
114. Mosinger JL, Yazulla S, Studholme KM. GABA-like immunoreactivity in the vertebrate retina: a species comparison. *Exp Eye Res*. 1986;42(6):631–644.
115. Wassle H, Chun MH. GABA-like immunoreactivity in the cat retina: light microscopy. *J Comp Neurol*. 1989;279(1):43–54.
116. Guo C, Hirano AA, Stella SL Jr, et al. Guinea pig horizontal cells express GABA, the GABA-synthesizing enzyme GAD 65, and the GABA vesicular transporter. *J Comp Neurol*. 2010;518(10):1647–1669.
117. Yazulla S, Studholme KM, Vitorica J, et al. Immunocytochemical localization of GABAA receptors in goldfish and chicken retinas. *J Comp Neurol*. 1989;280(1):15–26.
118. Picaud S, Pattnaik B, Hicks D, et al. GABAA and GABAC receptors in adult porcine cones: evidence from a photoreceptor-glia co-culture model. *J Physiol*. 1998;513(Pt

1):33–42.
119. Pattnaik B, Jellali A, Sahel J, et al. GABAC receptors are localized with microtubule-associated protein 1B in mammalian cone photoreceptors. *J Neurosci*. 2000;20(18):6789–6796.
120. Klooster J, Nunes Cardozo B, Yazulla S, et al. Postsynaptic localization of gamma-aminobutyric acid transporters and receptors in the outer plexiform layer of the goldfish retina: an ultrastructural study. *J Comp Neurol*. 2004;474(1):58–74.
121. Lee H, Brecha NC. Immunocytochemical evidence for SNARE protein-dependent transmitter release from guinea pig horizontal cells. *Eur J Neurosci*. 2010;31(8):1388–1401.
122. Hirano AA, Brandstatter JH, Morgans CW, et al. SNAP25 expression in mammalian retinal horizontal cells. *J Comp Neurol*. 2011;519(5):972–988.
123. Zampighi GA, Schietroma C, Zampighi LM, et al. Conical tomography of a ribbon synapse: structural evidence for vesicle fusion. *PLoS ONE*. 2011;6(3):e16944.
124. Murakami M, Shimoda Y, Nakatani K, et al. GABA-mediated negative feedback from horizontal cells to cones in carp retina. *Jpn J Physiol*. 1982;32(6):911–926.
125. Kamermans M, Fahrenfort I, Schultz K, et al. Hemichannel-mediated inhibition in the outer retina. *Science*. 2001;292(5519):1178–1180.
126. Hirasawa H, Kaneko A. pH changes in the invaginating synaptic cleft mediate feedback from horizontal cells to cone photoreceptors by modulating $Ca2^{+}$ channels. *J Gen Physiol*. 2003;122(6):657–671.
127. Babai N, Thoreson WB. Horizontal cell feedback regulates calcium currents and intracellular calcium levels in rod photoreceptors of salamander and mouse retina. *J Physiol*. 2009;587(Pt 10):2353–2364.
128. Endeman D, Fahrenfort I, Sjoerdsma T, et al. Chloride currents in cones modify feedback from horizontal cells to cones in goldfish retina. *J Physiol*. 2012;590(Pt 22):5581–5595.
129. Liu X, Hirano AA, Sun X, et al. Calcium channels in rat horizontal cells regulate feedback inhibition of photoreceptors through an unconventional GABA- and pH-

sensitive mechanism. *J Physiol*. 2013;591(Pt 13):3309–3324.
130. Byzov AL, Shura-Bura TM. Electrical feedback mechanism in the processing of signals in the outer plexiform layer of the retina. *Vision Res*. 1986;26(1):33–44.
131. Fahrenfort I, Steijaert M, Sjoerdsma T, et al. Hemichannel-mediated and pH-based feedback from horizontal cells to cones in the vertebrate retina. *PLoS ONE*. 2009;4(6):e6090.
132. Klaassen LJ, Sun Z, Steijaert MN, et al. Synaptic transmission from horizontal cells to cones is impaired by loss of connexin hemichannels. *PLoS Biol*. 2011;9(7):e1001107.
133. Barnes S, Bui Q. Modulation of calcium-activated chloride current via pH-induced changes of calcium channel properties in cone photoreceptors. *J Neurosci*. 1991;11(12):4015–4023.
134. Vroman R, Klaassen LJ, Howlett MH, et al. Extracellular ATP hydrolysis inhibits synaptic transmission by increasing ph buffering in the synaptic cleft. *PLoS Biol*. 2014;12(5):e1001864.
135. Wang TM, Holzhausen LC, Kramer RH. Imaging an optogenetic pH sensor reveals that protons mediate lateral inhibition in the retina. *Nat Neurosci*. 2014;17(2):262–268.
136. Yazulla S. Evoked efflux of [3H]GABA from goldfish retina in the dark. *Brain Res*. 1985;325(1–2):171–180.
137. Yang XL, Wu SM. Effects of prolonged light exposure, GABA, and glycine on horizontal cell responses in tiger salamander retina. *J Neurophysiol*. 1989;61(5):1025–1035.
138. Djamgoz MB, Downing JE, Kirsch M, et al. Plasticity of cone horizontal cell functioning in cyprinid fish retina: effects of background illumination of moderate intensity. *J Neurocytol*. 1988;17(5):701–710.
139. Greferath U, Grunert U, Muller F, et al. Localization of GABAA receptors in the rabbit retina. *Cell Tissue Res*. 1994;276(2):295–307.
140. Vardi N, Sterling P. Subcellular localization of GABAA receptor on bipolar cells in macaque and human retina. *Vision Res*. 1994;34(10):1235–1246.
141. Wassle H, Koulen P, Brandstatter JH, et al. Glycine and

GABA receptors in the mammalian retina. *Vision Res*. 1998;38(10):1411–1430.
142. Thoreson WB, Mangel SC. Lateral interactions in the outer retina. *Prog Retin Eye Res*. 2012;31(5):407–441.
143. Sterling P. How retinal circuits optimize the transfer of visual information. Chalupa LM. *The visual neurosciences*. Cambridge: Boston, MA; 2004:234–259.
144. Kraaij DA, Kamermans M, Spekreijse H. Spectral sensitivity of the feedback signal from horizontal cells to cones in goldfish retina. *Vis Neurosci*. 1998;15(5):799–808.
145. Kamermans M, Kraaij DA, Spekreijse H. The cone/horizontal cell network: a possible site for color constancy. *Vis Neurosci*. 1998;15(5):787–797.
146. Vanleeuwen MT, Joselevitch C, Fahrenfort I, et al. The contribution of the outer retina to color constancy: a general model for color constancy synthesized from primate and fish data. *Vis Neurosci*. 2007;24(3):277–290.
147. Boycott BB, Wassle H. Morphological classification of bipolar cells of the primate retina. *Eur J Neurosci*. 1991;3(11):1069–1088.
148. Ghosh KK, Bujan S, Haverkamp S, et al. Types of bipolar cells in the mouse retina. *J Comp Neurol*. 2004;469(1):70–82.
149. Grunert U, Martin PR, Wassle H. Immunocytochemical analysis of bipolar cells in the macaque monkey retina. *J Comp Neurol*. 1994;348(4):607–627.
150. MacNeil MA, Heussy JK, Dacheux RF, et al. The population of bipolar cells in the rabbit retina. *J Comp Neurol*. 2004;472(1):73–86.
151. Helmstaedter M, Briggman KL, Turaga SC, et al. Connectomic reconstruction of the inner plexiform layer in the mouse retina. *Nature*. 2013;500(7461):168–174.
152. Euler T, Haverkamp S, Schubert T, et al. Retinal bipolar cells: elementary building blocks of vision. *Nat Rev Neurosci*. 2014;15(8):507–519.
153. Wassle H, Puller C, Muller F, et al. Cone contacts, mosaics, and territories of bipolar cells in the mouse retina. *J Neurosci*. 2009;29(1):106–117.
154. Dhingra A, Sulaiman P, Xu Y, et al. Probing neurochemical

structure and function of retinal ON bipolar cells with a transgenic mouse. *J Comp Neurol*. 2008;510(5):484–496.
155. Schubert T, Kerschensteiner D, Eggers ED, et al. Development of presynaptic inhibition onto retinal bipolar cell axon terminals is subclass-specific. *J Neurophysiol*. 2008;100(1):304–316.
156. Wong GT, Ruiz-Avila L, Margolskee RF. Directing gene expression to gustducin-positive taste receptor cells. *J Neurosci*. 1999;19(14):5802–5809.
157. Murakami M, Otsuka T, Shimazaki H. Effects of aspartate and glutamate on the bipolar cells in the carp retina. *Vision Res*. 1975;15(3):456–458.
158. Slaughter MM, Miller RF. The role of excitatory amino acid transmitters in the mudpuppy retina: an analysis with kainic acid and N-methyl aspartate. *J Neurosci*. 1983;3(8):1701–1711.
159. DeVries SH. Bipolar cells use kainate and AMPA receptors to filter visual information into separate channels. *Neuron*. 2000;28(3):847–856.
160. Borghuis BG, Looger LL, Tomita S, et al. Kainate receptors mediate signaling in both transient and sustained OFF bipolar cell pathways in mouse retina. *J Neurosci*. 2014;34(18):6128–6139.
161. Puthussery T, Percival KA, Venkataramani S, et al. Kainate receptors mediate synaptic input to transient and sustained OFF visual pathways in primate retina. *J Neurosci*. 2014;34(22):7611–7621.
162. Lindstrom SH, Ryan DG, Shi J, et al. Kainate receptor subunit diversity underlying response diversity in retinal off bipolar cells. *J Physiol*. 2014;592(Pt 7):1457–1477.
163. Baden T, Berens P, Bethge M, et al. Spikes in mammalian bipolar cells support temporal layering of the inner retina. *Curr Biol*. 2013;23(1):48–52.
164. Borghuis BG, Marvin JS, Looger LL, et al. Two-photon imaging of nonlinear glutamate release dynamics at bipolar cell synapses in the mouse retina. *J Neurosci*. 2013;33(27):10972–10985.
165. Odermatt B, Nikolaev A, Lagnado L. Encoding of

luminance and contrast by linear and nonlinear synapses in the retina. *Neuron*. 2012;73(4):758–773.
166. Nomura A, Shigemoto R, Nakamura Y, et al. Developmentally regulated postsynaptic localization of a metabotropic glutamate receptor in rat rod bipolar cells. *Cell*. 1994;77(3):361–369.
167. Dhingra A, Lyubarsky A, Jiang M, et al. The light response of ON bipolar neurons requires G[alpha]o. *J Neurosci*. 2000;20(24):9053–9058.
168. Shen Y, Heimel JA, Kamermans M, et al. A transient receptor potential-like channel mediates synaptic transmission in rod bipolar cells. *J Neurosci*. 2009;29(19):6088–6093.
169. Morgans CW, Zhang J, Jeffrey BG, et al. TRPM1 is required for the depolarizing light response in retinal ON-bipolar cells. *Proc Natl Acad Sci USA*. 2009;106(45):19174–19178.
170. Koike C, Obara T, Uriu Y, et al. TRPM1 is a component of the retinal ON bipolar cell transduction channel in the mGluR6 cascade. *Proc Natl Acad Sci USA*. 2010;107(1):332–337.
171. Nawy S. The metabotropic receptor mGluR6 may signal through G(o), but not phosphodiesterase, in retinal bipolar cells. *J Neurosci*. 1999;19(8):2938–2944.
172. Dhingra A, Faurobert E, Dascal N, et al. A retinal-specific regulator of G-protein signaling interacts with Galpha(o) and accelerates an expressed metabotropic glutamate receptor 6 cascade. *J Neurosci*. 2004;24(25):5684–5693.
173. Martemyanov KA. G protein signaling in the retina and beyond: the Cogan lecture. *Invest Ophthalmol Vis Sci*. 2014;55(12):8201–8207.
174. Ichinose T, Fyk-Kolodziej B, Cohn J. Roles of ON cone bipolar cell subtypes in temporal coding in the mouse retina. *J Neurosci*. 2014;34(26):8761–8771.
175. Awatramani GB, Slaughter MM. Intensity-dependent, rapid activation of presynaptic metabotropic glutamate receptors at a central synapse. *J Neurosci*. 2001;21(2):741–749.
176. de la Villa P, Vaquero CF, Kaneko A. Two types of calcium currents of the mouse bipolar cells recorded in the retinal

slice preparation. *Eur J Neurosci*. 1998;10(1):317–323.
177. DeVries SH, Li W, Saszik S. Parallel processing in two transmitter microenvironments at the cone photoreceptor synapse. *Neuron*. 2006;50(5):735–748.
178. Cui J, Pan ZH. Two types of cone bipolar cells express voltage-gated Na+ channels in the rat retina. *Vis Neurosci*. 2008;25(5–6):635–645.
179. Hu C, Bi A, Pan ZH. Differential expression of three T-type calcium channels in retinal bipolar cells in rats. *Vis Neurosci*. 2009;26(2):177–187.
180. von Gersdorff H, Sakaba T, Berglund K, et al. Submillisecond kinetics of glutamate release from a sensory synapse. *Neuron*. 1998;21(5):1177–1188.
181. Singer JH, Diamond JS. Sustained $Ca2^{+}$ entry elicits transient postsynaptic currents at a retinal ribbon synapse. *J Neurosci*. 2003;23(34):10923–10933.
182. Werblin FS. Six different roles for crossover inhibition in the retina: correcting the nonlinearities of synaptic transmission. *Vis Neurosci*. 2010;27(1–2):1–8.
183. Eggers ED, Lukasiewicz PD. Multiple pathways of inhibition shape bipolar cell responses in the retina. *Vis Neurosci*. 2011;28(1):95–108.
184. Dacey DM. The mosaic of midget ganglion cells in the human retina. *J Neurosci*. 1993;13(12):5334–5355.
185. Mariani AP. Bipolar cells in monkey retina selective for the cones likely to be blue-sensitive. *Nature*. 1984;308(5955):184–186.
186. Kouyama N, Marshak DW. Bipolar cells specific for blue cones in the macaque retina. *J Neurosci*. 1992;12(4):1233–1252.
187. Bloomfield SA, Dacheux RF. Rod vision: pathways and processing in the mammalian retina. *Prog Retin Eye Res*. 2001;20(3):351–384.
188. Field GD, Rieke F. Nonlinear signal transfer from mouse rods to bipolar cells and implications for visual sensitivity. *Neuron*. 2002;34(5):773–785.
189. Sampath AP, Rieke F. Selective transmission of single photon responses by saturation at the rod-to-rod bipolar

synapse. *Neuron*. 2004;41(3):431–443.
190. Ghosh KK, Haverkamp S, Wassle H. Glutamate receptors in the rod pathway of the mammalian retina. *J Neurosci*. 2001;21(21):8636–8647.
191. Li W, Trexler EB, Massey SC. Glutamate receptors at rod bipolar ribbon synapses in the rabbit retina. *J Comp Neurol*. 2002;448(3):230–248.
192. Chavez AE, Singer JH, Diamond JS. Fast neurotransmitter release triggered by Ca influx through AMPA-type glutamate receptors. *Nature*. 2006;443(7112):705–708.
193. Eggers ED, McCall MA, Lukasiewicz PD. Presynaptic inhibition differentially shapes transmission in distinct circuits in the mouse retina. *J Physiol*. 2007;582(Pt 2):569–582.
194. Eggers ED, Lukasiewicz PD. Interneuron circuits tune inhibition in retinal bipolar cells. *J Neurophysiol*. 2010;103(1):25–37.
195. Grimes WN, Zhang J, Graydon CW, et al. Retinal parallel processors: more than 100 independent microcircuits operate within a single interneuron. *Neuron*. 2010;65(6):873–885.
196. Ivanova E, Muller U, Wassle H. Characterization of the glycinergic input to bipolar cells of the mouse retina. *Eur J Neurosci*. 2006;23(2):350–364.
197. Weiss J, O'Sullivan GA, Heinze L, et al. Glycinergic input of small-field amacrine cells in the retinas of wildtype and glycine receptor deficient mice. *Mol Cell Neurosci*. 2008;37(1):40–55.
198. Strettoi E, Dacheux RF, Raviola E. Cone bipolar cells as interneurons in the rod pathway of the rabbit retina. *J Comp Neurol*. 1994;347(1):139–149.
199. Mills SL, Massey SC. Differential properties of two gap junctional pathways made by AII amacrine cells. *Nature*. 1995;377(6551):734–737.
200. Field GD, Sampath AP, Rieke F. Retinal processing near absolute threshold: from behavior to mechanism. *Annu Rev Physiol*. 2005;67:491–514.
201. Demb JB, Singer JH. Intrinsic properties and functional

circuitry of the AII amacrine cell. *Vis Neurosci*. 2012;29(1):51–60.
202. Dunn FA, Doan T, Sampath AP, et al. Controlling the gain of rod-mediated signals in the mammalian retina. *J Neurosci*. 2006;26(15):3959–3970.
203. Nelson R. AII amacrine cells quicken time course of rod signals in the cat retina. *J Neurophysiol*. 1982;47(5):928–947.
204. Ke JB, Wang YV, Borghuis BG, et al. Adaptation to background light enables contrast coding at rod bipolar cell synapses. *Neuron*. 2014;81(2):388–401.
205. Oesch NW, Diamond JS. Ribbon synapses compute temporal contrast and encode luminance in retinal rod bipolar cells. *Nat Neurosci*. 2011;14:1555–1561.
206. Jarsky T, Cembrowski M, Logan SM, et al. A synaptic mechanism for retinal adaptation to luminance and contrast. *J Neurosci*. 2011;31(30):11003–11015.
207. Grimes WN, Hoon M, Briggman KL, et al. Cross-synaptic synchrony and transmission of signal and noise across the mouse retina. *Elife*. 2014;3:e03892.
208. Grimes WN, Schwartz GW, Rieke F. The synaptic and circuit mechanisms underlying a change in spatial encoding in the retina. *Neuron*. 2014;82(2):460–473.
209. Dunn FA, Rieke F. Single-photon absorptions evoke synaptic depression in the retina to extend the operational range of rod vision. *Neuron*. 2008;57(6):894–904.
210. Vaney DI, Nelson JC, Pow DV. Neurotransmitter coupling through gap junctions in the retina. *J Neurosci*. 1998;18(24):10594–10602.
211. Deans MR, Volgyi B, Goodenough DA, et al. Connexin36 is essential for transmission of rod-mediated visual signals in the mammalian retina. *Neuron*. 2002;36(4):703–712.
212. Hampson EC, Vaney DI, Weiler R. Dopaminergic modulation of gap junction permeability between amacrine cells in mammalian retina. *J Neurosci*. 1992;12(12):4911–4922.
213. Kothmann WW, Massey SC, O'Brien J. Dopamine-stimulated dephosphorylation of connexin 36 mediates AII amacrine cell uncoupling. *J Neurosci*. 2009;29(47):14903–14911.

214. Trexler EB, Li W, Mills SL, et al. Coupling from AII amacrine cells to ON cone bipolar cells is bidirectional. *J Comp Neurol*. 2001;437(4):408–422.
215. Veruki ML, Hartveit E. Electrical synapses mediate signal transmission in the rod pathway of the mammalian retina. *J Neurosci*. 2002;22(24):10558–10566.
216. Manookin MB, Beaudoin DL, Ernst ZR, et al. Disinhibition combines with excitation to extend the operating range of the OFF visual pathway in daylight. *J Neurosci*. 2008;28(16):4136–4150.
217. Munch TA, da Silveira RA, Siegert S, et al. Approach sensitivity in the retina processed by a multifunctional neural circuit. *Nat Neurosci*. 2009;12(10):1308–1316.
218. van Wyk M, Wassle H, Taylor WR. Receptive field properties of ON- and OFF-ganglion cells in the mouse retina. *Vis Neurosci*. 2009;26(3):297–308.
219. Mills SL, O'Brien JJ, Li W, et al. Rod pathways in the mammalian retina use connexin 36. *J Comp Neurol*. 2001;436(3):336–350.
220. Maxeiner S, Dedek K, Janssen-Bienhold U, et al. Deletion of connexin45 in mouse retinal neurons disrupts the rod/cone signaling pathway between AII amacrine and ON cone bipolar cells and leads to impaired visual transmission. *J Neurosci*. 2005;25(3):566–576.
221. DeVries SH, Baylor DA. An alternative pathway for signal flow from rod photoreceptors to ganglion cells in mammalian retina. *Proc Natl Acad Sci USA*. 1995;92(23):10658–10662.
222. Soucy E, Wang Y, Nirenberg S, et al. A novel signaling pathway from rod photoreceptors to ganglion cells in mammalian retina. *Neuron*. 1998;21(3):481–493.
223. Hack I, Frech M, Dick O, et al. Heterogeneous distribution of AMPA glutamate receptor subunits at the photoreceptor synapses of rodent retina. *Eur J Neurosci*. 2001;13(1):15–24.
224. Tsukamoto Y, Morigiwa K, Ueda M, et al. Microcircuits for night vision in mouse retina. *J Neurosci*. 2001;21(21):8616–8623.
225. Fyk-Kolodziej B, Qin P, Pourcho RG. Identification of a cone

bipolar cell in cat retina which has input from both rod and cone photoreceptors. *J Comp Neurol*. 2003;464(1):104–113.
226. Li W, Chen S, DeVries SH. A fast rod photoreceptor signaling pathway in the mammalian retina. *Nat Neurosci*. 2010;13(4):414–416.
227. MacNeil MA, Masland RH. Extreme diversity among amacrine cells: implications for function. *Neuron*. 1998;20(5):971–982.
228. MacNeil MA, Heussy JK, Dacheux RF, et al. The shapes and numbers of amacrine cells: matching of photofilled with Golgi-stained cells in the rabbit retina and comparison with other mammalian species. *J Comp Neurol*. 1999;413(2):305–326.
229. Lin B, Masland RH. Populations of wide-field amacrine cells in the mouse retina. *J Comp Neurol*. 2006;499(5):797–809.
230. Perez De Sevilla Muller L, Shelley J, Weiler R. Displaced amacrine cells of the mouse retina. *J Comp Neurol*. 2007;505(2):177–189.
231. Zhang C, Mccall MA. Receptor targets of amacrine cells. *Vis Neurosci*. 2012;29:11–29.
232. Hsueh HA, Molnar A, Werblin FS. Amacrine-to-amacrine cell inhibition in the rabbit retina. *J Neurophysiol*. 2008;100(4):2077–2088.
233. Badea TC, Nathans J. Quantitative analysis of neuronal morphologies in the mouse retina visualized by using a genetically directed reporter. *J Comp Neurol*. 2004;480(4):331–351.
234. Dedek K, Breuninger T, de Sevilla Muller LP, et al. A novel type of interplexiform amacrine cell in the mouse retina. *Eur J Neurosci*. 2009;30(2):217–228.
235. Majumdar S, Weiss J, Wassle H. Glycinergic input of widefield, displaced amacrine cells of the mouse retina. *J Physiol*. 2009;587(Pt 15):3831–3849.
236. Lukasiewicz PD. Synaptic mechanisms that shape visual signaling at the inner retina. *Prog Brain Res*. 2005;147:205–218.
237. Demb JB. Functional circuitry of visual adaptation in the retina. *J Physiol*. 2008;586(Pt 18):4377–4384.

238. Marc R. Retinal neurotransmitters. Claw JS. *The visual sciences. 1*. MIT Press: Cambridge, MA; 2004:301–319.
239. Li W, Zhang J, Massey SC. Coupling pattern of S1 and S2 amacrine cells in the rabbit retina. *Vis Neurosci*. 2002;19(2):119–131.
240. Xin D, Bloomfield SA. Tracer coupling pattern of amacrine and ganglion cells in the rabbit retina. *J Comp Neurol*. 1997;383(4):512–528.
241. Marc RE, Jones BW. Molecular phenotyping of retinal ganglion cells. *J Neurosci*. 2002;22(2):413–427.
242. Hu EH, Pan F, Volgyi B, et al. Light increases the gap junctional coupling of retinal ganglion cells. *J Physiol*. 2010;588(Pt 21):4145–4163.
243. Berry MJ 2nd, Brivanlou IH, Jordan TA, Meister M. Anticipation of moving stimuli by the retina. *Nature*. 1999;398(6725):334–338.
244. Olveczky BP, Baccus SA, Meister M. Segregation of object and background motion in the retina. *Nature*. 2003;423(6938):401–408.
245. Roska B, Werblin F. Rapid global shifts in natural scenes block spiking in specific ganglion cell types. *Nat Neurosci*. 2003;6(6):600–608.
246. Knop GC, Feigenspan A, Weiler R, et al. Inputs underlying the ON–OFF light responses of type 2 wide-field amacrine cells in TH:GFP mice. *J Neurosci*. 2011;31(13):4780–4791.
247. Massey SC, Mills SL. Antibody to calretinin stains AII amacrine cells in the rabbit retina: double-label and confocal analyses. *J Comp Neurol*. 1999;411(1):3–18.
248. Arman AC, Sampath AP. Dark-adapted response threshold of OFF ganglion cells is not set by OFF bipolar cells in the mouse retina. *J Neurophysiol*. 2012;107(10):2649–2659.
249. Smith RG, Vardi N. Simulation of the AII amacrine cell of mammalian retina: functional consequences of electrical coupling and regenerative membrane properties. *Vis Neurosci*. 1995;12(5):851–860.
250. Vardi N, Smith RG. The AII amacrine network: coupling can increase correlated activity. *Vision Res*. 1996;36(23):3743–3757.

251. Bloomfield SA, Volgyi B. Function and plasticity of homologous coupling between AII amacrine cells. *Vision Res*. 2004;44(28):3297–3306.
252. Oesch NW, Kothmann WW, Diamond JS. Illuminating synapses and circuitry in the retina. *Curr Opin Neurobiol*. 2011;21(2):238–244.
253. Vaney DI. Morphological identification of serotonin-accumulating neurons in the living retina. *Science*. 1986;233(4762):444–446.
254. Zhang J, Li W, Trexler EB, et al. Confocal analysis of reciprocal feedback at rod bipolar terminals in the rabbit retina. *J Neurosci*. 2002;22(24):10871–10882.
255. Fletcher EL, Wassle H. Indoleamine-accumulating amacrine cells are presynaptic to rod bipolar cells through GABA(C) receptors. *J Comp Neurol*. 1999;413(1):155–167.
256. Lukasiewicz PD, Eggers ED, Sagdullaev BT, et al. GABAC receptor-mediated inhibition in the retina. *Vision Res*. 2004;44(28):3289–3296.
257. Eggers ED, Lukasiewicz PD. Receptor and transmitter release properties set the time course of retinal inhibition. *J Neurosci*. 2006;26(37):9413–9425.
258. Eggers ED, Lukasiewicz PD. GABA(A), GABA(C) and glycine receptor-mediated inhibition differentially affects light-evoked signalling from mouse retinal rod bipolar cells. *J Physiol*. 2006;572(Pt 1):215–225.
259. Grimes WN, Li W, Chavez AE, et al. BK channels modulate pre- and postsynaptic signaling at reciprocal synapses in retina. *Nat Neurosci*. 2009;12(5):585–592.
260. Freed MA, Smith RG, Sterling P. Timing of quantal release from the retinal bipolar terminal is regulated by a feedback circuit. *Neuron*. 2003;38(1):89–101.
261. Sagdullaev BT, McCall MA, Lukasiewicz PD. Presynaptic inhibition modulates spillover, creating distinct dynamic response ranges of sensory output. *Neuron*. 2006;50(6):923–935.
262. Dacey DM. The dopaminergic amacrine cell. *J Comp Neurol*. 1990;301(3):461–489.
263. Hokoc JN, Mariani AP. Synapses from bipolar cells onto

dopaminergic amacrine cells in cat and rabbit retinas. *Brain Res*. 1988;461(1):17–26.
264. Contini M, Lin B, Kobayashi K, et al. Synaptic input of ON-bipolar cells onto the dopaminergic neurons of the mouse retina. *J Comp Neurol*. 2010;518(11):2035–2050.
265. Contini M, Raviola E. GABAergic synapses made by a retinal dopaminergic neuron. *Proc Natl Acad Sci USA*. 2003;100(3):1358–1363.
266. Feigenspan A, Gustincich S, Bean BP, et al. Spontaneous activity of solitary dopaminergic cells of the retina. *J Neurosci*. 1998;18(17):6776–6789.
267. Puopolo M, Hochstetler SE, Gustincich S, et al. Extrasynaptic release of dopamine in a retinal neuron: activity dependence and transmitter modulation. *Neuron*. 2001;30(1):211–225.
268. Witkovsky P, Veisenberger E, LeSauter J, et al. Cellular location and circadian rhythm of expression of the biological clock gene Period 1 in the mouse retina. *J Neurosci*. 2003;23(20):7670–7676.
269. Gustincich S, Contini M, Gariboldi M, et al. Gene discovery in genetically labeled single dopaminergic neurons of the retina. *Proc Natl Acad Sci USA*. 2004;101(14):5069–5074.
270. Dorenbos R, Contini M, Hirasawa H, et al. Expression of circadian clock genes in retinal dopaminergic cells. *Vis Neurosci*. 2007;24(4):573–580.
271. Pozdeyev N, Tosini G, Li L, et al. Dopamine modulates diurnal and circadian rhythms of protein phosphorylation in photoreceptor cells of mouse retina. *Eur J Neurosci*. 2008;27(10):2691–2700.
272. Witkovsky P. Dopamine and retinal function. *Doc Ophthalmol*. 2004;108(1):17–40.
273. Ribelayga C, Mangel SC. Identification of a circadian clock-controlled neural pathway in the rabbit retina. *PLoS ONE*. 2010;5(6):e11020.
274. Herrmann R, Heflin SJ, Hammond T, et al. Rod vision is controlled by dopamine-dependent sensitization of rod bipolar cells by GABA. *Neuron*. 2011;72(1):101–110.
275. Vaney DI, Pow DV. The dendritic architecture of the

cholinergic plexus in the rabbit retina: selective labeling by glycine accumulation in the presence of sarcosine. *J Comp Neurol*. 2000;421(1):1–13.
276. Dacheux RF, Chimento MF, Amthor FR. Synaptic input to the on–off directionally selective ganglion cell in the rabbit retina. *J Comp Neurol*. 2003;456(3):267–278.
277. Brecha N, Johnson D, Peichl L, et al. Cholinergic amacrine cells of the rabbit retina contain glutamate decarboxylase and gamma-aminobutyrate immunoreactivity. *Proc Natl Acad Sci USA*. 1988;85(16):6187–6191.
278. Lee S, Kim K, Zhou ZJ. Role of ACh-GABA cotransmission in detecting image motion and motion direction. *Neuron*. 2010;68(6):1159–1172.
279. Yoshida K, Watanabe D, Ishikane H, et al. A key role of starburst amacrine cells in originating retinal directional selectivity and optokinetic eye movement. *Neuron*. 2001;30(3):771–780.
280. Kittila CA, Massey SC. Pharmacology of directionally selective ganglion cells in the rabbit retina. *J Neurophysiol*. 1997;77(2):675–689.
281. Fried SI, Munch TA, Werblin FS. Mechanisms and circuitry underlying directional selectivity in the retina. *Nature*. 2002;420(6914):411–414.
282. Borg-Graham LJ. The computation of directional selectivity in the retina occurs presynaptic to the ganglion cell. *Nat Neurosci*. 2001;4(2):176–183.
283. Hausselt SE, Euler T, Detwiler PB, et al. A dendrite-autonomous mechanism for direction selectivity in retinal starburst amacrine cells. *PLoS Biol*. 2007;5(7):e185.
284. Kim JS, Greene MJ, Zlateski A, et al. Space–time wiring specificity supports direction selectivity in the retina. *Nature*. 2014;509(7500):331–336.
285. Briggman KL, Helmstaedter M, Denk W. Wiring specificity in the direction-selectivity circuit of the retina. *Nature*. 2011;471(7337):183–188.
286. Oesch N, Euler T, Taylor WR. Direction-selective dendritic action potentials in rabbit retina. *Neuron*. 2005;47(5):739–750.

287. Wei W, Feller MB. Organization and development of direction-selective circuits in the retina. *Trends Neurosci*. 2011;34(12):638–645.
288. Elstrott J, Anishchenko A, Greschner M, et al. Direction selectivity in the retina is established independent of visual experience and cholinergic retinal waves. *Neuron*. 2008;58(4):499–506.
289. Feller MB. The role of nAChR-mediated spontaneous retinal activity in visual system development. *J Neurobiol*. 2002;53(4):556–567.
290. Syed MM, Lee S, He S, et al. Spontaneous waves in the ventricular zone of developing mammalian retina. *J Neurophysiol*. 2004;91(5):1999–2009.
291. Syed MM, Lee S, Zheng J, et al. Stage-dependent dynamics and modulation of spontaneous waves in the developing rabbit retina. *J Physiol*. 2004;560(Pt 2):533–549.
292. Renna JM, Weng S, Berson DM. Light acts through melanopsin to alter retinal waves and segregation of retinogeniculate afferents. *Nat Neurosci*. 2011;14(7):827–829.
293. Lukasiewicz PD, Wilson JA, Lawrence JE. AMPA-preferring receptors mediate excitatory synaptic inputs to retinal ganglion cells. *J Neurophysiol*. 1997;77(1):57–64.
294. Vaney DI. A quantitative comparison between the ganglion cell populations and axonal outflows of the visual streak and periphery of the rabbit retina. *J Comp Neurol*. 1980;189(2):215–233.
295. Williams RW, Strom RC, Rice DS, et al. Genetic and environmental control of variation in retinal ganglion cell number in mice. *J Neurosci*. 1996;16(22):7193–7205.
296. Baden T, Berens P, Franke K, et al. The functional diversity of retinal ganglion cells in the mouse. *Nature*. 2016;529(7586):345–350.
297. Huberman AD, Wei W, Elstrott J, et al. Genetic identification of an On-Off direction-selective retinal ganglion cell subtype reveals a layer-specific subcortical map of posterior motion. *Neuron*. 2009;62(3):327–334.
298. Huberman AD, Manu M, Koch SM, et al. Architecture and activity-mediated refinement of axonal projections from a

mosaic of genetically identified retinal ganglion cells. *Neuron*. 2008;59(3):425–438.
299. Kim IJ, Zhang Y, Yamagata M, et al. Molecular identification of a retinal cell type that responds to upward motion. *Nature*. 2008;452(7186):478–482.
300. Yonehara K, Ishikane H, Sakuta H, et al. Identification of retinal ganglion cells and their projections involved in central transmission of information about upward and downward image motion. *PLoS ONE*. 2009;4(1):e4320.
301. Rivlin-Etzion M, Zhou K, Wei W, et al. Transgenic mice reveal unexpected diversity of on–off direction-selective retinal ganglion cell subtypes and brain structures involved in motion processing. *J Neurosci*. 2011;31(24):8760–8769.
302. Sanes JR, Masland RH. The types of retinal ganglion cells: current status and implications for neuronal classification. *Annu Rev Neurosci*. 2015;38:221–246.
303. Roska B, Molnar A, Werblin FS. Parallel processing in retinal ganglion cells: how integration of space-time patterns of excitation and inhibition form the spiking output. *J Neurophysiol*. 2006;95(6):3810–3822.
304. Roska B, Werblin F. Vertical interactions across ten parallel, stacked representations in the mammalian retina. *Nature*. 2001;410(6828):583–587.
305. Farrow K, Masland RH. Physiological clustering of visual channels in the mouse retina. *J Neurophysiol*. 2011;105(4):1516–1530.
306. Masland RH. The neuronal organization of the retina. *Neuron*. 2012;76(2):266–280.
307. Bolinger D, Gollisch T. Closed-loop measurements of iso-response stimuli reveal dynamic nonlinear stimulus integration in the retina. *Neuron*. 2012;73(2):333–346.
308. Kastner DB, Baccus SA. Coordinated dynamic encoding in the retina using opposing forms of plasticity. *Nat Neurosci*. 2011;14(10):1317–1322.
309. Nikolaev A, Leung KM, Odermatt B, et al. Synaptic mechanisms of adaptation and sensitization in the retina. *Nat Neurosci*. 2013;16(7):934–941.
310. Kastner DB, Baccus SA. Spatial segregation of adaptation

and predictive sensitization in retinal ganglion cells. *Neuron*. 2013;79(3):541–554.
311. Farrow K, Teixeira M, Szikra T, et al. Ambient illumination toggles a neuronal circuit switch in the retina and visual perception at cone threshold. *Neuron*. 2013;78(2):325–338.
312. Solomon SG, Kohn A. Moving sensory adaptation beyond suppressive effects in single neurons. *Curr Biol*. 2014;24(20):R1012–22.
313. Dacey DM. Morphology of a small-field bistratified ganglion cell type in the macaque and human retina. *Vis Neurosci*. 1993;10(6):1081–1098.
314. Rockhill RL, Daly FJ, MacNeil MA, et al. The diversity of ganglion cells in a mammalian retina. *J Neurosci*. 2002;22(9):3831–3843.
315. Peichl L. Alpha ganglion cells in mammalian retinae: common properties, species differences, and some comments on other ganglion cells. *Vis Neurosci*. 1991;7(1–2):155–169.
316. Yamada ES, Bordt AS, Marshak DW. Wide-field ganglion cells in macaque retinas. *Vis Neurosci*. 2005;22(4):383–393.
317. Barlow HB, Levick WR. The mechanism of directionally selective units in rabbit's retina. *J Physiol*. 1965;178(3):477–504.
318. Amthor FR, Oyster CW, Takahashi ES. Morphology of on–off direction-selective ganglion cells in the rabbit retina. *Brain Res*. 1984;298(1):187–190.
319. Wei W, Elstrott J, Feller MB. Two-photon targeted recording of GFP-expressing neurons for light responses and live-cell imaging in the mouse retina. *Nat Protoc*. 2010;5(7):1347–1352.
320. Vaney DI. Territorial organization of direction-selective ganglion cells in rabbit retina. *J Neurosci*. 1994;14(11 Pt 1):6301–6316.
321. Kay JN, De la Huerta I, Kim IJ, et al. Retinal ganglion cells with distinct directional preferences differ in molecular identity, structure, and central projections. *J Neurosci*. 2011;31(21):7753–7762.
322. Oyster CW, Barlow HB. Direction-selective units in rabbit

retina: distribution of preferred directions. *Science*. 1967;155(764):841–842.
323. Sun W, Li N, He S. Large-scale morphological survey of mouse retinal ganglion cells. *J Comp Neurol*. 2002;451(2):115–126.
324. Sun W, Li N, He S. Large-scale morphological survey of rat retinal ganglion cells. *Vis Neurosci*. 2002;19(4):483–493.
325. Isayama T, Berson DM, Pu M. Theta ganglion cell type of cat retina. *J Comp Neurol*. 2000;417(1):32–48.
326. Yonehara K, Balint K, Noda M, et al. Spatially asymmetric reorganization of inhibition establishes a motion-sensitive circuit. *Nature*. 2011;469(7330):407–410.
327. Oyster CW, Simpson JI, Takahashi ES, et al. Retinal ganglion cells projecting to the rabbit accessory optic system. *J Comp Neurol*. 1980;190(1):49–61.
328. Buhl EH, Peichl L. Morphology of rabbit retinal ganglion cells projecting to the medial terminal nucleus of the accessory optic system. *J Comp Neurol*. 1986;253(2):163–174.
329. Hoshi H, Tian LM, Massey SC, et al. Two distinct types of ON directionally selective ganglion cells in the rabbit retina. *J Comp Neurol*. 2011;519(13):2509–2521.
330. Kanjhan R, Sivyer B. Two types of ON direction-selective ganglion cells in rabbit retina. *Neurosci Lett*. 2010;483(2):105–109.
331. Ackert JM, Farajian R, Volgyi B, et al. GABA blockade unmasks an OFF response in ON direction selective ganglion cells in the mammalian retina. *J Physiol*. 2009;587(Pt 18):4481–4495.
332. Hoshi H, Mills SL. Components and properties of the G3 ganglion cell circuit in the rabbit retina. *J Comp Neurol*. 2009;513(1):69–82.
333. Venkataramani S, Taylor WR. Orientation selectivity in rabbit retinal ganglion cells is mediated by presynaptic inhibition. *J Neurosci*. 2010;30(46):15664–15676.
334. Trenholm S, Johnson K, Li X, et al. Parallel mechanisms encode direction in the retina. *Neuron*. 2011;71(4):683–694.
335. Klerman EB, Shanahan TL, Brotman DJ, et al. Photic resetting of the human circadian pacemaker in the absence

of conscious vision. *J Biol Rhythms*. 2002;17(6):548–555.
336. Berson DM. Strange vision: ganglion cells as circadian photoreceptors. *Trends Neurosci*. 2003;26(6):314–320.
337. Lucas RJ, Hattar S, Takao M, et al. Diminished pupillary light reflex at high irradiances in melanopsin-knockout mice. *Science*. 2003;299(5604):245–247.
338. Grunert U, Jusuf PR, Lee SC, et al. Bipolar input to melanopsin containing ganglion cells in primate retina. *Vis Neurosci*. 2011;28(1):39–50.
339. Hattar S, Lucas RJ, Mrosovsky N, et al. Melanopsin and rod-cone photoreceptive systems account for all major accessory visual functions in mice. *Nature*. 2003;424(6944):76–81.
340. Schmidt TM, Chen SK, Hattar S. Intrinsically photosensitive retinal ganglion cells: many subtypes, diverse functions. *Trends Neurosci*. 2011;34(11):572–580.
341. Schmidt TM, Do MT, Dacey D, et al. Melanopsin-positive intrinsically photosensitive retinal ganglion cells: from form to function. *J Neurosci*. 2011;31(45):16094–16101.
342. Berson DM, Castrucci AM, Provencio I. Morphology and mosaics of melanopsin-expressing retinal ganglion cell types in mice. *J Comp Neurol*. 2010;518(13):2405–2422.
343. Chen SK, Badea TC, Hattar S. Photoentrainment and pupillary light reflex are mediated by distinct populations of ipRGCs. *Nature*. 2011;476(7358):92–95.
344. Lennie P. Color vision: putting it together. *Curr Biol*. 2000;10(16):R589–91.
345. Crook JD, Manookin MB, Packer OS, et al. Horizontal cell feedback without cone type-selective inhibition mediates "red-green" color opponency in midget ganglion cells of the primate retina. *J Neurosci*. 2011;31(5):1762–1772.
346. Dacey DM. Circuitry for color coding in the primate retina. *Proc Natl Acad Sci USA*. 1996;93(2):582–588.
347. Field GD, Gauthier JL, Sher A, et al. Functional connectivity in the retina at the resolution of photoreceptors. *Nature*. 2010;467(7316):673–677.
348. Mariani AP. The neuronal organization of the outer plexiform layer of the primate retina. *Int Rev Cytol*. 1984;86:285–320.

349. Haverkamp S, Wassle H, Duebel J, et al. The primordial, blue-cone color system of the mouse retina. *J Neurosci*. 2005;25(22):5438–5445.
350. Dacey DM, Lee BB. The "blue-on" opponent pathway in primate retina originates from a distinct bistratified ganglion cell type. *Nature*. 1994;367(6465):731–735.
351. Field GD, Greschner M, Gauthier JL, et al. High-sensitivity rod photoreceptor input to the blue-yellow color opponent pathway in macaque retina. *Nat Neurosci*. 2009;12(9):1159–1164.
352. Field GD, Sher A, Gauthier JL, et al. Spatial properties and functional organization of small bistratified ganglion cells in primate retina. *J Neurosci*. 2007;27(48):13261–13272.
353. Crook JD, Davenport CM, Peterson BB, et al. Parallel ON and OFF cone bipolar inputs establish spatially coextensive receptive field structure of blue-yellow ganglion cells in primate retina. *J Neurosci*. 2009;29(26):8372–8387.
354. Packer OS, Verweij J, Li PH, et al. Blue–yellow opponency in primate S cone photoreceptors. *J Neurosci*. 2010;30(2):568–572.
355. Yin L, Smith RG, Sterling P, et al. Physiology and morphology of color-opponent ganglion cells in a retina expressing a dual gradient of S and M opsins. *J Neurosci*. 2009;29(9):2706–2724.
356. Jacobs GH, Williams GA, Cahill H, et al. Emergence of novel color vision in mice engineered to express a human cone photopigment. *Science*. 2007;315(5819):1723–1725.
357. Mancuso K, Hauswirth WW, Li Q, et al. Gene therapy for red-green colour blindness in adult primates. *Nature*. 2009;461(7265):784–787.
358. Osterhout JA, Josten N, Yamada J, et al. Cadherin-6 mediates axon-target matching in a non-image-forming visual circuit. *Neuron*. 2011;71(4):632–639.
359. Siegert S, Cabuy E, Gross Scherf B, et al. Transcriptional code and disease map for adult retinal cell types. *Nat Neurosci*. 2012;15:487–495.
360. Harwerth RS, Carter-Dawson L, Shen F, et al. Ganglion cell losses underlying visual field defects from experimental

glaucoma. *Invest Ophthalmol Vis Sci*. 1999;40(10):2242–2250.
361. Strettoi E. A survey of retinal remodeling. *Front Cell Neurosci*. 2015;9:494.
362. Miyake Y, Yagasaki K, Horiguchi M, et al. Congenital stationary night blindness with negative electroretinogram: a new classification. *Arch Ophthalmol*. 1986;104(7):1013–1020.
363. Chang B, Heckenlively JR, Bayley PR, et al. The nob2 mouse, a null mutation in Cacna1f: anatomical and functional abnormalities in the outer retina and their consequences on ganglion cell visual responses. *Vis Neurosci*. 2006;23(1):11–24.
364. Ishii M, Morigiwa K, Takao M, et al. Ectopic synaptic ribbons in dendrites of mouse retinal ON- and OFF-bipolar cells. *Cell Tissue Res*. 2009;338(3):355–375.

18

Cell Biology of the Retinal Pigment Epithelium

James T. Handa

Immune Privilege and the Immune Response
Transport of Nutrients, Ions, and Water
Secretion of Cytokines and Growth Factors

The retinal pigment epithelium (RPE) forms a monolayer of highly specialized neuroectodermally derived pigmented cells located between the neurosensory retina and the vascular choroid. The RPE mediates functions essential for normal outer retinal physiology, including participation in the visual cycle, phagocytosis of shed photoreceptor outer segments (OS), maintenance of the outer blood–retinal barrier, secretion of neurotrophic, inflammatory, and vasculotrophic growth factors, water transport out of the subretinal space, and regulation of bidirectional ion and metabolic transport between the retina and choroid. The RPE is a primary site of pathology in major blinding diseases, including age-related macular degeneration (AMD) and proliferative vitreoretinopathy (PVR).

Embryology

At day 27 postconception, the optic vesicles invaginate to form the optic cup and the neuroepithelium differentiates and thickens. By day 30, the basic cellular relationship of the outer retina is established with the prospective RPE layer closely apposed to the developing neural retina. Several transcription factors play a critical role in the determination and specification of RPE, among which are microphthalmia-associated transcription factor (Mitf), orthodenticle homeobox (Otx)1/2, and paired box (Pax) 6.[1] The Sonic hedgehog (Shh) signaling pathway is also critical; the distinct expression pattern of its members in central and peripheral RPE suggests multiple regulatory roles during RPE differentiation.[2] By day 35, melanin pigment granules are identified in the RPE; this is the earliest site of pigmentation in the body. By the 6th week of gestation, the RPE elaborates basement membrane material that initiates the formation of Bruch's membrane. Between 4 weeks and

6 months of gestation, RPE cells exhibit a high rate of proliferation, peaking at 4 months of gestation.[3] Meanwhile, the RPE develops polarity with apical microvilli that extend into the subretinal space, which coordinates photoreceptor differentiation.[4] Studies indicate that the Shh pathway,[5] retinoic acid,[6] bone morphogenetic protein (BMP),[7] Notch,[8] and Wnt/β-catenin[9] pathways all participate in RPE differentiation.[10] In addition, ezrin, a member of the ezrin/radixin/moesin (ERM) family, directs the morphogenesis of apical microvilli and basal infoldings.[11] RPE polarity is also required for choroid and scleral development.[12] Readers are referred to Chapter 15 (The development of the retina), for a more comprehensive review of the development of the RPE and retina.

Anatomy and Histology

The adult human eye contains approximately 3.5×10^6 RPE cells. Since they are postmitotic and do not remain in the cell cycle, this population remains stable during adult life in the absence of disease.[13] The RPE extends from the optic nerve to the ora serrata, and is continuous with the ciliary body pigment epithelium. The fovea contains the highest density of RPE cells, with a progressive decrease in density to the periphery. These cobblestone-shaped cells with highly polarized structure form a monolayer between the neurosensory retina and the choroid. Their apical microvilli interdigitate with photoreceptor outer segments, while their basal side attachs to the RPE basement membrane of Bruch's membrane. Readers are referred to Chapter 22 (Structure, function, and pathology of Bruch's membrane) for a detailed description of Bruch's membrane physiology and interaction with the RPE.

The RPE, with its brown melanin granules, contributes to the typical patterned fundus appearance due to variations in RPE pigmentation. Typically, the highest concentration of pigment in the RPE is found in the peripheral retina, while the lowest is in the macula.[14] With age, the RPE gradually loses melanin granules, in part from the effects of photo-oxidation.[15] The retina and RPE are separated by a potential space known as the subretinal space. Although the retina conforms to the shape of the adjacent RPE and underlying sclera, it is not firmly attached to the RPE except at the

optic disc and ora serrata; attachments elsewhere are weak and can be disrupted by relatively weak forces. Chapter 21 (Mechanisms of normal retinal adhesion) provides complete discussion of retinal adhesion.

Heterogeneity and Polarity of the RPE

RPE cells exhibit regional heterogeneity in morphology and function.[16] They have cuboidal morphology and appear polygonal in shape when viewed en face, a pattern that is maintained in culture when grown to confluence (Fig. 18.1). The morphology varies by fundus location. In the macula, the cells are tall and narrow, while they are flat, spread out, and may be binucleated in the periphery.[13] Due to regional differences in requirements for RPE function, RPE cells vary regionally in growth potential,[17] expression of vimentin and phosphotyrosine,[16] distribution of Na/K adenosine triphosphatase (ATPase) pumps,[18] and kinetics of rod OS binding and ingestion.[19] Age-related expression of lysosomal enzymes, superoxide dismutase-2, and accumulation of lipofuscin vary by fundus region,[20–22] suggesting that this heterogeneity contributes to pathologic changes in the RPE.

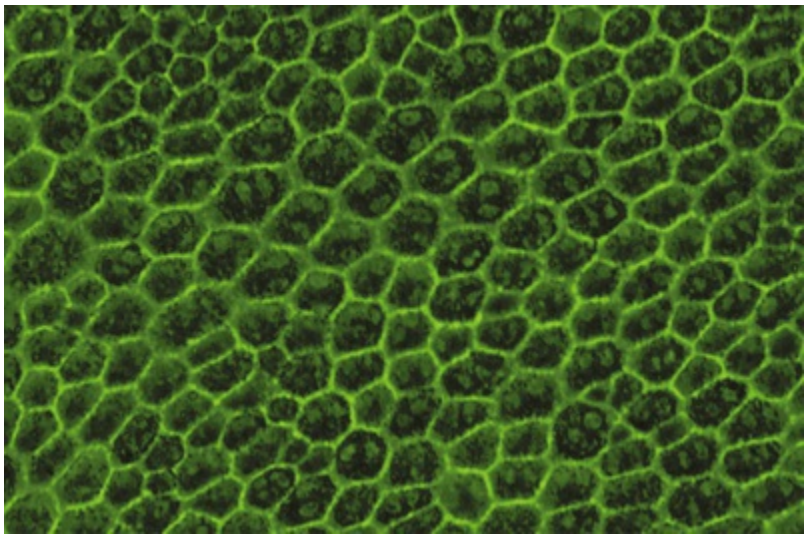

FIG. 18.1 Cultured human retinal pigment epithelium (RPE) cells. A monolayer of early-passage human RPE cells demonstrates the polygonal appearance of the cells when grown to confluence (phase microscopy, ×25).

RPE cell polarity is characterized by distinct ultrastructural features and specialized functions in the apical and basolateral domains (Fig. 18.2). The apical cell membrane elaborates numerous microvilli (3–7 μm in length) that interdigitate and ensheath photoreceptor OSs[23] (Figs. 18.3 and 18.4). These interdigitations, in conjunction with the extracellular matrix (ECM), and neural cell adhesion molecule (N-CAM) expressed on the RPE apical surface, allow adhesion between the retina and the RPE. Between 30 and 45 photoreceptors are in contact with each RPE cell.[24] The RPE engulfs and degrades nearly 30,000 shed OS each day such that one RPE cell will ingest and degrade hundreds of millions of discs during its lifetime.[25,26]

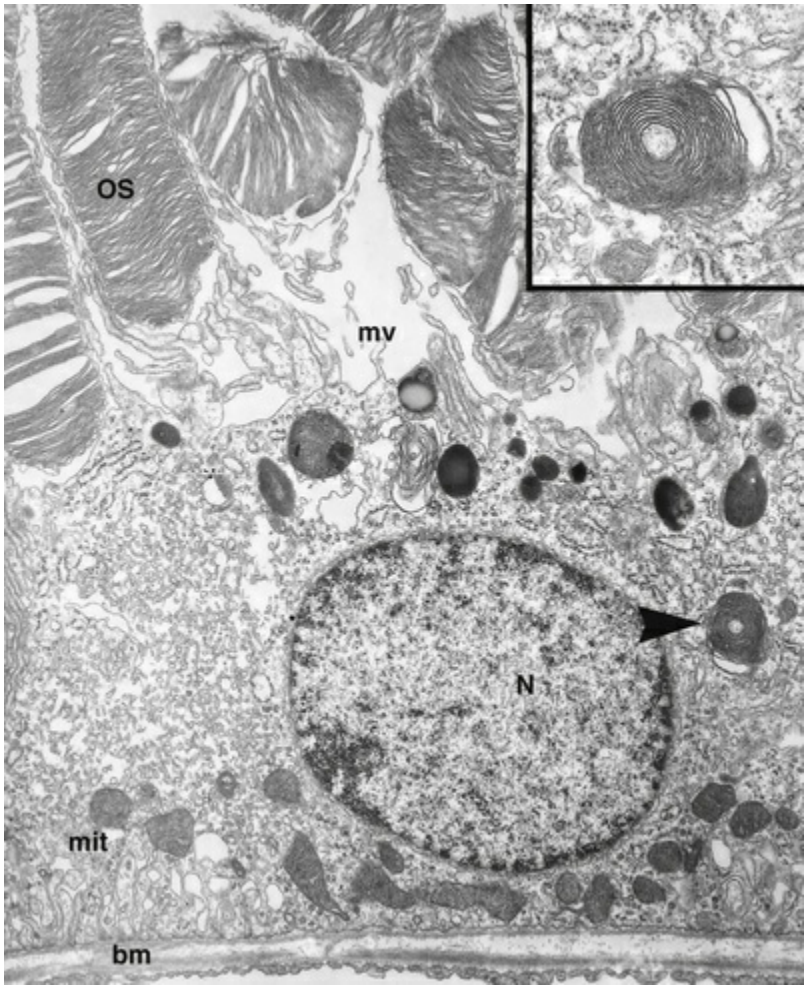

FIG. 18.2 Electron micrograph of a retinal pigment epithelium (RPE) cell and adjacent outer segments (OS) of the rod photoreceptor cells. Note the apical

microvilli (*mv*) of the RPE cell. Darkly stained melanin granules are seen apically, while mitochondria (*mit*) are predominantly basal. The cell rests on the basal Bruch's membrane (*bm*). The nucleus (*N*) is present in the basal third of the cytoplasm. A phagolysosome (*arrowhead*) containing degrading rod OS material is seen in the cytoplasm at low (×21,500) and high (inset, ×50,000) magnification.

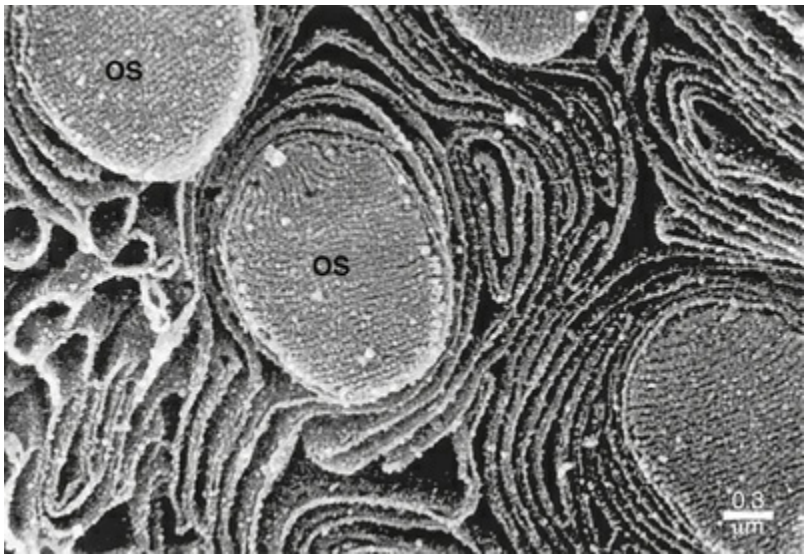

FIG. 18.3 Scanning electron micrograph of rod photoreceptor outer segments (OS) fractured across their long axis, surrounded by apical folds extending from the surface of the retinal pigment epithelium. The membrane forms a sheath around each of the rod OSs. (Reproduced with permission from Hollenberg MJ, Lea PJ. High resolution scanning electron microscopy of the retinal pigment epithelium and Bruch's layer. Invest Ophthalmol Vis Sci 1988;29:1380–9.)

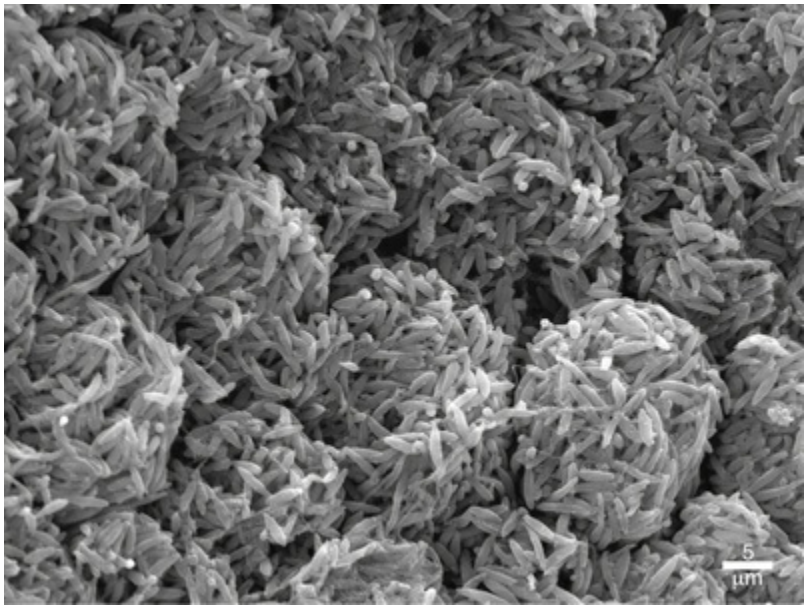

FIG. 18.4 Scanning electron micrograph of the apical surface of a bovine retinal pigment epithelium (RPE) explant. Note the abundant microvilli on the apical surface of the RPE cells. Approximately a dozen RPE are shown.

The functional polarity of RPE cells results from the differential apical–basal distribution of membrane proteins (Table 18.1). The RPE shares many common characteristics with other transporting epithelia, but uniquely exhibits "reversed polarity" of certain proteins, such as the Na/K-ATPase pump, ECM metalloproteinase inducer (EMMPRIN), and N-CAM. In contrast to other epithelia, these proteins are apically rather than basolaterally located. In a proteomic study of RPE apical microvilli,[27] 283 proteins were identified, which could be divided into different functional categories, including retinoid-metabolizing, cytoskeletal, enzymes, ECM components, membrane proteins, and transporters. $\alpha v\beta 5$ integrin (Fig. 18.5), mannose receptors, and CD36 are localized to the apical membrane domain, specifically in the microvilli, where they play critical roles in OS phagocytosis.[28–30] Na/K-ATPase is mainly apically located, where it is critical for trans-RPE ion transport.[31] The membrane protein chloride intracellular channel 4 (CLIC4) is enriched in apical RPE microvilli, possibly for modulating the activity of cell surface channels/transporters.[32] The RPE basal membrane domain is characterized by infoldings that are approximately 1 μm in length (Fig. 18.6). The basal membrane

contains α3β1, α6β1, and αvβ3 integrins, which mediate RPE attachment to Bruch's membrane (see Fig. 18.5). The basal infoldings also express Bestrophin-1, a chloride anion channel, that regulates voltage-dependent L-type Ca^{2+} channels by interacting with the beta-subunits of the Ca^{2+} channels.[33] Ezrin, localized to both apical and basolateral membranes, promotes morphogenesis of apical microvilli and basal infoldings, respectively.[34] A number of transporters work together in apical and basal domains. For example, glucose transport from the choroid to the photoreceptors is mediated by basally and apically located glucose transporter (GLUT) 1.[35] In contrast, elimination of lactic acid from the subretinal space is mediated by different monocarboxylate transporters in the apical (MCT1) and basolateral (MCT3) membranes.[36] The lateral membrane domain of the RPE cell demonstrates specialized junctions important for cell–cell attachment and communication, which will be discussed below.

TABLE 18.1

Polarized Cell Surface Molecule Expression in Retinal Pigment Epithelium

Location	Protein	Function
Apical membrane	Na/K-ATPase	Na flux
	N-CAM	Adhesion to retina, phagocytosis
	αvβ5 integrin	Phagocytosis
	CD36	Phagocytosis
	Ezrin	Apical microvilli
	CLIC4	Channels/transporters
	GLUT1	Glucose transport
	MCT1	Monocarboxylate transporter
Lateral membrane	Occludin	Tight junction
	Cadherin	Adherens junction
	Connexin	Gap junction
Basolateral membrane	α3β1, α6β1, αvβ3 integrin	Attachment to Bruch's membrane
	Ezrin	Basal infoldings
	GLUT1	Glucose transport
	MCT3	Monocarboxylate transporter
	Bestrophin-1	Chloride anion channel

Na/K-ATPase, Na/K adenosine triphosphatase; N-CAM, neural cell adhesion molecule; CLIC4, chloride intracellular channel 4; GLUT1, glucose transporter 1; MCT1, monocarboxylate transporter 1.

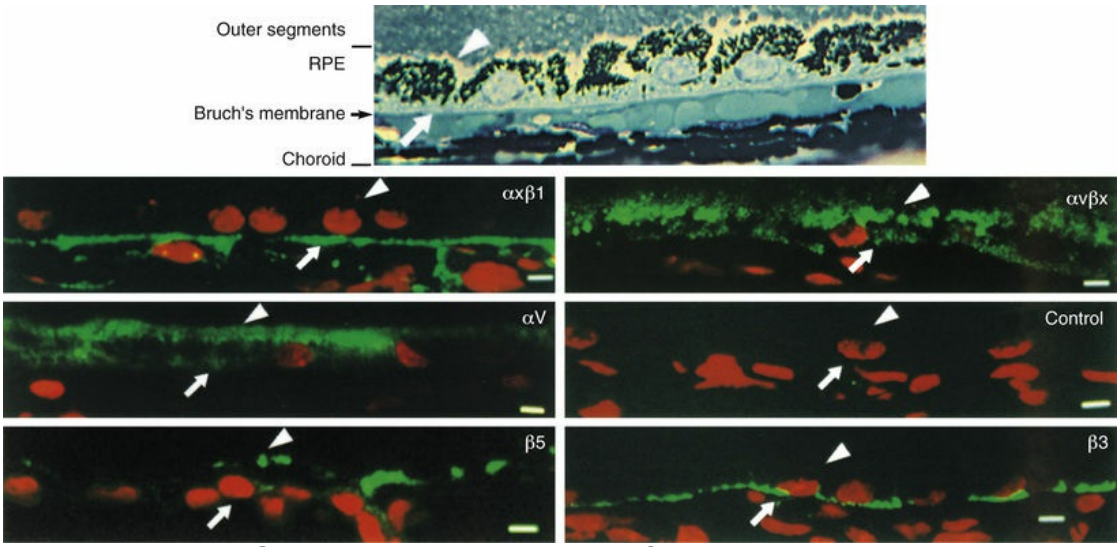

FIG. 18.5 Subcellular distribution of integrin receptors in adult rat retinal pigment epithelium by indirect immunofluorescence. For reference, a methylene blue-stained section of intact retina is shown at the top. β1 integrins are exclusively basal. αv integrin receptors are apical and basolateral and stain cytoplasmic vesicles. β5 integrins are located apically, and β3 integrins are restricted to a basal location. Scale bar: 5 μm. (Reproduced with permission from Finnemann SC, Bonilha VL, Mamorstein AD, et al. Phagocytosis of rod outer segments by retinal pigment epithelial cells requires αvβ5 integrin for binding but not for internalization. Proc Natl Acad Sci USA 1997;94:12932–7.)

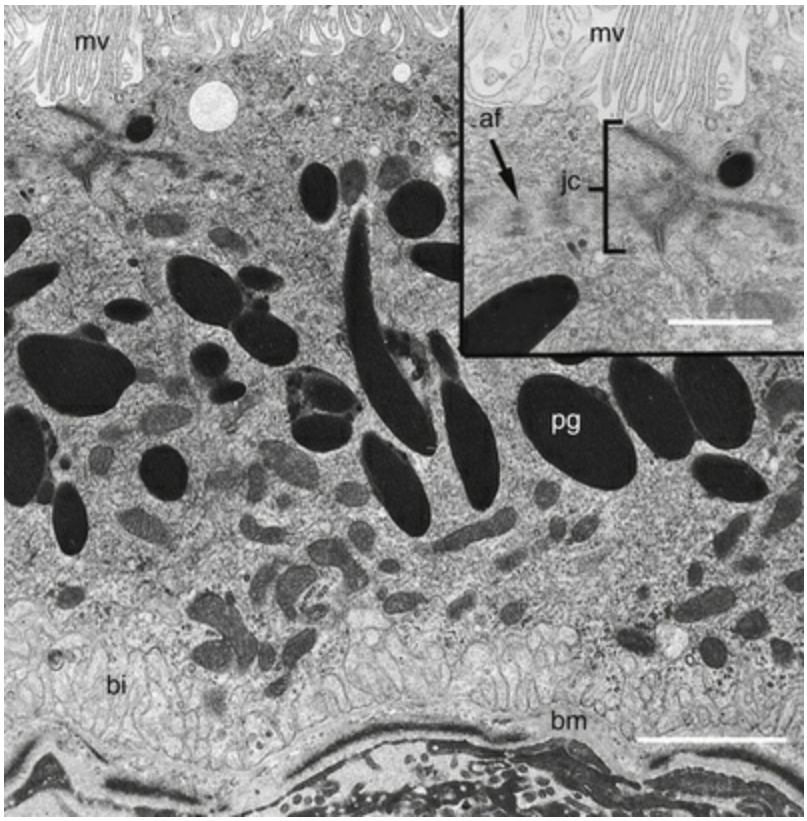

FIG. 18.6 Transmission electron micrograph of intact bovine retinal pigment epithelium (RPE) cells. Note the apical microvilli (*mv*), the pigment granules (*pg*) in the apical region of the RPE cytoplasm, and the basal infoldings (*bi*) in contact with Bruch's membrane (*bm*). In the upper left portion of the figure, the apically located junctional complex is seen between two retinal pigment epithelia, including the more apical zonula occludens (tight junction) and adjacent zonula adherens. The junctional complex (*jc*) is shown at higher magnification in the inset. The junctional complex is associated with a cytoplasmic band of actin filaments (*af*). Scale bar: 1.8 μm; bar in inset: 1 μm.

The intracellular distribution of cell organelles in the RPE also exhibits polarization and heterogeneity (see Figs. 18.2 and 18.6).[37] Melanin granules, which are 2–3 μm in diameter, are ovoid or spherically shaped, and are located in the apical region adjacent to the endoplasmic reticulum. At the ora serrata, the RPE contain many dense, round melanin granules throughout the cell while at the equator and macula, melanin granules are more apical, less abundant, and ovoid. The nucleus, with a diameter of 8–12 μm, is located in the basal aspect of the cell. Mitochondria also reside in

the basal RPE due to the high oxygen pressure originating from the choriocapillaris, and are most prominent in the macula.[38] Other cytoplasmic elements, such as microperoxisomes, lysosomes, autophagosomes, and phagosomes, do not have a distinct distribution. However, inhibition of lysosomal degradation in the RPE can induce exocytosis of phagocytic residual material at the basolateral plasma membrane.[39]

Cellular Junctions

The outer blood–retinal barrier is formed by the RPE, in which the lateral domains of adjacent cells are connected by apical zonulae occludens (tight junctions) and adjacent zonulae adherentes (adherens junctions), which form a barrier that regulates transepithelial diffusion through the paracellular spaces (Fig. 18.6).[40] These junctions seal off the subretinal space from the choriocapillaris, forming the so-called Verhoeff's membrane. The two major zonulae occludens proteins are the claudins and the occludins. The interaction between the extracellular domains of adjacent occludin molecules leads to high transepithelial resistance and an intact blood–retinal barrier. They maintain cell polarity by preventing the lateral diffusion of integral membrane proteins between the apical and lateral/basal surfaces, which compartmentalizes specialized functions, such as molecule transport.[41] The cytoplasmic domain of occludens interact with several other proteins, including zonula occludens (ZO)-1 and ZO-2, to form a complex that interacts with the actin cytoskeleton and components of various signal transduction pathways (Fig. 18.7). ZO-1 regulates cell proliferation and gene expression by inhibiting the activity of the Y-box transcription factor ZONAB, indicating they are critical for the differentiation and homeostasis of the RPE.[42] Early expression of the assembly proteins, including junctional adhesion molecule-A (JAM-A), AF-6, PAR-3, and PAR-6, corresponds to the initial establishment of the adherens and tight junctions,[43] whereas diffusible factors secreted by the neural retina act synergistically with basolateral stimulation to regulate the structure and function of RPE tight junctions.[44] Of the claudins, claudin 19 is the dominantly expressed isoform in human fetal RPE

cells.[45] JAM-C localizes specifically in the tight junctions of human fetal and adult native RPE, and regulates the recruitment of N-cadherin and ZO-1 to cell–cell contacts.[46] Under pathologic conditions such as oxidative stress,[47] inhibition of Na/K-ATPase,[48] matrix metalloproteinase (MMP)-9, interferon-gamma (IFN-γ), tumor necrosis factor,[49] and amyloid-beta(1–42)[50] could decrease tight junction protein expression, resulting in the disruption of the outer blood–retina barrier. In contrast, nitric oxide is involved in the maintenance of blood–retina barrier integrity.[49]

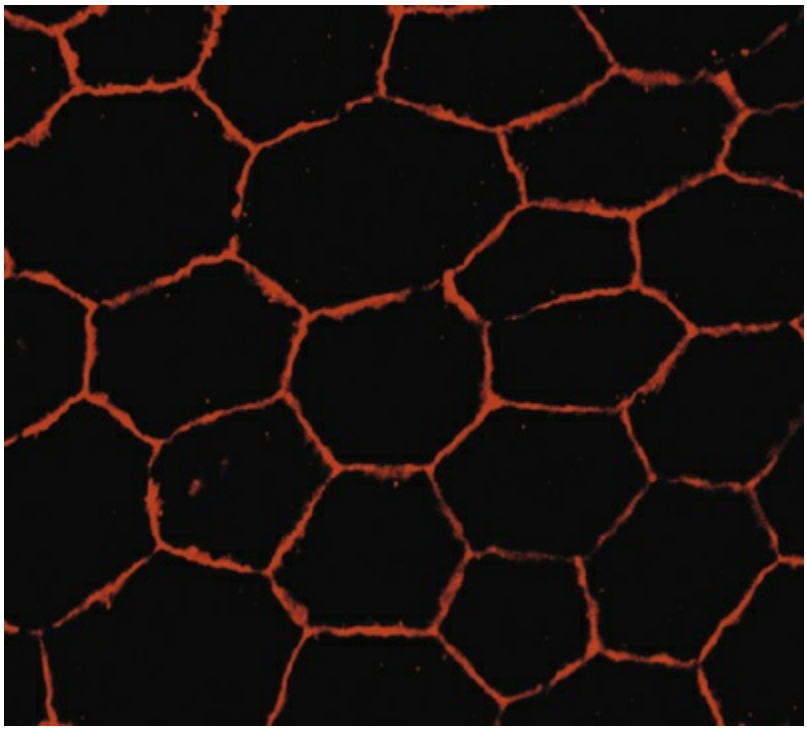

FIG. 18.7 Immunofluorescent stain of a bovine retinal pigment epithelium (RPE) monolayer explant stained with an antibody against the ZO-1 protein, a protein associated with the zonula occludens, or tight junction, demonstrating the polygonal shape and tight adherence of the RPE (×440).

The zonulae adherentes (adherens junction) form a 200 Å junction that are associated with circumferential microfilament bundles.[51] The transmembrane cadherins of the adherens junction require calcium to maintain cell-cell adhesion. Their cytoplasmic domains interact with catenins, which in turn, form a complex with α-actinin and vinculin. The adherens junctions organize the actin

cytoskeleton to maintain the cell's polygonal shape.[52] Gap junctions, which are also present in the lateral cell membranes, contain connexins which exchange ions and metabolites between cells. For example, connexin 43 mediates communication between the retina and RPE that is essential for the correct pacing of retinal organogenesis.[53] Connexin 43 participates in the release of ATP through hemichannels, influencing both neural retinal cell division and proliferation.[54] The basal cell membrane contains various integrins that are involved in focal adhesion points with the ECM.[55] Desmosomes, which are variably present in RPE cells among different species, are not necessary for establishment of a polar, functioning RPE layer.[56]

Cytoskeleton

Apart from the general role of the cytoskeleton, the RPE cytoskeleton has unique functions, including as melanosome transport and phagocytosis.[57,58] These vital functions are disrupted in diseases like PVR, caused by RPE cell proliferation and myofibroblastic transdifferentiation, where there are prominent rearrangements of the cytoskeleton.[59] The cytoskeleton is composed of three major elements: the actin microfilaments (diameter 7 nm), microtubules (diameter 25 nm), and intermediate filaments (diameter 10 nm). Microfilaments and microtubules are dynamic structures that undergo polymerization and depolymerization, and are critical for intracellular transport. Microtubules participate in mitosis, and the movement of subcellular organelles and pigment granules. Actin microfilaments are located in the microvilli and throughout the cytoplasm where they are arranged in loose arrays or bundles. They help to generate and maintain cellular shape and participate in cell migration.[60]

Myosins are cytoskeletal motors that generate the forces to establish cell structure and actin-dependent cell motility. Multiple myosin family members are expressed by the RPE.[61] In addition, myosins are involved in the movement and biogenesis of melanosomes.[62] Intermediate filaments provide a structural framework that links the nucleus with the cell membrane, as well as to microfilaments and microtubules. In human RPE cells,

intermediate filaments of type I (acidic keratins), type II (basic/neutral keratins), and type V (lamins) have been identified. In the RPE, cytokeratin filament expression varies with cellular differentiation, changes in cellular polarity, intercellular association, and cell culture conditions.[63,64] Human RPE cells in vivo express keratins 8 and 18.[65] In cell culture, the RPE coexpresses keratins 7 and 19. The presence of keratin 18/19 has been correlated with migration in cultured RPE cells.[65]

Role of RPE in Bruch's Membrane Synthesis and Remodeling

The basal surface of the RPE has elaborate basal infoldings that attach to Bruch's basement membrane, an acellular layer separating the RPE from the choriocapillaris.[66] Besides the attachment site for the RPE, Bruch's membrane serves as a selective conduit for nutrients transported to the retina from the choriocapillaris and for metabolic wastes transported from the retina to the circulation. Bruch's membrane is a pentalaminar matrix composed of consists of the RPE basement membrane, the inner collagenous layer, the middle elastic layer, the outer collagenous layer, and the choriocapillaris endothelium basement membrane.[67] In mice, the RPE basement membrane and the choriocapillaris endothelial basement membrane are synthesized first, followed by the deposition of a collagenous layer between the two basement membranes. Finally, the elastic layer is synthesized and deposited within the collagenous layer, eventually separating it into an inner and outer collagenous layer.[68]

The RPE and choriocapillaris endothelial basement membranes (1.4–1.5 μm thick) are similar to other basement membranes in composition, containing collagen type IV, laminin, fibronectin, and sulfated polysaccharides,[69–71] and serve to anchor subjacent cells, act as a barrier and a filter, and stabilize the tissue structure.[72] The choriocapillaris basement membrane also contains collagen type VI, which is not present in the RPE basement membrane, which is involved in capillary endothelial cell stabilization. The inner collagenous (1.4 μm thick) and outer collagenous (0.7 μm thick) layers are composed of collagens type I, II, and V, which are

organized in a lattice-like network embedded in an amorphous collection of glycosaminoglycans.[73]

Collagen XVIII,[74] which gives rise to the endostatin, an inhibitor of choroidal neovascularization, is distributed through all layers of Bruch's membrane.[75] Booij et al.[76] have shown that both the RPE and choroid express most of the genes necessary for the formation and maintenance of Bruch's membrane. Specifically, the RPE maintains its basement membrane while the choriocapillaris endothelium maintains its basement membrane, whereas the inner, outer collagenous, and the elastic layers are maintained cooperatively by both cell types. Age-related biochemical alterations in the composition and three-dimensional organization of ECM molecules in Bruch's membrane may affect this function, and are described in detail in Chapter 22 (Structure, function, and pathology of Bruch's membrane).

The apical domain of RPE cells is embedded in the interphotoreceptor matrix (IPM), which is produced by the RPE and photoreceptor inner segments. A major proportion of IPM proteins are involved in retinoid transport between the photoreceptors and the RPE, and include the interphotoreceptor-binding protein (IRBP), retinol-binding protein (RBP), and transthyretin (TTR).[77–80] Retinal adhesion to the RPE is mediated in part by RPE transport of water and ions from the IPM toward the choriocapillaris. The IPM contains the neurotrophic pigment epithelial-derived factor (PEDF) that is secreted by the RPE with a 1000-fold greater abundance than vascular endothelial growth factor (VEGF), which is mainly secreted to the basolateral side.[81] Proteomic analysis of the porcine IPM indicates the wide array of functions possible by the IPM, such as neuroprotective phosphoproteins enriched in astrocytes (PEA)-15, peroxiredoxin 5, αB crystallin, macrophage migration inhibitory factor, 78-kDa glucose-regulated protein (GRP78), protein disulfide isomerase (PDI), and PEP-19.[82] Notably, αB crystallin is secreted by the RPE and maintains a neuroprotective outer retinal microenvironment.[83]

Degradation of ECM is regulated in part by both matrix metalloproteinases (MMPs) and the urokinase-type plasminogen activator (uPA) cascade,[84] which are activated by multiple types of cells, including leukocytes, endothelial cells, and RPE. MMPs are a

family of zinc-binding, Ca^{+}-dependent endopeptidases that degrade both collagen and proteoglycans during physiologic and pathologic ECM remodeling. The MMPs are tightly regulated by their tissue inhibitors of metalloproteinases (TIMPs), whose impairment may lead to progressive alterations in Bruch's membrane.[85] Normal RPE express the membrane-bound type 1 (MT1-MMP), type 2 (MMP-2) metalloproteinase,[86] and the metalloproteinase inhibitors TIMP-1 and TIMP-3.[87] ECM degradation is also promoted by uPA, a serine protease that activates plasminogen to active plasmin, which degrades fibrin, fibronectin, laminin, and other ECM components.[88] uPA activity can be blocked by two endogenous inhibitors, plasminogen activator inhibitor-1 and -2 (PAI-1 and PAI-2),[89] which belong to the serpin protease superfamily.

Specialized Functions of the RPE

Absorption of Light

The RPE absorbs light that passes beyond the photoreceptors. This light absorption serves to both sharpen vision by removing stray photons of light and protect the RPE from photo-oxidative stress.[14] Within the RPE, the melanin pigment granules absorb the stray light photons (see Fig. 18.6).

Phagocytosis of Photoreceptor Outer Segments

The apical microvilli of the RPE interdigitate with the photoreceptor OS. This interaction enables the shedding of OS that are ingested and degraded by the RPE that renews the phototransduction machinery and maintains a constant OS length. In all vertebrates examined, nocturnal and diurnal, cold-blooded and warm-blooded, rod OS shedding occurs maximally at or shortly after light onset, a daily rhythm which is established early after birth, irrespective of the lighting conditions during development. In fact, in rats the daily rod OS shedding rhythm is established by 2 weeks postnatally, and is maintained even after optic nerve transection, indicating that the rhythmic process of OS

shedding is controlled by intrinsic, ocular signals.[90,91] The temporal pattern of cone OS shedding is variable since in some species it occurs at night,[92] whereas in others, cones and rod OS are shed just after light onset.[93]

The disposal of the continuously shed OS is accomplished by phagocytosis of the OS at the expense of heightened metabolic activity and energy expenditure.[94,95] It has been estimated that, during an 80-year span, one RPE cell has internalized and degraded about 200 million discs.[96] The phagocytosis of OS material can be visualized in normal rat eyes using confocal microscopy to visualize rhodopsin^{+} phagolysosomes by enucleating the eye 2 hours after onset of light (Fig. 18.8). As reviewed in reference 97, rod OS phagocytosis is a highly specialized receptor-mediated, multistep process that comprises recognition, attachment (receptor–ligand interactions), internalization (transmembrane signaling and contractile proteins), and degradation of the ingested OS. The first step in the phagocytosis is recognition, a receptor-mediated process through integrin $\alpha v\beta 5$, which interacts with phosphatidylserine of rod OS plasma membranes.[98] Although $\alpha v\beta 3$ and $\alpha v\beta 5$ are instrumental for substrate binding, they do not directly bind phosphatidylserine, but instead, they bind an opsonin that recognizes the "eat-me" signal of their phagocytic targets. Gas6, protein S, and milk fat globule epidermal growth factor (MFG)-E8 are soluble bridging elements.[99] Recently, Tubby and tubby-like protein (Tulp) 1, which are secreted by photoreceptors, have also been identified as bridging molecules that bind to MerTk (a member of the TAM receptor tyrosine kinase subfamily) at their N-terminal region and to the rod OS at their C-terminal region.[100]

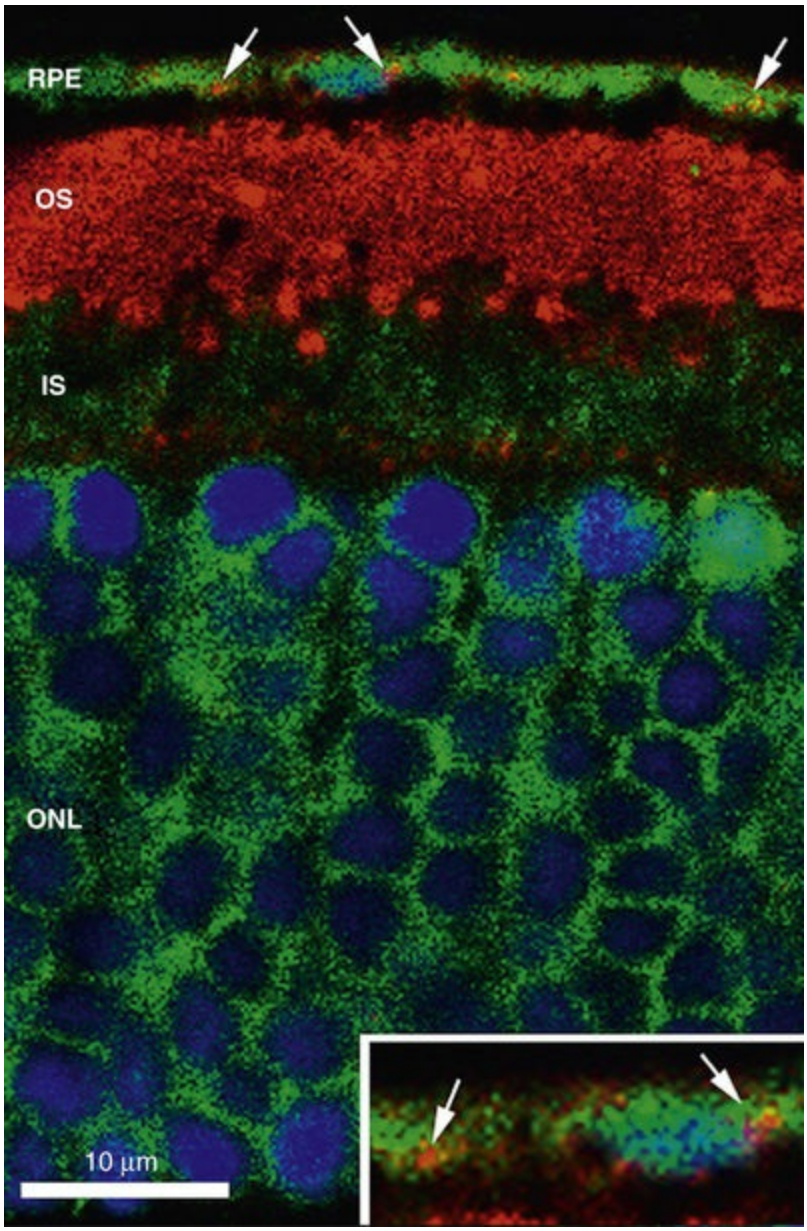

FIG. 18.8 Phagocytosis of rod outer segments. A section of outer retina was obtained from an eye enucleated 2 hours after light exposure in a pigmented rat. The section was evaluated using confocal microscopy after fluorescent labeling for rhodopsin (red), cytoplasm (green), and nuclei (blue). The figure shows the rhodopsin^{+} outer segment and punctate labeling of rhodopsin in the phagolysosomes within the retinal pigment epithelium (*arrows*); shown at higher magnification in insert. *IS*, inner segments of photoreceptors; *ONL*, outer nuclear layer; *OS*, outer segment; *RPE*, retinal pigment epithelium.

After binding the rod OS, the RPE plasma membrane invaginates

around the OS, leading to its ingestion into a phagosome. Cytoskeletal elements, particularly the microfilaments in the microvilli, reorganize during the initial stages of ingestion. An actin feltwork forms at the sites of attachment that extend into the pseudopods which surround and engulf the OS to form the phagosome.[101] This process includes an undefined, presumably G-protein-coupled transmembrane signal that stimulates the assembly of an appropriate contractile apparatus that, in turn, provides the motive force for internalization of the attached particle.[102] OS internalization is mediated by the receptor tyrosine kinase, c-mer, and its ligand Gas6.[103] Once inside the cytoplasm, phagosomes are transported to the basal aspect of the cell by microtubules.[104,105] Transport may also be partially mediated by myosin VIIa, an unconventional myosin that is mutated in patients with Usher syndrome.[106] Cytokines such as transforming growth factor (TGF)-β_1 and basic fibroblast growth factor (FGF) regulate rod OS phagocytosis.[107]

Basally transported phagosomes then fuse with lysosomes where they are degraded. The lysosome–phagosome interaction occurs in two steps. First, small lysosomes fuse with phagosomes. Subsequently, larger lysosomes appear to interact with phagosomes via pore-like structures. Following fusion, lysosomal enzymes hydrolyze the sequestered OS into small molecules that diffuse out of the RPE cell or are reused within the cell. Of the wide array of lysosomal enzymes capable of hydrolyzing photoreceptor OS, cathepsin D and S are among the most important because they degrade rhodopsin, the major protein in the OS.[108–110] With age and/or pathologic changes, degradation of OS within the phagolysosome leads to the formation of lipofuscin granules.[111,112]

Autophagy is a normal homeostatic process of cells that manages cellular stress by protein degradation and turnover of damaged organelles. The degradation products are then used as building blocks for continued cell survival. Recently, Kim et al. found that a form of autophagy designated LC3 associated phagocytosis (LAP) is central to the processing of engulfed OS.[113] RPE phagocytosis coincided with the enzymatic conversion of LC3 to its lipidated form, which initiated single-membrane phagosomes containing engulfed POS in an Atg5-dependent manner. This process required

Beclin1, which then enables the lysosome to fuse with the phagosome and form the phagolysosome, ultimately leading to degradation of the ingested OS. Degradation products are subsequently removed from the RPE by transport to the choroid, whereas some materials are recycled to the photoreceptors to maintain vision. LAP was found to be essential for the recovery of vitamin A for 11-*cis*-retinal (11-*cis*-RAL) synthesis. This finding demonstrates the interplay of phagocytosis and autophagy within the RPE that is required for both OS degradation and the maintenance of retinoid levels to support vision.

Role in Visual Cycle

The first step in the visual process is absorption of light by the opsins of rod and cone photoreceptors as well as by the melanopsin of retina ganglion cells. Melanopsin is involved in the regulation of circadian rhythms, pupillary light reflex, and other nonvisual responses to light,[114] although recently it has been shown that melanopsin in ganglion cells may contribute directly to pattern vision.[115] The light-absorbing chromophore of opsins is 11-*cis*-RAL, which is delivered to the rod photoreceptors by the RPE cells. The RPE cells possess the enzymatic mechanism to convert vitamin A to 11-*cis*-RAL and deliver it to the photoreceptors.

Light perception by the retina is initiated by the reaction of photons with light-sensitive pigments that are part of the membranes of photoreceptor OS. Cooperation between the photoreceptors and the RPE allows these visual pigments to be recycled through a complex series of oxidation–reduction reactions and transport mechanisms that are referred as the "visual cycle" (Fig. 18.9).

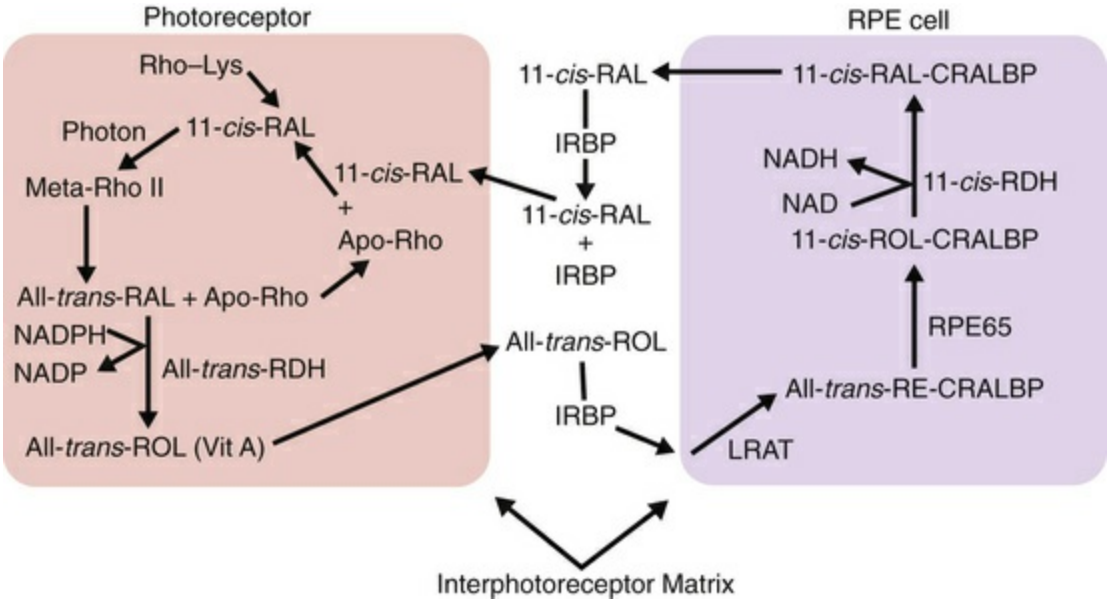

FIG. 18.9 The visual cycle takes place in the photoreceptors (left), the retinal pigment epithelium (right), and the intervening interphotoreceptor matrix. See text for description of components of the cycle: CRALBP, cellular retinal-binding protein; IRBP, interphotoreceptor-binding protein; LRAT, lecithin retinol acyltransferase; RAL, retinal; RDH, retinol dehydrogenase; RE, retinyl esters; Rho, rhodopsin; ROL, retinol.

The visual cycle is initiated by a photon reacting with rhodopsin, which comprises a G-coupled receptor protein, opsin (rods) or cone-opsin (cones), and the chromophore 11-*cis*-RAL. Reaction with light changes 11-*cis*-RAL into all-*trans*-RAL, which is released from the opsin and reduced to all-*trans* retinol (all-*trans*-ROL). ABCA4, a member of the A subfamily of ATP-binding cassette proteins, supports the processing of highly reactive all-*trans*-RAL and prevents the buildup of A2E, an insoluble toxic compound that is shed from the photoreceptors, phagocytosed by RPE, and accumulates as lipofuscin.[116] All-*trans*-ROL passes into the IPM, where it binds to IRBP and is transported into the adjacent RPE cells. IRBP is a 140-kDa glycoprotein secreted by the photoreceptors, which enhances the translocation of 11-*cis*-RAL from the RPE to the photoreceptors[117] and the translocation of all-*trans*-ROL from the photoreceptors to the RPE.[118] IRBP is essential for normal visual cycle function. In fact, mice that lack IRBP have significant photoreceptor degeneration.[119]

In the RPE, all-*trans*-ROL is esterified to fatty acids through the action of lecithin retinol acyltransferase (LRAT) to yield all-*trans* retinyl esters (all-*trans*-RE), which are the substrates for RPE65 isomerase. RPE65 isomerase converts the all-*trans*-RE to 11-*cis*-ROL, which is bound by cellular retinaldehyde-binding protein, reduced to 11-*cis*-RAL, transferred to the IPM where it binds to IRBP, and translocated to the photoreceptors where it binds to opsin to start the cycle anew.

Protection From Oxidative Stress

The RPE resides in a high oxidative stress environment due to a combination of unique factors. The retina obviously processes light for vision. As a result, photo-oxidative stress is a unique source of exogenous oxidative stress. Since the work of Ham et al. in 1978,[120] photo-oxidative stress has been linked with oxidative damage to the retina, RPE, and choroid. Vision is an energy-expensive process, which generates a high degree of reactive oxygen species (ROS).[121] To meet the energy demands, the retina requires a high level of oxygen. As a result, the RPE lives in high ambient oxygen partial pressures of 70–90 mm Hg.[122] The phagocytosis of outer segments is another unique source of ROS because H_2O_2 is produced by NADPH oxidase in phagosomes or from β-oxidation of OS lipids in peroxisomes.[123,124] Thus, the RPE is armed with a substantial antioxidant system to protect itself in this high oxidative stress environment.

A number of antioxidant systems are regulated through various transcription factors, including Nf-κB, AP1, the FoxO family, or PGC-1α. Central to the RPE's antioxidant response is the transcription factor nuclear factor-erythroid 2 p45-related factor 2 (Nrf2), which regulates a coordinated, comprehensive transcriptional program that maintains cellular redox homeostasis and protects the cell from oxidative injury[125–127] (Fig. 18.10). Under basal conditions, Nrf2 interacts with the negative regulator Kelch-like ECH-associated protein 1 (Keap1), keeping Nrf2 in the cytoplasm. Keap1 also functions as a substrate adaptor protein for a Cul3-dependent E3 ubiquitin ligase complex, which targets Nrf2 for proteolysis by the ubiquitin-proteasome pathway.[128] With oxidative

stress, Keap1 undergoes a conformational change of its multiple cysteine residues, which releases Nrf2 and prevents Keap1-mediated proteasomal degradation of Nrf2. Nrf2 then translocates to the nucleus where it dimerizes with Maf proteins, and binds to the antioxidant response element (ARE) in the promoters of antioxidant target genes to initiate the transcription.[129,130] Importantly, Nrf2 signaling plays an essential antioxidant role in the RPE.[131–134]

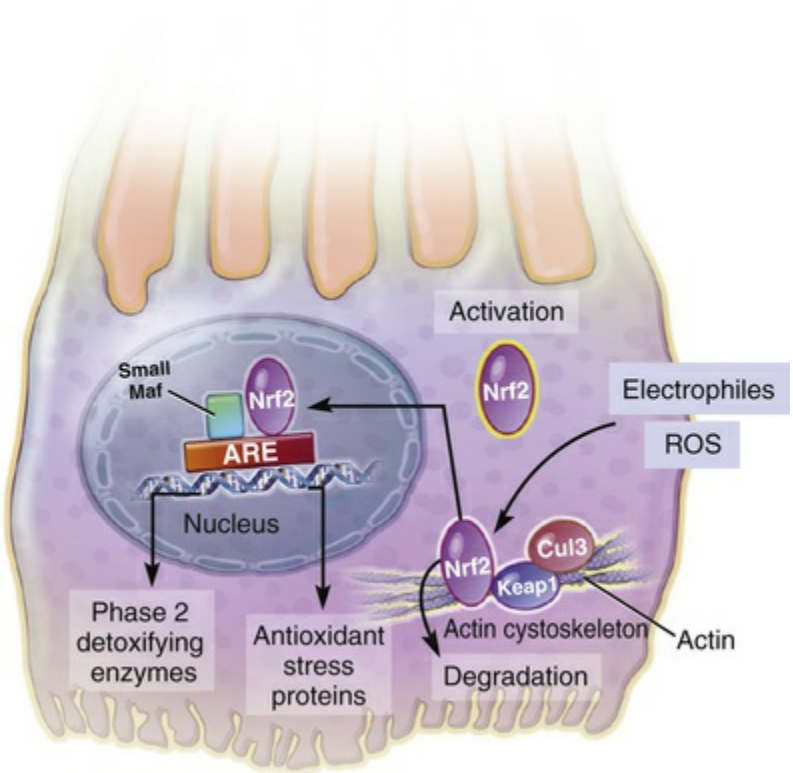

FIG. 18.10 Schematic of Nrf2 signaling. Normally, Nrf2 is sequestered in the cytoplasm by Keap1, which also functions as a substrate adaptor protein for a Cul3-dependent E3 ubiquitin ligase complex, which targets Nrf2 for proteolysis by the ubiquitin-proteasome pathway. Upon oxidative stress, reactive oxygen species (*ROS*) induce a conformational change to Keap1, which releases Nrf2. Nrf2 translocates to the nucleus where, along with Maf proteins, they bind to antioxidant response elements (*ARE*) to induce cytoprotective gene expression including phase 2 detoxifying enzymes and antioxidant stress proteins.

The Nrf2 signaling response regulates both an early acute phase to H_2O_2, 4-hydroxy-2-nonenal, hypoxia/hyperoxia, inflammation, and toxic drugs, as well as lipid signaling agents such as ceramide[135] through actions of the "direct" enzymes, such as catalase or SOD, which neutralize H_2O_2 and superoxide, respectively.[136,137] Nrf2 signaling regulates chronic oxidative stress by maintaining cellular glutathione and thioredoxin systems through glutathione (GSH),[138] thioredoxins (Trx),[139] glutaredoxins (Grx),[140] methionine sulfoxide reductases (Msrs),[141] and glutathione peroxidase.[142] Nrf2 also regulates the expression of xenobiotic metabolism enzymes that produce reducing equivalents, such as NADPH quinine oxidoreductase-1 (NQO-1).[143] In the cytosol, the glutathione and thioredoxin 1 systems are essential for maintaining normal cellular function. When ROS depletes cellular glutathione, Nrf2 signaling is activated with an accompanying compensatory upregulation of glutathione S-transferase, gamma glutamylcysteine synthetase, and glutathione peroxidase-1.[144,145] Trx1 also protects against oxidative stress in the cytoplasm; overexpression or intravenous injection of Trx1 protects RPE cells from oxidative injury.[140,146] Should glutathione or Trx1 levels drop sufficiently, cells can die from oxidatively induced apoptosis.[147,148]

Mitochondria continuously produce 90% of cellular ROS, an amount that can increase 10-fold when damaged.[149] Due to the high energy demands for vision, maintenance of the mitochondrial antioxidant pool is critical to prevent mitochondrial and cellular dysfunction. Mitochondrial antioxidants are pivotal, first line defense that protects mitochondria from excessive ROS to ensure cellular homeostasis. These include the thioredoxin 2 (Trx2) system including Trx reductase 2 (TrxR2), and peroxiredoxin 3 (Prx3) and the glutathione (GSH) system including glutathione reductase (GR), glutathione peroxidase (GPx-1 and -4).[150] Sulfiredoxin (Srx), a cytosolic protein, is an additional member of the Trx2 system after it translocates to the mitochondria.[151] Nrf2 is involved in the regulation of mitochondrial antioxidants including Trx2, Prx3, and Srx.[152–154] Most mitochondrial ROS are produced as superoxide anion (O_2-), which is rapidly converted to H_2O_2 by superoxide dismutase-2 (SOD2). Since mitochondrial catalase levels are very low, H_2O_2 is neutralized by the GSH and Trx2 systems, which

protect against retinal injury.[142,155] Despite 100-fold lower levels than GSH,[156] Trx2 redox regulation is essential for survival and is more sensitive than GSH to oxidative stress because enhanced ROS reduces Trx2 before GSH.[157]

Role in Maintaining Avascular Outer Retina

The avascularity of the subretinal space is dependent on the antiangiogenic activity of PEDF and endostatin, the 20-kDa C-terminal fragment derived from type XVIII collagen by proteolysis. PEDF is synthesized and secreted by the RPE into the IPM,[158,159] where it acts as a neuroprotective factor for photoreceptors and neural retina ganglion cells. PEDF is also a most potent and selective antiangiogenic factor that inhibits vascular growth, mediates regression of newly formed blood vessels without affecting preexisting vessels, and in the retina, prevents the growth of blood vessels into the subretinal space.[160–162] The importance of PEDF in maintaining the avascularity of the outer retina is apparent from its retinal distribution of PEDF. The expression of PEDF is highest in the developing fovea of mid-gestation human retinas and in the fovea of monkeys aged between fetal day 55 and 11 years of age.[163] In normal adult eyes, PEDF is 10-fold higher than VEGF in the macula, but not in the retinal periphery, strongly suggesting that PEDF is responsible for subretinal macular avascularity.[164]

In addition to PEDF, avascularity of the subretinal space is dependent on endostatin. Endostatin is cleaved from collagen XVIII in Bruch's membrane by the action of RPE-derived MMP-9 and cathepsin L. Laser-induced choroidal neovascular lesions in *Col18a1*$^{-/-}$ mice, which lack endostatin, develop marked vascular permeability and form large, confluent areas of subretinal neovascularization. In contrast, choroidal neovascular lesions in control mice remain small and clearly circumscribed. Administration of recombinant endostatin to *Col18a1*$^{-/-}$ mice decreases the lesion size to that observed in control mice.[165]

Immune Privilege and the Immune Response

Immune privilege refers to the fact that foreign-tissue grafts placed in the immune-privileged site are tolerated and survive for

prolonged, often indefinite, intervals, while placement of such grafts at conventional body sites leads to acute irreversible immune rejection. Ocular immune privilege was demonstrated by Sir Peter Medawar in 1948 when skin allografts survived when implanted into the anterior chamber of the eye.[166] Only in the past 20 years has research supported the subretinal space as a relatively immune-privileged space.[167,168] The RPE is a major source of subretinal immune privilege, evolving from a concept of passive physical barriers (tight junctions between RPE; lack of lymphatic drainage from the subretinal space; low levels of major histocompatibility antigen expression) to an active process. The RPE express both soluble (TGF-β, PEDF) and cell surface molecules (TGF-β, CD95 (FAS) ligand, CD59, CD46) that promote immune privilege. TGF-β has been identified as a major factor in the inhibition of T-cell proliferation and IFN-γ production, and the generation of T-regulatory cells (Tregs) in ocular immune-privileged sites.[168] Recently, immune privilege in the aqueous humor was shown to require a role for both TGF-β and retinoic acid in the generation of Tregs; however, whether this is also true for the subretinal space is currently unknown.[169]

The RPE possesses significant capability of eliciting an immune response. The RPE expresses many components of innate immunity. For example, the RPE expresses Toll-like receptors 1–7, 9, and 10, which participate in host defense response to either bacteria or damaged molecules.[170] The RPE expresses many components of the complement system, which can be induced in response to a stress as a protective early response.[171] Recently, the RPE has been found to produce the NLRP3 inflammasome in response to a number of inciting factors including Alu RNAs, ROS, and extracellular ATP.[172] These different arms of innate immunity are designed to eliminate dangerous molecules. They are an intricate, finely balanced network that responds definitively to an inciting trigger. Disruption of this delicate balance can result in a dysregulated response that causes tissue injury critical for maintaining the health of the RPE while a dysregulated response can impair RPE health. A full discussion of the blood–retinal barrier and immune privilege is found in Chapter 29 (Blood–retinal barrier, immune privilege, and autoimmunity).

Transport of Nutrients, Ions, and Water

RPE cells are responsible for delivering nutrients from the circulation to the photoreceptors, and water and metabolic waste from the photoreceptors to the circulation. Since the RPE forms a tight barrier to diffusion, nutrients are taken up by active transport mechanisms that are specific for each nutrient and ion.

Of the nutrients that the RPE must deliver, glucose is one of the most important. RPE cells express very high levels of the glucose transporters, GLUT1 and GLUT3.[173,174] GLUT1 glucose transport is dependent on metabolic demand, and its expression is regulated by the glucose level. Low glucose levels increase its expression whereas high glucose levels decrease it.[175] GLUT3 is a high-affinity glucose transporter that is responsible for the basal transport of glucose to maintain resting-level activity. GLUT1 also mediates the uptake of vitamin C. In RPE cells, this may be important since the high energy requirements of the retina produce ROS, which are neutralized by vitamin C.[176]

Vitamin A is essential for vision. Vitamin A is transported from the circulation to the RPE bound to a complex of RBP and TTR. Upon reaching the RPE basal membrane, retinol is released to the membrane retinol receptor STRA6 (stimulated by retinoic acid 6), which transfers vitamin A into the cell, where it is converted to the active chromophore 11-*cis*-retinal.[177]

Ions are transported in and out of RPE cells through selective channels. For example, calcium, which in the RPE is essential for growth factor secretion, phagocytosis, ion exchange, and water transport, is mediated by a number of channels. These include L-type and T-type voltage-gated calcium channels,[31,178,179] as well as calcium channels of the transient receptor potential canonical (TRPC), specifically TRPC1 and TRPC4.[180,181] Two calcium transport channels, TRPV5 and TRPV6, with a calcium–sodium selectivity of more than 100:1 for calcium, have also been identified in RPE cells.[182]

The RPE removes water, ions, and catabolites from the retina to the choriocapillaris. However, RPE cell tight junctions prevent the paracellular transport of water, ions, and other solutes between the subretinal space and the choriocapillaris. Instead, they are actively transported across the RPE. For example, lactic acid is removed

from the subretinal space by monocarboxylate transporters in the apical (MCT1) and basolateral (MCT3) membranes.[36,183] Apically located Na^+,K^+-ATPase provides the energy for transepithelial transport, and regulates sodium and potassium ion flux across the RPE plasma membrane, which maintains proper ion balance in the IPM and establishes membrane potentials. Water is formed during the high metabolism of vision in the retina, and is removed from the subretinal space through active transport of chloride ion channels across the RPE to the choroid.[182] Water movement across the RPE is also facilitated by Aquaporin-1 channels.[184,185] Impaired egress of water will result in macular edema, exudative retinal detachment, and if chronic, RPE and photoreceptor degeneration that results in blindness.

Secretion of Cytokines and Growth Factors

RPE cells secrete many cytokines and growth factors that regulate many of the cellular pathways necessary for function, survival, and response to injury. The best known of these factors are VEGF and PEDF. VEGF, which is constitutively secreted from the basal surface of the RPE towards the choriocapillaris, has two main functions: (1) to provide prosurvival signals to the choroidal vascular endothelial cells; and (2) to maintain the fenestrations of the choriocapillaris endothelium.[186] PEDF is predominantly secreted from the apical RPE surface where it promotes an antiangiogenic and neuroprotective environment for the photoreceptors.[81] Many of these factors show dysregulated expression in retinal diseases such as AMD, diabetic retinopathy, and PVR. The most common of these factors are listed in Table 18.2.

TABLE 18.2

Growth Factors Produced by Retinal Pigment Epithelium Cells

Factor	Function	References
Pigment epithelial-derived factor (PEDF)	Neuroprotection, neurogenesis, antiangiogenesis	81, 158, 159
Vascular endothelial growth factor (VEGF)	Angiogenesis, endothelial cell survival factor, maintenance of choriocapillaris fenestrations	81, 164, 186
Nerve growth factor (NGF)	Survival and maintenance of sympathetic and sensory neurons. Ocular immune response	187, 188
Brain-derived neurotrophic	Supports the survival of existing neurons, and	188, 189

factor (BDNF)	fosters the growth and differentiation of new neurons and synapses	
Neurotrophin-3 (NT-3)	Stimulation and control of neurogenesis	189
Insulin-like growth factor (IGF-1)	Regulation of neurogenesis, myelination, synaptogenesis, and dendritic branching and neuroprotection after neuronal damage	190, 191
Neuroprotectin 1 (NPD1)	Protects neural tissues from injury caused by free radicals and other oxidative stress	192
Transforming growth factor-β (TGFβ)	Regulation of many cellular processes in the adult and developing embryo, including cell growth and differentiation and cellular homeostasis	193
Granulocyte–macrophage colony-stimulating factor (GM-CSF)	Stimulation of stem cells to differentiate into granulocytes and monocytes	194
Monocyte chemotactic protein-1 (MCP-1)	Monocyte chemoattractant	195
Hepatocyte growth factor (HGF)	Hepatocyte growth factor regulates cell growth, cell adhesion, cell motility, and morphogenesis	196
Erythropoietin (EPO)	Regulates red blood cell production. EPO protects retina from physiologic and pathologic light-induced oxidative injury	197
Platelet-activating factor (PAF)	Phospholipid activator and mediator of platelet aggregation, inflammation, and anaphylaxis	198
Melanoma growth-stimulatory activity/growth-regulated protein (MGSA/GRO)	Enhances chemotaxis of neutrophils and enhances the secretion of elastase and other matrix-degrading enzymes	199
Endothelin 1	Vasoconstriction	200
Fibroblast growth factor	Mitogenic and cell survival activities. Involved in embryonic development, cell growth, morphogenesis, tissue repair, tumor growth, and invasion	201
Bone morphogenetic protein	Regulation of differentiation, senescence, and apoptosis	202
Interleukin-6	Pleiotropic cytokine with a role in inflammation, hematopoiesis, angiogenesis, cell differentiation, and neuronal survival	203
Interleukin-8	Interleukin-8 attracts and activates neutrophils	204
Connective tissue growth factor	Intraocular fibrosis	205

References

1. Martinez-Morales JR, Rodrigo I, Bovolenta P. Eye development: a view from the retina pigmented epithelium. *Bioessays*. 2004;26(7):766–777.
2. Perron M, Boy S, Amato MA, et al. A novel function for Hedgehog signalling in retinal pigment epithelium differentiation. *Development*. 2003;130(8):1565–1577.
3. Stroeva OG, Mitashov VI. Retinal pigment epithelium:

proliferation and differentiation during development and regeneration. *Int Rev Cytol*. 1983;83:221–293.
4. Marmorstein AD. The polarity of the retinal pigment epithelium. *Traffic*. 2001;2(12):867–872.
5. Zhang XM, Yang XJ. Temporal and spatial effects of Sonic hedgehog signaling in chick eye morphogenesis. *Dev Biol*. 2001;233(2):271–290.
6. Matt N, Ghyselinck NB, Pellerin I, et al. Impairing retinoic acid signalling in the neural crest cells is sufficient to alter entire eye morphogenesis. *Dev Biol*. 2008;320(1):140–148.
7. Adler R, Belecky-Adams TL. The role of bone morphogenetic proteins in the differentiation of the ventral optic cup. *Development*. 2002;129(13):3161–3171.
8. Schouwey K, Aydin IT, Radtke F, et al. RBP-Jkappa-dependent Notch signaling enhances retinal pigment epithelial cell proliferation in transgenic mice. *Oncogene*. 2011;30(3):313–322.
9. Burke JM. Epithelial phenotype and the RPE: is the answer blowing in the Wnt? *Prog Retin Eye Res*. 2008;27(6):579–595.
10. Fuhrmann S. Eye morphogenesis and patterning of the optic vesicle. *Curr Top Dev Biol*. 2010;93:61–84.
11. Bonilha VL, Rayborn ME, Saotome I, et al. Microvilli defects in retinas of ezrin knockout mice. *Exp Eye Res*. 2006;82(4):720–729.
12. Lawrence MS, Azar DT. Myopia and models and mechanisms of refractive error control. *Ophthalmol Clin North Am*. 2002;15(1):127–133.
13. Panda-Jonas S, Jonas JB, Jakobczyk-Zmija M. Retinal pigment epithelial cell count, distribution, and correlations in normal human eyes. *Am J Ophthalmol*. 1996;121(2):181–189.
14. Schmidt SY, Peisch RD. Melanin concentration in normal human retinal pigment epithelium. Regional variation and age-related reduction. *Invest Ophthalmol Vis Sci*. 1986;27(7):1063–1067.
15. Sarna T, Burke JM, Korytowski W, et al. Loss of melanin from human RPE with aging: possible role of melanin photooxidation. *Exp Eye Res*. 2003;76(1):89–98.

16. Burke JM, Skumatz CM, Irving PE, et al. Phenotypic heterogeneity of retinal pigment epithelial cells in vitro and in situ. *Exp Eye Res*. 1996;62(1):63–73.
17. Burke JM, Soref C. Topographical variation in growth in cultured bovine retinal pigment epithelium. *Invest Ophthalmol Vis Sci*. 1988;29(12):1784–1788.
18. Burke JM, McKay BS, Jaffe GJ. Retinal pigment epithelial cells of the posterior pole have fewer Na/K adenosine triphosphatase pumps than peripheral cells. *Invest Ophthalmol Vis Sci*. 1991;32(7):2042–2046.
19. McLaren MJ. Kinetics of rod outer segment phagocytosis by cultured retinal pigment epithelial cells. Relationship to cell morphology. *Invest Ophthalmol Vis Sci*. 1996;37(7):1213–1224.
20. Cabral L, Unger W, Boulton M, et al. Regional distribution of lysosomal enzymes in the canine retinal pigment epithelium. *Invest Ophthalmol Vis Sci*. 1990;31(4):670–676.
21. Hjelmeland LM, Fujikawa A, Oltjen SL, et al. Quantification of retinal pigment epithelial phenotypic variation using laser scanning cytometry. *Mol Vis*. 2010;16:1108–1121.
22. Gulcan HG, Alvarez RA, Maude MB, et al. Lipids of human retina, retinal pigment epithelium, and Bruch's membrane/choroid: comparison of macular and peripheral regions. *Invest Ophthalmol Vis Sci*. 1993;34(11):3187–3193.
23. Bonilha VL, Rayborn ME, Bhattacharya SK, et al. The retinal pigment epithelium apical microvilli and retinal function. *Adv Exp Med Biol*. 2006;572:519–524.
24. Young RW. The renewal of rod and cone outer segments in the rhesus monkey. *J Cell Biol*. 1971;49(2):303–318.
25. Bonnel S, Mohand-Said S, Sahel JA. The aging of the retina. *Exp Gerontol*. 2003;38(8):825–831.
26. Ershov AV, Bazan NG. Photoreceptor phagocytosis selectively activates PPARgamma expression in retinal pigment epithelial cells. *J Neurosci Res*. 2000;60(3):328–337.
27. Bonilha VL, Bhattacharya SK, West KA, et al. Proteomic characterization of isolated retinal pigment epithelium microvilli. *Mol Cell Proteomics*. 2004;3(11):1119–1127.
28. Finnemann SC, Bonilha VL, Marmorstein AD, et al. Phagocytosis of rod outer segments by retinal pigment

epithelial cells requires alpha(v)beta5 integrin for binding but not for internalization. *Proc Natl Acad Sci USA*. 1997;94(24):12932–12937.
29. Tarnowski BI, Shepherd VL, McLaughlin BJ. Mannose 6-phosphate receptors on the plasma membrane on rat retinal pigment epithelial cells. *Invest Ophthalmol Vis Sci*. 1988;29(2):291–297.
30. Ryeom SW, Sparrow JR, Silverstein RL. CD36 participates in the phagocytosis of rod outer segments by retinal pigment epithelium. *J Cell Sci*. 1996;109(Pt 2):387–395.
31. Wimmers S, Karl MO, Strauss O. Ion channels in the RPE. *Prog Retin Eye Res*. 2007;26(3):263–301.
32. Chuang JZ, Chou SY, Sung CH. Chloride intracellular channel 4 is critical for the epithelial morphogenesis of RPE cells and retinal attachment. *Mol Biol Cell*. 2010;21(17):3017–3028.
33. Milenkovic VM, Krejcova S, Reichhart N, et al. Interaction of bestrophin-1 and Ca^{2+} channel beta-subunits: identification of new binding domains on the bestrophin-1 C-terminus. *PLoS ONE*. 2011;6(4):e19364.
34. Bonilha VL, Finnemann SC, Rodriguez-Boulan E. Ezrin promotes morphogenesis of apical microvilli and basal infoldings in retinal pigment epithelium. *J Cell Biol*. 1999;147(7):1533–1548.
35. Senanayake P, Calabro A, Hu JG, et al. Glucose utilization by the retinal pigment epithelium: evidence for rapid uptake and storage in glycogen, followed by glycogen utilization. *Exp Eye Res*. 2006;83(2):235–246.
36. Philp NJ, Wang D, Yoon H, et al. Polarized expression of monocarboxylate transporters in human retinal pigment epithelium and ARPE-19 cells. *Invest Ophthalmol Vis Sci*. 2003;44(4):1716–1721.
37. Korte GE, Perlman JI, Pollack A. Regeneration of mammalian retinal pigment epithelium. *Int Rev Cytol*. 1994;152:223–263.
38. Gouras P, Ivert L, Neuringer M, et al. Topographic and age-related changes of the retinal epithelium and Bruch's membrane of rhesus monkeys. *Graefes Arch Clin Exp*

Ophthalmol. 2010;248(7):973–984.
39. Peters S, Reinthal E, Blitgen-Heinecke P, et al. Inhibition of lysosomal degradation in retinal pigment epithelium cells induces exocytosis of phagocytic residual material at the basolateral plasma membrane. *Ophthalmic Res*. 2006;38(2):83–88.
40. Fine BS. Limiting membranes of the sensory retina and pigment epithelium: an electron microscopic study. *Arch Ophthalmol*. 1961;66:847–860.
41. Rodriguez-Boulan E. Genesis of polarity in renal tubular cells. *Miner Electrolyte Metab*. 1986;12(1):20–24.
42. Georgiadis A, Tschernutter M, Bainbridge JW, et al. The tight junction associated signalling proteins ZO-1 and ZONAB regulate retinal pigment epithelium homeostasis in mice. *PLoS ONE*. 2010;5(12):e15730.
43. Luo Y, Fukuhara M, Weitzman M, et al. Expression of JAM-A, AF-6, PAR-3 and PAR-6 during the assembly and remodeling of RPE tight junctions. *Brain Res*. 2006;1110(1):55–63.
44. Peng S, Rahner C, Rizzolo LJ. Apical and basal regulation of the permeability of the retinal pigment epithelium. *Invest Ophthalmol Vis Sci*. 2003;44(2):808–817.
45. Peng S, Rao VS, Adelman RA, et al. Claudin-19 and the barrier properties of the human retinal pigment epithelium. *Invest Ophthalmol Vis Sci*. 2011;52(3):1392–1403.
46. Economopoulou M, Hammer J, Wang F, et al. Expression, localization, and function of junctional adhesion molecule-C (JAM-C) in human retinal pigment epithelium. *Invest Ophthalmol Vis Sci*. 2009;50(3):1454–1463.
47. Bailey TA, Kanuga N, Romero IA, et al. Oxidative stress affects the junctional integrity of retinal pigment epithelial cells. *Invest Ophthalmol Vis Sci*. 2004;45(2):675–684.
48. Rajasekaran SA, Hu J, Gopal J, et al. Na,K-ATPase inhibition alters tight junction structure and permeability in human retinal pigment epithelial cells. *Am J Physiol Cell Physiol*. 2003;284(6):C1497–507.
49. Zech JC, Pouvreau I, Cotinet A, et al. Effect of cytokines and nitric oxide on tight junctions in cultured rat retinal

pigment epithelium. *Invest Ophthalmol Vis Sci*. 1998;39(9):1600–1608.
50. Bruban J, Glotin AL, Dinet V, et al. Amyloid-beta(1-42) alters structure and function of retinal pigmented epithelial cells. *Aging Cell*. 2009;8(2):162–177.
51. Hudspeth AJ, Yee AG. The intercellular junctional complexes of retinal pigment epithelia. *Invest Ophthalmol*. 1973;12(5):354–365.
52. Sandig M, Kalnins VI. Subunits in zonulae adherentes and striations in the associated circumferential microfilament bundles in chicken retinal pigment epithelial cells in situ. *Exp Cell Res*. 1988;175(1):1–14.
53. Tibber MS, Becker D, Jeffery G. Levels of transient gap junctions between the retinal pigment epithelium and the neuroblastic retina are influenced by catecholamines and correlate with patterns of cell production. *J Comp Neurol*. 2007;503(1):128–134.
54. Pearson RA, Dale N, Llaudet E, et al. ATP released via gap junction hemichannels from the pigment epithelium regulates neural retinal progenitor proliferation. *Neuron*. 2005;46(5):731–744.
55. Opas M, Kalnins VI. Light-microscopical analysis of focal adhesions of retinal pigmented epithelial cells. *Invest Ophthalmol Vis Sci*. 1986;27(11):1622–1633.
56. Owaribe K, Kartenbeck J, Rungger-Brandle E, et al. Cytoskeletons of retinal pigment epithelial cells: interspecies differences of expression patterns indicate independence of cell function from the specific complement of cytoskeletal proteins. *Cell Tissue Res*. 1988;254(2):301–315.
57. Hunt RC, Davis AA. Altered expression of keratin and vimentin in human retinal pigment epithelial cells in vivo and in vitro. *J Cell Physiol*. 1990;145(2):187–199.
58. Grisanti S, Guidry C. Transdifferentiation of retinal pigment epithelial cells from epithelial to mesenchymal phenotype. *Invest Ophthalmol Vis Sci*. 1995;36(2):391–405.
59. Lee J, Ko M, Joo CK. Rho plays a key role in TGF-beta1-induced cytoskeletal rearrangement in human retinal pigment epithelium. *J Cell Physiol*. 2008;216(2):520–526.

60. Burnside B, Adler R, O'Connor P. Retinomotor pigment migration in the teleost retinal pigment epithelium. I. Roles for actin and microtubules in pigment granule transport and cone movement. *Invest Ophthalmol Vis Sci*. 1983;24(1):1–15.
61. Lin-Jones J, Sohlberg L, Dose A, et al. Identification and localization of myosin superfamily members in fish retina and retinal pigmented epithelium. *J Comp Neurol*. 2009;513(2):209–223.
62. Coudrier E. Myosins in melanocytes: to move or not to move? *Pigment Cell Res*. 2007;20(3):153–160.
63. Turksen K, Opas M, Aubin JE, et al. Microtubules, microfilaments and adhesion patterns in differentiating chick retinal pigment epithelial (RPE) cells in vitro. *Exp Cell Res*. 1983;147(2):379–391.
64. Korte GE. New ultrastructure of rat RPE cells: basal intracytoplasmic tubules. *Exp Eye Res*. 1984;38(4):399–409.
65. Robey HL, Hiscott PS, Grierson I. Cytokeratins and retinal epithelial cell behaviour. *J Cell Sci*. 1992;102(Pt 2):329–340.
66. Bok D. The retinal pigment epithelium: a versatile partner in vision. *J Cell Sci Suppl*. 1993;17:189–195.
67. Hogan MJ. Ultrastructure of the choroid: its role in the pathogenesis of chorioretinal disease. *Trans Pac Coast Otoophthalmol Soc Annu Meet*. 1961;42:61–87.
68. Hirabayashi Y, Fujimori O, Shimizu S. Bruch's membrane of the brachymorphic mouse. *Med Electron Microsc*. 2003;36(3):139–146.
69. Timpl R. Structure and biological activity of basement membrane proteins. *Eur J Biochem*. 1989;180(3):487–502.
70. Marshall GE, Konstas AG, Lee WR. Collagens in ocular tissues. *Br J Ophthalmol*. 1993;77(8):515–524.
71. Aisenbrey S, Zhang M, Bacher D, et al. Retinal pigment epithelial cells synthesize laminins, including laminin 5, and adhere to them through alpha3- and alpha6-containing integrins. *Invest Ophthalmol Vis Sci*. 2006;47(12):5537–5544.
72. Libby RT, Brunken WJ, Hunter DD. Roles of the extracellular matrix in retinal development and maintenance. *Results Probl Cell Differ*. 2000;31:115–140.

73. Hewitt AT, Nakazawa K, Newsome DA. Analysis of newly synthesized Bruch's membrane proteoglycans. *Invest Ophthalmol Vis Sci*. 1989;30(3):478–486.
74. Bhutto IA, Kim SY, McLeod DS, et al. Localization of collagen XVIII and the endostatin portion of collagen XVIII in aged human control eyes and eyes with age-related macular degeneration. *Invest Ophthalmol Vis Sci*. 2004;45(5):1544–1552.
75. Ma DH, Yao JY, Kuo MT, et al. Generation of endostatin by matrix metalloproteinase and cathepsin from human limbocorneal epithelial cells cultivated on amniotic membrane. *Invest Ophthalmol Vis Sci*. 2007;48(2):644–651.
76. Booij JC, Baas DC, Beisekeeva J, Gorgels TG, Bergen AA. The dynamic nature of Bruch's membrane. *Prog Retin Eye Res*. 2010;29(1):1–18.
77. Chader GJ. Interphotoreceptor retinoid-binding protein (IRBP): a model protein for molecular biological and clinically relevant studies. Friedenwald lecture. *Invest Ophthalmol Vis Sci*. 1989;30(1):7–22.
78. Adler AJ, Evans CD. Proteins of the bovine interphotoreceptor matrix: retinoid binding and other functions. *Prog Clin Biol Res*. 1985;190:65–88.
79. Semenova EM, Converse CA. Comparison between oleic acid and docosahexaenoic acid binding to interphotoreceptor retinoid-binding protein. *Vision Res*. 2003;43(28):3063–3067.
80. Cunningham LL, Gonzalez-Fernandez F. Internalization of interphotoreceptor retinoid-binding protein by the *Xenopus* retinal pigment epithelium. *J Comp Neurol*. 2003;466(3):331–342.
81. Sonoda S, Sreekumar PG, Kase S, et al. Attainment of polarity promotes growth factor secretion by retinal pigment epithelial cells: relevance to age-related macular degeneration. *Aging*. 2010;2(1):28–42.
82. Hauck SM, Schoeffmann S, Deeg CA, et al. Proteomic analysis of the porcine interphotoreceptor matrix. *Proteomics*. 2005;5(14):3623–3636.
83. Sreekumar PG, Kannan R, Kitamura M, et al. alphaB

crystallin is apically secreted within exosomes by polarized human retinal pigment epithelium and provides neuroprotection to adjacent cells. *PLoS ONE*. 2010;5(10):e12578.
84. Elner SG, Elner VM, Kindzelskii AL, et al. Human RPE cell lysis of extracellular matrix: functional urokinase plasminogen activator receptor (uPAR), collagenase and elastase. *Exp Eye Res*. 2003;76(5):585–595.
85. Alexander JP, Bradley JM, Gabourel JD, et al. Expression of matrix metalloproteinases and inhibitor by human retinal pigment epithelium. *Invest Ophthalmol Vis Sci*. 1990;31(12):2520–2528.
86. Smine A, Plantner JJ. Membrane type-1 matrix metalloproteinase in human ocular tissues. *Curr Eye Res*. 1997;16(9):925–929.
87. Jomary C, Neal MJ, Iwata K, et al. Localization of tissue inhibitor of metalloproteinases-3 in neurodegenerative retinal disease. *Neuroreport*. 1997;8(9-10):2169–2172.
88. Siren V, Immonen I. uPA, tPA and PAI-1 mRNA expression in periretinal membranes. *Curr Eye Res*. 2003;27(5):261–267.
89. Andreasen PA, Kjoller L, Christensen L, et al. The urokinase-type plasminogen activator system in cancer metastasis: a review. *Int J Cancer*. 1997;72(1):1–22.
90. Tamai M, Chader GJ. The early appearance of disc shedding in the rat retina. *Invest Ophthalmol Vis Sci*. 1979;18(9):913–917.
91. Tamai M, Teirstein P, Goldman A, et al. The pineal gland does not control rod outer segment shedding and phagocytosis in the rat retina and pigment epithelium. *Invest Ophthalmol Vis Sci*. 1978;17(6):558–562.
92. Anderson DH, Fisher SK. Disc shedding in rodlike and conelike photoreceptors of tree squirrels. *Science*. 1975;187(4180):953–955.
93. Anderson DH, Fisher SK, Erickson PA, et al. Rod and cone disc shedding in the rhesus monkey retina: a quantitative study. *Exp Eye Res*. 1980;30(5):559–574.
94. Young RW. The renewal of photoreceptor cell outer segments. *J Cell Biol*. 1967;33(1):61–72.

95. Young RW, Bok D. Participation of the retinal pigment epithelium in the rod outer segment renewal process. *J Cell Biol*. 1969;42(2):392–403.
96. Young RW. The Bowman Lecture, 1982. Biological renewal: applications to the eye. *Trans Ophthalmol Soc U K*. 1982;102(Pt 1):42–75.
97. Kevany BM, Palczewski K. Phagocytosis of retinal rod and cone photoreceptors. *Physiology (Bethesda)*. 2010;25(1):8–15.
98. Boesze-Battaglia K, Albert AD. Phospholipid distribution among bovine rod outer segment plasma membrane and disk membranes. *Exp Eye Res*. 1992;54(5):821–823.
99. Nandrot EF, Anand M, Almeida D, et al. Essential role for MFG-E8 as ligand for alphavbeta5 integrin in diurnal retinal phagocytosis. *Proc Natl Acad Sci USA*. 2007;104(29):12005–12010.
100. Caberoy NB, Maiguel D, Kim Y, et al. Identification of tubby and tubby-like protein 1 as eat-me signals by phage display. *Exp Cell Res*. 2010;316(2):245–257.
101. Chaitin MH, Hall MO. The distribution of actin in cultured normal and dystrophic rat pigment epithelial cells during the phagocytosis of rod outer segments. *Invest Ophthalmol Vis Sci*. 1983;24(7):821–831.
102. Hall MO, Abrams TA, Mittag TW. ROS ingestion by RPE cells is turned off by increased protein kinase C activity and by increased calcium. *Exp Eye Res*. 1991;52(5):591–598.
103. Hall MO, Obin MS, Prieto AL, et al. Gas6 binding to photoreceptor outer segments requires gamma-carboxyglutamic acid (Gla) and $Ca^{(2+)}$ and is required for OS phagocytosis by RPE cells in vitro. *Exp Eye Res*. 2002;75(4):391–400.
104. Besharse JC, Dunis DA. Rod photoreceptor disc shedding in vitro: inhibition by cytochalasins and activation by colchicine. Hollyfield JG. *The structure of the eye*. Elsevier Biomedical; 1982.
105. Herman KG, Steinberg RH. Phagosome movement and the diurnal pattern of phagocytosis in the tapetal retinal pigment epithelium of the opossum. *Invest Ophthalmol Vis Sci*. 1982;23(3):277–290.

106. Gibbs D, Kitamoto J, Williams DS. Abnormal phagocytosis by retinal pigmented epithelium that lacks myosin VIIa, the Usher syndrome 1B protein. *Proc Natl Acad Sci USA*. 2003;100(11):6481–6486.
107. Hayashi A, Nakae K, Naka H, et al. Cytokine effects on phagocytosis of rod outer segments by retinal pigment epithelial cells of normal and dystrophic rats. *Curr Eye Res*. 1996;15(5):487–499.
108. Regan CM, de Grip WJ, Daemen FJ, et al. Degradation of rhodopsin by a lysosomal fraction of retinal pigment epithelium: biochemical aspects of the visual process. XLI. *Exp Eye Res*. 1980;30(2):183–191.
109. Zimmerman WF, Godchaux W 3rd, Belkin M. The relative proportions of lysosomal enzyme activities in bovine retinal pigment epithelium. *Exp Eye Res*. 1983;36(1):151–158.
110. Rakoczy PE, Mann K, Cavaney DM, et al. Detection and possible functions of a cysteine protease involved in digestion of rod outer segments by retinal pigment epithelial cells. *Invest Ophthalmol Vis Sci*. 1994;35(12):4100–4108.
111. Feeney L, Mixon RN. An in vitro model of phagocytosis in bovine and human retinal pigment epithelium. *Exp Eye Res*. 1976;22(5):533–548.
112. Feeney-Burns L, Hilderbrand ES, Eldridge S. Aging human RPE: morphometric analysis of macular, equatorial, and peripheral cells. *Invest Ophthalmol Vis Sci*. 1984;25(2):195–200.
113. Kim JY, Zhao H, Martinez J, et al. Noncanonical autophagy promotes the visual cycle. *Cell*. 2013;154(2):365–376.
114. Hattar S, Liao HW, Takao M, et al. Melanopsin-containing retinal ganglion cells: architecture, projections, and intrinsic photosensitivity. *Science*. 2002;295(5557):1065–1070.
115. Allen AE, Cameron MA, Brown TM, et al. Visual responses in mice lacking critical components of all known retinal phototransduction cascades. *PLoS ONE*. 2010;5(11):e15063.
116. Pollock NL, Callaghan R. The lipid translocase, ABCA4: seeing is believing. *FEBS J*. 2011;278(18):3204–3214.
117. Edwards RB, Adler AJ. IRBP enhances removal of 11-*cis*-

retinaldehyde from isolated RPE membranes. *Exp Eye Res*. 2000;70(2):235–245.
118. Wu Q, Blakeley LR, Cornwall MC, et al. Interphotoreceptor retinoid-binding protein is the physiologically relevant carrier that removes retinol from rod photoreceptor outer segments. *Biochemistry*. 2007;46(29):8669–8679.
119. Jin M, Li S, Nusinowitz S, et al. The role of interphotoreceptor retinoid-binding protein on the translocation of visual retinoids and function of cone photoreceptors. *J Neurosci*. 2009;29(5):1486–1495.
120. Ham WT Jr, Ruffolo JJ Jr, Mueller HA, et al. Histologic analysis of photochemical lesions produced in rhesus retina by short-wavelength light. *Invest Ophthalmol Vis Sci*. 1978;17(10):1029–1035.
121. Cai J, Nelson KC, Wu M, et al. Oxidative damage and protection of the RPE. *Prog Retin Eye Res*. 2000;19(2):205–221.
122. Winkler BS, Boulton ME, Gottsch JD, et al. Oxidative damage and age-related macular degeneration. *Mol Vis*. 1999;5:32.
123. Miceli MV, Liles MR, Newsome DA. Evaluation of oxidative processes in human pigment epithelial cells associated with retinal outer segment phagocytosis. *Exp Cell Res*. 1994;214(1):242–249.
124. Tate DJ Jr, Miceli MV, Newsome DA. Phagocytosis and H2O2 induce catalase and metallothionein gene expression in human retinal pigment epithelial cells. *Invest Ophthalmol Vis Sci*. 1995;36(7):1271–1279.
125. Rangasamy T, Cho CY, Thimmulappa RK, et al. Genetic ablation of Nrf2 enhances susceptibility to cigarette smoke-induced emphysema in mice. *J Clin Invest*. 2004;114(9):1248–1259.
126. Thimmulappa RK, Mai KH, Srisuma S, et al. Identification of Nrf2-regulated genes induced by the chemopreventive agent sulforaphane by oligonucleotide microarray. *Cancer Res*. 2002;62(18):5196–5203.
127. Nguyen T, Sherratt PJ, Pickett CB. Regulatory mechanisms controlling gene expression mediated by the antioxidant

response element. *Annu Rev Pharmacol Toxicol*. 2003;43:233–260.
128. Adams J, Kelso R, Cooley L. The kelch repeat superfamily of proteins: propellers of cell function. *Trends Cell Biol*. 2000;10(1):17–24.
129. Wakabayashi N, Itoh K, Wakabayashi J, et al. Keap1-null mutation leads to postnatal lethality due to constitutive Nrf2 activation. *Nat Genet*. 2003;35(3):238–245.
130. Dinkova-Kostova AT, Holtzclaw WD, Kensler TW. The role of Keap1 in cellular protective responses. *Chem Res Toxicol*. 2005;18(12):1779–1791.
131. Nelson KC, Carlson JL, Newman ML, et al. Effect of dietary inducer dimethylfumarate on glutathione in cultured human retinal pigment epithelial cells. *Invest Ophthalmol Vis Sci*. 1999;40(9):1927–1935.
132. Nelson KC, Armstrong JS, Moriarty S, et al. Protection of retinal pigment epithelial cells from oxidative damage by oltipraz, a cancer chemopreventive agent. *Invest Ophthalmol Vis Sci*. 2002;43(11):3550–3554.
133. Cano M, Wang L, Wan J, et al. Oxidative stress induces mitochondrial dysfunction and a protective unfolded protein response in RPE cells. *Free Radic Biol Med*. 2014;69C:1–14.
134. Wang L, Kondo N, Cano M, et al. Nrf2 signaling modulates cigarette smoke-induced complement activation in retinal pigmented epithelial cells. *Free Radic Biol Med*. 2014;70:155–166.
135. Zhu D, Sreekumar PG, Hinton DR, et al. Expression and regulation of enzymes in the ceramide metabolic pathway in human retinal pigment epithelial cells and their relevance to retinal degeneration. *Vision Res*. 2010;50(7):643–651.
136. Kannan R, Jin M, Gamulescu MA, et al. Ceramide-induced apoptosis: role of catalase and hepatocyte growth factor. *Free Radic Biol Med*. 2004;37(2):166–175.
137. Dong A, Shen J, Krause M, et al. Superoxide dismutase 1 protects retinal cells from oxidative damage. *J Cell Physiol*. 2006;208(3):516–526.

138. Mari M, Morales A, Colell A, et al. Mitochondrial glutathione, a key survival antioxidant. *Antioxid Redox Signal*. 2009;11(11):2685–2700.
139. Holmgren A, Lu J. Thioredoxin and thioredoxin reductase: current research with special reference to human disease. *Biochem Biophys Res Commun*. 2010;396(1):120–124.
140. Sreekumar PG, Ding Y, Ryan SJ, et al. Regulation of thioredoxin by ceramide in retinal pigment epithelial cells. *Exp Eye Res*. 2009;88(3):410–417.
141. Sreekumar PG, Hinton DR, Kannan R. Methionine sulfoxide reductase A: structure, function and role in ocular pathology. *World J Biol Chem*. 2011;2(8):184–192.
142. Usui S, Oveson BC, Iwase T, et al. Overexpression of SOD in retina: need for increase in H_2O_2-detoxifying enzyme in same cellular compartment. *Free Radic Biol Med*. 2011;51(7):1347–1354.
143. Osburn WO, Yates MS, Dolan PD, et al. Genetic or pharmacologic amplification of nrf2 signaling inhibits acute inflammatory liver injury in mice. *Toxicol Sci*. 2008;104(1):218–227.
144. Jin M, Yaung J, Kannan R, et al. Hepatocyte growth factor protects RPE cells from apoptosis induced by glutathione depletion. *Invest Ophthalmol Vis Sci*. 2005;46(11):4311–4319.
145. Johnson J, Maher P, Hanneken A. The flavonoid, eriodictyol, induces long-term protection in ARPE-19 cells through its effects on Nrf2 activation and phase 2 gene expression. *Invest Ophthalmol Vis Sci*. 2009;50(5):2398–2406.
146. Inomata Y, Nakamura H, Tanito M, et al. Thioredoxin inhibits NMDA-induced neurotoxicity in the rat retina. *J Neurochem*. 2006;98(2):372–385.
147. Rahman I, Biswas SK, Jimenez LA, et al. Glutathione, stress responses, and redox signaling in lung inflammation. *Antioxid Redox Signal*. 2005;7(1-2):42–59.
148. Walsh AC, Michaud SG, Malossi JA, et al. Glutathione depletion in human T lymphocytes: analysis of activation-associated gene expression and the stress response. *Toxicol Appl Pharmacol*. 1995;133(2):249–261.
149. Grivennikova VG, Kareyeva AV, Vinogradov AD. What are

the sources of hydrogen peroxide production by heart mitochondria? *Biochim Biophys Acta*. 2010;1797(6-7):939–944.
150. Imai H, Nakagawa Y. Biological significance of phospholipid hydroperoxide glutathione peroxidase (PHGPx, GPx4) in mammalian cells. *Free Radic Biol Med*. 2003;34(2):145–169.
151. Noh YH, Baek JY, Jeong W, et al. Sulfiredoxin translocation into mitochondria plays a crucial role in reducing hyperoxidized peroxiredoxin III. *J Biol Chem*. 2009;284(13):8470–8477.
152. Arner ES. Focus on mammalian thioredoxin reductases – important selenoproteins with versatile functions. *Biochim Biophys Acta*. 2009;1790(6):495–526.
153. Niso-Santano M, Gonzalez-Polo RA, Bravo-San Pedro JM, et al. Activation of apoptosis signal-regulating kinase 1 is a key factor in paraquat-induced cell death: modulation by the Nrf2/Trx axis. *Free Radic Biol Med*. 2010;48(10):1370–1381.
154. Bae SH, Sung SH, Lee HE, et al. Peroxiredoxin III and sulfiredoxin together protect mice from pyrazole-induced oxidative liver injury. *Antioxid Redox Signal*. 2012;17(10):1351–1361.
155. Kowluru RA, Kowluru V, Xiong Y, et al. Overexpression of mitochondrial superoxide dismutase in mice protects the retina from diabetes-induced oxidative stress. *Free Radic Biol Med*. 2006;41(8):1191–1196.
156. Aon MA, Stanley BA, Sivakumaran V, et al. Glutathione/thioredoxin systems modulate mitochondrial H_2O_2 emission: an experimental-computational study. *J Gen Physiol*. 2012;139(6):479–491.
157. Han D, Canali R, Rettori D, et al. Effect of glutathione depletion on sites and topology of superoxide and hydrogen peroxide production in mitochondria. *Mol Pharmacol*. 2003;64(5):1136–1144.
158. Wu YQ, Notario V, Chader GJ, et al. Identification of pigment epithelium-derived factor in the interphotoreceptor matrix of bovine eyes. *Protein Expr Purif*. 1995;6(4):447–456.

159. Perez-Mediavilla LA, Chew C, Campochiaro PA, et al. Sequence and expression analysis of bovine pigment epithelium-derived factor. *Biochim Biophys Acta*. 1998;1398(2):203–214.
160. Filleur S, Volz K, Nelius T, et al. Two functional epitopes of pigment epithelial-derived factor block angiogenesis and induce differentiation in prostate cancer. *Cancer Res*. 2005;65(12):5144–5152.
161. Bouck N. PEDF: anti-angiogenic guardian of ocular function. *Trends Mol Med*. 2002;8(7):330–334.
162. Bhutto IA, McLeod DS, Hasegawa T, et al. Pigment epithelium-derived factor (PEDF) and vascular endothelial growth factor (VEGF) in aged human choroid and eyes with age-related macular degeneration. *Exp Eye Res*. 2006;82(1):99–110.
163. Kozulin P, Natoli R, Bumsted O'Brien KM, et al. The cellular expression of antiangiogenic factors in fetal primate macula. *Invest Ophthalmol Vis Sci*. 2010;51(8):4298–4306.
164. Kociok N, Joussen AM. Varied expression of functionally important genes of RPE and choroid in the macula and in the periphery of normal human eyes. *Graefes Arch Clin Exp Ophthalmol*. 2007;245(1):101–113.
165. Marneros AG, She H, Zambarakji H, et al. Endogenous endostatin inhibits choroidal neovascularization. *FASEB J*. 2007;21(14):3809–3818.
166. Medawar PB. Immunity to homologous grafted skin; the fate of skin homografts transplanted to the brain, to subcutaneous tissue, and to the anterior chamber of the eye. *Br J Exp Pathol*. 1948;29(1):58–69.
167. Streilein JW, Ma N, Wenkel H, et al. Immunobiology and privilege of neuronal retina and pigment epithelium transplants. *Vision Res*. 2002;42(4):487–495.
168. Masli S, Vega JL. Ocular immune privilege sites. *Methods Mol Biol*. 2011;677:449–458.
169. Zhou R, Horai R, Mattapallil MJ, et al. A new look at immune privilege of the eye: dual role for the vision-related molecule retinoic acid. *J Immunol*. 2011;187(8):4170–4177.
170. Kumar MV, Nagineni CN, Chin MS, et al. Innate immunity

in the retina: Toll-like receptor (TLR) signaling in human retinal pigment epithelial cells. *J Neuroimmunol*. 2004;153(1-2):7–15.
171. Anderson DH, Radeke MJ, Gallo NB, et al. The pivotal role of the complement system in aging and age-related macular degeneration: hypothesis re-visited. *Prog Retin Eye Res*. 2010;29(2):95–112.
172. Tarallo V, Hirano Y, Gelfand BD, et al. DICER1 loss and Alu RNA induce age-related macular degeneration via the NLRP3 inflammasome and MyD88. *Cell*. 2012;149(4):847–859.
173. Ban Y, Rizzolo LJ. Regulation of glucose transporters during development of the retinal pigment epithelium. *Brain Res Dev Brain Res*. 2000;121(1):89–95.
174. Bergersen L, Johannsson E, Veruki ML, et al. Cellular and subcellular expression of monocarboxylate transporters in the pigment epithelium and retina of the rat. *Neuroscience*. 1999;90(1):319–331.
175. Kim DI, Lim SK, Park MJ, et al. The involvement of phosphatidylinositol 3-kinase/Akt signaling in high glucose-induced downregulation of GLUT-1 expression in ARPE cells. *Life Sci*. 2007;80(7):626–632.
176. Montel-Hagen A, Kinet S, Manel N, et al. Erythrocyte Glut1 triggers dehydroascorbic acid uptake in mammals unable to synthesize vitamin C. *Cell*. 2008;132(6):1039–1048.
177. Bridges CD, Alvarez RA, Fong SL, et al. Visual cycle in the mammalian eye: retinoid-binding proteins and the distribution of 11-*cis* retinoids. *Vision Res*. 1984;24(11):1581–1594.
178. Wimmers S, Coeppicus L, Rosenthal R, et al. Expression profile of voltage-dependent Ca^{2+} channel subunits in the human retinal pigment epithelium. *Graefes Arch Clin Exp Ophthalmol*. 2008;246(5):685–692.
179. Wimmers S, Halsband C, Seyler S, et al. Voltage-dependent Ca^{2+} channels, not ryanodine receptors, activate Ca^{2+}-dependent BK potassium channels in human retinal pigment epithelial cells. *Mol Vis*. 2008;14:2340–2348.
180. Bollimuntha S, Cornatzer E, Singh BB. Plasma membrane

localization and function of TRPC1 is dependent on its interaction with beta-tubulin in retinal epithelium cells. *Vis Neurosci*. 2005;22(2):163–170.
181. Wimmers S, Strauss O. Basal calcium entry in retinal pigment epithelial cells is mediated by TRPC channels. *Invest Ophthalmol Vis Sci*. 2007;48(12):5767–5772.
182. Kennedy BG, Torabi AJ, Kurzawa R, et al. Expression of transient receptor potential vanilloid channels TRPV5 and TRPV6 in retinal pigment epithelium. *Mol Vis*. 2010;16:665–675.
183. Gallagher-Colombo S, Maminishkis A, Tate S, et al. Modulation of MCT3 expression during wound healing of the retinal pigment epithelium. *Invest Ophthalmol Vis Sci*. 2010;51(10):5343–5350.
184. Stamer WD, Bok D, Hu J, et al. Aquaporin-1 channels in human retinal pigment epithelium: role in transepithelial water movement. *Invest Ophthalmol Vis Sci*. 2003;44(6):2803–2808.
185. Motulsky E, Koch P, Janssens S, et al. Aquaporin expression in blood–retinal barrier cells during experimental autoimmune uveitis. *Mol Vis*. 2010;16:602–610.
186. Blaauwgeers HG, Holtkamp GM, Rutten H, et al. Polarized vascular endothelial growth factor secretion by human retinal pigment epithelium and localization of vascular endothelial growth factor receptors on the inner choriocapillaris: evidence for a trophic paracrine relation. *Am J Pathol*. 1999;155(2):421–428.
187. Dicou E, Nerriere V, Naud MC, et al. NGF involvement in ocular inflammation: secretion by rat resident retinal cells. *Neuroreport*. 1994;6(1):26–28.
188. Ishida K, Yoshimura N, Yoshida M, et al. Expression of neurotrophic factors in cultured human retinal pigment epithelial cells. *Curr Eye Res*. 1997;16(2):96–101.
189. Hackett SF, Friedman Z, Freund J, et al. A splice variant of trkB and brain-derived neurotrophic factor are co-expressed in retinal pigmented epithelial cells and promote differentiated characteristics. *Brain Res*. 1998;789(2):201–212.
190. Rosenthal R, Wohlleben H, Malek G, et al. Insulin-like

growth factor-1 contributes to neovascularization in age-related macular degeneration. *Biochem Biophys Res Commun*. 2004;323(4):1203–1208.
191. Lambooij AC, van Wely KH, Lindenbergh-Kortleve DJ, et al. Insulin-like growth factor-I and its receptor in neovascular age-related macular degeneration. *Invest Ophthalmol Vis Sci*. 2003;44(5):2192–2198.
192. Bazan NG. Cell survival matters: docosahexaenoic acid signaling, neuroprotection and photoreceptors. *Trends Neurosci*. 2006;29(5):263–271.
193. Nagineni CN, Cherukuri KS, Kutty V, et al. Interferon-gamma differentially regulates TGF-beta1 and TGF-beta2 expression in human retinal pigment epithelial cells through JAK-STAT pathway. *J Cell Physiol*. 2007;210(1):192–200.
194. Crane IJ, Wallace CA, Forrester JV. Regulation of granulocyte-macrophage colony-stimulating factor in human retinal pigment epithelial cells by IL-1beta and IFN-gamma. *Cell Immunol*. 2001;209(2):132–139.
195. Yang D, Elner SG, Chen X, et al. MCP-1-activated monocytes induce apoptosis in human retinal pigment epithelium. *Invest Ophthalmol Vis Sci*. 2011;52(8):6026–6034.
196. Jin M, Chen Y, He S, et al. Hepatocyte growth factor and its role in the pathogenesis of retinal detachment. *Invest Ophthalmol Vis Sci*. 2004;45(1):323–329.
197. Xie Z, Wu X, Qiu Q, et al. Expression pattern of erythropoietin and erythropoietin receptor in experimental model of retinal detachment. *Curr Eye Res*. 2007;32(9):757–764.
198. He YG, Wang H, Zhao B, et al. Functional analysis of platelet-activating factor in the retinal pigment epithelial cells and choroidal endothelial cells. *Curr Eye Res*. 2009;34(11):957–965.
199. Jaffe GJ, Richmond A, Van Le L, et al. Expression of three forms of melanoma growth stimulating activity (MGSA)/gro in human retinal pigment epithelial cells. *Invest Ophthalmol Vis Sci*. 1993;34(9):2776–2785.
200. Narayan S, Brun AM, Yorio T. Endothelin-1 distribution

and basolateral secretion in the retinal pigment epithelium. *Exp Eye Res*. 2004;79(1):11–19.
201. Bryckaert M, Guillonneau X, Hecquet C, et al. Both FGF1 and bcl-x synthesis are necessary for the reduction of apoptosis in retinal pigmented epithelial cells by FGF2: role of the extracellular signal-regulated kinase 2. *Oncogene*. 1999;18(52):7584–7593.
202. Zhu D, Wu J, Spee C, et al. BMP4 mediates oxidative stress-induced retinal pigment epithelial cell senescence and is overexpressed in age-related macular degeneration. *J Biol Chem*. 2009;284(14):9529–9539.
203. Benson MT, Shepherd L, Rees RC, et al. Production of interleukin-6 by human retinal pigment epithelium in vitro and its regulation by other cytokines. *Curr Eye Res*. 1992;11(Suppl):173–179.
204. Bian ZM, Elner SG, Yoshida A, et al. Differential involvement of phosphoinositide 3-kinase/Akt in human RPE MCP-1 and IL-8 expression. *Invest Ophthalmol Vis Sci*. 2004;45(6):1887–1896.
205. He S, Chen Y, Khankan R, et al. Connective tissue growth factor as a mediator of intraocular fibrosis. *Invest Ophthalmol Vis Sci*. 2008;49(9):4078–4088.

19

Cell Biology of Retinal Glia

Andreas Reichenbach, Andreas Bringmann

Introduction

The human retina contains three main types of glial cells: microglia and two types of macroglia, astrocytes and Müller cells (Fig. 19.1A). Microglial cells are the primary resident innate immune cells of the retina. They play (in close relationship to macroglial cells and blood-derived immune cells; Fig. 19.2A) important roles in the host defense against microorganisms, the initiation of inflammatory processes, and tissue repair. Astrocytes are associated with the nerve fibers and blood vessels of the superficial vascular plexus (Fig. 19.1A). Müller cells are the principal macroglia of the retina (Figs. 19.1A–B).[1] In virtually every retinopathy, activated glial cells contribute to neuroprotection and neurodegeneration in the retina.[2]

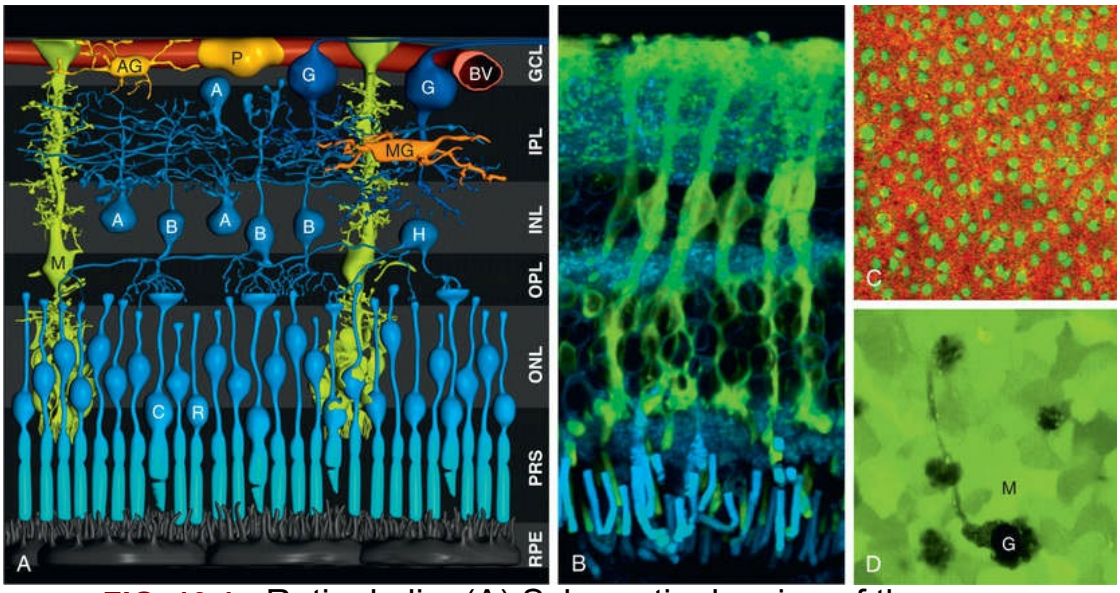

FIG. 19.1 Retinal glia. (A) Schematic drawing of the cellular constituents of a human retina. Müller cells (*M*) span the entire thickness of the neuroretina, and are arranged in a regular pattern. The perikarya of Müller cells are localized in the inner nuclear layer (*INL*). The funnel-shaped endfeet of Müller cells form the inner surface of the retina. In the outer (*OPL*) and inner plexiform layers (*IPL*), side branches which form perisynaptic membrane sheaths originate at the stem processes. Both astrocytes (*AG*) and Müller cells contact the superficial blood vessels and the inner surface of the retina. In the outer nuclear layer (*ONL*), the stem process of Müller cells forms membrane sheaths which envelop the perikarya of rods (*R*) and cones (*C*). Microvilli of Müller cells extend into the subretinal space which surrounds the photoreceptor segments (PRS). Microglia (*MG*) are located in both plexiform layers and the ganglion cell layer (*GCL*). *A*, amacrine cell; *B*, bipolar cell; *G*, ganglion cell; *H*, horizontal cell; *P*, pericyte; *RPE*, retinal pigment epithelium. Panels B–D: Confocal images of guinea pig retina preparations. (B) Retinal section. Müller cells are green-labeled; synapses and the outer segments of photoreceptor cells are blue-stained. (C,D) "Horizontal sections" through a flat-mounted retina, illustrating the regular pattern of Müller cell stem processes (green) in the inner plexiform layer (C) and the almost total occupation of the ganglion cell layer by the Müller cell endfeet (green; *M*); only the somata of the ganglion cells (*G*) appear "empty" (D).

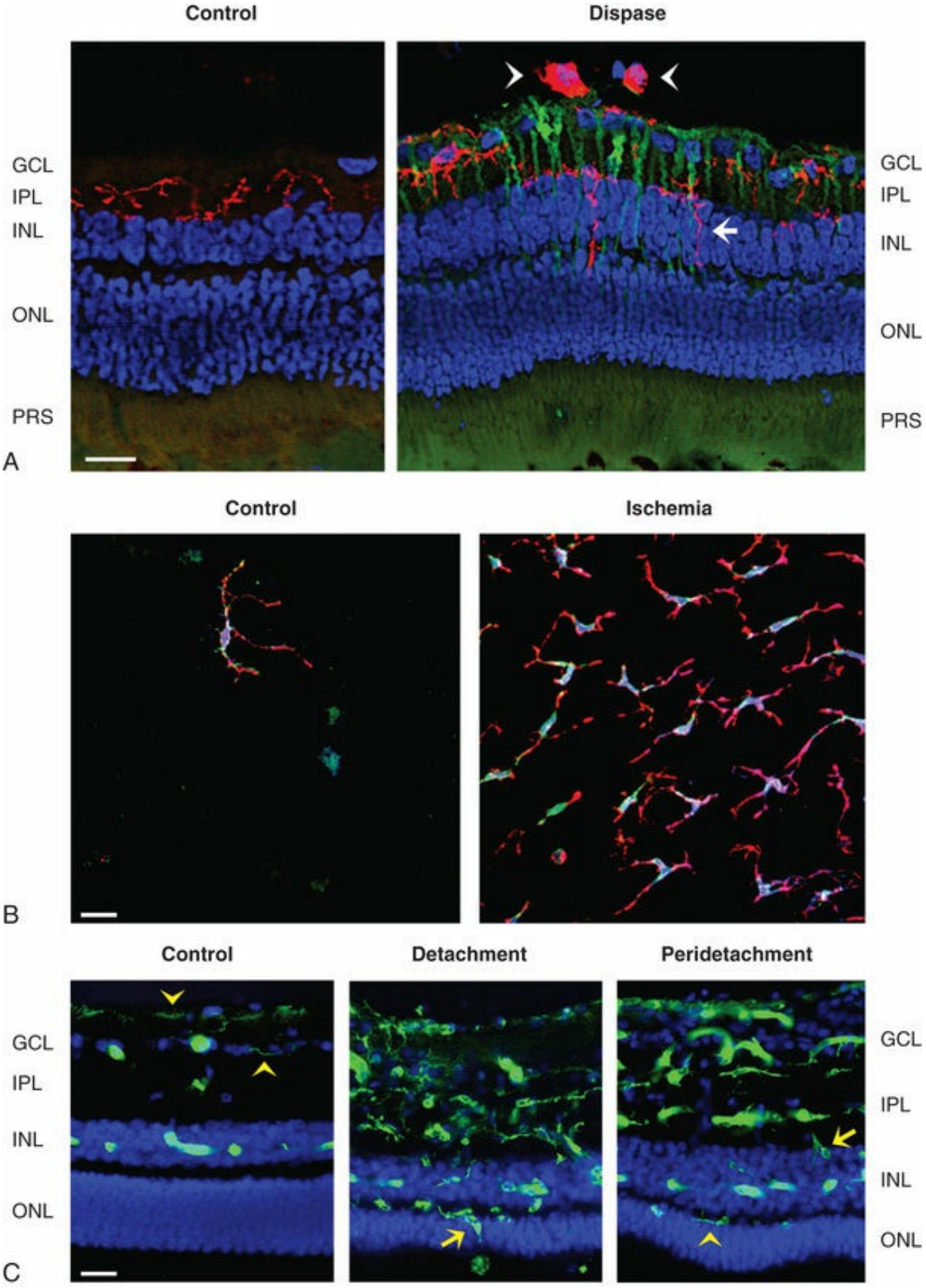

FIG. 19.2 Retinal microglia activation. (A) Interaction of blood-derived monocytes/macrophages and retinal glia in a rabbit model of early PVR induced by intravitreal

injection of the protease dispase. Retinal slices were stained against immune cells (red), glial fibrillary acidic protein (GFAP) (*green*; a marker of activated Müller cells), and cell nuclei (blue). Under control conditions, microglia (*red*) are restricted to the innermost retinal layers, and Müller cells do not express GFAP. The retina of the dispase-treated eye displays “hot spots” of glial reactivity characterized by upregulation of GFAP in Müller cells (green) and activated microglia that begin to migrate toward the outer retina (*arrow*). Blood-borne monocytes/macrophages adhere to the vitreal surface of such hot spots (*arrowheads*), suggesting a relationship between the attachment of macrophages and glial cell activation. (B) Microglia at the vitreal surface of a control rabbit retina (left) and a retina obtained 8 days after a 1-h transient retinal ischemia (right). Note the proliferation of microglial cells. (C) Microglia migration in the porcine retina after experimental local retinal detachment. Retinal slices were derived from a control retina, a detached retina 7 days after surgery, and a peridetached retinal area that surrounded the detached retina in situ. The slices were labeled with isolectin to stain blood vessels and microglial/immune cells (green). Cell nuclei are blue. *Arrows* and *arrowheads*: microglial cell bodies and processes, respectively. Note the migration of microglia from the inner to the outer retina after detachment and the thinner outer nuclear layer (*ONL*) in the detached retina compared to the control retina which reflects the degeneration of photoreceptor cells. *GCL*, ganglion cell layer; *INL*, inner nuclear layer; *IPL*, inner plexiform layer; *PRS*, photoreceptor segments. Scale bars: 20 μm.

Retinal Microglia

Microglial cells are blood-borne mononuclear phagocytes and antigen-presenting cells. Microglia enter the retina via the ciliary body and hyaloid vasculatures, and later via the optic nerve head, during embryonic and postnatal development (see reference 2 and references therein). Resting microglia are located in the plexiform

and nerve fiber/ganglion cell layers, and around the vessels (Figs. 19.1A and 19.2B–C). Resting microglia display a ramified morphology (Figs. 19.2A and 19.3C) and act as highly motile patrolling cells that constantly survey their microenvironment to clear metabolic products and cellular debris. Microglial process motility is dependent on neuronal activity; it is increased during glutamatergic neurotransmission and decreased during γ-aminobutyric acid (GABA)ergic neurotransmission.[3] Once a pathogenic stimulus is detected, microglia become activated, proliferate (Figs. 19.2A and 19.3C), and migrate towards the region of damage (Figs. 19.2A, C) where the cells kill bacteria, release cytotoxic agents, and phagocytize cellular debris. While activated microglia initially contribute to neuronal protection and tissue regeneration, excessive or prolonged activation of the cells by alarm signals from exogenous and endogenous sources can lead to chronic overactivation and loss of autoregulatory mechanisms which contribute to retinal inflammation and degeneration.[4,5]

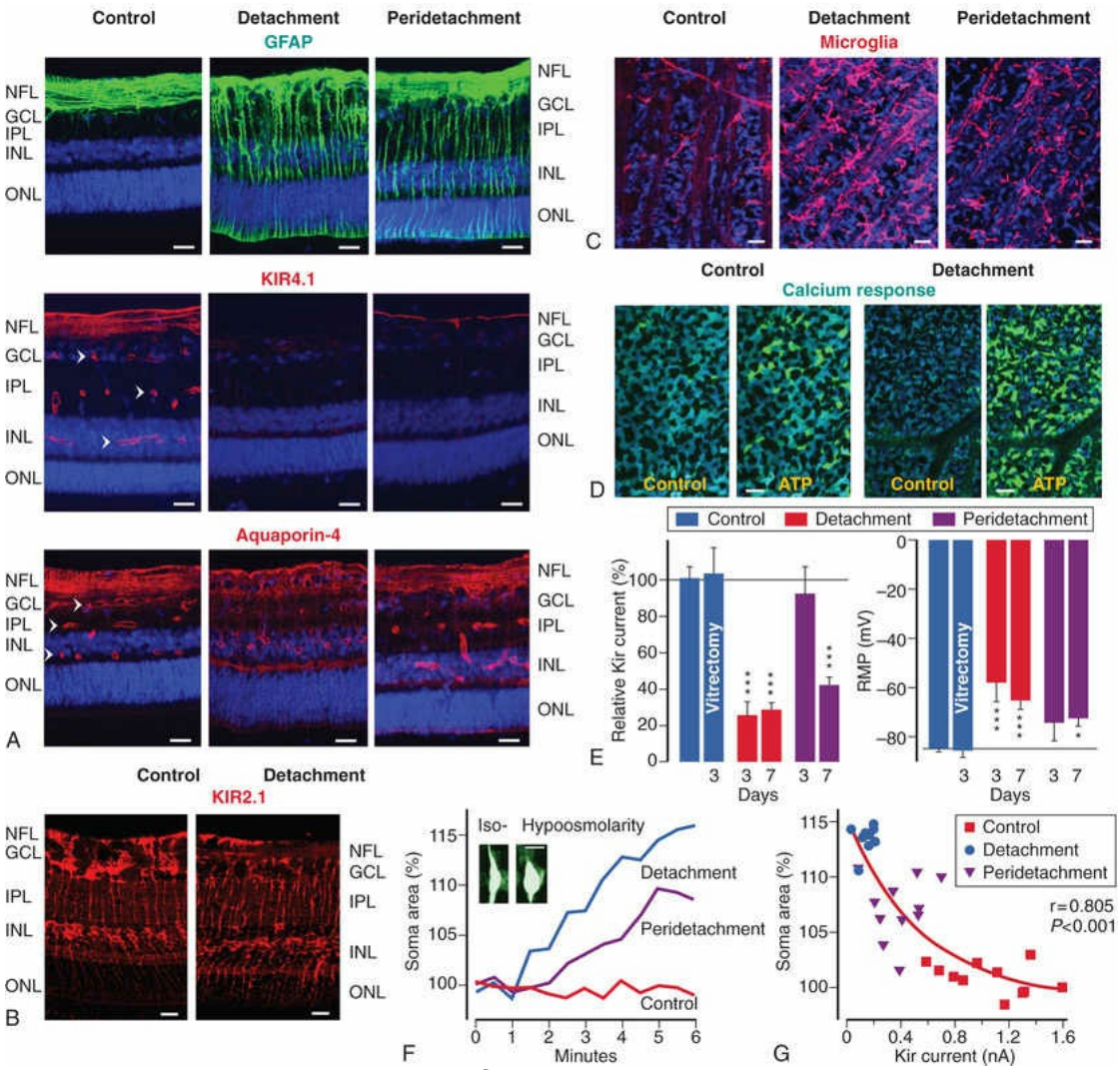

FIG. 19.3 Propagation of retinal gliosis in response to experimental focal detachment of the porcine retina. The tissues and cells were obtained from control retinas, from retinal areas that were detached for 3 and 7 days, respectively, and from nondetached retinal tissues that were localized around the focally detached retinal areas in situ (peridetachment). (A) Müller cell gliosis is reflected by the upregulation of the intermediate filament glial fibrillary acidic protein (GFAP; above) and the downregulation of Kir4.1 (middle) in the detached and peridetached retinal areas compared to the control retina. In contrast, the localization of the aquaporin-4 water channel remained unaltered after detachment (below). Retinal slices were obtained 7 days after surgery. Cell nuclei are blue. *Arrowheads*: perivascular staining. Note that GFAP expression is restricted to astrocytes in the nerve fiber (*NFL*)/ganglion cell layers (GCL) in the control retina

(above). (B) The distribution of Kir2.1 protein does not alter after detachment compared to control. (C) Staining of microglia (red) in the NFL/GCL in wholemounts of retinas 3 days after surgery. (D) Retinal detachment increases the ATP-induced calcium responsiveness in the endfeet of Müller cells. The calcium imaging records were obtained from the NFL/GCL of retinal wholemounts before (*control*) and during administration of ATP (*ATP*) (200 µM). The wholemounts were derived from a control retina and a 7-days-detached retina. In the control retina, single endfeet of Müller cells showed a calcium response (green) while in the detached retina, the majority of Müller cell endfeet displayed a response. (E) Kir currents (left) and resting membrane potential (*RMP*; right) of Müller cells derived from control (unoperated and vitrectomized), 3-days-detached, 7-days-detached, and attached retinal areas. Note the time-dependent decrease of the Kir currents in the cells of the attached retinal area. (F) Focal retinal detachment causes an alteration in the osmotic swelling properties of Müller cells in the detached and peridetached retinal areas. The cross-sectional area of Müller cell somata was measured in retinal slices. Acute exposure of retinal slices to a hypoosmotic extracellular solution (60% osmolarity) induced a time-dependent swelling of Müller cell bodies in detached and peridetached retinal areas, and had no effect on the size of Müller cell bodies in control retinas. The images display original records of a Müller cell body in a slice of a detached retina, obtained before (left) and during (right) hypoosmotic exposure. (G) Relation between the amplitude of the Kir currents and the severity of osmotic cell swelling in Müller cells derived from control, 7-days-detached, and peridetached retinas. *INL*, inner nuclear layer; *IPL*, inner plexiform layer; *ONL*, outer nuclear layer. Scale bars: (A–D) 20 µm; (F) 5 µm.

Resting Microglia

Resting microglia are programmed for immunologic tolerance and

display an antiinflammatory phenotype characterized, for example, by low nitric oxide (NO) and superoxide anion production.[6] The quiescence of microglia requires the presence of antiinflammatory cytokines such as thrombospondin-1, transforming growth factor (TGF)-β, and interleukin (IL)-10 which downregulate antigen-presenting molecules like major histocompatibility (MHC) class II, block inflammatory gene expression, and inhibit microglial migration and phagocytic activity.[7] Thrombospondin-1 is essential for the immune privilege of the retina.[8] Further soluble and cell-contact factors such as CD200 and fractalkine (CX3CL1) contribute to microglia quiescence.[2]

Microglia Activation

Microglial cells become activated early under pathologic conditions (Figs. 19.2A–C and 19.3C). Microgliosis is associated with and often precedes retinal degeneration (see reference 2 and references therein). Many retinopathies, like retinal detachment and proliferative vitreoretinopathy (PVR) (Fig. 19.2A), are characterized by a tripartite process involving inflammation, immune response, and coagulation/fibrinolysis, which is mediated by activation of immune cells (microglia in the retinal parenchyma, blood-derived monocytes/macrophages and neutrophils in the subretinal space and/or vitreous, and leukostasis in blood vessels).[9]

Microglia activation is associated with a morphologic transition from a stellate, ramified morphology to an ameboid cell shape; activated microglia display enlarged somata and shortened and thickened processes (Fig. 19.3C). Microgliosis is triggered by various molecules, including bacterial lipopolysaccharide, complement components, thrombin, inflammatory cytokines and chemokines such as IL-1β, IL-6, tumor necrosis factor-α (TNF-α), vascular endothelial growth factor (VEGF), fractalkine, macrophage colony-stimulating factor, and monocyte chemoattractant protein-1 (MCP-1; Ccl2), advanced glycation endproducts, glycated albumin, and adenosine 5'-triphosphate (ATP) released from damaged neurons (see reference 2 and references therein). MCP-1 also recruits bone marrow-derived monocytic precursor cells into the retina that replace resident microglia.[10]

Microglial Contribution to Neuronal Degeneration

Although inflammation normally protects from dangerous stimuli and restores tissue homeostasis, chronic, overstimulated, and dysregulated inflammation is a major cause of secondary tissue damage.[4,5] Activated microglia generate reactive oxygen and nitrogen species, produce prostaglandins and matrix metalloproteinases (MMPs), and secrete Fas-ligand and proinflammatory cytokines like TNF-α and IL-1β.[2] The majority of these microglia-secreted molecules can cause progressive neurodegeneration upon chronic exposure.[4] Damage-associated molecular patterns released from degenerating neurons trigger Toll-like receptor (TLR)-dependent microglia activation which may lead to attacks against healthy neurons by the release of cytotoxic cytokines like TNF-α, the production of reactive oxygen and nitrogen species, and the initiation of immune responses against retinal antigens.[4] Activated microglia may also exacerbate photoreceptor and neuronal degeneration by the production of chemotactic factors such as MCP-1 that recruits monocytes/macrophages and polymorphonuclear leukocytes to the retinal tissue.[11] Activated microglia produce endothelin-2 which induces astrogliosis, retinal ganglion cell death, and vasoconstriction; microglia-induced vascular dysfunction is a pathogenic factor of glaucoma, for example.[12] Activated microglia also exacerbate retinal pathologies after systemic viral, bacterial, and fungal infections.[2] The spread of retinal gliosis and retinal degeneration from a local retinal injury to the surrounding noninjured tissue (Figs. 19.3A, D–F) is mediated by the diffusion of growth and inflammatory factors, and by migrating activated microglia (Fig. 19.3C). Inhibition of microglia activation was shown to slow hereditary and light-induced retinal degeneration, and to have protective effects in glaucomatous eyes, and in the ischemic-hypoxic and diabetic retina.[2]

Microglial Contribution to Neuronal Survival

Microglia activation can also promote neuroprotection and

regeneration. Resting and activated microglia produce neurotrophic factors such as brain-derived neurotrophic factor (BDNF), ciliary neurotrophic factor (CNTF), glial cell line-derived neurotrophic factor (GDNF), and basic fibroblast growth factor (bFGF), as well as antiinflammatory cytokines that facilitate neuronal and photoreceptor survival (see reference 2 and references therein).[4] Activated microglia also benefit surviving cells by removing toxic byproducts, pathogens, extravasated serum proteins, and cell debris. Photoreceptor degeneration in mice was shown to be promoted by activated resident microglia, but inhibited by bone marrow-derived microglial precursors.[13,14] Activated microglia may also limit retinal inflammation by directing T cells toward the Th2 pathway and the release of immunosuppressive cytokines like TGF-β.[15] Astrocytes and Müller cells may limit the magnitude of retinal inflammation by facilitating the quiescence of microglia.[16] At present, it is unclear why microglia are sometimes damaging and other times protective.

Microglia in the Aging Retina

With advancing age, micro- and macroglial cells display increased signs of gliosis. Microglia undergo age-related changes in gene expression which give rise to pathogenic phenotypes and to a dysregulation of immune responses.[17] Breakdown of the blood–retinal barrier, MHC class II expression, microglia activation, and trafficking of activated T cells are characteristics of physiologic aging.[18] In the young adult retina, the outer retina is devoid of microglia (Fig. 19.2C). In the aging retina, a subretinal accumulation of microglia is triggered by the inefficient clearance of oxidized photoreceptor lipoproteins by the retinal pigment epithelium (RPE).[5] Microglia migrate from the inner retina to the subretinal space to clear oxidized lipoproteins.[2,5] The subretinal microglia was suggested to activate the RPE and to form “crystallization” points for cellular deposits and complement-containing immune complexes.[19] Infiltrating macrophages and resident microglia are major sources of the complement factors C3 and CFB, complement activators associated with retinal light damage and the pathogenesis of age-related macular degeneration (AMD).[2]

Activated microglia containing photoreceptor debris may actively exit the retina, and may reach the spleen, where they act as antigen-presenting cells and elicit systemic immune responses against retinal antigens.[20] Autoantibodies against retinal antigens play pathogenic roles in various retinopathies including AMD, diabetic retinopathy, light-induced retinal degeneration, and glaucoma (see reference 2 and references therein).

Activated microglia also contribute to the progression of AMD to the neovascular stage. In experimental choroidal neovascularization, infiltrating monocytes/macrophages and resident microglia express VEGF, the major angiogenic factor implicated in wet AMD, prior to the increased VEGF expression in the RPE.[2] By the release of blood–retinal barrier-dissolving factors like VEGF, NO, and MMPs, activated microglia also contribute to the breakdown of the barrier resulting in retinal edema, a characteristic of wet AMD and diabetic retinopathy. In human subjects with diabetic macular edema, assumed to be primarily caused by vascular leakage, oral administration of the microglia-inhibitory agent minocycline improves visual function, macular edema, and vascular leakage.[21]

Retinal Astrocytes

Astrocytes are localized in the nerve fiber/ganglion cells layers (Figs. 19.1A and 19.3A); their processes contact the retinal ganglion cell somata and axons, and the superficial blood vessels (Figs. 19.4A–B). Both astrocytes and microglia play crucial roles in retinal vascularization (see reference 2 and references therein). Astrocytes, vascular endothelial cells, and pericytes are immigrants from the brain. In the mature retina, astrocytes, microglia, pericytes, and Müller cells normally inhibit vascular endothelial cell proliferation, maintain vascular stability, and contribute to the formation of the inner blood–retinal barrier which is constituted by tight junctions between vascular endothelial cells.[2] In the developing retina, astrocytes promote the capability of retinal ganglion cells to receive synaptic input and the growth of ganglion cell axons.[22,23] In the mature retina, the growth of ganglion cell axons is inhibited by astrocytes.[24] Retinal astrocytes contribute to various glial

homeostatic functions which are also carried out by Müller cells, e.g., removal of carbon dioxide (CO_2), regulation of extracellular pH, and clearance of the extracellular fluid from neurotransmitters and excess potassium (see below). The gap junctional coupling of astrocytes creates a functional syncytium which allows the intercellular propagation of intracellular signals, the control of the ionic and metabolic homeostasis of retinal ganglion cell somata and axons, the neurovascular coupling, and the propagation of intercellular glial calcium waves.[2]

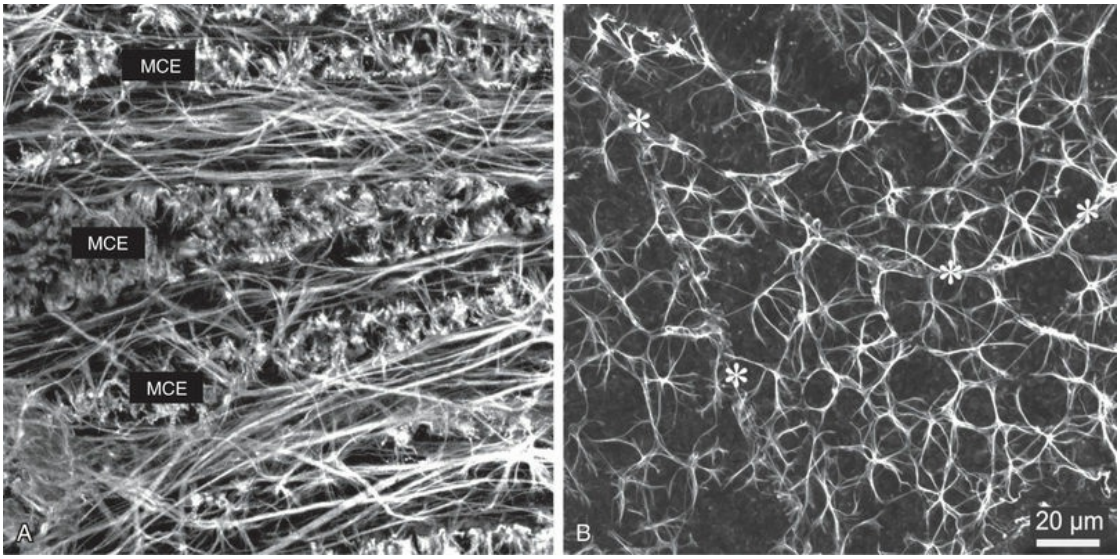

FIG. 19.4 Astrocytes in the murine retina. (A) In the central retina, the processes of many astrocytes run parallel to the bundles of ganglion cell axons and form (together with Müller cell endfeet, *MCE*) perivascular endfeet. (B) In the periphery of the same retina, the density of nerve fibers is low; accordingly, the pattern of astrocytic processes is rather irregular but still these processes form endfeet at the blood vessels (*asterisks*).

Astrocytes in the Aging Retina

Decreases in astrocyte number and gliotic changes of astrocytes were observed in the aged human retina and in AMD.[25] These changes will impair the capacity of astrocytes to maintain tissue homeostasis and the support of neuronal function in old age, and

will predispose the retina to age-related diseases such as glaucoma and AMD.[26] The age-related degeneration of astrocytes is associated with a breakdown of the blood–retinal barrier and inflammation.[18] On the other hand, inflammatory astrogliosis was also suggested to be required for the survival of retinal ganglion cells in the aged and diseased retina.[27]

Astrocytes in the Diseased Retina

After retinal injury, astrocytes become activated, proliferate, migrate, exhibit enlarged somata and processes, and upregulate intermediate filaments such as glial fibrillary acidic protein (GFAP), but often to a lesser extent than Müller cells (see reference 2 and references therein). Elevation of the intraocular pressure results in deleterious changes of astrocytes in the optic nerve head and the retina.[28] Activation of astrocytes initially represents a cellular attempt to limit the extent of neuronal injury, but reactive astrocytes also have noxious effects on retinal ganglion cell axons by creating mechanical injury and changing the neuronal microenvironment, resulting in activation of the autonomous self-destruction of ganglion cells.[29] Astrocytes are suggested to contribute to the secondary death of retinal ganglion cells in glaucoma via a spread of oxidative stress through the astrocytic network from the injured axons to the ganglion cell somata.[30] The inflammatory response of astrocytes in experimental glaucoma, which involves the upregulation of soluble inflammatory and neurotoxic factors like TNF-α, prostaglandins, reactive oxygen and nitrogen species, and MMPs, is thought to mediate the glial toxicity in retinal ganglion cells.[2,31]

Malfunction and degeneration of astrocytes may also play a key role in vascular degeneration and retinal dysfunction in diabetic retinopathy.[2] The hyperplasia and malfunction of astrocytes in experimental diabetes coincides with the inner retinal hypoxia and ganglion cell dysfunction.[32] Under ischemic–hypoxic conditions, upregulation of VEGF and TGF-β in astrocytes and Müller cells, and downregulation of antipermeability factors like atrial natriuretic peptide (ANP) in astrocytes, contribute to the breakdown of the blood–retinal barrier and the development of

retinal edema.[2,33,34] A malfunction of astrocytes in glaucoma and diabetic retinopathy may lead to an impaired neurovascular coupling (the hyperemia in response to neuronal activity; see below) and may thus contribute to hypoxic conditions. Upregulation of proangiogenic factors and enzymes like VEGF, platelet-derived growth factor, placental growth factor, NO synthases, and cyclooxygenase-2, and downregulation of antiangiogenic factors like ANP contribute to the development of retinal neovascularization (see reference 2 and references therein).

Bacterial and viral infections are important cofactors of autoimmune uveitis. In addition to infiltrating and resident microglia/macrophages, activated astrocytes have the potential to act as antigen-presenting cells.[35] Various pathogenic conditions like oxidative stress, hypoxia, and elevated intraocular pressure, as well as inflammatory factors stimulate the antigen presentation by astrocytes, via upregulation of MHC class I and II molecules.[2] Pathogen-associated molecular patterns which activate microbial recognition receptors like TLRs trigger alterations in retinal astrocytes required to activate T cells.[36] T-cell-derived IL-17 induces increased production of inflammatory cytokines and chemokines in retinal astrocytes which stimulate the migration of granulocytes.[37]

Activation of astrocytes also has neuroprotective and regenerative effects. Astrocytes protect retinal ganglion cells from injury by various mechanisms including the uptake of excess glutamate, the production of neurotrophic factors like bFGF, BDNF, and CNTF, the restoration of the blood–retinal barrier, and the inhibition of retinal neovascularization.[2] Astrocyte-derived BDNF and CNTF also stimulate the regeneration of retinal ganglion cell axons after injury.[2,38]

Müller Glial Cells

Müller cells are specialized radial glial cells which span the entire thickness of the neural retina, from the vitreal surface to the subretinal space (Figs. 19.1A–B). Their somata are localized in the inner nuclear layer; two stem processes radiate from the soma in opposite directions. The outer stem process draws towards the subretinal space; here, microvilli of Müller cells surround the

photoreceptor inner segments (Figs. 19.5A–B). Zonulae adherentes between Müller and photoreceptor cells form the outer limiting membrane of the retina. The inner stem process projects towards the vitreous chamber; the end of this process is expanded into a funnel-shaped endfoot (Fig. 19.5A). The basement membrane at the inner retinal surface and Müller cell endfoot membranes (Fig. 19.1D) constitute the inner limiting membrane. Lateral processes expand into the plexiform layers where they form sheaths around the synapses, as well as into the nuclear layers where they embed neuronal perikarya (Fig. 19.5A). In the macula, Müller cells display a "Z-shaped" morphology because the outer processes accompany the centrifugally running cone axons in the Henle fiber layer (Figs. 19.6A–B).

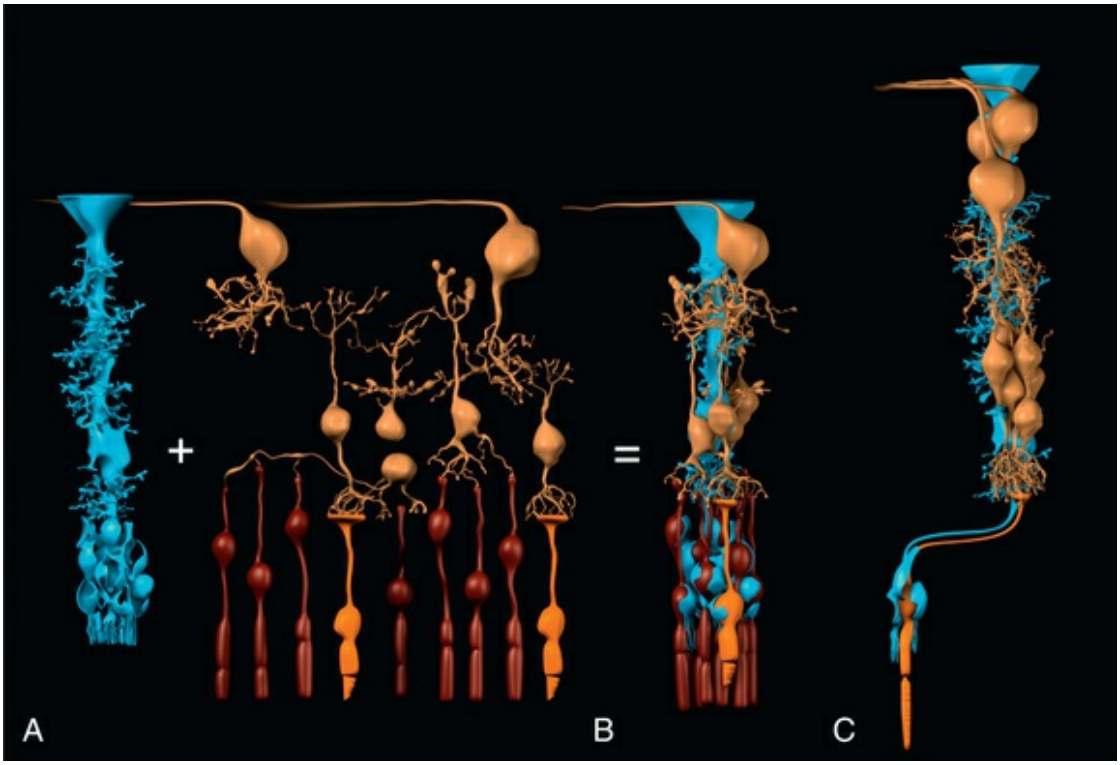

FIG. 19.5 Müller cells form the cores of radial units of retinal neurons. Every Müller cell is surrounded by a distinct group of retinal neurons (A) with which it interacts specifically during development, mature functioning, and injury of the retina. These repetitive radial units are almost identical throughout most regions of the retina (B) but differ in the (peri-)fovea (C) by the lack of rods, an increased number of neurons of

the inner nuclear and ganglion cell layers, and by an elongation and a Z-shaped course of the outer processes of Müller cells (cf. Fig. 19.6). Blue, Müller cells; yellow, retinal neurons; orange, cones; brown, rods.

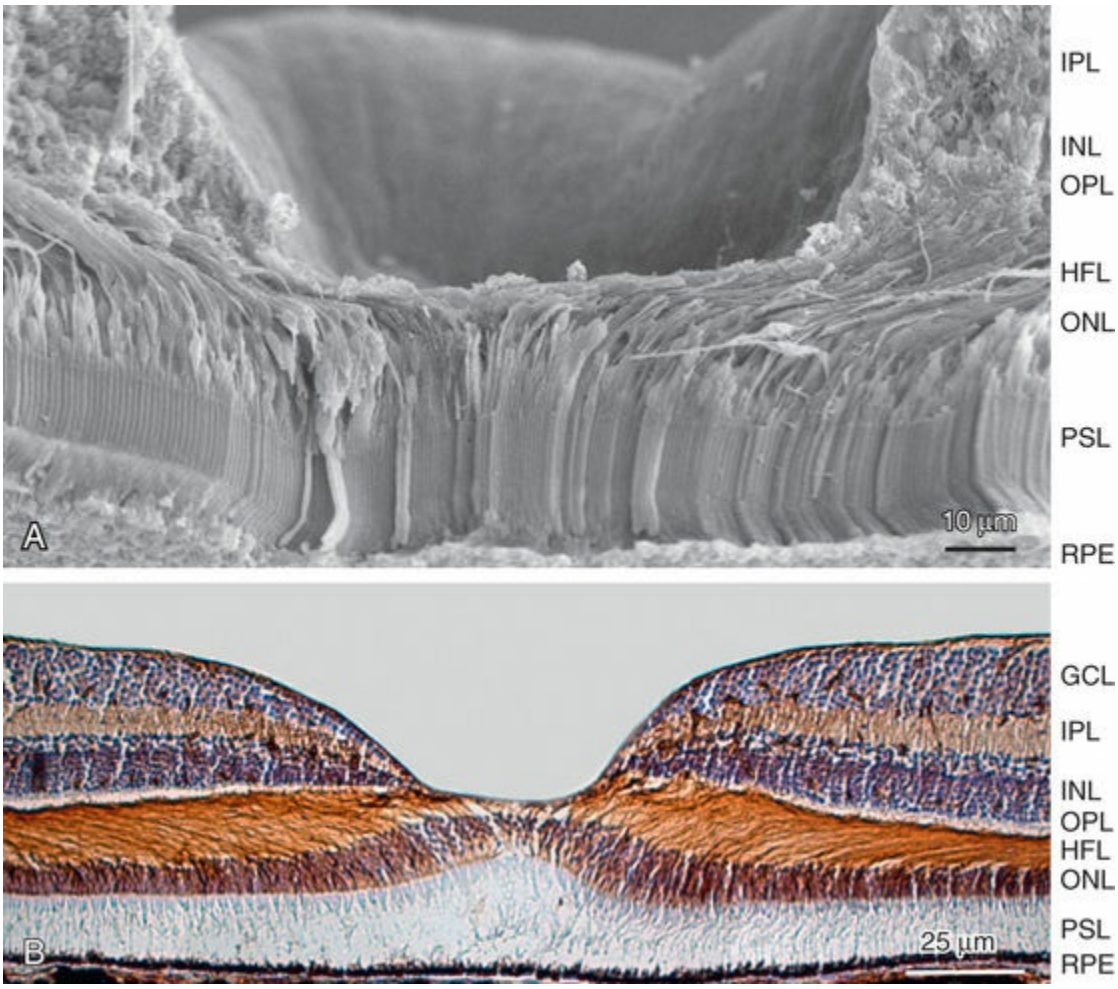

FIG. 19.6 Müller cells of the primate macula are elongated and run in parallel with the Henle fibers. (A) Scanning electron microphotograph of the fovea of a macaque. The extremely high packing density of cone inner and outer segments in the photoreceptor segment layer (*PSL*), the complex centrifugal course of their axons crowded in the Henle fiber layer (*HFL*), and the absence of the ganglion cell (*GCL*), inner plexiform (*IPL*), inner nuclear layer (*INL*) and outer plexiform layer (*OPL*) are illustrated. The outer processes of Müller cells run among the Henle fibers but can not be reliably identified. (B) When the Müller cell processes

are visualized by vimentin immunohistochemistry (brown; cell nuclei are blue-stained; siamang retina), they can be traced along their path from the outer margin of the outer nuclear layer (*ONL*) up to their endfeet; it becomes obvious that they run in parallel to the Henle fibers.

The human retina contains 4–5 million regularly arranged Müller cells (Figs. 19.1C and 19.7C). Each Müller cell constitutes the core of a column of retinal neurons which represents the smallest functional unit for the "forward information processing."[39] Such a column contains one cone per Müller cell (Figs. 19.5A–C and 19.7C–D) and up to 10 rods, as well as 6 (fovea) and 4 (periphery) inner nuclear layer neurons, and 2.5 (fovea) and 0.3 (periphery) ganglion cell layer neurons, respectively.[1]

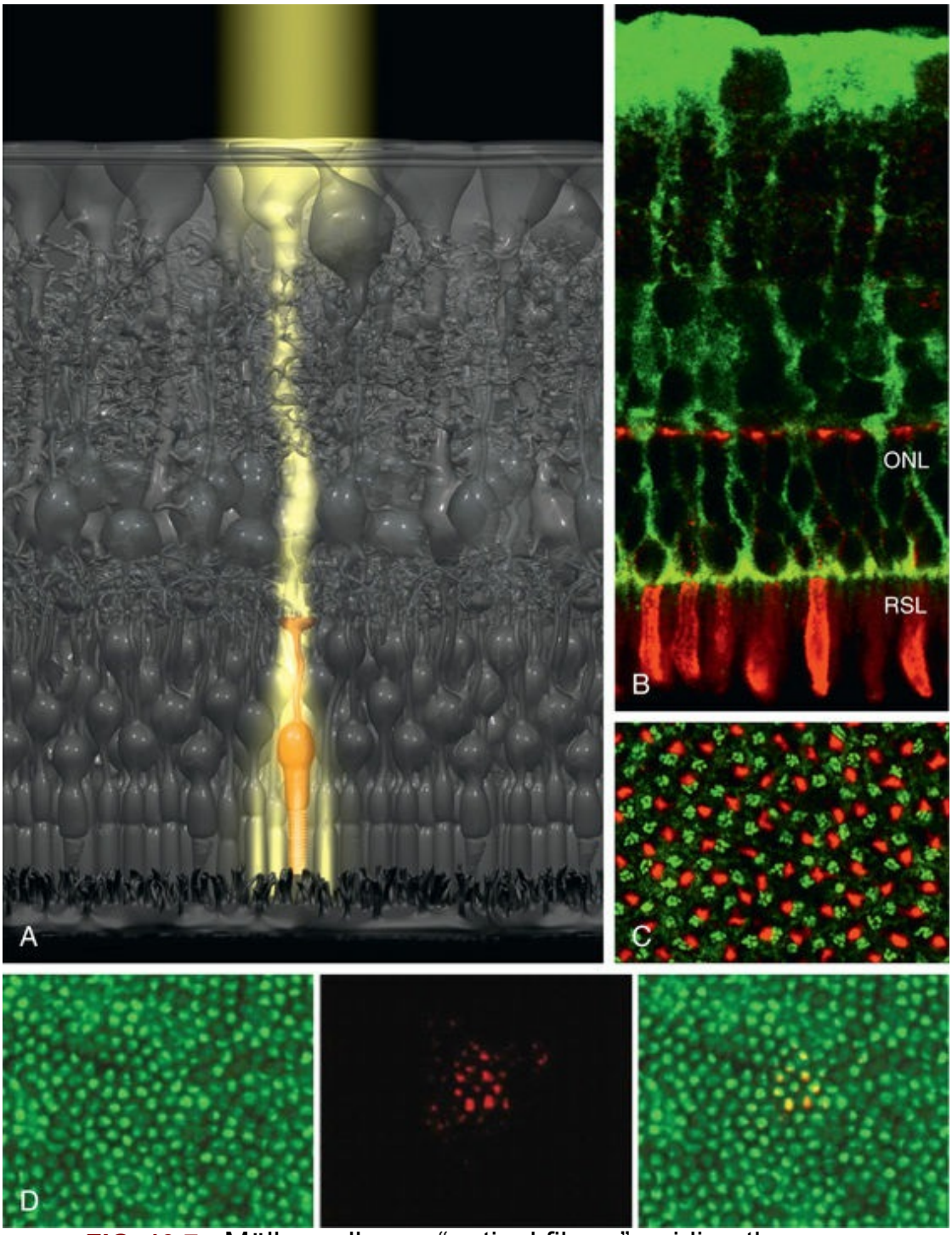

FIG. 19.7 Müller cells are “optical fibers” guiding the incoming light to the photoreceptor cells. (A) Artist's view of the optical path through the retina. Light arrives at the inner retinal surface where it hits the Müller cell endfeet. Then it propagates through the Müller cell stem processes (thus bypassing the light-scattering retinal structures, particularly the synapses in the two plexiform layers) until it arrives at the photoreceptor cells. (B,C) Vertical (B) and horizontal (C) sections

through the guinea pig retina. Müller cells were immunolabeled for vimentin (green), and cones were red-stained. (B) The cone inner segments in the photoreceptor segment layer (*RSL*) appear as "continuous" with the outer processes of Müller cells which envelop the cone perikarya in the outer nuclear layer (*ONL*). (C) The focus of the image is on the outer plexiform layer. The number of cone pedicles (red) roughly equals that of Müller cell processes (green); often the two elements appear as pairs. Thus, each cone receives its part of the image of the outside world by its "individual" light-guiding Müller cell. (D) Every Müller cell illuminates a distinct group of photoreceptors, about 10 rods and 1 cone, in the guinea pig retina.

Müller cells provide crucial homeostatic, metabolic, and functional support to the neurons of their columns. They constitute an anatomical and functional link between neurons and the compartments with which they need to exchange molecules (blood vessels, vitreous chamber, subretinal space). Most nutrients, "waste" products, ions, water, and other molecules are transported through Müller cells between the vessels and neurons. Müller cells play crucial roles in the regulation of the extracellular space volume, ion and water homeostasis, and the maintenance of the inner blood–retinal barrier. They release gliotransmitters and other neuroactive molecules, and impact synaptic activity by neurotransmitter recycling which involves the supply of neurons with the precursor of the transmitters. All of these functions directly or indirectly modify the neuronal activity. The Müller cell-mediated homeostasis of the extracellular space composition and volume has a great impact for the setting of the signal-to-noise ratio of the synaptic transmission and the spatial distribution of light-induced signaling. Müller cells support the survival of photoreceptors and neurons, are responsible for the structural stabilization of the retina, and are modulators of immune and inflammatory responses. They guide the light to the photoreceptors and buffer mechanical tissue deformations. Müller cells become activated upon virtually all pathogenic stimuli. Reactive Müller cells are neuroprotective but may also quit supporting the neurons,

and rather contribute to neuronal degeneration. Currently, the many roles of Müller cells in the regulation of retinal function are still not resolved, and are the subject of ongoing intensive research. Noteworthy, much of the current knowledge about Müller cell (dys-)functions was obtained in animal models and thus awaits confirmation on human cells.

Light Guidance

Because the retina is inverted, light has to pass the entire depth of the neuroretina before it arrives at the photoreceptors. In the retina as in any other organ, cells and their processes and organelles are phase objects which scatter the incoming light. In particular, the synapses in the plexiform layers have dimensions close to 500 nm, i.e., within the wavelength range of visible light; this makes them light-scattering structures.[40] The backscattering of light from the retinal cell structures is clinically used by optical coherence tomography. However, light scattering will reduce visual sensitivity and acuity, particularly outside the fovea (where the inner layers are shifted aside, and the light directly hits the cones; Figs. 19.6A–B).

To reduce light scattering, nonfoveal Müller cells act as living optical fibers that guide the light through the inner retinal layers toward the photoreceptors (Fig. 19.7A).[40] The funnel-shaped endfeet of Müller cells act as light collectors at the vitreal surface of the retina. The refractory index of Müller cells is slightly lower than that of photoreceptor segments (which are also light-guiding structures) but higher than that of the surrounding retinal tissue.[40] The refractory index of the Müller cell endfeet is about halfway between that of Müller cell stem processes and that of the vitreous.[40] This allows a "soft coupling" of the light path between the vitreous and the retina, and reduces light reflection at the inner retinal surface. By light guidance, Müller cells transport an image (like a fiberoptic plate) with minimal loss of light intensity from the inner retinal surface to the photoreceptors; this image is resolved in "pixels" corresponding to individual Müller cells (Fig. 19.7A). Because the local densities of cones and Müller cells are roughly equal (Figs. 19.7B–C), every cone has its "private" Müller cell which

delivers its part of the image, while several (up to 10) rods are illuminated by 1 Müller cell (Fig. 19.7D).

Glial Support to Photoreceptor Function

There exist two metabolic cycles in the retina that regenerate photopigments, the rod and the cone visual cycle.[41] In the photoreceptor outer segments, all-*trans* retinal is reduced to all-*trans* retinol. Rod-derived all-*trans* retinol is regenerated to 11-*cis*-retinal in the RPE while cone-derived all-*trans* retinol is processed by Müller cells. Müller cells convert all-*trans* retinol to 11-*cis* retinal, which is released for the uptake by cone photoreceptors. Müller cells phagocytose outer-segment discs shed from cones and contribute to the assembly and renewal of photoreceptor outer segments by the delivery of lactose, pigment epithelium-derived factor (PEDF), and docosahexaenoic acid.[2,42,43]

Regulation of Synaptic Activity by Neurotransmitter Uptake

Precise "shaping" (i.e., control in time and space) of synaptic activity depends on the kinetics of the presynaptic neurotransmitter release and the reuptake of transmitter molecules into the cells. In the neuroretina, photoreceptor cells, neurons, and glial cells express high-affinity transporters for neurotransmitters. Müller cells possess uptake and exchange systems for various neurotransmitters, including glutamate and GABA (Fig. 19.8). By the uptake of neurotransmitters, Müller cells are involved in the regulation of the synaptic activity in the inner retina.

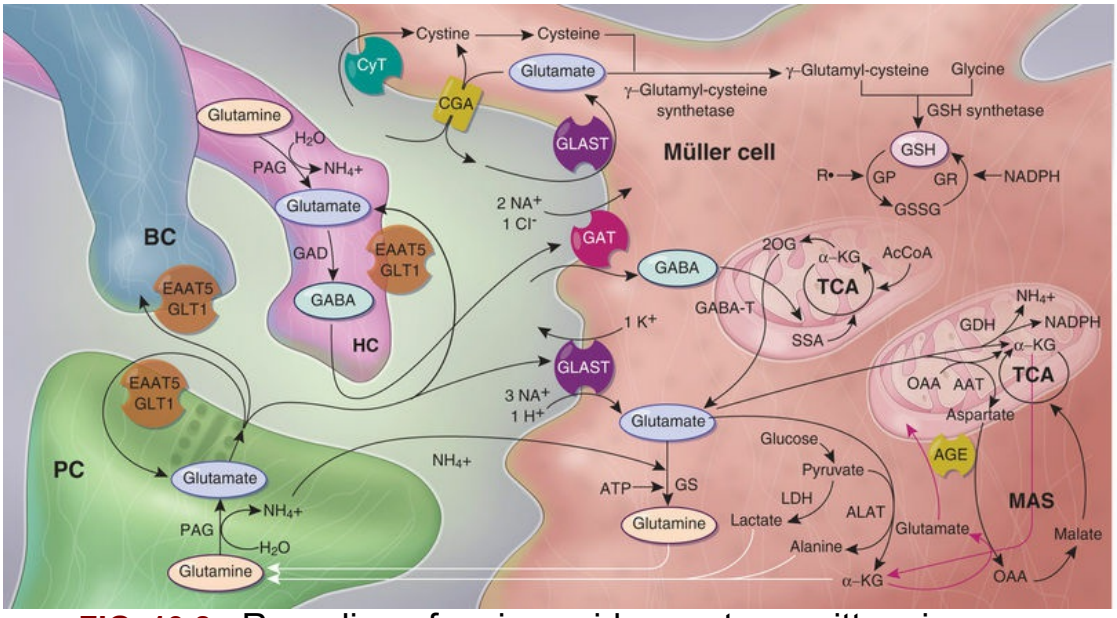

FIG. 19.8 Recycling of amino acid neurotransmitters in the outer plexiform (synaptic) layer. The ribbon synapse of a photoreceptor cell (PC) synthesizes glutamate which is continuously released in the dark. The postsynaptic elements are dendrites of bipolar (BC) and horizontal cells (HC). Horizontal cells release GABA which is formed from glutamate. The synaptic complexes are surrounded by Müller cell sheets. The right side of the figure shows neurotransmitter uptake systems and some metabolic pathways of Müller cells. Glutamate, GABA, and ammonia (NH_4^+) are transported into Müller cells and transformed to glutamine, alanine, and α-ketoglutarate (α-KG). Glutamine is released from Müller cells and serves as precursor for the transmitter synthesis in neurons (glutamate–glutamine cycle). Lactate, alanine, pyruvate, α-ketoglutarate, and glutamine are utilized by neurons as substrates for their energy metabolism. The mitochondrial enzyme GABA transaminase (GABA-T) catalyzes the formation of glutamate from 2-oxoglutarate (2OG), coupled to a conversion of GABA to succinate semialdehyde (SSA). Glutamate is also used for the production of reduced glutathione (GSH) which is an antioxidant, released from Müller cells and taken up by neurons under oxidative stress conditions. Abbreviations: AcCoA, acetyl coenzyme A; AGC, aspartate-glutamate carrier; ALAT, alanine aminotransferase; AAT, aspartate aminotransferase; CGA, cystine-glutamate antiporter; CyT, cystine

transporter; EAAC1, excitatory amino acid carrier 1; EAAT5, excitatory amino acid transporter 5; GAD, glutamic acid decarboxylase; GAT, GABA transporter; GDH, glutamate dehydrogenase; GLAST, glutamate-aspartate transporter; GLT-1, glutamate transporter-1; GlyT, glycine transporter; GP, glutathione peroxidase; GR, glutathione reductase; GS, glutamine synthetase; GSSG, glutathione disulfide; LDH, lactate dehydrogenase; MAS, malate–aspartate shuttle; OAA, oxaloacetate; PAG, phosphate-activated glutaminase; $R^{\bullet}$, free radicals; TCA, tricarboxylic acid cycle.

The major glutamate uptake carrier of Müller cells is the glutamate-aspartate transporter (GLAST, or excitatory amino acid transporter-1, EAAT1).[44,45] In addition, EAAT2 (GLT1) and EAAT3 were found in human Müller cells.[46,47] EAATs mediate a cotransport of three sodium ions and one proton, and the countertransport of one potassium ion, with each glutamate anion.[48] The transport of an excess of sodium into the cell generates an inward current (Figs. 19.9A–B, E, G) and cellular depolarization. The amplitude of the glutamate transporter currents is voltage-dependent (Fig. 19.9A); a very negative membrane potential is essential for the efficient uptake of glutamate.[49] Sodium-dependent carriers allow uphill transport of substrates into the cells against a concentration gradient. The driving force for the transport is the electrochemical sodium gradient across the plasma membrane generated by the Na^+, K^+-ATPase. Other transporters, e.g., for GABA, are also electrogenic (Figs. 19.9C–D). The subcellular distribution of the GABA transporter currents (Fig. 19.9C) corresponds with the observation that GABA is taken up by amacrine and Müller cells in the inner retina but exclusively by Müller cells in the outer retina.[50]

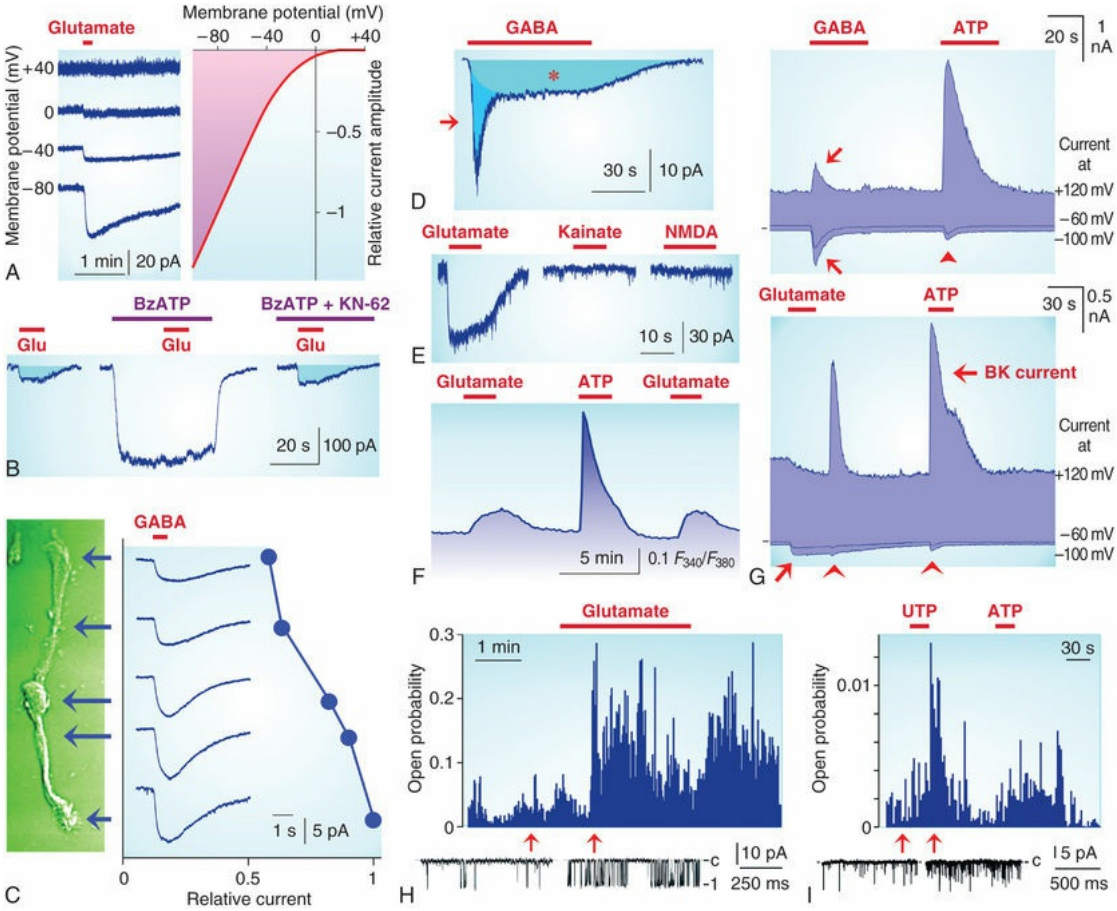

FIG. 19.9 Glutamate and GABA receptors and transporters of Müller cells. (A) Administration of glutamate (1 mM) to a rabbit Müller cell induces inward currents at negative membrane potentials (left). The current-voltage relation of the glutamate transporter currents in guinea pig Müller cells (right) shows that the efficiency of the glutamate transport increases with increasing (i.e., more negative) membrane potentials. (B) Activation of ionotropic $P2X_7$ receptors (which mediate cation currents and thus induce a depolarization of the cells) decreases the electrogenic uptake of glutamate in human Müller cells. The glutamate transporter currents induced by glutamate (Glu; 100 μM) were diminished in the presence of the $P2X_7$ receptor agonist BzATP (10 μM). Inhibition of $P2X_7$ activation by KN-62 (1 μM) suppressed the BzATP-induced current (and cell depolarization), resulting in glutamate transporter currents similar in amplitude as under control conditions. (C) Subcellular distribution of the GABA transporter currents in a guinea pig Müller cell. The distribution of the currents was determined by focal ejections of GABA (1 mM)

onto the following cell membrane domains: endfoot, inner stem process, soma, and inner and outer parts of the outer stem process. (D) GABA (100 μM) induces two kinds of inward currents in human Müller cells: a transient, rapidly inactivating chloride current mediated by $GABA_A$ receptors (*arrow*) and a sustained current mediated by electrogenic GABA transporters (*asterisk*). (E) In a rat Müller cell, glutamate (100 μM) induces inward currents through electrogenic glutamate transporters while the glutamate receptor agonists kainate (500 μM) and NMDA (100 μM, in the presence of 10 μM glycine and the absence of magnesium) do not induce membrane currents. (F) Administration of glutamate (100 μM) and ATP (500 μM) to a human Müller cell induces intracellular calcium responses, suggesting the presence of metabotropic glutamate receptors. The calcium imaging record was done in a cell from a patient with PVR. (G) (Above) A subpopulation of human Müller cells express $GABA_A$ receptors. GABA (500 μM) induced a transient increase of the inward and outward membrane currents (*arrows*). ATP (500 μM) induced a transient increase of the BK channel-mediated potassium currents (at +120 mV). (Below) In human Müller cells, glutamate (500 μM) induces a delayed transient increase of the BK currents. The increase in the currents at −60 and −100 mV during the exposure of glutamate (*arrow*) reflects the activation of electrogenic glutamate transporters. P2Y receptor activation by ATP (500 μM) induces an immediate transient activation of BK channels and of calcium-induced cation channels (*arrowhead*). (H,I) Agonists of metabotropic glutamate receptors (200 μM glutamate; H) and P2Y receptors (100 μM UTP and ATP, respectively; I) induce activation of single BK channels in human Müller cells. The diagrams show the time-dependent open probability of single BK channels. *c*, closed state; *1*, open state of the channels.

In the outer plexiform layer, photoreceptor-derived glutamate is mainly removed by photoreceptor, horizontal, and bipolar cells[44,51] while Müller cells prevent the lateral spread of glutamate beyond the synapses, thus ensuring visual resolution (Fig. 19.8). In the inner

plexiform layer, Müller cell-provided glutamate uptake takes a more active part in shaping the synaptic responses. The rapid termination of the synaptic glutamate action in nonspiking inner retinal neurons and in retinal ganglion cells is predominantly mediated by the uptake of glutamate into Müller cells.[52,53] Generally, Müller cells remove the bulk of extracellular glutamate in the inner retina.[45,54]

Malfunction of Glial Glutamate Uptake Contributes to Retinal Degeneration

Glutamate toxicity is a major cause of neuronal loss in many retinal disorders including glaucoma, ischemia, diabetes, and inherited photoreceptor degeneration. A malfunction and/or downregulation of GLAST may cause, or contribute to, a rise in extracellular glutamate toward excitotoxic levels.[55–57] Hypoxia facilitates the formation of free radicals in mitochondria; the resulting lipid peroxidation disrupts the glutamate transport into Müller cells.[58] This mechanism is one cause of neuronal dysfunction and degeneration in various retinopathies including diabetic retinopathy and Leber hereditary optic neuropathy.[59,60] Inflammatory lipids like arachidonic acid and a reduction of the extracellular pH as occurs in ischemia also inhibit the glial glutamate uptake.[61]

Because the glutamate transport is voltage-dependent (Fig. 19.9A), depolarization decreases the efficiency of the glial glutamate uptake.[49,62] Depolarization of Müller cells occurs in response to pathologic rises in extracellular potassium (as in ischemia and glaucoma), to the opening of cation channels in Müller cells, e.g., of $P2X_7$ receptor channels (Fig. 19.10C), and to a decrease in the potassium permeability of glial membranes which results from an inactivation and/or downregulation of inwardly rectifying potassium (Kir) channels (Figs. 19.3A, E, G, 19.10A, 19.11B–D and 19.12D, G). An inactivation of Kir channels was observed in animal models of various retinopathies (see below). Cellular depolarization can also be induced by inflammatory lipids like arachidonic acid and prostaglandins that potently inhibit the Na^+, K^+-ATPase. Depolarization of Müller cells may even result in a reversal of the

glutamate transport.[63] A nonvesicular release of glutamate and aspartate via reversed operation of glial glutamate transporters was suggested to be implicated in the excitotoxic damage of retinal ganglion cells.[64,65] A release of glial glutamate might also be mediated by the cysteine glutamate antiporter (which is activated under oxidative stress conditions when an elevated production of glutathione requires an increased uptake of cystine; Fig. 19.8) and by exocytosis of glutamate-containing secretory vesicles.[66–68] Under various pathologic conditions including ischemia, glaucoma, retinal detachment, and proliferative retinopathies, an enhanced expression or activity of GLAST was observed.[69,70] This may counterbalance the depolarization-induced malfunction of the glial glutamate uptake.

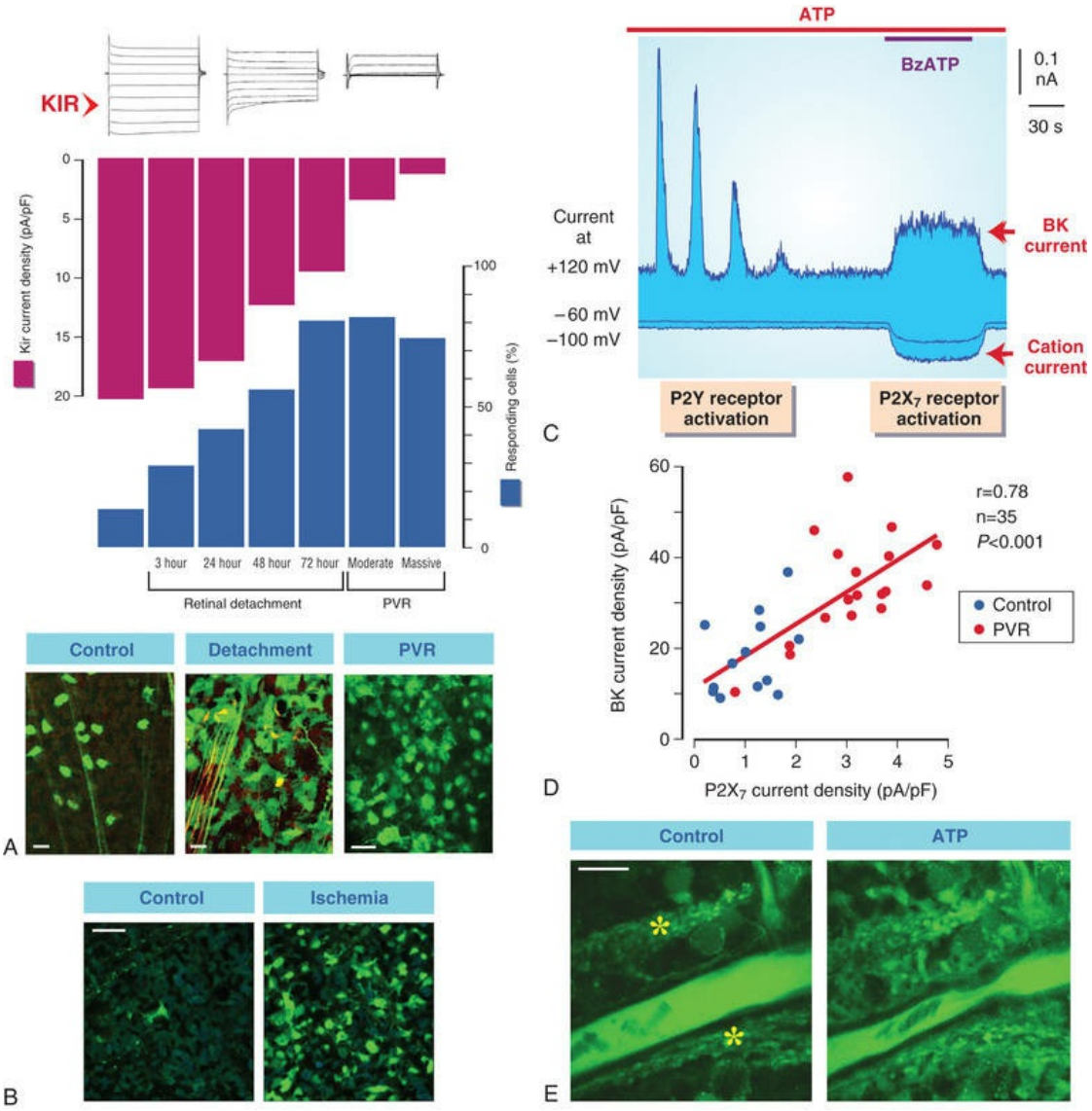

FIG. 19.10 Purinergic signaling in Müller cell gliosis. (A,B) Upregulation of glial calcium responsiveness in response to P2Y receptor activation in animal models of different retinopathies. (A) The incidence of rabbit Müller cells that respond to exogenous ATP (200 μM) with a rise in the cytosolic free calcium level (bar chart, below) is inversely related to the density of Kir potassium currents (bar chart, above). This relation was observed after experimental retinal detachment and in moderate and massive proliferative vitreoretinopathy (PVR). The traces shown above represent examples of potassium current records in single Müller cells. The images below show examples of peak calcium responses (green areas) to ATP (200 μM) at the inner surface of the retinas. While nearly all Müller cell endfeet displayed a calcium response in the retinas of rabbits with retinal detachment and PVR,

only some Müller cell endfeet responded in the retina of the control animal. (B) Ischemia–reperfusion increases the P2Y-induced calcium responsiveness in Müller cell endfeet recorded in wholemounts of the porcine retina. The calcium responses were recorded 1 min after beginning of the administration of ATP (200 μM). Tissues of a control retina and a retina 3 days after a 1-h transient retinal ischemia were investigated. (C) Activation of P2Y and $P2X_7$ receptors alters the membrane conductance of a human Müller cell. Activation of P2Y receptors by extracellular ATP (100 μM) induced repetitive transient calcium-induced activation of BK currents while activation of $P2X_7$ receptors by BzATP (50 μM) induced a sustained calcium-induced activation of BK currents and cation currents through $P2X_7$ receptor channels. (D) Müller cells of human subjects with PVR exhibit a greater density of $P2X_7$-mediated cation currents than cells from healthy donor eyes. The density of the BzATP (50 μM)-induced $P2X_7$-mediated currents in cells of each subject is plotted against the density of the BK currents activated by calcium ions which flow through $P2X_7$ receptor channels. (E) Peak calcium responses in Müller cell endfeet on the vitreal surface of a control rat retinal wholemount induced by ATP (500 μM). Note the constriction of the arteriole in response to ATP. Müller cell endfeet fill the spaces between the arteriole and nerve fiber bundles (*asterisk*). Scale bars: 20 μm.

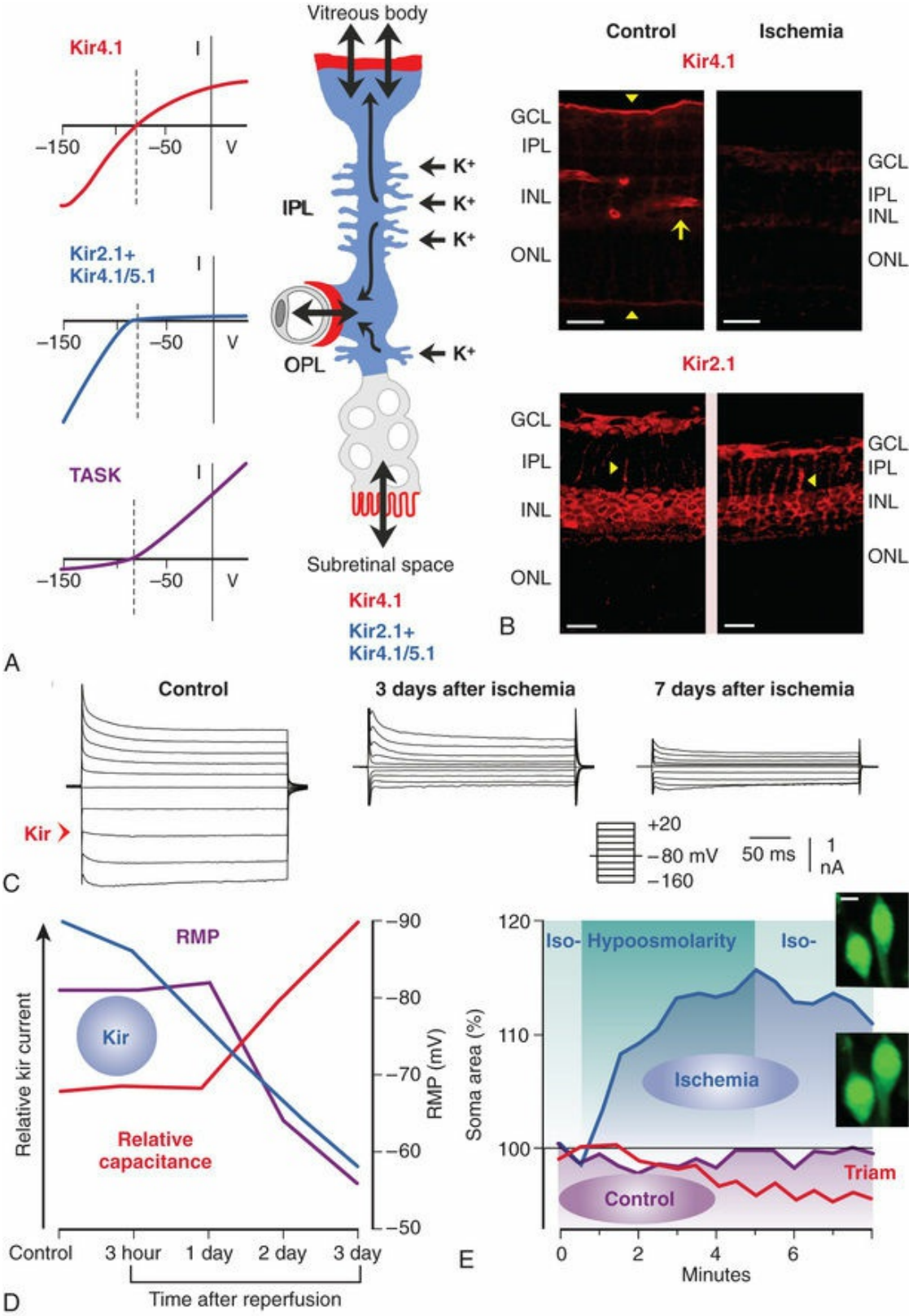

FIG. 19.11 Müller cell gliosis is associated with alterations of Kir channel expression and osmotic cell swelling. (A) The subcellular localization of Kir channel subtypes determines the direction of the spatial buffering potassium currents through Müller cells. Left:

Current–voltage (I–V) relations of different potassium channels. Kir4.1 channels mediate inward and outward potassium currents with similar amplitudes, whereas Kir2.1 channels mediate inward currents but almost no outward currents. Two-pore domain (TASK) channels mediate outward potassium currents. Right: Schematic drawing of the potassium buffering currents flowing through Müller cells during neuronal activity. Activated neurons release potassium which is absorbed by Müller cells through Kir2.1 and Kir5.1/4.1 channels, and distributed into the blood vessels, the vitreous, and the subretinal space through Kir4.1 channels. Kir4.1 channels mediate in- and outward currents and thus contribute to the osmohomeostasis between the neuroretina and extraretinal fluid-filled spaces. (B) Immunolocalization of glial Kir channels in slices of the normal and postischemic rat retina. The Kir4.1 protein is predominantly localized at the limiting membranes of the neuroretina (*arrowheads*) and around the vessels (*arrow*). Kir2.1 protein is localized in glial membrane domains that abut neuronal compartments of the inner retina such as processes that traverse the inner plexiform layer (IPL) (*arrowheads*). Seven days after a 1-h transient retinal ischemia, the Kir4.1 protein is largely downregulated whereas the localization of the Kir2.1 protein remains unaltered. Note the decrease in the thickness of the inner retina which is a characteristic of retinal ischemia–reperfusion injury. (C) Examples of whole-cell potassium currents of single Müller cells isolated from a control retina, and from retinas 3 and 7 days after a 1-h transient retinal ischemia. (D) The amplitude of the Kir currents decreases time-dependently after transient retinal ischemia. Simultaneously, the resting membrane potential (RMP) of the cells decreases and the whole-cell capacitance (that is proportional to the cell membrane area) increases, indicating cellular hypertrophy. The parameters were measured at different periods (3 hours to 3 days) after transient ischemia. (E) Under hypoosmotic stress, Müller cells in slices of 3-days-postischemic retinas display a rapid swelling which is not observed in Müller cells in slices of control retinas. Administration of triamcinolone acetonide (*Triam*; 100 μM) simultaneously with the

hypoosmotic solution fully inhibited the Müller cell swelling. The time-dependent alterations in the cross-sectional area of Müller cell somata are shown. The images on the right display Müller cell somata in a postischemic retina before (above) and after (below) hypoosmotic swelling. *GCL*, ganglion cell layer; *INL*, inner nuclear layer; *ONL*, outer nuclear layer; *OPL*, outer plexiform layer. Scale bars: (B) 20 μm and (E) 5 μm.

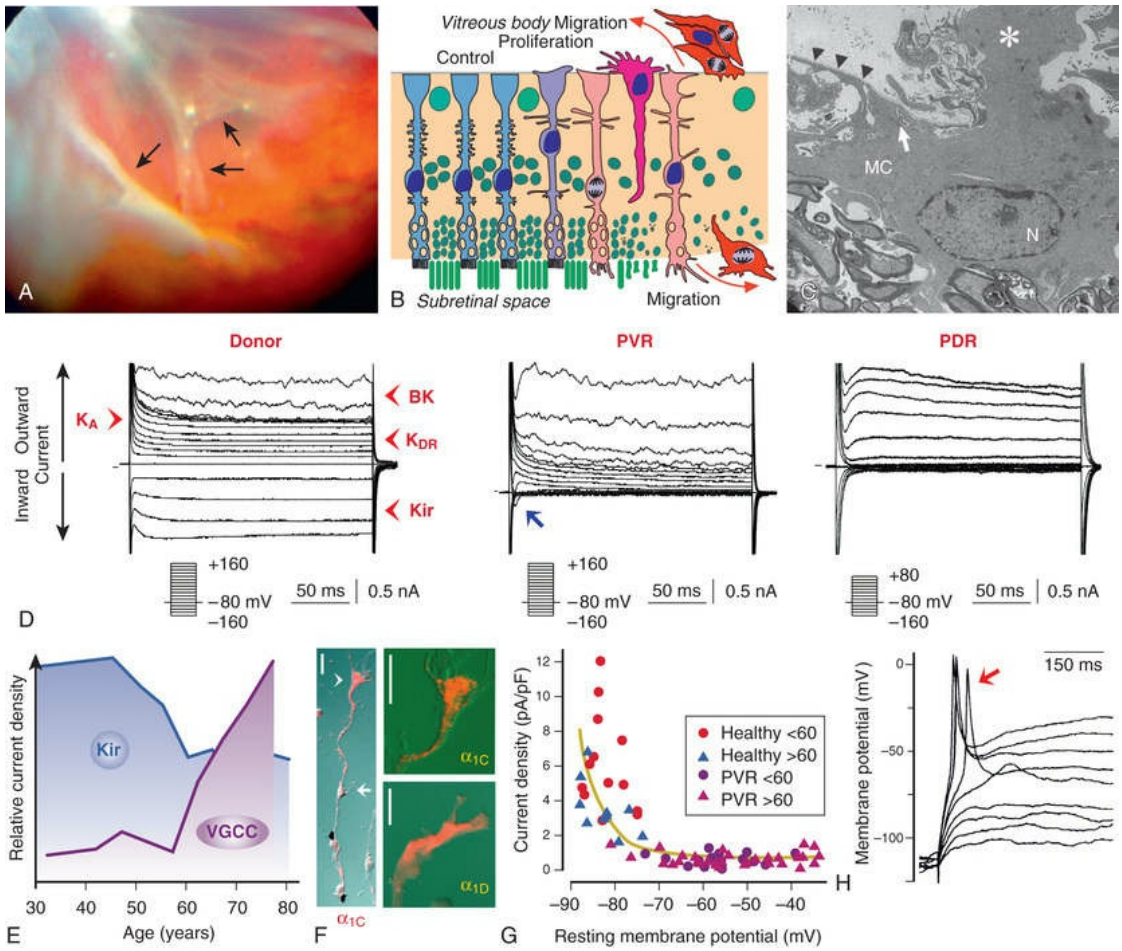

FIG. 19.12 Age- and disease-related Müller cell reactivity. (A–C) Müller cell reactivity in experimental proliferative vitreoretinopathy (PVR). (A) Ophthalmoscopic image of an experimentally induced PVR in the rabbit eye. Note the large, folded cellular masses on the vitreal surface of the retina (*arrows*). (B) Schematic drawing of increasing degrees of Müller cell reactivity in PVR (from left to right). Müller cells reenter the proliferation cycle, migrate out of the neural retina,

and participate in the formation of periretinal fibrocellular membranes. (C) Transmission electron micrograph of a reactive Müller cell (*MC*) of the rabbit retina which migrates through a hole in the inner limiting membrane (*arrowheads*) into the vitreous body (*asterisk*). The nucleus (*N*) of the Müller cell is translocated to the innermost retinal layer. (D) Alterations in the membrane conductance of human Müller cells in proliferative retinopathies. Four different types of potassium currents can be recorded in Müller cells of postmortem donors without apparent eye diseases: *BK*, currents mediated by big-conductance potassium channels; K_A, fast transient (A-type) potassium currents; K_{DR}, delayed rectifying potassium currents; *Kir*, inwardly rectifying potassium currents. Müller cells obtained from patients with proliferative vitreo- (*PVR*) and diabetic retinopathies (*PDR*) display an almost complete absence of Kir currents. The *arrow* indicates transient inward currents through voltage-gated sodium channels. (E) Age-dependent alterations in the densities of Kir and L-type voltage-gated calcium channel (*VGCC*) currents in human Müller cells. While the Kir currents display an age-dependent decrease, the currents through L-type calcium channels increase in the course of aging. (F) Immunolabeling of isolated human Müller cells for the α_{1C}- and α_{1D}-subunits of voltage-gated calcium channels (*red-orange*). Right: Müller cell endfeet at higher magnification. *Arrow*, cell soma. *Arrowhead*, cell endfoot. Scale bars: 20 µm. (G) Relation between the Kir current density and the resting membrane potential of Müller cells from human donors of different age. The cells were derived from donors without apparent retinal disease (*Healthy*) and from patients with PVR. Note the great variability of the membrane potential in the cells of the patients. (H) Single action potential-like discharges (*arrow*) can be induced in the current-clamp mode by large depolarizing current steps in a Müller cell of a patient with PVR. Depolarizing currents from 40 to 200 pA (increment, 20 pA) were applied after administration of a hyperpolarizing current of 250 pA (resulting in a membrane potential between −100 and −125 mV).

Glutamate–Glutamine Cycle

To ensure synaptic transmitter recycling, Müller cells are endowed with specific enzymes. After GABA is taken up by Müller cells, it is readily converted to glutamate by GABA transaminase; glutamate is converted to glutamine by glutamine synthetase (Fig. 19.8). Glutamine synthetase is exclusively localized to glial cells.[71] Glutamine is released from Müller cells and taken up by neurons as a precursor for the resynthesis of glutamate and GABA (Fig. 19.8).[72] While photoreceptor cells produce only a part of glutamate from glia-derived glutamine (and also take up glutamate from the synaptic cleft and produce glutamate from other substrates), the production of glutamate in bipolar and ganglion cells depends almost entirely on glia-derived glutamine.[51,73] Pharmacologic blockade of glutamine synthetase in Müller cells causes a loss of the glutamate content of bipolar and ganglion cells, and the animals become functionally blind.[73] Likewise, a significant amount of GABA in amacrine cells is synthesized from glia-derived glutamine.[73]

Downregulation of glial glutamine synthetase contributes to neuronal dysfunction and glutamate toxicity, for example in inherited photoreceptor degeneration and after retinal detachment.[74,75] bFGF is one factor that induces a downregulation of glutamine synthetase.[76] bFGF is rapidly released in the retina after detachment, and it is increasingly expressed under ischemic conditions, after light and mechanical injuries, and in inherited photoreceptor degeneration (see reference 2 and references therein). Although bFGF is a neurotrophic factor that supports the survival of photoreceptors and neurons,[77–79] the bFGF-induced downregulation of glutamine synthetase may aggravate neuronal degeneration.

Trophic and Antioxidative Support to Photoreceptors and Neurons

The uptake of glutamate by Müller cells links neuronal excitation with the release of metabolic substrates and the defense against oxidative stress. Müller cells produce various substrates of

oxidative neuronal metabolism such as glutamine, lactate, alanine, and α-ketoglutarate (Fig. 19.8);[80] these substrates are used by photoreceptors and neurons in periods of metabolic stress in the dark. The metabolic support is regulated by neuron-derived glutamate (which stimulates the uptake of glucose and the production of lactate) and potassium (which induces hydrolyzation of glycogen in Müller cells).[2,81]

Glutamate in Müller cells is also utilized for the production of the antioxidant, glutathione (Fig. 19.8).[82] The retina has a high need of antioxidant protection; this results from the light exposure together with the high oxygen consumption and the high level of polyunsaturated fatty acids in photoreceptors. The outer retina underlies circadian periods of hypoxia (dark) and hyperoxia (light);[83] both increase the oxidative stress level. Usually, retinal glutathione is confined to glial and horizontal cells.[82,84] In response to oxidative stress, for instance during ischemia, glutathione is rapidly released from Müller cells and provided to neurons[84] where it acts as cofactor of reducing enzymes, the glutathione peroxidases. The glial release of antioxidants like glutathione, and of neuroprotective factors like bFGF and adenosine, protects the photoreceptors from the harmful effects of circadian light exposure.

Müller cells from aged animals contain reduced levels of glutathione; this is associated with mitochondrial damage, membrane depolarization, and reduced cell viability.[85] The decrease in retinal glutathione may accelerate the development of age-related retinopathies. In diabetic retinopathy, the decreased glutamate uptake of Müller cells results in a reduced glutathione synthesis and in an upregulation of glutaredoxin which catalyzes the deglutathionylation of proteins; this leads to an increased expression of inflammatory factors.[86,87]

Removal of CO_2 and Regulation of pH

Photoreceptor cells have the highest rate of oxidative metabolism of all cells in the body.[88] This high metabolic activity is associated with high oxygen and glucose demands. The glucose metabolism generates CO_2 and water which are redistributed into the blood and vitreous by a transcellular transport through Müller cells. CO_2 is

rapidly hydrated to bicarbonate and protons by carbonic anhydrases[89] which are localized to Müller and amacrine cells, and the vascular endothelia.[90–92] Bicarbonate is transported to the blood and vitreous by sodium-bicarbonate cotransporters and anion exchangers; both are enriched in glial endfoot membranes.[92]

By the removal of CO_2, Müller cells also regulate the extracellular pH. Light-induced neuronal activity is associated with extracellular alkalinization.[93] The pH shift is balanced by an efflux of protons from photoreceptors and the consecutive action of carbonic anhydrases and glial sodium-bicarbonate cotransporters.[94,95] Because sodium-bicarbonate transporters are electrogenic, depolarization of Müller cells by potassium released from active neurons causes an influx of bicarbonate into the cells.[95] The carbonic anhydrase-generated protons remain outside the cells and cause an extracellular acidification.[95] Because extracellular acidification inhibits synaptic transmission,[96] Müller cell-mediated pH regulation may protect neurons from overexcitation. A subpopulation of human Müller cells express ionotropic $GABA_A$ receptors (Figs. 19.9D, G).[2] Because $GABA_A$ receptors are permeable for bicarbonate, they may be implicated in the regulation of the extracellular pH. In addition, $GABA_A$ receptor activation may compensate the decrease in the extracellular chloride level caused by the chloride influx into activated neurons.

Spatial Potassium Buffering

Neuronal activity is associated with rapid ion shifts between the intra- and extracellular spaces. Sodium, chloride, and calcium ions flow into active neurons, and potassium ions are released from neurons. Light onset causes increases in the extracellular potassium level within the plexiform layers, and a decrease in the subretinal space.[97] If not corrected, excess extracellular potassium will cause neuronal hyperexcitation. Müller cells buffer imbalances in the local extracellular potassium level via permission of transcellular potassium currents, a process termed “spatial potassium buffering” or “potassium siphoning.”[98] Müller cells take up excess potassium from the extracellular fluid, and release equal amounts of potassium into fluid-filled spaces outside the neuroretina where the

potassium concentration is constant or decreased, i.e., blood vessels, vitreous, and subretinal space (Fig. 19.11A).

Because Müller cell membranes are highly permeable to potassium, Müller cells have a very negative resting membrane potential close to the potassium equilibrium potential, around −80 mV.[99] The potassium permeability is mainly mediated by potassium channels of the Kir channel subfamily.[100] In particular, Kir4.1 (which mediate bidirectional potassium currents; Fig. 19.11A) and Kir2.1 channels (which mediate inward potassium currents) are implicated in potassium siphoning.[101,102] The channel proteins are localized in a polarized fashion in the Müller cell membrane (Fig. 19.11A). Homomeric Kir4.1 channels are mainly localized in membrane domains across which the cells extrude potassium into spaces outside the neuroretina, i.e., in perivascular and vitreal endfoot membranes, and in the microvilli that extend into the subretinal space (Figs. 19.3A, 19.11B and 19.13).[101,103] Membranes that abut neuronal cell structures contain predominantly Kir channels which mediate inward potassium currents, i.e., Kir2.1 (Figs. 19.3B and 19.11B) and heterotetrameric Kir4.1/Kir5.1 channels.[102,104] Thus, the direction of the transcellular potassium currents is determined by the subcellular localization of different Kir channel subtypes, while the local increases in extracellular potassium cause the driving force for the passive currents through the channels. Müller cells also express other types of potassium channels which may contribute to potassium buffering, including voltage-gated potassium (K_A, K_{DR}) channels, calcium-activated big-conductance potassium (BK) channels (Figs. 19.9G–I, 19.10C and 19.12D), and tandem-pore domain potassium channels. In addition, the Na^+, K^+-ATPase, and transporter molecules, e.g., the K/Na/2Cl cotransporter, contribute to the Müller cell-mediated potassium homeostasis (see reference 2 and references therein).

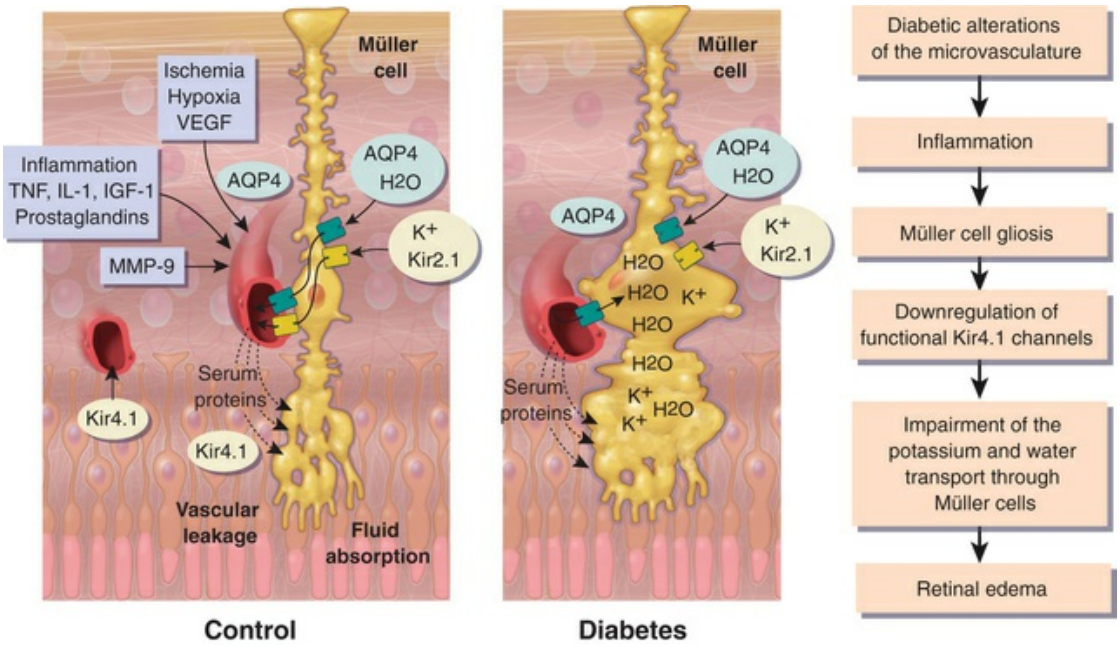

FIG. 19.13 Disruption of the Müller cell-mediated fluid clearance and (under conditions of osmotic imbalances) Müller cell swelling may contribute to the development of diabetic retinal edema. Retinal edema develops from an imbalance between the fluid influx into the retina mainly caused by vascular leakage and the fluid clearance from the retinal tissue mainly mediated by the water transport through Müller cells coupled to the potassium transport. In diabetic retinopathy, the major potassium channel of Müller cells (*Kir4.1*), which is predominantly expressed around the retinal vessels and at the inner limiting membrane, is downregulated. This disrupts the water transport through the cells which is facilitated by water channels (*AQP4*) and normally coupled to potassium currents through potassium channels (*Kir2.1*, *Kir4.1*). Accumulation of potassium within the cells increases the intracellular osmotic pressure, resulting in a water flux into the cells and cellular swelling.

Many of the homeostatic functions of Müller cells, including potassium siphoning and neurotransmitter uptake, depend on the very negative membrane potential constituted by Kir4.1 channels.[101] Kir4.1 channels are also involved in the cell volume regulation that compensates for changes in the osmotic conditions (see below). Under various pathologic conditions, Kir4.1 channels of Müller cells are downregulated and/or dislocated (Figs. 19.3A, 19.11B and 19.13)

resulting in a decrease of the potassium currents through Müller cells. Such alterations have been observed in animal models of various ischemic–hypoxic and inflammatory diseases including ischemia–reperfusion (Figs. 19.11C–D), ocular inflammation, diabetic retinopathy, blue light injury, retinal detachment (Figs. 19.3E and 19.10A), retinal vein occlusion, and proliferative vitreoretinopathy (Fig. 19.10A), as well as in Müller cells from patients with proliferative retinopathies (Figs. 19.12D, G).[2,105] The impaired transcellular potassium transport and the depolarization of the cells (Figs. 19.3E, 19.11D and 19.12G), which impairs the glutamate uptake, contribute to neuronal hyperexcitation and glutamate toxicity.[62] Human Müller cells display an age-dependent decrease of the Kir currents, on average by 50% between the ages of 40 and 80 years (Fig. 19.12E). This may enhance the susceptibility for age-related retinopathies.

Water Clearance

Water accumulates in the retinal tissue resulting from a water influx from the blood coupled to the glucose uptake, a water influx from the vitreous, and the metabolic water production by the oxidative degradation of glucose. The accumulation of metabolic water is especially abundant in the macular tissue which displays a high metabolic activity and a high density of cells. This generates the necessity of a substantial constitutive efflux of water out of the retina into the blood. In addition, the transmembrane ion shifts associated with neuronal activity (in particular, with ionotropic glutamatergic signaling) needs, for osmotical reasons, to be buffered by a rapid water transport across glial membranes.

The retinal water clearance is mediated by an osmotically driven transcellular water transport coupled to a transport of osmolytes, in particular, to potassium currents.[2,103] The Müller cell-mediated clearance of the retinal tissue from excess potassium will simultaneously redistribute metabolic water out of the neuroretina. The transmembrane water transport is facilitated by aquaporin-4 water channels which are mainly localized in glial membranes in the inner retina and the outer plexiform layer (Fig. 19.3A).[2,103] In Müller cell membranes that contact fluid-filled spaces outside the

neuroretina, aquaporin-4 and Kir4.1 channels are colocalized (Fig. 19.3A).[103] This suggests that osmotic gradients between the neuroretina on the one hand and the blood, vitreal fluid, and subretinal fluid on the other hand are compensated by a bidirectional potassium and water flux across Müller cell membranes. Müller cells also express aquaporin-4 in the perisynaptic membranes within the plexiform layers (Fig. 19.3A). Because the plexiform layers are high-resistance barriers for the paracellular fluid movement,[106] any water flowing into neurons (associated with the ion flux) will be delivered from Müller cells through aquaporin-4.[2] Aquaporin-4 knockout mice display reduced electroretinogram b-waves,[107] suggesting that the Müller cell-mediated water transport is implicated in the maintenance of the regular neuronal activity. Ischemia-reperfusion results in a decreased thickness of the inner retina (Fig. 19.11B) due to a neuronal degeneration mainly caused by reactive oxygen radicals and glutamate toxicity.[108] Deletion of aquaporin-4 in mice protects against ischemic injury of the retina,[109] suggesting that Müller cell-mediated water transport is implicated in the pathomechanisms of neuronal cell death after ischemia.

Contribution to Edema Development and Resolution

Dysfunctional Müller cells may contribute to the development of retinal edema. Edema is characterized by a thickening of the retinal tissue due to extra- and/or intracellular water accumulation. Extracellular edema is caused by vascular leakage in association with a dysfunctional glial water clearance. Retinal capillaries are closely ensheathed by glial processes. Usually, Müller cells enhance the barrier function of vascular endothelia by the secretion of factors such as PEDF, thrombospondin-1, and GDNF.[110–112] However, in response to hypoxia, inflammation, or glucose-deprivation, Müller cells produce factors such as VEGF and TNF that increase the vascular permeability.[111,113,114] Müller cells are also a source of MMPs[33,114] which degrade the tight junction protein, occludin.[115]

Intracellular water accumulation may result in cellular swelling.

While neuronal cell swelling is observed early after ischemia–hypoxia, and is mainly caused by overexcitation of ionotropic receptors (Figs. 19.14A–B),[108] Müller cell edema occurs within days after hypoxia.[116] Müller cells release glutamate[67,68] and ATP,[117] e.g., during mechanical stress; Müller cell-derived glutamate (acting at ionotropic glutamate receptors) and ATP (acting at ionotropic $P2X_7$ receptors) may contribute to the swelling and degeneration of retinal ganglion cells, e.g., in glaucoma.[2,118,119] Because the water transport through Müller cells is coupled to potassium currents,[103] the downregulation or functional inactivation of Kir4.1 channels observed under pathologic conditions (Figs. 19.3A, E, 19.10A, 19.11B, 19.12D, G and 19.13) will also disturb the transcellular water transport. Indeed, Müller cell bodies in slices of diseased retinas swell upon hypoosmotic challenge which is not observed in control tissues (Figs. 19.3F–G and 19.11E). In the absence of functional Kir4.1 channels, the cells are not capable of rapidly releasing potassium and thus to compensate the osmotic gradient between the Müller cell interior and the hypoosmotic environment. This results in a water influx and cellular swelling. Because Müller cells are still capable of taking up excess potassium from the extracellular space through Kir2.1 channels which are not altered in their expression (Figs. 19.3B and 19.11B), the impairment in the release of potassium from Müller cells will result in a potassium accumulation within the cells which increases the intracellular osmotic pressure.[105] The increased osmotic pressure draws water from fluid-filled spaces outside the neuroretina (blood, vitreous) into the perivascular and endfeet regions of Müller cells, resulting in Müller cell edema. The water influx from the blood and vitreous is supported by aquaporin-4 water channels which are not altered, or even increased, in their expression (Fig. 19.3A).[116] Thus, dysfunctional glial water clearance and possibly Müller cell swelling, may contribute to the development of edema (Fig. 19.13).

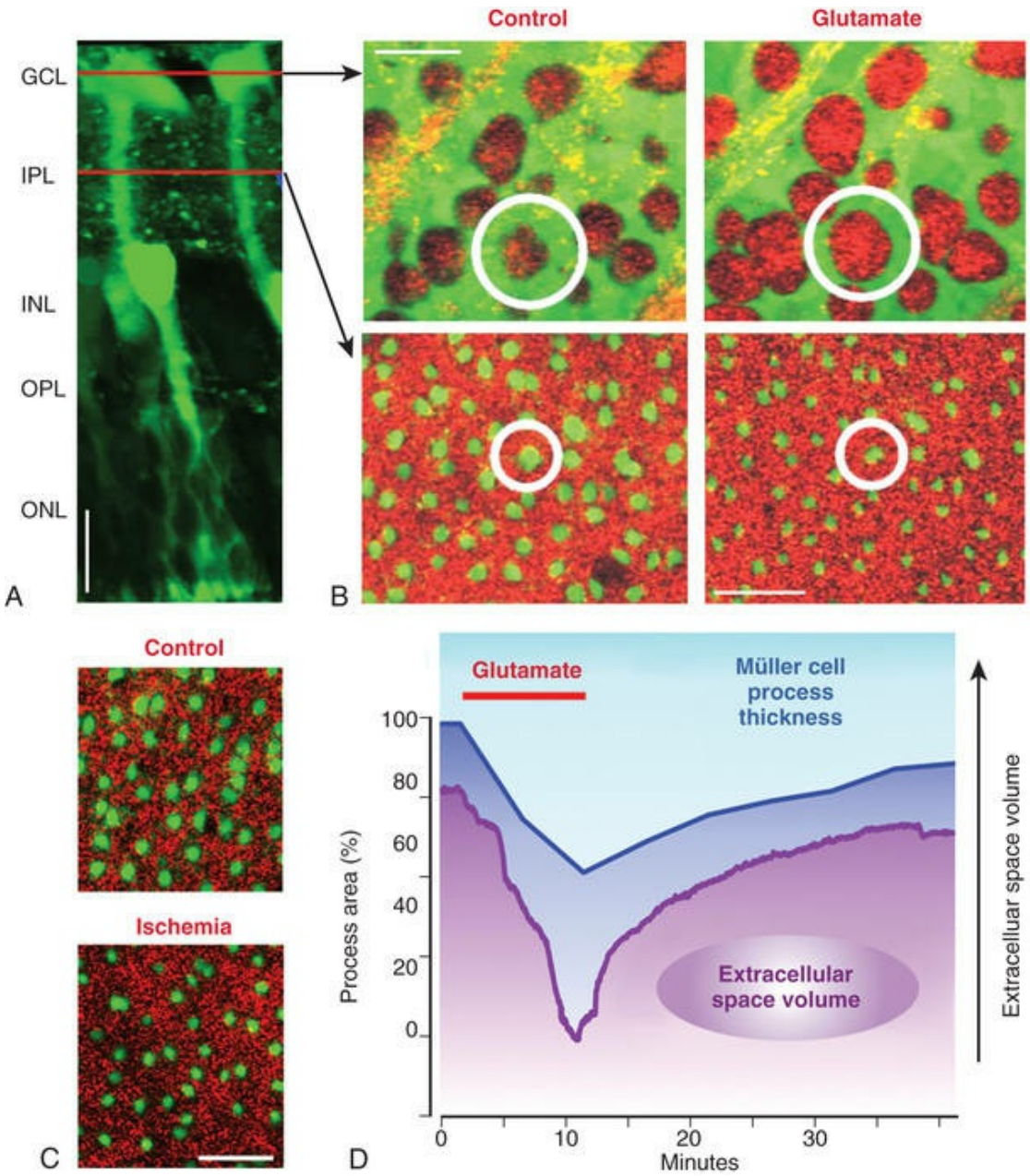

FIG. 19.14 Glutamate and ischemia induce morphological alterations of neurons and Müller cells in the guinea pig retina. (A) The retinal slice displays Müller cells and the optical planes in the ganglion cell layer (*GCL*) and inner plexiform layer (*IPL*) which were used to record the morphological alterations of the cells. Müller cells are selectively green stained, while neuronal structures are dark. (B) The retinal wholemount was exposed to glutamate (1 mM) for 10 min. Above: Glutamate exposure results in a swelling of the neuronal cell bodies in the GCL (red). The elongated structures are nerve fiber bundles. Below: Glutamate causes a reduction in the thickness of

Müller cell stem processes that traverse the IPL (green) resulting from a swelling of the synapses between the Müller cell processes (red). (C) A decrease of the thickness of Müller cell processes (and an increase in the size of neuronal cell bodies; not shown) was also observed shortly after a 1-h ischemia of the retina. (D) Glutamate (1 mM) induces a decrease of the extracellular space volume in the IPL. This is associated with a decrease of the cross-sectional area of Müller cell processes that traverse the IPL. *INL*, inner nuclear layer; *ONL*, outer nuclear layer; *OPL*, outer plexiform layer. Scale bars: 20 μm.

Neurovascular Coupling

In order to meet the extremely high metabolic demands and oxygen consumption of the retina,[88] the ability to regulate the local blood flow is critical for retinal function.[120] Light stimulation induces functional hyperemia via dilation of retinal arterioles.[120] Purinergic neuron-to-glia signaling and glial calcium waves are involved in the activity-dependent regulation of the blood flow rate in the superficial vascular plexus in dependence on the synaptic activity in the inner plexiform layer.[120] In response to light, retinal neurons release ATP in the inner plexiform layer which induces calcium responses in Müller cells (Figs. 19.3D and 19.9F).[121] The blood flow-regulatory signals transmit to the inner surface of the retina (where arterioles are localized) via propagation of ATP-mediated[117] calcium waves in Müller cells and astrocytes.[121,122] Calcium responses activate phospholipases A_2 in glial cells resulting in the production of arachidonic acid metabolites that cause dilation (epoxyeicosatrienoic acids and prostaglandins) or constriction (20-hydroxyeicosatetraenoic acid) of arterioles.[121] Whether vasodilating or vasoconstricting responses are produced by glial cells is dependent on the production of NO; increased NO reduces vasodilation.[121,123] ATP and adenosine released from neurons and/or glial cells[124] induce constriction (Fig. 19.10E) and relaxation, respectively, of arteriolar vascular smooth muscle cells and capillary-surrounding pericytes.[125,126] It was shown that the functional hyperemia is dramatically reduced in the retina of

diabetic patients, possibly resulting in retinal hypoxia that contributes to the development of diabetic retinopathy.[127] The glia-induced vasodilation is reduced early in experimental diabetic retinopathy, likely resulting from an overproduction of NO which alters the glia-to-vessel signaling.[123] Because activation of purinergic receptors on retinal glial cells induces glial calcium waves that lead to vasodilation,[120] it is conceivable but remains to be proven that the increase in the glial calcium responsiveness observed under pathologic conditions (Figs. 19.3D and 19.10A–B, D) may contribute to the impaired neurovascular coupling in the diabetic retina.

Regulation of the Extracellular Space Volume

The ion flux into activated neurons is (for osmotic reasons) coupled to a water flux which may result in a swelling of neuronal cell bodies and synapses (Fig. 19.14B), and thus in a decrease of the extracellular space volume (Fig. 19.14D).[2] The ion flux into neurons also decreases the osmolarity of the extracellular fluid.[128] In order to avoid detrimental decreases in the extracellular space volume (which otherwise will cause neuronal hyperexcitation), Müller cells inhibit a swelling of their cell bodies even when the extracellular fluid becomes hypoosmotic, which normally favors a water influx (Figs. 19.3F and 19.11E). In addition, Müller cells elongate and reduce the thickness of their inner stem processes (Figs. 19.14B–D).[2] The rapid, activity-dependent alterations in cell shape are supported by the viscoelastic properties of Müller cells (see below).

To regulate the cellular volume, Müller cells possess a purinergic signaling mechanism that is triggered by glutamate released from neurons or Müller cells.[2] The final step of this autocrine cascade is the release of adenosine from Müller cells, which activates adenosine A_1 receptors resulting in the opening of potassium and chloride channels. The ion efflux compensates the osmotic gradient across the Müller cell membrane and thus prevents cellular swelling. This mechanism may also accelerate the clearance of excess fluid from the retina through Müller cells.[2] The antiinflammatory corticosteroid triamcinolone acetonide, which is clinically used to rapidly clear retinal edema, was shown to inhibit

the osmotic swelling of Müller cells (Fig. 19.11E), via inducing a release of endogenous adenosine.[129] The adenosine-induced opening of ion channels may reestablish the ion and water transport through Müller cells under conditions when the Kir4.1 channels are inactivated, and may thus support the resolution of extra- and intracellular edema.

Responses to Mechanical Stress

The activity-depending reshaping of Müller cell processes (Figs. 19.14B–D) is supported by the viscoelastic properties of the cells. Müller cells are softer than neurons; in particular, the processes within the plexiform layers are very soft.[130] Because growing neurites prefer soft substrates,[131] soft glial processes may support the growth of neuronal processes implicated in the synaptic plasticity.[130] Müller cell gliosis is associated with an increase of the cell stiffness mainly resulting from the upregulation of intermediate filaments like GFAP (Figs. 19.2A and 19.3A); this will inhibit the neurite growth and might be one reason for the aberrant tissue repair after retinal injury.[132] The increased stiffness of gliotic Müller cells may also be responsible for the fact that, in retinal neovascularization, new blood vessels grow towards the vitreous rather than within the retinal tissue.[133]

Müller cells sense mechanical deformations of the retina by calcium-dependent mechanisms. Stretching of the retinal tissue induces calcium responses and upregulation of bFGF in Müller cells.[134] This may have implications for postnatal eye growth. Because bFGF counteracts the development of form deprivation-induced axial myopia,[135] Müller cell-derived bFGF may prevent retinal overstretching and the development of myopia during ocular growth.[134] Stretch-induced Müller cell responses may also be implicated in epiretinal membrane formation. Vitreous fibers, which adhere to Müller cell endfeet at sites of vitreoretinal attachments, exert tractional forces onto the cells; this activates Müller cells and results in cellular hypertrophy and proliferation, as well as vascular leakage.[136] Mechanically stressed Müller cells release growth factors (e.g., bFGF) and ATP.[117,134] Calcium influx (through stretch-activated and/or voltage-gated channels;

Figs.19.12E–F) and activation of BK channels (Figs. 19.9G, I and 19.10C–D) are required for the growth factor- and ATP-induced proliferation of Müller cells.[2,137] An increased expression of calcium-permeable $P2X_7$ receptors (Fig. 19.10D), which induce upon activation opening of BK channels (Fig. 19.10C), are a characteristic of proliferating Müller cells in PVR.[2]

Müller Cell Gliosis

Müller cells become activated in response to virtually every pathologic stimulus (see reference 2 and references therein). Reactive gliosis is thought to represent a cellular attempt to protect the tissue from further damage, to promote tissue repair, and to limit tissue remodeling. An upregulation of intermediate filaments like GFAP in glial cells (Fig. 19.3A) is a very sensitive and early "retinal stress" indicator.[2,138] Müller cell gliosis has both neuroprotective and neurotoxic effects (see reference 2 and references therein). Particularly under conditions of massive (proliferative) gliosis (Fig. 19.12A), the regular glial-neuronal interactions are disrupted and the retina degenerates (Figs. 19.12B–C). An inverse relation between Müller cell proliferation and the expression of neuron-glia symbiosis-mediating proteins has been observed. However, also in the case of "conservative" gliosis (associated with short-term, or low-level, Müller cell proliferation), a dysfunction of Müller cells may contribute to neurodegeneration. After retinal detachment, for example, the downregulation of cellular retinal binding protein and glutamine synthetase[139] disrupts glioneuronal interactions involved in photopigment and neurotransmitter recycling. The downregulation of carbonic anhydrases[139] and Kir channels (Figs. 19.3A, E, 19.10A, 19.11B–D and 19.12D, G)[2] results in disturbances of the retinal acid–base, potassium, and water homeostasis. Because the electrogenic uptake carriers are voltage-dependent (Fig. 19.9A), membrane depolarization (Figs. 19.3E, 19.11D and 19.12G) reduces the efficiency of the glial neurotransmitter recycling which, together with an increase in extracellular potassium, will aggravate neurotoxicity. Because the potassium currents of Müller cells are also a major driving force for the water transport through the cells,

downregulation of functional Kir channels also impairs retinal water homeostasis, contributing to the development of edema (Fig. 19.13).

Inflammatory responses of reactive Müller cells may contribute to retinal degeneration. After retinal detachment, Müller cells upregulate inflammatory factors like MCP-1 which recruit phagocytotic monocytes/macrophages and microglial cells to the injured area (Fig. 19.2A).[9,140] Blood-derived monocytes/macrophages and neutrophils release oxygen-free radicals and cytotoxic cytokines which play critical roles in photoreceptor apoptosis after retinal detachment and neuronal degeneration after ischemia–reperfusion, for example.[141,142] Mice deficient in vimentin and GFAP display attenuated detachment-induced glial cell responses (e.g., a lowered expression of MCP-1) and, as a consequence, a decrease in monocyte infiltration and photoreceptor apoptosis.[143]

Contrariwise, reactive Müller cells may also protect photoreceptors and neurons from cell death by various mechanisms, including the secretion of neurotrophic factors, in particular bFGF, which enhance the neuronal survival.[2,79,144] GDNF produced by photoreceptor and glial cells protects photoreceptors and ganglion cells from apoptosis through upregulation of the glial glutamate transporter GLAST.[145,146] Retinal preconditioning with bright light or mechanical stress protects photoreceptors from apoptosis because these stimuli induce an upregulation of bFGF and CNTF in Müller cells.[78,144] Likewise, argon laser photocoagulation slows photoreceptor degeneration by the induction of bFGF in Müller cells.[147]

Müller Stem Cells

As a precondition for proliferation and migration, Müller cells reactivate distinct cellular programs normally used during ontogenetic development. In the injured retina, a subpopulation of Müller cells dedifferentiates to cells with properties similar to pluripotent retinal progenitor/stem cells, and may even express distinct neuronal and photoreceptor markers.[148,149] The decrease of the Kir currents (Figs. 19.12D, G) and the increase of voltage-gated

sodium currents (Figs. 19.12D, H) observed in Müller cells from patients with proliferative retinopathies[70] may reflect such a transdifferentiation of the cells. However, the neuron-regenerating capability of mammalian Müller cells in situ is very restricted. Attempts to facilitate the neurogenic program of Müller cells, e.g., by transdifferentiation of cultured Müller cells, are ongoing.[149,150] The tedious progress of this approach underlines the general issue that a better understanding of the gliotic mechanisms is essential for the development of efficient therapeutic strategies which increase the protective and regenerative, and decrease the destructive, roles of reactive Müller cells.

References

1. Reichenbach A, Bringmann A. *Müller cells in the healthy and diseased retina*. Springer: New York; 2010.
2. Reichenbach A, Bringmann A. Retinal glia. Verkhratsky A, Parpura V. *Colloquium series on neuroglia in biology and medicine: from physiology to disease*. Morgan & Claypool Life Sciences: Philadelphia; 2015.
3. Fontainhas AM, Wang M, Liang KJ, et al. Microglial morphology and dynamic behavior is regulated by ionotropic glutamatergic and GABAergic neurotransmission. *PLoS ONE*. 2011;6:e15973.
4. Langmann T. Microglia activation in retinal degeneration. *J Leukoc Biol*. 2007;81:1345–1351.
5. Buschini E, Piras A, Nuzzi R, et al. Age related macular degeneration and drusen: neuroinflammation in the retina. *Prog Neurobiol*. 2011;95:14–25.
6. Forrester JV, Xu H, Kuffová L, et al. Dendritic cell physiology and function in the eye. *Immunol Rev*. 2010;234:282–304.
7. D'Orazio TJ, Niederkorn JY. A novel role for TGF-β and IL-10 in the induction of immune privilege. *J Immunol*. 1998;160:2089–2098.
8. Ng TF, Turpie B, Masli S. Thrombospondin-1-mediated regulation of microglia activation after retinal injury. *Invest Ophthalmol Vis Sci*. 2009;50:5472–5478.

9. Hollborn M, Francke M, Iandiev I, et al. Early activation of inflammation- and immune response-related genes after experimental detachment of the porcine retina. *Invest Ophthalmol Vis Sci*. 2008;49:1262–1273.
10. Chen M, Zhao J, Luo C, et al. Para-inflammation-mediated retinal recruitment of bone marrow-derived myeloid cells following whole-body irradiation is CCL2 dependent. *Glia*. 2012;60:833–842.
11. Kohno H, Maeda T, Perusek L, et al. CCL3 production by microglial cells modulates disease severity in murine models of retinal degeneration. *J Immunol*. 2014;192:3816–3827.
12. Howell GR, Macalinao DG, Sousa GL, et al. Molecular clustering identifies complement and endothelin induction as early events in a mouse model of glaucoma. *J Clin Invest*. 2011;121:1429–1444.
13. Sasahara M, Otani A, Oishi A, et al. Activation of bone marrow-derived microglia promotes photoreceptor survival in inherited retinal degeneration. *Am J Pathol*. 2008;172:1693–1703.
14. Wang NK, Lai CC, Liu CH, et al. Origin of fundus hyperautofluorescent spots and their role in retinal degeneration in a mouse model of Goldmann–Favre syndrome. *Dis Model Mech*. 2013;6:1113–1122.
15. Ma N, Streilein JW. T cell immunity induced by allogeneic microglia in relation to neuronal retina transplantation. *J Immunol*. 1999;162:4482–4489.
16. Wang M, Wang X, Zhao L, et al. Macroglia–microglia interactions via TSPO signaling regulates microglial activation in the mouse retina. *J Neurosci*. 2014;34:3793–3806.
17. Ma W, Cojocaru R, Gotoh N, et al. Gene expression changes in aging retinal microglia: relationship to microglial support functions and regulation of activation. *Neurobiol Aging*. 2013;34:2310–2321.
18. Chan-Ling T, Hughes S, Baxter L, et al. Inflammation and breakdown of the blood–retinal barrier during "physiological aging" in the rat retina: a model for CNS aging. *Microcirculation*. 2007;14:63–76.

19. Xu H, Chen M, Forrester JV. Para-inflammation in the aging retina. *Prog Retin Eye Res*. 2009;28:348–368.
20. Raoul W, Keller N, Rodéro M, et al. Role of the chemokine receptor CX3CR1 in the mobilization of phagocytic retinal microglial cells. *J Neuroimmunol*. 2008;198:56–61.
21. Cukras CA, Petrou P, Chew EY, et al. Oral minocycline for the treatment of diabetic macular edema (DME): results of a phase I/II clinical study. *Invest Ophthalmol Vis Sci*. 2012;53:3865–3874.
22. Barker AJ, Koch SM, Reed J, et al. Developmental control of synaptic receptivity. *J Neurosci*. 2008;28:8150–8160.
23. Lorber B, Berry M, Douglas MR, et al. Activated retinal glia promote neurite outgrowth of retinal ganglion cells via apolipoprotein E. *J Neurosci Res*. 2009;87:2645–2652.
24. Steinbach K, Bauch H, Stier H, et al. Tissue-specific neuro-glia interactions determine neurite differentiation in ganglion cells. *Eur J Cell Biol*. 2001;80:245–255.
25. Ramírez JM, Ramírez AI, Salazar JJ, et al. of astrocytes in retinal ageing and age-related macular degeneration. *Exp Eye Res*. 2001;73:601–615.
26. Mansour H, Chamberlain CG, Weible MW 2nd, et al. Aging-related changes in astrocytes in the rat retina: imbalance between cell proliferation and cell death reduces astrocyte availability. *Aging Cell*. 2008;7:526–540.
27. Takahashi Y, Katai N, Murata T, et al. Development of spontaneous optic neuropathy in NF-κBp50-deficient mice: requirement for NF-κBp50 in ganglion cell survival. *Neuropathol Appl Neurobiol*. 2007;33:692–705.
28. Ganesh BS, Chintala SK. Inhibition of reactive gliosis attenuates excitotoxicity-mediated death of retinal ganglion cells. *PLoS ONE*. 2011;6:e18305.
29. Calandrella N, Scarsella G, Pescosolido N, et al. Degenerative and apoptotic events at retinal and optic nerve level after experimental induction of ocular hypertension. *Mol Cell Biochem*. 2007;301:155–163.
30. Fitzgerald M, Bartlett CA, Harvey AR, et al. Early events of secondary degeneration after partial optic nerve transection: an immunohistochemical study. *J Neurotrauma*.

2010;27:439–452.
31. Dvoriantchikova G, Barakat D, Brambilla R, et al. Inactivation of astroglial NF-κB promotes survival of retinal neurons following ischemic injury. *Eur J Neurosci*. 2009;30:175–185.
32. Ly A, Yee P, Vessey KA, et al. Early inner retinal astrocyte dysfunction during diabetes and development of hypoxia, retinal stress, and neuronal functional loss. *Invest Ophthalmol Vis Sci*. 2011;52:9316–9326.
33. Behzadian MA, Wang XL, Windsor LJ, et al. TGF-β increases retinal endothelial cell permeability by increasing MMP-9: possible role of glial cells in endothelial barrier function. *Invest Ophthalmol Vis Sci*. 2001;42:853–859.
34. Rollín R, Mediero A, Fernández-Cruz A, et al. Downregulation of the atrial natriuretic peptide/natriuretic peptide receptor-C system in the early stages of diabetic retinopathy in the rat. *Mol Vis*. 2005;11:216–224.
35. Jiang G, Ke Y, Sun D, et al. Reactivation of uveitogenic T cells by retinal astrocytes derived from experimental autoimmune uveitis-prone B10RIII mice. *Invest Ophthalmol Vis Sci*. 2008;49:282–289.
36. Jiang G, Sun D, Kaplan HJ, et al. Retinal astrocytes pretreated with NOD2 and TLR2 ligands activate uveitogenic T cells. *PLoS ONE*. 2012;7:e40510.
37. Ke Y, Jiang G, Sun D, et al. Retinal astrocytes respond to IL-17 differently than retinal pigment epithelial cells. *J Leukoc Biol*. 2009;86:1377–1384.
38. Berry M, Ahmed Z, Lorber B, et al. Regeneration of axons in the visual system. *Restor Neurol Neurosci*. 2008;26:147–174.
39. Reichenbach A, Robinson SR. Phylogenetic constraints on retinal organization and development: an Haeckelian perspective. *Prog Retin Eye Res*. 1995;15:139–171.
40. Franze K, Grosche J, Skatchkov SN, et al. Müller cells are living optical fibers in the vertebrate retina. *Proc Natl Acad Sci USA*. 2007;104:8287–8292.
41. Muniz A, Villazana-Espinoza ET, Hatch AL, et al. A novel cone visual cycle in the cone-dominated retina. *Exp Eye Res*. 2007;85:175–184.

42. Long KO, Fisher SK, Fariss RN, et al. Disc shedding and autophagy in the cone-dominant ground squirrel retina. *Exp Eye Res*. 1986;43:193–205.
43. Jablonski MM, Iannaccone A. Targeted disruption of Müller cell metabolism induces photoreceptor dysmorphogenesis. *Glia*. 2000;32:192–204.
44. Rauen T, Rothstein JD, Wässle H. Differential expression of three glutamate transporter subtypes in the rat retina. *Cell Tissue Res*. 1996;286:325–336.
45. Rauen T, Taylor WR, Kuhlbrodt K, et al. High-affinity glutamate transporters in the rat retina: a major role of the glial glutamate transporter GLAST-1 in transmitter clearance. *Cell Tissue Res*. 1998;291:19–31.
46. Kugler P, Beyer A. Expression of glutamate transporters in human and rat retina and rat optic nerve. *Histochem Cell Biol*. 2003;120:199–212.
47. Ward MM, Jobling AI, Kalloniatis M, et al. Glutamate uptake in retinal glial cells during diabetes. *Diabetologia*. 2005;48:351–360.
48. Barbour B, Brew H, Attwell D. Electrogenic glutamate uptake in glial cells is activated by intracellular potassium. *Nature*. 1988;335:433–435.
49. Brew H, Attwell D. Electrogenic glutamate uptake is a major current carrier in the membrane of axolotl retinal glial cells. *Nature*. 1987;327:707–709.
50. Marc RE. Structural organization of GABAergic circuitry in ectotherm retinas. *Prog Brain Res*. 1992;90:61–92.
51. Hasegawa J, Obara T, Tanaka K, et al. High-density presynaptic transporters are required for glutamate removal from the first visual synapse. *Neuron*. 2006;50:63–74.
52. Matsui K, Hosoi N, Tachibana M. Active role of glutamate uptake in the synaptic transmission from retinal nonspiking neurons. *J Neurosci*. 1999;19:6755–6766.
53. Higgs MH, Lukasiewicz PD. Glutamate uptake limits synaptic excitation of retinal ganglion cells. *J Neurosci*. 2002;19:3691–3700.
54. Pow DV, Barnett NL, Penfold P. Are neuronal transporters

relevant in retinal glutamate homeostasis? *Neurochem Int*. 2000;37:191–198.
55. Naskar R, Vorwerk CK, Dreyer EB. Concurrent downregulation of a glutamate transporter and receptor in glaucoma. *Invest Ophthalmol Vis Sci*. 2000;41:1940–1944.
56. Barnett NL, Pow DV, Bull ND. Differential perturbation of neuronal and glial glutamate transport systems in retinal ischaemia. *Neurochem Int*. 2001;39:291–299.
57. Holcombe DJ, Lengefeld N, Gole GA, et al. The effects of acute intraocular pressure elevation on rat retinal glutamate transport. *Acta Ophthalmol Scand*. 2008;86:408–414.
58. Muller A, Maurin L, Bonne C. Free radicals and glutamate uptake in the retina. *Gen Pharmacol*. 1998;30:315–318.
59. Li Q, Puro DG. Diabetes-induced dysfunction of the glutamate transporter in retinal Muller cells. *Invest Ophthalmol Vis Sci*. 2002;43:3109–3116.
60. Beretta S, Wood JP, Derham B, et al. Partial mitochondrial complex I inhibition induces oxidative damage and perturbs glutamate transport in primary retinal cultures: relevance to Leber hereditary optic neuropathy (LHON). *Neurobiol Dis*. 2006;24:308–317.
61. Barbour B, Szatkowski M, Ingledew N, et al. Arachidonic acid induces a prolonged inhibition of glutamate uptake into glial cells. *Nature*. 1989;342:918–920.
62. Napper GA, Pianta MJ, Kalloniatis M. Reduced glutamate uptake by retinal glial cells under ischemic/hypoxic conditions. *Vis Neurosci*. 1999;16:149–158.
63. Szatkowski M, Barbour B, Attwell D. Non-vesicular release of glutamate from glial cells by reversed electrogenic glutamate uptake. *Nature*. 1990;348:443–446.
64. Maguire G, Simko H, Weinreb RN, et al. Transport-mediated release of endogenous glutamate in the vertebrate retina. *Pflügers Arch*. 1998;436:481–484.
65. Marcaggi P, Hirji N, Attwell D. Release of L-aspartate by reversal of glutamate transporters. *Neuropharmacology*. 2005;49:843–849.
66. Kato S, Ishita S, Sugawara K, et al. Cystine/glutamate antiporter expression in retinal Müller glial cells:

implications for DL-α-aminoadipate toxicity. *Neuroscience*. 1993;57:473–482.
67. Linnertz R, Wurm A, Pannicke T, et al. Activation of voltage-gated Na^+ and Ca^{2+} channels is required for vesicular release of glutamate from retinal glial cells implicated in cell volume regulation. *Neuroscience*. 2011;188:23–34.
68. Slezak M, Grosche A, Niemiec A, et al. Relevance of exocytotic glutamate release from retinal glia. *Neuron*. 2012;74:504–516.
69. Otori Y, Shimada S, Tanaka K, et al. Marked increase in glutamate-aspartate transporter (GLAST/GluT-1) mRNA following transient retinal ischemia. *Mol Brain Res*. 1994;27:310–314.
70. Reichelt W, Pannicke T, Biedermann B, et al. Comparison between functional characteristics of healthy and pathological human retinal Müller glial cells. *Surv Ophthalmol*. 1997;42:S105–17.
71. Riepe RE, Norenburg MD. Müller cell localisation of glutamine synthetase in rat retina. *Nature*. 1977;268:654–655.
72. Pow DV, Crook DK. Direct immunocytochemical evidence for the transfer of glutamine from glial cells to neurons: use of specific antibodies directed against the D-stereoisomers of glutamate and glutamine. *Neuroscience*. 1996;70:295–302.
73. Pow DV, Robinson SR. Glutamate in some retinal neurons is derived solely from glia. *Neuroscience*. 1994;60:355–366.
74. Fletcher EL, Kalloniatis M. Neurochemical architecture of the normal and degenerating rat retina. *J Comp Neurol*. 1996;376:343–360.
75. Marc RE, Murry RF, Fisher SK, et al. Amino acid signatures in the detached cat retina. *Invest Ophthalmol Vis Sci*. 1998;39:1694–1702.
76. Kruchkova Y, Ben-Dror I, Herschkovitz A, et al. Basic fibroblast growth factor: a potential inhibitor of glutamine synthetase expression in injured neural tissue. *J Neurochem*. 2001;77:1641–1649.
77. Faktorovich EG, Steinberg RH, Yasumura D, et al. Photoreceptor degeneration in inherited retinal dystrophy

delayed by basic fibroblast growth factor. *Nature*. 1990;347:83–86.
78. Liu C, Peng M, Laties AM, et al. Preconditioning with bright light evokes a protective response against light damage in the rat retina. *J Neurosci*. 1998;18:1337–1344.
79. Harada T, Harada C, Nakayama N, et al. Modification of glial-neuronal cell interactions prevents photoreceptor apoptosis during light-induced retinal degeneration. *Neuron*. 2000;26:533–541.
80. Poitry S, Poitry-Yamate C, Ueberfeld J, et al. Mechanisms of glutamate metabolic signaling in retinal glial (Müller) cells. *J Neurosci*. 2000;20:1809–1821.
81. Poitry-Yamate CL, Poitry S, Tsacopoulos M. Lactate released by Müller glial cells is metabolized by photoreceptors from mammalian retina. *J Neurosci*. 1995;15:5179–5191.
82. Pow DV, Crook DK. Immunocytochemical evidence for the presence of high levels of reduced glutathione in radial glial cells and horizontal cells in the rabbit retina. *Neurosci Lett*. 1995;193:25–28.
83. Linsenmeier RA. Effects of light and darkness on oxygen distribution and consumption in the cat retina. *J Gen Physiol*. 1986;88:521–542.
84. Schütte M, Werner P. Redistribution of glutathione in the ischemic rat retina. *Neurosci Lett*. 1998;246:53–56.
85. Paasche G, Gärtner U, Germer A, et al. Mitochondria of retinal Müller (glial) cells: the effects of aging and of application of free radical scavengers. *Ophthalmic Res*. 2000;32:229–236.
86. Kern TS, Kowluru RA, Engerman RL. Abnormalities of retinal metabolism in diabetes or galactosemia: ATPases and glutathione. *Invest Ophthalmol Vis Sci*. 1994;35:2962–2967.
87. Shelton MD, Kern TS, Mieyal JJ. Glutaredoxin regulates nuclear factor κ-B and intercellular adhesion molecule in Müller cells: model of diabetic retinopathy. *J Biol Chem*. 2007;282:12467–12474.
88. Warburg O. Über die Klassifizierung tierischer Gewebe nach ihrem Stoffwechsel. *Biochem Z*. 1928;184:484–488.

89. Oakley B, Wen R. Extracellular pH in the isolated retina of the toad in darkness and during illumination. *J Physiol*. 1989;419:353–378.
90. Linser PJ, Moscona AA. Carbonic anhydrase-C in the neural retina: transition from generalized to glia-specific cell localization during embryonic development. *Proc Natl Acad Sci USA*. 1981;78:7190–7194.
91. Nagelhus EA, Mathiisen TM, Bateman AC, et al. Carbonic anhydrase XIV is enriched in specific membrane domains of retinal pigment epithelium, Müller cells, and astrocytes. *Proc Natl Acad Sci USA*. 2005;102:8030–8035.
92. Newman EA. A physiological measure of carbonic anhydrase in Müller cells. *Glia*. 1994;11:291–299.
93. Borgula GA, Karwoski CJ, Steinberg RH. Light-evoked changes in extracellular pH in frog retina. *Vision Res*. 1989;29:1069–1077.
94. DeVries SH. Exocytosed protons feedback to suppress the Ca^{2+} current in mammalian cone photoreceptors. *Neuron*. 2001;32:1107–1117.
95. Newman EA. Acid efflux from retinal glial cells generated by sodium bicarbonate cotransport. *J Neurosci*. 1996;16:159–168.
96. Barnes S, Merchant V, Mahmud F. Modulation of transmission gain by protons at the photoreceptor output synapse. *Proc Natl Acad Sci USA*. 1993;90:10081–10085.
97. Steinberg RH, Oakley B II, Niemeyer G. Light-evoked changes in $[K^+]_0$ in retina of intact cat eye. *J Neurophysiol*. 1980;44:897–921.
98. Karwoski CJ, Lu HK, Newman EA. Spatial buffering of light-evoked potassium increases by retinal Müller (glial) cells. *Science*. 1989;244:578–580.
99. Newman EA. Regional specialization of retinal glial cell membrane. *Nature*. 1984;309:155–157.
100. Newman EA. Inward-rectifying potassium channels in retinal glial (Müller) cells. *J Neurosci*. 1993;13:3333–3345.
101. Kofuji P, Ceelen P, Zahs KR, et al. Genetic inactivation of an inwardly rectifying potassium channel (Kir4.1 subunit) in mice: phenotypic impact in retina. *J Neurosci*. 2000;20:5733–

5740.
102. Kofuji P, Biedermann B, Siddharthan V, et al. Kir potassium channel subunit expression in retinal glial cells: implications for spatial potassium buffering. *Glia*. 2002;39:292–303.
103. Nagelhus EA, Horio Y, Inanobe A, et al. Immunogold evidence suggests that coupling of K^+ siphoning and water transport in rat retinal Müller cells is mediated by a coenrichment of Kir4.1 and AQP4 in specific membrane domains. *Glia*. 1999;26:47–54.
104. Ishii M, Fujita A, Iwai K, et al. Differential expression and distribution of Kir5.1 and Kir4.1 inwardly rectifying K^+ channels in retina. *Am J Physiol*. 2003;285:C260–7.
105. Pannicke T, Iandiev I, Uckermann O, et al. A potassium channel-linked mechanism of glial cell swelling in the postischemic retina. *Mol Cell Neurosci*. 2004;26:493–502.
106. Antcliff RJ, Hussain AA, Marshall J. Hydraulic conductivity of fixed retinal tissue after sequential excimer laser ablation: barriers limiting fluid distribution and implications for cystoid macular edema. *Arch Ophthalmol*. 2001;119:539–544.
107. Li J, Patil RV, Verkman AS. Mildly abnormal retinal function in transgenic mice without Müller cell aquaporin-4 water channels. *Invest Ophthalmol Vis Sci*. 2002;43:573–579.
108. Osborne NN, Casson RJ, Wood JP, et al. Retinal ischemia: mechanisms of damage and potential therapeutic strategies. *Prog Retin Eye Res*. 2004;23:91–147.
109. Da T, Verkman AS. Aquaporin-4 gene disruption in mice protects against impaired retinal function and cell death after ischemia. *Invest Ophthalmol Vis Sci*. 2004;45:4477–4483.
110. Tout S, Chan-Ling T, Hollander H, et al. The role of Müller cells in the formation of the blood–retinal barrier. *Neuroscience*. 1993;55:291–301.
111. Eichler W, Yafai Y, Wiedemann P, et al. Angiogenesis-related factors derived from retinal glial (Müller) cells in hypoxia. *Neuroreport*. 2004;15:1633–1637.
112. Nishikiori N, Osanai M, Chiba H, et al. Glial cell-derived cytokines attenuate the breakdown of vascular integrity in diabetic retinopathy. *Diabetes*. 2007;56:1333–1340.

113. Aiello LP, Northrup JM, Keyt BA, et al. Hypoxic regulation of vascular endothelial growth factor in retinal cells. *Arch Ophthalmol*. 1995;113:1538–1544.
114. Noda K, Ishida S, Shinoda H, et al. Hypoxia induces the expression of membrane-type 1 matrix metalloproteinase in retinal glial cells. *Invest Ophthalmol Vis Sci*. 2005;46:3817–3824.
115. Giebel SJ, Menicucci G, McGuire PG, et al. Matrix metalloproteinases in early diabetic retinopathy and their role in alteration of the blood–retinal barrier. *Lab Invest*. 2005;85:597–607.
116. Kaur C, Sivakumar V, Yong Z, et al. Blood–retinal barrier disruption and ultrastructural changes in the hypoxic retina in adult rats: the beneficial effect of melatonin administration. *J Pathol*. 2007;212:429–439.
117. Newman EA. Propagation of intercellular calcium waves in retinal astrocytes and Müller cells. *J Neurosci*. 2001;21:2215–2223.
118. Zhang X, Zhang M, Laties AM, et al. Stimulation of $P2X_7$ receptors elevates Ca^{2+} and kills retinal ganglion cells. *Invest Ophthalmol Vis Sci*. 2005;46:2183–2191.
119. Resta V, Novelli E, Vozzi G, et al. Acute retinal ganglion cell injury caused by intraocular pressure spikes is mediated by endogenous extracellular ATP. *Eur J Neurosci*. 2007;25:2741–2754.
120. Newman EA. Functional hyperemia and mechanisms of neurovascular coupling in the retinal vasculature. *J Cereb Blood Flow Metab*. 2013;33:1685–1695.
121. Metea MR, Newman EA. Glial cells dilate and constrict blood vessels: a mechanism of neurovascular coupling. *J Neurosci*. 2006;26:2862–2870.
122. Newman EA. Calcium increases in retinal glial cells evoked by light-induced neuronal activity. *J Neurosci*. 2005;25:5502–5510.
123. Mishra A, Newman EA. Inhibition of inducible nitric oxide synthase reverses the loss of functional hyperemia in diabetic retinopathy. *Glia*. 2010;58:1996–2004.
124. Housley GD, Bringmann A, Reichenbach A. Purinergic

signaling in special senses. *Trends Neurosci*. 2009;32:128–141.
125. Li Q, Puro DG. Adenosine activates ATP-sensitive K^+ currents in pericytes of rat retinal microvessels: role of A_1 and A_{2A} receptors. *Brain Res*. 2001;907:93–99.
126. Kur J, Newman EA. Purinergic control of vascular tone in the retina. *J Physiol*. 2014;592:491–504.
127. Garhöfer G, Zawinka C, Resch H, et al. Reduced response of retinal vessel diameters to flicker stimulation in patients with diabetes. *Br J Ophthalmol*. 2004;88:887–891.
128. Dmitriev AV, Govardovskii VI, Schwahn HN, et al. Light-induced changes of extracellular ions and volume in the isolated chick retina-pigment epithelium preparation. *Vis Neurosci*. 1999;16:1157–1167.
129. Uckermann O, Kutzera F, Wolf A, et al. The glucocorticoid triamcinolone acetonide inhibits osmotic swelling of retinal glial cells via stimulation of endogenous adenosine signaling. *J Pharmacol Exp Ther*. 2005;315:1036–1045.
130. Lu Y-B, Franze K, Seifert G, et al. Viscoelastic properties of individual glial cells and neurons in the CNS. *Proc Natl Acad Sci USA*. 2006;103:17759–17764.
131. Flanagan LA, Ju YE, Marg B, et al. Neurite branching on deformable substrates. *Neuroreport*. 2002;13:2411–2415.
132. Lu YB, Iandiev I, Hollborn M, et al. Reactive glial cells: increased stiffness correlates with increased intermediate filament expression. *FASEB J*. 2011;25:624–631.
133. Lundkvist A, Reichenbach A, Betsholtz C, et al. Under stress, the absence of intermediate filaments from Müller cells in the retina has structural and functional consequences. *J Cell Sci*. 2004;117:3481–3488.
134. Lindqvist N, Liu Q, Zajadacz J, et al. Retinal glial (Müller) cells: sensing and responding to tissue stretch. *Invest Ophthalmol Vis Sci*. 2010;51:1683–1690.
135. Rohrer B, Stell WK. Basic fibroblast growth factor (bFGF) and transforming growth factor β (TGF-β) act as stop and go signals to modulate postnatal ocular growth in the chick. *Exp Eye Res*. 1994;58:553–561.
136. Schubert HD. Cystoid macular edema: the apparent role of mechanical factors. *Prog Clin Biol Res*. 1989;312:277–291.

137. Puro DG, Roberge F, Chan C-C. Retinal glial cell proliferation and ion channels: a possible link. *Invest Ophthalmol Vis Sci*. 1989;30:521–529.
138. Bignami A, Dahl D. The radial glia of Müller in the rat retina and their response to injury: an immunofluorescence study with antibodies to the glial fibrillary acidic (GFA) protein. *Exp Eye Res*. 1979;28:63–69.
139. Lewis GP, Erickson PA, Guerin CJ, et al. Changes in the expression of specific Müller cell proteins during long-term retinal detachment. *Exp Eye Res*. 1989;49:93–111.
140. Nakazawa T, Matsubara A, Noda K, et al. Characterization of cytokine responses to retinal detachment in rats. *Mol Vis*. 2006;12:867–878.
141. Nakazawa T, Hisatomi T, Nakazawa C, et al. Monocyte chemoattractant protein 1 mediates retinal detachment-induced photoreceptor apoptosis. *Proc Natl Acad Sci USA*. 2007;104:2425–2430.
142. Neufeld AH, Kawai S, Das S, et al. Loss of retinal ganglion cells following retinal ischemia: the role of inducible nitric oxide synthase. *Exp Eye Res*. 2002;75:521–528.
143. Nakazawa T, Takeda M, Lewis GP, et al. Attenuated glial reactions and photoreceptor degeneration after retinal detachment in mice deficient in glial fibrillary acidic protein and vimentin. *Invest Ophthalmol Vis Sci*. 2007;48:2760–2768.
144. Wen R, Song Y, Cheng T, et al. Injury-induced upregulation of bFGF and CNTF mRNAs in the rat retina. *J Neurosci*. 1995;15:7377–7385.
145. Delyfer MN, Simonutti M, Neveux N, et al. Does GDNF exert its neuroprotective effects on photoreceptors in the *rd1* retina through the glial glutamate transporter GLAST? *Mol Vis*. 2005;11:677–687.
146. Koeberle PD, Bähr M. The upregulation of GLAST-1 is an indirect antiapoptotic mechanism of GDNF and neurturin in the adult CNS. *Cell Death Differ*. 2008;15:471–483.
147. Chu Y, Humphrey MF, Alder VV, et al. Immunocytochemical localization of basic fibroblast growth factor and glial fibrillary acidic protein after laser photocoagulation in the Royal College of Surgeons rat. *Aust*

N Z J Ophthalmol. 1998;26:87–96.
148. Fischer AJ, Reh TA. Müller glia are a potential source of neural regeneration in the postnatal chicken retina. *Nat Neurosci*. 2001;4:247–252.
149. Ooto S, Akagi T, Kageyama R, et al. Potential for neural regeneration after neurotoxic injury in the adult mammalian retina. *Proc Natl Acad Sci USA*. 2004;101:13654–13659.
150. Lawrence JM, Singhal S, Bhatia B, et al. MOI-M1 cells and similar Müller glial cell lines derived from adult human retina exhibit neural stem cell characteristics. *Stem Cells*. 2007;25:2033–2043.

20

Retinal and Choroidal Vasculature

Retinal Oxygenation

Maria B. Grant, Gerard A. Lutty

Introduction

Oxygen is necessary for the existence of mammals because it is required to generate adenosine triphosphate (ATP) oxidatively. Although the partial pressure of oxygen (PO_2) is 149 mmHg (21% of atmospheric oxygen) at sea level, arterial oxygen content is as low as 75–100 mmHg (10–14%) and tissue PO_2 is much lower. The oxygen level in inner segments of photoreceptors (mitochondria-rich) after dark adaptation plunges to zero but measures up to 20 mmHg in the light. Inner retinal oxygen is normally 10–20 mmHg, thus normoxia depends on the area of retina and dark/light state.[1,2] Hypoxia is an oxygen level below normoxia, while hyperoxia is achieved by inhaling high levels of oxygen as in the isolette of the

neonatal intensive care unit.

The retina, one of the most metabolically active tissues in the body, has two unique zones of oxygenation.[1] The inner retina is supplied with oxygen by the retinal vasculature. The retinal vasculature is autoregulated because it is responsive to changes in systemic oxygen levels, keeping the inner retina at a relatively constant level. If the retinal vasculature is compromised, as in ischemic retinopathies, the retina becomes hypoxic in that area. The outer retina is supplied solely by the choroidal vasculature. Unlike retina, choroidal vessels are not autoregulated, so systemic levels of oxygen control the level of oxygen in choroid. Blood flow in the choroidal vasculature, at least in bird and rat, is parasympathetically baroregulated.[3] Supply of oxygen to choroid is diminished by stenosis of the ophthalmic artery, which is the branch off the internal carotid that is most likely to be stenosed because it arises as a right-angled branch.

Comparison of Retinal and Choroidal Vasculatures

Although less than 300 μm apart in distance, the retinal and choroidal vasculatures are vastly different in many attributes in addition to autoregulation. The initial superficial retinal vasculature in human starts forming around 14 weeks' gestation (WG) by vasculogenesis, development by differentiation and assembly of vascular precursors, angioblasts.[4–6] The deep capillary network forms after 20 WG by angiogenesis, development by migration, and proliferation of endothelial cells from existing blood vessels. The driving force for vascular development is physiologic hypoxia; metabolic requirements of developing neurons are met only by stimulating the development of a retinal vasculature.[7,8] It is mostly a bilayered system, a superficial network, and a deep capillary plexus; however, there are multiple layers of capillaries in the peripapillary region, the radial peripapillary capillaries. There is only one layer of blood vessels in the periphery at the ora serrata where the retina thins to 100 μm. The retinal vasculature is supplied with blood directly by the central retinal artery in humans.

The retinal vasculature has a traditional end-arterial hierarchy:

arteries branch to arterioles, which supply a capillary network that is drained by venules, and then veins remove the blood from the retina (Fig. 20.1). The retinal vasculature forms the inner blood–retinal barrier (BRB), restricting passage of molecules that do not have receptors or transporters on the luminal surface of the endothelial cells. Capillaries have a lumenal diameter of 3.5–6 μm, permitting passage of red blood cells only after deformation of their disc shape. The retinal capillaries and venules have perivascular pericytes, and the retina has the highest endothelial cell-to-pericyte ratio in the body, 1 : 1.[9]

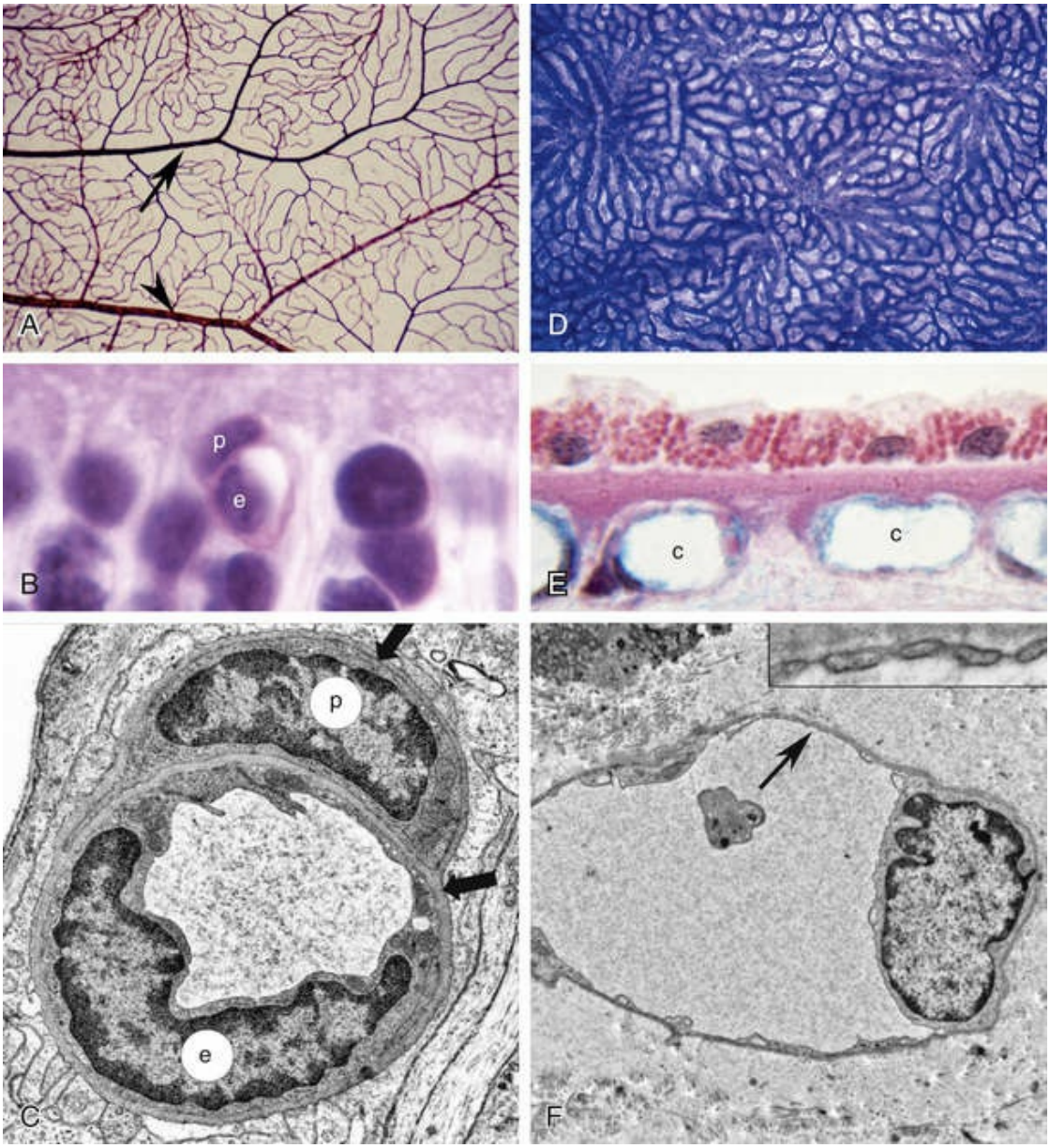

FIG. 20.1 Comparison of retinal (A–C) and choroidal

(D–F) vasculatures. (A) The retinal vasculature, stained here with adenosine diphosphatase (ADPase) enzyme histochemistry, has an end-arterial hierarchy: arteries (*arrow*) have a capillary-free zone, and arterioles and then capillaries, which are drained by venules, and then veins (*arrowhead*). (B) A capillary in the deep capillary network has a pericyte and endothelial cell. (C) Transmission electron microscopy (TEM) of a retinal capillary shows a pericyte (*p)* within the shared basement membrane (*arrow*) with an endothelial cell (*e*). (D) The choriocapillaris, stained by alkaline phosphatase (APase) enzyme histochemistry, has a lobular hierarchy. (E) When sectioned, the endothelial cell APase activity in choriocapillaris (*c*) shows the broad flat lumens of the choriocapillaris, which are positioned under retinal pigment epithelial cells (top), and Bruch's membrane between them. (F) With TEM the thin processes of the choriocapillaris endothelial cells (*arrow*) are apparent and, at higher magnification (inset), the fenestrations in these endothelial cells are visible. (Panel C courtesy of DB Archer, TA Gardiner, and AW Stitt.)

The choroidal vasculature forms well before the retinal vessels (6–9 WG), although its maturation is only completed after 20 WG.[10] It develops by hemovasculogenesis, formation of blood cells and blood vessel cells from a common progenitor, the hemangioblast.[11] The choroidal vasculature provides oxygen and nutrients to the photoreceptors. The capillary system, the choriocapillaris, lies directly under the Bruch's membrane, while intermediate and large blood vessels of the system lie posterior to the capillaries. The short and long ciliary arteries supply blood to the choroidal vasculature while 4–6 vortex veins remove blood from this vast system. Unlike the retina, the hierarchy in choroid is lobular, similar to kidney glomeruli (Fig. 20.1). The lobules change in shape, vascular density, and size depending upon area; the location of feeding arterioles and draining venules also varies by geographic location of the lobule.[12] The capillaries are broad and flat, having luminal diameters ranging from 10 to 38 μm in diameter. Another major difference from retina is that the capillaries are fenestrated, allowing the passage of small molecules and solutes through these 60–70-nm

pores. The choriocapillaris is sided in that the majority of the fenestrations are on the retinal side as well as all three types of vascular endothelial growth factor (VEGF) receptors.[13] Pericytes, however, are mostly on the scleral side of these capillaries. Control of vascular tone in choroid may be accomplished by mast cells, which lie abluminal to arteries and arterioles,[14,15] or choroidal ganglion cells.[16]

History of Retinal Ischemia

Ischemia is the restriction in oxygen supply without considering actual levels of oxygen. Michaelson[17,18] and Wise[19] hypothesized that areas of vascular loss in retina must be hypoxic because the high metabolic rate requires a continuous supply of oxygen. They observed that neovascularization always formed adjacent to these nonperfused areas and, therefore, an angiogenic factor must be produced by the hypoxic retina. They hypothesized that this factor X must be hypoxia-inducible and diffusible. Subsequently, oxygen was measured directly in retinas of several species and it demonstrated that nonperfused areas were indeed hypoxic.[1,2] It was not until 1989 that factor X was discovered, purified, and characterized as VEGF.[20] This factor was first shown to be responsible for the increased vascular permeability seen in some retinopathies.[21]

Normoxia

The studies of Wangsa-Wirawan and Linsenmeier[1] and Yu and Cringle[2] using oxygen electrodes directly assessed oxygen levels from choroid to vitreous in various species. The oxygen tension is approximately 70 mmHg in choroid and plummets to zero at the inner segments in the dark (Fig. 20.2). Inner retina is around 10–20 mmHg. There are regional variations in oxygen concentration within the retina. Yu et al.[22] showed that oxygen consumption in outer retina is highest in the parafoveal region while inner retinal oxygen in the fovea (approximately 5 mmHg) reflected the lack of a retinal vasculature and the predominantly choroidal source of oxygen.

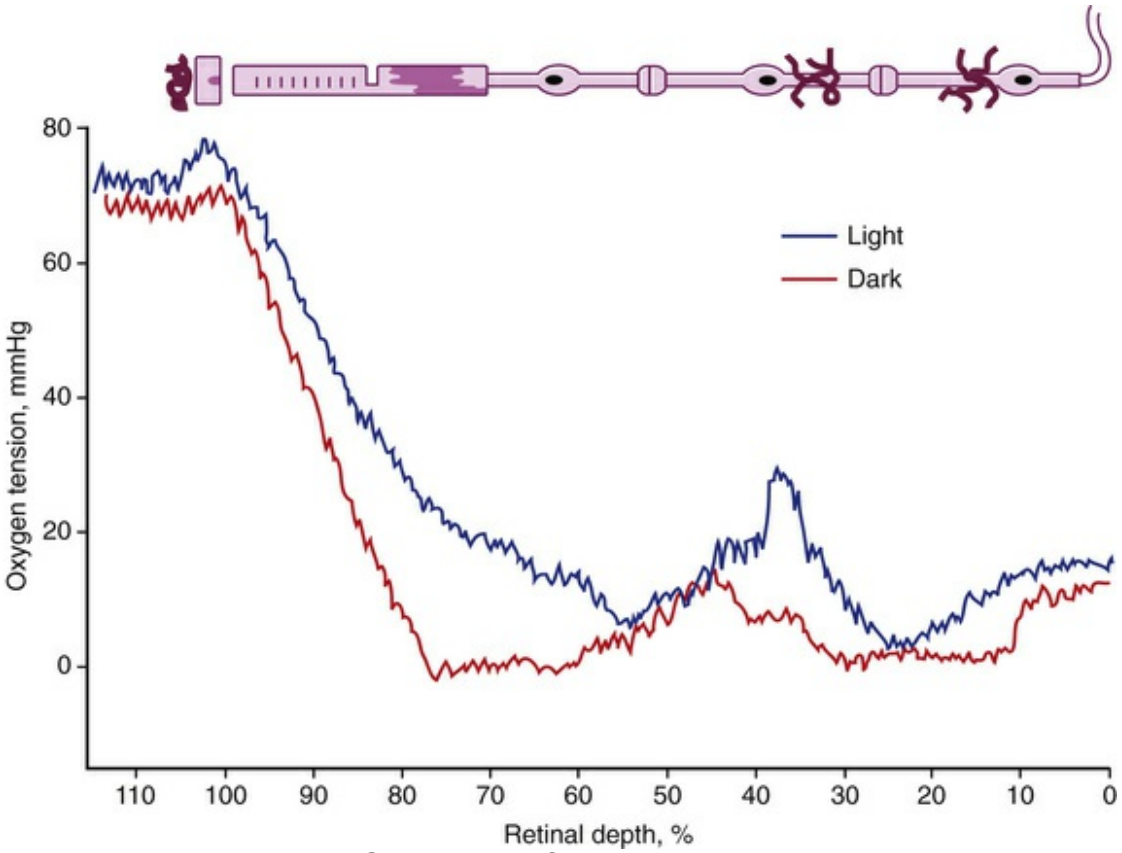

FIG. 20.2 Oxygen profile measured with microelectrodes in cat retina during light and dark adaptations. The schematic at the top shows where, anatomically, the measurements were taken from choriocapillaris (left, retinal depth = 100) to the internal limiting membrane (right, retinal depth = 0). (Reproduced with permission from Wangsa-Wirawan ND, Linsenmeier RA. Retinal oxygen. Arch Ophthalmol 2003;121:547–55.)

Hyperoxia

Life in utero is hypoxic, so when a child is born prematurely, the normoxic environment is actually hyperoxic. Prematurely born children are placed in 40% oxygen, making their tissue further hyperoxic, which yields vaso-obliteration (endothelial cells die and pericytes and progenitors survive).[23] The only direct measurements of oxygen in a model of retinopathy of prematurity (ROP) were performed by Ernest and Goldstick.[24] They found in kittens after 80–90% O_2 that preretinal PO_2 over avascular retina was close to zero but was normal over vascularized retina. Vaso-obliteration

from hyperoxia does not occur in the choroid of humans and dogs[23] but does occur when rats are exposed to hyperoxia.[25] Loss of vasculature in vaso-obliteration makes the retina hypoxic when the child is returned to room air. Exposure of the adult vasculature to hyperoxia causes constriction but not vaso-obliteration. During hyperoxia breathing (100% oxygen), the inner retinal PO_2 remains unchanged due to autoregulation while the choroidal PO_2 rises to 250 mmHg in cat[26] and 220 mmHg in the minipig, due to a lack of metabolic control of the choroidal vasculature.[27]

Hypoxia

Complex homeostatic mechanisms are designed to maintain O_2 concentration in each cell within a narrow range. While O_2 consumption increases with the metabolic activity of the organism, exposure to O_2 must be limited due to the potentially damaging effects of reactive oxygen species (ROS). Hypoxia, the state of low oxygen concentration, promotes the formation of blood vessels and is important for the formation of a vascular system in embryos.[28] Disease occurs when the retina and choroid are deprived of adequate oxygen supply; this can also be described as a mismatch of oxygen supply versus demand at the cellular level within ocular tissues.

The blood O_2-carrying capacity is maintained by the O_2-regulated production of erythropoietin (EPO), which stimulates the proliferation and survival of red blood cell progenitors. In 1991, Semenza and coworkers[29,30] performed seminal studies to identify hypoxia-inducible factor 1 (HIF-1). HIF-1 orchestrates a pleiotropic adaptive response to hypoxia by inducing the expression of more than 100 genes encoding glycolytic enzymes and glucose transporters (thereby facilitating the glycolytic switch in energy metabolism typically observed under hypoxic conditions), matrix metalloproteinases, and angiogenic, mitogenic, and survival factors, including EPO.[31,32] Other molecules upregulated by HIF-1 that have profound effects on vasculature include 5′ nucleotidase, an enzyme that is the major source of the potent vasodilator adenosine in the body, VEGF, and angiopoietin-like 4 (ANGPTL4).[33] HIFs are vital to

development and, in mammals, deletion of the HIF-1 genes results in perinatal death. HIF-1 is expressed in all cell types and functions as a master regulator of oxygen homeostasis by playing critical roles in embryonic development and postnatal physiology.

Hypoxia-Inducible Factor

HIF is a highly conserved transcriptional complex that is a heterodimer composed of an alpha and a beta subunit. HIF-1 belongs to the PER-ARNT-SIM (PAS) subfamily of the basic helix–loop–helix (bHLH) family of transcription factors. The alpha- and beta-subunit both contain an N-terminus bHLH domain for DNA binding, a central region with PAS domain, which facilitates heterodimerization, and a C-terminus, which recruits transcriptional coregulatory proteins.

The activity of HIF depends on the intracellular levels of its inducible alpha-subunit. In the presence of oxygen, HIF-1α is hydroxylated on two critical proline residues (Pro_{402} and Pro_{564}) in the so-called oxygen-dependent degradation domain. Three prolyl hydroxylases have been identified in mammalian cells and use O_2 as a substrate to generate 4-hydroxyproline at residues 402 and/or 564 of HIF-1α. The hydroxylation reaction also requires 2-oxoglutarate (α-ketoglutarate) as a substrate and generates succinate as a side product. These prolyl hydroxylases have a high K_m for O_2 that is slightly above atmospheric concentration; thus O_2 is rate-limiting for enzymatic activity under physiologic conditions, and any change in cellular O_2 concentration is directly transduced into changes in the rate of HIF-1α hydroxylation.[34]

Factor-inhibiting HIF-1 (FIH-1), which was identified in a yeast two-hybrid screen as a protein that interacts with, and inhibits the activity of, the HIF-1α transactivation domain,[35] functions as an asparaginyl hydroxylase.[36] As in the case of the prolyl hydroxylases, FIH-1 appears to use O_2 and 2-oxoglutarate,[37] although it has a K_m for O_2 that is three times lower than the prolyl hydroxylases.[38] Hydroxylation provides a mechanism for regulating protein–protein interactions, similar to the effect of phosphorylation and other posttranslational modifications. However, this

hydroxylation occurs in an O_2-dependent manner, thus establishing a direct link between cellular oxygenation and HIF-1 activity. Following HIF-1α hydroxylation, the protein becomes targeted for ubiquitination by an E3 ligase complex (including the von Hippel–Lindau [VHL] tumor suppressor protein) and subsequent proteasomal degradation.

Under hypoxic conditions, the HIF prolyl hydroxylases are inhibited, because these HIF prolyl hydroxylases utilize oxygen as a cosubstrate. Hypoxia results in an increase in succinate, due to inhibition of the electron transport chain in the mitochondria, which serves to inhibit further HIF prolyl-hydroxylase activity. When stabilized by hypoxic conditions, HIF increases the expression of critical genes that promote survival in low-oxygen conditions, including glycolytic enzymes, which allow ATP synthesis in an oxygen-independent manner. HIF activates the transcription of genes encoding secreted signaling molecules, including angiogenic growth factors and survival factors, cell surface receptors, extracellular matrix proteins and modifying enzymes, transcription factors, cytoskeletal proteins, proapoptotic proteins, and glucose transporters and glycolytic enzymes (Fig. 20.3).[34]

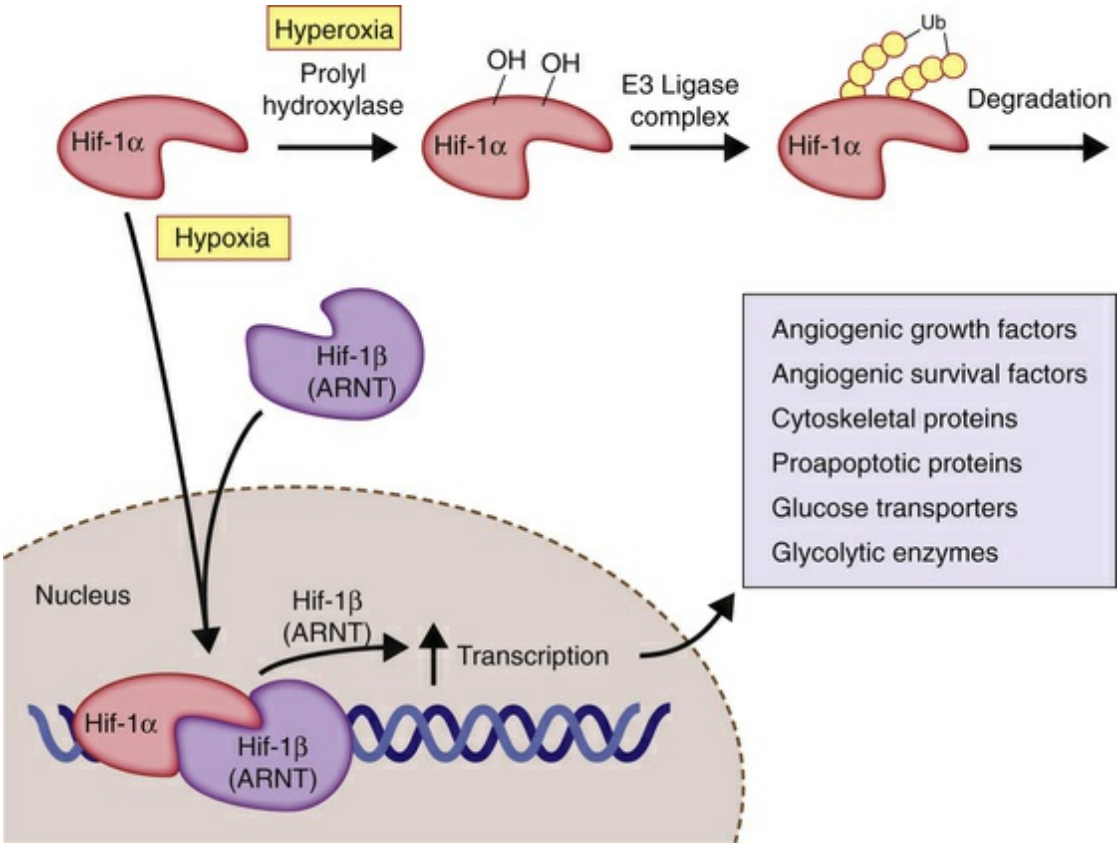

FIG. 20.3 Hypoxia-inducible factor 1 (Hif-1α) in hypoxia and hyperoxia. ARNT, aryl hydrocarbon receptor nuclear translocator.

HIF-induced VEGF, stromal-derived factor 1 (SDF-1), and EPO promote neovascularization. HIF-1 acts by binding to HIF-responsive elements in promoters that contain the sequence NCGTG, which is present in the promoters for VEGF, SDF-1, EPO, and many other genes. In addition to hypoxia, other factors such as nuclear factor κB (NF-κB) modulate HIF-1*α* expression in the presence of normal oxygen pressure. Thus, conditions such as tissue inflammation can lead to local HIF-1*α* expression.[39] HIF-1 DNA-binding activity and target gene expression are induced in cells exposed not only to hypoxia but also to the iron chelator desferrioxamine or to cobalt chloride.[40]

A structurally and functionally related protein to HIF-1*α*, designated HIF-2*α*, is the product of the *EPAS1* gene. HIF-2*α* can also heterodimerize with HIF-1ß.[41] HIF-1*α*:HIF-1β and HIF-2*α*:HIF-1β heterodimers have overlapping yet distinct target gene specificities.[42] HIF-2*α*, unlike HIF-1*α*, is not expressed in all cell types, and HIF-2*α* can be inactivated by cytoplasmic sequestration.

This "compartmentalization" of oxygen-sensitive signaling components also influences the hypoxic response.[43,44]

Interestingly, recent studies by Shelby et al. demonstrate another novel function of HIF-1α. HIF-1α, but not HIF-2α, was shown to be required in regulating photoreceptor autophagy and that silencing of HIF-1α in rat retinas resulted in increased photoreceptor cell death.[45] Their data support that HIF-1α serves as an early response signal to induce autophagy and reduce photoreceptor cell death.

High throughput screening of a drug library with a reporter cell line for HIF-1 transcriptional activity has identified digoxin and doxorubicin as strong inhibitors of HIF-1 activity.[46,47] Subcutaneous injections or intraocular injections of digoxin reduce levels of VEGF, PDGF-B, SDF-1 and their receptors in ischemic retina and resulted in a dose-dependent reduction in retinal neovascularization.[48]

HIF Deficiency and Its Resultant Pathology

O_2 delivery to cells of the developing embryo becomes limited by diffusion such that establishment of a functioning circulatory system is required for embryonic survival by embryonic day 9 (E9) in the mouse. In wild-type mouse embryos, HIF-1α expression increases dramatically between E8.5 and E9.5, whereas embryos that lack HIF-1α expression die between E9.5 and E10.5 and show cardiac malformations, vascular regression, and massive cell death.[49] Complete HIF-2α deficiency is also associated with embryonic lethality,[50] and because the embryos survive longer than HIF-1$\alpha^{-/-}$ mice, effects on multiple organ systems can be demonstrated.[51]

Complete HIF-1α deficiency results in developmental defects; however, partial HIF-1α deficiency is sufficient to result in impaired responses to physiologic stimuli. A particularly dramatic example is the loss of O_2 sensing in the carotid body of HIF-1$\alpha^{+/-}$ mice.[52] Although the carotid bodies are anatomically and histologically normal and depolarize normally in response to cyanide application, they show essentially no response to hypoxia. Thus partial HIF-1α deficiency in the carotid body results in a complete loss of the ability to sense and/or respond to changes in the arterial PO_2 by stimulation of the central nervous system

cardiorespiratory centers. The HIF-1 target genes that are critical for O_2 sensing and/or efferent responses by the carotid body have not been identified.

Mice with HIF-1α conditionally knocked out using PAX6-Cre have delayed development of the outer retinal plexus but not the superficial or deep plexus.[53] However, when HIF-1α was knocked down only in Müller cells using a Cre-LOX system, and the animals were made diabetic with streptozotocin, vascular permeability in retina was reduced and leukostasis and overproduction of VEGF and intercellular adhesion molecule (ICAM)-1 were attenuated in adult mice.[54] Xin et al. suggested that expression of hypoxia-inducible ANGPTL4 by Müller cells promoted increased vascular permeability.[33] Sears and associates prevented OIR by inhibiting prolyl hydroxylases during the hyperoxia.[55,56] Furthermore, they demonstrated that stabilizing hepatic HIF-1α prevented OIR as well, so stabilizing HIF-1α in visceral organs may be a simple strategy to protect capillary beds in retina.[57]

Another dramatic phenotype is the complete inability of HIF-1$\alpha^{-/-}$ myeloid cells (granulocytes and macrophages) to respond to inflammatory stimuli.[58] Myeloid cells are dependent on glycolysis for ATP generation, perhaps reflecting the hypoxic microenvironment that is often associated with inflammation and infection. HIF-1α deficiency results in ATP deficiency, which impairs critical myeloid cell functions such as aggregation, motility, invasion, and bacterial killing. HIF-1 also plays critical roles in B-lymphocyte development[59] and T-lymphocyte activation.[60] Hoppe and associates demonstrated a twofold increase in circulating bone marrow-derived endothelial precursors when hepatic HIF-1α was stabilized with dimethyloxalylglycine (DMOG).[57]

HIF-Activated Genes Relevant to Physiologic and Pathologic Ocular Angiogenesis

The paragraphs above provide a brief summary of the critical role of HIF-1α in oxygen sensing, development, and physiology. HIF-1α plays an equally important role in disease pathophysiology, including retinal diseases. As a result, there is considerable interest in HIF-1α as a therapeutic target.[61] In cardiovascular diseases,

increased HIF-1α activity induced as a result of HIF-1α gene therapy,[62] small-molecule inhibitors of prolyl hydroxylase activity,[63] or inhibitors of HIF-1α–VHL interaction[64] may provide a means to stimulate neovascularization in ischemic tissue. Sears and Hoppe have found novel hypoxia mimetics that stabilize HIF-1α and may provide new strategies in protecting the retinal vasculature from hyperoxia.[65] In contrast, small-molecule inhibitors of HIF-1α activity may be useful as antiangiogenic agents. However, because HIF-1α functions as a global regulator of oxygen homeostasis, it may not be a useful therapeutic target if the treatment results in unintended and undesirable side-effects.

An alternative therapeutic approach that may be particularly relevant to the treatment of ocular pathology is to focus on modulation of HIF-1α target genes. However, the protein products of these target genes must also be delivered in a precise and perfectly timed manner. EPO is an oxygen-regulated hormone stimulating erythrocyte production and is critical for retinal angiogenesis. Increasing EPO expression in phase 1 of the murine ROP model (postnatal days 7–12) is protective and results in less neovascularization during phase 2 (postnatal days 12–17).[66] In contrast, EPO mRNA expression levels in retina are highly elevated during the hypoxia-induced proliferation phase of retinopathy (phase 2) and inhibition of retinal EPO mRNA expression with RNA interference results in suppressed retinal neovascularization.[66]

The best-known gene activated by HIF-1α is *Vegfa*, first identified as a potent promoter of vascular permeability[21] and endothelial cell proliferation.[19] VEGF has become known as a master regulator of angiogenesis.[67] Tight control of physiologic VEGF levels is required for proper embryologic development.[68] Although it was initially thought that the postembryonic role of VEGF was restricted to a few processes, it is now quite clear that VEGF acts as a pluripotent growth factor essential for a wide variety of physiologic processes,[69] including maintenance of the adult microvasculature,[70] neuronal survival,[71] and trophic maintenance of ocular tissues.

VEGF in Health and in Ocular Disease

VEGF is produced by many cell types in the retina, including

retinal pigment epithelium (RPE),[72] vascular endothelial cells,[73] pericytes,[73] retinal neurons,[74] Müller cells,[74] and astrocytes,[75] suggesting that VEGF has important functions in ocular homeostasis. RPE-secreted VEGF plays an important role in maintaining the choriocapillaris.[13,76,77] VEGF secretion by retinal cells and the RPE is stimulated in response to hypoxia.[73] VEGF administration protects retinal neurons from apoptosis.[78] Moreover, chronic VEGF inhibition can lead to a significant loss of retinal ganglion cells in normal adult animals.[78]

While VEGF is critical to maintaining normal ocular function, overproduction of VEGF is deleterious. Elevated levels of VEGF have been strongly implicated in the pathogenesis of ocular neovascular diseases such as neovascular age-related macular degeneration (NV in AMD)[79] and proliferative diabetic retinopathy[80] as well as diabetic macular edema.[81] Elevated VEGF levels are observed in central and branch retinal vein occlusion (CRVO and BRVO),[82] neovascular glaucoma,[83] and ROP.[84] Blocking VEGF action is now an established strategy for the treatment of NV in AMD, with three agents (VEGF trap or Eylea, Avastin, and the humanized murine monoclonal antibody antigen-binding fragment ranibizumab[85]) having received regulatory approval for the intravitreal treatment of NV in AMD.

While current standard of care for NV in AMD uses intravitreal delivery of an anti-VEGF agent on a repeated basis, this routine clinical practice does not address all the nuances of VEGF biology. The biology of the VEGF proteins is extremely complex. The VEGF family members are part of a superfamily of cysteine knot proteins and include VEGF-B, -C, -D, and placental growth factor (PlGF). Alternative splicing events for VEGFA give rise to at least 14 subtypes of VEGF, namely, $VEGF_{111}$, $VEGF_{121}$, $VEGF_{121b}$, $VEGF_{145}$, $VEGF_{145b}$, $VEGF_{148}$, $VEGF_{162}$, $VEGF_{165}$, $VEGF_{165b}$, $VEGF_{183}$, $VEGF_{183b}$, $VEGF_{189}$, $VEGF_{189b}$,[86] and $VEGF_{206}$.[87,88] Following the discovery of the antiangiogenic isoform of VEGF, $VEGF_{165b}$, and its associated family of isoforms, a further layer of complexity was added to understanding the regulation of VEGF.[89]

All VEGF isoforms are essential regulators of angiogenesis and vascular permeability. VEGFs elicit their intracellular activities via the activation of two receptor tyrosine kinases (RTKs): VEGFR-1

and -2. VEGFR-1, a high-affinity fms-like tyrosine kinase-1,[90] and VEGFR-2, a kinase insert domain-containing receptor,[91] are transmembrane glycoproteins consisting of a seven-tandem immunoglobulin-like domains, which serves as the extracellular ligand-binding region, a single-transmembrane domain, and a cytoplasmic domain consisting of two tyrosine kinase catalytic domains. Moreover, it has also been reported that a family of cell surface glycoproteins, particularly neuropilin-1(NP-1), act as isoform-specific coreceptors for VEGF-A.[92] The VEGF family and their respective receptors are outlined in Fig. 20.4.

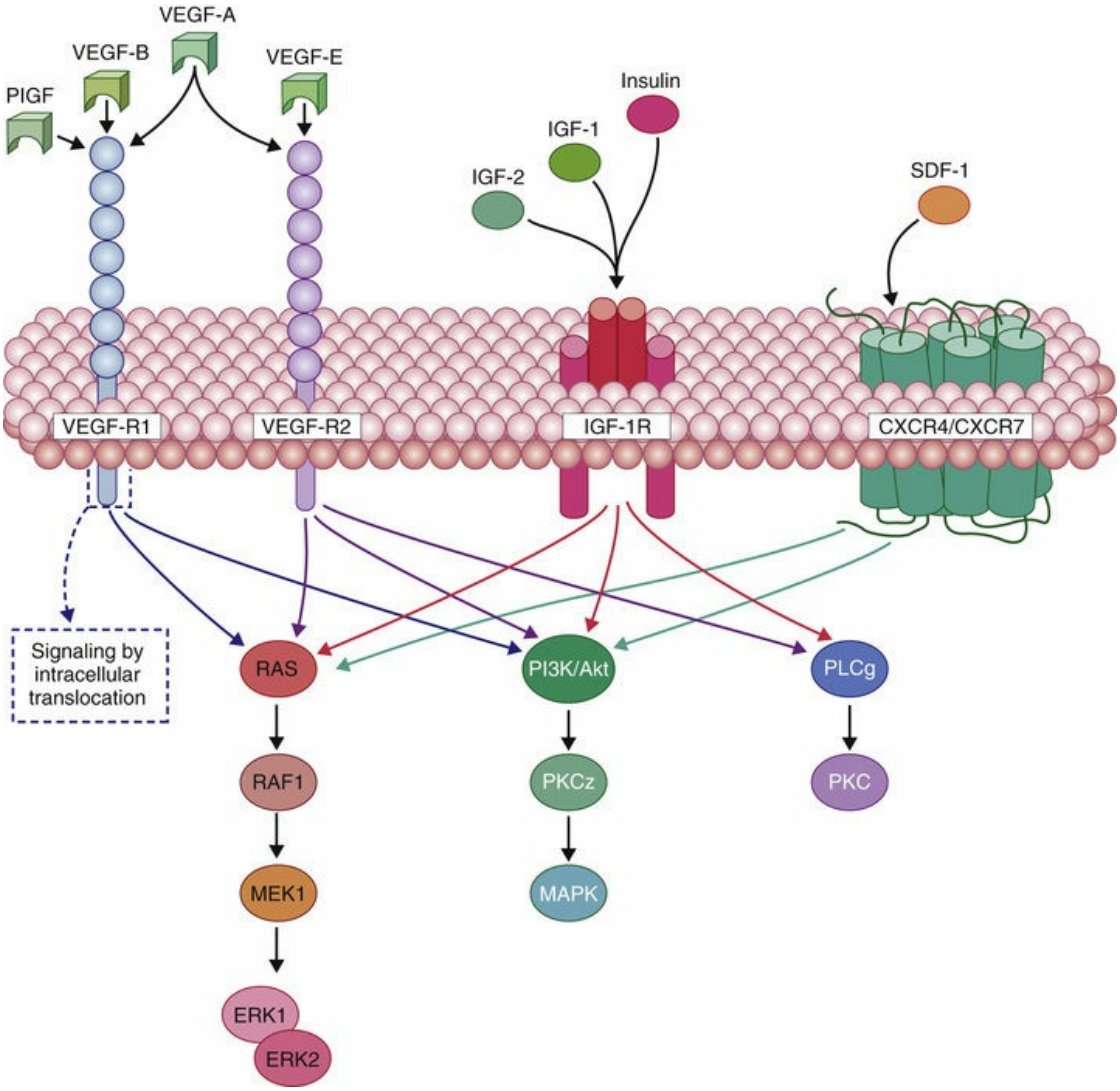

FIG. 20.4 Vascular endothelial growth factor (VEGF) family and its receptors. IGF, insulin-like growth factor; PIGF, placental growth factor; SDF, stromal-derived factor.

Ligand binding to the extracellular domain of VEGFR-2 results in a maximal increase of kinase activity following the induction of receptor dimerization and subsequent phosphorylation of tyrosine residues on the intracellular domain of the receptor.[93] This event is crucial for the recruitment of additional signaling molecules that contain Src homology 2 or phosphotyrosine binding domains, which mediate further downstream signaling cascades.[94] The association of RTKs with coreceptors, such as NP-1, in the case of VEGFR-2:$VEGF_{165}$ signaling/interaction, can enhance the functional signal transduction and facilitate diverse cellular responses.[93] VEGFR-1/R2 signaling activates RAS, raf1, MEK1, and ERK1/ERK2 and stimulates PI3K/AKT/PKCz/MAPK pathways to mediate proliferation, migration, and cell survival (Fig. 20.4).

VEGFR-2 is the major mediator of angiogenic signaling in endothelial cells and is required for de novo vessel formation, vasculogenesis, and for angiogenesis, the formation of vessels from preexisting vasculature.[95] The pathways leading to VEGFR internalization and the role of receptor degradation in VEGF signaling remain controversial and differ for VEGFR-1 and -2. VEGFRs generate signal output at the plasma membrane and on their way to degradation through endocytic vesicles,[96] whereas, in unstimulated cells, VEGFR-2 is predominantly located in recycling endosomes identified by Rab4 and/or Rab5.[97] VEGFR internalization is clathrin-mediated, and transport is further directed by the endosomal sorting complex required for transport proteins.[98] VEGFR signaling is also regulated by ubiquitination, not only of the receptor itself, but also of receptor-associated signaling molecules.[99] Specific VEGFR trafficking regulates biol output, as shown for arterial morphogenesis, for example.[100]

The molecular basis for ligand specificity of VEGFR signaling is poorly understood. It is well accepted, however, that VEGF receptors can associate with distinct coreceptors such as neuropilins, integrins, semaphorins, or heparan sulfate glycosaminoglycans, and engage distinct signaling molecules giving rise to specific signal output. Ligand-specific signaling may also result from receptor trafficking to specific cellular compartments, including the nucleus,[101] where receptors encounter distinct signaling molecules.[102]

Do et al. have recently identified a conserved binding site for estrogen-related receptor γ (ERRγ) on the promoter of the *Vegfa* gene. ERRγ is a constitutively active orphan nuclear receptor, and its expression is increased by hypoxic stimuli in metabolically active tissues. Using the oxygen-induced retinopathy (OIR) mouse model, they show by immunohistochemistry increased ERRγ expression in the ganglion cell layer at postnatal day (P) 17. They also use a novel pharmacologic suppressor of ERRγ, GSK5182, to reduce hypoxia-induced VEGF expression, supporting that ERRγ could be a treatment target for ischemic retinopathies.[103]

In addition to EPO and VEGF, SDF-1 is hypoxia-regulated and ischemic tissues express high levels of SDF-1 to recruit reparative cells to the injured region. SDF-1 activation of either CXCR-4 or CXCR-7 results in stimulation of the Ras/Raf/Mek/ERK pathway and the PI3K/Akt pathway to promote endothelial cell proliferation and neovascularization. Thus ligand–receptor interaction of VEGF to VEGFR-1 and VEGFR-2 and SDF-1 to CXCR4/CXCR-7 and their subsequent internalization sets in motion the cascade of cellular effects of VEGF and SDF-1 (Fig. 20.4). The VEGF and SDF-1 signaling pathways appear to be intimately connected with HIF-1 activation (see Fig. 20.3), as the promoters of each of these factors contain a HIF response element. Because hypoxic tissue releases SDF-1 and VEGF, varying O_2 concentrations would be expected to also influence the expression of the receptors for these ligands, CXCR-4 and VEGFR.

Bone Marrow-Derived Progenitor Cells (BMPC) and Vascular Repair

In conditions like diabetic retinopathy and ROP, areas of retinal vasodegeneration occur and ultimately lead to retinal ischemia, which in turn induces the expression of hypoxia-regulated angiogenic factors. Typically, BMPCs robustly respond to these factors, including VEGF and SDF-1.[104]

Importantly, all hypoxia-regulated angiogenic factors are modulators of bone marrow-derived stem cells. Specifically, hematopoietic stem cells and other BMPCs reside in the bone marrow and are mobilized into the peripheral circulation by

increased levels of EPO, SDF-1, and VEGF released by the ischemic tissue. Hematopoietic stem cell/BMPC mobilization occurs in response to vascular injury throughout the body and, when functioning properly, leads to revascularization of injured areas.[105] In healthy individuals, bone marrow-derived $CD34^+$ endothelial progenitor cells as well as other BMPC successfully orchestrate the reparative process. BMPC do not demonstrate an ability to differentiate directly into endothelial cells and form components of new blood vessels by vasculogenesis, but show marked ability to provide paracrine support for the resident vasculature. This paracrine support facilitates resident endothelial cell recovery.

D'Amico et al. have recently demonstrated the protective role of pituitary adenylate cyclase-activating peptide (PACAP) in early diabetes, after 3 weeks of hyperglycemia.[106] They found that the expression of HIF-1α and HIF-2α was significantly increased in diabetic rats as compared to controls and that expression levels were significantly decreased after PACAP intraocular administration. The results suggest that the protective effect of the peptide in diabetic retina are mediated through modulation of HIFs' expression.

Disease-Associated BMPC Dysfunction

In diabetes, for example, BMPC are dramatically altered and cannot facilitate the repair process. Diabetic individuals have fewer circulating $CD34^+$ cells and an increased number of inflammatory BMPC such as $CD14^+$ cells compared to nondiabetics.[107–109] This diabetes-related bone marrow dysfunction is closely linked to the impaired healing response experienced by many diabetic individuals and to the vasodegenerative aspect of diabetic macro- and microvascular complications.[109–111] Diabetes-induced BMPC defects occur in part due to uncoupling of nitric oxide synthases, enhanced NADPH oxidase activity, and increased generation of ROS such as superoxide and peroxynitrite (ONOO-)[112] within BMPC. While stem and progenitor cells are deemed more resistant to oxidative stress,[113] the highly oxidative diabetic milieu has a clearly detrimental effect on the function of these cells.[114] Prolonged oxidant exposure reduces reparative function[115] by impairing

antioxidant defense enzymes. Previously, we and others have shown that diabetic $CD34^+$ cells exhibit decreased migration and adhesion activities in vitro and consequently reduce recruitment to areas of injury.[111] In addition to oxidative stress, other key mechanisms implicated in diabetes-induced BMPC dysfunction include a reduction of cathepsin L activity[116] and an upregulation of thrombospondin-1.[115,117] While these functional defects are profound, strategies that successfully reverse BMPC defects in diabetics have included (1) enhancement of angiogenic stimulus by increasing BMPC mobilization using granulocyte colony-stimulating factor and targeting SDF-1;[118] (2) use of nitric oxide donors to correct migration and promote cell deformability;[119] (3) enhancing cell interactions with substrate proteins to increase attachment to basement membranes;[120] (4) reducing high levels of endogenous transforming growth factor-β to normal levels;[121] and (5) treatment with rosiglitazone[122] or atorvastatin.[123]

In addition to $CD34^+$ cells, other populations of bone marrow cells may attempt vascular repair, such as $CD14^+$ cells, discussed above, which can, under select circumstances, form endothelial-like cells;[124] however, the blood vessels formed by the endothelial cells of $CD14^+$ origin eventually generate pathological blood vessels with increased permeability and contribute to the pathology of diabetic retinopathy.

We and others have been particularly interested in a novel factor expressed in increased concentrations in hypoxic tissue, insulin-like growth factor-binding protein 3 (IGFBP-3). While the standard IGF-dependent actions of the family of IGF-binding proteins have been well described, recently several IGF-independent actions have been discovered for IGFBPs, including IGFBP-3. These IGF-1-independent actions have been characterized as regulating cell fate and apoptosis.[125–128] The role of IGFBP-3 in the control of cell growth remains an area under intense study, since IGFBP-3 may enhance or suppress cell growth, depending on specific conditions.[127,129] In the retina, multiple forms of IGFBP (2–5) are secreted by retinal endothelial cells.[128] IGFBP-3 has been shown to enhance cell proliferation in retinal endothelial cells and to decrease the formation of neovascular tufts in a murine model of oxygen-induced retinopathy.[130,131] These studies suggest that IGFBP-3 may

be vascular-protective in the retina. Recently, we also have demonstrated that IGFBP-3 is neuroprotective in the retina and reduces injury-induced retinal inflammation.[132]

Key Factors That Modulate VEGF Function in the Retina

The retina is one of the last organs to become vascularized in the fetus. The vasculogenic part of the process of human retinal vascularization begins at about gestational week 14 and appears to depend on a physiologic hypoxia[8,133] brought about by an increase in metabolic demand within the developing retina.[4–6] This physiologic hypoxia induces the local release of VEGF which, together with IGF-1, regulates angiogenesis and therefore normal vascularization of the retina.[133,134] Retinal vascularization is complete by 36–40 WG.

ROP is a two-phase disease in which the phases are mirror images; the controlling growth factors are deficient in phase 1 and in excess in phase 2. Phase 2 involves uncontrolled proliferative growth of retinal blood vessels in response to hypoxia. The therapeutic intention would be to prevent the first phase of cessation of vessel and neural retinal development and then the second destructive phase would be prevented. This has been successfully performed using exogenous EPO, VEGF, and IGFBP-3 during phase 1 to prevent phase 2. These two phases, seen in premature infants, can be duplicated in animal models of ROP. Hyperoxia causes vaso-obliteration and cessation of normal retinal blood vessel development, which mimics phase 1 of ROP. IGF-1 levels rise in the third trimester of pregnancy but not in the preterm infant. The low IGF-1 in the preterm infant is due to the infant no longer being exposed to the support of the maternal environment, including maternal sources of IGF-1. IGF-1 levels rise slowly after preterm birth, as these babies are unable to produce adequate IGF-1 compared to term infants.[135] In these premature infants, IGF-1 is further reduced by poor nutrition,[136] acidosis, hypothyroxinemia, and sepsis.[137] IGF-1 appears important for retinal and brain growth.[134] Low levels of IGF-1 appear to play an important role in the early cessation of retinal growth that precipitates ROP.

IGF-1 mediates its effects through activation of the IGF-1 receptor (IGF-1R) (see Fig. 20.3). IGF-1R is a receptor tyrosine kinase and is well established as a key regulator of cell growth and survival with activation of Ras-ERK pathway, the PI3K/Akt pathway, and PKC (see Fig. 20.4). Insulin and IGF-2 can also signal using the IGF-R. There is also a growing body of data to support a role for the structurally and functionally related insulin receptor (IR) in cell survival, even though its major function has been to modulate metabolism. Bidirectional cross-talk between IGF-1R and IR is observed, where specific inhibition of either receptor confers a compensatory increase in activity for the reciprocal receptor.

Although fluctuating oxygen has long been associated with the development of ROP, oxygen-regulated factors like VEGF appear to be directly modulated by IGF-1. IGF-1 is a key growth factor in early retinal development. IGF-1 controls maximum VEGF activation of the Akt endothelial cell survival pathway (see Fig. 20.3). Thus loss of IGF-1 leads to loss of VEGF signaling and retinal vaso-obliteration. This vaso-obliteration leads to phase 2 of ROP which is the proliferative phase. At this point, suppression of IGF-1 and VEGF can reduce neovascularization. Thus IGF-1 is critical to normal retinal vascular development, and a lack of IGF-1 in the early neonatal period is associated with lack of vascular growth and with subsequent proliferative ROP. In IGF-1-null mice, the retinal blood vessels grow more slowly than in those of normal mice, a pattern very similar to that seen in premature babies with ROP.

Adult Retinal Hypoxia and Etiology

Diabetic Retinopathy

Much like ROP, diabetic retinopathy has a vaso-obliteration phase that leads to a proliferative phase. The vaso-obliteration is not due to hyperoxia but rather to vaso-occlusion and vasodegeneration of the microvasculature, setting up the ischemic environment that leads to the vasoproliferative end-stage condition. Clinically the early pathology has been classified as nonproliferative (microaneurysms, exudates, leakage, capillary nonperfusion) resulting in hypoxia and the endstage pathology as proliferative

(preretinal neovascularization). The purely vasodegenerative, nonproliferative form of the disease is by far the most common and represents a disease of the neurovascular unit, resulting in dysfunction and eventual death of several of the key cells that maintain the BRB: pericytes, vascular endothelial cells, Müller glia, and neurons. Kohner and Henkind elegantly demonstrated that, in diabetic individuals, areas of nonperfusion on fluorescein angiography are associated with acellular capillaries in trypsin digests.[138] Direct measurement of oxygen in diabetic cat retinas demonstrated that even small aneurysms can result in a decrease in retinal interstitial oxygen.[139]

There are many mechanisms implicated in the pathogenesis of diabetic retinopathy but one that has gained considerable attention in the last decade is inflammation. The environment of hyperglycemia, abnormal lipids, increased oxidative stress, elevated serum and tissue advanced glycation endproducts (AGE)/receptor for AGE, increased serum/tissue cytokines, elevated blood pressure, and endoplasmic reticulum stress are the likely initiators of inflammation.[140] Pathways of inflammation converge with pathways of endothelial dysfunction and coagulation to accelerate the pathogenesis of this disease.[141] Initially, nonspecific indicators of inflammation such as white-cell count and fibrinogen were found to be predictive of incident diabetes.[142] Subsequently, plasminogen activator inhibitor-1 (PAI-1), C-reactive protein, and fibrinogen were shown to be independent predictors.[143] These observations are supported by several other prospective studies, in which tissue plasminogen activator, another marker of reduced fibrinolysis,[144] and von Willebrand factor, a marker of endothelial injury, were predictive.[145] In one clinical study of type 2 diabetics, adhesion molecules were higher in subjects with retinopathy than those without,[146] and in another population-based cohort, composite scores of both inflammatory and endothelial function markers were strongly associated with the presence of diabetic retinopathy.[147] Similarly, E-selectin values were found to be increased in a group with type 1 diabetes and retinopathy.[148] Adiponectin was increased in the advanced stages of retinopathy.[149] These results should be interpreted cautiously, however, as serum markers are not necessarily indicators of tissue events. However, P-

selectin, ICAM-1, and polymorphonuclear leukocyte numbers are all elevated in human diabetic retina.[150] Experimental work in diabetic rat retinas later demonstrated that inflammatory cytokine-mediated leukostasis occurs early in diabetic retina and neutralizing ICAM-1 and CD-18 prevents it.[151–153] From these studies it appears that inflammation-mediated EC injury and vaso-occlusion may cause nonperfusion and subsequent hypoxia in diabetic retina.[154,155]

The hypothesis that inflammation is critical to the development of diabetic retinopathy arose from initial reports that diabetic patients taking salicylates to treat rheumatoid arthritis had a lower-than-expected incidence of diabetic retinopathy.[156] The subsequent decades demonstrated an increase in inflammatory markers and growth factors in the diabetic vitreous and retina. Recently microarray analyses substantiated a marked inflammatory response in the retinas of diabetic rodents.[157] Confirmation of the importance of inflammatory factors and growth factors is supported by additional rodent studies that show that blocking these factors prevents the development of lesions characteristic of the retinopathy in animals. Specific inflammatory molecules that have been shown to contribute to structural or functional alterations that are characteristic of the retinopathy include NF-κβ;[158] inducible nitric oxide synthase;[159] cytochrome c oxidase;[159] ICAM;[155] 5-lipoxygenase;[159] interleukin-1β;[160] tumor necrosis factor (TNF)-α;[161] and VEGF.[80,162] Inflammation can intensify the generation of AGEs that are produced in response to hyperglycemia and increased oxidative stress.

Retinal Vein Occlusion (RVO)

Occlusion of large retinal blood vessels is a common occurrence, which results in retinal hypoxia. RVO is the second most common sight-threatening retinal vascular disorder after diabetic retinopathy.[163] RVO represents an obstruction of the retinal venous system that involves either the central retinal vein or a branch retinal vein. RVO is typically due to external compression or disease of the vein wall, such as is seen in vasculitis.[164] Central retinal artery occlusion (CRAO) results in sudden, catastrophic

visual loss, and branch retinal arteriolar occlusion (BRAO) causes sudden segmental visual loss and may recur to involve other branch retinal arterioles. CRAO studies have shown that the ischemic retinal whitish opacity and swelling are essentially located in the perifoveolar region of the macula. Oxygen supply and nutrition from the choroidal vascular bed to the thinner peripheral retina help in its much longer survival and the maintenance of peripheral visual fields. The diagnosis is clinical and based on the observation of the ocular fundus: venous dilation and tortuosity, flame-shaped retinal hemorrhages, retinal edema, and cotton-wool exudates affecting all the retinal sectors (in CRVO) or the sector of the retina drained by the affected vein in BRVO. Open angle glaucoma is the most frequent local alteration predisposing to RVO as it compromises venous outflow by increasing intraocular pressure. Raised intraocular pressure causes external compression of the central retinal vein as it passes through the lamina cribrosa, resulting in turbulent blood flow distal to the compression leading to thrombus formation.

The natural history of RVO is highly variable; in some cases the retinal findings progressively disappear and there is a good visual outcome, while in other cases severe complications like ocular neovascularization (proliferative retinopathy), vitreous hemorrhage, neovascular glaucoma, and macular edema develop. Using retinal oximetry in BRVO, venular saturation was found to be highly variable between patients (12–93%);[165] this was attributed to variable severity of the disease, recanalization, degree of occlusion, collateral vasculature, or tissue atrophy. The majority of patients with CRVO have signs of macular edema at presentation whereas only 5–15% of eyes with BRVO develop macular edema over the first year. Venous collateral channels represent tortuous vessels that develop locally, mainly around the optic disc, and are usually associated with a long-standing vascular obstruction. Vitreous hemorrhage develops in 10% of eyes with CRVO within 9 months of presentation and in about 40% of eyes with BRVO.[163] If there is restoration of circulation in the central retinal artery, the retinal capillaries in the central, thickest part of the macular region do not refill because of compression by the surrounding swollen superficial retinal tissue, resulting in the “no-reflow

phenomenon,"[166] and consequently in permanent ganglion cell death in the nonperfused retina; the area of central retinal capillary nonfilling may vary from eye to eye depending upon the severity of retinal swelling in the macular region. This results in the variable size of the permanent central scotoma. In considering the outcome of CRAO, it is important to consider retinal tolerance time to acute retinal ischemia. The chance of recovery of vision only exists as long as the retina has reversible ischemic damage. The retina suffers no detectable damage with CRAO of up to 97 minutes, but after that, the longer the CRAO, the more extensive the irreversible ischemic retinal damage.

It is generally believed that the CRAO is always either embolic or thrombotic in origin. Embolism is far more common than thrombosis,[167] as was pointed out almost a century ago by Coats.[168,169] If diagnosis is made within 15 days from onset of clinical manifestations, low molecular weight heparins at anticoagulant doses are typically used 10–15 days followed by half dose for a total of 90 days.[170] An inflammatory etiology is also postulated in RVO, as RVO is associated with immunologic diseases in young patients. To support this contention, patients can experience prompt resolution of symptoms with the use of periocular steroids.[171]

Giant cell arteritis is an important and well-known cause of CRAO and is an ophthalmic emergency because of the high risk of bilateral visual loss, which is preventable.

Elevated levels of PAI-1, lipoprotein(a), and hyperhomocysteinemia and low circulating levels of folic acid, vitamin B_{12} and vitamin B_6 have been implicated in the pathogenesis of this disease.[172] While the pathogenesis is complex and largely unknown, medical treatment includes identification and correction of vascular risk factors. The use of fluorescein fundus angiography before (showing occlusion of the central retinal artery) and immediately after thrombolysis may show improvement in and/or restoration of retinal circulation and retinal function. It is also important to consider that fibrinolytic agents can dissolve only platelet fibrin emboli.[173] Retinal emboli are made of 74% cholesterol, 10.5% calcific material, and only 15.5% of platelet fibrin. Fibrinolytic agents cannot dissolve cholesterol or calcified material. Therefore, there is no scientific rationale for the use of

fibrinolytic agents in at least 85% of CRAO cases. Of Virchow's three classical factors that play a role in thrombogenesis – stasis, vessel wall damage, and hypercoagulability – the first two have long been reported in patients with RVO, whereas the third has not been sufficiently investigated until recently.

Sickle-Cell Disease (SCD)

The pathologic processes involved in SCD can affect virtually every vascular bed in the body including the retina, and in its advanced stages, SCD has the potential to cause blindness.[174] Classification of ophthalmic manifestations of SCD in the retina is based on the presence or absence of vascular proliferation, which is the most important precursor of blinding complications and precedes development of a vitreous hemorrhage or retinal detachment. Ischemia occurs due to obstruction of capillaries with sickle red blood cells and subsequent thrombus formation. The subsequent scenario for disease pathogenesis is similar to that for ROP, diabetic retinopathy, and RVO, described above, except that there is no retinal leakage of retinal blood vessels only from preretinal neovascularization, even though there is loss of peripheral vasculature and elevation of VEGF.[175] Neovascularization that occurs can lead to fibrosis that can then result in retinal detachment. See Chapter 60 (Hemoglobinopathies) for a complete discussion of sickle-cell retinopathy.

Ocular Ischemic Syndrome (OIS)

OIS occurs at a mean age of 65 years and is rare before the age of 50. Men are affected twice as often as women,[176] reflecting their higher incidence of atherosclerotic disease; however, no racial predilection exists. Bilateral involvement may occur in up to 22% of cases.[177,178] Sturrock and Mueller estimated 7.5 cases per million persons every year,[179] but this is likely an underestimation as OIS can be easily misdiagnosed. Kearns[180] reported that, of patients with occlusion of the internal carotid artery undergoing surgical anastomosis between the superficial temporal artery and the middle cerebral artery, 18% presented with OIS. Up to 29% of patients with a symptomatic carotid artery occlusion manifest retinal vascular

changes that are usually asymptomatic; however, 1.5% of them progress per year to symptomatic OIS.[181] OIS develops especially in patients with poor collateral circulation between the internal and external carotid arterial systems. Insufficient collateral vascular flow in OIS patients explains the frequent association with cerebral infarctions and the poor neurologic outcomes.[182] Degree of internal carotid artery stenosis, presence of collateral vessels, and compensation by collaterals are important in assessing OIS disease severity. Also if the OIS is bilateral or there are associated systemic vascular diseases, this tends to worsen the prognosis.

Retinal Detachment

Retinal detachment causes the sensory retina to be distant from choriocapillaris, thus reducing its oxygen supply and resulting in photoreceptor degeneration. Linsenmeier and Padnick-Silver[183] demonstrated in cat that retinal detachment resulted in a significant decrease in outer retinal oxygen, having a serious metabolic effect on photoreceptors. In subsequent work, Linsenmeier demonstrated that hyperoxia may have clinical benefit after retinal detachment because it normalized photoreceptor oxygen consumption and prevented photoreceptor dysfunction.[184] Furthermore, hyperoxia prevents proliferation and reactivity of retinal Müller cells in the detached feline retina, limiting retinal injury.[185]

Consequences of Retinal Ischemia

In 1971, Judah Folkman reported in the *New England Journal of Medicine* that all cancer tumors are angiogenesis-dependent.[186] If a tumor could be stopped from growing its own blood supply, he surmised, it would wither and die. Though his hypothesis was initially disregarded by most experts in the field, Folkman persisted with his research. After more than a decade, his theory became widely accepted and is now at the center of our understanding of ocular angiogenesis. Retinal neovascularization is defined as a state where new pathologic vessels originate from the existing retinal veins and extend along the inner surface of the retina.

Vascular Permeability

Growth factors such as VEGF have been implicated in both retinal neovascularization and vascular hyperpermeability.[187] Antibodies to VEGF improve visual function in patients with diabetic macular edema.[188] In experimental diabetes and in VEGF-induced permeability, alterations of the tight junction (TJ) complex of microvascular endothelial cells alters the BRB.[189] A role of classical PKC isoforms (cPKCs) but especially PKCβ in regulating VEGF-induced vascular permeability is well accepted.[190] VEGF activation of PKCβ leads to phosphorylation and reorganization of the TJ complex, increasing vessel wall permeability.[191] VEGF increases the phosphorylation of the TJ protein, occludin, at multiple sites,[192] including Ser490.[193] Phosphorylation at Ser490 allows subsequent ubiquitination and endocytosis of occludin and fosters breaks in the TJ.[194] Despite this well-supported mechanism, the PKCβ inhibitor ruboxistaurin failed to achieve Food and Drug Administration approval for diabetic retinopathy. cPKC inhibition also failed to prevent TNF-α-induced permeability,[195] a proinflammatory cytokine also implicated in diabetic retinopathy. Thus targeting permeability in the retina continues to be a difficult clinical problem.

Adult Choroidal Ischemia

The choroidal vasculature is an expansive vascular plexus that handles 90% of the blood from the ophthalmic artery. It was often assumed that the choriocapillaris was so vast that generation of choroidal ischemia rarely occurred. However, there are several diseases in which the loss of choroidal vasculature is extensive, resulting in apparent choroidal ischemia.

Diabetic choroidopathy was first described by Hidiyat and Fine.[196] The use of alkaline phosphatase enzyme histochemistry on human choroid permitted quantification of vascular loss in choroid. Viable vessels were positive for alkaline phosphatase while acellular, dysfunctional capillaries lacked it, and choroidal neovascularization had the greatest activity.[12] This technique demonstrated that there was four times greater loss in

choriocapillaris in diabetic subjects than in aged control subjects.[197] Loss of alkaline phosphatase activity was associated with the presence of polymorphonuclear leukocytes.[198] Areas of choriocapillaris loss were also associated with choroidal neovascularization and Bruch's membrane deposits. A consequence of choriocapillaris dropout is loss of outer retinal oxygenation. This may be the reason for loss of blue cones and other cones in diabetic retina when there is no retinopathy present.[199,200]

Decreased choroidal blood flow has been measured in AMD.[201–204] Using alkaline phosphatase activity and quantification of RPE in AMD, the loss of choriocapillaris has been demonstrated in exudative or wet AMD as well as geographic atrophy (Fig. 20.5). RPE loss occurs first in geographic atrophy and then choriocapillaris degeneration occurs. Although some capillaries survive in the area of RPE atrophy, a 50% loss of vasculature occurs and the surviving capillaries are highly constricted.[205,206] This undoubtedly contributes to photoreceptor loss in the area of degeneration. Capillary loss occurs in exudative AMD as well, but in the presence of a complete RPE monolayer (Fig. 20.5). This suggests that the RPE in this area are hypoxic and VEGF production may be increased, causing choroidal neovascularization. Large-vessel stenosis is also often observed in AMD choroid, suggesting that the choriocapillaris blood supply may be limited as well. Unfortunately, we have no way of measuring oxygen directly in the choroid, so we can only assume ischemia occurs when there is loss of viable choriocapillaris and stenosis of large and intermediate choroidal blood vessel.

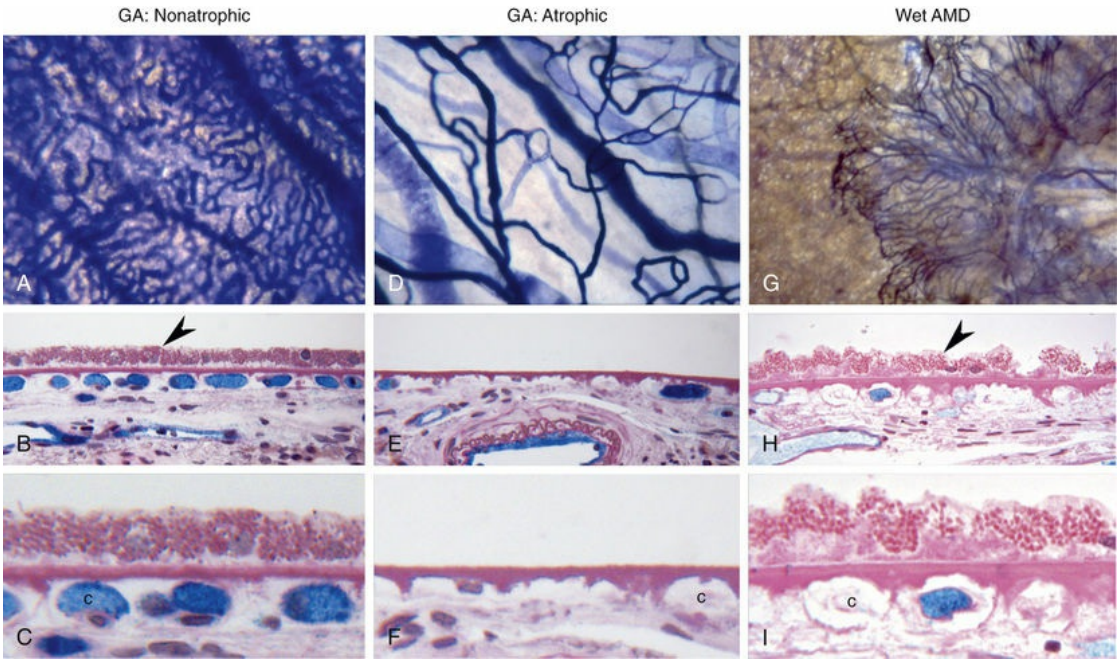

FIG. 20.5 The choroid and retinal pigment epithelium (RPE) in geographic atrophy (A–F) and wet (neovascular) age-related macular degeneration (AMD) (G–I). (A) Alkaline phosphatase (APase)-stained choroidal blood vessels in a nonatrophic region of geographic atrophy (GA) choroid. (B) When sectioned, this area has normal-appearing RPE cells (*arrowhead*) and viable choriocapillaris lumens filled with serum APase. (C) Higher magnification shows the intimate relationship between RPE, Bruch's membrane, and choriocapillaris (*c*). (D) The atrophic region of this GA choroid has no RPE and an attenuated choriocapillaris with narrow lumens. (E) Cross-sections of this area demonstrate the APase reaction product in a few remaining choriocapillaris lumens and the endothelial cells of artery (bottom). (F) At higher magnification it is apparent that the $APase^{-}$ capillaries (*c*) are only collagenous tubes between intercapillary septa. (G) In a flat choroid preparation of a wet AMD subject, a large fan-shaped choroidal neovascular formation is present and the RPE monolayer to the left appears normal. (H) A section of this subject immediately in advance of the choroidal neovascularization demonstrates viable hypertrophic RPE (*arrowhead*) over an attenuated choriocapillaris. (I) At higher magnification, the remnants of atrophic choriocapillaris lumens (*c*) are present between intercapillary septa and a single $APase^{+}$ lumen

remains, yet RPE are still present.

Conclusions

Both too little and too much oxygen can be damaging to the retina. Retina cannot function properly nor survive without the support of two vasculatures: retinal and choroidal. If either vasculature is dysfunctional, retinal hypoxia occurs and HIF-1α becomes stable and induces expression of key factors to assist in retinal cell survival. Reduced retinal oxygenation causes impaired neuroretinal activity in young healthy persons.[207] One key factor upregulated by HIF-1α is VEGF, which stimulates new angiogenesis and increased vascular permeability. These pathol events can be controlled by destroying ischemic retina (photocoagulation), inhibiting VEGF, or reducing levels of HIF-1α.

References

1. Wangsa-Wirawan ND, Linsenmeier RA. Retinal oxygen. Fundamental and clinical aspects. *Arch Ophthalmol*. 2003;121:547–557.
2. Yu DY, Cringle SJ. Oxygen distribution and consumption within the retina in vascularised and avascular retinas and in animal models of retinal disease. *Prog Retin Eye Res*. 2001;20:175–208.
3. Li C, Fitzgerald ME, Del Mar N, et al. The identification and neurochemical characterization of central neurons that target parasympathetic preganglionic neurons involved in the regulation of choroidal blood flow in the rat eye using pseudorabies virus, immunolabeling and conventional pathway tracing methods. *Front Neuroanat*. 2015;9:65.
4. Chan-Ling T, McLeod DS, Hughes S, et al. Astrocyte–endothelial cell relationships during human retinal vascular development. *Invest Ophthalmol Vis Sci*. 2004;45:2020–2032.
5. Hasegawa T, McLeod DS, Prow T, et al. Vascular precursors in developing human retina. *Invest Ophthalmol Vis Sci*. 2008;49:2178–2192.

6. McLeod DS, Hasegawa T, Prow T, et al. The initial fetal human retinal vasculature develops by vasculogenesis. *Dev Dyn*. 2006;235:3336–3347.
7. Stone J, Itin A, Alon T, et al. Development of retinal vasculature is mediated by hypoxia-induced vascular endothelial growth factor (VEGF) expression by neuroglia. *J Neurosci*. 1995;15:4738–4747.
8. Chan-Ling T, Gock B, Stone J. The effect of oxygen on vasoformative cell division: Evidence that 'physiol hypoxia' is the stimulus for normal retinal vasculogenesis. *Invest Ophthalmol Vis Sci*. 1995;36:1201–1214.
9. Cogan DG, Kuwabara T. The mural cell in perspective. *Arch Ophthalmol*. 1967;78:133–139.
10. Baba T, Grebe R, Hasegawa T, et al. Maturation of the fetal human vasculature. *Invest Ophthalmol Vis Sci*. 2009;50:3503–3511.
11. Hasegawa T, McLeod DS, Bhutto IA, et al. The embryonic human choriocapillaris develops by hemo-vasculogenesis. *Dev Dyn*. 2007;236:2089–2100.
12. McLeod DS, Lutty GA. High resolution histologic analysis of the human choroidal vasculature. *Invest Ophthalmol Vis Sci*. 1994;35:3799–3811.
13. Blaauwgeers HG, Holtkamp GM, Rutten H, et al. Polarized vascular endothelial growth factor secretion by human retinal pigment epithelium and localization of vascular endothelial growth factor receptors on the inner choriocapillaris. Evidence for a trophic paracrine relation. *Am J Pathol*. 1999;155:421–428.
14. Steptoe R, McMenamin PG, McMenamin C. Distribution and characterisation of rat choroidal mast cells. *Br J Ophthalmol*. 1994;78:211–218.
15. Godfrey W. Characterization of the choroidal mast cell. *Trans Am Ophthalmol Soc*. 1987;85:557–599.
16. Lutjen-Drecoll E. Choroidal innervation in primate eyes. *Exp Eye Res*. 2006;82:357–361.
17. Michaelson IC. The mode of development of the vascular system of the retina, with some observations on its significance for certain retinal diseases. *Trans Ophthalmol*

Soc U K. 1948;68:137–180.
18. Michaelson IC. *Retinal circulation in man and animals*. CC Thomas: Springfield, IL; 1954.
19. Wise GN. Retinal neovascularization. *Trans Am Ophthalmol Soc*. 1956;96:729–826.
20. Leung DW, Cachianes G, Kuang WJ, et al. Vascular endothelial growth factor is a secreted angiogenic mitogen. *Science*. 1989;246:1306–1309.
21. Senger DR, Galli SJ, Dvorak AM, et al. Tumor cells secrete a vascular permeability factor that promotes accumulation of ascites fluid. *Science*. 1983;219:983–985.
22. Yu DY, Cringle SJ, Su EN. Intraretinal oxygen distribution in the monkey retina and the response to systemic hyperoxia. *Invest Ophthalmol Vis Sci*. 2005;46:4728–4733.
23. McLeod DS, Brownstein R, Lutty GA. Vaso-obliteration in the canine model of oxygen-induced retinopathy. *Invest Ophthalmol Vis Sci*. 1996;37:300–311.
24. Ernest JT, Goldstick TK. Retinal oxygen tension and oxygen reactivity in retinopathy of prematurity in kittens. *Invest Ophthalmol Vis Sci*. 1984;25:1129–1134.
25. Hardy P, Peri KG, Lahaie I, et al. Increased nitric oxide synthesis and action preclude choroidal vasoconstriction to hyperoxia in newborn pigs. *Circ Res*. 1996;79:504–511.
26. Linsenmeier RA, Yancy CM. Effects of hyperoxia on the oxygen distribution in the intact cat retina. *Invest Ophthalmol Vis Sci*. 1989;30:612–618.
27. Pournaras CJ, Riva CE, Tsacopoulos M, et al. Diffusion of O_2 in the retina of anesthetized miniature pigs in normoxia and hyperoxia. *Exp Eye Res*. 1989;49:347–360.
28. Benizri E, Ginouves A, Berra E. The magic of the hypoxia-signaling cascade. *Cell Mol Life Sci*. 2008;65:1133–1149.
29. Semenza GL, Wang GL. A nuclear factor induced by hypoxia via de novo protein synthesis binds to the human erythropoietin gene enhancer at a site required for transcriptional activation. *Mol Cell Biol*. 1992;12:5447–5454.
30. Wang GL, Jiang BH, Rue EA, et al. Hypoxia-inducible factor 1 is a basic-helix-loop-helix-PAS heterodimer regulated by cellular O_2 tension. *Proc Natl Acad Sci USA*. 1995;92:5510–

5514.
31. Gariboldi MB, Ravizza R, Monti E. The IGFR1 inhibitor NVP-AEW541 disrupts a pro-survival and pro-angiogenic IGF-STAT3-HIF1 pathway in human glioblastoma cells. *Biochem Pharmacol*. 2010;80:455–462.
32. Jiang BH, Zheng JZ, Leung SW, et al. Transactivation and inhibitory domains of hypoxia-inducible factor 1alpha. Modulation of transcriptional activity by oxygen tension. *J Biol Chem*. 1997;272:19253–19260.
33. Xin X, Rodrigues M, Umapathi M, et al. Hypoxic retinal Muller cells promote vascular permeability by HIF-1-dependent up-regulation of angiopoietin-like 4. *Proc Natl Acad Sci USA*. 2013;110(36):E3425–34.
34. Semenza GL. Hydroxylation of HIF-1: oxygen sensing at the molecular level. *Physiology (Bethesda)*. 2004;19:176–182.
35. Mahon PC, Hirota K, Semenza GL. FIH-1: a novel protein that interacts with HIF-1alpha and VHL to mediate repression of HIF-1 transcriptional activity. *Genes Dev*. 2001;15:2675–2686.
36. Lando D, Peet DJ, Whelan DA, et al. Asparagine hydroxylation of the HIF transactivation domain a hypoxic switch. *Science*. 2002;295:858–861.
37. Lee C, Kim SJ, Jeong DG, et al. Structure of human FIH-1 reveals a unique active site pocket and interaction sites for HIF-1 and von Hippel–Lindau. *J Biol Chem*. 2003;278:7558–7563.
38. Kukkola L, Koivunen P, Pakkanen O, et al. Collagen prolyl 4-hydroxylase tetramers and dimers show identical decreases in K_m values for peptide substrates with increasing chain length: mutation of one of the two catalytic sites in the tetramer inactivates the enzyme by more than half. *J Biol Chem*. 2004;279:18656–18661.
39. van Uden P, Kenneth NS, Rocha S. Regulation of hypoxia-inducible factor-1alpha by NF-kappaB. *Biochem J*. 2008;412:477–484.
40. Wang GL, Semenza GL. Desferrioxamine induces erythropoietin gene expression and hypoxia-inducible factor 1 DNA-binding activity: implications for models of

hypoxia signal transduction. *Blood*. 1993;82:3610–3615.
41. Tian H, McKnight SL, Russell DW. Endothelial PAS domain protein 1 (EPAS1), a transcription factor selectively expressed in endothelial cells. *Genes Dev*. 1997;11:72–82.
42. Sowter HM, Raval RR, Moore JW, et al. Predominant role of hypoxia-inducible transcription factor (Hif)-1alpha versus Hif-2alpha in regulation of the transcriptional response to hypoxia. *Cancer Res*. 2003;63:6130–6134.
43. Park SK, Dadak AM, Haase VH, et al. Hypoxia-induced gene expression occurs solely through the action of hypoxia-inducible factor 1alpha (HIF-1alpha): role of cytoplasmic trapping of HIF-2alpha. *Mol Cell Biol*. 2003;23:4959–4971.
44. Makino Y, Cao R, Svensson K, et al. Inhibitory PAS domain protein is a negative regulator of hypoxia-inducible gene expression. *Nature*. 2001;414:550–554.
45. Shelby S, Angadi PS, Zheng QD, et al. Hypoxia inducible factor 1α contributes to regulation of autophagy in retinal detachment. *Exp Eye Res*. 2015;137:84–93.
46. Lee K, Qian DZ, Rey S, et al. Anthracycline chemotherapy inhibits HIF-1 transcriptional activity and tumor-induced mobilization of circulating angiogenic cells. *Proc Natl Acad Sci USA*. 2009;106(7):2353–2358.
47. Zhang H, Qian DZ, Tan YS, et al. Digoxin and other cardiac glycosides inhibit HIF-1alpha synthesis and block tumor growth. *Proc Natl Acad Sci USA*. 2008;105(50):19579–19586.
48. Yoshida T, Zhang H, Iwase T, et al. Digoxin inhibits retinal ischemia-induced HIF-1alpha expression and ocular neovascularization. *FASEB J*. 2010;24(6):1759–1767.
49. Compernolle V, Brusselmans K, Franco D, et al. Cardia bifida, defective heart development and abnormal neural crest migration in embryos lacking hypoxia-inducible factor-1alpha. *Cardiovasc Res*. 2003;60:569–579.
50. Peng J, Zhang L, Drysdale L, et al. The transcription factor EPAS-1/hypoxia-inducible factor 2alpha plays an important role in vascular remodeling. *Proc Natl Acad Sci USA*. 2000;97:8386–8391.
51. Scortegagna M, Morris MA, Oktay Y, et al. The HIF family

member EPAS1/HIF-2alpha is required for normal hematopoiesis in mice. *Blood*. 2003;102:1634–1640.
52. Kline DD, Peng YJ, Manalo DJ, et al. Defective carotid body function and impaired ventilatory responses to chronic hypoxia in mice partially deficient for hypoxia-inducible factor 1 alpha. *Proc Natl Acad Sci USA*. 2002;99:821–826.
53. Caprara C, Thiersch M, Lange C, et al. HIF1A is essential for the development of the intermediate plexus of the retinal vasculature. *Invest Ophthalmol Vis Sci*. 2011;52:2109–2117.
54. Lin M, Chen Y, Jin J, et al. Ischaemia-induced retinal neovascularisation and diabetic retinopathy in mice with conditional knockout of hypoxia-inducible factor-1 in retinal Müller cells. *Diabetologia*. 2011;54:1554–1566.
55. Sears JE, Hoppe G, Ebrahem Q, et al. Prolyl hydroxylase inhibition during hyperoxia prevents oxygen-induced retinopathy. *Proc Natl Acad Sci USA*. 2008;105(50):19898–19903.
56. Trichonas G, Lee TJ, Hoppe G, et al. Prolyl hydroxylase inhibition during hyperoxia prevents oxygen-induced retinopathy in the rat 50/10 model. *Invest Ophthalmol Vis Sci*. 2013;54(7):4919–4926.
57. Hoppe G, Lee TJ, Yoon S, et al. Inducing a visceral organ to protect a peripheral capillary bed: stabilizing hepatic HIF-1α prevents oxygen-induced retinopathy. *Am J Pathol*. 2014;184:1890–1899.
58. Cramer T, Yamanishi Y, Clausen BE, et al. HIF-1alpha is essential for myeloid cell-mediated inflammation. *Cell*. 2003;112:645–657.
59. Kojima H, Gu H, Nomura S, et al. Abnormal B lymphocyte development and autoimmunity in hypoxia-inducible factor 1alpha -deficient chimeric mice. *Proc Natl Acad Sci USA*. 2002;99:2170–2174.
60. Makino Y, Nakamura H, Ikeda E, et al. Hypoxia-inducible factor regulates survival of antigen receptor-driven T cells. *J Immunol*. 2003;171:6534–6540.
61. Giaccia A, Siim BG, Johnson RS. HIF-1 as a target for drug development. *Nat Rev Drug Discov*. 2003;2:803–811.
62. Kelly BD, Hackett SF, Hirota K, et al. Cell type-specific

regulation of angiogenic growth factor gene expression and induction of angiogenesis in nonischemic tissue by a constitutively active form of hypoxia-inducible factor 1. *Circ Res*. 2003;93:1074–1081.
63. Hirsila M, Koivunen P, Gunzler V, et al. Characterization of the human prolyl 4-hydroxylases that modify the hypoxia-inducible factor. *J Biol Chem*. 2003;278:30772–30780.
64. Willam C, Masson N, Tian YM, et al. Peptide blockade of HIFalpha degradation modulates cellular metabolism and angiogenesis. *Proc Natl Acad Sci USA*. 2002;99:10423–10428.
65. Sears J, Hoppe G. Stimulating retinal blood vessel protection with hypoxia-inducible factor stabilization: identification of novel small-molecule hydrazones to inhibit hypoxia-inducible factor prolyl hydroxylase (an American Ophthalmol Society thesis). *Trans Am Ophthalmol Soc*. 2013;111:169–179.
66. Chen J, Smith LE. A double-edged sword: erythropoietin eyed in retinopathy of prematurity. *J AAPOS*. 2008;12:221–222.
67. Ferrara N. Vascular endothelial growth factor as a target for anticancer therapy. *Oncologist*. 2004;9(Suppl. 1):2–10.
68. Carmeliet P, Ferreira V, Breier G, et al. Abnormal blood vessel development and lethality in embryos lacking a single VEGF allele. *Nature*. 1996;380:435–439.
69. Alon T, Hemo I, Itin A, et al. Vascular endothelial growth factor acts as a survival factor for newly formed retinal vessels and has implications for retinopathy of prematurity. *Nat Med*. 1995;1:1024–1028.
70. Baffert F, Le T, Thurston G, et al. Angiopoietin-1 decreases plasma leakage by reducing number and size of endothelial gaps in venules. *Am J Physiol Heart Circ Physiol*. 2006;290:H107–18.
71. Saint-Geniez M, Maharaj AS, Walshe TE, et al. Endogenous VEGF is required for visual function: evidence for a survival role on muller cells and photoreceptors. *PLoS ONE*. 2008;3:e3554.
72. Adamis AP, Shima DT, Yeo KT, et al. Synthesis and secretion of vascular permeability factor/vascular

endothelial growth factor by human retinal pigment epithelial cells. *Biochem Biophys Res Commun*. 1993;193:631–638.
73. Aiello LP, Northrup JM, Keyt BA, et al. Hypoxic regulation of vascular endothelial growth factor in retinal cells. *Arch Ophthalmol*. 1995;113:1538–1544.
74. Famiglietti EV, Stopa EG, McGookin ED, et al. Immunocytochemical localization of vascular endothelial growth factor in neurons and glial cells of human retina. *Brain Res*. 2003;969:195–204.
75. Sandercoe TM, Geller SF, Hendrickson AE, et al. VEGF expression by ganglion cells in central retina before formation of the foveal depression in monkey retina: evidence of developmental hypoxia. *J Comp Neurol*. 2003;462:42–54.
76. Marneros AG, Fan J, Yokoyama Y, et al. Vascular endothelial growth factor expression in the retinal pigment epithelium is essential for choriocapillaris development and visual function. *Am J Pathol*. 2005;167:1451–1459.
77. Saint-Geniez M, Kurihara T, Sekiyama E, et al. An essential role for RPE-derived soluble VEGF in the maintenance of the choriocapillaris. *Proc Natl Acad Sci USA*. 2009;106:18751–18756.
78. Nishijima K, Ng YS, Zhong L, et al. Vascular endothelial growth factor-A is a survival factor for retinal neurons and a critical neuroprotectant during the adaptive response to ischemic injury. *Am J Pathol*. 2007;171:53–67.
79. Ng EW, Adamis AP. Targeting angiogenesis, the underlying disorder in neovascular age-related macular degeneration. *Can J Ophthalmol*. 2005;40:352–368.
80. Kunz Mathews M, Merges C, McLeod DS, et al. Vascular endothelial growth factor (VEGF) and vascular permeability changes in human diabetic retinopathy. *Invest Ophthalmol Vis Sci*. 1997;38:2729–2741.
81. Starita C, Patel M, Katz B, et al. Vascular endothelial growth factor and the potential therapeutic use of pegaptanib (Macugen) in diabetic retinopathy. *Dev Ophthalmol*. 2007;39:122–148.

82. Aiello LP, Cahill MT, Cavallerano JD. Growth factors and protein kinase C inhibitors as novel therapies for the medical management diabetic retinopathy. *Eye (Lond)*. 2004;18:117–125.
83. Tripathi RC, Li J, Tripathi BJ, et al. Increased level of vascular endothelial growth factor in aqueous humor of patients with neovascular glaucoma. *Ophthalmology*. 1998;105:232–237.
84. Lashkari K, Hirose T, Yazdany J, et al. Vascular endothelial growth factor and hepatocyte growth factor levels are differentially elevated in patients with advanced retinopathy of prematurity. *Am J Pathol*. 2000;156:1337–1344.
85. Rosenfeld PJ, Brown DM, Heier JS, et al. Ranibizumab for neovascular age-related macular degeneration. *N Engl J Med*. 2006;355:1419–1431.
86. Miller-Kasprzak E, Jagodzinski PP. 5-Aza-2'-deoxycytidine increases the expression of anti-angiogenic vascular endothelial growth factor 189b variant in human lung microvascular endothelial cells. *Biomed Pharmacother*. 2008;62:158–163.
87. Anthony FW, Wheeler T, Elcock CL, et al. Short report: identification of a specific pattern of vascular endothelial growth factor mRNA expression in human placenta and cultured placental fibroblasts. *Placenta*. 1994;15:557–561.
88. Woolard J, Bevan HS, Harper SJ, et al. Molecular diversity of VEGF-A as a regulator of its biol activity. *Microcirculation*. 2009;16:572–592.
89. Harper SJ, Bates DO. VEGF-A splicing: the key to anti-angiogenic therapeutics? *Nat Rev Cancer*. 2008;8(11):880–887.
90. de Vries C, Escobedo JA, Ueno H, et al. The fms-like tyrosine kinase, a receptor for vascular endothelial growth factor. *Science*. 1992;255:989–991.
91. Quinn TP, Peters KG, De Vries C, et al. Fetal liver kinase 1 is a receptor for vascular endothelial growth factor and is selectively expressed in vascular endothelium. *Proc Natl Acad Sci USA*. 1993;90:7533–7537.
92. Soker S, Takashima S, Miao HQ, et al. Neuropilin-1 is

expressed by endothelial and tumor cells as an isoform-specific receptor for vascular endothelial growth factor. *Cell*. 1998;92:735–745.
93. Schlessinger J. New roles for Src kinases in control of cell survival and angiogenesis. *Cell*. 2000;100:293–296.
94. Hubbard SR. Structural analysis of receptor tyrosine kinases. *Prog Biophys Mol Biol*. 1999;71:343–358.
95. Shalaby F, Rossant J, Yamaguchi TP, et al. Failure of blood-island formation and vasculogenesis in Flk-1-deficient mice. *Nature*. 1995;376:62–66.
96. Scott A, Mellor H. VEGF receptor trafficking in angiogenesis. *Biochem Soc Trans*. 2009;37:1184–1188.
97. Jopling HM, Odell AF, Hooper NM, et al. Rab GTPase regulation of VEGFR2 trafficking and signaling in endothelial cells. *Arterioscler Thromb Vasc Biol*. 2009;29:1119–1124.
98. Salikhova A, Wang L, Lanahan AA, et al. Vascular endothelial growth factor and semaphorin induce neuropilin-1 endocytosis via separate pathways. *Circ Res*. 2008;103:e71–9.
99. Ewan LC, Jopling HM, Jia H, et al. Intrinsic tyrosine kinase activity is required for vascular endothelial growth factor receptor 2 ubiquitination, sorting and degradation in endothelial cells. *Traffic*. 2006;7:1270–1282.
100. Lanahan AA, Hermans K, Claes F, et al. VEGF receptor 2 endocytic trafficking regulates arterial morphogenesis. *Dev Cell*. 2010;18:713–724.
101. Cai J, Jiang WG, Ahmed A, et al. Vascular endothelial growth factor-induced endothelial cell proliferation is regulated by interaction between VEGFR-2, SH-PTP1 and eNOS. *Microvasc Res*. 2006;71:20–31.
102. Chen J, Braet F, Brodsky S, et al. VEGF-induced mobilization of caveolae and increase in permeability of endothelial cells. *Am J Physiol Cell Physiol*. 2002;282:C1053–63.
103. Do JY, Choi YK, Kook H, et al. Retinal hypoxia induces vascular endothelial growth factor through induction of estrogen-related receptor γ. *Biochem Biophys Res Commun*.

2015;460(2):457–463.
104. Grant MB, Boulton ME, Ljubimov AV. Erythropoietin: when liability becomes asset in neurovascular repair. *J Clin Invest*. 2008;118:467–470.
105. Takahashi T, Ueno H, Shibuya M. VEGF activates protein kinase C-dependent, but Ras-independent Raf-MEK-MAP kinase pathway for DNA synthesis in primary endothelial cells. *Oncogene*. 1999;18:2221–2230.
106. D'Amico AG, Maugeri G, Reitano R, et al. PACAP Modulates expression of hypoxia-inducible factors in streptozotocin-induced diabetic rat retina. *J Mol Neurosci*. 2015;57(4):501–509.
107. Fadini GP, Miorin M, Facco M, et al. Circulating endothelial progenitor cells are reduced in peripheral vascular complications of type 2 diabetes mellitus. *J Am Coll Cardiol*. 2005;45:1449–1457.
108. Tepper OM, Galiano RD, Capla JM, et al. Human endothelial progenitor cells from type II diabetics exhibit impaired proliferation, adhesion, and incorporation into vascular structures. *Circulation*. 2002;106:2781–2786.
109. Loomans CJ, de Koning EJ, Staal FJ, et al. Endothelial progenitor cell dysfunction: a novel concept in the pathogenesis of vascular complications of type 1 diabetes. *Diabetes*. 2004;53:195–199.
110. Schatteman GC, Hanlon HD, Jiao C, et al. Blood-derived angioblasts accelerate blood-flow restoration in diabetic mice. *J Clin Invest*. 2000;106:571–578.
111. Caballero S, Sengupta N, Afzal A, et al. Ischemic vascular damage can be repaired by healthy, but not diabetic, endothelial progenitor cells. *Diabetes*. 2007;56:960–967.
112. Jarajapu YP, Caballero S, Verma A, et al. Blockade of NADPH oxidase restores vasoreparative function in diabetic $CD34^+$ cells. *Invest Ophthalmol Vis Sci*. 2011;52:5093–5104.
113. Case J, Ingram DA, Haneline LS. Oxidative stress impairs endothelial progenitor cell function. *Antioxid Redox Signal*. 2008;10:1895–1907.
114. Togliatto G, Trombetta A, Dentelli P, et al. Unacylated

ghrelin rescues endothelial progenitor cell function in individuals with type 2 diabetes. *Diabetes*. 2010;59:1016–1025.
115. Ingram DA, Lien IZ, Mead LE, et al. In vitro hyperglycemia or a diabetic intrauterine environment reduces neonatal endothelial colony-forming cell numbers and function. *Diabetes*. 2008;57:724–731.
116. Urbich C, Dernbach E, Rossig L, et al. High glucose reduces cathepsin L activity and impairs invasion of circulating progenitor cells. *J Mol Cell Cardiol*. 2008;45:429–436.
117. Li SS, Liu Z, Uzunel M, et al. Endogenous thrombospondin-1 is a cell-surface ligand for regulation of integrin-dependent T-lymphocyte adhesion. *Blood*. 2006;108:3112–3120.
118. Butler JM, Guthrie SM, Koc M, et al. SDF-1 is both necessary and sufficient to promote proliferative retinopathy. *J Clin Invest*. 2005;115:86–93.
119. Segal MS, Shah R, Afzal A, et al. Nitric oxide cytoskeletal-induced alterations reverse the endothelial progenitor cell migratory defect associated with diabetes. *Diabetes*. 2006;55:102–109.
120. Bhatwadekar AD, Glenn JV, Li G, et al. Advanced glycation of fibronectin impairs vascular repair by endothelial progenitor cells: implications for vasodegeneration in diabetic retinopathy. *Invest Ophthalmol Vis Sci*. 2008;49:1232–1241.
121. Bhatwadekar AD, Guerin EP, Jarajapu YP, et al. Transient inhibition of transforming growth factor-beta1 in human diabetic $CD34^+$ cells enhances vascular reparative functions. *Diabetes*. 2010;59:2010–2019.
122. Sorrentino SA, Bahlmann FH, Besler C, et al. Oxidant stress impairs in vivo reendothelialization capacity of endothelial progenitor cells from patients with type 2 diabetes mellitus: restoration by the peroxisome proliferator-activated receptor-gamma agonist rosiglitazone. *Circulation*. 2007;116:163–173.
123. Mohler ER 3rd, Shi Y, Moore J, et al. Diabetes reduces bone marrow and circulating porcine endothelial progenitor

cells, an effect ameliorated by atorvastatin and independent of cholesterol. *Cytometry A*. 2009;75:75–82.
124. Anghelina M, Krishnan P, Moldovan L, et al. Monocytes/macrophages cooperate with progenitor cells during neovascularization and tissue repair: conversion of cell columns into fibrovascular bundles. *Am J Pathol*. 2006;168:529–541.
125. Chang KH, Chan-Ling T, McFarland EL, et al. IGF binding protein-3 regulates hematopoietic stem cell and endothelial precursor cell function during vascular development. *Proc Natl Acad Sci USA*. 2007;104:10595–10600.
126. Granata R, Trovato L, Garbarino G, et al. Dual effects of IGFBP-3 on endothelial cell apoptosis and survival: involvement of the sphingolipid signaling pathways. *FASEB J*. 2004;18:1456–1458.
127. Franklin SL, Ferry RJ Jr, Cohen P. Rapid insulin-like growth factor (IGF)-independent effects of IGF binding protein-3 on endothelial cell survival. *J Clin Endocrinol Metab*. 2003;88:900–907.
128. Liu LQ, Sposato M, Liu HY, et al. Functional cloning of IGFBP-3 from human microvascular endothelial cells reveals its novel role in promoting proliferation of primitive CD34+CD38– hematopoietic cells in vitro. *Oncol Res*. 2003;13:359–371.
129. Vasylyeva TL, Chen X, Ferry RJ Jr. Insulin-like growth factor binding protein-3 mediates cytokine-induced mesangial cell apoptosis. *Growth Horm IGF Res*. 2005;15:207–214.
130. Lofqvist C, Chen J, Connor KM, et al. IGFBP3 suppresses retinopathy through suppression of oxygen-induced vessel loss and promotion of vascular regrowth. *Proc Natl Acad Sci USA*. 2007;104:10589–10594.
131. Giannini S, Cresci B, Pala L, et al. IGFBPs modulate IGF-I- and high glucose-controlled growth of human retinal endothelial cells. *J Endocrinol*. 2001;171:273–284.
132. Kielczewski JL, Hu P, Shaw LC, et al. Novel protective properties of IGFBP-3 result in enhanced pericyte ensheathment, reduced microglial activation, increased

microglial apoptosis, and neuronal protection after ischemic retinal injury. *Am J Pathol*. 2011;178:1517–1528.
133. Chan-Ling TL, Halasz P, Stone J. Development of retinal vasculature in the cat: processes and mechanisms. *Curr Eye Res*. 1990;9:459–478.
134. Hellstrom A, Engstrom E, Hard AL, et al. Postnatal serum insulin-like growth factor I deficiency is associated with retinopathy of prematurity and other complications of premature birth. *Pediatrics*. 2003;112:1016–1020.
135. Giudice LC, de Zegher F, Gargosky SE, et al. Insulin-like growth factors and their binding proteins in the term and preterm human fetus and neonate with normal and extremes of intrauterine growth. *J Clin Endocrinol Metab*. 1995;80:1548–1555.
136. Smith WJ, Underwood LE, Keyes L, et al. Use of insulin-like growth factor I (IGF-I) and IGF-binding protein measurements to monitor feeding of premature infants. *J Clin Endocrinol Metab*. 1997;82:3982–3988.
137. Smith LE. IGF-1 and retinopathy of prematurity in the preterm infant. *Biol Neonate*. 2005;88:237–244.
138. Kohner EM, Henkind P. Correlation of fluorescein angiogram and retinal digest in diabetic retinopathy. *Am J Ophthalmol*. 1970;69:403–414.
139. Linsenmeier RA, Braun RD, McRipley MA, et al. Retinal hypoxia in long term diabetic cats. *Invest Ophthalmol Vis Sci*. 1998;39:1647–1657.
140. Tang J, Kern TS. Inflammation in diabetic retinopathy. *Prog Retin Eye Res*. 2011;30:343–358.
141. Kern TS. Contributions of inflammatory processes to the development of the early stages of diabetic retinopathy. *Exp Diabetes Res*. 2007;2007:95103.
142. Schmidt MI, Duncan BB, Sharrett AR, et al. Markers of inflammation and prediction of diabetes mellitus in adults (Atherosclerosis Risk in Communities study): a cohort study. *Lancet*. 1999;353:1649–1652.
143. Festa A, D'Agostino R Jr, Tracy RP, et al. Elevated levels of acute-phase proteins and plasminogen activator inhibitor-1 predict the development of type 2 diabetes: the insulin

resistance atherosclerosis study. *Diabetes*. 2002;51:1131–1137.
144. Eliasson MC, Jansson JH, Lindahl B, et al. High levels of tissue plasminogen activator (tPA) antigen precede the development of type 2 diabetes in a longitudinal population study. The Northern Sweden MONICA study. *Cardiovasc Diabetol*. 2003;2:19.
145. Meigs JB, Dupuis J, Liu C, et al. PAI-1 gene 4G/5G polymorphism and risk of type 2 diabetes in a population-based sample. *Obesity (Silver Spring)*. 2006;14:753–758.
146. Orasanu G, Plutzky J. The pathologic continuum of diabetic vascular disease. *J Am Coll Cardiol*. 2009;53:S35–42.
147. van Hecke MV, Dekker JM, Nijpels G, et al. Inflammation and endothelial dysfunction are associated with retinopathy: the Hoorn study. *Diabetologia*. 2005;48:1300–1306.
148. Spijkerman AM, Gall MA, Tarnow L, et al. Endothelial dysfunction and low-grade inflammation and the progression of retinopathy in type 2 diabetes. *Diabet Med*. 2007;24:969–976.
149. Hadjadj S, Aubert R, Fumeron F, et al. Increased plasma adiponectin concentrations are associated with microangiopathy in type 1 diabetic subjects. *Diabetologia*. 2005;48:1088–1092.
150. McLeod DS, Lefer DJ, Merges C, et al. Enhanced expression of intracellular adhesion molecule-1 and P-selectin in the diabetic human retina and choroid. *Am J Pathol*. 1995;147:642–653.
151. Joussen AM, Murata T, Tsujikawa A, et al. Leukocyte-mediated endothelial cell injury and death in the diabetic retina. *Am J Pathol*. 2001;158:147–152.
152. Joussen AM, Poulaki V, Qin W, et al. Retinal vascular endothelial growth factor induces intracellular adhesion molecule-1 and endothelial nitric oxude synthase expression and initiates early diabetic retinal leukocyte adhesion in vivo. *Am J Pathol*. 2002;160:501–509.
153. Joussen AM, Poulaki V, Mitsiades N, et al. Nonsteroidal anti-inflammatory drugs prevent early diabetic retinopathy

via TNF-α suppression. *FASEB J*. 2002;16:438–440.
154. Adamis AP. Is diabetic retinopathy an inflammatory disease? *Br J Ophthalmol*. 2002;86:363–365.
155. Joussen AM, Poulaki V, Le ML, et al. A central role for inflammation in the pathogenesis of diabetic retinopathy. *FASEB J*. 2004;18:1450–1452.
156. Powell ED, Field RA. Diabetic retinopathy and rheumatoid arthritis. *Lancet*. 1964;2:17–18.
157. Brucklacher RM, Patel KM, VanGuilder HD, et al. Whole genome assessment of the retinal response to diabetes reveals a progressive neurovascular inflammatory response. *BMC Med Genomics*. 2008;1:26.
158. Kern TS, Miller CM, Du Y, et al. Topical administration of nepafenac inhibits diabetes-induced retinal microvascular disease and underlying abnormalities of retinal metabolism and physiology. *Diabetes*. 2007;56:373–379.
159. Gubitosi-Klug RA, Talahalli R, Du Y, et al. 5-Lipoxygenase, but not 12/15- lipoxygenase, contributes to degeneration of retinal capillaries in a mouse model of diabetic retinopathy. *Diabetes*. 2008;57:1387–1393.
160. Vincent JA, Mohr S. Inhibition of caspase-1/interleukin-1beta signaling prevents degeneration of retinal capillaries in diabetes and galactosemia. *Diabetes*. 2007;56:224–230.
161. Behl Y, Krothapalli P, Desta T, et al. Diabetes-enhanced tumor necrosis factor-alpha production promotes apoptosis and the loss of retinal microvascular cells in type 1 and type 2 models of diabetic retinopathy. *Am J Pathol*. 2008;172:1411–1418.
162. Lutty GA, McLeod DS, Merges C, et al. Localization of VEGF in human retina and choroid. *Arch Ophthalmol*. 1996;114:971–977.
163. Rogers SL, McIntosh RL, Lim L, et al. Natural history of branch retinal vein occlusion: an evidence-based systematic review. *Ophthalmology*. 2010;117:1094–1101.e5.
164. Laouri M, Chen E, Looman M, et al. The burden of disease of retinal vein occlusion: review of the literature. *Eye (Lond)*. 2011;25(8):981–988.
165. Hardarson HS, Stefansson E. Oxygen saturation in branch

retinal vein occlusion. *Acta Ophthalmol*. 2012;90(5):466–470.
166. Hayreh SS, Weingeist TA. Experimental occlusion of the central artery of the retina. IV: retinal tolerance time to acute ischaemia. *Br J Ophthalmol*. 1980;64:818–825.
167. Hayreh SS, Podhajsky P. Ocular neovascularization with retinal vascular occlusion. II. Occurrence in central and branch retinal artery occlusion. *Arch Ophthalmol*. 1982;100:1585–1596.
168. Coats G. Obstruction of the central artery of the retina. *R Lond Ophthalmic Hosp Rep*. 1905;16:262–306.
169. Coats G. Pathology of obstruction of the centeral artery of the retina. *R Lond Ophthalmic Hosp Rep*. 1913;19:45–70.
170. Ageno W, Cattaneo R, Manfredi E, et al. Parnaparin versus aspirin in the treatment of retinal vein occlusion. A randomized, double blind, controlled study. *Thromb Res*. 2010;125:137–141.
171. Fong AC, Schatz H, McDonald HR, et al. Central retinal vein occlusion in young adults (papillophlebitis). *Retina*. 1992;12:3–11.
172. Sofi F, Marcucci R, Fedi S, et al. High lipoprotein (a) levels are associated with an increased risk of retinal vein occlusion. *Atherosclerosis*. 2010;210:278–281.
173. Arruga J, Sanders MD. Ophthalmologic findings in 70 patients with evidence of retinal embolism. *Ophthalmology*. 1982;89:1336–1347.
174. Nagpal KC, Goldberg MF, Rabb MF. Ocular manifestations of sickle hemoglobinopathies. *Surv Ophthalmol*. 1977;21:391–411.
175. Cao J, Kunz Mathews M, McLeod DS, et al. Angiogenic factors in human proliferative sickle cell retinopathy. *Br J Ophthalmol*. 1999;83:838–846.
176. Brown GC, Magargal LE. The ocular ischemic syndrome. Clinical, fluorescein angiographic and carotid angiographic features. *Int Ophthalmol*. 1988;11:239–251.
177. Boto de los Bueis A, Fernandez-Prieto A, Ruiz-Martin MM, et al. Bilateral carotid occlusion in young woman. Clinical and hemodynamic ocular results. *Arch Soc Esp Oftalmol*. 2003;78:227–230.

178. Baatz H, Lange S, Buchner H, et al. Pseudoangiitis in bilateral ocular ischemia. *Ophthalmologe*. 2007;104:243–245.
179. Sturrock GD, Mueller HR. Chronic ocular ischaemia. *Br J Ophthalmol*. 1984;68:716–723.
180. Kearns TP. Differential diagnosis of central retinal vein obstruction. *Ophthalmology*. 1983;90:475–480.
181. Klijn CJ, Kappelle LJ, van Schooneveld MJ, et al. Venous stasis retinopathy in symptomatic carotid artery occlusion: prevalence, cause, and outcome. *Stroke*. 2002;33:695–701.
182. Costa VP, Kuzniec S, Molnar LJ, et al. Clinical findings and hemodynamic changes associated with severe occlusive carotid artery disease. *Ophthalmology*. 1997;104:1994–2002.
183. Linsenmeier RA, Padnick-Silver L. Mtabolic dependence of photoreceptors on the choroid in the normal and detached retina. *Invest Ophthalmol Vis Sci*. 2000;41:3117–3123.
184. Wang S, Linsenmeier RA. Hyperoxia improves oxygen consumption in the detached feline retina. *Invest Ophthalmol Vis Sci*. 2007;48:1335–1341.
185. Lewis G, Mervin K, Valter K, et al. Limiting the proliferation and reactivity of retinal Müller cells during experimental retinal detachment: the value of oxygen supplementation. *Am J Ophthalmol*. 1999;128:165–172.
186. Folkman J. Tumor angiogenesis: therapeutic implications. *N Engl J Med*. 1971;285:1182–1186.
187. Penn JS, Madan A, Caldwell RB, et al. Vascular endothelial growth factor in eye disease. *Prog Retin Eye Res*. 2008;27:331–371.
188. Salam A, Mathew R, Sivaprasad S. Treatment of proliferative diabetic retinopathy with anti-VEGF agents. *Acta Ophthalmol*. 2011;89:405–411.
189. Antonetti DA, Barber AJ, Khin S, et al. Vascular permeability in experimental diabetes is associated with reduced endothelial occludin content: vascular endothelial growth factor decreases occludin in retinal endothelial cells. Penn State Retina Research Group. *Diabetes*. 1998;47:1953–1959.
190. Aiello L, Bursell S, Clermont A, et al. Vascular endothelial growth factor-induced retinal permeability is mediated by

protein kinase C in vivo and suppressed by an orally effective beta-isoform-selective inhibitor. *Diabetes*. 1997;46:1473–1480.
191. Barber AJ, Antonetti DA, Gardner TW. Altered expression of retinal occludin and glial fibrillary acidic protein in experimental diabetes. The Penn State Retina Research Group. *Invest Ophthalmol Vis Sci*. 2000;41:3561–3568.
192. Harhaj NS, Felinski EA, Wolpert EB, et al. VEGF activation of protein kinase C stimulates occludin phosphorylation and contributes to endothelial permeability. *Invest Ophthalmol Vis Sci*. 2006;47:5106–5115.
193. Sundstrom JM, Sundstrom CJ, Sundstrom SA, et al. Phosphorylation site mapping of endogenous proteins: a combined MS and bioinformatics approach. *J Proteome Res*. 2009;8:798–807.
194. Murakami T, Felinski EA, Antonetti DA. Occludin phosphorylation and ubiquitination regulate tight junction trafficking and vascular endothelial growth factor-induced permeability. *J Biol Chem*. 2009;284:21036–21046.
195. Aveleira CA, Lin CM, Abcouwer SF, et al. TNF-alpha signals through PKCzeta/NF-kappaB to alter the tight junction complex and increase retinal endothelial cell permeability. *Diabetes*. 2010;59:2872–2882.
196. Hidayat A, Fine B. Diabetic choroidopathy: light and electron microscopic observations of seven cases. *Ophthalmology*. 1985;67:512–522.
197. Cao J, McLeod S, Merges CA, et al. Choriocapillaris degeneration and related pathologic changes in human diabetic eyes. *Arch Ophthalmol*. 1998;116:589–597.
198. Lutty GA, Cao J, McLeod DS. Relationship of polymorphonuclear leukocytes (PMNs) to capillary dropout in the human diabetic choroid. *Am J Pathol*. 1997;151:707–714.
199. Lovasik J, Kergoat H. Electroretinographic results and ocular vascular perfusion in type I diabetes. *Invest Ophthalmol Vis Sci*. 1993;34:1731–1743.
200. Holopigian K, Greenstein VC, Seiple W, et al. Evidence for photoreceptor changes in patients with diabetic

retinopathy. *Invest Ophthalmol Vis Sci*. 1997;38:2355–2365.
201. Grunwald J, Hariprasad S, DuPont J, et al. Foveolar choroidal blood flow in age-related macular degeneration. *Invest Ophthalmol Vis Sci*. 1998;39:385–390.
202. Grunwald JE, Metelitsina TI, Dupont JC, et al. Reduced foveolar choroidal blood flow in eyes with increasing AMD severity. *Invest Ophthalmol Vis Sci*. 2005;46:1033–1038.
203. Metelitsina TI, Grunwald JE, DuPont JC, et al. Foveolar choroidal circulation and choroidal neovascularization in age-related macular degeneration. *Invest Ophthalmol Vis Sci*. 2008;49:358–363.
204. Pournaras CJ, Rungger-Brandle E, Riva CE, et al. Regulation of retinal blood flow in health and disease. *Prog Retin Eye Res*. 2008;27:284–330.
205. McLeod DS, Taomoto M, Otsuji T, et al. Quantifying changes in RPE and choriocapillaris in eyes with age-related macular degeneration. *Invest Ophthalmol Vis Sci*. 2002;43:1986–1993.
206. McLeod DS, Grebe R, Bhutto I, et al. Relationship between RPE and choriocapillaris in age-related macular degeneration. *Invest Ophthalmol Vis Sci*. 2009;50:4982–4991.
207. Feigl B. Age-related maculopathy-linking aetiology and pathophysiol changes to the ischaemia hypothesis. *Prog Retin Eye Res*. 2009;28:63–86.

21

Mechanisms of Normal Retinal Adhesion

Michael F. Marmor

In some cases of retinal detachment, the reasons for retinal separation are obvious, such as penetrating trauma that snags the retina or gross vitreous traction bands that pull the retina from the retinal pigment epithelium (RPE). Any physiologic mechanism of adhesion would be overwhelmed by such forces. However, detachment is also caused by less dramatic forces and under

conditions in which stronger adhesion might prevent, or at least delay, the separation and its spread. The physiology of attachment is especially important with respect to nonrhegmatogenous detachments that cannot develop unless local mechanisms for keeping the subretinal space dry are overwhelmed.

Independent of its clinical relevance, the study of retinal adhesion is also of considerable physiologic interest. No anatomic junctions bridge the mammalian subretinal space,[1] yet this primordial dural cavity remains collapsed and, indeed, tightly closed throughout a lifetime of ocular movement and tugging from the vitreous. Our current knowledge of this system is still incomplete, but evidence suggests that adhesion depends on a mixture of anatomic, physical, and metabolic factors.[2] This chapter reviews these factors and considers clinical and therapeutic implications.

Models for Measuring Retinal Adhesion

The strength of the adhesion between the sensory retina and the RPE can be measured with in vitro and in vivo methods.

In Vitro Methods

Adhesive force falls rapidly after enucleation or death,[3,4] as is discussed later, and this puts a constraint of time on techniques for measuring adhesiveness in vitro.[5,6] One approach is to peel the retina within a fluid bath while recording the required force with a transducer.[3] A faster method is to measure the amount of RPE pigment that remains attached to the retina after separation as the index of adhesiveness.[7] An eye can be enucleated and small strips of the eyecup prepared within 30 seconds, after which the retina is gently peeled by hand from the RPE. The stronger the adhesive force, the more pigment adheres to the peeled retina.

In Vivo Methods

Kita et al.[8] developed the most direct technique for quantifying adhesiveness within the living eye. A small detachment is made in

the eye by injecting fluid into the subretinal space through a micropipette, and a second micropipette is inserted simultaneously into the detachment cavity to measure fluid pressure. The pressure that is required to expand the detachment can be converted mathematically, by Laplace's law, into a value for adhesive force at the margin of the detachment (where the separation is taking place). This technique allows the evaluation in living animals of the effects of drugs and other agents that modify retinal adhesion.[9,10]

Adhesive Force and Environmental Factors

A substantial force maintains attachment of the sensory retina to the underlying RPE. This force can be altered by environmental factors.

Magnitude of Adhesive Force

In vitro measurements, 5–20 minutes after enucleation, have shown that about 25 mg of force is required to peel a 5-mm strip of rabbit retina from the RPE.[3,11,12] Pressure measurements in living eyes have shown an adhesive force in the rabbit of 100–180 dyn/cm.[8,9] Adhesion is stronger in cats and monkeys, which show mean values for adhesive force that are 180% (for cats) and 140% (for monkeys) of that in the rabbits.[9]

Sensitivity to Temperature and Ionic Environment

Retinal adhesiveness drops rapidly postmortem at 37°C, but remains near control levels for hours at 4°C[7,13–15] (Fig. 21.1A). These effects of temperature are reversible. Fig. 21.1B shows that changing the temperature from 37°C to 4°C or vice versa causes retinal adherence in the rabbit[16] to rise or fall, respectively, and repeatedly. This reversibility has also been documented in primate and human tissue.[14,15,17] The mechanism of these reversible temperature effects is still obscure. Temperature could act directly on physicochemical

components of adhesion or modulate metabolic systems. Some of the adhesion-enhancing effect of cold temperature may result from sodium pump inhibition and secondary tissue swelling, which would make the interdigitated outer segments and RPE microvilli harder to separate.[3,13] Because cellular swelling is a pathologic event, the actions of cold temperature may not be entirely relevant to normal adhesive processes.

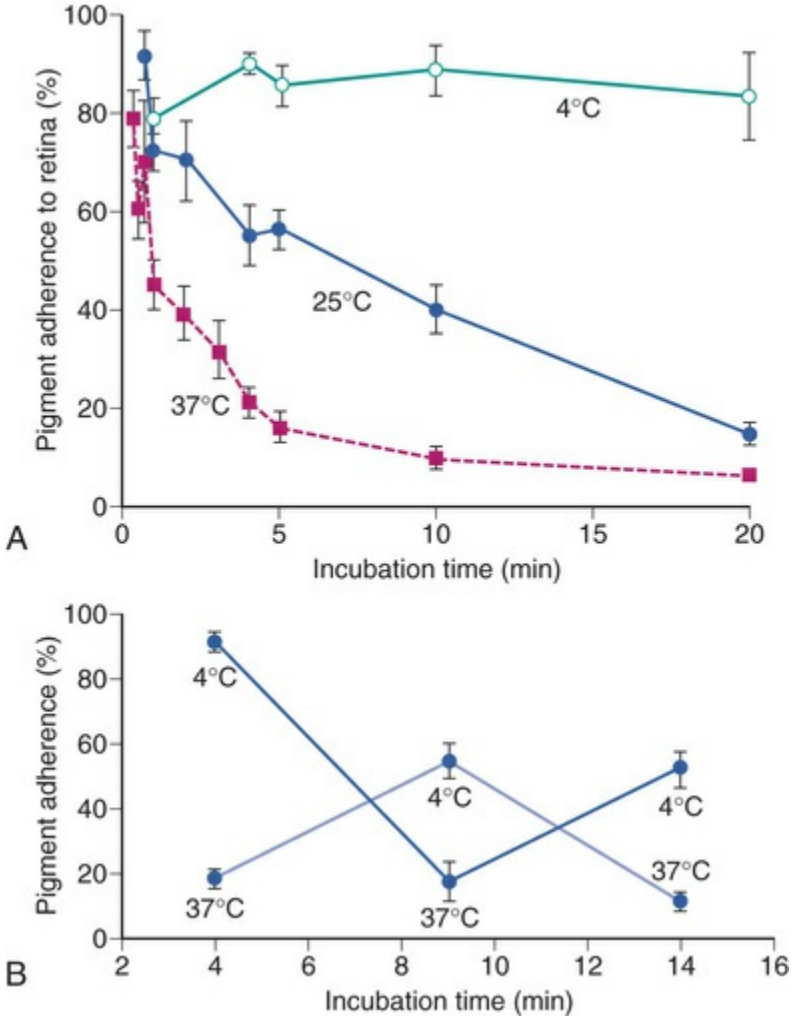

FIG. 21.1 Relationship between retinal adhesiveness and temperature in the rabbit. (A) Cold temperatures slow down the postmortem failure in adhesiveness to the point that firm adhesion is maintained at 4°C for many hours. (B) The effects of temperature on retinal adhesion are reversible within minutes, and adhesiveness can be repeatedly strengthened or weakened by cooling or warming the same piece of tissue. (Panel A modified with permission from Endo EG, Yao XY, Marmor MF.

Pigment adherence as a measure of retinal adhesion: dependence on temperature. Invest Ophthalmol Vis Sci 1988;29:1390–6. Panel B modified with permission from Yao XY, Endo EG, Marmor MF. Reversibility of retinal adhesion in the rabbit. Invest Ophthalmol Vis Sci 1989;30:220–4.)

The ionic environment appears to be critical to adhesive strength. In in vitro experiments using tissue from rabbits, humans, and other primates, lowering the pH from 7.4 to 5.5, or removing calcium and magnesium ions from the bathing solution, weakened adhesive force and accelerated the rate at which adhesion falls postmortem[11,13,15,17] (Fig. 21.2A). These changes can be rapidly reversible[16] (Fig. 21.2B), although cold temperature will block or mask the effects of pH and calcium ions. In vivo, the removal of calcium ions from the subretinal space weakens retinal adhesion in rabbits to about 30% of normal.[18] In other words, calcium appears to be a necessary element for the maintenance of normal adhesiveness in the living eye.

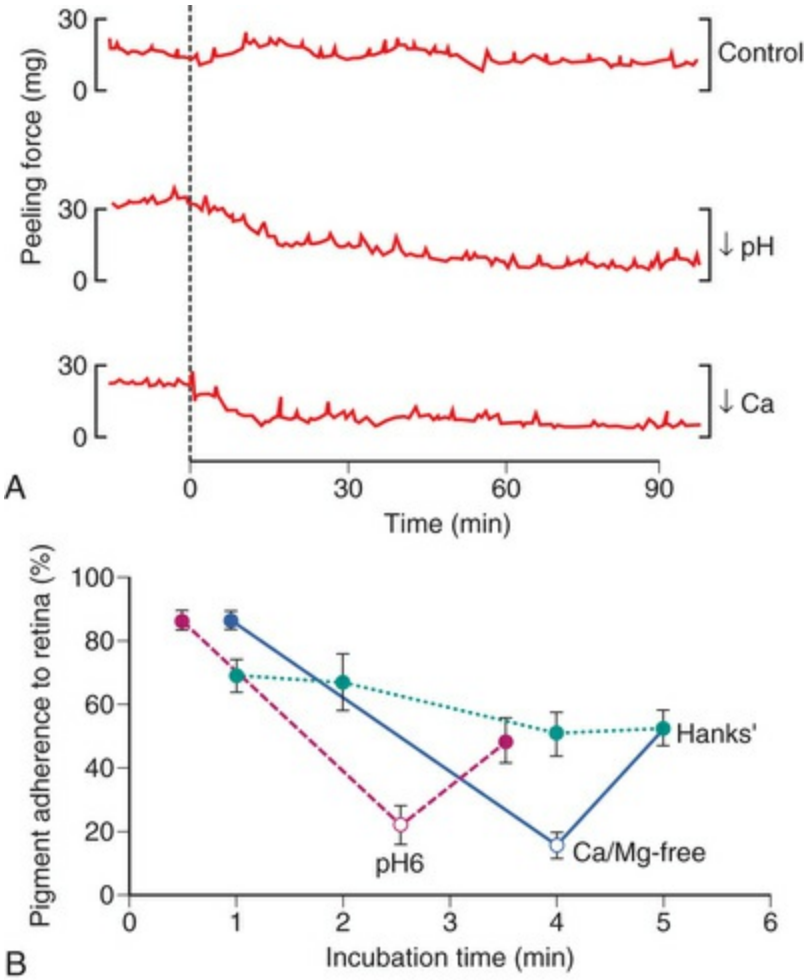

FIG. 21.2 Effects of pH and calcium/magnesium ion concentration on retinal adhesiveness in the rabbit. (A) The force required to peel retina from retinal pigment epithelium (RPE) drops within seconds after lowering pH (by injecting 1 mL of 1 mol/L HCl near the tissue) or lowering external Ca/Mg-free solution. The tracings represent a continuous measurement of the peeling force; chemical changes were made at time 0. (B) The effects of changing pH or Ca/Mg concentration are rapidly reversible. Pigment adherence was used as an index of adhesiveness. *Dotted line*, tissue maintained in Hanks balanced salt solution; *dashed line*, pH changed from 7.4 to 6.0 and back again; *solid line*, Hanks solution changed to Ca/Mg-free solution and back again. (Panel A modified with permission from Marmor MF, Maack T. Local environmental factors and retinal adhesion in the rabbit. Exp Eye Res 1982;34:727–33. Panel B modified with permission from Yao XY, Endo EG, Marmor MF. Reversibility of retinal adhesion in the rabbit. Invest Ophthalmol Vis Sci 1989;30:220–4.)

Mechanical Forces Outside the Subretinal Space

A number of forces play upon the retina from outside the subretinal space, strengthening or weakening retinal adhesion. Most important are fluid and vitreous pressure, not only because they contribute to adhesion, but also because they may cause detachment when altered by pathologic conditions.

Fluid Pressure: Hydrostatic and Osmotic

Fluid is driven passively from vitreous to choroid by both intraocular pressure and the osmotic pressure of the extracellular fluid in the choroid (estimated to be about 12 mmHg in the rabbit,[19] but possibly lower in humans[20]). However, under normal conditions there appears to be relatively little posterior flow, and most of the fluid that enters the eye as aqueous leaves the eye through anterior drainage channels.[19,21] The posterior route is limited because the retina and RPE[22,23] provide a substantial resistance to water movement, and little fluid can cross these layers under the available heads of pressure. A side-effect of this retinal flow resistance is that the outward movement of fluid acts to push the retina against the RPE (Fig. 21.3). This is one mechanism contributing to normal retinal attachment. The actual pressure difference across retina or RPE is probably small because intraocular pressure is ultimately contained by the sclera, and tissue pressures will therefore equalize to a large degree between the vitreous and choroid. However, Fatt and Shantinath[22] have calculated that even a very small pressure difference (only 0.52×10^{-3} mmHg) across the retina would generate a force sufficient to keep the retina firmly fixed against the wall of the eye. This low value may explain the fact that no one[14,19] has been able to measure a pressure difference between the vitreous cavity and subretinal space.

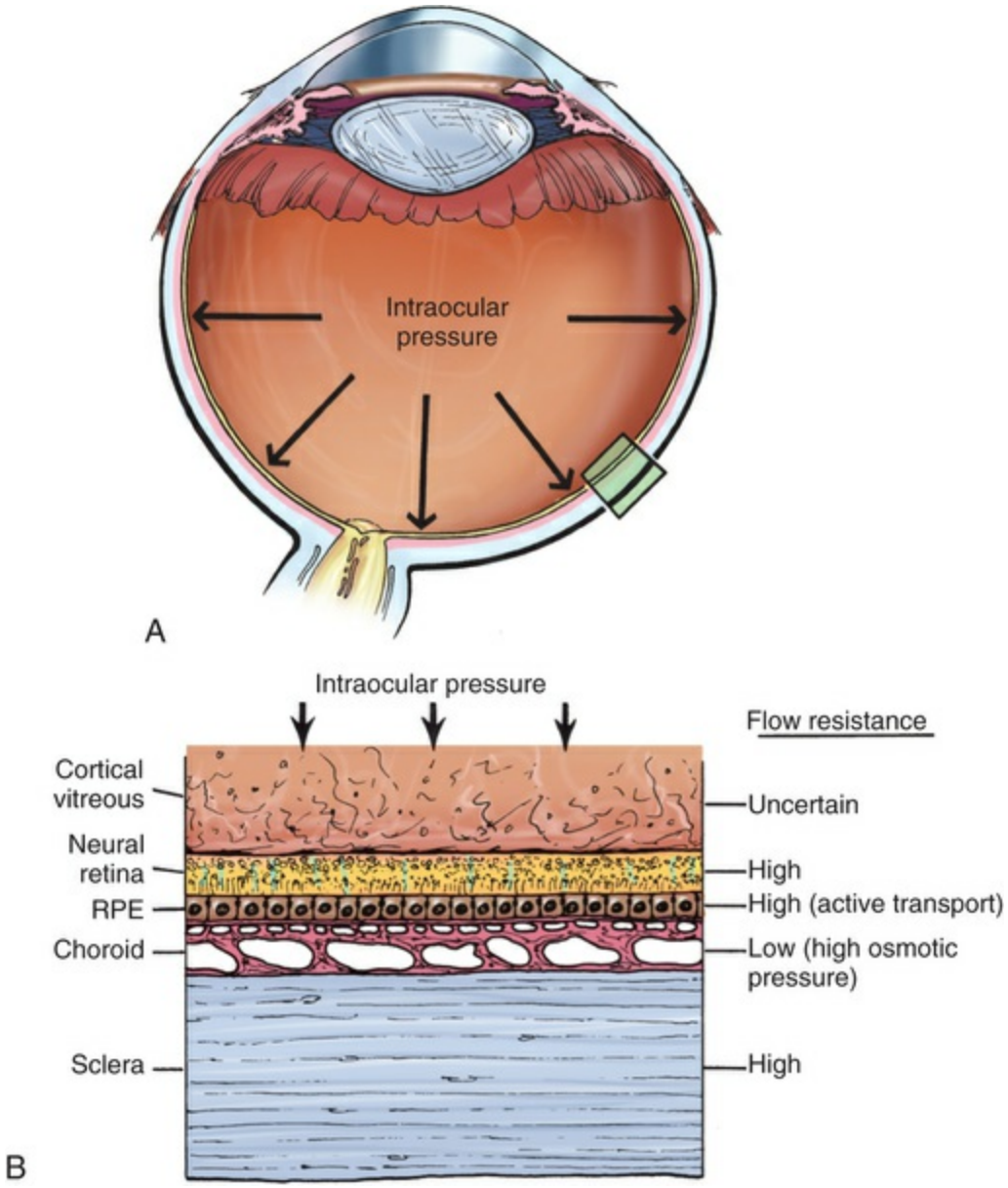

FIG. 21.3 Intraocular pressure and retinal flow resistance as a factor in retinal adhesion. (A) Intraocular pressure is evenly distributed within the vitreous cavity so that fluid is continually being pushed through the coats of the eye. (B) Magnified view of the tissue layers in the posterior of the eye, including cortical vitreous. The flow resistance of each layer is indicated on the right; note that the retinal pigment epithelium (*RPE*) and choroid can also modify fluid movement by active transport and osmotic pressure, respectively.

These physical forces can also work in the other direction and cause retinal detachment. For example, if hyperosmotic fluid is

introduced into the vitreous cavity, fluid moving from the choroid into the vitreous will elevate the retina[24,25] (Fig. 21.4). This is an important concern in the evaluation or use of intravitreal drugs that may damage the retina osmotically independently of pharmacologic effects.

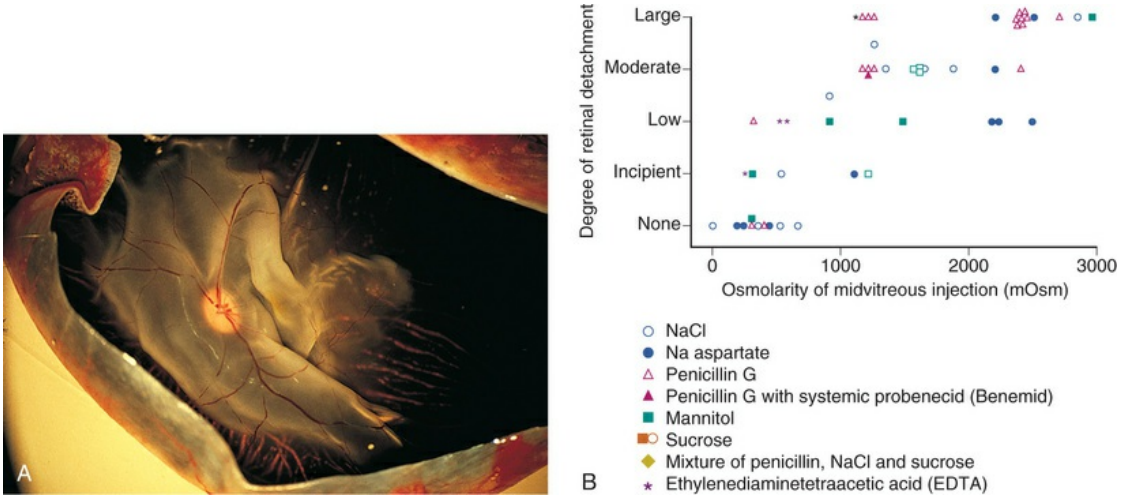

FIG. 21.4 Effects of injecting hyperosmolar solution into the vitreous. (A) Monkey eye enucleated after a midvitreal hyperosmolar injection. Bullous detachment was present in the posterior pole and peripapillary region. (B) Degree of serous retinal detachment in rabbit eyes 15 minutes after injecting 0.05 mL of different solutions and osmolarities into the vitreous: incipient detachment, the vitreoretinal interface glistened but did not visibly separate; low detachment, separation occurred without bullous elevation; moderate detachment, the bullae were confined to the posterior pole; large detachment, there was extension near or beyond the equator. (Reproduced with permission from Marmor MF. Retinal detachment from hyperosmotic intravitreal injection. Invest Ophthalmol Vis Sci 1979;18:1237–44.)

It may seem puzzling that, although most intraocular fluid leaves the eye anteriorly rather than posteriorly, ample animal data[26–30] indicated that the RPE can pump fluid from the subretinal space to choroid at a very high rate (about 0.3 μL/h/mm^2 of RPE) comparable with that of aqueous secretion. How can the RPE have such enormous power for fluid removal, yet very little fluid leaves the normal eye by a posterior route? The answer probably lies in

the flow resistance of the retina. Under normal conditions, given the flow resistance of the tissue and the tiny pressure differential across it,[22,23] water will cross the retina only at a very slow rate. In other words, the tissue resistance is rate-limiting, and most aqueous fluid must leave by the anterior route. Under pathologic conditions of retinal detachment (whether rhegmatogenous or nonrhegmatogenous), fluid is present within the subretinal space and is thus available for transport at a maximal rate. Measurements in humans for the resorption of detachments showed a rate of 0.11 $\mu L/h/mm^2$ of RPE, and the rate may well be higher in eyes without pathology.[31] This translates into roughly 3.5 mL of fluid per day, which explains why a rhegmatogenous detachment can settle within 24 hours, and emphasizes the power of RPE fluid transport.

The clinical importance of fluid pressure as a factor in preventing retinal detachment is uncertain. It undoubtedly helps to keep the retina in place when the retina is intact, but raising intraocular pressure in rabbits to 38 mmHg or lowering it to 0 mmHg had only a modest effect on the rate of subretinal fluid absorption.[32] Furthermore, clinical retinal (as opposed to choroidal) detachment is uncommon in hypotonus eyes, and even a small hole in the retina would theoretically allow fluid to reach the subretinal space and circumvent fluid pressure mechanisms of adhesion. Retinal holes are, in fact, found in about 10% of autopsy eyes without detachment,[33] but many of these holes may not be functionally open because of surrounding pigmentation or because of "tamponade" by the cortical vitreous gel.[34]

Once the retina has detached and adhesion mechanisms that depend on retina–RPE contact can no longer work, fluid dynamics become much more important, even in the presence of a hole. Hammer[35] has calculated that fluid entering a retinal hole over a scleral buckle will, by its flow pattern, create a suction force that pulls the retina backward against the buckle.

Osmotic pressure can be manipulated more easily and may turn out to have therapeutic applications. Both in vitro and in vivo experiments, using rabbits and primates,[9,36,37] have shown that an intravenous injection of mannitol will increase retinal adhesiveness by roughly 50% within 1–2 hours of injection (Fig. 21.5). The magnitude of the effect correlates rather closely with blood

osmolality. Mannitol is known to enhance the absorption of fluid out of the subretinal space.[38] Some of the adhesive effect may come from fluid absorption "pulling" the retina against the RPE; however, most of the effect probably comes from dehydration of the subretinal space (which enhances the binding properties of the interphotoreceptor matrix [IPM]), because the mannitol effect is still evident in excised tissue where there is no flow toward the choriocapillaris.

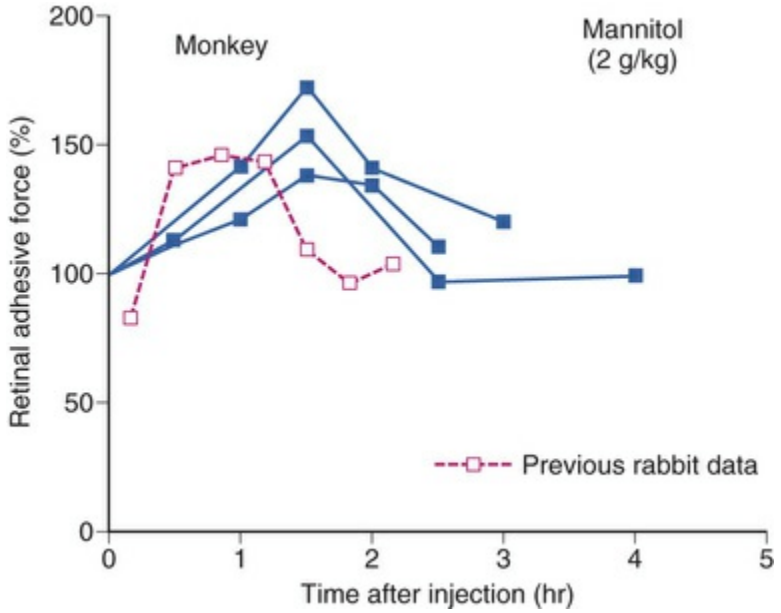

FIG. 21.5 Time course of change in retinal adhesive force after intravenous injection of mannitol in rabbits (*broken line*, 2.5 g/kg) and monkeys (*solid lines*, 2.0 g/kg). (Reproduced with permission from Kita M, Marmor MF. Retinal adhesive force in living rabbit, cat, and monkey eyes: normative data and enhancement by mannitol and acetazolamide. Invest Ophthalmol Vis Sci 1992;33:1879–82.)

Vitreous Support and Other Physical Aspects of Adhesion

The role of the vitreous in creating retinal detachments through traction and contraction is well known. The role of the vitreous in maintaining retinal attachment is less clear. Vitreous gel has a physical structure that may help to keep the retina in place,[34,39] although retinas do not just come off when vitreous detachment or

syneresis occurs. A thin cortical layer of vitreous might remain after vitreous detachment or syneresis and serve as a seal or tamponade for retinal holes,[34] thus aiding the action of fluid pressure in keeping the retina apposed (Fig. 21.3).

There is other, indirect, evidence for a vitreous role in adhesion. It is very difficult to produce and maintain an experimental rhegmatogenous detachment if the vitreous body remains intact.[24,40] Vitreous removal (either mechanical or with hyaluronidase) presumably weakens the tamponade and the structural qualities of the gel, but it also allows liquid vitreous to reach the subretinal space. The status of the gel may help account for the vastly different incidence of retinal detachment among young individuals, in whom the gel is largely intact, and among older individuals, in whom syneresis and vitreous detachment have occurred. A retinal hole in a young eye is blocked by gel pressure and can seal uneventfully; a hole in an old eye is more likely to allow fluid to enter the subretinal space and cause detachment. On the other hand, the integrity of the vitreous gel seems of little consequence to the formation or persistence of experimental nonrhegmatogenous detachments[32] or to the retinal adhesive force measured by peeling,[11] so the role of the vitreous gel in attachment may be more one of preventing pathologic fluid access to the subretinal space than one of providing a direct adhesive support or force.

The weight of retina is potentially a factor in attachment and detachment, as influenced by gravity and ocular movement. Once a detachment has occurred, the influence of gravity is well known, because appropriate positioning of the patient can be enormously effective in inducing retina to settle. However, it is hard to envision retinal weight as a major factor in retinal attachment under normal conditions[27,32] because our upright posture and eye movements would dictate that benefits and adverse effects be simultaneously present in different parts of the eye.

Mechanical Forces Inside the Subretinal Space

Anatomic bridges do not exist between retina and RPE,[1] but it is

reasonable to ask to what extent matrix material between the layers serves as "glue" and to what extent the physical interdigitation of photoreceptor outer segments and RPE microvilli serves to hold the tissues together.

Mechanical Interdigitation

RPE microvilli wrap closely around the tips of the outer segments (Fig. 21.6), and this connection is strong enough to allow for daily phagocytosis of outer-segment fragments as the photoreceptors renew their disc material.[1,41,42] However, as a factor in adhesion, interdigitation seems of variable importance. The RPE microvilli are subject to continuous cellular remodeling during the outer-segment renewal cycle. After surgical repair of a retinal detachment, reattachment takes place rather promptly, before the outer segments have regenerated and microvillous connections have been reestablished.[43,44] Interdigitation begins to develop within 3 days of reattachment, but retinal adhesiveness does not return to normal until 5–6 weeks after reapposition of experimentally detached retina in the rabbit[45] (Fig. 21.7).

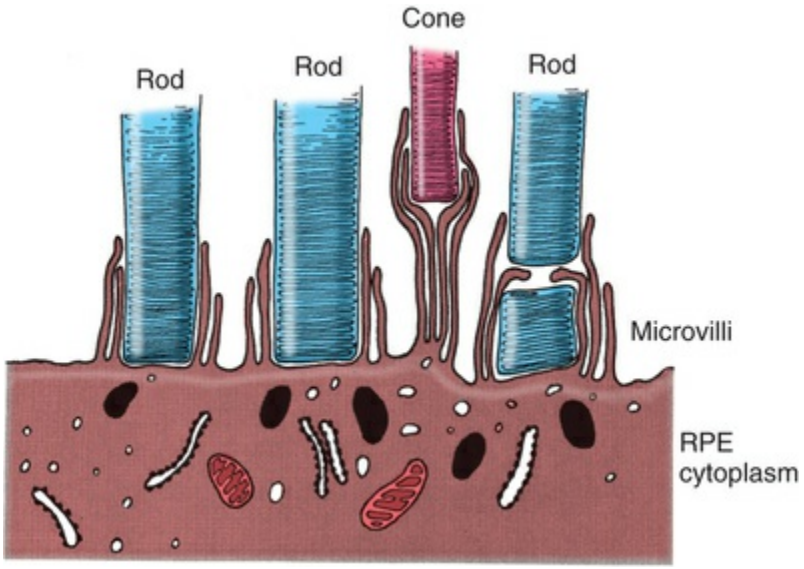

FIG. 21.6 Interdigitation between photoreceptor outer segments and the microvilli of the retinal pigment epithelium (RPE). Note that the microvilli actually indent the outer segments during phagocytosis of "outdated" discs. The cone outer segments are shorter,

and the microvilli form long pedicles in order to reach them.

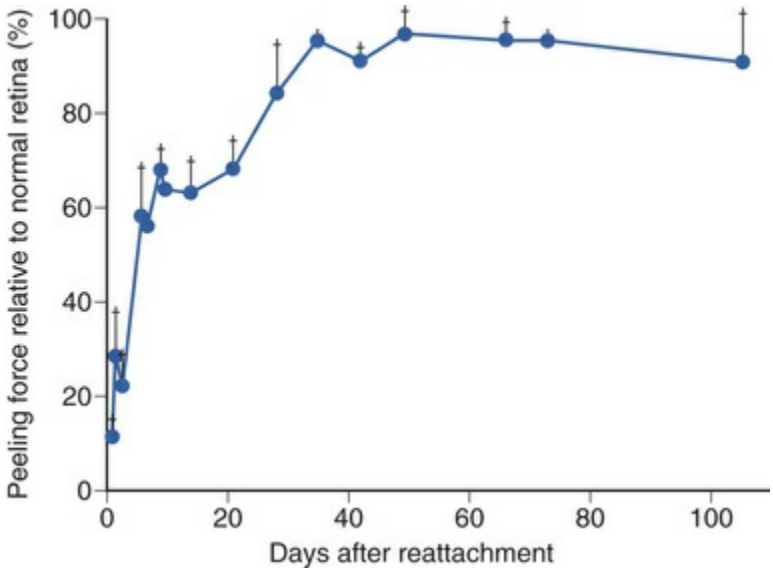

FIG. 21.7 Time course of the recovery of adhesive strength after separated retina becomes reattached. Experimental detachments were made in rabbit eyes by injecting a balanced salt solution into the subretinal space; the fluid absorbed within several hours, and at intervals after settling of the detachment, a comparison was made between the force required to peel the retina from normal and reattached areas of retinal pigment epithelium. (Reproduced with permission from Yoon YH, Marmor MF. Rapid enhancement of retinal adhesion by laser photocoagulation. Ophthalmology 1988;95:1385–8. Copyright © 1988, with permission from the American Academy of Ophthalmology.)

The mechanisms by which interdigitation could produce adhesion are not known. During outer-segment phagocytosis, the microvilli indent the outer segments and must physically impede attempts to withdraw them. Close ensheathment might also provide a frictional resistance to withdrawal, just as a finger is hard to pull from a narrow tube. There may be electrostatic forces that oppose separation of the membranes.[46] The magnitude of all of these effects will also depend on other factors, such as the composition of the intervening matrix and capability of the RPE microvilli for motility and remodeling.

Interphotoreceptor Matrix Properties

The IPM is a viscous material composed largely of proteins, glycoproteins, and proteoglycans[47,48] but containing a substantial concentration of glycosaminoglycans.[49] The idea that IPM might serve as a viscous glue was proposed many years ago by Berman,[50] but current evidence indicates the IPM is not just a layer of glue but has component structures that play a role in the adhesive process. For example, the cones are surrounded by a specialized sheath of matrix[51,52] that can be recognized histochemically by the binding of peanut agglutinin (PNA) (Fig. 21.8A). These cone matrix sheaths remain attached to both RPE and photoreceptor cells when the neural retina is peeled from the RPE.[48,51,53] If fresh primate or human retina is peeled from the RPE, the matrix material will stretch markedly before breaking (Fig. 21.8B), suggesting a rather strong bonding at both the outer-segment and RPE interfaces.[17,54] The evidence for a bonding function of the IPM is strongest with respect to the cone matrix sheaths, but the structural material that surrounds the rods may play a similar role. It can be recognized histochemically by staining with wheatgerm agglutinin (WGA) or other lectins,[55,56] and stretching of WGA-staining material may be observed on peeling freshly enucleated eyecup material.[17,54,57] The role of newly recognized matrix components such as galectins and IPM proteoglycans remains to be determined.[58,59]

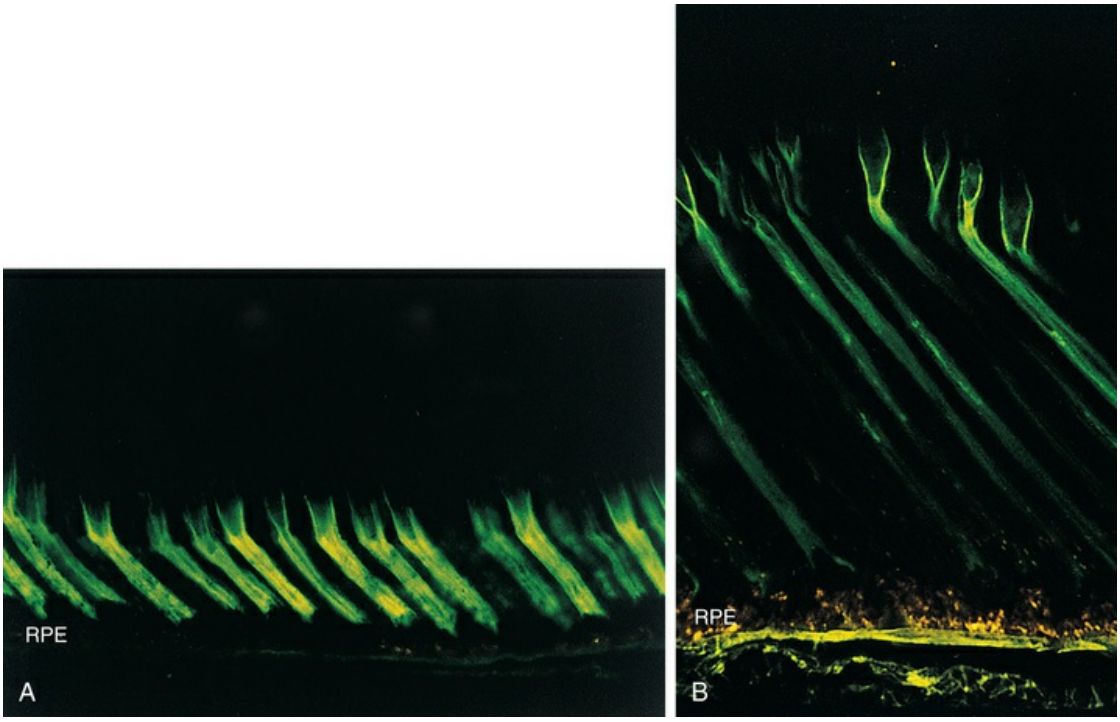

FIG. 21.8 Fluorescence micrographs of monkey retina showing cone sheaths of the interphotoreceptor matrix (IPM) stained with peanut agglutinin. Photoreceptors are above and retinal pigment epithelium (RPE) below. (A) Normal retina. The cone sheaths are short and thick. (B) Partially peeled retina. The cone sheaths have been stretched markedly between the photoreceptors and the RPE surface, showing the strength of IPM bonding to both sides. (Original magnification ×130). (Reproduced with permission from Hageman GS, Marmor MF, Yao XY, et al. The interphotoreceptor matrix mediates primate retinal adhesion. Arch Ophthalmol 1995;113:655–60. Copyright © 1995 American Medical Association. All rights reserved.)

The ability of cone or rod matrix sheaths to serve as a structural bond between retina and RPE may well depend on the presence of specific receptors that bind IPM components to the cell membranes. ("Cell adhesion molecules" represent a group of substances that mediate adhesion between individual cells or between cells and substrates.[60]) Experiments have shown that extracted IPM material does not automatically stick cells to one another,[61] but adhesion is unlikely unless specific receptors are present to bind the macromolecular substances. Several receptor systems, including sites for fibronectin, integrins, and mannose, have been proposed and disputed as being involved with retinal adhesion.[48,62–66] There is

functional evidence that inhibition of chondroitin sulfate proteoglycan synthesis with xylosides causes spontaneous detachments in primates.[48,67] Fibulin 2, an extracellular matrix protein, is upregulated in RPE after retinal detachment.[68]

Other types of evidence support the concept that IPM contributes significantly to retinal adhesion. Physical factors that affect adhesiveness, such as temperature, pH, and calcium concentration, are known to be modulators of the physicochemical properties of IPM macromolecules and may also affect the bonding of large-molecular species at receptoral sites.[69,70] There is also a marked loss of retinal adhesiveness when the subretinal space is exposed to enzymes that degrade matrix components,[15,71] such as chondroitinase ABC (which degrades chondroitin sulfate[72]) or neuraminidase (which breaks sialic acid bonds[73]). These enzymes, given intravitreally or into the subretinal space itself, weaken adhesiveness markedly in correlation with cytochemical evidence of damage to the IPM (Figs. 21.9 and 21.10). It is unknown whether the effects of these enzymes on adhesiveness are a result of changes in viscosity or damage to the structural elements of the IPM. However, adhesiveness returns to normal roughly 3 weeks after exposure of an eye to neuraminidase or chondroitinase ABC, and the recovery of adhesiveness correlates closely with the recovery of normal PNA-binding properties in the IPM.[74]

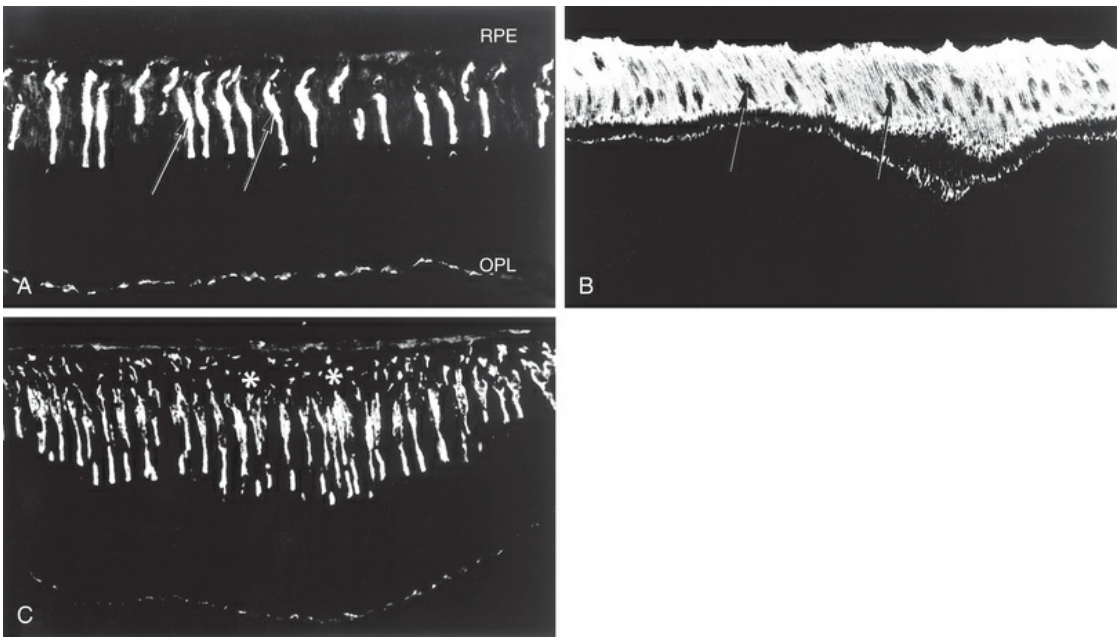

FIG. 21.9 Fluorescence light micrographs depicting binding of peanut agglutinin (PNA) to rabbit retinas in the region between the retinal pigment epithelium (RPE) and outer plexiform layer (OPL). (A) In a normal eye, PNA bound intensely and specifically to cone matrix sheaths (*arrows*). (B) After injection of neuraminidase, PNA binds throughout the interphotoreceptor matrix, with binding in the region of cones being diminished (note gaps indicated by *arrows*). (C) After intravitreal injection of testicular hyaluronidase, cone matrix sheaths were disrupted, especially at their apices (*asterisks*), and shallow separations between the photoreceptors and RPE were commonly observed. (Reproduced with permission from Yao XY, Hageman GS, Marmor MF. Retinal adhesiveness is weakened by enzymatic modification of the interphotoreceptor matrix in vivo. Invest Ophthalmol Vis Sci 1990;31:2051–8.)

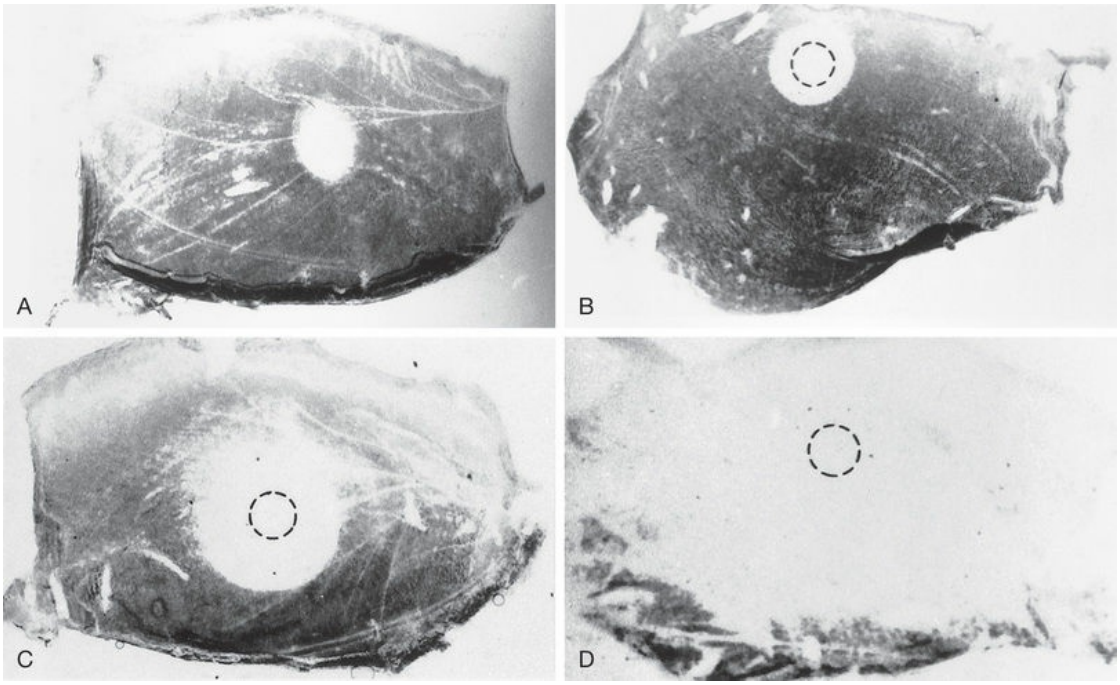

FIG. 21.10 Peeled whole-mount retinas after subretinal injection of enzymes. The areas of strong adhesion show retinal pigment epithelium pigment adherent to the retina after peeling; the areas of weak adhesion are clear of pigment. (A) Three days after injection of control (Hanks) solution, adhesion is normal (strong) except at the injection site. At (B) 1 day, (C) 2 days,

and (D) 3 days after testicular hyaluronidase, there was a progressive increase in the area of weakened adhesion beyond the injection site. A similar progression of adhesive loss was observed after neuraminidase. (Reproduced with permission from Yao XY, Hageman GS, Marmor MF. Retinal adhesiveness is weakened by enzymatic modification of the interphotoreceptor matrix in vivo. Invest Ophthalmol Vis Sci 1990;31:2051–8.)

Experiments have shown that the chemical nature of the IPM may change with light and dark adaptation.[75] To the extent that photic effects might modify the viscosity or bonding properties of the IPM, light could be a modulating factor of retinal adhesion. However, experimental data on adhesion in the light and dark have been contradictory and of uncertain significance.[11,76,77]

Subcellular Components and Mobility

Subcellular components of the RPE, such as microtubules and microfilaments, will be relevant to retinal adhesion to the extent that they influence remodeling and movement of the RPE microvilli.[78] Actin filaments control melanin movement in the amphibian RPE[11] and are present in mammalian RPE,[79,80] but a movement of melanin granules has never been observed in mammals. A few attempts have been made to alter adhesion by inhibiting subcellular components of the RPE. Cytochalasin B, which blocks microfilaments, was found to have no effect on adhesion when the drug was presented to excised tissue briefly after enucleation.[12] However, injecting cytochalasin into the vitreous 4–72 hours before enucleation caused a 70–90% reduction in pigment adherence as a measure of adhesiveness.[81]

When retina detaches, the surface morphology of the RPE changes literally within minutes.[23] The evolution of these changes can be altered by both colchicine (which dissembles microtubules) and cytochalasin,[82] suggesting that microtubules and microfilaments are important to apical RPE morphology. Actin filament contraction and subcellular motility are known to require calcium,[83] the absence of which is severely detrimental to retinal adhesion. However, we do not know whether the action of calcium in weakening adhesiveness relates to this mechanism or to effects

that calcium may have on transport systems and matrix-binding properties.

Metabolic Factors

The question of whether or why metabolic activity is necessary or even contributory to retinal adhesion is extremely important. From a physiologic standpoint, we would like to know the interaction between RPE transport, IPM properties, and the passive physical forces that impinge on the subretinal space. From a clinical standpoint, if adhesion is purely passive (i.e., dependent on pressure, or "glue"), therapy for clinical detachments would be primarily mechanical, whereas if active metabolism is necessary for adhesion, physicians may have a very different range of therapeutic options.

Critical Dependence on Oxygen

It was noted previously that adhesiveness in living rabbit eyes falls severely within a few minutes of death[5] (see Fig. 21.1A). Furthermore, just 1 minute of ocular ischemia in living rabbits weakens adhesion dramatically, whereas restoration of circulation restores adhesiveness.[84,85] The postmortem adhesive loss appears to be slower in primates and humans, and under similar in vitro conditions, at least a moderate adhesive force was measurable for 30 minutes or more after enucleation of primate and human tissue[15,17,85] (Fig. 21.11A).

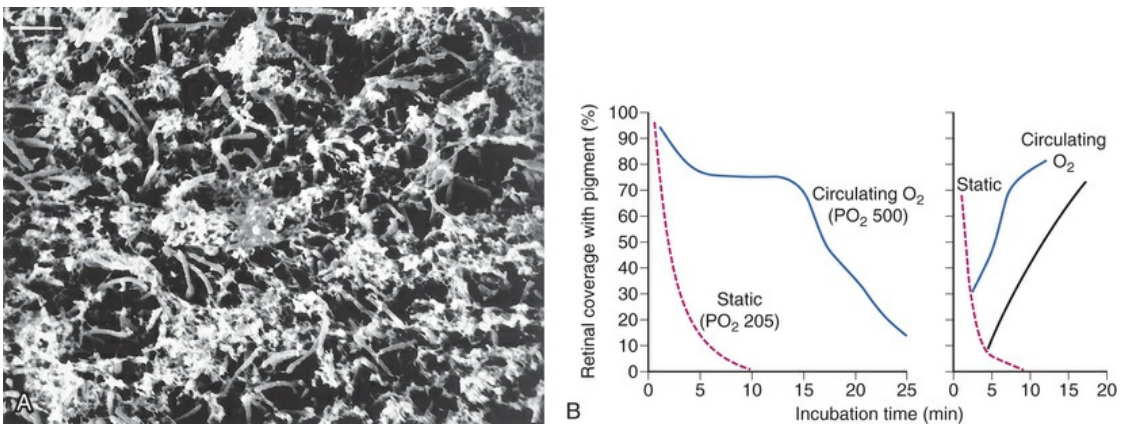

FIG. 21.11 Dependence of retinal adhesion on

metabolic activity. (A) Scanning electron micrograph of the photoreceptor surface of human retina peeled from the retinal pigment epithelium (RPE) within 4 minutes of enucleation. The outer segments are largely covered by apical fragments of RPE cells, indicating that the strength of retinal adhesion in living or fresh tissue is greater than that of the RPE cell membrane. Retinas peeled 1 hour after enucleation showed little or no adherence of RPE fragments. Bar = 10 μm. (B) Effect of oxygenation on the adhesiveness of rabbit retina in vitro. Left, Postmortem adhesive failure was delayed markedly by the incubation of tissue in an oxygenated rather than static bath. Right, Switching tissue from a static bath to an oxygenated one caused a prompt recovery of adhesive strength. (Panel A reproduced with permission from Marmor MF, Yao XY. The metabolic dependency of retinal adhesion in rabbit and primate. Arch Ophthalmol 1995;113:232–8. Panel B modified with permission from Marmor MF, Yao XY. The metabolic dependency of retinal adhesion in rabbit and primate. Arch Ophthalmol 1995;113:232–8.)

One possible explanation for the post-enucleation loss of adhesion is that the rapid release of lysosomal enzymes by injured RPE alters the IPM.[86] Enzyme release can occur quickly after injury,[86,87] and lysosomal enzyme activity is generally enhanced by warm temperature, low pH, and low calcium levels, all of which reduce retinal adhesiveness. However, the loss of adhesion under warm temperature, low pH, and low calcium conditions is rapidly reversible by restoring normal environmental conditions,[16] which would seem unlikely if irreversible degradation of the IPM had taken place. We have also been unable to find any cytochemical or morphologic changes in the IPM that correlate with the postmortem period loss of adhesion.

The postmortem failure can be retarded or even reversed simply by improving or restoring oxygenation.[84] With enhanced oxygenation, retinal adhesion in excised rabbit tissue can be maintained for 15–30 minutes (instead of 1–2 minutes) without postmortem failure (Fig. 21.11B); adhesive failure that occurred after a few minutes without oxygen was rapidly reversed by oxygenating the bath. In monkeys, adhesiveness may persist in oxygenated Ames solution for 1 hour or more.[85]

These results are extremely important with respect to the

mechanisms of adhesion because they show that, although IPM may account for much of the mechanical bond between retina and RPE, continuous oxygenation and active metabolic activity by RPE and photoreceptors are vital to the maintenance of adhesive strength. The critical activity might be subretinal fluid transport, which dehydrates the subretinal space, or it might be the metabolic control of membrane systems that modulate local pH, calcium concentration, or other factors that influence the bonding properties of the IPM. Metabolic failure could also affect the synthesis of IPM components and the function of subcellular organelles that influence microvillous motility.

Metabolic Inhibitors and Other Agents

A number of experiments have shown that general metabolic inhibitors have a deleterious effect on the process of retinal adhesion. For example, the introduction of cyanide into the experimental bath reduces the measured adhesive force and hastens the postmortem failure of adhesion.[3] In vivo experiments with dinitrophenol placed in the subretinal space showed that retinal adhesiveness was rapidly reduced to an unmeasurable level[10] (Fig. 21.12). Sodium iodate and hemicholinium-3 also cause retinal adhesiveness to fall rapidly to a low level,[88–91] but these effects may involve a variety of mechanisms because these agents affect not only metabolic functions of the RPE (and, more slowly, the photoreceptors) but also the physical integrity of the RPE cells and blood–retinal barrier.[89,92]

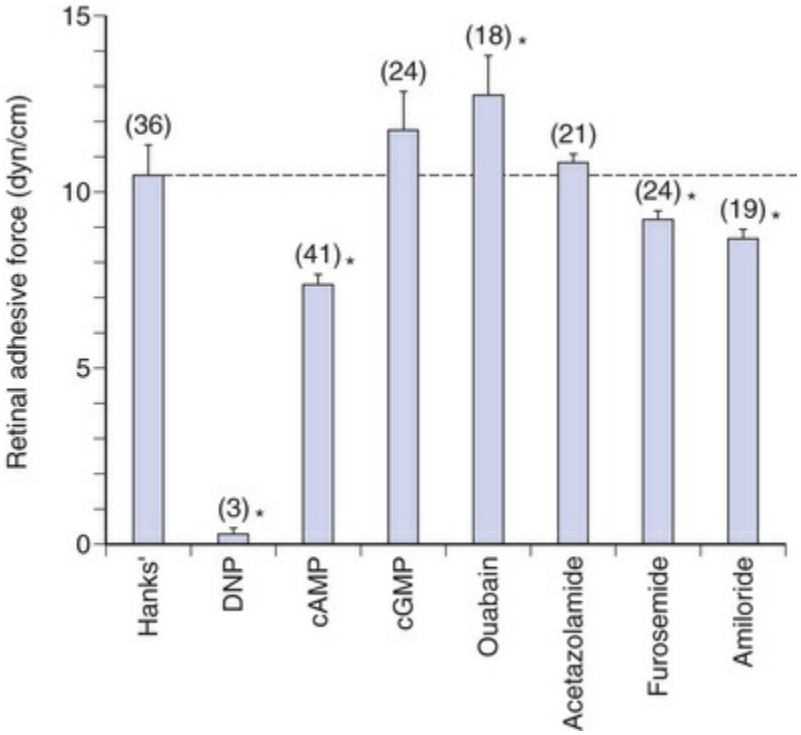

FIG. 21.12 The retinal adhesive force after injection of active agents into the subretinal space. Columns show mean value; bars show standard error; the numbers of experiments are in parentheses; asterisks indicate a significant difference from control ($p \leq .05$). *cAMP*, cyclic adenosine monophosphate; *cGMP*, cyclic guanosine monophosphate; *DNP*, dinitrophenol. (Reproduced with permission from Kita M, Marmor MF. Retinal adhesive force in living rabbit, cat, and monkey eyes: normative data and enhancement by mannitol and acetazolamide. Invest Ophthalmol Vis Sci 1992;33:1879–82.)

Specific transport inhibitors, in contrast, may act very selectively on different aspects of the adhesive process. For example, ouabain, which blocks the electrogenic sodium pump, will ultimately kill photoreceptor and RPE cells. However, in the short term its effect is to strengthen adhesiveness[3,10] (Fig. 21.12) because sodium entry causes cellular swelling that tightens (presumably) the interdigitation between RPE microvilli and outer segments.[13] This is a pathologic effect, of course, and is probably of little relevance to normal mechanisms of adhesion. Acetazolamide, which inhibits carbonic anhydrase, causes an increase in retinal adhesiveness, measured in vitro in rabbits[93] and in vivo in rabbit and monkey[9] (Fig. 21.13). The drug is effective only when given systemically and does not enhance adhesion if placed in the subretinal space or in an

experimental bath.[3,93] Acetazolamide enhances the apical-to-basal transport of fluid across the RPE,[93] and its effects on adhesion may well be a result of fluid movement, since the enhancement of outward fluid movement by other means such as mannitol[36] also increases adhesiveness.[36,37]

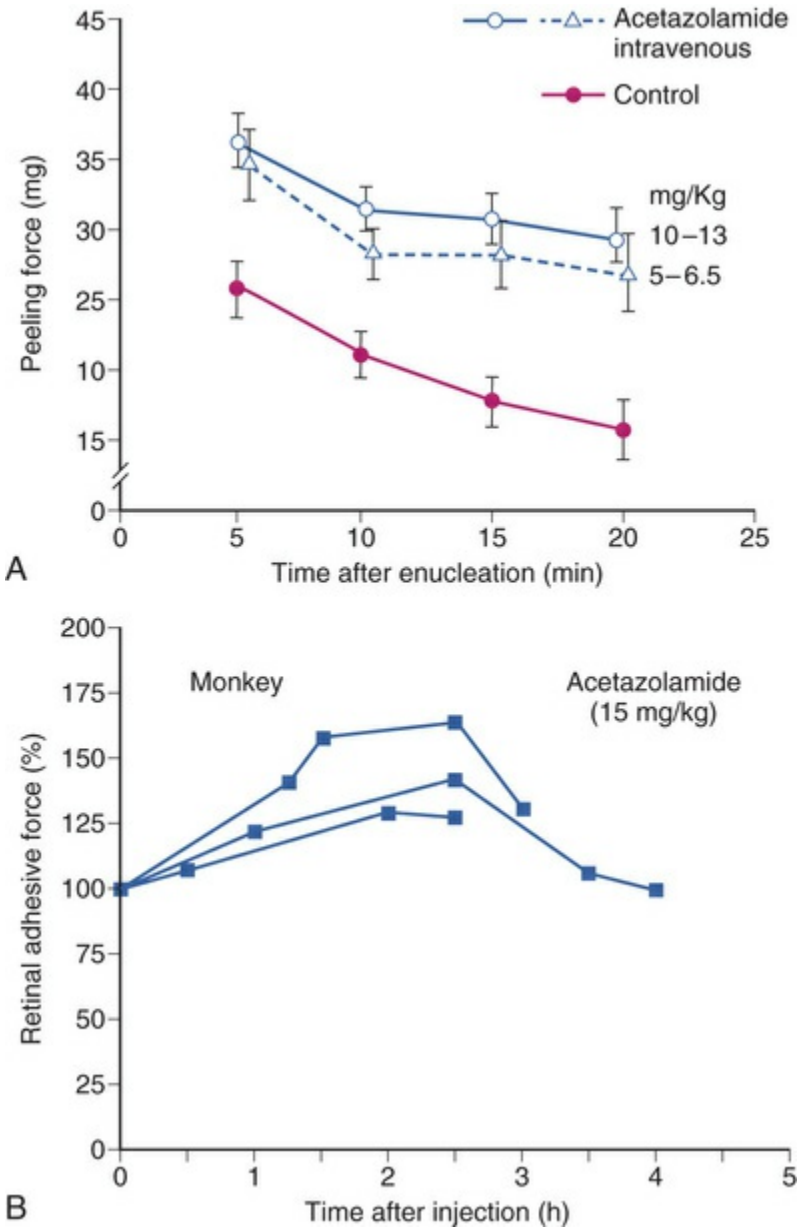

FIG. 21.13 Effects of acetazolamide on retinal adhesiveness. (A) Retinal adhesion in the rabbit is increased by systemically administered acetazolamide. The graph shows the force required to peel retina from the retinal pigment epithelium at four time intervals after enucleation, with and without acetazolamide. (B)

The time course of change in retinal adhesive force in three monkeys after intravenous injection of a clinical dose (15 mg/kg) of acetazolamide. A control value (100%) was derived from each eye before administration of the drug. (Panel A modified with permission from Marmor MF, Maack T. Enhancement of retinal adhesion and subretinal fluid resorption by acetazolamide. Invest Ophthalmol Vis Sci 1982;23:121–4. Panel B reproduced with permission from Kita M, Marmor MF. Retinal adhesive force in living rabbit, cat, and monkey eyes: normative data and enhancement by mannitol and acetazolamide. Invest Ophthalmol Vis Sci 1992;33:1879–82.)

Cyclic adenosine monophosphate (cAMP), which has been shown by several groups to inhibit the outward transport of fluid from the subretinal space,[94–96] reversibly weakens retinal adhesive force in vitro[12] (Fig. 21.14). cAMP is present in the RPE, but it is not known whether it actively modulates adhesive force in the living eye. In rabbits with experimental detachments, cyclic guanosine monophosphate (cGMP) has the opposite effect of cAMP on RPE fluid transport (i.e., it facilitates outward movement),[95,97] but it has not been shown to have an effect on retinal adhesiveness.

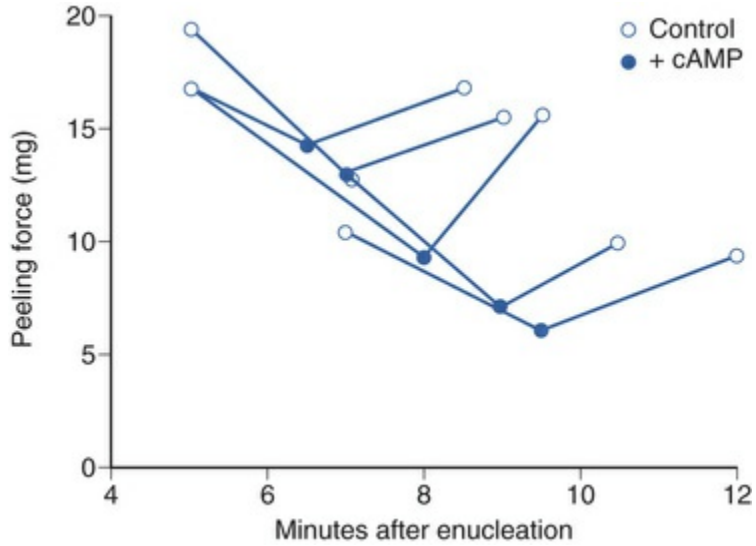

FIG. 21.14 Retinal adhesive force is weakened by exposure to cyclic adenosine monophosphate (cAMP). The graph shows the force required to peel rabbit retina from the retinal pigment epithelium (RPE) at various times after enucleation. For each strip of eyecup, three measurements of peeling force were made: one in control solution, one after cAMP was

added to the bath, and one after the tissue was returned to control solution. The addition of cAMP always weakened adhesion, but the effect was reversible on removing it from the bath. (Modified with permission from Yoon YH, Marmor MF. Effects on retinal adhesion of temperature, cyclic AMP, cytochalasin B, and enzymes. Invest Ophthalmol Vis Sci 1988;29:910–14.)

Retinal adhesiveness in vivo in the rabbit was also decreased, relative to normal, to 86% with furosemide and 81% with amiloride[10] (Fig. 21.12). Both these agents reduce apical–basal fluid transport across epithelial cells.[98,99]

Relationship of Adhesion to Subretinal Fluid Transport and Subretinal Protein

The RPE actively transports water from the subretinal space to the choroid[23,94,100] and experiments on the control of subretinal fluid transport[3,27,28,32,93,95,97,101] show that many of the factors affecting adhesion also influence transport in a similar direction. This concurrence may, in part, be fortuitous, since both physiologic processes involve the RPE; thus, conditions that nonspecifically stimulate or inhibit the RPE will have a similar effect on adhesion and fluid absorption. However, there may also be a more direct connection insofar as conditions that dehydrate the subretinal space should serve to keep the retina closely apposed, the matrix viscous, and the matrix molecules tightly interactive at ionic or receptor-binding sites. Conversely, conditions that block subretinal fluid transport and allow the subretinal space to become hydrated would seem intuitively to weaken adhesiveness. Thus, part of the metabolic requirement for retinal adhesion is almost certainly a direct result of the fact that subretinal fluid transport under normal conditions takes place primarily by active metabolic transport across the RPE. Adhesiveness is also increased by raising systemic osmolality with mannitol,[9,36,37] which passively enhances the absorption of subretinal fluid.[38]

In certain conditions the efficacy of subretinal fluid transport is clearly a critical factor in maintaining adhesion. For example, under conditions where defects occur in the RPE barrier and choroidal

pressure is relatively elevated (e.g., through venous obstruction, ocular hypotony, systemic hypertension, or other causes), there will be a risk of fluid following the pressure gradient to enter the subretinal space and cause a nonrhegmatogenous (serous) detachment. Passive adhesive systems are important to minimize the spread of fluid laterally, but the critical determinant of whether a detachment forms and how large it grows will be the ability of the RPE surrounding the "leak" to remove fluid as quickly as it enters the subretinal space. This concept of serous detachment[2] is discussed later.

Since the subretinal fluid of both serous and rhegmatogenous detachments has a high concentration of protein, the question may be asked whether oncotic pressure from this protein contributes to the formation or persistence of detachments by drawing in fluid. However, in experiments that introduced albumin (serum) or larger molecules into the subretinal space of rabbits (Fig. 21.15), fluid was absorbed within a few hours regardless of whether protein or other larger molecules remained in the subretinal space.[102–104] Furthermore, retina is sufficiently permeable to ions and water that the osmotic pressure of the subretinal space is continuously equilibrating with that of the vitreous to neutralize gradients[104,105] (Fig. 21.15B). In fact, albumin can also diffuse slowly across the retina. When serum is injected into the subretinal space, the subretinal fluid loses roughly 5% of its protein concentration per hour into the vitreous (Figs. 21.15A, C). Thus, the high protein content of subretinal fluid is not self-maintaining and is not the cause of detachment; rather it is the result of continued protein influx from the RPE or vitreous. Faulty RPE transport may also contribute to the retention of fluid within the retina, i.e., macular edema.[106]

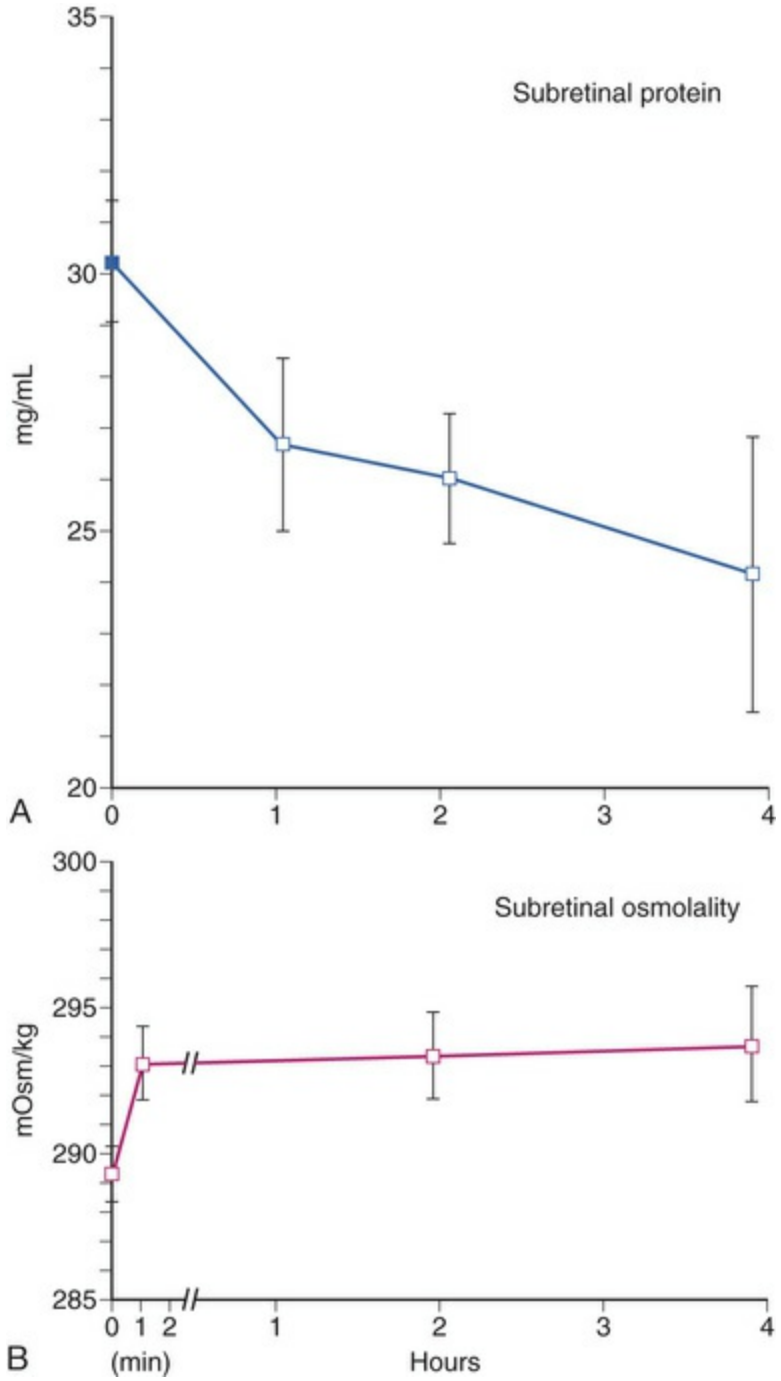
Subretinal protein
mg/mL
35
30
25
20
0
1
2
3
4
A
Subretinal osmolality
mOsm/kg
300
295
290
285
0 1 2
1
2
3
4
(min)
Hours
B

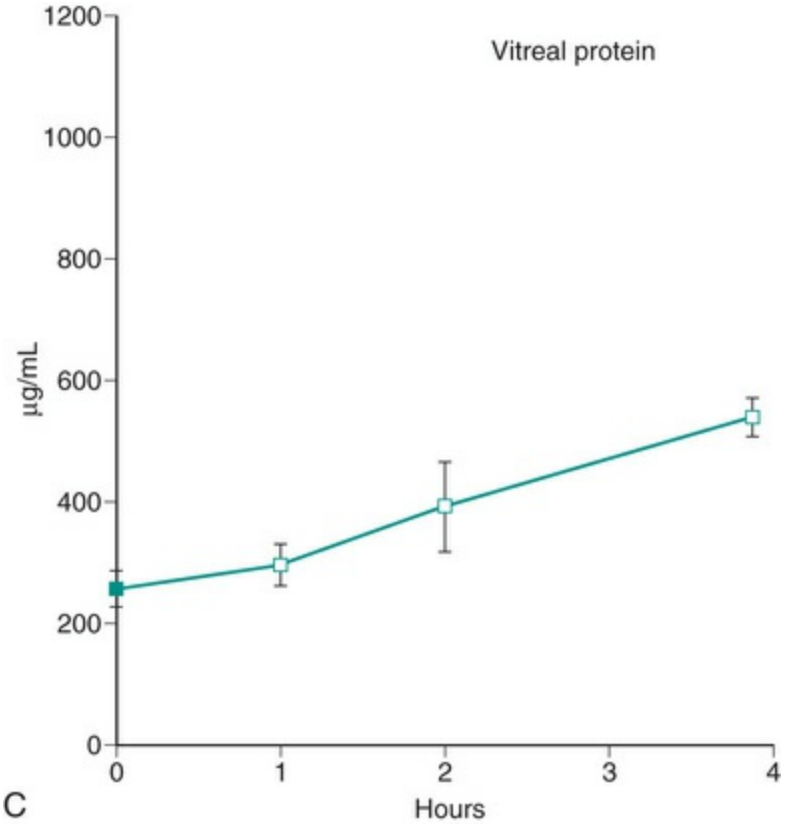

FIG. 21.15 Changes in protein concentration and osmolality after injecting highly proteinaceous fluid into the subretinal space of rabbit eyes. (A) Protein concentration of subretinal fluid. There is a steady decrease despite simultaneous water absorption. (B) Osmolality of the subretinal fluid. The osmolality of the injected fluid was initially low, but it equilibrated to vitreous levels (293 mosmol/kg) within 2 minutes and then remained steady despite the changing subretinal protein concentration. (C) Protein concentration of vitreous. There was a steady increase as protein diffused from the subretinal space. (Modified with permission from Takeuchi A, Kricorian G, Marmor MF. Albumin movement out of the subretinal space after experimental retinal detachment. Invest Ophthalmol Vis Sci 1995;36:1298–305.)

Pharmacologic Modification of Adhesion

Pharmacologic agents that modify retinal adhesive force could be useful clinically in several ways. Agents that enhance adhesion

could help reduce the risk of retinal detachment in high-risk eyes. They might minimize the spread of an existing detachment while awaiting surgical repair. They could improve or hasten the healing process after surgical repair of a detachment. To the extent that they enhance the absorption of subretinal fluid, they would speed the recovery of nonrhegmatogenous, as well as rhegmatogenous, detachments and minimize the risk of redetachment. If drugs can compensate in part for metabolic factors that fail in older eyes (which are more susceptible to detachment than younger ones) or in specific diseases that are predisposed to detachment, the risk of detachment might be decreased in these selected populations. Agents that reduce adhesion could facilitate an atraumatic separation of the retina in surgical procedures such as the removal of subretinal lesions, macular translocation, RPE transplantation, and injections of therapeutic agents such as a viral vector for gene transfer or stem cells for retinal regeneration.[107,108]

Mannitol

Mannitol is an accepted therapeutic agent in humans for glaucoma and cerebral edema. In systemic doses that are used clinically, it causes a 50% increase in retinal adhesiveness, measured both in excised tissue in vitro[37] and in the living eyes of primates and rabbits[9,36] (Fig. 21.5). The magnitude and duration (2–3 hours) of the mannitol effect are directly related to the increase in blood osmolality. However, the effect is not simply a result of fluid movement "pulling" the retina against the RPE, because it is measurable in vitro (where there is no transretinal flow). More likely, it depends on dehydration of the IPM, which strengthens bonding characteristics.

Intravenous mannitol might be useful preoperatively for short-term stabilization of retinal attachment (in a case with partial detachment) or postoperatively to enhance the absorption of fluid and increase the initial strength of bonding of retina to RPE. The drug might even be given intraoperatively to help minimize retinal separation during vitrectomy. The benefits are limited, however, because the drug cannot be given repeatedly over long periods. This would seem to reduce its value in the management of serous

nonrhegmatogenous detachments, although it might help to clear the accumulated fluid in cases where the source of leakage is no longer active.

When hyperosmotic solutions are injected into the vitreous cavity,[25] the gradient is in the opposite direction and retinal detachment can be induced (Fig. 21.4). This is a risk with certain drugs, but could in theory be used to produce or facilitate retinal separation in conjunction with procedures that require surgical elevation of the macula. Limitations are the minutes required for detachment to develop and the associated cellular damage if the osmotic load is too great.

Acetazolamide

The acetazolamide effect is slightly weaker than mannitol in the clinical doses we have used, causing a 30–45% increase in retinal adhesiveness in primates and rabbits[9,17] (Fig. 21.13). The acetazolamide effect lasts for 3–4 hours after a single injection, but acetazolamide can be given safely over long periods (although currently it is unknown whether the positive effects on adhesion would persist). Acetazolamide increases subretinal fluid transport[93] and thus could theoretically help to absorb fluid postoperatively or in cases of serous detachment. However, judging by anecdotal reports, researchers have not found acetazolamide to be dramatically effective in the management of central serous retinopathy. The problem may be that the effect of acetazolamide on subretinal fluid transport is not very strong and can only occur when the RPE is basically healthy and receptive to metabolic stimulation.[109] In a disorder such as central serous retinopathy, where RPE transport is probably compromised as a part of the disease, there may not be a normal substrate of RPE on which the acetazolamide can work.

Although acetazolamide and related carbonic anhydrase inhibitors have not been clinically useful for detachment disorders, they have proved quite useful for the removal of foveal cystic fluid in a number of disorders. They have not been of great use in postcataract cystoid edema and diabetic macular edema, where fluid continuously enters from vascular sources, but they can clear

intraretinal cysts dramatically where the fluid is relatively static in disorders such as retinitis pigmentosa, X-linked juvenile retinoschisis, enhanced S-cone syndrome, and sometimes macular epiretinal membrane formation.[106,109–113] The effectiveness probably depends on reasonable preservation of RPE metabolic function under the fovea, so that the drug can augment transport. One limitation to its use for retinal edema is the systemic side-effects, which may relate in part to its action on intracellular carbonic anhydrase throughout the body. Agents like benzolamide, which affect only the membrane-bound enzymes that are relevant to RPE transport, may have fewer side-effects.[114] Recent work has shown that enough drug may enter from topical carbonic anhydrase drops to produce a clinical effect, although the onset may take months instead of days.[115,116] The action of both oral and topical carbonic anhydrase inhibitors seems subject to tachyphylaxis (rebound of cystic edema), and cysts may return after roughly a year of usage; however, the effects will usually return after several months off treatment.[117,118]

Cold Temperature and Ouabain

Both cold temperature and ouabain increase retinal adhesiveness,[3,7] but their action depends on pathologic changes (cellular swelling) rather than a true enhancement of the mechanisms of adhesion.[13] Neither cold nor ouabain therefore can be used for any long-term clinical applications, but they may be valuable in special situations. For example, cooling the irrigating solution during vitrectomy might reduce the risk of retinal separation during the manipulation of surgery.

Ionic Changes

The removal of local calcium and magnesium ions, or lowering the pH, causes a dramatic fall in retinal adhesive force. Thus transient irrigation of the retina with calcium-free solution, or a solution of low pH, might facilitate the production of atraumatic surgical separation in association with submacular surgery. Alternatively a small amount of such solution might be injected into the subretinal space to weaken adhesion and make enlargement of the surgical

detachment easier. Preliminary studies on this approach have been reported,[75,107] but RPE or retinal toxicity is a risk, and guidelines for safe administration still need to be established.

Implications for Vitreoretinal Surgery

Understanding mechanisms of retinal adhesion, both positive and negative, is relevant to vitreoretinal surgery. During procedures of repair, or whenever retinal detachment would be a complication, it may be useful to create conditions that maximize adhesiveness. Conversely, when detachment is created surgically such as during macular translocation, it may be useful to create conditions that weaken adhesiveness to make the procedure as atraumatic as possible.

Two agents have already been documented to enhance retinal adhesiveness to a significant degree – mannitol and acetazolamide. cGMP might theoretically be of use, and a study of related agents may reveal some that are clinically beneficial. Other options for the future include agents that modify local pH or calcium concentration, strengthen the binding properties of adhesion molecules within the IPM, or stimulate microvillous growth and ensheathment of outer segments. Even a "pathologic" effect of cold temperature in strengthening adhesion through cellular edema might prove useful in temporary clinical situations such as vitreous surgery.

Conversely, conditions that reduce adhesiveness, such as intravitreal hyperosmolarity, metabolic inhibition, low Ca^{2+}, and low pH, might prove useful in subretinal surgery where retinal separation needs to be produced transiently and with little cellular damage. Low-Ca^{2+}, low-Mg^{2+} solutions have already been shown to weaken adhesion and facilitate experimental detachment in rabbits.[75,107,119] Metabolic inhibitors, such as dinitrophenol, should in theory also be effective if their effects could be made transient and nontoxic. Another agent that might reduce adhesiveness is cAMP. Some of these approaches are likely to reach clinical practice within the next few years.

Recovery After Rhegmatogenous Retinal Detachment

Retinal reattachment forces return following reapproximation of the sensory retina and RPE. This is observed both without retinopexy and following such therapy, which augments the adhesion.

Recovery of Adhesiveness Without Retinopexy

Recovery after retinal detachment depends on a variety of factors, including the length of detachment (which may affect the survival of cells) and effectiveness with which adhesive mechanisms can be reestablished. We have measured in rabbits the retinal peeling force in vitro[45] after making small experimental detachments that spontaneously settled within hours to a few days. The results show that restoration of normal adhesive strength requires 4–6 weeks (Fig. 21.7). Keep in mind that these experiments involved the injection of a small amount of balanced salt solution into the subretinal space; in clinical detachments, where the fluid is serous and the retina is separated for longer periods, there could well be more trauma to the RPE or outer segments and thus an even more prolonged recovery period. It remains to be shown which adhesive factors are rate-limiting for the recovery process, considering that full recovery involves the restoration of anatomic interdigitation, RPE synthetic capabilities, IPM structure and binding, and subretinal fluid transport. These data show how clinical recovery after retinal detachment is possible without retinopexy,[120–122] although it is slow and would only be advisable when mechanical (vitreous) traction forces have been fully relieved.

Effects of Retinopexy

Retinal surgeons frequently use retinopexy (i.e., scarification of the retina and RPE with laser photocoagulation, diathermy, or cryotherapy) as a means of creating an extra-strong adhesion between retina and RPE that will strengthen attachment and prevent the lateral movement of subretinal fluid. Experiments on

the in vitro peeling force[45] and the in vivo adhesive force[122] show that laser photocoagulation produces a bond that approaches normal adhesive strength within 24 hours, possibly from local effects such as fibrin formation (Fig. 21.16). The adhesive strength continues to increase gradually and reaches levels roughly twice normal by 2–3 weeks after the photocoagulation.[45,123,124] Diathermy effects, measured in vivo, have a similar time course. Cryotherapy, however, weakens adhesion for the first week, after which the adhesive force rises to the same levels as with other forms of retinopexy. The initial weakening after cryotherapy probably relates to local inflammation or edema. Thus, all forms of retinopexy appear to be effective in the long run, presumably by inducing scar formation; however, if a rapid bond is required, laser photocoagulation or diathermy is preferable.

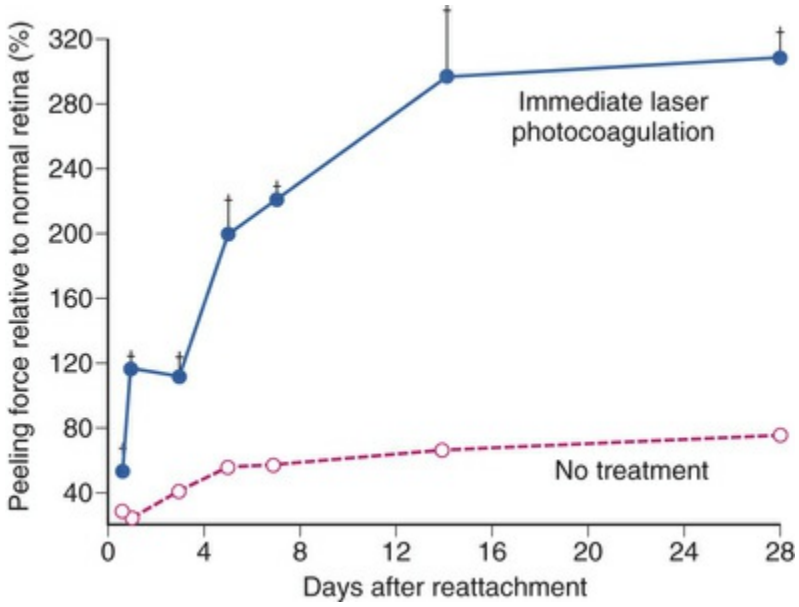

FIG. 21.16 Laser photocoagulation of freshly reattached retina can rapidly enhance the strength of retinal adhesion. Two experimental detachments were made in each eye (Fig. 19.7), and after the subretinal fluid had spontaneously absorbed, the base of one detachment was covered with laser photocoagulation. The force required to peel retina from the reattached areas, with or without photocoagulation, was compared to the force required in the intervening normal areas. The adhesive force in the photocoagulated regions exceeded normal within hours and reached an

apparent maximum after about 2 weeks (although at these levels of force the retina frequently tore rather than separated, and the "true" adhesive strength may be even greater). (Reproduced from Yoon YH, Marmor MF. Rapid enhancement of retinal adhesion by laser photocoagulation. Ophthalmology 1988;95:1385–8. Copyright © 1988, with permission from the American Academy of Ophthalmology.)

Effects of Vitreous in the Subretinal Space

One of the factors contributing to many rhegmatogenous detachments is vitreous syneresis and liquefaction, which allow fluid to percolate through the retinal tear and expand or maintain the elevation of retina. Although there is some evidence that hyaluronic acid may be toxic in high concentrations to RPE,[125] clinical data indicate that liquid vitreous is tolerated insofar as a reasonable recovery of retinal function generally occurs if detachments are repaired within a few days or weeks. The presence of liquefied vitreous in the subretinal space has no immediate effect on the rate of fluid transport across the RPE.[126] The concentration of protein in normal vitreous is only about 1% of that in serum, but when vitreous enters the subretinal space, the concentration of subretinal protein rises slowly.[126] This occurs because water is pumped out faster than the protein can be removed, whereas the continued entry of liquid vitreous brings in more protein. This mechanism may contribute to the high protein concentration of subretinal fluid in chronic rhegmatogenous detachments. Serum and protein may also leak in from the choroid to the extent that the RPE has been damaged under the conditions of detachment.

Pathophysiology of Serous Detachment

For detachment to occur there must be forces that cause the retina to separate and also conditions that allow subretinal fluid to persist. The clinical condition of serous detachment (considered in detail in Chapter 32, Pathogenesis of serous detachment of the retina and

pigment epithelium) provides a case in point. In central serous chorioretinopathy (CSC), fluorescein angiography demonstrates apparent "leaks" through the RPE, defects through which fluid enters the subretinal space from the choroid. However, experimental work has clearly shown that subretinal fluid overlying an intact RPE is removed very actively by active metabolic transport and that damage to the RPE barrier in general makes the absorption of fluid faster rather than slower (Fig. 21.17). For example, damaging the RPE focally by mechanical micropipette injury or laser burns or diffusely by the systemic administration of sodium iodate hastens the absorption of subretinal fluid.[127,128] This occurs because intraocular pressure and the osmotic absorption of the choroid both move fluid in an outward direction, and their effectiveness is increased when the RPE flow barrier is removed. Even serous fluid is absorbed at least as fast over damaged as over intact RPE.[103,105] Furthermore, to cause detachment the entering fluid must overcome the retinal adhesive forces at the margin of the leak. Thus the mere presence of a focal defect in the RPE does not "cause" serous detachment.[129]

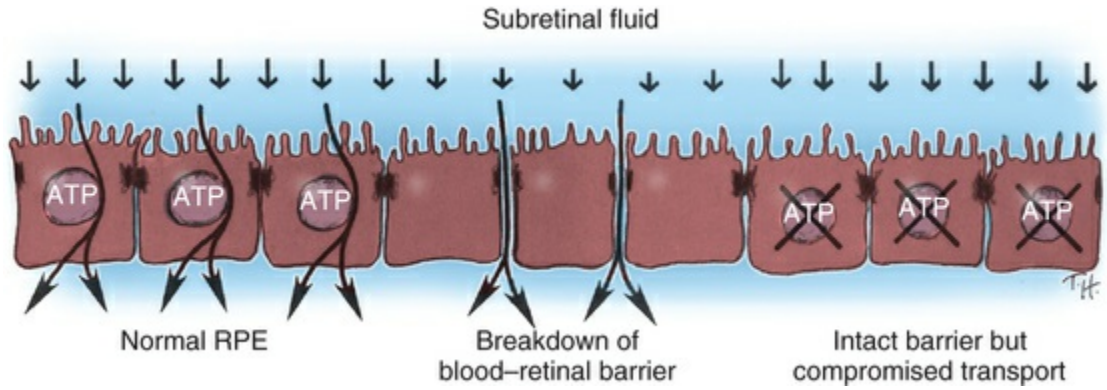

FIG. 21.17 Conditions that control the movement of fluid across the retinal pigment epithelium (RPE). Left, When the tight junctions are intact between normal RPE cells, fluid is transported across by active transport. Middle, If the tight junctions are damaged, fluid can cross passively under the influence of hydrostatic and osmotic pressure. Right, If the tight junctions are intact and the metabolic transport capability of the RPE has been compromised, then fluid is unable to cross. *ATP*, adenosine triphosphate.

How then do serous detachments form?[2,130,131] The question is not whether the leaks are the source of fluid – they must be – but why the fluid accumulates when entry is slow and one would expect subretinal fluid to be cleared rapidly by active transport (across a normal RPE) or by passive mechanisms (across damaged RPE). On reflection, the one condition that would allow fluid to accumulate is when the RPE barrier function remains intact around the leak, whereas active fluid transport is impaired (Fig. 21.18). In this situation fluid cannot leave passively or actively. The present author's conjecture is that many serous detachments form because there is widespread functional damage to the process of transport across the RPE (either from RPE disease directly or from disease of the underlying choroid and choriocapillaris). For example, the absorption of subretinal fluid in rabbits is slowed by the ligation of vortex veins,[132] and the choroid is typically thickened in CSC, which may signify increased hydrostatic pressure.[108] When fluid absorption is compromised, fluid that enters from a focal leak may persist and accumulate within the subretinal space (Fig. 21.19). One may ask whether the persistence of serous detachment can be accounted for simply by oncotic pressure when protein-rich fluid leaks into the subretinal space. However, as noted earlier, protein in the subretinal space does not prevent fluid absorption: it is osmotically neutralized by the diffusion of water and ions from the vitreous, and it will not persist unless there is a continual influx of new proteinaceous fluid.

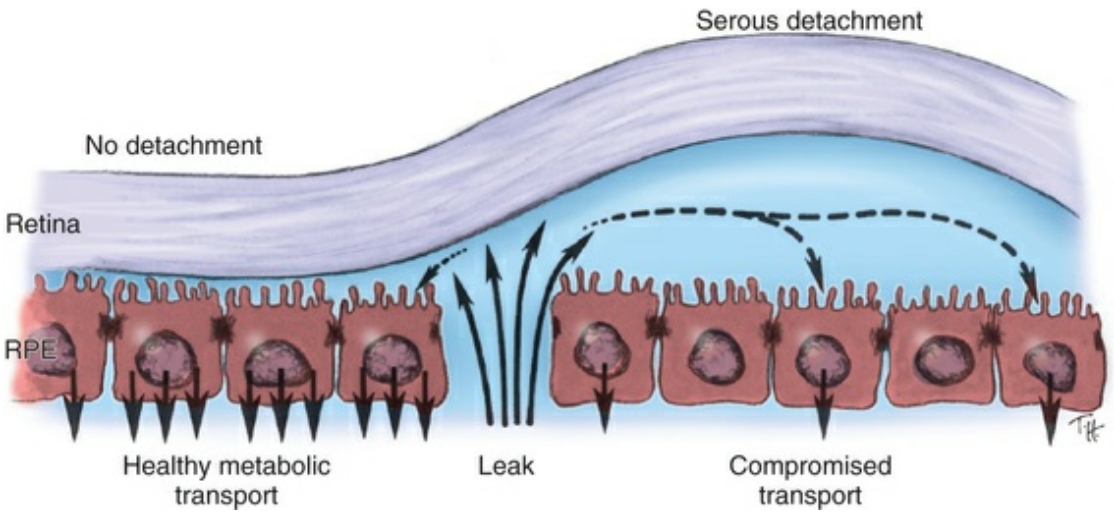

FIG. 21.18 Transport capabilities of the retinal pigment epithelium (RPE) can determine whether or not a serous detachment will form in the presence of fluid leakage through an RPE defect. Left, When the active systems are working at normal efficiency, fluid can be pumped out as fast as it enters the subretinal space, and little or no detachment will develop. Right, When RPE transport has been compromised, then a serous detachment will form until a large enough area of RPE is exposed to subretinal fluid to allow outward transport to balance the inward leakage of fluid.

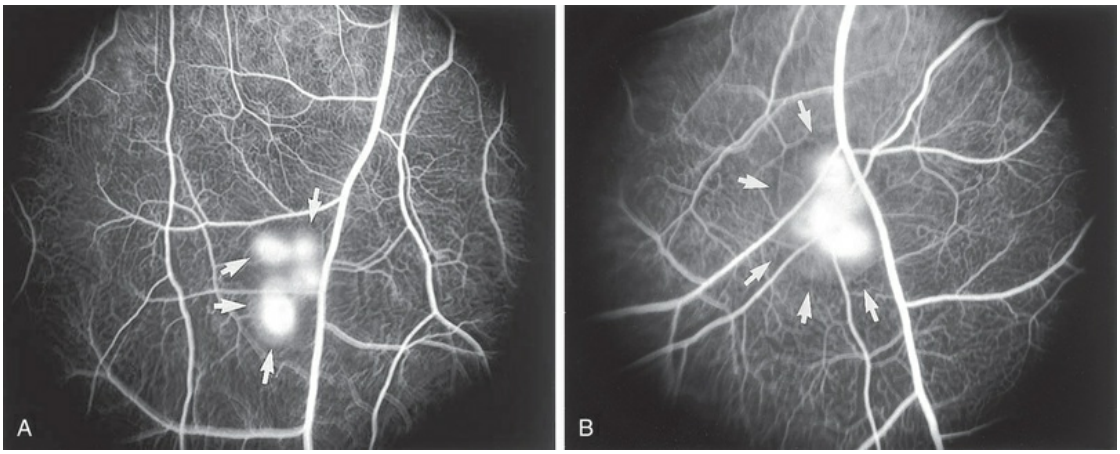

FIG. 21.19 Fluorescein angiograms from different fundus regions of the same cat, showing the effects of diffuse retinal pigment epithelium (RPE) damage on the accumulation of serous fluid. (A) Control region. Weak laser burns were applied after the animal was given intravenous rose Bengal to photosensitize the choriocapillaris. Fluorescein leaks from the burn sites but spreads very little. (B) RPE-damaged region. This area was pretreated with intense white light to injure the RPE diffusely before giving the rose Bengal and laser burns. The dye leakage extends much farther beyond the burn sites and slowly fills an overlying detachment. (Unpublished data reproduced with permission from Marmor MF, Yao XY. Conditions necessary for the formation of serous detachment: experimental evidence from the cat. Arch Ophthalmol 1994;112:830–8.)

Three conditions appear to be necessary for serous fluid to accumulate:[131,132] (1) a defect in the RPE barrier that allows access to

the subretinal space; (2) a source of fluid pressure, to move fluid in; and (3) an impairment of outward fluid transport (or a broad area of leakage), so fluid spreads and persists in the subretinal space. Weakness of retinal adhesion or retinal tension may be an additional facilitating factor. Unless all three basic conditions are present, detachment will not occur, and the balance of these forces has been modeled mathematically.[133] For example, attempts to induce serous detachment in rabbits by damaging the RPE focally while altering intraocular pressure (conditions 1 and 2 only) have been largely unsuccessful.[120] However, diffuse injury to the RPE and underlying choriocapillaris (by photosensitization with rose Bengal dye[134] or by toxic effects of *N*-ethylmaleimide[135]) leads to the formation of bullae (Fig. 21.20), since the damaged capillaries not only serve as a source of fluid, but also compromise RPE transport and barrier functions. In clinical practice, choroidal vascular damage is probably the most frequent primary cause of serous detachments and may underlie even the focal RPE defects of CSC.[108,130]

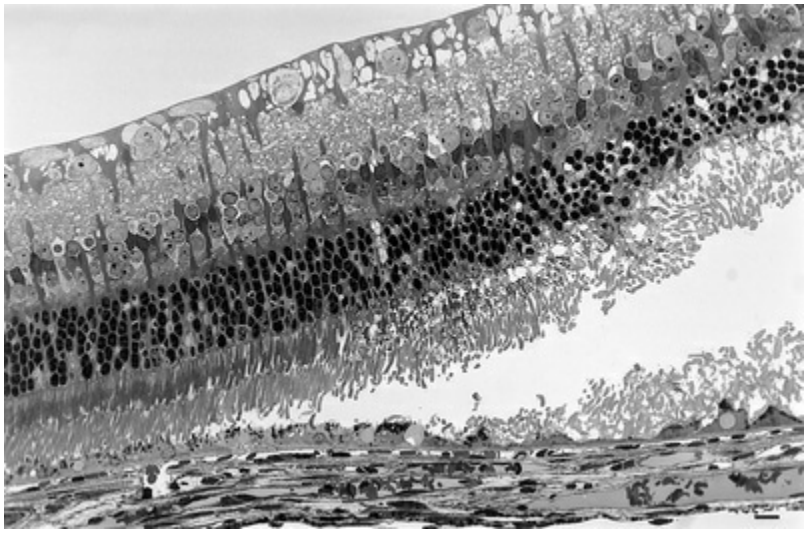

FIG. 21.20 Histology from the margin of an experimental serous detachment in the rabbit, induced by illumination of the fundus after injection of the photosensitizing dye, rose Bengal. This treatment causes vascular injury, and the animal was cooled to prevent choroidal thrombosis. There was diffuse fluorescein leakage across the base of the detachment, and the detached area (right) shows

retinal pigment epithelium damage over patent (but presumably injured) choriocapillaris. (Reproduced with permission from Yao XY, Marmor MF. Induction of serous retinal detachment in rabbit eyes by pigment epithelial and choriocapillary injury. Arch Ophthalmol 1992;110:541–6. Copyright © 1982 American Medical Association. All rights reserved.)

If CSC is more a disease of diffuse transport dysfunction than a result of the focal "leak" seen on angiography,[2] why does laser photocoagulation of the leak help to clear the fluid? Because the laser seals a leak so that the existing fluid can slowly absorb. However, recurrences will be common as long as the underlying transport dysfunction persists, and this is indeed the clinical course of the disease. In further support of the concept of diffuse dysfunction, serous retinopathy is often associated with systemic disease, including vascular disorders, inflammatory disease, abnormal blood protein, corticosteroid usage, and emotional stress (chronic administration of epinephrine can produce serous detachments in experimental animals[136]). And the serous fluid accumulations are often bilateral and multifocal. Unfortunately, treatment with carbonic anyhdrase inhibitors that enhance RPE transport has not shown great value in most serous detachment, presumably because the RPE transport system is already compromised by disease. However, as noted earlier, these agents can be very effective in clearing cystic intraretinal fluid, especially in retinal dystrophies including retinitis pigmentosa, X-linked retinoschisis, and enhanced S-cone syndrome.

Conclusions and General Implications

One important conclusion to be derived from the evidence reviewed in this chapter is that retina "wants" to adhere. A variety of systems, including passive hydrostatic forces, the interdigitation of outer segments and RPE microvilli, the active transport of subretinal fluid, and the complex structure and binding properties of the IPM, all work to keep the retina properly apposed to the wall of the eye. Thus retinas do not detach simply because there is a hole or a tear or even a leak in the RPE; there must be positive traction pulling it off or a positive force pushing fluid into the subretinal

space (often in conjunction with underlying pathologic conditions of the RPE or choriocapillaris that block the normal transport processes that remove subretinal fluid). Retinal detachment is not simply a disease of physical separation but is the result of a vital battle between a destructive influence and the collection of forces routinely at work constructively to maintain attachment.

This multifactorial nature of retinal adhesiveness is important clinically, as well as physiologically. To function optimally, adhesive systems require proper anatomic relations, healthy metabolic activity, and an appropriate local environment (pH, temperature, Ca^{2+} concentration) in the subretinal space. This means that adhesion may be weakened by diseases with various sites and modes of action; at the same time, the complementary mechanisms for attachment undoubtedly provide safety coverage for one another, so injury or illness of one adhesive system does not necessarily doom the eye to total detachment. The multiplicity of factors also allows us to consider a variety of therapeutic options that might otherwise not be available. For example, the presence of holes in the retina obviates the use of fluid pressure to aid retinal apposition but leaves open options for encouraging fluid transport pharmacologically or for creating scars as a means of restoring local adhesion. As the different mechanisms of adhesion become better understood, more specific medical and surgical approaches to the prevention, as well as the management, of detachments should become available.

The importance of metabolic activity in maintaining retinal adhesion cannot be emphasized too strongly. If retinal attachment were solely a passive process, then detachment would be solely at the mercy of passive forces and physical means of repair. To the extent that the metabolic health of the RPE appears to be critical to adhesion, we can better understand the failure of adhesion in certain disease states or ocular locations, and we may ultimately realize more effective means of treatment. The propensity of aged eyes to suffer detachment much more than younger ones, for example, may in part lie in the gradual metabolic failure of the RPE. The retinal periphery has a less effective vascular supply than the posterior pole, and this, too, is where most detachments begin. This discussion is not intended to minimize the well-documented role of

vitreous syneresis and vitreous traction in creating detachments. However, by improving the metabolic status of peripheral retina and RPE, we might be able to reduce the incidence of detachment and improve the success rate of surgical repair. Cutting vitreous bands and sealing holes manage only one aspect of the disease; we will treat the whole disease only when we can also treat the pathologic conditions within the subretinal space.

References

1. Steinberg RH, Wood I. Pigment epithelial cell ensheathment of cone outer segments in the retina of the domestic cat. *Proc R Soc Lond B Biol Sci*. 1974;187:461–478.
2. Marmor MF. New hypothesis on the pathogenesis and treatment of serous retinal detachment. *Graefes Arch Clin Exp Ophthalmol*. 1988;226:548–552.
3. Marmor MF, Abdul-Rahim AS, Cohen DS. The effect of metabolic inhibitors on retinal adhesion and subretinal fluid resorption. *Invest Ophthalmol Vis Sci*. 1980;19:893–903.
4. Zauberman H, DeGuillebon H. Retinal traction in vivo and postmortem. *Arch Ophthalmol*. 1972;87:549–554.
5. De Guillebon H, De la Tribonniere MM, Pomerantzeff O. Adhesion between retina and pigment epithelium. *Arch Ophthalmol*. 1971;86:679–684.
6. De Guillebon H, Zauberman H. Experimental retinal detachment: biophysical aspects of retinal peeling and stretching. *Arch Ophthalmol*. 1972;87:545–548.
7. Endo EG, Yao XY, Marmor MF. Pigment adherence as a measure of retinal adhesion: dependence on temperature. *Invest Ophthalmol Vis Sci*. 1988;29:1390–1396.
8. Kita M, Negi A, Kawano SI, et al. Measurement of retinal adhesive force in the in vivo rabbit eye. *Invest Ophthalmol Vis Sci*. 1990;31:624–628.
9. Kita M, Marmor MF. Retinal adhesive force in living rabbit, cat, and monkey eyes: normative data and enhancement by mannitol and acetazolamide. *Invest Ophthalmol Vis Sci*. 1992;33:1879–1882.
10. Kita M, Marmor MF. Effects on retinal adhesive force in vivo

of metabolically active agents in the subretinal space. *Invest Ophthalmol Vis Sci*. 1992;33:1883–1887.
11. Marmor MF, Maack T. Local environmental factors and retinal adhesion in the rabbit. *Exp Eye Res*. 1982;34:727–733.
12. Yoon YH, Marmor MF. Effects on retinal adhesion of temperature, cyclic AMP, cytochalasin B, and enzymes. *Invest Ophthalmol Vis Sci*. 1988;29:910–914.
13. Marmor MF, Yao XY. The enhancement of retinal adhesiveness by ouabain appears to involve cellular edema. *Invest Ophthalmol Vis Sci*. 1989;30:1511–1514.
14. Maurice DM, Salmon J, Zauberman H. Subretinal pressure and retinal adhesion. *Exp Eye Res*. 1971;12:212–217.
15. Yao XY, Hageman GS, Marmor MF. Retinal adhesiveness in the monkey. *Invest Ophthalmol Vis Sci*. 1994;35:744–748.
16. Yao XY, Endo EG, Marmor MF. Reversibility of retinal adhesion in the rabbit. *Invest Ophthalmol Vis Sci*. 1989;30:220–224.
17. Marmor MF, Yao XY, Hageman GS. Retinal adhesiveness in surgically enucleated human eyes. *Retina*. 1994;14:181–186.
18. Kita M, Negi A, Marmor MF. Lowering the calcium concentration in the subretinal space in vivo loosens retinal adhesion. *Invest Ophthalmol Vis Sci*. 1992;33:23–29.
19. Bill A. Some aspects of tissue fluid dynamics in the eye. Cant JS. *Vision and circulation*. Mosby: St. Louis; 1976.
20. Toris CB, Pederson JE, Tsuboi S, et al. Extravascular albumin concentration of the uvea. *Invest Ophthalmol Vis Sci*. 1990;31:43–53.
21. Maurice DM. Flow of water between aqueous and vitreous compartments in the rabbit eye. *Am J Physiol*. 1987;252:104–108.
22. Fatt I, Shantinath K. Flow conductivity of retina and its role in retinal adhesion. *Exp Eye Res*. 1971;12:218–226.
23. Tsuboi S. Measurement of the volume flow and hydraulic conductivity across the isolated dog retinal pigment epithelium. *Invest Ophthalmol Vis Sci*. 1987;28:1776–1782.
24. Marmor MF. Retinal detachment from hyperosmotic intravitreal injection. *Invest Ophthalmol Vis Sci*. 1979;18:1237–1244.

25. Marmor MF, Martin LJ, Tharpe S. Osmotically induced retinal detachment in the rabbit and primate: electron microscopy of the retinal pigment epithelium. *Invest Ophthalmol Vis Sci*. 1980;19:1016–1029.
26. Cantrill HL, Pederson JE. Experimental retinal detachment. VI. The permeability of the blood–retinal barrier. *Arch Ophthalmol*. 1984;102:747–751.
27. Frambach DA, Marmor MF. The rate and route of fluid resorption from the subretinal space of the rabbit. *Invest Ophthalmol Vis Sci*. 1982;22:292–302.
28. Negi A, Marmor MF. Quantitative estimation of metabolic transport of subretinal fluid. *Invest Ophthalmol Vis Sci*. 1986;27:1564–1568.
29. Pederson JE, Cantrill HL. Experimental retinal detachment. V. Fluid movement through the retinal hole. *Arch Ophthalmol*. 1984;102:136–139.
30. Hamann S, Kiilgaard JF, la Cour M, et al. Cotransport of H^+, lactate, and H_2O in porcine retinal pigment epithelial cells. *Exp Eye Res*. 2003;76:493–504.
31. Chihara E, Nao-i N. Resorption of subretinal fluid by transepithelial flow of the retinal pigment epithelium. *Graefes Arch Clin Exp Ophthalmol*. 1985;223:202–204.
32. Negi A, Kawano S, Marmor MF. Effects of intraocular pressure and other factors on subretinal fluid resorption. *Invest Ophthalmol Vis Sci*. 1987;28:2099–2102.
33. Rutnin U, Schepens CL. Fundus appearance in normal eyes. IV. Retinal breaks and other findings. *Am J Ophthalmol*. 1978;64:1063–1078.
34. Foulds WS. The vitreous in retinal detachment. *Trans Ophthalmol Soc U K*. 1975;95:412–416.
35. Hammer ME. Retinal re-attachment forces created by absorption of subretinal fluid. *Doc Ophthalmol*. 1981;25:61–75.
36. Kita M, Marmor MF. Systemic mannitol increases the retinal adhesive force in vivo. *Arch Ophthalmol*. 1991;109:1449–1450.
37. Yao XY, Moore KT, Marmor MF. Systemic mannitol increases retinal adhesiveness measured in vitro. *Arch Ophthalmol*. 1991;109:275–277.

38. Negi A, Marmor MF. Effects of subretinal and systemic osmolality on the rate of subretinal fluid resorption. *Invest Ophthalmol Vis Sci*. 1984;25:616–620.
39. Osterlin S. On the molecular biology of the vitreous in the aphakic eye. *Acta Ophthalmol*. 1977;55:353–361.
40. Foulds WS. Experimental retinal detachment. *Trans Ophthalmol Soc U K*. 1963;83:153–170.
41. Anderson DH, Fisher SK. The relationship of primate foveal cones to the pigment epithelium. *J Ultrastruct Res*. 1986;67:23–32.
42. Young RW. Visual cells and the concept of renewal. *Invest Ophthalmol*. 1976;15:700–725.
43. Anderson DH, Guerin CJ, Erickson PA, et al. Morphological recovery in the reattached retina. *Invest Ophthalmol Vis Sci*. 1986;227:168–183.
44. Kroll AJ, Machemer R. Experimental retinal detachment in the owl monkey. V. Electron microscopy of the reattached retina. *Am J Ophthalmol*. 1969;67:117–130.
45. Yoon YH, Marmor MF. Rapid enhancement of retinal adhesion by laser photocoagulation. *Ophthalmology*. 1988;95:1385–1388.
46. Gingell D, Fornes JA. Demonstration of intermolecular forces in cell adhesion using a new electrochemical technique. *Nature*. 1975;256:210–211.
47. Adler AJ, Klucznik KM. Proteins and glycoproteins of the bovine interphotoreceptor matrix: composition and fractionation. *Exp Eye Res*. 1982;34:423–434.
48. Hageman GS, Kirchoff MA, Anderson DH. Biochemical characterization and distribution of retinal interphotoreceptor matrix glycoconjugates. *Glycoconj J*. 1990;7:512.
49. Porello K, LaVail MM. Histochemical demonstration of spatial heterogeneity in the interphotoreceptor matrix of the rat retina. *Invest Ophthalmol Vis Sci*. 1986;27:1577–1586.
50. Berman ER. Mucopolysaccharides (glycosaminoglycans) of the retina: identification, distribution, and possible biological role. *Mod Probl Ophthalmol*. 1969;8:5–31.
51. Hollyfield JG, Varner H, Rayborn ME, et al. Retinal

attachment to the pigment epithelium. *Retina*. 1989;9:59–68.
52. Johnson LV, Hageman GS, Blanks MC. Interphotoreceptor matrix domains ensheath vertebrate cone photoreceptor cells. *Invest Ophthalmol Vis Sci*. 1986;27:129–135.
53. Hageman GS, Marmor MF, Yao XY, et al. The interphotoreceptor matrix mediates primate retinal adhesion. *Arch Ophthalmol*. 1995;113:655–660.
54. Hageman GS, Johnson LV. Structure, composition, and function of the retinal interphotoreceptor matrix. Osborne N, Chader J. *Progress in retinal research*. Pergamon Press: Oxford; 1991.
55. Hageman GS, Johnson LV. The "cone matrix sheath": structural, compositional, and functional analyses. *Invest Ophthalmol Vis Sci*. 1988;29(Suppl.):108.
56. Kirchoff MA, Anderson K, Johnson LF, et al. Composition and distribution of insoluble interphotoreceptor matrix components. *Invest Ophthalmol Vis Sci*. 1990;31(Suppl.):153.
57. Marmor MF. Mechanisms of retinal adhesion. Osborne NN, Chader GJ. *Progress in retinal research*. Pergamon Press: Oxford; 1993.
58. Kuehn MH, Wietecki DT, Hageman GS. Molecular characterization of the murine orthologue of the human retinal proteoglycan IPM 150. *Mol Vis*. 2000;6:148–156.
59. Uebara F, Ohba N, Ozawa M. Isolation and characterization of galectins in the mammalian retina. *Invest Ophthalmol Vis Sci*. 2001;42:2164–2172.
60. Edelman GM. Cell adhesion molecules. *Science*. 1983;219:450–457.
61. Adler AJ, Klucznik KM. Interaction of bovine pigment epithelium cells, photoreceptor outer segments, and interphotoreceptor matrix: a model for retinal adhesion. *Curr Eye Res*. 1982;1:579–589.
62. Kohno T, Sorgente N, Ishibashi T, et al. Immunofluorescent studies of fibronectin and laminin in the human eye. *Invest Ophthalmol Vis Sci*. 1987;28:506–514.
63. Philp NJ, Nachmias VT. Polarized distribution of integrins and fibronectin in retinal pigment epithelium. *Invest Ophthalmol Vis Sci*. 1987;28:1275–1280.

64. Shirakawa H, Ishiguro SI, Itoh Y, et al. Are sugars involved in the binding of rhodopsin-membranes by the retinal pigment epithelium? *Invest Ophthalmol Vis Sci*. 1987;28:628–632.
65. Opas M, Kalnins VI. Distribution of spectrin and lectin-binding materials in surface lamina of RPE cells. *Invest Ophthalmol Vis Sci*. 1985;26:621–627.
66. Nandrot ER, Yongen C, Finnermann SC. αvβ5 integrin receptors at the apical surface of the RPE: one receptor, two functions. *Adv Exp Med Biol*. 2008;613:369–375.
67. Lazarus HS, Hageman GS. Xyloside-induced disruption of interphotoreceptor matrix proteoglycans results in retinal detachment. *Invest Ophthalmol Vis Sci*. 1992;33:364–376.
68. Kanan Y, Brobst D, Han Z, et al. Fibulin 2, a tyrosine O-sulfated protein, is up-regulated following retinal detachment. *J Biol Chem*. 2014;289:13419–13433.
69. Ishikawa M, Johnson LV, DeWing MD, et al. pH-Dependent changes in interphotoreceptor matrix domains surrounding cone photoreceptors. *Ophthalmic Res*. 1996;28:117–124.
70. Ishikawa M, Fujiwara T, Yoshitomi T. Temperature-dependent ultrastructural changes in the cone interphotoreceptor matrix. *Jpn J Ophthalmol*. 2009;53:536–540.
71. Yao XY, Hageman GS, Marmor MF. Retinal adhesiveness is weakened by enzymatic modification of the interphotoreceptor matrix in vivo. *Invest Ophthalmol Vis Sci*. 1990;31:2051–2058.
72. Yamada K. The effect of digestion with chondroitinases upon certain histochemical reactions of mucosaccharide-containing tissues. *J Histochem Cytochem*. 1974;22:266.
73. Uehara F, Muramatsu T, Sameshima M, et al. Effects of neuraminidase on lectin binding sites in photoreceptor cells of monkey retina. *Jpn J Ophthalmol*. 1985;29:54.
74. Yao XY, Hageman GS, Marmor MF. Recovery of retinal adhesion after enzymatic perturbation of the interphotoreceptor matrix. *Invest Ophthalmol Vis Sci*. 1992;33:498–503.
75. Uehara F, Yasumura D, LaVail MM. Rod- and cone-

associated interphotoreceptor matrix in the rat retina. *Invest Ophthalmol Vis Sci*. 1991;32:285–292.
76. Owczarek FR, Marak GE, Pilkerton AR. Retinal adhesion in light- and dark-adapted rabbits. *Invest Ophthalmol*. 1975;14:353–358.
77. Faude F, Wendt S, Biedermann B, et al. Facilitation of artificial retinal detachment for macular translocation surgery tested in rabbits. *Invest Ophthalmol Vis Sci*. 2001;42:1328–1337.
78. Burnside MB. Possible roles of microtubules and actin filaments in retinal pigmented epithelium. *Exp Eye Res*. 1976;23:257–275.
79. Burnside B, Laties AM. Actin filaments in apical projections of the primate pigmented epithelial cell. *Invest Ophthalmol*. 1976;15:570–575.
80. Burnside B, Adler R, O'Connor P. Retinomotor pigment migration in the teleost retinal pigment epithelium. I. Roles for actin and microtubules in pigment granule transport and cone movement. *Invest Ophthalmol Vis Sci*. 1983;24:1–15.
81. Moore KT, Yao XY, Marmor MF. Intravitreal cytochalasin D decreases retinal adhesion. *Invest Ophthalmol Vis Sci*. 1991;32(Suppl.):772.
82. Immel J, Negi A, Marmor MF. Acute changes in RPE apical morphology after retinal detachment in rabbit: a SEM study. *Invest Ophthalmol Vis Sci*. 1986;27:1770–1776.
83. Dearry A, Burnside B. Effects of extracellular Ca^{++}, K^{+}, and Na^{+} on cone and retinal pigment epithelium retinomotor movements in isolated teleost retinas. *J Gen Physiol*. 1984;83:589–611.
84. Kim RY, Yao XY, Marmor MF. Oxygen dependency of retinal adhesion. *Invest Ophthalmol Vis Sci*. 1993;34:2074–2078.
85. Marmor MF, Yao XY. The metabolic dependency of retinal adhesion in rabbit and primate. *Arch Ophthalmol*. 1995;113:232–238.
86. Kain HL, Libondi T. Experimentelle Netzhautabldaung-Untersuchungen zum Pathomechanismus. *Fortschr Ophthalmol*. 1986;83:590–596.

87. Adler AJ, Martin KJ. Lysosomal enzymes in the interphotoreceptor matrix: acid protease. *Curr Eye Res*. 1983;2:359–366.
88. Ashburn FS Jr, Pilkerton A, Rao NA, et al. The effects of iodate and iodoacetate on the retinal adhesion. *Invest Ophthalmol Vis Sci*. 1980;19:1427–1432.
89. Negi A, White MP, Marmor MF. Effects of hemicholinium-3, a photoreceptor and pigment epithelial toxin, on retinal adhesiveness and subretinal fluid absorption. *Doc Ophthalmol*. 1993;83:331–336.
90. Takeuchi A, Negi A, Yamamoto F, et al. Effects of sodium iodate on retinal adhesive force in vivo. *Invest Ophthalmol Vis Sci*. 1991;32(Suppl.):667.
91. Yoon YH, Marmor MF. Effects of hemicholinium-3 and sodium iodate on RPE and retinal adhesiveness. *Invest Ophthalmol Vis Sci*. 1991;32(Suppl.):667.
92. Nilsson SEG, Knave B, Persson HE. Changes in ultrastructure and function of the sheep pigment epithelium and retina induced by sodium iodate. II. Early effects. *Acta Ophthalmol*. 1977;55:1007–1026.
93. Marmor MF, Maack T. Enhancement of retinal adhesion and subretinal fluid resorption by acetazolamide. *Invest Ophthalmol Vis Sci*. 1982;23:121–124.
94. Hughes BA, Miller SS, Machen TE. Effects of cyclic AMP on fluid absorption and ion transport across frog retinal pigment epithelium: measurements in the open-circuit state. *J Gen Physiol*. 1984;83:875–899.
95. Marmor MF, Negi A. Pharmacologic modification of subretinal fluid absorption in the rabbit eye. *Arch Ophthalmol*. 1986;104:1674–1677.
96. Miller S, Farber D. Cyclic AMP modulation of ion transport across frog retinal pigment epithelium: measurements in the short-circuit state. *J Gen Physiol*. 1984;83:853–874.
97. Kawano SI, Marmor MF. Metabolic influences on the absorption of serous subretinal fluid. *Invest Ophthalmol Vis Sci*. 1988;29:1255–1257.
98. Frambach DA, Misfeldt DS. Furosemide-sensitive Cl transport in embryonic chicken retinal pigment epithelium.

Am J Physiol. 1983;244:679–685.
99. Tsuboi S, Pederson JE. Experimental retinal detachment. XI. Furosemide-inhibitable fluid absorption across retinal pigment epithelium in vivo. *Arch Ophthalmol*. 1986;104:602–603.
100. Frambach DA, Weiter JJ, Adler AJ. A photogrammetric method to measure fluid movement across isolated frog retinal pigment epithelium. *Biophys J*. 1985;47:547–552.
101. Negi A, Marmor MF. Mechanisms of subretinal fluid resorption in the cat eye. *Invest Ophthalmol Vis Sci*. 1986;27:1560–1563.
102. Marmor MF, Negi A, Maurice DM. Kinetics of macromolecules injected into the subretinal space. *Exp Eye Res*. 1985;40:687–696.
103. Negi A, Marmor MF. Healing of photocoagulation lesions affects the rate of subretinal fluid resorption. *Ophthalmology*. 1984;91:1678–1683.
104. Takeuchi A, Kricorian G, Marmor MF. Albumin movement out of the subretinal space after experimental retinal detachment. *Invest Ophthalmol Vis Sci*. 1995;36:1298–1305.
105. Takeuchi A, Kricorian G, Yao XY, et al. The rate and source of albumin entry into saline-filled experimental retinal detachments. *Invest Ophthalmol Vis Sci*. 1994;35:3792–3798.
106. Wolfensberger TJ, Gregor ZJ. Macular edema – rationale for therapy. Karger: Basel; 2010:49–58. Coscas G. *Macular edema*. vol. 47.
107. Szurman P, Roters S, Grisanti S, et al. Ultrastructural changes after artificial retinal detachment with modified retinal adhesion. *Invest Ophthalmol Vis Sci*. 2006;47:4983–4989.
108. Imamura Y, Fujiwara T, Margolis R, et al. Enhanced depth imaging optical coherence tomography of the choroid in central serous chorioretinopathy. *Retina*. 2009;29:1469–1473.
109. Marmor MF. Hypothesis concerning carbonic anhydrase treatment of CME: example with epiretinal membrane. *Arch Ophthalmol*. 1990;108:1524–1525.
110. Cox SN, Hay E, Bird AC. Treatment of chronic macular edema with acetazolamide. *Arch Ophthalmol*. 1988;106:1190–

1195.
111. Fishman GA, Gilbert COT, Fiscella RG, et al. Acetazolamide for treatment of chronic macular edema in retinitis pigmentosa. *Arch Ophthalmol*. 1989;107:1445–1452.
112. Apushkin MA, Fishman GA. Use of dorzolamide for patients with X-linked retinoschisis. *Retina*. 2006;26:741–745.
113. Genead MA, Fishman GA, McAnany JJ. Efficacy of topical dorzolamide for treatment of cystic macular lesions in a patient with enhanced S-cone syndrome. *Doc Ophthalmol*. 2010;121:231–240.
114. Wolfensberger TJ, Chiang R, Takeuchi A, et al. Inhibition of membrane-bound carbonic anhydrase enhances subretinal fluid absorption and retinal adhesiveness. *Graefes Arch Clin Exp Ophthalmol*. 2000;238:76–80.
115. Fishman GA, Apushkin MA. Continued use of dorzolamide for the treatment of cystoid macular oedema in patients with retinitis pigmentosa. *Br J Ophthalmol*. 2007;91:743–745.
116. Genead MA, Fishman GA. Efficacy of sustained topical dorzolamide therapy for cystic macular lesions in patients with retinitis pigmentosa and usher syndrome. *Arch Ophthalmol*. 2010;128:1146–1150.
117. Apushkin MA, Fishman GA, Grover S, et al. Rebound of cystoid macular edema with continued use of acetazolamide in patients with retinitis pigmentosa. *Retina*. 2007;27:1112–1118.
118. Thobani A, Fishman GA. The use of carbonic anhydrase inhibitors in the retreatment of cystic macular lesions in retinitis pigmentosa and X-linked retinoschisis. *Retina*. 2011;31:312–315.
119. Fang XY, Hayashi A, Cekic O, et al. Effect of Ca^{2+}-free and Mg^{2+}-free BSS plus solution on the retinal pigment epithelium and retina in rabbits. *Am J Ophthalmol*. 2001;131:481–488.
120. Chignell AH, Markham RHC. Retinal detachment surgery without cryotherapy. *Br J Ophthalmol*. 1981;65:371–373.
121. Machemer R. The importance of fluid absorption, traction, intraocular currents, and chorioretinal scars in the therapy of rhegmatogenous retinal detachments. *Am J Ophthalmol*.

1984;98:681–693.
122. Zauberman H, Rosell FG. Treatment of retinal detachment without inducing chorioretinal lesions. *Trans Am Acad Ophthalmol Otolaryngol*. 1975;79:835–844.
123. Kita M, Negi A, Kawano SI, et al. Photothermal, cryogenic, and diathermic effects on retinal adhesive force in vivo. *Retina*. 1991;11:441–444.
124. Kwon OW, Kim SY. Changes in adhesive force between the retina and the retinal pigment epithelium by laser photocoagulation in rabbits. *Yonsei Med J*. 1995;36:243–250.
125. Zhu ZR, Goodnight R, Sorgente N, et al. Cellular proliferation induced by subretinal injection of vitreous in the rabbit. *Arch Ophthalmol*. 1988;106:406–411.
126. Takeuchi A, Kricorian G, Marmor MF. When vitreous enters the subretinal space: implications for subretinal fluid protein. *Retina*. 1996;16:426–430.
127. Negi A, Marmor MF. The resorption of subretinal fluid after diffuse damage to the retinal pigment epithelium. *Invest Ophthalmol Vis Sci*. 1983;24:1475–1479.
128. Negi A, Marmor MF. Experimental serous retinal detachment and focal pigment epithelial damage. *Arch Ophthalmol*. 1984;102:445–449.
129. Tsukahara Y, Marmor MF. Experimental studies on the accumulation of subretinal fluid. *Ophthalmologica*. 1991;202:202–207.
130. Marmor MF. On the cause of serous detachments and acute central serous chorioretinopathy. *Br J Ophthalmol*. 1997;81:812–813.
131. Marmor MF, Yao XY. Conditions necessary for the formation of serous detachment: Experimental evidence from the cat. *Arch Ophthalmol*. 1994;112:830–838.
132. Kita M, Negi A, Kawano S, et al. Lamellar scleral resection enhances subretinal fluid absorption in eyes with choroidal congestion. *Jpn J Ophthalmol*. 1991;35:394–401.
133. Chou T, Siegel M. A mechanical model of retinal detachment. *Phys Biol*. 2012;9:046001.
134. Yao XY, Marmor MF. Induction of serous retinal detachment in rabbit eyes by pigment epithelial and

choriocapillary injury. *Arch Ophthalmol*. 1992;110:541–546.
135. Chon CH, Yao XY, Dalal R, et al. An experimental model of retinal pigment epithelial and serous detachment. *Retina*. 1996;16:139–144.
136. Yoshioka H, Katsume Y, Akune H. Experimental central serous chorioretinopathy in monkey eyes: fluorescein angiographic findings. *Ophthalmologica*. 1982;185:168–178.

22

Structure, Function, and Pathology of Bruch's Membrane

Christine A. Curcio, Mark Johnson

Introduction, History, Embryology

Bruch's membrane is a thin (2–4 μm), acellular, five-layered

extracellular matrix located between the retina and choroid.[1,2] It extends anteriorly to the ora serrata, interrupted only by the optic nerve. Tissue resembling Bruch's membrane is visible anterior to the ora serrata extending forward to the pigmented epithelium of the ciliary body. Bruch's membrane lies between the metabolically active retinal pigment epithelium (RPE) and a capillary bed (choriocapillaris) and thus serves two major functions as the substratum of the RPE and a vessel wall. It has major clinical significance because of its involvement in age-related macular degeneration (AMD) and other chorioretinal diseases.

Early History

Carl Ludwig Wilhelm Bruch (1819–1884) (Fig. 22.1 online) first isolated the "lamina vitrea" that we now know as Bruch's membrane and described it in his 1844 doctoral thesis[3,4] where he also first described the tapetum found in many mammals. By light microscopy, Bruch's membrane appeared transparent, with little internal structure. Later studies by A.E. Smirnow[5] divided this membrane into an outer elastic layer (first described by Sattler in 1877) and an inner cuticular layer, separated by a dense plexus of very fine elastic fibers.[6,7]

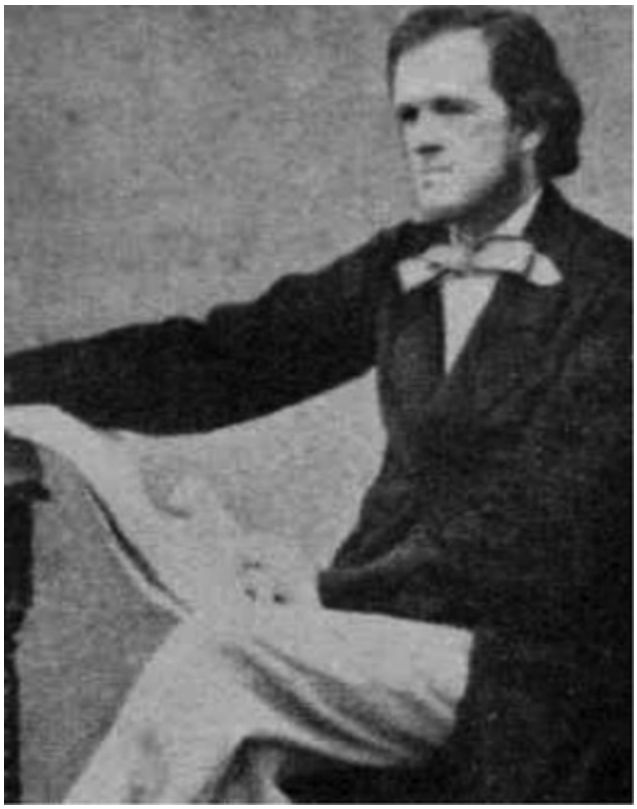

FIG. 22.1 Carl Bruch (1819–1884). (With permission from the Archives of the University of Heidelberg. http://www.ub.uni-heidelberg.de/helios/digi/anatomie/bruch.html.)

Development of Bruch's Membrane

The bipartite character of Bruch's membrane arises from the embryology of its tissue. When the optic cup invaginates and folds, its inner layer forms the neural retina, and its outer layer, the RPE. The RPE lies in contact with mesenchyme. At this apposition, Bruch's membrane forms by 6–7 weeks' gestation. Thus, its inner layer is composed of ectodermal tissue and its outer, mesodermal. At the border of two layers, the elastic layer forms last, becoming histologically visible by 11–12 weeks.[8–10]

The collagen that fills the extracellular space, and the later appearing elastin, appear to be made by invading fibroblasts and the filopodia of endothelial cells lining the adjacent choriocapillaris. The two basal laminas are produced by their associated cell layers.[11] In addition to collagen IV subunits specific to specialized basal lamina, RPE expresses genes for structural collagen III and angiostatic collagen XVIII in a developmentally regulated manner

linked to photoreceptor maturation.[12]

By week 13, fenestrations are apparent in the endothelium facing Bruch's membrane,[10] indicating that at this stage, transport across this tissue may be functional. Choroidal endothelial cells originate from paraocular mesenchyme. Development of the choroidal vasculature, and Bruch's as part of it, depends on differentiated RPE and its production of inductive signals, including basic fibroblast growth factor (bFGF) and vascular endothelial growth factor (VEGF).[13]

Structure of Bruch's Membrane in the Young Adult Eye

Hogan's five-layer nomenclature for Bruch's membrane[14,15] is commonly used. Gass proposed a three-layer system that did not include the cellular basal laminas as part of Bruch's proper.[16] These layers are shown in Fig. 22.2 and their constituents in Table 22.1. Important components in specific layers are structural collagens, elastin, and proteoglycans with negatively charged glycosaminoglycan side-chains.

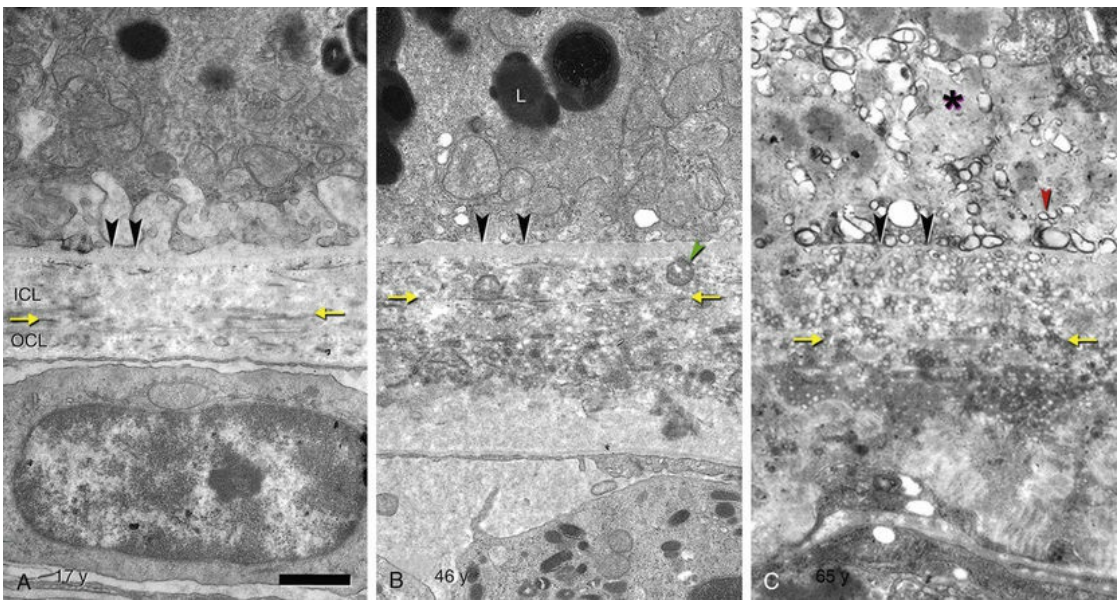

FIG. 22.2 Macular Bruch's membrane throughout the lifespan. Retinal pigment epithelium (RPE) is at the top of all panels. RPE basal lamina (*arrowheads*) and

elastic layer (EL, *yellow arrows*, discontinuous in macula) are shown. (A) 17 years: Electron-dense amorphous debris and lipoproteins are absent. Scale bar: 1 μm. (B) 46 years: Electron-dense amorphous debris and lipoproteins are present. A coated membrane bounded body (*green arrow*) contains lipoproteins. L, lipofuscin. (C) 65 years: Electron-dense amorphous debris and lipoproteins are abundant. Membranous debris, also called lipoprotein-derived debris (*red arrow*) has electron-dense exteriors within BLamD (*). Within OCL, banded material is type VI collagen, often found in BLamD.

TABLE 22.1

Structural and Molecular Components of Bruch's Membrane

Layer (Common Abbreviation)	Component; Age Change	References
Basal laminar deposit (BlamD)	**+ Fibronectin, laminin, IV α4-5, VI, endostatin, EFEMP1**	220, 223, 277–280
RPE–Basal lamina (RPE–BL)	IV α1–5, V, laminins 1, 5, 10, and 11, nidogen-1, heparan sulfate, chondroitin sulfate	19, 22, 23, 78, 281,282
Lipid Wall/ Basal linear deposit (BlinD)	**+ Lipoproteins**	52, 53, 283
Inner collagenous layer (ICL)	I, III, V, fibronectin, chondroitin sulfate, dermatan sulfate, **lipoproteins**↑, apoE, heme, clusterin, vitronectin	44, 47, 52, 53, 78, 189, 197, 281, 284–287
Elastic layer (EL)	**Elastin**↑, **calcium phosphate**↑	78–81, 281, 288
Outer collagenous layer (OCL)	I, III, V, fibulin-5, fibronectin, chondroitin sulfate, dermatan sulfate, **lipoproteins**↑, apoE, clusterin	19, 53, 189, 281, 285, 289
ChC–Basal lamina	IV α1,2, V, VI, laminin, heparan sulfate, chondroitin sulfate, endostatin	22, 279, 281, 292, 290
Bruch's, throughout or layer not specified	**I**↑, **collagen solubility**↓, perlecan, **MMP-2**↑, **MMP-9**↑, **TIMP-2; TIMP-3**↑, **pentosidine**↑, **CML**↑, **GA-AGE**↑, RGR-d, apoB, oxidized apoB-100, 7-KCh, MDA, LHP, **HHE**↑, **DHP-lys**↑, **FHL-1, C3d**↑, **C5b-9**↑, **pentraxin-3**↑, thrombospondin-1, zinc	74, 78, 85, 174, 183, 198, 290–302

Table shows definitely localized components. Most determinations were made in macula. Studies showing histochemical/ immunohistochemical verification of biochemistry and ultrastructural validation of structures identified by light microscopy

techniques were given greater weight. Localizations were assigned to specific layers if immunogold-electron microscopy or high magnification confocal microscopy images were available. Roman numerals denote collagens. Components are ordered within each layer: structural components, lipoproteins, extracellular matrix and its regulation, modified lipids and proteins, complement/immunity, cellular response/activity, metals. Known changes with advancing age are **bold** with an arrow indicating direction of change. New additions with age are shown with a plus (**+**). Plain text means no change or not tested.

Abbreviations: 7-KCh, 7 keto-cholesterol;[301] CML, carboxymethyl-lysine;[298] DHP-Lys, dihydropyridine lysine;[78] GA-AGE, glycolaldehyde derived AGE;[293] HHE, 4-hydroxyhexenal;[78] MDA, malondialdehyde.[78,290]

RPE Basal Lamina (RPE-BL)

This ~0.15-µm thick layer is a meshwork of fine fibers like other basal laminas in the body.[17,18] The RPE-BL resembles that of the choriocapillaris endothelium (ChC-BL) in containing heparan sulfate proteoglycans with several sulfation motifs.[19–21] Unlike ChC-BL, RPE-BL does not contain collagen VI. The RPE-BL contains collagen IV α3-5,[22] like that of kidney glomerulus, another organ with specialized filtration and transport functions. The RPE synthesizes specific laminins that preferentially adhere Bruch's membrane to the RPE through interaction with integrins.[23]

Inner Collagenous Layer (ICL)

The ICL is ~1.4 µm thick and contains 70-nm-diameter fibers of collagens I, III, and V in a multilayered crisscross, parallel to the plane of Bruch's membrane.[1] The collagen grid is associated with interacting molecules, particularly chondroitin sulfate and dermatan sulfate proteoglycans.[19,21,24]

Elastic Layer (EL)

The EL consists of stacked layers of linear elastin fibers, crisscrossing to form a 0.8-µm thick sheet with interfibrillary spaces of ~1 µm. This sheet extends from the edge of the optic nerve to the ciliary body pars plana.[1] In addition to elastin fibers, the EL contains collagen VI, fibronectin, and other proteins, and collagen fibers from the two collagenous layers can cross the EL. Some EL

elastin fibers cross the tissue space between the choriocapillaris and join bundles of choroidal elastic tissue.[25] The EL confers biomechanical properties, vascular compliance, and antiangiogenic barrier functions. It is discontinuous in the macula, perhaps explaining why choroidal neovascularization is more prominent there.[26] This concept is supported by the extensive laser-induced neovascularization in mice deficient in lysyl oxidase-like 1, an enzyme required for elastin polymerization.[27]

Outer Collagenous Layer (OCL)

The OCL contains many of the same molecular components as the ICL, and the collagen fibrils running parallel to the choriocapillaris additionally form prominent bundles. This layer, unlike the ICL, has periodic outward extensions between individual choriocapillary lumens called intercapillary pillars, where thickness cannot be determined due to the lack of a boundary. Between pillars, OCL thickness can range from 1 to 5 μm.[28]

Choriocapillaris Basal Lamina (ChC-BL)

This 0.07-μm-thick layer is discontinuous with respect to Bruch's membrane due to the interruptions of the intercapillary pillars of the choroid. It is continuous with respect to the complex network of spaces defined by the choriocapillary lumens because the basal lamina envelops the complete circumference of the endothelium. A remarkable structural feature of the adjacent choriocapillary endothelium is fenestrations that are permeable to macromolecules (Fig. 22.3).[29] This basal lamina may inhibit endothelial cell migration into Bruch's membrane, as do basal laminas associated with retinal capillaries.[30]

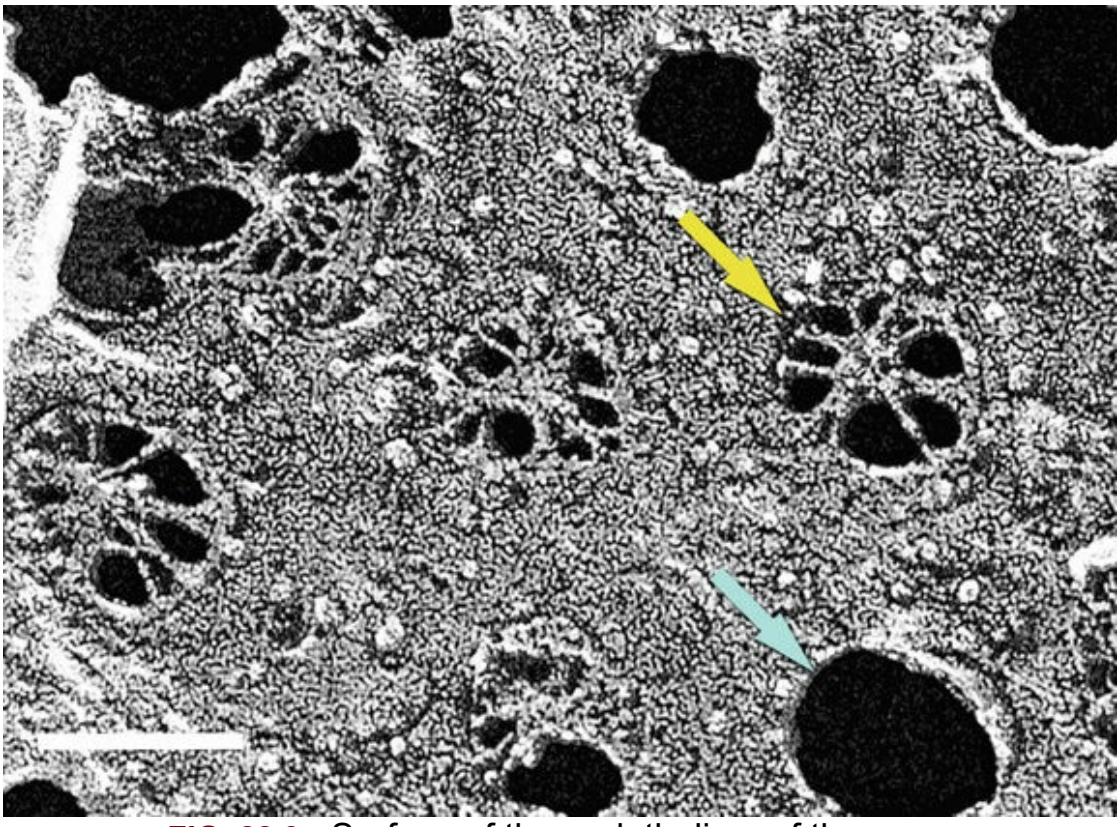

FIG. 22.3 Surface of the endothelium of the choriocapillaris showing fenestrations with a bicycle-spoke pattern (*yellow arrow*) and presumed artifactual openings arising from tissue preparation (*cyan arrow*); quick-freeze/deep-etch, 64-year-old eye, macula. Scale bar: 100 nm. (Reproduced with permission from Johnson M, Huang J-D, Presley JB, et al. Comparison of morphology of human macular and peripheral Bruch's membrane in older eyes. Curr Eye Res 2007;32:791-9.)

Bruch's Membrane in an Aged Eye

Aging is the largest risk factor for developing AMD,[31] and Bruch's membrane undergoes significant age-related changes. Identification of factors predisposing to disease progression is a priority. This task has been challenged by difficulty imposed by the thinness of the tissue, and the closely integrated functions of RPE, Bruch's membrane, and choriocapillaris. Current opinion holds that RPE and Bruch's membrane age in concert, and normal Bruch's membrane aging transforms insidiously into AMD pathology.[1,17,18,32] This section covers aging, to inform the following section on function.

Lipid Accumulation: Bruch's Membrane Lipoproteins

Early electron microscopists described aged Bruch's membrane as being filled with debris, including amorphous electron dense material, membrane fragments, vesicles, and calcification.[33,34] Debris deposition in ICL and OCL begins in the second decade of life in the macula and is delayed in equatorial regions.[35] Verhoeff speculated that calcification of aging Bruch's membrane might follow lipoidal deposition[36] as it does in atherosclerosis. Later investigators described aged Bruch's membrane as sudanophilic (i.e., histochemically detectable lipid).[37,38] Histochemical, ultrastructural, biochemical, gene expression, cell biologic, and epidemiologic evidence have converged to indicate that the lipid-rich material accumulating with age in Bruch's membrane is cholesterol-rich lipoprotein particles containing apolipoproteins B and E that are assembled and secreted by the RPE.[39] This process, ongoing throughout life yet first revealed by aging, has implications for formation of AMD-specific lesions, RPE physiology, nutrient and waste product transport to and from the outer retina, and maintenance of photoreceptor health. The physicochemical properties, physiologic roles, and distribution of cholesterol in relation to AMD pathology has been reviewed.[40]

Clinical observations on fluid-filled RPE detachments in older adults led to Bird and Marshall's hypothesis that a lipophilic barrier in Bruch's membrane blocked a normal, outwardly directed fluid efflux from the RPE[41] (as opposed to leakage from neovascularization). This hypothesis motivated a seminal histochemical study by Pauliekhoff[42] that demonstrated oil red O-binding material (EC, esterified cholesterol; TG, triglyceride; FA, fatty acid) localized exclusively to Bruch's membrane, unlike other stains. This lipid was absent <30 years, variably present at 31–60 years, and abundant at ≥61 years.[43,44] Biochemical studies confirmed the strongly age-related nature of the deposition.[45,46]

The oil red O-binding material proved to be EC, which with unesterified cholesterol (UC) accumulates markedly in Bruch's membrane, in sevenfold higher quantities in macula than periphery.[44,47] Key techniques were use of the fluorescent marker

filipin, which binds the 3-β-hydroxy group of sterols to reveal unesterified (free) cholesterol (UC) or EC depending on tissue pretreatment[47] and hot stage polarizing microscopy,[44] which showed very few birefringent crystals signifying the neutral lipid TG. Among lipids, EC is confined exclusively to Bruch's membrane,[48] focusing attention on lipoproteins, the only means by which EC is released by cells. Human RPE expresses apoB gene and protein, along with microsomal triglyceride transfer protein, required for apoB lipidation and secretion.[49] This suggests that RPE is a constitutive lipoprotein secretor. Indeed, human- and rat-derived RPE cell lines secrete full-length apoB.[50,51]

Lipid-preserving ultrastructure and analytic biochemistry support this concept. Ultrastructural studies described, in Bruch's membrane of older eyes,[39] numerous small (<100 nm), round, electron-lucent vesicular profiles, implying aqueous interiors. These so-called vesicles are actually solid, lipid-containing particles (Fig. 22.4B**)** when prepared by lipid-preserving methods including postfixation in osmium paraphenylenediamine (OTAP)[47] and, strikingly, quick-freeze/deep-etch (QFDE), a freeze fracture method with etching to remove frozen water.[52–54] Particles vary in size from 60 to 100 nm and occasionally appeared to coalesce (Fig. 22.4). Particles of comparable diameter with lipoprotein-like flotation properties and spherical shapes indicating neutral lipid cores are isolable from normal human Bruch's membrane[50,55] (Fig. 22.5**)**. These fractions include apolipoproteins B, A-I, and E. Bruch's membrane cholesterol is EC-enriched (EC/total cholesterol = 0.56)[47,50,55,56] and there is little triglyceride (EC/TG = 4-11), unlike hepatic very-low-density lipoprotein (VLDL), of similar diameter. An early report of TG-enriched Bruch's membrane[46] was not replicated. Thus, Bruch's membrane apoB-lipoproteins are unusual because they are large like VLDL yet EC-rich like atherogenic LDL (Fig. 22.5).

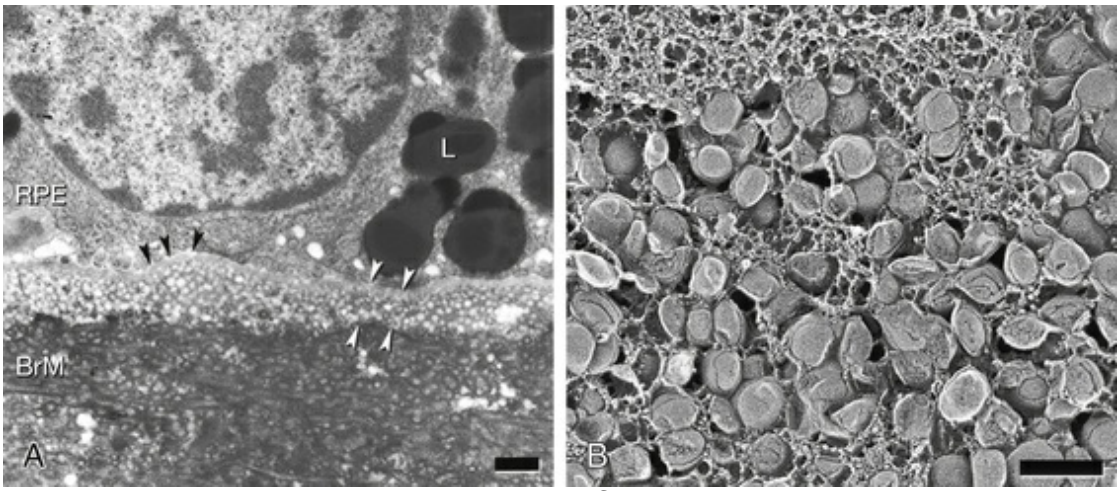

FIG. 22.4 Lipid Wall, a layer of lipoproteins on the inner surface of Bruch's membrane. (A) Lipoproteins (spherical vesicles of uniform diameter) accumulate 3–4 deep between the RPE basal lamina (*black arrowheads*) and Bruch's membrane ICL (*white arrowheads*). Thin section transmission electron micrograph following osmium postfixation. *RPE*, retinal pigment epithelium; *BrM*, Bruch's membrane; *L*, lipofuscin. Sectioning plane is vertical; scale bar: 1 μm. (B) Quick-freeze deep-etch shows tightly packed Bruch's membrane lipoproteins in the Lipid Wall, and that lipoproteins have classic core and surface morphology.[53] Fracture plane is oblique; scale bar: 200 nm.

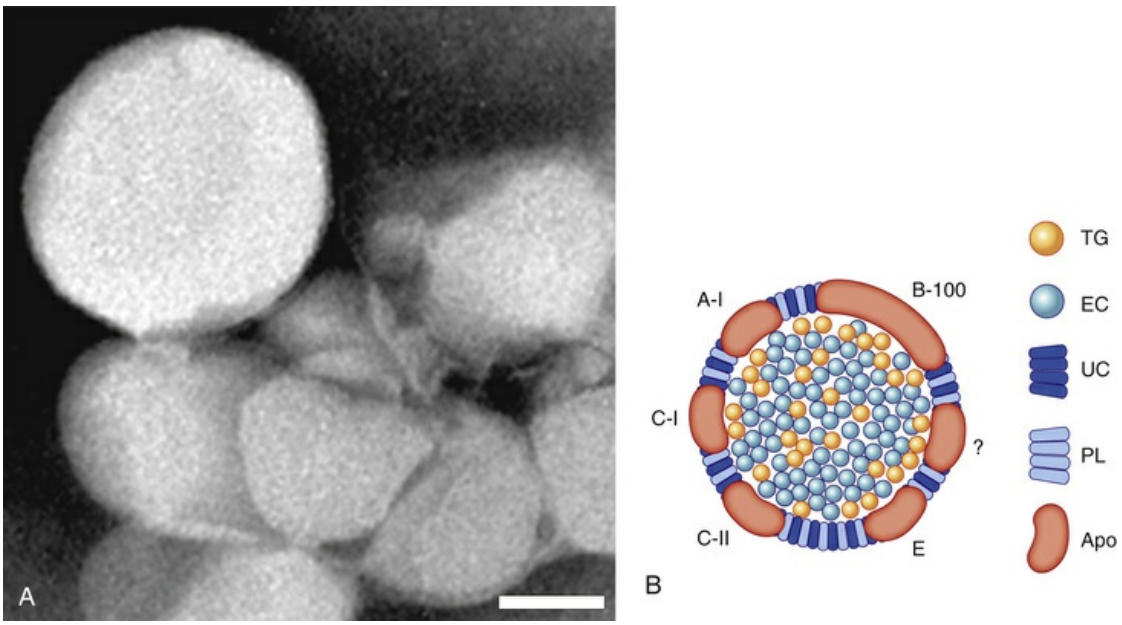

FIG. 22.5 Bruch's membrane lipoprotein composition. (A) Lipoprotein particles isolated from Bruch's membrane are large and spherical; negative stain.[190] Scale bar: 50 nm. (B) Bruch's membrane lipoprotein composition inferred from direct assay,[190,285] druse composition, and RPE gene expression.[174,191] *TG*, triglyceride; *EC*, esterified cholesterol; *UC*, unesterified cholesterol; *PL*, phospholipid; *Apo*, apolipoproteins. The question mark signifies that not all apolipoproteins are known.

A natural history of Bruch's membrane lipid deposition obtained with quick-freeze deep etch showed lipoprotein particles first gathering among fibrils of the elastic layer in early adulthood.[57,58] This accumulation then extends toward RPE to fill the ICL by the seventh decade of life,[54,57] consistent with an RPE origin. In many older eyes, a new layer, the Lipid Wall,[52]forms between RPE basal lamina and OCL, and this is considered a precursor to basal linear deposits, a specific lesion of AMD (see below). With solid lipoprotein particles occupying nearly 100% of this sub-RPE space, the Lipid Wall displaces ICL collagen fibrils that anchor the RPE basal lamina (Fig. 22.4).

The fatty acid composition of Bruch's membrane lipids implicates diet as a driving force in RPE lipoprotein secretion. A longstanding hypothesis that debris in aging Bruch's membrane originates as outer segment membranes phagocytosed by RPE[59] was tested through fatty acid profiling of Bruch's membrane lipoproteins and lipid extracts.[50,56] Outer segment membranes have characteristically high concentrations of docosahexaenoate.[60] In contrast, all lipid classes in Bruch's membrane were dominated by linoleate, the most abundant fatty acid in plasma, with little (<2%) docosahexaenoate. Bruch's membrane lipid deposition is thus proposed as a recycling system whereby plasma lipoproteins delivering dietary essentials (vitamins A, E, lutein, UC) are taken up by RPE, stripped of cargo destined for photoreceptors, and excess fatty acids and UC repackaged as lipoproteins for basolateral secretion and choroidal clearance.[61]

If the proposed primacy of diet is true, then cells in culture medium should be able to create deposits without supplementation

by outer segments. A landmark study by Johnson et al. confirmed these predictions,[62] demonstrating that highly differentiated and polarized human fetal RPE, supplemented only by culture medium, secreted apoE-immunoreactive particles resembling native Bruch's membrane lipoproteins. While the source of cholesterol in Bruch's membrane lipoproteins has not been determined to date, endogenous synthesis, taken-up plasma lipoproteins, and phagocytosed outer segments are obvious choices (see below).

It is informative to contrast Bruch's membrane lipid deposition with the systemic process whereby extracellular oil red O-binding lipids increase with age in normal human connective tissues. In arterial intima, tendons, sclera, and cornea, perifibrous lipid provides the background to atherosclerosis, xanthomas, and lipid keratopathy.[44,63–66] The source of extracellular EC in these locations is LDL translocated from plasma and trapped via binding to proteoglycans.[67,68] After apolipoproteins degrade, the remaining lipid components fuse.[67] The evidence that lipid deposition in aging Bruch's membrane is a distinct process dictated by photoreceptor physiology and not simply an ocular manifestation of this systemic process is compelling[40] (see below, AMD lesions). Indirect evidence also emerges from epidemiology. If EC deposition in Bruch's membrane and AMD-associated lesions were a manifestation of systemic perifibrous lipid and atherosclerosis, then a strong positive correlation between disease status and plasma lipoprotein levels, like that in cardiovascular disease,[69] might be expected. Such an association has not emerged despite many studies.[70] Nevertheless, the commonality of cholesterol-rich lipoproteins in a vessel wall is a rationale for seeking guidance in cardiovascular disease for AMD pathogenesis and treatments.

Other Aging Changes

Bruch's membrane thickens throughout adulthood (20–100 years), two- to threefold under the macula and becoming more variable between individuals at older ages.[28,71,72] Equatorial Bruch's membrane changes little while Bruch's membrane near the ora serrata increases twofold during this time.[28] In the macula, the OCL thickens more prominently than the ICL.[73] A large ultrastructural

study of 121 human donor eyes demonstrated that the macular EL is three to six times thinner than peripheral EL at all ages.[26]

Unbalanced regulation of extracellular matrix molecules and their modulators are thought to result in Bruch's membrane thickening. Increased histochemical reactivity for glycoconjugates, glycosaminoglycans, collagen, and elastin is seen in the macula relative to equator and near the ora serrata.[28] Collagen solubility declines with age.[74] Metalloproteinases MMP-2 and MMP-3 increase with age as does a potent inhibitor of metalloproteinases, TIMP-3. TIMP-3 immunoreactivity reaches mature levels at 30 years of age near vasculature in lung, kidney, and in Bruch's membrane, signifying the end of developmental organogenesis.[75] The reduction or absence of TIMP-3 is proangiogenic, as this protein not only regulates metalloproteinases during the normal turnover of Bruch's membrane matrix components but it also binds to VEGF.[76,77]

The EL thickens with age but decreases relative to overall thickening of Bruch's membrane.[26] Thus elastin referenced to other Bruch's constituents, as detected by Raman spectroscopy, decreases with age.[78] Similar arguments can be made for collagen III and IV. A prominent age-change,[79] noted early,[36] is calcification and ensuing brittleness. This process involves deposition of fine electron-dense particulate matter[80] confirmed as calcium phosphate[81] on individual elastin fibrils.

Long-lived proteins like collagens are modified *in vivo* by nonenzymatic Maillard and free radical reactions to yield advanced glycation end products (AGEs) and the formation of lipid-derived reactive carbonyl species like malondialdehyde (MDA), and 4-hydroxyhexenal (HHE), collectively called age-related lipoperoxidation end products (ALEs). Accumulation of AGEs and ALEs, characteristic of diabetes and atherosclerosis, also occurs in aging Bruch's membrane (Table 22.1). Finally, other components prominent in aged eyes include complement components C3d, C5b-9, and pentraxin-3, a homolog of the acute phase respondent C-reactive protein. Thus, at the molecular level, aging Bruch's membrane contains evidence of many biologic activities including remodeling, oxidative damage, and inflammation, in addition to lipoprotein accumulation.

New evidence from Clark, Bishop, Day, and associates indicates

that variations in proteoglycan sulfation in Bruch's membrane have potential pathogenic significance for AMD.[21,82–86] Bruch's membrane has many heparan sulfate (HS) proteoglycan structures and motifs, as determined with antibodies to specific full-length and enzymatically truncated forms.[21] Sequence variants in the gene encoding the fluid phase regulator of complement factor H (CFH) are highly associated with risk for AMD.[87] Key in innate immunity, CFH can discriminate self from nonself for clearing by recognizing polyanionic structures such GAG chains of proteoglycans (e.g., HS and dermatan sulfate), thereby inhibiting complement activation on host cell surfaces. CFH of molecular weight 155 kD comprises 20 complement control protein (CCP) domains and contains main GAG-binding regions in CCP7 and CCP20. The Y402H polymorphism, in CCP7, alters CFH binding to sulfated GAGs. This polymorphism also affects factor H-like protein-1 (FHL-1), a 43 kD protein containing the CCP7 module that is generated by a splice variant of the CFH gene. The disease-associated 402H polymorphic variant of CFH was found to require 2-O- and/or 6-O-sulfation for binding to HS and dermatan sulfate in human Bruch's membrane tissue slices. In contrast, the non-disease-associated 402Y form binds to a broader range of proteoglycans, suggesting that it is overall more tightly bound and thus potentially more effective as an inhibitor. Importantly, in aged human Bruch's membrane, HS is reduced 50% overall and in the macula.[86] This change, attributed to either decreased production or increased turnover of HS core proteins, is one way in which disease-associated sequence variants could promote complement activation, lipoprotein binding to extracellular matrix,[88] and AMD progression in Bruch's membrane.

Function of Bruch's Membrane

As a vessel wall of the choroid, Bruch's membrane primary function is structural, like other vessel walls. Its architecture is similar to vascular intima, with a sub-endothelial extracellular matrix and elastic layer corresponding to the internal elastic lamina. The abluminal surface of Bruch's membrane differs from other vessel walls in that it abuts a basal lamina, that of the RPE. Essentially, Bruch's membrane is comprised of two epithelial membranes in

apposition, consistent with its embryologic origin The luminal surface faces a fenestrated vascular endothelium and basal lamina, making Bruch's membrane structurally analogous to the renal glomerulus and providing a basis for commonality between retinal and kidney disease.[89–91] The importance of fluid and macromolecular transport across the renal glomerulus is well known.[92] Transport is a second important function of Bruch's membrane.

Structural Role of Bruch's Membrane

Bruch's membrane encircles more than half the eye and stretches with the corneoscleral envelope as intraocular pressure (IOP) increases. It withstands this stretch and return to its original shape when IOP decreases. This tissue also stretches to accommodate changes in choroidal blood volume. Finally, the choroid (and Bruch's membrane with it) may act as a spring that pulls the lens during accommodation.[93,94] For these reasons, then, Bruch's membrane requires elasticity.

Marshall and Hussain's group estimated the modulus of elasticity in Bruch's membrane-choroid preparations to be 7–19 MPa.[95] These values are similar to those of sclera (although sclera is much thicker and thus can support more load) consistent with the notion that Bruch's membrane contributes to load bearing. After early adulthood, the modulus of elasticity of human Bruch's membrane-choroid complex increases ($p<.001$) at a rate of ~1% per year. Bruch's membrane stiffness in AMD eyes does not differ from age-matched normals.[96]

Transport Role of Bruch's Membrane

The choroid services the metabolic needs of the outer retina, facilitated in part by fenestrated endothelium (Fig. 22.3). Oxygen, electrolytes, nutrients, and cytokines destined for the RPE and photoreceptors pass from the choriocapillaris and through Bruch's membrane, and waste products travel back in the opposite direction for elimination. Vitamins, signaling molecules, and other factors needed for photoreceptor function are carried to the RPE by lipoprotein particles passing through Bruch's membrane, as do the

RPE-produced lipoproteins that are eliminated in the opposite direction. The RPE pumps water from the subretinal space to counter the swelling of the interphotoreceptor matrix glycosaminoglycans (GAGs). This fluid flows across Bruch's membrane to reach the circulation. Thus, many transport processes involve Bruch's membrane, as reviewed here.

Hydraulic Conductivity of Bruch's Membrane

GAGs are concentrated in the interphotoreceptor matrix[97,98] and corneal stroma.[99] In both locations, these highly charged macromolecules maintain geometric fidelity essential for vision (periodic collagen spacing for corneal transparency, orderly photoreceptor spacing for visual sampling).[98,100,101] GAGs generate significant swelling pressure (up to 50 mm Hg in cornea).[102,103] Without a mechanism to maintain tissue deturgescence, GAGs would imbibe fluid, swell, destroy tissue geometry, and interfere with visual function. Corneal endothelium forestalls swelling by continuously pumping fluid out. This function is accomplished for retina by the RPE, and its failure can lead to retinal detachment.

The fluid pumped by the RPE must then flow from the basal surface of the RPE, across Bruch's membrane, and through the endothelial lining of the choriocapillaris to be adsorbed by the vasculature. A driving force adequate to overcome the collective flow resistance of these tissues is provided by a gradient in fluid pressure and oncotic pressure (the osmotic pressure generated by plasma proteins). This balance is embodied by Starling's Law that characterizes the relationship between fluid flux (q: flow per unit area; positive when flow is out of the blood vessel) across a capillary vessel wall and the forces driving this flow:

$$q = L_p * (\Delta P - \sigma \Delta \Pi) \qquad \textbf{[22.1]}$$

L_p is hydraulic conductivity, which characterizes the ease with which fluids flow cross the vessel wall. If the surface area of the blood vessel is A, then $1/(L_p A)$ is the flow resistance of the vessel wall. ΔP is the difference between the fluid pressure within the blood vessel (P_{cc}) and the pressure at the basal surface of the RPE

(P_{RPE}). $\Delta\Pi$ is the difference between the oncotic pressure within the blood vessel (Π_{cc}) and that at the basal surface of the RPE (Π_{RPE}). σ is the reflection coefficient that characterizes the extent to which the vessel wall rejects the plasma proteins species generating $\Delta\Pi$. σ ranges from 0 for a freely permeable species to 1 when a species is completely rejected by the membrane.

We can estimate the magnitude of $\Delta P - \sigma \Delta\Pi$ using measured value of q and L_p. The fluid pumping rate by human RPE has been measured as q=11 μL h^{-1} cm^{-2}, similar to that in other animals (Table 22.2). The hydraulic conductivity of macular Bruch's membrane/choroid of healthy young humans ranges from 20 to 100×10^{-10} m s^{-1} Pa^{-1}.[104] Then, using q=11 μL h^{-1} cm^{-2} and L_p=50×10^{-10} m s^{-1} Pa^{-1},[a] we can calculate that the magnitude of $(\Delta P - \sigma \Delta\Pi)$ necessary to drive this flow through Bruch's membrane is roughly 0.05 mm Hg.

TABLE 22.2
Retinal Pigment Epithelium Fluid Pumping Rates

Species	Fluid Transport Rate Across RPE (μL h^{-1} cm^{-2})	References
Frog	4.8-7.6	303, 304
Rabbit	12±4	305, 306
Canine	6.4	307
Primate[a]	14±3	308, 309
Human	11	310

[a]Cantrell and Pederson measured a much higher transport rate than that reported here,[308] but used fluorescein as a tracer which likely does not track fluid flow due to its high diffusion coefficient.

Retinal pigment epithelium (RPE) pumping rates were measured by reabsorption of subretinal fluid or by direct measurement in culture.

σ can be roughly estimated by assuming that the fluid in the suprachoroidal space is in equilibrium with blood in the choroid. Using measurements in monkeys of plasma protein concentration inside and outside of choriocapillaries (82.1 and 23.7 mg/ml, respectively),[107] and the Landis Pappenheimer equation[108] for osmotic pressure, the osmotic pressure difference, in this species, across the choroid can be estimated to be 33 mmHg − 6 mmHg=27 mmHg. The pressure in suprachoroidal fluid was measured by Emi[107] to be 4.7 mmHg below IOP while that in the choriocapillaris

was measured at 8 mmHg higher than IOP[109] giving a pressure difference across this wall of 12.7 mmHg. Then, Eq. 22.1 is used to estimate that σ=0.5, assuming equilibrium conditions.

Using Π_{cc}=33 mmHg, P_{cc}=IOP+8 mmHg, Π_{RPE}=0 mmHg (fluid pumped by the RPE is assumed protein-free), and we take P_{RPE}=IOP (assuming no pressure is generated by the RPE above that necessary for crossing Bruch's), we find that $\Delta P - \sigma \Delta \Pi$ is approximately 8.5 mmHg pulling fluid into the choroid. Thus, in normal young adults, oncotic pressure within the choroid is more than sufficient to adsorb all the fluid pumped by the RPE. We can also use Eq. 22.1 to calculate that the lowest value of L_p that still adsorbs fluid pumped by the RPE without generating an elevated pressure at the RPE basal surface is $L_p > 0.3 \times 10^{-10}$ m s^{-1} Pa^{-1}.

Experiments using laser ablation of Bruch's membrane/choroid explants allowed Starita et al.[110] to conclude that the ICL was responsible for most of the flow resistance in Bruch's membrane. Attempts to further localize the flow resistance using morphometric methods are complicated by (i) stereologic issues[111] and (ii) the loss of ultrastructural fidelity from connective tissue conventionally processed for electron microscopy.[52] Failure to appreciate the former difficulty can lead to unphysiologically low estimates for tissue porosity and thereby hydraulic conductivity.[1]

Age-Related Changes in Hydraulic Conductivity and Disease

Fisher was the first to measure L_p of human Bruch's membrane,[112] finding that L_p decreased significantly with age. However, his values for L_p of Bruch's membrane and other tissues are much lower than those found by later investigators.[106,113,114] Marshall and Hussain carefully revisited these measurements using Bruch's membrane/choroid with RPE removed, a preparation that was simpler to create. They showed using laser ablation that the flow resistance of these preparations was entirely due to Bruch's membrane.[110] They also found that flow rate increased linearly with driving pressure, indicating that L_p of Bruch's membrane is relatively insensitive to pressure up to 25 mmHg.

They reported that L_p of macular Bruch's membrane exhibited a dramatic, exponential decline throughout life (Fig. 22.6), dropping from 130×10^{-10} m s^{-1} Pa^{-1} in young children to 0.52×10^{-10} m s^{-1} Pa^{-1} in old age. L_p of macular Bruch's membrane dropped more rapidly with age than did that of the periphery, consistent with an accelerated process occurring in the macula.[1,104,105,115,116] Note that the lowest value measured for L_p of Bruch's membrane in normal eyes is similar to the calculated minimum value of L_p (0.4×10^{-10} m s^{-1} Pa^{-1}, see above) that allows complete resorption of fluid pumped by the RPE without need of an elevated pressure at the basal surface of the RPE. Marshall and Hussain reached similar conclusions regarding this process.[115]

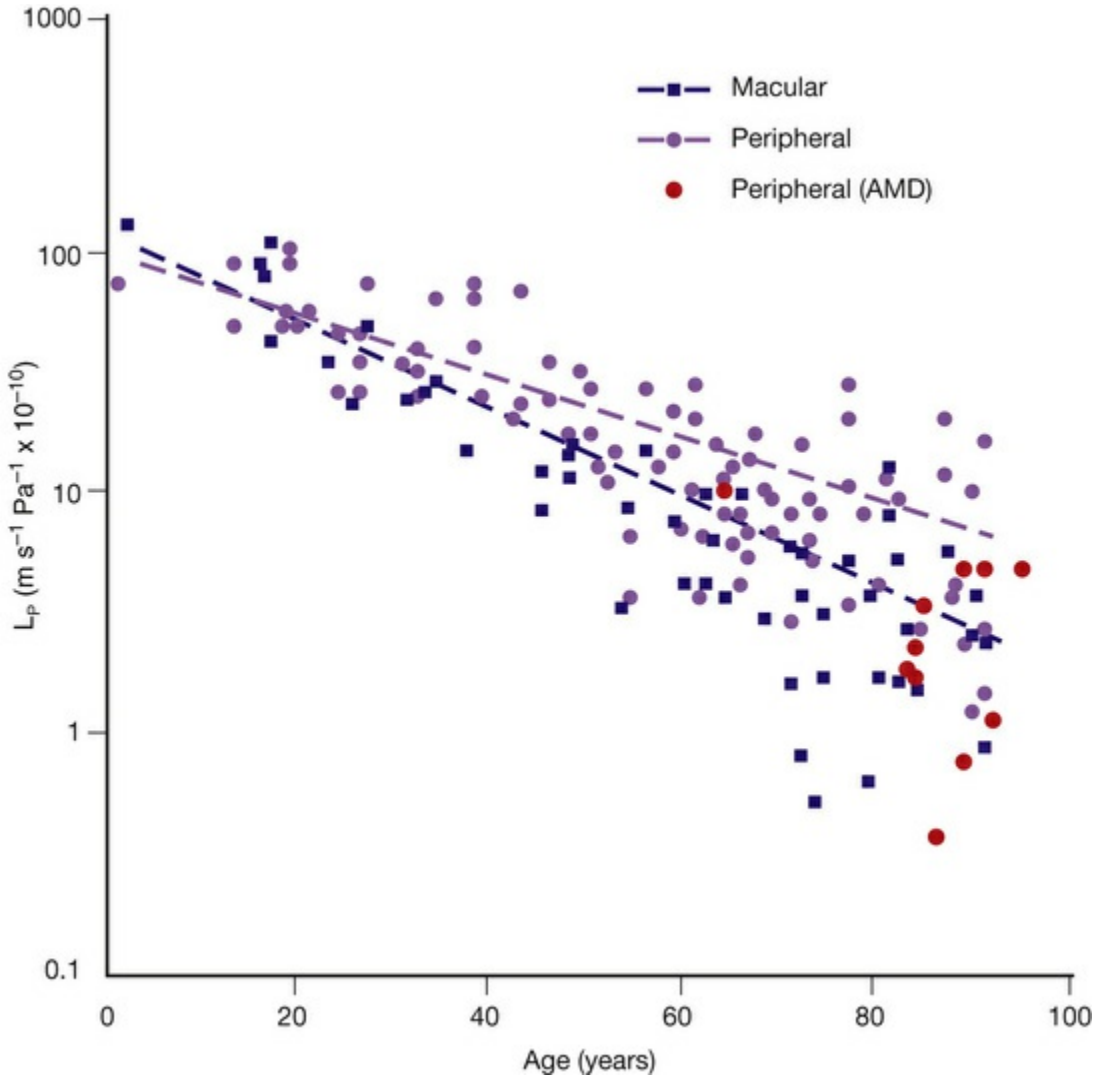

FIG. 22.6 Hydraulic conductivity (L_p) of Bruch's

membrane as a function of age. Dotted lines are exponential fits to data from macular and peripheral regions, respectively. Note that all of the data from eyes with AMD (taken only in peripheral region) have lower values of L_p than the best fit to data taken from peripheral Bruch's membrane of nondiseased eyes.[115]

Determining L_p of Bruch's membrane in isolated macular samples of AMD eyes is difficult due to scar formation and other changes.[115] However, Marshall and Hussein's group showed that in the periphery, L_p of Bruch's membrane is decreased in AMD eyes as compared to age-matched normal eyes (Fig. 22.6).[115] Assuming that similar processes occur in macular Bruch's membrane due to the profound lipid accumulation in this region, then in diseased eyes, the RPE must generate higher pressures at its basal surface to drive fluid into the choriocapillaris, with further pathologic consequences.[41] Above an unknown threshold level, higher pressure will cause the RPE-EL to separate from the ICL, leading to RPE detachment and fluid accumulation, as seen in 12–20% of AMD patients.[115]

What causes the dramatic age-related decrease in L_p of Bruch's membrane? It is natural to suspect the age-related lipid accumulation. In fact, McCarty et al.[117] showed that lipid particles trapped in an extracellular matrix can generate very significant flow resistance, more than would be expected based simply on their size and number. However, Marshall and Hussain observed that most of the marked change in L_p occurred before age 40 (Fig. 22.7A) while the increase in Bruch's membrane lipid content occurred largely after this age. They thus concluded that other age-related changes must be responsible for changes in L_p.[1,104]

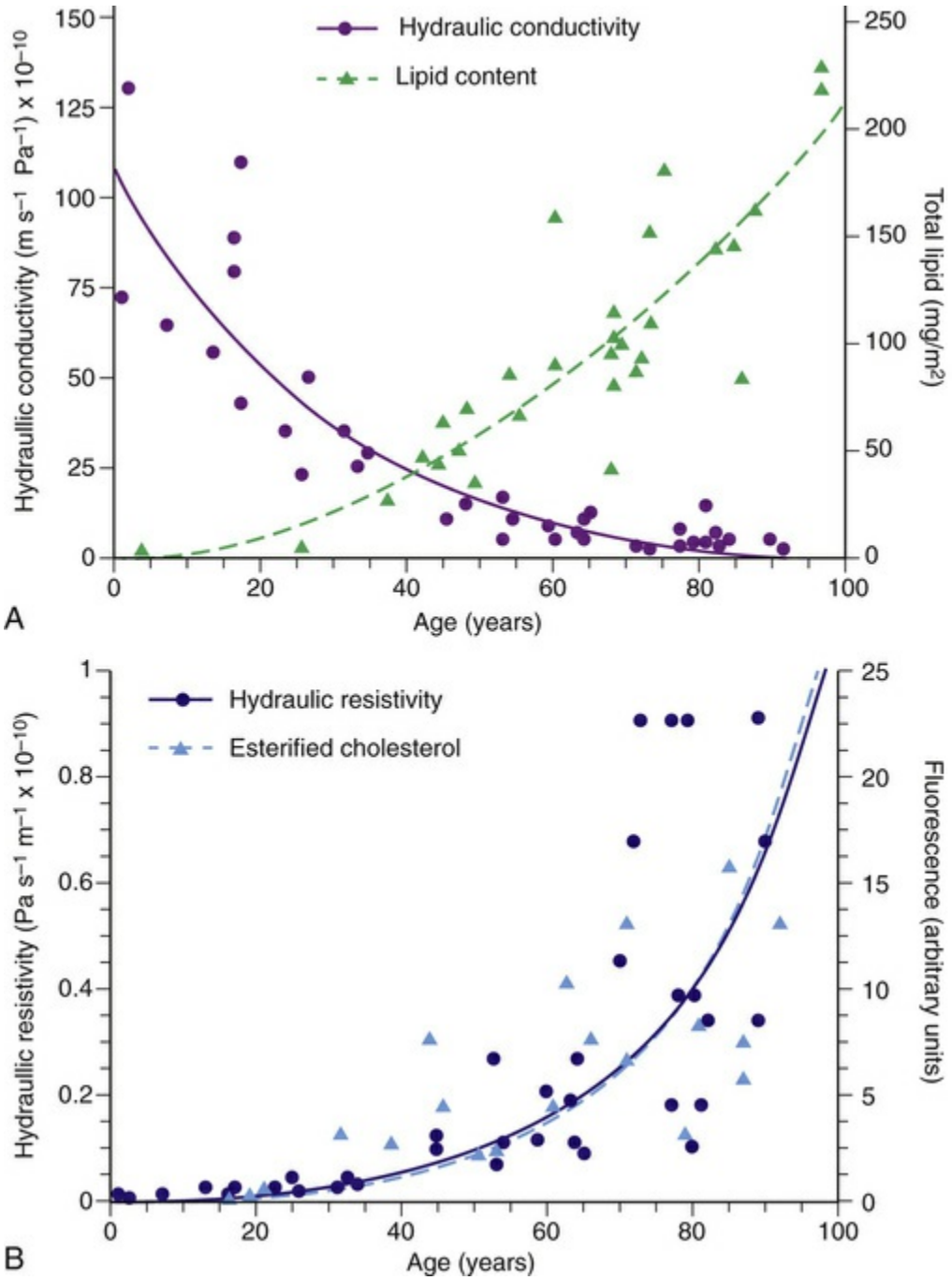

FIG. 22.7 (A) Hydraulic conductivity of human macular Bruch's membrane/choroidal preparations as a function of age, as compared to lipid accumulation in human macular Bruch's membrane; lines as exponential fits to the data. (B) Hydraulic resistivity of human macular Bruch's membrane/choroidal preparations as a function of age,[1] as compared to esterified cholesterol accumulation in human macular Bruch's membrane;[47] lines are exponential fits to the data (the fits nearly overlie one another). (Panel A modified from Marshall J, Hussain AA, Starita C, et al. Aging and Bruch's membrane. In:

A different conclusion can be reached from examining age-effects on flow *resistivity*, the *inverse* of L_p. Resistivity increases from a low of roughly $R=10^8$ Pa m^{-1} s^{-1} for young individuals to $R=10^{10}$ Pa m^{-1} s^{-1} for aged persons. Thus, when hydraulic conductivity L_p drops from roughly 100×10^{-10} m s^{-1} Pa^{-1} to 25×10^{-10} m s^{-1} Pa^{-1} between the ages of birth and 40 years of age, 75% of its total possible decrease, resistivity R increases from 1×10^8 Pa m^{-1} s^{-1} to 4×10^8 Pa m^{-1} s^{-1}, only 4% of the ultimate increase. Simply put, hydraulic conductivity drops more rapidly with age at young ages because its value is high to start with. Fig. 22.7B plots resistivity and histochemically detected EC against age for Bruch's membrane.[118] The agreement between the trends and the fits to the data are striking. This is strong evidence that the increasing lipid content and progressively hydrophobic character of Bruch's membrane are responsible for impairing fluid transfer with age, as postulated.[41] The strong correlation between flow *resistivity* of Bruch's membrane and lipid content was likewise found by Marshall and Hussain.[1,104,116] Laser ablation studies localizing flow resistance to the ICL[110] further supports this conclusion, because lipids accumulate prominently in the ICL with aging.[53] Further, more laser pulses were required to abolish flow resistance in the oldest eyes, consistent with presence of a Lipid Wall, requiring prior removal.

Thus, it appears that decreased L_p and increased resistivity of Bruch's membrane with aging is closely related to the age-related accumulation of lipids, primarily EC. Lipids accumulate more rapidly in the macular Bruch's membrane than in the periphery.[47,119] Thus, L_p of the macula decreases more rapidly with age than it does in the periphery.

L_p in Other Species

L_p of dog Bruch's membrane was measured as 3.7×10^{-10} m s^{-1} Pa^{-1},[120,121] similar to the value found in an older human. Hillenkamp et al.[122] reported a very low value of $L_p=0.345\times10^{-10}$ m s^{-1} Pa^{-1}in cow eyes, lower than that found in any human eyes. Cankova et al.[123]

examined calf eyes and found a much higher value of L_p (14.2×10^{-10} m s^{-1} Pa^{-1}) that was threefold lower in the cow eyes that they examined (4.9×10^{-10} m s^{-1} Pa^{-1}), although not as low as measured by Hillenkamp et al. Cankova et al.[123] concluded that, as in humans, L_p decreases with age.

Permeability of Bruch's Membrane to Solute Transport

Along with bulk fluid flow, there is significant transport of individual molecular species across Bruch's membrane, including dissolved gases, nutrients, cytokines, and waste products driven by passive diffusion. Flow crossing Bruch's membrane is too slow to influence this process. This can be seen through calculation of the Peclet number, the relative magnitude of convection of a species due to bulk flow to that of diffusion:[124]

$$\frac{VL}{D_0} \qquad \textbf{[22.2]}$$

where V is the velocity of the flow, L is the transport path length, and D_0 the free diffusion coefficient of the species being transported. (The free diffusion coefficient in saline is used rather than its value in tissue, since the species carried by flow is constrained to the same extent by the tissue as is its diffusion). Using the RPE pumping rate (Table 22.2) for V, Bruch's membrane thickness (average of 3 μm[71]) for L, and a range of diffusion coefficients of species crossing Bruch's membrane (2×10^{-7} cm^2/sec for LDL to 2×10^{-5} cm^2/sec for oxygen)[124,125] we find that the Peclet number ranges in value from 5×10^{-5} to 5×10^{-3}. Thus, convection is negligible in transporting species across Bruch's membrane under physiologic conditions.

Diffusion follows Fick's law whereby the diffusive flux per unit area (j) is proportional to the diffusion coefficient (D) of that species in the medium through which it passes and to the concentration difference across the medium (ΔC), and inversely proportional to the diffusion length:

$$j = D\,\Delta C/L \qquad \textbf{[22.3]}$$

The *permeability* of a tissue to a given species is defined as $P = j/\Delta C$. We see then that $P=D/L$. For example, the permeability of Bruch's membrane to oxygen is ~0.067 cm/sec. Note that since diffusion moves down a concentration gradient, one species might be diffusing across Bruch's membrane toward the RPE (e.g., oxygen) while another species (e.g., carbon dioxide) diffuses simultaneously in the other direction.

With high diffusion coefficient and little interaction with extracellular matrix, small molecules (e.g., oxygen, cytosine, RNAaseA) diffuse quickly across Bruch's membrane with diffusion coefficients nearly the same as in free solution.[126] However, macromolecules have much smaller free solution diffusion coefficients due to their larger size. Their diffusion coefficients are further reduced by interactions with extracellular matrix and/or lipoproteins that accumulate with age. For example, the diffusion coefficients of albumin and ferritin are an order of magnitude smaller in Bruch's membrane than their values in free solution.[126]

The transport of amino acids,[127] serum proteins,[128] drugs,[129] and LDL[123,130] across Bruch's membrane has been examined. Transport experiments by Clark and associates[85] suggest that FHL-1 (43 kDa) crosses Bruch's membrane more readily than CFH (155 kDa) and is in fact the major CHF form in native aged Bruch's membrane.

There are technical challenges to these transport experiments. First, as indicated in Eq. 22.3, diffusional flux depends on the length of the tissue. Since the diffusion coefficient of the transported species is likely different in Bruch's membrane than in the choroid in a combined preparation, but the path lengths of both tissue components are usually not determined, it is difficult to use the measured values to determine absolute values of permeability. Instead the more easily measured flux rate (j: see Eq. 22.3) is usually presented. Second, an unstirred layer can develop near the membrane thereby complicating the results, and this can occur even in cases when the solutions are stirred.[131] Nonetheless, useful comparative results can be generated.

The transport rate across human Bruch's membrane declines linearly with age for all molecules measured. Amino acids exhibited permeabilities of 0.6×10^{-4} cm/sec (phenylalanine) to 1.2×10^{-4} cm/sec

(glycine) for young Bruch's membrane and exhibited a modest decline (twofold or less) with aging.[127] Serum proteins decrease more markedly, dropping from $3.5x10^{-6}$ cm/sec in the first decade to $0.2x10^{-6}$ cm/sec in the ninth decade, a >10-fold decrease.[128] In particular, proteins larger than 100 kDa have significantly decreased flux through Bruch's membrane of older individuals. Macular Bruch's membrane showed a steeper decrease with age than did the periphery.[132] Permeability was reduced in eyes with AMD relative to age-matched normal eyes.[132]

Decreased permeability of Bruch's membrane to transport is likely due to a decrease in diffusion coefficients, especially for the larger species affected by interaction with extracellular matrix and lipoproteins. As indicated in Eq. 22.3, increased path length due to age-related thickening of Bruch's membrane[71] could also have a significant effect.

An original proposal of a molecular weight (MW) exclusion limit to Bruch's membrane macromolecule transport of 66–200 kD[127,128] has been questioned by more recent work suggesting that if such a limits exists, it is much higher.[132] Because of the importance of lipoproteins in transporting lipophilic nutrients to the RPE for ultimate use by the photoreceptors, and also because lipoproteins accumulate with age in Bruch's membrane, Cankova et al.[123] specifically examined the reflection coefficient of bovine Bruch's membrane to plasma LDL. They measured a reflection coefficient of 0.62 (compared to a reflection coefficient of arterial endothelium to LDL of 0.998 and arterial intima to LDL of 0.827[133]). Thus, while LDL did not pass freely through Bruch's membrane, it could nonetheless pass. Hussain et al.[132] also concluded that particles as large as LDL could cross Bruch's membrane. Accordingly, RPE cells have been shown to internalize plasma LDL from the choroid.[134–136]

These considerations are relevant not only to understanding mass transfer between the choriocapillaris and the RPE, but also for transcleral drug delivery strategies including antiangiogenic agents for treating AMD and steroids for treating diabetic retinopathy.[137,138] Cheruvu and Kompella[129] reported that the choroid–Bruch's layer is a more significant barrier to drug transport than is sclera. It hindered the transport of lipophilic solutes more than hydrophilic solutes and in a more dramatic way than does sclera. Importantly,

the reduction in transport across this layer directly correlated with solute binding to the tissue. Pitakänen et al. found significant lag times associated with transport of lipophilic beta blockers across the RPE-choroid, consistent with binding of these drug to the tissues; however, they found that the permeability of the lipophilic drugs across this tissue was greater than that of hydrophilic compounds or macromolecules.[139] Lipophilic substances are known to have both different transport characteristics in connective tissues and also bind to extracelluar matrix.[140]

Summary and Implications

Bruch's membrane's physiologic roles are structural and facilitating transport. Transport across Bruch's membrane is increasingly hindered with age, due at least partly to the marked age-related accumulation of EC-rich lipoproteins in this tissue, impeding pumping of fluid from RPE.[115] A ≥90% decrease in transport of some species from the choroid[128,132] may include lipophilic essentials delivered by lipoproteins. This decline in transport capability is thought to have functional consequences for photoreceptors.[141] A well-characterized change occurring through the lifespan of individuals with healthy maculas is slowed dark adaptation,[142] attributed to impaired translocation of retinoids across the RPE-Bruch's interface. This slowing, worse in AMD patients,[143,144] can be partly ameliorated by short-term administration of high-dose vitamin A,[145] presumably overcoming the translocation deficit via mass action.

However, it is important to recognize that except for the studies on tissue from individuals with AMD, all of the results in human summarized here were from eyes that did not have retinal disease. As such, while the age-related decline in the transport capability of Bruch's membrane has functional consequences on photoreceptor function it is not likely that this represents disease, but instead, is part of the aging process. Accordingly, a prospective study has shown that slowed dark adaption is detectable in 22% of older adults with maculas considered normal by color fundus photography and that these persons are two times more likely to have incident early AMD 3 years later.[146,147] Thus the overall model of photoreceptor nutritional insufficiency, due to impaired

transport, at the interface of aging and disease has strong *in vivo* validation.

Pathology of Bruch's Membrane

AMD Lesions

In aging and AMD, characteristic extracellular lesions accumulate in tissue compartments between the RPE-BL and ICL (Fig. 22.8). Known as drusen and basal linear deposits (BLinD),[32,148] these lipid-containing aggregations ultimately impact RPE and photoreceptor health by impairing transport, causing inflammation, and predisposing to choroidal neovascularization. Basal laminar deposit (BLamD), a stereotypic thickening of RPE basal lamina, forms in parallel with lipid deposition in Bruch's and may indicate RPE stressed by it. Since 2010, clinical optical coherence tomography (OCT) has revealed that AMD lesions include a major new component, called subretinal drusenoid deposits (SDD) by cross-sectional OCT and histology[149] and reticular pseudodrusen by en face imaging such as color fundus photography.[150] These solid space-filling lesions located between the photoreceptors and RPE (Fig. 22.8) are common in AMD but are not unique to AMD. In the section below, we refer to retinal regions as foveal (central 1 mm), perifoveal (0.5–3 mm from the foveal center), and extramacular (>3 mm).

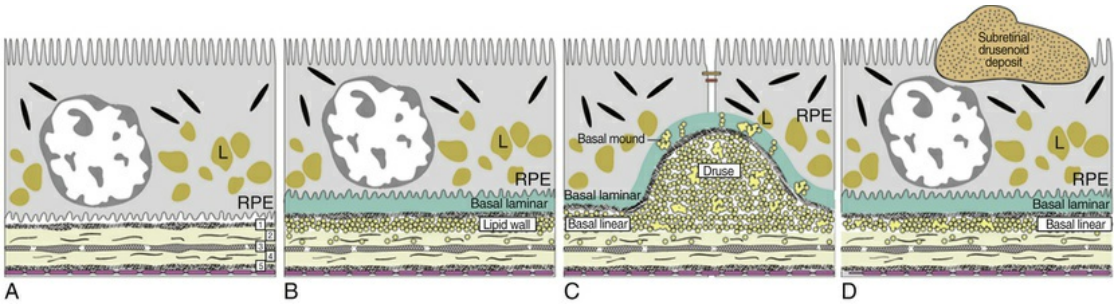

FIG. 22.8 Bruch's membrane and characteristic AMD lesions. (A) Bruch's membrane has five layers in a normal eye: 1, basal lamina of the retinal pigment epithelium (RPE); 2, inner collagenous layer; 3, elastic layer; 4, outer collagenous layer; 5, basal lamina of the

choriocapillary endothelium (fenestrated cells, pink). *L*, lipofuscin. (B) Older eyes have basal laminar deposit (BlamD) and the Lipid Wall, precursor to basal linear deposit and soft drusen. (C) Drusen, basal linear deposit, and the Lipid Wall occupy the same tissue compartment. Basal mounds are soft druse material within BlamD. (D) Subretinal drusenoid deposit is an extracellular lesion compositionally distinct from drusen, located between the photoreceptors (not shown) and the RPE. (Modified from Curcio CA, Johnson M, Huang J-D, et al. Apolipoprotein B-containing lipoproteins in retinal aging and age-related maculopathy. J Lipid Res. 2010;51(3):451-67.)

Drusen

In a fundus view, drusen are 30–300 μm-diameter yellow–white deposits posterior to the RPE. By OCT, they appear as variably hyporeflective spaces in the same location.[151–153] Found in most older adults,[79,154] drusen are more numerous in extramacular retina than in macula.[155–157] Drusen are typically classified as "hard" and "soft" by the appearance of their borders. Other rare druse types exist and are less well characterized.[158] Soft drusen confer high risk of advanced disease.[159–162] Histologically, drusen are focal, domed lesions between the RPE basal lamina and the ICL (Fig. 22.8), as illustrated[163] and established[148,164] using transmission electron microscopy.

In separate 1854 publications, Donders (a Dutch ophthalmologist) and Wedl (an Austrian pathologist) described "colloid bodies" (*Colloidkugeln*) or "hyaline deposits" on the inner surface of the choroid in older or diseased human eyes[3,165,166] (translated by Busk). Both authors interpreted droplets filling these deposits as "fat-globules." The term drusen originated with Müller in 1856, from the German word for geode (not to be confused with *drüse*, meaning gland).[167] The name drusen was adopted by English writers early in the 20th century[168] yet "colloid body" was used by Verhoeff into the 1920s.[169] Lauber[170] (cited in reference 171) noted that deposits between the lamina vitrea and the RPE were sudanophilic in 1924. Wolter and Falls[38] stated that "hyaline bodies [drusen] … stain reddish with … oil red O" in 1962. Soft drusen

were termed serogranular and hard druse hyaline (glassy) by S. Sarks,[159] implying different composition. Soft drusen are oily, difficult to isolate individually, biomechanically more fragile than hard drusen, and found only in the macula.[157] Friability upon processing for conventional paraffin histology was noted early.[172] Due to this and other technical challenges, few recent drusen compositional studies (Table 22.3 online) included true macular soft drusen.[173–177] Many studies analyzed peripheral drusen, combined macular and peripheral drusen, or did not specify location.

TABLE 22.3
Localized Components of Drusen

Component	Phase	Direct Assay	Abundance	References
Lipoproteins (EC, UC, phospholipid)	P	✓	All drusen; >40% of hard druse volume; EC pools in soft drusen	157,194,311
Modified lipids (7-ketocholesterol, isolevuglandin)	D	✓	All drusen	185,312
Apolipoproteins (apoB, A-I, C-I, E)	P	apoE ✓	60–100% of hard drusen; higher rates in periphery than macula	189,191,311
Melanin/lipofuscin granules	P		6% of hard and soft drusen	157
Cells (dendritic, others)	P		3–6% of hard drusen only	157, 313
Amyloid vesicles (0.25–10 μm)	P		2% of hard drusen, 40% of compound drusen, frequent in eyes with many drusen, some AMD eyes	157, 173, 194, 200
Hydroxyapatite (calcium phosphate)	P	✓	43% of macular hard drusen, 1.6% of soft drusen, 2% of peripheral hard drusen by light microscopy; all drusen by specific label	157, 215
Clusterin, TIMP3, vitronectin, apolipoprotein E, complement factor H, membrane attack complex (complement components 8, 9), C-reactive protein	D	✓	Reliably detected; abundance inferred	186, 198, 314–317
Components of classic, lectin, alternative, terminal complement pathways; C3 fragments indicating activation	D	Some ✓	Many pathway components evidence key role of complement	318
RGR-d	D		All drusen	319
αA- and αB-crystallin	D	✓	N.A.; higher in BrM, more in AMD drusen	201, 202
Ubiquitin	D		Most drusen in most eyes	196, 320

Carbohydrates	D		All drusen	181
Zinc	D	✓	Many drusen	18, 321
Iron	D	✓	Many drusen	321
Exosome markers CD63, CD81, and LAMP2	P		N.A.	322
Bestrophin, membrane-bound	P		N.A.	323

P, particulate; D, dispersed; BrM, Bruch's membrane; Localization methods: immunohistochemistry, histochemistry, immunogold transmission electron microscopy; Direct assays: proteomics, Western blot, microprobe synchrotron X-ray fluorescence for zinc; N.A. not available. Varying estimates of particulate druse components are due to differences in location of samples and druse types examined. "All drusen" means "all drusen sampled." Many studies did not specify the location of drusen studied or pooled macula and periphery.

Extant theories for druse formation, extending back to their discovery,[167] fit into two general categories: transformation of the overlying RPE and deposition of materials onto Bruch's membrane. The latter is now accepted.[166] The RPE has been implicated as a source of many druse components, via budding of membrane-bound packets of cytoplasm or secretion of lipoproteins with retention by aged Bruch's membrane,[39] as experimentally confirmed.[178] BLinD and soft drusen are two physical forms (layer and lump) of the same AMD-specific lesion, located only in the macula. BLinD forms consequent to lipoprotein accumulation in Bruch's membrane and formation of the Lipid Wall, likely involving lipoprotein aggregation, oxidation of individual lipid classes, and local inflammation. Soft drusen involves these and other processes that cause the distinctive dome shape of these lesions. RPE expresses genes for many druse components, including lipoproteins.[18,179,180] The contribution of plasma-derived components, in contrast, has not been well characterized. The existence of druse subregions additionally suggest remodeling in the extracellular compartment, such as cellular invasion and enzymatic activity[181–183] and uplifting of the Lipid Wall.[174]

Most prominent among druse constituents are lipids (Table 22.3 online), as noted early. All drusen contain EC and UC, in addition to phosphatidylcholine, other phospholipids, ceramides, and 7-ketocholesterol, an oxidation product of UC that is angiogenic and proinflammatory.[44,47,163,174,182,184,185] Extractable lipids account for ≥40% of hard druse volume[186] and likely more for macular soft drusen.[174] This includes large EC-rich lakes in soft drusen (Figs. 22.9A–B), as in atherosclerotic plaques.[187] Apolipoprotein

immunoreactivity appears in drusen with high frequency (100%, apoE; >80% apoB; 60%, A-I).[174,188–191] Importantly, hard drusen contain many solid, Folch-extractable electron-dense particles of the same diameter as the lipoproteins in Bruch's membrane. These observations together with the appearance of membranous debris in soft drusen (below) make an RPE-secreted apoB,E-containing lipoprotein particle an efficient mechanism to place multiple lipids and apolipoproteins within lesion compartments. Only half of macular drusen take up hydrophilic fluorescein in angiography,[192] possibly reflecting differing proportions of lipid classes in individual lesions.[184]

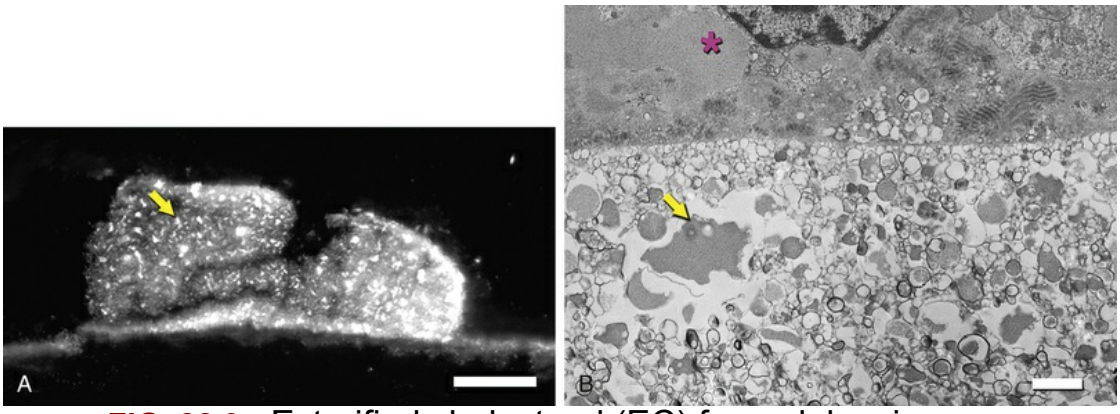

FIG. 22.9 Esterified cholesterol (EC) forms lakes in macular soft drusen. (A) EC lakes in a macular soft druse revealed by filipin fluorescence (*arrow*). Scale bar: 25 μm. (B) Macular soft druse from an AMD eye has lakes of homogeneous electron-dense lipid (*arrow*) among partially preserved lipoprotein-like material. Basal laminar deposit (*asterisk*) overlying the druse has similar material, called membranous- or lipoprotein-derived debris (to the right of the asterisk). Scale bar: 1 μm. (Panel A modified from Malek G, Li C-M, Guidry C, et al. Apolipoprotein B in cholesterol-containing drusen and basal deposits in eyes with age-related maculopathy. Am J Pathol. 2003;162(2):413-25.)

Discrete nonlipid components in some drusen granules of lipofuscin or melanin indicate cellular origin (Table 22.3 online). Spherical β-amyloid assemblies[173,193,194] now appear to be due to nonspecific binding of proteins to hydroxyapatite spherules (see below), consistent with immunohistochemistry.[195,196] Other

constituents present in all drusen include vitronectin, TIMP-3, complement factor H, complement components C3 and C8, crystallins, ubiquitin, and zinc.[26,183,193,197–201] Many druse components are found also in retina IL-1[177] and/or choroid (carboxypyrrhole adducts[202]) of the same eyes and thus are less specific for these lesions than other components.

The principal lipid-containing component of soft drusen and BLinD was called "membranous debris" by the Sarks[159,203,204] and "lipoprotein-derived debris" was suggested as an alternative, for two reasons.[39] First, these lesions are richer in histochemically detectable UC than surrounding cellular membranes.[184,205] By transmission electron microscopy following osmium tetroxide postfixation, membranous debris appears as variably sized, contiguous coils of uncoated membranes consisting of uni- or multilamellar electron dense lines, that are denser than cellular membranes and surround an electron-lucent center (Fig. 22.2). Since conventional ultrastructural preparation methods can remove lipids, the building blocks of membranous debris are likely the UC-rich exteriors of lipoproteins (native and fused) whose neutral lipid interiors are not well preserved in postmortem tissue.[53,190,206] Second, all drusen have abundant EC that can only be explained by lipoprotein particles in addition to cellular membranes.

By ophthalmoscopy, refractile or glistening deposits thought to be calcified drusen[172] regularly appear in areas where drusen regress, before the onset of geographic atrophy.[207,208] Recent investigation has confirmed that glistening drusen in fact contain calcium phosphate in the form of hydroxyapatite spherules, culminating a five-decade quest. Studies included detection of refractile nodules by light microscopy,[32,209–212] phosphate detection via von Kossa histochemistry,[172,208] confirmation of calcium and phosphate signals in nodules by energy dispersive X-ray analysis,[213,214] and identification of hydroxyapatite mineral by synchrotron micro-X-ray diffraction.[215] Most drusen contain 0.5–20 μm diameter spherules that become clinically visible when the RPE degenerates.[208] Concentric shells within the spherules account for the refractility.[208] Spherules also have UC within them.[215] As hydroxyapatite binds proteins well and is widely used as a stationary phase for chromatography, these nodules are strong

candidates for nucleation sites for further protein deposition and druse enlargement.[215] Calcification in drusen differs from that within Bruch's membrane itself by not requiring the presence of elastin fibers. The source and mechanism of high calcium and phosphate concentration in the sub-RPE space, likely reflecting RPE physiology, are important areas for future research.

Basal Linear Deposit

BLinD is a thin (0.4–2 μm) layer located in the same sub-RPE compartment as soft drusen (Fig. 22.8). BLinD is not visible clinically except as associated with other pathology. By lipid-preserving ultrastructural techniques, BLinD is rich in solid lipoprotein particles and lipid pools (Figs. 22.10A,C) and can contain hydroxyapatite.[203] BLinD and soft drusen are considered alternate forms of the same entity.[216] ApoE and apoB are present in BLinD and its precursor, the Lipid Wall.[174,188,189] Transitional morphologies between Lipid Wall and BLinD have been reported.[217] BLinD is thicker in the fovea than in the perifovea, unlike SDD, consistent with these lesions reflecting differential aspects of cone and rod physiology[61] (see below).

Basal Laminar Deposit

BLamD forms small pockets between the RPE and the RPE-BL in many older normal eyes or a continuous layer as thick as 15 μm in AMD eyes[204,205,218] (Fig. 22.8). The presence and abundance of BLamD has been used to stage AMD.[32,219] Ultrastructurally, BLamD resembles basement membrane material (Fig. 22.10B), containing laminin, fibronectin, type IV, and type VI collagen.[220–223] The latter is a distinctive banded material with 120 nm periodicity, called wide- or long-spacing collagen, which also appears in other ocular locations like epiretinal membranes. Thick BlamD, associated with advanced AMD risk,[204] contains histochemically detectable lipid including UC and EC[184,205] and is a classically described site for membranous debris (Fig. 22.2**)**. By lipid-preserving methods, solid particles are seen in BLamD (Figs. 22.10A–B). Especially enriched in basal mounds[204] (Fig. 22.8C), lipoprotein-derived debris in BLamD may be considered as retained in transit from the RPE to BLinD and/or drusen.[174,184,205] Morphologically heterogeneous BLamD also

contains vitronectin, MMP-7, TIMP-3, C3, and C5b-9,[218] EC, and UC.[205] Evoked in numerous mouse models of aging, stress, and genetic manipulation, BLamD is a reliable marker of RPE stress.[224,225]

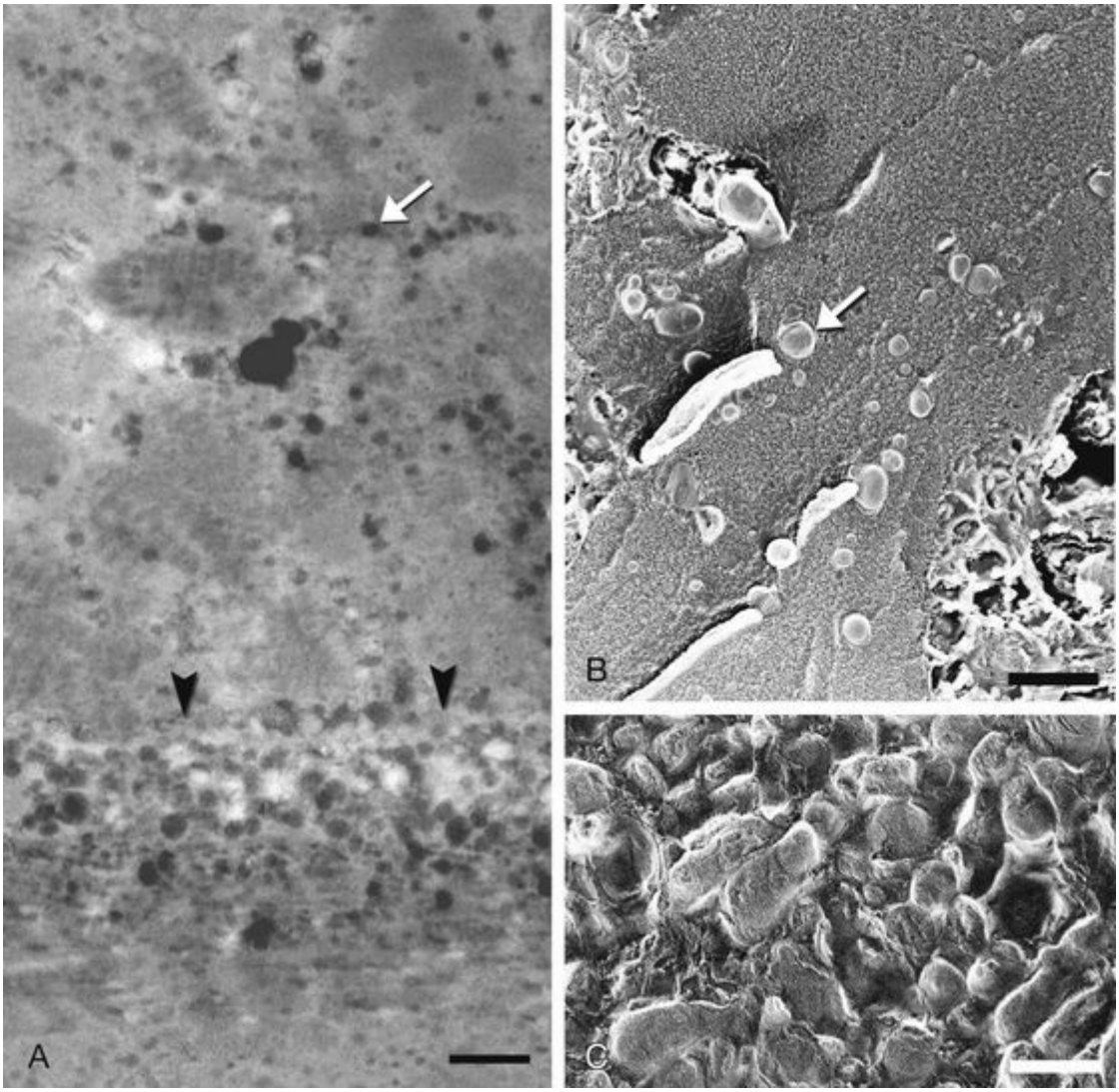

FIG. 22.10 Lipoprotein-derived debris and lipid pools in AMD lesions are solid rather than vesicular material. (A) Above retinal pigment epithelium (RPE) basal lamina (*arrowheads*) is basal laminar deposit (BlamD) with individual particles indicated (*arrow*). Below RPE basal lamina are numerous solid particles in basal linear deposit (BlinD). Transmission electron microscopy, OTAP fixation; scale bar: 500 nm. (B) BlamD appears as a solid column of basal lamina-like material, with solid particles embedded within (*arrow*). Scale bar = 500 nm. (C) BlinD has lipoproteins of

heterogeneous sizes and shapes as well as pooled lipid, consistent with a model of surface degradation and particle fusion. Scale bar = 200 nm. (Panel A Curcio CA, Presley JB, Millican CL, Medeiros NE. Basal deposits and drusen in eyes with age-related maculopathy: evidence for solid lipid particles. Exp Eye Res 2005;80(6):761–75. Panel B image courtesy of J.-D. Huang, PhD. Panel C Curcio CA, Johnson M, Rudolf M, Huang J-D. The oil spill in ageing Bruch's membrane. Br J Ophthalmol 2011;95(12):1638–45.)

Subretinal Drusenoid Deposit

Hypotheses of druse formation must eventually also account for SDD, the extracellular deposits between RPE and photoreceptors (Fig. 22.8). These lesions were first illustrated histologically in AMD by the Sarks[203] and independently described as drusen "visible en lumière bleu" by Mimoun et al.[226] Conferring risk for late AMD,[227] SDD appear in 60% or more of eyes with geographic atrophy,[227,228] 49% of early AMD eyes, and 23% of older eyes considered normal by color fundus photography.[229] SDD are also detectable in several Mendelian inherited disorders affecting the RPE–Bruch's membrane complex.[230–232] Comprehensive histology, clinicopathologic correlation, and adaptive optics scanning laser ophthalmoscopy[61,233–235] have definitively localized these lesions in the subretinal space, after some early debate. SDD lack markers for cells bounding this space (photoreceptors, Müller cells, RPE).[175,205] SDD share protein components with drusen,[175] and importantly, SDD lipid composition differs from drusen (UC only vs. UC and EC, respectively[236]). SDD are abundant in the perifovea and peripapillary area[149,150,229,237–239] and sparse in central macula, whereas BLinD is thickest under the fovea.[61] Cones are numerous in the fovea, and rods are numerous in the perifoveal region and just beyond.[240] Thus drusen and SDD have been linked in a system of outer retinal lipid recycling serving the differential lipid requirements of rod and cone photoreceptor outer segment membranes.[61,241] The low content of EC relative to drusen has been explained by invoking a hypothetical high-density lipoprotein particle, rich in UC, that shuttles UC from and docosahexanoate to rod outer segments selectively.[61] If this hypothesis is true, SDD might be also rich in docosahexanoate and its derivatives, an

important question to address experimentally.

Summary

Levels of significance ascribed to molecules sequestered in drusen (Table 22.3 online), and by inference, BLinD, include toxicity to the overlying RPE, stigmata of formative processes (extrusion of cellular materials, secretion, extracellular enzymatic processing, cellular activity), and markers of a diffusely distributed disease process affecting RPE and Bruch's membrane. Additional significance can be ascribed to these lesions as physical objects that increase path length between choriocapillaries and retina and provide a biomechanically unstable cleavage plane between RPE-BL and ICL. Many of these processes likely also occur in the subretinal space in relation to SDD.[149]

Response-to-Retention Hypothesis of AMD

The parallels between the pathology of arterial intima of large arteries in atherosclerosis and that of Bruch's membrane in AMD are striking. Both diseases feature cholesterol-rich lesions in subendothelial compartments within the systemic circulation, involving many of the same molecules and biologic processes at multiple steps, as long anticipated.[242,243] According to the Response-to-Retention theory of atherosclerosis, plasma lipoproteins cross the vascular endothelium of large arteries, and bind to extracellular matrix. By itself, this process is not pathologic. However, lipoprotein components become modified via oxidative and nonoxidative processes and launch numerous downstream deleterious events, including inflammation, macrophage recruitment, and neovascularization leading to disease.[244,245] Parallel with apoB-lipoprotein-instigated disease in arterial intima, an intraocular Response-to-Retention involving the RPE and Bruch's membrane in aging and AMD would begin with age-related accumulation of lipoproteins, but *of local origin.* Oxidation, perhaps driven by reactive oxygen species from adjacent RPE mitochondria, would then initiate a pathologic process resembling that in the vascular system with inflammation-driven downstream events including complement activation and structurally unstable

lesions.[39] New model systems such as highly differentiated and polarized cultured RPE[178] and mice with genetically modified lipoprotein pathways[246] will allow rigorous experimental test of these concepts.

Neovascular AMD

Choroidal neovascularization (CNV), the major sight-threatening complication of AMD, involves angiogenesis along vertical and horizontal vectors: vertically across Bruch's membrane, and either laterally external to the RPE (type 1 CNV,[247]), laterally within the subretinal space (type 2 CNV), or further anteriorly into the retina (type 3 CNV).[247–249] Of 40+ conditions involving CNV, AMD is the most prevalent, followed by ocular histoplasmosis,[247] and including angioid streaks (below). CNV is a multifactorial nonspecific wound healing response to various specific stimuli, involving VEGF stimulation of choriocapillaris endothelium, compromise to Bruch's membrane, and participation of macrophages.[247] Impaired transport across Bruch's membrane in AMD increasingly isolates the RPE from its metabolic source in the choriocapillaries and enhances the challenge in waste product disposal. VEGF released by RPE as a stress signal initiates an angiogenic response by the endothelium. However, Bruch's membrane compromise is essential for CNV to proceed, as evidenced by intrachoroidal neovascularization without CNV in a mouse overexpressing VEGF in the setting of an intact Bruch's membrane.[250]

Bruch's membrane in a state of compromise can be breached easily by new vessels in AMD. It is notable that the EL is thinner and more interrupted in eyes with neovascular AMD.[26] The length of gaps in the EL is greater in eyes with early AMD and any CNV.[26] In paired donor eyes with and without CNV secondary to AMD, progressed eyes are distinguished by calcification and breaks in Bruch's membrane.[251] In contrast, calcification in a small number of geographic atrophy eyes is unremarkable.[252]

BLinD and soft drusen together further this process by presenting a horizontal cleavage plane for vessel formation to exploit. The lipid-rich composition, relative lack of structural elements like collagen fibrils, lesion biomechanical instability,[157] and

proinflammatory, proangiogenic compounds like 7-ketocholesterol and linoleate hydroperoxide[247,253,254] likely promote vessel growth in this plane.[253] Interestingly, SDD is strongly associated with type 3 neovascularization,[255,256] suggesting that this lesion also plays a similarly important proangiogenic role.

Angioid Streaks (*ABCC6*, *MTP* Genes)

Angioid streaks are ruptures in Bruch's membrane associated with multiple disorders, caused by excess calcification of the elastic layer[257] and often accompanied by CNV. They are prominent ocular manifestation of pseudoxanthoma elasticum (PXE), a systemic connective tissue disorder. PXE patients harbor mutations of a hepatically expressed lipid transporter ABCC6.[258] Clinical presentation includes, in addition to streaks and CNV, peau d'orange (flat, yellow, drusen-like lesions), optic nerve head drusen, outer retinal tubulations, subretinal fluid, and pigmentary changes.[230] PXE clinical manifestations are believed related to ectopic mineralization of nonhepatic tissues, suggesting a defect in the transport of antimineralization agents.[259]

Angioid streaks are associated with abetalipoproteinemia,[260–263] an extremely rare disorder with low plasma apoB-containing lipoproteins, acanthocytosis of erythrocytes, neuropathy, and pigmentary retinopathy. It is historically attributed to lack of lipophilic vitamins delivered by plasma LDL.[264] The RPE expresses the abetalipoproteinemia gene (microsomal triglyceride transfer protein),[265] which cotranslationally lipidates apoB (see above). How this deficiency leads to angioid streaks is unknown. The finding, however, highlights that *lack* of apoB lipoproteins has negative consequences for Bruch's membrane health, likely by impacting RPE health, just as an *excess* of retained apoB lipoproteins has negative consequences via lesion formation and impaired transport (see above). Good chorioretinal function thus requires an optimal balance between these extremes.

Thick Basal Laminar Deposits (*TIMP-3*, *CTRP5*, *EFEMP1* Genes)

Three autosomal dominant-inherited disorders with adult onset – Sorsby fundus dystrophy, late-onset retinal degeneration (LORD) and Malattia Leventinese–Doyne honeycomb retinal dystrophy (ML–DH) – share phenotypic similarities with AMD and provide mechanistic support for many aspects of Bruch's membrane physiology and pathophysiology discussed above. All three conditions result from mutations in genes encoding extracellular matrix proteins or their regulators (Sorsby – *TIMP3*[266], LORD – *CTRP5*[267], and ML–DH – *EFEMP1*[268]). All three can progress to CNV. All three have visual dysfunction, especially rods, attributed to a nutritional night blindness that is responsive to short-term administration of high-dose vitamin A.[269–271] Sorsby and LORD are notable for panretinal thick BLamD and areas of RPE atrophy,[272] while ML–DL is notable for radially distributed drusen and peripapillary deposits. In Sorsby mutant *TIMP-3* localizes to BLamD. In ML–DL, *EFEMP1* localizes to BLamD and not to the pathognomonic drusen themselves, suggesting an important role of BLamD in druse formation. Notably drusen in ML–DL are immunoreactive for fibulin-3 and collagen IV unlike drusen associated with aging and AMD.[273]

BLamD in Sorsby and LORD, like that in AMD, is notably rich in oil red O-binding lipid.[274–276] In LORD eyes[276] deposits contain EC, UC, and apoB, and lipid-preserving ultrastructural methods revealed solid electron-dense particles tracking in intersecting networks across the BLamD. Although not initially apparent, these may represent native lipoproteins in transit from RPE to the choriocapillaris. Lipid particle disposition within these thick deposits has been replicated in a mouse model expressing the R345W *EFEMP1* mutation.[224]

Conclusion

Bruch's membrane serves essential functions as substrate to the RPE and vessel wall of the outer retina. Its layers and constituent proteins collectively represent a barrier that keeps choroidal vessels at bay, provides a route for water, solutes, and macromolecules that transfer between RPE and choroid while supporting the structural integrity of both. It is unusual among human tissues in

accumulating a high content of EC-rich neutral lipid over the lifespan. A natural history and biochemical model now suggests this lipid is due to apoB lipoprotein secretion by RPE, which may be part of an outer retinal nutrition system with an second component possibly also involving lipoproteins in the subretinal space. This deposition can account for the impaired outward movement of fluid from RPE, increasing risk for RPE detachments more common in older persons, and impaired macromolecular transport also leading to RPE stress. Oxidation of these lipid deposits in Bruch's membrane likely initiates an inflammatory process that leads to lesion formation and choroidal neovascularization in AMD.

References

1. Marshall J, Hussain AA, Starita C, Moore DJ, Patmore AL. Aging and Bruch's membrane. Marmor MF, Wolfensberger TJ. *The retinal pigment epithelium: function and disease*. Oxford University Press: New York; 1998:669–692.
2. Harris A, Moss A, Erhlich R. The choroid. Tasman W, Jaeger EA. *Duane's ophthalmology*. 18th ed. Lippincott Williams & Wilkins: Philadelphia, PA; 2011.
3. Wedl C. *Grundzüge der pathologischen Histologie*. Carl Gerold & Sohn: Vienna; 1854.
4. Bruch CLW. *Untersuchungen zur Kenntniss des Kornigen Pigments der Wirbelthiere*. University of Zurich: Zurich; 1844.
5. Smirnow AE. Zum Baue der Chorioidea propia des erwachsenen Menschen (Stratum elasticum supracapillare). *Graefes Arch*. 1899;57:451.
6. Salzmann M. *The anatomy and histology of the human eye in the normal state. its development and senescence*. University of Chicago: Chicago; 1912.
7. Wolfensberger TJ. The historical discovery of the retinal pigment epithelium. Marmor MF, Wolfensberger TJ. *The retinal pigment epithelium: function and disease*. Oxford University Press: New York; 1998:13–22.
8. Duke-Elder S, Cook C. *Part 1, Embryology*. Mosby: St. Louis; 1967.
9. Mann I. *The development of the human eye*. Grune and

Stratton: New York; 1964.
10. Scales D, Fryczkowski A, Opremcak E. The choroid. WB Saunders: Philadelphia; 1994:252–261. Albert D, Jakoviec F. *Principle and practices of ophthalmology*. vol. 1.
11. Takei Y, Ozanics V. Origin and development of Bruch's membrane in monkey fetuses: an electron microscopic study. *Invest Ophthalmol*. 1975;14(12):903–916.
12. Rizzolo LJ, Chen X, Weitzman M, Sun R, Zhang H. Analysis of the RPE transcriptome reveals dynamic changes during the development of the outer blood–retinal barrier. *Mol Vis*. 2007;13:1259–1273.
13. Saint-Geniez M, D'Amore PA. Development and pathology of the hyaloid, choroidal and retinal vasculature. *Int J Dev Biol*. 2004;48(8–9):1045–1058.
14. Hogan MJ. Bruch's membrane and disease of the macula. Role of elastic tissue and collagen. *Trans Ophthalmol Soc U K*. 1967;87:113–161.
15. Hogan MJ, Alvarado JA, Weddel J. *Histology of the human eye: an atlas and textbook*. W.B. Saunders Co.: Philadelphia, PA; 1971.
16. Gass JDM. *Stereoscopic atlas of macular diseases: diagnosis and treatment*. 4th ed. Mosby: St. Louis; 1997.
17. Guymer R, Bird A. Age changes in Bruch's membrane and related structures. Ryan SJ. *Retina. II*. Mosby: St Louis; 2006:1030–1039.
18. Booij JC, Baas DC, Beisekeeva J, Gorgels TG, Bergen AA. The dynamic nature of Bruch's membrane. *Prog Retin Eye Res*. 2009;29(1):1–18.
19. Call TW, Hollyfield JG. Sulfated proteoglycans in Bruch's membrane of the human eye: localization and characterization using cupromeronic blue. *Exp Eye Res*. 1990;51:451–462.
20. Kelly U, Yu L, Kumar P, et al. Heparan sulfate, including that in Bruch's membrane, inhibits the complement alternative pathway: implications for age-related macular degeneration. *J Immunol*. 2010;185(9):5486–5494.
21. Clark SJ, Keenan TD, Fielder HL, et al. Mapping the differential distribution of glycosaminoglycans in the adult

human retina, choroid, and sclera. *Invest Ophthalmol Vis Sci*. 2011;52(9):6511–6521.
22. Chen L, Miyamura N, Ninomiya Y, Handa JT. Distribution of the collagen IV isoforms in human Bruch's membrane. *Br J Ophthalmol*. 2003;87(2):212–215.
23. Aisenbrey S, Zhang M, Bacher D, Yee J, Brunken WJ, Hunter DD. Retinal pigment epithelial cells synthesize laminins, including laminin 5, and adhere to them through alpha3- and alpha6-containing integrins. *Invest Ophthalmol Vis Sci*. 2006;47(12):5537–5544.
24. Hewitt TA, Nakasawa K, Newsome DA. Analysis of newly synthesized Bruch's membrane proteoglycans. *Invest Ophthalmol Vis Sci*. 1989;30:478–486.
25. Korte GE, D'Aversa G. The elastic tissue of Bruch's membrane. *Arch Ophthalmol*. 1989;107:1654–1658.
26. Chong NH, Keonin J, Luthert PJ, et al. Decreased thickness and integrity of the macular elastic layer of Bruch's membrane correspond to the distribution of lesions associated with age-related macular degeneration. *Am J Pathol*. 2005;166(1):241–251.
27. Yu HG, Liu X, Kiss S, et al. Increased choroidal neovascularization following laser induction in mice lacking lysyl oxidase-like 1. *Invest Ophthalmol Vis Sci*. 2008;49(6):2599–2605.
28. Newsome DA, Huh W, Green WR. Bruch's membrane age-related changes vary by region. *Curr Eye Res*. 1987;6:1211–1221.
29. Lutty GA, Hasegawa T, Baba T, Grebe R, Bhutto I, McLeod DS. Development of the human choriocapillaris. *Eye (Lond)*. 2010;24(3):408–415.
30. Roberts JM, Forrester JV. Factors affecting the migration and growth of endothelial cells from microvessels of bovine retina. *Exp Eye Res*. 1990;50(2):165–172.
31. Smith W, Assink J, Klein R, et al. Risk factors for age-related macular degeneration: pooled findings from three continents. *Ophthalmology*. 2001;108:697–704.
32. Sarks SH. Ageing and degeneration in the macular region: a clinico-pathological study. *Br J Ophthalmol*. 1976;60(5):324–

341.
33. Bairaiti A, Orzalesi N. The ultrastructure of the pigment epithelium and of the photoreceptor-pigment epithelium interface. *J Ultrastruct Res*. 1963;9:484–496.
34. Nakaizumi Y. The ultrastructure of Bruch's membrane. II. Eyes with a tapetum. *Arch Ophthalmol*. 1964;72:388–394.
35. Johnson M, Huang J-D, Presley JB, Chimento MF, Curcio CA. Comparison of morphology of human macular and peripheral Bruch's membrane in older eyes. *Curr Eye Res*. 2007;32:791–799.
36. Verhoeff FH, Sisson RJ. Basophilic staining of Bruch's membrane. *Arch Ophthalmol*. 1926;55:125–127.
37. Streeten BW. The sudanophilic granules of the human retinal pigment epithelium. *Arch Ophthalmol*. 1961;66:391–398.
38. Wolter JR, Falls HF. Bilateral confluent drusen. *Arch Ophthalmol*. 1962;68:219–226.
39. Curcio CA, Johnson M, Huang J-D, Rudolf M. Aging, age-related macular degeneration, and the Response-to-Retention of apolipoprotein B-containing lipoproteins. *Prog Retin Eye Res*. 2009;28(6):393–422.
40. Pikuleva I, Curcio CA. Cholesterol in the retina: the best is yet to come. *Prog Retin Eye Res*. 2014;41:64–89.
41. Bird AC, Marshall J. Retinal pigment epithelial detachments in the elderly. *Trans Ophthalmol Soc U K*. 1986;105:674–682.
42. Pauleikhoff D, Harper CA, Marshall J, Bird AC. Aging changes in Bruch's membrane: a histochemical and morphological study. *Ophthalmology*. 1990;97(2):171–178.
43. Pauleikhoff D, Wojteki S, Muller D, Bornfeld N, Heiligenhaus A. [Adhesive properties of basal membranes of Bruch's membrane. Immunohistochemical studies of age-dependent changes in adhesive molecules and lipid deposits]. *Ophthalmologe*. 2000;97(4):243–250.
44. Haimovici R, Gantz DL, Rumelt S, Freddo TF, Small DM. The lipid composition of drusen, Bruch's membrane, and sclera by hot stage polarizing microscopy. *Invest Ophthalmol Vis Sci*. 2001;42(7):1592–1599.
45. Sheraidah G, Steinmetz R, Maguire J, Pauleikhoff D,

Marshall J, Bird AC. Correlation between lipids extracted from Bruch's membrane and age. *Ophthalmology*. 1993;100:47–51.
46. Holz FG, Sheraidah G, Pauleikhoff D, Bird AC. Analysis of lipid deposits extracted from human macular and peripheral Bruch's membrane. *Arch Ophthalmol*. 1994;112:402–406.
47. Curcio CA, Millican CL, Bailey T, Kruth HS. Accumulation of cholesterol with age in human Bruch's membrane. *Invest Ophthalmol Vis Sci*. 2001;42(1):265–274.
48. Rudolf M, Curcio CA. Esterified cholesterol is highly localized to Bruch's membrane, as revealed by lipid histochemistry in wholemounts of human choroid. *J Histochem Cytochem*. 2009;57(8):731–739.
49. Li CM, Presley JB, Zhang X, et al. Retina expresses microsomal triglyceride transfer protein: implications for age-related maculopathy. *J Lipid Res*. 2005;46(4):628–640.
50. Wang L, Li C-M, Rudolf M, et al. Lipoprotein particles of intra-ocular origin in human Bruch membrane: an unusual lipid profile. *Invest Ophthalmol Vis Sci*. 2009;50:870–877.
51. Wu T, Fujihara M, Tian J, et al. Apolipoprotein B100 secretion by cultured ARPE-19 cells is modulated by alteration of cholesterol levels. *J Neurochem*. 2010;114(6):1734–1744.
52. Ruberti JW, Curcio CA, Millican CL, Menco BP, Huang JD, Johnson M. Quick-freeze/deep-etch visualization of age-related lipid accumulation in Bruch's membrane. *Invest Ophthalmol Vis Sci*. 2003;44(4):1753–1759.
53. Huang J-D, Presley JB, Chimento MF, Curcio CA, Johnson M. Age-related changes in human macular Bruch's membrane as seen by quick-freeze/deep-etch. *Exp Eye Res*. 2007;85(2):202–218.
54. Huang J-D, Curcio CA, Johnson M. Morphometric analysis of lipoprotein-like particle accumulation in aging human macular Bruch's membrane. *Invest Ophthalmol Vis Sci*. 2008;49(6):2721–2727.
55. Li CM, Chung BH, Presley JB, et al. Lipoprotein-like particles and cholesteryl esters in human Bruch's

membrane: initial characterization. *Invest Ophthalmol Vis Sci*. 2005;46(7):2576–2586.
56. Bretillon L, Thuret G, Gregoire S, et al. Lipid and fatty acid profile of the retina, retinal pigment epithelium/choroid, and the lacrimal gland, and associations with adipose tissue fatty acids in human subjects. *Exp Eye Res*. 2008;87(6):521–528.
57. Huang J-D, Presley JB, Chimento MF, Curcio CA, Johnson M. Age-related changes in human macular Bruch's membrane as seen by quick-freeze/deep-etch. *Exp Eye Res*. 2007;85(2):202–218.
58. Ruberti JW, Curcio CA, Millican CL, Menco BP, Huang JD, Johnson M. Quick-freeze/deep-etch visualization of age-related lipid accumulation in Bruch's membrane. *Invest Ophthalmol Vis Sci*. 2003;44(4):1753–1759.
59. Hogan MJ. Role of the retinal pigment epithelium in macular disease. *Trans Am Acad Ophthalmol Otolaryngol*. 1972;76(1):64–80.
60. Fliesler SJ, Anderson RE. Chemistry and metabolism of lipids in the vertebrate retina. *Prog Lipid Res*. 1983;22(2):79–131.
61. Curcio CA, Messinger JD, Sloan KR, McGwin G Jr, Medeiros NE, Spaide RF. Subretinal drusenoid deposits in non-neovascular age-related macular degeneration: morphology, prevalence, topography, and biogenesis model. *Retina*. 2013;33(2):265–276.
62. Johnson LV, Forest DL, Banna CD, et al. Cell culture model that mimics drusen formation and triggers complement activation associated with age-related macular degeneration. *Proc Natl Acad Sci USA*. 2011;108(45):18277–18282.
63. Smith EB. The relationship between plasma and tissue lipids in human atherosclerosis. *Adv Lipid Res*. 1974;12:1–49.
64. Guyton JR, Bocan TMA, Schifani TA. Quantitative ultrastructural analysis of perifibrous lipid and its association with elastin in nonatherosclerotic human aorta. *Arteriosclerosis*. 1985;5:644–652.
65. Gaynor PM, Zhang WY, Salehizadeh B, Pettiford B, Kruth

HS. Cholesterol accumulation in human cornea: evidence that extracellular cholesteryl ester-rich lipid particles deposit independently of foam cells. *J Lipid Res*. 1996;37:1849–1861.
66. Crispin S. Ocular lipid deposition and hyperlipoproteinaemia. *Prog Retin Eye Res*. 2002;21(2):169–224.
67. Kruth HS. The fate of lipoprotein cholesterol entering the arterial wall. *Curr Opin Lipidol*. 1997;8(5):246–252.
68. Williams KJ, Tabas I. The Response-to-Retention hypothesis of atherogenesis reinforced. *Curr Opin Lipidol*. 1998;9(5):471–474.
69. Contois JH, McConnell JP, Sethi AA, et al. Apolipoprotein B and cardiovascular disease risk: position statement from the AACC Lipoproteins and Vascular Diseases Division Working Group on Best Practices. *Clin Chem*. 2009;55(3):407–419.
70. Dashti N, McGwin G Jr, Owsley C, Curcio CA. Plasma apolipoproteins and risk for age-related maculopathy. *Br J Ophthalmol*. 2006;90:1028–1033.
71. Ramrattan RS, van der Schaft TL, Mooy CM, de Bruijn WC, Mulder PGH, de Jong PTVM. Morphometric analysis of Bruch's membrane, the choriocapillaris, and the choroid in aging. *Invest Ophthalmol Vis Sci*. 1994;35:2857–2864.
72. Okubo A, Rosa RH Jr, Bunce CV, et al. The relationships of age changes in retinal pigment epithelium and Bruch's membrane. *Invest Ophthalmol Vis Sci*. 1999;40(2):443–449.
73. Killingsworth MC. Age-related components of Bruch's membrane. *Graefes Arch Clin Exp Ophthalmol*. 1987;225(6):406–412.
74. Karwatowski WSS, Jeffried TE, Duance VC, Albon J, Bailey AJ, Easty DL. Preparation of Bruch's membrane and analysis of the age-related changes in the structural collagens. *Br J Ophthalmol*. 1995;79:944–952.
75. Macgregor AM, Eberhart CG, Fraig M, Lu J, Halushka MK. Tissue inhibitor of matrix metalloproteinase-3 levels in the extracellular matrix of lung, kidney, and eye increase with age. *J Histochem Cytochem*. 2009;57(3):207–213.

76. Qi JH, Ebrahem Q, Moore N, et al. A novel function for tissue inhibitor of metalloproteinases-3 (TIMP3): inhibition of angiogenesis by blockage of VEGF binding to VEGF receptor-2. *Nat Med*. 2003;9(4):407–415.
77. Ebrahem Q, Qi JH, Sugimoto M, et al. Increased neovascularization in mice lacking tissue inhibitor of metalloproteinases-3. *Invest Ophthalmol Vis Sci*. 2011;52(9):6117–6123.
78. Beattie JR, Pawlak AM, Boulton ME, et al. Multiplex analysis of age-related protein and lipid modifications in human Bruch's membrane. *FASEB J*. 2010;24(12):4816–4824.
79. van der Schaft TL, Mooy CM, de Bruijn WC, Oron FG, Mulder PGH, de Jong PTVM. Histologic features of the early stages of age-related macular degeneration. *Ophthalmology*. 1992;99(2):278–286.
80. Hogan MJ, Alvarado JA, Weddell JE. *Histology of the human eye: an atlas and textbook*. WB Saunders: Philadelphia; 1971:328–363.
81. Davis WL, Jones RG, Hagler HK. An electron microscopic histochemical and analytical X-ray microprobe study of calcification in Bruch's membrane from human eyes. *J Histochem Cytochem*. 1981;29(5):601–608.
82. Clark SJ, Higman VA, Mulloy B, et al. His-384 allotypic variant of factor H associated with age-related macular degeneration has different heparin binding properties from the non-disease-associated form. *J Biol Chem*. 2006;281(34):24713–24720.
83. Clark SJ, Bishop PN, Day AJ. Complement factor H and age-related macular degeneration: the role of glycosaminoglycan recognition in disease pathology. *Biochem Soc Trans*. 2010;38(5):1342–1348.
84. Clark SJ, Perveen R, Hakobyan S, et al. Impaired binding of the AMD-associated complement factor H 402H allotype to Bruch's membrane in human retina. *J Biol Chem*. 2010;285(39):30192–30202.
85. Clark SJ, Schmidt CQ, White AM, Hakobyan S, Morgan BP, Bishop PN. Identification of Factor H-like protein 1 as the predominant complement regulator in Bruch's membrane:

implications for age-related macular degeneration. *J Immunol*. 2014;193(10):4962–4970.
86. Keenan TD, Pickford CE, Holley RJ, et al. Age-dependent changes in heparan sulfate in human Bruch's membrane: implications for age-related macular degeneration. *Invest Ophthalmol Vis Sci*. 2014;55(8):5370–5379.
87. Fritsche LG, Fariss RN, Stambolian D, Abecasis G, Curcio CA, Swaroop A. Age-related macular degeneration: genetics and biology coming together. *Annu Rev Genomics Hum Genet*. 2014;15:151–171.
88. Toomey CB, Kelly U, Saban DR, Bowes Rickman C. Regulation of age-related macular degeneration-like pathology by complement factor H. *Proc Natl Acad Sci USA*. 2015;112(23):E3040–9.
89. Colville D, Savige J. Alport syndrome. Review of the ocular manifestations. *Ophthalmic Genet*. 1997;18:161–173.
90. Kim RY, Faktorovich EG, Kuo CY, Olson JL. Retinal function abnormalities in membranoproliferative glomerulonephritis type II. *Am J Ophthalmol*. 1997;123:619–628.
91. Weiner DE, Tighiouart H, Reynolds R, Seddon JM. Kidney function, albuminuria and age-related macular degeneration in NHANES III. *Nephrol Dial Transplant*. 2011;26(10):3159–3165.
92. Maddox DA, Brenner BM. Glomerular filtration of fluid and macromolecules: the renal response to injury. *Annu Rev Med*. 1977;28:91–102.
93. Beers APA, Van Der Heijde GL. In vivo determination of the biomechanical properties of the component elements of the accommodation mechanism. *Vision Res*. 1994;34(21):2897–2905.
94. Charman WN. The eye in focus: accommodation and presbyopia. *Clin Exp Optom*. 2008;91(3):207–225.
95. Chan WH, Hussain AA, Marshall J. Youngs modulus of Bruch's membrane: implications for AMD. *Invest Ophthalmol Vis Sci*. 2007;48(5):2187.
96. Ugarte M, Hussain AA, Marshall J. An experimental study of the elastic properties of the human Bruch's membrane-choroid complex: relevance to ageing. *Br J Ophthalmol*.

2006;90(5):621–626.
97. Tawara A, Varner HH, Hollyfield JG. Proteoglycans in the mouse interphotoreceptor matrix. I. Histochemical studies using cuprolinic blue. *Exp Eye Res*. 1988;46(5):689–704.
98. Hollyfield JG. Hyaluronan and the functional organization of the interphotoreceptor matrix. *Invest Ophthalmol Vis Sci*. 1999;40:2767–2769.
99. Klintworth GK. The cornea: structure and macromolecules in health and disease. A review. *Am J Pathol*. 1977;89(3):718–808.
100. Maurice DM. The structure and transparency of the cornea. *J Physiol*. 1957;136(2):263–286.
101. Hassell JR, Birk DE. The molecular basis of corneal transparency. *Exp Eye Res*. 2010;91(3):326–335.
102. Dohlman CH, Hedbys BO, Mishima S. The swelling pressure of the corneal stroma. *Invest Ophthalmol*. 1962;1:158–162.
103. Wiig H. Cornea fluid dynamics. I: measurement of hydrostatic and colloid osmotic pressure in rabbits. *Exp Eye Res*. 1989;49(6):1015–1030.
104. Moore DJ, Hussain AA, Marshall J. Age-related variation in the hydraulic conductivity of Bruch's membrane. *Invest Ophthalmol Vis Sci*. 1995;36(7):1290–1297.
105. Shimomura Y, Hirata A, Ishikawa S, Okinami S. Changes in choriocapillaris fenestration of rat eyes after intravitreal bevacizumab injection. *Graefes Arch Clin Exp Ophthalmol*. 2009;247(8):1089–1094.
106. Levick JR, Smaje LH. An analysis of the permeability of a fenestra. *Microvasc Res*. 1987;33:233–256.
107. Emi K, Pederson JE, Toris CB. Hydrostatic pressure of the suprachoroidal space. *Invest Ophthalmol Vis Sci*. 1989;30:233.
108. Navar PD, Navar LG. Relationship between colloid osmotic pressure and plasma protein concentration in the dog. *Am J Physiol*. 1977;233(2):H295–8.
109. Maepea O. Pressures in the anterior ciliary arteries, choroidal veins and choriocapillaris. *Exp Eye Res*. 1992;54(5):731–736.
110. Starita C, Hussain AA, Patmore A, Marshall J. Localization

of the site of major resistance to fluid transport in Bruch's membrane. *Invest Ophthalmol Vis Sci*. 1997;38(3):762–767.
111. Overby D, Johnson M. Studies of depth-of-field effects in microscopy supported by numerical simulations. *J Microsc*. 2005;220(3):176–189.
112. Fisher RF. The influence of age on some ocular basement membranes. *Eye (Lond)*. 1987;1(Pt 2):184–189.
113. Daniels BS, Hauser EB, Deen WN, Hostetter TH. Glomerular basement membrane: in vitro studies of water and protein permeability. *Am J Physiol*. 1992;262:F919–26.
114. Renkin EM. Multiple pathways of capillary permeability. *Circ Res*. 1977;41:735–743.
115. Hussain AA, Starita C, Marshall J. Transport characteristics of ageing human Bruch's membrane: implications for age-related macular degeneration (AMD). Ioseliani OR. *Focus on macular degeneration research*. Nova Biomedical Books: Hauppauge, NY; 2004.
116. Starita C, Hussain AA, Pagliarini S, Marshall J. Hydrodynamics of ageing Bruch's membrane: implications for macular disease. *Exp Eye Res*. 1996;62(5):565–572.
117. McCarty WJ, Chimento MF, Curcio CA, Johnson M. Effects of particulates and lipids on the hydraulic conductivity of Matrigel. *J Appl Physiol*. 2008;105(8):621–628.
118. Ethier CR, Johnson M, Ruberti J. Ocular biomechanics and biotransport. *Annu Rev Biomed Eng*. 2004;6:249–273.
119. Holz FG, Piguet B, Minassian DC, Bird AC, Weale RA. Decreasing stromal iris pigmentation as a risk factor for age-related macular degeneration. *Am J Ophthalmol*. 1994;117(1):19–23.
120. Lyda W, Eriksen N, Krishna N. Studies of Bruch's membrane; flow and permeability studies in a Bruch's membrane-choroid preparation. *Am J Ophthalmol*. 1957;44(5 Pt 2):362–369 [discussion 9-70].
121. Moore DJ, Hussain AA, Marshall J. Age-related variation in the hydraulic conductivity of Bruch's membrane. *Invest Ophthalmol Vis Sci*. 1995;36:1290–1297.
122. Hillenkamp J, Hussain AA, Jackson TL, Cunningham JR, Marshall J. The influence of path length and matrix

components on ageing characteristics of transport between the choroid and outer retina. *Invest Ophthalmol Vis Sci*. 2004;45(5):1493–1498.
123. Cankova Z, Huang JD, Kruth HS, Johnson M. Passage of low-density lipoproteins through Bruch's membrane and choroid. *Exp Eye Res*. 2011;93(6):947–955.
124. Truskey GA, Yuan F, Katz DF. *Transport phenomena in biological systems*. Pearson Prentice Hall: Upper Saddle River, NJ; 2004.
125. Fisher WR, Granade ME, Mauldin JL. Hydrodynamic studies of human low density lipoproteins. Evaluation of the diffusion coefficient and the preferential hydration. *Biochemistry*. 1971;10(9):1622–1629.
126. Zayas-Santiago A, Marmorstein AD, Marmorstein LY. Relationship of stokes radius to the rate of diffusion across Bruch's membrane. *Invest Ophthalmol Vis Sci*. 2011;52(7):4907–4913.
127. Hussain AA, Rowe L, Marshall J. Age-related alterations in the diffusional transport of amino acids across the human Bruch's-choroid complex. *J Opt Soc Am A*. 2002;19:166–172.
128. Moore DJ, Clover GM. The effect of age on the macromolecular permeability of human Bruch's membrane. *Invest Ophthalmol Vis Sci*. 2001;42:2970–2975.
129. Cheruvu NP, Kompella UB. Bovine and porcine transscleral solute transport: influence of lipophilicity and the choroid–Bruch's layer. *Invest Ophthalmol Vis Sci*. 2006;47(10):4513–4522.
130. Cankova Z, Huang J-D, Kruth H, Johnson M. Passage of low-density lipoproteins through Bruch's membrane and choroid. *Exp Eye Res*. 2011;93(6):947–955.
131. Pedley TJ. Calculation of unstirred layer thickness in membrane transport experiments: a survey. *Q Rev Biophys*. 1983;16(2):115–150.
132. Hussain AA, Starita C, Hodgetts A, Marshall J. Macromolecular diffusion characteristics of ageing human Bruch's membrane: implications for age-related macular degeneration (AMD). *Exp Eye Res*. 2010;90(6):703–710.
133. Yang N, Vafai K. Modeling of low-density lipoprotein

(LDL) transport in the artery - effects of hypertension. *Int J Heat Mass Transfer*. 2006;49:850–867.
134. Elner VM. Retinal pigment epithelial acid lipase activity and lipoprotein receptors: effects of dietary omega-3 fatty acids. *Trans Am Ophthalmol Soc*. 2002;100:301–338.
135. Gordiyenko N, Campos M, Lee JW, Fariss RN, Sztein J, Rodriguez IR. RPE cells internalize low-density lipoprotein (LDL) and oxidized LDL (oxLDL) in large quantities in vitro and in vivo. *Invest Ophthalmol Vis Sci*. 2004;45(8):2822–2829.
136. Tserentsoodol N, Sztein J, Campos M, et al. Uptake of cholesterol by the retina occurs primarily via a low density lipoprotein receptor-mediated process. *Mol Vis*. 2006;12:1306–1318.
137. Martidis A, Duker JS, Greenberg PB, et al. Intravitreal triamcinolone for refractory diabetic macular edema. *Ophthalmology*. 2002;109(5):920–927.
138. Anderson OA, Bainbridge JW, Shima DT. Delivery of anti-angiogenic molecular therapies for retinal disease. *Drug Discov Today*. 2010;15(7–8):272–282.
139. Pitkanen L, Ranta VP, Moilanen H, Urtti A. Permeability of retinal pigment epithelium: effects of permeant molecular weight and lipophilicity. *Invest Ophthalmol Vis Sci*. 2005;46(2):641–646.
140. Lovich MA, Creel C, Hong K, Hwang CW, Edelman ER. Carrier proteins determine local pharmacokinetics and arterial distribution of paclitaxel. *J Pharm Sci*. 2001;90(9):1324–1335.
141. Jackson GR, Curcio CA, Sloan KR, Owsley C. Photoreceptor degeneration in aging and age-related maculopathy. Penfold PL, Provis JM. *Macular degeneration*. Springer-Verlag: Berlin; 2005:45–62.
142. Jackson GR, Owsley C, McGwin G. Aging and dark adaptation. *Vision Res*. 1999;39:3975–3982.
143. Owsley C, McGwin G Jr, Jackson GR, Kallies K, Clark M. Cone- and rod-mediated dark adaptation impairment in age-related maculopathy. *Ophthalmology*. 2007;114(9):1728–1735.

144. Steinmetz RL, Haimovici R, Jubb C, Fitzke FW, Bird AC. Symptomatic abnormalities of dark adaptation in patients with age-related Bruch's membrane change. *Br J Ophthalmol*. 1993;77:549–554.
145. Owsley C, McGwin G Jr, Jackson GR, et al. Effect of short-term, high-dose retinol on dark adaptation in aging and early age-related maculopathy. *Invest Ophthalmol Vis Sci*. 2006;47(4):1310–1318.
146. Owsley C, Huisingh C, Jackson GR, et al. Associations between abnormal rod-mediated dark adaptation and health and functioning in older adults in normal macular health. *Invest Ophthalmol Vis Sci*. 2014;55(8):4776–4789.
147. Owsley C, McGwin G Jr, Clark ME, et al. Delayed rod-mediated dark adaptation is a functional biomarker for incident early age-related macular degeneration. *Ophthalmology*. 2016;123(2):344–351.
148. Green WR, Enger C. Age-related macular degeneration histopathologic studies: the 1992 Lorenz E. Zimmerman Lecture. *Ophthalmology*. 1993;100(10):1519–1535.
149. Zweifel SA, Spaide RF, Curcio CA, Malek G, Imamura Y. Reticular pseudodrusen are subretinal drusenoid deposits. *Ophthalmology*. 2010;117(2):303–312.e.1.
150. Arnold JJ, Sarks SH, Killingsworth MC, Sarks JP. Reticular pseudodrusen: a risk factor in age-related maculopathy. *Retina*. 1995;15(3):183–191.
151. Khanifar AA, Koreishi AF, Izatt JA, Toth CA. Drusen ultrastructure imaging with spectral domain optical coherence tomography in age-related macular degeneration. *Ophthalmology*. 2008;115(11):1883–1890.
152. Spaide RF, Curcio CA. Drusen characterization with multimodal imaging. *Retina*. 2010;30(9):1441–1454.
153. Ouyang Y, Heussen FM, Hariri A, Keane PA, Sadda SR. Optical coherence tomography-based observation of the natural history of drusenoid lesion in eyes with dry age-related macular degeneration. *Ophthalmology*. 2013;120(12):2656–2665.
154. Klein R, Klein BE, Linton KL. Prevalence of age-related maculopathy. The Beaver Dam Eye Study. *Ophthalmology*.

1992;99(6):933–943.
155. Friedman E, van Buskirk EM, Fineberg E, Messner K, Schinazi H. Pathogenesis of senile disciform degeneration of the macula. Elsevier: XXI Concilium Ophthalmologicum Mexico; 1971:454–458. *I.* .
156. Lengyel I, Tufail A, Hosaini HA, Luthert P, Bird AC, Jeffery G. Association of drusen deposition with choroidal intercapillary pillars in the aging human eye. *Invest Ophthalmol Vis Sci*. 2004;45(9):2886–2892.
157. Rudolf M, Clark ME, Chimento M, Li C-M, Medeiros NE, Curcio CA. Prevalence and morphology of druse types in the macula and periphery of eyes with age-related maculopathy. *Invest Ophthalmol Vis Sci*. 2008;49(3):1200–1209.
158. Querques G, Guigui B, Leveziel N, et al. Insights into pathology of cuticular drusen from integrated confocal scanning laser ophthalmoscopy imaging and corresponding spectral domain optical coherence tomography. *Graefes Arch Clin Exp Ophthalmol*. 2011;249(11):1617–1625.
159. Sarks SH. Council Lecture: Drusen and their relationship to senile macular degeneration. *Aust J Ophthalmol*. 1980;8(2):117–130.
160. Klein R, Davis MD, Magli YL, Segal P, Klein BEK, Hubbard L. The Wisconsin Age-Related Maculopathy Grading System. *Ophthalmology*. 1991;98:1128–1134.
161. Davis MD, Gangnon RE, Lee LY, et al. The Age-Related Eye Disease Study severity scale for age-related macular degeneration: AREDS Report No. 17. *Arch Ophthalmol*. 2005;123(11):1484–1498.
162. Klein R, Klein BE, Knudtson MD, Meuer SM, Swift M, Gangnon RE. Fifteen-year cumulative incidence of age-related macular degeneration: the Beaver Dam Eye Study. *Ophthalmology*. 2007;114(2):253–262.
163. Farkas TG, Sylvester V, Archer D. The ultrastructure of drusen. *Am J Ophthalmol*. 1971;71(6):1196–1205.
164. Sarks JP, Sarks SH, Killingsworth MC. Evolution of soft drusen in age-related macular degeneration. *Eye (Lond)*. 1994;8:269–283.

165. Donders F. Beitrage zur pathologischen Anatomie des Auges. *Arch Ophthalmologie*. 1854;1:106–118.
166. Hageman GS, Mullins RF. Molecular composition of drusen as related to substructural phenotype. *Mol Vis*. 1999;5:28–37.
167. Müller H. Anatomische Beiträge zur Ophthalmologie. *Graefes Arch Klin Exp Ophthalmol*. 1856;2(2):1–69.
168. Oatman EL. *Diagnostics of the fundus oculi*. The Southworth Company: Troy, NY; 1913.
169. Holloway TB, Verhoeff FH. Disc-like degeneration of the macula with microscopic report concerning a tumor-like mass in the macular region. *Trans Am Ophthalmol Soc*. 1928;26:206–228.
170. Lauber H. The origin of hyaline formations within the eye. *Ber ü d deutsch ophth Gesellsch*. 1924;44:216.
171. Rones B. Formation of drusen of the lamina vitrea. *Arch Ophthalmol*. 1937;18:288–402.
172. Green WR, Key SN 3rd. Senile macular degeneration: a histopathologic study. *Trans Am Ophthalmol Soc*. 1977;75:180–254.
173. Dentchev T, Milam AH, Lee VM, Trojanowski JQ, Dunaief JL. Amyloid-beta is found in drusen from some age-related macular degeneration retinas, but not in drusen from normal retinas. *Mol Vis*. 2003;9:184–190.
174. Malek G, Li C-M, Guidry C, Medeiros NE, Curcio CA. Apolipoprotein B in cholesterol-containing drusen and basal deposits in eyes with age-related maculopathy. *Am J Pathol*. 2003;162(2):413–425.
175. Rudolf M, Malek G, Messinger JD, Wang L, Clark ME, Curcio CA. Sub-retinal drusenoid deposits in human retina: organization and composition. *Exp Eye Res*. 2008;87(11):402–408.
176. Curcio CA, Johnson M, Rudolf M, Huang J-D. The oil spill in ageing Bruch's membrane. *Br J Ophthalmol*. 2011;95(12):1638–1645.
177. Jiang K, To E, Cui JZ, Cao S, Gao J, Matsubara JA. Drusen and pro-inflammatory mediators in the post-mortem human eye. *J Clin Exp Ophthalmol*. 2012;3:208.
178. Johnson LV, Forest DL, Banna CD, et al. Cell culture model

that mimics drusen formation and triggers complement activation associated with age-related macular degeneration. *Proc Natl Acad Sci USA*. 2011;108(45):18277–18282.
179. Zheng W, Reem R, Omarova S, et al. Spatial distribution of the pathways of cholesterol homeostasis in human retina. *PLoS ONE*. 2012;7(5):e37926.
180. Li M, Jia C, Kazmierkiewicz KL, et al. Comprehensive analysis of gene expression in human retina and supporting tissues. *Hum Mol Genet*. 2014;23(15):4001–4014.
181. Mullins RF, Hageman GS. Human ocular drusen possess novel core domains with a distinct carbohydrate composition. *J Histochem Cytochem*. 1999;47(12):1533–1539.
182. Li C-M, Clark M, Rudolf M, Curcio CA. Distribution and composition of esterified and unesterified cholesterol in extra-macular drusen. *Exp Eye Res*. 2007;85(2):192–201.
183. Lengyel I, Flinn JM, Peto T, et al. High concentration of zinc in sub-retinal pigment epithelial deposits. *Exp Eye Res*. 2007;84(4):772–780.
184. Pauleikhoff D, Zuels S, Sheraidah GS, Marshall J, Wessing A, Bird AC. Correlation between biochemical composition and fluorescein binding of deposits in Bruch's membrane. *Ophthalmology*. 1992;99(10):1548–1553.
185. Rodriguez IR, Clark ME, Lee JW, Curcio CA. 7-ketocholesterol accumulates in ocular tissues as a consequence of aging and is present in high levels in drusen. *Exp Eye Res*. 2014;128:151–155.
186. Wang L, Clark ME, Crossman DK, et al. Abundant lipid and protein components of drusen. *PLoS ONE*. 2010;5(4):e10329.
187. Guyton JR, Klemp KF. The lipid-rich core region of human atherosclerotic fibrous plaques. Prevalence of small lipid droplets and vesicles by electron microscopy. *Am J Pathol*. 1989;134:705–717.
188. Klaver CC, Kliffen M, van Duijn CM, et al. Genetic association of apolipoprotein E with age-related macular degeneration. *Am J Hum Genet*. 1998;63(1):200–206.
189. Anderson DH, Ozaki S, Nealon M, et al. Local cellular sources of apolipoprotein E in the human retina and retinal

pigmented epithelium: implications for the process of drusen formation. *Am J Ophthalmol*. 2001;131:767–781.
190. Li C-M, Chung BH, Presley JB, et al. Lipoprotein-like particles and cholesteryl esters in human Bruch's membrane: initial characterization. *Invest Ophthalmol Vis Sci*. 2005;46(7):2576–2586.
191. Li C-M, Clark ME, Chimento MF, Curcio CA. Apolipoprotein localization in isolated drusen and retinal apolipoprotein gene expression. *Invest Ophthalmol Vis Sci*. 2006;47:3119–3128.
192. Friedman DA, Parker JS, Kimble JA, Delori FC, McGwin G Jr, Curcio CA. Quantification of fluorescein localization in drusen associated with age-related macular degeneration. *Retina*. 2012;32(1):19–24.
193. Johnson LV, Leitner WP, Rivest AJ, Staples MK, Radeke MJ, Anderson DH. The Alzheimer's Aβ-peptide is deposited at sites of complement activation in pathologic deposits associated with aging and age-related macular degeneration. *Proc Natl Acad Sci USA*. 2002;99(18):11830–11835.
194. Anderson DH, Talaga KC, Rivest AJ, Barron E, Hageman GS, Johnson LV. Characterization of beta amyloid assemblies in drusen: the deposits associated with aging and age-related macular degeneration. *Exp Eye Res*. 2004;78(2):243–256.
195. Isas JM, Luibl V, Johnson LV, et al. Soluble and mature amyloid fibrils in drusen deposits. *Invest Ophthalmol Vis Sci*. 2010;51(3):1304–1310.
196. Leger F, Fernagut PO, Canron MH, et al. Protein aggregation in the aging retina. *J Neuropathol Exp Neurol*. 2011;70(1):63–68.
197. Hageman GS, Mullins RG, Russell SR, Johnson LV, Anderson DH. Vitronectin is a constituent of ocular drusen and the vitronectin gene is expressed in human retinal pigmented epithelial cells. *FASEB J*. 1999;13:477–484.
198. Fariss RN, Apte SS, Olsen BR, Iwata K, Milam AH. Tissue inhibitor of metalloproteinases-3 is a component of Bruch's membrane of the eye. *Am J Pathol*. 1997;150:323–328.

199. Hageman GS, Anderson DH, Johnson LV, et al. A common haplotype in the complement regulatory gene factor H (HF1/CFH) predisposes individuals to age-related macular degeneration. *Proc Natl Acad Sci USA*. 2005;102:7227–7232.
200. Luibl V, Isas JM, Kayed R, Glabe CG, Langen R, Chen J. Drusen deposits associated with aging and age-related macular degeneration contain nonfibrillar amyloid oligomers. *J Clin Invest*. 2006;116(2):378–385.
201. Nakata K, Crabb JW, Hollyfield JG. Crystallin distribution in Bruch's membrane-choroid complex from AMD and age-matched donor eyes. *Exp Eye Res*. 2005;80(6):821–826.
202. Crabb JW, Miyagi M, Gu X, et al. Drusen proteome analysis: an approach to the etiology of age-related macular degeneration. *Proc Natl Acad Sci USA*. 2002;99(23):14682–14687.
203. Sarks JP, Sarks SH, Killingsworth MC. Evolution of geographic atrophy of the retinal pigment epithelium. *Eye (Lond)*. 1988;2:552–577.
204. Sarks S, Cherepanoff S, Killingsworth M, Sarks J. Relationship of basal laminar deposit and membranous debris to the clinical presentation of early age-related macular degeneration. *Invest Ophthalmol Vis Sci*. 2007;48(3):968–977.
205. Curcio CA, Presley JB, Malek G, Medeiros NE, Avery DV, Kruth HS. Esterified and unesterified cholesterol in drusen and basal deposits of eyes with age-related maculopathy. *Exp Eye Res*. 2005;81(6):731–741.
206. Curcio CA, Presley JB, Millican CL, Medeiros NE. Basal deposits and drusen in eyes with age-related maculopathy: evidence for solid lipid particles. *Exp Eye Res*. 2005;80(6):761–775.
207. Klein ML, Ferris FL 3rd, Armstrong J, et al. Retinal precursors and the development of geographic atrophy in age-related macular degeneration. *Ophthalmology*. 2008;115(6):1026–1031.
208. Suzuki M, Curcio CA, Mullins RF, Spaide RF. Refractile drusen: clinical imaging and candidate histology. *Retina*. 2015;35(5):859–865.

209. Gass JDM. Pathogenesis of disciform detachment of the neuroepithelium. III. Senile disciform macular degeneration. *Am J Ophthalmol*. 1967;63:617–644.
210. Bressler NM, Silva JC, Bressler SB, Fine SL, Green WR. Clinicopathological correlation of drusen and retinal pigment epithelial abnormalities in age-related macular degeneration. *Retina*. 1994;14(2):130–142.
211. Curcio CA, Medeiros NE, Millican CL. The Alabama age-related macular degeneration grading system for donor eyes. *Invest Ophthalmol Vis Sci*. 1998;39(7):1085–1096.
212. Ooto S, Vongkulsiri S, Sato T, Suzuki M, Curcio CA, Spaide RF. Outer retinal corrugations in age-related macular degeneration. *JAMA Ophthalmol*. 2014;132(7):806–813.
213. Ulshafer RJ, Allen CB, Nicolaissen B Jr, Rubin ML. Scanning electron microscopy of human drusen. *Invest Ophthalmol Vis Sci*. 1987;28(4):683–689.
214. van der Schaft TL, de Bruijn WC, Mooy CM, Ketelaars DA, de Jong PT. Element analysis of the early stages of age-related macular degeneration. *Arch Ophthalmol*. 1992;110(3):389–394.
215. Thompson RB, Reffatto V, Bundy JG, et al. Identification of hydroxyapatite spherules provides new insight into subretinal pigment epithelial deposit formation in the aging eye. *Proc Natl Acad Sci USA*. 2015;112(5):1565–1570.
216. Curcio CA, Millican CL. Basal linear deposit and large drusen are specific for early age-related maculopathy. *Arch Ophthalmol*. 1999;117(3):329–339.
217. Messinger JD, Johnson M, Medeiros NE, Curcio CA. Transition from Lipid Wall to basal linear deposit in age-related maculopathy (ARM). *Invest Ophthalmol Vis Sci*. 2009;50:4933.
218. Lommatzsch A, Hermans P, Muller KD, Bornfeld N, Bird AC, Pauleikhoff D. Are low inflammatory reactions involved in exudative age-related macular degeneration? Morphological and immunhistochemical analysis of AMD associated with basal deposits. *Graefes Arch Clin Exp Ophthalmol*. 2008;246(6):803–810.
219. Yamada Y, Ishibashi K, Ishibashi K, et al. The expression of

advanced glycation endproduct receptors in RPE cells associated with basal deposits in human maculas. *Exp Eye Res*. 2006;82(5):840–848.
220. Löffler KU, Lee WR. Basal linear deposit in the human macula. *Graefes Arch Clin Exp Ophthalmol*. 1986;224:493–501.
221. Marshall GE, Konstas AGP, Reid GG, Edwards JG, Lee WR. Type IV collagen and laminin in Bruch's membrane and basal linear deposit in the human macula. *Br J Ophthalmol*. 1992;76:607–614.
222. Knupp C, Munro PM, Luther PK, Ezra E, Squire JM. Structure of abnormal molecular assemblies (collagen VI) associated with human full thickness macular holes. *J Struct Biol*. 2000;129(1):38–47.
223. Reale E, Groos S, Eckardt U, Eckardt C, Luciano L. New components of 'basal laminar deposits' in age-related macular degeneration. *Cells Tissues Organs*. 2008;190(3):170–181.
224. Marmorstein LY, McLaughlin PJ, Peachey NS, Sasaki T, Marmorstein AD. Formation and progression of sub-retinal pigment epithelium deposits in Efemp1 mutation knock-in mice: a model for the early pathogenic course of macular degeneration. *Hum Mol Genet*. 2007;16(20):2423–2432.
225. Garland DL, Fernandez-Godino R, Kaur I, et al. Mouse genetics and proteomic analyses demonstrate a critical role for complement in a model of DHRD/ML, an inherited macular degeneration. *Hum Mol Genet*. 2014;23(1):52–68.
226. Mimoun G, Soubrane G, Coscas G. Macular drusen. *J Fr Ophtalmol*. 1990;13(10):511–530.
227. Zweifel SA, Imamura Y, Spaide TC, Fujiwara T, Spaide RF. Prevalence and significance of subretinal drusenoid deposits (reticular pseudodrusen) in age-related macular degeneration. *Ophthalmology*. 2010;117(9):1775–1781.
228. Schmitz-Valckenberg S, Alten F, Steinberg JS, et al. Reticular drusen associated with geographic atrophy in age-related macular degeneration. *Invest Ophthalmol Vis Sci*. 2011;52:5009–5015.
229. Zarubina AV, Neely D, Clark ME, et al. Prevalence of subretinal drusenoid deposits in older persons with and

without age-related macular degeneration, by multimodal imaging. *Ophthalmology*. 2016;123(5):1090–1100.
230. Zweifel SA, Imamura Y, Freund KB, Spaide RF. Multimodal fundus imaging of pseudoxanthoma elasticum. *Retina*. 2011;31(3):482–491.
231. Schatz P, Preising M, Lorenz B, et al. Lack of autofluorescence in fundus albipunctatus associated with mutations in RDH5. *Retina*. 2010;30(10):1704–1713.
232. Gliem M, Muller PL, Mangold E, et al. Reticular pseudodrusen in Sorsby fundus dystrophy. *Ophthalmology*. 2015;122(8):1555–1562.
233. Sarks J, Arnold J, Ho IV, Sarks S, Killingsworth M. Evolution of reticular pseudodrusen. *Br J Ophthalmol*. 2011;95(7):979–985.
234. Mrejen S, Sato T, Curcio CA, Spaide RF. Assessing the cone photoreceptor mosaic in eyes with pseudodrusen and soft drusen in vivo using adaptive optics imaging. *Ophthalmology*. 2014;121(2):545–551.
235. Zhang Y, Wang X, Blanco E, et al. Photoreceptor perturbation around subretinal drusenoid deposits revealed by adaptive optics scanning laser ophthalmoscopy. *Am J Ophthalmol*. 2014;158(3):584–596.e1.
236. Oak ASW, Messinger JD, Curcio CA. Subretinal drusenoid deposits: further characterization by lipid histochemistry. *Retina*. 2014;34(4):825–826.
237. Klein R, Meuer SM, Knudtson MD, Iyengar SK, Klein BE. The epidemiology of retinal reticular drusen. *Am J Ophthalmol*. 2007;145(2):317–326.
238. Smith RT, Sohrab MA, Busuioc M, Barile G. Reticular macular disease. *Am J Ophthalmol*. 2009;148(5):733–743.e2.
239. Schmitz-Valckenberg S, Steinberg JS, Fleckenstein M, Visvalingam S, Brinkmann CK, Holz FG. Combined confocal scanning laser ophthalmoscopy and spectral-domain optical coherence tomography imaging of reticular drusen associated with age-related macular degeneration. *Ophthalmology*. 2010;117(6):1169–1176.
240. Curcio CA, Sloan KR, Kalina RE, Hendrickson AE. Human photoreceptor topography. *J Comp Neurol*. 1990;292(4):497–

523.
241. Albert AD, Boesze-Battaglia K. The role of cholesterol in rod outer segment membranes. *Prog Lipid Res*. 2005;44(2–3):99–124.
242. Verhoeff FH, Grossman HP. The pathogenesis of disciform degeneration of the macula. *Trans Am Ophthalmol Soc*. 1937;35:262–294.
243. Friedman E. The role of the atherosclerotic process in the pathogenesis of age-related macular degeneration. *Am J Ophthalmol*. 2000;130(5):658–663.
244. Williams KJ, Tabas I. The response-to-retention hypothesis of early atherogenesis. *Arterioscler Thromb Vasc Biol*. 1995;15(5):551–561.
245. Tabas I, Williams KJ, Boren J. Subendothelial lipoprotein retention as the initiating process in atherosclerosis: update and therapeutic implications. *Circulation*. 2007;116(16):1832–1844.
246. Curcio CA. Mice with cholesterol in Bruch's membrane: have we arrived? *Invest Ophthalmol Vis Sci*. 2014;55(11):7296.
247. Grossniklaus HE, Green WR. Choroidal neovascularization. *Am J Ophthalmol*. 2004;137(3):496–503.
248. Yannuzzi LA, Freund KB, Takahashi BS. Review of retinal angiomatous proliferation or type 3 neovascularization. *Retina*. 2008;28(3):375–384.
249. Klein ML, Wilson DJ. Clinicopathologic correlation of choroidal and retinal neovascular lesions in age-related macular degeneration. *Am J Ophthalmol*. 2011;151(1):161–169.
250. Schwesinger C, Yee C, Rohan RM, et al. Intrachoroidal neovascularization in transgenic mice overexpressing vascular endothelial growth factor in the retinal pigment epithelium. *Am J Pathol*. 2001;158(3):1161–1172.
251. Spraul CW, Grossniklaus HE. Characteristics of drusen and Bruch's membrane in postmortem eyes with age-related macular degeneration. *Arch Ophthalmol*. 1997;115(2):267–273.
252. Vogt SD, Curcio CA, Wang L, et al. Retinal pigment epithelial expression of complement regulator CD46 is

altered early in the course of geographic atrophy. *Exp Eye Res*. 2011;93(4):413–423.
253. Sarks JP, Sarks SH, Killingsworth MC. Morphology of early choroidal neovascularization in age-related macular degeneration: correlation with activity. *Eye (Lond)*. 1997;11:515–522.
254. Spaide RF, Armstrong D, Browne R. Continuing medical education review: choroidal neovascularization in age-related macular degeneration –what is the cause? *Retina*. 2003;23(5):595–614.
255. Ueda-Arakawa N, Ooto S, Nakata I, et al. Prevalence and genomic association of reticular pseudodrusen in age-related macular degeneration. *Am J Ophthalmol*. 2012;155(2):260–269.e2.
256. Querques G, Souied EH, Freund KB. How has high-resolution multimodal imaging refined our understanding of the vasogenic process in type 3 neovascularization? *Retina*. 2015;35(4):603–613.
257. Jampol LM, Acheson R, Eagle RC, Serjeant G, O'Grady R. Calcification of Bruch's membrane in angioid streaks with homozygous sickle cell disease. *Arch Ophthalmol*. 1987;105:93–98.
258. Bergen AA, Plomp AS, Schuurman EJ, et al. Mutations in ABCC6 cause pseudoxanthoma elasticum. *Nat Genet*. 2000;25(2):228–231.
259. Le Saux O, Martin L, Aherrahrou Z, Leftheriotis G, Varadi A, Brampton CN. The molecular and physiological roles of ABCC6: more than meets the eye. *Front Genet*. 2012;3:289.
260. Runge P, Muller DP, McAllister J, Calver D, Lloyd JK, Taylor D. Oral vitamin E supplements can prevent the retinopathy of abetalipoproteinaemia. *Br J Ophthalmol*. 1986;70(3):166–173.
261. Duker JS, Belmont J, Bosley TM. Angioid streaks associated with abetalipoproteinemia. Case report. *Arch Ophthalmol*. 1987;105(9):1173–1174.
262. Dieckert J, White M, Christmann L, Lambert HM. Angioid streaks associated with abetalipoproteinemia. *Ann Ophthalmol*. 1989;21:172–175.

263. Gorin MB, Paul TO, Rader DJ. Angioid streaks associated with abetalipoproteinemia. *Ophthalmic Genet*. 1994;15(3–4):151–159.
264. Chowers I, Banin E, Merin S, Cooper M, Granot E. Long-term assessment of combined vitamin A and E treatment for the prevention of retinal degeneration in abetalipoproteinaemia and hypobetalipoproteinaemia patients. *Eye (Lond)*. 2001;15(Pt 4):525–530.
265. Li C-M, Presley JB, Zhang X, et al. Retina expresses microsomal triglyceride transfer protein: implications for age-related maculopathy. *J Lipid Res*. 2005;46:628–640.
266. Weber BHF, Vogt G, Pruett RC, Stöhr H, Felbor U. Mutations in the tissue inhibitor of metalloproteinases-3 (TIMP3) in patients with Sorsby's fundus dystrophy. *Nat Genet*. 1994;8:352–365.
267. Hayward C, Shu X, Cideciyan AV, et al. Mutation in a short-chain collagen gene, CTRP5, results in extracellular deposit formation in late-onset retinal degeneration: a genetic model for age-related macular degeneration. *Hum Mol Genet*. 2003;12(20):2657–2667.
268. Stone E, Lotery A, Munier F, et al. A single EFEMP1 mutation associated with both Leventinese and Doyne honeycomb retinal dystrophy. *Nat Genet*. 1999;22(2):199–202.
269. Jacobson SG, Cideciyan AV, Regunath G, et al. Night blindness in Sorsby's fundus dystrophy reversed by vitamin A. *Nat Genet*. 1995;11(1):27–32.
270. Jacobson SG, Cideciyan AV, Wright E, Wright AF. Phenotypic marker for early disease detection in dominant late-onset retinal degeneration. *Invest Ophthalmol Vis Sci*. 2001;42(8):1882–1890.
271. Michaelides M, Jenkins SA, Brantley MA Jr, et al. Maculopathy due to the R345W substitution in fibulin-3: distinct clinical features, disease variability, and extent of retinal dysfunction. *Invest Ophthalmol Vis Sci*. 2006;47(7):3085–3097.
272. Isashiki Y, Tabata Y, Kamimura K, Ohba N. Sorsby's fundus dystrophy in two Japanese families with unusual clinical

features. *Jpn J Ophthalmol*. 1999;43(6):472–480.
273. Sohn EH, Wang K, Thompson S, et al. Comparison of drusen and modifying genes in autosomal dominant radial drusen and age-related macular degeneration. *Retina*. 2015;35(1):48–57.
274. Capon MRC, Marshall J, Krafft JI, Alexander RA, Hiscott PS, Bird AC. Sorsby's fundus dystrophy: a light and electron microscopic study. *Ophthalmology*. 1989;96(12):1769–1777.
275. Kuntz CA, Jacobson SG, Cideciyan AV, et al. Sub-retinal pigment epithelial deposits in a dominant late-onset retinal degeneration. *Invest Ophthalmol Vis Sci*. 1996;37(9):1772–1782.
276. Milam AH, Curcio CA, Cideciyan AV, et al. Dominant late-onset retinal degeneration with regional variation of sub-RPE deposits, retinal function, and photoreceptor degeneration. *Ophthalmology*. 2000;107:2256–2266.
277. Curcio CA, Mayne R, Ninomiya H. *Localization of type IV collagen chains in AMD eyes*. 1999 [Unpublished].
278. Knupp C, Chong NH, Munro PM, Luthert PJ, Squire JM. Analysis of the collagen VI assemblies associated with Sorsby's fundus dystrophy. *J Struct Biol*. 2002;137(1–2):31–40.
279. Bhutto IA, Kim SY, McLeod DS, et al. Localization of collagen XVIII and the endostatin portion of collagen XVIII in aged human control eyes and eyes with age-related macular degeneration. *Invest Ophthalmol Vis Sci*. 2004;45(5):1544–1552.
280. Marmorstein LY, Munier FL, Arsenijevic Y, et al. Aberrant accumulation of EFEMP1 underlies drusen formation in Malattia Leventinese and age-related macular degeneration. *Proc Natl Acad Sci USA*. 2002;99(20):13067–13072.
281. Das A, Frank RN, Zhang NL, Turczyn TJ. Ultrastructural localization of extracellular matrix components in human retinal vessels and Bruch's membrane. *Arch Ophthalmol*. 1990;108:421–429.
282. Lin WL, Essner E, McCarthy KJ, Couchman JR. Ultrastructural immunocytochemical localization of chondroitin sulfate proteoglycan in Bruch's membrane of

the rat. *Invest Ophthalmol Vis Sci*. 1992;33:2072–2075.
283. Curcio C, Millican C, Kruth H. Cholesterol accumulates with age in human Bruch's membrane. *Invest Ophthalmol Vis Sci*. 2000;41:S115.
284. Liu A, Chang J, Lin Y, Shen Z, Bernstein PS. Long-chain and very long-chain polyunsaturated fatty acids in ocular aging and age-related macular degeneration. *J Lipid Res*. 2011;51:3217–3229.
285. Wang L, Li C-M, Rudolf M, et al. Lipoprotein particles of intra-ocular origin in human Bruch membrane: an unusual lipid profile. *Invest Ophthalmol Vis Sci*. 2009;50:870–877.
286. Tezel TH, Geng L, Lato EB, et al. Synthesis and secretion of hemoglobin by retinal pigment epithelium. *Invest Ophthalmol Vis Sci*. 2009;50(4):1911–1919.
287. Sakaguchi H, Miyagi M, Shadrach KG, Rayborn ME, Crabb JW, Hollyfield JG. Clusterin is present in drusen in age-related macular degeneration. *Exp Eye Res*. 2002;74:547–549.
288. Chong NH, Keonin J, Luthert PJ, et al. Decreased thickness and integrity of the macular elastic layer of Bruch's membrane correspond to the distribution of lesions associated with age-related macular degeneration. *Am J Pathol*. 2005;166(1):241–251.
289. Mullins RF, Olvera MA, Clark AF, Stone EM. Fibulin-5 distribution in human eyes: relevance to age-related macular degeneration. *Exp Eye Res*. 2007;84(2):378–380.
290. Yamada Y, Tian J, Yang Y, et al. Oxidized low density lipoproteins induce a pathologic response by retinal pigmented epithelial cells. *J Neurochem*. 2008;105(4):1187–1197.
291. Kamei M, Hollyfield JG. TIMP-3 in Bruch's membrane: changes during aging and in age-related macular degeneration. *Invest Ophthalmol Vis Sci*. 1999;40(10):2367–2375.
292. Xu H, Chen M, Forrester JV. Para-inflammation in the aging retina. *Prog Retin Eye Res*. 2009;28(5):348–368.
293. Glenn JV, Mahaffy H, Wu K, et al. Advanced glycation end product (AGE) accumulation on Bruch's membrane: links to age-related RPE dysfunction. *Invest Ophthalmol Vis Sci*.

2009;50(1):441–451.
294. Guo L, Hussain AA, Limb GA, Marshall J. Age-dependent variation in metalloproteinase activity of isolated human Bruch's membrane and choroid. *Invest Ophthalmol Vis Sci*. 1999;40:2676–2682.
295. Bhutto IA, Uno K, Merges C, Zhang L, McLeod DS, Lutty GA. Reduction of endogenous angiogenesis inhibitors in Bruch's membrane of the submacular region in eyes with age-related macular degeneration. *Arch Ophthalmol*. 2008;126(5):670–678.
296. Lin MY, Kochounian H, Moore RE, Lee TD, Rao N, Fong HK. Deposition of exon-skipping splice isoform of human retinal G protein-coupled receptor from retinal pigment epithelium into Bruch's membrane. *Mol Vis*. 2007;13:1203–1214.
297. Handa JT, Verzijl N, Matsunaga H, et al. Increase in the advanced glycation end product pentosidine in Bruch's membrane with age. *Invest Ophthalmol Vis Sci*. 1999;40:775–779.
298. Glenn JV, Beattie JR, Barrett L, et al. Confocal Raman microscopy can quantify advanced glycation end product (AGE) modifications in Bruch's membrane leading to accurate, nondestructive prediction of ocular aging. *FASEB J*. 2007;21(13):3542–3552.
299. Johnson PT, Betts KE, Radeke MJ, Hageman GS, Anderson DH, Johnson LV. Individuals homozygous for the age-related macular degeneration risk-conferring variant of complement factor H have elevated levels of CRP in the choroid. *Proc Natl Acad Sci USA*. 2006;103(46):17456–17461.
300. Spaide R, Ho-Spaide W, Browne R, Armstrong D. Characterization of peroxidized lipids in Bruch's membrane. *Retina*. 1999;19:141–147.
301. Moreira EF, Larrayoz IM, Lee JW, Rodriguez IR. 7-Ketocholesterol is present in lipid deposits in the primate retina: potential implication in the induction of VEGF and CNV formation. *Invest Ophthalmol Vis Sci*. 2009;50(2):523–532.
302. Vranka JA, Johnson E, Zhu X, et al. Discrete expression and

distribution pattern of TIMP-3 in the human retina and choroid. *Curr Eye Res*. 1997;16(2):102–110.
303. Hughes BA, Miller SS, Machen TE. Effects of cyclic AMP on fluid absorption and ion transport across frog retinal pigment epithelium: measurements in the open-circuit state. *J Gen Physiol*. 1984;83(6):875–899.
304. Frambach DA, Weiter JJ, Adler AJ. A photogrammetric method to measure fluid movement across isolated frog retinal pigment epithelium. *Biophys J*. 1985;47(4):547–552.
305. Negi A, Marmor MF. Quantitative estimation of metabolic transport of subretinal fluid. *Invest Ophthalmol Vis Sci*. 1986;27(11):1564–1568.
306. Marmor MF, Negi A. Pharmacologic modification of subretinal fluid absorption in the rabbit eye. *Arch Ophthalmol*. 1986;104(11):1674–1677.
307. Tsuboi S. Measurement of the volume flow and hydraulic conductivity across the isolated dog retinal pigment epithelium. *Invest Ophthalmol Vis Sci*. 1987;28(11):1776–1782.
308. Cantrill HL, Pederson JE. Experimental retinal detachment: VI. The permeability of the blood–retinal barrier. *Arch Ophthalmol*. 1984;102(5):747–751.
309. Pederson JE, Cantrill HL. Experimental retinal detachment: V. Fluid movement through the retinal hole. *Arch Ophthalmol*. 1984;102(1):136–139.
310. Chihara E, Nao-i N. Resorption of subretinal fluid by transepithelial flow of the retinal pigment epithelium. *Graefes Arch Clin Exp Ophthalmol*. 1985;223(4):202–204.
311. Malek G, Johnson LV, Mace BE, et al. Apolipoprotein E allele-dependent pathogenesis: amodel for age-related retinal degeneration. *Proc Natl Acad Sci USA*. 2005;102(33):11900–11905.
312. Charvet CD, Saadane A, Wang M, et al. Pretreatment with pyridoxamine mitigates isolevuglandin-associated retinal effects in mice exposed to bright light. *J Biol Chem*. 2013;288(41):29267–29280.
313. Hageman GS, Luthert PJ, Chong NHC, Johnson LV, Anderson DH, Mullins RF. An integrated hypothesis that considers drusen as biomarkers of immune-mediated

processes at the RPE-Bruch's membrane interface in aging and age-related macular degeneration. *Prog Retin Eye Res*. 2001;20:705–732.
314. Mullins RF, Russell SR, Anderson DH, Hageman GS. Drusen associated with aging and age-related macular degeneration contain proteins common to extracellular deposits associated with atherosclerosis, elastosis, amyloidosis, and dense deposit disease. *FASEB J*. 2000;14(7):835–846.
315. Anderson DH, Mullins RF, Hageman GS, Johnson LV. A role for local inflammation in the formation of drusen in the aging eye. *Am J Ophthalmol*. 2002;134(3):411–431.
316. Bhutto IA, Baba T, Merges C, Juriasinghani V, McLeod DS, Lutty GA. C-reactive protein and complement factor H in aged human eyes and eyes with age-related macular degeneration. *Br J Ophthalmol*. 2011;95(9):1323–1330.
317. Mullins RF, Schoo DP, Sohn EH, et al. The membrane attack complex in aging human choriocapillaris: relationship to macular degeneration and choroidal thinning. *Am J Pathol*. 2014;184(11):3142–3153.
318. Anderson DH, Radeke MJ, Gallo NB, et al. The pivotal role of the complement system in aging and age-related macular degeneration: hypothesis re-visited. *Prog Retin Eye Res*. 2010;29(2):95–112.
319. Kochounian H, Johnson LV, Fong HK. Accumulation of extracellular RGR-d in Bruch's membrane and close association with drusen at intercapillary regions. *Exp Eye Res*. 2009;88(6):1129–1136.
320. Loeffler KU, Mangini NJ. Immunolocalization of ubiquitin and related enzymes in human retina and retinal pigment epithelium. *Graefes Arch Clin Exp Ophthalmol*. 1997;235(4):248–254.
321. Flinn JM, Kakalec P, Tappero R, Jones B, Lengyel I. Correlations in distribution and concentration of calcium, copper and iron with zinc in isolated extracellular deposits associated with age-related macular degeneration. *Metallomics*. 2014;6(7):1223–1228.
322. Wang AL, Lukas TJ, Yuan M, Du N, Tso MO, Neufeld AH.

Autophagy and exosomes in the aged retinal pigment epithelium: possible relevance to drusen formation and age-related macular degeneration. *PLoS ONE*. 2009;4(1):e4160.

323. Gouras P, Braun K, Ivert L, Neuringer M, Mattison JA. Bestrophin detected in the basal membrane of the retinal epithelium and drusen of monkeys with drusenoid maculopathy. *Graefes Arch Clin Exp Ophthalmol*. 2009;247(8):1051–1056.

[a]This does not include the flow resistance of the choriocapillaris endothelium, which is not measured when L_p of a Bruch's membrane/choroidal preparation is determined. For this highly fenestrated endothelium with fenestra taking up roughly 80% of luminal surface area,[105] L_p can be estimated as roughly 25×10^{-10} m s^{-1} Pa^{-1},[106] which does not affect our conclusions.

23

Vitreous and Vitreoretinal Interface*

J. Sebag

Biochemistry
Anatomy And Histology
Physiology
Pathology

Biochemistry

Vitreous is 98% water and 2% structural proteins,[1] extracellular matrix components, and miscellaneous compounds.[2]

Collagen

Collagen is the major structural protein, consisting of heterotypic fibrils (Fig. 23.1) similar to cartilage.[3,4] Following vitrectomy, a type II procollagen is secreted in humans,[5] but an actual vitreous body is not reformed, since reoperations reveal that the gel state of vitreous is not reestablished.

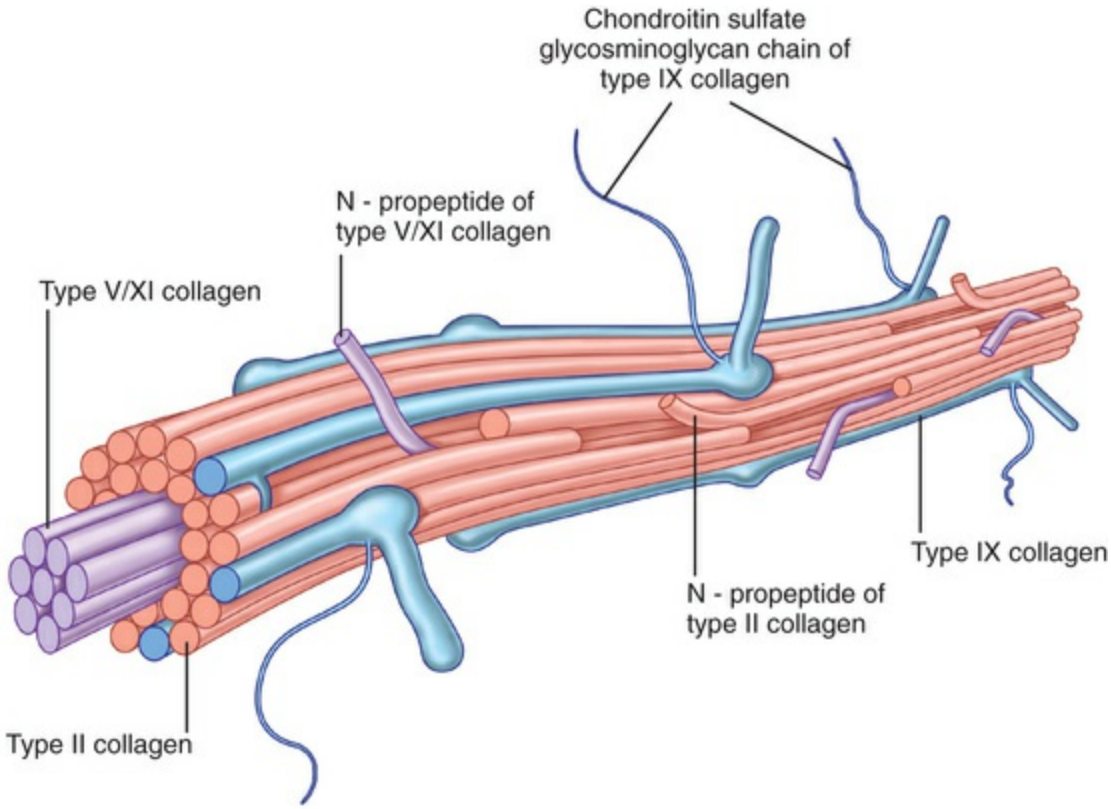

FIG. 23.1 Fibrillar structure of human vitreous collagen. Schematic diagram of the major heterotypic collagen fibrils of vitreous based upon the current knowledge of the structure and biophysical attributes of the constituent molecules. (Reproduced with permission from Bishop P. The biochemical structure of mammalian vitreous. Eye 1996;10:64.)

Type II collagen[6] comprises 75% of the total collagen content in vitreous. There are considerable similarities between vitreous and cartilage collagens,[7,8] perhaps explaining why inborn errors of type II collagen metabolism result in "arthro-ophthalmopathies,"[9] manifesting similar phenotypic expression in joints and vitreous. Type IX collagen accounts for up to 15% of vitreous collagen,[10] where it always contains a chondroitin sulfate glycosaminoglycan chain[11] covalently linked to the α_2 (IX) chain at the NC3 domain, enabling the molecule to assume a proteoglycan form.

An important function of vitreous is maintaining transparency within the eye (Fig. 23.2).[4] Studies[12] have shown that one of the minor collagens of vitreous is type XVIII, progenitor of endostatin, a potent inhibitor of angiogenesis.[13]

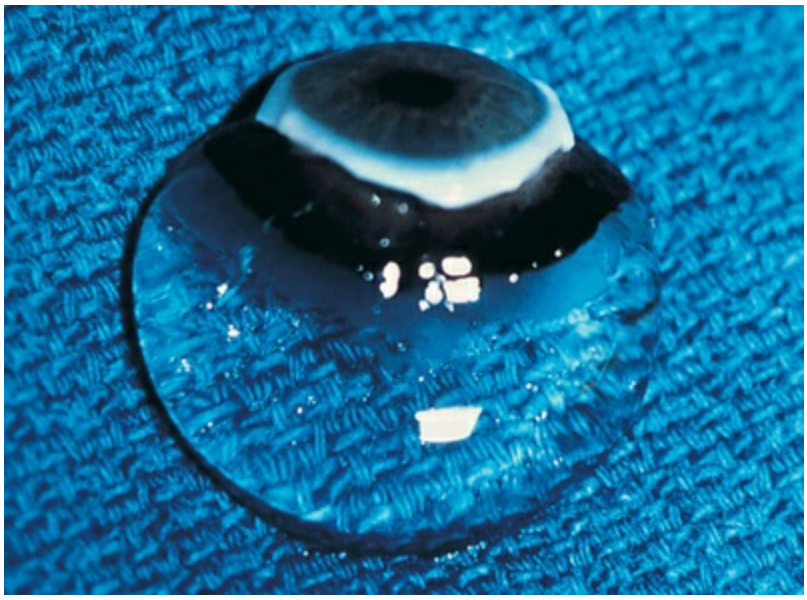

FIG. 23.2 Dissected human vitreous. Vitreous body dissected of the sclera, choroid, and retina in a 9-month old girl. The vitreous body is attached to the anterior segment, and the specimen is placed on a surgical towel in room air. The exquisite gel state of the vitreous body and the crystal-clear transparency are evident. (Specimen courtesy of the New England Eye Bank; originally published as cover photo in Sebag J. The vitreous: structure, function, and pathobiology. New York: Springer-Verlag; 1989.)

Hyaluronan

Hyaluronan (HA) was first isolated from bovine vitreous in 1934. HA appears after birth, perhaps synthesized by hyalocytes,[4] the ciliary body, and/or Müller cells. It is a large polyanion, which can influence the diffusion of drugs through vitreous.[14,15] As a result of HA's entanglement within the vitreous collagen fibril matrix, the mechanical force of HA's extension and contraction can be transmitted to the retina, optic disc, and neovascular complexes, inducing untoward effects in conditions that have fluctuations in ionic balance and hydration, such as diabetes.[16]

Chondroitin Sulfate

Most vitreous chondroitin sulfate is in the form of versican,[17] believed to form complexes with HA as well as with microfibrillar

proteins such as fibulin-1 and fibullin-2 and play a crucial role in maintaining the molecular morphology of vitreous.[18] Mutations that alter the splicing of the central chondroitin sulfate-bearing domains of versican have been implicated in Wagner syndrome, a condition with excess vitreous liquefaction.[19]

Noncollagenous Structural Proteins

Fibrillins

In Marfan syndrome, defects in the gene encoding fibrillin-1 (*FBN1* on chromosome 15q21) result in both ectopia lentis and vitreous liquefaction,[20] an important cause of rhegmatogenous retinal detachment (RD) in these patients.

Opticin

A major noncollagenous protein of vitreous is opticin (formerly called vitrican).[21] It is bound to the surface of the heterotypic collagen fibrils and prevents aggregation of adjacent collagen fibrils into bundles. Opticin binds heparan and chondroitin sulfates, suggesting that it may play a role in vitreoretinal adhesion.[22,23] Similar to its role in articular cartilage,[24] opticin may also stabilize vitreous gel structure by binding chondroitin sulfate proteoglycans.

Anatomy and Histology

Vitreous Body

Vitreous is a clear gel-like structure with a volume of about 4.0 mL. During invagination of the optic vesicle, the "primary" vitreous forms between the lens and the inner limiting membrane (ILM) of the retina. It is noteworthy that the ILM is continuous with Bruch's membrane (Fig. 23.3A), demonstrating a common embryologic origin with analogous molecular composition and structure, suggesting important similarities later in life.[25]

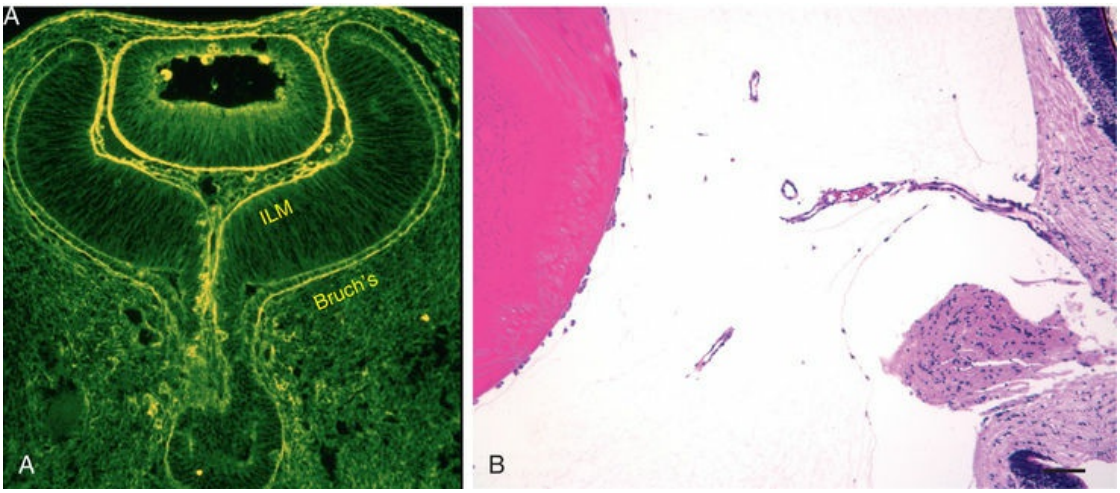

FIG. 23.3 Fetal human vitreous. (A) Human embryo eye stained with immunofluorescent anti-ABA (basement membrane lectin) antibodies revealing the continuity of the inner limiting membrane (*ILM*) and Bruch's membrane (*Bruch's*), demonstrating a common embryologic origin with an analogous molecular composition and structure. This suggests similarities during aging and as participants in various disease processes, especially those that feature cell migration and proliferation: biologic processes that will occur along these interfaces. (B) Photomicrograph of human fetal eye aged 13 gestational weeks. A prominent hyaloid artery and vasa hyaloidea propria can be seen arising from the optic nerve and extending anteriorly towards the lens to anastomose with the tunica vasculosa lentis (hematoxylin and eosin; scale bar: 100 μm). (Panel A reproduced with permission from Sebag J, Hageman GS. Interfaces. Eur J Ophthalmol 2000;10:1. Panel B courtesy of Kenneth MP Yee and Fred Ross-Cisneros, Doheny Eye Institute/UCLA.)

The "secondary" vitreous begins to develop at the 13-mm stage of embryogenesis and is derived from the retina and mesoderm of the hyaloid vascular system (Fig. 23.3B). Recent proteomic studies of human embryonic vitreous have identified changes in protein expression during the second trimester that may play a role in regression of the hyaloid vasculature.[26] Confirmatory studies may thus open new avenues of drug development to prevent or treat pathologic neovascularization in the eye and elsewhere.

Classic depictions of human vitreous structure are shown in Fig. 23.4. Modern concepts proposed membranous (Fig. 23.5A)[27] and

cisternal (Fig. 23.5B)[28] systems. Sebag and Balazs[29] performed dark-field slit microscopy to define the posterior vitreous cortex as a thin, membranous structure continuous from the ora serrata to the posterior pole. Two round holes are present in the prepapillary and premacular areas (Fig. 23.6). Anteroposterior fibers (Fig. 23.7) comprised of parallel collagen fibrils (Fig. 23.8) arise from the vitreous base (Fig. 23.9A), where Gartner[30] found "lateral aggregation" in older individuals. Vitreous base collagen fibers insert anterior to the ora serrata forming the anterior loop (Fig. 23.9B), important in anterior proliferative vitreoretinopathy (PVR).[31] In the posterior pole, fibers extend through the premacular hole (Figs. 23.6 and 23.7A), but a few attach to the rim of the hole. Condensed bundles of fibers insert into the vitreous cortex in the midperiphery and equator (Fig. 23.10).

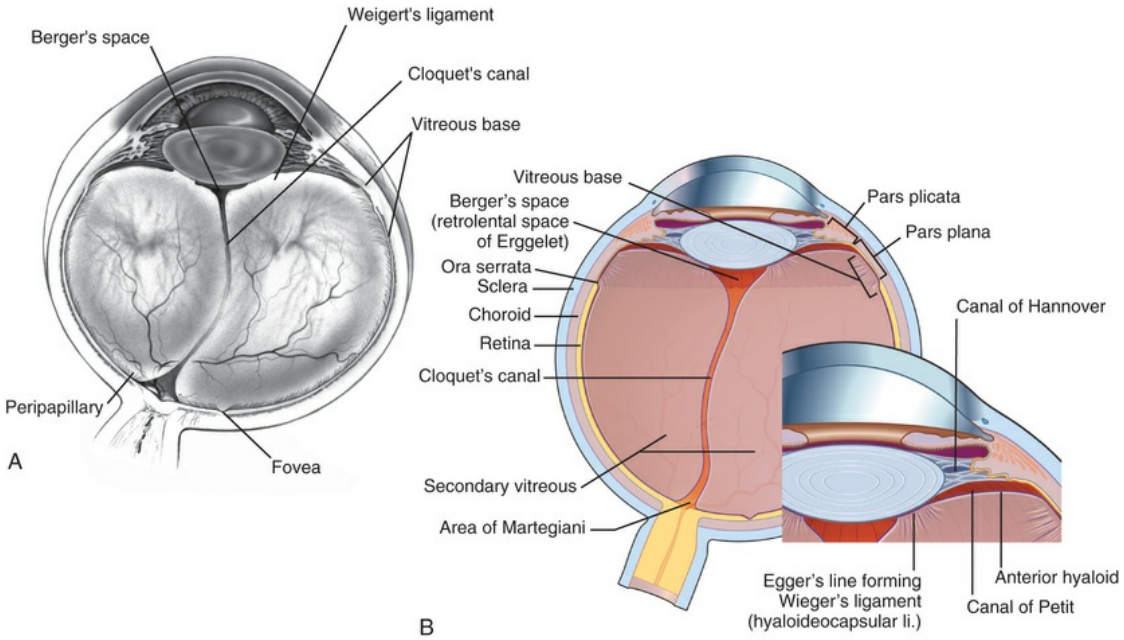

FIG. 23.4 Classic depictions of vitreous structure. (A) Schematic representation of vitreous structure. (B) Schematic diagram of vitreous structure with classic nomenclature of internal and interface structures. (Panel A redrawn with permission from Green WR. Pathology of the vitreous. In: Frayer WC, editor. Lancaster course in ophthalmic histopathology, unit 8. Philadelphia: FA Davis; 1981. Panel B reproduced with permission from Sang DN. Embryology of the vitreous. Congenital and developmental abnormalities. In: Schepens CL, Neetens A, editors. The vitreous and vitreoretinal interface. New York: Springer-Verlag; 1987. p. 20.)

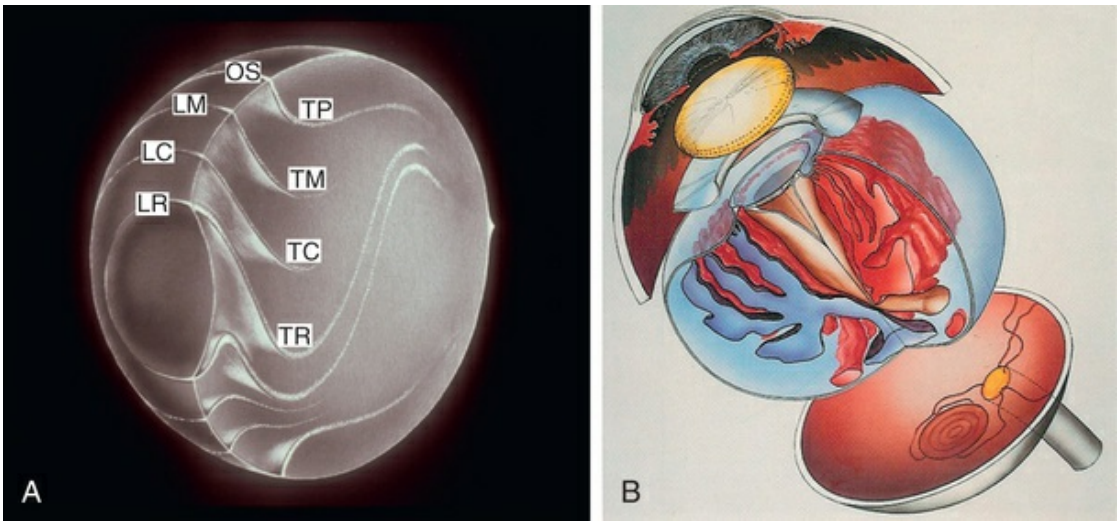

FIG. 23.5 Vitreous structure. (A) Membranelles, called tractae, course from the area of the ciliary body to the posterior pole. *LC*, ligamentum coronarium; *LM*, ligamentum medianum; *LR*, ligamentum retrolentalis; *OS*, ora serrata; *TC*, tractus coronarius; *TM*, tractus medianus; *TP*, tractus preretinalis; *TR*, tractus retrolentalis. (B) Cisterns are identified by injecting with colored India ink. Light brown, Cloquet's canal opening into the prepapillary area of Martegiani; light purple, equatorial cistern opening into the bursa premacularis.

(Panel A reproduced with permission from Eisner G. Clinical anatomy of the vitreous. In: Duane TD, Jaeger EA, editors. Biomedical foundations of ophthalmology, vol. 1. Philadelphia: JB Lippincott; 1984. p. 21. Panel B reproduced with permission from Jongbloed WL, Worst JGF. The cisternal anatomy of the vitreous body. Doc Ophthalmol 1987;67:183–96.)

FIG. 23.6 The two “holes” in the posterior vitreous cortex correspond to the prepapillary (smaller, to left) and premacular (larger “hole,” to right) regions. Vitreous can be seen extruding through these holes. The bright pin-point foci of intense light-scattering are hyalocytes embedded in the posterior vitreous cortex.

(Reproduced with permission from Sebag J, Balazs EA. Human vitreous fibres and vitreoretinal disease. Trans Ophthalmol Soc U K 1985;104:123–8.)

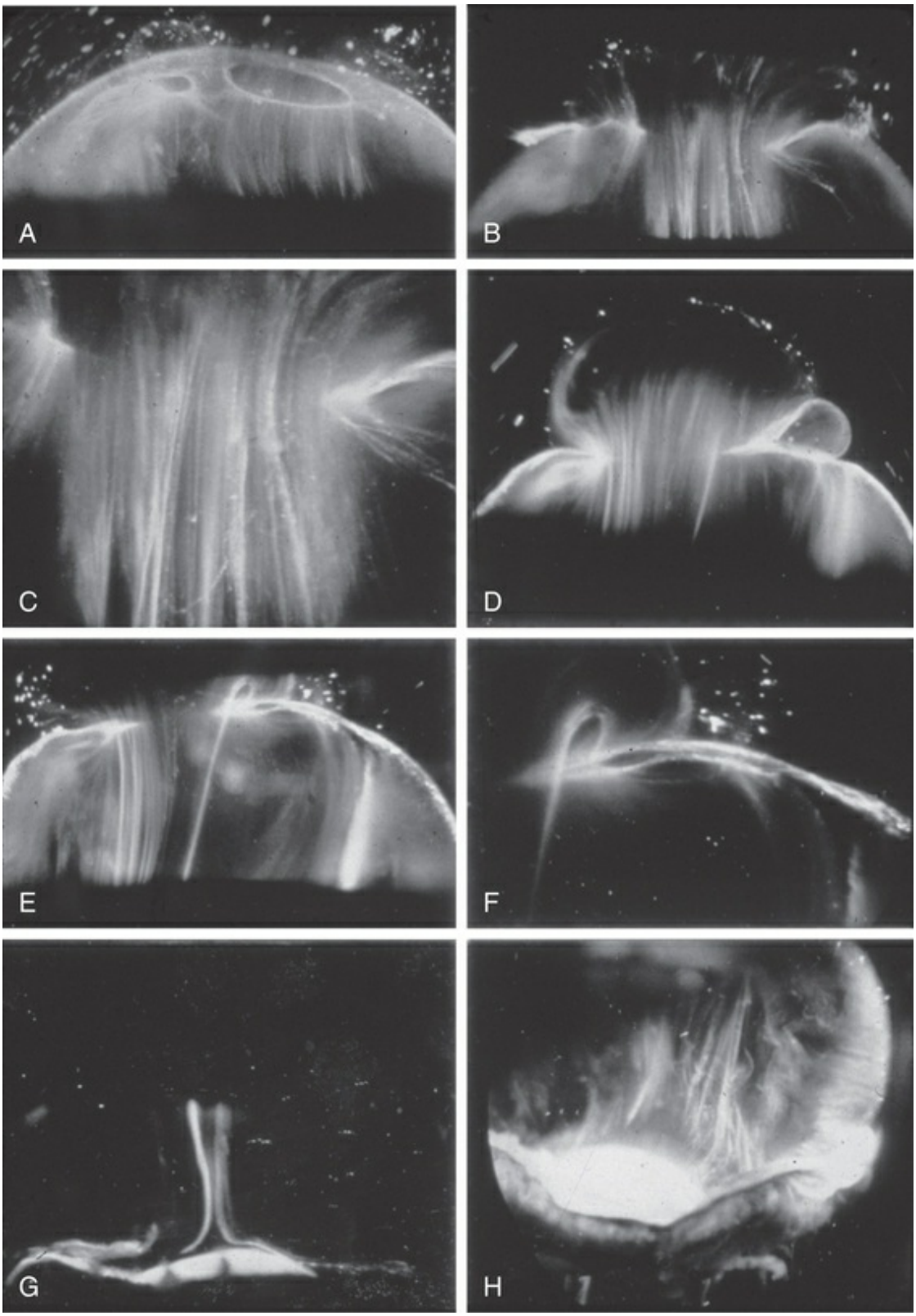

FIG. 23.7 Human vitreous morphology. Human vitreous structure visualized by dark-field slit illumination. All photographs are oriented with the anterior segment below and the posterior pole above. (A) Posterior vitreous in the left eye of a 52-year-old man. The vitreous body is enclosed by the vitreous

cortex. There is a hole in the prepapillary (small, to the left) vitreous cortex. Vitreous fibers are oriented toward the premacular region. (B) Posterior vitreous in a 57-year-old man. A large bundle of prominent fibers is seen coursing anteroposteriorly and entering the retrocortical space by way of the premacular vitreous cortex. (C) Same photograph as (B), at higher magnification. (D) Posterior vitreous in the right eye of a 53-year-old woman. There is posterior extrusion of vitreous out of the prepapillary hole (to the right) and premacular (large extrusion to the left) vitreous cortex. Fibers course anteroposteriorly out into the retrocortical space. (E) Horizontal optical section of the same specimen as (D), at a different level. A large fiber courses posteriorly from the central vitreous and inserts into the premacular vitreous cortex. (F) Same view as (E), at higher magnification. The large fiber has a curvilinear appearance because of traction by the vitreous extruding into the retrocortical space (see D). However, because of its attachment to the posterior vitreous cortex, the fiber arcs back to its point of insertion. (G) Anterior and central vitreous in a 33-year-old woman. Cloquet's canal is seen forming the retrolental space of Berger. (H) Anterior and peripheral vitreous in a 57-year-old man. The specimen is tilted forward to enable visualization of the posterior aspect of the lens and the peripheral anterior vitreous. To the right of the lens there are fibers coursing anteroposteriorly that insert into the vitreous base. These fibers “splay out” to insert anterior and posterior to the ora serrata. (Panels A, E, and F reproduced with permission from Sebag J, Balazs EA. Pathogenesis of CME: anatomic consideration of vitreo-retinal adhesions. Surv Ophthalmol 1984;28 (Suppl):493. Panels and C from Sebag J, Balazs EA. Morphology and ultrastructure of human vitreous fibers. Invest Ophthalmol Vis Sci 1989;30:187. Panels D, G, and H from Sebag J. The vitreous: structure, function, and pathobiology. New York: Springer-Verlag; 1989. Specimens were courtesy of the New York Bank for Sight and Restoration, New York, NY.)

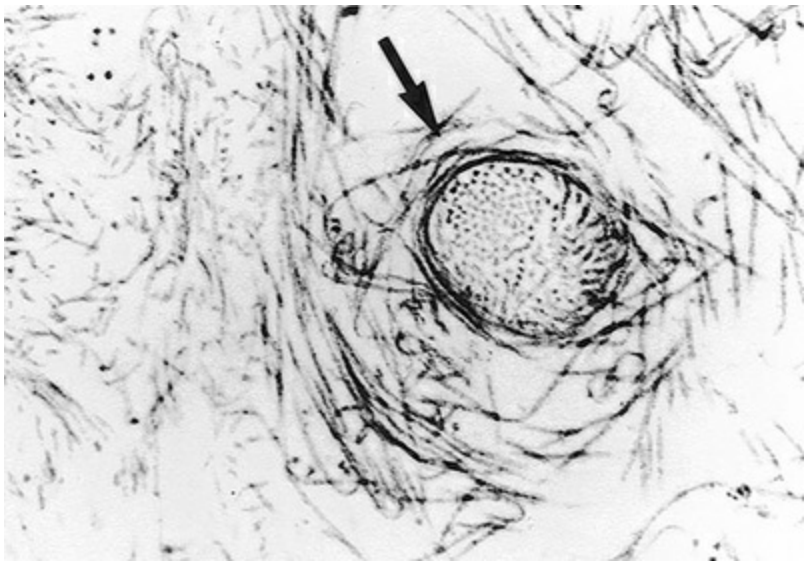

FIG. 23.8 Ultrastructure of human vitreous fiber. The fibers of the human vitreous visible by dark-field microscopy result from bundles of parallel collagen fibrils such as the one shown here in cross-section (*arrow*). (Reproduced with permission from Sebag J, Balazs EA. Morphology and ultrastructure of human vitreous fibers. Invest Ophthalmol Vis Sci 1989;30:187.)

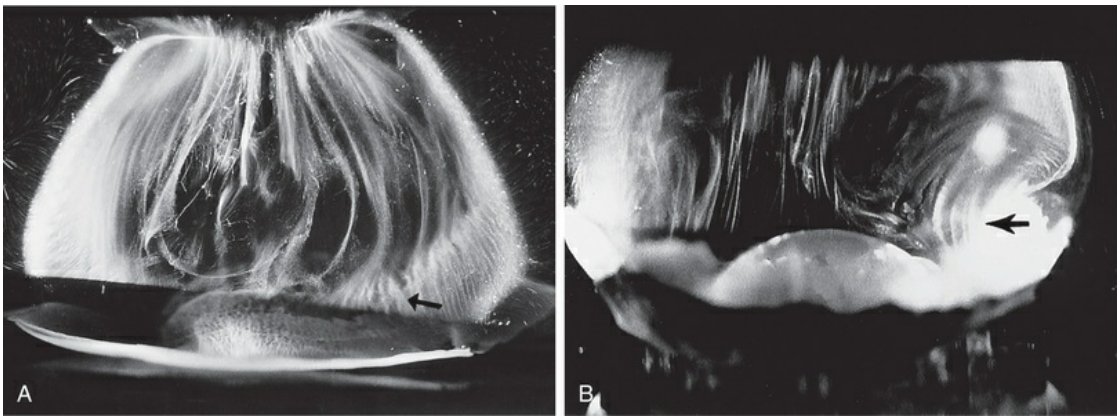

FIG. 23.9 (A) Vitreous base morphology. In this eye of a 58-year-old woman, postmortem dark-field slit microscopy studies showed vitreous fibers that are continuous from the posterior vitreous cortex (at the top of the photo) to the vitreous base, where they "splay out" to insert into the vitreous base (*arrow*). (B) Anterior loop of the vitreous base. Central, anterior, and peripheral vitreous structure in a 76-year-old man. The posterior aspect of the lens is seen below. Fibers course antero-posteriorly in the central vitreous and

insert into the vitreous base. The “anterior loop” configuration of those fibers inserting into the vitreous base anterior to the ora serrata is seen on the right side of the specimen (*arrow*). (Panel A reproduced with permission from Sebag J, Balazs EA. Pathogenesis of CME: anatomic consideration of vitreoretinal adhesions. Surv Ophthalmol 1984;28 (Suppl):493–8.)

FIG. 23.10 Fibers condense into bundles and insert into the vitreous cortex (*arrows*). Between these insertions are spaces seemingly devoid of structure, but probably filled with liquid vitreous. (Reproduced with permission from Sebag J, Balazs EA. Human vitreous fibres and vitreoretinal disease. Trans Ophthalmol Soc U K 1985;104:123–8.)

Vitreoretinal Interface

The equatorial and posterior vitreoretinal interfaces consist of the posterior vitreous cortex, the ILM of the retina, and an intervening extracellular matrix.[32]

Posterior Vitreous Cortex

The posterior vitreous cortex is 100–110 μm thick and consists of densely packed collagen fibrils[33] (Fig. 23.11). There is no vitreous cortex over the optic disc (Figs. 23.6 and 23.7A), and the cortex is

thin over the macula. The prepapillary hole can sometimes be visualized clinically following posterior vitreous detachment (PVD). If peripapillary tissue is torn away during PVD and remains attached around the prepapillary hole, it is called a Vogt or Weiss ring. Hageman[34] demonstrated a lamellar organization of the posterior vitreous cortex (Fig. 23.12), confirmed in humans by three-dimensional optical coherence tomography (OCT) (Fig. 23.13).[35] During anomalous PVD (APVD),[36,37] this lamellar structure predisposes to splitting along the potential cleavage planes between the lamellae, resulting in vitreoschisis.[38]

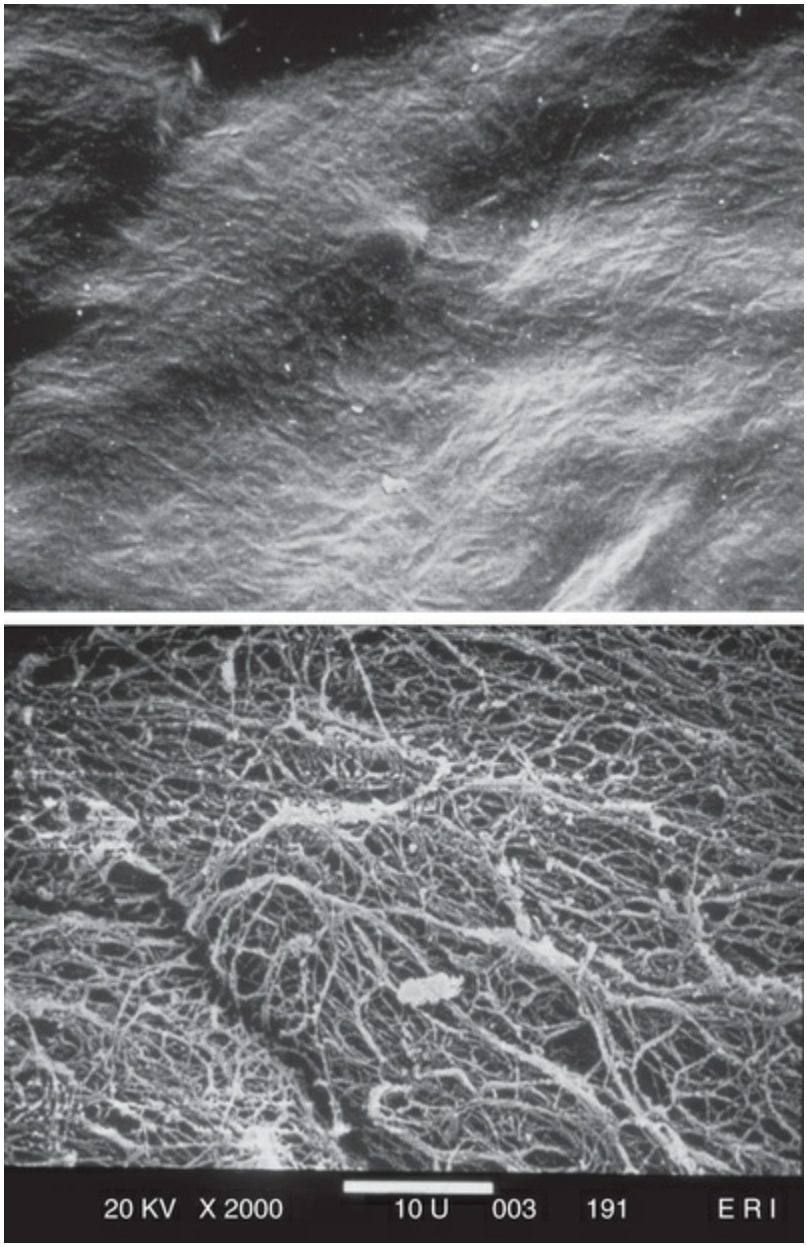

FIG. 23.11 Ultrastructure of human vitreoretinal interface. Scanning electron microscopy of anterior surface of the human retina (top) and the posterior surface of the posterior vitreous cortex (bottom).

(Reproduced with permission from Sebag J. The vitreous: structure, function, and pathobiology. New York: Springer-Verlag; 1989.)

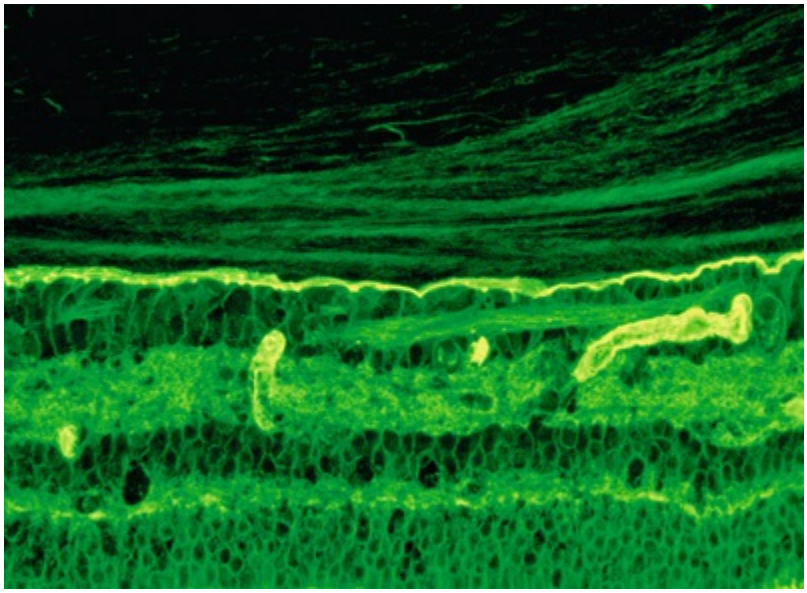

FIG. 23.12 Lamellar structure of the posterior vitreous cortex. Immunohistochemistry with anti-ABA lectin antibodies of the monkey vitreoretinal interface demonstrates lamellae in the posterior vitreous cortex just above the inner limiting membrane of the retina (intensely staining yellow line). These lamellae represent potential cleavage planes during anomalous posterior vitreous detachment with vitreoschisis.

(Reproduced with permission from Gupta P, Yee KMP, Garcia P, et al. Vitreoschisis in macular diseases. Br J Ophthalmol 2011;95:376–80.)

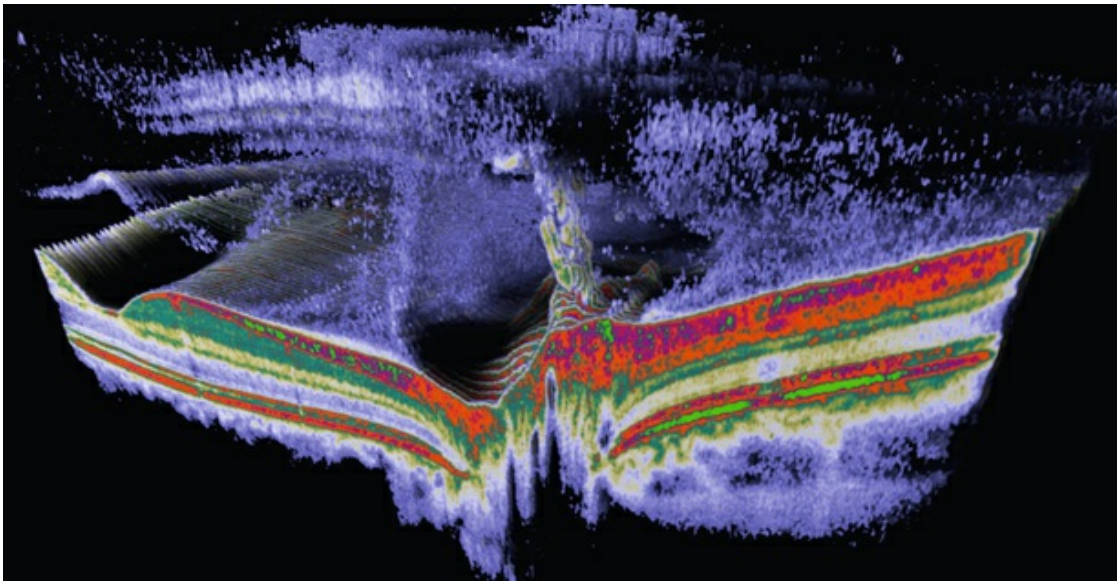

FIG. 23.13 Human posterior vitreous cortex. Three-dimensional spectral domain optical coherence tomography imaging of human posterior vitreous cortex demonstrates the lamellar structure that predisposes to vitreoschisis. (Reproduced with permission from Sebag J. Vitreous – the resplendent enigma. Br J Ophthalmol 2009;93:989–91. Image courtesy of Dr. Carl Glittenberg and Prof. Susanne Binder, Vienna.)

Hyalocytes.

Hyalocytes are mononuclear cells embedded in the posterior vitreous cortex 20–50 μm from the ILM posteriorly (Figs. 23.6 and 23.14). The highest density of hyalocytes is in the vitreous base followed by the posterior pole, with the lowest density at the equator.[39,40] Balazs[41] suggested that these cells synthesize vitreous HA,[42–45] but Swann[7] disagreed. Evidence suggests that hyalocytes maintain ongoing synthesis and metabolism of glycoproteins[46,47] and may also synthesize collagen[48] and enzymes.[49]

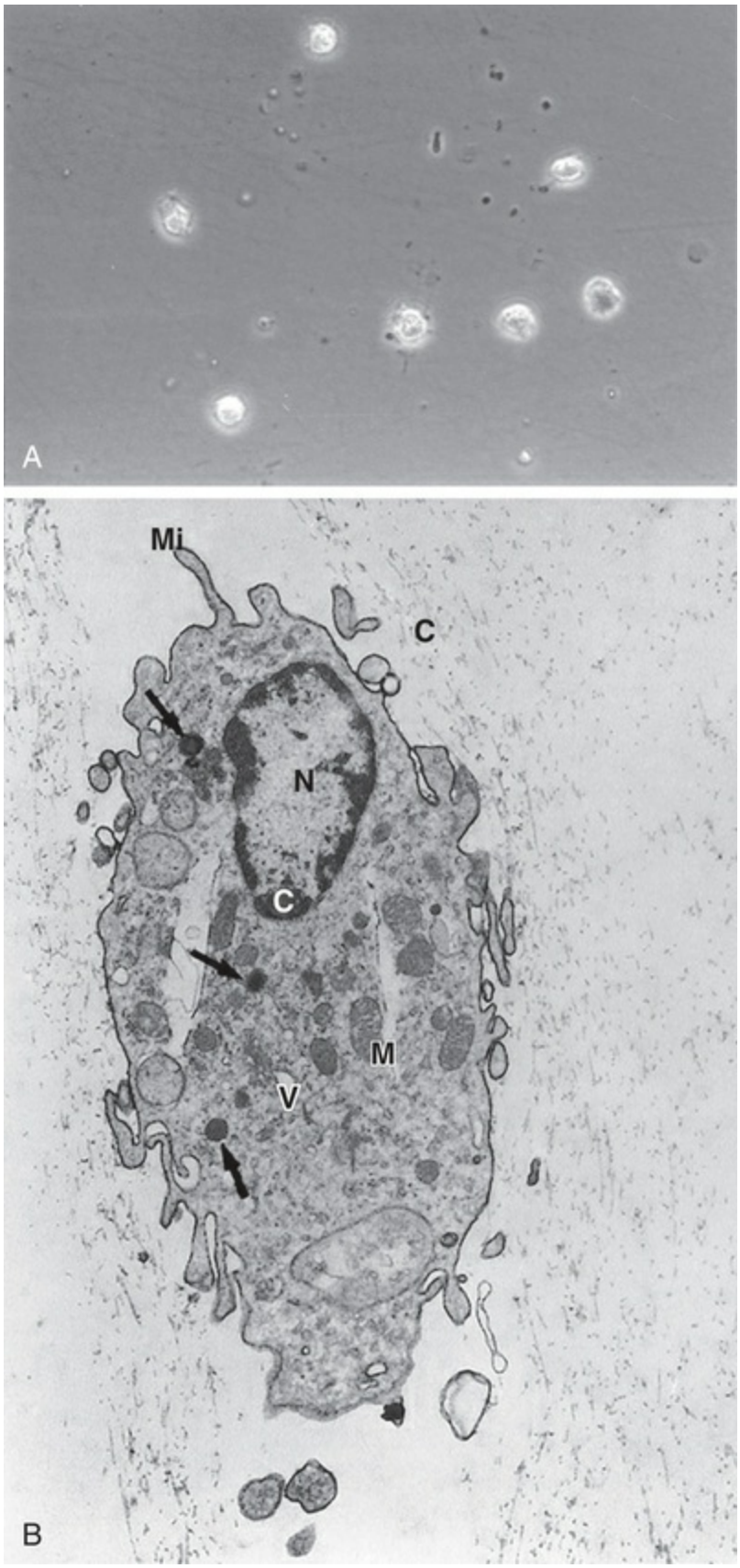

FIG. 23.14 Human hyalocytes. (A) Phase contrast microscopy of human hyalocytes in situ. (B) A mononuclear cell is seen embedded within the dense

collagen fibril (*black C*) network of the vitreous cortex. There is a lobulated nucleus (*N*) with a dense marginal chromatin (*white C*). In the cytoplasm there are mitochondria (*M*), dense granules (*arrows*), vacuoles (*V*), and microvilli (*MI*) (magnification = ×11 ,670). (Panel A reproduced with permission from Sebag J. The vitreous: structure, function, and pathobiology. New York: Springer-Verlag; 1989, p. 49. Panel B courtesy of J.L. Craft and D.M. Albert, Harvard Medical School.)

The phagocytic capacity of hyalocytes has been described in vivo[50] and demonstrated in vitro.[51–53] Hyalocytes become phagocytic in response to inducting stimuli and are important in antigen processing and as initiators of the immune response, making it possible for intravitreal inoculation of antigens to promote systemic immunity.[54] HA may have a regulatory effect on hyalocyte phagocytic activity.[55,56] Various constituents of vitreous[57,58] may be immunogenic and play a role in ocular inflammatory diseases. Sakamoto and Ishibashi have recently published excellent reviews of hyalocytes.[59,60]

Hyalocytes are important in macular pucker when APVD[31] and vitreoschisis[29,33,61] leave these cells on the macula (Fig. 23.15). Under the influence of cytokines, hyalocytes proliferate[62] on the surface of the retina, resulting in hypercellular membranes. Hyalocytes also recruit cells from the circulation and the retina (glial cells) via the release of connective tissue growth factor and induce collagen gel contraction in response to platelet-derived growth factor and other cytokines,[63,64] causing tangential vitreoretinal contraction.[61]

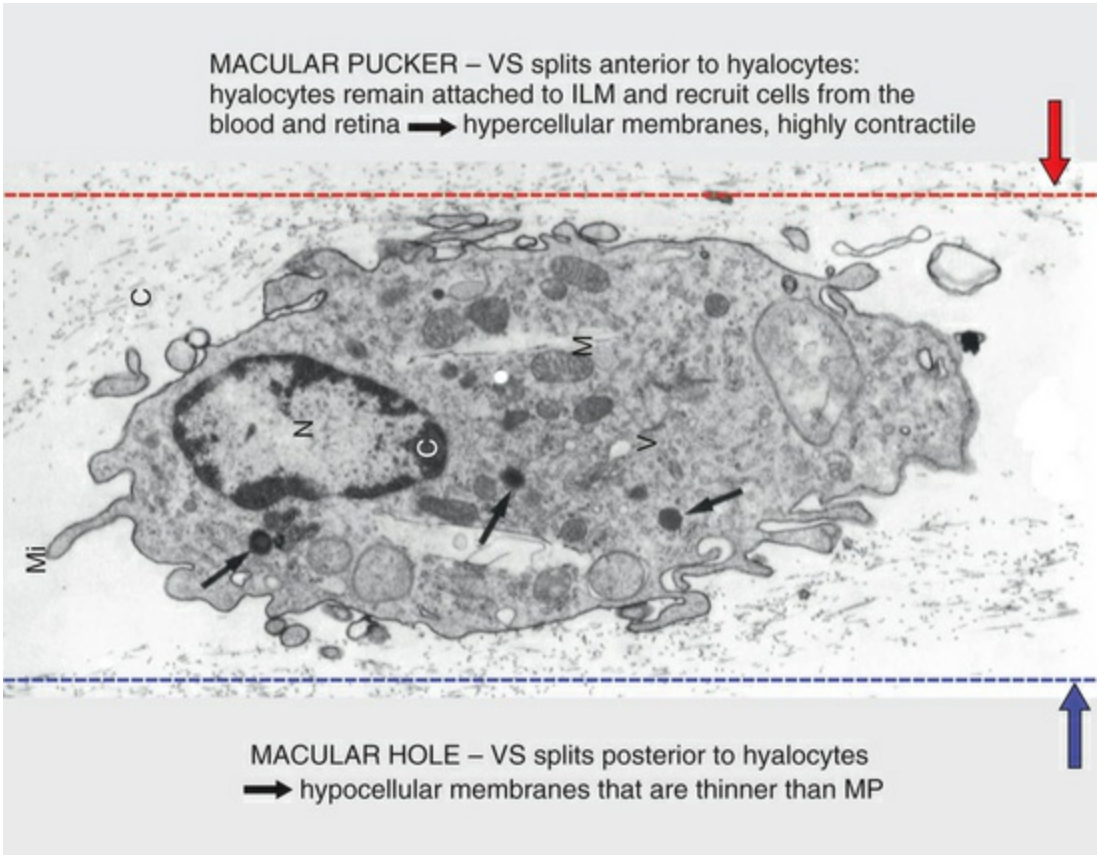

FIG. 23.15 Vitreoschisis. Transmission electron microscopy of human hyalocyte (same as in Fig. 23.14B) demonstrating two potential levels of splitting during vitreoschisis. Anomalous posterior vitreous detachment that induces vitreoschisis, which splits the posterior vitreous cortex anterior to the level of hyalocytes (*red dashes*) leaves these cells attached to the macula, resulting in a hypercellular membrane. The lack of attachment to the optic disc allows inward (centripetal) tangential traction and macular pucker. If vitreoschisis splits the posterior vitreous cortex posterior to the level of hyalocytes (*blue dashes*), the remaining membrane is thin and hypocellular. If there is also vitreopapillary attachment, the tangential forces will be outward (initially nasally), opening a central dehiscence and inducing a macular hole. *ILM*, inner limiting membrane; *MP*, macular pucker; *VS*, vitreoschisis; for other abbreviations see Fig. 23.14.

Inner Limiting Membrane of the Retina

The ILM is a multilaminar structure of variable thickness

topographically. Adjacent to Müller cell footplates is the lamina rara externa (0.03–0.06 μm) with no species variations or changes with topography or age. The lamina densa is thinnest at the fovea (0.01–0.02 μm) and thicker in the posterior pole (0.5–3.2 μm) than at the equator or vitreous base, where Foos[65] found the ILM to be uniformly thin (51 nm) and the lamina rara to be 40 nm thick with traversing fibrils that were denser at sites corresponding to attachment plaques in Müller cells. The ILM is very thin over major retinal vessels (Fig. 23.16) where defects allow glial cells to extend on to the inner retina.[66] Acquired ILM defects are in the foveola, retinal pits, retinal tufts, and retinal lattice. The ILM progressively thickens posteriorly to about 306 nm at the equator and about 1887 nm posteriorly. Müller footplates are less numerous at the equator than at the vitreous base. Posteriorly, no Müller footplates were observed and the inner aspect of the ILM remains smooth, while the outer aspect is irregular. Peripherally, both inner and outer surfaces are smooth.[2,58]

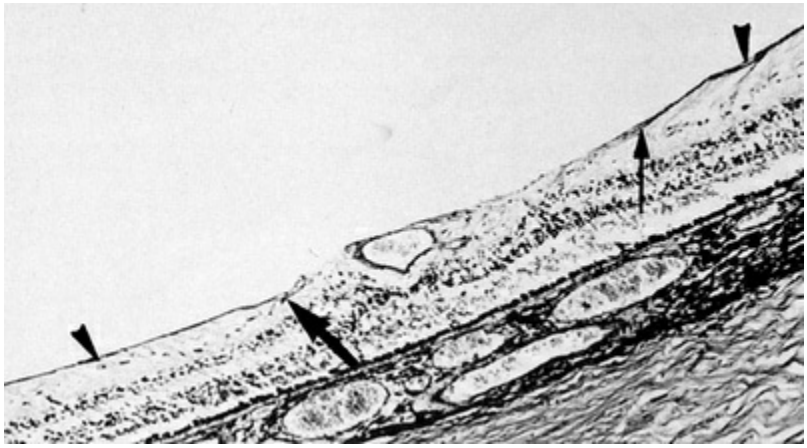

FIG. 23.16 Vitreoretinal vessel interface. A large gap (*between arrows*) in the inner limiting membrane (ILM) over and adjacent to a retinal artery is seen with a thin, fibroglial premacular membrane over the ILM (*arrowheads*) (periodic acid–Schiff; ×470).

The ILM consists of type IV collagen, more abundant on the vitreous side of the ILM, and laminin, which is more abundant on the retinal side of the ILM (Fig. 23.17). These are associated with glycoproteins,[25,67,68] type VI collagen, which may contribute to

vitreoretinal adhesion, and type XVIII,[69] which binds opticin.[70] Opticin binds to heparan sulfate, contributing to vitreoretinal adhesion.[71] Type XVIII collagen also prevents cell migration from the retina into vitreous.[72] Recent studies[32] have also identified agrin, a basement membrane-associated heparan sulfate proteoglycan similar to collagen XVIII that provides proteolytically cleaved bioactive fragments for modulating cellular behavior[73] at the vitreoretinal interface.

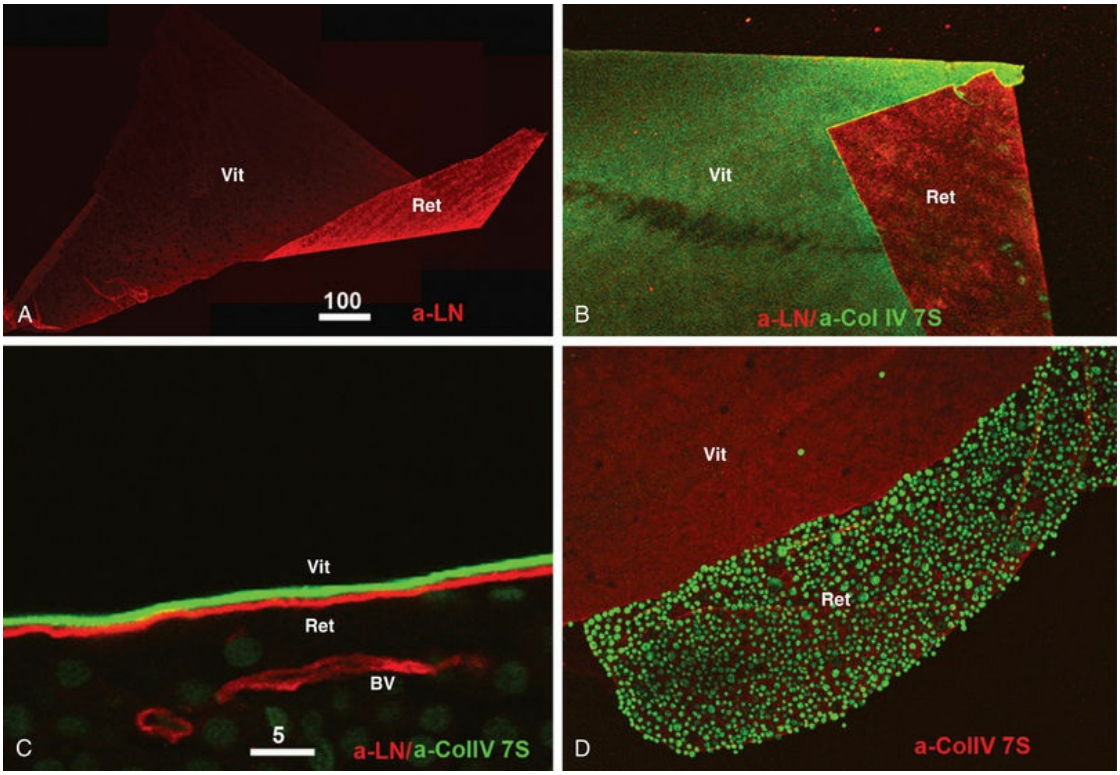

FIG. 23.17 Human inner limiting membrane (ILM) composition. The human ILM composition is detectable by side-specific labeling of a flat-mounted ILM using antibodies to laminin (A,B) or collagen IV (B,C). Laminin is most abundant on the retinal side of the ILM (A,B), whereas an antibody to collagen IV labels the vitread side (B,C, green). The abundance of both proteins on either the retinal or vitread side is best appreciated by double-labeling (B,C). When dissociated Madin-Darby Canine Kidney (MDCK) Epithelial Cells, corneal or retinal cells were plated on flat-mounted and folded ILMs, the cells adhere preferentially to the retinal side of the ILM (D). The vitread side of this preparation was labeled with an

antibody to the 7S domain of collagen IV a3 (red). The adherent cells were labeled green. (Reprinted with permission from Halfter W, Sebag J, Cunningham ET. Vitreoretinal interface and inner limiting membrane. In: Sebag J, editor. Vitreous – in health and disease. New York: Springer; 2014. p. 1792.)

Intervening Extracellular Matrix

The interface between vitreous and adjacent structures consists of a complex formed by the vitreous cortex and basal laminae, which are firmly attached to their cells.[74] The only part of vitreous not adjacent to a basal lamina is the annulus of the anterior vitreous cortex, which is directly exposed to the zonules and the aqueous humor of the posterior chamber, similar to the surface of articular cartilage, which is exposed to synovial fluid.[53] Zimmerman and Straatsma[75] claimed that there are fibrillar attachments between the posterior vitreous cortex and the ILM. The composition of these fibrillar structures is not known, and their presence has never been confirmed.

It is currently believed that an extracellular matrix "glue" of fibronectin, laminin, and other extracellular matrix components[76] exists between vitreous and retina, causing adhesion to be fascial, as opposed to focal.[62,63] Chondroitin sulfate is present at the sites of strong vitreoretinal adhesion such as the vitreous base and optic disc, forming the rationale for pharmacologic vitreolysis using avidin–biotin complex chondroitinase.[77,78]

Topographic Variations

Strength of Vitreoretinal Adhesion.

Vitreous is attached to all contiguous structures, but is most firmly adherent at the vitreous base,[79] which includes the posterior 2 mm of the pars plana and extends 1–4 mm posterior to the ora serrata, varying with age[80] and topography (more posterior temporally). There are also topographic differences posteriorly, with greater adhesion at the posterior pole than the equator[67] (Fig. 23.18).

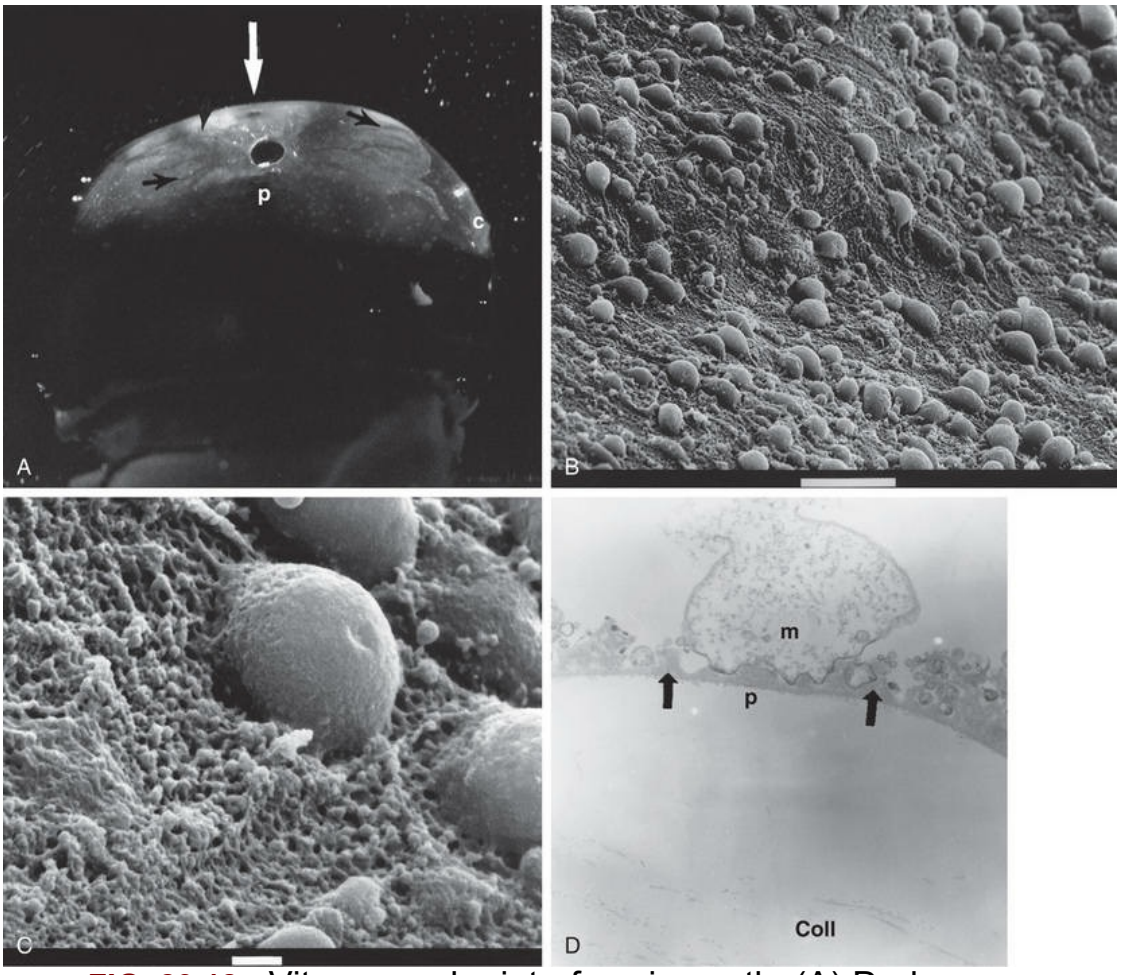

FIG. 23.18 Vitreomacular interface in youth. (A) Dark-field microscopy of the posterior vitreous from a 14-year-old boy. The sclera, choroid, and retina were dissected off the vitreous, which remains attached to the anterior segment. In contrast to adults, there is an extra layer of tissue that remained adherent to the posterior vitreous cortex when the retina was dissected off. The *white arrow* indicates the location of the fovea. The circular structure below this is the prepapillary hole in the posterior vitreous cortex. Emanating from this hole are linear, branching structures (*black arrows*) that correspond to the location of the retinal vessels. *p*, Prepapillary hole; *c*, vitreous cortex. (B) Scanning electron microscopy of the tissue shown in (A) demonstrates round structures adherent to the posterior aspect of this tissue (scale bar: 1 μm). (C) Higher magnification of structures shown in (B). (D) Transmission electron microscopy of this specimen identified this tissue as the inner limiting membrane (ILM) of the retina (*arrows*) attached to the posterior vitreous cortex (*p*). The round structures shown in (B)

are identified as the inner portion of Müller (*m*) cells that remained adherent to the posterior aspect of the ILM. The hole on the posterior aspect of these round structures is where the anterior portion of the Müller cell was torn away from the rest of the cell body. At the bottom of the photomicrograph are the collagen fibrils of the vitreous (*Coll*) (original magnification ×20 ,800).

(Reproduced with permission from Sebag J. Age-related differences in the human vitreoretinal interface. Arch Ophthalmol 1991;109:966–71.)

Peripheral Fundus and Vitreous Base.

The vitreous base is a three-dimensional structure that straddles the ora serrata. There is a high density of collagen fibrils oriented at right-angles to the inner surface of the ciliary epithelium and peripheral retina. The fibrils attach to the basement membrane of the nonpigmented epithelium of the pars plana and the ILM of the peripheral retina,[81] intimately interwoven with the intervening extracellular matrix. Within the vitreous base, there are several anatomic variations where vitreoretinal adhesion is firm,[82] adhesions that predispose to retinal breaks[83,84] [see below]

Interface Along Major Retinal Blood Vessels.

The ILM thins and is sometimes absent over major retinal vessels[85,86] (Fig. 23.19). At such points, vitreous may be incarcerated into retina, directly continuous with perivascular tissue, attachments called "vitreoretino-vascular bands,"[87] or "spider-like bodies,"[88] purported to be vitreous fibrils that traverse the ILM and coil about retinal blood vessels. It is common for retinal vessels to be associated with paravascular rarefaction (cystic degeneration), retinal pits and tears, and avulsion of retinal vessels.

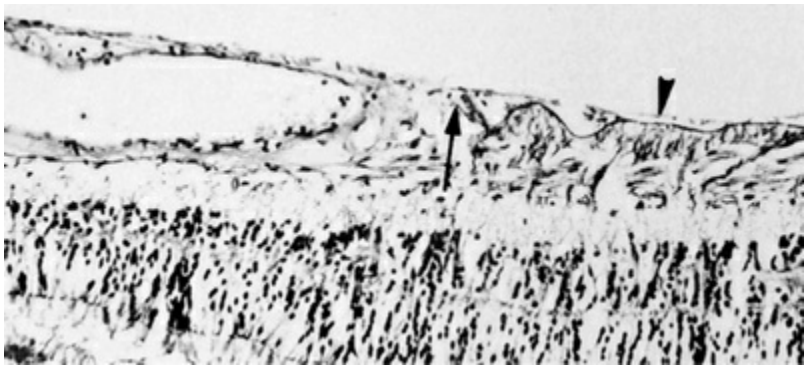

FIG. 23.19 Vitreous interface over retinal vessels. There is a large gap in the inner limiting membrane (ILM) over and adjacent to retinal artery. A glial preretinal membrane (*arrowhead*) originates at a defect in the ILM overlying the retinal vessel. *Arrow* indicates one end of the discontinuous ILM (periodic acid–Schiff stain; ×170). (Reproduced with permission from Clarkson JG, Green WR, Massof D. A histopathologic review of 168 cases of preretinal membrane. Am J Ophthalmol 1977;84:1–17.)

Retinal Sheen Dystrophy.[89]

This ILM dystrophy has cystic spaces under the ILM and in the inner nuclear layer, and numerous areas of separation of the ILM from the retina with filamentous material (Fig. 23.20). Endothelial cell swelling and degeneration, pericyte degeneration, and basement membrane thickening of retinal capillaries suggest that this condition is primarily a retinal vasculopathy with edema, swelling, and degeneration of Müller cells. Alternatively, the primary defect could be in Müller cells.

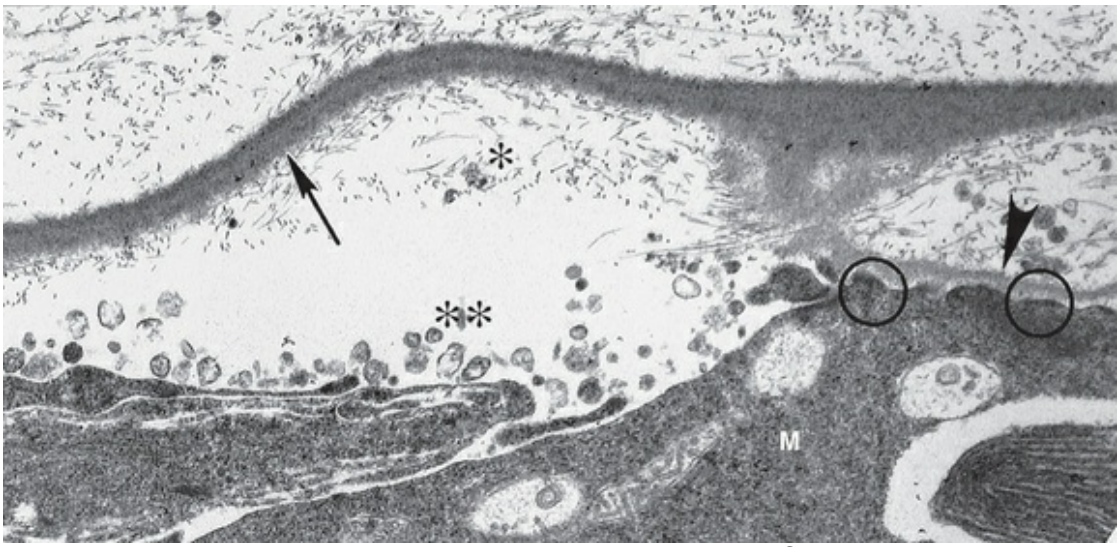

FIG. 23.20 Retinal sheen dystrophy. Inferior midperipheral area where the inner limiting membrane (*arrow*) is separated from Müller cells (*M*), and filaments (*asterisk*) and cellular debris (*two asterisks*) are interposed. The outer portion of the inner limiting membrane (*arrowhead*) is separated and remains attached to Müller cells with junctional densities (*circles*) (×15,000).

Vitreomacular Interface.

Attachment of vitreous to the macula occurs in an irregular, annular zone of 3–4 mm diameter,[4] generally not visible by clinical examination in normal adults but possibly evident in fetal and young adult eyes and in pathologic conditions. The posterior vitreous cortex is thinner over the macula in a disc-shaped area about 4–5 mm in diameter. Discontinuity of the ILM in the fovea may be a site where glial cells extend onto the inner surface of the retina (Fig. 23.21).

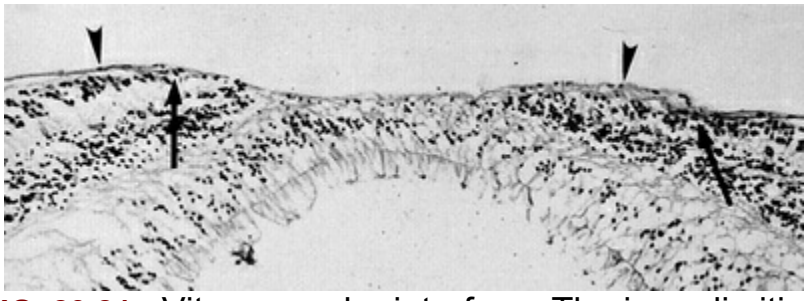

FIG. 23.21 Vitreomacular interface. The inner limiting

membrane is discontinuous (*between arrows*), at which point glial cells extend on to the inner surface of the retina and form a thin, fibroglial premacular membrane (*arrowheads*) with no apparent contraction (periodic acid–Schiff stain; ×100).

Vitreopapillary Interface.

At the rim of the optic disc the ILM ceases, although the basement membrane continues as the inner limiting membrane of Elschnig.[90] This membrane is 50 nm thick and is believed to be the basal lamina of the astroglia in the optic nerve head. At the centralmost portion of the optic disc the membrane thins to 20 nm, follows the irregularities of the underlying cells of the optic disc, and is composed only of glycosaminoglycans and no collagen (central meniscus of Kuhnt). Given that the ILM prevents the passage of cells,[52] the thinness and chemical composition of the central meniscus of Kuhnt and the membrane of Elschnig may account for frequent cell proliferation from or near the optic disc.

Vitreous attachment to the optic disc may persist even though the vitreous is detached elsewhere[91] (Fig. 23.22). This adhesion may be fortified by epipapillary membranes.[92] The entire complex may subsequently detach, resulting in a ring (Weiss) of tissue composed of fibrous astrocytes and collagen (Fig. 23.23) that flutters in and out of the visual axis, causing "floaters." Vitreopapillary adhesion contributes to macular holes[93] and any vitreomaculopathy that features intraretinal cystoid spaces,[94] presumably due to the influence of vitreopapillary adhesion upon the vectors of tangential traction at the macula.

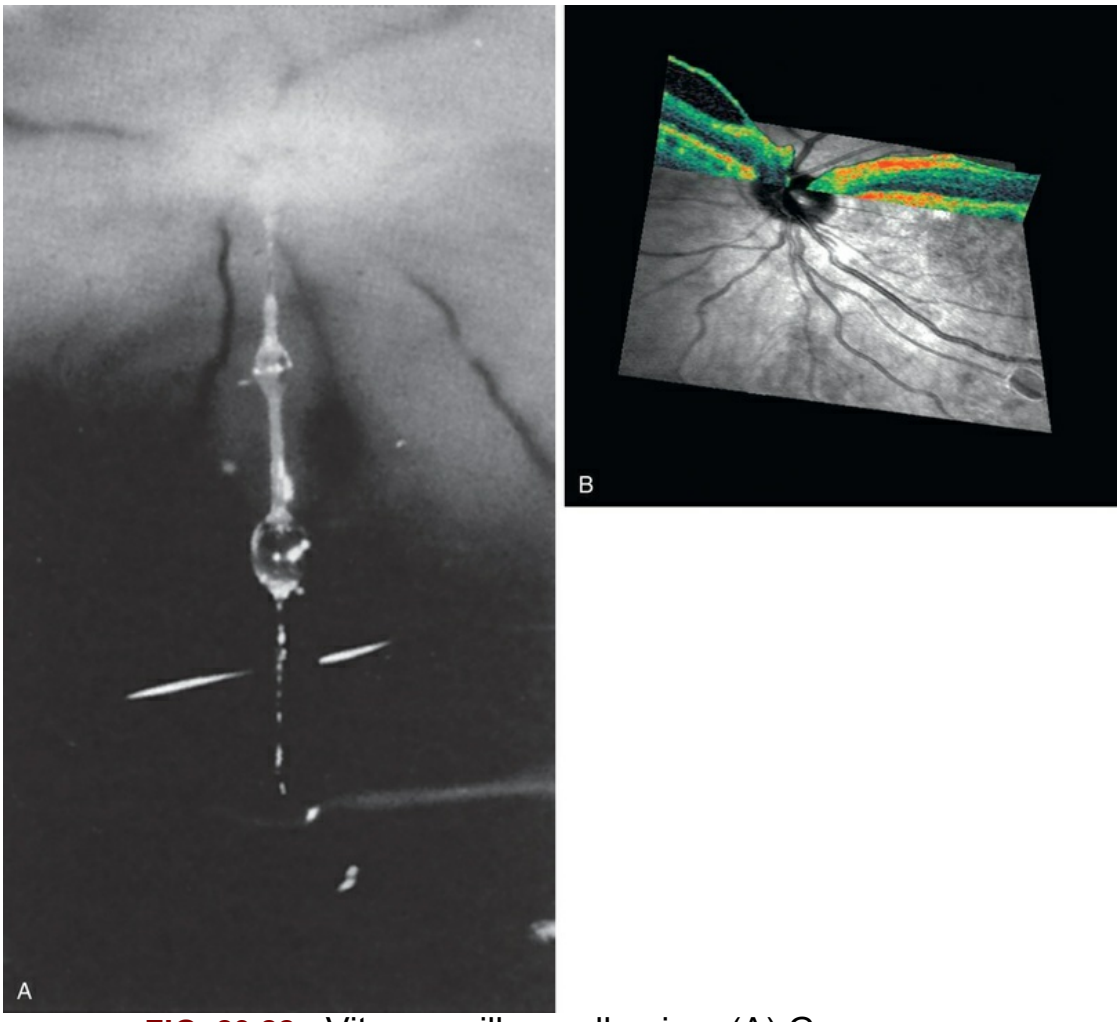

FIG. 23.22 Vitreopapillary adhesion. (A) Gross appearance illustrates partial posterior vitreous detachment with strand of vitreous remaining attached to the optic nerve head. Light reflexes in photograph taken with specimen out of fluid to depict the findings more clearly. (B) Combined optical coherence tomography-scanning laser ophthalmoscopy (OCT-SLO) imaging of vitreopapillary adhesion. The grayscale image is coronal plane imaging by SLO, and the color image is the transverse OCT image through the optic disc.

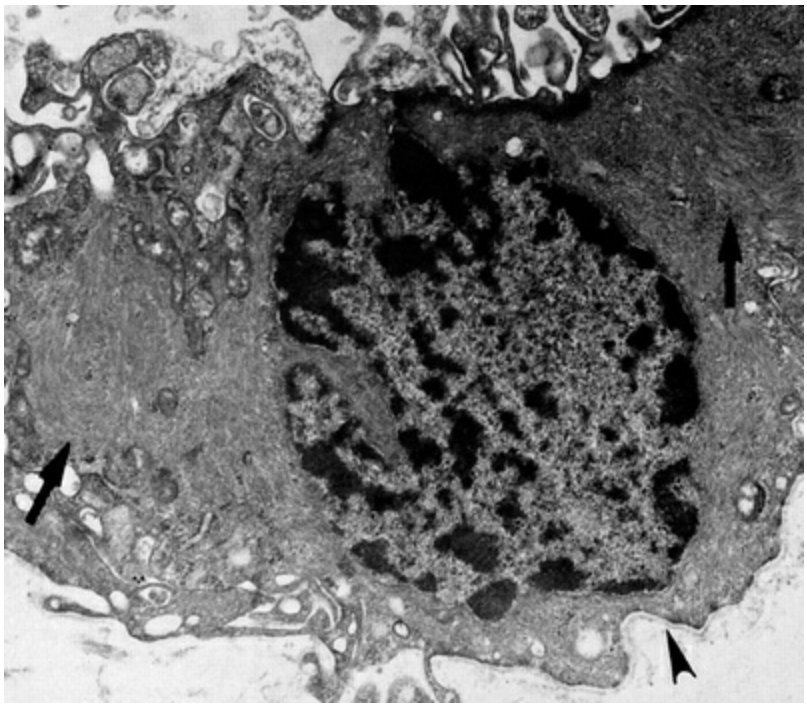

FIG. 23.23 Weiss ring. Surgically removed Weiss ring contains fibrous astrocytes that have polarity, basement membrane (*arrowhead*), and large bundles of 10-nm filaments (*arrows*) (×20,000).

Physiology

Biochemical

Vitreous is important in maintaining transparency for maximal photon transmission to the retina. Vitreous may also maintain lens transparency by mitigating the effects of reactive oxygen species on lens proteins and thus preventing cataracts.[95,96] This antioxidant effect is primarily the result of high concentrations of ascorbate in vitreous, an observation originally made in 1944 by Friedenwald and colleagues.[97]

Gisladottir et al.[98] recently emphasized the influence of vitreous on various physiologic processes and showed that vitrectomy can have considerable effects, both beneficial and harmful.[99] Vitrectomy reduces the risk of retinal neovascularization, but increases the risk of iris neovascularization, reduces macular edema, but stimulates cataract formation. In fact, one approach to mitigating cataract formation following vitrectomy is to leave 3–4 mm of retrolental

vitreous intact.[100,101]

Biophysical

During ocular saccades, the rotational force of the eye wall is transmitted to the vitreous body via attachments to adjacent structures.[102] During both acceleration and deceleration phases of saccades, vitreous movement lags behind the eye wall, resulting in markedly reduced acceleration.[103] This "slack and lag" results from vitreous viscoelasticity, dampening the force at any given internal vitreous attachment. The inferonasal displacement of the optic disc and the shorter distance between the disc and ora inferiorly and nasally make the relief of torsional strain on equatorial and anterior vitreoretinal attachments greater nasally and inferiorly. Accordingly, the greatest torsional strain on anterior and equatorial vitreous attachments should occur during lateral saccades, with the point of maximum strain located somewhere in the superotemporal quadrant, the site of most frequent retinal tears.[104]

Pathology

Age-Related Vitreous Degeneration

Liquefaction[105,106]

After age 40 years there is a significant decrease in the gel volume and a concurrent increase in the liquid volume of vitreous, primarily centrally.[107,108] In the posterior vitreous such changes form pockets of liquid vitreous, called "lacunae" (Fig. 23.24). When a single, large pocket forms, the terms "bursa"[27] or "precortical pocket"[109] have been employed. The large posterior lacuna that is present in young individuals is the bursa premacularis, as originally described by Jan Worst and now visualized on Swept Source OCT imaging. Indeed, Balazs and Denlinger[105] found evidence of liquid vitreous after the age of 4 years and observed that, by the time the human eye reaches adult size (ages 14–18 years), 20% of the total volume is liquid vitreous. By the age of 80–90 years more than half the vitreous body is liquid, which can collect in lacunae throughout or a 'pocket' posteriorly, a pocket,

sometimes referred to as the posterior precortical vitreous pocket (Fig. 23.24).[109]

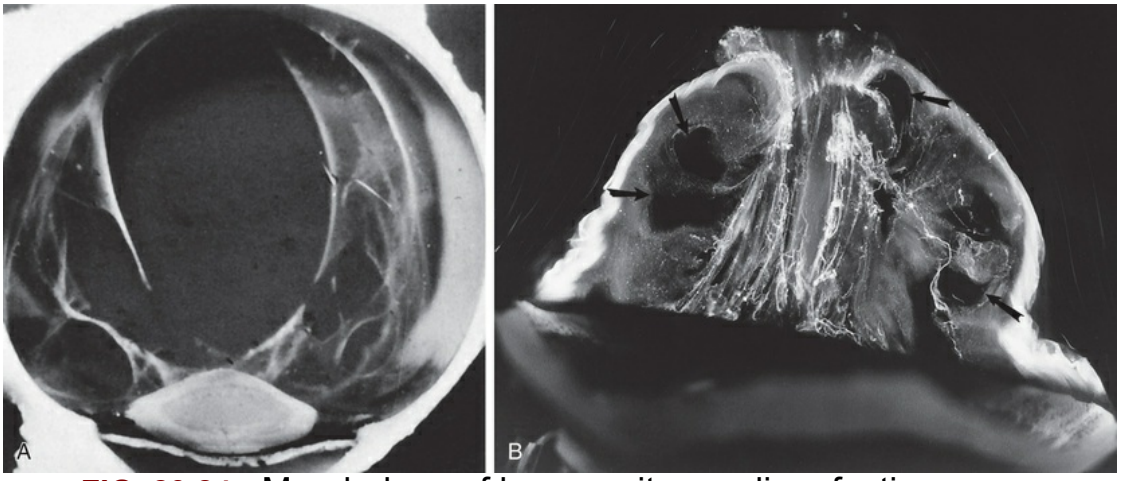

FIG. 23.24 Morphology of human vitreous liquefaction. (A) Gross appearance of central vitreous liquefaction. (B) Dark-field slit microscopy of human vitreous demonstrates the central vitreous has thickened, tortuous fibers. The peripheral vitreous has regions devoid of any structure, which contain liquid vitreous. These regions correspond to so-called lacunae (*arrows*).

Pathogenesis of Vitreous Liquefaction.

Changes in collagen[110,111] or the conformation of HA with subsequent crosslinking and aggregation of fibrils into bundles may result in vitreous liquefaction. Free radicals generated by metabolism and/or photons alter vitreous macromolecules and trigger dissociation of collagen from HA, leading to liquefaction.[112] Vitreous liquefaction may also result from changes in the minor glycosaminoglycans and chondroitin sulfate profile of vitreous.[113] Such mechanisms may be at play in myopic vitreopathy[114] where liquefaction occurs unrelated to aging.

Biochemical studies support the age-related rheologic observations described above. Total vitreous collagen content does not change after age 20–30 years. However, collagen concentration in gel vitreous at the ages of 70–90 years (0.1 mg/mL) was significantly greater than at the ages of 15–20 years (0.05 mg/mL;

$p<.05$).[105] Since the total collagen content does not change, this is likely due to the decreased volume of gel vitreous that occurs with aging and a consequent increase in the concentration of the collagen in the remaining gel. This concept is supported by the finding that vitreous HA concentration increases until about the age of 20, when adult levels are attained. Thereafter, until 70 years, there are no changes in the HA concentrations of either the liquid or gel compartments. This necessarily means that there is an increase in the HA content of liquid vitreous and a concomitant decrease in the HA content of gel vitreous, since the amount of liquid vitreous increases and the amount of gel vitreous decreases with age.

Structural Changes With Aging

Aging of the Vitreous Body.

The aforementioned rheologic and biochemical alterations induce significant structural changes during aging, consisting of a transition from a clear gel in youth (see Fig. 23.2) to a fibrous structure in adults (see Fig. 23.7A). In old age there is advanced liquefaction with thickening and tortuosity of vitreous fibers, and collapse of the vitreous body (Fig. 23.25). Postmortem studies[115] found such changes in 70% of subjects in the eighth decade. Gel liquefaction occurs earlier and is more extensive in myopic eyes,[114,116] and is accelerated with inflammation, trauma, and arthro-ophthalmopathies.[9,117]

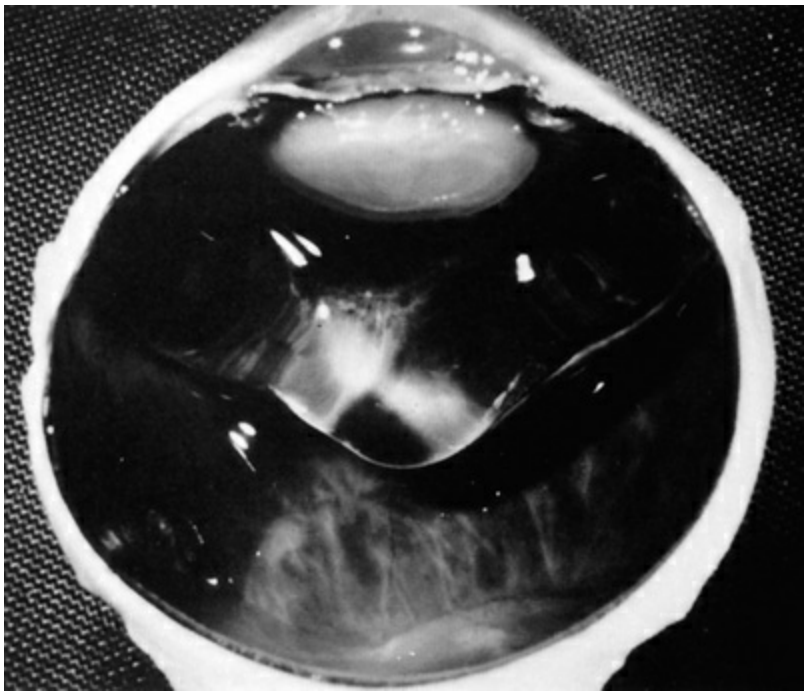

FIG. 23.25 Gross appearance of posterior vitreous detachment in a phakic eye.

Aging of the Vitreoretinal Interface.

With aging there is significant increase in ILM thickness (Fig. 23.26). This may play a role in weakening of vitreoretinal adhesion with age, although the mechanism of such a phenomenon is presently unclear.

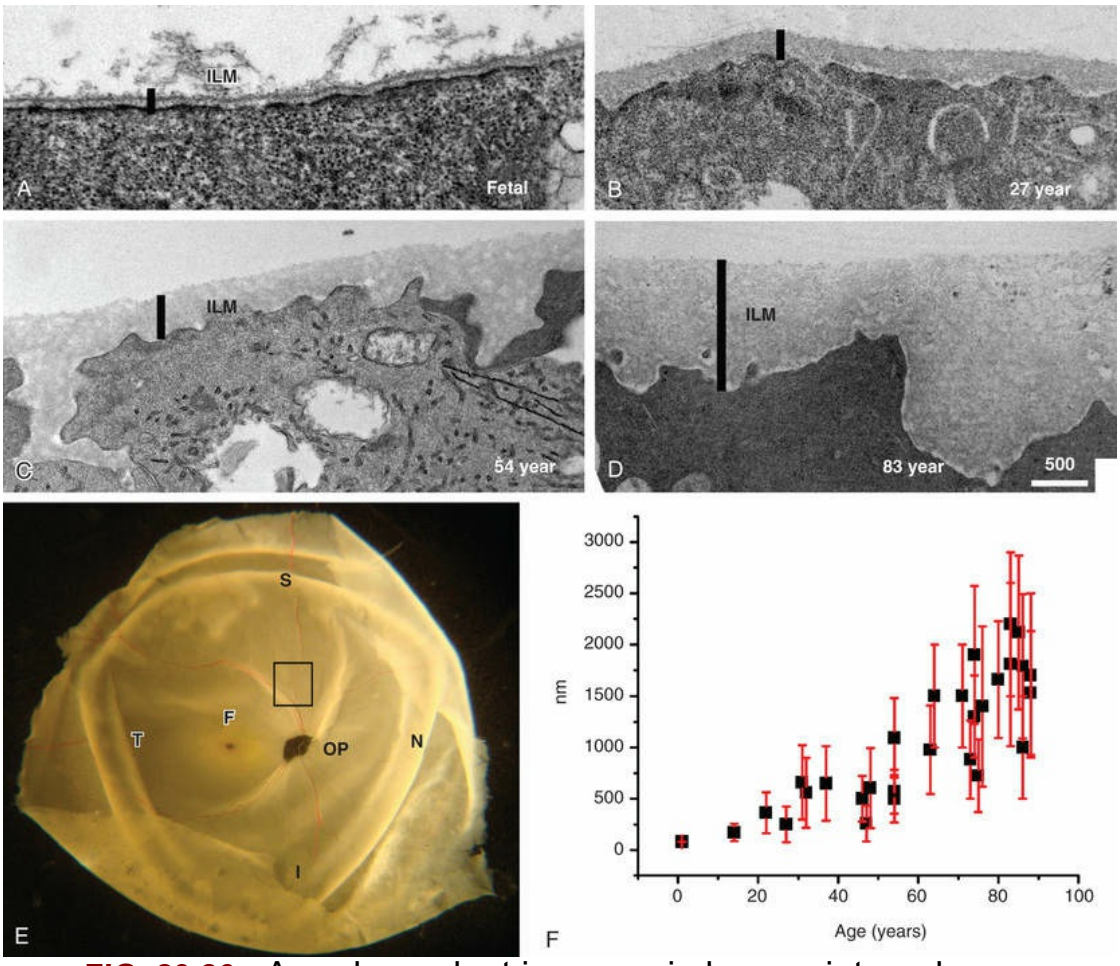

FIG. 23.26 Age-dependent increase in human internal limiting membrane (ILM) thickness. Transmission electron micrographs show the vitread surface of the retina from a 16-week fetal (A) and from 27-, 54-, and 83-year-old adult human eyes (B–D). The ILM in the fetal eye (A) is 70 nm thick with a typical lamina densa and three-layered ultrastructure. Between 22 and 83 years of age (B–D), the ILM dramatically increases in thickness, becomes highly irregular. The retinad surface no longer contains a distinct lamina densa. The vertical black bars in panels A–D indicate the thickness of the ILM. Panel E shows an adult human retina with the location in the superior posterior pole of the right eye (*boxed*) where the retina was sampled. The graph in panel F shows the age-dependent increase in ILM thickness. Each of the data points represents averages of measurements in one pair of eyes from a single patient. *F*, fovea; *I*, inferior; *N*, nasal; *OP*, optic papilla (disc); *S*, superior; *T*, temporal. Scale bar A–D: 500 nm. (Reprinted with permission from Halfter W, Sebag J, Cunningham ET. Vitreo-retinal interface and inner limiting membrane. In:

Peripheral Fundus.

Teng and Chi[80] found that the width (in the radial dimension) of the vitreous base posterior to the ora serrata increases with age to over 3.0 mm. There is also posterior migration of the posterior border of the vitreous base with age,[80,118] mostly temporally. In addition, Gartner[119] found "lateral aggregation" of the collagen fibrils in the vitreous base of older individuals. These and the changes listed below play important roles in the pathogenesis of peripheral retinal breaks and rhegmatogenous retinal detachmnent:

Ora bays[75,82,120] (Fig. 23.27)

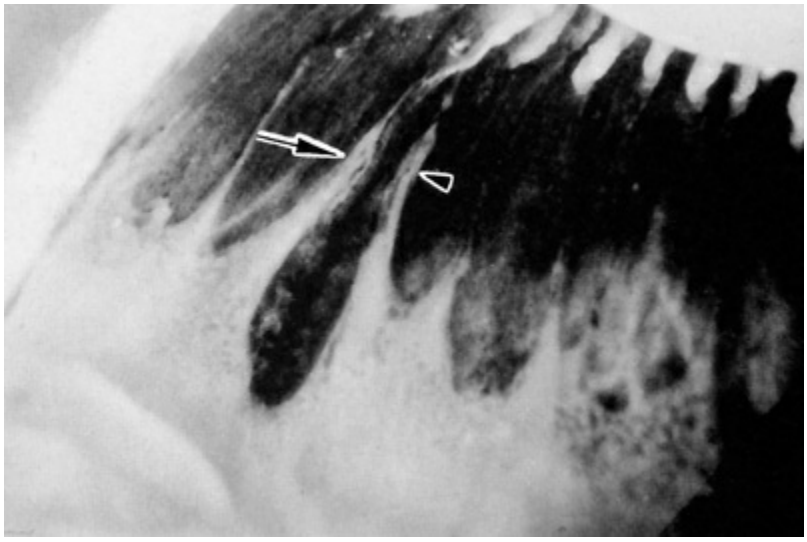

FIG. 23.27 A meridional complex (*arrow*) and dentate process (*arrowhead*) are located at the margin of a non-enclosed ora bay.

Meridional folds[84,121] (Fig. 23.28)

FIG. 23.28 Meridional folds, one in line with a meridional complex (*arrowhead*) and the other (*arrow*) in line with a meridional complex and enclosed ora bay (*asterisk*). (Reproduced with permission from Green WR. Pathology of the retina. In: Frayer WC, editor. Lancaster course in ophthalmic histopathology, unit 9. Philadelphia: FA Davis; 1981.)

Meridional complexes[84] (Figs. 23.27 and 23.29)

FIG. 23.29 Peripheral retinal excavation (*arrowhead*) in line with a meridional complex and an enclosed ora bay. (Reproduced with permission from Green WR. Pathology of the retina. In: Frayer WC, editor. Lancaster course in ophthalmic histopathology, unit 9. Philadelphia: FA Davis; 1981.)

Peripheral retinal excavations[84,122] (Fig. 23.29)

Retinal tufts

Noncystic retinal tufts[123–125] (Fig. 23.30)

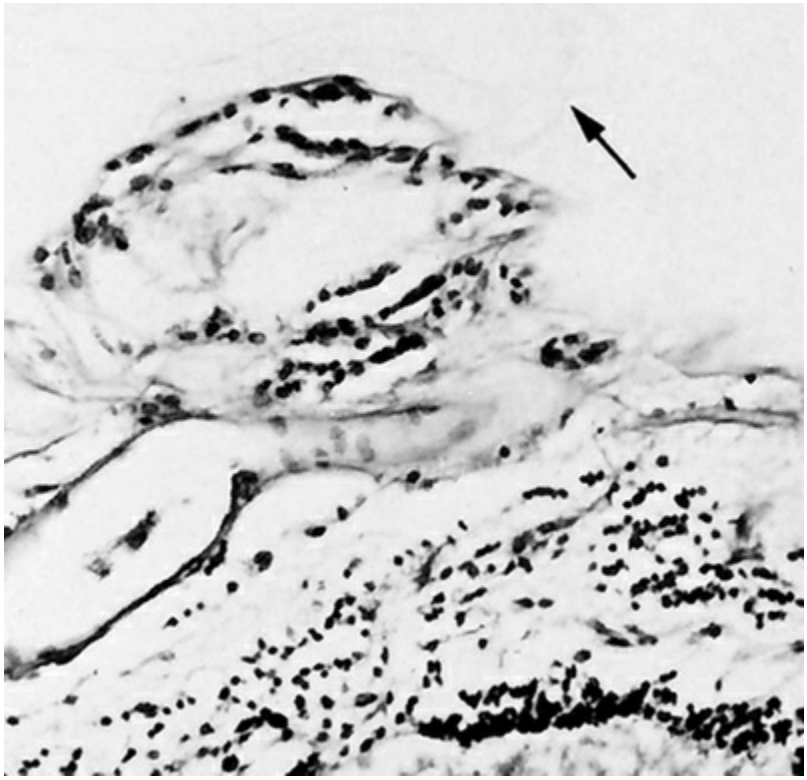

FIG. 23.30 Noncystic peripheral retinal tuft. Most tufts consist of glial cells, and some have strands of vitreous attached (*arrow*) (hematoxylin and eosin, ×215).

(Reproduced with permission from Green WR. Retina. In: Spencer WH, editor. Ophthalmic pathology: an atlas and textbook, vol. 2. Philadelphia: WB Saunders; 1985.)

Cystic retinal tufts[83,123,124,126](Fig. 23.31)

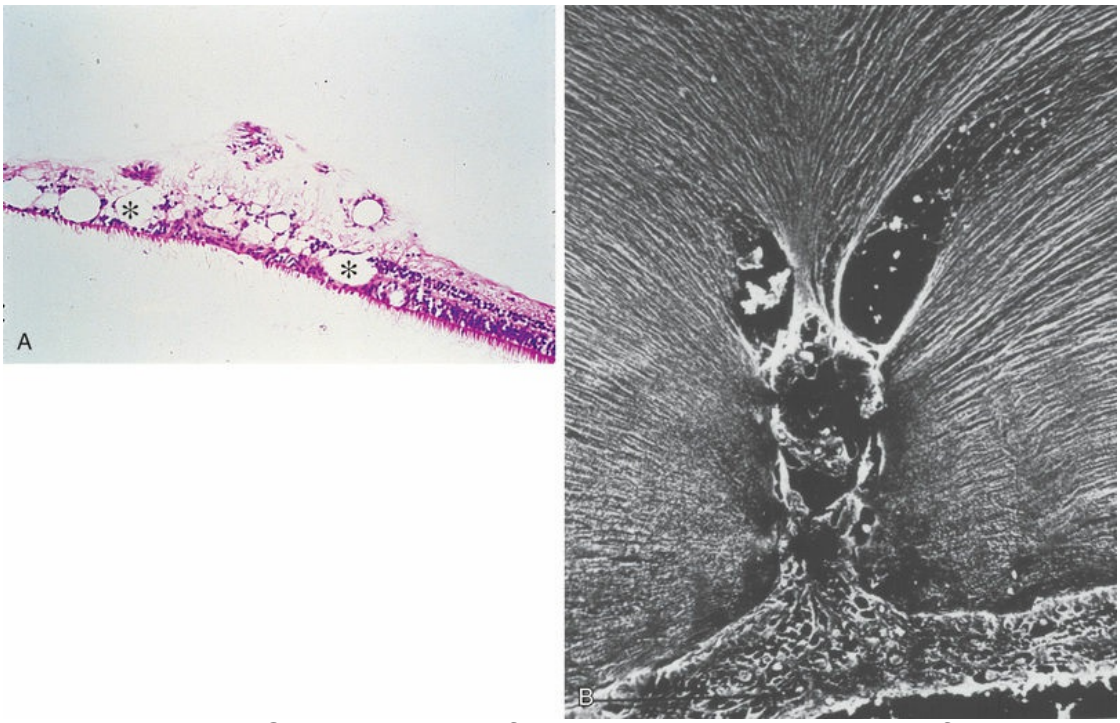

FIG. 23.31 Cystic retinal tuft. (A) The lesion consists of an area of retinal thickening caused by cystic changes (*asterisks*) and glial cell proliferation (hematoxylin and eosin, ×220). (B) Scanning electron microscopy (EM) demonstrates that the tuft is a cystoid formation of fibers, similar to those of the nerve fiber layer, and cells, similar to those found in the inner plexiform layer of the retina, that are connected to the inner limiting membrane of the retina. This scanning EM shows the insertion of the vitreous collagen fibers on the tuft's apical surface. (Panel B reproduced with permission from Dunker S, Glinz J, Faulborn J. Morphologic studies of the peripheral vitreoretinal interface in humans reveal structures implicated in the pathogenesis of retinal tears. Retina 1997;17:124–30.)

Zonular traction tufts[121,127–130] (Fig. 23.32)

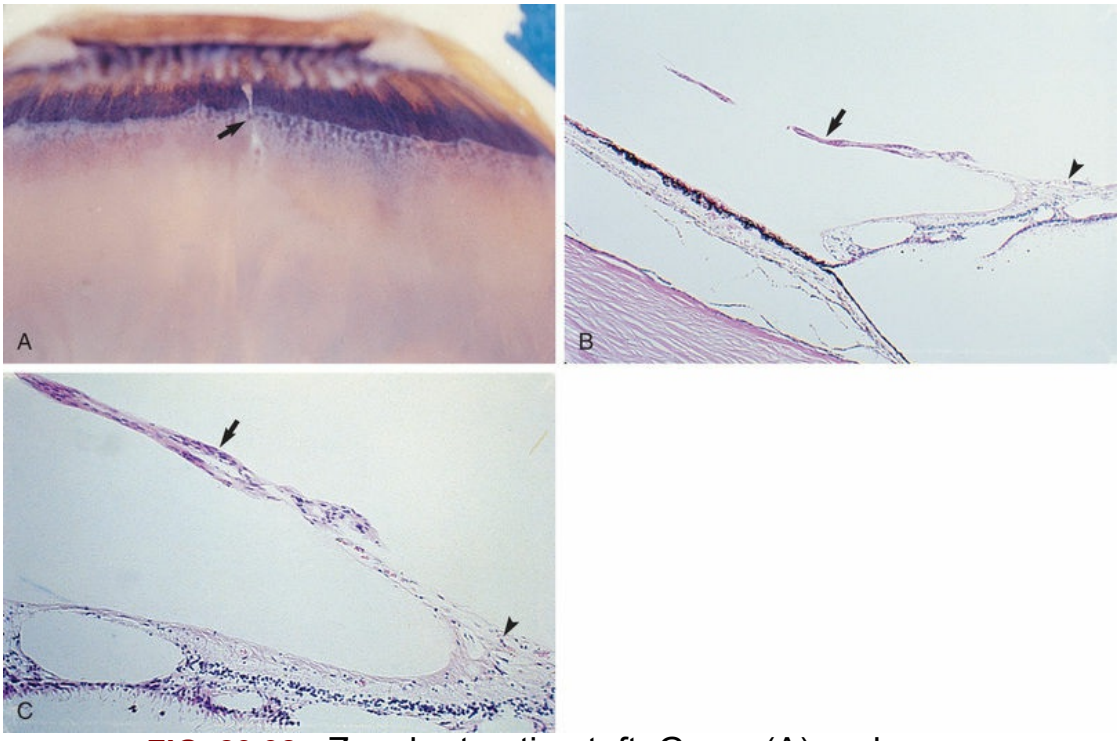

FIG. 23.32 Zonular traction tuft. Gross (A) and microscopic (B) appearances of zonular tractional tuft (*arrow* in panel A) composed of a strand of glial cells whose anterior part consists of two layers of embryonal-like epithelium (*arrows* in panels B and C; hematoxylin and eosin, ×65). (C) Higher magnification (hematoxylin and eosin, ×290). (Panels A and B reproduced with permission from Green WR. Pathology of the retina. In: Frayer WC, editor. Lancaster course in ophthalmic histopathology, unit 9. Philadelphia: FA Davis; 1981. Panel C reproduced with permission from Green WR. Retina. In: Spencer WH, editor. Ophthalmic pathology: an atlas and textbook, vol. 2. Philadelphia: WB Saunders; 1985.)

Spiculate and nodular pigment epithelial hyperplasia[129] (Fig. 23.33)

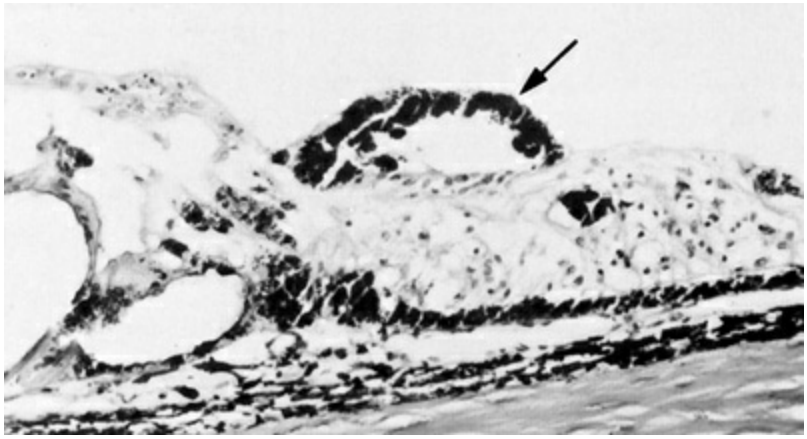

FIG. 23.33 Hyperplasia of pigment epithelium at ora serrata. Hyperplastic pigment epithelium (*arrow*) extends into the vitreous cavity at the ora serrata (periodic acid–Schiff; ×220). (Reproduced with permission from Green WR. Pathology of the retina. In: Frayer WC, editor. Lancaster course in ophthalmic histopathology, unit 9. Philadelphia: FA Davis; 1981.)

Retinal lattice[65,118,126,131–146] (Figs. 23.34–23.38)

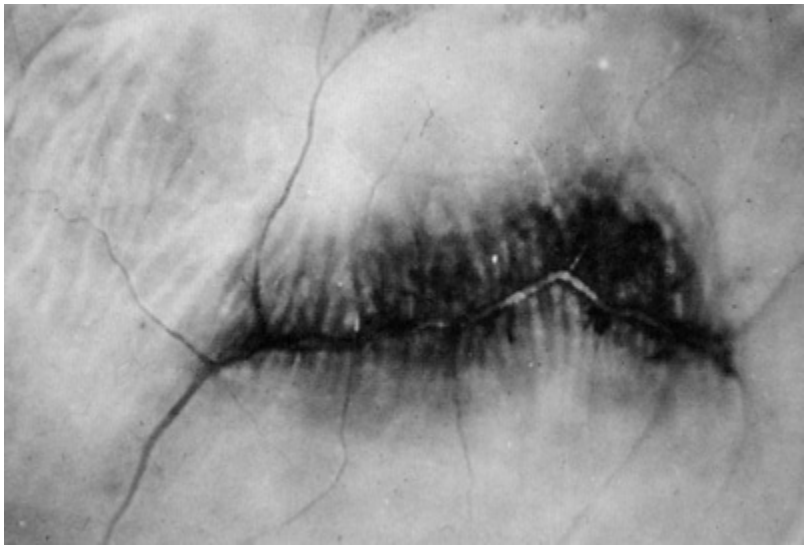

FIG. 23.34 Paravascular retinal lattice. Radial perivascular lattice with sclerotic vessel and hyperplastic retinal pigment epithelium, with migration into the retina in a paravascular location.

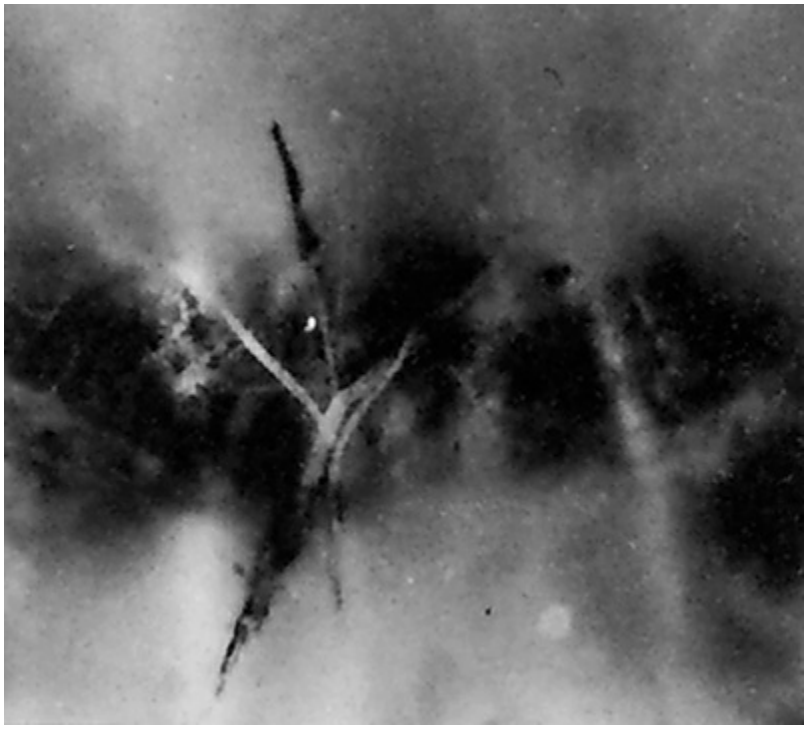

FIG. 23.35 Lattice wicker. Gross appearance of retinal lattice, with sclerotic vessels that have a wicker appearance.

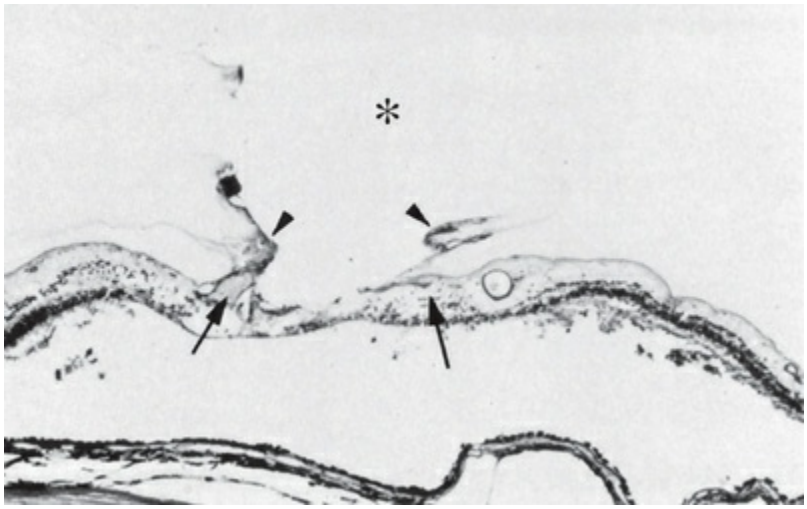

FIG. 23.36 Histopathology of retinal lattice. Lattice lesion with retinal thinning, discontinuity of inner limiting membrane (*arrows*), pocket of fluid vitreous (*asterisk*), and glial cell proliferation in vitreous at margin (*arrowheads*) (Alcian blue stain; ×145).

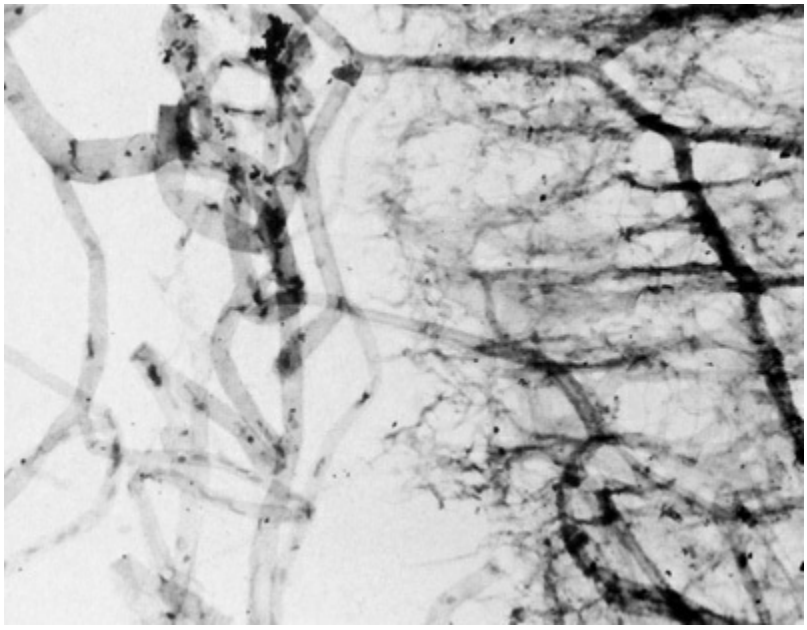

FIG. 23.37 Trypsin digestion preparation of retina discloses relatively acellular capillaries in area of lattice degeneration (right) (hematoxylin and eosin, and periodic acid–Schiff stains; ×185).

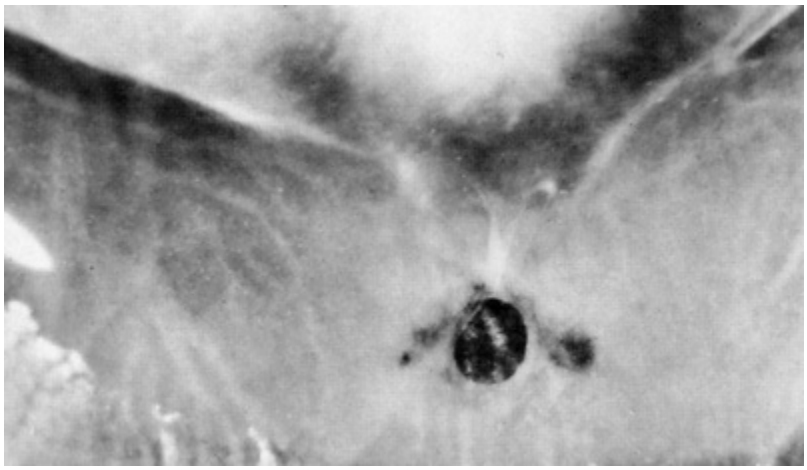

FIG. 23.38 Retinal tear at posterior margin of area of retinal lattice.

White with pressure, white without pressure[147–154]

Verruca[155] (Fig. 23.39).

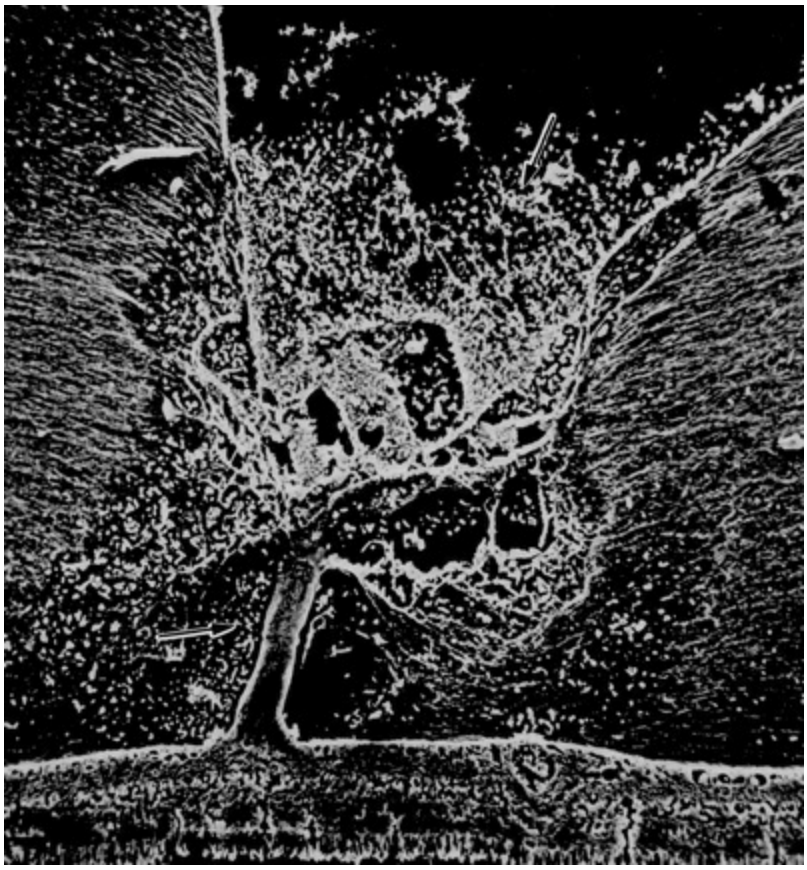

FIG. 23.39 Verruca. Scanning electron microscopy shows cellular elements resembling cells of the inner plexiform layer near the retinal surface. The "trunk" of the verruca extends from the retina to the vitreous cortex. The "branches" of the verruca are intertwined with vitreous collagen fibers. There is local collagen destruction (*arrows*) and interruption of the inner limiting membrane of the retina. (Reproduced with permission from Dunker S, Glinz J, Faulborn J. Morphologic studies of the peripheral vitreoretinal interface in humans reveal structures implicated in the pathogenesis of retinal tears. Retina 1997;17:124–30.)

Posterior Pole – Degenerative Remodeling.

Foos[156] defined a spectrum of changes in the ILM as "degenerative remodeling." Features include detachment and discontinuity of the ILM with vitreous collagen beneath the ILM (Fig. 23.40), cellular debris with macrophages, and absence of Müller cell attachment plaques. In larger lesions, vitreous may insinuate into degenerative crypts and adhere to the cell membrane of the lining Müller cells that have no basal lamina (Fig. 23.41). In the peripapillary area,

retinal glial cells extend from the optic disc and are continuous with a glial epipapillary membrane that has vitreous fiber incarceration. Roth and Foos[92] observed nasal epipapillary membranes associated with Bergmeister papillae in 27.6% of autopsy eyes.

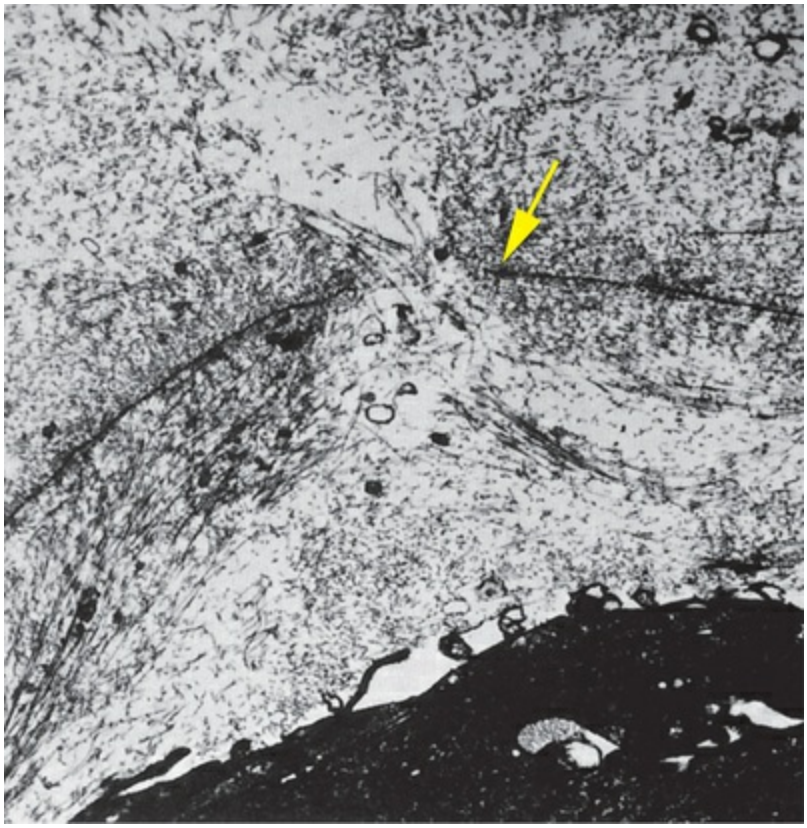

FIG. 23.40 Degenerative remodeling. Basal area with vitreous collagen located between detached inner limiting membrane (*arrow*) and glial cell process.
(Courtesy of Tsuyoshi Kimura.)

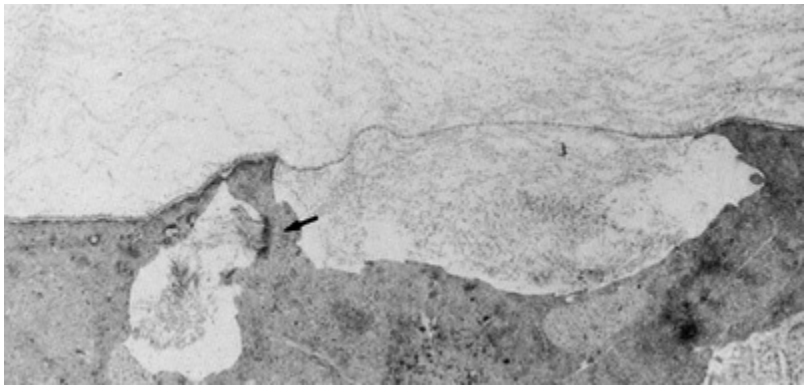

FIG. 23.41 Basal zone showing detached and degenerating inner limiting membrane under which the attachment plaques are missing in the surface of Müller cells and vitreous has become incarcerated. Vitreous in degeneration crypt has become firmly adherent to Müller cell (*arrow*) (×12,600). (Reproduced with permission from Foos RY. Vitreoretinal juncture: topographical variations. Invest Ophthalmol 1972;11:801–8.)

Posterior Vitreous Detachment (PVD)

Due to inadequate diagnostics,[157] PVD is an inaccurate diagnosis. PVD begins at the posterior pole, perhaps in the perifoveal region.[158] An innocuous PVD is clean separation between the ILM of the retina and the cortical vitreous.[159] Whereas it is widely held that PVD is an "abnormal" event, it is possible that PVD may be a preprogrammed event that mitigates the risks of an attached vitreous, which in patients with diabetic retinopathy or age-related macular degeneration are more dangerous than a PVD.[160] Fortunately, PVD is innocuous in most cases.

Epidemiology.

The incidence of PVD is 66% between the ages of 66 and 86 years,[161] and 53% after 50 years.[162] Clinical examination,[163] ultrasonography,[164] and monochromatic photography[165] have been standard, but nanotechnologies, such as dynamic light scattering,[166,167] are being developed to improve clinical evaluation.

In a postmortem study[168] of 786 subjects aged ≧20 years, an upside-down suspension-in-air technique detected a 41% incidence of PVD over 65 years of age. Of 62 aphakic eyes, 94% had partial or complete PVD.

Symptomatic PVD.

The sudden onset of "floaters" heralds the onset of PVD. A smartphone survey of 603 individuals recently determined that floaters are much more common than previously appreciated, with 76% reporting that they see floaters and 33% claiming visual impairment.[169] Other studies have found that floaters have a significant negative impact on the quality of life.[100,170] It has been

determined that the likely cause is a significant reduction in contrast sensitivity,[101] which is strongly correlated with the degree of vitreous opacification as measured by quantitative ultrasonography.[171] Fortunately, studies[100,101] have shown that within one week of limited vitrectomy contrast sensitivity levels return to normal and remain normal thereafter.

The incidence of retinal tears in patients with acute symptomatic PVD varies from 8 to 15%, to as high as 46%.[172] In a study[173] of 589 patients with "floaters," diffuse dots, vitreous cells, and hemorrhage were high-risk factors for a retinal tear, since 93 of 176 (52.8%) of eyes with one or more of these risk factors had retinal tears. Novak and Welch[174] reported that, in 172 eyes of 155 patients with acute symptomatic PVD, 31% had complications. Of these 155 patients, PVD developed in the fellow eye in 17 (11%) within 2 years.

Anomalous PVD (APVD)

APVD results from gel liquefaction without concurrent weakening of vitreoretinal adherence, causing various clinical manifestations based upon where vitreous is most liquefied and where the interface is most firmly adherent (Fig. 23.42).

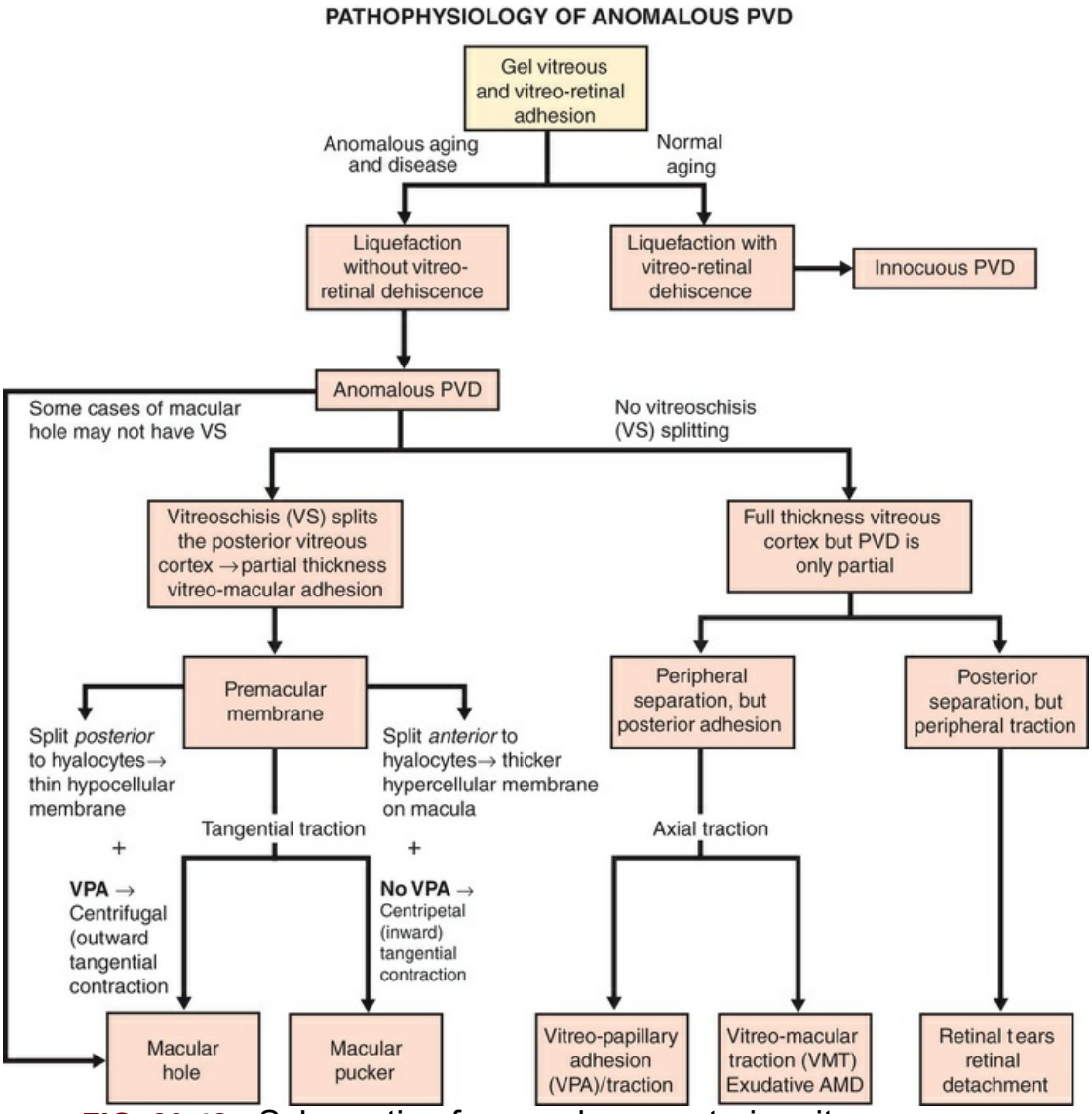

FIG. 23.42 Schematic of anomalous posterior vitreous detachment (APVD). This diagram demonstrates the various possible manifestations of anomalous PVD. When gel liquefaction and weakening of vitreoretinal adhesion occur concurrently, the vitreous body separates away from the retina without sequelae. If the gel liquefies without concurrent dehiscence at the vitreoretinal interface, there can be various untoward consequences, depending upon where the vitreous is most adherent. If separation of vitreous from retina is full-thickness but topographically incomplete, there can be different forms of partial PVD (right side of diagram). Posterior separation with persistent peripheral vitreoretinal attachment can induce retinal breaks and detachments. Peripheral vitreoretinal separation with persistent full-thickness attachment of vitreous to the retina posteriorly can induce traction

upon the macula, known as the vitreomacular traction syndrome (VMTS). This phenomenon appears to be highly associated with exudative age-related macular degeneration (EXUD AMD). Persistent attachment to the optic disc can induce vitreopapillopathies and also contribute to neovascularization and vitreous hemorrhage in ischemic retinopathies, as well as full-thickness macular hole. If, during PVD, the posterior vitreous cortex splits (vitreoschisis), there can be different effects depending upon the level of the split. Vitreoschisis anterior to the level of the hyalocytes leaves a relatively thick cellular membrane attached to the macula. If there is also separation from the optic disc (present in about 90% of cases), inward (centripetal) contraction of this premacular membrane induces macular pucker. If the split occurs at a level posterior to the hyalocytes, the remaining premacular membrane is relatively thin and hypocellular. Persistent vitreopapillary adhesion (VPA, present in 87.5% or more of cases) influences the vector of force in the tangential plane, resulting in outward (centrifugal) tangential traction (especially nasally), inducing a macular hole. Some cases of macular hole may develop in the absence of vitreoschisis. (Reproduced with permission from Sebag J, Niemeyer M, Koss MJ. Anomalous PVD and vitreoschisis. In: Sebag J, editor. Vitreous – in health and disease. New York: Springer; 2014. p. 252.)

Vitreous Effects of APVD

An important consequence of APVD is vitreoschisis[33,38] (Fig. 23.43) or splitting of the posterior vitreous cortex with forward displacement of the anterior portion of the cortex, leaving the posterior layer attached to the retina. Vitreoschisis has been detected in diabetic retinopathy,[16,175] macular pucker, and macular holes.[37,176,177]

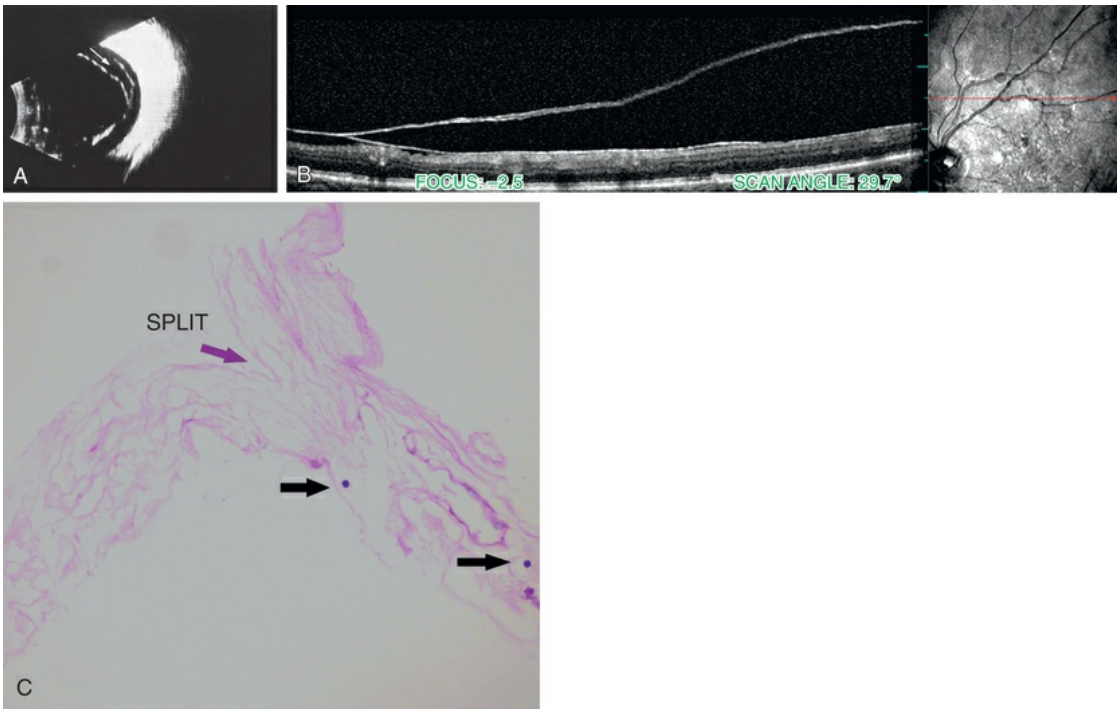

FIG. 23.43 Vitreoschisis. (A) Ultrasonography of posterior vitreoschisis demonstrates the two layers of the schisis cavity rejoining into full-thickness posterior vitreous cortex (below). (B) Optical coherence tomography-scanning laser ophthalmoscopy imaging of posterior vitreoschisis demonstrates the two walls of the schisis cavity rejoining into full-thickness posterior vitreous cortex (to left). (C) Histopathology of vitreoschisis. Surgical specimen removed from a patient with macular pucker demonstrates the split in the posterior vitreous cortex and rejoining of the two walls into full-thickness posterior vitreous cortex. Hyalocytes (*arrows*) are seen within the posterior vitreous cortex. Note the lack of any additional cellularity on the surfaces of the split posterior vitreous cortex. (Periodic acid–Schiff; ×300.) (Panel A reproduced with permission from Green RL, Byrne SF. Diagnostic ophthalmic ultrasound. In: Ryan SJ, editor. Retina. 1st ed. St Louis: Mosby; 1989. Panels B and C reproduced with permission from Gupta P, Yee KMP, Garcia P, et al. Vitreoschisis in macular diseases. Br J Ophthalmol 2011;95:376–80.)

Peripheral Retinal Effects of APVD

Retinal Breaks.

Retinal holes unrelated to PVD were observed in 326 (13.9%) of

2334 autopsy cases by Foos et al.[138] Retinal tears (Fig. 23.44) result from fluid movements.[178] Vitreous remains attached to the posterior margin of the retinal flap, which may be avulsed leaving a round or oval hole. The flap of retina remains attached to the posterior surface of the detached vitreous (operculum). Large detached flaps may form a cystic structure (Fig. 23.45).

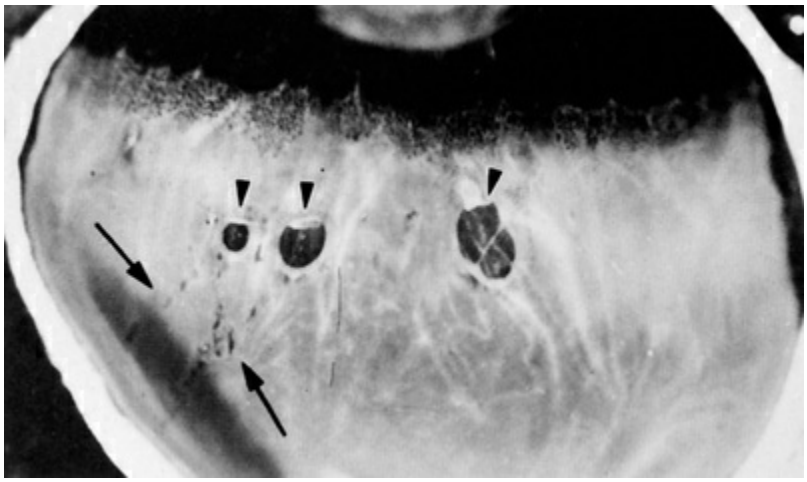

FIG. 23.44 Retinal pits and tears. Gross appearance of eye with posterior vitreous detachment, a string of retinal pits along vessels (*arrows*), and three horseshoe-shaped retinal tears (*arrowheads*). (Reproduced with permission from Green WR. Pathology of the vitreous. In: Frayer WC, editor. Lancaster Course in Ophthalmic Histopathology, unit 8. Philadelphia: FA Davis; 1981.)

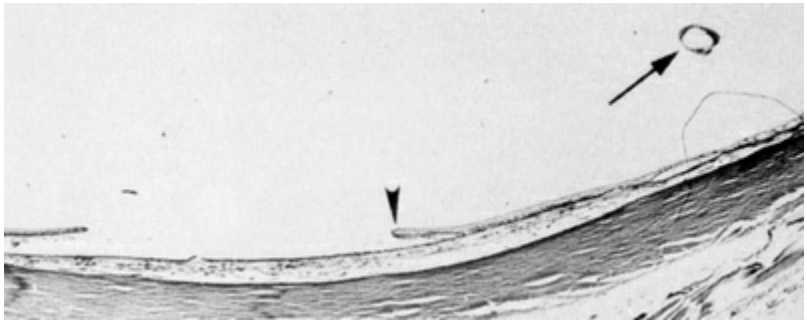

FIG. 23.45 Large retinal tear. Microscopic features include rounded anterior (*arrowheads*) and posterior margins of the hole and coiled-up, detached operculum (*arrow*) that remains attached to the posterior surface of the detached vitreous (periodic acid–Schiff stain;

×16). (Reproduced with permission from Green WR. Pathology of the vitreous. In: Frayer WC, editor. Lancaster course in ophthalmic histopathology, unit 8. Philadelphia: FA Davis; 1981.)

The clinical incidence of retinal tears[179] varies from 7.2%[180] to 5.8%,[181] with a high of 13.75%[121] and a low of 0.59%.[182] Postmortem incidences were 3.9%,[183] 8.6%,[184] 4.7%,[185] 8.8%,[196] 3.7%,[187] and 7.3%.[138] Although the role of retinal tears in causing retinal detachment (RD) is undisputed, management is controversial. Byer[188] concluded that prophylactic treatment is not justified for asymptomatic retinal breaks in phakic eyes. However, in a natural history study of 166 eyes with retinal breaks, Davis[146] observed that 31 (18%) progressed to RD. Neumann and Hyams[189] reported that 2% of 153 eyes with retinal breaks developed RD. The incidence of retinal tears is much greater than RD, which varies between 9 (0.009%)[190] and 24.4 (0.02%) per 100, 000 per year.[191] Benson[192] promoted patient education while Combs and Welch[193] concluded that prophylactic treatment of acute horseshoe tears with vitreous traction significantly reduces the incidence of RD. A particularly high-risk group are patients with vitreous hemorrhage that obscures fundus visualization. Ultrasound may be an effective means of identifying retinal tears in such eyes,[194] but misdiagnosis at presentation bodes poorly since there is a 67% incidence of retinal tears.[195]

Other Sequelae

Retinal tags[123]

Retinal folds

Traction retinoschisis (Fig. 23.46)

FIG. 23.46 Traction retinoschisis. Gross appearance of large retinoschisis caused by vitreous traction. A sheet of vitreous (*arrow*) extends across the eye and temporally is attached to the apex of the tented-up inner layer of the extensive areas of retinoschisis. Posteriorly a hole in the outer layer (*arrowhead*) is present and allows visualization of some interbridging strands of tissue between two layers of schisis.

(Reproduced with permission from Green WR. Retina. In: Spencer WH, editor. Ophthalmic pathology: an atlas and textbook, vol. 2. Philadelphia: WB Saunders; 1985.)

Traction on retinal vessels [85] (Fig. 23.47A)

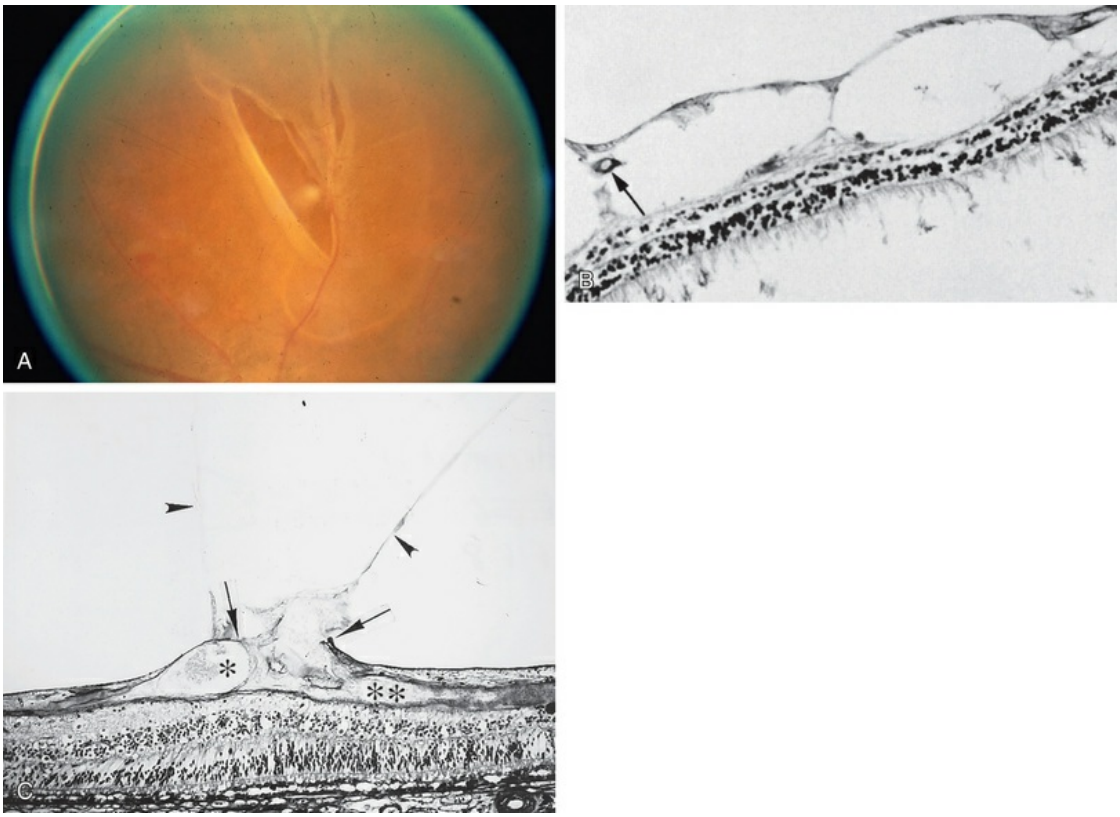

FIG. 23.47 Anomalous posterior vitreous detachment effects on retinal vessels. (A) Retinal tear with bridging retinal blood vessel. (B) There is cystic degeneration of the nerve fiber layer near the retinal vessel (*arrow*) (periodic acid–Schiff stain; ×120). (C) Section through a venous loop that is parallel to the axis of the vein shows the anterior (*asterisk*) and posterior (*double asterisks*) components of the loop as it extends through a discontinuity in the inner limiting membrane (*between arrows*). The wall of the loop is thin and tented at the points of attachment of thin delicate vitreous strands (*arrowheads*) anteriorly and posteriorly (periodic acid–Schiff stain; ×100). (Panel B reproduced with permission from Green WR. Pathology of the retina. In: Frayer WC, editor. Lancaster course in ophthalmic histopathology, unit 9. Philadelphia: FA Davis; 1981. Panel C reproduced with permission from Hersh PS, Green WR, Thomas JV. Tractional venous loops in diabetic retinopathy. Am J Ophthalmol 1981;92:661–71.)

Cystic degeneration[186,187] (Fig. 23.47B)

Avulsion of retinal vessels[196,197]

Retinal pits[186] (Fig. 23.48).

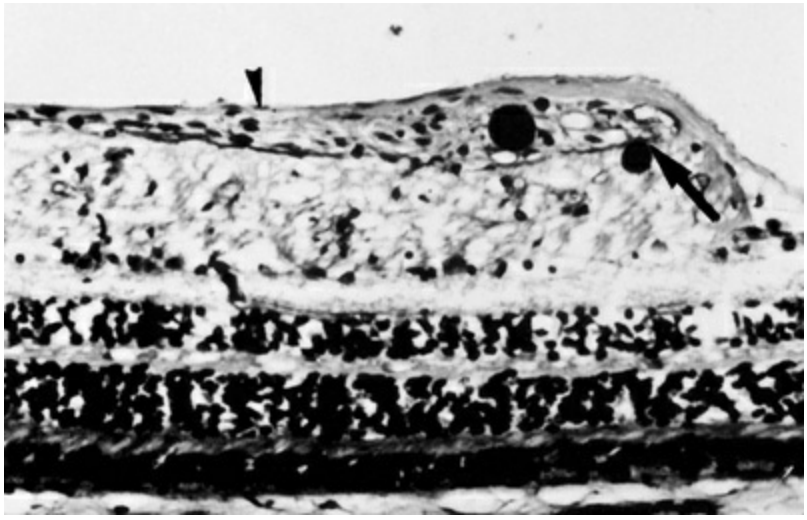

FIG. 23.48 Retinal pit. Margin of retinal pit with discontinuity of the inner limiting membrane (*arrow*) and a glial cell preretinal membrane (*arrowhead*). (Periodic acid–Schiff stain; ×185.) (Reproduced with permission from Clarkson JG, Green WR, Massof D. A histopathologic review of 168 cases of preretinal membrane. Am J Ophthalmol 1977;84:1–17.)

Macular Effects of APVD

Vitreomacular Traction.

For vitreomacular traction syndrome[4,31,36] see Fig. 23.49.

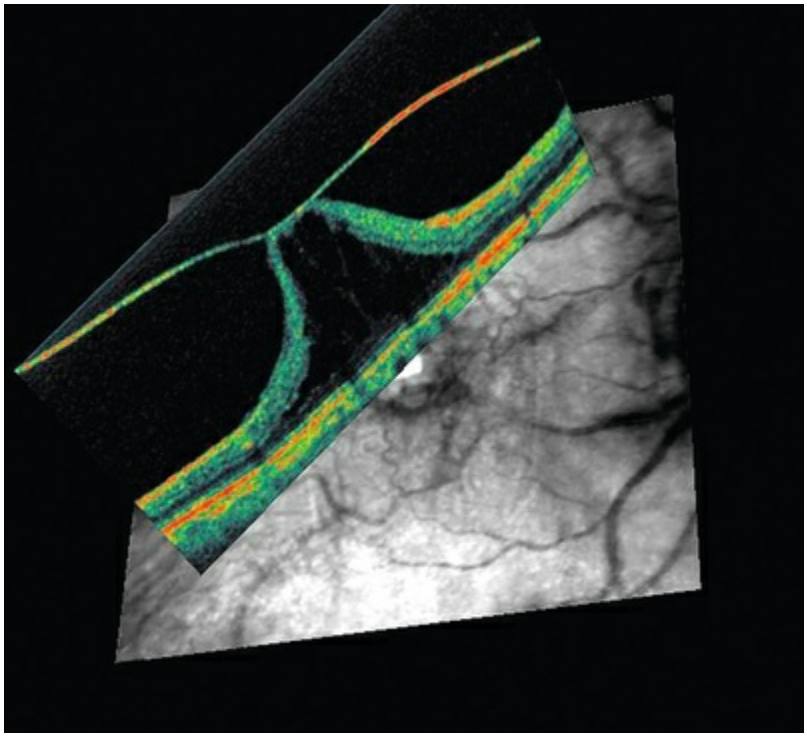

FIG. 23.49 Vitreomacular traction syndrome. This extreme example of anomalous posterior vitreous detachment with persistent full-thickness adhesion of the posterior vitreous cortex to the macula has induced sufficient traction upon the macula to induce prominent elevation of the central macula. Typically, there is only thickening of the macula without detachment.

Exudative Age-Related Macular Degeneration.

Recent studies[198–200] have determined that vitreomacular adhesion may be a risk factor for exudative age-related macular degeneration. Several subsequent studies have confirmed these findings. It has further been recently discovered that persistent vitreomacular adhesion increases the required number of intravitreal anti-VEGF injections and may limit efficacy.[201]

Cystoid Macular Edema.

For cystoid macular edema,[202–208] see Figs. 23.50 and 23.51.

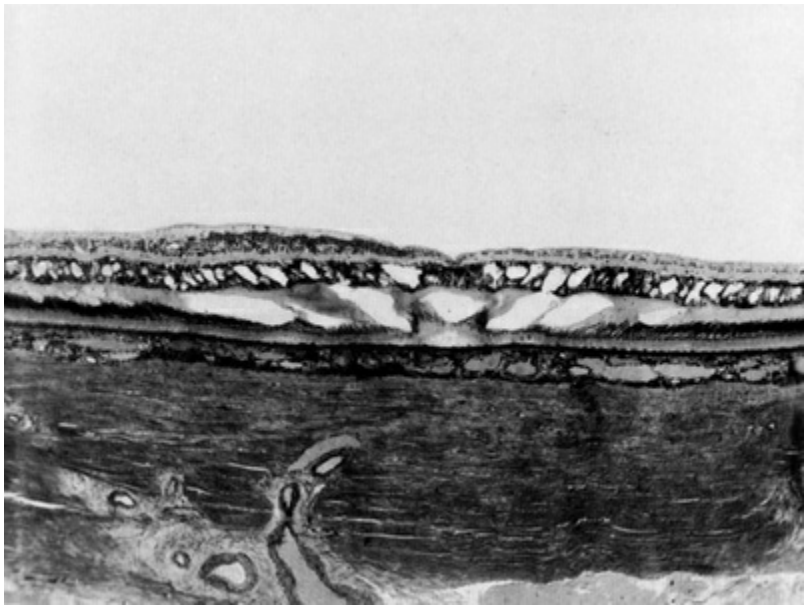

FIG. 23.50 Cystoid macular edema with cystic spaces in the outer plexiform and inner nuclear layers (hematoxylin and eosin, ×45).

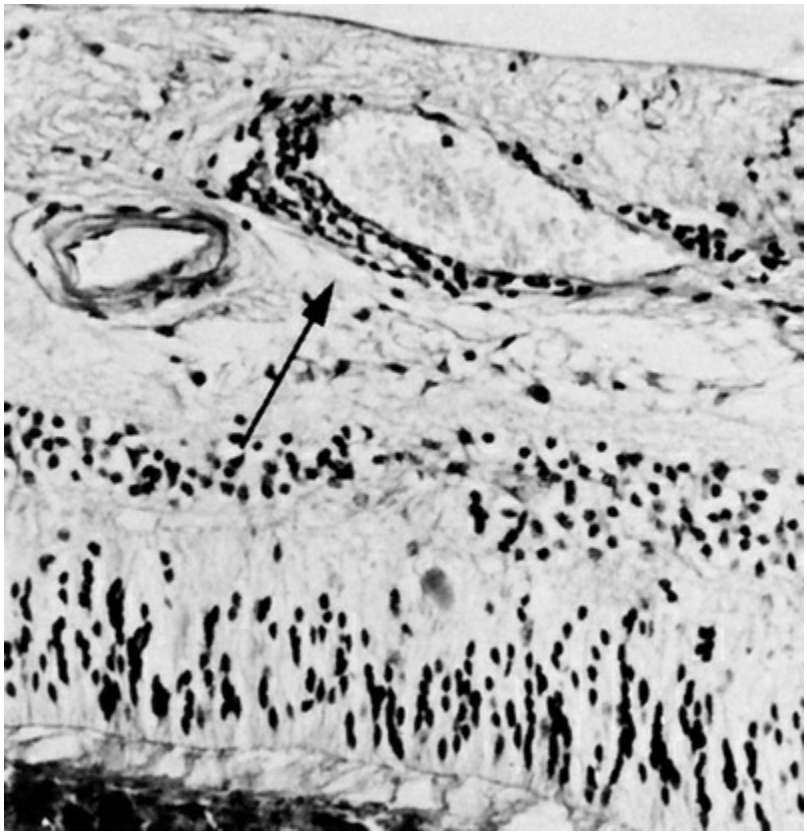

FIG. 23.51 Irvine–Gass syndrome. Area near posterior pole showing edema and retinal phlebitis (*arrow*) (hematoxylin and eosin, ×185). (Reproduced with permission from

Martin NF, Green WR, Martin LW. Retinal phlebitis in the Irvine–Gass syndrome. Am J Ophthalmol 1977;83:377–86.)

Macular Cysts.[209]

Macular cysts that result from chronic edema (Fig. 23.52) need to be distinguished from the cystoid spaces created by vitreous traction in macular holes (Figs. 23.53 and 23.54), and macular pucker with vitreopapillary adhesion.[93,94,210]

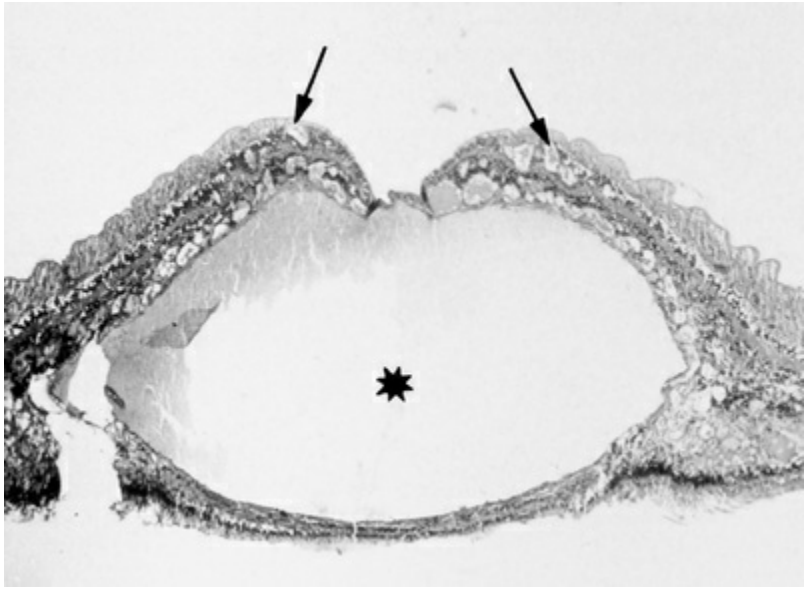

FIG. 23.52 Cystic edema (*arrows*) and a large cyst (*asterisk*) are present in the macula (hematoxylin and eosin, ×40). (Reproduced with permission from Green WR. Retina. In: Spencer WH, editor. Ophthalmic pathology: an atlas and textbook, vol. 2. Philadelphia: WB Saunders; 1985.)

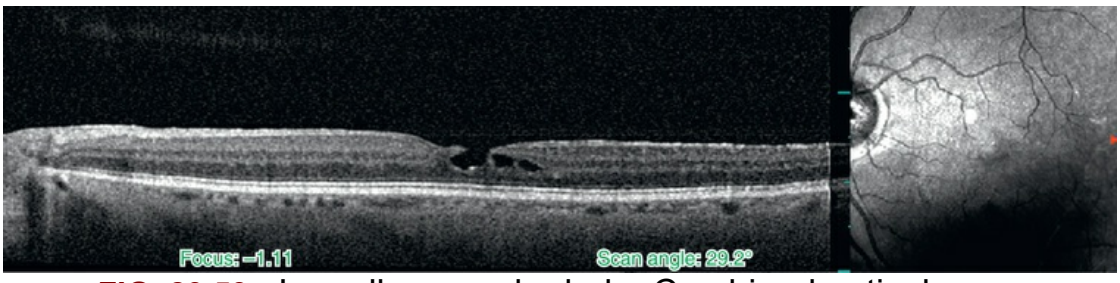

FIG. 23.53 Lamellar macular hole. Combined optical coherence tomography-scanning laser

ophthalmoscopy imaging of a partial-thickness macular hole with adjacent cystoid spaces.

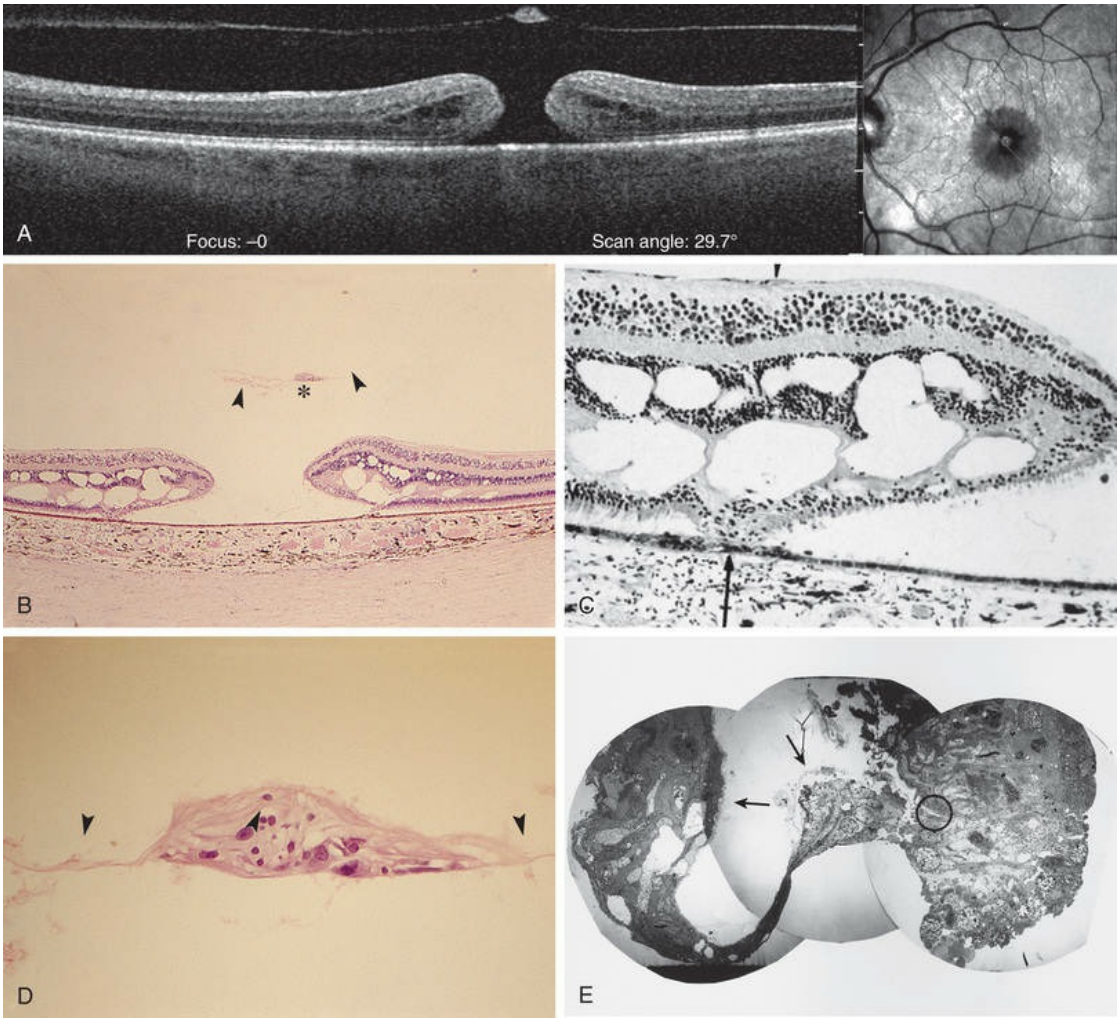

FIG. 23.54 Full-thickness macular hole. (A) Combined optical coherence tomography-scanning laser ophthalmoscopy imaging of macular hole demonstrating anomalous posterior vitreous detachment, a pseudo-operculum, pericentral intraretinal cystoid spaces, and a thin premacular membrane, particularly visible to the right. (B) Microscopy shows macular hole, detached posterior vitreous cortex *(arrowheads*) with adherent pseudo-operculum (*), cystoid spaces in outer plexiform and inner nuclear layers, a small area of surrounding retinal detachment, demarcation chorioretinal adhesions on both sides of the elevated retina, and a premacular membrane particularly visible to the right (hematoxylin

and eosin, ×55). (C) Higher-power view of panel B showing a thin hypocellular preretinal membrane (*arrowhead*), prominent cystoid spaces, and demarcation adhesion (*arrow*) (hematoxylin and eosin, ×140). (D) Detached pseudo-operculum demonstrating lack of neural retina elements. (E) Composite low-power view of operculum. Thicker cellular ends are connected by a thinner segment. A thin collagenous layer along this region (cortical vitreous) identified the inner vitreal surface (*arrows*) of the operculum. A short segment of ILM (*circle*) is present in an area of folding (×550). (Panel C reproduced with permission from Frangieh GT, Green WR, Engel HM. A histopathologic study of macular cysts and holes. Retina 1981;1:311–36. Panel E reproduced with permission from Madreperla SA, McCuen BW II, Hickingbotham D, et al. Clinicopathologic correlation of surgically removed macular hole opercula. Am J Ophthalmol 1995;120:197–207.)

Macular Holes.

Macular holes are surrounded by a gray ring of cystoid spaces and slightly elevated retina, thinning and depigmentation of the underlying retinal pigment epithelium (RPE), yellow nodular opacities at the level of the RPE, a preretinal membrane in all cases with eccentric retinal pucker in 40%, and an operculum in 25% of patients (see Fig. 23.54). Macular hole occurred in 8 of 37 (22%) fellow eyes in one study.[211] Avila et al.[212] reported axial traction as the cause, while Morgan and Schatz[213] proposed that involutional macular thinning predisposes to a macular hole.

Histopathology and Pseudo-Operculum.

Minor RPE hypertrophy and hyperplasia occur in the area of lamellar and full-thickness macular hole. At the onset of macular hole, there is likely vitreoschisis,[32] leaving a thin hypocellular layer of the posterior vitreous cortex attached to the macula[160,176,214] (Fig. 23.55). There is little cellular proliferation,[215] suggesting that fluid countercurrents or vitreoschisis (Fig. 23.56) may be important. Healing of macular hole following surgery[216] does, however, involve glial cell proliferation[217] and Müller cell processes.[218] Macular hole opercula are rarely composed of retinal tissue (see Fig. 23.54), hence the name "pseudo-operculum."

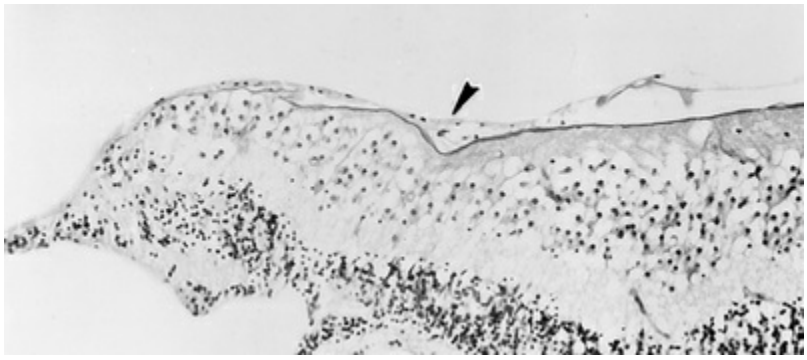

FIG. 23.55 Macular hole with extensive photoreceptor cell atrophy. A thin, tapered layer of cortical vitreous with a hypocellular membrane on its inner surface (*arrowhead*) apparently exerts tangential traction with elevation of the hole margins (periodic acid–Schiff, ×340). (Reproduced with permission from Guyer DR, Green WR. Idiopathic macular holes and precursor lesions. In: Franklin RM, editor. Proceedings of the 1992 New Orleans Academy of Ophthalmology. New York: Kugler; 1993.)

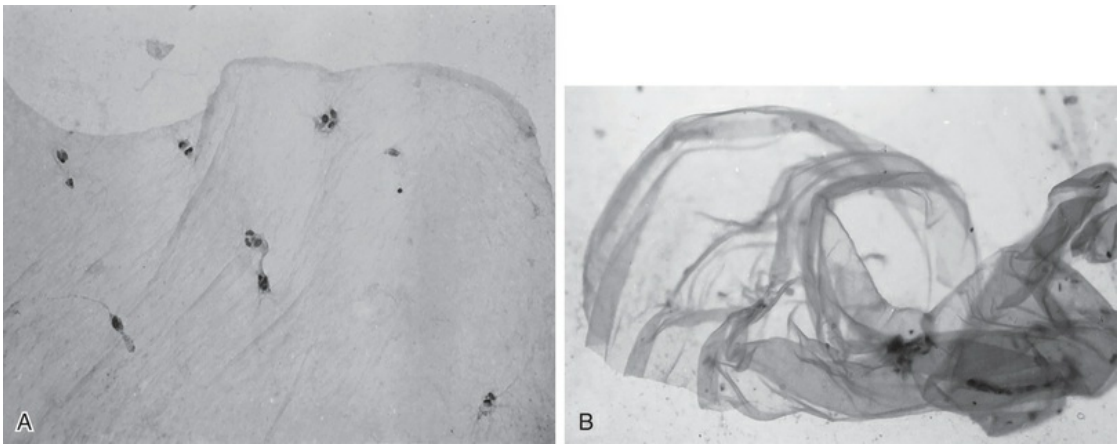

FIG. 23.56 Membranes removed during macular hole surgery. (A) Tissue removed at surgery for macular hole demonstrates a hypocellular membrane with spindle and stellate-shaped cells (Millipore filter, modified Papanicolaou; ×340). (B) Inner limiting membrane (ILM) of retina. After peeling off the retina, this tissue demonstrates the characteristic “scrolled” configuration of the ILM following chromodissection. This does not occur with preretinal membranes (A), only with the ILM. (Millipore filter, modified Papanicolaou stain; ×340.)

Pathogenesis.

There have been various theories of macular hole pathogenesis: trauma, foveal degeneration, vitreous traction, and involutional thinning with PVD. It is clear from surgical experience[219] that vitreous is the cause of macular hole. Johnson and Gass[220] formulated the tangential traction theory by suggesting that shrinkage of the prefoveal vitreous induces macular hole formation in four stages. There are three possible mechanisms of tangential vitreous traction: (1) fluid vitreous movements and countercurrents; (2) cellular remodeling of cortical vitreous; and (3) contraction of a cellular membrane on the tapered cortical vitreous after vitreoschisis.[30,35,36] Combined OCT-scanning laser ophthalmoscopy (OCT-SLO) imaging found vitreoschisis in half of eyes with macular hole[33,176] (Fig. 23.57). In an ultrastructural study of epiretinal tissue removed during vitrectomy for impending macular holes, Smiddy et al.[206] observed cortical vitreous in all eyes. VPA may be important, as this is present in 88.2% of macular hole eyes.[93,94] VPA influences the vector of tangential forces on the macula and induces outward (centrifugal) traction, opening a central dehiscence. In macular pucker, there is usually no VPA and the vector of tangential traction is inward (centripetal), causing a macular pucker.

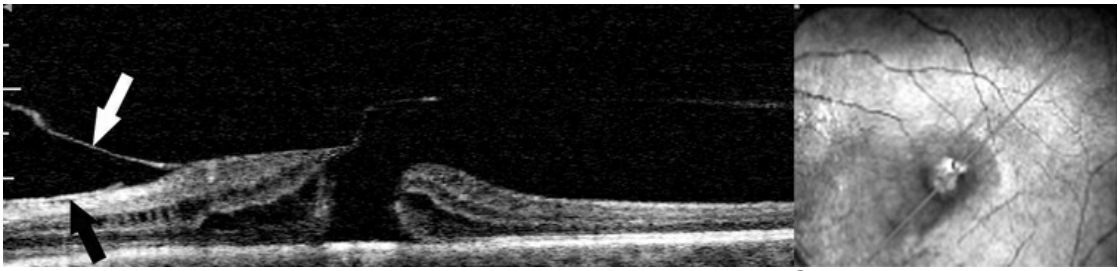

FIG. 23.57 Vitreoschisis in macular hole. Optical coherence tomography-scanning laser ophthalmoscopy imaging of vitreoschisis in a stage III macular hole. The inner wall of the schisis cavity (*white arrow*) is lifted off the retinal surface but remains adherent to the optic disc. The outer wall of the schisis cavity places centrifugal (outward) tangential traction of the macula opening a central dehiscence and inducing the macular hole. This layer must be removed at surgery, often done with chromodissection. *Black*

arrow indicates the outer layer of the vitreoschsis split in the posterior vitreous cortex, which is still attached to the retina.

Some surgeons[221] have advocated prophylactic surgery in symptomatic fellow eyes. However, a multicenter trial failed to demonstrate efficacy for vitrectomy in such eyes,[222] and thus surgery is not routinely performed.

Optic Disc Effects

Anomalous PVD with persistent adhesion to the optic disc can cause vitreopapillary traction inducing hemorrhage,[223] exacerbating neovascularization in proliferative diabetic vitreoretinopathy,[224] and even inducing gaze-evoked visual disturbances.[225] Vitreopapillary adhesion also plays a role in the formation of macular holes and cysts.[93,94,210]

Vitreoretinal Changes After Lens Extraction

Structural

Opacification[226]

Vitreous hemorrhage (APVD) with subsequent liquefaction

Vitreous incarceration with vitreoretinal traction[227] (Fig. 23.58).

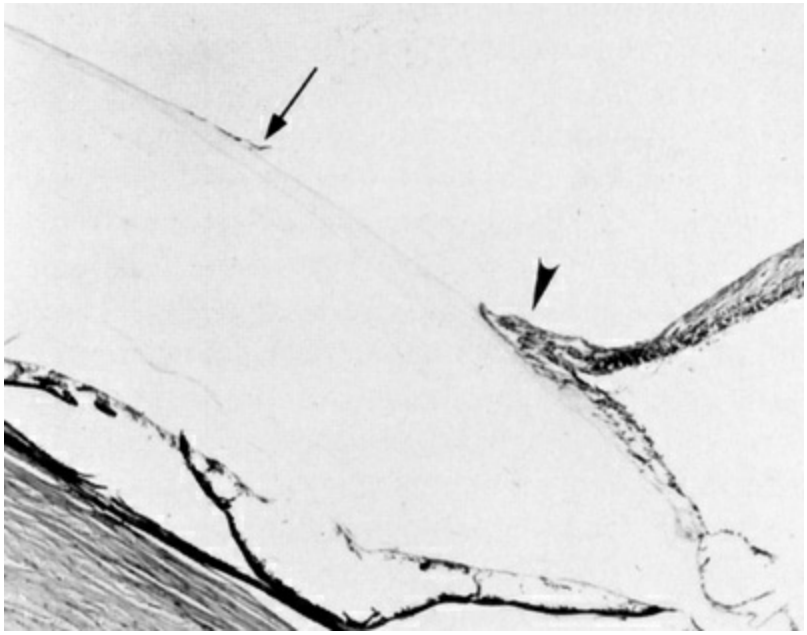

FIG. 23.58 Traction retinal detachment in eye of a 23-year-old man with a previous history of traumatic cataract who underwent surgery complicated by vitreous incarceration in the wound. A vitreous strand (*arrow*) is seen attached to the anterior retina that is under traction and "tented" (*arrowhead*) (periodic acid–Schiff, ×60). (Reproduced with permission from Smiddy WE, Green WR. Retinal dialysis: pathology and pathogenesis. Retina 1982;2:94–116.)

Biochemical

Reduction of vitreous HA concentration[228] results in decreased viscosity[229] and shock absorption. This can be prevented by maintaining an intact posterior capsule after lens surgery.

PVD Following Lens Extraction[230,231]

PVD occurred in 84% following intracapsular cataract extraction, 76% following extracapsular cataract extraction (ECCE) and surgical capsular discission, and in 40% of eyes following ECCE with an intact posterior capsule. The incidence of rhegmatogenous RD increases following YAG capsulotomy.[232]

Inflammatory

Iridovitreal synechiae have been associated with mild cyclitis, vitritis, retinal phlebitis, and cystoid macular edema.[231]

Vitreoretinal Effects of Trauma

Blunt Trauma

Blunt trauma may be transmitted to the retina in a direct and contrecoup fashion, resulting in a variety of rhegmatogenous sequelae (Fig. 23.59).[233] Dialysis at the anterior border of the vitreous base typically occurs inferonasally. Less common are avulsion of the vitreous base and retinal dialysis at the posterior border of the vitreous base. Concussive forces following blunt trauma can induce retinal edema, known as commotio retinae.

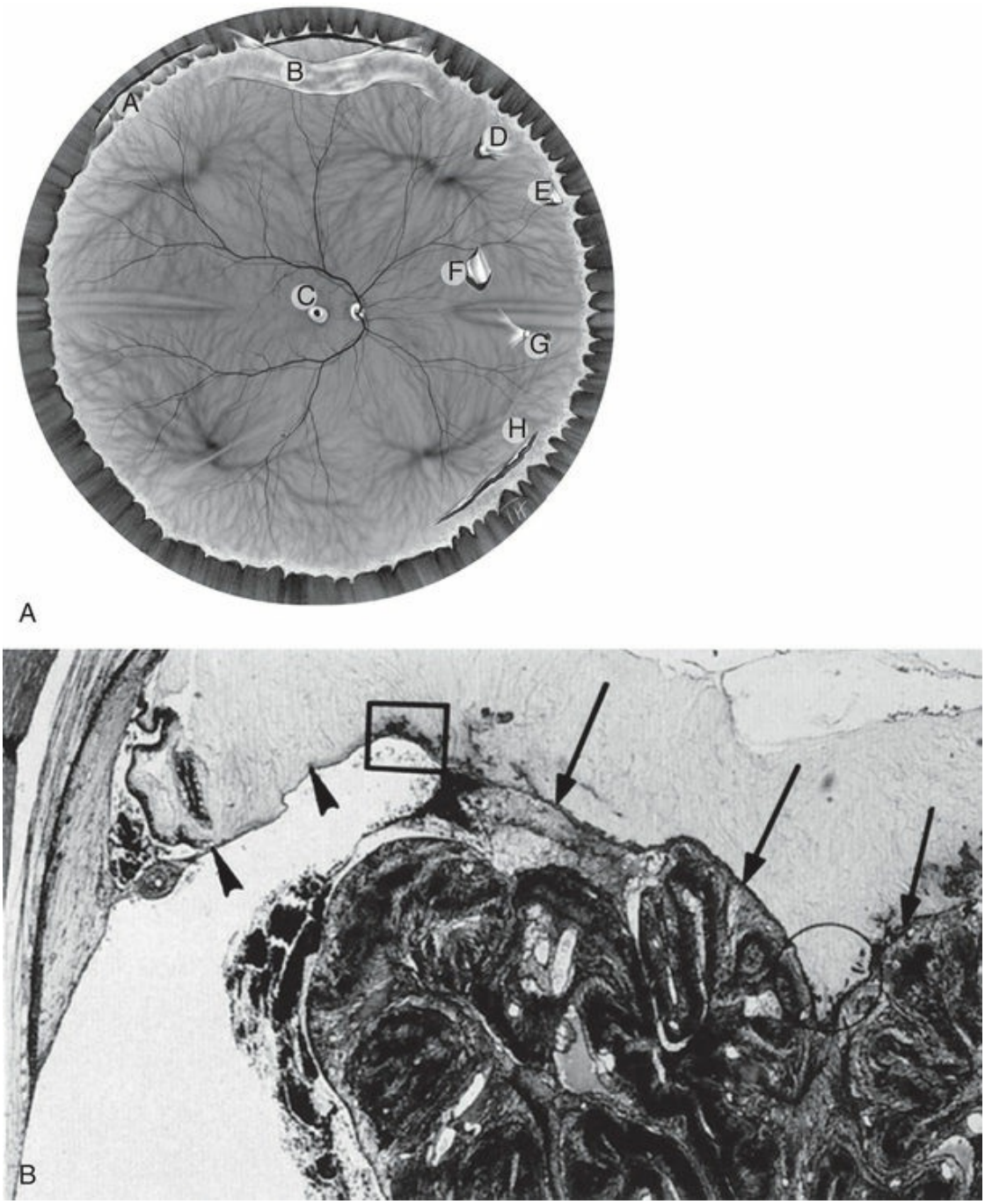

FIG. 23.59 (A) Retinal lesions caused by blunt trauma transmitted to retina. *A*, Dialysis at anterior border of vitreous base. *B*, Avulsion of vitreous base. *C*, Macular hole. *D*, Horseshoe-shaped tear on posterior margin of vitreous base. *E*, Horseshoe-shaped tear at posterior end of a meridional fold. *F*, Horseshoe-shaped tear at equator. *G*, Tear with operculum in overlying vitreous. *H*, Retinal dialysis at posterior border of vitreous base. (B) Retinal dialysis at posterior aspect of vitreous base with retinal pigment epithelium extending through the dialysis, along the posterior surface of vitreous

(*arrowheads*), and then along the anterior surface of the retina (*arrows)* (hematoxylin and eosin, ×20). (Panel A modified with permission from Cox MS, Schepens CL, Freeman HM. Retinal detachment due to ocular contusion. Arch Ophthalmol 1966;76:679–85. Panel B reproduced with permission from Clarkson JG, Green WR, Massof D. A histopathologic review of 168 cases of preretinal membrane. Am J Ophthalmol 1977;84:1–17.)

Shaken-Baby Syndrome (Fig. 23.60B)

Ocular effects are peripapillary hemorrhage, circular macular folds with a sub-ILM schisis cavity containing serosanguinous material[234], and vitreous detachment with ILM throughout the fundus (Fig. 23.60A), especially at the vitreous base.

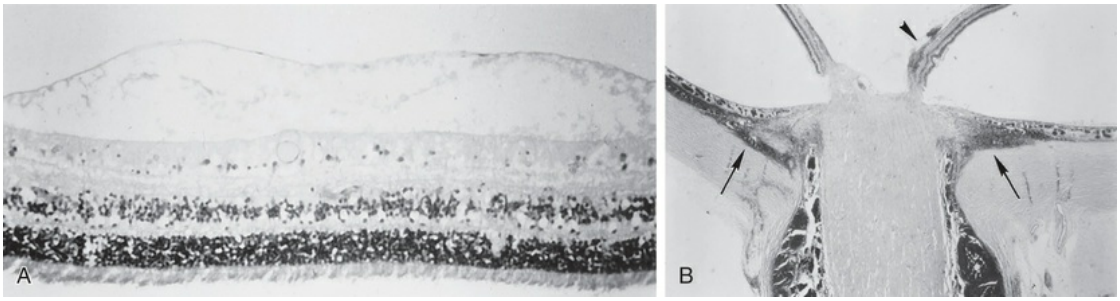

FIG. 23.60 Shaken-baby syndrome. (A) Sub-inner limiting membrane schisis cavity containing serosanguineous material results from severe trauma in a young individual with firm vitreoretinal adherence (hematoxylin and eosin, ×457). (B) Extensive subdural hemorrhage that extends from the adjacent sclera (*arrows*). A peripapillary retinal hemorrhage (*arrowhead*) is present (hematoxylin and eosin, ×183).

Posterior Penetrating and Perforating Trauma[235]

Wound healing at the perforation site allows fibrocellular proliferation into the eye, inducing traction RD (Fig. 23.61). Histopathologic studies revealed cyclitic and periretinal membranes.[236] Intraocular proliferation starts 2–4 days after injury,[237] PVD develops at 1–2 weeks,[238] and traction RD occurs at 7–11 weeks. Proliferation can be prevented by vitrectomy,[239] less

hazardous after 2 weeks because of the development of PVD[240,241] and more effective if complete.[242] Yet, Miller et al.[243] found that vitreous may play a role in normal healing of retinal wounds.

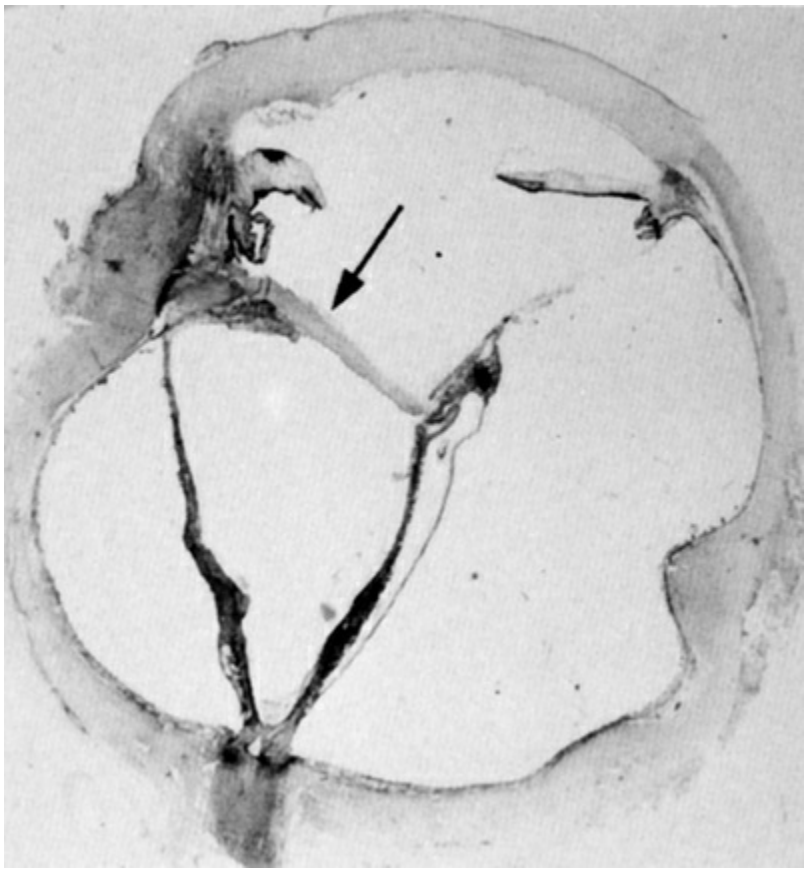

FIG. 23.61 Posterior perforation with fibrous tissue ingrowth (*arrow*) and traction retinal detachment (hematoxylin and eosin, ×25).

Periretinal Cell Proliferation

Premacular Membranes

Premacular membranes (PMMs) occur in the absence of associated conditions and are most often the result of vitreoschisis,[36] where APVD[35] splits the posterior vitreous cortex leaving the outermost layer attached to the macula. The level of this split can vary, as do the consequences (see Fig. 23.42) from no effects, such as in the case of "cellophane" premacular membranes (Fig. 23.62) that have no contractile features, to contractile premacular (previously called

"epiretinal") membranes that induce macular pucker.[61,160,176] Smiddy et al.[244] observed the principal cell to be RPE in these cases, although it is likely that many of these cells are actually hyalocytes (see Figs. 23.6 and 23.14) and circulating monocytes recruited from retinal and choroidal circulations.[34,176] Secondary premacular membranes occur in association with inflammation, accidental or surgical trauma, and retinovascular disease. Fibrous astrocytes are the predominant cell in secondary preretinal macular membranes (PMMs).

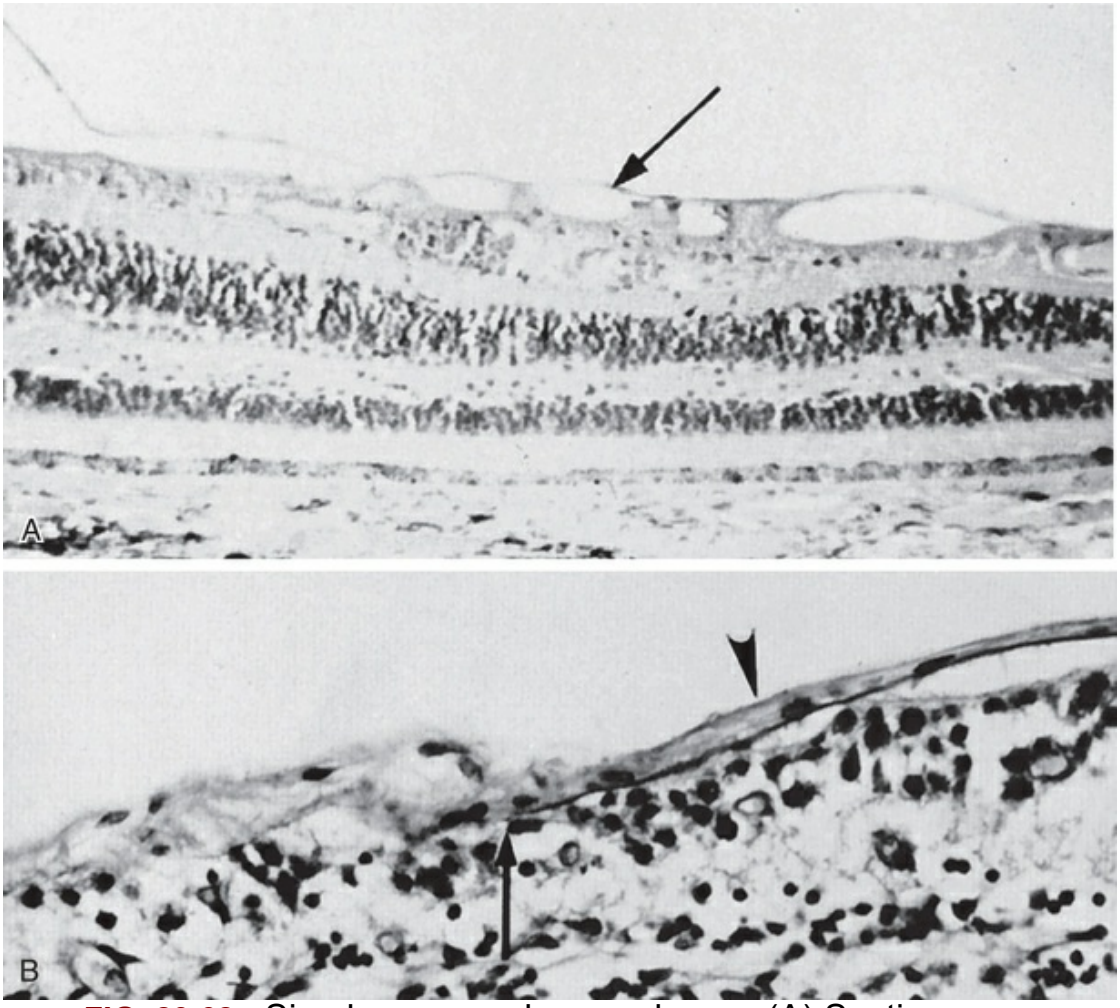

FIG. 23.62 Simple premacular membrane. (A) Section illustrates thin, hypocellular epiretinal membrane (*arrow*) and wrinkling of inner limiting membrane (ILM) (hematoxylin and eosin, ×310). (B) The ILM is discontinuous (*arrow*), at which point glial cells extend on to the inner surface of the retina and form a thin, fibroglial epiretinal membrane (*arrowhead*) with no

apparent contraction (periodic acid–Schiff, ×300). (Panel A reproduced with permission from Clarkson JG, Green WR, Massof D. A histopathologic review of 168 cases of preretinal membrane. Am J Ophthalmol 1977;84:1–17.)

Macular pucker (Fig. 23.63) results from PMMs that induce centripetal tangential (inward to the fovea) traction upon the macula. Macular pucker can have as many as four separate centers of retinal contraction[245] (Fig. 23.64). Eyes with three or four contraction centers had significantly more macular thickening and a higher prevalence of intraretinal cysts than eyes with one or two contraction centers.

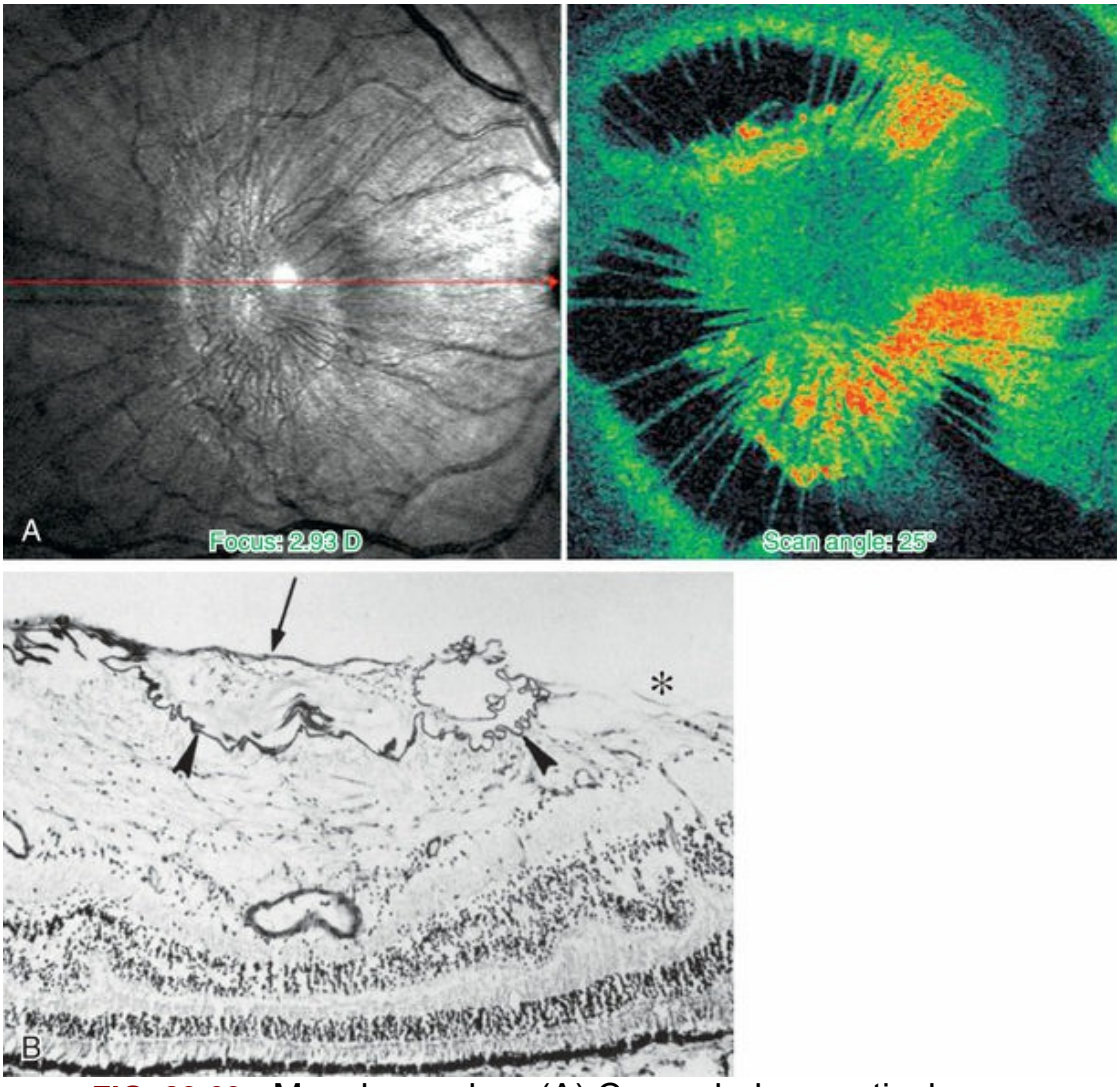

FIG. 23.63 Macular pucker. (A) Coronal-plane optical coherence tomography (color) and scanning laser ophthalmoscopy (grayscale) imaging of macular

pucker with prominent retinal striae in a radial configuration centered in the fovea. (B) Thick fibroglial membrane (*arrow*) that apparently contracted and produced wrinkling of the inner limiting membrane (ILM) (*arrowheads*) and a large gap (*asterisk*) in the ILM (periodic acid–Schiff, ×90). (Reproduced with permission from Clarkson JG, Green WR, Massof D. A histopathologic review of 168 cases of preretinal membrane. Am J Ophthalmol 1977;84:1–17.)

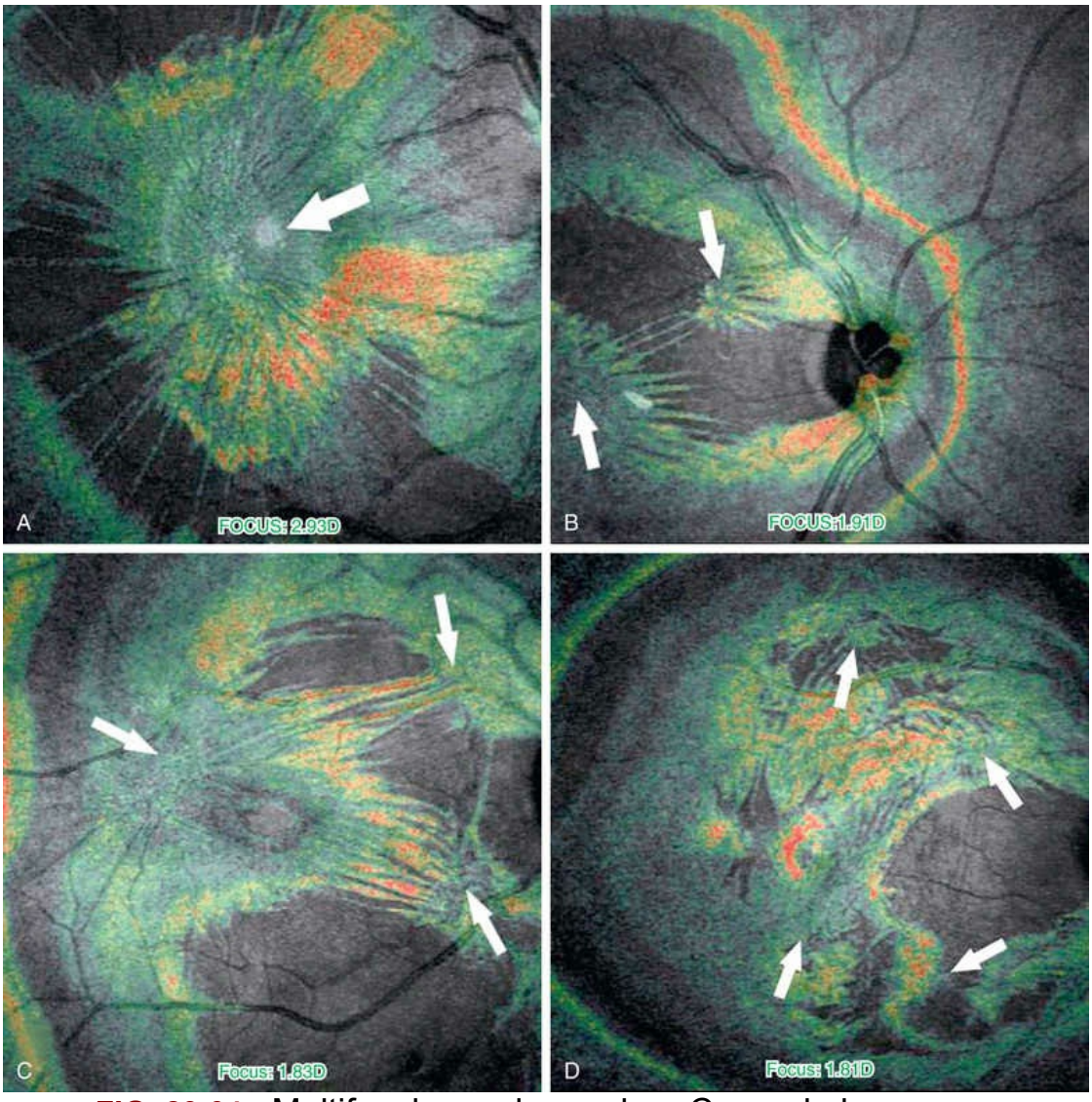

FIG. 23.64 Multifocal macular pucker. Coronal plane optical coherence tomography-scanning laser ophthalmoscopy (OCT-SLO) imaging with superimposition of OCT (color) onto SLO (grayscale) images. (A) Unifocal macular pucker. (B) Bifocal macular pucker with two centers (*arrows*) of retinal

contraction. (C) Trifocal macular pucker with three centers (*arrows*) of retinal contraction. (D) Four distinct centers (*arrows*) of retinal contraction are present.
(Panels A and C are reproduced with permission from Gupta P, Sadun AA, Sebag J. Multifocal retinal contraction in macular pucker analyzed by combined optical coherence tomography/scanning laser ophthalmoscopy. Retina 2008;28:447–52.)

Retroretinal Membranes

These membranes typically occur after RD when RPE grows in sheets over the undersurface of the retina. Strands of fibrous tissue contract and can prevent retinal reattachment.[246]

Complex Membranes

Complex membranes (Fig. 23.65) develop after RD surgery or after trauma. Most often the result of proliferative vitreoretinopathy (PVR),[247] contraction of this proliferative tissue causes traction RD. Anterior PVR features anterior-loop contraction[248] (see Fig. 23.9).

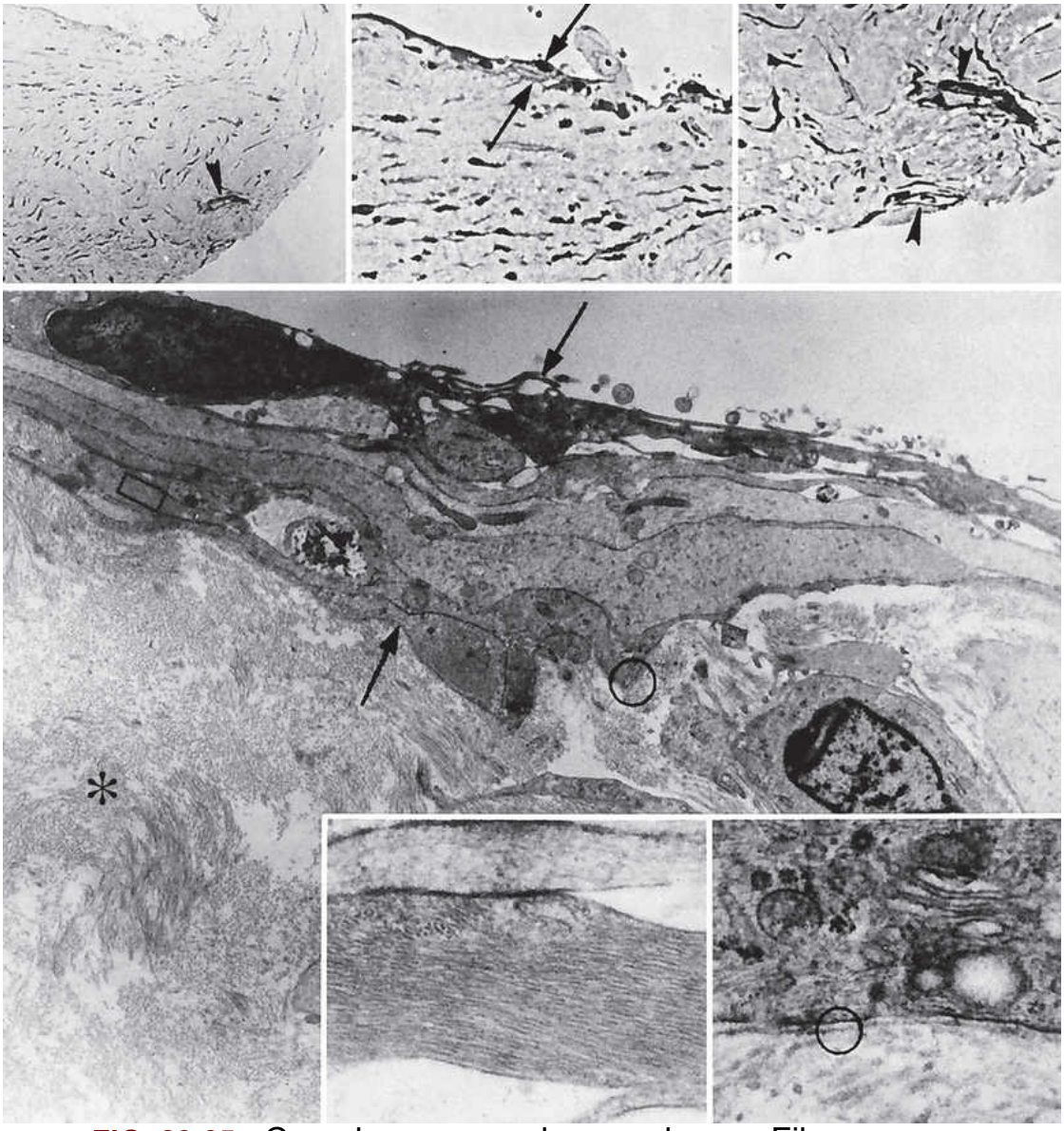

FIG. 23.65 Complex premacular membrane. Fibrous astrocytes in thick epiretinal membrane after anterior-segment surgery and severe intraocular inflammation. Membrane contains new collagen (*asterisk*) and fibrocytes in addition to fibrous astrocytes. Multiple layers of fibrous astrocytes line inner (vitreal) surface (*between arrows*). These cells show polarity with basement membrane (*circles* and bottom right inset), and cells contain numerous cytoplasmic filaments measuring 8–10 nm (rectangle and bottom left inset). Blood vessels (*arrowheads*) are also present in membrane (top left and top right insets). (Main figure ×6600; top insets, paraphenylenediamine hydrochloride stain; top left inset ×160; top middle and top right insets ×250; bottom left inset ×50,000; bottom right inset ×41,000.) (Reproduced with permission from Michels RG. A

clinical and histopathologic study of epiretinal membranes affecting the macula and removed by vitreous surgery. Trans Am Ophthalmol Soc 1982;80:580–656.)

Histopathologically, retinal glial cells gain access to the inner retinal surface via ILM discontinuities, such as at the optic disc, foveola, along major vessels, and at retinal tufts. Acquired sites of ILM discontinuity include retinal tags, pits (lamellar holes), holes, and tears (Fig. 23.66), avulsed retinal vessels, areas of degenerative remodeling, and retinal lattice. Retinal glial cells are the principal cells in membranes at the optic disc, in simple PMMs, in most secondary membranes associated with inflammatory diseases or retinovascular disease, after photocoagulation or RD surgery, and in retinitis pigmentosa. RPE gains access to the vitreous via retinal breaks, the ora serrata, and retinal lattice. RPE can also migrate through intact retina. RPE is the principal cell in PVR (Fig. 23.67), but glial cells are present in about 50% of cases. Myofibrocytes (Fig. 23.68) were observed by electron microscopy in 91% of membranes studied by Kampik et al.,[249] and actin has been observed in cells of PVR membranes.[250]

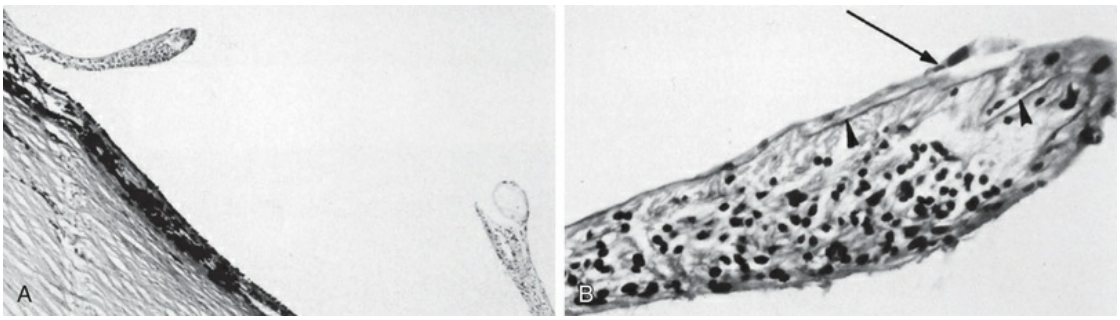

FIG. 23.66 Glial cell proliferation. (A) Peripheral retinal hole with glial membrane extending on the inner surface of the retina anteriorly and posteriorly (periodic acid–Schiff, ×65). (B) Higher-power view of anterior margin of retinal tear, showing glial preretinal membrane (*arrow*) extending along the inner surface of the inner limiting membrane (*arrowheads*) (periodic acid–Schiff; ×190). (Reproduced with permission from Clarkson JG, Green WR, Massof D. A histopathologic review of 168 cases of preretinal membrane. Am J Ophthalmol 1977;84:1–17.)

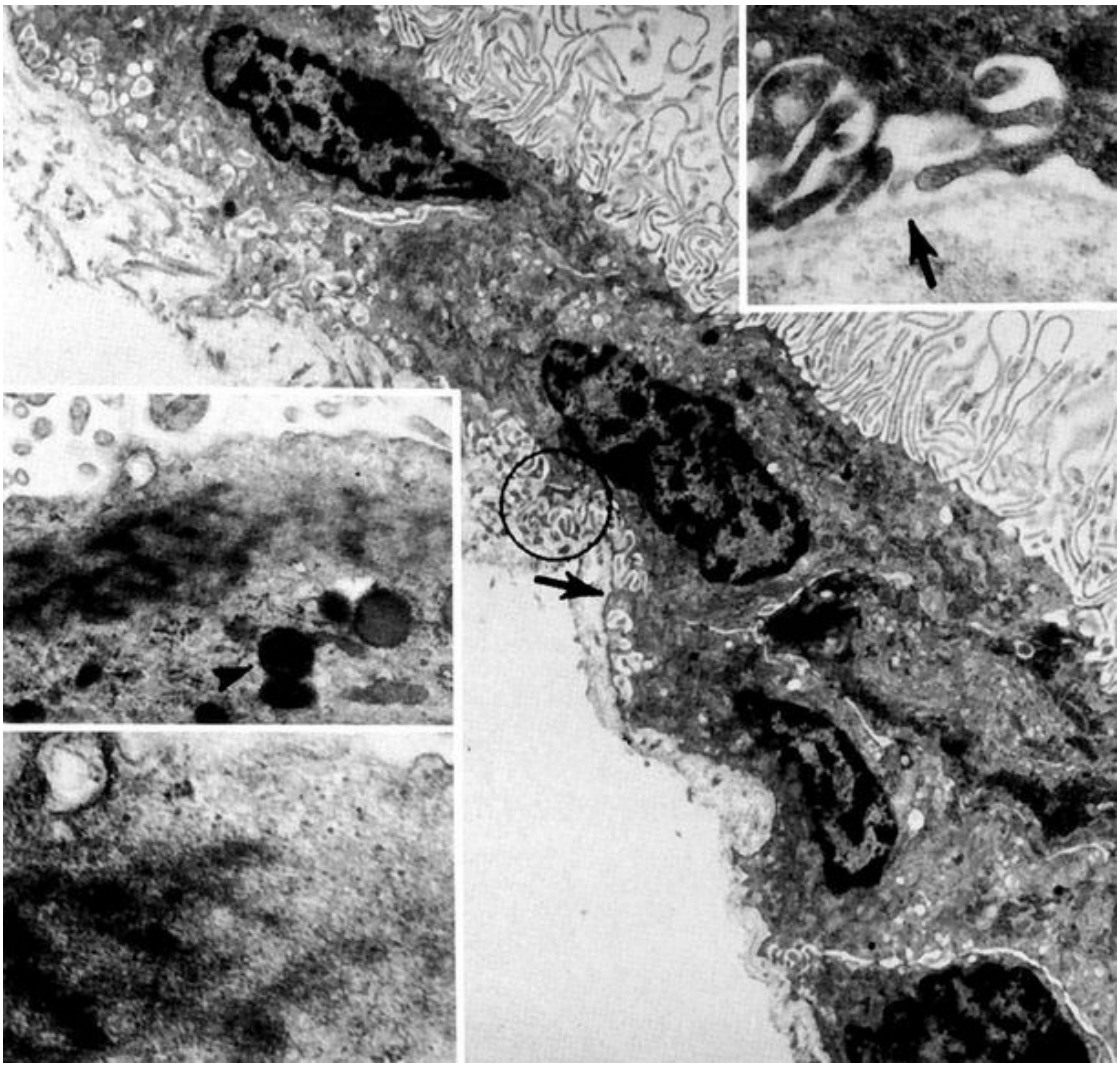

FIG. 23.67 Retinal pigment epithelium (RPE) cells in proliferative vitreoretinopathy. Pigmented membrane removed from the peripapillary area is composed of RPE arranged in a monolayer. Well-developed basement membrane (*arrows*) and basal laminar infoldings (*circle*, and top right inset) are present along the retinal surface. Extensive villous processes are present on the apical side of cells. Numerous apically located subplasmalemmal microfilaments that measure 4–5 nm and have fusiform densities are present (left insets). Occasional cytoplasmic lipid vacuoles are seen (*arrowhead*). (Main figure, ×4500; top left inset, ×17,000; top right inset, ×17,000; bottom left inset, ×36,000.) (Reproduced with permission from Michels RG. A clinical and histopathologic study of epiretinal membranes affecting the macula and removed by vitreous surgery. Trans Am Ophthalmol Soc 1982;80:580–656.)

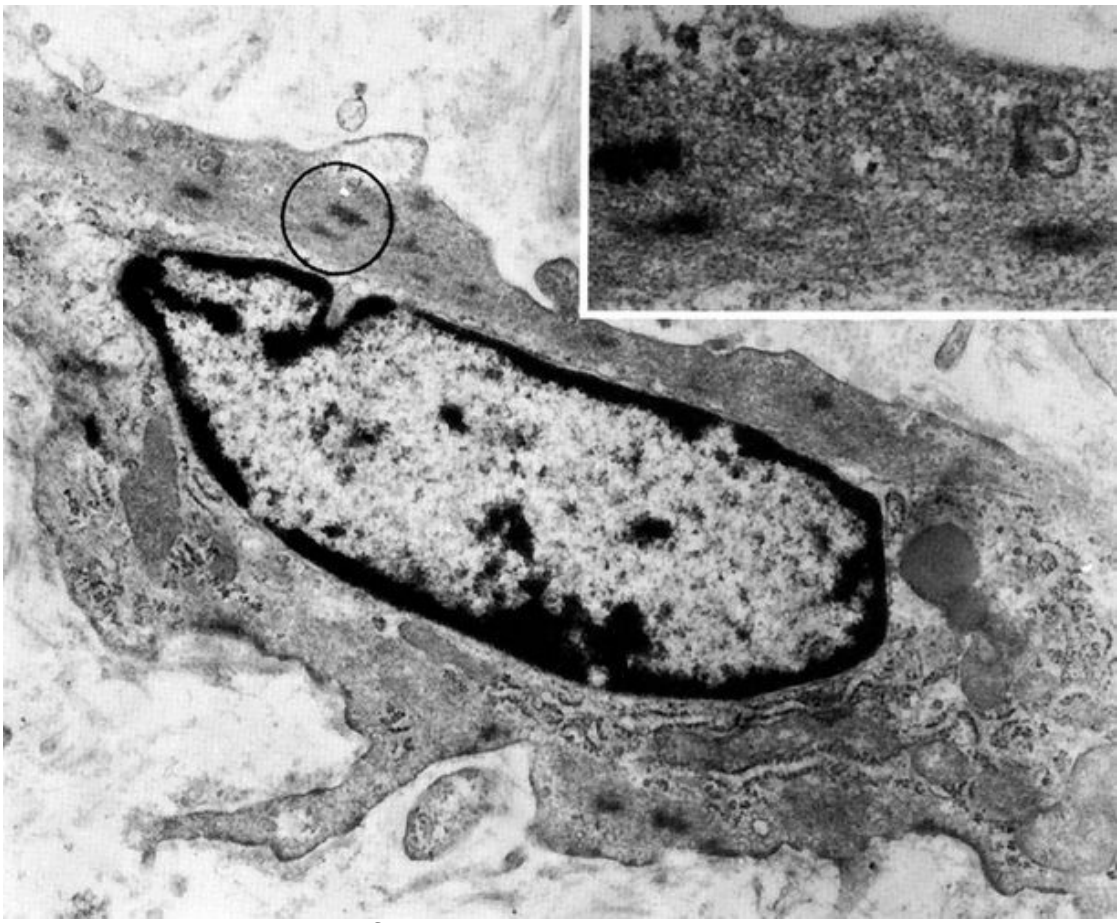

FIG. 23.68 Myofibrocyte. There is a characteristic spindle shape that contains large aggregates of subplasmalemmal microfilaments measuring 4–5 nm and small fusiform densities (*circle* and inset). (Main figure, ×14,000; inset, ×44,000.) (Reproduced with permission from Michels RG. A clinical and histopathologic study of epiretinal membranes affecting the macula and removed by vitreous surgery. Trans Am Ophthalmol Soc 1982;80:580–656.)

Incomplete vitrectomy, intraoperative hemorrhage,[237] and excessive cryopexy[251] render most cases of PVR an iatrogenic disease. Fibronectin and platelet-derived growth factor are the chemoattractants that stimulate migration of RPE[252] and glial cells.[253] Incomplete vitrectomy leaves behind hyalocytes (see Figs. 23.6 and 23.14), which are also the first cells to be exposed to these growth factors and other stimuli. When stimulated, these cells become phagocytic (Fig. 23.69). These resident macrophages play an important role in early PVR pathogenesis. Thus, targeting these cells for pharmacotherapy, similar to what has been done during vitrectomy for RD,[254] may significantly mitigate PVR. Alternatively,

eliminating the role of vitreous via pharmacologic vitreolysis[78,255] will have a great impact on PVR and many of the aforementioned conditions.

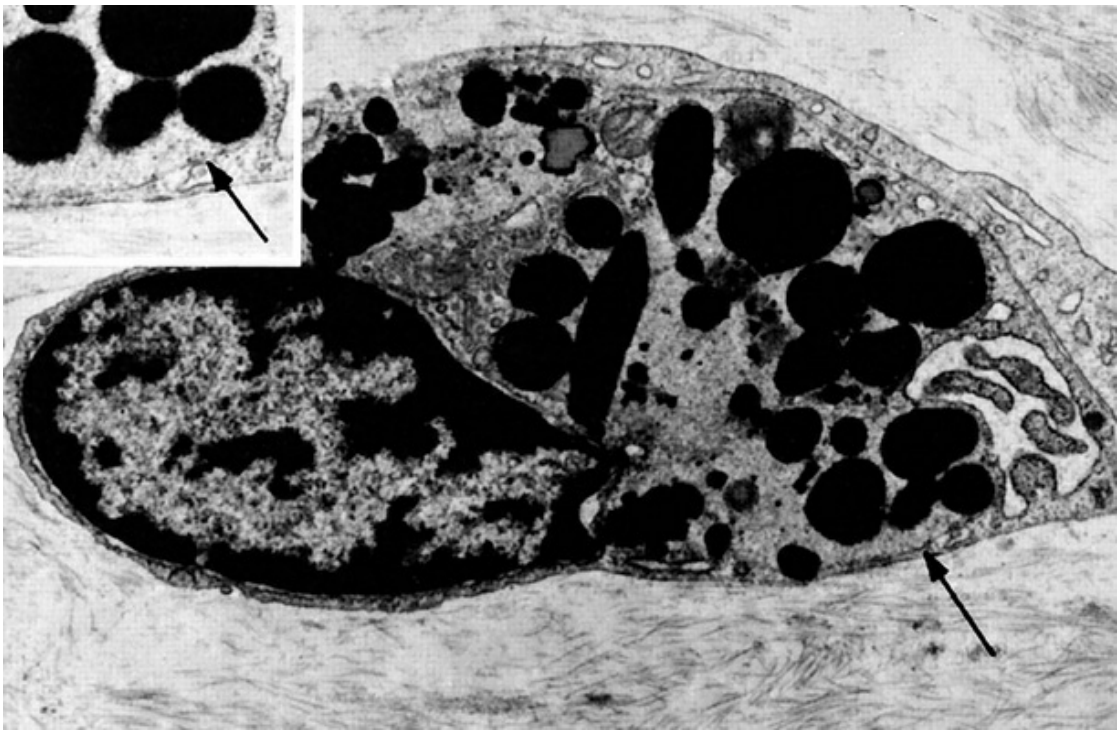

FIG. 23.69 Phagocytic hyalocyte. Macrophage-like cell with multiple pleomorphic inclusions contained in membrane-bound secondary lysosomes (*arrows*) is most likely a hyalocyte embedded within the collagen fibrils of the posterior vitreous cortex. (Main figure, ×12,000; inset, ×22,600.) (Reproduced with permission from Michels RG. A clinical and histopathologic study of epiretinal membranes affecting the macula and removed by vitreous surgery. Trans Am Ophthalmol Soc 1982;80:580–656.)

References

1. Bishop PB. Vitreous proteins. Sebag J. *Vitreous – in Health and Disease*. Springer: New York; 2014:3–13.
2. Crafoord S, Ghosh F, Sebag J. Vitreous biochemistry and artificial vitreous. Sebag J. *Vitreous – in Health and Disease*. Springer: New York; 2014:81–94.
3. Eyre DR, Apon S, Wu JJ, et al. Collagen type IX: Evidence

for covalent linkages to type II collagen in cartilage. *FEBS Lett*. 1987;220:337.
4. Sebag J. *The vitreous: structure, function, and pathobiology*. Springer-Verlag: New York, NY; 1989:63–64.
5. Itakura H, Kishi S, Kotajima N, et al. Embryonic synthesis of the inner limiting membrane and vitreous body. *Graefes Arch Clin Exp Ophthalmol*. 2005;243:994–998.
6. Schmut O, Mallinger R, Paschke E. Studies on a distinct fraction of bovine vitreous body collagen. *Graefes Arch Clin Exp Ophthalmol*. 1984;221:286.
7. Swann DA. Chemistry and biology of vitreous body. *Int Rev Exp Pathol*. 1980;22:1.
8. Snowden JM. The stabilization of in vivo assembled collagen fibrils by proteoglycans/glycosaminoglycans. *Biochem Biophys Acta*. 1982;703:21.
9. Maumenee IH. Vitreoretinal degeneration as a sign of generalized connective tissue diseases. *Am J Ophthalmol*. 1979;88:432–449.
10. Bishop PN, Crossman MV, McLeod D, et al. Extraction and characterisation of the tissue forms of collagen types II and IX from bovine vitreous. *Biochem J*. 1994;299:497–505.
11. Bishop PN, Reardon AJ, McLeod D, et al. Identification of alternatively spliced variants of type II procollagen in vitreous. *Biochem Biophys Res Commun*. 1994;203:289.
12. Bhutto IA, Kim SY, McLeod DS, et al. Localization of collagen XVIII and the endostatin portion of collagen XVIII in aged human control eyes and eyes with age-related macular degeneration. *Invest Ophthalmol Vis Sci*. 2004;45:1544–1552.
13. Ohlmann AV, Ohlmann A, Welge-Lussen U, et al. Localization of collagen XVIII and endostatin in the human eye. *Curr Eye Res*. 2005;30:27–34.
14. Kim H, Robison SB, Csaky KG. Investigating the movement of intravitreal human serum albumin nanoparticles in the vitreous and retina. *Pharm Res*. 2009;26:329–337.
15. Comper WD, Laurent TC. Physiological functions of connective tissue polysaccharides. *Physiol Rev*. 1978;58:255.
16. Sebag J. Diabetic vitreopathy. *Ophthalmology*. 1996;103:205.

17. Reardon A, Heinegard D, McLeod D, et al. The large chondroitin sulphate proteoglycans versican in mammalian vitreous. *Matrix Biol*. 1998;17:325–333.
18. Cain SA, Morgan A, Sherratt MJ, et al. Proteomics analysis of fibrillin-rich microfibrils. *Proteomics*. 2006;6:111–122.
19. Miyamoto T, Inoue H, Sakamoto Y, et al. Identification of a novel splice site mutation of the CSPG2 gene in a Japanese family with Wagner syndrome. *Invest Ophthalmol Vis Sci*. 2005;46:2726–2735.
20. Bishop PN. Structural macromolecules and supramolecular organization of the vitreous gel. *Prog Retin Eye Res*. 2000;19:323.
21. Reardon AJ, LeGoff M, Briggs MD, et al. Identification in vitreous and molecular cloning of opticin, a novel member of the family of leucine-rich repeat proteins of the extracellular matrix. *J Biol Chem*. 2000;275:2123.
22. Sanders EJ, Walter MA, Parker E, et al. Opticin binds retinal growth hormone in the embryonic vitreous. *Invest Ophthalmol Vis Sci*. 2003;44:5404–5409.
23. Hindson VJ, Gallagher JT, Halfter W, et al. Opticin binds to heparan and chondroitin sulphate proteoglycans. *Invest Ophthalmol Vis Sci*. 2005;46:4417–4423.
24. Monfort J, Tardif G, Roughley P, et al. Identification of opticin, a member of the small leucine-rich repeat proteoglycan family, in human articular tissues. *Osteoarthritis Cartilage*. 2008;16:749–755.
25. Sebag J, Hageman GS. Interfaces. *Eur J Ophthalmol*. 2000;10:1.
26. Yee KM, Feener EP, Madigan M, et al. Proteomic analysis of the embryonic and young human vitreous. *Invest Ophthalmol Vis Sci*. 2015;56(12):7036–7042.
27. Eisner G. *Biomicroscopy of the peripheral fundus*. Springer-Verlag: New York; 1979.
28. Worst JG. Cisternal systems of the fully developed vitreous body in the young adult. *Trans Ophthalmol Soc U K*. 1977;97:550–554.
29. Sebag J, Balazs EA. Human vitreous fibres and vitreoretinal disease. *Trans Ophthalmol Soc U K*. 1984;104:123–128.
30. Gartner J. Electron-microscopic study on the fibrillar

network and fibrocyte–collagen interactions in the vitreous cortex at the ora serrata of human eyes with special regard to the role of disintegrating cells. *Exp Eye Res*. 1986;42:21–23.
31. Sebag J. Surgical anatomy of vitreous and the vitreoretinal interface. JB Lippincott: Philadelphia; 1994. Tasman W, Jaeger EA. *Duane's clinical ophthalmology*. vol. 6 [updated 2008].
32. Halfter W, Sebag J, Cunningham ET. Vitreo-retinal interface and inner limiting membrane. Sebag J. *Vitreous – in Health and Disease*. Springer: New York; 2014:165–192.
33. Streeten BA. Disorders of the vitreous. Garner A, Klintworth GK. *Pathobiology of ocular disease – a dynamic approach*. Marcel Dekker: New York; 1982:1381–1419.
34. Gupta P, Yee KMP, Garcia P, et al. Vitreoschisis in macular diseases. *Br J Ophthalmol*. 2011;95:376–380.
35. Sebag J. Vitreous – the resplendent enigma. *Br J Ophthalmol*. 2009;93:989–991.
36. Sebag J. Anomalous PVD – a unifying concept in vitreo-retinal diseases. *Graefes Arch Clin Exp Ophthalmol*. 2004;242:690–698.
37. Sebag J, Niemeyer M, Koss MJ. Anomalous PVD and vitreoschisis. Sebag J. *Vitreous – in Health and Disease*. Springer: New York; 2014:241–265.
38. Sebag J. Vitreoschisis. *Graefes Arch Clin Exp Ophthalmol*. 2008;246:329–332.
39. Balazs EA, Toth LZ, Eckl EA, et al. Studies on the structure of the vitreous body. *Exp Eye Res*. 1964;3:57–71.
40. Gloor BP. Cellular proliferation on the vitreous surface after photocoagulation. *Graefes Arch Clin Exp Ophthalmol*. 1969;178:99.
41. Balazs EA. Structure of vitreous gel. *Acta XVII Concilium Ophthalmologicum*. 1954;11:1019.
42. Balazs EA, Sundblad L, Toth LZJ. In vitro formation of hyaluronic acid by cells in the vitreous body and by comb tissue. *Abstr Red Proc*. 1958;17:184.
43. Jacobson B, Osterlin S, Balazs EA. A soluble hyaluronic acid synthesizing system from calf vitreous. *Proc Fed Am Soc Exp Biol*. 1966;25:588.

44. Osterlin SE. The synthesis of hyaluronic acid in the vitreous. III. In vivo metabolism in the owl monkey. *Exp Eye Res*. 1968;7:524.
45. Osterlin SE. The synthesis of hyaluronic acid in the vitreous. IV. Regeneration in the owl monkey. *Exp Eye Res*. 1969;8:27.
46. Rhodes RH, Mandelbaum SH, Minckler DS, et al. Tritiated glucose incorporation in the vitreous body, lens and zonules of the pigmented rabbit. *Exp Eye Res*. 1982;34:921.
47. Jacobson B. Identification of sialyl and galactosyl transferase activities in calf vitreous hyalocytes. *Curr Eye Res*. 1984;3:1033.
48. Newsome DA, Linsemayer TF, Trelstad RJ. Vitreous body collagen: evidence for a dual origin from the neural retina and hyalocytes. *J Cell Biol*. 1976;71:59–67.
49. Hoffmann K, Baurwieg H, Riese K. Uber Gehalt und Verteilung niederund hoch molekularer Substanzen in Glaskorper. II. Hock molekulare Substanzen (LDH, MDH, GOT). *Graefes Arch Clin Exp Ophthalmol*. 1974;191:231.
50. Teng CC. An electron microscopic study of cells in the vitreous of the rabbit eye. Part I: The macrophage. *Eye Ear Nose Throat Monthly*. 1969;48:91.
51. Szirmai JA, Balazs EA. Studies on the structure of the vitreous body. III: Cells in the cortical layer. *Arch Ophthalmol*. 1958;59:34.
52. Grabner G, Baltz G, Forster O. Macrophage-like properties of human hyalocytes. *Invest Ophthalmol Vis Sci*. 1980;19:333.
53. Balazs EA. Functional anatomy of the vitreous. Harper and Row: Philadelphia; 1982:6–12. Duane TD, Jaeger EA. *Biomedical foundations of ophthalmology*. vol. 1.
54. Sonoda KH, Sakamoto T, Qiao H, et al. The analysis of systemic tolerance elicited by antigen inoculation into the vitreous cavity: vitreous cavity-associated immune deviation. *Immunology*. 2005;116:390–399.
55. Forrester JV, Balazs EA. Inhibition of phagocytosis by high molecular weight hyaluronate. *Immunology*. 1980;40:435.
56. Sebag J, Balazs EA, Eakins KE, et al. The effect of Na-hyaluronate on prostaglandin synthesis and phagocytosis by mononuclear phagocytes. *Invest Ophthalmol Vis Sci*.

1981;20:33.
57. Hultsch E. Vitreous structure and ocular inflammation. Silverstein AM, O'Connor GR. *Immunology and immunopathology of the eye*. Masson: New York; 1979.
58. Gartner J. The fine structure of the vitreous base of the human eye and pathogenesis of pars planitis. *Am J Ophthalmol*. 1971;71:1317–1327.
59. Sakamoto T, Ishibashi T. Hyalocytes: essential cells of the vitreous cavity in vitreoretinal pathophysiology? *Retina*. 2011;31:222–228.
60. Kita T, Sakamoto T, Ishibashi TE. Hyalocytes – essential vitreous cells in vitreo-retinal health and disease. Sebag J. *Vitreous – in Health and Disease*. Springer: New York; 2014:151–164.
61. Tozer K, Sebag JF. Vitreous in the pathobiology of macular pucker. Sebag J. *Vitreous – in Health and Disease*. Springer: New York; 2014:311–328.
62. Nishitsuka K, Kashiwagi Y, Tojo N, et al. Hyaluronan production regulation from porcine hyalocyte cell line by cytokines. *Exp Eye Res*. 2007;85:539–545.
63. Kita T, Hata Y, Kano K, et al. Transforming growth factor-beta2 and connective tissue growth factor in proliferative vitreoretinal diseases: possible involvement of hyalocytes and therapeutic potential of Rho kinase inhibitor. *Diabetes*. 2007;56:231–238.
64. Hiryama K, Hata Y, Noda Y, et al. The involvement of the rho-kinase pathway and its regulation in cytokine-induced collagen gel contraction by hyalocytes. *Invest Ophthalmol Vis Sci*. 2004;45:3896–3903.
65. Foos RY. Posterior peripheral retinal tears. *Ann Ophthalmol*. 1974;6:679–687.
66. Kishi S, Numaga T, Yoneya S, et al. Epivascular glia and paravascular holes in normal human retina. *Graefes Arch Clin Exp Ophthalmol*. 1986;224:124–130.
67. Sebag J. Age-related differences in the human vitreoretinal interface. *Arch Ophthalmol*. 1991;109:966.
68. Kefalides NA. The biology and chemistry of basement membranes. Kefalides NA. *Proceedings of the First*

International Symposium on the Biology and Chemistry of Basement Membranes. Academic Press: New York; 1978:215–228.
69. Fukai N, Eklund L, Marneros AG, et al. Lack of collagen XVIII/endostatin results in eye abnormalities. *EMBO J*. 2002;21:1535–1544.
70. Hindson VJ, Gallagher JT, Halfter W, et al. Opticin binds to heparan and chondroitin sulphate proteoglycans. *Invest Ophthalmol Vis Sci*. 2005;46:4417–4423.
71. Ramesh S, Bonshek RE, Bishop PN. Immunolocalisation of opticin in the human eye. *Br J Ophthalmol*. 2004;88:697–702.
72. Bhutto IA, Kim SY, McLeod DS, et al. Localization of collagen XVIII and the endostatin portion of collagen XVIII in aged human control eyes and eyes with age-related macular degeneration. *Invest Ophthalmol Vis Sci*. 2004;45:1544–1552.
73. Neill T, Schaefer L, Iozzo RV. Decoding the matrix: instructive roles of proteoglycan receptors. *Biochemistry*. 2015;54(30):4583–4598.
74. Cohen AI. Electron microscopic observations of the internal limiting membrane and optic fiber layer of the retina of the rhesus monkey. *Am J Anat*. 1961;108:179.
75. Zimmerman LE, Straatsma BR. Anatomic relationships of the retina to the vitreous body and to the pigment epithelium. Schepens CL. *Importance of the vitreous body in retina surgery with special emphasis on reoperation*. CV Mosby: St Louis; 1960:15–28.
76. Russell SR, Shepherd JD, Hageman GS. Distribution of glycoconjugates in the human internal limiting membrane. *Invest Ophthalmol Vis Sci*. 1991;32:1986.
77. Russell SR, Hageman G. Chondroitinase as a vitreous interfactant. Sebag J. *Vitreous – in Health and Disease*. Springer: New York; 2014:881–894.
78. Sebag J. Pharmacologic vitreolysis. Sebag J. *Vitreous – in Health and Disease*. Springer: New York; 2014:799–816.
79. Fine BS, Tousimus AJ. The structure of the vitreous body and the suspensory ligaments of the lens. *Arch Ophthalmol*. 1961;65:95–110.

80. Teng CC, Chi HH. Vitreous changes and the mechanism of retinal detachment. *Am J Ophthalmol*. 1957;44:335–356.
81. Hogan MJ. The vitreous, its structure and relation to the ciliary body and retina. *Invest Ophthalmol*. 1963;2:418–445.
82. Spencer LM, Foos RY, Straatsma BR. Meridional complexes and associated abnormalities of the peripheral retina. *Am J Ophthalmol*. 1970;70:697–713.
83. Byer NE. Cystic retinal tufts and their relationship to retinal detachment. *Arch Ophthalmol*. 1981;99:1788–1790.
84. Spencer LM, Straatsma BR, Foos RY. Tractional degenerations of the peripheral retina. *Transactions of the New Orleans Academy of Ophthalmology, Symposium on Retina and Retinal Surgery*. Mosby: St Louis; 1969.
85. Foos RY. Vitreoretinal juncture over retinal vessels. *Graefes Arch Clin Exp Ophthalmol*. 1977;204:223–234.
86. Wolter JR. Pores in the internal limiting membrane of the human retina. *Acta Ophthalmol*. 1964;42:971–974.
87. Kuwabara T, Cogan DG. Studies of retinal vascular patterns. I. Normal architecture. *Arch Ophthalmol*. 1960;64:904–911.
88. Mutlu F, Leopold IH. Structure of the human retinal vascular system. *Arch Ophthalmol*. 1964;71:93.
89. Polk TD, Gass DM, Green WR, et al. Familial internal limiting membrane dystrophy: a new sheen retinal dystrophy. *Arch Ophthalmol*. 1997;115:878–885.
90. Heergaard S, Jensen OA, Prause JU. Structure of the vitreal face of the monkey optic disc (*Macacca mulatta*): SEM on frozen resin-cracked optic nerve heads supplemented by TEM and immunohistochemistry. *Graefes Arch Clin Exp Ophthalmol*. 1988;226:377.
91. Foos RY, Roth AM. Surface structure of the optic nerve head. II: Vitreopapillary attachments and posterior vitreous detachment. *Am J Ophthalmol*. 1973;76:662–671.
92. Roth AM, Foos RY. Surface structure of the optic nerve head. I: Epipapillary membranes. *Am J Ophthalmol*. 1972;74:977–985.
93. Wang MY, Nguyen D, Hindoyan N, et al. Vitreopapillary adhesion in macular hole and macular pucker. *Retina*. 2009;29:644–650.

94. Sebag J, Wang M, Nguyen D, et al. Vitreopapillary adhesion in macular diseases. *Trans Am Ophthalmol Soc*. 2009;107:35–46.
95. Shui Y-B, Holekamp NM, Kramer BC, et al. The gel state of the vitreous and ascorbate-dependent oxygen consumption – relationship to the etiology of nuclear cataracts. *Arch Ophthalmol*. 2009;127:475–482.
96. Holekamp NM, Beebe DC, Shui Y-B. Oxygen in vitreo-retinal physiology and pathology. Sebag J. *Vitreous – in Health and Disease*. Springer: New York; 2014:459–476.
97. Friedenwald JS, Bushke W, Michel HO. Role of ascorbic acid in secretion of intraocular fluid. *Arch Ophthalmol*. 1944;29:535–574.
98. Gisladottir S, Loftsson T, Stefansson E. Diffusion characteristics of vitreous humour and saline solution follow the Stokes Einstein equation. *Graefes Arch Clin Exp Ophthalmol*. 2009;247:1677–1684.
99. Stefansson E. Physiology of vitreous surgery. *Graefes Arch Clin Exp Ophthalmol*. 2009;247:147–163.
100. Huang LC, Yee KMP, Wa CA, et al. Vitreous floaters and vision – current concepts and management paradigms. Sebag J. *Vitreous – in Health and Disease*. Springer: New York; 2014:771–788.
101. Sebag J, Yee KMP, Huang L, et al. Vitrectomy for floaters – prospective efficacy analyses and retrospective safety profile. *Retina*. 2014;34:1062–1068.
102. Balazs EA. Physiology of the vitreous body. Schepens CL. *Proceedings of the Second Conference of the Retina Foundation*. Mosby: St Louis; 1960.
103. Hilding AC. Alterations in the form, movement, and structure of the vitreous body in aphakic eyes. *Arch Ophthalmol*. 1954;52:699–709.
104. Schepens CL. Clinical aspects of pathologic changes of the vitreous body. *Am J Ophthalmol*. 1954;38:8–21.
105. Balazs EA, Denlinger JL. Aging changes in the vitreous. *Aging and human visual function*. Alan R Liss: New York; 1982.
106. O'Malley P. The pattern of vitreous syneresis: a study of 800

autopsy eyes. Irvine AR, O'Malley C. *Advances in vitreous surgery*. Charles C Thomas: Springfield, IL; 1976.
107. Eisner G. Zur Anatomie des Glaskorpers. *Graefes Arch Clin Exp Ophthalmol*. 1975;193:33–56.
108. Sebag J, Balazs EA. Morphology and ultrastructure of human vitreous fibers. *Invest Ophthalmol Vis Sci*. 1989;30:1867–1871.
109. Kishi S, Shimizu K. Posterior precortical vitreous pocket. *Arch Ophthalmol*. 1990;108:979–982.
110. Snowden JM. The stabilization of in vivo assembled collagen fibrils by proteoglycans/glycosaminoglycans. *Biochem Biophys Acta*. 1982;703:21–25.
111. Aguayo J, Glaser B, Mildvan A, et al. Study of vitreous liquefaction by NMR spectroscopy and imaging. *Invest Ophthalmol Vis Sci*. 1985;26:692.
112. Ueno N, Sebag J, Hirokawa H, et al. Effects of visible-light irradiation on vitreous structure in the presence of a photosensitizer. *Exp Eye Res*. 1987;44:863–870.
113. Kamei A, Totani A. Isolation and characterization of minor glycosaminoglycans in the rabbit vitreous body. *Biochem Biophys Res Commun*. 1982;109:881–887.
114. Gale J, Ikuno Y. Myopic vitreopathy. Sebag J. *Vitreous – in Health and Disease*. Springer: New York; 2014:113–130.
115. Foos RY, Wheeler NC. Vitreoretinal juncture: synchysis senilis and posterior vitreous detachment. *Ophthalmology*. 1982;89:1502–1512.
116. Goldmann H. Senile changes of the lens and the vitreous. *Am J Ophthalmol*. 1964;57:1–13.
117. Takahashi M, Jalkh A, Hoskins J, et al. Biomicroscopic evaluation and photography of liquefied vitreous in some vitreoretinal disorders. *Arch Ophthalmol*. 1981;99:1555–1559.
118. Wang J, McLeod D, Henson DB, et al. Age-dependent changes in the basal retinovitreous adhesion. *Invest Ophthalmol Vis Sci*. 2003;44:1793–1800.
119. Gartner J. Electron microscopic observations on the cilio-zonular border of the human eye with particular reference to the aging changes. *Z Anat Entwicklungsgesch*. 1970;131:263.

120. Spencer LM, Foos RY, Straatsma BR. Enclosed bays of the ora serrata: relationship to retinal tears. *Arch Ophthalmol*. 1970;83:421–425.
121. Rutnin U, Schepens CL. Fundus appearance in normal eyes. II: The standard peripheral fundus and developmental variations. *Am J Ophthalmol*. 1967;64:840–852.
122. Foos RY, Spencer LM, Straatsma BR. Trophic degenerations of the peripheral retina. *Transactions of the New Orleans Academy of Ophthalmology, Symposium on retina and retinal surgery*. Mosby: St Louis; 1969.
123. Streeten BW, Bert M. The retinal surface in lattice degeneration of the retina. *Am J Ophthalmol*. 1972;74:1201–1209.
124. Foos RY, Allen RA. Retinal tears and lesser lesions of the peripheral retina. *Am J Ophthalmol*. 1967;64:643–655.
125. Spencer LM, Straatsma BR, Foos RY. Tractional degenerations of the peripheral retina. *Transactions of the New Orleans Academy of Ophthalmology, Symposium on Retina and Retinal Surgery*. Mosby: St Louis; 1969.
126. Foos RY. Vitreous base, retinal tufts, and retinal tears: pathogenic relationships. Pruett RC, Regan CD. *Retina congress*. Appleton–Century–Crofts: New York; 1974.
127. Foos RY. Zonular traction tufts of the peripheral retina in cadaver eyes. *Arch Ophthalmol*. 1969;82:620–632.
128. Inomata H. Electron microscopic observations of cystoid degeneration in the peripheral retina. *Jpn J Ophthalmol*. 1966;10:26–40.
129. Green WR. Retina. Ryan SJ. *Ophthalmic pathology: an atlas and text*. 4th ed. WB Saunders: Philadelphia; 1996.
130. Bradford JD, Wilkinson CP, Fransen SR. Pseudophakic retinal detachment: the relationships between retinal tears and the time following cataract surgery at which they occur. *Retina*. 1989;9:181–186.
131. Byer NE. Lattice degeneration of the retina. *Surv Ophthalmol*. 1979;23:213–247.
132. Straatsma BR, Zeegen PD, Foos RY, et al. Lattice degeneration of the retina. *Trans Am Acad Ophthalmol Otolaryngol*. 1974;78:87–113.

133. Semes LP. Lattice degeneration of the retina and retinal detachment. *Optom Clin*. 1992;2:71–91.
134. Burton TC. The influence of refractive error and lattice degeneration on the incidence of retinal detachment. *Trans Am Ophthalmol Soc*. 1990;87:143–157.
135. Parelhoff ES, Wood WJ, Green WR, et al. Radial perivascular lattice degeneration of the retina. *Ann Ophthalmol*. 1980;12:25–32.
136. Schepens CL. Diagnostic and prognostic factors as found in pre-operative examination. *Trans Am Acad Ophthalmol Otolaryngol*. 1952;56:398–418.
137. Schepens CL. Subclinical retinal detachments. *Arch Ophthalmol*. 1952;47:593–606.
138. Foos RY, Simons KB, Wheeler NC. Comparison of lesions predisposing to rhegmatogenous retinal detachment by race and subjects. *Am J Ophthalmol*. 1983;96:644–649.
139. Byer NE. Clinical study of lattice degeneration of the retina. *Trans Am Acad Ophthalmol Otolaryngol*. 1965;69:1064–1077.
140. Byer NE. Changes in prognosis of lattice degeneration of the retina. *Trans Am Acad Ophthalmol Otolaryngol*. 1974;78:114–124.
141. Foos RY, Simons KB. Vitreous in lattice degeneration of retina. *Ophthalmology*. 1984;91:452–457.
142. Robinson MR, Streeten BW. The surface morphology of retinal breaks and lattice retinal degeneration: a scanning electron microscopic study. *Ophthalmology*. 1986;93:237–246.
143. Tillery WV, Lucier AC. Round atrophic holes in lattice degeneration: an important cause of phakic retinal detachment. *Trans Am Acad Ophthalmol Otolaryngol*. 1976;81:509–518.
144. Morse PH, Scheie HG. Prophylactic cryoretinopexy of retinal breaks. *Arch Ophthalmol*. 1974;92:204–207.
145. Byer NE. Lattice degeneration of the retina. *Surv Ophthalmol*. 1979;23:213–247.
146. Davis MD. Natural history of retinal breaks without detachment. *Arch Ophthalmol*. 1974;92:183–194.
147. Dobbie G. Discussion. New research on the aetiology and surgery of retinal detachment. *Mod Probl Ophthalmol*.

1975;15:113.
148. Schepens CL. Diagnostic and prognostic factors as found in preoperative examination. *Trans Am Acad Ophthalmol Otolaryngol*. 1952;56:398–418.
149. Tolentino FI, Schepens CL, Freeman HM. *Vitreoretinal disorders: diagnosis and management*. WB Saunders: Philadelphia; 1976.
150. Byer NE. *The peripheral retina in profile: a stereoscopic atlas*. Criterion Press: Torrence, CA; 1982.
151. Watzke RC. The ophthalmoscopic sign, "white with pressure": a clinicopathologic correlation. *Arch Ophthalmol*. 1961;66:812–823.
152. Daicker B. Sind die Symptome "weiss mit Druck" und weiss ohne Druck durch die Periphere Netzshantsklerose bedingt? *Mod Probl Ophthalmol*. 1975;15:82–90.
153. Gartner J. Discussion. New research on the aetiology and surgery of retinal detachment. *Mod Probl Ophthalmol*. 1975;15:112.
154. Freeman HM. Fellow eyes of giant retinal breaks. *Trans Am Ophthalmol Soc*. 1978;76:343–382.
155. Dunker S, Glinz J, Faulborn J. Morphologic studies of the peripheral vitreoretinal interface in humans reveal structures implicated in the pathogenesis of retinal tears. *Retina*. 1997;17:124–130.
156. Foos RY. Vitreoretinal juncture: topographical variations. *Invest Ophthalmol*. 1972;11:801–808.
157. Sebag J. To see the invisible: the quest of imaging vitreous. *Dev Ophthalmol*. 2008;42:5–28.
158. Johnson M. Perifoveal vitreous detachment and its macular complications. *Trans Am Ophthalmol Soc*. 2005;103:537–567.
159. Foos RY. Ultrastructural features of posterior vitreous detachment. *Graefes Arch Clin Exp Ophthalmol*. 1975;196:103–111.
160. Sebag J. Vitreous – the resplendent enigma. *Br J Ophthalmol*. 2009;93:989–991.
161. Favre M, Goldmann H. Zur Genese der hinteren Glaskorperabhebung. *Ophthalmologica*. 1956;132:86–97.
162. Pischel DK. Detachment of the vitreous as seen with slit-

lamp examination. *Trans Am Ophthalmol Soc*. 1952;50:329–346.
163. Buzney SM, Weiter JJ, Furukawa H, et al. Examination of the vitreous: a comparison of biomicroscopy using the Goldmann and El Bayadi-Kajiura lenses. *Ophthalmology*. 1985;92:1745–1748.
164. Fisher YL, Slakter JS, Friedman RA, et al. Kinetic ultrasound evaluation of the posterior vitreoretinal interface. *Ophthalmology*. 1991;98:1135–1138.
165. Ortiz RG, Lopez PF, Lambert HM, et al. Examination of macular vitreoretinal interface disorders with monochromatic photography. *Am J Ophthalmol*. 1992;113:243–247.
166. Ansari RR, Dunker S, Suh K. Quantitative molecular characterization of bovine vitreous and lens with non-invasive dynamic light scattering. *Exp Eye Res*. 2001;73:859–866.
167. Sebag J, Dunker S, Suh KI, et al. Dynamic light scattering measurements in vitreous. *Invest Ophthalmol Vis Sci*. 1997;38:662.
168. Foos RY. Posterior vitreous detachment. *Trans Am Acad Ophthalmol Otolaryngol*. 1972;76:480–497.
169. Webb BF, Webb JR, Schroeder MC, North CS. Prevalence of vitreous floaters in a community sample of smartphone users. *Int J Ophthalmol*. 2013;6(3):402–405.
170. Sebag J. Floaters and the quality of life. *Am J Ophthalmol*. 2011;152:3–4.
171. Mamou J, Wa CA, Yee KM, et al. Ultrasound-based quantification of vitreous floaters correlates with contrast sensitivity and quality of life. *Invest Ophthalmol Vis Sci*. 2015;56:1611–1617.
172. Tasman WS. Posterior vitreous detachment and peripheral retinal breaks. *Trans Am Acad Ophthalmol Otolaryngol*. 1968;72:217–224.
173. Boldrey EE. Risk of retinal tears in patients with vitreous floaters. *Am J Ophthalmol*. 1983;96:783–787.
174. Novak MA, Welch RB. Complications of acute symptomatic posterior vitreous detachment. *Am J Ophthalmol*.

1984;97:308–314.
175. Sebag J. Vitreoschisis in diabetic macular edema. *Invest Ophthalmol Vis Sci*. 2011;52(11):8455–8456.
176. Sebag J, Gupta P, Rosen R, et al. Macular holes and macular pucker: the role of vitreoschisis as imaged by optical coherence tomography/scanning laser ophthalmoscopy. *Trans Am Ophthalmol Soc*. 2007;105:121–131.
177. Gupta P, Yee KMP, Garcia P, et al. Vitreoschisis in macular diseases. *Br J Ophthalmol*. 2011;95(3):376–380.
178. Machemer R. The importance of fluid absorption, traction, intraocular currents, and chorioretinal scars in the therapy of rhegmatogenous retinal detachments. *Am J Ophthalmol*. 1984;98:681–693.
179. Sigelman J. Vitreous base classification of retinal tears: clinical application. *Surv Ophthalmol*. 1980;25:59–74.
180. Halpern JI. Routine screening of the retinal periphery. *Am J Ophthalmol*. 1966;62:99–102.
181. Byer NE. Clinical study of retinal breaks. *Trans Am Acad Ophthalmol Otolaryngol*. 1967;71:461–473.
182. Smith RE, Ganley JP. Ophthalmic survey of a community. I: Abnormalities of the ocular fundus. *Am J Ophthalmol*. 1972;74:1126–1130.
183. Teng CC, Katzin KM. An anatomic study of the periphery of the retina. I: Nonpigmented epithelial cell proliferation and hole formation. *Am J Ophthalmol*. 1951;34:1237–1248.
184. Boniuk M, Butler FC. An autopsy study of lattice degeneration, retinal breaks, and retinal pits. McPherson A. *New and controversial aspects of retinal detachment*. Hoeber: New York; 1968.
185. Spencer LM, Foos RY. Paravascular vitreoretinal attachments: role in retinal tears. *Arch Ophthalmol*. 1970;84:557–564.
186. Barishak YR, Stein R. Retinal breaks without retinal detachment in autopsy eyes. *Acta Ophthalmol*. 1972;50:147–159.
187. Foos RY. Tears of the peripheral retina: pathogenesis, incidence, and classification in autopsy eyes. *Mod Probl Ophthalmol*. 1975;15:68–81.

188. Byer NE. The natural history of asymptomatic retinal breaks. *Ophthalmology*. 1982;89:1033–1039.
189. Neumann E, Hyams S. Conservative management of retinal breaks: a follow-up study of subsequent retinal detachment. *Br J Ophthalmol*. 1972;56:482–486.
190. Haimann MH, Burton TC, Brown CK. Epidemiology of retinal detachment. *Arch Ophthalmol*. 1982;100:289–292.
191. Bohringer HR. Statistiches zu Haufigkeit and Risiko der Netz-hautablosung. *Ophthalmologica*. 1956;131:331–334.
192. Benson WE. Prophylactic therapy of retinal breaks. *Surv Ophthalmol*. 1977;22:41–47.
193. Combs JL, Welch RB. Retinal breaks without detachment: natural history, management, and long-term follow-up. *Trans Am Ophthalmol Soc*. 1982;80:64–97.
194. DiBernardo C, Blodi B, Byrne SF. Echographic evaluation of retinal tears in patients with spontaneous vitreous hemorrhage. *Arch Ophthalmol*. 1992;110:511–514.
195. Sarrafizadeh R, Hassan T, Ruby AJ. Incidence of retinal detachment and visual outcome in eyes presenting with posterior vitreous separation and dense fundus-obscuring vitreous hemorrhage. *Ophthalmology*. 2001;108:2273–2278.
196. Theodossiadis GP, Velissatopoulos P, Magouritsas N, et al. Behandlung und Nachuntersuchung von Netzhautrissen ohne Netz-hautablosung mit den Riss uberlagerndem abgehobenem Netzhautgefass. *Klin Monatsbl Augenheilkd*. 1977;170:411–415.
197. Lincoff H, Kreissig I, Richard G. Treating avulsed vessels with a temporary balloon buckle. *Am J Ophthalmol*. 1986;101:90–94.
198. Krebs I, Brannath W, Glittenberg K, et al. Posterior vitreo-macular adhesion: a potential risk factor for exudative age-related macular degeneration. *Am J Ophthalmol*. 2007;144:741–746.
199. Robison C, Krebs I, Binder S, et al. Vitreo-macular adhesion in active and end-stage age-related macular degeneration. *Am J Ophthalmol*. 2009;148:79–82.
200. Krebs I, Glittenberg C, Binder S. Vitreous in age-related macular degeneration. Sebag J. *Vitreous – in Health and*

Disease. Springer: New York; 2014:329–346.
201. Sebag J. Vitreous in age-related macular degeneration therapy – the medium is the message. *Retina*. 2015;35(9):1715–1718.
202. Gass JDM, Norton WD. Cystoid macular edema and papilledema following cataract extraction: a fluorescein funduscopic and angiographic study. *Arch Ophthalmol*. 1966;76:646–661.
203. Irvine AR. Cystoid maculopathy. *Surv Ophthalmol*. 1976;21:1–17.
204. Jaffe NS. Vitreous traction at the posterior pole of the fundus due to alterations in the vitreous posterior. *Trans Am Acad Ophthalmol Otolaryngol*. 1967;71:642–652.
205. Sebag J, Balazs EA. Pathogenesis of cystoid macular edema: an anatomic consideration of vitreoretinal adhesions. *Surv Ophthalmol*. 1984;28(Suppl.):493–498.
206. Smiddy WE, Green WR, Michels RG, et al. Ultrastructural studies of vitreomacular traction syndrome. *Am J Ophthalmol*. 1989;107:177–185.
207. Patel A, de Bustros S, Michels RG. Pars plana vitrectomy for aphakic cystoid macular edema. *Retina*. 1985;5:11–15.
208. Fung WE, Vitrectomy–ACME Study Group. Vitrectomy for chronic aphakic cystoid macular edema: results of a national, collaborative, prospective, randomized investigation. *Ophthalmology*. 1985;92:1102–1111.
209. McDonnell PJ, Fine SL, Hillis AI. Clinical features of idiopathic macular cysts and holes. *Am J Ophthalmol*. 1982;93:777–786.
210. Wang MY, Sadun AA, Sebag J. Vitreo-papillary adhesion and traction. Sebag J. *Vitreous – in Health and Disease*. Springer: New York; 2014:299–310.
211. Bronstein MA, Trempe CL, Freeman HM. Fellow eyes of eyes with macular holes. *Am J Ophthalmol*. 1981;92:757–761.
212. Avila MP, Jalkh AE, Murakami K, et al. Biomicroscopic study of the vitreous in macular breaks. *Ophthalmology*. 1983;90:1277–1283.
213. Morgan CM, Schatz H. Involutional macular thinning: a premacular hole condition. *Ophthalmology*. 1986;93:153–161.

214. Guyer DR, Green WR. Idiopathic macular holes and precursor lesions. Franklin RM. *Symposium on vitreous and retinal disease. Proceedings of the 1992 New Orleans Academy of Ophthalmology*. Kugler: New York; 1993.
215. Sadda SR, Campochiaro PA, de Juan E Jr, et al. Histopathological features of vitreous removed at macular hole surgery. *Arch Ophthalmol*. 1999;117:478–484.
216. Kelly NE, Wendel RT. Vitreous surgery for idiopathic macular holes: results of a pilot study. *Arch Ophthalmol*. 1991;109:654–659.
217. Funata M, Wendel RT, de la Cruz Z, et al. Clinicopathologic study of bilateral macular holes treated with pars plana vitrectomy and gas tamponade. *Retina*. 1992;12:289–298.
218. Madreperla SA, Geiger GL, Funata M, et al. Clinicopathologic correlation of a macular hole treated by cortical vitreous peeling and gas tamponade. *Ophthalmology*. 1994;101:682–686.
219. Haritoglou C, Reiniger IW, Schaumberger M, et al. Five-year follow-up of macular hole surgery with peeling of the internal limiting membrane: update of a prospective study. *Retina*. 2006;26:618–622.
220. Johnson RN, Gass JDM. Idiopathic macular holes: observations, stages of formation, and implications for surgical intervention. *Ophthalmology*. 1988;95:917–924.
221. Jost BF, Hutton WL, Fuller DG, et al. Vitrectomy in eyes at risk for macular hole formation. *Ophthalmology*. 1990;97:843–847.
222. de Bustros S. Vitrectomy for prevention of macular holes: results of a randomized multicenter clinical trial. Vitrectomy for Prevention of Macular Hole Study Group. *Ophthalmology*. 1994;101:1055–1059.
223. Cibis GW, Watzke RC, Chua J. Retinal hemorrhages in posterior vitreous detachment. *Am J Ophthalmol*. 1975;80:1043–1046.
224. Kroll P, Wiegand W, Schmidt J. Vitreopapillary traction in proliferative diabetic vitreoretinopathy. *Br J Ophthalmol*. 1999;83:261–264.
225. Katz B, Hoyt C. Gaze-evoked amaurosis from

vitreopapillary traction. *Am J Ophthalmol*. 2005;139:631–637.
226. Bradford RH, Wilkinson CP. Vitreous opacification after cataract extraction. *Am J Ophthalmol*. 1987;103:276–280.
227. McDonnell PJ, de la Cruz ZC, Green WR. Vitreous incarceration complicating cataract surgery: a light and electron microscopic study. *Ophthalmology*. 1986;93:247–253.
228. Osterlin S. Macromolecular composition of the vitreous in the aphakic owl monkey eye. *Exp Eye Res*. 1978;26:77–84.
229. Kawano SI, Honda Y, Negi A. Effects of biological stimuli on the viscosity of the vitreous. *Acta Ophthalmol*. 1982;60:977–991.
230. Heller MD, Straatsma BR, Foos RY. Detachment of the posterior vitreous in phakic and aphakic eyes. *Mod Probl Ophthalmol*. 1972;10:23–36.
231. McDonnell PJ, Patel A, Green WR. Comparison of intracapsular and extracapsular cataract surgery: histopathologic study of eyes obtained postmortem. *Ophthalmology*. 1985;92:1208–1223.
232. Erie JC, Raecker ME, Baratz KH, et al. Risk of retinal detachment after cataract extraction, 1980–2004: a population-based study. *Trans Am Ophthalmol Soc*. 2006;104:167–175.
233. Cox MS, Schepens CL, Freeman HM. Retinal detachment due to ocular contusion. *Arch Ophthalmol*. 1966;76:678–685.
234. Massicotte SJ, Folberg R, Torczynski E, et al. Vitreoretinal traction and perimacular retinal folds in the eyes of deliberately traumatized children. *Ophthalmology*. 1991;98:1124–1127.
235. de Juan E, Sternberg P, Michels RG. Penetrating ocular injuries: types of injuries and visual results. *Ophthalmology*. 1983;90:1318–1322.
236. Winthrop SR, Cleary PE, Minckler DS, et al. Penetrating eye injuries: a histopathological review. *Br J Ophthalmol*. 1980;64:809–817.
237. Faulborn J, Topping TM. Proliferations in the vitreous cavity after perforating injuries: a histopathological study. *Graefes Arch Clin Exp Ophthalmol*. 1978;205:157–166.
238. Cleary PE, Ryan SJ. Histology of wound, vitreous and retina

in experimental posterior penetrating eye injury in the rhesus monkey. *Am J Ophthalmol*. 1979;88:221–231.
239. Abrams GW, Topping TM, Machemer R. Vitrectomy for injury: the effect on intraocular proliferation following perforation of the posterior segment of the rabbit eye. *Arch Ophthalmol*. 1979;97:743–748.
240. Cleary PE, Ryan SJ. Vitrectomy in penetrating eye injury: results of a controlled trial of vitrectomy in an experimental posterior penetrating eye injury in the rhesus monkey. *Arch Ophthalmol*. 1981;99:287–292.
241. Spalding SC, Sternberg P. Controversies in the management of posterior segment ocular trauma. *Retina*. 1990;10:76–82.
242. Gregor Z, Ryan SJ. Complete and core vitrectomies in the treatment of epiretinal posterior penetrating eye injury in the rhesus monkey. II: Histologic features. *Arch Ophthalmol*. 1983;101:446–450.
243. Miller B, Miller H, Patterson R, et al. Effect of the vitreous on retinal wound-healing. *Graefes Arch Clin Exp Ophthalmol*. 1986;224:576–579.
244. Smiddy WE, Maguire AM, Green WR, et al. Idiopathic epiretinal membranes: ultrastructural characteristics and clinicopathologic correlation. *Ophthalmology*. 1989;96:811–821.
245. Gupta P, Sadun AA, Sebag J. Multifocal retinal contraction in macular pucker analyzed by combined optical coherence tomography/scanning laser ophthalmoscopy. *Retina*. 2008;28:447–452.
246. Wilkes SR, Mansour AM, Green WR. Proliferative vitreoretinopathy: histopathology of retroretinal membranes. *Retina*. 1987;7:94–101.
247. The Retina Society Terminology Committee. The classification of retinal detachment with proliferative vitreoretinopathy. *Ophthalmology*. 1983;90:121–125.
248. Charles S. *Vitreous microsurgery*. Williams and Wilkins: Baltimore, MD; 1981.
249. Kampik A, Kenyon KR, Michels RG, et al. Epiretinal and vitreous membranes: a comparative study of 56 cases. *Arch Ophthalmol*. 1981;99:1445–1454.

250. Wallow IHL, Stevens TS, Greaser ML, et al. Actin filaments in contracting preretinal membranes. *Arch Ophthalmol*. 1984;102:1370–1375.
251. Campochiaro PA, Gaskin HC, Vinores SA. Retinal cryopexy stimulates traction retinal detachment formation in the presence of an ocular wound. *Arch Ophthalmol*. 1987;105:1567–1570.
252. Campochiaro PA, Glaser BM. Platelet-derived growth factor is chemotactic for human retinal pigment epithelial cells. *Arch Ophthalmol*. 1985;103:576–579.
253. Harvey AK, Roberge F, Hjelmeland LM. Chemotaxis of rat retinal glia to growth factors found in repairing wounds. *Invest Ophthalmol Vis Sci*. 1987;28:1092–1099.
254. Sebag J. Shaken not stirred. *Ophthalmology*. 2001;108:1177–1178.
255. Sebag J. Pharmacologic vitreolysis – premise and promise of the first decade. *Retina*. 2009;29:871–874.

[*] **W. Richard Green, MD** was first author of this chapter for the first four editions of this book. His monumental contributions to this field are reflected in the histopathologic images and content of this chapter, which continues to teach long after his parting on July 5, 2010.

SECTION 2

Basic Mechanisms of Injury in the Retina

OUTLINE

24

Mechanisms of Oxidative Stress in Retinal Injury

Milam A. Brantley Jr., Allison C. Umfress, Paul Sternberg Jr.

Oxidative stress has been implicated in the development and progression of retinal diseases. This chapter will focus on three forms of retinal pathology that are related to oxidative stress: age-related macular degeneration (AMD), diabetic retinopathy (DR), and inherited retinal degenerations. We will discuss specific mechanisms of oxidative stress that affect the retinal pigment epithelium (RPE), retinal vasculature, photoreceptors, and mitochondria. We will also consider the evidence linking oxidative stress and inflammation in the pathogenesis of retinal disease. Finally, we will explore potential therapies targeting oxidative stress in the retina.

Overview of Oxidative Stress in the Retina

Reactive oxygen species (ROS) are a major source of retinal oxidative stress. These highly reactive particles include free radicals and nonradical oxidants such as peroxides and singlet oxygen. Free radicals such as the hydroxyl radical (OH•), hydroperoxyl radicals (HO_2•), superoxide anion (O_2^-•), and lipid peroxyl radicals, are strong oxidizing agents with an unpaired electron in their outer shells. Peroxides (e.g., hydrogen peroxide [H_2O_2], lipid peroxides) and singlet oxygen ($^1O_2$) have a full complement of electrons in an unstable state.[1]

Under physiologic conditions, the body produces ROS through normal metabolic processes such as glycolysis and the Krebs cycle. Aging and disease may disturb the balance between ROS generation and clearance, resulting in oxidative damage to macromolecules.[2] The majority of endogenous ROS are produced

by mitochondria through the electron transport chain, which converts 2–3% of all utilized oxygen into ROS.[3] Stimuli such as aging, inflammation, irradiation, air pollutants, and cigarette smoke lead to increased ROS, and thus increased cellular oxidative injury.[1,4,5]

The body's defenses against increasing oxidative stress consist of small antioxidant molecules including vitamin C, vitamin E, and carotenoids, as well as larger antioxidant enzymes, such as superoxide dismutase (SOD), glutathione peroxidase (GSHPx), and catalase. Most ROS are eliminated immediately by these antioxidant enzymes. For example, the superoxide anion, produced by mitochondria during the electron transport stage of cellular respiration, is converted to the less noxious hydrogen peroxide molecule (H_2O_2) by SOD.[1] The smaller antioxidant molecules (e.g., vitamin C [ascorbate], vitamin E [tocopherol], and carotenoids) reduce ROS by acting directly on free radicals.

As most free radical chain reactions are prevented by free radical-scavenging molecules, it appears that free radicals are often not the direct cause of oxidative damage but rather act to initiate further oxidative damage by nonradical oxidants. The redox hypothesis describes radical-free oxidative stress in which disrupted thiol redox circuits interfere with regulation of cellular redox status, affecting cell signaling and homeostasis. Redox-sensitive thiols include the amino acid cysteine (Cys), the Cys-derived disulfide cystine (CySS), the Cys-containing tripeptide glutathione (GSH), and glutathione disulfide (GSSG). Sulfur redox couples act as "on/off" switches regulating gene expression and protein function. Because the Cys/CySS and GSH/GSSG couples are not in equilibrium, it is plausible that abnormal levels of nonradical oxidants could be sufficient to disrupt normal function.[6]

The retina is particularly vulnerable to oxidative stress because of its high oxygen consumption and high proportion of polyunsaturated fatty acids (PUFAs).[1,2] High light exposure and phagocytosis in the RPE contribute to the oxidative burden of the retina. The turnover rate of photoreceptors is high, with these cells shedding about 10% of their outer segment discs each day. The disc membranes, in particular the PUFAs, are subject to peroxidation, which is highly damaging to the RPE. This can be more impactful in

the central retina, the macula, where there is a high level of metabolic activity and where light exposures are higher. There the macular pigment, which protects against ROS in the retina, is composed of two carotenoids: lutein, which exists as a single stereoisomer, and zeaxanthin, which exists in two predominant isomeric forms, zeaxanthin and meso-zeaxanthin. Lutein and zeaxanthin can quench the reactive singlet oxygen and form an optical filter that blocks highly damaging blue light from reaching the photoreceptors.[1]

Retinal Diseases Related to Oxidative Stress

Oxidative stress contributes to diseases of the retina, including age-related macular degeneration, diabetic retinopathy, and inherited retinal degenerations (Table 24.1). To set the stage for detailed discussion of the underlying mechanisms of oxidative damage to the retina, we will discuss the pathology and evidence for a role of oxidative stress in each of these diseases.

TABLE 24.1

Oxidative Stress in the Pathophysiology of Common Retinal Diseases

Disease	Supporting Evidence
AMD	AMD risk factors (e.g., aging, smoking) linked to increased systemic oxidative stress[1,2,4,74,75] Oxidative modifications to proteins and DNA in Bruch's membrane, drusen, and RPE cells[23–26] Light exposure associated with increased generation of ROS and AGEs[74,75] and increased risk of AMD[1,2] Colocalization of RAGE with AGE deposits and macular disease in AMD retinas[77] RAGE-induced secretion of VEGF in RPE cells[77] Low macular pigment associated with AMD[27–29] Dietary or supplemental intake of antioxidants (e.g., vitamins, carotenoids) and zinc linked to lower risk of AMD progression[21,22,30,32] Decreased viability and increased proliferation in cultured RPE and choroidal endothelial cells exposed to the oxidant *t*-BHP[90] Increased proliferation and VEGF upregulation in choroidal endothelial cells exposed to AGEs[76,77,91]
Diabetic retinopathy	Mitochondrial overproduction of superoxide potentially disruptive to multiple pathways implicated in diabetes (e.g., polyol, AGE, protein kinase C, hexosamine)[44,45]

	Prevention of early retinal cell death by superoxide inhibition[41,42] Involvement of oxidative stress-activated caspases and NF-κB in retinal cell death[37–39] Increased expression of oxidative stress markers in endothelial cells and pericytes in high-glucose environment[38] Impaired glucose transport in H_2O_2-exposed retinal endothelial cells[89] Link between the oxidant peroxynitrite and upregulated VEGF expression in endothelial cells[82,83,85,88]
Inherited retinal degenerations	Increased oxygen concentration in outer retina of multiple animal models of retinal degeneration[92-94] Cone damage due to increased retinal oxygen levels[95,105,106] Link between thioredoxin antioxidant defense and a rod-derived cone survival factor[64,109,110] Increased ROS and decreased GSH in an in vitro model of photoreceptor apoptosis[65,102] Downregulation of DNA repair mediators in the *rd1* mouse retina[104] Reduction in cone cell loss and preservation of cone ERGs seen in *rd1* mice treated with antioxidants[107] Decreased antioxidant defense (e.g., GST and GSHPx) in *rd1* mice[102,103]

AGE, advanced glycation endproduct; AMD, age-related macular degeneration; ERGs, electroretinograms; GSH, glutathione; GSHPx, glutathione peroxidase; GST, glutathione-*S*-transferase; NF-κB, nuclear factor-κB;RPE, retinal pigment epithelium; ROS, reactive oxygen species; RAGE, receptor of AGEs; *t*-BHP, tert-butyl hydroperoxide; VEGF, vascular endothelial growth factor.

Age-Related Macular Degeneration

AMD, the leading cause of irreversible vision loss in older individuals in the Western world, is a complex disease influenced by factors such as genetics, demographics, and environmental exposures. Approximately 6.5% of individuals in the United States over the age of 40 (7.2 million people) show signs of any AMD, and 0.8% have sight-threatening advanced stages of the disease.[7] With the prevalence of AMD increasing with older age, and the anticipated aging of the American population, cases of advanced AMD are expected to increase to over 3 million by 2050.[8]

AMD can be divided into an early, typically asymptomatic, form and a late form that often results in severe central vision loss. In the early stages of AMD, whitish-yellow waste deposits called drusen accumulate in the macula, usually localized between the RPE and Bruch's membrane. These deposits may be small and discrete (hard drusen) or larger and more confluent (soft drusen). Drusen may also be present between the photoreceptors and RPE or within the photoreceptor cell layer (reticular drusen).[9,10] Histologically, drusen consist of numerous proteins (e.g., complement, immunoglobulins,

amyloid-β) and lipids (e.g., phospholipids, cholesterol, apolipoproteins).[11,12] Early dry AMD may develop into advanced dry or advanced wet AMD. Advanced dry AMD (geographic atrophy) is marked by cell death in the choriocapillaris and overlying RPE. Advanced wet AMD is characterized by choroidal neovascularization, in which abnormal choroidal vessels extend into the subretinal space.

Demographic and environmental risk factors for AMD include older age, smoking, high body mass index (BMI), and high light exposure.[13,14] Smoking, the strongest environmental risk factor for AMD, has been linked to disease onset and progression in multiple large, epidemiologic studies.[15–20] Additionally, high dietary intake of carotenoids and antioxidant supplementation has been associated with lower risk of AMD.[21,22]

Multiple lines of evidence point to the role of oxidative stress in the pathogenesis of AMD. Several AMD risk factors, particularly aging, smoking, and light exposure, have been linked to increased levels of oxidative stress.[1] Additionally, proteomic analysis of human donor eyes revealed oxidative modifications to proteins and DNA in Bruch's membrane, drusen, and RPE.[23] Subsequent proteomic analyses of AMD donor eyes have demonstrated early stage changes in expression of chaperone proteins that aid in microtubule regulation,[24] protect against stress-induced protein unfolding,[24,25] aid in mitochondrial trafficking, and regulate apoptosis.[25] The higher prevalence of these oxidative changes[23] and decreased expression of proteins protective against oxidative stress-induced damage[24–26] in AMD patients versus controls suggest an increased oxidative state in AMD retinas.

Impairment of the retinal antioxidant defense system may also play a role in AMD, as some studies have reported decreased macular pigment in AMD patients.[27–29] Significantly lower levels of macular pigment (lutein and zeaxanthin) were found by direct measurement in AMD versus control eyes at autopsy.[27] The Age-Related Eye Disease Study (AREDS), conducted from 1992 to 2001, demonstrated that supplementation with antioxidants (vitamin C, vitamin E, and β-carotene) and zinc decreased the risk of progression from early to advanced AMD.[30] In past observational studies, high dietary intake of lutein/zeaxanthin and omega-3 fatty

acids such as docosahexaenoic acid (DHA) and eicosapentaenoic acid (EPA) has corresponded to reduced prevalence and incidence of AMD.[31] These compounds were investigated in AREDS2, conducted from 2006 to 2012, which concluded that the addition of the xanthophylls lutein and zeaxanthin to the original AREDS formula had no additional effect on reducing progression of AMD. However, these compounds were recommended as an alternative to β-carotene in the original formulation due to association of β-carotene supplementation with lung cancer.[32]

Diabetic Retinopathy

DR, a common microvascular complication of both type 1 and type 2 diabetes mellitus (DM), is the leading cause of vision loss in working-age adults.[33] In the United States, approximately 26 million people have diabetes, and the number of diabetic adults with retinopathy is projected to triple to 16 million by the year 2050.[34] The majority of DM (90–95%) is represented by type 2 diabetes (T2DM), which involves impaired insulin action at target tissues and impaired insulin release. In contrast, the primary cause of type 1 diabetes (T1DM) is the autoimmune destruction of pancreatic β-cells.

Clinically, DR is defined by the presence of specific retinal microvascular signs in an individual with DM. The nonproliferative form is characterized by microaneurysms, hemorrhages, hard exudates, cotton-wool spots, venous dilation and beading, and intraretinal microvascular abnormalities. The more severe proliferative form is characterized by retinal neovascularization, which can lead to vitreous hemorrhage and traction retinal detachment. Intraretinal macular edema, which may be present in either form of retinopathy, can also lead to severe vision loss.

Interestingly, retinal capillary cells in diabetics undergo accelerated apoptosis that precedes the detection of any histopathologic changes characteristic of DR.[35,36] Although the exact mechanism for this accelerated apoptosis remains uncertain, studies have pointed to the involvement of oxidative stress-activated caspases and the activation of the proinflammatory transcription factor NF-κB via Raf-1 kinase in retinal cell death.[37–39] Treatment

with Raf-1 kinase inhibitors resulted in decreased capillary cell death, prevented Raf-1 activation of NF-κB, and reduced the development of DR in rats.[37,39,40] Additional experiments revealed that inhibition of superoxide accumulation in diabetes prevented this early retinal cell death.[41,42]

Oxidative stress appears to be a major risk factor for the onset and progression of diabetes. Many of the common DM risk factors, including obesity and age, foster an oxidative environment that may alter insulin sensitivity by increasing insulin resistance or impairing glucose tolerance. Hyperglycemia, a common result of both types of diabetes, contributes in turn to the progression and maintenance of an overall oxidative environment.[43]

Hyperglycemia may contribute to oxidative stress by generating ROS directly or by disrupting the cellular redox balance. This hyperglycemia-induced oxidative stress can occur via several well-studied mechanisms, including increased polyol pathway flux, increased intracellular formation of advanced glycation endproducts (AGE), activation of protein kinase C (PKC), and disturbance of the hexosamine biosynthesis pathway. The overproduction of superoxide by the mitochondrial transport chain has been proposed as a possible root cause for these metabolic changes.[44,45]

The polyol pathway reduces sugars to their respective sugar alcohols (polyols) via reaction with aldose reductase in an NADPH-dependent manner. Both glucose and the glycolytic metabolites of glucose, such as glyceraldehyde-3-phosphate, serve as substrates for aldose reductase. Hyperglycemia thus leads to increased polyol pathway flux and increased redox stress through consumption of NADPH, an essential cofactor for regenerating the intracellular antioxidant glutathione (GSH). By decreasing the amount of free GSH, the polyol pathway may increase the susceptibility of cells to oxidative injury.[44]

AGEs are modifications of proteins or lipids that become nonenzymatically glycated and oxidized after contact with aldose sugars. Early glycation and oxidation of proteins and lipids result in the formation of intermediate Schiff bases and Amadori products, which then undergo further molecular rearrangements that lead to the generation of AGEs.[46] In diabetes, AGEs are found at increased

concentration in the extracellular matrix. AGEs appear to damage cells by modifying intracellular proteins such as transcription factors, extracellular proteins, and matrix molecules. These modified proteins can then bind and activate the receptor of AGEs (RAGE), inducing the production of ROS, which results in upregulation of NF-κB.[44] In endothelial cells, RAGE activation induces the expression of procoagulant genes including thrombomodulin, tissue factor, and vascular cell adhesion molecule (VCAM)-1.[47–50] Recently, additional ligands for RAGE have been identified, including members of the calgranulin and HMGB1 (high-mobility group box 1) families. Hyperglycemia-induced overexpression of these ligands and resultant activation of RAGE induce pro-inflammatory interaction with the innate immune system via TLR-4 (toll-like receptor 4).[51–53]

The activation of PKC leads to multiple characteristics of DR including increased vascular permeability, endothelial cell proliferation and apoptosis, and neovascularization.[54] Hyperglycemia-induced ROS inhibit the key glycolytic enzyme glyceraldehyde 3-phosphate dehydrogenase (GAPDH), leading to an increase in glycolytic pathway precursors. Inhibition of GADPH leads to increased levels of triose phosphate, which results in enhanced de novo synthesis of diacylglycerol (DAG), the primary activator of PKC, from glucose.[54,55] Activated PKC can induce expression of vascular endothelial growth factor (VEGF),[56] a major effector of vessel permeability and a primary stimulator of neovascularization. Activation of PKC induces expression of the protein tyrosine phosphatase SHP-1, which leads to a reduction in downstream signaling of platelet-derived growth factor (PDGF) and resultant pericyte apoptosis.[57] PKC also leads to synthesis of NF-κB and transforming growth factor-β1 (TGF-β), which results in accumulation of microvascular matrix proteins that can contribute to the occlusion of capillaries seen in DR.[44,54,58,59]

The hexosamine biosynthesis pathway may also mediate some of the toxic effects of hyperglycemia. The inhibition of GADPH by ROS causes diversion of glycolytic metabolites to the hexosamine pathway, producing UDP-N-acetylglucosamine. N-acetylglucosamine is added to serine and threonine residues of transcription factors, often resulting in pathologic changes in gene

expression. Examples include increased expression of TGF-β and plasminogen activator inhibitor-1 (PAI-1).[44]

Hyperglycemia-induced alterations in each of these DM-associated pathways can be linked to oxidative stress. Toward that end, Brownlee has proposed a "unifying mechanism" hypothesizing that all of these pathway changes are a result of mitochondrial superoxide overproduction in the endothelial cells of both large and small blood vessels.[45,60] In this model, diabetic hyperglycemia causes increased production of ROS by mitochondria. Greater concentration of ROS in the body induces nuclear DNA strand breaks. This DNA damage activates the DNA repair enzyme poly(ADP-ribose) polymerase (PARP), which reduces GADPH activity by the addition of ADP-ribose polymers. Decreased GAPDH activity results in a backup of the glycolytic pathway and activation of the polyol, AGE, PKC, and hexosamine pathways discussed above.[44]

Inherited Retinal Degenerations

Inherited retinal degenerations comprise a group of disorders characterized by primary and progressive loss of photoreceptor cells, leading to irreversible vision loss. Over 230 genes and greater than 270 loci have been associated with inherited retinal degenerations (www.sph.uth.tmc.edu/retnet). The proteins encoded by these genes are diverse in function, including not only proteins required for phototransduction but also structural proteins, RNA splicing factors, intracellular trafficking molecules, and proteins involved in phagocytosis and regulation of intracellular pH.[61]

The most common form of these diseases, retinitis pigmentosa (RP), which has an estimated prevalence of around 1 in 4000,[62] involves a primary insult to rods that initiates rod cell death followed by cone cell death (rod–cone dystrophy). Other forms of inherited retinal degeneration include cone dystrophy, cone–rod dystrophy, and macular dystrophy. The most common inherited macular dystrophy is Stargardt macular dystrophy, an autosomal recessive disease with a carrier frequency of approximately 1 in 50.[63]

The first symptom of RP is typically night blindness, followed by

progressive loss of the peripheral visual field. Funduscopic exam classically demonstrates a pale optic nerve, attenuated retinal vessels, and "bone-spicule" pigmentation in the retinal midperiphery. The widespread retinal degeneration leads to diminution or abolishment of the a-waves and b-waves on electroretinogram (ERG). Various molecular defects have been identified in individuals with RP, including mutations in genes encoding rhodopsin, peripherin, and cGMP phosphodiesterase. These genes are typically rod-specific, but some also code for more general proteins, such as structural proteins in cilia and their associated transport molecules.

The unifying feature in animal models and human cases of RP seems to be the apoptotic cell death of rod photoreceptors, although the mechanisms that lead to photoreceptor cell death in RP remain poorly defined. While most mutations in RP specifically affect rods, both rods and cones die. Several mechanisms have been proposed for the dependence of cone survival on the presence of functioning rods. One theory is that rods produce a survival factor that is required by cones and that modulates the thioredoxin antioxidant defense system in the retina.[64] Several groups have also proposed oxidative stress or alterations in the cellular redox state as a common mediator of photoreceptor cell death.[65,66] Various lines of evidence support this hypothesis, including the induction of apoptosis by oxidants like H_2O_2[66,67] and the inhibition of apoptosis by antioxidants.[68]

Oxidative Injury to the Retina

Specific mechanisms of oxidative damage to the retina are unique to the affected retinal cell types. Morphology and function of the RPE, retinal vasculature, and photoreceptors can be severely impaired by the increased oxidative stress associated with disease. Growing evidence suggests that the mitochondria of retinal cells contribute to oxidative stress-related pathology and that inflammatory processes are closely tied to pathologic oxidative stress in the retina.

Retinal Pigment Epithelium

Oxidative stress can lead to the accumulation of debris and ultimately cell death in the RPE, as manifest by the drusen and geographic atrophy of AMD. Abnormally high concentrations of oxidized products may also interfere with the ability of RPE cells to regulate key angiogenic factors, resulting in retinal neovascularization.

Oxidative damage to the RPE can be induced by oxidizing agents or light. Under normal conditions, phagocytosis of photoreceptor outer segments by the RPE generates ROS via the NADPH oxidase system, leading to increased intracellular H_2O_2 and increased catalase activity.[69] The phosphoinositide 3-kinase (PI3K)-Akt pathway may protect RPE cells from such oxidative stress. The oxidant H_2O_2 was demonstrated to induce PI3K-dependent Akt activation in cultured RPE cells. Akt activation can enhance RPE survival by phosphorylating, and thus inactivating, multiple proapoptotic factors.[70] Cultured human RPE cells exhibited signs of senescence when treated with the oxidizing agents tert-Butyl hydroperoxide (t-BHP)[71] or H_2O_2,[72] suggesting that oxidative stress may contribute to the RPE senescence seen in AMD. Oxidative stress induced by hypoxia/reoxygenation in cultured human RPE cells led to the accumulation of extracellular matrix and may be linked to the thickening of Bruch's membrane seen in early AMD.[73] Additionally, animal and laboratory studies have shown that blue light damages the RPE through ROS generation.[74] RPE cells treated with subapoptotic levels of UV light showed increases in both ROS and AGEs.[75]

The AGE-induced activation of RAGE may play a key role in RPE apoptosis. In human donor eyes, RAGE were found to colocalize with AGE deposits and macular disease in AMD retinas, while normal retinas displayed little or no immunolabeling for either AGE or RAGE. This study also showed that AGEs stimulate RAGE-mediated activation in cultured RPE cells in a dose-dependent fashion.[76] RAGE increased secretion of VEGF in cultured RPE cells, suggesting that AGE-mediated activation of the RAGE axis in RPE cells could contribute to neovascular macular disease.[77]

Further evidence supports the idea that oxidative stress in the

RPE has a significant influence on VEGF regulation. Treatment of cultured human RPE cells with the oxidant DL-buthionine-(S,R)-sulfoximine (BSO) caused a significant decrease in intracellular GSH and GSH/GSSG ratios. This change in thiol redox status was associated with increased VEGF-A secretion as well as significant induction of VEGF receptors VEGFR-1 and VEGFR-2.[78] In cultured RPE cells treated with t-BHP, both VEGF-A and VEGF-C were upregulated, with secretion higher to the apical side than to the basal side,[79] suggesting that VEGF may directly affect the photoreceptors. VEGF secretion in RPE cells is regulated, in part, by the mitogen-activated protein kinases (MAPK), including c-Jun-activated kinase (JNK), p38, and extracellular signal-regulated kinases (ERK). Studies in cultured RPE cells demonstrated that constitutive VEGF secretion is regulated by p38, while oxidative stress-induced VEGF secretion is regulated by both p38 and ERK.[80] Finally, it appears that autocrine VEGF-A can enhance RPE cell survival under oxidative stress, utilizing the autocrine VEGF-A/VEGFR-2/PI3K/Akt pathway.[81]

Retinal Vasculature

Increased oxidative stress can lead to alterations in both the retinal and choroidal vasculature. In diabetes, hyperglycemia-induced ROS may link elevated glucose and multiple metabolic abnormalities associated with the development of retinopathy.[60] Retinal capillary cell cultures containing endothelial cells and pericytes incubated in high-glucose medium exhibited increased oxidative stress markers. In these cells, increased caspase-3 expression and apoptosis were seen after five days in culture.[38]

Oxidative stress has been correlated with the increased production of VEGF and may be involved in the upregulation of endothelial cell VEGF expression seen in diabetes.[82] The increased expression of VEGF in DR may be driven by elevated levels of peroxynitrite,[83] a highly-reactive oxidant formed by the combination of superoxide anion with nitric oxide (NO). In early DR, NF-κB activation and subsequent NO synthesis generate elevated levels of NO that promote peroxynitrite formation.[37,84] Treatment of microvascular endothelial cells with peroxynitrite

demonstrated a dose-dependent increase in VEGF mRNA expression via activation of STAT3.[83] In addition, peroxynitrite mediates a variety of biologic processes including inhibition of key metabolic enzymes, lipid peroxidation, nitration of protein tyrosine residues, and oxidation of thiol pools.[85] The reaction of peroxynitrite with DNA results in the formation of 8-hydroxy deoxyguanosine, a marker of oxidative DNA damage, and high levels of intracellular peroxynitrite deplete glutathione stores, further contributing to oxidative stress and inducing apoptosis.[85]

A hyperglycemic environment may promote the damaging effects of VEGF observed in diabetes. Interestingly, VEGF has been shown to be a potent survival factor for endothelial cells in vitro and in vivo.[86] Despite its antiapoptotic properties, the increased levels of VEGF seen in diabetic retinas[87] are associated with increased retinal endothelial cell death. Cultured endothelial cells subjected to serum withdrawal-induced apoptosis were protected by VEGF in normal glucose but not in high glucose or peroxynitrite media.[85] Further experiments determined that high glucose treatment blocks the pro-survival effect of VEGF and causes accelerated endothelial cell apoptosis via the action of peroxynitrite.[85] Hyperglycemia-induced peroxynitrite accumulation in the retinal vasculature persists even with reversal of poor glycemic control, suggesting that peroxynitrite may contribute to the failure of retinopathy to improve after good glycemic control is attained.[88]

Oxidative stress can also affect retinal endothelial cells' ability to transport glucose into the cell. Exposure of endothelial cells to sustained oxidative stress in the form of H_2O_2 resulted in decreased glucose transport activity due to increased internalization of GLUT1, the most common retinal glucose transporter.[89] H_2O_2-induced oxidative stress was also found to increase the rate of GLUT1 internalization by a proteasome-dependent mechanism involving inactivation of Akt.

Oxidative stress may have direct and indirect effects on the choroidal endothelial cells (CEC), and thus may contribute to the choroidal neovascularization seen in AMD. Treatment of cultured RPE and CEC with the oxidant t-BHP resulted in decreased viability and increased proliferation of both cell types.[90] RPE cells

exposed to t-BHP for 24 hours were found to release basic fibroblast growth factor (bFGF), a prominent proangiogenic factor. This finding suggests that oxidative stress may stimulate choroidal neovascularization via RPE-mediated growth factor release. Interestingly, CECs exposed to oxidative stress-induced AGEs in culture demonstrated increased proliferation as well as upregulation of VEGF, suggesting that AGEs may also promote choroidal neovascularization.[91]

Photoreceptors

The process of retinal degeneration disrupts the physiologic balance between oxidants and antioxidants in the retinal spaces. As a source of ROS, photoreceptors contribute to the oxidative burden of the retina, particularly in a pathologic oxidative environment. The vitality of rods and cones is directly affected by the redox status of surrounding tissue.

Loss of photoreceptor cells or reduction of energy-demanding activities such as phototransduction can lead to elevated tissue oxygen concentrations because choroidal blood vessels are not autoregulated by local oxygen levels. Accordingly, increases in outer retinal oxygen concentrations have been confirmed in multiple animal models of photoreceptor loss.[92–94] In contrast, the inner retinal arterioles do autoregulate, leading to their attenuation in the presence of high oxygen concentrations.[95] This oxygen imbalance induced by photoreceptor dysfunction and degeneration is manifest by the thinned retinal vessels observed clinically in RP.

Alterations in the cellular redox state appear to mediate photoreceptor cell death. An in vitro model of photoreceptor apoptosis demonstrated an early and sustained increase in intracellular ROS accompanied by a rapid depletion of intracellular GSH.[65] Evidence suggests that multiple oxidative-stress related mechanisms underlie the programmed cell death (PCD) of photoreceptors. Classically, caspase-dependent apoptotic pathways have been described.[96,97] More recently, it has been shown that PCD can also be accomplished through caspase-independent apoptosis,[66,98,99] as well as via autophagy.[100] In a photoreceptor cell line treated with the nitric oxide donor sodium nitroprusside,

cytosolic calcium levels increased during photoreceptor apoptosis, leading to activation of caspases as well as the calcium-dependent proteases calpains.[68] Inhibitors of both caspases[68] and calpains,[101] applied independently to the same photoreceptor cell line, failed to prevent apoptosis. These results indicate that, in addition to the classic caspase-dependent pathways of apoptosis, calpain activity may be crucial for apoptosis.

Calpains may lead to retinal oxidative damage by impairing DNA repair mechanisms. Studies in retinal degeneration (*rd1*) mice, which have a mutation in exon 7 of the beta-subunit of the rod photoreceptor *PDE6* gene, have demonstrated downregulation in defensive mechanisms against oxidative stress (e.g., glutathione-S-transferase and glutathione peroxidase), potentially allowing an increase in intracellular ROS.[102,103] Reactions between ROS and DNA can produce the highly mutagenic oxidated nucleotide 8-oxo-guanosine (8-oxoG). Mismatches of 8-oxoG with adenine or cytosine are corrected by the specific DNA repair enzyme 8-oxoG DNA glycosylase (OGG1).[104] OGG1 is regulated by cAMP response element binding protein (CREB), and OGG1 and CREB have both been found to be downregulated in the *rd1* retina. Since OGG1 can be inactivated by calpains, an increase in calpain activity could severely compromise a cell's ability to repair oxidative stress-induced DNA damage.

Cones appear to be sensitive to retinal oxygen concentration. In multiple animal models of RP, increased levels of oxygen in the retina resulted in progressive oxidative damage to cones.[95,105,106] Treatment of *rd1*$^{-/-}$ mice with a cocktail of antioxidants resulted in downregulation of markers of oxidative damage in cones, reduced cone cell loss, and preserved the cone ERGs. These results suggest that oxidative damage is important in cone death regardless of the underlying mechanism that kills rods.[107] Most recently, studies in *rd1*$^{-/-}$ mice showed that NADPH oxidase plays a critical role in generation of the oxidative stress that leads to cone death in RP.[107]

Initial experiments investigating the progressive death of cones after rod cell death showed that grafting of normal photoreceptors (97% rods) into the eye of the rodless *rd1*$^{-/-}$ mouse before the cones degenerated had a positive effect on the host cones, even at some distance from the transplant.[108] Further studies identified a protein

that allowed for cone survival termed Rod-derived Cone Viability Factor (RdCVF).[64] RdCVF, encoded by the exon1 of the nucleoredoxin-like 1 gene (*Nxnl1*), corresponds to a truncated thioredoxin (TRX)-like protein. Because TRX proteins are key to maintaining a reducing intracellular environment (109), disruption of TRXs can lead to conditions of increased oxidative stress. *Nxnl1* knockout mice have been shown to be sensitive to oxidative stress,[109] and the delivery of RdCVF through viral vectors to *Nxnl1*-/- mice was protective against light-induced photoreceptor damage,[110] suggesting that RdCVF is part of an endogenous redox-based signaling pathway involved in retinal maintenance.

Mitochondria

Cumulative oxidative damage to mitochondria appears to play a role in aging and retinal diseases[111] (see also Chapter 34, Mitochondrial genetics of retinal disease). Mitochondria are especially susceptible to oxidative injury due to the high concentration of ROS produced by the electron transport chain and the limited capacity for mitochondrial DNA (mtDNA) repair.[112] RPE cells treated with UV light demonstrated conformational changes in mitochondria,[75] and oxidized photoreceptor outer segments in vitro damaged RPE mtDNA.[113] Additionally, variations in the mitochondrial genome may modulate ROS production and thus susceptibility to disease.

Accumulating evidence, reviewed in Table 24.2, suggests a role for mitochondrial damage in the pathophysiology of both AMD and DR.[111] Abnormalities in the number and structure of mitochondria in the RPE have been reported in studies of AMD donor eyes.[114] Proteomic analyses have suggested that mitochondrial proteins[25] and mtDNA[26] are altered in AMD, and long-extension polymerase chain reaction (PCR) confirmed that mtDNA is increasingly damaged with AMD progression.[115] Characterization of mtDNA from retina and blood of AMD patients and controls demonstrated that AMD mtDNA has an increased number of large deletions, rearrangements, and amino acid-altering single nucleotide polymorphisms (SNPs).[116] Oxidative damage to mitochondria can lead to apoptosis in human RPE cells,[117] and

decreased levels of the mitochondrial antioxidant manganese superoxide dismutase (MnSOD) led to the development of dry AMD-like lesions in mice.[118]

TABLE 24.2

Evidence of Mitochondrial Oxidative Stress in Age-Related Macular Degeneration and Diabetic Retinopathy

Disease	Supporting Evidence
AMD	Light-induced conformational changes in mitochondria of RPE cells[75] Damage to RPE mtDNA by oxidized photoreceptor outer segments[114] Alterations in mitochondrial proteins[25] and mtDNA[26,115] in AMD Apoptosis in human RPE cells induced by oxidative damage to mitochondria[117] Development of dry AMD-like lesions in mice with decreased levels of MnSOD[118] Association of multiple mitochondrial haplogroups (H, J, U, T) with AMD[121–125]
Diabetic retinopathy	Enhanced permeability of the mitochondrial membrane due to hyperglycemia-induced oxidative stress in retinal endothelial cells and pericytes[119] Protective effects of MnSOD on retinal antioxidant capacity[120] and vascular pathology[41] Association of mtDNA haplogroup T with risk of retinopathy among type 2 diabetics[126] Association of mtDNA haplogroup H with risk of proliferative retinopathy among patients with diabetic retinopathy[127]

AMD, age-related macular degeneration; MnSOD, manganese superoxide dismutase; mtDNA, mitochondrial DNA; RPE, retinal pigment epithelium.

In the case of diabetes, hyperglycemia causes excess production of superoxide by the mitochondrial electron transport chain, inhibiting GAPDH activity.[44] As mentioned previously, Brownlee has proposed that this excess of mitochondrial superoxide in endothelial cells of both large and small blood vessels leads to an array of complications seen in diabetes, including increased activity of the polyol pathway and increased production of AGEs. Specifically, hyperglycemia causes increased oxidation of glucose, leading to an elevation in the voltage gradient across the mitochondrial membrane. Once a critical threshold in voltage gradient is reached, electron transfer inside complex III of the electron transport chain is blocked. The electrons accumulate at coenzyme Q, which donates them to molecular oxygen, creating large amounts of superoxide. Ultimately, the increased number of ROS in diabetes can alter the mitochondrial membrane potential, leading to cell death.[44]

Animal studies have demonstrated the effects of hyperglycemia-induced impairment of the mitochondrial membrane. Increased

levels of cytochrome *c*, a key component of the electron transport chain and the precursor to caspase-9 in the apoptotic cascade, were detected in rats after 8 months of diabetes. These rats also had increased levels of the proapoptotic Bcl-2-associated X protein (BAX) in the mitochondria. In retinal endothelial cells and pericytes, high concentrations of glucose enhanced the permeability of the mitochondrial membrane, increasing levels of cytochrome *c* in the cytosol and BAX in the mitochondria.[119] These glucose-mediated responses were inhibited by the antioxidant MnSOD. A subsequent study by the same group showed that increased expression of MnSOD can prevent the reduction of GSH levels and total antioxidant capacity caused by diabetes.[120] In nontransgenic diabetic mice, upregulation of MnSOD protected against diabetes-related changes in the mitochondria and reduced vascular pathology.[41]

Genetic association studies have indicated that polymorphisms in mtDNA influence the risk of developing AMD and diabetic retinopathy. In the Blue Mountain Eye Study, mitochondrial haplogroup H was associated with a reduced prevalence of any AMD (OR 0.75, 95% CI 0.58–0.97) and early AMD (OR 0.75, 95% CI 0.57–0.98), whereas haplogroups J and U were associated with early AMD only.[121,122] More recent analysis reported a higher frequency of haplogroup J and a lower frequency of haplogroup H in patients with CNV compared to controls without AMD, suggesting that haplogroup H is protective against AMD.[123] A US study determined that individuals with the T2 haplogroup were 2.5 times more likely to have advanced AMD than those without the haplogroup (OR 2.54, 95% CI 1.36–4.80).[124] This finding was supported by studies showing that the mtDNA 4917G polymorphism associated with haplogroup T independently predicted the presence of AMD (OR 2.16, 95% CI 1.21–3.91).[125] Subsequently, PCR analysis of mtDNA from AMD and control donor retinas found that SNPs T16126C and A73G, associated with haplogroups J and T, were more frequent in AMD retinas than in normal retinas.[122] The authors then replicated these associations in blood DNA from 99 cases and 92 controls. The mitochondrial haplogroup T was also associated with risk of retinopathy among type 2 diabetics.[126] As this haplogroup has been associated with multifactorial age-related diseases such as coronary

artery disease[126] and AMD,[125] it seems plausible that carriers of haplogroup T may be exposed to greater oxidative stress or have greater susceptibility to oxidative damage than individuals with other haplogroups. Mitochondrial haplogroups have also been associated with severity of DR. In two independent cohorts of DR patients, those with the haplogroup H were more likely to have proliferative DR, while those with haplogroup Uk were less likely to have proliferative disease.[127]

Oxidative Stress and Inflammation

Growing evidence from both cell culture and animal studies points to a mechanistic link between oxidative stress and inflammation (Table 24.3). (See detailed discussion of inflammation in Chapter 27, Inflammation and immune responses in retinal health and disease.) Decreased superoxide dismutase 2 (SOD2) and increased superoxide production were associated with mononuclear phagocyte-induced apoptosis of the RPE in *sod2*$^{+/-}$ mice.[128] In mice with oxygen-induced retinopathy, injections of the serine proteinase inhibitor SERPINA3K reduced expression of proinflammatory factors (e.g., VEGF, tumor necrosis factor (TNF)-α, and intercellular adhesion molecule (ICAM)-1), decreased ROS production, and increased SOD and GSH levels.[129] The antiinflammatory effect of SERPINA3K was also demonstrated in cultured retinal cells exposed to hypoxia.[129]

TABLE 24.3

Inflammation and Its Relationship With Oxidative Stress in Age-Related Macular Degeneration (AMD) and Diabetic Retinopathy

	Evidence in AMD	Evidence in Diabetic Retinopathy
Inflammation	Presence of complement proteins in drusen[11,12] Associations of genetic variants in multiple complement genes (*CFH*, *C2/BF*, *C3*, *CFI*) with AMD[131–139] High blood complement protein levels associated with AMD[143,144]. Development of retinal deposits similar to AMD drusen in young patients with systemic complement activation[145]	Increased vitreous levels of IL-1, IL-6, and IL-8 increased in patients with PDR[156] Link between IL-1β and retinal capillary cell apoptosis[157] Involvement of the inflammatory mediators COX-2 and PGE_2 in the development of diabetic retinopathy via VEGF modulation[158]

Link between inflammation and oxidative stress	Decreased *CFH* mRNA expression in the presence of oxidized photoreceptor outer segments[147] Reduced *CFH* expression in RPE cells in response to H_2O_2[146] Disruption in RPE function in presence of both H_2O_2 and complement-sufficient serum[154] Development of AMD-like lesions in mice treated with CEP adducts[155] Association of increased superoxide and decreased SOD2 with mononuclear phagocyte-induced apoptosis of the RPE in *sod2*$^{+/-}$ mice[128]	Increased superoxide leading to endothelial cell damage, increased microvascular permeability, and recruitment of neutrophils[54] Increased ROS leading to activation of the transcription factor NF-κB, which upregulates cytokines, nitric oxide, and prostaglandins[60]

CEP, carboxyethylpyrrole; COX-2, cyclooxygenase-2; IL, interleukin; NF-κB, nuclear factor-κB; PDR, proliferative diabetic retinopathy; PGE_2, prostaglandin E_2; ROS, reactive oxygen species; RPE, retinal pigment epithelium; SOD2, superoxide dismutase 2;VEGF, vascular endothelial growth factor.

Immunologic and inflammatory processes appear to play a major role in AMD, including drusen formation, complement activation, recruitment of tissue-destructive macrophages, and microglial activation and accumulation.[130] The association of multiple complement gene polymorphisms with AMD,[131–139] the presence of complement proteins in drusen,[140–142] and the link between systemic complement activation and AMD[143–145] suggest that innate immunity plays a critical role in AMD pathogenesis. These discoveries have led to experiments designed to define the role of oxidative stress in complement activation in the RPE.

Cell culture studies have linked oxidative stress to reduced expression of the complement factor H (*CFH*) gene in RPE cells.[146] Investigation of constitutive CFH production in a stable RPE cell line demonstrated that long-term treatment of RPE cells with oxidized photoreceptor outer segments (POS), but not normal POS, markedly downregulated *CFH* mRNA expression. Furthermore, phagocytosis of both oxidized and normal POS reduced CFH protein expression.[147] These results suggest that the phagocytosis of POS, particularly if oxidized, impairs synthesis and secretion of CFH, resulting in reduced regulatory control of complement activation and its proinflammatory effects.[147] Additionally, the introduction of H_2O_2 to RPE cells was shown to reduce the normal interferon (IFN)-γ-induced stimulation of *CFH* expression via acetylation of FOXO3, which interrupts STAT1 binding to the *CFH*

promoter.[146]

Various polymorphisms in the *ARMS2* gene have been associated with increased risk of AMD.[148,149] The presence of risk variants in *ARMS2* has been associated with high serum CRP levels[150,151] and inflammatory markers such as interleukin (IL)-6, IL-8, TNF-α, C3, and C5, suggesting a proinflammatory role for *ARMS2* in the pathogenesis of AMD.[152,153] However, further investigation is necessary to clarify the function of *ARMS2* and its involvement in AMD pathophysiology.

The dynamic interplay between oxidative stress and inflammation may contribute to the abnormalities in RPE function evident in AMD. A combination of H_2O_2 and complement-sufficient serum was shown to disrupt the barrier function of RPE monolayers in culture and to evoke polarized secretion of VEGF, although introduction of either H_2O_2 or serum alone did not cause these changes.[154] These results suggest that oxidative stress and complement together impair RPE function. They also point to a common pathway that relates an oxidizing environment and complement activation with VEGF production. Such a pathway could play a role in the neovascularization seen in late AMD.

A close link between oxidative stress and inflammation in AMD is also supported by recent animal work in which mice immunized with mouse serum albumin adducted with the lipid peroxidation product carboxyethylpyrole (CEP) developed AMD-like lesions in the retina.[155] Specifically, these mice produced antibodies to the hapten, fixed complement component 3 in Bruch's membrane, and accumulated drusen below the RPE.[155] Taken together, these studies demonstrate a molecular link between oxidative stress and complement in RPE cells and suggest that the interaction between oxidative stress and inflammatory mediators plays a key role in the development of AMD.

Oxidative stress-related inflammation may also play a key role in the pathogenesis of DR. Increased superoxide can promote inflammation by damaging endothelial cells, increasing microvascular permeability, and recruiting neutrophils.[54] ROS activate the transcription factor NF-κB, which can increase proinflammatory mediators, such as cytokines, nitric oxide, and prostaglandins. The cytokines IL-1β, IL-6, and IL-8 have been

reported to be increased in the vitreous of patients with proliferative DR.[156] Interestingly, it appears that IL-1β increases retinal capillary cell apoptosis.[157] Additionally, IL-1 induces the production of cyclooxygenase-2 (COX-2), a catalyst for prostaglandin E_2 (PGE_2) formation. The inflammatory mediators COX-2 and PGE_2 are reported to contribute to the development of DR by modulating VEGF-mediated vascular permeability and angiogenesis.[158]

Retinal Therapies Targeting Oxidative Stress

In this section, we will discuss oxidative stress-related therapies for retinal diseases. We will then explore potential avenues for the development of future treatments that protect against oxidative damage in the retina, including antioxidant therapy, AGE inhibitors, and genetic modification (Fig. 24.1). These potential therapies are outlined in Table 24.4.

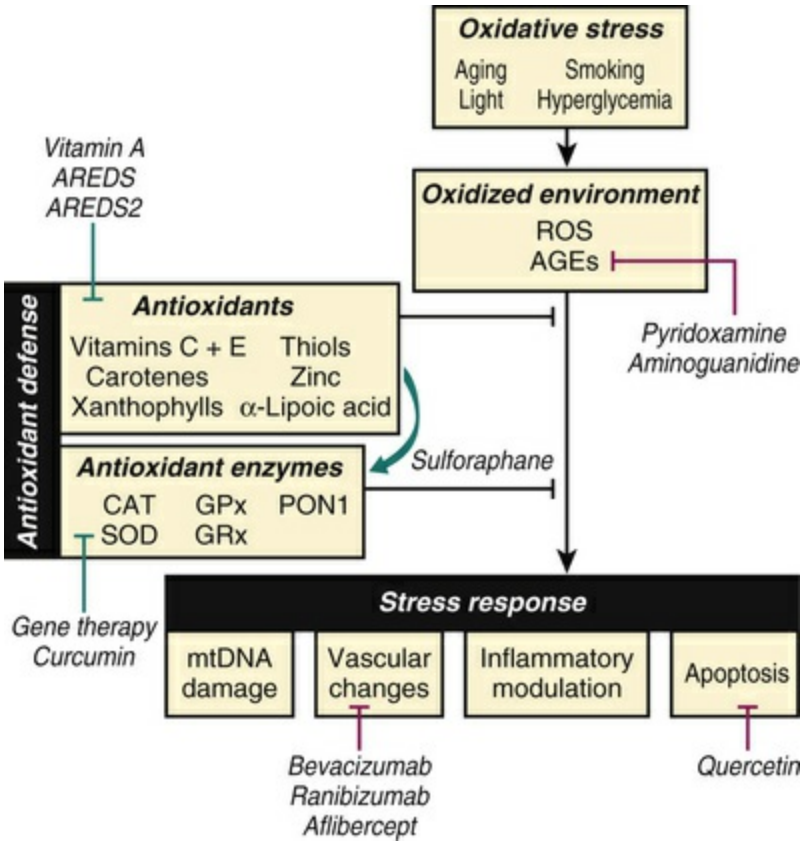

FIG. 24.1 Oxidative stress, brought on by factors such as aging, smoking, light exposure, and hyperglycemia, leads to an oxidized cellular environment that is marked by the accumulation of reactive oxygen species (ROS) and advanced glycation endproducts (AGEs). This oxidized environment triggers stress responses, such as damage to mitochondrial (mt) DNA, vascular changes, inflammatory modulation, and apoptosis. Concurrently, the cellular antioxidant defense system, comprised of both antioxidants and antioxidant enzymes, is activated, mitigating the damage of oxidative stress. The mechanisms of current and potential treatments for retinal diseases are depicted above, with green representing activation and red representing inhibition. *AREDS*, Age-Related Eye Disease Study; *CAT*, catalase; *GPx*, glutathione peroxidase; *GRx*, glutathione reductase; *PON1*, paraoxonase 1; *SOD*, superoxide dismutase.

TABLE 24.4

Retinal Therapies Targeting Oxidative Stress

Potential Avenues for Retinal Therapy	Specific Treatments Under Investigation
Antiinflammatory agents	Resveratrol to decrease oxidative damage and RPE proliferation via inhibition of the NF-κB pathway[178] Curcumin to decrease expression of inflammatory mediators[173] and inhibit the NF-κB pathway[172]
Boost in antioxidant defense	Vitamin A palmitate supplementation to slow rate of retinal degeneration (e.g., RP)[164] Supplementation with xanthophylls and omega-3 fatty acids for treatment of AMD in AREDS2 clinical trial[31,32] Sulforaphane to protect against retinal oxidative damage via activation of the Nrf2-thioredoxin system[184–186] Curcumin to prevent retinal oxidative damage via activation of the Nrf2-thioredoxin system[1] and increased antioxidant expression (e.g., GST)[174] Lipoic acid to reduce oxidative stress and photoreceptor cell death[95,171]
Genetic modification	Modulation of *SOD2* and *CAT* gene expression to protect against oxidative damage to retinal cells[193,194]
Inhibition of AGEs	Pyridoxamine to protect against retinal vascular lesions in diabetics[188] Aminoguanidine to prevent capillary closure, microaneurysm formation, and NOS depletion[190,191]
Inhibition of apoptotic pathways	Quercetin to protect against oxidative damage and senescence in the retina through inhibition of caspase-3 activity[180,181,183]

AGEs, advanced glycation endproducts; AMD, age-related macular degeneration; AREDS2, Age-Related Eye Disease Study 2; CAT, catalase GST, glutathione-*S*-transferase; NF-κB, nuclear factor-κB; NOS, nitric oxide synthase; RP, retinitis pigmentosa; RPE, retinal pigment epithelium; SOD2, superoxide dismutase 2.

Supplemental Antioxidants

Currently, care of patients with dry AMD is centered on antioxidant and zinc supplementation, as there are no direct interventions for drusen or geographic atrophy. AREDS, a multicenter, randomized clinical trial sponsored by the National Eye Institute, demonstrated that daily intake of supplemental antioxidants (β-carotene, vitamin C, vitamin E) and zinc reduced the risk of progression to advanced AMD by 25% over 5 years.[159]

Supplemental carotenoids have also been associated with decreased AMD risk. Two smaller studies linked xanthophylls (lutein and zeaxanthin) and/or omega-3 fatty acids with improved visual acuity[160] and central retinal function (as measured by multifocal ERG).[161] In the Rotterdam Study, high dietary intake of zinc, omega-3 fatty acids, β-carotene, and lutein/zeaxanthin corresponded to decreased risk of early AMD onset.[162]

A recent study investigated the relationship between short-term AREDS supplementation and oxidative stress. AMD patients and

controls were placed on a controlled diet supplemented with the AREDS formula for five days. This brief treatment significantly lowered plasma concentrations of the oxidative stress marker cystine, suggesting that the antioxidant and zinc combination directly affects redox status.[163]

The AREDS2 study investigated the effect of oral supplementation of xanthophylls and omega-3 fatty acids (DHA and eicosapentaenoic acid [EPA]) on the risk of AMD progression. In this clinical trial, completed in 2012, AMD patients were randomly assigned to four treatment groups: (1) xanthophylls only (10 mg lutein and 2 mg zeaxanthin); (2) omega-3 fatty acids only (350 mg DHA and 650 mg EPA); (3) xanthophylls and omega-3 fatty acids; and (4) placebo.[32] The addition of xanthophylls, omega-3 fatty acids, or both to the original AREDS formulation did not further reduce the observed risk of progression to advanced AMD. This study also examined the effect of eliminating β-carotene or reducing the zinc doses in the original AREDS formula. There was again no apparent effect of either β-carotene elimination or zinc reduction on progression to advanced AMD. However, a higher incidence of lung cancer was noted in the group receiving β-carotene supplementation, particularly in current and former smokers. Therefore, lutein and zeaxanthin supplementation was recommended as an alternative to β-carotene in the original AREDS formula.[32]

A phase II study investigated topical application of OT-551, a di-substituted hydroxylamine with antioxidant properties for the ability to stop GA progression in AMD. No significant treatment effects were observed, and no further trials were carried out for this agent.

Studies have suggested the benefit of nutritional and drug supplements in preserving photoreceptor function. The most widely recognized supplement for RP patients is vitamin A palmitate, which has been suggested to slow the rate of retinal degeneration by an unknown mechanism.[164] These same studies suggested that vitamin E may be associated with an increase in the deterioration rate of the electroretinogram in RP patients,[164] possibly by reducing the availability of other vitamins in the retina. More recently, studies from the same group investigated the role of

docosahexaenoic acid (DHA)[165] and lutein[166] in the treatment of RP, concluding that these supplements may have positive effects on the disease. However, letters to the journal editor have questioned the clinical conclusions that were drawn based on the experimental data for each of these studies.[167–169] Also, a more recent randomized controlled trial demonstrated no significant difference in the loss of cone cell ERG function with DHA supplementation as compared to placebo.[170]

In preclinical studies, the naturally occurring antioxidant α-lipoic acid has been demonstrated to reduce oxidative stress and photoreceptor cell death in mouse models of retinitis pigmentosa[95] and light-induced photoreceptor damage.[171] A number of small clinical trials are currently underway to evaluate the ability of α-lipoic acid to preserve photoreceptor function in retinal diseases.

Dietary Antioxidants

Naturally occurring compounds found in food may protect against retinal degenerations. Curcumin, from the spice turmeric, has been shown to inhibit the NF-κB pathway, which is involved in immune response,[172] and to decrease expression of inflammatory mediators.[173] Curcumin also increases expression of antioxidants, such as heme oxygenase-1, quinone reductase, and glutathione S-transferase.[174,175] A 2-week diet supplemented with curcumin protected rats from light-induced retinal damage.[176] Similarly, treatment of cultured retinal cells with curcumin protected against H_2O_2-induced cell death by increasing production of antioxidant enzymes, such as thioredoxin, and activating the Nrf2 antioxidant pathway.[176] Treatment of diabetic rats with curcumin was protective against Müller cell loss and prevented downregulation of glutamine synthetase compared with untreated rats.[177]

Another member of the plant-derived polyphenol family, resveratrol, a compound in red wine, has been shown to decrease oxidative damage and RPE proliferation in vitro.[178] Evidence suggests that resveratrol may take effect by inhibiting the NF-κB pathway involved in inflammatory response. In diabetic mice, resveratrol prevented diabetes-induced retinal ganglion cell (RGC) apoptosis via downregulation of calmodulin-dependent protein

kinase II.[179]

The flavonoid quercetin, found in green tea and red onion, is a free radical scavenger and a chelating agent that can reduce iron-driven lipid peroxidation.[180] Quercetin has been reported to protect against H_2O_2-induced oxidative damage and senescence in cultured RPE cells by inhibiting caspase-3 activity.[181,182] In diabetic rats, retinas treated with quercetin demonstrated significantly lower levels of inflammatory cytokines, NF-κB, and caspase-3 expression compared to untreated rats.[183]

Sulforaphane, an isothiocyanate found in cruciferous vegetables, appears to exert neuroprotective effects through activation of the Nrf2-thioredoxin system. The antioxidant transcription factor Nrf2 binds to the antioxidant response element (ARE), activating the antioxidant defense system in response to oxidative stress.[184] Thioredoxin has been shown to protect against H_2O_2-induced damage in photoreceptor cells and light damage in mice.[185] Sulforaphane induces thioredoxin in light-exposed RPE cells via the Nrf2-ARE pathway,[186] thus protecting against photo-oxidative damage to the retina.

Anti-Advanced Glycation Endproduct Treatment

One possible avenue for treatment of DR targets the accumulation of AGEs, which can disturb retinal vascular cell function. More recently, sulforaphane has been demonstrated to inhibit AGE-induced pericyte damage via downregulation of RAGE, suggesting a protective role for sulforaphane in DR.[187] The AGE inhibitor pyridoxamine protected against diabetes-induced retinal vascular lesions, thickening of the basement membrane, and acellular capillaries in diabetic rats.[188] Treatment of diabetic rats with pyridoxamine decreaed the accumulation of AGEs in retinal cells compared to untreated controls.[189] Aminoguanidine, which acts as an inhibitor of inducible nitric oxide synthase and AGE crosslinking, may prevent capillary closure, microaneurysm formation, and nitric oxide synthase (NOS) depletion.[190,191] This inhibition of NOS has been linked to inhibition of apoptosis in mice with oxygen-induced retinopathy.[192] The efficacy of pyridoxamine

and aminoguanidine has yet to be investigated for the treatment of DR in clinical trials.

Genetic Modification

Gene therapy is being explored for the treatment of retinal degenerations. Toward this end, genes involved in the regulation of cellular oxidative stress are being targeted in animal studies to reduce ROS production, bolster antioxidant defenses, and/or increase cellular repair capacity. In mice with ischemia-induced retinal injury, plasmids encoding the human *SOD2* (MnSOD) or *CAT* (catalase) genes significantly decreased ROS generation and retinal endothelial cell.[193] Another study showed that an adenovirus carrying the *CAT* gene protected against H_2O_2-induced damage to RPE cells and light-induced damage to RPE and photoreceptors in mice.[194]

Conclusions

Oxidative stress plays a significant role in the pathogenesis of multiple retinal diseases, including AMD, DR, and inherited retinal degenerations. ROS, derived primarily from the mitochondria, can adversely affect health and survival of RPE cells, retinal vascular endothelial cells, and photoreceptors. Regardless of a condition's primary insult, oxidative stress often contributes to retinal cell death via instigation of DNA damage, modulation of alternative metabolic pathways, and stimulation of proapoptotic reactions. Because oxidative stress appears to be a common mechanism of retinal cell damage, the development of therapy that protects against retinal oxidative damage has the potential to significantly reduce vision loss from retinal diseases (Fig. 24.1).

References

1. Beatty S, Koh H, Phil M, Henson D, Boulton M. The role of oxidative stress in the pathogenesis of age-related macular degeneration. *Surv Ophthalmol*. 2000;45(2):115–134.
2. Cai J, Nelson KC, Wu M, Sternberg P Jr, Jones DP.

Oxidative damage and protection of the RPE. *Prog Retin Eye Res*. 2000;19(2):205–221.
3. Chance B, Sies H, Boveris A. Hydroperoxide metabolism in mammalian organs. *Physiol Rev*. 1979;59(3):527–605.
4. Borish ET, Pryor WA, Venugopal S, Deutsch WA. DNA synthesis is blocked by cigarette tar-induced DNA single-strand breaks. *Carcinogenesis*. 1987;8(10):1517–1520.
5. Jones DP, Mody VC Jr, Carlson JL, Lynn MJ, Sternberg P Jr. Redox analysis of human plasma allows separation of pro-oxidant events of aging from decline in antioxidant defenses. *Free Radic Biol Med*. 2002;33(9):1290–1300.
6. Jones DP. Radical-free biology of oxidative stress. *Am J Physiol Cell Physiol*. 2008;295(4):C849–68.
7. Klein R, Chou CF, Klein BE, Zhang X, Meuer SM, Saaddine JB. Prevalence of age-related macular degeneration in the US population. *Arch Ophthalmol*. 2011;129(1):75–80.
8. Rein DB, Wittenborn JS, Zhang X, et al. Forecasting age-related macular degeneration through the year 2050: the potential impact of new treatments. *Arch Ophthalmol*. 2009;127(4):533–540.
9. Sarks J, Arnold J, Ho IV, Sarks S, Killingsworth M. Evolution of reticular pseudodrusen. *Br J Ophthalmol*. 2011;95(7):979–985.
10. Zweifel SA, Spaide RF, Curcio CA, Malek G, Imamura Y. Reticular pseudodrusen are subretinal drusenoid deposits. *Ophthalmology*. 2010;117(2):303–312.e1.
11. Mullins RF, Russell SR, Anderson DH, Hageman GS. Drusen associated with aging and age-related macular degeneration contain proteins common to extracellular deposits associated with atherosclerosis, elastosis, amyloidosis, and dense deposit disease. *FASEB J*. 2000;14(7):835–846.
12. Wang L, Clark ME, Crossman DK, et al. Abundant lipid and protein components of drusen. *PLoS ONE*. 2010;5(4):e10329.
13. Seddon JM, Cote J, Davis N, Rosner B. Progression of age-related macular degeneration: association with body mass index, waist circumference, and waist-hip ratio. *Arch Ophthalmol*. 2003;121(6):785–792.

14. Clemons TE, Milton RC, Klein R, Seddon JM, Ferris FL 3rd. Risk factors for the incidence of Advanced Age-Related Macular Degeneration in the Age-Related Eye Disease Study (AREDS) AREDS report no. 19. *Ophthalmology*. 2005;112(4):533–539.
15. Tan JS, Mitchell P, Kifley A, Flood V, Smith W, Wang JJ. Smoking and the long-term incidence of age-related macular degeneration: the Blue Mountains Eye Study. *Arch Ophthalmol*. 2007;125(8):1089–1095.
16. Cackett P, Wong TY, Aung T, et al. Smoking, cardiovascular risk factors, and age-related macular degeneration in Asians: the Singapore Malay Eye Study. *Am J Ophthalmol*. 2008;146(6):960–967.e1.
17. Chakravarthy U, Augood C, Bentham GC, et al. Cigarette smoking and age-related macular degeneration in the EUREYE Study. *Ophthalmology*. 2007;114(6):1157–1163.
18. Fraser-Bell S, Wu J, Klein R, Azen SP, Varma R. Smoking, alcohol intake, estrogen use, and age-related macular degeneration in Latinos: the Los Angeles Latino Eye Study. *Am J Ophthalmol*. 2006;141(1):79–87.
19. Klein R, Knudtson MD, Cruickshanks KJ, Klein BE. Further observations on the association between smoking and the long-term incidence and progression of age-related macular degeneration: the Beaver Dam Eye Study. *Arch Ophthalmol*. 2008;126(1):115–121.
20. Tomany SC, Wang JJ, Van Leeuwen R, et al. Risk factors for incident age-related macular degeneration: pooled findings from 3 continents. *Ophthalmology*. 2004;111(7):1280–1287.
21. Seddon JM, Ajani UA, Sperduto RD, et al. Dietary carotenoids, vitamins A, C, and E, and advanced age-related macular degeneration. Eye Disease Case-Control Study Group. *JAMA*. 1994;272(18):1413–1420.
22. van Leeuwen R, Boekhoorn S, Vingerling JR, et al. Dietary intake of antioxidants and risk of age-related macular degeneration. *JAMA*. 2005;294(24):3101–3107.
23. Crabb JW, Miyagi M, Gu X, et al. Drusen proteome analysis: an approach to the etiology of age-related macular degeneration. *Proc Natl Acad Sci USA*. 2002;99(23):14682–

14687.
24. Ethen CM, Reilly C, Feng X, Olsen TW, Ferrington DA. The proteome of central and peripheral retina with progression of age-related macular degeneration. *Invest Ophthalmol Vis Sci*. 2006;47(6):2280–2290.
25. Nordgaard CL, Berg KM, Kapphahn RJ, et al. Proteomics of the retinal pigment epithelium reveals altered protein expression at progressive stages of age-related macular degeneration. *Invest Ophthalmol Vis Sci*. 2006;47(3):815–822.
26. Nordgaard CL, Karunadharma PP, Feng X, Olsen TW, Ferrington DA. Mitochondrial proteomics of the retinal pigment epithelium at progressive stages of age-related macular degeneration. *Invest Ophthalmol Vis Sci*. 2008;49(7):2848–2855.
27. Bone RA, Landrum JT, Mayne ST, Gomez CM, Tibor SE, Twaroska EE. Macular pigment in donor eyes with and without AMD: a case-control study. *Invest Ophthalmol Vis Sci*. 2001;42(1):235–240.
28. Bernstein PS, Zhao DY, Wintch SW, Ermakov IV, McClane RW, Gellermann W. Resonance Raman measurement of macular carotenoids in normal subjects and in age-related macular degeneration patients. *Ophthalmology*. 2002;109(10):1780–1787.
29. Obana A, Hiramitsu T, Gohto Y, et al. Macular carotenoid levels of normal subjects and age-related maculopathy patients in a Japanese population. *Ophthalmology*. 2008;115(1):147–157.
30. Age-Related Eye Disease Study Research Group. A randomized, placebo-controlled, clinical trial of high-dose supplementation with vitamins C and E, beta carotene, and zinc for age-related macular degeneration and vision loss: AREDS report no. 8. *Arch Ophthalmol*. 2001;119(10):1417–1436.
31. Krishnadev N, Meleth AD, Chew EY. Nutritional supplements for age-related macular degeneration. *Curr Opin Ophthalmol*. 2010;21(3):184–189.
32. Age-Related Eye Disease Study 2 Research G. Lutein + zeaxanthin and omega-3 fatty acids for age-related macular

degeneration: the Age-Related Eye Disease Study 2 (AREDS2) randomized clinical trial. *JAMA*. 2013;309(19):2005–2015.
33. Cheung N, Mitchell P, Wong TY. Diabetic retinopathy. *Lancet*. 2010;376(9735):124–136.
34. Saaddine JB, Honeycutt AA, Narayan KM, Zhang X, Klein R, Boyle JP. Projection of diabetic retinopathy and other major eye diseases among people with diabetes mellitus: United States, 2005–2050. *Arch Ophthalmol*. 2008;126(12):1740–1747.
35. Mizutani M, Kern TS, Lorenzi M. Accelerated death of retinal microvascular cells in human and experimental diabetic retinopathy. *J Clin Invest*. 1996;97(12):2883–2890.
36. Li W, Yanoff M, Liu X, Ye X. Retinal capillary pericyte apoptosis in early human diabetic retinopathy. *Chin Med J*. 1997;110(9):659–663.
37. Kowluru RA, Koppolu P, Chakrabarti S, Chen S. Diabetes-induced activation of nuclear transcriptional factor in the retina, and its inhibition by antioxidants. *Free Radic Res*. 2003;37(11):1169–1180.
38. Kowluru RA, Koppolu P. Diabetes-induced activation of caspase-3 in retina: effect of antioxidant therapy. *Free Radic Res*. 2002;36(9):993–999.
39. Rayappa SP, Kowluru RA. Role of raf-1 kinase in diabetes-induced accelerated apoptosis of retinal capillary cells. International journal of biomedical science. *Int J Biomed Sci*. 2008;4(1):20–28.
40. Kowluru RA, Kowluru A, Chakrabarti S, Khan Z. Potential contributory role of H-Ras, a small G-protein, in the development of retinopathy in diabetic rats. *Diabetes*. 2004;53(3):775–783.
41. Kanwar M, Chan PS, Kern TS, Kowluru RA. Oxidative damage in the retinal mitochondria of diabetic mice: possible protection by superoxide dismutase. *Invest Ophthalmol Vis Sci*. 2007;48(8):3805–3811.
42. Kowluru RA, Atasi L, Ho YS. Role of mitochondrial superoxide dismutase in the development of diabetic retinopathy. *Invest Ophthalmol Vis Sci*. 2006;47(4):1594–1599.

43. Rains JL, Jain SK. Oxidative stress, insulin signaling, and diabetes. *Free Radic Biol Med*. 2011;50(5):567–575.
44. Brownlee M. The pathobiology of diabetic complications: a unifying mechanism. *Diabetes*. 2005;54(6):1615–1625.
45. Giacco F, Brownlee M. Oxidative stress and diabetic complications. *Circ Res*. 2010;107(9):1058–1070.
46. Goldin A, Beckman JA, Schmidt AM, Creager MA. Advanced glycation end products: sparking the development of diabetic vascular injury. *Circulation*. 2006;114(6):597–605.
47. Vlassara H, Fuh H, Donnelly T, Cybulsky M. Advanced glycation endproducts promote adhesion molecule (VCAM-1, ICAM-1) expression and atheroma formation in normal rabbits. *Mol Med*. 1995;1(4):447–456.
48. Schmidt AM, Hori O, Chen JX, et al. Advanced glycation endproducts interacting with their endothelial receptor induce expression of vascular cell adhesion molecule-1 (VCAM-1) in cultured human endothelial cells and in mice: a potential mechanism for the accelerated vasculopathy of diabetes. *J Clin Invest*. 1995;96(3):1395–1403.
49. Schmidt AM, Crandall J, Hori O, Cao R, Lakatta E. Elevated plasma levels of vascular cell adhesion molecule-1 (VCAM-1) in diabetic patients with microalbuminuria: a marker of vascular dysfunction and progressive vascular disease. *Br J Haematol*. 1996;92(3):747–750.
50. Sengoelge G, Fodinger M, Skoupy S, et al. Endothelial cell adhesion molecule and PMNL response to inflammatory stimuli and AGE-modified fibronectin. *Kidney Int*. 1998;54(5):1637–1651.
51. Rong LL, Gooch C, Szabolcs M, et al. RAGE: a journey from the complications of diabetes to disorders of the nervous system – striking a fine balance between injury and repair. *Restor Neurol Neurosci*. 2005;23(5–6):355–365.
52. Koya D, King GL. Protein kinase C activation and the development of diabetic complications. *Diabetes*. 1998;47(6):859–866.
53. Bierhaus A, Humpert PM, Morcos M, et al. Understanding RAGE, the receptor for advanced glycation end products. *J*

Mol Med. 2005;83(11):876–886.
54. Kowluru RA, Chan PS. Oxidative stress and diabetic retinopathy. *Exp Diabetes Res*. 2007;2007:43603.
55. Shiba T, Inoguchi T, Sportsman JR, Heath WF, Bursell S, King GL. Correlation of diacylglycerol level and protein kinase C activity in rat retina to retinal circulation. *Am J Physiol*. 1993;265(5 Pt 1):E783–93.
56. Williams B, Gallacher B, Patel H, Orme C. Glucose-induced protein kinase C activation regulates vascular permeability factor mRNA expression and peptide production by human vascular smooth muscle cells in vitro. *Diabetes*. 1997;46(9):1497–1503.
57. Geraldes P, Hiraoka-Yamamoto J, Matsumoto M, et al. Activation of PKC-delta and SHP-1 by hyperglycemia causes vascular cell apoptosis and diabetic retinopathy. *Nat Med*. 2009;15(11):1298–1306.
58. Pugliese G, Pricci F, Pugliese F, et al. Mechanisms of glucose-enhanced extracellular matrix accumulation in rat glomerular mesangial cells. *Diabetes*. 1994;43(3):478–490.
59. Craven PA, Studer RK, Felder J, Phillips S, DeRubertis FR. Nitric oxide inhibition of transforming growth factor-beta and collagen synthesis in mesangial cells. *Diabetes*. 1997;46(4):671–681.
60. Brownlee M. Biochemistry and molecular cell biology of diabetic complications. *Nature*. 2001;414(6865):813–820.
61. Bramall AN, Wright AF, Jacobson SG, McInnes RR. The genomic, biochemical, and cellular responses of the retina in inherited photoreceptor degenerations and prospects for the treatment of these disorders. *Annu Rev Neurosci*. 2010;33:441–472.
62. Ayuso C, Millan JM. Retinitis pigmentosa and allied conditions today: a paradigm of translational research. *Genome Med*. 2010;2(5):34.
63. Allikmets R, Shroyer NF, Singh N, et al. Mutation of the Stargardt disease gene (ABCR) in age-related macular degeneration. *Science*. 1997;277(5333):1805–1807.
64. Leveillard T, Mohand-Said S, Lorentz O, et al. Identification and characterization of rod-derived cone viability factor.

Nat Genet. 2004;36(7):755–759.
65. Carmody RJ, McGowan AJ, Cotter TG. Reactive oxygen species as mediators of photoreceptor apoptosis in vitro. *Exp Cell Res*. 1999;248(2):520–530.
66. Carmody RJ, Cotter TG. Oxidative stress induces caspase-independent retinal apoptosis in vitro. *Cell Death Differ*. 2000;7(3):282–291.
67. Sharma AK, Rohrer B. Sustained elevation of intracellular cGMP causes oxidative stress triggering calpain-mediated apoptosis in photoreceptor degeneration. *Curr Eye Res*. 2007;32(3):259–269.
68. Sanvicens N, Gomez-Vicente V, Masip I, Messeguer A, Cotter TG. Oxidative stress-induced apoptosis in retinal photoreceptor cells is mediated by calpains and caspases and blocked by the oxygen radical scavenger CR-6. *J Biol Chem*. 2004;279(38):39268–39278.
69. Miceli MV, Liles MR, Newsome DA. Evaluation of oxidative processes in human pigment epithelial cells associated with retinal outer segment phagocytosis. *Exp Cell Res*. 1994;214(1):242–249.
70. Yang P, Peairs JJ, Tano R, Jaffe GJ. Oxidant-mediated Akt activation in human RPE cells. *Invest Ophthalmol Vis Sci*. 2006;47(10):4598–4606.
71. Yu AL, Fuchshofer R, Kook D, Kampik A, Bloemendal H, Welge-Lussen U. Subtoxic oxidative stress induces senescence in retinal pigment epithelial cells via TGF-beta release. *Invest Ophthalmol Vis Sci*. 2009;50(2):926–935.
72. Glotin AL, Debacq-Chainiaux F, Brossas JY, et al. Prematurely senescent ARPE-19 cells display features of age-related macular degeneration. *Free Radic Biol Med*. 2008;44(7):1348–1361.
73. Fuchshofer R, Yu AL, Teng HH, Strauss R, Kampik A, Welge-Lussen U. Hypoxia/reoxygenation induces CTGF and PAI-1 in cultured human retinal pigment epithelium cells. *Exp Eye Res*. 2009;88(5):889–899.
74. Winkler BS, Boulton ME, Gottsch JD, Sternberg P. Oxidative damage and age-related macular degeneration. *Mol Vis*. 1999;5:32.

75. Roehlecke C, Schaller A, Knels L, Funk RH. The influence of sublethal blue light exposure on human RPE cells. *Mol Vis*. 2009;15:1929–1938.
76. Howes KA, Liu Y, Dunaief JL, et al. Receptor for advanced glycation end products and age-related macular degeneration. *Invest Ophthalmol Vis Sci*. 2004;45(10):3713–3720.
77. Ma W, Lee SE, Guo J, et al. RAGE ligand upregulation of VEGF secretion in ARPE-19 cells. *Invest Ophthalmol Vis Sci*. 2007;48(3):1355–1361.
78. Sreekumar PG, Kannan R, de Silva AT, Burton R, Ryan SJ, Hinton DR. Thiol regulation of vascular endothelial growth factor-A and its receptors in human retinal pigment epithelial cells. *Biochem Biophys Res Commun*. 2006;346(4):1200–1206.
79. Kannan R, Zhang N, Sreekumar PG, et al. Stimulation of apical and basolateral VEGF-A and VEGF-C secretion by oxidative stress in polarized retinal pigment epithelial cells. *Mol Vis*. 2006;12:1649–1659.
80. Klettner A, Roider J. Constitutive and oxidative-stress-induced expression of VEGF in the RPE are differently regulated by different Mitogen-activated protein kinases. *Graefes Arch Clin Exp Ophthalmol*. 2009;247(11):1487–1492.
81. Byeon SH, Lee SC, Choi SH, et al. Vascular endothelial growth factor as an autocrine survival factor for retinal pigment epithelial cells under oxidative stress via the VEGF-R2/PI3K/Akt. *Invest Ophthalmol Vis Sci*. 2010;51(2):1190–1197.
82. Kuroki M, Voest EE, Amano S, et al. Reactive oxygen intermediates increase vascular endothelial growth factor expression in vitro and in vivo. *J Clin Invest*. 1996;98(7):1667–1675.
83. Platt DH, Bartoli M, El-Remessy AB, et al. Peroxynitrite increases VEGF expression in vascular endothelial cells via STAT3. *Free Radic Biol Med*. 2005;39(10):1353–1361.
84. Griscavage JM, Wilk S, Ignarro LJ. Inhibitors of the proteasome pathway interfere with induction of nitric oxide synthase in macrophages by blocking activation of

transcription factor NF-kappa B. *Proc Natl Acad Sci USA*. 1996;93(8):3308–3312.
85. Abou-Mohamed G, Johnson JA, Jin L, et al. Roles of superoxide, peroxynitrite, and protein kinase C in the development of tolerance to nitroglycerin. *J Pharmacol Exp Ther*. 2004;308(1):289–299.
86. Gerber HP, McMurtrey A, Kowalski J, et al. Vascular endothelial growth factor regulates endothelial cell survival through the phosphatidylinositol 3'-kinase/Akt signal transduction pathway. Requirement for Flk-1/KDR activation. *J Biol Chem*. 1998;273(46):30336–30343.
87. Duh E, Aiello LP. Vascular endothelial growth factor and diabetes: the agonist versus antagonist paradox. *Diabetes*. 1999;48(10):1899–1906.
88. Kowluru RA, Kanwar M, Kennedy A. Metabolic memory phenomenon and accumulation of peroxynitrite in retinal capillaries. *Exp Diabetes Res*.2007;2007:21976.
89. Fernandes R, Hosoya K, Pereira P. Reactive oxygen species downregulate glucose transport system in retinal endothelial cells. *Am J Physiol Cell Physiol*. 2011;300(4):C927–36.
90. Eichler W, Reiche A, Yafai Y, Lange J, Wiedemann P. Growth-related effects of oxidant-induced stress on cultured RPE and choroidal endothelial cells. *Exp Eye Res*. 2008;87(4):342–348.
91. Hoffmann S, Friedrichs U, Eichler W, Rosenthal A, Wiedemann P. Advanced glycation end products induce choroidal endothelial cell proliferation, matrix metalloproteinase-2 and VEGF upregulation in vitro. *Graefes Arch Clin Exp Ophthalmol*. 2002;240(12):996–1002.
92. Yu DY, Cringle SJ, Su EN, Yu PK. Intraretinal oxygen levels before and after photoreceptor loss in the RCS rat. *Invest Ophthalmol Vis Sci*. 2000;41(12):3999–4006.
93. Yu DY, Cringle S, Valter K, Walsh N, Lee D, Stone J. Photoreceptor death, trophic factor expression, retinal oxygen status, and photoreceptor function in the P23H rat. *Invest Ophthalmol Vis Sci*. 2004;45(6):2013–2019.
94. Padnick-Silver L, Kang Derwent JJ, Giuliano E, Narfstrom K,

Linsenmeier RA. Retinal oxygenation and oxygen metabolism in Abyssinian cats with a hereditary retinal degeneration. *Invest Ophthalmol Vis Sci*. 2006;47(8):3683–3689.
95. Komeima K, Rogers BS, Lu L, Campochiaro PA. Antioxidants reduce cone cell death in a model of retinitis pigmentosa. *Proc Natl Acad Sci USA*. 2006;103(30):11300–11305.
96. Chang GQ, Hao Y, Wong F. Apoptosis: final common pathway of photoreceptor death in rd, rds, and rhodopsin mutant mice. *Neuron*. 1993;11(4):595–605.
97. Tso MO, Zhang C, Abler AS, et al. Apoptosis leads to photoreceptor degeneration in inherited retinal dystrophy of RCS rats. *Invest Ophthalmol Vis Sci*. 1994;35(6):2693–2699.
98. Donovan M, Cotter TG. Caspase-independent photoreceptor apoptosis in vivo and differential expression of apoptotic protease activating factor-1 and caspase-3 during retinal development. *Cell Death Differ*. 2002;9(11):1220–1231.
99. Doonan F, Donovan M, Cotter TG. Caspase-independent photoreceptor apoptosis in mouse models of retinal degeneration. *J Neurosci*. 2003;23(13):5723–5731.
100. Kunchithapautham K, Rohrer B. Autophagy is one of the multiple mechanisms active in photoreceptor degeneration. *Autophagy*. 2007;3(1):65–66.
101. Doonan F, Donovan M, Cotter TG. Activation of multiple pathways during photoreceptor apoptosis in the rd mouse. *Invest Ophthalmol Vis Sci*. 2005;46(10):3530–3538.
102. Ahuja P, Caffe AR, Ahuja S, Ekstrom P, van Veen T. Decreased glutathione transferase levels in rd1/rd1 mouse retina: replenishment protects photoreceptors in retinal explants. *Neuroscience*. 2005;131(4):935–943.
103. Ahuja-Jensen P, Johnsen-Soriano S, Ahuja S, et al. Low glutathione peroxidase in rd1 mouse retina increases oxidative stress and proteases. *Neuroreport*. 2007;18(8):797–801.
104. Hill JW, Hu JJ, Evans MK. OGG1 is degraded by calpain following oxidative stress and cisplatin exposure. *DNA Repair (Amst)*. 2008;7(4):648–654.

105. Shen J, Yang X, Dong A, et al. Oxidative damage is a potential cause of cone cell death in retinitis pigmentosa. *J Cell Physiol*. 2005;203(3):457–464.
106. Komeima K, Rogers BS, Campochiaro PA. Antioxidants slow photoreceptor cell death in mouse models of retinitis pigmentosa. *J Cell Physiol*. 2007;213(3):809–815.
107. Usui S, Oveson BC, Lee SY, et al. NADPH oxidase plays a central role in cone cell death in retinitis pigmentosa. *J Neurochem*. 2009;110(3):1028–1037.
108. Leveillard T, Sahel JA. Rod-derived cone viability factor for treating blinding diseases: from clinic to redox signaling. *Sci Transl Med*. 2010;2(26):26ps16.
109. Cronin T, Raffelsberger W, Lee-Rivera I, et al. The disruption of the rod-derived cone viability gene leads to photoreceptor dysfunction and susceptibility to oxidative stress. *Cell Death Differ*. 2010;17(7):1199–1210.
110. Elachouri G, Lee-Rivera I, Clerin E, et al. Thioredoxin rod-derived cone viability factor protects against photooxidative retinal damage. *Free Radic Biol Med*. 2015;81:22–29.
111. Jarrett SG, Lewin AS, Boulton ME. The importance of mitochondria in age-related and inherited eye disorders. *Ophthalmic Res*. 2010;44(3):179–190.
112. Wallace DC. Mitochondrial diseases in man and mouse. *Science*. 1999;283(5407):1482–1488.
113. Jin GF, Hurst JS, Godley BF. Rod outer segments mediate mitochondrial DNA damage and apoptosis in human retinal pigment epithelium. *Curr Eye Res*. 2001;23(1):11–19.
114. Feher J, Kovacs I, Artico M, Cavallotti C, Papale A, Balacco Gabrieli C. Mitochondrial alterations of retinal pigment epithelium in age-related macular degeneration. *Neurobiol Aging*. 2006;27(7):983–993.
115. Karunadharma PP, Nordgaard CL, Olsen TW, Ferrington DA. Mitochondrial DNA damage as a potential mechanism for age-related macular degeneration. *Invest Ophthalmol Vis Sci*. 2010;51(11):5470–5479.
116. Kenney MC, Atilano SR, Boyer D, et al. Characterization of retinal and blood mitochondrial DNA from age-related

macular degeneration patients. *Invest Ophthalmol Vis Sci*. 2010;51(8):4289–4297.
117. Jiang S, Moriarty-Craige SE, Orr M, Cai J, Sternberg P Jr, Jones DP. Oxidant-induced apoptosis in human retinal pigment epithelial cells: dependence on extracellular redox state. *Invest Ophthalmol Vis Sci*. 2005;46(3):1054–1061.
118. Justilien V, Pang JJ, Renganathan K, et al. SOD2 knockdown mouse model of early AMD. *Invest Ophthalmol Vis Sci*. 2007;48(10):4407–4420.
119. Kowluru RA, Abbas SN. Diabetes-induced mitochondrial dysfunction in the retina. *Invest Ophthalmol Vis Sci*. 2003;44(12):5327–5334.
120. Kowluru RA, Kowluru V, Xiong Y, Ho YS. Overexpression of mitochondrial superoxide dismutase in mice protects the retina from diabetes-induced oxidative stress. *Free Radic Biol Med*. 2006;41(8):1191–1196.
121. Jones MM, Manwaring N, Wang JJ, Rochtchina E, Mitchell P, Sue CM. Mitochondrial DNA haplogroups and age-related maculopathy. *Arch Ophthalmol*. 2007;125(9):1235–1240.
122. Udar N, Atilano SR, Memarzadeh M, et al. Mitochondrial DNA haplogroups associated with age-related macular degeneration. *Invest Ophthalmol Vis Sci*. 2009;50(6):2966–2974.
123. Mueller EE, Schaier E, Brunner SM, et al. Mitochondrial haplogroups and control region polymorphisms in age-related macular degeneration: a case-control study. *PLoS ONE*. 2012;7(2):e30874.
124. SanGiovanni JP, Arking DE, Iyengar SK, et al. Mitochondrial DNA variants of respiratory complex I that uniquely characterize haplogroup T2 are associated with increased risk of age-related macular degeneration. *PLoS ONE*. 2009;4(5):e5508.
125. Canter JA, Olson LM, Spencer K, et al. Mitochondrial DNA polymorphism A4917G is independently associated with age-related macular degeneration. *PLoS ONE*. 2008;3(5):e2091.
126. Kofler B, Mueller EE, Eder W, et al. Mitochondrial DNA

haplogroup T is associated with coronary artery disease and diabetic retinopathy: a case control study. *BMC Med Genet*. 2009;10:35.
127. Estopinal CB, Chocron IM, Parks MB, et al. Mitochondrial haplogroups are associated with severity of diabetic retinopathy. *Invest Ophthalmol Vis Sci*. 2014;55(9):5589–5595.
128. Yang D, Elner SG, Lin LR, Reddy VN, Petty HR, Elner VM. Association of superoxide anions with retinal pigment epithelial cell apoptosis induced by mononuclear phagocytes. *Invest Ophthalmol Vis Sci*. 2009;50(10):4998–5005.
129. Zhang B, Hu Y, Ma JX. Anti-inflammatory and antioxidant effects of SERPINA3K in the retina. *Invest Ophthalmol Vis Sci*. 2009;50(8):3943–3952.
130. Patel M, Chan CC. Immunopathological aspects of age-related macular degeneration. *Semin Immunopathol*. 2008;30(2):97–110.
131. Edwards AO, Ritter R 3rd, Abel KJ, Manning A, Panhuysen C, Farrer LA. Complement factor H polymorphism and age-related macular degeneration. *Science*. 2005;308(5720):421–424.
132. Haines JL, Hauser MA, Schmidt S, et al. Complement factor H variant increases the risk of age-related macular degeneration. *Science*. 2005;308(5720):419–421.
133. Klein RJ, Zeiss C, Chew EY, et al. Complement factor H polymorphism in age-related macular degeneration. *Science*. 2005;308(5720):385–389.
134. Hageman GS, Anderson DH, Johnson LV, et al. A common haplotype in the complement regulatory gene factor H (HF1/CFH) predisposes individuals to age-related macular degeneration. *Proc Natl Acad Sci USA*. 2005;102(20):7227–7232.
135. Gold B, Merriam JE, Zernant J, et al. Variation in factor B (BF) and complement component 2 (C2) genes is associated with age-related macular degeneration. *Nat Genet*. 2006;38(4):458–462.
136. Hughes AE, Orr N, Esfandiary H, Diaz-Torres M, Goodship T, Chakravarthy U. A common CFH haplotype, with deletion of CFHR1 and CFHR3, is associated with lower

risk of age-related macular degeneration. *Nat Genet*. 2006;38(10):1173–1177.
137. Li M, Atmaca-Sonmez P, Othman M, et al. CFH haplotypes without the Y402H coding variant show strong association with susceptibility to age-related macular degeneration. *Nat Genet*. 2006;38(9):1049–1054.
138. Yates JR, Sepp T, Matharu BK, et al. Complement C3 variant and the risk of age-related macular degeneration. *N Engl J Med*. 2007;357(6):553–561.
139. Fagerness JA, Maller JB, Neale BM, Reynolds RC, Daly MJ, Seddon JM. Variation near complement factor I is associated with risk of advanced AMD. *Eur J Human Genet*. 2009;17(1):100–104.
140. Johnson LV, Leitner WP, Staples MK, Anderson DH. Complement activation and inflammatory processes in Drusen formation and age related macular degeneration. *Exp Eye Res*. 2001;73(6):887–896.
141. Johnson LV, Ozaki S, Staples MK, Erickson PA, Anderson DH. A potential role for immune complex pathogenesis in drusen formation. *Exp Eye Res*. 2000;70(4):441–449.
142. Nozaki M, Raisler BJ, Sakurai E, et al. Drusen complement components C3a and C5a promote choroidal neovascularization. *Proc Natl Acad Sci USA*. 2006;103(7):2328–2333.
143. Reynolds R, Hartnett ME, Atkinson JP, Giclas PC, Rosner B, Seddon JM. Plasma complement components and activation fragments: associations with age-related macular degeneration genotypes and phenotypes. *Invest Ophthalmol Vis Sci*. 2009;50(12):5818–5827.
144. Scholl HP, Charbel Issa P, Walier M, et al. Systemic complement activation in age-related macular degeneration. *PLoS ONE*. 2008;3(7):e2593.
145. Huang SJ, Costa DL, Gross NE, Yannuzzi LA. Peripheral drusen in membranoproliferative glomerulonephritis type II. *Retina*. 2003;23(3):429–431.
146. Wu Z, Lauer TW, Sick A, Hackett SF, Campochiaro PA. Oxidative stress modulates complement factor H expression in retinal pigmented epithelial cells by

acetylation of FOXO3. *J Biol Chem*. 2007;282(31):22414–22425.
147. Chen M, Forrester JV, Xu H. Synthesis of complement factor H by retinal pigment epithelial cells is down-regulated by oxidized photoreceptor outer segments. *Exp Eye Res*. 2007;84(4):635–645.
148. Rivera A, Fisher SA, Fritsche LG, et al. Hypothetical LOC387715 is a second major susceptibility gene for age-related macular degeneration, contributing independently of complement factor H to disease risk. *Hum Mol Genet*. 2005;14(21):3227–3236.
149. Fritsche LG, Loenhardt T, Janssen A, et al. Age-related macular degeneration is associated with an unstable ARMS2 (LOC387715) mRNA. *Nat Genet*. 2008;40(7):892–896.
150. Yasuma TR, Nakamura M, Nishiguchi KM, et al. Elevated C-reactive protein levels and ARMS2/HTRA1 gene variants in subjects without age-related macular degeneration. *Mol Vis*. 2010;16:2923–2930.
151. Seddon JM, Gensler G, Rosner B. C-reactive protein and CFH, ARMS2/HTRA1 gene variants are independently associated with risk of macular degeneration. *Ophthalmology*. 2010;117(8):1560–1566.
152. Seddon JM, George S, Rosner B, Rifai N. Progression of age-related macular degeneration: prospective assessment of C-reactive protein, interleukin 6, and other cardiovascular biomarkers. *Arch Ophthalmol*. 2005;123(6):774–782.
153. Zeng F, Zhang M, Xu Y, Xu H. ARMS2 interference leads to decrease of proinflammatory mediators. *Graefes Arch Clin Exp Ophthalmol*. 2013;251(11):2539–2544.
154. Thurman JM, Renner B, Kunchithapautham K, et al. Oxidative stress renders retinal pigment epithelial cells susceptible to complement-mediated injury. *J Biol Chem*. 2009;284(25):16939–16947.
155. Hollyfield JG, Bonilha VL, Rayborn ME, et al. Oxidative damage-induced inflammation initiates age-related macular degeneration. *Nat Med*. 2008;14(2):194–198.
156. Yuuki T, Kanda T, Kimura Y, et al. Inflammatory cytokines in vitreous fluid and serum of patients with diabetic

vitreoretinopathy. *J Diabetes Complications*. 2001;15(5):257–259.
157. Kowluru RA, Odenbach S. Role of interleukin-1beta in the pathogenesis of diabetic retinopathy. *Br J Ophthalmol*. 2004;88(10):1343–1347.
158. Wilkinson-Berka JL. Vasoactive factors and diabetic retinopathy: vascular endothelial growth factor, cycoloxygenase-2 and nitric oxide. *Curr Pharm Des*. 2004;10(27):3331–3348.
159. Age-Related Eye Disease Study Research Group. A randomized, placebo-controlled, clinical trial of high-dose supplementation with vitamins C and E and beta carotene for age-related cataract and vision loss: AREDS report no. 9. *Arch Ophthalmol*. 2001;119(10):1439–1452.
160. Cangemi FE. TOZAL Study: an open case control study of an oral antioxidant and omega-3 supplement for dry AMD. *BMC Ophthalmol*. 2007;7:3.
161. Parisi V, Tedeschi M, Gallinaro G, Varano M, Saviano S, Piermarocchi S. Carotenoids and antioxidants in age-related maculopathy italian study: multifocal electroretinogram modifications after 1 year. *Ophthalmology*. 2008;115(2):324–333.e2.
162. Ho L, van Leeuwen R, Witteman JC, et al. Reducing the Genetic risk of age-related macular degeneration with dietary antioxidants, zinc, and {omega}-3 fatty acids: the Rotterdam Study. *Arch Ophthalmol*. 2011;129(6):758–766.
163. Brantley MA Jr, Osborn MP, Sanders BJ, et al. The short-term effects of antioxidant and zinc supplements on oxidative stress biomarker levels in plasma: a pilot investigation. *Am J Ophthalmol*. 2012;153(6):1104–1109.e2.
164. Berson EL, Rosner B, Sandberg MA, et al. A randomized trial of vitamin A and vitamin E supplementation for retinitis pigmentosa. *Arch Ophthalmol*. 1993;111(6):761–772.
165. Berson EL, Rosner B, Sandberg MA, et al. Clinical trial of docosahexaenoic acid in patients with retinitis pigmentosa receiving vitamin A treatment. *Arch Ophthalmol*. 2004;122(9):1297–1305.
166. Berson EL, Rosner B, Sandberg MA, et al. Clinical trial of

lutein in patients with retinitis pigmentosa receiving vitamin A. *Arch Ophthalmol*. 2010;128(4):403–411.
167. Massof RW, Finkelstein D. Supplemental vitamin A retards loss of ERG amplitude in retinitis pigmentosa. *Arch Ophthalmol*. 1993;111(6):751–754.
168. Massof RW, Fishman GA. How strong is the evidence that nutritional supplements slow the progression of retinitis pigmentosa? *Arch Ophthalmol*. 2010;128(4):493–495.
169. Wittes J, Gorin MB, Mayne ST, McCarthy CS, Sternberg P Jr, Wall M. Letter from the DSMC regarding a clinical trial of lutein in patients with retinitis pigmentosa. *Arch Ophthalmol*. 2011;129(5):675 [author reply -6].
170. Hoffman DR, Hughbanks-Wheaton DK, Pearson NS, et al. Four-year placebo-controlled trial of docosahexaenoic acid in X-linked retinitis pigmentosa (DHAX trial): a randomized clinical trial. *JAMA Ophthalmol*. 2014;132(7):866–873.
171. Zhao L, Wang C, Song D, et al. Systemic administration of the antioxidant/iron chelator alpha-lipoic acid protects against light-induced photoreceptor degeneration in the mouse retina. *Invest Ophthalmol Vis Sci*. 2014;55(9):5979–5988.
172. Singh S, Aggarwal BB. Activation of transcription factor NF-kappa B is suppressed by curcumin (diferuloylmethane) [corrected]. *J Biol Chem*. 1995;270(42):24995–25000.
173. Abe Y, Hashimoto S, Horie T. Curcumin inhibition of inflammatory cytokine production by human peripheral blood monocytes and alveolar macrophages. *Pharmacol Res*. 1999;39(1):41–47.
174. Scapagnini G, Colombrita C, Amadio M, et al. Curcumin activates defensive genes and protects neurons against oxidative stress. *Antioxid Redox Signal*. 2006;8(3–4):395–403.
175. Woo JM, Shin DY, Lee SJ, et al. Curcumin protects retinal pigment epithelial cells against oxidative stress via induction of heme oxygenase-1 expression and reduction of reactive oxygen. *Mol Vis*. 2012;18:901–908.
176. Mandal MN, Patlolla JM, Zheng L, et al. Curcumin protects retinal cells from light-and oxidant stress-induced cell

death. *Free Radic Biol Med*. 2009;46(5):672–679.
177. Zuo ZF, Zhang Q, Liu XZ. Protective effects of curcumin on retinal Muller cell in early diabetic rats. *Int J Ophthalmol*. 2013;6(4):422–424.
178. King RE, Kent KD, Bomser JA. Resveratrol reduces oxidation and proliferation of human retinal pigment epithelial cells via extracellular signal-regulated kinase inhibition. *Chem Biol Interact*. 2005;151(2):143–149.
179. Kim YH, Kim YS, Kang SS, Cho GJ, Choi WS. Resveratrol inhibits neuronal apoptosis and elevated Ca^{2+}/calmodulin-dependent protein kinase II activity in diabetic mouse retina. *Diabetes*. 2010;59(7):1825–1835.
180. Murota K, Mitsukuni Y, Ichikawa M, Tsushida T, Miyamoto S, Terao J. Quercetin-4'-glucoside is more potent than quercetin-3-glucoside in protection of rat intestinal mucosa homogenates against iron ion-induced lipid peroxidation. *J Agric Food Chem*. 2004;52(7):1907–1912.
181. Kook D, Wolf AH, Yu AL, et al. The protective effect of quercetin against oxidative stress in the human RPE in vitro. *Invest Ophthalmol Vis Sci*. 2008;49(4):1712–1720.
182. Cao X, Liu M, Tuo J, Shen D, Chan CC. The effects of quercetin in cultured human RPE cells under oxidative stress and in Ccl2/Cx3cr1 double deficient mice. *Exp Eye Res*. 2010;91(1):15–25.
183. Kumar B, Gupta SK, Nag TC, et al. Retinal neuroprotective effects of quercetin in streptozotocin-induced diabetic rats. *Exp Eye Res*. 2014;125:193–202.
184. Nguyen T, Sherratt PJ, Pickett CB. Regulatory mechanisms controlling gene expression mediated by the antioxidant response element. *Annu Rev Pharmacol Toxicol*. 2003;43:233–260.
185. Tanito M, Agbaga MP, Anderson RE. Upregulation of thioredoxin system via Nrf2-antioxidant responsive element pathway in adaptive-retinal neuroprotection in vivo and in vitro. *Free Radic Biol Med*. 2007;42(12):1838–1850.
186. Tanito M, Masutani H, Kim YC, Nishikawa M, Ohira A, Yodoi J. Sulforaphane induces thioredoxin through the antioxidant-responsive element and attenuates retinal light

damage in mice. *Invest Ophthalmol Vis Sci*. 2005;46(3):979–987.
187. Maeda S, Matsui T, Ojima A, Takeuchi M, Yamagishi S. Sulforaphane inhibits advanced glycation end product-induced pericyte damage by reducing expression of receptor for advanced glycation end products. *Nutr Res*. 2014;34(9):807–813.
188. Stitt A, Gardiner TA, Alderson NL, et al. The AGE inhibitor pyridoxamine inhibits development of retinopathy in experimental diabetes. *Diabetes*. 2002;51(9):2826–2832.
189. Curtis TM, Hamilton R, Yong PH, et al. Muller glial dysfunction during diabetic retinopathy in rats is linked to accumulation of advanced glycation end-products and advanced lipoxidation end-products. *Diabetologia*. 2011;54(3):690–698.
190. Edelstein D, Brownlee M. Mechanistic studies of advanced glycosylation end product inhibition by aminoguanidine. *Diabetes*. 1992;41(1):26–29.
191. Friedman EA. Advanced glycosylated end products and hyperglycemia in the pathogenesis of diabetic complications. *Diabetes Care*. 1999;22(Suppl. 2):B65–71.
192. Du AJ, Ren B, Gao XW, Yang L, Fu Y, Zhao XD. Effects of aminoguanidine on retinal apoptosis in mice with oxygen-induced retinopathy. *Int J Ophthalmol*. 2013;6(4):436–441.
193. Chen B, Caballero S, Seo S, Grant MB, Lewin AS. Delivery of antioxidant enzyme genes to protect against ischemia/reperfusion-induced injury to retinal microvasculature. *Invest Ophthalmol Vis Sci*. 2009;50(12):5587–5595.
194. Rex TS, Tsui I, Hahn P, et al. Adenovirus-mediated delivery of catalase to retinal pigment epithelial cells protects neighboring photoreceptors from photo-oxidative stress. *Hum Gene Ther*. 2004;15(10):960–967.

25

Mechanisms of Endoplasmic Reticulum Stress in Retinal Disease

Sylvia B. Smith

Introduction

Basic science and clinical investigations aimed at understanding mechanisms of retinal disease frequently focus on retinal tissue, specific retinal cell types (such as photoreceptor cells, ganglion cells, Müller cells), and genes/proteins specific to the retina. An emerging approach to understanding retinal disease examines pathogenesis at the level of an intracellular organelle, the endoplasmic reticulum. In this chapter, a brief overview of the field of endoplasmic reticulum stress (ER stress) and the unfolded protein response (UPR) is provided followed by information linking these processes to retinal disease.

The Endoplasmic Reticulum

As its name suggests, the endoplasmic reticulum or ER is a

membrane-bound labyrinth of tubes and sacs, where virtually all plasma membrane and secreted proteins begin their progression to the cellular surface. The ER is the largest membrane compartment within eukaryotic cells, frequently comprising more than half of the total membrane composition. The ER has a number of major physiologic functions.[1] It plays a key role in lipid and protein biosynthesis; it functions as a Ca^{2+} storage organelle; and importantly, it is the site where most secretory and transmembrane proteins fold into their native conformation. When proteins enter the ER, they may undergo formation of disulfide bonds through the action of folding enzymes such as protein disulfide isomerase (PDI).[2] Proteins that are processed through the ER frequently undergo glycosylation, a posttranslational modification involving the addition of asparagine-linked oligosaccharides. There are two known chaperone systems in the ER: the calnexin/calreticulin system and binding immunoglobulin protein/78-kDa glucose-regulated protein (BiP/GRP78). The calnexin/calreticulin system is particularly relevant to folding of glycoproteins although some calnexin/calreticulin substrates can also bind BiP/GRP78. Protein folding is essential for protein function; therefore, sophisticated mechanisms have evolved to ensure that proper folding occurs or that irreversibly misfolded proteins are eliminated. Quality control is an ER surveillance mechanism to permit only properly folded proteins to exit the ER en route to other organelles.

When there is perturbation of ER function (such as inhibition of glycosylation or disulfide bond formation, disruption of Ca^{2+} homeostasis, hypoxia, infection, etc.), unfolded or misfolded proteins accumulate. This situation, termed ER stress, is defined as an imbalance between the cellular demand for ER function and ER capacity.[2–5] When the influx of nascent unfolded polypeptides exceeds the folding and processing capacity of the ER, the normal physiologic state of the ER is perturbed, activating signaling pathways, termed the ER stress response or the unfolded protein response (UPR), to return the ER to its normal physiologic state.[2–4] The possible fates for a protein in the ER are shown in Fig. 25.1 and include either (1) proper folding and exit through the ER; or in the case of misfolded proteins, (2) translational attenuation whereby protein synthesis halts temporarily to prevent accumulation of

unfolded proteins; (3) transcriptional induction of ER chaperone genes to increase protein folding capacity; (4) transcriptional induction of ER-associated degradation (ERAD) activity. If these strategies fail and protein aggregation is excessive, (5) apoptosis is induced to dispose of cells injured by ER stress thereby ensuring survival of the organism. Recent studies implicate dysregulation of the UPR in neurodegenerative diseases, including retinal diseases.

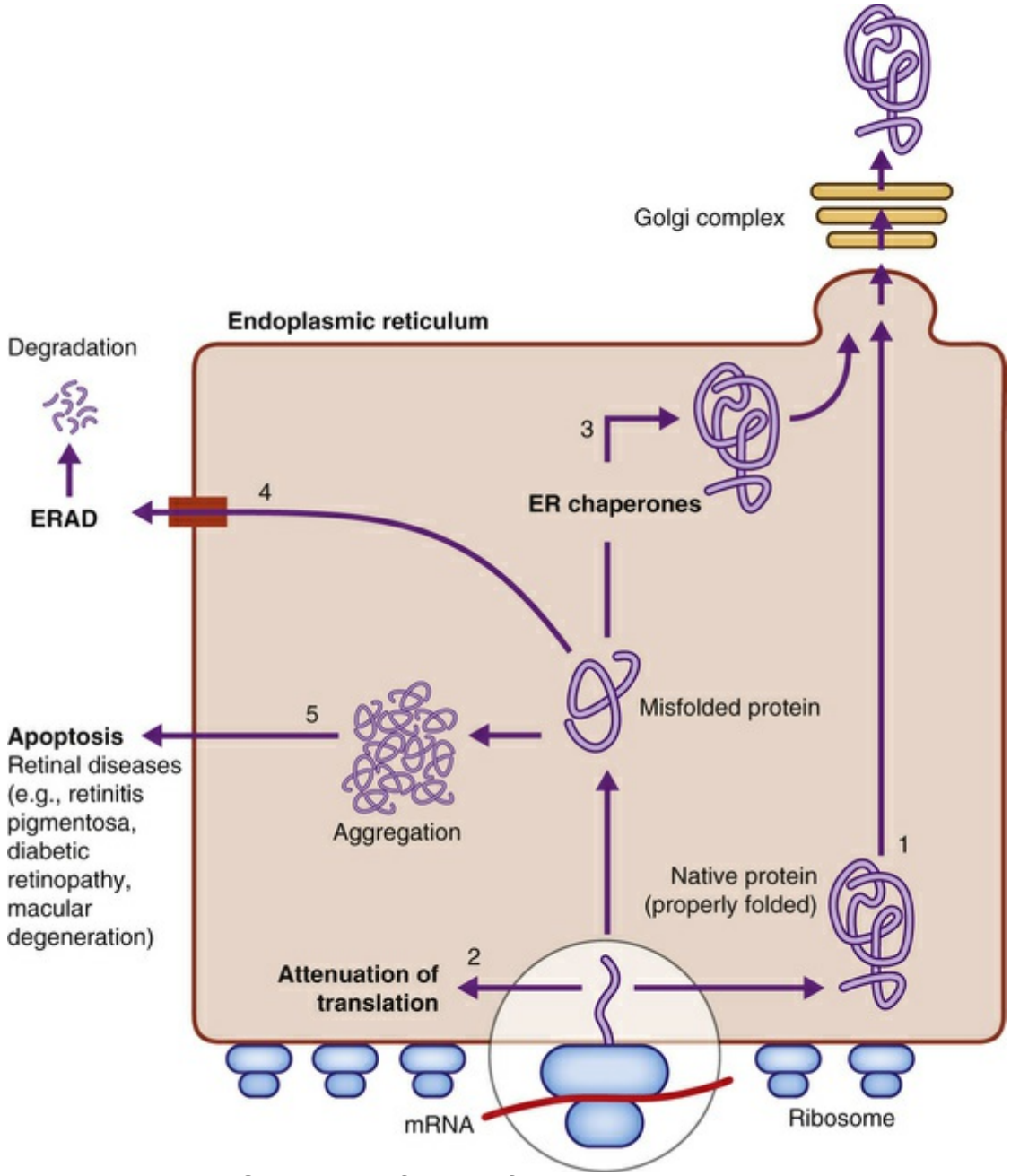

FIG. 25.1 Overview of the unfolded protein response (UPR). The ribosome sits at the endoplasmic reticulum

(ER) membrane and the nascent protein is translated. If the protein is folded properly (*1*), it will typically exit the ER to the Golgi apparatus for further modifications before being secreted or inserted into plasma membrane. If the protein is misfolded, several outcomes are possible that comprise the UPR: (*2*) Protein translation may be attenuated halting protein synthesis temporarily to prevent further accumulation of unfolded or misfolded proteins; (*3*) transcriptional induction of ER chaperone genes may occur, which will increase protein folding capacity within the cell; or (*4*) transcriptional induction of ER-associated degradation (ERAD) activity will dispose of the misfolded protein. If these mechanisms are not successful in managing the misfolded protein, genes that trigger apoptosis (*5*) may be upregulated leading to cellular death. Excessive accumulation of misfolded proteins is toxic to cells and incompatible with long-term survival.

ER Stress and Unfolded Protein Response Signaling

The UPR is a complex cellular signaling pathway that attempts to restore cellular homeostasis, but in the face of prolonged ER stress, pathways may be activated that lead to cell death.[6] The UPR involves three signaling pathways governed by three integral ER membrane proteins: PERK (protein kinase-like ER kinase, pancreatic ER eukaryotic translation initiation factor (eIF)-2a kinase; official name: EIF2AK3), IRE-1 (inositol-requiring protein 1; official name: ERN1), and ATF6 (activating transcription factor 6). Research related to ER stress and retinal disease has focused on investigations of BiP/GRP78 and these downstream effector proteins.

Binding Protein/Glucose-Regulated Protein 78

BiP/GRP78 is a calcium-dependent resident ER protein that

facilitates the transfer of proteins into the ER through the ER translocator.[2,3,7] It is a heat shock protein with a molecular weight of 78 kD. As a key ER stress regulatory protein, it binds to exposed hydrophobic amino acid sequences of polypeptides that would normally be buried in the interior of correctly folded proteins. Under nonstress conditions, BiP/GRP78 binds to the luminal domains PERK, IRE1, and ATF6, maintaining them in an inactive state (Fig. 25.2). When misfolded proteins accumulate, BiP/GRP78 preferentially binds to these misfolded proteins and dissociates from the UPR sensor proteins allowing their activation. BiP/GRP78 and other UPR gene targets such as GRP94 and calreticulin contain an ER stress response element (ERSE, CCAAT(N_9)CCACG) that is required and sufficient to activate the UPR. The absolute requirement for BiP/GRP78 for survival is underscored by evidence that absence of BiP/GRP78 results in perimplantation embryonic lethality in mice.[8] Upregulation of *BiP* gene expression is considered by some investigators as a marker for ER stress induction.

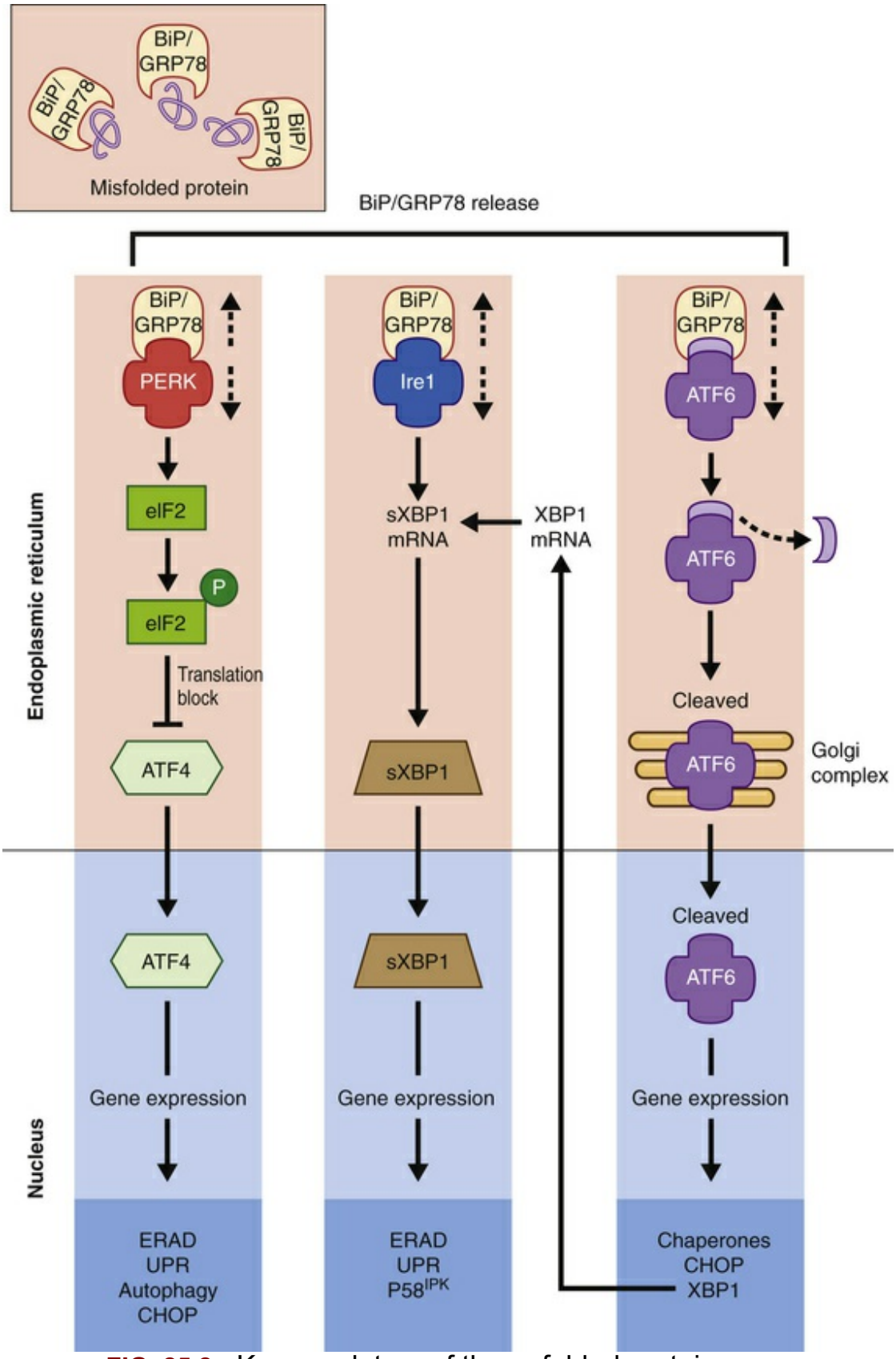

FIG. 25.2 Key regulators of the unfolded protein response. When misfolded proteins aggregate, BiP/GRP78 dissociates from the three ER stress receptors, PERK, ATF6, and IRE1, which permits their

activation. Activation of PERK blocks general protein synthesis by phosphorylating eukaryotic initiation factor 2α (eIF2α), which enables translation of ATF4 (through an eIF2α-independent translation pathway). ATF4 translocates to the nucleus and induces the transcription of genes required to restore ER homeostasis. When IRE1 is released from BiP/GRP78, it dimerizes and autophosphorylates to activate its RNase activity removing a 26-nucleotide intron from X-box binding protein (XBP1) mRNA. Spliced XBP1 activates many UPR target genes and can activate genes required for ER-associated degradation (ERAD). ATF6 is activated by limited proteolysis after its translocation from the ER to the Golgi apparatus. Active ATF6 can regulate the expression of ER chaperones and XBP1. The combined action of these three ER stress receptors is to attenuate translation to prevent further accumulation of misfolded proteins, to enhance proper protein folding, and to degrade misfolded proteins.

PERK

The signaling events mediated by PERK represent the most immediate response to ER stress in metazoan cells. PERK is a 125-kDa ER-associated transmembrane serine/threonine protein kinase. When unfolded proteins accumulate in the ER lumen, BiP/GRP78 dissociates from PERK, which then dimerizes and is subsequently autophosphorylated triggering phosphorylation of eukaryotic translation initiation factor 2 on the alpha-subunit (eIF2α). Phosphorylation of eIF2α attenuates mRNA translation, thereby preventing influx of newly synthesized polypeptides into the ER lumen of the stressed cell.[7] This reduces the assembly and folding activities of the ER. Interestingly, although phosphorylation of eIF2α inhibits translation initiation in general, it is required for selective translation of several mRNAs such as activating transcription factor 4 (ATF4). Activation of ATF4 can increase levels of chaperones, restore cellular redox homeostasis, and help the ER to fold proteins or degrade them. However, it has been reported that excess ATF4 expression can evoke oxidative stress and increase

cell death in mouse embryonic fibroblasts.[9] Besides elF2α, PERK can also phosphorylate nuclear erythroid 2 p45-related factor 2 (NRF2), which contributes to dissociation of the NRF2-Keap1 complex and promotes expression of genes containing antioxidant response elements (ARE), preventing oxidative stress by induction of antioxidant genes such as heme oxygenase 1 (HO-1).[10] Lack of the gene encoding PERK is not lethal but does result in increased hypersensitivity to ER stress.[11] Activation of PERK induces transcription of ~1/3 of UPR-dependent genes.[12] Recent data suggest that PERK initially mediates a prosurvival response, which switches into a proapoptotic response under conditions of prolonged ER stress.[13]

IRE1

IRE1 is a 100-kDa bifunctional transmembrane protein with kinase and endoribonuclease (RNase) activity. It was the first component in the UPR pathway to be identified[14] and is evolutionarily the oldest branch of the UPR. Under nonstress conditions, the protein kinase is maintained in a monomeric form through its interactions with BiP/GRP78. IRE1 can bind members of the tumor necrosis factor (TNF) receptor family and can activate protein kinases that are implicated in immunity, inflammation, and apoptosis. Under conditions of ER stress, when unfolded proteins are accumulating, IRE1 is released from BiP/GRP78, dimerizes, and autophosphorylates to activate its RNase activity.[2–4] Indeed, IRE1 mediates the degradation of many other mRNAs through a pathway referred to as regulated IRE1-dependent decay, or RIDD.[15]

In mammals there are two forms of the protein, IRE1α and IRE1β. IRE1α is expressed in most cells and tissues (including retina), while IRE1β is primarily in intestinal epithelial cells. Upon activation of the UPR, IRE1 RNase activity initiates removal of a 26-nucleotide intron from XBP1 (X-box binding protein) mRNA. Spliced XBP1 is a transcriptional activator that activates many UPR target genes through its interaction with ERSE, and it can activate genes required for ER-associated degradation (ERAD). IRE1 may be a focal point for the BCL-2 family of proteins that regulates cell death. BCL-2-associated X protein (BAX) and BCL-2

antagonist/killer (BAK) interact physically with IRE1α modulating the UPR. If either IRE1 or XBP1 are absent in mouse models, the result is embryonic lethality. Recent studies note that IRE1 can sense ER stress by directly monitoring the concentration of unfolded proteins.[16] Thus, it may be that BiP/GRP78 buffers UPR activity and helps turn IRE1 off, while direct binding to unfolded proteins switches IRE1 on.[17]

ATF6

ATF6α and ATF6β are bZIP family transcription factors with calculated molecular weights of ~90 kDa. In the absence of ER stress, BiP/GRP78 binds to the luminal domain of ATF6 tethering it to the ER membrane. When unfolded proteins accumulate, BiP/GRP78 releases ATF6, which then translocates to the Golgi apparatus by vesicular transport.[3,7] Unlike PERK and IRE1α, ATF6α and ATF6β do not undergo oligomerization, rather in the Golgi ATF6 is cleaved by proteases and the resultant cytoplasmic portion translocates to the nucleus, where it (like XBP1) binds to an ER stress element (ERSE) to activate transcription of ER chaperone genes such as BiP/GRP78, GRP94, and calreticulin. It is noteworthy that ATF6 transcriptionally upregulates *Xbp1* IRE1 activation. Thus, ATF6 activation can increase ER chaperone activity. If both ATF6α and ATF6β are deleted in mouse, the result is early embryonic lethality.

ER-Associated Degradation

The ER employs ERAD to clear aggregated, misfolded, or unassembled proteins. Target proteins are selected through the ER quality control system, are retrotranslocated to the cytosol, and degraded by the ubiquitin-proteasome system. The four steps associated with ERAD are recognition, retrotranslocation, ubiquitination, and degradation.[3] In the recognition step, glycosylated proteins are bound to ER degradation-enhancing α-mannosidase-like (EDEM) protein that can discriminate folded from unfolded proteins. Misfolded proteins destined for the retrotranslocation machinery associate with PDI and BiP/GRP78 to cleave disulfide bonds and to unfold the partially folded protein.

Proteins are translocated to the cytoplasm where they undergo ubiquitination by the E1–E2–E3 ubiquitin system. The proteins are then deglycosylated and degraded by the proteasome.

Apoptosis-Inducing Pathways

If PERK, ATF6, and IRE1 pathways cannot suppress ER stress, and if the ERAD pathway does not rectify the unfolded protein accumulation, an apoptotic pathway will be triggered so that the cell will die allowing the organism (or tissue) to survive since accumulation of unfolded proteins is toxic to cells. Apoptosis is signaled through mitochondrial-dependent and -independent pathways. In the ER, apoptosis is signaled through several mechanisms, the most significant of which is the PERK/eIF2α/ATF4-dependent or ATF6-dependent transcriptional induction of CHOP (CCAAT-enhancer-binding protein homologous protein). CHOP activates transcription of several genes that potentiate apoptosis including *GADD34*, *ER01*, *DR5*, *TRB3*, *carbonic anhydrase VI*. One mechanism of CHOP-induced apoptosis is to suppress the prosurvival protein BCL-2. Additionally, GADD34 (growth arrest and DNA damage-inducible protein-34) is a particularly important transcriptional target of CHOP as it can dephosphorylate eIF2α, restoring global protein translation and suppressing ATF4 translation.

Retinal Diseases Associated With ER Stress

The UPR has been referred to as a "double-edged sword" because it can restore cellular homeostasis, but if unchecked may lead to chronic, overwhelming stress that can cause apoptotic cell death.[18] ER stress and the UPR have been implicated in a number of retinal diseases, including retinitis pigmentosa, achromatopsia, diabetic retinopathy, and macular degeneration.

To investigate the role of ER stress genes and proteins in retina, a number of research tools (antibodies, molecular probes, etc.) are available commercially or have been developed by individual

laboratories. Fig. 25.3 shows immunocytochemical studies performed in freshly isolated mouse retinal Müller cells to detect two ER proteins. Protein disulphide isomerase is a known ER resident protein and hence an excellent marker of this organelle (Fig. 25.3A). In this dual-label experiment, a second antibody was used to detect BiP/GRP78, the key ER stress regulatory protein (Fig. 25.3B). The final panel shows the merged image of PDI and BiP/GRP78; there is considerable overlap in the expression of these two proteins (Fig. 25.3C). Immunodetection methods, gene expression analysis, and elegant genetic manipulation methods have formed the basis of investigations of the ER stress genes/proteins in various retinal diseases.

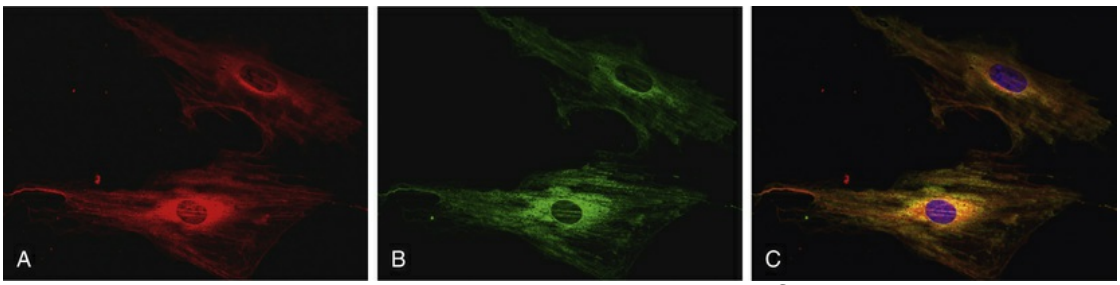

FIG. 25.3 Immunocytochemical analysis of PDI and BiP/GRP78 in retinal Müller cells. Primary Müller cells were isolated from neonatal mouse retina using methods established in the author's lab and were subjected to immunocytochemical methods to detect two proteins: protein disulphide isomerase (PDI), a known ER protein, and BiP/GRP78, the major ER stress regulatory protein. The anti-PDI antibody was detected with a secondary antibody that fluoresces red (panel A); the anti-BiP/GRP78 antibody was detected with a secondary antibody that fluoresces green (panel B). When the cells were viewed by epifluorescence using filters to detect green and red fluorescence simultaneously, the areas of colocalization appear yellow in the merged image (panel C). The cells were also labeled with a dye 4′-6-diamidino-2-phenylindole (DAPI), which forms fluorescent complexes with natural double-stranded DNA, hence the nucleus stains blue in the merged image. (Studies performed by Dr. Yonju Ha in the author's lab.)

Retinitis Pigmentosa and Other Photoreceptor Dystrophies

Retinitis pigmentosa (RP) is an inherited retinal dystrophy in which loss of photoreceptors leads to progressive vision loss. The prevalence of nonsyndromic RP is ~1/3500–4000. The most common form of RP is a rod–cone dystrophy, characterized initially by night blindness, followed by progressive loss in the peripheral visual field in daylight, eventually leading to blindness after several decades.[19] To date, mutations in over 40 genes have been implicated in RP.[20] In some cases the genes are specific to photoreceptor cells, including rhodopsin, rod cGMP phosphodiesterase, peripherin, and rod outer-segment membrane protein-1, while others are expressed in retinal and nonretinal cells. ER stress is implicated in RP due to mutations in several genes, as described below.

Rhodopsin Mutations

Among the genes associated with RP, mutations within the rhodopsin gene account for approximately 25% of cases of autosomal dominantly inherited RP (adRP). Rhodopsin is the visual pigment initially made in the ER and eventually located in the outer-segment discs until used in the visual transduction cascade. AdRP is a human protein folding disease that is frequently caused by a proline-to-histidine mutation at position 23 of rhodopsin (P23H rhodopsin) that leads to its retention in the ER.[21,22] In vitro studies have shown that cells transfected with P23H rhodopsin increased expression of *BiP* mRNA to a level greater than in cells transfected with wild-type rhodopsin.[21,22] Interestingly, activation of the IRE1α pathway was protective, while prolonged PERK activation was associated with cell death. Elegant studies by Gorbatyuk and colleagues[22] provide immunohistochemical data showing that when HeLa cells are transfected with mutant rhodopsin (P23H) the protein was not able to traffic to the cell membrane and was localized in the cytoplasm, clear evidence of the retention in the ER of a misfolded protein (see figures 1A and B of reference article 14). These cell culture observations have been extended to studies in an animal model of adRP (transgenic rat expressing P23H rhodopsin at high levels). During retinal

development, levels of *BiP* mRNA were high, but diminished with age; however, levels of *Chop* indicative of apoptosis increased significantly with age as the retinopathy advanced in the adRP rat model.[21] Additional experiments, in which *BiP/GRP78* was over expressed using adenoviral vector-mediated delivery in the rat adRP model, resulted in improved a- and b-wave amplitudes of the scotopic electroretinogram and a reduction in photoreceptor cell loss.[22] The field of microribonucleic acid (microRNA) (miRNA) expression profiling and bioinformatics has identified miR-708 in the homeostatic regulation of ER function in photoreceptor cells, specifically preventing excess rhodopsin from entering the ER. Investigators speculate that miR-708 may function analogously to UPR control proteins such as PERK and IRE1α.[23] In contrast to these studies in the rat adRP model, there have been studies in which the P23H rhodopsin has been genetically expressed in mice. These mice with P23H rhodopsin knocked-in closely mimic the photoreceptor death observed in humans with the P23H mutation. Interestingly in this model, IRE1 significantly upregulated ERAD, triggering pronounced P23H rhodopsin degradation, with minimal activation of PERK and no increase in ATF4 or CHOP.[24] It appears that in this mouse model at least, loss of rhodopsin precedes photoreceptor cell death, underscoring the role of ERAD in this form of RP.[25] In addition to P23H rhodopsin mutations, other mutations of rhodopsin have now been shown to involve increased ER stress, including the single amino acid substitution in amino acid 181 of glutamic acid (E) to lysine (K) (E181K)[26] and the substitution in amino acid 7 of threonine (T) to methionine (M) (T7M).[27,28]

cGMP-PDE Mutations

Mutations of the gene coding for the beta-subunit of the rod photoreceptor-specific cGMP phosphodiesterase 6 (*PDE6B*) underlie cases of autosomal recessive RP (arRP) and account for ~1–2% of all cases of human RP.[29] The *rd1* mouse carries a non-sense mutation of this gene and has proven to be a very useful model for understanding the pathogenic mechanisms of this form of RP. The absence of phosphodiesterase activity leads to increased accumulation of cGMP in photoreceptors, which leads to increased influx of Na^+ and Ca^{2+} through cGMP-gated cation channels. The

uncontrolled influx of Ca^{2+} triggers apoptosis of photoreceptor cell nuclei so that between postnatal day 10 and postnatal day 21, rod photoreceptor cells are lost. The number of rows of cells in the retinal outer nuclear layer decreases from ~10–12 to ~1–2, representing remaining cones. Interestingly, as the rod cells are lost, there is an increase in expression of BiP/GRP78, phosphorylated eIF2α, phosphorylated PERK, and caspase-12 over postnatal days 10–14, but levels decrease by postnatal day 21.[30] These data clearly implicate ER stress in the pathogenesis of RP caused by mutations of the PDE-β gene.

Carbonic Anhydrase Mutation

Carbonic anhydrase IV (*CA4*) is another gene which, when mutated, leads to human adRP that involves ER stress. This form of RP (RP17) is caused by an arginine to tryptophan (R14W) mutation in the signal sequence of carbonic anhydrase IV.[31–33] Carbonic anhydrase is a GPI-anchored membrane protein expressed in the choriocapillaris of the eye and in the renal epithelium. Interestingly, the mutation results in an exclusively ocular phenotype. In vitro studies have shown that in cells R14W mutation, which is the RP17 form of adRP, leads to accumulation of carbonic anhydrase IV as unfolded protein in the ER. This gene defect is associated with increased expression of BiP/GRP78, PERK, and CHOP, leading to cell death.[32]

LRAT Mutations

An inherited retinal dystrophy that preferentially affects cones before rods is Leber congenital amaurosis (LCA), the most severe retinal dystrophy in early childhood.[34] Mutations in *RPE65* or the lecithin-retinol acyltransferase gene (*LRAT*) disrupt 11-*cis*-retinal recycling, causing this devastating disease. LRAT catalyzes the esterification of all-*trans* retinol (vitamin A) to all-*trans*-retinyl esters, which are the substrate for RPE65, to produce 11-*cis* retinol. In studies of a murine model of LCA ($Lrat^{-/-}$ mouse), large quantities of M and S opsins are mislocalized to the inner regions of cones, creating an extra burden on the cell.[35] Interestingly, mislocalized M opsin is degraded, whereas S opsin is resistant to proteasome degradation, resulting in far more toxic aggregation of

S opsin in the ventral and central retina than of M opsin in the dorsal retina. Furthermore, aggregation of S opsin leads to CHOP activation. The UPR in cones copes with mislocalized M opsin more effectively than mislocalized S opsin. Thus, M opsin is degraded by the ERAD pathway, which relieves ER stress. S opsin was resistant to ERAD, resulting in aggregation/accumulation, which induces apoptosis.

IRBP Mutations

Interphotoreceptor retinoid-binding protein (IRBP) is a 140–145-kDa glycoprotein of ~300 amino acid residues that is secreted by photoreceptors into the interphotoreceptor matrix. It protects and solubilizes the visual cycle retinoids by physically binding with 11-*cis* retinaldehyde, 11-*cis* retinol, and all-*trans* retinol.[36] In 2009, the first mutation of the (*IRBP*) gene responsible for RP was reported in patients with the autosomal recessive form of the disease.[37] The mutation was due to an aspartate (D) to asparagine (N) substitution at position 1080 (D1080N) of IRBP. The precise pathogenic mechanisms underlying this form of RP are not known, but recent work demonstrated that the mutant IRBP was not transported to the Golgi apparatus, rather it accumulated in the ER, bound to BiP/GRP78 and PDI.[38] Splicing of ATF4 and cleavage of ATF6 increased significantly in cells that express the D1080N IRBP compared to wild-type IRBP. Additionally, D1080N IRBP induced upregulation and nuclear translocation of CHOP.[38]

The apparent role of ER stress and UPR in some forms of photoreceptor disease has prompted suggestions that therapeutic approaches, which modulate these pathways, may prove beneficial.[35,39,40]

USH2A

Mutations in the *USH2A* gene are the most common cause of Usher syndrome type I,[41] a genetically heterogeneous autosomal recessive disorder characterized by early-onset sensorineural hearing loss and later onset RP. Recent analysis of *USH2A* transcripts revealed that one of the patient's mutations causes exonification of intron 40, a translation frameshift, and a premature stop codon. Western blotting revealed upregulation of GRP78 and GRP94, suggesting

that the patient's other USH2A variant (Arg4192His) caused disease through protein misfolding and ER stress.[42]

Achromatopsia

In addition to rod dystrophies, cone photoreceptor cells are also vulnerable to genetic defects that compromise function. Congenital achromatopsia is a rare, autosomal recessively inherited condition characterized by lack of cone photoreceptor function.[43] Patients present with pendular nystagmus, absence of color vision, marked photophobia/hemeralopia, and severely reduced visual acuity. Rod responses detected by electroretinography (ERG) are normal; however, cone responses are absent.[44] Until recently, five genes had been associated with achromatopsia, which encode the cone-specific phototransduction cascade (reviewed by Aboshiha and colleagues[45]). The most commonly mutated genes include *CNGA3*, *CNGB3*, which encode the alpha-subunits and beta-subunits of the cGMP-gated cation channel, respectively. Very recently, work from the Lin lab provides compelling evidence that mutations in *ATF6*, the basic leucine-zipper (bZIP) transcription factor that is a key regulator of the UPR, are responsible for some forms of achromatopsia.[46] The highly collaborative study provides the first evidence implicating dysfunction of an ER stress gene in achromatopsia. It used homozygosity mapping and whole-exome and candidate gene sequencing and identified 10 families carrying six homozygous and two compound-heterozygous mutations in the *ATF6* gene. Patients demonstrated foveal hypoplasia and disruption of the cone photoreceptor layer. The findings suggest a crucial and unexpected role for ATF6 in human foveal development and cone function and are particularly noteworthy because, despite the ubiquitous expression of ATF6, when mutated it results in an isolated retinal phenotype.

Diabetic Retinopathy

Diabetic retinopathy is a major complication of diabetes mellitus, a complex metabolic disorder characterized by deficiency of or insensitivity to insulin. Diabetic retinopathy is a neurovascular disease.[47,48] The microvascular characteristics, which are visible clinically, include pericyte dropout, microaneurysms, intraretinal

hemorrhages, capillary nonperfusion, intraretinal microvascular abnormalities, and neovascularization. The neuronal component is characterized by death of ganglion cells, loss of cells in the inner nuclear layer,[49,50] and functional changes detected particularly using multifocal ERG.[51] ER stress has been implicated in diabetic retinopathy, and investigations have examined features of ER stress in retinal vascular cells and retinal neurons.[52–54]

Regarding the vasculature, retinal homeostasis is regulated in part by the blood–retinal barrier. The outer barrier is comprised of the tight junctions between retinal pigment epithelial (RPE) cells, while the inner blood–retinal barrier is composed of tight junctions between vascular endothelial cells. Breakdown of this barrier is characteristic of diabetic retinopathy. TNF-α is a major proinflammatory cytokine induced by diabetes that plays a key role in endothelial cell injury in diabetic retinopathy. Investigators have shown that ER stress plays a pathogenic role in retinal inflammation and vascular leakage in diabetic retinopathy.[55–57] Interestingly, preconditioning human retinal endothelial cells with very low levels of ER stress-inducing agents such as tunicamycin actually alleviate TNF-α-induced endothelial adhesion molecule expression, retinal leukostasis, and vascular leakage in vitro.[58] The beneficial effects of ER stress preconditioning require that XBP1, a major regulator of the adaptive response to ER, must be activated if ER stress is to be protective of endothelial cell function.[58] There are reports showing that $P58^{IPK}$, a 58-kilodalton inhibitor of protein kinase, which has been shown to be important in ER stress, reduced the level of TNF-α in endothelial cells.[59] Thus, the potential role of modulating ER stress may prove therapeutically useful for the endothelial cell alterations observed in diabetic retinopathy.

Vascular endothelial growth factor (VEGF) plays a key role in the development and progression of diabetic retinopathy.[60] Investigators have shown that homocysteine, which induces ER stress, increased expression of VEGF along with BiP/GRP78.[61] Incubating RPE cells with homocysteine in vitro caused transient phosphorylation of eIF2α and increased ATF4 protein level. In addition to its effects on vasculature, excess homocysteine induces death of ganglion cells. In a mouse model of hyperhomocysteinemia, diabetes accelerates the loss of these retinal

neurons.[62]

Retinal neurons die in diabetic retinopathy as evidenced by decreased contrast sensitivity,[51] decreased blue–yellow color sensitivity,[63] and reduced electrical responses in full-field and multifocal ERG.[64] ER stress has been implicated in the death of retinal neurons, particularly ganglion cells. Studies subjecting a retinal neuronal cell line to oxidative stress, as observed in diabetic retinopathy, demonstrated increased expression of the ER stress gene BiP/GRP78 as well as PERK, IRE1-α, ATF6, and the apoptosis gene, *CHOP*.[65] Upregulation of several of these ER stress markers has been detected in neural retinas of the *Ins2*$^{Akita/+}$ mouse.[55,65] The *Ins2*$^{Akita/+}$ mouse is an endogenous model of diabetic retinopathy characterized by marked apoptosis of retinal neurons, including ganglion cells and cells of the inner nuclear layer and vasculopathy.[66,67] Interestingly, treatment of this mouse with a ligand for sigma receptor 1 (σR1), a molecular chaperone that binds BiP/GRP78, provided marked neuroprotection against neuronal cell death when it was administered over a period of several weeks.[68] Examination of the ER stress genes in retinas of these mice (using quantitative reverse transcriptase polymerase chain reaction [RT-qPCR]) showed that BiP/GRP78 expression increased in diabetic mice compared with wild-type mice, as did PERK, ATF6, IRE1, ATF4, and CHOP (Fig. 25.4). The retinas of *Ins2*$^{Akita/+}$ diabetic mice treated with the σR1 ligand (+)-pentazocine showed ER stress gene expression levels that were very similar to the age-matched wild-type mice (Fig. 25.4). The data suggest that targeting ER stress may hold promise in treatment of diabetic retinopathy.

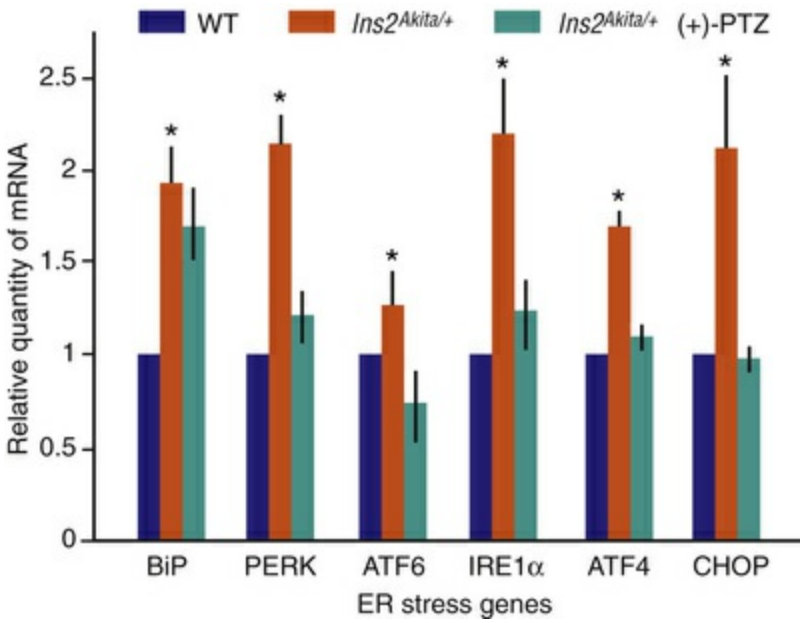

FIG 25.4 Quantitative analysis of ER stress genes in retinas of wild-type versus diabetic mice. Total RNA was isolated from neural retinas of wild-type (WT), C57Bl/6-Ins2Akita/+ mice, and C57Bl/6-Ins2Akita/+ administered (+)-pentazocine, a ligand for the molecular chaperone protein sigma receptor 1 (σR1). The expression of ER stress genes was analyzed by RT-qPCR. There was a significant increase in expression of these genes in diabetic mice (*asterisk*), but expression levels were similar to wild-type mouse retinas when treated with the ligand for σR1. (Figure adapted from Ha Y, Dun Y, Thangaraju M, et al. Sigma receptor 1 modulates endoplasmic reticulum stress in retinal neurons. Invest Ophthalmol Vis Sci 2011;52:527-40; copyright held by Association for Research in Vision and Ophthalmology.)

Macular Degeneration

The macula is the cone photoreceptor-dense region of the retina; dystrophy of this area is collectively termed macular degeneration. Macular degeneration can develop at an early age through single gene mutations or can present later in life as the much more common multifactorial age-related macular degeneration (AMD).[20] Clinically, patients present with progressive loss of visual acuity, abnormal color vision, and central scotomas. ER stress has been implicated in the pathogenesis of both genetically inherited, early-onset macular dystrophies and multifactorial age-related macular

degenerations.

Early-Onset Macular Dystrophies

Mutations of at least two genes leading to juvenile macular dystrophy are associated with ER stress, *ELOVL4* and *EFEMP1*. *ELOVL4* encodes a 314 amino acid ER-bound transmembrane protein associated with the long-chain fatty acid synthesis machinery. Retinal tissue has a unique fatty acid composition; the lipid environment is critical for normal retinal functions. While the precise role of ELOVL4 in photoreceptors is not known, mutations of *ELOVL4* result in an autosomal dominant atrophic macular dystrophy resembling Stargardt macular degeneration, hence the disease is referred to as Stargardt-like macular dystrophy. Wild-type ELOVL4 is localized to the ER; however, the mutant form of the protein accumulates in the Golgi apparatus.[69] Investigators have transfected cells with the mutant forms of ELOVL4, known to cause Stargardt-like macular dystrophy, and observed an increase in the expression of BiP/GRP78 and the UPR apoptosis-associated gene, *CHOP*.[70]

EFEMP1 (epithelial growth factor [EGF]-containing fibulin-like extracellular matrix protein 1) encodes an extracellular matrix protein, fibulin-3. Fibulin-3 is a glycoprotein that typically undergoes proper folding in the ER is then transported to the Golgi and then secreted. A missense point mutation (arginine-to-tryptophan [Arg345Trp]) results in an early-onset autosomal dominant maculopathy known as Doyne honeycomb retinal dystrophy (also termed malattia leventinese). Mutant forms of the protein accumulate aberrantly in the ER of retinal pigment epithelial (RPE) cells hindering proper secretion to the extracellular milieu.[71,72] To determine the consequences of the Arg345Trp mutation on ER stress, investigators transfected the human ARPE-19 cell line with the mutated *EFEMP1* and demonstrated an upregulation of BiP/GRP78; indeed the level of BiP/GRP78 expression paralleled the intracellular levels of fibulin-3. Additional evidence that the UPR was activated by this mutation was increased IRE-1 endonuclease activity and XBP-2 mRNA processing.[71]

Age-Related Macular Degeneration

AMD is the leading cause of visual impairment in elderly persons. The macula is the photoreceptor-dense retinal region, which when affected by this disease results in central vision loss. The RPE cells sustain photoreceptor cells through myriad activities including the transport of needed vitamins such as vitamin A and folate, removal of waste, and phagocytosis of shed outer segment discs. RPE cells are vascularized via the choriocapillaris. A hallmark of AMD is the accumulation of lipofuscin and extracellular deposits known as drusen. The retina and RPE are exposed constantly to oxidative stress through intense light exposure, high metabolic activity, oxygen consumption, and the high concentration of polyunsaturated fatty acids making them particularly susceptible to ER stress.[73]

Clinically, AMD is classified as either atrophic (dry) AMD or exudative (wet) AMD,[74] based upon whether neovascularization has developed. A major trigger for exudative AMD is upregulation of VEGF expression and ER stress can trigger this upregulation.[61,72,75] Also implicated in the development of AMD is smoking;[76,77] cigarette smoke extract contains benzopyrene, a potent inducer of ER stress via the PERK pathway.[78] A number of studies performed using human ARPE-19 cells have implicated cigarette smoke in VEGF upregulation and in induction of ER stress.[79–81] Another pathogenic mechanism implicated in AMD is accumulation of age-related lipofuscin N-retinylidene-N-retinylethanolamine (A2E) in RPE, which can confer susceptibility to blue light-mediated damage in the cells. Recent work has shown elevation of GRP78 and CHOP after A2E and blue light-induced damage in human RPE cells.[82]

In vivo studies of AMD implicate ER stress in the disease pathogenesis. For example Dr. C. Chan (National Eye Institute, NIH) developed a mouse model of AMD that has defects in two genes that are involved in immunologic processes.[83] One gene encodes CX3C chemokine receptor 1 (CX3CR1), the receptor for CX3CL1/fractalkine chemokine, which is expressed in RPE, Müller cells, and microglia. Two single nucleotide polymorphisms (SNPs) of CX3CR1 coupled with a decreased number of CX3CR1 transcripts and protein in AMD macula are associated with AMD.[84]

The second gene, *Ccl2* (MCP-1, a CC chemokine), is thought to play a homeostatic, immunoregulatory role in AMD pathogenesis.[85] Aged mice with deficient *Ccl2* or *Ccr2*, the corresponding receptor, develop many cardinal features of AMD, including drusen formation, RPE accumulation of lipofuscin and complement factors, and choroidal neovascularization.[86] To mimic closely the pathologic features of AMD, mice with mutations in these two genes have been crossed to generate *Ccl2*/*Cx3cr1* mice.[87] These double-knockout (DKO) mice were established in mice that harbor the Crb^{rd8} mutation and recent data show that DKO^{rd8} mice recapitulate some human AMD-like features in addition to the retinal dystrophy observed in *rd8* mice.[88] Fundoscopic examination of $Ccl2^{-/-}/Cx3cr1^{-/-}$ (DKO^{rd8}) mice as early as 4–6 weeks of age revealed drusen-like lesions that progressed to large, confluent areas of yellow deposits in the deep retina and subretinal space by 4–6 months of age and flattened atrophic areas by 6 months of age. Studies of the retinas of these mice suggest that the pathogenesis of AMD may be mediated by ER stress and protein misfolding. Indeed, there is decreased expression at the mRNA and protein level of ERp29, a molecular chaperone protein.[83] Given that AMD is multifactorial and there is no single mutated protein to be targeted, Tuo and colleagues hypothesized that enhancing chaperone activity through the use of chemical and/or pharmacologic chaperone compounds may prove beneficial to many individuals suffering from this devastating sight-threatening disease.[73] A promising example of this concerns the chaperone protein αB crystallin, a 20-kD member of the small heat shock protein (HSP) family. HSPs prevent aggregation of folded proteins and facilitate intracellular protein trafficking. αB crystallin is secreted from RPE cells and is taken up by adjacent photoreceptor cells conferring neuroprotection.[89] As increased αB crystallin is a biomarker for AMD, it may be fruitful to exploit increased secretion toward neuroprotective effects. More recent studies suggest that αB crystallin is an important regulator of ER stress in RPE.[90] Indeed, RPE cells from αB crystallin (−/−) mice and from human RPE cells transfected with αB crystallin siRNA are more vulnerable to ER stress induced by tunicamycin.[91] These studies also demonstrated that prolonged ER stress decreases levels of αB crystallin, thereby exacerbating mitochondrial dysfunction.

Summary

In summary, ER stress is implicated in a number of retinal diseases, including RP, diabetic retinopathy, early-onset maculopathies, and AMD. It is paradoxical that the UPR, which is triggered by ER stress, can induce cytoprotective effects that restore homeostasis but can also induce cell destructive effects that promote apoptosis. It is not clear how the UPR integrates these opposing outcomes to progress toward survival or death. It has been postulated that the duration of expression of specific branches of the UPR process (i.e., the PERK, IRE1α or ATF-6 branches) dictates this outcome. Understanding ER stress in retinal diseases is emerging as an area of intense investigation.[92–94] It is hoped that the outcome of these studies will lead to discovery and development of innovative therapeutic intervention strategies for retinopathies.

References

1. Chen X, Karnovsky A, Sans MD, et al. Molecular characterization of the endoplasmic reticulum: insights from proteomic studies. *Proteomics*. 2010;10:4040–4052.
2. Malhotra JD, Kaufman RJ. The endoplasmic reticulum and the unfolded protein response. *Semin Cell Dev Biol*. 2007;18:716–731.
3. Yoshida H. ER stress and diseases. *FEBS J*. 2007;274:630–658.
4. Ni M, Lee AS. ER chaperones in mammalian development and human diseases. *FEBS Lett*. 2007;581:3641–3651.
5. Sano R, Reed JC. ER stress-induced cell death mechanisms. *Biochim Biophys Acta*. 2013;1833:3460–3470.
6. Tsai YC, Weissman AM. The unfolded protein response, degradation from endoplasmic reticulum and cancer. *Genes Cancer*. 2010;1:764–778.
7. Kaufman RJ. Regulation of mRNA translation by protein folding the endoplasmic reticulum. *Trends Biochem Sci*. 2004;29:152–158.
8. Luo S, Mao C, Lee B, et al. GRP78/BiP is required for cell proliferation and protecting the inner cell mass from

apoptosis during early mouse embryonic development. *Mol Cell Biol*. 2006;26:5688–5697.
9. Han J, Back SH, Hur J, et al. ER-stress-induced transcriptional regulation increases protein synthesis leading to cell death. *Nat Cell Biol*. 2013;15:481–490.
10. Cullinan SB, Diehl JA. PERK-dependent activation of Nrf2 contributes to redox homeostasis and cell survival following endoplasmic reticulum stress. *J Biol Chem*. 2004;279:20108–20117.
11. Harding HP, Zhang Y, Bertolotti A, et al. Perk is essential for translational regulation and cell survival during the unfolded protein response. *Mol Cell*. 2000;5:897–904.
12. Harding HP, Zhang Y, Ron D. Protein translation and folding are coupled by an endoplasmic-reticulum-resident kinase. *Nature*. 1999;397:271–274.
13. Walter P, Ron D. The unfolded protein response: from stress pathway to homeostatic regulation. *Science*. 2011;334:1081–1086.
14. Cox JS, Walter P. A novel mechanism for regulating activity of a transcription factor that controls the unfolded protein response. *Cell*. 1996;87:391–404.
15. Hollien J. Evolution of the unfolded protein response. *Biochim Biophys Acta*. 2013;1833:2458–2463.
16. Gardner BM, Walter P. Unfolded proteins are Ire1-activating ligands that directly induce the unfolded protein response. *Science*. 2011;333:1891–1894.
17. Gardner BM, Pincus D, Gotthardt K, et al. Endoplasmic reticulum stress sensing in the unfolded protein response. *Cold Spring Harb Perspect Biol*. 2013;5:a013169.
18. Rutkowski DT, Kaufman RJ. That which does not kill me makes me stronger: adapting to chronic ER stress. *Trends Biochem Sci*. 2007;32:469–476.
19. Hamel C. Retinitis pigmentosa. *Orphanet J Rare Dis*. 2006;1:40.
20. Berger W, Kloeckener-Gruissem B, Neidhardt J. The molecular basis of human retinal and vitreoretinal diseases. *Prog Retin Eye Res*. 2010;29:335–375.
21. Lin JH, Li H, Yasumura D, et al. IRE1 signaling affects cell

fate during the unfolded protein response. *Science*. 2007;318:944–949.
22. Gorbatyuk MS, Knox T, LaVail MM, et al. Restoration of visual function in P23H rhodopsin transgenic rats by gene delivery of BiP/Grp78. *Proc Natl Acad Sci USA*. 2010;107:5961–5966.
23. Behrman S, Acosta-Alvear D, Walter P. A CHOP-regulated microRNA controls rhodopsin expression. *J Cell Biol*. 2011;192:919–927.
24. Chiang WC, Kroeger H, Sakami S, et al. Robust endoplasmic reticulum-associated degradation of rhodopsin precedes retinal degeneration. *Mol Neurobiol*. 2015;52:679–695.
25. Hiramatsu N, Chiang WC, Kurt TD, et al. Multiple mechanisms of unfolded protein response-induced cell death. *Am J Pathol*. 2015;185:1800–1808.
26. Yoshida T, Ozawa Y, Suzuki K, et al. The use of induced pluripotent stem cells to reveal pathogenic gene mutations and explore treatments for retinitis pigmentosa. *Mol Brain*. 2014;7:45.
27. Jiang H, Xiong S, Xia X. Retinitis pigmentosa-associated rhodopsin mutant T17M induces endoplasmic reticulum (ER) stress and sensitizes cells to ER stress-induced cell death. *Mol Med Rep*. 2014;9:1737–1742.
28. Kunte MM, Choudhury S, Manheim JF, et al. ER stress is involved in T17M rhodopsin-induced retinal degeneration. *Invest Ophthalmol Vis Sci*. 2012;53:3792–3800.
29. Bowes C, Li T, Danciger M, et al. Retinal degeneration in the rd mouse is caused by a defect in the beta-subunit of rod cGMP-phosphodiesterase. *Nature*. 1990;347:677–680.
30. Yang LP, Wu LM, Guo XJ, et al. Activation of endoplasmic reticulum stress in degenerating photoreceptors of the rd1 mouse. *Invest Ophthalmol Vis Sci*. 2007;48:5191–5198.
31. Rebello G, Ramesar R, Vorster A, et al. Apoptosis inducing signal sequence mutation in carbonic anhydrase IV identified in patients with the RP17 form of retinitis pigmentosa. *Proc Natl Acad Sci USA*. 2004;101:6617–6622.
32. Stams T, Nair SK, Okuyama Pandor A, et al. Cell-specific differences in the processing of the R14W CAIV mutant

associated with retinitis pigmentosa 17. *J Cell Biochem*. 2010;111:735–741.
33. Datta R, Waheed A, Bonapace G, et al. Pathogenesis of retinitis pigmentosa associated with apoptosis-inducing mutations in carbonic anhydrase IV. *Proc Natl Acad Sci USA*. 2009;106:3437–3442.
34. den Hollander AI, Roepman R, Koenekoop RK, et al. Leber congenital amaurosis: genes, proteins and disease mechanisms. *Prog Retin Eye Res*. 2008;27:391–419.
35. Zhang T, Zhang N, Baehr W, et al. Cone opsin determines the time course of cone photoreceptor degeneration in Leber congenital amaurosis. *Proc Natl Acad Sci USA*. 2011;108:8879–8884.
36. Borst DE, Redmond TM, Elser JE, et al. Interphotoreceptor retinoid-binding protein: gene characterization, protein repeat structure, and its evolution. *J Biol Chem*. 1989;264:1115–1123.
37. den Hollander AI, McGee TL, Ziviello C, et al. A homozygous missense mutation in the IRBP gene (RBP3) associated with autosomal recessive retinitis pigmentosa. *Invest Ophthalmol Vis Sci*. 2009;50:1864–1872.
38. Li S, Yang Z, Hu J, et al. Secretory defect and cytotoxicity: the potential disease mechanisms for the retinitis pigmentosa (RP)-associated interphotoreceptor retinoid-binding protein (IRBP). *J Biol Chem*. 2013;288:11395–11406.
39. Mendes CS, Levet C, Chatelain G, et al. ER stress protects from retinal degeneration. *EMBO J*. 2009;28:1296–1307.
40. Farrar GJ, Palfi A, O'Reilly M. Gene therapeutic approaches for dominant retinopathies: 3. *Curr Gene Ther*. 2010;10:381–388.
41. Aller E, Jaijo T, Beneyto M, et al. Identification of 14 novel mutations in the long isoform of USH2A in Spanish patients with Usher syndrome type II. *J Med Genet*. 2006;43:e55.
42. Tucker BA, Mullins RF, Streb LM, et al. Patient-specific iPSC-derived photoreceptor precursor cells as a means to investigate retinitis pigmentosa. *Elife*. 2013;2:e00824.
43. Sharpe LT, Stockman A, Jagle H, et al. Opsin genes, cone photopigments and colour blindness. Gegenfurtner KR,

Sharpe LT. *Color vision: from genes to perception*. Cambridge University Press: Cambridge; 2001:48–52.
44. Andréasson S, Tornqvist K. Electroretinograms in patients with achromatopsia. *Acta Ophthalmol*. 1991;69:711–716.
45. Aboshiha J, Dubis AM, Carroll J, et al. The cone dysfunction syndromes. *Br J Ophthalmol*. 2016;100(1):115–121.
46. Kohl S, Zobor D, Chiang WC, et al. Mutations in the unfolded protein response regulator ATF6 cause the cone dysfunction disorder achromatopsia. *Nat Genet*. 2015;47:757–765.
47. Gardner TW, Abcouwer SF, Barber AJ, et al. An integrated approach to diabetic retinopathy research. *Arch Ophthalmol*. 2011;129:230–235.
48. Barber AJ, Gardner TW, Abcouwer SF. The significance of vascular and neural apoptosis to the pathology of diabetic retinopathy. *Invest Ophthalmol Vis Sci*. 2011;52:1156–1163.
49. Barber AJ, Lieth E, Khin SA, et al. Neural apoptosis in the retina during experimental and human diabetes: early onset and effect of insulin. *J Clin Invest*. 1998;102:783–791.
50. Abu-El-Asrar AM, Dralands L, Missotten L, et al. Expression of apoptosis markers in the retinas of human subjects with diabetes. *Invest Ophthalmol Vis Sci*. 2004;45:2760–2766.
51. Ng JS, Bearse MA Jr, Schneck ME, et al. Local diabetic retinopathy prediction by multifocal ERG delays over 3 years. *Invest Ophthalmol Vis Sci*. 2008;49:1622–1628.
52. Oshitari T, Hata N, Yamamoto S. Endoplasmic reticulum stress and diabetic retinopathy. *Vasc Health Risk Manag*. 2008;4:115–122.
53. Roy S, Trudeau K, Roy S, et al. Mitochondrial dysfunction and endoplasmic reticulum stress in diabetic retinopathy: mechanistic insights into high glucose-induced retinal cell death. *Curr Clin Pharmacol*. 2013;8:278–284.
54. Ma JH, Wang JJ, Zhang SX. The unfolded protein response and diabetic retinopathy. *J Diabetes Res*. 2014;2014:160140.
55. Li J, Wang JJ, Yu Q, et al. Endoplasmic reticulum stress is implicated in retinal inflammation and diabetic retinopathy. *FEBS Lett*. 2009;583:1521–1527.
56. Yang H, Liu R, Cui Z, et al. Functional characterization of

58-kilodalton inhibitor of protein kinase in protecting against diabetic retinopathy via the endoplasmic reticulum stress pathway. *Mol Vis*. 2011;17:78–84.
57. Ikesugi K, Mulhern ML, Madson CJ, et al. Induction of endoplasmic reticulum stress in retinal pericytes by glucose deprivation. *Curr Eye Res*. 2006;31:947–953.
58. Li J, Wang JJ, Zhang SX. Preconditioning with endoplasmic reticulum stress mitigates retinal endothelial inflammation via activation of X-box binding protein 1. *J Biol Chem*. 2011;286:4912–4921.
59. Yang H, Liu R, Cui Z, et al. Functional characterization of 58-kilodalton inhibitor of protein kinase in protecting against diabetic retinopathy via the endoplasmic reticulum stress pathway. *Mol Vis*. 2011;17:78–84.
60. Praidou A, Androudi S, Brazitikos P, et al. Angiogenic growth factors and their inhibitors in diabetic retinopathy. *Curr Diabetes Rev*. 2010;6:304–312.
61. Roybal CN, Yang S, Sun CW, et al. Homocysteine increases the expression of vascular endothelial growth factor by a mechanism involving endoplasmic reticulum stress and transcription factor ATF4. *J Biol Chem*. 2004;279:14844–14852.
62. Ganapathy PS, Roon P, Moister TK, et al. Diabetes accelerates retinal neuronal cell death in a mouse model of endogenous hyperhomocysteinemia. *Ophthalmol Eye Dis*. 2009;1:3–11.
63. Daley ML, Watzke RC, Riddle MC. Early loss of blue-sensitive color vision in patients with type I diabetes. *Diabetes Care*. 1987;10:777–781.
64. Fortune B, Schneck ME, Adams AJ. Multifocal electroretinogram delays reveal local retinal dysfunction in early diabetic retinopathy. *Invest Ophthalmol Vis Sci*. 1999;40:2638–2651.
65. Ha Y, Dun Y, Thangaraju M, et al. Sigma receptor 1 modulates endoplasmic reticulum stress in retinal neurons. *Invest Ophthalmol Vis Sci*. 2011;52:527–540.
66. Barber AJ, Antonetti DA, Kern TS, et al. The Ins2Akita mouse as a model of early retinal complications in diabetes.

Invest Ophthalmol Vis Sci. 2005;46:2210–2218.
67. Gastinger MJ, Kunselman AR, Conboy EE, et al. Dendrite remodeling and other abnormalities in the retinal ganglion cells of Ins2Akita diabetic mice. *Invest Ophthalmol Vis Sci*. 2008;49:2635–2642.
68. Smith SB, Duplantier JN, Dun Y, et al. In vivo protection against retinal neurodegeneration by the sigma receptor 1 ligand (+)-pentazocine. *Invest Ophthalmol Vis Sci*. 2008;49:4154–4161.
69. Ambasudhan R, Wang X, Jablonski MM, et al. Atrophic macular degeneration mutations in ELOVL4 result in the intracellular misrouting of the protein. *Genomics*. 2004;83:615–625.
70. Karan G, Yang Z, Howes K, et al. Loss of ER retention and sequestration of the wild-type ELOVL4 by Stargardt disease dominant negative mutants. *Mol Vis*. 2005;11:657–664.
71. Marmorstein LY, Munier FL, Arsenijevic Y, et al. Aberrant accumulation of EFEMP1 underlies drusen formation in malattia leventinese and age-related macular degeneration. *Proc Natl Acad Sci USA*. 2002;99:13067–13072.
72. Roybal CN, Marmorstein LY, Vander Jagt DL, et al. Aberrant accumulation of fibulin-3 in the endoplasmic reticulum leads to activation of the unfolded protein response and VEGF expression. *Invest Ophthalmol Vis Sci*. 2005;46:3973–3979.
73. Sauer T, Patel M, Chan CC, et al. Unfolding the therapeutic potential of chemical chaperones for age-related macular degeneration. *Expert Rev Ophthalmol*. 2008;3:29–42.
74. Jager RD, Mieler WF, Miller JW. Age-related macular degeneration. *N Engl J Med*. 2008;358:2606–2617.
75. Salminen A, Kauppinen A, Hyttinen JM, et al. Endoplasmic reticulum stress in age-related macular degeneration: trigger for neovascularization. *Mol Med*. 2010;16:535–542.
76. Klein R, Peto T, Bird A, et al. The epidemiology of age-related macular degeneration. *Am J Ophthalmol*. 2004;137:486–495.
77. Kabasawa S, Mori K, Horie-Inoue K, et al. Associations of cigarette smoking but not serum fatty acids with age-

related macular degeneration in a Japanese population. *Ophthalmology*. 2011;118:1082–1088.
78. Hengstermann A, Muller T. Endoplasmic reticulum stress induced by aqueous extracts of cigarette smoke in 3T3 cells activates the unfolded protein-response-dependent PERK pathway of cell survival. *Free Radic Biol Med*. 2008;44:1097–1107.
79. Bertram KM, Baglole CJ, Phipps RP, et al. Molecular regulation of cigarette smoke induced oxidative stress in human retinal pigment epithelial cells: implications for age-related macular degeneration. *Am J Physiol Cell Physiol*. 2009;297:C1200–10.
80. Pons M, Marin-Castaño ME. Cigarette smoke-related hydroquinone dysregulates MCP-1, VEGF and PEDF expression in retinal pigment epithelium in vitro and in vivo. *PLoS ONE*. 2011;6:e16722.
81. Pons M, Cousins SW, Csaky KG, et al. Cigarette smoke-related hydroquinone induces filamentous actin reorganization and heat shock protein 27 phosphorylation through p38 and extracellular signal-regulated kinase 1/2 in retinal pigment epithelium: implications for age-related macular degeneration. *Am J Pathol*. 2010;177:1198–1213.
82. Feng J, Chen X, Sun X, et al. Expression of endoplasmic reticulum stress markers GRP78 and CHOP induced by oxidative stress in blue light-mediated damage of A2E-containing retinal pigment epithelium cells. *Ophthalmic Res*. 2014;52:224–233.
83. Tuo J, Bojanowski CM, Zhou M, et al. Murine ccl2/cx3cr1 deficiency results in retinal lesions mimicking human age-related macular degeneration. *Invest Ophthalmol Vis Sci*. 2007;48:3827–3836.
84. Tuo J, Smith B, Bojanowski CM, et al. The involvement of sequence variation and expression of CX3CR1 in the pathogenesis of age-related macular degeneration. *FASEB J*. 2004;18:1297–1299.
85. Forrester JV. Macrophages eyed in macular degeneration. *Nat Med*. 2003;9:1350–1351.
86. Ambati J, Anand A, Fernandez S, et al. An animal model of

age-related macular degeneration in senescent Ccl-2- or Ccr-2-deficient mice. *Nat Med*. 2003;9:1390–1397.
87. Chan CC, Ross RJ, Shen D, et al. Ccl2/Cx3cr1-deficient mice: an animal model for age-related macular degeneration. *Ophthalmic Res*. 2008;40:124–128.
88. Popp N, Chu XK, Shen D, et al. Evaluating potential therapies in a mouse model of focal retinal degeneration with age-related macular degeneration (AMD)-like lesions. *J Clin Exp Ophthalmol*. 2013;4(5):1000296.
89. Sreekumar PG, Kannan R, Kitamura M, et al. αB crystallin is apically secreted within exosomes by polarized human retinal pigment epithelium and provides neuroprotection to adjacent cells. *PLoS ONE*. 2010;5(10):e12578.
90. Kannan R, Sreekumar PG, Hinton DR. Alpha crystallins in the retinal pigment epithelium and implications for the pathogenesis and treatment of age-related macular degeneration. *Biochim Biophys Acta*. 2016;1860(1 Pt B):258–268.
91. Dou G, Sreekumar PG, Spee C, et al. Deficiency of αB crystallin augments ER stress-induced apoptosis by enhancing mitochondrial dysfunction. *Free Radic Biol Med*. 2012;53:1111–1122.
92. Zhang SX, Sanders E, Fliesler SJ, et al. Endoplasmic reticulum stress and the unfolded protein responses in retinal degeneration. *Exp Eye Res*. 2014;125:30–40.
93. Griciuc A, Aron L, Ueffing M. ER stress in retinal degeneration: a target for rational therapy? *Trends Mol Med*. 2011;8:442–451.
94. Haeri M, Knox BE. Endoplasmic reticulum stress and unfolded protein response pathways: potential for treating age-related retinal degeneration. *J Ophthalmic Vis Res*. 2012;7:45–59.

26

Cell Death, Apoptosis, and Autophagy in Retinal Injury

Michael E. Boulton, Sayak K. Mitter, S. Louise Pay

Introduction

Cell death is an inevitable consequence of life. It plays a critical role in development by eliminating transitory organs and tissues (e.g., hyaloid vessels) and tissue remodeling where cell death allows the removal of excess or unwanted cells (e.g., death of oligodendrocytes in the optic nerve). During life, dead and damaged cells are constantly being replaced to ensure homeostasis and normal functioning of multicellular organisms. However, with increasing age, cell death can exceed replacement, leading to loss of tissue/organ function. Furthermore, injury and disease can lead to excessive cell loss, which overwhelms the organism and leads to functional impairment and even death. The majority of cell death in the retina occurs by apoptosis, which has the big advantage over necrosis that it is self-contained and does not result in an overt inflammatory response. Autophagy, a housekeeping process to maintain cellular homeostasis, can result in cell death when it exceeds a certain threshold. The following chapter will discuss cell death in the retina in detail in the context of development, aging, and diseases such as glaucoma, diabetic retinopathy (DR), and age-

related macular degeneration (AMD). It will further consider the initiating factors in retinal apoptosis and discuss potential therapeutic strategies for preventing retinal cell death and preserving or restoring vision.

Modes of Cell Death

The Nomenclature Committee on Cell Death (NCCD) has made two subsequent recommendations on guidelines for the identification of modes of cell death since 2005, each time incorporating the latest findings in the area.[1,2] The NCCD concludes that: "Cell death can be classified according to its morphological appearance (which may be apoptotic, necrotic, autophagic or associated with mitosis), enzymological criteria (with and without the involvement of nucleases or of distinct classes of proteases, such as caspases, calpains, cathepsins, and transglutaminases), functional aspects (programmed or accidental, physiological or pathological) or immunological characteristics (immunogenic or non-immunogenic)." While death associated pathways may be "turned on" transiently during several unrelated biologic processes, a cell is normally only considered dead once it has passed an irreversible phase in the "death process."

Apoptosis

Apoptosis, or programmed cell death, has been extensively studied due to its critical role in development, tissue homeostasis, and pathology.[3,4] Importantly, apoptosis does not elicit an inflammatory response, thus allowing "physiologic" cell death to take place without pathologic consequences. Morphologic features of apoptosis include rounding up of the cell, reduction in cellular and nuclear volume (pyknosis), nuclear fragmentation, modification of cytoplasmic organelles, plasma membrane blebbing, and engulfment by neighboring cells (Fig. 26.1).[2] Apoptosis can be initiated by a variety of stimuli through two distinct pathways – extrinsic and intrinsic.[5] The extrinsic pathway is triggered by interaction of death receptors present on the cell surface with their cognate ligands (e.g., Fas/CD95 ligand, tumor necrosis factor-alpha

[TNF-α], TNF ligand superfamily, and TNF-related apoptosis-inducing ligand [TRAIL]) and which can initiate the downstream executioner caspase (cysteine aspartic acid proteases) cascade within seconds of ligand binding.[6] Additionally, dependence receptors including Netrin-1 receptors, DCC (deleted in colorectal cancer) and UNCH5, neogenin, RET (prototypical oncogene tyrosine-protein kinase receptor), TrkC (tropomyosin-related kinase C), ALK (anaplastic lymphoma kinase), ephrin A4 (EphA4), Patched, MET, and some integrins have been identified to participate in alternative extrinsic apoptotic signaling whereby cell death or subapoptotic events may ensue.[7–10] By contrast, the intrinsic pathway is initiated by "stress signals" including oxidative damage, DNA damage, loss of cell–cell contact, growth factor withdrawal, hypoxia, cytosolic Ca^{++} overload, and endoplasmic reticulum stress. These signals target the mitochondria and induce the release of proapoptotic factors to the cytosol that activates caspases via mitochondrial outer membrane permeabilization. Excessive or deficient apoptosis is involved in numerous disease states. Readers requiring more detail are directed to the work of Green and Reed.[3,4]

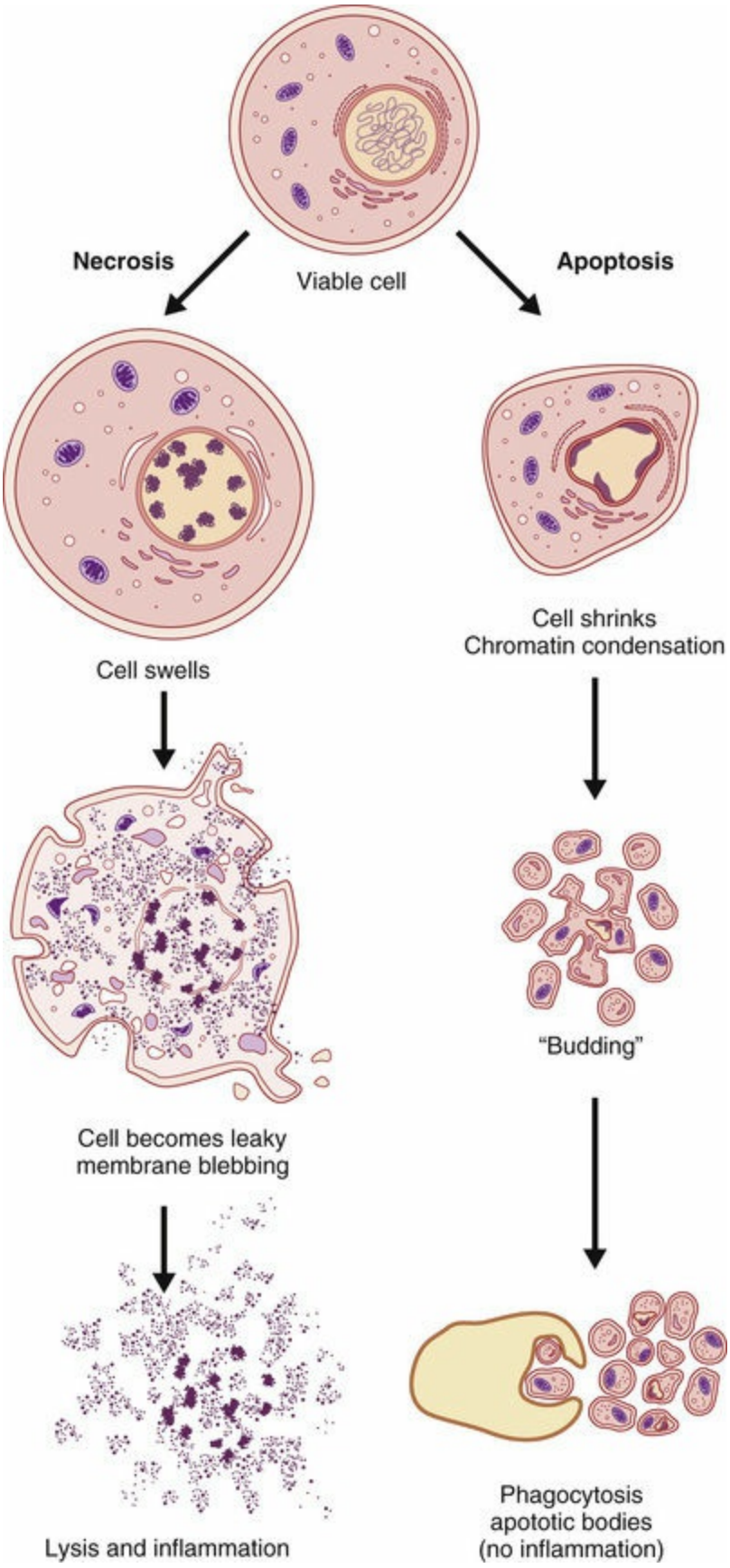

FIG. 26.1 Apoptotic versus necrotic morphology.

Necrosis

Necrosis has been defined as a type of uncontrolled cell death occurring in response to alkylating DNA damage, infection, toxins, chemicals, injury, or lack of blood supply.[3,11] Morphologically, necrosis is associated with cytoplasmic swelling (oncosis), rupture of the plasma membrane, swelling of cytoplasmic organelles, and moderate chromatin condensation (Fig. 26.1). The critical pathophysiologic difference between necrosis and apoptosis is inflammation. Necrosis culminates in the uncontrolled release of antigens that activate the immune system and promote inflammation, whereas in apoptosis, cell-bound bodies are formed that are phagocytosed by neighboring cells and there is an absence of inflammation. Recent studies suggest that there is a molecular signaling network that can regulate the necrotic cell death pathway.[12] Specific necrotic signaling mechanisms consist of RIP Kinase homologs 1 and 3 interacting with FAS-associated death domain (FADD), FLIP (FLICE-like inhibitory protein long isoform), and pro-caspase 8. Readers are advised to consult Humphries et al. for a deeper understanding of the process.[13]

Other

A number of other cell death pathways have been identified, of which autophagic cell death has gained some prominence.[14] Increased autophagy (see below), such as that occurring under starvation, leads to self-destruction of intracellular organelles for provision of nutrients which, if starvation is not reversed, will culminate in self-destruction of cells and tissues.[15] Autophagic cell death is morphologically defined as occurring in the absence of chromatin condensation, massive autophagic vacuolization, and little or no uptake by neighboring cells.[16] Interestingly, autophagy is upregulated in a number of neurodegenerative diseases and thus may contribute to cell loss associated with these conditions. Several other atypical cell death modalities have also been identified, and these are reviewed in Galluzzi et al.[17]

Cross-Talk Between Cell Death Pathways

Until recently, a requirement for gene expression was documented only for apoptotic and autophagic cell death. Interestingly, certain genes and their products, e.g., p53, Bcl-2 family proteins, and calpain, are important for both these modes of cell death.[11,12,14] Basal p53 activity suppresses autophagy, whereas p53 activation by some stimuli induces autophagy as well as apoptosis mediated by the Bcl-2 family proteins.[12,14] Atg5 is essential for autophagy; however, its truncated form, produced as a result of calpain cleavage, interacts with Bcl-xL to promote cytochrome c release and caspase-dependent apoptosis.[18] Accumulating evidence now suggests that necrotic cell death can also be mediated by a specific set of signal transduction pathways and degradative mechanisms that can contribute to embryonic development and adult tissue homeostasis.[19] Some gene products, such as TNFR, CD95, TRAIL-R, and RIP1, might trigger both apoptosis and necrosis, depending on interaction with other proteins.[11] Moreover, there is cross-talk between these two cell death modalities. For example, inactivation of caspases might cause a shift from apoptosis to necrosis, or a mixture of the two.[11] Thus cell death is not as easily defined as generally believed, and there is considerable cross-talk between the different cell death mechanisms.

Is Cell Death Bad?

Cell death is often considered as a pathologic endpoint, but is this really the case? During normal development and differentiation we produce an excess of many cell types that undergo apoptosis.[20] Cells are constantly dying and being replaced as part of the overall homeostatic process to remove dysfunctional and damaged cells. In this context cell death is beneficial as it maintains optimal function in multicellular organisms. Provided the balance between loss and replacement remains constant, all is good; however, this is not always the case in aging or pathology where cell death increases and cell replacement decreases, resulting in an impaired organism. One therapeutic approach is to inhibit cell death. While laudable, this may not always be the best option as keeping alive damaged, mutated, or dysregulated cells will be to the detriment of the organism.

Autophagy and Cell Maintenance

Autophagy is essential for cellular housekeeping and homeostasis through the sequestration and transfer of intracellular components (e.g., protein aggregates, organelles) to lysosomes for degradation.[21,22] In mammalian cells, three primary types of autophagy have been reported: macroautophagy, chaperone-mediated autophagy (CMA), and microautophagy (Fig. 26.2).[23–27]

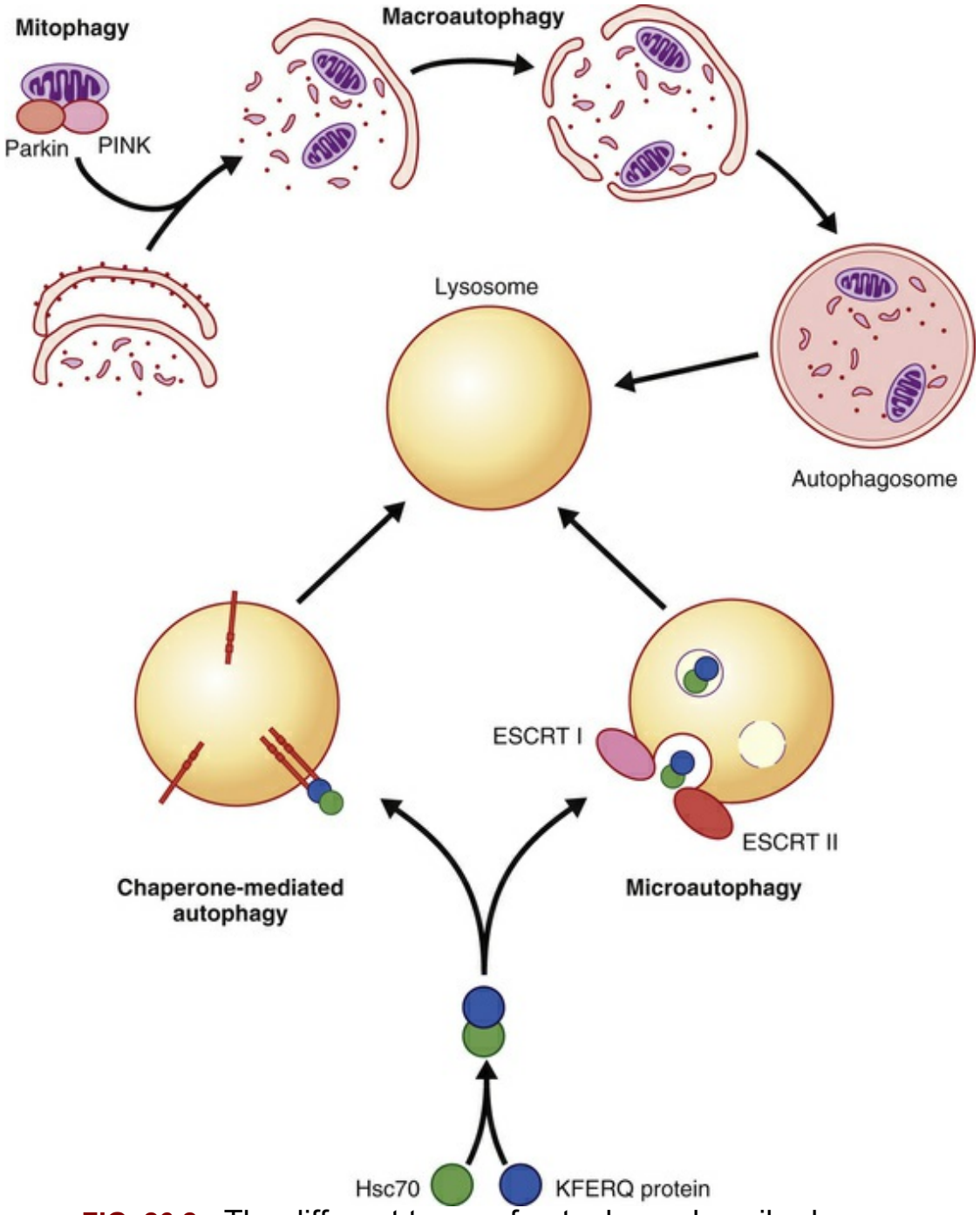

FIG. 26.2 The different types of autophagy described in the text.

Macroautophagy is the best-characterized autophagy pathway that targets larger substrates such as protein aggregates, intracellular pathogens, and dysfunctional organelles such as mitochondria for degradation (Fig. 26.2).[21,22,28] The process of macroautophagy involves over 37 autophagy-related proteins (ATGs), which regulate different stages of the autophagic response (Fig. 26.3).[29] Macroautophagy is initiated by the sequestration of the

cytosolic substrate into double membrane-bound phagophores that predominantly originate from the rough endoplasmic reticulum with possible contributions from the plasma membrane or mitochondria.[30–33] The resulting autophagosome acquires endosomal and lysosomal proteins, ultimately maturing into a degradative autolysosome. The mTOR kinase complex is considered central to the signaling pathway of autophagy and can sense regulating conditions such as nutrient abundance, energy state, and growth factor levels.[34,35] The PI3K-III complex, consisting of Vps34 and p150 and activators such as Beclin-1, Ambra1, ATG14, and UVRAG, plays a crucial role in the induction of autophagy by generating PtdIns(3)P-rich membranes, which act as platforms for ATG protein recruitment and autophagosome nucleation.[36] Antiapoptotic BH3 proteins such as Bcl-xL and Bcl-2 bind to Beclin-1, negatively regulating PI3K-III activity and autophagy. Initiation of the mammalian autophagosome membrane formation depends on the ULK1-mAtg13-FIP200-Atg101 complex.[37] Elongation and completion of the phagophore are brought about by two ubiquitin-like conjugation systems: the Atg12-Atg5-Atg16 system and the Atg8-phosphatidylethanolamine (PE) system. Atg7 functions as an E1 enzyme in both systems, while Atg10 and Atg3 act as E2 enzymes for Atg12 and Atg8, respectively.[38,39] The C-terminus of Atg8 is cleaved by Atg4, which primes the protein for conjugation to PE. The Atg12–Atg5–Atg16 complex recruits Atg8-PE to the elongating phagophore.[39,40] At least eight different Atg8 orthologs belonging to two subfamilies (LC3 and GATE-16/GABARAP) occur in mammalian cells.[41,42] LC3s are involved in elongation of the phagophore membrane, whereas the GABARAP/GATE-16 subfamily is essential for a later stage in autophagosome maturation. The N-termini of LC3 and GATE-16 are required for autophagosome–lysosome fusion.[42] Once in the lysosomes, substrates are degraded by the repertoire of lysosomal enzymes.[43] It has been proposed that the autophagic elimination of mitochondria has its own specialized pathway.[26] Critical to this process are the proteins PINK1, the E3 ubiquitin ligase, Parkin, BNIP3, NIX, and possibly p62, a protein that binds to ubiquitin and LC3. PINK1 binds to uncoupled mitochondria, which then facilitates the recruitment of Parkin, which leads to ubiquitination of

mitochondrial surface proteins. The ubiquitinated mitochondrion is then sequestered into the autophagosome, likely through the actions of p62 and LC3.

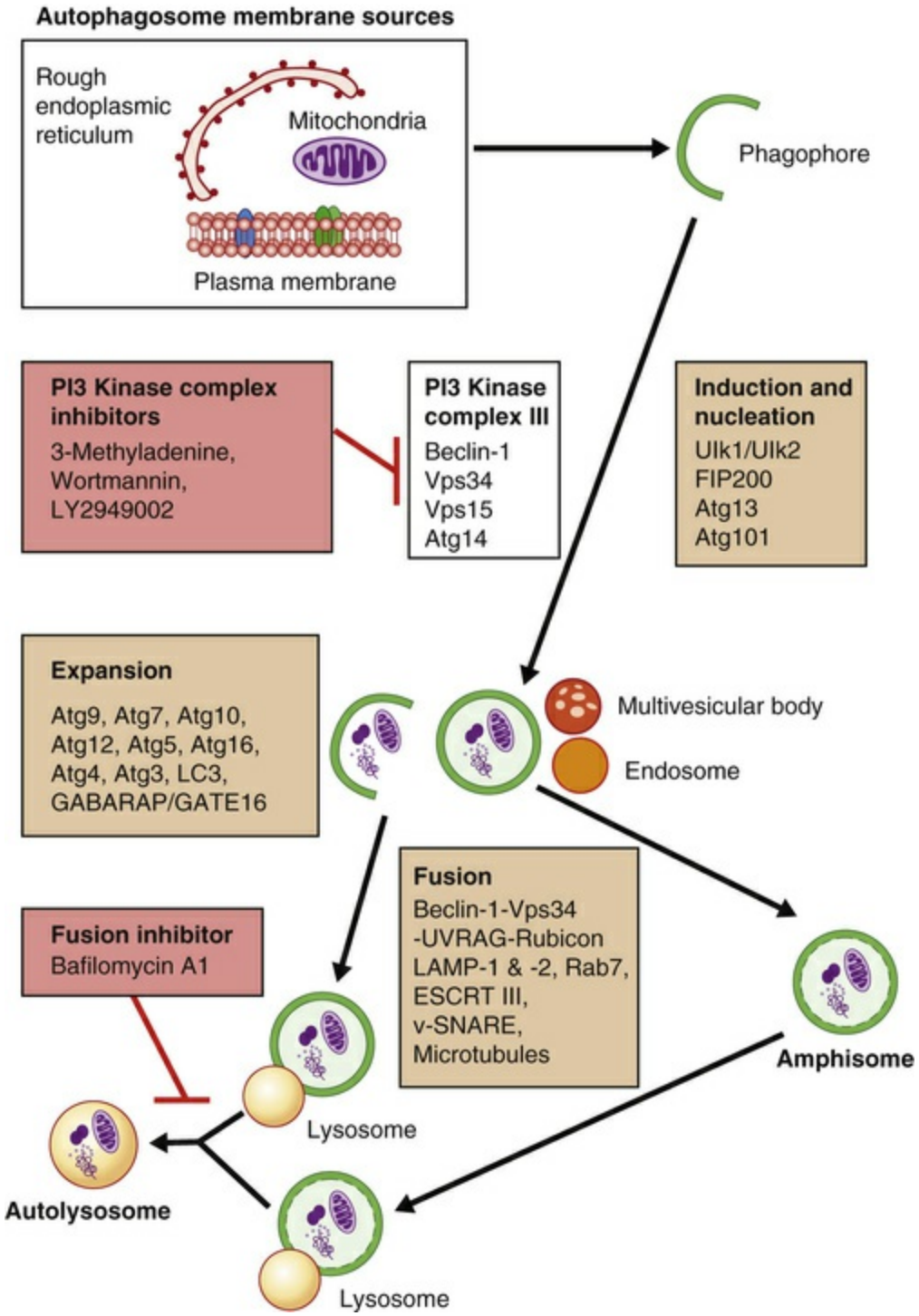

FIG. 26.3 The regulatory molecules involved in the different steps of the mammalian macroautophagy pathway. Potential pharmacologic inhibitors used to

block autophagy at different steps are also shown.

Autophagy can be activated by nutrient deprivation and environmental stress. For example, amino acid starvation and reactive oxygen species (ROS) can stimulate autophagy.[44,45] Recently, a distinction has been made between starvation- and stress-induced macroautophagy, also referred to as "quality control" autophagy. It has been observed that autophagic deficient cells tend to accumulate p62-rich aggregates, which in turn cause Nrf2 to be activated after separation from its interacting partner Keap1, which allows Nrf2 to mount an antioxidant response.[46] In addition, histone deacetylase 6 (HDAC6) stands out as a key regulator in the autophagic response to oxidative damage, as it is recruited to ubiquitinated autophagic substrates, where it stimulates autophagosome–lysosome fusion by promoting F-actin remodeling in a cortactin-dependent manner.[47] However, HDAC6 and cortactin are dispensable for starvation-induced autophagy.

CMA differs from the other types of autophagy as it does not involve vesicle formation but, rather, a direct translocation of a specific set of soluble proteins across the lysosomal membrane for subsequent degradation (Fig. 26.2).[48] CMA cargo substrates include enzymes, transcription factors, binding proteins, subunits of the proteasome, and proteins involved in vesicular trafficking and contain a KFERQ-like motif, which is recognized by the cytosolic chaperone, Hsc70. Binding of the chaperone/substrate to the cytosolic tail of lysosome-associated membrane protein type 2A (LAMP-2A), which spans the lysosomal membrane, leads to translocation of the cargo across the membrane and into the lysosomal lumen for degradation.[23] This pathway has been shown to be progressively ineffective with age because of the age-related loss of LAMP-2A.[49]

Microautophagy involves internalization of cytosolic cargo such as cytosolic proteins, glycogen, and ribosomes through invaginations of the lysosomal membrane,[50,51] resembling multivesicular body formation (Fig. 26.2).[24,48,52] Although the molecular mechanisms in mammalian cells are poorly understood, a recent study by Sahu et al. proposes that microautophagy relies on endosomal sorting complexes required for transport (ESCRT) I

and III, which are necessary for the formation of the vesicles in which the cytosolic cargo is internalized.[53] It appears that this pathway also involves Hsc70 interaction with a substrate containing a KFERQ-like motif, also found in CMA, and that mitophagy and CMA may share common upstream pathways.[48,53]

As will be discussed below, autophagy plays a critical role in maintaining retinal homeostasis, together with the proteosomal system, in the removal of damaged proteins and organelles in highly metabolic nondividing cells that exist in a pro-oxidative retinal environment. Autophagy proteins are strongly expressed in the retina (Fig. 26.4). However, problems occur when basal levels of autophagy become dysregulated as either a decrease or increase in autophagy flux will have significantly detrimental effects on cell function.[54]

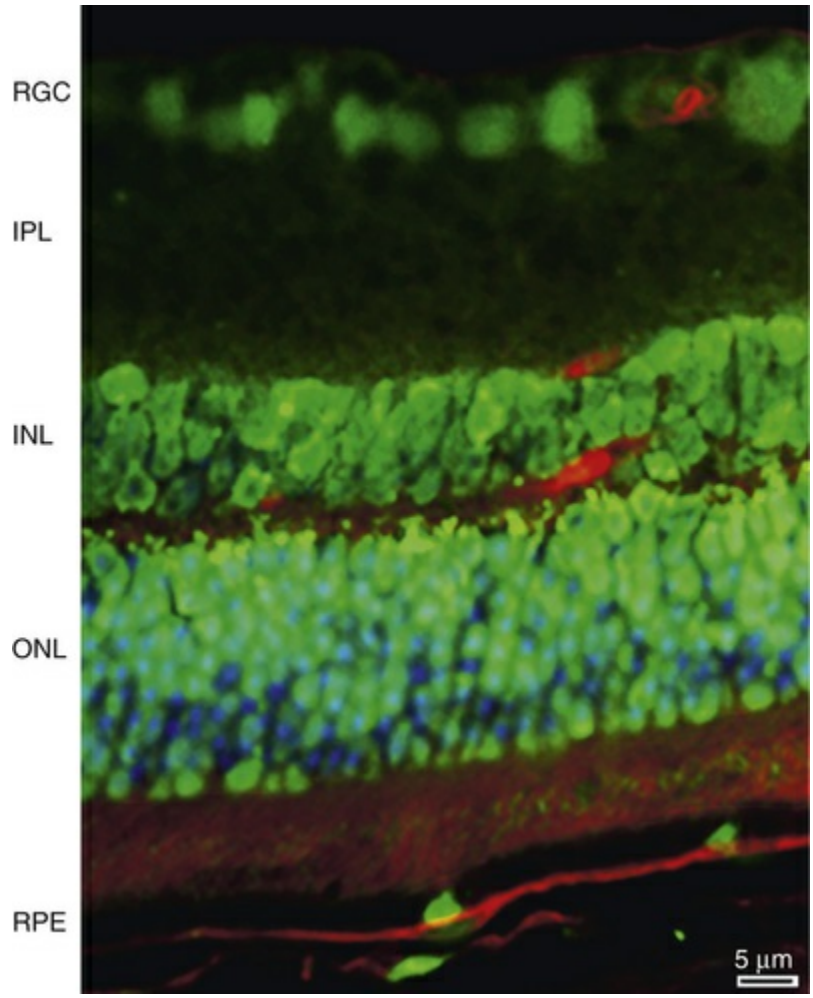

FIG. 26.4 Immunolocalization of the autophagy protein LC3 (green) in normal mouse retina. Nuclei are stained

with 4′,6-diamidino-2-phenylindole (DAPI: blue) and blood with agglutinin (red). LC3 is strongly expressed in the retinal ganglion cell layer (*RGC*), retinal vessels, a subpopulation of the inner nuclear layer (*INL*), the outer nuclear layer (*ONL*) of rods and cones, and the retinal pigment epithelium (*RPE*) but is only very weakly expressed in the inner plexiform layer (*IPL*).
(Courtesy of Xiaoping Qi, University of Florida.)

Age-Related Retinal Cell Loss

It is well recognized that the human retina undergoes numerous age-related changes that result in altered morphology, reduced function, and cell loss. Not surprisingly, this is associated with a significant reduction of retinal thickness as a function of age.[55–57] Mean retinal thickness is reported to decrease by 0.53 μM/year[55] and, in the macula, retinal thickness and macular volume decrease by around 0.35 μM and 0.01 mm^3/year.[57] Changes in cell morphology include nodular excrescences in rod outer segments;[58] accumulation of lipofuscin in photoreceptor inner segments and the retinal pigment epithelium (RPE);[59,60] displacement of nuclei from the outer nuclear layer (ONL);[61] and extension of ON-cone bipolar cell and horizontal cell processes into the ONL. Such evidence of retinal reorganization and plasticity has also been corroborated by animal studies.[62,63] Reorganization of the dendrites could be an adaptive attempt to compensate for the lost circuitry due to photoreceptor loss and/or to make up for existing, yet dysfunctional, synapses.

There is an age-related decrease in the density of photoreceptor cells in the human retina, with rods appearing to be more vulnerable than cones.[64] In the equatorial retina, cones decrease uniformly at a rate of approximately 16 cells/mm^2 per year while the decrease in equatorial rods is greatest, 970 cells/mm^2 per year, between the second and fourth decades.[65] By contrast, cone density remains relatively constant at the fovea up to the ninth decade.[64–66] It therefore appears that rod photoreceptors are more vulnerable to loss during aging than cones and that photoreceptors in the fovea are less susceptible to attrition. Furthermore, compensatory

adaptations have been reported following rod cell degeneration where the space vacated by dying rods is filled by enlarged rod inner segments from neighboring photoreceptors, resulting in similar rod coverage at all ages.[64,67–69] Evidence that cones depend on survival factors secreted by rods may explain the differential vulnerability between rods and cones,[70–72] but this remains a matter of intense debate.

Photoreceptor loss appears to precede the loss of associated neural cells. Retinal nerve fiber layer thickness decreases dramatically with age[73] and is associated with significant retinal ganglion cells (RGC) loss by as much as 150/mm^2 over a period of 40+ years.[56] RGC death at the equatorial regions follows a similar trend to photoreceptor death during aging, thus maintaining a constant photoreceptor-to-RGC ratio.[69] Age-associated degeneration of the rod bipolar cells in the inner nuclear layer (INL) has been reported.[74] Although rod cell death can initiate as early as the second decade of life, the bipolar cells start to degenerate only after the fourth decade and appreciably reduce by the ninth decade[65] indicating that this phenomenon is secondary to rod cell loss. In a more comprehensive study using multiphoton confocal microscopy to quantify neuron densities in the RGC layer, INL, and ONL, the greatest neuronal loss occurred in the RGC layer and ONL in human aging retinas, whereas the INL is relatively preserved.[75] It must also be remembered that RGCs are classified into a number of subtypes and so even a seemingly mild loss of RGC in the initial phases could imply the loss of a major subtype of RGC that could start affecting visual perception.[69]

Despite numerous studies to determine age-related changes in RPE cell density, outcomes vary and are highly dependent on retinal location. Two studies have reported that RPE density decreases with age in the equatorial retina and is greatest in the periphery,[65,76] with an estimated loss of 0.3% per year.[76] By contrast, no significant age-related decrease in RPE cell density was observed at the foveal center, suggesting that, like foveal cones, the RPE cells in this region are more resistant to attrition than those outside the fovea.[65] However, a further study reported that the macular region in aged eyes contained a significant number of apoptotic cells and these were greatest in the fovea.[67] Given the disparity between

studies on age-related changes in RPE cell density, it is not surprising that there is no clear agreement to what extent the RPE-to-photoreceptor ratio changes with age, if at all.[65,76]

Evidence would suggest that age-related cell loss in the retina occurs by apoptosis since occasional apoptotic cells are observed in retinal sections and without the typical inflammatory response that would occur via necrosis. The stimulus for age-related cell loss is also unclear, but since the majority of cells affected are postmitotic or terminally differentiated, the accumulation of stochastic damage as occurs with aging in other tissues is plausible. In particular, oxidative damage is likely to play a significant role since the retina has high oxygen levels, is exposed to light, and has a number of highly metabolically active cell types, making it an ideal environment for the generation of ROS.[77] As previously mentioned, the retina undergoes considerable remodeling throughout life to adapt to age-related cell loss. In addition, there is likely to be a basal level of limited cellular replacement through resident and bone marrow-derived stem or progenitor cells that have the capacity to differentiate into a number of retinal cell types.[78]

Retinal Damage: Death and Repair

Introduction

Retinal cell dysfunction and loss are common features of most retinal diseases (e.g., glaucoma, diabetic retinopathy [DR], age-related macular degeneration [AMD]) as well as tissue injury (e.g., retinal detachment, light damage). Such cell loss has a major negative impact on retinal function and can lead to significant visual loss.

Glaucoma and Ganglion Cell Loss

Glaucoma is a heterogeneous group of diseases that lead to RGC death.[79–81] Pathology is associated with "cupping" of the optic disc due to loss of ganglion cell axons. Analysis of both postmortem specimens and experimental animal models show that RGC death occurs by apoptosis.[82–84] Analysis of retinas from human donors

suffering primary open angle glaucoma demonstrated greater than 15 times more apoptotic cells than the controls.[84] Interestingly, apoptosis also accounts for the selective elimination of about 50% of excess RGCs during developmental organization of the visual pathway.[85] Apoptosis of RGCs in glaucoma has generally been considered to occur as a result of mechanical damage due to an increase in intraocular pressure, but damage to RGCs can also occur in normal-pressure glaucoma.[86] Other insults that have been reported to induce RGC apoptosis are neurotrophin deprivation, glial activation, ischemia, glutamate excitotoxicity, and oxidative stress.[81] Confirmatory data that RGC apoptosis occurs by the intrinsic pathway involving mitochondria come from backcrossing DBA/2J mice that exhibit a spontaneous secondary glaucoma with Bax (one of several BH3 family death proteins) knockout mice resulting in a mouse strain in which glaucomatous neurodegeneration was reduced.[87]

Despite the strong association between oxidative stress, mitochondrial damage, and RGC death, there have been only limited studies on the role of autophagy in RGC maintenance and glaucoma. Rodriguez-Muela and colleagues recently reported that autophagy promotes survival of RGCs after optic nerve axotomy in mice.[88] Calpain-mediated cleavage of Beclin-1 and autophagy deregulation have been reported in a rat model of retinal ischemic injury that recapitulates features of glaucoma.[89] Furthermore, blockade of autophagy increased cell death in cultured RGC, suggesting a prosurvival role for the autophagic process. Activation of autophagy in RGCs occurs after optic nerve transection and increased autophagy offers a protective role in cultured RGCs.[90] Sternberg and colleagues demonstrated that autophagy provided a survival mechanism against caspase-dependent death of neonatal RGCs induced by axon damage.[91] However, some reports fail to support the hypothesis that autophagy is protective to RGCs. Piras et al. recently reported that following ischemia/reperfusion, 3-MA mediated inhibition of autophagy resulted in reduced RGC death,[92] and Park et al. made a similar observation in a chronic hypertensive glaucoma rat model where autophagy inhibition resulted in lower RGC death.[93]

Diabetic Retinopathy

It has long been recognized that diabetes leads to a loss of pericytes and endothelial cells in the retinal vasculature (Fig. 26.5).[94,95] Cogan and colleagues identified intramural pockets in the vascular basement membrane lacking normal cell contents, referred to as pericyte "ghosts," as one of the earliest changes in DR.[96] Pericyte loss is accompanied by loss of endothelial cells from the retinal vasculature, leading to "acellular" capillaries (intact vessel basement membrane devoid of cells lining the lumen) and loss of blood–retinal barrier function. Cell death in these populations appears to occur predominantly via the intrinsic apoptotic pathway.[97] These characteristic changes have long been considered a hallmark of DR. However, studies by Barber and others reveal that diabetes is also associated with increased loss of retinal neurons.[98,99] STZ-diabetic rat retinas after 30 weeks of diabetes showed a 22% reduction in the thickness of the inner plexiform layer, a 10% reduction in RGCs, and a 14% reduction in the thickness of the INL.[100] Clinical studies of diabetic patients using scanning laser polarimetry and optical coherence tomography have largely confirmed these findings.[101–103] It is also likely that other neuronal populations such as amacrine cells undergo apoptosis in diabetes.[104] There are many potential initiators of retinal cell apoptosis including hyperglycemia, oxidative stress, reduced blood flow, ischemia, neuroinflammation, and, specifically in the case of retinal neurons, glutamate excitotoxicity.[97,98] Light and electron microscopy have revealed a significant number of pericytes in human and rodent diabetic retinas to have necrotic cell characteristics.[105] While apoptosis is the predominant death pathway of pericytes,[106,107] it is possible that a selective population of these dying cells may undergo programmed necrosis.

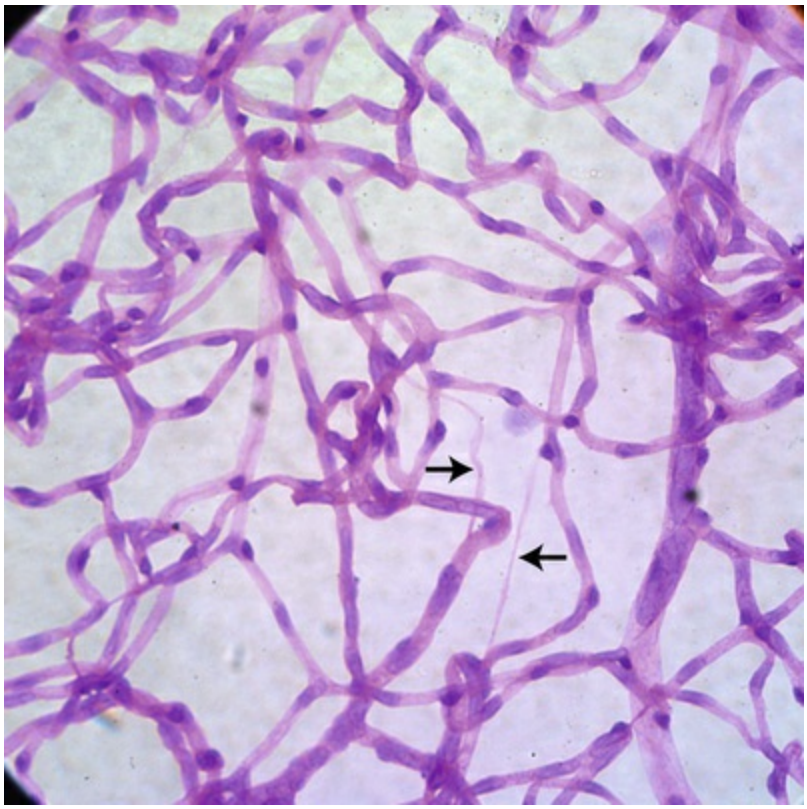

FIG. 26.5 A retinal digest showing pericyte dropout and areas of avascular capillaries in the rat retina (*arrows*). (Courtesy of Ashay Bhatwadekar, University of Florida.)

There is surprisingly little information currently available on the potential role of autophagy in the pathogenesis of DR, even though there is extensive evidence that (1) autophagy is dysregulated in other diabetic tissues[108,109] and (2) damaged mitochondria are associated with the pathogenesis of DR.[97] We have recently reported that autophagy flux is decreased in the retinal cells of diabetic rats compared to controls.[110] Although DR had been originally thought to be purely a microvascular disease, several new findings indicate a role of inflammation in the form of activation of caspase-1 and IL-1β production in the retina of diabetic rodent models.[111–114] In vitro studies indicate increased caspase-1 activity and IL-1β secretion in Müller cells following exposure to hyperglycemic conditions. Kusner et al. demonstrated that inhibition of caspase-1/IL-1β activation prevented Müller cell loss suggesting a possible role of the caspase-1 dependent death pathway in the diabetic retina namely, pyroptosis.[115]

The impact of cell death in the diabetic retina and the order in which different cell types die during the progression of DR remain

unclear. For example, pericyte dropout and acellular capillaries are observed in many diabetic animal models, yet they do not progress to the sight-threatening proliferative stage. Furthermore, the duration of diabetes in many patients may be 15 years or more before clinical abnormalities are observed in the retina, even though vascular and neuronal cell death will be occurring. A possible explanation for this chronic, rather than acute, attrition in the retina is a low level of cellular replacement from resident and bone marrow-derived stem or progenitor cells.[78] Bone marrow-derived progenitor cells have the capacity to differentiate in a range of retinal vascular and neuronal cell types in response to retinal injury and in the case of the retinal vasculature can repopulate acellular capillaries in rodent models of DR.[116,117] However, these bone marrow-derived progenitors are reduced and appear to be dysfunctional in diabetics and thus repair potential is attenuated.[118,119]

Macular Degeneration

The challenge in studying retinal cell loss mechanisms in AMD is to be able to differentiate between cell loss resulting from disease and that observed in the normal course of aging. However, reports concur that loss of photoreceptors, RPE, and choroidal cells are accelerated in AMD and that this is regional and often focal. Clinically, areas of geographic atrophy (GA) can be observed within the retinal arcades of patients with dry AMD, and these lesions will increase in size with lengthening duration of AMD (Fig. 26.6). Areas of GA show a continuous enlargement over time with a median growth rate of between 1 and 13 mm^2/year and linear progression.[120,121] The considerable variability between patients is unexplained but could reflect genetic susceptibility, diet, smoking, and light exposure. However, there is concordance of disease progression in bilateral GA.[122] RPE loss is normally associated with a reduction in the choroidal vasculature. Evidence of the degree of choroidal capillary loss and its relationship with RPE loss has been elegantly described by McLeod and colleagues.[123] They observed a linear relationship between the loss of RPE and loss of the choriocapillaris in GA. The vascular area was reduced by 50% in

regions of complete RPE atrophy, and there was extreme constriction of remaining viable capillaries. Adjacent to active choroidal neovascularization, choriocapillaris dropout was evident in the absence of RPE atrophy, resulting in a 50% decrease in vascular area. The authors concluded that the close association observed between degenerating RPE and choriocapillaris suggests that, at least in GA, RPE atrophy occurs first, followed by choriocapillaris degeneration.

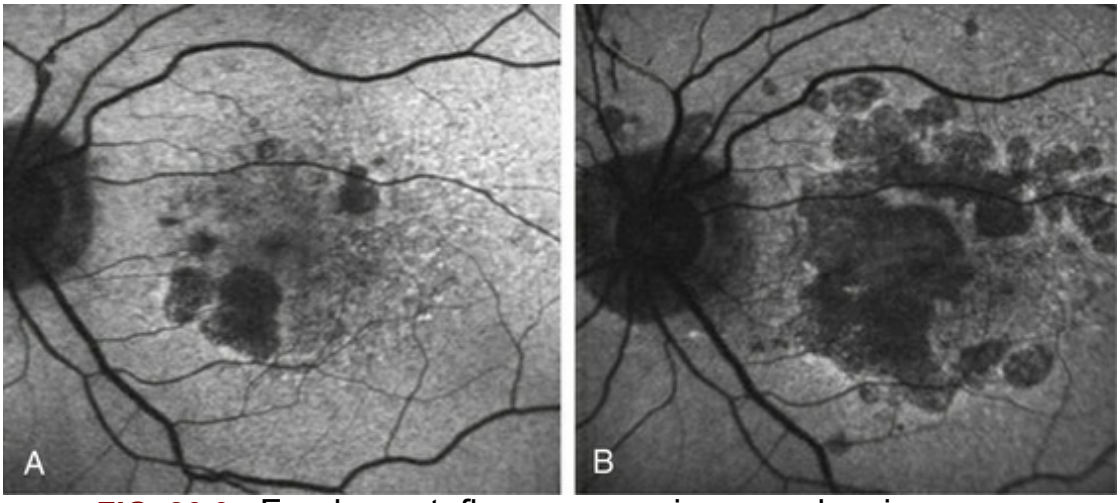

FIG. 26.6 Fundus autofluorescence images showing geographic atrophy in a 74-year-old patient. (A) The patient presented with visual acuity of 20/40 and several areas of retinal pigment epithelial atrophy. (B) Two years later the same patient was re-examined: visual acuity had decreased to 20/200, and there was extensive geographic atrophy, including the foveal area. (Courtesy of Erik Van Kuijk, Ophthalmology and Visual Sciences, UTMB, Galveston, Texas.)

It has largely been considered that photoreceptor cell death occurs as a result of dysfunction or death of the underlying RPE. However, as mentioned earlier, there is significant rod photoreceptor loss as a function of age even in the presence of an apparently healthy RPE.[64] Photoreceptor topography in both dry and wet AMD shows preferential loss of rods over cones.[124] The total number of foveal cones in eyes with large drusen and basal deposits was similar to that of age-matched controls, and the foveal cone mosaic appeared normal. By contrast, cones appeared large

and misshapen with few rods remaining in the parafovea and, by late-stage AMD, virtually all surviving photoreceptors in the macula were cones.[124] In eyes from wet AMD donors, photoreceptors surviving on, or at the margins of, disciform scars were largely cones. Subsequent functional studies supported the histologic evidence for preferential vulnerability of rods in aging and AMD.[125] Although Jackson and colleagues concluded from these histologic studies that photoreceptor loss is secondary to RPE dysfunction or death in AMD, it still remains possible that a photoreceptor abnormality could be the primary effect in AMD and that this leads to subsequent loss of the underlying RPE.

Despite the overwhelming evidence of retinal cell loss in AMD, there are surprisingly few reports on the type of cell death, or the initiating insult(s), in human AMD tissue. Most studies have relied on cell culture assays and animal models with an AMD phenotype, which indicate that cell death occurs primarily by apoptosis. The most detailed report is from Dunaief and colleagues who observed a statistically significant increase in TUNEL-positive apoptotic cells in the inner choroid, RPE, ONL, and INL of AMD donor eyes.[126] This increase in the number of apoptotic cells was evident in 5 of 6 eyes with GA and all eyes with exudative AMD. Interestingly, in eyes with drusen, only a few TUNEL-positive cells were observed in each nuclear layer except the RGC layer. From the same study TUNEL-positive photoreceptors are also evident over an area of disorganized RPE near an edge of atrophy. TUNEL-positive RPE cells were found most commonly near areas of atrophy and occurred more often in AMD eyes than in controls.[126] While an interesting and informative study on cell death in AMD, the number of apoptotic cells seems high, especially in the neural retina, for a slowly progressive condition. By contrast, Xu et al. only observed apoptotic cells in the retina of 4 of 16 AMD donor eyes and the overall numbers of apoptotic cells appeared relatively low.[127] Nordgaard and colleagues undertook proteomic analysis of the RPE from donor eyes at progressive stages of AMD.[128] Several components of apoptotic signaling pathways (αA crystallin, VDAC1, HSP70, GST-π) demonstrated changes in expression early in AMD or changed linearly with AMD progression. Surprisingly, information on death mechanisms in the AMD is scarce, but there is

evidence from cell culture and animal models for both intrinsic and extrinsic apoptosis pathways. FAS-mediated apoptosis has been observed in retinal cells, which could explain the role of inflammation in AMD,[129] and studies have reported oxidative stress-induced apoptosis by the classic mitochondrial route.[130–132] Recent reports indicate the alternative possibility of both RIP kinase-mediated programmed necrosis as well as the NLRP3 inflammasome-mediated sterile inflammation in RPE subjected to oxidative stress. Hanus et al. reported that oxidative stress-mediated RPE death in vitro could be effectively prevented when RIP kinases that are involved in programmed necrosis are inhibited.[133] The recent finding of Alu RNA accumulation leading to RPE cytotoxicity in geographic atrophy suggests a completely new mechanism of RPE degeneration.[134] Although Alu RNA accumulation stimulates "sterile inflammation" via the NLRP3 inflammasome/MyD88 signaling in the RPE, follow-up experiments suggested that the RPE degeneration does not ensue by the expected caspase-1 mediated pyroptosis.[135] More recent reports suggest the role of programmed necrosis in Alu RNA-mediated cytotoxicity.[133] We and others have recently reported that autophagy flux may be dysregulated in the RPE in AMD.[136–142] Studies in mouse models of AMD as well as human AMD donor samples suggest a decline in established autophagy markers while there is a marked accumulation of p62/Sqstm1, which (amongst its other functions) is a cargo for degradation via autophagy.[137,138] The decline in autophagy is likely due to multiple factors affecting autophagic initiation and/or the fusion of autophagosomes with lysosomes. These include lipofuscin accumulation, susceptibility to oxidative stress, mitochondrial damage, and lysosomal dysregulation, all of which have a strong association with AMD.[140,143] We and others have shown that inhibition of autophagy in RPE leads to lipofuscin accumulation.[138,144] To what extent changes in autophagy flux reflect alterations in the formation or elimination of autophagosomes remains to be determined, and it is unclear whether or not these changes are a cause or consequence of AMD. Lipid peroxidation products reduce autophagy flux and increase lipofuscin accumulation in cultured RPE cells.[145] An increase in lysosomal pH that is associated with the lipofuscin

constituent A2E[146] may impair autophagosome–lysosome fusion, as may the accumulation of lipofuscin granules within the lysosomal vacuome. It has been reported that drusen formation may reflect an increase in both mitochondrial damage and autophagy in the RPE.[142] The researchers speculated that increased autophagy and the release of intracellular proteins via exosomes by the aged RPE may contribute to the formation of drusen. It is important to note that there is substantial cross-talk between autophagy and proteasomal degradation pathways that may also affect the status of the RPE.[136] Nevertheless, elements of the autophagic pathway have been shown to be required for phagocytic degradation of photoreceptor outer segments within the RPE.[147] Silencing of RB1CC1/FIP200, an essential protein for autophagy initiation, results in degeneration of mouse RPE.[139] The current overall opinion on the role of autophagy in AMD is that it is a housekeeping process absolutely essential for RPE function and survival rather than a mode of cellular demise.

A key point to be considered is that cellular repair, cellular replacement, and damage control are critical in retinal homeostasis and a declining antioxidant system together with increased oxidative damage will play a major etiologic role in AMD, and that once the threshold for damage is reached, multiple cellular processes for repair and regeneration will be impacted.[148–151]

Retinal Detachment

Retinal detachment resulting from full-thickness retinal breaks, subretinal exudation, and/or vitreoretinal traction is a common cause of photoreceptor loss.[152] Cell death is highly dependent on the area and duration of the detachment. Analysis of tissue samples from patients with retinal detachment showed significant numbers of apoptotic cells by 24 hours, which peaked by 2 days and dropped to a low level by 7 days after detachment.[153] These observations have been largely supported by experimental retinal detachment in cats and rats, both of which show a peak of apoptosis between 1 and 3 days postdetachment, which then declines.[154,155] Some apoptotic cells were still evident at 28 days postdetachment. However, there is some debate as to whether apoptosis following

retinal detachment occurs via the intrinsic or extrinsic pathways.[152,156,157] The enzymatic activities of both initiator and effector caspases are elevated in rat retinas following detachment.[158] Paradoxically, pan-caspase inhibition does not completely reverse photoreceptor degeneration postdetachment indicating a possible role of additional caspase-independent cell death modes.[154] For example, RIP3 expression is dramatically elevated in retina after detachment suggesting a role of programmed necrosis.[159] Interestingly, retina RPE separation in rats causes a Fas-dependent activation of autophagy in injured photoreceptors and, if autophagy is inhibited, the time course and number of apoptotic cells is accelerated.[160] Furthermore, prolonging autophagy in detached retina by inhibiting upregulated calpain 1, which cleaves Atg5, can reduce the number of apoptotic cells.[161] Thus it appears that autophagy is activated to regulate the level of receptor apoptosis. The readers are advised to read an excellent review on the subject by Murakami et al.[162]

Retinal Dystrophies

Retinal dystrophies encompass a heterogeneous group of inherited conditions, with more than 100 genes or loci identified to date.[163] The most common subtype is retinitis pigmentosa (RP), which is characterized by progressive death of retinal rod and cone photoreceptors in which the disease proceeds toward reduction of peripheral field with tunnel vision and finally loss of sight.[163,164] One of the major barriers in the comprehensive identification of the degenerative mechanisms underlying retinal dystrophies is the involvement of multiple causal genes in their pathogenesis.[165] The mode of rod cell death in several animal models of RP suggests death by apoptosis, which is in agreement with findings in RP retinas from donor eyes[166] (reviewed by Travis[167]). Cone cells usually die as a secondary response to rod cell death, possibly because they depend on rod-secreted neurotrophic factors for survival.[70,72]

Studies of apoptotic mechanisms in the photoreceptors of RP models imply the involvement of caspase-dependent as well as independent pathways.[168–170] DNA fragmentation was a regular

feature encountered in the mouse models, indicating that photoreceptors in mouse models die of apoptosis. Administration of caspase-3 inhibitors inhibited photoreceptor apoptosis in the tubby mouse model of Usher syndrome.[171] Caspase-independent modes of apoptosis may involve calpain and Ca^{2+} excess in RP.[172] In recent years it has been suggested that, although apoptosis is the primary cell death mode, other modes of cell removal could be involved, including autophagy and complement-mediated lysis.[173] Investigation of different cell death pathways in three independent mouse models of photoreceptor degeneration – the *rd/rd* mouse, the *rds/rds* mouse, and the light-damage model in albino mice – shows that, apart from apoptotic cell death, several oxidative stress markers as well as elements of the autophagic and complement pathways are upregulated. While the induction of oxidative stress response genes is early, the induction of autophagy was only seen in damaged retinas when compared to controls.[173] The authors concluded that autophagy specifically removes damaged photoreceptors from the retina. However, the data may also be interpreted as an attempt in the damaged retina to salvage the photoreceptors from initial stress which, when overwhelming, gives rise to autophagic death. The evidence of upregulation of high-mobility group box 1 (HMGB1) protein in human eyes with retinal detachment suggests that necrosis could also be a mode of photoreceptor death.[174] It could well be this mode of cell death that accounts for some of the caspase-independent photoreceptor death pathways that have hitherto been thought to be apoptosis. Recent findings further support the theory that cone photoreceptors die by a programmed necrotic pathway. Murakami et al. showed that in $Rip3^{-/-}$ *rd10* mice, cone photoreceptors do not degenerate although the rods die at the same rate as in control *rd10* mice.[175] Furthermore, RIP kinase inhibitor prevented cone cell degeneration in *rd10* mice. It is possible that necrosis is initiated in the photoreceptors as a secondary response to apoptosis in rod cells. Nevertheless, the heterogeneity of RP and similar retinal dystrophies necessitates the understanding of the earliest mechanisms of disease inception such that customized treatments may be catered according to the nature of disease pathology in a patient. Attempts to block cell death by one strategy may prove to be futile as the protective effect may be

successful for only a short duration, after which the cell might proceed through another death mode.

Light Damage

The retina is vulnerable to damage from ultraviolet radiation, visible light (400–700 nm), and infrared radiation.[77,176,177] The extent and type of damage are highly dependent upon the wavelength, power, duration, area of coverage, cumulative exposure, and location (e.g., macular versus periphery). Light-induced retinal damage can occur via at least one of three mechanisms: (1) mechanical (high irradiances of short duration that cause sonic shock waves disrupting the tissue irreversibly); (2) photothermal (when incident energy is trapped, causing a rise of temperature 10°C or more); and (3) photochemical (shorter-wavelength visible light is absorbed and dissipated away, causing molecular alterations).[77] Retinal photodamage is highly dependent on the presence of chromophores, of which the most obvious are the visual pigments, and in most species prolonged intense light exposure will lead to significant photoreceptor cell damage.[178] Other important chromophores include hemoglobin, melanin, lipofuscin, macular pigment, and flavins.[77] Photochemical damage has been the most extensively studied form of light damage because it causes retinal damage within the intensity range of ambient visible light.[77,179,180] There are two well-defined types of retinal light damage. Class 1 damage has an action spectrum that is identical to the absorption spectrum of the visual pigment and the initial damage is in the photoreceptors.[77,179,181] Class 2 damage has an action spectrum that peaks at shorter wavelengths, is generally confined to the RPE, and is often referred to as the blue light hazard.[77,179,181]

Most mechanistic studies on retinal photochemical damage have been undertaken in experimental animal models and all show that cell death occurs via apoptosis. Excess light has been shown to trigger apoptosis in rat retinas.[182,183] Low-intensity light exposure for long durations as well as intense light exposure (3000 lux) for short durations up to 2 hours can cause severe photoreceptor degeneration by apoptosis followed by RPE degeneration.[184,185] Higher intensity light (5000 lux for 1 hour) has been shown to

induce RPE permeability and increased secretion of vascular endothelial growth factor (VEGF), which when blocked is neuroprotective to the photoreceptors.[186] Both types of retinal photodamage, induced by exposure to either low- or high-intensity light, are dependent on the presence of, and regeneration of, rhodopsin in the retina.[187–191] The extent of photodamage correlates to the amount of rhodopsin present in the retina prior to the light damage,[192,193] although direct evidence of rhodopsin causing damage is absent. Several rhodopsin intermediates have been implicated as mediators of photo-oxidation, in particular all-*trans*-retinal, which accumulates in the photoreceptor membrane due to decreased reduction by retinol dehydrogenase.[194] Decrease of intracellular calcium levels during the phototransduction cycle has also been suggested to contribute to rhodopsin-mediated injury causing photoreceptor apoptosis.[195] Light-induced photoreceptor apoptosis can either be caspase-mediated or caspase-independent.[196,197] Cellular response will vary according to lighting conditions and all of the discovered pathways may contribute to photoreceptor cell fate depending on the prevalence and type of light damage during an individual's lifetime, contributing to a difference of opinion regarding the mechanisms of cell death observed, and the involvement of caspase and signal transduction pathways. Melanosomes and lipofuscin granules are the most significant fluorophores implicated in RPE damage. Irradiated lipofuscin granules or their constituents can generate high levels of ROS.[198–200] Several models of retinal degeneration in vitro and in vivo demonstrate the role of calcium in inducing cell death by activating degradative proteases such as calpain.[201,202] Adaptor protein 1 (AP-1) signal transduction has also been implicated in bright light-induced photoreceptor death where there is an increase of AP-1 gene expression.[203] Light can also damage RGCs[204] and a subpopulation of RGCs contain the chromophore melanopsin, suggesting that light damage could impact this specific subset of RGCs and contribute to the pathogenesis of glaucoma.[205] The role of autophagy in retinal light damage has only received limited attention, but Kunchithapautham and colleagues have shown that upregulation of autophagy can protect against light damage and oxidative stress in the retina.[206–210]

Therapeutic Options

Neuroprotection

Neuroprotection offers a promising approach for preventing or slowing retinal cell loss and is broadly defined as the use of therapeutic agents to prevent, hinder, and, in some instances, reverse neuronal cell death whatever the primary injury.[207,211,212] The strategies for neuroprotection vary considerably dependent upon the target cell, the nature of the factors initiating cell loss, and the stage of disease. Clearly, the ideal time for neuroprotection is in the early stages of the disease before any significant cell death has occurred. Three broad approaches have evolved: (1) blocking the pathways involved in the cellular damage (e.g., antioxidants); (2) inhibiting the cell death path directly (e.g., upregulation of Bcl-2 and inhibition of caspases); and (3) treatment with neurotrophic factors that suppress the intrinsic apoptosis pathway (e.g., brain-derived neurotrophic factor (BDNF), glial-derived neurotrophic factor (GDNF), pigment epithelial-derived factor (PEDF)). A summary of potential neuroprotective agents, their retinal cell targets, and their proposed mechanisms of action is shown in Table 26.1.

TABLE 26.1

A Summary of Potential Neuroprotective Agents, Their Retinal Cell Targets, and Their Proposed Mechanisms of Action

Target Cell	Mechanistic Target	Therapeutic Approaches
Retinal ganglion cells	Excitotoxicity	Memantine, taurine
	Oxidative stress	Vitamin E
	Mitochondrial damage	Coenzyme Q10
	Neurotrophin deprivation	BDNF, gene therapy
Photoreceptors	Apoptosis	Survival and growth factors (e.g., BDNF, GDNF)
RPE	Apoptosis	Survival and growth factors
	Autophagy	Rapamycin
	Oxidative damage	Antioxidants, lutein, zeaxanthin, zinc
	Lipofuscin system	Reducing the retinoid cycle, glutathione-S-transferase
	Mitochondrial damage	Antioxidants, resveratrol
	Lysosomal system	Elevated pH (A_{2A} adenosine receptor agonist)
	Bruch's membrane	Subthreshold laser, MMP upregulation, microbial enzymes

Choroid	Endothelial cell loss	Growth factors (e.g., VEGF)
Inflammation	Alternative complement pathway	Complement pathway inhibitors

BDNF, brain-derived neurotrophic factor; GDNF, glial-derived neurotrophic factor; MMP, matrix metalloproteinase; RPE, retinal pigment epithelium; VEGF, vascular endothelial growth factor.

Light damage in rodents, which results in extensive photoreceptor and RPE cell loss, has been extensively studied in the search for effective neuroprotective agents.[176] Light-induced photoreceptor apoptosis is dependent on the availability of 11-*cis* retinal for rhodopsin regeneration.[187] Acute bright light-induced photoreceptor apoptosis involves activation of nitric oxide synthase (NOS) and generation of nitric oxide (NO), increased intracellular calcium, oxidative damage, and alterations in mitochondrial function.[176,213] Inhibition of NOS activity by NG-nitro-L-arginine methyl ester (LNAME)[213,214] or application of the calcium channel blockers D-diltiazem, nilvadipine, or nicardipine[197] protected photoreceptor cells following cell death in light-damaged retinas. Inhibition of the apoptotic cascade by reduction of the proapoptotic Bcl-2 family members Bax and Bak also protects the retina against light damage.[215] The use of antioxidants that quench ROS such as dimethylthiourea and *N*-phenyl-2-naphthylamine and the administration of exogenous neurotrophic factors including BDNF, ciliary neurotrophic factor (CNTF), basic fibroblast growth factor (bFGF), erythropoietin (Epo), and PEDF have all been shown to be protective against light damage (reviewed by Wenzel et al.[176]). bFGF plays an important role in the endogenous defense against stress of retinal cells. Preconditioning with light[216] or ischemic preconditioning[217,218] increases the expression of bFGF and protects retinal cells against damaging doses of light or increased intraocular pressure. The neuroprotective effect could be enhanced by a combination of bFGF and PEDF.[219] In contrast, no protection resulted against constant light exposure for 1 week when bFGF was expressed locally from a transgene delivered by an adeno-associated viral vector[220] or a simian immunodeficiency viral vector.[221] However, intravitreal injection of recombinant BDNF protein or its release from transgenic cell transplants[222] protects the retina against 1–2 weeks of constant light exposure.

Inhibition of apoptotic pathways in a light-damaged neuron is

relatively straightforward as the cell is otherwise healthy. However, in retinal cells harboring mutations, as is the case in retinal dystrophies, the cell has more than just the apoptotic cascade to address as the cause of the dystrophy and associated cell death will remain unless also treated. Photoreceptors are the target cells as these are the predominant cell type lost in the retinal dystrophies. Studies in animal models with inherited retinal diseases have used similar strategies to those described above for light damage. While considerable success has been achieved, this has not translated to clinical care and gene therapy to reverse the mutation, as in Leber congenital amaurosis, is perhaps a preferable option.[223] Both PEDF and CNTF have shown considerable promise in slowing photoreceptor degeneration, whether provided by intraocular injection or gene transfer, in rd1, rd2, rds P216L, rhodopsin S334ter, and P23H rodent models of inherited degeneration.[224–228] CNTF, released by engineered cells, slowed retinal degeneration in the rcd1 dog model[229] and, after intravitreal injection, in an autosomal dominant feline model of rod–cone dystrophy.[230] Neurotrophin-3 can induce upregulation of bFGF, and thereby neuroprotection, by activation of TrkC in Müller cells.[231] Viral delivery of a BDNF transgene delayed degeneration induced by the Q344ter mutation in rhodopsin[232] and prolonged release of BDNF from transgenic cell transplants into the eye slowed degeneration in RCS rats.[233] Capsase-3 inhibition is protective in the *rd1* degeneration by delaying cell death[234,235] and preservation of retinal morphology.[236] Caspase-3 inhibitors also provided protection in two other models of inherited retinal degeneration: the S334ter rat[169] and the tubby mouse.[171] Alternative approaches that have reduced photoreceptor loss and slowed the progression of retinal degeneration in animal models include (1) overexpression of the X-linked inhibitor of apoptosis using gene therapy;[237,238] (2) sustained intravitreal delivery of fluocinolone acetonide, which suppresses microglial activation and inflammation;[239] (3) GDNF either given by subretinal injection or conjugated to nanoparticles;[240] and (4) neuroprotectin D1 (NPD1).[130]

Rodent and canine models of glaucoma have shown that agents that block glutamate excitotoxicity, prevent mitochondrial dysfunction, reduce oxidative stress, or enhance neurotrophic

factors all decrease or prevent the loss of RGCs (Table 26.1). The *N*-methyl-D-aspartate receptor antagonist was shown to be a highly effective neuroprotective agent in animal models of RGC death (reviewed by Cheung et al.[241] and Danesh-Meyer[242]). However, the outcome of clinical trials was inconclusive, though a trend for improvement was observed. An alternative agent is brimonidine tartrate, which is a highly selective alpha-2-adrenergic agonist that increases RGC survival in animal models.[243] Coenzyme Q10, which is an essential cofactor of the electron transport chain, has been shown to have some neuroprotective effect on RGCs based on its antioxidant properties.[244] Treatment with exogenous neurotrophins such as BNDF, nerve growth factor, and CNTF have all been shown to slow the loss of RGCs but not to inhibit RGC death in the long term. To improve outcomes, researchers have investigated sustained release of neurotrophic factors via either gene therapy[245] or encapsulated cell technology, which allows the intravitreal implantation of a chamber containing live cells programmed to release CNTF.[246] More direct antiapoptotic strategies have included activation of the Bcl-2 pathways using cilostazol or 5-*S*-GAD, which increases RGC survival in animal models.[247,248] The retina (and particularly the photoreceptors) is rich in taurine,[249,250] a sulfonic acid that has been widely studied for its cytoprotective properties.[251] Taurine deficiency has been associated with retinal neurodegeneration.[252] The beneficial effect of taurine results from a number of modes: (1) antioxidant properties; (2) inhibition of glutamate-induced calpain activation; (3) inhibition of Ca^{2+} influx through voltage-gated calcium channels; and (4) prevention of Bcl-2 downregulation. It has also been shown that taurine may prevent apoptosome activation that results in intrinsic apoptosis activation.[253] Recent reports suggest taurine to be neuroprotective against RGC degeneration and that taurine supplementation increases RGC density in rodent models of glaucoma and retinitis pigmentosa.[254]

RPE cell loss is a hallmark feature of dry AMD. In vitro studies have identified a plethora of agents capable of either directly inhibiting apoptosis with, for example, caspase inhibitors, or indirectly by neutralizing the initiating factors leading to cell death. Macular carotenoids, NPD1, eEpo, resveratrol, and PEDF have all

been shown to confer protection against oxidative stress-induced apoptosis.[255–262] αB crystallin is apically secreted within exosomes by polarized human RPE and provides neuroprotection to adjacent cells.[263] An alternative approach has been to upregulate antioxidants or molecular chaperones to cope with the increased oxidative stress.[264] Neurotrophic protection of the RPE has been more difficult to model in vivo because there are no reliable models of GA. However, the Age-Related Eye Disease Study demonstrated that oral supplementation with high levels of antioxidants and zinc can reduce the risk of disease progression to advanced AMD.[265] With reports establishing necrosis as a possible mode of RPE degeneration,[133] use of inhibitors that target molecules crucial to both apoptosis and necrosis or the use of a synergistic mixture of apoptosis and necrosis inhibitors may be considered as novel therapeutic modes.

The strategies described above are likely to be equally effective in other retinal conditions resulting in cell death. Imai and colleagues emphasize the importance of exogenous neurotrophic factors in reducing cell loss in DR[266] while BDNF, bFGF, and inhibition of the FAS receptor impede apoptosis following retinal detachment.[154,156]

Modulating Autophagy

As discussed earlier, autophagy is dysregulated in a number of retinal conditions. However, dependent on the type and stage of the disease, this dysregulation could reflect as decreased or increased autophagy. A similar trend is also observed in cancer and neurodegenerative diseases. Autophagy plays a role in tumor suppression or oncogenesis but can desensitize cells to chemotherapeutic agents.[267] Similarly, upregulation of autophagy can protect against Huntington's disease in mouse models, whereas enhancing autophagosome formation in Alzheimer's disease can exacerbate the accumulation of Aβ.[267] Therefore any therapy must ensure the correct balance of autophagy flux is attained for the targeted disease or cell type.

Many autophagy-related proteins and signaling molecules have been implicated in a number of events of autophagy, including signaling, sequestration, maturation, and degradation. The primary

regulation of autophagy proceeds by mTOR, GCN2, and PI3K-III signaling pathways. Autophagy is negatively regulated by mTOR and Bcl-2/Bcl-xL and positively regulated by PI3K class III and GCN2/eIF2α. Compounds that inhibit mTOR phosphorylation (rapamycin) or Bcl-2 interaction with Beclin-1 (ABT737) promote autophagy.[268] PI3K-III can be activated by inhibiting the interactions between Bcl-2 and Beclin/Atg6 or by overexpressing Beclin-1 or Beclin-1-BD (Bcl-2 binding defective mutant) and suppression by Vps34 inhibitors, 3-methyladenine, or wortmannin.[269,270] Several mTOR-dependent and mTOR-independent agents have been identified that stimulate autophagy. Rapamycin is a well-established compound for inducing autophagy and attenuating neuronal cell death in a number of in vitro and in vivo experimental models. Other stimulators of autophagy include lithium and trehalose, which enhance autophagy via an mTOR-independent mechanism.[271] Unfortunately, despite their potency, rapamycin and lithium have significant side-effects that lessen enthusiasm for clinical application in chronic neurodegenerative diseases.[272,273] In an attempt to address this, researchers are screening for small-molecule enhancers of rapamycin (SMERs) and small molecule inhibitors of rapamycin (SMIRs) with less cytotoxicity. The efficacy and specificity of compounds that activate autophagy in an mTOR-independent fashion have yet to be established.[272,273] Gene therapy is also a possibility and overexpression of Atg7 can protect against anoxia/reoxygenation injury.[274]

Given the realization of the importance of autophagy in cancer and neurodegenerative diseases, there has been an extensive effort to identify potential therapeutic regulators of autophagy. Those under development include HDAC inhibitors, mTOR inhibitors, BH3 domain mimetics, glycolytic inhibitors, inositol-lowering agents, and protein kinase inhibitors.[271,274–276] Of particular interest in cancer has been the use of the antimalarial drug hydroxychloroquine (HCQ), which serves to inhibit autophagy by perturbing lysosomal function. HCQ is now being assessed in combination with a number of chemotherapy agents in phase I and II clinical trials.[274,275] However, it has long been recognized that HCQ can cause ocular toxicity, with the most serious being an irreversible retinopathy. The dosage parameters associated with

retinopathy are still uncertain, but it has been suggested that, for doses of HCQ less than 6.5 mg/kg, the incidence of retinopathy is minimal.[277] Nevertheless, some clinical trials are testing dosages that exceed these levels. Furthermore, shutting down lysosomal functions, whether it be autophagy or endocytosis, can dramatically alter cellular homeostasis and defense.

Proteins other than the autophagic pathway proteins have been implicated in autophagy. Caspases and calpains play key roles in cleavage and activation or inactivation of autophagy proteins (summarized by Kaminskyy and Zhivotovsky[278]). Cross-talk between the autophagy and apoptosis pathways is regulated by caspase cleavage of Beclin-1[279] and also by p62/Sqstm1-Keap1 signaling.[280] Similarly, modulation of the Sirt-1-Foxo pathway also modulates autophagy.[281,282] Modulating reactive oxygen species levels with antioxidant compounds such as resveratrol and curcumin or overexpressing antioxidant enzymes can negatively modulate autophagy. Quenching reactive oxygen species will decrease mitochondrial damage and autophagy initiation. In addition, a lowering of reactive oxygen species will preserve the activity of lysosomal enzymes (reviewed by Scherz-Shouval and Elazar[283]). It is important to keep in mind that, when one type of autophagy is altered, the other types will also be affected. Chronic blockage of CMA promotes upregulation of macroautophagy,[284] whereas acute blockage leads to macroautophagic dysregulation.[285] Cells respond to blockage of macroautophagy by increasing CMA.[285] Acute blockage of the proteasome upregulates macroautophagy,[286] whereas chronic blockage leads to macroautophagic dysregulation.[287] Some subunits of the proteasome are degraded by CMA,[288] which may explain why blockage of CMA is associated with proteasome dysregulation.[284] Interactions of microautophagy with other proteolytic systems remain undiscovered. Futhermore, recent findings suggest that autophagy may be inhibited in AMD both in the initiation as well as in the lysosomal maturation.[137,138] Enhancing autophagy in the initiation stages may not prove to be beneficial if lysosomal function itself is compromised. Hence, therapeutic strategies based in autophagy-modulation in retinal diseases like AMD need to be carefully designed keeping the lysosomal aspect under

consideration.

Cellular Replacement

Replacement of dead or dysfunctional cells in the retina is vital to preserve and/or restore tissue and organ function. While amphibians and fish exhibit robust retinal regeneration, arising from the RPE and intrinsic Müller glial cell-derived progenitors respectively, this is not observed in mammals, where cellular replacement in the retina is limited even in response to injury.[289–294] A number of endogenous retinal stem and progenitor populations have been reported but many, such as those observed in the ciliary margin zone, remain controversial.[290] Progenitor gene expression in Müller glia following retinal injury has been observed in rodents, for example expression of bipolar and photoreceptor markers,[294] though there is no definitive evidence that these cells have regenerative function. The bone marrow may be an alternative source of endogenous reparative cells. Using chimeric mice transplanted with bone marrow cells expressing green fluorescent protein, it has been shown that bone marrow-derived cells would home to the site of retinal injury and differentiate into astrocytes, macrophages/microglia, endothelial cells, pericytes, and RPE.[116,117] However, recruitment and integration is limited.

Transplantation of RPE cells has been extensively investigated, as these cells can be readily generated from embryonic stem cells (ESC) or induced pluripotent stem cells (iPSC).[295–297] ESC and iPSC-derived cells have been successfully transplanted into animal models of retinal degeneration and have been shown to restore vision. Additionally, a number of phase I/II clinical trials have been initiated involving transplantation of RPE derived from hESC and hiPSC in humans. Schwartz et al.[298] published preliminary reports of two phase I/II clinical trials involving hESC-derived RPE transplant in patients with Stargardt macular dystrophy and AMD.[299] The cells were not found to exhibit abnormal hyperproliferation, and some recovery of vision was observed, though limited.[298,299] An ongoing clinical trial in Japan investigating transplant of RPE sheets as opposed to cells may result in greater recovery of vision.[300] Central nervous system stem cells (HuCNS-

SC) have been found to protect the photoreceptor layer following subretinal injection into rats[301] and are currently being investigated in a phase I/II clinical trial (NCT01632527).

While a promising strategy, there remain concerns that (1) ESC may result in teratoma formation;[302] (2) iPSC contain protein-coding point mutations;[303] (3) success with RPE transplantation in humans has been modest;[298,299,304,305] and (4) transplantation is normally into a severely degenerated retina with late-stage disease.[304,305] Replacing the RPE may be insufficient in late-stage disease, as the overlying photoreceptor layer and neural retina are likely already too dysfunctional for visual recovery as a result of RPE regeneration alone. Additionally, subretinal transplant of cells may also lead to damage, such as intraocular hemorrhage or retinal detachment. To overcome this, a recent study infected bone marrow-derived cells ex vivo with lentiviral vector expressing the RPE-specific gene *RPE65* and injected these cells into the circulation of mice in which the RPE had been destroyed by sodium iodate.[306] These systemically delivered cells homed to the neural retina/Bruch's membrane interface in large numbers and showed restoration of a functional RPE layer, with typical RPE phenotype, including coexpression of another RPE-specific marker, CRALBP, and photoreceptor outer-segment phagocytosis. Most importantly, retinal degeneration was prevented and visual function was restored to levels similar to those found in normal animals.[306]

Critically, the systemic delivery of the modified cells is noninvasive, allowing for delivery without disruption of the subretinal space necessary for transplantation of ESC, iPSC, and HuCNS-SC-derived cells. Due to the decreased risk, if applicable in humans, systemic delivery of therapeutic cells potentially allows for treatment in the early stages of disease where damage to the neural retina is limited. Human bone marrow-derived $CD34^+$ cells have been shown to be tolerated in NOD/SCID mice and in humans following intravitreal injection in two phase I/II clinical trials, with no worsening of vision and no evidence of intraocular inflammation.[307–309] Incorporation of the cells into the damaged macula was also observed, indicating a promising therapeutic potential for bone marrow-derived cells in RPE replacement.[308]

Repair of the neural retina is more complicated due to the need to

form the requisite neural connections to perform vision. The most cited study is that of MacLaren and colleagues, who showed that donor cells can integrate into the adult or degenerating mouse retina provided the donor cells are derived from the developing retina at a time coincident with the peak of rod genesis.[310] Importantly, these transplanted cells integrated and differentiated into functional rod photoreceptors that formed synaptic connections, and improved visual function in the host animals. Human ESC or iPS have been shown, under the right conditions, to be able to differentiate into rods and cones[311,312]and when transplanted into the adult mouse retina can differentiate into photoreceptors and restore light responses in Crx-deficient mice.[313] Since it is not the intention of this chapter to provide a detailed review of regenerative medicine for retinal repair, the reader is pointed to the following reviews[290,311] and Chapter 37 (Stem cells and cellular therapy).

Conclusions

Cell death is a major feature of retinal injury and disease. Preventing cell loss or replacing the lost cells is now becoming a realistic option with a number of pharmacologic agents in clinical trials and Food and Drug Administration approval for cell replacement therapies. The last 20 years have seen an exponential increase in our knowledge of cell death pathways in the retina and the identification of targets for therapeutic intervention. However, while considerable improvement has been observed in animal models of retinal cell loss, translation into the clinic has, to date, only shown modest success. It is likely that different approaches will be required for different retinal conditions as preserving a cell with a debilitating genetic mutation is likely to be detrimental to the retina, while preventing apoptosis of normal cells following retinal detachment or light damage would be beneficial. Similarly, autophagy has been shown to play a protective role in a number of retinal diseases, but the balance is critical as excess autophagy will lead to removal of essential organelles and loss of cell function while too little autophagy will lead to the buildup of damaged organelles. A further problem is that all these therapeutic

approaches will remain limited if the initiating factors resulting in cell loss are not also addressed. Finally, we have to address the clinical limitation that intervention is often not until the late stage of disease when extensive cell death has already taken place, and thus we need to consider strategies for treating much earlier if we are to prevent significant retinal cell loss. Despite these hurdles, our ever-increasing understanding of retinal pathogenesis and cell death, together with improved pharmacologic screening for novel therapeutic agents, will almost certainly result in major advances in clinical treatment over the next decade.

References

1. Kroemer G, El-Deiry WS, Golstein P, et al. Classification of cell death: recommendations of the Nomenclature Committee on Cell Death. *Cell Death Differ*. 2005;12(Suppl. 2):1463–1467.
2. Kroemer G, Galluzzi L, Vandenabeele P, et al. Classification of cell death: recommendations of the Nomenclature Committee on Cell Death 2009. *Cell Death Differ*. 2009;16(1):3–11.
3. Green DR. *Means to an end: apoptosis and other cell death mechanisms*. Cold Spring Harbor Laboratory Press: New York; 2011.
4. Green DR, Reed JC. *Apoptosis: physiology and pathology*. Cambridge University Press: Cambridge; 2011.
5. Pereira WO, Amarante-Mendes GP. Apoptosis: a programme of cell death or cell disposal? *Scand J Immunol*. 2011;73(5):401–407.
6. Koff JL, Ramachandiran S, Bernal-Mizrachi L. A time to kill: targeting apoptosis in cancer. *Int J Mol Sci*. 2015;16(2):2942–2955.
7. Forcet C, Ye X, Granger L, et al. The dependence receptor DCC (deleted in colorectal cancer) defines an alternative mechanism for caspase activation. *Proc Natl Acad Sci USA*. 2001;98(6):3416–3421.
8. Nicolini V, Cassinelli G, Cuccuru G, et al. Interplay between Ret and Fap-1 regulates CD95-mediated apoptosis in

medullary thyroid cancer cells. *Biochem Pharmacol*. 2011;82(7):778–788.
9. Stupack DG, Cheresh DA. Get a ligand, get a life: integrins, signaling and cell survival. *J Cell Sci*. 2002;115(Pt 19):3729–3738.
10. Fombonne J, Bissey PA, Guix C, Sadoul R, Thibert C, Mehlen P. Patched dependence receptor triggers apoptosis through ubiquitination of caspase-9. *Proc Natl Acad Sci USA*. 2012;109(26):10510–10515.
11. Golstein P, Kroemer G. Cell death by necrosis: towards a molecular definition. *Trends Biochem Sci*. 2007;32(1):37–43.
12. Hitomi J, Christofferson DE, Ng A, et al. Identification of a molecular signaling network that regulates a cellular necrotic cell death pathway. *Cell*. 2008;135(7):1311–1323.
13. Humphries F, Yang S, Wang B, Moynagh PN. RIP kinases: key decision makers in cell death and innate immunity. *Cell Death Differ*. 2015;22(2):225–236.
14. Zhivotovsky B, Orrenius S. Cell death mechanisms: cross-talk and role in disease. *Exp Cell Res*. 2010;316(8):1374–1383.
15. Liu Y, Levine B. Autosis and autophagic cell death: the dark side of autophagy. *Cell Death Differ*. 2015;22(3):367–376.
16. Parzych KR, Klionsky DJ. An overview of autophagy: morphology, mechanism, and regulation. *Antioxid Redox Signal*. 2014;20(3):460–473.
17. Galluzzi L, Vitale I, Abrams JM, et al. Molecular definitions of cell death subroutines: recommendations of the Nomenclature Committee on Cell Death 2012. *Cell Death Differ*. 2012;19(1):107–120.
18. Yousefi S, Perozzo R, Schmid I, et al. Calpain-mediated cleavage of Atg5 switches autophagy to apoptosis. *Nat Cell Biol*. 2006;8(10):1124–1132.
19. Galluzzi L, Vanden Berghe T, Vanlangenakker N, et al. Programmed necrosis from molecules to health and disease. *Int Rev Cell Mol Biol*. 2011;289:1–35.
20. Haanen C, Vermes I. Apoptosis: programmed cell death in fetal development. *Eur J Obstet Gynecol Reprod Biol*. 1996;64(1):129–133.
21. Chen Y, Klionsky DJ. The regulation of autophagy –

unanswered questions. *J Cell Sci*. 2011;124(Pt 2):161–170.
22. Hubbard VM, Valdor R, Macian F, Cuervo AM. Selective autophagy in the maintenance of cellular homeostasis in aging organisms. *Biogerontology*. 2012;13(1):21–35.
23. Arias E, Cuervo AM. Chaperone-mediated autophagy in protein quality control. *Curr Opin Cell Biol*. 2011;23(2):184–189.
24. Mijaljica D, Prescott M, Devenish RJ. Microautophagy in mammalian cells: revisiting a 40-year-old conundrum. *Autophagy*. 2011;7(7):673–682.
25. Mizushima N, Levine B, Cuervo AM, Klionsky DJ. Autophagy fights disease through cellular self-digestion. *Nature*. 2008;451(7182):1069–1075.
26. Youle RJ, Narendra DP. Mechanisms of mitophagy. *Nat Rev Mol Cell Biol*. 2011;12(1):9–14.
27. Yang Z, Klionsky DJ. Mammalian autophagy: core molecular machinery and signaling regulation. *Curr Opin Cell Biol*. 2010;22(2):124–131.
28. Wong E, Cuervo AM. Autophagy gone awry in neurodegenerative diseases. *Nat Neurosci*. 2010;13(7):805–811.
29. Ohsumi Y. Historical landmarks of autophagy research. *Cell Res*. 2014;24(1):9–23.
30. Hailey DW, Rambold AS, Satpute-Krishnan P, et al. Mitochondria supply membranes for autophagosome biogenesis during starvation. *Cell*. 2010;141(4):656–667.
31. Ravikumar B, Moreau K, Jahreiss L, Puri C, Rubinsztein DC. Plasma membrane contributes to the formation of pre-autophagosomal structures. *Nat Cell Biol*. 2010;12(8):747–757.
32. Ravikumar B, Moreau K, Rubinsztein DC. Plasma membrane helps autophagosomes grow. *Autophagy*. 2010;6(8):1184–1186.
33. Dunn WA Jr. Studies on the mechanisms of autophagy: formation of the autophagic vacuole. *J Cell Biol*. 1990;110(6):1923–1933.
34. Nobukuni T, Joaquin M, Roccio M, et al. Amino acids mediate mTOR/raptor signaling through activation of class

3 phosphatidylinositol 3OH-kinase. *Proc Natl Acad Sci USA*. 2005;102(40):14238–14243.
35. Corradetti MN, Guan KL. Upstream of the mammalian target of rapamycin: do all roads pass through mTOR? *Oncogene*. 2006;25(48):6347–6360.
36. Fimia GM, Di Bartolomeo S, Piacentini M, Cecconi F. Unleashing the Ambra1-Beclin 1 complex from dynein chains: Ulk1 sets Ambra1 free to induce autophagy. *Autophagy*. 2011;7(1):115–117.
37. Mizushima N. The role of the Atg1/ULK1 complex in autophagy regulation. *Curr Opin Cell Biol*. 2010;22(2):132–139.
38. Geng J, Klionsky DJ. The Atg8 and Atg12 ubiquitin-like conjugation systems in macroautophagy. 'Protein modifications: beyond the usual suspects' review series. *EMBO Rep*. 2008;9(9):859–864.
39. Hanada T, Noda NN, Satomi Y, et al. The Atg12-Atg5 conjugate has a novel E3-like activity for protein lipidation in autophagy. *J Biol Chem*. 2007;282(52):37298–37302.
40. Fujita N, Itoh T, Omori H, Fukuda M, Noda T, Yoshimori T. The Atg16L complex specifies the site of LC3 lipidation for membrane biogenesis in autophagy. *Mol Biol Cell*. 2008;19(5):2092–2100.
41. Kabeya Y, Mizushima N, Yamamoto A, Oshitani-Okamoto S, Ohsumi Y, Yoshimori T. LC3, GABARAP and GATE16 localize to autophagosomal membrane depending on form-II formation. *J Cell Sci*. 2004;117(Pt 13):2805–2812.
42. Weidberg H, Shvets E, Shpilka T, Shimron F, Shinder V, Elazar Z. LC3 and GATE-16/GABARAP subfamilies are both essential yet act differently in autophagosome biogenesis. *EMBO J*. 2010;29(11):1792–1802.
43. Saftig P. Physiology of the lysosome. Mehta A, Beck M, Sunder-Plassmann G. *Fabry Disease: Perspectives from 5 Years of FOS*. Oxford PharmaGenesis: Oxford; 2006 [chapter 3; ISBN-10: 1-903539-03-X].
44. Mortimore GE, Poso AR. Intracellular protein catabolism and its control during nutrient deprivation and supply. *Annu Rev Nutr*. 1987;7:539–564.

45. Scherz-Shouval R, Shvets E, Fass E, Shorer H, Gil L, Elazar Z. Reactive oxygen species are essential for autophagy and specifically regulate the activity of Atg4. *EMBO J*. 2007;26(7):1749–1760.
46. Komatsu M, Kurokawa H, Waguri S, et al. The selective autophagy substrate p62 activates the stress responsive transcription factor Nrf2 through inactivation of Keap1. *Nat Cell Biol*. 2010;12(3):213–223.
47. Lee JY, Koga H, Kawaguchi Y, et al. HDAC6 controls autophagosome maturation essential for ubiquitin-selective quality-control autophagy. *EMBO J*. 2010;29(5):969–980.
48. Shpilka T, Elazar Z. Shedding light on mammalian microautophagy. *Dev Cell*. 2011;20(1):1–2.
49. Cuervo AM, Dice JF. Age-related decline in chaperone-mediated autophagy. *J Biol Chem*. 2000;275(40):31505–31513.
50. Farre JC, Krick R, Subramani S, Thumm M. Turnover of organelles by autophagy in yeast. *Curr Opin Cell Biol*. 2009;21(4):522–530.
51. Marzella L, Ahlberg J, Glaumann H. Autophagy, heterophagy, microautophagy and crinophagy as the means for intracellular degradation. *Virchows Arch B Cell Pathol Incl Mol Pathol*. 1981;36(2–3):219–234.
52. Eliasieh K, Liets LC, Chalupa LM. Cellular reorganization in the human retina during normal aging. *Invest Ophthalmol Vis Sci*. 2007;48(6):2824–2830.
53. Sahu R, Kaushik S, Clement CC, et al. Microautophagy of cytosolic proteins by late endosomes. *Dev Cell*. 2011;20(1):131–139.
54. Banerjee R, Beal MF, Thomas B. Autophagy in neurodegenerative disorders: pathogenic roles and therapeutic implications. *Trends Neurosci*. 2010;33(12):541–549.
55. Alamouti B, Funk J. Retinal thickness decreases with age: an OCT study. *Br J Ophthalmol*. 2003;87(7):899–901.
56. Cavallotti C, Artico M, Pescosolido N, Leali FM, Feher J. Age-related changes in the human retina. *Can J Ophthalmol*. 2004;39(1):61–68.
57. Eriksson U, Alm A. Macular thickness decreases with age in

normal eyes: a study on the macular thickness map protocol in the Stratus OCT. *Br J Ophthalmol*. 2009;93(11):1448–1452.
58. Marshall J, Grindle J, Ansell PL, Borwein B. Convolution in human rods: an ageing process. *Br J Ophthalmol*. 1979;63(3):181–187.
59. Tucker GS. Refractile bodies in the inner segments of cones in the aging human retina. *Invest Ophthalmol Vis Sci*. 1986;27(5):708–715.
60. Boulton ME. Lipofuscin of the retinal pigment epithelium. Lois N, Forrester JV. *Fundus autofluorescence*. Wolters Kluwer/Lippincott Williams & Wilkins: Philadelphia; 2009:14–26.
61. Gartner S, Henkind P. Aging and degeneration of the human macula. 1. Outer nuclear layer and photoreceptors. *Br J Ophthalmol*. 1981;65(1):23–28.
62. Mansergh F, Orton NC, Vessey JP, et al. Mutation of the calcium channel gene Cacna1f disrupts calcium signaling, synaptic transmission and cellular organization in mouse retina. *Hum Mol Genet*. 2005;14(20):3035–3046.
63. Liets LC, Eliasieh K, van der List DA, Chalupa LM. Dendrites of rod bipolar cells sprout in normal aging retina. *Proc Natl Acad Sci USA*. 2006;103(32):12156–12160.
64. Curcio CA, Millican CL, Allen KA, Kalina RE. Aging of the human photoreceptor mosaic: evidence for selective vulnerability of rods in central retina. *Invest Ophthalmol Vis Sci*. 1993;34(12):3278–3296.
65. Gao H, Hollyfield JG. Aging of the human retina: differential loss of neurons and retinal pigment epithelial cells. *Invest Ophthalmol Vis Sci*. 1992;33(1):1–17.
66. Curcio CA, Owsley C, Jackson GR. Spare the rods, save the cones in aging and age-related maculopathy. *Invest Ophthalmol Vis Sci*. 2000;41(8):2015–2018.
67. Sanyal S, Hawkins RK, Jansen HG, Zeilmaker GH. Compensatory synaptic growth in the rod terminals as a sequel to partial photoreceptor cell loss in the retina of chimaeric mice. *Development*. 1992;114(3):797–803.
68. Jansen HG, Sanyal S. Synaptic plasticity in the rod terminals after partial photoreceptor cell loss in the heterozygous rds

mutant mouse. *J Comp Neurol*. 1992;316(1):117–125.
69. Spear PD. Neural bases of visual deficits during aging. *Vision Res*. 1993;33(18):2589–2609.
70. Leveillard T, Mohand-Said S, Fintz AC, Lambrou G, Sahel JA. The search for rod-dependent cone viability factors, secreted factors promoting cone viability. *Novartis Found Symp*. 2004;255:117–127 [discussion 27-30, 77-8].
71. Chalmel F, Leveillard T, Jaillard C, et al. Rod-derived Cone Viability Factor-2 is a novel bifunctional-thioredoxin-like protein with therapeutic potential. *BMC Mol Biol*. 2007;8:74.
72. Yang Y, Mohand-Said S, Danan A, et al. Functional cone rescue by RdCVF protein in a dominant model of retinitis pigmentosa. *Mol Ther*. 2009;17(5):787–795.
73. Feuer WJ, Budenz DL, Anderson DR, et al. Topographic differences in the age-related changes in the retinal nerve fiber layer of normal eyes measured by Stratus optical coherence tomography. *J Glaucoma*. 2011;20(3):133–138.
74. Aggarwal P, Nag TC, Wadhwa S. Age-related decrease in rod bipolar cell density of the human retina: an immunohistochemical study. *J Biosci*. 2007;32(2):293–298.
75. Lei Y, Garrahan N, Hermann B, et al. Transretinal degeneration in ageing human retina: a multiphoton microscopy analysis. *Br J Ophthalmol*. 2011;95(5):727–730.
76. Panda-Jonas S, Jonas JB, Jakobczyk-Zmija M. Retinal pigment epithelial cell count, distribution, and correlations in normal human eyes. *Am J Ophthalmol*. 1996;121(2):181–189.
77. Boulton M, Rozanowska M, Rozanowski B. Retinal photodamage. *J Photochem Photobiol B*. 2001;64(2–3):144–161.
78. Boulton M, Albon J. Stem cells in the eye. *Int J Biochem Cell Biol*. 2004;36(4):643–657.
79. Agarwal R, Gupta SK, Agarwal P, Saxena R, Agrawal SS. Current concepts in the pathophysiology of glaucoma. *Indian J Ophthalmol*. 2009;57(4):257–266.
80. Kisiswa L, Dervan AG, Albon J, Morgan JE, Wride MA. Retinal ganglion cell death postponed: giving apoptosis a break? *Ophthalmic Res*. 2010;43(2):61–78.
81. Qu J, Wang D, Grosskreutz CL. Mechanisms of retinal

ganglion cell injury and defense in glaucoma. *Exp Eye Res*. 2010;91(1):48–53.
82. Pease ME, McKinnon SJ, Quigley HA, Kerrigan-Baumrind LA, Zack DJ. Obstructed axonal transport of BDNF and its receptor TrkB in experimental glaucoma. *Invest Ophthalmol Vis Sci*. 2000;41(3):764–774.
83. Quigley HA, McKinnon SJ, Zack DJ, et al. Retrograde axonal transport of BDNF in retinal ganglion cells is blocked by acute IOP elevation in rats. *Invest Ophthalmol Vis Sci*. 2000;41(11):3460–3466.
84. Kerrigan LA, Zack DJ, Quigley HA, Smith SD, Pease ME. TUNEL-positive ganglion cells in human primary open-angle glaucoma. *Arch Ophthalmol*. 1997;115(8):1031–1035.
85. Levin LA. Mechanisms of optic neuropathy. *Curr Opin Ophthalmol*. 1997;8(6):9–15.
86. Baltmr A, Duggan J, Nizari S, Salt TE, Cordeiro MF. Neuroprotection in glaucoma – Is there a future role? *Exp Eye Res*. 2010;91(5):554–566.
87. Libby RT, Li Y, Savinova OV, et al. Susceptibility to neurodegeneration in a glaucoma is modified by Bax gene dosage. *PLoS Genet*. 2005;1(1):17–26.
88. Rodriguez-Muela N, Germain F, Marino G, Fitze PS, Boya P. Autophagy promotes survival of retinal ganglion cells after optic nerve axotomy in mice. *Cell Death Differ*. 2012;19:162–169.
89. Russo R, Berliocchi L, Adornetto A, et al. Calpain-mediated cleavage of Beclin-1 and autophagy deregulation following retinal ischemic injury in vivo. *Cell Death Dis*. 2011;2:e144.
90. Kim SH, Munemasa Y, Kwong JM, et al. Activation of autophagy in retinal ganglion cells. *J Neurosci Res*. 2008;86(13):2943–2951.
91. Sternberg C, Benchimol M, Linden R. Caspase dependence of the death of neonatal retinal ganglion cells induced by axon damage and induction of autophagy as a survival mechanism. *Braz J Med Biol Res*. 2010;43(10):950–956.
92. Piras A, Gianetto D, Conte D, Bosone A, Vercelli A. Activation of autophagy in a rat model of retinal ischemia following high intraocular pressure. *PLoS ONE*.

2011;6(7):e22514.
93. Park HY, Kim JH, Park CK. Activation of autophagy induces retinal ganglion cell death in a chronic hypertensive glaucoma model. *Cell Death Dis*. 2012;3:e290.
94. Hammes HP, Lin J, Renner O, et al. Pericytes and the pathogenesis of diabetic retinopathy. *Diabetes*. 2002;51(10):3107–3112.
95. Porta M. The importance of endothelial damage: Diabetic retinopathy. *Adv Stud Med*. 2005;5:S150–8.
96. Cogan DG, Toussaint D, Kuwabara T. Retinal vascular patterns. IV. Diabetic retinopathy. *Arch Ophthalmol*. 1961;66:366–378.
97. Kowluru RA. Diabetic retinopathy: mitochondrial dysfunction and retinal capillary cell death. *Antioxid Redox Signal*. 2005;7(11–12):1581–1587.
98. Barber AJ, Gardner TW, Abcouwer SF. The significance of vascular and neural apoptosis to the pathology of diabetic retinopathy. *Invest Ophthalmol Vis Sci*. 2011;52(2):1156–1163.
99. El-Remessy AB, Al-Shabrawey M, Khalifa Y, Tsai NT, Caldwell RB, Liou GI. Neuroprotective and blood–retinal barrier-preserving effects of cannabidiol in experimental diabetes. *Am J Pathol*. 2006;168(1):235–244.
100. Barber AJ, Lieth E, Khin SA, Antonetti DA, Buchanan AG, Gardner TW. Neural apoptosis in the retina during experimental and human diabetes: early onset and effect of insulin. *J Clin Invest*. 1998;102(4):783–791.
101. Lopes de Faria JM, Russ H, Costa VP. Retinal nerve fibre layer loss in patients with type 1 diabetes mellitus without retinopathy. *Br J Ophthalmol*. 2002;86(7):725–728.
102. van Dijk HW, Verbraak FD, Kok PH, et al. Decreased retinal ganglion cell layer thickness in patients with type 1 diabetes. *Invest Ophthalmol Vis Sci*. 2010;51(7):3660–3665.
103. van Dijk HW, Kok PH, Garvin M, et al. Selective loss of inner retinal layer thickness in type 1 diabetic patients with minimal diabetic retinopathy. *Invest Ophthalmol Vis Sci*. 2009;50(7):3404–3409.
104. Gastinger MJ, Singh RS, Barber AJ. Loss of cholinergic and dopaminergic amacrine cells in streptozotocin-diabetic rat

and Ins2Akita-diabetic mouse retinas. *Invest Ophthalmol Vis Sci*. 2006;47(7):3143–3150.
105. Feenstra DJ, Yego EC, Mohr S. Modes of retinal cell death in diabetic retinopathy. *J Clin Exp Ophthalmol*. 2013;4(5):298.
106. Park SH, Park JW, Park SJ, et al. Apoptotic death of photoreceptors in the streptozotocin-induced diabetic rat retina. *Diabetologia*. 2003;46(9):1260–1268.
107. Li W, Yanoff M, Liu X, Ye X. Retinal capillary pericyte apoptosis in early human diabetic retinopathy. *Chin Med J*. 1997;110(9):659–663.
108. Chen ZF, Li YB, Han JY, et al. The double-edged effect of autophagy in pancreatic beta cells and diabetes. *Autophagy*. 2011;7(1):12–16.
109. Gonzalez CD, Lee MS, Marchetti P, et al. The emerging role of autophagy in the pathophysiology of diabetes mellitus. *Autophagy*. 2011;7(1):2–11.
110. Qi X, Cai J, Dunn WA, et al. Circadian rhythmicity in the expression of autophagy proteins in normal and diabetic retinas. *Invest Ophthalmol Vis Sci*. 2010;51 [ARVO E-Abstract 5614].
111. Tang J, Kern TS. Inflammation in diabetic retinopathy. *Prog Retin Eye Res*. 2011;30(5):343–358.
112. Liu Y, Biarnes Costa M, Gerhardinger C. IL-1beta is upregulated in the diabetic retina and retinal vessels: cell-specific effect of high glucose and IL-1beta autostimulation. *PLoS ONE*. 2012;7(5):e36949.
113. Yuuki T, Kanda T, Kimura Y, et al. Inflammatory cytokines in vitreous fluid and serum of patients with diabetic vitreoretinopathy. *J Diabetes Complications*. 2001;15(5):257–259.
114. Kern TS. Contributions of inflammatory processes to the development of the early stages of diabetic retinopathy. *Exp Diabetes Res*. 2007;2007:95103.
115. Kusner LL, Sarthy VP, Mohr S. Nuclear translocation of glyceraldehyde-3-phosphate dehydrogenase: a role in high glucose-induced apoptosis in retinal Müller cells. *Invest Ophthalmol Vis Sci*. 2004;45(5):1553–1561.
116. Chan-Ling T, Baxter L, Afzal A, et al. Hematopoietic stem

cells provide repair functions after laser-induced Bruch's membrane rupture model of choroidal neovascularization. *Am J Pathol*. 2006;168(3):1031–1044.
117. Grant MB, May WS, Caballero S, et al. Adult hematopoietic stem cells provide functional hemangioblast activity during retinal neovascularization. *Nat Med*. 2002;8(6):607–612.
118. Busik JV, Tikhonenko M, Bhatwadekar A, et al. Diabetic retinopathy is associated with bone marrow neuropathy and a depressed peripheral clock. *J Exp Med*. 2009;206(13):2897–2906.
119. Caballero S, Sengupta N, Afzal A, et al. Ischemic vascular damage can be repaired by healthy, but not diabetic, endothelial progenitor cells. *Diabetes*. 2007;56(4):960–967.
120. Holz FG, Bindewald-Wittich A, Fleckenstein M, Dreyhaupt J, Scholl HP, Schmitz-Valckenberg S. Progression of geographic atrophy and impact of fundus autofluorescence patterns in age-related macular degeneration. *Am J Ophthalmol*. 2007;143(3):463–472.
121. Schatz H, McDonald HR. Atrophic macular degeneration: rate of spread of geographic atrophy and visual loss. *Ophthalmology*. 1989;96(10):1541–1551.
122. Fleckenstein M, Adrion C, Schmitz-Valckenberg S, et al. Concordance of disease progression in bilateral geographic atrophy due to AMD. *Invest Ophthalmol Vis Sci*. 2010;51(2):637–642.
123. McLeod DS, Grebe R, Bhutto I, Merges C, Baba T, Lutty GA. Relationship between RPE and choriocapillaris in age-related macular degeneration. *Invest Ophthalmol Vis Sci*. 2009;50(10):4982–4991.
124. Curcio CA, Medeiros NE, Millican CL. Photoreceptor loss in age-related macular degeneration. *Invest Ophthalmol Vis Sci*. 1996;37(7):1236–1249.
125. Jackson GR, Owsley C, Curcio CA. Photoreceptor degeneration and dysfunction in aging and age-related maculopathy. *Ageing Res Rev*. 2002;1(3):381–396.
126. Dunaief JL, Dentchev T, Ying GS, Milam AH. The role of apoptosis in age-related macular degeneration. *Arch Ophthalmol*. 2002;120(11):1435–1442.

127. Xu GZ, Li WW, Tso MO. Apoptosis in human retinal degenerations. *Trans Am Ophthalmol Soc*. 1996;94:411–430 [discussion 30-1].
128. Nordgaard CL, Berg KM, Kapphahn RJ, et al. Proteomics of the retinal pigment epithelium reveals altered protein expression at progressive stages of age-related macular degeneration. *Invest Ophthalmol Vis Sci*. 2006;47(3):815–822.
129. Jiang S, Wu MW, Sternberg P, Jones DP. Fas mediates apoptosis and oxidant-induced cell death in cultured hRPE cells. *Invest Ophthalmol Vis Sci*. 2000;41(3):645–655.
130. Bazan NG. Cell survival matters: docosahexaenoic acid signaling, neuroprotection and photoreceptors. *Trends Neurosci*. 2006;29(5):263–271.
131. Cai J, Nelson KC, Wu M, Sternberg P Jr, Jones DP. Oxidative damage and protection of the RPE. *Prog Retin Eye Res*. 2000;19(2):205–221.
132. Kasahara E, Lin LR, Ho YS, Reddy VN. SOD2 protects against oxidation-induced apoptosis in mouse retinal pigment epithelium: implications for age-related macular degeneration. *Invest Ophthalmol Vis Sci*. 2005;46(9):3426–3434.
133. Hanus J, Zhang H, Wang Z, Liu Q, Zhou Q, Wang S. Induction of necrotic cell death by oxidative stress in retinal pigment epithelial cells. *Cell Death Dis*. 2013;4:e965.
134. Kaneko H, Dridi S, Tarallo V, et al. DICER1 deficit induces Alu RNA toxicity in age-related macular degeneration. *Nature*. 2011;471(7338):325–330.
135. Tarallo V, Hirano Y, Gelfand BD, et al. DICER1 loss and Alu RNA induce age-related macular degeneration via the NLRP3 inflammasome and MyD88. *Cell*. 2012;149(4):847–859.
136. Kaarniranta K. Autophagy – hot topic in AMD. *Acta Ophthalmol*. 2010;88(4):387–388.
137. Viiri J, Amadio M, Marchesi N, et al. Autophagy activation clears ELAVL1/HuR-mediated accumulation of SQSTM1/p62 during proteasomal inhibition in human retinal pigment epithelial cells. *PLoS ONE*. 2013;8(7):e69563.
138. Mitter SK, Song C, Qi X, et al. Dysregulated autophagy in

the RPE is associated with increased susceptibility to oxidative stress and AMD. *Autophagy*. 2014;10(11):1989–2005.
139. Yao J, Jia L, Khan N, et al. Deletion of autophagy inducer RB1CC1 results in degeneration of the retinal pigment epithelium. *Autophagy*. 2015;11(6):939–953.
140. Mitter SK, Rao HV, Qi X, et al. Autophagy in the retina: a potential role in age-related macular degeneration. *Adv Exp Med Biol*. 2012;723:83–90.
141. Ferrington DA, Sinha D, Kaarniranta K. Defects in retinal pigment epithelial cell proteolysis and the pathology associated with age-related macular degeneration. *Prog Retin Eye Res*. 2016;51:69–89.
142. Wang AL, Lukas TJ, Yuan M, Du N, Tso MO, Neufeld AH. Autophagy, exosomes and drusen formation in age-related macular degeneration. *Autophagy*. 2009;5(4):563–564.
143. Blasiak J, Petrovski G, Vereb Z, Facsko A, Kaarniranta K. Oxidative stress, hypoxia, and autophagy in the neovascular processes of age-related macular degeneration. *Biomed Res Int*. 2014;2014:768026.
144. Saadat KA, Murakami Y, Tan X, et al. Inhibition of autophagy induces retinal pigment epithelial cell damage by the lipofuscin fluorophore A2E. *FEBS Open Bio*. 2014;4:1007–1014.
145. Krohne TU, Stratmann NK, Kopitz J, Holz FG. Effects of lipid peroxidation products on lipofuscinogenesis and autophagy in human retinal pigment epithelial cells. *Exp Eye Res*. 2010;90(3):465–471.
146. Liu J, Lu W, Reigada D, Nguyen J, Laties AM, Mitchell CH. Restoration of lysosomal pH in RPE cells from cultured human and ABCA4($^{-/-}$) mice: pharmacologic approaches and functional recovery. *Invest Ophthalmol Vis Sci*. 2008;49(2):772–780.
147. Kim JY, Zhao H, Martinez J, et al. Noncanonical autophagy promotes the visual cycle. *Cell*. 2013;154(2):365–376.
148. Shamsi FA, Boulton M. Inhibition of RPE lysosomal and antioxidant activity by the age pigment lipofuscin. *Invest Ophthalmol Vis Sci*. 2001;42(12):3041–3046.

149. Jarrett SG, Boulton ME. Antioxidant up-regulation and increased nuclear DNA protection play key roles in adaptation to oxidative stress in epithelial cells. *Free Radic Biol Med*. 2005;38(10):1382–1391.
150. Liang FQ, Godley BF. Oxidative stress-induced mitochondrial DNA damage in human retinal pigment epithelial cells: a possible mechanism for RPE aging and age-related macular degeneration. *Exp Eye Res*. 2003;76(4):397–403.
151. Winkler BS, Boulton ME, Gottsch JD, Sternberg P. Oxidative damage and age-related macular degeneration. *Mol Vis*. 1999;5:32.
152. Yang L, Bula D, Arroyo JG, Chen DF. Preventing retinal detachment-associated photoreceptor cell loss in Bax-deficient mice. *Invest Ophthalmol Vis Sci*. 2004;45(2):648–654.
153. Arroyo JG, Yang L, Bula D, Chen DF. Photoreceptor apoptosis in human retinal detachment. *Am J Ophthalmol*. 2005;139(4):605–610.
154. Hisatomi T, Sakamoto T, Goto Y, et al. Critical role of photoreceptor apoptosis in functional damage after retinal detachment. *Curr Eye Res*. 2002;24(3):161–172.
155. Cook B, Lewis GP, Fisher SK, Adler R. Apoptotic photoreceptor degeneration in experimental retinal detachment. *Invest Ophthalmol Vis Sci*. 1995;36(6):990–996.
156. Besirli CG, Chinskey ND, Zheng QD, Zacks DN. Inhibition of retinal detachment-induced apoptosis in photoreceptors by a small peptide inhibitor of the fas receptor. *Invest Ophthalmol Vis Sci*. 2010;51(4):2177–2184.
157. Dong K, Sun X. Targeting death receptor induced apoptosis and necroptosis: a novel therapeutic strategy to prevent neuronal damage in retinal detachment. *Med Hypotheses*. 2011;77(1):144–146.
158. Zacks DN, Zheng QD, Han Y, Bakhru R, Miller JW. FAS-mediated apoptosis and its relation to intrinsic pathway activation in an experimental model of retinal detachment. *Invest Ophthalmol Vis Sci*. 2004;45(12):4563–4569.
159. Trichonas G, Murakami Y, Thanos A, et al. Receptor interacting protein kinases mediate retinal detachment-

induced photoreceptor necrosis and compensate for inhibition of apoptosis. *Proc Natl Acad Sci USA*. 2010;107(50):21695–21700.
160. Besirli CG, Chinskey ND, Zheng QD, Zacks DN. Autophagy activation in the injured photoreceptor inhibits fas-mediated apoptosis. *Invest Ophthalmol Vis Sci*. 2011;52(7):4193–4199.
161. Chinskey ND, Zheng QD, Zacks DN. Control of photoreceptor autophagy after retinal detachment: the switch from survival to death. *Invest Ophthalmol Vis Sci*. 2014;55(2):688–695.
162. Murakami Y, Notomi S, Hisatomi T, et al. Photoreceptor cell death and rescue in retinal detachment and degenerations. *Prog Retin Eye Res*. 2013;37:114–140.
163. Hartong DT, Berson EL, Dryja TP. Retinitis pigmentosa. *Lancet*. 2006;368(9549):1795–1809.
164. Marigo V. Programmed cell death in retinal degeneration: targeting apoptosis in photoreceptors as potential therapy for retinal degeneration. *Cell Cycle*. 2007;6(6):652–655.
165. Ferrari S, Di Iorio E, Barbaro V, Ponzin D, Sorrentino FS, Parmeggiani F. Retinitis pigmentosa: genes and disease mechanisms. *Curr Genomics*. 2011;12:238–249.
166. Portera-Cailliau C, Sung CH, Nathans J, Adler R. Apoptotic photoreceptor cell death in mouse models of retinitis pigmentosa. *Proc Natl Acad Sci USA*. 1994;91(3):974–978.
167. Travis GH. Mechanisms of cell death in the inherited retinal degenerations. *Am J Hum Genet*. 1998;62(3):503–508.
168. Cottet S, Schorderet DF. Mechanisms of apoptosis in retinitis pigmentosa. *Curr Mol Med*. 2009;9(3):375–383.
169. Liu C, Li Y, Peng M, Laties AM, Wen R. Activation of caspase-3 in the retina of transgenic rats with the rhodopsin mutation s334ter during photoreceptor degeneration. *J Neurosci*. 1999;19(12):4778–4785.
170. Chang GQ, Hao Y, Wong F. Apoptosis: final common pathway of photoreceptor death in rd, rds, and rhodopsin mutant mice. *Neuron*. 1993;11(4):595–605.
171. Bode C, Wolfrum U. Caspase-3 inhibitor reduces apoptotic photoreceptor cell death during inherited retinal

degeneration in tubby mice. *Mol Vis*. 2003;9:144–150.
172. Doonan F, Donovan M, Cotter TG. Caspase-independent photoreceptor apoptosis in mouse models of retinal degeneration. *J Neurosci*. 2003;23(13):5723–5731.
173. Lohr HR, Kuntchithapautham K, Sharma AK, Rohrer B. Multiple, parallel cellular suicide mechanisms participate in photoreceptor cell death. *Exp Eye Res*. 2006;83(2):380–389.
174. Arimura N, Ki-i Y, Hashiguchi T, et al. Intraocular expression and release of high-mobility group box 1 protein in retinal detachment. *Lab Invest*. 2009;89(3):278–289.
175. Murakami Y, Matsumoto H, Roh M, et al. Receptor interacting protein kinase mediates necrotic cone but not rod cell death in a mouse model of inherited degeneration. *Proc Natl Acad Sci USA*. 2012;109(36):14598–14603.
176. Wenzel A, Grimm C, Samardzija M, Reme CE. Molecular mechanisms of light-induced photoreceptor apoptosis and neuroprotection for retinal degeneration. *Prog Retin Eye Res*. 2005;24(2):275–306.
177. Mainster MA, Boulton ME. Retinal toxicity. Albert DM, Miller JW, Blodi BA, Azar DT. *Principles and practice of ophthalmology*. 3rd ed. Elsevier: London; 2008:2195–2205.
178. Organisciak DT, Vaughan DK. Retinal light damage: mechanisms and protection. *Prog Retin Eye Res*. 2010;29(2):113–134.
179. Wu J, Seregard S, Algvere PV. Photochemical damage of the retina. *Surv Ophthalmol*. 2006;51(5):461–481.
180. Wu J, Seregard S, Spangberg B, Oskarsson M, Chen E. Blue light induced apoptosis in rat retina. *Eye (Lond)*. 1999;13(Pt 4):577–583.
181. Noell WK, Walker VS, Kang BS, Berman S. Retinal damage by light in rats. *Invest Ophthalmol*. 1966;5(5):450–473.
182. Abler AS, Chang CJ, Ful J, Tso MO, Lam TT. Photic injury triggers apoptosis of photoreceptor cells. *Res Commun Mol Pathol Pharmacol*. 1996;92(2):177–189.
183. Zhang SR, Li SH, Abler A, Fu J, Tso MO, Lam TT. Tissue transglutaminase in apoptosis of photoreceptor cells in rat retina. *Invest Ophthalmol Vis Sci*. 1996;37(9):1793–1799.
184. Hafezi F, Marti A, Munz K, Reme CE. Light-induced

apoptosis: differential timing in the retina and pigment epithelium. *Exp Eye Res*. 1997;64(6):963–970.
185. Hafezi F, Steinbach JP, Marti A, et al. The absence of c-fos prevents light-induced apoptotic cell death of photoreceptors in retinal degeneration in vivo. *Nat Med*. 1997;3(3):346–349.
186. Cachafeiro M, Bemelmans AP, Samardzija M, et al. Hyperactivation of retina by light in mice leads to photoreceptor cell death mediated by VEGF and retinal pigment epithelium permeability. *Cell Death Dis*. 2013;4:e781.
187. Grimm C, Wenzel A, Hafezi F, Yu S, Redmond TM, Reme CE. Protection of Rpe65-deficient mice identifies rhodopsin as a mediator of light-induced retinal degeneration. *Nat Genet*. 2000;25(1):63–66.
188. Grimm C, Wenzel A, Williams T, Rol P, Hafezi F, Reme C. Rhodopsin-mediated blue-light damage to the rat retina: effect of photoreversal of bleaching. *Invest Ophthalmol Vis Sci*. 2001;42(2):497–505.
189. Keller C, Grimm C, Wenzel A, Hafezi F, Reme C. Protective effect of halothane anesthesia on retinal light damage: inhibition of metabolic rhodopsin regeneration. *Invest Ophthalmol Vis Sci*. 2001;42(2):476–480.
190. Wenzel A, Reme CE, Williams TP, Hafezi F, Grimm C. The Rpe65 Leu450Met variation increases retinal resistance against light-induced degeneration by slowing rhodopsin regeneration. *J Neurosci*. 2001;21(1):53–58.
191. Rozanowska M, Sarna T. Light-induced damage to the retina: role of rhodopsin chromophore revisited. *Photochem Photobiol*. 2005;81(6):1305–1330.
192. Farber DB, Danciger JS, Organisciak DT. Levels of mRNA encoding proteins of the cGMP cascade as a function of light environment. *Exp Eye Res*. 1991;53(6):781–786.
193. Organisciak DT, Xie A, Wang HM, Jiang YL, Darrow RM, Donoso LA. Adaptive changes in visual cell transduction protein levels: effect of light. *Exp Eye Res*. 1991;53(6):773–779.
194. Kennedy MJ, Lee KA, Niemi GA, et al. Multiple

phosphorylation of rhodopsin and the in vivo chemistry underlying rod photoreceptor dark adaptation. *Neuron*. 2001;31(1):87–101.
195. Fain GL, Lisman JE. Light, $Ca^{2+,}$ and photoreceptor death: new evidence for the equivalent-light hypothesis from arrestin knockout mice. *Invest Ophthalmol Vis Sci*. 1999;40(12):2770–2772.
196. Tezel G, Kolker AE, Kass MA, Wax MB, Gordon M, Siegmund KD. Parapapillary chorioretinal atrophy in patients with ocular hypertension. I: An evaluation as a predictive factor for the development of glaucomatous damage. *Arch Ophthalmol*. 1997;115(12):1503–1508.
197. Donovan M, Cotter TG. Caspase-independent photoreceptor apoptosis in vivo and differential expression of apoptotic protease activating factor-1 and caspase-3 during retinal development. *Cell Death Differ*. 2002;9(11):1220–1231.
198. Gaillard ER, Atherton SJ, Eldred G, Dillon J. Photophysical studies on human retinal lipofuscin. *Photochem Photobiol*. 1995;61(5):448–453.
199. Rozanowska M, Jarvis-Evans J, Korytowski W, Boulton ME, Burke JM, Sarna T. Blue light-induced reactivity of retinal age pigment. In vitro generation of oxygen-reactive species. *J Biol Chem*. 1995;270(32):18825–18830.
200. Rozanowska M, Wessels J, Boulton M, et al. Blue light-induced singlet oxygen generation by retinal lipofuscin in non-polar media. *Free Radic Biol Med*. 1998;24(7–8):1107–1112.
201. Paquet-Durand F, Azadi S, Hauck SM, Ueffing M, van Veen T, Ekstrom P. Calpain is activated in degenerating photoreceptors in the rd1 mouse. *J Neurochem*. 2006;96(3):802–814.
202. Sharma AK, Rohrer B. Calcium-induced calpain mediates apoptosis via caspase-3 in a mouse photoreceptor cell line. *J Biol Chem*. 2004;279(34):35564–35572.
203. Hafezi F, Marti A, Grimm C, Wenzel A, Reme CE. Differential DNA binding activities of the transcription factors AP-1 and Oct-1 during light-induced apoptosis of

photoreceptors. *Vision Res*. 1999;39(15):2511–2518.
204. Sang A, Cheng Y, Lu H, Chen D, Gao R, Shen A. Light-induced retinal ganglion cell damage in vivo involves Dexras1. *Mol Vis*. 2011;17:134–143.
205. Dacey DM, Liao HW, Peterson BB, et al. Melanopsin-expressing ganglion cells in primate retina signal colour and irradiance and project to the LGN. *Nature*. 2005;433(7027):749–754.
206. Kunchithapautham K, Coughlin B, Lemasters JJ, Rohrer B. Differential effects of rapamycin on rods and cones during light-induced stress in albino mice. *Invest Ophthalmol Vis Sci*. 2011;52(6):2967–2975.
207. Bahr M. *Neuroprotection: models, mechanisms, and therapies*. Wiley–VCH: Weinheim; 2004.
208. Chen Y, Sawada O, Kohno H, et al. Autophagy protects the retina from light-induced degeneration. *J Biol Chem*. 2013;288(11):7506–7518.
209. Chen Y, Perusek L, Maeda A. Autophagy in light-induced retinal damage. *Exp Eye Res*. 2016;144:64–72.
210. Li CP, Yao J, Tao ZF, Li XM, Jiang Q, Yan B. Epigallocatechin-gallate (EGCG) regulates autophagy in human retinal pigment epithelial cells: a potential role for reducing UVB light-induced retinal damage. *Biochem Biophys Res Commun*. 2013;438(4):739–745.
211. Faden AI, Stoica B. Neuroprotection: challenges and opportunities. *Arch Neurol*. 2007;64(6):794–800.
212. Whitcup SM. Clinical trials in neuroprotection. *Prog Brain Res*. 2008;173:323–335.
213. Donovan M, Carmody RJ, Cotter TG. Light-induced photoreceptor apoptosis in vivo requires neuronal nitric-oxide synthase and guanylate cyclase activity and is caspase-3-independent. *J Biol Chem*. 2001;276(25):23000–23008.
214. Goureau O, Jeanny JC, Becquet F, Hartmann MP, Courtois Y. Protection against light-induced retinal degeneration by an inhibitor of NO synthase. *Neuroreport*. 1993;5(3):233–236.
215. Hahn P, Lindsten T, Lyubarsky A, et al. Deficiency of Bax and Bak protects photoreceptors from light damage in vivo.

Cell Death Differ. 2004;11(11):1192–1197.
216. Li F, Cao W, Anderson RE. Alleviation of constant-light-induced photoreceptor degeneration by adaptation of adult albino rat to bright cyclic light. *Invest Ophthalmol Vis Sci*. 2003;44(11):4968–4975.
217. Casson RJ, Chidlow G, Wood JP, Vidal-Sanz M, Osborne NN. The effect of retinal ganglion cell injury on light-induced photoreceptor degeneration. *Invest Ophthalmol Vis Sci*. 2004;45(2):685–693.
218. Casson RJ, Wood JP, Melena J, Chidlow G, Osborne NN. The effect of ischemic preconditioning on light-induced photoreceptor injury. *Invest Ophthalmol Vis Sci*. 2003;44(3):1348–1354.
219. Cao W, Tombran-Tink J, Elias R, Sezate S, Mrazek D, McGinnis JF. In vivo protection of photoreceptors from light damage by pigment epithelium-derived factor. *Invest Ophthalmol Vis Sci*. 2001;42(7):1646–1652.
220. Lau D, Flannery J. Viral-mediated FGF-2 treatment of the constant light damage model of photoreceptor degeneration. *Doc Ophthalmol*. 2003;106(1):89–98.
221. Spencer B, Agarwala S, Gentry L, Brandt CR. HSV-1 vector-delivered FGF2 to the retina is neuroprotective but does not preserve functional responses. *Mol Ther*. 2001;3(5 Pt 1):746–756.
222. Kano T, Abe T, Tomita H, Sakata T, Ishiguro S, Tamai M. Protective effect against ischemia and light damage of iris pigment epithelial cells transfected with the BDNF gene. *Invest Ophthalmol Vis Sci*. 2002;43(12):3744–3753.
223. Bainbridge JW, Ali RR. Success in sight: The eyes have it! Ocular gene therapy trials for LCA look promising. *Gene Ther*. 2008;15(17):1191–1192.
224. Bok D, Yasumura D, Matthes MT, et al. Effects of adeno-associated virus-vectored ciliary neurotrophic factor on retinal structure and function in mice with a P216L rds/peripherin mutation. *Exp Eye Res*. 2002;74(6):719–735.
225. Cayouette M, Smith SB, Becerra SP, Gravel C. Pigment epithelium-derived factor delays the death of photoreceptors in mouse models of inherited retinal

degenerations. *Neurobiol Dis*. 1999;6(6):523–532.
226. Huang SP, Lin PK, Liu JH, Khor CN, Lee YJ. Intraocular gene transfer of ciliary neurotrophic factor rescues photoreceptor degeneration in RCS rats. *J Biomed Sci*. 2004;11(1):37–48.
227. Schlichtenbrede FC, MacNeil A, Bainbridge JW, et al. Intraocular gene delivery of ciliary neurotrophic factor results in significant loss of retinal function in normal mice and in the Prph2Rd2/Rd2 model of retinal degeneration. *Gene Ther*. 2003;10(6):523–527.
228. Miyazaki M, Ikeda Y, Yonemitsu Y, et al. Simian lentiviral vector-mediated retinal gene transfer of pigment epithelium-derived factor protects retinal degeneration and electrical defect in Royal College of Surgeons rats. *Gene Ther*. 2003;10(17):1503–1511.
229. Tao W, Wen R, Goddard MB, et al. Encapsulated cell-based delivery of CNTF reduces photoreceptor degeneration in animal models of retinitis pigmentosa. *Invest Ophthalmol Vis Sci*. 2002;43(10):3292–3298.
230. Chong NH, Alexander RA, Waters L, Barnett KC, Bird AC, Luthert PJ. Repeated injections of a ciliary neurotrophic factor analogue leading to long-term photoreceptor survival in hereditary retinal degeneration. *Invest Ophthalmol Vis Sci*. 1999;40(6):1298–1305.
231. Harada T, Harada C, Nakayama N, et al. Modification of glial-neuronal cell interactions prevents photoreceptor apoptosis during light-induced retinal degeneration. *Neuron*. 2000;26(2):533–541.
232. Okoye G, Zimmer J, Sung J, et al. Increased expression of brain-derived neurotrophic factor preserves retinal function and slows cell death from rhodopsin mutation or oxidative damage. *J Neurosci*. 2003;23(10):4164–4172.
233. Lawrence JM, Keegan DJ, Muir EM, et al. Transplantation of Schwann cell line clones secreting GDNF or BDNF into the retinas of dystrophic Royal College of Surgeons rats. *Invest Ophthalmol Vis Sci*. 2004;45(1):267–274.
234. Yoshizawa K, Kiuchi K, Nambu H, et al. Caspase-3 inhibitor transiently delays inherited retinal degeneration in C3H

mice carrying the rd gene. *Graefes Arch Clin Exp Ophthalmol*. 2002;240(3):214–219.
235. Osborne NN, Li GY, Ji D, Mortiboys HJ, Jackson S. Light affects mitochondria to cause apoptosis to cultured cells: possible relevance to ganglion cell death in certain optic neuropathies. *J Neurochem*. 2008;105(5):2013–2028.
236. Zeiss CJ, Neal J, Johnson EA. Caspase-3 in postnatal retinal development and degeneration. *Invest Ophthalmol Vis Sci*. 2004;45(3):964–970.
237. Leonard KC, Petrin D, Coupland SG, et al. XIAP protection of photoreceptors in animal models of retinitis pigmentosa. *PLoS ONE*. 2007;2(3):e314.
238. Renwick J, Narang MA, Coupland SG, et al. XIAP-mediated neuroprotection in retinal ischemia. *Gene Ther*. 2006;13(4):339–347.
239. Glybina IV, Kennedy A, Ashton P, Abrams GW, Iezzi R. Photoreceptor neuroprotection in RCS rats via low-dose intravitreal sustained-delivery of fluocinolone acetonide. *Invest Ophthalmol Vis Sci*. 2009;50(10):4847–4857.
240. Read SP, Cashman SM, Kumar-Singh R. POD nanoparticles expressing GDNF provide structural and functional rescue of light-induced retinal degeneration in an adult mouse. *Mol Ther*. 2010;18(11):1917–1926.
241. Cheung W, Guo L, Cordeiro MF. Neuroprotection in glaucoma: drug-based approaches. *Optom Vis Sci*. 2008;85(6):406–416.
242. Danesh-Meyer HV. Neuroprotection in glaucoma: recent and future directions. *Curr Opin Ophthalmol*. 2011;22(2):78–86.
243. Dong CJ, Guo Y, Agey P, Wheeler L, Hare WA. Alpha2 adrenergic modulation of NMDA receptor function as a major mechanism of RGC protection in experimental glaucoma and retinal excitotoxicity. *Invest Ophthalmol Vis Sci*. 2008;49(10):4515–4522.
244. Russo R, Cavaliere F, Rombola L, et al. Rational basis for the development of coenzyme Q10 as a neurotherapeutic agent for retinal protection. *Prog Brain Res*. 2008;173:575–582.
245. Pease ME, Zack DJ, Berlinicke C, et al. Effect of CNTF on

retinal ganglion cell survival in experimental glaucoma. *Invest Ophthalmol Vis Sci*. 2009;50(5):2194–2200.
246. Tao W. Application of encapsulated cell technology for retinal degenerative diseases. *Expert Opin Biol Ther*. 2006;6(7):717–726.
247. Kashimoto R, Kurimoto T, Miyoshi T, et al. Cilostazol promotes survival of axotomized retinal ganglion cells in adult rats. *Neurosci Lett*. 2008;436(2):116–119.
248. Koriyama Y, Tanii H, Ohno M, Kimura T, Kato S. A novel neuroprotective role of a small peptide from flesh fly, 5-S-GAD in the rat retina in vivo. *Brain Res*. 2008;1240:196–203.
249. Lombardini JB. Taurine: retinal function. *Brain Res Brain Res Rev*. 1991;16(2):151–169.
250. Militante JD, Lombardini JB. Taurine: evidence of physiological function in the retina. *Nutr Neurosci*. 2002;5(2):75–90.
251. Schaffer S, Azuma J, Takahashi K, Mozaffari M. Why is taurine cytoprotective? *Adv Exp Med Biol*. 2003;526:307–321.
252. Heller-Stilb B, van Roeyen C, Rascher K, et al. Disruption of the taurine transporter gene (taut) leads to retinal degeneration in mice. *FASEB J*. 2002;16(2):231–233.
253. Takatani T, Takahashi K, Uozumi Y, et al. Taurine inhibits apoptosis by preventing formation of the Apaf-1/caspase-9 apoptosome. *Am J Physiol Cell Physiol*. 2004;287(4):C949–53.
254. Froger N, Cadetti L, Lorach H, et al. Taurine provides neuroprotection against retinal ganglion cell degeneration. *PLoS ONE*. 2012;7(10):e42017.
255. Mansoor S, Gupta N, Patil AJ, et al. Inhibition of apoptosis in human retinal pigment epithelial cells treated with benzo(e)pyrene, a toxic component of cigarette smoke. *Invest Ophthalmol Vis Sci*. 2010;51(5):2601–2607.
256. Bazan NG. Neurotrophins induce neuroprotective signaling in the retinal pigment epithelial cell by activating the synthesis of the anti-inflammatory and anti-apoptotic neuroprotectin D1. *Adv Exp Med Biol*. 2008;613:39–44.
257. Mukherjee PK, Marcheselli VL, Barreiro S, Hu J, Bok D, Bazan NG. Neurotrophins enhance retinal pigment epithelial cell survival through neuroprotectin D1 signaling.

Proc Natl Acad Sci USA. 2007;104(32):13152–13157.
258. Wang ZY, Shen LJ, Tu L, et al. Erythropoietin protects retinal pigment epithelial cells from oxidative damage. *Free Radic Biol Med*. 2009;46(8):1032–1041.
259. Wrona M, Rozanowska M, Sarna T. Zeaxanthin in combination with ascorbic acid or alpha-tocopherol protects ARPE-19 cells against photosensitized peroxidation of lipids. *Free Radic Biol Med*. 2004;36(9):1094–1101.
260. Bryckaert M, Guillonneau X, Hecquet C, Courtois Y, Mascarelli F. Both FGF1 and bcl-x synthesis are necessary for the reduction of apoptosis in retinal pigmented epithelial cells by FGF2: role of the extracellular signal-regulated kinase 2. *Oncogene*. 1999;18(52):7584–7593.
261. Elner SG, Yoshida A, Bian ZM, Kindezelskii AL, Petty HR, Elner VM. Human RPE cell apoptosis induced by activated monocytes is mediated by caspase-3 activation. *Trans Am Ophthalmol Soc*. 2003;101:77–89 [discussion -91].
262. Ferrington DA, Tran TN, Lew KL, Van Remmen H, Gregerson DS. Different death stimuli evoke apoptosis via multiple pathways in retinal pigment epithelial cells. *Exp Eye Res*. 2006;83(3):638–650.
263. Sreekumar PG, Kannan R, Kitamura M, et al. alphaB crystallin is apically secreted within exosomes by polarized human retinal pigment epithelium and provides neuroprotection to adjacent cells. *PLoS ONE*. 2010;5(10):e12578.
264. Alge CS, Priglinger SG, Neubauer AS, et al. Retinal pigment epithelium is protected against apoptosis by alphaB-crystallin. *Invest Ophthalmol Vis Sci*. 2002;43(11):3575–3582.
265. AREDS. A randomized, placebo-controlled, clinical trial of high-dose supplementation with vitamins C and E, beta carotene, and zinc for age-related macular degeneration and vision loss: AREDS report no. 8. *Arch Ophthalmol*. 2001;119(10):1417–1436.
266. Imai H, Singh RS, Fort PE, Gardner TW. Neuroprotection for diabetic retinopathy. *Dev Ophthalmol*. 2009;44:56–68.
267. Bao XH, Naomoto Y, Hao HF, et al. Autophagy: can it become a potential therapeutic target? *Int J Mol Med*.

2010;25(4):493–503.
268. Codogno P, Meijer AJ. Autophagy and signaling: their role in cell survival and cell death. *Cell Death Differ*. 2005;12(Suppl. 2):1509–1518.
269. Pattingre S, Tassa A, Qu X, et al. Bcl-2 antiapoptotic proteins inhibit Beclin 1-dependent autophagy. *Cell*. 2005;122(6):927–939.
270. Petiot A, Ogier-Denis E, Blommaart EF, Meijer AJ, Codogno P. Distinct classes of phosphatidylinositol 3'-kinases are involved in signaling pathways that control macroautophagy in HT-29 cells. *J Biol Chem*. 2000;275(2):992–998.
271. Sarkar S, Rubinsztein DC. Small molecule enhancers of autophagy for neurodegenerative diseases. *Mol Biosyst*. 2008;4(9):895–901.
272. Shacka JJ, Roth KA, Zhang J. The autophagy-lysosomal degradation pathway: role in neurodegenerative disease and therapy. *Front Biosci*. 2008;13:718–736.
273. Winslow AR, Rubinsztein DC. Autophagy in neurodegeneration and development. *Biochim Biophys Acta*. 2008;1782(12):723–729.
274. Carew JS, Nawrocki ST, Giles FJ, Cleveland JL. Targeting autophagy: a novel anticancer strategy with therapeutic implications for imatinib resistance. *Biologics*. 2008;2(2):201–204.
275. Amaravadi RK, Lippincott-Schwartz J, Yin XM, et al. Principles and current strategies for targeting autophagy for cancer treatment. *Clin Cancer Res*. 2011;17(4):654–666.
276. Dalby KN, Tekedereli I, Lopez-Berestein G, Ozpolat B. Targeting the prodeath and prosurvival functions of autophagy as novel therapeutic strategies in cancer. *Autophagy*. 2010;6(3):322–329.
277. Spalton DJ. Retinopathy and antimalarial drugs – the British experience. *Lupus*. 1996;5(Suppl. 1):S70–2.
278. Kaminskyy V, Zhivotovsky B. Proteases in autophagy. *Biochim Biophys Acta*. 2012;1824(1):44–50.
279. Kang R, Zeh HJ, Lotze MT, Tang D. The Beclin 1 network regulates autophagy and apoptosis. *Cell Death Differ*.

2011;18(4):571–580.
280. Stepkowski TM, Kruszewski MK. Molecular cross-talk between the NRF2/KEAP1 signaling pathway, autophagy, and apoptosis. *Free Radic Biol Med*. 2011;50(9):1186–1195.
281. Goligorsky MS. SIRTing out the link between autophagy and ageing. *Nephrol Dial Transplant*. 2010;25(8):2434–2436.
282. Hariharan N, Maejima Y, Nakae J, Paik J, Depinho RA, Sadoshima J. Deacetylation of FoxO by Sirt1 Plays an essential role in mediating starvation-induced autophagy in cardiac myocytes. *Circ Res*. 2010;107(12):1470–1482.
283. Scherz-Shouval R, Elazar Z. Regulation of autophagy by ROS: physiology and pathology. *Trends Biochem Sci*. 2011;36(1):30–38.
284. Massey AC, Follenzi A, Kiffin R, Zhang C, Cuervo AM. Early cellular changes after blockage of chaperone-mediated autophagy. *Autophagy*. 2008;4(4):442–456.
285. Kaushik S, Massey AC, Mizushima N, Cuervo AM. Constitutive activation of chaperone-mediated autophagy in cells with impaired macroautophagy. *Mol Biol Cell*. 2008;19(5):2179–2192.
286. Iwata A, Christianson JC, Bucci M, et al. Increased susceptibility of cytoplasmic over nuclear polyglutamine aggregates to autophagic degradation. *Proc Natl Acad Sci USA*. 2005;102(37):13135–13140.
287. Ding Q, Dimayuga E, Martin S, et al. Characterization of chronic low-level proteasome inhibition on neural homeostasis. *J Neurochem*. 2003;86(2):489–497.
288. Cuervo AM, Palmer A, Rivett AJ, Knecht E. Degradation of proteasomes by lysosomes in rat liver. *Eur J Biochem*. 1995;227(3):792–800.
289. Araki M. Regeneration of the amphibian retina: role of tissue interaction and related signaling molecules on RPE transdifferentiation. *Dev Growth Differ*. 2007;49(2):109–120.
290. Karl MO, Reh TA. Regenerative medicine for retinal diseases: activating endogenous repair mechanisms. *Trends Mol Med*. 2010;16(4):193–202.
291. Bernardos RL, Barthel LK, Meyers JR, Raymond PA. Late-stage neuronal progenitors in the retina are radial Muller

glia that function as retinal stem cells. *J Neurosci*. 2007;27(26):7028–7040.
292. Raymond PA, Hitchcock PF. How the neural retina regenerates. *Results Probl Cell Differ*. 2000;31:197–218.
293. Fischer AJ, Reh TA. Müller glia are a potential source of neural regeneration in the postnatal chicken retina. *Nat Neurosci*. 2001;4(3):247–252.
294. Ooto S, Akagi T, Kageyama R, et al. Potential for neural regeneration after neurotoxic injury in the adult mammalian retina. *Proc Natl Acad Sci USA*. 2004;101(37):13654–13659.
295. Carr AJ, Vugler AA, Hikita ST, et al. Protective effects of human iPS-derived retinal pigment epithelium cell transplantation in the retinal dystrophic rat. *PLoS ONE*. 2009;4(12):e8152.
296. Du H, Lim SL, Grob S, Zhang K. Induced pluripotent stem cell therapies for geographic atrophy of age-related macular degeneration. *Semin Ophthalmol*. 2011;26(3):216–224.
297. Lu B, Malcuit C, Wang S, et al. Long-term safety and function of RPE from human embryonic stem cells in preclinical models of macular degeneration. *Stem Cells*. 2009;27(9):2126–2135.
298. Schwartz SD, Hubschman JP, Heilwell G, et al. Embryonic stem cell trials for macular degeneration: a preliminary report. *Lancet*. 2012;379(9817):713–720.
299. Schwartz SD, Regillo CD, Lam BL, et al. Human embryonic stem cell-derived retinal pigment epithelium in patients with age-related macular degeneration and Stargardt's macular dystrophy: follow-up of two open-label phase 1/2 studies. *Lancet*. 2015;385(9967):509–516.
300. Kamao H, Mandai M, Okamoto S, et al. Characterization of human induced pluripotent stem cell-derived retinal pigment epithelium cell sheets aiming for clinical application. *Stem Cell Reports*. 2014;2(2):205–218.
301. McGill TJ, Cottam B, Lu B, et al. Transplantation of human central nervous system stem cells - neuroprotection in retinal degeneration. *Eur J Neurosci*. 2012;35(3):468–477.
302. Fong CY, Gauthaman K, Bongso A. Teratomas from

pluripotent stem cells: a clinical hurdle. *J Cell Biochem*. 2010;111(4):769–781.
303. Gore A, Li Z, Fung HL, et al. Somatic coding mutations in human induced pluripotent stem cells. *Nature*. 2011;471(7336):63–67.
304. Binder S, Stanzel BV, Krebs I, Glittenberg C. Transplantation of the RPE in AMD. *Prog Retin Eye Res*. 2007;26(5):516–554.
305. da Cruz L, Chen FK, Ahmado A, Greenwood J, Coffey P. RPE transplantation and its role in retinal disease. *Prog Retin Eye Res*. 2007;26(6):598–635.
306. Sengupta N, Caballero S, Sullivan SM, et al. Regulation of adult hematopoietic stem cells fate for enhanced tissue-specific repair. *Mol Ther*. 2009;17(9):1594–1604.
307. Park SS, Caballero S, Bauer G, et al. Long-term effects of intravitreal injection of GMP-grade bone-marrow-derived $CD34^+$ cells in NOD-SCID mice with acute ischemia-reperfusion injury. *Invest Ophthalmol Vis Sci*. 2012;53(2):986–994.
308. Park SS, Bauer G, Abedi M, et al. Intravitreal autologous bone marrow $CD34^+$ cell therapy for ischemic and degenerative retinal disorders: preliminary phase 1 clinical trial findings. *Invest Ophthalmol Vis Sci*. 2015;56(1):81–89.
309. Siqueira RC. Stem cell therapy for retinal diseases: update. *Stem Cell Res Ther*. 2011;2(6):50.
310. MacLaren RE, Pearson RA, MacNeil A, et al. Retinal repair by transplantation of photoreceptor precursors. *Nature*. 2006;444(7116):203–207.
311. Bi YY, Feng DF, Pan DC. Stem/progenitor cells: a potential source of retina-specific cells for retinal repair. *Neurosci Res*. 2009;65(3):215–221.
312. Ikeda H, Osakada F, Watanabe K, et al. Generation of $Rx^+/Pax6^+$ neural retinal precursors from embryonic stem cells. *Proc Natl Acad Sci USA*. 2005;102(32):11331–11336.
313. Lamba DA, Gust J, Reh TA. Transplantation of human embryonic stem cell-derived photoreceptors restores some visual function in Crx-deficient mice. *Cell Stem Cell*. 2009;4(1):73–79.

27

Inflammation and Immune Responses in Retinal Health and Disease

Andrew D. Dick, Richard W.J. Lee, Robert B. Nussenblatt, (posthumously)

Introduction

The eye has been long recognized as an immune privileged site.[1,2] Yet many disorders of the retina are driven by inflammation or by significantly altered immune responses. In addition to the archetypical immune-mediated disorders such as uveitis, examples include aging degenerative conditions, diabetic retinopathy (DR), and vascular ischemic events with immune consequences. This chapter will introduce the notion of immune regulation in the eye, rather than the historical strict definition of privilege; the latter evokes concepts of immune sequestration and relative immune incompetence, which is not the case. Instead, like most tissues and organs, the eye is bestowed with mechanisms that regulate immune responses and contain inflammation, the function of which is to protect and sustain tissue function in the face of constant insult and potential damage. This understanding of immunologic activities in the eye, particularly regarding the regulation of immune cell activation, regulation of vascular barriers, and interactions with systemic immunity, sets the stage for appreciating when immune responses are beneficial to maintain function during disease, and when immune responses require to be dampened to prevent ensuing damage.[3,4]

The historical idea that the retina is sequestered from systemic immunity and has "immunologic ignorance" has been largely dispelled. We now know that both the retina and choroid (including the ciliary body) are bestowed with a network of immune competent cells, such as microglia and choroidal macrophages, dendritic cells, and mast cell populations.[5] Further, there is active regulation of vascular barriers with perivascular macrophages and interaction with Müller glia.[6] A multitude of cognate and soluble mediators control cell activation in the eye,[3] including contributions from traditional nonimmune cells such as retinal pigment epithelium and astroglia[7] (Fig. 27.1). Not surprisingly, mechanisms of immune regulation (immune privilege) are implied by the need to combat against persistent damaging events such as oxidative stress, aging, and lifestyle events (e.g., smoking and obesity). These insults are compounded by genetic polymorphisms and epigenetic regulation of gene

expression, as illustrated by age-related macular degeneration (AMD).[8,9] By examining specific disorders, this chapter will highlight the immune regulatory mechanisms that operate in the eye, as well as the role of tissue-specific and system-wide immune responses in the context of uveitis, multifactorial degenerative conditions such as AMD, and dysregulation during angiogenesis.

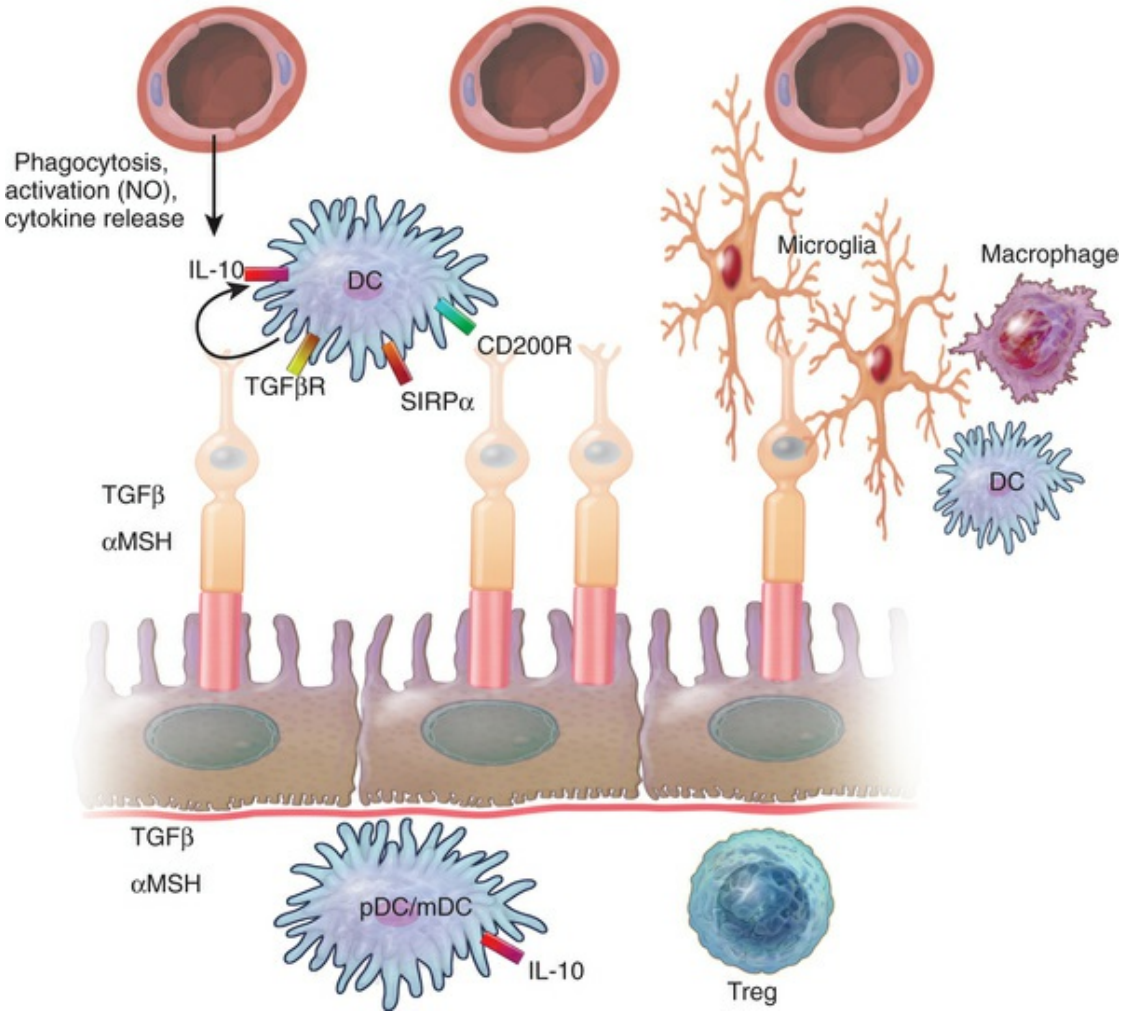

FIG. 27.1 Immune regulation within the retina. The retina is endowed with many immunoregulatory mechanisms. The retinal pigment epithelium (RPE) monolayer extends across the bottom of the figure. The apical microvilli of the RPE interdigitate with the outer segments of the photoreceptors. Multiple star-shaped microglia are shown within the retina, as are elongated, vertically oriented Müller cells. Perivascular macrophages are shown in the upper left. Microglia and choroidal myeloid cells (dendritic cells and

macrophages) sense the environment and regulate inflammatory responses. The healthy tissue sets the threshold for responses through inhibitory receptors (e.g., CD200R, SIRPα) or via the TGF-β or α-MSH rich environment. Regulation via neuronal cognate interactions is augmented by the regulatory functions of FasL expressing-RPE, in addition to mediators such as PD-1–PD-L1 interactions, TGF-β secretion, and inhibitory peptides. Activation of myeloid cells in the eye results primarily in IL-10 release; while other proinflammatory cytokines are also produced, the default response is regulation. Müller cells and microglia interact to maintain neuronal health, as well as the integrity of the inner blood–retinal barrier. DC, dendritic cell; NO, nitric oxide; pDC/mDC, plasmacytoid DC/myeloid DC; Treg, T regulatory cell.

Innate Defenses in the Maintenance of Retinal Health

As Fig. 27.1 illustrates, there are numerous cellular, cognate, and soluble mediators that regulate unnecessary and unwanted cellular activation, attenuate heightened immune responses, and maintain the vascular barrier. The innate immune defenses in this system are comprised of myeloid cells such as dendritic cells, monocytes, and macrophages, and the closely related microglia. These cells present antigen to T cells and may produce cytokines in response to nonspecific stimuli such as bacterial lipopolysaccharide (LPS). In the eye, myeloid cells are prone to producing regulatory cytokines such as IL-10, rather than inflammatory cytokines. This feature may aid in preserving tissue and cellular homeostasis, and limit inflammatory damage.

In the face of an aging process that includes tissue, cellular, and immune senescence, the retina may be vulnerable to a variety of noxious challenges that also activate host defense systems. From an immunologic perspective, the eye is endowed with a variety of immune response strategies that activate in response to insults, sometimes to excess, but also serve to counteract excessive immune

activation and control pathologic damage. The major components will be considered briefly.

Tissue Resident Macrophages

Microglia initially populate the developing retina and are derived from the yolk sac.[10,11] These cells are capable of division in the tissue, and maintain a signature transcriptome[12,13] that differentiates them from tissue macrophages and recent immigrant monocyte-macrophage populations. However, bone marrow-derived cells that become tissue macrophages may replenish the microglia population of the retina.[14] Populations of macrophages are found around the inner retinal vasculature (within the glial limitans), while microglia are generally situated in the inner and outer plexiform layers. However, when microglia are activated they can divide and become highly motile, migrating to the areas of tissue damage. There they may act as antigen-presenting cells, thus assisting to bridge and engage adaptive immune responses.[15–19]

The phenotype of microglia is typical of resident macrophage populations (Fig. 27.2 and Table 27.1). Their function is to maintain homeostasis, through cognate receptors that downregulate their activation (e.g., CD200-CD200R);[20–22] to secrete neurotrophins to support glial and neuronal function;[23] phagocytosis;[24] and to secrete immunomodulatory cytokines such as IL-10, produce indoleamine 2,3-dioxygenase (IDO), and express B7-H1.[25,26] In contrast, fully activated microglia can behave akin to recent monocyte-macrophage immigrants and potentiate inflammatory responses.[27] Unchecked innate activation proceeds to inflammasome activation and secretion of potent inflammatory mediators. Also of note, the monocyte-macrophage population, including microglia, is very plastic. This property results in a range of behaviors and responses that depend on the environmental context, and on the cognate and soluble cues that monocytes receive.[28,29] Monocyte-macrophages have been classified into subtypes (Table 27.1) in an effort to correlate phenotype with function, but these designations must be taken in the context of ongoing cell plasticity.

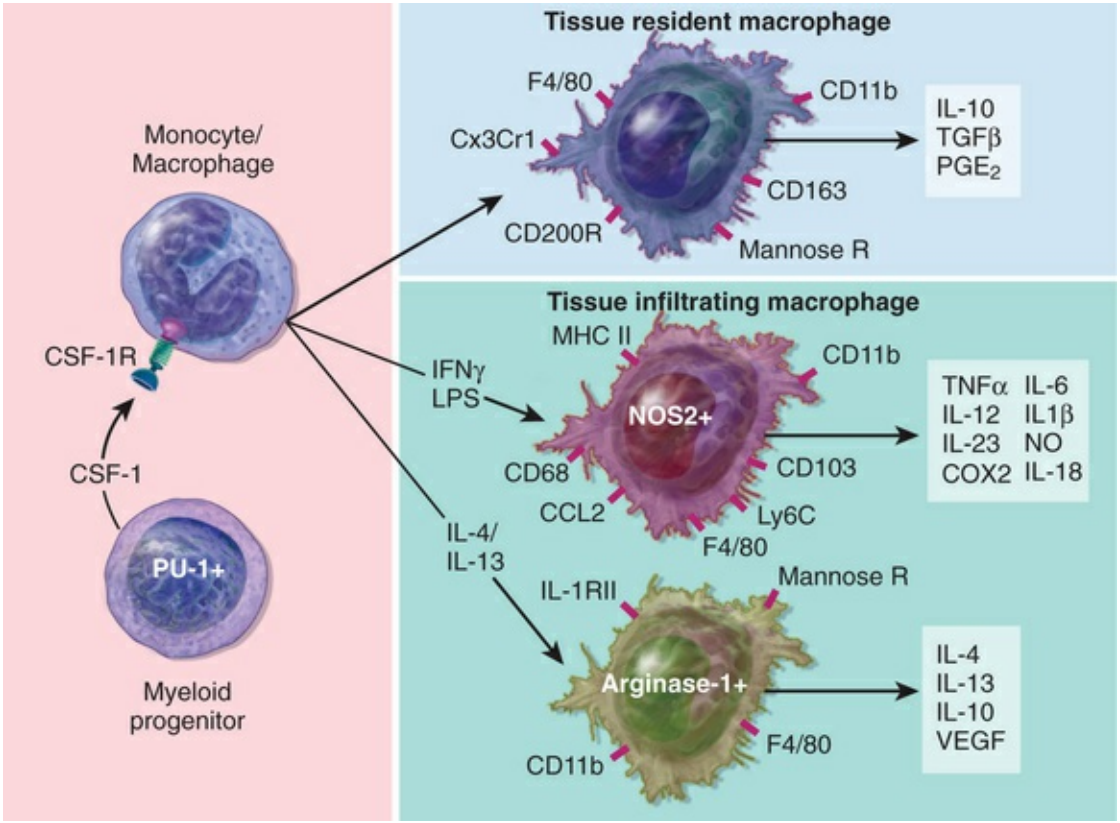

FIG. 27.2 The many subtypes of macrophages. Microglia are derived from yolk sac during development and may self-renew independently of bone marrow hemopoietic precursors.[11] Nonetheless, macrophages are derived from a common bone marrow progenitor; both in the bone marrow and in the tissues, macrophages require CSF-1 for viability. Upon entering tissues, microglia and macrophages respond to their environment and are plastic. This has led to a classification of tissue resident macrophages versus classically and alternatively activated macrophages (also termed M1 and M2). The development of these subtypes depends on the cognate and soluble signals that condition the cells. The resulting phenotypes lead to production of signature cytokines that effect their function as either cytopathic (when conditioned by IFN-γ and LPS) versus wound healing (when conditioned by IL-4/IL-13). NOS2+, enzyme Nitric Oxide Synthase 2+. (Modified from Schewitz LP, Lee RW, Dayan CM, et al. Glucocorticoids and the emerging importance of T cell subsets in steroid refractory diseases. Immunopharmacol Immunotoxicol. 2009;31(1):1-22.)

TABLE 27.1

Phenotypic Characteristics of Macrophage Subtypes

Classification	M1	M2		
		M2a	*M2b*	*M2c*
	CLASSICAL	ALTERNATIVE		
Stimulus	LPS, IFN, and TNF	IL-4, IL-13	TLR/IL-1 ligands	IL-10 glucocorticoids
Phenotype	CD68 MHC class II IL-12 high IL-10 low	MHC class II Mannose receptor	MHC class II CD68 IL-10 high IL-12 low	Mannose receptor
Gene	*NOS2*	*Arg*	*Arg, Ym-1*	*Arg-1, Ym-1*
Secretion	IL-1 TNF IL-6 VEGF	IL-10 IL-1RA	TNF IL-1 IL-6 IL-10 VEGF	IL-10 TGF-β
Function	TH1 responses Killing Tumor resistance	Killing of parasites Allergy	Th2 activation Immunoregulation	Immunoregulation Matrix remodeling Tissue restoration

The inflammasome is a multiprotein complex comprising a sensor protein, the adaptor protein ASC (apoptosis-associated speck-like domain containing caspase recruitment domain), and the inflammatory protease caspase-1. This complex is responsible for activation of many inflammatory processes. The assembly of the inflammasome signaling platform occurs due to conformational changes in the sensor protein, which in turn recruits caspase-1 to the complex and promotes the activation of caspase-1. Once activated, caspase-1 cleaves the inactive precursors of two proinflammatory cytokines, interleukin (IL)-1β and IL-18, the mature forms of which are secreted from cells.[30–33] The eye is endowed with inflammasome-forming sensors as receptors on cell surfaces, within cytoplasm, and on the nucleus.[34] These include the NLRP receptor molecules (nucleotide binding domain and leucine-rich repeat containing pyrin domain family), which belong to the Nod-like receptor family of proteins, such as NLRP1, NLRP3, and NLRC4; or Absent In Melanoma (AIM 2), a receptor of the HIN (interferon [IFN] inducible nuclear proteins) family of proteins. The NLRP3 inflammasome is clearly involved in host defense. For example, activation of IL-1β by an inflammasome is required to control certain pathogenic viral, bacterial, and fungal infections efficiently. However, excess IL-1β activity contributes to a variety of

diseases.[35] The NLRP3 inflammasome is also central in the pathogenesis of autoinflammatory disorders; its activity has been implicated in pathologies such as Alzheimer's disease, cancer, type 2 diabetes, and most recently AMD. Regulation of the NLRP3 inflammasome is poorly understood, but probably involves the integration of signals from a number of stimuli, such as cellular damage and stress. Inflammasome-dependent biologic effects may be mediated not only by IL-1β and IL-18, but also by the multifaceted activities of caspase-1. Thus, there may be secondary effects of protecting against inflammasome activation, such as when autophagy is increased.[36,37]

Immune Regulation by the Nonimmune Cell Compartment

The retinal pigment epithelium (RPE) not only comprises the outer retinal barrier, but is also a key contributor to immunoregulatory properties of the eye. This includes canonical features such as Fas Ligand (FasL) expression,[38,39] and secretion of immunomodulatory cytokines such as TGF-β and immunoregulatory neuropeptides, including α-melanocyte stimulating hormone (α-MSH).[40] In experimental models, α-MSH modulates macrophage-monocyte populations toward an alternatively activated pathway. Adaptive immunity is attenuated via FasL expression, resulting in the death of Fas-expressing T cells. Programmed cell death of T cells may also be induced through RPE PD-L1 expression,[41] or through generation of Treg cells supported, in part, by RPE-derived CTLA-4.[42,43] The RPE also protects against complement-induced damage[44–47] through membrane complement regulatory proteins (CD46, CD59) and generation of Complement Factor H (CFH).

Müller cells are the predominant glial cell type in the retina and are immune competent: they secrete cytokines, regulate immunity, and respond to danger signals through pathogen recognition receptors such as Toll-like receptors (TLR).[48] Under certain conditions, the Müller glia may induce suppression of T-cell responses. However, they also promote T-cell responses by producing IL-1 and by acting as antigen-presenting cells.[49,50] Moreover, experimental studies indicate that intercellular

interactions between Müller cells and both the inner retinal barrier (glial limitans) and microglia are essential for immune health. For example, activated microglia secrete neurotrophins (including CNTF, NT-3, and NGF) detected by Müller glia (which express neurotrophin receptor $p75^{ntr}$ and TrkC), with reciprocal effects on photoreceptor survival.[23]

Blood–Retinal Barriers

The well-described anatomic barriers, namely the inner retinal vasculature and the outer retinal RPE barrier, regulate immune traffic. Both the retinal endothelium and the RPE have well-formed junctional complexes, including tight junctions and adherens.[51] During experimental autoimmune uveitis (EAU), inflammation is accompanied by upregulation of adhesion molecules (e.g., p-selectin and ICAM-1), loss of junctional complexes, and transendothelial migration of leukocytes.[52,53] Further, compelling data support the conclusion that endothelium also regulates T-cell traffic. This occurs through "classic" migratory pathways such as chemotaxis, rolling, adhesion, and transmigration. In addition, B-cell secretion of a peptide initiates a regulatory cascade that results in production of sphingosine-1-phosphate by endothelial cells, which inhibits trafficking of T cells.[54] Similarly, endothelial cells express molecules such as CD200 that also influence the migration and activation of innate cells.[19] Together, the available data suggest a complex role for retinal endothelium, in which blood–retinal barriers are not absolute but allow trafficking of cells and immune surveillance;[25] yet the endothelium maintains the ability to control cell traffic, unless overwhelmed through systemic immune activation.[55]

The Role and Limits of Persistent Immune Activation in Maintaining Eye Health

Medzhitov first introduced the idea of parainflammation as a tissue-adaptive response to noxious stress or malfunction that is intermediate between basal and inflammatory states.[56] Briefly, in the basal state, tissue resident macrophages (principally retinal

microglia, and retinal perivascular macrophages or choroidal macrophages) are largely quiescent, but when activated promote an adaptive change with short-term benefits, providing ongoing tissue homeostasis. In contrast, parainflammatory responses are low level but ongoing and chronic. The purpose of parainflammation is to regulate homeostasis and tissue function in the face of persistent tissue insult with cell and immune activation responses. When a tissue is exposed to prolonged stress or malfunction, immune activation and inflammation ensues, and parainflammatory regulatory mechanisms are overwhelmed. Dysregulated or absent parainflammation has been proposed to play an important role in the progression of diabetes, atherosclerosis, and obesity, as well as AMD. Parainflammation has been illuminated experimentally in the aging retina and during degeneration.[4] These observations and concepts add complexity to the notion that immune activation and recruitment of macrophages may be required to help process photoreceptor and RPE byproducts, and thereby control overt inflammation, tissue dysfunction, and ultimately cell death. Moreover, in other models, it appears that the organ/tissue-specific regulatory threshold to maintain tissue homeostasis may be reset following every insult.[57]

The Aging Influence

Because the prevalence of retinal disease increases with age, the effect of aging and senescence on regulation of immune responses is important. Senescence is a loss of cellular potential to divide and grow, with consequences that influence immune responses. For example, senescence induces a p38 MAPK-mediated senescent-associated secretory phenotype that is proinflammatory,[58–60] with increased secretion of chemokines and proinflammatory cytokines (e.g., IL-6 and IL-1α); increase in mTOR-dependent autophagy; oxLDL secretion; and mROS upregulation. These activities potentiate inflammation, particularly innate immune activation and tissue infiltration. Cellular senescence in the eye is manifest in specific cellular responses. Hallmarks include changes in cell morphology (e.g., altered astrocyte and microglial morphology[61,62]); phenotypic changes that include altered telomerase and β-

galactosidase activities; release and cell loss of HMGB1; decline in lamin B1 (a nucleus stabilizer); and gH2AX nucleolar expression. While senescence may be present in retinal disorders, aging also influences the immune response. Adaptive T-cell immune responses exhibit both exhaustion and senescence. The mechanisms underlying each are independent, although both are compounded by age,[63,64] and both are central to individuals' response to chronic and persistent tissue damage and infection.

Autoinflammation and Autoimmunity

In health, appropriate immune responses protect the eye and maintain tissue homeostasis, but direct tissue destruction occurs when responses are aberrant. If immune responses ensue in the absence of foreign pathogens, the term “auto” is used to indicate that the consequent harm to host tissues is driven by a response against self. When the mediators of these inappropriate responses are cells of the innate immune system, this is described as “autoinflammation.” Conversely, damage caused by self-directed cells of the adaptive immune system (T and B lymphocytes) is called “autoimmunity.” Neither phenomenon occurs in isolation; once initiated, the full immune repertoire with varying contributions from each of its elements is brought into play. The magnitude of immune responses and accompanying tissue destruction are consequences of the underlying health of affected ocular tissues, the immune status of the host (both at a systemic and tissue level), and the balance of other homeostatic mechanisms. The latter include metabolic factors such as lipid profiles, control of glucose storage and action, and levels of tissue oxidative stress.[65,66]

At its most extreme, autoimmune and autoinflammatory intraocular inflammation is explosive, acute, and potentially rapidly devastating for vision. Conversely, when chronic, low-grade, subclinical tissue inflammation exceeds homeostatic (i.e., parainflammatory) levels, this can gradually progress over years to cause loss of retinal function. Importantly, chronic inflammation creates a local environment that is conducive to neovascularization. These pathologies further illustrate the idea that ocular immune privilege is a relative, rather than absolute, phenomenon. Once

immune responses are triggered, they can affect a variety of neural, vascular, endothelial, and epithelial components of the eye. Autoimmune responses ultimately exhibit all the features of conventional inflammatory cascades in other organs, and cause irreversible loss of vision through damage to the tissues responsible for sight.[25]

Erosion of Eye Health in the Absence of Infectious Disease

Autoinflammation and Autoimmunity as Classic Paradigms of Immune-Mediated Damage to Host Retinal Tissues

The most canonical examples of retinal autoinflammation and autoimmunity are in genetic diseases, which present in childhood. These have helped to reveal the mechanisms that underlie the dysregulation of both innate and adaptive immune responses. Blau disease is caused by gain-of-function mutations in *NOD2*, which regulates inflammasomes (see Tissue Resident Macrophages). This results in loss of tissue homeostasis in a range of organs, and is principally manifest clinically in the eye, skin, and joints.[67] Heightened responses to tissue danger signals trigger the secretion of IL-1β and IL-18 through a caspase-1-controlled intracellular cascade. This creates a proinflammatory environment in which adaptive immune cells are inappropriately recruited to healthy tissues, in the absence of pathogens that would normally trigger these immune responses.[68] If these immune responses continue unabated, pathologic tissue destruction occurs. Similarly, in IPEX syndrome, regulatory T cells (Tregs) have a loss-of-function mutation affecting their master transcription factor FoxP3. In health, Tregs suppress adaptive immune responses to self-tissues, and their loss unleashes multiorgan autoimmunity. The most complete clinical manifestation of IPEX leads to death in infancy.[69]

Experimental models of both autoimmune and autoinflammatory diseases that are similar to these human diseases and that affect a range of organs have further uncovered the principles of these immune abnormalities. However, in man the exact triggers for

pathologic autoinflammatory and autoimmune diseases are rarely well defined, and the consensus is that both autoinflammation and autoimmunity often contribute.[70] Pure noninfectious pathologies may result from heightened innate tissue inflammatory tone (either due to genetic polymorphisms or to environmental triggers), or adaptive immune responses against self-antigens which have escaped regulatory control. In addition, immune deviations triggered by previous infections may contribute, or bystander damage to self-tissues may take place during clearance of an infectious agent.[71] However, even in the most typical examples of noninfectious uveitis such as birdshot chorioretinopathy, there is no definitive serologic evidence of autoantibodies to self-antigens. This contrasts with classic autoimmune conditions affecting nonocular tissues, such as rheumatoid factor and anticitrullinated protein antibodies in rheumatoid arthritis, and antinuclear antibodies in systemic lupus erythematosus. Hence, although a wide range of well-characterized human uveitic entities have no known infectious trigger, their etiology remains unknown but putatively autoimmune. These diseases are often phenotypically similar to animal models of ocular autoimmunity, which are stimulated by specific retinal antigens. This circumstantial evidence therefore suggests they are caused by aberrant immune responses against self.[72] There are also well-defined associations between certain uveitic entities and major histocompatibility complex (MHC) class II human leukocyte antigens (HLAs), such as the link between Vogt–Koyanagi–Harada's syndrome and HLA-DR4. These observations further support the notion of underlying self-directed $CD4^+$ helper T-cell responses, similar to that in other MHC class II polymorphism-associated diseases.[73] However, the majority of reported HLA associations in intraocular inflammation are with MHC class I alleles, the most common of which is HLA-B27-associated anterior uveitis. Because class I HLAs primarily present antigen to $CD8^+$ T cells, the possibility of an undiagnosed viral infectious cause remains.

Nonuveitic Diseases of the Retina That Have Autoimmune or Autoinflammatory

Components

Abnormal inflammatory responses directed against self-tissues are most readily recognized in uveitis, where there are frank clinical signs of breakdown of the blood–ocular barrier. These include white cells suspended in the aqueous and vitreous humor and overt features of retinal vasculitis, retinal pigment epithelitis, edema within the neuroretina, and choroidal infiltrates that are clearly visible with a slit-lamp biomicroscope. However, the ocular tissue destruction that results during other more common diseases, such as AMD and DR, also has a major inflammatory drive. In these cases, inflammation takes place at a tissue level that is beyond the optical resolution achievable with current instruments used for clinical observation.

The chronic onslaught of environmental stresses with aging heightens the readiness of tissue resident innate immune cells, such as retinal microglia, to proceed to overt inflammation.[56] Although not a frank dysregulation of innate immunity as is seen in Blau syndrome, parainflammation (see The Role and Limits of Persistent Immune Activation in Maintaining Eye Health) provides the immunologic context for altered tissue homeostasis and a chronic inflammatory environment. Additional insults such as oxidative stress, or an increased level of proinflammatory metabolites, can potentiate this. Stress at this level induces an insidious recruitment of monocytes and T cells from the peripheral circulation, contributing to an emerging milieu of soluble mediators. These immune responses may harm self-tissues either directly, or indirectly through the induction of choroidal neovascularization.[74,75] In DR, leukostasis occurs in the retinal circulation, when immune cells adhere to an activated retinal vascular endothelium. Further, hyperglycemia affects innate immune cell function. These two factors, coupled with the breakdown of the blood–ocular barrier and neovascularization of the retinal circulation, generate a proinflammatory drive that is harmful to retinal tissue.[76,77] Although neither AMD nor DR fit the definitions of inflammasome-mediated inflammation or antigen-specific inflammation seen in classic autoinflammatory and autoimmune syndromes, they still represent nonuveitic immune-mediated retinal diseases resulting from secondary immune responses that destroy self-tissues.

The Potential for Nonocular Infections to Augment Immune Responses Directed Against Self-Tissues in the Eye

In theory, autoimmunity against ocular proteins can be driven by infections at nonocular sites. This is best illustrated in animal models of uveitis, where an adaptive immune response in the eye is elicited by systemic immunization using retinal proteins.[78] However, intraocular inflammation does not result if the animal is injected with retinal antigens alone. This is because antigen-specific T cells are not activated through antigen recognition in the absence of a second signal from antigen-presenting immune cells. In experimental models, antigen-presenting cells need to be nonspecifically stimulated by pattern recognition receptors, such as by engagement of either evolutionarily conserved proteins that are common to a range of infectious pathogens (e.g., lipopolysaccharide), or indirectly by host-tissue derived danger signals.[79,80] In the case of direct ocular infection, such as in exogenous bacterial endophthalmitis following cataract surgery, both innate and adaptive immune responses are triggered by bacteria present in the eye; in this case, autoimmune disease does not follow, presumably due to the destructive outcome of the profound infection. However, the infectious innate immune stimulus can be nonocular, followed by consequent antigen-specific autoimmune responses in the eye. Hence, an autoimmune response is only observed in the retina of an experimental animal immunized with interretinal binding protein if tubercular proteins and often pertussis toxin are also injected intraperitoneally.[72] Although there is no direct proof of this paradigm in human disease, anecdotes suggest that intraocular inflammation, which improves with immunosuppressive therapy, can go into remission following treatment of latent tuberculosis infection.[81] These observations imply that removing systemic nonocular innate immune triggers leads to resolution of associated adaptive immune responses in the eye. The relevance of this phenomenon may extend equally to other nonuveitic retinal pathologies. There are many features in common with the neurodegeneration observed in Alzheimer's disease and AMD. It is well documented that an acute deterioration in the

cognitive ability of Alzheimer's patients can be precipitated by a bacterial urinary tract infection, and acute systemic inflammation exacerbates neurodegeneration both experimentally and in patients.[82,83] By implication, a parallel acceleration of inflammatory pathology associated with AMD may accompany nonocular systemic infectious disease.

Inflammation, Vascular Regulation, and Pathologic Angiogenesis (Neovascularization)

Pathologic angiogenesis occurs in numerous ocular disorders, particularly retinal disorders. To some extent, altered immune responses occur in all pathologic angiogenesis. In considering mechanisms, it is important to distinguish between types of inflammation in any of these conditions, whether retinopathy of prematurity, diabetes, or AMD. Altered immune responses may be apparent in the activation of constituent cell populations (e.g., microglia, Müller glia, and endothelial cells) without evidence of pathologic inflammation, or be obvious, such as when immune cells infiltrate from the periphery. The absence of infiltrating cells does not mean absence of inflammation, absence of altered immunity, or absence of defects in immune homeostasis.

The degree of contribution of inflammation during angiogenesis depends upon the pathology. In uveitis (intraocular inflammation), altered vasculature is common, but pathologic angiogenesis occurs infrequently. Despite this, neovascularization occurs from the retinal circulation[84] (not always as a consequence of ischemia), and via the choroid as choroidal neovascularization (CNV).[85] Neovascularization can be prevalent in some low-grade persistent inflammatory uveitic conditions.[86] Its link with inflammation has been corroborated in experimental models, where angiogenesis is frequently observed with persistent inflammation.[87] In uveitis, breakdown of barriers provided by capillary and postcapillary venular architecture is common, accompanied by uveitic macular edema. Studies of the HIF-driven vascular endothelial growth factor (VEGF)-mediated CNV in neovascular AMD indicate a role

for inflammation, further illustrating the close interplay between inflammation, vascular health, and the potential for pathologic angiogenesis when inflammation is present.

Role of Macrophage Subtypes in Pathologic Angiogenesis

As introduced above, the function and phenotype of macrophage subtypes is conditioned by signals encountered within the tissue microenvironment. In mice, the paradigm of M1 and M2 macrophages (Table 27.1) has been studied with respect to angiogenesis in other fields as well as in the retina.[88–91] Classic activation generates M1 macrophages, which have proinflammatory functions. Alternatively, activated M2 macrophages confer responses related to wound healing, and are capable of generating VEGF and promoting angiogenesis. However, pathologic angiogenesis is observed most commonly in the presence of M2 macrophages.[92] The role of macrophages in driving a VEGF-dependent angiogenic response is supported by recent evidence from studies using the laser-induced CNV model. These studies demonstrate that early initiation of choroidal angiogenesis is dependent upon macrophage phagocytosis of damaged RPE components. This in turn elicits an Arg-1$^+$, VEGF$^+$ M2 phenotype. On the other hand, macrophage subtypes are plastic, and functional outcomes may not be straightforward. For example, IFN-γ and TLR4 ligation (with LPS) can generate VEGF$^+$ M1 macrophages, but prostaglandin (PG) E_2 remains a potent stimulus for the generation VEGF$^+$ M2 macrophages as well. Similarly, macrophages that are alternatively activated via IL-4 can result in a sFlt-1-secreting M2 cell in mouse and man[93] (Fig. 27.3). In man, macrophages associated with CNV or in specimens of AMD retina that are assessed using immunohistochemistry confirm the nature of VEGF-expressing CD68$^+$ cells[94] (Fig. 27.2). Finally, as noted elsewhere, perturbing macrophage function can attenuate neovascularization in experimental models.[95]

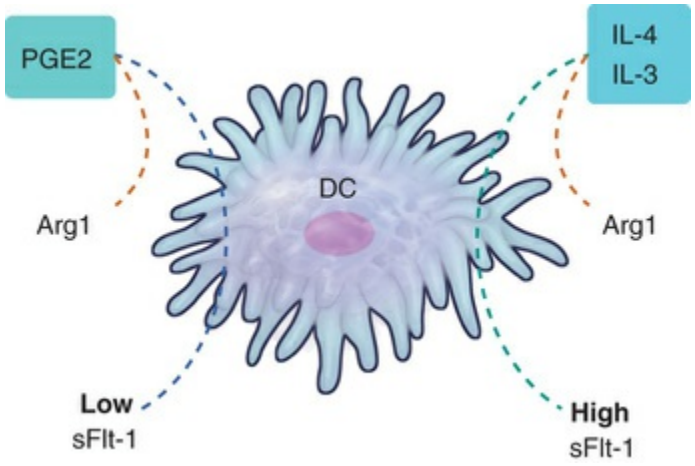

FIG. 27.3 M2 macrophages can serve divergent functions. The contribution of alternatively activated M2 (Arg-1$^+$) macrophages to angiogenesis is polarized, depending on signals and conditioning they receive. Both PGE_2 and IL-4 (Th2 cytokines) may drive macrophages toward an M2 phenotype, but the functional response to each is quite discrete. PGE_2 generates proinflammatory cells that secrete high levels of VEGF and low levels of sFlt-1; in contrast, IL-4 generates M2 cells that secrete high levels of sFlt-1 secretion, and as a result are antiangiogenic.

Role of Pathologic Angiogenesis in DR

In DR, advanced glycation endproducts (AGE) are recognized and accumulate at endothelium. This, along with loss of pericytes and capillary occlusion, are all instrumental in the progression of disease that leads to a breakdown of vascular integrity. Ischemia, edema, and finally neovascularization are also associated with changes in microglial distribution[96] and infiltration of VEGF-secreting monocyte-macrophage populations. Inflammation also plays a central role in the progression of DR.[97] For example, receptors for AGE (RAGE)[98] are widely expressed on retinal cells in DR, and upregulate proinflammatory pathways. A proinflammatory environment has been described in animal models and human studies, which is exacerbated by DR's hypoxic–ischemic environment. The central role of inflammation in DR is further reflected in the upregulation of tumor necrosis factor (TNF)-α, IL-1β, monocyte chemotactic protein 1 (MCP-1/CCL2), and

macrophage inflammatory protein (MIP)/CCL3. Transcripts for all of these have been detected in the ischemic–hypoxic retina. These proinflammatory cytokines, particularly TNF-α and IL-1β, are thought to play a major role in the breakdown of the blood–retinal barrier and in the degeneration of retinal capillaries. CCL2 and RANTES/CCL5 are significantly elevated in sera of patients with severe nonproliferative diabetic retinopathy, compared with those who have less severe retinopathy. Increased C-reactive protein (CRP), IL-6, TNF-α, and especially the adhesion molecules intercellular adhesion molecule (ICAM)-1, vascular cell adhesion molecule (VCAM)-1, and E-selectin are associated with nephropathy, retinopathy, and cardiovascular disease in both type 1 and type 2 diabetes. In proliferative diabetic retinopathy, vitreous cytokine levels of IL-6, IL-8, and CCL2 are strongly correlated with elevated VEGF.

Thus, the pathogenesis of diabetic retinopathy is a highly complex and multifactorial process. Hyperglycemia perturbs the metabolic and hemodynamic equilibrium, affecting multiple cell types. Their signature molecular responses lead ultimately to the formation of AGE, oxidative stress, glial activation, and inflammation. These conditions result in neural and vascular damage. As with the CNS, maintaining the health of retinal neurons depends on functional interactions between neurons, glial, microglia, and blood vessels, termed the "neurovascular unit." When these functional interactions are impaired in DR, such as when driven by ischemic inflammation, regulation is impaired correspondingly. This includes impaired remodeling via endothelial progenitor cell (EPC) recruitment. Recently, therefore, the available evidence has suggested that diabetic retinopathy is a neurovascular complication that results from changes to the neurovascular unit, rather than from isolated neuroglial or vascular alterations.[99] Neural apoptosis and gliosis (activation of glial cells, including astrocytes and Müller cells with a resulting proinflammatory environment) are thus the final, canonical histologic features of diabetic neurodegeneration.[100]

Inflammation and AGE-Related

Macular Degeneration

For many years, the term degeneration denoted numerous mechanisms of cellular decay, but none of them intoned immune mechanisms. Immune mechanisms have come to the forefront recently as a possible explanation for the underlying changes noted in the degenerative diseases, including those in the eye.[101] Atherosclerosis, heart disease, and Alzheimer's disease are examples of diseases where immune mechanisms appear to be centrally important to the disease process. Importantly, it appears that changes can be seen in the systemic immune system as well as in the eye. Here, AMD, a major public health problem, will be used as an example of a disease affected by both systemic and local degenerative changes in inflammatory responses. For convenience, these will be addressed separately.

Systemic Inflammatory Changes During AMD

Patients with ocular inflammatory disorders such as uveitis, while clearly demonstrating alterations within the eye, have demonstrable and characteristic alterations in the circulating immune system. This is being noted now in many degenerative conditions. Perhaps the best known example is that of CFH. CFH is a regulatory protein, which suppresses formation of the C3 cleavage enzyme and inhibits the alternative pathway of complement activation. Complement gene polymorphisms have been clearly implicated in the development of AMD.[102–104] However, it is important to remember that about a third of whites, most of whom have healthy eyes, have the Y402H variant that is most often linked to AMD. Further, while differences in complement regulation between those with the variant and the wild type alleles have been reported,[105] no functional immune mechanism has been found to explain this association, at least in the canonical pathways of complement activation. Further, the same CFH variant has been reported in patients with sarcoidosis, most of whom were black,[106] as well as those with multifocal choroiditis.[107] As a group, blacks do not develop advanced AMD. However, CFH may play an important role in RPE homeostasis. Genomewide associations have

now demonstrated DNA variants in several other genes, many of which involve the complement system (Table 27.2).

TABLE 27.2

Genetic Risk Factors Associated With Age-Related Macular Degeneration[a]

Gene Symbol	Gene Name	Major Function	Location	Variant
CFH	Complement factor H	Regulation of complement activation	1q32	rs380390, rs1061170, rs1410996, rs10737680
CFB	Complement factor B	Alternative pathway of complement activation	6p21	rs641153, rs415667, rs541862
C2	Complement component 2	Classic pathway of the complement system	6p21	rs9332739, rs9380272
C3	Complement component 3	Activation of both classic and alternative complement pathways	19p13	rs2230199, rs1047286
CFI[b]	Complement factor I	A serine proteinase regulating the complement cascade	4q25	rs10033900
ARMS2	Age-related maculopathy susceptibility 2	Retina homeostasis	10q26	rs10490924
HTRA1	HtrA serine peptidase 1	Proteolysis, negative regulation of BMP and TGFb signaling pathway	10q26	rs11200638, rs3793917
APOE	Apolipoprotein E	Cholesterol homeostasis and cell apoptosis	19q13	APOε4, APOε2
TIMP3	TIMP metallopeptidase inhibitor 3	Metalloendopeptidase inhibitor	22q12	rs9621532
HLA	Major histocompatibility complex	Antigen processing and presentation, immune response	6q21	Cw-0701, B-4001, DRB1-1301
IL8	Interleukin 8	Neutrophil chemotactic and activating factor	4q13-q21	rs4073
CX3CR1	Chemokine (C-X3-C motif) receptor 1	Macrophage chemotaxis and microglial cell activation	3q21	T280M
TLR3[b]	Toll-like receptor 3	Pathogen recognition and activation of innate immunity	4q35	rs3775291
TLR4[b]	Toll-like receptor 4	Pathogen recognition and activation of innate immunity	9q33	rs4986790
CETP	Cholesteryl ester transfer protein, plasma	Cholesterol homeostasis	16q21	rs3764261
LIPC	Hepatic lipase	Triglyceride hydrolase and ligand/bridging factor for receptor-mediated lipoprotein uptake	15q21-q23	rs10468017
VEGFA	Vascular endothelial growth factor A	Angiogenesis, artery morphogenesis, blood coagulation	6q12	rs4711751
COL10A1	Collagen, type X, alpha 1	Extracellular matrix organization	6q21-q22	rs1999930

TNFRSF10A	Tumor necrosis factor receptor superfamily, member 10a	Transduces cell death signal and induces cell apoptosis	8q21	rs13278062

[a]For references please see the original publication cited below.

[b]Conflicting results were obtained from different studies.

Reproduced with permission from Nussenblatt RB, Liu B, Wei L, Sen HN. The immunological basis of degenerative diseases of the eye. Int Rev Immunol 2013; 32:1563.

Systemic Complement C5a and TH17-Mediated Immune Responses in AMD

Mouse studies suggested that C5a provides both an activating and survival stimulus to T cells.[108,109] T cells from peripheral blood of AMD patients have larger numbers of the receptor for C5a on their cell surfaces when compared to control subjects.[110] This increased number of receptors is associated with several observations that demonstrate immune activation. In vitro experiments with T cells from both AMD patients and control subjects, in which C5a was added to the cultures, resulted in enhanced production of IL-22 and IL-17. Blocking the C5a receptor reversed this enhancement. Of interest, both control subjects and AMD patients with higher IL-17 and IL-22 production had the risk allele.[110] These findings invite speculation that CFH's role in controlling responses is at the level of the adaptive immune system. In addition, enhanced cytokine responses were noted when monocytes were added to the in vitro cultures, and neutralization of IL-1γ or IL-6 markedly dampened these responses. Further, and similar to mouse studies, an enhanced number of C5aR on human T cells protected them from undergoing apoptosis. In addition, the peripheral blood cells from AMD patients often demonstrate anamnestic responses to retinal antigens. The development of choroidal neovascularization in AMD patients in association with activated macrophages found in peripheral blood has also been reported.[111]

Systemic Cytokines and Autoantibodies

Altered T-cell responses are not the only systemic differences in AMD patients. When circulating cytokines were assessed, IL-22 and

Il-17 levels were significantly elevated in patients as compared to controls; further, these changes were seen early in the disease process. The higher cytokine levels in patients were particularly notable in those with the CFH variant. Penfold et al.[112] reported the presence of antiglial fibrillary acid protein (GFAP) in the sera of AMD patients. This is a marker for activities of retinal astrocytes, which help to maintain the blood–ocular barrier. In addition, other antibodies directed to retinal antigens have been found circulating in AMD sera. These include antibodies to CEP adducts, alpha-crystallin, alpha-enolase, and annexin II.[113–115] Hollyfield et al. connected in vitro experiments and in vivo observations by producing AMD-like lesions in mice exposed to an oxidative product.[116,117] In these studies, mice were immunized with CEP adducts formed by the covalent interaction with an oxidation fragment of docosahexanoic acid (DHA), resulting in antibodies against CEP and development of retinal pathology.

Inflammatory Changes Seen in the AMD Eye

In addition to the systemic alterations which are readily detected in AMD, various inflammatory processes are found directly in the eye itself as well. These are considered in detail below.

Oxidative Stress in the Eye

Oxidative processes occur through the removal of electrons from molecules. In biologic systems, energy is released when lipids, proteins, and carbohydrates are oxidized to form carbon dioxide and water. Oxidative reactions may also result in the production of reactive oxygen intermediates (ROIs), such as free radicals, hydrogen peroxide, and singlet oxygen. ROIs, which can damage other molecules, increase under conditions of irradiation, aging, reperfusion, inflammation, increased partial pressure of oxygen, cigarette smoke, and air pollution.[118] The biologic mechanisms that prevent the detrimental effects of ROIs include cellular compartmentalization, repair of DNA and proteins, and neutralization by antioxidant compounds. The retina is an ideal environment for the generation of ROIs for several reasons: (1) high oxygen consumption; (2) high levels of cumulative irradiation; (3)

RPE phagocytosis, which is an oxidative stress that produces ROIs; (4) high levels of polyunsaturated fatty acids in the photoreceptor outer-segment membranes; and (5) abundant photosensitizers in the neurosensory retina and RPE.[118]

Oxidative stress results when there is an imbalance between prooxidants and antioxidants, leading to molecular damage and/or a disruption of redox signaling.[119] Inflammation and oxidative stress are closely interrelated: inflammatory cells can generate ROIs, and oxidative stress can induce inflammation through nuclear factor-kappa B (NF-κB)-mediated inflammatory gene expression.[119] Oxidative stress plays a role in the pathogenesis of several retinal disorders, including AMD. Multiple changes are associated with the aging eye, including thickening of Bruch's membrane, accumulation of lipofuscin in the RPE, and loss of parafoveal rods. In a model outlined by Curcio et al.[120] and others, the RPE and Bruch's membrane are modified or damaged by oxidative stress and enzymatic processes over time. The materials retained at these sites, including lipoproteins, may be modified by oxidative stress, and then become stimuli for inflammation.[120]

Oxidative Stress and Inflammation in AMD

Several studies have provided further evidence that oxidative stress is involved in AMD pathogenesis. Crabb et al. performed a proteomic analysis of drusen from normal and AMD donor eyes.[121] These studies identified multiple proteins modified by oxidation that were found more frequently in drusen from AMD eyes. These oxidation-related products included cross-linked molecules of carboxyethyl pyrrole (CEP) protein adducts, tissue metalloproteinase inhibitor 3, and vitronectin. Carboxymethyl lysine, an AGE produced through oxidation of carbohydrate, was also isolated. Significant elevation of an oxidation product-related receptor was also found in eyes with the advanced dry form of AMD. In another general proteome study by Yuan et al.,[122] approximately 60% of the elevated proteins were involved in immune responses or host defense, including complement factors C5 and C7, α-crystallin A, α-crystallin B, and major histocompatibility complex (MHC) class II molecule DRα.

Other Immune Alterations in the AMD Eye

Cells from eyes with inflammatory diseases, including AMD, exhibit upregulated expression of immune receptors and molecules.[123,124] Enhanced receptor expression has been noted, particularly at the outer retina, especially the expression of IL-17RC. This is a receptor for a dimer of IL-17A and IL-17F. Clearly immune activation can occur via this receptor, altering RPE function. In addition to IL-17RC, IL-17, and IL-22 transcripts are also increased in the eye. Interestingly, IL-22 has a negative effect on human RPE cells, decreasing total tissue resistance and increasing apoptosis.[125] As discussed above, the NLRP-3 inflammasome promotes cleavage of pro-IL-1beta and IL-18, and may play a role in negatively regulating angiogenesis.[126]

Numerous histopathologic studies of AMD eyes have documented the presence of macrophages and multinucleated giant cells, mainly associated with vascular channels and breaks in Bruch's membrane (Fig. 27.4).[127–132] Macrophage subtype changes have been noted in the eyes of patients with AMD, including a change in the M1/M2 ratio in AMD eyes compared to that in control eyes of the same age.[132]

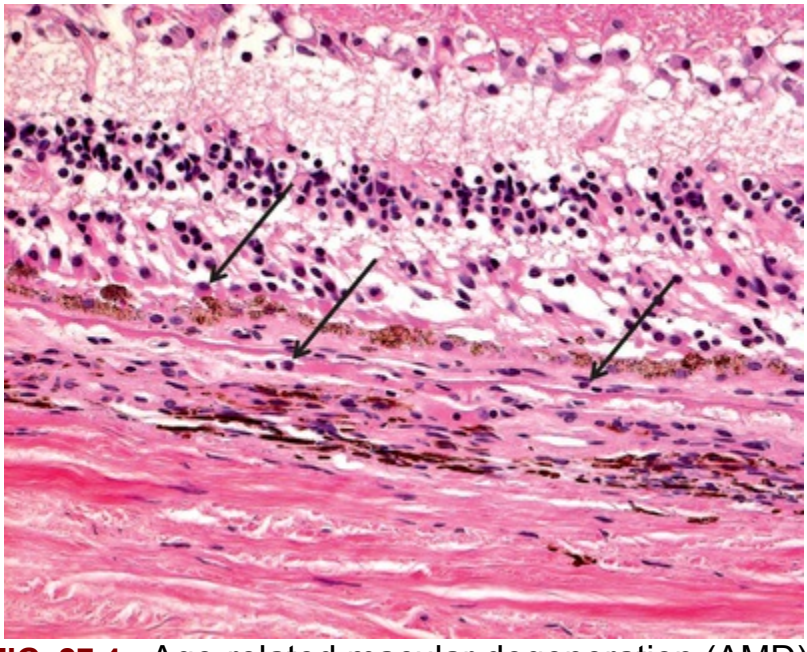

FIG. 27.4 Age-related macular degeneration (AMD). Scattered inflammatory cells (*arrows*) are found in an AMD lesion. (Hematoxylin and eosin, ×200.)

While the systemic alterations noted are an indication of general immune activation, many of these changes would also be observed specifically in the cluster of characteristics termed immunosenescence.[133] Some of the cardinal features of immunosenescence include an impaired ability to respond to new antigens, while at the same time unsustained memory responses appear to be coupled with a greater propensity for autoimmune responses. These factors are believed to lead to a lingering, low-grade inflammation, and possibly are major contributors to the development of rheumatoid arthritis.[134] It is therefore plausible that the phenomenon of immunosenescence also contributes to the pathogenesis of inflammation in the aging eye.

Targeting Inflammation Through Molecular Stratification: Genetics and Beyond

Clearly one major impetus to better understand the underlying mechanisms that lead to degenerative disorders such as AMD is to prevent or reverse these. It is likely that AMD results from many mechanisms. A large randomized and controlled clinical trial, the Age-Related Eye Disease Study (AREDS), demonstrated that vitamin and mineral supplementation reduced the risk progression from intermediate to advanced AMD.[135] Although the exact mechanism is unknown, one hypothesis is that the AREDS vitamin formulation counteracts oxidative stresses in the retina. Understanding the mechanistic role of CFH may unlock new strategies as well. Other genetic alterations may also help define the various paths that lead to this disorder. Gene therapy for eye diseases has gained considerable interest in the past years, and the potential approaches continue to change and improve.[136] An alternative strategy is to evaluate the epigenetic alterations associated with the genes that lead to degenerative disorders. Epigenetic studies could target the mechanisms that lead to expression of gene products, separately from the gene sequence itself. Epigenetic therapy is already effective in treating some

cancers, and is beginning to be used in autoimmune diseases such as juvenile idiopathic arthritis.[137] We have shown that epigenetic therapy provides benefit, decreasing the development of disease in a uveitis model (Nussenblatt et al., unpublished data). Silencing or activating genes either by affecting the promoter site, or via histones, will certainly be a future therapeutic approach.

An AMD clinical trial demonstrated the benefits of immunomodulatory medications such as sirolimus and daclizumab;[138] ongoing studies are now investigating complement component inhibitors.[139] While systemic immunomodulation did appear to have an effect on the course of advanced AMD, this is not a viable long-term strategy for multiple reasons, including cost and the age of the patients. However, anti-IL-17 and IL-22 therapy administered locally to the eye may be useful in preventing changes that appear to result from the presence of these respective cytokines. A larger goal would be to reverse systemic immunosenescent changes. Finally, from a public health perspective it would be far more attractive to prevent AMD than to treat it. Developing treatments based on oral tolerance could be one such approach,[140] which showed promise in treating uveitis patients.[141] In an inflammatory disease model, oral tolerance downregulated IL-17 expression,[142] and such therapy with appropriate fragments could be continued for long periods of time.[143]

Conclusion

Retinal disease results from an intricate mixture of factors that include direct and indirect effects of inflammation and immune responses. Many of the recent findings that help explain immune-mediated pathogenesis suggest opportunities for interventions. In the future, treatment and preferably prevention of retinal diseases will likely use combinations of options. These include local and systemic immunomodulation, targeting senescent changes, epigenetic remodeling, and tolerance. Such multipronged approaches might best attack the many complex interacting pathways associated with aging, oxidative stress, and inflammation.

References

1. Niederkorn JY. See no evil, hear no evil, do no evil: the lessons of immune privilege. *Nat Immunol*. 2006;7(4):354–359.
2. Stein-Streilein J, Caspi RR. Immune privilege and the philosophy of immunology. *Front Immunol*. 2014;5:110.
3. Dick AD, Carter D, Robertson M, et al. Control of myeloid activity during retinal inflammation. *J Leukoc Biol*. 2003;74(2):161–166.
4. Xu H, Chen M, Forrester JV. Para-inflammation in the aging retina. *Prog Retin Eye Res*. 2009;28(5):348–368.
5. Forrester JV, Xu H, Kuffova L, Dick AD, McMenamin PG. Dendritic cell physiology and function in the eye. *Immunol Rev*. 2010;234(1):282–304.
6. Guillemin GJ, Brew BJ. Microglia, macrophages, perivascular macrophages, and pericytes: a review of function and identification. *J Leukoc Biol*. 2004;75(3):388–397.
7. Detrick B, Hooks JJ. Immune regulation in the retina. *Immunol Res*. 2010;47(1–3):153–161.
8. Black JR, Clark SJ. Age-related macular degeneration: genome-wide association studies to translation. *Genet Med*. 2016;18(4):283–289.
9. Fritsche LG, Chen W, Schu M, et al. Seven new loci associated with age-related macular degeneration. *Nat Genet*. 2013;45(4):433–439 [439e1-2].
10. Alliot F, Godin I, Pessac B. Microglia derive from progenitors, originating from the yolk sac, and which proliferate in the brain. *Brain Res Dev Brain Res*. 1999;117(2):145–152.
11. Gomez Perdiguero E, Klapproth K, Schulz C, et al. Tissue-resident macrophages originate from yolk-sac-derived erythro-myeloid progenitors. *Nature*. 2015;518(7540):547–551.
12. Beutner C, Lepperhof V, Dann A, et al. Engineered stem cell-derived microglia as therapeutic vehicle for experimental autoimmune encephalomyelitis. *Gene Ther*. 2013;20(8):797–806.

13. Gautier EL, Shay T, Miller J, et al. Gene-expression profiles and transcriptional regulatory pathways that underlie the identity and diversity of mouse tissue macrophages. *Nat Immunol*. 2012;13(11):1118–1128.
14. Xu H, Chen M, Mayer EJ, Forrester JV, Dick AD. Turnover of resident retinal microglia in the normal adult mouse. *Glia*. 2007;55(11):1189–1198.
15. Wang M, Wong WT. Microglia-Müller cell interactions in the retina. *Adv Exp Med Biol*. 2014;801:333–338.
16. Karlstetter M, Langmann T. Microglia in the aging retina. *Adv Exp Med Biol*. 2014;801:207–212.
17. Gregerson DS, Sam TN, McPherson SW. The antigen-presenting activity of fresh, adult parenchymal microglia and perivascular cells from retina. *J Immunol*. 2004;172(11):6587–6597.
18. Omri S, Behar-Cohen F, de Kozak Y, et al. Microglia/macrophages migrate through retinal epithelium barrier by a transcellular route in diabetic retinopathy: role of PKCzeta in the Goto Kakizaki rat model. *Am J Pathol*. 2011;179(2):942–953.
19. Carter DA, Dick AD. CD200 maintains microglial potential to migrate in adult human retinal explant model. *Curr Eye Res*. 2004;28(6):427–436.
20. Copland DA, Calder CJ, Raveney BJ, et al. Monoclonal antibody-mediated CD200 receptor signaling suppresses macrophage activation and tissue damage in experimental autoimmune uveoretinitis. *Am J Pathol*. 2007;171(2):580–588.
21. Dick AD, Broderick C, Forrester JV, Wright GJ. Distribution of OX2 antigen and OX2 receptor within retina. *Invest Ophthalmol Vis Sci*. 2001;42(1):170–176.
22. Hoek RM, Ruuls SR, Murphy CA, et al. Downregulation of the macrophage lineage through interaction with OX2 (CD200). *Science*. 2000;290(5497):1768–1771.
23. Harada T, Harada C, Kohsaka S, et al. Microglia-Müller glia cell interactions control neurotrophic factor production during light-induced retinal degeneration. *J Neurosci*. 2002;22(21):9228–9236.
24. Karlstetter M, Nothdurfter C, Aslanidis A, et al. Translocator

protein (18 kDa) (TSPO) is expressed in reactive retinal microglia and modulates microglial inflammation and phagocytosis. *J Neuroinflammation*. 2014;11:3.
25. Wraith DC, Nicholson LB. The adaptive immune system in diseases of the central nervous system. *J Clin Invest*. 2012;122(4):1172–1179.
26. Broderick C, Duncan L, Taylor N, Dick AD. IFN-gamma and LPS-mediated IL-10-dependent suppression of retinal microglial activation. *Invest Ophthalmol Vis Sci*. 2000;41(9):2613–2622.
27. Robertson MJ, Erwig LP, Liversidge J, Forrester JV, Rees AJ, Dick AD. Retinal microenvironment controls resident and infiltrating macrophage function during uveoretinitis. *Invest Ophthalmol Vis Sci*. 2002;43(7):2250–2257.
28. Martinez FO, Gordon S. The evolution of our understanding of macrophages and translation of findings toward the clinic. *Expert Rev Clin Immunol*. 2015;11(1):5–13.
29. Gordon S. Alternative activation of macrophages. *Nat Rev Immunol*. 2003;3(1):23–35.
30. Gross O, Thomas CJ, Guarda G, Tschopp J. The inflammasome: an integrated view. *Immunol Rev*. 2011;243(1):136–151.
31. Dowling JK, O'Neill LA. Biochemical regulation of the inflammasome. *Crit Rev Biochem Mol Biol*. 2012;47(5):424–443.
32. Campbell M, Doyle S, Humphries P. IL-18: a new player in immunotherapy for age-related macular degeneration? *Expert Rev Clin Immunol*. 2014;10(10):1273–1275.
33. Doyle SL, Campbell M, Ozaki E, et al. NLRP3 has a protective role in age-related macular degeneration through the induction of IL-18 by drusen components. *Nat Med*. 2012;18(5):791–798.
34. Tseng WA, Thein T, Kinnunen K, et al. NLRP3 inflammasome activation in retinal pigment epithelial cells by lysosomal destabilization: implications for age-related macular degeneration. *Invest Ophthalmol Vis Sci*. 2013;54(1):110–120.
35. Mankan AK, Kubarenko A, Hornung V. Immunology in

clinic review series; focus on autoinflammatory diseases: inflammasomes: mechanisms of activation. *Clin Exp Immunol*. 2012;167(3):369–381.
36. Nakahira K, Haspel JA, Rathinam VA, et al. Autophagy proteins regulate innate immune responses by inhibiting the release of mitochondrial DNA mediated by the NALP3 inflammasome. *Nat Immunol*. 2011;12(3):222–230.
37. Shi CS, Shenderov K, Huang NN, et al. Activation of autophagy by inflammatory signals limits IL-1beta production by targeting ubiquitinated inflammasomes for destruction. *Nat Immunol*. 2012;13(3):255–263.
38. Lee HO, Ferguson TA. Biology of FasL. *Cytokine Growth Factor Rev*. 2003;14(3–4):325–335.
39. Griffith TS, Ferguson TA. The role of FasL-induced apoptosis in immune privilege. *Immunol Today*. 1997;18(5):240–244.
40. Taylor AW, Lee D. Applications of the role of alpha-MSH in ocular immune privilege. *Adv Exp Med Biol*. 2010;681:143–149.
41. Ke Y, Sun D, Jiang G, Kaplan HJ, Shao H. PD-L1(hi) retinal pigment epithelium (RPE) cells elicited by inflammatory cytokines induce regulatory activity in uveitogenic T cells. *J Leukoc Biol*. 2010;88(6):1241–1249.
42. Horie S, Sugita S, Futagami Y, Yamada Y, Mochizuki M. Human retinal pigment epithelium-induced $CD4^{+}CD25^{+}$ regulatory T cells suppress activation of intraocular effector T cells. *Clin Immunol*. 2010;136(1):83–95.
43. Sugita S, Horie S, Nakamura O, et al. Retinal pigment epithelium-derived CTLA-2alpha induces TGFbeta-producing T regulatory cells. *J Immunol*. 2008;181(11):7525–7536.
44. Luo C, Zhao J, Madden A, Chen M, Xu H. Complement expression in retinal pigment epithelial cells is modulated by activated macrophages. *Exp Eye Res*. 2013;112:93–101.
45. Chen M, Muckersie E, Luo C, Forrester JV, Xu H. Inhibition of the alternative pathway of complement activation reduces inflammation in experimental autoimmune uveoretinitis. *Eur J Immunol*. 2010;40(10):2870–2881.

46. Chen M, Muckersie E, Robertson M, Forrester JV, Xu H. Up-regulation of complement factor B in retinal pigment epithelial cells is accompanied by complement activation in the aged retina. *Exp Eye Res*. 2008;87(6):543–550.
47. Chen M, Forrester JV, Xu H. Synthesis of complement factor H by retinal pigment epithelial cells is down-regulated by oxidized photoreceptor outer segments. *Exp Eye Res*. 2007;84(4):635–645.
48. Kumar A, Pandey RK, Miller LJ, Singh PK, Kanwar M. Müller glia in retinal innate immunity: a perspective on their roles in endophthalmitis. *Crit Rev Immunol*. 2013;33(2):119–135.
49. Roberge FG, Caspi RR, Chan CC, Nussenblatt RB. Inhibition of T lymphocyte proliferation by retinal glial Muller cells: reversal of inhibition by glucocorticoids. *J Autoimmun*. 1991;4(2):307–314.
50. Roberge FG, Caspi RR, Nussenblatt RB. Glial retinal Müller cells produce IL-1 activity and have a dual effect on autoimmune T helper lymphocytes. Antigen presentation manifested after removal of suppressive activity. *J Immunol*. 1988;140(7):2193–2196.
51. Runkle EA, Antonetti DA. The blood–retinal barrier: structure and functional significance. *Methods Mol Biol*. 2011;686:133–148.
52. Xu H, Dawson R, Crane IJ, Liversidge J. Leukocyte diapedesis in vivo induces transient loss of tight junction protein at the blood–retina barrier. *Invest Ophthalmol Vis Sci*. 2005;46(7):2487–2494.
53. Xu H, Forrester JV, Liversidge J, Crane IJ. Leukocyte trafficking in experimental autoimmune uveitis: breakdown of blood-retinal barrier and upregulation of cellular adhesion molecules. *Invest Ophthalmol Vis Sci*. 2003;44(1):226–234.
54. Chimen M, McGettrick HM, Apta B, et al. Homeostatic regulation of T cell trafficking by a B cell-derived peptide is impaired in autoimmune and chronic inflammatory disease. *Nat Med*. 2015;21(5):467–475.
55. Crane IJ, Liversidge J. Mechanisms of leukocyte migration

across the blood–retina barrier. *Semin Immunopathol*. 2008;30(2):165–177.
56. Medzhitov R. Origin and physiological roles of inflammation. *Nature*. 2008;454(7203):428–435.
57. Snelgrove RJ, Goulding J, Didierlaurent AM, et al. A critical function for CD200 in lung immune homeostasis and the severity of influenza infection. *Nat Immunol*. 2008;9(9):1074–1083.
58. Mombach JC, Vendrusculo B, Bugs CA. A model for p38MAPK-induced astrocyte senescence. *PLoS ONE*. 2015;10(5):e0125217.
59. Tchkonia T, Zhu Y, van Deursen J, Campisi J, Kirkland JL. Cellular senescence and the senescent secretory phenotype: therapeutic opportunities. *J Clin Invest*. 2013;123(3):966–972.
60. Zarubin T, Han J. Activation and signaling of the p38 MAP kinase pathway. *Cell Res*. 2005;15(1):11–18.
61. Ma W, Cojocaru R, Gotoh N, et al. Gene expression changes in aging retinal microglia: relationship to microglial support functions and regulation of activation. *Neurobiol Aging*. 2013;34(10):2310–2321.
62. Ma W, Zhao L, Wong WT. Microglia in the outer retina and their relevance to pathogenesis of age-related macular degeneration. *Adv Exp Med Biol*. 2012;723:37–42.
63. Akbar AN, Henson SM. Are senescence and exhaustion intertwined or unrelated processes that compromise immunity? *Nat Rev Immunol*. 2011;11(4):289–295.
64. Lanna A, Henson SM, Escors D, Akbar AN. The kinase p38 activated by the metabolic regulator AMPK and scaffold TAB1 drives the senescence of human T cells. *Nat Immunol*. 2014;15(10):965–972.
65. Odegaard JI, Chawla A. The immune system as a sensor of the metabolic state. *Immunity*. 2013;38(4):644–654.
66. Chovatiya R, Medzhitov R. Stress, inflammation, and defense of homeostasis. *Mol Cell*. 2014;54(2):281–288.
67. Sfriso P, Caso F, Tognon S, Galozzi P, Gava A, Punzi L. Blau syndrome, clinical and genetic aspects. *Autoimmun Rev*. 2012;12(1):44–51.
68. Rosenzweig HL, Martin TM, Planck SR, et al. Activation of

NOD2 in vivo induces IL-1beta production in the eye via caspase-1 but results in ocular inflammation independently of IL-1 signaling. *J Leukoc Biol*. 2008;84(2):529–536.
69. Wildin RS, Freitas A. IPEX and FOXP3: clinical and research perspectives. *J Autoimmun*. 2005;25(Suppl.):56–62.
70. McGonagle D, McDermott MF. A proposed classification of the immunological diseases. *PLoS Med*. 2006;3(8):e297.
71. Lee RW, Nicholson LB, Sen HN, et al. Autoimmune and autoinflammatory mechanisms in uveitis. *Semin Immunopathol*. 2014;36(5):581–594.
72. Caspi RR. A look at autoimmunity and inflammation in the eye. *J Clin Invest*. 2010;120(9):3073–3083.
73. Shi T, Lv W, Zhang L, Chen J, Chen H. Association of HLA-DR4/HLA-DRB1*04 with Vogt–Koyanagi–Harada disease: a systematic review and meta-analysis. *Sci Rep*. 2014;4:6887.
74. Parmeggiani F, Romano MR, Costagliola C, et al. Mechanism of inflammation in age-related macular degeneration. *Mediators Inflamm*. 2012;2012:546786.
75. Whitcup SM, Sodhi A, Atkinson JP, et al. The role of the immune response in age-related macular degeneration. *Int J Inflam*. 2013;2013:348092.
76. Adamis AP, Berman AJ. Immunological mechanisms in the pathogenesis of diabetic retinopathy. *Semin Immunopathol*. 2008;30(2):65–84.
77. Devaraj S, Glaser N, Griffen S, Wang-Polagruto J, Miguelino E, Jialal I. Increased monocytic activity and biomarkers of inflammation in patients with type 1 diabetes. *Diabetes*. 2006;55(3):774–779.
78. Kerr EC, Copland DA, Dick AD, Nicholson LB. The dynamics of leukocyte infiltration in experimental autoimmune uveoretinitis. *Prog Retin Eye Res*. 2008;27(5):527–535.
79. Janeway CA Jr. Approaching the asymptote? Evolution and revolution in immunology. *Cold Spring Harb Symp Quant Biol*. 1989;54(Pt 1):1–13.
80. Matzinger P. Tolerance, danger, and the extended family. *Annu Rev Immunol*. 1994;12:991–1045.
81. Vos AG, Wassenberg MW, de Hoog J, Oosterheert JJ.

Diagnosis and treatment of tuberculous uveitis in a low endemic setting. *Int J Infect Dis*. 2013;17(11):e993–9.
82. Cunningham C, Wilcockson DC, Campion S, Lunnon K, Perry VH. Central and systemic endotoxin challenges exacerbate the local inflammatory response and increase neuronal death during chronic neurodegeneration. *J Neurosci*. 2005;25(40):9275–9284.
83. Perry VH, Cunningham C, Holmes C. Systemic infections and inflammation affect chronic neurodegeneration. *Nat Rev Immunol*. 2007;7(2):161–167.
84. Graham EM, Stanford MR, Shilling JS, Sanders MD. Neovascularisation associated with posterior uveitis. *Br J Ophthalmol*. 1987;71(11):826–833.
85. Baxter SL, Pistilli M, Pujari SS, et al. Risk of choroidal neovascularization among the uveitides. *Am J Ophthalmol*. 2013;156(3):468–477.e2.
86. Atan D, Fraser-Bell S, Plskova J, et al. Punctate inner choroidopathy and multifocal choroiditis with panuveitis share haplotypic associations with IL10 and TNF loci. *Invest Ophthalmol Vis Sci*. 2011;52(6):3573–3581.
87. Chen M, Copland DA, Zhao J, et al. Persistent inflammation subverts thrombospondin-1-induced regulation of retinal angiogenesis and is driven by CCR2 ligation. *Am J Pathol*. 2012;180(1):235–245.
88. Dace DS, Khan AA, Kelly J, Apte RS. Interleukin-10 promotes pathological angiogenesis by regulating macrophage response to hypoxia during development. *PLoS ONE*. 2008;3(10):e3381.
89. Grossniklaus HE, Ling JX, Wallace TM, et al. Macrophage and retinal pigment epithelium expression of angiogenic cytokines in choroidal neovascularization. *Mol Vis*. 2002;8:119–126.
90. Pugh CW, Ratcliffe PJ. Regulation of angiogenesis by hypoxia: role of the HIF system. *Nat Med*. 2003;9(6):677–684.
91. Wu WK, Llewellyn OP, Bates DO, Nicholson LB, Dick AD. IL-10 regulation of macrophage VEGF production is dependent on macrophage polarisation and hypoxia. *Immunobiology*. 2010;215(9–10):796–803.

92. Ferguson TA, Apte RS. Angiogenesis in eye disease: immunity gained or immunity lost? *Semin Immunopathol*. 2008;30(2):111–119.
93. Wu WK, Georgiadis A, Copland DA, et al. IL-4 Regulates specific Arg-1 macrophage sFlt-1-mediated inhibition of angiogenesis. *Am J Pathol*. 2015;185(8):2324–2335.
94. Skeie JM, Mullins RF. Macrophages in neovascular age-related macular degeneration: friends or foes? *Eye (Lond)*. 2009;23(4):747–755.
95. Horie S, Robbie SJ, Liu J, et al. CD200R signaling inhibits pro-angiogenic gene expression by macrophages and suppresses choroidal neovascularization. *Sci Rep*. 2013;3:3072.
96. Grigsby JG, Cardona SM, Pouw CE, et al. The role of microglia in diabetic retinopathy. *J Ophthalmol*. 2014;2014:705783.
97. Tang J, Kern TS. Inflammation in diabetic retinopathy. *Prog Retin Eye Res*. 2011;30(5):343–358.
98. Zong H, Ward M, Stitt AW. AGEs, RAGE, and diabetic retinopathy. *Curr Diab Rep*. 2011;11(4):244–252.
99. Feng Y, Busch S, Gretz N, Hoffmann S, Hammes HP. Crosstalk in the retinal neurovascular unit - lessons for the diabetic retina. *Exp Clin Endocrinol Diabetes*. 2012;120(4):199–201.
100. Simo R, Hernandez C, European Consortium for the Early Treatment of Diabetic Retinopathy. Neurodegeneration in the diabetic eye: new insights and therapeutic perspectives. *Trends Endocrinol Metab*. 2014;25(1):23–33.
101. Perez VL, Caspi RR. Immune mechanisms in inflammatory and degenerative eye disease. *Trends Immunol*. 2015;36(6):354–363.
102. Hageman GS, Hancox LS, Taiber AJ, et al. Extended haplotypes in the complement factor H (CFH) and CFH-related (CFHR) family of genes protect against age-related macular degeneration: characterization, ethnic distribution and evolutionary implications. *Ann Med*. 2006;38(8):592–604.
103. Edwards AO, Ritter R 3rd, Abel KJ, Manning A, Panhuysen

C, Farrer LA. Complement factor H polymorphism and age-related macular degeneration. *Science*. 2005;308(5720):421–424.
104. Klein RJ, Zeiss C, Chew EY, et al. Complement factor H polymorphism in age-related macular degeneration. *Science*. 2005;308(5720):385–389.
105. Clark SJ, Schmidt CQ, White AM, Hakobyan S, Morgan BP, Bishop PN. Identification of factor H-like protein 1 as the predominant complement regulator in Bruch's membrane: implications for age-related macular degeneration. *J Immunol*. 2014;193(10):4962–4970.
106. Thompson IA, Liu B, Sen HN, et al. Association of complement factor H tyrosine 402 histidine genotype with posterior involvement in sarcoid-related uveitis. *Am J Ophthalmol*. 2013;155(6):1068–1074.e1.
107. Ferrara DC, Merriam JE, Freund KB, et al. Analysis of major alleles associated with age-related macular degeneration in patients with multifocal choroiditis: strong association with complement factor H. *Arch Ophthalmol*. 2008;126(11):1562–1566.
108. Lalli PN, Strainic MG, Yang M, Lin F, Medof ME, Heeger PS. Locally produced C5a binds to T cell-expressed C5aR to enhance effector T-cell expansion by limiting antigen-induced apoptosis. *Blood*. 2008;112(5):1759–1766.
109. Strainic MG, Liu J, Huang D, et al. Locally produced complement fragments C5a and C3a provide both costimulatory and survival signals to naive $CD4^+$ T cells. *Immunity*. 2008;28(3):425–435.
110. Liu B, Wei L, Meyerle C, et al. Complement component C5a promotes expression of IL-22 and IL-17 from human T cells and its implication in age-related macular degeneration. *J Transl Med*. 2011;9:1–12.
111. Cousins SW, Espinosa-Heidmann DG, Csaky KG. Monocyte activation in patients with age-related macular degeneration: a biomarker of risk for choroidal neovascularization? *Arch Ophthalmol*. 2004;122(7):1013–1018.
112. Penfold PL, Provis JM, Furby JH, Gatenby PA, Billson FA. Autoantibodies to retinal astrocytes associated with age-

related macular degeneration. *Graefes Arch Clin Exp Ophthalmol*. 1990;228(3):270–274.
113. Gu X, Meer SG, Miyagi M, et al. Carboxyethylpyrrole protein adducts and autoantibodies, biomarkers for age-related macular degeneration. *J Biol Chem*. 2003;278(43):42027–42035.
114. Joachim SC, Bruns K, Lackner KJ, Pfeiffer N, Grus FH. Analysis of IgG antibody patterns against retinal antigens and antibodies to alpha-crystallin, GFAP, and alpha-enolase in sera of patients with "wet" age-related macular degeneration. *Graefes Arch Clin Exp Ophthalmol*. 2007;245(5):619–626.
115. Umeda S, Suzuki MT, Okamoto H, et al. Molecular composition of drusen and possible involvement of anti-retinal autoimmunity in two different forms of macular degeneration in cynomolgus monkey (Macaca fascicularis). *FASEB J*. 2005;19(12):1683–1685.
116. Hollyfield JG, Bonilha VL, Rayborn ME, et al. Oxidative damage-induced inflammation initiates age-related macular degeneration. *Nat Med*. 2008;14(2):194–198.
117. Hollyfield JG, Perez VL, Salomon RG. A hapten generated from an oxidation fragment of docosahexaenoic acid is sufficient to initiate age-related macular degeneration. *Mol Neurobiol*. 2010;41(2–3):290–298.
118. Beatty S, Koh H, Phil M, Henson D, Boulton M. The role of oxidative stress in the pathogenesis of age-related macular degeneration. *Surv Ophthalmol*. 2000;45(2):115–134.
119. Morgan MJ, Liu ZG. Crosstalk of reactive oxygen species and NF-kappaB signaling. *Cell Res*. 2011;21(1):103–115.
120. Curcio CA, Johnson M, Huang JD, Rudolf M. Apolipoprotein B-containing lipoproteins in retinal aging and age-related macular degeneration. *J Lipid Res*. 2010;51(3):451–467.
121. Crabb JW, Miyagi M, Gu X, et al. Drusen proteome analysis: an approach to the etiology of age-related macular degeneration. *Proc Natl Acad Sci USA*. 2002;99(23):14682–14687.
122. Yuan X, Gu X, Crabb JS, et al. Quantitative proteomics:

comparison of the macular Bruch membrane/choroid complex from age-related macular degeneration and normal eyes. *Mol Cell Proteomics*. 2010;9(6):1031–1046.
123. Nussenblatt RB, Liu B, Wei L, Sen HN. The immunological basis of degenerative diseases of the eye. *Int Rev Immunol*. 2013;32(1):97–112.
124. Wei L, Liu B, Tuo J, et al. Hypomethylation of the IL17RC promoter associates with age-related macular degeneration. *Cell Rep*. 2012;2(5):1151–1158.
125. Li Z, Liu B, Maminishkis A, et al. Gene expression profiling in autoimmune noninfectious uveitis disease. *J Immunol*. 2008;181(7):5147–5157.
126. Celkova L, Doyle SL, Campbell M. NLRP3 inflammasome and pathobiology in AMD. *J Clin Med*. 2015;4(1):172–192.
127. Killingsworth MC, Sarks JP, Sarks SH. Macrophages related to Bruch's membrane in age-related macular degeneration. *Eye (Lond)*. 1990;4(Pt 4):613–621.
128. Green WR, Enger C. Age-related macular degeneration histopathologic studies. The 1992 Lorenz E. Zimmerman Lecture. *Ophthalmology*. 1993;100(10):1519–1535.
129. Dastgheib K, Green WR. Granulomatous reaction to Bruch's membrane in age-related macular degeneration. *Arch Ophthalmol*. 1994;112(6):813–818.
130. Grossniklaus HE, Cingle KA, Yoon YD, Ketkar N, L'Hernault N, Brown S. Correlation of histologic 2-dimensional reconstruction and confocal scanning laser microscopic imaging of choroidal neovascularization in eyes with age-related maculopathy. *Arch Ophthalmol*. 2000;118(5):625–629.
131. Grossniklaus HE, Miskala PH, Green WR, et al. Histopathologic and ultrastructural features of surgically excised subfoveal choroidal neovascular lesions: submacular surgery trials report no. 7. *Arch Ophthalmol*. 2005;123(7):914–921.
132. Cao X, Shen D, Patel MM, et al. Macrophage polarization in the maculae of age-related macular degeneration: a pilot study. *Pathol Int*. 2011;61(9):528–535.
133. Muller L, Pawelec G. As we age: Does slippage of quality

control in the immune system lead to collateral damage? *Ageing Res Rev*. 2015;23(Pt A):116–123.
134. Lindstrom TM, Robinson WH. Rheumatoid arthritis: a role for immunosenescence? *J Am Geriatr Soc*. 2010;58(8):1565–1575.
135. Krishnadev N, Meleth AD, Chew EY. Nutritional supplements for age-related macular degeneration. *Curr Opin Ophthalmol*. 2010;21(3):184–189.
136. Sahel JA, Roska B. Gene therapy for blindness. *Annu Rev Neurosci*. 2013;36:467–488.
137. Vojinovic J, Damjanov N. HDAC inhibition in rheumatoid arthritis and juvenile idiopathic arthritis. *Mol Med*. 2011;17(5–6):397–403.
138. Nussenblatt RB, Byrnes G, Sen HN, et al. A randomized pilot study of systemic immunosuppression in the treatment of age-related macular degeneration with choroidal neovascularization. *Retina*. 2010;30(10):1579–1587.
139. Wang Y, Wang VM, Chan CC. The role of anti-inflammatory agents in age-related macular degeneration (AMD) treatment. *Eye (Lond)*. 2011;25(2):127–139.
140. Weiner HL, da Cunha AP, Quintana F, Wu H. Oral tolerance. *Immunol Rev*. 2011;241(1):241–259.
141. Nussenblatt RB, Gery I, Weiner HL, et al. Treatment of uveitis by oral administration of retinal antigens: results of a phase I/II randomized masked trial. *Am J Ophthalmol*. 1997;123(5):583–592.
142. Peron JP, Yang K, Chen ML, et al. Oral tolerance reduces Th17 cells as well as the overall inflammation in the central nervous system of EAE mice. *J Neuroimmunol*. 2010;227(1–2):10–17.
143. Nussenblatt RB, Lee RW, Chew E, et al. Immune responses in age-related macular degeneration and a possible long-term therapeutic strategy for prevention. *Am J Ophthalmol*. 2014;158(1):5–11.e2.

28

Basic Mechanisms of Pathologic Retinal and Choroidal Angiogenesis

Demetrios G. Vavvas, Aristomenis Thanos, Avni V. Patel, Joan W. Miller *

Introduction

The search to dissect the molecular mechanisms of ocular

angiogenesis dates back to 1948 when Michaelson postulated that a soluble and diffusible growth factor was responsible for retinal vascular growth in development and disease.[1] In the late 1980s and early 1990s vascular endothelial growth factor (VEGF) was identified as this diffusible growth factor, ushering a new paradigm in the understanding as well as treatment of ocular neovascular diseases.[2–6] Since then our knowledge of ocular neovascularization continues to grow as new molecules are discovered, new interactions between molecules are elucidated, and our understanding of the pathogenesis of specific retinal diseases evolves. The last step is essential for developing of new strategies with improved therapeutic targeting.

Retinal neovascularization occurs in diseases such as diabetic retinopathy (DR), retinopathy of prematurity (ROP), ischemic retinal vein occlusions (RVOs), and other retinopathies such as sickle-cell disease. On the other hand, choroidal neovascularization is the hallmark of exudative (wet) or neovascular age-related macular degeneration (nvAMD) but can also be encountered in a variety of other conditions, such as outer retinal retinochoroidopathies, trauma, myopia, angioid streaks, and macular dystrophies, or without any identifiable cause (idiopathic) (Fig. 28.1).

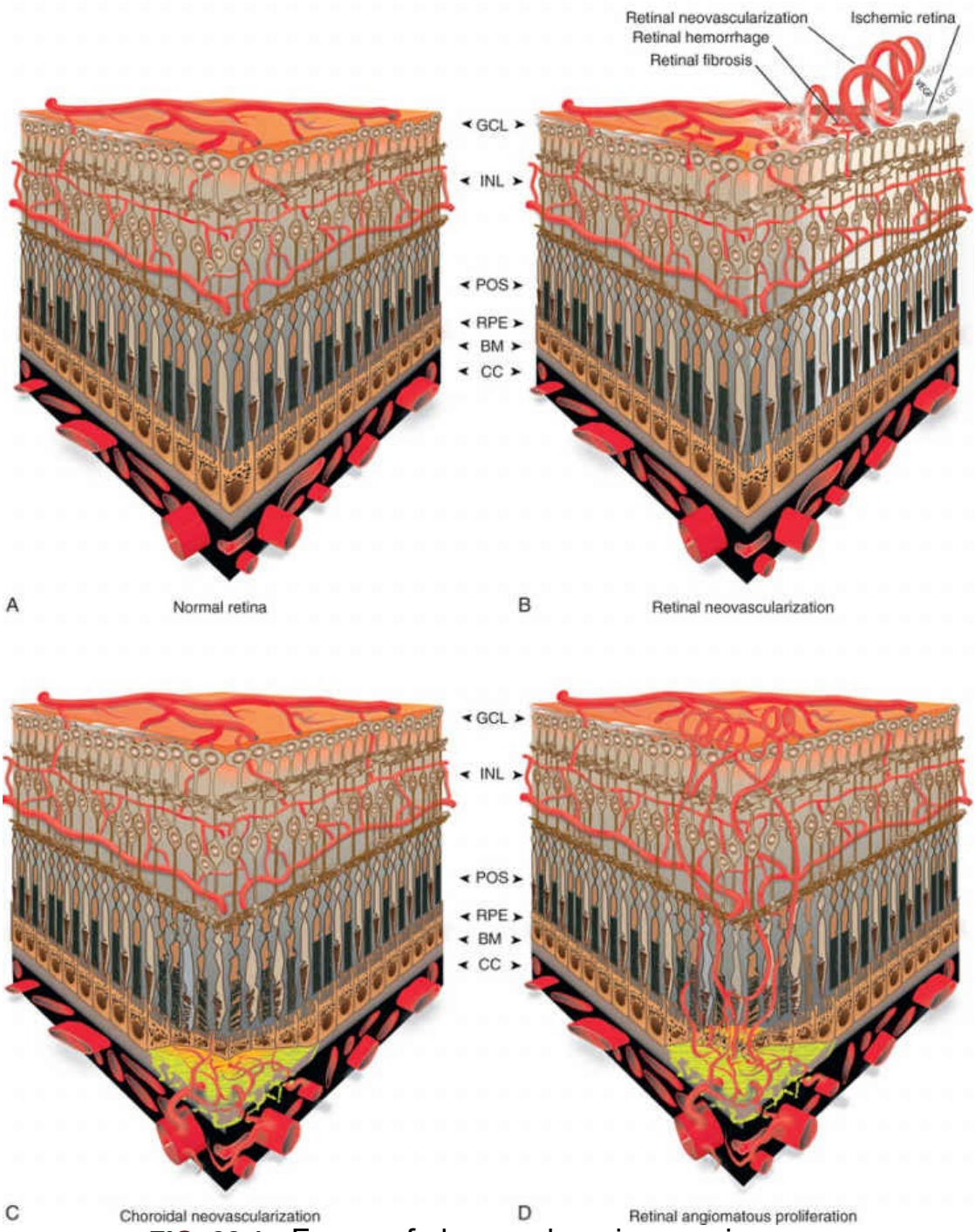

FIG. 28.1 Forms of abnormal angiogenesis encountered in ocular neovascular disorders. (A) The vascular network of the retina consists of the superficial and intraretinal vascular plexus, which provide oxygen and nutrients to the inner two-thirds of the retina. The outer one-third of the retina (photoreceptors and retinal pigment epithelium, RPE) receives its blood supply from the choroidal circulation. (B) Retinal neovascularization involves the proliferation of new vessels from the superficial retina at the

vitreoretinal interface. These fragile and tortuous neovessels often result in hemorrhage, fibrosis, and traction of the retina. (C) In choroidal neovascularization, new vessels arising from the choroidal circulation grow through breaks in Bruch's membrane under the RPE, neurosensory retina, or a combination of both. (D) In some cases, neovascularization forms in the neurosensory retina and at later stages may form anastomoses with the choroidal circulation, which is also known as retinal angiomatous proliferation or retinochoroidal anastomosis. *BM*, Bruch's membrane; *CC*, choroidal circulation; *GCL*, ganglion cell layer; *INL*, inner nuclear layer; *POS*, photoreceptor outer segments; *RPE*, retinal pigment epithelium. (Courtesy of Aristomenis Thanos, MD.)

Impact of Abnormal Retinal and Choroidal Angiogenesis

Neovascularization is part of the aberrant wound healing response occurring in response to continuous tissue injury occurring in diseases such as DR, nvAMD, RVOs, and ROP, all of which contribute to the major causes of blindness in developed countries. DR is the leading cause of blindness among the working-age population in industrialized countries. An estimated 93 million people worldwide have some form of DR and about 28 million have sight-threatening stages of DR.[7] About 50% of patients with diabetes develop various degrees of diabetic retinopathy after 25 years with the disease.[8] RVOs constitute the second most common cause of vision loss due to retinal vascular disease,[9] whereas ROP has become the leading cause of childhood blindness affecting up to 30% of premature infants in developing countries and 5–8% of infants in industrialized countries.[10] About 1.75 million people in the United States are estimated to have neovascular AMD, and this number is supposed to double to 3 million by 2020. Additionally, there are nearly 200,000 new cases of wet AMD each year.[11]

Normal Retinal Vascular Development

Vasculogenesis is the de novo formation of blood vessels from endothelial precursors. On the other hand, angiogenesis is the process by which new blood vessels are formed from preexisting blood vessels. Angiogenesis primarily occurs through "sprouting," whereby activated endothelial cells secrete proteolytic enzymes that dissolve basement membrane around the parent vessel and align themselves to form a new capillary sprout. By curving and elongating, the sprouts form tubes with lumens, which anastomose to form loops. Mesenchymal cells are recruited to form smooth-muscle cells, or pericytes, and new basement membrane is deposited.[12] More recently it has been demonstrated that hemangioblasts migrate to the human choroid during development and give rise to the choriocapillaris in a process called hemovasculogenesis (blood vessels and blood cells form simultaneously from common precursors).[13]

Normal retinal vascularization begins at the most superficial level of the inner retina at the optic nerve head and radiates outward, reaching the retinal periphery at about 40 weeks in humans.[1] A meshwork of astrocytes that enter the retina at the optic nerve and grow peripherally lay a road map for retinal vascularization.[14,15] The endothelial "tip cells" of growing retinal vessels extend along the processes of underlying astrocytes, which secrete VEGF.[16–18] Pericytes associated with retinal blood vessels also promote retinal vascular growth by secreting VEGF and inducing VEGF receptors in endothelial cells through transforming growth factor-beta 1 (TGF-β1).[19,20]

The vasculature of the eye is completely formed shortly after birth and is normally quiescent and nonproliferating in adults.[1] An active balance of pro- and antiangiogenic influences is required to maintain homeostasis. Abnormal angiogenesis occurs when environmental changes result in tissue expression of molecules that favor the growth of abnormal new vessels. In these ocular diseases, angiogenesis occurs chaotically and does not conform to normal retinal vascular anatomy, leading to vision-threatening disease with hemorrhage, exudation, and ultimately fibrosis and retinal cell death.

Pathogenesis of Retinal Angiogenesis

Abnormal or pathologic retinal vascularization usually occurs as a combination of two processes. The first process involves vascular injury and subsequent retinal capillary loss resulting in tissue hypoxia. The second process is characterized by deregulated vascular growth driven by a state of hypoxia. There are several experimental models supporting the idea that hypoxia is the primary stimulus for pathologic retinal angiogenesis and VEGF seems to be the cardinal growth factor to date mediating retinal angiogenesis. The first correlation of VEGF with ocular angiogenesis in vivo came from studies in monkey eyes with experimental retinal ischemia following laser vein occlusion, which demonstrated that VEGF levels correlated with the degree of neovascularization.[6,21,22]

In DR, sickle-cell retinopathy, and RVOs, neovascularization is a consequence of retinal capillary nonperfusion and tissue ischemia.[23,24] The cellular response to reduced oxygen levels is mediated by the transcriptional regulator hypoxia-inducible factor 1 (HIF-1). This is a heterodimeric complex protein made up of an oxygen-dependent alpha unit and a constitutively expressed nuclear beta unit. Hypoxia prevents the ubiquitin proteasome system degradation of the transcription factor HIF-1-alpha (HIF-1α). Stable HIF-1α binds to the promoter region of its major target genes, resulting in upregulation of factors such as VEGF, placental growth factor (PlGF), angiopoietin-1 (ANGPT1) and angiopoietin-2 (ANGPT2), erythropoietin (Epo), and platelet derived growth factor (PDGF)-B, which are key molecules in angiogenesis (Fig. 28.2).[25–27] VEGF acts as a potent endothelial cell mitogen, stimulating their proliferation.[28,29]

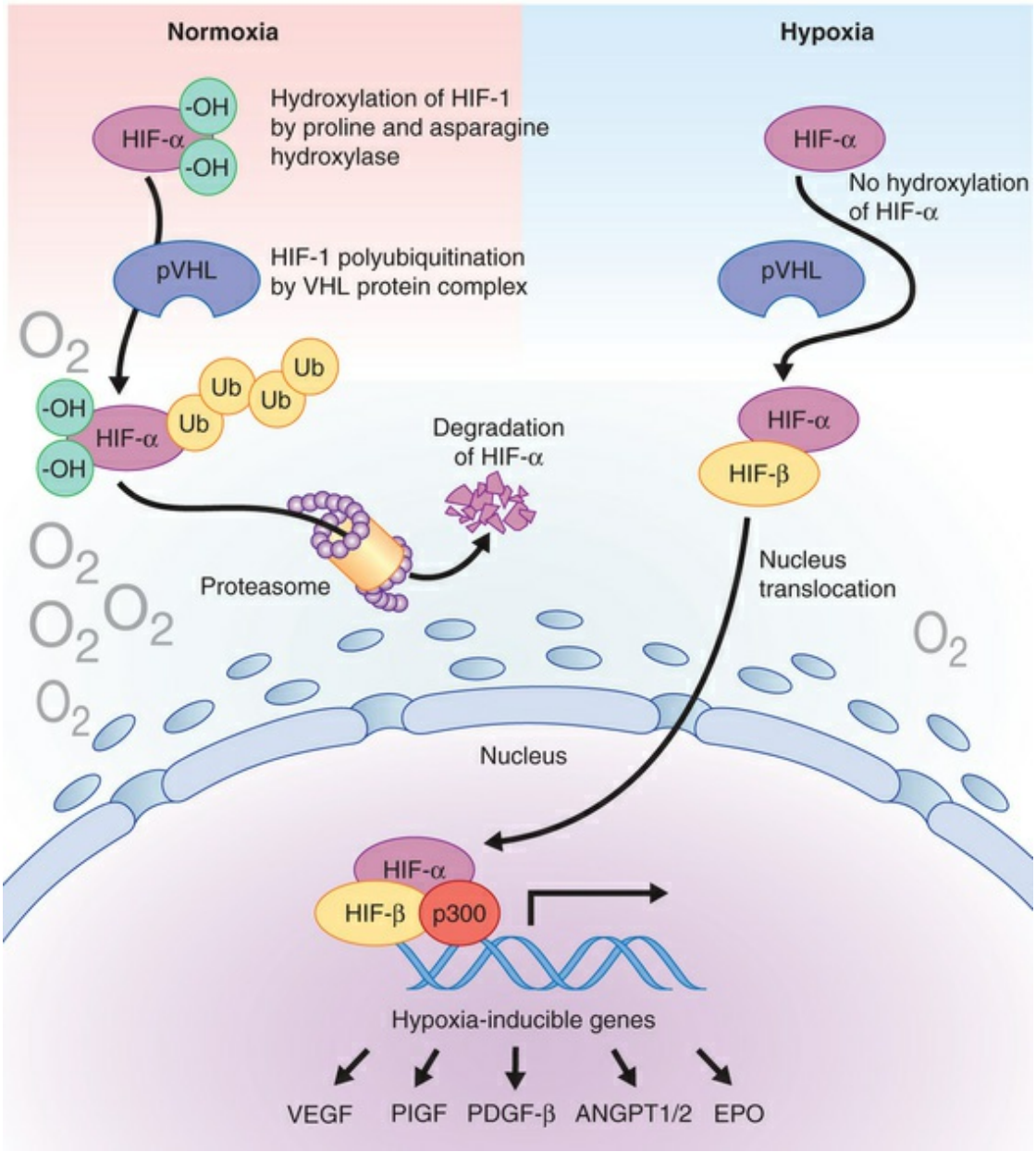

FIG. 28.2 The hypoxia-inducible factor (HIF) pathway. Simplified representation of HIF regulation under normoxia and hypoxia. Under normoxic conditions (left), HIF is degraded by the proteasome through a process involving hydroxylation and then ubiquitination of HIF molecules by von Hippel–Lindau (VHL) protein complex. Under hypoxic conditions, HIF-1αaccumulates in the cytoplasm and dimerizes with HIF-1β. The dimer then translocates to the nucleus, upregulating a number of proangiogenic molecules, including VEGF, vascular endothelial growth factor; PlGF, placental growth factor, PDGF-β, platelet-derived growth factor-β; ANGPT1/2, angiopoietins 1 and 2; and EPO, erythropoietin. (Courtesy of Aristomenis Thanos,

In addition to endothelial cells, several key cells involved in normal retinal vascularization, including pericytes, astrocytes, and Müller glial cells, also play a role in abnormal retinal angiogenesis. Pericyte loss is among the first pathologic changes in DR and is thought to contribute to multiple vascular changes including the loss of formed vessels, the loss of normally growing vessels, and abnormal angiogenesis.[20,30] Experimental models suggest astrocytes may stabilize vessels and restrict growth of normal vessels to the appropriate retinal layers. Müller cells influence retinal neovascularization as they may secrete more proangiogenic factors such as VEGF rather than antiangiogenic factors such as pigment epithelium-derived factor, also now known as Serpin peptidase inhibitor, Clade F, member 1; SERPINF1 (PEDF/SERPINF1) in the setting of retinal ischemia.[31] Lastly, hypoxia leads to degeneration and focal disruptions in the glial sheath surrounding retinal blood vessels, allowing neovascularization to extend beyond the retinal surface and into the vitreous cavity.[32]

It is widely accepted that the vitreous plays a significant role in the pathogenesis and propagation of retinal angiogenesis. The posterior vitreous cortex consists of densely packed type II collagen fibrils and other extracellular matrix components, which offer an ideal scaffold for endothelial cell proliferation and new blood vessel development. The attachment of the cortical vitreous to the retina is mediated primarily through the proteins laminin and fibronectin, which have critical roles in angiogenesis.[33] Histologic analysis of neovascular tissue from patients with proliferative DR (PDR) reveals it is intertwined with vitreous collagen.[34] Moreover, clinical evidence confirms that eyes with DR and central RVO and concurrent posterior vitreous detachment are less likely to develop posterior segment neovascularization compared to eyes with intact posterior cortical vitreous.[35]

DR, ROP, and RVOs are among the ischemic diseases leading to retinal neovascularization and are discussed below so that through these disease processes we may understand more about mechanisms of retinal angiogenesis.

Retinal Neovascularization in Diabetes

Pathologic retinal neovascularization in DR takes place in two phases: an initial vascular dropout/occlusion phase is followed by abnormal vascular growth. Chronic hyperglycemia leads to vascular injury with basement membrane thickening, pericyte loss, microaneurysms, and vascular leakage.[36,37] While the exact mechanism remains ill defined, many biochemical pathways (protein kinase C, nuclear factor (NF)-κB, mitogen-activated protein kinase) have been involved in the pathogenesis of early DR. Oxidative injury, microthrombi formation, inflammatory mediator upregulation, and leukostasis have all been observed to aggravate vessel loss.

DR behaves as chronic inflammatory disease in many ways, and there is a growing body of evidence suggesting a key role for inflammation in vascular dropout and neovascularization. Early inflammation promotes increased vasopermeability and leukostasis, while persistent inflammation is accompanied by the rise of proinflammatory cytokines.[38–40] Specifically, cytokines such as tumor necrosis factor-alpha (TNF-α), interleukin (IL)-1β, intercellular adhesion molecule (ICAM), inducible nitric oxide synthase (iNOS), and IL-6 are elevated in patients with PDR.[40–43] Localized inflammation is thought to lead to leukostasis through the interaction of ICAM and CD18.[44–47] Leukostasis leads to microvascular occlusion, nonperfusion, and ischemia, which induces the upregulation of angiogenic factors. IL-1β can promote endothelial cell proliferation, propagate inflammation, and upregulate HIF-1α.[48,49] TNF-α can promote angiogenesis, endothelial cell sprouting, and macrophage-induced angiogenesis is mediated through TNF-α.[50,51] TNF-receptor p55-deficient animals are protected from retinal neovascularization in animal models.[52] Inhibitors of inflammation such as cyclooxygenase 2 inhibitors and aspirin have been shown to curtail vascular pathology and neovascularization.[38,44,53]

The proinflammatory environment is characterized by elevated matrix metalloproteinases (MMPs), which degrade the extracellular matrix, a step necessary for angiogenesis. Additionally, MMP-9 is not only induced by IL-8[54] but also activates IL-8,[55] which recruits more inflammatory cells, feeding a destructive positive-feedback

loop. Insulin[56] and PEDF[57] are degraded by MMP-9, leading to a state of more insulin resistance and neuronal peril. Beránek et al. in 2008 showed MMP-2 and MMP-9 to be elevated in patients with PDR.[58]

As a consequence of vascular degeneration and dropout there is inadequate supply of oxygen and nutrients for proper cellular metabolism. This state of hypoxia leads neurons and supporting astrocytes to secrete proangiogenic factors such as VEGF and insulin-like growth factor (IGF)-1. Clinical studies have substantiated the role of VEGF in DR.[59,60] VEGF levels are elevated in patients with PDR and anti-VEGF intervention is of immediate benefit.[61–72] Panretinal photocoagulation may not decrease VEGF levels in the short term (and may increase proinflammatory cytokines);[73,74] however, successful laser retinal ablation decreases VEGF over the long term.[60]

Before the discovery of VEGF and its important role in DR, hypophysectomy studies had revealed a role of growth hormone (GH) and associated factors in DR. IGF-1 levels have been shown to be elevated in the vitreous of patients with PDR relative to control eyes.[75–77] Although there may be a role for IGF-1 in retinal neovascularization, our understanding of IGF-1 in DR remains unclear.[78] IGF-1 may act indirectly via VEGF. Studies of cultured RPE cells demonstrated that adding IGF-1 in vitro increased VEGF mRNA and secreted protein.[79] The accumulation of advanced glycation endproducts (AGE) after long-term exposure to hyperglycemia caused an increase in IGF-1 synthesis in human monocytes, suggesting a role for inflammatory pathways.[80]

Another proangiogenic factor, erythropoietin (Epo), has also been shown to play a role in DR.[81] Epo is involved in the generation of red blood cells but has been shown to be synthesized in astrocytes and its receptors have been detected in photoreceptors. In the adult mouse retina, acute hypoxia stimulates Epo expression via HIF-1α.[82] Epo has been shown to have neuroprotective effects in various models.[83,84] Epo levels are higher in the vitreous of patients with PDR, and inhibition of both Epo and VEGF leads to greater inhibition of neovascularization.[81] However, since Epo has neuroprotective effects, its inhibition for neovascularization may come with significant collateral damage.

Angiopoietins are molecules that bind endothelial Tie receptors and are involved in developmental as well as pathologic angiogenesis, such as in the case of PDR. Vitreous level of Ang 2 and VEGF were significantly higher in patients with PDR than in controls or those with inactive PDR and the levels of Ang 2 correlated significantly with that of VEGF, suggesting an association of Ang 2 and VEGF with angiogenic activity in PDR.[85] A nuclease-resistant RNA aptamer that binds and inhibits Ang 2 but not the related Tie2 agonist, Ang 1, inhibited basic fibroblast growth factor (FGF)-mediated neovascularization in the rat corneal micropocket angiogenesis assay, demonstrating that a specific inhibitor of Ang 2 can act as an antiangiogenic agent.[86]

More recently another potent angiogenic factor, angiopoietin-like 4 (ANGPTL4), was identified in patients with PDR. ANGPTL4 is upregulated in hypoxic retinal Müller cells in vitro and the ischemic retina in vivo. Expression of ANGPLT4 was increased in the aqueous and vitreous of patients with PDR, independent of VEGF levels, and localized to areas of retinal neovascularization. In a recent study, inhibiting the effects of ANGPLT4 was additive to anti-VEGF treatment.[87]

In addition to elevation of proangiogenic factors, there is also an imbalance of antiangiogenic factors in diabetic retinopathy. PEDF, now known as serpin peptidase inhibitor clade F member 1 (SERPINF1), is considered to be the most potent inhibitor of neovascularization, inhibiting endothelial cell migration with a median effective dose of 0.4 nM.[88] It specifically interferes with neovasculature and not with established vessels due to its mechanism of action through Fas/FasL and its cooperation with angiogenic factors. SERPINF1 upregulates FasL on endothelial cells, whereas angiogenic factors induce its essential partner Fas receptor on neovessels but not on established vessels.[89] In PDR, it has been found that PEDF levels are downregulated compared to controls.[90] PEDF also has neuroprotective effects, and thus seems to be an ideal candidate for therapeutic intervention.

Neovascularization in Vascular Occlusions

Similar to diabetic retinopathy, tissue ischemia and subsequent

elevation of angiogenic factors are thought to be of major importance in neovascularization after RVOs. The role of VEGF in particular has been well established. Aiello et al. in 1994 showed increased VEGF levels in the vitreous of patients with active neovascular central RVO (CRVO);[60] in the same year, Miller et al. showed evidence that VEGF is temporally and spatially correlated with ocular angiogenesis in a primate model of CRVO and that blockade of VEGF could inhibit iris neovascularization.[91] Most recently the clinical benefit of anti-VEGF in CRVO has been established.[92–97] Several proinflammatory cytokines have been shown to be elevated in CRVO, including monocyte chemoattractant protein (MCP)-1, IL-6,[98] and ICAM-1.[99–101] Additionally, antiangiogenic factors such as PEDF have been shown to be downregulated in CRVO with macular edema.[102] The alterations of cytokines seen in CRVO not only lead to potential neovascularization but are also major contributors to vascular leakage and macular edema. To this aim, combination treatment approaches with anti-VEGF and corticosteroids have been suggested.[103,104]

Neovascularization Associated With Retinopathy of Prematurity

Retinal neovascularization in ROP is a complex phenomenon, where genetic, developmental, environmental, and disease-associated factors come into play. First, retinal vasculature development begins at about the fourth month of gestation and is complete at about 40 weeks. Therefore, full retinal vascular development is accomplished mostly in utero, where the fetus is in a relatively hypoxic environment (average PaO_2 is 25–35) and exposed to the placental and maternal cytokines and growth factors.[105,106] The placenta is known to be secreting several proangiogenic cytokines, including VEGF, and PlGF.[107] Several pivotal cell signaling pathways and growth factors are involved in retinal vascularization, including the VEGF-signaling pathway, IGF-1, and the Wnt-signaling pathway, among others.[108] Premature birth disrupts this well orchestrated process, as the fetus is exposed into a new environment, which renders the developing vascular

endothelial cells unresponsive to the normal developmental stimuli.

During retinal vascular development, VEGF expression is regulated by retinal oxygen tension and therefore VEGF mRNA is upregulated in astrocytes of the nonvascularized (hypoxic) retina and downregulated in vascularized areas.[108] VEGF acts through VEGFR2 on the filopodia of tip cells to guide blood vessel development.[18] In ROP, VEGF has been shown to be elevated, and the importance of VEGF upregulation in the proliferative phase of this disease has been shown in humans, since blockade of VEGF with anti-VEGF antibodies showed significant efficacy in infants with less development of myopia.[109–115] It should be noted that due to the dual role of VEGF in development and disease concerns about timing and safety of VEGF inhibition in ROP have been raised.[116–118]

In addition to VEGF, IGF-1 as was mentioned before plays an important role in ROP by allowing VEGF to enhance endothelial cell survival and promote early vascular development.[119] Infants with low IGF-1 levels 3 weeks postpartum had higher risk for developing ROP.[120,121] A clinical trial investigating the effect of recombinant human IGF-1 administration in premature infants in increasing normal retinal vascular development and preventing neovascular ROP is currently in phase II clinical trials in the United States and in Europe (NCT01096784).

High oxygen administration at birth was among the first factors to be found critical in the pathogenesis of ROP. Excessively high levels of oxygen in incubators, used to save the lives of premature infants, led to an ROP epidemic and the realization that reducing the level of oxygen given to premature babies reduces the incidence of ROP.[122,123] The detrimental effects of high and/or fluctuating oxygen concentrations were validated in the oxygen-induced retinopathy (OIR) models, where alternating oxygen concentrations induce retinal neovascularization.[124–126] Although these models lack significant features of human ROP (absence of ridge tissue, involution of RNV, and absence of neovascular complications such as hemorrhage and traction retinal detachment), they have been instrumental in the dissection of the molecular mechanisms involved in ROP and retinal neovascular diseases in general. The association between high oxygen levels and ROP led to the

development of the 2-phase hypothesis for ROP almost 30 years before the classification of human ROP in zones and stages. According to this, in the first phase there is a delay or halting in physiologic retinal vascular development due to prematurity as well as hyperoxia-induced endothelial cell damage and subsequent vasoattenuation. As the peripheral avascular retina continues to develop in the absence of a developing vascular bed, it becomes relatively hypoxic and secretes proangiogenic factors, which promote retinal neovascularization and abnormal vasoproliferation into the vitreous (second phase). It is possible that the rate of change of oxygenation rather than the absolute level may be more important for disease progression, and there have been reports that return to high oxygen levels for prolonged time with gradual decline to normal oxygen levels may halt and reverse the disease.[127–129]

Oxygen level changes cannot fully account for disease progression and other factors have been implicated in RNV seen in ROP. Evidence from OIR models shows that oxidative stress and reactive oxygen species (ROS) play a role in the pathologic neovascularization.[130] Clinical trials for lutein[131] and N-acetyl cysteine[132] supplementation failed to show any significant benefit; however, a meta-analysis for vitamin-E supplementation concluded that it can reduce the risk of stage 3 ROP by 52%.[133] The discrepancy between treatment efficacies between the OIR model and human ROP underlines the limitation of our animal models and the complex pathophysiology of human disease.

Neovascularization in Uveitis

Inflammatory eye diseases may be complicated by neovascularization, which occurs due to two primary mechanisms: occlusive retinopathy (resulting in retinal ischemia) and inflammation. Occlusive retinopathy is the prominent characteristic in diseases with retinal vasculitis. These include Eales disease, Behçet disease, sarcoidosis, lupus, and retinitis associated with infectious such as cytomegalovirus (CMV), syphilis, tuberculosis, and herpes simplex virus (HSV), which can result in necrotizing vasculitis.[134] However, neovascularization of the disc has been seen

in other uveitic cases without apparent ischemia.[135] Given the fact that neovascularization can regress with corticosteroid and other immune-suppressive treatments, it seems that inflammation alone may be sufficient for retinal neovascularization in this heterogeneous group of diseases.[136–138] In the setting of uveitis, the breakdown of the blood–ocular barrier results in the accumulation of inflammatory cells, cytokines, and growth factors in the vitreous, which significantly alter the retinal microenvironment. The transcription factor NF-κB is critical for the inflammatory response and has been found to affect the expression of a variety of proinflammatory and proangiogenic cytokines and growth factors, including VEGF, IL-1β, IL-6, and TNF-α. These cytokines have been found to be elevated in the vitreous of patients with uveitis.[139] VEGF is still a key molecule in uveitis-associated neovascularization, and several studies have shown benefit (albeit partial) of anti-VEGF therapy.[140,141]

Mechanisms of Choroidal Angiogenesis

Choroidal neovascularization (CNV) denotes the growth of new blood vessels that originate from the choriocapillaris into the subretinal pigment epithelium (sub-RPE) or subretinal space. A *sine qua non* for the development of CNV is the disruption of Bruch's membrane (BM), which can occur with prolonged inflammation (nvAMD, outer retinal retinochoroidopathies, infectious etiologies), trauma (choroidal rupture, myopia, iatrogenic), defective BM secondary to systemic disease (angioid streaks), or without any identifiable cause (idiopathic). However, CNV lesions in pathologic myopia are associated with considerably less retinal edema, subretinal fluid (SRF), and pigment epithelial detachments (PEDs) compared with CNV associated with AMD.[142] In addition, myopic CNVM is usually smaller in size and has less need for chronic anti-VEGF suppression. This underlines that the development of CNVM in myopia may share some signaling pathways with CNVM seen in AMD, but with different root causes and pathogenetic mechanisms.

The development of the laser-induced model of CNV originally

described by Ryan has had a significant impact in our understanding of the molecular events involved in choroidal angiogenesis and has become the most widely used model in nvAMD research.[143] Although this model does not fully recapitulate the stages of nvAMD, it has been widely used in the preclinical testing of several antiangiogenic drugs.[144] Additionally, the surgical extraction of choroidal neovascular membranes from patients with nvAMD and their subsequent histopathologic examination increased our understanding about the complex pathways leading to CNV in nvAMD.[145] Below we will discuss the components involved in CNV, especially in the context of nvAMD (Fig. 28.3).

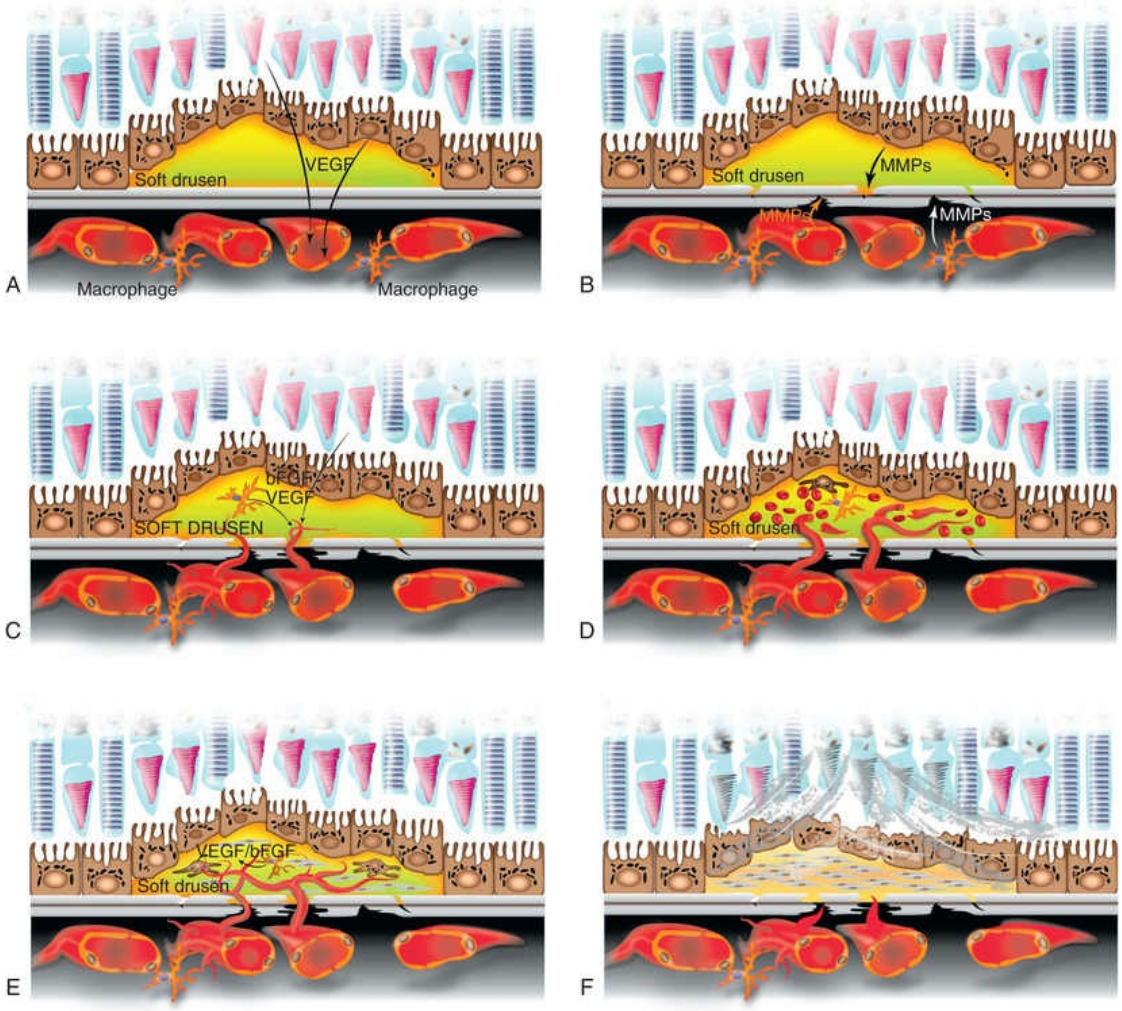

FIG. 28.3 Choroidal neovascularization (CNV). Presumed pathologic stages required for the development and progression of CNV. (A) Low-grade inflammation and tissue hypoxia at the sites of soft

drusen trigger the secretion of vascular endothelial growth factor (VEGF) by retinal pigment epithelium (RPE) and photoreceptor cells. Macrophages are attracted to the area in response to locally secreted chemoattractants or drusen components (e.g., monocyte chemoattractant protein-1, complement factor H). Accumulation of proangiogenic M2-macrophages. (B) Rupture of Bruch's membrane as a prerequisite for the development of CNV, which is thought to occur due to the local secretion of matrix metalloproteinases by RPE, choroidal endothelial cells, or macrophages. This proteolytic degradation of Bruch's membrane activates the wound-healing response at the choroidal–RPE interface. (C) Angiogenic cytokines such as VEGF and basic fibroblast growth factor induce the activation and proliferation of choroidal endothelial cells through the breaks in Bruch's membrane. Macrophages migrate into the subretinal space and promote the angiogenic response. (D) The newly formed vessels lack pericytes, are leaky and fragile, and often result in subretinal fluid accumulation or hemorrhage. (E) Growth factors secreted locally induce the transdifferentiation of RPE cells and its further migration from the monolayer into the stroma of the lesion. Maturation of the neovascular membrane with recruitment of fibroblasts, transdifferentiated RPE cells, and inflammatory cells. (F) The endpoint of this wound-healing response is the formation of a disciform lesion, characterized by aberrant fibrous tissue proliferation severely affecting the function of overlying photoreceptors. *bFGF*, Basic fibroblast growth factor; *MMPs*, matrix metalloproteinases. (Courtesy of Aristomenis Thanos, MD.)

Aging and Senescence of the Retinal Pigment Epithelium (RPE)

The incidence and progression of nearly every feature of AMD, including CNV, relates to age.[146] Lipofuscin, a byproduct of photoreceptor outer-segment digestion by lysosomes, increases

with age in RPE as lysosomal activity decreases in RPE with aging. Progressive accumulation of lipofuscin is thought to result in disturbance of RPE function. Aged RPE cells may decrease production of antiangiogenic molecules such as PEDF as successive passage of cultured RPE cells results in diminished production of PEDF.[147–149]

Drusen, Basal Laminar/Linear Deposit Formation

Soft drusen, unlike hard drusen, appear to be an important associated and predisposing feature of CNV. It is thought that membranous accumulation of debris as part of a diffuse disturbance of the RPE, softening of hard drusen, and cleavage in basal laminar/linear deposits may aid in the formation of soft drusen.[150–154] Histopathologic studies also reveal that basal laminar deposits (accumulating between the plasma and basement membrane of the RPE) and basal linear deposits (with a thickening of the inner collagenous zone of the Bruch's membrane) also have important associations with CNV.[155] Therefore, abnormal deposits that occur with diffuse distribution pattern between the RPE layer and Bruch's membrane are predisposing features of CNV. It is hypothesized that deposits between the RPE layer and Bruch's membrane may block the diffusion of oxygen and nutrients from choriocapillaris to the RPE monolayer and photoreceptors.[156] This speculative localized cellular hypoxia could result in overexpression of angiogenic growth factors such as VEGF, which, in turn, induce neovascularization from the choroidal vasculature. Additionally, the deposits are known to contain components of the immune response, and thus may act as initiators of inflammation.[157–160] The deposits may also serve as a reservoir for sequestration of factors such as advanced glycation end-products (AGE)[161,162] that may affect the function of adjacent RPE and choroidal endothelial cells.

Enzymatic and Mechanical Disruption of Bruch's Membrane

In CNV, activated endothelial cells migrate through Bruch's membrane; this process occurs by degradation of an intact Bruch's membrane, or growth through an existing Bruch's membrane break. Clinicopathologic studies suggest that occult CNV (type 1) is neovascularization proliferating under the RPE and is less permeable/active than classic CNV (type 2) in which the neovascularization has penetrated the BM/RPE complex.[163] It is also important to note that there is yet a third type of neovascularization (type 3) in which there is proliferation of new vessels within the retina itself with a perfusing arteriole and draining venule that can be accompanied by compensatory retinal telangiectatic changes and formation of a retinal–choroidal anastomosis (RCA) through breaks in the BM/RPE complex.[164] Bruch's membrane may be disrupted when the balance between proteolytic enzymes such as matrix MMPs and their inhibitors, the tissue inhibitors of metalloproteinases (TIMPs), favors a proteolytic environment. RPE cells express MMP-1 (interstitial collagenase),[165] MMP-2 (72-kDa gelatinase),[165,166] MMP-3 (stromelysin), and MMP-9 (92-kDa gelatinase),[165] as well as TIMP-1,[166,167] TIMP-2, and TIMP-3.[167] Thus, proteolysis of Bruch's membrane may potentially result from reduced expression of TIMPs or increased expression of MMPs. MMPs also play an important role in degrading the extracellular matrix at the leading edge of neovascular fronds. It has been shown that decreases in thickness and integrity of the elastic layer of Bruch's membrane are seen in the macula of eyes with AMD but not in controls.[168] Lysyl oxidase-like (LOXL) protein 1 has been shown to guide the spatially defined deposition of elastin and is essential for the maintenance of elastic fibers. LOXL1-deficient mice have been shown to develop increased neovascularization after laser injury.[169] Impairment in other components of the Bruch's membrane such as collagen XVIII has been shown to affect CNV formation in animals. Collagen XVIII knockout mice develop normal choroidal vasculature; however, they demonstrate increased size and leakage of laser-induced CNV.[170]

Transgenic mice with an intact Bruch's membrane that overexpress VEGF in photoreceptors develop subretinal neovascularization; however, the subretinal vessels extend from retinal vessels rather than the choroidal vasculature.[171] In contrast,

transgenic mice that overexpress VEGF in RPE cells show intrachoroidal CNV.[172] These findings support the notion that CNV requires both the expression of an angiogenic factor and a break in Bruch's membrane (by proteolysis, physical disruption, or preexisting break).

Macrophages are an alternative source of enzymes (such as MMPs) that could cause focal disruption of Bruch's membrane.[173] Histopathologic studies reveal that macrophages accumulate near thinned segments of Bruch's membrane.[174] In AMD, the RPE shows increased expression of MCP-1, a factor critical for macrophage recruitment.[175] Macrophages in the choroid may subsequently degrade Bruch's membrane, thus forming a passage that can be used by activated choroidal endothelial cells to gain entrance to the sub-RPE space.

Macrophages and Microglial Cells, and CNV

Macrophages (Mϕs) are an additional source of angiogenic growth factors that may promote the development of CNV and pharmacologic depletion of macrophages diminishes the lesion size and severity in experimental laser-induced CNV.[176,177] Activated Mϕs show increased expression of inflammatory cytokines such as TNF-α and IL-1β, which may promote angiogenesis by stimulating VEGF expression in RPE.[178] Polarization of Mϕs into classical proinflammatory M1-like and alternative proangiogenic M2-like, two extremes in a continuum of polarization states,[179] seems to be crucial for the angiogenic switch in nvAMD degeneration.[180] Rho-associated kinase (ROCK) signaling is involved in Mϕ polarization and ROCK inhibitors have been tested in neovascular disease.[180,181] It has been shown that the number of M2 Mϕs are increased compared to M1 macrophages in normal aging eyes,[182] and furthermore, aging macrophages show impaired cholesterol efflux and switch to angiogenic phenotype promoting neovascular AMD,[183] which partially supports the fact why age is the most crucial risk factor for nvAMD.[184]

Microglial cells (MC) – the resident Mϕs of the retina – are involved in phagocytosis of injured and dead cells.[185] Dysfunction of phagocytosis of accumulating debris may lead to further

inflammation.[186] In addition, accumulation of microglia in the subretinal space has been reported in animal models of AMD.[187] CX3CR1 is a cytokine produced by MC, and an association between AMD and CX3CR1 has been reported.[188,189] In CX3CR1-deficient mice, accumulation of MCs in the subretinal space has been observed, contributing to drusen formation and photoreceptor degeneration,[190] whereas a double knockout of MCP1 and CX3CR1 in an animal model leads to an AMD phenotype with spontaneous CNV formation.[191,192]

Complement, AMD, and CNV

Studies of human donor eyes have shown increased levels of C-reactive protein and decreased complement factor H (CFH) in the RPE/Bruch's membrane/choriocapillaris region of eyes with AMD compared to controls, suggesting a role of complement and inflammation in the progression of the disease.[193] Complement components have been detected in drusen,[151,152,157–160] and an animal model of CD59 knockout leads to increased CNV.[194] Most recently, a Y402H polymorphism in complement factor H (CFH) has been associated with increased risk of AMD and likely wet AMD.[195–198] This particular allele of CFH leads to decrease in its activity and thus an increased complement-mediated inflammation since CFH is a negative regulator of the alternative pathway. Other human studies have identified protective haplotypes in two other genes encoding complement proteins, factor B (abbreviated as BF, fB, or Fb) and complement component 2 (C2).[199] The alternative complement regulates pathologic angiogenesis, and Fb($^{-/-}$) mice show an increased number of neovessels at postnatal day 17 in the OIR model,[200] and mice deficient in the central complement component C3 displayed increased neovascularization in the same model.[201] However, another study showed that fB deficiency was protective in a laser model of CNVM.[202] In that same study they showed the antiangiogenic role of a soluble factor consisting of the N terminus of mouse factor H, containing the AP-inhibitory domain, linked to a complement receptor-2 targeting fragment. CFH polymorphisms were reported to affect response to anti-VEGF with CFH Y402H CC being accompanied with a poor response to

anti-VEGF therapy,[203,204] yet the CATT trial reported that although specific alleles for CFH, ARMS2, HTRA1, and C3 may predict the development of AMD, they did not predict response to anti-VEGF therapy.[205] Complement-based therapies have been mostly targeting dry AMD, but early clinical trials have not been encouraging.[206]

Angiogenic and Antiangiogenic Factors in Neovascularization

Angiogenic Factors

Vascular Endothelial Growth Factor

VEGF, also known as VEGF-A or VEGF-1, is expressed as five mRNA splice variants in humans: isoforms 121, 145, 165, 189, and 206.[207] VEGF is a heparin-binding dimeric glycoprotein with disulfide-linked subunits, which share significant sequence homology with the A and B chains of PDGF.[208] VEGF 121 is entirely soluble and unbound to extracellular matrix. VEGF 165 is intermediate and binds somewhat to extracellular matrix. VEGF 189 is almost entirely sequestered to extracellular matrix and cell surface sites.[209,210] VEGF 165 is the predominantly expressed isoform when human cDNA libraries are screened, and is optimal for bioavailability and biologic potency. It is the critical isoform for both developmental and pathologic retinal angiogenesis.[16,210,211] Two other related endothelial growth factors, VEGF-B and VEGF-C, have structural homology to VEGF and appear to play roles in tumor angiogenesis and in the development of the lymphatic system, as does VEGF-D.[212] VEGF-C, also known as VEGF-2, has been shown to promote angiogenesis in the rabbit ischemic hindlimb model.[213] VEGF-E has similar angiogenic activity to VEGF-A, primarily through VEGF receptor 2.[214]

VEGF was first identified in tumor models as a vasopermeability factor and initiator of angiogenesis upregulated by hypoxia. In addition to being the strongest endothelial cell mitogen, VEGF has been shown to induce the expression of plasminogen activators in microvascular endothelial cells, which is important in the extracellular proteolysis necessary for capillary formation.[215] VEGF

induces the expression of endothelial cell $\alpha_1\beta_1$ and $\alpha_2\beta_1$ integrins, which are important in migration.[216] There is also in vitro evidence that VEGF upregulates endothelial cell fenestrations in kidney glomerulus, choroid plexus, and even the choriocapillaris.[217] Leukocyte adhesion has been shown to be important in vascular leakage. VEGF increases the expression of ICAM-1 on endothelial cells, resulting in increased leukostasis, which mediates the breakdown of the blood–retinal barrier.[45,218]

Both high- and low-affinity VEGF receptors have been identified on not only endothelial cells, but also on bone marrow-derived and retinal epithelial cells.[219–221] They belong to the family of tyrosine kinases requiring phosphorylation to be activated upon ligand binding. VEGFR-1 (FMS-like tyrosine kinase or FLT-1 in human) and VEGFR-2 (fetal liver kinase 1 or Flk-1 in the mouse; TKR-C in the rat; kinase insert domain receptor or KDR in the human) are expressed on endothelial cells, whereas VEGFR-3 (FLT4) is primarily found on lymphatic endothelial cells.[222] Although VEGF binds to both VEGFR-1 and VEGFR-2, the latter is primarily responsible for endothelial cell mitogenesis, survival, and permeability.[223] VEGFR-1 may be important in development by sequestering VEGF, preventing it from interacting with VEGFR-2.[224] VEGFR-1 has an established role in monocyte chemotaxis.[225,226] VEGF-C has also been shown to be a ligand for VEGFR-2 and VEGFR-3.[213] Synergism between FGF-2 and VEGF has been demonstrated by the finding that FGF-2 increases VEGFR-2 expression in microvascular endothelial and aortic endothelial cells.[227] In addition to the receptor tyrosine kinases, VEGF also interacts with a family of coreceptors, the neuropilins, which may enhance its angiogenic function.[228]

Several growth factors cause upregulation of VEGF gene expression, including epidermal growth factor, TGF-α and β, IGF-1, FGF, and PDGF, implicating both paracrine and autocrine release of these factors in the hypoxic regulation of VEGF.[219,229] It has been shown that TGF-β is upregulated in RPE cells in CNV and hypothesized to play a role in modulating the effects of VEGF and basic FGF.[230] Both TGF-β and IL-1 induce VEGF expression in cultured choroidal fibroblasts.[231] VEGF and TGF-β can upregulate connective tissue growth factor (CTGF), a proangiogenic and

profibrotic growth factor found in CNV.[232] However, the relative importance of these growth factors, in comparison with VEGF, has not been determined.

Fibroblast Growth Factor-2

Acidic and basic fibroblast growth factor are prototype members of the FGF family. Basic FGF or FGF-2 is a fibroblast mitogen, and one of the first angiogenic factors identified and suspected in ocular neovascularization. FGF-2 has been called "the stored growth factor" because much of the cell-associated FGF-2 is found in the extracellular matrix.[233]

FGF-2 has been implicated in various aspects of angiogenesis. It stimulates endothelial cell proliferation and migration and induces the production of proteases.[234] FGF-2 is angiogenic in vivo in the chick chorioallantoic membrane (CAM) and corneal micropocket bioassays at very low levels.[235,236] FGF-2 has been isolated from many normal tissues and tumors of mesodermal and neuroectodermal origin, as well as in CNV membranes.[230,237–239]

One of the arguments against FGF-2's role in pathologic angiogenesis is its lack of a definitive signal peptide for secretion.[240] However, a number of alternative pathways for FGF-2 release have been postulated, including the ATP-binding cassette (ABC) transport proteins, selective exocytosis, and cell death or injury.[241–243] During sublethal injury, cells may transiently release FGF-2. Using cultured aortic endothelial cells, McNeil and colleagues have demonstrated that mechanical wounding by scraping leads to efficient release of FGF-2 from injured cells[241] (also reviewed by D'Amore[242]). In an experimental model of optic nerve crush in the mouse, FGF-2 immunostaining is dramatically increased in the retinal photoreceptor layer.[244] Finally, injury to the corneal epithelium leads to release of FGF-2, which binds to basement membrane.[243] These and other observations suggest that FGF-2 may act as a "wound hormone" both in maintenance of tissue integrity and repair after injury.

Integrins

The integrins are a family of cell adhesion proteins that are heterodimer combinations of 15 α and 8 β subunits, and are

important regulators of angiogenesis. They mediate endothelial cell adhesion to the extracellular matrix, which facilitates proliferation, migration, and response to prosurvival or apoptotic signals in the formation of new vessels.[245] Different integrins can bind to the same ligand, but initiate different intracellular signaling pathways. Also, one integrin can bind to multiple ligands; in addition to extracellular matrix components, ICAMs important for leukocyte adhesion can also be bound to integrins.[246]

$\alpha_v\beta_3$ has been demonstrated to inhibit endothelial cell apoptosis in newly sprouting blood vessels through the regulation of NF-κB.[247] $\alpha_v\beta_3$ and $\alpha_v\beta_5$ are highly expressed on angiogenic endothelial cells and have been demonstrated in neovascular tissue of experimental models and in clinical specimens.[248,249] Friedlander and colleagues found both $\alpha_v\beta_3$ and $\alpha_v\beta_5$ expressed in neovascular tissue from eyes with proliferative DR, whereas only $\alpha_v\beta_3$ was expressed in neovascular tissue from AMD and ocular histoplasmosis syndrome.[249] Blocking the integrins halts angiogenesis in the chick CAM and corneal neovascularization models, and integrin binding also partially suppresses retinal neovascularization.[250,251]

Ang and Tie2

Ang-1 is a 70-kDa glycoprotein that is chemotactic for endothelial cells, and is postulated to play a role in the assembly of nonendothelial cell components and the formation of capillary sprouts.[252,253] Ang-1 binds to Tie2, a tyrosine kinase receptor, which is expressed on endothelial cells and early hematopoietic cells.[254,255] Knockouts of the gene encoding Ang-1 or its receptor Tie2 are embryologically lethal, with failure to recruit smooth-muscle and pericyte precursors. Tie2 has also been demonstrated in quiescent and angiogenic vasculature in adults and may play a role in vascular maintenance.[255,256] Ang-2 also binds strongly to Tie2 but does not result in phosphorylation of the receptor; instead, it acts as a competitive inhibitor preventing Ang-1 binding.[257] It has been postulated that Ang-2 binding mediates endothelial cell survival signals by making them more responsive to VEGF, resulting in neovascularization. However, with VEGF inhibition, Ang-2 binding

results in apoptosis.[257] In the rabbit cornea micropocket model, neither Ang-1 or Ang-2 alone induced corneal neovascularization, but either Ang-1 or Ang-2 added to VEGF promoted neovascularization, with Ang-2 having the more potent effect.[258] Transgenic mice overexpressing Ang-2 demonstrate disruption of blood vessel formation and are similar in phenotype to Ang-1-deficient mice.[257] A phase II study of the angiopoietin 1 and 2 peptibody trebananib for the treatment of angiosarcoma, a rare malignant endothelial cell tumor with upregulation of the angiopoietin system (Tie2 and Ang2), was well tolerated, but lack of response led to closure of this study.[259] A more recent study of treatment of diabetic macular edema with an inhibitor of vascular endothelial-protein tyrosine phosphatase that activates Tie2 showed preliminary positive results.[260] Additional studies are needed to understand better the role of the Ang and Tie2 in ocular angiogenesis.

Matrix Metalloproteinases

The extracellular matrix of the microvasculature is a highly dynamic structure containing collagens, laminins, fibronectins, proteoglycans, and other proteins. Growth factors such as FGF-2 are localized there, and integrins mediate interactions between cells and the extracellular matrix. The extracellular matrix is remodeled during development and angiogenesis, with degradation of existing matrix and synthesis of new matrix material permitting migration and proliferation of endothelial cells. Degradation is accomplished by 16 known MMPs and plasmin. Plasmin is synthesized as a latent proenzyme, plasminogen, which requires proteolytic activation by enzymes such as urokinase-type plasminogen activator. This activation can be inhibited by plasminogen activator inhibitors. The MMPs are likewise synthesized as latent proenzymes and require proteolytic activation. The active MMPs can be inhibited by four known specific tissue inhibitors (TIMPS) and α-macroglobulin. For a review of the MMPs and their inhibitors, see Hadler-Olsen et al.[261]

VEGF has been shown to induce tissue factor and MMP production in endothelial cells, and MMP production in smooth-muscle cells via Flt-1.[262,263] AGE also caused increased MMP-2 mRNA in choroidal endothelial cells in vitro.[264] Another interaction

has been demonstrated between MMP-2 and the integrin $\alpha_v\beta_3$, which are functionally associated on the surface of angiogenic blood vessels; upon their binding, collagenolytic activity is increased. A naturally occurring fragment of MMP-2, termed PEX, has also been shown to prevent binding of MMP-2 to $\alpha_v\beta_3$, acting to decrease the proteolytic activity.[265] Thus, endogenous MMP fragments and TIMPs serve to regulate the invasive new vessels. MMP-9 is one of the major inducible MMPs. Its levels in the basal state seem to be suppressed by the energy sensor AMP-activated protein kinase (AMPK).[266] Human neutrophils have been shown uniquely to release TIMP-free MMP-9 to provide a potent catalytic stimulator of angiogenesis.[267]

Antiangiogenic Factors

Pigment Epithelium-Derived Factor (PEDF); Serpin Peptidase Inhibitor, Clade F, Member 1 (SERPINF1)

PEDF is a 50-kDa serpin protease that was first discovered as a secreted protein from human fetal RPE cells.[268] PEDF is the most potent antiangiogenic growth factor identified to date.[88] PEDF has been demonstrated to promote apoptosis in proliferating endothelial cells through increasing the interaction of Fas ligand with its receptor Fas. This seems to be the only cell type where PEDF promotes apoptosis.[89] PEDF has also been shown to signal cellular differentiation of retinoblastoma cells in vitro.[268] Furthermore, a neuroprotective role for PEDF has been identified in neural cerebellar granule cells where PEDF caused the expression of antiapoptotic genes through the activation of NF-κB.[269] In retinal degeneration slow (RDS) mutant mice, PEDF was shown to protect photoreceptors from undergoing apoptosis.[270] Thus, the signaling cascades that are activated by PEDF lead to cell-specific actions to promote both survival and cell death.

Immunohistochemical studies have shown PEDF to be expressed in the RPE cells, the interphotoreceptor matrix, ganglion cells, and in the ciliary neuroepithelium.[271,272] PEDF is also bound to components of the extracellular matrix. In vitro, hypoxia causes a decrease in PEDF expression while VEGF is increased.[88] In vivo, levels of PEDF were shown to be decreased in the vitreous of

patients with proliferative DR and wet AMD, such that PEDF levels correlated inversely with neovascularization.[273–275]

PEDF may have therapeutic potential as both a neuroprotective and antiangiogenic agent. The fact that it is both differentiation-promoting and antiangiogenic has popularized its study in tumor research. Using gene therapy approaches to administer PEDF may also be important in treating ocular neovascularization. Both intravitreal and subretinal adenoviral-associated PEDF have been used to treat retinal ischemia and CNV in mouse models, and overexpression of PEDF has been shown to inhibit neovascularization and inflammation.[276–278] However, there has been no follow-up of an early phase I dose-escalation study of adenovirus mediated PEDF study in neovascular age-related macular degeneration (AMD).[279]

Angiostatin and Endostatin

Angiostatin is a 38-kDa peptide identified in a murine model of Lewis lung carcinoma, where it was thought to inhibit tumor metastasis at distant sites.[280] It was found to be an internal fragment of plasminogen.[280]

Endostatin is a 20-kDa peptide isolated from murine hemangioendothelioma and has been identified as the C-terminal fragment of collagen XVIII.[281] Mice that lack collagen XVIII form larger and leakier laser-induced CNV.[170] Finally, circulating endostatin has been identified in human plasma.[282] Both angiostatin and endostatin have been proposed as potential therapeutic agents to treat ocular neovascularization; however, up to now they have not found success in clinical use and there has been controversy over their perceived biological effects.

Other Factors With Recent Interest in Angiogenesis

Recent studies have focused on the role of interleukin-18 (IL-18).[283–287] Initially termed interferon-gamma-inducing factor, IL-18 induces IFN-γ expression in responsive cells. IFN-γ was shown to be antiangiogenic[288,289] and to prevent laser-induced CNV in mice.[290] Doyle et al. have shown IL-18 to be protective in models of

neovascular AMD,[286] a point contested by Hirano et al.,[291] although Hirano et al. used a less bioactive molecule and at different dosage. Further studies by Doyle et al. using primates continue to show protective role in CNV at physiologic levels of the cytokine.[283,292] Shen et al. showed that intraocular IL-18 levels increased significantly after treatment with ranibizumab particularly and correlated with good visual outcome, in addition intraocular injection of IL-18 reduced VEGF-induced leakage and neovascularization.[293] A clinical trial will be able to give more definitive answers.

PDGF is a dimeric glycoprotein composed of two A (-AA) or two B (-BB) chains or a combination of the two (-AB) and is a potent mesenchymal cell mitogen involved in angiogenesis and is overexpressed in atherosclerotic plaques.[294–296] PDGF has been very important in embryo development and studies from transgenic mice have also pointed out to its importance in vascular pericytes. In 1997 Lindahl et al.[297] discovered that that deficiency in Pdgfb results in loss of microvascular pericytes and development of numerous capillary microaneurysms. Lack of Pdgfb resulted in embryonic lethality but also the inability of sprouting capillary endothelial cells to attract PDGF-receptor-beta-positive pericyte progenitor cells.[297] Endothelial cell specific loss of Pdgfb resulted in viable mice but with abnormal density of pericytes and a strong inverse correlation between their density and the formation of microvascular abnormalities all the way to proliferative retinopathy when pericyte density was less than 50% of normal.[30] PDGF-BB and FGF2, but not PDGF-BB and VEGF or VEGF and FGF2, synergistically induced angiogenesis and long-lasting functional vessels in a model of hindlimb ischemia.[298] Because of its somewhat distinct role in angiogenesis (pericytes, compared to endothelial cells) compared to VEGF, investigators have studied the potential synergistic treatment in angiogenesis. Its expression has been reported in the outer nuclear layer of the macula from patients with AMD and in the serum.[299,300] Clinical trials have progressed and results from Phase III have shown no benefit compared to anti-VEGF monotherapy. It should be noted that hypomorphic *Pdgfb* alleles has been associated with idiopathic basal ganglia calcification in both humans and mice and it is thought to be related

to the loss of endothelial PDGF-B and correlates with the degree of pericyte and blood–brain barrier deficiency.[301]

Conclusions

Ever since Michelson's hypothesis about a soluble and diffusible growth factor mediating ocular neovascularization, our knowledge about retinal and choroidal angiogenesis has expanded considerably. Undoubtedly, anti-VEGF agents revolutionized the treatment of ocular neovascular diseases and provided the proof of concept for molecular targeting as a therapeutic approach. The continuous discovery of new molecules and signaling pathways involved in these processes revealed the complexity of their pathogenesis, but also offers new candidate therapeutic targets. Given the redundancy of cellular signaling pathways, combination treatments with multiple agents may be needed for optimal therapy although the anti-leakage efficacy of anti-VEGF treatment seem to leave little room for short term efficacy improvement in many of these diseases.

References

1. Michaelson I. The mode of development of the vascular system of the retina, with some observations on its significance for certain retinal disease. *Trans Ophthalmol Soc U K*. 1948;68:137–180.
2. Senger DR, Galli SJ, Dvorak AM, Perruzzi CA, Harvey VS, Dvorak HF. Tumor cells secrete a vascular permeability factor that promotes accumulation of ascites fluid. *Science*. 1983;219(4587):983–985.
3. Shima DT, Adamis AP, Ferrara N, et al. Hypoxic induction of endothelial cell growth factors in retinal cells: identification and characterization of vascular endothelial growth factor (VEGF) as the mitogen. *Mol Med*. 1995;1(2):182–193.
4. Shima DT, Gougos A, Miller JW, et al. Cloning and mRNA expression of vascular endothelial growth factor in ischemic retinas of *Macaca fascicularis*. *Invest Ophthalmol Vis Sci*.

1996;37(7):1334–1340.
5. Aiello LP, Northrup JM, Keyt BA, Takagi H, Iwamoto MA. Hypoxic regulation of vascular endothelial growth factor in retinal cells. *Arch Ophthalmol*. 1995;113(12):1538–1544.
6. Miller JW, Le Couter J, Strauss EC, Ferrara N. Vascular endothelial growth factor a in intraocular vascular disease. *Ophthalmology*. 2013;120(1):106–114.
7. Yau JWY, Rogers SL, Kawasaki R, et al. Global prevalence and major risk factors of diabetic retinopathy. *Diabetes Care*. 2012;35(3):556–564.
8. Kempen JH, O'Colmain BJ, Leske MC, et al. The prevalence of diabetic retinopathy among adults in the United States. *Arch Ophthalmol*. 2004;122(4):552–563.
9. Rogers SL, McIntosh RL, Lim L, et al. Natural history of branch retinal vein occlusion: an evidence-based systematic review. *Ophthalmology*. 2010;117(6):1094–1101.e5.
10. Gergely K, Gerinec A. Retinopathy of prematurity – epidemics, incidence, prevalence, blindness. *Bratisl Lek Listy*. 2010;111(9):514–517.
11. Friedman DS, O'Colmain BJ, Muñoz B, et al. Prevalence of age-related macular degeneration in the United States. *Arch Ophthalmol*. 2004;122(4):564–572.
12. Ausprunk DH, Folkman J. Migration and proliferation of endothelial cells in preformed and newly formed blood vessels during tumor angiogenesis. *Microvasc Res*. 1977;14(1):53–65.
13. Lutty GA, Hasegawa T, Carol M, Prow T, McLeod DS. The human choriocapillaris develops by hemovasculogenesis. *FASEB J*. 2007;21(5):A379.
14. Watanabe T, Raff MC. Retinal astrocytes are immigrants from the optic nerve. *Nature*. 1988;332(6167):834–837.
15. Gariano RF, Kalina RE, Hendrickson AE. Normal and pathological mechanisms in retinal vascular development. *Surv Ophthalmol*. 1996;40(6):481–490.
16. Stalmans I, Ng Y-S, Rohan R, et al. Arteriolar and venular patterning in retinas of mice selectively expressing VEGF isoforms. *J Clin Invest*. 2002;109(3):327–336.
17. Dorrell MI, Aguilar E, Friedlander M. Retinal vascular

development is mediated by endothelial filopodia, a preexisting astrocytic template and specific R-cadherin adhesion. *Invest Ophthalmol Vis Sci*. 2002;43(11):3500–3510.
18. Gerhardt H, Golding M, Fruttiger M, et al. VEGF guides angiogenic sprouting utilizing endothelial tip cell filopodia. *J Cell Biol*. 2003;161(6):1163–1177.
19. Darland DC, Massingham LJ, Smith SR, Piek E, Saint-Geniez M, D'Amore PA. Pericyte production of cell-associated VEGF is differentiation-dependent and is associated with endothelial survival. *Dev Biol*. 2003;264(1):275–288.
20. Shih S-C, Ju M, Liu N, Mo J-R, Ney JJ, Smith LEH. Transforming growth factor beta1 induction of vascular endothelial growth factor receptor 1: mechanism of pericyte-induced vascular survival in vivo. *Proc Natl Acad Sci USA*. 2003;100(26):15859–15864.
21. Pournaras CJ. Systemic hyperoxia decreases vascular endothelial growth factor gene expression in ischemic primate retina. *Arch Ophthalmol*. 1997;115(12):1553.
22. Pournaras CJ, Tsacopoulos M, Strommer K, Gilodi N, Leuenberger PM. Experimental retinal branch vein occlusion in miniature pigs induces local tissue hypoxia and vasoproliferative microangiopathy. *Ophthalmology*. 1990;97(10):1321–1328.
23. Henkind P. Ocular neovascularization. *Am J Ophthalmol*. 1978;85(3):287–301.
24. Wise G. Retinal neovascularization. *Trans Ophthalmol Soc U K*. 1956;54:729–826.
25. Liu Y, Cox SR, Morita T, Kourembanas S. Hypoxia regulates vascular endothelial growth factor gene expression in endothelial cells: identification of a 5' enhancer. *Circ Res*. 1995;77(3):638–643.
26. Maxwell PH, Dachs GU, Gleadle JM, et al. Hypoxia-inducible factor-1 modulates gene expression in solid tumors and influences both angiogenesis and tumor growth. *Proc Natl Acad Sci USA*. 1997;94(15):8104–8109.
27. Tsuzuki Y, Fukumura D, Oosthuyse B. Vascular endothelial growth factor (VEGF) modulation by targeting hypoxia-inducible factor-1alpha – hypoxia response element – VEGF

cascade differentially regulates vascular response and growth rate in tumors. *Cancer Res*. 2000;60:6248–6252.
28. Jośko J, Gwóźdź B, Jedrzejowska-Szypułka H, Hendryk S. Vascular endothelial growth factor (VEGF) and its effect on angiogenesis. *Med Sci Monit*. 2000;6(5):1047–1052.
29. Neufeld G, Cohen T, Gengrinovitch S. Vascular endothelial growth factor (VEGF) and its receptors. *FASEB J*. 1999;13:9–22.
30. Enge M, Bjarnegård M, Gerhardt H, et al. Endothelium-specific platelet-derived growth factor-B ablation mimics diabetic retinopathy. *EMBO J*. 2002;21(16):4307–4316.
31. Eichler W, Yafai Y, Wiedemann P, Reichenbach A. Angiogenesis-related factors derived from retinal glial (Müller) cells in hypoxia. *Neuroreport*. 2004;15(10):1633–1637.
32. Stone J, Chan-Ling T, Pe'er J, Itin A, Gnessin H, Keshet E. Roles of vascular endothelial growth factor and astrocyte degeneration in the genesis of retinopathy of prematurity. *Invest Ophthalmol Vis Sci*. 1996;37(2):290–299.
33. Bishop PN. The role of extracellular matrix in retinal vascular development and preretinal neovascularization. *Exp Eye Res*. 2015;133:30–36.
34. Hosoda Y, Okada M, Matsumura M, Ogino N, Honda Y, Nagai Y. Intravitreal neovascular tissue of proliferative diabetic retinopathy: an immunohistochemical study. *Ophthalmic Res*. 1992;24(5):260–264.
35. Kado M, Hirokawa H, Yoshida A. [Role of the vitreous in retinal neovascularization evaluated by a comparison of central retinal vein occlusion and branch retinal vein occlusion]. *Nippon Ganka Gakkai Zasshi*. 1989;93(8):812–816.
36. Engerman RL. Pathogenesis of diabetic retinopathy. *Diabetes*. 1989;38(10):1203–1206.
37. Engerman RL, Kern TS. Retinopathy in animal models of diabetes. *Diabetes Metab Rev*. 1995;11(2):109–120.
38. Joussen AM, Poulaki V, Le ML, et al. A central role for inflammation in the pathogenesis of diabetic retinopathy. *FASEB J*. 2004;18(12):1450–1452.
39. Kowluru RA, Odenbach S. Role of interleukin-1beta in the

pathogenesis of diabetic retinopathy. *Br J Ophthalmol*. 2004;88(10):1343–1347.
40. Meleth AD, Agrón E, Chan C-C, et al. Serum inflammatory markers in diabetic retinopathy. *Invest Ophthalmol Vis Sci*. 2005;46(11):4295–4301.
41. Spranger J, Meyer-Schwickerath R, Klein M. TNF-alpha level in the vitreous body. Increase in neovascular eye diseases and proliferative diabetic retinopathy. *Med Klin*. 1995;90:134–137.
42. Abu El Asrar AM, Maimone D, Morse PH, Gregory S, Reder AT. Cytokines in the vitreous of patients with proliferative diabetic retinopathy. *Am J Ophthalmol*. 1992;114(6):731–736.
43. Funatsu H, Yamashita H, Shimizu E, Kojima R, Hori S. Relationship between vascular endothelial growth factor and interleukin-6 in diabetic retinopathy. *Retina*. 2001;21(5):469–477.
44. Joussen A, Poulaki V, Mitsiades N. Nonsteroidal anti-inflammatory drugs prevent early diabetic retinopathy via TNF-alpha suppression. *FASEB J*. 2002;16:438–440.
45. Miyamoto K, Khosrof S, Bursell S-E, et al. Prevention of leukostasis and vascular leakage in streptozotocin-induced diabetic retinopathy via intercellular adhesion molecule-1 inhibition. *Proc Natl Acad Sci USA*. 1999;96(19):10836–10841.
46. Kern TS. Contributions of inflammatory processes to the development of the early stages of diabetic retinopathy. *Exp Diabetes Res*. 2007;2007:95103.
47. Iliaki E, Poulaki V, Mitsiades N, Mitsiades CS, Miller JW, Gragoudas ES. Role of alpha 4 integrin (CD49d) in the pathogenesis of diabetic retinopathy. *Invest Ophthalmol Vis Sci*. 2009;50(10):4898–4904.
48. Dinarello CA. Biologic basis for interleukin-1 in disease. *Blood*. 1996;87(6):2095–2147.
49. Jung Y-J, Isaacs JS, Lee S, Trepel J, Neckers L. IL-1beta-mediated up-regulation of HIF-1alpha via an NFkappaB/COX-2 pathway identifies HIF-1 as a critical link between inflammation and oncogenesis. *FASEB J*. 2003;17(14):2115–2117.
50. Frater-Schroder M, Risau W, Hallmann R, Gautschi P,

Bohlen P. Tumor necrosis factor type alpha, a potent inhibitor of endothelial cell growth in vitro, is angiogenic in vivo. *Proc Natl Acad Sci USA*. 1987;84(15):5277–5281.
51. Leibovich SJ, Polverini PJ, Shepard HM, Wiseman DM, Shively V, Nuseir N. Macrophage-induced angiogenesis is mediated by tumour necrosis factor-alpha. *Nature*. 1987;329(6140):630–632.
52. Kociok N, Radetzky S, Krohne TU, Gavranic C, Joussen AM. Pathological but not physiological retinal neovascularization is altered in TNF-Rp55-receptor-deficient mice. *Invest Ophthalmol Vis Sci*. 2006;47(11):5057–5065.
53. Joussen AM, Poulaki V, Qin W, et al. Retinal vascular endothelial growth factor induces intercellular adhesion molecule-1 and endothelial nitric oxide synthase expression and initiates early diabetic retinal leukocyte adhesion in vivo. *Am J Pathol*. 2002;160(2):501–509.
54. Pruijt JF, Fibbe WE, Laterveer L, et al. Prevention of interleukin-8-induced mobilization of hematopoietic progenitor cells in rhesus monkeys by inhibitory antibodies against the metalloproteinase gelatinase B (MMP-9). *Proc Natl Acad Sci USA*. 1999;96(19):10863–10868.
55. Van den Steen PE, Proost P, Wuyts A, Van Damme J, Opdenakker G. Neutrophil gelatinase B potentiates interleukin-8 tenfold by aminoterminal processing, whereas it degrades CTAP-III, PF-4, and GRO-alpha and leaves RANTES and MCP-2 intact. *Blood*. 2000;96(8):2673–2681.
56. Descamps FJ, Van den Steen PE, Martens E, Ballaux F, Geboes K, Opdenakker G. Gelatinase B is diabetogenic in acute and chronic pancreatitis by cleaving insulin. *FASEB J*. 2003;17(8):887–889.
57. Notari L, Miller A, Martínez A, et al. Pigment epithelium-derived factor is a substrate for matrix metalloproteinase type 2 and type 9: implications for downregulation in hypoxia. *Invest Ophthalmol Vis Sci*. 2005;46(8):2736–2747.
58. Beránek M, Kolar P, Tschoplova S, Kankova K, Vasku A. Genetic variations and plasma levels of gelatinase A (matrix metalloproteinase-2) and gelatinase B (matrix

metalloproteinase-9) in proliferative diabetic retinopathy. *Mol Vis*. 2008;14:1114–1121.
59. Adamis AP, Miller JW, Bernal M-T, et al. Increased vascular endothelial growth factor levels in the vitreous of eyes with proliferative diabetic retinopathy. *Am J Ophthalmol*. 1994;118(4):445–450.
60. Aiello LP, Avery RL, Arrigg PG, et al. Vascular endothelial growth factor in ocular fluid of patients with diabetic retinopathy and other retinal disorders. *N Engl J Med*. 1994;331(22):1480–1487.
61. Moradian S, Ahmadieh H, Malihi M, Soheilian M, Dehghan MH, Azarmina M. Intravitreal bevacizumab in active progressive proliferative diabetic retinopathy. *Graefes Arch Clin Exp Ophthalmol*. 2008;246(12):1699–1705.
62. Cho WB, Oh SB, Moon JW, Kim HC. Panretinal photocoagulation combined with intravitreal bevacizumab in high-risk proliferative diabetic retinopathy. *Retina*. 2009;29(4):516–522.
63. Tonello M, Costa RA, Almeida FPP, Barbosa JC, Scott IU, Jorge R. Panretinal photocoagulation versus PRP plus intravitreal bevacizumab for high-risk proliferative diabetic retinopathy (IBeHi study). *Acta Ophthalmol*. 2008;86(4):385–389.
64. Jorge R, Costa RA, Calucci D, Cintra LP, Scott IU. Intravitreal bevacizumab (Avastin) for persistent new vessels in diabetic retinopathy (IBEPE study). *Retina*. 2006;26(9):1006–1013.
65. Mirshahi A, Roohipoor R, Lashay A, Mohammadi S-F, Abdoallahi A, Faghihi H. Bevacizumab-augmented retinal laser photocoagulation in proliferative diabetic retinopathy: a randomized double-masked clinical trial. *Eur J Ophthalmol*. 2008;18(2):263–269.
66. Spaide RF, Fisher YL. Intravitreal bevacizumab (Avastin) treatment of proliferative diabetic retinopathy complicated by vitreous hemorrhage. *Retina*. 2006;26(3):275–278.
67. Avery RL. Regression of retinal and iris neovascularization after intravitreal bevacizumab (Avastin) treatment. *Retina*. 2006;26(3):352–354.

68. Avery RL, Pearlman J, Pieramici DJ, et al. Intravitreal bevacizumab (Avastin) in the treatment of proliferative diabetic retinopathy. *Ophthalmology*. 2006;113(10):1695–1705.e6.
69. Hattori T, Shimada H, Nakashizuka H, Mizutani Y, Mori R, Yuzawa M. Dose of intravitreal bevacizumab (Avastin) used as preoperative adjunct therapy for proliferative diabetic retinopathy. *Retina*. 2010;30(5):761–764.
70. Mendrinos E, Donati G, Pournaras CJ. Rapid and persistent regression of severe new vessels on the disc in proliferative diabetic retinopathy after a single intravitreal injection of pegaptanib. *Acta Ophthalmol*. 2009;87(6):683–684.
71. Adamis AP, Altaweel M, Bressler NM, et al. Changes in retinal neovascularization after pegaptanib (Macugen) therapy in diabetic individuals. *Ophthalmology*. 2006;113(1):23–28.
72. Schmidinger G, Maar N, Bolz M, Scholda C, Schmidt-Erfurth U. Repeated intravitreal bevacizumab (Avastin(®)) treatment of persistent new vessels in proliferative diabetic retinopathy after complete panretinal photocoagulation. *Acta Ophthalmol*. 2011;89(1):76–81.
73. Shimura M, Yasuda K, Nakazawa T, et al. Panretinal photocoagulation induces pro-inflammatory cytokines and macular thickening in high-risk proliferative diabetic retinopathy. *Graefes Arch Clin Exp Ophthalmol*. 2009;247(12):1617–1624.
74. Shimura M, Yasuda K, Nakazawa T, Shiono T, Nishida K. Panretinal-photocoagulation before pars plana vitrectomy influences vitreous level of interleukin-6 but not of vascular endothelial growth factor in patients with diabetic retinopathy. *Int J Biomed Sci*. 2007;3(1):31–37.
75. Boulton M, Gregor Z, McLeod D, et al. Intravitreal growth factors in proliferative diabetic retinopathy: correlation with neovascular activity and glycaemic management. *Br J Ophthalmol*. 1997;81(3):228–233.
76. Dills DG, Moss SE, Klein R, Klein BEK. Association of elevated IGF-I levels with increased retinopathy in late-onset diabetes. *Diabetes*. 1991;40(12):1725–1730.

77. Grant M, Russell B, Fitzgerald C, Merimee TJ. Insulin-like growth factors in vitreous: studies in control and diabetic subjects with neovascularization. *Diabetes*. 1986;35(4):416–420.
78. Wang Q, Dills DG, Klein R, Klein BEK, Moss SE. Does insulin-like growth factor I predict incidence and progression of diabetic retinopathy? *Diabetes*. 1995;44(2):161–164.
79. Punglia RS, Lu M, Hsu J, et al. Regulation of vascular endothelial growth factor expression by insulin-like growth factor I. *Diabetes*. 1997;46(10):1619–1626.
80. Kirstein M, Aston C, Hintz R, Vlassara H. Receptor-specific induction of insulin-like growth factor I in human monocytes by advanced glycosylation end product-modified proteins. *J Clin Invest*. 1992;90(2):439–446.
81. Watanabe D, Suzuma K, Matsui S, et al. Erythropoietin as a retinal angiogenic factor in proliferative diabetic retinopathy. *N Engl J Med*. 2005;353(8):782–792.
82. Grimm C, Wenzel A, Groszer M, et al. HIF-1-induced erythropoietin in the hypoxic retina protects against light-induced retinal degeneration. *Nat Med*. 2002;8(7):718–724.
83. Sakanaka M, Wen T-C, Matsuda S, et al. In vivo evidence that erythropoietin protects neurons from ischemic damage. *Proc Natl Acad Sci USA*. 1998;95(8):4635–4640.
84. Becerra SP, Amaral J. Erythropoietin – an endogenous retinal survival factor. *N Engl J Med*. 2002;347(24):1968–1970.
85. Watanabe D, Suzuma K, Suzuma I, et al. Vitreous levels of angiopoietin 2 and vascular endothelial growth factor in patients with proliferative diabetic retinopathy. *Am J Ophthalmol*. 2005;139(3):476–481.
86. White RR, Shan S, Rusconi CP, et al. Inhibition of rat corneal angiogenesis by a nuclease-resistant RNA aptamer specific for angiopoietin-2. *Proc Natl Acad Sci USA*. 2003;100(9):5028–5033.
87. Babapoor-Farrokhran S, Jee K, Puchner B, et al. Angiopoietin-like 4 is a potent angiogenic factor and a novel therapeutic target for patients with proliferative diabetic retinopathy. *Proc Natl Acad Sci USA*.

2015;112(23):E3030–9.
88. Dawson DW. Pigment epithelium-derived factor: a potent inhibitor of angiogenesis. *Science*. 1999;285(5425):245–248.
89. Volpert OV, Zaichuk T, Zhou W, et al. Inducer-stimulated Fas targets activated endothelium for destruction by anti-angiogenic thrombospondin-1 and pigment epithelium-derived factor. *Nat Med*. 2002;8(4):349–357.
90. Ogata N, Matsuoka M, Matsuyama K, et al. Plasma concentration of pigment epithelium-derived factor in patients with diabetic retinopathy. *J Clin Endocrinol Metab*. 2007;92(3):1176–1179.
91. Miller JW, Adamis AP, Shima DT, et al. Vascular endothelial growth factor/vascular permeability factor is temporally and spatially correlated with ocular angiogenesis in a primate model. *Am J Pathol*. 1994;145(3):574–584.
92. Brown DM, Heier JS, Clark WL, et al. Intravitreal aflibercept injection for macular edema secondary to central retinal vein occlusion: 1-year results from the phase 3 COPERNICUS study. *Am J Ophthalmol*. 2013;155(3):429–437.e7.
93. Holz FG, Roider J, Ogura Y, et al. VEGF Trap-Eye for macular oedema secondary to central retinal vein occlusion: 6-month results of the phase III GALILEO study. *Br J Ophthalmol*. 2013;97(3):278–284.
94. Campochiaro PA, Sophie R, Pearlman J, et al. Long-term outcomes in patients with retinal vein occlusion treated with ranibizumab: the RETAIN study. *Ophthalmology*. 2014;121(1):209–219.
95. Campochiaro PA, Brown DM, Awh CC, et al. Sustained benefits from ranibizumab for macular edema following central retinal vein occlusion: twelve-month outcomes of a phase III study. *Ophthalmology*. 2011;118(10):2041–2049.
96. Yuzbasioglu E, Artunay O, Rasier R, Sengul A, Bahcecioglu H. Simultaneous intravitreal and intracameral injection of bevacizumab (Avastin) in neovascular glaucoma. *J Ocul Pharmacol Ther*. 2009;25(3):259–264.
97. Brynskov T, Kemp H, Sørensen TL. Intravitreal ranibizumab for retinal vein occlusion through 1 year in clinical practice.

Retina. 2014;34(8):1637–1643.
98. Koss MJ, Pfister M, Rothweiler F, et al. Comparison of cytokine levels from undiluted vitreous of untreated patients with retinal vein occlusion. *Acta Ophthalmol*. 2012;90(2):e98–103.
99. Noma H, Funatsu H, Mimura T, Harino S, Hori S. Vitreous levels of interleukin-6 and vascular endothelial growth factor in macular edema with central retinal vein occlusion. *Ophthalmology*. 2009;116(1):87–93.
100. Suzuki Y, Nakazawa M, Suzuki K, Yamazaki H, Miyagawa Y. Expression profiles of cytokines and chemokines in vitreous fluid in diabetic retinopathy and central retinal vein occlusion. *Jpn J Ophthalmol*. 2011;55(3):256–263.
101. Noma H, Funatsu H, Harino S, Mimura T, Eguchi S, Hori S. Vitreous inflammatory factors in macular edema with central retinal vein occlusion. *Jpn J Ophthalmol*. 2011;55(3):248–255.
102. Noma H, Funatsu H, Mimura T, Eguchi S, Shimada K, Hori S. Vitreous levels of pigment epithelium-derived factor and vascular endothelial growth factor in macular edema with central retinal vein occlusion. *Curr Eye Res*. 2011;36(3):256–263.
103. Mayer WJ, Wolf A, Kernt M, et al. Twelve-month experience with Ozurdex for the treatment of macular edema associated with retinal vein occlusion. *Eye (Lond)*. 2013;27(7):816–822.
104. Fan C, Wang Y, Ji Q, Zhao B, Xie J. Comparison of clinical efficacy of intravitreal ranibizumab with and without triamcinolone acetonide in macular edema secondary to central retinal vein occlusion. *Curr Eye Res*. 2014;39(9):938–943.
105. Bell E, Klein J. Comments on oxygen toxicity and retinopathy (ROP) in the premature infant. Bell EF, Segar JL. *Iowa neonatology handbook: pulmonary*. I. Iowa University, Children's Hospital Department of Pediatrics; 1994.
106. Ashton N. Oxygen and the growth and development of retinal vessels. *Am J Ophthalmol*. 1966;62(3):412–435.
107. Vrachnis N, Kalampokas E, Sifakis S, et al. Placental growth

factor (PlGF): a key to optimizing fetal growth. *J Matern Fetal Neonatal Med*. 2013;26(10):995–1002.
108. Fruttiger M. Development of the retinal vasculature. *Angiogenesis*. 2007;10(2):77–88.
109. Wu W-C, Kuo H-K, Yeh P-T, Yang C-M, Lai C-C, Chen S-N. An updated study of the use of bevacizumab in the treatment of patients with prethreshold retinopathy of prematurity in Taiwan. *Am J Ophthalmol*. 2013;155(1):150–158.e1.
110. Lepore D, Quinn GE, Molle F, et al. Intravitreal bevacizumab versus laser treatment in type 1 retinopathy of prematurity: report on fluorescein angiographic findings. *Ophthalmology*. 2014;121(11):2212–2219.
111. Geloneck MM, Chuang AZ, Clark WL, et al. Refractive outcomes following bevacizumab monotherapy compared with conventional laser treatment: a randomized clinical trial. *JAMA Ophthalmol*. 2014;132(11):1327–1333.
112. Chen Y-H, Chen S-N, Lien R-I, et al. Refractive errors after the use of bevacizumab for the treatment of retinopathy of prematurity: 2-year outcomes. *Eye (Lond)*. 2014;28(9):1080–1086 [quiz 1087].
113. Mintz-Hittner HA. Intravitreal pegaptanib as adjunctive treatment for stage 3+ ROP shown to be effective in a prospective, randomized, controlled multicenter clinical trial. *Eur J Ophthalmol*. 2012;22(5):685–686.
114. Wu W-C, Yeh P-T, Chen S-N, Yang C-M, Lai C-C, Kuo H-K. Effects and complications of bevacizumab use in patients with retinopathy of prematurity: a multicenter study in Taiwan. *Ophthalmology*. 2011;118(1):176–183.
115. Mintz-Hittner HA, Kennedy KA, Chuang AZ. Efficacy of intravitreal bevacizumab for stage 3+ retinopathy of prematurity. *N Engl J Med*. 2011;364(7):603–615.
116. Azad R, Dave V, Jalali S. Use of intravitreal anti-VEGF: retinopathy of prematurity surgeons in Hamlet's dilemma? *Indian J Ophthalmol*. 2011;59(6):421–422.
117. McCloskey M, Wang H, Jiang Y, Smith GW, Strange J, Hartnett ME. Anti-VEGF antibody leads to later atypical intravitreous neovascularization and activation of

angiogenic pathways in a rat model of retinopathy of prematurity. *Invest Ophthalmol Vis Sci*. 2013;54(3):2020–2026.
118. Vavvas DG. Anti-VEGF in retinopathy of prematurity, need to titrate. *Invest Ophthalmol Vis Sci*. 2013;54(3).
119. Hellstrom A, Perruzzi C, Ju M, et al. Low IGF-I suppresses VEGF-survival signaling in retinal endothelial cells: direct correlation with clinical retinopathy of prematurity. *Proc Natl Acad Sci USA*. 2001;98(10):5804–5808.
120. Pérez-Muñuzuri A, Fernández-Lorenzo JR, Couce-Pico ML, Blanco-Teijeiro MJ, Fraga-Bermúdez JM. Serum levels of IGF1 are a useful predictor of retinopathy of prematurity. *Acta Paediatr*. 2010;99(4):519–525.
121. Pérez-Muñuzuri A, Couce-Pico ML, Baña-Souto A, et al. Preclinical screening for retinopathy of prematurity risk using IGF1 levels at 3 weeks post-partum. *PLoS ONE*. 2014;9(2):e88781.
122. Campbell K. Intensive oxygen therapy as a possible cause of retrolental fibroplasia: a clinical approach. *Med J Aust*. 1951;2(2):48–50.
123. Patz A, Hoeck LE, De La Cruz E. Studies on the effect of high oxygen administration in retrolental fibroplasia. I. Nursery observations. *Am J Ophthalmol*. 1952;35(9):1248–1253.
124. Smith LE, Wesolowski E, McLellan A, et al. Oxygen-induced retinopathy in the mouse. *Invest Ophthalmol Vis Sci*. 1994;35(1):101–111.
125. Hartnett ME, Penn JS. Mechanisms and management of retinopathy of prematurity. *N Engl J Med*. 2012;367(26):2515–2526.
126. Patz A, Eastham A, Higginbotham DH, Kleh T. Oxygen studies in retrolental fibroplasia. II. The production of the microscopic changes of retrolental fibroplasia in experimental animals. *Am J Ophthalmol*. 1953;36(11):1511–1522.
127. Szewczyk TS. Retrolental fibroplasia: etiology and prophylaxis; a preliminary report. *Am J Ophthalmol*. 1951;34(12):1649–1650.
128. Bedrossian RH, Carmichael P, Ritter J. Retinopathy of

prematurity (retrolental fibroplasia) and oxygen. *Am J Ophthalmol*. 1954;37(1):78–86.
129. Kinsey VE. Retrolental fibroplasia; cooperative study of retrolental fibroplasia and the use of oxygen. *AMA Arch Ophthalmol*. 1956;56(4):481–543.
130. Saito Y, Geisen P, Uppal A, Hartnett ME. Inhibition of NAD(P)H oxidase reduces apoptosis and avascular retina in an animal model of retinopathy of prematurity. *Mol Vis*. 2007;13:840–853.
131. Manzoni P, Guardione R, Bonetti P, et al. Lutein and zeaxanthin supplementation in preterm very low-birth-weight neonates in neonatal intensive care units: a multicenter randomized controlled trial. *Am J Perinatol*. 2013;30(1):25–32.
132. Soghier LM, Brion LP. Cysteine, cystine or N-acetylcysteine supplementation in parenterally fed neonates. *Cochrane Database Syst Rev*. 2006;(4) [CD004869].
133. Brion LP, Bell EF, Raghuveer TS. Vitamin E supplementation for prevention of morbidity and mortality in preterm infants. *Cochrane Database Syst Rev*. 2003;(4) [CD003665].
134. Kuo IC, Cunningham ET. Ocular neovascularization in patients with uveitis. *Int Ophthalmol Clin*. 2000;40(2):111–126.
135. Shorb SR, Irvine AR, Kimura SJ, Morris BW. Optic disk neovascularization associated with chronic uveitis. *Am J Ophthalmol*. 1976;82(2):175–178.
136. Dees C. Immunosuppressive treatment of choroidal neovascularization associated with endogenous posterior uveitis. *Arch Ophthalmol*. 1998;116(11):1456.
137. Flaxel CJ, Owens SL, Mulholland B, Schwartz SD, Gregor ZJ. The use of corticosteroids for choroidal neovascularisation in young patients. *Eye (Lond)*. 1998;12(Pt 2):266–272.
138. Martidis A, Miller DG, Ciulla TA, Danis RP, Moorthy RS. Corticosteroids as an antiangiogenic agent for histoplasmosis-related subfoveal choroidal neovascularization. *J Ocul Pharmacol Ther*. 1999;15(5):425–

428.
139. Ooi KG-J, Galatowicz G, Calder VL, Lightman SL. Cytokines and chemokines in uveitis: is there a correlation with clinical phenotype? *Clin Med Res*. 2006;4(4):294–309.
140. Adan A, Mateo C, Navarro R, Bitrian E, Casaroli-Marano RP. Intravitreal bevacizumab (Avastin) injection as primary treatment of inflammatory choroidal neovascularization. *Retina*. 2007;27(9):1180–1186.
141. Chan W-M, Lai TYY, Liu DTL, Lam DSC. Intravitreal bevacizumab (Avastin) for choroidal neovascularization secondary to central serous chorioretinopathy, secondary to punctate inner choroidopathy, or of idiopathic origin. *Am J Ophthalmol*. 2007;143(6):977–983.
142. Sadda SR, Keane PA, Joeres SA, et al. Quantitative comparison of the morphology of choroidal neovascularization in pathologic myopia versus that in age-related macular degeneration, using optical coherence tomography subanalysis. *Invest Ophthalmol Vis Sci*. 2008;49(13):263.
143. Ryan SJ. Subretinal neovascularization after argon laser photocoagulation. *Albrecht Von Graefes Arch Klin Exp Ophthalmol*. 1980;215(1):29–42.
144. Gragoudas ES, Adamis AP, Cunningham ET, Feinsod M, Guyer DR. Pegaptanib for neovascular age-related macular degeneration. *N Engl J Med*. 2004;351(27):2805–2816.
145. Gass JD. Biomicroscopic and histopathologic considerations regarding the feasibility of surgical excision of subfoveal neovascular membranes. *Am J Ophthalmol*. 1994;118(3):285–298.
146. Klein R, Klein BEK, Jensen SC, Meuer SM. The five-year incidence and progression of age-related maculopathy. *Ophthalmology*. 1997;104(1):7–21.
147. Wilcox DK. Vectorial accumulation of cathepsin D in retinal pigmented epithelium: effects of age. *Invest Ophthalmol Vis Sci*. 1988;29:1205–1212.
148. Kennedy CJ, Rakoczy PE, Constable IJ. Lipofuscin of the retinal pigment epithelium: a review. *Eye (Lond)*. 1995;9(Pt 6):763–771.

149. Tombran-Tink J, Shivaram SM, Chader GJ, Johnson LV, Bok D. Expression, secretion, and age-related downregulation of pigment epithelium-derived factor, a serpin with neurotrophic activity. *J Neurosci*. 1995;15(7 Pt 1):4992–5003.
150. Rakoczy PE, Zhang D, Robertson T, et al. Progressive age-related changes similar to age-related macular degeneration in a transgenic mouse model. *Am J Pathol*. 2002;161(4):1515–1524.
151. Hageman GS, Mullins RF. Molecular composition of drusen as related to substructural phenotype. *Mol Vis*. 1999;5:28.
152. Mullins RF, Russell SR, Anderson DH, Hageman GS. Drusen associated with aging and age-related macular degeneration contain proteins common to extracellular deposits associated with atherosclerosis, elastosis, amyloidosis, and dense deposit disease. *FASEB J*. 2000;14(7):835–846.
153. Sarks JP, Sarks SH, Killingsworth MC. Evolution of soft drusen in age-related macular degeneration. *Eye (Lond)*. 1994;8(Pt 3):269–283.
154. Abdelsalam A, Del Priore L, Zarbin MA. Drusen in age-related macular degeneration. *Surv Ophthalmol*. 1999;44(1):1–29.
155. Green WR, Enger C. Age-related macular degeneration histopathologic studies. *Ophthalmology*. 1993;100(10):1519–1535.
156. Starita C, Hussain A, Patmore A. Localization of the site of major resistance to fluid transport in Bruch's membrane. *Invest Ophthalmol Vis Sci*. 1997;38:762–767.
157. Russell SR, Mullins RF, Schneider BL, Hageman GS. Location, substructure, and composition of basal laminar drusen compared with drusen associated with aging and age-related macular degeneration. *Am J Ophthalmol*. 2000;129(2):205–214.
158. Mullins RF, Aptsiauri N, Hageman GS. Structure and composition of drusen associated with glomerulonephritis: implications for the role of complement activation in drusen biogenesis. *Eye (Lond)*. 2001;15(Pt 3):390–395.
159. Hageman G. An Integrated hypothesis that considers

drusen as biomarkers of immune-mediated processes at the RPE-Bruch's membrane interface in aging and age-related macular degeneration. *Prog Retin Eye Res*. 2001;20(6):705–732.
160. Anderson DH, Mullins RF, Hageman GS, Johnson LV. A role for local inflammation in the formation of drusen in the aging eye. *Am J Ophthalmol*. 2002;134(3):411–431.
161. Lutty GA. Localization of vascular endothelial growth factor in human retina and choroid. *Arch Ophthalmol*. 1996;114(8):971.
162. Ishibashi T. Advanced glycation end products in age-related macular degeneration. *Arch Ophthalmol*. 1998;116(12):1629.
163. Lafaut BA. Clinicopathological correlation in exudative age related macular degeneration: histological differentiation between classic and occult choroidal neovascularisation. *Br J Ophthalmol*. 2000;84(3):239–243.
164. Freund KB, Ho I-V, Barbazetto IA, et al. Type 3 neovascularization: the expanded spectrum of retinal angiomatous proliferation. *Retina*. 2008;28(2):201–211.
165. Alexander JP, Bradley JM, Gabourel JD, Acott TS. Expression of matrix metalloproteinases and inhibitor by human retinal pigment epithelium. *Invest Ophthalmol Vis Sci*. 1990;31(12):2520–2528.
166. Padgett LC, Lui GM, Werb Z, LaVail MM. Matrix metalloproteinase-2 and tissue inhibitor of metalloproteinase-1 in the retinal pigment epithelium and interphotoreceptor matrix: vectorial secretion and regulation. *Exp Eye Res*. 1997;64(6):927–938.
167. Vranka JA, Johnson E, Zhu X, et al. Discrete expression and distribution pattern of TIMP-3 in the human retina and choroid. *Curr Eye Res*. 1997;16(2):102–110.
168. Chong NHV, Keonin J, Luthert PJ, et al. Decreased thickness and integrity of the macular elastic layer of Bruch's membrane correspond to the distribution of lesions associated with age-related macular degeneration. *Am J Pathol*. 2005;166(1):241–251.
169. Yu HG, Liu X, Kiss S, et al. Increased choroidal neovascularization following laser induction in mice

lacking lysyl oxidase-like 1. *Invest Ophthalmol Vis Sci*. 2008;49(6):2599–2605.
170. Marneros AG, She H, Zambarakji H, et al. Endogenous endostatin inhibits choroidal neovascularization. *FASEB J*. 2007;21(14):3809–3818.
171. Okamoto N, Tobe T, Hackett SF, et al. Transgenic mice with increased expression of vascular endothelial growth factor in the retina: a new model of intraretinal and subretinal neovascularization. *Am J Pathol*. 1997;151(1):281–291.
172. Schwesinger C, Yee C, Rohan RM, et al. Intrachoroidal neovascularization in transgenic mice overexpressing vascular endothelial growth factor in the retinal pigment epithelium. *Am J Pathol*. 2001;158(3):1161–1172.
173. Goetzl EJ, Banda MJ, Leppert D. Matrix metalloproteinases in immunity. *J Immunol*. 1996;156(1):1–4.
174. Killingsworth MC, Sarks JP, Sarks SH. Macrophages related to Bruch's membrane in age-related macular degeneration. *Eye (Lond)*. 1990;4(Pt 4):613–621.
175. Grossniklaus HE, Ling JX, Wallace TM, et al. Macrophage and retinal pigment epithelium expression of angiogenic cytokines in choroidal neovascularization. *Mol Vis*. 2002;8:119–126.
176. Espinosa-Heidmann DG, Suner IJ, Hernandez EP, Monroy D, Csaky KG, Cousins SW. Macrophage depletion diminishes lesion size and severity in experimental choroidal neovascularization. *Invest Ophthalmol Vis Sci*. 2003;44(8):3586.
177. Sakurai E, Anand A, Ambati BK, van Rooijen N, Ambati J. Macrophage depletion inhibits experimental choroidal neovascularization. *Invest Ophthalmol Vis Sci*. 2003;44(8):3578.
178. Oh H, Takagi H, Takagi C. The potential angiogenic role of macrophages in the formation of choroidal neovascular membranes. *Invest Ophthalmol Vis Sci*. 1999;40:1891–1898.
179. Sica A, Mantovani A. Macrophage plasticity and polarization: in vivo veritas. *J Clin Invest*. 2012;122(3):787–795.
180. Zandi S, Nakao S, Chun K-H, et al. ROCK-isoform-specific

polarization of macrophages associated with age-related macular degeneration. *Cell Rep*. 2015;10(7):1173–1186.
181. Hollanders K, Van Bergen T, Kindt N, et al. The effect of AMA0428, a novel and potent ROCK inhibitor, in a model of neovascular age-related macular degeneration. *Invest Ophthalmol Vis Sci*. 2015;56(2):1335–1348.
182. Cao X, Shen D, Patel MM, et al. Macrophage polarization in the maculae of age-related macular degeneration: a pilot study. *Pathol Int*. 2011;61(9):528–535.
183. Sene A, Khan AA, Cox D, et al. Impaired cholesterol efflux in senescent macrophages promotes age-related macular degeneration. *Cell Metab*. 2013;17(4):549–561.
184. Klein R, Klein BE, Jensen SC, Meuer SM. The five-year incidence and progression of age-related maculopathy: the Beaver Dam Eye Study. *Ophthalmology*. 1997;104(1):7–21.
185. Thanos A, Morizane Y, Murakami Y, et al. Evidence for baseline retinal pigment epithelium pathology in the Trp1-Cre mouse. *Am J Pathol*. 2012;180(5):1917–1927.
186. Gupta N, Brown KE, Milam AH. Activated microglia in human retinitis pigmentosa, late-onset retinal degeneration, and age-related macular degeneration. *Exp Eye Res*. 2003;76(4):463–471.
187. Cruz-Guilloty F, Saeed AM, Echegaray JJ, et al. Infiltration of proinflammatory m1 macrophages into the outer retina precedes damage in a mouse model of age-related macular degeneration. *Int J Inflam*. 2013;2013:503725.
188. Chan C-C, Tuo J, Bojanowski CM, Csaky KG, Green WR. Detection of CX3CR1 single nucleotide polymorphism and expression on archived eyes with age-related macular degeneration. *Histol Histopathol*. 2005;20(3):857–863.
189. Combadière C, Feumi C, Raoul W, et al. CX3CR1-dependent subretinal microglia cell accumulation is associated with cardinal features of age-related macular degeneration. *J Clin Invest*. 2007;117(10):2920–2928.
190. Sennlaub F, Auvynet C, Calippe B, et al. CCR2($^{+}$) monocytes infiltrate atrophic lesions in age-related macular disease and mediate photoreceptor degeneration in experimental subretinal inflammation in Cx3cr1 deficient mice. *EMBO*

Mol Med. 2013;5(11):1775–1793.
191. Tuo J, Bojanowski CM, Zhou M, et al. Murine ccl2/cx3cr1 deficiency results in retinal lesions mimicking human age-related macular degeneration. *Invest Ophthalmol Vis Sci*. 2007;48(8):3827–3836.
192. Chan C-C, Ross RJ, Shen D, et al. Ccl2/Cx3cr1-deficient mice: an animal model for age-related macular degeneration. *Ophthalmic Res*. 2008;40(3–4):124–128.
193. Johnson PT, Betts KE, Radeke MJ, Hageman GS, Anderson DH, Johnson LV. Individuals homozygous for the age-related macular degeneration risk-conferring variant of complement factor H have elevated levels of CRP in the choroid. *Proc Natl Acad Sci USA*. 2006;103(46):17456–17461.
194. Bora NS, Kaliappan S, Jha P, et al. CD59, a complement regulatory protein, controls choroidal neovascularization in a mouse model of wet-type age-related macular degeneration. *J Immunol*. 2007;178(3):1783–1790.
195. Klein RJ, Zeiss C, Chew EY, et al. Complement factor H polymorphism in age-related macular degeneration. *Science*. 2005;308(5720):385–389.
196. Edwards AO, Ritter R, Abel KJ, Manning A, Panhuysen C, Farrer LA. Complement factor H polymorphism and age-related macular degeneration. *Science*. 2005;308(5720):421–424.
197. Hageman GS, Anderson DH, Johnson LV, et al. A common haplotype in the complement regulatory gene factor H (HF1/CFH) predisposes individuals to age-related macular degeneration. *Proc Natl Acad Sci USA*. 2005;102(20):7227–7232.
198. Haines JL, Hauser MA, Schmidt S, et al. Complement factor H variant increases the risk of age-related macular degeneration. *Science*. 2005;308(5720):419–421.
199. Gold B, Merriam JE, Zernant J, et al. Variation in factor B (BF) and complement component 2 (C2) genes is associated with age-related macular degeneration. *Nat Genet*. 2006;38(4):458–462.
200. Sweigard JH, Yanai R, Gaissert P, et al. The alternative complement pathway regulates pathological angiogenesis

in the retina. *FASEB J*. 2014;28(7):3171–3182.
201. Langer HF, Chung K-J, Orlova VV, et al. Complement-mediated inhibition of neovascularization reveals a point of convergence between innate immunity and angiogenesis. *Blood*. 2010;116(22):4395–4403.
202. Rohrer B, Long Q, Coughlin B, et al. A targeted inhibitor of the alternative complement pathway reduces angiogenesis in a mouse model of age-related macular degeneration. *Invest Ophthalmol Vis Sci*. 2009;50(7):3056–3064.
203. Dikmetas O, Kadayıfcılar S, Eldem B. The effect of CFH polymorphisms on the response to the treatment of age-related macular degeneration (AMD) with intravitreal ranibizumab. *Mol Vis*. 2013;19:2571–2578.
204. Veloso CE, de Almeida LNF, Nehemy MB. CFH Y402H polymorphism and response to intravitreal ranibizumab in Brazilian patients with neovascular age-related macular degeneration. *Rev Col Bras Cir*. 2014;41(6):386–392.
205. Hagstrom SA, Ying G-S, Pauer GJT, et al. Pharmacogenetics for genes associated with age-related macular degeneration in the Comparison of AMD Treatments Trials (CATT). *Ophthalmology*. 2013;120(3):593–599.
206. Yehoshua Z, de Amorim Garcia Filho CA, Nunes RP, et al. Systemic complement inhibition with eculizumab for geographic atrophy in age-related macular degeneration: the COMPLETE study. *Ophthalmology*. 2014;121(3):693–701.
207. Hutchings H, Ortega N, Plouet J. Extracellular matrix-bound vascular endothelial growth factor promotes endothelial cell adhesion, migration, and survival through integrin ligation. *FASEB J*. 2003;17:1520–1522.
208. Tischer E, Gospodarowicz D, Mitchell R, et al. Vascular endothelial growth factor: A new member of the platelet-derived growth factor gene family. *Biochem Biophys Res Commun*. 1989;165(3):1198–1206.
209. Ferrara N, Houck K, Jakeman L, Leung DW. Molecular and biological properties of the vascular endothelial growth factor family of proteins. *Endocr Rev*. 1992;13(1):18–32.
210. Houck KA, Leung DW, Rowland AM, Winer J, Ferrara N. Dual regulation of vascular endothelial growth factor

bioavailability by genetic and proteolytic mechanisms. *J Biol Chem*. 1992;267(36):26031–26037.
211. Carmeliet P, Ng YS, Nuyens D, et al. Impaired myocardial angiogenesis and ischemic cardiomyopathy in mice lacking the vascular endothelial growth factor isoforms VEGF164 and VEGF188. *Nat Med*. 1999;5(5):495–502.
212. Salven P, Lymboussaki A, Heikkilä P, et al. Vascular endothelial growth factors VEGF-B and VEGF-C are expressed in human tumors. *Am J Pathol*. 1998;153(1):103–108.
213. Witzenbichler B, Asahara T, Murohara T, et al. Vascular endothelial growth factor-C (VEGF-C/VEGF-2) promotes angiogenesis in the setting of tissue ischemia. *Am J Pathol*. 1998;153(2):381–394.
214. Meyer M, Clauss M, Lepple-Wienhues A, et al. A novel vascular endothelial growth factor encoded by Orf virus, VEGF-E, mediates angiogenesis via signalling through VEGFR-2 (KDR) but not VEGFR-1 (Flt-1) receptor tyrosine kinases. *EMBO J*. 1999;18(2):363–374.
215. Pepper MS, Ferrara N, Orci L, Montesano R. Vascular endothelial growth factor (VEGF) induces plasminogen activators and plasminogen activator inhibitor-1 in microvascular endothelial cells. *Biochem Biophys Res Commun*. 1991;181(2):902–906.
216. Senger DR, Claffey KP, Benes JE, Perruzzi CA, Sergiou AP, Detmar M. Angiogenesis promoted by vascular endothelial growth factor: regulation through $\alpha 1\beta 1$ and $\alpha 2\beta 1$ integrins. *Proc Natl Acad Sci USA*. 1997;94(25):13612–13617.
217. Esser S. Vascular endothelial growth factor induces endothelial fenestrations in vitro. *J Cell Biol*. 1998;140(4):947–959.
218. Lu M, Perez VL, Ma N, et al. VEGF increases retinal vascular ICAM-1 expression in vivo. *Invest Ophthalmol Vis Sci*. 1999;40(8):1808–1812.
219. Ferrara N, Davis-Smyth T. The biology of vascular endothelial growth factor. *Endocr Rev*. 1997;18(1):4–25.
220. Jakeman LB, Winer J, Bennett GL, Altar CA, Ferrara N. Binding sites for vascular endothelial growth factor are

localized on endothelial cells in adult rat tissues. *J Clin Invest*. 1992;89(1):244–253.
221. Kim I, Ryan AM, Rohan R, et al. Constitutive expression of VEGF, VEGFR-1, and VEGFR-2 in normal eyes. *Invest Ophthalmol Vis Sci*. 1999;40(9):2115–2121.
222. Ferrara N, Gerber H-P, LeCouter J. The biology of VEGF and its receptors. *Nat Med*. 2003;9(6):669–676.
223. Matsumoto T, Claesson-Welsh L. VEGF receptor signal transduction. *Sci STKE*. 2001;2001(112):re21.
224. Park JE, Chen HH, Winer J, Houck KA, Ferrara N. Placenta growth factor: potentiation of vascular endothelial growth factor bioactivity, in vitro and in vivo, and high affinity binding to Flt-1 but not to Flk-1/KDR. *J Biol Chem*. 1994;269(41):25646–25654.
225. Barleon B, Sozzani S, Zhou D, Weich HA, Mantovani A, Marmé D. Migration of human monocytes in response to vascular endothelial growth factor (VEGF) is mediated via the VEGF receptor flt-1. *Blood*. 1996;87(8):3336–3343.
226. Hiratsuka S, Minowa O, Kuno J, Noda T, Shibuya M. Flt-1 lacking the tyrosine kinase domain is sufficient for normal development and angiogenesis in mice. *Proc Natl Acad Sci USA*. 1998;95(16):9349–9354.
227. Pepper MS, Mandriota SJ. Regulation of vascular endothelial growth factor receptor-2 (Flk-1) expression in vascular endothelial cells. *Exp Cell Res*. 1998;241(2):414–425.
228. Lee P, Goishi K, Davidson AJ, Mannix R, Zon L, Klagsbrun M. Neuropilin-1 is required for vascular development and is a mediator of VEGF-dependent angiogenesis in zebrafish. *Proc Natl Acad Sci USA*. 2002;99(16):10470–10475.
229. Neufeld G, Cohen T, Gengrinovitch S, Poltorak Z. Vascular endothelial growth factor (VEGF) and its receptors. *FASEB J*. 1999;13(1):9–22.
230. Amin R, Puklin JE, Frank RN. Growth factor localization in choroidal neovascular membranes of age-related macular degeneration. *Invest Ophthalmol Vis Sci*. 1994;35(8):3178–3188.
231. Kvanta A. Expression and regulation of vascular endothelial growth factor in choroidal fibroblasts. *Curr Eye Res*.

1995;14(11):1015–1020.
232. He S, Jin ML, Worpel V, Hinton DR. A role for connective tissue growth factor in the pathogenesis of choroidal neovascularization. *Arch Ophthalmol*. 2003;121(9):1283–1288.
233. Vlodavsky I, Folkman J, Sullivan R, et al. Endothelial cell-derived basic fibroblast growth factor: synthesis and deposition into subendothelial extracellular matrix. *Proc Natl Acad Sci USA*. 1987;84(8):2292–2296.
234. Mignatti P. In vitro angiogenesis on the human amniotic membrane: requirement for basic fibroblast growth factor-induced proteinases. *J Cell Biol*. 1989;108(2):671–682.
235. Lobb RR, Alderman EM, Fett JW. Induction of angiogenesis by bovine brain derived class 1 heparin-binding growth factor. *Biochemistry*. 1985;24(19):4969–4973.
236. Shing Y, Folkman J, Haudenschild C, Lund D, Crum R, Klagsbrun M. Angiogenesis is stimulated by a tumor-derived endothelial cell growth factor. *J Cell Biochem*. 1985;29(4):275–287.
237. Baird A. Peptide growth factors and their receptors. Roberts A. *Handbook of experimental pharmacology*. Springer-Verlag: Berlin; 1990.
238. Gospodarowicz D. Fibroblast growth factors. Pimentel E, Perucho M. *Critical reviews in oncogenesis*. CRC Press: Boca Raton, FL; 1989.
239. Kitaoka T, Morse LS, Schneeberger S, Ishigooka H, Hjelmeland LM. Expression of FGF5 in choroidal neovascular membranes associated with ARMD. *Curr Eye Res*. 1997;16(4):396–399.
240. Abraham JA, Mergia A, Whang JL, et al. Nucleotide sequence of a bovine clone encoding the angiogenic protein, basic fibroblast growth factor. *Science*. 1986;233(4763):545–548.
241. McNeil PL. Growth factors are released by mechanically wounded endothelial cells. *J Cell Biol*. 1989;109(2):811–822.
242. D'Amore PA. Modes of FGF release in vivo and in vitro. *Cancer Metastasis Rev*. 1990;9(3):227–238.
243. Adamis AP, Meklir B, Joyce NC. In situ injury-induced release of basic-fibroblast growth factor from corneal

epithelial cells. *Am J Pathol*. 1991;139(5):961–967.
244. Kostyk S, D'Amore P, Herman I, Wagner J. Optic nerve injury alters basic fibroblast growth factor localization in the retina and optic tract. *J Neurosci*. 1994;14(3):1441–1449.
245. Silverstein J, Silverstein RL. Cell adhesion molecules: an overview. *Cancer Invest*. 2015;16:176–182.
246. McEver RP. Adhesive interactions of leukocytes, platelets, and the vessel wall during hemostasis and inflammation. *Thromb Haemost*. 2001;86(3):746–756.
247. Scatena M. NF-kappa B mediates alpha vbeta 3 integrin-induced endothelial cell survival. *J Cell Biol*. 1998;141(4):1083–1093.
248. Brooks PC, Clark RA, Cheresh DA. Requirement of vascular integrin alpha v beta 3 for angiogenesis. *Science*. 1994;264(5158):569–571.
249. Friedlander M, Theesfeld CL, Sugita M, et al. Involvement of integrins alpha v beta 3 and alpha v beta 5 in ocular neovascular diseases. *Proc Natl Acad Sci USA*. 1996;93(18):9764–9769.
250. Friedlander M, Brooks P, Shaffer R. Definition of two angiogenic pathways by distinct alpha v integrins. *Science*. 1995;270:1500–1502.
251. Hammes H-P, Brownlee M, Jonczyk A, Sutter A, Preissner KT. Subcutaneous injection of a cyclic peptide antagonist of vitronectin receptor-type integrins inhibits retinal neovascularization. *Nat Med*. 1996;2(5):529–533.
252. Folkman J, D'Amore PA. Blood vessel formation: what is its molecular basis? *Cell*. 1996;87(7):1153–1155.
253. Koblizek TI, Weiss C, Yancopoulos GD, Deutsch U, Risau W. Angiopoietin-1 induces sprouting angiogenesis in vitro. *Curr Biol*. 1998;8(9):529–532.
254. Davis S, Aldrich TH, Jones PF, et al. Isolation of angiopoietin-1, a ligand for the TIE2 receptor, by secretion-trap expression cloning. *Cell*. 1996;87(7):1161–1169.
255. Witzenbichler B, Maisonpierre PC, Jones P, Yancopoulos GD, Isner JM. Chemotactic properties of angiopoietin-1 and -2, ligands for the endothelial-specific receptor tyrosine kinase Tie2. *J Biol Chem*. 1998;273(29):18514–18521.

256. Wong AL, Haroon ZA, Werner S, Dewhirst MW, Greenberg CS, Peters KG. Tie2 expression and phosphorylation in angiogenic and quiescent adult tissues. *Circ Res*. 1997;81(4):567–574.
257. Maisonpierre PC, Suri C, Jones PF, et al. Angiopoietin-2, a natural antagonist for Tie2 that disrupts in vivo angiogenesis. *Science*. 1997;277(5322):55–60.
258. Asahara T, Chen D, Takahashi T, et al. Tie2 Receptor ligands, angiopoietin-1 and angiopoietin-2, modulate vegf-induced postnatal neovascularization. *Circ Res*. 1998;83(3):233–240.
259. D'Angelo SP, Mahoney MR, Van Tine BA, et al. Alliance A091103 a phase II study of the angiopoietin 1 and 2 peptibody trebananib for the treatment of angiosarcoma. *Cancer Chemother Pharmacol*. 2015;75(3):629–638.
260. Campochiaro PA, Sophie R, Tolentino M, et al. Treatment of diabetic macular edema with an inhibitor of vascular endothelial-protein tyrosine phosphatase that activates Tie2. *Ophthalmology*. 2015;122(3):545–554.
261. Hadler-Olsen E, Fadnes B, Sylte I, Uhlin-Hansen L, Winberg J-O. Regulation of matrix metalloproteinase activity in health and disease. *FEBS J*. 2011;278(1):28–45.
262. Wang H, Keiser JA. Vascular endothelial growth factor upregulates the expression of matrix metalloproteinases in vascular smooth muscle cells: role of flt-1. *Circ Res*. 1998;83(8):832–840.
263. Zucker S, Mirza H, Conner CE, et al. Vascular endothelial growth factor induces tissue factor and matrix metalloproteinase production in endothelial cells: conversion of prothrombin to thrombin results in progelatinase A activation and cell proliferation. *Int J Cancer*. 1998;75(5):780–786.
264. Hoffmann S, Friedrichs U, Eichler W, Rosenthal A, Wiedemann P. Advanced glycation end products induce choroidal endothelial cell proliferation, matrix metalloproteinase-2 and VEGF upregulation in vitro. *Graefes Arch Clin Exp Ophthalmol*. 2002;240(12):996–1002.
265. Brooks PC, Silletti S, von Schalscha TL, Friedlander M,

Cheresh DA. Disruption of angiogenesis by PEX, a noncatalytic metalloproteinase fragment with integrin binding activity. *Cell*. 1998;92(3):391–400.
266. Morizane Y, Thanos A, Takeuchi K, et al. AMP-activated protein kinase suppresses matrix metalloproteinase-9 expression in mouse embryonic fibroblasts. *J Biol Chem*. 2011;286(18):16030–16038.
267. Ardi VC, Kupriyanova TA, Deryugina EI, Quigley JP. Human neutrophils uniquely release TIMP-free MMP-9 to provide a potent catalytic stimulator of angiogenesis. *Proc Natl Acad Sci USA*. 2007;104(51):20262–20267.
268. Tombran-Tink J, Johnson LV. Neuronal differentiation of retinoblastoma cells induced by medium conditioned by human RPE cells. *Invest Ophthalmol Vis Sci*. 1989;30(8):1700–1707.
269. Yabe T, Wilson D, Schwartz JP. NF-kappaB activation is required for the neuroprotective effects of pigment epithelium-derived factor (PEDF) on cerebellar granule neurons. *J Biol Chem*. 2001;276(46):43313–43319.
270. Cayouette M, Smith SB, Becerra SP, Gravel C. Pigment epithelium-derived factor delays the death of photoreceptors in mouse models of inherited retinal degenerations. *Neurobiol Dis*. 1999;6(6):523–532.
271. Karakousis PC, John SK, Behling KC, et al. Localization of pigment epithelium derived factor (PEDF) in developing and adult human ocular tissues. *Mol Vis*. 2001;7:154–163.
272. Ogata N, Wada M, Otsuji T, Jo N, Tombran-Tink J, Matsumura M. Expression of pigment epithelium-derived factor in normal adult rat eye and experimental choroidal neovascularization. *Invest Ophthalmol Vis Sci*. 2002;43(4):1168–1175.
273. Holekamp NM, Bouck N, Volpert O. Pigment epithelium-derived factor is deficient in the vitreous of patients with choroidal neovascularization due to age-related macular degeneration. *Am J Ophthalmol*. 2002;134(2):220–227.
274. Ogata N, Nishikawa M, Nishimura T, Mitsuma Y, Matsumura M. Inverse levels of pigment epithelium-derived factor and vascular endothelial growth factor in the

vitreous of eyes with rhegmatogenous retinal detachment and proliferative vitreoretinopathy. *Am J Ophthalmol*. 2002;133(6):851–852.
275. Ogata N, Tombran-Tink J, Nishikawa M, et al. Pigment epithelium-derived factor in the vitreous is low in diabetic retinopathy and high in rhegmatogenous retinal detachment. *Am J Ophthalmol*. 2001;132(3):378–382.
276. Mori K, Gehlbach P, Yamamoto S, et al. AAV-mediated gene transfer of pigment epithelium-derived factor inhibits choroidal neovascularization. *Invest Ophthalmol Vis Sci*. 2002;43(6):1994–2000.
277. Raisler BJ, Berns KI, Grant MB, Beliaev D, Hauswirth WW. Adeno-associated virus type-2 expression of pigmented epithelium-derived factor or Kringles 1-3 of angiostatin reduce retinal neovascularization. *Proc Natl Acad Sci USA*. 2002;99(13):8909–8914.
278. Park K, Jin J, Hu Y, Zhou K, Ma J. Overexpression of pigment epithelium-derived factor inhibits retinal inflammation and neovascularization. *Am J Pathol*. 2011;178(2):688–698.
279. Rasmussen H, Chu KW, Campochiaro P, et al. Clinical protocol: an open-label, phase I, single administration, dose-escalation study of ADGVPEDF.11D (ADPEDF) in neovascular age-related macular degeneration (AMD). *Hum Gene Ther*. 2001;12(16):2029–2032.
280. O'Reilly M. Angiostatin: aA novel angiogenesis inhibitor that mediates the suppression of metastases by a lewis lung carcinoma. *Cell*. 1994;79(2):315–328.
281. O'Reilly MS, Boehm T, Shing Y, et al. Endostatin: an endogenous inhibitor of angiogenesis and tumor growth. *Cell*. 1997;88(2):277–285.
282. Ständker L, Schrader M, Kanse SM, Jürgens M, Forssmann W-G, Preissner KT. Isolation and characterization of the circulating form of human endostatin. *FEBS Lett*. 1997;420(2–3):129–133.
283. Doyle SL, Adamson P, López FJ, Humphries P, Campbell M. Reply to IL-18 is not therapeutic for neovascular age-related macular degeneration. *Nat Med*. 2014;20(12):1376–

1377.
284. Campbell M, Doyle S, Humphries P. IL-18: a new player in immunotherapy for age-related macular degeneration? *Expert Rev Clin Immunol*. 2014;10(10):1273–1275.
285. Bray N. Eye diseases: a new use for interleukin-18 in sight. *Nat Rev Drug Discov*. 2014;13(6):418.
286. Doyle SL, Ozaki E, Brennan K, et al. IL-18 attenuates experimental choroidal neovascularization as a potential therapy for wet age-related macular degeneration. *Sci Transl Med*. 2014;6(230):230ra44.
287. Volin MV, Koch AE. Interleukin-18: a mediator of inflammation and angiogenesis in rheumatoid arthritis. *J Interferon Cytokine Res*. 2011;31(10):745–751.
288. Sato N, Nariuchi H, Tsuruoka N, et al. Actions of TNF and IFN-gamma on angiogenesis in vitro. *J Invest Dermatol*. 1990;95(6 Suppl.):85S–89S.
289. Beatty G, Paterson Y. IFN-gamma-dependent inhibition of tumor angiogenesis by tumor-infiltrating $CD4^+$ T cells requires tumor responsiveness to IFN-gamma. *J Immunol*. 2001;166(4):2276–2282.
290. Kleinman ME, Yamada K, Takeda A, et al. Sequence- and target-independent angiogenesis suppression by siRNA via TLR3. *Nature*. 2008;452(7187):591–597.
291. Hirano Y, Yasuma T, Mizutani T, et al. IL-18 is not therapeutic for neovascular age-related macular degeneration. *Nat Med*. 2014;20(12):1372–1375.
292. Doyle SL, López FJ, Celkova L, et al. IL-18 immunotherapy for neovascular AMD: tolerability and efficacy in nonhuman primates. *Invest Ophthalmol Vis Sci*. 2015;56(9):5424–5430.
293. Shen J, Choy DF, Yoshida T, et al. Interleukin-18 has antipermeablity and antiangiogenic activities in the eye: reciprocal suppression with VEGF. *J Cell Physiol*. 2014;229(8):974–983.
294. Hannink M, Donoghue DJ. Structure and function of platelet-derived growth factor (PDGF) and related proteins. *Biochim Biophys Acta*. 1989;989(1):1–10.
295. Heldin CH. Structural and functional studies on platelet-

derived growth factor. *EMBO J*. 1992;11(12):4251–4259.
296. Wilcox JN, Smith KM, Williams LT, Schwartz SM, Gordon D. Platelet-derived growth factor mRNA detection in human atherosclerotic plaques by in situ hybridization. *J Clin Invest*. 1988;82(3):1134–1143.
297. Lindahl P, Johansson BR, Levéen P, Betsholtz C. Pericyte loss and microaneurysm formation in PDGF-B-deficient mice. *Science*. 1997;277(5323):242–245.
298. Cao R, Bråkenhielm E, Pawliuk R, et al. Angiogenic synergism, vascular stability and improvement of hind-limb ischemia by a combination of PDGF-BB and FGF-2. *Nat Med*. 2003;9(5):604–613.
299. Kliffen M, Sharma HS, Mooy CM, Kerkvliet S, de Jong PTVM. Increased expression of angiogenic growth factors in age-related maculopathy. *Br J Ophthalmol*. 1997;81(2):154–162.
300. Zehetner C, Kirchmair R, Neururer SB, Kralinger MT, Bechrakis NE, Kieselbach GF. Systemic upregulation of PDGF-B in patients with neovascular AMD. *Invest Ophthalmol Vis Sci*. 2014;55(1):337–344.
301. Keller A, Westenberger A, Sobrido MJ, et al. Mutations in the gene encoding PDGF-B cause brain calcifications in humans and mice. *Nat Genet*. 2013;45(9):1077–1082.

*With acknowledgement to prior authors of this chapter, Stephen J. Ryan, David R. Hinton, and Toshinori Murata.

29

Blood–Retinal Barrier, Immune Privilege, and Autoimmunity

Karen R. Armbrust, Robert B. Nussenblatt, (posthumously)

Introduction

More than 100 years ago a fascinating discovery was made. Different tissue samples were placed into the anterior chamber of dogs or rabbits and then were observed for 4 months. Surprisingly, the induced intraocular inflammation was limited, and most of the tissue samples placed in the anterior chamber were not rejected. In contrast, heterografts placed in other parts of the body did not survive.[1] This experiment was the first to identify the eye as a site of immune privilege, although the significance of this finding was not appreciated until many years later: it was not until the 1940s that Sir Peter Medawar correctly identified the connection between these

results and the immune system.[2]

Today, we know that the eye is a unique and complex organ that has developed multiple mechanisms to protect itself against frivolous immunologic attacks and inflammation in order to maintain its delicate structure and function. The blood–ocular barrier system, which is formed by the blood–aqueous barrier and the inner and outer blood–retinal barriers, limits the passage of ions and proteins to maintain homeostasis and to sequester tissue-specific antigens. The pathogenesis of diabetic retinopathy provides evidence for the importance of an intact blood–retinal barrier: one of the earliest changes detected in diabetic retinopathy is dysfunction of the inner blood–retinal barrier.[3,4] Furthermore, in addition to the blood–ocular barrier, many active factors within the eye contribute to a downregulatory immune environment (DIE).[5] The blood–ocular barrier and the DIE are mechanisms that depend on each other's proper function and together are central to preserving the immune privilege of the eye. Immune privilege is instrumental in curbing excessive inflammation and preserving normal function. However, immune privilege may be lost under certain conditions and situations, resulting in retinal autoimmunity and ocular inflammation. A breakdown of the blood–retinal barrier can be found in cystoid macular edema, while a loss of the DIE occurs in many forms of uveitis and now is thought to play a critical role in the development of age-related macular degeneration (AMD).[6]

In the past, all retinal autoimmunity was perceived as pathogenic, and active suppression of retinal immunity was presumed necessary to maintain the health of the eye. However, studies have shown that retinal autoantibodies are present in normal controls,[7a] and constitutive expression of proinflammatory ligands have been found in the normal retina in high concentration.[7b] Moreover, animal optic nerve injury studies have revealed that retinal autoimmunity may be beneficial in limiting collateral damage to the retinal ganglion cells.[8] Thus, retinal autoimmunity can be viewed as a “double-edged sword,” with both protective and destructive effects.

Blood–Ocular Barrier

At the end of the 19th century the German bacteriologist and immunologist Paul Ehrlich experimented with staining tissues in animal models. When he injected dyes into the bloodstream, almost all tissues became intensely colored, though notably the brain remained unstained.[9] A few decades later, one of Ehrlich's students, Edwin Goldmann, performed the experiment the other way around, by injecting dyes into the cerebrospinal fluid. This time the brain became stained and the rest of the body remained dye-free.[10] Goldmann correctly concluded that there is a barrier restricting the passage of soluble material between the two compartments – the blood and the cerebrospinal fluid. In the same year, in 1913, Schnaudigel used trypan blue to demonstrate a similar barrier between the bloodstream and the retina of rabbits.[11]

Today we know that anatomic structures within the eye limit flux between the blood and much of the eye itself.[12] The blood–ocular barrier consists of two main components: the blood–aqueous barrier and the blood–retinal barrier. The blood–aqueous barrier is formed by the ciliary body nonpigmented epithelium, Schlemm's canal endothelium, and the endothelium of the iridal capillaries.[13] The blood–retinal barrier is located at two levels. The nonfenestrated capillaries of the retinal vessels form the inner blood–retinal barrier, and tight junctions of the retinal pigment epithelium (RPE) form the outer blood–retinal barrier.[14]

Together, these blood–ocular barriers limit the passage of ions to maintain homeostasis in the aqueous humor and vitreous, while they also prevent other blood-borne molecules from entering the eye. Hydrophilic molecules in particular have a low permeability across the blood–ocular barrier.[15] Conditions that involve breakdown of the blood–ocular barrier characteristically lead to inflammation and allow drugs and other molecules to penetrate more easily into the eye. It is not surprising that many eye diseases are associated with alterations of the blood–ocular barrier, although it may be difficult to distinguish whether blood–ocular barrier dysfunction is more of a cause or an effect of disease.

Blood–Retinal Barrier in Cystoid Macular

Edema

Cystoid macular edema and the potential for subsequent vision loss is associated with many different etiologies, since ocular trauma, intraocular inflammation, and vascular degeneration all may cause increased permeability of the blood–retinal barrier. The inner and outer plexiform layers of the retina act as diffusion barriers against continuous fluid distribution. Therefore, a breakdown of the inner blood–retinal barrier causes cysts mainly in the inner nuclear layer, whereas serum leakage from the outer blood–retinal barrier pools into cystic spaces in the Henle fiber layer.[16]

Blood–Retinal Barrier in Diabetic Retinopathy

The initial insult in both nonproliferative and proliferative diabetic retinopathy is chronic hyperglycemia, which leads to retinal hypoxia. Compensatory mechanisms like vasodilation provide a temporizing means to increase retinal blood flow under hypoxic conditions. However, after exhaustion of autoregulation, loss of retinal vascular pericytes and disruption of the pericyte-endothelial-cell complex may occur, which then leads to a disruption of endothelial tight junctions in the retinal vasculature.[4,17] Plasma leakage from the now permeable inner blood–retinal barrier may cause retinal edema and subsequent vision loss. Furthermore, chronic hyperglycemia induces hypoxia-mediated expression of growth factors and cytokines that upregulate pathways resulting in leukocyte adhesion, endothelial cell injury, and increased permeability of endothelial cells, as well as the abnormal blood vessel growth of proliferative diabetic retinopathy.[18–20]

Basic Concepts of Immunology

Early work on ocular immune privilege focused on the importance of the blood–ocular barrier and the lack of direct lymphatic drainage from the eye.[2] Although an intact blood–ocular barrier is undeniably important for ocular immune privilege, today we know

that ocular immune privilege is more complex than simply isolating tissue-specific antigens. To more fully understand the concepts of ocular immune privilege and retinal autoimmunity, we have to understand basic concepts in immunology and then examine how these immunologic components actively function in the eye.

Innate Immunity

There are two systems of immunity, innate and adaptive, coexisting to keep pathogens out. Innate immunity, the more primitive system, is nonspecific and immediate in response. A variety of pattern recognition receptors (PRR) recognize conserved microbial patterns – for example, Toll-like receptors recognize lipopolysaccharides (LPS) on gram-negative bacterial outer membranes – and trigger a nonspecific inflammatory response.[21] The key components of innate immunity are epithelial barriers, monocytes, macrophages, natural killer (NK) cells, polymorphonuclear cells, eosinophils, basophils, and plasma proteins belonging to families of the complement cascade, clotting cascade, and acute-phase reactants.

Adaptive Immunity

In contrast, adaptive immunity, as the name implies, changes depending on prior and current environments. The key cellular components of adaptive immunity are the B and T lymphocytes, which possess unique receptors for recognizing billions of different antigenic epitopes, to encompass most molecules of biologic interest.[22] Immunoglobulins, expressed by B cells, and T-cell receptors (TCR), expressed by T cells, form in the absence of exogenous stimulation and have unique configurations that confer specificity in antigen recognition. Each clone of lymphocyte expresses molecularly identical receptors on the cell surface; hence, in order to recognize billions of different epitopes, there are billions of unique lymphocytes. After maturation in the thymus (T cells) and the bone marrow (B cells), cells remain quiescent in G0 of the cell cycle until they encounter a complementary antigen with sufficient affinity to their receptors. A molecule binding one of these B- or T-cell receptors in the presence of appropriate

costimulation is the initiating event to trigger a specific immune response targeting elimination of the bound molecule, or antigen. If this molecule is pathogen-derived, immune activation will lead to the elimination of the pathogen, but if the molecule is self-derived, then immune activation may lead to autoimmunity, tissue injury, disease, and destruction of host tissue. It is important to realize that the random process for creating antibodies and T-cell receptors will generate lymphocyte receptors that bind to self antigens with high affinity;[23] we will examine the processes to protect the body from these potentially self-reactive lymphocytes in more detail in the following sections of this chapter.

Activation of a naive lymphocyte results in proliferation of that lymphocyte to produce clones, each with that same unique receptor that recognizes a single epitope of the inciting antigen. There are two major classes of T cells: $CD4^+$ T cells and $CD8^+$ T cells. Activated $CD8^+$ T cells become effector cytotoxic T cells, while the cytokine environment during activation of naive $CD4^+$ T cells is responsible for differentiation into three major types of effector T cells: Th1, Th2, and Th17 cells. Interleukin (IL)-12 expression leads to Th1 cell production, IL-4 leads to Th2 production,[24] and IL-1 and IL-23 lead to Th17 differentiation.[25] Some Th1 and Th2 cell clones will become memory cells that drive the enhanced immune response if the antigen is re-encountered. The rest of the Th1 cells will secrete cytokines targeted at macrophages and other cells that mediate cellular immunity. In contrast, Th2 cells will stimulate B cells to proliferate and produce antibody, mediating humoral immunity. Th17 cells are a recently discovered family of T-helper cells that are capable of producing IL-17.[26] Th17 cells play an important role in combating various bacterial and fungal species by producing IL-23, but increased numbers of Th17 cells also can be found in patients with autoimmune diseases like uveitis, multiple sclerosis, and rheumatoid arthritis.

The immune response can be compared to the neural reflex arc, which has an afferent limb, a central process, and an efferent limb. In the immune afferent limb, antigens are captured, processed, transported, and presented to the lymphocytes. Dendritic cells and macrophages, both bone marrow-derived, act as antigen presenting cells (APCs) by phagocytosing and endocytosing antigens,

processing the antigens, and then presenting the processed antigens in conjunction with special major histocompatibility complex (MHC) molecules on the cell surface. There are differences in B and T lymphocytes antigen presentation: B-cell receptors can engage a naive antigen directly, while TCRs only can recognize peptide fragments presented on special surface molecules (MHC classes I and II). MHC class I molecules, which are present in most cells, present peptides derived from protein degradation in the cytoplasm (intracellular antigens such as viral and other intracellular microbial products), while MHC class II molecules, which are present in APCs and lymphocytes, present peptides from phagocytic vesicles (extracellular antigens from the microenvironment).

The central limb of the immune response consists of antigen-specific lymphocyte activation and differentiation. Activation of naive lymphocytes requires APCs and only occurs in the organized lymph tissues in secondary lymphoid organs such as lymph nodes, spleen, tonsils, and Peyer's patches. After an APC-antigen complex engages a lymphocyte, costimulation is required for full lymphocyte activation.[27] APCs themselves provide the necessary costimulation needed for lymphocyte activation by upregulating an array of surface molecules (CD80, CD86, intercellular adhesion molecule-1, lymphocyte function-associated molecule-3, and CD40) that function as ligands for lymphocyte receptors. Costimulation also involves APCs secreting soluble cytokines such as IL-12, IL-6, IL-10, and IL-1β.

Upon $CD4^+$ T-cell activation, the $CD4^+$ lymphocytes proliferate and secrete an array of cytokines, including IL-2, IL-3, granulocyte–macrophage colony-stimulating factor, interferon-gamma (IFN-γ), and IL-4, that serve as growth and stimulation factors for the lymphocytes and APCs, hence amplifying the proliferation process. In addition, IL-2, IFN-γ, and IL-4 promote the differentiation of $CD8^+$ T lymphocytes to mature cytotoxic T lymphocytes (CTLs). The cytokine production by $CD4^+$ T cells also promotes activation and differentiation of B lymphocytes with IFN-γ and IL-2 stimulating B cells to produce complement-fixing immunoglobulin G (IgG) antibodies, while IL-4, IL-5, IL-6, and IL-10 stimulate production of noncomplement-fixing IgG, IgE, or IgA antibodies.

The final products after central processing in the lymphoid tissues are activated effector $CD4^+$, $CD8^+$, and B cells that have receptors specific for the inciting antigen.

These effector cells are transported, predominantly via a hematogenous route, to the site of the inciting antigens to execute the efferent limb of the immune response. While the engagement and activation of B cells can be direct, T cells require APCs for antigen recognition. Activated lymphocytes may engage the targeted antigen and also may recruit other components of the immune system. Activated B cells secrete antigen-specific antibodies to directly kill/lyse the target and also recruit polymorphonuclear cells, in a complement-dependent manner. Activated $CD4^+$ T cells secrete cytokines such as IFN-γ and tumor necrosis factor-alpha (TNF-α), which in turn recruit the cells of the innate immune system, such as monocytes, macrophages, and NK cells, to the site to effect the actual destruction of the antigen or pathogen. Activated $CD8^+$ CTLs lyse targeted cells and produce proinflammatory cytokines, especially IFN-γ. In this way, the adaptive immune system directs the innate immune system components to target the inciting antigen or pathogen. Cytokines involved in this inflammatory response then perpetuate a positive feedback loop: at the target sites, vessels become leaky, the vascular endothelial cells display ligands that bind to receptors on the immune cells, and chemokines secreted by the local inflammatory cells attract more immune effector cells to the site.

Immune Regulation

Since the genome has the capability to generate both self- and nonself-recognizing antibodies and TCRs, mechanisms must be in place to contain and/or prevent the activation of self-reactive lymphocytes. The first line of defense against autoimmunity targets T lymphocytes within the thymus and B cells within the bone marrow, before such cells enter the bloodstream. APCs within the thymus present a variety of self-peptides to developing T cells; those T cells with receptors that recognize self molecules with high affinity are clonally deleted via apoptosis, a mechanism known as central tolerance.[28] A similar selection process to eliminate self-

reactive B cells occurs in the bone marrow.[29] Central tolerance is a well-described mechanism to prevent autoimmunity, but we now know that there is an alternate pathway to apoptosis for T cells identified as self-reactive within the thymus; a subset of these self-reactive T cells differentiate into regulatory T cells.

The $CD4^+$ CD25high forkhead box protein 3 $(Foxp3)^+$ regulatory T cell, otherwise known as the Treg cell, is crucial for maintaining immune homeostasis by preventing autoimmunity.[30] Mouse studies show that peripheral $Foxp3^+$ T-cell depletion quickly leads to a fatal lymphoproliferative autoimmune response.[31] A related human disease, immune dysfunction, polyendocrinopathy and enteropathy (IPEX) syndrome, is an X-linked recessive disorder caused by *Foxp3* mutations; IPEX patients exhibit T-cell hyperactivation and severe autoimmune disease, likely as a result of Treg cell dysfunction.[32] Treg cells help maintain peripheral self-tolerance by modifying the functions of both $CD4^+$ and $CD8^+$ cells, either directly through T-cell to T-cell interactions or indirectly through APCs.[33] Treg cells may develop in the thymus, during negative clonal selection, or in the periphery when a $CD4^+$ T cell encounters its corresponding antigen-APC in an environment unfavorable for T cell activation, such as a low level of antigen, inadequate costimulation, mucosal antigen administration, or an environment high in IL-2, transforming growth factor-beta (TGF)-β, IL-10, and/or retinoic acid.[34] The molecular mechanisms underpinning Treg cell development and function are an active area of research.

Not all self-reactive lymphocytes are detected before entering the peripheral bloodstream, and in fact, peripheral autoreactive T cells and B cells exist even in normal individuals. Many tissue-specific antigens, like the eye-restricted molecules, may not be expressed in the thymus or bone marrow, or self-reactive cells may have escaped the selection process by other mechanisms. Hence, an immunologic response triggered by a self-reactive lymphocyte remains a potential threat, and mechanisms to contain these autoreactive immune cells are crucial to prevent autoimmunity.[35,36]

The functional properties of the APCs offer many opportunities for modulation. First, the antigen can be sequestrated from APCs by physical barriers or by rendering APCs incapable of antigen capture in the antigen's microenvironment (sequestration). Second, the

ability of the APC to degrade, process, and express the antigen can be inhibited. Third, the antigen-bearing APC may be prevented from migrating to the lymphoid tissues. Lastly, either inadequate costimulation or too much costimulation can inhibit lymphocyte activation, even in the presence of an APC with a high-affinity epitope.[37] Effector T cells need costimulatory signals both centrally and peripherally, and the expression of cytokines such as IL-10 or TGF-β can lead to anergy or reprogramming of the lymphocytes into cells that secrete immunosuppressive cytokines, thereby further suppressing autoimmunity.[38,39]

Another type of immune regulation targets antigen-specific immune effector cells such as Fas ligand-induced apoptosis of lymphocytes.[40,41] The immune-reactive lymphocytes express the CD95 receptor (Fas receptor). On encountering the Fas ligand, which is expressed in immunoprivileged eye tissues such as the cornea and retina, Fas receptor-expressing lymphocytes undergo apoptosis. Other molecular mechanisms, such as TNF-α production by immune and accessory cells, such as Müller cells and RPE cells during antigen encounter, also may result in lymphocyte apoptosis, thereby deleting these immune-reactive cells.

The Eye as an Immune-Privileged Site

The eye has been recognized as an immune-privileged site for more than 100 years, with heterogenous tissue grafts surviving within the eye but not in other parts of the body. In the 1940s Sir Peter Medawar demonstrated prolonged, often indefinite, survival of skin grafts in the anterior chamber of the eye only if the skin graft remains unvascularized.[2] Others have expanded on Medawar's work to show that (1) various tissues, including allogeneic skin grafts, thyroid tissues, neuronal retinal tissue, and allogeneic tumor cells, also can survive in the anterior chamber of the eye for prolonged periods,[42] and (2) a similar immune privilege occurs when allogeneic tissue was placed in the vitreous cavity and the subretinal space.[43,44] Although Medawar and others attributed this immune privilege to an intact blood–ocular barrier and absence of direct lymphatic drainage, now we know that ocular immune privilege involves more than tissue-specific antigen sequestration.

Many studies show that ocular immune privilege is a complex, dynamic process involving immunoregulatory mechanisms as well as anatomic factors.

After all, even immune privilege is influenced by the immunogenic strength of the antigens expressed by the cells. Tumors expressing MHC-encoded alloantigens had limited survival in the anterior chamber of recipient mice; whereas tumors that expressed weaker transplantation alloantigens showed much longer survival.[45] Additionally, certain eye tissues are known to be immune-privileged, i.e., these tissues themselves elicit an altered immune response and less rejection when transplanted elsewhere in the body. Such ocular tissues include the cornea, the RPE, and probably the retina. When transplanted beneath the capsule of the kidney, a nonimmune-privileged site, cornea demonstrated extended survival compared with other ocular tissues like the conjunctiva.[46] Both passive factors, such as the blood–retinal barrier, and active factors, such as the DIE, are essential to establish and maintain ocular immune privilege (Table 29.1).

TABLE 29.1
Components Contributing to Ocular Immune Privilege

PASSIVE	
Blood–retinal barrier	Nonfenestrated vascular endothelium of the retinal vessels and tight junctions among the retinal pigment epithelium
Lack of lymphatic drainage	Absence of lymphatics in the retina – lymphatics are present in the choroid
Tissue fluid drainage	Tissue fluid drains via the hematogenous route
Reduced expression of MHC	Antigen presentation is reduced by reduction of MHC class I and II molecules and APCs. The APCs are altered by the microenvironment to promote immune regulation
Reduced APCs in the retina	
APCs with altered function	
ACTIVE	
Immunosuppressive	TGF-β, α-MSH, VIP, CGRP, MIF, IL-1 receptor antagonist and free cortisol microenvironment
Factors expressed on cell surface	CD95 ligand, CD59, CD55, CD46

APC, antigen-presenting cell; CD, nomenclature for surface proteins of human leukocytes; CGRP, calcitonin gene-related peptide; IL, interleukin; MHC, major histocompatibility complex; MIF, migration inhibitory factor; MSH, melanocyte-stimulating hormone; TGF, transforming growth factor; VIP, vasoactive intestinal

peptide.

Transportation of Antigens

As first identified by Medawar,[2] the blood–ocular barrier keeps tissue-specific antigens sequestrated. There is an absence of lymphatics in the retina, although there is evidence that antigen may still be able to be transported to the lymph nodes.[47] However, tissue drainage via the hematogenous route, instead of via the lymphatic route, may alter ocular APC function.[48]

Downregulatory Immune Environment

The DIE is an evolutionary adaptation of the eye to protect itself against excessive inflammation. A small focus of inflammation in the eye has a far greater impact than one of similar size in most other areas of the body. The posterior segment utilizes several active factors that help maintain the local immunoenvironmental balance in a downregulatory state. Active factors include the downregulatory effect of Müller cells in cell-to-cell contact with lymphocytes.[49] Furthermore, there are many other factors that affect the DIE, including ocular cells (NK T cells, RPE, microglia, $F4/80^{+}$ macrophages) as well as cell surface and soluble factors in the ocular microenvironment (CD95 ligand, CD55, CD59, CD46, IL-10, IL-11, TGF-β, α-melanocyte-stimulating hormone, vasoactive intestinal peptide, calcitonin gene-related peptide, macrophage migration-inhibitory factor, IL-1-receptor antagonist, and free cortisol). Normal retina has reduced expression of MHC class I and II molecules and an absence of bone marrow-derived cells that function within tissues as APCs.[50a] Cultured RPE cells expressing sCD54 and PGE2 can downregulate T lymphocyte production of CCL3 and CCL4, which dampens the immune response.[50b] All of these factors contribute to actively downregulate immunologic activity in an attempt to prevent autoimmunity.[5]

Downregulatory Immune Environment in Age-Related Macular Degeneration

Several findings in patients with AMD (e.g., variants of CFH, HTRA-1, PLEKHA1 and Toll-like receptors, activated macrophages in the blood, autoantibodies to retinal components) point to a role for the immune system in AMD.[6] Neovascular AMD is associated with loss of the DIE,[51] and results from a masked, randomized pilot study indicate that systemic antiinflammatory therapy may be beneficial in treating wet AMD, in combination with anti-vascular endothelial growth factor (VEGF) agents.[52]

Anterior-Chamber-Associated Immune Deviation

Anterior-chamber-associated immune deviation (ACAID) is the best-studied immune-privilege phenomenon in the eye[53] and clearly demonstrates that immune privilege involves more than tissue-specific antigen sequestration. In animal models of ACAID, antigen inoculation into the anterior chamber induces peripheral tolerance to the antigen. Although its name implies that it is a phenomenon unique to the anterior chamber, there is evidence that the same mechanisms are at work in the vitreous and subretinal space.[44] There are many bone marrow-derived APCs in the iris, trabecular meshwork, and ciliary body,[54] and these APCs reach the spleen via the hematogenous route, bypassing the afferent lymphatics and the lymph nodes. These ocular APCs are different from APCs in other parts of the body, since the ocular APCs show reduced capacity to activate cell-mediated immune mechanisms and in fact, drive differentiation of suppressor cells to induce tolerance to the ocular antigen. The microenvironment of the eye also contains factors such as TGF-β_2 that are able to reprogram APCs from conventional sites, if exposed to the eye microenvironment, to secrete less IL-2, express less CD40 (a costimulatory signal for T-cell activation), and produce more mature TGF-β, which suppresses T-cell activation.[55a] Disruption of the ocular environment may interfere with ACAID. For instance, experiments in mice show that after laser retinal burn treatments in one eye, anterior chamber antigen inoculation of either the treated or the untreated eye does not lead to the peripheral tolerance seen in mice without laser treatment.[55b]

Although there are active soluble factors in the aqueous humor

that can inhibit T-cell activation in vitro, decrease the ability of NK cells to lyse their target,[56] and block complement activation,[57] the eye is not left defenseless against pathogens. It still retains certain immune functions to deter pathogenic invasion. Antibodies in the aqueous are capable of neutralizing viruses, and terminally differentiated cytotoxic T cells can bind and kill their target cells as they do elsewhere in the body.[58]

Retinal Antigens and Experimental Autoimmune Uveoretinitis

Animal experimentation allows in vivo study of ocular immunology. Several animal models for autoimmune posterior uveitis have been described (Table 29.2). Wacker and Lipton developed the experimental autoimmune uveoretinitis (EAU) model in 1968,[59] which still is commonly used today, since it is a good animal model for human ocular autoimmunity. This model is mostly self-limited and requires administration of an adjuvant, as well as the pathogenic antigen, for disease induction. The EAU model has been instrumental in eliciting immune mechanisms, identifying pathogenic epitopes of autoantigens within the eye, and evaluating therapeutic strategies with clinical relevance.

TABLE 29.2

Animal Models for Autoimmune Posterior Uveitis

Model	Antigen	Target	Clinical Disease
Experimental autoimmune uveoretinitis (EAU)	S-antigen	Photoreceptor layer of the retina	Posterior uveitis and retinal vasculitis, like sympathetic ophthalmia, VKH, and Behçet disease
	IRBP		
	Rhodopsin		
	Recoverin		
	Phosducin		
Experimental melanin protein-induced uveitis (EMIU)	Melanin proteins		
	Tyrosinase-related proteins 1 and 2	Choroid	Chronic panuveitis and posterior uveitis, like SO and VKH
Experimental autoimmune pigment epithelial uveitis (EAPU)	Retinal pigment epithelium membrane protein-induced	Retinal pigment epithelial cells	Posterior uveitis

IRBP, interphotoreceptor retinoid-binding protein; SO, sympathetic ophthalmia; VKH, Vogt–Koyanagi–Harada.

Using the EAU animal model, several retinal antigens, including S-antigen (arrestin), interphotoreceptor retinoid-binding protein (IRBP), rhodopsin, recoverin, and phosducin, have been shown to have uveitogenic properties. Immunization with these antigens or fragments of these antigens can induce ocular inflammation in susceptible guinea-pigs, rats, mice, rabbits, and monkeys. The resulting disease resembles various human uveitic conditions, such as ocular sarcoidosis (Fig. 29.1), Vogt–Koyanagi–Harada disease, sympathetic ophthalmia, and Behçet disease (Fig. 29.2). Much of our understanding of retinal autoantigens is derived from EAU models using S-antigen, IRBP-derived peptides, and, to a lesser extent, rhodopsin, recoverin, and phosducin.

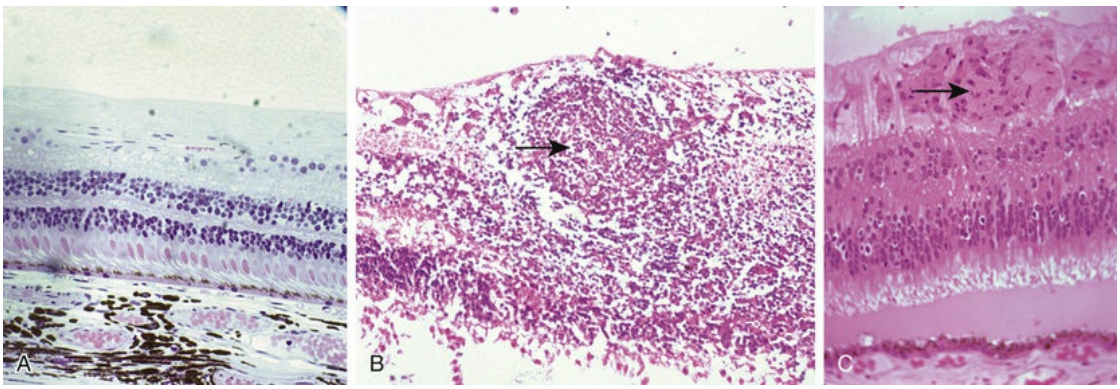

FIG. 29.1 Photomicrograph of (A) normal retina in monkey; (B) retinal vasculitis (*arrow*) in experimental autoimmune uveoretinitis in monkey; (C) retinal vasculitis (*arrow)* in a patient with sarcoidosis. (Courtesy of Dr Chi-Chao Chan, Laboratory of Immunology, National Eye Institute.)

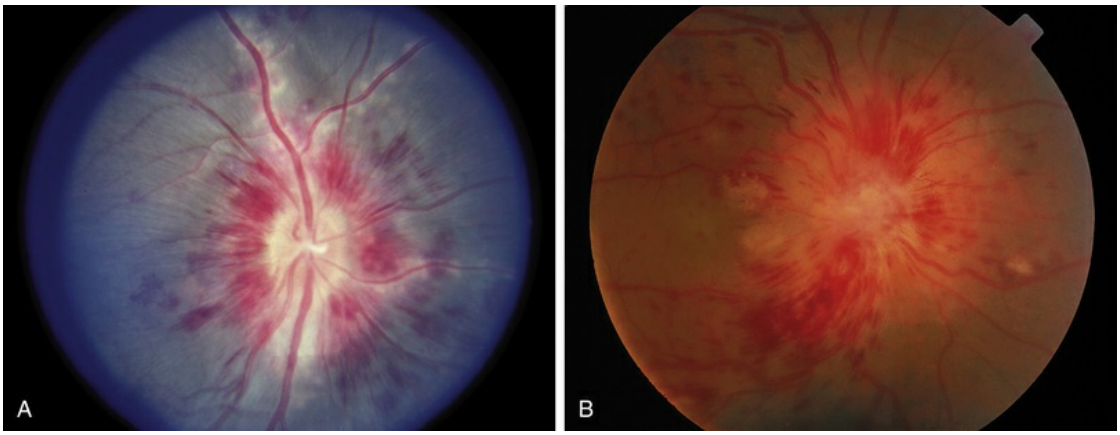

FIG. 29.2 (A) Color fundus photograph of experimental autoimmune uveoretinitis in nonhuman primate. (B) Color fundus photograph of retinal vasculitis in a patient with Behçet disease. (Panel A courtesy of Dr Chi-Chao Chan, Laboratory of Immunology, National Eye Institute. Panel B courtesy of Associate Professor Soon-Phaik Chee, Singapore National Eye Center.)

S-Antigen

S-antigen, a 48-kDa protein also known as arrestin, was first identified in the soluble fraction of retinal extracts and is one of the antigens most commonly used to induce EAU.[60] As S-antigen was the first autoretinal antigen implicated in the pathogenesis of uveitis,[61] its sequence and role in normal retinal function have been studied extensively.[62,63] S-antigen is a highly conserved protein expressed in retinal photoreceptor cells and in pinealocytes, the melatonin-secreting cells of the pineal gland. In photoreceptor cells, the main function of S-antigen (or arrestin) is to drive recovery of the rod phototransduction cascade by inactivating light-activated phosphorylated rhodopsin; arrestin-bound rhodopsin is unable to bind the G protein transducin, which halts downstream G protein signaling.[64] Immunization of susceptible animals (such as Lewis rats but not mice) with S-antigen induces a predominantly $CD4^+$ T-cell-mediated inflammatory response in the retina, uveal tract, and pineal gland.[65] Six peptide fragments of S-antigen have been identified as uveitogenic, including the major uveitogenic peptide M (sequence 303–320).[62] Some of the fragments are species-specific in their uveitogenicity.[65] Although studying uveitogenic properties of S-antigen in animal models has provided understanding of general uveitis mechanisms, the relevance to human uveitis needs

to be more fully explored. S-antigen also has been implicated in the pathogenesis of uveitis through molecular mimicry. Several exogenous (baker's yeast, *Escherichia coli*, hepatitis B virus, streptococcal M5 protein, Moloney murine sarcoma virus, and baboon endogenous virus) and endogenous (human leukocyte antigen (HLA) B-derived peptide, tropomyosin) antigens share sequence homology with peptide M of S-antigen.[66] Some of these homologous antigens have been shown to be uveitogenic in the EAU models, and lymphocytes from animals immunized with M peptide cross-reacted and proliferated when stimulated with peptides derived from some of these other antigens. Antistreptococcal monoclonal antibodies were found to recognize several uveitogenic peptides of S-antigen,[67] which further suggests that immunologic mimicry between self and exogenous antigens from an infectious agent may be a potential mechanism in the pathogenesis of uveitis in humans.

Interphotoreceptor Retinoid-Binding Protein

IRBP is a major protein of the interphotoreceptor matrix, functioning as a transporter of retinoids between the retina and RPE, and it can induce EAU in both mouse and rat.[68] Similar to S-antigen, IRBP also is found in both the retina and the pineal gland, and induction of EAU with IRBP will cause disease in both locations. Depending on the dose of antigen used and the species of model animal, a spectrum of disease ranging from hyperacute to chronic relapsing disease has been induced. The inflammatory response targets the photoreceptor layer, producing histopathology similar to lesions seen in human uveitis, with retinal vasculitis, retinal and choroidal granulomas, focal serous retinal detachments, photoreceptor loss, and formation of sub-RPE infiltrates that resemble the Dalen–Fuchs nodules seen in patients with Vogt–Koyanagi–Harada disease and sympathetic ophthalmia.[69] Disease activity in the murine IRBP EAU model peaks at 5 and 10 weeks after immunization, with apparent disease remission between 6 and 8 weeks after immunization, simulating the relapsing course of human uveitis.[70] The relatively long duration of disease activity and the relapsing course of disease in this model make it a preferred model for evaluating therapeutic strategies in chronic uveitis.

Rhodopsin

Rhodopsin is the visual pigment of rod photoreceptor cells, belonging to the larger family of G-protein-coupled receptors.[71] It is a membrane-bound protein comprised of a polypeptide chain, the opsin, and a covalently bound chromophore, 11-*cis* retinal. The function of rhodopsin is to capture photons and trigger the phototransduction cascade, and its function is blocked by binding to S-antigen, as described above. The uveitis induced in susceptible animals such as guinea-pigs, rabbits, rats, and monkeys is typically a retinitis with multifocal destruction of photoreceptor cells, showing dense mononuclear and polymorphonuclear cell infiltrates in the retina and anterior uvea in severe disease.[72] There are three distinct immunopathogenic sites on the molecule; sequence 230–250 (extracellular loop V–VI) is the most uveitogenic and is comparable to S-antigen and IRBP in terms of induced disease severity.[73] The role of rhodopsin autoantigens in human diseases is still unclear. Romano and coworkers have demonstrated an elevated antirhodopsin antibody titer in patients with normal-pressure glaucoma, which suggests the possibility that an antiretinal antibody and autoimmunity may play a role in the optic neuropathy of normal-pressure glaucoma.[74]

Recoverin

Recoverin is a 23-kDa calcium-binding protein that controls photoreceptor light adaptation by functioning as a calcium sensor, although the underlying mechanisms differ somewhat between rods and cones.[75] Recoverin also is found in bipolar cells, pinealocytes, and certain tumor cells, though recoverin's function in these nonphotoreceptor cells is unknown.[76] Immunization of Lewis rats with high doses of recoverin, as well as with the major immunopathogenic epitope of recoverin, sequence 62–81, produced EAU similar in severity, histology, and duration to other retinal autoantigens such as S-antigen.[77,78] In humans, recoverin has been identified as an self-antigen in cancer-associated retinopathy.[79] Anti-recoverin autoantibodies have been demonstrated to induce apoptosis of photoreceptors, which is further suggestive of a pathogenic role for these autoantibodies.[80] It is important to note that in some cases of human disease, retinal dysfunction and high

levels of antirecoverin antibodies occur prior to the cancer diagnosis, but can help point to the underlying malignancy. Having a low threshold for detecting this condition with antiretinal antibodies may improve prognosis in the case of a life-threatening disease.

Phosducin

Phosducin is a 33-kDa protein, a cytosolic regulator of G-protein-mediated signaling, found in the retina and also in nonretinal tissues such as liver, lung, heart, and brain.[81] Immunization with phosducin in Lewis rats produces mild to moderate EAU characterized by late onset, relatively mild ocular inflammation that primarily affects the posterior segment.[82] It is unclear whether phosducin autoantibodies play a role in human disease.

Novel Ocular Autoantigens

Researchers have used a variety of in vitro techniques to identify novel ocular autoantigens with the potential for pathogenicity. For instance, uveal autoantigen with coiled coil domains and ankyrin repeats (UACA) in patients with Vogt–Koyanagi–Harada disease,[83] a retinal autoantigen targeting the connecting cilium region of photoreceptors in a patient with Waldenström macroglobulinemia and retinal dysfunction similar to cancer-associated retinopathy,[84] and heat shock protein 27 (HSP27) in Behçet disease[85] all have been identified as autoantigens. Additional testing, often in animal models, to determine pathogenicity is the next logical step.

Retinal Autoimmunity

Autoimmunity in Human Uveitis

Although nearly five decades have elapsed since the first EAU model was published, translating EAU model findings to human uveitis and determining the extent of the role of retinal autoimmunity in human uveitis remains a work in progress. Since lymphocytes reactive to retinal antigens have been demonstrated in normal individuals,[86] as well as in those with retinal disease,[87] immunoregulatory mechanisms must exist to prevent pathologic

retinal autoimmunity in normal individuals. To further these investigations, multiple clinical studies have examined human lymphocyte proliferative responses to S-antigen, IRBP, and peptides derived from patients with uveitis. Increased lymphocyte proliferative responses to S-antigen were reported in patients with Behcet's disease during periods of active ocular inflammation compared to periods of disease quiescence.[88] Lymphocyte proliferative responses to S-antigen, S-antigen-derived peptides (peptides M and G), and uveitogenic peptide derived from IRBP (R16) were found in patients with idiopathic uveitis but not in healthy controls or patients with systemic connective tissue disease.[89] A lymphocyte proliferation response was mounted to at least one of the 20 tested peptides spanning the entire sequence of S-antigen in half of the patients with idiopathic uveitis, whereas there was no response to the peptides in the normal controls.[90] A study evaluating oral tolerance by feeding S-antigen to uveitis patients showed a good clinical response, with less immunosuppression required.[91] Together, these studies provide further support for the possible pathogenic roles of retinal autoantigen in uveitis.

Although both EAU animal models and human uveitis can result from a $CD4^+$ Th1 or a Th17 effector response driving autoimmunity, there are differences in the T-cell specificities in antigen response between animals and humans.[92] Patients with uveitis, due to epitope spread, may respond to more than one peptide, i.e., several epitopes are recognized in the same patient, while animals with EAU tend to respond only to the inciting antigen. There is no common pattern of lymphocyte response in clinical studies reported so far. Early clinical studies on the humoral response showed the presence of antiretinal autoantibodies, including anti-S-antigen antibodies in the sera of some uveitis patients (Fig. 29.3),[93,94] but there was no good correlation between presence or levels of autoantibodies and clinical disease. Moreover, anti-IRBP antibody was reported to occur in the same frequency in the sera of patients with uveitis and normal controls, with the only noted difference being the stronger affinity of the antibodies in patients with uveitis.[95]

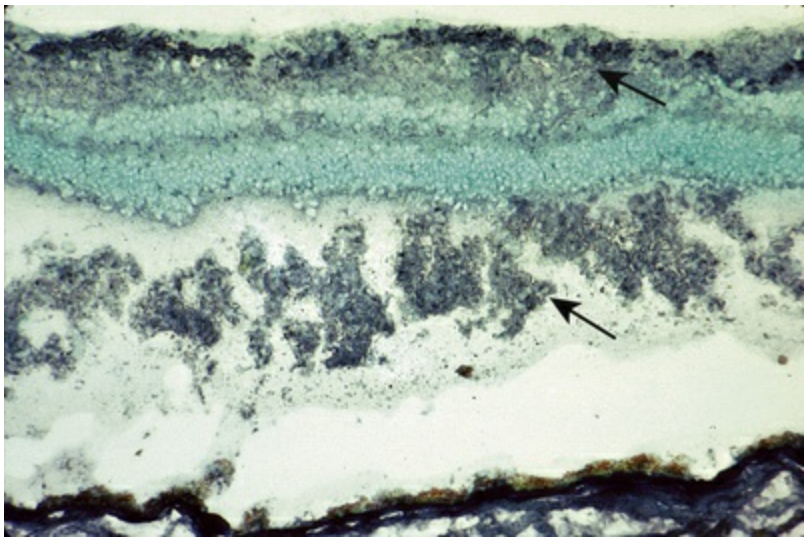

FIG. 29.3 Photomicrograph showing antiretinal antibodies in the serum of a patient with Vogt–Koyanagi–Harada disease reacting immunohistochemically to the photoreceptor layer of the monkey retina (*arrows*). (Courtesy of Dr Chi-Chao Chan, Laboratory of Immunology, National Eye Institute.)

The relationship between humoral and cellular responses to these autoantigens was studied in a group of patients with endogenous uveitis such as birdshot retinochoroidopathy, retinal vasculitis, and Behçet disease. The antibody titers to S-antigen and IRBP were found to be decreased during active inflammation periods and the lymphocyte responses to S-antigen were found to be more frequent in the period preceding a relapse of ocular inflammation, supporting the pathogenic roles of these lymphocytes in retinal autoimmunity.[96] The role of humoral and cellular responses to retinal autoantigens remains unclear, and it is possible that different subsets of patients with uveitis respond to different epitopes and antigens, resulting in the wide spectrum of clinical disease encountered.

Role of Retinal Autoimmunity in Protection

Retinal autoimmunity may not always be pathogenic. Studies on central nervous system (CNS) injury and its reparative process have revealed a possible beneficial role of autoimmunity in limiting self-injury during insults to the CNS. Axonal injury in the CNS leads not only to the degeneration of the affected axon but also the

neighboring axon through self-destructive compounds released by the degenerating axon into the microenvironment.[97] Studies have revealed that autoreactive T cells directed against myelin antigens have beneficial effects on CNS myelinated axons after a mechanical crush injury,[98] and it has been proposed that this neuroprotective activity exhibited by autoimmune T cells may be a physiologic process to cope with stressful conditions.[99] Interestingly, rodent strains that are more resilient against developing experimental CNS autoimmune disease also are better able to mount an autoimmune response after CNS injury that results in a better outcome.[100] Extrapolating these CNS observations to the retina provides a possible explanation for the protective effect of vaccination on retinal ganglion cells, when vaccination with peptides derived from IRBP is performed prior to optic nerve injury.[8] It appears that the immune system not only protects the body against invading pathogens but also protects it from toxic substances released by self tissues during trauma and stress.[101] The autoreactive cells that induce neuroprotection and those that induce autoimmune disease may share the same specificity and phenotype, thus having the potential to be protective and destructive at the same time. From these findings, it appears that the ability to protect the eye from inflammation and injury does not solely depend on mechanisms conferring immune privilege but rather on a precise regulation of autoimmunity.

Role of Retinal Autoimmunity in Infection

The role of infection in the pathogenesis of eye autoimmunity has long been suspected, but there is no conclusive validative study. Possible causative relationships have been hypothesized between infections and ocular autoimmunity such as streptococcus, herpesvirus, and Behçet disease;[102] gram-negative bacteria and HLA B27-associated uveitis;[103] and herpesviruses and serpiginous choroiditis.[104] Infection as an exogenous trigger for inflammation in the eye is an enticing possibility as infections have been linked to the pathogenesis of many other autoimmune diseases such as rheumatic fever,[105] inflammatory bowel disease,[106] and sarcoidosis.[107] Antiretinal antibodies in the serum of patients with

toxoplasmosis retinochoroiditis[108] and antiretinal and anti-RPE antibodies in murine coronavirus retinopathy[109] have been reported. Taken together, these reports provide support for a role of infection in retinal autoimmunity. Even in the current EAU animal models, bacterial-derived products like mycobacteria in complete Freund's adjuvant, LPS, and pertussis toxin are used as adjuvants to promote the development of autoimmune disease.[110] The adjuvant in EAU has been shown to effect many changes that could sensitize the animal's immune system to the antigen, including changing the blood–tissue barrier to allow infiltration of inflammatory cells,[111] promoting the Th1 response,[112] stimulating APCs,[113] and enhancing the innate immune response.[114] It is feasible that similar infection-related mechanisms may drive pathogenesis of human uveitis, by sensitizing the immune system to eye-restricted antigens, which are expressed systemically in low levels below the immune activation threshold.

On the other hand, there is evidence that immunologic mimicry may play a role in uveitis pathogenesis as molecular homology exists between certain retinal autoantigens and peptides derived from microbes, such as the M peptide derived from S-antigen and the streptococcal cell wall peptide, the yeast's histone peptide, and certain viral agents.[67,115] Molecular mimicry has also been suspected of playing a role in disease susceptibility with certain HLA haplotypes, like HLA B27 for acute anterior uveitis,[116] HLA B51 for Behçet disease,[117] and HLA-A29 for birdshot retinochoroidopathy.[118] Synthetic peptides derived from HLA-B molecules such as B27 and B51 have amino acid sequence homology with an S-antigen peptide that was reported to induce EAU in animals.[119] Lymphocytes from Behçet disease patients with uveitis respond to peptides derived from both HLA-B molecules and S-antigen, again demonstrating possible immunologic mimicry.[120] Further studies showed sequence homology between this same S-antigen peptide, a rotavirus peptide, and a casein protein, and cross-reaction in cellular immunity between these peptides was demonstrated in animal studies.[121] Together these studies present the possibility that exogenous factors like infection or foreign proteins may break down tolerance and induce autoimmunity via immunologic mimicry.

Another proposed mechanism for sensitizing the immune system to eye-restricted antigens involves the microbiota, the community of microorganisms that colonize the body surface. Intestinal microbes can activate Th17 cells.[122] Recent work with a type of IRBP EAU mice that develop spontaneous uveitis shows that activated Th17 cells are present in gut mucosa prior to development of uveitis. Modifying the components of the intestinal microbiota in these animals with administration of a broad-spectrum antibiotic delays the onset of uveitis and alleviates the disease course, raising the possibility that interactions with the intestinal microbiota also may be a trigger for uveitis in humans.[123]

The guardian that prevents pathologic autoimmunity is immunologic tolerance to self antigens. Immune tolerance, usually maintained by mechanisms described earlier, can be lost or modulated. Work examining heat shock protein (HSP) in an animal model shows that HSPs can modulate APC function, resulting in loss of immune tolerance.[124] HSPs, especially microbial HSPs, have been implicated in the pathogenesis of Behçet disease[125] and have been shown to worsen inflammation in the eye in animal studies.[126] Therefore, one may speculate that an infection and the subsequent release of microbial HSPs could be the initial triggering event, resulting in altered APC function and a subsequent loss of immune tolerance, leading to autoimmunity.

All of the pathogenic hypotheses discussed above are difficult to test for a number of reasons. First, uveitis is a heterogeneous disease. Second, evidence of the initial triggering event usually is difficult to identify, given the delay between the trigger and disease presentation. Lastly, a single disease may have multiple triggering mechanisms, and different triggers may lead to the same disease.

Conclusion

Retinal autoimmunity may be a physiologic process as well as a pathologic one, given its role in organ- and tissue-specific protection from injury and stress in the normal retina. The physiologic role of retinal autoimmunity may account for the lymphocyte proliferative responses to retinal antigens detected in normal subjects, but there still is much that is unknown about the

maintenance of the fine balance between protection and destruction in retinal autoimmunity, given that these paradoxical roles may reside in the same group of cells. With rapid technologic advances in molecular immunology, new tools are available to help unravel the roles of retinal autoimmunity in both physiologic and pathologic states. The subsequent elucidation of molecular mechanisms should assist in developing novel targeted therapeutic strategies for the management of retinal autoimmunity-induced diseases in the near future.

References

1. van Dooremaal JC. Die Entwicklung der in fremden Grund versetzten lebenden Gewebe. *Graefes Arch Ophthalmol*. 1873;19:359–373.
2. Medawar PB. Immunity to homologous grafted skin; the fate of skin homografts transplanted to the brain, to subcutaneous tissue, and to the anterior chamber of the eye. *Br J Exp Pathol*. 1948;29(1):58–69.
3. Cunha-Vaz J, Faria de Abreu JR, Campos AJ. Early breakdown of the blood–retinal barrier in diabetes. *Br J Ophthalmol*. 1975;59(11):649–656.
4. Wallow IH, Engerman RL. Permeability and patency of retinal blood vessels in experimental diabetes. *Invest Ophthalmol Vis Sci*. 1977;16(5):447–461.
5. Taylor AW. Ocular immunosuppressive microenvironment. *Chem Immunol*. 1999;73:72–89.
6. Nussenblatt RB, Liu B, Li Z. Age-related macular degeneration: an immunologically driven disease. *Curr Opin Investig Drugs*. 2009;10(5):434–442.

7a. Shimazaki K, Jirawuthiworavong GV, Heckenlively JR, et al. Frequency of anti-retinal antibodies in normal human serum. *J Neuroophthalmol*. 2008;28(1):5–11.

7b. Kim BJ, Li Z, Fariss RN, Shen DF, et al. Constitutive and cytokine-induced GITR ligand expression on human retinal pigment epithelium and photoreceptors. *Invest Ophthalmol Vis Sci*. 2004;45(9):3170–3176.

8. Mizrahi T, Hauben E, Schwartz M. The tissue-specific self-

pathogen is the protective self-antigen: the case of uveitis. *J Immunol*. 2002;169(10):5971–5977.
9. Ehrlich P. *Das Sauerstoffbedürfnis des Organismus, eine farbenanalytische Studie*. Hirschwald: Berlin; 1885.
10. Goldmann EE. *Vitalfärbung am Zentralnervensystem*. [Abh Preuss Akd Wiss Phys – Math K1/1] 1913:1–3.
11. Schnaudigel O. Die Vitalfarbung mit Trypanblau am Auge. *Graefes Arch Ophthalmol*. 1913;86:93–97.
12. Cunha-Vaz JG, Shakib M, Ashton N. Studies on the permeability of the blood–retinal barrier. I. On the existence, development, and site of a blood–retinal barrier. *Br J Ophthalmol*. 1966;50(8):441–453.
13. Coca-Prados M. The blood–aqueous barrier in health and disease. *J Glaucoma*. 2014;23:S36–8.
14. Runkle EA, Antonetti DA. The blood–retinal barrier: structure and functional significance. *Methods Mol Biol*. 2011;686:133–148.
15. Toda R, Kawazu K, Oyabu M, et al. Comparison of drug permeabilities across the blood-retinal barrier, blood–aqueous humor barrier, and blood–brain barrier. *J Pharm Sci*. 2011;100(9):3904–3911.
16. Bringmann A, Reichenbach A, Wiedemann P. Pathomechanisms of cystoid macular edema. *Ophthalmic Res*. 2004;36(5):241–249.
17. Willard AL, Herman IM. Vascular complications and diabetes: current therapies and future challenges. *J Ophthalmol*. 2012;2012:209538.
18. Haurigot V, Villacampa P, Ribera A, et al. Increased intraocular insulin-like growth factor-I triggers blood–retinal barrier breakdown. *J Biol Chem*. 2009;284(34):22961–22969.
19. Rangasamy S, Srinivasan R, Maestas J, et al. A potential role for angiopoietin 2 in the regulation of the blood–retinal barrier in diabetic retinopathy. *Invest Ophthalmol Vis Sci*. 2011;52(6):3784–3791.
20. Joussen AM, Poulaki V, Mitsiades N, et al. Nonsteroidal anti-inflammatory drugs prevent early diabetic retinopathy via TNF-alpha suppression. *FASEB J*. 2002;16(3):438–440.

21. Janeway CA Jr, Medzhitov R. Innate immune recognition. *Annu Rev Immunol*. 2002;20:197–216.
22. Davis MM. T cell receptor gene diversity and selection. *Annu Rev Biochem*. 1990;59:475–496.
23. Schatz DG, Oettinger MA, Schlissel MS. V(D)J recombination: molecular biology and regulation. *Annu Rev Immunol*. 1992;10:359–383.
24. Amsen D, Spilianakis CG, Flavell RA. How are T(H)1 and T(H)2 effector cells made? *Curr Opin Immunol*. 2009;21(2):153–160.
25. Romagnani S, Maggi E, Liotta F, et al. Properties and origin of human Th17 cells. *Mol Immunol*. 2009;47(1):3–7.
26. Amadi-Obi A, Yu CR, Liu X, et al. TH17 cells contribute to uveitis and scleritis and are expanded by IL-2 and inhibited by IL-27/STAT1. *Nat Med*. 2007;13(6):711–718.
27. Croft M, Dubey C. Accessory molecule and costimulation requirements for CD4 T cell response. *Crit Rev Immunol*. 1997;17(1):89–118.
28. Sprent J. Central tolerance of T cells. *Int Rev Immunol*. 1995;13(2):95–105.
29. Liu J, Cao X. Regulatory dendritic cells in autoimmunity: a comprehensive review. *J Autoimmun*. 2015;63:1–12.
30. Sakaguchi S, Miyara M, Costantino CM, et al. $FOXP3^+$ regulatory T cells in the human immune system. *Nat Rev Immunol*. 2010;10(7):490–500.
31. Lahl K, Loddenkemper C, Drouin C, et al. Selective depletion of $Foxp3^+$ regulatory T cells induces a scurfy-like disease. *J Exp Med*. 2007;204(1):57–63.
32. Tommasini A, Ferrari S, Moratto D, et al. X-chromosome inactivation analysis in a female carrier of FOXP3 mutation. *Clin Exp Immunol*. 2002;130(1):127–130.
33. Sakaguchi S, Sakaguchi N, Asano M, et al. Immunologic self-tolerance maintained by activated T cells expressing IL-2 receptor alpha-chains (CD25). Breakdown of a single mechanism of self-tolerance causes various autoimmune diseases. *J Immunol*. 1995;155(3):1151–1164.
34. Safinia N, Scotta C, Vaikunthanathan T, et al. Regulatory T cells: serious contenders in the promise for immunological

tolerance in transplantation. *Front Immunol*. 2015;6:438.
35. Arnold B, Schonrich G, Hammerling GJ. Multiple levels of peripheral tolerance. *Immunol Today*. 1993;14(1):12–14.
36. Moudgil KD, Ametani A, Grewal IS, et al. Processing of self-proteins and its impact on shaping the T cell repertoire, autoimmunity and immune regulation. *Int Rev Immunol*. 1993;10(4):365–377.
37. Sinclair NR, Anderson CC. Co-stimulation and co-inhibition: equal partners in regulation. *Scand J Immunol*. 1996;43(6):597–603.
38. de Vries JE. Immunosuppressive and anti-inflammatory properties of interleukin 10. *Ann Med*. 1995;27(5):537–541.
39. Sosroseno W, Herminajeng E. The immunoregulatory roles of transforming growth factor beta. *Br J Biomed Sci*. 1995;52(2):142–148.
40. Van Parijs L, Abbas AK. Role of Fas-mediated cell death in the regulation of immune responses. *Curr Opin Immunol*. 1996;8(3):355–361.
41. Griffith TS, Ferguson TA. The role of FasL-induced apoptosis in immune privilege. *Immunol Today*. 1997;18(5):240–244.
42. Niederkorn J, Streilein JW, Shadduck JA. Deviant immune responses to allogeneic tumors injected intracamerally and subcutaneously in mice. *Invest Ophthalmol Vis Sci*. 1981;20(3):355–363.
43. Wenkel H, Streilein JW. Analysis of immune deviation elicited by antigens injected into the subretinal space. *Invest Ophthalmol Vis Sci*. 1998;39(10):1823–1834.
44. Jiang LQ, Jorquera M, Streilein JW. Subretinal space and vitreous cavity as immunologically privileged sites for retinal allografts. *Invest Ophthalmol Vis Sci*. 1993;34(12):3347–3354.
45. Niederkorn JY, Shadduck JA, Streilein JW. Immunogenetic basis for immunologic privilege in the anterior chamber of the eye. *Immunogenetics*. 1981;13(3):227–236.
46. Streilein J. *Immune privilege and the cornea*. [In: Press BA, editor. Proceedings of symposium on bullous oculo-muco-cutaneous disorders] 1997:43–52.

47. Egan RM, Yorkey C, Black R, et al. Peptide-specific T cell clonal expansion in vivo following immunization in the eye, an immune-privileged site. *J Immunol*. 1996;157(6):2262–2271.
48. McMenamin PG. Dendritic cells in the central nervous system and eye and their associated supporting tissues. Lotze MY. *Dendritic cells: biology and clinical applications*. Academic Press: San Diego; 1999:205–254.
49. Caspi RR, Roberge FG, Nussenblatt RB. Organ-resident, nonlymphoid cells suppress proliferation of autoimmune T-helper lymphocytes. *Science*. 1987;237(4818):1029–1032.
50a. Zhang J, Wu GS, Ishimoto S, et al. Expression of major histocompatibility complex molecules in rodent retina: immunohistochemical study. *Invest Ophthalmol Vis Sci*. 1997;38(9):1848–1857.
50b. Wallace CA, Moir G, Malone DF, et al. Regulation of T-lymphocyte CCL3 and CCL4 production by retinal pigment epithelial cells. *Invest Ophthalmol Vis Sci*. 2013;54(1):722–730.
51. Nussenblatt RB, Ferris F 3rd. Age-related macular degeneration and the immune response: implications for therapy. *Am J Ophthalmol*. 2007;144(4):618–626.
52. Nussenblatt RB, Byrnes G, Sen HN, et al. A randomized pilot study of systemic immunosuppression in the treatment of age-related macular degeneration with choroidal neovascularization. *Retina*. 2010;30(10):1579–1587.
53. Stein-Streilein J, Streilein JW. Anterior chamber associated immune deviation (ACAID): regulation, biological relevance, and implications for therapy. *Int Rev Immunol*. 2002;21(2–3):123–152.
54. Kaplan HJ, Streilein JW. Do immunologically privileged sites require a functioning spleen? *Nature*. 1974;251(5475):553–554.
55a. Takeuchi M, Alard P, Streilein JW. TGF-beta promotes immune deviation by altering accessory signals of antigen-presenting cells. *J Immunol*. 1998;160(4):1589–1597.
55b. Niederkorn JY. The induction of anterior chamber-associated immune deviation. *Chem Immunol Allergy*. 2007;92:27–35.

56. Apte RS, Niederkorn JY. Isolation and characterization of a unique natural killer cell inhibitory factor present in the anterior chamber of the eye. *J Immunol*. 1996;156(8):2667–2673.
57. Sohn JH, Kaplan HJ, Suk HJ, et al. Complement regulatory activity of normal human intraocular fluid is mediated by MCP, DAF, and CD59. *Invest Ophthalmol Vis Sci*. 2000;41(13):4195–4202.
58. Koevary SB, Beaudry K. Effect of anterior chamber-associated immune deviation (ACAID) on rat islet allograft rejection. *Ocul Immunol Inflamm*. 2000;8(1):39–47.
59. Wacker WB, Lipton MM. Experimental allergic uveitis. II. Serologic and hypersensitive responses of the guinea pig following immunization with homologous retina. *J Immunol*. 1968;101(1):157–165.
60. Singh VK, Nussenblatt RB, Donoso LA, et al. Identification of a uveitopathogenic and lymphocyte proliferation site in bovine S-antigen. *Cell Immunol*. 1988;115(2):413–419.
61. Wacker WB, Donoso LA, Kalsow CM, et al. Experimental allergic uveitis: isolation, characterization, and localization of a soluble uveitopathogenic antigen from bovine retina. *J Immunol*. 1977;119(6):1949–1958.
62. Hirose S, Singh VK, Donoso LA, et al. An 18-mer peptide derived from the retinal S antigen induces uveitis and pinealitis in primates. *Clin Exp Immunol*. 1989;77(1):106–111.
63. Merryman CF, Donoso LA, Zhang XM, et al. Characterization of a new, potent, immunopathogenic epitope in S-antigen that elicits T cells expressing V beta 8 and V alpha 2-like genes. *J Immunol*. 1991;146(1):75–80.
64. Gurevich VV, Hanson SM, Song X, et al. The functional cycle of visual arrestins in photoreceptor cells. *Prog Retin Eye Res*. 2011;30(6):405–430.
65. Gregerson DS, Fling SP, Obritsch WF, et al. A new perspective of S-antigen from immunochemical analysis. *Curr Eye Res*. 1990;9(Suppl.):145–153.
66. Shinohara T, Singh VK, Tsuda M, et al. S-antigen: from gene to autoimmune uveitis. *Exp Eye Res*. 1990;50(6):751–757.
67. Lerner MP, Donoso LA, Nordquist RE, Cunningham MW.

Immunological mimicry between retinal S-antigen and group A streptococcal M proteins. *Autoimmunity*. 1995;22(2):95–106.
68. Broekhuyse RM, Winkens HJ, Kuhlmann ED. Induction of experimental autoimmune uveoretinitis and pinealitis by IRBP: comparison to uveoretinitis induced by S-antigen and opsin. *Curr Eye Res*. 1986;5(3):231–240.
69. Caspi RR, Roberge FG, Chan CC, et al. A new model of autoimmune disease. Experimental autoimmune uveoretinitis induced in mice with two different retinal antigens. *J Immunol*. 1988;140(5):1490–1495.
70. Chan CC, Caspi RR, Ni M, et al. Pathology of experimental autoimmune uveoretinitis in mice. *J Autoimmun*. 1990;3(3):247–255.
71. Hargrave PA, McDowell JH. Rhodopsin and phototransduction. *Int Rev Cytol*. 1992;137B:49–97.
72. Adamus G, Arendt A, Hargrave PA. Genetic control of antibody response to bovine rhodopsin in mice: epitope mapping of rhodopsin structure. *J Neuroimmunol*. 1991;34(2–3):89–97.
73. Adamus G, Schmied JL, Hargrave PA, et al. Induction of experimental autoimmune uveitis with rhodopsin synthetic peptides in Lewis rats. *Curr Eye Res*. 1992;11(7):657–667.
74. Romano C, Barrett DA, Li Z, et al. Anti-rhodopsin antibodies in sera from patients with normal-pressure glaucoma. *Invest Ophthalmol Vis Sci*. 1995;36(10):1968–1975.
75. Sakurai K, Chen J, Khani SC, et al. Regulation of mammalian cone phototransduction by recoverin and rhodopsin kinase. *J Biol Chem*. 2015;290(14):9239–9250.
76. Kawamura S, Cox JA, Nef P. Inhibition of rhodopsin phosphorylation by non-myristoylated recombinant recoverin. *Biochem Biophys Res Commun*. 1994;203(1):121–127.
77. Adamus G, Ortega H, Witkowska D, et al. Recoverin: a potent uveitogen for the induction of photoreceptor degeneration in Lewis rats. *Exp Eye Res*. 1994;59(4):447–455.
78. Gery I, Chanaud NP 3rd, Anglade E. Recoverin is highly uveitogenic in Lewis rats. *Invest Ophthalmol Vis Sci*.

1994;35(8):3342–3345.
79. Adamus G, Guy J, Schmied JL, et al. Role of anti-recoverin autoantibodies in cancer-associated retinopathy. *Invest Ophthalmol Vis Sci*. 1993;34(9):2626–2633.
80. Adamus G. Autoantibody-induced apoptosis as a possible mechanism of autoimmune retinopathy. *Autoimmun Rev*. 2003;2(2):63–68.
81. Danner S, Lohse MJ. Phosducin is a ubiquitous G-protein regulator. *Proc Natl Acad Sci USA*. 1996;93(19):10145–10150.
82. Dua HS, Lee RH, Lolley RN, et al. Induction of experimental autoimmune uveitis by the retinal photoreceptor cell protein, phosducin. *Curr Eye Res*. 1992;11(Suppl.):107–111.
83. Yamada K, Senju S, Nakatsura T, et al. Identification of a novel autoantigen UACA in patients with panuveitis. *Biochem Biophys Res Commun*. 2001;280(4):1169–1176.
84. Sen HN, Chan CC, Caruso RC, et al. Waldenstrom's macroglobulinemia-associated retinopathy. *Ophthalmology*. 2004;111(3):535–539.
85. Chen P, Shi L, Jiang Y, et al. Identification of heat shock protein 27 as a novel autoantigen of Behçet's disease. *Biochem Biophys Res Commun*. 2015;456(4):866–871.
86. Yamamoto JH, Minami M, Inaba G, et al. Cellular autoimmunity to retinal specific antigens in patients with Behçet's disease. *Br J Ophthalmol*. 1993;77(9):584–589.
87. Nussenblatt RB, Gery I, Ballintine EJ, et al. Cellular immune responsiveness of uveitis patients to retinal S-antigen. *Am J Ophthalmol*. 1980;89(2):173–179.
88. de Smet MD, Dayan M. Prospective determination of T-cell responses to S-antigen in Behcet's disease patients and controls. *Invest Ophthalmol Vis Sci*. 2000;41(11):3480–3484.
89. Rajasingh J, Singh VK, Singh V, et al. Cellular immune response to retinal S-antigen and interphotoreceptor retinoid binding protein fragments in idiopathic human uveitis. *Indian J Med Res*. 1996;103:222–226.
90. Rai G, Saxena S, Kumar H, et al. Human retinal S-antigen: T cell epitope mapping in posterior uveitis patients. *Exp Mol Pathol*. 2001;70(2):140–145.
91. Nussenblatt RB, Gery I, Weiner HL, et al. Treatment of

uveitis by oral administration of retinal antigens: results of a phase I/II randomized masked trial. *Am J Ophthalmol*. 1997;123(5):583–592.
92. Luger D, Silver PB, Tang J, et al. Either a Th17 or a Th1 effector response can drive autoimmunity: conditions of disease induction affect dominant effector category. *J Exp Med*. 2008;205(4):799–810.
93. Chan CC, Palestine AG, Nussenblatt RB, et al. Anti-retinal auto-antibodies in Vogt–Koyanagi–Harada syndrome, Behçet's disease, and sympathetic ophthalmia. *Ophthalmology*. 1985;92(8):1025–1028.
94. Doekes G, Luyendijk L, Gerritsen MJ, et al. Anti-retinal S-antigen antibodies in human sera: a comparison of reactivity in ELISA with human or bovine S-antigen. *Int Ophthalmol*. 1992;16(3):147–152.
95. Hoekzema R, Hwan SB, Rothova A, et al. Serum antibody response to human and bovine IRBP in uveitis. *Curr Eye Res*. 1990;9(12):1177–1183.
96. Jobin D, Thillaye B, de Kozak Y, et al. Severe retinochoroidopathy: variations of humoral and cellular immunity to S-antigen in a longitudinal study. *Curr Eye Res*. 1990;9(Suppl.):91–96.
97. Liu D, Yang R, Yan X, et al. Hydroxyl radicals generated in vivo kill neurons in the rat spinal cord: electrophysiological, histological, and neurochemical results. *J Neurochem*. 1994;62(1):37–44.
98. Hauben E, Nevo U, Yoles E, et al. Autoimmune T cells as potential neuroprotective therapy for spinal cord injury. *Lancet*. 2000;355(9200):286–287.
99. Yoles E, Hauben E, Palgi O, et al. Protective autoimmunity is a physiological response to CNS trauma. *J Neurosci*. 2001;21(11):3740–3748.
100. Kipnis J, Yoles E, Schori H, et al. Neuronal survival after CNS insult is determined by a genetically encoded autoimmune response. *J Neurosci*. 2001;21(13):4564–4571.
101. Kipnis J, Mizrahi T, Yoles E, et al. Myelin specific Th1 cells are necessary for post-traumatic protective autoimmunity. *J Neuroimmunol*. 2002;130(1–2):78–85.

102. Zouboulis CC, May T. Pathogenesis of Adamantiades–Behcet's disease. *Med Microbiol Immunol*. 2003;192(3):149–155.
103. Sahly H, Podschun R, Kekow J, et al. Humoral immune response to *Klebsiella* capsular polysaccharides in HLA-B27-positive patients with acute anterior uveitis and ankylosing spondylitis. *Autoimmunity*. 1998;28(4):209–215.
104. Priya K, Madhavan HN, Reiser BJ, et al. Association of herpesviruses in the aqueous humor of patients with serpiginous choroiditis: a polymerase chain reaction-based study. *Ocul Immunol Inflamm*. 2002;10(4):253–261.
105. Guilherme L, Kalil J. Rheumatic fever: the T cell response leading to autoimmune aggression in the heart. *Autoimmun Rev*. 2002;1(5):261–266.
106. Cummings JH, Macfarlane GT, Macfarlane S. Intestinal bacteria and ulcerative colitis. *Curr Issues Intest Microbiol*. 2003;4(1):9–20.
107. Ishige I, Usui Y, Takemura T, et al. Quantitative PCR of mycobacterial and propionibacterial DNA in lymph nodes of Japanese patients with sarcoidosis. *Lancet*. 1999;354(9173):120–123.
108. Whittle RM, Wallace GR, Whiston RA, et al. Human antiretinal antibodies in toxoplasma retinochoroiditis. *Br J Ophthalmol*. 1998;82(9):1017–1021.
109. Hooks JJ, Percopo C, Wang Y, et al. Retina and retinal pigment epithelial cell autoantibodies are produced during murine coronavirus retinopathy. *J Immunol*. 1993;151(6):3381–3389.
110. Sasamoto Y, Kawano YI, Bouligny R, et al. Immunomodulation of experimental autoimmune uveoretinitis by intravenous injection of uveitogenic peptides. *Invest Ophthalmol Vis Sci*. 1992;33(9):2641–2649.
111. Linthicum DS, Munoz JJ, Blaskett A. Acute experimental autoimmune encephalomyelitis in mice. I. Adjuvant action of *Bordetella pertussis* is due to vasoactive amine sensitization and increased vascular permeability of the central nervous system. *Cell Immunol*. 1982;73(2):299–310.
112. Silver PB, Chan CC, Wiggert B, et al. The requirement for

pertussis to induce EAU is strain-dependent: B10.RIII, but not B10.A mice, develop EAU and Th1 responses to IRBP without pertussis treatment. *Invest Ophthalmol Vis Sci*. 1999;40(12):2898–2905.
113. Hofstetter HH, Shive CL, Forsthuber TG. Pertussis toxin modulates the immune response to neuroantigens injected in incomplete Freund's adjuvant: induction of Th1 cells and experimental autoimmune encephalomyelitis in the presence of high frequencies of Th2 cells. *J Immunol*. 2002;169(1):117–125.
114. Agarwal RK, Sun SH, Su SB, et al. Pertussis toxin alters the innate and the adaptive immune responses in a pertussis-dependent model of autoimmunity. *J Neuroimmunol*. 2002;129(1–2):133–140.
115. Singh VK, Kalra HK, Yamaki K, et al. Molecular mimicry between a uveitopathogenic site of S-antigen and viral peptides: induction of experimental autoimmune uveitis in Lewis rats. *J Immunol*. 1990;144(4):1282–1287.
116. Suhler EB, Martin TM, Rosenbaum JT. HLA-B27-associated uveitis: overview and current perspectives. *Curr Opin Ophthalmol*. 2003;14(6):378–383.
117. Mizuki N, Inoko H, Mizuki N, et al. Human leukocyte antigen serologic and DNA typing of Behçet's disease and its primary association with B51. *Invest Ophthalmol Vis Sci*. 1992;33(12):3332–3340.
118. LeHoang P, Ozdemir N, Benhamou A, et al. HLA-A29.2 subtype associated with birdshot retinochoroidopathy. *Am J Ophthalmol*. 1992;113(1):33–35.
119. Wildner G, Thurau SR. Cross-reactivity between an HLA-B27-derived peptide and a retinal autoantigen peptide: a clue to major histocompatibility complex association with autoimmune disease. *Eur J Immunol*. 1994;24(11):2579–2585.
120. Kurhan-Yavuz S, Direskeneli H, Bozkurt N, et al. Anti-MHC autoimmunity in Behçet's disease: T cell responses to an HLA-B-derived peptide cross-reactive with retinal-S antigen in patients with uveitis. *Clin Exp Immunol*. 2000;120(1):162–166.
121. Wildner G, Diedrichs-Mohring M. Autoimmune uveitis

induced by molecular mimicry of peptides from rotavirus, bovine casein and retinal S-antigen. *Eur J Immunol*. 2003;33(9):2577–2587.
122. Hooper LV, Littman DR, Macpherson AJ. Interactions between the microbiota and the immune system. *Science*. 2012;336(6086):1268–1273.
123. Horai R, Zarate-Blades CR, Dillenburg-Pilla P, et al. Microbiota-dependent activation of an autoreactive T cell receptor provokes autoimmunity in an immunologically privileged site. *Immunity*. 2015;43(2):343–353.
124. Millar DG, Garza KM, Odermatt B, et al. Hsp70 promotes antigen-presenting cell function and converts T-cell tolerance to autoimmunity in vivo. *Nat Med*. 2003;9(12):1469–1476.
125. Zierhut M, Mizuki N, Ohno S, et al. Immunology and functional genomics of Behçet's disease. *Cell Mol Life Sci*. 2003;60(9):1903–1922.
126. Marengo EB, Commodaro AG, Peron JPS, et al. Administration of *Mycobacterium leprae* rHsp65 aggravates experimental autoimmune uveitis in mice. *PLoS ONE*. 2009;4(11):e7912.

30

Mechanisms of Macular Edema and Therapeutic Approaches

Antonia M. Joussen, Alan Stitt, Noemi Lois

1993

Introduction

Macular edema is a common phenomenon in various diseases where fluid accumulates in the extracellular space within the retinal neuropile. This phenomenon relates to Starling's law which predicts that macular edema will develop if the hydrostatic pressure gradient between capillary and retinal tissue is increased. In the retina this can occur in the presence of elevated blood pressure, or if

the osmotic pressure gradient is decreased by excessive protein accumulation in the extracellular space.[1] The edema is also related to concomitant breakdown of the inner and outer blood–retinal barriers (BRBs) which are modulated by imbalances in cytokines and growth factors that disturb the integrity of the tight junctions of the capillary endothelium and retinal pigment epithelium (RPE).[2]

Both focal, diffuse, and the cystic forms of edema are characterized by extracellular accumulation of fluid, specifically in Henle's layer and the inner nuclear layer of the retina, but also in the subretinal space. The compartmentalization of the accumulated fluid is likely to be due in part to the slow dispersal of accumulated extracellular fluid that occurs within the plexiform layers as a consequence of the tightly packed neuronal and glial parenchyma combined with impaired fluid clearance mechanisms. Recent evidence indicates that edematous changes to the inner retina can also occur as a consequence of disruption of the normal homeostatic function of the Müller glia. This can lead to intracellular, cytoplasmic swelling of these cells that span the entire inner retina, which exacerbates disruption of the retinal interstitium and contributes to the development of edema and neurodegeneration.

Macular Edema as a Result of Various Disease Mechanisms

Causes of Macular Edema

In general, formation of macular edema is related to metabolic changes, ischemia, hydrostatic forces, inflammatory and toxic mechanisms, or mechanical forces that occur to various degrees in the different conditions (Table 30.1 online).

TABLE 30.1

Causes of Macular Edema in Relation to the Underlying Disorders

Disease Group	Disorder	Pathogenesis
Metabolic alterations	Diabetes	Abnormal glucose metabolism Aldose reductase Both inner and outer BRB are affected

	Retinitis pigmentosa	CME: leakage at the level of RPE
	Inherited CME (autosomal dominant)	Müller cell disease: leakage from perifoveolar capillaries
Ischemia	Vein occlusion Diabetic retinopathy	Predominantly inner BRB (retinal capillary hypoperfusion)
	Severe hypertensive retinopathy HELLP syndrome Vasculitis, collagenosis	Outer BRB (ischemic hypoperfusion of the choroid: serous detachment)
Hydrostatic forces	Retinal vascular occlusions Venous occlusion Arterial hypertension Low IOP	Increased intravascular pressure Failure of the BRB
Mechanical forces	Vitreous traction on the macula	Epiretinal membranes with tangential traction Vitreomacular traction syndrome
Inflammation	Intermediate uveitis	Mediated by prostaglandins CME is considered indication for treatment
	Postoperative CME	Perivascular leukocytic infiltrates
	DME	Diabetic leukostasis mediates vascular leakage by endothelial cell apoptosis
	Choroidal inflammatory diseases Vogt–Koyanagi–Harada syndrome Birdshot retinochoroidopathy	Lymphocytes: T-cells, microglia activation
Pharmacotoxic effects	For example: Epinephrine (in aphakia) Betaxolol Latanoprost	Mostly via prostaglandins

BRB, blood–retinal barrier; CME, cystoid macular edema; DME, diabetic macular edema; HELLP syndrome, Hemolytic anemia, Elevated Liver enzymes, and Low Platelet count; IOP, intraocular pressure.

The classic pattern of cystoid macular edema (CME) with a petaloid appearance originating from the fluorescein leakage from perifoveal capillaries may be seen in cases of advanced edema of various origins (Fig. 30.1A). This includes postsurgical CME as well as CME associated with one of the following conditions: diabetes, vascular occlusion, hypertensive retinopathy, epiretinal membranes, intraocular tumors (e.g., melanoma, choroidal hemangioma), intraocular inflammation (e.g., pars planitis), arterial macroaneurysm, inherited retinal disorders such as retinitis pigmentosa, choroidal neovascularization, and radiation retinopathy.

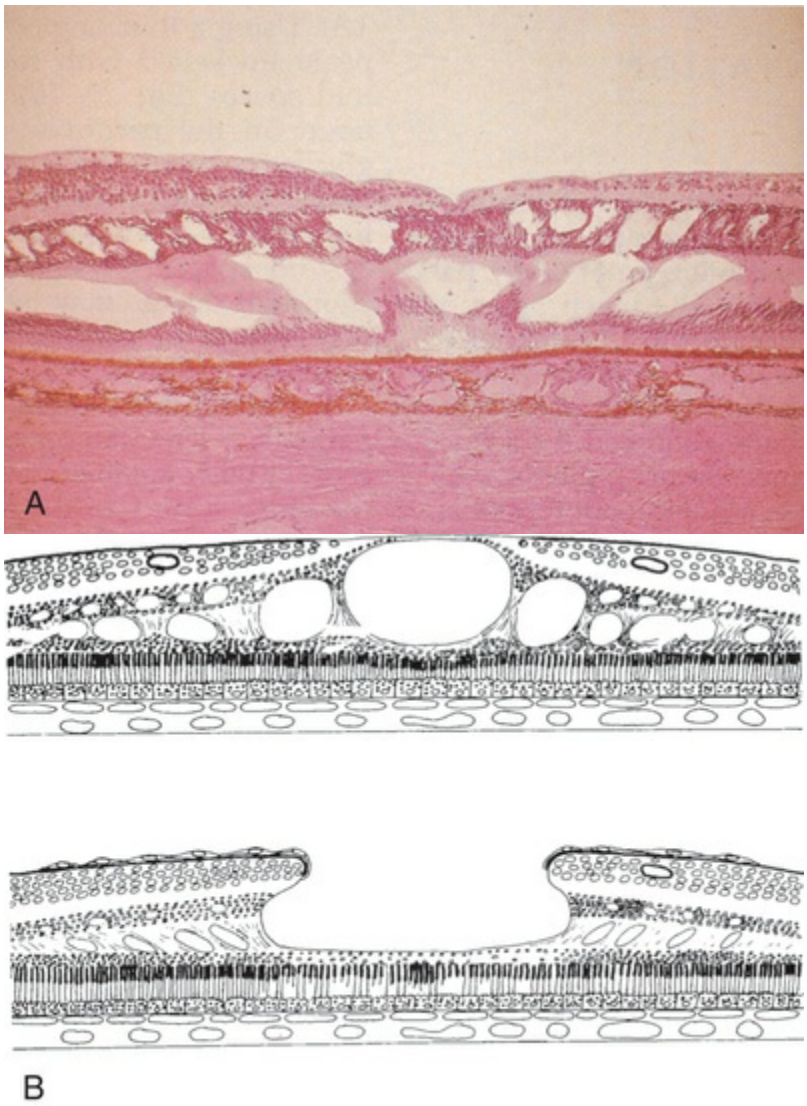

FIG. 30.1 (A) Histologic section of the fovea area demonstrating cystoid macular edema with large cystic spaces in the outer nuclear and plexiform layer as well as in the inner nuclear layer. (B) Schematic drawing.

Given the heterogeneous etiology of macular edema, its effective treatment depends upon a better understanding of the underlying pathogenesis.

Metabolic alterations have a causal role in diabetic maculopathy, but also in inherited diseases such as the autosomal dominant form of macular edema or macular edema in retinitis pigmentosa. Furthermore, ischemia of the peripheral retina leads to formation of macular edema. Decreased perfusion of the retinal capillaries on the arterial side is seen, for example, in vein occlusion and diabetic retinopathy, whereas ischemia plus decreased perfusion of the choroid with associated serous retinal detachment occurs in severe

hypertensive retinopathy, in eclampsia, or in rheumatoid disorders. Following retinal vein occlusion, the intravascular pressure increases and leads to dysfunction of the BRB. Similarly, hydrostatic forces are effective in arterial hypertension or in eyes with low intraocular pressure and may cause fluid accumulation in the macula. Mechanical traction such as in epiretinal membranes or in vitreomacular traction syndrome may also promote macular edema by physical forces.

Inflammation is important in the pathogenesis of macular edema in conditions such as posterior uveitis, postoperative CME (Irvine–Gass syndrome), diabetic macular edema (DME), and various diseases linked to choroidal inflammation such as Vogt–Koyanagi–Harada disease and birdshot retinochoroidopathy. All prostaglandin-like pharmacologic agents, even if applied topically for treatment of glaucoma, can induce macular edema via a cytokine response similar to inflammatory conditions.

The knowledge of the basic mechanisms involved in vascular leakage is essential for the development of an effective clinical treatment. Development of optimal strategies for treating retinal edema may depend on determining the ratio of the contribution of intra- and extracellular mechanisms to edema and measuring how this ratio changes among patients, retinal disease, and even during disease progression. It should also take into account the site of disturbance (i.e., breakdown of inner or outer BRB or both).With the growing understanding of the pathophysiology of the macular edema, the therapeutic thinking is likely to change from a merely symptomatic treatment (either surgical or medical) to a treatment that targets specifically the causal factors involved in its formation (e.g., cytokine or growth factor inhibition).

Molecular and Cellular Alterations Leading to Macular Edema

Much of the knowledge on the pathophysiology of macular edema has been determined from extensive studies based on animal models, especially relating to early-stage diabetic retinopathy, experimental autoimmune uveitis, and ischemia-induced leakage. A variety of techniques measuring accumulation of material from

plasma in the neural retina have been investigated as indicators of permeability. Such accumulation seems diffuse in nature, and focal defects have not been reproducibly described in diabetic mice; as well, interpretations of techniques involving tracer accumulation have not been validated in terms of "gold standard" permeability surface area product.[3] Interestingly, edema has not been demonstrated in the retina of diabetic mice based on retinal thickness measurements despite the indication of increased permeability.

The BRB consists of the retinal pigment epithelium (RPE) layer (outer BRB), and the vascular endothelium (inner BRB), that prohibit the passage of macromolecules and circulating cells from the vascular compartment to the extracellular compartment and therefore to the intraretinal or subretinal space.[4] Intracellular edema (formerly also referred to as "cytotoxic edema") is defined as cellular swelling that occurs independent of the BRB. Extracellular edema (sometimes referred to as "vasogenic edema") is characterized by retinal thickening in association with loss of BRB integrity (Fig. 30.2). Combinations thereof are possible.

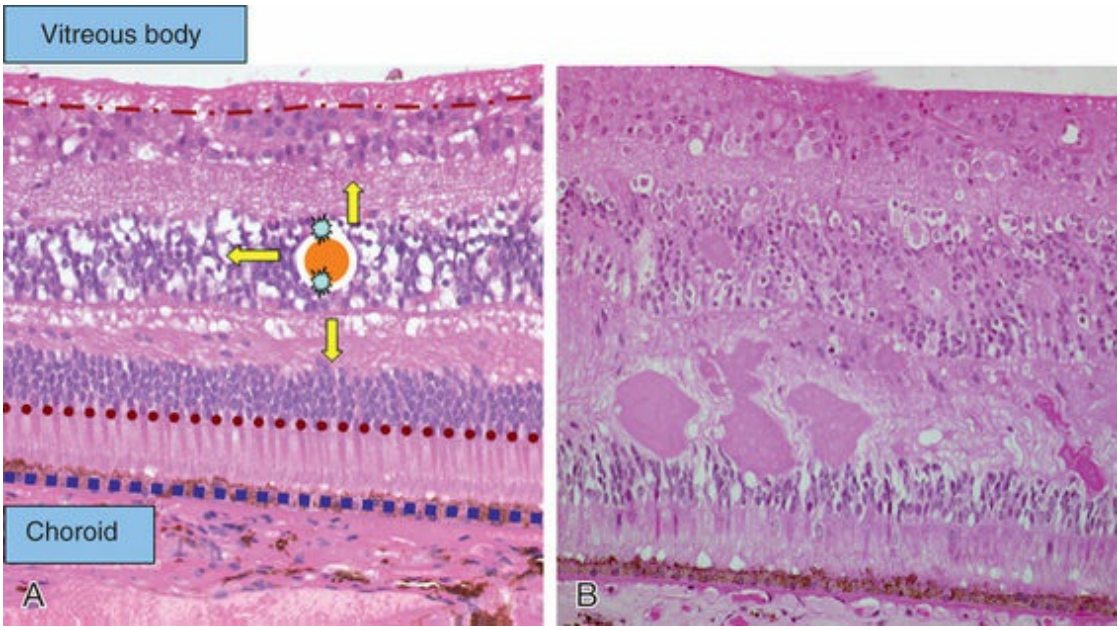

FIG. 30.2 Blood–retinal barrier (BRB) and breakdown in vascular disease. (A) Normal retinal tissue. Dotted line marks the outer BRB at the level of the retinal pigment epithelial cells. The inner BRB is at the level of the endothelial cells of retinal vessels. Further

structural guidance is given by Müller cells. (B) Diabetic retinopathy: note the large caveolae of fluid and accumulation of blood cells in the retinal tissue resulting of a breakdown of the inner BRB. (Courtesy of Sarah Coupland, MD, Liverpool.)

The breakdown of the inner BRB, as a result of a variable contribution of dysfunction of intercellular junctions, increased transcellular transport, or endothelial cell and pericyte dysfunction/loss, leads to an increased vascular permeability (Fig. 30.3 online). The initial site of damage that results in the increased vascular permeability is controversial to date. Although impairment of the perivascular supporting cells such as pericytes and glial cells might play a role, endothelial cell dysfunction and injury seems more likely to be the first pathogenetic step towards the breakdown of the BRB early in the course of the disease. In order to dissect the molecular and pathophysiologic mechanisms that lead to the accumulation of fluid in the macular area, most knowledge from preclinical models is related to diabetic models.

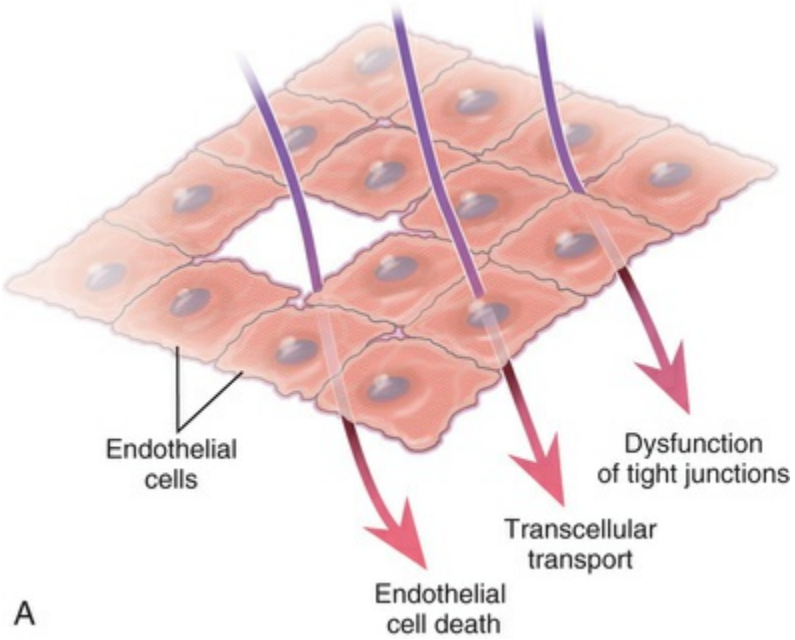

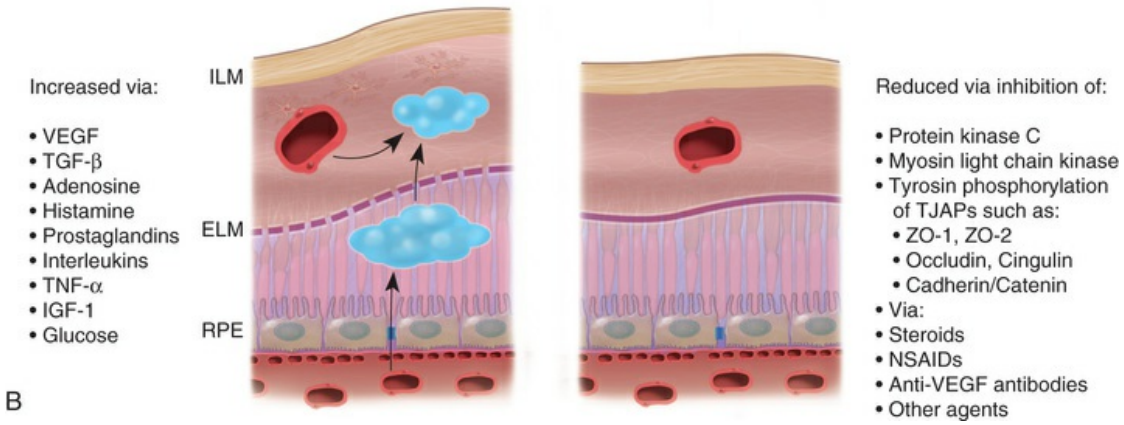

FIG. 30.3 Pathogenesis of macular edema and vascular leakage. (A) In general, water outflow through vessels is possible via three major routes: paracellular via dysfunction of tight junctions, transcellular via increased transport, e.g., mediated via growth factors, and finally directly via endothelial gaps after cell death. (B) Vascular leakage is increased by a variety of factors including growth factors and inflammatory cytokines. Leakage in turn is decreased by steroids, inhibition of tight-junction formation or antibodies to factors inducing leakage. *ELM,* external limiting membrane; *ILM,* internal limiting membrane; *RPE,* retinal pigment epithelium; *TJAPs,* tight junction-associated proteins. Other abbreviations, see text.

While for diabetes and ischemic retinopathies the inner-BRB is believed to play a dominant role in vascular leakage, the importance of the outer BRB has recently been supported.[5] The outer BRB separates the neural retina from the choroidal vasculature, which is responsible for approximately 80% of the blood supply in the eye (Fig. 30.4).

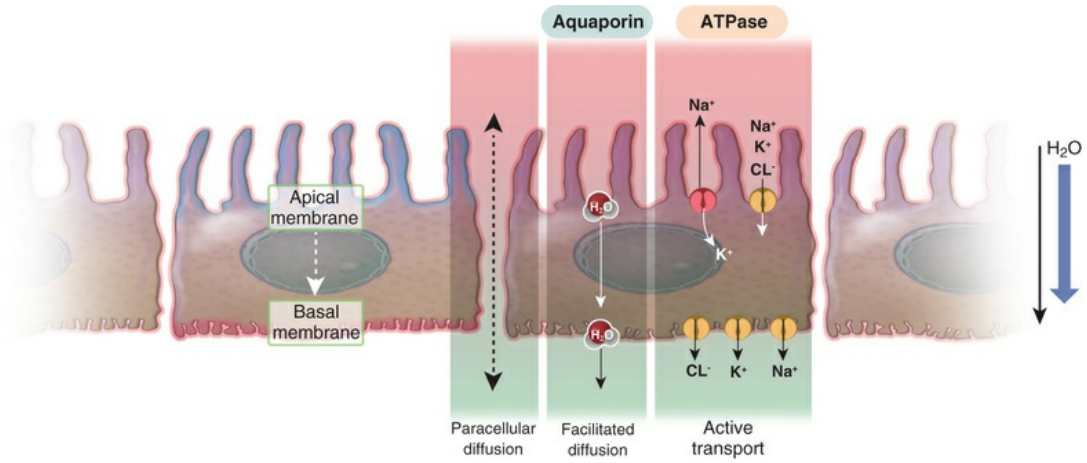

FIG. 30.4 The retinal pigment epithelial (RPE) cells represent the outer blood–retina barrier (BRB). In the normal healthy retina, the transretinal water fluxes are mediated by Müller cells and pigment epithelial cells. These water fluxes are inevitably coupled to fluxes of osmolytes; to K(+) clearance currents. For this purpose, the cells express a complex, microtopographically optimized pattern of transporters and channels for osmolytes and water in their plasma membrane. Aquaporin-4 is a water channel that is abundantly expressed in Muller cells, but also in the RPE cells, and that permits the flow of water into the cell. In conditions of ischemia or inflammation, aquaporin-4 levels rise, and more fluid will enter the cells as described in previous slide. Ischemic/hypoxic alterations of the retinal microvasculature involve a downregulation of K(+) channels in the perivascular Müller cell end-feet and in the RPE cells. This means a closure of the main pathway that normally generates the osmotic drive for the redistribution of water from the inner retina into the blood. The result is an intracellular K(+) accumulation which, then, osmotically drives water from the blood into cells (i.e., in the opposite direction) and causes cell swelling, edema, and finally results in cyst formation.

The outer BRB-specific leakage of fluorescent macromolecules can be visualized in diabetic and ischemic rodents, and substantial leakage of macromolecules through the outer BRB can be detected. The role of the outer BRB is largely underestimated but has significant clinical implications.

Cell-to-Cell Junctions and Vascular Permeability

Fluid homeostasis and capillary permeability are regulated by the complex intercellular communications within the cells of the neurovascular unit which comprises endothelial cells, pericytes and closely associated macro- and microglia and neurons. This cellular unit responds dynamically to complex circulatory and neural cues to control blood flow and regulate the intercellular junctions of the inner BRB. Intercellular junctions are complex structures formed by the assembly of transmembrane and cytoplasmic/cytoskeletal protein components. At least four different types of endothelial junctions have been described: tight junctions, gap junctions, adherence junctions, and syndesmos. Tight junctions are the most apical component of the intercellular cleft and are most relevant for the BRB (Fig. 30.5 online). Although the molecular structure of tight junctions generally appears to be similar in all barrier systems, there are some differences between epithelial and endothelial tight junctions, and between tight junctions of peripheral and retinal endothelial cells.[6] Expression of selected endothelial cell tight-junction genes and particularly that of occludin and claudin-5 are reduced in the diabetic retina.[7] In contrast to tight junctions in epithelial systems, structural and functional characteristics of tight junctions in endothelial cells respond promptly to ambient factors. It is likely that inflammatory agents increase permeability by binding to specific receptors that transduce intercellular signals, which in turn cause cytoskeletal reorganization and widening of the interendothelial clefts. For example, tumor necrosis factor (TNF)-α signals through protein kinase C (PKC)ζ/nuclear factor (NF)-κB alter the tight-junction complex and increase retinal endothelial cell permeability.[8] Endothelial junctions also regulate leukocyte extravasation. Once leukocytes have adhered to the endothelium, a coordinated opening of interendothelial cell junctions occurs.

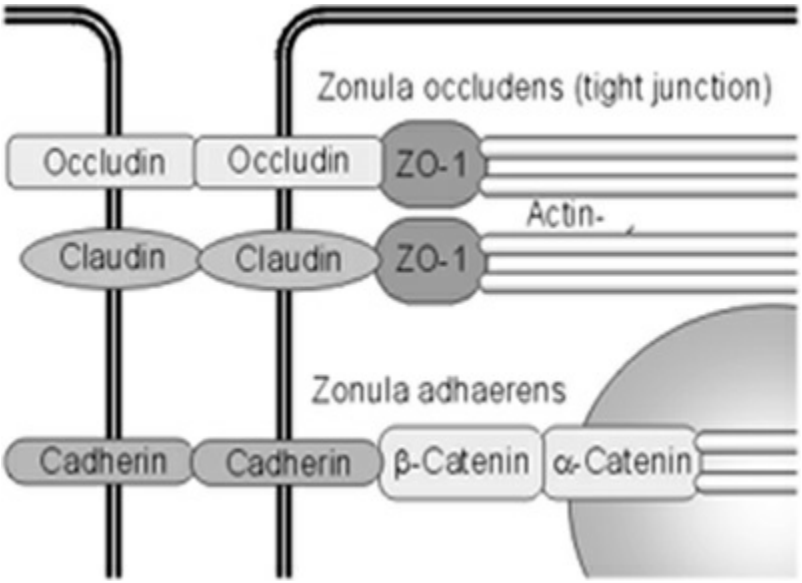

FIG. 30.5 Intercellular junctions in endothelial cells: Endothelial cells are connected and communicate with each other by tight junctions and adherens junctions. Tight junctions resemble a major part of the inner blood–retinal barrier. They are built by different proteins including occludin, ZO-1, and the claudin family.

Fluid moves from the retina to the choroid largely due to the osmotic pressure exerted by the proteins in the choroidal stroma and disruption of this normal flow can lead to significant edema. Especially in the context of ischemia and diabetic retinopathy, there is evidence that the RPE becomes dysfunctional and that leakage from the choriocapillaris occurs in unison with impaired fluid clearance contributing to retinal edema. When the RPE shows stress responses resulting from oxidative or nitrosative damage, this can result in significant loss of fluid control and damage to junctional integrity. Similar to the breakdown of the inner BRB, the breakdown of the outer BRB is associated with a significant depletion of the occludin in the RPE of ischemic and diabetic rodents.

Inflammation and Vascular Permeability

"Inflammation" comprises a broad range of reactions from intravascular leukostasis and reactive glial activation as seen in diabetic retinopathy to overt inflammatory responses as in pars planitis, or choroidal inflammatory diseases.

Diseases not primarily called inflammatory such as diabetes present with activated leukocytes with abnormal adherence to the retinal vascular endothelium.[9,10] So-called leukostasis is initiated by activation of vascular endothelium and circulating myeloid cells such as neutrophils and monocytes. In diabetes, for example, the leukostasis phenomenon is typified by immune cells becoming trapped in narrow-channel retinal capillaries leading to occlusion and nonperfusion which is one of the first histologic changes in diabetic retinopathy and occurs prior to any apparent clinical pathology. Adherent leukocytes play a crucial role in diabetic retinopathy by directly inducing endothelial cell death in capillaries[11] causing vascular obstruction and vascular leakage. Endothelial cell death precedes the formation of acellular capillaries.[3] With time, however, acellular capillaries prevail and become widespread. Although the mechanism of this destructive process remains elusive, it is clear that the interaction between the altered leukocytes and the endothelial cells and the subsequent endothelial damage represents a crucial pathogenic step[9,11,12] (Fig. 30.6 online). This process is triggered by various growth factors and inflammatory cytokines. Inflammatory cytokines such as TNF-α decrease the protein and mRNA content of the tight-junction proteins zonula occludens (ZO)-1 and claudin-5.[8] TNF-α and interleukin-1 beta (IL-1β) are elevated in the vitreous of diabetic patients and in the retina of diabetic rats associated with increased retinal vascular permeability and leukostasis[13,14] (Fig. 30.7 online). Furthermore, TNF-α is involved in ischemic vascular changes.[15] While a variety of cells may express these cytokines including endothelial cells, perivascular cells, and Müller glia, a bulk of expression is probably linked to activation of retina-resident microglia and infiltrating monocytes.

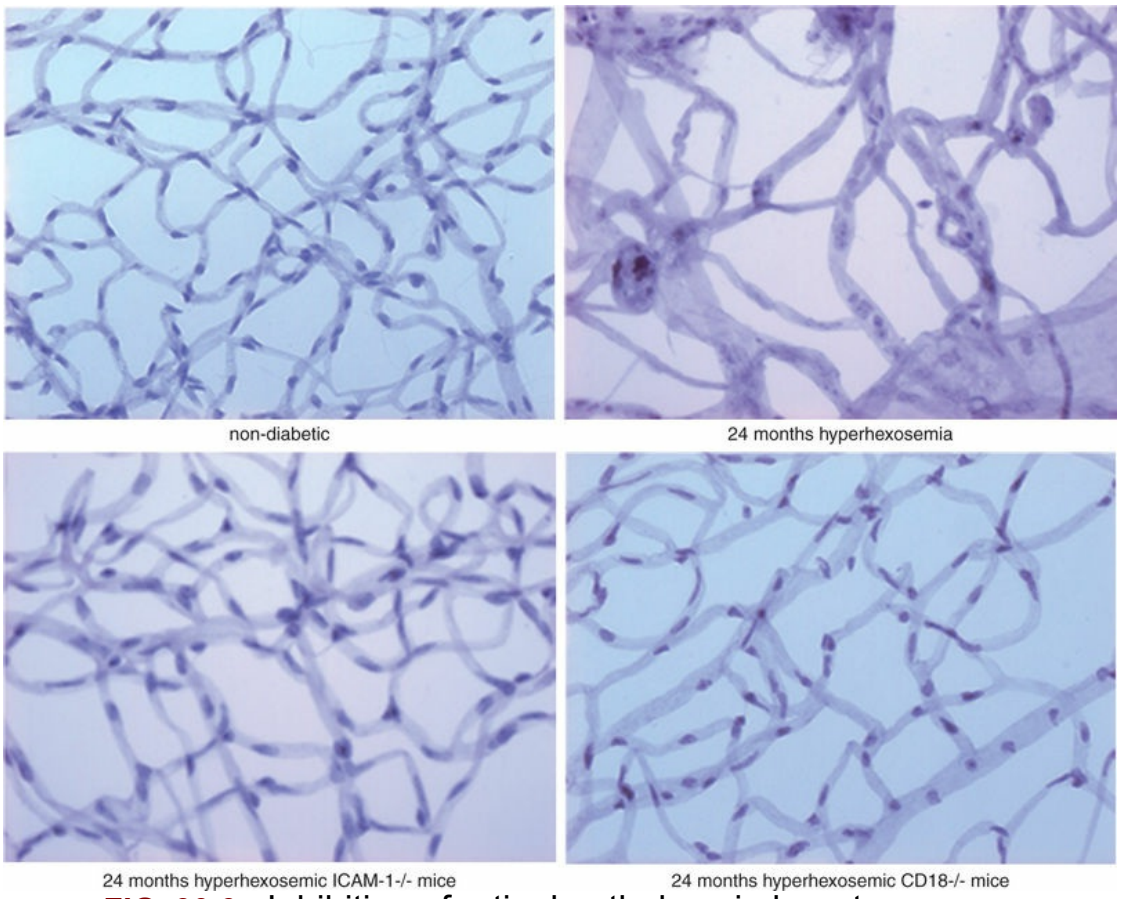

FIG. 30.6 Inhibition of retinal pathology in long-term hyperhexosemic ICAM-1- and CD-18-deficient mice: trypsin digests demonstrating a large destruction of the capillary network comparable to nonproliferative diabetic retinopathy with acellular capillaries and microaneurysms in 24-months hyperhexosemic mice. The capillary network in mice with a “noninflammatory” phenotype (CD-18- or ICAM-1-deficient) demonstrates almost normal capillaries. (Reproduced with permission from Joussen AM, Poulaki V, Le ML, et al. A central role for inflammation in the pathogenesis of diabetic retinopathy. FASEB J 2004;18:1450–2.)

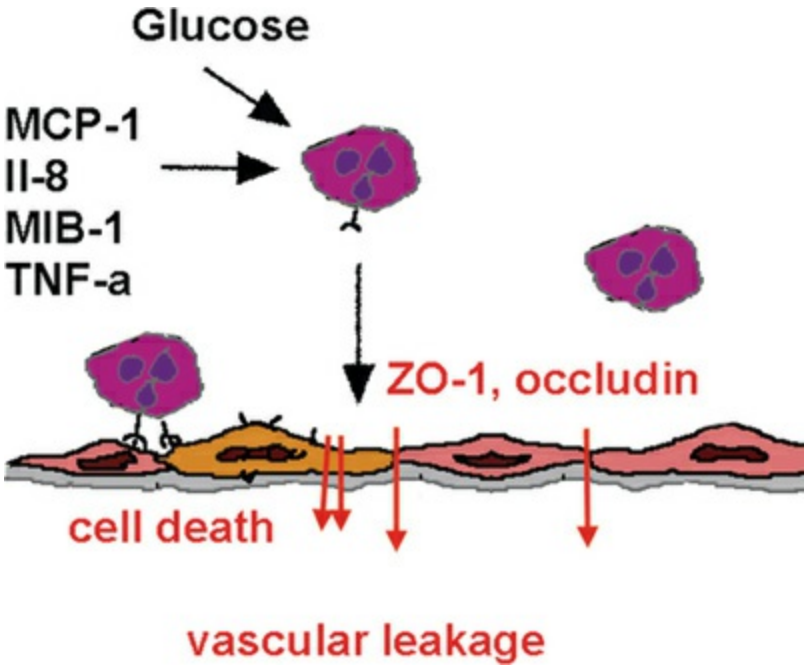

FIG. 30.7 Inflammatory mediators are involved in leukocyte-endothelial interaction that via reduction of tight junction protein expression and induction of apoptosis results in vascular leakage.

While this is typical for overt inflammatory retinal disorders such as uveitis, such cell activation responses are now known to also be central to inflammatory responses developing during diabetic retinopathy. For example, a number of in vitro studies and in vivo investigations of animal models and human postmortem specimens indicate that activation of retinal microglia could play an important regulatory role in diabetes-mediated retinal inflammation by modulating cytokine expression and other pathologic responses. Monocytes that infiltrate the retina are distinct from microglia, and they reside in proximity to blood vessels (perivascular macrophages) or within various layers of the neuropile. While both monocytes and microglia have important roles in retinal homeostasis, they are also central to neuroinflammation responses that lead to retinal edema.[16,17]

In the inner retina, metabolic substrates, such as glucose, flow from vascular endothelium to astrocytes to neurons. In the outer retina, substrates reach Müller cells and photoreceptors from the choroid via the RPE[18] (Fig. 30.8).

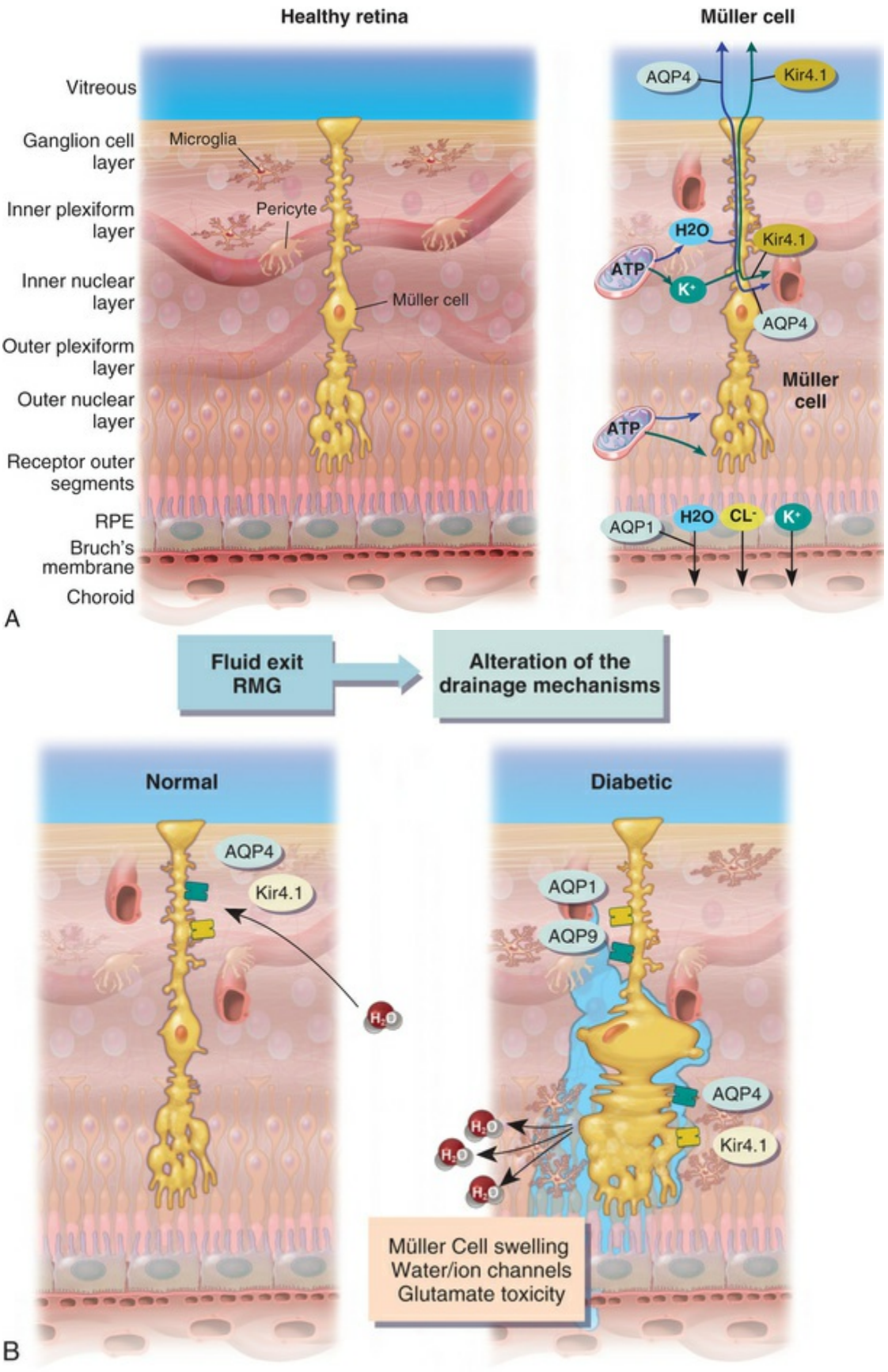

FIG. 30.8 (A) Müller cells are the communicators of the retina and are one of the principal locations for

intracellular fluid accumulation in patients with macular edema. The image on the left shows in orange the Müller cell in the healthy retina stretching through the retina from the ganglion cell layer to the retinal pigment epithelium. Some of the early changes are due to changes of the Müller cells and ionic channels as they control the tight junctions. (B) Alteration of the drainage mechanisms. *RMG*, retinal Müller glia.

Microglia associate intimately with neurons that express molecules, such as CX3CL1 (fractalkine) and CD20, that negatively regulate microglial activation through their respective receptors. As such, perturbation of expression of ligand or receptor during stress would activate microglia to produce proinflammatory cytokines and acquire an activated morphology. Activated microglia produce chemokines such as monocyte chemoattractant protein-1, inducing expression of adhesion molecules, which can promote the leukostasis of neutrophils on endothelium, and potentially inducing the extravasation of inflammatory macrophages.[18,19] Induction of glial fibrillary acidic protein (GFAP) is a marker of glial activation and increased expression of this protein occurs in Müller cells from the retinas of diabetic patients, but also after ischemic injury. The importance of Müller cells on the formation of neuronal and vascular pathology has been confirmed in transgenic models recently.[20]

Growth Factors, Vasoactive Factors, and Vascular Permeability

The disruption of endothelial integrity leads to retinal ischemia with an ensuing hypoxia response by the oxygen-deprived retina. At a molecular level this is typified by stabilization and nuclear translocation of hypoxia-inducible factor-1 alpha (HIF-1α) in the neurons and glia. HIF-1α is one of a family of hypoxia-inducible transcription factors that bind to hypoxia response elements in inducible target genes and control gene expression of proteins such as erythropoietin (EPO), vascular endothelial growth factor (VEGF), and glucose transporters. VEGF is most well appreciated in the ophthalmology field since it drives iris and retinal neovascularization.[9,21,22] Also known as vascular permeability factor

(VPF), VEGF is 50,000 times more potent than histamine in causing increased vascular permeability.[23–25] Previous work has shown that retinal VEGF levels correlate with diabetic BRB breakdown in rodents[26] and humans.[27] Flt-1(1-3Ig)F_c, a soluble VEGF receptor, reverses early diabetic BRB breakdown and diabetic leukostasis in a dose-dependent manner.[21] Early BRB breakdown localizes, in part, to retinal venules and capillaries of the superficial inner retinal circulation[28] and can be sufficiently reduced by VEGF inhibition (Fig. 30.9 online). Although VEGF is only one of the cytokines involved in the pathogenesis of the vascular leakage, it is likely to be one of the most effective therapeutic targets.

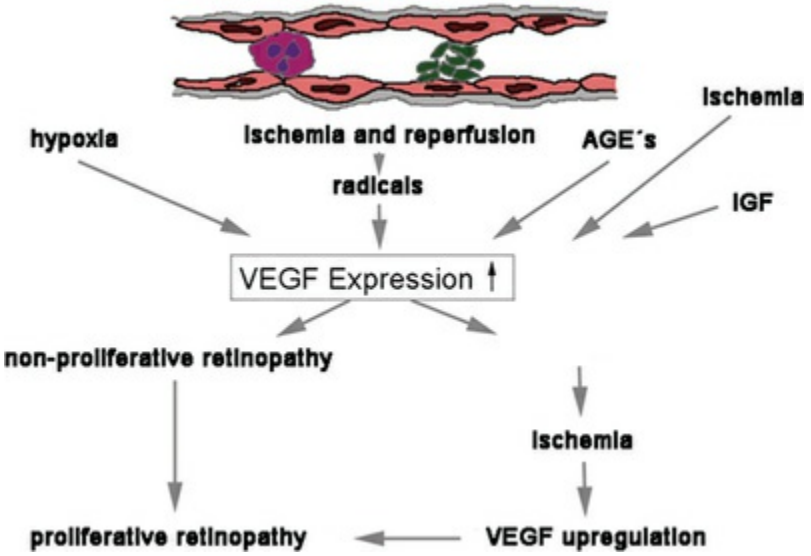

FIG. 30.9 Vascular endothelial growth factor (VEGF) is the key mediator of vascular damage and finally proliferation in the diabetic retina.

On a cellular level, VEGF has been implicated in many different mechanisms that lead to macular edema. VEGF has, for example, been shown to decrease the proteins responsible for the tightness of the intercellular junctions and induces rapid phosphorylation of the tight-junction proteins occludin and ZO- 1 resulting in the breakdown of the BRB.[29] VEGF-induced BRB breakdown appears to be effected via nitric oxide.[22] VEGF also increases paracellular transport without altering the solvent drag reflection coefficient.[30] Furthermore, VEGF activation of PKC stimulates occludin phosphorylation and contributes to endothelial permeability.[31]

There are established tight connections between inflammation and VEGF expression.[22] Müller-cell derived VEGF has been shown to be essential for diabetes-induced retinal inflammation and vascular leakage.[32]

To determine the significance of Müller cell-derived VEGF in diabetic retinopathy, VEGF expression in Müller cells was disrupted with an inducible Cre/lox system and diabetes-induced retinal inflammation and vascular leakage was examined in these conditional VEGF knockout (KO) mice. Diabetic conditional VEGF KO mice exhibited significantly reduced leukostasis expression of inflammatory biomarkers, a reduced depletion of tight-junction proteins, reduced numbers of acellular capillaries, and reduced vascular leakage compared to diabetic control mice.

In vitro investigations on cell–cell interactions by D'Amore and coworkers demonstrated an inhibitory effect of transforming growth factor (TGF)-ß secreted by pericytes on endothelial cell growth. In diabetic retinopathy formation of sorbitol via aldose reductase leads to PKC activation resulting in pericyte damage and subsequently a loss of the inhibitory balance via TGF-ß secretion[33] (Fig. 30.10).

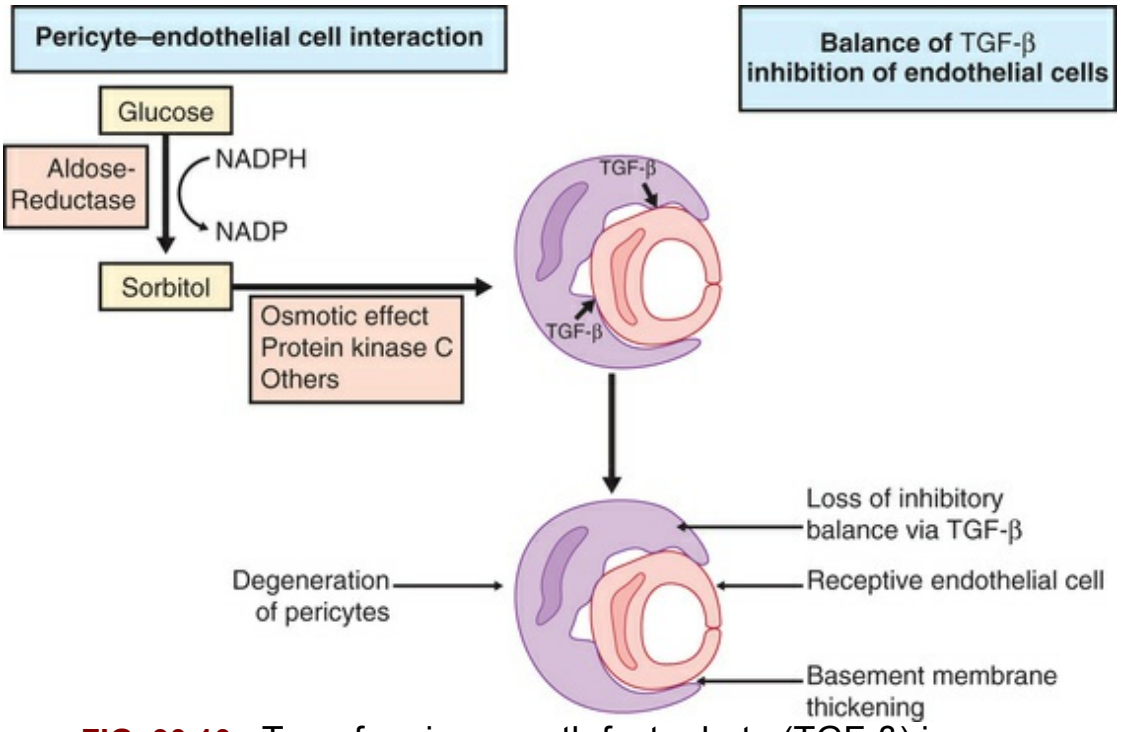

FIG. 30.10 Transforming growth factor beta (TGF-ß) is

involved in an inhibitory balance between pericytes and endothelial cells.

High glucose concentration leads to increased diacylglycerol (DAG) by two pathways: de novo synthesis and through dehydrogenation of phosphatidylcholine (PC). Increased levels of DAG mediate PKC activation. Several studies have shown that a decrease in retinal blood flow occurs with PKC activation. Conversely, inhibition of PKC with LY333531 (Eli Lilly, Indianapolis, IN) normalized decreased retinal blood flow in diabetic rats.[34,35]

PKC activation causes vasoconstriction by increasing the expression of endothelins (ET), especially ET-1. The expression of endothelins can be induced by a variety of growth factors and cytokines including thrombin, TNF-α, TGF-β, insulin, and vasoactive substances including: angiotensin II, vasopressin, and bradykinin.

Furthermore, retinal vascular endothelial cells are very sensitive to histamine. Several studies have documented increased vascular histamine synthesis in diabetic rats and humans.[36–38] The administration of histamine reduces ZO-1 protein expression and thus correlates with vascular permeability. The H1 receptor stimulates PKC that has been implicated in increased retinal vascular permeability.[39] Interestingly, Aiello and coworkers showed that administration of LY333531, a PKC-β isoform-selective inhibitor, does not significantly decrease histamine-induced permeability but rather VEGF-induced permeability. In contrast, administration of non-isoform-selective PKC inhibitors did significantly suppress histamine-induced permeability.[40]

Furthermore, in vascular endothelial cells, advanced glycation endproducts (AGE) may affect the gene expression of ET-1 and modify VEGF expression. The AGE-stimulated increased VEGF expression is dose- and time-dependent and additive to hypoxia.[41,42]

Endothelial Cell Death and Vascular Permeability

Where intraluminal pressure falls below a critical closing pressure, the tone of the arteriolar wall cannot be maintained and the downstream capillary bed collapses and endothelial cells may

become “fibrin locked.” Endothelial cells deprived of their circulation and nutrition die and only acellular basement membranes persist. Similarly, a reduction in retinal perfusion pressure, often linked to carotid/ophthalmic artery insufficiency, can have similar retinal manifestations, and in extreme circumstances, there may be retrograde filling of arteries from fellow veins. Stasis of the blood flow in capillaries after venous or arterial occlusions results in rapid apoptosis of endothelial cells.[43]

Similarly, in diabetes, BRB breakdown is at least in part due to endothelial cell damage and apoptosis. The proapoptotic molecule Fas-ligand (FasL) induces apoptosis in cells that carry its receptor Fas (CD 95).[44] There is evidence that FasL is expressed on vascular endothelium where it functions to inhibit leukocyte extravasation. The expression of FasL on vascular endothelial cells might thus prevent detrimental inflammation by inducing apoptosis in leukocytes as they attempt to enter the vessel. In fact, during inflammation and ensuing TNF-α release, the retinal endothelium upregulates several adhesion molecules[45] that mediate the adherence of the leukocytes, but also downregulates FasL thus allowing leukocyte survival and migration to active sites of inflammation. In experimental diabetic retinopathy, inhibition of Fas-mediated apoptotic cell death reduces vascular leakage.[46] The cumulative endothelial cell death during the course of diabetes plays a causal role in the pathogenesis of the diabetic vascular leakage and maculopathy.

Extracellular Matrix Alterations and Vascular Permeability

In diabetic retinopathy matrix changes are mostly related to basement membrane thickening of the capillaries which arises because of increased synthesis of protein components such as collagen IV, fibronectin, and laminin in combination with reduced degradation by catabolic enzymes. Degradation of the extracellular matrix affects endothelial cell function at many levels causing endothelial cell lability, which is required for cellular invasion and proliferation, or influencing the cellular resistance and therefore the vascular permeability. The degradation and modulation of the extracellular matrix is exerted by matrix metalloproteinases

(MMPs), a family of zinc-binding, calcium-dependent enzymes.[47] Elevation of MMP-9 and MMP-2 expression has been shown in diabetic neovascular membranes,[48,49], although a direct effect of glucose on MMP-9 expression in vascular endothelial cells could not be shown.[50] It is probable that MMPs participate at various stages during the course of the BRB dysfunction and breakdown. Their actions include early changes of the endothelial cell resistance with influence on intercellular junction formation and function[51] to active participation in endothelial and pericyte cell death[52] that occurs late in the course of the disease. Taken together, the degradation of extracellular matrix affect the blood vessels not just because then the blood vessels do not have support (i.e., mechanical effect) but also via altered interactions between endothelial cells and perivascular cells and an altered distribution of soluble growth factors and cytokines.

Although basement membrane thickening is a hallmark lesion in diabetic retinopathy it is still uncertain if it is of primary or secondary importance in the development of microvasculopathy. In the context of vasopermeability abnormalities, changes to this extracellular matrix impact the integrity of the neurovascular unit and normal cell–cell communication. Even from a structural perspective, changes in protein and proteoglycan composition of the basement membrane, as occurs in diabetes, influence charge selectivity which contributes to capillary barrier function.

Transcellular Transport and Vascular Permeability

Disruption of the BRB is an early phenomenon in preclinical diabetic retinopathy (PCDR). Two vascular permeability pathways may be affected: the paracellular pathway involving endothelial cell tight junctions, and the endothelial transcellular pathway mediated by endocytotic vesicles (caveolae and pinocytic transport). Despite the fact that pinocytic transport is critically involved in the transepithelial fluid exchange, its role in the pathogenesis of increased vascular leakage in diabetes is just emerging.[53,54] The importance of the regulation of fluid homeostasis by active cellular transport of nutrients and fluid via pinocytosis is underlined by recent data suggesting a transient induction of the paracellular pathway and prolonged involvement of transcellular endothelial

transport mechanisms in the increased permeability of retinal capillaries in diabetes.[7]

It is currently known that one of the factors involved in the regulation of pinocytic transport is VEGF. VEGF increases vascular permeability not only by disrupting the intercellular tight junctions between the retinal endothelial cells but also by inducing the formation of fenestrations and vesiculo-vacuolar organelles. The role of VEGF in the disruption of the pinocytic transport that is translated into increased vascular permeability in disease states is still controversial.[55] Whereas in highly permeable blood vessels the number of pinocytotic vesicles at the endothelial luminal membrane transporting plasma IgG is significantly increased, no fenestrations or vesicles were found in the endothelial cells of the VEGF affected eyes when examined by electron microscopy.

Neurovascular Coupling

Neuronal degeneration is a common feature of long-standing macular edema but has been recently shown to occur early in the pathogenesis of various origins of macular edema.

The retina consists of a network of neurons and specialized sensory cells (photoreceptors, bipolar cells, horizontal cells, amacrine cells, and ganglion cells) and glia (astrocytes, Müller cells, and microglial cells) that comprise approximately 95% of the tissue, with blood vessels representing less than 5% of the retinal mass.[56] As the network of retinal neurons and glia are intimately linked, there is no doubt that the neural and vascular components of the retina are closely associated by metabolic synergy and paracrine communication.[18,57]

There are complex neural, glial and vascular cell interactions occurring with both large and small retinal vessels and these play important roles in controlling retina homeostasis, including blood flow, water balance, and vasopermeability. The phenomenon called neurovascular coupling refers to the process by which retinal blood flow and vasoreactivity is matched to the metabolic (particularly oxygen) demands of the neuropile.[58] This interplay between the cell-types can become dysfunctional in disease states. For example, in the diabetic retina, regulation of vascular smooth muscle reactivity is depressed and this correlates with the severity of

retinopathy.[59–61] In an animal model of diabetes, the impairment of neurovascular coupling in the retina has been attributed to alterations in the NO signaling pathway since the response could be restored by inhibition of the enzyme inducible nitric oxide synthase (iNOS).[62,63] Such interactions can increase or decrease blood flow depending on local oxygen concentration, but how this switch occurs remains unclear.[62,64]

Mechanical Factors Involved in the Formation of Macular Edema

Clinical and anatomic evidence indicates that abnormalities in the structure of the vitreoretinal interface may play an important role in the pathogenesis of DME.[65–67]It was suggested that vitreoretinal adhesions in diabetic eyes are stronger than the shear forces of traction from vitreous shrinkage and this in turn may lead to the development of vitreomacular traction and subsequently to macular edema.[68] The risk of developing diffuse macular edema was 3.4-fold lower in the group of eyes with complete posterior vitreous attachment or complete vitreoretinal separation compared to the eyes with vitreomacular adhesion.[69]

The vitreous humor is a gel-like structure composed mostly of water (99%), hyaluronic acid, and collagen. A structural barrier between the vitreous cavity and the retina is formed by the internal limiting membrane (ILM), which is localized between the innermost layer of the retina and the outer boundary of the vitreous. The ILM shows typical ultrastructural characteristics of a basal lamina, is found in close contact with the foot processes of Müller cells, and contains proteins that are typically found in basal laminae such as collagen type IV and laminin.[70] Striated collagen fibrils of the vitreous cortex insert into the inner portion of the ILM,[71] which is also known as the hyaloid membrane of the vitreous. Detachment of the posterior hyaloid membrane with aging or pathology results in a condensation of the posterior vitreous surface (membrana hyaloidea posterior). In youth, there is adhesion between the vitreous cortex and the ILM that is stronger than Müller cells themselves and Müller cell foot processes become separated from their main cell body and remain connected to the posterior aspect of

the ILM when this is separated from the retinal surface.[72]

There has been a controversial discussion regarding the embryonic origin of the ILM, which can be demonstrated as early as 4 weeks after gestation in the human eye.[73,74] Traditionally, the ILM has been considered to be synthesized by Müller cells. This concept has been challenged by data presented from Sarthy and coworkers, who investigated the expression of collagen type IV during development of the mouse eye.[75] ILM proteins appear to originate largely from lens and ciliary body, although a contribution of retinal glial cells in ILM synthesis cannot be excluded. In support of this are data that show that also other ILM proteins such as perlecan, laminin-1, nidogen, and collagen XVIII are expressed predominantly in lens and ciliary body, but are not detected in the retina.[76]

Diffuse DME has been found in association with an attached, thickened, and taut posterior hyaloids.[77] As immunocytochemical staining for cytokeratin (found in RPE) and GFAP (found in astrocytes and Müller cells) demonstrated the existence of RPE and Müller cells or astrocytes in the premacular posterior hyaloid, it suggested a possible role for cell infiltration in the development or maintenance of macular edema. It remains to be elucidated whether these cells in the posterior vitreous cause macular edema physiologically rather than mechanically through the production of cytokines.

Fig. 30.11 is a schematic illustration of macular edema of different origins.

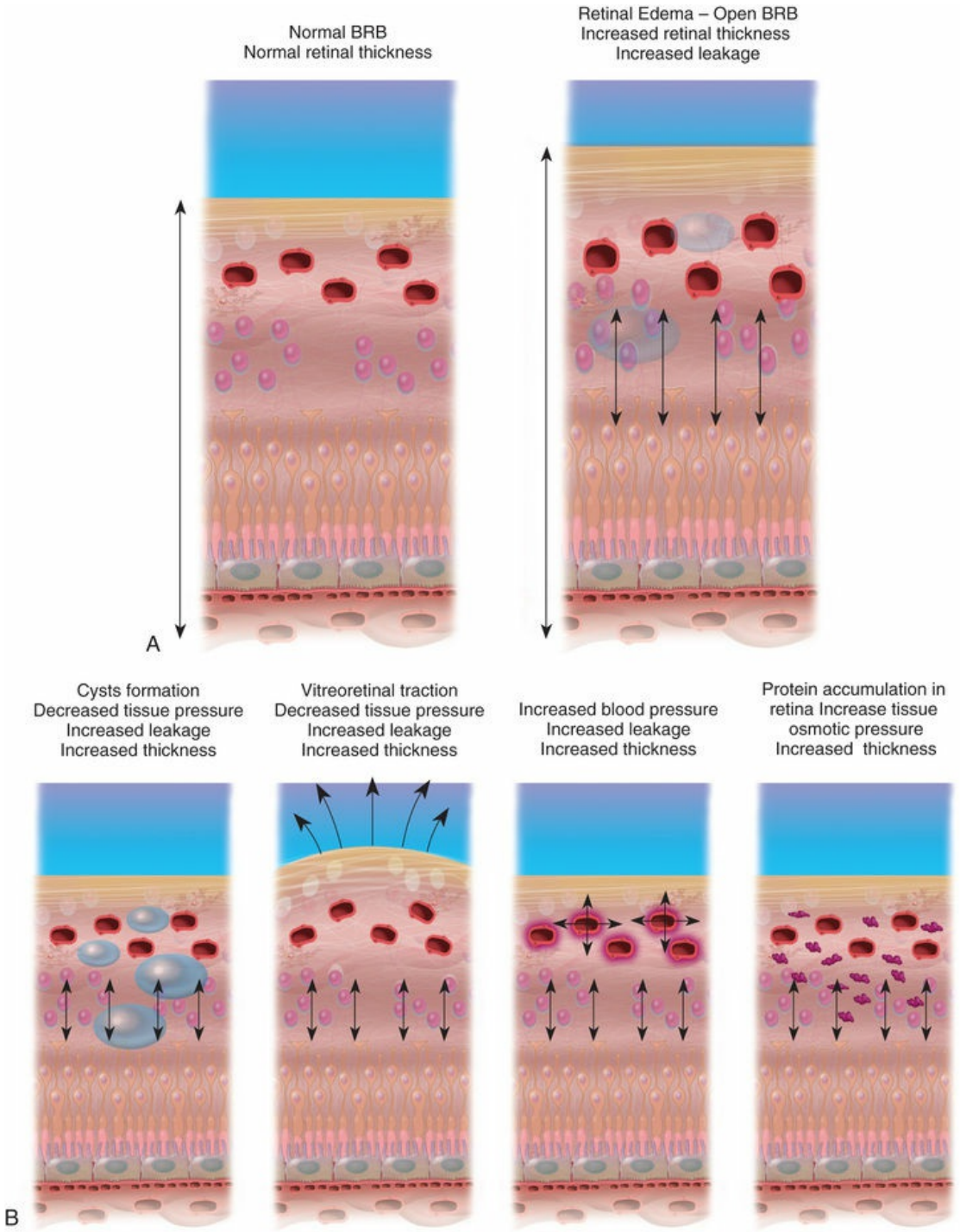

FIG. 30.11 (A) Schematic illustration of macular edema. *BRB*, blood–retinal barrier. (B) Pathophysiologic changes in macular edema of different origin.

Clinical Endpoints in Macular Edema

Best corrected visual acuity (BCVA) is the only endpoint that has

gained acceptance by regulatory and health technology agencies as being patient-relevant. BCVA, for example, has been used as primary outcome measure in all landmark clinical trials on new treatments for macular edema.[78–85]

However, BCVA alone does not provide a good indication of the visual function and potential restrictions patients may experience as a result of disease. Indeed, several eye disorders may adversely affect the visual function and the quality of life of individuals without impacting on BCVA. Furthermore, in certain diseases, BCVA is only affected once irreversible damage has taken place. Thus, new validated endpoints able to better capture functional deficits that affect and restrict patients as well as incipient changes related to early disease are needed. This may comprise distinct psychophysical tests, e.g., low luminance acuity, retinal sensitivity by microperimetry (photopic and scotopic) as a surrogate for topographic localization of retinal deficits.

Structural outcomes related to patient-reported outcomes or predictive of future functional loss and disease progression should be also sought. Besides an improvement of current imaging protocols (spectral domain optical coherence tomography SD-OCT) new approaches may include active eye-tracking technology. Phase variance OCT (PV-OCT) allows for volumetric imaging of the retinal vasculature of the eye. This novel approach, also referred to as OCT-angiography, has the added advantage of a noninvasive imaging technique not requiring potentially toxic contrast agents such as fluorescein, however not presenting vascular perfusion, but rather the outer vascular outlines. To overcome this problem and to better assess perfusion Doppler-OCT technology is currently being developed. Oximetry in diabetic retinopathy has extensively been reported.[86] Longitudinal data on oxygenation, perfusion, and oxygen extraction of the retina is currently lacking in diabetic retinopathy and is currently been generated. In the future, combination of Doppler-OCT with oximetry measures will allow determination of oxygen concentration and tissue metabolism as well as delineation of normoxic and hypoxic retina. All the above imaging technologies require validation and, in the context of macular edema, would need to demonstrate their value on this particular disorder.

Ideally, in order to identify the most adequate outcome measures, an integrated approach should be conducted, which should include a visual function and structural assessment, an evaluation of patients' perception of the impact of the disease in their daily living through patient reported outcomes (PROs), and, importantly, a study of molecular markers at the different stages of the disease process. Given the high output that such an approach would generate, a robust data management would be needed to allow integrating data of the individual patient and compare them with data from peer groups. To achieve this, a system medicine approach could be used which, by integrating all data generated, would allow improved characterization of disease phenotypes, better understanding of disease mechanisms, establishment of predictive models of disease progression and response to treatment. Advanced machine learning/statistics procedures need to be used to identify correlations between different parameters to gain insights into disease mechanisms and to identify and validate biomarkers: computational models of disease status within individual patients are required. For this reason object-oriented modeling systems, based on standard human pathway information, need to be adapted to the situation in the eye. As models become more complex and parameters become better defined, unknown mechanisms can be identified as systematic mismatches between prediction and measurement, accelerating progress in the identification of disease mechanisms, clinical endpoints, and biomarkers, revealing matches between different biomarkers that show relevance for prognosis of disease progression or susceptibility to treatment approaches.

Treatment of Macular Edema

The current therapy for macular edema targets conditions where mechanical traction, hydrostatic force, or inflammation play a pathogenetic role. Laser photocoagulation, pharmacologic approaches, and surgical measures are the most frequently used therapies.

Laser Treatment

Many studies have demonstrated a beneficial effect of photocoagulation therapy for DME.[87–92]

Traditionally argon laser photocoagulation was used to treat DME in an attempt to stabilize vision and prevent further visual loss. The Early Treatment of Diabetic Retinopathy Study (ETDRS) showed that laser treatment reduced the risk of moderate visual loss by 50% during 3 years of follow-up; however, only a small proportion of patients (<3%) experienced visual improvement of ≥15 letters.[88]

Recent randomized trials have shown that a much higher proportion (about 30%) of patients with DME can experience a clinically relevant (≥10 ETDRS letters) improvement in visual acuity following laser treatment. Thus, in a study conducted by the (US–Canadian) Diabetic Retinopathy Clinical Research network (DRCR.net), laser treatment for "center-involving DME" achieved gains of ≥10 letters in 32% of patients at 2 years.[93,94]

The probability of improvement was similar in naive eyes and those that had previously received ≥3 laser treatments. Similarly, in a more recently conducted study by DRCR.net, an improvement in visual acuity of ≥10 letters was observed in 28% of patients who had received laser treatment after one year.[85,95,96] Thus, it is clear that laser treatment can actually improve, not just stabilize, vision in some patients. Appropriate selection of patients, however, is required. It is likely that people with "thinner" retinas would respond better to laser treatment that those with "thicker" retinas, and thus, be clinically effective and cost-effective in the former, as suggested by the UK National Institute for Health and Care Excellence (NICE) Single Technology Assessments for anti-VEGF therapies.[97] There may be other factors that modulate clinical response; and ability to identify the "responders" in advance would be of great benefit to patients and to health services.

Laser treatment to areas of peripheral retinal ischemia, as determined by wide-angle fluorescein angiography, has been evaluated in small studies with good preliminary success (Tornambe PE, personal communication).

The exact mechanism of action of laser photocoagulation-induced resolution of DME still remains unknown. A laser-induced

destruction of oxygen-consuming photoreceptors has been discussed as well as cell death and scarring (involving gliosis and RPE hyperplasia) induced by the temporary raise in tissue temperature. Oxygen that normally diffuses from the choriocapillaris into the outer retina can now diffuse through the laser scar to the inner retina, thus relieving inner retinal hypoxia.[98,99] There are contrasting data whether an increased preretinal oxygen partial pressure is involved and allows for microvascular repair in the treated areas.[100,101]

When studying the diameter of retinal arterioles, venules, and their macular branches before and after macular laser photocoagulation in eyes with DME, the macular arteriolar branches were found to be constricted by 20.2% and the venular branches 13.8%. This was attributed to an improved retinal oxygenation caused by the laser treatment leading to autoregulatory vasoconstriction, improving the DME.[102]

According to another theory, the beneficial effect of laser photocoagulation is due to an enhanced proliferation of RPE and endothelial cells leading to a repair and restoration of the BRB.[103] RPE cells may respond to the injury in several ways: if the lesion is relatively small, the RPE defect can be filled by cell spreading; if the defect is relatively large, the cells can proliferate to resurface the area, and the RPE can produce cytokines (e.g., TGF-β) that antagonize the permeabilizing effects of VEGF.[104,105]

While focal laser coagulation reduces hypoxic areas and directly occludes leaky microaneurysms, the rationale for grid laser treatment in DME is not yet well established. Potentially, grid laser may have its beneficial effect by thinning the retina, bringing retinal vessels closer to choroidal vessels, permitting the retinal vessels to constrict by autoregulation, thereby decreasing retinal blood flow and consequently decreasing edema formation.[106] This theory, however, cannot be reconciled with the fact that current techniques used for focal/grid laser treatment for DME, including subthreshold laser (as opposed to what was used initially, which implied applying a much stronger laser) do not cause cell death. The effect of the laser can be observed even when damage is not detected by current imaging modalities including fundus autofluorescence imaging. Similarly, by using this milder form of treatment, reported

side-effects of laser, such as choroidal neovascularization (CNV) are no longer seen (Fig. 30.12). A lack of an effect of laser treatment in cases of diffuse edema, especially when causing large increases in retinal thickness, may occur (Fig. 30.13).

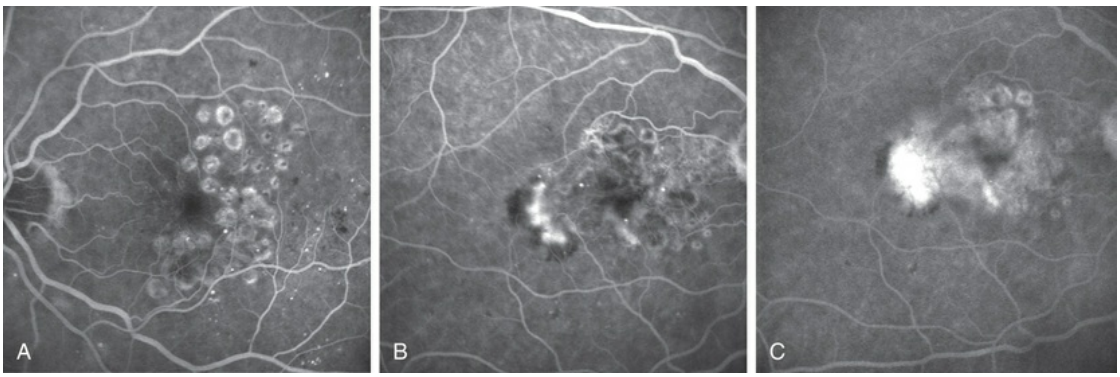

FIG. 30.12 (A) Complications after grid laser coagulation: enlarged central retinal pigment epithelial scars of the left eye, no obvious macula edema. (B) Early phase fluorescein angiography demonstrates choroidal neovascularization lesion growing from earlier photocoagulation scars at the right eye. (C) Late phase with increased leakage of fluorescein.

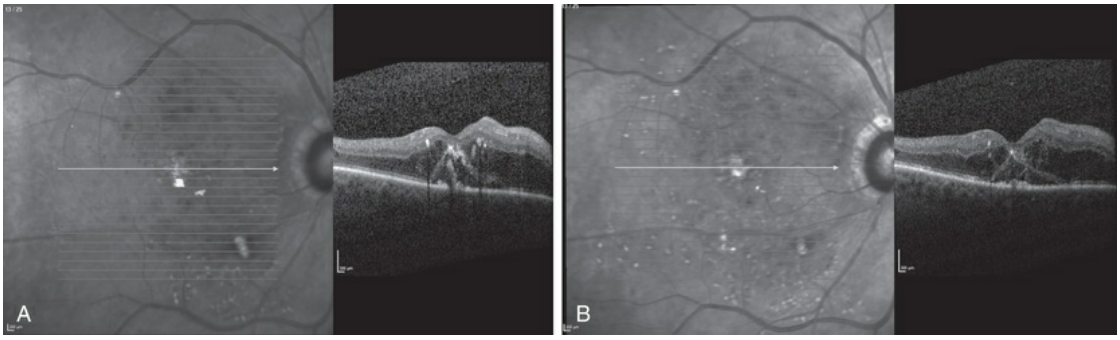

FIG. 30.13 (A) Grid laser treatment in persistent diffuse diabetic macular edema has limited effects. (B) The optical coherence tomography imaging demonstrates no difference in retinal thickness prior to and 3 months after grid laser treatment.

Medical Treatment

General Aspects of Systemic and Topical Medical Therapy

In many cases, macular edema is caused by a generalized health problem such as diabetes, high blood pressure or inflammatory conditions.[107] These systemic diseases need to be treated prior to undertaking any other therapeutic measures. There have been several reports in the literature that such treatments – particularly in diabetes, high blood pressure, and inflammatory diseases – can cure macular edema without any additional specific ocular treatment.[108]

Modification of the systemic blood flow including hyperbaric oxygen treatment is thought to alter blood flow via vasoconstriction, and facilitates the reformation of damaged junctional complexes in the vessel wall. However, despite an improvement in visual acuity in patients with chronic CME after cataract extraction, there was no correlation to macular edema.[109] In uveitis-associated CME hyperbaric oxygen had no significant effect. Other rheologic treatments, such as plasma membrane filtration, demonstrated good effects in initial studies; however, these treatments did not enter large-scale prospective studies.[110] Still there is no evidence that rheologic measures have any effect on inflammatory macular edema or DME.

Medical treatment of macular edema so far is best established in postsurgical and predominantly inflammatory edema, e.g., in uveitis, but gaining importance in the treatment of DME. The majority of the therapeutic strategies inhibit the release of inflammatory mediators and therefore target the pathogenetic factors responsible for the altered vascular permeability.

Medical treatment for macular edema consists of therapeutic agents that are collectively categorized into four groups: carbonic anhydrase inhibitors, nonsteroidal antiinflammatory drugs, corticosteroids, and anti-VEGF therapies.

Carbonic Anhydrase Inhibitors

Carbonic anhydrase (CA) inhibitors have been used clinically for over 20 years in the treatment of macular edema. The initial observation on its therapeutic efficacy was reported in 1988 in a

study of 41 patients with CME of various etiologies.[111] The rationale of CA inhibitors as a therapeutic agent in the treatment of macular edema is to improve the ability of the RPE to pump fluid out of the retina by modulation of the polarized distribution of CA at the level of the RPE.[112]

In the retina, CA is found in the cytoplasm of red/green cones (albeit not in rods) and especially inside Müller cells. The RPE, however, appears to contain almost exclusively the membrane-bound form of CA.[113] The latter appears to regulate and modulate the extracellular pH gradients created by the metabolic activity of cells and may act as a bicarbonate channel.[113,114] The CA activity in the RPE shows a clear-cut polarized distribution with a large amount of enzyme on the apical surface of the cell, whereas there is less CA activity on the basolateral portion of the cell membrane.[115] Further immunohistochemical differentiation has shown the isozyme IV is responsible for apical CA activity in the RPE.[113] Intravenous injection of acetazolamide has been shown to decrease the pH in the subretinal space in both chicks and cats.[113,116] This acidification was followed immediately by a reduction of the subretinal volume, and it has been postulated that it is the acidification that induces changes in ion and consequent fluid transport through the RPE[115] (Fig. 30.14).

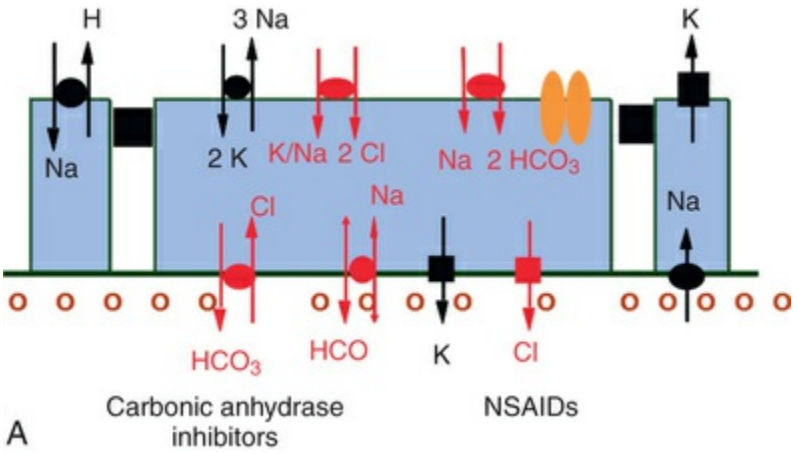

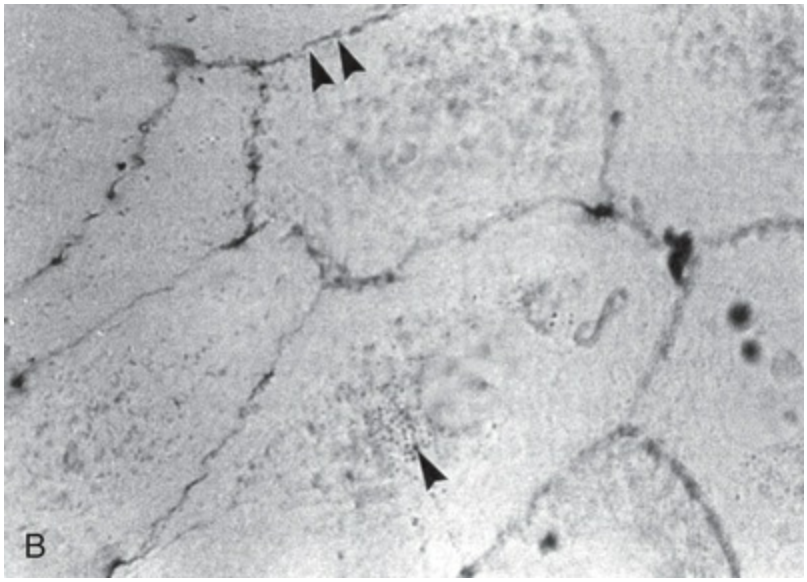

FIG. 30.14 (A) Schematic diagram showing selected ion channels in the retinal pigment epithelium. Note that carbonic anhydrase inhibitors act on the bicarbonate/chloride exchange channel in the basal membrane, and nonsteroidal antiinflammatory drugs (NSAIDs) have been shown to act on the chloride channel in the basal membrane of the retinal pigment epithelium. Both channels are associated with transcellular fluid transport. (B) Membrane-bound carbonic anhydrase (CA IV) 55 kDa.

Under normal conditions, roughly 70% of the subretinal fluid is removed by metabolic transport to the choroid. In an in vivo rabbit model, this fluid transport, which is driven to a large extent by active ion transport through the RPE, can be enhanced by acetazolamide.[117,118] Furthermore, experiments in an animal model of iatrogenically induced retinal detachments showed that the disappearance of fluorescein through the RPE increased by 25% after intravenous injection of acetazolamide.[119] The same authors also observed a marked increase in resorption of subretinal fluid at a higher dosage of 50–65 mg/kg body weight. Further studies on the frog RPE demonstrated that active chloride and bicarbonate transport probably occurs at the basal surface, which faces the choroidal blood supply, and it was postulated that subretinal fluid absorption occurs at this level.[114]

Currently, there are no randomized clinical trials available, confirming the beneficial effect of CA inhibitors in the treatment of macular edema. However, evidence from nonrandomized studies

suggests improved visual function in patients with postsurgical macular edema (e.g., after cataract surgery or buckling procedures) following this therapy.[111,120] The effect lasts only as long as the patient takes the drug (on–off-effect, tachyphylaxis).[120] Similarly, the favorable reports that were described regarding the application of CA inhibition in patients with macular edema secondary to retinitis pigmentosa are not supported by long-term observations. With the continuous use of methazolamide a rebound phenomenon is observed, but might also be attributed to disease progression.[121]

While there is no indication for the application of topical CA inhibitors (e.g., dorzolamide) for prophylaxis or treatment of macular edema, the systemic treatment with CA inhibitors is worthwhile when the edema is proven to come from the RPE (as determined by stereoangiography). Contrary to tenacious clinical habit, the use of CA inhibition for intraretinal macular edema as a result of inner blood–retinal barrier breakdown is not based upon scientific evidence to date. The use of CA inhibitors for diabetic macular edema is not recommended.

Nonsteroidal Antiinflammatory Drugs (NSAIDs)

As cyclooxygenase inhibitors block the synthesis and release of prostaglandins, nonsteroidal drugs have been investigated in the prophylaxis and therapy of postsurgical CME. The action is based on the inhibition of the enzyme cyclooxygenase, which in turn inhibits the production of prostaglandins, a degradation product of arachidonic acid in the eye.[122] Diclofenac sodium in high doses inhibits the formation of leukotrienes, which amplify cellular infiltration during an inflammatory reaction. Other NSAIDs have been shown to modulate chloride movement, and, as a consequence, fluid movement through the RPE.[123] The effect of COX-inhibitors on inflammatory aspects of DME was only demonstrated in preclinical studies[13] (Fig. 30.15).

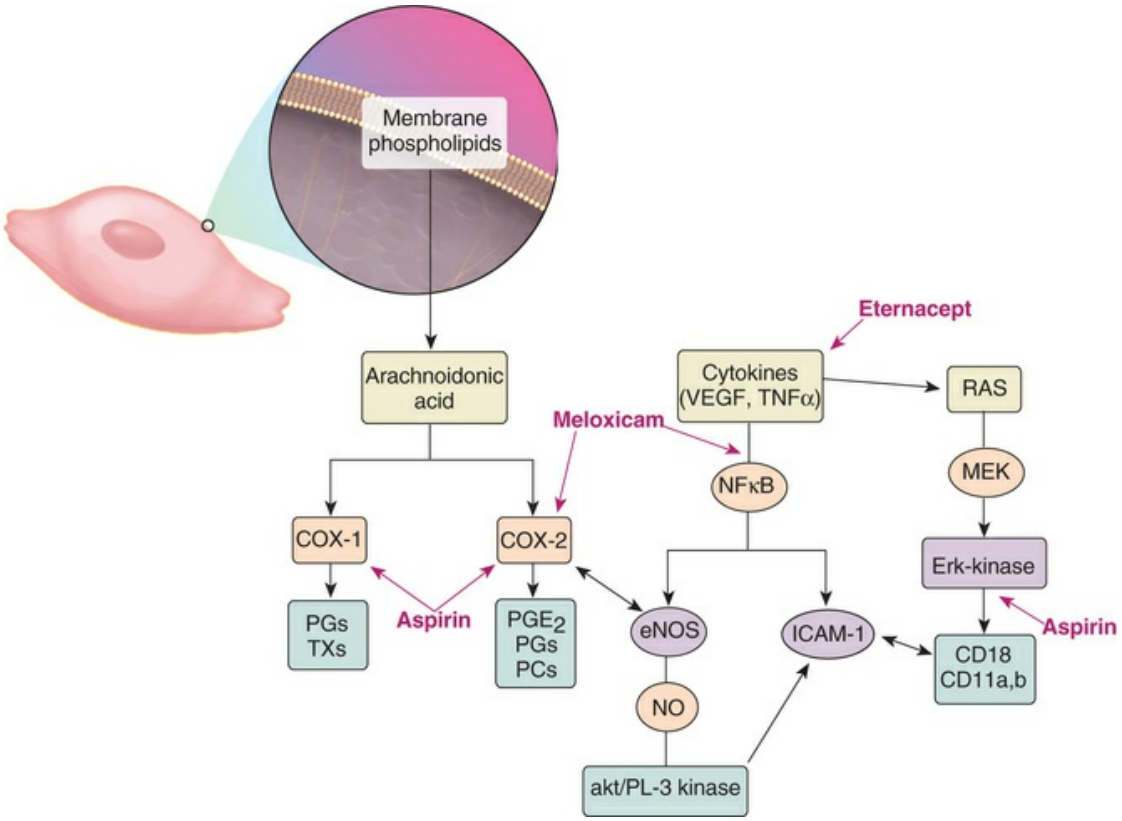

FIG. 30.15 Interaction of nonsteroidal antiinflammatory drugs with vascular endothelial growth factor (VEGF) and inflammatory cytokines and their signaling pathways.

Thus, NSAIDS target the inflammatory mediators that are responsible for the edema formation, and although they may not be an optimal stand-alone treatment, they can be used as steroid-sparing agents. Topical NSAIDs have become the mainstay in the treatment of inflammatory CME.[124] The clinical efficacy of topical NSAIDs has been shown to be of value both in the prevention[125–127] and in the treatment[128,129] of inflammatory CME, particularly when related to cataract surgery. Two double-masked, placebo-controlled studies in which corticosteroids were not used demonstrated that ketorolac 0.5% ophthalmic solution, administered for up to 3 months, improves vision in some patients with chronic CME after cataract surgery.[130,131] A meta-analysis of the results from several randomized controlled trials (RCTs) suggested that NSAIDs are beneficial as a medical prophylaxis for aphakic and pseudophakic CME and as medical treatment for chronic CME.[132]

On the basis of these findings, it has been suggested to employ topical NSAIDs in the treatment of inflammatory CME, especially

when related to ocular surgery. This effect is independent of the presence of DME.[133]

There may be several explanations for why NSAIDs are unlikely to improve vision in DME, such as chronic edema, inflammation, and ischemia that induce permanent structural alterations. Although effects on diabetic vascular leakage were achieved in preclinical studies,[13] there is so far no evidence for an effect of NSAIDs in DME. A recent Cochrane review did not identify any RCTs investigating the effects of topical NSAIDs in the treatment of diabetic CME.[133] The review has identified the need for well-designed, adequately powered RCTs that should aim to include a large sample size with an adequate follow-up period of up to one year.[134]

Corticosteroids

Steroids are currently regaining attention for the treatment of various forms of macular edema. Corticosteroids block the release of arachidonic acid from cell membranes by inhibiting the enzyme cyclooxygenase and thus reduce the synthesis of prostaglandins, but they also have a multitude of other antiinflammatory effects by acting, among others, on IL-1 and by reducing vascular permeability[135] (Fig. 30.16A). Their additive antiinflammatory effect to NSAIDs has been shown to be useful in the treatment of various postoperative inflammatory conditions. One potential mode of action is the increased resorption of fluid through the RPE, although the exact mechanism of this is not as yet clear. Steroids specifically stabilize endothelial tight junctions and increase their numbers.[136,137] Another action of steroids is the downregulation of the production of the VEGF, which, in turn, renders the BRB tighter (Fig. 30.16B). Steroids also downregulate VEGF production,[138] specifically in the retina,[139,140] and this explains the clinical observation that the application of steroids both intravitreally and into the sub-Tenon space can reduce macular edema considerably. Furthermore, steroids have been shown to prevent the induction of VEGF production by platelet-activating factor and platelet-derived growth factor.[141] Triamcinolone also inhibits IL-6- and VEGF-induced angiogenesis downstream of the IL-6 and VEGF receptors.[142] Leukocyte adhesion plays an important role in macular

edema – particularly so in diabetic maculopathy.[11,12] The endothelial damage resulting from this leukocyte adherence to vessel walls is mediated by nitric oxide, adhesion molecules, and other inflammatory mediators.[22,143] Sub-Tenon triamcinolone inhibits leukocyte-endothelium interactions in the retina and downregulates adhesion molecules of retinal vascular endothelium[144] and thus decreases the retinal thickness.

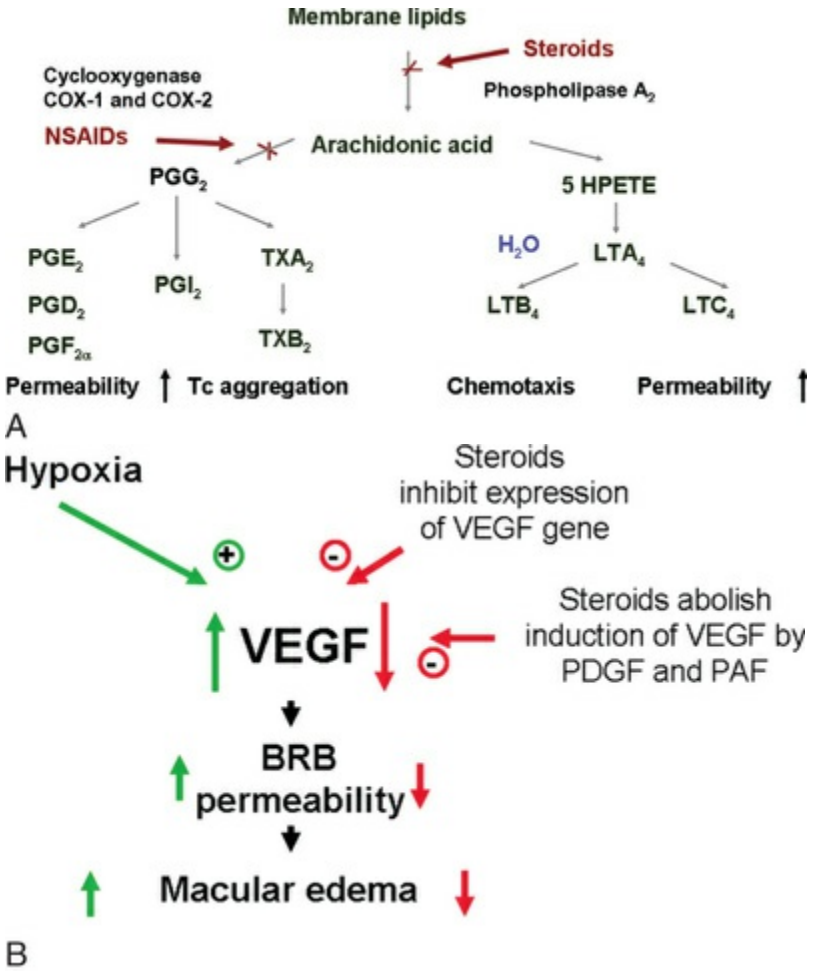

FIG. 30.16 (A) Action of steroids on arachidonic acid. (B) Action of steroids on growth factor release. *BRB*, blood–retinal barrier; *PAF*, platelet-activating factor; *PDGF*, platelet-derived growth factor; *VEGF*, vascular endothelial growth factor.

The Müller cells represent a further site of action of steroids.[145] Macular edema is thought to be partly linked to the downregulation of the Müller cell protein Kir4.1.[145] The resultant

increase in intracellular K+ leads to the uptake of proteins and osmotic swelling of the Müller cells via aquaporin 4 channels. The administration of triamcinolone reduces the production of VEGF, arachidonic acid, and prostaglandins, allowing the reactivation of fluid clearance by Müller cells via endogenous adenosine and an increase in TWIK-related acid-sensitive potassium (TASK) channels. These processes lead to an efflux of potassium thus correcting the downregulation of the Kir4.1 protein.[145]

Corticosteroids have different potency levels depending on their chemical composition,[146] and the newer synthetically produced compounds show an up to 25-fold increase in activity, as compared to cortisone. These new agents, such as triamcinolone, dexamethasone, and fluocinolone acetonide, have fluor at the 9α position, which increases corticosteroid receptor binding. Routes of clinical administrations are manifold, including topical, periocular, intraocular, oral, and intravenous routes. Sub-Tenon injections of corticosteroids are widely used in patients with asymmetric or unilateral uveitis. The advantages of the periocular injections are high concentrations of corticosteroids in the posterior segment of the eye, and reduction of the adverse effects compared to systemic administration. Intraocular levels of corticosteroids are identical between sub-Tenon and retrobulbar administration.[147] For oral administration, the initial high dose (1–1.5 mg/kg) is subsequently decreased according to clinical effect.[148]

Another therapeutic option is the administration of steroids as intravitreal injections or sustained release implants in order to obtain high local concentrations, maximizing their antiinflammatory, angiostatic, and antipermeability effects while minimizing systemic toxicity.[149]

Depending on the cause of the macular edema, local or systemic routes may be chosen (e.g., in posterior uveitis, systemic steroids may be required to control the systemic inflammation whereas in macular edema secondary to vein occlusion local therapies may be more appropriate).

Several randomized trials have evaluated the use of fluocinolone, dexamethasone, and triamcinolone in patients with DME and vein occlusion, as summarized below.

Triamcinolone.

Triamcinolone is a corticosteroid which can be delivered by intravitreal bolus injection. It has been widely used in macular edema of various origins including DME and edema secondary to vein occlusion. For DME, there have been several randomized trials comparing triamcinolone with laser; none showed benefit of triamcinolone. However, as stated below (see anti-VEGF section, ranibizumab) subgroup analysis of the DRCR.net demonstrated similar gains in pseudophakic eyes in patients with DME receiving triamcinolone to those observed in patients receiving ranibizumab.[150]

Furthermore, in this group, triamcinolone appeared to be cost-effective when compared with ranibizumab.[151] The use of currently available triamcinolone formulations, however, has not been licensed for intraocular use. Despite not being licensed, triamcinolone is still used in postsurgical CME that does not respond to NSAIDs although there is no RCT evidence supporting this use.

Fluocinolone.

Fluocinolone acetonide is delivered intravitreally as a sustained release implant (Iluvien, Alimera Sciences). It is a small intravitreal implant for DME. The efficacy of this fluocinolone acetonide implant was assessed in two randomized, multicenter, double-masked, parallel, 36-month clinical trials in patients with DME. There were 956 patients in the "Fluocinolone Acetonide for Diabetic Macular Edema" studies which compared fluocinolone acetonide with sham control.[152]

As in RISE and RIDE (see below), despite the fact that the standard of care treatment for DME at the time this trial was initiated was laser (focal/grid) photocoagulation, the fluocinolone comparator arm was sham. "Rescue laser" was allowed after week 6 and retreatments could be performed after month 12. At 3 years, ~28% of patients gained ≥15 in letters in the fluocinolone group compared with 18.9% in the sham group. The benefit doubled in patients who reported duration of DME ≥3 years at baseline. Almost all phakic patients in the fluocinolone acetonide insert groups developed cataract, but their visual benefit after cataract

surgery was similar to that in pseudophakic patients. Rescue laser was required in ~37% of patients in the fluocinolone group and 60.7% in the sham. As anticipated, in phakic eyes cataract surgery extraction rates were found to be 80% in the fluocinolone group vs. 27.3% in the sham group. In the overall clinical trial population (excluding subjects with baseline IOP>21 mmHg), the proportion of fluocinolone-treated subjects requiring treatment with IOP-lowering drops was 38% compared to 14% in the sham-treated group. The incidence of incisional glaucoma surgery at month 36 was 4.8% in the low-dose group and 8.1% in the high-dose insert group.

The microimplant has been approved in 17 European countries as well as in the United States. In the UK, NICE has recommended the use of fluocinolone in pseudophakic patients with DME that show an insufficient response to other medications.[153] In Germany fluocinolone acetonide is indicated for treating DME in patients "who are insufficiently responsive to first line therapy."

Fluocinolone acetonide has been used for the treatment of uveitis[154,155] as well as vein occlusion.[155] Data on Iluvien from RCTs in these indications are still pending. Similar to Ozurdex (see below), there is evidence that Iluvien is of value to vitrectomized patients as the release is independent of the presence of the vitreous.[156]

Dexamethasone.

Dexamethasone has the highest relative strength of any corticosteroid used in ophthalmic practice. Dexamethasone (Ozurdex; dexamethasone 700 μg intravitreal implant, Allergan), is a commercially available implant which can be delivered to the vitreous cavity by means of an injectable device.[157]

It is approved in most European countries and the United States for the treatment of DME, macular edema secondary to posterior uveitis and vein occlusion.

There were two initial studies assessing the efficacy of dexamethasone implants for DME; one compared two doses of dexamethasone with no treatment; the other compared an unspecified dose of dexamethasone vs. dexamethasone plus laser vs. laser alone.[158,159]

Both studies found dexamethasone gave an improvement in visual acuity, regressing to baseline after 3 months. Cataract and raised intraocular pressure were the main side-effects. In October 2014, members of the MEAD (Macular Edema: Assessment of Implantable Dexamethasone in Diabetes) study group published the results of their 3-year, randomized, sham-controlled trial of dexamethasone intravitreal implant (DEX) in patients with DME.[160]

The mean number of treatments given over 3 years was 4.1, 4.4, and 3.3 with DEX implant 0.7 mg, DEX implant 0.35 mg, and sham, respectively. The percentage of patients with ≥15-letter improvement in best corrected visual acuity (BCVA) from baseline at study end was greater with DEX implant 0.7 mg (22.2%) and DEX implant 0.35 mg (18.4%) than sham (12.0%; $p \leq .018$). The study also reported a greater mean average reduction in central retinal thickness (CRT) from baseline in both the 0.7 mg and 0.35 mg dexamethasone implant compared to sham. As with all steroid compounds, the rates of cataract-related adverse events in phakic eyes were higher in the dexamethasone groups (threefold) when compared to those in the sham arm. The investigators stated that increases in IOP were usually controllable with medication or no therapy within the 3 years. In the UK NICE has recently approved the use of the dexamethasone intravitreal implant for DME in eyes with an artificial lens (pseudophakic) where other treatments were ineffective or not suitable.[161]

The Geneva Study assessed patients with macular edema secondary to branch or central retinal vein occlusion receiving DEX implant 0.7 mg (n=421), DEX implant 0.35 mg (n=412), or sham (n=423) in the study eye. At day 180, patients could receive DEX implant 0.7 mg if BCVA was <84 letters or retinal thickness was >250 μm. Single and repeated treatment with DEX implant had a favorable safety profile over 12 months. A ≥15-letter improvement in BCVA from baseline was achieved by 30% and 32% of patients 60 days after the first and second DEX implant. The IOP increases were usually transient and controlled with medication or observation; an additional 10.3% of patients initiated IOP-lowering medications after the second treatment.[162]

The slow release effect of Ozurdex is independent of the presence of the vitreous and clinical findings do not differ between

nonvitrectomized and vitrectomized eyes[163] (Fig. 30.17 online).

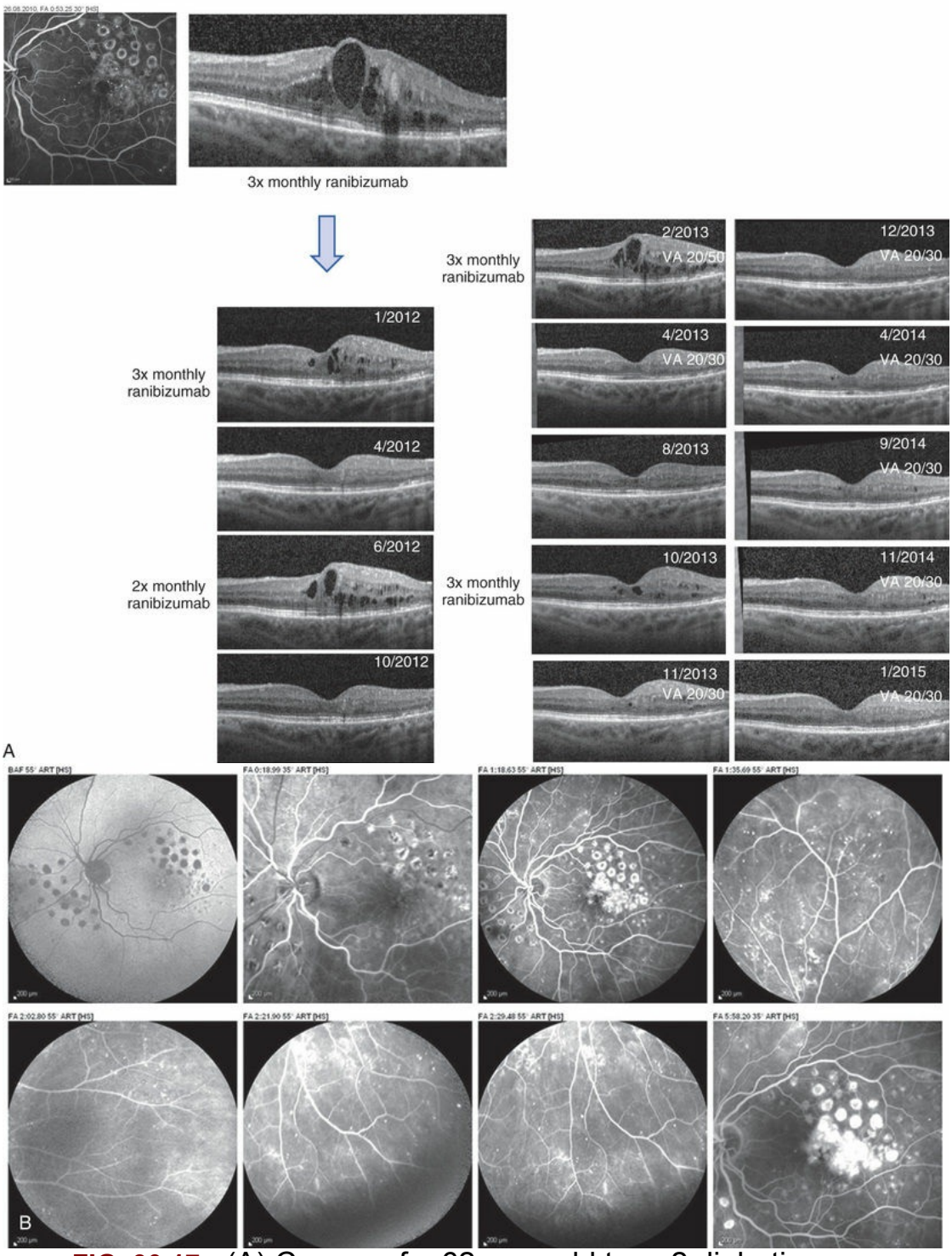

FIG. 30.17 (A) Course of a 62-year-old type 2 diabetic patient. Insulin therapy since 2004; HbA1c 7.2, hypertension. Medication: insulin, enalapril, statin, aspirin. All horizontal scans of the left eye. During 3 years, 15 injections with ranibizumab. Finally stable

situation over 18 months after last injection. (B) Angiogram of the patient in panel A demonstrating few areas of capillary nonperfusion in the midperiphery, but no proliferation.

Antiangiogenic Treatment

Several clinical trials have assessed the effectiveness of anti-VEGF therapies, including bevacizumab, ranibizumab, and aflibercept, for the treatment of DME and edema secondary to vein occlusion. Anti-VEGFs are administered by intraocular (intravitreal) injection. A summary of the evidence available from the largest trials on these therapies is provided below.

Ranibizumab.

Ranibizumab (Lucentis, Novartis Europharm Limited, Camberley, UK) is a recombinant humanized IgG1 kappa isotype monoclonal antibody fragment (Fab) designed for intraocular use. It binds to and inhibits the biologic activity of human VEGF-A. It has a half-life of approximately 9 days.

RESTORE randomized 354 patients with "center-involving DME" to receive one of the three following treatments: ranibizumab (0.5 mg) + sham laser, ranibizumab (0.5 mg) + laser, or sham injection + laser. Participants in the ranibizumab arms had a minimum of three monthly injections, after which injections were continued until stable BCVA or BCVA of 6/6 was achieved on two consecutive visits. Treatment was reinitiated if VA decreased due to recurrence of DME. The primary outcome was mean average change in VA from baseline to months 1–12.[164]

After one year, there was a greater gain in BCVA in the ranibizumab groups (37% and 23% of patients with ≥10 and ≥15 letter gain, respectively, in the ranibizumab + sham laser arm; and 43% and 23% of patients with ≥10 and ≥15 letter gain, respectively, in the ranibizumab + laser arm) than in those receiving laser only. The median number of injections was seven.

In the RISE and RIDE trials, patients were randomized to one of three arms: ranibizumab 0.3 mg monthly, ranibizumab 0.5 mg monthly, or sham injection. Monthly treatments with ranibizumab

were given for the whole duration of the study (24 months). "Rescue" laser was allowed, but there was not an active laser arm, despite the fact that laser was the standard of care for eligible patients when the studies were initiated. In RISE and RIDE, 377 and 382 patients were randomized, and the primary outcome of both trials was the percentage of patients with a ≥15 letters gain at 24 months.[165]

The trial showed that ~45%, 40%, and 18% of patients in the 0.3-mg ranibizumab, 0.5-mg ranibizumab, and sham arms, respectively, gained ≥15 letters. Also, in patients receiving ranibizumab, there was less retinopathy progression. Interestingly, "rescue" laser was required in ~40% of patients in the 0.3-mg ranibizumab arm and ~35% in the 0.5-mg ranibizumab arm, suggesting that in these patients, monthly ranibizumab injections were not sufficient to control DME. Laser treatment was also given to 74% of patients in the sham group; thus, 26% of patients appear not to have received any treatment.

In a randomized trial conducted by the Diabetic Retinopathy Clinical Research Network patients with "center-involving DME" were randomized to one of four arms: sham injection + prompt laser; ranibizumab (0.5 mg) + prompt (3–10 days after injection) laser; triamcinolone (intraocular) + prompt laser; or ranibizumab (0.5 mg) + deferred (≥24 weeks after injection) laser. The study included 691 patients (854 eyes). Intravitreal injections of ranibizumab (or sham) were given monthly through the first 12 weeks of the study; from Week 16 onwards a complex algorithm for retreatment was used. The primary outcome was the mean change in BCVA from baseline to year 1. At 1 year a significant gain in BCVA was achieved in the ranibizumab + prompt and deferred laser arms vs. the non-ranibizumab groups ($p<.001$), with ~50% of patients experiencing ≥10 letter gain and ~30% of patients achieving gains of ≥15 letter after a median of 8–9 injections. This occurred even though a high proportion of cases (72% of eyes) in the deferred laser group did not receive any laser.[150] It should be noted, however, that although at 1 year only 28% of patients in the deferred laser group had received laser, this percentage increased to 42% at 2 years and 46% at 3 years suggesting that, in a considerable number of patients, ranibizumab alone did not

suffice.[166]

A meta-analysis of these studies undertaken by Ford et al. concluded that ranibizumab improved results obtained with laser alone, considering both mean change in BCVA and the proportion of patients with ≥15 letter gain. Surprisingly, there was no benefit of adding laser to ranibizumab by either of these outcome measures.[167]

Several studies have demonstrated the value of ranibizumab in vein occlusion. A meta-analysis by the Cochrane group of the available RCT evidence suggests that repeated treatment of nonischemic macular edema secondary to branch retinal vein occlusion (BRVO) with the anti-VEGF agent ranibizumab may improve clinical and visual outcomes at 6 and 12 months. However, the frequency of retreatment has not yet been determined, and the impact of prior or combined treatment with laser photocoagulation on the primary outcome is unclear.[168]

A posthoc analysis of the two phase III clinical trials conducted for vein occlusion demonstrated the relevance of OCT as a predictive measure for early versus late or incomplete ranibizumab response. Among ranibizumab-treated patients, 71.2% (0.3 mg) and 78.5% (0.5 mg) in the CRUISE study and 79.1% (0.3 mg) and 84.7% (0.5 mg) in the BRAVO study had central foveal thickness (CFT) of 250 μm or less at month 3 and therefore were categorized as early ranibizumab responders. Visual outcome at months 6 and 12 was reduced in 0.5 mg ranibizumab-treated patients with central retinal vein occlusion (CRVO) who had persistent CME at month 3. It also was reduced in CRVO for those with CFT of more than 250 μm at month 3 who were treated with 0.3 mg ranibizumab. This suggests that late or incomplete responders do need careful follow-up.[169]

Currently several RCTs are ongoing that determine the use of ranibizumab in macular edema of other origin including radiation retinopathy.

Bevacizumab.

Bevacizumab (Avastin, Genetech Inc., San Francisco, CA) is a full-length humanized antibody that binds to all types of VEGF and is used successfully in cancer therapy as a systemic drug. Despite its widespread use for intravitreal therapy around the world, it is not licensed for this application.

Its potential usefulness in DME was tested in the BOLT trial, in which patients were randomized to receive bevacizumab or laser.[170]

BOLT was a small RCT that included 80 patients; people with macular ischemia were excluded because they were considered unsuitable for laser treatment. Laser was performed according to the modified ETDRS criteria; focal or grid laser treatment for DME was applied to treat all leaking microaneurysms in areas of retinal thickening or to areas of edema or nonperfusion (based on fluorescein angiography) located at least at 500 μm from the fovea (only rarely is treatment applied closer) in order to obtain mild "gray" burns. Bevacizumab was given every 6 weeks until week 18, after which it was continued until retinal status was considered stable if the central retinal thickness was >270 μm. The main outcome measure was BCVA at 1 year.[170]

A greater gain in BCVA was observed in the bevacizumab vs. laser arm, with 31% and 12% of patients having a ≥10 letter and ≥15 letter gain, respectively, following bevacizumab, compared with 5% and 8% following laser. The median number of injections required was nine. Interestingly, in this trial, success of laser treatment was much lower than that observed in the ranibizumab studies described above. Similarly, studies demonstrating a long-term benefit of bevacizumab in vein occlusions have been published.[171]

Head-to-head trials for age-related macular degeneration (AMD) demonstrated similar effects on visual acuity for both ranibizumab and bevacizumab over extended periods.[172–174]

It is likely there is no difference in the effectiveness and safety profile when used for the treatment of macular edema. This is supported by recently published systematic reviews. Compared to no treatment, repeated intravitreal injection of anti-VEGF agents (ranibizumab, aflibercept, and bevacizumab) in eyes with CRVO and macular edema improved visual outcomes. All agents were relatively well tolerated, with a low incidence of adverse effects in the short term; however, the number of injections differed slightly among the different anti-VEGF agents.[175,176]

Aflibercept.

Aflibercept (Eylea, Regeneron-Bayer HealthCare) is the most recent addition to the anti-VEGF family of drugs. It is a fully human

recombinant fusion protein designed to bind all isoforms of VEGF-A as well as placental growth factor (PlGF), thereby inhibiting the activation of VEGF receptors.

Its suitability and efficacy in treating DME was assessed in the DA VINCI trial[177,178] and in the VISTA and VIVID trials.[81] The 221 patients in the DA VINCI trial were randomized to either laser only or to one of four regimens of intravitreal aflibercept; 0.5 mg every 4 weeks; 2 mg every 4 weeks; 2 mg every 4 weeks for 3 months then every 8 weeks; 2 mg every 4 weeks for 3 months, then PRN ("as needed"). The mean change in BCVA at 6 months (primary outcome) demonstrated superior visual gain in all aflibercept arms compared to laser.[13] The ≥10 letters gain was highest in the 2-mg-every-4-weeks subgroup, at 64%, whereas the 0.5-mg-every-4-weeks group demonstrated 34% of patients gaining ≥15 letters. After one year, data from 79% of patients were available and showed that the 6-month gain of ≥10 letters in the 2-mg-every-4-weeks group had risen to 71 %. This group also had the highest percentage of patients with ≥15 letters gain; this gain compared to 30% and 11% gain of ≥10 letters and ≥15 letters, respectively, in the laser arm at this time point.[86]

A total of 872 patients (eyes) with type 1 or type 2 diabetes mellitus and "center-involving DME" were randomized to receive intravitreal aflibercept injection (IAI) 2 mg every 4 weeks (2q4), IAI 2 mg every 8 weeks after five initial monthly doses (2q8), or to macular laser photocoagulation. The primary outcome was the change from baseline in BCVA at one year. The proportion of eyes gaining ≥15 letters was 41.6% and 31.1% vs. 7.8% in VISTA, and 32.4% and 33.3% vs. 9.1% in VIVID in the 2q4, 2q8 vs. laser arms, respectively. The mean reduction in central macular thickness was also significantly greater in the two IAI arms. The study concluded that IAI demonstrated significant superiority in functional and anatomic endpoints over laser, with similar efficacy in the 2q4 and 2q8 groups.

Similarly there is data demonstrating the effectiveness of aflibercept in retinal vein occlusion. The Galileo study is the phase III trial investigating patients with CRVO receiving either 2 mg intravitreal aflibercept or sham injections every 4 weeks for 20 weeks. At week 52, the mean percentage of patients gaining 15

letters or more was 60.2% in the aflibercept group and 32.4% in the sham group.[83,179]

The mean central retinal thickness in DME eyes treated with anti-VEGFs was high (405 μm DRCR.net; >460 μm RISE and RIDE; 412–426 μm RESTORE; >479 μm VISTA and VIVID). As evidence suggests that patients with central retinal thickness of less than 400 μm appear to be the best candidates for laser, the high central retinal thickness in RCTs of anti-VEGF could have potentially favored anti-VEGF groups.

The VIBRANT study represents the pendant in branch vein occlusion: a total of 183 patients received either 2 mg intravitreal aflibercept injection every 4 weeks from baseline to week 20 or grid laser at baseline with a single grid laser rescue treatment, if needed, from weeks 12 through 20. The mean improvement from baseline BCVA at week 24 was 17.0 ETDRS letters in the intravitreal aflibercept group and 6.9 ETDRS letters in the laser group.[180]

Other Medical Treatments

There are several active areas of investigation in the DME research field. These include novel therapies and potential new biologic targets.

Steroid-sparing immunosuppressive drugs are frequently used as additional, second-line agents, particularly in patients with severe intraocular inflammation and CME.[2] The rationale for these treatments relies on the inhibition of several different proinflammatory cytokines, which are specifically involved in causing macular edema by breaking down the BRB in intraocular inflammatory disorders.

Apart from the well-known agents such as VEGF, prostaglandins, and leukotrienes, these cytokines also include insulin-like growth factor 1, IL-6, stromal cell-derived factor 1, and hepatocyte growth factor. Particularly elevated levels of intraocular VEGF and IL-6 have been correlated with the severity of uveitic macular edema[181] and treatments directed specifically against these factors have been proposed.

Promising results have also been reported using interferon $\alpha 2$[182] as a treatment for long-standing refractory CME in uveitis. In addition, a beneficial effect of interferon on inflammatory CME was

noted in a retrospective study of patients with multiple sclerosis-associated intermediate uveitis.[183] Others reported comparable efficacy of cyclosporine A to prednisolone in the treatment of macular edema in patients with endogenous uveitis.[184] Anti-TNF therapy has also been demonstrated as a promising therapy for uveitic macular edema.[185] Somatostatin analogs such as octreotide may also be effective in the treatment of CME by blocking the local and systemic production of growth hormone, insulin-like growth factor, and VEGF.[186] Treatment with octreotide resulted in marked improvement, or even complete resolution of CME in uveitic patients.[187] Similarly, Ca-Dobesilate prevents the BRB breakdown induced by diabetes, by restoring tight-junction protein levels and organization and decreasing leukocyte adhesion to retinal vessels. The protective effects of Ca-Dobesilate is likely to involve the inhibition of p38 MAPK and NF-κB activation, possibly through the inhibition of oxidative/nitrosative stress.

A major goal of treating patients with diabetic retinopathy should be a good control of blood glucose, blood pressure, and plasma lipids.

Fenofibrate has been shown to retard significantly the rate of diabetic retinopathy (DR) progression in adults with type 2 diabetes (T2D), including the development of macular edema. Fenofibrate as an oral agent is effective in preventing progression of established diabetic retinopathy in type 2 diabetes. Thus, in the FIELD study, fenofibrate (200 mg/day) reduced the requirement for laser therapy and prevented disease progression in patients with preexisting diabetic retinopathy.[188]

In the ACCORD study, fenofibrate (160 mg daily) with simvastatin resulted in a 40% reduction in the odds of retinopathy progressing over 4 years, compared with simvastatin alone. This occurred with an increase in HDL-cholesterol and a decrease in the serum triglyceride level in the fenofibrate group, as compared with the placebo group, and was independent of glycemic control.[189]

Surgical Approaches

Vitrectomy with or without peeling of the posterior hyaloid membrane may be beneficial for the treatment of DME in eyes with

vitreomacular traction that are resistant to laser photocoagulation and/or steroid injection.

There is clinical evidence that traction forces at the vitreoretinal interface may play an important role in the pathogenesis of macular edema. Several authors have studied vitrectomy for persistent macular edema and have suggested that release of the tractional forces at the vitreomacular interface may improve resolution of the macular edema and restore visual acuity (Fig. 30.18).

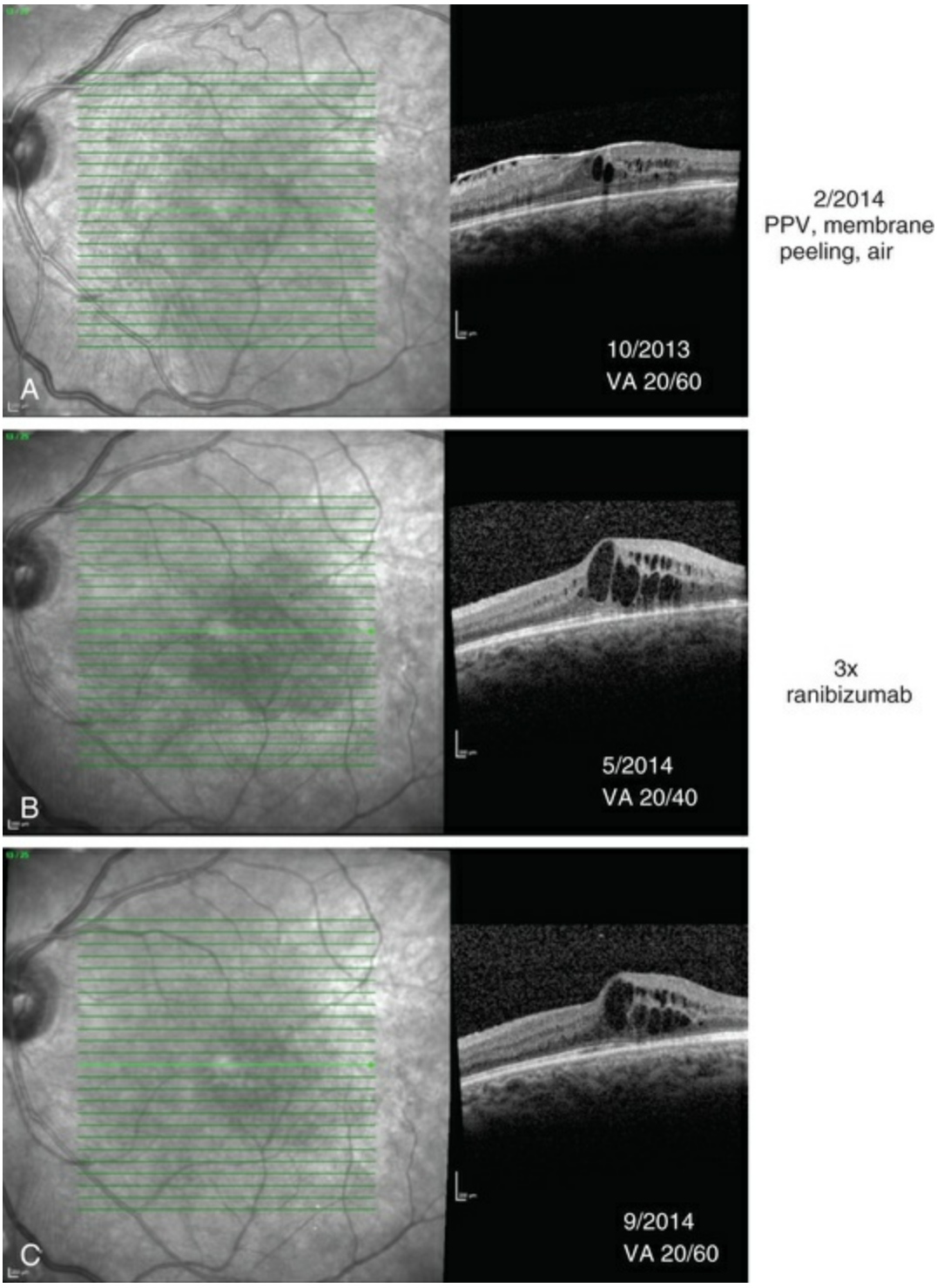

FIG. 30.18 Type 1 diabetic patient, 38 years old, HbA1c 6.5, previous mild proliferative retinopathy. Epiretinal membrane with macular edema. Epiretinal membrane on the horizontal scan with macular edema. After removal of the epiretinal traction, persistent edema which was nonresponsive to injections with ranibizumab.

Although pars plana vitrectomy may be considered as a very simple surgical procedure, its manifold effects on a cellular level are becoming better understood.[2]

The initial rationale for using vitrectomy in cases of macular edema was entirely structural, i.e., aimed at the removal of vitreous traction on the macula.[65,190] The effect of traction on retinal structures becomes more understandable using Newton's third law: to any action there is always an equal reaction in the opposite direction. The force of vitreoretinal traction will thus be met by an equal and opposite force in the retina, resulting in the retinal tissues being pulled apart. Eventually this results in the lowering of the tissue pressure within the retina, which in turn increases the difference between the hydrostatic pressure in the blood vessels and the tissue and contributes thus to edema formation (Starling's law). Releasing the traction will increase tissue pressure and lower the hydrostatic pressure gradient, reducing the water flux from blood vessels into retinal tissue.[1]

Vitreoretinal traction associated with macular edema has been identified in diabetic retinopathy, following complicated cataract surgery (Irvine–Gass syndrome), and in several other disease entities. The removal of such traction by vitreoretinal surgery has been found to be beneficial.[65,190,191] Peeling of the ILM of the retina ensures complete release of tractional forces, removes a potential diffusional barrier, and inhibits reproliferation of fibrous astrocytes.[192] The rationale for vitrectomy (removal of the hyaloid) plus peeling of the ILM is the postulated improvement of fluid diffusion from the retina to the vitreous cavity.

To evaluate the effect of ILM peeling on the long-term visual outcomes in eyes with diffuse, nontractional DME, 116 eyes of 58 patients were randomized to either ILM peeling or vitrectomy without peeling (fellow eye). Differences in BCVA between the two groups were not significant at any time point. Thus, ILM peeling does not affect the postoperative vision significantly, while vitrectomy alone seems to be beneficial.[193]

The beneficial effect of vitrectomy is thought to be based – at least in part – on two mechanisms. Firstly, it has been found, for example, that oxygen transport between the anterior and posterior segments of the eye is increased in the vitrectomized-lensectomized

eyes.[194,195] Others have shown that pharmacologic vitreolysis also improves oxygen diffusion within the vitreous cavity.[196] This means that following vitrectomy and/or posterior vitreous detachment, the transport of molecules to and from the retina is increased.

Secondly, it has been shown that several growth factors such as VEGF, IL-6, platelet-derived growth factor, and others are secreted in large amounts into the vitreous during proliferative vasculopathies such as diabetic retinopathy or retinal vein occlusion,[197,198] and it is conceivable that a complete vitrectomy will remove this excess of growth factors mechanically with the desired effect of a restitution of the BRB. The rapid clearance of VEGF and other cytokines may thus help to prevent macular edema and retinal neovascularization in ischemic retinopathies, such as diabetic retinopathy and retinal vein occlusions. Vitreous clearance of growth factors may indeed have the same effect as the presence of, for example, VEGF antibodies in the vitreous cavity.[1,199,200] This part of the effect will be only temporary as those growth factors would be released again as a result of the disease into the vitreous fluid.

Discussion and Conclusion

In DME, with anti-VEGF intravitreal injections clinically relevant visual acuity improvements (of 10 ETDRS letters or more) are likely to be achieved, at best, in 50–60% of patients and long-term treatment is required. This is similar in the case of RVO. Steroids are less than ideal given their side-effects. Therefore, there is an obvious need for the development of more effective and targeted treatments that can be satisfied only by a better understanding of the pathophysiology of macular edema. There is a need to determine which core outcome measures should be used, both in clinical trials determining the clinical effectiveness and cost-effectiveness of new treatments for macular edema and in clinical practice. Furthermore, clinically feasible retreatment criteria need to be determined.

Ischemic maculopathy remains untreatable. A foveal avascular zone of more than 500 μm should be considered ischemic. The value of current treatments for ischemic maculopathy is uncertain.

Early intervention in macular edema is undoubtedly advantageous, as the risk of ultrastructural alterations induced by a persistent macular edema increases with time. To date, however, most surgical approaches (except in patients with tractional membranes) will only be considered for persistent macular edema that is not responsive to laser treatment or pharmacologic approaches. Earlier intervention could be possibly more advantageous.

The different treatment approaches are likely to affect the clinical course of macular edema at variable time points and for different time periods. While the effect of intravitreal steroids is known to wear off with time, this may be also the case for other treatments. Any therapeutic approach should be evaluated for the duration of its anticipated beneficial effect and beyond. As macular edema requiring treatment appears to be mostly chronic, a follow-up period of one year is unlikely to suffice. It is unlikely that one treatment will fit all patients, even with the same condition. Recognizing patients' characteristics that may predict who will respond to which treatment is essential: i.e., a stratified system medicine approach is required.

References

1. Stefansson E. Physiology of vitreous surgery. *Graefes Arch Clin Exp Ophthalmol*. 2009;247:147–163.
2. Tranos PG, Wickremasinghe SS, Stangos NT, et al. Macular edema. *Surv Ophthalmol*. 2004;49:470–490.
3. Kern TS, Tang J, Berkowitz BA. Validation of structural and functional lesions of diabetic retinopathy in mice. *Mol Vis*. 2010;16:2121–2131.
4. Antcliff RJ, Marshall J. The pathogenesis of edema in diabetic maculopathy. *Semin Ophthalmol*. 1999;14:223–232.
5. Xu HZ, Le YZ. Significance of outer blood–retina barrier breakdown in diabetes and ischemia. *Invest Ophthalmol Vis Sci*. 2011;52:2160–2164.
6. Schulze C, Firth JA. Immunohistochemical localization of adherens junction components in blood–brain barrier microvessels of the rat. *J Cell Sci*. 1993;104:773–782.

7. Klaassen I, Hughes JM, Vogels IM, Schalkwijk CG, Van Noorden CJ, Schlingemann RO. Altered expression of genes related to blood–retina barrier disruption in streptozotocin-induced diabetes. *Exp Eye Res*. 2009;89:4–15.
8. Aveleira CA, Lin CM, Abcouwer SF, et al. TNF-α signals through PKCζ/NF-κB to alter the tight junction complex and increase retinal endothelial cell permeability. *Diabetes*. 2010;59:2872–2882.
9. Miyamoto K, Khosrof S, Bursell S-E, et al. Prevention of leukostasis and vascular leakage in streptozotocin-induced diabetic retinopathy via intercellular adhesion molecule-1 inhibition. *Proc Natl Acad Sci USA*. 1999;96:10836–10841.
10. Schröder S, Palinski W, Schmidt-Schönbein GW. Activated monocytes and granulocytes, capillary nonperfusion, and neovascularization in diabetic retinopathy. *Am J Pathol*. 1991;139:81–100.
11. Joussen AM, Murata T, Tsujikawa A, et al. Leukocyte-mediated endothelial cell injury and death in the diabetic retina. *Am J Pathol*. 2001;158:147–152.
12. Joussen AM, Poulaki V, Le ML, et al. A central role for inflammation in the pathogenesis of diabetic retinopathy. *FASEB J*. 2004;18:1450–1452.
13. Joussen AM, Poulaki V, Mitsiades N, et al. Potential use of non-steroidal anti-inflammatory drugs for prevention of diabetic vascular changes: aspirin prevents diabetic leakage and leukocyte adhesion through inhibition of TNF-a. *FASEB J*. 2002;16:438–440.
14. Joussen AM, Doehmen S, Le ML, et al. TNF-alpha mediated apoptosis plays an important role in the development of early diabetic retinopathy and long-term histopathological alterations. *Mol Vis*. 2009;15:1418–1428.
15. Kociok N, Radetzky S, Krohne TU, et al. Pathological but not physiological retinal neovascularization is altered in TNF-Rp55-receptor-deficient mice. *Invest Ophthalmol Vis Sci*. 2006;47:5057–5065.
16. Karlstetter M, Scholz R, Rutar M, et al. Retinal microglia: just bystander or target for therapy? *Prog Retin Eye Res*. 2015;45:30–57.

17. Rivera JC, Sitaras N, Noueihed B, et al. Microglia and interleukin-1β in ischemic retinopathy elicit microvascular degeneration through neuronal semaphorin-3A. *Arterioscler Thromb Vasc Biol*. 2013;33(8):1881–1891.
18. Antonetti DA, Barber AJ, Bronson SK, JDRF Diabetic Retinopathy Center Group, et al. Diabetic retinopathy: seeing beyond glucose-induced microvascular disease. *Diabetes*. 2006;55:2401–2411.
19. Müther PS, Semkova I, Schmidt K, et al. Conditions of retinal glial and inflammatory cell activation after irradiation in a GFP-chimeric mouse model. *Invest Ophthalmol Vis Sci*. 2010;51:4831–4839.
20. Chen W, Lee SR, Araujo J, et al. Effect of glucocorticoids on neuronal and vascular pathology in a transgenic model of selective Müller cell ablation. *Glia*. 2014;62(7):1110–1124.
21. Mizutani M, Kern TS, Lorenzi M. Accelerated death of retinal microvascular cells in human and experimental diabetic retinopathy. *J Clin Invest*. 1996;97:2883–2890.
22. Joussen AM, Qin W, Poulaki V, et al. Endogenous VEGF induces retinal ICAM-1 and eNOS expression and initiates early diabetic retinal leukostasis. *Am J Pathol*. 2002;160:501–509.
23. Senger DR, Van De Water L, Brown LF, et al. Vascular permeability factor (VPF, VEGF) in tumor biology. *Cancer Metastasis Rev*. 1993;12:303–324.
24. Keck PJ, Hauser SD, Krivi G, et al. Vascular permeability factor, an endothelial cell mitogen related to PDGF. *Science*. 1989;246:1309–1312.
25. Ferrara N, Houck K, Jakeman L, Leung DW. Molecular and biological properties of the vascular endothelial growth factor family of proteins. *Endocr Rev*. 1992;13:18–32.
26. Engerman RL, Kern TS. Retinopathy and tissue hexose in drug-treated animals. *Arch Ophthalmol*. 1998;116:543–544.
27. Amin RH, Frank RN, Kennedy A, et al. Vascular endothelial growth factor is present in glial cells of the retina and optic nerve of human subjects with nonproliferative diabetic retinopathy. *Invest Ophthalmol Vis Sci*. 1999;38:36–47.
28. Qaum T, Xu Q, Joussen AM, et al. Early diabetic blood-

retinal barrier breakdown is VEGF-dependent. *Invest Ophthalmol Vis Sci*. 2001;42:2408–2413.
29. Antonetti DA, Barber AJ, Khin S, et al. Vascular permeability in experimental diabetes is associated with reduced endothelial occludin content: vascular endothelial growth factor decreases occludin in retinal endothelial cells; Penn State Retina Research Group. *Diabetes*. 1998;47:1953–1959.
30. DeMaio L, Antonetti DA, Scaduto RC Jr, et al. VEGF increases paracellular transport without altering the solvent-drag reflection coefficient. *Microvasc Res*. 2004;68(3):295–302.
31. Harhaj NS, Felinski EA, Wolpert EB, et al. VEGF activation of protein kinase C stimulates occludin phosphorylation and contributes to endothelial permeability. *Invest Ophthalmol Vis Sci*. 2006;47:5106–5115.
32. Wang J, Xu X, Elliott MH, et al. Müller cell-derived VEGF is essential for diabetes-induced retinal inflammation and vascular leakage. *Diabetes*. 2010;59:2297–2305.
33. Antonelli-Orlidge A, Saunders KB, Smith SR, et al. An activated form of transforming growth factor beta is produced by cocultures of endothelial cells and pericytes. *Proc Natl Acad Sci USA*. 1989;86:4544–4548.
34. Ishii H, Jirousek MR, Koya D, et al. Amelioration of vascular dysfunction in diabetic rats by an oral PKC beta inhibitor. *Science*. 1996;272:728–731.
35. Whiteside C, Dlugosz J. Mesangial cell protein kinase C isozyme activation in diabetic milieu. *Am J Physiol Renal Physiol*. 2002;282:F975–80.
36. Orlidge A, Hollis TM. Aortic endothelial and smooth muscle histamine metabolism in experimental diabetes. *Atherosclerosis*. 1982;2:142–150.
37. Gilbert RE, Kelly DJ, Cox AJ, et al. Angiotensin converting enzyme inhibition reduces retinal overexpression of vascular endothelial growth factor and hyperpermeability in experimental diabetes. *Diabetologia*. 2000;43:1360–1367.
38. Gill DS, Barradas MA, Fonseca VA, et al. Plasma histamine concentrations are elevated in patients with diabetes mellitus and peripheral vascular disease. *Metabolism*.

1989;38:243–247.
39. Gardner T. Histamine, ZO-1 and increased blood retinal permeability in diabetic retinopathy. *Trans Am Ophthalmol Soc*. 1995;93:583–621.
40. Aiello LP, Bursell S-E, Clermont A, et al. Vascular endothelial growth factor-induced retinal permeability is mediated by protein kinase C in vivo and suppressed by an orally effective beta isoform selective inhibitor. *Diabetes*. 1997;46:1473–1480.
41. Vlassara H. Recent progress in advanced glycation end products and diabetic complications. *Diabetes*. 1997;46:S19–25.
42. Lu M, Kuroki M, Amano S, et al. Advanced glycation end products increase retinal vascular endothelial growth factor expression. *J Clin Invest*. 1998;101:1219–1224.
43. Donati G, Kapetanios A, Dubois-Dauphin M, et al. Caspase-related apoptosis in chronic ischaemic microangiopathy following experimental vein occlusion in mini-pigs. *Acta Ophthalmol*. 2008;86:302–306.
44. Cardier JE, Schulte T, Kammer H, et al. Fas (CD95-Apo-1) antigen expression and function in murine liver endothelial cells: implications for the regulation of apoptosis in liver endothelial cells. *FASEB J*. 1999;13:1950–1960.
45. Walsh K, Sata M. Is extravasation a Fas-regulated process? *Mol Med Today*. 1999;5:61–67.
46. Joussen AM, Poulaki V, Mitsiades N, et al. Suppression of Fas-FasL-induced endothelial cell apoptosis prevents diabetic blood–retinal barrier breakdown in a model of streptozotocin-induced diabetes. *FASEB J*. 2003;17:76–78.
47. Matrisian LM. The matrix-degrading metalloproteinases. *Bio Assays*. 1992;14:455–463.
48. Das A, McGuire PG, Eriqat C, et al. Human diabetic neovascular membranes contain high levels of urokinase and metalloproteinase enzymes. *Invest Ophthalmol Vis Sci*. 1999;40:809–813.
49. Salzmann J, Limb GA, Khaw PT, et al. Matrix metalloproteinases and their natural inhibitors in fibrovascular membranes of proliferative diabetic

retinopathy. *Br J Ophthalmol*. 2000;84:1091–1096.
50. Grant MB, Caballero S, Tarnuzzer RT, et al. Matrix metalloproteinases expression in human retinal microvascular cells. *Diabetes*. 1998;47:1311–1317.
51. Fernandez-Patron C, Zouki C, Whittal R, et al. Matrix metalloproteinases regulate neutrophil-endothelial cell adhesion through generation of endothelin-1. *FASEB J*. 2001;15:2230–2240.
52. Behzadian MA, Wang XL, Windsor LJ, et al. TGF-beta increases retinal endothelial cell permeability by increasing MMP-9: possible role of glial cells in endothelial barrier function. *Invest Ophthalmol Vis Sci*. 2001;42:853–859.
53. Abrass CK. Measurement of the rates of basal pinocytosis of horseradish peroxidase and internalization of heat-aggregated IgG by macrophages from normal and streptozotocin-induced diabetic rats. *Immunology*. 1998;65:411–415.
54. Fitzgerald ME, Caldwell RB. The retinal microvasculature of spontaneously diabetic BB rats: structure and luminal surface properties. *Microvasc Res*. 1990;39:15–27.
55. Hofman P, Blauwegers HG, Tolentino MJ, et al. VEGF-A induced hyperpermeability of blood–retinal barrier endothelium in vivo is predominantly associated with pinocytotic vesicular transport and not with formation of fenestrations. Vascular endothelial growth factor-A. *Curr Eye Res*. 2000;21:637–645.
56. Gardner TW, Abcouwer SF, Barber AJ, et al. An integrated approach to diabetic retinopathy research. *Arch Ophthalmol*. 2011;129:230–235.
57. Masland RH. The fundamental plan of the retina. *Nat Neurosci*. 2001;4:877–886.
58. Kur J, Newman EA, Chan-Ling T, et al. Cellular and physiological mechanisms underlying blood flow regulation in the retina and choroid in health and disease. *Prog Retin Eye Res*. 2012;31:377–406.
59. Nguyen TT, Kawasaki R, Kreis AJ, et al. Correlation of light-flicker-induced retinal vasodilation and retinal vascular caliber measurements in diabetes. *Invest Ophthalmol Vis Sci*.

2009;50:5609–5613.
60. Nguyen TT, Kawasaki R, Wang JJ, et al. Flicker light-induced retinal vasodilation in diabetes and diabetic retinopathy. *Diabetes Care*. 2009;32:2075–2080.
61. Pemp B, Garhofer G, Weigert G, et al. Reduced retinal vessel response to flicker stimulation but not to exogenous nitric oxide in type 1 diabetes. *Invest Ophthalmol Vis Sci*. 2009;50:4029–4032.
62. Mishra A, Hamid A, Newman EA. Oxygen modulation of neurovascular coupling in the retina. *Proc Natl Acad Sci USA*. 2011;108:17827–17831.
63. Mishra A, Newman EA. Inhibition of inducible nitric oxide synthase reverses the loss of functional hyperemia in diabetic retinopathy. *Glia*. 2010;58:1996–2004.
64. Attwell D, Buchan AM, Charpak S, et al. Glial and neuronal control of brain blood flow. *Nature*. 2010;468:232–243.
65. Lewis H, Abrams GW, Blumenkranz MS, et al. Vitrectomy for diabetic macular traction and edema associated with posterior hyaloidal traction. *Ophthalmology*. 1992;99:753–759.
66. Harbour JW, Smiddy WE, Flynn HW Jr, et al. Vitrectomy for diabetic macular edema associated with a thickened and taut posterior hyaloid membrane. *Am J Ophthalmol*. 1996;121:405–413.
67. Tachi N, Ogino N. Vitrectomy for diffuse macular edema in cases of diabetic retinopathy. *Am J Ophthalmol*. 1996;8:258–260.
68. Tagawa H, McMeel JW, Furukawa H, et al. Role of the vitreous in diabetic retinopathy. I. Vitreous changes in diabetic retinopathy and in physiologic aging. *Ophthalmology*. 1986;93:596–601.
69. Lopes de Faria JM, Jalkh AE, Trempe CL, et al. Diabetic macular edema: risk factors and concomitants. *Acta Ophthalmol Scand*. 1999;77:170–175.
70. Bron AJ, Tripathi RC, Tripathi BJ. The inner limiting membrane. *Wolff's Anatomy of the eye*. Chapman & Hall: London; 1997:488.
71. Hogan MJ, Alvaroda JA, Weddell JE. Retina. *Histology of the human eye*. W.B. Saunders.: Philadelphia; 1971:393–522.

72. Sebag J. Age-related differences in the human vitreoretinal interface. *Arch Ophthalmol*. 1991;109:966–971.
73. Rhodes RH. A light microscopic study of the developing human neural retina. *Am J Anat*. 1979;154:195–209.
74. Spira AW, Hollenberg MJ. Human retinal development: ultrastructure of the inner retinal layers. *Dev Biol*. 1973;31:1–21.
75. Sarthy V. Collagen IV mRNA expression during development of the mouse retina: an in situ hybridization study. *Invest Ophthalmol Vis Sci*. 1993;34:145–152.
76. Halfter W, Dong S, Schurer B, et al. Embryonic synthesis of the inner limiting membrane and vitreous body. *Invest Ophthalmol Vis Sci*. 2005;46:2202–2209.
77. Jumper JM, Embabi SN, Toth CA, et al. Electron immunocytochemical analysis of posterior hyaloid associated with diabetic macular edema. *Retina*. 2000;20:63–68.
78. Schmidt-Erfurth U, Lang GE, Holz FG, RESTORE Extension Study Group, et al. Three-year outcomes of individualized ranibizumab treatment in patients with diabetic macular edema: the RESTORE Extension Study. *Ophthalmology*. 2014;121(5):1045–1053.
79. Lang GE, Berta A, Eldem BM, RESTORE Extension Study Group. Two-year safety and efficacy of ranibizumab 0.5 mg in diabetic macular edema: interim analysis of the RESTORE Extension Study. *Ophthalmology*. 2013;120(10):2004–2012.
80. Brown DM, Schmidt-Erfurth U, Do DV, et al. Intravitreal aflibercept for diabetic macular edema: 100-week results from the VISTA and VIVID studies. *Ophthalmology*. 2015;122(10):2044–2052.
81. Korobelnik JF, Do DV, Schmidt-Erfurth U, et al. Intravitreal aflibercept for diabetic macular edema. *Ophthalmology*. 2014;121(11):2247–2254.
82. Heier JS, Clark WL, Boyer DS, et al. Intravitreal aflibercept injection for macular edema due to central retinal vein occlusion: two-year results from the COPERNICUS study. *Ophthalmology*. 2014;121(7):1414–1420.

83. Ogura Y, Roider J, Korobelnik JF, GALILEO Study Group, et al. Intravitreal aflibercept for macular edema secondary to central retinal vein occlusion: 18-month results of the phase 3 GALILEO study. *Am J Ophthalmol*. 2014;158(5):1032–1038.
84. Bressler SB, Melia M, Glassman AR, Diabetic Retinopathy Clinical Research Network, et al. Ranibizumab plus prompt or deferred laser for diabetic macular edema in eyes with vitrectomy before anti-vascular endothelial growth factor therapy. *Retina*. 2015;35(12):2516–2528.
85. Beck RW, Edwards AR, Aiello LP, Diabetic Retinopathy Clinical Research Network (DRCR.net), et al. Three-year follow-up of a randomized trial comparing focal/grid photocoagulation and intravitreal triamcinolone for diabetic macular edema. *Arch Ophthalmol*. 2009;127(3):245–251.
86. Hardarson SH, Stefánsson E. Retinal oxygen saturation is altered in diabetic retinopathy. *Br J Ophthalmol*. 2012;96(4):560–563.
87. Blankenship GW. Diabetic macular edema and argon laser photocoagulation: a prospective randomized study. *Ophthalmology*. 1979;86:69–76.
88. Early Treatment Diabetic Retinopathy Study Research Group. Photocoagulation for diabetic macular edema. Early Treatment Diabetic Retinopathy Study report number 1. *Arch Ophthalmol*. 1985;103:1796–1806.
89. Early Treatment Diabetic Retinopathy Study Research Group. Treatment techniques and clinical guidelines for photocoagulation of diabetic macular edema. Early Treatment Diabetic Retinopathy Study report number 2. *Ophthalmology*. 1987;94:761–774.
90. Early Treatment Diabetic Retinopathy Study Research Group. Techniques for scatter and local photocoagulation treatment of diabetic retinopathy: Early Treatment Diabetic Retinopathy Study report number 3. *Int Ophthalmol Clin*. 1987;27:254–264.
91. Early Treatment Diabetic Retinopathy Study Research Group. Photocoagulation for diabetic macular edema. Early Treatment Diabetic Retinopathy Study report number 4.*Int Ophthalmol Clin*. 1987;27:265–272.

92. Early Treatment Diabetic Retinopathy Study Research Group. Early photocoagulation for diabetic retinopathy. ETDRS report number 9. *Ophthalmology*. 1991;98:766–785.
93. Diabetic Retinopathy Clinical Research Network; Writing Committee, Aiello LP, Beck RW, et al. Rationale for the diabetic retinopathy clinical research network treatment protocol for center-involved diabetic macular edema. *Ophthalmology*. 2011;118(12):e5–14.
94. Elman MJ, Ayala A, Bressler NM, Diabetic Retinopathy Clinical Research Network, et al. Intravitreal ranibizumab for diabetic macular edema with prompt versus deferred laser treatment: 5-year randomized trial results. *Ophthalmology*. 2015;122(2):375–381.
95. Aiello LP, Edwards AR, Beck RW, Diabetic Retinopathy Clinical Research Network, et al. Factors associated with improvement and worsening of visual acuity 2 years after focal/grid photocoagulation for diabetic macular edema. *Ophthalmology*. 2010;117(5):946–953.
96. Diabetic Retinopathy Clinical Research Network, Elman MJ, Qin H, et al. Intravitreal ranibizumab for diabetic macular edema with prompt versus deferred laser treatment: three-year randomized trial results. *Ophthalmology*. 2012;119(11):2312–2318.
97. National Institute for Health and Care Excellence. *Guidance in Practice – Diabetic Retinopathy: Drug Therapy*. [London:NICE] 2011.
98. Weiter JJ, Zuckerman R. The influence of the photoreceptor-RPE complex on the inner retina. An explanation for the beneficial effects of photocoagulation. *Ophthalmology*. 1980;87:1133–1139.
99. Bresnick GH. Diabetic maculopathy: a critical review highlighting diffuse macular edema. *Ophthalmology*. 1983;90:1301–1317.
100. Molnar I, Poitry S, Tsacopoulos M, et al. Effect of laser photocoagulation on oxygenation of the retina in miniature pigs. *Invest Ophthalmol Vis Sci*. 1985;26:1410–1414.
101. Perry DD, Risco JM. Choroidal microvascular repair after argon photocoagulation. *Am J Ophthalmol*. 1982;93:787–793.

102. Gottfredsdottir MS, Stefansson E, Jonasson F, et al. Retinal vasoconstriction after laser treatment for diabetic macular edema. *Am J Ophthalmol*. 1993;115:64–67.
103. Wallow IH, Sponsel WE, Stevens TS. Clinicopathologic correlation of diode laser burns in monkeys. *Arch Ophthalmol*. 1991;109:648–653.
104. Glaser BM, Campochiaro PA, Davis JL Jr, et al. Retinal pigment epithelial cells release inhibitors of neovascularization. *Ophthalmology*. 1987;94:780–784.
105. Boulton ME, Xiao M, Khaki A. Changes in growth factor expression in pig eyes following scatter laser photocoagulation. *Invest Ophthalmol Vis Sci*. 1995;36(Suppl.):95.
106. Wilson D, Finkelstein D, Quingley H, et al. Macular grid photocoagulation: an experimental animal study on the primate retina. *Arch Ophthalmol*. 1988;106:100–105.
107. Gardner TW, Gabbay RA. Diabetes and obesity: a challenge for every ophthalmologist. *Arch Ophthalmol*. 2009;127:328–329.
108. Liew G, Mitchell P, Wong TY. Systemic management of diabetic retinopathy. *BMJ*. 2009;338:b441.
109. Pfoff DS, Thom SR. Preliminary report on the effect of hyperbaric oxygen on cystoid macular edema. *J Cataract Refract Surg*. 1987;13:136–140.
110. Widder RA, Brunner R, Walter P, et al. Improvement of visual acuity in patients suffering from diabetic retinopathy after membrane differential filtration: a pilot study. *Transfus Sci*. 1999;21:201–206.
111. Cox SN, Hay E, Bird AC. Treatment of chronic macular edema with acetazolamide. *Arch Ophthalmol*. 1988;106:1190–1195.
112. Marmor MF, Maak T. Enhancement of retinal adhesion and subretinal fluid absorption by acetacolamide. *Invest Ophthalmol Vis Sci*. 1982;23:121–124.
113. Wolfensberger TJ, Dmitriev AV, Govardovskii VI. Inhibition of membrane-bound carbonic anhydrase decreases subretinal pH and volume. *Doc Ophthalmol*. 1999;97:261–271.

114. Miller SS, Steinberg RH. Active transport of ions across frog retinal pigment epithelium. *Exp Eye Res*. 1977;25:235.
115. Wolfensberger TJ, Gregor ZJ. Macular edema – rationale for therapy. *Dev Ophthalmol*. 2010;47:49–58.
116. Yamamoto F, Steinberg RH. Effects of intravenous acetazolamide on retinal pH in the cat. *Exp Eye Res*. 1992;54:711–718.
117. Wolfensberger TJ, Chiang RK, Takeuchi A, et al. Inhibition of membrane-bound carbonic anhydrase enhances subretinal fluid absorption and retinal adhesiveness. *Graefes Arch Clin Exp Ophthalmol*. 2000;238:76–80.
118. Marmor MF, Negi A. Pharmacologic modification of subretinal fluid absorption in the rabbit eye. *Arch Ophthalmol*. 1986;104:1674–1677.
119. Tsuboi S, Pederson JE. Experimental retinal detachment. 10. Effect of acetazolamide on vitreous fluorescein disappearance. *Arch Ophthalmol*. 1985;103:1557–1558.
120. Weene LE. Cystoid macular edema after scleral buckling responsive to acetazolamide. *Ann Ophthalmol*. 1992;24:423–424.
121. Fishman GA, Gilbert LD, Anderson RJ, et al. Effects of methazolamidine on chronic macular edema in patients with retinitis pigmentosa. *Ophthalmology*. 1994;101:687–693.
122. Colin J. The role of NSAIDs in the management of postoperative ophthalmic inflammation. *Drugs*. 2007;67:1291–1308.
123. Bialek S, Quong JN, Yu K, et al. Nonsteroidal anti-inflammatory drugs alter chloride and fluid transport in bovine retinal pigment epithelium. *Am J Physiol*. 1996;270:C1175–89.
124. Wolfensberger TJ, Herbort CP. Treatment of cystoid macular edema with non-steroidal anti-inflammatory drugs and corticosteroids. *Doc Ophthalmol*. 1999;97:381–386.
125. Flach AJ, Stegman RC, Graham J, et al. Prophylaxis of aphakic cystoid macular edema without corticosteroids. A paired-comparison, placebo-controlled double-masked study. *Ophthalmology*. 1990;97:1253–1258.
126. Almeida DR, Johnson D, Hollands H, et al. Effect of

prophylactic nonsteroidal antiinflammatory drugs on cystoid macular edema assessed using optical coherence tomography quantification of total macular volume after cataract surgery. *J Cataract Refract Surg*. 2008;34:64–69.
127. DeCroos FC, Afshari NA. Perioperative antibiotics and anti-inflammatory agents in cataract surgery. *Curr Opin Ophthalmol*. 2008;19:22–26.
128. Nelson ML, Martidis A. Managing cystoid macular edema after cataract surgery. *Curr Opin Ophthalmol*. 2003;14:39–43.
129. Sivaprasad S, Bunce C, Patel N. Non-steroidal anti-inflammatory agents for treating cystoid macular edema following cataract surgery. *Cochrane Database Syst Rev*. 2005; (1) [CD004239].
130. Flach AJ, Dolan BJ, Irvine AR. Effectiveness of ketorolac tromethamine 0.5% ophthalmic solution for chronic aphakic and pseudophakic cystoid macular edema. *Am J Ophthalmol*. 1987;103:479–486.
131. Flach AJ, Jampol LM, Weinberg D, et al. Improvement in visual acuity in chronic aphakic and pseudophakic cystoid macular edema after treatment with topical 0.5% ketorolac tromethamine. *Am J Ophthalmol*. 1991;112:514–519.
132. Rossetti L, Chaudhuri J, Dickersin K. Medical prophylaxis and treatment of cystoid macular edema after cataract surgery. The results of a meta-analysis. *Ophthalmology*. 1998;105:397–405.
133. Sahoo S, Barua A, Myint KT, et al. Topical non-steroidal anti-inflammatory agents for diabetic cystoid macular edema. *Cochrane Database Syst Rev*. 2015;(2) [CD010009].
134. Wielders LH, Lambermont VA, Schouten JS, et al. Prevention of cystoid macular edema after cataract surgery in non-diabetic and diabetic patients: a systematic review and meta-analysis. *Am J Ophthalmol*. 2015;160(5):968–981.
135. Nehme A, Edelman J. Dexamethasone inhibits high glucose-, TNF-α-, and IL-1β-induced secretion of inflammatory and angiogenic mediators from retinal microvascular pericytes. *Invest Ophthalmol Vis Sci*. 2008;49:2030–2038.
136. Romero IA, Radewicz K, Jubin E, et al. Changes in cytoskeletal and tight junctional proteins correlate with

decreased permeability induced by dexamethasone in cultured rat brain endothelial cells. *Neurosci Lett*. 2003;334:112–116.
137. Antonetti DA, Wolpert EB, DeMaio L, et al. Hydrocortisone decreases retinal endothelial cell water and solute flux coincident with increased content and decreased phosphorylation of occludin. *J Neurochem*. 2002;80:667–677.
138. Edelman JL, Lutz D, Castro MR. Corticosteroids inhibit VEGF-induced vascular leakage in a rabbit model of blood–retinal and blood–aqueous barrier breakdown. *Exp Eye Res*. 2005;80:249–258.
139. Wang K, Wang Y, Gao L, et al. Dexamethasone inhibits leukocyte accumulation and vascular permeability in retina of streptozotocin-induced diabetic rats via reducing vascular endothelial growth factor and intercellular adhesion molecule-1 expression. *Biol Pharm Bull*. 2008;31:1541–1546.
140. Zhang X, Bao S, Lai D, et al. Intravitreal triamcinolone acetonide inhibits breakdown of the blood–retinal barrier through differential regulation of VEGF-A and its receptors in early diabetic rat retinas. *Diabetes*. 2008;57:1026–1033.
141. Nauck M, Roth M, Tamm M, et al. Induction of vascular endothelial growth factor by platelet-activating factor and platelet-derived growth factor is downregulated by corticosteroids. *Am J Respir Cell Mol Biol*. 1997;16:398–406.
142. Ebrahem Q, Minamoto A, Hoppe G, et al. Triamcinolone acetonide inhibits IL-6- and VEGF-induced angiogenesis downstream of the IL-6 and VEGF receptors. *Invest Ophthalmol Vis Sci*. 2006;47:4935–4941.
143. Leal EC, Manivannan A, Hosoya K, et al. Inducible nitric oxide synthase isoform is a key mediator of leukostasis and blood–retinal barrier breakdown in diabetic retinopathy. *Invest Ophthalmol Vis Sci*. 2007;48:5257–5265.
144. Mizuno S, Nishiwaki A, Morita H, et al. Effects of periocular administration of triamcinolone acetonide on leukocyte-endothelium interactions in the ischemic retina. *Invest Ophthalmol Vis Sci*. 2007;48:2831–2836.
145. Reichenbach A, Wurm A, Pannicke T, et al. Müller cells as

players in retinal degeneration and edema. *Graefes Arch Clin Exp Ophthalmol*. 2007;245:627–636.
146. Haynes RC Jr, Murad F. Adrenocorticotropic hormone: adrenocortical steroids and their synthetic analogs: inhibitors of adrenocortical steroid biosynthesis. Gilman AG, Goodman LS, Rall TW, et al. *Goodman and Gilman's The pharmacological basis of therapeutics*. Macmillan.: New York; 1985:1459–1489.
147. Thach AB, Dugel PU, Flindall RJ, et al. A comparison of retrobulbar versus subtenon's corticosteroid therapy for cystoid macular edema refractory to topical medications. *Ophthalmology*. 1997;104:2003–2008.
148. Freeman G. Cystoid macular edema in uveitis: an unsolved problem. *Eye (Lond)*. 2001;15:12–17.
149. Kuppermann BD, Chou C, Weiberg DV, et al. Intravitreous dexamethasone effects on different patterns of diabetic macular edema. *Arch Ophthalmol*. 2010;128:642–643.
150. Diabetic Retinopathy Clinical Research Network, Elman MJ, Aiello LP, et al. Randomized trial evaluating ranibizumab plus prompt or deferred laser or triamcinolone plus prompt laser for diabetic macular edema. *Ophthalmology*. 2010;117(6):1064–1077.
151. Dewan V, Lambert D, Edler J, et al. Cost-effectiveness analysis of ranibizumab plus prompt or deferred laser or triamcinolone plus prompt laser for diabetic macular edema. *Ophthalmology*. 2012;119(8):1679–1684.
152. Campochiaro PA, Brown DM, Pearson A, FAME Study Group, et al. Sustained delivery fluocinolone acetonide vitreous inserts provide benefit for at least 3 years in patients with diabetic macular edema. *Ophthalmology*. 2012;119(10):2125–2132.
153. National Institute for Health and Care Excellence (NICE). *Fluocinolone acetonide intravitreal implant for treating chronic diabetic macular edema after an inadequate response to prior therapy*. [2013 NICE technology appraisal guidance 301; Nov 27] https://www.nice.org.uk/guidance/ta301; 2013.
154. Sangwan VS, Pearson PA, Paul H, et al. Use of the fluocinolone acetonide intravitreal implant for the

treatment of noninfectious posterior uveitis: 3-year results of a randomized clinical trial in a predominantly Asian population. *Ophthalmol Ther*. 2015;4(1):1–19.
155. Sallam A, Taylor SR, Lightman S. Review and update of intraocular therapy in noninfectious uveitis. *Curr Opin Ophthalmol*. 2011;22(6):517–522.
156. Lim JI, Fung AE, Wieland M, et al. Sustained-release intravitreal liquid drug delivery using triamcinolone acetonide for cystoid macular edema in retinal vein occlusion. *Ophthalmology*. 2011;118(7):1416–1422.
157. Campochiaro PA, Brown DM, Pearso A, et al. Long-term benefit of sustained-delivery fluocinolone acetonide vitreous inserts for diabetic macular edema. *Ophthalmology*. 2011;118:626–635.
158. Haller JA, Kuppermann BD, Blumenkranz MS, Dexamethasone DDS Phase II Study Group, et al. Randomized controlled trial of an intravitreous dexamethasone drug delivery system in patients with diabetic macular edema. *Arch Ophthalmol*. 2010;128:289–296.
159. Callanan DG, Gupta S, Boyer DS, Ozurdex PLACID Study Group, et al. Dexamethasone intravitreal implant in combination with laser photocoagulation for the treatment of diffuse diabetic macular edema. *Ophthalmology*. 2013;120:1843–1851.
160. Boyer DS, Young HY, Belfort R Jr, et al. Three-year, randomized, sham-controlled trial of dexamethasone intravitreal implant in patients with diabetic macular edema. *Ophthalmology*. 2014;121(10):1904–1914.
161. National Institute for Health and Care Excellence (NICE). Macular edema (diabetic) – dexamethasone intravitreal implant. Technology Apraisal Guidance (TA349). ISBN: 978-1-4731-1317-6.
162. Haller JA, Bandello F, Belfort R Jr, et al. Dexamethasone intravitreal implant in patients with macular edema related to branch or central retinal vein occlusion twelve-month study results. *Ophthalmology*. 2011;118(12):2453–2460.
163. Medeiros MD, Alkabes M, Navarro R, et al. Dexamethasone intravitreal implant in vitrectomized versus

nonvitrectomized eyes for treatment of patients with persistent diabetic macular edema. *J Ocul Pharmacol Ther*. 2014;30(9):709–716.
164. Mitchell P, Bandello F, Schmidt-Erfurth U, et al. The RESTORE study: ranibizumab monotherapy or combined with laser versus laser monotherapy for diabetic macular edema. *Ophthalmology*. 2011;118:615–625.
165. Nguyen QD, Brown DM, Marcus DM, et al. Ranibizumab for diabetic macular edema: results from 2 phase III randomized trials: RISE and RIDE. *Ophthalmology*. 2012;119:789–801.
166. Elman MJ, Bressler NM, Qin H, et al. Expanded 2-year follow-up of ranibizumab plus prompt or deferred laser or triamcinolone plus prompt laser for diabetic macular edema. *Ophthalmology*. 2011;118:609–614.
167. Ford JA, Lois N, Royle P, et al. Current treatments in diabetic macular edema: systematic review and meta-analysis. *BMJ Open*. 2013;3(3):e002269.
168. Mitry D, Bunce C, Charteris D. Anti-vascular endothelial growth factor for macular edema secondary to branch retinal vein occlusion. *Cochrane Database Syst Rev*. 2013;(1) [CD009510].
169. Bhisitkul RB, Campochiaro PA, Shapiro H, et al. Predictive value in retinal vein occlusions of early versus late or incomplete ranibizumab response defined by optical coherence tomography. *Ophthalmology*. 2013;120(5):1057–1063.
170. Michaelides M, Kaines A, Hamilton RD, et al. A prospective randomized trial of intravitreal bevacizumab or laser therapy in the management of diabetic macular edema (BOLT study) 12-month data: report 2. *Ophthalmology*. 2010;117:1078–1086.
171. Kornhauser T, Schwartz R, Goldstein M, et al. Bevacizumab treatment of macular edema in CRVO and BRVO: long-term follow-up. (BERVOLT study: Bevacizumab for RVO long-term follow-up). *Graefes Arch Clin Exp Ophthalmol*. 2016;254(5):835–844.
172. CATT Research Group, Martin DF, Maguire MG, et al.

Ranibizumab and bevacizumab for neovascular age-related macular degeneration. *N Engl J Med*. 2011;364(20):1897–1908.
173. Comparison of Age-related Macular Degeneration Treatments Trials (CATT) Research Group, Martin DF, Maguire MG, et al. Ranibizumab and bevacizumab for treatment of neovascular age-related macular degeneration: two-year results. *Ophthalmology*. 2012;119(7):1388–1398.
174. Chakravarthy U, Harding SP, Rogers CA, IVAN study investigators, et al. Alternative treatments to inhibit VEGF in age-related choroidal neovascularisation: 2-year findings of the IVAN randomised controlled trial. *Lancet*. 2013;382(9900):1258–1267.
175. Pielen A, Feltgen N, Isserstedt C, et al. Efficacy and safety of intravitreal therapy in macular edema due to branch and central retinal vein occlusion: a systematic review. *PLoS ONE*. 2013;8(10):e78538.
176. Braithwaite T, Nanji AA, Lindsley K, et al. Anti-vascular endothelial growth factor for macular edema secondary to central retinal vein occlusion. *Cochrane Database Syst Rev*. 2014;(5) [CD007325].
177. Do DV, Schmidt-Erfurth U, Gonzalez VH, et al. The DA VINCI Study: phase 2 primary results of VEGF Trap-Eye in patients with diabetic macular edema. *Ophthalmology*. 2011;118:1819–1826.
178. Do DV, Nguyen QD, Boyer D, et al. One-year outcomes of the DA VINCI Study of VEGF Trap-Eye in eyes with diabetic macular edema. *Ophthalmology*. 2012;119:1658–1665.
179. Korobelnik JF, Holz FG, Roider J, GALILEO Study Group, et al. Intravitreal aflibercept injection for macular edema resulting from central retinal vein occlusion: one-year results of the phase 3 GALILEO Study. *Ophthalmology*. 2014;121(1):202–208.
180. Campochiaro PA, Clark WL, Boyer DS, et al. Intravitreal aflibercept for macular edema following branch retinal vein occlusion: the 24-week results of the VIBRANT study. *Ophthalmology*. 2015;122(3):538–544.
181. van Kooij B, Rothova A, Rijkers GT, et al. Distinct cytokine

and chemokine profiles in the aqueous of patients with uveitis and cystoid macular edema. *Am J Ophthalmol*. 2006;142:192–194.
182. Deuter CM, Koetter I, Guenaydin I, et al. Interferon alfa-2a: a new treatment option for long lasting refractory cystoid macular edema in uveitis? A pilot study. *Retina*. 2006;26:786–791.
183. Becker MD, Heiligenhaus A, Hudde T, et al. Interferon as a treatment for uveitis associated with multiple sclerosis. *Br J Ophthalmol*. 2005;89:1254–1257.
184. Nussenblatt RB, Palestine AG, Chan CC, et al. Randomized, double-masked study of cyclosporine compared to prednisolone in the treatment of endogenous uveitis. *Am J Ophthalmol*. 1991;112:138–146.
185. Theodossiadis PG, Markomichelakis NN, Sfikakis PP. Tumor necrosis factor antagonists: preliminary evidence for an emerging approach in the treatment of ocular inflammation. *Retina*. 2007;27:399–413.
186. Rothova A. Inflammatory cystoid macular edema. *Curr Opin Ophthalmol*. 2007;18:487–492.
187. Kafkala C, Choi JY, Choopong P, et al. Octreotide as a treatment for uveitic cystoid macular edema. *Arch Ophthalmol*. 2006;124:1353–1355.
188. Davis TM, Ting R, Best JD, Fenofibrate Intervention and Event Lowering in Diabetes Study investigators, et al. Effects of fenofibrate on renal function in patients with type 2 diabetes mellitus: the Fenofibrate Intervention and Event Lowering in Diabetes (FIELD) Study. *Diabetologia*. 2011;54(2):280–290.
189. ACCORD Study Group: ACCORD Eye Study Group, Chew EY, Ambrosius WT, et al. Effects of medical therapies on retinopathy progression in type 2 diabetes. *N Engl J Med*. 2010;363(3):233–244.
190. Fung WE. Vitrectomy for chronic aphakic cystoid macular edema. Results of a national, collaborative, prospective, randomized investigation. *Ophthalmology*. 1985;92:1102–1111.
191. Margherio RR, Trese MT, Margherio AR, Cartright K.

Surgical management of vitreomacular traction syndromes. *Ophthalmology*. 1989;96:1437–1445.
192. Gandorfer A, Messmer EM, Ulbig MW, et al. Resolution of diabetic macular edema after surgical removal of the posterior hyaloid and the inner limiting membrane. *Retina*. 2000;20:126–133.
193. Kumagai K, Hangai M, Ogino N, et al. Effect of internal limiting membrane peeling on long-term visual outcomes for diabetic macular edema. *Retina*. 2015;35(7):1422–1428.
194. Stefansson E, Novack RL, Hatchell DL. Vitrectomy prevents retinal hypoxia in branch retinal vein occlusion. *Invest Ophthalmol Vis Sci*. 1990;31:284–289.
195. Holekamp NM, Shui YB, Beebe DC. Vitrectomy surgery increases oxygen exposure to the lens: a possible mechanism for nuclear cataract formation. *Am J Ophthalmol*. 2005;139:302–310.
196. Giblin FJ, Quiram PA, Leverenz VR, et al. Enzyme-induced posterior vitreous detachment in the rat produces increased lens nuclear pO2 levels. *Exp Eye Res*. 2009;88:286–292.
197. Noma H, Funatsu H, Mimura T, et al. Vitreous levels of interleukin-6 and vascular endothelial growth factor in macular edema with central retinal vein occlusion. *Ophthalmology*. 2009;116:87–93.
198. Praidou A, Klangas I, Papakonstantinou E, et al. Vitreous and serum levels of platelet-derived growth factor and their correlation in patients with proliferative diabetic retinopathy. *Curr Eye Res*. 2009;34:152–161.
199. Stefansson E. The therapeutic effects of retinal laser treatment and vitrectomy: a theory based on oxygen and vascular physiology. *Acta Ophthalmol Scand*. 2001;79:435–440.
200. Stefansson E. Ocular oxygenation and the treatment of diabetic retinopathy. *Surv Ophthalmol*. 2006;4:364–380.

31

Cellular Effects of Detachment and Reattachment on the Neural Retina and the Retinal Pigment Epithelium

Louisa Wickham, Geoffrey P. Lewis, David G. Charteris, Steven K. Fisher

Introduction

In rhegmatogenous retinal detachment (RRD) the separation of the neural retina from the retinal pigment epithelium (RPE) initiates a complex series of cellular and molecular changes.[1] Left untreated, RRD results in permanent visual loss; however, early intervention may be associated with good visual outcomes, suggesting that some of these molecular changes may be arrested or reversed.[2,3]

By studying the cellular and molecular changes that occur after detachment and/or reattachment, clinicians may gain a more precise understanding of the degenerative processes within the retina that lead to visual impairment and the mechanisms underlying the serious complications of detachment, such as proliferative vitreoretinopathy (PVR). In addition, these insights may aid the development of future treatment strategies and adjunctive therapies aimed at improving visual outcomes.

This chapter reviews the many changes that occur in retinal cells following RRD and the ensuing process of morphologic recovery following reattachment, as revealed by human case series and studies of experimental retinal detachment and reattachment in animal models.

Use and Limitations of Animal Models in the Study of Retinal Detachment

Human studies of cellular changes following acute RRD are limited to isolated case reports as surgical management does not routinely involve removal of retinal tissue. More recently data have become available from patients undergoing macular translocation surgery in which the retina is detached as part of the procedure, allowing sampling of the retina as early as 1 hour following detachment.[4] In patients with advanced stages of RRD and PVR, surgical management may involve excising areas of scarred retinal tissue, allowing histopathologic analysis. However, the data from human studies is still limited by small numbers, the challenges of sampling and analyzing small retinal specimens, and an inability to study cellular recovery following reattachment.[4–7]

This difficulty in obtaining retinal tissue from patients with RRD has led to the use of animal models. Animal models have been developed in a variety of mammalian species from rodents to primates, most commonly in rabbits and cats, and more recently in mice. The feline retina is rod-dominant, and has an intraretinal circulation that is excluded from the photoreceptor layer and a choroidal circulation that supplies the photoreceptor layer. The rabbit retina is also rod-dominant but has no intraretinal vasculature, with the inner retina being supplied by vessels that lie on the vitreal surface. The rabbit retina has proved to be a more difficult animal model in long-term experiments because the retina tends to degenerate very rapidly following detachment; for short-term studies, however, (i.e., 3–7 days) rabbits continue to be a valuable model.

Ideally the characteristics of an experimental detachment should closely mimic those found in humans while allowing for precise control over the extent of separation between the two layers (detachment height), the location of the detachment, its surface area, and the onset of detachment (or reattachment) time. A number of methods have been used to simulate human RRD in animal models. These range from creating large retinal tears to subretinal injections of fluid or viscous substances. Experiments where retinal detachment induction is standardized with a micropipette provide a controlled environment for analysis; however, they differ from the clinical pattern of events in which acute retinal tears of variable size are induced by vitreoretinal traction at the time of posterior

vitreous detachment. It is possible that retinal tearing may act as a more potent stimulus for cellular disorganization, loss, and remodeling, leading more rapidly to the advanced pathology usually seen following longer periods of retinal detachment in animal models. Although experiments involving animal models may differ in methodology, species used, and outcome measures, they have yielded similar results to give a relatively detailed profile of the changes that occur after detachment. Retinal tissue removed from human postmortem specimens and from patients undergoing retinal detachment surgery has demonstrated changes similar to those seen in animal models.[6–8]

Animal models have proved invaluable in providing insight into the regenerative capacity of photoreceptor cells and the ability of reattachment to slow, stop, or reverse changes induced by detachment. They also continue to provide opportunities to test adjunctive agents targeting neuroprotection and wound healing before progressing to human surgical trials. Further, in mouse models the large variety of genetic mutations that exist provides additional scope to the study of retinal detachment and potential gene therapies.

Cellular Changes in Response to Retinal Detachment

Descriptions of the cellular response to RRD are frequently divided into those observed in the early stages of retinal detachment and those observed in more chronic cases and in PVR. There is, however, a continuous progression of pathologic change.

Acute Retinal Detachment

Acute RRD, i.e., changes occurring within the first 3 days, has been extensively documented.

A rapid response to retinal detachment has been shown to occur within 15 minutes, including phosphorylation of fibroblast growth factor receptor (FGFR-1) and increased expression by RPE and Müller cells of extracellular signal-regulated kinase and activator

protein transcription factor.[9] This initiates a cascade of events that leads to a number of molecular and cellular changes within the retina and RPE.

RPE–Photoreceptor Interface

The earliest structural effects of retinal detachment are seen at the interface of photoreceptor outer segments and the RPE.[10] The mature RPE is a polarized monolayer of neuroepithelial cells that rests on Bruch's membrane, between the choriocapillaris and the neural retina.[11] The relationship of the apical surface of the RPE to differentiated photoreceptors is anatomically complex. There are no actual cellular junctions between the two layers in the mature eye, but the two are adherent, with the degree of adhesion varying among species.[12] With the onset of retinal detachment changes to this interface include alterations in the RPE apical surface, proliferation of RPE cells, migration of cells into the subretinal space, degeneration of photoreceptor outer segments, and changes in photoreceptor outer-segment renewal.[1]

Within a few hours of retinal detachment, the long and elaborate sheet-like and villous processes that normally ensheath the outer segments are lost and replaced by a “fringe” of short microvilli (Fig. 31.1).[13] At the same time, the overall surface morphology of the RPE cells changes into a rounded contour, as cytoplasm protrudes past the normal limits of the apical surface into the subretinal space, and the nucleus becomes displaced to a more apical position[10,14] (Fig. 31.2).

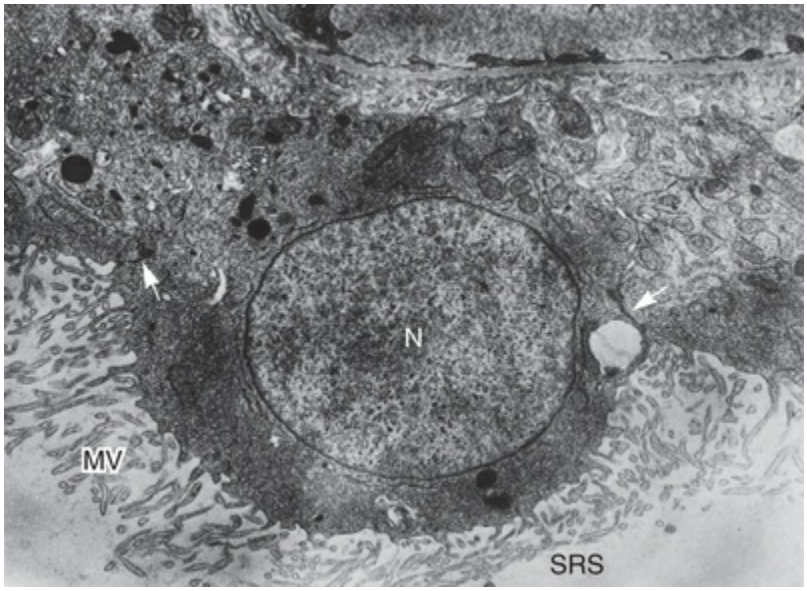

FIG. 31.1 Electron micrograph of the retinal pigment epithelium (RPE) 1 day after production of a retinal detachment. Compared with normal RPE cells, the apical surface is mounded. The sheet-like apical projections that normally ensheath the outer segments have been replaced by a homogeneous fringe of short, microvillous processes (*MV*). In this particular cell, the nucleus (*N*) is displaced into the mounded region. The cells' lateral junctions are indicated by arrows. *SRS*, subretinal space. (Reproduced with permission from Anderson DH, Stern WH, Fisher SK, et al. Retinal detachment in the cat: The pigment epithelial–photoreceptor interface. Invest Ophthalmol Vis Sci 1983;24:909.)

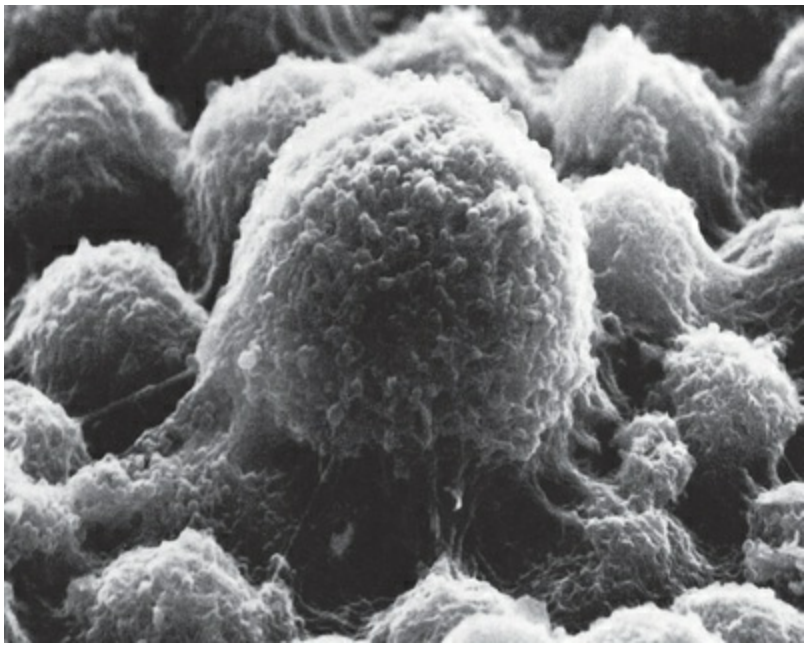

FIG. 31.2 Scanning electron micrograph of the apical surface of the retinal pigment epithelium 6 weeks after production of an experimental detachment, demonstrating the pronounced mounding response of the epithelial cells. (Reproduced with permission from Anderson DH, Stern WH, Fisher SK, et al. Retinal detachment in the cat: The pigment epithelial–photoreceptor interface. Invest Ophthalmol Vis Sci 1983;24:910.)

In the feline model, experiments using ^{3}H-thymidine have shown that within 72 hours of retinal detachment the RPE has begun to proliferate and may be observed as areas of hyperplasia within the RPE monolayer.[10] This proliferative response transforms the RPE's uniform monolayer into a heterogeneous morphology in which strands of cells extend from the original monolayer into the subretinal space or result in the formation of multiple layers of cells whose polarity does not necessarily match that of the original monolayer (Fig. 31.3). This effect is limited to the region of detachment; in attached regions the RPE remains mitotically quiet, suggesting that attachment to the neural retina acts to keep the RPE mitotically inactive and its apical surface highly differentiated.[15–17] The proliferative response of the RPE cells also appears to be self-limiting with only low levels of proliferation observed after long detachment intervals (e.g., 12–14 months) in owl, monkey, and cat retinas[10,16] (Box 31.1 and Fig. 31.4).

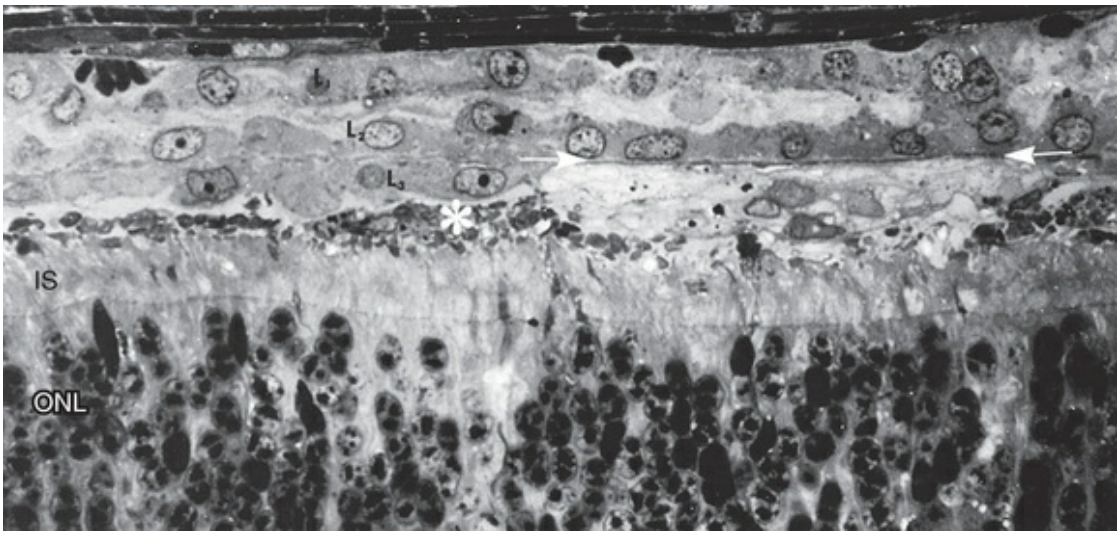

FIG. 31.3 Light micrograph of an area of retinal pigment epithelium (RPE) cell proliferation in a cat retina detached for 14 days and reattached for 30 days. Three layers of RPE cells are present (*L1–L3*), each displaying different surface polarity. The apical surfaces of L1 and L2 face each other, as do the basal surfaces of L2 and L3. The basal lamina of L2 is clearly evident (*arrow*). Only outer-segment fragments (*asterisk*) appear near the inner segment (*IS*) tips (×800). *ONL*, outer nuclear layer. (Reproduced with permission from Anderson DH, Guerin CJ, Erickson PA, et al. Morphological recovery in the reattached retina. Invest Ophthalmol Vis Sci 1986;27:174.)

Box 31.1

Clinical Correlates

Retinal pigment epithelial (RPE) proliferation can be seen as subretinal pigment deposition in chronic retinal detachments. It is likely that the demarcation lines noted in human retinal detachments represent zones of proliferated RPE occurring at transitions between detached and attached regions of the eye (Fig. 31.4).

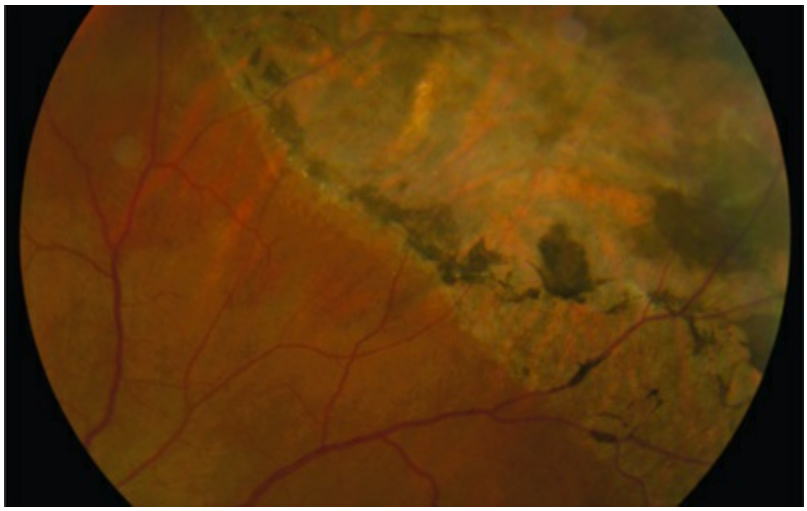

FIG. 31.4 Color fundus photograph of a chronic retinal detachment with a pigmented demarcation line indicating the interface between attached and detached retina.

The subretinal space is usually free of cells; however within 24 hours of retinal detachment a number of cell types (polymorphonuclear neutrophils, monocytes, and macrophages) migrate into this space from the choroidal and retinal capillaries.[10,18] Free RPE cells are also seen in the subretinal space within 72 hours of retinal detachment and frequently contain outer-segment fragments, indicating that they may play a role in phagocytosis of cellular debris.[10,18]

Photoreceptors

Within 12 hours of experimental retinal detachment, photoreceptor outer segments show evidence of structural damage. Initially, the distal end of the outer segment becomes vacuolated or distorted, and by 24–72 hours, all rod and cone outer segments are significantly shorter and distorted with disoriented discs.[19] The degeneration of outer segments may proceed until those in the zone of detachment appear only as empty sacs of membrane attached to the connecting cilium.[10]

Outer-segment debris is shed into the subretinal space where it is phagocytosed by RPE cells and macrophages that have migrated into the area.[10,18]

Although retinal detachment interrupts the process of disc production and shedding, outer-segment-specific proteins continue

to be produced but localize to abnormal cellular locations. Opsin, normally concentrated in the outer segment, begins to accumulate in the plasma membrane vitread to the outer segment within a day following experimental retinal detachment (Fig. 31.5).[19] Peripherin/rds, another outer-segment protein specific to the disc rims, is also redistributed and begins to appear in cytoplasmic vesicles.[20] Cone outer-segment proteins appear to be more susceptible to damage, with redistributed cone opsins persisting for just 1 week following retinal detachment, after which their expression is downregulated.[21]

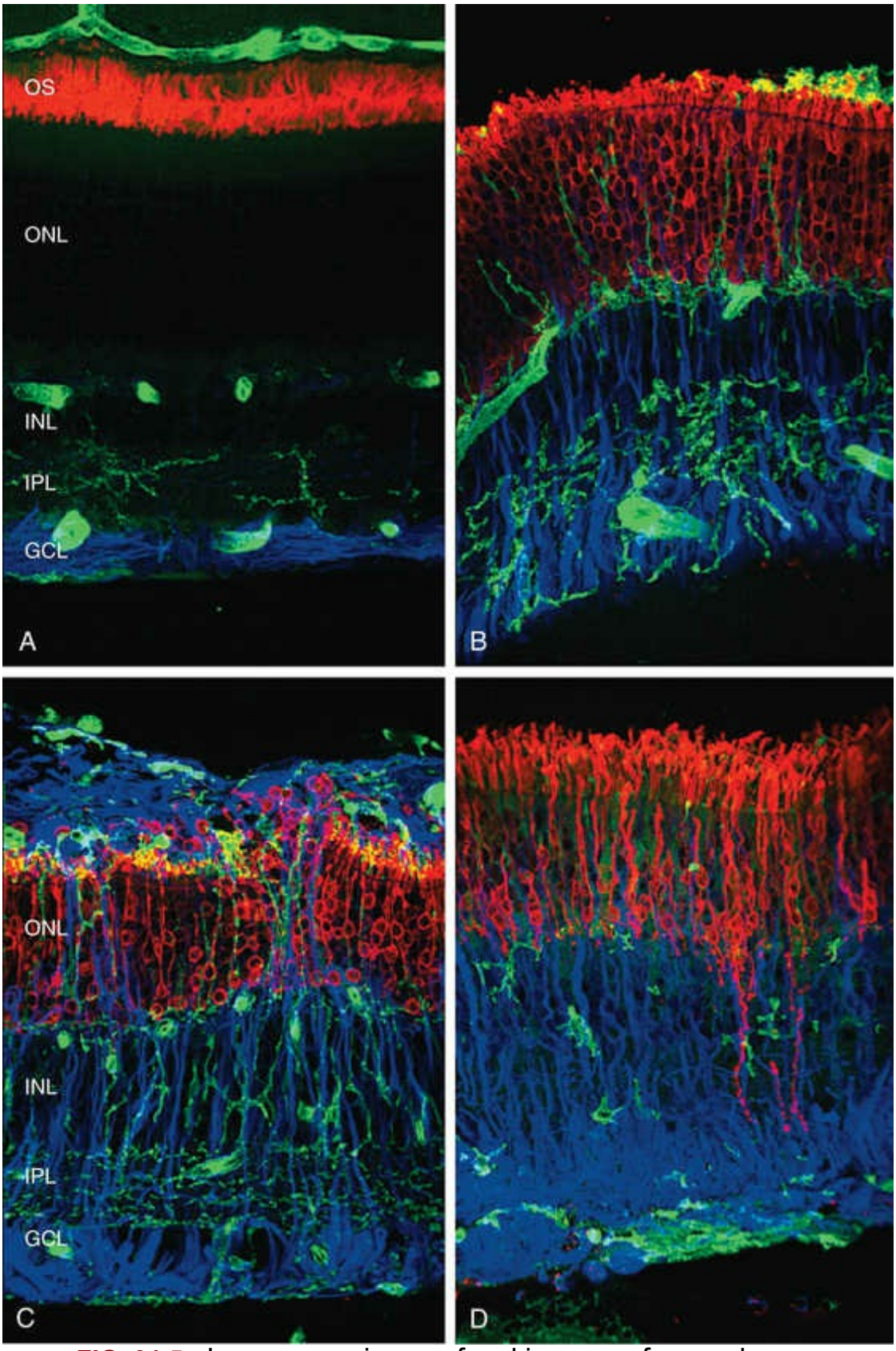

FIG. 31.5 Laser scanning confocal images of normal (A), 7-day (B), and 28-day (C) cat retinas, as well as a human detached retina (D), labeled with isolectin B4 (green), antiglial fibrillary acidic protein (anti-GFAP)

(blue), and antirod opsin (red). In the normal retina, isolectin B4 labels microglia in the inner plexiform layer (*IPL*) (and blood vessels), anti-GFAP labels astrocytes and Müller cell endfeet, and antirod opsin labels rod outer segments (*OS*) (A). Following 7 days of detachment isolectin B4 labeling illustrates an overall increase in the number of microglia and their presence in the outer retina, rod opsin becomes mislocalized to the photoreceptor cell bodies, and GFAP increases in Müller cells (B). At 28 days numerous microglia can be observed throughout the retina, photoreceptor cell bodies are extruded out of the retina, and Müller cell processes extend into the subretinal space (C). A similar pattern of increased numbers of microglia, rod opsin mislocalization, and increased GFAP labeling is observed in human detached retinas (D). Note rod axons extending into the inner retina in (D), a common phenomenon in cat retinas following detachment and reattachment. *GCL*, ganglion cell layer; *INL*, inner nuclear layer; *ONL*, outer nuclear layer.

During the first day of a detachment, the inner segments appear essentially normal, but between the first and third days, they begin to show signs of degeneration: most commonly swelling, disruption, and loss of mitochondria (and loss of anticytochrome oxidase labeling) in the ellipsoid region,[2,22] an overall disruption of the organized rough endoplasmic reticulum and Golgi apparatus in the myoid region, and, within a few days, an overall size reduction of the inner segment. It is interesting to note that the connecting cilium, which is essential for production of the outer segment, is retained even in severely affected inner segments in long-term detachments. This is crucial as its loss would prevent regeneration of outer segments following reattachment. Similarly, the loss of mitochondria also has the potential to affect the photoreceptors' ability to regenerate significantly, because the metabolic rate in these cells is among the highest of any in the body.

The outer nuclear layer contains the cell bodies of the photoreceptor cells. These cell bodies extend a process toward the outer plexiform layer, where they form synapses with second-order neurons. Rods and cones have characteristic synaptic terminals called spherules and pedicles respectively.[23] The outer plexiform

layer also contains the processes of second-order neurons, the cell bodies of which lie in the inner nuclear layer. These processes synapse with each other and with the photoreceptors. The photoreceptor cell bodies and synaptic terminals show a rapid response to detachment with extensive vacuolization, degeneration of mitochondria, and disorganization of the microtubules and actin filaments. Cell death via the apoptotic pathway peaks at day 3 following retinal detachment but continues at low levels for as long as the retina is detached. Photoreceptor death has been shown to differ significantly in different mouse strains, suggesting that genetic factors also play a role in cellular response to retinal detachment.[24] Photoreceptor apoptosis appears to be mediated via caspases 3, 7, and 9.[25,26] Recent studies have shown that, when caspase pathways are blocked, receptor interacting protein (RIP) kinases promote necrosis and overcome apoptosis inhibition. Therefore, targeting of both caspase and RIP kinase pathways is required for effective photoreceptor protection[27] (Box 31.2).

Box 31.2

Clinical Correlates

More recently, photoreceptor apoptosis has also been demonstrated in human retinal specimens, with a peak at day 2 following RRD.[28] Ethnic variations in severity of retinal detachment have been demonstrated and may also reflect genetic differences in cellular response to injury.[29]

Following cell death, some photoreceptors are extruded into the subretinal space where they are phagocytosed by macrophages while others appear to undergo degeneration and phagocytosis within the outer nuclear layer.[30]

Not all photoreceptors degenerate at the same rate; areas of extensive degeneration coexist with areas of relatively intact photoreceptors.[19] Rod cell bodies appear to degenerate quicker than cones following retinal detachment.[21] In a region in which nearly all of the rod cell bodies show signs of degeneration and even cell death, neighboring cone cell bodies may look relatively intact. Consistent with this observation, the rod spherules appear to be particularly susceptible to the effects of detachment. These synaptic terminals are normally filled with synaptic vesicles and contain one

or two large presynaptic ribbons. When the retina has been detached for 3 days, many of these terminals appear depleted of vesicles, except for a few that remain as a halo around a greatly truncated or fragmented ribbon.[31] Many terminals appear as if they have "retracted" into the cell body, and some synaptic structures generally associated with the outer plexiform layer now occur within the outer nuclear layer (Fig. 31.6).[31,32] As with the cone and rod photoreceptor cell bodies, the cone synaptic terminals seem to survive the early effects of detachment better than the rod terminals do. Although their shape can change fairly dramatically, they do not appear to retract and by electron microscopy they remain filled with synaptic vesicles.[32,33]

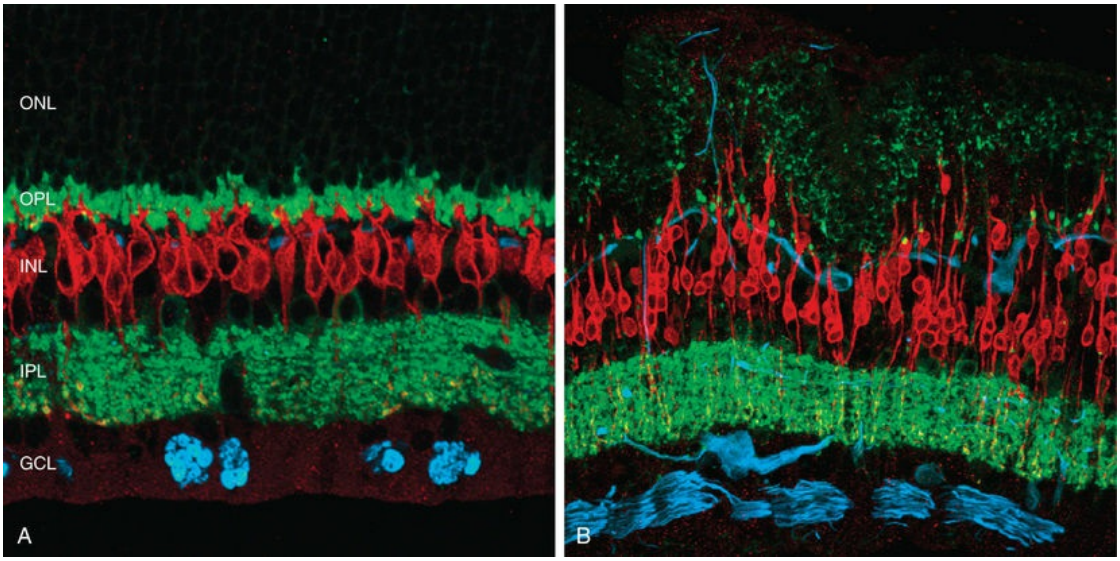

FIG. 31.6 Laser scanning confocal images of normal (A) and 28-day detached (B) cat retinas labeled with antisynaptophysin (green), antiprotein kinase C (anti-PKC) (red), and antineurofilament (blue). In the normal retina, antisynaptophysin labels synaptic vesicles in the rod and cone terminals in the outer plexiform layer as well as synaptic terminals in the inner plexiform layer, anti-PKC labels rod bipolar cells, and antineurofilament labels ganglion cell axons and horizontal cell processes (A). After detachment, rod terminals retract into the outer nuclear layer (*ONL*), as evidenced by the synaptophysin labeling, the dendrites of rod bipolar cells extend into the ONL, while horizontal cell processes grow through the ONL into

the subretinal space (B). Neurofilament labeling also increases in some ganglion cell bodies (B). *GCL*, ganglion cell layer; *INL*, inner nuclear layer; *IPL*, inner plexiform layer; *OPL*, outer plexiform layer.

Second-Order Neurons and Nonneuronal Cell Types

At the same time as rod spherules are retracting, processes from the rod bipolar cells and horizontal cells (labeled with antibodies to protein kinase C, and neurofilament protein, respectively) appear to retract from the rod spherules and then begin to grow beyond the normal layer of photoreceptor synaptic terminals, into the outer nuclear layer and even beyond, sometimes extending into the subretinal space (Fig. 31.7).[32]

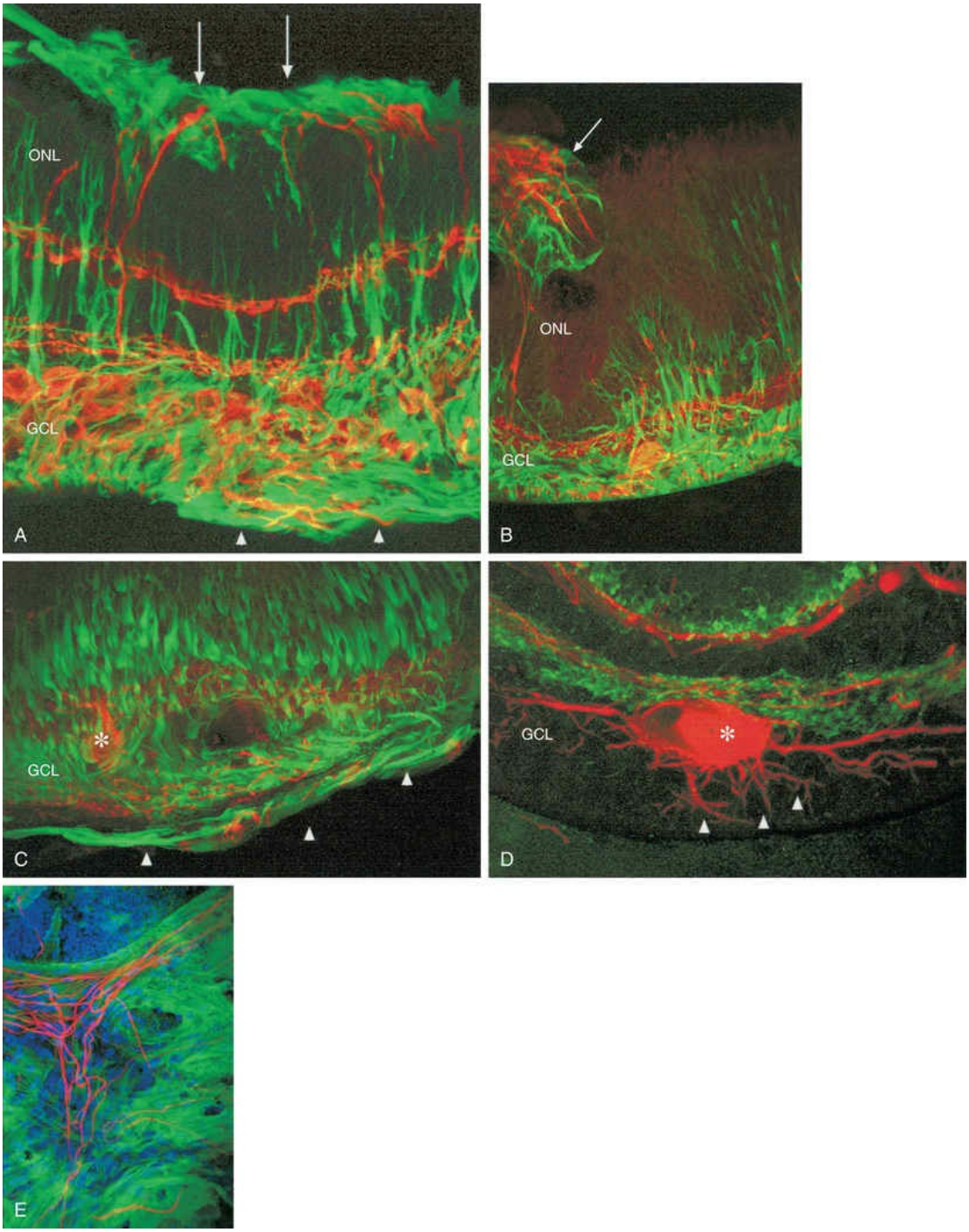

FIG. 31.7 Laser scanning confocal images illustrating the neurite sprouting of second- and third-order neurons as well as the formation of sub- and epiretinal Müller cell scars in the feline retina following a 28-day detachment. (A) An antibody to neurofilament protein (red) labels ganglion cell bodies in the ganglion cell layer (*GCL*) and neurites from ganglion cells within an epiretinal membrane (*arrowheads*) as well as horizontal cell bodies and neurites from these cells

extending through the outer nuclear layer (*ONL*) into a subretinal glial scar (green; *arrows*). An antibody to glial fibrillary acidic protein (GFAP; green) labels intermediate filaments in Müller cells throughout the retina as well as those in the subretinal (*arrow* in panel B) and epiretinal membranes. (B,C) An antibody to GAP 43 (red) labels activated ganglion cell bodies (*asterisks* in panels C and D), dendrites in the inner plexiform layer, and neurites that extend through the retina into subretinal (green; *arrow* in panel B) and epiretinal (*arrowheads* in panel C) glial scars. An antibody to GFAP (green) labels intermediate filaments in Müller cells throughout the retina and in the subretinal scar. (D) An antibody to neurofilament protein (red) labels an activated ganglion cell (*asterisk*) and newly formed neurites extending from the base of its cell body (*arrowheads*). An antibody to synaptophysin (green) labels synaptic terminals in the outer and inner plexiform layers. (E) An antibody to neurofilament protein (red) labels horizontal cell neurites within a glial scar (green; labeled with anti-GFAP) in the subretinal space in a retinal flat-mount preparation. "ToPro" labeling (blue) shows the presence of photoreceptor nuclei just below the glial scar. (Panel B reproduced with permission from Lewis GP, Fisher SK. Upregulation of glial fibrillary acidic protein in response to retinal injury: its potential role in glial remodelling and a comparison of vimentin expression. Int Rev Cytol 2003;230:263.)

Just as changes in the synaptic terminals are accompanied by the growth of processes from the rod bipolar cells and horizontal cells into the outer nuclear layer,[31,32] ganglion cells also become reactive and begin to reexpress growth-associated protein (GAP)-43, a protein expressed early in cell body development for the formation of synaptic connections between ganglion cell axons and the brain.[34] As in the case of horizontal cells, ganglion cells show dramatic and extensive remodeling, growing processes that appear to be attracted to Müller cells.[35] By contrast, rod bipolar cell dendrite growth is less aggressive, being targeted towards the retracted terminals of the rod photoreceptors.

Within 24 hours of retinal detachment nonneuronal cell types, for example, astrocytes, Müller cells, pericytes, capillary endothelial

cells, and microglia, also display signs of proliferation.[16,17] By 2 days, some labeled Müller cell nuclei are translocated from their normal positions on the vitreal border of the inner nuclear layer into the outer plexiform and outer nuclear layers (Fig. 31.8).[36] The proliferative response peaks 3–4 days after detachment and declines slowly to very low levels several weeks later. Microglia, a form of macrophage in the central nervous system that usually lie dormant in the retina, are activated and begin to divide and migrate to the outer retina (see Fig. 31.5). Microglial proliferation is observed to differing degrees in different species and is thought to play a role in photoreceptor cell death, possibly by modifying the production of neuroprotective trophic factors by Müller cells.[30]

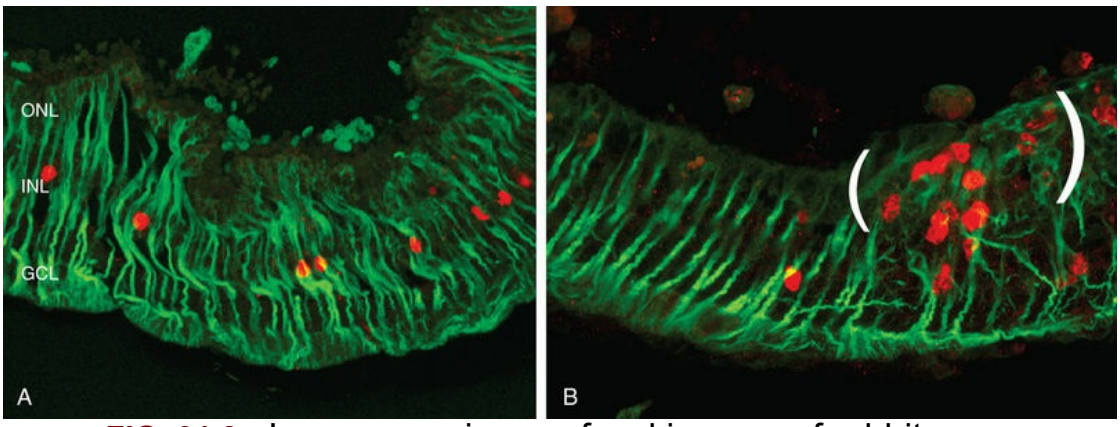

FIG. 31.8 Laser scanning confocal images of rabbit retinas detached for 3 days (A) and 7 days (B), and immunolabeled with antivimentin (green) and anti-BrdU (red). An intravitreal injection of bromodeoxyuridine (BrdU) was given on day 3, and the animals were euthanized either 4 hours later or 4 days later on day 7. BrdU labeling is present in Müller cell nuclei in the inner nuclear layer on day 3, after which they migrate to the outer retina and contribute to the formation of subretinal scars (*brackets*) at day 7 (B). *GCL*, ganglion cell layer; *INL*, inner nuclear layer; *ONL*, outer nuclear layer.

Changes in the Müller cell are seen within 1 day of retinal detachment, including changes in protein expression and early growth of their processes.[37] Within 3 days Müller cell bodies have migrated to the outer nuclear and outer plexiform layers (Fig. 31.9)

and processes begin to extend into the subretinal space through localized disruptions in the outer limiting membrane. Müller cell processes within the feline retina express both vimentin and glial fibrillary acidic protein (GFAP); however, segments of the processes extending through the outer limiting membrane into the subretinal space preferentially express vimentin (Fig. 31.10).[37] These processes appear to penetrate the outer limiting membrane preferentially adjacent to cone photoreceptors, often growing for long distances on the photoreceptor border.[37] Müller cells stimulated to divide on day 3 appear to ultimately contribute to the formation of subretinal scars.[36]

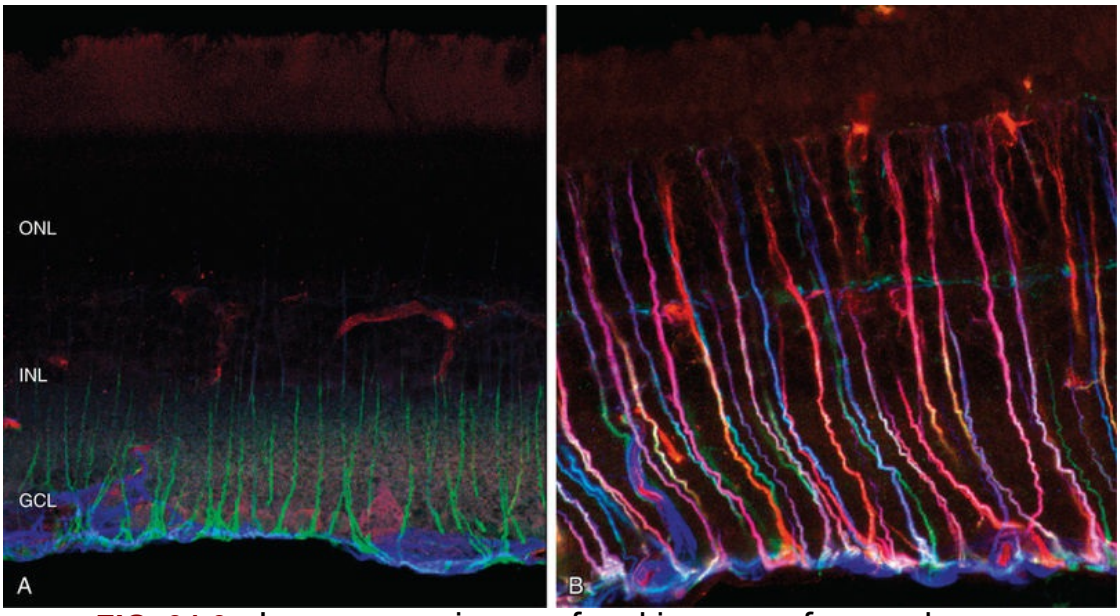

FIG. 31.9 Laser scanning confocal images of normal (A) and 3-day detached (B) rat retinas immunolabeled with antiglial fibrillary acidic protein (GFAP) (blue), antivimentin (green), and antinestin (red). In the normal retina GFAP is present only in the astrocytes and vimentin is present only in Müller cells; no nestin labeling is apparent. After retinal detachment, there is a dramatic upregulation of all three proteins. They are expressed throughout the Müller cells' cytoplasm but at different levels, giving the “rainbow” appearance of the labeling. *GCL*, ganglion cell layer; *INL*, inner nuclear layer; *ONL*, outer nuclear layer.

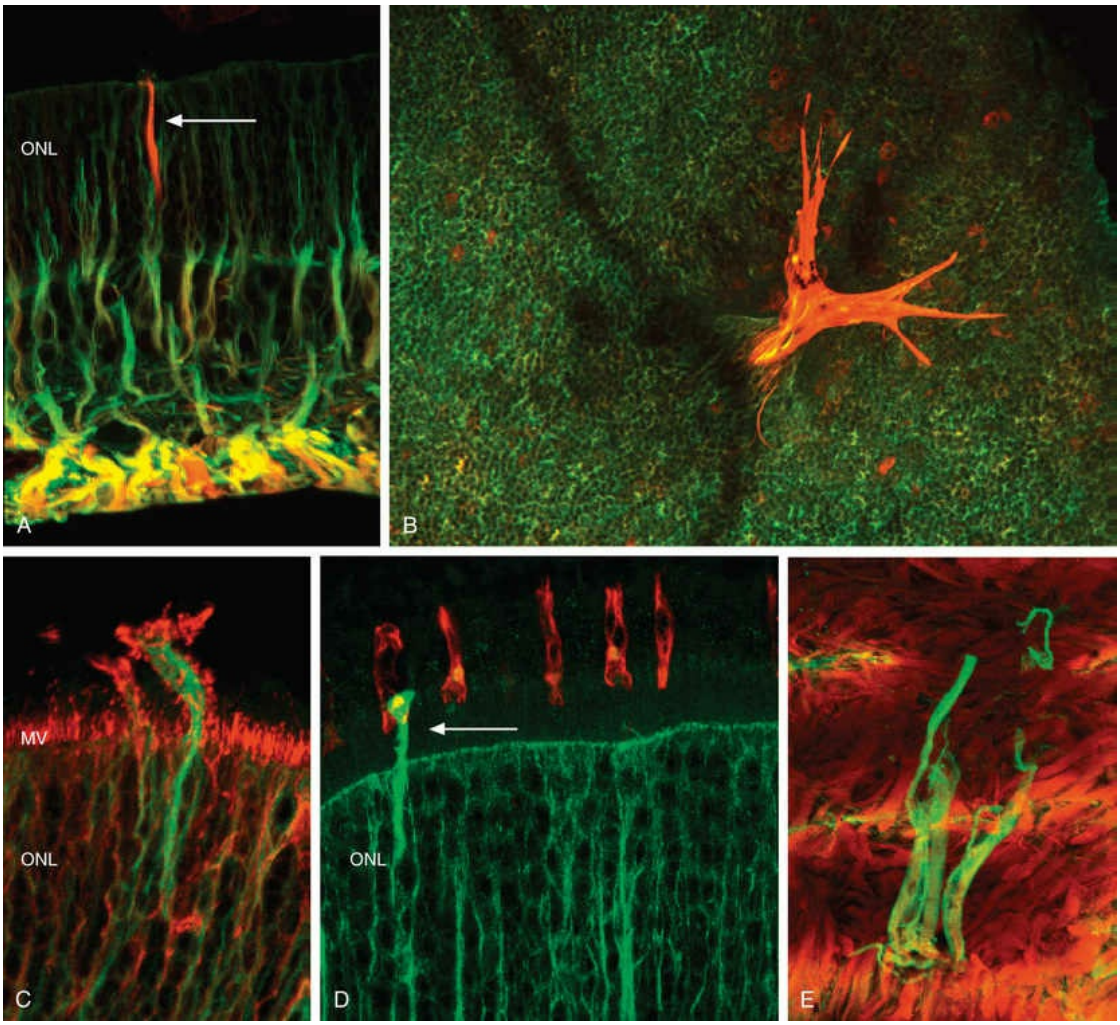

FIG. 31.10 Laser scanning confocal images illustrating the early stages of Müller cell growth on to the subretinal and epiretinal surfaces of the feline retina. (A) Antibodies to glial fibrillary acidic protein (GFAP) (green) and vimentin (red) label intermediate filaments within Müller cells throughout the retina. The red process (*arrow*) in the outer nuclear layer is labeled predominantly with the antibody to vimentin and represents a Müller cell that is just beginning to extend into the subretinal space. (B) A flat-mounted preparation, viewed from the photoreceptor surface and labeled with antibodies to GFAP (green) and vimentin (red). It shows the predominance of vimentin in a Müller cell process in the very early stages of extending into the subretinal space. (C) An antibody to GFAP (green) labels a Müller cell process just entering the subretinal space. An antibody to CD44 (red) labels fine filopodia on this process as well as the Müller cell microvilli (*MV*). (D) An antibody to GFAP (green) labels

a Müller cell's process entering the subretinal space (*arrow*) directly adjacent to a peanut agglutinin-labeled cone photoreceptor (red). (E) A flat-mounted preparation, viewed from the vitreal side of the retina, labeled with antibodies to GFAP (green) and vimentin (red). It shows a predominantly GFAP-labeled Müller cell process in the earliest stage of extending on to the vitreal surface of the retina. (The vimentin labeling in the background is in the Müller cells' endfeet.) *ONL*, outer nuclear layer. (Reproduced with permission from Lewis GP, Fisher SK. Up-regulation of glial fibrillary acidic protein in response to retinal injury: its potential role in glial remodeling and a comparison to vimentin expression. Int Rev Cytol 2003;230:263. Copyright 2003, with permission from Elsevier.)

Astrocytes, the other glial cell type in the retina, also undergo their own remodeling response following retinal detachment, albeit less prominent than Müller cells. This is more readily seen in the mouse retina, where the Müller cell response does not overwhelm that of the astrocytes as it can in the feline or human retina. Indeed, astrocyte processes become highly jagged and irregular after detachment compared to those in normal retina.[38] While the processes do not appear to grow laterally across the retina in the mouse retina, they can often be observed extending deep into the inner retina, often along blood vessels (Fig. 31.11).

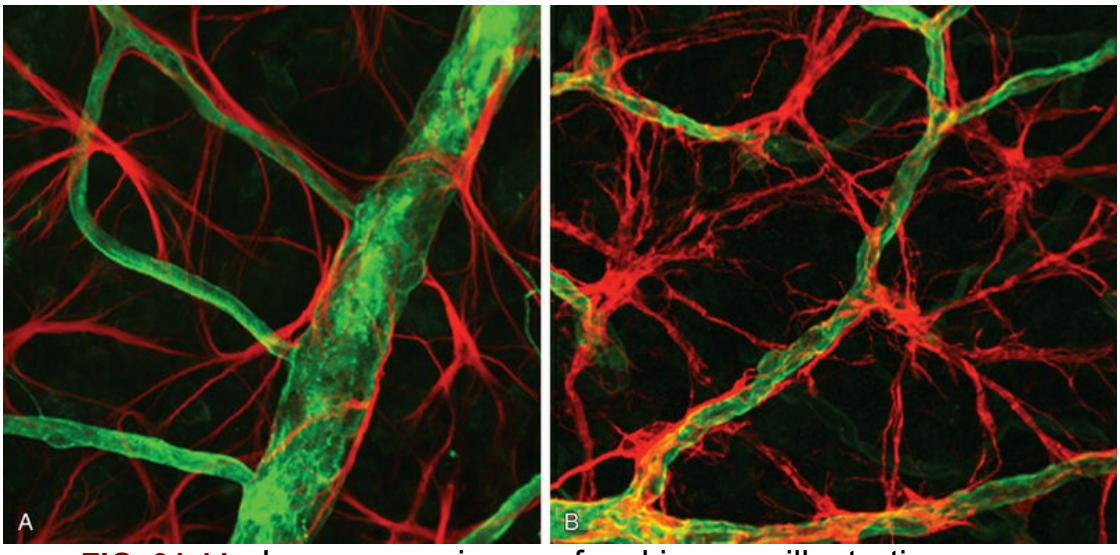

FIG. 31.11 Laser scanning confocal images illustrating astrocytes in a mouse retina (wholemount orientation). (A) Normal mouse retina showing relationship between

astrocytes (red; anti-GFAP) and retinal blood vessels (green; collagen IV). (B) Following 5 weeks of retinal detachment the astrocytes (red; anti-GFAP) appear more irregular and jagged compared with normal retina.

A number of pharmacologic agents, working through different mechanisms, have been shown to slow cell proliferation and glial scar formation following experimental RRD. These therapies include akylphosphocholines,[39] an inhibitor of the Akt/mTOR pathway,[40] anti-VEGF agents such as ranibizumab,[41] and an inhibitor of the alpha5Beta1-fibronectin interactions.[42] At present these have not been used outside animal models.

Chronic Retinal Detachment and Proliferative Vitreoretinopathy

Although animal models remain the main source of data regarding more long-term neuronal remodeling following RRD, human studies of retinectomy specimens removed at the time of surgery also exist.[6] These studies show close correlation with results from feline and primate models.

Photoreceptors

The degree of photoreceptor cell death and its timing are species-dependent. In the feline model, there is a significant decrease in the number of photoreceptor cells by 1 month after detachment, and this number continues to decline until the outer nuclear layer loses about 80% of its cell population by 90 days after detachment.[19] In regions severely affected by photoreceptor degeneration, the outer nuclear layer can be reduced in thickness to one or two cell layers. In humans, a histopathologic study by Wilson and Green of retinal detachment in postmortem eyes also showed atrophy of the photoreceptor layer in 26.5% of retinas examined[7] (Box 31.3).

Box 31.3

Clinical Correlates

Cell death in the photoreceptor cell layer is likely to be a significant factor in visual recovery after reattachment, particularly in

detachments of more than a few days' duration. Finding a strategy for preserving photoreceptors may lead to an improvement of the visual outcome after reattachment surgery. A number of factors have been successful at reducing cell death in animal models including brain-derived neurotrophic factor (BDNF), ciliary neurotrophic factor (CNTF), and basic fibroblast growth factors (FGF-1, FGF-2), the free radical scavenger edaravone, the antibiotic minocycline, and the Fas receptor inhibitor MET12.[43-49] Increasing the concentration of environmental oxygen breathed has also yielded positive results.[22,50]

The loss of cells from the photoreceptor layer occurs by cell death and the extrusion of photoreceptor cell bodies past the outer limiting membrane into the subretinal space. Photoreceptor cell death by apoptosis and necrosis[25,27,51,52] has also been documented in human studies.[8,53,54] The mechanism by which cells are extruded into the subretinal space is not understood, but they have clearly lost their differentiated phenotype, appearing as rounded cells with very little cytoplasm. With increasing chronicity of retinal detachment, disorganized lamellar debris rather than discrete packets of outer-segment discs are found in the subretinal space, providing additional evidence that discs are not shed and phagocytosed in the normal manner.

Second-Order Neurons and Nonneuronal Cell Types

Beyond 3 days of detachment, Müller cell processes often extend into the subretinal space through localized disruptions in the outer limiting membrane. These processes become more commonplace and elaborate as detachment time lengthens. Immunocytochemical labeling and confocal imaging studies demonstrate their unique nature. In felines, Müller cell processes within the retina that preferentially express vimentin in the outer portion of the cell grow into the subretinal space.[37] At the presumed earliest stage of their growth, the vimentin-expressing processes beyond the outer limiting membrane assume the appearance of filopodia while retaining their preferential expression of vimentin over GFAP.

Microvilli normally extend from the apical surface of the Müller cells, just beyond the outer limiting membrane. These processes are richly decorated with the protein CD-44. As the Müller cell filopodia intrude into the subretinal space, their surface remains decorated with "microspikes" of CD-44. The presence of CD-44 on the apical microvilli and subretinal outgrowths may provide for sites of molecular interaction between the growing processes and components of the subretinal space, perhaps providing some clue to their preference for growing adjacent to cone photoreceptors.[55] These Müller cell processes can grow for long distances on the photoreceptor border, often forming a multilayered "glial scar" within the subretinal space (see Fig. 31.5C and Box 31.4).

Box 31.4

Clinical Correlates

Subretinal Müller cell processes are responsible for the formation of subretinal membranes often seen in patients with chronic retinal detachment and proliferative vitreoretinopathy. These may subsequently inhibit photoreceptor recovery and limit visual acuity. Subretinal membranes may also cause visual distortion by preventing proper flattening of the retina or by disturbing the contour of the overlying retina. Clinically, subretinal membranes differ in nature to those seen on the retinal surface, and this may be partly explained by the different expression of proteins on their surface.

In a study of 16 retinectomy specimens taken from patients with PVR, Sethi et al. demonstrated that the response to prolonged RRD with PVR in humans was similar to that observed in chronic detachment in animal models.[6] In humans, as in animal models, photoreceptors were degenerate and intracellular redistribution of opsin proteins to the plasma membrane was observed. In cones, labeling with anti-M/L cone opsin showed degenerate outer segments and faint staining of swollen inner segments and, in severe PVR, staining of cone opsins was absent. Rod synaptic terminals showed remodeling with extension of rod bipolar cell dendrites and horizontal cell processes into the outer nuclear layer. There was also upregulation of neurofilament and GAP-43 expression in large ganglion cells with neurite sprouting. All

retinectomy specimens showed a marked upregulation of Müller cell and astrocyte expression of GFAP and vimentin, with areas of increased glial tissue replacing degenerated retinal neurons (Fig. 31.12).[6] In some sections Müller cells, together with microglia, breached the inner limiting membrane and extended onto the retinal surface where they formed one of the components of an epiretinal membrane (see Fig. 31.5D). Müller cell processes also formed confluent subretinal membranes (Fig. 31.12). Ongoing photoreceptor apoptosis has also been demonstrated in human PVR.[54]

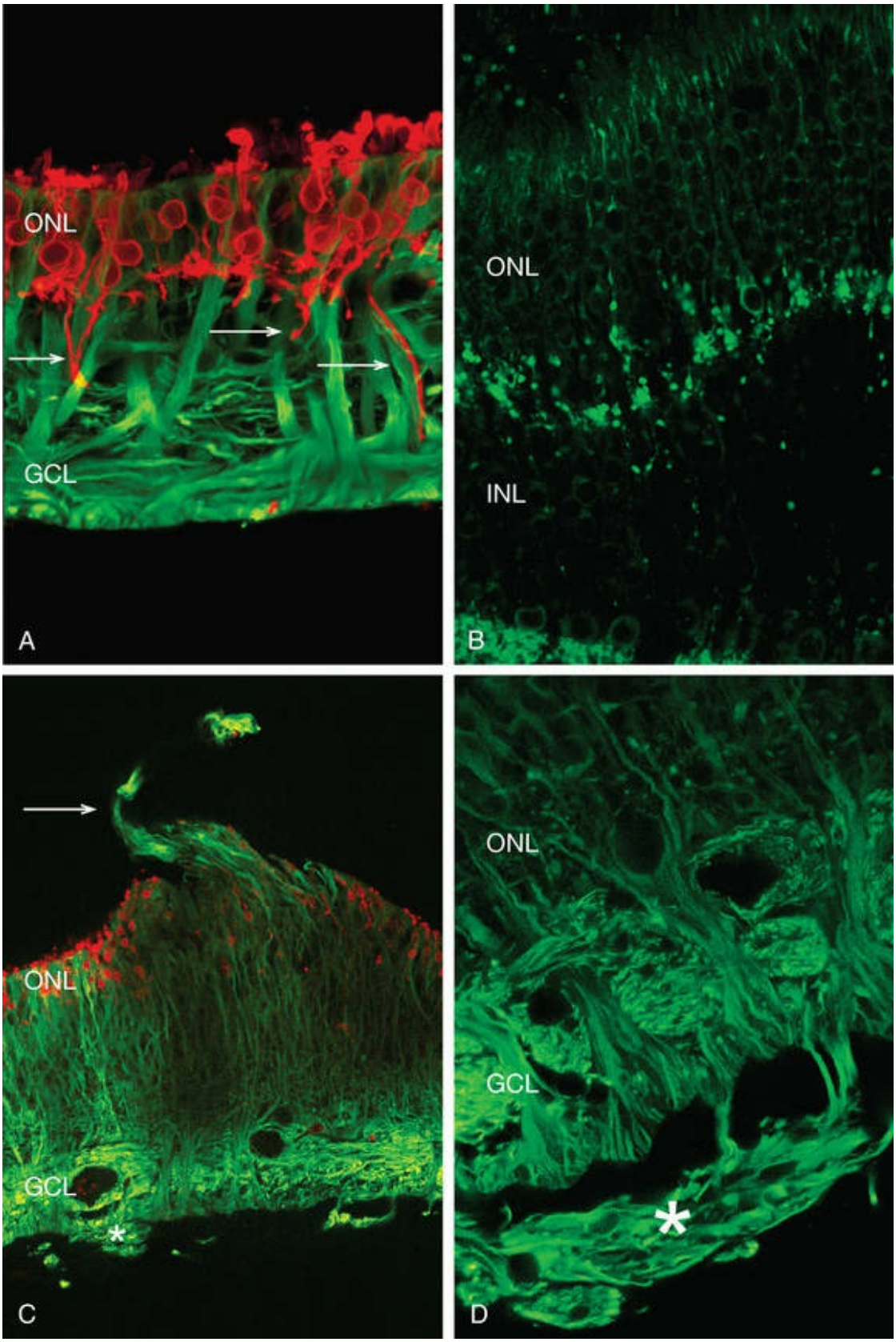

FIG. 31.12 Laser scanning confocal images of human retinas that had been previously reattached, illustrating similar responses to detachment as those observed in the feline model. (A) Rod axons (*arrows*; red; antirod

opsin) extend into the inner retina, and Müller cells upregulate their expression of glial fibrillary acidic protein (*GFAP*) (green). (B) Synaptic terminals (green "dots"; antisynaptophysin) become scattered within the outer nuclear layer (*ONL*), indicating the presence of retracted rod terminals, while the green "dots" in the inner nuclear layer (*INL*) represent terminals of "overgrown" rod axons. (C) Müller cells (green; anti-GFAP) grow on to the subretinal surface (*arrow*) and on to the vitreal surface (*asterisk*). In the absence of outer segments, antirod opsin (red) labels rod cell bodies. (D) Müller cell outgrowths (green; anti-GFAP) grow beyond the inner limiting membrane to form an epiretinal membrane on the vitreal surface of the retina (*asterisk*). *GCL*, ganglion cell layer. (Panels C and D reproduced with permission from Sethi CS, Lewis GP, Fisher SK. Glial remodelling and neuronal plasticity in human retinal detachment with proliferative vitreoretinopathy. Invest Ophthalmol Vis Sci 2005;46:329–42.)

Retinal Reattachment

Clinical evidence shows that retinal reattachment is associated with good visual outcomes, particularly if the macula is rapidly reattached, and that visual recovery may continue for some time following surgery.[56,57] This suggests that some of the changes described above may be reversible or have little effect on visual function, when measured by Snellen acuities and patient reported outcomes.[58] A number of factors are associated with poor visual outcomes, including involvement of the macula, the duration and extent of the detachment, and the development of PVR.[3] Development of PVR is associated with a significant deterioration in visual outcomes, and this is likely to reflect more than just the length of detachment as good outcomes can still be achieved in patients who undergo multiple operations for retinal detachment with no clinical PVR.[2,56]

Feline models have shown that rapid retinal reattachment is associated with a good but not complete restoration of neural circuitry.[2,19] This has also been observed clinically in human case series, for example in patients undergoing translocation surgery:

despite only minor changes in neuronal remodeling being observed prior to reattachment, some patients still developed PVR postoperatively.[4] This suggests that the retina had been primed or activated by retinal detachment and that this process remained active despite subsequent rapid reattachment.[4] This is consistent with the observation that within 15 minutes of retinal detachment there are changes in growth factor expression that may lead to irreversible changes in cellular structure.[9] For example, in rabbits and cats a single intravitreal injection of 1 μg of basic fibroblast growth factor (bFGF) leads to FGFR internalization, Müller cell proliferation, an increased expression of GFAP and vimentin, and the growth of Müller cell processes onto the vitreal surface of the retina.[59,60] It is possible therefore that, in some patients, the cellular events initiated by this rapid response to retinal detachment may persist despite reattachment, resulting in the development of PVR following retinal reattachment or translocation surgery.

Animal models have given us a clearer understanding of cellular recovery following retinal reattachment. In the feline model, retinal reattachment within 1–3 days is very effective at reversing the cellular changes induced by retinal detachment.[2,19] Retinal recovery relies on reestablishing the cell-to-cell contact of RPE cells and photoreceptors. This involves redifferentiation of the RPE apical surface, re-ensheathment of the regenerating outer segments (which differs for rods and cones), and probably synthesis of interphotoreceptor matrix components. Finally, the photoreceptors and RPE must also reestablish a functional relationship. For example, a normal balance between disc addition and disc shedding must be restored if the outer segments are going to attain normal length. Clinical evidence indicates that this process may occur over months or even years.[57] In addition, the transport of ions and molecules between the retina and RPE, which is affected to an unknown degree when the two cell layers are separated from each other, must also be restored. For example, retinoids (chemically distinct forms of vitamin A), coupled with their binding proteins, must be transported back and forth between the neural retina and the RPE as part of the visual cycle.[61]

In the feline model, retinal reattachment following a 3-day detachment results in recovery of the outer segments to

approximately 70% of their length at 28 days, arrested photoreceptor apoptosis, and a reduction in cellular proliferation.[62] Regenerating outer segments may appear shortened and misaligned with respect to each other and stacking of the disc membranes is often abnormal. In monkey retinas detached for 1 week, rod and cone outer segments regain approximately 30% of their normal mean length within 7 days of reattachment, 60% of their length after 30 days, and 100% by 150 days.[63] In the first 30-day interval, the mean disc membrane assembly rate in rods is approximately one-third slower than the normal rate. Disc shedding, on the other hand, appears to engage after the first reattachment week. Photoreceptor recovery may also be determined by the duration of retinal detachment prior to reattachment. In cat retinas detached for periods longer than 7 days, many outer segments remained shorter than normal several months after reattachment,[64] implying that defects in the assembly or shedding phases (or both) of the renewal process may persist well beyond 30 days of reattachment in retinas detached for longer durations. Long-term reattachment experiments are expensive because of the cost of maintaining experimental animals, but they may be highly informative given our lack of understanding of long-term recovery and indications that visual recovery may continue for a very long time after reattachment in humans.

Retinal reattachment may also stimulate the formation of scar tissue. The development of PVR following retinal reattachment surgery remains the major cause of surgical failure. In the feline model, reattachment induces growth into the vitreous of Müller cell processes, that form epiretinal membranes.[19,35] These have a different structure and a different intermediate filament composition compared to those that grow into the subretinal space.[37] The initial outgrowths into the vitreous occur as thin "wispy" extensions of the endfoot region and have an intermediate filament population that is dominated by GFAP instead of vimentin. These Müller cell processes then act as a substrate for ganglion cell neurite growth.[35,65,66] In humans and animal models rod axons are also stimulated to grow by retinal reattachment, and this may be seen as neurite extensions into the inner retina and beyond to the vitreal surface within epiretinal membranes (Fig.

31.13).[6,19,65]

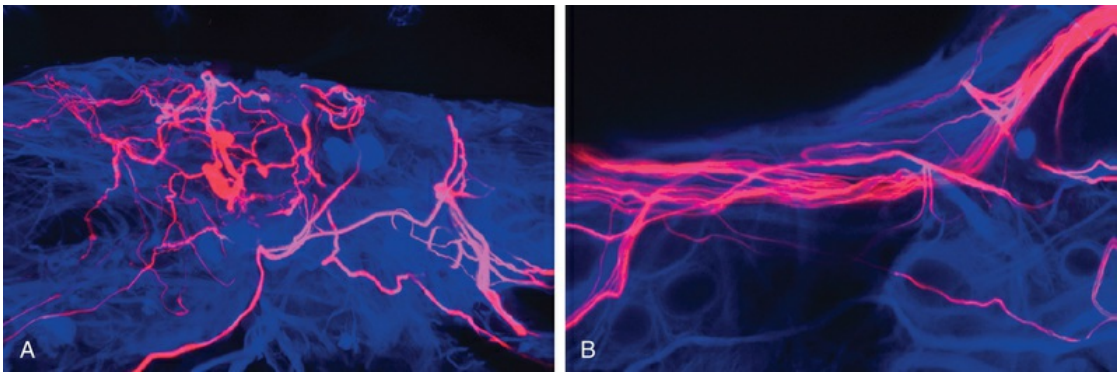

FIG. 31.13 Laser scanning confocal images of two different epiretinal membranes removed from human patients with proliferative vitreoretinopathy and immunolabeled with antineurofilament, for neurites (red) and antiglial fibrillary acidic protein for glial cells (blue). Neurites were invariably observed in all membranes examined but only in regions containing glial cells.

Restoration of retinal anatomy following reattachment is not uniform. The morphologic appearance has been described as a "patchwork," with areas of variability in outer-segment length and levels of protein expression within the same retina (Fig. 31.14).[19,62] There is also variability between different retinas.[19,62] Although this may reflect the variations in the extent (detachment height) and duration of detachment seen clinically in humans, this patchwork appearance is still observed in controlled detachment experiments. In the feline model, in areas where the apposition of the retina with the apical surface of the RPE is restored, photoreceptors are quick to regenerate. In some areas where RPE cells may have proliferated with rounded apical surfaces and/or reversal of cellular polarity, bearing little resemblance to normal RPE, photoreceptor outer-segment regeneration following retinal reattachment is far more likely to be abnormal.[67] In areas where photoreceptor recovery is poor, microglia remain activated, suggesting that they may play a role in modulating recovery.[30] Similarly, in areas where Müller cell hypertrophy has led to the formation of a subretinal scar, photoreceptors only show limited signs of recovery with no outer-

segment regeneration.

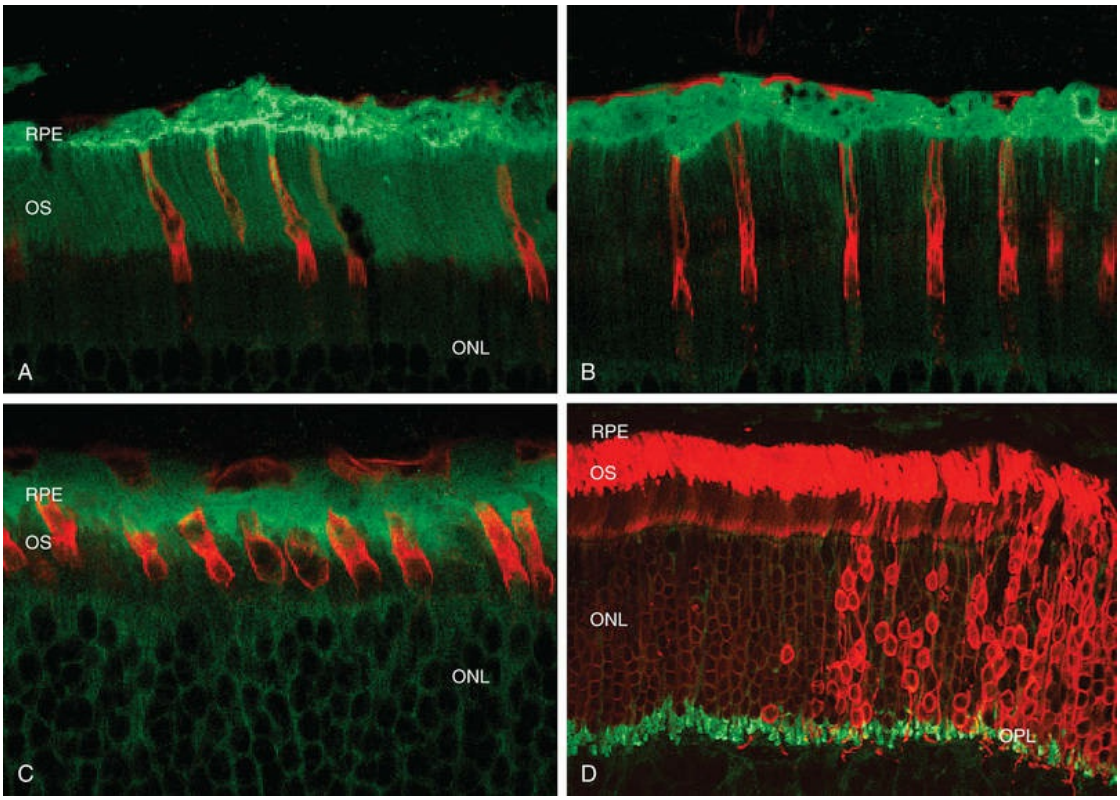

FIG. 31.14 Laser scanning confocal images illustrating the "patchy" recovery that occurs in the feline retina following reattachment. (A–C) Retinas are labeled with biotinylated peanut agglutinin lectin (red; labels cone matrix sheaths) and anticellular retinaldehyde-binding protein (green; labels the retinal pigment epithelium [RPE]). (A) Normal, control retina. (B–D) Retinas detached for 3 days and reattached for 28 days. (B) In many areas of the reattached retina, the cone matrix sheath appears similar to that observed in normal (A) retina. (C) In some regions, however, the cone matrix sheaths appear greatly truncated. In these areas the RPE sits adjacent to the inner segments, indicating little regeneration of either rod or cone outer segments (*OS*). (D) When the reattached retina is labeled with antirod opsin (red), regions within the reattached area can show different levels of OS regeneration. In some regions, rod OS are quite long and there is no rod opsin labeling in the outer nuclear layer (*ONL*) (left half of micrograph), while in an adjacent region, rod OS are truncated and rod opsin is redistributed to the rod cell

bodies (right half of micrograph). The green in (D) represents labeling of the photoreceptor synaptic terminals with an antibody to synaptophysin. *OPL*, outer plexiform layer. (Reproduced with permission from Lewis GP, Sethi CS, Linberg KA, et al. Experimental retinal reattachment – a new perspective. Mol Neurobiol 2003;28:159.)

At present it seems reasonable to conclude that a return towards completely normal retinal morphology occurs gradually over a timespan of months or years, even after brief episodes of detachment.[57,64] Incomplete morphologic recovery may, however, be sufficient to subserve near-normal vision, although functional correlates in humans are lacking.

References

1. Fisher SK, Lewis GP, Linberg KA, Verardo M. Cellular remodelling in mammalian retina: results from studies of experimental retinal detachment. *Prog Retin Eye Res*. 2005;24:395–431.
2. Lewis GP, Charteris DG, Sethi CS, Leitner WP, Linberg KA, Fisher SK. The ability of rapid retinal reattachment to stop or reverse the cellular and molecular events initiated by detachment. *Invest Ophthalmol Vis Sci*. 2002;43:2412–2420.
3. Burton TC. Recovery of visual acuity after retinal detachment involving the macula. *Trans Am Ophthalmol Soc*. 1982;80:475–497.
4. Wickham L, Lewis GP, Charteris DG, Fisher SK, Da Cruz L. Histological analysis of retinas sampled during translocation surgery: a comparison with normal and transplantation retinas. *Br J Ophthalmol*. 2009;93:969–973.
5. Wickham L, Sethi CS, Lewis GP, Fisher SK, McLeod DC, Charteris DG. Glial and neural response in short-term human retinal detachment. *Arch Ophthalmol*. 2006;124:1779–1782.
6. Sethi CS, Lewis GP, Fisher SK, Leitner WP, Mann DL, Luthert PJ, Charteris DG. Glial remodelling and neuronal plasticity in human retinal detachment with proliferative vitreoretinopathy. *Invest Ophthalmol Vis Sci*. 2005;46:329–

342.
7. Wilson DJ, Green WR. Histopathological study of the effect of retinal detachment surgery on 49 eyes obtained post mortem. *Am J Ophthalmol*. 1987;103:167–179.
8. Chang CJ, Lai WW, Edward DP, Tso MO. Apoptotic photoreceptor cell death after traumatic retinal detachment in humans. *Arch Ophthalmol*. 1995;113:880–886.
9. Geller SF, Lewis GP, Fisher SK. FGFR1 signaling and AP-1 expression after retinal detachment: reactive Müller and RPE cells. *Invest Ophthalmol Vis Sci*. 2001;42:1363–1369.
10. Anderson DH, Stern WH, Fisher SK, Erickson PA, Borgula GA. Retinal detachment in the cat: the pigment epithelial-photoreceptor interface. *Invest Ophthalmol Vis Sci*. 1983;24:906–926.
11. Campochiaro PA, Jerdan JA, Glaser BM. The extracellular matrix of human retinal pigment epithelial cells in vivo and its synthesis in vitro. *Invest Ophthalmol Vis Sci*. 1986;27:1615–1621.
12. Steinberg RH, Wood I. The relationship of the retinal pigment epithelium to photoreceptor outer segments in the human retina. Zimm KM, Marmor ME. *The retinal pigment epithelium*. Harvard University Press: Cambridge, MA; 1979.
13. Fisher SK, Anderson DH. Cellular responses of the RPE to retinal detachment and reattachment. Marmor MF, Wolfensberger TJ. *The retinal pigment epithelium*. Oxford University Press: Oxford; 1999.
14. Immel J, Negi A, Marmor MF. Acute changes in RPE apical morphology after retinal detachment in rabbit: a SEM study. *Invest Ophthalmol Vis Sci*. 1986;27:1770–1776.
15. Anderson DH, Stern WH, Fisher SK, Erickson PA, Borgula GA. The onset of pigment epithelial proliferation after retinal detachment. *Invest Ophthalmol Vis Sci*. 1981;21:10–16.
16. Fisher SK, Erickson PA, Lewis GP, Anderson DH. Intraretinal proliferation induced by retinal detachment. *Invest Ophthalmol Vis Sci*. 1991;32:1739–1748.
17. Geller SF, Lewis GP, Anderson DH, Fisher SK. Use of the MIB-1 antibody for detecting proliferating cells in the retina. *Invest Ophthalmol Vis Sci*. 1995;36:737–744.

18. Johnson NF, Foulds WS. Observations on the retinal pigment epithelium and retinal macrophages in experimental retinal detachment. *Br J Ophthalmol*. 1977;61:564–572.
19. Lewis GP, Sethi CS, Linberg KA, Charteris DG, Fisher SK. Experimental retinal reattachment – a new perspective. *Mol Neurobiol*. 2003;28:159–175.
20. Fariss RN, Molday RS, Fisher SK, Matsumoto B. Evidence from normal and degenerating photoreceptors that two outer segment integral membrane proteins have separate transport pathways. *J Comp Neurol*. 1997;387:148–156.
21. Rex TS, Fariss RN, Lewis GP, Linberg KA, Sokal I, Fisher SK. A survey of molecular expression by photoreceptors after experimental retinal detachment. *Invest Ophthalmol Vis Sci*. 2002;43:1234–1247.
22. Mervin K, Valter K, Maslim J, Lewis GP, Fisher SK, Stone J. Limiting photoreceptor death and deconstruction during experimental retinal detachment: the value of oxygen supplementation. *Am J Ophthalmol*. 1999;128:155–164.
23. Rodieck RW. *The vertebrate retina*. WH Freeman: San Francisco; 1973.
24. Matsumoto H, Kataoka K, Tsoka P, Connor KM, Miller JW, Vavvas DG. Strain difference in photoreceptor cell death after retinal detachment in mice. *Invest Ophthalmol Vis Sci*. 2014;55:4165–4174.
25. Cook B, Lewis GP, Fisher SK, Adler R. Apoptotic photoreceptor degeneration in experimental retinal detachment. *Invest Ophthalmol Vis Sci*. 1995;36:990–996.
26. Zacks DN, Hanninen V, Pantcheva M, Ezra E, Grosskreutz C, Miller JW. Caspase activation in an experimental model of retinal detachment. *Invest Ophthalmol Vis Sci*. 2003;44:1262–1267.
27. Murakami Y, Miller JW, Vavvas DG. RIP Kinase-mediated necrosis as an alternative mechanism of photoreceptor death. *Oncotarget*. 2011;2(6):497–509.
28. Arroyo JG, Yang L, Bula D, Chen DF. Photoreceptor apoptosis in human retinal detachment. *Am J Ophthalmol*. 2005;139:605–610.

29. Chandra A, Banerjee P, Davis D, Charteris D. Ethnic variation in rhegmatogenous retinal detachments. *Eye (Lond)*. 2015;29:803–807.
30. Lewis GP, Sethi CS, Carter KM, Charteris DG, Fisher SK. Microglial cell activation following retinal detachment: a comparison between species. *Mol Vis*. 2005;11:491–500.
31. Lewis GP, Linberg KA, Fisher SK. Neurite outgrowth from bipolar and horizontal cells after experimental retinal detachment. *Invest Ophthalmol Vis Sci*. 1998;39:424–434.
32. Linberg KA, Lewis GP, Fisher SK. Retraction and remodeling of rod spherules are early events following experimental retinal detachment: an ultrastructural study using serial sections. *Mol Vis*. 2009;15:10–25.
33. Erickson PA, Fisher SK, Anderson DH, Stern W, Borgula GA. Retinal detachment in the cat: the outer nuclear and outer plexiform layers. *Invest Ophthalmol Vis Sci*. 1983;24:927–942.
34. Coblentz FE, Radeke MJ, Lewis GP, Fisher SK. Evidence that ganglion cells react to retinal detachment. *Exp Eye Res*. 2003;76:333–342.
35. Fisher SK, Lewis GP. Mueller cell and neuronal remodelling in retinal detachment and reattachment and their potential consequences for visual recovery: a review and reconsideration of recent data. *Vision Res*. 2003;43:887–897.
36. Lewis GP, Chapin EA, Luna G, Linberg KA, Fisher SK. The fate of Muller's glia following experimental retinal detachment: nuclear migration, cell division, and subretinal glial scar formation. *Mol Vis*. 2010;16:1361–1372.
37. Lewis GP, Fisher SK. Upregulation of glial fibrillary acidic protein in response to retinal injury: its potential role in glial remodelling and a comparison of vimentin expression. *Int Rev Cytol*. 2003;230:263–290.
38. Luna G, Lewis GP, Banna CD, Skalli O, Fisher SK. Expression profiles of nestin and synemin in reactive astrocytes and Müller cells following retinal injury: a comparison with glial fibrillar acidic protein and vimentin. *Mol Vis*. 2010;16:2511–2523.
39. Eibl KH, Lewis GP, Betts K, et al. The effect of

alkylphosphocholines on intraretinal proliferation initiated by experimental retinal detachment. *Invest Ophthalmol Vis Sci*. 2007;48:1305–1311.
40. Lewis GP, Chapin EA, Byun J, Luna G, Sherris D, Fisher SK. Müller cell reactivity and photoreceptor cell death are reduced after experimental retinal detachment using an inhibitor of the Akt/mTOR pathway. *Invest Ophthalmol Vis Sci*. 2009;50:4429–4435.
41. Pennock S, Kim D, Mukai S, et al. Ranibizumab is a potential prophylaxis for proliferative vitreoretinopathy, a nonangiogenic blinding disease. *Am J Pathol*. 2013;182:1659–1670.
42. Zahn G, Volk K, Lewis GP, et al. Assessment of the integrin alpha5beta1 antagonist JSM6427 in proliferative vitreoretinopathy using in vitro assays and a rabbit model of retinal detachment. *Invest Ophthalmol Vis Sci*. 2010;51:1028–1035.
43. Lewis GP, Linberg KA, Geller SF, Guerin CJ, Fisher SK. Effects of the neurotrophin brain-derived neurotrophic factor in an experimental model of retinal detachment. *Invest Ophthalmol Vis Sci*. 1999;40:1530–1544.
44. Faktorovich EG, Steinberg RH, Yasumura D, Matthes MT, LaVail MM. Basic fibroblast growth factor and local injury protect photoreceptors from light damage in the rat. *J Neurosci*. 1992;12:3554–3567.
45. LaVail MM, Unoki K, Yasumura D, Matthes MT, Yancopoulos GD, Steinberg RH. Multiple growth factors, cytokines, and neurotrophins rescue photoreceptors from the damaging effects of constant light. *Proc Natl Acad Sci USA*. 1992;89:11249–11253.
46. LaVail MM, Yasumura D, Matthes MT, et al. Protection of mouse photoreceptors by survival factors in retinal degenerations. *Invest Ophthalmol Vis Sci*. 1998;39:592–602.
47. Roh MI, Murakami Y, Thanos A, Vavvas DG, Miller JW. Edaravone, an ROS scavenger, ameliorates photoreceptor cell death after experimental retinal detachment. *Invest Ophthalmol Vis Sci*. 2011;52:3825–3831.
48. Yang L, Kim JH, Kovacs KD, Arroyo JG, Chen DF.

Minocycline inhibition of photoreceptor degeneration. *Arch Ophthalmol*. 2009;127:1475–1480.
49. Besirli CG, Chinskey ND, Zheng QD, Zacks DN. Inhibition of retinal detachment-induced apoptosis in photoreceptors by a small peptide inhibitor of the fas receptor. *Invest Ophthalmol Vis Sci*. 2010;51:2177–2184.
50. Lewis GP, Talaga KC, Linberg KA, Avery RL, Fisher SK. The efficacy of delayed oxygen therapy in the treatment of experimental retinal detachment. *Am J Ophthalmol*. 2004;137:1085–1095.
51. Sakai T, Lewis GP, Linberg KA, Fisher SK. The ability of hyperoxia to limit the effects of experimental detachment in cone-dominated retina. *Invest Ophthalmol Vis Sci*. 2001;42:3264–3273.
52. Linberg KA, Sakai T, Lewis GP, Fisher SK. Experimental retinal detachment in the cone-dominant ground squirrel retina: morphology and basic immunocytochemistry. *Vis Neurosci*. 2002;19:603–619.
53. Xu GZ, Li WW, Tso MO. Apoptosis in human retinal degenerations. *Trans Am Ophthalmol Soc*. 1996;94:411–430.
54. Charteris DG, Downie J, Aylward GW, Sethi C, Luthert P. Intraretinal and periretinal pathology in anterior proliferative vitreoretinopathy. *Graefes Arch Clin Exp Ophthalmol*. 2007;245:93–100.
55. Lewis GP, Fisher SK. Müller cell outgrowth after retinal detachment: association with cone photoreceptors. *Invest Ophthalmol Vis Sci*. 2000;41:1542–1545.
56. Wickham L, Bunce C, Wong D, Charteris DG. Retinal detachment repair by vitrectomy: simplified formulae to estimate the risk of failure. *Br J Ophthalmol*. 2011;95(9):1239–1244.
57. Kusaka S, Toshino A, Ohashi Y, Sakaue E. Long-term visual recovery after scleral buckling for macular-off retinal detachments. *Jpn J Ophthalmol*. 1998;42:218–222.
58. Sullivan P, Luff AJ, Julious SA, Canning CR. Patient satisfaction following vitreoretinal surgery. *Eye (Lond)*. 1993;7:433–435.
59. Lewis GP, Fisher SK, Anderson DH. Fate of biotinylated

basic fibroblast growth factor in the retina following intravitreal injection. *Exp Eye Res*. 1996;62:309–324.
60. Lewis GP, Erickson PA, Guerin CJ, Anderson DH, Fisher SK. Basic fibroblast growth factor: a potential regulator of proliferation and intermediate filament expression in the retina. *J Neurosci*. 1992;12:3968–3978.
61. Bunt-Milam AH, Saari JC. Immunocytochemical localization of two retinoid-binding proteins in vertebrate retina. *J Cell Biol*. 1983;97:703–712.
62. Lewis GP, Charteris DG, Sethi CS, Fisher SK. Animal models of retinal detachment and reattachment: identifying cellular events that may affect visual recovery. *Eye (Lond)*. 2002;16:375–387.
63. Guerin CJ, Lewis GP, Fisher SK, Anderson DH. Recovery of photoreceptor outer segment length and analysis of membrane assembly rates in regenerating primate photoreceptor outer segments. *Invest Ophthalmol Vis Sci*. 1993;34:175–183.
64. Anderson DH, Guerin CJ, Erickson PA, Stern WH, Fisher SK. Morphological recovery in the reattached retina. *Invest Ophthalmol Vis Sci*. 1986;27:168–183.
65. Lewis GP, Betts KE, Sethi CS, et al. Identification of ganglion cell neurites in human subretinal and epiretinal membranes. *Br J Ophthalmol*. 2007;91:1234–1238.
66. Lesnik Oberstein SY, Lewis GP, Chapin EA, Fisher SK. Ganglion cell neurites in human idiopathic epiretinal membranes. *Br J Ophthalmol*. 2008;92:981–985.
67. Guerin CJ, Anderson DH, Fariss RN, Fisher SK. Retinal reattachment of the primate macula: photoreceptor recovery after short-term detachment. *Invest Ophthalmol Vis Sci*. 1989;30:1708–1725.

32

Serous and Hemorrhagic Detachment of the Sensory Retina and Pigment Epithelium

Gisèle Soubrane-Daguet, Gabriel Coscas

Introduction

Retinal detachment is defined as the accumulation of fluid between the neurosensory retina (NSR) and the underlying retinal pigment epithelium (RPE) in the remnant of the embryonic optic vesicle.[1] The different layers involved can presently be analyzed in vivo by optical coherence tomography (OCT). Retinal pigment epithelial detachment (PED) results from a separation between the RPE basement membrane and the inner collagenous layer of Bruch's membrane.[2] These abnormalities imply a dysfunction of the RPE that may be caused by choroidal or retinal diseases or both. The term “central” refers to the form of the disease causing visual symptoms due to the presence of serous detachments in the macular area.

Anatomic Constituents

Retinal Barrier

The RPE forms the outer retinal barrier (BRB), composed of a single polarized monolayer of cells. (The inner BRB being formed of tight junctions between retinal capillary endothelial cells.) The outer BRB is located at the tight junctions between the apical lateral membranes of the RPE cells. Tight junctions are complex structures that are dynamically regulated. The integrity of the BRB is fundamentally important for the health and function of the inner and the outer retina.[3] It is a particularly restrictive physiologic barrier. BRB regulates the flow of nutrients, metabolic waste products, ions, proteins, the movement of solutes, and water flux between the fenestrated capillaries of the choroid and the photoreceptor layer into and out of the retina. Various mechanisms to accomplish its tasks are used including membrane pumps, transporters, and channels, transcytosis, metabolic alteration of solutes in transit, and passive but selective diffusion. The last category includes tight junctions, which regulate transepithelial diffusion through the spaces between neighboring cells.

Bruch's Membrane

Bruch's membrane (BM) is a unique pentalaminar structure, which

is strategically located between the RPE and the choroidal capillaries. It is believed there are structural connections between the RPE and Bruch's membrane. The inner portion of Bruch's membrane is the basement membrane of the pigment epithelial cells, to which the cells adhere. Local electron-dense areas can be seen in this basement membrane, and it is thought these represent sites of insertion of collagen fibers from the inner collagenous layer of Bruch's membrane into the basement membrane. The outer limit of Bruch's membrane is the basement membrane of the choriocapillaris, the collagenous and elastic layers lying in front. BM is an elastin- and collagen-rich extracellular matrix that acts as a molecular sieve partly regulating the reciprocal exchange of products between the retina and the general circulation.

The Choriocapillaris

The choriocapillaris is a continuous plexus of large capillaries (50 μm in diameter) that lies in a single plane beneath the RPE. The wall of the choriocapillaris facing Bruch's membrane is fenestrated with circular openings (fenestrae) measuring approximately 800 Å. The fenestrae of the choriocapillaris are unique in that they have a diaphragm covering them, unlike those seen in the renal glomerulus.

These fenestrae allow easy movement of macromolecules into the extracapillary compartment. Fluid and macromolecules escaping from these leaky vessels percolate through Bruch's membrane and have access to the basal side of the RPE.[4]

Mechanism of Normal Attachment

The RPE plays a critical role in the visual cycle and photoreceptor outer-segment phagocytosis. Furthermore, it is the main transport pathway between the inner retina and the choriocapillaris through the Müller cells.[5] The mechanisms by which the retina is normally maintained in apposition to the pigment epithelium, and the pigment epithelium to Bruch's membrane, have not been defined, although many factors have been identified. Mechanical and metabolic factors intervene in the attachment from the RPE to the

photoreceptors on one side and to Bruch's membrane on the other side.

Mechanical Factors

The physiologic mechanisms of adhesion of the neural retina to the RPE are highly synergistic and complex and involve mechanical and metabolic factors.[6] Briefly, these include the active and passive metabolism of the RPE, the properties of the interphotoreceptor matrix (IPM), and established pressure gradients between the retina and choroid.

Adhesion

Mechanical forces inside the subretinal space (SRS) include the matrix material between the NSR and RPE and the complex anatomic relationship with the outer segments of the photoreceptors.[7]

The IPM is a highly organized structure with interconnected domains surrounding cone and rod photoreceptor cells and extends throughout the subretinal space. The IPM is thought to have several prominent functions including serving as a receptor for growth factors, regulating retinoid transport, participating in cytoskeletal organization in surrounding cells, and regulation of oxygen and nutrient transport.[8] The IPM occupies the interface between the matrix **and** may act as a glue binding the NSR and the RPE. The IPM has structural components that remain attached to both the RPE and the cones and become apparent when the RPE is peeled off.[9] Cones and rods are surrounded by a specific matrix.[10,11] Cell adhesion molecules or receptors may be involved in this interaction between the matrix and the cellular membranes.[12,13]

Factors that affect the physicochemical properties of the IPM and enzymes that degrade some of its components such as proteoglycan-degrading enzymes (given intravitreally or directly into the IPM in primate eyes) weaken retinal adhesion.[14] Similarly, hyaluronidase and neuraminidase degrade chondroitin sulfate proteoglycan and sialoglycoconjugates, respectively. This decreased adhesion suggests that the IPM plays a role in normal retina–RPE adhesion.[15]

No data are available on the influence of repeated intravitreal injections of any compound on RPE and IPM adhesion and intracellular RPE transport in humans and animals.

The mechanism by which interdigitations of RPE apical villous processes and photoreceptor outer segments contribute to retinal adhesion is still not yet clear. They play a crucial role in disc phagocytosis and renewal, but their role in adhesion is uncertain.[16] They may provide a frictional resistance or an electrostatic force that opposes separation, but the magnitude of this is unknown.[16] However, three mechanisms have been proposed. These include the continuous process of phagocytosis of photoreceptor outer segments by RPE cells during which the two cells are intimately connected,[17] the frictional forces that result from the interdigitations, and the possible presence of electrostatic interaction between the cell membranes.[18]

Intercellular adhesion molecule-1 (ICAM-1) is an endothelial- and leukocyte-associated transmembrane protein long known for its importance in stabilizing cell–cell interactions and facilitating leukocyte endothelial transmigration. Upon cytokine stimulation, i.e., interleukin-1 (IL-1β) and tumor necrosis factor-alpha, the concentrations of ICAM-1 greatly increase.[19] The role of interphotoreceptor retinoid-binding protein (IRBP)'s function in promoting Müller cell delivery and retrieval of retinols may be critical to photoreceptor and RPE function and integrity.

Pressure Gradient

Passage of fluid from the vitreous, across the retina and RPE, and out of the SRS is associated with a pressure gradient from the vitreous.

Mechanical forces include active transport across the RPE, and passive hydrostatic and oncotic forces. Fluid is driven towards the choroid by active transport across the RPE and by passive hydrostatic and oncotic forces, which is blocked in the normal eye by the RPE tight junction barrier.

The high oncotic pressure in the choroid, when compared to the vitreous, maintains the necessary fluid dynamics for intact retinal attachment in causing outward movement of the water. In addition, osmolarity modifies the spontaneous resolution speed in

experimental nonrhegmatogenous retinal detachments induced by subretinal injection.

Formed vitreous acts in maintaining adhesion between the retina and RPE.[20] Whether the vitreous plays a direct role in retinal adhesion is yet to be determined, although some studies suggest the physical structure of the vitreous might be of importance in maintaining retinal apposition.[20,21]

Metabolic Factors

Metabolic factors that affect retinal adhesion are intricate.

Oxygenation

Retinal adhesion is markedly decreased during ischemia[22,23] and is restored with oxygenation.[24] This can either be due to the effect of released RPE lysosomal enzymes on IPM[25] or due to the effect of ischemia on active RPE fluid transport.[26] The importance of metabolic factors in retinal adhesion is also inferred from the effect of many drugs that interfere with the pH and RPE fluid transport activity.

Water Movement

The RPE actively transports water from the SRS to the choroid. This active transport, as well as dehydrating the SRS, is a crucial factor in maintaining adhesion. RPE fluid transport is normally limited by the retina, which resists water flow from the vitreous. Fluid exits partially through the trabecular meshwork and the uveo scleral route; however, a small proportion tends to exit from the vitreous to the choroid by virtue of the intraocular and choroidal oncotic pressures.[27]

In addition, the high osmotic pressure in the choroid causes outward movement of water.[28–30] Also, the RPE is continuously moving ions toward the choroid with the associated movement of water.[31]

This constant water movement induces the apposition of the tissues. In human fetal (hf) RPE cells, acute exposure to interferon (IFN)-γ increased transepithelial fluid absorption from the retinal to the choroidal side of the tissue.[5] In addition, the IFN-cystic fibrosis

transmembrane conductance regulator (CFTR) pathway in RPE is also activated by nitric oxide, which is continually produced in large amounts by the inner retina and perhaps by the choriocapillaris. Therefore, normal retinal metabolism helps dehydrate the SRS and maintain a close anatomic relationship between the photoreceptors and RPE.

An inward movement of fluid from the choroid into the vitreous could lead to retinal separation from the RPE because of retinal resistance to flow.[32,33]

Mechanisms of Impairment

Impairment of Water Movement

The retina will stay attached whether or not the RPE is intact, but retinal function requires the RPE barrier. Clinical serous detachments are unlikely to form solely as a result of small RPE defects or leaks, since the active and passive transport systems for removing subretinal fluid are both strong. The primary pathology in most cases of serous retinopathy is a diffuse metabolic or vascular abnormality of RPE fluid transport, and RPE defects or leaks are necessary and represent only secondary components of the disease.[34]

The development of a retinal PED is related to disorders in fluid outflow between the sensory retina and Bruch's membrane.[35] The normal nonvascular nature of Bruch's membrane is due to suppression by RPE of inward growth of choroidal blood vessels. The stimulus to change in growth factor production by RPE is unknown, but it is surmised that it may be due to lack of metabolic supply from plasma as a result of reduced diffusion of material through the thickened Bruch's membrane, or from reduced oxygen supply consequent upon changes in the choroidal capillaries.[36]

Detachment of the RPE is likely to be the consequence of increased resistance of Bruch's membrane to water flow. The mechanisms underlying this process are attributed to increased deposition of lipids,[37] enhanced collagen crosslinking, and alteration in the ratio of tissue-dissolving enzymes and their inhibitors.

In hypotony, in which it is assumed that water movement across the retina is severely reduced, clinically detectable detachment of the neuroretina from the pigment epithelium is extremely rare; it is much more characteristic under these circumstances for fluid to accumulate within the choroid.

In choroidal effusion syndrome, fluid accumulates between the choroid and the neuroretina in the absence of a retinal hole. In rhegmatogenous retinal detachment accumulation of fluid between the neuroretina and pigment epithelium is most commonly associated with retinal hole; in this instance the subretinal fluid is thought to be derived from the hyaloid cavity and to enter the SRS through the hole.

An intricate synergy of these factors is primarily responsible for maintaining retinal adhesion under normal conditions.

Occurrence of Detachment

A serous detachment will form if there are conditions that drive fluid against the normal gradients into the SRS and that limit its subsequent removal by active and passive transport. As long as the RPE is able to pump the leaking fluid into the choroidal circulation, no fluid accumulates in the SRS and no retinal detachment occurs. However, if the process continues and the normal RPE pump activity becomes overwhelmed, or if the RPE activity decreases because of RPE loss or decreased metabolic supply (e.g., ischemia), then fluid starts to accumulate and a retinal detachment occurs.[38] This type of retinal detachment can be also due to accumulation of blood in the SRS (hemorrhagic retinal detachment).

A continued influx and a reduced absorptive capacity of the surrounding RPE maintain the detachment. Protein will diffuse continuously out of the SRS, and high subretinal protein content will be maintained only if there is continued entry of new fluid with protein.

Most subretinal fluid is absorbed rapidly by active transport across the RPE. However, in the presence of damage to the RPE BRB, subretinal fluid is rapidly cleared by IFN-γ receptors localized to the basolateral membrane of human RPE which inhibit, when activated, cell proliferation and migration, decrease RPE

mitochondrial membrane potential, alter transepithelial potential and resistance, but also significantly increase transepithelial fluid absorption. In vivo experiments showed that IFN-γ can remove extra fluid deposited in the extracellular or SRS between the retinal photoreceptors and RPE.[5] Removal of this extra fluid can be blocked by a combination of inhibitors injected into the SRS. In addition, the IFN-CFTR pathway in RPE is activated by nitric oxide, which is continually produced in large amounts by the inner retina and, perhaps, by the choriocapillaris. IFN-γ regulates retinal hydration across the outer BRB, helps dehydrate the SRS, and maintains a close anatomic relationship between the photoreceptors and RPE.[39]

Persistence and Resorption of Serous Detachments

When the retina separates from the RPE secondary to retinal detachment of any type, the outer retina becomes ischemic due to loss of its blood supply from the choroid. Photoreceptor cell degeneration has been shown to increase as the distance between the RPE layer and the photoreceptor layer increases. The earliest light microscopic manifestations include accumulation of subretinal fluid with loss of photoreceptor outer segments, and if the process persists, the entire photoreceptor cell layer becomes atrophic.[40–42]

Apoptosis appears to play an important role in the time-dependent photoreceptor cell degeneration that occurs following retinal detachment.[43] In cases of chronic detachment, more prominent changes occur, including cystic and macrocystic retinal degeneration, retinal thinning, RPE alterations, demarcation lines, large drusen, choroidal neovascularization (CNV) at the ora serrata, and iris neovascularization secondary to angiogenic factor elaboration by the ischemic detached retina. As the detachment is mostly centered on the macula, the foveal cones at a distance from the RPE are less likely to receive adequate oxygenation and other nutrients from the choriocapillaris. After retinal reattachment, photoreceptor atrophy in the fovea typically occurs after a long duration.[44]

Subretinal fluid is removed both by active transport across the

RPE and by passive hydrostatic and oncotic forces that work most effectively when the RPE barrier has been damaged. Saline subretinal fluid is removed across the RPE into the choroidal space primarily by RPE metabolic activity.[45] cGMP, acetazolamide, and hyperosmotic agents experimentally facilitate its resorption. Clinical retinal detachments invariably contain protein, which slows the absorption of fluid. The biochemical interplay between the RPE and the retinal photoreceptors is affected.[45]

Potential sources of variation in the dynamics of precipitation and resorption of subretinal lipid include the surface area of the source of leakage and its effective pore size, the surface area of the site(s) of resorption, the active fluid and salt resorption capacity of the RPE, the phagocytic activity of the RPE and infiltrating macrophages, and the degree of infiltration of phagocytic cells in the SRS.[46]

The effects of intraocular pressure, vitreous pressure, and gravity on the resorption of small experimental retinal detachments (blebs) made with Hanks' solution or autologous serum was shown to be limited to normal subretinal fluid absorption. Neither liquefaction of the vitreous nor intra ocular pressure has a significant influence on fluid absorption.[47]

Clinical Manifestations of PED and Serous Retinal Detachments

Serous detachments, with elevation of the retina, occur in a variety of diseases. Regardless of the mechanism, all types of exudative or transudative retinal detachments, are characterized by fluid accumulation in the SRS, in the absence of retinal breaks or traction.

The source of the fluid is the vessels of the choroid, or *of* the retina, or *of* both. This can occur in a variety of vascular, inflammatory, or neoplastic diseases of the retina, RPE, and choroid[48] in which fluid leaks outside the vessels and accumulates under the retina. It is suggested that the primary pathology in most serous retinopathies is a diffuse metabolic or vascular abnormality of fluid transport, and that RPE defects or leaks are necessary but only secondary components of the disease.

Serous detachment of the neuroretina is observed under multiple circumstances: vascular diseases include malignant hypertension, toxemia of pregnancy, retinal vein occlusion, Coats' disease, retinal angiomatous diseases, and polypoidal choroidal vasculopathies. It is a characteristic of central serous retinopathy, which appears to be associated with focal dysfunction of the RPE secondary to dysregulation of the choroidal vasculature. Detachment of the retina from the RPE is also seen in primary choroidal disorders such as tumors, choroidal inflammation, ischemia, and in a variety of other conditions falling into the category of uveal effusion syndrome.

Accumulation of fluid between Bruch's membrane and the RPE is seen consistently in only one situation: PED. This occurs in the young as a manifestation of central serous retinopathy and in the elderly as a manifestation of age-related macular disease (AMD). The differentiation between various kinds of PEDs is essential because each PED type is a distinct entity that has a specific pathogenesis, natural history, prognosis, and optimal treatment strategy. Multimodal imaging of PED, enhanced depth imaging optical coherence tomography, and indocyanine green angiography allow a better analysis of the subretinal pigment epithelium compartment and could even enable visualization and localization of the entire branching neovascular network of CNV within fibrovascular (FV)-PED without dye injection.[49,50]

Serous Retinal Detachment Associated With Choroidal Dysregulation

Central Serous Chorioretinopathy

The separation of the outer segments of photoreceptors from the RPE by subretinal fluid should slow down the exchange of all-*trans* and 11-*cis* retinal. The RPE–photoreceptor visual cycle serves mainly the rods, and cone function is supported by a separate visual cycle within the sensory retina[51] and is thus less affected by the separation from the RPE.

Central serous chorioretinopathy (CSC) is a disease in which the NSR becomes detached, supposedly due to a single or multiple focal lesions within the RPE, which leaks into the SRS overlying

dysregulation of the choroidal vasculature. With indocyanine green angiography (ICGA), it has been demonstrated that CSC primarily affects the choroidal circulation and causes multifocal areas of choroidal vascular hyperpermeability.[52,53] PED shown by biomicroscopy, fluorescein angiography (FA), ICGA, and optical coherence tomography (OCT) can be seen in early stages of CSC, under the SRD. The location of these PEDs is the same as the location of the leakage in FA. Spontaneous resolution is the usual outcome.[54] The serous detachment extends significantly beyond the leak if the tight junctional RPE barrier under the elevated retina (except directly over the areas of leakage) is intact, since fluid would otherwise leave under hydrostatic and osmotic pressure.[55]

Chronic forms of CSC, defined as a persistent choroid anomaly demonstrated on ICGA, are not the rule. In those cases, PEDs do not always accompany **a** SRD.[56] ICGA has demonstrated the presence of "multiple presumed occult" PEDs in both acute and chronic stages.[57]

Chronic CSCR often resembles age-related macular degeneration (AMD) or can be complicated by CNV. Enhanced visualization of the choroid with spectral-domain optical coherence tomography (SD-OCT) has facilitated the assessment of the role played by the choroid in CSCR. Based on these observations, it was proposed that "pachychoroid pigment epitheliopathy" could be a subclinical phenotype potentially complicated by serous detachments and/or choroidal vasculopathy, including subepithelial CNV and polypoidal vasculopathy.[58] Although the possible occurrence of subepithelial CNV complicating the course of chronic CSC should not be ignored, all cases of flat irregular PED should not be mistaken for active CNV and systematically treated with anti-vascular endothelial growth factor (VEGF) drugs. Nevertheless, in some cases with worsened vision not responding to usual CSC therapy, use of anti-VEGF drugs could be considered as a therapeutic test to rule out the presence of secondary CNV.[59]

There are multiple theories on the origin of CSC, none of which has been proven. Neither RPE nor choroidal dysfunction can be effectively pointed out as the sole causative mechanism. The leakage rate corresponds to bulk fluid flow, rather than secretion and diffusion,[60] which indicates that the underlying choroid is

possibly responsible and not the RPE. Focal areas of hyperpermeability visualized as tiny punctuate spots in the inner choroid may be involved in the development of SRD.[61] During the period of time in which the retina remains detached, many events occur that have to do with the change in metabolism and intercellular processes. The outer segments of photoreceptors overlying the detached area are no longer phagocytosed, the photoreceptors elongate,[62] and finally, outer segments begin to accumulate, resulting in the deposit of multiple dot-like yellow precipitates and material. This material is demonstrated by high reflectivity on OCT and hyperautofluorescence.[63] The autofluorescent fluorophores in the photoreceptor outer segments may be concentrated in precipitates or settled into the inferior SRD.[64] This could correspond to the described acute hypertrophic outer retinal changes.[65]

The structure of the detached NSR in eyes with CSC remains preserved.[66] Photoreceptor apoptosis may be implicated in visual function in CSC, since apoptosis has been reported in experimental retinal detachment and human retinal detachment within a few days.[67]

Upon resolution the fluid will be reabsorbed rapidly for water and ions, whereas macromolecules will remain in the SRS and precipitate. After resolution of a long lasting episode, a hyperautofluorescent aspect remains on retinal imaging.[68]

Recently, significant progress has been made in the understanding of the molecular events triggering choroidal vasodilation in CSC. Inappropriate activation of the mineralocorticoid receptor (MR) by glucocorticoids, induces upregulation of the vasodilator potassium channel KCa2.3 (calcium-dependent channel) and smooth muscle cells relaxation in the choroidal vasculature.[69]

Serous Retinal Detachment in Idiopathic Polypoidal Choroidal Vasculopathy

Idiopathic polypoidal choroidal vasculopathy (PCV) is a distinct exudative disorder in which the SRD is thought to be of choroidal origin.[70] PCV is a disease in which the primary abnormality involves the inner choroidal circulation,[71,72] where thin capillary

vessels dilate within Bruch's membrane, immediately under the RPE, where they form cavernous vascular channels.[73] It is distinguishable from more typical proliferations of abnormal choroidal vessels.[74]

These lesions cause serosanguineous RPE detachments via damage to the overlying Bruch's membrane and/or RPE. The histopathologic findings suggest that these lesions can be more accurately considered as a degenerated RPE–Bruch's membrane–choriocapillaris complex and inner choroid dilated venules and arterioles, rather than an intra-Bruch's fibrovascular membrane.[75–77]

Age-Related Macular Degeneration

In the early stages of AMD, inflammation may help keep the RPE barrier intact by preventing RPE proliferation and migration, and, at the same time, choroidal cell growth may increase blood flow to the retina and the clearance of pathogens or drusen.

In chronic inflammatory diseases such as in AMD, the IFN-induced dehydration of the SRS would increase the activity of already accumulating chemokines and, thereby, help draw monocytes and neutrophils across the RPE to the SRS. Inhibition of RPE proliferation and migration by IFN also protects and maintains the RPE barrier. However, over long periods of unresolved inflammation, chronic exposure to IFN and other cytokines (e.g., IL-1 and tumor necrosis factor) could induce a significant decrease in transepithelial paracellular resistance and the loss of transport potential (fluid absorption).

These persistent changes, coupled with an IFN-driven increase in choroidal cell proliferation, suggest a pathway for the entry of choroidal neovascular blood vessels into the SRS via the RPE. Neovascular AMD results in an alteration of the outer BRB. These mechanisms provide a possible basis for understanding the role of inflammation in CNV and AMD.

Presently, fluid accumulation under the RPE, under and within the NSR, evidenced on OCT examination is considered clinically as an indicator of CNV activity. Its presence results in treatment indication.[78]

Serous Retinal Detachment in Uveitis: Exudative

Retinal Detachment

During inflammation, loss of the BRB and a diminished outflow of the choroid and choriocapillaris result in the accumulation of liquid in the SRS. The sustained pressure exerted from the choroid is responsible for the accumulation of fluid between the RPE and the retina and then may evolve into edema of the inner retinal layers.

Later, when more inflammatory damage develops and/or fluid volume increases, retinal resistance may become insufficient, and the fluid may enter the neuroretinal tissue and form cysts. The transient aspect of a subfoveal SRD in uveitis and favorable response to treatment support this hypothesis. A subfoveal SRD may also be documented in patients with normal neuroretinal tissue and without intraretinal edema.[79] In the acute phase of Vogt–Koyanagi–Harada disease, fluorescein angiography has shown increased permeability of the chorioretinal vessels and of the BRB, and delayed circulation of choroidal arteries, veins, and choriocapillaris.[80,81] This delayed perfusion has been related to massive infiltration of the choroid, resulting in the thickening of the choroid and delayed arterial choroidal flow.

NSR serous detachment of the macula resulting from focal retinochoroiditis has been reported previously in patients with *Bartonella*-associated neuroretinitis. SRD may precede the formation of a macular star in a minority of patients with neuroretinitis.[82] The macular exudates may take months to resolve.[83]

Detachment of Retinal Origin

Serous Retinal Detachment in Diabetic Retinopathy

Diabetic macular edema (DME) is thought to be caused by hyperpermeability in the retinal vasculature, leading to dysfunction of the neuroglial cells and concomitant visual disturbance. Macular SRD occurs in 15–30% of patients with diabetic maculopathy.[84,85] SRD in DME is diagnosed on OCT even when the neuroretinal tissue above the SRD is normal.[86] Retinal functionality in these types of SRD is controversial.[87] It has been reported that macular SRD in diabetic patients is more often correlated with high levels of HbA1c, and that this might break both the inner and the outer BRB.[88]

Transient SRD may represent a step in the process of macular edema resorption. Its evolution is not related to the severity of DME, and it sometimes disappears before resorption of retinal fluid. The elongation of the photoreceptors is not visualized in diabetic retinopathy-associated SRD, suggesting that the pathogenesis of this disease might be different.[89] The high protein content of the fluid in these SRDs could alter the oxygenation and elimination of metabolites from the photoreceptor layer, thus decreasing retinal sensibility.

The involvement of the RPE is also thought to play a role in the hydrodynamics of fluid accumulation into the SRS, where hypoxia might impede its normal pump function. RPE impairment has already been proven in human and experimental diabetes.[90] Thus SRD in diabetic maculopathy is linked not only to the limited drainage of the vascular system (both retinal and choroidal) but also to impairment in the function of the RPE.

Severe Retinal Detachment in Central or Branch Retinal Vein Occlusion

Severe retinal vein occlusion may be accompanied by extensive SRD.[91] The occurrence of SRD has been related to inflammatory reaction that is associated with hyperreflective material on OCT. SRD can be demonstrated in approximately 80% of central retinal vein occlusion patients with cystoid macular edema.[92] It appears that SRD is more frequent in major branch retinal vein occlusion (BRVO) than in macular BRVO.[93] In cases of major BRVO, a positive correlation with VEGF and the presence of SRD has been reported.[94] The major complication of serous detachment is the deposit of macular hard exudates, which may result in poor visual outcome.[95]

Other Causes

A large number of diseases, both ocular and systemic, have been associated with SRD. Different immunogammopathies have been associated with serous macular detachments: multiple myeloma, Waldenström macroglobulinemia, and immunoglobulin M paraproteinemia. SRD has been described in patients with acute leukemias while on chemotherapy or during a relapse.[96] The

mechanism of SRD in hypertensive choroidopathy as well as in eclampsia is more linked to renal failure and subsequent uremia.[97]

Choroidal effusion syndrome is thought to be due to the reduced porosity of the sclera and to the compression of the vortex veins by a rigid sclera, impeding the normal outflow of fluid within the choriocapillaris. Choroidal melanomas and retinoblastoma have been associated with SRD.[98] Vascular malformations such as retinal capillary hemangioma, phacomatoses, and carotid–cavernous fistula have all been associated with SRD.

Conclusion

Detachment of the neuroretina and/or of the pigment epithelium is not pathognomonic of a single disease. Detachments may result either from a primary choroidal alteration, with or without RPE secondary disturbances, or from an abnormality of the retinal circulation. The triggering mechanism remains, however, unknown most of the time, requiring not only the dissection of the biochemical cascades but in addition a detailed analysis of all clinical data available.

References

1. Green WR, McDonnell PJ, Yeo JH. Pathologic features of senile macular degeneration. *Ophthalmology*. 1985;92:615–621.
2. Murphy RP, Yeo JH, Green WR, et al. Dehiscences of the pigment epithelium. *Trans Am Ophthalmol Soc*. 1985;83:63–81.
3. Cunha-Vaz J, Bernardes R, Lobo C. Blood–retinal barrier. *Eur J Ophthalmol*. 2010;21:3–9.
4. Anand-Apte B, Hollyfield JG. *Developmental anatomy of the retinal and choroidal vasculature*. Elsevier: Cleveland, OH; 2010.
5. Li R, Maminishkis A, Banzon T, et al. IFNγ regulates retinal pigment epithelial fluid transport. IFNγ regulates retinal pigment epithelial fluid transport. *Am J Physiol Cell Physiol*. 2009;297:C1452–65.

6. Marmor MF. Mechanisms of retinal adhesion. Ryan SJ. *Retina*. 4th ed. Mosby: St. Louis; 2006:1891–1908.
7. Campochiaro PA, Jerdon JA, Glaser BM. The extracellular matrix of human retinal pigment epithelial cells in vivo and its synthesis in vitro. *Invest Ophthalmol Vis Sci*. 1986;27:1615–1621.
8. Ishikawa M, Sawada Y, Yoshitomi T. Structure and function of the interphotoreceptor matrix surrounding retinal photoreceptor cells. *Exp Eye Res*. 2015;133:3–18.
9. Porrello K, LaVail MM. Histochemical demonstration of spatial heterogeneity in the interphotoreceptor matrix of the rat retina. *Invest Ophthalmol Vis Sci*. 1986;27:1577–1586.
10. Hollyfield JG, Varner HH, Rayborn ME, et al. Retinal attachment to the pigment epithelium. Linkage through an extracellular sheath surrounding cone photoreceptors. *Retina*. 1989;9:59–68.
11. Hageman GS, Marmor MF, Yao XY, et al. The interphotoreceptor matrix mediates primate retinal adhesion. *Arch Ophthalmol*. 1995;113:655–660.
12. Johnson LV, Hageman GS. Characterization of molecules bound by the cone photoreceptor-specific monoclonal antibody CSA-1. *Invest Ophthalmol Vis Sci*. 1988;29:550–557.
13. Opas M, Kalnins VI. Distribution of spectrin and lectin binding materials in surface lamina of RPE cells. *Invest Ophthalmol Vis Sci*. 1985;26:621–627.
14. Yao XY, Hageman GS, Marmor MF. Retinal adhesiveness is weakened by enzymatic modification of the interphotoreceptor matrix in vivo. *Invest Ophthalmol Vis Sci*. 1990;31:2051–2058.
15. Yoon YH, Marmor MF. Effects of retinal adhesion of temperature, cyclic AMP, cytochalasin, and enzymes. *Invest Ophthalmol Vis Sci*. 1988;29:910–914.
16. Fisher SK, Lewis GP. Cellular effects of detachment and reattachment on the neural retina and retinal pigment epithelium. Ryan SJ. *Retina*. 4th ed. Mosby: St. Louis; 2006:1991–2012.
17. Marmor MF. Mechanisms of normal retinal adhesion. Ryan SJ, Wilkinson CP. *Retina*. 3rd ed. Mosby: St. Louis;

2001:1849–1869.
18. Gingell D, Fornes JA. Demonstration of intermolecular forces in cell adhesion using a new electrochemical technique. *Nature*. 1975;256:210–211.
19. Betts-Obregon BS, Gonzalez-Fernandez F, Tsin AT. Interphotoreceptor retinoid-binding protein (IRBP) promotes retinol uptake and release by rat Müller cells (rMC-1) in vitro: implications for the cone visual cycle. *Invest Ophthalmol Vis Sci*. 2014;55(10):6265–6271.
20. Foulds WS. The vitreous in retinal detachment. *Trans Ophthalmol Soc U K*. 1975;95:412–416.
21. Osterlin S. On the molecular biology of the vitreous in the phakic eye. *Acta Ophthalmol*. 1977;55:353–361.
22. Yao XY, Hageman GS, Marmor MF. Retinal adhesiveness in the monkey. *Invest Ophthalmol Vis Sci*. 1994;35:744–748.
23. Marmor MF, Yao XY. The metabolic dependency of retinal adhesion in rabbit and primate. *Arch Ophthalmol*. 1995;113:232–238.
24. Kim R, Yao XY, Marmor MF. Oxygen dependency of retinal adhesion. *Invest Ophthalmol Vis Sci*. 1993;34:2074–2078.
25. Kain HL, Libondi T. Experimentelle Netzhautablosung-untersuchungen zum Pathomechanismus. *Fortschr Ophthalmol*. 1986;83:590–596.
26. Marmor MF. Mechanisms of retinal adhesion. Ryan SJ. *Retina*. 4th ed. Mosby: St. Louis; 2006:1891–1908.
27. Orr G, Goodnight R, Lean JS. Relative permeability of retina and retinal pigment epithelium to the diffusion of tritiated water from vitreous to choroid. *Arch Ophthalmol*. 1986;104:1678–1680.
28. Casswell AG, Gregor ZJ, Bird AC. The surgical management of uveal effusion syndrome. *Eye (Lond)*. 1987;1:115–119.
29. Machemer R. The importance of fluid absorption, traction, intraocular currents, and chorioretinal scars in the therapy of rhegmatogenous retinal detachments. *Am J Ophthalmol*. 1984;98:681–693.
30. Negi A, Marmor MF. Experimental serous retinal detachment and focal pigment epithelial damage. *Arch Ophthalmol*. 1984;102:445–449.

31. Van Buskirk EM, Lessell S, Friedman E. Pigmentary epitheliopathy and erythema nodosum. *Arch Ophthalmol*. 1971;85:369–372.
32. Marmor MF. Retinal detachment from hyperosmotic intravitreal injection. *Invest Ophthalmol Vis Sci*. 1979;18:1237–1244.
33. Marmor MF, Martin LJ, Tharpe S. Osmotically induced retinal detachment in the rabbit and primate. *Invest Ophthalmol Vis Sci*. 1980;19:1016–1029.
34. Marmor MF. Control of subretinal fluid: experimental and clinical studies. *Eye (Lond)*. 1990;4:340–344.
35. Bird AC, Marshall J. Retinal pigment epithelial detachments in the elderly. *Trans Ophthalmol Soc U K*. 1986;105:614–668.
36. Holtz FG, Sheraidah G, Pauleikhoff D, et al. Analysis of lipid deposits extracted from human macular and peripheral Bruch's membrane. *Arch Ophthalmol*. 1994;112:402–406.
37. Curcio C, Baily T, Knuth HS, et al. Accumulation of cholesterol with age in human Bruch's membrane. *Invest Ophthalmol Vis Sci*. 2001;42:265–274.
38. Marmor MF. New hypothesis on the pathogenesis and treatment of serous retinal detachment. *Graefe's Arch Klin Exp Ophthalmol*. 1988;226:548–552.
39. Marmor MF. Control of subretinal fluid: experimental and clinical studies. *Eye (Lond)*. 1990;4:340–344.
40. Green WR. Retina. 4th ed. Saunders: Philadelphia; 1996:667–1313. Spencer WH. *Ophthalmic pathology: an atlas and textbook*. vol. 2.
41. Yamana T, Kita M, Ozaki S, et al. The process of closure of experimental retinal holes in rabbit eyes. *Graefes Arch Klin Exp Ophthalmol*. 2000;238:81–87.
42. Guerin CJ, Anderson DH, Fariss RN, et al. Retinal reattachment of the primate macula. Photoreceptor recovery after short-term detachment. *Invest Ophthalmol Vis Sci*. 1989;30:1708–1725.
43. Arroyo JG, Yang L, Bula D, et al. Photoreceptor apoptosis in human retinal detachment. *Am J Ophthalmol*. 2005;139:605–610.
44. Gemenetzi M, De Salvo G, Lotery AJ. Central serous

retinopathy: an update on pathogenesis and treatment. *Eye (Lond)*. 2010;24:1743–1756.
45. Kawano S, Marmor MF. Metabolic influences on the absorption of serous subretinal fluid. *Invest Ophthalmol Vis Sci*. 1988;29:1255–1257.
46. Taarnhoj NC, Kjeka O, Larsen M. Kinetics of retinal lipoprotein precipitation and elimination after closure of subretinal new vessels. *Invest Ophthalmol Vis Sci*. 2003;44:1680–1685.
47. Negi A, Kawano S-I, Marmor MF. Effects of intraocular pressure and other factors on subretinal fluid resorption. *Invest Ophthalmol Vis Sci*. 1987;28:2099–2102.
48. Anand R, Tasman WS. Nonrhegmatogenous retinal detachment. Ryan SJ, Wilkinson CP. *Retina*. 3rd ed. Mosby: St. Louis, MO; 2001:2076–2099.
49. Mrejen S, Sarraf D, Mukkamala SK, et al. Multimodal imaging of pigment epithelial detachment: a guide to evaluation. *Retina*. 2013;33:1735–1762.
50. Coscas F, Coscas G, Querques G, et al. En face enhanced depth imaging optical coherence tomography of fibrovascular pigmentepitheliumdetachment. *Invest Ophthalmol Vis Sci*. 2012;28:4147–4151.
51. Rando RR, Bangerter FW. The rapid intermembraneous transfer of retinoids. *Biochem Biophys Res Commun*. 1982;104:430.
52. Piccolino FC, Borgia L. Central serous chorioretinopathy and indocyanine green angiography. *Retina*. 1994;14:231–242.
53. Lai TY, Chan WM, Li H, et al. Safety enhanced photodynamic therapy with half dose verteporfin for chronic central serous chorioretinopathy: a short term pilot study. *Br J Ophthalmol*. 2006;90:869–874.
54. Gass JDM. *Stereoscopic atlas of macular diseases: diagnosis and treatment*. Mosby: St. Louis; 1997:49–70.
55. Marmor MF. New hypothesis on the pathogenesis and treatment of serous retinal detachment. *Graefes Arch Klin Exp Ophthalmol*. 1988;226:548–552.
56. van Velthoven ME, Verbraak FD, Garcia PM, et al. Evaluation of central serous retinopathy with en face optical

coherence tomography. *Br J Ophthalmol*. 2005;89:1483–1488.
57. Guyer DR, Yannuzzi LA, Slakter JS, et al. Digital indocyanine green video angiography of central serous chorioretinopathy. *Arch Ophthalmol*. 1994;112:1057–1062.
58. Pang CE, Freund KB. Pachychoroid neovasculopathy. *Retina*. 2015;35:1–9.
59. Hage R, Mrejen S, Krivosic V, et al. Flat irregular retinal pigment epithelium detachments in chronic central serous chorioretinopathy and choroidal neovascularization. *Am J Ophthalmol*. 2015;159:890–903.
60. Pryds A, Sander B, Larsen M. Characterization of subretinal fluid leakage in central serous chorioretinopathy. *Invest Ophthalmol Vis Sci*. 2010;51:5853–5857.
61. Tsujikawa A, Ojima Y, Yamashiro K, et al. Punctate hyperfluorescent spots associated with central serous chorioretinopathy as seen on indocyanine green angiography. *Retina*. 2010;30:801–809.
62. Matsumoto H, Kishi S, Otani T, et al. Elongation of photoreceptor outer segment in central serous chorioretinopathy. *Am J Ophthalmol*. 2008;145:162–168.
63. Maruko I, Iida T, Ojima A, et al. Subretinal dot-like precipitates and yellow material in central serous chorioretinopathy. *Retina*. 2011;4:759–765.
64. Matsumoto H, Kishi S, Sato T, et al. Fundus autofluorescence of elongated photoreceptor outer segments in central serous chorioretinopathy. *Am J Ophthalmol*. 2011;151:617–623.
65. Cho M, Athanikar A, Paccione J, et al. Optical coherence tomography features of acute central serous chorioretinopathy versus neovascular age-related macular degeneration. *Br J Ophthalmol*. 2010;94:597–599.
66. Maruko I, Iida T, Sekiryu T, et al. Morphologic changes in the outer layer of the detached retina in rhegmatogenous retinal detachment and central serous chorioretinopathy. *Am J Ophthalmol*. 2009;147:489–494.
67. Ojima A, Iida T, Sekiryu T, et al. Photopigments in central serous chorioretinopathy. *Am J Ophthalmol*. 2011;151:940–952.

68. Ayata A, Tatlipinar S, Kar T, et al. Near-infrared and short-wavelength autofluorescence imaging in central serous chorioretinopathy. *Br J Ophthalmol*. 2009;93:79–82.
69. Daruich A, Matet A, Dirani A, et al. Central serous chorioretinopathy: recent findings and new physiopathology hypothesis. *Progr Retinal Eye Res*. 2015;1-37.
70. Yannuzzi LA, Sorenson J, Spaide RF, et al. Idiopathic polypoidal choroidal vasculopathy (IPCV). *Retina*. 1990;10:1–8.
71. Yuzawa M, Mori R, Kawamura A. The origins of polypoidal choroidal vasculopathy. *Br J Ophthalmol*. 2005;89:602–607.
72. Coscas G, Lupidi M, Coscas F, et al. Toward a specific classification of polypoidal choroidal vasculopathy: idiopathic disease or subtype of age-related macular degeneration. *Invest Ophthalmol Vis Sci*. 2015;56(5):3187–3195.
73. Lafaut BA, Aisenbrey S, Van den Broecke C, et al. Polypoidal choroidal vasculopathy pattern in age-related macular degeneration: a clinicopathologic correlation. *Retina*. 2000;20:650–654.
74. Imamura Y, Engelbert M, Iida T, et al. Polypoidal choroidal vasculopathy: a review. *Surv Ophthalmol*. 2010;55:501–515.
75. Okubo A, Sameshima M, Uemura A, et al. Clinicopathological correlation of polypoidal choroidal vasculopathy revealed by ultrastructural study. *Br J Ophthalmol*. 2002;86:1093–1098.
76. Ojima Y, Hangai M, Sakamoto A, et al. Improved visualization of polypoidal choroidal vasculopathy lesions using spectral-domain optical coherence tomography. *Retina*. 2009;29:52–59.
77. Sasahara M, Tsujikawa A, Musashi K, et al. Polypoidal choroidal vasculopathy with choroidal vascular hyperpermeability. *Am J Ophthalmol*. 2006;142:601–607.
78. Chae JB, Lee JY, Yang SJ, et al. Time-lag between subretinal fluid and pigment epithelial detachment reduction after polypoidal choroidal vasculopathy treatment. *Korean J Ophthalmol*. 2011;25:98–104.

79. Ossewaarde-van Norel J, Berg EM, Sijssens KM, et al. Subfoveal serous retinal detachment in patients with uveitic macular edema. *Arch Ophthalmol*. 2011;129:158–162.
80. Yamanaka E, Ohguro N, Yamamoto S, et al. Evaluation of pulse corticosteroid therapy for Vogt–Koyanagi–Harada disease assessed by optical coherence tomography. *Am J Ophthalmol*. 2002;134:454–456.
81. Fardeau C, Tran THC, Gharbi B, et al. Retinal fluorescein and indocyanine green angiography and optical coherence tomography in successive stages of Vogt–Koyanagi–Harada disease. *Int Ophthalmol*. 2007;27(2–3):163–172.
82. Pollock SC, Kristinsson J. Cat-scratch disease manifesting as unifocal helioid choroiditis. *Arch Ophthalmol*. 1998;116:1249–1251.
83. Kalogeropoulos C, Koumpoulis I, Mentis A, et al. Bartonella and intraocular inflammation: a series of cases and review of literature. *Clin Ophthalmol*. 2011;5:817–829.
84. Ozdemir H, Karacorlu M, Karacorlu S. Serous macular detachment in diabetic cystoid macular oedema. *Acta Ophthalmol Scand*. 2005;83:63–66.
85. Catier A, Tadayoni R, Paques M, et al. Characterization of macular edema from various etiologies by optical coherence tomography. *Am J Ophthalmol*. 2005;140:200–206.
86. Gaucher D, Sebah C, Erginay A, et al. Optical coherence tomography features during the evolution of serous retinal detachment in patients with diabetic macular edema. *Am J Ophthalmol*. 2008;145:289–296.
87. Deak GG, Bolz M, Ritter M, et al. A systematic correlation between morphology and functional alterations in diabetic macular edema. *Invest Ophthalmol Vis Sci*. 2010;51:6710–6714.
88. Turgut B, Gul FC, Ilhan N, et al. Comparison of serum glycosylated hemoglobin levels in patients with diabetic cystoid macular edema with and without serous macular detachment. *Indian J Ophthalmol*. 2010;58:381–384.
89. Murakami T, Nishijima K, Sakamoto A, et al. Association of pathomorphology, photoreceptor status, and retinal thickness with visual acuity in diabetic retinopathy. *Am J*

Ophthalmol. 2011;151:310–317.
90. Kirber WM, Nichols CW, Grimes PA, et al. A permeability defect of the retinal pigment epithelium: occurrence in early streptozocin diabetes. *Arch Ophthalmol*. 1980;98:725–728.
91. Tsujikawa A, Sakamoto A, Ota M, et al. Serous retinal detachment associated with retinal vein occlusion. *Am J Ophthalmol*. 2010;149:291–301.
92. Ozdemir H, Karacorlu M, Karacorlu S. Serous macular detachment in central retinal vein occlusion. *Retina*. 2005;25:561–563.
93. Yamaguchi Y, Otani T, Kishi S. Serous macular detachment in branch retinal vein occlusion. *Retina*. 2006;26:1029–1033.
94. Park SP, Ahn JK, Mun GH. Aqueous vascular endothelial growth factor levels are associated with serous macular detachment secondary to branch retinal vein occlusion. *Retina*. 2010;30:281–286.
95. Takahashi K, Kashima T, Kishi S. Serous macular detachment combined with branch retinal vein occlusion. *Nihon Ganka Gakkai Zasshi*. 2005;109:362–367.
96. Dhar-Munshi S, Alton P, Ayliffe WH. Masquerade syndrome: T-cell prolymphocytic leukemia presenting as panuveitis. *Am J Ophthalmol*. 2001;132:275–277.
97. Gass JD. Bullous retinal detachment and multiple retinal pigment epithelial detachments in patients receiving hemodialysis. *Graefes Arch Klin Exp Ophthalmol*. 1992;230:454–458.
98. Muscat S, Parks S, Kemp E, et al. Secondary retinal changes associated with choroidal naevi and melanomas documented by optical coherence tomography. *Br J Ophthalmol*. 2004;88:120–124.

SECTION 3

Genetics

OUTLINE

33

Genetic Mechanisms of Retinal Disease

Stephen P. Daiger, Lori S. Sullivan, Sara J. Bowne

Introduction

The purpose of this chapter is to provide an overview of concepts underlying our current understanding of the genetic basis of inherited retinal diseases (iRDs). iRDs are perhaps the best understood of human hereditary disorders. In part this is because diseases that affect vision are easily recognized and the retina is an accessible and well-characterized tissue. In many ways, though, we are still at an early stage of understanding the causes and consequences of these diseases. In fact, the causes of iRDs are highly varied: many different types of retinal disease are known, many different genes are involved, and there may be dozens of disease-causing mutations reported within a single gene. For example, currently at least 256 genes are known that can cause one or another form of retinal disease,[1] and over 12,000 mutations have been reported, in total, in these genes.[2] In spite of the underlying complexity, it is now possible to identify the disease-causing gene and mutation, or mutations, in a substantial fraction of affected individuals and families.[3,4]

A useful concept in medical genetics is the distinction between single-gene diseases and multifactorial diseases. Inherited diseases such as retinitis pigmentosa (RP) are considered to be single-gene because there is a specific, underlying cause in each affected individual, that is, an inherited difference in DNA sequence that has a direct cause-and-effect relationship to the disease. There may be one DNA difference for dominant diseases, or two for recessive diseases, but only one gene is involved. These are also referred to as monogenic or Mendelian diseases. In contrast, for diseases such as age-related macular degeneration (AMD), genetic differences play a role in lifetime risk and/or clinical expression, but the differences are merely contributory and do not have a clear cause-and-effect relationship to the disease. These are "multifactorial" diseases because multiple factors, genetic, environmental, and stochastic, play a role in determining who is affected and who is not.

Therefore the cause of disease in an individual with an inherited condition such as RP is "simple," in the sense that only one gene is affected (and usually affected in an obvious way), whereas there may be multiple contributory factors in an individual with AMD and the differences may be subtle. We already know exceptions to this rule – for example, there are digenic forms of RP with two affected genes[5] – but the exceptions are rare.

This chapter focuses on genetic differences that are single-gene in nature and have a direct cause-and-effect relationship with disease, that is, inherited diseases of the retina. Genetic factors contributing to AMD are discussed in Chapter 66 (Epidemiology and risk factors for age-related macular degeneration).

Basic Concepts in Human Genetics

Inheritance

Fig. 33.1 shows pedigrees illustrating autosomal dominant, autosomal recessive, and X-linked recessive inheritance (see Nussbaum et al.[6] for details).

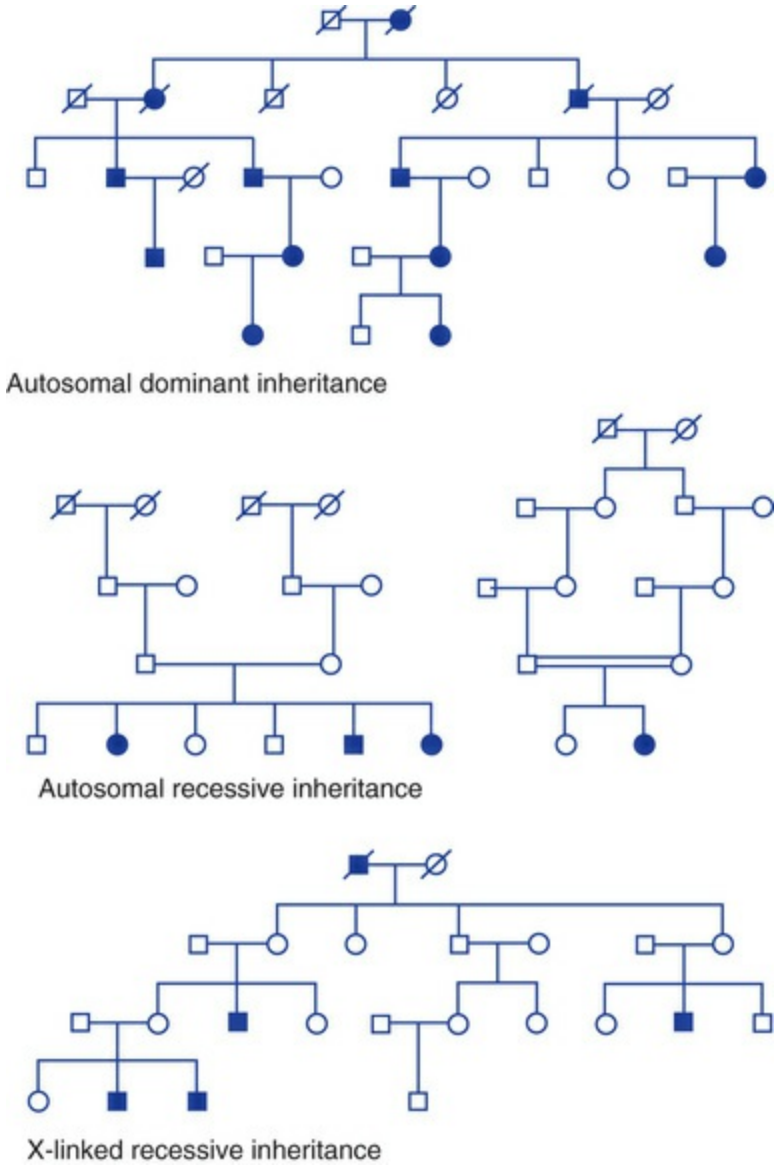

FIG. 33.1 Pedigrees illustrating autosomal dominant, autosomal recessive, and X-linked recessive inheritance.

iRDs follow textbook patterns of Mendelian inheritance: autosomal dominant, autosomal recessive, or X-linked. However, real families are often more complicated, especially for late-onset, progressive forms of retinal disease. This section reviews the conventional modes of inheritance and possible complexities.

Autosomal Dominant Inheritance

Autosomal dominant inheritance occurs when a single copy of a mutation on an autosomal chromosome is sufficient to cause disease. That is, an affected individual is heterozygous for the

mutation. Diseases caused by dominant mutations pass from generation to generation, i.e., most families have affected individuals in multiple generations. Males are as likely to be affected as females, and approximately 50% of children of an affected individual will be affected. Forms of retinal disease that are often autosomal dominant include maculopathies such as Best disease.

Two phenomena that can confuse the picture of autosomal dominant disease are variable expression and incomplete penetrance.

Variable clinical expression means that individuals with the same mutation may vary in onset, progression, or severity of disease or, in some cases, may have distinctly different clinical findings. Autosomal dominant RP is notoriously variable in expression. For example, mutations in one autosomal gene, *PRPH2* (also known as *RDS*), can cause dominant RP, dominant macular degeneration, or dominant panretinal maculopathy, even among members of the same family.[7–11]

Variable expression is a problem in determining mode of inheritance because some individuals may not show symptoms until late in life, and individuals with different symptoms may be diagnosed with different diseases even if the underlying cause is the same.

Incomplete penetrance, or nonpenetrance, means that some individuals with a disease-causing mutation will not be affected. For instance, 20% of individuals with a dominant-acting mutation in *PRPF31* will have normal vision by age 60 even though relatives with the same mutation may have RP by age 20.[12–15] One indicator of nonpenetrance in a multigenerational family is a "skipped generation," that is, an unaffected individual with an affected parent and an affected child. This is often seen in families with *PRPF31* mutations.[16,17]

Although variable expression and incomplete penetrance are seen as distinct phenomena, they are actually part of a continuum, with nonpenetrance just the extreme. The difference between late onset and no onset may simply be the age of the patient when examined. Whatever the terminology, the underlying finding is that dominant retinal disease mutations may have highly variable

consequences, confounding diagnosis.

An additional rare but confounding possibility has been observed in large, multigenerational families with inherited retinal disease: mutations in more than one gene may be segregating independently in the family. This occurs because families with late onset, nonlethal diseases are likely to meet and socialize with similar families. Descendants of these families are at risk of inheriting mutations in more than one gene. This is "assortative mating."

Autosomal Recessive Inheritance

Autosomal recessive inheritance occurs when both copies of an autosomal gene must be affected to cause disease. An affected individual can be either homozygous for a single mutation or heterozygous for two distinct mutations. An individual with two distinct recessive mutations is also called a compound heterozygote. Note that a pair of recessive mutations must be on opposite chromosomes. If two variants are in the same gene on the same chromosome, they are in *cis* to each other; if they are on opposite chromosomes, they are in *trans*. Recessive mutations must be in *trans* to cause disease

Examples of autosomal recessive retinopathies include Leber congenital amaurosis and Usher syndrome.

Unless one of the two mutations in a recessive case is a new mutation, the parents must be carriers of the mutation or mutations, that is, they must be heterozygous. Carriers are usually not affected. Approximately one-fourth of children of carrier parents are affected and one-half of children are carriers. Many recessive cases are isolated or simplex cases, i.e., one affected family member only. Families with multiple affected sibs are "multiplex."

Finally, in consanguineous families with marriage between relatives, an identical recessive mutation may be passed to multiple family members. Affected individuals may occur in more than one generation and in more than one branch of these families. Two identical mutations that derive from a recent ancestor are identical by descent (IBD). Marriage between relatives is more common in some cultures than others, hence IBD inheritance of retinal diseases is more frequent in those societies.

Because carriers are not self-evident, the mode of inheritance is often hard to assign in recessive families.

X-Linked or Sex-Linked Inheritance

X-linked or sex-linked inheritance is a single mutation on the X chromosome that causes disease. Males, who are hemizygous for the X chromosome, are always affected, often severely affected. For many inherited diseases, female carriers of an X-linked mutation are not affected. Since females have two Xs, this implies that most X-linked mutations will be recessive in females. For a truly recessive X-linked mutation, one-half of the sons of a carrier female are affected, one-half of her daughters are unaffected carriers, and none of the sons of an affected male are affected. This produces a notable pattern of inheritance, with the salient feature that male-to-male transmission of an X-linked mutation is not possible.

The disease status of female carriers is more complex. Although females have two Xs, one of the Xs, selected at random in each cell, is inactivated in most tissues. This is X-inactivation or Lyonization, named for Mary Lyon, who first described the phenomenon.[18,19] Lyonization increases the likelihood that a female carrier will be affected since some cells will express only the mutant protein. In fact, many female carriers of X-linked RP mutations show clinical symptoms. Females are less severely affected than males with the same mutation, but female carriers of X-linked RP mutations may have significant loss of vision by midlife or earlier.[20–24]

One consequence of clinical disease in carrier females is that families with X-linked RP may appear to have autosomal dominant RP if several females are affected.[25] This is an example of complexities that arise in determining the mode of inheritance of iRDs.

Isolated Cases

Isolated cases deserve an entry of their own because the mode of inheritance is often unclear. A practical definition of an isolated case is an affected individual with no affected first-degree relatives (parents, sibs, and children) and no reports of more distant affected relatives. One immediate concern is that there may be other affected family members but the person describing the family is unaware of

the disease status in these individuals. Clinical examination of first-degree relatives is often informative in these cases.

Assuming a case is genuinely isolated, there are several possibilities. The most likely prospect is that this is an autosomal recessive case and the parents are carriers. Or, perhaps one parent is a carrier but the other mutation is de novo (new). Alternatively, this may be a new dominant-acting or X-linked mutation. Another possibility is autosomal dominant or X-linked inheritance with nonpenetrance in prior generations. Ultimately, for most isolated cases the mode of inheritance must be determined at a molecular level by genetic testing.

Digenic and Polygenic Inheritance

Nearly all iRDs are monogenic, with only one gene affected per person. This is based on empirical observation, but it may be misleading since more complex forms of inheritance are hard to prove. Two counterexamples are known for iRDs. First, one form of RP is caused by a combination of one mutation in the *PRPH2* (*RDS*) gene and another mutation in the *ROM1* gene.[5,24] These two mutations are benign alone but pathogenic in combination. This is digenic inheritance. Secondly, Bardet–Biedl syndrome (BBS), a form of RP combined with congenital abnormalities, is in most instances a recessive disease with mutations in any one of at least 22 known BBS genes.[1,26] Some cases of BBS, though, require a third mutation in a second BBS gene for disease expression.[27,28] This is called trigenic or triallelic inheritance. Whether these examples of polygenic inheritance of iRDs are just rare anomalies or hint at greater complexity of retinal diseases is uncertain.

Chromosomes

Chromosomes are dark-staining bodies seen in the nucleus of dividing eukaryotic cells. In diploid organisms, such as humans, the earliest diploid cell before division results from fusion of a haploid cell from the male parent and a haploid cell from the female parent. That is, the first human cell has a diploid count of 23 pairs of chromosomes (n), or 46 total chromosomes (2n), and derives from fusion of a haploid sperm and haploid ovum. This is

the primary germline cell and contains the germline genetic information in the nucleus. All subsequent cells, known as somatic cells, contain a nearly perfect copy of the original chromosomes and genetic information. Exceptions in humans are sperm- and ovum-producing cells (also known as germline cells), which produce haploid cells, and certain blood cells that do not contain a nucleus.

Eukaryotic chromosomes have been referred to as "information-carrying organelles" because they are highly structured, ultra-compressed complexes of proteins, RNAs, DNA, and other factors, with the primary function of transmitting genetic information from one generation to the next, or from a parent cell to a daughter cell. However, at the heart of each chromosome is a single, double-stranded DNA molecule. DNA length is measured in basepairs (bp): each single strand of DNA is composed of nucleotide bases, and each base interacts (pairs) with an alternate base in double-stranded DNA, so bp are the natural units. DNA is also measured in kilobases (kb), megabases (Mb), and gigabases (Gb). The DNA molecule within a chromosome may be hundreds of Mb in length. This is, by far, the largest single biomolecule known. One reason for the chromosomal superstructure may simply be to keep this giant molecule intact. However, chromosomes also participate directly in DNA duplication and expression.

DNA, RNA, and Proteins

Fig. 33.2 shows the steps in DNA duplication, RNA translation, and protein synthesis.[29]

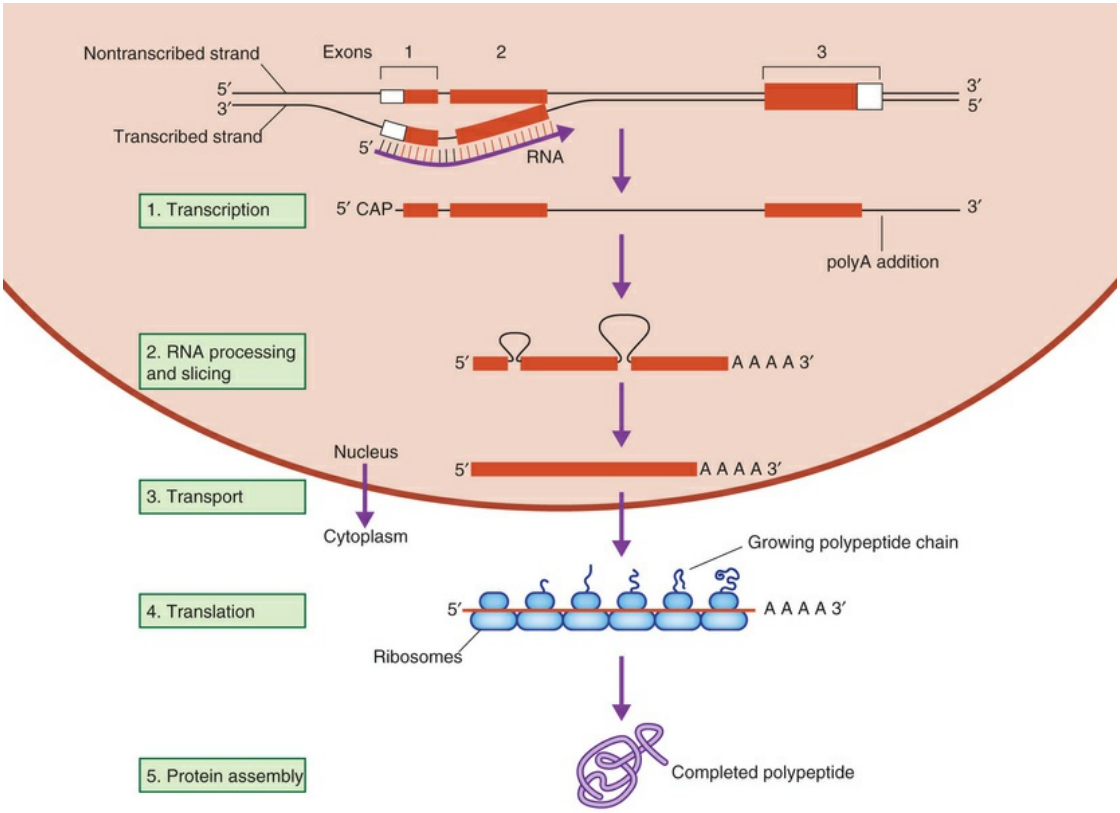

FIG. 33.2 Steps in DNA duplication, RNA translation, and protein synthesis. (Reproduced from Nussbaum RL, McInness RR, Willard HF. Thompson and Thompson's Genetics in medicine. 7th ed. Philadelphia, PA: Saunders Elsevier; 2007. p. 31. With permission from Elsevier.)

DNA is deoxyribonucleic acid, a linear molecule composed of four monomers: adenine (A), thymine (T), guanine (G), and cytosine (C). Two antiparallel DNA strands pair through hydrogen bonds to form a double-stranded molecule that carries genetic information.

RNA is ribonucleic acid, a linear molecule, like DNA, composed of adenine, uracil (U), guanine, and cytosine. RNA is single-stranded in most circumstances, but it can form complex folded shapes by pair bonding within the linear strand. Messenger RNA (mRNA) transfers genetic information within cells, but other RNA molecules play diverse roles in many biologic processes.

Proteins, composed of various combinations of 20 amino acids, are linear molecules that can fold into many shapes, and can play essential and highly diverse roles in all biologic processes.

DNA function is called the central dogma of DNA in recognition of the landmark explanation of DNA structure and function by

Watson and Crick in 1953, and subsequent unraveling of the genetic code over the next decade.[30,31] DNA is comprised of a phosphate backbone with nucleotide bases, A, T, G, or C, in linear array along the backbone. The backbone is conventionally drawn from the 5′ phosphate on one end to the 3′ phosphate on the other end. The opposite strand forms by pairing of cognate bases, A to T and G to C, on the parent strand. The opposite strand naturally aligns in a helical, antiparallel fashion, from 3′ to 5′ phosphates. This arrangement essentially explains inheritance in all living things.

In DNA *duplication*, the two antiparallel strands unwind, and a nearly exact antiparallel copy is synthesized on each single strand. The principal enzyme involved is DNA polymerase, but additional enzymes are involved in unwinding, patching, and repairing the DNA. DNA duplication occurs in the nucleus of cells only.

In DNA-RNA *transcription*, the DNA strands unwind, and a single-stranded RNA molecule is synthesized as an antiparallel copy of one of the DNA strands, pairing each DNA nucleotide with the corresponding RNA nucleotide. The primary enzyme involved is RNA polymerase, and the first steps occur in the nucleus. Thereafter the RNA molecule is processed through many steps and eventually exported from the nucleus to the protein-forming machinery. The final molecule in this process is mRNA since it carries the DNA message to the cytoplasm.

In protein *translation*, mRNA is read by the protein-forming machinery and the corresponding protein is built by adding one amino acid to the next in succession, from the amino (NH_2-) end of the protein to the carboxy terminus (-COOH). Each amino acid is coded for by three RNA bases, that is, a nucleotide triplet or codon. After synthesis, most proteins are further modified through posttranslational modification, then the linear protein folds into its active shape, often with the assistance of proteins known as chaperones.

It is now recognized that RNA plays many additional roles than simply carrying genetic information through mRNA. Functional RNA that does not code for a protein is called nontranslated (or noncoding) RNA and is a major focus of contemporary research.

Gene Structure

Fig. 33.3 shows gene structure based on the relationship between the protein sequence, mRNA intermediate, and original DNA gene sequence.[29]

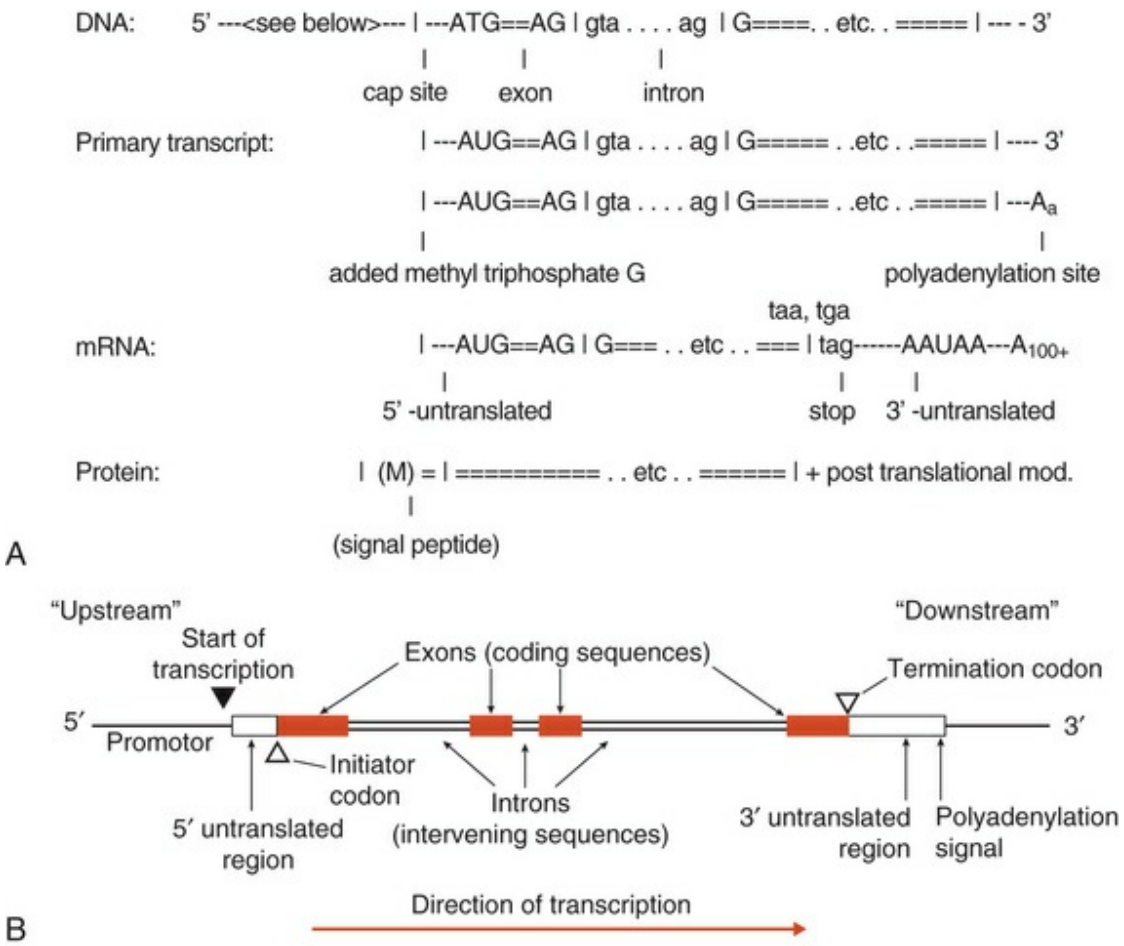

FIG. 33.3 (A,B) Gene structure based on the relationship between the protein sequence, mRNA intermediate, and original DNA gene sequence. (Panel B, reproduced from Nussbaum RL, McInness RR, Willard HF. Thompson and Thompson's Genetics in medicine. 7th ed. Saunders Elsevier; 2007. p. 29. With permission from Elsevier.)

The modern concept of a gene is clouded by arguments as to where a gene starts and stops, and whether segments of DNA that do not code for proteins but still influence traits are "genes." The discussion here is limited to defining a gene in terms of proteins while acknowledging the broader complexities, e.g., noncoding RNAs.

Gene expression is principally the steps from DNA transcription

to protein translation. Gene expression starts with separation of double-stranded DNA, exposing a single-stranded sequence on which DNA-to-RNA transcription can occur. This is accompanied by binding of a complex set of proteins, "expression factors," that facilitate binding and activity of RNA polymerase.

The primary RNA strand begins at the start of transcription and ends far beyond the length sufficient to code for a protein. The first RNA-processing steps add a methyl cap to the first RNA nucleotide, trim the 3′ end, and add a polyadenosine tail (poly-A tail). Next the RNA moves to a complex assembly of proteins and small, functional RNAs, known as a splicesome. The splicesome then removes anywhere from one to many internal segments of the RNA transcript and reassembles the remainder. This is, largely, the finished mRNA, which is then exported from the nucleus to the protein synthesis machinery in the cytoplasm.

RNA splicing has profound consequences for gene structure and protein variation. Splicing occurs in nearly all eukaryotes, and almost all human genes are spliced. The spliced-out segments are called introns, and the remaining, reassembled segments are exons. The splice sites are defined by short, canonical sequences, highly conserved across species, known respectively as splice-donor and splice-acceptor sites.

The evolutionary significance of splicing is still disputed, but its functional consequence is clear: it vastly increases the number of distinct proteins. This is because when splicing occurs, alternate combinations of introns may be removed. Alternate splicing is the norm in human genes, not the exception, and usually results in alternate mRNAs and alternate protein isoforms – all from a "single" gene. There are many examples of alternately spliced retinal genes producing multiple protein isoforms.[32,33]

Following splicing and export from the nucleus, mRNA is translated into protein by ribosomes in the endoplasmic reticulum. The start of translation is usually not at the beginning of the mRNA, and the end is not at the end. The segment upstream of the start of translation is the 5′ untranslated region (5′-UTR). Similarly, the segment downstream of the end of translation is the 3′ untranslated region (3′-UTR). The 5′ and 3′-UTRs may sit within the first and last exons, respectively, or may stretch across exons.

In addition to alternate splicing and alternate protein isoforms, there are alternate starts of transcription, alternate starts of translation, alternate ends of translation, and alternate poly-A sites.

Mitosis, Meiosis, and Linkage

Fig. 33.4 shows the steps in meiosis.[6]

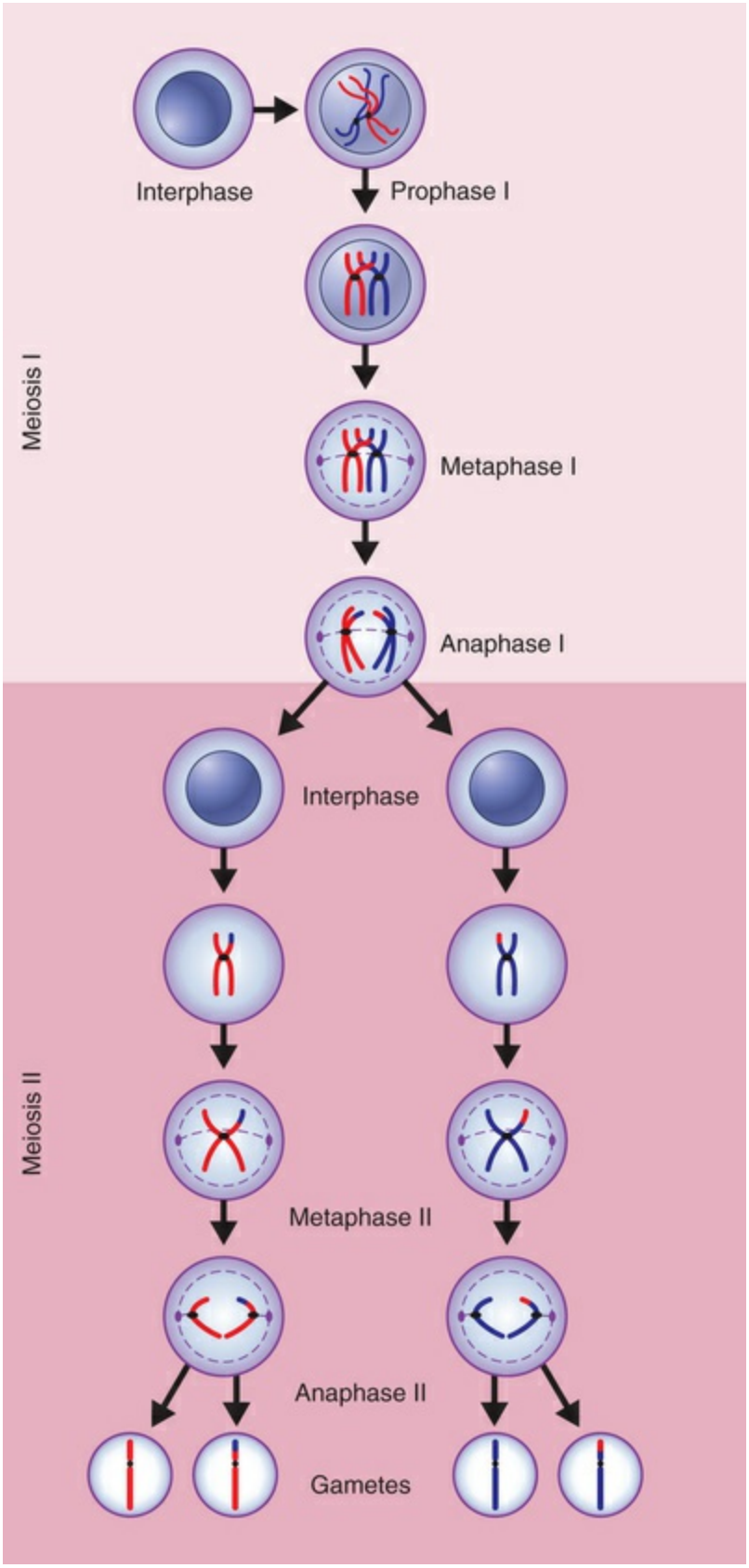

FIG. 33.4 The steps in meiosis. (Reproduced from Nussbaum RL, McInness RR, Willard HF. Thompson and Thompson's Genetics in medicine. 7th ed. Philadelphia, PA: Saunders Elsevier; 2007. p. 19. With permission from Elsevier.)

In normal cell division, in which a somatic cell divides to produce a daughter cell, the DNA in all 46 human chromosomes is copied and a complete copy is passed to each of the two resulting cells. This is mitosis, and it provides a nearly perfect copy of the DNA sequence to each somatic cell.

Chromosome distribution and DNA processing are substantially different in meiosis. Meiosis occurs in cells producing sperm and ova. In the first phase of meiosis chromosomal DNA is duplicated as in mitosis, but the duplicated DNA strands do not separate. Then, in subsequent phases, homologous chromosomes bind to each other and exchange DNA strands. Homologous chromosomes are pairs of similar chromosomes from each parent, e.g., the maternal and paternal chromosome 1. The result of homologous exchange or recombination is to produce novel DNA sequences that are mixed linear combinations of chromosomal segments from each parent. The resulting duplicated, recombined chromosomes are then separated into four haploid-containing cells, which eventually become sperm or ovum.

The result is, first, that each sperm or ovum contains only a haploid set of chromosomes. However, when a sperm fertilizes an ovum, the resulting cell has the full diploid set of chromosomes. Second, each chromosome in the offspring is a recombined mix of the chromosomes of each parent. Thus the chromosomes in each individual are a unique, one-of-a-kind combination of previous generations (excepting identical twins).

As a result, genes on different chromosomes segregate independently, but genes that are close together on a chromosome segregate together. More generally, the further a pair of genes are apart on a chromosome, the more likely a recombination will have occurred between them during meiosis. Two loci that are close enough on a chromosome such that recombination is unlikely are "linked." The phenomenon of genes that do not segregate independently is linkage.

To put this in context, the average chromosome is 100 Mb in length. Genes that are 50 Mb apart are unlinked, and genes within 10 Mb of each other show linkage. If genes are within 1 Mb of each other, the chance of recombination is less than 1% per generation.

There are roughly 5–20 genes per Mb in the human genome, so hundreds of contiguous genes on a chromosome may show linkage to each other.[34]

Linkage has significant evolutionary and functional consequences, but its importance in medical genetics is as a tool to locate disease-causing genes. If a neutral genetic variant is found in association with an inherited disease in a family, then the variant, called a marker in this case, may be physically close to the disease gene, that is, they may be linked. If so, then knowing the location of the marker fixes the location of the disease gene.

Evolution

Theodosius Dobzhansky said "nothing in biology makes sense except in the light of evolution."[35] This observation serves to emphasize the fundamental organizing principal of biology. Without evolution, biology is largely a random collection of facts and principles; with evolution, biology (and medicine) is a coherent science. Evolution explains why the central dogma is true for all species, why all eukaryotic cells share a common architecture, why animal models are useful in understanding and treating human diseases, why human DNA variants are evaluated by comparison to other species. Evolution is so central to biology and medicine that we often forget its impact, but modern, 21st-century biomedicine is unimaginable without it.

The Human Genome

Overview

The human genome is the combined DNA sequence of the haploid set of all chromosomes. Humans have 23 pairs of chromosomes; these consist of 22 pairs shared by males and females (autosomes) and a pair of Xs in females or an X and Y in males (sex chromosomes). Autosomes are labeled from the largest, 1, to the smallest, 22. Thus the human genome is the sequence from the top of chromosome 1 through the bottom of chromosome 22, plus the X and Y chromosomes.

In one of the greatest scientific achievements in modern history, the Human Genome Project produced the first human genome sequences in 2001.[36,37] Since then thousands of complete human genomes have been sequenced, and the genomes of thousands of other species are known.[38]

There is a distinction between the generic human genome and the genome of a specific person. "The" human genome, or "the" genome of any species, is neither an average nor a consensus. It is simply a sampling of the first individuals sequenced. Therefore the reference human sequence and reference gene sequences are just examples, not definitive sequences. In contrast, the genome of a specific human would cover all 46 chromosomes and be unique to that person. Thus, in this sense, there are billions of human genomes and no two are alike.

Nonetheless, both the generic human genome sequence and the many specific sequences are extremely valuable contributions to medicine and biology.

The human haploid genome is 3.3 Gb in length; the complete genome of an individual is 6.6 Gb. There are 21,000–25,000 protein-producing genes in the generic human genome. This is far fewer than expected, but the discrepancy is partly explained by alternate splicing and multiple protein isoforms.

Most genes, including introns, exons, and regulatory elements, are 10–100 kb in length. Therefore the portion of the genome devoted to genes is less than 10% of the total. Considering exons only, the fraction of the genome actually coding for proteins is only 1.5% of the total.

Roughly 50% of the human genome consists of thousands or millions of short, repetitive DNAs. For example, there are more than one million copies of *Alu* sequences dispersed throughout the genome. *Alu*'s are short retrotransposon-related sequences that have the capacity to copy themselves into new locations in the genome. Some repetitive DNAs are functional in that they play a role in chromosome structure and protein activity. However, it is fair to say that this is principally "junk DNA," at least in relation to actual genes.

The remaining 50% consists of single-copy DNA (that is, not repetitive), including coding sequences. Most of this single-copy

DNA is transcribed into RNA but not translated into proteins. This noncoding RNA (ncRNA) must play a role in normal biologic processes, and probably contributes to human diseases, but it is poorly understood at present.

Polymorphisms

Humans are 99.9% identical to each other at a DNA level. Since there are 6.6 Gb in the human diploid genome, this means that one person differs from another at millions of sites. Some of these differences contribute to diseases, both simple and complex, but the vast majority are neutral or only slightly advantageous or disadvantageous. This is the extremely varied "genetic background" that distinguishes one individual from another.

An identifiable site in a genome, usually a gene, is called a locus, and any variant at this site is an allele. If there is more than one allele at a locus in a group of people, and the second most common allele has a frequency of 1% or greater, then this is called a genetic polymorphism. If there are only two alleles at a locus, then the less common allele is the minor allele. Note that locus and allele apply to an individual, whereas polymorphism only makes sense in the context of a population in which more than one allele is found.

The 1% criterion is arbitrary. A specific allele may occur only once in one individual or may range up to 100% of all chromosomes in a population. One percent was chosen because this frequency can be measured in a realistic survey and it was presumed that any more common allele must be largely benign. (The latter is definitely not true; for instance, the sickle-cell and cystic fibrosis mutations are both polymorphic in their respective populations.) Polymorphism is a useful concept, though, despite the arbitrary definition.

A person who has identical alleles at a locus is homozygous at that site; a person with two different alleles is heterozygous. (This applies to autosomal chromosomes and the Xs in a female. Alleles on the male Y are hemizygous.) The frequency of heterozygotes in a population is predicted from Hardy–Weinberg equilibrium: if there are two alleles with frequencies p and q, then the frequency of the two homozygote types is p^2 and q^2, respectively, and the

heterozygote type is $2 \times p \times q$. The total fraction of heterozygotes at a locus in a population is heterozygosity, basically the sum of all heterozygote combinations.

Several broad classes of polymorphism are found in the human genome.

Single Nucleotide Polymorphisms

Single nucleotide polymorphisms (SNPs) are sites at which more than one nucleotide is found in a population. There are usually only two alleles at a SNP locus, e.g., an A or a T. Millions of SNP sites have been identified in humans.[39] Some are found in only one major population, such as Africans, but many are polymorphic in all major human groups. A SNP site at which the nucleotide substitution leads to an amino acid substitution, or otherwise affects a protein, is a coding SNP (cSNP). There are tens of thousands of cSNPs, at least one in almost every gene.

If a pair of human chromosomes are compared base by base, each of us is heterozygous for a nucleotide substitution roughly every 1000 bp. Not all of these are at polymorphic sites; some are private or rare variants (often called single nucleotide variants). However, most are true SNPs.

Short Tandem Repeats

Another type of polymorphism is short tandem repeats (STRs). STRs are short stretches of DNA, typically 2–5 bp in length, which are repeated a variable number of times, say from 10 to 20 times. Alleles differ in the number of repeats. Because many different lengths are possible, there are usually several or many alleles at a locus. These are also called microsatellites.

Copy Number Variants (CNVs)

The number of copies of a gene or genetic region may also differ between individuals and the differences may be polymorphic. These are copy number variants (CNVs). CNV differences may range between zero copies up to several copies in tandem. An absent or deleted gene may have obvious functional consequences, but multiple copies of a gene may also have consequences, through

overexpression, for example. CNVs are not as numerous as SNPs, but there are at least 100s of sites in humans.[40]

Other Polymorphisms

There are many other human DNA polymorphisms. There are large polymorphic elements called minisatellites or VNTRs (variable number tandem repeats); *Alu* insertions may be polymorphic; chromosome deletions and rearrangements are polymorphic in humans. The extent of polymorphic variation in humans is exceptional, reflecting our high mobility, heterogeneous habitats, and variable mating patterns.

Finally, in addition to polymorphic variants, there are many private or rare variants. Some, but not all, of these are deleterious, e.g., mutations causing retinal diseases. The extent of rare variants is not well known, and it is often difficult to determine which are benign and which are pathogenic. However, it is clear that each of us harbors millions of variants in our genomes that are rare or unique to us or our families, some of which affect our health and wellbeing.

Mutations

Fig. 33.5 illustrates several of the types of mutation that cause iRDs.

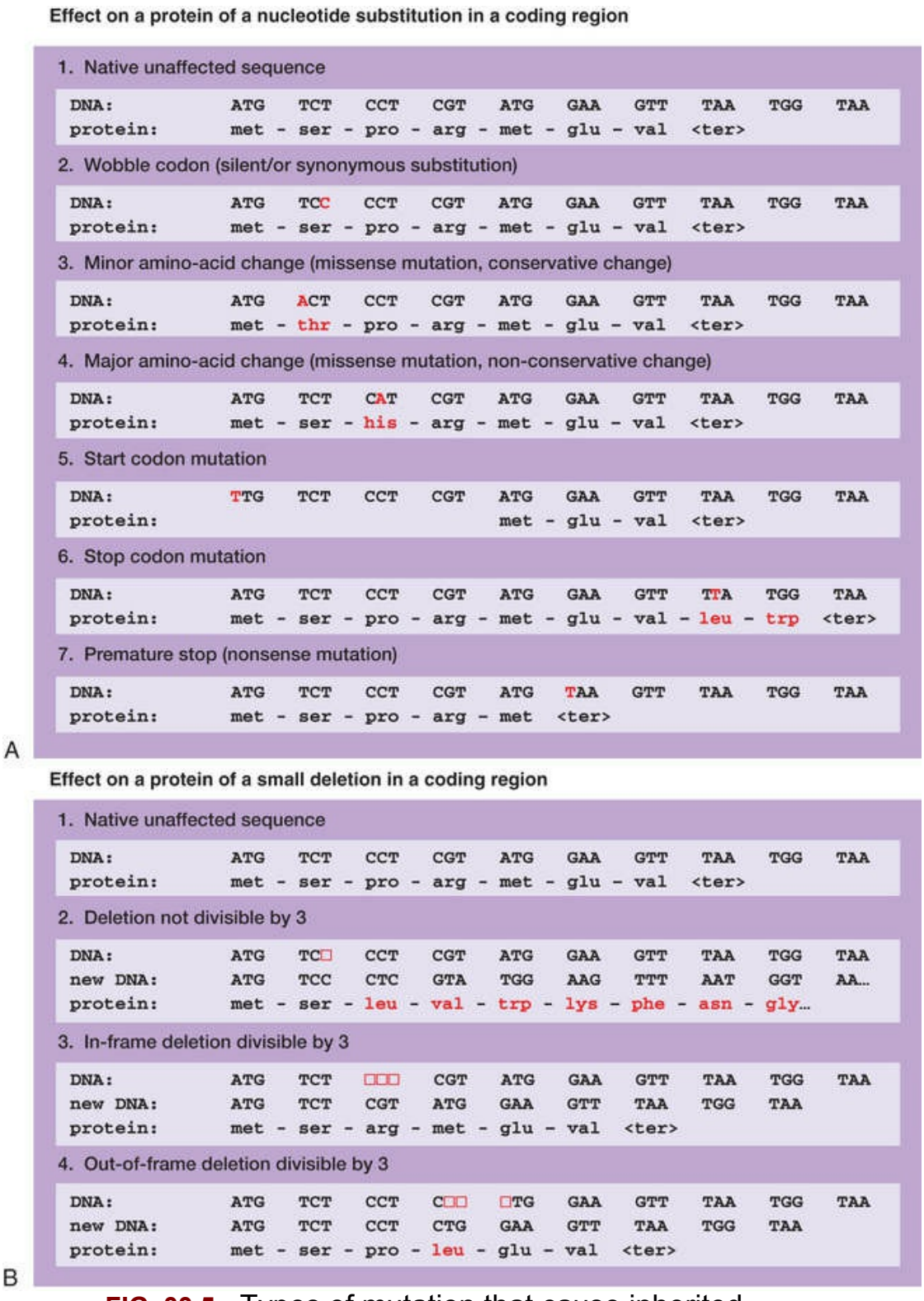

FIG. 33.5 Types of mutation that cause inherited retinal diseases.

Technically, a mutation is a change in DNA from one generation to the next. In practice, the word often refers to any damaging, deleterious DNA variant, one that acts in either a dominant or

recessive fashion. This chapter uses the word largely in the second sense, that is, a mutation is "bad." However, it is important to recognize that a rare, novel variant is not necessarily pathogenic and a polymorphic variant with an allele frequency of 1% or greater is not necessarily benign.

Most disease-causing mutations affect a protein, either directly or indirectly. However, this observation may simply reflect the fact that only proteins have been well studied.

A mutation may eliminate a protein, reduce or eliminate its function, alter or add to its function, or convert the protein into a toxic factor. One way of describing mutations is by their consequences: an absent protein, a functional null, a gain or loss of function, or a toxic protein. Dominant mutations may also be described as dominant negative: the mutant protein interferes with the wild-type protein. As a sweeping generalization, with many exceptions, autosomal recessive mutations often lead to an absence of a protein or a functional null, and autosomal dominant mutations often result in a gain of function, toxic protein, or dominant negative effect. X-linked mutations are less predictable because of the differential effect in males and females.

Another way to categorize mutations is to work from DNA to mRNA to proteins:

1. DNA deletions or rearrangements may result in the absence of a protein or a critical part of a protein. Surprisingly, humans harbor large, polymorphic deletions, some 100 kb in length or longer.[40] In apparently healthy people, these are in a heterozygous state: one chromosome segment is deleted, and the matching segment on the homologous chromosome is intact. Large, homozygous deletions are severely deleterious. Smaller deletions, usually the size of a gene or less, affecting one or a few proteins, may cause autosomal dominant, autosomal recessive, or X-linked retinal diseases.[14,41,42]

2. DNA changes 5′ to the start of transcription may block synthesis of mRNA or may affect timing or amounts of mRNA. These are promoter or expression mutations. Further, any changes to the canonical nucleotides that define the donor or acceptor slice sites of introns may profoundly affect mRNA splicing. These are splice site mutations. Splice site mutations typically result in a structurally

abnormal protein or no protein at all.

3. Finally, mutations can alter proteins directly in a myriad of ways. Mutations in DNA that directly affect proteins are broadly classed into nucleotide substitutions in contrast to small insertions or deletions, typically 1–15 bp in length, called indels. A nucleotide substitution that causes replacement of one amino acid with another is a missense mutation. Missense mutations may alter protein function or produce a toxic protein or a dominant negative protein. (A nucleotide substitution that changes a codon but does not alter an amino acid is a silent substitution. Most silent substitutions are benign.) An indel that alters the order of codons is a frameshift mutation or an in-frame amino acid deletion. A nucleotide substitution that introduces a signal to stop translation of a message prior to the normal stop is a nonsense mutation or a premature-stop mutation. Indels and premature-stop mutations produce a severely abnormal protein or no protein.

It is likely that new ways in which mutations can cause disease will be revealed in the future as the complexity of the human genome and inherited diseases is better understood.

Genetic Testing Methods

The primary purpose of genetic testing for iRDs is to determine the underlying cause of disease in an affected individual and in his or her family. A broader goal is to use genetic testing for research purposes, e.g., to find novel mutations, to discover new disease-causing genes, to identify patients for clinical trials, or to study the natural history of disease. There is no clear demarcation between diagnostic testing and research, but there are practical distinctions. Diagnostic testing is often limited to testing affected individuals, screening known genes only, and is usually conducted in a certified laboratory. (Diagnostic laboratories in the USA have Clinical Laboratory Improvement Amendments (CLIA)[43] and/or College of American Pathologists (CAP)[44] certification.) Research testing may involve other family members, may screen novel genes, and is often conducted in facilities that are not certified.

However, for this section, no distinction is made between diagnostic testing and research testing, in part because the boundary between them is frequently shifting. In general, diagnostic testing and research are highly interdependent activities.

Current methods for genetic testing can be grouped into three categories: (1) screening known genes and mutations; (2) mapping to localize the disease-causing gene; and (3) high-throughput DNA sequencing. However, the essential first step is an informed clinical examination, which must precede testing.

Informed Clinical Examination

The clinical examination is critical in selecting the correct tests and in making sense of the results. An effective examination and good family history are necessary to establish the mode of inheritance, may identify subtle clinical findings suggesting possible causes, and may rule out certain genes and diseases. The examination may involve additional affected and unaffected family members, which will facilitate follow-up studies. Finally, without good clinical and family information it may be difficult or impossible to interpret and explain the testing results.

Screening Known Genes and Mutations

For each category of disease there is a set of known, possible disease-causing genes and a set of known mutations within each gene. Among the known genes and mutations, some are more common causes of disease than others. For example, mutations in 27 genes are known to cause autosomal dominant RP,[1] and more than 1000 mutations have been reported in these genes.[2] However, mutations in one gene, rhodopsin, account for at least 25% of cases of autosomal dominant RP in the United States.[4] Also, more than 195 mutations have been reported in rhodopsin alone, but six of these mutations account for more than half of all cases.[24]

As a consequence, the natural next step is to test the most likely disease-causing genes in an affected individual, based on clinical findings and family history. One approach uses polymerase chain reaction-based di-deoxy chain termination cycle sequencing, also called Sanger sequencing.[45,46] Sequencing laboratories and services

in the United States for iRDs include commercial facilities, university-based services, and federally supported programs.[47] A current list of testing facilities in Europe and the United States is maintained by GeneTests.[48,49]

An alternative to DNA sequencing is to detect known mutations only. One approach is to use microarrays with short single-stranded DNA sequences that bind to the region containing the targeted mutation and detect the presence or absence of the mutation. An example of this technology is arrayed primer extension.[50,51] The advantage of DNA sequencing is that it detects both known and unknown mutations in the genes tested. The advantage of testing known mutations only is that it is much less expensive than sequencing.

Additional possible tests include sequencing all the known disease-causing genes, even the rare causes of disease, and using methods other than sequencing to detect mutations. An example of the latter is the use of multiplex ligation-dependent probe amplification to detect large deletions.[14,52,53]

Linkage and Homozygosity Mapping

If sequencing known genes fails to detect a disease-causing mutation in an affected individual, then an alternative approach is to determine the chromosomal site of the disease locus using linkage mapping. This does not immediately identify the disease gene, but it can reduce the location harboring the gene from the entire genome to a region containing, at most, a few hundred genes. From this information, other methods can be used to find the specific gene.

Linkage testing is the principal approach used to map disease genes. This involves determining whether a neutral allele at a polymorphic site is tracking with disease in a family, taking into consideration the proposed mode of inheritance. A large number of polymorphic sites are assayed, and alleles at each locus are tested for association with the putative disease mutation or mutations in each family member. If a particular allele is segregating with disease in the family, then the polymorphic locus and the disease gene are linked, that is, close together on the same chromosome.

The chromosomal location of each polymorphic site is known exactly (an outcome of the Human Genome Project), so the location of the disease gene is also fixed.

In practice, linkage testing is most useful in large families with autosomal dominant or X-linked disease since more affected family members are available for testing. Currently, linkage testing is often done using microarrays that assay up to a million SNPs, made by Affymetrix, among others.[54,55] Several computer programs are available for analysis of linkage data.[56–58] Once linkage is established, genes in the linkage region are sequenced, by a variety of methods, looking for mutations. Determining whether a rare variant in the linkage region is pathogenic can be challenging.[54]

In some cases, linkage can be useful in small recessive families, too. One effective approach is homozygosity mapping (also called autozygosity mapping).[59] If the mutations in a family with recessive disease are IBD, then not only are the mutations themselves identical, but DNA sequences within thousands of basepairs of the mutations are also identical, because of linkage. This manifests as long chromosomal segments surrounding the disease gene that contain no variant sites, for example, no heterozygous SNP sites. Long, homozygous DNA sequences are rare in humans and often indicative of IBD. They can be detected using the same SNP-testing arrays used for conventional linkage testing. Once the region containing the disease gene is located by homozygosity mapping, strategies to identify mapped genes can be applied. This has been a fruitful approach to finding genes causing recessive iRDs.[60,61]

High-Throughput DNA Sequencing

In recent years, novel methods for very rapid DNA sequencing have become available. This is referred to as next-generation sequencing (NGS) or deep sequencing.[62,63] These approaches can be up to 10, 000 times as fast as conventional di-deoxy cycle sequencing. The principle is to shear human DNA into short fragments and to sequence these fragments, up to 1 million simultaneously, in micron-sized wells or slots. The isolated sequences are then assembled computationally by comparison to the reference human genome. This is called “shotgun sequencing”

because many short, random fragments are sequenced and later assembled into long, useful sequences. Next-generation sequencing is more error-prone than conventional sequencing, but it more than compensates by the extremely high sequencing rate.

With next-generation sequencing it is practical and inexpensive to sequence large tracts of the genome in individual patients. One application is to sequence the coding regions of all human genes. This is referred to as whole-exome sequencing – the "exome" is all known exons. Another application is whole-genome sequencing, that is, sequencing the entire genome of an individual. Since exons are only 1.5% of the genome, whole-exome sequencing is currently faster and cheaper than whole-genome sequencing, but whole-genome sequencing will be common within a few years. Already, whole-exome and whole-genome sequencing have shown promise in finding novel iRD genes and mutations.[54,64–66]

A variant of whole-exome sequencing is to target only genes known to cause disease followed by next-generation sequencing. For retinal diseases this is retinal targeted-capture NGS.[67] This has the advantage of limiting analysis to known causes only, increasing the likelihood of identifying truly pathogenic mutations, but perforce excludes detection of novel disease-causing genes.

Future Prospects

Currently, high-throughput sequencing, and even faster sequencing methods, are beginning to dominate genetic testing. One problem now, and for the foreseeable future, is distinguishing pathogenic mutations from the exceptional number of rare variants in each of us – variants that help define our individuality. Also, the sheer amount of DNA sequence data per patient is potentially overwhelming. At the same time, though, robust computational methods are under development to address these problems. The divide between diagnostic testing and research is likely to fade further. Genetic testing will play an increasingly important role in the diagnosis and treatment of iRDs, with clinical ophthalmology serving as the indispensable link between patients, families, and testing facilities.

References

1. RetNet. *The Retinal Information Network*. http://www.sph.uth.tmc.edu/RetNet/.
2. HGMD. *Human Gene Mutation Database*. http://www.hgmd.cf.ac.uk/.
3. Berger W, Kloeckener-Gruissem B, Neidhardt J. The molecular basis of human retinal and vitreoretinal diseases. *Prog Retin Eye Res*. 2010;29:335–375.
4. Daiger SP, Bowne SJ, Sullivan LS. Genes and mutations causing autosomal dominant retinitis pigmentosa. *Cold Spring Harb Perspect Med*. 2014;5(10) [pii: a017129].
5. Dryja TP, Hahn LB, Kajiwara K, et al. Dominant and digenic mutations in the peripherin/RDS and ROM1 genes in retinitis pigmentosa. *Invest Ophthalmol Vis Sci*. 1997;38:1972–1982.
6. Nussbaum RL, McInnes RR, Williard HF. *Thompson and Thompson Genetics in medicine*. 8th ed. Saunders Elsevier: Philadelphia, PA; 2015.
7. Weleber RG, Carr RE, Murphey WH, et al. Phenotypic variation including retinitis pigmentosa, pattern dystrophy, and fundus flavimaculatus in a single family with a deletion of codon 153 or 154 of the peripherin/RDS gene. *Arch Ophthalmol*. 1993;111:1531–1542.
8. Wells J, Wroblewski J, Keen J, et al. Mutations in the human retinal degeneration slow (RDS) gene can cause either retinitis pigmentosa or macular dystrophy. *Nat Genet*. 1993;3:213–218.
9. Felbor U, Schilling H, Weber BH. Adult vitelliform macular dystrophy is frequently associated with mutations in the peripherin/RDS gene. *Hum Mutat*. 1997;10:301–309.
10. Shankar SP, Birch DG, Ruiz RS, et al. Founder effect of a c.828+3A>T splice site mutation in peripherin 2 (PRPH2) causing autosomal dominant retinal dystrophies. *JAMA Ophthalmol*. 2015;133:511–517.
11. Boon CJ, van Schooneveld MJ, den Hollander AI, et al. Mutations in the peripherin/RDS gene are an important cause of multifocal pattern dystrophy simulating

STGD1/fundus flavimaculatus. *Br J Ophthalmol*. 2007;91:1504–1511.
12. Shankar SP, Hughbanks-Wheaton DK, Birch DG, et al. Autosomal dominant retinal dystrophies caused by a founder splice site mutation, c.828+3A>T, in PRPH2 and protein haplotypes in trans as modifiers. *Invest Ophthalmol Vis Sci*. 2016;57:349–359.
13. Rivolta C, McGee TL, Frio TR, et al. Variation in retinitis pigmentosa-11 (PRPF31 or RP11) gene expression between symptomatic and asymptomatic patients with dominant RP11 mutations. *Hum Mutat*. 2006;27:644–653.
14. Sullivan LS, Bowne SJ, Seaman CR, et al. Genomic rearrangements of the PRPF31 gene account for 2.5% of autosomal dominant retinitis pigmentosa. *Invest Ophthalmol Vis Sci*. 2006;47:4579–4588.
15. Vithana EN, Abu-Safieh L, Pelosini L, et al. Expression of PRPF31 mRNA in patients with autosomal dominant retinitis pigmentosa: a molecular clue for incomplete penetrance? *Invest Ophthalmol Vis Sci*. 2003;44:4204–4209.
16. Rose AM, Shah AZ, Venturini G, et al. Transcriptional regulation of PRPF31 gene expression by MSR1 repeat elements causes incomplete penetrance in retinitis pigmentosa. *Sci Rep*. 2016;6:19450.
17. Rose AM, Shah AZ, Venturini G, et al. Dominant PRPF31 mutations are hypostatic to a recessive CNOT3 polymorphism in retinitis pigmentosa: a novel phenomenon of "linked trans-acting epistasis". *Ann Hum Genet*. 2014;78:62–71.
18. Lyon MF. Gene action in the X-chromosome of the mouse (Mus musculus L.). *Nature*. 1961;190:372–373.
19. Lyon MF. The Lyon and the LINE hypothesis. *Semin Cell Dev Biol*. 2003;14:313–318.
20. Fahim AT, Bowne SJ, Sullivan LS, et al. Allelic heterogeneity and genetic modifier loci contribute to clinical variation in males with X-linked retinitis pigmentosa due to RPGR mutations. *PLoS ONE*. 2011;6:ie23021.
21. Pelletier V, Jambou M, Delphin N, et al. Comprehensive survey of mutations in RP2 and RPGR in patients affected

with distinct retinal dystrophies: genotype–phenotype correlations and impact on genetic counseling. *Hum Mutat*. 2007;28:81–91.
22. Rozet JM, Perrault I, Gigarel N, et al. Dominant X-linked retinitis pigmentosa is frequently accounted for by truncating mutations in exon ORF15 of the RPGR gene. *J Med Genet*. 2002;39:284–285.
23. Comander J, Weigel-DiFranco C, Sandberg MA, et al. Visual function in carriers of X-linked retinitis pigmentosa. *Ophthalmology*. 2015;122:1899–1906.
24. Sullivan LS, Bowne SJ, Birch DG, et al. Prevalence of disease-causing mutations in families with autosomal dominant retinitis pigmentosa (adRP): a screen of known genes in 200 families. *Invest Ophthalmol Vis Sci*. 2006;47:3052–3064.
25. Churchill JD, Bowne SJ, Sullivan LS, et al. Mutations in the X-linked retinitis pigmentosa genes RPGR and RP2 found in 8.5% of families with a provisional diagnosis of autosomal dominant retinitis pigmentosa. *Invest Ophthalmol Vis Sci*. 2013;54:1411–1416.
26. Chen J, Smaoui N, Hammer MB, et al. Molecular analysis of Bardet–Biedl syndrome families: report of 21 novel mutations in 10 genes. *Invest Ophthalmol Vis Sci*. 2011;52:5317–5324.
27. Badano JL, Leitch CC, Ansley SJ, et al. Dissection of epistasis in oligogenic Bardet–Biedl syndrome. *Nature*. 2006;439:326–330.
28. Katsanis N. The oligogenic properties of Bardet–Biedl syndrome. *Hum Mol Genet*. 2004;13:R65–71.
29. Krebs JE, Goldstein ES, Kilpatrick ST. *Lewin's GENES XI*. 11th ed. Jones and Bartlett Publishers Inc.; 2013.
30. Watson JD, Crick FHC. A structure for deoxyribose nucleic acid. *Nature*. 1953;171:737–738.
31. Crick F. Central dogma of molecular biology. *Nature*. 1970;227:561–563.
32. Bowne SJ, Liu Q, Sullivan LS, et al. Why do mutations in the ubiquitously expressed housekeeping gene IMPDH1 cause retina-specific photoreceptor degeneration? *Invest Ophthalmol Vis Sci*. 2006;47:3754–3765.

33. Schmid F, Glaus E, Cremers FP, et al. Mutation- and tissue-specific alterations of RPGR transcripts. *Invest Ophthalmol Vis Sci*. 2010;51:1628–1635.
34. Matise TC, Chen F, Chen W, et al. A second-generation combined linkage physical map of the human genome. *Genome Res*. 2007;17:1783–1786.
35. Dobzhansky T. Nothing in biology makes sense except in the light of evolution. *Am Biol Teach*. 1973;35:125–129.
36. Lander ES, Linton LM, Birren B, et al. Initial sequencing and analysis of the human genome. *Nature*. 2001;409:860–921.
37. Venter JC, Adams MD, Myers EW, et al. The sequence of the human genome. *Science*. 2001;291:1304–1351.
38. Lander ES. Initial impact of the sequencing of the human genome. *Nature*. 2011;470:187–197.
39. 1000 Genomes Project Consortium, Auton A, Brooks LD, et al. A global reference for human genetic variation. *Nature*. 2015;526:68–74.
40. Sudmant PH, Rausch T, Gardner EJ, et al. An integrated map of structural variation in 2,504 human genomes. *Nature*. 2015;526:75–81.
41. Stone EM. Leber congenital amaurosis – a model for efficient genetic testing of heterogeneous disorders: LXIV Edward Jackson Memorial Lecture. *Am J Ophthalmol*. 2007;144:791–811.
42. Travaglini L, Brancati F, Attie-Bitach T, et al. Expanding CEP290 mutational spectrum in ciliopathies. *Am J Med Genet A*. 2009;149A:2173–2180.
43. CLIA. *Clinical Laboratory Improvement Amendments (CLIA)*. https://www.cms.gov/clia/; 2011 [US Departments of Health and Human Services, Centers for Medicare and Medical Services].
44. CAP. *College of American Pathologists (CAP) Accreditation*. http://www.cap.org/accreditation/.
45. Pettersson E, Lundeberg J, Ahmadian A. Generations of sequencing technologies. *Genomics*. 2009;93:105–111.
46. Sanger F, Nicklen S, Coulson AR. DNA sequencing with chain-terminating inhibitors. *Proc Natl Acad Sci USA*. 1977;74:5463–5467.

47. EyeGENE. *National Ophthalmic Disease Genotyping Network*. http://www.nei.nih.gov/resources/eyegene.asp.
48. GeneTests. *geneTests*. http://www.genetests.org/.
49. *NCBI NH Genetic Testing Registry*. http://www.ncbi.nlm.nih.gov/gtr/.
50. Clark GR, Crowe P, Muszynska D, et al. Development of a diagnostic genetic test for simplex and autosomal recessive retinitis pigmentosa. *Ophthalmology*. 2010;117:2169–2177.e3.
51. Jaakson K, Zernant J, Kulm M, et al. Genotyping microarray (gene chip) for the ABCR (ABCA4) gene. *Hum Mutat*. 2003;22:395–403.
52. Aguirre-Lamban J, Riveiro-Alvarez R, Maia-Lopes S, et al. Molecular analysis of the ABCA4 gene for reliable detection of allelic variations in Spanish patients: identification of 21 novel variants. *Br J Ophthalmol*. 2009;93:614–621.
53. Pieras JI, Barragan I, Borrego S, et al. Copy-number variations in EYS: a significant event in the appearance of arRP. *Invest Ophthalmol Vis Sci*. 2011;52:5625–5631.
54. Sullivan LS, Koboldt DC, Bowne SJ, et al. A dominant mutation in hexokinase 1 (HK1) causes retinitis 2 pigmentosa. *Invest Ophthalmol Vis Sci*. 2014;55:7147–7158.
55. Thermo Fisher Scientific. *Affymetrix*. http://www.affymetrix.com/.
56. Abecasis GR, Cherny SS, Cookson WO, et al. Merlin–rapid analysis of dense genetic maps using sparse gene flow trees. *Nat Genet*. 2002;30:97–101.
57. Lathrop GM, Lalouel JM, Julier C, et al. Strategies for multilocus linkage analysis in humans. *Proc Natl Acad Sci USA*. 1984;81:3443–3446.
58. Purcell S, Neale B, Todd-Brown K, et al. PLINK: a tool set for whole-genome association and population-based linkage analyses. *Am J Hum Genet*. 2007;81:559–575.
59. Lander ES, Botstein D. Homozygosity mapping: a way to map human recessive traits with the DNA of inbred children. *Science*. 1987;236:1567–1570.
60. Collin RW, van den Born LI, Klevering BJ, et al. High-resolution homozygosity mapping is a powerful tool to detect novel mutations causative of autosomal recessive RP

in the Dutch population. *Invest Ophthalmol Vis Sci*. 2011;52:2227–2239.
61. Littink KW, Koenekoop RK, van den Born LI, et al. Homozygosity mapping in patients with cone–rod dystrophy: novel mutations and clinical characterizations. *Invest Ophthalmol Vis Sci*. 2010;51:5943–5951.
62. Mardis ER. Next-generation DNA sequencing methods. *Annu Rev Genomics Hum Genet*. 2008;9:387–402.
63. Schuster SC. Next-generation sequencing transforms today's biology. *Nat Methods*. 2008;5:16–18.
64. Ozgul RK, Siemiatkowska AM, Yucel D, et al. Exome sequencing and cis-regulatory mapping identify mutations in MAK, a gene encoding a regulator of ciliary length, as a cause of retinitis pigmentosa. *Am J Hum Genet*. 2011;89:253–264.
65. Tucker BA, Scheetz TE, Mullins RF, et al. Exome sequencing and analysis of induced pluripotent stem cells identify the cilia-related gene male germ cell-associated kinase (MAK) as a cause of retinitis pigmentosa. *Proc Natl Acad Sci USA*. 2011;108:E569–76.
66. Zuchner S, Dallman J, Wen R, et al. Whole-exome sequencing links a variant in DHDDS to retinitis pigmentosa. *Am J Hum Genet*. 2011;88:201–206.
67. Consugar MB, Navarro-Gomez D, Place EM, et al. Panel-based genetic diagnostic testing for inherited eye diseases is highly accurate and reproducible, and more sensitive for variant detection, than exome sequencing. *Genet Med*. 2015;7:253–261.

34

Mitochondrial Genetics of Retinal Disease

M. Cristina Kenney, Deborah A. Ferrington, Nitin Udar

Mitochondrial Origins

It is now accepted that the origin of mitochondria within eukaryotes is the result of an endosymbiotic relationship and that mitochondrial (mt) DNAs can be traced to an α-proteobacterial genome.[1,2] This theory has been supported by phylogenetic patterns of gene arrangements, small subunit ribosomal RNAs (rRNA) and protein data.[3,4] The DNA sequencing studies have shown that tremendous variations still remain, with the genome of the protozoan *Reclinomonas americana* having the most bacteria-like mitochondrial genome and *Rickettsia prowazekii* the most mitochondria-like eubacterial genome.[1] The mtDNA from eukaryote species show remarkable differences in size, ranging from 6 kb to 60 kb. They also vary in shape, with some eukaryotes having linear mtDNA while others have circular mtDNA. Although there is no recombination of mtDNA in humans, mitochondrial genomes of some plant species, such as *Arabidopsis thaliana*, have become recombinantly active.

Mitochondrial Structure

Depending on the energy requirement of each cell, the number of mitochondria varies from one to several thousand. Each mitochondrion is divided into compartments that are contained within the outer membrane and include the intermembrane space, the inner membrane, cristae, and the matrix (Fig. 34.1). The outer

membrane is permeable to molecules smaller than 5000 Daltons, which pass through the lipid bilayer through channels called porins (voltage-dependent anion channel, VDAC) into the intermembrane space. It also contains a translocase of the outer membrane (TOM) complex that is involved in the import of resident mitochondrial proteins that are encoded by the nuclear genome and produced in the cytosol.[5] The inner membrane has a high content of cardiolipin, and its selective permeability allows only specific molecules into the matrix. The surface area is greatly expanded as a result of the numerous invaginations of the inner membrane, known as cristae. Embedded within the inner membrane are many of the enzyme complexes required for adenosine triphosphate (ATP) production and the translocase of the inner membrane (TIM) complex that is responsible for the import of nuclear-encoded proteins into the matrix. The matrix contains numerous proteins, ribosomes, tRNA, and the mtDNA.

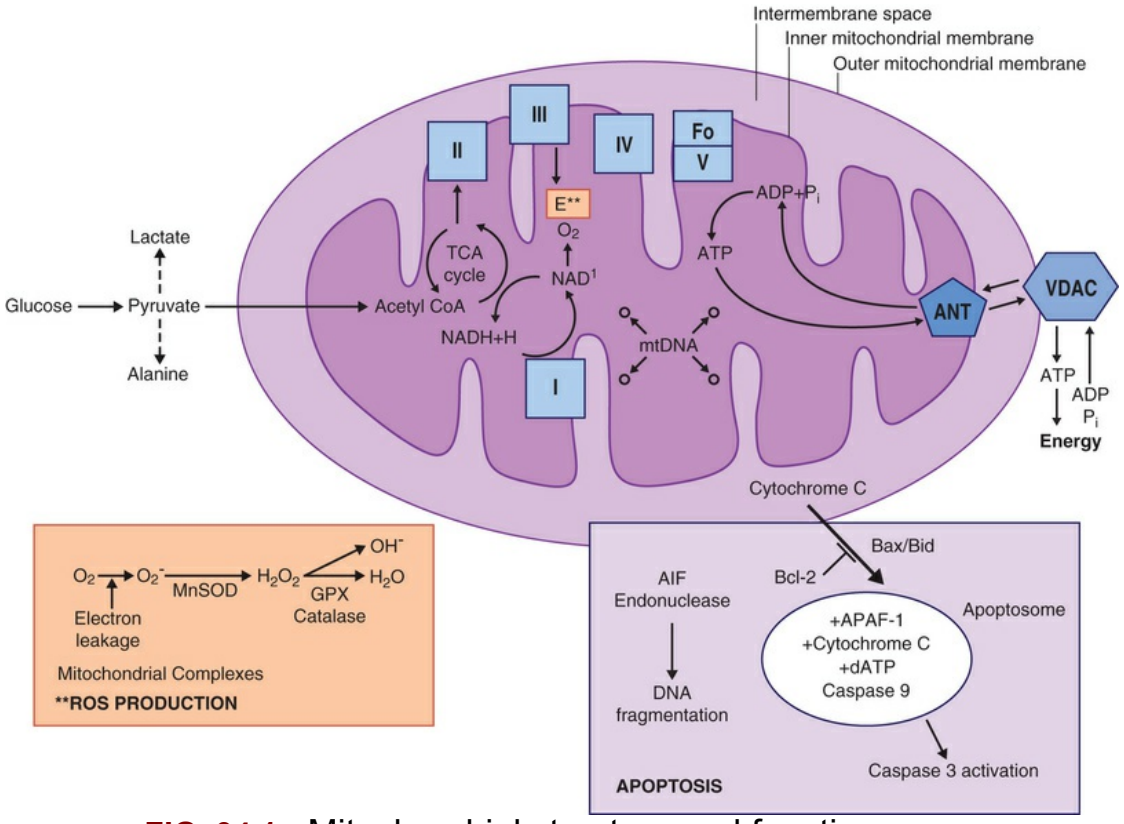

FIG. 34.1 Mitochondrial structure and function. Schematic showing the mitochondrial structure and summarizing the three important functions of energy production, ROS production, and apoptosis. *AIF*

Endonuclease, apoptosis-inducing factor; *ANT,* adenine nucleotide translocase; *APAf-1,* apoptotic protease activating factor; *GPX,* glutathione peroxides; *MnSOD,* manganese superoxide dismutase; *mtDNA,* mitochondrial DNA; *ROS,* reactive oxygen species; *VDAC,* voltage dependent anion channel. (Modified from www.mitomap.org, illustration by S. Atilano.)

Mitochondrial DNA (mtDNA)

Mitochondria are unique in that they have their own DNA that is inherited through the maternal lineage. The human mtDNA forms a closed circle of double-stranded DNA, with 16,569 nucleotide pairs, comprised of two strands that are differentiated by their nucleotide content. The heavy strand is guanine-rich and encodes for 28 genes while the light strand is cytosine-rich and encodes for nine genes. Unlike the nuclear genome, mtDNA contains a unique noncoding Control Region but no introns. The noncoding mtDNA D-loop has within it the 1121 nucleotide control region that is important for replication and transcription. The coding region of mtDNA codes for 37 genes including 13 protein subunits essential for oxidative phosphorylation (OXPHOS), 2 ribosomal RNAs, and 22 transfer RNAs (Fig. 34.2A).[6–8] Recently, small biologically active mitochondrial derived peptides (MDPs) that are encoded from the mtDNA genome have been reported. The vast majority of mitochondrial proteins (~1500–2000), many of which contribute to energy biogenesis,[4,9] are encoded by nuclear DNA and imported into the mitochondria.

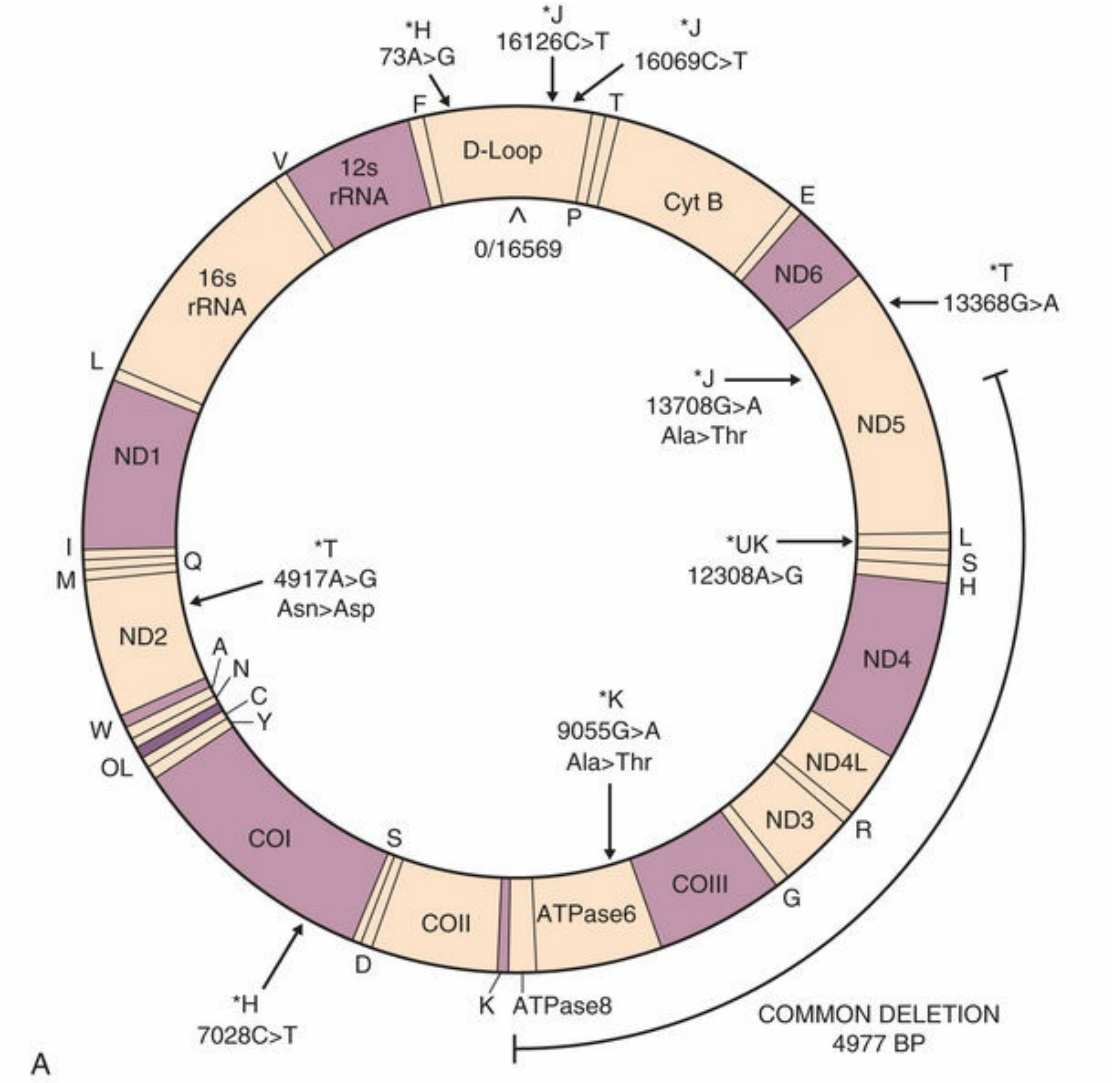

A

Human mtDNA Migrations
http://www.mitomap.org

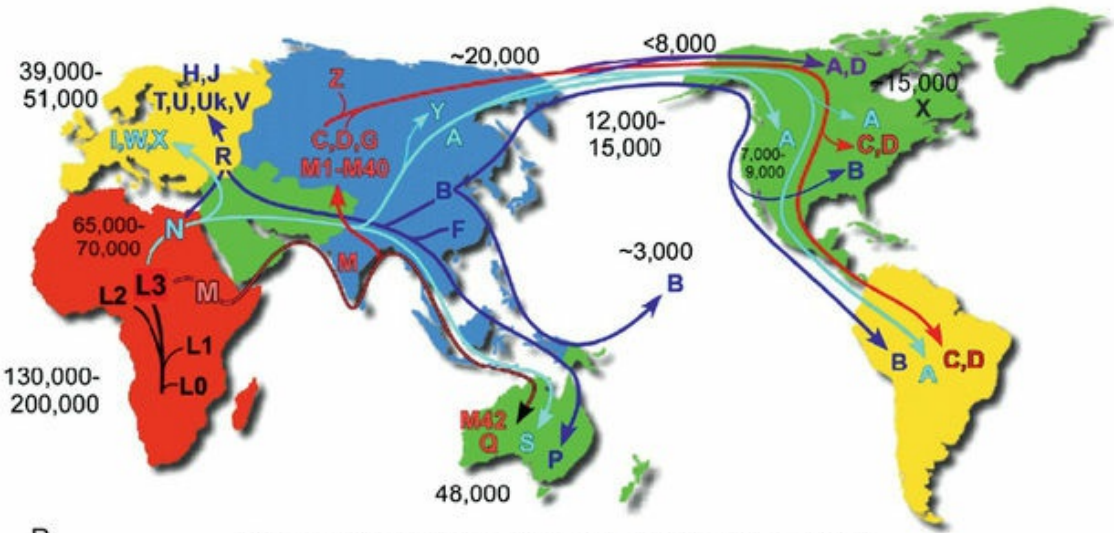

B

Time estimates are years before present

FIG. 34.2 Haplogroups' associated mt single nucleotide polymorphisms (SNPs) and global origins of mtDNA. (A) Schematic of circular mtDNA showing noncoding D-loop region and coding genome. SNPs that define the H haplogroup (73A>G, 7028C>T), the J haplogroup (13708 G>A, 16126 C>T, 16069 C>T), T haplogroup (4917 A>G, 13368 G>A), UK haplogroup (12308 A>G), and K haplogroup (9055 G>A) are shown. Note that some are nonsynonymous SNPs that lead to amino acid changes that may alter bioenergetic functions. The 4977 bp common deletion spans coding regions for subunits of complexes I, IV, and V. Cells that have this common deletion will have decreased bioenergetic efficiency. (B) Map of the haplogroup origins showing mtDNA distribution worldwide. *MYR*, million years; *YBP*, years before present. (Panel A modified from www.mitomap.org; illustration by S. Atilano. Panel B image from www.mitomap.org.)

Within a cell there is a single DNA copy of the nuclear genome (nDNA) but multiple copies of mtDNA because there can be thousands of mitochondria per cell, and within each mitochondrion, 1 to 10 copies of mtDNA. With aging and exposure to oxidative stress, mtDNA molecules can be damaged, which results in a mixture of nonmutated (wild-type) and mutant mtDNA within the same cell. This mixture of damaged and undamaged mtDNA is termed heteroplasmy. When cells with heteroplasmic mitochondria divide, the two types of mtDNA are randomly or in some instances nonrandomly distributed into the daughter cells.[10–14] Alternatively, cells may have either a pure mutant mtDNA or pure nonmutant (wild-type) mtDNA population, in which case it is referred to as homoplasmic mtDNA.[15] Homoplasmy within a cell indicates that all mtDNA copies are identical. Cells can function only with relatively low levels of heteroplasmy, but once this threshold is breached, abnormal function and disease can occur. Although low levels of heteroplasmic mtDNA defects may have an effect on function, the mtDNA changes are not always obvious and special technical approaches are required to ensure their detection. Correlating a phenotype with mtDNA defects can be difficult

because the complexity of the phenotype can be influenced by when (time during embryogenesis) and where (tissue-type) the mutation arises.[16–18] In addition, environmental factors, such as oxidative stress, can modulate the expression of the phenotype. mtDNA is particularly susceptible to oxidative damage because it resides in the matrix in close proximity to sites of ROS formation. In addition, the mitochondrion has a poor DNA repair process and a high transcription rate. Oxidative damage to mtDNA is especially prevalent in very metabolically active tissues such as the retina, brain, and muscle.

Mitochondrial Function

The mitochondria perform many essential roles, such as heme biosynthesis, calcium buffering, iron homeostasis, and regulation of apoptosis. The mitochondria are also the major site of cellular energy production, which includes contributions from beta-oxidation of fatty acids, the tricarboxylic acid (TCA) cycle, and OXPHOS. The initial molecular processes occur within the intermembrane space and mitochondrial matrix to produce acetyl COA, which is then taken up into the TCA cycle. In addition to producing ATP, the TCA cycle also supplies reducing equivalents for OXPHOS via enzymes of the electron transport chain (ETC). The ETC consist of five multi-subunit respiratory complexes (complexes I–V) that are embedded in the mitochondrial inner membrane. Thirteen critical protein subunits of the respiratory complexes I, III, IV, and V are encoded by mtDNA and produced within the mitochondria. The remaining ETC subunits, including the four subunits of respiratory complex II, are encoded by the nuclear genome, produced in the cytosol, and imported into the mitochondria.

Electron Leakage and ROS Formation

Under normal conditions, ATP is produced via a series of oxidation-reduction reactions that involve the flow of electrons through complex I to IV of the ETC. Electron transfer generates the energy required to transport protons across the inner mt membrane

into the inner membrane space. The flow of the protons down their concentration gradient from the inner membrane space into the matrix through complex V, also known as the ATP synthase, provides the energy to generate ATP from ADP. Under optimal conditions, each molecular oxygen captures two electrons released from complex IV to form water. However, partial reduction of oxygen can produce potentially harmful intermediates, such as superoxide, peroxide, and hydroxyl radicals, collectively known as reactive oxygen species (ROS). Additionally, ineffective transfer of electrons between ETC complexes can permit partial reduction of oxygen and production of ROS as byproducts during normal oxidative metabolism. In fact, approximately 2% to 5% of the oxygen we consume is only partially reduced and forms ROS.[19]

Localization of Mitochondria Within the Retina and Optic Nerve

The retina has one of the highest oxygen consumption rates in the body due, in part, to the high concentration of mitochondria in nearly all cells. Mitochondria are distributed toward the source of oxygen, which in the outer retina are toward the choriocapillaris and for the inner retina toward the inner retinal vessels. To meet the energy demand for vision, the photoreceptor cells have a high concentration of mitochondria within the inner segments and at the axon terminals, thus receiving oxygen from both the choriocapillaris and the deep capillaries of the inner retinal vasculature (Fig. 34.3). In RGCs, the mitochondria are present in the soma around the nucleus and along the axons, but they tend to accumulate just anterior to the lamina cribrosa (Fig. 34.3).[20] For Müller cells, mitochondria congregate along the outer limiting membrane toward their oxygen source from the choriocapillaris. Mitochondria in the RPE cluster at the basal surface of the cell, which is adjacent to the choriocapillaris.

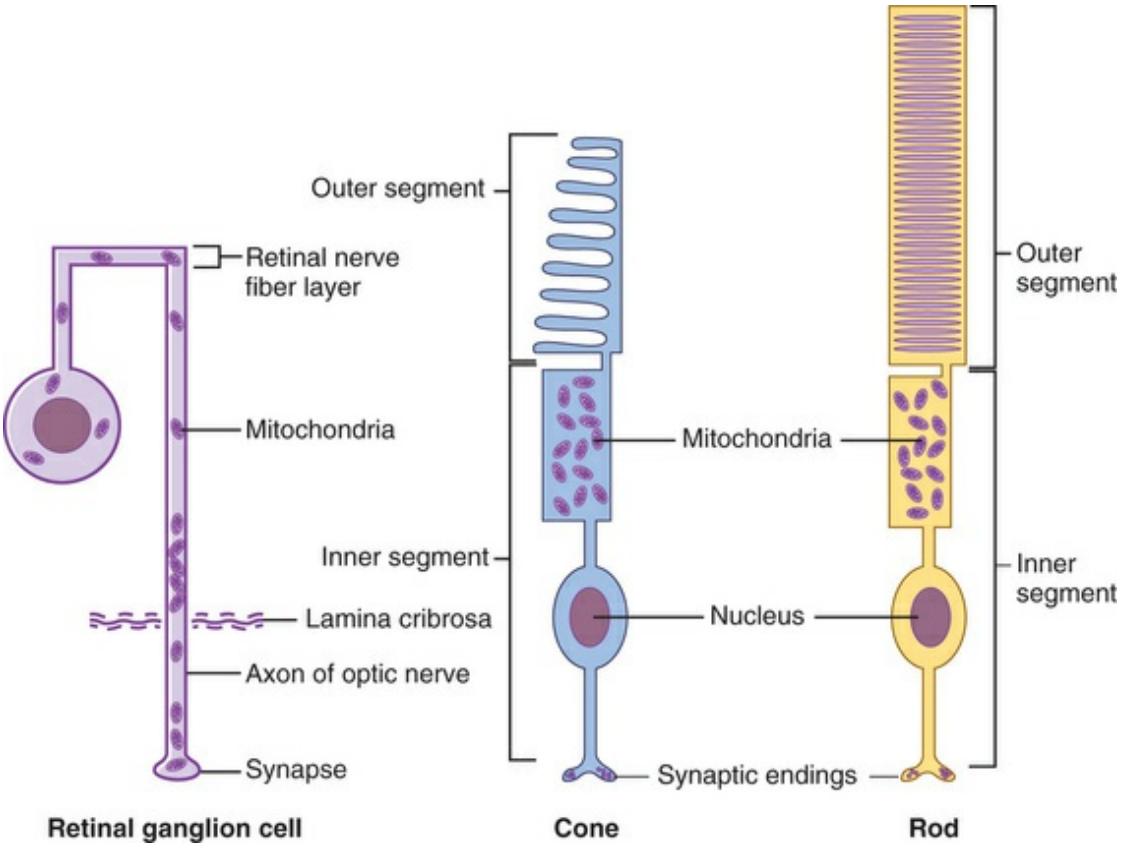

FIG. 34.3 Mitochondrial localization within retinal cells. Schematic showing sites with high density of mitochondria within retinal ganglion cells, cone photoreceptors, and rod photoreceptors. (Illustration by S. Atilano.)

Influences of mtDNA on Cell Function

Influences of mtDNA upon cell function can be classified into hereditary (ancient adaptive polymorphism changes/haplogroups versus recent mutations) and somatic mtDNA changes.[21] Examples of each are presented below.

Ancient Inherited mtDNA Variants Representing Populations (Haplogroups)

Definition of Haplogroups

Haplogroups are mtDNA sequence polymorphism variations that have occurred over more than 150,000 years and correlate to the

geographic origins of populations traced through the maternal lineages (Fig. 34.2B). The oldest haplogroups are from Africa, and with migration and climate adaptations, European, Asian, and Native American haplogroups have evolved.[4] Each haplogroup has related patterns of mtDNA sequences (haplotypes) that represent that population. If the specific single nucleotide polymorphism (SNP) variants representing the haplogroup are found in the mtDNA D-loop, it can affect the replication and transcription rates. If within the coding region, the SNP variants can be nonsynonymous (amino acid changing), which can alter efficiencies of energy production, causing ROS formation, apoptosis, and cell death. This means that each haplogroup, with its different set of SNPs, can produce unique bioenergetic properties.

Association of Haplogroups With Retinal Diseases

Haplogroups increasingly are being correlated to a broad spectrum of age-related diseases, such as Parkinson's disease and Alzheimer's disease.[22–32] Additionally, there are a number of ocular diseases that exhibit an increased disease risk among individuals in a specific haplogroup. For example, AMD is associated with specific mtDNA SNPs that define northern European haplogroups.[33–36] Studies of European mtDNA variants have revealed that J, T, and U haplogroups are associated with AMD,[33–38] while the H haplogroup has a protective effect.[37] Large soft drusen and retinal pigment abnormalities, which are characteristics of AMD retinas, have been associated with J and U haplogroups.[33] The haplogroup T-associated SNP A4917G located in the NADH dehydrogenase subunit 2 of complex I is an independent predictor of AMD.[34] Udar and coworkers found that patients with late AMD showed strong association with noncoding mtDNA D-loop SNPs (Fig. 34.2A).[35] Two variants of the T2 haplogroup, A11812G of MT-ND4 and A14233G of MT-ND6 located in respiratory complex I, are 2.5 times more likely to be associated with advanced AMD than the age-matched control subjects.[36]

Multiple studies have shown that a person's mtDNA background can play a role in the clinical phenotype of diseases, such as diabetes and glaucoma. In an Austrian cohort, type 2 diabetic patients with the mtDNA T haplogroup background have a higher

prevalence of diabetic retinopathy.[39] In an Italian population, the H haplogroup was associated with diabetic retinopathy, the H3 subgroup with neuropathy, U3 haplogroup with nephropathy, and the V haplogroup with renal failure.[40] In an American population, diabetic subjects who had the H haplogroup were more likely to develop proliferative diabetic retinopathy, while the UK haplogroup patients were protected.[41] In addition, the mtDNA haplogroups were a strong predictive risk factor for those that had elevated HgbA1c.[41] The manifestation of glaucoma has also been linked to specific haplogroups. Recent studies have reported that susceptibility to pseudoexfoliation glaucoma is decreased in patients with a U haplogroup but increased with T or L2 haplogroups.[42,43] In a Saudi Arabian population, the African L haplogroups, excluding L2 haplogroup, have been associated with increased risk of primary open angle glaucoma.[44]

Haplogroups may also influence diseases via interaction with nuclear genes to increase the severity of or protect against disease. It has been shown that an individual harboring the milder Leber hereditary optic neuropathy (LHON) mutations at positions 11778, 14484, and 10663 has increased probability of blindness if they have a J haplogroup background.[45,46] In contrast, human immunodeficiency virus (HIV)-infected patients with a J haplogroup background were protected against progression of neuroretinal disorder (NRD).[47]

The mechanism behind how mtDNA haplogroups influence disease risk is an area of active investigation. One of the prominent ideas is that mtDNA variants alter cellular bioenergetics. This idea is supported by results showing that mtDNA SNPs defining haplogroups can cause partial uncoupling of OXPHOS and decreased efficiency of ATP production.[31,32,48] If mitochondrial energy production levels fall below a specific bioenergetic threshold, the mitochondrial permeability transition pore (mtPTP) can be activated and photoreceptors or RGCs destroyed through apoptosis. This scenario of mitochondrial dysfunction playing a role in retinal or neuronal diseases may offer an array of new therapeutic approaches targeted toward increasing mitochondrial energy production, decreasing mitochondrial ROS, and stabilizing the mtPTP.

Our knowledge for understanding the effects of mtDNA upon cellular homeostasis has been advanced through the use of the transmitochondrial cybrid model, which are cell lines with identical nuclei, but the mtDNA from different subjects. Using human retinal pigment epithelial cell cybrids, it has been demonstrated that mtDNA can greatly affect growth rates of cells, bioenergetics and expression levels of complement, inflammation, and angiogenesis genes, pathways which are important in human retinal diseases.[49–55] In addition, cybrids with H (protective against AMD) versus J (high risk for AMD) mtDNA haplogroups have different responses to heat stress, hydrogen peroxide, and ultraviolet (UV) radiation.[49,54,56,57] Osteosarcoma cybrids with K mtDNA have lower mitochondrial potential, consistent with decreased endogenous leaking and uncoupled respiration compared to the H cybrids.[58] These studies support the hypothesis that an individual's mtDNA background sets up baseline cellular homeostasis, making the cells differentially susceptible to identical stressors.

Recent Maternally Transmitted mtDNA Mutations Associated With Retinal Diseases

This category refers to true pathology-creating mtDNA mutations that are inherited over recent generations rather than mtDNA adaptation (haplogroups) that occur over thousands of years in response to environmental challenges. Defects or mutations in the mtDNA genes can decrease OXPHOS and ATP production, which results in energy deficiency diseases. Tissues that are very metabolically active, such as brain, heart, muscle, retina, kidney, and the endocrine organs, can be significantly affected by these changes. Therefore, many of these patients have not only retinal abnormalities but also neurologic, cardiac, metabolic, and skeletal muscle dysfunctions related to damage in these high-energy requiring organs systems. It is now apparent that patients with mtDNA mutations that cause mitochondrial dysfunction can have a wide range of clinically abnormal ocular and systemic phenotypes.[59] Table 34.1 lists mtDNA defects that result in diseases involving the retina and optic nerve. While there are many diseases caused by nuclear gene defects encoding mitochondrial proteins,

they are not addressed here but are covered in an excellent review by Yu-Wai-Man and coworkers.[60]

TABLE 34.1
Mitochondrial DNA Defects That Result in Diseases Involving the Retina

Disease	Mutation	OMIM#	Site of Action	Retinal Phenotype
Cytochrome c oxidase deficiency	T7587C, G7896A, *MT-CO2* gene	516040	Complex IV deficiency	Pigmentary retinopathy, decreased color vision, bilateral optic atrophy
Kearns–Sayre syndrome (KSS)/chronic progressive external ophthalmoplegia (CPEO)	Large mtDNA deletions	530000	Depends on site of deletion	Pigmentary degeneration of retina, altered electroretinogram, ophthalmoplegia
Leber hereditary optic neuropathy (LHON)	G11778G, *MT-ND4* gene; G3460A, *MT-ND1* gene; T14484C, *MT-ND6* gene; and others[a]	516003	Complex I deficiency	Acute-optic disc hyperemia, pseudoedema, circumpapillary telangiectatic microangiopathy, swollen nerve fiber layer, temporal optic nerve pallor, optic atrophy
Maternally inherited diabetes and deafness (MIDD)	A3243G, T14709C, *MT-TE* gene; mtDNA, deletions, duplication, point mutations	520000	tRNA-glu	Salt and pepper retinopathy, pigmentary degeneration, diabetic retinopathy, macular pattern dystrophy
Mitochondrial encephalopathy lactic acidosis and stroke-like episodes (MELAS)	T3271C, C3256T, A3243G *MT-TL1* gene	590050	tRNA-leu	Retinal pigment epithelium atrophy
Myoclonic epilepsy and ragged red fibers (MERRF)	C3256T, *MT-TL1* gene; G8313A, *MT-TK* gene	590060	tRNA-leu tRNA-lys	Pigmentary retinopathy
Neuropathy, ataxia, and retinitis pigmentosa (NARP)/Leigh syndrome	T8993G, T8993C, *MT-ATP6* gene	516060	Complex V deficiency	Retinitis pigmentosa, bone spicules, loss of foveal reflex, optic atrophy, ophthalmoplegia, strabismus, nystagmus
Renal tubulopathy, diabetes mellitus, and cerebellar ataxia	mtDNA duplication between ATPase6 and cytochrome b genes	560000	Complex III deficiency	Pigmentary deposits of the retina, extinguished electroretinogram

[a]There are 18 other allelic variants with varying phenotypes.

Somatic mtDNA Variations Associated With Retinal Diseases

Mechanisms of mtDNA Damage

The hydroxyl radical is most reactive with mtDNA and can produce multiple DNA modifications, such as strand breaks, cleavage of bases from the deoxyribose backbone to form abasic sites, and addition of oxygen to DNA forming many different mutagenic molecules (e.g., 8-hydroxydeoxyguanosine [8-OHdG] and thymine glycol). Compared with nuclear DNA, mtDNA is particularly susceptible to oxidative damage due in part to its close proximity to the ETC, the major cellular source of ROS. Additionally, mtDNA lacks protective histones and has a limited capacity for repair, which includes only a mechanism for base excision repair.[61] Enzymes involved in base excision repair that are present in the mitochondria include glycosylases, endonucleases, and GTPases. Of great importance for ocular tissue, proteins involved in nucleotide excision repair that repair UV damage are abundant in the nucleus but are absent from the mitochondria.[61]

The most frequent oxidative damage to mtDNA is 8-hydroxylation/oxidation of a guanine base to 8-OHdG[62,63] (Fig. 34.4). This oxidative modification is mutagenic because it inhibits methylation and can pair with adenosine (rather than cytosine) during DNA replication, leading to a GC to AT conversion, which is the most frequent type of spontaneous mutation. In postmitotic tissue, such as skeletal muscle, neurons, and retina, 8-OHdG accumulates with age and disease.[64–66] Abasic sites, which have neither purines (adenine and guanine) nor pyrimidines (cytosine and thymine), are also produced due to DNA damage and can lead to somatic mutations. Thymine is also susceptible to oxidative modification and produces a variety of modified thymines that are mutagenic.

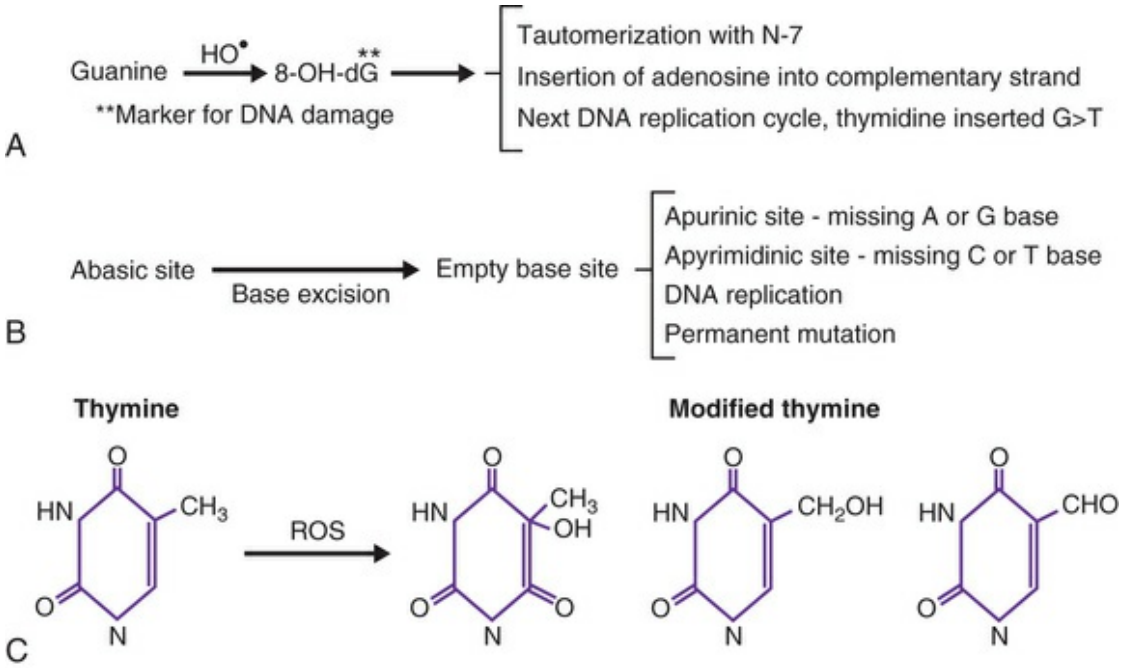

FIG. 34.4 Common mtDNA base modifications caused by oxidative damage. (A) Oxidation of guanine to 8-OHdG results in the mispairing of guanine with adenosine during DNA replication. (B) An abasic site can be either an apurinic site (missing the A or G base) or apyrimidinic site (missing the C or T base). (C) Oxidation of thymine can produce multiple forms of modified thymine.

In addition to DNA mutations, oxidative damage to mtDNA can also lead to mtDNA deletions by causing double-strand breaks in the DNA.[67,68] Damage from UV light can also cause double-strand breaks.[69] In general, mtDNA deletions occur more frequently than somatic mutations in aged postmitotic tissue.[70,71] There is a frequently encountered 4977 bp deletion known as the "common deletion." It is located in the major arc between the two origins of replication (O_H and O_L) and is flanked by short direct repeats (Fig. 34.2A). This region of the mtDNA genome is eliminated with increasing frequency in aged postmitotic cells, such as neurons, muscle, cochlear tissue, retina, and retinal pigment epithelium (RPE) and thus is considered a hallmark of aging.[64,70,72–75] In a comparison of the amount of common deletion 4977 in ocular tissue, the occurrence is highest in the cornea > iris > retina and accumulates with age.[76] The common deletion encompasses the coding region for subunits of complex I (ND3, ND4, ND4L, ND5),

complex IV (cytochrome oxidase III), and complex V (ATPase 6, ATPase 8). Therefore, high levels of common deletion should have a functional impact on the cell. However, each cell contains multiple mtDNA copy numbers, which may be a mixture of damaged and undamaged mtDNA (heteroplasmic). As the damaged mtDNA continues to accumulate, a "critical threshold" is reached, whereby extensive mitochondrial dysfunction causes detrimental consequences for the cell. Importantly, the "critical threshold" is tissue-specific. For example, the abundance of mtDNA deletions must reach >85% in muscles of Kearns–Sayre syndrome patients for disease phenotype to manifest.[77] In aged substantia nigra neurons, the critical threshold for functional defects is between 48% and 67%.[66] In RPE from elderly donors, deletion levels of ~40% were tolerated since the donors had no clinically obvious signs of retinal degeneration.[75] This may explain why clinical signs of diseases (such as drusen and RPE cell loss) may take decades to present in AMD patients. Of note, the content of RPE mtDNA deletions was not significantly increased in age-related macular degeneration (AMD) eyes compared with age-matched controls, suggesting that the presence of the common deletion does not contribute to AMD pathology.[75]

Two opposing models involving either replication or repair have been proposed as the mechanism for deletion formation.[78] While both models are supported by strong evidence, the presence of high levels of deletions in postmitotic cells compared with actively replicating mitotic cells favors defects in the process of repair as the mechanism responsible for generating deletions. In brief, double-stranded breaks that occur as a consequence of oxidative or UV damage stimulates activation likely of a 3′-5′ exonuclease that removes base pairs that are directly adjacent to the double-stranded break.[78] This action exposes homologous regions of 10–15 bp and allows them to anneal with direct repeats on the opposite strand. The unbound single strands are degraded and double strands are ligated. This results in production of mtDNA containing a partially deleted sequence. Thus, the age-dependent accumulation of mtDNA deletions is likely a byproduct of a lifetime of ongoing repair.

In vitro studies show that oxidative stress leads to preferential

damage of mtDNA compared to nuclear DNA.[79] There are numerous reports of mitochondrial abnormalities, including mtDNA damage, in aging, and AMD retinas.[75,79–84] Animal models also support the idea that mtDNA is particularly vulnerable to damage, as demonstrated by increased mtDNA deletions and damage in aging and degenerating retinas.[82,85] In some studies, specific regions of damage have been identified. In diabetic retinas and in retinas from donors with AMD, the mtDNA D-loop region has increased levels of damage compared to other regions.[84,86] The retinal ganglion cells (RGC) with their long axons are also susceptible to mitochondria damage. The numbers of RGCs and their axons are significantly decreased in Leber hereditary optic neuropathy and glaucoma.[87,88] This may be related to lower energy production caused by mtDNA damage and dysfunction.

mtDNA Damage and AMD

Three studies using a long-extension polymerase chain reaction technique testing for mtDNA damage in the RPE from human donor eyes provided evidence that mtDNA damage is increased with AMD. Karunadharma and colleagues showed marked differences in damage accumulation with aging and disease.[75] Age-related damage in the RPE appeared to be limited to the common deletion, whereas AMD was associated with global damage, which includes deletions and oxidative damage to mtDNA, throughout the mt genome. Corroborating data was also provided by Lin and colleagues, who showed that the increased DNA damage in RPE cultured from donors with AMD was accompanied by a fivefold increase in somatic mutations compared with age-matched controls.[89] Terluk and colleagues showed increased mtDNA damage with AMD progression occurred in the RPE but not the neural retina, and also localized the damage to specific regions of the mt genome, including the regulatory D-loop.[84] This result was consistent with a previous study where the sequence analyses of the mtDNA D-loop showed a significantly greater number of SNPs per person in the AMD population compared to either older or younger normal groups.[80] Increased oxidative DNA damage in retinas from donors with AMD was also shown from immunohistochemical staining with antibodies that recognize 8-OH-dG.[35] These results

support the hypothesis that defects in the mitochondria are hallmark, and most probably pathologic, events in AMD and other retinal diseases.

The potential consequences provoked by mtDNA damage has been suggested from studies using an animal model, where increased accumulation of mtDNA deletions and mutations impaired the cellular function and left the cells more susceptible to external stresses.[90] Additionally, damaged cells can release mtDNA, eliciting an inflammatory reaction because mtDNA contains "damage-associated molecular patterns," or DAMPs, that bind to toll-like receptors and activate the NLRP3 inflammasomes,[91] alter innate immunity, and generate chronic, low-grade inflammation.[92] Inflammation and inflammasome activation play an important role in several retinal diseases, including AMD.

Epigenetics and mtDNA

"Epigenetics" describes mechanisms by which gene expression and cellular functions are modified without alterations in the gene sequence. Epigenetic changes can be inherited but are also subject to environmental factors and are reversible. The most common epigenetic modification occurs at CpG dinucleotides where the 5′ position cytosine becomes methylated to become 5-methylcytosine (5-mc). Another epigenetics event includes histone modifications through methylation, acetylation, phosphorylation, ubiquitylation, and SUMOylation, which ultimately activates or inhibits transcription, thereby regulating gene expression.[93]

Recent studies have shown that altered epigenetic profiles play a role in human retinal diseases including AMD, diabetic retinopathy, retinitis pigmentosa, proliferative vitreoretinopathy, retinoblastoma, and uveal melanoma.[94–98] There is a close association between mitochondria and methylation status. For example, DNA methylation levels are affected if mitochondria are depleted from cells.[99] High glucose levels, as seen in diabetes, lead to hypermethylation of mtDNA and mitochondrial dysfunction.[95] In addition, cybrids with the J mtDNA haplogroup have elevated total global methylation levels and higher expression levels of genes associated with acetylation and methylation compared to cybrids

with H mtDNA.[100,101] Furthermore, methylation inhibitor studies show the mtDNA variants can influence transcription for inflammation, signaling and angiogenesis genes, which are important pathways in retinal diseases.[101] It has been suggested that epigenetic changes of the nDNA and mtDNA leads to long-term "metabolic memory," which causes pathologic conditions leading to retinal diseases.[102] Investigating the role of epigenetics in retinal diseases has provided a new area for developing therapeutics and drugs that target this malleable condition within the human genome.

Mitochondria as a Target for Retinal Diseases

The importance of mtDNA damage and mitochondrial dysfunction to the development and progression of retinal diseases has become increasingly recognized. This is true not only for eye diseases but also for neurodegenerative diseases, cancers, diabetes, obesity, and cardiovascular diseases. Therefore, the mitochondria have become a target for a new field of drug development. While there are currently no ongoing clinical trials using mitochondrial-targeting drugs for retinal diseases, this represents an exciting, novel area of research with great therapeutic potential.

Two different approaches to protecting the mitochondria included either capitalizing on endogenously produced compounds (i.e., mitochondrial derived peptides) or targeting specific pathways that are involved in maintaining mitochondrial function. Mitochondrial-derived peptides (MDPs) are recently identified biologically active, short peptides (20–27 AAs) that are encoded from short open reading frames (sORF) in the mtDNA genome.[103–106] In 2001, Humanin (MT-RNR2), a 24 amino acid peptide, was the first MDP described,[107] is encoded from the 16S rRNA region of the mtDNA and has been shown in vitro and in vivo to have antiapoptotic, neuroprotective properties supporting cell survival.[103,105,106,108,109] Humanin levels decline with aging, and it has been associated with many age-related and metabolic diseases.[103,110] A second MDP, called MOTS-c, is coded from the 12S rRNA region of mtDNA and plays a role in regulation of metabolic

homeostasis and insulin sensitivity.[111] The MDPs represent a new class of biologically active molecules with tremendous potential to protect retinal cells from aging and oxidative stress associated with retinal pathology.

Another approach for maintaining mitochondrial function includes targeting specific pathways that are altered with aging and disease. The decrease in mitochondrial function is often paralleled by increased oxidative stress and high levels of ROS. Therefore antioxidant drugs, (e.g., α-lipoic acid, α-tocopherol, genistein, resveratrol, memantine, MitoQ, and Mito-CP) have been tested in vitro and in vivo for their protective effects with some encouraging results.[112–114] However, the positive outcome of a vitamin/mineral supplement in slowing the progression to blindness in some AMD patients support the notion that suppressing ROS damage is a viable therapeutic approach for AMD.[115–118] Attempts to attenuate the decrease in energy production have been to supplement with substrates or regulators of energy metabolism (e.g., creatine, EPI-743, coenzyme Q10, and its analogs such as Idebenone, or quinone analogs, such as SkQ1, SkQR1).[119–121] Some positive results have been obtained with this approach. In a small open-label trial for five patients with Leber hereditary optic neuropathy, EPI-743 arrested disease progression and reversed vision loss in all but one participant.[122] Preventing apoptosis by stabilizing the mitochondrial permeability transition pore with cyclosporine A or by inhibiting the mitochondrial fission protein Drp1 with the drug MDIV-1 or molecular manipulation have shown protective effects in the in vitro and in vivo models.[123–127] Another promising drug, known as MTP-131, was effective in reversing the visual decline associated with diabetes induced by either streptozotocin or a high fat diet in mice and protecting ocular cells against oxidative stress in vitro.[128,129] MTP-131(SS-31) is a soluble peptide that has high affinity for cardiolipin and selectively partitions into the inner mitochondrial membrane.[130,131] Some of these drugs have been tested clinically for cardiovascular and neurodegenerative disorders, but none has been performed on a large-scale clinical scale for retinal diseases.[112,113,119,120,126,132,133] The field of mitochondria-targeting drugs to treated retinal and other ocular diseases has shown tremendous promise and will be expanding in the future.

References

1. Gray MW, Burger G, Lang BF. Mitochondrial evolution. *Science*. 1999;283:1476–1481.
2. Burger G, Gray MW, Lang BF. Mitochondrial genomes: anything goes. *Trends Genet*. 2003;19:709–716.
3. Gray MW, Lang BF, Cedergren R, et al. Genome structure and gene content in protist mitochondrial DNAs. *Nucleic Acids Res*. 1998;26:865–878.
4. Wallace DC. A mitochondrial paradigm of metabolic and degenerative diseases, aging, and cancer: a dawn for evolutionary medicine. *Annu Rev Genet*. 2005;39:359–407.
5. Schmidt O, Pfanner N, Meisinger C. Mitochondrial protein import: from proteomics to functional mechanisms. *Nat Rev Mol Cell Biol*. 2010;11:655–667.
6. Wallace DC. Diseases of the mitochondrial DNA. *Annu Rev Biochem*. 1992;61:1175–1212.
7. Wallace DC. Mitochondrial DNA mutations in diseases of energy metabolism. *J Bioenerg Biomembr*. 1994;26:241–250.
8. McFarland R, Turnbull DM. Batteries not included: diagnosis and management of mitochondrial disease. *J Intern Med*. 2009;265:210–228.
9. Yates JR 3rd, Gilchrist A, Howell KE, Bergeron JJ. Proteomics of organelles and large cellular structures. *Nat Rev Mol Cell Biol*. 2005;6:702–714.
10. Shoubridge EA, Karpati G, Hastings KE. Deletion mutants are functionally dominant over wild-type mitochondrial genomes in skeletal muscle fiber segments in mitochondrial disease. *Cell*. 1990;62:43–49.
11. Bua E, Johnson J, Herbst A, et al. Mitochondrial DNA-deletion mutations accumulate intracellularly to detrimental levels in aged human skeletal muscle fibers. *Am J Hum Genet*. 2006;79:469–480.
12. Durham SE, Samuels DC, Cree LM, Chinnery PF. Normal levels of wild-type mitochondrial DNA maintain cytochrome c oxidase activity for two pathogenic mitochondrial DNA mutations but not for m.3243A–>G. *Am J Hum Genet*. 2007;81:189–195.

13. Chinnery PF, Zwijnenburg PJ, Walker M, et al. Nonrandom tissue distribution of mutant mtDNA. *Am J Med Genet*. 1999;85:498–501.
14. Fan W, Waymire KG, Narula N, et al. A mouse model of mitochondrial disease reveals germline selection against severe mtDNA mutations. *Science*. 2008;319:958–962.
15. Wallace DC, Lott MT, Procaccio V. *Mitochondrial genes in degenerative diseases, cancer and aging*. Churchill Livingstone Elsevier: Philadelphia, PA; 2007.
16. Corral-Debrinski M, Horton T, Lott MT, et al. Mitochondrial DNA deletions in human brain: regional variability and increase with advanced age. *Nat Genet*. 1992;2:324–329.
17. Wang Y, Michikawa Y, Mallidis C, et al. Muscle-specific mutations accumulate with aging in critical human mtDNA control sites for replication. *Proc Natl Acad Sci USA*. 2001;98:4022–4027.
18. Nekhaeva E, Bodyak ND, Kraytsberg Y, et al. Clonally expanded mtDNA point mutations are abundant in individual cells of human tissues. *Proc Natl Acad Sci USA*. 2002;99:5521–5526.
19. Chance B, Sies H, Boveris A. Hydroperoxide metabolism in mammalian organs. *Physiol Rev*. 1979;59:527–605.
20. Sadun AA, Carelli V, Salomao SR, et al. A very large Brazilian pedigree with 11778 Leber's hereditary optic neuropathy. *Trans Am Ophthalmol Soc*. 2002;100:169–178 [discussion 178-169].
21. Wallace DC, Fan W. Energetics, epigenetics, mitochondrial genetics. *Mitochondrion*. 2010;10:12–31.
22. van der Walt JM, Nicodemus KK, Martin ER, et al. Mitochondrial polymorphisms significantly reduce the risk of Parkinson disease. *Am J Hum Genet*. 2003;72:804–811.
23. van der Walt JM, Dementieva YA, Martin ER, et al. Analysis of European mitochondrial haplogroups with Alzheimer disease risk. *Neurosci Lett*. 2004;365:28–32.
24. Fesahat F, Houshmand M, Panahi MS, et al. Do haplogroups H and U act to increase the penetrance of Alzheimer's disease? *Cell Mol Neurobiol*. 2007;27:329–334.
25. Hassani-Kumleh H, Houshmand M, Panahi MS, et al.

Mitochondrial D-loop variation in Persian multiple sclerosis patients: K and A haplogroups as a risk factor!. *Cell Mol Neurobiol*. 2006;26:119–125.
26. Dunaief JL, Dentchev T, Ying GS, Milam AH. The role of apoptosis in age-related macular degeneration. *Arch Ophthalmol*. 2002;120:1435–1442.
27. Huerta C, Castro MG, Coto E, et al. Mitochondrial DNA polymorphisms and risk of Parkinson's disease in Spanish population. *J Neurol Sci*. 2005;236:49–54.
28. Castro MG, Huerta C, Reguero JR, et al. Mitochondrial DNA haplogroups in Spanish patients with hypertrophic cardiomyopathy. *Int J Cardiol*. 2006;112:202–206.
29. Torroni A, Huoponen K, Francalacci P, et al. Classification of European mtDNAs from an analysis of three European populations. *Genetics*. 1996;144:1835–1850.
30. Torroni A, Schurr TG, Cabell MF, et al. Asian affinities and continental radiation of the four founding Native American mtDNAs. *Am J Hum Genet*. 1993;53:563–590.
31. Ruiz-Pesini E, Mishmar D, Brandon M, et al. Effects of purifying and adaptive selection on regional variation in human mtDNA. *Science*. 2004;303:223–226.
32. Mishmar D, Ruiz-Pesini E, Golik P, et al. Natural selection shaped regional mtDNA variation in humans. *Proc Natl Acad Sci USA*. 2003;100:171–176.
33. Jones MM, Manwaring N, Wang JJ, et al. Mitochondrial DNA haplogroups and age-related maculopathy. *Arch Ophthalmol*. 2007;125:1235–1240.
34. Canter JA, Olson LM, Spencer K, et al. Mitochondrial DNA polymorphism A4917G is independently associated with age-related macular degeneration. *PLoS ONE*. 2008;3:e2091.
35. Udar N, Atilano SR, Memarzadeh M, et al. Mitochondrial DNA haplogroups associated with age-related macular degeneration. *Invest Ophthalmol Vis Sci*. 2009;50:2966–2974.
36. SanGiovanni JP, Arking DE, Iyengar SK, et al. Mitochondrial DNA variants of respiratory complex I that uniquely characterize haplogroup T2 are associated with increased risk of age-related macular degeneration. *PLoS ONE*. 2009;4:e5508.

37. Mueller EE, Schaier E, Brunner SM, et al. Mitochondrial haplogroups and control region polymorphisms in age-related macular degeneration: a case-control study. *PLoS ONE*. 2012;7:e30874.
38. Kenney MC, Hertzog D, Chak G, et al. Mitochondrial DNA haplogroups confer differences in risk for age-related macular degeneration: a case control study. *BMC Med Genet*. 2013;14:4.
39. Kofler B, Mueller EE, Eder W, et al. Mitochondrial DNA haplogroup T is associated with coronary artery disease and diabetic retinopathy: a case control study. *BMC Med Genet*. 2009;10:35.
40. Achilli A, Olivieri A, Pala M, et al. Mitochondrial DNA backgrounds might modulate diabetes complications rather than T2DM as a whole. *PLoS ONE*. 2011;6:e21029.
41. Estopinal CB, Chocron IM, Parks MB, et al. Mitochondrial haplogroups are associated with severity of diabetic retinopathy. *Invest Ophthalmol Vis Sci*. 2014;55:5589–5595.
42. Wolf C, Gramer E, Muller-Myhsok B, et al. Mitochondrial haplogroup U is associated with a reduced risk to develop exfoliation glaucoma in the German population. *BMC Genet*. 2010;11:8.
43. Abu-Amero KK, Cabrera VM, Larruga JM, et al. Eurasian and Sub-Saharan African mitochondrial DNA haplogroup influences pseudoexfoliation glaucoma development in Saudi patients. *Mol Vis*. 2011;17:543–547.
44. Abu-Amero KK, Gonzalez AM, Osman EA, et al. Mitochondrial DNA lineages of African origin confer susceptibility to primary open-angle glaucoma in Saudi patients. *Mol Vis*. 2011;17:1468–1472.
45. Hofmann S, Bezold R, Jaksch M, et al. Wolfram (DIDMOAD) syndrome and Leber hereditary optic neuropathy (LHON) are associated with distinct mitochondrial DNA haplotypes. *Genomics*. 1997;39:8–18.
46. Brown MD, Sun F, Wallace DC. Clustering of Caucasian Leber hereditary optic neuropathy patients containing the 11778 or 14484 mutations on an mtDNA lineage. *Am J Hum Genet*. 1997;60:381–387.

47. Hendrickson SL, Jabs DA, Van Natta M, et al. Mitochondrial haplogroups are associated with risk of neuroretinal disorder in HIV-positive patients. *J Acquir Immune Defic Syndr*. 2010;53:451–455.
48. Coskun PE, Beal MF, Wallace DC. Alzheimer's brains harbor somatic mtDNA control-region mutations that suppress mitochondrial transcription and replication. *Proc Natl Acad Sci USA*. 2004;101:10726–10731.
49. Bellizzi D, Taverna D, D'Aquila P, et al. Mitochondrial DNA variability modulates mRNA and intra-mitochondrial protein levels of HSP60 and HSP75: experimental evidence from cybrid lines. *Cell Stress Chaperones*. 2009;14:265–271.
50. Chen A, Raule N, Chomyn A, et al. Decreased reactive oxygen species production in cells with mitochondrial haplogroups associated with longevity. *PLoS ONE*. 2012;7:e46473.
51. Kenney MC, Chwa M, Atilano SR, et al. Mitochondrial DNA variants mediate energy production and expression levels for CFH, C3 and EFEMP1 genes: implications for age-related macular degeneration. *PLoS ONE*. 2013;8:e54339.
52. Kenney MC, Chwa M, Atilano SR, et al. Inherited mitochondrial DNA variants can affect complement, inflammation and apoptosis pathways: insights into mitochondrial-nuclear interactions. *Hum Mol Genet*. 2014;23:3537–3551.
53. Kenney MC, Chwa M, Atilano SR, et al. Molecular and bioenergetic differences between cells with African versus European inherited mitochondrial DNA haplogroups: implications for population susceptibility to diseases. *Biochim Biophys Acta*. 2014;1842:208–219.
54. Malik D, Hsu T, Falatoonzadeh P, et al. Human retinal transmitochondrial cybrids with J or H mtDNA haplogroups respond differently to ultraviolet radiation: implications for retinal diseases. *PLoS ONE*. 2014;9:e99003.
55. Pacheu-Grau D, Gomez-Duran A, Iglesias E, et al. Mitochondrial antibiograms in personalized medicine. *Hum Mol Genet*. 2013;22:1132–1139.
56. Mueller EE, Brunner SM, Mayr JA, et al. Functional

differences between mitochondrial haplogroup T and haplogroup H in HEK293 cybrid cells. *PLoS ONE*. 2012;7:e52367.
57. Lin TK, Lin HY, Chen SD, et al. The creation of cybrids harboring mitochondrial haplogroups in the Taiwanese population of ethnic Chinese background: an extensive in vitro tool for the study of mitochondrial genomic variations. *Oxid Med Cell Longev*. 2012;2012:824275.
58. Gomez-Duran A, Pacheu-Grau D, Lopez-Gallardo E, et al. Unmasking the causes of multifactorial disorders: OXPHOS differences between mitochondrial haplogroups. *Hum Mol Genet*. 2010;19:3343–3353.
59. Chinnery PF. *Mitochondrial disorders overview*. [Seattle, WA: NCBI Bookshelf. National Library of Medicine, National Institutes of Health] 2010.
60. Yu-Wai-Man P, Griffiths PG, Chinnery PF. Mitochondrial optic neuropathies – disease mechanisms and therapeutic strategies. *Prog Retin Eye Res*. 2011;30:81–114.
61. LeDoux SP, Druzhyna NM, Hollensworth SB, et al. Mitochondrial DNA repair: a critical player in the response of cells of the CNS to genotoxic insults. *Neuroscience*. 2007;145:1249–1259.
62. Barja G, Herrero A. Oxidative damage to mitochondrial DNA is inversely related to maximum life span in the heart and brain of mammals. *FASEB J*. 2000;14:312–318.
63. Dizdaroglu M. Oxidative damage to DNA in mammalian chromatin. *Mutat Res*. 1992;275:331–342.
64. Wang AL, Lukas TJ, Yuan M, et al. Increased mitochondrial DNA damage and down-regulation of DNA repair enzymes in aged rodent retinal pigment epithelium and choroid. *Mol Vis*. 2008;14:644–651.
65. Short KR, Bigelow ML, Kahl J, et al. Decline in skeletal muscle mitochondrial function with aging in humans. *Proc Natl Acad Sci USA*. 2005;102:5618–5623.
66. Bender A, Krishnan KJ, Morris CM, et al. High levels of mitochondrial DNA deletions in substantia nigra neurons in aging and Parkinson disease. *Nat Genet*. 2006;38:515–517.
67. Wei YH, Lee HC. Oxidative stress, mitochondrial DNA

mutation, and impairment of antioxidant enzymes in aging. *Exp Biol Med (Maywood)*. 2002;227:671–682.
68. Breen AP, Murphy JA. Reactions of oxyl radicals with DNA. *Free Radic Biol Med*. 1995;18:1033–1077.
69. Berneburg M, Plettenberg H, Medve-Konig K, et al. Induction of the photoaging-associated mitochondrial common deletion in vivo in normal human skin. *J Invest Dermatol*. 2004;122:1277–1283.
70. Meissner C, Bruse P, Mohamed SA, et al. The 4977 bp deletion of mitochondrial DNA in human skeletal muscle, heart and different areas of the brain: a useful biomarker or more? *Exp Gerontol*. 2008;43:645–652.
71. Kraytsberg Y, Kudryavtseva E, McKee AC, et al. Mitochondrial DNA deletions are abundant and cause functional impairment in aged human substantia nigra neurons. *Nat Genet*. 2006;38:518–520.
72. Markaryan A, Nelson EG, Hinojosa R. Quantification of the mitochondrial DNA common deletion in presbycusis. *Laryngoscope*. 2009;119:1184–1189.
73. Barreau E, Brossas JY, Courtois Y, et al. Accumulation of mitochondrial DNA deletions in human retina during aging. *Invest Ophthalmol Vis Sci*. 1996;37:384–391.
74. Barron MJ, Johnson MA, Andrews RM, et al. Mitochondrial abnormalities in ageing macular photoreceptors. *Invest Ophthalmol Vis Sci*. 2001;42:3016–3022.
75. Karunadharma PP, Nordgaard CL, Olsen TW, et al. Mitochondrial DNA damage as a potential mechanism for age-related macular degeneration. *Invest Ophthalmol Vis Sci*. 2010;51:5470–5479.
76. Gendron SP, Mallet JD, Bastien N, et al. Mitochondrial DNA common deletion in the human eye: a relation with corneal aging. *Mech Ageing Dev*. 2012;133:68–74.
77. Sciacco M, Bonilla E, Schon EA, et al. Distribution of wild-type and common deletion forms of mtDNA in normal and respiration-deficient muscle fibers from patients with mitochondrial myopathy. *Hum Mol Genet*. 1994;3:13–19.
78. Krishnan KJ, Reeve AK, Samuels DC, et al. What causes mitochondrial DNA deletions in human cells? *Nat Genet*.

2008;40:275–279.
79. Liang FQ, Godley BF. Oxidative stress-induced mitochondrial DNA damage in human retinal pigment epithelial cells: a possible mechanism for RPE aging and age-related macular degeneration. *Exp Eye Res*. 2003;76:397–403.
80. Kenney MC, Atilano SR, Boyer D, et al. Characterization of retinal and blood mitochondrial DNA from age-related macular degeneration patients. *Invest Ophthalmol Vis Sci*. 2010;51:4289–4297.
81. Nag TC, Wadhwa S, Chaudhury S. The occurrence of cone inclusions in the ageing human retina and their possible effect upon vision: an electron microscope study. *Brain Res Bull*. 2006;71:224–232.
82. Bravo-Nuevo A, Williams N, Geller S, et al. Mitochondrial deletions in normal and degenerating rat retina. *Adv Exp Med Biol*. 2003;533:241–248.
83. Nordgaard CL, Karunadharma PP, Feng X, et al. Mitochondrial proteomics of the retinal pigment epithelium at progressive stages of age-related macular degeneration. *Invest Ophthalmol Vis Sci*. 2008;49:2848–2855.
84. Terluk MR, Kapphahn RJ, Soukup LM, et al. Investigating mitochondria as a target for treating age-related macular degeneration. *J Neurosci*. 2015;35:7304–7311.
85. Wang AL, Lukas TJ, Yuan M, et al. Age-related increase in mitochondrial DNA damage and loss of DNA repair capacity in the neural retina. *Neurobiol Aging*. 2009;31(11):2002–2010.
86. Tewari S, Santos JM, Kowluru RA. Damaged mitochondrial DNA replication system and the development of diabetic retinopathy. *Antioxid Redox Signal*. 2012;17:492–504.
87. Carelli V. *Leber's hereditary optic neuropathy*. Butterworth–Heinemann: Boston, MA; 2002.
88. Kong GY, Van Bergen NJ, Trounce IA, et al. Mitochondrial dysfunction and glaucoma. *J Glaucoma*. 2009;18:93–100.
89. Lin H, Xu H, Liang FQ, et al. Mitochondrial DNA damage and repair in RPE associated with aging and age-related macular degeneration. *Invest Ophthalmol Vis Sci*.

2011;52:3521–3529.
90. Kong YX, Van Bergen N, Trounce IA, et al. Increase in mitochondrial DNA mutations impairs retinal function and renders the retina vulnerable to injury. *Aging Cell*. 2011;10:572–583.
91. Shimada K, Crother TR, Karlin J, et al. Oxidized mitochondrial DNA activates the NLRP3 inflammasome during apoptosis. *Immunity*. 2012;36:401–414.
92. Kapetanovic R, Bokil NJ, Sweet MJ. Innate immune perturbations, accumulating DAMPs and inflammasome dysregulation: a ticking time bomb in ageing. *Ageing Res Rev*. 2015;24(Pt A):40–53.
93. Hjelmeland LM. Dark matters in AMD genetics: epigenetics and stochasticity. *Invest Ophthalmol Vis Sci*. 2011;52:1622–1631.
94. Tewari S, Zhong Q, Santos JM, et al. Mitochondria DNA replication and DNA methylation in the metabolic memory associated with continued progression of diabetic retinopathy. *Invest Ophthalmol Vis Sci*. 2012;53:4881–4888.
95. Mishra M, Kowluru RA. Epigenetic modification of mitochondrial DNA in the development of diabetic retinopathy. *Invest Ophthalmol Vis Sci*. 2015;56:5133–5142.
96. VanderJagt TA, Neugebauer MH, Morgan M, et al. Epigenetic profiles of pre-diabetes transitioning to type 2 diabetes and nephropathy. *World J Diabetes*. 2015;6:1113–1121.
97. Oliver VF, Jaffe AE, Song J, et al. Differential DNA methylation identified in the blood and retina of AMD patients. *Epigenetics*. 2015;10:698–707.
98. He S, Li X, Chan N, et al. Review: Epigenetic mechanisms in ocular disease. *Mol Vis*. 2013;19:665–674.
99. Smiraglia DJ, Kulawiec M, Bistulfi GL, et al. A novel role for mitochondria in regulating epigenetic modification in the nucleus. *Cancer Biol Ther*. 2008;7:1182–1190.
100. Bellizzi D, D'Aquila P, Giordano M, et al. Global DNA methylation levels are modulated by mitochondrial DNA variants. *Epigenomics*. 2012;4:17–27.
101. Atilano SR, Malik D, Chwa M, et al. Mitochondrial DNA

variants can mediate methylation status of inflammation, angiogenesis and signaling genes. *Hum Mol Genet*. 2015;24:4491–4503.
102. Kowluru RA. Mitochondria damage in the pathogenesis of diabetic retinopathy and in the metabolic memory associated with its continued progression. *Curr Med Chem*. 2013;20:3226–3233.
103. Gong Z, Tas E, Muzumdar R. Humanin and age-related diseases: a new link? *Front Endocrinol (Lausanne)*. 2014;5:210.
104. Guo B, Zhai D, Cabezas E, et al. Humanin peptide suppresses apoptosis by interfering with Bax activation. *Nature*. 2003;423:456–461.
105. Tajima H, Niikura T, Hashimoto Y, et al. Evidence for in vivo production of Humanin peptide, a neuroprotective factor against Alzheimer's disease-related insults. *Neurosci Lett*. 2002;324:227–231.
106. Lee C, Wan J, Miyazaki B, et al. IGF-I regulates the age-dependent signaling peptide humanin. *Aging Cell*. 2014;13:958–961.
107. Hashimoto Y, Niikura T, Tajima H, et al. A rescue factor abolishing neuronal cell death by a wide spectrum of familial Alzheimer's disease genes and Abeta. *Proc Natl Acad Sci USA*. 2001;98:6336–6341.
108. Niikura T, Chiba T, Aiso S, et al. Humanin: after the discovery. *Mol Neurobiol*. 2004;30:327–340.
109. Men J, Zhang X, Yang Y, et al. An AD-related neuroprotector rescues transformed rat retinal ganglion cells from CoCl(2)-induced apoptosis. *J Mol Neurosci*. 2012;47:144–149.
110. Lee C, Yen K, Cohen P. Humanin: a harbinger of mitochondrial-derived peptides? *Trends Endocrinol Metab*. 2013;24:222–228.
111. Lee C, Zeng J, Drew BG, et al. The mitochondrial-derived peptide MOTS-c promotes metabolic homeostasis and reduces obesity and insulin resistance. *Cell Metab*. 2015;21:443–454.
112. Miller TJ, Phelka AD, Tjalkens RB, et al. CI-1010 induced opening of the mitochondrial permeability transition pore

precedes oxidative stress and apoptosis in SY5Y neuroblastoma cells. *Brain Res*. 2003;963:43–56.
113. Chaturvedi RK, Beal MF. Mitochondrial approaches for neuroprotection. *Ann N Y Acad Sci*. 2008;1147:395–412.
114. Mansoor S, Gupta N, Patil AJ, et al. Inhibition of apoptosis in human retinal pigment epithelial cells treated with benzo(e)pyrene, a toxic component of cigarette smoke. *Invest Ophthalmol Vis Sci*. 2010;51:2601–2607.
115. Age-Related Eye Disease Study Research G. A randomized, placebo-controlled, clinical trial of high-dose supplementation with vitamins C and E, beta carotene, and zinc for age-related macular degeneration and vision loss: AREDS report no. 8. *Arch Ophthalmol*. 2001;119:1417–1436.
116. Age-Related Eye Disease Study 2 Research G. Lutein + zeaxanthin and omega-3 fatty acids for age-related macular degeneration: the Age-Related Eye Disease Study 2 (AREDS2) randomized clinical trial. *JAMA*. 2013;309:2005–2015.
117. Krishnadev N, Meleth AD, Chew EY. Nutritional supplements for age-related macular degeneration. *Curr Opin Ophthalmol*. 2010;21:184–189.
118. Andreatta W, El-Sherbiny S. Evidence-based nutritional advice for patients affected by age-related macular degeneration. *Ophthalmologica*. 2014;231:185–190.
119. Tabara LC, Poveda J, Martin-Cleary C, et al. Mitochondria-targeted therapies for acute kidney injury. *Expert Rev Mol Med*. 2014;16:e13.
120. Ajith TA, Jayakumar TG. Mitochondria-targeted agents: future perspectives of mitochondrial pharmaceutics in cardiovascular diseases. *World J Cardiol*. 2014;6:1091–1099.
121. Lee D, Kim KY, Shim MS, et al. Coenzyme Q10 ameliorates oxidative stress and prevents mitochondrial alteration in ischemic retinal injury. *Apoptosis*. 2014;19:603–614.
122. Sadun AA, Chicani CF, Ross-Cisneros FN, et al. Effect of EPI-743 on the clinical course of the mitochondrial disease Leber hereditary optic neuropathy. *Arch Neurol*. 2012;69:331–338.
123. Kim SY, Shim MS, Kim KY, et al. Inhibition of cyclophilin D

by cyclosporin A promotes retinal ganglion cell survival by preventing mitochondrial alteration in ischemic injury. *Cell Death Dis*. 2014;5:e1105.
124. Zhao YX, Cui M, Chen SF, et al. Amelioration of ischemic mitochondrial injury and Bax-dependent outer membrane permeabilization by Mdivi-1. *CNS Neurosci Ther*. 2014;20:528–538.
125. Srivastava A, McGinniss J, Wong Y, et al. MKK3 deletion improves mitochondrial quality. *Free Radic Biol Med*. 2015 [FRBMD1500388].
126. Zhang N, Wang S, Li Y, et al. A selective inhibitor of Drp1, mdivi-1, acts against cerebral ischemia/reperfusion injury via an anti-apoptotic pathway in rats. *Neurosci Lett*. 2013;535:104–109.
127. Kim KY, Perkins GA, Shim MS, et al. DRP1 inhibition rescues retinal ganglion cells and their axons by preserving mitochondrial integrity in a mouse model of glaucoma. *Cell Death Dis*. 2015;6:e1839.
128. Alam NM, Mills WC, Wong AA, et al. A mitochondrial therapeutic reverses visual decline in mouse models of diabetes. *Dis Model Mech*. 2015;8:701–710.
129. Chen M, Liu B, Gao Q, et al. Mitochondria-targeted peptide MTP-131 alleviates mitochondrial dysfunction and oxidative damage in human trabecular meshwork cells. *Invest Ophthalmol Vis Sci*. 2011;52:7027–7037.
130. Szeto HH, Birk AV. Serendipity and the discovery of novel compounds that restore mitochondrial plasticity. *Clin Pharmacol Ther*. 2014;96:672–683.
131. Birk AV, Chao WM, Bracken C, et al. Targeting mitochondrial cardiolipin and the cytochrome c/cardiolipin complex to promote electron transport and optimize mitochondrial ATP synthesis. *Br J Pharmacol*. 2014;171:2017–2028.
132. Liu Z, Guo J, Sun H, et al. alpha-Lipoic acid attenuates LPS-induced liver injury by improving mitochondrial function in association with GR mitochondrial DNA occupancy. *Biochimie*. 2015;116:52–60.
133. Lulli M, Witort E, Papucci L, et al. Coenzyme Q10 instilled

as eye drops on the cornea reaches the retina and protects retinal layers from apoptosis in a mouse model of kainate-induced retinal damage. *Invest Ophthalmol Vis Sci*. 2012;53:8295–8302.

35

Epigenetic Mechanisms of Retinal Disease

Shikun He, Renu Kowluru

Introduction

The term "epigenetics" was coined by C.H. Waddington in the 1940s, fusing the word "genetics" with "epigenesis," the latter indicating the theory by which the adult form develops from the embryo through gradual steps, as opposed to being fully preformed as a zygote.[1,2] Epigenetics refers to the modifications of external factors to DNA that turn genes "on" or "off" by which the functions and behaviors of an organism are modified, these modifications do not cause a change of the DNA sequence but are inheritable. Since

the 1990s, with the expansion of epigenetic research, several new concepts and terms such as the epigenome, epigenetic epidemiology, epigenetic pathology, epigenetic disease, epimutation, and epigenetic therapy have been created. In order to promote epigenetic research, the Association for the Study of the Epigenome in Europe was established in 1999, and launched the Human Epigenome Project (HEP) in 2003. The Genome Research Institute (NHGRI) launched a public research consortium named ENCODE, the Encyclopedia of DNA Elements, in September 2003 to carry out a project to identify all functional elements in the human genome sequence. In 2010, the International Human Epigenome Consortium (IHEC) was launched to coordinate international collaborative efforts to produce reference maps of epigenomes for cellular states relevant to human health and disease. Recent reports from the ENCODE project consortium show that 80% of the genome is functional; the significance of research into epigenetic mechanisms has become even more important. With the inspiration of genome-wide association studies (GWAS), epigenome-wide association studies (EWAS), primarily focused on evaluating DNA methylation across the entire genome, are identifying associations between variation in DNA methylation and common diseases or related traits.[3] Most recently, scientists from NIH have summarized epigenome studies and published their data from mature cells from healthy human tissues, various stem cell populations, cancer cells, and patients with neurodegenerative diseases and autoimmune diseases.[4] Mapping of epigenomic marks in healthy and diseased human tissues may provide new understanding into epigenetic variation and disease. Notably, the possibility of predicting the human epigenome from DNA motifs has been published.[5] The field of epigenetics has garnered increasing attention over recent years; therefore, the importance of epigenetic research to human health has coined the term “the epigenetic era.”

Major Factors of Epigenetic Regulation

DNA Methylation

Traditionally, DNA methylation involves the addition of a methyl group to the 5′ position of the cytosine pyrimidine ring or the number 6 nitrogen of the adenine purine ring, and typically occurs in a CpG dinucleotide context. Recently, 5-(hydroxymethyl) cytosine (5-hmc), the sixth base of the genome, and 5-formylcytosine and 5-carboxylcytosine, the seventh and eighth bases, were discovered. CpG islands are regions with high frequency of CpG sites often at or near transcription start sites of genes. Lower CpG density regions are termed CpG "island shores."

The CpG dinucleotide is the most important site of DNA methylation. In general, CpG methylation silences genes while demethylation activates them; however, recent studies have shown that the functional effects of DNA methylation can vary according to the genomic context. In mammals, 60–90% of all CpGs are methylated in the nonpromoter area.[6] DNA methylation may affect the transcription of genes in two ways. First, the methylation of DNA may itself physically impede the binding of transcriptional factors to the gene, and second, and likely more important, methylated DNA may be bound by proteins known as methyl-CpG-binding domain (MBD) proteins. MBD proteins then recruit additional proteins to the locus, such as histone deacetylases (HDACs) and other chromatin remodeling proteins that can modify histones, thereby forming compact, inactive chromatin. This process has been termed silent gene expression.[7] On the other hand, more recently methyl CpG binding protein 2 (MeCP2), a reader of DNA methylation, has been found to bind not only methylated CpG islands related to gene silencing but also to sites of active gene transcription. MeCP2 may act as a transcriptional repressor or as a gene activator depending on its specific modification and the microenvironment.[8]

Although CpG dinucleotides are the primary site of DNA methylation in mammals, there is new evidence to show that up to 7.5% of all non-CpG cytosines (CPA, CPT, and CPC) exist in the tissue of many mammals.[9] Importantly, non-CpG methylation plays a unique role in the regulation of gene expression for genes such as *PGC1*, *IFN*, and *SYT11*.[10] Genome-wide analysis showed that non-CpG methylation is abundant in the adult brain.

Histone Methylation

Histone methylation is the modification of certain amino acids in a histone protein by the addition of one, two, or three methyl groups, and is catalyzed by histone methyltransferases (HMTs). The regulation of gene expression by histone methylation is bifunctional and can either increase or decrease transcription of the gene, depending on the location of the histone protein. Histone lysine methylation has been well studied at the K4, K9, and K27 residues. These lysine residues can be monomethylated, dimethylated, or trimethylated. Generally, trimethylation of lysine 4 on histone H3 (H3K4me3) is associated with a fully activated promoter, which correlates with gene transcription activities, whereas dimethylation (H3K4me2) occurs at both inactive and active euchromatic genes. H3K9 is a major negative regulator of the H3K4 mark. Dimethylation at lysine 9 (H3K9me2) marks the silence of gene expression in euchromatin, whereas H3K9me3 is enriched in regions of "gene-poor" pericentric heterochromatin. Methylation at lysine 27 on histone H3 (H3K27me) is associated with transcriptional repression in many developmental processes.

Histone Acetylation and Deacetylation

The histones can also be acetylated on lysine residues in the N-terminal tail, and this serves as an important regulatory factor of gene expression. Steady-state levels of histone acetylation are maintained by a balance between the opposing activities of histone acetyltransferases (HATs) and HDACs. Acetylation brings in a negative charge, which acts to neutralize the positive charge on the histones and decreases the interaction of the N termini of histones with the negatively charged phosphate groups of DNA. As a consequence, the condensed chromatin is transformed to a more relaxed structure, which allows transcription factors access for DNA binding and gene transcription. Aberrant histone acetylation/deacetylation and other epigenetic modulations have been implicated in cell division, growth, DNA damage, genome stability, cell fate determination, higher-level cognitive behaviors such as learning and memory[11] and many pathologic conditions, including inflammatory diseases characterized by expression of

inflammatory factors such as nuclear factor-kappa B (NF-κB) and activator protein (AP)-1 transcription factor, wound healing, degenerative and neurologic disease, cancer development, and multiple sclerosis.

Histone acetylases are broadly classified in two different types: types A and B, based on their functional localization. While type A HATs are nuclear and catalyze transcription-related acetylation events, type B HATs are cytoplasmic and catalyze acetylation events linked to the transport of newly synthesized histones from the cytoplasm to the nucleus for deposition on to newly replicated DNA. There are five main classes of HATs (GNAT, MYST, p300/CBP, transcription factor, and nuclear hormone-related), which are characterized by specific functions controlled by its specific structural folding.

The process of histone acetylation is reversed by the HDACs, which catalyze acetyl group removal, and there are four main classes (I–IV) of HDACs. HDAC1–3 and 8 are members of class I, and are located in the nucleus and involved in epigenetic regulation. HDAC4–6, 7, 9, and 10 are members of class II, and are characterized by nucleocytoplasmic shuttling. Class III HDACs are characterized by their NAD dependence. HDAC 11 has been categorized into its own group, a class IV deacetylase. These molecules have been implicated in aging and calorie restriction as well as disease.

Noncoding RNA

A noncoding RNA (ncRNA) is a functional RNA molecule that is not translated into a protein. ncRNA genes include highly abundant and functionally important RNAs such as transfer RNA (tRNA) and ribosomal RNA (rRNA), as well as RNAs such as miRNA, siRNAs, piRNAs, and long noncoding RNAs (lncRNAs). Recently, roughly 1300 short RNA sequencing datasets from 13 distinct human tissues have documented 3707 novel mature miRNAs arising from 3494 novel precursors. The current estimates are that the human genome likely has over 25,000 miRNAs.[12]

miRNAs are a class of small (on average 22 nucleotides long), ncRNA molecules that regulate gene expression and are implicated

in many cellular processes, including development, tissue morphogenesis, apoptosis, and tumor growth. Genes encoding primary miRNAs are scattered throughout the genomes of eukaryotes and are transcribed to generate RNA species that are cleaved to 60–70-nucleotide stem–loop miRNA precursors (pre-miRNAs) by a microprocessor complex containing the nuclear RNaseIII Drosha and DiGeorge syndrome critical region protein. After export from the nucleus, the pre-miRNAs are cleaved by a cytoplasmic RNase III (Dicer). After strand selection and separation, mature 22-basepair miRNAs are incorporated into an RNA-induced silencing complex to act as target recognition sequences. miRNAs may contain target sequences and can undergo cleavage.

miRNAs have been implicated in the regulation of growth and development, cell differentiation and diseases by modification of chromatin structure, and regulation of transcription.[13]

Epigenetic Factors in the Retina

DNA Methylation in Mammalian Retina

DNA methylation is catalyzed by DNA methyl transferases (DNMTs), a five-member family consisting of DNMT1, 2, 3a, 3b, and 3L. Among these, DNMT1, 3a, and 3b are the catalytically active enzymes. While DNMT3a and 3b are de novo enzymes, DNMT1 is a maintenance enzyme important in regulating tissue-specific patterns of methylated cytosine residues DNMT3a methylates CpG sites at a rate much slower than that of DNMT1 but greater than that of DNMT3b. DMNT1 is expressed in human retinal pigment epithelium (RPE) cells and in endothelial cells, and DNMT3a is weakly expressed in some inner nuclear layer cells in the adult mouse retina.[14] DNA methylation regulates the expression of genes in mammalian retina; the gene encoding interphotoreceptor retinoid-binding protein (IRBP), a major soluble component of the interphotoreceptor matrix, which is secreted into this matrix by both rods and cones, and is hypomethylated in retinas. Methylation of IRBP promoter suppresses transcription in nonphotoreceptor cells by precluding specific DNA protein-binding events, whereas the lack of methylation in photoreceptors allows

for its transcription. In the retina of the adult mouse, EphA5, a member of the ephrin receptor subfamily of the protein-tyrosine kinase family, mediates 1.2 ± 0.3% of CpG methylation.[15] This represents a relatively low level of promoter methylation. Although methylation of major CpG sites results in the silencing of EphA5 promoter activity, lower levels of methylation can produce differential activation or repression of EphA5 promoter activity, depending on the sites methylated. Methyl-CpG binding protein 2 (MECP2), a protein that specifically binds methylated DNA, thus regulating transcription and chromatin organization, is expressed in all retinal neurons, except rods, and the onset of its expression coincides with neuronal differentiation, in particular, with massive formation of neural synapses in the inner and outer plexiform layers.[16]

In the adult murine retina, H3K4me3, a mark associated with active transcription, is observed in all layers of the neural retina, including rhodopsin-positive photoreceptors, Müller glia, and retinal ganglion cells (RGCs). H3K27me3, a mark associated with transcriptional repression, is enriched in the inner nuclear layers and in a subset of outer nuclear layer in the adult murine retina. However, H3K9me2, another repressive mark, is not observed in the inner layers of the adult retina. Histone methylation, a dynamic and reversible process, is maintained by the balance between HMTs and histone demethylases (HDMs). Although the majority of HMTs contain a Su(var)3-9, Enhancer of Zeste, Trithorax (SET) domain, which catalyzes the addition of methyl groups to lysine residues, a small group consists of non-SET domain-containing enzymes. The Ezh2 and G9a HMTases are the two best-characterized HMTases, which catalyze H3K27me3 and H3K9me2 modifications, respectively, and are found in the fetal murine retina,[17] suggesting a crucial role of gene transcription by Ezh2- and G9a-mediated histone lysine methylation in retinal neuronal differentiation and survival. Although the enzymes responsible for demethylation are not well defined, a lysine-specific histone demethylase, LSD1, which specifically removes methyl group from H3K4me and H3K9me, is shown to be present in the retina and its capillary cells.[18]

As with histone methylation, a group of enzymes with opposing

functions maintain the required acetylation status; while HATs insert acetyl groups on the lysine residues, HDACs remove them.[19,20] Acetylated histone 3 and 4 are found in fetal and adult retina; however, their levels are reduced in dry age-related macular degeneration (AMD). HATs and HDACs are expressed in mammalian retina, and in contrast to the decrease of acetylated histones, HDAC1 is highly upregulated in human AMD retinal sections. In addition, exposure of adult murine retina to trichostatin A (TSA) induces upregulation of apoptotic genes. Activation of HDAC may decrease the retina's resistance to ischemic injury.[21]

miRNA in Mammalian Retina

Gene regulation by miRNAs has been associated with normal retinal development and function and with many retinal diseases, and more than 250 miRNAs have been identified in the retina. Retinal miRNAs have different levels of expression across different layers, and some are regulated directly by light.[22] The most highly expressed adult mouse retinal miRNAs are miR-181a, 182, 183, 204, 125b, 126a, and 124a. Among these, miR182 is expressed throughout all layers of the retina, miR-181 is in the ganglion cell, inner plexiform and inner nuclear layers; and miR-183 is expressed only in the outer nuclear layer. Strong expression of miR-204 is detected in the RPE and the ciliary body, and miR-124a is expressed in all layers of the neural retina except the RPE. miRNA-132, miR-204, and 211 are also expressed in the RPE. Transforming growth factor-beta (TGF-β) receptor-2 and SNAIL2 are direct targets of miR-204. Notably, anti-miR-204/211 decreases transepithelial resistance and reduces cell membrane voltage and conductance, suggesting a critical role of miR-204/211 in maintaining epithelial barrier function and cell physiology.

Epigenetic Mechanisms in Retinal Development

Although epigenetic mechanisms have been shown to regulate neural stem cell renewal and differentiation, it was not until recent

years that their involvement in retinal development has been realized. The retina is composed of specialized glia and neuronal cells which are generated from multipotent retinal progenitor cells in a highly conserved temporal sequence with overlapping phases during development. RGCs, horizontal cells, and cone photoreceptors appear in the early phases, while rod photoreceptors, bipolar cells, and Müller glial cells appear in the late phases. The cell fate decision of the progenitor cells depends on both intrinsic and environmental cues, and these are regulated by specific networks of transcription factors. Through covalent modifications of DNA and histone, chromatin remodeling regulates the interactions of these transcription factors and their effector genes, and is an important epigenetic mechanism in retinal development.

DNA and Histone Methylation in Retinal Development

DNA and histone methylation are mediated by DNMT and HMTases. In zebrafish retina, antisense-based morpholino knockdown of DNMT3 and H3K9 HMTases Suv39h1 and G9a lead to defects in retinal cell differentiation, supporting a role of both DNA and histone methylation in zebrafish retinal development. In mice, immunohistochemical analysis shows changing patterns of histone methylation marks in the developing retina. Specifically, the transcriptionally activating H3K4me3 and repressive H3K27me3 histone marks are found in differentiated neurons from embryo to adulthood, corresponding to the expression of the HMTase Ezh2 that catalyzes the H3K27me3 mark. In contrast to Jmjd3, Ezh2 is expressed in the embryonic retina, but its expression decreases rapidly after birth, suggesting an important role for histone H3K27me3 modification in regulating the proliferation and maturation of certain subsets of interneurons in the retina.[23] In contrast, the repressive H3K9me2 mark and the corresponding HMTase G9a are seen primarily in early differentiating RGCs, and decrease after birth. These changing patterns of histone methylation may, at least in part, account for the temporal sequence of retinal progenitor cell differentiation during development. Evidence also

implicates DNA methylation in regulating the expression of genes involved in the topographic patterning of RGC axons, such as EphA5 receptor.[15] These studies have suggested that DNA and histone modifications may regulate both temporal and spatial expression of these genes in different populations of retinal progenitor cells to orchestrate the precise timing of cell proliferation and differentiation during development.

Histone Acetylation in Retinal Development

During photoreceptor differentiation, HAT-containing coactivators, such as general control nondepressible 5 (Gcn5) and CREB-binding protein (Cbp), interact with cone–rod homeobox (Crx) transcription factor to promote the transcription of opsin genes The role of the histone acetyltransferase-containing Tip60 is shown in the developing mouse retina by acting as a coactivator in the Nrl-dependent transcriptional regulation of the rhodopsin and Ppp2r5c gene.[24] In addition to HATs, HDACs have been also studied extensively and are implicated in retinal development. HDAC1 is recruited by the retinoblastoma protein (Rb) and related family members to promoters with E2F-binding sites, resulting in transcriptional repression of cell cycle genes and suppression of cell growth. In zebrafish, *hdac1*-deficient mutants exhibit retinal cell proliferation and differentiation defects, resulting in severe reduction in the inner and outer plexiform layers and absence of RGC, rod and cone photoreceptors, and Müller glia. These defects result from failure in downregulation of cyclin D and E transcription and the canonical Wnt and Notch signaling pathways, which are necessary for retinal progenitor cells to exit the cell cycle, suggesting that histone deacetylation may be a regulatory mechanism to switch off stem cell proliferation and initiate a program for retinal differentiation. In mouse retinal explants, pharmacologic inhibition of HDAC with TSA also results in defects in rod differentiation, but unlike in zebrafish, causes a reduction in retinal progenitor cell proliferation. In vivo knockdown of HDAC4 by RNA interference leads to apoptosis of rod photoreceptors and bipolar cells, and overexpression of HDAC4 reduces naturally occurring cell death of bipolar cells, supporting a role of HDAC4 in

promoting the survival of developing retinal neurons as well.[25] Further work is needed to help clarify the specific downstream effectors regulated by HATs and HDACs during the various stages of retinal development.

Chromatin Remodeling Complexes in Retinal Development

While covalent DNA and histone modifications decondense chromatin and promoter regions, adenosine triphosphate (ATP)-dependent displacement from promoters and enhancer regions requires the action of chromatin-remodeling complexes. These include the SWItch/Sucrose NonFermentable (SWI/SNF) and the Imitation SWItch (ISWI) families. Zebrafish mutants lacking the brahma-related gene 1 (*BRG1*), the catalytic ATPase subunit of SWI/SNF chromatin remodeling complex, show defects in retinal differentiation, suggesting that *BRG1* is involved in triggering retinal cell differentiation. In mice, however, loss of *BRG1* in neural stem cells results in precocious neuronal differentiation, suggesting that it represses differentiation and maintains neural stem and progenitor cells. These differences may be related to changes in the composition of accessory units known as BRG1-associated factors (BAFs) in the SWI/SNF complexes in different cell states. Nevertheless, chromatin-remodeling complexes are likely to be critically involved in regulating retinal cell differentiation during development.

microRNAs in Retinal Development

Recently, miRNAs have also been implicated in retinal development. Early studies using a conditional knockout mouse lacking the RNA endonuclease Dicer in the retina has shown no defects in the retina before the second postnatal week, suggesting that miRNAs are not required for mouse retinal development. However, subsequent research using a different strain of Dicer conditional knockout mouse have documented increased production of early generated cell types such as RGC and horizontal cells, and failure to generate late-born cell types such as

rod photoreceptors and Müller glia. This is also supported by data from *Xenopus* morpholinos, where Dicer inactivation results in defects in cell cycle, lamination, and timing of retinal differentiation. Thus Dicer and miRNAs may provide a common regulatory mechanism to signal changes in retinal progenitor cell competence.[26]

Microarray analysis of the miRNA transcriptome in mouse retina has revealed at least 78 miRNAs, 21 of which are potentially retina-specific.[27] The miRNA transcriptome of the mouse retina is similar to that of humans, and shows dozens of miRNAs that are differentially expressed during different stages of development. In *Xenopus*, miRNAs have been found to inhibit the translation of homeodomain transcription factors (Xotx2 and Xvsx1) involved in bipolar cell differentiation by binding the 3′ untranslated region of mRNAs. Inactivation of these miRNAs in vivo releases the inhibition and supports the generation of additional bipolar cells. Another miRNA, miR-24a, negatively regulates proapoptotic factors caspase-9 and apoptotic protease-activating factor 1 (apaf1) in *Xenopus* retina. Inhibition of miR-24a leads to increased apoptosis during retina development and reduction in eye size. miR-7a is shown to regulate Müller glia differentiation, possibly, via attenuation of Notch3 expression, and miR410 in RPE differentiation program.[28,29] Target prediction and in vitro functional studies have indicated that the microphthalmia-associated transcription factor (MITF), a transcription factor necessary for the development and function of RPE, is directly inhibited by miR-96 and miR-182, supporting a role of miRNAs in RPE maintenance also. MiR-124a, which is expressed in all neuronal subtypes in the adult retina, has also been shown to repress retinol dehydrogenase 10 (Rdh10), which is selectively expressed in Müller glia and RPE. Hence, some miRNAs may impact retinal development not by affecting neuronal proliferation and differentiation, but via effects on supporting glial and RPE cells. MicroRNA research is still in its infancy, and more work is necessary to determine the landscape of noncoding RNAs in different retinal cell populations.

Epigenetic Mechanisms in Retinal Diseases

Epigenetic Factors in Retinal Fibrosis

It is known that RPE cells are key players in the pathogenesis of proliferative vitreoretinopathy (PVR). In PVR, RPE cells undergo epithelial–mesenchymal transition (EMT) characterized by an increase in mesenchymal cell components and the manifestation of a migratory and proliferative phenotype. Transdifferentiation of RPE cells into myofibroblast-like cells has been exclusively demonstrated in tissue repair during several retinal pathologic conditions, including choroidal neovascularization, diabetic retinopathy, and PVR. A major feature of RPE transdifferentiation is the increased expression of alpha smooth-muscle actin (α-SMA), and α-SMA-positive RPE cells have been shown to be the major cells that promote contraction and induce retinal detachment in PVR. Although a variety of inflammatory cytokines and growth factors (in particular, TGF-β and PDGF) are involved in the regulation of RPE transdifferentiation, the basic mechanisms of the RPE transdifferentiation from an epithelial cell to a myofibroblast-like cell is still under investigation. TGF-β is the major inducer of α-SMA expression in transdifferentiated cells,[30] and increased TGF-β activity is associated with the downregulation of the genes of transdifferentiation inhibitors such as Smad7, IκBα, and peroxisome proliferator-activated receptor-gamma (PPAR-γ).[31]

DNA Methylation

Recent studies suggest that the wound-healing process is also regulated by epigenetic factors, including DNA methylation and histone acetylation.[32] In terms of DNA methylation, MeCP2 has been demonstrated to be an orchestrator of epithelial myofibroblastic transdifferentiation and play a pivotal role in EMT and/or fibrosis.[32] We have recently shown that RPE EMT and the pathogenesis of PVR are tightly regulated by MeCP2.[33] MeCP2 is highly expressed in human PVR membranes (Fig. 35.1) and MeCP2 colocalized with cytokeratin and α-SMA in human PVR

membranes. Knockdown of MeCP2 by specific siRNA inhibits TGFβ-receptor 2 and Smad2/3 activation and α-SMA, fibronectin expression induced by TGF-β. The regulation of α-SMA by MeCP2 is mediated through the Ras GTPase activating-like protein (RASAL1). 5-aza-2′deoxycytidine (5-AZA, a DNA methylation inhibitor) suppressed *RASAL1* gene promote methylation while increasing the gene expression of *RASAL1*.[33] More importantly, we have shown that PPAR-γ expression is almost absent in human PVR membranes; the upregulation of PPAR-γ is associated with the decreased expression of MeCP2 after methylation inhibitor 5-AZA exposure. These observations support the suggestion that MeCP2 is an important factor in the regulation of fibrosis in general and that the pathogenesis of PVR may be under complex epigenetic regulation. More importantly, EMT is reversible from mesenchymal-to-epithelial transition (MET). MeCP2 and DNA methylation may be targets for therapeutic intervention in PVR (Fig. 35.1).

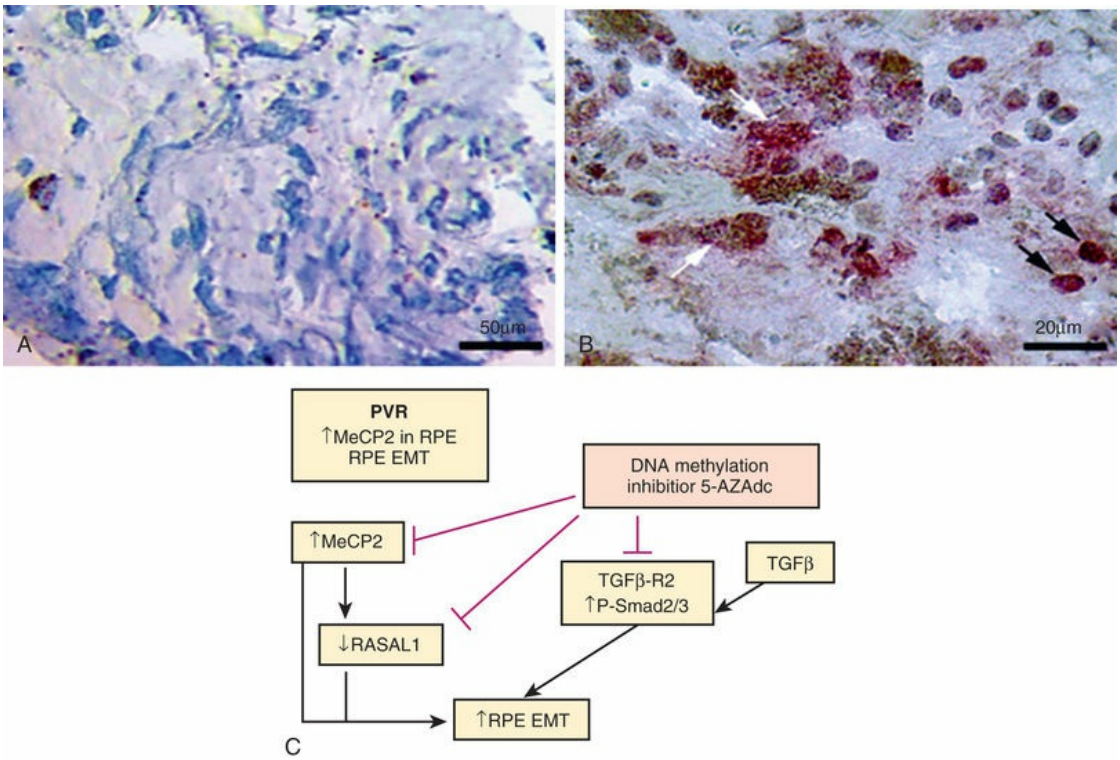

FIG. 35.1 MeCP2 expression in human proliferative vitreoretinopathy (PVR) membranes. Negative control without primary antibody (A), abundant MeCP2 expression was seen within cellular regions of a

human PVR membrane (B). *Black arrows* indicate MeCP2 staining in nuclei and *white arrows* show cytoplasmic MeCP2 immunoreactivity. (C) MeCP2 is increased in human PVR membranes, which is associated with retinal pigment epithelium (RPE) epithelial–mesenchymal transition (EMT). Application of 5-AZAdc inhibits the RPE EMT by the following mechanisms: (1) Inhibition of the expression of MeCP2 leads to increased expression of RASAL1; (2) reduction of methylation level of the RASAL1 promotor leads to upregulation of RASAL1 expression; (3) inhibition of TGFβ-R2 expression leads to decrease of TGFβ Smad2/3 phosphorylation; (4) increased RASAL1 expression and decreased Smad2/3 phosphorylation both lead to inhibition of RPE EMT.

(Panels A and B modified from He S, Barron E., Ishikawa K. et al. Inhibition of DNA Methylation and Methyl-CpG-Binding Protein 2 Suppresses RPE Transdifferentiation: Relevance to Proliferative Vitreoretinopathy. Invest Ophthalmol Vis Sci 2015;56:5579-89. © Association for Research in Vision and Ophthalmology.)

Histone Acetylation/Deacetylation

Besides DNA methylation, the other epigenetic mechanism that regulates EMT or fibrosis is histone acetylation/deacetylation. Although there are few reports of the effect of histone acetylation on RPE EMT and retinal fibrosis, the involvement of histone acetylation has been extensively studied in a number of systemic diseases.[34] Recent reports reveal that histone acetylation and HDAC activity are also correlated with the development and progression of some fibrotic diseases, such as cardiac hypertrophy, kidney fibrosis, idiopathic pulmonary fibrosis, and liver fibrosis. Hyunjin et al. found that HDAC inhibition suppressed both diabetes- and TGF-β_1-induced renal fibrosis.[34] Inhibition of HDAC activity by TSA decreased platelet-derived growth factor (PDGF)-induced fibroblast proliferation; importantly, it was found that activation of STAT3 is required for the induction of HDAC activity; renal fibroblast activation also is blocked by the inhibition of STAT3 pathway. Interestingly, TSA is able to inhibit the TGF-β-mediated transdifferentiation of corneal stromal cell. Furthermore, silencing

of matrix metalloproteinase (MMP) genes is under epigenetic regulation, especially by HDAC-4 during liver cell fibrogenesis. More specifically, Hyunjin et al. have demonstrated an important role of HDAC-2 in the development of EMT, and extracellular matrix (ECM) accumulation in diabetic kidney.[34] In the laser-induced model of choroidal neovascularization (CNV) systemic administration of TSA significantly reduces expression of vascular endothelial growth factor (VEGF), and smooth muscle actin in CNV lesions.[35]

Finally, alterations in DNA methylation and histone acetylation/deacetylation are required for the development and progression of tissue fibrosis. It seems that manipulation of DNA methylation and histone acetylation may suppress major profibrotic growth factors such as TGF-β. However, the mechanisms of epigenetic-mediated EMT and fibrosis formation remain largely under investigation. Further study is required to establish the profile of DNA methylation and HDAC-mediated genes in the initiation of EMT and fibrosis, especially, the regulation of the expression of NF-κB, Snai1, and Twist by epigenetic factors in the process of development of RPE EMT and how the RPE EMT could be reversed to MET by increases of the MET inducer factors such as BMP7,OCT4, and SOX2 expression because the switch between EMT and MET is a dynamic process.[36] This knowledge is not only important for further understanding of the mechanism by which DNA methylation and histone acetylation regulates tissue fibrosis, but also is critical for the potential pharmacologic epigenetic approach for the treatment of PVR and other fibrotic retinal diseases.

Epigenetic Factors in Retinitis Pigmentosa

Retinitis pigmentosa (RP) is an inherited retinal degeneration that is characterized by selective cell death of photoreceptors. At least 40 gene mutations involved in human RP have been identified so far,[37] although the metabolic pathways leading to photoreceptor cell death remain unknown, and no cure is as yet available. In the well-studied retinal degeneration 1 (rd1) mouse model for RP, where a rod photoreceptor cGMP phosphodiesterase-6 mutation leads to

cGMP accumulation and photoreceptor cell death, increased HDAC activity was found to precede photoreceptor degeneration. More importantly, pharmacologic inhibition of HDAC activity reduces photoreceptor cell death, an effect that may be mediated by transcriptional regulation through the poly-ADP-ribose-polymerase family of proteins, or through upregulating peroxisome proliferator-activated receptor-gamma in an animal model.[38]

Interestingly, overexpression of HDAC4, which regulates retinal neuronal survival, can prolong photoreceptor survival in *rd1* mouse retina,[25] suggesting different roles of HDAC family members in the pathogenesis of retinal degeneration. Beside the abnormal histone acetylation/deacetylation, Farinelli et al. have demonstrated that cytosine hypermethylation is revealed in dying photoreceptors in the rodent models of RP; importantly, inhibition of DNA methylation suppressed photoreceptor death.[39] Recently, valproic acid, an HDAC inhibitor, has been used for treating patients with retinitis pigmentosa.[40] Although encouraging preliminary results are available, the benefit of this drug in RP needs to be confirmed in a placebo-controlled clinical trial.

Studies in recent years are beginning to unveil a role for miRNAs in retinal degenerative diseases. miRNAs typically enriched in the mouse retina, such as miR-96, miR-182, and miR-183, are reduced several fold in *rd1* mice where rod photoreceptors have degenerated.[27] A mouse model of RP carrying a mutant Pro347Ser rhodopsin transgene demonstrates altered expression of miR-96, miR-183, miR-1, and miR-133 in the retina when compared with wild-type animals. A similar miRNA signature is confirmed in three other mouse models of RP. Predicted targets of these miRNAs include antiapoptotic factors such as Fas apoptotic inhibitor molecule, which offers a possible mechanism whereby defects in miRNAs expression may lead to photoreceptor degeneration through apoptosis.

Epigenetic Factors in Age-Related Macular Degeneration

Age-related macular degeneration (AMD) is a leading cause of vision loss among people age 50 and older. Though AMD is an age-

related disease, several genetic components have also been identified, and the extent to which epigenetic modifications contribute to the phenotype heritability remains unclear. Emerging evidence has clearly suggested that epigenetic changes could be playing an important role in the disease process and is implicated in various aspects of the disease, including inflammatory responses and gliosis.[41] In addition, significant DNA methylation differences are observed in the blood of neovascular AMD patients near age-related maculopathy susceptibility 2, a top-ranked GWAS locus preferentially associated with neovascular AMD, and also in the promoter region of protease serine 50.[42] Clusterin (also known as apolipoprotein J), a major component of drusen that accumulates with age, has a promoter with a CpG-rich methylation domain that may be epigenetically regulated.[43] In human RPE cell culture, pharmacologic induction of DNA hypomethylation or histone hyperacetylation leads to increased expression of clusterin. Another recent study showed that Dicer may also be involved in the pathogenesis of geographic atrophy in AMD. Dicer is reduced in the RPE of human patients with geographic atrophy, and conditional knockout of Dicer reproduces the RPE degeneration phenotype in mice. Surprisingly, the role of Dicer in the pathogenesis of macular degeneration does not appear to involve miRNAs, but instead the degradation of *Alu* elements, common noncoding, repetitive DNA sequences in the human genome which may be toxic to the RPE.[44] miRNAs are implicated in various aspects of the disease pathogenesis; miR-22, miR-26, miR-30, miR-92, miR-124, and let-7 families are associated with the survival of rods.[45] miR-23a is considered to serve as a regulator of macular RPE cell survival in response to oxidative stress, and miR-31 and -150, that code for proteins that have proangiogenic activity, have altered in AMD, and are associated with choroidal neovascularization. Although how much epigenetic changes contribute to AMD is still unknown, there is a great need to study the role of epigenetics in its pathogenesis in the future. If similar findings can be demonstrated in vivo, epigenetic mechanisms may potentially be exploited as targets for treating this chronic eye disease.

Epigenetic Factors in Retinoblastoma

Retinoblastoma is the most common intraocular tumor of childhood. Although the disease is initiated by the loss of both alleles of the prototypic tumor suppressor gene, *RB1*, subsequent changes in other tumor suppressor and DNA repair genes have been implicated in the pathogenesis of the disease. The retinoblastoma protein (pRb) is the founding member of the pocket protein family of tumor suppressors, including p107 and p130, which have been implicated in numerous cellular processes, including cell cycle regulation, DNA repair, DNA replication, differentiation, and apoptosis. *RB1* has been shown to regulate numbers of epigenetic events, such as miRNA, DNA methylation histone acetylation, and chromatin remodeling. The inactivation of *RB1* gene in retinoblastoma and other tumor genesis is found to be the major force of tumor development without other genetic abnormal. pRb regulates cell cycle progression by binding to the E2F family of transcription factors and inducing repression of E2F-regulated cell cycle genes.[46] The action of this repression involves two mechanisms – direct binding and blockage of the transactivation domain of E2F, and recruitment of chromatin-modifying molecules. All three pocket protein family members have been shown to associate with HDAC1 through the "pocket" domain to repress cell cycle genes by E2F-regulated promoters.[47] In addition, pRb associates with the HMTase Suv39H1, DNMT1, and heterochromatin protein 1 (HP1) via its pocket domain.[48] Finally, pRb also influences the accessibility of chromatin through interactions with the ATP-dependent helicase *BRG1*, the catalytic subunit of the SNF/SWI chromatin remodeling complex. Together, DNMT1, HMTases, HDACs, HP1, and *BRG1* are all recruited by pRb to form a multiprotein chromatin remodeling complex that can heterochromatinize promoters regulated by the E2F family, and epigenetically silence transcriptional activation of cell cycle genes.

There is increasing evidence that, in addition to mutations in the *RB1* gene, epigenetic changes involving aberrant DNA methylation of other tumor suppressor gene promoters may be involved. Researchers found that there is hypermethylation in RB1 promoter which is associated with suppression of *RB1* gene expression.[49] Besides *RB1*, examination of the promotor methylation of other tumor suppressor genes such as *p16INK4A*, *MGMT*, *GSTP1*, *APC*,

DAPK, *RARB*, *CDH11*, and *CDH13* in retinoblastoma have also been revealed.[50] It is found that 118 genes are differentially expressed in their promoter methylation from19 primary retinoblastoma tumor samples by a genome-wide analysis.[46] In retinoblastoma tissues there is promoter hypermethylation of O_6-methylguanine-DNA methyltransferase,[51] which encodes a DNA repair enzyme and is also hypermethylated in breast and prostate cancer, lymphoma, and gliomas. *RASSF1A* (the RAS-association domain family 1, isoform A, tumor suppressor gene involved in microtubule stability, apoptosis, and cell cycle regulation), is also methylated and inactivated in multiple pediatric tumors, including retinoblastoma. Finally, promoter methylation of caspase 8, which is involved in Fas-mediated apoptosis, and *MLH1*, a DNA mismatch repair gene, may provide mechanistic explanations for loss of cell cycle regulation in retinoblastoma tumors. It remains unclear to what degree aberrant methylation contributes to the pathogenesis of tumor growth in patients with retinoblastoma. For example, does hypermethylation of tumor suppressor genes represent the second or third "hit" required for tumor genesis, or are they merely compensatory changes that occur in response to tumor growth? Furthermore, the involvement of miRNA in the pathogenesis of retinoblastoma is also being studied. It was found that the level of miRNA-17 92a is high in retinoblastoma, which means it may be a therapeutic target.[49] Further work will be necessary to delineate the roles of complex epigenetic factors including single nucleotide polymorphisms (SNPs) of p53 rs1042522 involved in this childhood cancer.[52]

Epigenetic Factors in Uveal Melanomas

Uveal melanoma is the most common primary intraocular tumor in adults, with a high mortality rate and frequent metastases. Similar to retinoblastoma, aberrant DNA methylation of the *RASSF1A* promoter has also been implicated in uveal melanoma.[53] In addition, there are a number of tumor suppression gens silenced by promoter methylation, including *pINK4a*, *TIMP3*, *RASEF*, and *EFS*.[54] Interestingly, the expression of a number of histone-modifying genes and polycomb family members are decreased in

the tissues of uveal melanoma with monosomy 3/class 2, and more importantly abnormality of those epigenetic modifiers is associated with a worse prognosis.[55] However, other investigations of promoter methylation in several tumor suppressor genes in uveal melanoma tissues identified only the human telomerase reverse transcriptase (*hTERT*) gene, but not *RASSF1A*, to be abnormally methylated. Such discrepancies may be related to the genetic heterogeneity of uveal melanomas in humans, and additional research is needed to identify these different patterns of DNA methylation.

The involvement of histone acetylation in uveal melanoma remains unclear. In vitro, inhibition of HDAC activity in both primary and metastatic uveal melanoma cell lines results in inhibition of cell growth and induction of apoptosis, an effect likely mediated by Fas-dependent pathways.[56] It is not known, however, whether HDACs are involved in the pathogenesis of the disease in humans. Nevertheless, these findings implicate a potential role of HDAC inhibitors in the treatment of this devastating cancer.

Recent evidence also points to a role of microRNAs in uveal melanoma. miRNAs such as miR-34a and miR-137, which have been implicated in tumor suppression, are expressed in melanocytes, but not in uveal melanoma cells.[57,58] Transfection of miR-34a or miR-137 into uveal melanoma cells led to decreased cell growth and migration. miR-34a is a potential key effector of the p53 tumor suppressor gene, while miR-137 is involved in downregulation of MITF, a master regulator of melanocyte cell growth, maturation, apoptosis, and pigmentation.[59] miR-144 acts as a tumor suppressor in uveal melanoma. Identifying other miRNAs involved in tumor suppression may provide novel targets for uveal melanoma therapy.

Notably, application of DNA methylation inhibitor-5-AZA can suppress the migration and proliferation of uveal and cutaneous melanoma cells,[60] suggesting the involvement of a methylation mechanism in the pathogenesis of uveal melanoma.

Epigenetic Factors in Retinal Angiogenesis

Angiogenesis is controlled by a balance between pro- and

antiangiogenic factors. Epigenetic changes caused by aberrant DNA methylation or histone acetylation of antiangiogenic molecules have been shown to control angiogenesis. Initial studies revealed a crucial role for miRNAs in stimulating or reducing angiogenesis. These research efforts improved our understanding of how epigenetic factors control angiogenesis. Importantly, these epigenetic insights may also be of important clinical relevance for the use of antiangiogenic strategies in diabetic retinopathy or AMD.

Diabetic Retinopathy

Diabetes is now considered as the epidemic of the 21st century, and diabetic retinopathy is emerging as a major public health concern. The vasculature and neuronal cells components of the retina are damaged, but the exact mechanism responsible for the pathogenesis of this blinding disease, however, remains unclear. A cross-sectional study with over 1000 type 2 diabetic patients has identified a possible genetic and epigenetic basis for the development of diabetic retinopathy. Diabetic patients have shown a strong association between the polymorphism in the gene that encodes histone methyltransferases, *SUV39H2,* and retinopathy.[61] Experimental studies have shown a role of increased H4K20 methylation at the promoter and enhancer regions of *SOD2*, the gene that encodes mitochondrial superoxide dismutate in its downregulation in diabetes.[18,20,62] Increased histone methyltransferase Set7 recruitment at the promoter of NF-κB in hyperglycemic milieu is associated with its increased transcription.[61,63] Altered histone acetylation machinery (HATs and HDACs) is observed in the in vitro and in vivo models of diabetic retinopathy. Increased acetyl H3K9 at the promoter of matrix metalloproteinsase-9, an enzyme implicated in retinal mitochondrial damage in diabetes, is considered to facilitate its binding with NF-κB, resulting in its increased expression in diabetes, but that at the promoter of *SOD2*, is implicated in its downregulation.[64,65] In addition, hypoxia is a major stimulus for the retinal neovascularization observed in diabetes;[66] ischemia and hypoxia also stimulate HDAC activity, thus the activation of retinal HDAC by increased retinal hypoxia in diabetes remains a strong

possibility. In addition, in the development of diabetic retinopathy, epigenetic modifications are considered to play a significant role in the decreased transcriptional activity of the master regulator Nrf2.[67] The modification of histone H3 at lysine 9 (H3K9) at the proximal Cox2 promoter bearing the NF-κB-binding site has been shown to modulate hyperglycemia-induced thioredoxin-interacting protein-mediated inflammation in retinal capillary endothelial cells. The mechanism of histone modification in diabetes may include increased oxidative stress and hypoxia, as in diabetes the retina experiences increased oxidative stress, and hyperglycemia-induced superoxide overproduction activates the major pathways in the development of diabetic retinopathy.[18,20,62] Global DNA methylation status in a case–control study of 168 patients with type II diabetes has shown a strong correlation with the progression of retinopathy[68] and 19 potential CpG sites undergoing methylation have been identified in the blood cells from type 1 diabetic patients that undergo DNA methylation in diabetes. Animal models have shown the role of DNA methylation in retinal mitochondrial homeostasis in diabetes: hypermethylation of the mitochondrial DNA biogenesis enzyme, DNA polymerase-gamma, downregulates its expression, impairs mtDNA transcription, and compromises the electron transport system.[14,69] The role of miRNAs in diabetic retinopathy is still in its incipient stage. miRNA-expression profiling and established miRNA transcriptomes of the retina have shown dysregulation of many miRNAs associated with the pathogenetic pathways of diabetic retinopathy, especially upregulation of a NF-κB-responsive miRNA, miR-146, in the retina and retinal endothelial cells of diabetic rats. Altered levels of miR-21, miR-181c, and miR-1179 are observed in the serum of patients with proliferative and nonproliferative diabetic retinopathy. Models of diabetic retinopathy have shown an association between downregulation of miR-126, miR-146a, and miR-200b and the upregulation of VEGF, and upregulation of miR-29b and protection of apoptosis of the retinal ganglion cells.[62,70] Thus, epigenetic modifications appear to play an important role in the development of diabetic retinopathy (Fig. 35.2), and could be targeted to combat this blinding disease.

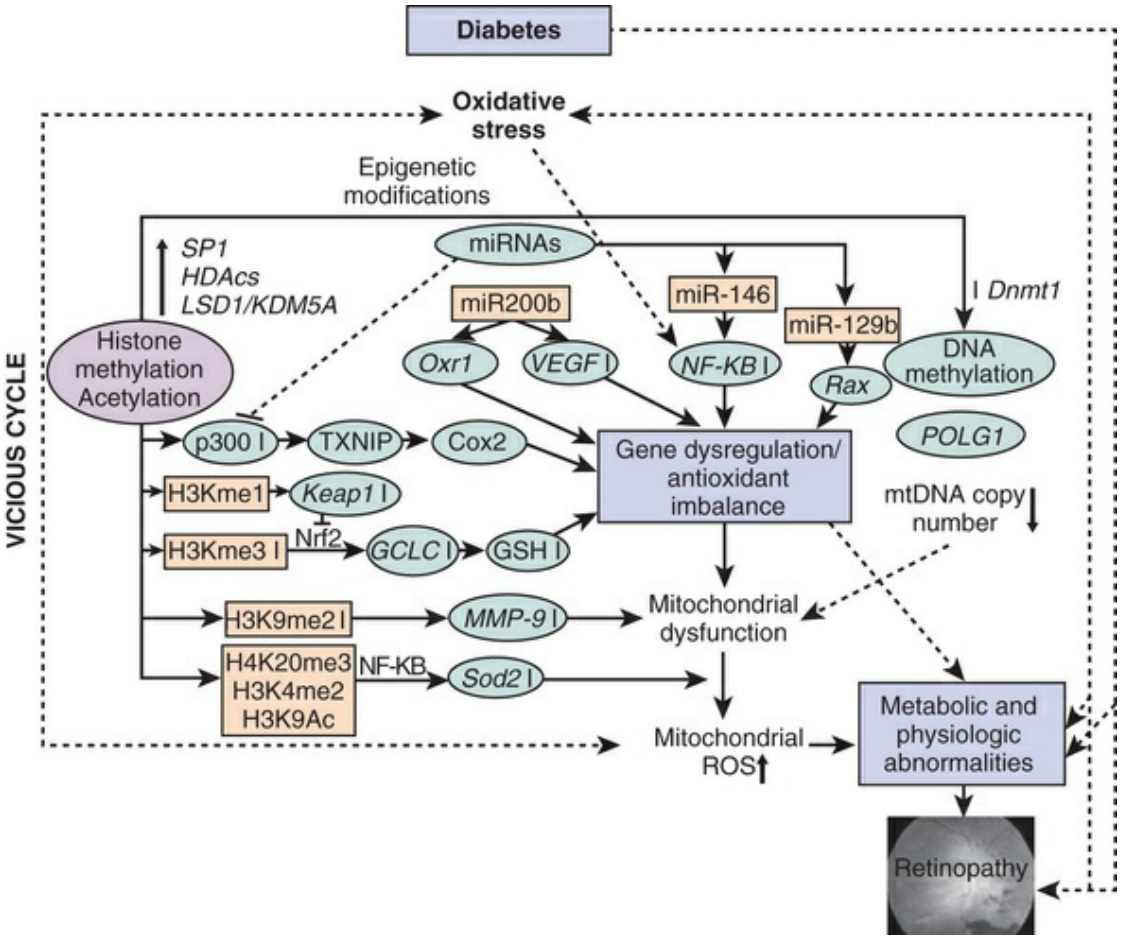

FIG. 35.2 Diabetes increases oxidative stress, and this, by altering the expression of genes involved in histone (LSD1, KDM5A, HDACs) and DNA (Dnmts) modifications, brings about a number of epigenetic changes. Due to alterations in histone methylation (e.g., H3K4, H3K9, and H4K20) and acetylation (H3K9-Ac, p300), the binding of transcription factor (Nrf2, Sp1, NF-κB-p65) is altered resulting in dysregulation (*GCLC, Keap1, MMP-9, Sod2, TXNIP*). Activation of DNMTs methylates *POLG1* promoter, suppressing its expression and altering mtDNA biogenesis. In addition, the levels of number of microRNAs (miR-200b, miR-129b, miR-149) are also changed, dysregulating transcription of various genes (*Oxr1*, *VEGF*, *Rax*, *NF-kB*). These epigenetic modifications, by altering the gene expressions of proteins associated with the oxidative damage and antioxidant defense and miRNA levels, also dysfunction mitochondria and impair mtDNA transcription, and the vicious cycle of ROS continues to fuel in. Although a number of modifications are

shown here, there are many other, yet unidentified, epigenetic modifications, that could also be contributing to the development of diabetic retinopathy. Cox2, cytochrome c oxidase subunit 2; Dnmt1, DNMT1: DNA methyl transferase 1; Gclc, glutamate cysteine ligase, catalytic subunit; GSH, glutathione-reduced form; H3K4me1, histone H3 lysine 4 monomethyl; H3K4me3, histone H3 lysine 4 trimethyl; H3K9Ac, histone H3 lysine 9 acetylation; H3K9me2, histone H3 lysine 9 dimethyl; H4K20me3, histone H3 lysine 20 trimethyl; HDAC, histone deacetylases; KDM5A, lysine-specific demethylase 5A; Keap1, Kelch-Like ECH-associated protein 1; LSD1, lysine specific demethylase 1; MMP-9, matrix metalloproteinase 9; NF-κB, nuclear transcriptional factor-κB; NRF2, nuclear factor-erythroid 2-Like 2; Oxr1, oxidation resistance protein 1; POLG1, polymerase gamma 1; Rax, retina and anterior neural fold homeobox; Sod2, superoxide dismutase 2; SP1, specificity protein 1.

Choroidal Neovascularization (CNV)

CNV describes the growth of new blood vessels that originate from the choroid through a break in Bruch's membrane into the sub-RPE or subretinal space.[71] CNV is a major cause of central visual loss.

The pathogenesis of CNV is mediated by a multitude of factors. Epigenetics can potentially participate in various pathologic aspects of CNV. miR-155, which is expressed in immune cells, was demonstrated to activate macrophages. Macrophages facilitate the inflammatory response that promotes angiogenesis, for instance, through the production of tumor necrosis factor, which induces the expression of VEGF and MMPs.[72] However, retinal production of tumor necrosis factor and its stimulatory effects on MMPs can be reversed by an HDAC inhibitor.[21] The expression of pro- and antiinflammatory genes, such as interleukin genes *IL2*, *IL8*, and *IL10*, can also be regulated by HDAC activity.[72] Furthermore, oxidative stress can also induce expression of the major player in angiogenesis, VEGF, as well as expression of HIF-1α, which stimulates VEGF production. HIF-1α can also be downregulated by

the HDAC inhibitor,[73] TSA, whereas the antiangiogenic and neuroprotective molecule pigment epithelium-derived factor is upregulated by TSA.[73] TSA can also inhibit the proliferation and migration of RPE cells, implying the potential regulation of pro- and antiproliferative, ECM-modifying genes by HDACs.

In a study mapping promoter DNA methylation in AMD and age-matched normal RPE/choroid samples, the antioxidants glutathione S-transferase isoforms mu1 and mu2 have been shown to be downregulated and heavily methylated in their promoter regions in AMD samples. Additionally, the proangiogenic angiopoietin-like protein 2 had less methylation in its promoter in the AMD samples.[74] Notably, hypomethylation of the interleukin-17 receptor C (IL17RC) promoter has recently been identified in peripheral blood cells from patients with AMD and was associated with increased expression of IL17RC in their peripheral blood and affected retina and choroid. These results suggest that epigenetic regulation of IL17RC may play a role in the pathogenesis of AMD.[75]

Previous studies described the key role of SIRT1 as a critical regulator of angiogenesis. The expression of SIRT1 was found more frequently in human CNV membranes than non-AMD donor eyes. Another experiment revealed that the SIRT1 pathway is involved in the mechanism of resveratrol inhibiting hypoxic-induced choroidal vascular endothelial cells proliferation through downregulating the levels of HIF-1a. Thus, RSV inhibits the HIF-1α/VEGF/VEGFR2 signaling axis in choroidal neovascularization-related cells, at least in part, through SIRT1.[76] The discrepancy of effects of SIRT1 may be due to the different activators or inhibitors used in the experiments. Further studies should be performed to identify the accurate effect of SIRT1 on CNV formation.

Perspectives and Challenges of Epigenetics

The epigenome plays a pivotal role as the interface between genome and environment, and over years, an individual may accumulate various intrinsic insults caused by chronic diseases such as diabetes mellitus or accumulate environmental alterations that

could affect the epigenome, and participate in the induction of age-related diseases. Understanding the pathologic epigenetic alterations should help reveal additional insights into their etiology and how possible environmental modulations may contribute to the disease process and may be targeted through pharmacologic intervention on chromatin-modifying enzymes. The class III family of HDACs, sirtuins, specifically SIRT1, has been demonstrated to inhibit cell death.[77] It acts to prevent the overactivation of p53 in causing apoptosis due to DNA damage, resulting in DNA repair and cell survival.

Epigenetics has become an important area of biomedical research and it may be able to explain phenotypic changes in many complex retinal diseases. Epigenetic therapies may offer additional options for the treatment of some retinal diseases. However, there are some important challenges, including nonspecific activation of imprinted genes, which are normally regulated by methylation, unwanted expression of transposable elements, which may contribute to pathology, persistence of the reversible nature of methylation patterns after drug treatment, and remethylation and resilencing issues. Due to the dynamic nature of epigenetics, and lack of detailed knowledge about its role in retina, some critical questions need to be addressed:

1. What is the detailed mechanism of epigenetic regulation of retinal development?

2. In the physiologic condition, how do epigenetic factors contribute to normal retinal function?

3. How is retinal inflammation regulated by epigenetic factors?

4. How much of a role does epigenetics play in the pathogenesis of retinal angiogenesis and fibrosis?

5. How do cytokines and growth factors regulate epigenetic factor expression and vice versa?

6. How is epigenetics involved in the process of retinal degeneration, including AMD?

7. What is the role of epigenetics in mitochondrial, endoplasmic reticulum, and Golgi stress in retinal disease?

8. What is the role of crosstalk among epigenetic factors in retinal development and disease?

9. What is the epigenome of retinal cells in the normal and diseased condition?

Treatment of Retinal Disease With Epigenetic-Modifying Drugs

As detailed above, ongoing research has clearly documented a major role of epigenetics in the retinal development and diseases. Since the epigenetic modifications are dynamic and can be reversed, they are evolving as attractive targets for therapeutic interventions. Many small molecule compounds have been designed to modulate the activity of histone modifying enzymes and DNMTs, and some of them are in clinical trials. Preclinical studies using epigenetic modifying drugs are in progress and some epigenetic modifying drugs, such as 5-AZA and suberoylanilide hydroxamic acid, are in clinical trials.[78–80] However, the major concern about epigenetic drugs is lack of target specificity. The DNA methylation inhibitors result in global demethylation; similarly, the HDAC inhibitors can affect many isoforms of HDAC and nonhistone proteins. Since miRNAs are considered as potential diagnostic biomarkers for disease, double-stranded miRNA mimics and anti-mRNA antisense oligo-deoxyribonucleotide could be used to target specific miRNAs. But one miRNA can act on multiple targets, so the development of compounds with higher specificity and greater efficacy is essential, and the possibility of their access to the posterior part of the eye is another important aspect that needs major consideration.

Although several epigenetic inhibitors have been approved, or are in clinical trials, for cancer treatment, the use of combinations of inhibitors targeting different regulatory components of the epigenetic machinery, and/or with other traditional therapies, may be considered to improve therapeutic efficacy for patients suffering

from retinal diseases.

References

1. Waddington CH. The epigenotype. *Endeavour*. 1942;1:18–20.
2. Bonasio R, Tu S, Reinberg D. Molecular signals of epigenetic states. *Science*. 2010;330:612–616.
3. Romanosk CE, Glass ChK, Stunnenberg HG, et al. Epigenomics: Roadmap for regulation. *Nature*. 2015;518:314–316.
4. Orozco LD, Morselli M, Rubbi L, et al. Epigenome-wide association of liver methylation patterns and complex metabolic traits in mice. *Cell Metab*. 2015;21(6):905–991.
5. Whitaker JW, Chen Z, Wang W. Predicting the human epigenome from DNA motifs. *Nat Methods*. 2015;12(3):265–272.
6. Ehrlich M, Gama-Sosa MA, Huang LH, et al. Amount and distribution of 5-methylcytosine in human DNA from different types of tissues of cells. *Nucleic Acids Res*. 1982;10:2709–2721.
7. Boyes J, Bird A. DNA methylation inhibits transcription indirectly via a methyl-CpG binding protein. *Cell*. 1991;64:1123–1134.
8. Hu B, Gharaee-Kermani M, Wu Z, et al. Essential role of MeCP2 in the regulation of myofibroblast differentiation during pulmonary fibrosis. *Am J Pathol*. 2011;178:1500.
9. Patil V, Ward RL, Hesson LB. The evidence for functional non-CpG methylation in mammalian cells. *Epigenetics*. 2014;9(6):823–828.
10. Pinney SE. Mammalian non-CpG methylation: stem cells and beyond. *Biology (Basel)*. 2014;3:739–751.
11. Rudenko A, Tsai LH. Epigenetic modifications in the nervous system and their impact upon cognitive impairments. *Neuropharmacology*. 2014;80:70–82.
12. Londin E, Loher P. Reply to Backes and Keller: Identification of novel tissue-specific and primate-specific human microRNAs. *Proc Natl Acad Sci USA*. 2015;112(22):E2851.
13. Ha M, Kim VN. Regulation of microRNA biogenesis. *Nat*

Rev Mol Cell Biol. 2014;15:509–524.
14. Mishra M, Kowluru RA. Epigenetic modification of mitochondrial DNA in the development of diabetic retinopathy. *Invest Ophthalmol Vis Sci*. 2015;56:5133–5142.
15. Petkova TD, Seigel GM, Otteson DC. A role for DNA methylation in regulation of EphA5 receptor expression in the mouse retina. *Vision Res*. 2011;51:260–268.
16. Song C, Feodorova Y, Guy J, et al. DNA methylation reader MECP2: cell type- and differentiation stage-specific protein distribution. *Epigenetics Chromatin*. 2014;7:17.
17. Gillette TG, Hill JA. Readers, writers, and erasers: chromatin as the whiteboard of heart disease. *Circ Res*. 2015;116:1245–1253.
18. Zhong Q, Kowluru RA. Epigenetic changes in mitochondrial superoxide dismutase in the retina and the development of diabetic retinopathy. *Diabetes*. 2011;60:1304–1313.
19. Haery L, Thompson RC, Gilmore TD. Histone acetyltransferases and histone deacetylases in B- and T-cell development, physiology and malignancy. *Genes Cancer*. 2015;6(5–6):184–213.
20. Zhong Q, Kowluru RA. Role of histone acetylation in the development of diabetic retinopathy and the metabolic memory phenomenon. *J Cell Biochem*. 2010;110(6):1306–1313.
21. Crosson CE, Mani SK, Husain S, et al. Inhibition of histone deacetylase protects the retina from ischemic injury. *Invest Ophthalmol Vis Sci*. 2010;51:3639–3645.
22. Sundermeier TR, Palczewski K. The physiological impact of microRNA gene regulation in the retina. *Cell Mol Life Sci*. 2012;69:2739–2750.
23. Iida A, Iwagawa T, Baba Y, et al. Roles of histone H3K27 trimethylase Ezh2 in retinal proliferation and differentiation. *Dev Neurobiol*. 2015;75(9):947–960.
24. Kim JW, Jang SM, Kim CH, et al. Transcriptional activity of neural retina leucine zipper (Nrl) is regulated by c-Jun N-terminal kinase and Tip60 during retina development. *Mol Cell Biol*. 2012;32:1720–1732.
25. Chen B, Cepko CL. HDAC4 regulates neuronal survival in

normal and diseased retinas. *Science*. 2009;323:256–259.
26. Akhtar S, Patnaik SR, Kotapati Raghupathy R, et al. Histological characterization of the Dicer1 mutant zebrafish retina. *J Ophthalmol*. 2015;2015:309510.
27. Xu S, Witmer PD, Lumayag S, et al. MicroRNA (miRNA) transcriptome of mouse retina and identification of a sensory organ-specific miRNA cluster. *J Biol Chem*. 2007;282:25053–25066.
28. Baba Y, Aihara Y, Watanabe S. MicroRNA-7a regulates Müller glia differentiation by attenuating Notch3 expression. *Exp Eye Res*. 2015;138:59–65.
29. Choi SW, Kim JJ, Seo MS, et al. miR-410 inhibition induces RPE differentiation of amniotic epithelial stem cells via overexpression of OTX2 and RPE65. *Stem Cell Rev*. 2015;11:376–386.
30. Feng Z, Li R, Shi H, et al. Combined silencing of TGF-β2 and Snai1 genes inhibit epithelial-mesenchymal transition of retinal pigment epithelial cells under hypoxia. *Graefes Arch Clin Exp Ophthalmol*. 2015;253(6):875–884.
31. Burgess HA, Daugherty LE, Thatcher TH, et al. PPARg agonist inhibit TGF-β induced pulmonary myofibroblast differentiation and collagen production: implications for therapy of lung fibrosis. *Am J Physiol Lung Cell Mol Physiol*. 2005;288(6):L1146–53.
32. Mann J, Chu DC, Maxwell A, et al. MeCP2 controls an epigenetic pathway that promotes myofibroblast transdifferentiation and fibrosis. *Gastroenterology*. 2010;138:705–714.
33. He S, Barron E, Ishikawa K, et al. Inhibition of DNA methylation and methyl-CpG-binding protein 2 suppresses RPE transdifferentiation: relevance to proliferative vitreoretinopathy. *Invest Ophthalmol Vis Sci*. 2015;56:5579–5589.
34. Noh H, Oh EY, Seo JY, et al. Histone deacetylase-2 is a key regulator of diabetes- and transforming growth factor-β_1-induced renal injury. *Am J Physiol Renal Physiol*. 2009;297:F729–39.
35. Chan N, He S, Spee CK, et al. Attenuation of choroidal

neovascularization by histone deacetylase inhibitor. *PLoS ONE*. 2015;10(3):e0120587.
36. Cicchini C, de Nonno V, Battistelli C, et al. Epigenetic control of EMT/MET dynamics: HNF4α impacts DNMT3s through miRs-29. *Biochim Biophys Acta*. 2015;1849(8):919–929.
37. Sancho-Pelluz J, Arango-Gonzalez B, Kustermann S, et al. Photoreceptor cell death mechanisms in inherited retinal degeneration. *Mol Neurobiol*. 2008;38:253–269.
38. Sancho-Pelluz J, Alavi MV, Sahaboglu A, et al. Excessive HDAC activation is critical for neurodegeneration in the rd1 mouse. *Cell Death Dis*. 2010;1:e24.
39. Farinelli P, Perera A, Arango-Gonzalez B, et al. DNA methylation and differential gene regulation in photoreceptor cell death. *Cell Death Dis*. 2014;5:e1558.
40. Clemson CM, Tzekov R, Krebs M, et al. Therapeutic potential of valproic acid for retinitis pigmentosa. *Br J Ophthalmol*. 2011;95:89–93.
41. Hutchinson JN, Fagerness J, Kirby A, et al. Epi)Genetic analyses of age-related macular degeneration: case-control and discordant twin studies. *Hum Hered*. 2014;78:59–72.
42. Oliver V, Jaffe AE, Song J, et al. Differential DNA methylation identified in the blood and retina of AMD patients. *Epigenetics*. 2015;10(8):698–707.
43. Rosemblit N, Chen CL. Regulators for the rat clusterin gene: DNA methylation and *cis*-acting regulatory elements. *J Mol Endocrinol*. 1994;13:69–76.
44. Kaneko H, Dridi S, Tarallo V, et al. DICER1 deficit induces Alu RNA toxicity in age-related macular degeneration. *Nature*. 2011;471:325–330.
45. Sundermeier TR, Zhang N, Vinberg F, et al. DICER1 is essential for survival of postmitotic rod photoreceptor cells in mice. *FASEB J*. 2014;28:3780–3791.
46. Zhang J, Benavente CA, McEvoy J, et al. A novel retinoblastoma therapy from genomic and epigenetic analyses. *Nature*. 2012;481(7381):329–334.
47. Luo RX, Postigo AA, Dean DC. Rb interacts with histone deacetylase to repress transcription. *Cell*. 1998;92:463–473.

48. Robertson KD, Ait-Si-Ali S, Yokochi T, et al. DNMT1 forms a complex with Rb, E2F1 and HDAC1 and represses transcription from E2F-responsive promoters. *Nat Genet*. 2000;25:338–342.
49. Benavente CA, Dyer MA. Genetics and epigenetics of human retinoblastoma. *Annu Rev Pathol*. 2015;10:547–562.
50. Harada K, Toyooka S, Maitra A, et al. Aberrant promoter methylation and silencing of the RASSF1A gene in pediatric tumors and cell lines. *Oncogene*. 2002;21(27):4345–4349.
51. Choy KW, Pang CP, To KF, et al. Impaired expression and promotor hypermethylation of O6-methylguanine-DNA methyltransferase in retinoblastoma tissues. *Invest Ophthalmol Vis Sci*. 2002;43:1344–1349.
52. Chen R, Liu S, Ye H, et al. Association of p53 rs1042522, MDM2 rs2279744, and p21 rs1801270 polymorphisms with retinoblastoma risk and invasion in a Chinese population. *Sci Rep*. 2015;5:13300.
53. Maat W, van der Velden PA, Out-Luiting C, et al. Epigenetic inactivation of RASSF1a in uveal melanoma. *Invest Ophthalmol Vis Sci*. 2007;48:486–490.
54. Herlihy N, Dogrusöz M, van Essen TH, et al. Skewed expression of the genes encoding epigenetic modifiers in high-risk uveal melanoma. *Invest Ophthalmol Vis Sci*. 2015;56:1447–1458.
55. Venza M, Visalli M, Beninati C, et al. Role of genetics and epigenetics in mucosal, uveal, and cutaneous melanomagenesis. *Anticancer Agents Med Chem*. 2016;16(5):528–538.
56. Klisovic DD, Katz SE, Effron D, et al. Depsipeptide (FR901228) inhibits proliferation and induces apoptosis in primary and metastatic human uveal melanoma cell lines. *Invest Ophthalmol Vis Sci*. 2003;44:2390–2398.
57. Yan D, Zhou X, Chen X, et al. MicroRNA-34a inhibits uveal melanoma cell proliferation and migration through downregulation of c-Met. *Invest Ophthalmol Vis Sci*. 2009;50:1559–1565.
58. Chen X, Wang J, Shen H, et al. Epigenetics, microRNAs, and carcinogenesis: functional role of microRNA-137 in uveal

melanoma. *Invest Ophthalmol Vis Sci*. 2011;52:1193–1199.
59. Levy C, Khaled M, Fisher DE. MITF: master regulator of melanocyte development and melanoma oncogene. *Trends Mol Med*. 2006;12:406–414.
60. Rajaii F, Asnaghi L, Enke R, et al. The demethylating agent 5-Aza reduces the growth, invasiveness, and clonogenicity of uveal and cutaneous melanoma. *Invest Ophthalmol Vis Sci*. 2014;55(10):6178–6186.
61. Keating ST, El-Osta A. Epigenetic changes in diabetes. *Clin Genet*. 2013;84:1–10.
62. Kowluru RA, Kowluru A, Mishra M, et al. Oxidative stress and epigenetic modifications in the pathogenesis of diabetic retinopathy. *Prog Retin Eye Res*. 2015;48:40–61.
63. Paneni F, Costantino S, Battista R, et al. Adverse epigenetic signatures by histone methyltransferase Set7 contribute to vascular dysfunction in patients with type 2 diabetes mellitus. *Circ Cardiovasc Genet*. 2015;8(1):150–158.
64. Zhong Q, Kowluru RA. Regulation of matrix metalloproteinase-9 by epigenetic modifications and the development of diabetic retinopathy. *Diabetes*. 2013;62:2559–2568.
65. Kowluru RA, Santos JM, Zhong Q. Sirt1, a negative regulator of matrix metalloproteinase-9 in diabetic retinopathy. *Invest Ophthalmol Vis Sci*. 2014;55(9):5653–5660.
66. Frank RN. Diabetic retinopathy. *N Engl J Med*. 2004;350:48–58.
67. Mishra M, Zhong Q, Kowluru RA. Epigenetic modifications of Nrf2-mediated glutamate-cysteine ligase: implications for the development of diabetic retinopathy and the metabolic memory phenomenon associated with its continued progression. *Free Radic Biol Med*. 2014;75:129–139.
68. Maghbooli Z, Hossein-Nezhad A, Larijani B, et al. Global DNA methylation as a possible biomarker for diabetic retinopathy. *Diabetes Metab Res Rev*. 2015;31:183–189.
69. Tewari S, Zhong Q, Santos JM, et al. Mitochondria DNA replication and DNA methylation in the metabolic memory associated with continued progression of diabetic retinopathy. *Invest Ophthalmol Vis Sci*. 2012;53(8):4881–4888.

70. Mastropasqua R, Toto L, Cipollone F, et al. Role of microRNAs in the modulation of diabetic retinopathy. *Prog Retin Eye Res*. 2014;43C:92–107.
71. Yonekawa Y, Miller JW, Kim IK. Age-related macular degeneration: advances in management and diagnosis. *J Clin Med*. 2015;4(2):343–359.
72. Campa C, Harding SP. Two-year visual results for older Asian women treated with photodynamic therapy or bevacizumab for myopic choroidal neovascularization. *Am J Ophthalmol*. 2010;149:1014–1015.
73. Chen S, Sang N. Histone deacetylase inhibitors: the epigenetic therapeutics that repress hypoxia-inducible factors. *J Biomed Biotechnol*. 2011;2011:197946.
74. Hunter A, Spechler PA, Cwanger A, et al. DNA methylation is associated with altered gene expression in AMD. *Invest Ophthalmol Vis Sci*. 2012;53:2089–2105.
75. Wei L, Liu B, Tuo J, et al. Hypomethylation of the IL-17RC promoter associates with age-related macular degeneration. *Cell Rep*. 2012;2:1151.
76. Zhang H, He S, Spee C, et al. SIRT1 mediated inhibition of VEGF/VEGFR2 signaling by Resveratrol and its relevance to choroidal neovascularization. *Cytokine*. 2015;76(2):549–552.
77. Ozawa Y, Kubota S, Narimatsu T, et al. Retinal aging and sirtuins. *Ophthalmic Res*. 2010;44:199–203.
78. Fandy TE. Development of DNA methyltransferase inhibitors for the treatment of neoplastic diseases. *Curr Med Chem*. 2009;16:2075–2085.
79. Santini V, Gozzini A, Ferrari G. Histone deacetylase inhibitors: molecular and biological activity as a premise to clinical application. *Curr Drug Metab*. 2007;8:383–393.
80. Morales L, Madrid A, Hashizume R, et al. Future clinical trials in DIPG: bringing epigenetics to the clinic. *Front Oncol*. 2015;1(5):148.

SECTION 4

Translational Basic Science

OUTLINE

36

Gene Therapy for Retinal Disease

Jean Bennett, Albert M. Maguire

Background: Preclinical Gene Therapy Studies

Gene therapy holds great promise for the treatment of inherited and acquired blinding retinal diseases. There has been much progress over the past two decades in identifying disease-causing genes in humans and in animal models and this, in turn, has expedited our understanding of disease pathogenesis. For diseases that lack naturally occurring animal models, additional models have been generated through genetic-engineering techniques or through somatic gene transfer. Simultaneous with the increase in knowledge of the genetic bases of retinal diseases, there have been great technical developments in delivering genes efficiently and stably to retinal cells. Because of its ease of access, its favorable immunologic response to gene transfer, and the ability to perform noninvasive functional and structural studies, the mammalian eye has been intensely studied as a target for gene therapy. Gene transfer strategies have been used in both small- and large-animal models to demonstrate proof of concept. These preclinical studies have allowed the field to reach the point where gene therapy to treat several forms of inherited blindness have been tested in clinical trials. A phase III trial (aimed at obtaining approval of a gene therapy reagent as a drug) is also underway for one of these diseases. Tremendous challenges lie ahead to extrapolate these results to other retinal diseases. These challenges include the need to develop individualized treatment strategies for a vast array of different genetic diseases, studies of the natural history of the disease so that appropriate outcome measures/timing of studies can be planned, identification of appropriate candidates for clinical trials through genetic testing and phenotypic characterization, and development of outcome measures appropriate for identifying a therapeutic benefit in a reasonable period of time. Despite the challenges, these efforts bring hope for patients with a variety of blinding diseases which, until recently, have been considered to be untreatable and incurable.

Definitions

Nucleic acids do not readily cross cell membranes due to their charge and size. Vectors are therefore used to deliver DNA or RNA into the cell, where they can then access the cell nucleus. Over the past two decades, there has been great progress in developing vectors with which to deliver nucleic acids to a variety of retinal cell types. Delivery of genes by a virus and subsequent expression of the gene is termed "transduction" and the infected cells are described as "transduced." Usually the complementary deoxyribonucleic acid (cDNA) is delivered with a recombinant virus due to the large size of genomic DNA. The DNA is not expressed unless the appropriate regulatory elements are present. The transgene cassette generally consists of regulatory elements (promoter, etc.), the cDNA, and a poly(A) sequence. There are both physicochemical methods for delivering genes as well as a large toolkit of recombinant virus vectors, complete with modifications of capsids, envelopes, and surface proteins designed to achieve the desired transduction parameters.

Nonviral Gene Delivery

There are several nonviral methods of delivering nucleic acids to cells, and those include use of physicochemical agents to compact the DNA and/or transport it across the membrane lipid bilayer.[1,2] There are several potential advantages of nonviral approaches: First, they can be used to deliver DNA of unlimited size. Second, there is a smaller chance of detrimental immune response since the only antigen would be the nucleic acid itself plus any protein that is used as a condensation agent. The main obstacle faced with most physicochemical methods is the difficulty in applying the technique to *in vivo* conditions and in achieving an extended duration of gene expression. Several studies have demonstrated proof of concept of retinal gene therapy using nonviral DNA delivery[1,3,4] and additional studies will reveal the long-term safety, stability, and efficacy of this approach.

Viral Vector-Mediated Gene Delivery

Recombinant viruses are genetically engineered so that they cannot reproduce and cause an infectious disease once they infect a target

cell. There is a host of recombinant viruses that have been tested in the retina (Table 36.1). Different viruses have varying attributes and challenges, including cargo capacity, ease of purification, cellular specificity, and immune response. However, a large cohort of these have been used to demonstrate efficacy in animal models of retinal disease (see Table 36.2).

TABLE 36.1

Vectors Tested for Transduction Characteristics in Animal Models[a]

Delivery Approach	Cargo Limits	Integration	Stability (Large-Animal Models)	Retinal Cell Targets	Risk of Toxic Immune Response	Used in Human Ocular Studies	Requires Further Development Prior to Human Application
Electroporation	Unlimited	No	Unknown (unlikely)	RPE, PRs; BP	Low	No	Yes
Compact nanoparticles; POD	Unlimited	No	Unknown	PRs, RPE; GC, IR	Low	No	Yes
Adenovirus	7.5 kb	No	No	RPE, Müller	High	Yes	No
Helper-independent ("gutted") adenovirus	36 kb	No	Unknown	RPE, PRs	Unknown	No	No
Adeno-associated virus	4.8 kb	No	Stable	RPE, Müller, PRs, GCs	Low	Yes	No
Lentivirus	7.5 kb	Yes	Stable	RPE, PRs	Low	Yes	No

[a]Various retinal cell targets are listed; however, the exact targets depend on the route of administration, dose, species, and modifications to the vector.

BP, bipolar cells; GC, ganglion cell; IR, inner retinal cells; Müller, Müller cells; POD, peptide for ocular delivery; PRs, photoreceptor cells; RPE, retinal pigment epithelium. References for the use of these vectors are provided in Table 36.2.

TABLE 36.2

Examples of Recent Studies Showing Proof of Concept of Retinal Gene Therapy Strategies Using (A) Selected Approaches Targeting a Specific Gene and (B) "Generic" Approaches That Could Potentially Be Used Regardless of the Disease-Causing

Genetic Defect[a]

A. Approaches Targeting a Specific Gene				
Human Gene	**Disease**	**Delivery**	**Target Species for Gene Therapy**	**Gene Therapy Strateg**
4-sulfatase	Mucopolysaccharidosis VI	SR	MPS VI cats	Augmentation
ABCA4	STGD1, CRD, RP (AR)	SR	Abcr$^{-/-}$ mice	Augmentation
AIPL1	LCA, RP, cone dystrophy	SR	Aipl1 hypomorphic mice; Aipl1$^{-/-}$	Augmentation
BBS-4	Bardet–Beidl RP	SR	Bbs-4$^{-/-}$ mice	Augmentation
CHM	Choroideremia	SR	NP	Augmentation
CNGA3	ACHM, CD	SR	Cnga3$^{-/-}$ mice	Augmentation
CNGB3	ACHM, CRD	SR	Cngb3$^{-/-}$ mice	Augmentation
GNAT2	ACHM	SR	Gnat2 (cpfl3) mice	Augmentation
GUCY2D	LCA	SR	GC1$^{-/-}$ mice; rd chick	Augmentation
IMPDH1	AD RP (RP10)	SR	Impdh1$^{-/-}$ mice	RNAi
L-opsin	Red–green color blindness (XL)	SR	Squirrel monkey (*Saimiri sciureus*)	Augmentation
LRAT	LCA, RP	SR	Lrat$^{-/-}$ mice	Augmentation
MERTK	LCA, RP	SR	RCS rat	Augmentation
MYO7A	Usher syndrome 1B (RP)	SR	Shaker1 mice (Myo7a-null)	Augmentation
ND4	Leber's hereditary optic neuropathy	Intravitreal	Mice, rats	Augmentation
TYR	Oculocutaneous albinism 1	SR	Tyr(c-2j) mice; Gpr143$^{-/-}$ mice	Augmentation
PDE6B	AR RP	SR	Rd1; rd10 mice	Augmentation; single-stranded oligonucleoti mediated repair
Peripherin/RDS	Macular dystrophy; AD RP	SR	Rds$^{-/-}$; rds$^{+/-}$; R172W tg mouse	Augmentation; knockdown using miR based hairpins
RHO	AD RP	SR	Rho$^{-/-}$; P367S, Pro23H mice	Augmentation, augmentation/suppres zinc finger-based transcriptional repress
RPE65	LCA, RP	SR	Rpe65$^{-/-}$ mice; RPE65$^{-/-}$ dogs	Augmentation

RPGRIP1	LCA, CRD	SR	Rpgrip$^{-/-}$ mice	Augmentation
RS1 (XL juvenile retinoschisis)	XL juvenile retinoschisis	IV, SR	Rs1$^{-/-}$ mice	Augmentation
VEGF (S-FLT)	Ret NV	SR; IV	Oxygen-induced retinopathy mouse; trVEGF029 mice; laser photocoagulation monkeys	VEGF decoy
Whirlin	Usher syndrome 2D (RP)	SR	Whirlin$^{-/-}$mouse	Augmentation
B. GENERIC GENE THERAPY APPROACHES				
BiP/Grp78 (ER localized chaperone)	AD RP	SR	P23H Rho rat	Antiapoptosis
BCL2	AR RP	SR	Rd1 mouse	Antiapoptosis
BDNF	Light damage	SR	Light-damaged rats	Antiapoptosis
bFGF	AD RP; AR RP	SR	S336ter Rho rat; RCS rat	Antiapoptosis
Channel rhodopsin-2 (ChRd)	AR RP	SR	Rd1, rd10, rd16 mice; RCS rats	Optogenetics
Catalase	Light damage	SR	Light-damaged mice	Antioxidant
CNTF	AR RP, AD RP; cancer-related retinopathy	SR; IV	Rds, rd	Antiapoptosis
Endostatin	Ocular NV	SR	Oxygen-induced retinopathy mouse	Antineovascular
EPO	AR RP	IM, IV, SR	Prph2/rds; rd10	Antiapoptosis
GDNF	AR RP; light damage	SR	Rds, rd double check	Antiapoptosis
Halorhodopsin	AR RP	SR	Cnga3$^{-/-}$/Rho$^{-/-}$; rd1 mice	Optogenetics
LiGluR light-gated ionotropic glutamate receptor	AR RP	IV	Rd1 mouse	Optogenetics
NXNL1 (Rod-derived cone viability factor)	AR RP	SR	Rd1 mouse	Antiapoptosis
PEDF	CNV	IV, P-O	Oxygen-induced retinopathy mouse; VEGF transgenic mice	Antineovascularizatio
Retinostat (angiostatin	CNV	SR	Laser photocoagulation	Antineovascular factor

and endostatin)			in mice	
TIMP3	Ocular NV	SR	Oxygen-induced retinopathy mouse	Antineovascular
XIAP	AD RP	SR	P23H and S336ter RHO transgenic rats	Antiapoptosis
Herpes simplex thymidine kinase (and ganciclovir)	Retinoblastoma	IV	Intravitreal injection of Y79Rb cells in immunodeficient mice	Suicide gene therapy

[a]This list highlights many of the recent studies aiming to treat animal models of retinal degeneration, retinal development anomalies, and retinal neovascularization. Several of these studies have been carried forward to human clinical trial, and those references are listed as well.

AAV, recombinant adeno-associated virus vector; ACHM, achromatopsia; AD, autosomal dominant; Adeno, recombinant adenovirus vector; AR, autosomal recessive; CD, cone dystrophy; CNV, choroidal neovascularization; CRD, cone–rod dystrophy; EIAV, equine infectious anemia virus; IM, intramuscular; IV, intravitreal; LCA, Leber congenital amaurosis; Lenti, recombinant lentivirus vector; MPS, mucopolysaccharidosis; NP, not published; NXNL1, nucleoredoxin-like 1; P-O, periocular; POD, peptide for ocular delivery; Ret NV, retinal neovascularization; RP, retinitis pigmentosa; SR, subretinal; STGD1, recessive Stargardt disease; VEGF, vascular endothelial growth factor; XL, X-linked: strategies aiming at treating glaucoma or optic nerve disease are not included.

The first recombinant adenovirus vectors, generated from the common respiratory virus, carried deletions in the adenoviral E1, E3 genes, and these Ad type 5 (Ad5) vectors were the first to be evaluated for retinal gene transfer in the differentiated retina.[5,6] Adenovirus vectors result in high levels of gene expression within 24–48 hours. When injected subretinally, they target retinal pigment epithelial (RPE) cells efficiently in the adult eye and also Müller cells.[5,6] When injected intravitreally, they target Müller cells and cells in the anterior segment, including corneal endothelium, lens and iris epithelium, and cells in the outflow tract (such as trabecular meshwork cells).[7] Similar results are found when recombinant adenovirus is injected into the undifferentiated (early postnatal) retina; however, in addition to RPE cells, progenitor cells are targeted in the neonatal mouse eye.[8,9] Additional manipulations of adenovirus vectors have yielded reagents that target photoreceptors more efficiently.[10–13]

A disadvantage of the early generations of E1, E3-deleted

adenovirus is that it still carries viral open reading frames. These can enhance its immunogenicity, even in the immune-privileged environment of the eye. This characteristic of adenoviral vectors has in fact been utilized to probe the nature of the intraocular immune response. When these vectors were injected subretinally, transgene expression persisted for several weeks to months. However, when injected intravitreally, transgene expression ceased within 2 weeks. Expression could be prolonged by incorporating immune-suppressant molecules, however.[14,15]

Adeno-associated virus (AAV) vectors do not carry any virus open reading frames (and thus encode any virus-specific proteins) and therefore are generally more favorable from an immunologic standpoint than adenovirus vectors (Table 36.1). There is abundant safety data related to AAV administration in animals and in humans, both systemically and intraocularly. Recombinant AAV (rAAV) vectors have an added benefit in that they target a more diverse set of cell types than adenoviral (or other) vectors. Unlike lentiviral vectors, AAV vectors do not integrate into host cell genomic DNA, or do so only rarely (Table 36.1). However, since the transgene persists in episomal fashion in the target retinal cells, rAAV vectors result in stable transgene expression. Expression persists for the life of small animals (mice and rats) and at least for many years in large animals and humans.[16–20] rAAV vectors are useful for delivering genes efficiently to many types of retinal cells. A major disadvantage of these vectors is their relatively limited cargo capacity (a maximum of 4.8 kb) (Table 36.1).

AAV vectors can be modified in several ways in order to optimize their behavior for specific gene therapy applications. In AAV vectors, the transgene cassette is bordered by the inverted terminal repeats (ITRs) from an AAV2 genome. The original AAV vectors were generated by packaging the transgene cassette ITRs into an AAV serotype 2 capsid and this resulted in "AAV2/2" vectors, i.e., ITRs of an AAV serotype 2 genome packaged into an AAV2 serotype 2 capsid. Often, investigators skip the reference to the ITR serotype and refer to the capsid serotype alone as will be done henceforth in this chapter (i.e., AAV2 vectors instead of AAV2/2 vectors.) More than a dozen AAVs of different serotypes have been described. Many cross-packaged AAVs differ

significantly from rAAV2 vectors with respect to cellular specificity, efficiency of transduction, and onset of transgene expression. While rAAV2 targets RPE cells efficiently (and photoreceptors less efficiently), it takes up to 6 weeks for transgene expression mediated by this vector to plateau.[21–23] In comparison, rAAV5 and rAAV8 vectors transduce photoreceptors with much higher efficiency and result in transgene expression within 5–10 days of delivery.[21,22] This information is helpful in selecting vectors for particular applications. For example, in a relatively slowly progressive retinal degenerative disease (Leber congenital amaurosis (LCA) due to *RPE65* mutations), rAAV2 performs well in delivering a therapeutic transgene to RPE cells. For an animal model with a much faster rate of degeneration (e.g., LCA due to *AIPL1* mutations[24,25]), it is necessary to use a vector with a much faster onset of expression and which targets photoreceptors efficiently (such as a rAAV5 or 8 vector; Table 36.2). Efforts have also been made to reengineer the virus by altering specific molecules in the capsid or by "directed evolution." The latter strategy screens large numbers of variants for desirable properties such as the ability to reach the outer nuclear layer from the vitreous or the ability to transduce specific cells (such as ON-bipolar cells).[26,27] More recently, two different groups have reconstructed ancestral AAVs as an approach to generate novel gene therapy vectors.[28,29]

Vectors originally based on the human immunodeficiency virus, lentiviral vectors, have been shown to be safe in animal models and their safety in humans is currently being tested (Table 36.2). A number of groups have since generated vectors based on viruses that were identified in nonhuman species, such as equine lentivirus.[30,31] Transgene expression is stable after lentiviral administration, because these vectors mediate integration into the host chromosome (Table 36.1). Lentiviral vectors target RPE cells efficiently after subretinal injection and, in undifferentiated retina, also target neural progenitor cells. They have thus been used to demonstrate efficacy in animal models of RPE disease, such as LCA-RPE65 or autosomal recessive (AR) retinitis pigmentosa (RP) due to *PDE6B* mutations[32] (Table 36.2). Lentiviral vectors are also attractive in that they can carry a relatively large cargo of up to 7.5

kb (Table 36.1). Specific modifications also allow lentiviral vectors to target mature photoreceptors.[23,33] Since lentiviral vectors are integrating vectors, there is a concern about the potential for insertional mutagenesis. To date there has been no report of such an effect after retinal administration in animal models.

Surgical Delivery

With the exception of the engineered AAV, AAV7m8, which penetrates the retina efficiently after intravitreal injection (at least in the mouse),[26] the currently available viral vectors used in retinal gene therapy have very limited ability to diffuse across tissue interfaces. While intravitreal administration by pars plana injection may be adequate to transduce cells of the inner retina and uveal tract, this simple technique is inadequate for treatment of the outer retina and RPE. In animals with anatomically large eyes such as canines and primates, viral vectors must come into direct contact with photoreceptor and RPE cells to result in successful transduction. In this case, gene therapy agents need to be delivered to the subretinal space.

There are several methods whereby subretinal delivery can be achieved. First, diffusion may potentially occur across the choriocapillaris and RPE layers after systemic administration. This has not been observed, however, and has several theoretical disadvantages, including the need for increased dosing due to larger volumes of distribution, as well as exposure of nontarget tissues to immunogenic and potentially toxic viral vectors or transgene products. Delivery to the subretinal space can be achieved using a transchoroidal approach. This requires manipulations through the choriocapillaris layer which lacks the diffusion barrier present in retinal vasculature. Presence of immunogenic material in this area may be undesirable due to increased exposure to the systemic vasculature. In addition, visualization of the injection procedure is problematic using this surgical approach since it is often difficult to monitor the position of the injection apparatus through several intervening tissue layers.

Most investigators have employed a transvitreal, transretinal approach to subretinal injection in large-animal eyes. This approach

has several practical and theoretical advantages. First, there is a wealth of experience with three-port pars plana vitrectomy for human retinal surgery. This approach allows direct visualization of the retina throughout the procedure and real-time monitoring of the injection. The instrumentation for subretinal injection is easily available having been developed for other subretinal applications. Additional maneuvers such as fluid–gas exchange and laserpexy can be employed with the pars plana approach in order to manipulate the subretinal bleb or to manage potential complications.

When a subretinal injection is performed through a small retinotomy, a retinal detachment or "bleb" is raised (Fig. 36.1). Most if not all of the volume of injected material is trapped between the outer retina and RPE as a localized retinal detachment. There is negligible escape of material back through the retinotomy site into the vitreous, as evidenced by the fact that, initially, the size of the bleb does not change once it is formed. There is apparently little pressure differential between the subretinal space and vitreous once the bleb is established and this is especially so when the scleral incisions are closed. In addition, the small-gauge cannulas used for the subretinal injection appear to be self-sealing, especially when a gas tamponade or formed vitreous is present. Since a bleb raised by subretinal injection tends not to expand beyond the border of the initial injection, the volume of distribution of the administered agent is limited, especially when compared to an intravitreal injection or systemic administration. The concentration of the compound contained in the bleb remains high and may even increase as the RPE cells extract free water from the vehicle used to dilute the agent. Limiting the volume of distribution in this manner may serve both to increase the efficiency of drug delivery and to decrease local and systemic toxicities by restricting diffusion of the drug. The location of the original subretinal detachment cannot be appreciated in most species (including humans) after it has flattened, though occasionally the most dependent border of a bleb is later outlined by pigment fallout.[18,34] (The location of a bleb raised in the tapetal retina of dogs is often visible years after the injection, however, because of alterations in reflectivity of the underlying tapetum due to the procedure; see Fig. 36.1.)

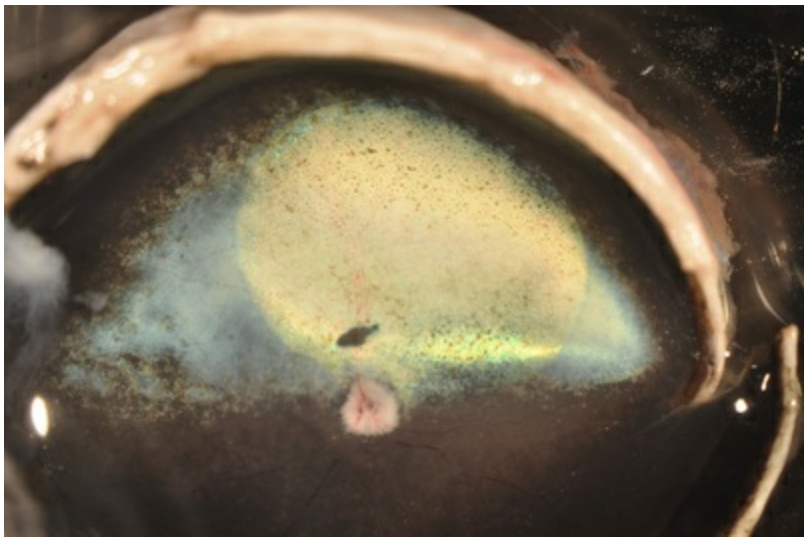

FIG. 36.1 Subretinal injection of gene therapy vector results in a “bleb,” the position of which is often visible in the dog retina years after the injection has occurred, due to alterations in the reflective properties of the underlying tapetum. Such changes are not observed in the human retina.

Since the RPE and Bruch's membrane are typically not violated when subretinal injection is performed by the pars plana approach, there is further protection against systemic exposure of antigens via the highly vascular choroidal circulation. In addition, there is minimal disruption of retinal vasculature since the placement of the injection cannula is done under direct visualization. Therefore, the integrity of the blood–ocular barrier remains intact when subretinal delivery is performed in this manner. There is in addition an immunologic compartmentalization when antigenic material is delivered to the subretinal space. Limiting exposure to this area may result not only in characteristic immunoprivileged behavior evident with intraocular delivery but, when delivery is confined to the subretinal space, antigenic tolerance can be induced due to immune-deviant response.[35,36] This unique property of the subretinal space is of great significance in the delivery of biologics and in gene therapy in particular as the development of antibody/immune response to both viral antigens and foreign transgene products may limit the effectiveness of treatment.

While several methods for subretinal injection of gene therapy agents have been described in human clinical trials, the basic elements of the procedure are similar. All surgical maneuvers are

done using standard three-port pars plana vitrectomy techniques and instrumentation. In all instances, a core vitrectomy is performed and subretinal injection is delivered using a small-gauge cannula. Spontaneous resorption of the subretinal bleb is allowed to occur without the need for laser or tamponade for posterior retinotomy sites.

The major differences in surgical methods between various investigators who have carried out gene transfer in humans so far[15,18,34,37–39] involve (1) use of perioperative systemic corticosteroid therapy; (2) the removal of posterior cortical vitreous prior to subretinal injection; and (3) placement of a gas (air) bubble after the injection is performed. With regard to systemic corticosteroid use, there appears to be no important difference in efficacy. It should be noted that all studies employ the use of topical and periocular corticosteroid to suppress surgical inflammation.

The surgical protocols for the phase I/II and III Children's Hospital of Philadelphia (CHOP) gene therapy trial for LCA2 and the phase I University of Pennsylvania (UPenn)/CHOP trial for choroideremia specify removal of the posterior hyaloid.[18,34] In many instances, a complete posterior vitreous detachment (PVD) is already present despite the young age of the subjects enrolled in the LCA2 trial. This is not unexpected as vitreous abnormalities, including the presence of debris or posterior separation, are characteristic features of eyes with retinal degeneration. In cases without PVD, the posterior cortical vitreous is engaged with active suction and the hyaloid face is gently separated to create a complete PVD, as evidenced by the presence of a glial ring separating from the optic nerve head (Weiss ring). Once the presence of a PVD is confirmed, the mobilized vitreous is removed as completely as possible, with special attention to pare back any gel in the vicinity of the active sclerotomy sites. This is done both to avoid vitreoretinal traction induced by instruments passing into and out of the eye, and also to prevent vitreous traction which can bend the tip of the 39-gauge (and smaller) subretinal injection cannula. Most investigators recommend the removal of epiretinal membrane (ERM) if present in the macular area in order to prevent interference with the injection cannula and to avoid late-occurring complications such as macular hole resulting from membrane

contraction.

Prior to subretinal injection, the infusion pressure is reduced in order to accommodate the additional intraocular volume added by the injection. Removal of vitreous gel from the vicinity of the infusion cannula allows reflux of infusate during the injection, though a small amount of fluid may escape around the active instruments at the other sclerotomy sites.

When directing the injection into the posterior pole or macula, the cannula tip is usually placed in the vicinity of the papillomacular bundle. Even in eyes with advanced retinal degeneration, the retina in this area is usually thick enough to allow for successful placement of the cannula tip and the injection into the subretinal space. The cannula tip is positioned so as to avoid direct injury to retinal arterioles. The UPenn/CHOP protocols specify that the site of injection be a minimum of 3 mm from the foveal center in order to avoid development of a foveal dehiscence from fluid tracking directly to the central macula in a fistula-like manner. In addition, a small bubble of perfluoro-octane liquid is placed over the fovea to counteract the hydrodynamic force created during the subretinal injection in the CHOP LCA2 trial, thereby buttressing this anatomically vulnerable area (Fig. 36.2; Video 36.1 online). In contrast, injection directly under the fovea is clearly necessary to treat diseases such as choroideremia (CHM) where the remaining viable tissue is in the central macular area. Typically, an area at the border of atrophic and intact retina is chosen as the entry site for the subretinal cannula.

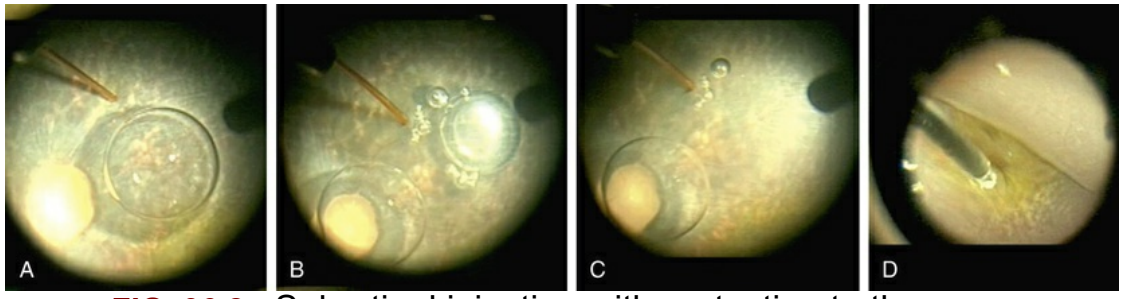

FIG. 36.2 Subretinal injection with protection to the fovea. (A) Subretinal injection cannula is apposed to the retina. Perfluoron had already been layered over the fovea. (B) The injection was initiated. A few small bubbles were expressed initially from the cannula (and

are in the subretinal space). (C) The bleb has expanded. (D) The cannula has been removed and the Perfluoron is being removed. The inferior border of the bleb is visible. (See Video 36.1 online, showing subretinal injection of AAV2-hRPE65v2 in a human.[34])

The subretinal injection is performed in two steps. First, the cannula is positioned so as to indent the retina over the tip. When the cannula is inserted near a blood vessel, the vessel can be used as a landmark to visualize the tip as it passes underneath. Blanching of the choroid is sometimes observed as the retina is imbricated by the cannula. This indicates significant downward force being exerted on the RPE and the need to avoid further advancement of the cannula tip. At this point, the surgeon directs the assistant to inject a small amount of the gene therapy agent. If a small bleb is raised during the test injection, the remainder of the material is injected. If no bleb is created during the test injection, the cannula tip is repositioned and the sequence is repeated until a bleb is created. If a volume of 0.15 mL or more is placed in the subretinal space near the macula, a smooth-domed retinal detachment is created which typically encompasses the temporal posterior pole extending just beyond the major vascular arcades. As mentioned above, the injection site is self-sealing and reflux of the injected material is not observed.

The retina is inspected with indirect ophthalmoscopy. Any retinal breaks identified are treated with retinopexy prior to fluid–air exchange. If bleeding is seen at the injection site, intraocular pressure is raised with closed sclerotomy sites until hemostasis is achieved.

The CHOP/UPenn protocols specify that fluid–air exchange is performed, carefully avoiding draining through the retinotomy created for the subretinal injection. Air exchange is principally done to compartmentalize the subretinal injection so that the vector does not come into contact with anterior uveal structures and remains central to the area of the retina-RPE. A 55% exchange is adequate for this purpose. In cases where it is desirable to change the position of the bleb, a more complete air exchange can be performed. The subretinal fluid in the bleb then migrates in a gravity-assisted fashion to settle in the most dependent region of

retina. Head positioning is instituted in the postoperative period to orient the eye such that the desired area of retina-RPE treatment is placed in the most dependent position. A complete air exchange also serves to tamponade the posterior retinotomy site if any reflux of the subretinal injection is observed.

One unique feature of subretinal injection in retinal gene therapy when compared to other surgical indications is that the subretinal fluid, i.e., gene therapy agent, is not evacuated and the retina flattened at the time of fluid–air exchange. This is done in order to maximize the time of exposure to the subretinal injection, something that is not necessary, for example, after the extraction of a subretinal hemorrhage or translocation of the macula. Indeed, the creation of retinal detachment by subretinal injection is of itself a concern with respect to possible retinal toxicity. Fortunately, the extent of injury after acute retinal detachment created by injection of physiologic solutions appears to be small based on both laboratory and clinical data. Resorption of volumes less than 0.45 mL typically occurs in less than 24 hours.[15–18,34,40,41] In the CHOP trial, resorption of 0.3 mL of fluid was observed within 6 hours of injection. Bainbridge et al.[37] reported a longer period of detachment >24 hours after subretinal injection using a two-step injection technique where vector was administered into a bleb raised first with a physiologic solution. The longer period required for reattachment is likely due to the large volume of injection, i.e., 1.0 mL.[37]

Development of macular hole is a complication that appears to be unique to the subretinal injection procedure. Although creation of macular hole has been described in subretinal surgery for choroidal neovascularization (CNV), this typically occurs as a CNV is extracted in the presence of an adhesion to the overlying retina. In the phase I CHOP trial for LCA2, macular hole developed in one patient not during the surgical manipulation but rather several days postoperatively. Although ultimately the ophthalmoscopic appearance of the defect was typical for an idiopathic macular hole, several key differences were noted. First, prior to the development of a full-thickness defect, inner lamellar thinning was demonstrated on optical coherence tomography.[18] In addition, intraretinal edema or cystoid macular edema was never present either during

evolution of the hole or after hole formation. Finally, a subretinal fluid cuff was never apparent before or after hole formation. In the absence of inflammation, vasculopathy, or acute tissue injury, it was felt that the macular hole was unlikely to have been caused by drug toxicity. The appearance of the lamellar defect was reminiscent of pseudohole caused by ERM contracture. Since the ERM was recognized preoperatively and the posterior cortical vitreous was removed at surgery, it was thought that surgery-induced contraction of the pre-existing ERM was the most likely cause of macular hole formation. A second patient was observed to develop a foveal dehiscence at the time of subretinal injection as fluid channeled directly from the cannula through the fovea through a fistula-like tract.[34] This phenomenon has been observed to occur infrequently during subretinal injection in nonhuman primates.[42] Occurrence of a foveal dehiscence is presumably induced by intense hydrodynamic stress from injection in the vicinity of the fovea. No ERM was present in this case. Air tamponade with face-down positioning resulted in complete resolution of this induced hole within days. Since instituting a protocol modification specifying a minimum distance from the fovea for injection and use of perfluorocarbon liquid prior to injection, intraoperative foveal dehiscence has not occurred. In addition, foveal complications were not reported in CHM patients who received subretinal injection in the macular center.[43] This latter finding suggests that the foveal changes that can occur after creating a subretinal bleb may in fact be disease-specific and less likely to occur when the remaining tissue is relatively normal in thickness.[34]

History of Retinal Gene Therapy

Preclinical Studies: Retinal Transduction Characteristics of Different Vectors

Initial gene transfer studies in animals generally evaluated the safety and stability of delivery of "reporter genes," genes whose activity in terms of protein products can be evaluated noninvasively or in tissue samples through either

histochemical/immunohistochemical measures or through a bioassay. A popular reporter gene encodes enhanced green fluorescent protein (EGFP), a bioluminescent, intracellular protein normally produced by the jellyfish *Aequorea victoria*. EGFP's absorption/fluorescence characteristics are very similar to those of fluorescein, which is used in the clinic to measure blood vessel integrity in the eye. Thus, EGFP can be measured using the same instruments/optics that are used in the clinic to measure fluorescein (Fig. 36.3). The only difference is that fluorescence with EGFP is not transient (as in the case with fluorescein angiography) as intracellular EGFP does not wash out with time.

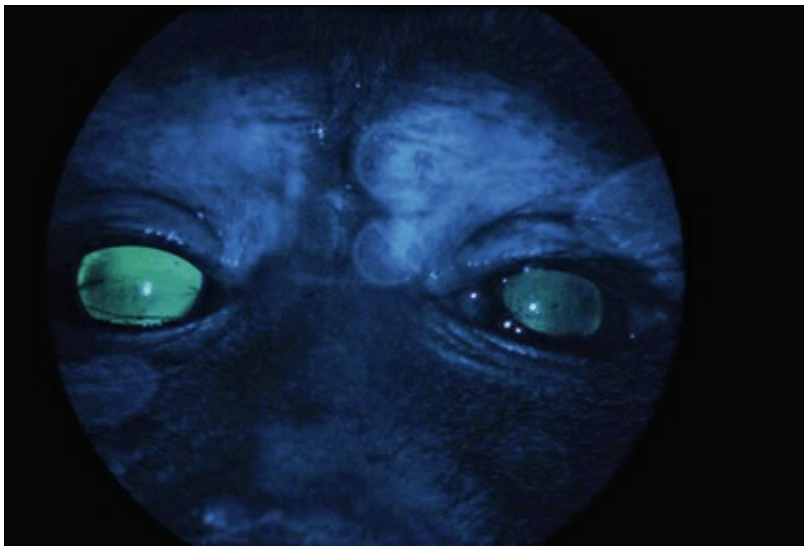

FIG. 36.3 Green fluorescent protein (GFP) is visible through illumination with blue light with an ophthalmoscope in this nonhuman primate that had received subretinal injection of 1E11 vector genomes (vg) AAV2/8.CMV.EGFP in its right eye. The left eye had received subretinal injection of the same material but with a dose that was 2 log units lower than the right eye.[44]

Evaluation of Different Vectors

Numerous studies in small and large animals have relied on vector-mediated delivery of reporter genes to elucidate the characteristics of one vector versus another.[21–23,44] The transduction characteristics

are affected by dose and age (or stage of development) of the animal. In the fetal mouse, one can deliver vector to retinal progenitor cells and carry out "birthday studies" by looking later in adulthood at which types of photoreceptor cells were being "born" at the time of injection.[45,46] This led to an approach that reversed blindness in utero in LCA-rpe65 mice.[47]

The majority of studies published to date involve postnatal delivery. Transduction characteristics are dependent on the surgical approach and the dose. Intravitreal injection of particular recombinant viruses can lead to transduction of ganglion cells and/or Müller glia. For example, intravitreal injection of AAV2 leads to ganglion cell transduction (and expression in the optic nerve, optic chiasms, and brain) in species ranging from mouse to dog to human, whereas intravitreal injection of AAV5 does not.[48,49] Except for AAV7m8, intravitreal injection of recombinant viral vectors does not usually result in transduction of the photoreceptors in the outer retina or the RPE (Table 36.1).[7,16,17,22,26]

Most vectors target RPE cells efficiently even at low dose (Table 36.1). As the dose is increased and depending on the vector, photoreceptors and Müller cells can also be transduced (Fig. 36.4).[44] Cellular transduction characteristics can also differ from species to species. A very active area of research continues to involve engineering of AAV capsids in order to expand their cargo capacity and enhance their transduction properties.[23,50,51]

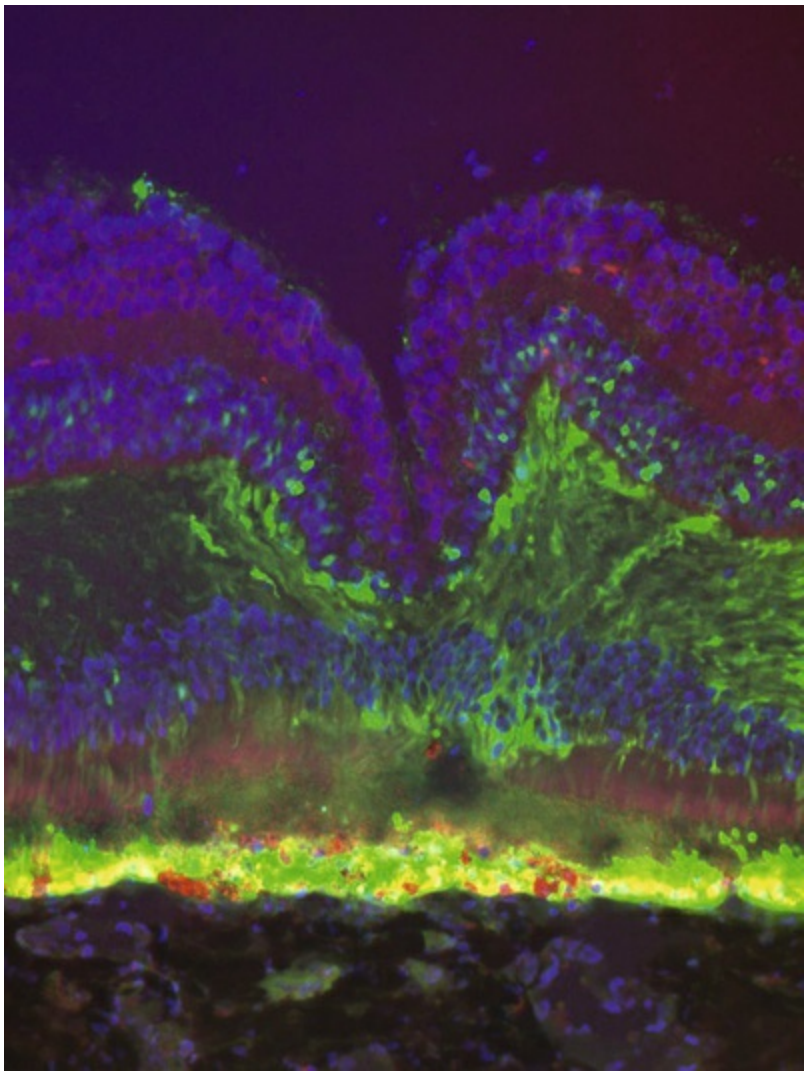

FIG. 36.4 Histologic section from a monkey injected subretinally in the macula with 1E11 vg AAV2.CMV.EGFP. This shows very strong enhanced green fluorescent protein (EGFP) expression in retinal pigment epithelium cells and also (lesser) expression in photoreceptors (including inner-segment, outer nuclear layer, and outer plexiform layers). There are also occasional inner retinal cells which express EGFP. Nuclei are labeled blue and background fluorescence is shown with red.

Proof-of-Concept Studies

With progress in delineating the molecular genetic bases of inherited retinal degenerations in humans and in animals and the development of recombinant viral vectors with which to deliver

transgenes to different retinal cell types, the logical next step is to determine how this information can be used to correct the diseases. Gene augmentation strategies, whereby a wild-type copy of a gene is delivered, have been tested successfully now in animal models of more than a dozen different conditions (Table 36.2). The animal model conditions have included AR RP, autosomal dominant (AD) RP, LCA, cone–rod dystrophy, macular dystrophy, oculocutaneous albinism, Leber hereditary optic neuropathy (LHON), X-linked retinoschisis (XLRS), mucopolysaccharidosis VI, AR Stargardt disease, choroideremia, and RP found in syndromes such as Bardet–Biedl and Usher syndrome (Table 36.2).[3,8,14,16,17,24,25,32,33,30,52–89] Gene augmentation therapy has also been used to restore function to a nonhuman primate model of red–green color blindness (Table 36.2).[90] There are a number of details that affect the success of retinal gene augmentation, including selection of the appropriate vector (see above), and when and where to deliver the vectors. The outcome measures used in the various studies include physiologic assays such as electroretinograms (ERGs), evaluations of pupillary light reflexes and optokinetic responses, visual behavior (ability to swim through a water maze or to select light or dark areas and, in the monkey model of color blindness, to identify specific colors),[90] and histology (including immunohistochemical demonstration of expression of the appropriate transgenic protein).

There has also been success with strategies aimed at rescuing disease due to toxic gain-of-function mutations.[91–99] Such strategies are necessarily more complex than gene augmentation strategies. The best-studied examples of intervention with gain-of-function gene defects include rhodopsin mutations found in AD RP. Such defects result in abnormal cellular trafficking as well as altered functional properties. Deleterious effects of the endogenous mutant genes can be minimized by a knockdown or knockdown/gene augmentation strategy. The mutant messenger ribonucleic acid (mRNA) can be specifically targeted, leaving the wild-type mRNA (either endogenous or delivered via gene augmentation) intact. Knockdown has been achieved successfully by using ribozymes, RNA interference (RNAi), delivery of microRNAs, and use of zinc finger nucleases (Table 36.2 part A).

Gene therapy strategies have also been used successfully to target

specific genes/proteins which may not be the primary cause of disease, but which are known to be involved in downstream pathways. An example involves manipulation of the vascular endothelial growth factor (VEGF) pathway implicated in ocular neovascularization (Table 36.2 part A).

Several groups have evaluated the possibility of ameliorating neovascularization by delivery of a gene that encodes a soluble decoy VEGF receptor, s-FLT.[100–105] Such an approach has been used successfully in animal models of both retinal and CNV. These studies led to two different phase I human clinical trials to test the safety and efficacy of intraocular delivery of an AAV2-sFLT vector in humans with CNV (Table 36.2 part A).

There are gene therapy strategies that can be used that are not specific to the disease-causing gene and could potentially be applied to a diverse set of conditions. One approach that has been used to evaluate development of a "generic" strategy with which to treat RP has been to use growth or neurotrophic factors or hormones to maintain the health of the diseased photoreceptors (Table 36.2 part B). Because growth factor proteins have very short half-lives (some as short as seconds), generation of a constant supply through a gene therapy approach is attractive. A growth factor could potentially be used to maintain the health of these cells until a disease-specific vector can be developed. Alternatively, such factors could be delivered as part of a cocktail.[106] An additional set of factors that has attracted interest in recent years consists of molecules that could protect against oxidative stress. Protection using a variety of different growth factors has been tested through direct viral gene transfer in animal models, including brain-derived neurotrophic factor, basic fibroblast growth factor, ciliary neurotrophic factor (CNTF), glial cell-derived neurotrophic factor, pigment epithelium-derived factor (PEDF), and X-linked inhibitor of apoptosis (Table 36.2 part B).[4,106–122] The majority of these have ameliorated structure and function, although CNTF, while ameliorating structure, has been shown to diminish retinal function at high doses in some animal models.[114,117,123] Sustained delivery of CNTF through use of a device that encapsulates CNTF-transfected cells (encapsulated cell therapy) has resulted in structural improvement without adverse functional effects (and in some cases,

improvement in function), both in animals and in humans (Table 36.2 part B).[112,124–129] The encapsulated cell therapy approach entails placement of a capsule containing a grid occupied by cells, transfected with a CNTF-encoding plasmid, into the vitreous. Another neurotrophic factor that has attracted great interest due to data showing that it rescues cone photoreceptors in animal models is rod-derived neurotrophic factor (RdCVF, whose gene is known as *NXNL1*).[130] Alternative splicing of *NXNL1* results in two isoforms of RdCVF, and the two isoforms appear to have distinct protective properties. This long isoform appears to protect against hyperoxia and the short form appears to protect cones from degeneration through stimulation of aerobic glycolysis.[131,132] Evaluation of the results in all of these growth/neurotrophic factor therapies reveals that, with the majority of these factors, efficacy is dependent on them being expressed in/by the retina. Interestingly, there is a hormone, erythropoietin, that can also delay retinal degeneration in certain animal models through gene therapy-mediated delivery, but this is only effective if it is delivered outside the eye (intramuscularly: Table 36.2 part B).[110] Finally, there are a number of factors that appear to reduce reactive oxygen and resultant oxidative stress and these are also "generic" candidates for therapy of retinal degeneration. Such factors include the transcription factors NRF2 and PGC1a, which regulate a network of genes involved in oxidative stress pathways, and superoxide dismutase 2 (SOD2) or catalase, enzymes which break down oxidants.[111]

Approaches using a generic gene therapy strategy to bring vision to retinas in which photoreceptor cells have been lost or severely damaged are also under investigation. These involve delivering light-sensitive channels, originally isolated from single-celled organisms, to either inner retinal neurons or remaining diseased cone photoreceptors. The gene encoding channel rhodopsin-2 (*ChRd*), originally identified in the algae *Chlamydomonas reinhardtii*, has been delivered to either bipolar cells or ganglion cells; Halorhodopsin (*NpHR*), originally identified in halobacteria, has been delivered to diseased cone photoreceptors (Table 36.2 part B). Unlike mammalian opsins, however, these light-activated proteins directly form ion channels that polarize (*NpHR*) or depolarize (*ChRd*) upon photostimulation in a single molecule. Other groups

have developed synthetic optogenetic molecules, including a light-gated excitatory mammalian ion channel light-gated ionotropic glutamate receptor (LiGluR). A second generation of the LiGluR receptor was recently tested in both mice and dogs.. With all of these molecules, optogenetic gene therapy rendered animals that were previously insensitive to light responsive to light as judged by retinal/visual behavior.[51,133–138]

Current Status of Retinal Gene Therapy Trials: Retinal Diseases Evaluated in Human Clinical Trials

Studies That Were Completed, but Discontinued

Retinoblastoma

Gene therapy has been used for treating tumor cells in the eye with the ultimate goal of avoiding the need to perform enucleation (and then chemotherapy and radiation therapy) in young children. If gene therapy were used to reduce the tumor burden, this would allow more control. Such an approach could potentially spare the patient disfigurement and loss of vision. Hurwitz and colleagues transduced murine retinoblastomas in vivo with an adenoviral vector containing the herpes simplex thymidine kinase gene followed by treatment with the prodrug ganciclovir (Table 36.2 part B).[139,140] This resulted in a complete ablation of detectable tumors in 70% of animals and a significant prolongation of progression-free survival compared with untreated controls. The study proceeded to clinical trial: seven patients had resolution of their vitreous tumors and one patient remained free of active vitreous tumors 38 months after therapy.[139,141]

CNV Using AdPEDF

Campochiaro and colleagues[142] carried out a phase I clinical trial in individuals with advanced neovascular age-related macular degeneration (AMD). In this dose escalation study, a serotype 5

(Ad5), E1, partial E3-, E4-deleted adenoviral vector carrying human *PEDF* (AdPEDF.11) was injected intravitreally into one eye of each of 28 individuals (Table 36.2 part B). PEDF is an endogenous protein with potent antiangiogenic activity. It also has antiapoptotic activity. There were no serious adverse events or dose-limiting toxicities through the highest dose. There was evidence that injection of doses greater than 10E8 particle units of AdPEDF.11 resulted in antiangiogenic activity persisting for several months.

Encapsulated Cell Therapy

Results of a phase I study of delivery of CNTF through encapsulated cell therapy (see above) were reported by Sieving et al.[129] in 10 subjects with retinal degeneration. The implants were removed after 6 months. The delivery was safe save for one surgically related choroidal detachment. Three of the individuals showed improved visual acuity. A phase II study followed and results showed the outer retinal layers were thicker in CNTF-treated eye, and cone spacing and density increased as judged with adaptive optics scanning laser ophthalmoscopy.[128] The results of a multicenter, dose-ranging phase II study followed selected subjects with geographic atrophy and the results indicated that the implant slowed the progression of vision loss.[125] In a recent study individuals with achromatopsia due to *CNGB3* mutations were tested for efficacy of CNTF-encapsulated cell therapy after promising results were found in CNGB3 mutant dogs.[126] Although the subjects reported beneficial changes of visual function in the treated eyes, no objectively measurable enhancement of cone function was found.[127]

Studies in Progress

Gene Augmentation Therapy for Leber Congenital Amaurosis

Three different clinical trials involving gene augmentation therapy for LCA due to *RPE65* mutations were initiated near simultaneously in 2007. The disease in LCA-RPE65 is due to lack of a function of RPE 65 kDa (RPE65) protein in the RPE. RPE65 is an isomerohydrolase and breaks down retinyl ester, thereby allowing

production of 11-*cis* retinal, the chromophore which contributes to the visual pigment rhodopsin.[143] Each of the three studies used an AAV serotype 2 vector delivering the wild-type human *RPE65* cDNA subretinally to the RPE in one eye, but the studies differed in terms of dose, inclusion criteria, type of promoter, location of injection, and outcome measures. The early reports from all three trials revealed a high degree of safety and demonstrated efficacy as judged by increase in light sensitivity, improved visual acuity and visual fields, improved pupillary light reflex, and improved mobility.[18,37,144]

The entire set of results of the phase I/II study were reported from the group at CHOP and indicated that not only was the AAV delivery safe, but also each one of the 12 clinical trial subjects, ages 8–45 years, showed evidence of improved retinal and visual function as judged by any of several different test paradigms.[34] The children in the study showed particularly large improvements, now being able to read books and play sports.[15] The older individuals also showed evidence of gain in function but not surprisingly (since this is a degenerative disease), had worse vision outcomes compared to the younger cohort. A follow-on study reported the results of readministration of the AAV to the contralateral eye in the first three subjects. There was no inflammation and there were no safety concerns with readministration and there was evidence of benefit.[145] The safety and efficacy data from these phase I/II studies prompted initiation of a phase III clinical trial at CHOP. Enrollment has been completed in this phase III study and the initial results show robust improvement in the primary endpoint (a multi-luminance mobility test) as well as secondary endpoints (http://ir.sparktx.com/phoenix.zhtml?c=253900&p=irol-newsArticle&ID=2211949). The full set of results will be reviewed by the Food and Drug Administration (FDA) in 2017. This could potentially lead to the first approved gene therapy in the United States and the first approved gene therapy for retinal disease in the entire world.

The set of results from a second phase I (single eye) study were recently reported and were complementary yet did not describe any age-related effects of treatment.[146] The authors also described retinal sensitivity testing in 3 of the 16 subjects and showed

significant benefit of retinal and visual function, but the authors believe there is in focal retinal sensitivity in the injected areas of the retina, although sensitivity was still significantly higher than it was at baseline.[147] The set of results from the third phase I (single eye) study initiated in 2007 were published in 2015, and the authors concluded that it will be important in the future to use more efficient delivery of RPE65 at an early stage of the disease.[148]

Two other clinical trials for LCA-RPE65 were initiated several years ago (www.clinicaltrials.gov) but neither has provided results (except for one report from one patient).[15]

CNV and AAV-sFLT

Wet AMD is currently under consideration as a target for development of gene therapy. In this disease people can go blind overnight due to leakage in blood vessels. Anti-VEGF therapies have been shown to be effective for the treatment of neovascular AMD. The downside of anti-VEGF therapies is that they must be readministered frequently, with the result that doctors are overburdened and patients must return frequently to receive intravitreal injections. There is a clear need for long-lasting production of a VEGF decoy in the eye – a stable product that could be delivered through a one-time injection. A strategy with which to interfere with proangiogenic activities of VEGF involves intravitreal delivery of an AAV-carrying soluble VEGF receptor (sFLT). This strategy is currently being tested in two different dose escalation studies in individuals with AMD (Table 36.2 part A). Recent results of one of the phase IIa studies (run by Avalanche Biotechnologies) indicated that the test compound, AVA-101, met its 12-month primary endpoint, based on ophthalmic and systemic safety. AVA-101 also showed an improvement on best corrected visual acuity (BCVA) compared with the control group and a positive trend in response rate (stable vision with few rescue injections; http://investors.avalanchebiotech.com/).

CNV and Lentivirus-Mediated Delivery of Angiostatin and Endostatin

Another strategy that is being tested in clinical trial for wet AMD is

subretinal delivery of RetinoStat, a lentiviral vector delivering angiostatin and endostatin.[30,149] Both angiostatin and endostatin have strong and well-documented antineovascularization effects.

Gene Augmentation Therapy for X-Linked Juvenile Retinoschisis (XLRS)

Mutations in the *RS1* gene cause abnormal function of the retina protein, retinoschisin. A lack of retinoschisin causes the layers of the retina to split apart, resulting in the loss of vision. Studies in rodent models have shown that delivery of the normal copy of the *RS1* cDNA can improve retinal structure and function.[82–85] A clinical trial evaluating safety and efficacy of intravitreal delivery of AAV2.RS1 in adults with XLRS is in progress at the National Eye Institute, National Institutes of Health, USA.

Gene Augmentation Therapy for Choroideremia (CHM)

Two different phase I/II trials are underway to test safety and efficacy of subretinally delivered AAV2 carrying the wild-type human *CHM* cDNA. Both studies enroll affected men, aged 18 years and older (www.clinicaltrials.gov). The ultimate goals of a CHM gene augmentation trial are different than those of an LCA2 trial. CHM have fairly good vision early in life whereas individuals with LCA2 do not. Retinal degeneration proceeds in CHM in a peripheral-to-central fashion, leaving few viable cells in the periphery late in the disease. Central vision is the last to remain intact. Gene augmentation therapy requires that viable cells be present (even if dysfunctional) in order of having a chance of benefitting, and so there is little hope that peripheral vision can be rescued late in the course of CHM. The goal in CHM is thus to preserve central vision (and to halt further progression of the disease). Ultimately, it may be possible to treat the entire retina of a boy affected with CHM and prevent any disease symptoms.

Gene Augmentation Therapy for Leber Hereditary Optic Neuropathy (LHON)

Two different phase I/II trials are underway and one additional trial is planned to test safety and efficacy of intravitreally injected AAV2

carrying a synthetic nuclear DNA encoding one of the three NADH dehydrogenase mitochondrial genes implicated in LHON, the *ND4* gene. LHON is caused by mitochondrial defects in retinal ganglion cells, which are efficiently transduced through intravitreal injection of AAV2. A challenge inherent with mitochondrial disorders, such as those implicated in LHON, is that the mitochondrial DNA encodes proteins localized to this organelle. Since viruses deliver genes to the cell's nucleus, a challenge is how to intervene to target the gene/protein to the mitochondria. One solution is to deliver the corrective gene to the nucleus, but to tag it with a mitochondrial targeting sequence, a signal that guides the cell to shuttle proteins into the mitochondrion. This approach was used to develop proof-of-concept data to support clinical trials run by two different groups targeting the G11778A ND4 mutation.[150,151] Interestingly, the rodent models were generated by injecting either DNA (followed by electroporation) or AAV encoding the mutant G11788A human *ND4* cDNA.[150,151] A second injection allowed the allotopically expressed wild-type ND4 to ameliorate the phenotype induced by the G11778A mitochondrial DNA. A third group, directed by Dr. G. Farrar, generated the disease model by giving animals a drug that inhibits Complex I proteins normally encoded by mitochondrial DNA.[152] This team tested a novel strategy for intervening with LHON by delivering a gene from yeast, *ND11,* which encodes a protein that functions similarly as mammalian Complex I. The therapeutic protein compensated for the dysfunctional Complex I in the rodent mitochondria.[152] Whether the synthetic mitochondrial targeting sequence or the yeast-derived protein may result in a harmful immune response in the primate retina is unknown. Additional challenges include the fact that most affected individuals are initially unaware that they are affected until they experience loss of vision in the first eye and it is difficult to predict when there will be vision loss in the second eye, although the delay is usually only a few months. Thus, one of the current goals of LHON gene therapy is to develop a rational strategy to prevent vision loss in the second eye after symptoms initially manifest in the first eye.

Promises and Challenges of Bringing Retinal Gene Transfer From Bench to Bedside

Safety/Efficacy/Stability Issues

Numerous studies have been carried out showing that retinal gene transfer can be both safe and effective. The successes of the first human gene augmentation therapy studies involving LCA-RPE65,[15,18,34,37,144,145,147,148,153] provide the foundation for gene therapy approaches for the treatment of other forms of inherited retinal degenerative diseases. LCA-RPE65 may well be the easiest target for study as it is slowly progressive, is caused by a gene whose cDNA fits within the limited AAV cargo capacity, and is caused by a defect in RPE cells. The latter are easy to target using AAV vectors. In predicting what other disease(s) could be targeted using a similar approach, one confronts the following challenges:

1. Not all transgene cassettes fit within the cargo confines of the AAV vector (Table 36.1). Studies in progress aim to modify AAV capsids so that they can carry larger cargo or, alternatively, deliver different portions of large transgenes in multiple AAVs so that, after infection has taken place, the cargo recombines in the target cell and leads to the production of a full-length therapeutic protein. Alternative strategies to packaging large transgene cassettes into rAAVs include delivery of a cDNA encoding a truncated but functional protein, or delivering the cDNA in segments through a "trans-splicing" approach. For the latter approach, the cDNA is split into two separate rAAV vectors using an engineered intron to mediate splicing of the two cDNA segments within the cell. Feasibility of this approach has been demonstrated in vivo in the mouse retina.[154] With new gene editing techniques using CRISPR/CAS, it may also be possible to correct the specific source of the disease.[155] There are concerns with this approach, however, about potential "off-target" effects[156] that could lead to additional malfunction or even oncogenesis.

2. Photoreceptors – not RPE cells – are the primarily diseased cells

in many retinal degenerative diseases and those cells are not targeted as efficiently by AAV2 or by most forms of lentivirus (Table 36.1). Fortunately, a number of hybrid vectors are now available that can target these cells efficiently and this work continues (Fig. 36.4; see above). Further, some of them result in transgene expression using 10-fold less vector than AAV2.[44] Additional modifications of capsids, envelopes, and surface proteins will continue to provide improved toolkits with which to deliver these large genes efficiently to photoreceptors and other retinal cell types.

3. Some diseases progress very quickly and there will be challenges making sure that the gene is delivered before the cells have died. In some cases (such as in diseases that involve mutation in a gene expressed early in development), the optimal result will likely require delivery early in infancy, or even prenatally. In those cases, besides the need to identify the disease early in life, there will be difficult ethical issues to consider, in addition to risk-to-benefit ratios.

4. There are formidable economic challenges. For many of the potential disease targets, very few patients have been identified. Even though the cost of carrying out genotyping has decreased considerably over the years, it is still expensive. It would be possible to establish widespread genetic screening programs to identify the disease-causing gene in every individual with retinal degeneration, but who will pay for this? Another challenge involves unavailability or lack of an appropriate animal model. It is possible to engineer rodent models but, again, this is costly and time-consuming. Also, rodent models do not mirror some of the unique issues of the primate (human retina), for example, presence of a macula. It may be possible to carry out proof-of-concept studies in cell models for which animal models are unavailable or irrelevant, and then carry out safety studies in animals with normal vision. Such a strategy was used successfully by Vasireddy et al.[89] Finally, the costs of establishing and running clinical trials will limit the number of therapies that can be tested. It is possible, however, that once the first gene therapy reagent is designated as a FDA-approved drug in the USA or in Europe, the regulatory (and thus

financial) burden for developing additional drugs will decrease. For example, data from development of one particular vector could be used to support the development of another.

5. Gene therapy is not going to be effective for every retinal disease. There are some diseases in which the efficiency of transduction and/or levels of gene expression are going to be critical. Delivery of either too much or too little of the reagent will be either ineffective or possibly even toxic. There may also be immune responses to particular vectors/gene products that could limit efficacy. The recent successes in retinal gene therapy are very exciting but we have much to learn about the safety limitations not only with respect to type of gene, route of delivery, and dose, but also with respect to readministration.

Outcome Measures in Human Clinical Trials

A number of outcome measures (visual acuity, visual field, color vision, and area of nonseeing retina) have been used or accepted in the development of drugs for ophthalmologic indications. Except for visual acuity, however, there is no generally accepted level of improvement considered "clinically meaningful" in FDA parlance. For visual acuity, the precedent of 15 letters, or three lines on an ETDRS eye chart corresponding to 0.3 logMAR or 50% improvement, has been accepted as clinically meaningful. For some of the diseases that are being considered for treatment with gene therapy, individuals may only have light perception vision and so an ETDRS chart is irrelevant. In addition, there are many diseases, e.g., choroideremia, where visual acuity remains intact long after patients become severely disabled from nyctalopia and legally blind from visual field loss. Furthermore, endpoints that are used in adults may not be applicable for small children, who do not have the attention span or cognitive abilities to participate in the study procedures. Some endpoints may not have enough sensitivity to detect a change in clinical status. While it has been argued that improvement on visual field testing can be considered clinically meaningful when results of multiple points in the visual field meet specific criteria, this test cannot be completed accurately by an individual who cannot fixate due to nystagmus, such as individuals

with LCA or cone–rod dystrophy. Thus, it will be essential to do correlation analyses that will provide surrogate measures for clinically meaningful outcomes and thus expand and validate additional efficacy outcome measures such as pupillometry (Fig. 36.5) for particular target populations.

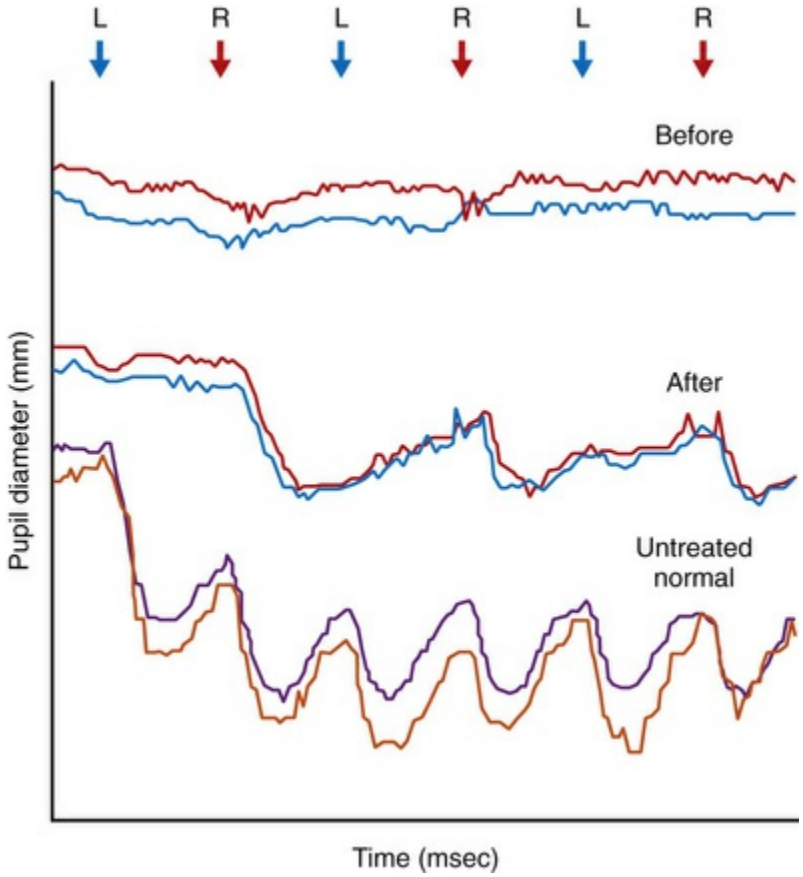

FIG. 36.5 Example of improvement of the pupillary light reflex after a unilateral subretinal injection of AAV2-hRPE65v2. There is minimal response to light in either eye in the subject prior to injection. After injection, there is a brisk pupillary response after the (treated) right eye (but not the untreated left eye) is illuminated. This gives the appearance of a relative afferent pupillary defect except that this reflects correction of the defect in the treated eye. Shown for comparison is the pupillary light reflex of a normal-sighted individual.

Window of Opportunity

In order to attain the maximal therapeutic effect for any retinal disease, it is important that the transgene be delivered within the appropriate timeframe. In the case of degenerative diseases, gene augmentation therapy will only be effective if the target cells are still present. For example, gene augmentation strategies for RP will only be effective if the photoreceptors are still present (even if they are dysfunctional).

There is also the issue of whether the goal is to reverse blindness or simply to prevent the disease from worsening (i.e., to hold it in place). For a disease such as LCA due to *RPE65* mutations, there is a biochemical deficit that can be remedied and thus allow previously functional photoreceptors to respond to light. In AR Stargardt disease, however, there may be toxicity due to the disease-associated accumulation of toxic byproducts of the retinoid cycle. Delivery of the normal version of the Stargardt disease gene, *ABCA4*, may prevent additional toxic byproducts from accumulating but will not remove those that have already accumulated. In other diseases, the gene mutation may affect a structural component in photoreceptor cells and thus may affect the development of the retina and prevent formed vision very early in life. In such cases, the disease initiates and thus must be corrected very early in life (i.e., it has a developmental component). In addition, there is the significant risk that if the retina is "corrected" too late in life, the individual will not be able to benefit from vision because of amblyopia. In cases where there is formed vision early in life, this may not be as significant a concern (see below).

Plasticity of the Visual System

Nearly 40% of the human brain is involved with the processing and perception of vision.[157] Of all sensory systems, vision provides the most information to the human brain. Both laboratory and clinical studies have demonstrated that early onset of blindness can lead to structural and functional brain changes. Severe impairment of the visual pathway early in life due to developmental or retinal degenerative diseases is likely to limit the responsiveness of neurons in the visual cortex. Thus, while gene therapy for some early-onset retinal degenerative diseases may be able to rescue

retinal function, it may not necessarily allow vision. The limits to restoration of the retinal-cortical pathways are not well defined, however, as shown by recent results from a functional magnetic resonance imaging (fMRI) study in children and young adults who had been treated at CHOP with gene therapy for LCA-RPE65 mutations. Ashtari and colleagues[158] carried out an fMRI study in such patients to investigate how the cortex responds to the recovery of function after gene therapy in specific areas of the retina after prolonged visual deprivation. That study employed only dim light stimuli, since it is known that young LCA-RPE65 patients are able to see and function (albeit poorly) when their environment is brightly lit. Functional analyses were carried out separately for each individual patient to account for disease stage and treatment area in each of the subjects. The untreated eyes served as an internal control for each subject. The results showed that the visual cortex could become responsive to visual input, even after prolonged (up to 35 years in the oldest patient) visual deprivation (Fig. 36.6).[158] Treatment of the retina also resulted in myelination of the corresponding visual tracts in the brain.[159] The plasticity data provide hope for being able to use gene therapy to resuscitate not just the retina (and potentially also other sensory organs) but also the visual cortex even after chronic visual deprivation.

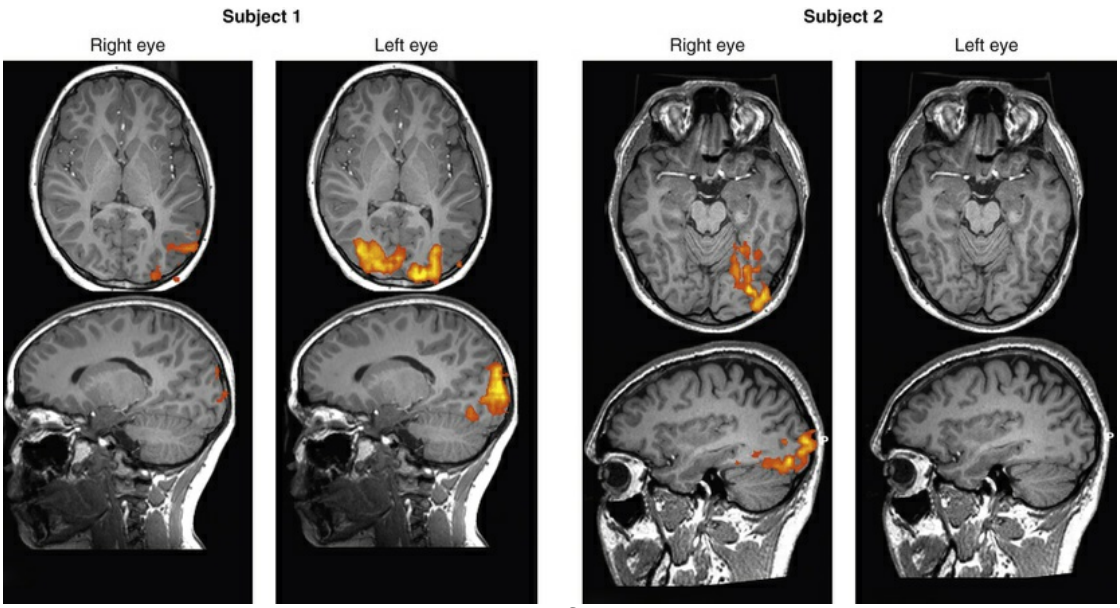

FIG. 36.6 The visual cortex of individuals with Leber congenital amaurosis due to *RPE65* mutations

responds to visual stimuli as predicted by the site of injection of AAV2-hRPE65v2. Cortical activations are appreciated after presentation of stimuli to the injected, but not the uninjected, eye. Subject 1 had received an injection in his left macula; subject 2 had received a superotemporal injection in his right retina. (For full details, see Ashtari M, Cyckowski LL, Monroe JF, et al. The human visual cortex responds to gene therapy-mediated recovery of retinal function. J Clin Invest 2011;121:2160–8.)

Genotyping Issues

Over the past two decades, more than 238 different genes have been identified which, when mutated, cause retinal disease (http://www.sph.uth.tmc.edu/RetNet). Molecular diagnostics of inherited retinal diseases is performed in order to provide a definitive disease diagnosis and to be able to provide prognostic information to patients as well as genetic counseling. With the progress in developing gene therapy for retinal diseases, genotyping has become increasingly more important as patients want to know whether they are eligible for certain trials. In addition, genotype/phenotype data have become very important in planning ahead for other clinical trials. This information is invaluable for determining the optimal age for intervention, selecting appropriate outcome measures, and predicting how long it would take to document an improvement in the phenotype given the appropriate gene therapy intervention.

While genetic testing has become more commonplace, there is still not a routine, standardized test. There are large technologic and economic challenges associated with genetic testing because of allelic and genetic heterogeneity, and further, we still do not know the genes responsible for a large number of the diseases. As a result, only a minority of patients know their genetic defect. The decision as to what path to take in order to obtain a genetic diagnosis is often guided by economic issues, including insurance coverage. Good phenotype analysis can shorten the list of suspect genes on a differential diagnosis list considerably. That, the initiation of other retinal gene therapy trials for genetic disease, and the development of cost-effective strategies for identifying and sequencing disease-

causing genes will continue to transform the clinical workup of retinal degeneration and other patients.

A Treatment Versus a Cure?

One of the questions that is being and continues to be evaluated in various clinical trials is whether gene therapy can result in a permanent improvement in retinal and visual function. Results reported by two of the groups carrying out human clinical trials for LCA2 show long-lasting (on the order of 3–6 years so far) improvements in retinal and visual function,[20,145,153] although one group reported on 3 of the 15 subjects treated and found large improvements followed after 3 years by a slow decline.[147] In that study, even with the decline, retinal sensitivity is increased significantly over baseline at the 6-year timepoint. The phase I clinical trials in which the data were collected using different doses of AAV are complicated by numerous additional variables, including stage of degeneration, volume of AAV injected, area of retina injected, complications, age of the subject, surgical details, type of outcome measures used, etc. With time, it should be possible to determine the optimal parameters for intervention and to determine whether a cure is possible. In the meantime, even with a slow decline in retinal sensitivity over years, the improvements could be meaningful to the subjects suffering from these otherwise untreatable conditions (see also http://www.medscape.com/viewarticle/844151#vp_2). It may be possible to further boost efficacy by readministration to additional portions of the retina, however safety of such strategies will need to be tested in animal models prior to testing in humans.

Generic Strategies for Reversing Blindness in "Dead" Retinas

A major challenge for retinal gene therapy is, who will pay for the costs of generating and validating clinical vectors, carrying out preclinical safety studies, screening potential clinical trial candidates for the relevant gene defect, conducting the appropriate regulatory oversight, and paying for the clinical trial itself –

particularly if potentially over 230 different gene therapy products (each specific for a different retinal gene) could be developed? Studies involving proof of concept of a given gene therapy often can be covered by conventional funding mechanisms – government grants, private foundations. It is much more difficult, however, to find funding for the costlier clinical trials. Safety data from one approach and then applied to another may provide shortcuts for some portions of product development but still, the economic challenges alone are enormous.

It is for that reason that generic strategies to treat retinal disease are appealing. As described above, there has long been an interest in using growth factors or neurotrophic factors to maintain the health of the retina for longer (Table 36.2 part B). In many diseases, a stabilization of the disease progression would be clinically meaningful. In "dead" retinas, it may be feasible to harness the remaining circuitry to provide some useful vision using "optogenetic therapy". There are many technical challenges associated with this endeavor, including the desirability of engineering the molecules so that they would be useful with typical indoor lighting parameters. There are also potential biologic challenges with this approach. Will the mammalian retina recognize optogenetic (algal or bacterial) proteins produced in inner retinal cells as foreign? Nevertheless, the ability to deliver clinically meaningful vision to individuals who have none is very exciting and could supply hope to millions of patients with endstage retinal or macular degeneration.

Conclusion

State of the Art of Retinal Gene Therapy

There has been a huge amount of progress in developing proof-of-concept of retinal gene therapy and proof-of-concept data for several approaches that have led to the initiation of clinical trials. It may not be long before the first gene therapy product is approved for human use in the Western world and this may be a product intended for use in the retina. The early successes will likely fuel the development of gene therapy for other retinal disease targets.

With the rapid development of engineered vectors, the swift progress in our understanding of the genetics of retinal diseases, and finetuning of surgical delivery procedures, this field has never been more promising. With continued successes with ocular gene therapy, there may be a day when gene-based approaches can be used to treat blinding diseases which are currently untreatable.

References

1. Farjo R, Skaggs J, Quiambao AB, et al. Efficient non-viral ocular gene transfer with compacted DNA nanoparticles. *PLoS ONE*. 2006;1:e38.
2. Johnson LN, Cashman SM, Kumar-Singh R. Cell-penetrating peptide for enhanced delivery of nucleic acids and drugs to ocular tissues including retina and cornea. *Mol Ther*. 2008;16:107–114.
3. Cai X, Nash Z, Conley SM, et al. A partial structural and functional rescue of a retinitis pigmentosa model with compacted DNA nanoparticles. *PLoS ONE*. 2009;4:e5290.
4. Read SP, Cashman SM, Kumar-Singh R. POD nanoparticles expressing GDNF provide structural and functional rescue of light-induced retinal degeneration in an adult mouse. *Mol Ther*. 2010;18:1917–1926.
5. Bennett J, Wilson J, Sun D, et al. Adenovirus vector-mediated in vivo gene transfer into adult murine retina. *Invest Ophthalmol Vis Sci*. 1994;35:2535–2542.
6. Li T, Adamian M, Roof DJ, et al. In vivo transfer of a reporter gene to the retina mediated by an adenoviral vector. *Invest Ophthalmol Vis Sci*. 1994;35:2543–2549.
7. Budenz D, Bennett J, Alonso L, et al. In vivo gene transfer into murine trabecular meshwork and corneal endothelial cells. *Invest Ophthalmol Vis Sci*. 1995;36:2211–2215.
8. Bennett J, Tanabe T, Sun D, et al. Photoreceptor cell rescue in retinal degeneration (rd) mice by in vivo gene therapy. *Nat Med*. 1996;2:649–654.
9. Bennett J, Zeng Y, Bajwa R, et al. Adenovirus-mediated delivery of rhodopsin-promoted bcl-2 results in a delay in photoreceptor cell death in the rd/rd mouse. *Gene Ther*.

1998;5:1156–1164.
10. Von Seggern D, Aguilar E, Kinder K, et al. In vivo transduction of photoreceptors or ciliary body by intravitreal injection of pseudotyped adenoviral vectors. *Mol Ther*. 2003;7:27–36.
11. Cashman SM, McCullough L, Kumar-Singh R. Improved retinal transduction in vivo and photoreceptor-specific transgene expression using adenovirus vectors with modified penton base. *Mol Ther*. 2007;15:1640–1646.
12. Kumar-Singh R, Chamberlain JS. Encapsidated adenovirus minichromosomes allow delivery and expression of a 14 kb dystrophin cDNA to muscle cells. *Hum Mol Genet*. 1996;5:913–921.
13. Kumar-Singh R, Yamashita C, Tran K, et al. Construction of encapsidated (gutted) adenovirus minichromosomes and their application to rescue of photoreceptor degeneration. *Methods Enzymol*. 2000;316:724–743.
14. Hoffman LM, Maguire AM, Bennett J. Cell-mediated immune response and stability of intraocular transgene expression after adenovirus-mediated delivery. *Invest Ophthalmol Vis Sci*. 1997;38:2224–2233.
15. Bennett J, Maguire AM, Cideciyan AV, et al. Recombinant adeno-associated virus-mediated gene transfer to the monkey retina. *Proc Natl Acad Sci USA*. 1999;96:9920–9925.
16. Acland GM, Aguirre GD, Bennett J, et al. Long-term restoration of rod and cone vision by single dose rAAV-mediated gene transfer to the retina in a canine model of childhood blindness. *Mol Ther*. 2005;12:1072–1082.
17. Acland GM, Aguirre GD, Ray J, et al. Gene therapy restores vision in a canine model of childhood blindness. *Nat Genet*. 2001;28:92–95.
18. Maguire AM, Simonelli F, Pierce EA, et al. Safety and efficacy of gene transfer for Leber's congenital amaurosis. *N Engl J Med*. 2008;358:2240–2248.
19. Lebherz C, Auricchio A, Maguire AM, et al. Long-term inducible gene expression in the eye via adeno-associated virus gene transfer in nonhuman primates. *Hum Gene Ther*. 2005;16:178–186.

20. Cideciyan AV, Jacobson SG, Beltran WA, et al. Human retinal gene therapy for Leber congenital amaurosis shows advancing retinal degeneration despite enduring visual improvement. *Proc Natl Acad Sci USA*. 2013;110:517–525.
21. Allocca M, Mussolino C, Garcia-Hoyos M, et al. Novel adeno-associated virus serotypes efficiently transduce murine photoreceptors. *J Virol*. 2007;81:11372–11380.
22. Lebherz C, Maguire A, Tang W, et al. Novel AAV serotypes for improved ocular gene transfer. *J Gene Med*. 2008;10:375–382.
23. Auricchio A, Kobinger G, Anand V, et al. Exchange of surface proteins impacts on viral vector cellular specificity and transduction characteristics: the retina as a model. *Hum Mol Genet*. 2001;10:3075–3081.
24. Sun X, Pawlyk B, Xu X, et al. Gene therapy with a promoter targeting both rods and cones rescues retinal degeneration caused by AIPL1 mutations. *Gene Ther*. 2011;17:117–131.
25. Tan M, Smith AJ, Pawlyk B, et al. Gene therapy for retinitis pigmentosa and Leber congenital amaurosis caused by defects in AIPL1: effective rescue of mouse models of partial and complete Aipl1 deficiency. *Hum Mol Genet*. 2009;18:2099–2114.
26. Dalkara D, Byrne LC, Klimczak RR, et al. In vivo-directed evolution of a new adeno-associated virus for therapeutic outer retinal gene delivery from the vitreous. *Sci Transl Med*. 2013;5:189ra76.
27. Cronin T, Vandenberghe LH, Hantz P, et al. Efficient transduction and optogenetic stimulation of retinal bipolar cells by a synthetic adeno-associated virus capsid and promoter. *EMBO Mol Med*. 2014;6:1175–1190.
28. Santiago-Ortiz J, Ojala DS, Westesson O, et al. AAV ancestral reconstruction library enables selection of broadly infectious viral variants. *Gene Ther*. 2015;22(12):934–946.
29. Zinn E, Pacouret S, Khaychuk V, et al. In silico reconstruction of the viral evolutionary lineage yields a potent gene therapy vector. *Cell Rep*. 2015;12:1056–1068.
30. Kachi S, Binley K, Yokoi K, et al. EIAV vector-mediated co-delivery of endostatin and angiostatin driven by the RPE-

specific VMD2 promoter inhibits choroidal neovascularization. *Hum Gene Ther*. 2008;20:31–39.
31. Balaggan KS, Binley K, Esapa M, et al. Stable and efficient intraocular gene transfer using pseudotyped EIAV lentiviral vectors. *J Gene Med*. 2006;8:275–285.
32. Takahashi M, Miyoshi H, Verma IM, et al. Rescue from photoreceptor degeneration in the rd mouse by human immunodeficiency virus vector-mediated gene transfer. *J Virol*. 1999;73:7812–7816.
33. Kong J, Kim SR, Binley K, et al. Correction of the disease phenotype in the mouse model of Stargardt disease by lentiviral gene therapy. *Gene Ther*. 2008;15:1311–1320.
34. Maguire AM, High KA, Auricchio A, et al. Age-dependent effects of RPE65 gene therapy for Leber's congenital amaurosis: a phase I dose-escalation trial. *Lancet*. 2009;374:1597–1605.
35. Jiang LG, Jorquera M, Streilein JW. Subretinal space and vitreous cavity as immunologically privileged sites for retinal allografts. *Invest Ophthalmol Vis Sci*. 1993;36:3347–3354.
36. Anand V, Chirmule N, Maguire AM, et al. Induction of immune deviant response in the subretinal space is dependent on the nature of antigen introduced. *Invest Ophthalmol Vis Sci*. 2000;41:S117.
37. Bainbridge JW, Smith AJ, Barker SS, et al. Effect of gene therapy on visual function in Leber's congenital amaurosis. *N Engl J Med*. 2008;358:2231–2239.
38. Hauswirth WW, Aleman TS, Kaushal S, et al. Treatment of leber congenital amaurosis due to RPE65 mutations by ocular subretinal injection of adeno-associated virus gene vector: short-term results of a phase I trial. *Hum Gene Ther*. 2008;19:979–990.
39. Banin E, Bandah-Rozenfeld D, Obolensky A, et al. Molecular anthropology meets genetic medicine to treat blindness in the north African Jewish population: human gene therapy initiated in Israel. *Hum Gene Ther*. 2010;21:1749–1757.
40. Bennicelli J, Wright JF, Komaromy A, et al. Reversal of blindness in animal models of Leber congenital amaurosis

using optimized AAV2-mediated gene transfer. *Mol Ther*. 2008;16:458–465.
41. Amado D, Mingozzi F, Hui D, et al. Safety and efficacy of subretinal re-administration of an AAV2 vector in large animal models: implications for studies in humans. *Sci Transl Med*. 2010;2:21ra16.
42. Vandenberghe L, Bell P, Maguire A, et al. AAV9 targets cone photoreceptors in non-human primates. *PLoS ONE*. 2013;8(1):e53463.
43. MacLaren RE, Groppe M, Barnard AR, et al. Initial observations in patients undergoing retinal gene therapy for choroideremia. *Lancet*. 2014;383:1129–1137.
44. Vandenberghe L, Bell P, Maguire A, et al. Dosage thresholds for AAV2 and AAV8 photoreceptor gene therapy in monkey. *Sci Transl Med*. 2011;3:88ra54.
45. Surace EM, Auricchio A, Reich SJ, et al. Delivery of adeno-associated virus vectors to the fetal retina: impact of viral capsid proteins on retinal neuronal progenitor transduction. *J Virol*. 2003;77:7957–7963.
46. Cepko C, Ryder E, Austin C, et al. Lineage analysis using retroviral vectors. *Methods*. 1998;14:393–406.
47. Dejneka NS, Surace EM, Aleman TS, et al. In utero gene therapy rescues vision in a murine model of congenital blindness. *Mol Ther*. 2004;9:182–188.
48. Dudus L, Anand V, Acland G, et al. Persistent transgene product in retina, optic nerve and brain after intraocular injection of rAAV. *Vis Res*. 1999;39:2545–2553.
49. Bennett J, Anand V, Acland GM, et al. Cross-species comparison of in vivo reporter gene expression after recombinant adeno-associated virus-mediated retinal transduction. *Methods Enzymol*. 2000;316:777–789.
50. Petrs-Silva H, Dinculescu A, Li Q, et al. Novel properties of tyrosine-mutant AAV2 vectors in the mouse retina. *Mol Ther*. 2011;19:293–301.
51. Caporale N, Kolstad KD, Lee T, et al. LiGluR restores visual responses in rodent models of inherited blindness. *Mol Ther*. 2011;19:1212–1219.
52. Ho TT, Maguire AM, Aguirre GD, et al. Phenotypic rescue

after adeno-associated virus-mediated delivery of 4-sulfatase to the retinal pigment epithelium of feline mucopolysaccharidosis VI. *J Gene Med*. 2002;4:613–621.
53. Allocca M, Doria M, Petrillo M, et al. Serotype-dependent packaging of large genes in adeno-associated viral vectors results in effective gene delivery in mice. *J Clin Invest*. 2008;118:1955–1964.
54. Simons DL, Boye SL, Hauswirth WW, et al. Gene therapy prevents photoreceptor death and preserves retinal function in a Bardet–Biedl syndrome mouse model. *Proc Natl Acad Sci USA*. 2011;108:6276–6281.
55. Michalakis S, Muhlfriedel R, Tanimoto N, et al. Restoration of cone vision in the CNGA3$^{-/-}$ mouse model of congenital complete lack of cone photoreceptor function. *Mol Ther*. 2010;18:2057–2063.
56. Pang JJ, Alexander J, Lei B, et al. Achromatopsia as a potential candidate for gene therapy. *Adv Exp Med Biol*. 2010;664:639–646.
57. Carvalho LS, Xu J, Pearson RA, et al. Long-term and age-dependent restoration of visual function in a mouse model of CNGB3-associated achromatopsia following gene therapy. *Hum Mol Genet*. 2011;20:3161–3175.
58. Alexander JJ, Umino Y, Everhart D, et al. Restoration of cone vision in a mouse model of achromatopsia. *Nat Med*. 2007;13:685–687.
59. Mihelec M, Pearson RA, Robbie SJ, et al. Long-term preservation of cones and improvement in visual function following gene therapy in a mouse model of Leber congenital amaurosis (LCA) caused by GC1 deficiency. *Hum Gene Ther*. 2011;22:1179–1190.
60. Boye SE, Boye SL, Pang J, et al. Functional and behavioral restoration of vision by gene therapy in the guanylate cyclase-1 (GC1) knockout mouse. *PLoS ONE*. 2010;5:e11306.
61. Williams ML, Coleman JE, Haire SE, et al. Lentiviral expression of retinal guanylate cyclase-1 (RetGC1) restores vision in an avian model of childhood blindness. *PLoS Med*. 2006;3:e201.
62. Batten ML, Imanishi Y, Tu DC, et al. Pharmacological and

rAAV gene therapy rescue of visual functions in a blind mouse model of Leber congenital amaurosis. *PLoS Med*. 2005;2:e333.
63. Gargiulo A, Bonetti C, Montefusco S, et al. AAV-mediated tyrosinase gene transfer restores melanogenesis and retinal function in a model of oculo-cutaneous albinism type I (OCA1). *Mol Ther*. 2009;17:1347–1354.
64. Surace EM, Domenici L, Cortese K, et al. Amelioration of both functional and morphological abnormalities in the retina of a mouse model of ocular albinism following AAV-mediated gene transfer. *Mol Ther*. 2005;12:652–658.
65. Pang JJ, Boye SL, Kumar A, et al. AAV-mediated gene therapy for retinal degeneration in the rd10 mouse containing a recessive PDEbeta mutation. *Invest Ophthalmol Vis Sci*. 2008;49:4278–4283.
66. Pang JJ, Dai X, Boye SE, et al. Long-term retinal function and structure rescue using capsid mutant AAV8 vector in the rd10 mouse, a model of recessive retinitis pigmentosa. *Mol Ther*. 2011;19:236–242.
67. Andrieu-Soler C, Halhal M, Boatright JH, et al. Single-stranded oligonucleotide-mediated in vivo gene repair in the rd1 retina. *Mol Vis*. 2007;13:682–706.
68. Allocca M, Manfredi A, Iodice C, et al. AAV-mediated gene replacement either alone or in combination with physical and pharmacological agents results in partial and transient protection from photoreceptor degeneration associated with β-PDE deficiency. *Invest Ophthalmol Vis Sci*. 2011;52(8):5713–5719.
69. Cai X, Conley SM, Naash MI. Gene therapy in the retinal degeneration slow model of retinitis pigmentosa. *Adv Exp Med Biol*. 2010;664:611–619.
70. Georgiadis A, Tschernutter M, Bainbridge JW, et al. AAV-mediated knockdown of peripherin-2 in vivo using miRNA-based hairpins. *Gene Ther*. 2010;17:486–493.
71. Conley SM, Naash MI. Nanoparticles for retinal gene therapy. *Prog Retin Eye Res*. 2010;29:376–397.
72. Ali R, Sarra G-M, Stephens C, et al. Restoration of photoreceptor ultrastructure and function in retinal

degeneration slow mice by gene therapy. *Nature Genet*. 2000;25:306–310.
73. Sarra G-M, Stephens C, de Alwis M, et al. Gene replacement therapy in the retinal degeneration slow (rds) mouse: the effect on retinal degeneration following partial transduction of the retina. *Hum Mol Genet*. 2001;10:2353–2361.
74. Mao H, James T Jr, Schwein A, et al. AAV delivery of wild-type rhodopsin preserves retinal function in a mouse model of autosomal dominant retinitis pigmentosa. *Hum Gene Ther*. 2011;22:567–575.
75. Pang J, Boye SE, Lei B, et al. Self-complementary AAV-mediated gene therapy restores cone function and prevents cone degeneration in two models of Rpe65 deficiency. *Gene Ther*. 2010;17:815–826.
76. Pang JJ, Chang B, Kumar A, et al. Gene therapy restores vision-dependent behavior as well as retinal structure and function in a mouse model of RPE65 Leber congenital amaurosis. *Mol Ther*. 2006;13:565–572.
77. Dejneka N, Surace E, Aleman T, et al. Fetal virus-mediated delivery of the human RPE65 gene rescues vision in a murine model of congenital retinal blindness. *Mol Ther*. 2004;9:182–188.
78. Narfstrom K, Bragadottir R, Redmond TM, et al. Functional and structural evaluation after AAV.RPE65 gene transfer in the canine model of Leber's congenital amaurosis. *Adv Exp Med Biol*. 2003;533:423–430.
79. Narfstrom K, Katz ML, Bragadottir R, et al. Functional and structural recovery of the retina after gene therapy in the RPE65 null mutation dog. *Invest Ophthalmol Vis Sci*. 2003;44:1663–1672.
80. Narfstrom K, Katz ML, Ford M, et al. In vivo gene therapy in young and adult RPE65$^{-/-}$ dogs produces long-term visual improvement. *J Hered*. 2003;94:31–37.
81. Pawlyk BS, Smith AJ, Buch PK, et al. Gene replacement therapy rescues photoreceptor degeneration in a murine model of Leber congenital amaurosis lacking RPGRIP. *Invest Ophthalmol Vis Sci*. 2005;46:3039–3045.
82. Kjellstrom S, Bush RA, Zeng Y, et al. Retinoschisin gene

therapy and natural history in the Rs1h-KO mouse: long-term rescue from retinal degeneration. *Invest Ophthalmol Vis Sci*. 2007;48:3837–3845.
83. Zeng Y, Takada Y, Kjellstrom S, et al. RS-1 gene delivery to an adult Rs1h knockout mouse model restores ERG b-wave with reversal of the electronegative waveform of X-linked retinoschisis. *Invest Ophthalmol Vis Sci*. 2004;45:3279–3285.
84. Janssen A, Min SH, Molday LL, et al. Effect of late-stage therapy on disease progression in AAV-mediated rescue of photoreceptor cells in the retinoschisin-deficient mouse. *Mol Ther*. 2008;16:1010–1017.
85. Min SH, Molday LL, Seeliger MW, et al. Prolonged recovery of retinal structure/function after gene therapy in an Rs1h-deficient mouse model of X-linked juvenile retinoschisis. *Mol Ther*. 2005;12:644–651.
86. Zou J, Luo L, Shen Z, et al. Whirlin replacement restores the formation of the USH2 protein complex in whirlin knockout photoreceptors. *Invest Ophthalmol Vis Sci*. 2011;52:2343–2351.
87. Tolmachova T, Tolmachov OE, Barnard AR, et al. Functional expression of Rab escort protein 1 following AAV2-mediated delivery in the retina of choroideremia mice and human cells ex vivo. *J Mol Med*. 2013;91:825–837.
88. Black A, Vasireddy V, Chung DC, et al. Adeno-associated virus 8-mediated gene therapy for choroideremia: preclinical studies in vitro and in vivo models. *J Gene Med*. 2014;16:122–130.
89. Vasireddy V, Mills JA, Gaddameedi R, et al. AAV-mediated gene therapy for choroideremia: preclinical studies in personalized models. *PLoS ONE*. 2013;8:e61396.
90. Mancuso K, Hauswirth WW, Li Q, et al. Gene therapy for red–green colour blindness in adult primates. *Nature*. 2009;461:784–787.
91. Tam LC, Kiang AS, Chadderton N, et al. Protection of photoreceptors in a mouse model of RP10. *Adv Exp Med Biol*. 2010;664:559–565.
92. Tam LC, Kiang AS, Kennan A, et al. Therapeutic benefit derived from RNAi-mediated ablation of IMPDH1 transcripts in a murine model of autosomal dominant

retinitis pigmentosa (RP10). *Hum Mol Genet*. 2008;17:2084–2100.
93. Millington-Ward S, Chadderton N, O'Reilly M, et al. Suppression and replacement gene therapy for autosomal dominant disease in a murine model of dominant retinitis pigmentosa. *Mol Ther*. 2011;19:642–649.
94. Palfi A, Ader M, Kiang AS, et al. RNAi-based suppression and replacement of rds-peripherin in retinal organotypic culture. *Hum Mutat*. 2006;27:260–268.
95. Chadderton N, Millington-Ward S, Palfi A, et al. Improved retinal function in a mouse model of dominant retinitis pigmentosa following AAV-delivered gene therapy. *Mol Ther*. 2009;17:593–599.
96. O'Reilly M, Palfi A, Chadderton N, et al. RNA interference-mediated suppression and replacement of human rhodopsin in vivo. *Am J Hum Genet*. 2007;81:127–135.
97. Mussolino C, Sanges D, Marrocco E, et al. Zinc-finger-based transcriptional repression of rhodopsin in a model of dominant retinitis pigmentosa. *EMBO Mol Med*. 2011;3:118–128.
98. LaVail MM, Yasumura D, Matthes MT, et al. Ribozyme rescue of photoreceptor cells in P23H transgenic rats: long-term survival and late stage therapy. *Proc Natl Acad Sci USA*. 2000;97:11488–11493.
99. Lewin AS, Drenser KA, Hauswirth WW, et al. Ribozyme rescue of photoreceptor cells in a transgenic rat model of autosomal dominant retinitis pigmentosa. *Nat Med*. 1998;4:967–971.
100. Lai CM, Estcourt MJ, Wikstrom M, et al. rAAV.sFlt-1 gene therapy achieves lasting reversal of retinal neovascularization in the absence of a strong immune response to the viral vector. *Invest Ophthalmol Vis Sci*. 2009;50:4279–4287.
101. Lai CM, Shen WY, Brankov M, et al. Long-term evaluation of AAV-mediated sFlt-1 gene therapy for ocular neovascularization in mice and monkeys. *Mol Ther*. 2005;12:659–668.
102. Maclachlan TK, Lukason M, Collins M, et al. Preclinical

safety evaluation of AAV2-sFLT01 – a gene therapy for age-related macular degeneration. *Mol Ther*. 2011;19:326–336.
103. Pechan P, Rubin H, Lukason M, et al. Novel anti-VEGF chimeric molecules delivered by AAV vectors for inhibition of retinal neovascularization. *Gene Ther*. 2009;16:10–16.
104. Tuo J, Pang JJ, Cao X, et al. AAV5-mediated sFLT01 gene therapy arrests retinal lesions in Ccl2($^{-/-}$)/Cx3cr1($^{-/-}$) mice. *Neurobiol Aging*. 2012;33:433.e1–433.e10.
105. Lukason M, DuFresne E, Rubin H, et al. Inhibition of choroidal neovascularization in a nonhuman primate model by intravitreal administration of an AAV2 vector expressing a novel anti-VEGF molecule. *Mol Ther*. 2011;19:260–265.
106. Buch PK, MacLaren RE, Duran Y, et al. In contrast to AAV-mediated CNTF expression, AAV-mediated GDNF expression enhances gene replacement therapy in rodent models of retinal degeneration. *Mol Ther*. 2006;14:700–709.
107. Gauthier R, Joly S, Pernet V, et al. Brain-derived neurotrophic factor gene delivery to Müller glia preserves structure and function of light-damaged photoreceptors. *Invest Ophthalmol Vis Sci*. 2005;46:3383–3392.
108. McGee LH, Lau D, Zhou S, et al. Rescue of photoreceptor degeneration in S336ter(4) mutant rhodopsin transgenic rats by adeno-associated virus (AAV)-mediated delivery of basic fibroblast growth factor. *Invest Ophthalmol Vis Sci*. 1999;40:S936.
109. Akimoto M, Miyatake S-I, Kogishi J-I, et al. Adenovirally expressed basic fibroblast growth factor rescues photoreceptor cells in RCS rats. *Invest Ophthalmol Vis Sci*. 1999;40:273–279.
110. Rex TS, Allocca M, Domenici L, et al. Systemic but not intraocular Epo gene transfer protects the retina from light- and genetic-induced degeneration. *Mol Ther*. 2004;10:855–861.
111. Xiong W, MacColl Garfinkel AE, Li Y, et al. NRF2 promotes neuronal survival in neurodegeneration and acute nerve damage. *J Clin Invest*. 2015;125:1433–1445.
112. Bush RA, Lei B, Tao W, et al. Encapsulated cell-based intraocular delivery of ciliary neurotrophic factor in normal

rabbit: dose-dependent effects on ERG and retinal histology. *Invest Ophthalmol Vis Sci*. 2004;45:2420–2430.
113. Adamus G, Sugden B, Shiraga S, et al. Anti-apoptotic effects of CNTF gene transfer on photoreceptor degeneration in experimental antibody-induced retinopathy. *J Autoimmun*. 2003;21:121–129.
114. Bok D, Yasumura D, Matthes MT, et al. Effects of adeno-associated virus-vectored ciliary neurotrophic factor on retinal structure and function in mice with a P216L rds/peripherin mutation. *Exp Eye Res*. 2002;74:719–735.
115. Cayouette M, Gravel C. Adenovirus-mediated gene transfer of ciliary neurotrophic factor can prevent photoreceptor degeneration in the retinal degeneration (rd) mouse. *Hum Gene Ther*. 1997;8:423–430.
116. Huang SP, Lin PK, Liu JH, et al. Intraocular gene transfer of ciliary neurotrophic factor rescues photoreceptor degeneration in RCS rats. *J Biomed Sci*. 2004;11:37–48.
117. Liang F-Q, Aleman TS, Dejneka NS, et al. Long-term protection of retinal structure but not function using rAAV.CNTF in animal models of retinitis pigmentosa. *Mol Ther*. 2001;4:461–472.
118. Pearce-Kelling SE, Rein D, Acland GM, et al. Encapsulated cell-based intraocular delivery of CNTF slows inherited retinal degeneration in the rcd1 dog model. *Invest Ophthalmol Vis Sci*. 2000;41:S542.
119. Peterson WM, Flannery JG, Hauswirth WW, et al. Enhanced survival of photoreceptors in P23H mutant rhodopsin transgenic rats by adeno-associated virus (AAV)-mediated delivery of neurotrophic genes. *Invest Ophthalmol Vis Sci*. 1998;39:S1117.
120. Liang F-Q, Dejneka NS, Cohen DR, et al. AAV-mediated delivery of ciliary neurotrophic factor prolongs photoreceptor survival in the rhodopsin knockout mouse. *Mol Ther*. 2001;3:241–248.
121. Dalkara D, Kolstad KD, Guerin KI, et al. AAV mediated GDNF secretion from retinal glia slows down retinal degeneration in a rat model of retinitis pigmentosa. *Mol Ther*. 2011;19:1602–1608.

122. Leonard KC, Petrin D, Coupland SG, et al. XIAP protection of photoreceptors in animal models of retinitis pigmentosa. *PLoS ONE*. 2007;2:e314.
123. Schlichtenbrede FC, MacNeil A, Bainbridge JW, et al. Intraocular gene delivery of ciliary neurotrophic factor results in significant loss of retinal function in normal mice and in the Prph2Rd2/Rd2 model of retinal degeneration. *Gene Ther*. 2003;10:523–527.
124. MacDonald IM, Sauve Y, Sieving PA. Preventing blindness in retinal disease: ciliary neurotrophic factor intraocular implants. *Can J Ophthalmol*. 2007;42:399–402.
125. Zhang K, Hopkins JJ, Heier JS, et al. Ciliary neurotrophic factor delivered by encapsulated cell intraocular implants for treatment of geographic atrophy in age-related macular degeneration. *Proc Natl Acad Sci USA*. 2011;108:6241–6245.
126. Komáromy AM, Rowlan JS, Corr AT, et al. Transient photoreceptor deconstruction by CNTF enhances rAAV-mediated cone functional rescue in late state CNGB3-achromatopsia. *Mol Ther*. 2013;21:1131–1141.
127. Zein WM, Jeffrey BG, Wiley HE, et al. CNGB3 achromatopsia clinical trial with CNTF: diminished rod pathway responses with no evidence of improvement in cone function. *Invest Ophthalmol Vis Sci*. 2014;55:6301–6308.
128. Talcott KE, Ratnam K, Sundquist SM, et al. Longitudinal study of cone photoreceptors during retinal degeneration and in response to ciliary neurotrophic factor treatment. *Invest Ophthalmol Vis Sci*. 2011;52:2219–2226.
129. Sieving PA, Caruso RC, Tao W, et al. Ciliary neurotrophic factor (CNTF) for human retinal degeneration: phase I trial of CNTF delivered by encapsulated cell intraocular implants. *Proc Natl Acad Sci USA*. 2006;103:3896–3901.
130. Leveillard T, Mohand-Said S, Lorentz O, et al. Identification and characterization of rod-derived cone viability factor. *Nat Genet*. 2004;36:755–759.
131. Aït-Ali N, Fridlich R, Millet-Puel G, et al. Rod-derived cone viability factor promotes cone survival by stimulating aerobic glycolysis. *Cell*. 2015;161:817–832.
132. Byrne LC, Dalkara D, Luna G, et al. Viral-mediated RdCVF

and RdCVFL expression protects cone and rod photoreceptors in retinal degeneration. *J Clin Invest*. 2015;125:105–116.
133. Lagali PS, Balya D, Awatramani GB, et al. Light-activated channels targeted to ON bipolar cells restore visual function in retinal degeneration. *Nat Neurosci*. 2008;11:667–675.
134. Tomita H, Sugano E, Yawo H, et al. Restoration of visual response in aged dystrophic RCS rats using AAV mediated channelopsin-2 gene transfer. *Invest Ophthalmol Vis Sci*. 2007;48:3821–3826.
135. Bi A, Cui J, Ma YP, et al. Ectopic expression of a microbial-type rhodopsin restores visual responses in mice with photoreceptor degeneration. *Neuron*. 2006;50:23–33.
136. Doroudchi MM, Greenberg KP, Liu J, et al. Virally delivered Channelrhodopsin-2 safely and effectively restores visual function in multiple mouse models of blindness. *Mol Ther*. 2011;19:1220–1229.
137. Busskamp V, Duebel J, Balya D, et al. Genetic reactivation of cone photoreceptors restores visual responses in retinitis pigmentosa. *Science*. 2010;329:413–417.
138. Gaub BM, Berry MH, Holt AE, et al. Restoration of visual function by expression of a light-gated mammalian ion channel in retinal ganglion cells or ON-bipolar cells. *Proc Natl Acad Sci USA*. 2014;111:5574–5583.
139. Hurwitz M, Marcus K, Chevez-Barrios P, et al. Suicide gene therapy for treatment of retinoblastoma in a murine model. *Hum Gene Ther*. 1999;10:441–448.
140. Hurwitz RL, Marcus KT, Chevez-Barrios P, et al. Suicide gene therapy of retinoblastoma in a murine model. *Invest Ophthalmol Vis Sci*. 1998;39:S1118.
141. Chevez-Barrios P, Chintagumpala M, Mieler W, et al. Response of retinoblastoma with vitreous tumor seeding to adenovirus-mediated delivery of thymidine kinase followed by ganciclovir. *J Clin Oncol*. 2005;23:7927–7935.
142. Campochiaro PA, Nguyen QD, Shah SM, et al. Adenoviral vector-delivered pigment epithelium-derived factor for neovascular age-related macular degeneration: results of a phase I clinical trial. *Hum Gene Ther*. 2006;17:167–176.

143. Redmond TM, Poliakov E, Yu S, et al. Mutation of key residues of RPE65 abolishes its enzymatic role as isomerohydrolase in the visual cycle. *Proc Natl Acad Sci USA*. 2005;102:13658–13663.
144. Hauswirth W, Aleman T, Kaushal S, et al. Treatment of Leber congenital amaurosis due to RPE65 mutations by ocular subretinal injection of adeno-associated virus gene vector: short-term results of a phase I trial. *Hum Gene Ther*. 2008;19:979–990.
145. Bennett J, Ashtari M, Wellman J. AAV gene therapy readministration in three adults with congenital blindness. *Sci Transl Med*. 2012;4:120ra15.
146. Jacobson SG, Cideciyan AV, Ratnakaram R, et al. Gene therapy for Leber congenital amaurosis caused by RPE65 mutations: safety and efficacy in 15 children and adults followed up to 3 years. *Arch Ophthalmol*. 2012;130:9–24.
147. Jacobson SG, Cideciyan AV, Roman AJ, et al. Improvement and decline in vision with gene therapy in childhood blindness. *N Engl J Med*. 2015;372:1920–1926.
148. Bainbridge JW, Mehat MS, Sundaram V, et al. Long-term effect of gene therapy on Leber's congenital amaurosis. *N Engl J Med*. 2015;372:1887–1897.
149. Kachi S, Binley K, Yokoi K, et al. Equine infectious anemia viral vector-mediated codelivery of endostatin and angiostatin driven by retinal pigmented epithelium-specific VMD2 promoter inhibits choroidal neovascularization. *Hum Gene Ther*. 2009;20:31–39.
150. Koilkonda R, Yu H, Talla V, et al. LHON gene therapy vector prevents visual loss and optic neuropathy induced by G11778A mutant mitochondrial DNA: biodistribution and toxicology profile. *Invest Ophthalmol Vis Sci*. 2014;55:7739–7753.
151. Ellouze S, Augustin S, Bouaita A, et al. Optimized allotropic expression of the human mitochondrial ND4 prevents blindness in a rat model of mitochondrial dysfunction. *Am J Hum Genet*. 2008;63:373–387.
152. Chadderton N, Palfi A, Millington-Ward S, et al. Intravitreal delivery of AAV-NDI1 provides functional benefit in a

murine model of Leber hereditary optic neuropathy. *Eur J Hum Genet*. 2013;21:62–68.
153. Simonelli F, Maguire AM, Testa F, et al. Gene therapy for Leber's congenital amaurosis is safe and effective through 1.5 years after vector administration. *Mol Ther*. 2010;18:643–650.
154. Reich SJ, Auricchio A, Hildinger M, et al. Efficient trans-splicing in the retina expands the utility of adeno-associated virus as a vector for gene therapy. *Hum Gene Ther*. 2003;14:37–44.
155. Young S. *CRISPR and other genome editing tools boost medical research and gene therapy's reach*. [MIT Technology Review] 11 February 2014 [Cambridge, MA].
156. Liang P, Xu Y, Zhang X. CRISPR/Cas9-mediated gene editing in human tripronuclear zygotes. *Protein Cell*. 2015;6:363–372.
157. Mather G. *Foundations of sensation and perception*. 2nd ed. Psychology Press: London; 2008 [Chapter 2].
158. Ashtari M, Cyckowski LL, Monroe JF, et al. The human visual cortex responds to gene therapy-mediated recovery of retinal function. *J Clin Invest*. 2011;121:2160–2168.
159. Ashtari M, Zhang H, Cook PA, et al. Plasticity of the human visual system after retinal gene therapy with Leber's congenital amaurosis. *Sci Transl Med*. 2015;7:296ra110.
160. Vollrath D, Feng W, Duncan J, et al. Correction of the retinal dystrophy phenotype of the RCS rat by viral gene transfer of Mertk. *Proc Natl Acad Sci USA*. 2001;98:12584–12589.
161. Smith AJ, Schlichtenbrede FC, Tschernutter M, et al. AAV-mediated gene transfer slows photoreceptor loss in the RCS rat model of retinitis pigmentosa. *Mol Ther*. 2003;8:188–195.
162. Gorbatyuk MS, Knox T, LaVail MM, et al. Restoration of visual function in P23H rhodopsin transgenic rats by gene delivery of BiP/Grp78. *Proc Natl Acad Sci USA*. 2010;107:5961–5966.
163. Rex T, Bennett J, Maguire A, et al. *Adeno-catalase protects the Balb/C mouse retina from light damage*. ARVO: Ft. Lauderdale, FL; 2003.
164. Auricchio A, Behling KC, Maguire AM, et al. Inhibition of

retinal neovascularization by intraocular viral-mediated delivery of anti-angiogenic agents. *Mol Ther*. 2002;6:490–494.
165. Gehlbach P, Demetriades AM, Yamamoto S, et al. Periocular injection of an adenoviral vector encoding pigment epithelium-derived factor inhibits choroidal neovascularization. *Gene Ther*. 2003;10:637–646.
166. Miyazaki M, Ikeda Y, Yonemitsu Y, et al. Simian lentiviral vector-mediated retinal gene transfer of pigment epithelium-derived factor protects retinal degeneration and electrical defect in Royal College of Surgeons rats. *Gene Ther*. 2003;10:1503–1511.
167. Gehlbach P, Demetriades AM, Yamamoto S, et al. Periocular gene transfer of sFlt-1 suppresses ocular neovascularization and vascular endothelial growth factor-induced breakdown of the blood–retinal barrier. *Hum Gene Ther*. 2003;14:129–141.
168. Saishin Y, Silva RL, Kachi S, et al. Periocular gene transfer of pigment epithelium-derived factor inhibits choroidal neovascularization in a human-sized eye. *Hum Gene Ther*. 2005;16:473–478.
169. Behling K, Auricchio A, O'Connor E, et al. AAV-mediated retinal transfer of anti-angiogenic genes in a murine model of retinopathy of prematurity (ROP). *Invest Ophthalmol Vis Sci*. 2002;6:490–494.
170. Mori K, Gehlbach P, Ando A, et al. Regression of ocular neovascularization in response to increased expression of pigment epithelium-derived factor. *Invest Ophthalmol Vis Sci*. 2002;43:2428–2436.
171. Mori K, Gehlbach P, Yamamoto S, et al. AAV-mediated gene transfer of pigment epithelium-derived factor inhibits choroidal neovascularization. *Invest Ophthalmol Vis Sci*. 2002;43:1994–2000.
172. Li Q, Miller R, Han PY, et al. Intraocular route of AAV2 vector administration defines humoral immune response and therapeutic potential. *Mol Vis*. 2008;14:1760–1769.
173. Mori K, Duh E, Gehlbach P, et al. Pigment epithelium-derived factor inhibits retinal and choroidal neovascularization. *J Cell Physiol*. 2001;188:253–263.

37

Stem Cells and Cellular Therapy

Teisha J. Rowland, Martin Friedlander, David R. Hinton, David M. Gamm, Dennis O. Clegg

Stem Cells as Therapeutics to Treat Retinal Disease

Nothing more dramatically captures the imagination of visually impaired patients or the ophthalmologist treating them than the possibility of rebuilding a damaged retina using stem cells. Since many retinal neuro- and vasculodegenerative diseases progress slowly, it may be possible to use stem cell-derived "replacement cells" to prevent visual loss if such therapies are performed at an early stage of disease. Stem cells are defined as cells that are able to self-renew (i.e., create more stem cells) and differentiate into (i.e., become) specialized, more mature cell types. The three main types of stem cells that will be explored in this chapter, and that are of most interest as potential therapeutics to treat retinal disease, are human embryonic stem cells (hESCs), human induced pluripotent stem cells (hiPSCs), and adult stem cells. hESCs are derived from early embryos, specifically called blastocysts, and are pluripotent, which means they can differentiate into all of the mature cell types in the human body, including retinal cell types. hiPSCs are also pluripotent stem cells, making them similar to hESCs in appearance and behavior, but hiPSCs can be derived from adult somatic tissues, which makes it possible to create patient-specific pluripotent stem

cells when autologous replacement tissues for treating ocular, and other, diseases is desirable. Many different subtypes of adult stem cells have been identified and isolated; these adult stem cells presumably represent a pool of progenitor cells in the specific tissues in which they are found and may supply cells to maintain those tissues as well as repair the tissue following injury or stress. Overall, there are now several populations of stem cells that have been described and each may have relative benefits for the treatment of different diseases.[1] Readers are referred to Chapter 128 (Transplantation frontiers) for further discussion of clinical applications of retinal progenitor and adult transplantation therapies.

Definitions

Stem cells can be generally divided into those that are isolated from early embryonic cell populations (i.e., embryonic stem cells [ESCs]) and those that are isolated from adult tissue (i.e., adult stem cells). (hiPSCs are often grouped together with ESCs based on their behavioral similarities.) ESCs are typically isolated from blastocysts, which are at an early embryonic stage of development, and exhibit pluripotency, meaning they have the ability to differentiate into any of the mature cell types of the adult body (when cultured under appropriate conditions). Adult stem cells typically reside in adult tissues in a quiescent, undifferentiated state and, under appropriate stimuli, will divide and differentiate into the cell type of the tissue in which they reside or, if appropriately stimulated, into other cell types.[2] The mechanism whereby an undifferentiated, quiescent stem cell can give rise to a multitude of differentiated, postmitotic cell types is an area of active investigation, and large-scale genomic analysis[3] and transcriptional profiling[4] of stem cells have led to the discovery that different types of stem cells have varying degrees of "stemness," or potency (i.e., limitations on the types of cells that they can differentiate into).[5] For example, while truly pluripotent ESCs can give rise to a multitude of differentiated cell types, adult stem cells are more limited in their differentiation potential and are usually considered "multipotent," meaning they can typically differentiate into more than one mature cell type, but the variety of

cell types is usually restricted to an interrelated group.

Embryonic Stem Cells

ESCs are derived from cells in the early embryo, specifically at the late blastocyst stage, and are characterized by being pluripotent and having the capacity to self-renew indefinitely. Pluripotency is defined as the ability to differentiate into cell types belonging to the three germ layers (ectoderm, endoderm, and mesoderm; the three different tissue types that exist during development in the embryo and that later, together, comprise the adult body). Their pluripotency is the reason why ESCs are theoretically able to become any of the mature cell types found in the adult body.

The first ESCs created were murine ESCs (mESCs), derived and cultured from mouse blastocysts in 1981,[6,7] and have become important research tools for the creation of transgenic and knockout mice, and for the study of early development in mammals (Table 37.1).[8] In 1995, James Thomson's team generated nonhuman primate ESCs for the first time – cultured from rhesus monkey blastocysts[9] – and then later, in 1998, Thomson's group was also the first to derive hESCs.[10] hESCs are generated from late-stage human blastocysts that are allowed to develop for approximately 4–5 days post-fertilization. At this point, the blastocyst has not yet been implanted in the uterus and consists of a hollow sphere made up of approximately 150 cells in total and three distinct areas: the trophoblast (the surrounding outer layer that later becomes the placenta), the blastocoel (a fluid-filled cavity within the blastocyst), and the inner cell mass (also known as the embryoblast; it has the potential to become the embryo proper, or fetus). hESCs are created from cells taken from the inner cell mass, which consists of 20–50 cells at days 5 and 6 (Fig. 37.1).[11] In 2006, a method for deriving hESCs from single blastomeres without destruction of the embryo was reported.[12] Methods for culturing hESCs have typically utilized a feeder layer of inactivated mouse embryonic fibroblasts (MEFs) to facilitate the growth and survival of the stem cells, although in recent years there has been a transition towards employing feeder-free and serum-free culture methods, which are more ideal for generating cells in xenogeneic-free (xeno-free) conditions for use in

cellular transplantation therapies.[8]

TABLE 37.1
Embryonic Stem Cell (ESC) Time Lines

1981	Mouse ESCs first derived
1995	Primate ESCs isolated and grown in culture
1998	Human ESCs isolated and grown in culture
2007	Differentiated adult cells reprogrammed to ESC-like cells (iPSCs)
2009	First human ESC clinical trial approved by US FDA for spinal cord injury
2010	FDA approval for phase I/II clinical trial to treat Stargardt disease
2011	FDA approval for phase I/II clinical trial to treat advanced dry age-related macular degeneration

ESC, embryonic stem cell; FDA, Food and Drug Administration; iPSC, induced pluripotent stem cells.

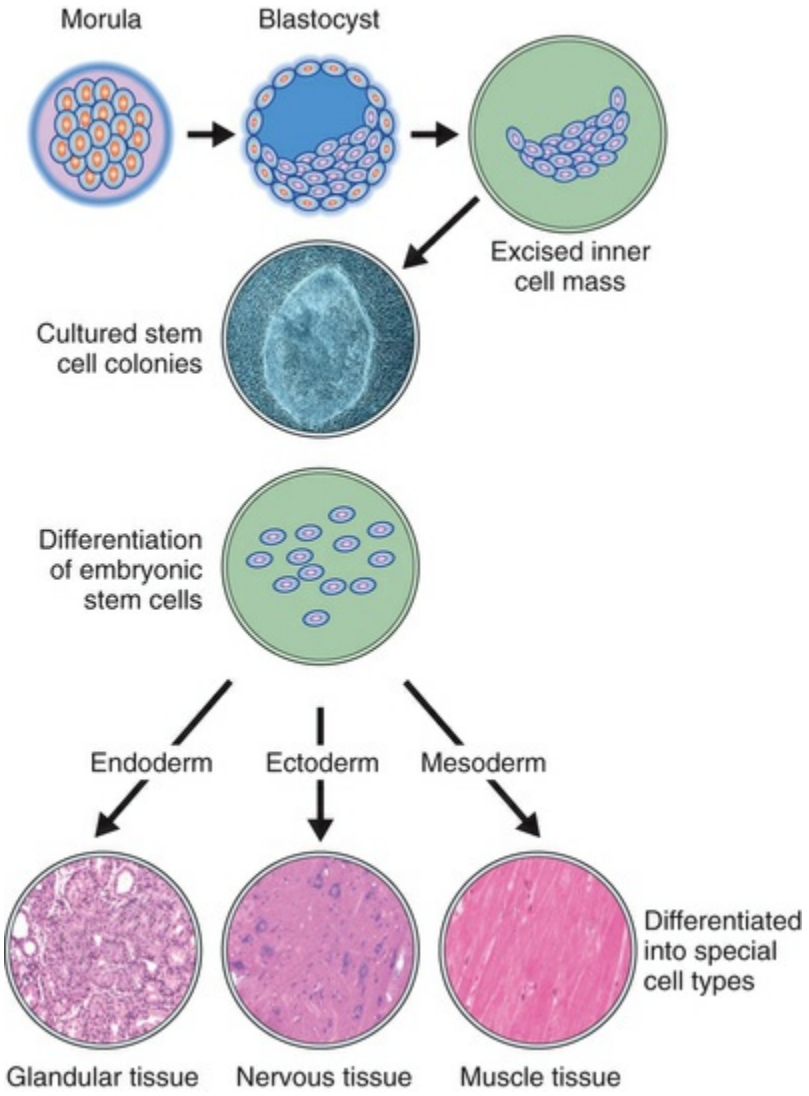

FIG. 37.1 Culture of human embryonic stem cells and their differentiation into endoderm, ectoderm, and mesoderm.

The National Institutes for Health (NIH) has developed guidelines to establish policy and procedures under which hESC-based research will be funded to ensure that NIH-sponsored research in this area is ethically responsible, scientifically worthy, and conducted in accordance with applicable law. These guidelines were developed in response to Executive Order 13505, were issued on March 9, 2009, and became effective on July 7, 2009. As of September 2016, there were 369 hESC lines eligible for use in NIH-supported research, as listed in the NIH Human Embryonic Stem Cell Registry (http://stemcells.nih.gov/research/registry/). The National Academy of Sciences has also released extensive guidelines for the ethical conduct of hESC research (http://nas-sites.org/stemcells/).

Induced Pluripotent Stem Cells

The creation of induced pluripotent stem cells (iPSCs) – pluripotent stem cells that are similar in appearance and function to ESCs but that can be generated from adult tissues – was one of the most significant advances in the field of stem cell biology. The idea that an adult, somatic cell could become a reprogrammed embryonic-like cell gained more attention in the scientific community after the creation of the first cloned animal in 1997 (i.e., Dolly the sheep) and the cloning of several other animals in the late 1990s. These cloned animals were generated using somatic cell nuclear transfer, a technique wherein the nucleus from a somatic cell is inserted into an enucleated egg cell, which is then implanted into, and develops in, a surrogate mother.[13] Similarly, the creation of iPSCs came with the finding that forcing adult somatic cells (e.g., skin keratinocytes, fibroblasts, or T or B cells from blood) to produce key ESC transcription factors could induce, or reprogram, the adult cells to a pluripotent state. In 2006, Shinya Yamanaka's group created the first iPSCs this way using mouse fibroblasts.[14] Expression of these embryonic transcription factors was accomplished by transducing the fibroblasts with a viral vector encoding the factors. Only a year

later, the same principles were independently applied by Thomson's and Yamanaka's teams to generate the first human iPSCs (hiPSCs; using human fibroblasts).[15,16] Yamanaka utilized the same transcription factors that were used for mice (Oct-4, Sox2, Klf4, and c-Myc), while Thomson used a different, but overlapping, set of factors (Oct-4, Sox2, Nanog, and Lin28). Since the creation of hiPSCs, researchers have found ways of making hiPSCs using nonintegrating vectors and systems that deliver the key reprogramming proteins to cells without directly altering the cell's genome. The creation of hiPSCs may enable the production of grafts that are autologous or donor-matched (i.e., human leukocyte antigen [HLA]-typed to assure immune system compatibility) for use in treating a variety of diseases, including those of the retina.[14,17] This is discussed in greater detail below.

Adult Stem Cells

The concept that adult tissues contain stem cells that can serve as a source of regenerative tissue is an important advancement in our way of thinking about normal mechanisms for repairing aging adult organ systems and how to apply these processes in the field of regenerative medicine.[18] While adult stem cells (specifically hematopoietic stem cells [HSCs]) were first used to treat patients during World War II – in the form of bone marrow transplants for people who had received lethal doses of radiation – these adult stem cells were not identified and characterized until decades later. Today, while there is an extensive literature on adult stem cells giving rise to nervous,[19] muscle,[20] vascular,[21,22] and hematopoietic tissue, work on retinal stem cells is more limited. Nonetheless, a literature has emerged over the past decade that strongly supports the potential for exploiting progenitor cells to maintain, and perhaps regenerate, abnormal retinal tissue. These studies describe four basic populations of cells that may contain dormant progenitor cells which, under appropriate circumstances, may have therapeutic application in the treatment of retinal disease: (1) retinal stem cells that can give rise to photoreceptors and other retinal neurons; (2) Müller glial stem cells that can differentiate into retinal neurons; (3) retinal pigment epithelial (RPE) stem cells that can not

only serve to replace diseased RPE but perhaps also be stimulated to differentiate into photoreceptors; and (4) endothelial progenitor cells (EPC) that can contribute to the retinal vasculature and exert a neurotrophic effect. Since there are a large number of reviews on retinal stem cells, this topic will not be discussed in great detail here. Müller glial cells, RPE stem cell biology, and adult bone marrow-derived HSC containing EPCs have great therapeutic potential, and are discussed below in more detail.

Retinal Stem and Müller Glial Cells

It has long been known from classic studies in developmental biology that the retina of amphibians and chick embryos regenerates after injury and that this regenerative capacity derives from quiescent stem cells that reside in the adult retina of these species.[23,24] Given that such potential exists in lower vertebrates, there have been numerous efforts to demonstrate similar regenerative capacity in the mammalian retina. For a population of retinal stem cells to exist in the adult retina, it would be necessary for such a cell population to remain quiescent after the retina has fully differentiated. Studies that give us a better understanding of gene expression during retinal development, such as by employing large-scale genomic analysis[25] or serial analysis of gene expression in combination with in situ hybridization[26] to localize gene expression temporally and spatially to individual retinal cell types, have assisted in the search for adult retinal progenitor cells by providing a kind of "molecular atlas." Such efforts have served as a starting point for the evaluation of numerous genes and their potential roles – as they are progressively switched on and off in an orderly manner – in the regulation of retinal cell developmental determination. The regulation of cell proliferation,[27] various transcription factors and signaling molecules,[28] and the surrounding microenvironment[29] have all been found to play roles during this process, providing insight into putative mechanisms whereby the mammalian retina holds in reserve a subset of progenitor cells that theoretically could be used to regenerate damaged tissue in the adult. Transcriptional profiling studies of retinas at different states of development coupled with in vitro

studies of progenitor cell populations[30] should continue to be important for providing information necessary to analyze and determine what conditions help maintain quiescence and what conditions stimulate proliferation and subsequent differentiation of retinal progenitor cell populations.

Retinal progenitor cells are purported to exist in the ciliary margin; single pigmented epithelial cells can be isolated from the ciliary margin (but not the central or peripheral pigmented epithelium) and clonally expanded in culture. However, the potential utility of these cells and their characterization have come under scrutiny and are discussed extensively in a number of excellent recent reviews and book chapters.[31–34] Retinal neuronal phenotypes[35] and neuroepithelial-like clusters of retinal progenitors[36] have also been generated via the differentiation of ESCs using factors including insulin-like growth factor (IGF)-1 and retinoic acid or the formation of self-organizing, 3-D optic vesicle-like structures from hESCs and hiPSCs. The development of such 3-D structures is explored in further detail later in this chapter.

Müller glial cells hold particular interest as an endogenous cell source due to their ability to potentially convert to a progenitor state under certain conditions, usually related to disease or injury.[33] In lower vertebrates (e.g., chickens), adult, differentiated Müller glia can, in response to injury or exogenously added cytokines or transcription factors, dedifferentiate, proliferate, and redifferentiate into additional glial cells or neurons.[37–39] Müller glia are also known to be activated in a variety of retinal vascular and neurodegenerative diseases, and in response to similar vascular changes.[40,41] Further supporting their role as stem cell-like cells are molecular profiling studies of developing mammalian retinas that show a high degree of similarity between the gene expression profiles of Müller glia and mitotic retinal progenitor cells in the mouse.[26] One study has expanded this concept significantly: amacrine, horizontal, and photoreceptor phenotypes have been found to be expressed by Müller glial cells following toxic injury to the adult mammalian retina in the presence of extrinsic factors (e.g., retinoic acid) or activation of intrinsic genes.[39] Similarly, Müller glial cells have also been shown to be capable of transdifferentiating to retinal interneurons after the introduction of a proneural

transcription factor (i.e., Ascl1) in a damaged mammalian retina.[38] These studies provide additional insight into retinal regeneration in mammals and potential rationale for targeting Müller glia in certain inherited and acquired retinal degenerative disorders. Additional studies are needed to improve our understanding of the development of mammalian Müller glial cells and their ability to revert to a stem cell-like state.

Müller glial cells may also be utilized for the targeted delivery of certain factors in the retina. These are the only cells that span the entire neurosensory retina; Müller cell processes extend anteriorly to the ganglion cell layer as well as posteriorly to the RPE. These processes form intimate contacts with retinal blood vessels, photoreceptors, and other retinal neurons. In animal models of outer retinal neovascular disease, the appearance and location of activated Müller glial cells precisely correlate, both temporally and spatially, with subretinal neovascularization and associated neuronal degeneration in the outer retina.[42] Activated Müller cell-targeted adeno-associated viral vectors containing a transgene encoding a neurotrophic molecule have been shown to target the outer retina in vasculodegenerative[42] and neurodegenerative disorders[43] characterized by photoreceptor degeneration. This strategy could be useful clinically to avoid the need for subretinal injections of the viral vector, a procedure that can have deleterious effects on already diseased retinas.

Differentiation of hESCs and hiPSCs Into Photoreceptors

Studies evaluating the in vivo efficacy of photoreceptors derived from pluripotent stem cells are at an early stage of development. Differentiation of hESCs into retinal progenitor cells has been achieved, as has further in vitro differentiation into photoreceptor-like cells.[44,45] However, while enrichment of RPE derived from human pluripotent stem cells is relatively straightforward, no equivalent protocol for purifying photoreceptors from these stem cell sources exists yet, and contamination of multiple retinal and perhaps other cell types is a significant concern.[46] Initial differentiation studies showed that Noggin (inhibitor of BMP

pathway) or Dickkopf (Dkk)-1 (an antagonist of the Wnt signaling pathway) promote anterior neural identity and then IGF-1 promotes the formation of retinal progenitor cells.[45,47] Tom Reh's lab reported differentiation of retinal and photoreceptor-like cells from hESC-derived embryoid bodies grown in suspension culture, through addition of Noggin, Dkk-1, and IGF-1 into neuronal differentiation medium in adherent culture[44,48] that, after 21 days of differentiation, expressed retinal progenitor cell-related transcription factors such as Rx, Otx2, Pax6, Chx10, and Crx.[48] When further cultured, these cells formed neural rosettes that, when allowed to self-aggregate, formed retinal progenitors and differentiated cells expressing photoreceptor and RPE markers.[48] Microarray analysis of hESC-derived retinal cells showed a very high correlation between genes expressed in human fetal retina and hESC-derived retinal cells.[49] Thereafter, investigators from the RIKEN Research Institute reported the successful derivation of retinal progenitor cell and photoreceptors from both mouse and human ESC using an even more highly defined stepwise method.[50,51] The final steps included use of retinoic acid and taurine to induce photoreceptor differentiation. With this induction method, they found that hESCs can be differentiated into photoreceptors showing both rhodopsin and recoverin immunoreactivity in 150 days.[51] The Gamm lab subsequently found that retinal differentiation from hESCs and hiPSCs can also occur through a near default pathway due to endogenous production of appropriate proanterior neuroectoderm and proteinogenic factors.[45]

Most recently, the Gamm, Sasai, and Canto-Soler labs have shown that photoreceptors can be generated from 3D retinal cultures using hESCs and hiPSCs, and these cells possess typical electrophysiologic features as well as primitive inner and outer segments, and are also light-responsive,[36,46,52,53] making such 3D approaches a promising route for generating photoreceptors derived from human pluripotent stem cells. These 3D structures are further explored in the following section of this chapter.

As compared to RPE, photoreceptor transplants would likely require integration into – or reformation of – the existing outer nuclear layer and establishment of functional synapses to act as a replacement therapy. Conversely, there may be some therapeutic

benefit by providing neurotrophic support to adjacent cells without true synaptic integration. When hESC-derived retinal progenitor cells were co-cultured with explants from retinal degeneration mice (*Aipl1*$^{-/-}$), they showed incorporation into the retinas, had morphologic characteristics of photoreceptor cells, and were immunoreactive for recoverin – a finding that was only rarely found when cells were cocultured with wild-type retinas.[44] Subsequent experiments showed that when these cells were injected into the subretinal space of adult Crx$^{-/-}$ mice (a model of Leber congenital amaurosis), the hESC-derived retinal cells differentiated into photoreceptor-like cells that were immunoreactive for recoverin and rhodopsin and restored light responses with an electroretinogram-like signal in the transplanted eye.[54] While the integration of hESC-derived photoreceptors may be a relatively rare event, these results demonstrate in principle that hESCs can be used as a source of cells for photoreceptor replacement therapy. Rod precursor cells generated from mESCs have also been transplanted into various mouse models in multiple studies.[55–58] Integration of the transplanted precursor cells in the investigated mouse models was found to depend upon disease progression and the specific genetic defect in the model, although significant integration was possible even in some late-stage models.[55] Integration of these cells was also shown to lead to the development of mature outer segment-bearing photoreceptors.[56] Of particular note, in a mouse model of severe retinitis pigmentosa that had no remaining rod cells, transplantation of precursor cells resulted in a polarized outer nuclear layer with mature rods and light-sensitive outer segments that restored visual function.[57] Fewer retinal integration and functional studies have been performed using photoreceptors derived from hiPSCs.

Differentiation of hESCs and hiPSCs Into Three-Dimensional Retinal Tissues

In 2003, murine ESCs were shown to be able to differentiate into eye-like structures with cells that have properties of the crystalline lens, neural retina, and RPE.[59] Later, in 2008, dissociated cells from these eye-like structures were shown to integrate into the retina,

especially after retinal injury.[60] Then, in 2011, investigators reported the remarkable discovery that murine ESC aggregates grown in the presence of added basement membrane components formed hollow spheres that underwent evagination into vesicles and then invagination into 3-D, optic cup-like structures containing RPE and neural retinal domains, and stratified neural retinal tissues[61] (Fig. 37.2). Later in 2011, populations of human retinal progenitor were isolated from 3-D optic vesicle-like structures (OVs) derived from hESCs and hiPSCs.[36] Since this discovery, several studies have reproduced and characterized human pluripotent stem cell-derived OVs.[46,52,53] These OVs, which are separated from early forebrain neurospheres, have been shown to be able to differentiate into all neuronal retinal cell types, including RPE and photoreceptors.[36] The timeframe for the generation of different cell types in human OVs is similar to human retinogenesis, with cones being the earliest photoreceptor cell type to appear and rods being produced in greater numbers later.[52] In addition, these OVs possess clearly delineated apical-basal orientation and self-organized tissue layers mimicking those found in the developing human retina, having a neuroblastic layer that gives rise to an inner ganglion layer, an intermediate layer containing retinal interneurons, and an outer layer comprised of photoreceptor cells.[52,53] Human OVs hold much potential for use in retinal disease research (such as by creating patient-specific hiPSC-derived OVs as retinal models) and clinical applications to regenerate diseased retinas.

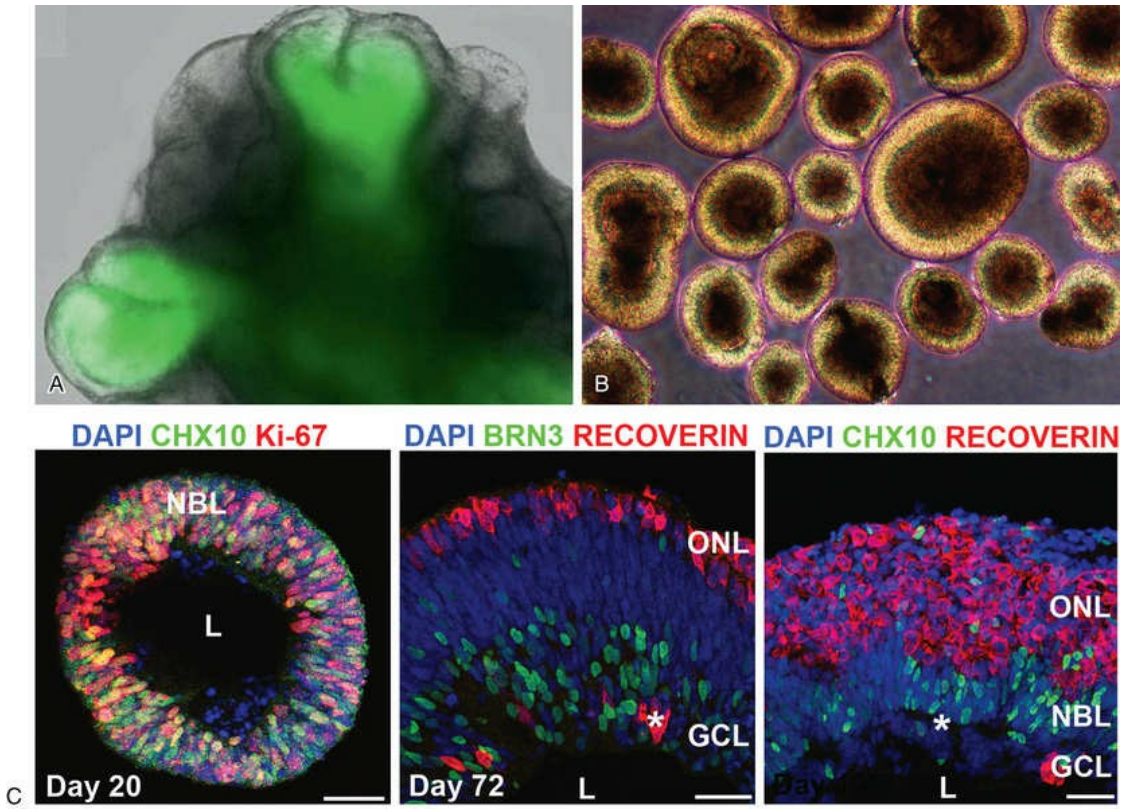

FIG. 37.2 (A) Murine embryonic stem cells can self-assemble into optic cup-like structures. These complex primitive retinal structures are engineered to express green fluorescence protein. (B,C) Similarly, hESCs and hiPSCs can differentiate and self-organize into optic vesicle-like structures, as shown here in phase-contrast (B) and immunostained (C) images that reveal structures that, over time, spontaneously organized into primitive retina-like tissues. (Panel A reproduced with permission from The Scientist – Magazine of the Life Sciences. classic.the-scientist.com/news/display/58105/ © The Scientist. Panel B © ARVO. From Phillips MJ, Wallace KA, Dickerson SJ, et al. Blood-derived human iPS cells generate optic vesicle-like structures with the capacity to form retinal laminae and develop synapses. Invest Opthalmol Vis Sci 2012;53:2007-2019.)

RPE Cells

RPE cells enjoy an intimate relationship both anatomically and functionally with their neighboring cells in the retina, forming a monolayer of pigmented, hexagonal cells situated between the overlying photoreceptors and the underlying choriocapillaris (which comprise part of an extracellular matrix layer called the

Bruch's membrane). The RPE cells are highly polarized, with their apical sides interacting with photoreceptor outer segment tips and their basal sides attaching to the Bruch's membrane.[62a] This interdependence has historically contributed to the difficulty in determining where the principal defect lies in many inherited retinal degenerations – the photoreceptor or underlying RPE cell. With the advent of molecular genetics this confusion has lessened, but the interdependence between these two cell types remains, and there is often concomitant degeneration of both cell types observed in a variety of inherited and acquired degenerative diseases of the retina. In this regard, RPE cell transplantation has been evaluated both for its potential to replace diseased RPE as well as to provide a source of cells whose phenotypic differentiation may be manipulated by various cytokines and trophic substances. Thus, RPE cell lines have been developed for use as RPE cell transplants, and as cell-based drug delivery platforms.

Because the RPE cells are unable to self-renew, replenishing diseased RPE cells with various sources of healthy RPE cells has been explored. In a number of macular and retinal degenerative disorders there is atrophy of the RPE and associated malfunctioning in the phototransducing cellular machinery. Damaged RPE cells and associated atrophy are hallmarks of age-related macular degeneration (AMD). Heroic surgical approaches have been undertaken in individuals with healthier, RPE-rich regions of the retina to translocate and insert such autologous extramacular RPE sheets below the fovea, and these efforts have been associated with visual improvement, serving as a proof-of-principle that such cell sheet transplantations are a potential treatment strategy.[62a] A limitation of this approach is the availability of cell sources; autologous peripheral RPE cells may be non-ideal due to sharing the same genetic defects.

Allogeneic adult RPE cells, some of which have been shown to have stem cell characteristics, are also being pursued for use in therapy.[62b,62c] Methods have been developed for expansion of adult RPE cells from donor eyes, which could be used to replace dysfunctional or dying RPE cells in patients. One limitation of using adult and fetal RPE is their limited ability to expand, however. Consequently, deriving RPE cells from potentially unlimited stem

cell sources is an appealing option.

RPE Cell-Based Delivery of Trophic (and Other) Factors

Immortalized human RPE cell lines have been created by stable transfection with a plasmid encoding the simian virus 40 large T antigen and many of the trophic (derived from the Greek word for "nourishment") or growth factors expressed by functional RPE cells in vivo are observed to be expressed by these transformed cell lines.[63] When these cells are transplanted subretinally into a rat model of retinal degeneration (the Royal College of Surgeons (RCS) rat), loss of visual function is attenuated[64] and cortically dependent visual function is preserved long-term.[65] These RPE cell lines can be transfected with plasmids encoding a variety of trophic factors shown to have protective effects on photoreceptors[66,67] and then encapsulated into polymer devices that permit diffusion of cell products into the tissue into which they are transplanted. When transformed RPE cell lines are transfected with a plasmid encoding one such factor, ciliary neurotrophic factor (CNTF), and transplanted directly into the vitreous of dogs with retinal degeneration, photoreceptor degeneration is reduced.[68] While multiple human clinical trials have been performed using transplantation of CNTF-transfected encapsulated RPE cells to treat different retinal degenerative diseases, the efficacy of this approach is unclear; patients with retinitis pigmentosa (RP) who received the implant showed no improvement in two clinical trials and some patients experienced reduced visual field sensitivity that was reversed upon removal of the implant.[62a,69] In contrast, vision was found to be significantly improved in a trial to treat AMD.[62a,70] Overall, implanted encapsulated cell devices utilizing trophic factors may provide factors critical to the prevention of, or recovery from, retinal degenerative disease.

Differentiation of hESCs and hiPSCs Into RPE

Over the past decade, a number of methods have been reported to

achieve the differentiation of hESCs and hiPSCs into retinal cells.[44,51,71–73] Some of these methods were developed for the differentiation of these stem cells into one type of retinal cell, such as the RPE[51,71–73] or photoreceptors,[51,72,73] while other methods have focused on the efficient generation of retinal progenitor cells.[44]

Spontaneous differentiation of hESCs and hiPSCs into RPE is the simplest and most commonly used method to produce RPE from these pluripotent stem cells.[72] hESC colonies are first allowed to overgrow in growth factor-supplemented hESC medium until the borders of the colonies contact each other. The medium is then changed to basic hESC medium without basic fibroblast growth factor supplementation and is changed every other day for several months until the RPE cells appear (visible as small pigmented colonies in the culture dish) and are then mechanically enriched (Fig. 37.3). RPE cells can also be derived from hESCs and hiPSCs using a two-stage induction method: the stem cells are first differentiated towards a neuroectodermal fate in suspension culture (i.e., embryoid bodies) using neural differentiation medium, and then differentiated into RPE through adhesive culture on cell culture plates.[36] During these stages of induction and differentiation, the RPE cells appear as early as 4 weeks and reach a large enough number of cells for subculture at approximately 8–10 weeks.[72] Nicotinamide and Activin A (a member of the transforming growth factor-beta superfamily) can also be used to direct the induction of RPE from hESCs.[36,74] Additionally, while RPE differentiation protocols have typically employed culture on MEFs and the addition of animal-derived soluble factors, efforts have been made to explore and adopt feeder-free and serum-free culture methods, as generating cells in such xeno-free conditions may be more ideal for use in cellular transplantation therapies.[62a,75]

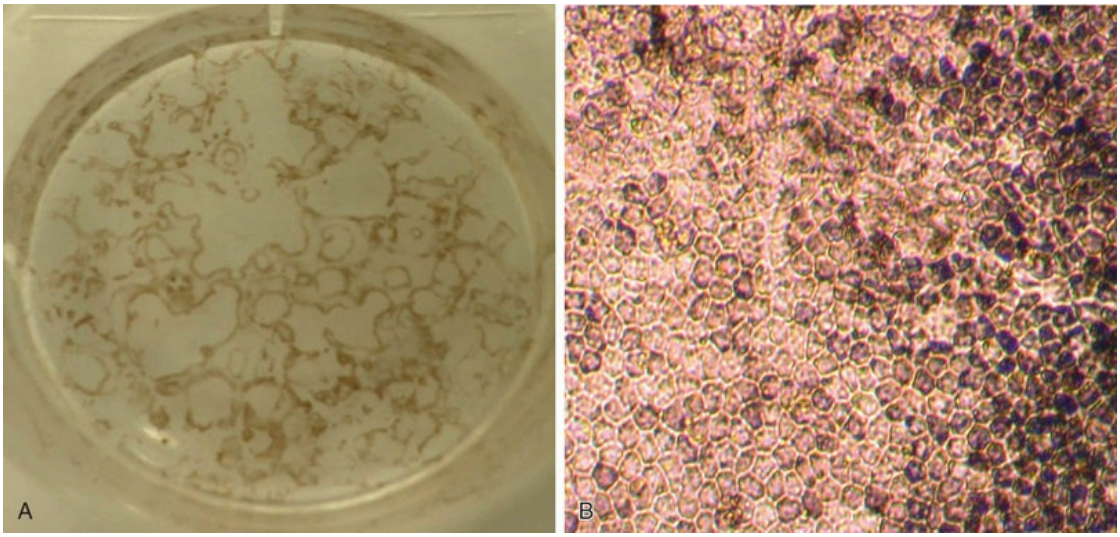

FIG. 37.3 Spontaneous differentiation of pigmented retinal pigment epithelium from human embryonic stem cells after withdrawal of basic fibroblast growth factor. In dish on left (A), multiple foci of pigmented cells are seen. These colonies can be picked, enriched, and expanded to pure populations of retinal pigment epithelium, as shown on right (B). (Panel A courtesy of Dennis Clegg, PhD, University of California Santa Barbara.)

RPE cells can be relatively easily identified, isolated, and enriched apart from other differentiated cells in these cultures because of their unique pigmentation, hexagonal shape, and pattern of growth. The RPE patches can be either mechanically incised out of the cultures through microdissection or enzymatically dissociated from the cultures. The enriched cells can then be grown to confluence, passaged, and retain typical pigmentation and morphology (Fig. 37.3).[76]

Characterization of hESC- and hiPSC-RPE in Vitro

The characteristics that define human RPE cells have been outlined in Chapter 18 (Cell biology of the retinal pigment epithelium) and reviewed by others.[71] hESC- and hiPSC-derived RPE (hESC-RPE and hiPSC-RPE, respectively) develop a typical hexagonal shape and become highly pigmented when they attain confluence (Fig. 37.3B). The cells can further differentiate and become highly polarized when grown for extended periods of time on Transwell

inserts and other substrates (Fig. 37.4).[76–78] Polarized hESC-RPE show apical microvilli, are joined in the apical regions by tight junctions, show apically distributed sodium/potassium ATPase (Na^+/K^+ATPase), and have a high transepithelial resistance.[78] hESC-RPE express a host of characteristic RPE genes, including visual cycle genes (*RPE65*, *RDH 11*, *CRALBP*); RPE membrane channel and transporter genes (*BEST1*, *SLC*); pigment biosynthesis and melanin biosynthesis genes (*GPR143*, *TYRP1*, dopachrome tautomerase gene *DCT*, *SILV*); and phagocytosis-associated genes (*LAMP2*, *VDP*, *Mertk*, *GULP1*).[72,79] hiPSC-RPE cells have been found to express RPE markers similarly to hESC-RPE cells, and both hESC-RPE and hiPSC-RPE can perform RPE functions as well, including being able to phagocytose rod outer segments.[72,79,80,81] However, transcriptomic studies have revealed significant differences in gene transcription between pluripotent stem cell-derived RPE and native human RPE,[82] emphasizing the importance of analyzing the functional consequences of transcriptional activity through metabolomic-based analyses (which can quantitatively measure the activities of endogenous biochemical pathways)[83–85] and sophisticated in vivo imaging techniques, such as scanning laser ophthalmoscopy, optical coherence tomography, and adaptive optics, coupled with focal electroretinography, which will altogether permit the detailed evaluation of therapeutic stem cell treatments.

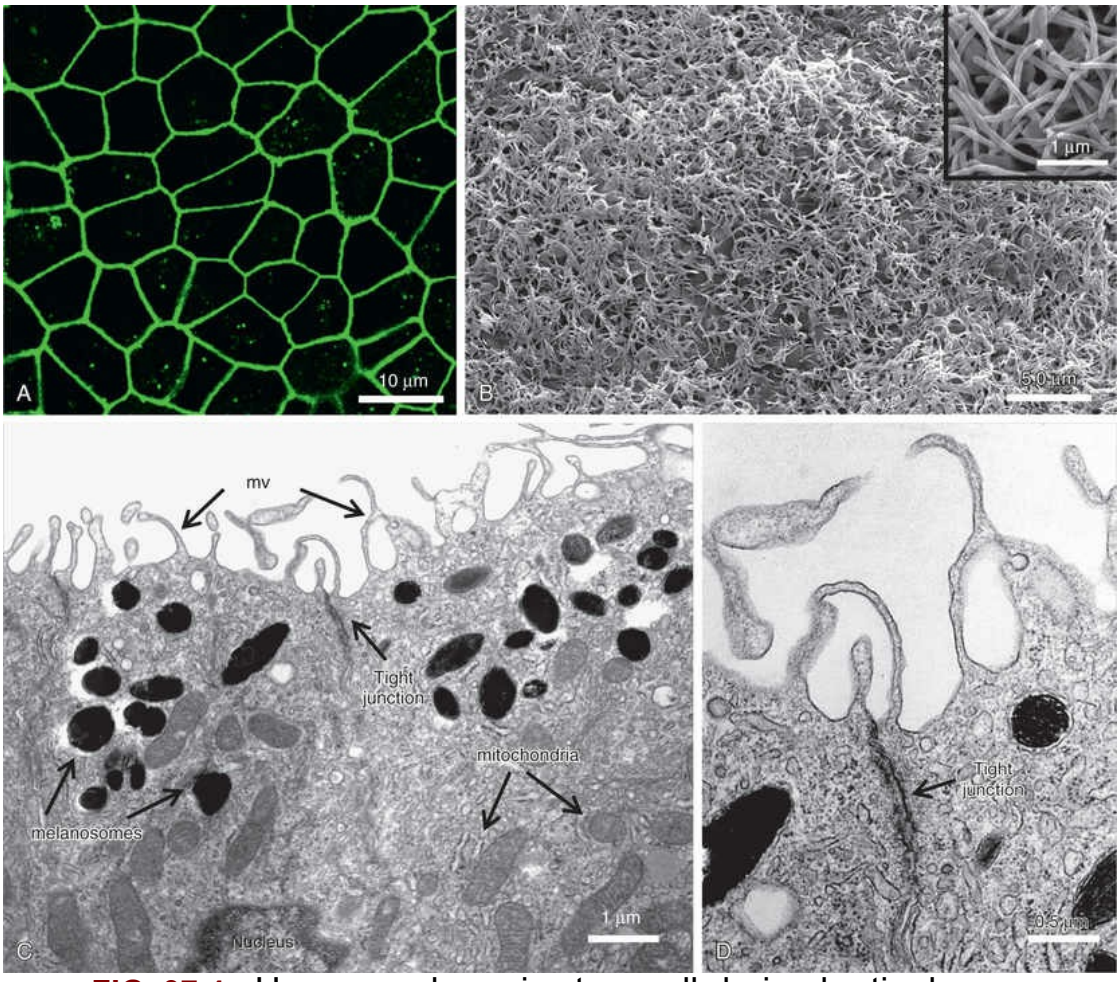

FIG. 37.4 Human embryonic stem cell-derived retinal pigment epithelium can be differentiated into a polarized monolayer. These monolayers show tight junction proteins (ZO-1), as shown by confocal microscopy (A), apical microvilli, as shown by scanning electron microscopy (B), and apical microvilli, apical melanosomes, and tight junctions, as shown by transmission electron microscopy (C,D). *MV,* microvilli.

Efficacy of hESC- and hiPSC-RPE in Vivo

The most commonly used model to evaluate therapeutic efficacy of hESC-RPE and hiPSC-RPE is the RCS rat. The primary defect in the RCS rat is in the RPE; thus this model provides the ability to evaluate the effectiveness of RPE cell replacement therapy. The RCS rat has a recessively inherited mutation in the receptor tyrosine kinase gene *Mertk,* leading to impaired phagocytosis of shed photoreceptor outer segments with buildup of outer-segment

material in the subretinal space, and subsequent secondary degeneration of photoreceptors between postnatal days 20 and 60.[86]

The two main transplantation approaches being pursued in the RCS rat, other model animals, and human trials are injecting a suspension of stem cell-derived RPE cells into the subretinal space and implanting the cells as a monolayer cultured on a membrane.[62a] Using subretinal injections of cell suspensions of hESC-RPE, several groups have shown reproducible survival of the transplanted hESC-RPE in the subretinal space of the RCS rat (>220 days in one study), and positive labeling of these cells with human-specific markers and RPE-specific genes (e.g., *RPE65*).[74,80,87–89] The cells appear to disperse in the subretinal space and, while clumps of cells or multilayered grafts are often formed, in some cases they were arranged in an apparent monolayer. Cells showed focal rhodopsin staining, suggesting that they are phagocytosing photoreceptor outer segments.[74,88,89] The transplanted hESC-RPE were associated with histologic and functional rescue of the photoreceptors, as measured by delay in the loss of nuclei in the outer nuclear layer, and retention of electroretinogram and optomotor responses in the treated eye compared to untreated eye.[74,87–89] Each of these studies utilized immune suppression (typically systemic cyclosporine, with or without systemic corticosteroid) to prevent immune rejection of the xenograft. Although the subretinal space is thought to be an immune-privileged site, such privilege may be compromised at the time of surgery or by the disease process.[90,91] hiPSC-RPE cell suspensions have also been injected into the subretinal space of RCS rats with similar in vivo results: they phagocytose photoreceptor outer segments, functionally rescue photoreceptors, and maintain long-term visual function.[72,80]

The main alternative approach to the use of hESC-RPE cell suspensions is to transplant monolayer sheets of highly differentiated and polarized RPE resting on a biodegradable or biostable scaffold. The reasoning for such an approach is that it is essential for RPE cells to become a polarized monolayer to carry out their normal functions, and implanting these cells as a monolayer should allow them to better integrate with the host photoreceptor outer segments and thus improve the functionality of the graft.[77] It has been shown that hESC-RPE can be polarized in vitro to develop

tight junctions with high transepithelial resistance and elaborate extensive apical microvilli (Fig. 37.4) and that highly polarized hESC-RPE show increased secretion of pigment epithelial-derived growth factor (a factor with neurotrophic and antiangiogenic activity).[78] hESC-RPE are capable of phagocytosing photoreceptor outer segments,[79] and polarized hESC–RPE specifically show increased phagocytosis of bovine rod outer segments in vitro compared to nonpolarized cultures.[78] Studies implanting polarized hESC-RPE grown on a nonbiodegradable substrate (e.g., parylene) show retention of an intact monolayer in vivo and prominent integration with host photoreceptors (Fig. 37.5).[77]

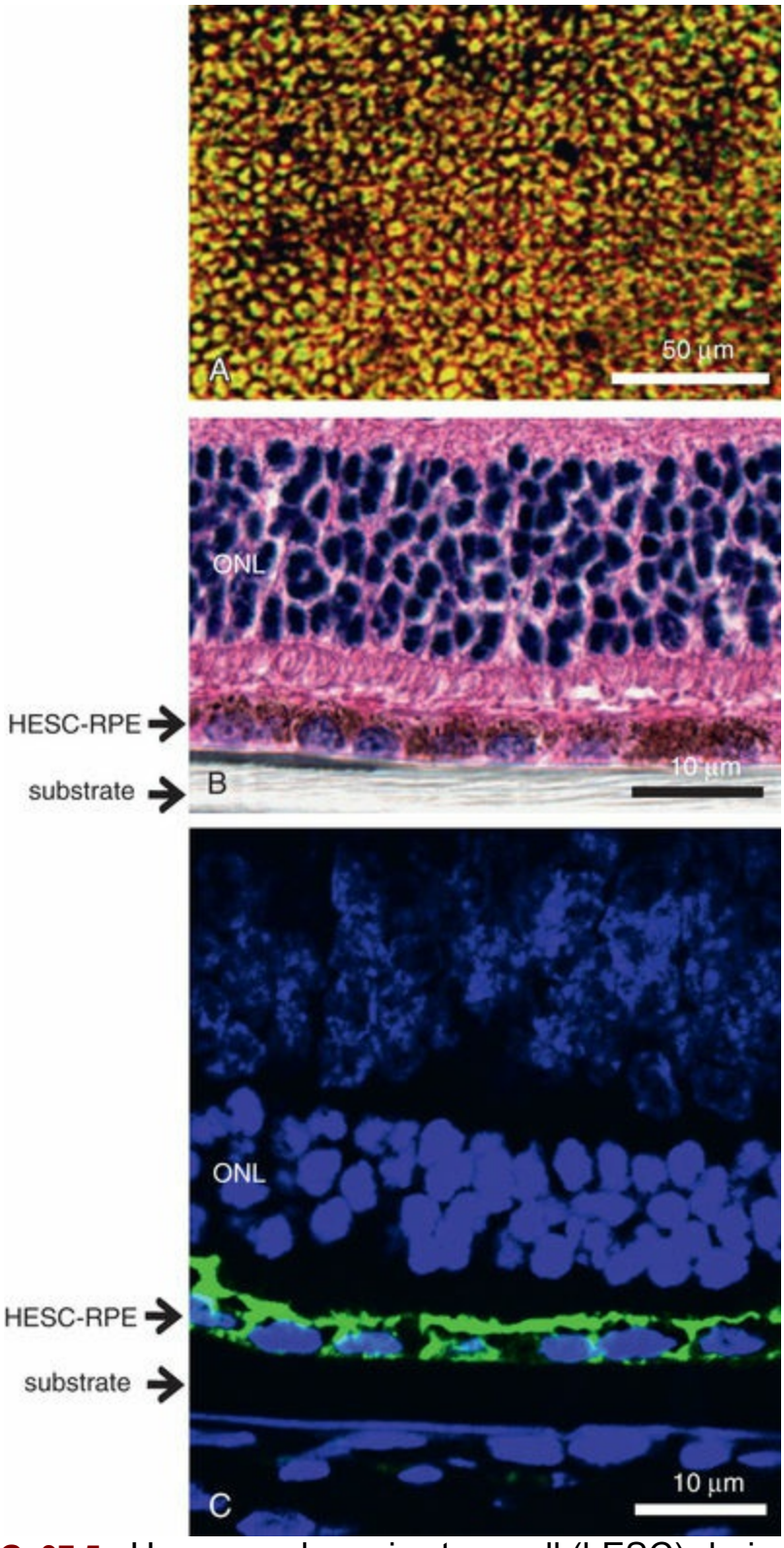

FIG. 37.5 Human embryonic stem cell (hESC)-derived retinal pigment epithelium (RPE) can be grown to confluence and polarized on a nonbiodegradable substrate. In (A), the pigment cells form an intact monolayer. The cells with substrate can be implanted in the subretinal space of Royal College of Surgeons

rats where they survive and protect host photoreceptors from degeneration. In (B) (hematoxylin and eosin stain), the hESC-RPE sitting on the nonbiodegradable membrane integrate into the host retina. Note the interface between the transplanted RPE and the host photoreceptor outer segments (*arrows*). In (C), the transplanted hESC-RPE can be identified using the human-specific marker TRA-1–85 (immunofluorescence microscopy with human marker TRA-1–85 in green, and nuclear counterstain 6′-diamidino-2-pheninlindole hydrochloride (DAPI) in blue). *ONL*, outer nuclear layer.

The relative efficacy of hESC-RPE cell suspensions versus polarized sheets is under active investigation by several groups. Injections of subretinal suspensions have been shown to rescue photoreceptors and preserve visual function, although problems and concerns have been reported with cell survivability, placement, and formation of a polarized monolayer. For example, hiPSC-RPE suspension injections into the subretinal space of monkeys created blebs of accumulated cells that compromised monolayer formation. At the same time, reflux of the injected hiPSC-RPE into the vitreous can result in severely damaging proliferative vitreoretinopathy.[92] On the other hand, some studies have shown that monolayer transplantations may improve photoreceptor function and survival compared to cell suspension injections.[80] For example, when hiPSC-RPE sheets were transplanted into the subretinal space of monkeys, the sheets were found to remain in place after implantation.[92]

The effect of the local tissue microenvironment on transplant survival is an important issue when considering how best to deliver stem cells and cells derived from stem cells. Cross-talk between cells and extracellular matrix is critical to maintaining the differentiated cell type as well as insuring appropriate function. Many studies, in the retina as well as other tissues, have identified a number of factors that may be critical to the successful engraftment of stem cell-derived, and other, cell types, including cardiomyocytes,[93] spinal cord,[94] and brain[95] neurons and photoreceptors.[96]

Pivotal safety studies are necessary prior to receiving approval from the FDA for a specific clinical trial, although there has been

increasing evidence that short-term safety of implanting pluripotent stem cell-derived RPE is not a major concern.[62a] Studies using hESC-RPE cell suspensions under good manufacturing practices and good laboratory practice have been performed to establish karyotypic stability in the cells, lack of infectious and adventitious agents in the product, and lack of teratoma and/or tumor formation by the cells in immune-deficient mice.[88] It should be noted that G-banding karyotypic analysis may not show any significant abnormalities while high-resolution DNA analysis may show culture-induced copy number changes and loss of heterozygosity; the significance of these changes for the purpose of cell therapy is unknown.[12] Importantly, none of the studies that utilized highly differentiated hESC-RPE in immune-deficient animals found evidence of teratoma formation.[74,87–89] However, long-term survival, function, and safety studies are still needed to achieve clinical application of stem cell-based therapeutics for AMD.[62a]

Using hiPSCs as a Source of RPE Grafts

Although it is possible that patients with hiPSC-derived autologous transplants may not require immunosuppressive treatment to prevent graft rejection, there are still major safety concerns regarding using hiPSC-RPE in transplantations. Post-translational modifications in hiPSCs may occur during dedifferentiation and/or differentiation, which may cause even autologous hiPSC-RPEs to elicit an immune reaction. However, studies investigating multiple hiPSC lines have detected only negligible immune responses following transplantations of hiPSC-derived cells, including hiPSC-RPEs.[62a,92] There have also been concerns that transplanted hiPSC-derived cells could undergo malignant transformation resulting from reactivation of the reprogramming transcription factors (e.g., *c-MYC*) that can be randomly integrated into the genome at multiple loci following retroviral transduction,[97–101] although this situation may be circumvented by using efficient, high-fidelity reprogramming methods that do not cause the reprogramming factors to become integrated into the genome. Such nonintegrating reprogramming systems – including sendai-viral, episomal, and mRNA transfection methods – are becoming more commonly

employed, and are thoroughly reviewed elsewhere.[102] Additionally, while epigenetic markers (some associated with cancer and/or pluripotency) may remain on both hiPSC- and hESC-derived cells after differentiation,[103] hiPSCs have been found to differ from hESCs by retaining additional epigenetic patterns that are typical of the somatic cells from which the hiPSCs were reprogrammed.[104] These epigenetic remnants may cause cells to undergo dedifferentiation, or drift away from the final, target cell type. To overcome this, efforts have been made to modify differentiation protocols[105] and screen the final cell product to detect and eliminate cells that are not the desired cell type, such as undifferentiated cells or cells that resemble ones from the hiPSCs' somatic origins (via flow cytometry and/or qRT-PCR).[62a,106]

It is also debated whether hiPSC-derived autologous cells are actually ideal or not for use in transplantations to treat a disease with a genetic basis, such as retinitis pigmentosa, because the derived cells would still contain the genetic abnormality (or abnormalities) that predispose the individual to the disease. While several genetic risk alleles for AMD have been identified,[107] manifestation age of AMD even in the presence of these risk alleles is above 55 years. Hence, hiPSC-RPE cell grafts from AMD patients would be expected to represent younger, and presumably healthier, RPE that have not yet themselves become damaged by the aging processes. Furthermore, patient-derived hiPSCs could be modified genetically to “fix” or replace the faulty genes, and then be differentiated into the desired hiPSC-RPE cells for use in transplantation.[62a] With the rapid development and continual improvements of the CRISPR/Cas9 gene-editing technique, such approaches are becoming more feasible, although it may not be a practical approach for the near future.[108] New methods to combine somatic cell reprogramming with gene correction offer a more time- and cost-effective means to harness the potential benefits of autologous hiPSC therapies.[109] Alternatively, the production of homozygous HLA-matched banks of hiPSCs could provide an off-the-shelf supply of partially immune matched stem cells for therapeutic use.

Exhaustive comparative analyses of multiple human hiPSCs and hESC lines reveal that, while many hiPSCs and hESCs lines share

very similar transcriptomic and epigenetic profiles, others are heterogeneous. The differences observed are randomly distributed and limit the differentiation capacity of the cells.[110] Furthermore, recent evidence shows that, in hiPSCs, reprogramming and selection pressure to obtain rapidly proliferating cell lines may induce chromosomal aneuploidy in nonrandomly distributed loci that may further limit the differentiation capacity and promote tumorigenicity of hiPSCs.[111–113] Genetic instability in hiPSCs is correlated with higher passage numbers, so reprogramming methods that are inefficient and require multiple passages may increase the risk of tumorigenesis.[111,112]

Generating patient-specific hiPSC-RPE is more time- and resource-intensive compared to creating hESC-RPE, which represents an economical challenge for patients and healthcare systems. To generate patient-specific hiPSCs, a cellular sample (commonly a skin fibroblast punch biopsy or, increasingly, a blood sample) must first be collected and cultured from patients, then the somatic cells are reprogrammed into hiPSCs, and finally the resultant hiPSC clones undergo careful screening, with all of this happening prior to RPE differentiation, which in itself is a time-consuming process. Therefore, to generate any tissue of interest, including RPE from hiPSCs, one or two specific reprogramming protocols may need to be adopted and optimized to ensure reliable, safe, and efficient derivations of that cell type.

Adult Bone Marrow-Derived Endothelial Progenitor Cells

Emerging evidence suggests an important role for endothelial cells in promoting interactions, self-renewal, and possibly the "rescuing" of severely stressed cells, all in surrounding vascular networks. The vast majority of diseases that lead to vision loss in industrialized nations, such as AMD, diabetic retinopathy, and neovascular glaucoma, do so at least in part as a result of abnormalities in the retinal or choroidal vasculature (i.e., macula edema, retinal and vitreous hemorrhage, and fibrovascular scarring). Most inherited retinal degenerations, such as retinitis pigmentosa, exhibit vascular

abnormalities traditionally attributed to the loss of neuronal elements and accompanying decreased metabolic demand, leading to vascular atrophy. "Cross-talk" between local vascular networks and the tissues they supply almost certainly helps maintain a functional state in a variety of organ systems.[114–116] Endothelial cells specifically are known to provide trophic substances that greatly stimulate self-renewal and expand neural differentiation of neural stem cells,[117] which has led to the idea of using EPCs to rescue surrounding tissues in the face of severe stress, such as hypoxia or cellular degenerations.

Adult bone marrow-derived EPCs, which consist of a lineage-negative (Lin^-) population of HSCs,[118] mobilize from the bone marrow in response to a variety of signaling molecules.[119,120] These EPCs can specifically target sites of angiogenesis in induced ocular injury,[121] where they can incorporate into forming blood vessels and potentially help relieve ischemia. While there is strong evidence supporting the concept that bone marrow contains progenitor cells capable of participating in the repair of a variety of injured tissues,[21] there is significant controversy as to how commonly such developmental plasticity is observed in adult HSCs[122] and even whether these EPCs are derived from HSCs or, in fact, are derived from an entirely distinct population of bone marrow-derived stem cells. While many reports in the literature demonstrate that HSCs can differentiate into a variety of cell types other than hematopoietic cells, including neurons, glia, and muscle, depending on their microenvironment,[123] the precise identity of the precursor cell remains unclear.[124,125]

The potential clinical utility of bone marrow-derived EPCs[21] falls into three broad categories. First, if these cells target sites of ischemia during circulation and, thus, contribute to pathologic neovascularization, it seems reasonable to inhibit their targeting or differentiation, thereby inhibiting angiopathies of the type seen in retinal and choroidal neovascularization. Second, and alternatively, enhancing their participation in functional, ischemia-relieving angiogenesis may be of benefit in ischemic retinopathies such as diabetes. Third, if EPCs do, indeed, target to sites of neovascularization, it should be possible first to transfect these cells ex vivo with plasmids encoding angiostatic or angio/neurotrophic

proteins and, thus, inhibit abnormal angiogenesis or enhance trophic activity of EPCs through a form of cell-based therapy. Each of these approaches will be explored below.

Potential Clinical Utility of Bone Marrow-Derived EPCs

Several groups have recently demonstrated that HSCs contain a pool of EPC capable of incorporating into areas of retinal and choroidal neovascularization. The study by Grant and colleagues was the first direct demonstration that systemically administered HSC can function as hemangioblasts during hypoxia-stimulated retinal neovascularization.[126] In these studies, GFP-expressing HSCs were injected intravenously into mice that had been sublethally irradiated (to destroy host bone marrow), mouse retinal neovascularization was stimulated (via thermal laser), and the injected GFP-expressing HSCs were found to contribute to the neovascularization. Other studies using the same irradiation/bone marrow reconstitution model have shown that circulating stem cells can also contribute to choroidal neovascularization.[127–129] This work shows that circulating, undifferentiated HSCs can be recruited to sites of retinal or choroidal neovascularization and, along with proliferation of local endothelial cells, can contribute to new blood vessel growth and development. While the experiments of Grant and colleagues demonstrate that circulating cells can incorporate into laser-stimulated retinal neovascularization, the relative contribution of circulating HSCs and endogenous retinal vascular endothelial cells to newly forming vasculature in normal conditions – when the proliferation of local cells is not impaired by irradiation – remains unknown.[121]

If circulating EPCs contribute to pathologic neovascularization in ischemic and inflammatory retinopathies, such as diabetic retinopathy and AMD, would inhibition of their targeting to these sites reduce abnormal angiogenesis? One study found that when R-cadherin (an adhesion molecule suspected to be involved in the targeting of HSCs to the retinal vasculature) was functionally blocked in HSCs prior to intravitreal injection, the cells did not target sites of angiogenesis.[130] However, all of the molecular signals

involved in HSC "homing" have not yet been identified (although R-cadherin is clearly involved); identification of these signals would be of immense benefit for exploiting the potential use of HSCs in therapeutic angiogenesis and directed cell therapy. Other adhesion molecules, such as integrins, likely play roles in targeting circulating EPC to sites of abnormal angiogenesis (e.g., tumor vascularization), and these molecules may be potential therapeutic targets if circulating EPCs do indeed contribute to pathologic ocular angiogenesis. Unfortunately, inhibition of neovascularization under ischemic conditions may serve to promote ongoing ischemia: would it be better to coax the newly forming vessels into functional ones that could alleviate hypoxia, or make the endogenous vasculature and neurons more resistant to hypoxic damage?

To address the potential utility of these cells in relieving hypoxia and exerting a vasculotrophic rescue of a damaged retinal vasculature, HSCs have been injected directly into the eyes of newborn mice while they were forming their retinal vasculature (Fig. 37.6); in this environment, these cells can target activated astrocytes, a hallmark of many ocular vascular and degenerative diseases, and participate in normal developmental angiogenesis in both neonatal mice and injury-induced neovascularization in adult mice.[131] An HSC fraction has also been found to "stabilize" degenerative, abnormal retinal vasculature by inhibiting angiogenesis when engineered to express an antiangiogenic and rescuing degenerating vessels.[131] More surprisingly, it was also observed that by preventing vascular degeneration there is a trophic rescue effect on the photoreceptors themselves,[115] suggesting that autologous bone marrow grafts of HSC fractions containing EPCs may provide trophic effects that go beyond simple nutrition, providing a rationale for the use of HSCs in treating a variety of inherited retinal degenerations, such as retinitis pigmentosa.

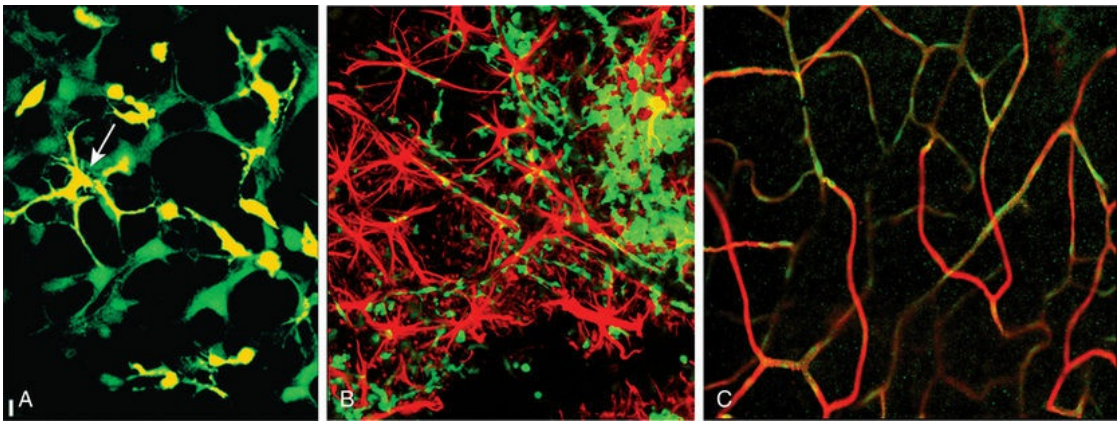

FIG. 37.6 Bone marrow-derived endothelial progenitor cells target sites of retinal gliosis and incorporate into developing blood vessels to form mosaic vessels. When these cells are taken from the bone marrow of adult mice transgenic for enhanced green fluorescent protein (eGFP, yellow) and injected into mice transgenic for GFP-glial fibrillary acidic protein (a marker of astrocytes, green), the stem cells selectively target to the underlying astrocytes (A). This also happens when these cells are injected into adult mice (B), in which a needle or laser is used to scar the retina and stimulate a focal gliosis (red), suggesting that these cells (green) may also be useful to treat injured adult retinas. Two weeks after injection of adult bone marrow-derived stem cells into the neonatal mouse retina (C), mosaic blood vessels (orange–yellow) consisting of stem cells and endogenous retinal vascular endothelial cells are observed along with vessels consisting only of endogenous vessels (red). (Adapted with permission from Otani A, Kinder K, Ewalt K, et al. Bone marrow-derived stem cells target retinal astrocytes and can promote or inhibit retinal angiogenesis. Nat Med 2002;8:1004–10.)

The use of EPCs and other stem cells as drug delivery vehicles has the potential to deliver drugs selectively and potently to the back of the eye in physiologically meaningful doses. Thus, genetically modified, autologous EPCs transplanted into ischemic or abnormally vascularized eyes may stably incorporate into new vessels and continuously deliver therapeutic molecules locally for prolonged periods of time.

Lastly, bone marrow-derived EPCs can exert a neurotrophic rescue in retinal degeneration and inhibit abnormal angiogenesis.

Despite having identified mutations in over 110 different genes involved in inherited degenerations of the retina,[132–137] there are still no effective treatments to slow or reverse the progression of these diseases. Recent advances in gene therapy have led to successful reversal of the *rds*[138] and *rd*[139] phenotypes in mice and the *RPE65* phenotype in dogs[140] when the wild-type transgene is delivered to photoreceptors or the RPE in animals with a specific mutation. The potential use of calcium channel blockers,[141] trophic factors,[142] and dietary supplements[143] has also been explored. Most inherited human retinal degenerations have concomitant loss of cones, the principal cellular component of the macula. Consequently cone-specific survival factors have been described[144] and may facilitate cone survival in mouse models of retinal degeneration. In addition to the vasculotrophic properties described above, these cells have also been reported to prevent retinal vascular degeneration, which correlates with neuronal rescue (Fig. 37.7). The inner nuclear layer remains nearly normal and the outer nuclear layer containing photoreceptors is significantly preserved, with the rescued cells being predominantly cones. This rescue effect is also observed when human bone marrow-derived Lin^- HSCs are used to treat severe combined immunodeficient mice with retinal degeneration. Large-scale genomic analysis of rescued and nonrescued eyes revealed significant upregulation of antiapoptotic genes. Of note, the injected (GFP-labeled) bone marrow-derived progenitor cells were not observed anywhere but in or near blood vessels. The fact that the neurotrophic effect correlates with preservation of the vasculature suggests that autologous bone marrow-derived EPCs may be useful in treating retinal degenerative diseases in which abnormal angiogenesis is the cause of vision loss. Furthermore, other reports support the concept that tissue-specific vasculature has trophic effects that go beyond that expected from simply providing vascular "nourishment";[114,116] in individuals with retinal degeneration, the presence of EPCs may make the vasculature more resistant to degeneration and at the same time facilitate retinal neuronal survival, potentially slowing the rate of degeneration to provide years of additional sight.

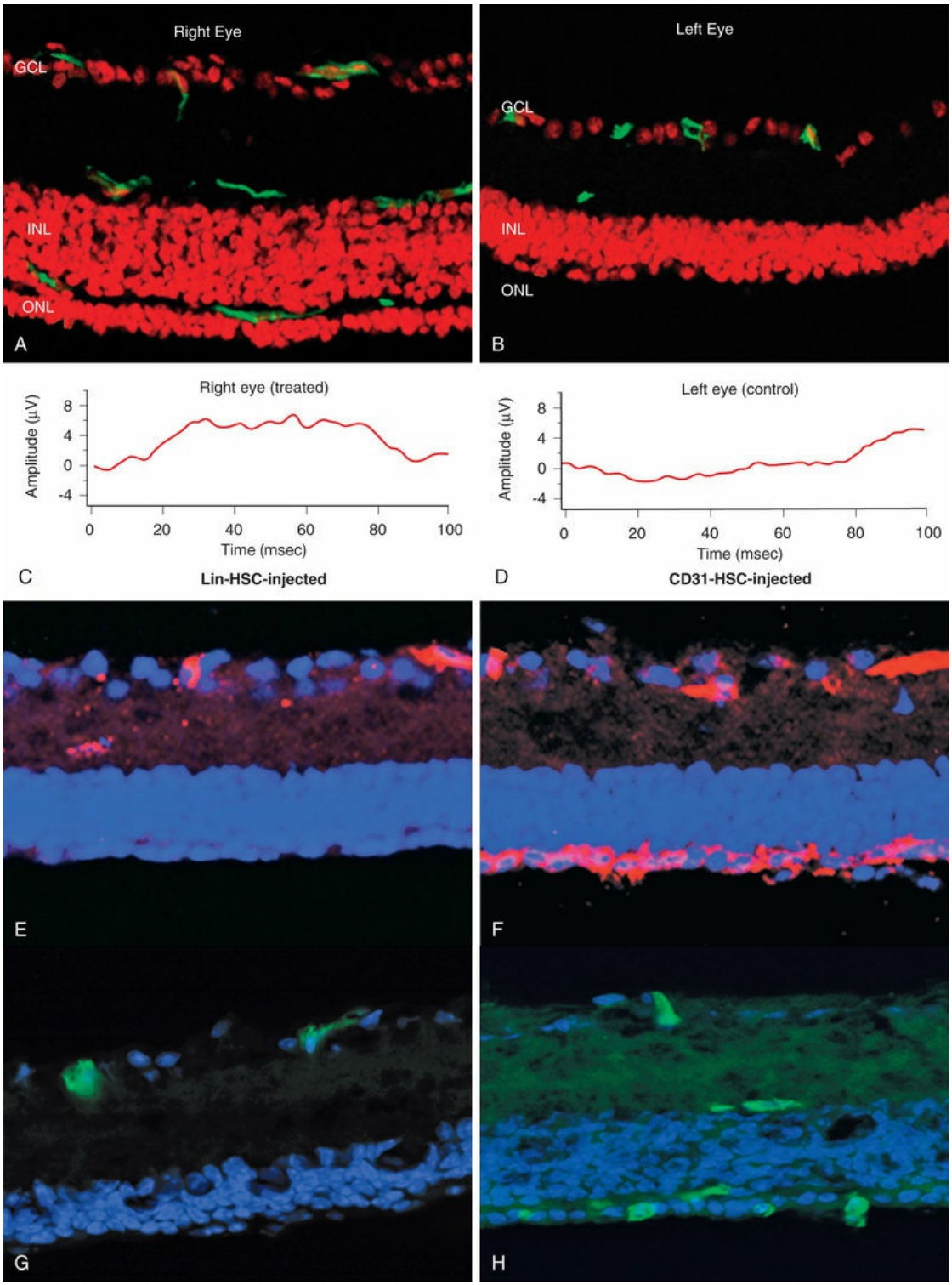

FIG. 37.7 Adult bone marrow-derived stem cells rescue degenerating blood vessels and retinal function, and exert a profound neurotrophic rescue effect in a mouse model of retinal degeneration. (A,B) Representative cases of rescued and nonrescued retinas 2 months after injection. Retinal section of stem cell-injected right eye (A) and control cell-injected left eye (B) of the same animal are shown (green: CD31-

stained vasculature, red: 6′-diamidino-2-pheninlindole hydrochloride (DAPI)-stained nuclei). (C,D) Electroretinographic recordings were used to measure the function of stem cell- or control cell-injected retinas from the same eyes shown in panels A and B. (E–H) Rescued outer nuclear layer (*ONL*) in a mouse model of retinal degeneration (rd1/rd1) following intravitreal injection of adult bone marrow-derived stem cells consists predominantly of cones. Control (CD31 hematopoietic stem cell-injected) eyes are identical to noninjected rd1/rd1 retinas, without any staining for cone (E) or rod (G) opsin. Stem cell-treated contralateral eyes in the same animals have a markedly reduced, but clearly present, ONL that is predominantly comprised of cones, as evidenced by positive immunoreactivity for cone red/green opsin (F). A small number of rods are also observed (H). *GCL*, ganglion cell layer; *INL*, inner nuclear layer. (Adapted with permission from Otani A, Kinder K, Ewalt K, et al. Bone marrow-derived stem cells target retinal astrocytes and can promote or inhibit retinal angiogenesis. Nat Med 2002;8:1004–10 and Otani A, Dorrell MI, Kinder K, et al. Rescue of retinal degeneration by intravitreally injected adult bone marrow-derived lineage negative hematopoietic stem cells. J Clin Invest 2004;114:765–74.)

Overall, adult bone marrow-derived stem cells may have wide utility in the treatment of retinal vascular diseases and perhaps even inherited retinal degenerations. Potential applications of these cells include not only use as cell-based therapeutic delivery vehicles, but also possible use as stabilizing elements in an otherwise unstable neovasculature of the type observed in ischemic retinopathies. In fact, these cells will selectively target sites of hypoxia-driven neovascularization, as demonstrated in mouse models of these diseases. While current retinal vascular disease therapy is based largely on ablating the new vessels with angiostatics or thermal and nonthermal lasers, a novel paradigm would include the use of these stem cells to target, incorporate into, and stabilize neovasculature.

Human Clinical Trials Using Stem Cells for the Treatment of Retinal

Diseases

In recent years, many groups[62a,145–147] have proposed using hESC- and/or hiPSC-derived cells for the therapy of retinal diseases such as retinitis pigmentosa, Usher syndrome, AMD and Stargardt disease. Human trials using hESCs became a reality in 2009 (Table 37.1) with the approval by the FDA for a phase I trial (NCT01217008). In this trial, hESCs differentiated into oligodendrocyte precursor cells (GRNOPC1) were injected into the spinal cord of patients with acute, severe spinal cord injury.

In November 2010, FDA approval was given for a phase I/II clinical trial to treat Stargardt disease using subretinal injection of cell suspensions of hESC-derived RPE (NCT01345006). Then, in January 2011 FDA approval was granted for a phase I/II clinical trial (NCT01344993) to treat advanced dry AMD using subretinal injection of cell suspensions of hESC-derived RPE (50, 000–200 ,000 cells/eye). No evidence of adverse reaction or serious safety issues related to the transplanted RPE tissue itself, including tumor formation or rejection, was reported although adverse events possibly related to immunosuppression were apparent in nearly all patients. Modest visual benefits for some study subjects were also claimed, although different interpretations of those results have been put forth.[62a,148]

Several other stem cell-based clinical trials for treating AMD and other retinal diseases – including retinitis pigmentosa, optic nerve disease, retinal vein occlusion, and diabetic retinopathy – are also being pursued. As of early 2015, there are at least 14 ongoing clinical trials registered in the International Clinical Trials Registry Platform of the World Health Organization for treating macular degeneration alone. A clinical trial using hiPSC-RPE sheets to treat patients with advanced wet AMD has begun in Japan, after approval by Japan's Ministry of Health in July 2013, which is the first approved clinical study for using hiPSC-RPE for the treatment of AMD (JPRN-UMIN000011929). This trial utilizes cell sheets cultured on a collagen-based scaffold that is enzymatically dissolved prior to implantation, creating a sheet of cells without a potentially immunogenic scaffold. For certain eligible patients with wet AMD, a phase I clinical trial (NCT01691261) to test the safety

and efficacy of hESC-RPE sheets (on a polyester membrane[149]) was initiated by Pfizer/University College London.[62a] This group is also investigating hiPSC-RPE on the same scaffold system.[62a] For treating patients with geographic atrophy involving the central fovea, a human phase I/IIa clinical trial using hESC-RPE monolayer implants (on a Parylene membrane) was initiated at the University of Southern California Eye Institute. This trial, supported by funding from the California Institute for Regenerative Medicine (CIRM), is the result of a collaboration between researchers at USC and researchers at the University of California, Santa Barbara, the City of Hope, and Caltech. Other stem cell types – including bone marrow-derived stem cells, human umbilical tissue-derived cells, human central nervous stem cells, human fetal retinal cells, and adipose-derived stroll cells – are being pursued in clinical trials to treat retinal diseases. Many of these rely on paracrine effects rather that cell replacement, as is discussed elsewhere in this volume[62a,150] In current clinical trials so far, patients are placed on a thorough systemic immunosuppressive regimen, involving pre- and postoperative immunomodulatory therapy along with oral and topical corticosteroids.[62a,148,151] For a more detailed review of recent and current clinical trials, see Nazari et al., 2015.[62a]

Discerning the Legitimacy of A Human Stem Cell Treatment

When approached by a patient inquiring about the legitimacy of a specific human stem cell-based treatment, it can be a challenge to investigate the treatment and address the many concerns that naturally accompany such a treatment. Table 37.2 provides a list of the basic questions that should be initially answered to help evaluate the legitimacy of a human stem cell-based treatment, although this list should only be used as a starting point for further investigation. For additional information, the International Society for Stem Cell Research (ISSCR) provides several useful resources online, including the "Patient Handbook on Stem Cell Therapies," "Stem Cell Treatments: What to Ask," and "Guidelines for Stem Cell Research and Clinical Translation" (http://www.isscr.org/).

TABLE 37.2

Initial Questions for Discerning the Legitimacy of a Human Stem Cell Treatment

Oversight and Safety	Scientific Evidence	The Treatment
• Is the treatment part of an approved clinical trial? • If the treatment is "approved," is the approving body official? For example, has approval been received from a national or regional regulatory agency, such as the European Medicines Agency (EMA), the US FDA, or Japan's PMDA? • Is the clinic conducting the treatment accredited? • What independent oversight is there for the clinic conducting the treatment and the facility that will prepare the cells? • Is there an ethics committee that has independent oversight of the treatment?	• What peer-reviewed scientific data supports the validity of the treatment? • Were there earlier preclinical or clinical trials? • What were the findings of earlier preclinical or clinical trials? • How many people have already been successfully treated at the clinic? What were their outcomes, and were these results published?	• Is the treatment specific for the retinal disease? • What are the potential benefits of the treatment? • What are the potential side-effects and risks of the treatment, both short-term and long-term? • How will the clinic handle emergencies (e.g., severe adverse reactions)? • What additional special care or medications will the treatment require? • How is the actual procedure conducted? Specifically: • What is the stem cell source? • How are the stem cells isolated and cultured? • How are the stem cells differentiated and purified into the final cell type? • How are the cells correctly delivered to the specific retinal location? • What is the specialized training of the

		doctor performing the procedure? • How is a potential immune response mitigated?

FDA, Food and Drug Administration; PMDA, Pharmaceuticals and Medical Devices Agency.

Adapted with permission from the International Society for Stem Cell Research from their informational website, "A Closer Look at Stem Cells" (www.closerlookatstemcells.org; accessed October 18, 2015).

Concluding Remarks

The potential use of stem cells in the treatment of a variety of human retinal diseases remains tremendously exciting, with multiple potential approaches. Recently initiated clinical trials using RPE derived from human pluripotent stem cells to treat patients with Stargardt disease and AMD are first steps in taking this technology into the clinics and will continue to be followed very closely while treatments for other retinal diseases, including optic nerve disease, retinal vein occlusion, and diabetic retinopathy, are nearing clinical trials. The recent development of 3D optic vesicle-like structures (OVs) from human pluripotent stem cells is of particular interest because of the ability of these OVs to generate a wide variety of retinal cell types and self-organize into the layers found in the human retina. hiPSCs may be of particular interest for generating autologous, patient-specific retinal cell types for disease modeling or regenerative therapeutics, in situations where this is desirable. Even if such tissue reconstruction from stem cells could be successfully completed, reestablishing functional visual pathways will be an even greater challenge. Clearly, prevention of retinal degeneration and vascular abnormalities would preserve established visual pathways and provide a better chance of preserving vision. In this regard, vasculo- and neurotrophic rescue effects of adult bone marrow and neonatal cord blood-derived progenitor cells may offer great promise, and the potential involvement of bone marrow-derived EPCs in the progression of

retinal neovascularization warrants additional study. Challenges remain in successfully identifying clinically useful progenitor cell types, optimizing differentiation protocols using these cells as well as human pluripotent stem cells to generate target retinal cell types, and developing strategies to surgically deliver and integrate healthy retinal cells into patient retinas to safely rescue and improve visual functionality.

Acknowledgments

TR: I am very grateful for my time spent in the laboratory of Dennis O. Clegg, where I became exposed to and passionately interested in the stem cell field, with a particular focus on how the microenvironment affects the differentiation of hESCs and hiPSCs into RPE cells.

DMG: I would like to recognize the Foundation Fighting Blindness Wynn-Gund Translational Research Award, NIH R01 EY021218, UW-Madison McPherson Eye Research Institute (Emmett A. Humble Distinguished Directorship and the Sandra Lemke Trout Chair in Eye Research), David Walsh Family Foundation, Reeves Foundation, Choroideremia Research Foundation, and Muskingum County Community Foundation (DMG) for supporting this work.

DOC: I would like to recognize the Garland Initiative for Vision, the California Institute for Regenerative Medicine (CIRM; grants DR1-01444, CL1-00521, TB1-01177, and TG2-01151) Fight for Sight, the Foundation Fighting Blindness Wynn-Gund Translational Research Acceleration Program, the University of California Santa Barbara Institute for Collaborative Biotechnologies from the US Army Research Office (Grant W911NF-09-0001), CIRM Major Facilities Grant (FA1-00616), The Vermont Community Foundation, the Breaux Foundation, and the Wilcox Family Foundation for supporting this work.

We would like to thank Dr. Lyndsay Leach for her comments on the chapter.

References

1. Zacharias DG, Nelson TJ, Mueller PS, et al. The science and ethics of induced pluripotency: what will become of embryonic stem cells? *Mayo Clin Proc*. 2011;86(7):634–640.
2. Rumman M, Dhawan J, Kassem M. Concise Review: Quiescence in adult stem cells: biological significance and relevance to tissue regeneration. *Stem Cells*. 2015;33(10):2903–2912.
3. Ivanova NB, Dimos JT, Schaniel C, et al. A stem cell molecular signature. *Science*. 2002;298:601–604.
4. Ramalho-Santos M, Yoon S, Matsuzaki Y, et al. Stemness": transcriptional profiling of embryonic and adult stem cells. *Science*. 2002;298:597–600.
5. Cai J, Weiss ML, Rao MS. In search of "stemness. *Exp Hematol*. 2004;32:585–598.
6. Evans MJ, Kaufman MH. Establishment in culture of pluripotential cells from mouse embryos. *Nature*. 1981;292:154–156.
7. Martin GR. Isolation of a pluripotent cell line from early mouse embryos cultured in medium conditioned by teratocarcinoma stem cells. *Proc Natl Acad Sci USA*. 1981;78:7634–7638.
8. Lin S, Talbot P. Methods for culturing mouse and human embryonic stem cells. *Methods Mol Biol*. 2011;690:31–56.
9. Thomson JA, Kalishman J, Golos TG, et al. Isolation of a primate embryonic stem cell line. *Proc Natl Acad Sci USA*. 1995;92:7844–7848.
10. Thomson JA, Itskovitz-Eldor J, Shapiro SS, et al. Embryonic stem cell lines derived from human blastocysts. *Science*. 1998;282:1145–1147.
11. Hardy K, Handyside AH, Winston RM. The human blastocyst: cell number, death and allocation during late preimplantation development in vitro. *Development*. 1989;107:597–604.
12. Klimanskaya I, Young C, Becker S, et al. Derivation of human embryonic stem cells from single blastomeres. *Nat Protoc*. 2007;2:1963–1972.
13. Cibelli J, Gurdon J, Wilmut I, et al. *Principles of cloning*. 2nd ed. Academic Press: New York; 2014.

14. Yamanaka S. Induced pluripotent stem cells: past, present, and future. *Cell Stem Cell*. 2012;10:678–684.
15. Yu J, Vodyanik MA, Smuga-Otto K, et al. Induced pluripotent stem cell lines derived from human somatic cells. *Science*. 2007;318(5858):1917–1920.
16. Takahashi K, Tanabe K, Ohnuki M, et al. Induction of pluripotent stem cells from adult human fibroblasts by defined factors. *Cell*. 2007;131:861–872.
17. Wright LS, Phillips MJ, Pinilla I, et al. Induced pluripotent stem cells as custom therapeutics for retinal repair: progress and rationale. *Exp Eye Res*. 2014;123:161–172.
18. Korbling M, Estrov Z. Adult stem cells for tissue repair – a new therapeutic concept? *N Engl J Med*. 2003;349:570–582.
19. McKay RD. Stem cell biology and neurodegenerative disease. *Philos Trans R Soc Lond B Biol Sci*. 2004;359:851–856.
20. Asakura A. Stem cells in adult skeletal muscle. *Trends Cardiovasc Med*. 2003;13:123–128.
21. Rafii S, Lyden D. Therapeutic stem and progenitor cell transplantation for organ vascularization and regeneration. *Nat Med*. 2003;9:702–712.
22. Yamashita JK. Differentiation and diversification of vascular cells from embryonic stem cells. *Int J Hematol*. 2004;80:1–6.
23. Reh TA, Levine EM. Multipotential stem cells and progenitors in the vertebrate retina. *J Neurobiol*. 1998;36:206–220.
24. Reh TA, Fischer AJ. Stem cells in the vertebrate retina. *Brain Behav Evol*. 2001;58:296–305.
25. Livesey FJ, Young TL, Cepko CL. An analysis of the gene expression program of mammalian neural progenitor cells. *Proc Natl Acad Sci USA*. 2004;101:1374–1379.
26. Blackshaw S, Harpavat S, Trimarchi J, et al. Genomic analysis of mouse retinal development. *PLoS Biol*. 2004;2:E247.
27. Dyer MA, Cepko CL. Regulating proliferation during retinal development. *Nat Rev Neurosci*. 2001;2:333–342.
28. Das AV, James J, Zhao X, et al. Identification of c-Kit receptor as a regulator of adult neural stem cells in the mammalian eye: interactions with Notch signaling. *Dev*

Biol. 2004;273:87–105.
29. James J, Das AV, Bhattacharya S, et al. In vitro generation of early-born neurons from late retinal progenitors. *J Neurosci*. 2003;23:8193–8203.
30. James J, Das AV, Rahnenfuhrer J, et al. Cellular and molecular characterization of early and late retinal stem cells/progenitors: differential regulation of proliferation and context dependent role of Notch signaling. *J Neurobiol*. 2004;61:359–376.
31. Cicero SA, Johnson D, Reyntjens S, et al. Cells previously identified as retinal stem cells are pigmented ciliary epithelial cells. *Proc Natl Acad Sci USA*. 2009;106:6685–6690.
32. Gualdoni S, Baron M, Lakowski J, et al. Adult ciliary epithelial cells, previously identified as retinal stem cells with potential for retinal repair, fail to differentiate into new rod photoreceptors. *Stem Cells*. 2010;28:1048–1059.
33. Ader M, Enzmann V, Francke M. Potential of Müller glia and stem/progenitor cells to regenerate retinal tissue. *Regen Biol Eye*. 2014;161–175.
34. Yu H, Vu THK, Cho K, et al. Mobilizing endogenous stem cells for retinal repair. *Transl Res*. 2014;163(4):387–398.
35. Bain G, Kitchens D, Yao M, et al. Embryonic stem cells express neuronal properties in vitro. *Dev Biol*. 1995;168:342–357.
36. Meyer JS, Howden SE, Wallace KA, et al. Optic vesicle-like structures derived from human pluripotent stem cells facilitate a customized approach to retinal disease treatment. *Stem Cells*. 2011;29:1206–1218.
37. Fischer AJ, Reh TA. Potential of Müller glia to become neurogenic retinal progenitor cells. *Glia*. 2003;43:70–76.
38. Pollak J, Wilken MS, Ueki Y, et al. ASCL1 reprograms mouse Müller glia into neurogenic retinal progenitors. *Development*. 2013;140:2619–2631.
39. Ooto S, Akagi T, Kageyama R, et al. Potential for neural regeneration after neurotoxic injury in the adult mammalian retina. *Proc Natl Acad Sci USA*. 2004;101:13654–13659.
40. Harada C, Guo X, Namekata K, et al. Glia- and neuron-

specific functions of TrkB signalling during retinal degeneration and regeneration. *Nat Commun*. 2011;2:189.
41. Karl MO, Reh TA. Regenerative medicine for retinal diseases: activating endogenous repair mechanisms. *Trends Mol Med*. 2010;16:193–202.
42. Dorrell MI, Aguilar E, Jacobson R, et al. Antioxidant or neurotrophic factor treatment preserves function in a mouse model of neovascularization-associated oxidative stress. *J Clin Invest*. 2009;119:611–623.
43. Dalkara D, Kolstad KD, Guerin KI, et al. AAV mediated GDNF secretion from retinal glia slows down retinal degeneration in a rat model of retinitis pigmentosa. *Mol Ther*. 2011;19:1602–1608.
44. Lamba DA, Karl MO, Ware CB, et al. Efficient generation of retinal progenitor cells from human embryonic stem cells. *Proc Natl Acad Sci USA*. 2006;103:12769–12774.
45. Meyer JS, Shearer RL, Capowski EE, et al. Modeling early retinal development with human embryonic and induced pluripotent stem cells. *Proc Natl Acad Sci USA*. 2009;106(39):16698–16703.
46. Zhong X, Gutierrez C, Xue T, et al. Generation of three-dimensional retinal tissue with functional photoreceptors from human iPSCs. *Nat Commun*. 2014;5(4047):1–14.
47. Mukhopadhyay M, Gorivodsky M, Shtrom S, et al. Dkk2 plays an essential role in the corneal fate of the ocular surface epithelium. *Development*. 2006;133:2149–2154.
48. Reh TA, Lamba D, Gust J. Directing human embryonic stem cells to a retinal fate. *Methods Mol Biol*. 2010;636:139–153.
49. Lamba DA, Reh TA. Microarray characterization of human embryonic stem cell-derived retinal cultures. *Invest Ophthalmol Vis Sci*. 2011;52:4897–4906.
50. Osakada F, Ikeda H, Mandai M, et al. Toward the generation of rod and cone photoreceptors from mouse, monkey and human embryonic stem cells. *Nat Biotechnol*. 2008;26:215–224.
51. Osakada F, Ikeda H, Sasai Y, et al. Stepwise differentiation of pluripotent stem cells into retinal cells. *Nat Protoc*. 2009;4:811–824.

52. Phillips MJ, Wallace KA, Dickerson SJ, et al. Blood-derived human iPS cells generate optic vesicle-like structures with the capacity to form retinal laminae and develop synapses. *Invest Opthalmol Vis Sci*. 2012;53:2007–2019.
53. Nakano T, Ando S, Takata N, et al. Self-formation of optic cups and storable stratified neural retina from human ESCs. *Cell Stem Cell*. 2012;10(6):771–785.
54. Lamba DA, Gust J, Reh TA. Transplantation of human embryonic stem cell-derived photoreceptors restores some visual function in Crx-deficient mice. *Cell Stem Cell*. 2009;4:73–79.
55. Barber AC, Hippert C, Duran Y, et al. Repair of the degenerate retina by photoreceptor transplantation. *Proc Natl Acad Sci USA*. 2012;110(1):354–359.
56. Gonzalez-Cordero A, West EL, Pearson RA, et al. Photoreceptor precursors derived from three-dimensional embryonic stem cell cultures integrate and mature within adult degenerate retina. *Nat Biotechnol*. 2013;31:741–747.
57. Singh MS, Issa PC, Butler R, et al. Reversal of end-stage retinal degeneration and restoration of visual function by photoreceptor transplantation. *Proc Natl Acad Sci USA*. 2012;110(3):1101–1106.
58. Homma K, Okamoto S, Mandai M, et al. Developing rods transplanted into the degenerating retina of Crx-knockout mice exhibit neural activity similar to native photoreceptors. *Regen Med*. 2013;31(6):1149–1159.
59. Hirano M, Yamamoto A, Yoshimura N, et al. Generation of structures formed by lens and retinal cells differentiating from embryonic stem cells. *Dev Dyn*. 2003;228:664–671.
60. Aoki H, Hara A, Niwa M, et al. Transplantation of cells from eye-like structures differentiated from embryonic stem cells in vitro and in vivo regeneration of retinal ganglion-like cells. *Graefes Arch Clin Exp Ophthalmol*. 2008;246:255–265.
61. Eiraku M, Takata N, Ishibashi H, et al. Self-organizing optic-cup morphogenesis in three-dimensional culture. *Nature*. 2011;472:51–56.
62a. Nazari H, Zhang L, Zhu D, et al. Stem cell based therapies for age-related macular degeneration: the promises and the

challenges. *Prog Retin Eye Res*. 2015;48:1–39.
62b. Davis RJ, Blenkinsop TA, Campbell M, et al. Human RPE Stem Cell-Derived RPE Preserves Photoreceptors in the Royal College of Surgeons Rat: Method for Quantifying the Area of Photoreceptor Sparing. *J Ocul Pharmacol Ther*. 2016;32(5):304–309.
62c. Saini JS, Temple S, Stern JH. Human Retinal Pigment Epithelium Stem Cell (RPESC). *Adv Exp Med Biol*. 2016;854:557–562.
63. Kanuga N, Winton HL, Beauchene L, et al. Characterization of genetically modified human retinal pigment epithelial cells developed for in vitro and transplantation studies. *Invest Ophthalmol Vis Sci*. 2002;43:546–555.
64. Lund RD, Adamson P, Sauve Y, et al. Subretinal transplantation of genetically modified human cell lines attenuates loss of visual function in dystrophic rats. *Proc Natl Acad Sci USA*. 2001;98:9942–9947.
65. Coffey PJ, Girman S, Wang SM, et al. Long-term preservation of cortically dependent visual function in RCS rats by transplantation. *Nat Neurosci*. 2002;5:53–56.
66. LaVail MM, Yasumura D, Matthes MT, et al. Protection of mouse photoreceptors by survival factors in retinal degenerations. *Invest Ophthalmol Vis Sci*. 1998;39:592–602.
67. Faktorovich EG, Steinberg RH, Yasumura D, et al. Photoreceptor degeneration in inherited retinal dystrophy delayed by basic fibroblast growth factor. *Nature*. 1990;347:83–86.
68. Tao W, Wen R, Goddard MB, et al. Encapsulated cell-based delivery of CNTF reduces photoreceptor degeneration in animal models of retinitis pigmentosa. *Invest Ophthalmol Vis Sci*. 2002;43:3292–3298.
69. Birch DG, Weleber RG, Duncan JL, et al. Randomized trial of ciliary neurotrophic factor delivered by encapsulated cell intraocular implants for retinitis pigmentosa. *Am J Ophthalmol*. 2013;156(2):283–292.
70. Kolomeyer AM, Zarbin MA. Trophic factors in the pathogenesis and therapy for retinal degenerative diseases. *Surv Ophthalmol*. 2014;59(2):134–165.

71. Bharti K, Miller SS, Arnheiter H. The new paradigm: retinal pigment epithelium cells generated from embryonic or induced pluripotent stem cells. *Pigment Cell Melanoma Res*. 2011;24:21–34.
72. Rowland TJ, Buchholz DE, Clegg DO. Pluripotent human stem cells for the treatment of retinal disease. *J Cell Physiol*. 2012;227:457–466.
73. Vugler A, Lawrence J, Walsh J, et al. Embryonic stem cells and retinal repair. *Mech Dev*. 2007;124:807–829.
74. Idelson M, Alper R, Obolensky A, et al. Directed differentiation of human embryonic stem cells into functional retinal pigment epithelium cells. *Cell Stem Cell*. 2009;5:396–408.
75. Rowland TJ, Blaschke AJ, Buchholz DE, et al. Differentiation of human pluripotent stem cells to retinal pigmented epithelium in defined conditions using purified extracellular matrix proteins. *J Tissue Eng Regen Med*. 2013;7(8):642–653.
76. Singh R, Phillips JM, Kuai D, et al. Functional analysis of serially expanded human iPS cell-derived RPE cultures. *Invest Ophthalmol Vis Sci*. 2013;54(10):6767–6778.
77. Sonoda S, Spee C, Barron E, et al. A protocol for the culture and differentiation of highly polarized human retinal pigment epithelial cells. *Nat Protocols*. 2009;4:662–673.
78. Zhu D, Deng X, Spee C, et al. Polarized secretion of PEDF from human embryonic stem cell-derived RPE promotes retinal progenitor cell survival. *Invest Ophthalmol Vis Sci*. 2011;52:1573–1585.
79. Carr AJ, Vugler A, Lawrence J, et al. Molecular characterization and functional analysis of phagocytosis by human embryonic stem cell-derived RPE cells using a novel human retinal assay. *Mol Vis*. 2009;15:283–295.
80. Leach LL, Clegg DO. Concise Review: Making stem cells retinal: methods for deriving retinal pigment epithelium and implications for patients with ocular disease. *Stem Cells*. 2015;33(8):2363–2373.
81. Kamao H, Mandai M, Goto K, et al. Evaluation of degree of pigmentation as an indicator of maturation status in human

iPSC-RPE. *Invest Ophthalmol Vis Sci*. 2014;55(13):1364.
82. Liao J-L, Yu J, Huang K, et al. Molecular signature of primary retinal pigment epithelium and stem-cell-derived RPE cells. *Hum Mol Genet*. 2010;19:4229–4238.
83. Baker M. Metabolomics: from small molecules to big ideas. *Nat Meth*. 2011;8:117–121.
84. Wikoff WR, Kalisak E, Trauger S, et al. Response and recovery in the plasma metabolome tracks the acute LCMV-induced immune response. *J Proteome Res*. 2009;8:3578–3587.
85. Yanes O, Clark J, Wong DM, et al. Metabolic oxidation regulates embryonic stem cell differentiation. *Nat Chem Biol*. 2010;6:411–417.
86. D'Cruz PM, Yasumura D, Weir J, et al. Mutation of the receptor tyrosine kinase gene Mertk in the retinal dystrophic RCS rat. *Hum Mol Genet*. 2000;9:645–651.
87. Lund RD, Wang S, Klimanskaya I, et al. Human embryonic stem cell-derived cells rescue visual function in dystrophic RCS rats. *Cloning Stem Cells*. 2006;8:189–199.
88. Lu B, Malcuit C, Wang S, et al. Long-term safety and function of RPE from human embryonic stem cells in preclinical models of macular degeneration. *Stem Cells*. 2009;27:2126–2135.
89. Vugler A, Carr AJ, Lawrence J, et al. Elucidating the phenomenon of HESC-derived RPE: anatomy of cell genesis, expansion and retinal transplantation. *Exp Neurol*. 2008;214:347–361.
90. Zhou R, Caspi RR. Ocular immune privilege. *F1000 Biol Rep*. 2010;2.
91. Masli S, Vega JL. Ocular immune privilege sites. *Methods Mol Biol*. 2011;677:449–458.
92. Kamao H, Mandai M, Okamoto S, et al. Characterization of human induced pluripotent stem cell-derived retinal pigment epithelium cell sheets aiming for clinical application. *Stem Cell Reports*. 2014;2(2):205–218.
93. Li TS, Cheng K, Lee ST, et al. Cardiospheres recapitulate a niche-like microenvironment rich in stemness and cell–matrix interactions, rationalizing their enhanced functional potency for myocardial repair. *Stem Cells*. 2010;28:2088–

2098.
94. Salazar DL, Uchida N, Hamers FP, et al. Human neural stem cells differentiate and promote locomotor recovery in an early chronic spinal cord injury NOD-scid mouse model. *PLoS ONE*. 2010;5:e12272.
95. Monnier PP, Sierra A, Schwab JM, et al. The Rho/ROCK pathway mediates neurite growth-inhibitory activity associated with the chondroitin sulfate proteoglycans of the CNS glial scar. *Mol Cell Neurosci*. 2003;22:319–330.
96. Tucker B, Klassen H, Yang L, et al. Elevated MMP expression in the MRL mouse retina creates a permissive environment for retinal regeneration. *Invest Ophthalmol Vis Sci*. 2008;49:1686–1695.
97. Aoi T, Yae K, Nakagawa M, et al. Generation of pluripotent stem cells from adult mouse liver and stomach cells. *Science*. 2008;321:699–702.
98. Okita K, Ichisaka T, Yamanaka S. Generation of germline-competent induced pluripotent stem cells. *Nature*. 2007;448:313–317.
99. Kim D, Kim CH, Moon JI, et al. Generation of human induced pluripotent stem cells by direct delivery of reprogramming proteins. *Cell Stem Cell*. 2009;4:472–476.
100. Markoulaki S, Hanna J, Beard C, et al. Transgenic mice with defined combinations of drug-inducible reprogramming factors. *Nat Biotechnol*. 2009;27:169–171.
101. Miura K, Okada Y, Aoi T, et al. Variation in the safety of induced pluripotent stem cell lines. *Nat Biotechnol*. 2009;27:743–745.
102. Schlaeger TM, Daheron L, Brickler TR, et al. A comparison of non-integrating reprogramming methods. *Nat Biotechnol*. 2014;33:58–63.
103. Huo JS, Baylin SB, Zambidis ET. Cancer-like epigenetic derangements of human pluripotent stem cells and their impact on applications in regeneration and repair. *Curr Opin Genet Dev*. 2014;28C:43–49.
104. Ma H, Morey R, O'Neil RC, et al. Abnormalities in human pluripotent cells due to reprogramming mechanisms. *Nature*. 2014;511:177–183.

105. Tomoda K, Takahashi K, Leung K, et al. Derivation conditions impact X inactivation status in female human induced pluripotent stem cells. *Cell Stem Cell*. 2012;11(1):91–99.
106. Kuroda T, Yasuda S, Kusakawa S, et al. Highly sensitive in vitro methods for detection of residual undifferentiated cells in retinal pigment epithelial cells derived from human iPS cells. *PLoS ONE*. 2012;7(5):e37342.
107. Seddon JM, Reynolds R, Maller J, et al. Prediction model for prevalence and incidence of advanced age-related macular degeneration based on genetic, demographic, and environmental variables. *Invest Ophthalmol Vis Sci*. 2009;50:2044–2053.
108. Nguyen HV, Li Y, Tsang SH. Patient-specific iPSC-derived RPE for modeling of retinal diseases. *J Clin Med*. 2015;4(4):567–578.
109. Howden SE, Maufort JP, Duffin BM, et al. Simultaneous reprogramming and gene correction of patient fibroblasts. *Stem Cell Reports*. 2015;5:1–10.
110. Bock C, Kiskinis E, Verstappen G, et al. Reference maps of human ES and iPS cell variation enable high-throughput characterization of pluripotent cell lines. *Cell*. 2011;144:439–452.
111. Hussein SM, Batada NN, Vuoristo S, et al. Copy number variation and selection during reprogramming to pluripotency. *Nature*. 2011;471:58–62.
112. Laurent LC, Ulitsky I, Slavin I, et al. Dynamic changes in the copy number of pluripotency and cell proliferation genes in human ESCs and iPSCs during reprogramming and time in culture. *Cell Stem Cell*. 2011;8:106–118.
113. Mayshar Y, Ben-David U, Lavon N, et al. Identification and classification of chromosomal aberrations in human induced pluripotent stem cells. *Cell Stem Cell*. 2010;7:521–531.
114. LeCouter J, Moritz DR, Li B, et al. Angiogenesis-independent endothelial protection of liver: role of VEGFR-1. *Science*. 2003;299:890–893.
115. Otani A, Dorrell MI, Kinder K, et al. Rescue of retinal

degeneration by intravitreally injected adult bone marrow-derived lineage negative hematopoietic stem cells. *J Clin Invest*. 2004;114:765–774.
116. Matsumoto K, Yoshitomi H, Rossant J, et al. Liver organogenesis promoted by endothelial cells prior to vascular function. *Science*. 2001;294:559–563.
117. Shen Q, Goderie SK, Jin L, et al. Endothelial cells stimulate self-renewal and expand neurogenesis of neural stem cells. *Science*. 2004;304:1338–1340.
118. Asahara T, Murohara T, Sullivan A, et al. Isolation of putative progenitor endothelial cells for angiogenesis. *Science*. 1997;275:964–967.
119. Kalka C, Tehrani H, Laudenberg B, et al. VEGF gene transfer mobilizes endothelial progenitor cells in patients with inoperable coronary disease. *Ann Thorac Surg*. 2000;70:829–834.
120. Gill M, Dias S, Hattori K, et al. Vascular trauma induces rapid but transient mobilization of VEGFR2(+)AC133(+) endothelial precursor cells. *Circ Res*. 2001;88:167–174.
121. Grant MB, May WS, Caballero S, et al. Adult hematopoietic stem cells provide functional hemangioblast activity during retinal neovascularization. *Nat Med*. 2002;8:607–612.
122. Wagers AJ, Sherwood RI, Christensen JL, et al. Little evidence for developmental plasticity of adult hematopoietic stem cells. *Science*. 2002;297:2256–2259.
123. Krause DS, Theise ND, Collector MI, et al. Multi-organ, multi-lineage engraftment by a single bone marrow-derived stem cell. *Cell*. 2001;105:369–377.
124. Morshead CM, Benveniste P, Iscove NN, et al. Hematopoietic competence is a rare property of neural stem cells that may depend on genetic and epigenetic alterations. *Nat Med*. 2002;8:268–273.
125. Wurmser AE, Nakashima K, Summers RG, et al. Cell fusion-independent differentiation of neural stem cells to the endothelial lineage. *Nature*. 2004;430:350–356.
126. Grant MB, Caballero S, Brown GA, et al. The contribution of adult hematopoietic stem cells to retinal neovascularization. *Adv Exp Med Biol*. 2003;522:37–45.

127. Espinosa-Heidmann DG, Caicedo A, Hernandez EP, et al. Bone marrow-derived progenitor cells contribute to experimental choroidal neovascularization. *Invest Ophthalmol Vis Sci*. 2003;44:4914–4919.
128. Sengupta N, Caballero S, Mames RN, et al. The role of adult bone marrow-derived stem cells in choroidal neovascularization. *Invest Ophthalmol Vis Sci*. 2003;44:4908–4913.
129. Csaky KG, Baffi JZ, Byrnes GA, et al. Recruitment of marrow-derived endothelial cells to experimental choroidal neovascularization by local expression of vascular endothelial growth factor. *Exp Eye Res*. 2004;78:1107–1116.
130. Dorrell MI, Otani A, Aguilar E, et al. Adult bone marrow-derived stem cells use R-cadherin to target sites of neovascularization in the developing retina. *Blood*. 2004;103:3420–3427.
131. Otani A, Kinder K, Ewalt K, et al. Bone marrow-derived stem cells target retinal astrocytes and can promote or inhibit retinal angiogenesis. *Nat Med*. 2002;8:1004–1010.
132. Humphries P, Kenna P, Farrar GJ. On the molecular genetics of retinitis pigmentosa. *Science*. 1992;256:804–808.
133. Farrar GJ, Kenna PF, Humphries P. On the genetics of retinitis pigmentosa and on mutation-independent approaches to therapeutic intervention. *EMBO J*. 2002;21:857–864.
134. Dryja TP, McGee TL, Reichel E, et al. A point mutation of the rhodopsin gene in one form of retinitis pigmentosa. *Nature*. 1990;343:364–366.
135. Bowes C, Li T, Danciger M, et al. Retinal degeneration in the rd mouse is caused by a defect in the beta subunit of rod cGMP-phosphodiesterase. *Nature*. 1990;347:677–680.
136. Kajiwara K, Hahn LB, Mukai S, et al. Mutations in the human retinal degeneration slow gene in autosomal dominant retinitis pigmentosa. *Nature*. 1991;354:480–483.
137. Gu SM, Thompson DA, Srikumari CR, et al. Mutations in RPE65 cause autosomal recessive childhood-onset severe retinal dystrophy. *Nat Genet*. 1997;17:194–197.
138. Ali RR, Sarra GM, Stephens C, et al. Restoration of

photoreceptor ultrastructure and function in retinal degeneration slow mice by gene therapy. *Nat Genet*. 2000;25:306–310.
139. Takahashi M, Miyoshi H, Verma IM, et al. Rescue from photoreceptor degeneration in the rd mouse by human immunodeficiency virus vector-mediated gene transfer. *J Virol*. 1999;73:7812–7816.
140. Acland GM, Aguirre GD, Ray J, et al. Gene therapy restores vision in a canine model of childhood blindness. *Nat Genet*. 2001;28:92–95.
141. Frasson M, Sahel JA, Fabre M, et al. Retinitis pigmentosa: rod photoreceptor rescue by a calcium-channel blocker in the rd mouse. *Nat Med*. 1999;5:1183–1187.
142. Frasson M, Picaud S, Leveillard T, et al. Glial cell line-derived neurotrophic factor induces histologic and functional protection of rod photoreceptors in the rd/rd mouse. *Invest Ophthalmol Vis Sci*. 1999;40:2724–2734.
143. Berson EL, Rosner B, Sandberg GA, et al. A randomized trial of vitamin A and vitamin E supplementation for retinitis pigmentosa. *Arch Ophthalmol*. 1993;111:761–772.
144. Mohand-Said S, et al. Normal retina releases a diffusible factor stimulating cone survival in the retinal degeneration mouse. *Proc Natl Acad Sci USA*. 1998;95:8357–8362.
145. Singh MS, MacLaren RE. Stem cells as a therapeutic tool for the blind: biology and future prospects. *Proc Biol Sci*. 2011;278:3009–3016.
146. Stern JH, Temple S. Stem cells for retinal replacement therapy. *Neurother*. 2011;8:736–743.
147. Marchetti V, Krohne TU, Friedlander DF, et al. Stemming vision loss with stem cells. *J Clin Invest*. 2010;120:3012–3021.
148. Schwartz SD, Regillo CD, Lam BL, et al. Human embryonic stem cell-derived retinal pigment epithelium in patients with age-related macular degeneration and Stargardt's macular dystrophy: follow-up of two open-label phase 1/2 studies. *Lancet*. 2015;9967:509–516.
149. Stanzel BV, Liu Z, Somboonthanakij S, et al. Human RPE stem cells grown into polarized RPE monolayers on a polyester matrix are maintained after grafting into rabbit

subretinal space. *Stem Cell Reports*. 2014;2(1):64–77.
150. Klassen H. Stem cells in clinical trials for treatment of retinal degeneration. *Expert Opin Biol Ther*. 2016;16:7–14.
151. Schwartz SD, Hubschman JP, Heilwell G, et al. Embryonic stem cell trials for macular degeneration: a preliminary report. *Lancet*. 2012;379(9817):713–720.

38

Nanomedicine in Ophthalmology

Marco A. Zarbin, James F. Leary, Carlo Montemagno, Robert Ritch, Mark S. Humayun

- Immune-Suppressive Therapy
- Gene Therapy
- Nonviral Vectors
- Viral Vectors
- Ocular Applications
- Imaging
- Minimally Invasive Physiologic Monitoring
- Coupling Diagnostics and Therapeutics
- Theranostics
- Prosthetics: Molecules as Machines (e.g., Light-Sensitive Ion Channels), Abiotic–Biotic Interfaces
- Induced Photosensitivity
- Bionic Retina
- Regenerative Medicine: Nanostructured Scaffolds to Control Cell Phenotype
- Engineering Scaffolds to Support Cell Transplants
- Scaffolds for Cell Transplantation to the Subretinal Space
- Surgical Technology

Obstacles to Incorporation of Nanotechnology Into Ophthalmology

- Persistence of Nanoparticles Despite Immune Surveillance
- Safe Manufacturing Techniques
- Cell-by-Cell Dose Delivery and Control

Introduction

Nanotechnology provides an important new set of tools for the diagnosis and treatment of ocular diseases. Miniaturization of devices, chip-based technologies, and novel nanosized materials and chemical assemblies already provide novel tools that are contributing to improved healthcare in the 21st century and will impinge directly on ophthalmology.[1–4] In this chapter, we review general principles of nanotechnology and nanomedicine as well as properties of nanomachines. We also consider specific and potential applications of nanotechnology to ophthalmology, including drug, peptide, and gene delivery; imaging; minimally invasive physiologic monitoring; prosthetics; regenerative medicine; and surgical technology. Finally, we consider obstacles to incorporation of nanotechnology into ophthalmology. Each of these topics has been reviewed in detail previously.[5–7]

General Principles of Nanotechnology and Nanomedicine

Nanotechnology

Nanotechnology involves the creation and use of materials and devices at the size scale of intracellular structures and molecules. The systems and constructs deployed typically are on the order of <100 nm. (Recall that an average man is 1.6 meters [1.6 billion nanometers (nm)] tall; an erythrocyte is 7 μm [7×10^3 nm] wide; and a strand of deoxyribonucleic acid [DNA] is 2 nm wide.) Transformational opportunities in information storage, computation, and mechanical efficiency are available through nanotechnology.

Regarding information storage, Richard Feynman, who is credited with conceiving the field of nanotechnology, calculated

that it was possible to write the entire 24 volumes of the *Encyclopedia Britannica* on the head of a pin.[8] If one did not simply etch the letters on to the surface of the pin but used the interior of the material also, he calculated that one could fit all the information that humans had accumulated up to December 1959 (estimated at 10^{15} bits) in a cube of material 1/200 inch wide, comparable to the size of a piece of dust.[8] Today, through nanotechnology-based precision assembly of matter, storage densities of 10^{11} bits per cm^2 have been demonstrated, which closely approximates Feynman's vision.[9] Efficient information storage is crucial for the complexity of biological systems, as each eukaryotic cell stores an enormous amount of information. A retinal pigment epithelial (RPE) cell has a diameter of approximately 4×10^{-4} inches (1×10^{-3} cm), and each cell stores the blueprint to create an entire human in DNA molecules (3 billion chemical basepairs, ~25,000 genes).

Regarding computation, Feynman also noted that biological systems do not simply store information, they create measurable outputs. The human brain has the capacity to make judgments, e.g., recognize a person's face (even if shown at different distances, under different lighting conditions, at different angles), or play chess. Feynman reasoned that if computers could have as many computational elements as our brains, they could make judgments as well.[8] Today sophisticated facial recognition can be accomplished with a powerful laptop computer (versus poorly in 1959, with a much larger computer), due to the development of microprocessors and sophisticated software. Defeating a grand master at chess, however, requires a supercomputer. A Cray XT5 supercomputer uses ~40 kW power/cabinet, and each cabinet measures ~81 × 23 × 57 $inches^3$ (larger than a refrigerator) and weighs ~1530 lb (694 kg) (http://www.cray.com/downloads/CrayXT5Blade.pdf). It is remarkable that the "computer" in our cranium does not require the amount of rare elements, generate the heat, or have the energy requirements of a supercomputer. Thus, the evolution of our cognitive capacities from infancy to adulthood (derived from the interaction between a DNA template-guided, manufactured neuronal network and the external environment) is one demonstration that it is possible to develop nanoscale mechanical systems that create complex, measurable outputs.

Nanomachines are highly efficient.[10] When organized in massively parallel structures, for example, nanomotors can generate large forces (e.g., muscles that move massive animals such as whales) or large electrical currents (e.g., those generated by the Hunter's organ of electric eels). Nanomotors also can direct delicate processes such as ion transport and chromosomal migration during mitosis. Nanomachines are not only highly efficient, they typically have long operational half-lives and are mass-produced easily.

Nanomedicine

The aim of nanomedicine is the comprehensive monitoring, control, construction, repair, defense, and improvement of human biological systems at the molecular level, using engineered nanodevices and nanostructures, operating massively in parallel at the single-cell level, performing "single-cell medicine," ultimately to achieve medical benefit.[11] Integration of nanoscale technologies with the practice of medicine will alter profoundly our approach to the diagnosis, treatment, and prevention of disease.[12] We will begin to diagnose and treat diseases at the single-cell level, for example, rather than just at the organ level.

General principles of nanotechnology as applied to nanomedicine include:

1. Biomimicry: the approach that cells use to direct molecules within a cell and/or direct molecules/machines to the proper cells in the body.

2. Size and location drive biocompatibility and biological efficacy.

3. Engineer feedback control into therapeutic systems (e.g., therapeutic gene synthesis).[3,4,13–15]

4. Molecules as machines: engineer molecules to perform specific physical tasks, such as opening ion channels, to alter cell and organism behavior.[16–18]

5. "Pseudointelligence" resulting from intelligent design, e.g., self-assembly of extracellular matrix (ECM) molecules.[15,19–23]

6. Highly interdisciplinary undertaking: development of nanotechnologies typically involves expertise in biology, engineering, chemistry, and physics.[18,24–26]

The functional properties of living systems arise not only from their component parts, but also from how these parts are assembled, which dictates interactions between the parts, the nature and flow of information within the system, and the outputs that the system produces.[6] Thus, one concept from biology that may be important for development of nanomachines in medicine is that spatial control of the distribution of nanomachines directly affects the efficiency of the macromolecular assembly and nature of this assembly's work product.[27] Spatial control can be achieved through the use of membranes and anchoring molecules that place enzymes and substrates in proximity (e.g., as occurs in the endoplasmic reticulum for synthesis of ECM proteins, in the mitochondrial membrane for electron transport, and on the cell surface for ECM ligand integrin-mediated changes in intracellular signaling).[28] This concept is exploited in the area of neural prosthetics, as described later in this chapter. Conversely, this engineering approach also permits segregation of molecules (e.g., segregation of lysosomal enzymes from the cytoplasm). Microelectromechanical systems (MEMS) or nanoelectromechanical systems (NEMS)-based techniques can be used to create engineered scaffolds (see next paragraph) that achieve this spatial control. One might also use a synthesized lipid bilayer or block co-polymer membranes to create artificial organelles as occurs in nature.

One can produce nanomachines by assembling naturally occurring ones.[10,29–32] M/NEMS-based engineering, however, permits the construction of small devices using computer-aided design and by the repeated application of a number of procedures, including oxidation, photolithography, etching, diffusion, sputtering, chemical vapor deposition, ion implantation, and epitaxy, as illustrated by the devices described later in this chapter. Control of features down to the submicron level permits production of mechanical structures at length scales ranging from 100 nm or less to greater than 1 cm. The ability to create complex microfabricated biomaterial substrates using these techniques enables one to define

surface microarchitecture, topography, and feature size. By engineering the microenvironment, one can control individual cell responses utilizing structures at the micro- and nanoscale to alter cellular attachment and motility, attenuate the foreign-body response, simulate tissue organization, and promote cell differentiation.[33–40]

A straightforward application of nanomachines to nanomedicine is the use of error-prone polymerase chain reaction and transposons to nanoengineer novel structures (e.g., viral capsids) as vectors for gene and drug delivery (as discussed later in this chapter). A somewhat less obvious application of nanomachines exploits their capacity for energy transduction. Motor proteins, for example, transduce the following forms of energy: (1) optical and electroosmotic; (2) optical and electronic; (3) chemical and electroosmotic; (4) chemical and electronic; (5) mechanical and electroosmotic; and (6) mechanical and chemical. By exploiting the transducing properties of nanomotors, one might be able to develop nanomachines that measure biological variables: oxygen tension, pH, glucose concentration, the redox state of a cell or subcellular organelle, temperature, intraocular pressure (IOP), or blood pressure. Alternatively, one can use nanomachines to induce energy sensitivity where it does not normally exist, e.g., creation of light-sensitive retinal ganglion cells (RGCs) or bipolar cells (described later in this chapter) or to provide therapeutic molecules to cells, e.g., wild-type alleles of retinal proteins to blind mutants (described later in this chapter). Finally, one might couple the measuring and therapeutic capacity of nanomachines to create devices that measure critical biological variables (e.g., redox state) for diagnostics and provide therapy (e.g., antioxidant therapy) at the appropriate time and place and in the appropriate quantity, a concept termed theranostics (discussed later in this chapter).

Properties of Nanomachines[8]

Physical Properties

Feynman noted that, at the size scale of intracellular structures and molecules, materials acquire seemingly surprising properties that

are predictable based on the principles of quantum physics.[8] For instance, carbon becomes stronger than steel; gold melts at room temperature, and aluminum becomes highly explosive. Quantities such as weight and inertia are of relatively little importance.

Inhomogeneity of materials (e.g., metals versus plastics) might limit their utility.[8] Magnetic properties on a very small scale are not the same as on a large scale. Lubrication is not needed if the machine is small enough because heat loss is rapid (due to the large surface area : volume ratio). Some of these properties produce unexpected results. For example, rapid heat loss might prevent gasoline from exploding, which would make a nanoscale internal combustion engine impossible.[8]

The influence of gravity on the function of true nanomachines is negligible because their mass is that of atoms ($F_g = Gm_Am_B/r^2$).[8] On the other hand, the distance between the elements is in nanometers. Because of van der Waals forces, parts of nanomachines might adhere to each other, which might not be desirable. Electrical resistance may be very large with nanocircuits, a feature that might be useful in biological systems. Another problem with nanocircuits is the inverse relationship between the size of the device and the amount of noise generated (Hooge's rule). The development of stacked graphene sheets may provide a solution to this problem and facilitate the development of circuits much smaller than those in conventional silicone-based computer chips.[41] However, when working on the scale of atoms, circuits might not be needed, and quantized energy levels might be manipulated for energy transfer according to the laws of quantum mechanics. This property is exploited in some nanoparticle-based imaging technologies.

Axial ratio is the ratio of the magnitude of the axes (e.g., length and width in the case of a two-dimensional object), the greater being divided by the lesser. Nanotubes and nanofibers have very large axial ratios. Synthetic methods exist to alter the length-to-volume ratio and thus the physical properties of the material. Conductivity, for example, is enhanced as the diameter of semiconducting nanotubes is reduced.

A key property of nanomaterials is that they are surface-rich objects in relation to volume. The following analogy illustrates this concept. A baseball filled with membrane surface-active enzymes

would have only a minimal number of these extending to the surface of the ball, so the vast majority would be inactive. A pea filled with enzymes would have a greater proportion extending to the surface. A sphere 100 nm in diameter would have the majority of the enzymes it contains in an active state. This property results in a situation in which there is relatively limited unutilized surface area on to which one might attach molecules to the nanoparticle surface. The net effect is to create structures that accelerate many chemical reactions at their surfaces and act in some ways like very active enzymes.

Vacancy-engineered mixed-valence state cerium oxide (CeO_2) nanoparticles (nanoceria) illustrate the useful properties that materials can develop at the nanoscale. Alteration in the oxidation state of CeO_2 creates defects in its lattice structure via loss of oxygen or its electrons. As their size decreases, nanoceria (3–5 nm diameter) demonstrate formation of more oxygen vacancies in the crystal structure.[42,43] As described later in this chapter, vacancy-engineered nanoceria may function as a highly effective treatment for ocular conditions associated with oxidative damage.

Manufacture

At each step in the process of manufacturing smaller and smaller machines, one must improve the accuracy of the equipment.[8] Feynman speculated that if devices are built on the scale of 5–10 atoms, then it should be possible to mass-produce them such that they are perfect copies of each other.[8] One useful outcome of a "nanomanufacturing" process is that the material costs of billions of these machines would be minimal since each is so small that minimal material is used. Nanomachines can have the capacity to repair and build themselves. Indeed, most nanoparticle structures are self-assembling under the proper thermodynamic conditions, allowing for production of a large number of virtually identical nanostructures.

Some properties of nanomachines are illustrated by the design and manufacture of an axon surgery platform. Using microtechnology, electrokinetic axon manipulation (i.e., dielectrophoresis), and cell fusion (i.e., electrofusion), Sretavan et

al.[24] developed a paradigm of direct axon repair involving the substitution of damaged axon regions with healthy segments from donor axons. This multidisciplinary group developed a multifunctional axon surgery platform that is ~1 mm^3 (Figs. 38.1 and 38.2). The cutting device consists of a silicon nitride knife with an ultrasharp knife-edge mounted on to a silicon-based compliant knife suspension (Fig. 38.1). The knife edge's radius of curvature (~20 nm) is similar to the diameter of a single microtubule. Because the knife is manufactured from a silicon nitride membrane, it is nearly transparent, which permits visualization of axons during the cutting procedure. The mechanical compliance of the suspension can be varied to deliver sufficient force for cutting different tissues (e.g., single axons) or for harvesting specific cell populations from histologic tissue sections. The authors envision future improvements such as sensors as well as force-generating actuation mechanisms that automatically deliver a controlled cutting stroke, and they indicate that both piezoelectric and thermal expansion actuation mechanisms can deliver forces in the range needed for axon cutting. A femtosecond laser might also be used for axotomy.[44] The goal is to develop a microcutting device with on-board sensing and actuation that can function as a semiautonomous instrument, requiring only initiating commands from the surgeon. Important limitations to the practical application of this invention remain. The authors estimate, for example, that ~20 seconds are required to repair a single axon using dielectrophoresis and electrofusion.[24] Cutting and fusing multiple axons simultaneously might enable relatively rapid repair of several thousand axons.

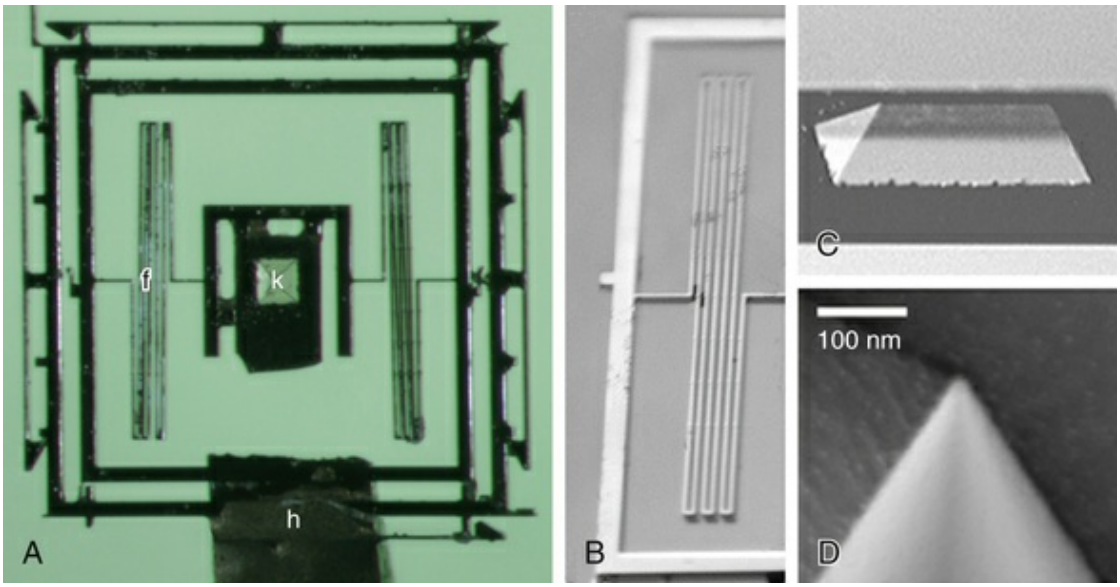

FIG. 38.1 Microfabricated axon surgery platform, an example of a nanomachine. (A) Axon knife assembled within a compliant suspension frame. The pyramidal structure in the center is an optically transparent axon knife with a 10-μm cutting edge. *f*, silicon suspension flexures; *k*, axon knife; *h*, handle to micromanipulator. The footprint of the frame is 1 mm^2. Scale = 200 μm. Devices with substantially smaller footprints can be fabricated. (B) Detail of the silicon suspension flexure on each side of the axon knife that provides mechanical compliance during cutting. The number of switchbacks in the flexure can be modified to obtain devices with different mechanical compliances that deliver a range of cutting forces. The compliance of the flexures allows it to act as a suspension, maximizing the durability of the knife edge. (C) Oblique view of the silicon nitride knife. Knives with edges from 5 to 200 μm have been fabricated and tested. A 200-μm-long knife is shown. (D) Scanning electron micrograph showing a cross-section of the silicon nitride knife at its very edge. The radius of curvature at the edge is roughly 20 nm. (Reproduced with permission from Sretavan DW, Chang W, Hawkes E, et al. Microscale surgery on single axons. Neurosurgery 2005;57:635–46, discussion 646; and from Zarbin MA, Montemagno C, Leary JF, et al. Nanomedicine in ophthalmology: the new frontier. Am J Ophthalmol 2010;150:144–62.)

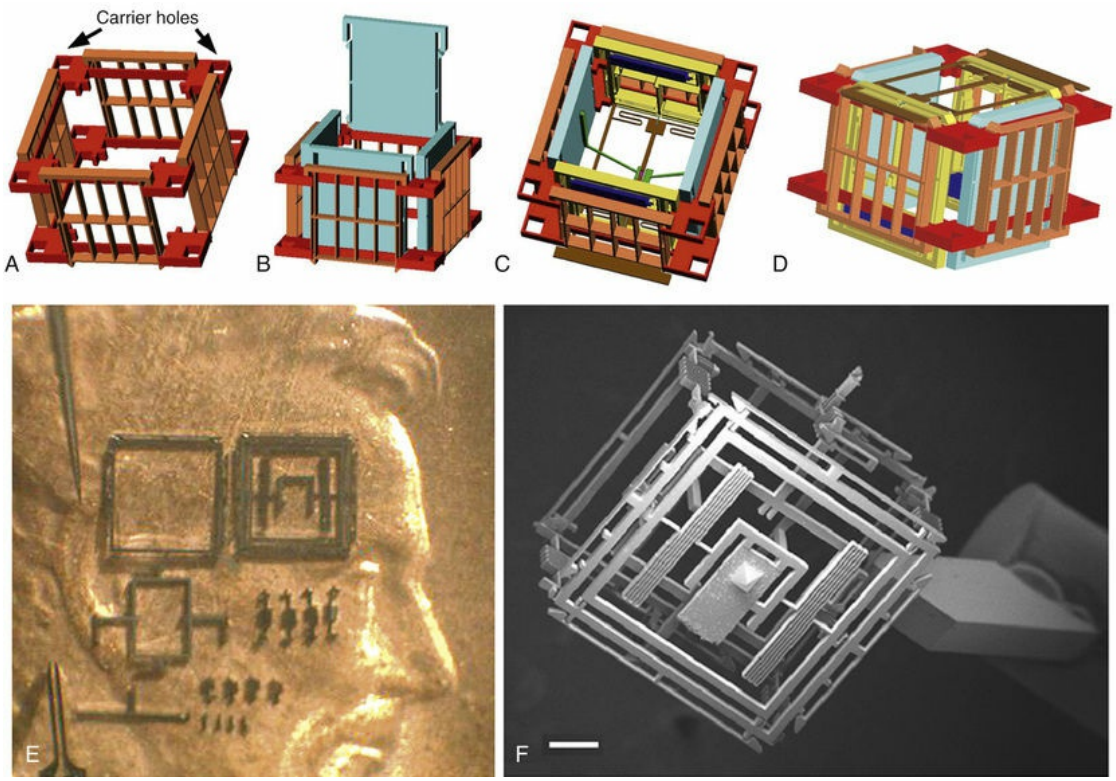

FIG. 38.2 Diagrams showing the design, assembly, and scale of a prototype multifunctional axon surgery platform. (A) Schematic representation of the space frame. Carrier holes are used for positioning the platform. (B) Modular axon repair components such as cutting devices and electrode arrays are inserted into the space frame to preposition their functional elements for efficient axon repair. (Generic components are shown here.) The space frame also contains a force generation (actuation) mechanism to execute the up–down motion of the axon knife during cutting. (C) Oblique view of platform assembled with a microcutting device and electrode arrays. (D) View from bottom. (E) Sixteen individual microfabricated parts on display on a penny. A microgripper and a microprobe are shown on the left. (F) Scanning electron microscope image of the assembled axon surgery device prototype containing a functioning axon microcutting device and supporting pieces locked in place to form a 1-mm^3 superstructure. Scale bar = 200 μm. (Reproduced with permission from Sretavan DW, Chang W, Hawkes E, et al. Microscale surgery on single axons. Neurosurgery 2005;57:635–46, discussion 646; and from Zarbin MA, Montemagno C, Leary JF, et al. Nanomedicine in ophthalmology: the new frontier. Am J Ophthalmol 2010;150:144–62.)

Applications to Ophthalmology

Nanomedicine will foster revolutionary advances in the diagnosis and treatment of disease. Nanomedicine is likely to have a major impact on biopharmaceuticals (e.g., drug delivery, drug discovery),[45] implantable materials (e.g., tissue regeneration scaffolds, bioresorbable materials), implantable devices (e.g., IOP monitors,[46] glaucoma drainage valves[47]), and diagnostic tools (e.g., infectious disease diagnosis, genetic testing, imaging, IOP monitoring). Nanotechnology will bring about the development of regenerative medicine (i.e., replacement and improvement of cells, tissues, and organs), ultrahigh resolution in vivo imaging, microsensors and feedback devices, and artificial vision. "Regenerative nanomedicine," a new subfield of nanomedicine, uses nanoparticles containing gene transcription factors and other modulating molecules that allow reprogramming of cells in vivo.

Delivery of Drugs, Peptides, and Genes

General Considerations Regarding Nanoparticles

Nanoparticles are colloidal carrier systems that can improve the efficacy of drug delivery by overcoming diffusion barriers, permitting reduced dosing (through more efficient tissue targeting) as well as sustained delivery (Fig. 38.3). These features are attractive for drug treatment of chronic conditions such as glaucoma,[48] uveitis,[49] or retinal edema (due to venous occlusion or choroidal neovascularization [CNV]) as well as for treatment of intraocular tumors and other conditions associated with cell proliferation such as capsular fibrosis after cataract surgery, ocular neovascularization, and proliferative vitreoretinopathy. Nanoscale-engineered cell substrata (e.g., nanowires) and carbon nanotubes also can be used for gene and drug delivery.[50–52]

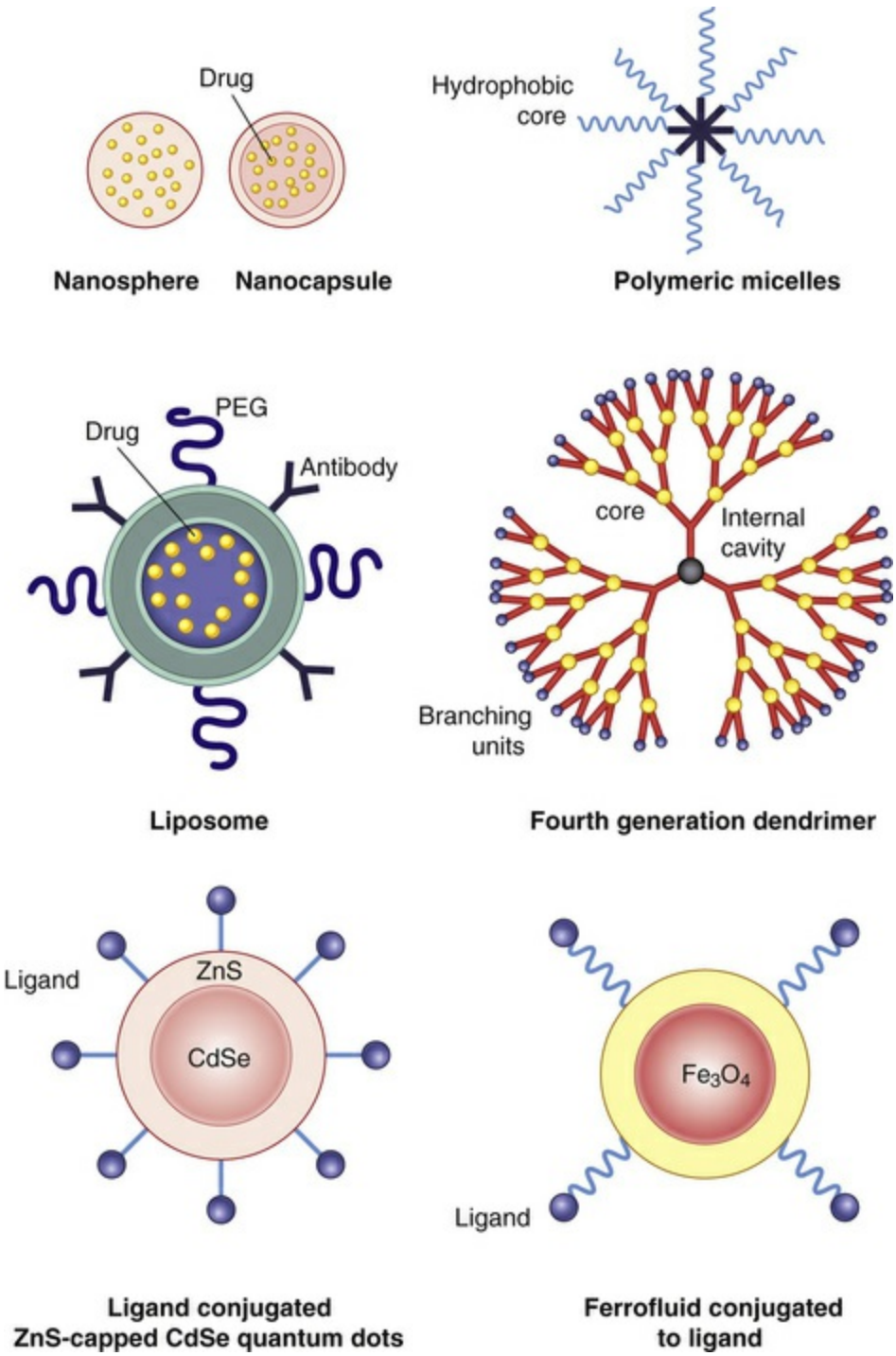

FIG. 38.3 Schematics of different nanotechnology-based drug delivery systems. Nanoparticles are small polymeric colloidal particles with a therapeutic agent either dispersed in polymer matrix or encapsulated in polymer. Polymeric micelles are self-assembled block copolymers, which in aqueous solution arrange to form an outer hydrophilic layer and an inner hydrophobic core. The micellar core can be loaded with a water-insoluble therapeutic agent. Liposomes are lipid structures that can be made “stealth” by PEGylation

and further conjugated to antibodies for targeting. Dendrimers are monodispersed symmetric macromolecules built around a small molecule with an internal cavity surrounded by a large number of reactive end groups. Quantum dots are fluorescent nanocrystals that can be conjugated to a ligand and thus can be used for imaging purposes. Ferrofluids are colloidal solutions of iron oxide magnetic nanoparticles surrounded by a polymeric layer, which can be further coated with affinity molecules such as antibodies. *PEG*, poly(ethylene glycol). (Reproduced with permission from Sahoo SK, Labhasetwar V. Nanotech approaches to drug delivery and imaging. Drug Discov Today 2003;8:1112–20 with permission from Elsevier; and from Zarbin MA, Montemagno C, Leary JF, et al. Nanomedicine in ophthalmology: the new frontier. Am J Ophthalmol 2010;150:144–62.)

Strategies in the design of nanoparticles for therapeutic purposes have been reviewed thoroughly by Petros and DeSimone,[53] Moghimi et al.[54] and Kompella et al.[55] Particle size, shape, and surface properties influence nanoparticle biodistribution. Particle size, for example, affects whether the particle is internalized via phagocytosis, macropinocytosis, caveolae-mediated endocytosis, or clathrin-mediated endocytosis, which in turn results in exposure of the nanoparticle to different intracellular environments.[56] The cell surface receptor, nucleolin, transports compacted polylysine DNA nanoparticles into cells and directly to the nucleus.[57]

One can target nanoparticles to specific cells by attaching to the particle surface ligands/antibodies/peptides/aptamers for receptors/molecules that are abundant on the surface of the target cell/tissue.[53] This approach can have complications. Receptor aggregation on the cell surface, for example, can induce unintended events, such as apoptosis.[58] One can engineer the nanoparticle for a particular mode of intracellular entry depending on the choice of nanoparticle targeting molecules, e.g., cholesterol favors uptake via caveolin-mediated endocytosis, and transactivating transcriptional activator peptide favors macropinocytosis.[59,60] Nanoparticle surface chemistry also can be manipulated to trigger cargo release under specific circumstances. For example, when exposed to a reducing environment such as is present in the cytosol, reductively labile disulfide-based crosslinks between the carrier and cargo are

broken.[61,62] Approaches for targeting nanoparticles to particular subcellular organelles, e.g., mitochondria[63] or the nucleus,[64] also have been developed.

Liposomes and polymer–drug conjugates are among the most frequently used nanoparticles for therapeutic purposes. Liposomes, which carry hydrophobic or hydrophilic cargo, can be coated with ligands that direct them to specific cell surface receptors for cell targeting as well as with polymers that prolong their half-life in the circulatory system. Poly(ethylene glycol) (PEG) can be conjugated with different molecules to enhance their solubility and stability in plasma and to reduce immunogenicity.[53] Opsonization by immunoglobulin and/or complement proteins can lead to recognition of the nanoparticle as foreign and induce a hypersensitivity reaction.[65,66] Coating a nanoparticle with albumin and/or PEG can create a hydrophilic surface that temporarily resists protein adsorption, thus prolonging the particle's bioavailability.[53,67,68] This approach allows for much longer drug circulation and concomitant lowering of therapeutic-level drug doses, which in turn can reduce many unintended side-effects.

Dendrimers are synthetic, highly branched polymers that have precisely controllable nanoscale scaffolding and nanocontainer properties, which in some senses mimic the properties of macromolecules such as DNA and ribonucleic acid (RNA).[69] The diameter of poly(amidoamine) dendrimer ranges from 1.5 to 14.5 nm.[70] As generation (G) number increases, the number of active terminal groups doubles. G3 dendrimers, for example, contain 32 terminal groups, and G4 dendrimers contain 64 terminal groups. In poly(amidoamine) dendrimers, full generations (e.g., G3) have terminal amine or hydroxyl groups while half-generation dendrimers (e.g., G3.5) have carboxylic acid terminal groups. Dendrimers have been explored as vehicles for controlled drug delivery, including cancer therapy, pilocarpine, gatifloxacin, and for vascular endothelial growth factor (VEGF) inhibition.[71–74] Marano et al.,[72] for example, used a lipophilic amino acid dendrimer to deliver an anti-VEGF oligonucleotide into rats' eyes with laser-induced CNV. The dendrimer–oligonucleotide conjugate inhibited CNV development for 4–6 months by up to 95%, whereas eyes injected with oligonucleotide alone showed no treatment benefit compared

to vehicle-injected controls at these times. The dendrimer–oligonucleotide conjugate was well tolerated in vivo. Ideta et al.[75] used dendrimer porphyrin encapsulated by a polymeric micelle to treat laser-induced CNV in rodents and found significant enhancement of photodynamic therapy efficacy with less light energy required for CNV occlusion.

Antibiotic Therapy

Typically, only a small fraction (<5%) of topically administered medications is biologically available due to limited ocular penetration and rapid clearance from the aqueous humor. Because dendrimers contain surface functional groups as well as void spaces within and between their branches, they can serve as delivery vehicles for therapeutic modalities such as carboplatin.[74] Dendrimeric polyguanidilyated translocators (DPT) are nanosized dendrimers that translocate molecules across biological barriers efficiently. Durairaj et al.[71] used a six-guanidine group-containing dendrimer to enhance gatifloxacin solubility (fourfold) and delivery to the anterior and posterior segment of rabbits. The DPT–gatifloxacin complexes (346 nm) enhanced tissue concentration in the conjunctiva (13-fold) and cornea (twofold). A single dose resulted in sustained aqueous humor levels ($t_{1/2}$ = 9 hours), potentially allowing decreased frequency of administration (e.g., once-daily dosing). After multiple dosing, DPT–gatifloxacin achieved therapeutic levels in the vitreous humor for 12 hours (versus no drug levels detectable at 12 hours after topical gatifloxacin alone).

Antimetabolite Therapy

Shaunak et al.[76] used anionic, polyamidoamine, generation 3.5 dendrimers to make novel water-soluble conjugates of D(+)-glucosamine and D(+)-glucosamine 6-sulfate with immunomodulatory and antiangiogenic properties, respectively. Dendrimer glucosamine inhibited Toll-like receptor 4-mediated lipopolysaccharide-induced synthesis of proinflammatory chemokines (i.e., macrophage inflammatory protein (MIP)-1α, MIP-1β, interleukin (IL)-8) and proinflammatory cytokines (i.e., tumor

necrosis factor-α, IL-1β, IL-6) primarily from immature human monocyte-derived dendritic cells and monocyte-derived macrophages, but allowed upregulation of the costimulatory molecules CD25, CD80, CD83, and CD86. Dendrimer glucosamine 6-sulfate blocked fibroblast growth factor-2-mediated human umbilical vein endothelial cell proliferation, but not VEGF-mediated proliferation, and neoangiogenesis in human Matrigel and placental angiogenesis assays. When dendrimer glucosamine and dendrimer glucosamine 6-sulfate were used together in a validated, clinically relevant rabbit model of scar tissue formation after glaucoma filtration surgery,[77,78] they increased the long-term success of the surgery from 30% to 80% (p=.029). A clinical trial of this modality to reduce scarring after trabeculectomy, however, was not successful (P Khaw, R Ritch, personal communication).

Neurotrophic Factor Therapy

Nanoparticles can deliver growth and neurotrophic factors to cells.[79] Intravitreal nanoparticle-based basic fibroblast growth factor (bFGF) delivery, for example, provides sustained retinal rescue in Royal College of Surgeons (RCS) rats.[80] In RCS rats, the RPE cells have a mutation that prevents proper outer-segment phagocytosis, with secondary rod and cone photoreceptor degeneration.[81] Some patients with retinitis pigmentosa (RP) have this same mutation.[82–84] Sakai et al.[80] prepared bFGF nanoparticles using gelatin isolated from bovine bone collagen and human recombinant bFGF. The nanoparticle diameter, assessed using dynamic light scattering, was ~585 nm.

Glaucoma, a leading cause of blindness worldwide, is associated with progressive RGC death and optic nerve atrophy.[85] Intravitreal glial cell line-derived neurotrophic factor (GDNF)-loaded biodegradable (poly)lactic-co-glycolic acid (PLGA) microspheres provide sustained RGC protection in a rodent model of glaucoma.[86] Microspheres (~8 µm diameter) containing GDNF were fabricated using a modification of a spontaneous emulsion technique.[87] Since adeno-associated virus (AAV)-mediated GDNF secretion from glia delays retinal degeneration in a rat model of RP,[88] it is possible that nanoparticle-mediated GDNF delivery can be applied to treating RP-like diseases.

Optic nerve injury (crush) has been treated using nanoparticles to deliver neurotrophic factors. Kim et al.[89] demonstrated that human serum albumin nanoparticles (150 nm diameter) conjugated with brimonidine released brimonidine for 5 days and improved retinal ganglion cell density after injury by almost 400% compared to control 14 days after optic nerve injury in rats. Brimonidine was loaded into the hydrophobic pockets of the human serum albumin nanoparticles. The nanoparticles seemed to reduce amyloid-beta deposition in the retinal ganglion cell layer. In view of the pore size of the internal limiting membrane (10–20 nm) and the outer limiting membrane (3–4 nm), it seems likely that the nanoparticles penetrated the retina by a receptor mediated endocytosis mechanism, possibly the transforming growth factor-beta receptor.[89]

Antioxidant Therapy

Age-related macular degeneration (AMD), RP, diabetic retinopathy, and retinopathy of prematurity are characterized, in part, by the presence of oxidative damage.[90–95] As noted above, alteration in the oxidation state of CeO_2 nanoparticles creates defects in its lattice structure via loss of oxygen or its electrons. Chen et al.[96] posited that engineered nanoceria can scavenge reactive oxygen intermediates because the large surface area-to-volume ratio at 5 nm diameter enables CeO_2 to regenerate its activity and thereby act catalytically. (Unlike nanoceria, most free-radical scavengers require repetitive dosing.) Chen et al.[96] showed that intravitreal injection of nanoceria prevents light-induced photoreceptor damage in rodents, even if injected after the initiation of light exposure. Vacancy-engineered nanoceria also inhibit the development of and promote regression of pathologic retinal neovascularization in the *Vldlr* knockout mouse, which carries a loss-of-function mutation in the very low-density lipoprotein receptor gene and whose phenotype resembles a clinical entity known as retinal angiomatous proliferation (Figs. 38.4 and 38.5).[97,98] This regression occurs even if nanoceria are injected intravitreally after the mutant retinal phenotypes are established (Fig. 38.6). Because nanoceria are a catalytic and regenerative antioxidant, a single injection has a prolonged effect (measured in weeks).

Nanoceria inhibition of increased VEGF levels in this model[97] may mean that CeO_2 nanoparticles will be effective in treating macular edema in diabetic eyes and CNV-induced retinal edema in AMD eyes.[99–101]

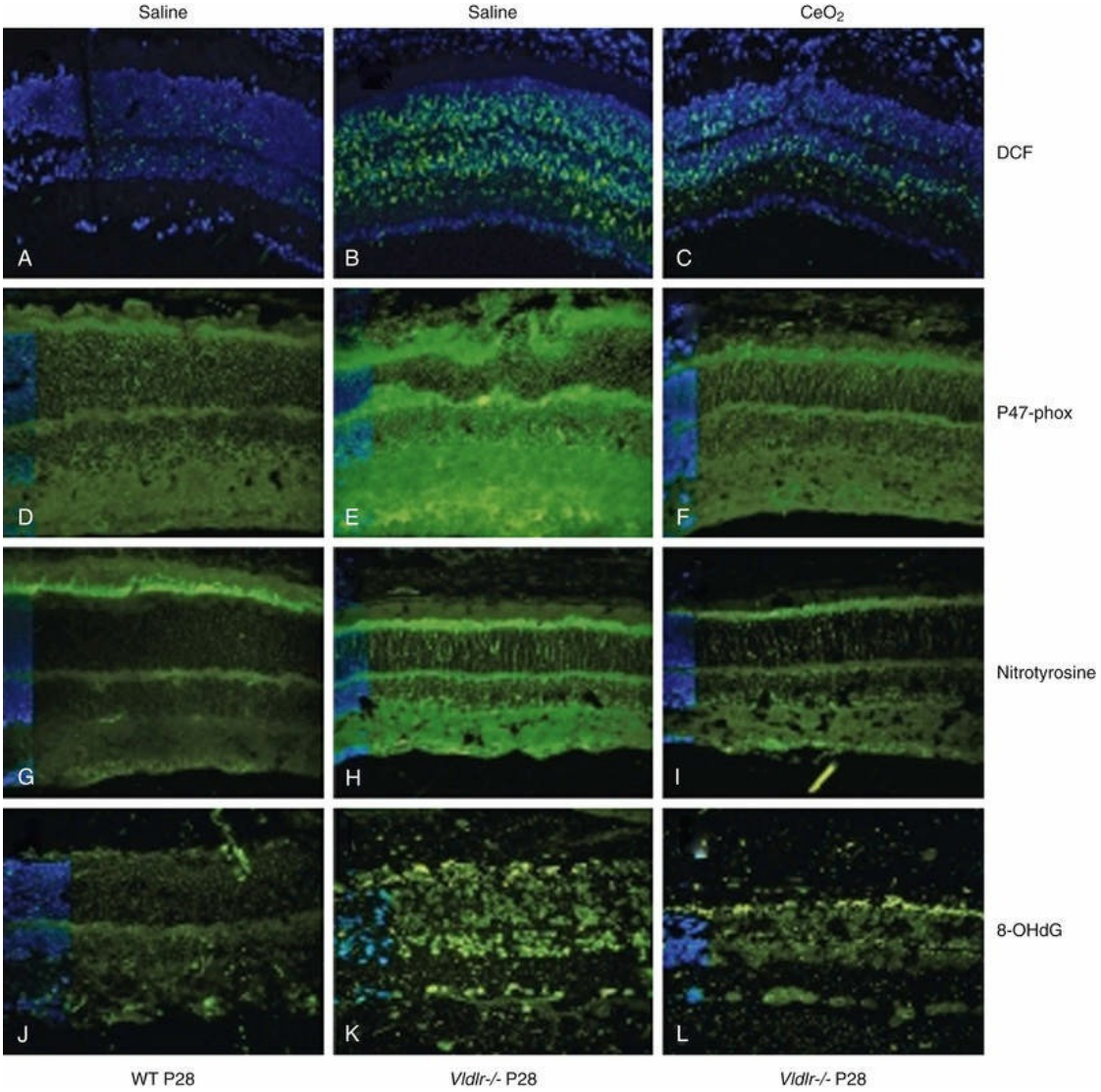

FIG. 38.4 Nanoceria reduce oxidative stress in the *Vldlr*$^{-/-}$ retina. Retinal sections from saline-injected wild-type (WT) mice (panels A, D, G, J); saline-injected *Vldlr*$^{-/-}$ mice (panels B, E, H, K), and CeO_2-injected (panels C, F, I, L) *Vldlr*$^{-/-}$ mice are shown as imaged by confocal microscopy. The 2′,7′-dicholoro-dihydro-fluorescein-diacetate (DCF) assay (A–C) visualizes reactive oxygen species (ROS) as punctuate fluorescence and demonstrates a very low level of ROS in the normal retina (A), a considerable amount in

the *Vldlr*$^{-/-}$ retina (B), and a greatly reduced amount in the retina of the *Vldlr*$^{-/-}$ mice injected with CeO_2 (C). Similar results were obtained with the other three assays. NADPH-oxidase (P47-phox; D–F), a major producer of ROS, was very high in the *Vldlr*$^{-/-}$ retina and almost reduced to control levels in the CeO_2-injected mice. Nitrotyrosine (G–I), a reflection of oxidative activity due to increases in nitric oxide concentration, was highest in the *Vldlr*$^{-/-}$ retina and significantly reduced in the nanoceria-injected mice. ROS-mediated damage to DNA was indicated by the labeling of the retina with an antibody against a DNA adduct, 8-hydroxy-29-deoxyguanosine (8-OHdG; J–L), which showed little labeling in the control, significant labeling in the saline-injected *Vldlr*$^{-/-}$ retina, and a greatly reduced amount in the nanoceria-treated retina. DAPI (blue) was used to visualize the nuclei. (Reproduced with permission from Zhou X, Wong LL, Karakoti AS, et al. Nanoceria inhibit the development and promote the regression of pathologic retinal neovascularization in the *Vldlr* knockout mouse. PLoS One 2011;6:e16733; and from Zarbin MA, Montemagno C, Leary JF, et al. Regenerative nanomedicine and the treatment of degenerative retinal diseases. Wiley Interdiscip Rev Nanomed Nanobiotechnol 2012;4:113–37.)

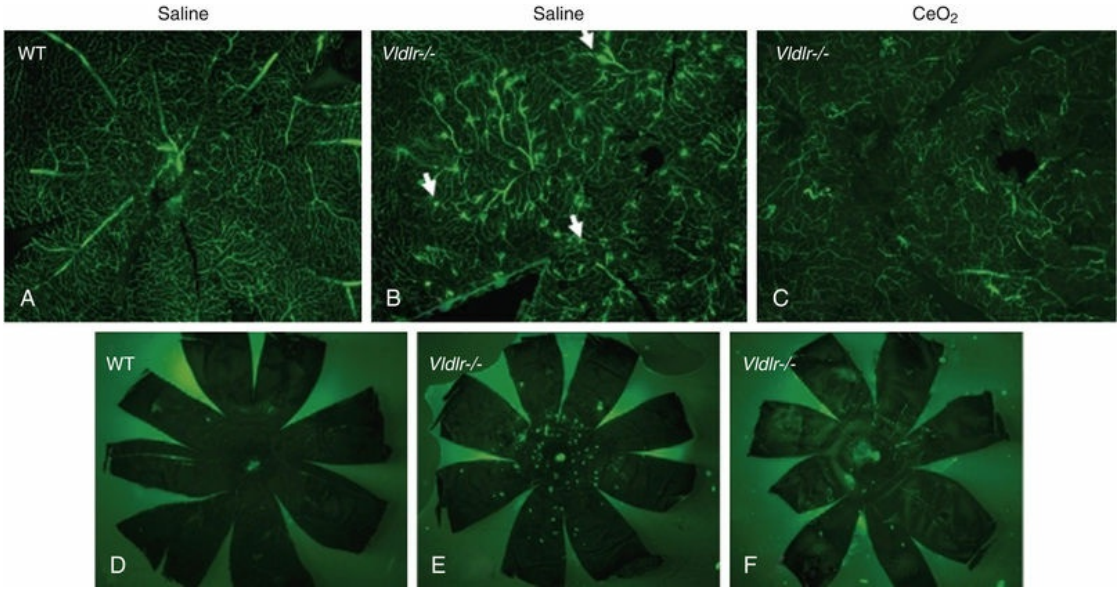

FIG. 38.5 Nanoceria inhibit the development of pathologic intra- and subretinal vascular lesions in the *Vldlr*$^{-/-}$ retina. Photomicrographs of whole-mount

retinas (A–C) and eyecups (retinal pigment epithelium, choroid, and sclera) (D–F) from P28 animals are shown. All retinal blood vessels were labeled green by the vascular filling assay. Wild-type (WT) retinas (A) showed the normal web-like retinal vasculature whereas those from the *Vldlr*$^{-/-}$ mice (B) showed numerous intraretinal vascular lesions or "blebs." See *white arrows* for examples. A single injection of nanoceria at P7 (C) inhibited the appearance of these lesions. Eyecups from WT mice (D) showed no subretinal neovascular (SRN) "tufts"' but those from *Vldlr*$^{-/-}$ mice (E) had many bright SRN tufts. A single injection of nanoceria on P7 inhibited the appearance of these SRN tufts (F). (Reproduced with permission from Zhou X, Wong LL, Karakoti AS, et al. Nanoceria inhibit the development and promote the regression of pathologic retinal neovascularization in the *Vldlr* knockout mouse. PLoS One 2011;6:e16733; and from Zarbin MA, Montemagno C, Leary JF, et al. Regenerative nanomedicine and the treatment of degenerative retinal diseases. Wiley Interdiscip Rev Nanomed Nanobiotechnol 2012;4:113–37.)

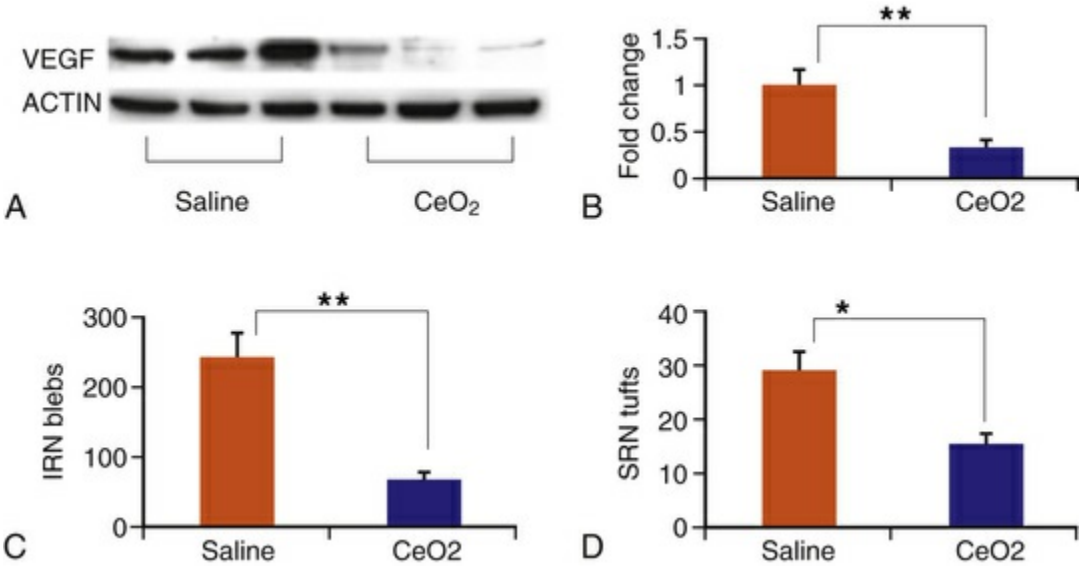

FIG. 38.6 Retinal vascular lesions in the *Vldlr*$^{-/-}$ retinas require continual production of excess reactive oxygen species. *Vldlr*$^{-/-}$ mice were injected at P28 with saline or nanoceria and killed 1 week later on P35. Analysis of vascular endothelial growth factor (VEGF) levels by Western blots (A) showed a fourfold reduction (B) within 1 week of nanoceria injection. The numbers of

intraretinal neovascular (IRN) blebs (C) and subretinal neovascular (SRN) tufts (D) were also dramatically reduced. *p=.05; **p=.01. (Reproduced with permission from Zhou X, Wong LL, Karakoti AS, et al. Nanoceria inhibit the development and promote the regression of pathologic retinal neovascularization in the *Vldlr* knockout mouse. PLoS One 2011;6:e16733; and from Zarbin MA, Montemagno C, Leary JF, et al. Regenerative nanomedicine and the treatment of degenerative retinal diseases. Wiley Interdiscip Rev Nanomed Nanobiotechnol 2012;4:113–37.)

C-60 fullerenes are cage-like structures (truncated icosahedron) of carbon atoms with antioxidant properties.[102] Malonic acid C-60 derivatives (carboxyfullerenes) can eliminate superoxide anion and H_2O_2, and inhibit lipid peroxidation.[8] Systemic administration of the C-3 carboxyfullerene isomer delayed motor deterioration and death in a mouse model of familial amyotrophic lateral sclerosis.[92,103] It might be useful in the treatment of retinal diseases associated with oxidative damage.

Iron is an essential element for enzymes involved in the phototransduction cascade, in outer-segment disc membrane synthesis, and in the conversion of all-*trans*-retinyl ester to 11-*cis*-retinol in the RPE.[104–106] Free Fe^{2+} catalyzes the conversion of hydrogen peroxide to hydroxyl radical, which is a highly reactive species that causes oxidative damage (e.g., lipid peroxidation, DNA strand breaks).[107] Increased intracellular iron causes oxidative photoreceptor damage.[108] Polymeric nanoparticles can be used to chelate metals. Liu et al.[109] showed that a chelator-nanoparticle system complexed with iron, when incubated with human plasma, preferentially adsorbs apolipoprotein E and apolipoprotein A–I, which should facilitate transport into and out of the brain via mechanisms used for transporting low-density lipoprotein. Iron accumulation in the RPE and Bruch's membrane is greater in AMD eyes than in controls, including cases with early AMD and late stages of the disease (i.e., geographic atrophy, CNV).[110] Some of this iron is chelatable.[110] Although it is not proven that iron overload is a cause of AMD,[111–114] iron chelation might have a therapeutic effect. Thus, the technology developed by Liu et al.[109] might have utility for treating AMD eyes.

Immune-Suppressive Therapy

Cell-based therapy might be sight-restoring for patients with degenerative retinal diseases such as RP and AMD. An immune response to transplanted cells may depend upon the cell types included in the cellular therapy.[115] Nanotechnology provides immune-suppressive therapy (local or systemic) in selected cases where its need is anticipated.[115–117] In preclinical models, for example, nanoparticles are helpful in managing corneal allograft rejection. Yuan et al.[118] manufactured 300-nm-diameter rapamycin-loaded chitosan/polylactic acid nanoparticles and demonstrated that they extended median allograft survival by 17% in rabbits compared with aqueous rapamycin eye drops. Topical chitosan particles were well tolerated in this study, but intraocular chitosan nanoparticles may not be well tolerated.[119]

Studies of experimental autoimmune uveoretinitis (EAU) demonstrate that nanoparticles can be used to modulate the inflammatory response in the retina and choroid. EAU is a T-cell-mediated autoimmune disease that targets the retina and related tissues and serves as a model for human autoimmune ocular diseases.[120] Nanosuspensions of relatively insoluble glucocorticoids (developed using a high-pressure homogenization method) enhance the rate and extent of drug absorption as well as the intensity and duration of drug action, compared with conventional solutions and microcrystalline suspensions.[49] Rats with EAU clear poly(lactic acid) (PLA) nanoparticles rapidly from the systemic circulation.[121] As noted above, PEG can be used to modify the surface of the nanoparticles, which reduces opsonization and interactions with the mononuclear phagocyte system.[122,123] Sakai et al.[124] prepared polymeric nanoparticles with encapsulated betamethasone phosphate. These nanosteroid particles (~120 nm diameter) were composed of PLA homopolymer and a block copolymer of PEG.[124] In vivo imaging of inflamed eyes of rats with EAU demonstrated greater nanoparticle accumulation and higher betamethasone concentration in eyes of PLA-PEG nanoparticle-treated rats versus PLA nanoparticle-treated rats. PLA-PEG nanosteroid-treated EAU rats also had lower clinical and histopathologic scores for ocular inflammation. The stronger therapeutic effect of PLA-PEG nanosteroids versus PLA nanosteroids may be due to prolonged blood circulation and

sustained release in situ as well as due to targeting to inflamed eyes (the latter effect resulting from the small diameter of the nanoparticles).[124] EAU also responds very well to intravitreal liposomal tacrolimus (mean diameter = 200 nm) with no side-effects on retinal function or systemic cellular immunity.[125]

Gene Therapy

Nonviral Vectors

Viral vectors deliver genes efficiently but can be associated with risks such as immunogenicity and insertional mutagenesis. Nonviral vectors (e.g., polymers, lipids) and other methods (e.g., electroporation, nucleofection) have high gene-carrying capacity, low risk of immunogenicity, relatively low cost, and, possibly, greater ease of production.[126] Nanoparticles can deliver genes efficiently to stem cells[127] and have been explored as a means for gene delivery in the diagnosis and treatment of ocular disease.[3,128–130] As viruses do, nanoparticles can use transactivating sequences that allow them to deploy the host cell machinery to manufacture therapeutic molecules in situ. Because these sequences can contain an upstream biomolecular control sensor, therapeutic molecules can be manufactured *in situ* under tight feedback control.[3,4]

Electrostatic interaction of cationic polymers with negatively charged DNA/RNA molecules results in condensation of the material into particles ranging from 8 to 500 nm in diameter, protection of the genes from enzymes, and mediation of cellular entry.[26,131] Complexes of cationic polymers and plasmid DNA, termed polyplexes, can have transfection efficiency comparable to adenoviral vectors.[132] In addition to nanometer size, polyplexes have large vector capacity, are stable in nuclease-rich environments, and can have relatively high transfectivity for both dividing and nondividing cells.[130,132] For example, nanoparticles compacted with a lysine 30-mer linked to 10 kDa PEG-containing cytomegalovirus-cystic fibrosis transmembrane conductance regulator (CMV-CFTR) cDNA were used successfully in a phase I/II clinical trial for the treatment of cystic fibrosis.[133] Some particles, however, have low transfection efficiency, and the duration of gene expression can be

short. When it occurs, toxicity is related to nanoparticle chemistry.[26]

To some degree, compacted DNA nanoparticles can be targeted to different tissues in the eye through selection of an appropriate injection site (e.g., intravitreal injection can target the cornea, trabecular meshwork, lens, and inner retina; subretinal injection can target the outer retina and RPE).[130] Nanoparticle size and charge influence migration through the vitreous cavity.[134] Farjo et al.[130] demonstrated that after subretinal injection of compacted lysine 30-mer DNA nanoparticles, gene expression is observed throughout the retina and not just at the site of the injection. By choosing cell-specific promoters, one can achieve additional specificity in the locus of gene expression. The rhodopsin promoter, for example, drives expression in rod photoreceptors, and the human red opsin promoter drives expression in cone photoreceptors.[135–137] Interphotoreceptor retinoid-binding protein drives expression in both rods and cones.[138] The vitelliform macular dystrophy promoter drives expression in RPE cells.[139]

Cai et al.[135,140] used a specific formulation of DNA nanoparticles consisting of single molecules of DNA compacted with 10 kDa PEG-substituted lysine 30-mer peptides containing the wild-type retinal degeneration slow (*Rds*) gene, peripherin/rds, to induce cone photoreceptor rescue in an animal model ($rds^{+/-}$) of RP. After injection into the subretinal space, these particles did not induce a detectable immune response, cytotoxicity, or disruption of retinal function. These compacted plasmid DNA nanoparticles are small (8–20 nm), have rod or ellipsoid shape (depending on the counterion used), and have a large carrying capacity (at least up to 20 kilobases).[130,140] PLGA nanoparticles can deliver genes to RPE cells in vitro and in vivo relatively efficiently and safely,[141] and PLGA DNA nanoparticles can be associated with long-term gene expression.[142] PLGA DNA nanoparticles tend to be larger than polylysine DNA nanoparticles,[143,144] which may affect cellular uptake mechanism and delivery to the nucleus. PLGA DNA nanoparticles might be used to deliver therapeutic genes for conditions associated with RPE gene mutations, e.g., Best disease[145] and a form of Leber congenital amaurosis.[146–148]

Albumin has a highly charged amino acid content, which facilitates its action as a carrier for charged drugs and

oligonucleotides. Albumin-derived nanoparticles that deliver plasmids containing genes for the Flt receptor (VEGFR1) which binds free VEGF penetrate keratocyte cytoplasm, and provide sustained inhibition of injury-induced corneal neovascularization.[149]

Despite these promising results, concerns involving nanoparticle use remain. Although the immune response to polylysine-based nanoparticles seems to be less than that for capsid proteins, for example, the efficiency of gene transfer is not as high since most are degraded in the endosomal complexes.[150] As a result, one may generate an immune response because one must use large numbers of nanoparticles to achieve therapeutic useful transfection. Also, the apparent low immunogenicity observed in murine models of RP may not be observed in human patients because the immune response to both nanoparticles and viruses varies from one species to another.[150]

Viral Vectors

Critical issues for successful gene therapy include (1) vector uptake, transport, and uncoating; (2) vector genome persistence; (3) sustained transcriptional expression; (4) the host immune response; and (5) insertional mutagenesis and cancer.[150–152] Virus-based gene therapy can induce immune responses, including innate, humoral, and cell-mediated, that are directed against the vector and/or the transgene product.[150,153,154] Primary humoral responses directed against the vector can limit its capacity to deliver genes to the target cells as well as the ability to readminister the virus to the patient (e.g., when treating the fellow eye with a second surgical procedure).[150] An immediate innate immune response and a secondary antigen-dependent response to intravenous administration of recombinant adenoviral vectors, for example, caused death in a patient with ornithine transcarbamylase deficiency.[155,156] A humoral response against the transgene product may neutralize the therapeutic protein.[150] A cell-mediated immune response against the vector or transgene product can eliminate the transduced cells.[150] Two patients with hemophilia B, for example, developed vector dose-dependent transaminitis that limited hepatocyte-derived factor IX expression to less than 2 months due to $CD8^+$ memory T cells that recognized AAV serotype 2 (AAV2)

capsids and eliminated AAV2-transduced hepatocytes.[157,158] The innate immune response can cause local and/or systemic toxicity and amplify a secondary antigen-dependent immune response.[150] The likelihood of an immune response is influenced by the dose of viral particles,[159] which in turn is influenced by the efficiency of vector uptake and gene expression, as well as by the specificity of targeting. If dendritic cells or antigen-presenting cells take up the vector, for example, an immune response is more likely.

Nanoengineering of the viral capsid and transgene may provide a means to solve some of these problems. Recombinant AAVs (rAAVs) have been used successfully to treat preclinical models of human ocular disease and also have been used to treat humans with Leber congenital amaurosis.[146,147,160] Modifications of the virus to improve clinical effectiveness illustrate some of the nanoengineering strategies that have been employed in this area. AAVs are small (4.7 kilobase carrying capacity), nonpathogenic, single-stranded DNA parvoviruses that can transduce dividing and nondividing cells.[161] The capsid is critical for extracellular events related to the recognition of specific receptors, which influences cell tropism, as well as intracellular processes involving AAV trafficking and uncoating. In turn, the latter processes influence transduction kinetics and transgene expression efficiency.[162,163] Due to previous exposure to various AAV serotypes, a significant proportion of the population harbors neutralizing antibodies that can block gene delivery.[154,164,165] Because administration of low doses of viral vector might mitigate the severity of this problem, two nanoengineering techniques have been used to improve vector cellular tropism, transduction efficiency, and immunogenicity: directed evolution and site-directed mutagenesis. These are discussed below. Other nanoengineering devices (e.g., DNA transposons,[166] bacteriophage recombinases[167]) may provide clinically useful means to achieve stable, safe DNA integration in the host genome and sustained transgene expression in the future.

Directed evolution of AAV capsids has generated vectors that are highly resistant to neutralizing antibodies.[168,169] Maheshri et al.[169] used error-prone polymerase chain reaction and a staggered extension process[170] to generate an AAV2 library (>10^6 independent clones) with randomly distributed capsid mutations and then used

high-throughput approaches (i.e., exposure of mutants to heparin affinity chromatography [wild-type AAV2 binds to heparan sulphate] or repeated amplification of AAV2 mutants that retain infectivity in the presence of serum containing neutralizing antibodies) to identify mutant AAV2 capsids with altered receptor-binding properties and the capacity to bind with very low affinity to neutralizing antibodies. This approach can be quite powerful. One mutagenesis and three selection steps generated mutant capsids, for example, with a threefold improved neutralizing antibody titer (versus wild-type capsid) and a ~7.5% infectivity at serum levels that completely neutralized wild-type infectivity.[169] Directed evolution has been used to generate AAV variants that transduce Müller cells after intravitreal injection,[171,172] which may provide a means to deliver growth factors to photoreceptors and RPE cells. These growth factors retard the progression of retinal degeneration in preclinical models of RP[88,173,174] and possibly in human patients also.[175]

Zhong et al.[176] demonstrated that site-directed mutagenesis[177] of surface-exposed tyrosine residues increases vector transduction efficiency 30-fold in vivo at one log lower vector dose compared to wild-type AAV2. The increased transduction efficiency is due to impaired capsid ubiquitination and improved intracellular trafficking to the nucleus. (Epidermal growth factor receptor protein tyrosine kinase [EGFR-PTK] signaling impairs AAV2 vector transduction by impairing nuclear transport of the vectors;[178] EGFR-PTK can phosphorylate AAV2 capsids at tyrosine residues,[178,179] and tyrosine-phosphorylated AAV2 vectors enter cells efficiently but do not transduce well, in part because the AAV capsids are ubiquitinated and then degraded by the proteasome.[178,180]) Thus, the T-cell response to AAV2 capsids seems to be manageable by using surface-exposed tyrosine mutant vectors. Another rate-limiting step in transduction efficiency, the conversion of single-stranded viral genome to double-stranded AAV DNA, has been overcome by deleting the terminal resolution site from one rAAV inverted terminal repeat, which prevents replication initiation at the mutated end, to generate self-complementary AAV (scAAV) vectors.[181,182] (AAV has a tendency to package DNA dimers when the replicating genome is half the length of the wild type.)

Ocular Applications

Due to their relatively low immunogenicity, ability to target many nondividing cells, and capacity for sustained efficient therapeutic gene expression after a single treatment,[162] rAAV vectors have been used to treat preclinical models of human retinal disease.[183,184] Site-directed mutagenesis technology has been used to improve the treatment of degenerative retinal disease in these preclinical models. Vectors containing point mutations in surface-exposed capsid tyrosine residues in AAV serotypes 2, 8, and 9 display strong and widespread transgene expression in retinal cells after intravitreal or subretinal delivery.[185] Petrs-Silva et al.[185] demonstrated that tyrosine-to-phenylalanine capsid scAAV2 mutants showed much greater transduction efficiency (10–20-fold higher transgene expression) of the entire retina (including photoreceptors) after intravitreal injection compared to scAAV with wild-type capsids (Fig. 38.7). Mutants of scAAV2, scAAV8, and scAAV9 also enhanced transduction of RGCs compared to wild-type AAV2 (e.g., 10^6-fold reduction in the number of virus particles needed for RGC transfection with mutant scAAV2 compared to wild-type AAV2). Intravitreal delivery may offer an important clinical advantage over subretinal delivery. Subretinal virus delivery, which has been used in clinical studies,[146–148] requires pars plana vitrectomy in the operating room and has a higher likelihood of complications (e.g., retinal tear) than intravitreal delivery, which can be done in an office under topical anesthesia. On the other hand, the subretinal space is a relatively immune-privileged site,[186] which may reduce the likelihood of an immune response after repeat virus treatment. Li et al.[187] demonstrated that a humoral immune response against AAV2 capsid proteins occurs after intravitreal but not after subretinal vector delivery. Subretinal injection of one of the mutant scAAVs also transduced Müller cells. These studies demonstrate two strategies for reducing the immune response to viral vectors via site-directed mutagenesis: increasing transduction efficiency, which permits lower doses of vector, and creation of multiple effective serotypes, which can be used sequentially for subsequent therapy.

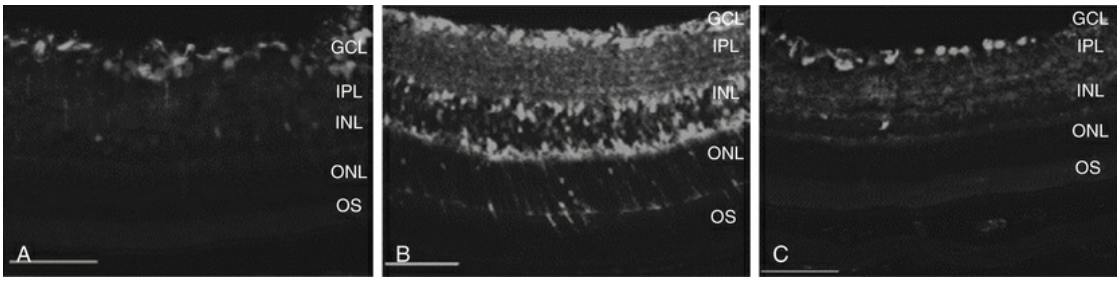

FIG. 38.7 Fluorescence microscopic evaluation of enhanced green fluorescent protein (EGFP) expression in transverse sections of retinal tissue 2 weeks after intravitreal injection. Immunostaining for EGFP in sections of the retina after delivery of (A) wild-type self-complementary adeno-associated virus 2 (WT scAAV2), (B) serotype 2 tyrosine-mutant Y444F, and (C) serotype 2 tyrosine-mutant Y730F. Note intense EGFP staining throughout all retinal layers with Y444F mutant and predominant EGFP staining in the ganglion cell layer with WT-2 and Y730F. Calibration bar = 100 μm. *GCL*, ganglion cell layer; *INL*, inner nuclear layer; *IPL*, inner plexiform layer; *ONL*, outer nuclear; *OS*, outer segment. (Reproduced with permission from Petrs-Silva H, Dinculescu A, Li Q, et al. High-efficiency transduction of the mouse retina by tyrosine-mutant AAV serotype vectors. Mol Ther 2009;17:463–71; and from Zarbin MA, Montemagno C, Leary JF, et al. Regenerative nanomedicine and the treatment of degenerative retinal diseases. Wiley Interdiscip Rev Nanomed Nanobiotechnol 2012;4:113–37.)

Imaging

The use of nanomaterials for biomedical imaging has been reviewed.[26,188,189] In addition to drug delivery, polyamidoamine dendrimer prototypes may be used as targeted diagnostic magnetic resonance imaging (MRI) contrast agents. Gold nanoparticles have been used to enhance tumor identification with computed tomography as well as for colorimetric biosensing. Colorimetric biosensing is based on the fact that the plasmon resonance frequency is a function of the average distance between the gold particles as well as their size, shape, and the dielectric properties of their environment. A plasmon is a quantum of plasma oscillation and can be viewed as the quantization of the oscillation of free electron density against the fixed positive charges in a metal. Gold

nanoparticles (5 nm), for example, are orange-red but turn blue-purple when aggregated to larger nanoparticles.[189] Colloids of gold nanoparticles impart vibrant colors to the stained-glass windows of some Gothic churches. If a gold nanoparticle–receptor complex is bound to a crosslinking molecule, nanoparticle clustering can occur with an associated colorimetric change.[190] Superparamagnetic iron oxide (SPIO) nanoparticles have been approved for use by the US Food and Drug Administration as MRI contrast agents.[191] Typically, an SPIO nanoparticle is composed of an iron oxide core coated with dextran, which renders it water-soluble.[192] For in vivo long-term imaging, the label is internalized by endocytosis or phagocytosis[193] with or without an excipient. These particles can have diameters of 60–150 nm and can be visualized using MRI. SPIO-labeled stem cells have been visualized in patients with brain trauma.[194] Limitations of this approach include the dilution of signal associated with cell replication and/or migration.[195] Also, no information is provided regarding the state of differentiation of the transplanted cells. Cytotoxicity (e.g., via iron-catalyzed generation of reactive oxygen species) might be a limitation of this approach.[26] Quantum dots (Qdots) are light-emitting nanocrystals (2–10 nm) composed of atoms from groups II–VI (e.g., CdSe, ZnSe) or III–V (e.g., InP) of the periodic table.[26] In contrast to SPIO nanoparticles, Qdots can be visualized with optical imaging (versus more complex MRI), including optical coherence tomography. In contrast to most organic dyes and fluorescent proteins, Qdots have durable fluorescence intensity, which helps one to distinguish the signal from background autofluorescence, and a broad excitation/narrow emission spectrum, which permits analysis of multiple cell targets with a single excitation wavelength.[196] Qdots can be used to monitor survival, distribution, and differentiation of stem cells in vivo.[197,198] Limitations can include signal dilution (due to cell proliferation and/or migration) as well as cytotoxicity.[26] In some cases, toxicity might arise from oxidative degradation of Qdots with subsequent Cd release and mitochondrial damage.[199,200] Coupling SPIO nanoparticles or Qdots to antibodies that recognize molecules such as components of the complement system or molecular constituents associated with AMD-induced changes in Bruch's membrane[201] might provide a means to image the biochemical and/or structural

abnormalities associated with AMD.[5,202] This capacity may help one assess the effectiveness of AMD treatments that target early molecular changes of the disease.

Nanowires are structures with a diameter of less than 100 nm and indefinite length. Semiconductor nanowires have unique electronic properties and sizes comparable with biological structures involved in cellular communication, thus making them promising nanostructures for establishing active interfaces with biological systems.[203] Cells can be grown on nanowire arrays, which can measure electrical functions in different parts of the same cell. Ophthalmic applications might include monitoring RGC survival/physiology in glaucoma patients or photoreceptor/RPE survival/physiology in transplant recipients.[5]

Minimally Invasive Physiologic Monitoring

We have reviewed this issue extensively[6] and recapitulate these observations here. Continuous measurement of critical biophysical properties can give insight into disease pathogenesis and the efficacy of a given treatment modality. An assembly of such monitors could be useful for telemedicine and remote patient monitoring, particularly for patients with chronic diseases such as glaucoma (e.g., detect elevated IOP, progressive optic nerve atrophy), diabetic retinopathy (e.g., detect macular edema, retinal neovascularization), and AMD (e.g., detect subretinal fluid/retinal edema associated with CNVs).[6] Ideally, the technology would permit repeated (if not continuous) noninvasive monitoring of preselected biomarkers. These platforms should function with minimal power (e.g., rather than incorporating a battery, utilize continuously available power sources) and provide accurate, precise information over an extended period of time (e.g., years). Recall that IOP is a dynamic quantity that fluctuates from moment to moment and diurnally (higher while asleep). It may be that nocturnal IOP (and blood pressure) measurement is more critical to glaucoma management rather than the daytime measurement performed in an outpatient setting.[204] When IOP is measured over 24 hours, the results often lead to a change in glaucoma management.[204–206] Thus, continuous, minimally invasive IOP

measurement could be an important innovation in glaucoma management. Finally, intraocular monitoring devices must be small because there is little unutilized space within the eye.

IOP measurement typically is done with a Goldmann tonometer. This device does not measure IOP directly but instead measures the force required to applanate a corneal surface whose circular area is 7.35 mm^2 ($[3.06/2]^2 \pi$). As a result, changes in corneal thickness as well as changes in corneal tension at different IOPs (Laplace's law for a thin-walled sphere: $T = (P \times R)/2\,h$, where T = tension in the wall, P = pressure difference across the sphere wall, R = sphere radius of curvature, and h = thickness of the wall) can affect the accuracy of IOP measurements done with the Goldmann tonometer.[207]

A number of nano-based IOP monitoring systems have been developed, but since this chapter is focused on retinal disease, they will only be briefly described. One noninvasive approach to IOP monitoring involves the use of a wireless contact lens.[208] Leonardi and coworkers developed a disposable silicone soft contact lens with an embedded sensor.[209]

An alternative approach that may be better suited for more invasive monitoring relies on capacitive pressure sensors (versus strain gauges).[210–212]

Chen et al.[213] developed a passive, biocompatible, micro-machined pressure sensor, based on the concept of a Bourdon tube (a thin-walled tube with an elliptical cross-sectional shape that can measure pressure quite accurately).

Challenges to the approaches mentioned above include short range (due to low signal-to-noise ratio), limited stability (e.g., due to variable mechanical contact with the cornea), high profile (despite use of MEMS technology), and high manufacturing costs. Rizq et al.[214] developed a piezoresistive IOP sensor that is implanted into the suprachoroidal space. The device is micro-machined and is fabricated with associated electronics (interface circuit, radiofrequency powering, and reverse telemetry) with full onboard electronics to provide active readout and superior signal-to-noise ratio, range, and accuracy. This device measured IOP accurately in human cadaver eyes. Dresher and Irazoqui[46] designed a compact, ultra-low-power operational amplifier that can be used to record

IOP. This CMOS operational amplifier can be incorporated with a wireless IOP monitoring system. It has a power consumption of 736 nW, chip area of 0.023 mm^2, and output impedance of 69 Ω to drive low-impedance loads. The authors envision implantation of the device into the suprachoroidal space and have designed and fabricated a high-frequency transmitter integrated circuit that has sufficient signal-to-noise ratio margin for a high data rate transmission wirelessly.[215] There is a possibility for choroid/retinal damage with suprachoroidal insertion and a likely need for a method to secure the device (e.g., sutures, glue) to ensure reproducible measurements. In addition it is not clear what the maximum distance between the sensor and the receiver antenna will be, which might place logistical constraints on the use of the device for continuous IOP monitoring.

Coupling Diagnostics and Therapeutics

Theranostics

Theranostics refers to a process in which diagnosis of a disease state, individualized for a particular patient (even to particular cells within a patient), is coupled with therapy that is targeted precisely in its amount, nature, and location.[6] Prow et al.,[3] for example, developed a biosensor DNA tethered to a magnetic nanoparticle. The biosensor uses an enhanced green fluorescent protein (EGFP) reporter gene driven by an antioxidant response element (ARE). The ARE is activated by oxidative stress and enhances the expression of genes downstream to it. Exposure of the cells to hyperoxia drives the expression of EFGP. This engineered nanoparticle penetrates endothelial cells (preferentially dividing cells), and after subretinal injection, these biosensor nanoparticles report the activation of the ARE in diabetic rat RPE.[216] The antioxidant biosensor could provide a means for clinicians to identify patients likely to need therapy (e.g., babies with retinopathy of prematurity who will need laser photocoagulation or other treatment) at a time before clinical manifestations of severe disease are evident. By coupling a therapeutic gene (e.g., catalase, peroxidase, superoxide dismutase) to the ARE (in addition to a reporter gene such as EGFP), one creates a combined diagnostic–

therapeutic device that enables endothelial cells (or any cells that take up the nanoparticle) to "treat themselves" in the setting of oxidative damage.[6] Therapeutic possibilities are limited primarily by one's knowledge of the pathways involved in disease pathogenesis. One could couple genes to manage angiogenesis, for example pigment epithelial-derived factor,[217] and to serve as a neurotrophin in eyes with AMD-associated CNV and geographic atrophy. Attractive features of this approach to gene therapy are (1) one uses the cell's endogenous metabolic machinery to drive the expression of exogenous genes that will enhance the cell's capacity to manage environmental stress; and (2) individual cells titer their own therapeutic enzyme/drug concentration in relation to their "toxic" exposure and endogenous capacity to respond to environmental stress. The concept and some experimental results are shown in Fig. 38.8.

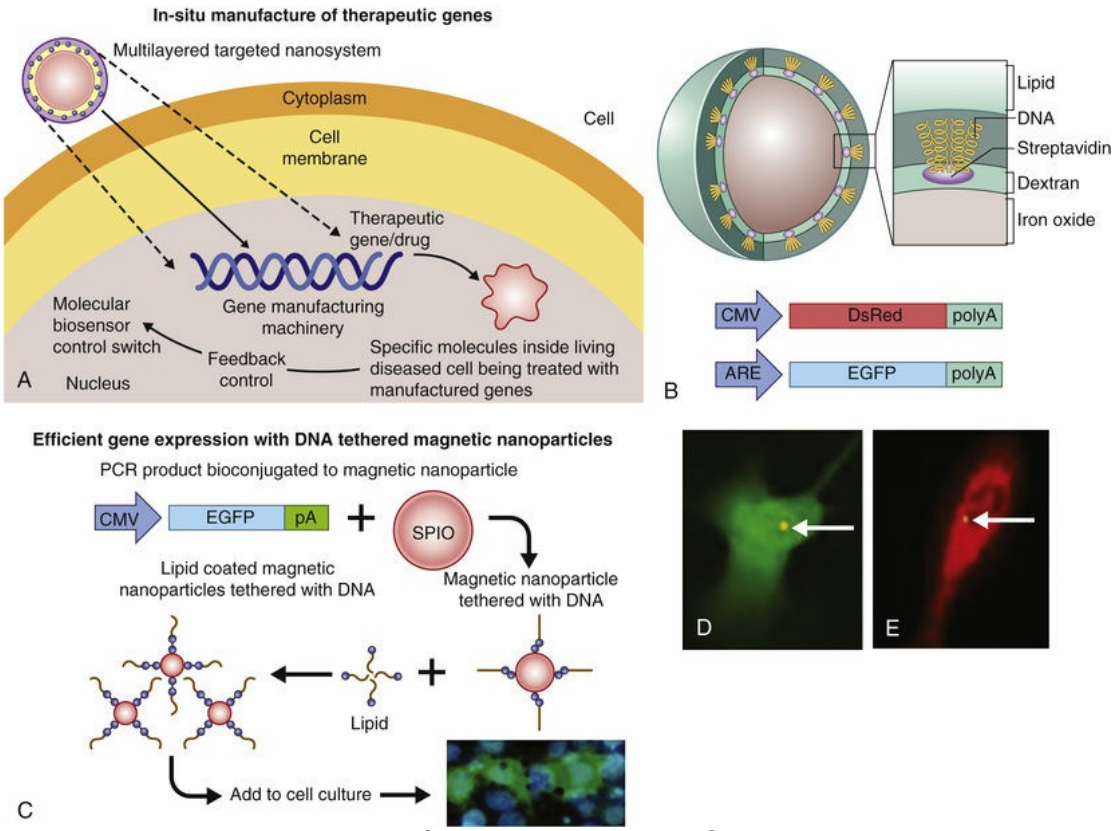

FIG. 38.8 Use of nanotechnology for health maintenance: design of a biomolecular control biosensor. (A) Gene templates containing upstream biomolecular feedback control sensors can be used to transcribe specific DNA sequences made by gene-

manufacturing machinery. This strategy may allow for in situ manufacture of peptide drugs within single cells under the control of upstream biomolecular control switches in a feedback loop suitable for treatment of chronic diseases. (B) Cytomegalovirus (CMV) or antioxidant response element (ARE) molecular bioswitches can be always ON (in the case of CMV) or OFF except when antioxidant proteins bind to the ARE biosensor and turn it ON. (C) Gene sequences can be expressed efficiently if they are tethered properly to the surface of super paramagnetic iron oxide (SPIO) nanoparticles. (D) As shown by efficient expression of the reporter gene, enhanced green fluorescent protein (EGFP), under control of the ARE, SPIO nanoparticles can transfect cells (*arrow*) and use the host cell machinery to manufacture GFP in response to oxidative stress. More importantly, genes can be expressed only when activated by oxidative stress proteins that bind to the ARE biosensor, which can be developed further to prevent damage therapeutically due to oxidative stress that can cause retinopathies and damage to the optic nerve. (E) Alternatively, the reporter gene product, DsRed, can simply be produced freely under control of a CMV promoter. *PCR*, polymerase chain reaction. (Adapted with permission from Seale M, Haglund E, Cooper CL, et al. Design of programmable multilayered nanoparticles with in situ manufacture of therapeutic genes for nanomedicine. Proc SPIE 2007;6430:643003-1-7 and Prow T, Grebe R, Merges C, et al. Nanoparticle tethered antioxidant responseelement as a biosensor for oxygen induced toxicity in retinal endothelial cells. Mol Vis 2006;12:616–25; and from Prow T, Smith JN, Grebe R, et al. Construction, gene delivery, and expression of DNA tethered nanoparticles. Mol Vis 2006;12:606–15; and from Zarbin MA, Montemagno C, Leary JF, et al. Nanomedicine in ophthalmology: the new frontier. Am J Ophthalmol 2010;150:144–62.)

Prosthetics: Molecules as Machines (e.g., Light-Sensitive Ion Channels), Abiotic–Biotic Interfaces

Induced Photosensitivity

The use of molecules as machines will revolutionize neural

prosthetics. The application of this concept to induced photosensitivity has been reviewed in detail elsewhere.[6,7] Here we recapitulate this analysis. Although rewiring of inner retinal circuits and inner retinal neuronal degeneration occur in association with photoreceptor degeneration in RP,[218,219] it is possible to create visually useful percepts by stimulating RGCs electrically.[220–223] Use of light-sensitive ion channels, rather than electrodes, to stimulate RGCs provides an alternative approach to retinal cell stimulation.[16–18,224] Induced light sensitivity has the potential for noninvasive neuronal stimulation with high spatial resolution.

Channelopsin-2 is a light-gated ion channel derived from green algae and is sensitive to blue light. When its attached chromophore, all-*trans* retinaldehyde, undergoes reversible photoisomerization, channelopsin-2 undergoes a conformational change that alters its permeability to mono- and divalent cations.[225] In contrast to mammalian rhodopsin, which loses its chromophore after 11-*cis* retinal-all-*trans* retinal isomerization, channelopsin-2 remains attached to its chromophore after all-*trans* to 11-*cis* retinal isomerization. Thus, there seems to be no need to provide chromophore to the transduced cells. The complex of channelopsin-2 and all-*trans* retinal is termed channelrhodopsin-2 (ChR2). Using a rAAV delivery system (rAAV serotype-2) in *rd1* mice, which have a null mutation in a cyclic GMP phosphodiesterase (PDE6b), and in RCS rats, which have a mutation in the tyrosine kinase, Mertk, ChR2 expression can be achieved in inner retinal neurons (primarily ON and OFF RGCs). Each of the latter mutations causes some form of RP in humans. ChR2 converts these neurons into cells that respond to light with membrane depolarization.[226–230] In addition, intraocular injection of rAAV2-ChR2 can restore the ability of the animals to encode light signals in the retina and transmit them to the visual cortex.

Recombinant AAV2 vectors have been used to deliver channelopsin-2 to retinal cells (primarily ganglion and amacrine cells) in wild-type adult mice stably for up to 18 months. Up to 20% of ganglion cells were infected (with normal morphology), and a sufficient number of functional ChR2 channels were maintained to drive robust ganglion cell membrane depolarization and spike firing in response to light.[231] These investigators estimated that, at

high viral concentrations, approximately 40% of all A-II amacrine cells were labeled. In mammals, rod signals are related through rod bipolar cells to A-II amacrine cells. These signals are coupled on to ON and OFF cone pathways by gap junctions and glycinergic synapses, respectively. Thus, the ability to target A-II amacrine cells with this vector may enable recovery of both ON and OFF light responses in RP retinas.[231] Restoration of both ON and OFF pathways probably will be important for achieving good contrast sensitivity and proper spatial and temporal signal processing.[232,233] Recombinant AAV2-mediated transfection of retinal neurons in nonhuman primates (marmoset) via intravitreal injection results in functional expression of ChR2 in all retinal neurons, but preferentially ganglion cells (all major types).[234] Regional variations in transfection efficiency seemed to correlate with the thickness of the inner limiting membrane. This potential barrier for rAAV2-mediated intravitreal gene delivery could, in principle, be overcome by internal limiting membrane peeling, a standard technique in vitreoretinal surgery, or by enzymatic digestion of the inner limiting membrane.[235]

Recently a new optogenetic tool has been bioengineered.[236] Opto-mGluR6 is a chimeric all-retinal G-protein-coupled-receptor (GPCR) consisting of the intracellular domains of the ON-bipolar cell-specific metabotropic glutamate receptor, mGluR6, and the light-sensing domains of melanopsin. Melanopsin, which also belongs to the GPCR protein family, is a blue-light-sensitive retinal photopigment present in a subpopulation of photosensitive retinal ganglion cells that control the pupillary light reflex as well as the circadian rhythm by signaling to the suprachiasmatic nucleus. The light-induced isomerization of this retinal chromophore is reversed while bound to the opsin. This property makes melanopsin highly resistant to bleaching by strong light and allows successive light activation without a response rundown.[236] Melanopsin is activated by moderate daylight as opposed to high intensity light (e.g., bright sunlight on a snow-covered field) required for activating the ion channel ChR2. The mGlu6 receptor normally mediates light responses in ON-bipolar cells by coupling glutamate signals from the photoreceptors to TRPM1 cation channels. Because it is a GPCR, mGluR6 greatly amplifies glutamate signal via the intracellular G-

protein coupled second messenger cascade. These features enable opto-mGluR6 coupling to bipolar cell-specific preexisting G-protein complexes, which include regulators of G-protein signaling essential for fast signal kinetics.[236] When illuminated, opto-mGluR6 causes cellular hyperpolarization as it does *in situ*. At light intensities that just begin to stimulate ChR2 rAAV (e.g., 10^{15} photons/cm^2/sec), opto-mGluR6 rAAV exhibits a maximal conductive response.[236]

Zhang et al.[237] showed that expression of halorhodopsin (HaloR), a yellow light-activated chloride ion pump from halobacteria, in inner retinal neurons converts them into OFF cells. In these experiments, HaloR was ~20-fold less sensitive to light than ChR2. HaloR and ChR2 coexpressing cells can produce ON, OFF, and ON–OFF responses, depending on the illumination wavelength.[237] Experiments in these preclinical models indicate that kinetics of ChR2- and HaloR-mediated light responses are compatible with temporal processing requirements of visual information in the retina. A current limitation of this approach is that ChR2 and HaloR both exhibit low light sensitivity, with threshold activation light intensities ~5–6 log units higher than those of cones.[226,237] Furthermore, the light intensity operating range of microbial rhodopsins is 2–3 log units, compared to normal retinal dynamic range of 10 log units. Doroudchi et al.[238] achieved stable, specific expression of ChR2 in ON bipolar cells using a rAAV vector packaged in a tyrosine-mutated capsid. Light levels that elicited visually guided behaviors were within the physiologic range of cone photoreceptors. There was no evidence of induced inflammation or toxicity. As indicated above, signal convergence from bipolar cells on to RGCs may mean that targeting ChR2 to rod bipolar cells will provide increased light sensitivity as well as higher spatial resolution, but this approach may be compromised by the alterations in synaptic circuitry that accompany photoreceptor degeneration.[218,219,239–241]

Greenberg et al.[242] reconstructed an excitatory center and antagonistic surround by targeting humanized ChR2 to the somata and enhanced HaloR to the dendrites of RGCs (Figs. 38.9 and 38.10). This approach to the deployment of optical neuromodulators retains crucial information processing (edge

detection) while being independent of the state of inner retinal circuit remodeling during degeneration. Fusion of the humanized ChR2 to ankyrin$_G$ polypeptide localized this opsin to the soma and proximal dendrites because ankyrins couple sodium channels to the spectrin-actin network. Fusion of enhanced HaloR to PSD-95 protein targeted this opsin to the dendritic regions in RGCs. As a result, Greenberg and coworkers nanoengineered RGCs with differential spatial and spectral photosensitivity. Depending on which opsin is fused to ankyrin$_G$ and which to PDS-95, both ON and OFF-center ganglion cells could be created. Because this approach generated nonphysiologic center surround dimensions, Greenberg et al.[242] preprocessed the visual image with gaussian blurring, such that when convolved with the dimensions of the soma and dendrites, the gaussians approximated the relative dimensions of the ganglion cells' center and surround receptive fields. Thus, imaging processing enabled extraction of edge information. These data and the above considerations indicate that ChR2/HaloR-based RGC prosthetics will require image preprocessing to perform light amplification, dynamic range compression, and local gain control operations.[242]

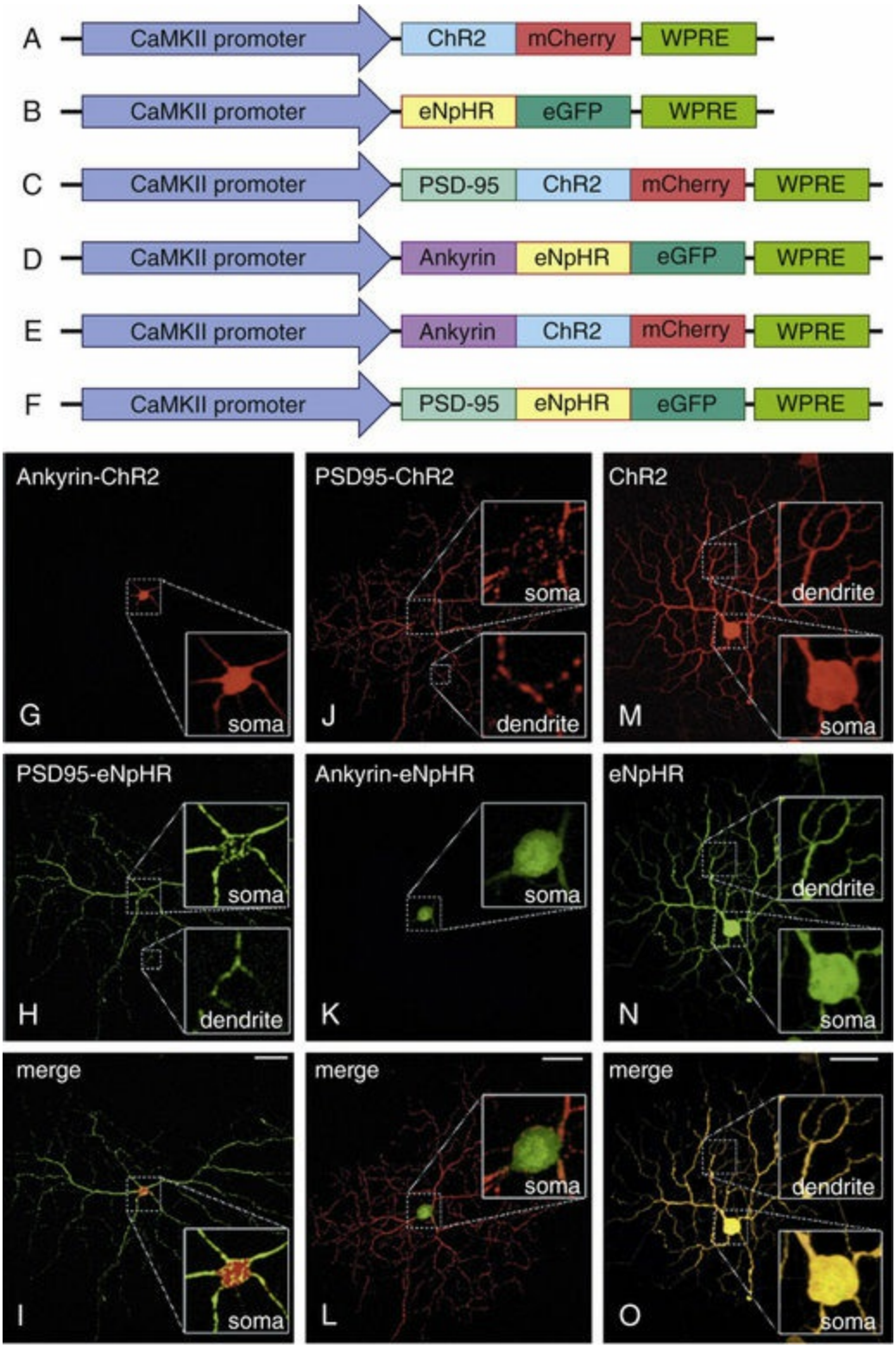

FIG. 38.9 Humanized ChR2 (hChR2) and enhanced HaloR (eNpHR) construct schematics and differential transgene expression in ganglion cell soma and dendrites of whole-mount rabbit retina. The calcium/calmodulin-dependent protein kinase II (CaMKIIa) promoter and woodchuck hepatitis virus posttranscriptional regulatory element (WPRE) to drive

high transgene expression levels in ganglion cells were used in all constructs. (A) Schematic of untargeted hChR2–mCherry fusion. (B) Untargeted eNpHR–enhanced green fluorescent protein (eGFP) fusion. (C) Postsynaptic density 95 (PSD-95) targeting motif fused with hChR2-mCherry for dendritic localization. (D) $Ankyrin_G$ motif fused with eNpHR-eGFP for somatic localization. (E) $Ankyrin_G$ motif fused with hChR2-mCherry. (F) PSD-95 fused with eNpHR-eGFP. (G) Confocal image of rabbit ganglion cell expressing $ankyrin_G$-hChR2-mCherry localized to the soma and proximal dendrites (red). (H) Same cell as (G) showing PSD95-eNpHR-eGFP localized primarily to the dendrites (green). (I) Merge of (G) and (H). Scale bar represents 100 μm. (J) PSD95-hChR2-mCherry localized to the dendrites. (K) $Ankyrin_G$-eNpHR-eGFP localized to the soma and proximal dendrites. (L) Merge of (J) and (K). Scale bar represents 100 μm. (M) Untargeted hChR2-mCherry is localized throughout the plasma membrane. (N) Untargeted eNpHR-eGFP is localized throughout the plasma membrane. (O) Merge of (M) and (N). Scale bar represents 100 μm. (Reproduced with permission from Greenberg KP, Pham A, Werblin FS. Differential targeting of optical neuromodulators to ganglion cell soma and dendrites allows dynamic control of center-surround antagonism. Neuron 2011;69:713–20; and from Zarbin MA, Montemagno C, Leary JF, et al. Regenerative nanomedicine and the treatment of degenerative retinal diseases. Wiley Interdiscip Rev Nanomed Nanobiotechnol 2012;4:113–37.)

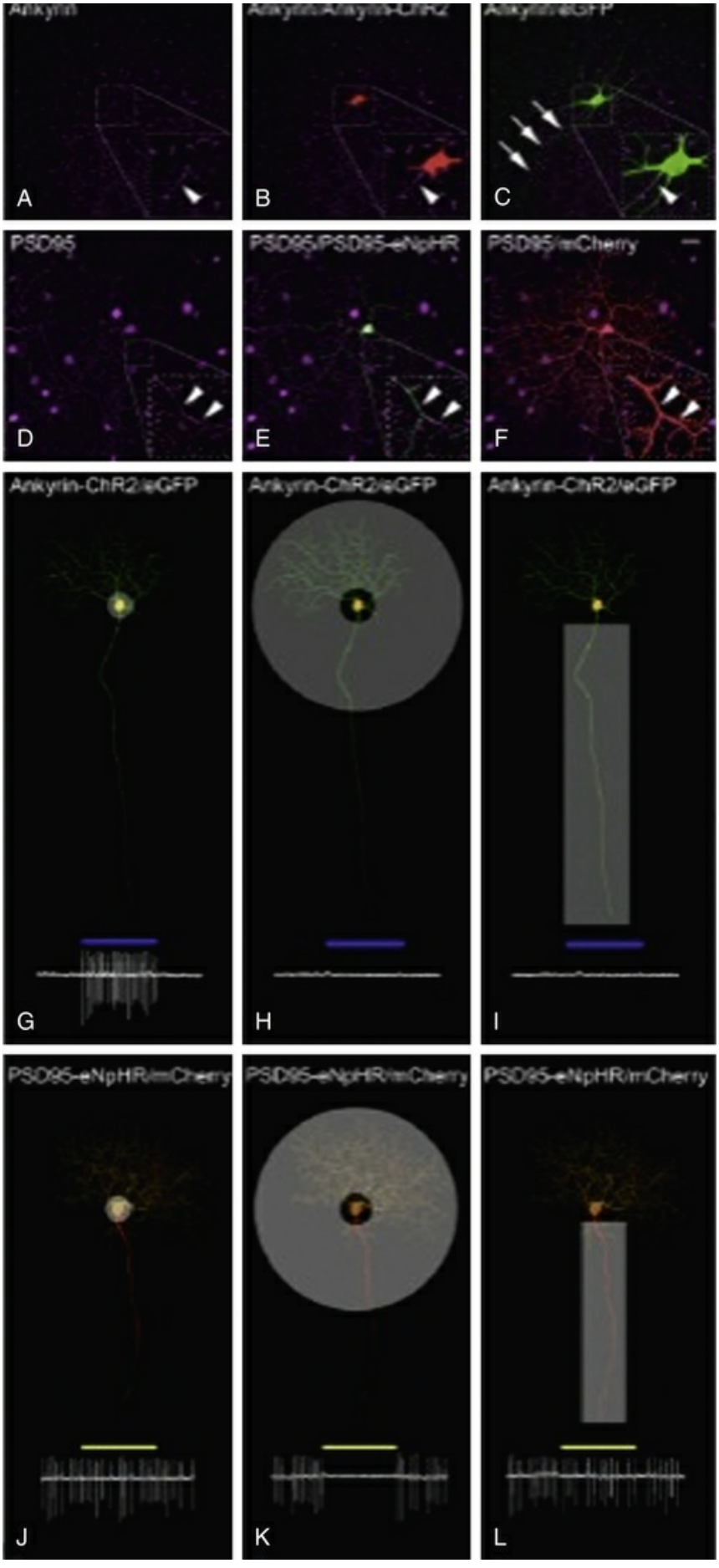
A
B
C
PSD95
D
PSD95/PSD95-eNpHR
E
PSD95/mCherry
F
Ankyrin-ChR2/eGFP
G
Ankyrin-ChR2/eGFP
H
Ankyrin-ChR2/eGFP
I
PSD95-eNpHR/mCherry
J
PSD95-eNpHR/mCherry
K
PSD95-eNpHR/mCherry
L

FIG. 38.10 Correlation of ankyrin$_G$-hChR2 and PSD95-eNpHR localization and function using immunostaining and electrophysiology. (A) Endogenous ankyrin$_G$-Cy5 (magenta) in flat-mount rabbit retina shown in the initial axon segment (*arrowhead*, inset) of ganglion cells. (B) Merge of ankyrin$_G$-Cy5 and transfected ankyrin$_G$-hChR2-mCherry (red). Ankyrin$_G$hChR2 is localized to the soma and proximal dendrites. Colocalization of endogenous ankyrin$_G$ *(arrowhead*) and mCherry is not apparent. (C) Cotransfection of untargeted enhanced green fluorescence protein (eGFP) (green) shows the complete cellular morphology (including axon, *arrows*). Scale bar represents 50 μm. (D) Endogenous PSD95-Cy5 (magenta) is present in ganglion cell somata and dendritic terminals (*arrowheads*, inset). (E) Merge of PSD95-Cy5 and transfected PSD95-eNpHR-eGFP (green). eNpHR-eGFP is observed to colocalize with endogenous PSD95 in dendrites. (F) Cotransfection of untargeted mCherry (red) shows complete dendritic morphology of cell. Scale bar represents 50 μm. (G) Illumination of ankyrin$_G$-hChR2-mCherry (yellow) in ganglion cell soma with 50 μm blue spot (10 mW/mm^2) elicits robust spiking. Untargeted eGFP (green) was cotransfected to show complete morphology. Extracellular spike recordings from whole-mount rabbit retina in the presence of l-AP4 (20 μM), CPP (10 μM), and CNQX (10 μM) cocktail designed to block all photoreceptor-driven synaptic transmission to ganglion cells. (H) Blue annulus (300 μm outer diameter (OD), 50 μm inner diameter (ID)) covering only the cell dendrites and partial axon fails to elicit spiking. (I) A blue rectangular stimulus (200 × 900 *μ*m) covering the entire axon also fails to elicit spiking. (J) Illumination of soma in ganglion cell expressing PSD95-eNpHR-eGFP (yellow) with 50 μm yellow spot (10 mW/mm^2) fails to silence spontaneous spiking. Untargeted mCherry (red) was cotransfected to show complete morphology. (K) Yellow annulus (300 μm OD, 50 μm ID) covering only the cell dendrites and partial axon effectively silences spikes. (L) Yellow rectangular stimulus (100 × 500 μm) covering the entire axon fails to silence spiking. (Reproduced with permission from Greenberg KP,

Pham A, Werblin FS. Differential targeting of optical neuromodulators to ganglion cell soma and dendrites allows dynamic control of center-surround antagonism. Neuron 2011;69:713–20; and from Zarbin MA, Montemagno C, Leary JF, et al. Regenerative nanomedicine and the treatment of degenerative retinal diseases. Wiley Interdiscip Rev Nanomed Nanobiotechnol 2012;4:113–37.)

In typical RP, the rod photoreceptors degenerate first, and cone degeneration follows.[219] Even after their outer segments are lost, cone cell bodies remain for a time. Busskamp et al.[243] demonstrated that enhanced HaloR expression in light-insensitive cones (via AAV transduction) can restore light sensitivity in mouse models of RP (i.e., the *rd1* mouse, which models fast forms of retinal degeneration, and *Cnga3*$^{-/-}$; *Rho*$^{-/-}$ double-knockout, which models a slow form of retinal degeneration). Targeted expression of enhanced HaloR in photoreceptors was achieved using human rhodopsin, human red opsin, and mouse cone arrestin promoters. In *rd1* mice, the resensitized cones activate all retinal cone pathways, drive directional selectivity, and activate cortical circuits. In *rd1* mice and, to a lesser degree, in *Cnga3*$^{-/-}$; *Rho*$^{-/-}$ mice, the resensitized cones mediate visually guided behaviors. Despite the synaptic reorganization of the inner retina that accompanies RP progression, when stimulated by light, HaloR-transfected photoreceptors seemed to convey information through bipolar cells to RGCs, including both ON and OFF pathways. These effects were obtained even when only ~25% of the cone cell bodies remained.

Allosteric photoswitches provide an alternative approach to using light-sensitive ion channels to stimulate RGCs.[16–18,224] To create the photoswitch, ion channels were reengineered using a light-sensitive azobenzene linker. Short-wavelength light (380 nm) drives the azobenzene moiety into a *cis* configuration, and longer-wavelength light (500 nm) as well as darkness (azobenzenes thermally isomerize to the lower-energy *trans* state) drive it into a ~0.7 nm more extended *trans* configuration. The active moiety can interact with the ion channel in only one of the isomeric states, which leads to a change in ion movement across the cell membrane. Coupling the azobenzene (AZO) moiety to maleimide (MAL) enables the photoswitch to be tethered to the Shaker potassium channel. Coupling the azobenzene moiety to a quaternary ammonium (QA) group enables the MAL-AZO-QA molecule to

block the potassium channel when in the *trans* configuration. To enable modulation of the ionotropic glutamate receptor subtype 6, a cysteine was introduced into the ligand-binding domain of the receptor, enabling the maleimide moiety to tether the photoswitch to the receptor. The quaternary ammonium group was replaced with a glutamate agonist. When in the *trans* configuration, the agonist is positioned outside the ligand-binding pocket, and when in the *cis* configuration, the agonist occupies the binding pocket and activates the channel (Fig. 38.11). Acrylamide azobenzene quaternary ammonium, a variant of the MAL-AZO-QA molecule, permits one to affinity-label endogenous potassium channels without receptor mutagenesis or genetic manipulation of the target cells (e.g., RGCs).[244] A genetically and chemically engineered light-gated mammalian ion channel, the light-activated glutamate receptor (LiGluR), has been expressed selectively in RGCs of the *rd1* mouse.[245] In this preclinical model of RP, the LiGluR restores light sensitivity to the RGCs, reinstates light responsiveness to the primary visual cortex, and restores both the pupillary reflex and a natural light avoidance behavior. Transducing photoreceptors with ChR2 and HaloR to induce light sensitivity is an example of using molecules to reengineer cells and their behavior. Here, one is using bionanotechnology to reengineer proteins first and to reengineer cell behavior second.[7]

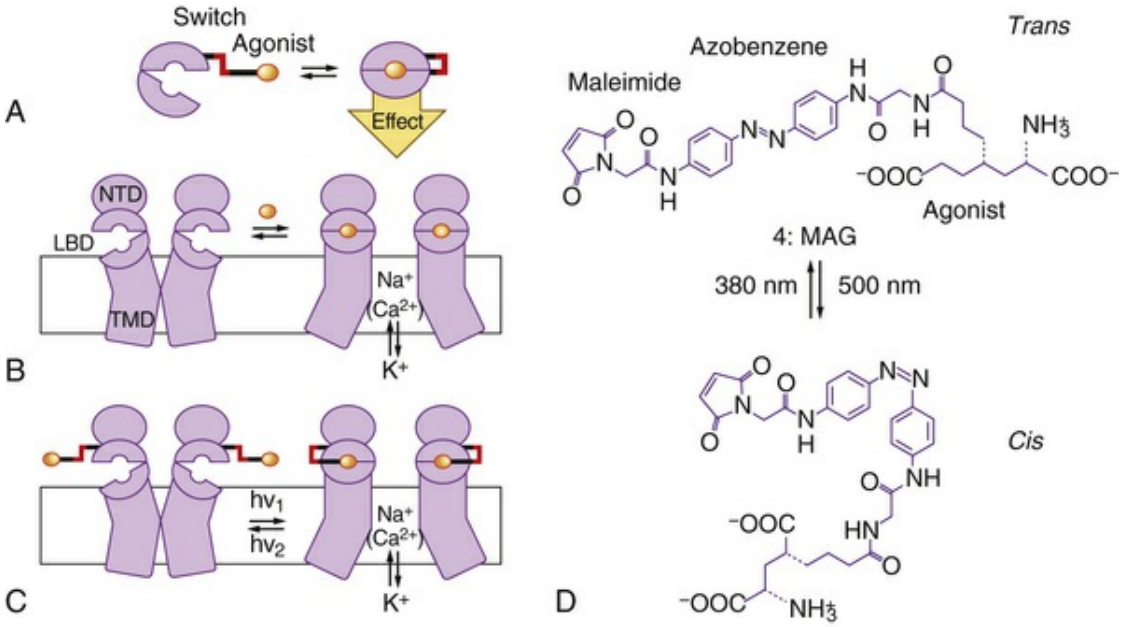

FIG. 38.11 Use of molecular engineering for the development of neural prosthetics: design of an allosteric photoswitch. (A) An agonist (orange) is tethered to a ligand-binding domain (LBD) through an optical switch (red) via linkers (black). In one state of the switch, the ligand cannot reach the binding pocket, whereas in the other state, the ligand docks and stabilizes the activated (closed) conformation of the LBD. (B) Schematic representation of the operating mode of ionotropic glutamate receptor switch (iGluRs). Binding of an agonist (orange) stabilizes the activated (closed) conformation of the LBD and allosterically opens the pore, allowing flow of Na^+, Ca^{2+}, and K^+. *NTD*, N-terminal domain; *TMD*, transmembrane domain. (C) The principle of light-activated glutamate receptor (LiGluR). Reversible optical switching of a tethered agonist on the LBD opens and closes the pore. (D) Structure of a photoswitched agonist. Structure of MAG 4 (which contains a cysteine-reactive maleimide (M), an azobenzene switch (A), and a glutamate head group (G)) in its *trans* state (dark and 500 nm) and *cis* state (380 nm). (Reproduced from Volgraf M, Gorostiza P, Numano R, et al. Allosteric control of an ionotropic glutamate receptor with an optical switch. Nature Chem Biol 2006;2:47–52, with permission from Macmillan Publishers, Copyright 2006; and from Zarbin MA, Montemagno C, Leary JF, et al. Nanomedicine in ophthalmology: the new frontier. Am J Ophthalmol 2010;150:144–62.)

Bionic Retina

Subretinal implants that provide precisely patterned electrical stimuli aim to restore vision in patients suffering from retinal degenerative disease. These devices convert a real-time video image of the world into electrical signals that are transmitted to the retina via a microelectrode array. Nanotechnology has played an important role in the progress in this field,[241–269] and this technology is reviewed in detail in Chapter 129 (Artificial vision). Ha et al.[270] have developed retinal prosthesis architecture that combines spatial optical addressing and pulsed electrical biasing for scalable high-resolution retinal stimulation by a photosensitive electrode array activated over a single inductive telemetry link (Fig. 38.12). The use

of a vertical silicon nanowire array supports electrode densities approaching the dimensions of retinal neural circuits, and in conjunction with the pulsed electrical biasing provides sufficient optoelectronic gain for neural stimulation at low light intensity.[270] This scalable architecture permits the use of high-density electrode arrays with ultra-high photosensitive silicon nanowires, which alleviates the need for extensive wiring and high-throughput data telemetry. The use of vertical silicon nanowires provides two main advantages over other types of phototransducers such as flat and thin-film microphotodiodes.[270] High light absorption efficiency in nanowires arises due to an increased light path length enhancement factor leading to better light trapping along the length of the nanowire. Also, nanowires can perform carrier collection and charge separation more efficiently than flat and thin microphotodiodes.[270] The nanowire geometry of a core-shell structure provides fast radial charge separation that allows for efficient carrier collection through band conduction. The nanowires are manufactured using nanoimprint lithography.

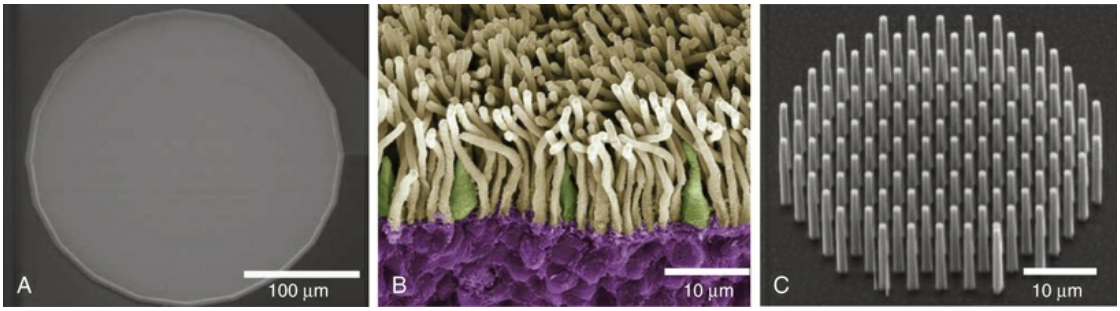

FIG. 38.12 Retina and electrode geometries. (A) Planar platinum gray electrodes of the Argus II retinal prosthesis. (B) Retinal photoreceptor cells with rods (yellow) and cones (green) [Image: Science Photo Library]. (C) Fabricated silicon nanowires at the same spatial magnification as (B). (Reproduced with permission from Ha S, Khraiche ML, Akinin A, et al. Towards high-resolution retinal prostheses with direct optical addressing and inductive telemetry. J Neural Eng 2016;13(5):056008.)

Regenerative Medicine: Nanostructured

Scaffolds to Control Cell Phenotype

Regenerative medicine deals with repairing or replacing tissues and organs by using advanced materials and methodologies. Transplantation of cultured autologous limbal stem cells, for example, has permitted recovery of corneal integrity and visual function following chemical corneal injury.[271] Regenerative nanomedicine can involve use of nanoparticles containing gene transcription factors and other modulating molecules that direct reprogramming of cells in vivo. Some examples of applications of these techniques have been described earlier, e.g., use of polyplexes to treat RP, restoring light sensitivity by transfecting cones with rAAV-HaloR, and the induction of light-sensitivity in neurons (i.e., ganglion cells) without viral transfection via acrylamide azobenzene quaternary ammonium. A further advance in regenerative ophthalmic medicine would be to replace damaged or dead retinal neurons in patients with chronic retinal detachment, RP, AMD, and allied diseases. Conditions such as retinal detachment, AMD, and RP cause blindness primarily through photoreceptor death. Reactive changes in the synaptic circuitry of second- and third-order neurons also occur,[218,272] but we suspect these changes will not decisively limit visual recovery, particularly if photoreceptor replacement can be achieved before atrophy is extensive. Cell-based therapy may be sight-preserving and/or sight-restoring for these patients.[273–281] Fetal retina sheet transplants, for example, have been effective in preclinical models.[282] Also, retinal progenitor cells and even adult photoreceptors can integrate into host retina and improve some aspects of visual function.[283,284] There is evidence, however, that cell isolation and bolus injection are associated with significant cell death.[282,285]

Strategies for neuronal replacement are nascent. Regeneration of damaged retina occurs readily in fish (from Müller cells) and amphibians (from RPE cells) via endogenous mechanisms.[286] Thus, one approach is to identify the genes needed to reprogram remaining neurons in the damaged adult to a more primitive state that enables reconstitution of intact neural tissue. Although mammals may possess a central marginal zone from which retinal progenitor cells can be harvested, this region does not readily support retinal regeneration. Müller cells, however, may be an

endogenous source of retinal progenitor cells. Transplantation of cells derived from human embryonic stem cells may provide an alternative means by which to provide sight-restoring therapy to patients with blindness arising from retinal degenerative disease. Retinal cells derived from human embryonic stem cells or induced pluripotent stem cells can be transplanted into mouse retina, differentiate into rod photoreceptors, integrate with the host retina, and, in some cases, mediate visual behavior.[273–281] Genes mediating the transformation of retinal progenitors to mature neurons are being identified.[286]

The ECM is dynamic, hierarchically organized at the nanoscale, and regulates cell differentiation, proliferation, adhesion, and migration.[287] Cells reorganize due to interactions with the ECM on the basis of topography, mechanical properties (e.g., matrix stiffness, elasticity, viscosity), and concentration gradients of immobilized growth factors or ECM molecules. Thus, biomimetic nanopatterns can be enabling tools for analysis and control of live cells.[288,289] Results from nanoscale patterning experiments demonstrate that specific surface patterns on which cells are cultured influences cell orientation,[290] neurite axonal extension,[291] bone deposition,[292] and gene expression patterns.[293,294] Nanofibers have been used to favorably modulate muscle replacement,[295] nerve repair,[296] wound healing,[297] and stem cell differentiation.[298] Gene-activated matrices combine tissue engineered scaffolds with plasmid DNA to modulate wound healing.[299] Cellular degradation of the ECM releases DNA that is taken up by cells locally, resulting in transient transfection of the cells and production of a therapeutic protein. Gene-activated matrices have been used to stimulate bone regeneration in preclinical models of bone fractures.[300]

The ECM may be crucial for successful retinal regeneration. The ECM can alter cell behavior by modulating the expression of genes that promote retinal regeneration. Keratocyte shape, alignment, and migration, for example, are guided by nanotopography.[301] These features might be altered to improve biointegration of prosthetic devices such as artificial corneas.[301] In addition, RPE survival on submacular Bruch's membrane from AMD eyes is improved substantially when a provisional, “healthy” ECM is present.[302] Stem cells are prevented from exiting the mitotic cycle by environments

called niches,[303] which comprise cellular and noncellular elements (i.e., ECM components). Physical features of the ECM that influence cell behavior and phenotype include the size, lateral spacing, surface chemistry, and geometry of ECM ligands.[304–306]

Engineering Scaffolds to Support Cell Transplants

Microscale topographical cues can influence retinal[307] and neural[308] progenitor cell attachment and differentiation independently of biochemical cues. The size, lateral spacing, surface chemistry, and geometry of ECM ligands are physical features of the ECM that influence cell behavior and phenotype.[304–306] Scaffolds with the proper nanoscale features might improve transplant efficacy by preventing anoikis (apoptosis due to absence of cell adhesion to the ECM substrate), promoting maintenance of a differentiated phenotype, providing proper three-dimensional organization of the cell–ECM assembly, and promoting a supportive host response to the transplant.[309] Nanofiber scaffolds might be used to create niches for stem cell self-renewal or as substrates supporting delivery of sheets of cells.[26] Nanofiber scaffolds have a high surface area-to-volume ratio and can present a high density of epitopes to cells, thus promoting neural progenitor cell differentiation.[310] These scaffolds can serve not only as a cell delivery platform; they can serve as a temporary ECM that maintains cell survival and differentiation while the transplanted cells elaborate their own ECM and degrade the scaffold. Ellis-Behnke et al.[311] reported that a designed self-assembling peptide nanofiber scaffold promoted axonal regeneration through the severed optic tract of hamsters. The regenerated axons reconnected to target tissues and promoted visual recovery.

Scaffolds for Cell Transplantation to the Subretinal Space

Instead of transplanting a cell suspension, some investigators advocate delivering the cells on a three-dimensional scaffold. These scaffolds can consist of hybrid nanomaterials with biocoatings. Potential advantages to this approach are threefold. First, one can transplant cells that are differentiated and organized anatomically,

resembling the in situ configuration. In the case of RPE cells, features such as hexagonal morphology, apical-basal polarization, intact cell–cell junctions (e.g., zonula adherens), and normal transepithelial electrical resistance (i.e., trans-RPE permeability) could exist at the time of scaffold transplantation. Highly differentiated transplanted cells may be better suited for subfoveal RPE transplantation, for example, than RPE suspensions. Once the foveal PRs are detached, they begin to degenerate. Clinically, this process is stopped by reapposition of the retina against functional RPE cells. When RPE cells are delivered as a suspension, time is required for them to attach to Bruch's membrane (the surface on which they reside normally in the eye) and to reacquire features of differentiation. In principle, this time interval (up to 1–2 weeks) can be eliminated by use of a scaffold delivering differentiated RPE cells. A second potential advantage is that scaffold delivery may be associated with a lower antigen load. Fewer cells are delivered with scaffolds than with cell suspensions. Although the subretinal space is an immune suppressive environment,[312] this privilege is not absolute, and there may be an advantage to reducing the antigen load with regard to stimulating immune surveillance of the transplanted cells.[313] Third, it may be possible to integrate growth factors, immunomodulatory molecules, or other useful moieties into the scaffold, thus prolonging RPE graft survival as well as photoreceptor survival.

Hynes and Lavik[314] have reviewed the materials, fabrication methods, and results of scaffold-assisted RPE and retinal cell transplantation in detail. Scaffolds can maintain proper three-dimensional organization of tissue (structural support), aid in cell delivery, influence cell behavior (e.g., differentiation), and deliver drugs or trophic molecules.[314] Naturally occurring materials (e.g., Descemet's membrane, lens capsule, Bruch's membrane, amniotic membrane) can serve as scaffolds, but, as Hynes and Lavik[314] point out, variations in material quality, availability, and infectious disease concerns probably supersede their attractive features, including biocompatibility and ease of handling. Naturally occurring polymers, such as collagen and fibrin, have the positive features of naturally occurring membranes and have been used as cell scaffolds, but product consistency, allergic response, and

infection risk remain as problems. Use of synthetic polymers enables one to regulate the biological properties (e.g., biodegradability, biocompatibility), mechanical properties (e.g., thickness, deformability), three-dimensional structure (e.g., porosity), and distribution of bioactive molecules (e.g., laminin, GDNF) precisely. Unfortunately, synthetic scaffolds may have undesirable features. For example, although poly(L-lactic acid)/poly(lactic-*co*-glycolide acid) (PLLA/PLGA) scaffolds improve cell delivery 10-fold, their use can be complicated by inflammation and fibrosis.[285,315] While thin (6 μm) and capable of promoting retinal progenitor cell differentiation,[25] spin-cast poly(methyl methacrylate) (PMMA) scaffolds are not biodegradable. PMMA scaffolds also require surface modification with either laminin or a combination of laminin and poly-L-lysine for retinal progenitor cells to attach. Poly(ε-caprolactone) (PCL), in contrast, is biodegradable, biocompatible, can be spin-cast to a thin film (5 μm) with controlled microtopography (that favors cell adherence), and promotes the differentiation of retinal progenitor cells.[307,316]

Most synthetic scaffolds for cell transplantation have been manufactured using techniques adapted from microchip fabrication methods, such as photolithography and soft lithography.[314] Microfabrication permits construction of scaffolds with precise architecture[25,317,318] (e.g., pore size, to improve cell retention; groove width, to improve cell morphology; and distribution of bioactive molecules,[25,307,316] to improve cell attachment and/or differentiation) (Figs. 38.13 and 38.14). Tao et al.[25] compared adhesion of retinal progenitor cells to polymer, as well as migration and differentiation in the host retina for PMMA laminin-coated scaffolds (6 μm thickness) with either smooth or porous (11 μm diameter) surface topography after transplantation into the subretinal space of C57BL/6 mice. Transplantation using porous scaffolds demonstrated enhanced retinal progenitor cell adherence during transplantation and allowed for greater process outgrowth and cell migration into the host retinal layers whereas transplantation with nonporous scaffolds showed limited retinal progenitor cell retention. A related strategy involves implantation of composite grafts. Redenti et al.[316] studied the survival, differentiation, and migration into the retina of mouse retinal progenitor cells cultured

on laminin-coated nanowire PCL scaffolds in C57bl/6 and rhodospsin$^{-/-}$ mouse retinal explants and transplant recipients. Retinal progenitor cells were cultured on smooth PCL and both short (2.5 μm) and long (27 μm) nanowire PCL scaffolds. Scaffolds with adherent mouse retinal progenitor cells were then either co-cultured with, or transplanted to, wild-type and rhodopsin$^{-/-}$ mouse retina. Robust retinal progenitor cell proliferation on each type of PCL scaffold was observed. Retinal progenitor cells cultured on nanowire scaffolds demonstrated increased expression of mature bipolar and photoreceptor markers. PCL-anchored retinal progenitor cells migrated into the retina of both wild-type and rhodopsin knockout mice. Using microfabrication processes, Sodha et al.[317] have manufactured a biodegradable thin-film cell encapsulation scaffold in PCL as a possible cell transplantation vehicle. Utilizing a modified spin-assisted solvent casting and melt templating technique, individual thin-film 2–2.5-D PCL layers (<10 μm) were structured with varying micro- and nanogeometries (protrusions, cavities, pores, particles). Thin-film layers were aligned and thermally bonded to form the three-dimensional cell encapsulation scaffold (<30 μm). These scaffolds promoted retinal progenitor cell retention and were appropriately permeable.

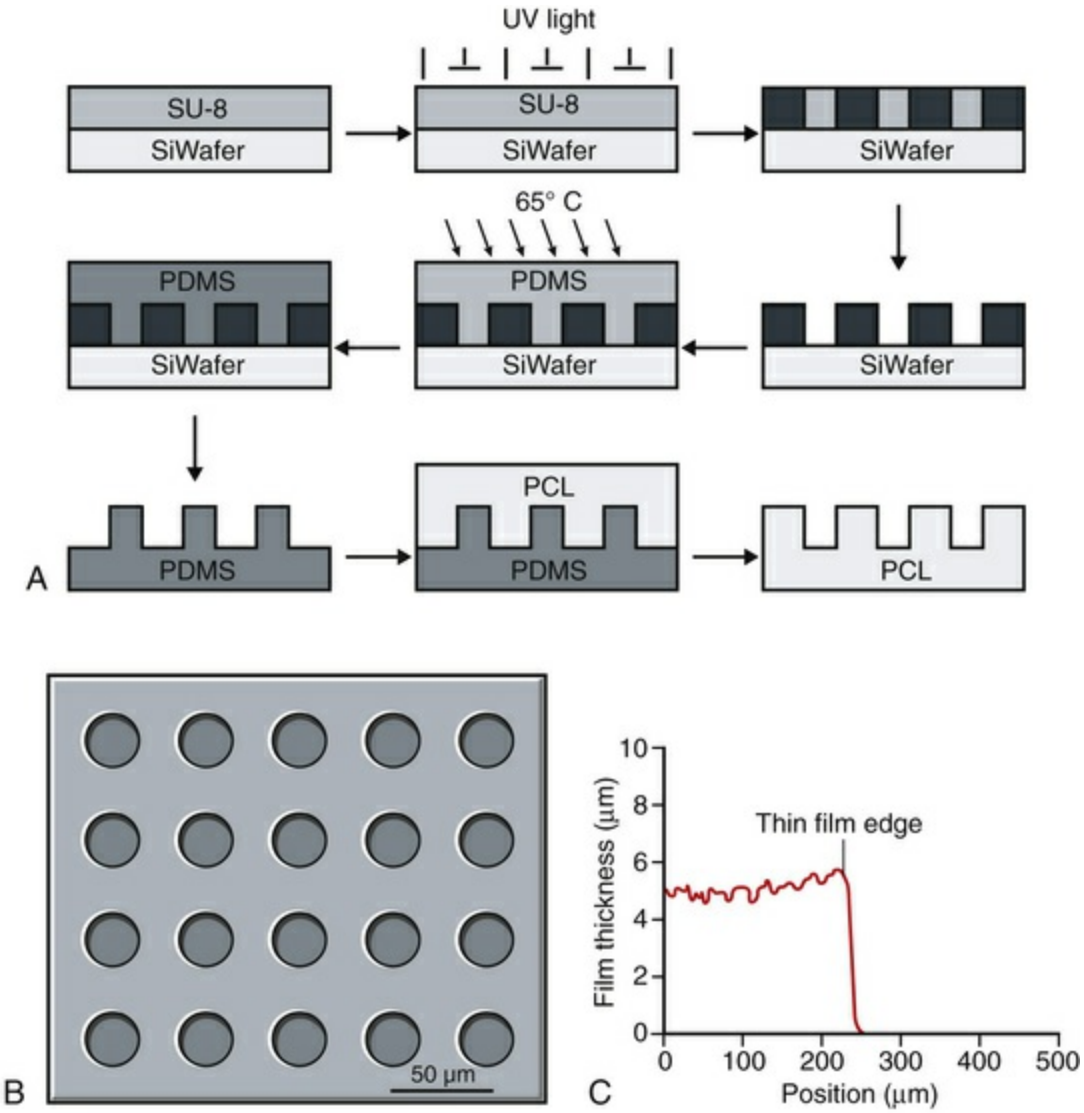

FIG. 38.13 Microfabrication of poly(ε-caprolactone) (PCL) thin film with photolithography and soft lithography. (A) Schematic of PCL thin-film scaffold fabrication. SU-8 photoresist is spin-cast onto a silicon wafer and exposed to ultraviolet (UV) light through a negative mask. Unexposed areas are not crosslinked and developed away, and polydimethylsiloxane (PDMS) is cured on the wafer. After peeling the PDMS mold from the wafer, PCL is spin-cast on the mold and peeled from the surface. (B) A scanning electron micrograph of a PCL thin film with 25 μm diameter wells. (C) Profile of PCL thin film. (Reproduced with permission from Steedman MR, Tao SL, Klassen H, et al. Enhanced differentiation of retinal progenitor cells using microfabricated topographical cues. Biomed Microdevices 2010;12:363–9; and from Zarbin MA, Montemagno C, Leary JF, et al. Regenerative nanomedicine and the treatment of degenerative retinal diseases. Wiley Interdiscip Rev Nanomed Nanobiotechnol 2012;4:113–37.)

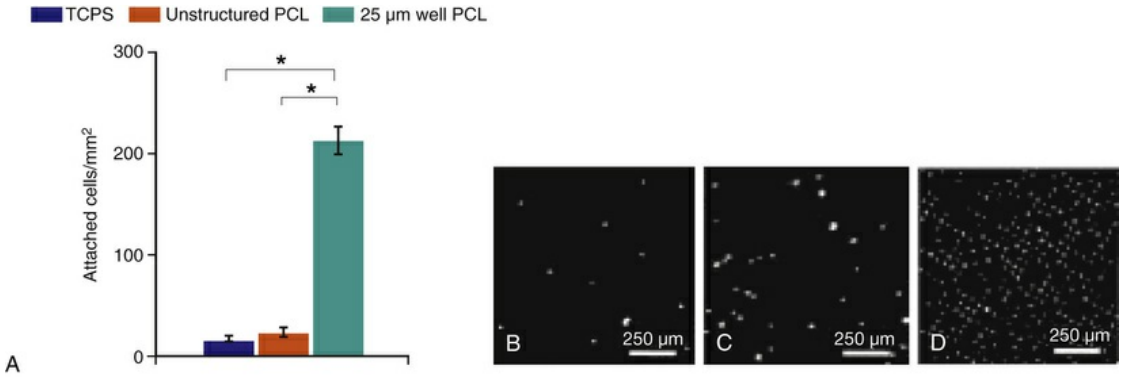

FIG. 38.14 Effect of structured surface on retinal progenitor cell behavior. (A) Attachment of retinal progenitor cells (RPCs) to substrate surfaces after 2 days' growth. Substrate microtopography of 25-µm well poly(ε-caprolactone) (PCL) leads to significantly more RPC attachment compared to unstructured PCL and tissue culture polystyrene (TCPS) surfaces. Fluorescence images of DAPI-stained RPC nuclei attached to (B) TCPS, (C) unstructured PCL, and (D) 25-µm well PCL. * $p<.05$, Student–Newman, Keuls test. Error bars indicate standard deviation over three independent experiments. (Reproduced with permission from Steedman MR, Tao SL, Klassen H, et al. Enhanced differentiation of retinal progenitor cells using microfabricated topographical cues. Biomed Microdevices 2010;12:363–9; and from Zarbin MA, Montemagno C, Leary JF, et al. Regenerative nanomedicine and the treatment of degenerative retinal diseases. Wiley Interdiscip Rev Nanomed Nanobiotechnol 2012;4:113–37.)

Lu and coworkers[319] have used nanotechnology to manufacture parylene C scaffolds for RPE transplantation (Figs. 38.15 and 38.16). The scaffolds are 6 µm thick to provide mechanical support and have 0.3 µm-thick diffusion zones to facilitate cell survival. These diffusion zones occupy 58% of the surface area of the scaffold and are 40 µm in diameter. A surgical instrument has been designed to facilitate scaffold delivery to the subretinal space (Fig. 38.17).

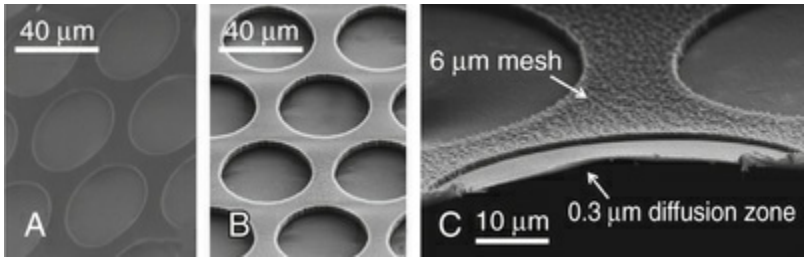

FIG. 38.15 Scanning electron microscopy images of (A) the front side, (B) the back side, and (C) the cross section of a mesh-supported submicron parylene C (MSPM) membrane with 0.30 µm parylene-C. (Reproduced with permission from Lu B, Tai YC, Humayun MS. Microdevice-based cell therapy for age-related macular degeneration. Dev Ophthalmol. 2014;53:155-66.)

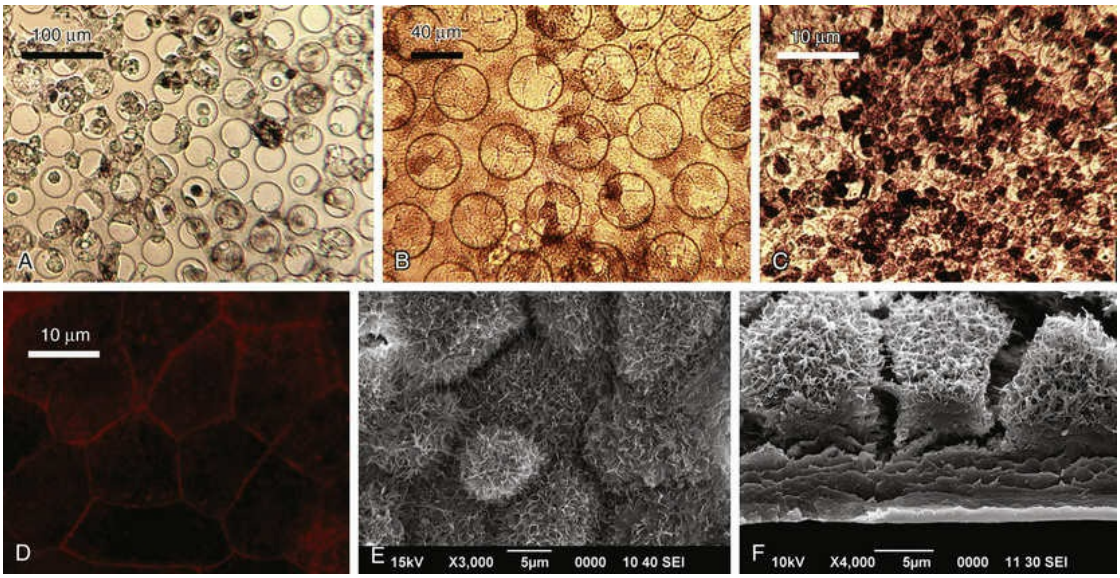

FIG. 38.16 H9-RPE cell culture on the MSPM. (A) One day after seeding, cells adhered and spread on the MSPM. (B) After 1 week, cells became confluent. (C) After 4 weeks, cells started to show pigmentation. (D) Anti-ZO-1 staining shows cells with hexagonal shapes and the tight junctions among cells. (E) and (F) the apical en face and cross-sectional SEM images show the formation of microvilli on well-polarized cells. (Reproduced with permission from Lu B, Tai YC, Humayun MS. Microdevice-based cell therapy for age-related macular degeneration. Dev Ophthalmol. 2014;53:155-66.)

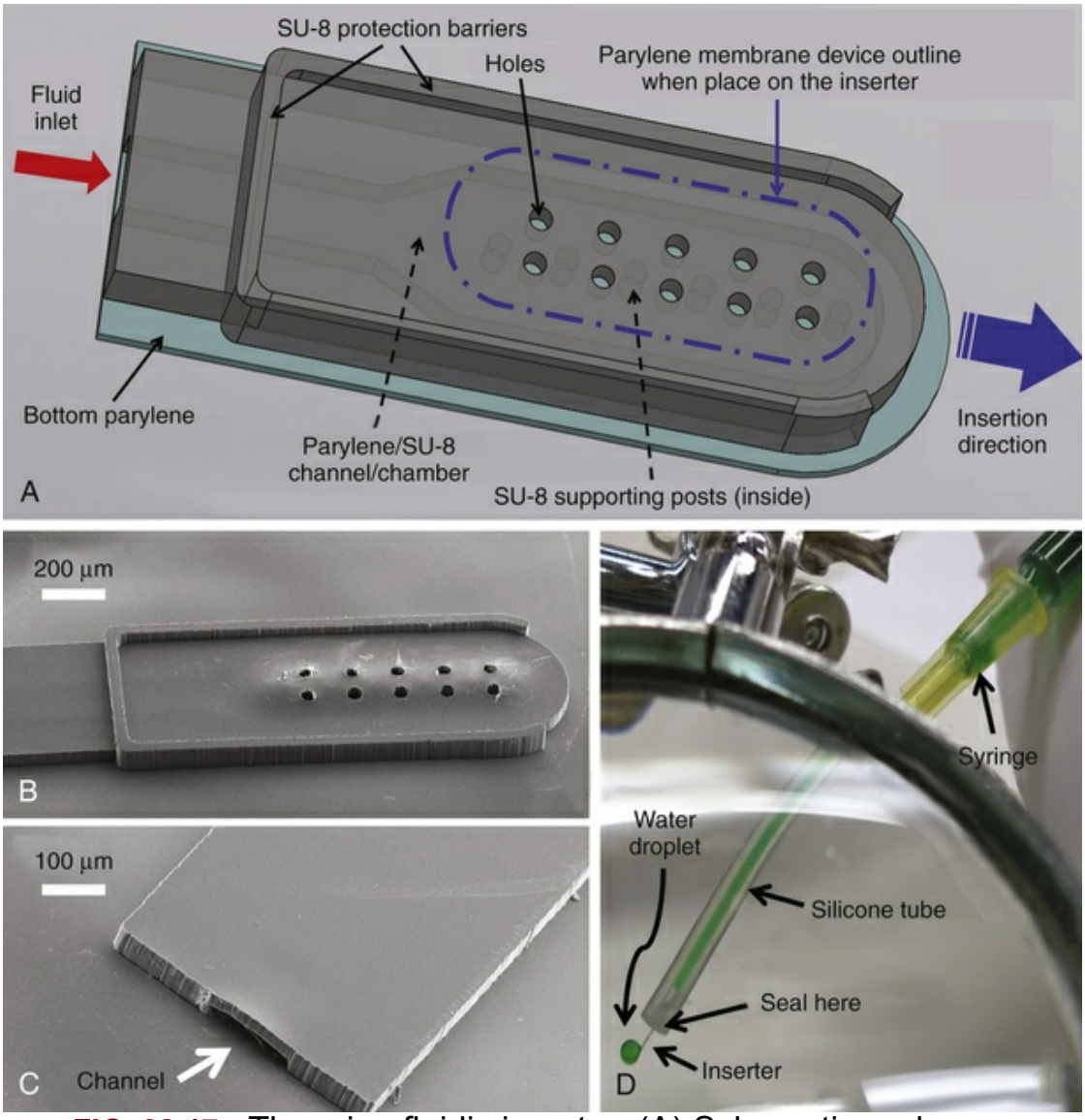

FIG. 38.17 The microfluidic inserter. (A) Schematic and working principle. (B,C) SEM images of the tip and tail. (D) Assembling and sealing method. (Reproduced with permission from Lu B, Tai YC, Humayun MS. Microdevice-based cell therapy for age-related macular degeneration. Dev Ophthalmol. 2014;53:155-66.)

Surgical Technology

Albert Hibbs suggested the notion of doing surgery by "swallowing the surgeon."[8] He proposed that this nanosurgeon could travel in blood vessels, identify areas of damaged tissue, and remove or repair them. The nanosurgical ophthalmic operating theater is in its infancy.[320–325] The axon surgery platform[24] was described earlier in this chapter. While peripheral nerve repair may be its first clinical

application, the availability of a microsurgical operating platform may render its introduction into ophthalmology relatively easy. Kim and Lieber[326] developed nanotweezers for the manipulation of nanostructures. Electrically conducting, mechanically robust carbon nanotubes were attached to electrodes fabricated on fine-glass micropipettes. The free ends of the nanotubes came into apposition as increasing voltage was applied across the electrodes (Fig. 38.18). Use of these nanotweezers for intraocular surgery would be difficult since the electric current that closes the tweezers might cause tissue coagulation, and the presence of a polar fluid environment might alter the properties of the tweezers. Alternatively, one can use MEMS technology to synthesize micromechanical forceps.[327] Robotic surgical manipulators would be needed to perform fine movements with true nanotweezers (humans have minimally a 50-μm tremor amplitude), and imaging systems providing very high magnification would be needed to enable the surgeon to visualize the target tissue and the instruments themselves.[5] Nanosurgical devices will enable performance of procedures such as internal recanalization of retinal artery and vein occlusions, dissection of complex epiretinal membranes, repair of retinal breaks (through tissue regeneration), and reanastomosis of severed optic nerves.[5]

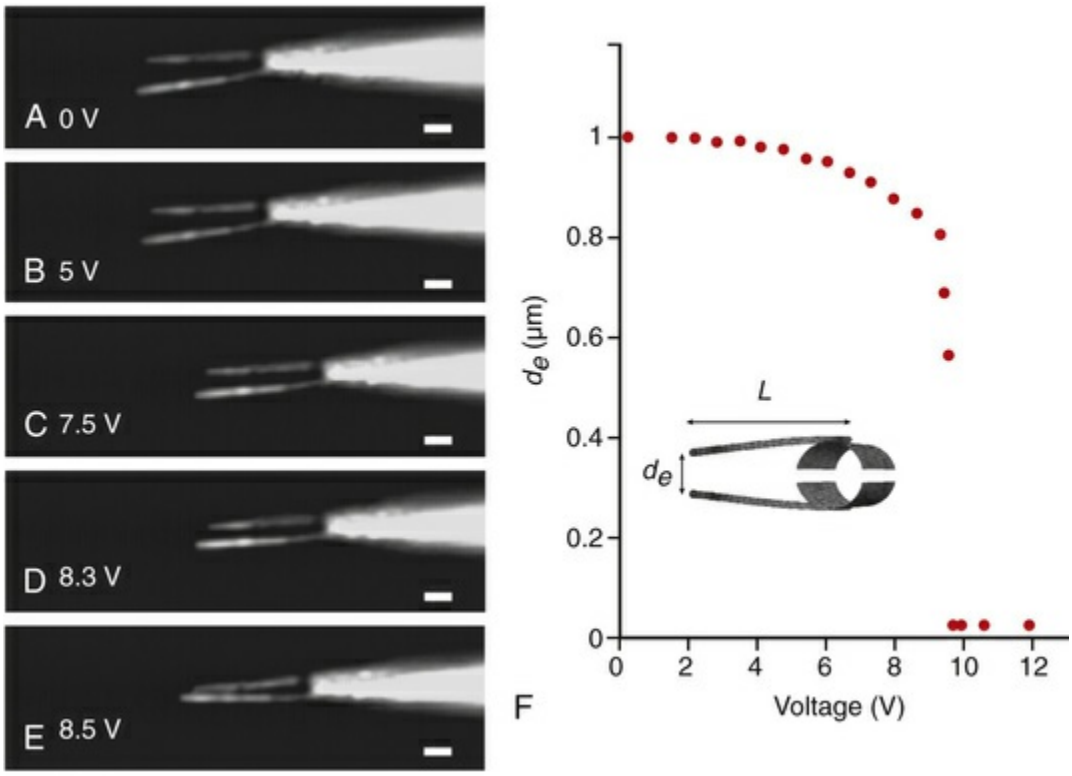

FIG. 38.18 Use of nanotechnology to create nanoinstruments for surgery. The electromechanical response of the nanotube nanotweezers is illustrated. The arms are made of carbon nanotubes, which have great tensile strength and also conduct electricity.[326] (A–E) Dark-field optical micrographs of the nanotube arms at potentials ranging from 0 to 8.5 V. Scale bars represent 1 μm. The arms are 50 nm wide and 4 μm long. Increasing deflection of the nanotweezers with increasing voltage is illustrated. (F) Calculated voltage response of the carbon nanotweezers. Separation of the ends of the nanotube arms, d_e, is plotted as a function of the applied voltage. (Reproduced from Kim P, Lieber CM. Nanotube nanotweezers. Science 1999;286:2148–21, with permission from the American Association for the Advancement of Science; and from Zarbin MA, Montemagno C, Leary JF, et al. Nanomedicine in ophthalmology: the new frontier. Am J Ophthalmol 2010;150:144–62.)

Obstacles to Incorporation of Nanotechnology Into Ophthalmology

Persistence of Nanoparticles Despite

Immune Surveillance

The biodistribution of nanoparticles and their persistence in tissues and organs are still not well known.[328] Locating and visualizing suboptical nanoparticles in large areas of tissues is an extremely difficult task. The ultimate confirmation of nanoparticle presence in organs and tissues is transmission electron microscopy, but it is impossible to scan large areas to find out where to look at this suboptical level.

Safe Manufacturing Techniques

Safe bionanomanufacturing is still a largely unexplored area since it requires not only the cleanroom processes similar to that of the manufacture of semiconductor devices, but also makes extreme demands on the manufacturing of biological components and their attachment to the nanoparticles. Nanomaterials are usually highly hydrophobic while biological molecules require aqueous environments. Thus, bionano cleanrooms must combine not only ultra-clean air and water but also containment of biological molecules capable of infecting humans.

Cell-by-Cell Dose Delivery and Control

Delivery of a precise amount of drug to individual cells in vivo is extremely difficult. One way to approach this problem has been suggested in an earlier section of this chapter, namely in situ production of therapeutic genes under the control of molecular biosensors that can regulate the amount of drug per cell according to what is needed, as detected in a feedback loop with an upstream molecular biosensor.

Unintended Biological Consequences

A major advantage of nanomedical approaches is that one can minimize unintended biological consequences by using highly targeted nano drug delivery systems. That targeting plus the fact that one to two orders of magnitude smaller amounts of drugs are delivered in vivo greatly reduce the possible unintended

consequences and adverse side-effects. Nonetheless, it is difficult to predict the biological response to a given nanomaterial in many cases. Test protocols to assess nanomaterial safety exist,[329] but hazards are identified on a case-by-case basis at this time. In general, the toxicity of nanoparticles reflects their chemistry.[26] Carbon nanotube toxicity, for example, depends on size, shape, surface coating, and concentration,[330] and the nanotubes can be genotoxic.[331] A variety of approaches can be taken to address these limitations (summarized by Cai et al.[129]).

Conclusion

Nanotechnology involves the creation and use of materials and devices at the size scale of intracellular structures and molecules, and involves systems and constructs on the order of <100 nm. Nanomedicine involves the comprehensive monitoring, control, construction, repair, defense, and improvement of human biological systems at the molecular level, using engineered nanodevices and nanostructures, operating massively in parallel at the single-cell level, ultimately to achieve medical benefit.[11] Individual atoms and molecules can be manipulated to form microscopic tubes, spheres, wires, and films for specific tasks, such as generating electricity or transporting drugs in the body.

The incorporation of nanotechnology in clinical medicine is a translational research endeavor. The earliest impact of nanomedicine is likely to involve the areas of biopharmaceuticals (e.g., drug delivery, drug discovery),[45] implantable materials (e.g., tissue regeneration scaffolds, bioresorbable materials), implantable devices (e.g., IOP monitors,[46] glaucoma drainage valves[47]), and diagnostic tools (e.g., genetic testing, imaging, IOP monitoring). Some applications of nanotechnology to ophthalmology are summarized in Table 38.1. Nanotechnology will bring about the development of regenerative medicine (i.e., replacement and improvement of cells, tissues, and organs), ultrahigh resolution in in vivo imaging, microsensors and feedback devices, and artificial vision. As illustrated in this chapter, nanotechnology will play an important role in both early- and late-stage intervention in the management of blinding diseases. “Regenerative nanomedicine,” a

new subfield of nanomedicine, uses nanoparticles containing gene transcription factors and other modulating molecules that allow for the reprogramming of cells in vivo. Nanotechnology already has been applied to the measurement and treatment of different disease states in ophthalmology, and many additional innovations will occur during the next century. These discoveries, as they are operationalized from preclinical models to clinical practice, are likely to have a major impact on the development of sight-preserving and sight-restoring treatments for conditions that currently lead to irreversible blindness.

TABLE 38.1
Applications of Nanotechnology to Ophthalmology

Nanotechnology Element	Application	Target Disease/Condition
Nanoparticles (carbon nanotube, dendrimer, fullerene, nanoceria, liposome, micelle, polypex)	Drug delivery Peptide delivery Gene delivery Antioxidant delivery	Choroidal neovascularization Glaucoma Lens capsule fibrosis (after phacoemulsification) Oxidative damage (e.g., AMD, diabetic retinopathy, retinitis pigmentosa) Proliferative vitreoretinopathy Retinal dystrophy (e.g., retinitis pigmentosa) Retinal edema Uveitis (including transplant rejection) Tumor therapy
Nanoparticles (dendrimer, gold nanoparticle, quantum dot, superparamagnetic iron oxide)	Biomedical imaging (e.g., contrast agents for MRI, CT, OCT) Genetic testing	Identification of tumor cells, transplanted cells, specific molecules
Nanoparticle (e.g., biosensor DNA tethered to magnetic nanoparticle), nanowires	Biosensor	Monitor and treat reactive oxygen species in conditions such as ROP, diabetic retinopathy, AMD
Nanomachine	Monitor cell/tissue physiology Prosthetics Nanosurgery	Monitor intraocular pressure, redox potential, oxygen tension (e.g., for ROP, diabetic retinopathy, AMD) Create light-sensitive ion channels to cure photoreceptor-based blindness Nanoneedles, nanotweezers, femtosecond laser
Nanostructured scaffolds (nanowires and other support matrices with defined nanoscale features)	Cell transplantation scaffold Induce cell differentiation Promote cell repair Drug delivery	Cell-based therapy for retinal disease Axonal regeneration after optic nerve injury

	Gene delivery	

AMD, age-related macular degeneration; CT, computed tomography; MRI, magnetic resonance imaging; OCT, optical coherence tomography; ROP, retinopathy of prematurity.

Reproduced with permission from Zarbin MA, Montemagno C, Leary JF, et al. Nanomedicine in ophthalmology: the new frontier. Am J Ophthalmol 2010;150:144–62.

References

1. Haglund EM, Seale-Goldsmith M-M, Leary JF. Design of multifunctional nanomedical systems. *Ann Biomed Eng*. 2009;37:2048–2063.
2. Seale M-M, Leary JF. Nanobiosystems. *Wiley Interdiscip Rev Nanomed Nanobiotechnol*. 2009;1:553–567.
3. Prow T, Grebe R, Merges C, et al. Nanoparticle tethered antioxidant response element as a biosensor for oxygen induced toxicity in retinal endothelial cells. *Mol Vis*. 2006;12:616–625.
4. Prow T, Smith JN, Grebe R, et al. Construction, gene delivery, and expression of DNA tethered nanoparticles. *Mol Vis*. 2006;12:606–615.
5. Zarbin MA, Montemagno C, Leary JF, et al. Nanomedicine in ophthalmology: the new frontier. *Am J Ophthalmol*. 2010;150:144–162.
6. Zarbin MA, Montemagno C, Leary JF, et al. Nanotechnology in ophthalmology. *Can J Ophthalmol*. 2010;45:457–476.
7. Zarbin MA, Montemagno C, Leary JF, et al. Regenerative nanomedicine and the treatment of degenerative retinal diseases. *Wiley Interdiscip Rev Nanomed Nanobiotechnol*. 2012;4:113–137.
8. Feynman R. There's plenty of room at the bottom. *Eng Sci*. 1960;23:22–36.
9. Ball P. High-density memory: a switch in time. *Nature*. 2007;445:362–363.
10. Soong RK, Bachand GD, Neves HP, et al. Powering an inorganic nanodevice with a biomolecular motor. *Science*.

2000;290:1555–1558.
11. Freitas RA Jr. What is nanomedicine? *Nanomedicine (Lond)*. 2005;1:2–9.
12. Morrow KJ Jr, Bawa R, Wei C. Recent advances in basic and clinical nanomedicine. *Med Clin North Am*. 2007;91:805–843.
13. Prow T, Salazar JH, Rose WA, et al. Nanomedicine – nanoparticles, molecular biosensors and targeted gene/drug delivery for combined single-cell diagnostics and therapeutics. *Proc SPIE*. 2004;5318:1–11.
14. Prow T, Rose WA, Wang NA, et al. Biosensor-controlled gene therapy/drug delivery with nanoparticles for nanomedicine. *Proc SPIE*. 2005;5692:199–208.
15. Seale M, Haglund E, Cooper CL, et al. Design of programmable multilayered nanoparticles with in situ manufacture of therapeutic genes for nanomedicine. *Proc SPIE*. 2007;6430:643003–1–7.
16. Banghart M, Borges K, Isacoff E, et al. Light-activated ion channels for remote control of neuronal firing. *Nat Neurosci*. 2004;7:1381–1386.
17. Volgraf M, Gorostiza P, Numano R, et al. Allosteric control of an ionotropic glutamate receptor with an optical switch. *Nature Chem Biol*. 2006;2:47–52.
18. Szobota S, Gorostiza P, Del Bene F, et al. Remote control of neuronal activity with a light-gated glutamate receptor. *Neuron*. 2007;54:535–545.
19. Barnes CP, Sell SA, Boland ED, et al. Nanofiber technology: designing the next generation of tissue engineering scaffolds. *Adv Drug Deliv Rev*. 2007;59:1413–1433.
20. Causa F, Netti PA, Ambrosio L. A multi-functional scaffold for tissue regeneration: the need to engineer a tissue analogue. *Biomaterials*. 2007;28:5093–5099.
21. Goldberg M, Langer R, Jia X. Nanostructured materials for applications in drug delivery and tissue engineering. *J Biomater Sci Polym Ed*. 2007;18:241–268.
22. Quondamatteo F. Assembly, stability and integrity of basement membranes in vivo. *Histochem J*. 2002;34:369–381.
23. Weigel T, Schinkel G, Lendlein A. Design and preparation of polymeric scaffolds for tissue engineering. *Expert Rev Med*

Devices. 2006;3:835–851.
24. Sretavan DW, Chang W, Hawkes E, et al. Microscale surgery on single axons. *Neurosurgery*. 2005;57:635–646 [discussion 646].
25. Tao S, Young C, Redenti S, et al. Survival, migration and differentiation of retinal progenitor cells transplanted on micro-machined poly(methyl methacrylate) scaffolds to the subretinal space. *Lab Chip*. 2007;7:695–701.
26. Ferreira L, Karp JM, Nobre L, et al. New opportunities: the use of nanotechnologies to manipulate and track stem cells. *Cell Stem Cell*. 2008;3:136–146.
27. Montemagno CD. Integrative technology for the twenty-first century. *Ann N Y Acad Sci*. 2004;1013:38–49.
28. Wendell DW, Patti J, Montemagno CD. Using biological inspiration to engineer functional nanostructured materials. *Small*. 2006;2:1324–1329.
29. Wendell D, Todd J, Montemagno C. Artificial photosynthesis in ranaspumin-2 based foam. *Nano Lett*. 2010;10:3231–3236.
30. Liu H, Schmidt JJ, Bachand GD, et al. Control of a biomolecular motor-powered nanodevice with an engineered chemical switch. *Nat Mater*. 2002;1:173–177.
31. Xi J, Schmidt JJ, Montemagno CD. Self-assembled microdevices driven by muscle. *Nat Mater*. 2005;4:180–184.
32. Bachand GD, Montemagno CD. Constructing organic/inorganic NEMS devices powered by biomolecular motors. *Biomed Microdevices*. 2000;3:179–184.
33. Ainslie KM, Tao SL, Popat KC, et al. In vitro immunogenicity of silicon-based micro- and nanostructured surfaces. *ACS Nano*. 2008;2:1076–1084.
34. Curtis AS, Gadegaard N, Dalby MJ, et al. Cells react to nanoscale order and symmetry in their surroundings. *IEEE Trans Nanobioscience*. 2004;3:61–65.
35. Dalby MJ, Riehle MO, Sutherland DS, et al. Changes in fibroblast morphology in response to nano-columns produced by colloidal lithography. *Biomaterials*. 2004;25:5415–5422.
36. Gallagher JO, McGhee KF, Wilkinson CD, et al. Interaction

of animal cells with ordered nanotopography. *IEEE Trans Nanobioscience*. 2002;1:24–28.
37. Huang NF, Patel S, Thakar RG, et al. Myotube assembly on nanofibrous and micropatterned polymers. *Nano Lett*. 2006;6:537–542.
38. Kim DHK, Suh KY, Choi SK, et al. *Modulation of adhesion and growth of cardiac myocytes by surface nanotopography. 27th Annual International Conference of the Engineering in Medicine and Biology Society*. 2005:4091–4094.
39. Popat KC, Leoni L, Grimes CA, et al. Influence of engineered titania nanotubular surfaces on bone cells. *Biomaterials*. 2007;28:3188–3197.
40. Yim EK, Reano RM, Pang SW, et al. Nanopattern-induced changes in morphology and motility of smooth muscle cells. *Biomaterials*. 2005;26:5405–5413.
41. Lin YM, Avouris P. Strong suppression of electrical noise in bilayer graphene nanodevices. *Nano Lett*. 2008;8:2119–2125.
42. Deshpande S, Patil S, Kuchibhatla SV, et al. Size dependency variation in lattice parameter and valency states in nanocrystalline cerium oxide. *Appl Phys Lett*. 2005;87:133113.
43. Tsunekawa S, Sahara R, Kawazoe Y, et al. Lattice relaxation of monosize CeO2-x nanocrystalline particles. *Appl Surf Sci*. 1999;152:53–56.
44. Yanik MF, Cinar H, Cinar HN, et al. Neurosurgery: functional regeneration after laser axotomy. *Nature*. 2004;432:822.
45. Wei C, Wei W, Morris M, et al. Nanomedicine and drug delivery. *Expert Rev Med Devices*. 2007;91:863–870.
46. Dresher RP, Irazoqui PP. A compact nanopower low output impedance CMOS operational amplifier for wireless intraocular pressure recordings. *Conf Proc IEEE Eng Med Biol Soc*. 2007;2007:6056–6059.
47. Pan T, Brown JD, Ziaie B. An artificial nano-drainage implant (ANDI) for glaucoma treatment. *Conf Proc IEEE Eng Med Biol Soc*. 2006;1:3174–3177.
48. Chu TC, He Q, Potter DE. Biodegradable calcium phosphate nanoparticles as a new vehicle for delivery of a potential

ocular hypotensive agent. *J Ocul Pharmacol Ther*. 2002;18:507–514.
49. Kassem MA, Abdel Rahman AA, Ghorab MM, et al. Nanosuspension as an ophthalmic delivery system for certain glucocorticoid drugs. *Int J Pharm*. 2007;340:126–133.
50. Kim W, Ng JK, Kunitake ME, et al. Interfacing silicon nanowires with mammalian cells. *J Am Chem Soc*. 2007;129:7228–7229.
51. Kostarelos K, Lacerda L, Pastorin G, et al. Cellular uptake of functionalized carbon nanotubes is independent of functional group and cell type. *Nat Nanotechnol*. 2007;2:108–113.
52. Bianco A, Kostarelos K, Prato M. Applications of carbon nanotubes in drug delivery. *Curr Opin Chem Biol*. 2005;9:674–679.
53. Petros RA, DeSimone JM. Strategies in the design of nanoparticles for therapeutic applications. *Nat Rev Drug Discov*. 2010;9:615–627.
54. Moghimi SM, Hunter AC, Andresen TL. Factors controlling nanoparticle pharmacokinetics: an integrated analysis and perspective. *Annu Rev Pharmacol Toxicol*. 2012;52:481–503.
55. Kompella UB, Amrite AC, Pacha Ravi R, et al. Nanomedicines for back of the eye drug delivery, gene delivery, and imaging. *Prog Retin Eye Res*. 2013;36:172–198.
56. Rejman J, Oberle V, Zuhorn IS, et al. Size-dependent internalization of particles via the pathways of clathrin- and caveolae-mediated endocytosis. *Biochem J*. 2004;377:159–169.
57. Chen X, Kube DM, Cooper MJ, et al. Cell surface nucleolin serves as receptor for DNA nanoparticles composed of pegylated polylysine and DNA. *Mol Ther*. 2008;16:333–342.
58. Renschler MF, Bhatt RR, Dower WJ, et al. Synthetic peptide ligands of the antigen binding receptor induce programmed cell death in a human B-cell lymphoma. *Proc Natl Acad Sci USA*. 1994;91:3623–3627.
59. Bareford LM, Swaan PW. Endocytic mechanisms for targeted drug delivery. *Adv Drug Deliv Rev*. 2007;59:748–758.
60. Torchilin VP. Cell penetrating peptide-modified

pharmaceutical nanocarriers for intracellular drug and gene delivery. *Biopolymers*. 2008;90:604–610.
61. Kirpotin D, Hong K, Mullah N, et al. Liposomes with detachable polymer coating: destabilization and fusion of dioleoylphosphatidylethanolamine vesicles triggered by cleavage of surface-grafted poly(ethylene glycol). *FEBS Lett*. 1996;388:115–118.
62. Saito G, Swanson JA, Lee KD. Drug delivery strategy utilizing conjugation via reversible disulfide linkages: role and site of cellular reducing activities. *Adv Drug Deliv Rev*. 2003;55:199–215.
63. Boddapati SV, D'Souza GG, Erdogan S, et al. Organelle-targeted nanocarriers: specific delivery of liposomal ceramide to mitochondria enhances its cytotoxicity in vitro and in vivo. *Nano Lett*. 2008;8:2559–2563.
64. Wagstaff KM, Jans DA. Importins and beyond: non-conventional nuclear transport mechanisms. *Traffic*. 2009;10:1188–1198.
65. Moghimi SM, Hamad I, Andresen TL, et al. Methylation of the phosphate oxygen moiety of phospholipid-methoxy(polyethylene glycol) conjugate prevents PEGylated liposome-mediated complement activation and anaphylatoxin production. *FASEB J*. 2006;20:2591–2593.
66. Hamad I, Christy Hunter A, Rutt KJ, et al. Complement activation by PEGylated single-walled carbon nanotubes is independent of C1q and alternative pathway turnover. *Mol Immunol*. 2008;45:3797–3803.
67. Yokoe J, Sakuragi S, Yamamoto K, et al. Albumin-conjugated PEG liposome enhances tumor distribution of liposomal doxorubicin in rats. *Int J Pharm*. 2008;353:28–34.
68. Furumoto K, Yokoe J, Ogawara K, et al. Effect of coupling of albumin on to surface of PEG liposome on its in vivo disposition. *Int J Pharm*. 2007;329:110–116.
69. Tomalia DA, Reyna LA, Svenson S. Dendrimers as multi-purpose nanodevices for oncology drug delivery and diagnostic imaging. *Biochem Soc Trans*. 2007;35:61–67.
70. Hahn U, Gorka M, Vogtle F, et al. Light-harvesting dendrimers: efficient intra- and intermolecular energy-

transfer processes in a species containing 65 chromophoric groups of four different types. *Angew Chem Int Ed Engl*. 2002;41:3595–3598 [3514].
71. Durairaj C, Kadam RS, Chandler JW, et al. Nanosized dendritic polyguanidilyated translocators for enhanced solubility, permeability, and delivery of gatifloxacin. *Invest Ophthalmol Vis Sci*. 2010;51:5804–5816.
72. Marano RJ, Toth I, Wimmer N, et al. Dendrimer delivery of an anti-VEGF oligonucleotide into the eye: a long-term study into inhibition of laser-induced CNV, distribution, uptake and toxicity. *Gene Ther*. 2005;12:1544–1550.
73. Vandamme TF, Brobeck L. Poly(amidoamine) dendrimers as ophthalmic vehicles for ocular delivery of pilocarpine nitrate and tropicamide. *J Control Release*. 2005;102:23–38.
74. Kang SJ, Durairaj C, Kompella UB, et al. Subconjunctival nanoparticle carboplatin in the treatment of murine retinoblastoma. *Arch Ophthalmol*. 2009;127:1043–1047.
75. Ideta R, Tasaka F, Jang WD, et al. Nanotechnology-based photodynamic therapy for neovascular disease using a supramolecular nanocarrier loaded with a dendritic photosensitizer. *Nano Lett*. 2005;5:2426–2431.
76. Shaunak S, Thomas S, Gianasi E, et al. Polyvalent dendrimer glucosamine conjugates prevent scar tissue formation. *Nat Biotechnol*. 2004;22:977–984.
77. Mead AL, Wong TT, Cordeiro MF, et al. Evaluation of anti-TGF-beta2 antibody as a new postoperative anti-scarring agent in glaucoma surgery. *Invest Ophthalmol Vis Sci*. 2003;44:3394–3401.
78. Siriwardena D, Khaw PT, King AJ, et al. Human antitransforming growth factor beta(2) monoclonal antibody – a new modulator of wound healing in trabeculectomy: a randomized placebo controlled clinical study. *Ophthalmology*. 2002;109:427–431.
79. Ferreira L, Park H, Choe H, et al. Human embryoid bodies containing nano- and micro-particulate delivery vehicles. *Adv Mater*. 2008;20:2285–2291.
80. Sakai T, Kuno N, Takamatsu F, et al. Prolonged protective effect of basic fibroblast growth factor-impregnated

nanoparticles in Royal College of Surgeons rats. *Invest Ophthalmol Vis Sci*. 2007;48:3381–3387.
81. Vollrath D, Feng W, Duncan JL, et al. Correction of the retinal dystrophy phenotype of the RCS rat by viral gene transfer of Mertk. *Proc Natl Acad Sci USA*. 2001;98:12584–12589.
82. Gal A, Li Y, Thompson DA, et al. Mutations in MERTK, the human orthologue of the RCS rat retinal dystrophy gene, cause retinitis pigmentosa. *Nat Genet*. 2000;26:270–271.
83. Charbel Issa P, Bolz HJ, Ebermann I, et al. Characterisation of severe rod–cone dystrophy in a consanguineous family with a splice site mutation in the MERTK gene. *Br J Ophthalmol*. 2009;93:920–925.
84. Mackay DS, Henderson RH, Sergouniotis PI, et al. Novel mutations in MERTK associated with childhood onset rod-cone dystrophy. *Mol Vis*. 2010;16:369–377.
85. Quigley HA, Broman AT. The number of people with glaucoma worldwide in 2010 and 2020. *Br J Ophthalmol*. 2006;90:262–267.
86. Jiang C, Moore MJ, Zhang X, et al. Intravitreal injections of GDNF-loaded biodegradable microspheres are neuroprotective in a rat model of glaucoma. *Mol Vis*. 2007;13:1783–1792.
87. Fu K, Harrell R, Zinski K, et al. A potential approach for decreasing the burst effect of protein from PLGA microspheres. *J Pharm Sci*. 2003;92:1582–1591.
88. Dalkara D, Kolstad KD, Guerin KI, et al. AAV mediated GDNF secretion from retinal glia slows down retinal degeneration in a rat model of retinitis pigmentosa. *Mol Ther*. 2011;19:1602–1608.
89. Kim KE, Jang I, Moon H, et al. Neuroprotective effects of human serum albumin nanoparticles loaded with brimonidine on retinal ganglion cells in optic nerve crush model. *Invest Ophthalmol Vis Sci*. 2015;56(9):5641–5649.
90. Brownlee M. A radical explanation for glucose-induced beta cell dysfunction. *J Clin Invest*. 2003;112:1788–1790.
91. Yorek MA. The role of oxidative stress in diabetic vascular and neural disease. *Free Radic Res*. 2003;37:471–480.

92. Dugan LL, Lovett EG, Quick KL, et al. Fullerene-based antioxidants and neurodegenerative disorders. *Parkinsonism Relat Disord*. 2001;7:243–246.
93. Shen JK, Dong A, Hackett SF, et al. Oxidative damage in age-related macular degeneration. *Histol Histopathol*. 2007;22:1301–1308.
94. Komeima K, Rogers BS, Campochiaro PA. Antioxidants slow photoreceptor cell death in mouse models of retinitis pigmentosa. *J Cell Physiol*. 2007;213:809–815.
95. Papp A, Nemeth I, Karg E, et al. Glutathione status in retinopathy of prematurity. *Free Radic Biol Med*. 1999;27:738–743.
96. Chen J, Patil S, Seal S, et al. Rare earth nanoparticles prevent retinal degeneration induced by intracellular peroxides. *Nat Nanotechnol*. 2006;1:142–150.
97. Zhou X, Wong LL, Karakoti AS, et al. Nanoceria inhibit the development and promote the regression of pathologic retinal neovascularization in the *Vldlr* knockout mouse. *PLoS ONE*. 2011;6:e16733.
98. Truong SN, Alam S, Zawadzki RJ, et al. High resolution Fourier-domain optical coherence tomography of retinal angiomatous proliferation. *Retina*. 2007;27:915–925.
99. Elman MJ, Aiello LP, Beck RW, et al. Randomized trial evaluating ranibizumab plus prompt or deferred laser or triamcinolone plus prompt laser for diabetic macular edema. *Ophthalmology*. 2010;117 [1064–77.e35].
100. Rosenfeld PJ, Brown DM, Heier JS, et al. Ranibizumab for neovascular age-related macular degeneration. *N Engl J Med*. 2006;355:1419–1431.
101. Brown DM, Kaiser PK, Michels M, et al. Ranibizumab versus verteporfin for neovascular age-related macular degeneration. *N Engl J Med*. 2006;355:1432–1444.
102. Kroto HW, Heath JR, O'Brien SC, et al. C60: Buckminsterfullerene. *Nature*. 1985;318:162–163.
103. Dugan LL, Turetsky DM, Du C, et al. Carboxyfullerenes as neuroprotective agents. *Proc Natl Acad Sci USA*. 1997;94:9434–9439.
104. Shichi H. Microsomal electron transfer system of bovine

retinal pigment epithelium. *Exp Eye Res*. 1969;8:60–68.
105. Yau KW, Baylor DA. Cyclic GMP-activated conductance of retinal photoreceptor cells. *Annu Rev Neurosci*. 1989;12:289–327.
106. Moiseyev G, Chen Y, Takahashi Y, et al. RPE65 is the isomerohydrolase in the retinoid visual cycle. *Proc Natl Acad Sci USA*. 2005;102:12413–12418.
107. Halliwell B, Gutteridge JM. Oxygen toxicity, oxygen radicals, transition metals and disease. *Biochem J*. 1984;219:1–14.
108. Rogers BS, Symons RC, Komeima K, et al. Differential sensitivity of cones to iron-mediated oxidative damage. *Invest Ophthalmol Vis Sci*. 2007;48:438–445.
109. Liu G, Men P, Harris PL, et al. Nanoparticle iron chelators: a new therapeutic approach in Alzheimer disease and other neurologic disorders associated with trace metal imbalance. *Neurosci Lett*. 2006;406:189–193.
110. Hahn P, Milam AH, Dunaief JL. Maculas affected by age-related macular degeneration contain increased chelatable iron in the retinal pigment epithelium and Bruch's membrane. *Arch Ophthalmol*. 2003;121:1099–1105.
111. Hahn P, Qian Y, Dentchev T, et al. Disruption of ceruloplasmin and hephaestin in mice causes retinal iron overload and retinal degeneration with features of age-related macular degeneration. *Proc Natl Acad Sci USA*. 2004;101:13850–13855.
112. Dunaief JL, Richa C, Franks EP, et al. Macular degeneration in a patient with aceruloplasminemia, a disease associated with retinal iron overload. *Ophthalmology*. 2005;112:1062–1065.
113. Chowers I, Wong R, Dentchev T, et al. The iron carrier transferrin is upregulated in retinas from patients with age-related macular degeneration. *Invest Ophthalmol Vis Sci*. 2006;47:2135–2140.
114. He X, Hahn P, Iacovelli J, et al. Iron homeostasis and toxicity in retinal degeneration. *Prog Retin Eye Res*. 2007;26:649–673.
115. Gullapalli VKKM, Wang H, Sugino IK, et al. Retinal

pigment epithelium and photoreceptor transplantation frontiers. Ryan SJ. *Retina*. 4th ed. Mosby: Philadelphia, PA; 2006:2597–2613.
116. Zarbin MA. Functionalizing cell-based therapy for age-related macular degeneration. *Am J Ophthalmol*. 2007;143:681–682.
117. Zarbin MA. Retinal pigment epithelium-retina transplantation for retinal degenerative disease. *Am J Ophthalmol*. 2008;146:151–153.
118. Yuan XB, Yuan YB, Jiang W, et al. Preparation of rapamycin-loaded chitosan/PLA nanoparticles for immunosuppression in corneal transplantation. *Int J Pharm*. 2008;349:241–248.
119. Prow TW, Bhutto I, Kim SY, et al. Ocular nanoparticle toxicity and transfection of the retina and retinal pigment epithelium. *Nanomedicine (Lond)*. 2008;4:340–349.
120. Caspi RR. Experimental autoimmune uveoretinitis in the rat and mouse. *Curr Protoc Immunol*. 2003 [Chapter 15:Unit 15 6].
121. Sakai T, Kohno H, Ishihara T, et al. Treatment of experimental autoimmune uveoretinitis with poly(lactic acid) nanoparticles encapsulating betamethasone phosphate. *Exp Eye Res*. 2006;82:657–663.
122. Bazile D, Prud'homme C, Bassoullet MT, et al. Stealth Me.PEG-PLA nanoparticles avoid uptake by the mononuclear phagocytes system. *J Pharm Sci*. 1995;84:493–498.
123. Ishihara T, Kubota T, Choi T, et al. Polymeric nanoparticles encapsulating betamethasone phosphate with different release profiles and stealthiness. *Int J Pharm*. 2009;375:148–154.
124. Sakai T, Ishihara T, Higaki M, et al. Therapeutic effect of stealth-type polymeric nanoparticles with encapsulated betamethasone phosphate on experimental autoimmune uveoretinitis. *Invest Ophthalmol Vis Sci*. 2011;52:1516–1521.
125. Zhang R, He R, Qian J, et al. Treatment of experimental autoimmune uveoretinitis with intravitreal injection of tacrolimus (FK506) encapsulated in liposomes. *Invest*

Ophthalmol Vis Sci. 2010;51:3575–3582.
126. Glover DJ, Lipps HJ, Jans DA. Towards safe, non-viral therapeutic gene expression in humans. *Nat Rev Genet*. 2005;6:299–310.
127. Kutsuzawa K, Chowdhury EH, Nagaoka M, et al. Surface functionalization of inorganic nano-crystals with fibronectin and E-cadherin chimera synergistically accelerates transgene delivery into embryonic stem cells. *Biochem Biophys Res Commun*. 2006;350:514–520.
128. Mo Y, Barnett ME, Takemoto D, et al. Human serum albumin nanoparticles for efficient delivery of Cu, Zn superoxide dismutase gene. *Mol Vis*. 2007;13:746–757.
129. Cai X, Conley S, Naash M. Nanoparticle applications in ocular gene therapy. *Vision Res*. 2008;48:319–324.
130. Farjo R, Skaggs J, Quiambao AB, et al. Efficient non-viral ocular gene transfer with compacted DNA nanoparticles. *PLoS ONE*. 2006;1:e38.
131. Pack DW, Hoffman AS, Pun S, et al. Design and development of polymers for gene delivery. *Nat Rev Drug Discov*. 2005;4:581–593.
132. Incani V, Tunis E, Clements BA, et al. Palmitic acid substitution on cationic polymers for effective delivery of plasmid DNA to bone marrow stromal cells. *J Biomed Mater Res A*. 2007;81:493–504.
133. Konstan MW, Davis PB, Wagener JS, et al. Compacted DNA nanoparticles administered to the nasal mucosa of cystic fibrosis subjects are safe and demonstrate partial to complete cystic fibrosis transmembrane regulator reconstitution. *Hum Gene Ther*. 2004;15:1255–1269.
134. Pitkanen L, Ruponen M, Nieminen J, et al. Vitreous is a barrier in nonviral gene transfer by cationic lipids and polymers. *Pharm Res*. 2003;20:576–583.
135. Cai X, Conley SM, Nash Z, et al. Gene delivery to mitotic and postmitotic photoreceptors via compacted DNA nanoparticles results in improved phenotype in a mouse model of retinitis pigmentosa. *FASEB J*. 2010;24:1178–1191.
136. Flannery JGZS, Vaquero MI, LaVail MM, et al. Efficient photoreceptor-targeted gene expression in vivo by

recombinant adeno-associated virus. *Proc Natl Acad Sci USA*. 1997;94:6916–6921.
137. Li Q, Timmers AM, Guy J, et al. Cone-specific expression using a human red opsin promoter in recombinant AAV. *Vision Res*. 2008;48:332–338.
138. Porrello K, Bhat SP, Bok D. Detection of interphotoreceptor retinoid binding protein (IRBP) mRNA in human and cone-dominant squirrel retinas by in situ hybridization. *J Histochem Cytochem*. 1991;39:171–176.
139. Esumi N, Oshima Y, Li Y, et al. Analysis of the VMD2 promoter and implication of E-box binding factors in its regulation. *J Biol Chem*. 2004;279:19064–19073.
140. Cai X, Nash Z, Conley SM, et al. A partial structural and functional rescue of a retinitis pigmentosa model with compacted DNA nanoparticles. *PLoS ONE*. 2009;4:e5290.
141. Bejjani RA, BenEzra D, Cohen H, et al. Nanoparticles for gene delivery to retinal pigment epithelial cells. *Mol Vis*. 2005;11:124–132.
142. Conley SM, Cai X, Naash MI. Nonviral ocular gene therapy: assessment and future directions. *Curr Opin Mol Ther*. 2008;10:456–463.
143. Conley SM, Naash MI. Nanoparticles for retinal gene therapy. *Prog Retin Eye Res*. 2010;29:376–397.
144. Ravi Kumar MN, Bakowsky U, Lehr CM. Preparation and characterization of cationic PLGA nanospheres as DNA carriers. *Biomaterials*. 2004;25:1771–1777.
145. Marmorstein AD, Marmorstein LY, Rayborn M, et al. Bestrophin, the product of the Best vitelliform macular dystrophy gene (VMD2), localizes to the basolateral plasma membrane of the retinal pigment epithelium. *Proc Natl Acad Sci USA*. 2000;97:12758–12763.
146. Maguire AM, Simonelli F, Pierce EA, et al. Safety and efficacy of gene transfer for Leber's congenital amaurosis. *N Engl J Med*. 2008;358:2240–2248.
147. Bainbridge JW, Smith AJ, Barker SS, et al. Effect of gene therapy on visual function in Leber's congenital amaurosis. *N Engl J Med*. 2008;358:2231–2239.
148. Cideciyan AV, Hauswirth WW, Aleman TS, et al. Human

RPE65 gene therapy for Leber congenital amaurosis: persistence of early visual improvements and safety at 1 year. *Hum Gene Ther*. 2009;20:999–1004.
149. Jani PD, Singh N, Jenkins C, et al. Nanoparticles sustain expression of Flt intraceptors in the cornea and inhibit injury-induced corneal angiogenesis. *Invest Ophthalmol Vis Sci*. 2007;48:2030–2036.
150. Kay MA. State-of-the-art gene-based therapies: the road ahead. *Nat Rev Genet*. 2011;12:316–328.
151. Donsante A, Miller DG, Li Y, et al. AAV vector integration sites in mouse hepatocellular carcinoma. *Science*. 2007;317:477.
152. Hacein-Bey-Abina S, Von Kalle C, Schmidt M, et al. LMO2-associated clonal T cell proliferation in two patients after gene therapy for SCID-X1. *Science*. 2003;302:415–419.
153. Boutin S, Monteilhet V, Veron P, et al. Prevalence of serum IgG and neutralizing factors against adeno-associated virus (AAV) types 1, 2, 5, 6, 8, and 9 in the healthy population: implications for gene therapy using AAV vectors. *Hum Gene Ther*. 2010;21:704–712.
154. Erles K, Sebokova P, Schlehofer JR. Update on the prevalence of serum antibodies (IgG and IgM) to adeno-associated virus (AAV). *J Med Virol*. 1999;59:406–411.
155. Raper SE, Chirmule N, Lee FS, et al. Fatal systemic inflammatory response syndrome in a ornithine transcarbamylase deficient patient following adenoviral gene transfer. *Mol Genet Metab*. 2003;80:148–158.
156. Zaiss AK, Machado HB, Herschman HR. The influence of innate and pre-existing immunity on adenovirus therapy. *J Cell Biochem*. 2009;108:778–790.
157. Manno CS, Pierce GF, Arruda VR, et al. Successful transduction of liver in hemophilia by AAV-factor IX and limitations imposed by the host immune response. *Nat Med*. 2006;12:342–347.
158. Mingozzi F, Maus MV, Hui DJ, et al. CD8(+) T-cell responses to adeno-associated virus capsid in humans. *Nat Med*. 2007;13:419–422.
159. Petry H, Brooks A, Orme A, et al. Effect of viral dose on

neutralizing antibody response and transgene expression after AAV1 vector re-administration in mice. *Gene Ther*. 2008;15:54–60.
160. Hauswirth WW, Aleman TS, Kaushal S, et al. Treatment of Leber congenital amaurosis due to RPE65 mutations by ocular subretinal injection of adeno-associated virus gene vector: short-term results of a phase I trial. *Hum Gene Ther*. 2008;19:979–990.
161. Goncalves MA. Adeno-associated virus: from defective virus to effective vector. *Virol J*. 2005;2:43.
162. Surace EM, Auricchio A. Versatility of AAV vectors for retinal gene transfer. *Vision Res*. 2008;48:353–359.
163. Yang GS, Schmidt M, Yan Z, et al. Virus-mediated transduction of murine retina with adeno-associated virus: effects of viral capsid and genome size. *J Virol*. 2002;76:7651–7660.
164. Zaiss AK, Muruve DA. Immunity to adeno-associated virus vectors in animals and humans: a continued challenge. *Gene Ther*. 2008;15:808–816.
165. Sun JY, Anand-Jawa V, Chatterjee S, et al. Immune responses to adeno-associated virus and its recombinant vectors. *Gene Ther*. 2003;10:964–976.
166. Ivics Z, Izsvak Z. The expanding universe of transposon technologies for gene and cell engineering. *Mob DNA*. 2010;1:25.
167. Calos MP. The phiC31 integrase system for gene therapy. *Curr Gene Ther*. 2006;6:633–645.
168. Kwon I, Schaffer DV. Designer gene delivery vectors: molecular engineering and evolution of adeno-associated viral vectors for enhanced gene transfer. *Pharm Res*. 2008;25:489–499.
169. Maheshri N, Koerber JT, Kaspar BK, et al. Directed evolution of adeno-associated virus yields enhanced gene delivery vectors. *Nat Biotechnol*. 2006;24:198–204.
170. Zhao H, Giver L, Shao Z, et al. Molecular evolution by staggered extension process (StEP) in vitro recombination. *Nat Biotechnol*. 1998;16:258–261.
171. Koerber JT, Klimczak R, Jang JH, et al. Molecular evolution

of adeno-associated virus for enhanced glial gene delivery. *Mol Ther*. 2009;17:2088–2095.
172. Klimczak RR, Koerber JT, Dalkara D, et al. A novel adeno-associated viral variant for efficient and selective intravitreal transduction of rat Müller cells. *PLoS ONE*. 2009;4:e7467.
173. LaVail MM, Yasumura D, Matthes MT, et al. Protection of mouse photoreceptors by survival factors in retinal degenerations. *Invest Ophthalmol Vis Sci*. 1998;39:592–602.
174. Chaum E. Retinal neuroprotection by growth factors: a mechanistic perspective. *J Cell Biochem*. 2003;88:57–75.
175. Sieving PA, Caruso RC, Tao W, et al. Ciliary neurotrophic factor (CNTF) for human retinal degeneration: phase I trial of CNTF delivered by encapsulated cell intraocular implants. *Proc Natl Acad Sci USA*. 2006;103:3896–3901.
176. Zhong L, Li B, Mah CS, et al. Next generation of adeno-associated virus 2 vectors: point mutations in tyrosines lead to high-efficiency transduction at lower doses. *Proc Natl Acad Sci USA*. 2008;105:7827–7832.
177. Wang W, Malcolm BA. Two-stage PCR protocol allowing introduction of multiple mutations, deletions and insertions using QuikChange site-directed mutagenesis. *Biotechniques*. 1999;26:680–682.
178. Zhong L, Zhao W, Wu J, et al. A dual role of EGFR protein tyrosine kinase signaling in ubiquitination of AAV2 capsids and viral second-strand DNA synthesis. *Mol Ther*. 2007;15:1323–1330.
179. Mah C, Qing K, Khuntirat B, et al. Adeno-associated virus type 2-mediated gene transfer: role of epidermal growth factor receptor protein tyrosine kinase in transgene expression. *J Virol*. 1998;72:9835–9843.
180. Zhong L, Zhou X, Li Y, et al. Single-polarity recombinant adeno-associated virus 2 vector-mediated transgene expression in vitro and in vivo: mechanism of transduction. *Mol Ther*. 2008;16:290–295.
181. McCarty DM, Fu H, Monahan PE, et al. Adeno-associated virus terminal repeat (TR) mutant generates self-complementary vectors to overcome the rate-limiting step

to transduction in vivo. *Gene Ther*. 2003;10:2112–2118.
182. Yokoi K, Kachi S, Zhang HS, et al. Ocular gene transfer with self-complementary AAV vectors. *Invest Ophthalmol Vis Sci*. 2007;48:3324–3328.
183. Acland GM, Aguirre GD, Bennett J, et al. Long-term restoration of rod and cone vision by single dose rAAV-mediated gene transfer to the retina in a canine model of childhood blindness. *Mol Ther*. 2005;12:1072–1082.
184. Min SH, Molday LL, Seeliger MW, et al. Prolonged recovery of retinal structure/function after gene therapy in an Rs1h-deficient mouse model of X-linked juvenile retinoschisis. *Mol Ther*. 2005;12:644–651.
185. Petrs-Silva H, Dinculescu A, Li Q, et al. High-efficiency transduction of the mouse retina by tyrosine-mutant AAV serotype vectors. *Mol Ther*. 2009;17:463–471.
186. Streilein JW. Limitations in the study of immune privilege in the subretinal space of the rodent. *Invest Ophthalmol Vis Sci*. 1999;40:3069.
187. Li Q, Miller R, Han PY, et al. Intraocular route of AAV2 vector administration defines humoral immune response and therapeutic potential. *Mol Vis*. 2008;14:1760–1769.
188. Nune SK, Gunda P, Thallapally PK, et al. Nanoparticles for biomedical imaging. *Expert Opin Drug Deliv*. 2009;6:1175–1194.
189. Boisselier E, Astruc D. Gold nanoparticles in nanomedicine: preparations, imaging, diagnostics, therapies and toxicity. *Chem Soc Rev*. 2009;38:1759–1782.
190. Elghanian R, Storhoff JJ, Mucic RC, et al. Selective colorimetric detection of polynucleotides based on the distance-dependent optical properties of gold nanoparticles. *Science*. 1997;277:1078–1081.
191. Reimer P, Balzer T. Ferucarbotran (Resovist): a new clinically approved RES-specific contrast agent for contrast-enhanced MRI of the liver: properties, clinical development, and applications. *Eur Radiol*. 2003;13:1266–1276.
192. Wang YX, Hussain SM, Krestin GP. Superparamagnetic iron oxide contrast agents: physicochemical characteristics and applications in MR imaging. *Eur Radiol*. 2001;11:2319–2331.

193. Hsiao JK, Tai MF, Chu HH, et al. Magnetic nanoparticle labeling of mesenchymal stem cells without transfection agent: cellular behavior and capability of detection with clinical 1.5 T magnetic resonance at the single cell level. *Magn Reson Med*. 2007;58:717–724.
194. Zhu J, Zhou L, XingWu F. Tracking neural stem cells in patients with brain trauma. *N Engl J Med*. 2006;355:2376–2378.
195. Guzman R, Uchida N, Bliss TM, et al. Long-term monitoring of transplanted human neural stem cells in developmental and pathological contexts with MRI. *Proc Natl Acad Sci USA*. 2007;104:10211–10216.
196. Michalet X, Pinaud FF, Bentolila LA, et al. Quantum dots for live cells, in vivo imaging, and diagnostics. *Science*. 2005;307:538–544.
197. Lei Y, Tang H, Yao L, et al. Applications of mesenchymal stem cells labeled with Tat peptide conjugated quantum dots to cell tracking in mouse body. *Bioconjug Chem*. 2008;19:421–427.
198. Slotkin JR, Chakrabarti L, Dai HN, et al. In vivo quantum dot labeling of mammalian stem and progenitor cells. *Dev Dyn*. 2007;236:3393–3401.
199. Derfus AM, Chan WCW, Bhatia SN. Probing the cytotoxicity of semiconductor quantum dots. *Adv Mater*. 2004;4:11–18.
200. Lovric J, Cho SJ, Winnik FM, et al. Unmodified cadmium telluride quantum dots induce reactive oxygen species formation leading to multiple organelle damage and cell death. *Chem Biol*. 2005;12:1227–1234.
201. Zarbin MA. Current concepts in the pathogenesis of age-related macular degeneration. *Arch Ophthalmol*. 2004;122:598–614.
202. Takeda A, Baffi JZ, Kleinman ME, et al. CCR3 is a target for age-related macular degeneration diagnosis and therapy. *Nature*. 2009;460:225–230.
203. Cohen-Karni T, Timko BP, Weiss LE, et al. Flexible electrical recording from cells using nanowire transistor arrays. *Proc Natl Acad Sci USA*. 2009;106:7309–7313.

204. Graham SL, Drance SM. Nocturnal hypotension: role in glaucoma progression. *Surv Ophthalmol*. 1999;43(Suppl. 1):S10–16.
205. Barkana Y, Anis S, Liebmann J, et al. Clinical utility of intraocular pressure monitoring outside of normal office hours in patients with glaucoma. *Arch Ophthalmol*. 2006;124:793–797.
206. Wax MB, Camras CB, Fiscella RG, et al. Emerging perspectives in glaucoma: optimizing 24-hour control of intraocular pressure. *Am J Ophthalmol*. 2002;133(Suppl.):S1–10.
207. Lee GA, Khaw PT, Ficker LA, et al. The corneal thickness and intraocular pressure story: where are we now? *Clin Experiment Ophthalmol*. 2002;30:334–337.
208. Leonardi M, Pitchon EM, Bertsch A, et al. Wireless contact lens sensor for intraocular pressure monitoring: assessment on enucleated pig eyes. *Acta Ophthalmol*. 2009;87:433–437.
209. Leonardi M, Leuenberger P, Bertrand D, et al. First steps toward noninvasive intraocular pressure monitoring with a sensing contact lens. *Invest Ophthalmol Vis Sci*. 2004;45:3113–3117.
210. Kakaday T, Hewitt AW, Voelcker NH, et al. Advances in telemetric continuous intraocular pressure assessment. *Br J Ophthalmol*. 2009;93:992–996.
211. Stangel K, Kolnsberg S, Hammerschmidt D, et al. A programmable intraocular CMOS pressure sensor system implant. *IEEE J Solid-State Circuits*. 2001;36:1094–1100.
212. Walter P, Schnakenberg U, vom Bogel G, et al. Development of a completely encapsulated intraocular pressure sensor. *Ophthalmic Res*. 2000;32:278–284.
213. Chen P-J, Rodger DC, Humayan MS, et al. Unpowered sprial-tube parylene pressure sensor for intraocular pressure sensing. *Sens Actuators A Phys*. 2006;127:276–282.
214. Rizq RN, Choi WH, Eilers D, et al. Intraocular pressure measurement at the choroid surface: a feasibility study with implications for implantable microsystems. *Br J Ophthalmol*. 2001;85:868–871.
215. Chow EY, Yang CL, Chlebowski A, et al. Implantable

wireless telemetry boards for in vivo transocular transmission. *IEEE Trans Microw Theory Tech*. 2008;56:3200–3208.
216. Prow TW, Bhutto I, Grebe R, et al. Nanoparticle-delivered biosensor for reactive oxygen species in diabetes. *Vision Res*. 2008;48:478–485.
217. Becerra SP. Focus on molecules: pigment epithelium-derived factor (PEDF). *Exp Eye Res*. 2006;82:739–740.
218. Jones BW, Watt CB, Frederick JM, et al. Retinal remodeling triggered by photoreceptor degenerations. *J Comp Neurol*. 2003;464:1–16.
219. Milam AH, Li ZY, Fariss RN. Histopathology of the human retina in retinitis pigmentosa. *Prog Retin Eye Res*. 1998;17:175–205.
220. Lakhanpal RR, Yanai D, Weiland JD, et al. Advances in the development of visual prostheses. *Curr Opin Ophthalmol*. 2003;14:122–127.
221. Chen SJ, Mahadevappa M, Roizenblatt R, et al. Neural responses elicited by electrical stimulation of the retina. *Trans Am Ophthalmol Soc*. 2006;104:252–259.
222. Zrenner E. Will retinal implants restore vision? *Science*. 2002;295:1022–1025.
223. Weiland JD, Liu W, Humayun MS. Retinal prosthesis. *Annu Rev Biomed Eng*. 2005;7:361–401.
224. Choi SY, Sheng Z, Kramer RH. Imaging light-modulated release of synaptic vesicles in the intact retina: retinal physiology at the dawn of the post-electrode era. *Vision Res*. 2005;45:3487–3495.
225. Nagel G, Szellas T, Huhn W, et al. Channelrhodopsin-2, a directly light-gated cation-selective membrane channel. *Proc Natl Acad Sci USA*. 2003;100:13940–13945.
226. Bi A, Cui J, Ma YP, et al. Ectopic expression of a microbial-type rhodopsin restores visual responses in mice with photoreceptor degeneration. *Neuron*. 2006;50:23–33.
227. Lagali PS, Balya D, Awatramani GB, et al. Light-activated channels targeted to ON bipolar cells restore visual function in retinal degeneration. *Nat Neurosci*. 2008;11:667–675.
228. Tomita H, Sugano E, Yawo H, et al. Restoration of visual

response in aged dystrophic RCS rats using AAV-mediated channelopsin-2 gene transfer. *Invest Ophthalmol Vis Sci*. 2007;48:3821–3826.
229. Bowes C, Li T, Danciger M, et al. Retinal degeneration in the rd mouse is caused by a defect in the beta subunit of rod cGMP-phosphodiesterase. *Nature*. 1990;347:677–680.
230. D'Cruz PM, Yasumura D, Weir J, et al. Mutation of the receptor tyrosine kinase gene Mertk in the retinal dystrophic RCS rat. *Hum Mol Genet*. 2000;9:645–651.
231. Ivanova E, Pan ZH. Evaluation of the adeno-associated virus mediated long-term expression of channelrhodopsin-2 in the mouse retina. *Mol Vis*. 2009;15:1680–1689.
232. Wassle H. Parallel processing in the mammalian retina. *Nat Rev Neurosci*. 2004;5:747–757.
233. Jacobs AL, Werblin FS. Spatiotemporal patterns at the retinal output. *J Neurophysiol*. 1998;80:447–451.
234. Ivanova E, Hwang GS, Pan ZH, et al. Evaluation of AAV-mediated expression of Chop2-GFP in the marmoset retina. *Invest Ophthalmol Vis Sci*. 2010;51:5288–5296.
235. Dalkara D, Kolstad KD, Caporale N, et al. Inner limiting membrane barriers to AAV-mediated retinal transduction from the vitreous. *Mol Ther*. 2009;17:2096–2102.
236. van Wyk M, Pielecka-Fortuna J, Lowel S, et al. Restoring the ON switch in blind retinas: opto-mglur6, a next-generation, cell-tailored optogenetic tool. *PLoS Biol*. 2015;13(5):e1002143.
237. Zhang Y, Ivanova E, Bi A, et al. Ectopic expression of multiple microbial rhodopsins restores ON and OFF light responses in retinas with photoreceptor degeneration. *J Neurosci*. 2009;29:9186–9196.
238. Doroudchi MM, Greenberg KP, Liu J, et al. Virally delivered channelrhodopsin-2 safely and effectively restores visual function in multiple mouse models of blindness. *Mol Ther*. 2011;19(7):1220–1229.
239. Marc RE, Jones BW, Watt CB, et al. Extreme retinal remodeling triggered by light damage: implications for age related macular degeneration. *Mol Vis*. 2008;14:782–806.
240. Strettoi E, Pignatelli V, Rossi C, et al. Remodeling of second-order neurons in the retina of rd/rd mutant mice. *Vision Res*.

2003;43:867–877.
241. Gargini C, Terzibasi E, Mazzoni F, et al. Retinal organization in the retinal degeneration 10 (rd10) mutant mouse: a morphological and ERG study. *J Comp Neurol*. 2007;500:222–238.
242. Greenberg KP, Pham A, Werblin FS. Differential targeting of optical neuromodulators to ganglion cell soma and dendrites allows dynamic control of center-surround antagonism. *Neuron*. 2011;69:713–720.
243. Busskamp V, Duebel J, Balya D, et al. Genetic reactivation of cone photoreceptors restores visual responses in retinitis pigmentosa. *Science*. 2010;329:413–417.
244. Fortin DL, Banghart MR, Dunn TW, et al. Photochemical control of endogenous ion channels and cellular excitability. *Nat Methods*. 2008;5:331–338.
245. Caporale N, Kolstad KD, Lee T, et al. LiGluR restores visual responses in rodent models of inherited blindness. *Mol Ther*. 2011;19:1212–1219.
246. Ahuja AK, Dorn JD, Caspi A, et al. Blind subjects implanted with the Argus II retinal prosthesis are able to improve performance in a spatial-motor task. *Br J Ophthalmol*. 2011;95:539–543.
247. Winter JO, Han N, Jensen R, et al. Adhesion molecules promote chronic neural interfaces following neurotrophin withdrawal. *Conf Proc IEEE Eng Med Biol Soc*. 2009;2009:7151–7154.
248. Kelly SK, Shire DB, Chen J, et al. Realization of a 15-channel, hermetically-encased wireless subretinal prosthesis for the blind. *Conf Proc IEEE Eng Med Biol Soc*. 2009;2009:200–203.
249. Zrenner E, Bartz-Schmidt KU, Benav H, et al. Subretinal electronic chips allow blind patients to read letters and combine them to words. *Proc Biol Sci*. 2011;278:1489–1497.
250. Julien S, Peters T, Ziemssen F, et al. Implantation of ultrathin, biofunctionalized polyimide membranes into the subretinal space of rats. *Biomaterials*. 2011;32:3890–3898.
251. Fujikado T, Kamei M, Sakaguchi H, et al. Testing of semichronically implanted retinal prosthesis by suprachoroidal-transretinal stimulation in patients with

retinitis pigmentosa. *Invest Ophthalmol Vis Sci*. 2011;52:4726–4733.
252. Finlayson PG, Iezzi R. Glutamate stimulation of retinal ganglion cells in normal and s334ter-4 rat retinas: a candidate for a neurotransmitter-based retinal prosthesis. *Invest Ophthalmol Vis Sci*. 2010;51:3619–3628.
253. Kotov NA, Winter JO, Jan E, et al. Nanomaterials for neural interfaces. *Adv Mater*. 2009;21:3970–4004.
254. Lovric J, Bazzi HS, Cuie Y, et al. Differences in subcellular distribution and toxicity of green and red emitting CdTe quantum dots. *J Mol Med*. 2005;83:377–385.
255. Chan WH, Shiao NH, Lu PZ. CdSe quantum dots induce apoptosis in human neuroblastoma cells via mitochondrial-dependent pathways and inhibition of survival signals. *Toxicol Lett*. 2006;167:191–200.
256. Choi AO, Cho SJ, Desbarats J, et al. Quantum dot-induced cell death involves Fas upregulation and lipid peroxidation in human neuroblastoma cells. *J Nanobiotechnology*. 2007;5:1.
257. Maysinger D, Behrendt M, Lalancette-Hebert M, et al. Real-time imaging of astrocyte response to quantum dots: in vivo screening model system for biocompatibility of nanoparticles. *Nano Lett*. 2007;7:2513–2520.
258. Oberdorster E. Manufactured nanomaterials (fullerenes, C60) induce oxidative stress in the brain of juvenile largemouth bass. *Environ Health Perspect*. 2004;112:1058–1062.
259. Kim DH, Martin DC. Sustained release of dexamethasone from hydrophilic matrices using PLGA nanoparticles for neural drug delivery. *Biomaterials*. 2006;27:3031–3037.
260. Bharali DJ, Klejbor I, Stachowiak EK, et al. Organically modified silica nanoparticles: a nonviral vector for in vivo gene delivery and expression in the brain. *Proc Natl Acad Sci USA*. 2005;102:11539–11544.
261. Zou LL, Huang L, Hayes RL, et al. Liposome-mediated NGF gene transfection following neuronal injury: potential therapeutic applications. *Gene Ther*. 1999;6:994–1005.
262. Green RA, Lovell NH, Wallace GG, et al. Conducting polymers for neural interfaces: challenges in developing an

effective long-term implant. *Biomaterials*. 2008;29:3393–3399.
263. Abidian MR, Kim D-H, Martin DC. Conducting-polymer nanotubes for controlled drug release. *Adv Mater*. 2006;18:405–409.
264. Kim D-H, Richardson-Burns SM, Hendricks JL, et al. Effect of immobilized nerve growth factor on conductive polymers: electrical properties and cellular responses. *Adv Funct Mater*. 2007;17:79–86.
265. Cui X, Lee VA, Raphael Y, et al. Surface modification of neural recording electrodes with conducting polymer/biomolecule blends. *J Biomed Mater Res*. 2001;56:261–272.
266. Decher G. Fuzzy nanoassemblies: toward layered polymeric multicomposites. *Science*. 1997;277:1232–1237.
267. Gheith MK, Pappas TC, Lioppo AV, et al. Stimulation of neural cells by lateral currents in conductive layer-by-layer films of single-walled carbon nanotubes. *Adv Mater*. 2006;18:2975–2979.
268. Sinani VA, Koktysh DS, Yun B-G, et al. Collagen coating promotes biocompatibility of semiconductor nanoparticles in stratified LBL films. *Nano Lett*. 2003;3:1177–1183.
269. Pappas TC, Wickramanyake WM, Jan E, et al. Nanoscale engineering of a cellular interface with semiconductor nanoparticle films for photoelectric stimulation of neurons. *Nano Lett*. 2007;7:513–519.
270. Ha S, Khraiche ML, Akinin A, et al. Towards high-resolution retinal prostheses with direct optical addressing and inductive telemetry. *J Neural Eng*. 2016;13(5):056008.
271. Rama P, Matuska S, Paganoni G, et al. Limbal stem-cell therapy and long-term corneal regeneration. *N Engl J Med*. 2010;363:147–155.
272. Lewis GP, Linberg KA, Fisher SK. Neurite outgrowth from bipolar and horizontal cells after experimental retinal detachment. *Invest Ophthalmol Vis Sci*. 1998;39:424–434.
273. Lamba DA, Gust J, Reh TA. Transplantation of human embryonic stem cell-derived photoreceptors restores some visual function in Crx-deficient mice. *Cell Stem Cell*. 2009;4:73–79.

274. Lamba DA, Karl MO, Reh TA. Strategies for retinal repair: cell replacement and regeneration. *Prog Brain Res*. 2009;175:23–31.
275. Lamba DA, Karl MO, Ware CB, et al. Efficient generation of retinal progenitor cells from human embryonic stem cells. *Proc Natl Acad Sci USA*. 2006;103:12769–12774.
276. Lamba DA, McUsic A, Hirata RK, et al. Generation, purification and transplantation of photoreceptors derived from human induced pluripotent stem cells. *PLoS ONE*. 2010;5:e8763.
277. Ikeda H, Osakada F, Watanabe K, et al. Generation of Rx+/Pax6+ neural retinal precursors from embryonic stem cells. *Proc Natl Acad Sci USA*. 2005;102:11331–11336.
278. Osakada F, Ikeda H, Mandai M, et al. Toward the generation of rod and cone photoreceptors from mouse, monkey and human embryonic stem cells. *Nat Biotechnol*. 2008;26:215–224.
279. Hirami Y, Osakada F, Takahashi K, et al. Generation of retinal cells from mouse and human induced pluripotent stem cells. *Neurosci Lett*. 2009;458:126–131.
280. Osakada F, Jin ZB, Hirami Y, et al. In vitro differentiation of retinal cells from human pluripotent stem cells by small-molecule induction. *J Cell Sci*. 2009;122:3169–3179.
281. Meyer JS, Katz ML, Maruniak JA, et al. Embryonic stem cell-derived neural progenitors incorporate into degenerating retina and enhance survival of host photoreceptors. *Stem Cells*. 2006;24:274–283.
282. Seiler MJ, Aramant RB, Thomas BB, et al. Visual restoration and transplant connectivity in degenerate rats implanted with retinal progenitor sheets. *Eur J Neurosci*. 2010;31:508–520.
283. MacLaren RE, Pearson RA, MacNeil A, et al. Retinal repair by transplantation of photoreceptor precursors. *Nature*. 2006;444:203–207.
284. Gust J, Reh TA. Adult donor rod photoreceptors integrate into the mature mouse retina. *Invest Ophthalmol Vis Sci*. 2011;52(8):5266–5272.
285. Tomita M, Lavik E, Klassen H, et al. Biodegradable polymer

composite grafts promote the survival and differentiation of retinal progenitor cells. *Stem Cells*. 2005;23:1579–1588.
286. Karl MO, Reh TA. Regenerative medicine for retinal diseases: activating endogenous repair mechanisms. *Trends Mol Med*. 2010;16:193–202.
287. Li JR, Shi L, Deng Z, et al. Nanostructures of designed geometry and functionality enable regulation of cellular signaling processes. *Biochemistry*. 2012;51(30):5876–5893.
288. Kim DH, Lee H, Lee YK, et al. Biomimetic nanopatterns as enabling tools for analysis and control of live cells. *Adv Mater*. 2010;22(41):4551–4566.
289. Kelleher CM, Vacanti JP. Engineering extracellular matrix through nanotechnology. *J R Soc Interface*. 2010;7(Suppl. 6):S717–29.
290. Heydarkhan-Hagvall S, Choi CH, Dunn J, et al. Influence of systematically varied nano-scale topography on cell morphology and adhesion. *Cell Commun Adhes*. 2007;14(5):181–194.
291. Johansson F, Carlberg P, Danielsen N, et al. Axonal outgrowth on nano-imprinted patterns. *Biomaterials*. 2006;27(8):1251–1258.
292. Kantawong F, Burgess KE, Jayawardena K, et al. Whole proteome analysis of osteoprogenitor differentiation induced by disordered nanotopography and mediated by ERK signalling. *Biomaterials*. 2009;30(27):4723–4731.
293. Dalby MJ, Gadegaard N, Wilkinson CD. The response of fibroblasts to hexagonal nanotopography fabricated by electron beam lithography. *J Biomed Mater Res A*. 2008;84(4):973–979.
294. Lamers E, Walboomers XF, Domanski M, et al. The influence of nanoscale grooved substrates on osteoblast behavior and extracellular matrix deposition. *Biomaterials*. 2010;31(12):3307–3316.
295. Choi JS, Lee SJ, Christ GJ, et al. The influence of electrospun aligned poly(epsilon-caprolactone)/collagen nanofiber meshes on the formation of self-aligned skeletal muscle myotubes. *Biomaterials*. 2008;29(19):2899–2906.
296. Panseri S, Cunha C, Lowery J, et al. Electrospun micro- and

nanofiber tubes for functional nervous regeneration in sciatic nerve transections. *BMC Biotechnol*. 2008;8:39.
297. Ma K, Liao S, He L, et al. Effects of nanofiber/stem cell composite on wound healing in acute full-thickness skin wounds. *Tissue Eng Part A*. 2011;17(9–10):1413–1424.
298. Xie J, Willerth SM, Li X, et al. The differentiation of embryonic stem cells seeded on electrospun nanofibers into neural lineages. *Biomaterials*. 2009;30(3):354–362.
299. Bonadio J. Tissue engineering via local gene delivery: update and future prospects for enhancing the technology. *Adv Drug Deliv Rev*. 2000;44(2–3):185–194.
300. Endo M, Kuroda S, Kondo H, et al. Bone regeneration by modified gene-activated matrix: effectiveness in segmental tibial defects in rats. *Tissue Eng*. 2006;12(3):489–497.
301. Pot SA, Liliensiek SJ, Myrna KE, et al. Nanoscale topography-induced modulation of fundamental cell behaviors of rabbit corneal keratocytes, fibroblasts, and myofibroblasts. *Invest Ophthalmol Vis Sci*. 2010;51:1373–1381.
302. Sugino IK, Gullapalli VK, Sun Q, et al. Cell-deposited matrix improves retinal pigment epithelium survival on aged submacular human Bruch's membrane. *Invest Ophthalmol Vis Sci*. 2011;52:1345–1358.
303. Scadden DT. The stem-cell niche as an entity of action. *Nature*. 2006;441:1075–1079.
304. Park J, Bauer S, von der Mark K, et al. Nanosize and vitality: TiO_2 nanotube diameter directs cell fate. *Nano Lett*. 2007;7:1686–1691.
305. Chua KN, Chai C, Lee PC, et al. Surface-aminated electrospun nanofibers enhance adhesion and expansion of human umbilical cord blood hematopoietic stem/progenitor cells. *Biomaterials*. 2006;27:6043–6051.
306. Dalby MJ, McCloy D, Robertson M, et al. Osteoprogenitor response to defined topographies with nanoscale depths. *Biomaterials*. 2006;27:1306–1315.
307. Steedman MR, Tao SL, Klassen H, et al. Enhanced differentiation of retinal progenitor cells using microfabricated topographical cues. *Biomed Microdevices*. 2010;12:363–369.

308. Recknor JB, Sakaguchi DS, Mallapragada SK. Directed growth and selective differentiation of neural progenitor cells on micropatterned polymer substrates. *Biomaterials*. 2006;27:4098–4108.
309. Mooney DJ, Vandenburgh H. Cell delivery mechanisms for tissue repair. *Cell Stem Cell*. 2008;2:205–213.
310. Silva GA, Czeisler C, Niece KL, et al. Selective differentiation of neural progenitor cells by high-epitope density nanofibers. *Science*. 2004;303:1352–1355.
311. Ellis-Behnke RG, Liang YX, You SW, et al. Nano neuro knitting: peptide nanofiber scaffold for brain repair and axon regeneration with functional return of vision. *Proc Natl Acad Sci USA*. 2006;103:5054–5059.
312. Streilein JW. Ocular immune privilege: the eye takes a dim but practical view of immunity and inflammation. *J Leukoc Biol*. 2003;74(2):179–185.
313. Zhang X, Bok D. Transplantation of retinal pigment epithelial cells and immune response in the subretinal space. *Invest Ophthalmol Vis Sci*. 1998;39(6):1021–1027.
314. Hynes SR, Lavik EB. A tissue-engineered approach towards retinal repair: scaffolds for cell transplantation to the subretinal space. *Graefes Arch Clin Exp Ophthalmol*. 2010;248:763–778.
315. Lavik EB, Klassen H, Warfvinge K, et al. Fabrication of degradable polymer scaffolds to direct the integration and differentiation of retinal progenitors. *Biomaterials*. 2005;26:3187–3196.
316. Redenti S, Tao S, Yang J, et al. Retinal tissue engineering using mouse retinal progenitor cells and a novel biodegradable, thin-film poly(e-caprolactone) nanowire scaffold. *J Ocul Biol Dis Infor*. 2008;1:19–29.
317. Sodha S, Wall K, Redenti S, et al. Microfabrication of a three-dimensional polycaprolactone thin-film scaffold for retinal progenitor cell encapsulation. *J Biomater Sci Polym Ed*. 2011;22:443–456.
318. Tao SL, Desai TA. Micromachined devices: the impact of controlled geometry from cell-targeting to bioavailability. *J Control Release*. 2005;109:127–138.

319. Lu B, Tai YC, Humayun MS. Microdevice-based cell therapy for age-related macular degeneration. *Dev Ophthalmol*. 2014;53:155–166.
320. Sacconi L, O'Connor RP, Jasaitis A, et al. In vivo multiphoton nanosurgery on cortical neurons. *J Biomed Opt*. 2007;12:050502.
321. Ellis-Behnke RG, Teather LA, Schneider GE, et al. Using nanotechnology to design potential therapies for CNS regeneration. *Curr Pharm Des*. 2007;13:2519–2528.
322. Wang BG, Halbhuber KJ. Corneal multiphoton microscopy and intratissue optical nanosurgery by nanojoule femtosecond near-infrared pulsed lasers. *Ann Anat*. 2006;188:395–409.
323. Leary SP, Liu CY, Apuzzo ML. Toward the emergence of nanoneurosurgery: part III – nanomedicine: targeted nanotherapy, nanosurgery, and progress toward the realization of nanoneurosurgery. *Neurosurgery*. 2006;58:1009–1026 [discussion-26].
324. Fankhauser F, Niederer PF, Kwasniewska S, et al. Supernormal vision, high-resolution retinal imaging, multiphoton imaging and nanosurgery of the cornea – a review. *Technol Health Care*. 2004;12:443–453.
325. Konig K. Robert Feulgen Prize Lecture. Laser tweezers and multiphoton microscopes in life sciences. *Histochem Cell Biol*. 2000;114:79–92.
326. Kim P, Lieber CM. Nanotube nanotweezers. *Science*. 1999;286:2148–2150.
327. Bhisitkul RB, Keller CG. Development of microelectromechanical systems (MEMS) forceps for intraocular surgery. *Br J Ophthalmol*. 2005;89:1586–1588.
328. Zhang LW, Monteiro-Riviere NA. Mechanisms of quantum dot nanoparticle cellular uptake. *Toxicol Sci*. 2009;110:138–155.
329. Hoet P, Legiest B, Geys J, et al. Do nanomedicines require novel safety assessments to ensure their safety for long-term human use? *Drug Saf*. 2009;32:625–636.
330. Magrez A, Kasas S, Salicio V, et al. Cellular toxicity of carbon-based nanomaterials. *Nano Lett*. 2006;6:1121–1125.

331. Zhu L, Chang DW, Dai L, et al. DNA damage induced by multiwalled carbon nanotubes in mouse embryonic stem cells. *Nano Lett*. 2007;7:3592–3597.

39

Neuroprotection

Benedetto Falsini, Ronald A. Bush, Paul A. Sieving

History and Definitions

The process of neuronal cell death following different types of

injury involves apoptosis. Blocking the apoptotic cascade leading to cell death may prevent cell death and consequent loss following neuronal injury (neuroprotection). Loss of neural visual cells means effective loss of vision. Hence, neuroprotection strategies are needed to maintain neuronal integrity or to keep damaged cells functioning. In glaucoma, intraocular pressure (IOP) lowering aims to prevent the insult that leads to retinal ganglion cell (RGC) injury. Neuroprotection aims to maintain function despite injury. Over the past 20 years, many laboratory studies of potential neuroprotective agents have yielded promising results. However, the same agents have subsequently failed to show significant neuroprotective activity in humans. Therefore, any evidence of neuroprotection in humans must be confirmed by controlled human clinical trials.

The present chapter will review the basic and clinical evidence in support of the action of different neuroprotective agents for retinal cells. Evidence will be reviewed on neuroprotection as applied to major fields of retinal pathology, glaucoma, and photoreceptor degenerations.

Retinal Ganglion Cell Glaucomatous Disease

Glaucoma is a degenerative optic neuropathy characterized by loss of RGCs and their axons and warrants consideration under retinal neuroprotection strategies. Elevated IOP is a principal risk factor. However, recent evidence indicates that IOP control does not prevent glaucomatous progression in all patients and that vision loss continues in some susceptible individuals despite lowering the IOP. RGCs are terminally differentiated neurons and cannot regenerate by cell division. Optic nerve damage is irreversible. The main goal of neuroprotection is to keep these cells alive to augment the therapeutic benefit achieved by lowering the IOP. Neuroprotection in glaucoma offers a means to prevent the irreversible loss of RGC and ideally should be efficacious irrespective of the specific pathophysiology of the disease.[1–3]

Three decades of work have established the causal relationship between elevated IOP and the development of optic nerve damage through a series of clinical treatment studies supported by the National Eye Institute (NEI), including the Advanced Glaucoma

Intervention Study trial, the Collaborative Initial Glaucoma Treatment Study Trial,[4] and the Early Manifest Glaucoma Trial.[5] However, glaucomatous optic neuropathy can occur despite having ocular pressures within a normal range. In some populations only half of glaucoma cases involve IOP elevated beyond the traditional demarcation of 20 mmHg pressure.[6] Even in this condition of "low-tension glaucoma," IOP remains a risk factor, as lowering the IOP further retards the loss of vision and presumptive retention of ganglion cells as monitored through nerve fiber volume in the optic nerve cup. This was shown in the Collaborative Normal Tension Glaucoma Study.[7] Nevertheless, a number of individuals continue to suffer progressive glaucomatous optic nerve damage and vision impairment despite appropriate regulation of IOPs. It is these cases in particular that would benefit from an alternate strategy of neuroprotection, aimed at preventing RGC death.

Among the first studies to demonstrate pharmacologic modulation of neural damage in glaucoma was that of Bernard Becker and colleagues using oral administration of diphenylhydantoin (phenytoin).[8] Diphenylhydantoin is an antiepileptic agent for controlling seizures but without the sedative effects of phenobarbital. It stabilizes the inactive state of voltage-gated sodium channels which could modulate glutamatergic transmission, and it is neuroprotective in a rat model with elevated IOP from cautery of episcleral veins.[9] Diphenylhydantoin has a wide range of actions on neurons and primarily involves cell excitability, and the potential protective action on RGCs could be through ameliorating excitotoxic *N*-methyl-D-aspartate (NMDA) action on third-order retinal neurons. While diphenylhydantoin has numerous neurologic effects and has been tried as a central nervous system (CNS) neuroprotective agent in a number of clinical trials, it has consistently failed to meet clinical endpoints in trial.

Two neuroactive drugs that have antiexcitotoxicity action currently have US Food and Drug Administration approval for CNS degenerative conditions, although clinical efficacy is limited. Riluzole extends life expectancy for amyotrophic lateral sclerosis patients by up to 3 months, and memantine is approved for advanced Alzheimer's disease and provides some improvement in cognition and behavior.[10] Riluzole blocks glutamatergic

neurotransmission in the CNS by inhibiting release of glutamic acid, possibly through inactivation of voltage-dependent sodium channels.[11] It may act at presynaptic NMDA receptors.[12]

Memantine is an antagonist at NMDA receptors[13] and was originally developed as a dopaminergic compound derivative from amantadine, which has approval for treatment of Parkinson disease. Memantine has therapeutic benefit against excitoneurotoxicity mediated by action of NMDA receptors. A broad-spectrum blockade of NMDA channels would not be physiologically attractive. However, memantine does not compete with glutamate for the binding site. Rather, memantine binds only to open-state NMDA channels. It does not impede neuronal synaptic signal transmission in the physiologic range, as it is competitive only for high levels of glutamate that lead to neuronal damage and death through excitotoxic mechanisms caused by excessive activation of NMDA receptors. The drug is well tolerated in treatment of Alzheimer's dementia without apparent side-effects, suggesting that, when applied to physiologic neuronal states, it does not impede neuronal activity. Studies indicate that memantine decreases the level of free glutamate in the vitreous of a dog glaucoma disease model[14] and in monkey and human glaucoma,[15] although some of this work is not fully accepted. This provides a basis for considering NMDA receptor antagonists in a neuroprotection strategy for glaucoma.

Large-scale formal studies of memantine have been conducted involving patients with chronic glaucoma. In 2000–2006, Allergan ran a phase III randomized, placebo-controlled trial to evaluate the efficacy of memantine in 1179 patients aged 18–82 years old.[4] Entry criteria required evidence of glaucomatous damage by examination of the optic nerve head accompanied by visual field loss. Subjects with all forms of open angle and chronic angle closure glaucoma were entered, including having prior glaucoma filtration surgery. Two treatment arms had different doses of memantine versus an oral placebo for glaucoma patients with otherwise controlled IOP. Visual fields were monitored every 6 months for evidence of progression as the outcome measure. Unfortunately, the trial failed to meet endpoint significance versus placebo control. As the outcome has not been formally submitted for publication,

information on the outcome is limited, but the memantine trials demonstrated statistically significant visual field benefit under high dose conditions compared to lower dose, although the overall trial significance failed at efficacy compared to control.[4] Precise reasons for failure are not understood, but it may have had to do with study design and handling of data acquisition at the point that a subject reached the clinical endpoint. The medical glaucoma field, nonetheless, remains optimistic that the strategy of neuroprotection for RGC degenerative disease remains important for study and will ultimately yield compounds that can augment lowering of IOP in glaucoma.[1,5]

Neurotrophic Factors in Glaucoma

Recent studies suggest that neurotrophic factors may have therapeutic benefit for individuals with advanced glaucoma. Lambiase and colleagues[2] demonstrated that application of nerve growth factor (NGF) in glaucomatous rats protects the RGCs from apoptotic cell death. Rats were made glaucomatous through injection of hypertonic saline into the episcleral vein, and NGF was applied topically in one of two doses (100 and 200 μg/mL). Cell biology studies indicated that molecules upstream of the apoptotic pathway, including Bax and BCL-2, were lower in treated animals, and morphometric analysis showed a significant preservation of RGC counts in the treated eyes.

These investigators then initiated a pilot human study of 3 patients with advanced glaucoma, who underwent careful electrophysiologic and psychophysical visual testing at baseline and after topical NGF eye drops applied four times daily for 3 months.[2] The subjects were evaluated by multiple parameters, including visual acuity, contrast sensitivity, pattern electroretinogram (ERG), and visual-evoked potentials, along with optic disc photography. While this study was too small to provide a definitive outcome, several of these test parameters indicated improved retinal function at the level of ganglion cells, consistent with inhibiting RGC apoptosis observed in the glaucomatous rats by NGF.

The pharmaceutical industry is considering other neurotrophic factors, including ciliary neurotrophic factors (CNTF) for glaucoma

rescue. Van Adel and colleagues have demonstrated that continuous administration of CNTF protects RGCs in animal models.[3] Neurotech has initiated preclinical studies using its encapsulated cell technology (ECT) devices in which epithelial cells transfected with the *CNTF* gene are sequestered and release low but therapeutic levels for months' to years' duration. Efficacy of other neurotrophic factors for RGC rescue has been demonstrated,[16] such as brain-derived neurotrophic factor (BDNF), which can protect RGCs following optic nerve crush in cat by intravitreal injection.[17] BDNF also promotes regeneration of spinal cord axons following axotomy.[18] Recently[19] the effectiveness of topical eye treatment with BDNF to preserve vision was shown in an experimental established model, the DBA/2J mouse, which develops progressive eye abnormalities mimicking human open angle glaucoma. Visual function was monitored using pattern electroretinogram (P-ERG) and visual cortical evoked potentials (VEP). RGC density was assessed using Brn-3 immunolabeling. Repeated application of human recombinant BDNF eye drops (12 µg/µl every 48 h for two weeks) was able to prevent P-ERG and VEP impairment in 7 month DBA/2J mice, also reducing the decline in Brn-3 immunopositive RGCs. Remarkably, BDNF eye application induced prominent increase of BDNF retinal level. Results suggested that topical eye treatment with BDNF represents a safe and feasible strategy to preserve visual function and diminish RGC vulnerability to ocular hypertension in glaucoma.

Neuroprotection Through the Serotonin Pathway

A promising area of neuroprotection research involves the serotonin (5HT) pathway. Memantine, in addition to its direct antiexcitotoxic effects as an NMDA receptor antagonist, is a noncompetitive antagonist at the 5HT3 receptor[20] which may be part of the memantine neuroprotection mechanism for Alzheimer's neural disease.[21] Recent literature indicates that serotonergic compounds, such as the selective serotonin reuptake inhibitor antidepressant agents, potentiate neurite sprouting by NGF.[22] The

retina has 5HT receptors, but whether this putative mechanism has relevance to retinal and/or glaucomatous disease is not currently known.

Agonists that stimulate the 5HT system are neuroprotective for RGCs.[23] Unfortunately, 5HT agonists have hallucinogenic action, and broad-action agonists at 5HT receptors would not be suitable for human glaucoma treatment. Among the interesting compounds in this regard is an indazole compound AL-34662 that is a selective 5HT receptor agonist at 5-HT-2A receptors and that lowers ocular pressure but which does not cross the blood–brain barrier.[24]

Neurotrophic Factors for Retinitis Pigmentosa

Roy Steinberg and Matthew LaVail and their group[25] made the seminal observation that neurotrophic factors could rescue photoreceptor cell death in an animal model of retinitis pigmentosa (RP). This observation in 1990 changed the face of research in photoreceptor neurodegenerative disease. Steinberg and LaVail and their colleagues showed that a single intraocular application of basic fibroblast growth factor (bFGF) delayed the loss of rod photoreceptors in the Royal College of Surgeons (RCS) rat. The rescue of the rods was panretinal, with a gradient of rescue highest near the injection site. This observation was subsequently extended to other genetic and environmental causes of photoreceptor cell death, including the light exposure damage model,[26] in which the protection was shown to extend to other cytokines and neurotrophic factors beyond bFGF alone. These observations occurred during a time of great explosion of the field of photoreceptor degeneration research, including the laboratory creation of genetic models, including the P23H rhodopsin transgenic rat that mimicked human RP.[27,28] Multiple neurotrophic factors have subsequently been found to rescue the rod cells in this rodent RP model.[26]

Exploration of this rescue proceeded along multiple lines, including cell biology of mechanisms,[29,30] and by multiple delivery approaches, including application using gene delivery with adeno-

associated virus (AAV) vector.[31] Experiments with control animals subjected to mechanical injury by insertion of a "dry" needle into the retina[32] also showed a surprising rescue of the rod photoreceptors. It was soon recognized that mechanical injury itself led to upregulation of expression of bFGF and CNTF. The precise mechanism of rescue was studied intensely but remained difficult to elucidate, and it is currently believed that the rescue is indirect and mediated through retinal glial cells which have receptors for neurotrophic factors, whereas the adult rods do not.[29] Several of the factors activate the Jak-STAT pathway.[29] Both NGF[30] and CNTF[31] were shown in other animal models to slow down photoreceptor loss quite significantly. NGF is the original neurotrophic factor identified in the 1950s by Rita Levi-Montalcini,[33,34] who subsequently received the Nobel Prize for demonstrating that NGF acts on morphologic differentiation of neural crest-derived cells and on peripheral and CNS neuronal cells. Cayouette and colleagues[35] demonstrated that CNTF rescued the "retinal degeneration slow" (rds) genetic mouse model of RP when applied by intraocular gene transfer that led to prolonged and stable CNTF expression in retina. They also showed that CNTF provided functional rescue of ERG potentials deriving from photoreceptor and bipolar cells and caused significant increase of the a-wave and b-wave of the rod-driven scotopic ERG.

CNTF Protein and Historical Selection

CNTF was first identified by Ruben Adler et al. as a factor in chick embryo extract that could support survival of chick ciliary neurons.[36] The factor was subsequently purified from the chick eye.[37] CNTF is a small 200-amino-acid 22-kDa protein that assembles into an α-helical tertiary structure. Adler[38] and McDonald et al.[39] subsequently proposed that CNTF expression is upregulated as a stress factor and released from cells, although the mechanism is not understood as the protein lacks a secretion sequence.[40]

Proteins interact with cells through a cellular receptor. The CNTF receptor is a trimeric construct that includes the CNTF α-receptor, the leukemia inhibitory factor receptor-β (LIFR-β), and gp130

component.[41] The CNTFRα soluble factor has been detected in cerebrospinal fluid and, consequently, a cell itself needs to express only LIFR-β and gp130. Subsequent binding of CNTF to this trimeric complex activates the Jak-STAT pathway[42] leading to gene transcription.[43] Ultimately, it is the upregulation of gene expression by CNTF that appears to be a crucial factor in human clinical trials of rod and cone rescue in photoreceptor degenerative diseases.

The effect of CNTF on nuclear activity was seen by AAV delivery of CNTF to RDS mice with peripherin mutation leading to slow death of rod photoreceptors.[44] There were several seminal observations in this study, including a further demonstration that vector-mediated gene therapy provided long-term and panretinal rescue of rod photoreceptors following a single intraocular application. Second, this particular study showed a potentially adverse consequence of CNTF, as ERG response amplitudes were diminished in the treated eyes compared to the fellow uninjected eyes. Third, the rod cell nuclei showed an increase in euchromatin and an increase in the size, resulting in increased thickness of the outer nuclear layer (ONL), which is composed exclusively of photoreceptor cell bodies containing the nuclei. They concluded that CNTF upregulated gene expression in the photoreceptor cell either directly or, more likely, indirectly. This interpretation was quickly replicated in the rabbit retina by application of CNTF using a novel delivery mode of encapsulated cell-based intraocular devices (the Neurotech ECT)[45] (Fig. 39.1). These devices release a continuous low level of CNTF protein into the vitreous, and hence, to the retina over weeks and months. Following implantation of ECT devices into the eye of normal rabbit, without retinal degeneration, the nuclear morphology changes, including dispersion of the nuclear chromatin, were consistent with DNA uncoiling that occurs during gene expression. The retinal function, as monitored by ERG recordings, was not affected, although high-dose CNTF suppressed the ERG for low-intensity stimuli. Cayouette et al. found that CNTF could augment retinal ERG function,[35] and Bush et al. observed[45] that CNTF did not adversely affect retinal function in lower dose, whereas the studies of Bok and colleagues[44] note that high-dose CNTF expression with a vigorous chick β actin promoter suppressed retinal ERG function: these

observations are consistent with CNTF having a safe biological range, beyond which it may cause potential retinal toxicity. A dose-ranging study in the rod–cone dystrophy 1 (RCD1) dog model of RP indicated that the ECT delivery approach spanned a sufficiently broad range of dosing that warranted safety study in a phase I human clinical trial for RP.

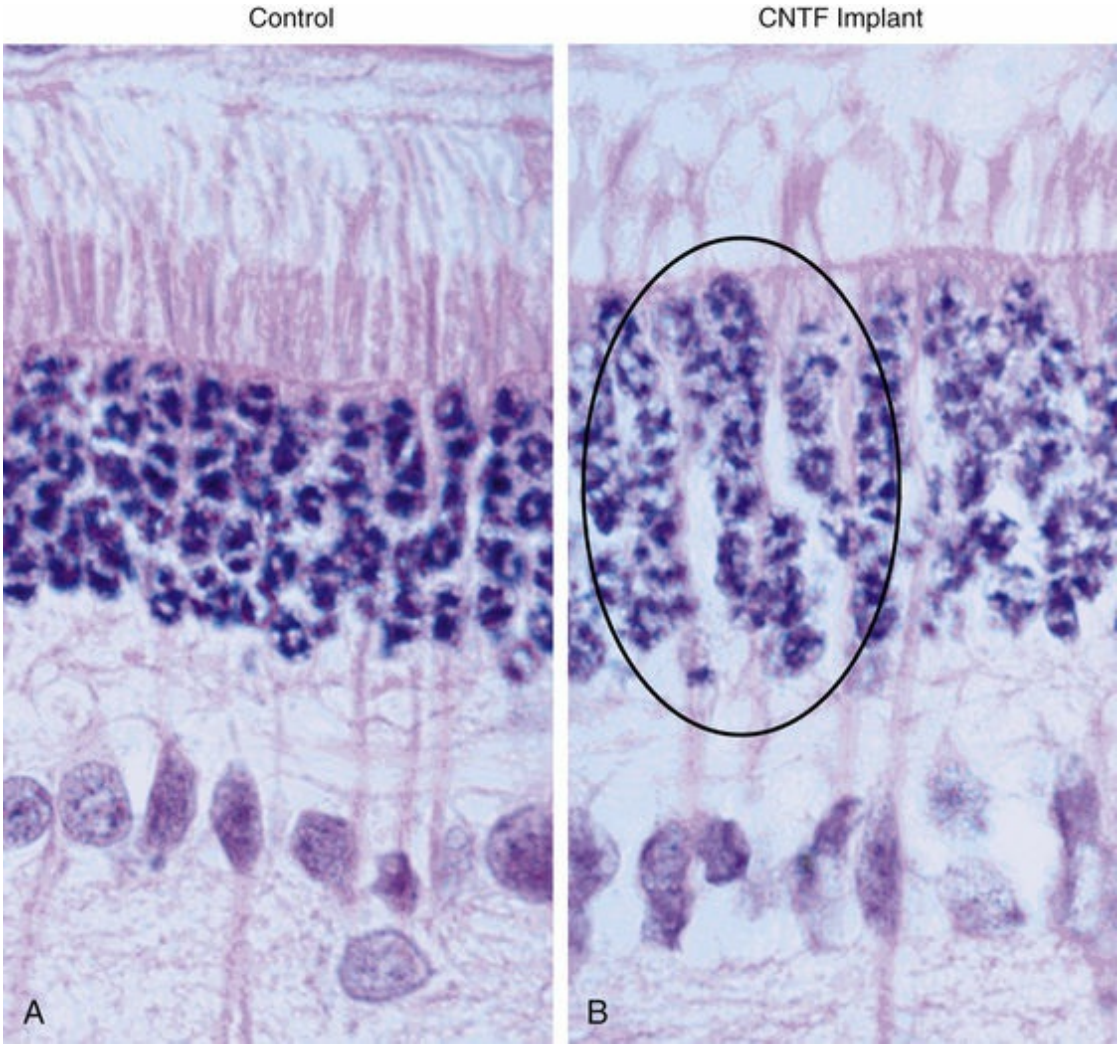

FIG. 39.1 (A,B) Ciliary neurotrophic factor (CNTF) intravitreal encapsulated cell technology implant releasing 1.5 ng/day in experimental rabbit P caused nuclear swelling and an increase in outer nuclear layer thickness due to rod photoreceptor nuclear chromatin uncoiling, indicating DNA transcriptional activity.

(Reproduced with permission from Bush RA, Lei B, Tao W, et al. Histology in dorsal central retina periphery. Encapsulated cell-based intraocular delivery of ciliary neurotrophic factor in normal rabbit: dose-dependent effects on ERG and retinal histology. Invest Ophthalmol Vis Sci 2004;45:2420–30.)

CNTF Phase I Trial for Human Photoreceptor Degeneration

A human phase I trial of CNTF for RP neurodegenerative diseases was conducted and reported in 2006 using the Neurotech ECT device for intraocular production and delivery of CNTF protein.[46] The device was surgically implanted in the eye of 10 study participants with advanced RP that severely limited their overall vision, including severe degradation of visual acuity (Fig. 39.2). The devices were implanted through a small pars plana incision which was closed by a single suture, causing minimal trauma to the eye, with the exception of one participant who had a transient choroidal effusion that resolved without ultimate reduction of baseline acuity. The devices were surgically explanted at the 6-month study conclusion. The initial 5 subjects received lower-dose implants delivering 0.28 ± 0.07 ng/day. The subsequent 5 participants received implants delivering 1.53 ± 0.54 ng/day, or about fivefold higher dose. The CNTF release levels were evaluated following explant. As this was a phase I safety study, the primary endpoints were safety parameters. No ocular or systemic complications ensued that met predetermined protocol adverse outcomes. The transfected cells derived from a human cultured retinal pigment epithelium (RPE) cell line. No serum antibodies to either CNTF or the transfected cells were detected in participants.

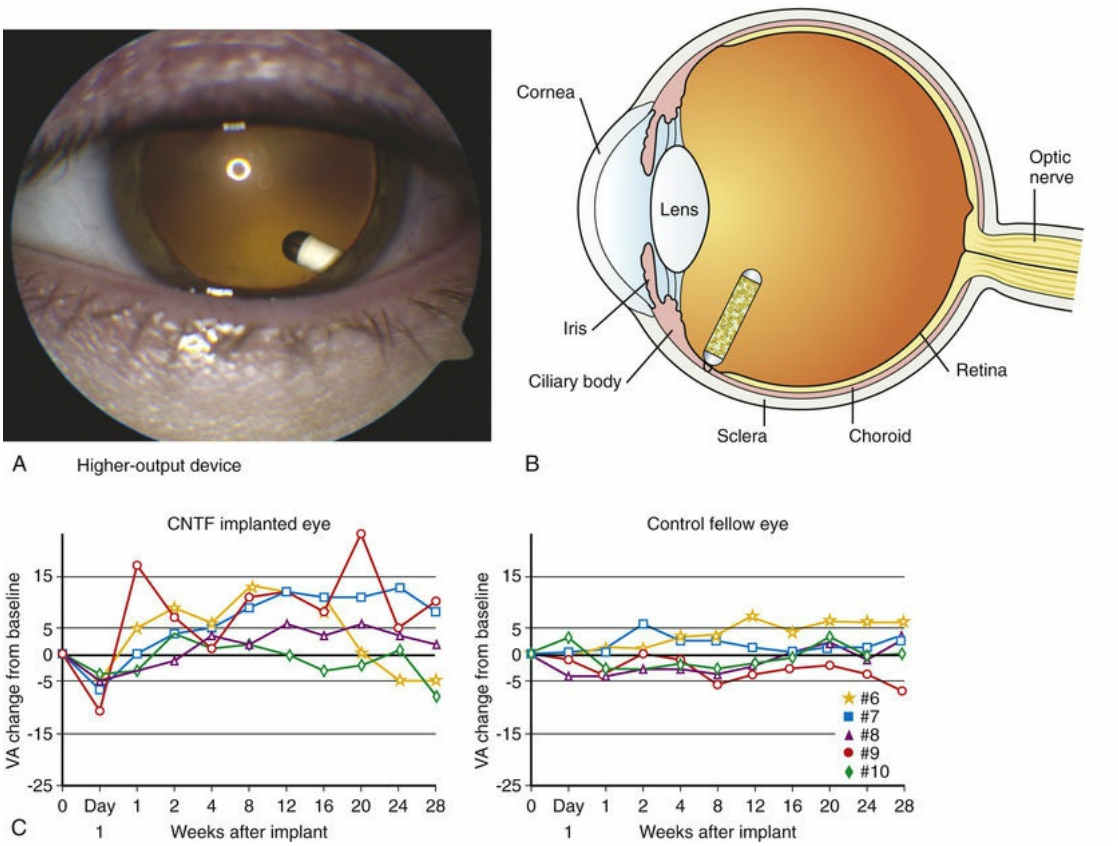

FIG. 39.2 (A,B) Intraocular ciliary neurotrophic factor (CNTF) encapsulated cell technology implant through dilated pupil of subject participating in phase I clinical safety study. (C) Visual acuity (VA) during the 6-month period of CNTF implant with higher-output device.

(Modified with permission from Sieving PA, Caruso RC, Tao W, et al. Ciliary neurotrophic factor (CNTF) for human retinal degeneration: phase I trial of CNTF delivered by encapsulated cell intraocular implants. Proc Natl Acad Sci USA 2006;103:3896–901.)

Because of preexisting retinal disease, only 7 of the 10 individuals had acuities that could be tracked on standard acuity charts at baseline and 3 of these recovered substantial acuity, to levels 10–15 letters above baseline. All 3 participants retained these improvements for 6 months or more after implants were removed. As the study was designed as a safety trial and was not powered to evaluate acuity, it remains speculative as to whether the acuity gains reflected a beneficial action of CNTF or whether this was within the bounds of normal acuity variation in RP disease.

We considered the possibility of true biological rescue by CNTF and proposed a hypothesis of plausible action, as follows: visual acuity requires both close spacing of many photoreceptors and that

these photoreceptors can functionally respond to light stimulation. We considered it unlikely that CNTF could "repopulate" the retina with new photoreceptors, but rather that CNTF might restore minimal function in cone photoreceptors that were present but were functionally dormant. Photoreceptors certainly can survive temporarily, even with no outer segments, in the rhodopsin knockout mouse model.[47] These rod cells cannot respond to light in the absence of photopigment in the outer segments, and ultimately they die by approximately 90 days from birth. Second, both Bok et al.[44] and Bush et al.[45] generated evidence that CNTF elicited transcriptional activity in photoreceptor cells, consistent with CNTF stimulating higher metabolic output of photoreceptors. Finally, it is well understood that even relatively few cone photoreceptors can support some degree of visual discrimination, as deduced from retinal histology of postmortem eyes of individuals with RP and through psychophysical experiments that modeled photoreceptor loss.[48] This chain of logic can be summarized as follows: first, photoreceptors become inactive before they die and go into a quiescent state and do not contribute to visual perception. Second, CNTF promotes photoreceptor transcriptional activity and metabolic function of cells, including elaboration of outer-segment material that supports photon capture and vision. Third, very few cone photoreceptors are required for a minimal level of visual acuity. Under these conditions, CNTF might partially restore visual function during a late stage of degeneration. This effect would be separate from CNTF preservation of photoreceptors in early stages of degeneration which was seen in at least 13 different animal models of degeneration, including phosphodiesterase (PDE) 6βmice, RDS peripherin mice, transgenic rats expressing P23H or S334ter mutant rhodopsin, RDY cat, RCD1 dog, rhodopsin knockout mice, and Q334ter rhodopsin transgenic mice. A study of CNTF in the S334ter rhodopsin transgenic rat model demonstrated regeneration of cone outer segments, consistent with the postulate of the CNTF phase I study group that CNTF may benefit vision by partially restoring or augmenting cone function.

Based on the successful safety study of CNTF protein released by encapsulated cell technology implants, phase II studies were developed to evaluate possible efficacy for age-related macular

degeneration (AMD) involving geographic atrophy and for RP (David Birch, Retinal Foundation of the Southwest; Rafael Caruso, NEI/NIH; Paul Sieving, NEI/NIH; Weng Tao, NeuroTech; Santa Tumminia, NEI/NIH; Ronald Bush, NIDCD/NIH; and Richard Weleber, Casey Eye Institute-OHSU). The scientific hypotheses were, first, whether one could demonstrate that CNTF slowed neurodegeneration and prolonged vision, and second, whether CNTF improves photoreceptor function in human RP. The CNTF-2 study for AMD trial had a principal outcome of visual acuity after 12 months' treatment.[49] The CNTF-3 and CNTF-4 were both for RP, with principal outcomes of visual acuity outcome at 12 months,[50] or visual field sensitivity at 24 months,[51] respectively. The trials involved about 60 subjects each, with asymmetric design, with 20 subjects receiving lower-dose implants and 40 subjects receiving higher-dose implants. All studies were fully enrolled.

The AMD trial (CNTF 2) reported results in 2011.[52] No serious adverse events related to the CNTF implant or to surgical procedures occurred during the study. Biological activity of the implant was indicated by an increase of retinal thickness on optical coherence tomography for both the lower-dose and higher-dose CNTF groups, but not in the sham control eyes. Unfortunately, visual acuity outcome did not reach significance for the endpoint, but the higher-dose group showed a trend towards stabilization of best corrected visual acuity (BCVA) at 12 months compared to sham treatment (p=.078). Neither the ERG amplitudes nor Humphrey visual field sensitivity showed significant change, either for better or worse.[52]

CNTF for CNGB3 Achromatopsia

Although CNTF continues to be a leading candidate for retinal neuroprotection, positive outcome data in humans are sparse to nonexistent thus far. An important new opportunity arose with the observation that CNTF rescues cone photoreceptor dysfunction in CNGB3 mutant dogs.[53] CNGB3 encodes the beta-subunit of the cyclic GMP-gated conductance channel on the cone outer segment and is essential for visual-signaling of cones. Human CNGB3 mutations cause achromatopsia, with loss of acuity and color

discrimination. Komaromy and colleagues found that intravitreal CNTF application restored cone function in CNGB3 achromatic dogs.[53] A human study was mounted with five achromatic subjects carrying CNGB3 mutations, with deficient color vision and acuity, using CNTF delivered by Neurotech encapsulated cell technology implants (Clinicaltrials.gov #NCT01408472).[54] Unfortunately none of the subjects showed improved cone function in testing for cone ERG responses, color discrimination, or visual acuity. One conclusion was that human cones with CNGB3 mutations responded differently to CNTF than do canine cones. The observation of a species difference was further reinforced by a study of CNTF effect on a CNGB3-knockout mouse model of achromatopsia.[55] In this model, injecting CNTF protein into the vitreous selectively augmented cone-mediated ERG responses, again confirming a difference between human and nonhuman response to CNTF. It may be important, however, that the CNTF action in the mouse appeared to act on inner retinal neurons rather than acting directly on the cone photoreceptors.

CNTF for Macular Telangiectasis Type 2

Studies are also ongoing with CNTF for type 2 macular telangiectasis (mac tel) (Clinicaltrials.gov #NCT01949324). Although mac tel clinically manifests abnormality of superficial retinal capillaries, current evidence suggests that photoreceptor cell changes occur early and are intrinsic to the disorder.[56] On this basis, CNTF intravitreal implants were studied in seven mac tel subjects.[57] The encapsulated cell implants were safe and well tolerated in mac tel eyes as also noted previously for other human retinopathies. The study was designed for safety and was not powered to demonstrate clinical efficacy in altering mac tel progression. However, by the 36-month study conclusion, no clinical impact was observed on dark adaptation or ERG responses nor on visual acuity. As previously found for other human CNTF studies, mean retinal thickness increased in study eyes, demonstrating some biological activity of the CNTF molecule.

CNTF for Glaucoma

A CNTF human clinical trial has been mounted for glaucoma using Neurotech NT-501 CNTF devices surgically implanted into the vitreous cavity (Clinicaltrials.gov # NCT01408472). Outcome metrics are broadly stated for this pilot study and involve both neuroprotection (prevention of vision loss) and also vision enhancement (possible visual acuity and peripheral visual field extent). No results are published to date.

In total, CNTF remains an attractive candidate for protection of neurons in the human retina during disease. Although this has been demonstrated clearly in multiple animal models of photoreceptor degeneration and for retinal ganglion cell rescue, current data are quite sparse on indicating that CNTF conveys protection to the human retinal neurons.

New Technology for Endpoints for Photoreceptor Degenerations

In considering future trials involving disease that causes demise of rod or cone photoreceptors, the selection of clinical endpoints to demonstrate significant rescue has received intense consideration. Psychophysical measures of visual acuity, visual sensitivity, or extent of visual field appear to be insensitive measures, as they persist even after objective measures of ERG amplitudes are greatly reduced. A new potential endpoint involves adaptive optics scanning laser ophthalmoscopy, in which cone photoreceptors can be imaged in vivo by sharpening image clarity upon correction of optical aberrations inherent in the lens and cornea. Talcott et al.[58] demonstrated the ability to image and count the cones in the foveal region of the human eye during CNTF treatment of two subjects. They found significant relative preservation of cone photoreceptors in the CNTF-treated eyes. While this approach currently is extremely labor-intensive, it may afford the best opportunity to track the natural history of photoreceptor loss by neuroprotective treatment trials in these slowly progressing diseases.

Delivery of Neurotrophins

Neurotrophic factors are proteins of substantial size, and controlled delivery to target ocular tissues presents a formidable challenge. None of the neurotrophic factors are particularly amenable to crossing the blood–retinal barrier, nor can they be administered from outside the eye and achieve substantial molecular flow to intraocular tissue. While delivery of neuroprotective factors will also be considered in a separate section of this chapter, some mention is warranted here of the major approaches to delivery. Direct delivery of CNTF protein by intravitreal injection has worked well in rodent models. This approach has major limitations, however. The first is the limited half-life of therapeutic effect. A single intravitreal application in the rat eye of CNTF has a rapid clearance time. Despite this, the effect is longer-lasting than expected, following a single bolus injection, indicating that CNTF acts through a secondary mechanism, possibly by upregulating gene expression in glial cells that release some currently unknown protective factor. Persistence of treatment duration can be extended by repeated injections, as is done for anti-vascular endothelial growth factor (VEGF) compounds to treat neovascular AMD.[59,60] However, even such heroic approaches are currently conducted only for 12–18 months, whereas neuroprotection for retinal photoreceptor degenerative diseases would need to continue for decades. Further, injecting a large bolus application of CNTF compound impacts retinal function and decreases the ERG amplitudes,[44] whereas low-dose continuous CNTF release had the possibility of augmenting rod cell function.[35]

An alternative promising approach is ECT, in which low-dose protein is released continuously into the vitreous cavity following surgical implantation of the encapsulated cells transfected with the gene of choice, as used for the CNTF phase I clinical trial.[46] Current indications from Neurotech are for continuous release in therapeutic quantity beyond 24 months' duration. While surgical insertion of the device is a potential limitation, conversely, it is attractive to be able to remove the device by surgical explant if it is necessary to terminate the drug application.

Vector-mediated gene transfer by intravitreal or subretinal application also holds the potential for long-term chronic therapy. While adenovirus-mediated transfer has limited duration of

expression of only many months, AAV vectors are capable of maintaining chronic release over the course of many years, as seen for the RPE65 trial in the dog.[61] The current limitations of AAV vector-mediated transfer involve potential immunogenicity, potential for mutagenesis, and a current lack of regulation of gene expression level, including genetic control to terminate protein production. Quite likely, these limitations will be overcome in the future.

Antioxidants

Oxidative Damage in Light-Induced and Inherited Photoreceptor Degenerations

Absorption of light (the normal function of photoreceptor outer segments) increases oxidation of their lipids, creating morphologic and functional damage as light exposure is increased.[62–64] Both death and damage appear to be caused by oxidative stress, i.e., by the damaging effects of partially reduced forms of oxygen, often called reactive oxygen species. The idea that light-induced damage is caused by oxidative stress is supported by evidence that levels of endogenous antioxidants increase following light damage,[64–66] and that exogenous antioxidants are protective[66–73] for cones[74,75] as well as rods.[76–78] The stress-induced death of photoreceptors is accompanied by damage to the survivors.[76,78]

In several inherited photoreceptor degenerations the starting event is a mutation that leads to the death of rod photoreceptors. After the death of rods, the major consumers of oxygen in the retina, the tissue oxygen level in the outer retina is substantially increased,[79] activating nicotinamide adenine dinucleotide phosphate (NADPH) oxidase and inducing accumulation of superoxide radicals.[80] Superoxide radicals attack macromolecules, causing oxidative damage and production of other molecules such as nitric oxide which generates peroxynitrite, a particularly damaging free radical that amplifies the damage.[81] Over time the antioxidant defense systems and repair mechanisms in cones cannot compensate for damage, leading to severe cell damage and apoptosis. According to cone density distribution, cone dysfunction and death are expected to occur first in the periphery and then

spread posteriorly, a process that is common to many inherited dystrophies. The generation of free radicals is relentless and, thus, any treatment directed at preserving cones must be provided continuously for the patient's entire life. The repair mechanisms can protect from a limited amount of damage. The aim of antioxidant treatment is to reduce the rate of oxidative damage below the rate of repair in order to prevent dysfunction and apoptosis. To determine if this can be achieved, long-term experiments are required. Alternatively, evidence of protection could be provided in a shorter time length by the rescuing effect of a candidate drug on damaged but still viable cells (Figs. 39.1 and 39.2).

Preclinical Evidence of Antioxidant Protection in Photoreceptor Degenerations

Inhibitors of NADPH Oxidase (Nox).

Usui et al.[80] investigated the hypothesis that Nox and/or xanthine oxidase serve as critical intermediaries between increased tissue oxygen and the generation of excessive reactive oxygen species that cause oxidative damage to cones. Apocynin, a blocker of Nox, but not allopurinol, a blocker of xanthine oxidase, markedly reduced the superoxide radicals in the outer retina of the retinal degeneration-1 ($rd1^{+/+}$) model of RP. Compared to $rd1^{+/+}$ mice treated with vehicle, those treated with apocynin, but not those treated with allopurinol, had significantly less oxidative damage in the retina. Apocynin-treated, but not allopurinol-treated, $rd1^{+/+}$ mice had preservation of cone cell density, increased mRNA levels for M- and S-cone opsin, and increased mean photopic b-wave amplitude. In Q344Ter mice, a model of dominant RP in which mutant rhodopsin is expressed, apocynin treatment preserved photopic ERG b-wave amplitude compared to vehicle-treated controls. These data indicated that Nox, but not xanthine oxidase, plays a critical role in the generation of oxidative stress leading to cone cell death in RP. Inhibition of Nox provides a new treatment strategy.

Nitric Oxide Synthase (NOS) Inhibitors.

Recent studies by Komeima et al.[81] have shown that treatment of

rd1 mice with a mixture of NOS inhibitors significantly increased cone survival, indicating that NO-derived peroxynitrite contributes to cone cell death. Treatment with 7-nitroindazole, a specific inhibitor of neuronal NOS, also significantly reduced cone cell death, but aminoguanidine, an inhibitor of inducible NOS, did not. These data suggest that NO generated by neuronal NOS exacerbates oxidative damage to cones in RP, and that combined therapy to reduce NO and oxidative stress should be considered.

Bolstering the Endogenous Antioxidant Defense System

In another study by the same group,[82] genetically engineered *rd10* mice with either inducible expression of superoxide dismutase (SOD) 2, catalase, or both in photoreceptor mitochondria were generated. Littermates with the same genetic background that did not have increased expression of SOD2 nor catalase served as controls. Coexpression of SOD2 and catalase, but not either alone, significantly reduced oxidative damage in the retinas of postnatal day (P) 50 *rd10* mice, as measured by protein carbonyl content. Cone density was significantly greater in P50 *rd10* mice with coexpression of SOD2 and catalase together than *rd10* mice that expressed SOD2 or catalase alone, or expressed neither. Coexpression of SOD2 and catalase in **rd10** mice did not slow rod cell death. These data supported the idea of bolstering the endogenous antioxidant defense system as a gene-based treatment strategy for RP, and also indicated that coexpression of multiple components may be needed for effective neuroprotection.

Following the same line of research, Lu et al.[83] explored the strategy of overexpressing components of the endogenous antioxidant defense system to combat oxidative damage in RPE cells and retina. In transfected cultured RPE cells with increased expression of SOD1 or SOD2, there was increased constitutive and stress-induced oxidative damage measured by the level of carbonyl adducts on proteins. In contrast, RPE cells with increased expression of glutathione peroxidase 1 (Gpx1) or Gpx4 did not show an increase in constitutive oxidative damage. An increase in Gpx4, and to a lesser extent in Gpx1, reduced oxidative stress-induced RPE cell damage. Coexpression of Gpx4 with SOD1 or 2

partially reversed the deleterious effects of the SODs. Transgenic mice with inducible expression of Gpx4 in photoreceptors were generated, and in three models of oxidative damage-induced retinal degeneration, increased expression of Gpx4 provided strong protection of retinal structure and function. These data suggest that gene therapy approaches to augment the activity of Gpx4 in the retina and RPE should be considered in patients with RP or AMD.

Hormone Influence on the Antioxidant Defense

Several studies have linked decreased circulating estrogens with development of AMD.[84,85] Estrogens are a group of steroid hormones that includes estradiol, estrone, and estriol. They are regulated by estrogen receptors which are found in various regions of the brain. Estrogens can penetrate the blood–brain barrier and can regulate neuronal functioning and behavior.[86,87]

Vina and colleagues[88] suggested that an inherent biological difference between men and women could be responsible for longer lifespan and possible protective effects against certain diseases. Vina showed that females were less likely to produce mitochondrial oxidants than males and that estradiol likely plays a role in induction of antioxidant genes.[88] The neuroprotective effects of estrogen have been studied in vivo for over a decade.[89] Estradiol was found to be the most effective and potent dose-dependent antioxidant, requiring only brief exposure to cell lines to prevent oxidative stress.

In 2011, Doonan et al. reported that norgestrel, a progestinic agonist, was neuroprotective in two distinct mouse models of retinal degeneration: the acute light induced degeneration model and the Pde6b chronic RP mouse model.[90] They found that norgestrel increased rhodopsin expression, and enhanced rod photoreceptor function. Norgestrel was beneficial even if administered after photoreceptor damage had already begun, preserving photoreceptor morphology and cell number[90] In an editorial in 2012, Doonan and Cotter proposed the potential utility of norgestrel in the treatment of RP and AMD.[91]

Carotenoids (Lutein, Zeaxanthin) in Combination With Other Antioxidants

Miranda et al.[92] have shown that the use of a combination of antioxidants delayed the degeneration process in *rd1* mouse retina. In an effort to understand the mechanism of action of these substances (zeaxanthin, lutein, α-lipoic acid, glutathione, and *Lycium barbarum* extract) the changes in the levels of several proteins and oxidative stress markers in the rd1 retina were studied. The treatment increased glutathione peroxidase activity and glutathione levels and decreased cystine concentrations in rd1 retinas. Considering all the results obtained from treated and untreated animals, a high correlation was present between glutathione concentration and glutathione peroxidase activity, and there was a negative correlation between glutathione retinal concentration and the number of TUNEL-positive cells. No difference was observed between the numbers of nNOS and NADPH diaphorase-positive cells in treated and untreated *rd1* mice. Thiol contents and thiol-dependent peroxide metabolism seem to be directly related to the survival of photoreceptors in *rd1* mouse retina.

Rac1

Rac1 is a component of NADPH oxidase that produces reactive oxygen species.[93] Rac1 is expressed abundantly in mammalian retinal photoreceptors, where it is activated in response to light stimuli.[94] Knocking down Rac1 expression, by conditional gene targeting, in mouse rod photoreceptors resulted in protection against light-induced photoreceptor death compared with wild-type (WT) littermates.[95] A similar protective effect on rods was also found by using apocynin, which inhibits NADPH oxidase activity. These results implicate both neuronal Rac1 and NADPH oxidase in cell death in this model of CNS degeneration. Diminished Rac1 expression in mouse rods had no effect on retinal structure or function examined by light microscopy, electron microscopy, rhodopsin measurement, ERG activity, and visual acuity, indicating that rod outer-segment morphogenesis proceeds normally in Rac1 conditional knockout mice. The lack of structural or functional effect of Rac1 depletion on photoreceptors, but protection under conditions of stress, indicates that the Rac1 pathway warrants exploration as a target for therapy in retinal neurodegenerative

diseases.

Rod-Derived Cone Viability Factor

A new signaling molecule that represents a potential therapy for these currently untreatable diseases has been identified over the past 12 years.[96] This protein, called rod-derived cone viability factor (RdCVF), maintains the function and consequently the viability of cone photoreceptor cells in the retina; mice that lack this factor exhibit a progressive loss of photoreceptor cells. The gene encoding RdCVF (nucleoredoxin-like gene, *Nxnl1*) also encodes, by differential splicing, a second product that has characteristics of a thioredoxin-like enzyme and protects both photoreceptor cells and, more specifically, its interacting protein partner, the tau protein, against oxidative damage. This signaling pathway potentially links environmental insults to an endogenous neuroprotective response. *Nxnl1* and, most likely, the paralogous gene *Nxnl2* are part of a newly discovered redox signaling pathway that involves an enzymatic product and a trophic factor, both encoded by the same gene. It has been suggested[82] that this therapy, by restoring a physiologic signal, may efficiently treat the effects of a broad range of RP mutations. Recently,[97] it has been demonstrated that the RdCVF promotes retinal cone survival by accelerating the entry of glucose into photoreceptors and enhancing aerobic glycolysis. RdCVF binds to the cell-surface complex basigin 1 (BSG1)/glucose transporter (GLUT1), resulting in increased glucose entry into cones and thereby promoting cone survival by stimulation of aerobic glycolysis. This pathway is also used by fast dividing cancer cells.

The delivery of RdCVF into the patient's eyes can be achieved through different routes, by injection of the protein into the eye, expression from viral vectors, or delivery of RdCVF-producing cells that are encapsulated in a semipermeable membrane to avoid attack by the immune system. RdCVF is now in translation into a possible therapeutic agent to treat a spectrum of degenerative eye diseases.

N-Acetylcysteine

Very recently, Lee et al.[98] determined whether orally administered *N*-acetylcysteine (NAC) reduced cone cell death and preserved cone function by reducing oxidative damage in two models of RP:

rd1 and *rd10* mice. In *rd10* mice, supplementation of drinking water with NAC promoted partial maintenance of cone structure and function for at least 6 months. Topical application of NAC to the cornea also reduced superoxide radicals in the retina and promoted survival and functioning of cones. Since oral and/or topical administration of NAC is feasible for long-term treatment in humans, and NAC has a good safety profile, it is reasonable to consider clinical trials to evaluate the effects of prolonged treatment with NAC in patients with RP.

Saffron (*Crocus sativus*) Extract

Among various antioxidants, the neuroprotective potential of the ancient spice saffron was explored.[99] To test whether the saffron extract (*Crocus sativus*) given as a dietary supplement counteracts the effects of continuous light exposure in the albino rat retina, Sprague–Dawley rats were prefed either saffron or beta-carotene (1 mg extract/kg per day) before they were exposed to bright continuous light (BCL) for 24 hours. Flash ERG amplitudes, the thickness of the ONL, and the amount of apoptotic figures in the ONL were the main outcome variables. The photoreceptor layer was largely preserved in saffron-treated animals as was the ERG response. In addition, the rate of photoreceptor death induced by BCL appeared to be drastically reduced in treated animals. In beta-carotene prefeeding experiments, morphologic analysis showed preservation of the ONL similar to that obtained with saffron prefeeding, whereas the ERG response was unrecordable. Western blot analysis showed that exposure to light induced a strong upregulation of fibroblastic growth factor in control and beta-carotene-treated rats, but no change was noted in saffron-treated rats. These results showed that saffron may protect photoreceptors from retinal stress, maintaining both morphology and function and probably acting as a regulator of programmed cell death. The stigmata of *C. sativus* contain powerful antioxidants (crocin, crocetin) in biologically high concentrations[100]; their multiple C=C bonds give the stigmata their color, fragrance, taste, and antioxidant potential. To identify the genes and noncoding RNAs (ncRNAs) involved in the neuroprotective actions of saffron, Natoli et al.[101] used a standardized assay of photoreceptor damage, in which

albino Sprague–Dawley rats raised in dim cyclic illumination (12 hours 5 lux, 12 hours darkness) were challenged by 24 hours' exposure to bright (1000 lux) light. Experimental groups were protected against light damage by pretreatment with dietary saffron (1 mg/kg per day for 21 days). RNA from the eye of exposed and unexposed animals was hybridized to Affymetrix rat genome ST arrays. Quantitative real-time polymerase chain reaction analysis of 14 selected genes was used to validate the microarray results. Light damage caused the regulation of 175 entities (genes and noncoding, ncRNAs) beyond criterion levels ($p<.05$ in comparison with controls, fold change >2). Saffron pretreatment reduced the expression of 53 entities. Saffron pretreatment regulated 122 entities not regulated by light damage. Saffron, given without light damage, regulated genes and ncRNAs beyond criterion levels, but in lesser numbers than during their protective action. A high proportion of the entities regulated by light damage (>90%) were known genes. By contrast, ncRNAs were prominent among the entities regulated by saffron in their neuroprotective roles (73% and 62%, respectively). Given before retinal exposure to damaging light, thus exerting its neuroprotective action, saffron regulated a large number of entities, among which ncRNAs were prominent.

Nanoceria

Cerium oxide nanoparticles, nanoceria, are inorganic antioxidants that have catalytic activities which mimic those of the neuroprotective enzymes SOD and catalase. Kong et al.[102] have shown that nanoceria preserves retinal morphology and prevents loss of retinal function in a rat light damage model. The homozygous tubby mutant mouse, which exhibits inherited early progressive cochlear and retinal degeneration, was used as a model to test the ability of nanoceria to slow the progression of retinal degeneration.[102] The results showed that nanoceria can protect the retina by decreasing reactive oxygen species, upregulating the expression of neuroprotection-associated genes, downregulating apoptosis signaling pathways and/or upregulating survival signaling pathways to slow photoreceptor degeneration. These data suggest that nanoceria has significant potential as global agents for

the therapeutic treatment of inherited retinal degeneration and most types of ocular disease.

Clinical Evidence of Antioxidant Protection in Photoreceptor Degenerations

Age-Related Eye Disease Study (AREDS).

The AREDS represents without doubt a milestone in the field of nutritional supplementation for AMD. Sponsored by the NEI and published in 2001,[103] AREDS was indeed the first large-scale, randomized and controlled clinical trial to demonstrate the protective role of high doses of vitamins and zinc on the progression of AMD and visual loss. AREDS was initially conceived as a long-term multicenter, prospective study designed to assess the clinical course, prognosis, and risk factors of both AMD and cataract. However, the widespread use and marketing of antioxidants and zinc in eye-targeted formulations, not supported by consistent scientific evidence, led the researchers to incorporate a clinical trial as part of the study, to evaluate the effect of high doses of zinc and selected antioxidant vitamins on the development of advanced AMD in a cohort of older persons. A total of 3641 participants, aged 55–80, were included in the study, and randomly selected to receive daily oral tablets for one of four treatments: (1) zinc alone; (2) antioxidants alone; (3) a combination of antioxidants and zinc; and (4) placebo. The antioxidant formulation consisted of 500 mg vitamin C, 400 IU vitamin E, and 15 mg beta-carotene. The specific daily amount of zinc was 80 mg as zinc oxide (formulations that included zinc also had 2 mg copper oxide added to offset potential zinc-induced copper-deficiency anemia). It should be noted that the formula was a type of active treatment, and therefore the dosages of ingredients were much higher than the current recommended daily allowance. These ingredients were thought to exert a protective effect on retinal cells by counteracting oxidative stresses. The beneficial effects of zinc supplementation were previously assessed in a small clinical trial as RPE normally has a particularly high zinc content. It was hypothesized that poor zinc intake in elderly persons might result in zinc deficiency and the loss of zinc-dependent coenzymes in the RPE, resulting in development

or worsening of AMD. After a mean follow-up period of 6.3 years, AREDS researchers concluded that people with intermediate AMD (extensive intermediate drusen in one or both eyes, one or more large drusen in at least one eye, or nonsubfoveal geographic atrophy in one eye), or advanced AMD (subfoveal geographic atrophy or choroidal neovascular membrane) in one eye, treated with the formulation of "antioxidants plus zinc," had a 25% risk reduction in progression to advanced AMD over 5 years, and the risk of losing vision of three or more lines (doubling of the visual angle) was reduced by 19%. No evidence of a direct benefit of the AREDS formulation in delaying disease progression was observed in patients with early AMD (multiple small drusen or intermediate drusen and/or pigment abnormalities in one or both eyes), and therefore AREDS supplementation was recommended only to people at high risk for developing advanced AMD.

Controlled Clinical Studies on Antioxidants in AMD and RP Employing Visual Function Endpoints

Carotenoids Alone or in Combination With Other Antioxidants

Age-Related Macular Degeneration.

In a double-masked, placebo-controlled, randomized trial of lutein and antioxidant supplementation for intervention in atrophic AMD (the Veterans Lutein Antioxidant Supplementation Trial), Richer et al.[104] determined whether nutritional supplementation with lutein or lutein together with antioxidants, vitamins, and minerals, improves visual function and symptoms in atrophic AMD. The study was a prospective, 12-month, randomized, double-masked, placebo-controlled trial. Visual function was evaluated by Snellen visual acuity, contrast sensitivity, Amsler grid, and VF-14 questionnaires. It was shown that visual function (acuity and contrast sensitivity) improved with lutein alone or lutein together with other nutrients, compared to placebo. In electrophysiologic pilot studies, Falsini et al.[105] and Parisi et al.[106] showed that short-

term supplementation of lutein or astaxanthin, in combination with other antioxidants (nicotinamide, vitamin C), significantly improved macular cone-mediated function as recorded by focal or multifocal ERGs in patients with early AMD (soft drusen and/or RPE defects) and moderately reduced visual acuity. More recently,[107] a randomized, double-blind, placebo-controlled study showed that 3 months of dietary saffron supplementation significantly improved the focal ERG-estimated retinal flicker sensitivity in early AMD patients (Fig. 39.3).

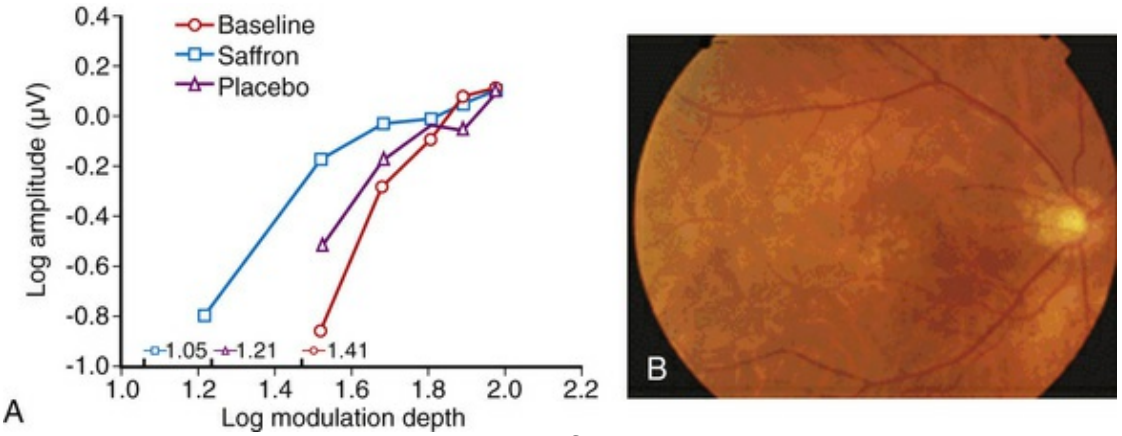

FIG. 39.3 (A) Representative flash electroretinogram (FERG) functions, recorded from one patient with age-related macular degeneration at baseline and after 90 days of saffron or placebo supplementation, are shown by plotting response amplitudes as a function of modulation depth. (B) Color fundus photograph from the study eye, showing confluent soft drusen in the foveal region. (Reproduced with permission from Falsini B, Piccardi M, Minnella A, et al. Influence of saffron supplementation on retinal flicker sensitivity in early age-related macular degeneration. Invest Ophthalmol Vis Sci 2010;51:6118–24.)

Retinitis Pigmentosa.

In a recent clinical trial of lutein supplementation in RP patients receiving vitamin A[108] it was determined whether lutein supplementation can slow visual function decline in patients with RP receiving vitamin A supplementation. The study was a randomized, controlled, double-masked trial of 225 nonsmoking

patients, aged 18–60 years, evaluated over a 4-year interval. Patients received 12 mg lutein or a placebo daily. All were given 15,000 IU/day vitamin A palmitate. Randomization took into account genetic type and baseline serum lutein level. The primary outcome was the total point score for the Humphrey field analyzer (HFA) 30–2 program; prespecified secondary outcomes were the total point scores for the 60–4 program and for the 30–2 and 60–4 programs combined, 30-Hz flicker ERG amplitude, and Early Treatment Diabetic Retinopathy Study acuity. The results showed that, for the HFA 60–4 program, a decrease in mean rate of sensitivity loss was observed in the lutein plus vitamin A group (p=.05). Mean decline with the 60–4 program was slower among those with the highest serum lutein level or with the highest increase in macular pigment optical density at follow-up (p=.01 and p=.006, respectively). Those with the highest increase in macular pigment optical density also had the slowest decline in HFA 30–2 and 60–4 combined field sensitivity (p=.005). No significant toxic effects of lutein supplementation were observed. These results indicated that lutein supplementation of 12 mg/day can slow loss of midperipheral visual field on average among nonsmoking adults with RP taking vitamin A, supporting its therapeutic use as neuroprotectant.

Other Antioxidants.

The safety and efficacy of OT-551, a disubstituted hydroxylamine with antioxidant properties, were evaluated[109] for the treatment of geographic atrophy, the advanced atrophic form of AMD. The study was a single-center, open-label phase II trial, enrolling 10 participants with bilateral geographic atrophy. Topical 0.45% OT-551 was administered in one randomly assigned eye three times daily for 2 years. Safety measures were assessed by complete ophthalmic examination, fundus photography, and review of symptoms. The primary efficacy outcome measure was the change in BCVA at 24 months. Secondary efficacy measures included changes in area of geographic atrophy, contrast sensitivity, microperimetry measurements, and total drusen area from baseline. The study drug was well tolerated and was associated with few adverse events. The mean change in BCVA at 2 years was +0.2 ±

13.3 letters in the study eyes and –11.3 ± 7.6 letters in fellow eyes (p=.0259). However, no statistically significant differences were found between the study and fellow eyes for all other secondary outcome measures. These results indicated that OT-551 was well tolerated by study participants and was not associated with any serious adverse effects. Efficacy measurements in this small study indicate a possible effect in maintaining visual acuity. However, the absence of significant effects on other outcome measures in this study suggests that OT-551, in the current concentration and mode of delivery, may have limited or no benefit as a treatment for geographic atrophy.

Neuroprotection With Small Molecules

Previous sections discussed neuroprotection by proteins such as growth and neurotrophic factors (e.g., CNTF) and antibodies (e.g., anti-VEGF), gene transfer, and antioxidants. In addition, neuroprotection by glutamate receptor antagonists (e.g., memantine) in treating glaucoma was described. This section will discuss neuroprotection by small molecules, many of which target specific intracellular pathways, particularly in photoreceptor degenerations, and have been tested primarily in animal models. Small molecules, for the purpose of this section, are considered to be those with molecular weights below the limit of diffusion across the inner limiting membrane and retina, which is 40–70 kDa or 4.5 nm in radius depending on their shape.[110] Thus, most can reach targets in the distal retina when injected into the vitreous. Table 39.1 includes only those discussed in this chapter, and indicates the striking variety of types of molecules and pathways explored for neuroprotection in animal models of retinal degeneration. They range in size from catecholamines, such as dopamine, and α_2-adrenergic agonists, to long-chain fatty acids and small heat shock proteins. Many, as is the case with the protein growth and neurotrophic factors already discussed, are naturally occurring molecules in the retina which help maintain retinal homeostasis but may have additional function in promoting or reducing neuron survival when the retina is stressed. Others are synthetic agonists or antagonists of naturally occurring compounds.

TABLE 39.1
Small Molecules in Retinal Neuroprotection

Class	Agent	Target	Model	Route
Neuromodulators	Melatonin receptor antagonist	GPCR	Rat photoreceptor light damage	Intravitreal
	Melatonin	Receptor-independent	Ischemic human RPE	In vitro
	Dopamine agonist	GPCR	Rat photoreceptor light damage	Systemic
	Alpha-2-adrenergic agonist	GPCR	Human retinal dystrophy	Topical
			Rat ganglion cell damage	Systemic
			Rat photoreceptor light damage	Systemic
Calcium overload blockers	Flunarizine hydrochloride	Internal calcium stores	Rat photoreceptor light damage	Systemic
	Diltiazem	L-type calcium channel	Rd1 mouse	Systemic
	Nilvadipine	L-type calcium channel	RCS rats	Systemic
	Verapamil	Calcium channel depletion	Rds mouse	Gene knockout
Retinoids	Isotretinoin (13-*cis* retinoic acid) 9-*cis* retinal	Visual cycle	Rat/mouse photoreceptor light damage Stargardt (*abcr*$^{-/-}$) mouse	Systemic
		Visual cycle	LCA (*rpe65*$^{-/-}$) mouse, dog	Systemic
	Vitamin A		*ldh*$^{-/-}$ mouse	
	9-*cis* retinal, 11-*cis* retinal analog, 11-*cis* retinal	Misfolded opsin Misfolded opsin	Pro23His mouse Cell culture expressing Pro23His	Diet In vitro
Intracellular neurotrophic pathway effector molecules	HSP27	Apoptosis pathway (cytochrome C)	Rat photoreceptor light damage	Intravitreal
	Ad-CMV-HSP27		RCS rat-inherited photoreceptor degeneration	Intravitreal
	17-allylamino-17-demethoxygeldanamycin (17-AAG)	HSP90/HSP70	RD10 mouse	Systemic
	Minocycline	Apoptosis pathway (mitogen-	RCS rat-inherited and light-induced	Systemic

		activated protein kinase (MAPK), nuclear factor-κB (NF-κB))	photoreceptor degeneration	
	Rac1	IL-6, AP-1	Rat photoreceptor light damage	Conditional gene knockdown
	ω-3 LCPUFA	Visual cycle, other unknown	Rat photoreceptor light damage, human AMD	Dietary depletion
	Neuroprotectin-D1		RPE	In vitro
Peptidomimetic agonists and antagonists of neurotrophic factor receptors	Synthetic peptides	TrkA and $p75^{ntr}$ neurotrophin receptors	Rat optic nerve axotomy	Intravitreal

Akt, protein kinase B; AMD, age-related macular degeneration; AP-1, activator protein-1; GPCR, G-protein-coupled receptor; HSP, heat shock protein; IL, interleukin; LCA, Leber congenital amaurosis; LCPUFA, long-chain polyunsaturated fatty acid; mTOR, mammalian target of rapamycin; PI3K, phosphatidylinositol 3-kinase; RCS, Royal College of Surgeons; RPE, retinal pigment epithelium.

Neuromodulators/Neurotransmitters

Retinal neuromodulators and neurotransmitters, particularly those that act on G-protein coupled (GPC) receptors, are being explored for their neuroprotective properties for retinal cells.[111] Two of these, melatonin and dopamine, negatively interact with each other in the maintenance of retinal diurnal and circadian function but also may perform various functions in the retinal response to stress. For melatonin especially, there is accumulating evidence for this dual role.[112,113] Exogenous systemic melatonin increased photoreceptor degeneration in the light damage rat, a model of acute stress-induced photoreceptor degeneration.[114,115] The rat retina is more susceptible to light damage during the dark period of the circadian cycle when retinal melatonin levels are high,[116] and intravitreal injection of the melatonin receptor (MT1/MT2) antagonist luzindole prior to exposure makes the rat retina less susceptible to light damage[117] (Fig. 39.4). These studies suggest that endogenous melatonin and retinal melatonin receptors play a role in photoreceptor degeneration due to acute light stress. On the other hand, loss of the melatonin MT1 receptor increased photoreceptor loss in aging mice,[118] suggesting a protective role for melatonin in age-related slow degenerations. Melatonin has been shown to

protect human RPE cells from ischemia-induced apoptosis by a melatonin receptor-independent mechanism,[119] and reduce blue light-induced caspase-mediated cell death in ARPE-19 cells,[120] indicating a possible therapeutic role in prolonging visual function in AMD.[121] It also performs a neuroprotective function in the CNS through its antiinflammatory and antioxidant action.[122]

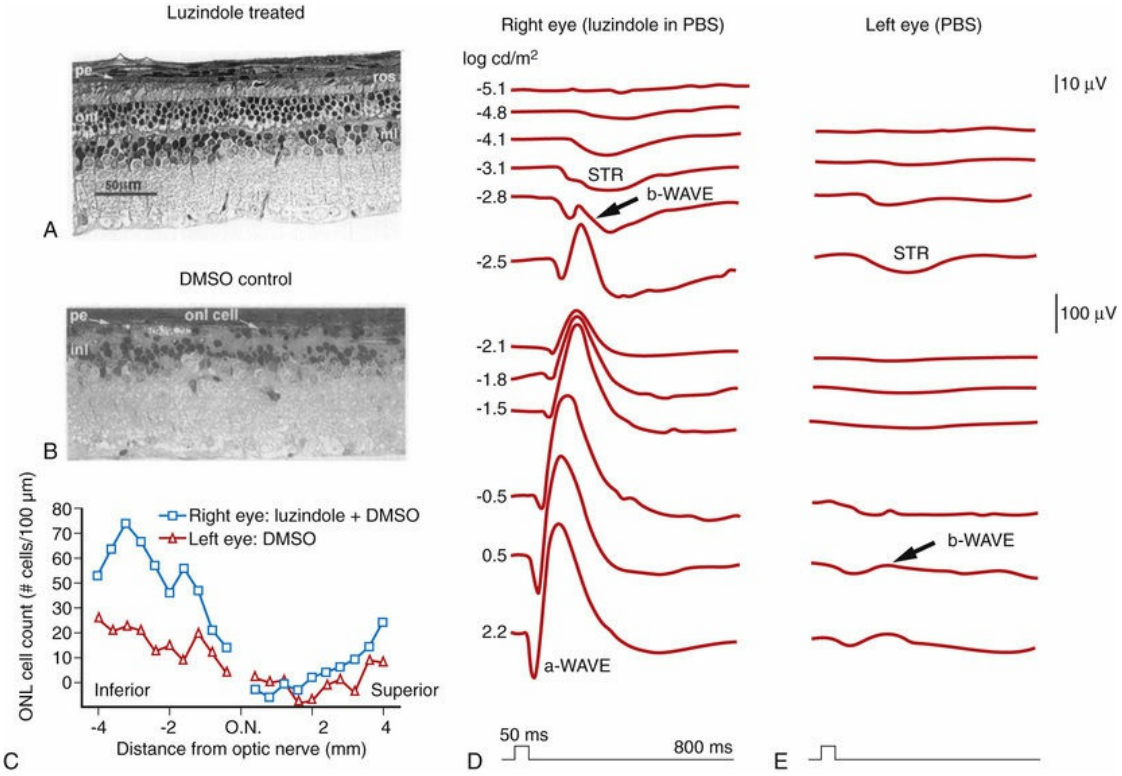

FIG. 39.4 Structural and functional photoreceptor protection from light damage by the melatonin antagonist luzindole. (A,B) Retinal sections show outer nuclear layer (ONL) preservation in eyes that received intravitreal luzindole (1 μl of 1 μM in dimethyl sulfoxide (DMSO)) 15 hours before light exposure compared to fellow eyes that received vehicle only. Images are from the superior central retina. (C) ONL cell counts per 100 μm at the specified positions across a retinal section through the vertical meridian. Protection by luzindole is most apparent in the inferior retina where overall damage is lowest. (D,E) Electroretinogram traces from the luzindole-treated and vehicle-injected eye of a single rat. The amplitudes of the traces indicate that the overall functional state of the luzindole-treated retina is much better than the control. *inl*, inner nuclear

layer; *onl*, outer nuclear layer; *PBS*, phosphate-buffered saline; *pe*, pigmented epithelium; *STR*, scotopic threshold response. (Reproduced with permission from Sugawara T, Sieving PA, Iuvone PM, et al. The melatonin antagonist luzindole protects retinal photoreceptors from light damage in the rat. Invest Ophthalmol Vis Sci 1998;39:2458–65.)

Dopamine, as well as being a neurotransmitter released in the light at inner retinal synapses, diffuses to the outer retina, activating receptors on photoreceptors that modulate cAMP levels through adenylate cyclase.[123] Activation of these receptors may lead to reduced light sensitivity and is known to downregulate photoreceptor melatonin production, which is low in the light. Melatonin release in darkness, in turn, acts on inner retinal neuron receptors to downregulate the production and release of dopamine and may increase retinal sensitivity to light.[112] Dopamine receptors are also found on Müller cells, however, and may affect photoreceptor survival through the release of neuroprotective factors from these cells.[124]

Recently, the serotonin (5HT) and adrenergic (AD) GPC receptors have been studied for their role in neuroprotection and damage using a mouse model of Stargardt disease (*Abca4*$^{-/-}$).[111] Light-induced photoreceptor cell death in this model is linked to GPC activation of phospholipase C leading to NADPH oxidase generated ROS.[125] Inhibition of this pathway via these GPC receptors reduced light-induced degeneration. In addition, adenylate cyclase was shown to play a central role in light-induced damage in this model and in wild-type mice. Thus, agonist of alpha-2-adrenergic receptors and antagonists of both alpha-1-adrenergic and 5HT receptors produced protection as did inhibition of this enzyme directly. Thus, small molecules that reduce GPC receptor activation of adenylate cyclase are potentially useful neuroprotectants.

These studies are consistent with previous work showing that the α_2-adrenergic receptor is linked to neuroprotection in other animal models. Topical administration of an α_2-adrenergic receptor agonist has also recently been tested for neuroprotective properties in a pilot study on humans with retinal dystrophies.[126] In optic nerve reperfusion injury, α_2-adrenergic agonists have been shown to

reduce ganglion cell degeneration,[127–130] and the mechanism probably involves reducing the excitotoxic influx of calcium.[131] Systemic administration of α_2-adrenergic agonists xylazine and clonidine can protect photoreceptors from damage due to light stress, perhaps by upregulation of bFGF and the activation of extracellular signal-regulated kinases in Müller cells.[132,133] Activation of neurotrophin/growth factor pathways to produce protection from light damage was also demonstrated for *N*-acetylserotonin (NAS), the precursor of serotonin.[134] However, in this case, protection was dependent on the neurotrophic receptor (tyrosine receptor kinase B) but independent of the neurotrophic factor itself (BDNF). Thus, a direct activation of the receptor by NAS was postulated, which would avoid simultaneous activation of the proapoptotic p75 neurotrophin receptor. Melatonin and serotonin and their receptors continue to be directly implicated in cell damage or neuroprotection for number of retinal cell types including pigment epithelium,[135,136] photoreceptors,[137,138] and ganglion cells.[139]

Calcium Channel Blockers

One of the earliest reports of neuroprotection in a photoreceptor degeneration model that offered hope for the treatment of a well-characterized form of RP using a small molecule showed that an L-type calcium channel blocker, D-*cis* diltiazem, could slow the course of photoreceptor cell death and loss of ERG function in the *Pde6b*^{rd1} mouse.[140] This followed an earlier report of protection of photoreceptors from light damage by a nonspecific Ca^{2+} channel blocker.[141] A mutation in *Pde6b*, a subunit of the light-activated PDE in rod outer segments, is responsible for 5–8% of cases of RP.[142] It results in a nonfunctional protein, high levels of cGMP in photoreceptors, and loss of ability to close the outer-segment light-gated cation channels. This leads to Na^+ and Ca^{2+} overload and photoreceptor cell death by apoptosis, though the precise link between elevated cGMP and cell death is not known.[143] Photoreceptor protection by D-*cis* diltiazem could not be replicated in other models of RP, including the Pro23His rat,[144] the *rcd1* dog that carries a stop codon in the *Pde6b* gene,[145] and a different strain of *rd1* mice.[146] A role for calcium overload in degeneration in *rd1*

mice was confirmed, however, by showing slowed cell loss in *rd1* mice crossed with L-type channel knockout mice.[147] Subsequently, another Ca^{2+} channel blocker, nilvadipine, slowed photoreceptor loss in RCS rats,[148] *Pde6b*^{rd1} mice,[149] and *rds* mice,[150] all of which have mutations in genes causing human RP. The bulk of the evidence indicates that Ca^{2+} overload mediated by calcium channels "potentiates" photoreceptor degeneration in some animal models, and successful use of strategies to counter these affects for therapeutic intervention will require a further understanding of the pathways and other molecules involved.[143]

Retinoids

Degeneration caused by the *Pde6B* mutation is the result of downstream activity related to a component of the transduction cascade, i.e., chronically elevated cGMP.[143] Likewise, some inherited photoreceptor degenerations result from mutations causing impairment of the first step in this cascade, the bleaching and regeneration of rhodopsin, i.e., the retinoid or visual cycle. Mutations in visual cycle enzymes result in a reduced capacity to regenerate visual pigment after bleaching. A second subset of diseases is caused by the accumulation of toxic derivatives of all-*trans*-retinaldehyde produced by isomerization of the visual pigment chromophore 11-*cis* retinaldehyde during normal photoactivation. Mutations in an ATP-binding cassette transporter called ABCR or ABCA4, which facilitates the tanslocation of all-*trans* retinaldehyde from disc membrane to the cytoplasmic space, is a cause of this subset of diseases. These retinal dystrophies can be treated pharmacologically with retinoids either to supplement or to inhibit visual cycle function, respectively.[151,152] An example of the former is the use of 9-*cis* retinaldehyde to recover function and preserve photoreceptors in animals with a mutation in the retinoid isomerase (*rpe65*)[153–155] and lecithin:retinol acyl transferase.[156] The validity of the strategy of blocking or inhibiting the retinoid cycle to protect photoreceptors was first demonstrated in the acute light-induced model; a single intraperitoneal injection of 40 mg/kg of isotretinoin (13-*cis* retinoic acid) given to rats prior to light exposure resulted in significant slowing of rhodopsin regeneration and reduction in photoreceptor cell loss due to light damage.[157] The

effect was reversible and long-term dosing had no effect on retinal morphology or function as measured by the ERG.

In contrast to the acute effects mediated by excessive light activation of the visual cycle, inherited retinal dystrophies may take years to result in significant photoreceptor and RPE damage due to the accumulation of toxic products. For example, the slow accumulation of autofluorescent lipofuscin containing A2E derived from the condensation of all-*trans* retinal and phosphatidylethanolamine in the lipid membranes of the outer-segment discs interferes with cellular metabolism and kills cells by apoptosis.[151,152] Evidence for A2E accumulation is found in multiple forms of retinal and macular degeneration, including Stargardt disease, AMD, and Best vitelliform macular dystrophy, and some rod–cone dystrophies. Even mutations in some genes coding for proteins not directly involved in retinoid processing result in A2E accumulation in animal models and human diseases, implying a wider applicability of pharmacologic strategies for visual cycle inhibition. Initially, the concept of modulating the visual cycle to counter the effects of A2E accumulation was done in a genetic model of Stargardt disease, the *abcr*$^{-/-}$ mouse, by raising them in darkness.[158] Dark-reared *abcr*$^{-/-}$ mice had levels of A2E equivalent to WT raised under cyclic light. Treatment of *abcr*$^{-/-}$ mice with isotretinoin completely blocked A2E synthesis and reduced lipofuscin deposits.[159] Though isotretinoin has unacceptable side-effects at doses necessary for human therapy in retinal dystrophies, these studies validated the concept of retinal protection by pharmacologically blocking the visual cycle. Other similar molecules that directly or indirectly reduce the level of all-*trans*-retinaldehyde and A2E production are being explored. Though treatment would necessarily slow rod dark adaptation, patients would not notice any difference in daylight vision mediated by cones.[160] Prolonging rod survival would help insure that cone vision is maintained in these rod dystrophies since the health of cones depends on the presence of rods.

Another possible application of retinoids in photoreceptor protection is as pharmacologic chaperones. The term "pharmacologic chaperone" refers to small molecules that bind to a protein at a specific site and help shift the folding equilibrium

toward the native structure.[161] These are often ligands, agonists or antagonists that bind in the ligand-binding pocket of the substrate polypeptides. Since about one-sixth of rhodopsin mutations that cause autosomal dominant RP are due to protein misfolding (see Heat shock proteins, below), retinoids are being investigated as therapy in these diseases. A series of in vitro[162–164] and in vivo[165] studies have demonstrated that retinoids can both stabilize the class II mutant opsin protein (e.g., Pro23His) to improve its movement through the secretory pathway and increase photoreceptor survival.

Modulation of Intracellular Neurotrophic Pathways

Heat Shock Proteins.

The use of neurotrophic factors, such as CNTF, in photoreceptor neuroprotection has been discussed. These proteins, released under conditions of cell stress and injury, produce their neuroprotective effect by activating intracellular pathways through cell surface receptors.[166] The intracellular effector molecules of these pathways are often transcription factors that promote DNA transcription leading to the production of antioxidant enzymes, calcium regulation proteins, cell cycle proteins, and metabolic enzymes.[167,168] One strategy for neuroprotection is to utilize the proteins and small molecules of these intracellular signaling pathways directly.[168] Lens epithelial-derived growth factor (LEDGF), for example, is a secreted cell survival factor expressed in response to stress signals.[169,170] Rather than binding to a cell surface receptor, it contains a Tat domain which allows it to enter cells and accumulate in the nucleus where it promotes the expression of smaller stress-related proteins, such as heat shock protein HSP27, which helps reduce caspase-dependent cell death. HSP27 binds to cytochrome c upon its release from mitochondria preventing its activation of caspase 3 and inhibiting apoptosis[169] (Fig. 39.5). LEDGF has been shown to promote cell survival under stress of many cell types in culture,[169] and intravitreal injection of the LEDGF protein protected photoreceptors in retinal light damage and the RCS rat model of inherited retinal degeneration.[171] In the retinas treated with LEDGF, HSP25 (the rat homolog of human HSP27), and the heat shock protein αB-crystallin expression was four- to fivefold higher

compared to the vehicle-injected eyes. To test whether upregulation of these small heat shock proteins could explain the protection by LEDGF, HSP25 was injected into the vitreous of RCS rats at 6 weeks of age and evaluated for retinal function by ERG and retinal morphology 4 weeks later (S Machida, PA Sieving, RA Bush, unpublished observations). HSP25 injection resulted in significantly better ERG responses and cellular preservation at 10 weeks of age than in vehicle-injected eyes (Fig. 39.6). The retinal level of HSP25 was higher in retinas from the HSP-injected eyes (data not shown). To confirm that intracellular HSP25 expression could rescue photoreceptors comparable to LEDGF, the genes for these proteins were transferred to the RCS rat retina using adenovirus HSP27 (the human homolog) and adeno-associated LEDGF viral vectors.[171] Both vectors resulted in similar degrees of rescue, which was similar to that seen with injection of the LEDGF and HSP25 protein. Protection only delayed the degeneration by about 2 weeks, however. But these results demonstrate that cell rescue can be achieved by exogenous administration of intracellular intermediates in endogenous survival-promoting pathways. Neuroprotection by small HSPs takes on added relevance with recent findings of the possible role of autoantibodies to HSP27 and HSP60 in the serum of glaucoma patients[172] and the production of a pattern of ganglion cell death in rats with induced autoimmunities to heat shock proteins.[173,174]

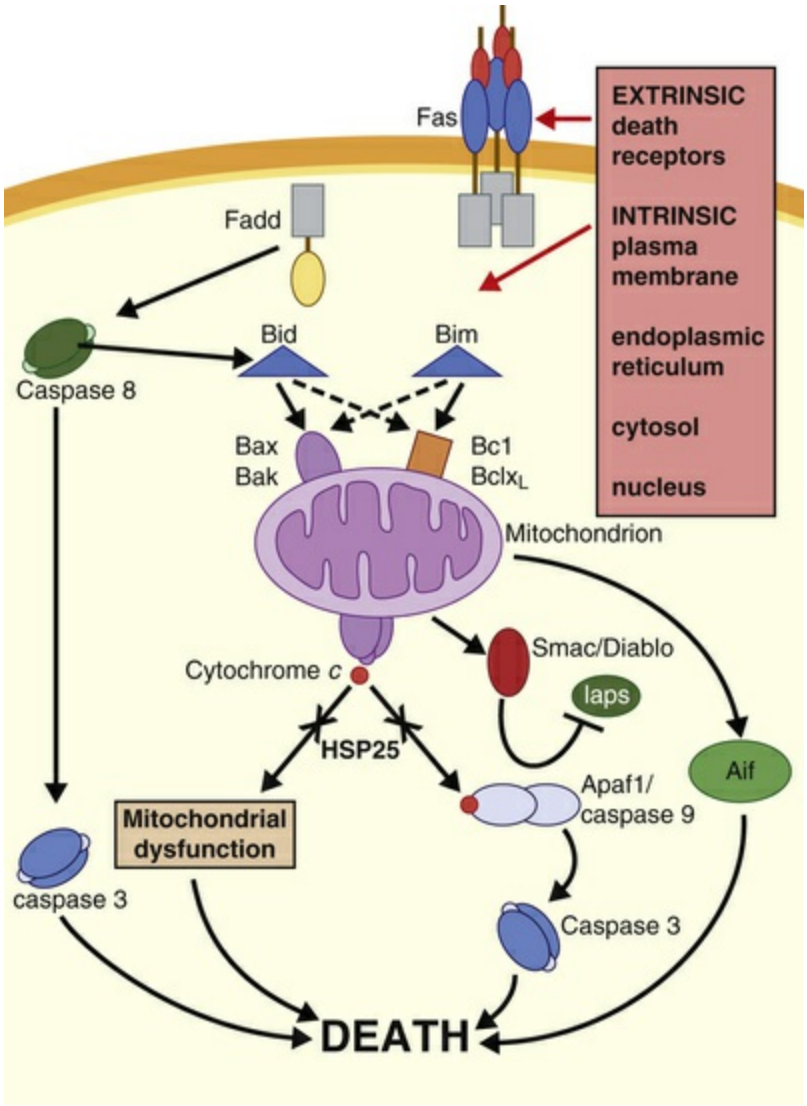

FIG. 39.5 The intracellular function of heat shock protein (HSP) 25 blocking cell death. (Reproduced with permission from Ranger AM, Malynn BA, Korsmeyer SJ. Mouse models of cell death. Nat Genet 2001;28:113–8.)

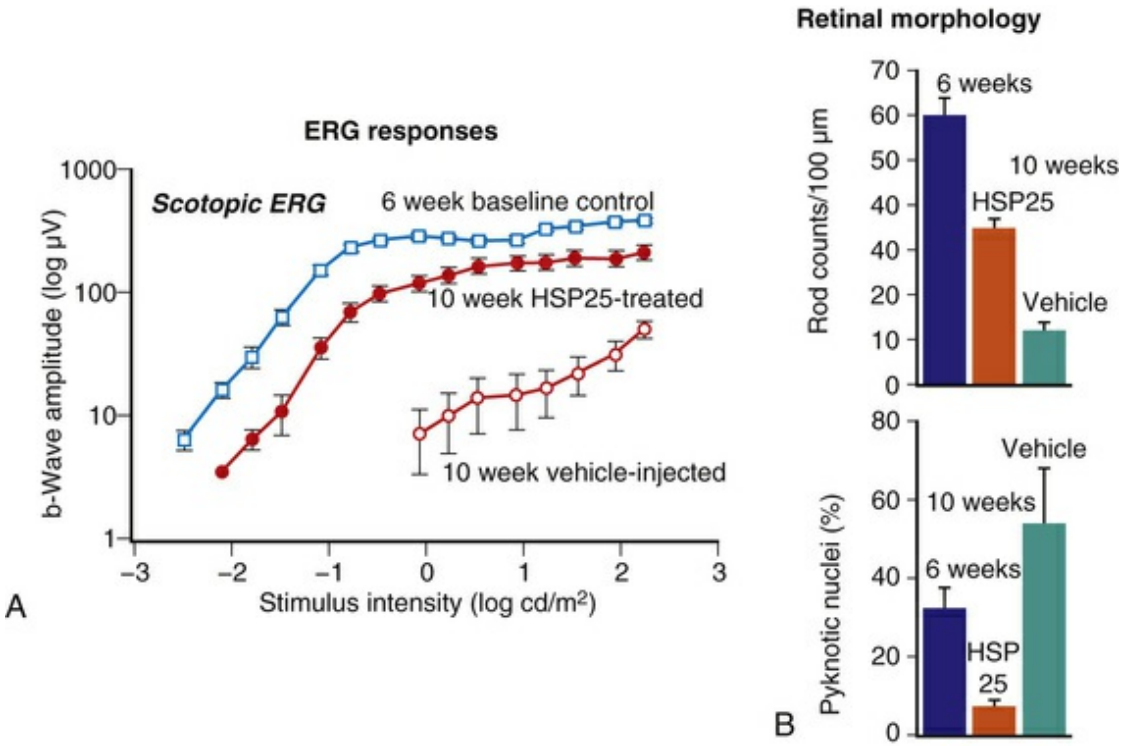

FIG. 39.6 (A,B) Photoreceptor functional and structural rescue by intravitreal injection of heat shock protein (HSP) 25 in the Royal College of Surgeons (RCS) rat. The RCS rat has a mutation in the MERTK gene in retinal pigment epithelial cells which prevents them from phagocytosing shed photoreceptor discs, resulting in death of rod and cone photoreceptors over several weeks. Rats received an intravitreal injection of 800 ng HSP25 in one eye and 1 µL buffer vehicle in the other eye at 6 weeks of age and were evaluated for electroretinogram response and retinal morphology at 10 weeks. The scotopic (rod) b-wave amplitude (log µv ± SEM) is shown over approximately 5 log units of stimulus intensity. HSP25-injected eyes (n=6) had a much higher b-wave amplitude at all intensities, had a lower threshold than the vehicle-injected eyes (n=6), and showed much less decline relative to the 6-week baseline (n=5). In retinal sections taken along the vertical meridian, the number of photoreceptors in the outer nuclear layer (nuclei/100 µm ± SD) was significantly greater in HSP25-treated eyes (n=6) than in vehicle-injected eyes (n=6; p<.0005). The proportion of these cells that were pyknotic (undergoing apoptosis) was significantly lower in HSP25-treated eyes than vehicle-injected eyes (n<.0001) and than eyes from the 6-week baseline control (n≤.0001). (Graphs

based on research by Machida S, Sieving PA, Bush RA, unpublished.)

Besides mediating the stress response, HSPs function as molecular chaperones to help regulate protein folding during synthesis and to keep misfolded proteins from aggregating by directing them to the proteosomal degradation machinery.[175] Many forms of autosomal dominant RP (adRP), for example, one-sixth of those caused by rhodopsin mutations, are due to mutations resulting in misfolded proteins and subsequent aggregation leading to photoreceptor cell death through a "gain of function" mechanism (e.g., Pro23His rhodopsin and Arg224Pro inosine 5′-monophosphate dehydrogenase type 1, IMPDH1, RP10, mutations).[176] Thus, enhancing HSP function either by vector-mediated overexpression or by pharmacologic means is being explored as a strategy for therapeutic intervention that could work in several kinds of adRP.[177] One such technique shown to be successful in several neurologic degeneration models is to produce an upregulation of HSP70 by pharmacologically inhibiting HSP90. This strategy has been effective in models of both Pro23His[178] and Rd10[179] using the partial geldanamycin derivative 17-allylamino-17demethoxygeldanamycin (17-AAG, molecular weight: 585.69). The former study was carried out in cell culture, while the latter was done using systemic administration in a mutant mouse. In addition to enhancing endogenous chaperone activity, small-molecule "pharmacologic chaperones," e.g., retinoids, are being studied for their ability to counteract both the gain of function and dominant negative phenotypes in adRP[178] (see Retinoids, above).

Minocycline.

Direct targeting of cell survival or death intracellular signaling pathways using small synthetic agonists or antagonists could be a valuable therapeutic approach in neuroprotection.[179] A good example is the recent research on the neuroprotective possibilities of minocycline, a semisynthetic broad-spectrum tetracycline antibiotic, in several neurodegenerative disorders. Since 2004 there have been more than 20 papers describing the neuroprotective effects of minocycline in animal and cell culture models of retinal degeneration. Minocycline can easily cross cell membranes, and

once in the cytoplasm, it modulates intracellular cytokine signaling pathways involving mitogen-activated kinases (MAPKs) or nuclear factor-kappa B (NF-κB). These pathways mediate cytokine responses to stress and injury and are linked to microglial activation in inflammation and the process of programmed cell death, or apoptosis, respectively.[180] Thus, minocycline may produce neuroprotection in the CNS by direct inhibition of apoptosis or by acting as an antiinflammatory agent through inhibition of microglial activation.[181] Several animal models of inherited photoreceptor degeneration show microglia activation and migration into the ONL, suggesting that microglia contribute to photoreceptor death.[182–185] Minocycline protected rods from degeneration in bright light-exposed mice and reduced the number of microglia entering the ONL.[186] It also delayed both photoreceptor degeneration and microglial activation in the rds mouse model of retinal degeneration.[181] In the latter study, however, depletion of microglia alone had no protective effect, suggesting the action of minocycline was microglia-independent and due to a direct effect on apoptosis pathways. Using an in vitro system of light-induced photoreceptor degeneration, Yang et al.[187] found that minocycline inhibited apoptosis, partly through an NF-κB-dependent mechanism, but not through the microglial-activating MAPK pathway. Recent research has focused on a possible role for minocycline treatment of diabetic retinopathy because of its ability to inhibit mitochondrial membrane permeability transition and Müller cell osmotic swelling[188] and reduce retinal edema[189] in the diabetic rat.

Rho GTPases.

As described earlier, activated Rac1 is a component of NADPH oxidase, which generates the superoxide anions thought to play a role in many forms of neurodegeneration.[190] Specific depletion of Rac1 in photoreceptors in a conditional knockout mouse resulted in photoreceptor protection from light-induced degeneration and a reduction in membrane-bound light-activated NADPH oxidase.[95] This is likely to be the mechanism of protection from light damage in the Rac1 conditional knockout. This is supported by the finding that a constitutively active Rac1 transgenic mouse showed

photoreceptor cell death and increased apoptosis.[191] However, inhibition of Rac1 may provide neuroprotection through other mechanisms. For example, persistent activation of Rac1 leads to autocrine production of the pleiotropic cytokine interleukin-6, which is involved in immune and inflammatory responses, and activation of STAT3.[192] It also stimulates activator protein-1 (AP-1), a regulator of apoptosis, through phosphorylation of c-jun.[193] Acute phototoxic insult involves the induction of AP-1 and members of the interleukin-6 family of cytokines in the neural retina and phosphorylation of STAT3 in Müller glial cells.[194] Small-molecule inhibitors of Rac1 that cross the blood–brain barrier have been shown to reduce the accumulation of Aβ peptide in animal models of Alzheimer's disease.[195] In addition, peptide inhibitors are being investigated for therapeutic effect in a variety of neurodegenerative disorders.[195–198]

Long-Chain Polyunsaturated Fatty Acids.

Long-chain polyunsaturated fatty acids (LCPUFAs) are usually thought of as structural components of cell membranes, but they also function in a number of intracellular signaling and metabolic pathways involved in the pathogenesis of vasoproliferative and retinal neurodegenerative disorders.[199] Dietary omega-3 LCPUFAs are important in normal retinal function as well as neuroprotection. Docosahexaenoic acid (DHA) in particular is important for photoreceptor metabolism and transduction mechanisms and it makes up the largest fraction of the LCPUFAs in the outer-segment disc membranes.[200] Lowered dietary intake of LCPUFAs reduced susceptibility of the rat retina to light-induced photoreceptor damage,[201] possibly through a slowing of the regeneration rate of rhodopsin.[202] Dietary effects on the levels of retinal LCPUFAs may affect a variety of retinal molecules and signaling pathways involved in neuroprotection, including dopamine, cyclic nucleotides, endocannabinoids, glutamate, and ionic transport and channel dynamics.[199] Metabolic and environmental activators of LCPUFAs, phospholipase A_2, cyclooxygenase, and lipoxygenase are associated with a number of retinal diseases, including diabetic retinopathy, AMD, and retinopathy of prematurity through modulation of neuronal and vascular function.[199] A major dietary

source of LCPUFAs is fish. Incidence of AMD was shown to decrease with increasing intake of DHA, tuna, or total fish.[203] Several other studies have shown similar trends,[199] but the neuroprotective mechanism is not known.

The natural recycling of membrane phospholipids produces neuroprotectin D1 (NPD1), the first known bioactive product of DHA. This molecule is produced by the action of phospholipase A_2 that releases free DHA from membrane phospholipids under conditions of oxidative stress and inflammation and promotes cell survival in animal models of stroke and Alzheimer's disease[204,205] and protects RPE cells from oxidative stress.[206,207] The latter effect is linked to activation of the phosphatidylinositol 3-kinase/Akt signaling pathway through increased phosphorylation.[206] Though a direct effect on photoreceptor neuroprotection has so far not been demonstrated, NPD1 produced in RPE upon daily phagocytosis of photoreceptor membranous discs, which contain large amounts of esterified DHA, may be released and promote the survival of other retinal cells in a paracrine fashion.[208]

Peptide Neurotrophin Receptor Agonists/Antagonists.

Neurotrophins, e.g., CNTF, and their receptors have proven to be useful as therapeutic targets in a variety of diseases, including retinal degenerations. They often fail to have the expected effect in vivo, however, in part because of their effect on multiple cell types and receptors. As members of the growth factor family of proteins, their size and complexity may also make them unstable and unable to reach the target tissues. Recently, small-molecule peptides have been designed to bind regulatory or activating subdomains of the Trk and $p75^{NTR}$ neurotrophin receptors to selectively activate or inhibit these receptors.[209] A potential therapeutic application for these compounds in retinal degeneration has been demonstrated in ganglion cell survival after axotomy.[210] While BDNF is a potent survival factor for injured ganglion cells,[211] NGF does not promote survival either in vitro[212] or in vivo.[213] It was found, however, that peptide agonists, which selectively activate the NGF TrkA receptor on ganglion cells, provided neuroprotection following axotomy.[210] Simultaneously treating with an antagonist to the proapoptotic $p75^{NTR}$ receptors further enhanced neuroprotection, even though

these receptors are found on Müller cells but not ganglion cells. This study, carried out using intravitreal injections in the rat, highlights the potential therapeutic benefits of using small molecules that mimic selected actions of larger molecules to achieve neuroprotection and avoid unwanted effects.

References

1. Osborne NN. Recent clinical findings with memantine should not mean that the idea of neuroprotection in glaucoma is abandoned. *Acta Ophthalmol*. 2009;87:450–454.
2. Lambiase A, Aloe L, Centofanti M, et al. Experimental and clinical evidence of neuroprotection by nerve growth factor eye drops: implications for glaucoma. *Proc Natl Acad Sci USA*. 2009;106:13469–13474.
3. van Adel BA, Kostic C, Deglon N, et al. Delivery of ciliary neurotrophic factor via lentiviral-mediated transfer protects axotomized retinal ganglion cells for an extended period of time. *Hum Gene Ther*. 2003;14:103–115.
4. Allergan Inc. *Press releases on memantine trials, fourth quarter operating results*. [Jan 30] http://agn.client.shareholder.com/releasedetail.cfm?ReleaseID=290764; 2008.
5. Belkin M. Nerve growth factor and glaucoma. *Glaucoma Today*. 2009;18–19.
6. Sommer A, Tielsch JM, Katz J, et al. Relationship between intraocular pressure and primary open angle glaucoma among white and black Americans. The Baltimore Eye Survey. *Arch Ophthalmol*. 1991;109:1090–1095.
7. Anderson DR. Collaborative normal tension glaucoma study. *Curr Opin Ophthalmol*. 2003;14:86–90.
8. Becker B, Stamper RL, Asseff C, et al. Effect of diphenylhydantoin on glaucomatous field loss: a preliminary report. *Trans Am Acad Ophthalmol Otolaryngol*. 1972;76:412–422.
9. Hains BC, Waxman SG. Neuroprotection by sodium channel blockade with phenytoin in an experimental model of glaucoma. *Invest Ophthalmol Vis Sci*. 2005;46:4164–4169.

10. Kerchner GA, Tartaglia MC, Boxer A. Abhorring the vacuum: use of Alzheimer's disease medications in frontotemporal dementia. *Expert Rev Neurother*. 2011;11:709–717.
11. Doble A. The pharmacology and mechanism of action of riluzole. *Neurology*. 1996;47:S233–41.
12. Lamanauskas N, Nistri A. Riluzole blocks persistent Na^+ and Ca^{2+} currents and modulates release of glutamate via presynaptic NMDA receptors on neonatal rat hypoglossal motoneurons in vitro. *Eur J Neurosci*. 2008;27:2501–2514.
13. Chen HS, Pellegrini JW, Aggarwal SK, et al. Open-channel block of *N*-methyl-D-aspartate (NMDA) responses by memantine: therapeutic advantage against NMDA receptor-mediated neurotoxicity. *J Neurosci*. 1992;12:4427–4436.
14. Brooks DE, Garcia GA, Dreyer EB, et al. Vitreous body glutamate concentration in dogs with glaucoma. *Am J Vet Res*. 1997;58:864–867.
15. Dreyer EB, Zurakowski D, Schumer RA, et al. Elevated glutamate levels in the vitreous body of humans and monkeys with glaucoma. *Arch Ophthalmol*. 1996;114:299–305.
16. Johnson EC, Guo Y, Cepurna WO, et al. Neurotrophin roles in retinal ganglion cell survival: lessons from rat glaucoma models. *Exp Eye Res*. 2009;88:808–815.
17. Chen H, Weber AJ. BDNF enhances retinal ganglion cell survival in cats with optic nerve damage. *Invest Ophthalmol Vis Sci*. 2001;42:966–974.
18. Song XY, Li F, Zhang FH, et al. Peripherally-derived BDNF promotes regeneration of ascending sensory neurons after spinal cord injury. *PLoS ONE*. 2008;3:e1707.
19. Domenici L, Origlia N, Falsini B, et al. Rescue of retinal function by BDNF in a mouse model of glaucoma. *PLoS ONE*. 2014;9(12):e115579.
20. Rammes G, Rupprecht R, Ferrari U, et al. The *N*-methyl-D-aspartate receptor channel blockers memantine, MRZ 2/579 and other amino-alkyl-cyclohexanes antagonise 5-HT(3) receptor currents in cultured HEK-293 and N1E-115 cell

systems in a non-competitive manner. *Neurosci Lett*. 2001;306:81–84.
21. Lipton SA. Pathologically activated therapeutics for neuroprotection. *Nat Rev Neurosci*. 2007;8:803–808.
22. Nishimura T, Ishima T, Iyo M, et al. Potentiation of nerve growth factor-induced neurite outgrowth by fluvoxamine: role of sigma-1 receptors, IP3 receptors and cellular signaling pathways. *PLoS ONE*. 2008;3:e2558.
23. May JA, Chen HH, Rusinko A, et al. A novel and selective 5-HT2 receptor agonist with ocular hypotensive activity: (S)-(+)-1-(2-aminopropyl)-8,9-dihydropyrano[3,2-e]indole. *J Med Chem*. 2003;46:4188–4195.
24. May JA, Dantanarayana AP, Zinke PW, et al. 1-((S)-2-aminopropyl)-1H-indazol-6-ol: a potent peripherally acting 5-HT2 receptor agonist with ocular hypotensive activity. *J Med Chem*. 2006;49:318–328.
25. Faktorovich EG, Steinberg RH, Yasumura D, et al. Photoreceptor degeneration in inherited retinal dystrophy delayed by basic fibroblast growth factor. *Nature*. 1990;347:83–86.
26. LaVail MM, Unoki K, Yasumura D, et al. Multiple growth factors, cytokines, and neurotrophins rescue photoreceptors from the damaging effects of constant light. *Proc Natl Acad Sci USA*. 1992;89:11249–11253.
27. Gorbatyuk MS, Knox T, LaVail MM, et al. Restoration of visual function in P23H rhodopsin transgenic rats by gene delivery of BiP/Grp78. *Proc Natl Acad Sci USA*. 2010;107:5961–5966.
28. LaVail MM, Yasumura D, Matthes MT, et al. Ribozyme rescue of photoreceptor cells in P23H transgenic rats: long-term survival and late-stage therapy. *Proc Natl Acad Sci USA*. 2000;97:11488–11493.
29. Peterson WM, Wang Q, Tzekova R, et al. Ciliary neurotrophic factor and stress stimuli activate the Jak-STAT pathway in retinal neurons and glia. *J Neurosci*. 2000;20:4081–4090.
30. Lambiase A, Aloe L. Nerve growth factor delays retinal degeneration in C3H mice. *Graefes Arch Clin Exp Ophthalmol*.

1996;234(Suppl. 1):S96–100.
31. Cayouette M, Gravel C. Adenovirus-mediated gene transfer of ciliary neurotrophic factor can prevent photoreceptor degeneration in the retinal degeneration (rd) mouse. *Hum Gene Ther*. 1997;8:423–430.
32. Cao W, Wen R, Li F, et al. Mechanical injury increases bFGF and CNTF mRNA expression in the mouse retina. *Exp Eye Res*. 1997;65:241–248.
33. Cohen S, Levi-Montalcini R, Hamburger V. A nerve growth-stimulating factor isolated from sarcomas 37 and 180. *Proc Natl Acad Sci USA*. 1954;40:1014–1018.
34. Levi-Montalcini R, Hamburger V. Selective growth stimulating effects of mouse sarcoma on the sensory and sympathetic nervous system of the chick embryo. *J Exp Zool*. 1951;116:321–361.
35. Cayouette M, Behn D, Sendtner M, et al. Intraocular gene transfer of ciliary neurotrophic factor prevents death and increases responsiveness of rod photoreceptors in the retinal degeneration slow mouse. *J Neurosci*. 1998;18:9282–9293.
36. Adler R, Landa KB, Manthorpe M, et al. Cholinergic neuronotrophic factors: intraocular distribution of trophic activity for ciliary neurons. *Science*. 1979;204:1434–1436.
37. Varon S, Manthorpe M, Adler R. Cholinergic neuronotrophic factors: I. Survival, neurite outgrowth and choline acetyltransferase activity in monolayer cultures from chick embryo ciliary ganglia. *Brain Res*. 1979;173:29–45.
38. Adler R. Ciliary neurotrophic factor as an injury factor. *Curr Opin Neurobiol*. 1993;3:785–789.
39. McDonald NQ, Panayotatos N, Hendrickson WA. Crystal structure of dimeric human ciliary neurotrophic factor determined by MAD phasing. *EMBO J*. 1995;14:2689–2699.
40. Sleeman MW, Anderson KD, Lambert PD, et al. The ciliary neurotrophic factor and its receptor, CNTFR alpha. *Pharm Acta Helv*. 2000;74:265–272.
41. Boulton TG, Stahl N, Yancopoulos GD. Ciliary neurotrophic factor/leukemia inhibitory factor/interleukin 6/oncostatin M

family of cytokines induces tyrosine phosphorylation of a common set of proteins overlapping those induced by other cytokines and growth factors. *J Biol Chem*. 1994;269:11648–11655.
42. Leonard WJ, O'Shea JJ. Jaks and STATs: biological implications. *Annu Rev Immunol*. 1998;16:293–322.
43. Heinrich PC, Behrmann I, Müller-Newen G, et al. Interleukin-6-type cytokine signalling through the gp130/Jak/STAT pathway. *Biochem J*. 1998;334:297–314.
44. Bok D, Yasumura D, Matthes MT, et al. Effects of adeno-associated virus-vectored ciliary neurotrophic factor on retinal structure and function in mice with a P216L rds/peripherin mutation. *Exp Eye Res*. 2002;74:719–735.
45. Bush RA, Lei B, Tao W, et al. Encapsulated cell-based intraocular delivery of ciliary neurotrophic factor in normal rabbit: dose-dependent effects on ERG and retinal histology. *Invest Ophthalmol Vis Sci*. 2004;45:2420–2430.
46. Sieving PA, Caruso RC, Tao W, et al. Ciliary neurotrophic factor (CNTF) for human retinal degeneration: phase I trial of CNTF delivered by encapsulated cell intraocular implants. *Proc Natl Acad Sci USA*. 2006;103:3896–3901.
47. Humphries MM, Rancourt D, Farrar GJ, et al. Retinopathy induced in mice by targeted disruption of the rhodopsin gene. *Nat Genet*. 1997;15:216–219.
48. Geller AM, Sieving PA. Assessment of foveal cone photoreceptors in Stargardt's macular dystrophy using a small dot detection task. *Vision Res*. 1993;33:1509–1524.
49. *A study of an encapsulated cell technology (ECT) implant for patients with atrophic macular degeneration (database on the Internet)*. http://clinicaltrials.gov/ct2/show/NCT00447954?term=CNTF+eye&rank=4.
50. *A study of encapsulated cell technology (ECT) implant for patients with late stage retinitis pigmentosa (database on the Internet)*. http://clinicaltrials.gov/ct2/show/NCT00447993?term=CNTF+eye&rank=3.
51. *A study of encapsulated cell technology (ECT) implant for participants with early stage retinitis pigmentosa (database on the Internet)*. http://clinicaltrials.gov/ct2/show/NCT00447980?

term=CNTF+eye&rank=2.
52. Zhang K, Hopkins JJ, Heier JS, et al. Ciliary neurotrophic factor delivered by encapsulated cell intraocular implants for treatment of geographic atrophy in age-related macular degeneration. *Proc Natl Acad Sci USA*. 2011;108:6241–6245.
53. Komaromy AM, Rowlan JS, Corr ATP, et al. Transient photoreceptor deconstruction by CNTF enhances rAAV-mediated cone functional rescue in late stage CNGB3-achromatopsia. *Mol Ther*. 2013;21:1131–1141.
54. Zein WM, Jeffrey BG, Wiley HE, et al. CNGB3-achromatopsia clinical trial with CNTF: diminished rod pathway responses with no evidence of improvement in cone function. *Invest Ophthalmol Vis Sci*. 2014;55:6301–6308.
55. Marangoni D, Vijayasarathy C, Bush RA, et al. Intravitreal ciliary neurotrophic factor transiently improves cone-mediated function in a CNGB3$^{-/-}$ mouse model of achromatopsia. *Invest Ophthalmol Vis Sci*. 2015;56:6810–6822.
56. Powner MB, Gillies MC, Tretiach M, et al. Perifoveal muller cell depletion in a case of macular telangiectasia type 2. *Ophthalmology*. 2010;117(12):2407–2416.
57. Chew EY, Clemons TE, Peto T, MacTel-CNTF Research Group, et al. Ciliary neurotrophic factor for macular telangiectasia type 2: results from a phase 1 safety trial. *Am J Ophthalmol*. 2015;159:659–666.
58. Talcott KE, Ratnam K, Sundquist SM, et al. Longitudinal study of cone photoreceptors during retinal degeneration and in response to ciliary neurotrophic factor treatment. *Invest Ophthalmol Vis Sci*. 2011;52:2219–2226.
59. Brown DM, Kaiser PK, Michels M, et al. Ranibizumab versus verteporfin for neovascular age-related macular degeneration. *N Engl J Med*. 2006;355:1432–1444.
60. Rosenfeld PJ, Brown DM, Heier JS, et al. Ranibizumab for neovascular age-related macular degeneration. *N Engl J Med*. 2006;355:1419–1431.
61. Acland GM, Aguirre GD, Ray J, et al. Gene therapy restores vision in a canine model of childhood blindness. *Nat Genet*. 2001;28:92–95.
62. Wiegand RD, Giusto NM, Rapp LM, et al. Evidence for rod

outer segment lipid peroxidation following constant illumination of the rat retina. *Invest Ophthalmol Vis Sci*. 1983;24:1433–1435.
63. Tanito M, Yoshida Y, Kaidzu S, et al. Detection of lipid peroxidation in light-exposed mouse retina assessed by oxidative stress markers, total hydroxyoctadecadienoic acid and 8-iso-prostaglandin F2alpha. *Neurosci Lett*. 2006;398:63–68.
64. Organisciak DT, Darrow RM, Jiang YI, et al. Protection by dimethylthiourea against retinal light damage in rats. *Invest Ophthalmol Vis Sci*. 1992;33:1599–1609.
65. Penn JS, Naash MI, Anderson RE. Effect of light history on retinal antioxidants and light damage susceptibility in the rat. *Exp Eye Res*. 1987;44:779–788.
66. Gosbell AD, Stefanovic N, Scurr LL, et al. Retinal light damage: structural and functional effects of the antioxidant glutathione peroxidase-1. *Invest Ophthalmol Vis Sci*. 2006;47:2613–2622.
67. Xie Z, Wu X, Gong Y, et al. Intraperitoneal injection of *Ginkgo biloba* extract enhances antioxidation ability of retina and protects photoreceptors after light-induced retinal damage in rats. *Curr Eye Res*. 2007;32:471–479.
68. Ranchon I, Gorrand JM, Cluzel J, et al. Functional protection of photoreceptors from light-induced damage by dimethylthiourea and *Ginkgo biloba* extract. *Invest Ophthalmol Vis Sci*. 1999;40:1191–1199.
69. Tomita H, Kotake Y, Anderson RE. Mechanism of protection from light-induced retinal degeneration by the synthetic antioxidant phenyl-*N*-tert-butylnitrone. *Invest Ophthalmol Vis Sci*. 2005;46:427–434.
70. Logvinov SV, Plotnikov MB, Varakuta EY, et al. Effect of ascovertin on morphological changes in rat retina exposed to high-intensity light. *Bull Exp Biol Med*. 2005;140:578–581.
71. Yilmaz T, Aydemir O, Ozercan IH, et al. Effects of vitamin E, pentoxifylline and aprotinin on light-induced retinal injury. *Ophthalmologica*. 2007;221:159–166.
72. Stahl W, Sies H. Bioactivity and protective effects of natural carotenoids. *Biochim Biophys Acta*. 2005;1740:101–107.

73. Costa BL, Fawcett R, Li GY, et al. Orally administered epigallocatechin gallate attenuates light-induced photoreceptor damage. *Brain Res Bull*. 2008;76:412–423.
74. Komeima K, Rogers BS, Lu L, et al. Antioxidants reduce cone cell death in a model of retinitis pigmentosa. *Proc Natl Acad Sci USA*. 2006;103:11300–11305.
75. Shen J, Yang X, Dong A, et al. Oxidative damage is a potential cause of cone cell death in retinitis pigmentosa. *J Cell Physiol*. 2005;203:457–464.
76. Jozwick C, Valter K, Stone J. Reversal of functional loss in the P23H-3 rat retina by management of ambient light. *Exp Eye Res*. 2006;83:1074–1080.
77. Chrysostomou V, Stone J, Stowe S, et al. The status of cones in the rhodopsin mutant P23H-3 retina: light-regulated damage and repair in parallel with rods. *Invest Ophthalmol Vis Sci*. 2008;49:1116–1125.
78. Valter K, Kirk DK, Stone J. Optimising the structure and function of the adult P23H-3 retina by light management in the juvenile and adult. *Exp Eye Res*. 2009;89:1003–1011.
79. Yu DY, Cringle SJ, Su EN, et al. Intraretinal oxygen levels before and after photoreceptor loss in the RCS rat. *Invest Ophthalmol Vis Sci*. 2000;41:3999–4006.
80. Usui S, Oveson BC, Lee SY, et al. NADPH oxidase plays a central role in cone cell death in retinitis pigmentosa. *J Neurochem*. 2009;110:1028–1037.
81. Komeima K, Usui S, Shen J, et al. Blockade of neuronal nitric oxide synthase reduces cone cell death in a model of retinitis pigmentosa. *Free Radic Biol Med*. 2008;45:905–912.
82. Usui S, Komeima K, Lee SY, et al. Increased expression of catalase and superoxide dismutase 2 reduces cone cell death in retinitis pigmentosa. *Mol Ther*. 2009;17:778–786.
83. Lu L, Oveson BC, Jo YJ, et al. Increased expression of glutathione peroxidase 4 strongly protects retina from oxidative damage. *Antioxid Redox Signal*. 2009;11:715–724.
84. Vingerling JR, Dielemans I, Witteman JC, et al. Macular degeneration and early menopause: a case-control study. *BMJ*. 1995;310:1570–1571.
85. Risk factors for neovascular age-related macular

degeneration. The Eye Disease Case-Control Study Group. *Arch Ophthalmol*. 1992;110:1701–1708.
86. Khayum MA, de Vries EF, Glaudemans AW, et al. In vivo imaging of brain estrogen receptors in rats: a 16alpha-18F-fluoro-17beta-estradiol PET study. *J Nucl Med*. 2014;55:481–487.
87. Azcoitia I, Yague JG, Garcia-Segura LM. Estradiol synthesis within the human brain. *Neuroscience*. 2011;191:139–147.
88. Vina J, Sastre J, Pallardo FV, et al. Modulation of longevity-associated genes by estrogens or phytoestrogens. *Biol Chem*. 2008;389:273–277.
89. Dubal DB, Wise PM. Neuroprotective effects of estradiol in middle-aged female rats. *Endocrinology*. 2001;142:43–48.
90. Doonan F, O'Driscoll C, Kenna P, et al. Enhancing survival of photoreceptor cells in vivo using the synthetic progestin Norgestrel. *J Neurochem*. 2011;118:915–927.
91. Doonan F, Cotter TG. Norgestrel may be a potential therapy for retinal degenerations. *Expert Opin Investig Drugs*. 2012;21:579–581.
92. Miranda M, Arnal E, Ahuja S, et al. Antioxidants rescue photoreceptors in rd1 mice: relationship with thiol metabolism. *Free Radic Biol Med*. 2010;48:216–222.
93. Ushio-Fukai M. Localizing NADPH oxidase-derived ROS. *Sci STKE*. 2006;2006:re8.
94. Balasubramanian N, Slepak VZ. Light-mediated activation of Rac-1 in photoreceptor outer segments. *Curr Biol*. 2003;13:1306–1310.
95. Haruta M, Bush RA, Kjellstrom S, et al. Depleting Rac1 in mouse rod photoreceptors protects them from photo-oxidative stress without affecting their structure or function. *Proc Natl Acad Sci USA*. 2009;106:9397–9402.
96. Leveillard T, Sahel JA. Rod-derived cone viability factor for treating blinding diseases: from clinic to redox signaling. *Sci Transl Med*. 2010;2:26ps16.
97. Ait-Ali N, Fridlich R, Millet-Puel G, et al. Rod-derived cone viability factor promotes cone survivial by stimulating aerobic glycolysis. *Cell*. 2015;161:817–832.
98. Lee SY, Usui S, Zafar AB, et al. *N*-Acetylcysteine promotes

long-term survival of cones in a model of retinitis pigmentosa. *J Cell Physiol*. 2011;226:1843–1849.
99. Maccarone R, Di Marco S, Bisti S. Saffron supplement maintains morphology and function after exposure to damaging light in mammalian retina. *Invest Ophthalmol Vis Sci*. 2008;49:1254–1261.
100. Giaccio M. Crocetin from saffron: an active component of an ancient spice. *Crit Rev Food Sci Nutr*. 2004;44:155–172.
101. Natoli R, Zhu Y, Valter K, et al. Gene and noncoding RNA regulation underlying photoreceptor protection: microarray study of dietary antioxidant saffron and photobiomodulation in rat retina. *Mol Vis*. 2010;16:1801–1822.
102. Kong L, Cai X, Zhou X, et al. Nanoceria extend photoreceptor cell lifespan in tubby mice by modulation of apoptosis/survival signaling pathways. *Neurobiol Dis*. 2011;42:514–523.
103. AREDS Research Group. A randomized, placebo-controlled, clinical trial of high-dose supplementation with vitamins C and E, beta carotene, and zinc for age-related macular degeneration and vision loss: AREDS Report No. 8. *Arch Ophthalmol*. 2001;119:1417–1436.
104. Richer S, Stiles W, Statkute L, et al. Double-masked, placebo-controlled, randomized trial of lutein and antioxidant supplementation in the intervention of atrophic age-related macular degeneration: the Veterans LAST study (Lutein Antioxidant Supplementation Trial). *Optometry*. 2004;75:216–230.
105. Falsini B, Piccardi M, Iarossi G, et al. Influence of short-term antioxidant supplementation on macular function in age-related maculopathy: a pilot study including electrophysiologic assessment. *Ophthalmology*. 2003;110:51–60 [discussion 1].
106. Parisi V, Tedeschi M, Gallinaro G, et al. Carotenoids and antioxidants in age-related maculopathy Italian study: multifocal electroretinogram modifications after 1 year. *Ophthalmology*. 2008;115 [324–33.e2].
107. Falsini B, Piccardi M, Minnella A, et al. Influence of saffron

supplementation on retinal flicker sensitivity in early age-related macular degeneration. *Invest Ophthalmol Vis Sci*. 2010;51:6118–6124.
108. Berson EL, Rosner B, Sandberg MA, et al. Clinical trial of lutein in patients with retinitis pigmentosa receiving vitamin A. *Arch Ophthalmol*. 2010;128:403–411.
109. Wong WT, Kam W, Cunningham D, et al. Treatment of geographic atrophy by the topical administration of OT-551: results of a phase II clinical trial. *Invest Ophthalmol Vis Sci*. 2010;51:6131–6139.
110. El Sanharawi M, Kowalczuk L, Touchard E, et al. Protein delivery for retinal diseases: from basic considerations to clinical applications. *Prog Retin Eye Res*. 2010;29:443–465.
111. Chen Y, Palczewska G, Mustafi D, et al. Systems pharmacology identifies drug targets for Stargardt disease-associated retinal degeneration. *J Clin Invest*. 2013;123:5119–5134.
112. Wiechmann AF, Summers JA. Circadian rhythms in the eye: the physiological significance of melatonin receptors in ocular tissues. *Prog Retin Eye Res*. 2008;27:137–160.
113. Tosini G, Baba K, Hwang CK, et al. Melatonin: an underappreciated player in retinal physiology and pathophysiology. *Exp Eye Res*. 2012;103:82–89.
114. Wiechmann AF, O'Steen WK. Melatonin increases photoreceptor susceptibility to light-induced damage. *Invest Ophthalmol Vis Sci*. 1992;33:1894–1902.
115. Wiechmann AF, Chignell CF, Roberts JE. Influence of dietary melatonin on photoreceptor survival in the rat retina: an ocular toxicity study. *Exp Eye Res*. 2008;86:241–250.
116. Grewal R, Organisciak D, Wong P. Factors underlying circadian dependent susceptibility to light induced retinal damage. *Adv Exp Med Biol*. 2006;572:411–416.
117. Sugawara T, Sieving PA, Iuvone PM, et al. The melatonin antagonist luzindole protects retinal photoreceptors from light damage in the rat. *Invest Ophthalmol Vis Sci*. 1998;39:2458–2465.
118. Baba K, Pozdeyev N, Mazzoni F, et al. Melatonin modulates

visual function and cell viability in the mouse retina via the MT1 melatonin receptor. *Proc Natl Acad Sci USA*. 2009;106:15043–15048.
119. Osborne NN, Nash MS, Wood JP. Melatonin counteracts ischemia-induced apoptosis in human retinal pigment epithelial cells. *Invest Ophthalmol Vis Sci*. 1998;39:2374–2383.
120. Argun M, Tok L, Uguz AC, et al. Melatonin and amfenac modulate calcium entry, apoptosis, and oxidative stress in ARPE-19 cell culture exposed to blue light irradiation (405 nm). *Eye (Lond)*. 2014;28:752–760.
121. Yi C, Pan X, Yan H, et al. Effects of melatonin in age-related macular degeneration. *Ann N Y Acad Sci*. 2005;1057:384–392.
122. Esposito E, Cuzzocrea S. Antiinflammatory activity of melatonin in central nervous system. *Curr Neuropharmacol*. 2010;8:228–242.
123. Jackson CR, Chaurasia SS, Zhou H, et al. Essential roles of dopamine D4 receptors and the type 1 adenylyl cyclase in photic control of cyclic AMP in photoreceptor cells. *J Neurochem*. 2009;109:148–157.
124. de Melo Reis RA, Ventura AL, Schitine CS, et al. Müller glia as an active compartment modulating nervous activity in the vertebrate retina: neurotransmitters and trophic factors. *Neurochem Res*. 2008;33:1466–1474.
125. Chen Y, Okano K, Maeda T, et al. Mechanism of all-*trans*-retinal toxicity with implications for Stargardt disease and age-related macular degeneration. *J Biol Chem*. 2012;287:5059–5069.
126. Merin S, Obolensky A, Farber MD, et al. A pilot study of topical treatment with an alpha-2-agonist in patients with retinal dystrophies. *J Ocul Pharmacol Ther*. 2008;24:80–86.
127. Ahmed FA, Hegazy K, Chaudhary P, et al. Neuroprotective effect of alpha(2) agonist (brimonidine) on adult rat retinal ganglion cells after increased intraocular pressure. *Brain Res*. 2001;913:133–139.
128. Chao HM, Osborne NN. Topically applied clonidine protects the rat retina from ischaemia/reperfusion by stimulating alpha(2)-adrenoceptors and not by an action on imidazoline receptors. *Brain Res*. 2001;904:126–136.

129. Lai RK, Chun T, Hasson D, et al. Alpha-2 adrenoceptor agonist protects retinal function after acute retinal ischemic injury in the rat. *Vis Neurosci*. 2002;19:175–185.
130. Yoles E, Wheeler LA, Schwartz M. Alpha-2-adrenoreceptor agonists are neuroprotective in a rat model of optic nerve degeneration. *Invest Ophthalmol Vis Sci*. 1999;40:65–73.
131. Dong CJ, Guo Y, Agey P, et al. Alpha-2 adrenergic modulation of NMDA receptor function as a major mechanism of RGC protection in experimental glaucoma and retinal excitotoxicity. *Invest Ophthalmol Vis Sci*. 2008;49:4515–4522.
132. Peng M, Li Y, Luo Z, et al. Alpha-2-adrenergic agonists selectively activate extracellular signal-regulated kinases in Müller cells in vivo. *Invest Ophthalmol Vis Sci*. 1998;39:1721–1726.
133. Wen R, Cheng T, Li Y, et al. Alpha-2-adrenergic agonists induce basic fibroblast growth factor expression in photoreceptors in vivo and ameliorate light damage. *J Neurosci*. 1996;16:5986–5992.
134. Iuvone PM, Boatright JH, Tosini G, et al. N-Acetylserotonin: circadian activation of the BDNF receptor and neuroprotection in the retina and brain. Ash JD, Grimm C, Hollyfield JG, et al. *Retinal degenerative diseases. Advances in experimental medicine and biology 801*. Springer: New York; 2014:765–771.
135. Thampi P, Rao HV, Mitter SK, et al. The 5HT Receptor agonist 8-Oh DPAT induces protection from lipofuscin accumulation and oxidative stress in the retinal pigment epithelium. *PLoS ONE*. 2012;7:e34468.
136. Rosen RB, Hu D-N, Chen M, et al. Effects of melatonin and its receptor antagonist on retinal pigment epithelial cells against hydrogen peroxide damage. *Mol Vis*. 2012;18:1640–1648.
137. Tullis BE, Ryals RC, Coyner AS, et al. Sarpogrelate, a 5-HT2A receptor antagonist, protects the retina from light-induced retinopathy. *Invest Ophthalmol Vis Sci*. 2015;56:4560–4569.
138. Salido EM, Bordone M, De Laurentiis A, et al. Therapeutic

efficacy of melatonin in reducing retinal damage in an experimental model of early type 2 diabetes in rats. *J Pineal Res*. 2013;54:179–189.
139. Kaur C, Sivakumar V, Robinson R, et al. Neuroprotective effect of melatonin against hypoxia-induced retinal ganglion cell death in neonatal rats. *J Pineal Res*. 2013;54:190–206.
140. Frasson M, Sahel JA, Fabre M, et al. Retinitis pigmentosa: rod photoreceptor rescue by a calcium-channel blocker in the rd mouse. *Nat Med*. 1999;5:1183–1187.
141. Edward DP, Lam TT, Shahinfar S, et al. Amelioration of light-induced retinal degeneration by a calcium overload blocker: flunarizine. *Arch Ophthalmol*. 1991;109:554–562.
142. McLaughlin ME, Ehrhart TL, Berson EL, et al. Mutation spectrum of the gene encoding the beta subunit of rod phosphodiesterase among patients with autosomal recessive retinitis pigmentosa. *Proc Natl Acad Sci USA*. 1995;92:3249–3253.
143. Barabas P, Cutler Peck C, Krizaj D. Do calcium channel blockers rescue dying photoreceptors in the Pde6b (rd1) mouse? *Adv Exp Med Biol*. 2010;664:491–499.
144. Bush RA, Kononen L, Machida S, et al. The effect of calcium channel blocker diltiazem on photoreceptor degeneration in the rhodopsin Pro213His rat. *Invest Ophthalmol Vis Sci*. 2000;41:2697–2701.
145. Pearce-Kelling SE, Aleman TS, Nickle A, et al. Calcium channel blocker D-*cis*-diltiazem does not slow retinal degeneration in the PDE6B mutant rcd1 canine model of retinitis pigmentosa. *Mol Vis*. 2001;7:42–47.
146. Pawlyk BS, Li T, Scimeca MS, et al. Absence of photoreceptor rescue with D-*cis*-diltiazem in the rd mouse. *Invest Ophthalmol Vis Sci*. 2002;43:1912–1915.
147. Read DS, McCall MA, Gregg RG. Absence of voltage-dependent calcium channels delays photoreceptor degeneration in rd mice. *Exp Eye Res*. 2002;75:415–420.
148. Yamazaki H, Ohguro H, Maeda T, et al. Preservation of retinal morphology and functions in Royal College Surgeons rat by nilvadipine, a Ca(2+) antagonist. *Invest*

Ophthalmol Vis Sci. 2002;43:919–926.
149. Takano Y, Ohguro H, Dezawa M, et al. Study of drug effects of calcium channel blockers on retinal degeneration of rd mouse. *Biochem Biophys Res Commun*. 2004;313:1015–1022.
150. Takeuchi K, Nakazawa M, Mizukoshi S. Systemic administration of nilvadipine delays photoreceptor degeneration of heterozygous retinal degeneration slow (rds) mouse. *Exp Eye Res*. 2008;86:60–69.
151. Palczewski K. Retinoids for treatment of retinal diseases. *Trends Pharmacol Sci*. 2010;31:284–295.
152. Travis GH, Golczak M, Moise AR, et al. Diseases caused by defects in the visual cycle: retinoids as potential therapeutic agents. *Annu Rev Pharmacol Toxicol*. 2007;47:469–512.
153. Gearhart PM, Gearhart C, Thompson DA, et al. Improvement of visual performance with intravitreal administration of 9-*cis*-retinal in Rpe65-mutant dogs. *Arch Ophthalmol*. 2010;128:1442–1448.
154. Van Hooser JP, Aleman TS, He YG, et al. Rapid restoration of visual pigment and function with oral retinoid in a mouse model of childhood blindness. *Proc Natl Acad Sci USA*. 2000;97:8623–8628.
155. Van Hooser JP, Liang Y, Maeda T, et al. Recovery of visual functions in a mouse model of Leber congenital amaurosis. *J Biol Chem*. 2002;277:19173–19182.
156. Batten ML, Imanishi Y, Tu DC, et al. Pharmacological and rAAV gene therapy rescue of visual functions in a blind mouse model of Leber congenital amaurosis. *PLoS Med*. 2005;2:e333.
157. Sieving PA, Chaudhry P, Kondo M, et al. Inhibition of the visual cycle in vivo by 13-*cis* retinoic acid protects from light damage and provides a mechanism for night blindness in isotretinoin therapy. *Proc Natl Acad Sci USA*. 2001;98:1835–1840.
158. Mata NL, Weng J, Travis GH. Biosynthesis of a major lipofuscin fluorophore in mice and humans with ABCR-mediated retinal and macular degeneration. *Proc Natl Acad Sci USA*. 2000;97:7154–7159.
159. Radu RA, Mata NL, Nusinowitz S, et al. Treatment with

isotretinoin inhibits lipofuscin accumulation in a mouse model of recessive Stargardt's macular degeneration. *Proc Natl Acad Sci USA*. 2003;100:4742–4747.
160. Travis GH, Golczak M, Moise AR, et al. Diseases caused by defects in the visual cycle: retinoids as potential therapeutic agents. *Annu Rev Pharmacol Toxicol*. 2007;47:469–512.
161. Mendes HF, Cheetham ME. Pharmacological manipulation of gain-of-function and dominant-negative mechanisms on rhodopsin retinitis pigmentosa. *Hum Mol Genet*. 2008;17:3043–3054.
162. Noorwez SM, Kuksa V, Imanishi Y, et al. Pharmacological chaperone-mediated in vivo folding and stabilization of the P23H-opsin mutant associated with autosomal dominant retinitis pigmentosa. *J Biol Chem*. 2003;278:14442–14450.
163. Noorwez SM, Malhotra R, McDowell JH, et al. Retinoids assist the cellular folding of the autosomal dominant retinitis pigmentosa opsin mutant P23H. *J Biol Chem*. 2004;279:16278–16284.
164. Saliba RS, Munro PM, Luthert PJ, et al. The cellular fate of mutant rhodopsin: quality control, degradation and aggresome formation. *J Cell Sci*. 2002;115:2907–2918.
165. Li T, Sandberg MA, Pawlyk BS, et al. Effect of vitamin A supplementation on rhodopsin mutants threonine-17 → methionine and proline-347 → serine in transgenic mice and in cell cultures. *Proc Natl Acad Sci USA*. 1998;95:11933–11938.
166. Wahlin KJ, Campochiaro PA, Zack DJ, et al. Neurotrophic factors cause activation of intracellular signaling pathways in Müller cells and other cells of the inner retina, but not photoreceptors. *Invest Ophthalmol Vis Sci*. 2000;41:927–936.
167. Mattson MP. Neuroprotective strategies based on targeting of postreceptor signaling events. Mattson MP. *Neuroprotective signal transduction*. Humana Press: Totowa, NJ; 1998:301–306.
168. Mattson MP. Glutamate and neurotrophic factors in neuronal plasticity and disease. *Ann N Y Acad Sci*. 2008;1144:97–112.
169. Shinohara T, Singh DP, Fatma N. LEDGF, a survival factor,

activates stress-related genes. *Prog Retin Eye Res*. 2002;21:341–358.
170. Raz-Prag D, Zeng Y, Sieving PA, et al. Photoreceptor protection by adeno-associated virus-mediated LEDGF expression in the RCS rat model of retinal degeneration: probing the mechanism. *Invest Ophthalmol Vis Sci*. 2009;50:3897–3906.
171. Machida S, Chaudhry P, Shinohara T, et al. Lens epithelium-derived growth factor promotes photoreceptor survival in light-damaged and RCS rats. *Invest Ophthalmol Vis Sci*. 2001;42:1087–1095.
172. Tezel G, Hernandez R, Wax MB. Immunostaining of heat shock proteins in the retina and optic nerve head of normal and glaucomatous eyes. *Arch Ophthalmol*. 2000;118:511–518.
173. Wax MB, Tezel G. Immunoregulation of retinal ganglion cell fate in glaucoma. *Exp Eye Res*. 2009;88:825–830.
174. Wax MB, Tezel G, Yang J, et al. Induced autoimmunity to heat shock proteins elicits glaucomatous loss of retinal ganglion cell neurons via activated T-cell-derived Fas-ligand. *J Neurosci*. 2008;28:12085–12096.
175. Kosmaoglou M, Schwarz N, Bett JS, et al. Molecular chaperones and photoreceptor function. *Prog Retin Eye Res*. 2008;27:434–449.
176. Mendes HF, van der Spuy J, Chapple JP, et al. Mechanisms of cell death in rhodopsin retinitis pigmentosa: implications for therapy. *Trends Mol Med*. 2005;11:177–185.
177. Tam LC, Kiang AS, Campbell M, et al. Prevention of autosomal dominant retinitis pigmentosa by systemic drug therapy targeting heat shock protein 90 (Hsp90). *Hum Mol Genet*. 2010;19:4421–4436.
178. Mendes HF, Cheetham ME. Pharmacological manipulation of gain-of-function and dominant-negative mechanisms in rhodopsin retinitis pigmentosa. *Hum Mol Genet*. 2008;17:3043–3054.
179. Martin D, Miller G, Fischer N. Neuroprotective strategies based on interleukin signaling. Mattson MP. *Neuroprotective signal transduction*. Humana Press: Totowa, NJ; 1998:185–196.

180. Plane JM, Shen Y, Pleasure DE, et al. Prospects for minocycline neuroprotection. *Arch Neurol*. 2010;67:1442–1448.
181. Hughes EH, Schlichtenbrede FC, Murphy CC, et al. Minocycline delays photoreceptor death in the rds mouse through a microglia-independent mechanism. *Exp Eye Res*. 2004;78:1077–1084.
182. Hughes EH, Schlichtenbrede FC, Murphy CC, et al. Generation of activated sialoadhesin-positive microglia during retinal degeneration. *Invest Ophthalmol Vis Sci*. 2003;44:2229–2234.
183. Thanos S. Sick photoreceptors attract activated microglia from the ganglion cell layer: a model to study the inflammatory cascades in rats with inherited retinal dystrophy. *Brain Res*. 1992;588:21–28.
184. Zeiss CJ, Johnson EA. Proliferation of microglia, but not photoreceptors, in the outer nuclear layer of the rd-1 mouse. *Invest Ophthalmol Vis Sci*. 2004;45:971–976.
185. Zeng HY, Zhu XA, Zhang C, et al. Identification of sequential events and factors associated with microglial activation, migration, and cytotoxicity in retinal degeneration in rd mice. *Invest Ophthalmol Vis Sci*. 2005;46:2992–2999.
186. Zhang C, Lei B, Lam TT, et al. Neuroprotection of photoreceptors by minocycline in light-induced retinal degeneration. *Invest Ophthalmol Vis Sci*. 2004;45:2753–2759.
187. Yang LP, Zhu XA, Tso MO. Role of NF-kappaB and MAPKs in light-induced photoreceptor apoptosis. *Invest Ophthalmol Vis Sci*. 2007;48:4766–4776.
188. Krugel K, Wurm A, Pannicke T, et al. Involvement of oxidative stress and mitochondrial dysfunction in the osmotic swelling of retinal glial cells from diabetic rats. *Exp Eye Res*. 2011;92:87–93.
189. Zhang Y, Xu G, Ling Q, et al. Expression of aquaporin 4 and kir4.1 in diabetic rat retina: treatment with minocycline. *J Int Med Res*. 2011;39:464–479.
190. Raz L, Zhang QG, Zhou CF, et al. Role of Rac1 GTPase in NADPH oxidase activation and cognitive impairment

following cerebral ischemia in the rat. *PLoS ONE*. 2010;5:e12606.
191. Song H, Bush RA, Vijayasarathy C, et al. Transgenic expression of constitutively active RAC1 disrupts mouse rod morphogenesis. *Invest Ophthalmol Vis Sci*. 2014;2659–2668.
192. Faruqi TR, Gomez D, Bustelo XR, et al. Rac1 mediates STAT3 activation by autocrine IL-6. *Proc Natl Acad Sci USA*. 2001;98:9014–9019.
193. Coso OA, Chiariello M, Yu JC, et al. The small GTP-binding proteins Rac1 and Cdc42 regulate the activity of the JNK/SAPK signaling pathway. *Cell*. 1995;81:1137–1146.
194. Wenzel A, Grimm C, Samardzija M, et al. Molecular mechanisms of light-induced photoreceptor apoptosis and neuroprotection for retinal degeneration. *Prog Retin Eye Res*. 2005;24:275–306.
195. Desire L, Bourdin J, Loiseau N, et al. RAC1 inhibition targets amyloid precursor protein processing by gamma-secretase and decreases Abeta production in vitro and in vivo. *J Biol Chem*. 2005;280:37516–37525.
196. Lu Q, Longo FM, Zhou H, et al. Signaling through Rho GTPase pathway as viable drug target. *Curr Med Chem*. 2009;16:1355–1365.
197. Marchioni F, Zheng Y. Targeting rho GTPases by peptidic structures. *Curr Pharm Des*. 2009;15:2481–2487.
198. Wang PL, Niidome T, Akaike A, et al. Rac1 inhibition negatively regulates transcriptional activity of the amyloid precursor protein gene. *J Neurosci Res*. 2009;87:2105–2114.
199. SanGiovanni JP, Chew EY. The role of omega-3 long-chain polyunsaturated fatty acids in health and disease of the retina. *Prog Retin Eye Res*. 2005;24:87–138.
200. Fliesler SJ, Anderson RE. Chemistry and metabolism of lipids in the vertebrate retina. *Prog Lipid Res*. 1983;22:79–131.
201. Bush RA, Remé CE, Malnoë A. Light damage in the rat retina: The effect of dietary deprivation of n-3 fatty acids on acute structural alterations. *Exp Eye Res*. 1991;53:741–752.
202. Bush RA, Malnoë A, Remé CE, et al. N-3 fatty acid deficiency alters rhodopsin content and function in the rat

retina. *Invest Ophthalmol Vis Sci*. 1994;35:91–100.
203. Cho E, Hung S, Willett WC, et al. Prospective study of dietary fat and the risk of age-related macular degeneration. *Am J Clin Nutr*. 2001;73:209–218.
204. Bazan NG. Neuroprotectin D1-mediated anti-inflammatory and survival signaling in stroke, retinal degenerations, and Alzheimer's disease. *J Lipid Res*. 2009;50(Suppl.):S400–5.
205. Stark DT, Bazan NG. Neuroprotectin D1 induces neuronal survival and downregulation of amyloidogenic processing in Alzheimer's disease cellular models. *Mol Neurobiol*. 2011;43:131–138.
206. Halapin NA, Bazan NG. NPD1 induction of retinal pigment epithelial cell survival involves PI3K/Akt phosphorylation signaling. *Neurochem Res*. 2010;35:1944–1947.
207. Mukherjee PK, Marcheselli VL, Serhan CN, et al. Neuroprotectin D1: a docosahexaenoic acid-derived docosatriene protects human retinal pigment epithelial cells from oxidative stress. *Proc Natl Acad Sci USA*. 2004;101:8491–8496.
208. Bazan NG. Cell survival matters: docosahexaenoic acid signaling, neuroprotection and photoreceptors. *Trends Neurosci*. 2006;29:263–271.
209. Zaccaro MC, Lee HB, Pattarawarapan M, et al. Selective small molecule peptidomimetic ligands of TrkC and TrkA receptors afford discrete or complete neurotrophic activities. *Chem Biol*. 2005;12:1015–1028.
210. Lebrun-Julien F, Morquette B, Douillette A, et al. Inhibition of p75(NTR) in glia potentiates TrkA-mediated survival of injured retinal ganglion cells. *Mol Cell Neurosci*. 2009;40:410–420.
211. Di Polo A, Aigner LJ, Dunn RJ, et al. Prolonged delivery of brain-derived neurotrophic factor by adenovirus-infected Müller cells temporarily rescues injured retinal ganglion cells. *Proc Natl Acad Sci USA*. 1998;95:3978–3983.
212. Johnson JE, Barde YA, Schwab M, et al. Brain-derived neurotrophic factor supports the survival of cultured rat retinal ganglion cells. *J Neurosci*. 1986;6:3031–3038.
213. Cui Q, Harvey AR. At least two mechanisms are involved in

the death of retinal ganglion cells following target ablation in neonatal rats. *J Neurosci*. 1995;15:8143–8155.

40

Drug Delivery

Erin B. Lavik, Baruch D. Kuppermann, Mark S. Humayun

Introduction

Drug delivery has the potential to have a tremendous impact on treatment of retinal diseases. There are a large number of drugs that are reasonably effective to treat retinal conditions, but those drugs are limited by delivery issues such as the need to have the molecule cross the blood–eye barrier or be present for long times, or the need to mitigate side-effects. The challenges of having drugs at a physiologically relevant concentration for extended periods or in a localized delivery system are challenges that can be solved with drug delivery technology, whether it is using cellular delivery systems, microelectromechanical (MEM)-based devices, polymer matrices, or gene delivery systems.

A Brief History of the Field of Drug

Delivery

The most common form of administration of a medication is the pill. There is evidence of the use of pills at least as early as ancient Egypt in the Ebers Papyrus (1500 BC). They consist, generally, of a medication mixed with a number of excipients or additives such as sugars and starches to protect and stabilize the formulation.[1] The basic concept is that one swallows the pill, it dissolves in the stomach, and the medication is absorbed in the intestines to the circulation. This approach works well for many drugs, but not for those that can break down in the stomach. Insulin is usually presented as a case in point, which must be injected because it cannot survive the environment of the stomach. Insulin is injected into the fatty tissue[2] and is then absorbed into the systemic circulation.

Systemic administration of medications by either route can be problematic for certain tissues, particularly those with strong barrier characteristics or those that are poorly vascularized. Early versions of local delivery systems to the eye involve ointments, which were described in ancient Mesopotamia.[3] Pilocarpine drops have been used for at least 100 years to lower intraocular pressure (IOP) and treat glaucoma.[4]

Drug delivery systems are a broad area that includes targeted systems as well as systems that provide controlled release of the drug. One of the earliest targeted systems was the liposome, which has been shown to build up in tumors due to the enhanced permeation effect.[5] Liposomes were discovered in the 1960s and the first US Food and Drug Administration (FDA) approval came with Doxil, the liposomal-encapsulated formulation of doxorubicin, an anticancer agent, in the 1990s.[6] More recent variants on targeted systems have focused on adding molecules on the outside of liposomes or other nanoparticles that can allow them to target the tissue of interest.[7] Targeted systems may allow the systemic delivery of a molecule that is released in the ocular tissues.[8] However, in and of themselves, targeted systems do not provide sustained delivery of drugs. They can be engineered to do so, but if one looks at the half-life of doxorubicin, it is still on the order of hours as opposed to days or weeks. This does not mean that

targeting cannot be combined with sustained delivery, but they are two components to consider.

Sustained delivery is better termed controlled delivery. The fundamental difference is that controlled delivery is dictated by the device and not the environment around the device.[9] This is fundamental to drug delivery. One does not want to administer a device to a patient and have different patients get the drug over different time courses, particularly in an unexpected way. One of the first controlled delivery systems was actually in the eye – the Ocusert system to deliver pilocarpine for glaucoma. The Ocusert system is a reservoir system that relies on the transport of the drug through a membrane. Membranes are effective for small molecules (less than 600 Da),[10] but are not suitable for delivering larger molecules such as antibodies, growth factors, and proteins more broadly.

The watershed in the drug delivery world occurred in 1976. Robert Langer and Judah Folkman showed that large molecules could be delivered over days and weeks from polymer matrices, and they showed that the release profile could be tailored based on the matrix.[11] The concept was not warmly received and there were huge questions about the mechanism and plausibility of the approach,[12] but the drug delivery field has grown from being nonexistent in the United States in the 1980s to being worth 11.5 billion dollars in 1996,[13] to an estimated worth of 85 billion dollars in 2010.[14] The economic impact is a reflection of a number of factors, including the ability to provide new patent protection for off-patent medications, but it also reflects the impact on human health.

Several of the applications of drug delivery technology have been in the eye, as discussed in this chapter, but we have barely begun to realize the potential. Drug delivery provides the means to improve patient compliance, increase efficacy, and reduce side-effects of ocular medications.

Drug Delivery

Formulating Sustained-Delivery Systems

There are five broad approaches for the sustained delivery of drugs

(Fig. 40.1). The first approach involves attaching molecules to the drug to increase its residence time. Poly(ethylene gycol) or PEG is the workhorse of this approach. PEGylating or attaching PEG molecules can increase the circulation time of a drug in the bloodstream by creating a highly hydrated volume around the drug.[15] The second broad approach is to encapsulate the drug of interest in a reservoir system that includes a membrane that allows the drug to diffuse through the device and into the surrounding tissue. This approach lies at the basis of drug delivery systems, including the Ocusert implant delivering pilocarpine.[16] Diffusion-based systems work for limited, typically small, molecules with molecular weights less than 600 Da.[10] There are great benefits to the membrane-based systems, such as the ability to deliver many drugs over very long timescales, but there are risks, including the rupture of the membrane, leading to spontaneous delivery of the entire reservoir.[9]

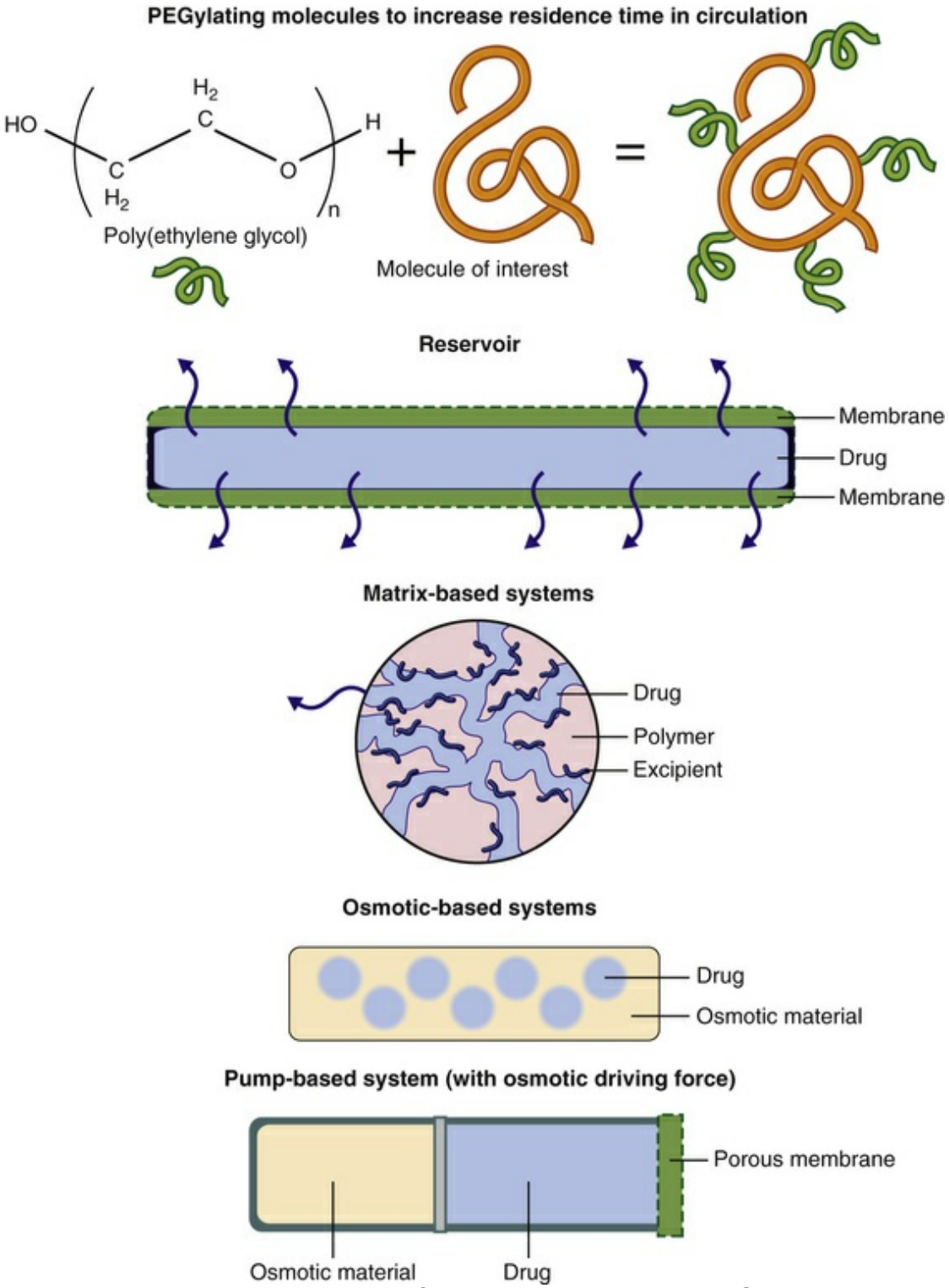

FIG. 40.1 Approaches for delivering drugs. *PEG*, poly(ethylene gycol).

The third approach involves mixing the drug with polymers that entrap the drug in a matrix. The drug typically phase separates on the micro- or nanoscale from the polymer, leading to veins of the drug in the polymer matrix. The tortuosity of the veins plays a

tremendous role in the release of the drug. With nondegradable polymers, the drug delivery profile is dictated by diffusion.[17] With degradable polymers, the drug delivery profile is dictated by a combination of diffusion and degradation events that occur over time.[17] The challenges in the matrix-based approaches involve achieving good mixing of the drug in the matrix to form tortuous pathways as well as promoting interactions between the drug and matrix. The closer the two associate with each other, the more likely one will achieve very long (weeks to months to years) release. Thinking about this interaction becomes part of the process of formulating drug delivery systems.

The fourth approach involves osmotic systems. In these systems the diffusion of water into the matrix leads to swelling and drives the release of the drug via diffusion. Typically, osmotic systems lead to relatively fast release of drugs with a significant burst effect. Investigators are developing asymmetric membranes to control the delivery in a more uniform manner over time,[18] but osmotic systems have not been used extensively other than as components to drive pump technologies that do have robust, long-term delivery.

Pump systems, the fifth approach, permit tight control of drug delivery over time for a wide range of medications. Pumps can either be continuous and passive or actively directed to deliver medications, and in some cases, pumps are refillable. The major limitation of pumps has been their size. Historically, they have been bulky and require more extensive implantation and placement than some of the other materials that are more amenable to delivery via small needles.

In thinking about which approach makes the most sense in formulating a drug delivery system, one needs to consider the following: the size, nature, and stability of the drug, the length of time one wants to deliver the drug, and the amount of the drug one wants to deliver over time. Regarding size, small molecules (<600 Da) can diffuse through polymers such as silicone.[10] Larger molecules, macromolecules such as proteins, are not able to diffuse through polymers on a useful timescale for most applications.[11] If one is hoping to deliver larger molecules, one will need to consider the methods outside of the membrane approach.

The nature of the drug refers to its charge and solubility. Most of the popular biodegradable polymers are extremely hydrophobic. If the drug of interest is very hydrophilic, it can be challenging to encapsulate the hydrophilic drug in the hydrophobic polymer matrix. One of the classic methods to overcome this challenge is to use excipients that interact with both the drug and the polymer. Fu et al. showed how excipients could greatly improve loading and delivery of glial cell line-derived neurotrophic factor (GDNF) through the use of excipients.[19] Likewise, charged molecules can interact poorly in uncharged or similarly charged polymer systems. Poly(lactic-co-glycolic acid) (PLGA) can be synthesized with a carboxyl group on the end that carries a negative charge depending on the pH. This can improve the encapsulation of positively charged molecules.

The stability of the drug is crucial. Delivery of a drug that has lost its bioactivity is fruitless. Large molecules, in particular, are susceptible to losing bioactivity via cleavage or conformational changes during encapsulation or storage. The techniques used to encapsulate molecules play a tremendous role in preserving their bioactivity. When water-soluble molecules are exposed to fewer organic solvents and less energy during processing, it is more likely that the bioactivity will be preserved; however, it is always critical to check bioactivity upon release. One of the exciting findings in the matrix-based approaches has been that, for many drugs, if the drug is active upon encapsulation, the activity can be maintained for long times with drugs that are released years after encapsulation.

Beyond the drug, one needs to consider the amount of the drug one needs to deliver and the time course. Matrix-based formulations have been shown to deliver medications for years, but they rely on relatively high polymer-to-drug ratios, which makes them more suitable for applications where one can either deliver a large volume of material (which is unlikely in the eye) or where one has a relatively potent medication. As we will see in the examples below, many of the commonly used drugs are effective at low concentrations, but it is an important consideration. Membrane and pump systems can both deliver larger amounts of drugs over time, but the volume they deliver determines the necessary reservoir size and overall device dimensions. The time course is the second

critical component. Membrane and pump approaches can both lead to very constant delivery depending on the geometry of the devices.[10] Careful formulation can lead to very constant delivery over time from matrix-based formulations, but they are prone to burst release due to drug adsorbed on or near the surface of the materials.[10]

There are clear benefits and challenges to all of these approaches, and multiple approaches may achieve the same desired effect. The key is to know one's drug and desired delivery profile and then to determine which approaches are likely to be the most effective. One must then consider the route of administration to narrow down the approach finally to the one that is the most likely to be effective. If one wants to inject a material through a 33-gauge needle into the intravitreal space, one will have a very different set of potential approaches than if one is looking for an implant to sit in or near the tear duct. The examples outlined in this chapter will help to provide specific, real-world examples of how the formulation challenges can be approached successfully to develop therapeutically viable treatments.

Delivering Drugs in a Targeted Manner

One simple way to achieve targeted drug delivery is to place the device in the area where one wants to deliver the drug. For a number of ocular conditions, this probably makes the most sense. If one wants long-term, local delivery of a drug that one is already injecting intravitreally every 4–6 weeks like the anti-vascular endothelial growth factor (VEGF) medications, being able to deliver the same drug with the same injection method but for several months or years would be very attractive. Injecting a device or matrix into the intravitreal space is a reasonable way to provide local delivery.

For some compounds, though, one may want either to deliver them systemically or to deliver them to a particular cell type in the eye and not to all cell types. A good example of this would be the delivery of a specific agent for a specific cell type, such as the retinal pigment epithelium (RPE).[20] The most common forms of targeting have involved creating particles, typically nanoparticles, from

either liposomes or other polymers that are covered in PEG arms to reduce their aggregation and promote transport, and attaching molecules to the particles that bind to receptors or molecules on the cells of interest. Antibodies,[21] peptides,[22] and aptamers[23,24] have all been used to facilitate targeting.

The key issues to consider in designing a targeting molecule are the specificity and affinity of the targeting moiety to the molecule of interest on the cell. Poor affinity or specificity will lead to poor targeting. Once one has identified targeting molecules with appropriate affinity and specificity, one needs to insure the stability of the targeting molecules in vivo. Larger molecules, such as antibodies, have the potential to be denatured or enzymatically cleaved in vivo, which has motivated the identification of smaller molecules with similar specificity and affinity such as aptamers.[23,24]

Targeting is primarily used to concentrate systemically administered particles in the tissue of interest. In the retina, much of the work has focused on targeting the choroidal vessels.[25,26] There is evidence that, when particles are small enough, they can cross through to the retina when administered systemically,[27] which opens up the possibility of delivering targeted nanoparticles to the retina via systemic administration.

The Role of Devices in Drug Delivery

The term "devices" can include everything from membrane-based depots to microparticles, implants, hydrogels, and MEMs-based systems.[28] In the novel delivery systems, a number of devices will be discussed along with their advantages and limitations.

Devices that are based on pumps and other microfluidic delivery systems have the potential to facilitate extremely well-controlled delivery of drugs over long times and, in some cases, may be refilled. The initial implantation of a device may be more involved than a simple injection of a drug, but that one-time invasiveness may be countered if a drug can be delivered for exceptionally long times in a controlled manner or if the device can be refilled and permit far fewer invasive injections.

The remaining classes of device rarely exhibit the ability to be refilled, with the one potential exception of affinity-based systems,

which are in the very early stage of preclinical testing. However, if one designs the geometry properly, many of the implant systems can be administered in a minimally invasive manner, and with careful formulation many implants achieve very well-controlled delivery of the drugs of interest.

Gene Delivery

Gene therapy has the potential to replace or restore function in the retina as well as produce growth factors that protect the eye. It is very challenging, though, to get the genetic material both to the cells and into the genome without breakdown of the material. There have been many studies looking at the transfection efficiency of deoxyribonucleic acid (DNA) through routes of administration, including drops, subconjunctival, intravitreal, and subretinal injections, and in all cases the transfection efficiency has been low to the retina and the subsequent protein expression is typically small and over a short duration.[29]

To facilitate more effective delivery of DNA and subsequent protein expression, a number of vectors have been pursued. The two basic approaches involve viral and nonviral delivery of constructs to the retina. Viruses have adapted over millions of years to deliver genes to cells efficiently, and viral delivery is generally efficient. Viral delivery does raise safety concerns and there were substantial complications and deaths in early viral-based gene therapy trials.[30,31] Nonviral gene delivery has sought to provide safer alternatives, but the challenge lies in getting efficient delivery and incorporation of the genetic material.

Viral Systems

There are three major classes of virus that have been used for transduction: retroviruses, lentiviruses, and adenoviruses. Retroviral vectors only infect dividing cells, making them relatively unattractive for ocular applications.[32] Lentiviral vectors are designed to infect nondividing cells in the G0 or G1 phase of the cell cycle.[32] There are significant safety concerns with both retroviral and lentiviral vectors because they have the potential to insert into

the genome. Of the three major classes, adenoviruses have drawn tremendous interest for gene therapy because they do not incorporate into the genome, which is thought to reduce their oncogenic potential, and they are extremely effective at transducing cells.[32] However, adenoviruses have been found to be very immunogenic, and one of the early clinical trials using an adenovirus had to be halted when an 18-year-old died due to a systemic inflammatory response syndrome.[31]

Adenovirus-based vectors have continued to be pursued in the eye because of the local delivery and immune-privileged nature. GenVec has used an adenovirus to deliver the gene for pigment epithelium-derived factor (PEDF) for the treatment of neovascular AMD in a phase I trial.[33] The adenovirus-based delivery system was well tolerated by patients with only transient, mild inflammation in some patients which was managed with topical medications. There was no control group in this phase I trial, but the size of the choroidal neovascular lesions was smaller in the high-dose group. Much of the follow-on research has focused on repeated administrations, longer-term expression of PEDF, and using inducible promoters to direct expression of the protein of interest.[34–36]

A variant on the adenovirus, first found as a contaminant of adenoviruses, the adeno-associated virus (AAV), has proven to be an effective alternative. Like adenoviruses, AAV vectors do not integrate into the genome. Furthermore, they do not elicit a strong immune response.[32] One of the first major successes for gene therapy with AAV vectors has been the treatment of Leber congenital amaurosis, a severe form of retinal degeneration that leads to vision loss in early childhood.[37] A replication-deficient AAV vector was used to deliver a gene for isomerohydrolase activity (AAV-hRPE65v2). The vector was injected subretinally, and vision gains were found in younger patients. Another company, Avalanche Biotechnologies, uses subretinally placed AAV to treat wet age-related macular degeneration. Avalanche's Ocular BioFactory™ platform uses the AAV vector to transduce a functional gene to the cells of the eye to promote continuous anti-VEGF protein production. The Ocular BioFactory platform features two key proprietary components: a novel vector screening and

optimization system referred to as directed evolution, and an industrialized manufacturing process. A recently completed phase IIa trial of AVA-101 showed signs of some benefit, however after further analyses of those results the company has announced it will not initiate a phase IIb clinical trial. Instead, the company will conduct additional preclinical studies to investigate optimal dose and delivery. This news led to a sharp drop in the company's stock and the resignation of the CEO. The company also changed its name to Adverum Biotechnologies.[38]

Nonviral Systems

Viruses are extraordinarily effective at delivering genetic material to cells, but there are safety concerns, and the size of the vector limits the amount of genetic material that can be delivered. Nonviral vectors have been pursued to address these issues.

There are five basic steps that have to be achieved to transfect a cell (Fig. 40.2). The genetic material must get to the cell, into the cell, out of the endosome, to the nucleus, and into the nucleus. Viruses have evolved a complex set of tools to achieve this. For example, the adenovirus has a targeting moiety for the cell of interest and leverages the pH drop in the endosome by having the capsid undergo a conformational change that opens the endosome. It is thought to bind to dynein, a molecular motor that moves along the microtubules to travel to the nucleus.[39]

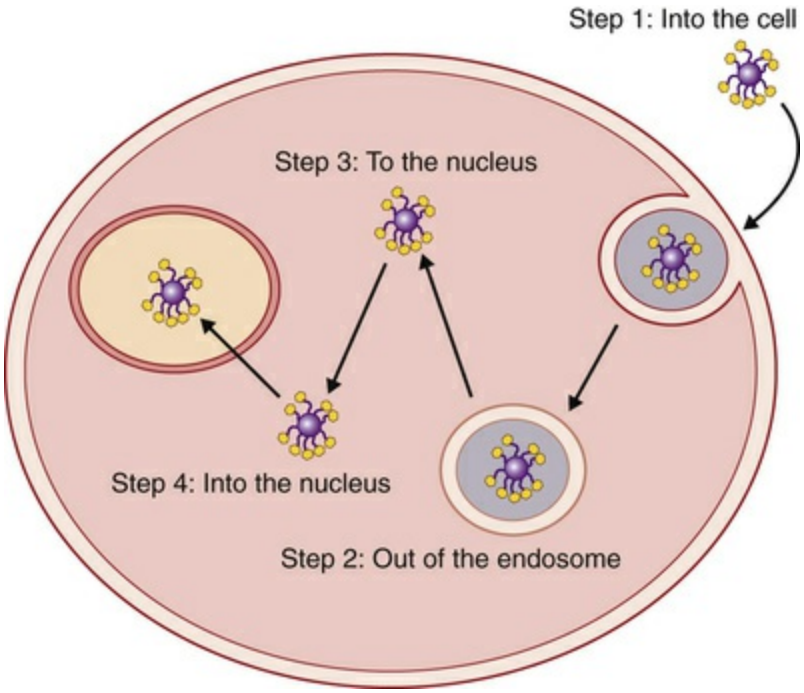

FIG. 40.2 The challenges involved in getting genes from outside cells to the nucleus.

Nonviral systems have been designed to address one or more of these issues, and the more recent systems have been designed to address several or all of these critical steps for transfection. Liposomes were among the earliest transfection agents. Liposomes are capable of shielding DNA from enzymatic breakdown until the material gets to the cell, but their fusion with the cell membranes is not efficient.[40] In 1987, however, the use of cationic liposomes was first identified as a means to facilitate high rates of transfection.[41] The cationic component of the system facilitates interactions with the negatively charged cell membranes and the subsequent cell fusion which delivers the DNA into the cell. While this is a tremendous improvement over previous nonviral approaches, the efficiency is still far lower than viral systems.

Positively charged polymers like polylysine and polyethylenimine (PEI) were very early in the nonviral vector development timeline. PEI, one of the major cationic polymers, was first shown to be an effective polymer for gene delivery in 1995.[42] It does two critical things. First, it is a positively charged polymer that complexes with negatively charged DNA to create positively charged nanoparticles that stick to the anionic membranes of cells. Second, it is a proton sponge, meaning that as the pH is lowered in

the endosome, the amines on the polymer take up the hydrogen ions and the polymer protonates. It does this to the point that it swells and bursts the endosome. The polymer, however, has no specific method for getting the DNA to or into the nucleus. PEI tends to be most effective in dividing cells where the organization of the mitotic spindles facilitates movement of the particles to the nucleus.[42,43] PEI has been used in animal models for transfection of retinal cells.[44] The particles were taken up primarily by what appear to be Müller glial cells but no quantification is discussed so it is not possible to assess what sort of efficiency was achieved.

In light of the complexities of getting DNA to the nucleus, more recent research has focused on developing multicomponent systems that incorporate protection of DNA with endosomal escape mechanisms and nuclear targeting moieties.[45–47] The challenges of specific transfection of retinal cells in the eye with nonviral vectors are significant, and it is likely that careful engineering of the vector will be needed for successful, long-term transfection, but the field is moving forward rapidly. It is likely to be a very different landscape in the next decade.

Cellular Delivery for Sustained Drug Delivery

Engineering Cells for Delivery

While using nonviral vectors for engineering cells in vivo in the retina may not be efficient, nonviral vectors can be very attractive for ex vivo engineering of cells where one can sort for the cells that produce the factor of interest. Viral vectors may also be more attractive because the safety of the cells can be well assessed before introduction in vivo.

The attraction of using cells for the delivery of therapeutic agents is that cells can deliver a molecule for very long periods of time, potentially years. Furthermore, cells have the potential to integrate into the retina and deliver molecules in layers that may not be easily reached by standard drug delivery of gene therapy approaches. For example, it can be challenging to deliver genes to the retina and to get robust expression of the molecule of interest

via intravitreal injections.[48] However, there are studies showing that certain cells may be able to migrate and integrate with the retina following intravitreal administration and produce molecules such as GDNF and brain-derived neurotrophic factor (BDNF) to preserve retinal cells in a number of models of retinal degeneration.[49,50] Mesenchymal stem cells,[50] embryonic stem cells,[49] Schwann cells,[51] and fibroblasts[52] have all been engineered as a means to promote neuroprotection and have all successfully been used for several months in animal models.

Engineering Materials for Immunologic Protection

While the eye is immune-privileged,[53,54] the presence of disease can alter this privilege, and long-term survival of transplanted cells is not guaranteed. Since the primary purpose of the engineered cells is to deliver their molecular payload, encapsulating them to protect them from the host while allowing their molecules to reach the retina makes a great deal of sense. It also facilitates their removal should complications arise.

As noted in the section on sustained delivery systems, solid polymer membranes do not allow large molecules (>600 Da) to diffuse through.[10] Most of the growth factors noted above are significantly greater than 600 Da. The solution, then, is to engineer the materials with higher-molecular-weight cutoffs that allow the growth factors through but still block the transport of antibodies and other larger molecules.

Alginate gels and variants on alginate gels have been one of the most used materials to encapsulate cells for this purpose since the early 1980s. Alginate is an attractive material in that it does not adsorb proteins, facilitating their transport, but the molecular weight of the transported molecules can be controlled by the crosslinking density.[55–57] Because alginate gels are crosslinked water-swollen gels, the encapsulated cells are able to remain hydrated and transport of nutrients and waste is maintained. Other materials, primarily synthetic hydrogels, have become popular because the permeability can be tightly controlled through crosslinking agents and density, membrane thickness, and the use

of multiple layers.[58,59] Kristi Anseth's group has shown that functionalizing hydrogels with moieties that interact with cells can still maintain the long-term delivery of the protein of interest while leading to higher and longer-term cell viability, the ultimate goal of these encapsulation systems.[60]

Routes of Delivery to the Retina

Traditional Routes of Administration

Oral Delivery

Oral delivery is the most preferred route of delivery of medications by patients. Drugs such as timolol maleate can be given orally and do have an ocular effect, namely the lowering of IOP.[61] However, the presence of the blood–retinal barrier makes transport to the eye difficult and the challenges of stabilizing drugs through the gut to systemic absorption and further on to the eye are possible but very difficult. Therefore, most ocular medications have been delivered topically.

Topical Delivery

A large range of medications are delivered topically either as solutions or as gels. Because a large portion of the drop or gel is cleared from the tear film quickly, topical delivery leads to significant (typically 80%) systemic absorption of the drug.[62] There is also relatively limited adsorption of the drug to the ocular tissues.[63] There are a number of models of pharmacokinetics of topically delivered medications, and the drug chemistry, particularly the hydrophobic versus hydrophilic nature of the drug, plays a role, but overall, there is very little drug delivered to the vitreous and the retina.[64] This makes topical administration challenging for retinal diseases.

There have been clinical trials in Europe looking at delivery of nerve growth factor (NGF) for neuroprotection of the retina, and in particular, there are trials looking at topical administration of NGF for glaucoma.[65] Three glaucoma patients who were losing vision received drops containing murine NGF four times daily for 3 months. There are no data from the human or animal studies

regarding the concentration of NGF that reaches the back of the eye, but some patients undergoing this treatment exhibited some signs of improvements in their electroretinograms.

Injections

When oral medications and drops are not effective, injections are typically considered. Subconjunctival injections are one of the least invasive injections but there are several barriers between the subconjunctival space and the retina, although a number of molecules can diffuse in low concentrations to the retina with this approach, depending on their size and chemistry.[66–68] Intravitreal injections, though more invasive, provide a means to put molecules near the retina. The vitreous is also capable of acting as a sink for many molecules, absorbing them and slowly releasing them, which can increase the residence time of these molecules in the intravitreal space.[69–71] Sub-Tenon injections have drawn more interest with the thought that the drug will be delivered over a prolonged period through this route.[72–74]

Novel Approaches for Administration

The ForSight VISION4 implantable ocular delivery technology port delivery system (PDS) is designed and validated specifically to work only with ranibizumab solution. Following initial implantation, refills can be performed in the office as needed, using a custom refill needle.

The PDS device provides continuous release of ranibizumab into the vitreous between refill procedures. A phase 1 study assessing the safety and efficacy of the PDS implant filled with 250 μg of ranibizumab was conducted in 20 newly diagnosed, treatment-naive patients with wet AMD. At 12 months patients gained on average 12 letters and 50% of patients gained 3 or more lines. Patients required a mean of 4.2 refills by 12 months. However, while the implantation and refill procedures were well tolerated, overall there were potentially sight-threatening adverse events in 4 of 20 patients (20%). One patient developed endophthalmitis, two developed persistent vitreous hemorrhage, and one developed traumatic cataract secondary to the implantation procedure. Six

implants were explanted per protocol at 12 months, and those explanted devices performed similarly to brand-new devices. A phase II a multicenter, randomized, active-treatment controlled study of the efficacy and safety of the PDS for sustained delivery of ranibizumab for wet AMD – the LADDER study – is being planned.[75]

Devices

Inserts.

The Ocusert system is one of the best-known and most widely studied membrane-based drug delivery systems. The device consists of two membranes of poly(ethylene-co-vinyl acetate) and a ring of the same material filled with pilocarpine to lower IOP.[76] The insert was designed to deliver the drug for 7 days when placed in the cul de sac of the eye. The system worked to manage IOP, but patients found that the device could be uncomfortable especially if it twisted, and it could fall out.[77] While follow-on designs sought to make the insert remain in the eye,[78] a fundamental problem was that patients had to be taught how to use the insert systems and older patients did not like the device.[9]

The landscape for inserts may be changing. Approximately 40 million people in the United States wear contact lenses and the contact lens market is expanding.[79] Modifying contact lenses makes sense in that many patients are familiar with them and their use.[80] Soft contact lenses, those primarily used at this point, are hydrogels, water-soluble polymers that are crosslinked to form networks, and hydrogels are a potential material for controlled drug delivery.[81] It should be noted, however, that when drug delivery researchers start looking at contact lenses or modified lenses as the solution to patient- and clinician-friendly inserts, they often forget that most patients remove their contact lenses at night. If one wants to use contact lenses as a depot for drug delivery, one needs either to account for the actual time patients wear the lenses or design a wearable long-term lens.

While hydrogels can be used as a drug delivery vehicle, water-soluble drugs, such as those likely to cross the conjunctiva most effectively, tend to elute very quickly from the highly hydrated

polymer networks, on the order of minutes or hours.[82] Timolol maleate, a water-soluble drug for lowering IOP, has been shown to be able to be delivered from contact lenses consisting of polymers of *N,N*-diethylacrylamide and methacrylic acid for approximately 24 hours.[83] A study of three patients using contact lenses delivering timolol showed the lenses controlled IOP as well as drops.[84] While this is promising, timolol, like pilocarpine, does not have to reach the retina. It only needs to be in a reasonable concentration near the ciliary body to affect aqueous production.

Getting molecules into lenses or inserts that then are delivered to the retina requires crossing many physical barriers in the eye. Liposomes, surfactants, and penetrating agents may facilitate transport through these barriers,[85] but a formulation that achieves this safely has yet to be demonstrated.

MEMs Devices.

Using a MEMs-based approach is exciting in that one can actively control the drug release by dictating the rate of electrolysis. An active delivery system allows the clinician to change the rate of delivery based on assessments. None of the other systems presented up to this point permits active control of the delivery of the drug. MEMS-based systems also have the potential for the delivery of multiple drugs with minor modifications, which increases the potential impact of these devices on treating retinal disease.

In the last few years, a number of MEMs-based systems have been developed that allow for remote, wireless delivery of drugs.[86–89] These systems range from implantable devices based on silicon technology to degradable systems that are designed to resorb once their payload is deployed. These systems are beginning to be reliable and small enough to open the possibility of application in the clinic.

Replenish External Scleral Fixated Refillable Device.

Implanting a reservoir system in the subconjunctival space opens the door to well-controlled long-term delivery of both small and large molecules without the need for repeated intravitreal injections. The MEMs device uses electrolysis to create bubbles that

push the drug out of the reservoir of the implantable device, and there is a port that facilitates loading of the drug into the system.[90] Implantation of the device is similar to a glaucoma drainage device in complexity and it can be reloaded several times and has been well tolerated in initial rabbit studies.[91]

Iontophoresis System.

EyeGate Pharma has developed a delivery system composed of an annular scleral iontophoresis reservoir which is filled with drug (Fig. 40.3). A potential is applied between an electrode on the forehead of the patient and the device to drive the charged drug into the anterior and posterior segments of the eye over 2–4 minutes. This device is currently in clinical trials, including a study to assess the safety and efficacy of a dexamethasone phosphate iontophoresis formulated solution (EGP-437) at two different dose levels for dry eye (NCT01129856), and a trial of four iontophoretic doses of EGP-437 in patients with noninfectious anterior-segment uveitis (NCT00694135). While the system has not yet been tested for diseases of the retina, it may be an alternative to different retinal pathologies due to the good penetration in human sclera of drugs like bevacizumab.[92]

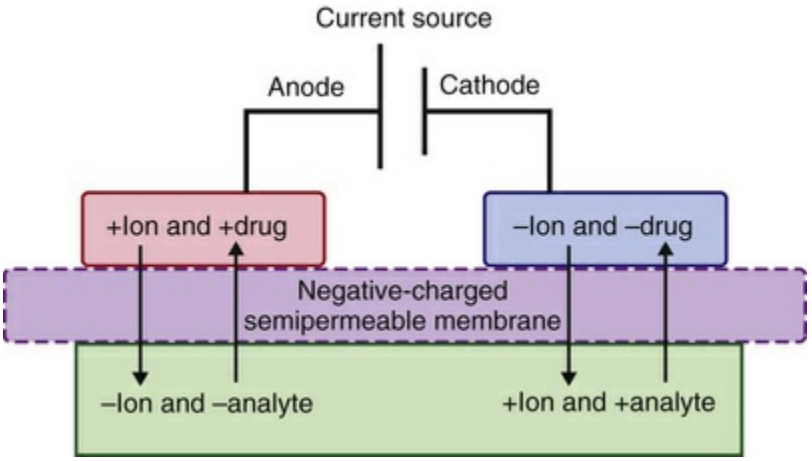

FIG. 40.3 A schematic of the design of the EyeGate Pharma® iontophoresis system for drug delivery through the sclera. (Courtesy of Juan Carlos Gutierrez MD, Research Fellow at the Doheny Retina Institute.)

Implants

Vitrasert Ganciclovir Implant.

There are several implants either in or through clinical trials which deliver drugs to the retina for long periods of time, up to several years. The Vitrasert implant was approved by the FDA in 1996 for the treatment of cytomegalovirus (CMV) retinitis.[93] The implant delivers ganciclovir, an antiviral drug, from an implant of poly(vinyl alcohol) and poly(ethylene vinyl acetate), one of the early workhorses of the controlled-release field.[9] The implant delivers the medication for approximately 32 weeks and has been shown to halt the progression of CMV.[94,95] One of the challenges with a nondegradable implant is removal, and to deal with this, the implant is sutured to the eye wall once inserted.[96] Fig. 40.4 shows a comparison of the sizes of the Iluvien, Retisert, and Vitrasert implants.

FIG. 40.4 Comparison of size of Iluvien, Retisert, and Vitrasert implants (left to right).

Retisert Fluocinolone Implant.

Retisert is an implant the size of a grain of rice that delivers fluocinolone acetonide intravitreally for 30 months for uveitis and was approved in 1995.[97] It has also been studied in trials for diabetic retinopathy.[97] The implant consists of a blend of the drug with poly(vinyl alcohol) and methylcellulose in a tablet geometry that is

secured with a suture once inserted into the vitreal space through a scleral incision, similarly to the Vitrasert implant. The implant is very effective at treating uveitis, but there are side-effects, including an increase in IOP associated with the steroid delivery and formation of cataracts.[98]

Iluvien Fluocinolone Implant.

The Iluvien implant is composed of the same materials and drug as the Retisert implant but is designed with a very different geometry (a narrow cylinder 3.5 × 0.37 mm) that can be injected into the intravitreal space through a 25-gauge needle.[99] The implant and injector are shown in Fig. 40.5. The system delivers a lower level of fluocinolone than the Retisert implant, and in clinical trials for diabetic macular edema there have been fewer complications. Two phase III pivotal trials were conducted which led to the approval of the 0.2 μg/day low-dose fluocinolone acetonide (FA) implant (Iluvien implant, Alimera Sciences, Alpharetta, GA) for the treatment of diabetic macular edema. The pivotal FAME studies showed that at 36 months the percentage of patients who had gained at least 15 ETDRS letters was 28.7% and 27.8% for patients treated with the low-dose 0.2 μg/day FA implant and high-dose 0.5 μg/day FA implant, respectively, compared with 18.9% (p=.018) in the sham group. Cataract development in subjects that were phakic at baseline was seen in 81.7% of the low-dose implant group, 88.7% of the high-dose implant group, and 5.4% of the sham group. The incidence of incisional glaucoma surgery at month 36 was 4.8% in the low-dose FA implant group and 8.1% in the high-dose implant group.[99]

FIG. 40.5 Iluvien implant and injector.

Ozurdex Dexamethasone Implant.

Ozurdex (Allergan) is a dexamethasone implant that delivers the steroid intravitreally for up to 6 months.[100,101] The implant consists of poly(lactic-co-glycolic acid), a degradable polyester and dexamethasone. It is inserted into the intravitreal space with a single-use applicator through a 22-gauge needle. The implant and applicator are shown in Fig. 40.6. The implant is not tethered in the vitreous, like many of the other devices. Because it degrades, it does not have to be removed. It has been approved for the treatment of diabetic macular edema, posterior noninfectious uveitis, and macular edema caused by retinal vein occlusion. The two pivotal phase III trials assessing the safety and efficacy of the Ozurdex dexamethasone (DEX) implant for the treatment of diabetic macular edema were called the MEAD trials. In those pivotal studies the percentage of patients at 36 months with ≥15-letter improvement was 22.2% in patients treated with the high-dose DEX implant 0.7 mg and 18.4% in patients treated with the low dose DEX implant 0.35 mg compared to 12.0% in the sham group ($p \leq .018$). Cataract-related adverse events occurred in 67.9% of phakic eyes in the DEX implant 0.7 mg group and 64.1% in the DEX implant 0.35 mg group compared to 20.4% in the sham group. Increases in IOP occurred in 40% of eyes in the DEX implant 0.7 group and were typically controlled with medication; however, two patients (0.6%) in the

DEX implant 0.7 mg group and one patient (0.3%) in the DEX implant 0.35 mg group required surgery for IOP control.[101]

FIG. 40.6 Ozurdex implant and applicator.

There is always a concern with implants and any delivery technology that if there is a problem, how will the implant or drug delivery system be removed? By using well-characterized drugs and well-defined delivery systems, that risk may be more limited, but careful assessment of side-effects in the clinical trials is critical. There are instances where drug delivery technologies have led to new side-effects not seen with the drug on its own due to the changes in pharmacokinetics associated with the new formulation. The classic example of this is Doxil, a PEGylated liposomal formulation of doxorubicin. The formulation is much more effective than free doxorubicin at treating cancer, but the longer circulation time due to the liposomal formulation and ability to circulate through the capillary beds of the hands and feet can lead to hand–foot syndrome.[102,103]

I-Vation Triamcinolone Implant.

Surmodics has developed the I-vation implant, a helical screw coated with triamcinolone acetonide that delivers the drug intravitreally for 36 months.[104,105] The implant is designed to be inserted through the sclera once a hole has been made with a 25-gauge needle. The implant and a schematic are shown in Fig. 40.7. The helical design increases the surface area from which the drug is released. One of the striking features of the implant is that the drug is entirely within the coating on the helical structure and not within the bulk of the device. Like the Retisert device, long-term usage is associated with an increase in IOP and cataracts. However this device is no longer in development at the current time.[104]

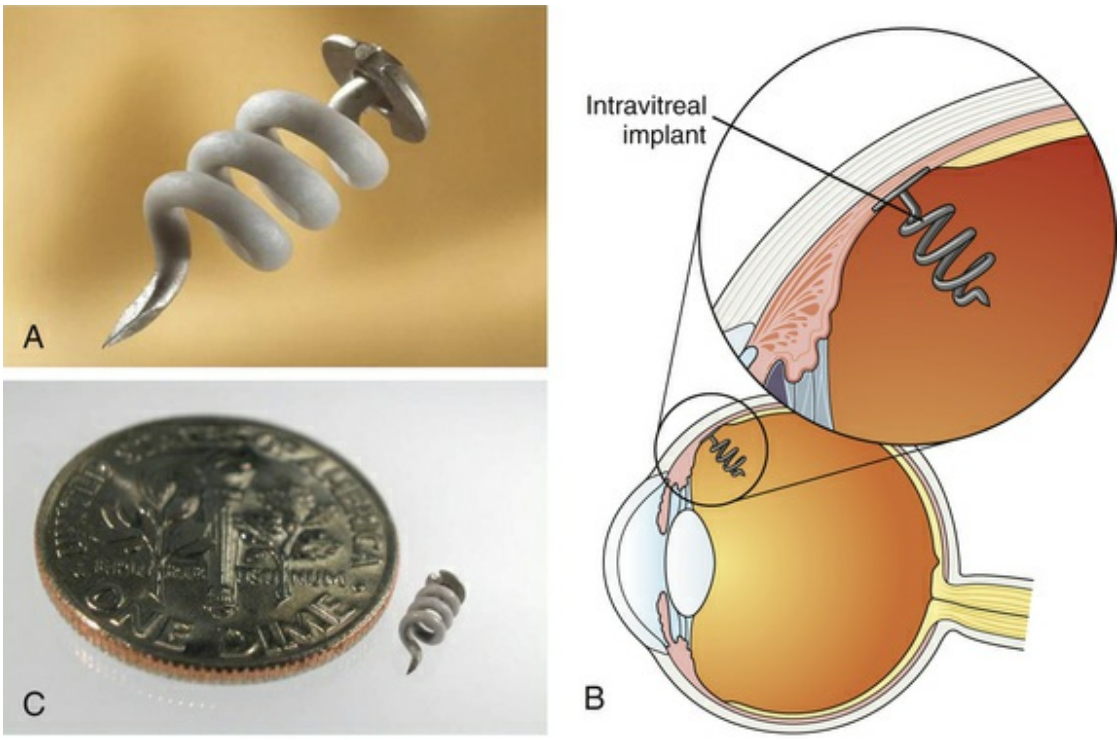

FIG. 40.7 I-vation implant.

Encapsulated Cell Technology (ECT) Ciliary Neurotropic Factor (CNTF) Implant.

CNTF can be delivered from a rice-sized implant via ECT for an estimated time of 2 years or more.[106] The implant contains immortalized RPE cells engineered to deliver CNTF in an encapsulated format, and it is inserted into the vitreous cavity and sutured to the eye wall. A schematic is shown in Fig. 40.8. The implant was studied in a phase I trial for retinitis pigmentosa, it was well tolerated by patients, and some patients showed improvements in visual acuity.[107] The implant (designated NT-501) was then studied in phase II trials for early- and late-stage retinitis pigmentosa. The retinal thickness was higher for those receiving the implant over a year, and Neurotech, the company developing the implant, has been given a fast-track designation by the FDA for the treatment of visual loss from retinitis pigmentosa.

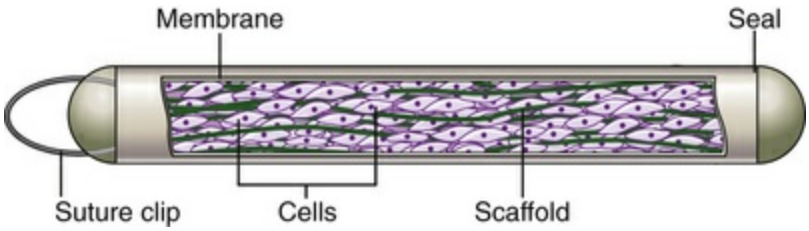

FIG. 40.8 Neurotech encapsulated cell technology implant.

ECT Technology Anti-VEGF Implant.

Neurotech is also developing an anti-VEGF ECT implant for the treatment of age-related macular degeneration (NT-503). Like the CNTF implant, the anti-VEGF implant uses human cells encapsulated to protect them from the immune system but allowing the release of the secreted molecule. Unfortunately, the clinical trials recently showed a suboptimal benefit, and the company is refocusing its efforts on developing the CNTF drug delivery system.

Injectables

Micro- and Nanoparticles.

The majority of micro- and nanoparticles used in the eye are based on the degradable polyesters poly(lactic acid) (PLA) and PLGA. These polymers degrade by hydrolysis and the rate of degradation is controlled by the ratio of lactic acid to glycolic acid subunits, the molecular weight of the polymers, and, in the case of poly(L-lactic acid) (PLLA), the crystallinity of the polymer. The FDA has approved a number of devices using these materials and there is a wealth of literature looking at these materials for use in the eye.[108]

Micro- and nanoparticles based on PLA and PLGA have been used for many years to deliver a range of drugs from small molecules to large proteins. One of the biggest challenges associated with these polymers in spherical form is that they tend to release the drug in multiple phases (typically triphasic) beginning with a burst phase.[109] However, by adding the appropriate excipients that interact with both the polymer and the drug, such as GDNF, one can achieve reduced burst and relatively constant

delivery over very long times up to several months from microparticles.[110] GDNF microspheres based on this approach have been used in vivo in the DBA/2 J mouse model of retinal ganglion cell (RGC) degeneration. The spheres delivering GDNF were injected intravitreally and led to significantly higher numbers of fluorogold-labeled RGCs as compared to the blank spheres or untreated animals.[111] The same formulation was shown to preserve RGC and function in the pig following a model of acute ocular ischemia and found that GDNF microspheres led to the preservation of a greater number of RGCs as well as improved function over time as measured by multifocal electroretinogram.[112]

A number of drugs have been formulated into microspheres for intravitreal and subconjunctival administration. PLGA microparticles delivering celecoxib have been administered subconjunctivally to reduce the concentration of VEGF in the retina and vascular leakage in a diabetic rat model.[113] Likewise, microparticles delivering the corticosteroid, budesonide, have been injected subconjunctivally in rats to alter VEGF expression.[114] Nanoparticles delivering carboplatin for a mouse model of retinoblastoma showed a reduction in tumors.[115] Nanoparticles delivering dexamethasone showed a reduction in choroidal neovascularization in a laser-induced rat model.[116] Intravitreal administration of microspheres delivering BDNF showed neuroprotective effects in a rat model of retinal ischemia.[117]

The difference between nanoparticles and microparticles in this format is really just one of size. The size does have effects, including obvious things like increasing the surface area of the delivery vehicle as the particle size shrinks, which tends to lead to faster release of the drug. Size also has an effect on the concentration of particles that can be administered through a small-gauge needle. Since one of the greatest attractions of the micro- and nanoparticle formulations is that they can be suspended in saline and injected using standard techniques, it is critical to be able to inject them at reasonable concentrations through fine-bore needles. When one is performing an intravitreal injection, in particular, there is very little volume that can be added safely, so one would like to be able to inject as much of the drug delivery system and as little saline as possible.

With careful formulation, and a few predictive models,[118] one can develop injectable formulations that facilitate long-term delivery (typically over several months) of the drug of interest at drug-loading efficiencies and with release kinetics that are suitable for long-term therapy for retinal diseases.

Nanoscale Systems.

Novagali Pharma is developing an emulsion-based delivery system called Eyeject for the sustained delivery of drugs to the intravitreal space. The system is currently in a phase I trial delivering corticosteroid prodrug for the treatment of diabetic macular edema (clinical trial identifier NCT00665106). The system involves combining the prodrug such as lipophilic ester of dexamethasone with an oil such as mineral or vegetable oil, a surfactant, and glycerol. The combination of these components leads to the formation of an emulsion that can be injected intravitreally and deliver the prodrug for 1–6 months. Novagali has been sold to Santen Pharmaceuticals and further development of the Eyeject delivery system is being re-assessed.[119]

Ocular Uptake of Systemically Delivered Nanoparticles

Size plays a critical role in whether nanoparticles can be delivered systemically and be found in the retina. While there is a blood–retina barrier, in one study, a small concentration of 20 nm gold nanoparticles was found in the retina in mice following intravenous administration;[120] 100 nm gold nanoparticles were not found. In another study, PLA-based nanoparticles encapsulating rhodamine (100–200 nm) were not found in normal rat retinas, but a few were seen in a rat model of experimental autoimmune uveoretinitis where the blood–retinal barrier is compromised.[25] Generally, few nanoparticles of any size make it to the retina. The vast majority are likely picked up by the reticuloendothelial system and cleared.[121,122]

Nanocomposites for Topical Delivery

Eye drops are far preferred by patients and clinicians to more invasive injections, and a great deal of research has focused on methods to make drops a viable system for delivery of drugs to the

posterior segment of the eye. Nanocomposites typically involve liposomes or other nanoscaled particles to deliver the drug. One of the primary objectives of nanocomposite research has been to increase the residence time of the solution on the eye to facilitate transport of the drug. The charge or lack thereof on the nanoparticles plays a critical role in their behavior. Neutrally charged liposomes delivering pilocarpine were shown to lead a drop in IOP for twice as long as free drug alone, suggesting that the liposomes increased the residence of the drug following administration.[123] Providing more direct evidence, rhodamine-loaded colloidal solutions of nanocapsules were administered as drops in the eye.[124] Neutral particles showed greater delivery of rhodamine than negatively charged particles.

The question, though, is whether these nanocomposite systems can lead to drug delivery in the back of the eye. Hironaka et al. investigated the delivery of coumarin-6 to the retina via nanocomposites of liposomes containing coumarin-6 as eye drops in mice.[125] Coumarin-6 was found in the inner plexiform layer over the first 60 minutes post administration. The group found that there was better delivery with smaller liposomes, and coating with mucoadhesive molecules increased the delivery of coumarin-6. The mechanism for delivery was not clear in this work, but the group hypothesized that conjunctival adsorption played a role. What is also not clear from this work is how much of the dose was absorbed and how much went into the systemic circulation. The group extended this work to rabbits and monkeys with similar results.[126]

It is impressive that any measurable amount of a molecule can reach the retina via topical administration. Whether enough drug could be delivered to be effective without substantial systemic or ocular side-effects remains to be seen, but the possibility does exist that nanocomposites could be formulated to permit delivery to the back of the eye.

Pharmacokinetics in the Eye

The delivery of a drug is dictated not only by the delivery device but also by the transport parameters in the tissue of interest. When in vitro release studies are conducted, they are almost always

conducted under unlimited or infinite sink conditions, meaning the sink into which the drug is delivered is not limited and does not put a boundary condition on the rate of delivery. In the eye there are several barriers to delivery as well as tissues and fluids that can act as drug sinks and delivery systems. Both the behavior of the drug delivery system and the transport of the drug in the eye need to be considered when predicting and understanding the kinetics of delivery to the retina.

Barriers to Delivery

The major barriers to delivery of molecules in the eye depending on route of administration include the conjunctiva, the sclera, the choriocapillaris, the RPE, the external limiting membrane, the internal limiting membrane, and the blood–retinal barrier. The conjunctiva is permeable to molecules up to ~26 kDa, the sclera is permeable to molecules up to 150 kDa, the choriocapillaris up to 55 kDa, the RPE up to 30 kDa, the external limiting membrane up to 70 kDa, the internal limiting membrane up to 150 kDa, and the blood–retinal barrier is not even permeable to 3 kDa dextran.[127]

Modeling Delivery

Impact of Drug Chemistry

There are good models for predicting drug release from nondegradable systems[105] There are also good models for the release of drugs from degradable polymers that are highly predictive and based on a combination of diffusion and degradation behaviors.[128] The one limitation of this model is that it does not consider the interaction between the polymer matrix and the drug.

This interaction is crucial for understanding release of many of the molecules of interest for the retina from polymer matrices. While size plays an important role in delivery, the drug chemistry is also critical. A good example of a place where the chemistry has a striking effect is in the delivery of NGF, BDNF, and neurotrophin-3. These molecules are from the same family of growth factors and are essentially identical in structure with minor changes in their amino

acid residues[129] and yet their delivery profiles from identically processed matrices can be extremely different.[130–134]

More models that consider the drug–polymer interactions are being developed[135–137] which can be combined with the diffusion and degradation-based models to predict release of drugs from matrices. This, however, is only the first step.

One must also consider how the drugs are absorbed by the surrounding tissues in vivo. Depending on the drug chemistry, several of the tissues of the eye can absorb the drug and, potentially, prolong the delivery.[138] When performing pharmacokinetic experiments, it is useful to look at not only the vitreous and aqueous concentrations, but if possible, to consider whether the lens, iris, and other tissues are acting as sinks for the drug.

Impact of Depot Placement

One will get a very different delivery profile of a drug to the retina if the depot is placed in the intravitreal, subconjunctival, or sub-Tenon space. What is becoming exciting is that more and more assessments of pharmacokinetics for the major drugs in the eye are being published, leading to more data regarding the diffusivities of the drugs through the major barriers in the eye. Often, simple compartment models based on traditional diffusion can be used to predict surprisingly well the potential pharmacokinetics of a drug delivery system placed in the subconjunctival versus intravitreal space.[139–142] The availability of this data increases the probability of efficiently designing delivery systems for treating the retina.

References

1. Royal Pharmaceutical Society of Great Britain. *History of pharmacy*. www.rpharms.com.
2. Frid A, Hirsch L, Gaspar R, et al. New injection recommendations for patients with diabetes. *Diabetes Metab*. 2010;36(Suppl. 2):S3–18.
3. Vogel WH, Berke A. *Brief history of vision and ocular medicine*. Kugler: Amsterdam; 2009.
4. Remis LL, Epstein DL. Treatment of glaucoma. *Annu Rev*

Med. 1984;35:195–205.
5. Gabizon A. Liposome circulation time and tumor targeting: implications for cancer chemotherapy. *Adv Drug Deliv Rev*. 1995;16:285–294.
6. Lian T, Ho RJ. Trends and developments in liposome drug delivery systems. *J Pharm Sci*. 2001;90:667–680.
7. Farokhzad OC, Cheng J, Teply BA, et al. Targeted nanoparticle-aptamer bioconjugates for cancer chemotherapy in vivo. *Proc Natl Acad Sci USA*. 2006;103:6315–6320.
8. Janoria KG, Gunda S, Boddu SH, et al. Novel approaches to retinal drug delivery. *Expert Opin Drug Deliv*. 2007;4:371–388.
9. Langer R. Implantable controlled release systems. *Pharmacol Ther*. 1983;21:35–51.
10. Langer RS, Peppas NA. Present and future applications of biomaterials in controlled drug delivery systems. *Biomaterials*. 1981;2:201–214.
11. Langer R, Folkman J. Polymers for the sustained release of proteins and other macromolecules. *Nature*. 1976;263:797–800.
12. Langer R. Drug delivery and targeting. *Nature*. 1998;392S:5–10.
13. Chess R. Economics of drug delivery. *Pharm Res*. 1998;15:172–174.
14. Takeda Pacific. *Drug delivery systems report*. Takeda Pacific: Fremont, CA; 2006.
15. Harris JM, Chess RB. Effect of PEGylation on pharmaceuticals. *Nat Rev Drug Discov*. 2003;2:214–221.
16. Stewart RH, Novak S. Introduction of the Ocusert ocular system to an ophthalmic practice. *Ann Ophthalmol*. 1978;10:325–330.
17. Langer R. New methods of drug delivery. *Science*. 1990;249:1527–1533.
18. Philip AK, Pathak K. Osmotic flow through asymmetric membrane: a means for controlled delivery of drugs with varying solubility. *AAPS PharmSciTech*. 2006;7:56.
19. Fu K, Harrell R, Zinski K, et al. A potential approach for

decreasing the burst effect of protein from PLGA microspheres. *J Pharm Sci*. 2003;92:1582–1591.
20. Kaneko H, Dridi S, Tarallo V, et al. DICER1 deficit induces Alu RNA toxicity in age-related macular degeneration. *Nature*. 2011;471:325–330.
21. Rudnick SI, Adams GP. Affinity and avidity in antibody-based tumor targeting. *Cancer Biother Radiopharm*. 2009;24:155–161.
22. Brown KC. New approaches for cell-specific targeting: identification of cell-selective peptides from combinatorial libraries. *Curr Opin Chem Biol*. 2000;4:16–21.
23. Cerchia L, de Franciscis V. Targeting cancer cells with nucleic acid aptamers. *Trends Biotechnol*. 2010;28:517–525.
24. Levy-Nissenbaum E, Radovic-Moreno AF, Wang AZ, et al. Nanotechnology and aptamers: applications in drug delivery. *Trends Biotechnol*. 2008;26:442–449.
25. Sakai T, Kohno H, Ishihara T, et al. Treatment of experimental autoimmune uveoretinitis with poly(lactic acid) nanoparticles encapsulating betamethasone phosphate. *Exp Eye Res*. 2006;82:657–663.
26. Sun D, Nakao S, Xie F, et al. Superior sensitivity of novel molecular imaging probe: simultaneously targeting two types of endothelial injury markers. *FASEB J*. 2010;24:1532–1540.
27. Kim JH, Kim KW, Kim MH, et al. Intravenously administered gold nanoparticles pass through the blood–retinal barrier depending on the particle size, and induce no retinal toxicity. *Nanotechnology*. 2009;20:505101.
28. Choonara YE, Pillay V, Danckwerts MP, et al. A review of implantable intravitreal drug delivery technologies for the treatment of posterior segment eye diseases. *J Pharm Sci*. 2010;99:2219–2239.
29. Bloquel C, Bourges JL, Touchard E, et al. Non-viral ocular gene therapy: potential ocular therapeutic avenues. *Adv Drug Deliv Rev*. 2006;58:1224–1242.
30. Friedmann T. A brief history of gene therapy. *Nat Genet*. 1992;2:93–98.
31. Raper SE, Chirmule N, Lee FS, et al. Fatal systemic

inflammatory response syndrome in a ornithine transcarbamylase deficient patient following adenoviral gene transfer. *Mol Genet Metab*. 2003;80:148–158.
32. Heilbronn R, Weger S. Viral vectors for gene transfer: current status of gene therapeutics. *Handb Exp Pharmacol*. 2010;197:143–170.
33. Campochiaro PA, Nguyen QD, Shah SM, et al. Adenoviral vector-delivered pigment epithelium-derived factor for neovascular age-related macular degeneration: results of a phase I clinical trial. *Hum Gene Ther*. 2006;17:167–176.
34. Chen P, Hamilton M, Thomas CA, et al. Persistent expression of PEDF in the eye using high-capacity adenovectors. *Mol Ther*. 2008;16:1986–1994.
35. Hamilton MM, Brough DE, McVey D, et al. Repeated administration of adenovector in the eye results in efficient gene delivery. *Invest Ophthalmol Vis Sci*. 2006;47:299–305.
36. McVey D, Hamilton MM, Hsu C, et al. Repeat administration of proteins to the eye with a single intraocular injection of an adenovirus vector. *Mol Ther*. 2008;16:1444–1449.
37. Sachetta R. *Avalanche Biotech CEO Chalberg resigns after disappointing trial*. [Bloomberg News July 23] http://bloom.bg/1HMmv15; 2015.
38. Maguire AM, High KA, Auricchio A, et al. Age-dependent effects of RPE65 gene therapy for Leber's congenital amaurosis: a phase 1 dose-escalation trial. *Lancet*. 2009;374:1597–1605.
39. Chailertvanitkul VA, Pouton CW. Adenovirus: a blueprint for non-viral gene delivery. *Curr Opin Biotechnol*. 2010;21:627–632.
40. Chonn A, Cullis PR. Recent advances in liposomal drug-delivery systems. *Curr Opin Biotechnol*. 1995;6:698–708.
41. Felgner PL, Gadek TR, Holm M, et al. Lipofection: a highly efficient, lipid-mediated DNA-transfection procedure. *Proc Natl Acad Sci USA*. 1987;84:7413–7417.
42. Boussif O, Lezoualc'h F, Zanta MA, et al. A versatile vector for gene and oligonucleotide transfer into cells in culture and in vivo: polyethylenimine. *Proc Natl Acad Sci USA*.

1995;92:7297–7301.
43. Horbinski C, Stachowiak MK, Higgins D, et al. Polyethyleneimine-mediated transfection of cultured postmitotic neurons from rat sympathetic ganglia and adult human retina. *BMC Neurosci*. 2001;2:2.
44. Gomes dos Santos AL, Bochot A, Tsapis N, et al. Oligonucleotide–polyethylenimine complexes targeting retinal cells: structural analysis and application to anti-TGFbeta-2 therapy. *Pharm Res*. 2006;23:770–781.
45. Won YW, Lim KS, Kim YH. Intracellular organelle-targeted non-viral gene delivery systems. *J Control Release*. 2011;152:99–109.
46. van Gaal EV, Oosting RS, van Eijk R, et al. DNA nuclear targeting sequences for non-viral gene delivery. *Pharm Res*. 2011;28:1707–1722.
47. Liechty WB, Caldorera-Moore M, Phillips MA, et al. Advanced molecular design of biopolymers for transmucosal and intracellular delivery of chemotherapeutic agents and biological therapeutics. *J Control Release*. 2011;30:119–127.
48. Dalkara D, Kolstad KD, Caporale N, et al. Inner limiting membrane barriers to AAV-mediated retinal transduction from the vitreous. *Mol Ther*. 2009;17:2096–2102.
49. Gregory-Evans K, Chang F, Hodges MD, et al. Ex vivo gene therapy using intravitreal injection of GDNF-secreting mouse embryonic stem cells in a rat model of retinal degeneration. *Mol Vis*. 2009;15:962–973.
50. Harper MM, Grozdanic SD, Blits B, et al. Transplantation of BDNF-secreting mesenchymal stem cells provides neuroprotection in chronically hypertensive rat eyes. *Invest Ophthalmol Vis Sci*. 2011;52:4506–4515.
51. Lawrence JM, Keegan DJ, Muir EM, et al. Transplantation of Schwann cell line clones secreting GDNF or BDNF into the retinas of dystrophic Royal College of Surgeons rats. *Invest Ophthalmol Vis Sci*. 2004;45:267–274.
52. Liu Y, Kim DH, Himes BT, et al. Transplants of fibroblasts genetically modified to express BDNF promote regeneration of adult rat rubrospinal axons and recovery of

forelimb function. *J Neurosci*. 1999;19:4370–4387.
53. Taylor AW. Ocular immune privilege. *Eye (Lond)*. 2009;23:1885–1889.
54. Taylor AW, Kaplan HJ. Ocular immune privilege in the year 2010: ocular immune privilege and uveitis. *Ocul Immunol Inflamm*. 2010;18:488–492.
55. Bjerkvig R, Read TA, Vajkoczy P, et al. Cell therapy using encapsulated cells producing endostatin. *Acta Neurochir Suppl*. 2003;88:137–141.
56. Siebers U, Horcher A, Bretzel RG, et al. Alginate-based microcapsules for immunoprotected islet transplantation. *Ann N Y Acad Sci*. 1997;831:304–312.
57. Kontturi LS, Yliperttula M, Toivanen P, et al. A laboratory-scale device for the straightforward production of uniform, small sized cell microcapsules with long-term cell viability. *J Control Release*. 2011;152:376–381.
58. Chong SF, Lee JH, Zelikin AN, et al. Tuning the permeability of polymer hydrogel capsules: an investigation of cross-linking density, membrane thickness, and cross-linkers. *Langmuir*. 2011;27:1724–1730.
59. Dusseault J, Leblond FA, Robitaille R, et al. Microencapsulation of living cells in semi-permeable membranes with covalently cross-linked layers. *Biomaterials*. 2005;26:1515–1522.
60. Lin CC, Anseth KS. Glucagon-like peptide-1 functionalized PEG hydrogels promote survival and function of encapsulated pancreatic beta-cells. *Biomacromolecules*. 2009;10:2460–2467.
61. Hoyng PF, van Beek LM. Pharmacological therapy for glaucoma: a review. *Drugs*. 2000;59:411–434.
62. Marquis RE, Whitson JT. Management of glaucoma: focus on pharmacological therapy. *Drugs Aging*. 2005;22:1–21.
63. Uusitalo H, Kahonen M, Ropo A, et al. Improved systemic safety and risk–benefit ratio of topical 0.1% timolol hydrogel compared with 0.5% timolol aqueous solution in the treatment of glaucoma. *Graefes Arch Clin Exp Ophthalmol*. 2006;244:1491–1496.
64. Worakul N, Robinson JR. Ocular

pharmacokinetics/pharmacodynamics. *Eur J Pharm Biopharm*. 1997;44:71–83.
65. Lambiase A, Aloe L, Centofanti M, et al. Experimental and clinical evidence of neuroprotection by nerve growth factor eye drops: implications for glaucoma. *Proc Natl Acad Sci USA*. 2009;106(32):13469–13474.
66. Amrite AC, Edelhauser HF, Kompella UB. Modeling of corneal and retinal pharmacokinetics after periocular drug administration. *Invest Ophthalmol Vis Sci*. 2008;49:320–332.
67. Kim TW, Lindsey JD, Aihara M, et al. Intraocular distribution of 70-kDa dextran after subconjunctival injection in mice. *Invest Ophthalmol Vis Sci*. 2002;43:1809–1816.
68. Lee TWY, Robinson JR. Drug delivery to the posterior segment of the eye: some insights on the penetration pathways after subconjunctival injection. *J Ocular Pharmacol Ther*. 2001;17:565–572.
69. Dureau P, Bonnel S, Menasche M, et al. Quantitative analysis of intravitreal injections in the rat. *Curr Eye Res*. 2001;22:74–77.
70. Kim H, Csaky KG, Chan CC, et al. The pharmacokinetics of rituximab following an intravitreal injection. *Exp Eye Res*. 2006;82:760–766.
71. Taylor SRJ, Habot-Wilner Z, Pacheco P, editors. Intraocular methotrexate in the treatment of uveitis and uveitic cystoid macular edema. 112th Annual Meeting of the American Academy of Ophthalmology; 2008 Nov 08–11; Atlanta, GA.
72. Byun YS, Park YH. Complications and safety profile of posterior subtenon injection of triamcinolone acetonide. *J Ocular Pharmacol Ther*. 2009;25:159–162.
73. Lee SJ, Kim ES, Geroski DH, et al. Pharmacokinetics of intraocular drug delivery of Oregon green 488-labeled triamcinolone by subtenon injection using ocular fluorophotometry in rabbit eyes. *Invest Ophthalmol Vis Sci*. 2008;49:4506–4514.
74. Verma LK, Vivek MB, Kumar A, et al. A prospective controlled trial to evaluate the adjunctive role of posterior subtenon triamcinolone in the treatment of diffuse diabetic

macular edema. *J Ocul Pharmacol Ther*. 2004;20:277–284.
75. Englander M, Shah CP, Heier JS. Extended release of ranibizumab with the port delivery system. *Retina Times*. 2015;33(2):20–21.
76. Macoul KL, Pavan-Langston D. Pilocarpine ocusert system for sustained control of ocular hypertension. *Arch Ophthalmol*. 1975;93:587–590.
77. Pollack IP, Quigley HA, Harbin TS. Ocusert pilocarpine system – advantages and disadvantages. *South Med J*. 1976;69:1296–1298.
78. Saettone MF, Salminen L. Ocular inserts for topical delivery. *Adv Drug Deliv Rev*. 1995;16:95–106.
79. American Academy of Ophthalmology. *Eye health statistics at a glance*. American Academy of Ophthalmology: San Francisco; 2009.
80. White CJ, Byrne ME. Molecularly imprinted therapeutic contact lenses. *Expert Opin Drug Deliv*. 2010;7:765–780.
81. Hoffman A. Hydrogels for biomedical applications. *Adv Drug Deliv Rev*. 2002;54:3–12.
82. Peppas N, Bures P, Leobandung W, et al. Hydrogels in pharmaceutical formulations. *Eur J Pharm Biopharm*. 2000;50:27–46.
83. Hiratani H, Alvarez-Lorenzo C. Timolol uptake and release by imprinted soft contact lenses made of N,N-diethylacrylamide and methacrylic acid. *J Control Release*. 2002;83:223–230.
84. Schultz CL, Poling TR, Mint JO. A medical device/drug delivery system for treatment of glaucoma. *Clin Exp Optom*. 2009;92:343–348.
85. Kompella UB, Kadam RS, Lee VH. Recent advances in ophthalmic drug delivery. *Ther Deliv*. 2010;1:435–456.
86. Fusco S, Ullrich F, Pokki J, et al. Microrobots: a new era in ocular drug delivery. *Expert Opin Drug Deliv*. 2014;11(11):1815–1826.
87. Jeong JW, McCall JG, Shin G, et al. Wireless optofluidic systems for programmable in vivo pharmacology and optogenetics. *Cell*. 2015;162(3):662–674.
88. Sheybani R, Cobo A, Meng E, et al. Wireless programmable

electrochemical drug delivery micropump with fully integrated electrochemical dosing sensors. *Biomed Microdevices*. 2015;17(4):74.
89. Tao H, Hwang SW, Marelli B, et al. Silk-based resorbable electronic devices for remotely controlled therapy and in vivo infection abatement. *Proc Natl Acad Sci USA*. 2014;111(49):17385–17389.
90. Saati S, Lo R, Li PY, et al. Mini drug pump for ophthalmic use. *Trans Am Ophthalmol Soc*. 2009;107:60–70.
91. Saati S, Lo R, Li PY, et al. Mini drug pump for ophthalmic use. *Curr Eye Res*. 2010;35:192–201.
92. Chopra P, Hao J, Li SK. Iontophoretic transport of charged macromolecules across human sclera. *Int J Pharm*. 2010;388:107–113.
93. First eye implant approved. *AIDS Alert*. 1996;11:59.
94. Chiron Vision files FDA application to market intraocular implant for CMV retinitis. Food and Drug Administration. *J Int Assoc Physicians AIDS Care*. 1995;1:37.
95. Ganciclovir implants (Vitrasert). *Treat Rev*. 1996;(21):10.
96. MacCumber MW, Sadeghi S, Cohen JA, et al. Suture loop to aid in ganciclovir implant removal. *Arch Ophthalmol*. 1999;117:1250–1254.
97. Schwartz SG, Flynn HW Jr. Fluocinolone acetonide implantable device for diabetic retinopathy. *Curr Pharm Biotechnol*. 2011;12:347–351.
98. Brumm MV, Nguyen QD. Fluocinolone acetonide intravitreal sustained release device – a new addition to the armamentarium of uveitic management. *Int J Nanomedicine*. 2007;2:55–64.
99. Campochiaro PA, Brown DM, Pearson A, et al. Sustained delivery fluocinolone acetonide vitreous inserts provide benefit for at least 3 years in patients with diabetic macular edema. *Ophthalmology*. 2012;119(10):2125–2132.
100. Kuno N, Fujii S. Biodegradable intraocular therapies for retinal disorders: progress to date. *Drugs Aging*. 2010;27:117–134.
101. Haller JA, Bandello F, Belfort R Jr, et al. Randomized, sham-controlled trial of dexamethasone intravitreal implant in

patients with macular edema due to retinal vein occlusion. *Ophthalmology*. 2010;117:1134–1146.
102. von Moos R, Thuerlimann BJ, Aapro M, et al. PEGylated liposomal doxorubicin-associated hand–foot syndrome: recommendations of an international panel of experts. *Eur J Cancer*. 2008;44:781–790.
103. Lorusso D, Di Stefano A, Carone V, et al. PEGylated liposomal doxorubicin-related palmar-plantar erythrodysesthesia ("hand–foot" syndrome). *Ann Oncol*. 2007;18:1159–1164.
104. Dugel PU, Eliott D, Cantrill HL, et al. I-VationTM TA: 24-month clinical results of the phase I safety and preliminary efficacy study. *Invest Ophthalmol Vis Sci*. 2009;50:4332.
105. Barnett PJ. Mathematical modeling of triamcinolone acetonide drug release from the I-vation intravitreal implant (a controlled release platform). *Conf Proc IEEE Eng Med Biol Soc*. 2009;2009:3087–3090.
106. Thanos CG, Bell WJ, O'Rourke P, et al. Sustained secretion of ciliary neurotrophic factor to the vitreous, using the encapsulated cell therapy-based NT-501 intraocular device. *Tissue Eng*. 2004;10:1617–1622.
107. Sieving PA, Caruso RC, Tao W, et al. Ciliary neurotrophic factor (CNTF) for human retinal degeneration: phase I trial of CNTF delivered by encapsulated cell intraocular implants. *Proc Natl Acad Sci USA*. 2006;103:3896–3901.
108. Shive M, Anderson J. Biodegradation and biocompatibility of PLA and PLGA microspheres. *Adv Drug Deliv Rev*. 1997;28:5–24.
109. Allison SD. Analysis of initial burst in PLGA microparticles. *Expert Opin Drug Deliv*. 2008;5:615–628.
110. Fu K, Harrell R, Zinski K, et al. A potential approach for decreasing the burst effect of protein from PLGA microspheres. *J Pharm Sci*. 2003;92:1582–1591.
111. Ward MS, Khoobehi A, Lavik EB, et al. Neuroprotection of retinal ganglion cells in DBA/2 J mice with GDNF-loaded biodegradable microspheres. *J Pharm Sci*. 2007;96:558–568.
112. Lavik EB, Warfvinge K, Scherfig E, et al. *Preservation of retinal ganglion cells via polymer microspheres delivering GDNF*

following low perfusion pressure in the pig. Society for Neuroscience: Washington, DC; 2005.
113. Amrite AC, Ayalasomayajula SP, Cheruvu NP, et al. Single periocular injection of celecoxib-PLGA microparticles inhibits diabetes-induced elevations in retinal PGE2, VEGF, and vascular leakage. *Invest Ophthalmol Vis Sci*. 2006;47:1149–1160.
114. Kompella UB, Bandi N, Ayalasomayajula SP. Subconjunctival nano- and microparticles sustain retinal delivery of budesonide, a corticosteroid capable of inhibiting VEGF expression. *Invest Ophthalmol Vis Sci*. 2003;44:1192–1201.
115. Kang SJ, Durairaj C, Kompella UB, et al. Subconjunctival nanoparticle carboplatin in the treatment of murine retinoblastoma. *Arch Ophthalmol*. 2009;127:1043–1047.
116. Xu J, Wang Y, Li Y, et al. Inhibitory efficacy of intravitreal dexamethasone acetate-loaded PLGA nanoparticles on choroidal neovascularization in a laser-induced rat model. *J Ocul Pharmacol Ther*. 2007;23:527–540.
117. Grozdanic SD, Lazic T, Kuehn MH, et al. Exogenous modulation of intrinsic optic nerve neuroprotective activity. *Graefes Arch Clin Exp Ophthalmol*. 2010;248:1105–1116.
118. Lemaire V, Belair J, Hildgen P. Structural modeling of drug release from biodegradable porous matrices based on a combined diffusion/erosion process. *Int J Pharm*. 2003;258:95–107.
119. Rabinovich-Guilatt L, Lambert G. *Methods for treating eye disease or conditions affecting the posterior segment of the eye*. [inventors; Novagali Pharma SA, assignee; USA patent 11/444,349] 2007.
120. Kim JH, Kim JH, Kim KW, et al. Intravenously administered gold nanoparticles pass through the blood–retinal barrier depending on the particle size, and induce no retinal toxicity. *Nanotechnology*. 2009;20:505101.
121. Caldorera-Moore M, Guimard N, Shi L, et al. Designer nanoparticles: incorporating size, shape and triggered release into nanoscale drug carriers. *Expert Opin Drug Deliv*. 2010;7:479–495.

122. Semete B, Booysen L, Lemmer Y, et al. In vivo evaluation of the biodistribution and safety of PLGA nanoparticles as drug delivery systems. *Nanomedicine (Lond)*. 2010;6:662–671.
123. Monem AS, Ali FM, Ismail MW. Prolonged effect of liposomes encapsulating pilocarpine HCl in normal and glaucomatous rabbits. *Int J Pharm*. 2000;198:29–38.
124. De Campos AM, Sanchez A, Gref R, et al. The effect of a PEG versus a chitosan coating on the interaction of drug colloidal carriers with the ocular mucosa. *Eur J Pharm Sci*. 2003;20:73–81.
125. Hironaka K, Inokuchi Y, Tozuka Y, et al. Design and evaluation of a liposomal delivery system targeting the posterior segment of the eye. *J Control Release*. 2009;136:247–253.
126. Inokuchi Y, Hironaka K, Fujisawa T, et al. Physicochemical properties affecting retinal drug/coumarin-6 delivery from nanocarrier systems via eyedrop administration. *Invest Ophthalmol Vis Sci*. 2010;51:3162–3170.
127. El Sanharawi M, Kowalczuk L, Touchard E, et al. Protein delivery for retinal diseases: from basic considerations to clinical applications. *Prog Retin Eye Res*. 2010;29:443–465.
128. Rothstein SN, Federspiel WJ, Little SR. A unified mathematical model for the prediction of controlled release from surface and bulk eroding polymer matrices. *Biomaterials*. 2009;30:1657–1664.
129. Ebendal T. Function and evolution in the NGF family and its receptors. *J Neurosci Res*. 1992;32:461–470.
130. Woodhall E, West AK, Chuah MI. Cultured olfactory ensheathing cells express nerve growth factor, brain-derived neurotrophic factor, glia cell line-derived neurotrophic factor and their receptors. *Brain Res Mol Brain Res*. 2001;88:203–213.
131. Aszmann OC, Korak KJ, Kropf N, et al. Simultaneous GDNF and BDNF application leads to increased motoneuron survival and improved functional outcome in an experimental model for obstetric brachial plexus lesions. *Plast Reconstr Surg*. 2002;110:1066–1072.
132. Bertram J, Rauch MF, Chang K, et al. Using polymer

chemistry to modulate the delivery of neurotrophic factors from degradable microspheres: Delivery of BDNF. *Pharm Res*. 2009;27:82–91.
133. Cao X. Schoichet M. Delivering neuroactive molecules from biodegradable microspheres for application in central nervous system disorders. *Biomaterials*. 1999;20:329–339.
134. Yang Y, De Laporte L, Rives CB, et al. Neurotrophin releasing single and multiple lumen nerve conduits. *J Control Release*. 2005;104:433–446.
135. Taylor SJ, McDonald JW 3rd, Sakiyama-Elbert SE. Controlled release of neurotrophin-3 from fibrin gels for spinal cord injury. *J Control Release*. 2004;98:281–294.
136. Park S, Kang S, Veach AJ, et al. Self-assembled nanoplatform for targeted delivery of chemotherapy agents via affinity-regulated molecular interactions. *Biomaterials*. 2010;31:7766–7775.
137. Fu AS, Thatiparti TR, Saidel GM, et al. Experimental studies and modeling of drug release from a tunable affinity-based drug delivery platform. *Ann Biomed Eng*. 2011;39:2466–2475.
138. Lee VHL, Luo AM, Li SY, et al. Pharmacokinetic basis for nonadditivity of intraocular pressure lowering in timolol combinations. *Invest Ophthalmol Vis Sci*. 1991;32:2948–2957.
139. Douglas LC, Yi NY, Davis JL, et al. Ocular toxicity and distribution of subconjunctival and intravitreal rapamycin in horses. *J Vet Pharmacol Ther*. 2008;31:511–516.
140. Hosseini K, Matsushima D, Johnson J, et al. Pharmacokinetic study of dexamethasone disodium phosphate using intravitreal, subconjunctival, and intravenous delivery routes in rabbits. *J Ocul Pharmacol Ther*. 2008;24:301–308.
141. Nomoto H, Shiraga F, Kuno N, et al. Pharmacokinetics of bevacizumab after topical, subconjunctival, and intravitreal administration in rabbits. *Invest Ophthalmol Vis Sci*. 2009;50:4807–4813.
142. Liu X, Li SK, Jeong EK. Ocular pharmacokinetic study of a corticosteroid by 19F MR. *Exp Eye Res*. 2010;91:347–352.

41

Retinal Laser Therapy

Biophysical Basis and Applications

Daniel Palanker, Mark S. Blumenkranz

Introduction

Historically, a number of light sources have been utilized for retinal phototherapy including the sun, various flash lamps, and lasers. The sun light is capable of producing a retinal burn either accidentally (e.g., in the case of solar eclipse gazing) or purposefully, as demonstrated first by Meyer-Schwickerath.[1] However, its dependence on weather conditions, its constant motion in the sky, and relatively large angular size (0.52°) make its use impractical for retinal therapy.

Arc lamps are very bright sources of light used in many therapeutic and imaging applications. In such lamps, a high-voltage discharge ionizes gas between an anode and cathode creating an electric arc – a high current density discharge. The ions emit light at specific wavelengths, and the spectrum of the plasma emission depends on the types of atoms involved, their temperatures and gas

pressure. Thus the spectrum of an arc lamp may have a distinct signature. The xenon arc lamp was the first to become widely used for retinal photocoagulation because of its strong visible and near-infrared emission, convenience, and low price. However, because of its large size, poorly collimated beam, and tendency to produce intense retinal burns, it was replaced in clinical practice by laser-based systems in the early 1970s.[2]

Lasers became the preferred light source for retinal photocoagulation due to their narrow spectrum, wide selection of wavelengths, excellent collimation (directionality), high brightness, and variable pulse duration. The highly collimated laser beam is easy to guide before its introduction into the eye, and to focus into very small spots. Its monochromaticity makes it possible to choose a wavelength for selective absorption in specific tissues of the eye. Adjustable pulse duration allows controlling the extent of thermal diffusion, thus producing very precise and selective interactions with minimal collateral damage.

The most widespread medical applications of lasers in medicine have been in ophthalmology. Since the introduction of the ruby laser more than three decades ago, ophthalmic laser applications have experienced rapid growth with the use of argon, krypton, argon-pumped dye, Nd : YAG, diode, Er : YAG, excimer, and Ti : Sapphire lasers. Lasers have been applied to a wide variety of slit lamp-based retinal therapies, as well as to vitreoretinal surgery, glaucoma therapy, posterior capsulotomy, and refractive surgery. These applications are based on different mechanisms of laser–tissue interactions, including photothermal, photodisruptive, and photochemical interactions. The most common vitreoretinal application is retinal photocoagulation. Additionally, a number of novel therapies have recently been introduced and are under active evaluation, including selective retinal pigmented epithelium (RPE) treatment (SRT) and nondamaging retinal therapy (NRT).

In the following sections we will describe the underlying principles of laser–tissue interactions and the types of lasers available and appropriate for various retinal applications.

Optical Properties of the Eye

The relaxed eye has an approximate optical power of 60 diopters (D) (i.e., its focal length is 16.7 mm), with the corneal power being about 40 D, or two-thirds of the total power.[3] Due to orderly arrangement of collagen fibrils in the cornea, it is highly transparent – with transmission above 95% in the spectral range of 400–900 nm.[4] The refractive index of the cornea is n≈1.3765± 0.0005.[4] The amount of light reaching the retina is regulated by the pupil size, which can vary between 1.5 and 8 mm. The anterior chamber of the eye, which is located between the cornea and lens capsule, is filled with a clear liquid – the aqueous humor having a refractive index n≈1.3335. The crystalline lens of the eye, located behind the iris is composed of specialized crystallin proteins with refractive index of n=1.40–1.42. The lens is about 4 mm in thickness and 10 mm in diameter and is enclosed in a elastic, thin (5–15 μm), transparent collagenous capsule. In the relaxed eye the lens has a power of about 20 D, while in the fully accommodated state it can temporarily increase to 33 D. The vitreous humor – a transparent jelly-like substance filling the large cavity posterior to the lens and anterior to the retina has a refractive index n≈1.335.[4]

Light entering the eye can be reflected, scattered, transmitted or absorbed. Reflected or scattered light contains information that can be used for noninvasive diagnostic purposes. The absorption characteristics of ocular tissues are determined by the chromophores resident within the tissue. In the visible part of the spectrum (400–750 nm) these chromophores include: (a) melanin located in the retinal and iris pigmented epithelia, choroid, uvea, trabecular meshwork; (b) hemoglobin, located in the red blood cells; (c) macular xanthophyll, which is located in the plexiform layers of the retina, especially in the macula; (d) rhodopsin and cone photopigments which are located in the photoreceptors; and (e) lipofuscin located primarily in the RPE layer. These pigments are of major importance in absorption of visible light in the retina from both a physiologic and pathologic standpoints. The absorption spectra of these pigments, as well as water and proteins are illustrated in Fig. 41.1. In the mid-infrared part of the spectrum (3–15 μm) the major absorber is water, while protein absorption is dominant in ultraviolet range (below 250 nm).

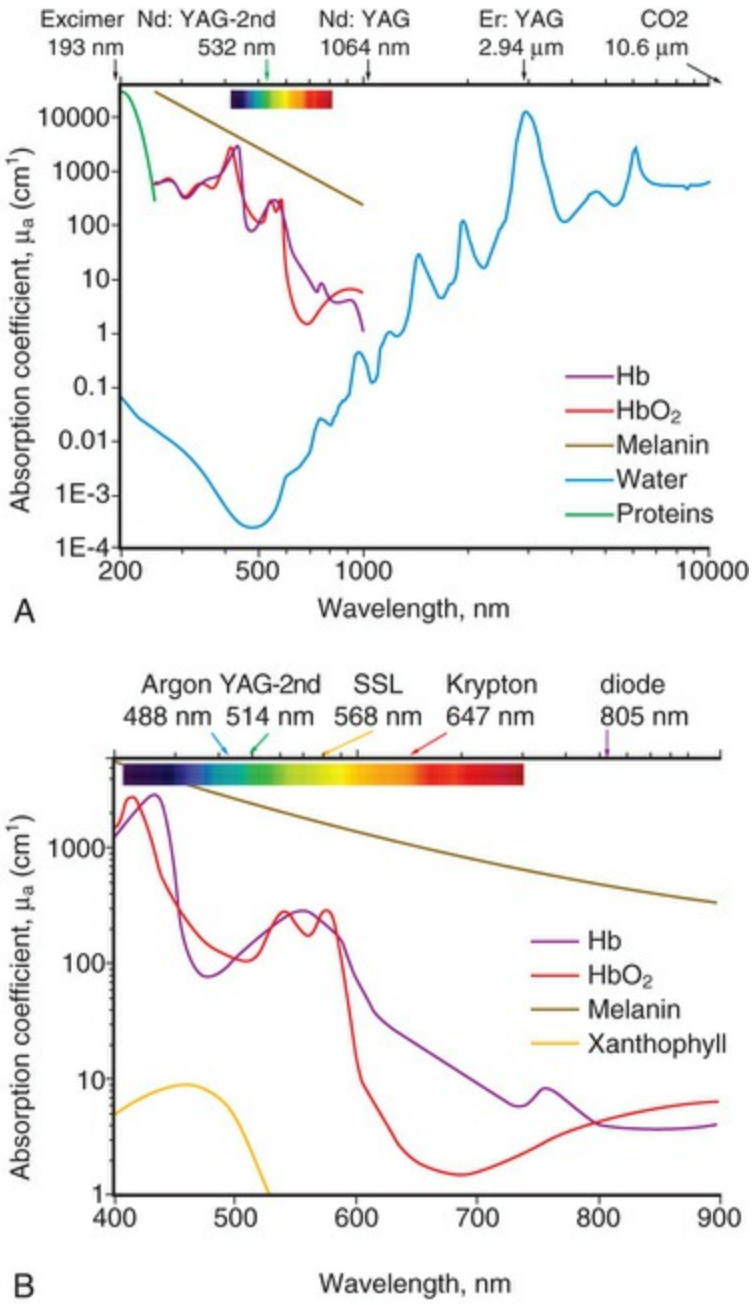

FIG. 41.1 (A) Absorption coefficients for major chromophores in a spectral range of 0.2–10 µm. Spectral location of some of the common laser lines are indicated above the plot. (B) Absorption coefficients of the major ocular chromophores in the visible part of the spectrum: 400–900 nm. Spectral location of some of the common laser lines in this range are indicated above the plot. *Hb*, hemoglobin.

Basics of Lasers

The term “laser” is an acronym for light amplification by stimulated emission of radiation. A beam of light is composed of individual packets of energy that are called quanta or photons. Each of these photons has a particular energy and direction of travel. The energy of a quantum of light is proportional to its frequency, i.e., it is a reciprocal of its wavelength. In the presence of a properly prepared laser material, it is possible for a quantum of light to trigger the release of other quanta with the same wavelength and direction of travel. This phenomenon is called stimulated emission, and it is an essential element in lasing. In thermal equilibrium the energy levels of atoms and molecules are populated according to the Boltzmann distribution, in which upper levels are always less populated than the lower levels. Stimulated emission requires an inverted population of energy levels, such that the upper levels are more populated than the lower ones. Therefore, lasing can occur only when material is not in thermal equilibrium. The nonequilibrium state of the population inversion is created in the lasing material by an excitation source or “pump.”

Generally, a laser is composed of three basic components: (1) a material that can store energy to be released by stimulated emission; (2) a means of replenishing the energy stored in the laser material; and (3) some method of retaining a fraction of the light emitted by the lasing material to stimulate further emission. Fig. 41.2 schematically illustrates a general configuration of a laser. An energy source is used to introduce energy into the lasing material. This energy is stored as atomic or molecular excitation waiting to be released by stimulated emission. Laser light emitted by the lasing material circulates between the two mirrors on either end of the laser cavity, with a fraction of the light escaping through one mirror to form the laser beam. The trapped light stimulates emission of new quanta of light from the laser material with the same wavelength and direction as the original quanta. This way laser produces a beam of light in which all of the quanta move “in phase” with one another. This property of light is called coherence. Duration of the synchronized emission multiplied by the speed of light is called the coherence length of the laser emission. This is the distance along which the photons are coherent, or moving “in step.” To remain in phase with one another, these quanta must have

approximately the same wavelength. Thus temporal coherence is related to the monochromaticity (or spectral width) of the light emitted from the laser: the broader is the spectrum the shorter is the temporal coherence. A laser may produce one or several discrete spectral lines in either the infrared, visible or ultraviolet domains, in contrast to conventional light sources (incandescent or arc lamps) which typically produce polychromatic (broad-band or white) light.

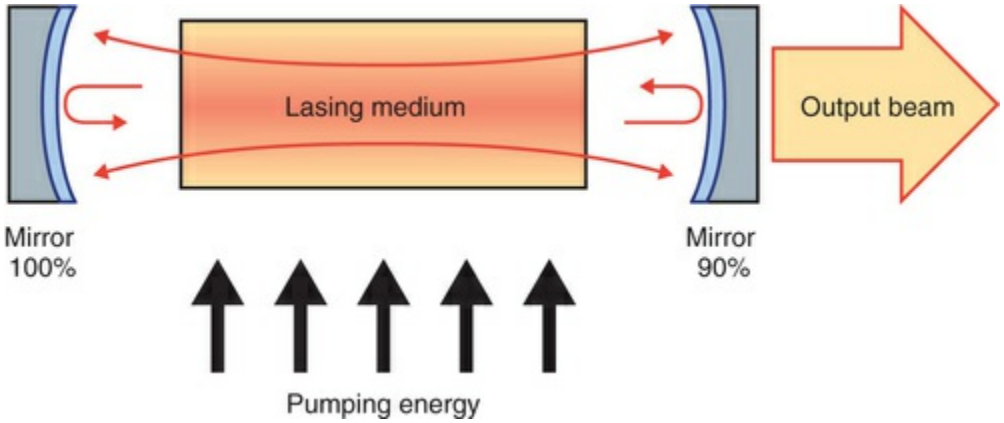

FIG. 41.2 Laser typically consists of the energy source (pump), the lasing medium, and the optical cavity with a partially transparent front mirror.

Collimation (directionality) of the emitted beam is governed by the mirror configuration of the laser cavity. In its simplest form, a cavity consists of two mirrors arranged such that light bounces back and forth, each time passing through the gain medium. One of the two mirrors, the output coupler, is partially transparent, allowing the output beam to exit through it (see Fig. 41.2). The reflection coefficient of the output coupler determines how many times photons are reflected back to circulate inside the cavity before exiting it. For example, with a reflection coefficient of 0.99, the photon will bounce, on average, 99 times before exiting the cavity. The structure of the laser cavity determines directionality (collimation) of the laser beam, which determines its ability to be focused into a small spot.

The lasing medium can be a gas, liquid, or solid. Lasers can be pumped by continuous discharge lamps and by pulsed flash lamps, by electric discharges in the laser medium, by chemical reactions, by an electron beam, by direct conversion of electric current into

photons in semiconductors, or by light from other lasers. Laser pulse durations can vary from femtoseconds to infinity. Pulsing techniques used for different ranges of pulse durations include electronic shutters (down to 1 ms), pulsed flash lamps (typically down to a few μs), Q-switching (down to a few ns), or mode-locking (down to fs).

Laser Beam Delivery to Tissue

Laser beams are typically very well collimated. Diffraction causes light waves to spread transversely as they propagate, and it is therefore impossible to have a perfectly collimated beam. The diffraction-limited divergence angle of a Gaussian beam with diameter D and wavelength λ is $\Theta = \frac{4 \cdot \lambda}{\pi \cdot D}$. As an example, for a laser emitting a 1 mm wide beam at 532 nm wavelength, the divergence (half-angle Θ) is about 0.66 mrad, i.e., the beam spreads by 1.3 mm over a distance of 1 meter.

Using a lens or a concave mirror with focal length f, a laser beam can be focused to a spot with a diameter $d = \frac{4 \cdot f}{\pi \cdot D} \lambda$. The depth of the focal region is: $F = \frac{8 \cdot f^2}{\pi \cdot D^2} \lambda$ (see Fig. 41.3). With a lens having focal distance f = 25 mm, the same 532 nm laser beam can be focused to a spot of 16 μm in diameter, having a focal depth of about 850 μm. It must be emphasized though that exact definition of the spot size depends on the beam profile, which varies with configurations of the laser cavities. For retinal photocoagulation such tight focusing is usually not required, and laser spots typically vary from 50 to 500 μm in diameter in various therapeutic applications.

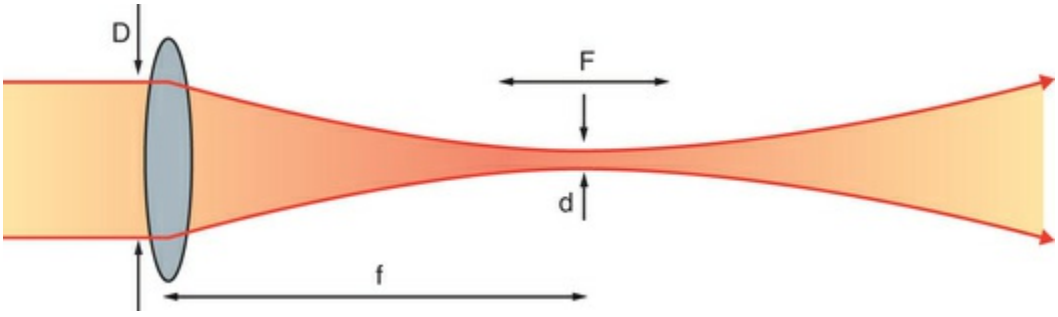

FIG. 41.3 Laser beam of diameter *D* focused with a lens of focal length *f* produces a waist with diameter *d* and a focal depth *F* (see equations in the text).

As an alternative to a free-propagating beam, laser light can be transported via optical fibers. An optical fiber, schematically shown in Fig. 41.4, typically consists of a core, cladding, and jacket. Light is trapped within the core due to total internal reflection at the interface of the core with cladding. To satisfy conditions of total internal reflection, the incidence angle of light at the core/cladding interface should not exceed the critical angle of total internal reflection: $\sin\Theta_{cr}=n_{core}/n_{clad}$, where n_{core} and n_{clad} are refractive indices of the core and cladding, respectively. To satisfy these criteria for total internal reflection, the light should be launched within a so-called acceptance cone, and the sine of its half-angle Θ_{ac} is defined as theNumerical Aperture of the fiber: $NA = \sin\Theta_{ac} = \sqrt{n_{core}^2 - n_{clad}^2}$. Typically the NA is within a range of 0.1–0.2. Optical fibers are often used for delivery of laser light to slit lamp-based systems (Fig. 41.5), and to the intraocular surgical probes (Fig. 41.6).

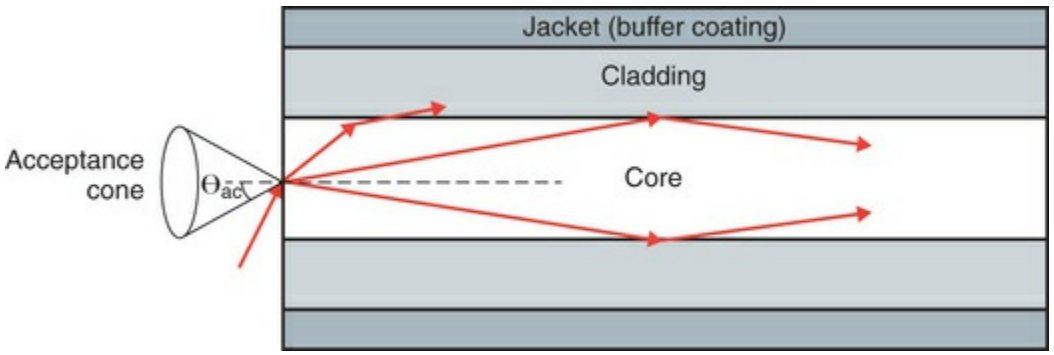

FIG. 41.4 Optical fiber typically consists of a core, cladding, and a jacket (buffer coating). Light launched into the fiber with its acceptance cone Θ_{ac} is trapped within a core due to the total internal reflection at the core/cladding interface.

FIG. 41.5 Laser photocoagulation on a slit lamp system. *1*, Optical fiber and electronic cable connecting laser with a slit lamp system. *2*, Optical coupler projecting the beam exiting from the fiber onto the retina. *3*, Contact lens.

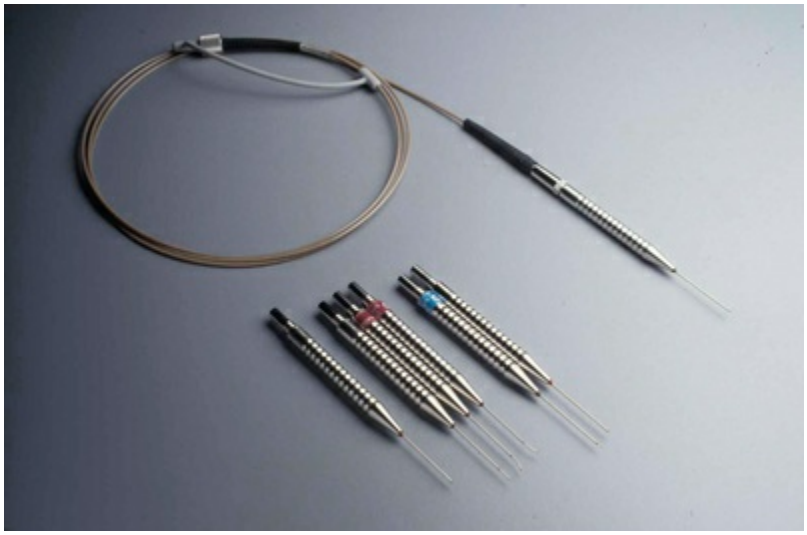

FIG. 41.6 Intraocular handpieces and optical fiber for vitreoretinal dissection with the Er : YAG laser.

Aberrations

With nonperfect focusing optics, the focal spot size of the laser beam is limited not only by diffraction, but also by aberrations.

Measurements of optical aberrations in the human eye demonstrate[5,6] that for pupillary dilation of up to 3 mm in diameter, an average emmetropic human eye is optically well corrected, and the focal spot is close to the diffraction limit. However, for pupils greater than 3 mm in diameter, the central aberrations increase, resulting in increases in the focal spot size. Peripheral field aberrations lead to rapidly increasing blur of the image with angle of visual field, strongly limiting the focusing capability of laser in the periphery of the retina.[6] In retinal photocoagulation, a flat contact lens is typically used to reduce the optical power of the front surface of the cornea. If the lens is used properly, it aids greatly in controlling peripheral aberrations during photocoagulation. Other methods include using an aspheric lens to control optical aberrations in the periphery during photocoagulation. Such lenses typically provide wide-field viewing, although aberrations are difficult to correct over the totality of fields of interest and additional reflections may be introduced by the lens surfaces.

Contact Lenses

Currently, retinal laser photocoagulation relies heavily on the use of contact lenses developed for this purpose, and the most common types are listed in Table 41.1. The universal (Goldmann) three-mirror contact lens provides a flat front surface that nearly cancels the positive refractive power of the front surface of the cornea. Mirrors at 59°, 67°, and 73° aid in visualization and photocoagulation of the periphery and anterior segment. To obtain the most reproducible results in photocoagulation the operator should hold the contact lens so that the flat surface is nearly normal (within ±5 degrees) to the laser beam (Fig. 41.5). The use of mirrors in contact lenses helps the operator keep the laser beam properly aligned to the lens while photocoagulating over a large field.

TABLE 41.1

List of Ocular Contact Lenses and Their Magnifications in a Human Eye

Lens	Image Magnification	Laser Beam Magnification

Ocular Mainster Std	0.95	1.05
Ocular Fundus Laser	0.93	1.08
Ocular Karichoff Laser	0.93	1.08
Ocular 3 Mirror Univ.	0.93	1.08
Ocular Mainster Wide	0.67	1.50
Ocular Mainster Ultra	0.53	1.90
Ocular Mainster 165	0.51	1.96
Rodenstock Panfundoscope	0.67	1.50
Volk G-3 Gonio	1.06	0.94
Volk Area Centralis	1.06	0.94
Volk TransEquator	0.69	1.44
Volk SuperQuad 160	0.5	2.00
Volk QuadrAspheric	0.51	1.97
Volk HRWF	0.5	2.00
Goldmann 3 mirror	1.00	1.00

Another useful photocoagulation lens is the inverted image lens system, typified by the Rodenstock, Quadraspheric, and Mainster photocoagulation lenses. These lenses contain a lens element in contact with the corneal surface and another positive lens element at a fixed distance from the cornea. These systems magnify the spot size on the retina, while increasing the field of view, requiring the operator to adjust the power accordingly. Magnification factors of the most common contact lenses are listed in Table 41.1. It is important to keep in mind that magnification of the retinal image demagnifies the beam size on the retina by the same amount, i.e., the higher magnification of the retina, the smaller is the laser spot on the retina.

Interactions of Light With Tissue

In linear interactions the irradiance (or power fluence) $I(z)$ [W/cm^2] of the beam propagating inside the tissue decreases exponentially with depth (Beer–Lambert law) due to absorption and scattering of light: $I(z) = (1-k_s)I_0\exp(-\mu z)$, where I_0 is the light intensity at the surface of tissue (z=0), k_s is the specular reflection coefficient at the tissue surface, $\mu=\mu_a+\mu_s$ is the attenuation coefficient combined of absorption and scattering components. The penetration depth (δ) of the beam into tissue is defined as a depth at which light intensity is reduced by a factor of e: $\delta=1/\mu$. Reflection of light from ocular tissue at normal incidence typically does not exceed 2%. As shown in Fig. 41.1, absorption of light by various chromophores in the eye

strongly varies with wavelength. Scattering of light is also a very strong function of the wavelength: scattering on subwavelength inhomogeneities of refractive index in ocular media (e.g., collagen fibrils) is reciprocal to the fourth power of the wavelength: $\mu_s \sim \lambda^{-4}$ (Rayleigh scattering). For example, the scattering coefficient for light at 1064 nm is 16 times lower than that at 532 nm. Scattering from structures larger than the wavelength (e.g., cellular organelles) is described by Mie theory and has more complex wavelength dependence and spatial distribution. Scaling of the Mie scattering coefficient with wavelength in various tissues can be approximated as $\mu_s \sim \lambda^{-b}$, with $b \approx 0.5–2$.[7,8]

Photochemical Interactions

Photochemical interactions are based on nonthermal light-induced chemical reactions. The common natural photochemical reactions are photosynthesis in plants and phototransduction in photoreceptors. Therapeutic photochemical interactions used in photodynamic therapy (PDT) take place at very low power densities (typically <1 W/cm^2) and long exposures – lasting tens of seconds. For PDT, special chromophores, called photosensitizers, are injected intravenously and allowed to accumulate in the target tissues. After excitation by laser radiation, the photosensitizer produces highly cytotoxic reactants – free radicals or singlet oxygen, which, in turn, produce irreversible oxidation of the nearby cell structures.

The concept to treat exudative age-related macular degeneration (AMD) by selectively targeting vascular endothelial cells using a specific photosensitizer-carrier complex (phthalocyanine, CASPc) activated by near-infrared laser was adapted from tumor therapy.[9,10] Closure of subretinal neovascularization using PDT with Rose Bengal was demonstrated a few years later.[11] Following upon the successful initial results with phthalocyanine, liposomal benzoporphyrin derivative (BPD) was developed, which selectively attaches to the endothelium of new blood vessels (verteporfin, or Visudyne™).[12,13]

Clinical Indication: Photodynamic Therapy for

Subfoveal Choroidal Neovascularization

Photodynamic therapy for subfoveal choroidal neovascularization (CNV) is performed as a two-step procedure. First, a specialized spectrally adapted photosensitizer, such as verteporfin is injected intravenously. Within minutes it is distributed via the bloodstream to tissues, including the retina and choroid. It selectively accumulates in neovascular tissue which is rich in low-density lipoprotein receptors, while it is rapidly cleared from the surrounding normal tissues. This differential accumulation and clearance is the basis for selectivity of PDT against neovascularization, compared with the normal choroidal and retinal vasculature. Increased presence of new blood vessels in tumors is also the reason for the use of PDT as a treatment for several ocular and nonocular tumors.

Upon absorption of a photon at the proper wavelength the porphyrin molecule undergoes a transition from the ground state into the singlet excited state ($^1P^*$). The singlet excited porphyrin can decay back to the ground state with release of energy in the form of fluorescence, which enables optical identification of tumor tissue (Fig. 41.7). The singlet can also be converted into the triplet excited state ($^3P^*$) which is able to transfer energy to another triplet. One of the very few molecules with a triplet ground state is dioxygen, which is found in most cells. Such energy transfer produces toxic singlet oxygen ($^1O_2$) from ground state dioxygen ($^3O_2$). Singlet oxygen is very reactive and therefore it has a very short diffusion path length – less than 20 nm, so all its interactions are highly localized. The photochemical processes and subsequent reactions are complex and vary for different sensitizers, which are also subject to the microenvironment. Singlet oxygen and other highly reactive species damage endothelial cells in close proximity to the adsorbed drug resulting in thrombosis and temporary closure of the neovascularization.

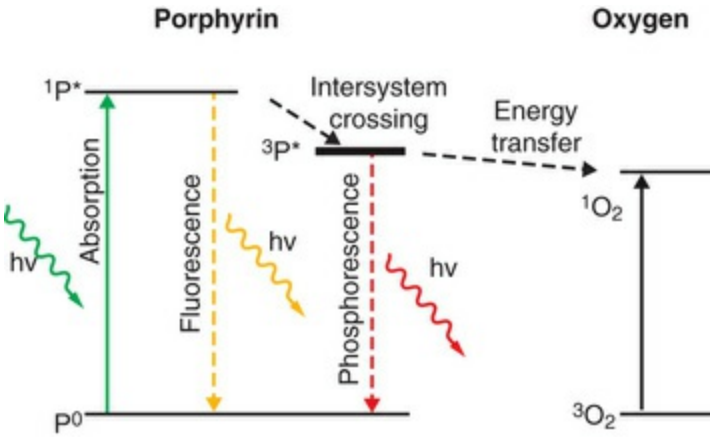

FIG. 41.7 Simplified diagram (with vibrational levels omitted) of the photoexcitation process in porphyrin and energy transfer to oxygen. Light causes excitation of porphyrin to the singlet excited state ($^1P^*$). It can decay back to the ground state with release of fluorescence or convert into excited state ($^3P^*$) which is able to transfer energy to a triplet ground state of oxygen. Such energy transfer results in highly toxic singlet oxygen ($^1O_2$).

Many photosensitizing dyes have been tested for PDT, including Rose Bengal, hematoporphyrin derivatives, lutetium texaphyrin Photofrin, and various benzoporphyrins. Only verteporfin (Visudyne™) has been approved for ophthalmic use in treatment of classic and occult CNV. Verteporfin has a very broad absorption spectrum, but only the far-red peak at 688–691 nm is typically utilized in clinical practice (Fig. 41.8). This is because of the lower sensitivity of retina to far-red light and its superior penetration into the choroid.[14]

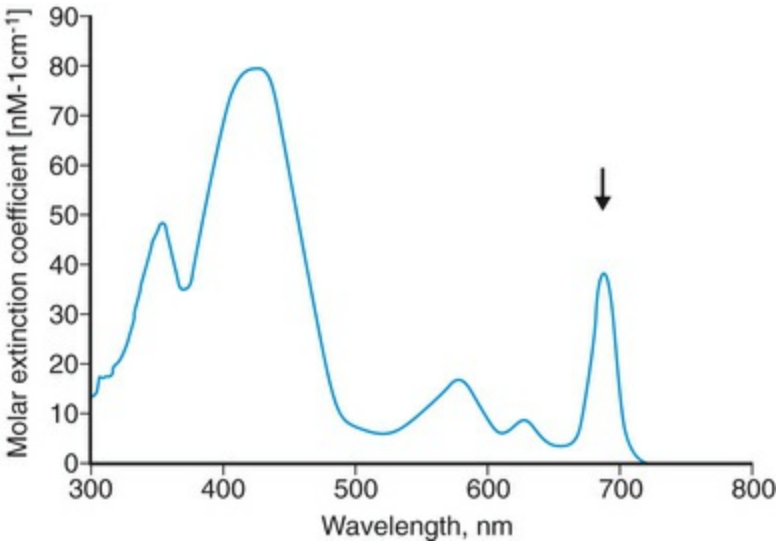

FIG. 41.8 Absorption spectrum of verteporfin. Arrow indicates the 689 nm peak typically used for PDT.

In PDT treatment with verteporfin, the activation by laser is typically performed 15–20 min after the intravenous injection of the dye. A beam of red laser light (689 nm diode laser) is applied to the retina via a slit lamp delivery system. The irradiated area on the retina is typically chosen to minimally exceed the dimension of the neovascularization, with light intensity of 600 mW/cm^2, for 83 seconds, resulting in a total radiant exposure of 50 J/cm^2.[15,16] Closure of the abnormal (leaking) blood vessels occurs within approximately 6–12 weeks in most patients. Reperfusion is common and multiple treatments are often required. Fluorescein angiography images shown in Fig. 41.9A (pretreatment) and 41.9B (1 week post treatment) demonstrate closure of a subfoveal CNV membrane after PDT.

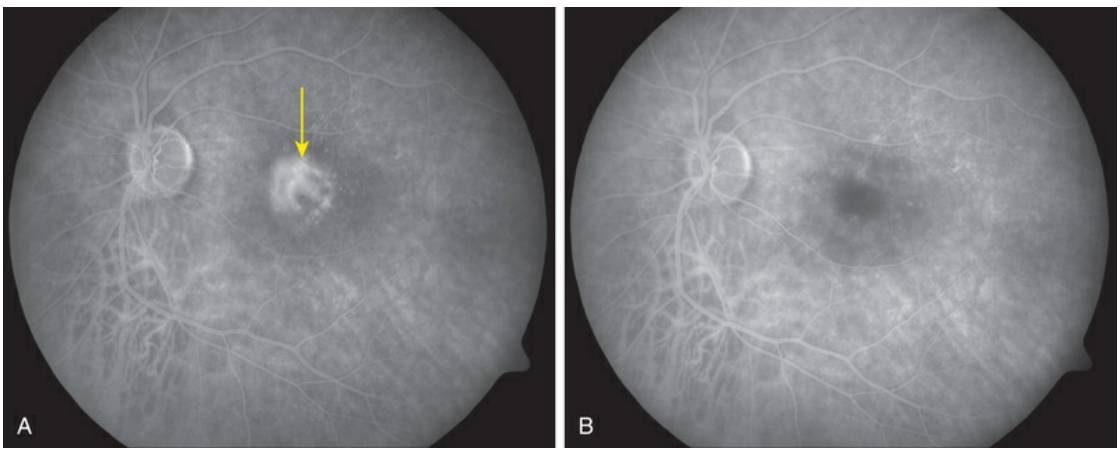

FIG. 41.9 (A) Fluorescein angiogram of a patient with predominantly occult subfoveal choroidal neovascular membrane in left eye (*arrow*). (B) Same eye 1 week following photodynamic therapy with verteporfin and intravitreal triamcinolone injection. Note absence of hyperfluorescence in the area of previous neovascularization and subtle darkening of choroid corresponding to area of photodynamic closure of the membrane.

Photothermal Interactions

Absorption of light in tissue leads to heating. Temperature is the governing parameter in all thermal laser–tissue interactions. Depending on duration and value of the temperature, different tissue effects may occur, including necrosis, coagulation, vaporization, and carbonization.

Heat generation in tissue is determined by the laser parameters and optical tissue properties – irradiance, exposure time, and the absorption coefficient, which depends on the laser wavelength. Heat transport is characterized by heat conductivity and heat capacity.

If heat diffusion is neglected, then at a constant beam power the temperature rise is linear with time: $T(z,t)=\frac{\mu_a \cdot I(z) \cdot t}{\rho \cdot c}$, where ϱ is tissue density, and c is its heat capacity (c = 4.2 J/g/K, ϱ=1 g/cm^3 for water). To assess whether heat diffusion plays a significant role during the laser pulse, one should compare pulse duration with a characteristic time it takes for heat to spread by the distance equal to the zone of initial heat deposition in tissue. For the heated zone (laser penetration depth) of length L, the heat diffusion time is: $\tau=L^2/4\alpha$, where α is thermal diffusivity (α=1.4 10^{-3} cm^2/s for water). For example, for L=1 μm in water the characteristic heat diffusion time is t=1.7 μs, while for L=1 mm, the diffusion time t=1.7 s. If the laser pulse duration is comparable or longer than the characteristic diffusion time across the light absorption zone, then proper estimation of the peak temperature in tissue should take heat diffusion into account.

Necrosis

Temperature rise induces conformational changes in various proteins, which denature at characteristic rates specific to protein species. These thermal processes, which may eventually lead to cell necrosis, depend on both the temperature and duration of the hyperthermia. Thermal damage to cells in a millisecond range of pulse durations can be approximated using the Arrhenius model.[17,18] It assumes a rate of decline in the concentration of a critical molecular component $D(t)$ with temperature $T(t)$:

$$dD(t) = -D(t) \cdot A \cdot \exp\left(-\frac{E^*}{R \cdot T(t)}\right) dt \qquad [1]$$

where E^* and A are the activation energy and rate constant parameterizing the process, and R=8.3 J/(K mol) is the gas constant. Tissue damage, i.e., decrease in critical molecular component $D(\tau)$, relative to its initial value D_0 over the pulse length τ is encapsulated in the Arrhenius integral Ω:

$$\Omega(\tau) = -\ln\left(\frac{D(\tau)}{D_0}\right) = A\int_0^{\tau} \exp\left(-\frac{E^*}{R \cdot T(t)}\right) dt \qquad [2]$$

The model assumes that irreversible tissue damage takes place when concentration of the critical molecular component drops below some threshold value. Conventionally, this threshold corresponds to a reduction in concentration by a factor of e, or an Arrhenius integral of unity. Thus for Ω=1, the remaining fraction of intact proteins is $1/e \approx 37\%$, or in other words, 63% of proteins have been damaged.

Measurement of the RPE damage at various irradiation conditions yields the following average values:[18] E^*=340 kJ/mol, A=1.6×10^{55}. It is important to keep in mind though that accurate estimation of cell survival under thermal stress is much more complex than just assessment of the denaturation rate of one type of protein or another. For example: (1) there are multiple types of proteins in cells and they denature at different rates; (2) different

proteins have different significance for cellular survival; (3) cellular repair mechanisms cannot be ignored at long exposures. Therefore the single values of the reaction rate A and activation energy E most likely represent characteristics of the "weak link" in cellular metabolism, the most susceptible to thermal damage, and may vary in different cell types.

Fig. 41.10 shows an example of the temperature rise in tissue for a hypothetical square pulse of heating, which is sufficient for cell death, according to the Arrhenius model. Cells exposed to temperatures above the threshold curve are coagulated and the tissue becomes necrotic. This curve is approximate, and the exact values depend on the shape of the actual pulse of temperature, type of cells, and tissues involved. The Arrhenius model fails to predict correct threshold temperatures at exposures longer than approximately 1 second, since cellular repair mechanisms should be taken into account at long exposures. At pulse durations shorter than 50 μs and temperatures below the vaporization threshold, the coagulation is insufficient for lethal damage, and therefore the dominant mechanism of damage at shorter pulses becomes mechanical – RPE cell rupture by vapor bubbles.[19]

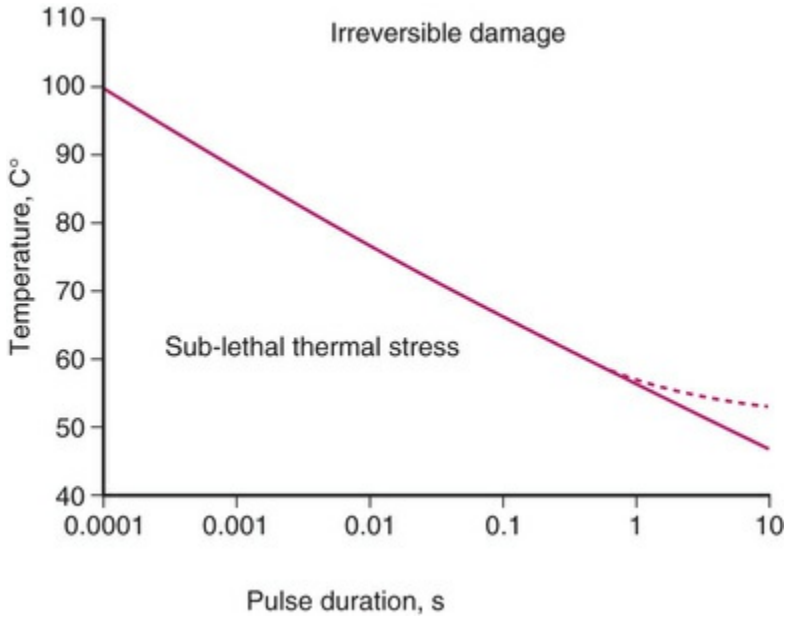

FIG. 41.10 Solid line depicts Arrhenius approximation of the cellular damage threshold as a function of duration of a hypothetical square pulse of heating. Dashed line indicates deviation of the damage

threshold from the Arrhenius model at long exposures.

Nondamaging Photothermal Therapy

There is a growing body of clinical evidence that many macular diseases, such as central serous chorioretinopathy, diabetic macular edema (DME), and branch retinal vein occlusion (BRVO), can be successfully treated without visible tissue damage.

A nondamaging approach to retinal laser therapy was initially attempted using a near-IR diode laser (810 nm) with very long exposures (60 s) and a millimeter-wide spot on the retina.[20] This approach, termed transpupillary thermotherapy or TTT,[21] has been tested in treatment of CNV in AMD.[20,21] Proponents of this approach have hypothesized a selective effect on the heating of actively dividing cells in newly formed blood vessels due to their higher susceptibility to thermal injury than nondividing cells in normal tissue. The estimated retinal temperature elevation with TTT at clinical settings (810 nm, 800 mW, 60 seconds, 3 mm spot size) is approximately 10 °C.[22] The mechanism of treatment of CNV by TTT may occur through vascular thrombosis, apoptosis, or the thermal inhibition of angiogenesis.[22] The use of TTT encountered difficulties with reliable titration, resulting in frequent occurrences of significant retinal damage.[23]

Later, a pulsed version of a similar laser with smaller spot sizes (125 μm) has been applied for nondamaging retinal therapy. The "micropulse" laser delivers 100–300 ms bursts of pulses of 100–300 μs in duration. Adjusting the pulse duty cycle and peak power, the average power should be set below the clinically detectable tissue damage. Clinical trials have shown that micropulse treatment of DME delivered with high spot density is equally efficient or superior to the standard mETDRS protocol.[24] A smaller clinical trial demonstrated that the micropulse laser treatment reduced the subretinal fluid and improved visual acuity in patients with central serous chorioretinopathy, compared to the untreated control group.[25] Micropulse laser also demonstrated equivalent clinical efficacy to conventional lasers in treatment of macular edema secondary to BRVO, but without the side effects of tissue damage.[26] However, the lack of a well-defined titration procedure is reflected

in the variable results of these studies.[27–29] In addition, high density coverage of the macula with relatively small spots and long pulses requires lengthy treatment, which is difficult to perform without a scanner.

Significant advantages of the retinal phototherapy with nondamaging endpoint are the absence of scotomas and scarring, the ability to treat foveal areas, as well as improved preservation of color vision and contrast sensitivity.[29] The lack of chorioretinal damage permits high-density therapy, which greatly improves therapeutic outcomes, compared to conventional sparse laser treatment protocols in the macula.[24] Nearly confluent laser applications could be safely delivered over the entire edematous areas if short pulse treatment and pattern scanning were to be applied. This approach would also allow retreatment of the same areas, even in a close proximity to the fovea.

Dynamic range of the retinal response to nondamaging hyperthermia has been established by monitoring expression of the heat shock protein HSP-70 in mice.[30] Based on these results, a titration protocol for adjustment of the laser power and duration was developed.[31] This protocol, called EndPoint Management (EpM), ties subvisible tissue effects to a visible titration point (Fig. 41.11). Experiments with heat shock protein expression following nondamaging retinal exposures in mice,[30] as well as a computational analysis of the clinical laser settings[32] indicated that nondamaging thermal therapy corresponds to Arrhenius values within the range of approximately $0.1<\Omega<1(-1<\mathrm{Log}\Omega<0)$. In this regime the RPE cells survive the hyperthermia, and respond to the thermal stress by expression of the heat shock proteins. Visible lesions produced at higher laser settings result in lethal damage to RPE and photoreceptors, and have calculated values of $\Omega \gg 1$, with the relevant range of Ω for retinal thermal therapy spanning several orders of magnitude. The EpM algorithm maps a range of calculated Arrhenius integral values to linear steps in pulse energy, normalized to a titration dose specified at a particular duration,[31] as shown in Fig. 41.11. The threshold of RPE damage was found to be 30% energy on the EpM scale. This protocol has been recently tested in treatment of chronic central serous retinopathy using 30% energy settings[33] (Fig. 41.12). The trial demonstrated lack of any visible

tissue damage and excellent response to the treatment, even after multiple retreatments.[33]

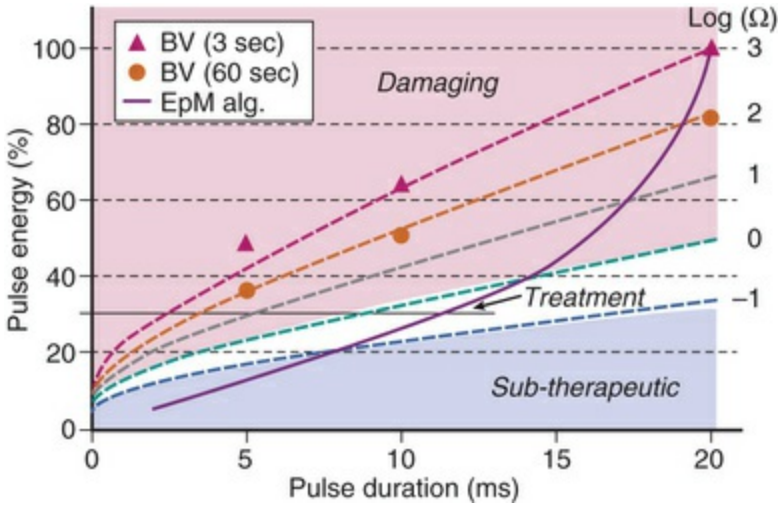

FIG. 41.11 EndPoint Management algorithm. Dashed lines correspond to various levels of Arrhenius integral: from 1000 (red, top) to 0.1 (blue, bottom). Threshold of the barely visible lesions visible within 3 seconds of exposures is plotted with red triangles, and it corresponds to Arrhenius integral of 1000 (LogΩ=3). Threshold of the lesions which become visible after 60 seconds is shown with circles, and it corresponds to Arrhenius integral of 100 (LogΩ=2). EndPoint Management algorithm(*EpM alg.*), plotted with a solid black line, adjusts power and duration such that it converts 10× steps of Ω into 20% steps of pulse energy. All settings above Ω=1 (Log Ω=0) are damaging, and all settings below Ω=0.1 (Log Ω=−1) are subtherapeutic.

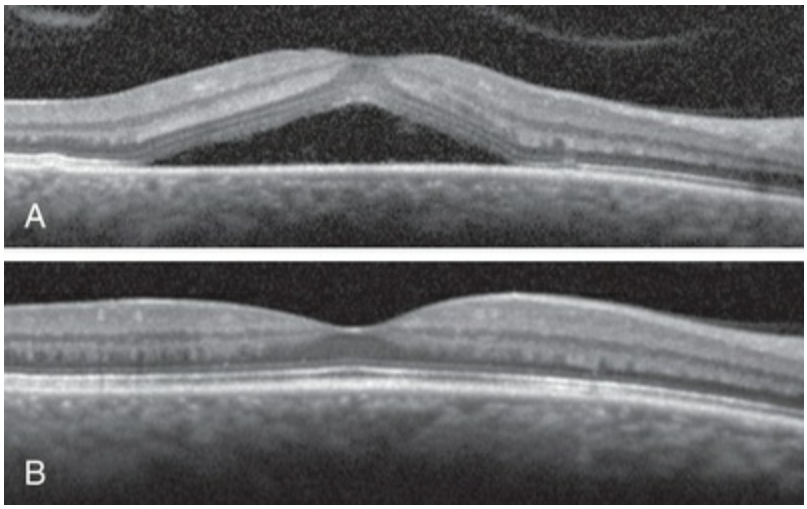

FIG. 41.12 Optical coherence tomography of a chronic central serous retinopathy patient (A) before and (B) 2 months after the nondamaging retinal laser therapy. Visual acuity improved from 20/100 at baseline to 20/20 at 2 months. No signs of tissue damage at the treatment locations could be seen with any fundus imaging modality. (A and B courtesy of Dr. Daniel Lavinsky.)

Photocoagulation

Retinal photocoagulation typically involves application of laser pulses with durations ranging from 10 to 200 ms, and transient hyperthermia by tens of degrees above body temperature. Various lasers have been used in the past: ruby (694 nm), argon (488, 514 nm), krypton (647 nm). Currently the most common lasers in photocoagulation are the frequency-doubled Nd : YAG (532 nm) and yellow semiconductor (577 nm) laser. The laser energy is absorbed primarily by melanin in the RPE and choroid, and by hemoglobin in blood. At a 532 nm wavelength, approximately half of the laser energy incident on the retina is absorbed in the RPE, and the rest in the choroid.[18] The generated heat diffuses from the RPE and choroid into the retina and causes coagulation of the photoreceptors and, sometimes, of the inner retina. During 100 ms applications, the heat diffuses distances of up to 200 μm thus "smoothing" the edge and extending the coagulated zone beyond the boundaries of the laser spot, termed "thermal blooming." Heat diffusion using shorter pulses and with smaller spot sizes can be limited to the photoreceptor layer, thereby avoiding the inner

retinal damage.

The left column in Fig. 41.13A demonstrates the acute effects of an intense burn in a rabbit retina produced by 100 ms laser applications, including full-thickness injury and early necrotic features 24 hours after treatment. The left column in Fig. 41.13B demonstrates a light lesion produced by 15 ms pulses. Damaged photoreceptors are pyknotic, but the inner nuclear layer and ganglion cell layer are very well preserved.

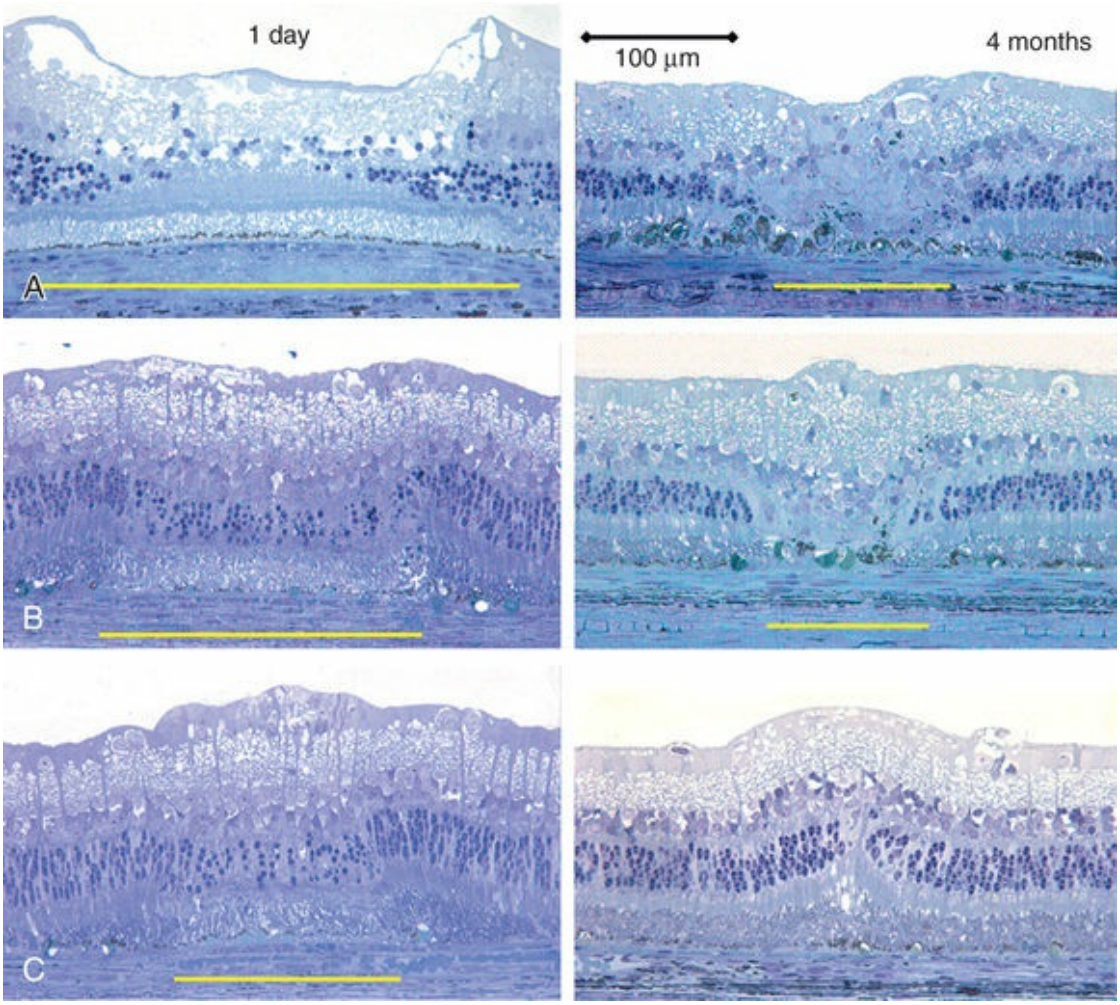

FIG. 41.13 Histology of the rabbit retina at 1 day (left column) and 4 months (right column) after photocoagulation. Retinal spot size is 330 µm, power 175 mW. (A) Intense retinal burn produced with 100-ms exposure. Yellow bar shows the lateral extent of the lesion. Note full-thickness retinal injury including the inner retinal layers. (B) Light burn produced with 15-ms exposure. Photoreceptors are coagulated, while

inner retina is well preserved. (C) Barely visible lesion produced with 7-ms pulse. Right column shows corresponding retinal scarring at 4 months. Note complete closure of the damage zone by shifting photoreceptors in the barely visible lesion (C).

Figs. 41.14A–B illustrate the effect of laser power and pulse duration on the size of the coagulated zone, in pigmented rabbits.[34] Table 41.2 lists the ratio of the lesion width to the retinal beam size for lesions of various clinical grades in human patients, as measured by optical coherence tomography (OCT) within 1 hour of treatment.[35] As one can see, lesion size increases relative to the beam width with more intense lesions and with longer pulses.

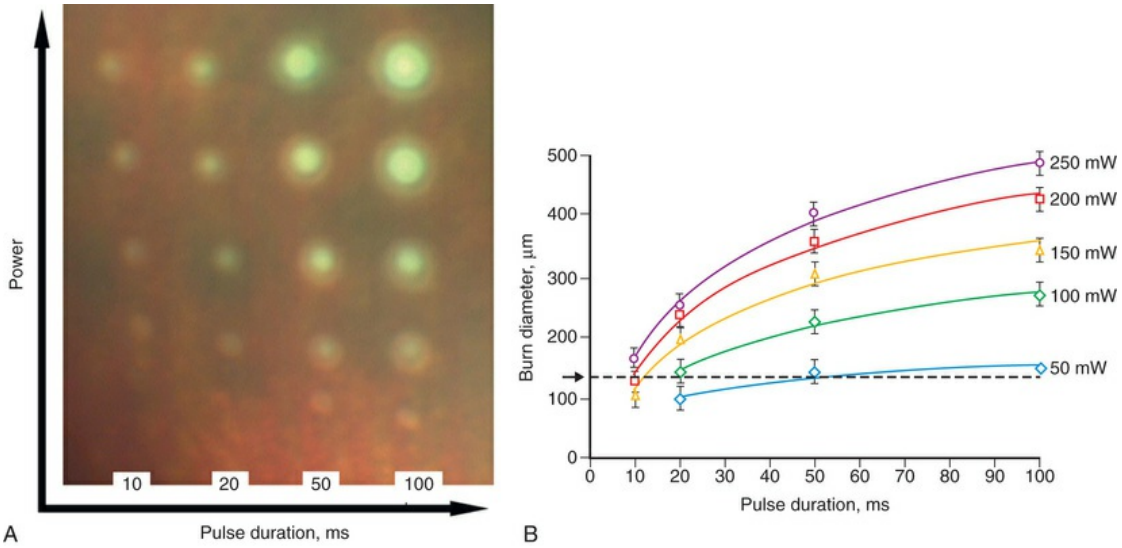

FIG. 41.14 (A) Retinal lesions in the rabbit eye with variable power and duration of exposure. Retinal beam size is 132 µm. (B) Lesion diameter as a function of laser power and duration of exposure. Laser beam size on the retina is 132 µm (indicated by the dashed line and the arrow).

TABLE 41.2

Ratio of the Lesion Width to the Retinal Beam Size for Various Pulse Durations and Clinical Grades, as Measured by OCT in Human Patients Within 1 Hour of Application

Beam Size		Lesion Clinical Grade					
		Moderate		Light		Barely Visible	
In Air	On Retina	100 ms	20 ms	100 ms	20 ms	100 ms	20 ms
100 μm	94 μm	3.81±0.98	2.50±0.30		2.08±0.24		
200 μm	188 μm	2.08±0.22	1.49±0.09		1.24±0.08		0.93±0.08
400 μm	376 μm	1.39±0.08	1.15±0.07	1.19±0.11	0.99±0.09	0.99±0.08	0.74±0.12

Coagulation was performed with Area Centralis lens (magnification ×0.94).

OCT, optical coherence tomography.

The threshold power required for the creation of retinal lesions increases with shorter pulses for two reasons: (a) energy should be delivered during shorter exposures, and (b) higher temperatures are required to reach the same Arrhenius integral of damage during a shorter period of hyperthermia. An example of the threshold powers for lesions of various grades is plotted in Fig. 41.15 as a function of pulse duration for a 132 μm retinal laser spot in the rabbit. If temperature exceeds the vaporization threshold, a transient vapor bubble may result in retinal rupture. For pulse durations of 20, 50, and 100 ms, all the grades (mild, moderate, intense, and very intense) could be created below the threshold of rupture with appropriate choice of power settings. At pulse durations below 10 ms it became increasingly difficult to reproducibly create intense lesions without inadvertently rupturing the retina. At 2 ms or less it was not possible to reproducibly create a moderate lesion without rupturing the retina. At 1 ms, there was little or no difference between the power required to create a mild retinal lesion or produce a rupture.

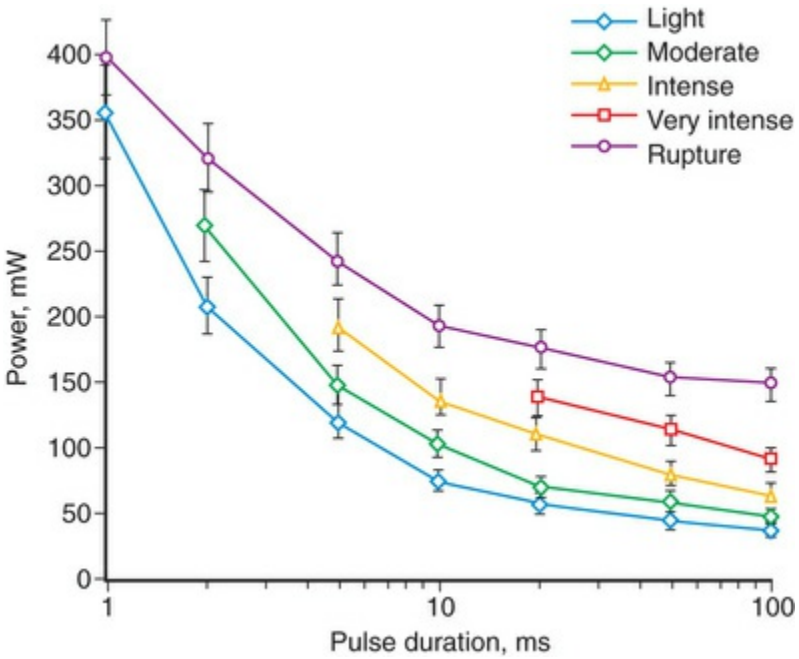

FIG. 41.15 Threshold power of retinal photocoagulation in rabbit eye, as a function of pulse duration. Laser beam size on the retina is 132 μm. Clinical grades indicated by the colors: light, moderate, intense, very intense, and rupture.

The ratio of the threshold power required to produce a rupture to that required to produce a mild lesion is defined as the therapeutic window, and represents one means of quantifying the relative safety (dynamic range) of retinal photocoagulation. The larger this ratio the greater the margin of safety to create a visible lesion without inadvertently inducing a retinal rupture. Fig. 41.16 depicts the width of this therapeutic window as a function of pulse duration for two different laser spot sizes. For a 132 μm retinal laser beam size, as pulse duration decreases from 100 to 20 ms, the width of the therapeutic window declines from 3.9 to 3.0. When pulse duration is further decreased to 10 ms, the therapeutic window decreases further to 2.5, and it approaches unity at a pulse durations of 1 ms. For a 330 μm retinal laser spot size the therapeutic window declines from 5.4 to 3.7 to 3.1 when pulse durations decrease from 100 to 20 to 10 ms, respectively. With both spot sizes, the therapeutic window decreases to unity as pulse durations decrease to 1 ms. At this point there is effectively no safe range of retinal photocoagulation: mild lesion and rupture are equally likely to occur at the same power.

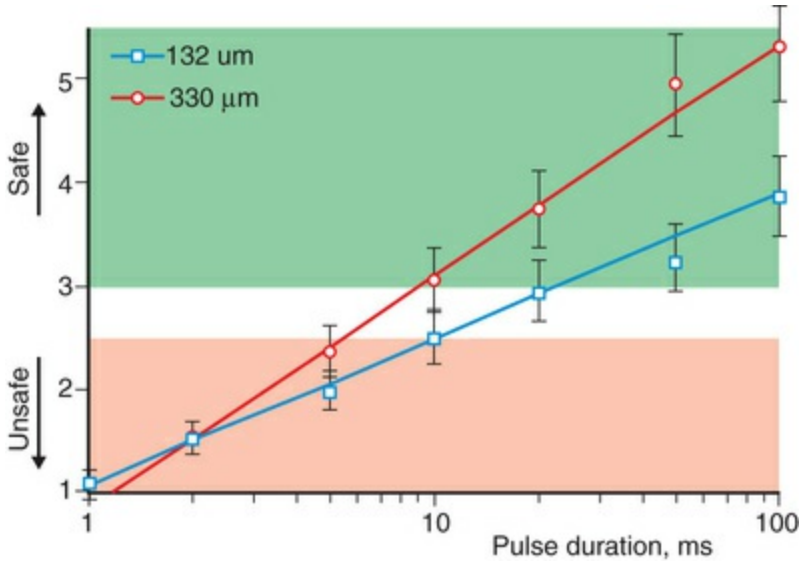

FIG. 41.16 Safe therapeutic window of retinal photocoagulation (ratio of the threshold of rupture to that of light coagulation) increases with pulse duration, and with a beam size on the retina (shown for 132 and 330 µm).

The width of the safe therapeutic window should suffice to accommodate for variations in fundus pigmentation, which typically do not exceed a factor of 2. To provide a safe therapeutic window larger than 2.5, pulse durations should equal or preferably exceed 10 ms for a beam of 330 µm, and 20 ms for the 132 µm spot size.

It is important to keep in mind that coagulation of blood vessels requires more energy than other tissue due to cooling by the blood flow. For example, if a spot size of 200 µm with exposure time of 200 ms is applied to occlude a blood vessel with flow velocity of 5 mm/s, the laser energy is effectively distributed over the column 5 times longer than the diameter of the laser spot. Thus the effective energy remaining at the photocoagulation site is 5 times lower than it would be in stationary tissue.

Healing of Retinal Lesions

Studies in rabbits demonstrate that in photocoagulation lesions the RPE layer is restored within a week, though its pigmentation may remain abnormal – either hyper- or hypopigmented.[36] In intense and moderate lesions gliotic scar filling the coagulated retinal layers stabilizes after one month, and the wound contracts to

approximately 40% of the original lesion diameter, as shown in the right column in Figs. 41.13A–B. However, in very light lesions (Barely Visible clinical grade) the photoreceptors continue to shift into the damage zone and completely refill it by 4 months, as shown in Fig. 41.13C, in the right column. Interestingly, the shifting photoreceptors rewire to local bipolar cells and restore ON and OFF retinal signal pathways.[37] As a result, scarring and scotomas typically associated with conventional photocoagulation may be minimized or even completely avoided.[36] A similar phenomenon of restorative retinal plasticity has been recently observed in rats[38] and in primates.[39]

It is important to keep in mind though that in order to maintain similar clinical efficacy of photocoagulation with smaller and lighter lesions a larger number of them should be applied, to keep the same total coagulated area.[35] For example, with 400 μm beam diameter on the retina, and 100 ms pulse duration, a lesion of the moderate clinical grade is 1.39 times larger than the beam, i.e., it is 1.39×400 μm = 556 μm in diameter (Table 41.2). The barely visible lesion produced with 20 ms exposure is only 0.74×400 μm = 296 μm in diameter. Therefore, the required number of lesions should increase by the ratio of the lesion diameters squared, i.e., by a factor 3.5.

Pattern Scanning Laser Photocoagulation

The first attempts to automate photocoagulation involved rather complex equipment, including image recognition software and eye tracking.[40] Complexity of such systems prevented their commercial introduction and acceptance in clinical practice.

A semiautomatic pattern scanning photocoagulator (PASCAL, Topcon Medical Laser Systems Inc.) was introduced by OptiMedica Corp. in 2005.[41] It delivered patterns of laser spots ranging from a single spot to 56 spots applied in a rapid sequence with a single depression of a foot pedal. The control of laser parameters was performed by means of a touch screen graphic user interface, facilitating selection of the different patterns of photocoagulation. The laser was activated by pressing a foot pedal, which was kept depressed until the entire pattern was completed. The physician can release the foot pedal and stop the laser at will prior to

completion of the pattern, if clinically indicated.

Patterns included square arrays with up to 5×5 spots, arcs with the number of concentric rows varying from 1 to 3, circular patterns for photocoagulation of small holes and other lesions in the retinal periphery. Patterns for macular photocoagulation included rings and arcs with an adjustable central exclusion zone to allow for laser application reducing the risk of inadvertent damage to the foveal avascular zone.

To deliver the whole pattern within the eye fixation time and avoid beam shift due to the eye movements, each exposure was required to be shorter than in conventional photocoagulation: 10–20 ms instead of 100–200 ms, traditionally applied with single spot exposures. Reduced heat diffusion into choroid during shorter exposures also resulted in patients experiencing less pain.[42,43] Short pulse lesions appear smaller and lighter than conventional burns produced with the same beam size (Table 41.2), and therefore a larger number of them are required to treat the same total area.[35]

An automatic laser delivery, guided by diagnostic imaging and stabilized using eye tracking, has been introduced in a Navilase™ system (OD-OS GmbH). This system includes retinal image acquisition, annotation of the images to create a detailed treatment plan, and then automated delivery of the laser to the retina according to the treatment plan.

Clinical Indications: Treatment of Diabetic Retinopathy

Photocoagulation has proven safe and effective in the treatment of proliferative diabetic retinopathy. In this disorder the retina becomes ischemic and releases a variety of chemical messengers, most importantly vascular endothelial growth factor (VEGF), that stimulate the growth of new blood vessels and also markedly increase retinal vascular permeability. The abnormal new vessels, and associated fibrous tissue and macular edema, are major causes of the sight-threatening complications in diabetic eye disease. By destroying a portion of the peripheral retina with laser, it has been hypothesized that retinal metabolic demands and available nutrients are better balanced and the stimulus for growth of the new blood vessels is decreased. This treatment has been termed panretinal photocoagulation (PRP) (Fig. 41.17), and it significantly

reduces the risk of central vision loss due to neovascularization. The side-effects of panretinal photocoagulation – mild nyctalopia and constriction of visual field – are felt to be outweighed by the preservation of the central vision, and have been confirmed in multiple large randomized clinical trials.[44] Similarly, the focal laser photocoagulation to actively leaking microaneurysms, and the grid photocoagulation to areas of diffuse retinal permeability (Fig. 41.18) have been shown to reduce clinically significant macular edema associated with diabetic retinopathy and slow the rate of vision loss. These effects have been confirmed in large randomized multicenter clinical trials.[45]

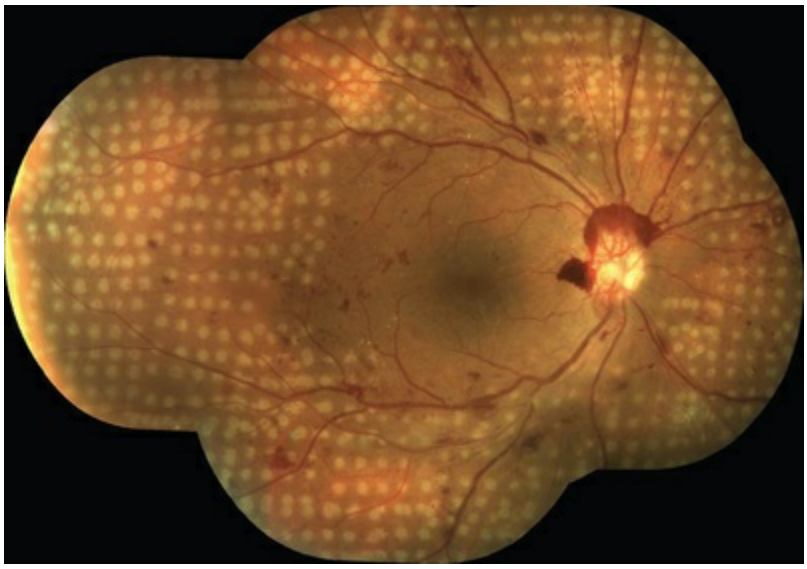

FIG. 41.17 Fundus photograph of a patient after panretinal photocoagulation with 532 nm laser. (Courtesy of Dr. Daniel Lavinsky.)

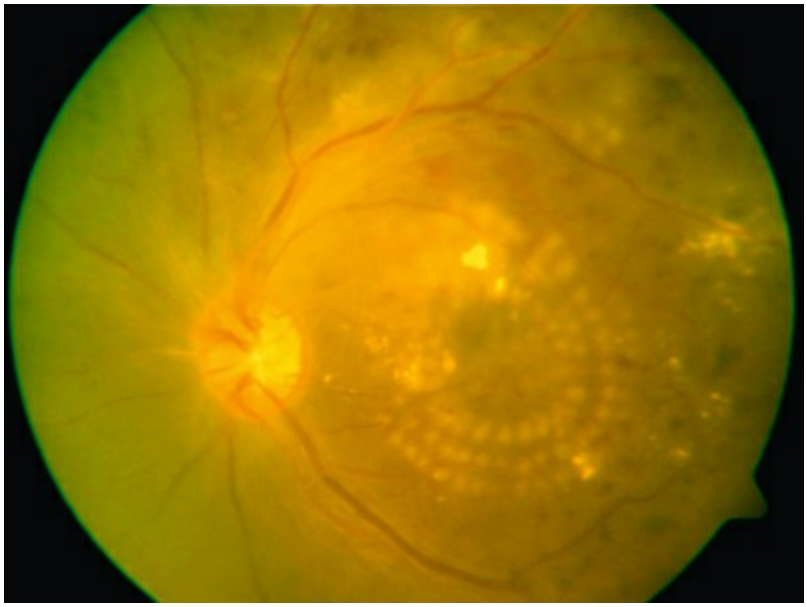

FIG. 41.18 Fundus photograph of a patient with clinically significant macular edema including central macular thickening and paramacular lipid exudates one week following grid photocoagulation. Note concentric rows of photocoagulation spots surrounding the macula, best seen inferiorly.

Age-Related Macular Degeneration: Extrafoveal Neovascular Lesions

Another application for laser photocoagulation in the past was for the treatment of extrafoveal CNV membranes that occur in AMD. Intense photocoagulation destroys the invading vascular membrane, but usually leaves a chorioretinal scar and a blind spot or scotoma. However, if the lesions are outside the center of the macula, the treatment is typically well tolerated by the patients. Currently, many physicians elect to use anti-VEGF pharmacotherapy since it avoids scarring and spread of the lesions into the macula.

Additional applications of retinal photocoagulation include grid and focal treatment of leaking microvascular abnormalities in branch-vein occlusion and radiation retinopathy, and treatment of retinal breaks and lattice degeneration to prevent retinal detachment.

Selection of Optimal Wavelengths for Coagulation

A number of important factors must be considered when choosing the best wavelength for a particular photocoagulation application. The first consideration is to determine what absorbers are present in the target tissue. Wavelengths that are highly absorbed by macular yellow (such as 488 nm) are relatively contraindicated when treating in or near the macula. Absorption of these wavelengths in macular pigments may cause heating and destruction of the nerve fiber layer, resulting in loss of vision. As shown in Fig. 41.1B, in the macular region, wavelengths longer than 500 nm should be chosen, such as the green argon (514 nm) or the frequency doubled YAG (532 nm) or yellow (577 nm) laser. Melanin provides good absorption at most photocoagulation wavelengths. Wavelength selection is therefore less important when melanin is the primary absorber. Scattering loss in cataract or in vitreous opacities can be minimized using longer wavelengths: yellow (577 nm) or red (640–680 nm). If scattering by the ocular tissues is not significant, the green wavelengths (514 or 532 nm) continue to serve well.

When hemoglobin is the primary absorber (see Fig. 41.1B), as in the treatment of vascular tumors, a wavelength shorter than 600 nm is preferable. Treatment of CNV may be effective using red light through indirect heat transfer from the surrounding melanin. In general, when the target structures contain a large quantity of hemoglobin, wavelengths between 520 and 580 nm are best suited. Ideally, for coagulation of blood vessels the photon penetration depth should be similar to the vessel diameter, thus providing uniform heating of the blood vessel without superficial damage and perforation.

Tunable lasers may provide the flexibility to select a wavelength of choice for required photothermal procedure. However, tunable lasers are costly, require more maintenance, and are now less commonly employed clinically than previously.

Photodisruption

When tissue temperature exceeds the vaporization threshold the vapor bubbles are produced, which may lead to tissue rupture within a zone comparable to the bubble size. This process of explosive vaporization is typically employed for tissue dissection.

The actual temperature required for vaporization varies between 100 and 305 °C depending on pulse duration and on presence of the bubble nucleation sites.[46] For efficient heating of the tissue the pulse energy should be delivered fast enough to avoid heat diffusion from the laser absorption zone during the pulse, a condition called "thermal confinement." In other words, the laser pulse duration should be shorter than the heat relaxation time, or the time of heat diffusion from the zone of laser absorption, L: $\tau < L^2/4\alpha$, where L is the penetration depth of light in tissue ($L=1/\mu_a$), and α is thermal diffusivity of tissue. For example, with light penetration depth of 1 μm, pulse duration should not exceed 1.7 μs. In this case the temperature rise ΔT in tissue with absorption coefficient μ_a achieved during laser pulse with duration τ at irradiance I [W/cm^2] is: $\Delta T = \frac{\mu_a \cdot I \cdot \tau}{\rho \cdot c}$, where ϱ and c are tissue density and heat capacity, respectively. A higher absorption coefficient μ_a facilitates reaching a vaporization threshold with lower total energy deposition ($E_{tot} = I\tau$). Precise tissue ablation requires the use of laser wavelengths corresponding to a small optical penetration depth in tissue in order to confine the energy deposition to a small volume.

Much shorter pulses may produce stress confinement – a condition when an acoustic wave produced by the thermal expansion of the material cannot escape from the heated zone during the laser pulse. Since the velocity of sound in water is about v=1.5 km/s the stress confinement conditions are achieved within the L=1 μm penetration depth if pulse duration does not exceed $t = L/v$=0.7 ns. In such conditions powerful stress waves may be generated which propagate with supersonic velocities and may result in significant damage to tissue, such as disruption and fragmentation.[46]

Vaporization of water in an overheated volume results in the formation of a short-living vapor bubble (a so-called cavitation bubble) which expands, cools down, and collapses during the time determined by its radius at maximum expansion. The lifetime of the spherical cavity with radius R_0 in free nonviscous liquid is described by the Rayleigh equation: $\tau = 0.91 R_0 \sqrt{\frac{\rho}{P_0}}$, where ϱ is liquid

density, and P_0 is the ambient pressure.[47] For example, in water at atmospheric pressure, a cavity of 0.1 mm in radius collapses in about 10 μs. (Growth and collapse of a spherical bubble take approximately the same time.) Symmetric collapse of a spherical cavity may lead to overheating of the liquid and formation of the secondary bubble. Due to the short lifetime, these bubbles are not visible to the eye during surgery, but they can be easily visualized using fast flash photography. As shown in Fig. 41.19, at the liquid–tissue interface the bubble might be deformed, and the secondary bubble is not created. Importantly, a collapsing cavitation bubble at the fiber probe or next to the tissue surface may produce a water jet which can damage tissue at distances exceeding the bubble radius by a factor of 4.[48]

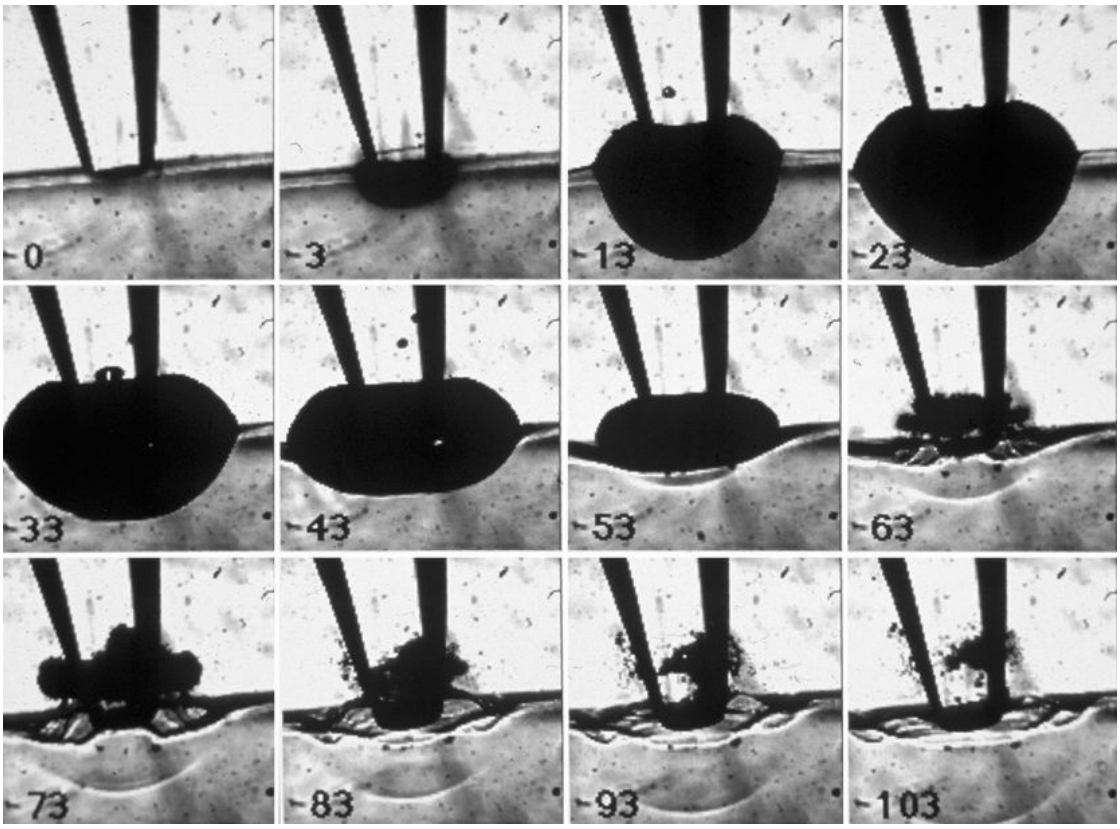

FIG. 41.19 Dynamics of the cavitation bubble at the gelatin–saline interface observed with fast flash photography. Bubble is created by a pulse of ArF excimer laser delivered via the tapered optical fiber. Numbers in each frame indicate a delay in μs between the laser pulse (10 ns) and a microsecond-long flash.

Explosive vaporization can be produced by absorption of laser radiation in water or in tissue. Strong absorption in water can be achieved at mid-infrared wavelengths. For example, penetration of the Er : YAG laser (λ=2.94 μm) in water is about 1 μm. Shallow penetration of these wavelengths necessitates the fiber-based delivery of this light into a liquid medium. A thin layer of water in front of the intraocular probe is overheated with the laser pulse, and the resulting vaporization leads to rupture of tissue in a proximity to the probe. This approach has been applied to dissection of epiretinal membranes using Er : YAG laser[49,50] (Fig. 41.20). Since a burst of closely spaced pulses, rather than a single pulse, was applied in that device, the actual vapor bubble had an elliptical shape and extended several hundred micrometers from the probe.[51]

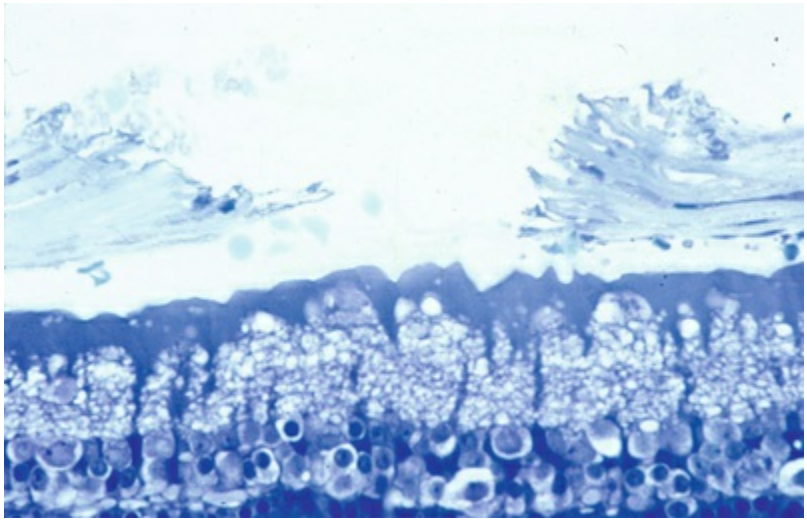

FIG. 41.20 Epiretinal membrane dissected by the Er : YAG laser. Note the absence of retinal damage despite close proximity of the membrane.

Alternatively, overheating of liquid can be achieved with a laser strongly absorbed in the tissue constituents. For example, a fiber-delivered ArF excimer laser (λ=193 nm), which is strongly absorbed by proteins (penetration depth 0.2 μm in tissue), has been applied for dissection of epiretinal and subretinal membranes.[52,53] In this case the laser light overheats the tissue and leads to vaporization of its water content with subsequent tissue rupture.[54,55] Despite the early promise of both of these devices (Er : YAG and ArF excimer

lasers) in clinical tests, both have failed to achieve widespread acceptance in medical practice due to the cost, fiber rigidity, and the lack of coagulation capability.

Another approach to dissection of transparent tissue utilizes ionization of the material and formation of plasma by a high-intensity laser beam. At extremely high irradiances (10^8–10^{11} W/cm^2), which can be achieved in a short pulsed (ns–fs) tightly focused laser beam, transparent material can be ionized, and ions absorbing the laser light reach very high temperatures.[56] This mechanism, called dielectric breakdown, allows for highly localized energy deposition in the middle of a transparent liquid or solid – at the focal point of the laser beam. This process is widely used in fragmentation of the opacified posterior lens capsule (secondary cataract) with nanosecond Nd : YAG lasers. At shorter pulse durations (1 ps to 100 fs) and lower energies this process is applied to intrastromal ablation – formation of a corneal flap for refractive surgery,[57] as well as in cataract surgery.[58] This approach has also been tested in the dissection of epiretinal membranes using the tightly focused beam directed from outside the eye.[59] Despite the fact that very low energy is required for this process (several microJoules with ps–fs lasers) its applicability in the posterior pole is limited due to the difficulty with axial discrimination between the epiretinal membranes and the retina located very close behind them. In addition, strong optical aberrations in the periphery of the posterior pole preclude tight focusing of the laser beam in these areas.

Selective RPE Therapy (SRT)

Light is strongly absorbed by melanosomes in the RPE ($\mu_a \approx 8000$ cm^{-1}).[60] Application of microsecond laser pulses allows for confinement of the thermal and mechanical effects of this absorption within the RPE layer, thus sparing the photoreceptors and the inner retina[61,62] (Fig. 41.21). It has been demonstrated that application of repetitive pulses of microsecond and sub-microsecond duration results in selective damage to RPE due to the formation of small cavitation bubbles around melanosomes.[19] Subsequent RPE proliferation and migration restores continuity of the RPE layer. Several small clinical studies have shown the efficacy

of SRT in diabetic maculopathy, central serous chorioretinopathy[63] and subfoveal fluid after rhegmatogenous retinal detachment.[64,65] Despite its clinical promise, this technique has not been commercialized yet. One of the difficulties with SRT is the lack of visible change in the retinal appearance making it difficult to assess adequate laser dosimetry in every patient. An acousto-optical system is being developed that may help to assess the cavitation threshold energy in RPE.[66] Microsecond exposures of RPE can be conveniently produced by rapid scanning of a continuous laser beam. For example, scanning a beam of d=100 μm in diameter with a speed v=10 m/s produces exposures $t=d/v$=10 μs in duration on the epithelial cells, sufficiently short for selective treatment of the RPE.[67,68]

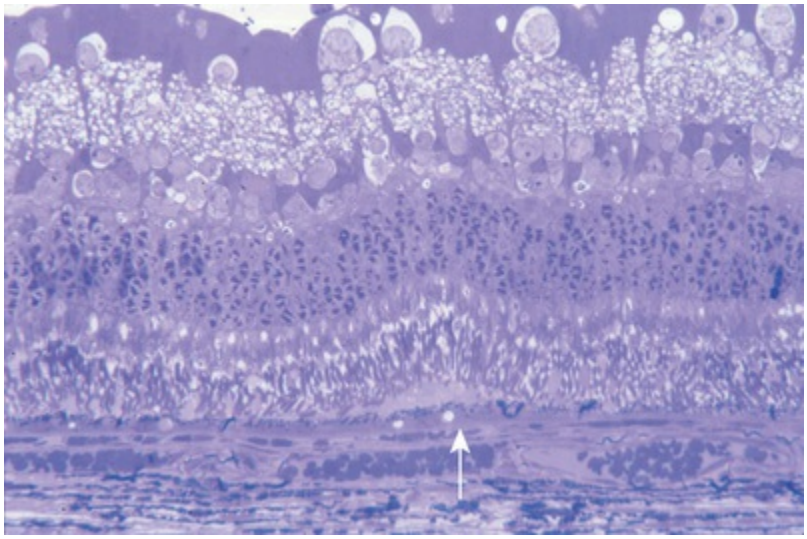

FIG. 41.21 Rabbit retina 24 hours after selective retinal pigment epithelium (RPE) treatment. Note that damage is confined almost exclusively to the RPE layer with preservation of the inner layer and even portions of the overlying photoreceptors. There is a small localized effusion between the RPE and photoreceptors (*arrow*).

Monitoring Retinal Temperature

Retinal thermal therapies utilizing the temperature rise below the threshold of immediately visible tissue response, such as

nondamaging hyperthermia, do not have as high a degree of control as conventional thermal photocoagulation methods. Due to the strong variation in fundus pigmentation the light absorption varies from patient to patient, and even between different areas in the same eye. Therefore, the same irradiation settings may lead to very different results in different patients, and so direct measurement of retinal temperature during such treatments is highly desirable. Similarly, it would be desirable to monitor retinal temperature in the treated spot during photocoagulation to provide uniform outcomes in areas with different pigmentation.

A noninvasive method of determination of retinal temperature has been recently developed, which is based on detection of acoustic waves generated in RPE irradiated with short laser pulses.[69] An acoustic transducer for the detection of the pressure waves is built into a contact lens attached to the treated eye during the procedure. The pressure waves are generated due to thermoelastic expansion of melanosomes upon absorption of the short (sub-microsecond) laser pulses. The key issue in this approach is that the thermoelastic expansion coefficient of water varies with temperature – by about 1% per 1 °C.[69] This effect allows for monitoring the changes in temperature of the RPE cells by monitoring the changes in amplitude of acoustic waves generated by the laser pulses of constant energy. The probing laser pulses are applied simultaneously with application of a therapeutic laser to detect temperature rise in tissue during the exposure. It has been demonstrated that precision of this method is on the order of 1 °C. Clinical testing of the system is currently in progress.

Optical Monitoring of Tissue Changes in Real Time

An optical approach to real-time feedback during retinal photocoagulation has recently been demonstrated.[70] It is based on OCT monitoring of the RPE expansion and changes in retinal scattering during coagulation. The system operates with millisecond temporal resolution, which should be fast enough for real-time monitoring of retinal photocoagulation.

Another technique for detection of tissue condition during slow

thermal therapy is based on spectroscopy of white light scattered from the tissue.[71] Cellular response to thermal stress involves expression of various proteins, as well as changes in their aggregation and concentration. All these effects result in changes of the refractive indices and/or the sizes and shapes of the cellular organelles, which can be detected using light scattering spectroscopy. Particle sizes down to 100 nm in diameter can be detected using light within the spectral range of 350–1000 nm. Since the information is obtained optically and without any staining this technique operates in real time and is noninvasive. It has been observed that scattering coefficients of some organelles in the heated cells change very strongly – up to 70%.[71]

References

1. Meyer-Schwickerath G. *Light coagulation*. Mosby: St Louis; 1960.
2. Palanker DV, Blumenkranz MS, Marmor MF. 50 years of ophthalmic laser therapy. *Arch Ophthalmol*. 2011;129(12):1613–1619.
3. Smith G, Atchinson DA. The eye. *The eye and visual optical instruments*. Cambridge University Press: Cambridge; 1996:291–316.
4. Thompson KP, Ren QS, Parel J-M. Therapeutic and diagnostic application of lasers in ophthalmology. Waynant RW. *Lasers in medicine*. CRC Press: Boca Raton, FL; 2002.
5. Pomerantzeff O, Pankratov M, Wang GJ, et al. Wide-angle optical-model of the eye. *Am J Optom Phys Opt*. 1984;61(3):166–176.
6. Walsh G, Charman WN, Howland HC. Objective technique for the determination of monochromatic aberrations of the human eye. *J Opt Soc Am A*. 1984;1(9):987–992.
7. Doornbos RMP, Lang R, Aalders MC, et al. The determination of in vivo human tissue optical properties and absolute chromophore concentrations using spatially resolved steady-state diffuse reflectance spectroscopy. *Phys Med Biol*. 1999;44(4):967–981.
8. Troy TL, Thennadil SN. Optical properties of human skin in

the near infrared wavelength range of 1000 to 2200 nm. *J Biomed Opt*. 2001;6(2):167–176.
9. Dougherty TJ, Mang TS. Characterization of intra-tumoral porphyrin following injection of hematoporphyrin derivative or its purified component. *Photochem Photobiol*. 1987;46(1):67–70.
10. Schmidt U, Birngruber R, Hasan T. Selective occlusion of ocular neovascularization by photodynamic therapy. *Ophthalmologe*. 1992;89(5):391–394.
11. Miller H, Miller B. Photodynamic therapy of subretinal neovascularization in the monkey eye. *Arch Ophthalmol*. 1993;111(6):855–860.
12. Kramer M, Miller JW, Michaud N, et al. Liposomal benzoporphyrin derivative verteporfin photodynamic therapy: selective treatment of choroidal neovascularization in monkeys. *Ophthalmology*. 1996;103(3):427–438.
13. Miller JW, Walsh AW, Kramer M, et al. Photodynamic therapy of experimental choroidal neovascularization using lipoprotein-delivered benzoporphyrin. *Arch Ophthalmol*. 1995;113(6):810–818.
14. Woodburn KW, Engelman CJ, Blumenkranz MS. Photodynamic therapy for choroidal neovascularization: a review. *Retina*. 2002;22(4):391–405.
15. Birngruber R, Indorf L, Soultanopoulos D, et al. Photodynamic occlusion of ocular neovascularization: preclinical evaluation of liposomal zinc phthalocyanine. *Invest Ophth Vis Sci*. 1996;37(3):4214.
16. Arnold J, Kilmartin D, Olson J, et al. Verteporfin therapy of subfoveal choroidal neovascularization in age-related macular degeneration: two-year results of a randomized clinical trial including lesions with occult with no classic choroidal neovascularization-verteporfin in photodynamic therapy report 2. *Am J Ophthalmol*. 2001;131(5):541–560.
17. Niemz M. *Laser–tissue interactions: fundamentals and applications*. Springer Verlag: Berlin; 2002.
18. Sramek C, Paulus Y, Nomoto H, et al. Dynamics of Retinal Photocoagulation and Rupture. *J Biomed Optics*. 2009;14(3) [034007].

19. Schuele G, Rumohr M, Huettmann G, et al. RPE damage thresholds and mechanisms for laser exposure in the microsecond-to-millisecond time regimen. *Invest Ophthalmol Vis Sci*. 2005;46(2):714–719.
20. Reichel E, Berrocal AM, Ip M, et al. Transpupillary thermotherapy of occult subfoveal choroidal neovascularization in patients with age-related macular degeneration. *Ophthalmology*. 1999;106(10):1908–1914.
21. Newsom RSB, McAlister JC, Saeed M, et al. Transpupillary thermotherapy (TTT) for the treatment of choroidal neovascularisation. *Br J Ophthalmol*. 2001;85(2):173–178.
22. Mainster MA, Reichel E. Transpupillary thermotherapy for age-related macular degeneration: Long-pulse photocoagulation, apoptosis, and heat shock proteins. *Ophthalmic Surg Las*. 2000;31(5):359–373.
23. Benner JD, Ahuja RM, Butler JW. Macular infarction after transpupillary thermotherapy for subfoveal choroidal neovascularization in age-related macular degeneration. *Am J Ophthalmol*. 2002;134(5):765–768.
24. Lavinsky D, Cardillo JA, Melo LA Jr, et al. Randomized clinical trial evaluating mETDRS versus normal or high-density micropulse photocoagulation for diabetic macular edema. *Invest Ophthalmol Vis Sci*. 2011;52(7):4314–4323.
25. Roisman L, Magalhaes FP, Lavinsky D, et al. Micropulse diode laser treatment for chronic central serous chorioretinopathy: a randomized pilot trial. *Ophthalmic Surgl Lasers Imaging Retina*. 2013;44(5):465–470.
26. Parodi MB, Spasse S, Iacono P, et al. Subthreshold grid laser treatment of macular edema secondary to branch retinal vein occlusion with micropulse infrared (810 nanometer) diode laser. *Ophthalmology*. 2006;113(12):2237–2242.
27. Figueira J, Khan J, Nunes S, et al. Prospective randomised controlled trial comparing sub-threshold micropulse diode laser photocoagulation and conventional green laser for clinically significant diabetic macular oedema. *Br J Ophthalmol*. 2009;93(10):1341–1344.
28. Venkatesh P, Ramanjulu R, Azad R, et al. Subthreshold micropulse diode laser and double frequency neodymium:

YAG laser in treatment of diabetic macular edema: a prospective, randomized study using multifocal electroretinography. *Photomed Laser Surg*. 2011;29(11):727–733.
29. Sivaprasad S, Elagouz M, McHugh D, et al. Micropulsed diode laser therapy: evolution and clinical applications. *Surv Ophthalmol*. 2010;55(6):516–530.
30. Sramek C, Mackanos M, Spitler R, et al. Non-damaging retinal phototherapy: dynamic range of heat shock protein expression. *Invest Ophthalmol Vis Sci*. 2011;52(3):1780–1787.
31. Lavinsky D, Sramek C, Wang J, et al. Subvisible retinal laser therapy: titration algorithm and tissue response. *Retina*. 2014;34(1):87–97.
32. Luttrull JK, Sramek C, Palanker D, et al. Long-term safety, high-resolution imaging, and tissue temperature modeling of sub-visible diode micropulse photocoagulation for retinovascular macular edema. *Retina*. 2012;32(2):375–386.
33. Lavinsky D, Palanker D. Nondamaging photothermal therapy for the retina: initial clinical experience with chronic central serous retinopathy. *Retina*. 2015;35(2):213–222.
34. Jain A, Blumenkranz MS, Paulus Y, et al. Effect of pulse duration on size and character of the lesion in retinal photocoagulation. *Arch Ophthalmol*. 2008;126(1):78–85.
35. Palanker D, Lavinsky D, Blumenkranz MS, et al. The Impact of pulse duration and burn grade on size of retinal photocoagulation lesion: implications for pattern density. *Retina*. 2011;31(8):1664–1669.
36. Paulus YM, Jain A, Gariano RF, et al. Healing of retinal photocoagulation lesions. *Invest Ophthalmol Vis Sci*. 2008;49(12):5540–5545.
37. Sher A, Jones BW, Huie P, et al. Restoration of retinal structure and function after selective photocoagulation. *J Neurosci*. 2013;33(16):6800–6808.
38. Belokopytov M, Belkin M, Dubinsky G, et al. Development and recovery of laser-induced retinal lesion in rats. *Retina*. 2010;30(4):662–670.
39. Merigan WH, Strazzeri J, DiLoreto DA Jr, et al. Visual

recovery after outer retinal damage in the macaque. *Invest Ophthalmol Vis Sci*. 2011;52(6):3202.
40. Wright CHG, Barrett SF, Ferguson RD, et al. Initial in vivo results of a hybrid retinal photocoagulation system. *J Biomed Opt*. 2000;5(1):56–61.
41. Blumenkranz MS, Yellachich D, Andersen DE, et al. Semiautomated patterned scanning laser for retinal photocoagulation. *Retina*. 2006;26(3):370–376.
42. Nagpal M, Marlecha S, Nagpal K. Comparison of laser photocoagulation for diabetic retinopathy using 532-nm standard laser versus multispot pattern scan laser. *Retina*. 2010;30(3):452–458.
43. Muqit MM, Marcellino GR, Gray JC, et al. Pain responses of Pascal 20 ms multi-spot and 100 ms single-spot panretinal photocoagulation: Manchester Pascal Study, MAPASS report 2. *Br J Ophthalmol*. 2010;94(11):1493–1498.
44. DRS_Study_Group. Photocoagulation Treatment for proliferative diabetic retinopathy. clinicial application of DRS findings, DRS Report Number 8. *Ophthalmology*. 1981;88:583–600.
45. Early Treatment Diabetic Retinopathy Study Research Group. Early photocoagulation for diabetic retinopathy. ETDRS report no. 9. *Ophthalmology*. 1991;98(5 Suppl.):766–785.
46. Vogel A, Venugopalan V. Mechanisms of pulsed laser ablation of biological tissues. *Chem Rev*. 2003;103(2):577–644.
47. Young FR. *Cavitation*. McGraw-Hill: Maidenhead; 1989:13–16.
48. Palanker D, Vankov A, Miller J, et al. Prevention of tissue damage by water jet during cavitation. *J Appl Phys*. 2003;94(4):2654–2661.
49. D'Amico DJ, Blumenkranz MS, Lavin MJ, et al. Multicenter clinical experience using an erbium:YAG laser for vitreoretinal surgery. *Ophthalmology*. 1996;103(10):1575–1585.
50. D'Amico DJ, Brazitikos PD, Marcellino GR, et al. Initial clinical experience with an erbium:YAG laser for vitreoretinal surgery. *Am J Ophthalmol*. 1996;121(4):414–425.

51. Lin CP, Stern D, Puliafito CA. High-speed photography of Er: YAG laser ablation in fluid. Implication for laser vitreous surgery. *Invest Ophth Vis Sci*. 1990;31(12):2546–2550.
52. Palanker D, Hemo I, Turovets I, et al. Vitreoretinal ablation with the 193-nm excimer laser in fluid media. *Invest Ophthalmol Vis Sci*. 1994;35(11):3835–3840.
53. Hemo I, Palanker D, Turovets I, et al. Vitreoretinal surgery assisted by the 193-nm excimer laser. *Invest Ophthalmol Vis Sci*. 1997;38(9):1825–1829.
54. Palanker D, Turovets I, Lewis A. Mechanisms of tissue damage during arf excimer endolaser microsurgery. laser–tissue interaction VII. *Proc SPIE.*1996;2681:220–225.
55. Palanker D, Turovets I, Lewis A. Dynamics of ArF excimer laser-induced cavitation bubbles in gel surrounded by a liquid medium. *Lasers Surg Med*. 1997;21(3):294–300.
56. Vogel A, Busch S, Jungnickel K, et al. Mechanisms of intraocular photodisruption with picosecond and nanosecond laser pulses. *Lasers Surg Med*. 1994;15(1):32–43.
57. Krueger RR, Quantock AJ, Juhasz T, et al. Ultrastructure of picosecond laser intrastromal photodisruption. *J Refract Surg*. 1996;12(5):607–612.
58. Palanker DV, Blumenkranz MS, Andersen D, et al. Femtosecond laser-assisted cataract surgery with integrated optical coherence tomography. *Sci Transl Med*. 2010;2(58):58ra85.
59. Cohen BZ, Wald KJ, Toyama K. Neodymium:YLF picosecond laser segmentation for retinal traction associated with proliferative diabetic retinopathy. *Am J Ophthalmol*. 1997;123(4):515–523.
60. Brinkmann R, Huttmann G, Rogener J, et al. Origin of retinal pigment epithelium cell damage by pulsed laser irradiance in the nanosecond to microsecond time regimen. *Laser Surg Med*. 2000;27(5):451–464.
61. Roider J, Hillenkamp F, Flotte T, et al. Microphotocoagulation: selective effects of repetitive short laser pulses. *Proc Natl Acad Sci USA*. 1993;90(18):8643–8647.
62. Roider J, Michaud NA, Flotte TJ, et al. Response of the

retinal pigment epithelium to selective photocoagulation. *Arch Ophthalmol*. 1992;110(12):1786–1792.
63. Elsner H, Porksen E, Klatt C, et al. Selective retina therapy in patients with central serous chorioretinopathy. *Graefes Arch Clin Exp Ophthalmol*. 2006;244(12):1638–1645.
64. Koinzer S, Elsner H, Klatt C, et al. Selective retina therapy (SRT) of chronic subfoveal fluid after surgery of rhegmatogenous retinal detachment: three case reports. *Graefes Arch Clin Exp Ophthalmol*. 2008;246(10):1373–1378.
65. Brinkmann R, Roider J, Birngruber R. Selective retina therapy (SRT): a review on methods, techniques, preclinical and first clinical results. *Bull Soc Belge Ophtalmol*. 2006;302:51–69.
66. Brinkmann R, Schuele G, Joachimmeyer E, et al. Determination of absolute fundus temperatures during retinal laser photocoagulation and selective RPE treatment. *Invest Ophthalmol Vis Sci*. 2001;42(4):S696.
67. Framme C, Alt C, Schnell S, Sherwood M, Brinkmann R, Lin CP. Selective targeting of the retinal pigment epithelium in rabbit eyes with a scanning laser beam. *Invest Ophthalmol Vis Sci*. 2007;48(4):1782–1792.
68. Paulus YM, Jain A, Gariano RF, et al. *Selective retinal therapy with a continuous line scanning laser*. SPIE Proceedings. 2010 [7550(Ophthalmic Technologies XX)].
69. Schule G, Huttmann G, Framme C, et al. Noninvasive optoacoustic temperature determination at the fundus of the eye during laser irradiation. *J Biomed Opt*. 2004;9(1):173–179.
70. Huttmann G, Muller H, Schlott K, et al. Investigating of retinal photocoagulation by high-speed oct in rabbits. *Invest Ophthalmol Vis Sci*. 2011;52(6):549.
71. Schuele G, Huie P, Vankov A, et al. *Non-invasive monitoring of the thermal stress in RPE using light scattering spectroscopy*. Ophthalmic Technologies, SPIE Proceedings. 2004 [5314].

VOLUME TWO

Medical Retina

OUTLINE

SECTION 1

Retinal Degenerations and Dystrophies

OUTLINE

42

Retinitis Pigmentosa and Allied Disorders

Kevin Gregory-Evans, Richard G. Weleber, Mark E. Pennesi

Introduction

The term "retinitis pigmentosa" (RP) implies that inflammation is a prominent part of the pathophysiology of the condition. Although a role of inflammation at some level in the retina is still discussed, RP is not considered a primary inflammatory disease. Vascular

permeability is greater in eyes of patients with RP, and trauma or surgery is accompanied by a greater incidence and severity of inflammation. Through the years, many terms have been used to describe RP, including "tapetoretinal degeneration" (by Leber in 1916), "primary pigmentary retinal degeneration," "pigmentary retinopathy," and "rod–cone dystrophy."

RP may be seen in isolation (typical RP) or in association with systemic disease (syndromic RP). The prevalence of typical RP is approximately 1 : 4000 worldwide. In Maine, USA, the prevalence of typical RP has been found to be 1 : 5200, and the birth incidence of those who will eventually be affected with RP has been calculated as 1 : 3500.[1] The prevalence of RP has been found to be 1 : 7000 in Switzerland,[2] 1 : 4800 in England,[3] 1 : 4500 in Israel,[4] 1 : 4000 in Denmark,[5] 1 : 3800–4000 in China,[6,7] and 1 : 3300 in Japan.[8] Some of the highest frequency of occurrence has been reported among the Navajo Indians (1 : 1878),[9] from Northern China (1 : 1000),[10] and from southern and central India (1 : 600-750).[11,12] The prevalence of syndromic forms of RP is less well documented. For example, the prevalence of Usher syndrome (RP with congenital deafness) is estimated to be from 1 : 60,000 to 1 : 30,000.[13–15]

The clinical aspects and basic science of RP and allied disorders are extensively documented in the published literature. A recent literature search (August 2015) using PubMed found more than 9100 articles on RP alone. Numerous scholarly reviews have been written, many of which are cited in previous versions of this chapter. Because the field is changing so rapidly, we recommend current reviews through major electronic journals as the best means of obtaining the most recent information.

Early History

The first description of the fundus findings and the use of the term "retinitis pigmentosa" are attributed to Donders in 1855 and 1857.[16–18] However, the diagnosis of complicated night blindness (presumably RP) has probably existed in all cultures for hundreds, if not thousands, of years. Ovelgün, in 1744, made observations on familial complicated hemeralopia (or night blindness), which probably represented RP.[16] Shortly after the discovery of the

ophthalmoscope by Helmholtz in 1851, van Trigt[19] in 1853 and Ruete[20] in 1854 described cases that most assuredly were RP.

Typical Retinitis Pigmentosa

Clinical Features

Nyctalopia

Difficulty with vision at night (night blindness) is one of the two hallmark symptoms of RP. Patients with typical RP usually attribute the beginning of night vision difficulties to the first or second decade of life. In some patients, especially those living in an urban setting, night vision problems may not be apparent until ocular disease is at an advanced stage. Tanino and Ohba[21] noted that the onset of symptoms of RP, most commonly nyctalopia, occurred at a median age of 10.7 years in autosomal recessive disease and 23.4 years in autosomal dominant disease. The symptom of nyctalopia should not be confused with the symptom of blurred vision with night myopia or uncorrected refractive error. People with RP have a narrowing of the visual field in the dark and may describe getting easily disoriented on dimly lit evenings when others are able to see adequately. Becoming accident-prone, especially at night, is a highly suggestive symptom.

Night blindness alone is not pathognomonic of RP and can be a feature of other retinal disorders, such as congenital stationary night blindness and age-related macular degeneration. Deteriorating night vision can also be a prominent feature of other ocular disease, such as high myopia.

Visual Field Loss

The second hallmark feature or symptom of RP is an insidious, progressive loss of peripheral visual field. In some patients, especially those with severe disease beginning in childhood, this may be manifested as a progressive contraction of the visual field (see also Perimetry, under Psychophysical findings). Loss of peripheral vision can be detected in early disease with small, dim test targets (Fig. 42.1). For many types of RP, field deficits are usually found first, and are most severe, in the superior visual field

(Fig. 42.2). This reflects the early involvement of the inferior retina in RP. Occasionally the visual field loss will be greater temporally, nasally, or inferiorly (Fig. 42.3). See the section on Perimetry for specifics about testing the visual field.

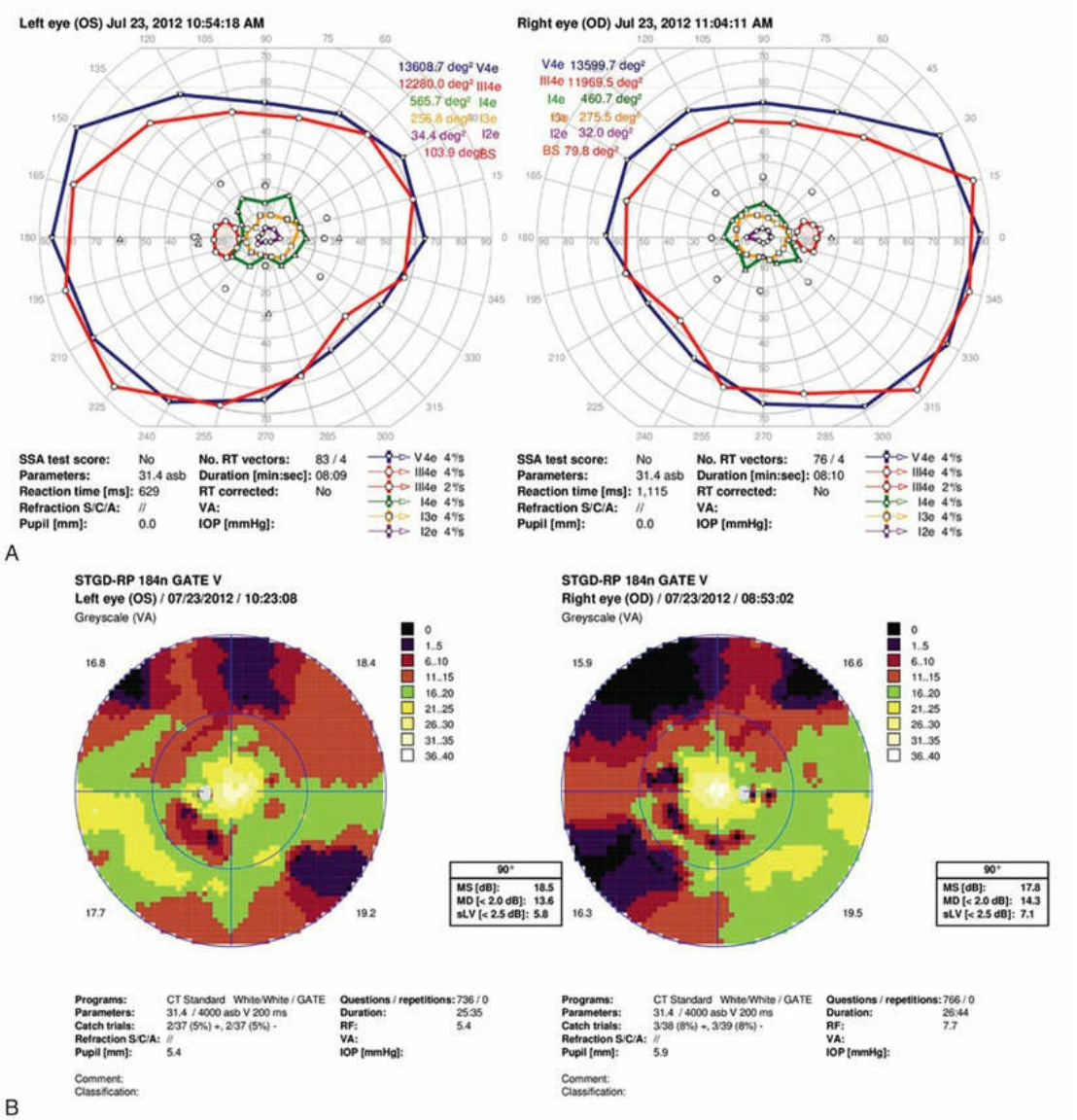

FIG. 42.1 (A) Visual fields in a 21-year-old woman with autosomal dominant retinitis pigmentosa. Note that the visual field is full to the IV4e and III4e test target are normal, but responses to smaller and dimmer targets are constricted creating a relative midperipheral scotoma. (B) Octopus static visual fields from the same patient using a 185-point radial grid, GATE algorithm, and Size V target. Note the decrease in retinal sensitivity in the midperiphery and far periphery. The

full-field electroretinogram demonstrated a severe and generalized rod–cone dystrophy.

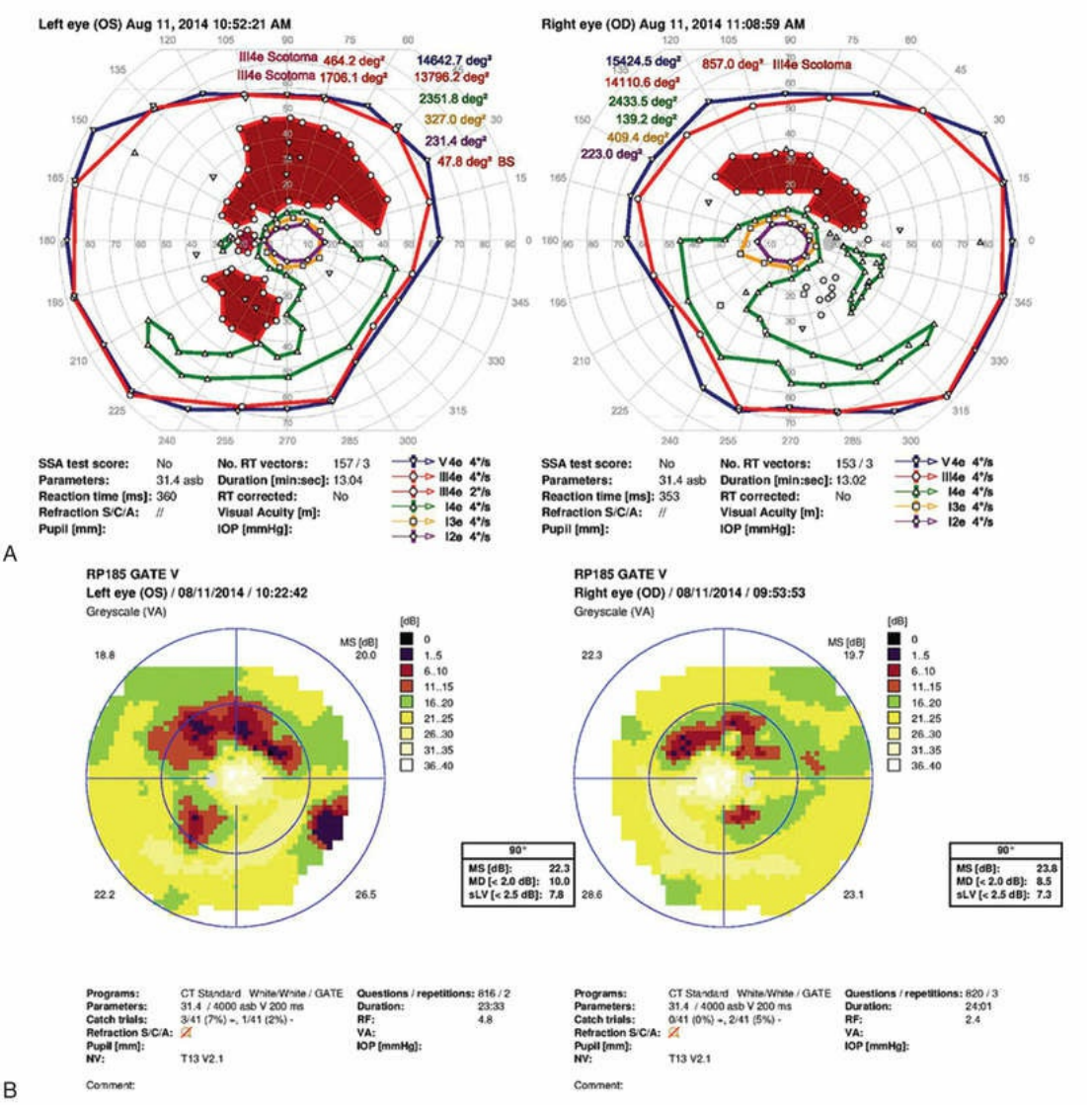

FIG. 42.2 (A) Octopus kinetic visual fields in a 18-year-old woman with autosomal dominant retinitis pigmentosa due to a *RHO* Pro23His mutation. Note that the visual field is full to the IV4e test target, but that there are midperipheral scotomas to the III4e target worse superiorly. Smaller and dimmer isopters are contracted. (B) Octopus static visual fields from the same patient using a 185-point radial grid, GATE algorithm, and Size V target. Note the decrease in retinal sensitivity in the midperiphery. The relatively worse sensitivity superiorly is typical of *RHO* Pro23His mutations, which often first show degeneration in the

inferior midperiphery. The electroretinogram demonstrated moderate to severe loss of rod-mediated responses and mild attenuation of cone responses.

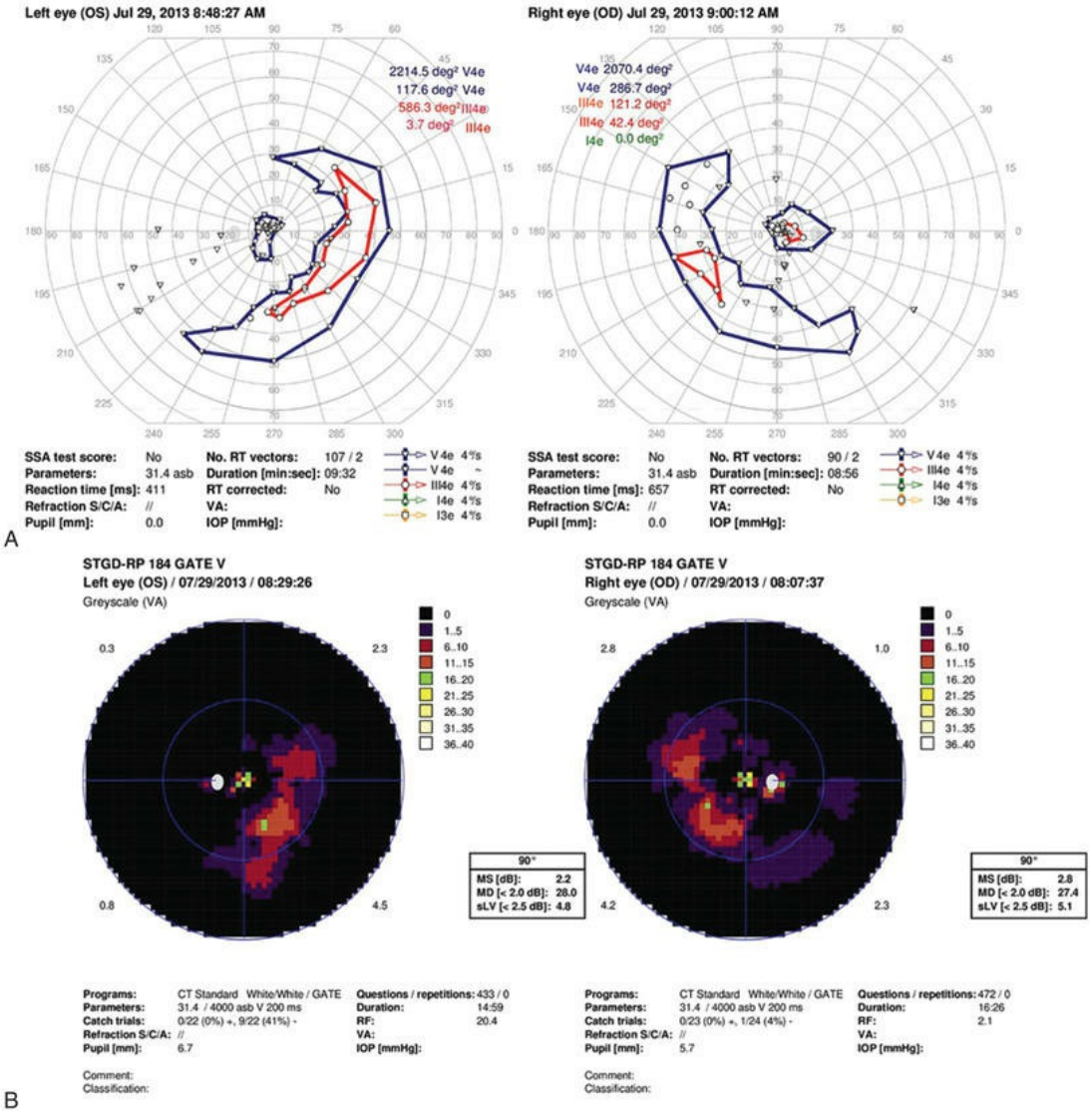

FIG. 42.3 (A) Octopus kinetic visual fields in a 65-year-old man with autosomal recessive retinitis pigmentosa. Note that relative preservation centrally and in the nasal midperiphery in each eye. (B) Octopus static visual fields from the same patient using a 185-point radial grid, GATE algorithm, and Size V target. The decreased sensitivity matches that observed with the kinetic visual fields.

In a group of patients with several types of RP, Berson et al.[22]

found that overall about 4.6% of the remaining visual field was lost per year. Massof et al.[23,24] found that, in most forms of generalized RP, the kinetic visual field shrank approximately 50% over 4.5 years. Massof and Finkelstein[24] argue that the time course for field loss in all major genetic and functional classes of RP is nearly identical if one corrects for the critical age, which is defined as the age when visual field loss is first detected by a test target of given size and brightness. In conjunction with this concept, they have proposed a two-stage hypothesis for the natural course of RP. The first stage is a predisposition for retinal degeneration, such as genetic or environmental factors, which would be different for the separate types of RP and possibly among individuals. The second stage involves the actual retinal degeneration, which proceeds on its own internal time course and which would be common to most forms of RP.

In general, there is a strong tendency for the visual field loss to be symmetric between the two eyes.[23,24] A notable exception to this is the phenotype expressed in female carriers of X-linked RP. In this situation, the distribution of mutant photoreceptors in the retina is determined by lyonization (X-chromosomal inactivation). This is a random event determining which genes of the two X chromosomes (the normal or mutant copy) are expressed in a particular cell. This leads not only to unusual, irregular patterns of visual field loss in individual eyes but also to quite striking differences in field loss between the two eyes.[25] However, even in these cases the visual fields usually correspond quite closely to the fundus appearance, with the greater visual field loss in the eye with greater pigmentary abnormalities.

In typical RP the rate of progression of visual field loss is usually slow and relentless, with changes best appreciated when observed over many years or even decades. However, the visual fields may change dramatically over a few months or years. A patient may not notice what may be a striking loss of peripheral visual field if the central field remains clear. As the visual field reaches the stage of "tunnel vision," the patient usually becomes acutely aware of subsequent change with time. This often leads the patient to the conclusion that the rate of degeneration is accelerating. In the United States, statutory legal blindness results when the remaining

central visual field measures 20° or less horizontally in the better eye, using the III-4-e test target on a Goldmann perimeter.[26] In the UK, most RP patients, with normal acuity, would be registered as partially sighted ("gross field defect"). Legal blindness occurs when fields become "very contracted" – a stage at which acuity loss has also usually occurred.

Central Vision Loss

There is a common misconception in RP (documented in older texts) that the central vision will remain good until most, if not all, the peripheral field is lost. Central visual function can, however, be seriously affected early in typical RP, while significant peripheral field remains.[27] Cystoid macular edema (CME),[28] diffuse retinal vascular leakage,[29] macular preretinal fibrosis[30] (Fig. 42.4), and retinal pigment epithelial (RPE) defects in the macula or fovea[31,32] can occur early in the disease. Macular edema is the topic of a section on treatment of RP later in this chapter.

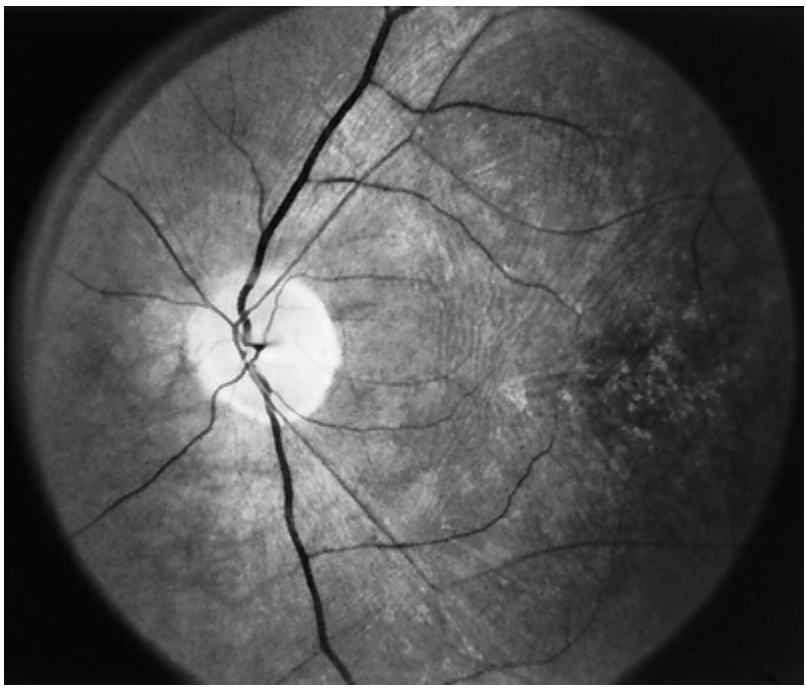

FIG. 42.4 Posterior pole of the left eye of a 33-year-old man with Bardet–Biedl syndrome from homozygosity for the common Met390Arg mutation of *BBS1*, demonstrating preretinal fibrosis with wrinkling of the internal limiting membrane. The acuity was 20/400.

The maculas developed atrophic lesions over the next 5 years with further reduction of visual acuity.

To a considerable extent, the likelihood of retaining "good vision" (central acuity) to a given age in life depends on the specific inheritance type of RP. Patients with regional ("sector") RP may retain good visual acuity all their life. Patients with autosomal dominant RP (adRP) are more likely than patients with autosomal recessive (arRP) or X-linked RP to retain good acuity beyond 60 years of age.[22] Marmor, in his study of visual loss in adRP and arRP,[33] found that when visual acuity began to fail, it generally dropped to 20/200 within 4–10 (median 6) years. Patients with X-linked RP are usually blind (acuity 20/200 or worse) by 30–40 years of age.[22,34,35] A good prognostic sign of retention of central acuity is electroretinography (ERG) amplitudes remaining quite large (e.g., greater than 100 μV).[33]

Color Vision Defects

In general, color vision in typical RP remains good until the visual acuity is 20/40 or worse. Color vision may fail early in cases where central cones appear to be abnormal from the beginning. In such cases, pericentral scotomas encroach very close to fixation early in the disease. These patients, even though they show a rod–cone loss on ERG, may show impressive color vision defects even when peripheral vision is relatively good.

Photopsia and Other Symptoms

Many patients with RP at some time during the course of their disease have light flashes, or photopsias. These are reported as occurring in the midperipheral field of vision, often adjacent to areas of relative or absolute scotomas. These photopsias are described as tiny, blinking or shimmering lights or as a coarse, sparkling graininess to vision. The phenomenon is similar to that reported by patients with ophthalmic migraine except that, although retinal disease involvement expands over the years, the photopsias are generally stationary within the field. Also, unlike ophthalmic migraine, the photopsias may be continuous rather than episodic. As the scotomas become denser over the years, the

photopsias decrease and finally disappear. In a retrospective survey of symptoms and findings in 500 patients with RP, Heckenlively et al.[36] reported light flashes in 170 (35%). Since eight patients in this series had retinal detachments, the symptom of light flashes must be considered an indication for careful fundus examination.

The cellular or tissue correlates that underlie photopsias in RP are unknown but may include photoreceptor dysfunction, neurite sprouting, aberrant synapse formation, and secondary remodeling of the retina, all of which occur as sequelae of photoreceptor degeneration (see section on Cell and tissue biology: Histopathology, for further discussion).

Fundus Appearance

The classically described fundus appearance of RP includes attenuated retinal vessels, mottling and granularity of the RPE, bone spicule intraretinal pigmentation, and optic nerve head pallor (Fig. 42.5). In general, when ophthalmoscopically detectable abnormalities of the fundus are present, there is a high degree of symmetry between the two eyes and fundus pigmentation is often greater in the midperiphery (Fig. 42.6). In advanced disease, atrophy of the RPE and choriocapillaris leads to fundus pallor and larger choroidal vessels become visible (Fig. 42.7). As the disease advances to late stages, vessel attenuation can become so severe that the retinal vessels appear thread-like (Fig. 42.8).

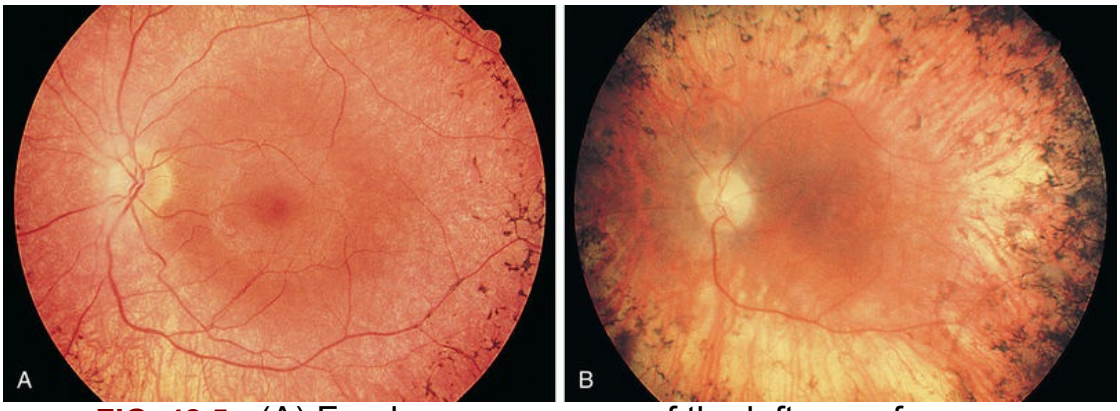

FIG. 42.5 (A) Fundus appearance of the left eye of a 13-year-old girl with autosomal recessive retinitis pigmentosa. Visual acuity was 20/20, but visual field was constricted to 20° diameter with the III-4-e test

target. (B) Advanced autosomal dominant retinitis pigmentosa in the left eye of a 57-year-old man from the Pro347Leu mutation of rhodopsin. Visual acuity was 20/100 right eye and 20/200 left eye and visual field constricted to 18° in both eyes with the III-4-e target.

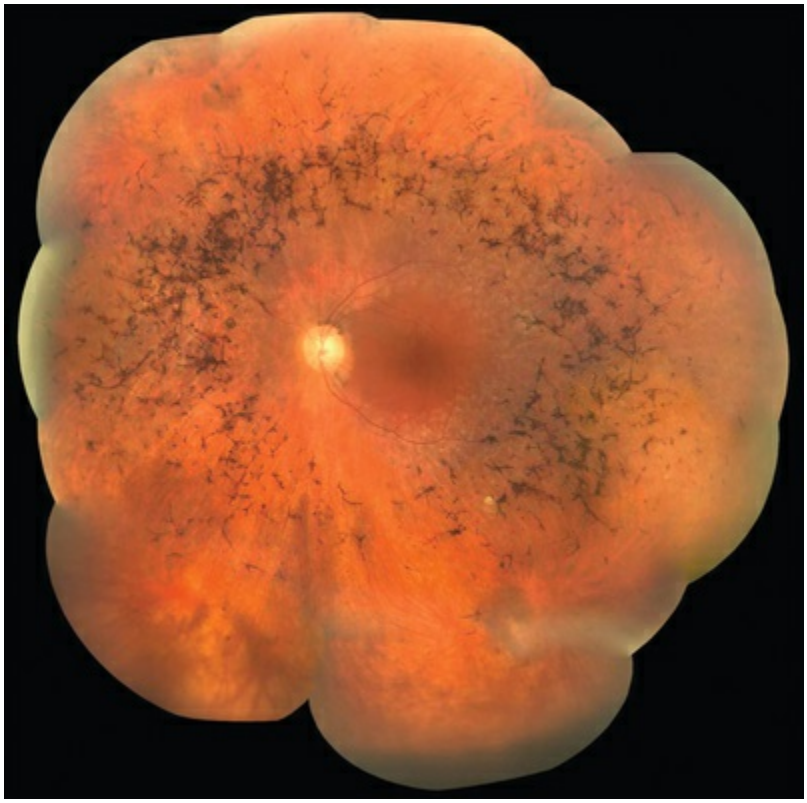

FIG. 42.6 Fundus appearance of the left eye of a 44-year-old patient with retinitis pigmentosa as part of Usher syndrome type 2. Note the midperipheral pigmentary changes, retinal pigment epithelium mottling, vascular attenuation, and optic nerve pallor.

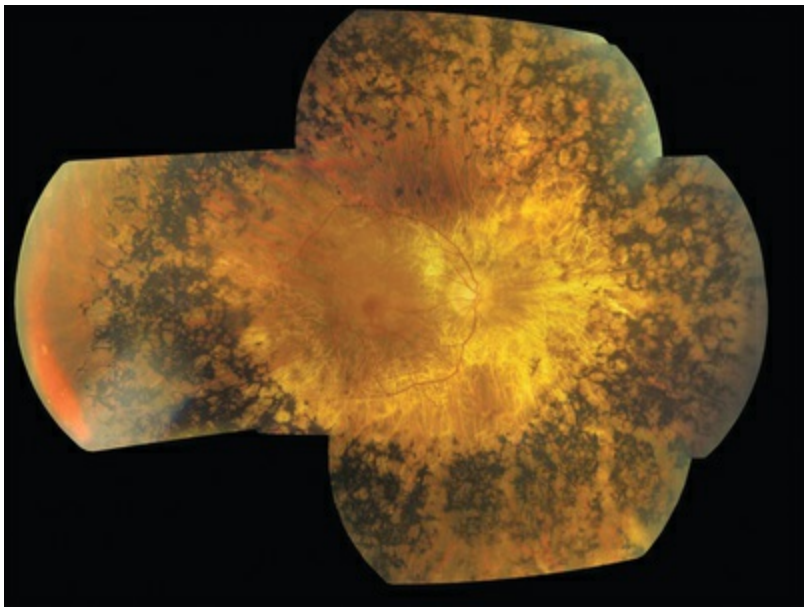

FIG. 42.7 Fundus appearance of the left eye of a 75-year-old patient with X-linked retinitis pigmentosa due to an *RPGR* mutation. Note the severe pigmentary changes, RPE atrophy revealing underlying choroidal vessels, attenuation, and optic nerve pallor.

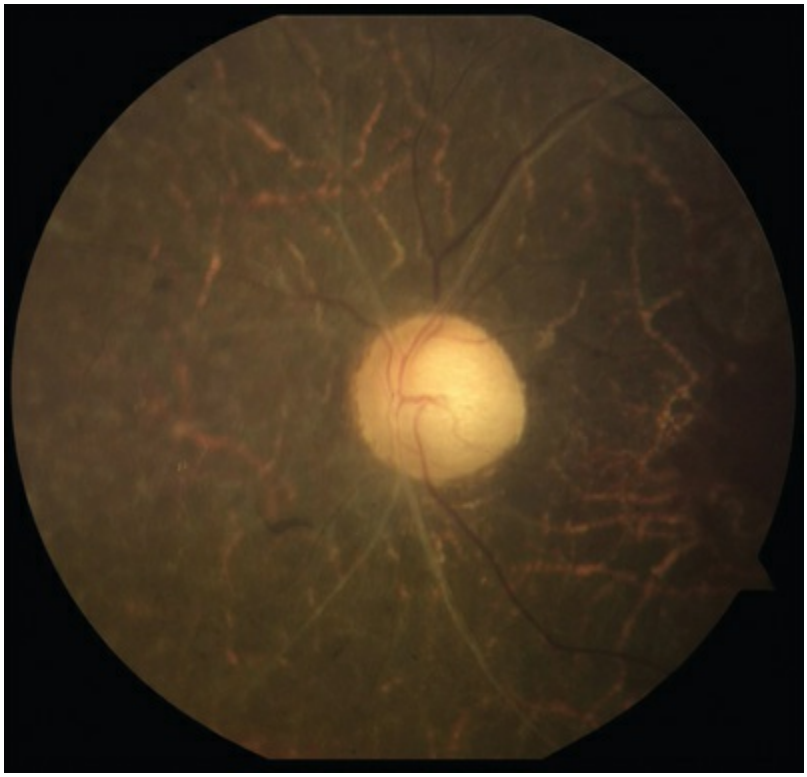

FIG. 42.8 Fundus appearance of the left eye of a 65-year-old patient with simplex retinitis pigmentosa. Note

the thread-like retinal vessels, pale, waxy optic discs, epiretinal membrane and mottling of retinal pigment epithelium. The patient was also a glaucoma suspect due to increased cup-to-disc ratios.

Almost all forms of RP go through a stage where the retina appears either normal or nearly normal, even though relative scotomas may be evident on visual field testing or areas of decreased retinal threshold may be present on static perimetry. Patients who have very early RP without fundus pigmentary abnormalities are often diagnosed as having RP sine pigmento or paucipigmentary RP. This is no longer considered a specific subtype of RP but a stage through which many, if not most, patients with RP pass. The sine pigmento stage may exist for decades before typical RP signs appear. For patients with high myopia and RP, the typical fundus features of high myopia may delay the appreciation of other retinal abnormalities (Fig. 42.9).

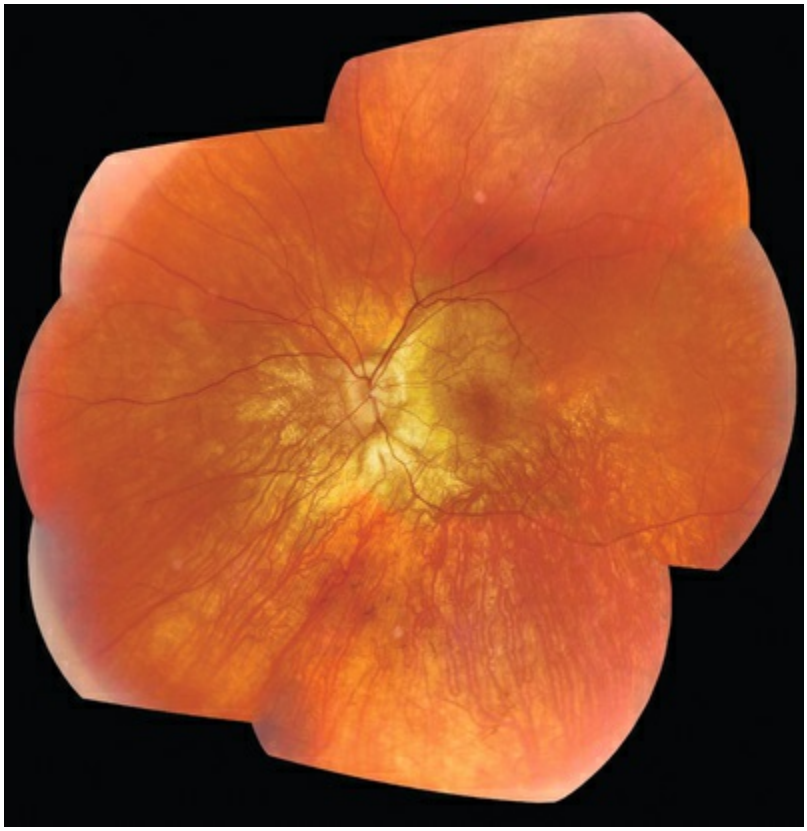

FIG. 42.9 Fundus of a 27-year-old man with high myopia and X-linked retinitis pigmentosa (same patient as in Fig. 42.2). Sparse but definite bone spicules were

present in the inferior mid- and far periphery. Discs showed a myopic tilt with peripapillary chorioretinal atrophy. The retinal pigment epithelium was diffusely hypopigmented.

When fundus abnormalities are evident, the earliest features are attenuation of retinal vessels and the appearance of fine mottling or granularity of the RPE in the mid- and far periphery (Fig. 42.10). Spectral domain optical coherence tomography (SD-OCT) imaging demonstrates that retinal thickness is decreased, particularly for outer layers, outside the macula and in areas of abnormal pigmentation with bone spicules.[37,38] The macular region may exhibit increased luster, abnormal highlights, or wrinkling, suggesting macular edema or early epiretinal membrane formation or preretinal fibrosis.[28,32] In advanced stages, patients with RP may exhibit atrophic macular lesions (Fig. 42.11) that simulate what some authors have called (perhaps inappropriately so) "macular coloboma."

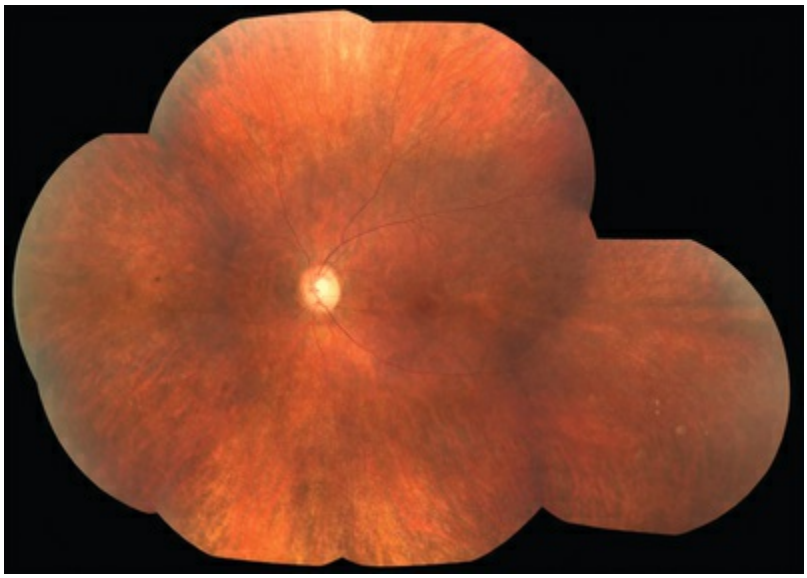

FIG. 42.10 Fundus appearance of the left eye of a 18-year-old female with simplex retinitis pigmentosa. Note the atrophy of retinal vessels and granular RPE changes in the mid- and far periphery. Bone spicules were not readily apparent.

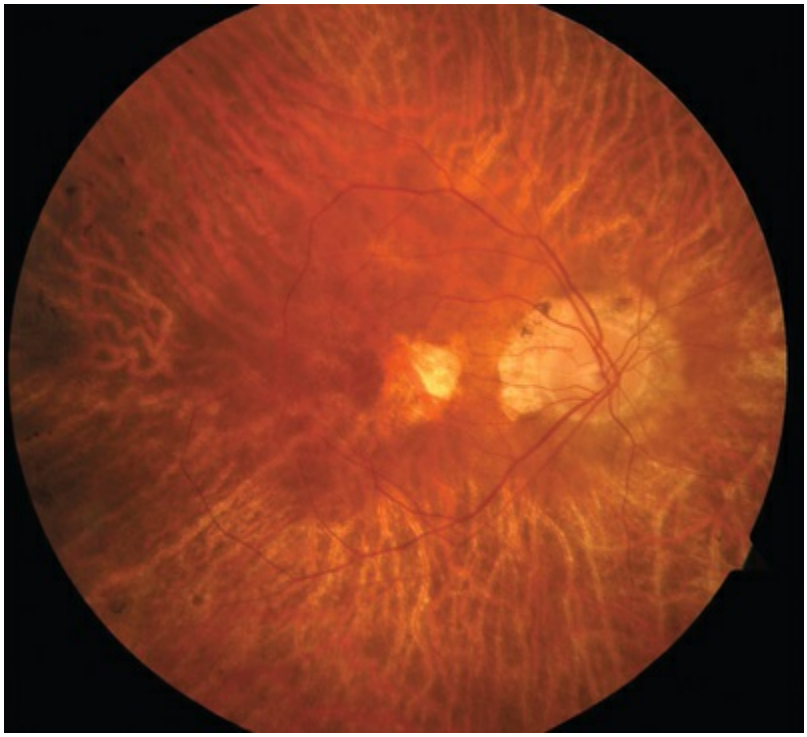

FIG. 42.11 The right eye of a 65-year-old man with simplex retinitis pigmentosa with notable peripapillary atrophy and an atrophic macular lesions.

Intraretinal, bone spicule pigment formations represent migration of pigment into the retina from disintegration of RPE cells with accumulation in the interstitial spaces surrounding retinal vessels. This process occurs most prominently at the junctions of vessels producing perivascular pigmentary cuffing and spicule-shaped deposits. The loss of pigment within the pigment epithelial cells often produces an overall gray, desaturated appearance to the retina with greater visibility of underlying choroidal vessels through the more transparent pigment epithelium. Eventually, the normal salmon-pink color of the entire mid- and far peripheral fundus is replaced by dense bone spicule pigmentary formations. Heckenlively[39] has described several patients with advanced RP with preservation of the RPE in a para-arteriolar distribution. Porta and colleagues described two additional cases. Van den Born et al.[40] reported a large consanguineous family with preserved para-arteriolar RP and confirmed the autosomal recessive inheritance. Almost all these patients were hyperopic. The gene for this form of RP (termed RP12) has been found to be the human homolog *CRB1* of the *Drosophila crumbs* gene.[41] Fig. 42.12 demonstrates this

phenomenon in a patient with heterozygous *CRB1* mutations.

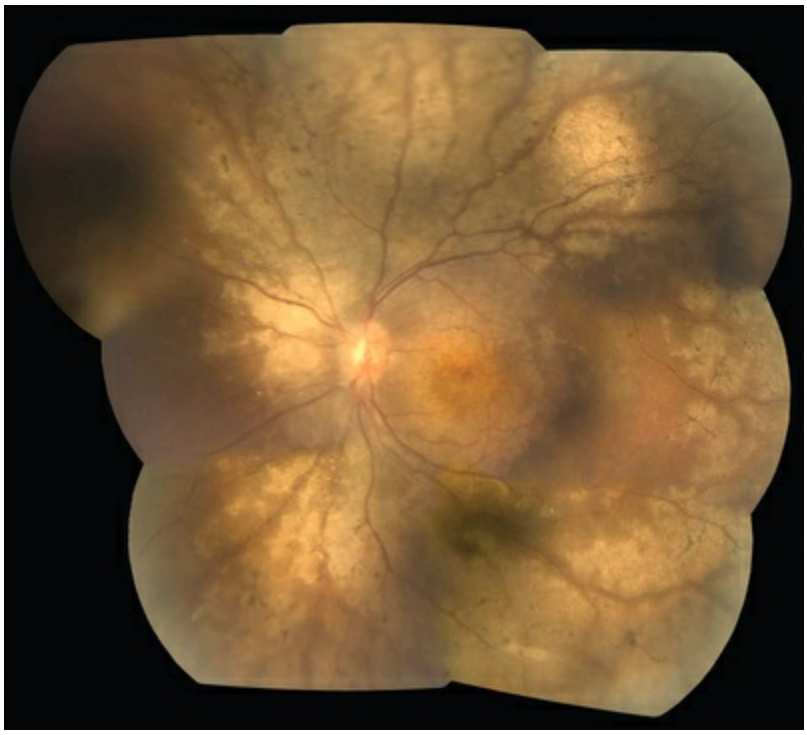

FIG. 42.12 Fundus photo montage of the left eye of an 11-year-old female with SECORD due to heterozygous mutations in *CRB1*. Note the relative preservation of the retinal pigment epithelium around the arterial vessels. (Photo courtesy of Dr. Paul Yang.)

In some patients abnormal pigmentation and atrophy are confined to one area of the retina. Such an appearance is termed "sector RP," a diagnosis that undoubtedly represents a heterogeneous group of disorders characterized by marked regionality of disease. Sector RP is discussed in further detail in the section Subdivision by distribution of retinal involvement or fundus appearance, below. However, since many patients with generalized disease present with localized pigmentary changes with regional functional loss, sector RP must always remain a provisional diagnosis until an adequate period of observation has occurred.

A golden (sometimes yellow/greenish) metallic tapetal-like reflex or sheen can occasionally be observed in women who are carriers for the X-linked form of RP[42] and rarely in young males with early

disease[43–45] (Fig. 42.13). With time, regional or diffuse mottling and atrophy of the RPE eventually replace the tapetal-like sheen. At least one form of dominant RP can show a tapetal-like reflex limited to the foveal and parafoveal region (Fig. 42.14). No histopathologic assessment has yet identified the source of this tapetal-like reflex. Cideciyan and Jacobson[46] suggested that abnormal cones may be the sources of the tapetal reflex. Berendschot et al.,[47] using spectral fundus reflectance, confirmed that outer segments of peripheral photoreceptor cells are the source of the abnormal reflex but that this abnormality was not confined to cones. SD-OCT studies of obligate X-linked RP carries have shown variable findings including outer retinal thinning and increased reflectivity of outer retinal structures.[48–50] A tapetal-like reflex is not pathognomonic of X-linked RP but has also been reported in occasional cases of X-linked retinoschisis,[51] and Oguchi disease.[52] The carrier state for X-linked RP appears to be a slowly progressive retinal dystrophy in its own right, with a patchy distribution of affected retina as determined by lyonization.[53,54] A number of studies have reported that the ERG is abnormal in most X-linked RP carriers.[25,55–58]

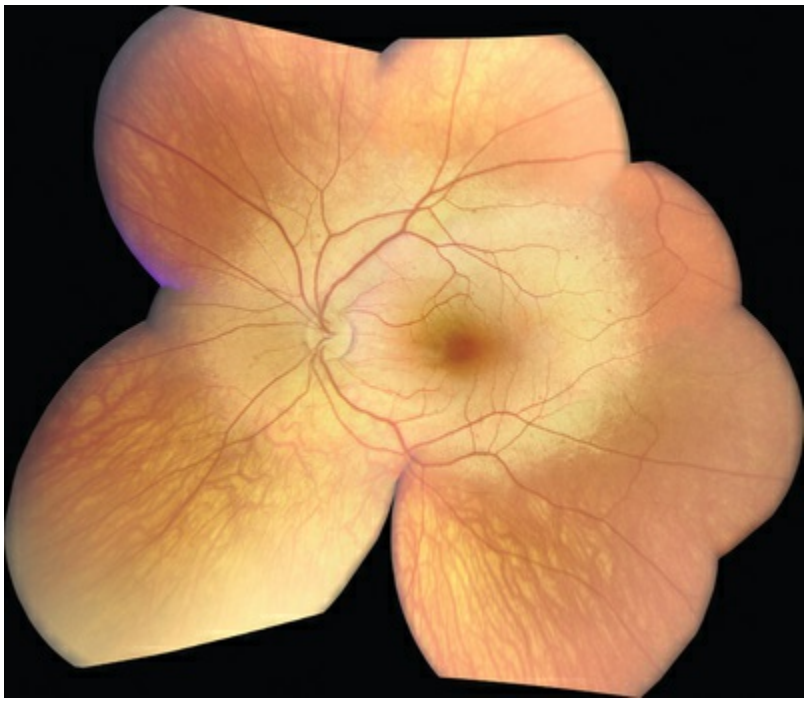

FIG. 42.13 Tapetal-like yellow–white reflex in a 13-year-old boy with X-linked retinitis pigmentosa.

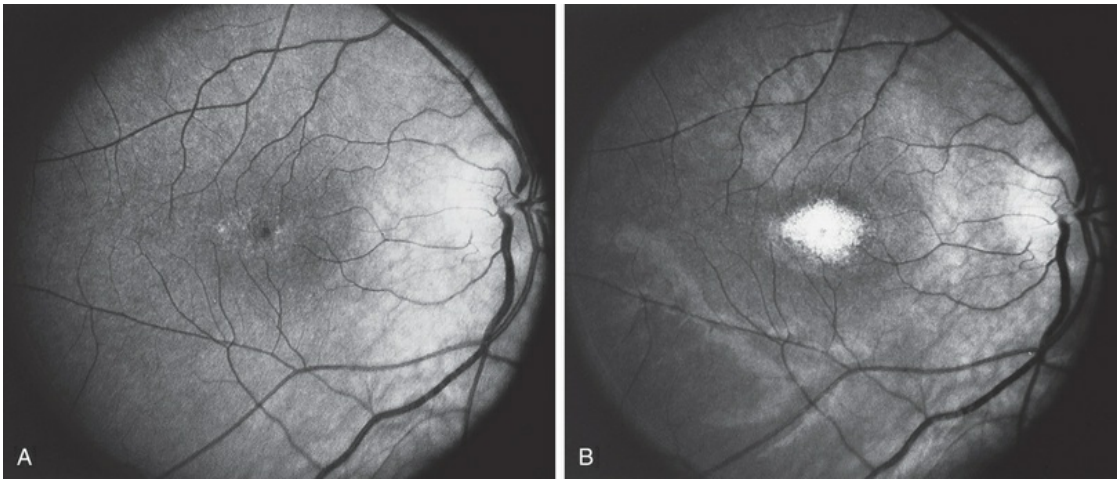

FIG. 42.14 Tapetal-like golden foveal reflex in an 11-year-old boy with autosomal dominant retinitis pigmentosa. Left (A) and right (B) stereo pair of right macula. In these and all stereo pairs for both eyes, the bright sheen was only visible in the photograph obtained through the nasal half of the pupil. This marked orientation dependency is similar to that seen in crystalline structures and may result from deformations of the outer photoreceptor segments.

The optic disc may be normal in early RP, show a waxy fullness with hyperemia, or appear waxy and pale (Fig. 42.15A). A "golden ring" or yellowish-white halo can often be seen surrounding the optic disc in early RP (Fig.42.15B). As disease progresses, this golden ring is replaced with peripapillary mottling, hyperpigmentation, and atrophy of the RPE (Fig.42.15C). The optic nerve head cup-to-disc ratio has been reported to be significantly smaller in RP patients of all types (0.19 compared to 0.35 in normal subjects).[59] In advanced disease, dense optic nerve head pallor results, in part from optic atrophy and in part from gliosis overlying the discs.[30] Drusen-like globular excrescences may develop on the optic nerve or adjacent retina (Fig. 42.16). These have been mistaken for astrocytic hamartomas[60] and are consistent with disc drusen due to aberrant axoplasmic transport.[61,62] In a survey of 117 RP patients,[63] 10% were found to have clinically apparent optic nerve head drusen. Edwards et al.[64] suggested that this phenomenon is particularly common in RP associated with Usher syndrome type 1.

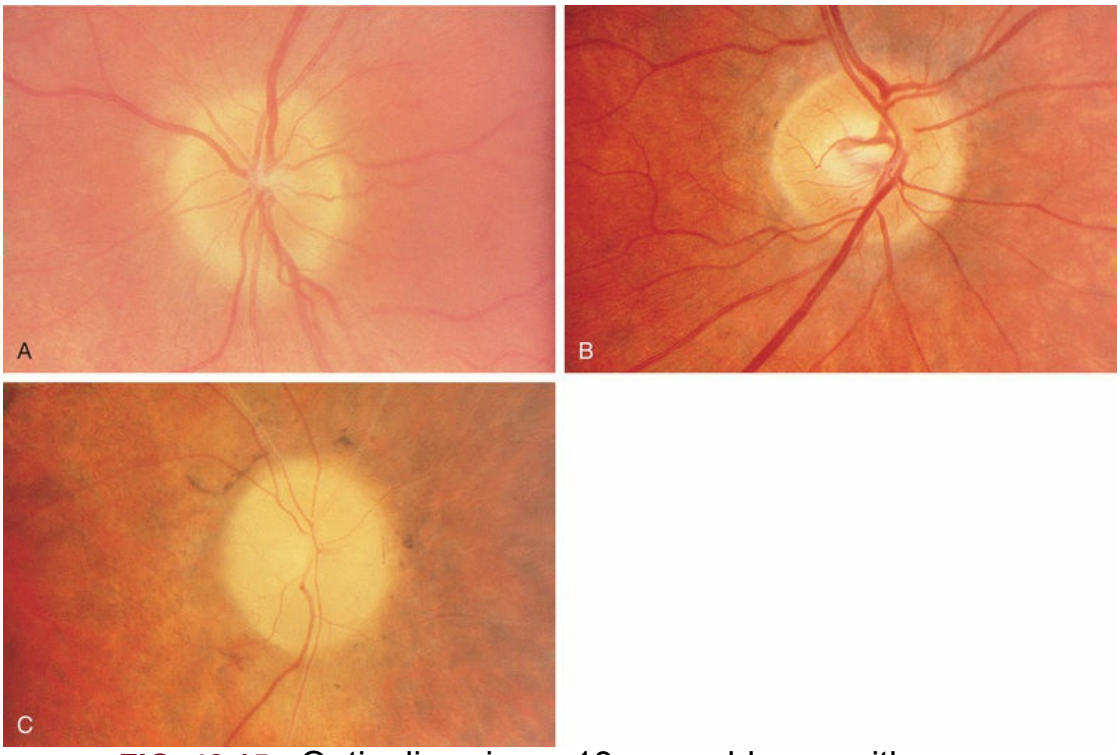

FIG. 42.15 Optic discs in an 18-year-old man with autosomal recessive retinitis pigmentosa as part of posterior column ataxia and retinitis pigmentosa syndrome (PCARP) (A) (same patient as in Fig. 42.3), a 32-year-old man (B), and his 55-year-old father (C), both of whom have autosomal dominant retinitis pigmentosa. The disc in (A) shows peripapillary chorioretinal pallor, or the "golden ring" sign, that is characteristic of early retinitis pigmentosa. Note that the disc is nearly normal in the son (B) but shows severe waxy pallor in the father (C).

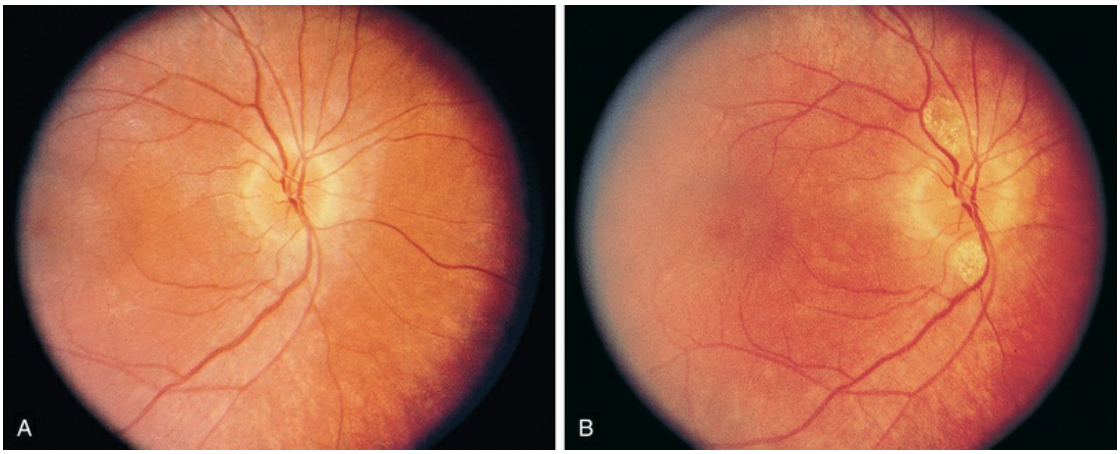

FIG. 42.16 Optic discs in the right eye of a patient with

type 1 Usher syndrome (retinitis pigmentosa and prelingual deafness) at age 16 (A) and 25 (B), demonstrating development of peripapillary drusen.

Flynn et al.[65] found that the presence or absence of macular RPE defects is of significant prognostic importance with regard to retention of visual acuity over the next 5 years. Specifically, the absence of macular lesion was associated with only one line of acuity loss over the 5-year period, whereas bull's-eye or geographic atrophy lesions were associated with a predicted acuity loss of 3 to 4 lines. The authors emphasize the importance of this type of information for prognostic counseling of patients with RP regarding the likelihood of preservation of visual acuity. Other maculopathies associated with RP include cellophane maculopathy, macular hole (complications of CME),[66] and a single report of RP with central serous retinopathy.[67]

Vitreous Abnormalities

The most common abnormality of the vitreous in RP is the presence of fine, dust-like pigmented cells released from degeneration of the RPE. In patients with RP, complete posterior detachment of the vitreous, “cotton-ball” opacities, interwoven filaments in the retrocortical space, and spindle-shaped vitreous condensations are seen more frequently than in normal subjects.[68,69] A single case is reported of vitreous opacity so dense that vitrectomy was required.[70] Vitreous abnormalities related to peripheral retinal ischemia and preretinal neovascularization have been reported in rare cases of adRP and arRP.[71] Uncommonly, a peripheral Coats-like retinal vasculopathy with lipid exudations and serous retinal elevation can be seen in RP.[72–74] Unlike idiopathic Coats syndrome, the retinal vasculopathy seen in RP is usually bilateral, shows no sex predilection, and typically occurs in older patients. Coats-like disease is seen in 3.6% of RP cases[75] and has been reported with adRP,[73,74] arRP,[40] and XLRP[76] (see Fig. 42.17). Coats-like changes that occur in children[75,77] may change over a relatively short period of months to years, must be monitored carefully, and may need to be considered for laser or cryocoagulation. Vitreous hemorrhage related to preretinal neovascularization has also been described in

rare cases.[71,78] Retinal edema in some cases may be caused by inflammation resulting from the degeneration of the outer retina.[71,79]

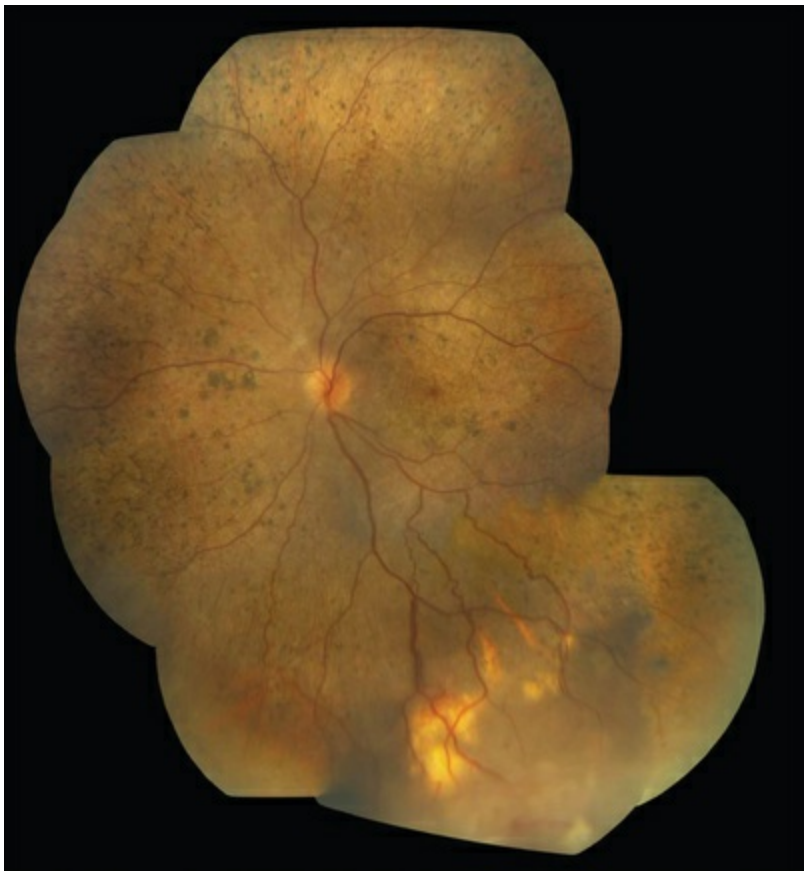

FIG. 42.17 Fundus photos from a 24-year-old female with LCA/SECORD due to heterozygous *CRB1* mutations demonstrating severe and generalized pigmentary changes throughout the macula and periphery as well as inferior exudate and a serous retinal detachment due to the Coats-like response. The patient received laser photocoagulation leading to resolution of the subretinal fluid.

Anterior Segment Abnormalities

Cataracts are frequent anterior segment complications of RP. The prevalence of cataracts in RP patients aged 20–39 years varied with the inheritance type, being roughly 52% for autosomal dominant, 39% for recessive, and 72% for X-linked cases.[80] The incidence of cataracts in RP is highly age-dependent.[80,81] The most frequent type of cataract is a posterior subcapsular lens opacity, which occurs in

35% to 51% of patients.[81,82] One study has suggested that posterior subcapsular opacities are most commonly associated with autosomal dominant inheritance (51%),[81,82] whereas another has suggested a more common association with X-linked inheritance.[83] Although keratoconus has been claimed to be more frequent among patients with RP,[84] the occurrence of keratoconus in typical juvenile- or adult-onset RP is extremely rare in our experience. Glaucoma, especially primary open angle glaucoma, is also allegedly more frequent in RP.[85] Sector RP appears to be associated with hyperopia and angle closure glaucoma.[86] Because of the other abnormalities of the disc and fundus, and because of the already abnormal visual fields, the diagnosis and management of glaucoma are quite challenging in RP patients.

Refractive Status

High myopia and astigmatism are frequently associated with RP.[80,87]

Psychophysical Findings

Perimetry.

Assessment of visual field is an important aspect of the management of RP. This is an invaluable tool in the diagnosis of RP, as well as being the most reliable method of quantifying real change in visual deficit. It should be remembered when assessing the results of visual field testing that the reproducibility of visual fields is significantly less in patients with RP than in normal subjects. Kinetic visual fields tested on separate days by the same examiner varied by 5–6% in normal subjects but by 11–13% in patients with RP (intraobserver variation); variability between examiners for the same patient was 4–6% for normal subjects but was 10–16% for patients with RP (interobserver variation).[88]

In the great majority of cases of RP, the earliest defects of the visual field, on kinetic perimetry, are relative scotomas in the mid-periphery, between 30 and 50° from fixation (Fig. 42.18). These enlarge, deepen, and coalesce to form a ring of visual field loss (Fig. 42.19). These midperipheral depressions of retinal sensitivity are readily documented as decreased retinal thresholds on static

perimetry. As ring scotomas enlarge toward the far periphery, islands of relatively normal visual field remain, usually temporal (Fig. 42.20) but occasionally inferior or nasal (see Fig. 42.3). The peripheral islands remnants of visual field are often lost before the central field contracts sufficiently to qualify the individual as legally blind.

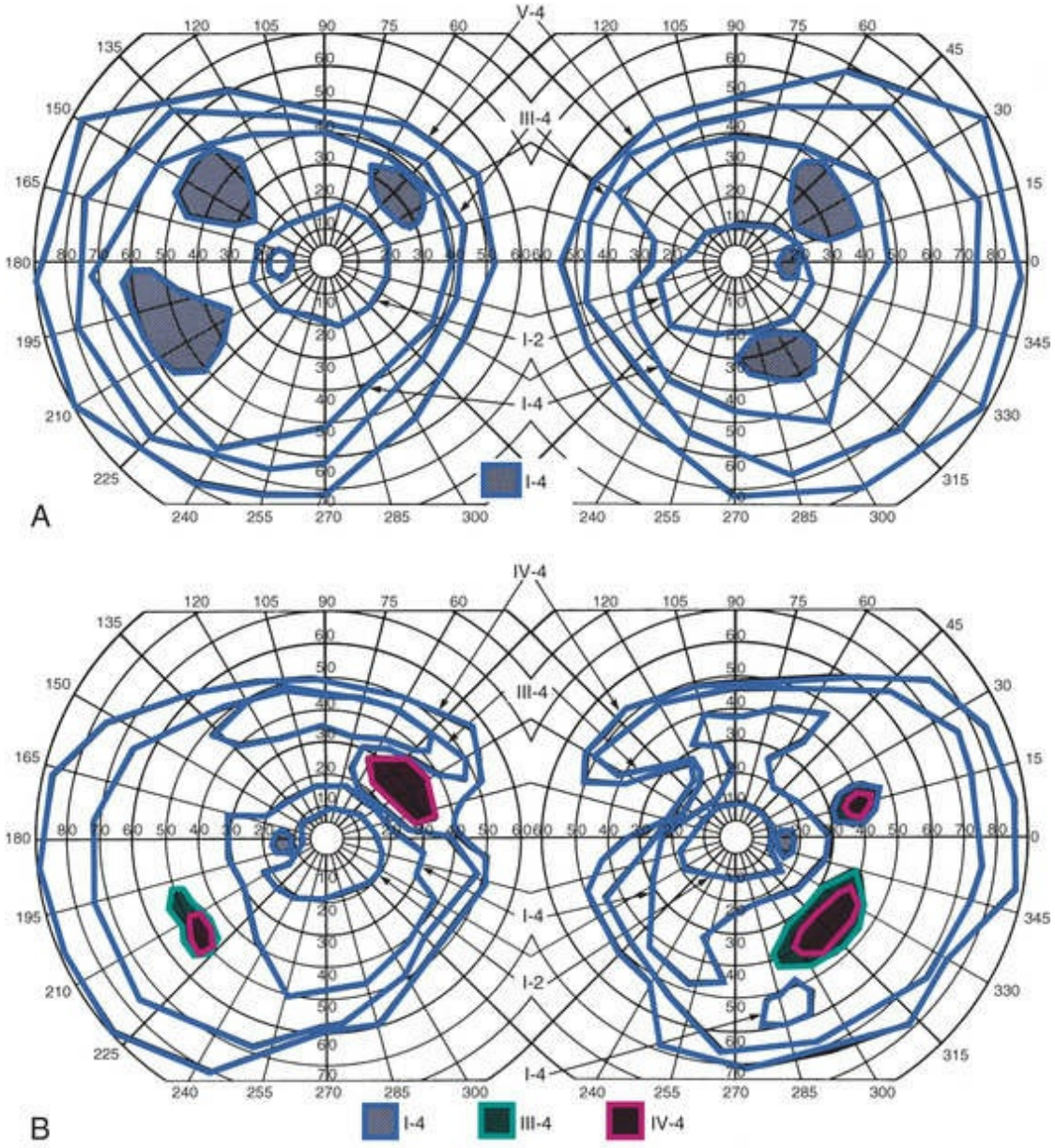

FIG. 42.18 Goldman kinetic perimeter for a patient with autosomal dominant retinitis pigmentosa from the Pro23His mutation at age 41 (A) and 47 years (B).

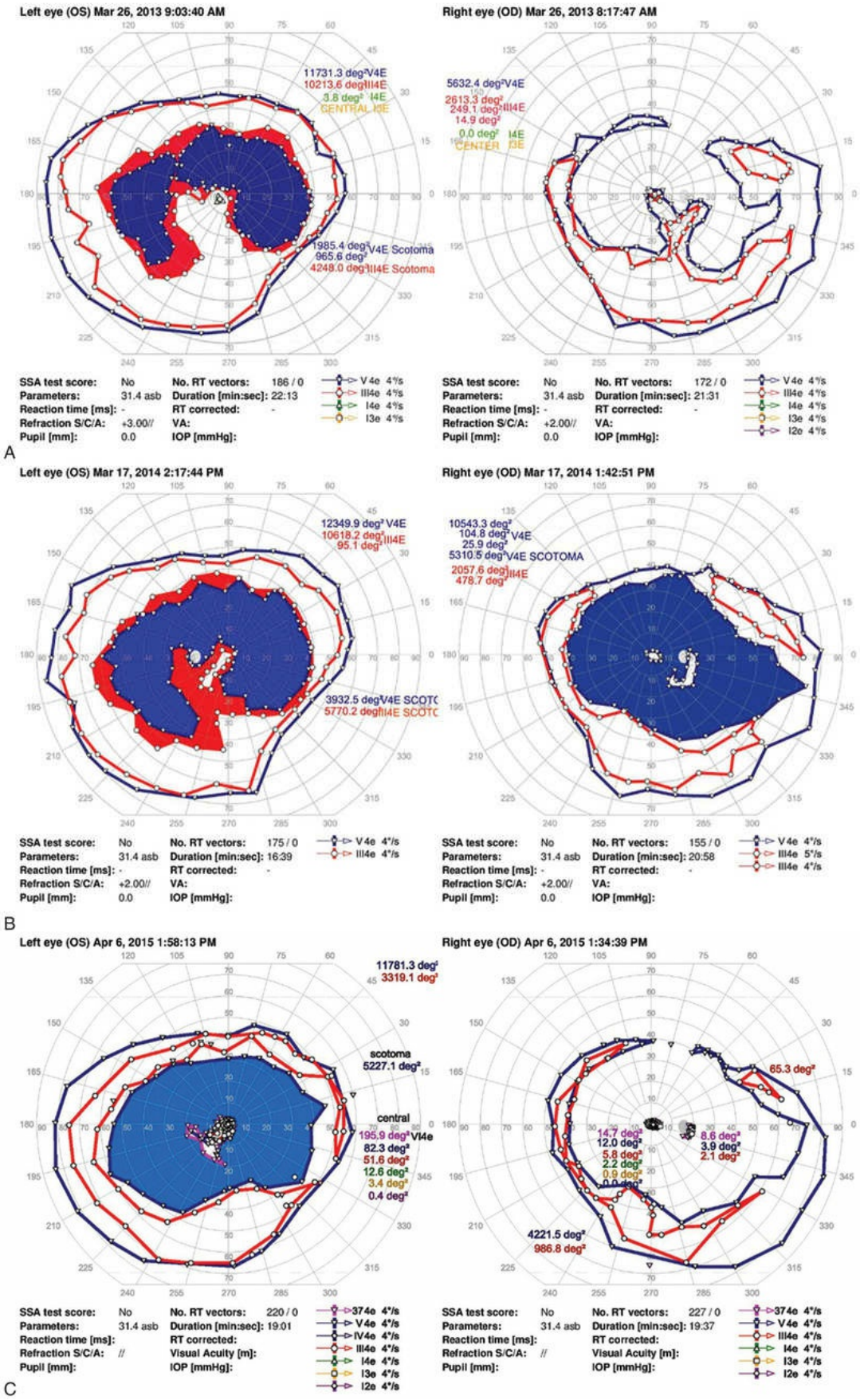

FIG. 42.19 Goldmann kinetic perimetry for a patient with simplex RP at 43 years (A), 44 years (B), and 45

years (C). Note enlargement and deepening of midperipheral scotomas.

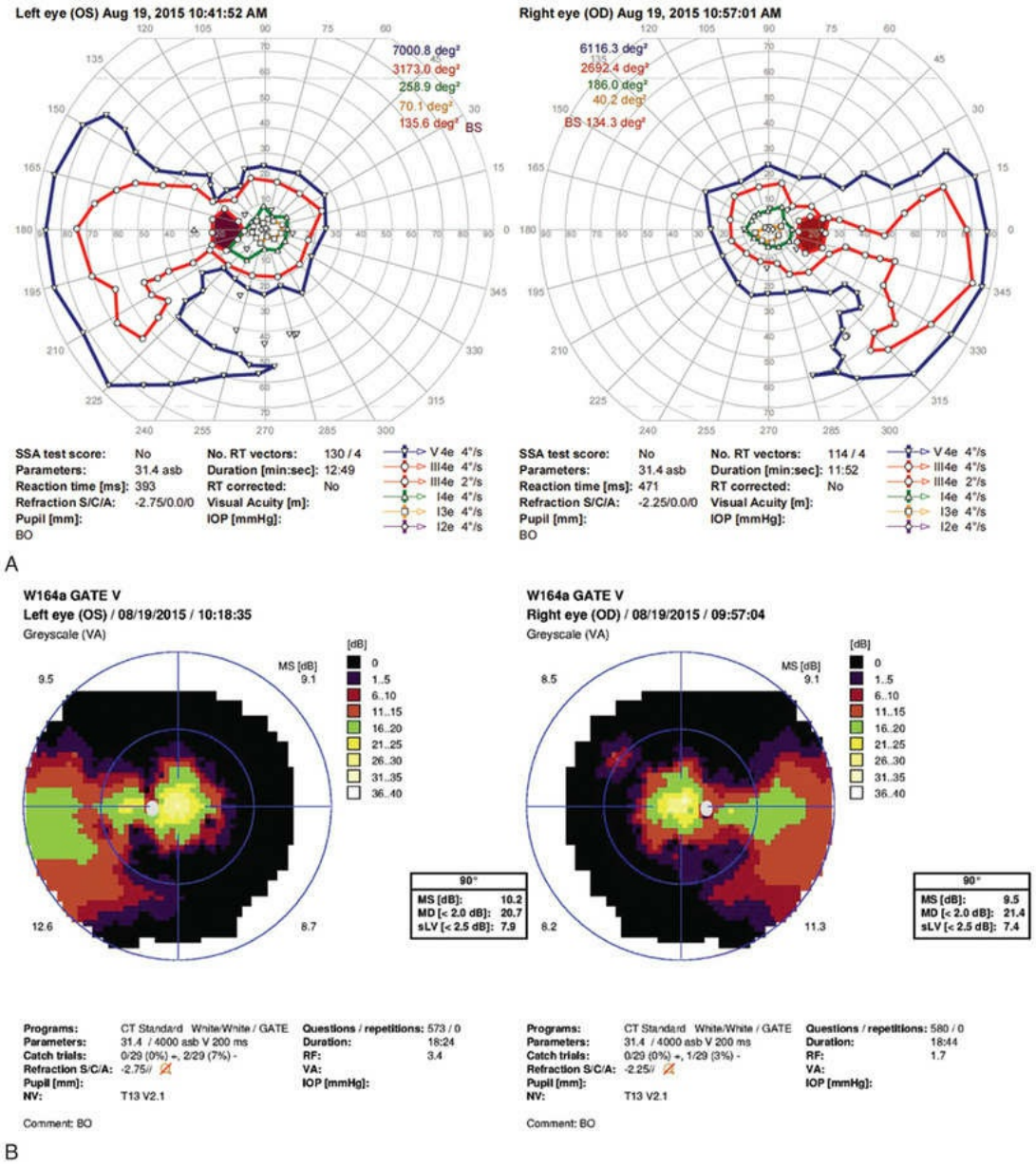

FIG. 42.20 Visual fields for a 43-year-old patient with simplex retinitis pigmentosa demonstrating relative temporal sparing of the kinetic (A) and static (B) visual fields.

Kinetic visual field testing has traditionally been performed with the manual Goldmann perimeter. Recent advances have occurred in both kinetic and static perimetry. Kinetic perimetry[89] as

implemented on the Octopus 101 and 900 perimeters (Haag-Streit, Köniz, Switzerland) (Fig. 42.21) automatically documents the testing and enables quantification of field by measurement of isopter area. A new fast thresholding algorithm known at German Adaptive Thresholding Estimation (GATE)[90] has enabled another advance in perimetry, that of full-field static perimetry to assess the entire visual field in a timeframe comparable to that required to test the central 30° field with the Standard 4-2-1 strategy (Fig. 42.21).[91] The static threshold data from such testing can be modeled as sensitivity values into a three-dimensional Hill of Vision from which the magnitude and extent of the total visual field can be determined as a volumetric measurement.[91]

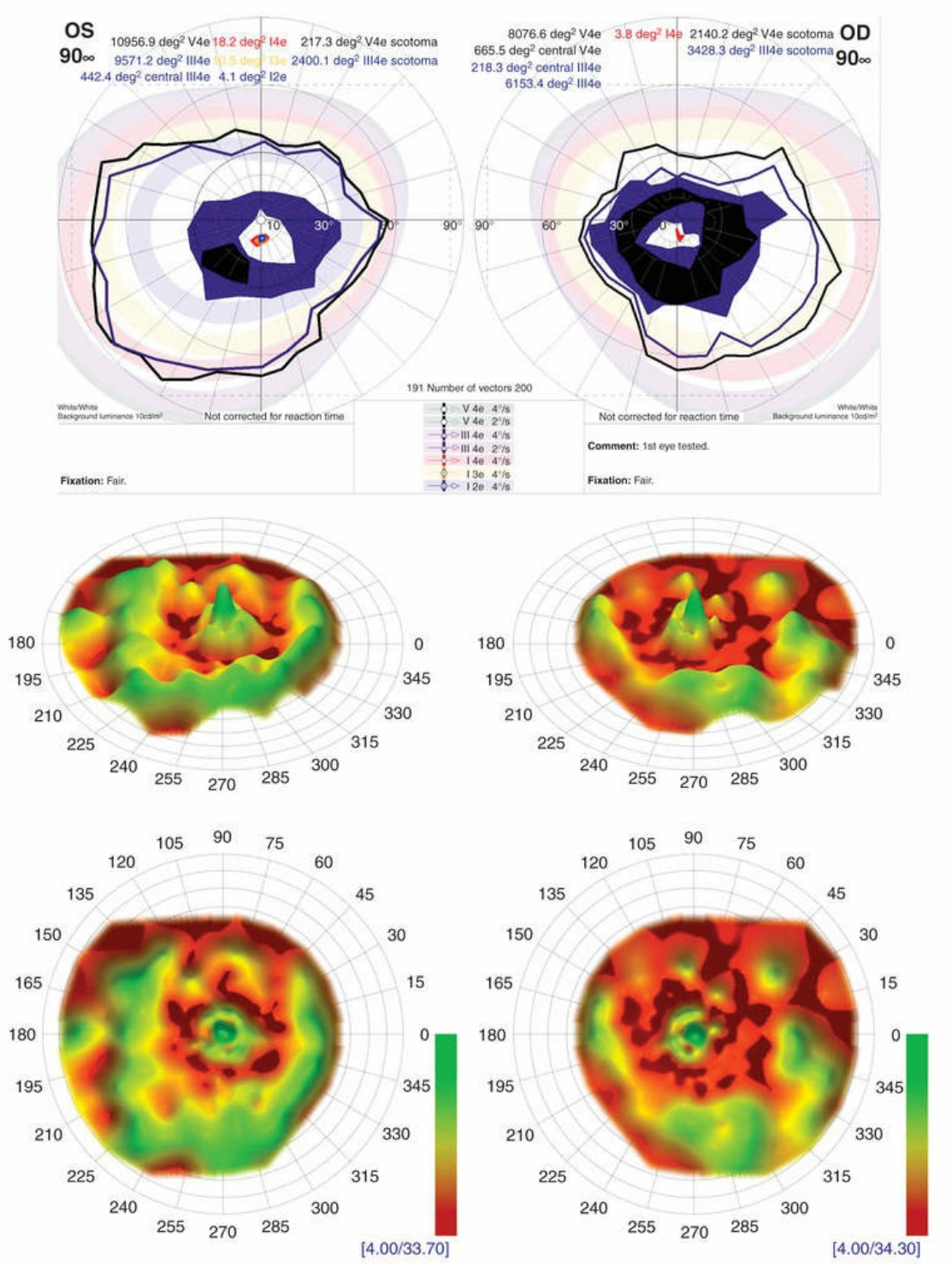

FIG. 42.21 Octopus kinetic perimetry in a 27-year-old woman with retinitis pigmentosa (top). The shaded areas depict the normal range for the isopters for the test targets presented. Three-dimensional model of the Hill of Vision for full-field static perimetry for this same subject (middle in tilted view, below en face view) using the size V test target and the GATE thresholding

algorithm.[90] The volume of this model, which was 40.2 dB-sr OD and 28.0 DB-sr OS (compared to a normal 112.5 dB-sr for a normal), reflects the magnitude and extent of the visual field for this subject. Thus, this patient has 35.7% OD and 24.9% OS of expected field volume for his age. Note that the 3D model provides much more topographical information on the location of the defects in the field of vision than does the kinetic perimetry. This is the same patient whose fundus autofluorescence image for the left eye is shown in Fig. 42.30A.

If an RP patient is driving a motor vehicle, regular visual field assessments are mandatory and should be undertaken at least every 2 years. Most centers perform kinetic visual fields using a Goldmann perimeter for clinical evaluation and for assessment for driving and for disability. Almost all patients with RP have to restrict their driving at night and eventually stop driving altogether. Periodic assessment of full-field kinetic perimetry helps to provide the patient with knowledge of his or her visual limitations and when to restrict and eventually stop driving.

Two-color static perimetry has been shown to be a useful tool in assessing the dark-adapted visual fields of patients with RP. Using this technique, Massof and Finkelstein[92–94] found that their patients with RP could be divided into two groups: (1) type I RP, which is associated with early diffuse loss of rod sensitivity relative to cone sensitivity and childhood-onset nyctalopia; and (2) type II RP, associated with regional and combined loss of both rod and cone retinal sensitivity and adult-onset nyctalopia. No patients have been observed to change from one type to the other.[95] No families have been reported that contain both types I and II in the same sibship.[24] An excess of type II RP over the type I form has been reported in simplex disease. Analysis of subgroups within simplex and multiplex RP suggest that a sizable proportion of type II patients may represent sporadic or acquired disease, and not true RP.[96]

Arden et al.[97] studied a series of cases of adRP both with ERGs and psychophysically with scotopic static thresholds. They found that the preservation of sizable rod responses on the ERG correlated perfectly with the Massof type II classification. Absence of rod ERG

did not always indicate type I disease, and both types were seen in this group. Lyness et al.[98] reported clinical, psychophysical, and ERG findings in 104 patients (from 44 families) with adRP. Subgroup D (13 patients in four families) had diffuse loss of rod function and night blindness before the age of 10. Subgroup R (28 patients in 13 families) had regional loss of rod function, and most of these patients were unaware of night blindness until after the age of 20. Both groups had regional loss of cone functions. In the R group the rod-mediated ERG was usually present and substantial, whereas in the D group the rod ERG was nondetectable. Although not identical, the D group bears similarities to Massof type I, and the R group bears similarities to type II. These studies suggest that the two types or groups may represent different pathophysiologic subtypes of RP. It should be emphasized, however, that a large proportion of patients (27 of the 44 families studied by Lyness et al.[98]) could not be incorporated into the D versus R type classification, partly because many patients with RP have almost undetectable electroretinographic responses at presentation.

The techniques of two-color scotopic static perimetry have been further developed to evaluate rod and cone retinal sensitivities in different regions of the retina.[99,100] Such testing allows the definition of which class of photoreceptor (rod or cone) is the determinant of retinal threshold in a particular region or area of the retina. This has allowed the characterization of the relative losses of rods and cones in various types of RP associated with specific mutations.[101,102] Equally important to the definition of early retinal abnormalities in retinal degenerations, two-color perimetry can be used for monitoring disease therapy or for testing hypothesis of disease pathophysiology. For example, the abnormal, thickened Bruch's membrane, which acts as a diffusion barrier between the retina and choroid, has been proposed as a major factor leading to night blindness in Sorsby fundus dystrophy.[103] The return of rod function after oral vitamin A supplements (50,000 IU/day) was elegantly demonstrated using these techniques.[103]

Dark Adaptometry.

Normal subjects, when placed in the dark after exposure to a strong adapting light, will rapidly reduce their retinal psychophysical

threshold using their cone system, reaching a plateau in about 5 minutes. Thereafter rod adaptation slowly increases, and rods determine retinal thresholds for another 3 log units of sensitivity before a second plateau occurs at about 30 minutes of dark adaptation. Patients with RP, when tested with dark adaptometry, may show elevation of the cone segment, the rod segment, or both, to varying degrees (Fig. 42.22) Also, in some patients there may be a delay in reaching what eventually for them is a relatively good final dark adaptation rod threshold[104] (Fig. 42.23A).

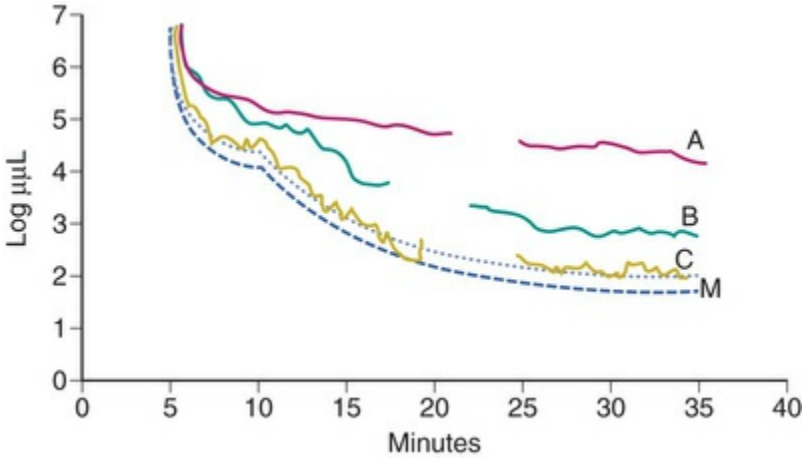

FIG. 42.22 Dark adaptometry showing marked elevation of both cone and rod thresholds with little or no cone–rod break in an 18-year-old woman *(broken solid curve A)*, with autosomal recessive retinitis pigmentosa and large-fiber sensory peripheral neuropathy (sister of patient shown in Figs. 42.3 and 42.17A). Mild elevation of cone threshold with greater elevation of rod threshold in a 15-year-old girl with Bardet–Biedl syndrome *(broken solid curve B)*. Borderline normal cone and rod segments in a 15-year-old girl with type 2 Usher syndrome *(broken solid curve C)*. Mean *(dashed curve M)* is shown for normals aged 10–20 years. *OD*, right eye. µµL = micromicrolambert.

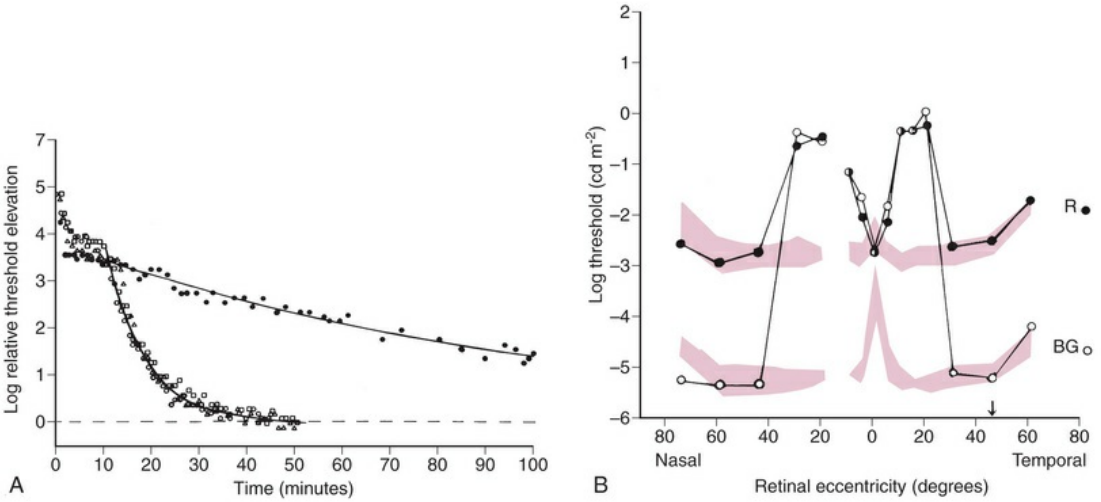

FIG. 42.23 (A) Delayed achievement of final dark-adaptation threshold in a patient with autosomal dominant retinitis pigmentosa. Filled circles are data from the patient; open triangles, circles, and squares are from three normals. The time constant for reduction of the rod retinal threshold by a factor of 1/2.718 of the threshold at the beginning of the curve was 8.5 min for the normal data and 101.6 min for the patient. Measurements were taken from a point approximately 45° temporal to the fovea. (B) Retinal thresholds measured at different points of retinal eccentricity for the same patient as in (A), showing zones of elevated thresholds in nasal and temporal midperiphery with lower thresholds centrally and more peripherally. The shaded regions represent the range of absolute thresholds for the long- (*R*) and middle-wavelength (*BG*) test flashes for 5 normal subjects. (The point used for A is noted with an arrow in B.)

(Reproduced from Alexander KR, Fishman GA. Prolonged rod dark adaptation in retinitis pigmentosa. Br J Ophthalmol 1984; 68:561–569.)

Time course analysis of dark adaptometry has been performed in patients with adRP, and prolonged dark adaptation is associated with rhodopsin mutations Thr17Met, Pro23His, Gly106Arg, and Thr58A.[101,102,105] The most characteristic feature of the Pro23His genotype was prolonged dark adaptation, which was present in all patients regardless of their stage of disease.[102] Jacobson et al.[101] also reported prolonged rod dark adaptation in patients with Thr58Arg and Thr17Met mutations of rhodopsin. Indeed, prolonged rod dark adaptation appears to be a characteristic finding of virtually all

rhodopsin mutations. These studies suggest that each of these mutations produces specific abnormalities in the rate of reactions within the rods that limit the recovery of scotopic sensitivity. For patients with regional forms of RP from other causes, zones of more normally functioning retina may allow reasonably good final rod thresholds (Fig. 42.23B). Minor abnormalities in cone thresholds are more likely to result in complaints of poor dark adaptation than mild to moderate elevation of rod thresholds. One study has indicated that abnormalities in the normal interactions between rods and cones may underlie the symptoms of poor night vision in some patients rather than isolated rod deficits.[106]

Electrophysiology.

Karpe[107] in 1945 first reported that the ERG was "extinguished" in RP. The standing, or resting, potential of the eye was first described by DuBois-Reymond in 1849. Riggs[108] in 1954 was the first to report that the resting potential was decreased in pigmentary degeneration of the eye. Arden et al.[109] in 1962 developed the currently widely used technique for measurement of the light-induced rise of the resting potential of the eye (the EOG), which is considered a function of the RPE. Fast oscillations of the resting potential can be recorded, and these offer another measure of RPE function.[110] Gouras[111] in 1970 based clinical ERG on the use of Ganzfeld stimulation. Standardized conditions and assessment protocols have now been established for electrodiagnostic investigations.[112]

Electrodiagnostic responses in an RP patient can range from normal to undetectable. In general, more sizable responses are seen with younger patients or at earlier stages of disease. Most patients with advanced RP have undetectable responses (typically less than 10 μV) to single-flash, nonaveraged techniques.[111] Computer averaging, however, can usually detect small ERG responses in even moderately advanced stages.[113,114] In studying the natural course of RP, Berson et al.[113] found that patients lost an average of 16% to 18.5% per year of remaining ERG amplitude to bright white flashes (a mixed rod–cone response).

Many studies have compared ERG responses in the different RP inheritance types. Tanino and Ohba[115] and Berson,[116] using

conventional techniques, found that the ERG is more likely to be recordable in older patients with adRP than arRP. Berson et al.[113] have also shown that progressive ERG loss of amplitude over a 3-year period is least in adRP. Birch and Fish[117] found that the rate of progression of rod loss, as indicated by the half-saturation coefficient of the rod stimulus–response curve, varied among the inheritance groups. This ranged from 0.3 log unit/year in elevation of rod threshold in X-linked RP to 0.12 log unit/year elevation in adRP.

Agreement exists that the cone-mediated implicit times can be significantly prolonged in various forms of RP. Berson[118] has also stressed the importance of delays in the implicit time for cone-mediated 30-Hz flicker responses. Berson and colleagues[119,120] found that the cone-mediated b-wave implicit time in their patients was characteristically prolonged in adRP with reduced penetrance but not in completely penetrant adRP. Sandberg et al.[121] suggested that this was due to an abnormal contribution of extrafoveal cones in adRP with incomplete penetrance. This may be due to abnormal cone light adaptation or a disturbance of normal rod–cone interactions.

Histopathologic study has indicated that in RP a postreceptor deficit may contribute to macular dysfunction.[122] Electroretinographic study has confirmed this. Falsini et al.[123] have assessed 8–10 Hz focal ERGs in 22 simplex and recessive RP cases. They found a loss of fundamental and second harmonic components and an increase in the fundamental–second harmonic ratio. This was interpreted as suggesting that both inner and outer retinal abnormalities contribute to visual deficit. Cideciyan and Jacobson[124] have documented electronegative b-waves in some cases of RP. This finding was seen with abnormalities of on/off components of cone ERGs and reduced oscillatory potentials[124] and was interpreted as indicative of significant inner retinal abnormalities in these RP cases.

Models of analysis of the ERG have been developed that attempt to isolate from the ERG the photoreceptor and bipolar contributions, specifically the original components of Granit's model of the cat ERG, termed P3 and P2[125] (Fig. 42.24A). These analysis methods have been developed to quantify the visual deficit

attributable to outer and inner retinal disease (Figs. 42.24B–D). P3 is the corneal-negative response of photoreceptor outer segments that contributes to the a-wave of the Ganzfeld ERG. The analysis involves subjecting the leading edge of the a-wave of the ERG at a range of intensities to a mathematical curve-fitting algorithm[126–128] (Fig. 42.24C) using equations that describe the kinetics of rod phototransduction activation.[129] The method of Hood and Birch[130] allows for estimation of two variables: *S*, which is a sensitivity factor, and R_{mp3}, which is the maximum amplitude. Such analysis can determine whether phototransduction is affected in a given disease.

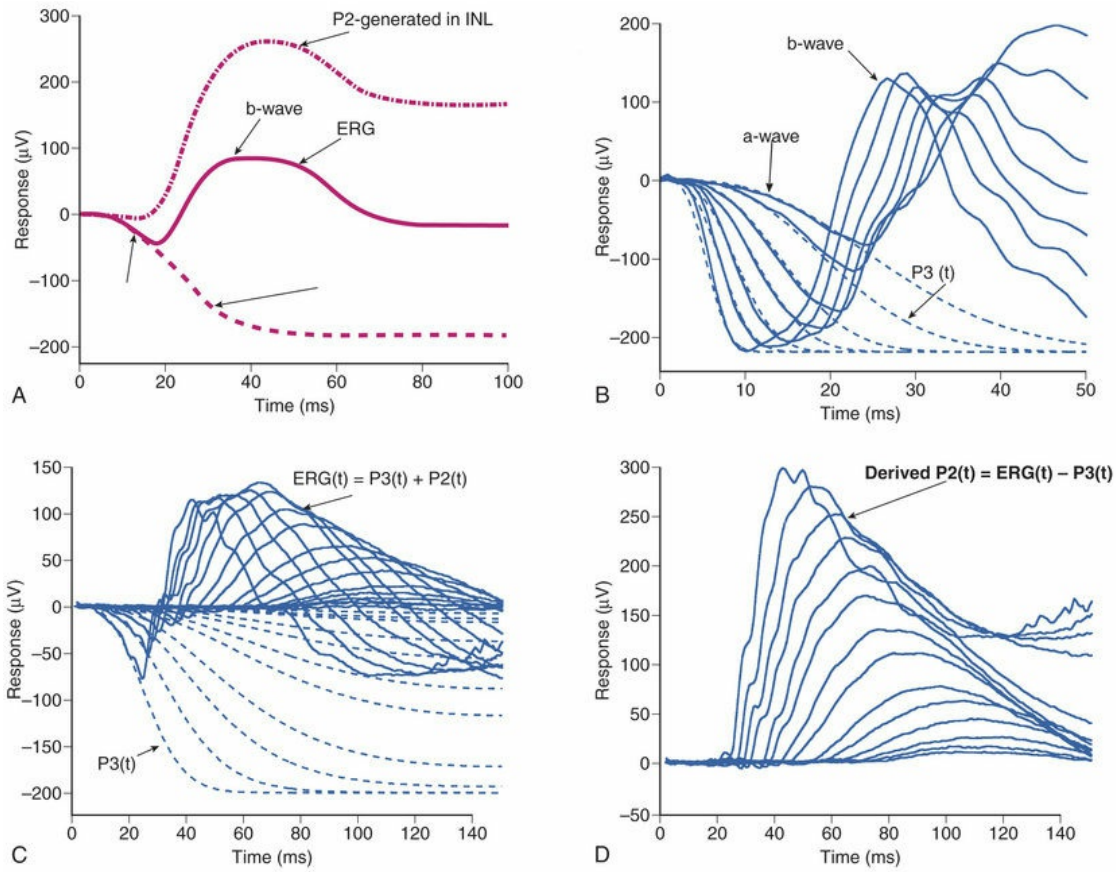

FIG. 42.24 (A) Simplified illustration of the retinal elements of the rod electroretinogram (ERG) based on Granit's model of the cat ERG. The b-wave of the corneal ERG *(solid line)* is the summation of a negative P3 generated by photoreceptors and a positive P2 generated in the inner layers of the retina. (B) Solid curves are the scotopic ERG responses elicited by a high-intensity series of flashes from a normal subject. *Dashed curves* are the predicted P3 responses from a

model of the receptor response fitted to the leading edge of the a-wave. (C) *Solid curves* are records from a normal subject to a series of brief flashes, up to about 2 log scotoma td-s in energy, with the underlying P3 (rod receptor) responses shown as dashed curves. (D) Derived P2 responses obtained by computer subtraction of the P3 responses from the ERGs. *INL*, inner nuclear layer. (Modified from Hood DC, Birch DG. A computational model of the amplitude and implicit time of the b-wave of the human ERG. Vis Neurosci 1992;8:107–126.)

P2 is the bipolar cell-derived component of the rod-isolated b-wave. The P2 component of the rod b-wave, derived from bipolar cells, can be isolated from the full-frequency ERG, using an algorithm whereby the P3 is first calculated for a given series of intensities, after which the P3 is subtracted from the series of rod responses[131,132] (Fig. 42.24D). This gives a much better estimate of the on-bipolar contribution to the b-wave, especially for patients in whom the on-bipolar cells are more affected than the photoreceptors.[131]

Application of these techniques to 15 patients with RP has shown that, for P3 analysis, all patients had significantly reduced values of R_{mp3}, indicating effective loss or damage of rods, and a wide spectrum of values for S.[133] Three patients had normal values for S. Four RP patients had subnormal S values but normal local retinal psychophysical thresholds in some regions of their retina. The rest had abnormal S values and abnormal visual fields with globally reduced thresholds. The rod b-wave amplitudes to a range of intensities for these RP patients were fitted with the Michaelis–Menten equation, generating the parameters K_{bw} (the semisaturation intensity, which is a sensitivity function) and V_{max} (the maximum amplitude). For all patients, the changes in K_{bw} and V_{max} followed the changes seen in S and R_{mp3}.[133] Hood and Birch[130] studied rod phototransduction in 11 patients with RP and four with cone–rod dystrophy (CRD). Their findings, which were similar to those above, supported the conclusion that the activation stage of rod phototransduction is affected in some forms of RP and CRD but not all.

Supernormal and delayed P2 responses were found by Hood et

al.[134] when they applied modeling analysis to an unusual retinal dystrophy, first reported by Gouras et al.[135] in 1983 as "cone dystrophy, nyctalopia, and supernormal rod responses." Although Gouras et al.[135] initially attributed this dystrophy to an abnormality in receptor cyclic guanosine monophosphate (cGMP) activity, P3 and P2 modeling by Hood et al.[134] showed that the delays in the rod and cone b-wave were not caused by the speed or amplification of phototransduction but resulted from delays beyond the outer segments involving a delay in activation of the inner nuclear layer activity. This disorder was subsequently clinically and electrophysiologically defined as the Enhanced S-Cone Syndrome (ESCS)[136,137] and was later shown to result from mutation of the gene *NR2E3*.[138]

Paradigms have been developed to study the kinetics of rod transduction deactivation.[139] This technique uses a bright conditioning flash followed by a probe flash. The recovery of the amplitude of the response to the probe, which is presented at varying intervals after the conditioning flash, provides a measure of the return to baseline of the response to the conditioning flash and, hence, the kinetics of transduction deactivation. The authors conclude that the lifetime of activated rhodopsin in normal human rods is 2.3 seconds. This technique has been applied to humans with the Pro23His rhodopsin mutation, demonstrating a reduction of the gain of activation and marked slowing of deactivation of rhodopsin (by a factor of at least 5).[139] Animal models of RP, for example, transgenic mice expressing the mutant Pro23His rhodopsin gene, have also demonstrated increases in the half-maximal recovery period, $T_{50\%}$, indicating abnormally prolonged recovery from the conditioning flash.[140]

Analysis of the a-wave leading edge has also shown that in RP, the efficiency of cone phototransduction is affected very early, even in some patients in whom the sensitivity of rod phototransduction is normal. X-linked inheritance seemed to be associated with greater phototransduction abnormalities in cones and rods at an age younger than seen in other modes of inheritance.[141]

Multifocal ERG techniques have been developed whereby, through patterned stimulation of the retina cross-correlated with recording of the ERG responses from a corneal electrode, very small

ERG responses can be obtained from precisely localized regions of the retina [142–144] (Fig. 42.25). Multifocal ERGs can be seen in advanced RP where the 30-Hz flicker response is barely detectable[145] (Fig. 42.26). Hood et al.[144] have shown that, in RP, amplitudes of ERG responses do not correspond as well as b-wave implicit times with the retinal sensitivity as measured by static perimetry (Fig. 42.27). This is most evident with the regional or sectorial types of RP. Thus the b-wave implicit time appears to reflect early involvement of the disease process in regions of the retina that still have relatively good retinal sensitivity. Robson et al.[146] compared pattern ERG changes in RP patients with abnormalities of fundus autofluorescence. In such patients, pattern ERG responses suggested that visual loss was attributable to dysfunction rather than cell death.

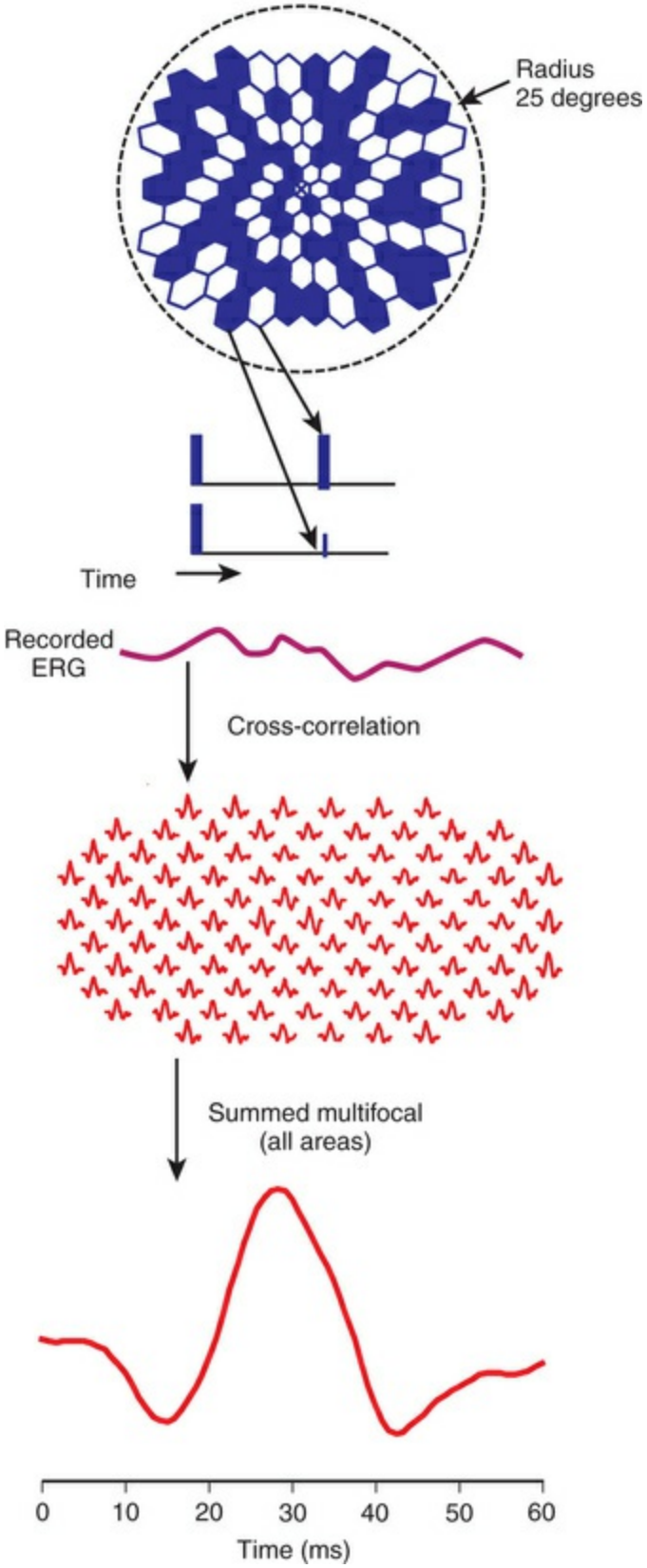

FIG. 42.25 Schematic of multifocal paradigm. The stimulus consists of a pattern of 103 hexagons contained within a 50°-diameter area. The subject fixates on the center of the pattern, while the hexagons

undergo changes from black to white and from white to black according to a mathematical sequence that allows the stimulation of various local areas of the retina to be cross-correlated with the electroretinogram (ERG) continuously recorded from the cornea. Within a few minutes (typically 4–8 min) one can record tiny submicrovolt ERGs corresponding to the changing pattern of each hexagon of the stimulus pattern. (Modified from Hood DC, Seiple W, Holopigian K et al. A comparison of the components of the multifocal and full-field ERGs. Vis Neurosci 1997;14:533–544.)

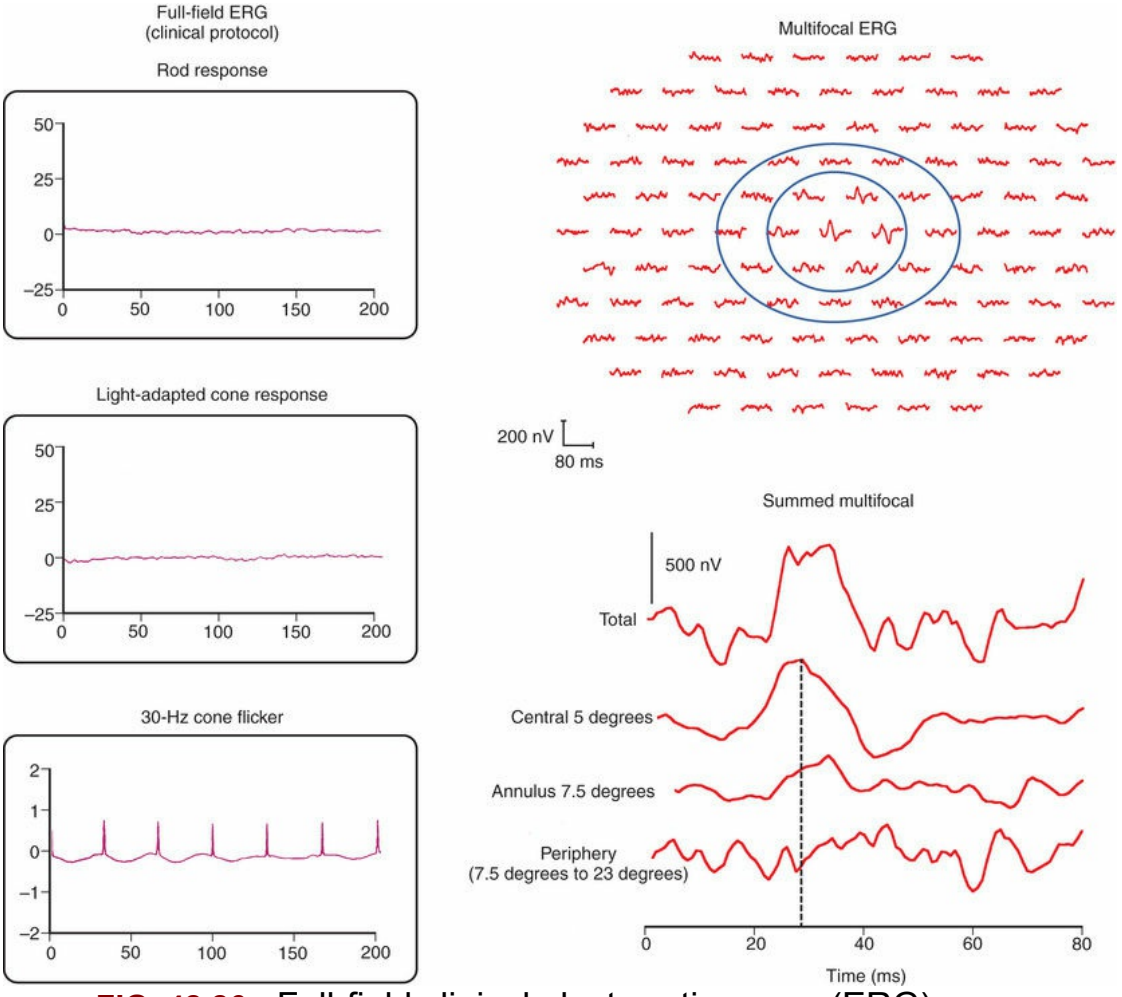

FIG. 42.26 Full-field clinical electroretinogram (ERG) protocol (left) and multifocal ERG (right) from a patient with retinitis pigmentosa. The full-field ERG showed no discernible rod or light-adapted cone response to single flash and a barely detectable 0.2-μV response to 30-Hz flicker response. However, sizable ERGs were detected within the central fields using the multifocal

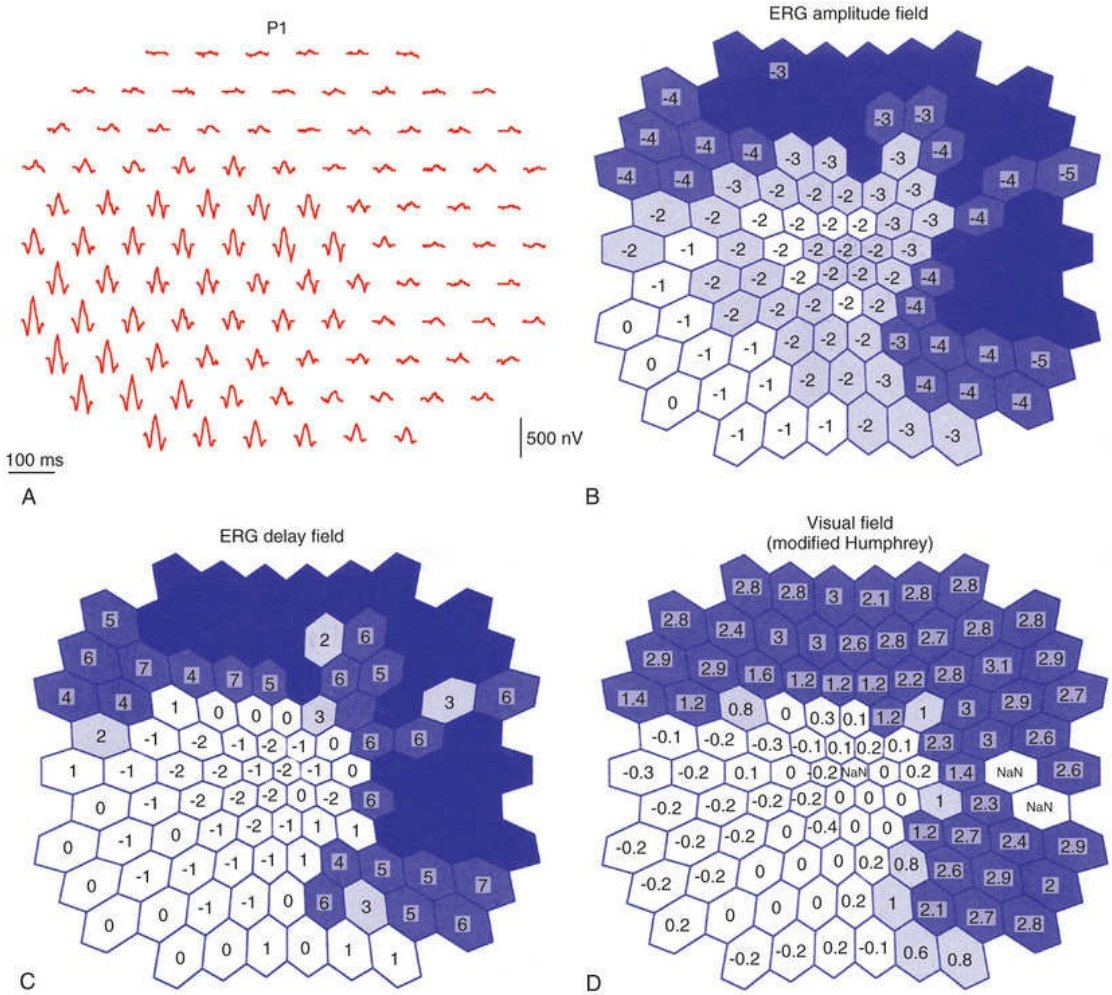

FIG. 42.27 (A) Multifocal electroretinograms (ERGs) from the right eye of a patient (P1) with autosomal recessive retinitis pigmentosa. The amplitude of the responses was decreased throughout the retina. However, this subject's disease was regional in distribution with marked preservation of function centrally and inferotemporally. (B) ERG amplitude loss field (in SD from normal) for the same subject calculated by subtracting the mean trough-to-peak amplitude for the controls from the trough-to-peak amplitude for the patient's response at each location. These differences were rounded and expressed in units of 100 nV. The clear regions indicate a decrease in amplitude of less than 162 nV (<−2 SD); the light-gray regions signify a decrease between 162 and 324

nV (−2 to −4 SD); and the darkest gray regions signify a decrease greater than 324 nV (>−4 SD). Black hexagons indicate that the response amplitude did not meet the criterion value of 90 nV. (C) ERG delay field for same subject, showing that regions that had subnormal amplitudes could be either normal or delayed in implicit time. The numbers in the hexagons were calculated by subtracting the mean implicit time for the controls from the implicit time for the patient's response at each location. The numbers in these fields are rounded to the nearest millisecond for presentation. The black hexagons indicate that the response amplitude did not meet the criterion value of 90 nV. The clear regions signify that the delay was less than 1.7 ms (<+2 SD); the light-gray regions signify that the delay was between 1.7 and 3.4 ms (+2 to +4 SD); and the darkest gray regions signify that the delay was greater than 3.4 ms (>+4 SD). (Note that, since the numbers in these figures have been rounded, the same delay, for example, 2 ms, can appear as clear or as light gray depending on whether it was less than or greater than 1.7 ms.) (D) Modified Humphrey visual field thresholds for the corresponding hexagons using a 40-min size target on a background luminance of 10 cd/m^2. The number at each point is the log of the ratio of the patient's threshold to the mean threshold of the control group for that point. The clear regions signify that the patient's threshold at that point was within 0.5 log unit (< +2 SD) of the mean; the light-gray regions signify values between 0.5 and 1.0 log unit (+2 to +4 SD); and the dark gray signify values greater than 1.0 log unit (> 4 SD). The regions designated NaN include the central point (which the Humphrey system does not allow to be measured with a custom program) and two points that fall within the blind spot of normals. Note that ERG delay field was a better predictor of visual field threshold loss than the ERG amplitude field. (Panel B reproduced from Hood DC, Holopigian K, Greenstein V, et al. Assessment of local retinal function in patients with retinitis pigmentosa using the multifocal ERG technique. Vis Res 1998;38:163–179.)

In general, the EOG is abnormal in diffuse hereditary rod–cone degenerations of the retina.[147] In typical RP, the slow and fast light-

induced oscillations of the resting potential are usually decreased simultaneously early in the disease (Fig. 42.28). In some patients the fast oscillations of the resting potential are diminished earlier than the slow oscillation.[110] In others the fast oscillations of the EOG are more preserved than the slow oscillation, a finding that also occurs in Best vitelliform macular dystrophy.[110,148] In most cases of RP the EOG is abnormal when the ERG is abnormal.

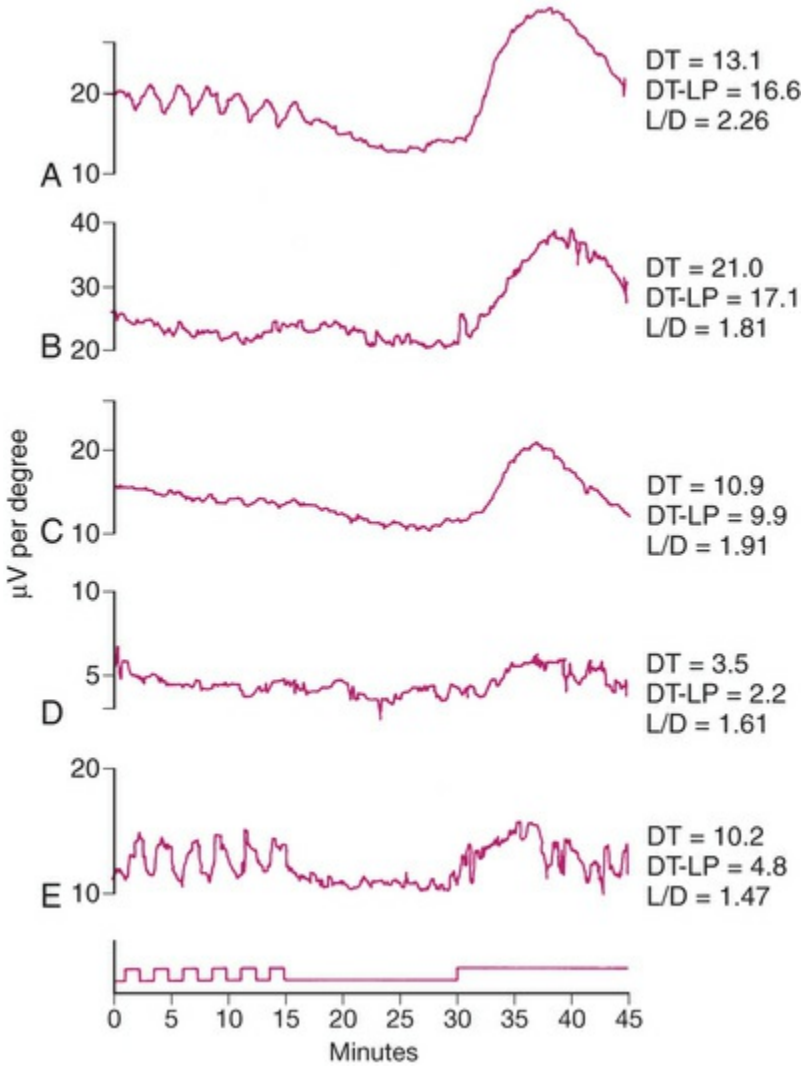

FIG. 42.28 Electro-oculogram (EOG) in (A) a normal subject; (B) a 24-year-old man with autosomal dominant retinitis pigmentosa; (C) a 25-year-old woman with autosomal recessive retinitis pigmentosa (Case 3); (D) a 30-year-old man with retinitis punctata albescens (Case 12); and (E) a 35-year-old woman with autosomal recessive pericentral retinitis pigmentosa. The event marker line below the tracings

indicates “on” (up) or “off” (down) in regard to the 68 cd/m^2 background light in the Ganzfeld stimulator. The ordinate is the indirectly measured amplitude of the corneofundal or standing potential of the eye (in microvolts per degree of fixation shift), as generated by alternating fixation between two red light-emitting diode fixation lights 30° apart. During the first 15 min of testing, the light alternates between dark and light periods of 75 s each to stimulate the so-called fast oscillations of the standing potential of the eye. The dark trough (*DT*) is the lowest point in the standing potential during the second 15 min of total darkness. During the third 15-min period, the background light is on continuously, stimulating a slow light-induced rise in the standing potential to a light peak (*LP*) 7–8 min later. As retinitis pigmentosa progresses, the light-induced rise of the resting potential (*DT-LP*), especially as indicated by the light-to-dark ratio (*L/D*), decreases. Note that, in all patients except E, the slow oscillation, as evidenced by the L/D ratio, is more preserved than the fast oscillations. (From Weleber RG. Fast and slow oscillations of the electro-oculogram in Best's macular dystrophy and retinitis pigmentosa. Arch Ophthalmol 1989; 107:530–537.)

Imaging Modalities in Retinitis Pigmentosa

Fundus Photography/Fluorescein Angiography

Documentation by fundus photography can assist in monitoring changes in patients with RP. Fluorescein angiography in patients with RP will demonstrate hyperfluorescence in areas of RPE atrophy and can highlight areas of cystoid macular edema (Fig. 42.29). However, fluorescein angiography has largely been supplanted by OCT for detecting cystoid maculopathy. In addition, concerns about light exposure accelerating certain forms of RP in animal models have prompted many ophthalmologists to exercise caution in obtaining excessive photographs.[149]

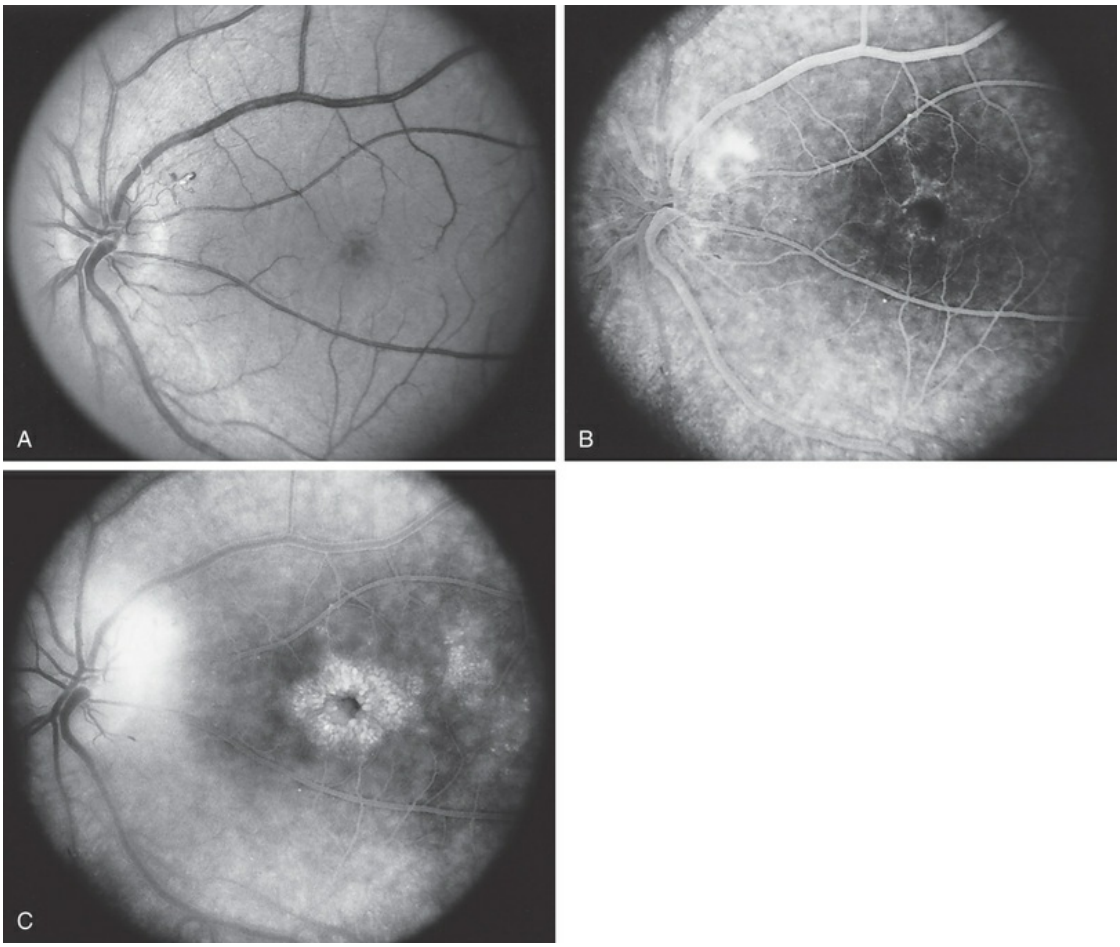

FIG. 42.29 Fundus appearance (A) and fluorescein angiograms (B and C) of the left eye of a patient with presumed autosomal recessive RP at 26 years of age. Note the vascular abnormality superotemporal to the disc, vascular leakage, and cystoid macular edema on the fluorescein angiogram.

In many cases of mild to moderate RP, fluorescein angiography reveals transmission defects of the RPE with later diffuse leakage.[150] In 78 of 82 patients with RP, Newsome[151] found extravasation of dye from perifoveal capillaries in only a few patients but frequent abnormalities of the blood–retinal barrier at the level of the RPE. Such angiographically significant CME can often be seen even in young patients at an early stage of disease who still retain good vision (20/25 or better). Macular edema is a significant cause of early loss of visual acuity in RP.[151,152]

Autofluorescence

Fundus autofluorescence (FAF) utilizes a scanning laser

ophthalmoscope to stimulate intrinsically autofluorescent molecules of lipofuscin to visualize the retinal pigment epithelium.[153] Studies from patients with RP have shown that lack of signal on FAF correlate well with areas of RPE atrophy, while areas of increased FAF can be seen in areas with persistent macular edema as well as within areas of surviving retina.[154] Most RP patients demonstrate a perifoveal ring (Fig. 42.30) of increased FAF within the macula, which denotes the border between functional and dysfunctional retina.[146,154–156] The border of the parafoveal ring of increased fundus autofluorescence has been shown to correlate with function measured by pattern ERG, multifocal ERG, scotopic fine matrix mapping, and microperimetry.[157,158] In addition, areas outside of the ring have been correlated with the loss of outer nuclear layer (ONL) thickness and disruption of the inner/outer-segment (IS/OS) junction, now referred to as the ellipsoid zone, on OCT.[159,160] Near-infrared autofluorescence (NIA) has also been used to image melanin present in the apical tips of the RPE.[161] Similar to FAF, increased rings with NIA are seen in patients with RP.[162] Combined NIA and FAF imaging suggest that the presence of NIA may correlate better with preserved cone function, while FAF indicates only preservation of RPE cells.[162]

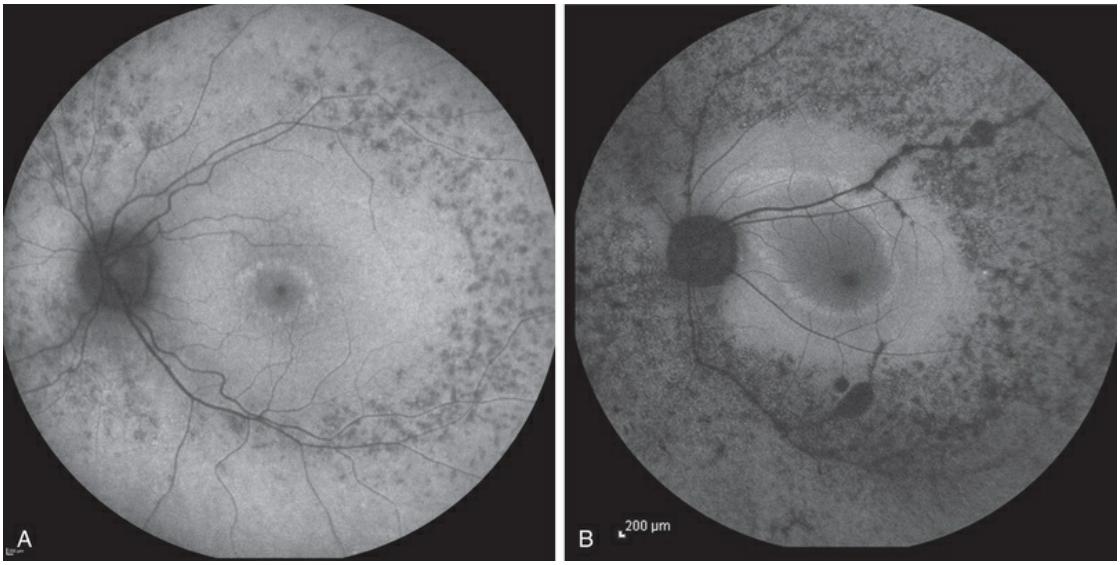

FIG. 42.30 Fundus autofluorescence image of left eye of patient with early (A) and more advanced (B) retinitis pigmentosa showing in each eye a central ring of hyperfluorescence and a region of mottled

hypofluorescence in the region along the arcades.

Optical Coherence Tomography

Optical coherence tomography (OCT) has become one of the most utilized imaging modalities for studying retinal disease in the past several years. Ultrahigh resolution OCT (UHR-OCT) and spectral domain OCT (SD-OCT) have been used to study retinal structures in patients with RP.[163,164] In these patients, such studies have demonstrated decreased thickness of the ONL and loss of the external limiting membrane (ELM) and IS/OS junctions, now called the ellipsoid zone. Loss of ONL thickness or of the IS/OS has been correlated with visual defects measured by visual fields, microperimetry, or multifocal ERG.[37,165–167] SD-OCT is especially useful for detecting cystoid macular edema (Fig. 42.31) or epiretinal membranes, which are common features in patients with RP.[168] The ability to detect cystoid macular edema by OCT ring often eliminates the need for fluorescein angiography. Most RP patients demonstrate a perifoveal ring of increased FAF that various in size.[162]

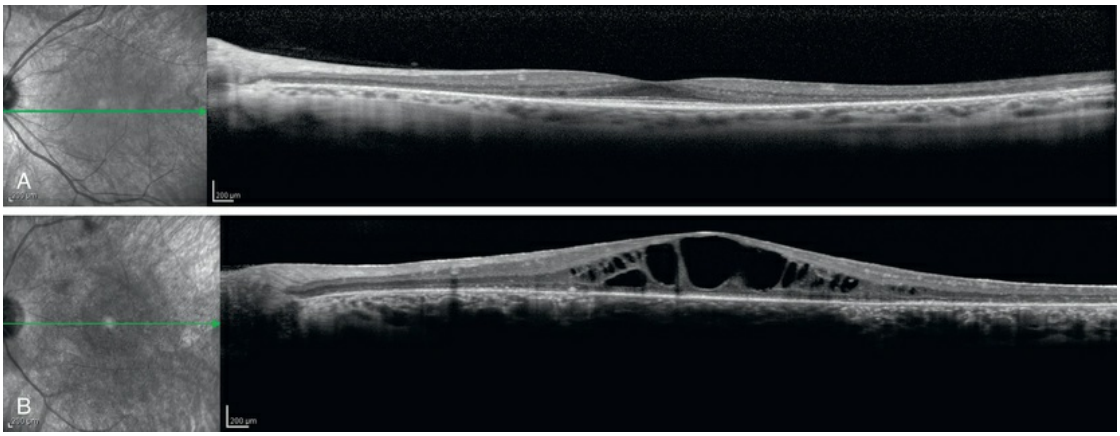

FIG. 42.31 Spectral domain foveal line scan of normal subject (A) and patient (B) with cystoid macular edema.

Adaptive Optics Scanning Laser Ophthalmoscopy

Traditional imaging modalities cannot resolve individual retina

cells due the optical limits imposed by the cornea and lens which create higher order aberrations resulting in image blur.[169] A combination of adaptive optics with flood illumination (AO-Flood) or scanning laser ophthalmoscopy (AO-SLO) can compensate for these factors and provide imaging of individual cone photoreceptors.[170] Adaptive optics studies from patients with both cone–rod dystrophies and RP have demonstrated increased cone spacing as well as qualitative areas where cone profiles could not be identified.[171–173] Recent advances have now enabled imaging of rod photoreceptors and foveal cones.[174] The ability to quantify cone photoreceptors has already been studied in one treatment trial for RP[175] and will undoubtedly play a role in future studies.

Classification

The ideal classification system would subdivide RP on the basis of molecular and biochemical abnormality and correlate this with useful, if not characteristic, clinical features. Despite the explosion of molecular genetic information that has become available in the past 15 years, a unified subclassification system that can be used by clinicians, cell biologists, and molecular geneticists is still lacking. Because of this, the different ways of classifying RP listed below are all still valid. The one used by an individual depends on that person's area of interest.

Subdivision by Inheritance Type

The most useful subclassification of RP both in the clinical and research setting is still subdivision on the basis of mode of inheritance. Typical RP can be inherited as an arRP, adRP, or X-linked recessive trait (X-linked RP). Although mitochondrial inheritance is associated with pigmentary retinopathy, typical nonsyndromic RP has yet to be reported with this type of inheritance. The percentage of each inheritance type has been found to vary from author to author and with country of origin of the study. Despite the fact that typical RP is always genetic, a lack of family history of retinal disease is often reported. Studies around the world have found that no other affected family member can be identified in 15–63% of cases. Such cases are labeled “simplex RP.”

Averaging results from different studies suggests that 35% of RP patients in the United States, 42% in the UK, and 48% in China are simplex. It is assumed that large proportions of these cases represent recessive inheritance. Jay[176] has estimated that no more than 70% of simplex cases are autosomal recessive.

Subdivision by Age of Onset

Early-onset RP may be subdivided into congenital and childhood-onset forms. Timing of onset of blindness, by the patient's parent(s), and the occurrence of nystagmus (usually suggestive of a congenital disease) can be used to differentiate between congenital and early-onset cases. Occasionally, a member of a family with otherwise typical RP may present in late infancy or early childhood, while other affected members present anywhere from the end of the first decade to the third decade. arRP is usually more consistent in the age of presentation among affected siblings.

The most common age for presentation of symptoms and subsequent diagnosis of RP is in the first three decades of life – juvenile-onset and early adult-onset RP. All three inheritance types may present in such a fashion. Often, children with juvenile-onset disease function quite well at home but have great difficulties navigating strange environments. Reliable testing of visual fields may be possible in some children as young as 6 or 7 years of age. Perimetry indicative of progression or improvement of visual field deficits should, however, be interpreted with caution in this age range.

Adult-onset and late-onset forms of RP are not uncommon but often go unrecognized as a retinal dystrophy. Some of these retinal degenerations may have a nongenetic basis, but those that are genetic are usually autosomal recessive.

Subdivision by Molecular Defect

The expanding discovery of gene mutations associated with forms of RP is leading to an ever-increasing understanding of these entities at the molecular level. We now recognize that a mutant allele for a gene can behave in different ways, depending on where the sequence change resides within the gene and the status of the other allele. Gene mutations that produce no gene product (so-

called *null* alleles) may exhibit autosomal recessive inheritance if one good copy of the gene is sufficient to produce enough product to maintain normal function. Null alleles can also be associated with dominant inheritance from "haploinsufficiency" if one good copy of the gene cannot produce enough product to maintain normal function. Dominant inheritance can be seen with "dominant-negative" alleles, where multiple products of the wild-type gene must normally interact to form a multimeric protein complex or supramolecular structure. Missense mutations can also behave as a dominant trait by producing a "toxic gain-of-function" whereby the mutant protein disables normal gene regulation to downregulate gene expression of the normal copy. Dominant inheritance can also occur if the mutant gene product either fails to bind or binds too tightly to another gene product, disabling normal regulation pathways or important biochemical systems. Eventually, information on both the gene and the specific mutation or combination of mutations at each allele will be essential for optimum care. Additionally, as more information is discovered about modifiers of genetic diseases, molecular information will be needed on the status of these genes as well.

Although diagnostic molecular genetic testing is becoming more accessible, information on the specific gene mutation in most patients is still not available. A classification based on molecular genetic defect has still therefore to supplant the need to consider subdivisions of RP on clinical or psychophysical grounds. However, such molecular information will eventually aid immensely in defining the true spectrum and natural history of specific types of RP. This refinement of classification will be particularly useful for prognostic counseling. The ability to detect the presence of the gene defect by examining DNA taken from blood or a mouth swab will allow earlier and more accurate diagnosis, facilitate genetic counseling, open the way for prenatal diagnosis, and eventually guide the patient toward specific gene defect-related therapies. Schemes for molecular classification of RP are given later in this text.

Subdivision by Distribution of Retinal Involvement or Fundus Appearance

A number of recognizable fundus appearances have been seen in certain cases of RP. RP sine pigmento – RP without signs of intraretinal pigmentation – is one. In almost all cases these represent early RP. In the early stages of RP, fine, whitish, punctate lesions in the mid- and far periphery at the level of the RPE can be seen. This fundus appearance is similar to that seen in retinitis punctata albescens.[177] White lesions or dots deep in the retina can be seen with RP in younger members of families with older affected members who have typical findings of RP. A myriad of tiny, irregularly shaped, gray–white, deep retinal lesions (Fig. 42.32) associated with lifelong stationary night blindness, minimally attenuated retinal vessels, and absence of pigment clumps or bone spicules are characteristic of fundus albipunctatus. Bilateral central scotomas can be present in later years. History of slow progressive visual loss with the macular atrophic degeneration is suggestive of the fleck retinal degeneration known as retinitis punctata albescens.[178] However, differentiation of fundus albipunctatus from retinitis punctata albescens can be difficult. Macular atrophic lesions have been reported by Miyake and colleagues to occur also in fundus albipunctatus.[179–181]

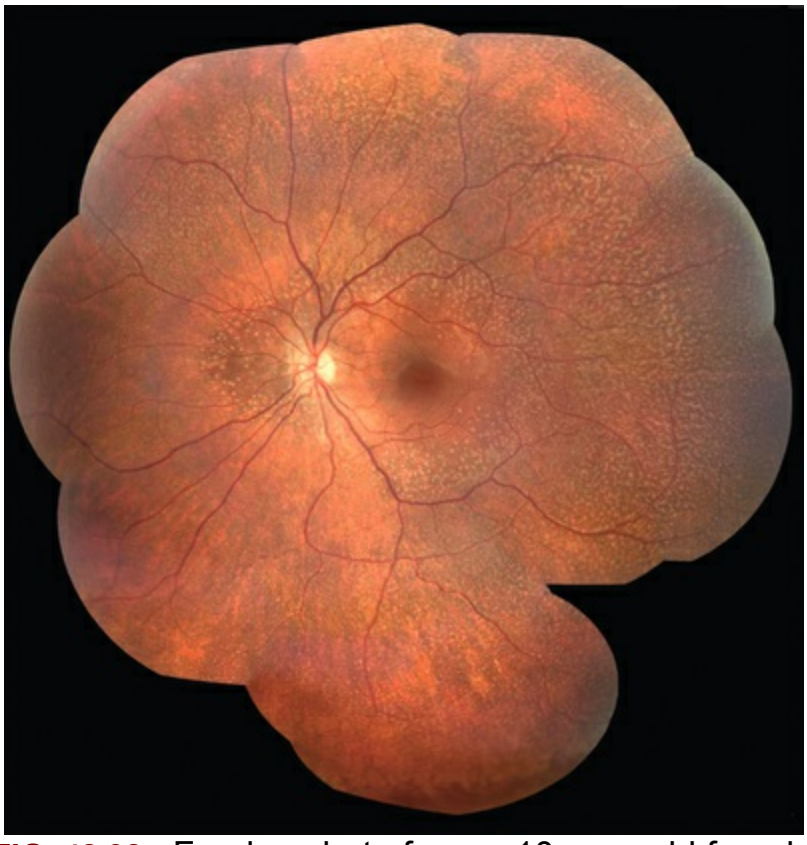

FIG. 42.32 Fundus photo from a 10-year-old female with fundus albipunctatus and heterozygous mutations in *RDH5*. Myriads of discrete white-yellow dots are present throughout the retina, but spare the central macula.

Sector and Sectorial Retinitis Pigmentosa

Sector RP, first described by Bietti[182] in 1937, refers to a specific subtype of RP. This is characterized by pigmentary changes limited to one or two quadrants, visual field defects usually only in the regions of retinal pigmentation, relatively good ERG responses, and minimal or no extension of the retinal area involved with time.

Patients may be minimally symptomatic. The area of retinal involvement is usually an arcuate swathe of retina just below the macula. In later years this involved region of the fundus may show almost a total regional atrophy of choroid and retina.[183] Occasionally the nasal retina[184] or inferior and nasal retina is involved.[183] Rarely, sector RP has been reported as affecting the temporal or superior quadrants.[185] True sector RP can be either autosomal dominant or autosomal recessive.[183] Although sector RP

has been reported with mutations of the rhodopsin gene[186,187] and with mutations of *USH1C*,[188] sporadic or isolated cases of sector retinal degeneration are common and may possibly result from nongenetic causes.

Massof and Finkelstein[92] have shown in autosomal dominant sector RP that the absolute retinal thresholds are elevated throughout the retina, including the fovea. Rods and cones appear to be equally affected. Over a period of years, the visual field defects worsen. Overall, however, visual prognosis is good. Using a combination of testing modalities, Fleckenstein et al.[158] studied the fundus autofluorescence associated with various forms of retinal dystrophy, including one case with sector RP. Microperimetry disclosed that the ring of hyperfluorescence sharply delineated the areas of severe impairment of sensitivity. In cases of true sector RP, the ERG demonstrates relative preservation of amplitudes, with mild to moderate subnormalities of both rod- and cone-mediated responses with normal implicit times.[184] One form of sector RP appears to be associated with angle closure glaucoma.[86]

Most cases of retinitis pigmentosa that begin or present in a sectorial distribution are, in fact, merely the sectorial presentation of what will become with time a more diffuse disease. One notable example of this is the brother of the patient shown in Figs. 17.2 and 17.18, who presented with a strikingly sectorial phenotype in association with RHO Pro23His retinitis pigmentosa. Although he had poor night vision from age 17, he began to notice areas of blindness in his upper visual fields at age 30 years. The diagnosis of RP was made at age 42 years. At age 50, his best corrected visual acuity was 20/20 J1 in each eye. His visual fields (Fig. 42.33) showed dense superior loss but good preservation of inferior field. Fundus appearance (Fig. 42.34) showed inferior and nasal pigmentary changes OD and well-demarcated inferior sectorial changes OS. The Ganzfeld ERG at age 51 showed small but measurable rod responses, markedly subnormal scotopic bright flash responses, and modestly subnormal photopic cone responses; rod and cone implicit times were normal. His acuity remains normal, and he was able to drive a car both during the day and at night until his mid 60s. This patient illustrates the phenotypic variability that can be evident with the age of onset of symptoms varying from early

adulthood to the fifth decade of life. The normal implicit times for rod and cone responses for his case are unusual but are consistent with the sectorial nature of the expression of his disease.

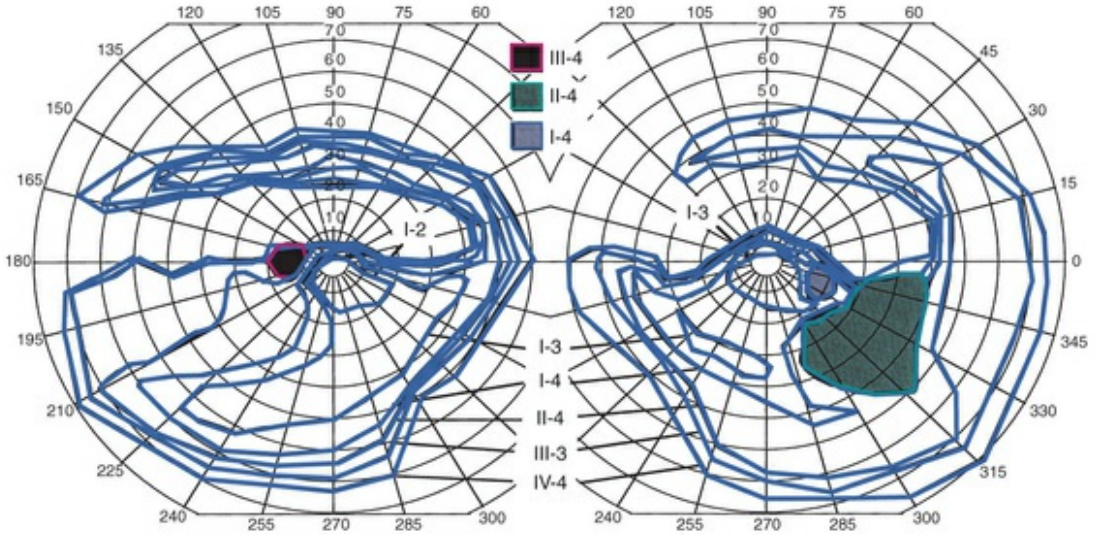

FIG. 42.33 Goldmann perimetry for a 51-year-old patient with autosomal dominant sectorial retinitis pigmentosa from the Pro23His mutation of rhodopsin. Note that the major visual field defect is superior.

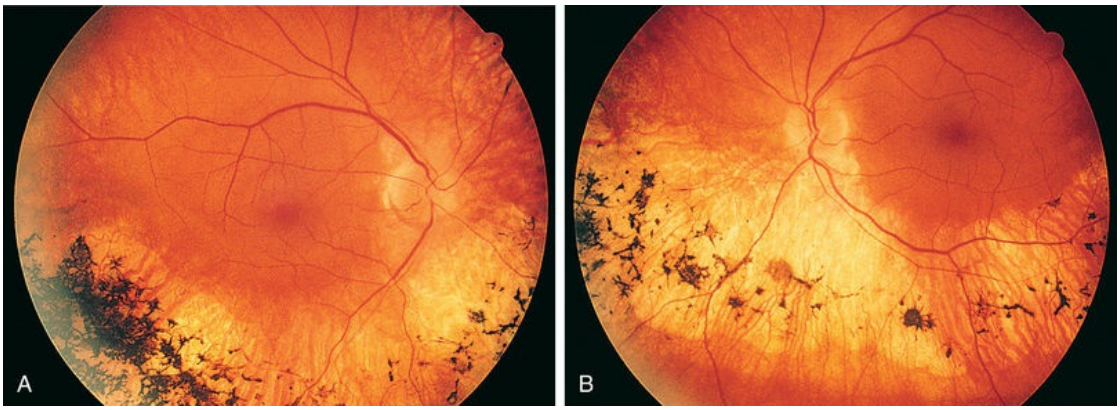

FIG. 42.34 Fundus appearance of the right (A) and left (B) eyes of the 51-year-old patient with autosomal dominant sectorial retinitis pigmentosa from the Pro23His mutation of rhodopsin. Note the discrete border between affected and normal-appearing retina and how well the fundus appearance correlates with the visual field in Fig. 42.33.

Pericentral Retinitis Pigmentosa

Pericentral retinitis pigmentosa is a special phenotype whereby the loss of visual field typically occurs between 5 and 15° (Fig. 42.35) from fixation rather than between 20–40° from fixation as is seen more commonly. Retinal diseases may commence inferiorly with commensurate superior field loss leading to the misconclusion that this is a form of sector RP. Pericentral RP is an important subtype because, as the areas of depressed field deepen, coalesce, and enlarge, they encroach more on the central region of seeing field and, thus, create greater disability at an earlier stage of disease.[189] Eventually, as the central region of retina becomes progressively smaller or if the macula develops cystoid edema or atrophic changes, the visual acuity can decrease rapidly from relatively good acuity to less than 20/400. Pericentral retinitis pigmentosa can occur in many genetic forms of RP and can even be seen in relatives whose other affected family members have a different pattern or a more limited form of disease, suggesting that modifying genes, other ocular conditions (e.g., high myopia), or environmental factors may contribute to this phenotype. Pericentral RP can occur as an autosomal recessive or dominant trait. Selmer et al.[190] reported a Norwegian family with autosomal dominant pericentral retinal dystrophy associated with a novel mutation of the gene *TOPORS*. More recently, Manes et al.[191] have reported pericentral RP in patients with *PRPH2* mutations.

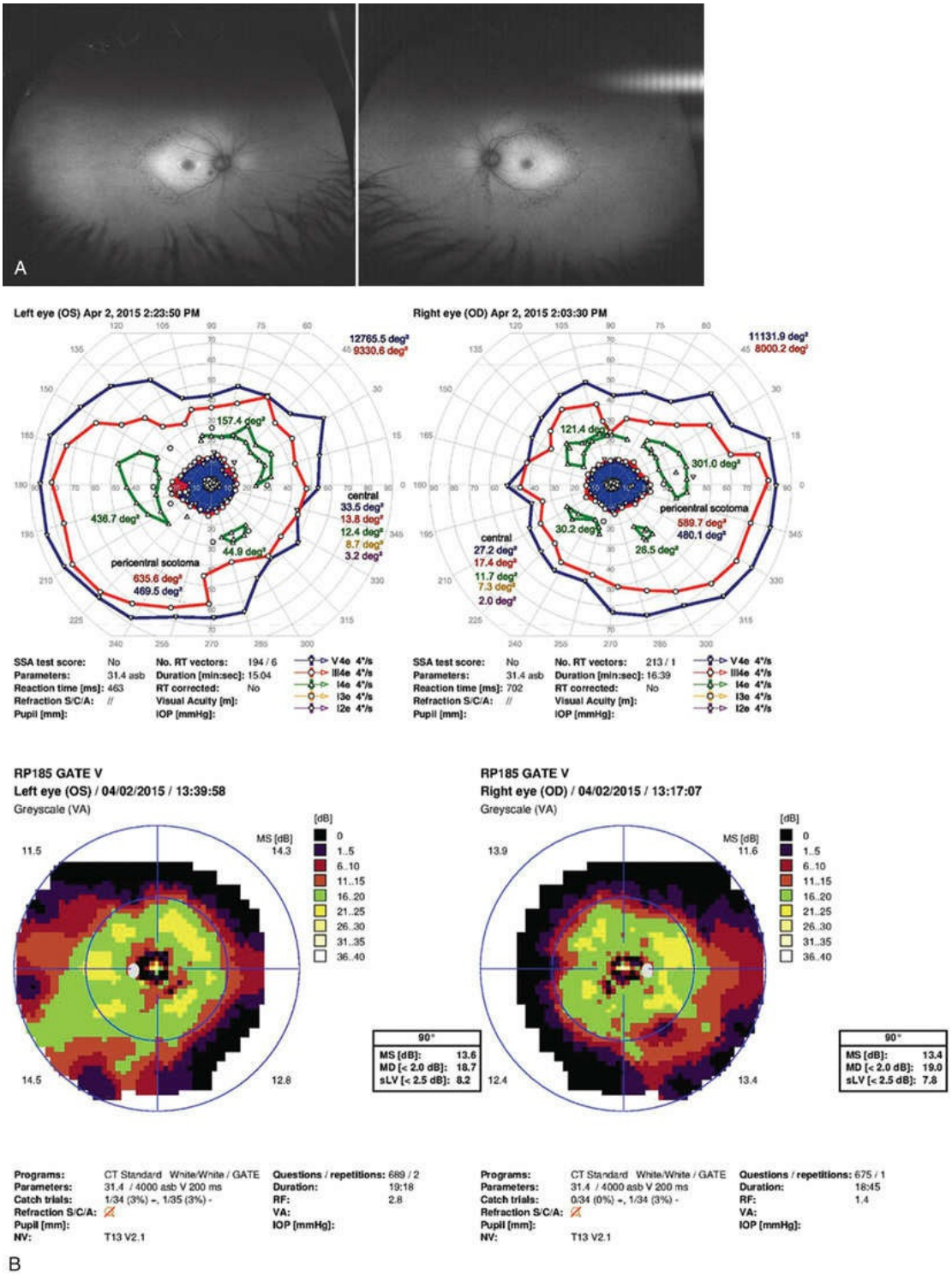

FIG. 42.35 (A) Optos autofluorescence images from a 18-year-old female with pericentral RP. The were hyperautofluorescent rings around the fovea with surrounding hyperautofluorescence through the macula. Hypoautofluorescent dots were located near the vascular arcades. Note the relatively normal structure in the mid- and far-periphery. (B) Kinetic and

static visual fields obtained with the Octopus 900 perimeter. Both tests demonstrate central preservation in fovea. The patient's visual acuity was 20/25 OU. However, just outside of the fovea there is a steep drop in sensitivity from the perifoveal macula to approximately 15–20°. Sensitivity in mid- and far-periphery were mildly reduced. (Panel A, photos courtesy of Dr. Paul Yang.)

Unilateral or Extremely Asymmetrical Retinitis Pigmentosa

The vast majority of cases of so-called unilateral RP are acquired rather than genetic unilateral disease. The most common form of unilateral pigmentary retinopathy that is referred to as unilateral RP is diffuse unilateral subacute neuroretinitis or DUSN. This will be covered in the section on forms of pseudoretinitis pigmentosa.

Extremely asymmetrical retinitis pigmentosa of genetic etiology can occur in two instances. One is the carrier state for X-linked retinitis pigmentosa. Lyonization, or X-chromosomal inactivation,[192] occurs close in time to lateralization during embryogenesis. Thus, if the number of cells undergoing inactivation of the X-chromosomes that contain the normal gene for retinitis pigmentosa is uneven at the time of lateralization and, by chance occurrence, a greater number of those cells are directed to one side of the developing embryo, the carrier will express an extremely asymmetrical phenotype with asymmetrical field loss (Fig. 42.36) and pigmentary changes (Fig. 42.37). The second mechanism by which unilateral retinitis pigmentosa can occur as a genetic trait is through somatic mosaicism of a dominant gene for retinitis pigmentosa. This mechanism has been reported as the cause of unilateral RP in a patient with somatic mosaicism of *RP1*.[193]

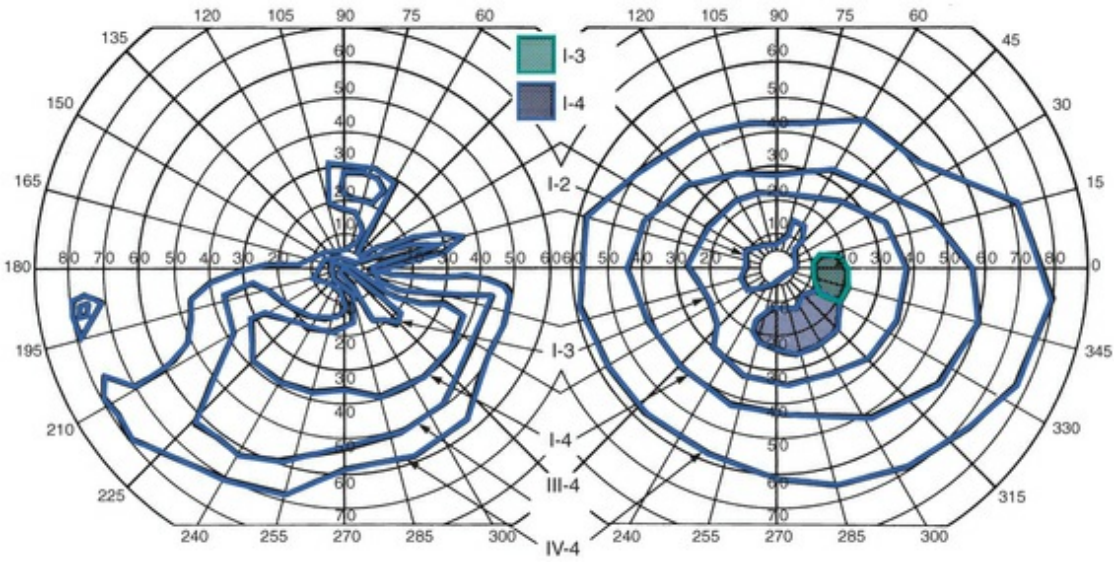

FIG. 42.36 Goldmann kinetic perimetry for the 64-year-old carrier of X-linked retinitis pigmentosa. She had mild, lifelong difficulty with night vision that was stable. The vision in her left eye began to fail as a young adult. At 64 years of age, the visual acuity was 20/25 OD and 20/60 OS, with −5.00 +1.00 axis 120° OD and −9.75 +0.75 axis 105° OS. Color vision was normal on the right and markedly disturbed on the left (AOHRR plates). Note the inferior arcuate defect in the right eye and severe irregular superior field loss in the left eye. The ERG was moderately subnormal OD and severely abnormal OS.

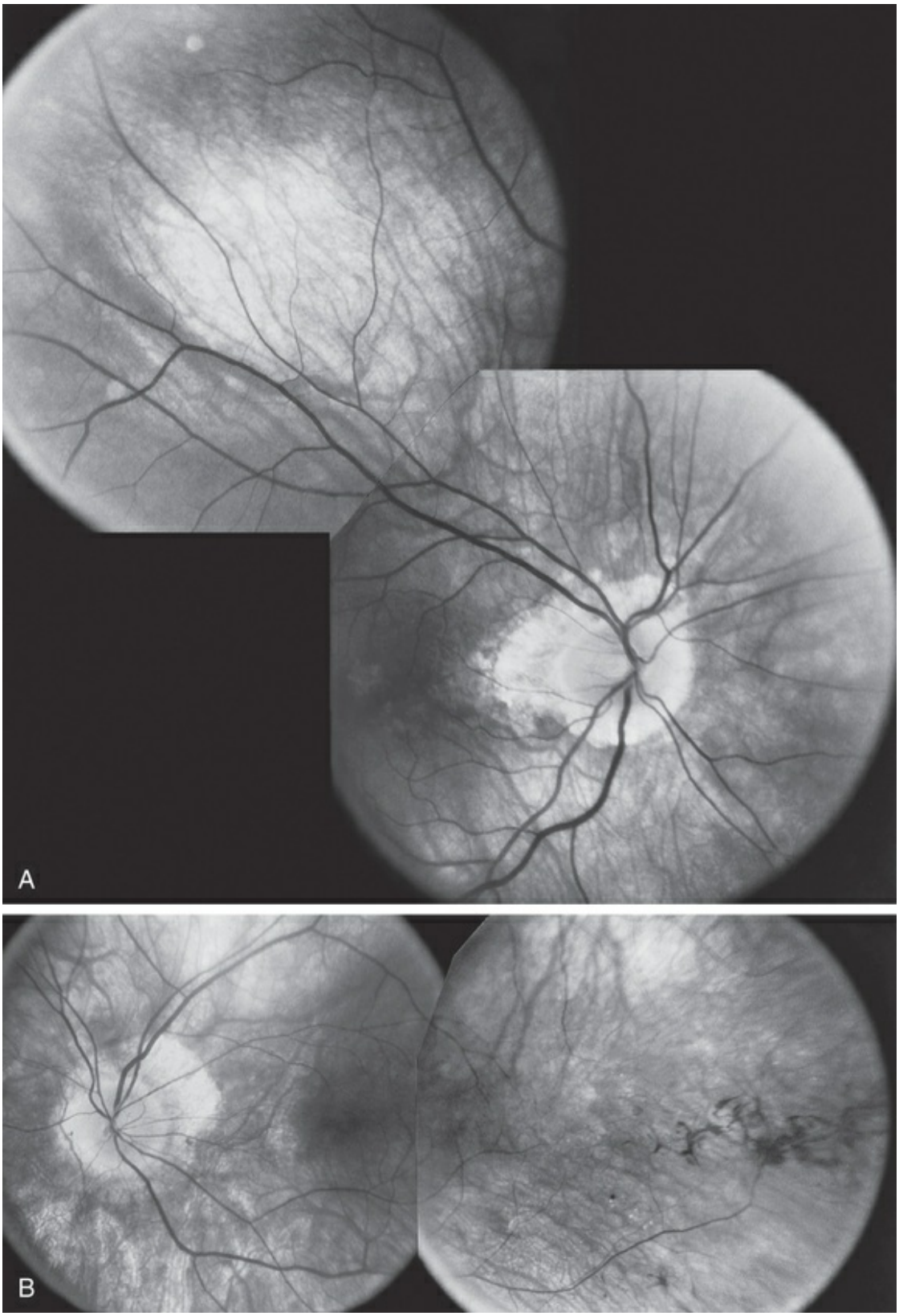

FIG. 42.37 Posterior pole and superotemporal retina of the right eye (A) and posterior pole and temporal retina of the left eye (B) of a 64-year-old carrier of a two basepair insertion in codon 99 of *RPGR*. Note the areas of retinal pigment epithelium (RPE) atrophy

around the discs and superotemporally in the right eye and RPE thinning inferiorly and nasally with bone-spicule pigmentation temporally in the left eye.

(Reproduced from Weleber RG, Butler NS, Murphey WH, et al. X-linked retinitis pigmentosa associated with a two base-pair insertion in codon 99 of the RP3 gene *RPGR*. Arch Ophthalmol 1997;115:1429-1435.)

Complicated Retinitis Pigmentosa

Systemic Associations

Most cases of RP are not associated with manifestations outside the eye. Patients with RP have been reported to have a greater than normal risk for thyroid disease.[194] Of 670 respondents to a questionnaire mailed to patients with RP, 7.3% reported mild and 1.3% reported severe thyroid conditions.[195,196] Several studies have reported immunologic abnormalities for patients with RP.[197] We suspect, however, that many of the psychiatric and other systemic associations with RP are either coincidental or epiphenomena.

However, approximately 30% of all patients with RP might experience mild to severe hearing loss as adults.[198] It is unknown what proportion of these are in fact cases of Usher syndrome and what proportion is coincidental or a feature of other genes associated with RP. Zito et al.[199] reported RP with a sensorineural and conductive hearing loss, recurrent ear infections, sinusitis, and chronic recurrent respiratory tract infections in a family with a 845-846delTG mutation of *RPGR*. This and other reports of similar systemic features in X-linked RP from mutation of *RPGR* may be related to the ubiquitous expression of elsewhere in the body. Kenna et al.[200] reported a large nonconsanguineous Irish family with a progressive pigmentary retinopathy (RP), deafness beginning in the third decade of life, and a subclinical myopathy, identified by skeletal muscle biopsy, electromyography, and electrocardiography. Mansergh et al.[201] identified a C12258A mutation in the mitochondrial gene *MTTS2* in this family; RetNet (http://www.sph.uth.tmc.edu/Retnet/home.htm) lists this mutation as affecting the serine tRNA 2 (AGU/C), nt 12207-12265.

Usher Syndrome

Usher syndrome is defined as autosomal recessive deafness (most commonly congenital) with retinopathy indistinguishable from typical RP. Although first described by von Graefe in 1858, credit is given to the British ophthalmologist Charles Usher for the appreciation that this condition was familial and represented a distinct entity.[202] He also recognized the existence of at least two types on the basis of severity of hearing loss, age of onset, and rate of vision loss. Usher syndrome is the most common of the syndromes associated with RP and accounts for about 18% of all patients with RP.[203] Although the prevalence has been estimated at between 1.8 and 6.2 cases per 100,000,[204,205] a more recent study found the population prevalence to be 1 : 6000.[206] Usher syndrome accounts for 50% of those persons in the USA who are both deaf and blind.[205,207] The Usher Consortium has recommended specific clinical criteria for the diagnosis of Usher syndrome.[208]

Usher syndrome can be divided clinically into three major groups. The two most frequent forms are type 1, with profound congenital sensorineural deafness and resultant prelingual deafness or severe speech impairment, vestibular symptoms, and childhood-onset retinopathy, and type 2, with congenital partial, nonprogressive deafness, absence of vestibular symptoms, and milder, later-onset retinopathy.[209] The least common is type 3 Usher syndrome, which is characterized by progressive deafness starting late in the second to fourth decades, adult-onset retinopathy, and hypermetropic astigmatism.[210–212] Another variant, Hallgren syndrome, was defined as congenital progressive deafness, vestibular ataxia, and retinopathy.[213] The validity of this as an entity distinct from Usher type 1 has been questioned.[209] Approximately 3–6% of those persons with profound prelingual deafness have type 1 Usher syndrome.[207] Piazza et al.,[214] in a study of 106 patients with Usher syndrome, found that 33% had type 1 and 67% had type 2 disease. No type 3 cases were identified. Most cases of type 3 disease are of Finnish descent.[215] As much as 40% of Usher syndrome cases are classified as type 3 in Finnish[212] and Ashkenazi Jewish[216] populations.

One of the earliest signs of type 1 Usher syndrome is vestibular dysfunction, which in infancy can manifest as a delay in motor

development in children and in adulthood as a nonprogressive ataxia.[209] Occasional ataxia is present in type 2 disease and has been attributed to cerebellar atrophy.[209] Because of vestibular dysfunction, almost all children with type 1 Usher syndrome fail to walk before the age of 18 months.[217] Patients with type 1 Usher syndrome almost invariably report onset of nyctalopia later, by age 15 years, whereas type 2 and type 3 patients report onset of nyctalopia over a greater range, up to the early 30s.[209,218] Visual acuity appears to be better retained in older patients with type 2 Usher syndrome as compared to type 1.[214] The cumulative percentage of patients retaining 20/40 visual acuity or better at age 29 was 69% for type 1 and 94% for type 2. For retention of 20/80 visual acuity at age 29, the figures were 89% for type 1 and 98% for type 2. Approximately 77% of type 1 patients and 95% of type 2 patients maintained 20/200 visual acuity at age 40. Foveal lesions were seen on fluorescein angiogram more frequently and at an earlier age in type 1 (14 of 35 with a mean age of 34.4 years) as compared with type 2 (19 of 71 with a mean age of 42.9 years). No difference in the prevalence of posterior subcapsular cataracts was noted between the two types in this study (roughly 50% in each).[214] No comparable figures are available for type 3 disease. The ERG is often profoundly abnormal to nondetectable by nonaveraging techniques in all types.

The dual impairments of deafness and severe visual impairment in all Usher syndrome patients necessitate a great deal of educational and sociopsychologic intervention to help them to maintain independence and productivity.[219,220] Cochlear implantation in profoundly deaf children has been successful in allowing these children to enter the world of the hearing. In order that the parents understand the importance of cochlear implantation, we believe that all infants with profound congenital deafness should be screened for Usher syndrome. Usher syndrome can be reliably diagnosed in infancy and early childhood with an ERG and more recently with genetic testing.[217] Because receptive and expressive language is most closely correlated with the precocity of cochlear implantation, the diagnosis of Usher syndrome should be established as early as feasible to optimize speech therapy.[217]

The diagnosis of Usher syndrome is missed in two common situations. The first is early disease, in which bone-spicule retinal pigmentation is not yet visible, and the second is in the patient with retinal disease that is described as fine pigment clumping and is misdiagnosed as rubella retinopathy. When the diagnosis is suspected, Usher syndrome must be confirmed with an ERG. Other syndromes that can be associated with deafness and pigmentary retinopathy must also be contemplated when considering a diagnosis of Usher syndrome. These include infantile Refsum disease (part of the Zellweger spectrum), adult Refsum disease, Cockayne syndrome, Bardet–Biedl syndrome (BBS), Alström disease, Flynn–Aird syndrome, Friedreich ataxia, and Kearns–Sayre syndrome.

Differential Diagnosis – Phenocopies of Retinitis Pigmentosa

Many other inherited retinal conditions may be confused with RP. These can be conditions confined to the retina or have associated systemic manifestations that may or may not be apparent at the time of examination. Misdiagnosis is common and causes the greatest problem in pediatric practice. Such phenocopies can usually be differentiated from RP on detailed retinal investigation and a thorough survey for systemic signs in the patient and relatives. This differentiation is important because it has a great bearing on the genetic and prognostic counseling given to the family. A great deal of anxiety and social problems can be avoided, for example, in families with BBS, if problems of obesity are predicted for a child who might otherwise be labeled as having an eating disorder as a result of the psychologic stress of blindness. When confronted with inherited retinal disease, especially when associated with systemic manifestations, the reader is encouraged to consult the phenotype catalog of "On-line Mendelian Inheritance in Man" (OMIM), which is available at http://www.ncbi.nlm.nih.gov/omim.

Cone–Rod and Cone Dystrophy

In the later stages of disease, many retinal dystrophies (e.g., choroideremia, Stargardt macular dystrophy, Sorsby fundus dystrophy, and others) involve the entire retina and can be confused with RP. Of these other retinal dystrophies, CRD is the one that is most frequently confused with RP.

CRD is characterized by early loss of visual acuity and color vision, with subsequent progressive peripheral visual field loss. There is little literature on the prevalence of CRD, although it has been suggested that the disease may be relatively common.[221] Moreover, some patients otherwise labeled as having RP may have a greater involvement of cones than rods. One study of 278 RP patients with recordable ERGs and fields large enough for rod threshold measurements reported that 41% had a cone–rod-type ERG deficit.[36] Macular pigmentation and atrophy precede variable degrees of peripheral pigmentary abnormality in CRD. In early disease, before peripheral field deficits or peripheral retinal abnormalities are apparent, a diagnosis of macular or cone dystrophy may be made.[221] Peripheral retinal bone-spicule pigmentation, in later disease, may resemble that seen in classic RP. Often the midperipheral retina is relatively spared or affected late in the evolution of disease.[222,223]

With such potential for diagnostic confusion, it has been suggested that a diagnosis of CRD should be made on the basis of marked reduction or absence of cone electroretinographic responses in the presence of quantitatively less reduction in rod responses.[224] However, this definition includes a range of phenotypes, and early attempts have subclassified CRD on the basis of fundus appearance[225] or visual field deficits.[226] Two studies have attempted to subclassify CRD on the basis of dark-adapted static threshold profiles[227] or differences in ERG responses.[228] Yagasaki and Jacobson[227] tested 14 autosomal recessive and simplex CRD cases using full-field ERGs, dark adaptometry, and modified perimetric techniques. They suggested that a subclassification could be based on three distinct patterns of visual field loss. Type 1 cases had central rod and cone functional loss, eccentric fixation, mild peripheral photoreceptor dysfunction, and slow progression. Type 2 was described as more severe, with a central scotoma, eccentric fixation, more cone than rod functional loss in the periphery, and

relatively normal midperipheral fields. Subjects classified as type 3 had central fixation, no measurable cone function, and patchy rod function loss. Szlyk and coworkers[228] studied 33 CRD patients, and reviewed the records of a further 150, and described four functionally distinct subtypes. Subjects were subdivided into type 1 (less rod than cone dysfunction) and type 2 (equal cone and rod dysfunction) on the basis of quantitative electroretinographic responses. These groups were further subdivided into type a (cone thresholds more elevated centrally, rod thresholds more peripherally) or b (matching areas of cone and rod threshold elevation mostly peripherally) on the basis of pattern of field loss and threshold elevation.

There is a tendency for the visual field defects in CRD to begin in the pericentral region between 5 and 30 degrees from fixation.[226] Many nonretinal conditions have been documented in association with CRD in certain patients, including optic nerve head atrophy and telangiectasia,[225,226] high myopia,[229] and macular coloboma.[230] Also, there have been associations with spinocerebellar ataxia,[231] dental amelogenesis imperfecta,[232] alopecia,[233] and hypertrichosis.[234] In the vast majority of cases, however, CRD is identified as the only genetic disease.

Autosomal dominant, recessive, and X-linked inheritance patterns have been described, as well as simplex cases implying genetic heterogeneity.[235] Recent molecular genetic studies have identified 16 different genomic regions, each of which contains a CRD-causing gene.

In the early stage of disease, an isolated cone dystrophy may be difficult to distinguish from a CRD. CRD can be associated with mutations in the gene *GUCY2D* for guanylate cyclase,[236] and cone dystrophy (COD3) has been associated with the functionally related gene *GUCA1A* encoding GCAP-1.[237,238] GCAPs play an important role in regulating the function of RETGC-1 in a calcium-dependent manner, but the reason why defects of these proteins result in degeneration limited to cones is difficult to explain. One suggested explanation focuses on the interactions of the defect of GCAPs at different levels of calcium.[238]

Leber Congenital Amaurosis/Severe Early

Childhood Onset Retinal Dystrophy (SECORD)

Leber congenital amaurosis (LCA) is not a single entity but a group of disorders due to mutation of at least 19 different genes. The disorder is characterized by severe visual impairment or blindness from infancy. In 1869, Theodor Leber originally described children with the condition as severely visually impaired before the age of 1 year, with nystagmus, poor pupillary reflexes, either normal or abnormal fundus appearance, and an autosomal recessive inheritance pattern.[239] In 1954, Franceschetti and Dieterlé[240] described a profoundly abnormal or absent ERG that has since become a requirement for the diagnosis of LCA. Eye-rubbing – the oculodigital sign – is a common association.[241] The vast majority of cases are autosomal recessive, although rare dominant families have been reported, which, when molecularly characterized, have been found to result from deletions within *CRX* and mutations of *IMPDH1*.[242–244]

In 1916 Leber wrote that in his experience the disorder that he originally described in infants (that now carries his name) merged into a continuum with children who presented later in early childhood, without the history of nystagmus or poor papillary responses from birth.[245] These cases typically presented at age 4–5 and had extremely poor vision by 30 years of age. Several names have been used for children presenting this second phenotype, including juvenile and early-onset RP,[246] childhood-onset severe retinal dystrophy,[247] early-onset severe retinal dystrophy,[248] and SECORD.[249]

Patients with LCA or SECORD may show either a normal fundus appearance or only subtle RPE granularity and mild vessel attenuation. More notable retinal abnormalities that have been described in LCA include so-called macular coloboma,[250,251] "salt and pepper" retinopathy,[252] retinitis punctata albescens,[253] and nummular pigmentation.[254] LCA is often associated with keratoconus.[255] Elder evaluated 35 children with LCA and found a prevalence of keratoconus of 29%. Elder suggested that keratoconus is not a consequence of the eye-rubbing frequently seen in LCA but may be due to other genetic factors.[256]

Systemic associations are commonly made. Several reports describe the association of LCA with deafness,[257] renal anomalies,[258] infantile cardiomyopathy (this case was later reclassified by Russell-Eggitt et al.[259] as Alström syndrome), hepatic dysfunction,[260] and skeletal abnormalities.[260,261] Neurologic abnormalities are the most common association and have been reported in 17–37% of LCA cases.[252,262] Nickel and Hoyt[263] have suggested that mental retardation is secondary to the visual impairment, although we believe this is unlikely to account for the severe intellectual impairment that can occur.[264] More recent studies suggest that up to 20% of LCA children without associated anomalies will develop mental retardation.[265,266] It is unknown whether these cases represent undiagnosed systemic disorders or a genetic subtype or subtypes of LCA. Walia et al.[267] studied 169 patients with LCA and 27 patients with early childhood-onset RP and found the visual acuity varied widely among those with mutations of *RPE65*, *RDH12*, and *CRB1*, whereas *AIPL1*, *GUCY2D*, *CRX*, and *RPGRIP* gene mutations were associated with severely decreased visual acuity commencing within the first year of life. Patients with either *RPE65* or *CRB1* mutations had progressive vision loss with age; those with onset of symptoms after infancy had better visual acuity. The gene *CEP290* is not only a frequent cause of LCA[268] but also is associated with the Joubert spectrum of diseases and with nephronophthisis.

Unfortunately, unless other diagnoses are considered and the correct tests are performed, several other entities can be confused with LCA,[269] including infantile Refsum disease,[270,271] congenital stationary night blindness,[272] early infantile neuronal ceroid lipofuscinosis (INCL) (Hagberg–Santavuori syndrome),[273,274] and any of several renal–retinal syndromes (Senior–Loken syndrome and Saldino–Mainzer syndrome).[258,275–277] There is the suggestion that the original report by Leber may have included cases of INCL.[278] Although, in the past, LCA has been considered synonymous with infantile blindness and a "flat ERG," LCA should be thought of as a clinical/electrophysiologic sign rather than a distinct pathologic entity. In the context of systemic anomalies, such misdiagnosis can be avoided if LCA is considered a diagnosis of exclusion.

Bardet–Biedl Syndrome

Bardet[279] in 1920 described a patient with retinopathy, polydactyly, and congenital obesity. Biedl[182] in 1922 added the fourth and fifth cardinal features, mental retardation and hypogenitalism, of the disorder now known as the BBS. A similar syndrome to BBS had been described by Laurence and Moon[280] in 1866 and Hutchinson[281] in 1900. As well as retinopathy and mental retardation, they described paraplegia as a prominent feature without polydactyly or obesity. Some authors classified all these cases together under the term *Laurence–Moon–Bardet–Biedl syndrome* until Ammann[282] in 1970 reasserted the separation of the two syndromes. The controversy continued, however, with some authors still recommending the combined term.[283,284] Most ophthalmologists today consider the features of Laurence–Moon within the spectrum of BBS. Beales et al. refined the diagnostic criteria in 1999 and proposed that the phenotype in the patients be renamed *polydactyly–obesity–kidney–eye syndrome*.[285] The prevalence has been placed at 1 in 160,000 in Switzerland.[282] Farag and Teebi[286] have found that Bardet–Biedl is more prevalent among the consanguineous Arab population of Kuwait and among the Bedouin, where the estimated minimum prevalence was 1 in 13,500.[287] Because of a founder effect, the prevalence of BBS in Newfoundland is approximately 1 in 17,500.[288]

Importantly, the retinopathy in BBS differs from typical RP in that visual acuity fails early in the course of the disease and usually the fundus shows little pigmentary dispersion until later stages. Macular lesions and atrophy of the RPE or choriocapillaris often develop early and prominently as the disease progresses.[289] These macular abnormalities may include macular wrinkling, preretinal membrane formation, and leakage on fluorescein angiogram from paramacular capillaries. When detectable, the ERG may show a rod–cone loss or, in many cases, even within the same family, a cone–rod loss pattern, the latter of which has led authors to call the retinal dystrophy in BBS a *cone–rod retinal degeneration*.[224,290,291] The absence of pigmentary deposits has also led to the retinopathy in Bardet–Biedl being called *RP sine pigmento,* or, when patchy whitish RPE lesions are evident, *retinitis punctata albescens*.[289] The onset of night blindness is recognized by a mean age of 8.5 years and legal blindness by a mean age of 15.5 years.[203] Approximately 73% of

patients reach legal blindness status by age 20 years and 86% by the age of 30 years.[289]

Incomplete manifestation of the five cardinal features is the rule rather than the exception in BBS. Prosperi et al.[292] estimated from previous reports that 40–45% of cases are incomplete. Another study of 102 cases showed only 24 with the complete syndrome.[293] Schachat and Maumenee[290] reviewed BBS and related disorders and suggested that at least four of the five cardinal features, of which retinopathy must be one, must be present to establish the diagnosis conclusively. Pigmentary retinopathy is reported in 90–100%[288,290] of cases, with ERG responses being abnormal in all cases. Most agree that mental retardation, which has been reported in 85–87% of cases,[290] is not an essential feature of this syndrome. Green et al.[288] found only 13 of 32 patients had mental retardation. When encountered, mental retardation is mild in slightly over 50% of cases.[289] Indeed, intelligence has been reported to be above normal in some patients. Although the tendency for obesity seems nearly universal, some patients have been able to control their weight by dieting and exercise. Polydactyly is present in 75% of cases, is postaxial, and may involve any or all extremities.[290] Syndactyly or brachydactyly is present in 14.4% of patients.[289] Both have been considered as equivalents of polydactyly with reference to determining the number of cardinal features present.[288,289,294] Hypogenitalism is present in roughly half of patients over the age of 15. Infertility is particularly prominent in male Bardet–Biedl patients,[291] although in our experience rare patients do remain fertile and father children. Vaginal atresia,[295] urogenital sinuses, uterine and ovarian hypoplasia,[295] and congenital hydrometrocolpos[296] have been described in female Bardet–Biedl patients. Many of these patients, however, have also met the cardinal diagnostic features (hydrometrocolpos and polydactyly) for McKusick–Kaufman syndrome, which is now recognized as having significant phenotypic overlap with the much more frequent disorder BBS.[297–299]

Of nonocular abnormalities not considered cardinal features of BBS, renal abnormalities are the most common, having been reported in 19 of 21 autopsied patients.[300] Hurley et al.[301] have observed radiologic abnormalities of the renal parenchyma or

collecting system in 11 of 11 patients. Since renal disease can be severe enough to lead to uremia and death, Churchill et al.[283] have argued for renal disease to be considered the sixth cardinal feature of BBS. Pagon et al.[302] reported a Bardet–Biedl child with renal failure and hepatic fibrosis. Cardiac abnormalities were identified on ultrasound in 50% of patients from Bedouin families.[303] Deafness is uncommonly associated with Bardet–Biedl, occurring in approximately 5% of patients.[290] Occasional cases with Hirschsprung's disease have been described.[304] Croft and Swift[305] suggested that even heterozygotes have an increased frequency of obesity, hypertension, diabetes mellitus, and renal disease.

Only subtle phenotypic differences between the different linkage types have been reported, the most striking of which was the finding of taller affected offspring compared with their parents in BBS1 families. Affected subjects in the BBS2 and BBS4 groups were significantly shorter than their parents. Carmi et al.[306] have shown that polydactyly of all four limbs seems associated with BBS3, whereas it is confined to the hands in BBS4. Early-onset obesity seems common in families with BBS4, whereas obesity is not associated with BBS2.[306] No confirmation of these correlations between phenotype and linkage loci has been reported with limited studies of molecularly confirmed genetic types of BBS.

In our experience, BBS fails to be recognized more frequently than any other syndrome associated with retinopathy, with the exception of the juvenile form of neuronal ceroid lipofuscinosis (NCL). This is either because patients are not asked about previously surgically corrected polydactyly or because the polydactyly is considered an isolated congenital birth defect unrelated to the manifest retinopathy.

Refsum Syndromes

Refsum name has been associated with two rare, autosomal recessive, peroxisomal diseases associated with progressive neurologic deficit, deafness, liver disease, skeletal abnormalities, and a pigmentary retinopathy. One, infantile Refsum disease, is a disorder of peroxisomal biogenesis that presents during infancy is part of the Zellweger spectrum. The other, adult (or classical)

Refsum disease, is a disorder of a single peroxisomal enzymatic function that presents as an early-to-middle-life adult-onset disease. Peroxisomes are cytoplasmic single-membrane-bound organelles present in almost all eukaryotic cells. They contain a number of enzymes such as catalases, hydroxylases, and oxidases involved in many oxidative reactions. Serum phytanic acid levels are elevated, either moderately (infantile form) or dramatically (adult form).

Infantile Refsum Disease

IRD was first reported in 1982 by Scotto et al.[307] in infants presenting with craniofacial malformation, severe hypotonia, psychomotor retardation, bleeding episodes, liver dysfunction by 6 months of age, and severe deafness within the first year of life. The ophthalmic manifestations were reported in 1984[270] to include nystagmus, poor vision, retinal degeneration with white flecks evident in the midperipheral retina (leopard spots) that fade and are replaced by coarse pigment clumping, optic atrophy, and eventually cataract. The ERG is profoundly abnormal early in the disease and can be electronegative.[270,271] Abnormalities of general peroxisomal biogenesis and function, similar to that seen with Zellweger's syndrome and neonatal adrenoleukodystrophy, were identified in IRD, and it is now classified as a milder variant of Zellweger syndrome (reviewed by Pennesi and Weleber[271]). The disease is often fatal by the second or third decade of life.[270,271]

Adult-Onset Refsum Disease

This autosomal recessive disease, also called *heredopathia atactica polyneuritiformis*, was first described in 1946,[308] with the ophthalmic features reviewed by Refsum in 1977.[309] This disease has been recently reviewed by Pennesi and Weleber.[271] The earliest symptoms in adult-onset Refsum syndrome are ataxia, weakness in the extremities, and nyctalopia presenting in later childhood. Progressive peripheral neuropathy and peripheral muscle wasting usually follow this, and cardiac conduction defects occur in early adulthood. Other common findings include paresthesia, anosmia, deafness, dry skin and ichthyosis, epiphyseal dysplasia, spondylitis, and kyphoscoliosis. Ocular features include cataract, miosis with poor pupil dilation, and retinopathy. Nyctalopia in the second

decade of life is followed by peripheral field defects. A pigmentary retinopathy is not evident until the third decade. ERG responses are severely abnormal or nonrecordable at all ages.

Phytanic acid levels in blood and urine are always very high due to a deficiency of phytanic acid oxidation. Protein levels in the cerebrospinal fluid are also characteristically elevated. Rather than a deficit of peroxisome biogenesis, as is seen in IRD, a specific peroxisomal enzyme, phytanoyl-coenzyme A hydroxylase, is deficient and inactivating mutations of the gene *PAHX*, also called *PHYH*, as well as mutations of the PTS2 receptor have been identified in Refsum syndrome patients.[310,311]

Restriction of dietary phytanic acid (which is present in dairy products and ruminant fat) can limit progression of disease and often improve the ichthyosis, neurologic deficits, and cardiac disease. There is limitation without improvement of visual or auditory deficits.[312,313]

Neuronal Ceroid Lipofuscinosis

The neuronal ceroid lipofuscinoses are a group of progressive neurodegenerative disorders characterized by accumulation of complex storage material within lysosomes. An extensive review by Mole and Williams is available at the website for GeneReview.[314] This class of conditions is the commonest neurodegenerative disorder to affect children, with a collective incidence worldwide of about 1 : 12 500 live births.[315] Characteristically, severe psychomotor deterioration eventually leads to a vegetative state, seizures, visual failure from retinal degeneration, and premature death.[316] Four classic forms exist: three childhood-onset forms, which are all autosomal recessive, and one adult-onset form, which may be autosomal recessive or dominant:

1. An infantile-onset form (INCL, *CLN1*), also called Haltia–Santavuori disease, Hagberg–Santavuori disease, or simply the Finnish form. This usually manifests at 8–24 months of age with severe psychomotor retardation, blindness, and microcephaly.[317]

2. A late infantile-onset form (LINCL, *CLN2*), also called Jansky–Bielschowsky disease. This condition manifests at 2–4 years of age

with ataxia, loss of speech, regression of development milestones, seizures, and later loss of vision.[318–320]

3. A juvenile-onset form (JNCL, *CLN3*), also called Batten–Mayou syndrome, Spielmeyer–Vogt disease, or Spielmeyer–Sjögren syndrome, which manifests at 4–8 years of age with visual acuity loss that progresses to loss of virtually all useful vision over a year or two.[316,321,322] The fundus appearance on presentation includes attenuated retinal vessels, a bull's-eye maculopathy, and fine pigmentary changes (Fig. 42.38).

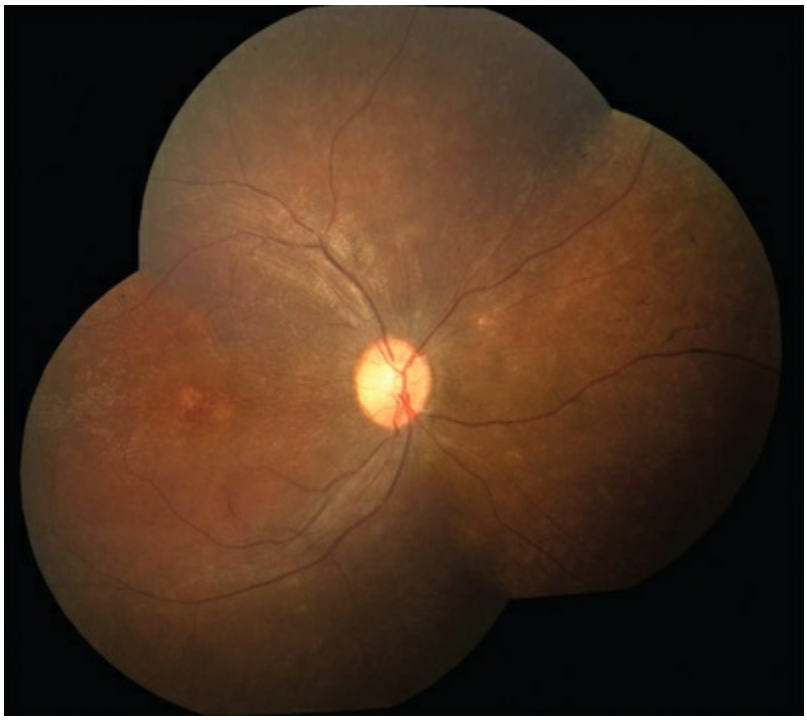

FIG. 42.38 Fundus appearance of the left eye of a girl with juvenile-onset neuronal ceroid lipofuscinosis at 11 years of age. Attenuated retinal vessels, bull's-eye maculopathy, and peripheral fine pigment clumping were evident.

4. The adult-onset disorder (ANCL, *CLN4*), also called Kufs' disease,[323] usually manifests as a motor disturbance without visual symptoms or findings. Although Kufs' disease is believed to be an autosomal recessive trait, autosomal dominant inheritance has been described.[324]

In addition, as many as 15 atypical forms have been described, some of which may be allelic to certain of the classical forms.[325] One of the variant forms (vLINCL, *CLN5*) occurs essentially only in the Finnish population and shows linkage to a site (13q22) distinct from the three classic forms of childhood NCL.[326] In Europe, the term *Batten disease* is often used collectively for all forms of NCL.[327,328]

INCL has an incidence of 1 in 13,000 to 20,000 in Finland, 1 in 50,000 in Scandinavia, and 1 in 100,000 worldwide.[316,329] LINCL has a frequency of 0.46 per 100,000 in Germany.[330] JNCL has an incidence of 1 in 21,000 in Finland and a frequency of 0.71 per 100,000 in Germany.[330]

The visual failure in the three classic childhood forms (1 to 3 above) involves central vision first and eventually results in profound visual loss, often with complete blindness, within a few years. The ERG becomes abnormal early in the course of all these disorders and within a few years is usually totally abolished to standard single-flash recording techniques. Goebel[316] states that the ERG becomes flat (undetectable to standard techniques) for LINCL between ages 3 to 4 years and for JNCL between 5 to 7 years of age. Visual symptoms and abnormalities on electrophysiologic testing are rare and even then occur late in the course of Kufs disease.[323]

Studies have examined the ERG in patients with INCL, LINCL, and JNCL.[273,274] The ERG is abnormal early in the course of all three disease types. For patients with INCL, rod responses were severely subnormal; the scotopic ERG to the 0.6 log cd-s/m^2 stimulus was normal for the a-wave and profoundly subnormal for the b-wave, indicating that the earliest manifestation of this disease appears not to affect phototransduction directly. Instead, this result was interpreted as an effect on neurotransmission from proximal photoreceptors to bipolar cells. This appeared to occur from one of three possible sites: (1) a disturbance of proximal photoreceptor function that interfered with presynaptic neurotransmission; (2) a disturbance of the postsynaptic plate region; or (3) some other effect on the bipolar cells, with subsequent reduction of the generation of the b-wave. The ERGs of three patients with LINCL were different in showing nearly normal rod amplitudes, mildly prolonged rod implicit times, and severely subnormal, prolonged cone responses. Patients with more advanced stages of LINCL had a greater deficit

of the b-wave than a-wave, suggesting development of loss of effective transmission of the signal from photoreceptor inner segments to bipolar cells. Unlike the ERG in either INCL or in JNCL, the rod responses in early LINCL were only mildly subnormal and prolonged but with much more preserved amplitude, even though cone responses were severely subnormal and prolonged. Three patients with JNCL had a third ERG phenotype (Fig. 42.39) with essentially no discernible rod responses and severely subnormal cone responses with normal to prolonged implicit times. The maximum scotopic a-waves in all three JNCL cases were subnormal, indicating loss of effective outer segments. The b-wave responses, however, were even more subnormal, creating an electronegative configuration. Oscillatory potentials were profoundly subnormal. The greater disturbance of the b-wave than that of the a-wave for patients with JNCL is consistent with the inner retinal localization of the *CLN3* gene product, which appears localized to mitochondria of Müller cells, inner retinal neurons, and the inner segments (but not the outer segments) of photoreceptors.[331]

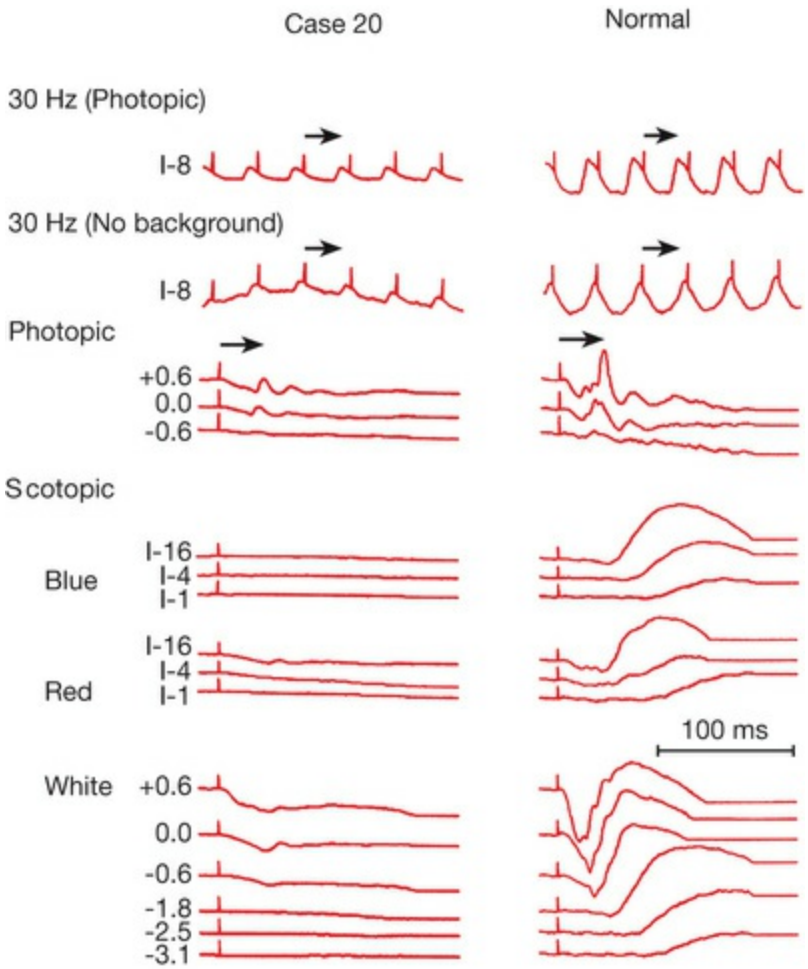

FIG. 42.39 Electroretinogram responses of a 6-year-old girl with juvenile-onset neuronal ceroid lipofuscinosis (Batten's disease) (left) compared with those of a normal subject (right). Note the absence of rod responses to the dark-adapted white light (−1.8 log cd-s/m^2) and blue I-16 stimuli. The scotopic response to +0.6 log cd-s/m^2 white light was electronegative in configuration with greater loss of the b-wave than the a-wave amplitude.

All forms of neuronal ceroid lipofuscinoses show accumulation of storage material that is autofluorescent, sudanophilic, and periodic acid–Schiff-positive within lysosomes in neurons and other cells. Because of its osmophilic nature and appearance on light microscopy, the storage material resembles ceroid and lipofuscin, but actually it is a complex mixture of lipoproteins and other hydrophobic peptides. The lipoprotein deposits within cells on electron microscopy take on characteristic patterns that are used for diagnosis and classification. Granular inclusions are seen in INCL,

Kufs disease, and some atypical forms of JNCL. Curvilinear inclusions predominate in LINCL (with occasional to rare fingerprint inclusions). Fingerprint inclusions are seen in JNCL (with occasional to rare curvilinear inclusions).[332,333]

Historically the diagnosis of this group of disorders has been established by looking for inclusion bodies in cells from brain biopsy or full-thickness rectal biopsy.[334,335] Skin or bulbar conjunctival biopsies typical shows fingerprint inclusions (Fig. 42.40), which have been valuable in establishing the diagnosis although genetic testing is starting to replace these procedures.[332,333] Buffy-coat leukocytes can be used but may include a wider range of inclusions that may represent other storage disorders, such as the mucopolysaccharidoses.[336,337] Fingerprint and tubular inclusions on electron microscopy of lymphocytes have been seen in children with LINCL and JNCL. These can also be seen in carriers of these conditions.[338,339] Rapola et al.[335] were unable to determine reliably the presence or absence of electron microscopic inclusions in lymphocytes from patients with INCL. Muscle biopsy may represent the best approach to ultrastructural diagnosis for ANCL.[340] However, since skeletal muscle fibers show only the curvilinear type of inclusions on electron microscopy, one cannot use muscle biopsy to differentiate the specific types of NCL.[341] Brain biopsies are no longer justifiable for establishment of the diagnosis of NCL.

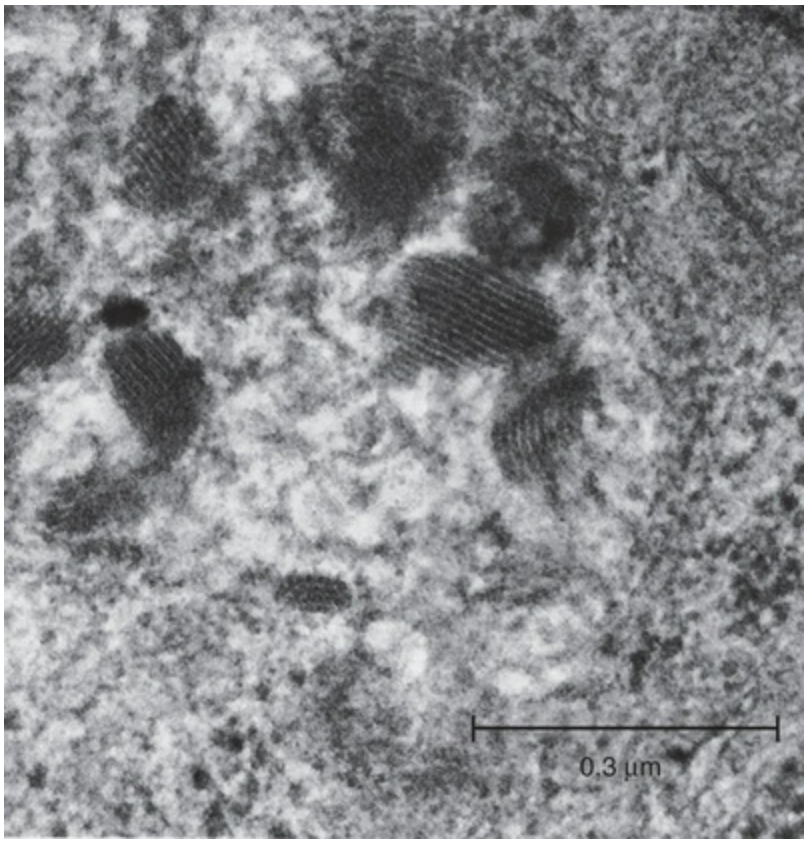

FIG. 42.40 Electron microscopy of endothelial cells from conjunctival biopsy taken from an 8-year-old girl with Batten's disease. Fingerprint inclusions were numerous, but one field showed curvilinear inclusions as well.

Differential Diagnosis: Pseudoretinitis Pigmentosa

To some extent, damage to the retina produces nonspecific symptoms and signs. This is especially true of panretinopathies. A number of acquired conditions can cause extensive chorioretinal atrophy that is difficult to distinguish from advanced RP. In such situations, specific details of the history or asymmetry of disease may be the most important differentiating factors. The accounts below summarize the acquired conditions most commonly confused with RP. More extensive descriptions of some of these are given elsewhere in the text.

Retinal Inflammatory Diseases

Rubella Retinopathy

The most common ocular manifestation of congenital rubella, rubella retinopathy,[342] is occasionally confused with RP. This confusion is especially likely in children with congenital deafness and a pigmentary retinopathy that are erroneously thought to represent both congenital rubella retinopathy and deafness rather than Usher syndrome. Uncommonly, the converse occurs, and the pigmentary disturbance of rubella retinopathy in a child with deafness triggers the suspicion or even the presumptive diagnosis of RP. Rubella retinopathy is one of the most characteristic manifestations of congenital rubella.[343] Rubella retinopathy may take any of several forms. In some, the macula is the only site of abnormality, with a speckling of fine pigment granules. In others, pigmentary changes can extend further into the peripheral retina. Usually the correct diagnosis can be established by a combination of clinical features and electroretinography, which is only mildly abnormal in rubella retinopathy but will be, almost invariably, severely abnormal in Usher syndrome. Rubella retinopathy is a disease that is capable of mild progressive increase in pigmentary changes[344] or the development of clinically significant subretinal neovascularization.[345]

Syphilis

Congenital or acquired syphilis can present as a pigmentary retinopathy that may appear similar in some respects to advanced RP,[346] but careful examination usually establishes the correct diagnosis. Interstitial keratitis is commonly seen in congenital syphilis, and the pigmentary retinal changes are more varied and patchy. Usually the pigment deposits are clumps or large patches of black pigment associated with chorioretinal scars; typical bone-spicule pigment formations are uncommon. The posterior pole may be as involved as the periphery. There may be evidence of past or present overlying vitreous reaction or uveitis. Acquired syphilis can also present with a diffuse retinal involvement.[346]

Infectious Retinitis

Rarely, toxoplasmosis or herpes infections of the retina may leave a pigmentary retinopathy that poses a diagnostic challenge. These entities usually produce extensive full-thickness chorioretinal scars but may in certain areas produce only mottling and granularity of the RPE. Usually, randomly arranged patches of severe retinopathy exclude a diagnosis of RP. Electroretinography is usually only minimally affected in postinfectious retinopathies, unless extensive areas of retina are severely damaged, in which case the ERG will be accordingly decreased in amplitude.

Autoimmune Paraneoplastic Retinopathy

Several reports have documented the existence of severe panretinal degeneration as a remote effect of cancer, usually either small-cell (oat-cell) carcinoma of the lung[347,348] or small-cell undifferentiated cervical carcinoma.[349] In several cases the vision loss preceded the diagnosis of the cancer.[279] Cancer-associated retinopathy (CAR) can progress rapidly or slowly with loss of vision over a period of months or years. Electroretinographic responses are usually severely abnormal. The fundus appearance may be normal even when the ERG is extinguished and the vision severely decreased. The first autoantigen in the human retina identified with a CAR is recoverin.[350,351] Antibodies to retinal enolase have also been reported in CAR.[352,353]

A paraneoplastic form of night blindness associated with "shimmering lights" and a characteristic ERG has been reported with malignant melanoma and has been called *melanoma-associated retinopathy* (*MAR*).[354,355] The scotopic ERG to maximum-intensity flash has a "negative" configuration, identical to that seen with congenital stationary night blindness. The a-wave amplitude is normal, and the b-wave amplitude is severely subnormal, distinguishing this form of paraneoplastic retinopathy from CAR. Alexander et al.[356] found a defect in the on response of the ERG, reflecting abnormal rod neurotransmission to depolarizing bipolar cells.

It has been suggested that in MAR there is a selective loss of function subserved by magnocellular cells with preservation of midget type 1 parvocellular cell function.[357] We have seen a patient

with acquired night blindness and a negative-configuration ERG typical for congenital stationary night blindness associated with an anaplastic squamous cell carcinoma of the nasopharynx (WT Shults and RG Weleber, unpublished observations, 1991). Other acquired cases of visual symptoms, field loss, and electronegative-configuration ERGs have been reported in the absence of either melanoma or other discernible cancer but with serum antiretinal antibodies that specifically labeled the inner plexiform layer of cadaver retina by indirect immunoperoxidase testing.[358] Presumably, these patients have produced an antibody to an antigen that is similar (by molecular mimicry) to one found in normal retina, producing the disturbance of retinal function and electrophysiology.

Drug Toxicity

See also Chapter 92, Drug toxicity of the posterior segment.

Thioridazine

This phenothiazine has been linked to severe, blinding retinal toxicity. In general, phenothiazines bind to melanin and concentrate in the uveal tract and RPE.[359,360] The retinal toxicity of thioridazine is believed to result from the presence of a piperidyl group. Thioridazine can cause a pigmentary retinopathy that can be confused with RP (in its early stages) or choroideremia (in its later stages).[361] In most patients with thioridazine retinopathy the drug has been taken at doses higher than 800 mg/day.[362]

The earliest symptoms include blurring of central vision, poor night vision, and a brownish discoloration to the vision. Early toxicity produces fine, deep retinal pigment posterior to the equator, which becomes coarser as the condition progresses. Large "signal" plaques of pigment deposition occur late. The characteristic appearance of advanced thioridazine retinopathy is diffuse, patchy atrophy of choriocapillaris, RPE, and overlying retina, simulating the fundus appearance of early choroideremia.[363] The ERG may show decreased amplitudes of both cone- and rod-mediated responses; responses of both a-waves and b-waves are subnormal.

Chlorpromazine

This drug has been reported to produce a pigmentary retinopathy when taken at high doses for prolonged periods.[364] The pigmentary retinopathy does not significantly affect retinal function, and the retinopathy appears to regress when the drug is stopped.

Chloroquine

Similar to the phenothiazines, chloroquine, if taken over a prolonged period, binds to melanin and causes a toxic retinal degeneration. Very few cases have been reported with patients taking a total dose of less than 300 g.[365] Early in the course of toxicity the ERG, EOG, and visual fields can be normal, although in late, severe toxicity, they can become markedly abnormal.[366,367] In advanced chloroquine retinopathy, unlike RP, the dark adaptometry may be either normal or only minimally abnormal.[366] The typical picture of advanced chloroquine toxicity is that of a bull's-eye maculopathy, although pigmentary changes with bone-spicule formations can occur in the mid- and far periphery.[286,366]

Hydroxychloroquine

This drug has mostly supplanted chloroquine usage for rheumatoid arthritis and systemic lupus erythematosus. However, toxicity can occur with chronic usage, and the current recommendation is periodic ophthalmologic examination with static perimetric visual fields (Humphrey Field Analyzer 10-2 or 24-2) when the duration of usage is over 5 years, particularly if the dosage is greater than 6.5 mg/kg per day.[368] The multifocal ERG appears to be a useful diagnostic tool to help differentiate pericentral visual field loss due to hydroxychloroquine from that due to optic nerve or other causes.[369]

Quinine

Retinopathy due to oral ingestion of quinine is usually a consequence of large doses taken either during a suicide attempt or to abort a pregnancy. Often, the diagnosis is aided by the history of acute loss of vision and the finding of characteristic pallor and edema of the retina early, with later development of attenuation of

retinal vessels and optic nerve head pallor.[370,371] At this stage, quinine toxicity may be misdiagnosed as RP sine pigmento.[370] The ERG in quinine toxicity is usually of a "negative" configuration, with far greater depression of the scotopic b-wave than a-wave.[372,373]

Pigmented Paravenous Retinochoroidal Atrophy

Pigmented paravenous retinochoroidal atrophy (PPRCA) was first described in 1937 as retinochoroiditis radiata.[374] PPRCA is a pigmentary retinopathy that is currently poorly understood but probably represents an acquired response pattern to an infectious or inflammatory disease.[183,375,376] It has been reported in association with meningoencephalitis,[377] tuberculosis,[183,375,377,378] syphilis,[183,379] and rubeola.[380,381] In most, the fundus appearance is first noticed on a routine examination. Three small pedigrees with PPRCA have been described.[382–384] These may, however, represent examples of infectious factors clustering in families rather than true genetic cases. As the name implies, the pigmentary changes are closely associated in distribution with retinal veins (Fig. 42.41). Most cases are relatively stable over time, although progression has been reported in one case.[385,386] Electroretinographic responses are only mildly to moderately abnormal, if at all,[183,375,387–389] but the EOG is usually affected, often significantly.[388]

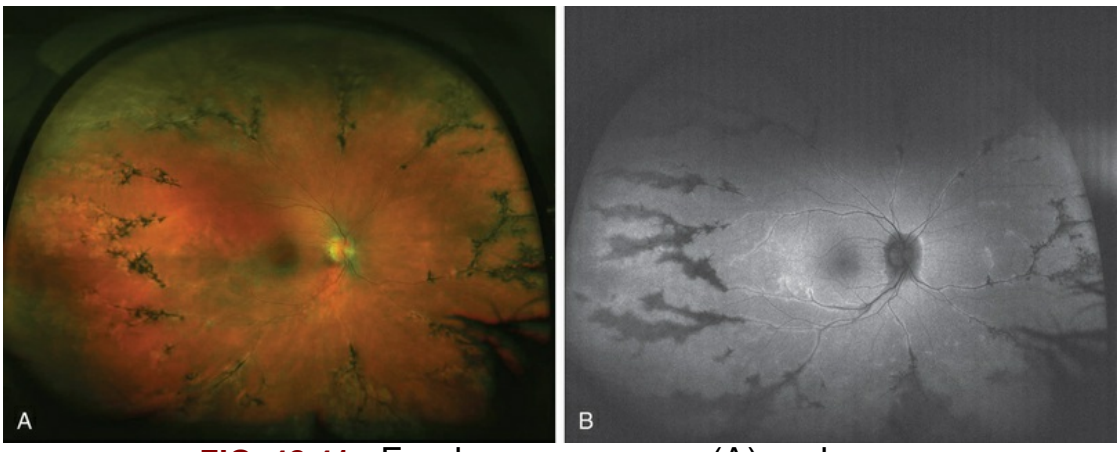

FIG. 42.41 Fundus appearance (A) and autofluorescence (B) of the right eye of a 20-year-old patient with PPRCA. (Photos courtesy of Dr. Paul Yang.)

Traumatic Retinopathy

Traumatic retinopathy is probably the commonest acquired retinopathy that is confused with RP and may, with diffuse unilateral subacute neuroretinitis (DUSN), account for many previously misnamed cases of "unilateral RP." The RPE and retina have only a limited range of responses to a traumatic insult. One of these is regional or generalized loss of the RPE with migration of melanin into the retinal layers where it accumulates along vessels, especially at branching points, creating a bone-spicule pattern. Thus patients with past traumatic injury to an eye can present with a fundus appearance in the traumatized eye that mimics RP.[390]

Diffuse Unilateral Subacute Neuroretinitis

DUSN is the term now used for the disorder previously called "unilateral wipe-out syndrome,"[391] and "unilateral RP."[183] True unilateral inherited RP is extremely rare and can occur with extreme lyonization of retinal involvement in a carrier of X-linked RP. DUSN is believed to result from the panretinal degeneration that takes place in eyes that have been infected by any of several possible worms. The raccoon nematode (*Baylisascaris procyonis*)[392,393] has been incriminated, but other worms such as *Toxocara canis*[394] have been suspected. Cases have been seen mainly in the United States and Caribbean, but a few cases have also been reported from Brazil[394] and Germany.[395] Cuhna de Souza et al.[396] described the first instance of bilateral acute neuroretinitis with documentation of the nematode in both eyes.

At the time of initial visual disturbance, the retina may either appear normal or show early signs of retinal degeneration (mottling, edema, narrowing of retinal vessels). Occasionally, one can see an elevated gliotic mass in the mid- or far periphery that may represent the encased worm. The visual field often shows abnormalities early in the course of the disease, but these are usually patchy. With time, the visual function usually deteriorates in the affected eye but remains normal in the fellow eye. Eventually the retina develops pigmentary clumping and scarring reminiscent of advanced RP (Fig. 42.42). The pigmentary abnormalities within

the retina in some patients may take the form of accumulation of medium to coarse clumps of pigment rather than bone spicules. ERG recordings show clinically significant abnormalities in the affected eye only. Retinal laser photocoagulation has been used in cases where the fundal view is clear.[391] Vitrectomy with surgical removal of the subretinal nematode has been achieved,[394] and oral tiabendazole or ivermectin is indicated when vitritis obscures retinal detail.[397]

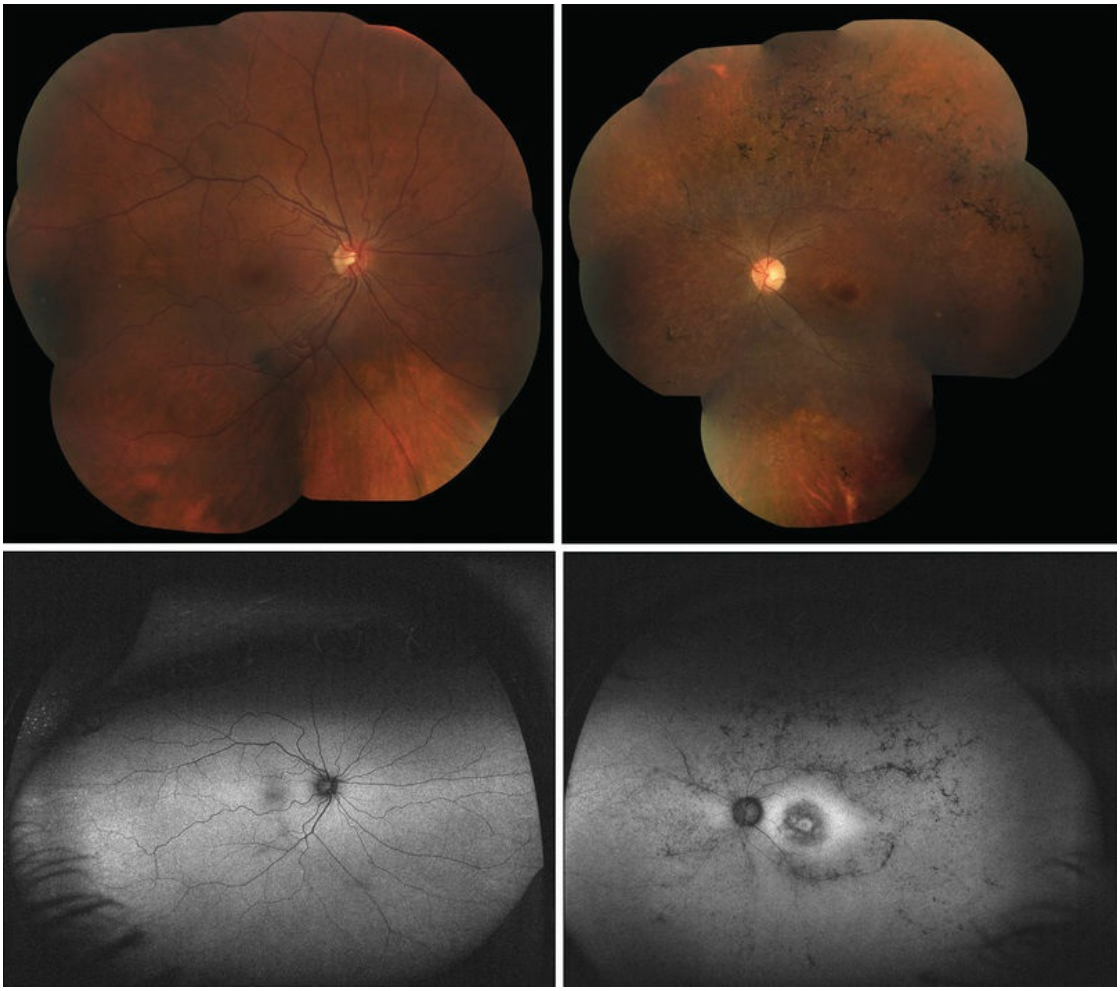

FIG. 42.42 Right (A) and left (B) fundi of a patient with suspected DUSN at age 27. Corresponding Optos autofluorescence images are shown below.

Grouped Pigmentation of the Retina

Grouped pigmentation of the retina, also called “bear-track”

pigmentation, is a benign congenital condition in which round and irregularly shaped lesions representing RPE hypertrophy are scattered throughout the retina[398] (Fig. 42.43). The condition does not appear to be hereditary. Usually the differentiation of this condition from more significant pigmentary retinopathies presents little difficulty. Retinal function and electrophysiologic tests are normal.

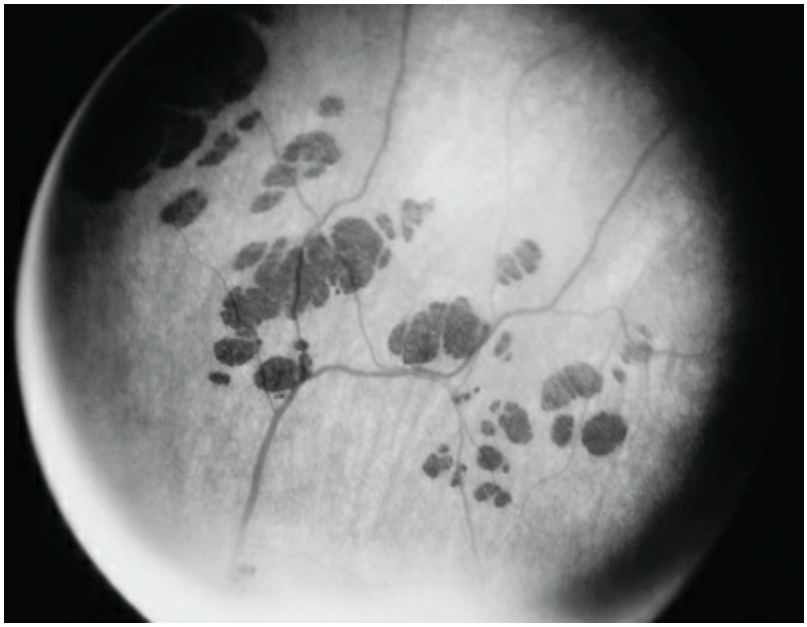

FIG. 42.43 Grouped pigmentation ("bear tracks") of the retina. (Reproduced from Buettner H. Congenital hypertrophy of the retinal pigment epithelium. Am J Ophthalmol 1975;79(2):177-189.)

Grouped pigmentation of the retina should be differentiated from multiple patches of congenital hypertrophy of the RPE, which are associated with familial adenomatous polyposis or Gardner's syndrome[399] (see Chapter 33, Genetic mechanisms of retinal disease).

Basic Science

Molecular Biology

Molecular Genetics

Retinal dystrophy research has been the subject of many important discoveries in ocular molecular genetics. This occurred because of the development of molecular genetic markers (DNA polymorphisms identified throughout the genome), DNA sequencing for mutation screening, and most recently, whole exome sequencing. Using current methodology, it is now possible to detect specific gene mutations in up to 80% of cases.[400]

Using molecular genetic analysis, 25 specific genes (and an additional one locus) have been associated with adRP, 55 specific genes associated with isolated arRP (with an additional three loci), three specific genes associated with X-linked RP (along with three more loci), and one with digenic inheritance. Additionally 20 genes (and a further four loci) have been associated with Usher syndrome (autosomal recessive). For those interested in the most recent gene assignments and localizations, a list of cloned and mapped genes causing retinal degenerations or allied disorders has been compiled by Dr. Stephen P. Daiger and is accessible at http://www.sph.uth.tmc.edu/Retnet/.

Autosomal Dominant RP Genes.

In rod photoreceptors, rhodopsin is the light-absorbing, conjugated photopigment found in outer-segment discs. It is composed of an apoprotein opsin molecule covalently bound to 11-*cis*-retinal (Figs. 42.44 and 42.45).[401] Incident light induces isomerization of the retinal and decay through a sequence of spectrally defined photoproducts. These light-induced changes result in a number of conformational changes in the opsin molecule, exposing G-protein-binding sites. A cascade of reactions (the phototransduction cascade; see (Fig. 42.46) is then set in motion and results in closing cGMP-dependent cation channels and relative transmembrane hyperpolarization.[402]

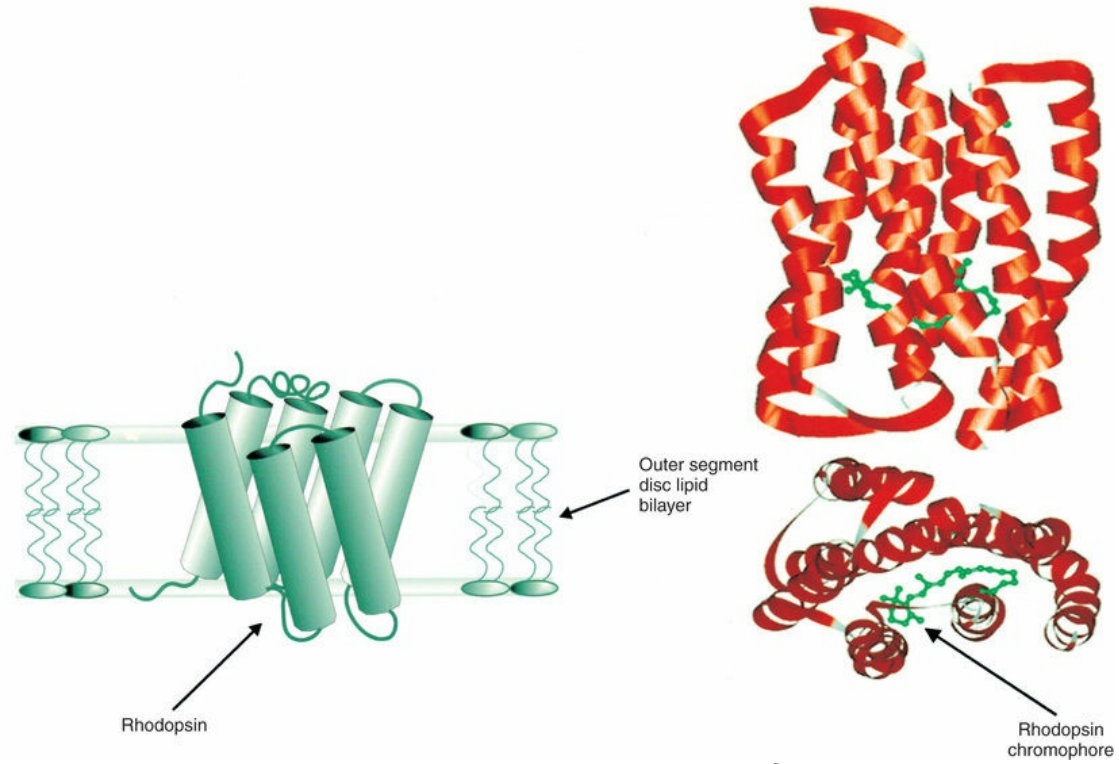

FIG. 42.44 Diagrammatic representations of rhodopsin protein. (Left) Positioning of rhodopsin within the rod outer-segment disc membrane. (Right) Three-dimensional representation of rhodopsin illustrating the central localization of the retinaldehyde chromophore.
(Courtesy of Dr. D. Farrens.)

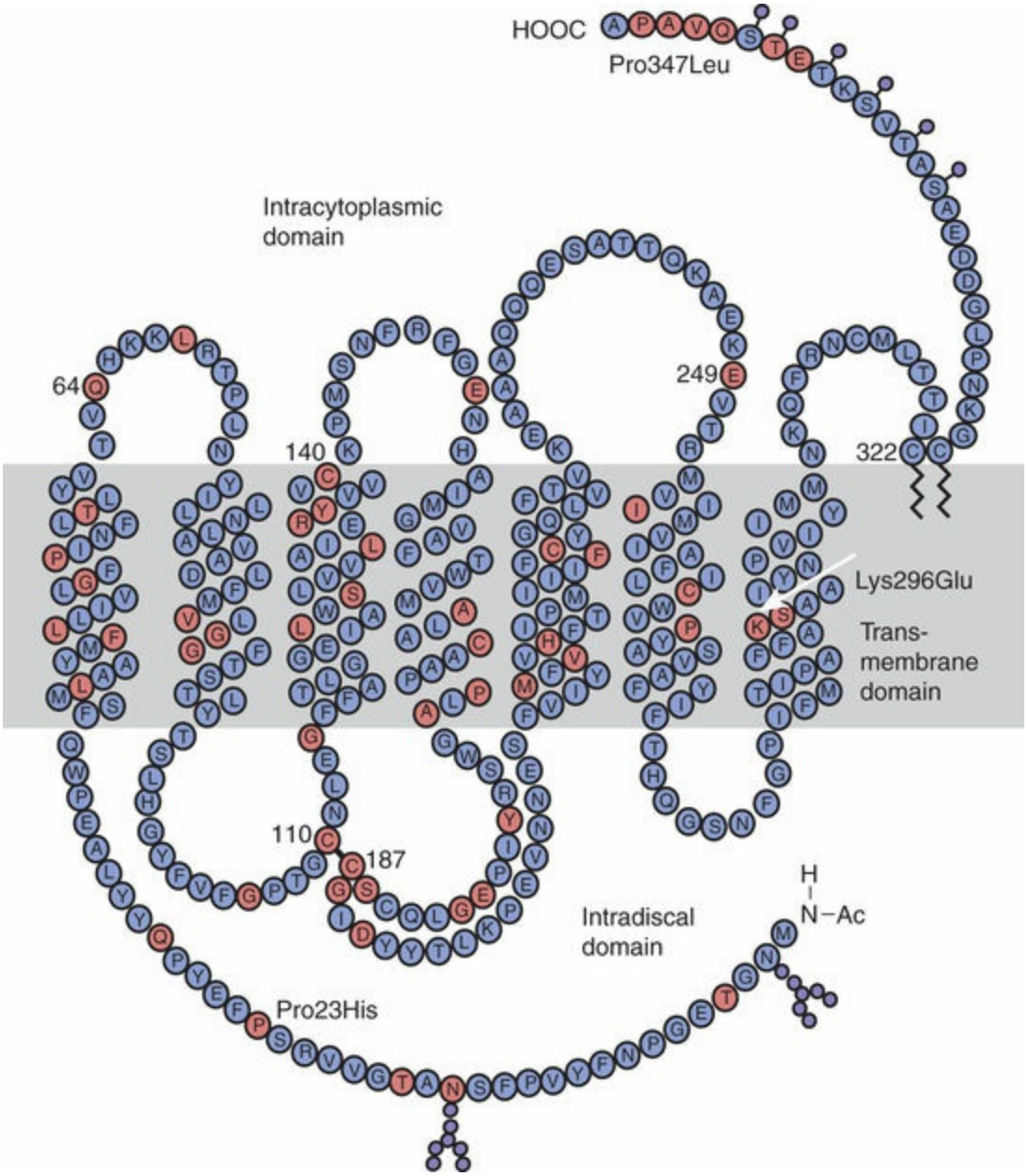

FIG. 42.45 Diagrammatic representation of rhodopsin. Amino acids mutated in retinitis pigmentosa are highlighted in red. There is a disulfide bridge important for the tertiary structure between the cysteines (*C*) at codons 110 and 187; palmitoylation sites exist at the cysteines at codons 322 and 323. The lysine (*K*) at codon 296 is the site of binding of retinal to rhodopsin; the glutamic acid (*E*) at codon 113 is the counter ion for the lysine at codon 296.

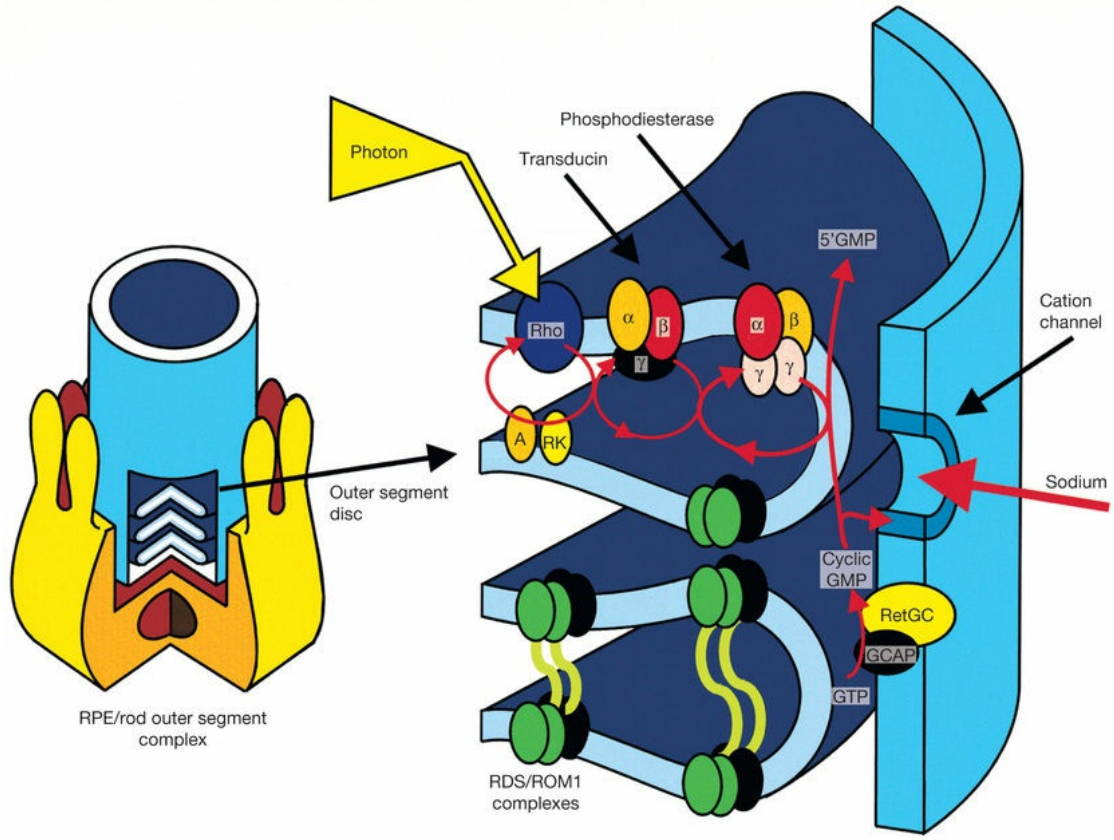

FIG. 42.46 Diagrammatic representation of the retinal pigment epithelium (RPE)–rod complex. Phototransduction and the role of rds/ROM-1 protein complexes in maintaining outer-segment discs are illustrated. *Rho*, Rhodopsin; *A*, arrestin; *RK*, rhodopsin kinase; *RetGC*, retinal guanylate cyclase; *GCAP*, guanylate cyclase-activating protein.

McWilliam et al.[403] were the first to detect linkage of adRP with an anonymous marker on the long arm of chromosome 3q. Shortly thereafter, Dryja et al.[404] reported a mutation of codon 23 (Pro23His) of the rhodopsin gene mapping to chromosome 3q (Fig. 42.44). A mutation in the third exon of rhodopsin, Met207Arg, has been found in the Irish family originally linked to chromosome 3q.[405]

It has been estimated that rhodopsin mutation accounts for approximately 25% of adRP.[406] In the United States, rhodopsin Pro23His is by far the most common of all rhodopsin mutations, being found in 12–15% of all American families with adRP.[407] It is interesting that the Pro23His mutation has rarely been reported anywhere else in the world.[408] In fact, the mutation rate of the rhodopsin gene appears to vary with ethnic background. For

instance, of *RHO* mutations in Asian populations, such as Japanese (5.9%),[409] Chinese (2.0–5.6%),[410] Indian (2.0%),[411] and Korean (2.0%)[412] are lower than that in the United States,[407] and Europe.[413]

From the occurrence of a rare, intron 1 polymorphism in all patients with Pro23His adRP, it has been suggested that all persons with this mutation have originated from a single mutation founder.[414] The phenotype associated with rhodopsin Pro23His is best described as Massof type II[92] or R-type RP.[97,98] Most rhodopsin adRP phenotypes have in fact been described as type II or R-type disease,[415–417] with a minority of mutations associated with type I or D-type disease.[418,419]

Pro347Leu is the next most frequent mutation of rhodopsin, accounting for approximately 5% of 148 adRP families in one series.[420] This form of adRP is a more severe, diffuse phenotype, with comparatively smaller visual fields with more ERG deficit than that seen in cases of Pro23His adRP.[421] The ophthalmologic findings of patients with Gly106Arg mutation of the rhodopsin gene[415] appear to be variable in expression, with patients rarely having normal cone and low-normal rod ERGs, a finding quite unusual among patients with RP. Sieving et al.[422] have reported the evaluations of seven affected members of a large family with a Gly90Asp rhodopsin mutation and described the condition for this family as autosomal dominant congenital nyctalopia to distinguish it from typical RP.

Sandberg et al.[423] have reported clinical details on patients with 27 different dominant rhodopsin mutations. They suggested that severity of disease, measured by visual acuity, visual field diameter, dark-adapted sensitivity, and ERG amplitudes, increased with increasing codon number (Fig. 42.45) Berson et al.[424] have suggested that the rate of progression of RP from mutation of rhodopsin is correlated with the site of mutation and that other modifying factors, genetic or environmental, may influence phenotypic expression. A “constant equivalent light” model, has been proposed for the severe adRP phenotype associated with rhodopsin codon 296 mutation. Lys296 is the chromophore-opsin attachment site and is also involved in holding the opsin in an inactive conformation. Theoretically this would lead to overstimulation of the phototransduction cascade, a situation

similar to constant light exposure. This situation is known to lead to photoreceptor cell death.[425] This explanation has been questioned, however, because the opsin appears to be inactivated by phosphorylation and arrestin binding in Lys296Glu transgenic mice.[426]

The *PRPH2* gene (formerly *peripherin/rds)* was first associated with RP in 1991,[427,428] and over 39 sequence variants have been associated with a range of autosomal dominant phenotypes, including RP, macular dystrophy, CRD, central areolar choroidal dystrophy, fundus flavimaculatus, and pattern dystrophy.[429] Most are missense mutations, but it is unlikely that *PRPH2* mutations account for more than 5% of adRP.[430] These reports do, however, represent the first instance of which an animal model of RP has been found to have a directly correlated human disease counterpart. Much of what we understand to be the role of peripherin/RDS in human photoreceptors (see Figs. 42.47 and 42.49) comes from initial studies on this naturally occurring mouse model (rds), which has a 10-kb insert in codon 230 of the disease gene, creating a null allele.[431] From this work and more recent human studies, it has been found that the peripherin/*rds* molecule accumulates in the rims of photoreceptor outer-segment discs and plays an important role in disc morphogenesis and stability.[432]

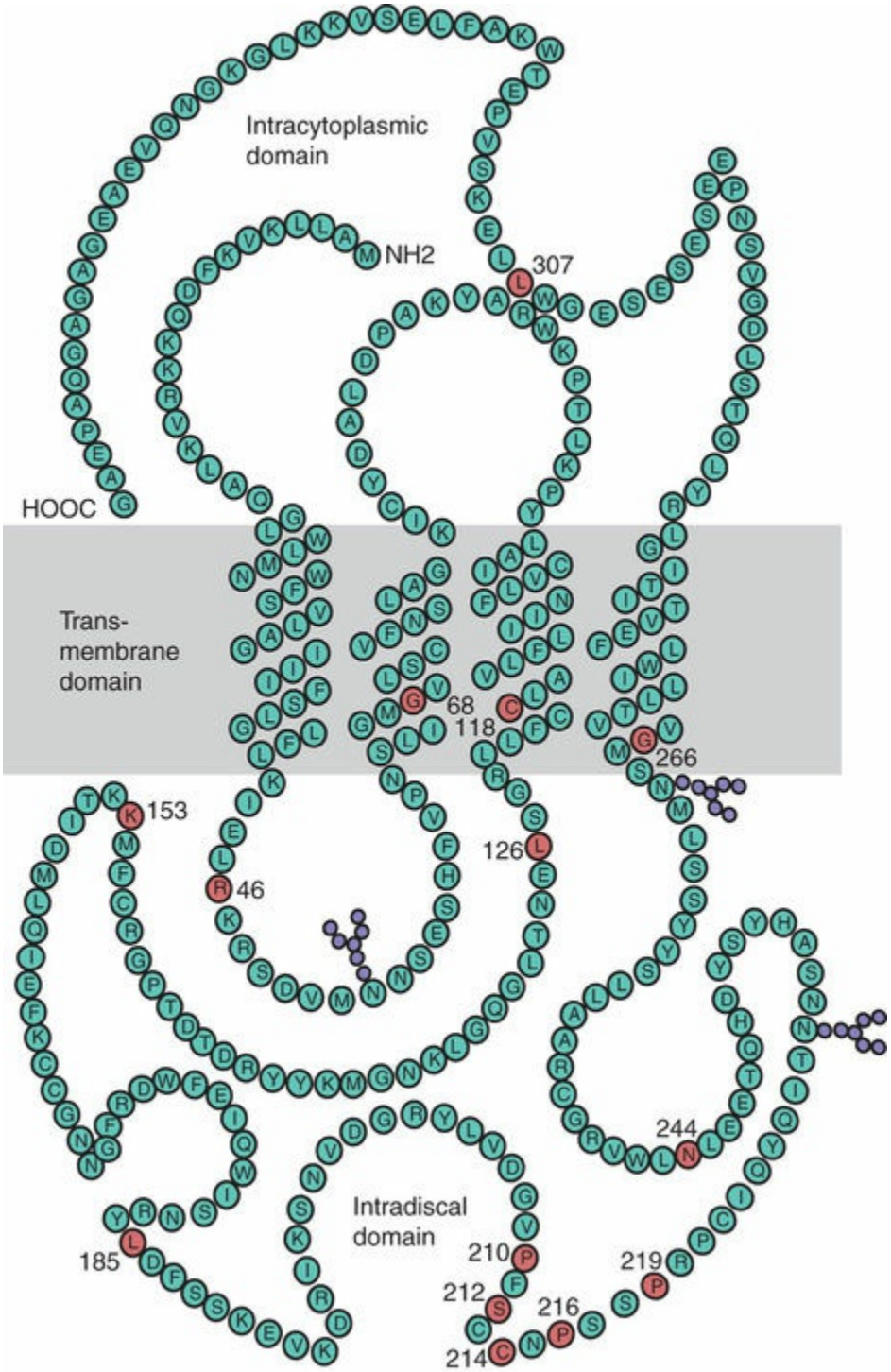

FIG. 42.47 Diagrammatic representation of peripherin/RDS protein. Amino acids mutated in retinitis pigmentosa are highlighted in red. Both the carboxyl-terminus and acetylated amino-terminus are cytoplasmic. Morphogenesis of the disc rims appears to involve interactions among tetramers of the large second intradiscal loop.

Bessant et al.[433] reported a large family with adRP previously

linked to chromosome 14q11 that is associated with a Ser50Thr mutation of *NRL*. The gene product NRL is a retinal-specific DNA-binding transcription factor that interacts with the cone–rod homeobox transcription factor CRX to promote and regulate transcription of rhodopsin and other retinal genes. The Ser50Thr NRL mutation, when coexpressed with CRX in transfection experiments, produced a marked increase in transactivation of the rhodopsin promoter, producing excessive transcription of rhodopsin. Other families with adRP have been reported with NRL mutations.[434]

A rare but remarkable regional (type II) phenotype with graded disease severity (variable expressivity) has been reported associated with mutations *PIM1*, on chromosome 7p.[435] This encodes a protein kinase involved in transcriptional control. The gene *FSCN2*, which encodes a photoreceptor-specific paralog of the actin-bundling protein fascin, with presumptive cytoskeletal formation functions, has been reported with autosomal dominant RP.[436] A common *FSCN2* mutation, 208delG, appears to account for 3.3% of adRP in Japan.[436]

Autosomal Recessive RP Genes.

Phenotypes associated with arRP loci can occur at any age, often tend to be early-onset and severe, and are usually consistent within a family.

The third phototransduction cascade protein (Fig. 42.47), cGMP phosphodiesterase (PDE), has been associated with a number of phenotypes.[437] PDE is a holoenzyme consisting of two large subunits, α and β, which become enzymatically active when the two γ-subunits are removed by activated transducin. Many nonsense and missense mutations of the α- and β-subunits of PDE (gene symbols *PDE6A* and *PDE6B*, respectively) have been associated with arRP, with the *PDE6A* mutations representing null alleles. No mutation of the PDEγ-subunit gene, *PDEG*, has yet been associated with human retinal disease. This might be due to the fact that *PDEG* has an exceptionally low mutation rate, that in humans the gene is expressed in other vital tissues and is lethal in utero, or the function of the mutant PDEγ may be taken over by some other protein. Most PDEβ-subunit mutations associated with arRP are

found in the C-terminal half of the molecule, which contains the catalytic domain. These mutations presumably directly affect the enzymatic activity of the protein. The His258Asp mutation, however, is near the N-terminal portion adjacent to the PDEγ-binding domain. This mutation has been reported in a Danish family associated with an autosomal dominant congenital stationary night blindness. It has been postulated that this mutation impedes complete inactivation of PDE in dark-adapted rod photoreceptors. This would result in rod desensitization and an inability to transduce at low light levels.[438]

Activated PDE hydrolyzes intracellular cGMP. This second-messenger molecule is generated from guanosine triphosphate by membrane-bound and soluble guanylate cyclase.[439] Increased intracellular cGMP leads to relative opening of membrane-bound cGMP-gated cation channels and cell hyperpolarization. The cGMP-gated cation channels are composed of three subunits, α, β, and γ. Mutations (usually null alleles) of the gene for the rod α subunit (*CNGA1*) have been associated with arRP.[440]

Recovery of active rod opsin, for further phototransduction, involves the regeneration of the 11-*cis* retinaldehyde chromophore from the *all-trans* isomer. In part, this process involves a cellular retinaldehyde binding protein (CRALBP), which binds and promotes 11-*cis* retinol oxidation to 11-*cis* retinaldehyde in the RPE.[441,442] A homozygous R150Q mutation of the gene for CRALBP (*RLBP1*) has recently been associated with childhood-onset arRP.[442] Nyctalopia was evident by 3–4 years of age. Optic atrophy, vascular attenuation, macular atrophy, and peripheral white dots without classic bone-spicule pigmentation were reported. Mutations of *RLBP1* have also been reported in autosomal recessive retinitis punctata albescens,[443] Bothnia dystrophy,[444] and Newfoundland rod-cone dystrophy.[445]

The tubby-like protein (TULP) gene family includes *TUB*, the human homolog of the mouse *tub* gene, *TULP1*, *TULP2*, and *TULP3*. All four are expressed in the retina but have unknown functions.[446] Mice, homozygous for a tub mutation, develop maturity-onset obesity, insulin resistance, cochlear degeneration, and a progressive retinal dystrophy. No mutations of *TUB* have yet been associated with human retinal disease, but mutations of *TULP1*, which is

retina-specific, have been associated with arRP.[447] Homozygous splice-site mutation IVS14+1, G→A, associated with severe early-onset retinal degeneration, has been reported in two families from the same Dominican Republic village.[447] Two North American individuals have been reported with compound heterozygous mutations, one patient with missense mutations Arg420Pro and Phe491Leu, and another with Ile459Lys and splice site mutation IVS14+1, G→A.[247]

One of the most studied of animal models for RP is the RCS rat, which is characterized by the inability of outer segments shed by photoreceptors to be recognized and phagocytized by RPE, leading to retinal degeneration. Recently, mutations in the receptor tyrosine kinase gene *Mertk* have been found to underlie the defect in the RCS rat.[448] Patients with arRP have been reported with mutations of the human ortholog *MERTK*.[449]

X-Linked RP Genes.

Positional cloning in X-linked RP at the RP3 locus has led to the discovery of mutations in *RPGR* (RP GTPase regulator).[450] A number of mutations have now been described. Detailed clinical assessments of families with a number of mutations[451,452] describe severe, early-onset RP in hemizygotes and variable but definite disease in most heterozygote carriers.[453] All the affected males have shown evidence of both rod and cone ERG loss consistent with the expression of the gene product of *RPGR* in both classes of photoreceptors. On the basis of poorer ERG responses in hemizygotes and severe symptoms and clinical findings in heterozygotes, Andréasson et al.[454] have suggested that microdeletion mutation of exons 8 through 10 is a more severe disease than that seen with splice site mutations. Despite a strong association between the tapetal-like reflex and the X-linked RP carrier state, this has been documented in few patients carrying an *RPGR* mutation.[452]

The predicted RPGR protein contains some sequence homology to RCC1 (regulator of chromosome condensations), which is a guanine nucleotide exchange factor for the small nuclear GTPase Ran. This enzyme is essential for nucleocytoplasmic transport, although it might also be involved in other cellular activities. Other

proteins with homology to RCC1 (e.g., ARF1) appear to be guanine nucleotide exchange factors for non-Ran GTPases. These enzymes are involved in protein trafficking through the Golgi apparatus. This has led to the proposition that the RPGR protein may have a similar function in intracellular trafficking.

Although studies suggested that 70–90% of X-linked pedigrees are linked to the RP3 locus, mutations of *RPGR* were initially identified in only about 10–20% of families with X-linked RP.[450,454,455] Recently, however, another retina-enriched transcript, called the ORF15 transcript, was discovered, which utilizes exons 1 to 13 as before but utilizes exon 14 through part of intron 15 as a large terminal exon (termed the ORF15 exon). This ORF15 exon has accounted for the remainder of families linked to RP3,[456] and amongst all *RPGR* mutations, males with mutations in the ORF15 usually have better visual fields and ERG responses.[453] Mutations of *RPGR* can result in other phenotypes, including cone–rod dystrophy,[457] cone dystrophy,[458] and even macular dystrophy.[459]

A disease gene has also been identified at the RP2 locus.[460] Most of the mutations cause truncation of the gene product.[461] Mutations of this gene, termed *RP2*, account for approximately 8–10% of families of X-linked RP.[462] The gene product has homology with human cofactor C, a protein involved in the ultimate step of β-tubulin folding, suggesting that this gene may act as a chaperone or in some way be involved in the structure or function of the cilium of photoreceptors.[460,461] Together mutations of *RP2* and *RPGR* account for the vast majority of cases of X-linked RP and differences in the RP phenotypes associated with these two genes are emerging. Males with XLRP due to *RP2* mutations tend to have lower visual acuities than those with *RPGR* mutations.[463,464]

Digenic Inheritance and RP.

In rod photoreceptors, two peripherin/*rds* molecules form homodimers that bind noncovalently to homodimers of the glycoprotein ROM-1[465,466] (Fig. 42.48). In cones, peripherin/*rds* homodimers form tetramers with homodimers of either ROM-1 or a homolog.[467] These tetramers may represent the "extracellular marginal templates" described by Corless and Fetter[468] (Fig. 42.49) that are crucial to the creation and structural integrity of the disc

rim.

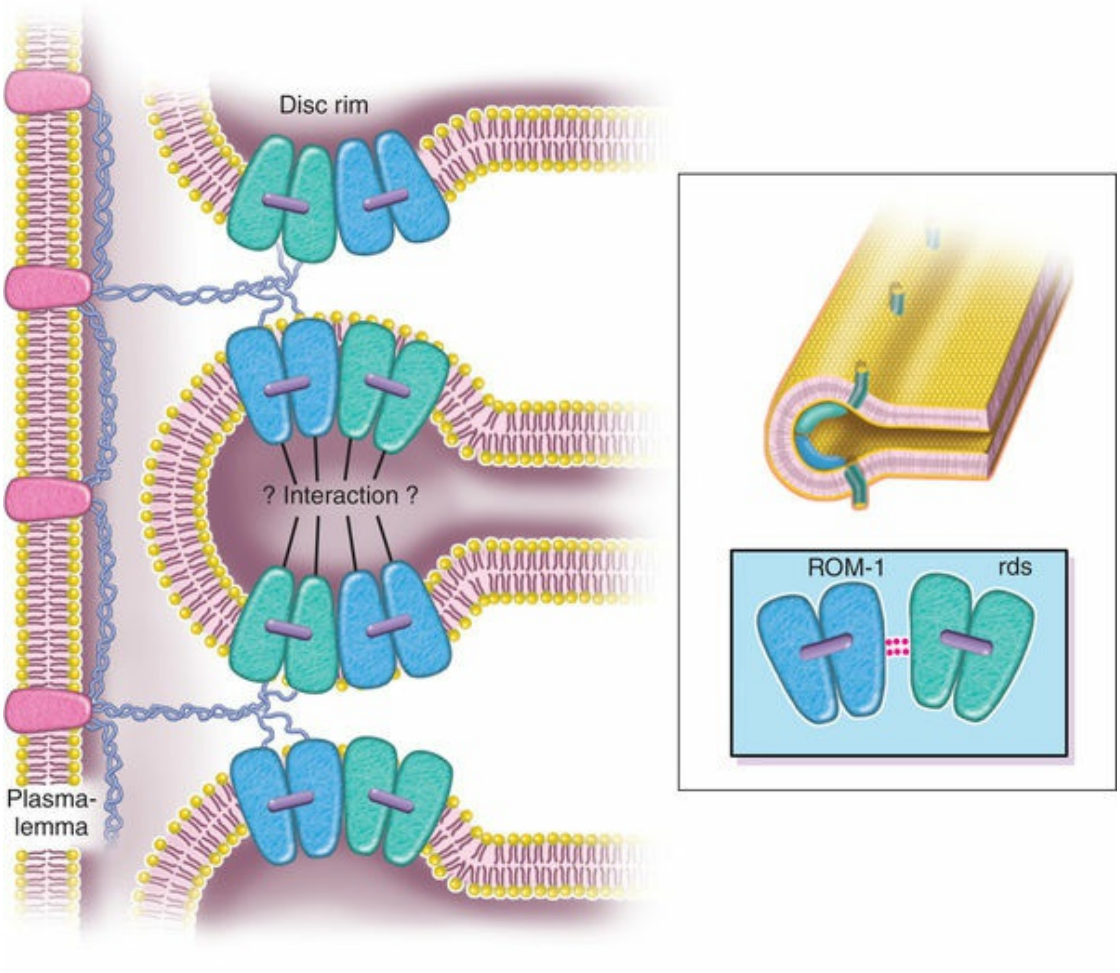

FIG. 42.48 rds/ROM-1 interactions at the disc rim, showing the homodimers of rds and ROM-1 forming tetramers by noncovalent bonds. These tetramers, which may represent the extracellular margin templates of Corless and Fetter, appear to interact across the intradiscal space at the rim margin to form the terminal loop complex (upper inset). (Reproduced from Weleber RG. Phenotypic variation in patients with mutations in the peripherin/RDS gene. Dig J Ophthalmol. 1999;5:1-8.)

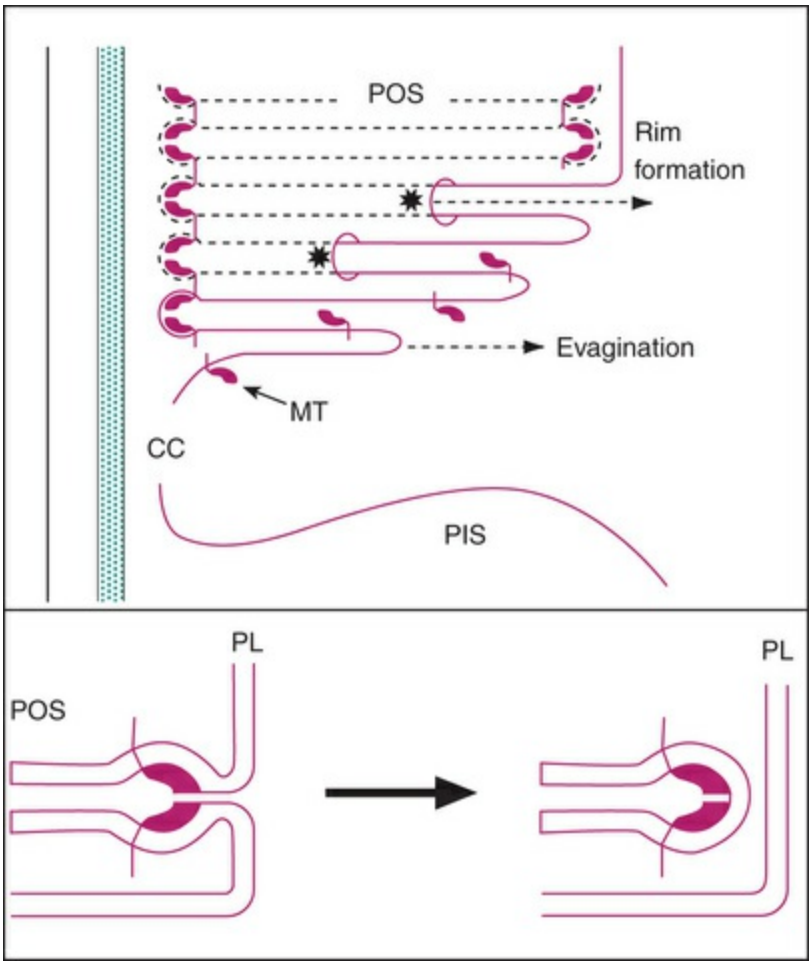

FIG. 42.49 Schematic illustration of the template theory of disc morphogenesis proposed by Corless and Fetter. Disc morphogenesis begins as a plate-like evagination from the plasma membrane in the region of the connecting cilium. The extracellular margin templates (*MT*) become aligned and assemble to form the terminal loop complexes that Corless and Fetter believe represent the primary morphogen of the disc rims. *Asterisk* denotes the leading edge of disc rim closure. *CC*, connecting cilium; *PIS*, photoreceptor inner segment; *PL*, plasmalemma; *POS*, photoreceptor outer segment. (Reproduced from Weleber RG. Phenotypic variation in patients with mutations in the peripherin/RDS gene. Dig J Ophthalmol. 1999;5:1-8.)

In a few families, three *rds* point mutations – Leu185Pro, Arg13Trp, and Leu45Phe[469] – have been seen in association with *ROM-1* mutations. The affected compound heterozygotes had a severe RP phenotype. This type of inheritance has been termed *digenic* and highlights the important structural relationship between

RDS and ROM-1 in the architecture of the rod photoreceptor. Despite studies around the world, very few RP families have been found to exhibit this phenomenon. Putative mutations of *ROM-1* in isolation have been reported in some small families.[470] As yet, isolated *ROM-1* mutations are not convincingly associated with retinal disease.[430] A paucity of recent reports on digenic inheritance would suggest that this genetic form of RP is quite rare.

Usher Syndrome Molecular Genetics.

Molecular genetic linkage analysis has shown that the three clinical subtypes of Usher syndrome are not only genetically distinct but also that there is notable genetic heterogeneity. Currently 17 chromosomal loci and three mitochondrial loci have been linked to Usher syndrome, and 16 of the associated disease genes have been identified (Table 42.1). The most severe and most common subtype, USH1B, has been associated with mutations of myosin VIIA *(MYO7A)*.[564] Mutation of *MYO7A* can also cause nonsyndromal deafness of either recessive (DFNB2) or dominant (DFNA22) type.

TABLE 42.1

Genetic Mutations Associated With Typical Retinitis Pigmentosa and Its Phenocopies

Disease	Inheritance	Genome Locus	Gene/Protein	Reference
RETINITIS PIGMENTOSA				
RP	AD	1p36.13	*EMC1*	471
RP	AR	1p36.1	*DHDDS*	472
RP32	AR	1p21.2	—	473
RP	AR	1p21.1	*ABCA4*	474
RP20	AD	1p31.2	*RPE65*	475
RP	AR	1p31.2	*RPE65*	475
RP12	AR	1q31.3	*CRB1*	476
RP18	AD	1q21.2	*PRP3*	477
RP35	AD	1q22	*SEMA4A*	478
RP	AR	1q32.2	*FLVCRI*/AXPC1	479
RP67	AR	1q32.3	*NEK2*	480
RP39	AR	1q41	*USH2A*	481
RP	AD	1q44	*OR2W3*	482
RP	AR	2p33.3	*IFT172*	483
RP	AR	2p23.2	*ZNF513*	484
RP54	AR	2p23.2	*C2ORF71*	485
RP28	AR	2p15	*FAM161A*	486
RP33	AD	2q11.2	*SNRNP200*	487
RP26	AR	2q31.3	*CERKL*	488

RP	AR	2q31.3	*NEUROD1*	489
RP47	AR	2q37.1	*SAG*/ARRESTIN	490
RP55	AR	3q11.2	*ARL6*	491
RP	AR	3q12.3	*IMPG2*/SPARCAN	492
RP68	AR	3q26.2	*SLC7A14*	493
RP38	AR	2q13	*MERTK*	449
RP	AD	3q21.1	*RHO* Pro23His	404
RP	AR	3q21.1	*RHO*	494
RP61	AR	3q25.1	*CLRN1*	495
RP40	AR	4p16.3	*PDE6B*	496
RP	AR	4p15.32	*PROML1*	497
RP	AR	4p15.33	*CC2D2A*	498
RP	AR	4p15.32	*GPR125*	471
RP49	AR	4p12	*CNGA1, CNCG*	440
RP29	AR	4q32	—	499
RP	AR	4q32.1	*LRAT*	498
RP	AR	4q35.5	*CYP4V2*	500
RP	AR	5q33.1	*PDE6A*	501
RP62	AR	6p24.2	*MAK*	502
RP14	AR	6p21.31	*TULP1*	503
RP7	AD	6p21.2	*PRPH2*	428
RP	AD	6p21	*GUCA1B*	504
RP25	AR	6q12	*EYS*/SPAM	505
RP63	AD	6q23	—	506
RP42	AD	7p14.3	*KLHL7*	406
RP9	AD	7p14.3	*PAP1*, PIM1K	435
RP10	AD	7q32.1	*IMPDH1*	507
RP	AR	7q34	*KIAA1549*	471
RP	AR	8p23.1	*RP1L1*	508
RP1	AD	8q12.1	*ORP1*	509
RP	AR	8q12.3	*TTPA*	510
RP64	AR	8q22.1	*C8ORF37*	511
RP31	AD	9p21.1	*TOPORS*	512
RP70	AD	9q32	*PRPF4*	513
RP	AR	10q11.22	*RBP3*, IRBP	514
RP	AD	10q22.1	*HK1*	515
RP44	AR	10q23.1	*RGR*	516
RP	Digenic	11q12.3	*ROM1*	469
RP	AR	11p11.2	*ZNF408*	517
RP	AD	11q12.3	*BEST1*	518
RP	AR	11q12.3	*BEST1*	518
RP	AR	11q13	*BBS1*	519
RP	AR	12q24.11	*MVK*	520
RP27	AD	14q11.2	*NRL*	433
RP53	AD	14q24.1	*RDH12*	521
RP	AR	14q31.3	*SPATA7*	522
RP51	AR	14q32.11	*TTC8*	523
RP22	AR	16p12.3	—	524
RP	AR	15p26.1	*RLBP1*, CRALBP	525
RP	AD	15q23	*NR2E3*	526
RP	AR	15q23	*NR2E3*	526
RP	AR	16q13.3	*IFT140*	527
RP	AR	16q12.2	*BBS2*	528
RP45	AR	16q13	*CNGB1*	529

RP	AR	16q13.3	*ARL2BP*	530
RP	AR	16q22.2	*DHX38*	531
RP13	AD	17p13.3	*PRPF8*	532
RP30	AD	17q25.3	*FSCN2*	436
RP	AR	17q25.3	*PDE6G*	533
RP17	AR	17q23.2	*CA4*	534
RP36	AR	17q25.1	*PRCD*	535
RP	AD	19q13.3	*CRX*	536
RP11	AD	19q13.42	*PRPF31*	537
RP	AD	20q13.33	*PRPF6*	538
RP69	AR	20p11.23	*KIZ*	539
RP	AR	20p13	*IDH3B*	540
RP23	XL	Xp22.2	OFD1	541
RP6	XL	Xp21.3-p21.2	—	542
RP3	XL	Xp11.4	*RPGR*	456
RP2	XL	Xp11.23	*RP2*	460
RP24	XL	Xq26-q27	—	543
RP34	XL	Xq28-qter	—	544
USHER SYNDROME				
USH1B	AR	11q13.5	*MYO7A*/myosin VIIa	545
USH1C	AR	11p15.1	*DFNB18*/harmonin	546
USH1D	AR	10q22.1	*CDH23*/*cadherin23*	547
USH1E	AR	21q21	—	548
USH1F	AR	10q21.1	*PCDH15*/procad.15	549
USH1G	AR	17q25.1	*USH1G*/SANS	550
USH1H	AR	10q21.1	—	551
USH1J	AR	15q25.1	*CIB2*	552
USH1K	AR	10q11.21	—	553
USH2A	AR	1q41	*USH2A*/usherin	554
USH2B	AR	3p24.2-p23	—	555
USH2C	AR	5q14.3	*GPR98*/mass1	556
USH2D	AR	9q32	*DFNB31*/whirlin	557
USH3A	AR	3q25.1	*CLRN1*/clarin-1	558
USH3B	AR	5q31.3	*HARS*	559
USH	AR	20p11.21	*ABHD12*	560
USH	AR	20q11.22	*CEP250*	561
RP + deafness	Maternal	mtDNA	*MT-TH*	562
RP + deafness	Maternal	mtDNA	*MT-TS2*	201
RP + deafness	Maternal	mtDNA	*MT-TP*	563

Nine other genes have been discovered for type 1 Usher syndrome. The gene for USH1C encodes harmonin, a novel PDZ-domain containing protein that functions in the organization and assembly of larger protein complexes for cell adhesion, signal transduction, and intracellular transport.[565] Mutations in the ear-specific exons of the gene for harmonin also called nonsyndromic recessive deafness (DFNB18).[566] The gene for USH1D is *CDH23*, which encodes cadherin 23, a novel member of a class of intercellular adhesion proteins.[547] Mutations in *CDH23* also cause autosomal recessive nonsyndromic deafness (DFNB12).[567] CDH23 is

expressed in the cochlea and retina and mutations in the mouse ortholog cause disorganization of inner ear stereocilia and deafness in the *waltzer* mouse animal model.[568] Two of the harmonin PDZ domains interact with MYO7A and CDH23, indicating that these three proteins form a complex important for organization, maintenance, and function of stereocilia in the cochlea.[569,570] The gene for USH1F is *PCDH15*, which encodes protocadherin 15.[549] Mutations in *PCDH15* have also been reported in nonsyndromic recessive deafness (DFNB23).[571] PCDH15 localizes to stereocilia in inner-ear hair cells and to the photoreceptors of the retina and is presumed to be essential for homeostasis. Mutation of the murine homolog causes vestibular dysfunction and deafness in the *Ames waltzer* mouse.[572] USH1G encodes the protein SANS, which is a novel scaffold-protein gene that is expressed in retina and cochlea and is associated with harmonin within stereocilia.[545] Thus, it appears that many of the genes for type 1 Usher syndrome (MYO7A, harmonin, CDH23, and SANS) function together in a complex essential for determining and maintaining cohesion of the stereocilia of the cochlea.[545]

The commonest gene association with type 2 Usher syndrome (*USH2A*),[554] encodes a protein called usherin which has motifs that show homology to thrombospondin, laminin epidermal growth factor, and to fibronectin type III. This indicates that the gene product may function as a cellular adhesion molecule or as a component of the basal lamina and extracellular matrix. Although discovered first in patients with type 2 Usher syndrome, a Cys759Phe mutation of USH2A was found in approximately 4.5% of 224 patients with arRP without hearing loss.

The first gene discovered for type 3 Usher syndrome (*USH3A*) was reported as encoding a 120-amino acid protein in 2001 by Joensuu et al.[558] A common termination mutation, Y100X, accounts for the majority of mutant alleles in Finnish cases.[558] The gene product, clarin-1, is believed to have a role in hair cell and photoreceptor cell synapses.[573] Pennings et al. have reported that type *USH3A* mutations can produce disease that mimics either type 1 or 2 Usher syndrome and that the fundus appearance may mimic retinitis punctata albescens or RP sine pigmento.[574]

Protein Chemistry

Considerable information has now accumulated on the molecular consequences of retinal dystrophy gene mutation. In turn that has lead to a much deeper understanding of the molecular physiology of the human retina. Readers are directed to a number of significant reviews on the subject.[575,576]

Some general principles can be applied to the molecular consequences of retinal gene mutation. Deficiency of gene product seems to be the most likely explanation for recessive disease. In two recessive RP pedigrees with rhodopsin mutations (a non-sense and splice-site mutation), for example, the aberrant alleles theoretically encode nonfunctional rhodopsin.[494,577] Haploinsufficiency is unlikely to be important in dominant rhodopsin disease though because carriers of at least one apparently null allele have been shown to be phenotypically normal.[577] Mutant rhodopsin expression in COS cells has shown that mutations in the intradiscal domain adversely influence normal rhodopsin folding.[578] Autosomal dominant mutations within the rhodopsin transmembrane helices still cause misfolding, but to a much lesser effect, and have a more profound effect on retinal binding.[579] In vitro studies have shown that mutant rhodopsin can accumulate within the rough endoplasmic reticulum of rod photoreceptors.[580] This could lead to inhibition of transport of the wild-type rhodopsin to the cytoplasmic membrane and loss of function and might explain pathogenesis in some cases of retinal dystrophy with rhodopsin mutations. However, different results in rhodopsin expression in in vitro studies in nonmammalian models and mammals have suggested that the true relevance of this mechanism in humans is as yet unproved. Truncation of the rhodopsin protein due to mutation of codon 343,[581] for example, is associated with expression of mutant and wild-type rhodopsin in the plasma membrane of tissue culture cells but leads to accumulation of the mutant in the rough endoplasmic reticulum in transgenic mice. The effect in humans is unknown.

Abnormal Pre-mRNA Splicing.

Proteins encoding three RP genes, *PRPF8* (RP13), *PRPF31* (RP11), and *PRPF3* (RP18), have been associated with RNA splicing. RNA

splicing is an essential process that removes intron sequences from pre-mRNA. This is carried out by the spliceosome, a high-molecular-weight ribonucleoprotein complex.[582] The vast majority of pre-mRNA introns (designated the U2-type) are spliced by the major spliceosome, which is composed of five uridine-rich small nuclear ribonucleoproteins, or snRNPs, termed U1, U2, U4, U5, and U6. Each snRNP is the central component of a protein complex that also contains seven Sm or Sm-like proteins, which are assembled by the so-called SMN (survival of motor neurons) protein. In addition to the Sm and Sm-like proteins, snRNPs also contain three to 10 particle-specific proteins.[583] The major spliceosome also contains a poorly defined number of other non-snRNP protein factors. The minor spliceosome is responsible for splicing a rare class of pre-mRNA introns, called the U12-type.[582] Minor spliceosomes contain the U5 snRNP and four nonabundant snRNPs: U11, U12, U4atac, and U6atac.

The *PRPF8* gene (chromosome 17p13.3) encodes PRPF8 (precursor RNA processing factor 8). The yeast homolog, Prp8p, is a U5 snRNP factor that is first required for assembly of the U4/U6 and U5 tri-snRNP[584] and then for facilitating the binding of the tri-snRNP to the 50 and 30 splice sites.[585] It functions as the catalytic core of the spliceosome, either by facilitating formation of the core and/or by stabilizing RNA interactions.[586] Seven different missense mutations of *PRPF8*, all clustered within a 14-codon stretch in the last exon, have been identified in five RP13-linked families.[587] *PRPF8* mutations are associated with early-onset adRP with diffuse retinal involvement and a severe prognosis in comparison with other forms of adRP.[587,588] Individuals experience night blindness beginning between 4 and 10 years of age and constricted visual field as teenagers.[588] Classic mid-equatorial bone spicule pigmentation is seen by middle age.[588] Typically, individuals are registered as blind or partially sighted by age 30.[586]*PRPF31* (chromosome 19q13.4) encodes protein 61K, the putative ortholog of the yeast pre-mRNA splicing factor Prp31p.[589] Protein 61K is specific to the U4/U6 snRNP and is required for pre-mRNA splicing in vitro.[590] Protein 61K participates in the formation of the tri-snRNP, possibly by physically tethering the U5 snRNP to the U4/U6 snRNP.

Haploinsufficiency appears to be the mechanism underlying the photoreceptor degeneration in the majority of alleles of the *PRPF31* gene associated with RP because most of these alleles are predicted to be protein truncation mutations. Families with *PRPF31* mutations are unique in showing bimodal expressivity of the phenotype, with asymptomatic carriers who have both affected parents and affected children.[591,592] Symptomatic individuals experience night blindness and loss of visual field in their teenage years and are typically registered as blind by their 30s.[591] Evans et al. suggested that the bimodal expressivity seen in these pedigrees may be explained by a second allelic genetic factor influencing phenotype. This idea was taken further by McGee et al.,[593] who confirmed that penetrance of the *PRPF31* mutations may be influenced in *trans* by otherwise silent *PRPF31* alleles or by a closely linked locus on the wild-type chromosome, because a statistically significant correlation was found between the development of RP in a carrier and the inheritance of the region around RP from the noncarrier parent.[593] Vithana et al.[589] have demonstrated that asymptomatic patients inherit a different wild-type allele to the one inherited by their symptomatic siblings. The third of the three known pre-mRNA splicing factors associated with adRP is encoded by the *PRPF3* gene (chromosome 1q21.1).[477] PRPF3 protein associates with the U4/U6 snRNP during pre-mRNA splicing.[594] Mutations in its yeast ortholog, Prp3p, cause instability of the U4/U6 snRNP and prevent assembly of the tri-snRNP, thereby preventing splicing.[595] Two different missense mutations have been identified in three individuals and three families.[595] Affected individuals suffer night blindness toward the end of the first decade of life.[477] Visual field defects are seen by the fourth decade of life, but the central field remains relatively spared. A few patients progress to total blindness by age 80.

Several mechanisms have been proposed to account for the fact that mutations in these three, ubiquitously expressed, splicing factor genes only cause adRP and not a more widespread abnormality. The loss of one functional copy of these splice factor genes may affect only rods because of their unusually high requirement for protein synthesis and, consequently, for pre-mRNA splicing.[596] Alternatively, the adRP-associated mutations may

decrease the rate at which spliceosome activation occurs,[597] making activation the rate-limiting step in rod photoreceptors but not other cells. Finally, it has also been suggested that the retina-specific phenotype may occur as a result of an unidentified retina-specific splicing cofactor that interacts with all three of these splicing factor proteins.[593]

RPGR Interactome.

An interactome is a complex representation of functional interactions between molecules either within a cell or within the organism as a whole. Often such interactomes reveal important interactions between molecules that at first would not appear to be functionally related. In this way, the functional consequences of genetic mutation can be predicted without the need for lengthy experimentation. An RPGR-interactome has also been proposed.[598] RPGR is a component of centrioles, ciliary axonemes, and microtubular transport complexes, although its precise function is unknown. It colocalizes with RPGRIP1 at the axonemes of connecting cilia in rod and cone photoreceptors[599] by binding to RPGRIP1. This localization is lost in Rpgrip1 knockout (KO) mice. Rpgr KO mice develop a slow retinal degeneration, with features resembling a cone–rod degeneration – cone photoreceptors degenerate faster than rods and there is partial mislocalization of cone opsins.[600] Some residual $Rpgr^{ORF15}$ expression has been reported in this model.[601] RPGR has been shown to coimmunoprecipitate in retinal extracts with a number of different axonemal, basal body and microtubular transport proteins.[602] These include nephrocystin-5 and calmodulin, which localize to photoreceptor connecting cilia; the microtubule-based transport proteins, kinesin II (KIF3A, KAP3 subunits), dynein (DIC subunit), SMC1, and SMC3; and two regulators of cytoplasmic dynein, p150Glued and p50-dynamitin, which tether cargoes to the dynein motor. Inhibition of dynein by overexpressing p50-dynamitin abrogates the localization of $RPGR^{ORF15}$ to basal bodies. RPGRORF15 can be coimmunoprecipitated from retinal extracts with other basal body proteins, including NPM, IFT88, 14-3-3ε, and γ-tubulin.[599,601] $RPGR^{ORF15}$ and RPGRIP1 colocalize at centrosomes in a wide variety of nonciliated cells and at basal bodies in ciliated

cells. Both proteins are core components of centrioles and basal bodies.[598] In summary, RPGRORF15 appears to have a role in microtubule-based transport to and from the basal bodies and within photoreceptor axonemes, perhaps concerned with movement of cargoes between IS and OS. $RPGR^{ORF15}$ is predominantly expressed in photoreceptor connecting cilia and basal bodies but expression has also been reported in OS in some species,[602] although this has been disputed.[599] RPGR is also expressed in the transitional zone of motile cilia in the epithelial lining of human bronchi and sinuses ($RPGR^{ex1–19}$ only) and within the human and monkey cochlea.[599,603–605]

USH Interactome.

The USH genes encode proteins of different classes and families, including motor proteins, scaffold proteins, cell adhesion molecules and transmembrane receptor proteins. In vitro direct interaction studies between USH proteins and also localization studies in mouse models have, however, suggested functional relationships between these proteins such that an "USH interactome" has been proposed.[606] In these studies, it should be noted, however, that although all the USH mouse models show severe hearing loss and vestibular dysfunction, only the $Ush2A^{-/-}$ mouse, shows signs of RP.[607] From such work, a "multiprotein scaffold complex" model has been proposed for harmonin, whirlin, and sans. There is also evidence that harmonin and whirlin can bind all other components of the USH network, including cadherin 23, protocadherin 15, usherin, VLGR1 and myosinVIIA.[569,603,608]

Myosin VIIa has also been found to interact with sans 11 and protocadherin 15.[570] Such findings suggest that the USH proteins form a transmembrane network that regulates hair bundle morphogenesis, particularly the growing stereocilia or the kinocilium, and may also have a role in the mechanoelectrical signal transduction and synaptic function of mature hair cells.[609] In the USH interactome model, it is proposed that the extracellular inter-stereocilia links are anchored intracellularly by the scaffold proteins, harmonin and whirlin, through direct binding to the actin cytoskeleton or through other proteins, including myosin VIIa.[569,603,610,611]

Additionally, it has been shown that the association of other proteins with the USH complex (through harmonin) may function in determining cell polarity and cell–cell interactions.[612] Also Myo7a is believed to use long filaments of actin as tracks along which to transport other USH complex molecules.[613] In photoreceptors, proteins of the USH interactome are localized in the connecting cilium and may participate in the ciliary transport, but are also arranged at the interface between the inner segment and the connecting cilium where they control cargo passage. USH protein complexes may also provide mechanical stabilization to membrane calycal processes and the connecting cilium.[614] Studies of coexpression of USH1 and USH2 proteins also show accumulation at synaptic endings of photoreceptor cells indicating that they are organized in an USH protein network there.[615]

Bardet–Biedl Syndrome and the "BBSome."

Recently it has been proposed that many of the proteins encoded by Bardet–Biedl genes form complexes, e.g., BBS1, BBS2, BBS4, BBS5,BBS7, BBS8, and BBS9 – the "BBSome."[616] The complex is important in the function of primary cilia, nonmotile projections found in numerous cell types. In particular BBSome complexes are thought to play a central role in vesicular trafficking of membrane proteins within cilla. The BBSome binds to Rab8 a GTP/GDP exchange factor involved in docking and fusion of rhodopsin carrier vesicles in the connecting cilium of photoreceptors.[617] It is also known that other Bardet–Biedl genes, e.g., BBS3 (Arl6) form functional relationships with this BBSome.[618] Others appear to function as chaperones, e.g., BBS6, BBS10, and BBS12 and in protein ubiquitination (BBS11/TRIM32).[619]

Abnormal Intracellular Trafficking.

An increasingly important consequence of retinal disease gene mutation has been the concept of abnormal intracellular trafficking.[407,620] For instance, rod damage is often associated with mutant rhodopsin accumulating in the outer segment.[407,621,622] It is thought that this interferes with normal phototransduction and triggers apoptotic cell death. It has been shown in transgenic mice that mutant rhodopsin is only transported to the rod outer segment

when the C-terminal region of the molecule is intact.[623] This observation has been corroborated in human eyes.[624]

Cell Death Pathways

A prevalent proposition in the last decade has been that since many different gene mutations result in a similar clinical outcome (retinitis pigmentosa), there must be a "final common cell death pathway" precipitated by these mutations.[625] Apoptosis, the first cell death biochemical pathway linked to retinitis pigmentosa, characteristically appears histologically as a rounding-up of the cell, reduction of cellular volume, chromatin condensation, and finally engulfment by resident phagocyte. Apoptosis is triggering of intrinsic and (to some extent) extrinsic pathways involving activation of caspases, which can be subclassified into both initiator (2,8,9,10) and effector (3, 6, 7) molecules. Studies with caspase inhibitors, however, have often produced only marginal neuroprotection in retinitis pigmentosa models.[626,627] Other studies have highlighted that caspase-independent inducers of cell death such as apoptosis-inducing factor (AIF), calpains, and poly(ADP-ribose) polymerases 1 (PARP-1) are activated during retinal degeneration.[628]

Previously, necrosis had not been considered a significant part of retinal degeneration. This passive, unregulated form of cell death, is now considered to be inducible by regulated signal transduction pathways such as those mediated by RIP kinases.[628] Such "necroptosis" may play a role in RP.[628,629.] Apoptosis and necroptosis mechanisms may act together or may form alternate pathways.

Cell and Tissue Biology

Histopathology

Early histopathologic studies found that the first degenerative abnormalities in RP occur in the photoreceptors. As more and more animal model histopathologic correlates of specific human genetic mutations become available our knowledge of both outer and inner retinal changes in RP is leading to new concepts for therapy.[575,630]

Photoreceptor Abnormalities.

The earliest histologic sign of retinal dystrophy is shortening of rod outer segments (Fig. 42.50).[631] With progression of disease, rod outer segments become more severely shortened, and eventually whole cells are lost. This is reflected in reduced numbers of nuclei in the outer nuclear layer. Rod cell loss is usually seen initially in the midperiphery. In certain cases cell loss is initially seen in the inferior retina. This is a typical finding in cases with rhodopsin mutation Pro23His.[186] In such cases there is a corresponding altitudinal field defect. Interestingly, a similar pattern of photoreceptor loss is seen in transgenic Pro23His mutant mice. In this model, if mutant mice were dark-reared, the resultant retinal degeneration was more uniform across the retina and was significantly milder.[632] This suggests that limiting light exposure in patients with this mutation may moderate the progression of disease.

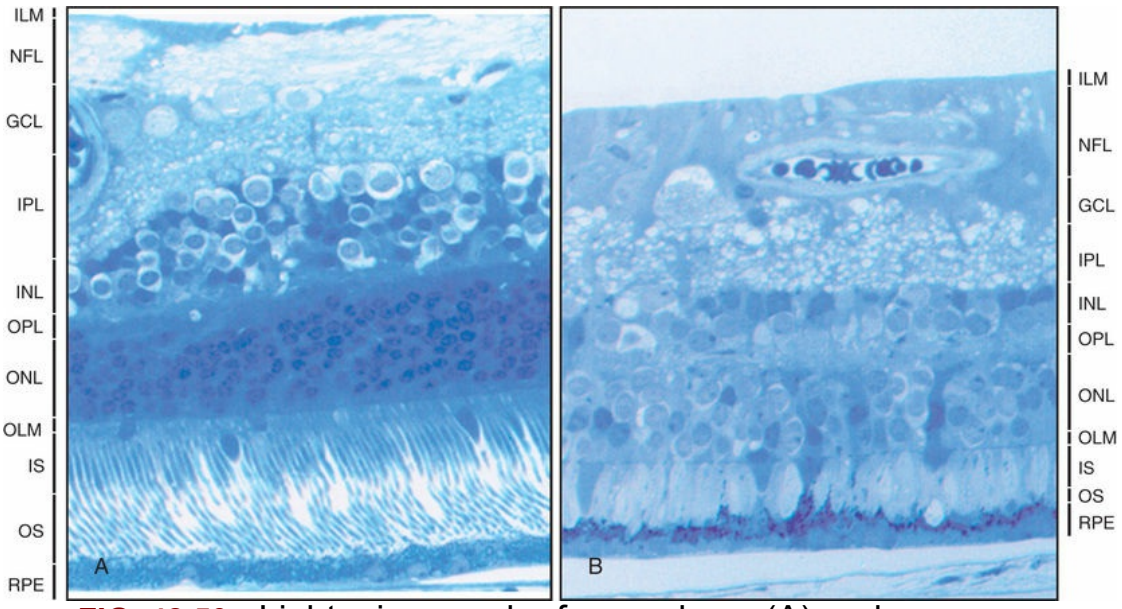

FIG. 42.50 Light micrograph of normal eye (A) and eye with retinitis pigmentosa (B). Richardson methylene blue/azure II stain. Note marked loss of outer segments in retinitis pigmentosa. *ILM*, internal limiting membrane; *NFL*, nerve fiber layer; *GCL*, ganglion cell layer; *IPL*, inner plexiform layer; *INL*, inner nuclear layer; *OPL*, outer plexiform layer; *ONL*, outer nuclear layer; *OLM*, outer limiting membrane; *IS*, inner segments and *OS*, outer segments of rod and cone

layer; *RPE*, retinal pigment epithelium. (×60.) (Courtesy of AH Milam.)

Using immunocytochemistry and antirhodopsin antibodies, extensive studies have been undertaken of cytopathologic abnormalities in photoreceptors. In normal rods, rhodopsin is concentrated in the outer segments. In a number of rhodopsin-mutant animal models, abnormal localization of mutant rhodopsin has been seen,[633] and this has also been seen in human eyes.[634,635] Such observations have led to interesting hypotheses as to how mutant protein may damage photoreceptors.[636] It has been proposed that certain mutant rhodopsin molecules accumulate in the endoplasmic reticulum or Golgi apparatus in the inner segment and lead to cell death by interfering with the function of these organelles. Clearly, though, there are species differences in the cytopathologic effects of particular mutations. In transgenic Pro347Ser mice, rhodopsin is seen to accumulate in extracellular vesicles attached to rod inner segments.[637] Alternatively, in the transgenic Pro347Ser pig, rhodopsin accumulates in the inner segments.[638,639] Such aberrant accumulation of rhodopsin in the inner segment has not, however, been seen in human cases of Pro347Ser.

Clarke et al.[640,641] studied 11 different animal models of outer retinal dystrophy. These authors noted that the kinetics of photoreceptor death fit an exponential model. This in turn suggests three important features: (1) the risk of death is constant throughout the lifetime of each mutant photoreceptor; (2) each mutant photoreceptor is at the same risk of death as every other mutant photoreceptor (other things being equal); (3) the time at which death will occur is random and independent of the time of death of other photoreceptors. The regional variation in photoreceptor death in RP is not inconsistent with the feature of equal risk because local geographic factors may be superimposed on the equal risk of death of all the photoreceptors, resulting in a higher risk in certain parts of the retina. In the animal model studies, the same region of the retina was always examined, eliminating any effect of regional variation. The identification of these three characteristics of outer retinal dystrophies is important for at least two reasons. First,

exponential kinetics refutes the major alternative model of photoreceptor death, the cumulative damage model, in which the risk of death increases with time (akin to the risk of death in an aging population of people) and the cell-death kinetics are sigmoidal, not exponential. Second, the recognition that mutant photoreceptors are at a constant risk of death requires that biochemical mechanisms proposed to underlie the photoreceptor death must explain both the exponential kinetics as well as other major characteristics of the disease. For example, this may mean that for all the different gene mutations, probably only a few pathways triggering apoptotic cell death are relevant to photoreceptor degeneration.[642]

Outer Retinal Disease.

After photoreceptor cell death, the RPE becomes detached from Bruch's membrane and migrates into the neurosensory retina. The subretinal space is abolished. Accumulation of RPE cells in a cuff around retinal vessels leads to bone-spicule pigmentation.[643] Bruch's membrane thickening has also been recorded under degenerate RP retina. In late-onset RP, material has been seen to accumulate between the RPE and the inner collagenous layer of Bruch's membrane.[644–646] This material was periodic acid-Schiff-positive and contained lipid, calcium, and iron. Choriocapillaris underlying areas of debrided RPE undergo atrophy.[647]

Inner Retinal Pathology.

Reactive changes have been reported in all cell types in the inner retina subsequent to photoreceptor cell death. Müller cells undergo reactive gliosis.[648,649] In advanced RP, entangled, thickened Müller cell processes result in extensive scarring in the remaining retina. Glial fibrillary acidic protein-positive astrocytes undergo reactive hyperplasia. This growth of astrocytes contributes to the pallor of the optic nerve head and epiretinal membrane formation.[650,651] Microglia migration into the outer retina has been documented in the Royal College of Surgeons (RCS) rat model of retinal dystrophy,[652] but the human and pathophysiologic significance of this is unknown.

Previously it has been suggested that RP has little effect on

ganglion cells.[653,654] Stone et al.[122] studied 41 RP retinas and found significant reductions in ganglion cell numbers in each inheritance type of RP. The most significant losses were in X-linked RP and adRP. Transneuronal degeneration[630,655] has been the explanation for this phenomenon. Compression of cell bodies by retinal vessels[656] and inner retinal ischemia has also been proposed as causes for ganglion cell loss. Inner retinal ischemia, a consequence of pigment epithelium perivascular cuffing,[643] may in part also explain the optic nerve head pallor that is observed clinically.[657]

More recent publications have expanded on the details of the anomalous remodeling and the misguided attempts at repair that take place within the retina in retinal degenerations following death and loss of the photoreceptors.[658,659] The changes appear in response to the stress of injury and cell death and progress through three stages: (1) the primary insult to the photoreceptors, which results in their dysfunction (and produces visual symptoms); (2) death of photoreceptors that ablates the sensory retina, by initial photoreceptor stress, phenotype deconstruction, and cell death of other cell types, through bystander effects or loss of trophic support; and (3) a protracted period of global remodeling and large-scale reorganization of the remaining neural retina.[660] These attempts at repair result in three major tranformations: (1) the reactive hypertrophy of Müller cells and the formation of a distal glial seal that essentially isolates the remaining neuroretina from the surviving RPE/choroids; (2) apparent neuronal migration along glial surfaces to ectopic sites; and (3) the establishment of aberrant rewiring through a complex formation of neurite fasicles, new synaptic foci, and aberrant connections within the retina.[657] It is also now known that bipolar and horizontal cells in particular undergo significant morphologic changes and changes in neurotransmitter receptor expression in response to outer retinal degeneration.[660] RP triggers permanent loss of bipolar cell glutamate receptor expression, though spontaneous iGluR-mediated signaling by amacrine and ganglion cells. It has been proposed that rod bipolar cell dendrite switching likely triggers new gene expression patterns and may impair cone pathway function.[661] These changes may place constraints on the concepts of cell or tissue transplantation or implantation of artificial retinas for regaining sight in advanced

retinal degenerations.

Cellular Remodeling and Vascular Changes

In the slowly degenerating dystrophic retina, peripheral rods sprout long, axon-like processes that can extend as far as the inner limiting membrane.[631,662] These neurites have been found in rhodopsin mutant eyes and in cases of X-linked RP. They are found in areas of marked cell death but have yet to be seen in the macula. Neurite processes bypass bipolar and horizontal cell synapses to become closely associated with hypertrophied Müller cell processes (Fig. 42.51). Neurites aggregate to form fascicles that arborize at the inner plexiform layer to form beaded processes under the internal limiting membrane. Although numerous vesicles similar to those seen in synapses are found in neurites, true synaptic connections have yet to be identified. Immunocytochemistry has shown that rhodopsin photopigment accumulates within neurites. It is still unknown whether these processes fulfill any functional role. Rod neurite sprouting does not seem to occur in dystrophic mouse models of RP. This suggests that the process occurs in retinas that undergo protracted degeneration over years rather than rapid degeneration over weeks to months that is typical of mouse models of retinal dystrophy. Such models therefore may not be suitable in retinal transplantation studies ultimately intended to justify human studies. The environment in which it is intended to re-establish synaptic contact between transplanted rods and second-order neurons must be very different in dystrophic mice as compared with humans.[662] Thus models of RP in larger animals, such as the transgenic pig,[638,663] are necessary.

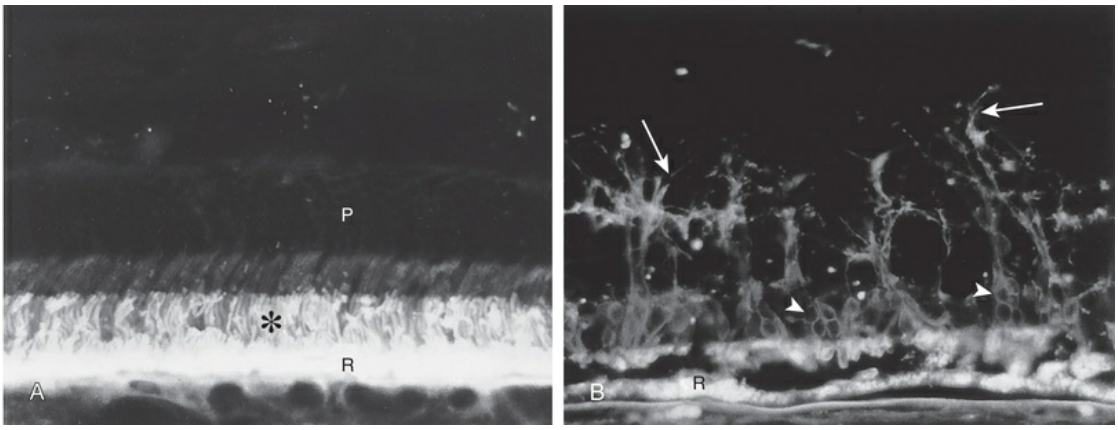

FIG. 42.51 Rhodopsin immunofluorescence in the retina in a normal (A) and a Q64ter rhodopsin mutant retinitis pigmentosa (B) subject. In the normal retina, rhodopsin immunolabeling is confined to the rod outer segments (*asterisk*). In the retinitis pigmentosa eye, rhodopsin is seen delocalized to processes (rod neurites) extending into the inner retina (*arrows*). *R*, Retinal pigment epithelium; *P*, photoreceptor somata. (×230.) (Courtesy of AH Milam.)

Cone degeneration may occur early or late in RP. The evolution of cone changes is similar to that seen in rods. Cytoplasmic densification, axon elongation, and eventual reduction in number of cell bodies indicative of cell death follow initial cone outer-segment shortening. In the peripheral retina, shortened cone outer segments become surrounded by pyramidal-shaped RPE processes.[664] Cones do not, however, undergo neurite sprouting to the extent seen in rods. In some RP eyes, peripheral cones occasionally evolve limited projections.[631,662] In an RP eye with a rhodopsin 64ter mutation, enlarged cone axons that extended into the inner plexiform layer were noted.[631] If cell death has been extensive, a monolayer of cone somata is still evident in the macula. Recently, a cell survival factor specifically elaborated by rods but important for cones has been discovered.[665] This factor, termed rod-derived cone viability factor, is a truncated thioredoxin-like protein that holds promise for the generation of potential new treatment possibilities for RP.

Retinal vascular abnormalities can be a prominent feature in cases of RP. Perivascular cuffing[643] and arteriolar attenuation are common features of advanced disease. Retinal blood flow decreases in advanced RP.[666] This may be caused by this perivascular cuffing,

which constitutes migrated pigment epithelium and deposited extracellular matrix, or it may be a phenomenon secondary to reduced metabolic need. Reduced cell density in the degenerating retina may lead to a reduced metabolic demand and therefore reduced flow.[666]

In a few RP patients, changes in retinal permeability can lead to exudative retinal detachment (Coats-like disease).[73] This can be associated with peripheral retinal telangiectasia.[667] Peripheral retinal ischemia and preretinal neovascularization have also been reported.[71] Histopathologic evaluations of these vascular changes in humans, however, have only been reported from eyes that were already at the end stage of disease.

Genetic Consultation

A diagnosis of RP always implies genetic disease. Therefore, once a diagnosis is suspected, further patient management is carried out within the special context of genetic consultation.[668] This can be subdivided into three areas: (1) diagnosis; (2) genetic counseling; and (3) management of therapeutic options. The first steps in the management of a patient with RP are to establish an accurate diagnosis and a mode of inheritance. Both involve the traditional methods of history-taking and clinical examination. Clinical investigations and molecular genetic diagnosis can augment information gathered in this way. The patient whose diagnosis brought the family to the attention of physicians is called the *proband* or *propositus*.[198]

A complete, detailed pedigree is an essential part of the workup before informed genetic counseling can begin. Examination of other family members may be essential not only to establish the correct diagnosis but also to gain a better appreciation of the range and extent of the manifestation shown by other family members and the expected rate of progression. For some retinal dystrophies, such as Usher syndrome and BBS, the inheritance, autosomal recessive in these examples, can be accurately predicted on the basis of the diagnosis. For others, such as typical RP, the family workup may be the only way an inheritance subtype may be uncovered.

The scope for molecular genetic diagnosis is clearly opening up,

and a number of centers around the world now offer molecular diagnostic testing for a growing number of RP genes. A list of laboratories can be obtained through www.genetests.org. For other genes, molecular diagnosis can only be obtained through research laboratories.

Counseling Family Groups

Genetic counseling may be defined as a communication process that deals with the human problems associated with the occurrence, or risk of genetic disease, in a family. After a diagnosis has been made, the first important issue is to determine who should undertake the genetic counseling of an RP patient. Traditionally this has been done by the ophthalmologist who establishes the diagnosis. With the recent advances in RP research, however, many ophthalmologists now refer such patients to specialist ophthalmologists more actively involved in the field. Recently it has been suggested that counseling should be undertaken by clinical medical geneticists, genetic counselors, or genetic nurses. This is in recognition of skills not formally within the training of ophthalmologists. There is increasing awareness of the need for more than just simple passing on of information about disease pathophysiology, mode of inheritance, and therapeutic options during the counseling process. The single most common patient complaint about genetic counseling is that the consultant does not address the problems that really concern the patient,[669] which are more often psychologic and social problems than specific details of disease. One of the most psychologically stressful periods in the life of an RP patient consists of the events surrounding the diagnosis of RP. Michie et al.,[670] in a survey of patients undergoing counseling, found that 50% expected direct advice, 30% expected help in making decisions, and 50% wanted simple reassurances about how the disease would affect their and their family's lives. The RP patient is often more concerned about how to cope, now that driving is prohibited because of peripheral field loss, than what actual percentage of field remains. No clinical trials have been undertaken to determine the best way to undertake the counseling of RP patients, but, with the promise of future advances in genetic

therapeutics, this is certainly an area that will change dramatically within the next decade.

A major principle of genetic counseling has been that it should be nondirective and supportive. However, it has been conceded that, to some extent, this is an ideal rather than a practical aim.[670,671] Most RP patients, for example, those who are given options to choose whether to undergo cataract surgery, act on the recommendation of the consulting physician. Similarly, many patients are influenced by the manner of presentation of risks and options for family planning. Reproductive counseling should always present the various options in as nondirective a manner as possible.

Predictions of severity of disease can be influenced by a number of nonmendelian factors that are becoming more recognized in ophthalmic genetics. Variable expressivity (variation in severity)[672] and incomplete penetrance (disease-gene carriers who are not symptomatic)[591] are particularly common in autosomal dominant disease. Digenic inheritance[469] (i.e., symptomatic individuals heterozygous for mutations in two separate genes) can also influence the predictions of severity. Other nonmendelian influences, such as meiotic drive,[673] anticipation,[674] and imprinting,[675] may also be relevant to predictions of disease severity in particular families.

After the discussion of symptoms and prognosis for vision with the patient, issues dealing with risk to the patient's children arise. Mode of inheritance will have already been assessed. An autosomal dominant trait with affected members in each generation and male-to-male transmission would imply a 50% risk to the offspring of affected individuals. In autosomal recessive families, in which both parents are carriers, each child of those parents has a 25% risk of being affected irrespective of the number of children already affected. An affected individual with an autosomal recessive disease has a small risk of having an affected offspring, depending on the frequency of carrier state in the population. Inheritance of autosomal recessive traits is influenced by traditions of consanguinity in the community. Information on such traditions should be sought, since consanguinity can be common in various populations.

Classically, X-linked traits are only symptomatic in affected

males (hemizygotes). However, female carriers of X-linked RP can be symptomatic even with minimal fundus abnormality.[676] Affected males cannot transmit the abnormal gene to their sons, but all daughters will be carriers (obligate heterozygotes). The variability and spectrum of clinical expression in heterozygotes are attributed to lyonization, the random inactivation of one of the two X chromosomes, with the extent of disease depending on the relative proportion of activity for the parental X chromosome that carries the mutant gene.[54,192] Rarely, because of extremes of lyonization, a carrier for an X-linked disorder, such as X-linked RP or choroideremia, may be moderately to severely affected. A common problem is the assessment of risk to offspring in simplex cases for which no family history of disease or limited pedigree information is available. In such cases the risk to offspring is likely quite small (e.g., < 5%) unless the proposed union is consanguineous.

In terms of ophthalmic genetic counseling, it is required to explain the severity of probable visual handicaps in terms that are understandable to the patient (e.g., relating loss of ability to read and to the extent of restriction of mobility rather than predicting probable Snellen visual acuity). To some extent comparisons can be made to the experience of another older affected family member. Many visually impaired individuals, despite severe visual deficit, are surprisingly well adjusted and lead highly productive lives. Such families may perceive the handicap as milder than would an outside observer, and support for affected children within these families may be so great that the risk of passing on the disease is not perceived as a large burden. When discussing such matters the practitioner needs to be particularly sensitive to racial, religious, and social influences. For instance, termination is rarely acceptable to Catholics or Muslims.[677]

No study has yet attempted to assess the requirements for prenatal diagnosis in ophthalmic genetics in the United States, although such studies have been undertaken in Europe. Members of the German Retinitis Pigmentosa Society participated in a questionnaire survey on attitudes toward prenatal diagnosis of RP.[678] Of the 414 respondents, 64% thought that prenatal diagnosis was appropriate. A similar study in Sweden found that 60% had a positive attitude toward prenatal diagnosis.[679] Both studies found

that, although most people would accept an offer of prenatal diagnosis, this did not imply that they would then proceed with the termination of an affected pregnancy. In the former study, over 32% responded that they would disagree with termination if the child were destined to be blind soon after birth, and 61% would decline if the onset of blindness would occur in adulthood. The latter study also found that, although prenatal diagnosis would be used, over 30% would not use this information to decide on termination. These attitudes were expressed even though the fetus is subjected to risk during such tests. However, despite the theoretical possibilities and some evidence to suggest a modicum of patient need, we are not aware of much demand for prenatal diagnosis of RP in the United States or UK.

The families of those with genetic diseases need to know their options for family planning. The most frequently considered options are proceeding with childbearing with the knowledge and acceptance of the risk, deciding against having children, and delaying childbearing with the hope of future options not yet available. If the mother is not a carrier for either a dominant or X-linked trait, parents who wish to have a normal child may consider artificial insemination from a normal donor. Other options that will become increasingly available are forms of prefertilization gamete selection (particularly applicable for traits inherited from the male) and a procedure referred to as preimplantation genetic diagnosis, which involves in vitro fertilization with implantation of only an embryo for which a cell taken from the 6- to 8-cell blastomere stage has been analyzed molecularly and has been shown not to carry the mutation in question. (Removal of a single cell at this stage appears to be tolerated by the embryo without consequence.)

A great deal of information is given to patients in genetic counseling sessions. For this reason, it should be normal practice to plan a number of visits rather than try to complete the process at one consultation. Also, a formal letter explaining the major points should be sent to the family members who attended the counseling session.

Support Services

Patients can benefit greatly from appropriate referral to local, regional, or national agencies that provide services and support to the visually impaired. These services may be for visually impaired individuals in general or to those specifically afflicted with RP. All patients should be offered referral. Coordination by Social Services personnel familiar with working with the visually handicapped is appropriate. This is particularly true when dealing with issues such as integrating the visually impaired child into the school system or coordinating vocational rehabilitation training.[680]

Specific societies for RP patients have been established in many countries. In the United States there is the Foundation Fighting Blindness, which was formerly called the Retinitis Pigmentosa Foundation (7168 Columbia Gateway Drive, Suite 100, Columbia, MD 21046, USA. Tel: +1 (800) 683-5555+. Web: http://blindness.org/). In the UK there is RP Fighting Blindness (PO Box 350, Buckingham, MK18 1GZ, UK. Tel: +44 01280 821334+. Fax: +44 1 712 723 862. Web: http://rpfightingblindness.org.uk). In Canada, there is The Foundation Fighting Blindness Canada (890 Yonge Street, 12th Floor, M4W 3P4, Ontario,Toronto, Tel: ++ 14163604200, Fax: ++14163600060. Web: www.ffb.ca). Addresses of some other RP societies are given below. The most updated addresses of RP societies in other countries may be found at http://www.retina-international.org/.

For deaf and blind RP patients the following contacts might be appropriate: in the United States, Helen Keller National Center, 141 Middle Neck Road, Sands Point, NY 11050, USA. Tel: +1 516 944 8900. Web:http://helenkeller.org. In the UK, Sense, Sense Head Office, 101 Pentonville Road, London N1 9LG. Tel: +44 0845 127 0060. Fax: +44 0845 127 0061. Web: info@sense.org.uk).

For problems of visual handicap in general, in the United States, Commissions for the Blind have been established in each state to help in vocational training of blind adults. State and regional programs for the visually impaired child also exist. In the UK, patients may be referred to the Royal National Institute of Blind People (RNIB), 105 Judd Street, London, WC1H 9NE, UK. Tel: +44 020 7388 1266. Web: http://www.rnib.org.uk/).

Treatment

A major fallacy in the management of RP is the common assertion that the condition is untreatable; it is more accurate to say that RP is incurable. The patient with RP can always be helped (treated), and after diagnosis, it is no longer acceptable to dismiss such patients with "I can't do anything for you." It should not be forgotten that aiding the patient to become adjusted to RP by supplying useful information and support can do a great deal of good. Other major options to consider as appropriate include careful refraction, cataract extraction when indicated, treatment of macular edema, and referral for low-vision aids.

It is mandatory to ensure that the patient has appropriate correction of refractive error and access to low-vision aids. The Night Vision Aid is a monocular, handheld device that amplifies low-level illumination to help patients with defective night vision see under dim illumination conditions.[681]Although such devices may be useful in specific instances, a wide-angle, powerful flashlight is usually more effective and far less expensive than the Night Vision Aid.[682]

Limiting ocular light exposure is a common theme in attempts to limit progression of RP.[683] This theory has been tested in several small clinic trials. In one study, a single patient with adRP and another with arRP were tested by occluding one eye with an opaque shell for 6–8 h/day for 5 years.[684] However, no significant difference was seen between the covered and uncovered eyes with respect to visual acuity, visual fields, fundus examination and photography, or ERG. In a similar study, 12 patients with RP wore a tinted contact lens for several years in one eye. The covered eye demonstrated a trend to having less visual field loss than the uncovered eye, but these results have not been replicated in a larger trial.

Periodic visual field examinations with compassionate explanation of visual field defects can help patients appreciate the rate of progression and hence plan for future disability. Furthermore, regular examinations can help to ensure that the patient is referred to specific community and legal support agencies where appropriate. Explanation of statutory visual requirements for

driving will help patients who are still driving to plan for when this will no longer be possible. Reassurance that the changes seen are typical or usual for patients with RP often allays fears that they are losing visual function at a rate faster than expected.

Cataract Extraction

Patients with RP often develop cataracts that are visually significant. Cataract surgery should be considered and recommended in many of these cases. The most frequent cataract type seen is a posterior subcapsular lens opacity (35–51% of adult RP patients).[81–83]. The greatest benefit from cataract surgery seems to occur in patients with posterior subcapsular opacities rather than other types of cataract.[685] Clinical examination of the macula, including high-resolution OCT, may help to assess the potential for improvement of acuity. Examination of the macula in the fellow eye can be helpful but is not an infallible assessor of potential in the cataract eye.[686] Laser interferometry[687] and the potential acuity meter may help to determine whether cataract extraction will improve vision. A 2-week trial of mydriasis may also help in this assessment.[82] Most RP patients with a cataract that warrants surgery are younger (approximately 35 years of age) than comparable cataract patients without other ocular disease.[82,688]

Studies have suggested significant improvement in acuity in appropriate patients after cataract extraction. Bastek et al.[82] reported that 83% of 30 RP eyes improved by two lines on the Snellen chart. Over 50% of the patients improved to 20/50 or better. Newsome et al.[688] studied 26 RP and Usher patients undergoing cataract extraction and found that visual acuity improved in 22. Two studies of RP patients undergoing cataract surgery have emphasized phacoemulsification extraction and posterior chamber intraocular lens.[685,689] Both reported results comparable with those published for cataract patients without other ocular disease. RP patients do not seem to be more predisposed to anterior or posterior segment complications,[688,689] except for posterior capsular opacification,[689] anterior capsulorhexis contracture,[689,690] and possible dislocation of the intraocular lens from loss of zonular support.[690,691] Because the eyes of patients with RP are more prone to inflammation from

intraocular surgery, particularly if manipulation of the iris is required, topical steroids and nonsteroidal antiinflammatory medication should be used for a longer extent following cataract surgery in patients to prevent the occurrence of cystoid macular edema. Anterior capsular contracture following cataract surgery should be treated promptly with radial relaxing incisions using the YAG laser.[692] Augmented use of corticosteroids is recommended to protect the remaining posterior pole from postoperative CME.

If surgery is planned, the patient must realize that any improvement in central acuity will not be associated with improvement in visual field[82,689,693] and that the cataract surgery will in no way affect the expected rate of progression of the disease.[688] It is important for patients to have a realistic expectation for visual improvement before surgery.

Macular Edema

Cystoid macular edema (CME) can significantly reduce visual acuity in patients with RP.[151,152] Loss of central vision is especially problematic for these patients, who may have already lost significant peripheral vision. The prevalence of CME has been reported to be 11–70% in patients with nonsyndromic RP, with most studies reporting an incidence around 20%.[694–699] While the incidence of CME in patients with Usher syndrome has been found to range from 8% to 60%.[700–702] The wide variability in incidence is likely due to varying definitions of significant CME, the development of newer technologies such as OCT, which more effectively detect CME, as well as population differences between the studies. Some reports suggested a higher incidence in autosomal dominant and recessive forms of RP and a lower incidence in X-linked forms, but other studies have demonstrated no difference.[79,168,697,698]

The exact origin of CME in RP is unclear and is likely multifactorial. Low-grade inflammation may lead to the breakdown of the blood–retinal barrier resulting in leakage from retinal or choroidal vessels.[703–707] Decreased pumping efficiency of RPE cells could also result in the accumulation of fluid in the macula.[708] The presence of antiretinal antibodies, such as antienolase and

anticarbonic anhydrase has been correlated with the occurrence of CME.[709–711] Epiretinal membranes are an additional source for CME and have been noted to be more prominent in patients with RP.[609] Cataract surgery can induce CME or worsen already present edema raising concern in RP patients, who frequently have posterior subcapsular cataracts. However, Jackson et al.[689] reported that most patients with RP who underwent cataract extraction benefited significantly and that the rate of CME was lower than expected.

CME in RP has traditionally been described as a nonleaking CME, which was detectable with careful stereoscopic fundus examination but showed little leakage on fluorescein angiography. The detection of CME in patients with RP has evolved and OCT, specifically spectral domain OCT, now appears to be the most sensitive method.[697,712–714] Hajali et al.[697] demonstrated that even in patients with no fundoscopic evidence, the rate of CME in at least one eye using spectral domain OCT was 32%.

While OCT is quite sensitive in detecting the presence of CME, the relationship between retinal thickness and visual acuity can be difficult. Thickness measurements can be confounded by the fact that patients with RP usually have significant parafoveal cell loss. Several studies have shown conflicting results between the relationship of visual acuity and central thickness on OCT.[696,712,713] In a larger study, Sandberg et al.[698] found that visually acuity was inversely related to retinal thickness at the foveal center as well as independently related to parafoveal thickness. Additionally, the presence of the IS/OS junction, now referred to as the ellipsoid zone, on OCT seems to be a more reliable indicator of visual potential.[163,695,715,716]

A number of treatment methods for CME in RP have been attempted, including vitrectomy,[717] laser grid photocoagulation,[718] intravitreal[719,720] or systemic steroids,[721] and anti-VEGF agents.[722–724] However, the most effective agents to date have been carbonic anhydrase inhibitors.[708,725] When assessing the results of treatment of CME in RP, it should be remembered that CME may improve spontaneously without intervention.[151,726] Laser photocoagulation is a commonly used, effective treatment for the exudative, Coats-like retinopathy that is sometimes seen in RP.[73,77] While treatment of grid photocoagulation for CME has been reported,[718]

Heckenlively,[726] has challenged the wisdom of treating, in a destructive manner, any retina within the central field in patients with RP.

Carbonic anhydrase inhibitors (CAIs), both oral and topical, remain the mainstay of treatment for CME in RP. Cox et al.[708] first undertook a prospective crossover study using oral acetazolamide. Four of six RP patients showed a significant, reproducible improvement in macular edema. A similar effect on visual acuity was found by Fishman et al.,[725] who undertook a similar study design in 12 RP patients over a 2-week period. Grover et al.[727] found that, while a topical CAI, dorzolamide, provided improvement in angiographic macular edema and subjective visual function, visual acuity did not improve. They concluded that oral acetazolamide was a more effective treatment. A repeat study with a larger cohort measured the OCT changes in RP patients with CME treated with topical dorzolamide.[728] They demonstrated that 13 out of 15 patients had reduced macular edema following treatment with topical dorzolamide. Rebound macular edema has been reported with continued use of CAIs.[728–730] Thobani et al.[731] have shown that a "vacation" from CAI therapy in patients with rebound phenomenon can restore the efficacy of these medicines.

A practical treatment approach is to start with a topical CAI, such as dorzolamide, three times a day and proceed to an oral CAI if no improvement is seen. It can take several months before a treatment effect is observed.[730] For acetazolamide, an induction dose of 500 mg/day, followed by a maintenance dose of 250 mg/day, is recommended. Side-effects, such as loss of appetite, fatigue, hand tingling, renal stones, and anemia, are major problems that often limit the length of time RP patients will tolerate treatment with acetazolamide. Because of these adverse side-effects, Fishman et al.[732] have assessed the efficacy of methazolamide 50 mg/day, another carbonic anhydrase inhibitor with milder side-effects. Although they found improvement in macular edema in nine of 17 patients, the improvements in both subjective and objective visual acuity were disappointing. It was concluded that acetazolamide was the more effective treatment.

A number of authors have noted that improvement in objective (Snellen acuity) and subjective vision may not correlate with

angiographic changes.[725,732,733] This may occur because angiographic changes correlate more with permeability in retinal vessels, and the major effect of carbonic anhydrase inhibitors may be to increase fluid passage through the RPE. It was also proposed that improving extrafoveal sensitivity might explain why many patients report subjective improvement in vision without supportive improvement in Snellen acuity. Chen et al.[734] studied the psychophysical effects of 500 mg/day acetazolamide on CME in one adRP patient. Despite little improvement in acuity (one Snellen line), a significant improvement in macular edema and extrafoveal retinal sensitivity, as measured by scotopic-threshold fine-matrix mapping, was seen. Overall, the best way to monitor the effectiveness of acetazolamide treatment is through the subjective report of the patient rather than relying on visual acuity assessment or angiography.

Intravitreal injections of triamcinolone have been used in refractory cases of CME not responsive to CAIs. These injections provide temporary resolution of macular thickening and can result in improved acuity.[694,719,720,735] Steroids have the benefit of delivering an antiinflammatory effect, which may counteract autoimmune antibodies, but also provide an antiangiogenic effect, which may reduce vascular leakage. One distinct disadvantage of intravitreal steroids is that the effect is limited and repeat injections would likely be needed. Subsequent injections increase the risk of accelerating the development of cataracts, inducing glaucoma, or causing endophthalmitis.

The anti-VEGF agents pegaptanib sodium (Macugen), ranibizumab (Lucentis), bevacizumab (Avastin), and aflibercept (Eylea) have been used to treat CME in small series of patients with RP.[722–724,736,737] While these agents appear effective in some patients at reducing macular thickness and improving vision, there are legitimate concerns that the chronic use of these agents may exacerbate the vascular attenuation that is already present in patients with RP.[738] Furthermore, since evidence suggests that VEGF can additionally act as a neurotrophic factor; chronic suppression could be deleterious to retinal neurons in genetic diseases such as RP.[739,740]

Dietary Supplements

Vitamin A Supplements

Vitamin A supplements effectively treat retinopathies that are associated with vitamin A deficiency resulting from intestinal malabsorption or defective transport, such as occurs in Bassen–Kornzweig syndrome (abetalipoproteinemia).[741] Between 1984 and 1991 a randomized, double-masked, prospective study was undertaken by Berson et al.[742] to determine the effects of oral vitamin A (retinyl palmitate) and E (*dl*-α-tocopherol) on the course of the more common form of RP. Patients with typical RP or Usher syndrome type 2 were assigned to one of four treatment groups: (1) 15,000 IU/day of vitamin A; (2) 15,000 IU/day of vitamin A plus 400 IU/day of vitamin E; (3) trace amounts of both vitamins; or (4) 400 IU/day of vitamin E.

Ninety-five percent (596) of 601 adult patients completed at least 4 years of follow-up. Although no significant difference occurred for the slow loss of visual field with time, the authors found that the two groups receiving 15,000 IU/day of vitamin A had, on average, a slightly slower rate of decline of cone ERG amplitudes. Interestingly, the two groups receiving 400 IU/day of vitamin E were found to be 42% more likely to have a decline in amplitude of 50% or more from baseline. No significant change in visual acuity was found between the two groups. It was speculated that the apparent adverse effect of vitamin E could result from secondary interference with vitamin A absorption. The authors recommended that most adult RP patients take vitamin A (retinyl palmitate) in 15,000 IU/day supplements under the supervision of an ophthalmologist and avoid high-dose supplemental vitamin E, such as the 400 IU/day vitamin E used for this trial.[743]

This study and its recommendation were controversial and led to a series of articles on the significance of this work on clinical practice. [744–747] In particular a number of issues were raised.[748,749] The positive outcome of vitamin A use was only reported in terms of reduced decline of 30-Hz, and to some extent 0.5-Hz, flash amplitudes. No improvement in psychophysical visual parameters, perceivable by patients, was detected. It has been suggested that the changes in cone ERG responses, rather than being a positive effect of vitamin A, might be caused by effects on background noise and were misinterpreted by idiosyncracies of the methodology. With

reference to this possibility, it should be remembered that very-low-amplitude responses (as little as 0.12 μV) were being recorded in the RP patients. No adverse effects of vitamin use were found in the cases studied. Side-effects such as increased intracranial pressure, hepatomegaly, bone disease in the young, and elevated blood lipids can, however, occur with this dose of vitamin A.[750] In addition, large doses of supplemental vitamin A are considered by many to be teratogenic, leading to congenital abnormalities such as cardiac defects and cleft palate.[751,752] One survey found that, among babies born to women who took more than 10,000 IU of preformed vitamin A per day in the form of supplements, an estimated one infant in 57 had a malformation attributable to the supplement.[753] Thus supplemental vitamin A at the 15,000 IU/day dose is of particular concern in women of childbearing potential. The argument was made that greater benefit needed to be proven before recommending the use of vitamin A in RP.[749] Additional concerns have been reported about increased risk of osteoporosis by high-dose vitamin A supplementation.[754–757]

Although no serious problems of safety in the recommended dose were encountered in the above-mentioned study, the long-term safety of taking high-dose vitamin A supplements for many decades is uncertain. Questions raised about the toxicity to the liver of high-dose vitamin A supplements[758] and the fact that similar beneficial results of such high-dose supplements of vitamin A on RP have yet to be reproduced led ophthalmologists in many parts of the world to adopt the view that vitamin A may be of marginal benefit, at best, in patients with RP and that this must be weighed against the somewhat uncertain risks associated with its use.[744]

Sibulesky et al.[759] have reported no clinical symptoms or signs of liver toxicity in 146 otherwise healthy adults 18–54 years of age with RP who took 15,000 IU/day of vitamin A for ≤ 12 years. Berson still advocates supplemental vitamin A as beneficial for most patients with RP, particularly those with the Pro23His mutation of rhodopsin (EL Berson, personal communication, 2004). If patients elect to take supplemental vitamin A, they should be periodically monitored for hepatic toxicity, warned of the teratogenic risk for pregnancies, and monitored for osteoporosis. If patients have initiated its use on their own, it is recommended that they undergo

regular assessment of vitamin A levels and liver function tests.

Docosahexaenoic Acid Supplements

Docosahexaenoic acid (DHA) is an abundant lipid in photoreceptors, accounting for 30–40% of lipids in rod photoreceptor outer segments.[760] DHA levels are reduced in plasma,[761] erythrocytes,[762,763] and sperm[764] of selected patients with RP. DHA synthesis appears to be impaired in at least some patients with X-linked RP.[765] Long-term supplementation of 400 mg/day DHA resulted in a 2.5-fold elevation of mean plasma DHA levels but was not associated with any significant adverse effects.[766]

A trial of oral supplementation with 400 mg/day DHA for 4 years for patients with X-linked RP demonstrated a correlation of preservation of cone ERG with red blood cell DHA level, suggesting that supplementation may be of possible benefit for patients.[767] However, a follow-up study that delivered DHA with a weight-adjusted dose failed to find a benefit in XLRP patients.[768]

Berson and colleagues[769] in 2004 reported the results of a 4-year randomized, double-masked trial 221 patients with RP who were give either 1200 mg/d of supplemental DHA or a placebo capsule. Because of the results of the previous trial of vitamin A, both the treated and the control groups were also give 15,000 units of vitamin-A palmitate per day. The primary outcome measure was the total point score for the Humphrey 30-2 visual fields, and secondary outcome measures were the total point score for the combined 30-2 and 30-60-1 kinetic visual fields and the 30-Hz ERG amplitudes. Of the original 221 patients, 208 completed the 4-year trial. No significance differences in decline of visual field sensitivity or ERG amplitudes were seen between the treated and control groups. The conclusion of this trial was that in patients receiving 15,000 IU/d of vitamin A, the addition of 1200 mg/day did not, on average, slow the course of field or ERG amplitude loss from PR.

A second report by the same authors described further evaluations of the data from subcohort analyses of the original study of DHA supplementation.[770] These evaluations focused on the finding that of the patients entering the study, some were naive to vitamin A whereas others were already taking supplemental vitamin A. In the subcohort analyses of these two groups, those

participants who were naive to vitamin A who received supplemental DHA and vitamin A were found to have a slower course of disease (slower decline in visual sensitivity and ERG amplitudes, at p=.01 and p=.03, respectively) for the first two years of monitoring during the trial compared to the control group, who were taking vitamin A at the time of entry into the study; no similar slowing was observed for the cohort already taking vitamin A when given DHA supplementation. For years 3 and 4, there was no significant benefit for either subcohort. However, dietary omega-3 fatty acid for the vitamin A control group was inversely correlated to loss of visual sensitivity over the 4 years of the trial (test for trend, p=.05) and similarly the duration of vitamin A supplementation prior to entry into the study was inversely correlated to the rate of decline in ERG amplitude (p=.008). The authors interpreted these findings of the subcohort analyses to be sufficient to make the recommendation that patients who are taking vitamin A should supplement their diet with DHA and those who are not taking vitamin A should take it as well as supplement their diet with additional DHA.

Lutein Supplements

Lutein and zeaxanthin are macular pigments that cannot be synthesized in the body and must be derived from dietary sources. Evidence suggests that, in quail, macular pigments convey protection from oxidative damage and light-induced photoreceptor cell death.[771] A study of oral supplementation with 20 mg/day lutein for 6 months demonstrated increased macular pigment in 50% of subjects with RP or Usher syndrome but no change in central vision.[772] The long-term effects of such supplementation are unknown.

In 2010, Berson et al.[773] reported a trial of supplementation of lutein for patients with retinitis pigmentosa. In the same issue, an editorial was published by Massof and Fishman[774] entitled "How strong is the evidence that nutritional supplements slow the progression of retinitis pigmentosa?" This article examined the evidence from the earlier trials on vitamin A as well as the current trials on DHA and lutein supplementation. The authors note that none of the studies produced simple, clear-cut benefits with

primary analyses. Only when the original study was divided in a post hoc fashion into subcohorts was there any significance. The study's Data and Safety Monitoring Committee reported in a letter to the editor that there was no difference between the vitamin A group and the control group or between the A+E and the control group and argued that much of the originally reported significant differences was a consequence of pooling of data and could be attributed to early and consistently large differences between the vitamin E and all of the other groups.

Criticisms of Dietary Studies for RP

With regard to the 2004 DHA supplementation study conducted by Berson, Massof and Fishman point out that no significance was obtained in analysis of the primary outcome data (p=.88) and there was no difference between treatment and control groups for any of the secondary outcomes (rate of loss of 30/60-2 HFA total point score, 30 Hz ERG $\log_e$ amplitude, and logMAR visual acuity). When subcohort analyses were applied to the data, a significance was found for years 1 and 2 but not years 3 and 4. Based on the subcohort analyses of these the first study, Berson and colleagues recommended that patients with RP consume 15,000 IU/d of vitamin A palmitate to slow the progression of disease. Based on the subcohort analyses of the second study, the authors concluded that supplementary DHA facilitates and hastens the benefit of high-dose vitamin A in the first 2 years of treatment.

Massof and Finkelstein then presented two important issues regarding these trials: (1) the misinterpretation of outcomes because of incorrect assumptions built into the data analyses, such as linear decline over time when this assumption may not hold true, and (2) the question of how much weight should be placed on clinical practice recommendation that are drawn from secondary subcohort analyses, which disrupt and unbalance the initial design of the study. Finally, the authors discuss the concept of the clinical trial as a special class of study that is highly formal in design, structure, and execution and is motivated by a clinical question that, when resolved, will set the new standard for clinical practice. They conclude that the primary outcome, which is agreed on in advance and which is the heart of the study design, should render the

verdict of the trial. Secondary analyses are useful to mine for potential other factors that may be operative and may lead into useful future studies but should not dictate the standard of patient care.

Purported "Cures" for RP

During consultation, RP patients often raise difficult questions on information and validation of less conventional therapies that have received media coverage, or which they have read about on the Internet. A recent online survey of patients with RP revealed that 95% of respondents had tried at least one form of complementary and alternative medicine for treatment of their RP, including acupuncture, massage, yoga, aromatherapy, mind–body therapies, and herbal therapies.[775] Some patients reported improvements in subjective visual acuity although there have not been any controlled scientific studies to assess vision with these treatments.

While many of the above-mentioned therapies are well intentioned and likely do provide some stress relief for patients, there exist other regimens, especially on the Internet, that claim to significantly improve vision in patients with RP. Testimonials from successfully "treated" patients often support such claims, but little objective data are provided. Such regimens usually have little scientific basis for their claims and often lead to great disappointment for patients.

Ophthalmologists involved in the care of RP patients are obliged to dissuade patients from subjecting themselves to the risks of unsubstantiated therapies and should warn patients that the pursuit of false hope can lead to significant emotional trauma and economic loss.[776]

Many unconventional treatments for RP have been proposed for many years. These have included therapeutic beestings,[777] vasodilators,[778] and injections of placental tissues.[779] In Russia, RP patients have been treated with intramuscular or peribulbar injections of ENCAD, an RNA extract of yeast.[780] A number of studies by outside agencies have, however, discredited this as an effective treatment for either halting or reversing RP.[781,782]

Patients attending a clinic in Cuba undergo electric stimulation to

the head, shoulders, and feet for 21 days; their blood is also drawn, ozonated, and reinjected on multiple days. A surgical procedure is then undertaken to transplant a flap of retrobulbar fat, with blood vessels, into a scleral pocket in the posterior globe. Some patients are also given oral vasodilator drugs and vitamins. Berson et al.[783] evaluated 10 RP patients over a 6- to 8-month period before and after they had undergone treatment in Cuba. Visual function testing, including assessment of acuity, visual field, and ERG changes, found no beneficial effect to the treatment. More worrisome was the fact that the magnitude of mean decline in ERG amplitude and visual field relative to those reported in other studies suggested that the intervention was associated with a worsening of the course of the disease. Similar poor results for this treatment have been published by others.[784,785] Diplopia requiring surgical correction has also been seen as a complication.[784,786] These reports conclude that this treatment protocol is of no benefit to RP patients.

Two studies have examined acupuncture for treatment of vision loss in retinitis pigmentosa, and while both studies reported impressive results, neither study was randomized or had a control group where patients receive "sham" acupuncture with needles placed at nontraditional locations thus raising questions about the validity of the data.[787,788] Determining whether or not acupuncture has value in preserving vision in retinitis pigmentosa will require larger, well-controlled randomized studies.

The previous studies looked at a heterogeneous population of RP patients, but there is evidence that light exposure may play an important role in a subset of RP patients, specifically those with autosomal dominant RP caused by class B1 rhodopsin mutations.[789] These patients can demonstrate greater loss in the inferior retina compared with the superior retina, which has been attributed to increasing light exposure from above.[186,790] Additionally, both canine and rodent models of autosomal dominant RP have demonstrated retinal degeneration that can be slowed by dark rearing and is worsened with exposure to bright light.[149,632,791–795] Therefore, although a direct relationship between light exposure and progression in RP has not been established, it seems reasonable to recommend patients (especially those with autosomal dominant

forms of RP) to wear tinted lenses when outside. Moreover, care should be taken when examining these patients to avoid unnecessary light exposure from photographic or surgical procedures.

Tinted lenses may provide comfort outdoors, and, for some patients with RP, may provide subjective vision improvement although more controlled subjective studies are needed.[796] Lenses with special tints, such as the Corning 550 lens, are appreciated as being subjectively better than ordinary sunglasses by some patients with RP, particularly those with a cone–rod pattern of dysfunction. We recommend that patients find an optician willing to allow an adequate trial period before purchasing these rather expensive tinted glasses.

Future Management

Much of the work on new therapeutic strategies for RP depends on animal models. Many such models are already available. Both transgenic[797] and knockout[798] rodent models of retinal dystrophy exist and, at the moment, are the most popular models for work in therapeutics. These have advantages over naturally occurring examples of retinal dystrophy of unknown genetic cause, in that the underlying molecular genetic defect can be chosen. For example, all work on disease due to mutant rhodopsin is based on such constructs, since, prior to 2002, no rhodopsin mutant animals, apart from humans, had been found in nature. The usefulness of these constructed rodent models is, however, limited by differences in the constitutional makeup of the rodent as compared to the human eye. The most pertinent differences are in the number and distribution of photoreceptors in the retina, especially cones, the absence of a true macula, and the fact that rodent eyes are much smaller than human globes.

By far the greatest visual handicap in human RP is caused by secondary loss of cone function.[663] The identification of a rod-derived cone viability factor offers hope for future therapeutic strategies to preserve cone survival and function in human RP.[665] It has also been suggested that cone death in RP is often a secondary phenomenon, due to the oxidative stress induced by primary rod

death.[799] Antioxidant therapies, most notably N-acetylcysteine have recently been shown to preserve cones in mouse models of RP.[800]

Further validation of such therapies will however require larger animals than the mouse or rat. Unfortunately rodent retinas have sparse, evenly distributed cone photoreceptors and so reflect the human situation only to a limited extent. The rodent eye is also very small, approximately 3–6 mm diameter, compared to a human globe (approximately 24 mm diameter) and the rodent lens is relatively large, almost filling the internal cavity of the globe. These two mechanical factors severely limit the usefulness of rodents in the evaluation of surgical techniques on the eye. Petters et al.[638] have developed a transgenic porcine animal model of RP that expresses a mutated rhodopsin gene (Pro347Leu). The pig eye is much more comparable in constitution and size (approximately 22 mm diameter) to the human eye. Although the pig also does not have a formed macular region, the number and gross distribution of cones are much more similar to human retina.[663] Other large animals of value to retinal degeneration work include the Briard dog (*RPE65* mutation),[801] the T4R rhodopsin mutant dog,[802] and the Siberian husky (*RPGR* mutation).[803]

Gene Therapy

As a target for genetic manipulation, the retina has some advantages. Target cells (usually photoreceptors) are more directly accessible than in most tissues, and the effects of manipulations can be directly observed. The cell population is static and nondividing. Once appropriate expression is obtained, it will be theoretically effective indefinitely.

The consequences of genetic mutation can be divided into two categories: (1) those abnormalities that lead to loss of function (e.g., most autosomal recessive disease, the majority of X-linked disorders, and some dominant conditions); and (2) those that lead to extra (usually detrimental) function (often seen in dominant disease). Examples of this are the deficits caused by PDE deficiency in autosomal recessive PDEβ mutations,[804] and the theoretical gain of function in some rhodopsin mutations in adRP.[580] Recognizing which is relevant to the disease process of interest is the starting

point of any gene therapy strategy, since dramatically different methods will be employed. In "loss-of-function"-type disease, replacing the mutant may be sufficient for cure. In "gain-of-function"-type disease it would be more appropriate to block, or "switch off," the disease gene (e.g., with complementary, antisense oligonucleotides).

The main problems associated with gene therapy in the retina are delivery of genetic material to cells and appropriate expression of that material in the target without adverse effects. Of the various gene transfer vectors used (e.g., ligand-DNA conjugates, DNA-loaded liposome vesicles, electroporation) adenovirus and adeno-associated virus have been the most extensively studied. Transfection with adeno- and adenoassociated virus[805] can be nonspecific. Intravitreal injection of adenovirus frequently leads to widespread expression in the lens, ciliary body, and the retina.[806] Subretinal injection leads to more confined gene expression.[807] Other major problems associated with the use of adenovirus are host immune response and theoretical problems of inhibition of host cell protein synthesis and neoplastic transformation. Adjuvant use of immunosuppressives is being studied to try to reduce immune responses.[808]

Landmark gene therapy studies in human retinal degeneration were undertaken in 2007.[809,810] A recombinant AAV2 vector was used by Bainbridge et al.[809] to deliver a human *RPE65* cDNA driven by elements of the endogenous RPE65 promoter in cases of Leber congenital amaurosis. Maguire et al.[810] used an AAV2 vector with a constitutive promoter to drive *RPE65* transgene expression and reported objective evidence of improved retinal function (e.g., by pupillometry) in all three patients. Both groups reported improvement in subjective measures of visual acuity, in four of the six participants in both trials. Maguire et al.[810] reported improvement in pupillometry. Neither group reported improvement in retinal function on electroretinography. After subretinal injection, Bainbridge et al.[809] reported one case of macular hole. Further follow-up has suggested stable clinical benefits and no unexpected complications.[811,812] Recently, Sparks Therapeutics released positive results from their phase III gene therapy study is treating patients with mutations in *RPE65* using an AAV2 vector.

The primary endpoint, which was met, measured improvement of change in mobility testing between baseline and one year in treated versus control groups.[813]

An innovative approach to the treatment of autosomal dominant disease has involved the use of hammerhead ribozymes.[814] Dominant disease is often associated with (adverse) gain of function by the mutant gene or a dominant-negative effect of the mutant allele's gene product. For example, mutant protein may accumulate in the Golgi apparatus or otherwise fail to be transported to the normal site within the cell, resulting in cell dysfunction and death. Mutant mRNA may accumulate in the nucleus, inhibiting normal mRNA maturation. If the mutant gene can be effectively suppressed by attacking its mRNA, the remaining wild gene may be sufficient for normal cell function. Ribozymes are RNA enzymes that induce sequence-specific cleavage of targeted RNA. In this way ribozymes can be designed to be mutation-specific and so destroy mutant RNA. “Proof of principle” for ribozyme therapy for Pro23His transgenic rats has been demonstrated.[815] In vivo expression in this rhodopsin mutant model is achieved by transduction with an rAAV incorporating a rod opsin promoter of either a hammerhead or hairpin ribozyme that targets the mutant message. The expression of the mutant-specific ribozyme and its effect on reduction of mutant mRNA significantly slowed the course of disease for 3 months. In a more recent innovation, Georgiadis et al.[816] used a virally transferred miRNA-based hairpin to silence peripherin/RDS in murine retina.

Another interesting gene therapy approach for dominant RP mutations is “combined gene knock-down and gene addition therapy,” Rather than targeting specific alleles, which in the case of rhodopsin would require target over a hundred different alleles, both endogenous rhodopsin alleles, regardless of whether mutated or not, are downregulated by siRNA technology, while at the same time, a codon modified rhodopsin cDNA that is not sensitive to siRNA interference is added by AAV mediated gene transfer.[817]

Cell Therapy

Tissue transplantation into the eye was first undertaken just over

100 years ago.[520,818] It is only recently though that cell therapeutics have become sufficiently understood to justify attempts to treat RP. Work in 1988[819] showed that transplanting normal RPE cells into the subretinal space of the RCS rat, an animal model of autosomal recessive retinal dystrophy, rescued photoreceptors in the immediate vicinity of the transplant. Such photoreceptor rescue in the RCS rat has also been documented using human fetal RPE cells[820] nonfetal human RPE,[821] and most recently using human-induced pluripotent stem cell-derived RPE.[822] Long-term effectiveness requires adjunctive immunosuppression (e.g., with cyclosporin).[820] Although most efforts in RPE transplantation have been directed toward macular diseases such as age-related macular degeneration,[823–825] this methodology may be useful in RP due to RPE-specific mutations.[826,827] Current tissue transplantation work in RP though is focused on replacing lost photoreceptors. Cells from three different sources lead this work: adult-derived human stem cells, human embryonic stem cells, and human-induced pluripotent stem cells.

A number of sources have been targeted for adult-derived stem cells including bone marrow[828] and adult brain-derived neural progenitor cells[829] but with very limited success. Others have focused on stem cell sources within the eye itself. A number of researchers have highlighted the potential for Müller glial cells to de-differentiate, proliferate, and produce new retinal neurons and glia.[830,831] In addition, considerable interest has emerged in stem cells derived from the epithelium of the ciliary body.[832,833] However, more recent studies have questioned the potential of these cells for retinal regeneration.[834] More promising work has been undertaken using embryonic stem cells (ESCs). These cells have been differentiated in vitro into photoreceptor-like cells[835] as well as retinal pigmented epithelium.[825,827] Currently though, these techniques have proven time-consuming, labor-intensive, and of low yield. Despite these technical limitations for widespread application, subretinal injection of ESC-derived photosensitive cells has been shown to restore visual function in Crx-deficient mice as detected by electroretinography.[836] A dramatic step forward in the manufacture of viable photoreceptors for transplantation work has been achieved using a technique involving 3D (rather than 2D)

culture methods.[837] Embryonic-stem-cell-derived retinal epithelium was found to spontaneously form hemispherical epithelial vesicles. These resembled embryonic optic cup, and it has been found that all retinal cell lineages can be derived from the cups.[838] It has now also been shown that photorecpeotrs derived from 3D culture can integrate somewhat into degenerating retina.[839] Recent embryonic stem cell clinical trials in humans with macular degeneration and Stargardt's disease suggest that such an approach might also be feasible in retinitis pigmentosa, although convincing clinical benefits have yet to be reported.[840]

Overcoming many of the ethical limitations and sourcing difficulties of using ESCs, the most intensively discussed stem cell source is induced pluripotent stem cells (iPSCs).[841,842] "Reprogramming" of adult, differentiated cells to recapture their pluripotency allows for versatile tissue regeneration from a plentiful source without immunogenic difficulties. Both mouse and human iPSC have been induced to differentiate into retinal progenitor cells in vitro.[843] Very recent work has shown histologic evidence that iPS-derived rhodopsin expressing cells can integrate into the iodoacetic acid-damaged pig retina.[844] Most recently, iPSCs have also been used in 3D culture systems to derive mutation specific photoreceptors for pathophysiology studies and to test new therapeutics in a preclinical setting.[845]

Another interesting approach in cell therapy has been to use cells not for their potential to regenerate lost cells but as a way to deliver therapeutic molecules long-term to the degenerating retina. This may be as an innate ability of the cells or by using cells genetically modified to deliver therapeutic molecules. Mesenchymal stem cells[846] have proven neuroprotective effects and have been used in animal models demonstrating neuroprotective effects in the retina after subretinal injection[847] and injection in the systemic circulation.[848] Mouse embryonic stem cells have been genetically modified to secrete glial-derived neurotrophic factor. A neurotrophic effect was reported following intravitreal injection of these cells in a rat rhodopsin-mutant.[849]

Apoptosis/Neuroprotection

It has been shown that in animal models of a number of retinal dystrophies, photoreceptor cell death occurs by a common mechanism known as apoptosis, or programmed cell death.[850,851] Apoptosis is as an alternative mode of cell death to necrosis and is part of normal cell turnover during embryogenesis (termed histogenetic cell death), as well as playing an important role in disease pathology. Apoptosis is biochemically characterized by cleavage of DNA at internucleosomal sites. Such DNA fragmentation can be observed at the single cell level by in situ labeling of apoptotic cell nuclei using a histochemical technique known as TUNEL (*T*dT-mediated d*U*TP-biotin *n*ick *e*nd *l*abeling).[840] Microscopically, apoptosis can be seen as cytoplasmic and nuclear condensation and fragmentation of cells into membrane-bound structures (apoptotic bodies). Inflammation and scarring do not occur.[839,840]

In animal models of RP such as the rd, rds, the RCS rat, and rhodopsin-mutant transgenic mice, apoptotic photoreceptor nuclei have been observed during normal retinal development and in periods of retinal degeneration.[850–852] The molecular triggering of apoptosis in the retina is a tightly controlled process that reflects the balance of pro-apoptotic versus antiapoptotic factors.[853] Due to the complexity and number of signals involved in the apoptotic cascade, there are many points for potential therapeutic intervention. One strategy has been to try to influence the balance of the proteins in the Bcl-2 family to tip the scale away from a commitment to apoptosis. For example, overexpression of the anti-apoptotic protein, Bcl-2, in the retina of several rodent models of RP was able to slow photoreceptor degeneration.[854,855] In a converse strategy, reducing the levels of the proapoptotic proteins, Bax and Bak, protected photoreceptors in a light damage model.[856] However, not all studies have shown a protective effect of the overexpression of Bcl-2 or Bcl- X_L,[857] and it has been suggested that alteration of Bcl-2 levels may actually be detrimental to cell survival.[858]

Elevated levels of calcium have long been known to play an integral role in photoreceptor degeneration in retinitis pigmentosa by triggering apoptosis.[859] Attempts to block calcium influx into photoreceptors to elicit neuroprotection have resulted in conflicting results. Administration of calcium channel blockers, such as

dilitiazem, in animal models of retinal degeneration has exhibited neuroprotection in some studies,[860–862] but other studies have demonstrated no effect.[863] More recently, there have been reports that the calcium channel blocker nilvadipine can provide a protective effect in animal models of retinal degeneration. One small study in patients with RP demonstrated that nilvidapine reduced visual field loss in RP patients treat with nilvadipine.[864] Larger-scale clinical trials are needed to confirm these results.

A different strategy to eliciting photoreceptor protection in retinitis pigmentosa is to block mediators of apoptosis further downstream, such as the caspase proteins. Increased caspase activity has been detected in photoreceptors undergoing apoptosis in animal models of retinitis pigmentosa.[865] Intraocular injection of caspase-3 inhibitors or ablation of caspase-1 have been shown to decrease photoreceptor death in some, but not all animal models of retinal degeneration.[866,867] However, such therapies have yet to be translated into human studies, and it is now realized that there are also non-caspase-dependent pathways that mediate apoptosis.[868] Another alternative approach is to deliver endogenous neurotrophic factors, which elicit cell protection by preventing apoptosis via multiple mechanisms. Through direct injection, viral-mediated delivery, nanoparticles, and encapsulated cell technology (ECT), a variety of different neurotrophic factors have been delivered in animal models of retinal degeneration, including basic fibroblast growth factor (bFGF),[869,870] brain-derived neurotrophic factor (BDNF),[871] ciliary neurotrophic factor (CNTF),[872,873] and glial-derived neurotrophic factor (GDNF).[849,874] In spite of the success of these agents in animal models, few have yet to be translated into the clinic setting.

An exception to this has been CNTF, which in humans has been delivered using ECT.[873] Animal models treated with CNTF have demonstrated protection of the photoreceptor cell bodies, but have also demonstrated no improvement and sometimes a worsening in the electroretinogram as well as a decrease in vision. It appears that CNTF downregulates proteins involved in rod phototransduction in a dose-dependent manner leading to a tradeoff between prolonged cell survival at the cost of immediate decreased vision.[875] The most recent clinical trials with CNTF/ECTs have been

disappointing.[876]

Electronic Prosthesis (Artificial Retina)

In 1929, Foerster showed that if the occipital pole is electrically stimulating the occipital pole, the subject will perceive "light" (phosphine).[877] In 1969, Potts and Inoue[878] also demonstrated that external electrical stimulation of the eye itself can also elicit the perception of light and a cortical response in patients with advanced RP. These results indicate that at least some retinal ganglion cells and more central elements of the visual system retain function even in very advanced RP. These studies form the basis for developing an electronic prosthesis in RP. Four different approaches are being studied. Subretinal implants are placed under the retina (between the degenerate photoreceptors and the RPE) and input into second-order neurons or ganglion cells. Epiretinal implants lie on the retina–vitreous interface and stimulate ganglion cells. Optic nerve implants stimulate the axons of ganglion cells, and cortical implants are implanted intracranially to stimulate the visual areas of the brain. (See Chapter 129, Artificial vision, for more details.)

Acknowledgment

The preparation of this chapter was supported in part by grants from the Foundation Fighting Blindness, Columbia, MD; The Grousbeck Family Foundation, Boston; Research to Prevent Blindness, New York; the TFC Frost Charitable Trust, Esher, Surrey, UK; and the British Retinitis Pigmentosa Society.

References

1. Bunker CH, Berson EL, Bromley WC, Hayes RP, Roderick TH. Prevalence of retinitis pigmentosa in Maine. *Am J Ophthalmol*. 1984;97(3):357–365.
2. Ammann F, Klein D, Franceschetti A. Genetic and epidemiological investigations on pigmentary degeneration of the retina and allied disorders in Switzerland. *J Neurol Sci*. 1965;2(2):183–196.
3. Bundey S, Crews SJ. A study of retinitis pigmentosa in the City of Birmingham. I Prevalence. *J Med Genet*. 1984;21(6):417–420.
4. Merin S, Auerbach E. Retinitis pigmentosa. *Surv Ophthalmol*. 1976;20(5):303–346.
5. Haim M. Epidemiology of retinitis pigmentosa in Denmark. *Acta Ophthalmol Scand Suppl*. 2002;(233):1–34.
6. You QS, Xu L, Wang YX, et al. Prevalence of retinitis pigmentosa in North China: the Beijing Eye Public Health Care Project. *Acta Ophthalmol*. 2013;91(6):e499–500.
7. Hu DN. Genetic aspects of retinitis pigmentosa in China. *Am J Med Genet*. 1982;12(1):51–56.
8. Iwase A, Araie M, Tomidokoro A, et al. Prevalence and causes of low vision and blindness in a Japanese adult population: the Tajimi Study. *Ophthalmology*. 2006;113(8):1354–1362.
9. Heckenlively J, Friederich R, Farson C, Pabalis G. Retinitis pigmentosa in the Navajo. *Metab Pediatr Ophthalmol*. 1981;5(3–4):201–206.
10. Xu L, Hu L, Ma K, Li J, Jonas JB. Prevalence of retinitis pigmentosa in urban and rural adult Chinese: The Beijing Eye Study. *Eur J Ophthalmol*. 2006;16(6):865–866.
11. Sen P, Bhargava A, George R, et al. Prevalence of retinitis pigmentosa in South Indian population aged above 40 years. *Ophthalmic Epidemiol*. 2008;15(4):279–281.
12. Nangia V, Jonas JB, Khare A, Sinha A. Prevalence of retinitis pigmentosa in India: the Central India Eye and Medical Study. *Acta Ophthalmol*. 2012;90(8):e649–50.

13. Kimberling WJ, Hildebrand MS, Shearer AE, et al. Frequency of Usher syndrome in two pediatric populations: Implications for genetic screening of deaf and hard of hearing children. *Genet Med*. 2010;12(8):512–516.
14. Nuutila A. Dystrophia retinae pigmentosa – dysacusis syndrome (DRD): a study of the Usher- or Hallgren syndrome. *J Genet Hum*. 1970;18(1):57–88.
15. Spandau UH, Rohrschneider K. Prevalence and geographical distribution of Usher syndrome in Germany. *Graefes Arch Clin Exp Ophthalmol*. 2002;240(6):495–498.
16. Ovelgün. Nyctalopia haerediotria. *Acta Physico Med (Nuremburg)*. 1744;7:76–77 [obs. 28].
17. Donders FC. Torpeur de la rétine congénital e héréditarie. *Ann Ocul (Paris)*. 1855;34:270–273.
18. Donders FC. Beiträge zur pathologischen Anatomie des Auges. II. Pigmentbildung in der Netzhaut. *Albrecht Von Graefes Arch Ophthalmol*. 1857;3(1):139–150.
19. van Trigt AC. De oogspiegel. 1852-1853.
20. Ruete CGT. *Bildliche Darstellung der Krankheiten des menschlichen Auges*. Teubner: Leipzig; 1854.
21. Tanino TO. Studies on pigmentary retinal dystrophy. II. Recordability of electroretinogram and the mode of inheritance. *Jpn J Ophthalmol*. 1976;20:482–486.
22. Berson EL, Sandberg MA, Rosner B, Birch DG, Hanson AH. Natural course of retinitis pigmentosa over a three-year interval. *Am J Ophthalmol*. 1985;99(3):240–251.
23. Massof RW, Benzschawel T, Emmel T, Palmer R, Finkelstein D. The spread of retinal degeneration in retinitis pigmentosa. *Invest Ophthalmol Vis Sci*. 1984;25(Suppl.):196.
24. Massof RW, Finkelstein D. A two-stage hypothesis for the natural course of retinitis pigmentosa. *Adv Biosci*. 1987;62:29–58.
25. Jacobson SG, Yagasaki K, Feuer WJ, Román AJ. Interocular asymmetry of visual function in heterozygotes of X-linked retinitis pigmentosa. *Exp Eye Res*. 1989;48(5):679–691.
26. *Social Security Laws: Aged, Blind, or Disabled Individual*. http://www.ssa.gov/OP_Home/ssact/title16b/1614.htm.
27. Grover S, Fishman GA, Anderson RJ, et al. Visual acuity

impairment in patients with retinitis pigmentosa at age 45 years or older. *Ophthalmology*. 1999;106(9):1780–1785.
28. Ffytche TJ. Cystoid maculopathy in retinitis pigmentosa. *Trans Ophthalmol Soc U K*. 1972;92:265–283.
29. Geltzer AI, Berson EL. Fluorescein angiography of hereditary retinal degenerations. *Arch Ophthalmol*. 1969;81(6):776–782.
30. Hansen RI, Friedman AH, Gartner S, Henkind P. The association of retinitis pigmentosa with preretinal macular gliosis. *Br J Ophthalmol*. 1977;61:597–600.
31. Fishman GA, Magianno J, Fishman M. Foveal lesions seen in retinitis pigmentosa. *Arch Ophthalmol*. 1977;95:1993–1996.
32. Fishman GA, Fishman M, Maggiano J. Macular lesions associated with retinitis pigmentosa. *Arch Ophthalmol*. 1977;95:798–803.
33. Marmor MF. The electroretinogram in retinitis pigmentosa. *Arch Ophthalmol*. 1979;97:1300–1304.
34. Fishman GA. Retinitis pigmentosa. Visual loss. *Arch Ophthalmol*. 1978;96(7):1185–1188.
35. Jay B, Bird A. X-linked retinitis pigmentosa. *Trans Am Acad Ophthalmol Otolaryngol*. 1973;77(5):OP641–51.
36. Heckenlively JR, Yoser SL, Friedman LH, Oversier JJ. Clinical findings and common symptoms in retinitis pigmentosa. *Am J Ophthalmol*. 1988;105:504–511.
37. Hood DC, Ramachandran R, Holopigian K, Lazow M, Birch DG, Greenstein VC. Method for deriving visual field boundaries from OCT scans of patients with retinitis pigmentosa. *Biomed Opt Express*. 2011;2(5):1106–1114.
38. Hood DC, Lin CE, Lazow MA, Locke KG, Zhang X, Birch DG. Thickness of receptor and post-receptor retinal layers in patients with retinitis pigmentosa measured with frequency-domain optical coherence tomography. *Invest Ophthalmol Vis Sci*. 2009;50(5):2328–2336.
39. Heckenlively JR. Preserved para-arteriolar retinal pigment epithelium (PPRPE) in retinitis pigmentosa. *Br J Ophthalmol*. 1982;66:26–30.
40. van den Born LI, van Soest S, van Schooneveld MJ, Riemslag FCC, de Jong PTVM, Bleeker-Wagemakers EM. Autosomal

recessive retinitis pigmentosa with preserved para-arteriolar retinal pigment epithelium. *Am J Ophthalmol*. 1994;118:430–439.
41. den Hollander AI, ten Brink JB, de Kok YJ, et al. Mutations in a human homologue of Drosophila crumbs cause retinitis pigmentosa (RP12). *Nat Genet*. 1999;23(2):217–221.
42. Cotterman CW, Falls HF, Neel JV. Some hereditary diseases having subclinical manifestations in carriers. *Genetics*. 1948;33(6):608.
43. Heckenlively JR. *Retinitis pigmentosa*. JP Lippincott Co.: Philadelphia; 1988.
44. Goodman G, Ripps H, Siegel IM. Sex-linked ocular disorders: trait expressivity in males and carrier females. *Arch Ophthalmol*. 1965;73:387–398.
45. Heckenlively JR, Weleber RG. X-linked recessive cone dystrophy with tapetal-like sheen. A newly recognized entity with Mizuo-Nakamura phenomenon. *Arch Ophthalmol*. 1986;104(9):1322–1328.
46. Cideciyan AV, Jacobson SG. Image analysis of the tapetal-like reflex in carriers of X-linked retinitis pigmentosa. *Invest Ophthalmol Vis Sci*. 1994;35(11):3812–3824.
47. Berendschot TT, DeLint PJ, van Norren D. Origin of tapetal-like reflexes in carriers of X-linked retinitis pigmentosa. *Invest Ophthalmol Vis Sci*. 1996;37(13):2716–2723.
48. Genead MA, Fishman GA, Lindeman M. Structural and functional characteristics in carriers of X-linked retinitis pigmentosa with a tapetal-like reflex. *Retina*. 2010;30(10):1726–1733.
49. Acton JH, Greenberg JP, Greenstein VC, et al. Evaluation of multimodal imaging in carriers of X-linked retinitis pigmentosa. *Exp Eye Res*. 2013;113:41–48.
50. Vingolo EM, Livani ML, Domanico D, Mendonca RH, Rispoli E. Optical coherence tomography and electro-oculogram abnormalities in X-linked retinitis pigmentosa. *Doc Ophthalmol*. 2006;113(1):5–10.
51. Miyake Y, Terasaki H. Golden tapetal-like fundus reflex and posterior hyaloid in a patient with x-linked juvenile retinoschisis. *Retina*. 1999;19(1):84–86.

52. Noble KG, Margolis S, Carr RE. The golden tapetal sheen reflex in retinal disease. *Am J Ophthalmol*. 1989;107(3):211–217.
53. Lyon MF. The William Allan memorial award address: X-chromosome inactivation and the location and expression of X-linked genes. *Am J Hum Genet*. 1988;42(1):8–16.
54. Szamier RB, Berson EL. Retinal histopathology of a carrier of X-chromosome-linked retinitis pigmentosa. *Ophthalmology*. 1985;92(2):271–278.
55. Berson EL, Rosen JB, Simonoff EA. Electroretinographic testing as an aid in detection of carriers of X-chromosome-linked retinitis pigmentosa. *Am J Ophthalmol*. 1979;87(4):460–468.
56. Arden GB, Carter RM, Hogg CR, et al. A modified ERG technique and the results obtained in X-linked retinitis pigmentosa. *Br J Ophthalmol*. 1983;67:419–430.
57. Fishman GA, Weinberg AB, McMahon TT. X-linked recessive retinitis pigmentosa. Clinical characteristics of carriers. *Arch Ophthalmol*. 1986;104(9):1329–1335.
58. Peachey NS, Fishman GA, Derlacki DJ, Alexander KR. Rod and cone dysfunction in carriers of X-linked retinitis pigmentosa. *Ophthalmology*. 1988;95(5):677–685.
59. Rajacich GM, Parelhoff ES, Heckenlively JR. The cup-disc ratio in retinitis pigmentosa subgroups. *Invest Ophthalmol Vis Sci*. 1982;22(Suppl.):55.
60. De Bustros S, Miller NR, Finkelstein D, Massof RF. Bilateral astrocytic hamartomas of the optic nerve heads in retinitis pigmentosa. *Retina*. 1983;3:21–23.
61. Novack RL, Foos RY. Drusen of the optic disc in retinitis pigmentosa. *Am J Ophthalmol*. 1987;103:44–47.
62. Spencer WH. Drusen of the optic disk and aberrant axoplasmic transport. The XXXIV Edward Jackson memorial lecture. *Am J Ophthalmol*. 1978;85(1):1–12.
63. Grover S, Fishman GA, Brown J Jr. Frequency of optic disc or parapapillary nerve fiber layer drusen in retinitis pigmentosa. *Ophthalmology*. 1997;104(2):295–298.
64. Edwards A, Grover S, Fishman GA. Frequency of photographically apparent optic disc and parapapillary

nerve fiber layer drusen in Usher syndrome. *Retina*. 1996;16(5):388–392.
65. Flynn MF, Fishman GA, Anderson RJ, Roberts DK. Retrospective longitudinal study of visual acuity change in patients with retinitis pigmentosa. *Retina*. 2001;21(6):639–646.
66. Giusti C, Forte R, Vingolo EM. Clinical pathogenesis of macular holes in patients affected by retinitis pigmentosa. *Eur Rev Med Pharmacol Sci*. 2002;6(2–3):45–48.
67. Dorenboim Y, Rehany U, Rumelt S. Central serous chorioretinopathy associated with retinitis pigmentosa. *Graefes Arch Clin Exp Ophthalmol*. 2004;242(4):346–349.
68. Takahashi M, Jalkh A, Hoskins J, Trempe CL, Schepens CL. Biomicroscopic evaluation and photography of liquefied vitreous in some vitreoretinal disorders. *Arch Ophthalmol*. 1981;99(9):1555–1559.
69. Vingolo EM, Giusti C, Forte R, Onori P. Vitreal alterations in retinitis pigmentosa: biomicroscopic appearance and statistical evaluation. *Ophthalmologica*. 1996;210(2):104–107.
70. Hong PH, Han DP, Burke JM, Wirostko WJ. Vitrectomy for large vitreous opacity in retinitis pigmentosa. *Am J Ophthalmol*. 2001;131(1):133–134.
71. Uliss AE, Gregor ZJ, Bird AC. Retinitis pigmentosa and retinal neovascularization. *Ophthalmology*. 1986;93(12):1599–1603.
72. Grizzard WS, Deutman AF, Pinckers AJ. Retinal dystrophies associated with peripheral retinal vasculopathy. *Br J Ophthalmol*. 1978;62(3):188–194.
73. Khan JA, Ide CH, Strickland MP. Coats'-type retinitis pigmentosa. *Surv Ophthalmol*. 1988;32(5):317–332.
74. Spallone A, Carlevaro G, Ridling P. Autosomal dominant retinitis pigmentosa and Coats'-like disease. *Int Ophthalmol*. 1985;8(3):147–151.
75. Pruett RC. Retinitis pigmentosa: Clinical observations and correlations. *Trans Am Ophthalmol Soc*. 1983;81:693–735.
76. Demirci FY, Rigatti BW, Mah TS, Gorin MB. A novel RPGR exon ORF15 mutation in a family with X-linked retinitis pigmentosa and Coats'-like exudative vasculopathy. *Am J*

Ophthalmol. 2006;141(1):208–210.
77. Kim RY, Kearney JJ. Coats-type retinitis pigmentosa in a 4-year-old child. *Am J Ophthalmol*. 1997;124(6):846–848.
78. Naoi N, Fukiyama J, Sawada A. Retinitis pigmentosa with recurrent vitreous hemorrhage. *Acta Ophthalmol Scand*. 1996;74(5):509–512.
79. Spalton DJ, Bird AC, Cleary PE. Retinitis pigmentosa and retinal oedema. *Br J Ophthalmol*. 1978;62(3):174–182.
80. Berson EL, Rosner B, Simonoff E. Risk factors for genetic typing and detection in retinitis pigmentosa. *Am J Ophthalmol*. 1980;89(6):763–775.
81. Heckenlively J. The frequency of posterior subcapsular cataract in the hereditary retinal degenerations. *Am J Ophthalmol*. 1982;93(6):733–738.
82. Bastek JV, Heckenlively JR, Straatsma BR, Carr RE. Cataract surgery in retinitis pigmentosa patients. *Ophthalmology*. 1982;89:880–884.
83. Fishman GA, Anderson RJ, Lourenco P. Prevalence of posterior subcapsular lens opacities in patients with retinitis pigmentosa. *Br J Ophthalmol*. 1985;69(4):263–266.
84. Franceschetti A, François J, Babel J. Tapetoretinal degeneration and keratoconus. Franceschetti A, François J, Babel J. *Chorioretinal heredodegenerations*. Charles C Thomas: Springfield, IL; 1974:855–859.
85. Franceschetti A, François J, Babel J. Glaucoma. Franceschetti A, François J, Babel J. *Chorioretinal heredodegenerations*. Charles C Thomas: Springfield, IL; 1974:851–852.
86. Omphroy CA. Sector retinitis pigmentosa and chronic angle-closure glaucoma: a new association. *Ophthalmologica*. 1984;189:12–20.
87. Sieving PA, Fishman GA. Refractive errors of retinitis pigmentoa patients. *Br J Ophthalmol*. 1978;62:163–167.
88. Ross DF, Fishman GA, Gilbert LD, Anderson RJ. Variability of visual fields measurements in normal subjects and patients with retinitis pigmentosa. *Arch Ophthalmol*. 1984;102(7):1004–1010.
89. Nowomiejska K, Vonthein R, Paetzold J, Zagorski Z, Kardon R, Schiefer U. Comparison between semiautomated kinetic

perimetry and conventional Goldmann manual kinetic perimetry in advanced visual field loss. *Ophthalmology*. 2005;112(8):1343–1354.
90. Schiefer U, Pascual JP, Edmunds B, et al. Comparison of the new perimetric GATE strategy with conventional full-threshold and SITA standard strategies. *Invest Ophthalmol Vis Sci*. 2009;50(1):488–494.
91. Weleber RG, Smith TB, Peters D, et al. VFMA: topographic analysis of sensitivity data from full-field static perimetry. *Transl Vis Sci Technol*. 2015;4(2):14.
92. Massof RW, Finkelstein D. Vision threshold profiles in sector retinitis pigmentosa. *Arch Ophthalmol*. 1979;97(10):1899–1904.
93. Massof RW, Finkelstein D. Rod sensitivity relative to cone sensitivity in retinitis pigmentosa. *Invest Ophthalmol Vis Sci*. 1979;18(3):263–272.
94. Massof RW, Finkelstein D. Subclassifications of retinitis pigmentosa from two-color scotopic static perimetry. *Doc Ophthalmol Proc Ser*. 1981;26:219–225.
95. Massof RW. Psychophysiological subclassifications of retinitis pigmentosa. LaVail MM, Hollyfield JG, Anderson RE. *Retinal degeneration, experimental and clinical studies*. Alan R Liss: New York; 1985:91–107.
96. Massof RW, Finkelstein D, Boughman JA. Genetic analysis of subgroups within simplex and multiplex retinitis pigmentosa. *Birth Defects Orig Artic Ser*. 1982;18(6):161–166.
97. Arden GB, Carter RM, Hogg CR, et al. Rod and cone activity in patients with dominantly inherited retinitis pigmentosa: comparisons between psychophysical and electroretinographic measurements. *Br J Ophthalmol*. 1983;67:405–418.
98. Lyness AL, Ernst W, Quinlan MP, et al. A clinical, psychophysical, and electroretinographic survey of patients with autosomal dominant retinitis pigmentosa. *Br J Ophthalmol*. 1985;69:326–339.
99. Ernst W, Faulkner DJ, Hogg CR, Powell DJ, Arden GB, Vaegan. An automated static perimeter/adaptometer using light emitting diodes. *Br J Ophthalmol*. 1983;67:431–442.

100. Jacobson SG, Voigt WJ, Parel J-M, et al. Automated light- and dark-adapted perimetry for evaluating retinitis pigmentosa. *Ophthalmology*. 1986;93(12):1604–1611.
101. Jacobson SG, Kemp CM, Sung C-H, Nathans J. Retinal function and rhodopsin levels in autosomal dominant retinitis pigmentosa with rhodopsin mutations. *Am J Ophthalmol*. 1991;112(3):256–271.
102. Kemp CM, Jacobson SG, Roman AJ, Sung C-H, Nathans J. Abnormal rod dark adaptation in autosomal dominant retinitis pigmentosa with proline-23-histidine rhodopsin mutation. *Am J Ophthalmol*. 1992;113(2):165–174.
103. Jacobson SG, Cideciyan AV, Regunath G, et al. Night blindness in Sorsby's fundus dystrophy reversed by vitamin A. *Nat Genet*. 1995;11:27–32.
104. Alexander KR, Fishman GA. Prolonged rod dark adaptation in retinitis pigmentosa. *Br J Ophthalmol*. 1984;68(8):561–569.
105. Moore AT, Fitzke FW, Kemp CM, et al. Abnormal dark adaptation kinetics in autosomal dominant sector retinitis pigmentosa due to rod opsin mutation. *Br J Ophthalmol*. 1992;76:465–469.
106. Arden GB. Rod–cone interactions in night-blinding disease. *Jpn J Ophthalmol*. 1987;31:6–19.
107. Karpe G. The basis of clinical electroretinography. *Acta Ophthalmol (Copenh)*. 1945;23(Suppl.):1–114.
108. Riggs LA. Electroretinography in cases of night blindness. *Am J Ophthalmol*. 1954;38:70–78.
109. Arden GB, Barrada A, Kelsey JH. New clinical test of retinal function based on the standing potential of the eye. *Br J Ophthalmol*. 1962;46:449–467.
110. Weleber RG. Fast and slow oscillations of the electro-oculogram in Best's macular dystrophy and retinitis pigmentosa. *Arch Ophthalmol*. 1989;107(4):530–537.
111. Gouras P. Electroretinography: some basic principals. *Invest Ophthalmol*. 1970;9:557–569.
112. McCulloch DL, Marmor MF, Brigell MG, et al. ISCEV Standard for full-field clinical electroretinography (2015 update). *Doc Ophthalmol*. 2015;130(1):1–12.
113. Berson EL, Sandberg MA, Rosner B, Birch DG, Hanson AH.

Natural course of retinitis pigmentosa over a three-year interval. *Am J Ophthalmol*. 1985;99(3):240–251.
114. Andréasson SOL, Sandberg MA, Berson EL. Narrow-band filtering for monitoring low-amplitude cone electroretinograms in retinitis pigmentosa. *Am J Ophthalmol*. 1988;105(5):500–503.
115. Tanino T, Ohba N. Studies on pigmentary retinal dystrophy. II. Recordability of electroretinogram and the mode of inheritance. *Jpn J Ophthalmol*. 1976;20:482–486.
116. Berson EL. Retinitis pigmentosa and allied disease: applications of electroretinographic testing. *Int Ophthalmol*. 1981;4:7–22.
117. Birch DG, Fish GF. Rod ERGs in retinitis pigmentosa and cone-rod degeneration. *Invest Ophthalmol Vis Sci*. 1987;28:140–150.
118. Berson EL. Electrical phenomena in the retina. Moses RA, Hart WM. *Adler's physiology of the eye: clinical application*. 8th ed. CV Mosby: St. Louis; 1987:506–567.
119. Berson EL, Simonoff EA. Dominant retinitis pigmentosa with reduced penetrance: further studies of the electroretinogram. *Arch Ophthalmol*. 1979;97:1286–1291.
120. Berson EL, Gouras P, Gunkel RD, Myrianthopoulos NC. Dominant retinitis pigmentosa with reduced penetrance. *Arch Ophthalmol*. 1969;81:226–234.
121. Sandberg MD, Effron MH, Berson EL. Focal cone electroretinograms in dominant retinitis pigmentosa with reduced penetrance. *Invest Ophthalmol Vis Sci*. 1978;17:1096–1101.
122. Stone JL, Barlow WE, Humayun MS, de Juan E Jr, Milam AH. Morphometric analysis of macular photoreceptors and ganglion cells in retinas with retinitis pigmentosa. *Arch Ophthalmol*. 1992;110:1634–1639.
123. Falsini B, Iarossi G, Porciatti V, et al. Postreceptoral contribution to macular dysfunction in retinitis pigmentosa. *Invest Ophthalmol Vis Sci*. 1994;35:4282–4290.
124. Cideciyan AV, Jacobson SG. Negative electroretinograms in retinitis pigmentosa. *Invest Ophthalmol Vis Sci*. 1993;34(12):3253–3263.

125. Granit R. The components of the retinal action potential in mammals and their relation to the discharge of the optic nerve. *J Physiol (Lond)*. 1933;77:207–239.
126. Breton ME, Quinn GE, Schueller AW. Development of electroretinogram and rod phototransduction response in human infants. *Invest Ophthalmol Vis Sci*. 1995;36:1588–1602.
127. Hood DC, Birch DG. A quantitative measure of the electrical activity of human rod photoreceptors using electroretinography. *Vis Neurosci*. 1990;5(4):379–387.
128. Hood DC, Birch DG. The a-wave of the human electroretinogram and rod receptor function. *Invest Ophthalmol Vis Sci*. 1990;31(10):2070–2081.
129. Lamb TD, Pugh EN Jr. A quantitative account of the activation steps involved in phototransduction in amphibian photoreceptors. *J Physiol*. 1992;449:749–757.
130. Hood DC, Birch DG. Rod phototransduction in retinitis pigmentosa: estimation and interpretation of parameters derived from the rod a-wave. *Invest Ophthalmol Vis Sci*. 1994;35(7):2948–2961.
131. Hood DC, Birch DG. A computational model of the amplitude and implicit time of the *b*-wave of the human ERG. *Vis Neurosci*. 1992;8(2):107–126.
132. Hood DC, Birch DG. *b*-wave of the scotopic (rod) electroretinogram as a measure of the activity of human on-bipolar cells. *J Opt Soc Am A*. 1996;13(3):623–633.
133. Shady S, Hood DC, Birch DG. Rod phototransduction in retinitis pigmentosa: distinguishing alternative mechanisms of degeneration. *Invest Ophthalmol Vis Sci*. 1995;36(6):1027–1037.
134. Hood DC, Cideciyan AV, Halevy DA, Jacobson SG. Sites of disease action in a retinal dystrophy with supernormal and delayed rod electroretinogram *b*-waves. *Vision Res*. 1996;36:889–901.
135. Gouras P, Eggers HM, MacKay CJ. Cone dystrophy, nyctalopia, and supernormal rod responses: a new retinal degeneration. *Arch Ophthalmol*. 1983;101:718–724.
136. Marmor MF, Jacobson SG, Foerster MH, Kellner U, Weleber RG. Diagnostic clinical findings of a new syndrome with

night blindness, maculopathy and enhanced S cone sensitivity. *Am J Ophthalmol*. 1990;110(2):124–134.
137. Jacobson SG, Marmor MF, Kemp CM, Knighton RW. SWS (blue) cone hypersensitivity in a newly identified retinal degeneration. *Invest Ophthalmol Vis Sci*. 1990;31(5):827–838.
138. Haider NB, Jacobson SG, Cideciyan AV, et al. Mutation of a nuclear receptor gene, NR2E3, causes enhanced S cone syndrome, a disorder of retinal cell fate. *Nat Genet*. 2000;24(2):127–131.
139. Birch DG, Hood DC, Nusinowitz S, Pepperberg DR. Abnormal activation and inactivation mechanisms of rod transduction in patients with autosomal dominant retinitis pigmentosa and the Pro-23-His mutation. *Invest Ophthalmol Vis Sci*. 1995;36(8):1603–1614.
140. Goto Y, Peachey NS, Ziroli NE, et al. Rod phototransduction in transgenic mice expressing a mutant opsin gene. *J Opt Soc Am A*. 1996;13:577–585.
141. Tzekov RT, Locke KG, Hood DC, Birch DG. Cone and rod ERG phototransduction parameters in retinitis pigmentosa. *Invest Ophthalmol Vis Sci*. 2003;44(9):3993–4000.
142. Sutter EE, Tran D. The field topography of ERG components in man – I. The photopic luminance response. *Vision Res*. 1992;32(3):433–446.
143. Bearse MA, Sutter EE, Lerner L. Imaging retinal damage with the multi-input electroretinogram. Vision science and its applications. Optical Society of America: Washingon, DC; 1994:358–361. *Technical Digest Series*. vol. 2.
144. Hood DC, Li J. A technique for measuring individual multifocal ERG records: non-invasive assessment of the visual system. Trends in Optical Photonics. *Proceedings of the Optical Society of America*. 1997;11:33–41.
145. Hood DC, Seiple W, Holopigian K, Greenstein V. A comparison of the components of the multifocal and full-field ERGs. *Vis Neurosci*. 1997;14(3):533–544.
146. Robson AG, El-Amir A, Bailey C, et al. Pattern ERG correlates of abnormal fundus autofluorescence in patients with retinitis pigmentosa and normal visual acuity. *Invest Ophthalmol Vis Sci*. 2003;44(8):3544–3550.

147. Arden GB, Fojas MR. Electrophysiological abnormalities in pigmentary degenerations of the retina. *Arch Ophthalmol*. 1962;68:369–389.
148. Weleber RG, Eisner A. Retinal function and physiological studies. Newsome DA. *Retinal dystrophies and degenerations*. Raven Press: New York, NY; 1988:21–69.
149. Cideciyan AV, Jacobson SG, Aleman TS, et al. In vivo dynamics of retinal injury and repair in the rhodopsin mutant dog model of human retinitis pigmentosa. *Proc Natl Acad Sci USA*. 2005;102(14):5233–5238.
150. Spalton DJ, Bird AC, Cleary PE. Retinitis pigmentosa and retinal oedema. *Br J Ophthalmol*. 1978;62:174–182.
151. Newsome DA. Retinal fluorescein leakage in retinitis pigmentosa. *Am J Ophthalmol*. 1986;101:354–360.
152. Fetkenhour CL, Choromokos E, Weinstein J, Shoch D. Cystoid macular edema in retinitis pigmentosa. *Trans Am Acad Ophthalmol Otolaryngol*. 1977;83:OP-515–21.
153. von Ruckmann A, Fitzke FW, Bird AC. Distribution of fundus autofluorescence with a scanning laser ophthalmoscope. *Br J Ophthalmol*. 1995;79(5):407–412.
154. Robson AG, Egan CA, Luong VA, Bird AC, Holder GE, Fitzke FW. Comparison of fundus autofluorescence with photopic and scotopic fine-matrix mapping in patients with retinitis pigmentosa and normal visual acuity. *Invest Ophthalmol Vis Sci*. 2004;45(11):4119–4125.
155. Popovic P, Jarc-Vidmar M, Hawlina M. Abnormal fundus autofluorescence in relation to retinal function in patients with retinitis pigmentosa. *Graefes Arch Clin Exp Ophthalmol*. 2005;243(10):1018–1027.
156. Robson AG, Saihan Z, Jenkins SA, et al. Functional characterisation and serial imaging of abnormal fundus autofluorescence in patients with retinitis pigmentosa and normal visual acuity. *Br J Ophthalmol*. 2006;90(4):472–479.
157. Robson AG, Michaelides M, Saihan Z, et al. Functional characteristics of patients with retinal dystrophy that manifest abnormal parafoveal annuli of high density fundus autofluorescence; a review and update. *Adv Ophthalmol*. 2008;116(2):79–89.

158. Fleckenstein M, Charbel Issa P, Fuchs HA, et al. Discrete arcs of increased fundus autofluorescence in retinal dystrophies and functional correlate on microperimetry. *Eye (Lond)*. 2009;23(3):567–575.
159. Robson AG, Tufail A, Fitzke F, et al. Serial imaging and structure-function correlates of high-density rings of fundus autofluorescence in retinitis pigmentosa. *Retina*. 2011;31(8):1670–1679.
160. Lima LH, Cella W, Greenstein VC, et al. Structural assessment of hyperautofluorescent ring in patients with retinitis pigmentosa. *Retina*. 2009;29(7):1025–1031.
161. Aleman TS, Cideciyan AV, Sumaroka A, et al. Retinal laminar architecture in human retinitis pigmentosa caused by Rhodopsin gene mutations. *Invest Ophthalmol Vis Sci*. 2008;49(4):1580–1590.
162. Kellner U, Kellner S, Weber BH, Fiebig B, Weinitz S, Ruether K. Lipofuscin- and melanin-related fundus autofluorescence visualize different retinal pigment epithelial alterations in patients with retinitis pigmentosa. *Eye (Lond)*. 2009;23(6):1349–1359.
163. Witkin AJ, Ko TH, Fujimoto JG, et al. Ultra-high resolution optical coherence tomography assessment of photoreceptors in retinitis pigmentosa and related diseases. *Am J Ophthalmol*. 2006;142(6):945–952.
164. Lim JI, Tan O, Fawzi AA, Hopkins JJ, Gil-Flamer JH, Huang D. A pilot study of Fourier-domain optical coherence tomography of retinal dystrophy patients. *Am J Ophthalmol*. 2008;146(3):417–426.
165. Wolsley CJ, Silvestri G, O'Neill J, Saunders KJ, Anderson RS. The association between multifocal electroretinograms and OCT retinal thickness in retinitis pigmentosa patients with good visual acuity. *Eye (Lond)*. 2009;23(7):1524–1531.
166. Lupo S, Grenga PL, Vingolo EM. Fourier-domain optical coherence tomography and microperimetry findings in retinitis pigmentosa. *Am J Ophthalmol*. 2011;151(1):106–111.
167. Fischer MD, Fleischhauer JC, Gillies MC, Sutter FK, Helbig H, Barthelmes D. A new method to monitor visual field defects caused by photoreceptor degeneration by

quantitative optical coherence tomography. *Invest Ophthalmol Vis Sci*. 2008;49(8):3617–3621.
168. Hajali M, Fishman GA, Anderson RJ. The prevalence of cystoid macular oedema in retinitis pigmentosa patients determined by optical coherence tomography. *Br J Ophthalmol*. 2008;92(8):1065–1068.
169. Liang J, Williams DR. Aberrations and retinal image quality of the normal human eye. *J Opt Soc Am A Opt Image Sci Vis*. 1997;14(11):2873–2883.
170. Roorda A, Romero-Borja F, Donnelly IW, Queener H, Hebert T, Campbell M. Adaptive optics scanning laser ophthalmoscopy. *Opt Express*. 2002;10(9):405–412.
171. Duncan JL, Zhang Y, Gandhi J, et al. High-resolution imaging with adaptive optics in patients with inherited retinal degeneration. *Invest Ophthalmol Vis Sci*. 2007;48(7):3283–3291.
172. Wolfing JI, Chung M, Carroll J, Roorda A, Williams DR. High-resolution retinal imaging of cone–rod dystrophy. *Ophthalmology*. 2006;113(6):1019.e1.
173. Choi SS, Doble N, Hardy JL, et al. In vivo imaging of the photoreceptor mosaic in retinal dystrophies and correlations with visual function. *Invest Ophthalmol Vis Sci*. 2006;47(5):2080–2092.
174. Dubra A, Sulai Y, Norris JL, et al. Noninvasive imaging of the human rod photoreceptor mosaic using a confocal adaptive optics scanning ophthalmoscope. *Biomed Opt Express*. 2011;2(7):1864–1876.
175. Talcott KE, Ratnam K, Sundquist SM, et al. Longitudinal study of cone photoreceptors during retinal degeneration and in response to ciliary neurotrophic factor treatment. *Invest Ophthalmol Vis Sci*. 2011;52(5):2219–2226.
176. Jay M. On the heredity of retinitis pigmentosa. *Br J Ophthalmol*. 1982;66:405–416.
177. Dryja TP. Molecular genetics of Oguchi disease, fundus albipunctatus, and other forms of stationary night blindness: LVII Edward Jackson Memorial Lecture. *Am J Ophthalmol*. 2000;130(5):547–563.
178. Franceschetti A, François J, Babel J. Retinitis punctata

albescens. Franceschetti A, François J, Babel J. *Chorioretinal heredodegenerations*. Charles C Thomas: Springfield, IL; 1974:222–231.
179. Miyake Y, Shiroyama N, Sugita S, Horiguchi M, Yagasaki K. Fundus albipunctatus associated with cone dystrophy. *Br J Ophthalmol*. 1992;76(6):375–379.
180. Nakamura M, Miyake Y. Macular dystrophy in a 9-year-old boy with fundus albipunctatus. *Am J Ophthalmol*. 2002;133(2):278–280.
181. Nakamura M, Hotta Y, Tanikawa A, Terasaki H, Miyake Y. A high association with cone dystrophy in fundus albipunctatus caused by mutations of the *RDH5* gene. *Invest Ophthalmol Vis Sci*. 2000;41(12):3925–3932.
182. Bietti G. Su alcune forme atipiche o rare di degenerazione retinica (degenerazioni tappeto-retiniche e quadri morbosi similari). *Boll Ocul*. 1937;16:1159–1244.
183. Krill AE. Incomplete rod–cone degenerations. Harper & Row: New York, NY; 1977:577–643. Krill AE. *Krill's Hereditary retinal and choroidal diseases*. vol. 2.
184. Berson EL, Howard J. Temporal aspects of the electroretinogram in sector retinitis pigmentosa. *Arch Ophthalmol*. 1971;86:653–665.
185. Deutman AF. Rod–cone dystrophy: primary, hereditary, pigmentary retinopathy, retinitis pigmentosa. Harper & Row: New York, NY; 1977:479–576. Krill AE. *Krill's Hereditary retinal and choroidal diseases*. vol. 2.
186. Heckenlively JR, Rodriguez JA, Daiger SP. Autosomal dominant sectoral retinitis pigmentosa: two families with transversion mutation in codon 23 of rhodopsin. *Arch Ophthalmol*. 1991;109:84–91.
187. Audo I, Friedrich A, Mohand-Said S, et al. An unusual retinal phenotype associated with a novel mutation in RHO. *Arch Ophthalmol*. 2010;128(8):1036–1045.
188. Saihan Z, Le Quesne Stabej P, Robson AG, et al. Mutations in the Ush1c gene associated with sector retinitis pigmentosa and hearing loss. *Retina*. 2011;31(8):1708–1716.
189. de Crecchio G, Alfieri MC, Cennamo G, D'Esposito F, Forte R. Pericentral pigmentary retinopathy: long-term follow-up.

Eye (Lond). 2006;20(12):1408–1410.
190. Selmer KK, Grondahl J, Riise R, et al. Autosomal dominant pericentral retinal dystrophy caused by a novel missense mutation in the TOPORS gene. *Acta Ophthalmol*. 2010;88(3):323–328.
191. Manes G, Guillaumie T, Vos WL, et al. High prevalence of PRPH2 in autosomal dominant retinitis pigmentosa in France and characterization of biochemical and clinical features. *Am J Ophthalmol*. 2015;159(2):302–314.
192. Lyon MF. The William Allan memorial award address: X-chromosome inactivation and the location and expression of X-linked genes. *Am J Hum Genet*. 1988;42(1):8–16.
193. Mukhopadhyay R, Holder GE, Moore AT, Webster AR. Unilateral retinitis pigmentosa occurring in an individual with a germline mutation in the RP1 gene. *Arch Ophthalmol*. 2011;129(7):954–956.
194. Whitcup SM, Iwata F, Podgor MJ, Valle D, Sran PK, Kaiser-Kupfer MI. Association of thyroid disease with retinitis pigmentosa and gyrate atrophy. *Am J Ophthalmol*. 1996;122(6):903–905.
195. Cowan CL, Grimes PE, Chakrabarti S, Minus HR, Kenney JA. Retinitis pigmentosa associated with hearing loss, thyroid disease, vitiligo, and alopecia areata. *Retina*. 1982;2(2):84–88.
196. Boughman JA. *Personal communication*. [January 28] 1988.
197. Newsome DA. The immune system in retinitis pigmentosa. LaVail MM, Hollyfield JG, Anderson RE. *Retinal degeneration: experimental and clinical studies*. Alan R Liss: New York; 1985:75–90.
198. Boughman JA, Caldwell RJ. Assessment of clinical variables and counseling needs in patients with retinitis pigmentosa. *Am J Med Genet*. 1982;12(2):185–193.
199. Zito I, Downes SM, Patel RJ, et al. *RPGR* mutation associated with retinitis pigmentosa, impaired hearing, and sinorespiratory infections. *J Med Genet*. 2003;40(8):609–615.
200. Kenna P, Mansergh F, Millington-Ward S, et al. Clinical and molecular genetic characterisation of a family segregating autosomal dominant retinitis pigmentosa and sensorineural

deafness. *Br J Ophthalmol*. 1997;81(3):207–213.
201. Mansergh FC, Millington-Ward S, Kennan A, et al. Retinitis pigmentosa and progressive sensorineural hearing loss caused by a C12258A mutation in the mitochondrial MTTS2 gene. *Am J Hum Genet*. 1999;64(4):971–985.
202. Usher CH. On the inheritance of retinitis pigmentosa, with notes of cases. *R Lond Ophthalmol Hosp Rep*. 1914;19:130–236.
203. Koenig R. Bardet–Biedl syndrome and Usher syndrome. *Dev Ophthalmol*. 2003;37:126–140.
204. Hope CI, Bundey S, Proops D, Fielder AR. Usher syndrome in the city of Birmingham – prevalence and clinical classification. *Br J Ophthalmol*. 1997;81(1):46–51.
205. Boughman JA, Vernon M, Shaver KA. Usher syndrome: definition and estimate of prevalence from two high-risk populations. *J Chronic Dis*. 1983;36(8):595–603.
206. Kimberling WJ, Hildebrand MS, Shearer AE, et al. Frequency of Usher syndrome in two pediatric populations: implications for genetic screening of deaf and hard of hearing children. *Genet Med*. 2010;12(8):512–516.
207. Vernon M. Usher's syndrome – deafness and progressive blindness: clinical cases, prevention, theory, and literature review. *J Chronic Dis*. 1969;22(3):133–151.
208. Smith RJH, Berlin CI, Hejtmancik JF, et al. Clinical diagnosis of the Usher syndromes. Usher Syndrome Consortium. *Am J Med Genet*. 1994;50(1):32–38.
209. Fishman GA, Kumar A, Joseph ME, Torok N, Anderson RJ. Usher's syndrome: ophthalmic and neuro-otologic findings suggesting genetic heterogeneity. *Arch Ophthalmol*. 1983;101(9):1367–1374.
210. Davenport SLH, Omenn GS. *The heterogeneity of Usher syndrome, publication 426*. [Excerpta Medica Foundation, International Congress Series, abstract 215. Amsterdam] 1977:87–88.
211. Pakarinen L, Karjalainen S, Simola KOJ, Laippala P, Kaitalo H. Usher's syndrome type 3 in Finland. *Laryngoscope*. 1995;105(6):613–617.
212. Pakarinen L, Tuppurainen K, Laippala P, Mäntyjärvi M, Puhakka H. The ophthalmological course of Usher

syndrome type III. *Int Ophthalmol*. 1996;19(5):307–311.
213. Merin S, Abraham FA, Auerbach E. Usher's and Hallgren's syndromes. *Acta Genet Med Gemellol (Roma)*. 1974;23:49–55.
214. Piazza L, Fishman GA, Farber M, Derlacki D, Anderson RJ. Visual acuity loss in patients with Usher's syndrome. *Arch Ophthalmol*. 1986;104:1336–1339.
215. Sankila E-M, Pakarinen L, Kääriäinen H, et al. Assignment of an Usher syndrome type III (USH3) gene to chromosome 3q. *Hum Mol Genet*. 1995;4(1):93–98.
216. Ness SL, Ben-Yosef T, Bar-Lev A, et al. Genetic homogeneity and phenotypic variability among Ashkenazi Jews with Usher syndrome type III. *J Med Genet*. 2003;40(10):767–772.
217. Loundon N, Marlin S, Busquet D, et al. Usher syndrome and cochlear implantation. *Otol Neurotol*. 2003;24(2):216–221.
218. Matthews TW, Poliquin J, Mount J, MacFie D. Is there genetic heterogeneity in Usher's syndrome? *J Otolaryngol*. 1987;16(2):61–66.
219. Szlyk JP, Fishman GA, Alexander KR, Revelins BI, Derlacki DJ, Anderson RJ. Relationship between difficulty in performing daily activities and clinical measures of visual function in patients with retinitis pigmentosa. *Arch Ophthalmol*. 1997;115:53–59.
220. Tamayo ML, Rodriguez A, Molina R, Martinez M, Bernal JE. Social, familial and medical aspects of Usher syndrome in Colombia. *Genet Couns*. 1997;8(3):235–240.
221. Krill AE, Deutman AF, Fishman M. The cone degenerations. *Doc Ophthalmol*. 1973;35:1–80.
222. Evans K, Duvall-Young J, Fitzke FW, Arden GB, Bhattacharya SS, Bird AC. Chromosome 19q cone–rod retinal dystrophy. *Arch Ophthalmol*. 1995;113:195–201.
223. Rabb MF, Tso MOM, Fishman GA. Cone–rod dystrophy: a clinical and histopathologic report. *Ophthalmology*. 1986;93:1443–1450.
224. Berson EL, Gouras P, Gunkel RD. Progressive cone–rod degeneration. *Arch Ophthalmol*. 1968;80:68–76.
225. Heckenlively JR, Martin DA, Rosales TO. Telangiectasia and optic atrophy in cone-rod degenerations. *Arch Ophthalmol*.

1981;99(11):1983–1991.
226. Krauss HR, Heckenlively JR. Visual field changes in cone-rod degenerations. *Arch Ophthalmol*. 1982;100(11):1784–1790.
227. Yagasaki K, Jacobson SG. Cone–rod dystrophy: phenotypic diversity by retinal function testing. *Arch Ophthalmol*. 1989;107:701–708.
228. Szlyk JP, Fishman GA, Alexander KR, Peachey NS, Derlacki DJ. Clinical subtypes of cone-rod dystrophy. *Arch Ophthalmol*. 1993;111(6):781–788.
229. Mäntyjärvi M, Tuppurainen K. Progressive cone–rod dystrophy and high myopia in a Finnish family. *Acta Ophthalmol (Copenh)*. 1989;67(3):234–242.
230. Heckenlively JR, Foxman SG, Parelhoff ES. Retinal dystrophy and macular coloboma. *Doc Ophthalmol*. 1988;68(3–4):257–271.
231. Aleman TS, Cideciyan AV, Volpe NJ, Stevanin G, Brice A, Jacobson SG. Spinocerebellar ataxia type 7 (*SCA7*) shows a cone–rod dystrophy phenotype. *Exp Eye Res*. 2002;74(6):737–745.
232. Jalili IK, Smith NJD. A progressive cone–rod dystrophy and amelogenesis imperfecta: a new syndrome. *J Med Genet*. 1988;25:738–740.
233. Samra D, Abraham FA, Treister G. Inherited progressive cone–rod dystrophy and alopecia. *Metab Pediatr Syst Ophthalmol*. 1988;11(1–2):83–85.
234. Jalili IK. Cone–rod congenital amaurosis associated with congenital hypertrichosis: an autosomal recessive condition. *J Med Genet*. 1989;26(8):504–510.
235. Moore AT. Cone and cone–rod dystrophies. *J Med Genet*. 1992;29(5):289–290.
236. Kelsell RE, Gregory-Evans K, Payne AM, et al. Mutations in the retinal guanylate cyclase (RETGC-1) gene in dominant cone–rod dystrophy. *Hum Mol Genet*. 1998;7(7):1179–1184.
237. Payne AM, Downes SM, Bessant DA, et al. A mutation in guanylate cyclase activator 1A (*GUCA1A*) in an autosomal dominant cone dystrophy pedigree mapping to a new locus on chromosome 6p21.1. *Hum Mol Genet*. 1998;7(2):273–277.
238. Wilkie SE, Li Y, Deery EC, et al. Identification and

functional consequences of a new mutation (E155G) in the gene for GCAP1 that causes autosomal dominant cone dystrophy. *Am J Hum Genet*. 2001;69(3):471–480.
239. Leber T. Ueber Retinitis pigmentosa und angeborene Amaurose. *Graefes Arch Clin Exp Ophthalmol*. 1869;15:1–25.
240. Franceschetti A, Dieterlé P. Importance diagnostique et pronostique de l'électrorétinogramme (ERG) dans les dégénérescences tapéto-rétiniennes avec rétrécissement du champ visuel et héméralopie. *Confin Neurol*. 1954;14:184–186.
241. Franceschetti A. Rubeola pendant la grossesse et cataracte congenitale chez l'enfant, accompagnee du phenomene digito-oculaire. *Ophthalmologica*. 1947;114:332–339.
242. Sohocki MM, Sullivan LS, Mintz-Hittner HA, et al. A range of clinical phenotypes associated with mutations in CRX, a photoreceptor transcription-factor gene. *Am J Hum Genet*. 1998;63(5):1307–1315.
243. Rivolta C, Berson EL, Dryja TP. Dominant Leber congenital amaurosis, cone–rod degeneration, and retinitis pigmentosa caused by mutant versions of the transcription factor CRX. *Hum Mutat*. 2001;18(6):488–498.
244. Bowne SJ, Sullivan LS, Mortimer SE, et al. Spectrum and frequency of mutations in IMPDH1 associated with autosomal dominant retinitis pigmentosa and leber congenital amaurosis. *Invest Ophthalmol Vis Sci*. 2006;47(1):34–42.
245. Leber T. *Die Krankheiten der Netzhaut*. W. Engelmen: Leipzig, Germany; 1916.
246. Foxman SG, Heckenlively JR, Bateman JB, Wirtschafter JD. Classification of congenital and early onset retinitis pigmentosa. *Arch Ophthalmol*. 1985;103(10):1502–1506.
247. Hagstrom SA, North MA, Nishina PM, Berson EL, Dryja TP. Recessive mutations in the gene encoding the tubby-like protein TULP1 in patients with retinitis pigmentosa. *Nat Genet*. 1998;18:174–176.
248. Lorenz B, Gyürüs P, Preising M, et al. Early-onset severe rod-cone dystrophy in young children with *RPE65* mutations. *Invest Ophthalmol Vis Sci*. 2000;41(9):2735–2742.

249. Weleber RG, Michaelides M, Trzupek KM, Stover NB, Stone EM. The phenotype of Severe Early Childhood Onset Retinal Dystrophy (SECORD) from mutation of RPE65 and differentiation from Leber congenital amaurosis. *Invest Ophthalmol Vis Sci*. 2011;52(1):292–302.
250. Leighton DA, Harris R. Retinal aplasia in association with macular coloboma, keratoconus and cataract. *Clin Genet*. 1973;4(3):270–274.
251. Margolis S, Scher BM, Carr RE. Macular colobomas in Leber's congenital amaurosis. *Am J Ophthalmol*. 1977;83(1):27–31.
252. Francois J. Choroideremia (progressive chorioretinal degeneration). *Int Ophthalmol Clin*. 1968;8(4):949–964.
253. Edwards WC, Macdonald R Jr, Price WD. Congenital amaurosis of retinal origin (Leber). *Am J Ophthalmol*. 1971;72(4):724–728.
254. Schroeder R, Mets MB, Maumenee IH. Leber's congenital amaurosis. Retrospective review of 43 cases and a new fundus finding in two cases. *Arch Ophthalmol*. 1987;105(3):356–359.
255. Flanders M, Lapointe ML, Brownstein S, Little JM. Keratoconus and Leber's congenital amaurosis: a clinicopathological correlation. *Can J Ophthalmol*. 1984;19(7):310–314.
256. Elder MJ. Leber congenital amaurosis and its association with keratoconus and keratoglobus. *J Pediatr Ophthalmol Strabismus*. 1994;31(1):38–40.
257. Lambert SR, Kriss A, Taylor D, Coffey R, Pembrey M. Follow-up and diagnostic reappraisal of 75 patients with Leber's congenital amaurosis. *Am J Ophthalmol*. 1989;107(6):624–631.
258. Senior B, Friedmann A, Braudo JL. Juvenile familial nephropathy with tapetoretinal degeneration. *Am J Ophthalmol*. 1961;52:625–633.
259. Russell-Eggitt IM, Clayton PT, Coffey R, Kriss A, Taylor DS, Taylor JF. Alström syndrome. Report of 22 cases and literature review. *Ophthalmology*. 1998;105(7):1274–1280.
260. Ehara H, Nakano C, Ohno K, Goto Y-I, Takeshita A. New

autosomal-recessive syndrome of Leber congenital amaurosis, short stature, growth hormone deficiency, mental retardation, hepatic dysfunction and metabolic acidosis. *Am J Med Genet*. 1997;71(3):258–266.
261. Schroeder R, Bets MB, Maumenee IH. Leber's congenital amaurosis: retrospective review of 43 cases and a new fundus finding in two cases. *Arch Ophthalmol*. 1987;105(3):356–359.
262. Alström CH, Olson OA. Heredoretinopathia congenitalis monohybrida recessiva autosomalis. *Hereditas*. 1957;43:1–177.
263. Nickel B, Hoyt CS. Leber's congenital amaurosis: Is mental retardation a frequent associated defect? *Arch Ophthalmol*. 1982;100:1089–1092.
264. Weinstein JM, Gleaton M, Weidner WA, Young RSK. Leber's congenital amaurosis: relationship of structural CNS anomalies to psychomotor retardation. *Arch Neurol*. 1984;41:204–206.
265. Schuil J, Meire FM, Delleman JW. Mental retardation in amaurosis congenita of Leber. *Neuropediatrics*. 1998;29(6):294–297.
266. Casteels I, Spileers W, Demaerel P, et al. Leber congenital amaurosis–differential diagnosis, ophthalmological and neuroradiological report of 18 patients. *Neuropediatrics*. 1996;27(4):189–193.
267. Walia S, Fishman GA, Jacobson SG, et al. Visual acuity in patients with Leber's congenital amaurosis and early childhood-onset retinitis pigmentosa. *Ophthalmology*. 2010;117(6):1190–1198.
268. den Hollander AI, Koenekoop RK, Yzer S, et al. Mutations in the CEP290 (NPHP6) gene are a frequent cause of Leber congenital amaurosis. *Am J Hum Genet*. 2006;79(3):556–561.
269. Weleber RG. Infantile and childhood retinal blindness: a molecular perspective (The Franceschetti Lecture). *Ophthalmic Genet*. 2002;23(2):71–97.
270. Weleber RG, Tongue AC, Kennaway NG, Budden SS, Buist NR. Ophthalmic manifestations of infantile phytanic acid storage disease. *Arch Ophthalmol*. 1984;102(9):1317–1321.

271. Pennesi ME, Weleber RG. Peroxisomal disorders. Traboulsi EI. *Genetic diseases of the eye*. Oxford University Press: Oxford; 2011:663–696.
272. Weleber RG, Tongue AT. Congenital stationary night blindness presenting as Leber's congenital amaurosis. *Arch Ophthalmol*. 1987;105:360–365.
273. Weleber RG. The dystrophic retina in multisystem disorders: the electroretinogram in neuronal ceroid lipofuscinoses. *Eye (Lond)*. 1998;12(Pt 3b):580–590.
274. Weleber RG, Gupta N, Trzupek KM, Wepner MS, Kurz DE, Milam AH. Electroretinographic and clinicopathologic correlations of retinal dysfunction in infantile neuronal ceroid lipofuscinosis (infantile Batten disease). *Mol Genet Metab*. 2004;83(1–2):128–137.
275. Loken AC, Hanssen O, Halvolsen S, Jolster NB. Hereditary renal dysplasia and blindness. *Acta Paediatr*. 1961;50:177–194.
276. Otto EA, Loeys B, Khanna H, et al. Nephrocystin-5, a ciliary IQ domain protein, is mutated in Senior–Loken syndrome and interacts with RPGR and calmodulin. *Nat Genet*. 2005;37(3):282–288.
277. Stone EM, Cideciyan AV, Aleman TS, et al. Variations in NPHP5 in patients with nonsyndromic leber congenital amaurosis and Senior–Loken syndrome. *Arch Ophthalmol*. 2011;129(1):81–87.
278. Pinckers AJL. Leber's congenital amaurosis as conceived by Leber. *Ophthalmologica*. 1979;179(1):48–51.
279. Bardet G. *Sur un syndrome d'obésité infantile avec polydactylie et rétinite pigmentaire (contributions à l'étude des formes cliniques de l'obésité hypophysaiare)*. [University of Paris] 1920.
280. Laurence JZ, Moon RC. Four cases of retinitis pigmentosa occurring in the same family and accompanied by general imperfection of development. *Obes Res*. 1995;3:400–403.
281. Hutchinson J. Slowly progressive paraplegia and disease of the choroids with defective intellect and arrested sexual development in several brothers and a sister. *Arch Surg (Lond)*. 1900;11:118–122.
282. Ammann F. Investigations cliniques et genetiques sur le

syndrome de Bardet–Biedl en Suisse. *J Genet Hum*. 1970;18(Suppl.):1–310.
283. Churchill DN, McManamon P, Hurley RM. Renal disease: a sixth cardinal feature of the Laurence–Moon–Biedl syndrome. *Clin Nephrol*. 1981;16:151–154.
284. Rizzo JF III, Berson EL, Lessell S. Retinal and neurological findings in the Laurence–Moon–Bardet–Biedl phenotype. *Ophthalmology*. 1986;93:1452–1456.
285. Beales PL, Elcioglu N, Woolf AS, Parker D, Flinter FA. New criteria for improved diagnosis of Bardet–Biedl syndrome: results of a population survey. *J Med Genet*. 1999;36(6):437–446.
286. Farag TI, Teebi AS. Bardet–Biedl and Laurence–Moon syndromes in a mixed Arab population. *Clin Genet*. 1988;33(2):78–82.
287. Farag TI, Teebi AS. High incidence of Bardet Biedl syndrome among the Bedouin. [Letter] *Clin Genet*. 1989;36(6):463–465.
288. Green JS, Parfrey PS, Harnett JD, et al. The cardinal manifestations of Bardet–Biedl syndrome, a form of Laurence–Moon–Biedl syndrome. *N Engl J Med*. 1989;321(15):1002–1009.
289. Klein D, Ammann F. The syndrome of Laurence–Moon–Bardet–Biedl and allied diseases in Switzerland: clinical, genetic and epidemiological studies. *J Neurol Sci*. 1969;9(3):479–513.
290. Schachat AP, Maumenee IH. The Bardet–Biedl syndrome and related disorders. *Arch Ophthalmol*. 1982;100(2):285–288.
291. Heckenlively JR. RP syndromes. Heckenlively JR. *Retinitis pigmentosa*. JB Lippincott Co: Philadelphia; 1988:221–252.
292. Prosperi L, Cordella M, Bernasconi S. Electroretinography and diagnosis of the Laurence–Moon–Bardet–Biedl syndrome in childhood. *J Pediatr Ophthalmol*. 1977;14:305–308.
293. Warkany J, Frauenberger GS, Mitchell AG. Heredofamilial deviations: I. The Laurence–Moon–Biedl syndrome. *Am J Dis Child*. 1937;53:455–470.
294. Bell J. The Laurence–Moon syndrome. Cambridge

University Press: Cambridge; 1958:51–96. Penrose LS. *The treasury of human inheritance*. vol. 5.
295. Stoler JM, Herrin JT, Holmes LB. Genital abnormalities in females with Bardet–Biedl syndrome. *Am J Med Genet*. 1995;55(3):276–278.
296. Mehrotra N, Taub S, Covert RF. Hydrometrocolpos as a neonatal manifestation of the Bardet–Biedl syndrome. [Letter] *Am J Med Genet*. 1997;69(2):220.
297. David A, Bitoun P, Lacombe D, et al. Hydrometrocolpos and polydactyly: a common neonatal presentation of Bardet–Biedl and McKusick–Kaufman syndromes. *J Med Genet*. 1999;36(8):599–603.
298. Katsanis N, Beales PL, Woods MO, et al. Mutations in MKKS cause obesity, retinal dystrophy and renal malformations associated with Bardet–Biedl syndrome. *Nat Genet*. 2000;26(1):67–70.
299. Schaap C, ten Tusscher MP, Schrander JJ, Kuijten RH, Schrander-Stumpel CT. Phenotypic overlap between McKusick–Kaufman and Bardet–Biedl syndromes: are they related? *Eur J Pediatr*. 1998;157(2):170–171.
300. Bauman ML, Hogan GR. Laurence–Moon–Biedl syndrome. *Am J Dis Child*. 1973;126:119–126.
301. Hurley RM, Dery P, Nogrady MB, Drummond KN. The renal lesion of the Laurence–Moon–Biedl syndrome. *J Pediatr*. 1975;87:206–209.
302. Pagon RA, Haas JE, Bunt AH, Rodaway KA. Hepatic involvement in the Bardet–Biedl syndrome. *Am J Med Genet*. 1982;13:373–381.
303. Elbedour K, Zucker N, Zalzstein E, Barki Y, Carmi R. Cardiac abnormalities in the Bardet–Biedl syndrome: echocardiographic studies of 22 patients. *Am J Med Genet*. 1994;52(2):164–169.
304. Islek I, Kucukoduk S, Erkan D, et al. Bardet–Biedl syndrome: delayed diagnosis in a child with Hirschsprung disease. [Letter] *Clin Dysmorphol*. 1996;5(3):271–273.
305. Croft JB, Swift M. Obesity, hypertension, and renal disease in relatives of Bardet–Biedl syndrome sibs. *Am J Med Genet*. 1990;36(1):37–42.

306. Carmi R, Elbedour K, Stone EM, Sheffield VC. Phenotypic differences among patients with Bardet–Biedl syndrome linked to three different chromosome loci. *Am J Med Genet*. 1995;59(2):199–203.
307. Scotto JM, Hadchouel M, Odievre M, et al. Infantile phytanic acid storage disease, a possible variant of Refsum's disease: three cases, including ultrastructural studies of the liver. *J Inherit Metab Dis*. 1982;5(2):83–90.
308. Refsum S. Heredopathia atactica polyneuritiformis: a familial syndrome not hitherto described. *Acta Psychiatr Scand Suppl*. 1946;38:1–303.
309. Refsum S. Heredopathia atactica polyneuritiformis: phytanic acid storage disease (Refsum's disease) with particular reference to ophthalmological disturbances. *Metabol Ophthalmol*. 1977;1:73–79.
310. Jansen GA, Ofman R, Ferdinandusse S, et al. Refsum disease is caused by mutations in the phytanolyl-CoA hydroxylase gene. *Nat Genet*. 1997;17(2):190–193.
311. Jansen GA, Waterham HR, Wanders RJ. Molecular basis of Refsum disease: sequence variations in phytanoyl-CoA hydroxylase (PHYH) and the PTS2 receptor (PEX7). *Hum Mutat*. 2004;23(3):209–218.
312. Hansen E, Bachen NI, Flage T. Refsum's disease. Eye manifestations in a patient treated with low phytol low phytanic acid diet. *Acta Ophthalmol*. 1979;57(5):899–913.
313. Djupesland G, Flottorp G, Refsum S. Phytanic acid storage disease: hearing maintained after 15 years of dietary treatment. *Neurology*. 1983;33(2):237–240.
314. Mole SE, Williams RE. *Neuronal ceroid–lipofuscinosis*. [GeneReviews] http://www.genetests.org; 2010 [2001 Oct 10 [updated 2010 Mar 2.].
315. Rider JA, Rider DL. Batten disease: past, present and future. *Am J Med Genet Suppl*. 1988;5:21–26.
316. Goebel HH. The neuronal ceroid–lipofuscinoses. *Semin Pediatr Neurol*. 1996;3(4):270–278.
317. Santavuori P, Vanhanen S-L, Sainio K, et al. Infantile neuronal ceroid-lipofuscinosis (INCL): diagnostic criteria. *J Inherit Metab Dis*. 1993;16(2):227–229.

318. Bielschowsky M. Über spät-infantile familiäre amaurotische Idiotie mit Kleinhirnsymptomen. *Dtsch Zschr Nervenheilk*. 1913;50:7–29.
319. Janský J. Dosud nepopsaný prípad familiárni amaurotické idiotie komplikovanés hypoplasii mozeckovou. *Sb Ved Pr Lek Fak Karlovy*. 1908;9:165–196.
320. Goebel HH, Gerhard L, Kominami E, Haltia M. Neuronal ceroid-lipofuscinosis – late-infantile or Jansky–Bielschowsky type – revisited. *Brain Pathol*. 1996;6:225–228.
321. Zeman W, Donahue S, Dyken P, Green J. The neuronal ceroid-lipofuscinosis (Batten–Vogt syndrome). North Holland Publishing Co: Amsterdam; 1970:588–679. Vinken PJ, Bruyn GW. *Handbook of clinical neurology*. vol. 10.
322. Zeman W. Batten disease: ocular features, differential diagnosis and diagnosis by enzyme analysis. *Birth Defects Orig Artic Ser*. 1976;12(3):441–453.
323. Kufs H. Über einen Fall von spätester Form der amaurotischen Idiotie mit dem Beginn im 42 und Tod im 59 Lebens-jahre in klinischer, histologischer und Vererbungs-pathologischer Beziehung. *Z ges Neurol*. 1931;137:432–448.
324. Boehme DH, Cottrell JC, Leonberg SC, Zeman W. A dominant form of neuronal ceroid–lipofuscinosis. *Brain*. 1971;94:745–756.
325. Dyken P, Wisniewski K. Classification of the neuronal ceroid–lipofuscinoses: expansion of the atypical forms. *Am J Med Genet*. 1995;57:150–154.
326. Tyynelä J, Suopanki J, Santavuori P, Baumann M, Haltia M. Variant late infantile neuronal ceroid-lipofuscinosis: pathology and biochemistry. *J Neuropathol Exp Neurol*. 1997;56:369–375.
327. Batten FE. Cerebral degeneration with symmetrical changes in the maculae in two members of a family. *Trans Ophthalmol Soc U K*. 1903;23:386–390.
328. Batten FE. Family cerebral degeneration with macular change (so-called juvenile form of family amaurotic idiocy). *Q J Med*. 1914;7:444–454.
329. Jongen PJH, Gabreëls FJM, Schuurmans Stekhoven JH, Renier WO, le Coultre R, Begeer JH. Early infantile form of

neuronal ceroid lipofuscinosis. *Clin Neurol Neurosurg*. 1987;89:161–167.
330. Claussen M, Heim P, Knispel J, Goebel HH, Kohlschütter A. Incidence of neuronal ceroid–lipofuscinoses in West Germany: variation of a method for studying autosomal recessive disorders. *Am J Med Genet*. 1992;42:536–538.
331. Katz ML, Gao C-L, Prabhakaram M, Shibuya H, Liu P-C, Johnson GS. Immunochemical localization of the Batten disease (CLN3) protein in retina. *Invest Ophthalmol Vis Sci*. 1997;38(11):2375–2386.
332. Libert J. Diagnosis of lysosomal storage diseases by the ultrastructural study of conjunctival biopsies. *Pathol Annu*. 1980;15(Pt 1):37–66.
333. Arsenio-Nunes ML, Goutieres F, Aicardi J. An ultramicroscopic study of skin and conjunctival biopsies in chronic neurological disorders of childhood. *Ann Neurol*. 1981;9(2):163–173.
334. Lake BD. The differential diagnosis of the various forms of Batten disease by rectal biopsy. *Birth Defects Orig Artic Ser*. 1976;12(3):441–453.
335. Rapola J, Santavuori P, Savilahti E. Suction biopsy of rectal mucosa in the diagnosis of infantile and juvenile types of neuronal ceroid–lipofuscinosis. *Hum Pathol*. 1984;15:352–360.
336. Markesbery WR, Shield LK, Egel RT, Jameson HD. Late-infantile neuronal ceroid–lipofuscinosis: an ultrastructural study of lymphocyte inclusions. *Arch Neurol*. 1976;33:630–635.
337. Schwendemann G. Lymphocyte inclusions in the juvenile type of generalized ceroid–lipofuscinosis. An electron microscopic study. *Acta Neuropathol*. 1976;36(4):327–338.
338. Dolman CL, MacLeod PM, Chang E. Skin punch biopsies and lymphocytes in the diagnosis of lipidoses. *Can J Neurol Sci*. 1975;2(1):67–73.
339. Brod RD, Packer AJ, Van Dyk HJ. Diagnosis of neuronal ceroid lipofuscinosis by ultrastructural examination of peripheral blood lymphocytes. *Arch Ophthalmol*. 1987;105(10):1388–1393.

340. Dom R, Brucher JM, Ceuterick C, Carton H, Martin JJ. Adult ceroid–lipofuscinosis (Kufs' disease) in two brothers. Retinal and visceral storage in one; diagnostic muscle biopsy in the other. *Acta Neuropathol*. 1979;45(1):67–72.
341. Becker K, Goebel HH, Svennerholm L, Wendel U, Bremer HJ. Clinical, morphological, and biochemical investigations on a patient with an unusual form of neuronal ceroid–lipofuscinosis. *Eur J Pediatr*. 1979;132(3):197–206.
342. Cooper LZ, Krugman S. Clinical manifestations of postnatal and congenital rubella. *Arch Ophthalmol*. 1967;77(4):434–439.
343. Hanshaw JB, Dudgeon JA, Marshall WC. *Viral diseases of the fetus and newborn*. 2nd ed. WB Saunders: Philadelphia; 1985.
344. Menne K. Congenital rubella retinopathy–a progressive disease. *Klin Monatsbl Augenheilkd*. 1986;189(4):326–329.
345. Slusher MM, Tyler ME. Rubella retinopathy and subretinal neovascularization. *Ann Ophthalmol*. 1982;14(3):292–294.
346. Heckenlively JR. Secondary retinitis pigmentosa (syphilis). *Doc Ophthalmol Proc Ser*. 1977;13:245–255.
347. Sawyer RA, Selhorst JB, Zimmerman LE, Hoyt WF. Blindness caused by photoreceptor degeneration as a remote effect of cancer. *Am J Ophthalmol*. 1976;81(5):606–613.
348. Thirkill CE, Roth AM, Keltner JL. Cancer-associated retinopathy. *Arch Ophthalmol*. 1987;105(3):372–375.
349. Keltner JL, Roth AM, Chang RS. Photoreceptor degeneration: possible autoimmune disorder. *Arch Ophthalmol*. 1983;101(4):564–569.
350. Polans AS, Buczylko J, Crabb J, Palczewski K. A photoreceptor calcium binding protein is recognized by autoantibodies obtained from patients with cancer-associated retinopathy. *J Cell Biol*. 1991;112(5):981–989.
351. Polans AS, Witkowska D, Haley TL, Amundson D, Baizer L, Adamus G. Recoverin, a photoreceptor-specific calcium-binding protein, is expressed by the tumor of a patient with cancer-associated retinopathy. *Proc Natl Acad Sci USA*. 1995;92(20):9176–9180.
352. Adamus G, Aptsiauri N, Guy J, Heckenlively J, Flannery J, Hargrave PA. The occurrence of serum autoantibodies against enolase in cancer-associated retinopathy. *Clin*

Immunol Immunopathol. 1996;78(2):120–129.
353. Borgstrom MK, Riise R, Tornqvist K, Granath L. Anomalies in the permanent dentition and other oral findings in 29 individuals with Laurence–Moon–Bardet–Biedl syndrome. *J Oral Pathol Med*. 1996;25(2):86–89.
354. Berson EL, Lessell S. Paraneoplastic night blindness with malignant melanoma. *Am J Ophthalmol*. 1988;106(3):307–311.
355. Boeck K, Hofmann S, Klopfer M, et al. Melanoma-associated paraneoplastic retinopathy: case report and review of the literature. *Br J Dermatol*. 1997;137(3):457–460.
356. Alexander KR, Fishman GA, Peachey NS, Marchese AL, Tso MO. "On" response defect in paraneoplastic night blindness with cutaneous malignant melanoma. *Invest Ophthalmol Vis Sci*. 1992;33(3):477–483.
357. Wolf JE, Arden GB. Selective magnocellular damage in melanoma-associated retinopathy: comparison with congenital stationary nightblindness. *Vision Res*. 1996;36(15):2369–2379.
358. Mizener JB, Kimura AE, Adamus G, Thirkill CE, Goeken JA, Kardon RH. Autoimmune retinopathy in the absence of cancer. *Am J Ophthalmol*. 1997;123(5):607–618.
359. Potts AM. The reaction of uveal pigment in vitro with polycyclic compounds. *Invest Ophthalmol*. 1964;3:405–416.
360. Potts AM. Further studies concerning the accumulation of polycyclic compounds on uveal melanin. *Invest Ophthalmol*. 1964;3:399–404.
361. Meredith TA, Aaberg TM, Willerson WD. Progressive chorioretinopathy after receiving thioridazine. *Arch Ophthalmol*. 1978;96(7):1172–1176.
362. Hamilton JD. Thioridazine retinopathy within the upper dosage limit. *Psychosomatics*. 1985;26(10):823–824.
363. Miller FS 3rd, Bunt-Milam AH, Kalina RE. Clinical-ultrastructural study of thioridazine retinopathy. *Ophthalmology*. 1982;89(12):1478–1488.
364. Mathalone MB. Eye and skin changes in psychiatric patients treated with chlorpromazine. *Br J Ophthalmol*. 1967;51(2):86–93.
365. Marks JS. Chloroquine retinopathy: is there a safe daily

dose? *Ann Rheum Dis*. 1982;41(1):52–58.
366. Krill AE, Potts AM, Johanson CE. Chloroquine retinopathy. Investigation of discrepancy between dark adaptation and electroretinographic findings in advanced stages. *Am J Ophthalmol*. 1971;71(2):530–543.
367. Michaelides M, Stover NB, Francis PJ, Weleber RG. Retinal toxicity associated with hydroxychloroquine and chloroquine: risk factors, screening, and progression despite cessation of therapy. *Arch Ophthalmol*. 2011;129(1):30–39.
368. Marmor MF, Carr RE, Easterbrook M, Farjo AA, Mieler WF. Recommendations on screening for chloroquine and hydroxychloroquine retinopathy: a report by the American Academy of Ophthalmology. *Ophthalmology*. 2002;109(7):1377–1382.
369. Maturi RK, Yu M, Weleber RG. Multifocal electroretinographic evaluation of long-term hydroxychloroquine users. *Arch Ophthalmol*. 2004;122(7):973–981.
370. Francois J, De Rouck A, Cambie E. Retinal and optic evaluation in quinine poisoning. *Ann Ophthalmol*. 1972;4(3):177–185.
371. Handelman IL, Robertson JE, Weleber RG, et al. Retinal toxicity of therapeutic agents. *J Toxicol Cutaneous Ocul Toxicol*. 1983;2–3:131–152.
372. Brinton GS, Norton EW, Zahn JR, Knighton RW. Ocular quinine toxicity. *Am J Ophthalmol*. 1980;90(3):403–410.
373. Hommer K. [On quinine poisoning of the retina. With a remark on experimental chloroquine poisoning]. *Klin Monatsbl Augenheilkd*. 1968;152(6):785–804.
374. Brown TH. Retino-choroiditis radiata. *Br J Ophthalmol*. 1937;21:645–648.
375. Noble KG, Carr RE. Pigmented paravenous chorioretinal atrophy. *Am J Ophthalmol*. 1983;96:338–344.
376. Krill AE. *Krill's Hereditary retinal and choroidal diseases. Clinical characteristics*. Harper and Row: New York; 1977.
377. Breageat P, Amalric P. Postmeningoencephalitis bilateral paravenous chorioretinal degeneration. Henkind P, Shimizu K, Blodi FC, et al. *Acta XXIV International Congress*

of Ophthalmology. JB Lippincott: Philadelphia; 1983.
378. Takei Y, Harada M, Mizuno K. Pigmented paravenous retinochoroidal atrophy. *Jpn J Ophthalmol*. 1977;21:311–317.
379. Chi HH. Retinochoroiditis radiata. *Am J Ophthalmol*. 1948;31(11):1485–1487.
380. Foxman SG, Heckenlively JR, Sinclair SH. Rubeola retinopathy and pigmented paravenous retinochoroidal atrophy. *Am J Ophthalmol*. 1985;99:605–606.
381. Peduzzi M, Guerrieri F, Torlai F, Prampolini ML. Bilateral pigmented paravenous retino-choroidal degeneration following measles. *Int Ophthalmol*. 1984;7(1):11–14.
382. Noble KG. Hereditary pigmented paravenous chorioretinal atrophy. *Am J Ophthalmol*. 1989;108(4):365–369.
383. Skalka HW. Hereditary pigmented paravenous retinochoroidal atrophy. *Am J Ophthalmol*. 1979;87:286–291.
384. Traboulsi EI, Maumenee IH. Hereditary pigmented paravenous chorioretinal atrophy. *Arch Ophthalmol*. 1986;104:1636–1640.
385. Pearlman JT, Heckenlively JR, Bastek JV. Progressive nature of pigmented paravenous retinochoroidal atrophy. *Am J Ophthalmol*. 1978;85(2):215–217.
386. Karmous-Benailly H, Martinovic J, Gubler MC, et al. Antenatal presentation of Bardet–Biedl syndrome may mimic Meckel syndrome. *Am J Hum Genet*. 2005;76(3):493–504.
387. Hirose T, Miyake Y. Pigmentary paravenous chorioretinal degeneration: fundus appearance and retinal functions. *Ann Ophthalmol*. 1979;11(5):709–718.
388. Lessel MR, Thaler A, Heilig P. ERG and EOG in progressive paravenous retinochoroidal atrophy. *Adv Ophthalmol*. 1986;62(1):25–29.
389. Miller SA, Stevens TS, Myers F, Nieder M. Pigmented paravenous retinochoroidal atrophy. *Ann Ophthalmol*. 1978;10(7):867–871.
390. Bastek JV, Foos RY, Heckenlively J. Traumatic pigmentary retinopathy. *Am J Ophthalmol*. 1981;92(5):621–624.
391. Gass JD, Braunstein RA. Further observations concerning the diffuse unilateral subacute neuroretinitis syndrome.

Arch Ophthalmol. 1983;101(11):1689–1697.
392. Goldberg MA, Kazacos KR, Boyce WM, Ai E, Katz B. Diffuse unilateral subacute neuroretinitis: morphometric, serologic, and epidemiologic support for Baylisascaris as a causative agent. *Ophthalmology*. 1993;100:1695–1701.
393. Kazacos KR, Raymond LA, Kazacos EA, Vestre WA. The raccoon ascarid: a probable cause of human ocular larva migrans. *Ophthalmology*. 1985;92(12):1735–1744.
394. de Souza EC, Nakashima Y. Diffuse unilateral subacute neuroretinitis. Report of transvitreal surgical removal of a subretinal nematode. *Ophthalmology*. 1995;102(8):1183–1186.
395. Naumann GO, Knorr HL. DUSN occurs in Europe. *Ophthalmology*. 1994;101(6):971–972.
396. de Souza EC, Abujamra S, Nakashima Y, Gass JD. Diffuse bilateral subacute neuroretinitis: first patient with documented nematodes in both eyes. *Arch Ophthalmol*. 1999;117(10):1349–1351.
397. Gass JD, Callanan DG, Bowman CB. Oral therapy in diffuse unilateral subacute neuroretinitis. *Arch Ophthalmol*. 1992;110(5):675–680.
398. Buettner H. Congenital hypertrophy of the retinal pigment epithelium. *Am J Ophthalmol*. 1975;79(2):177–189.
399. Traboulsi EI, Maumenee IH, Krush AJ, et al. Congenital hypertrophy of the retinal pigment epithelium predicts colorectal polyposis in Gardner's syndrome. *Arch Ophthalmol*. 1990;108(4):525–526.
400. Daiger SP, Sullivan LS, Bowne SJ. Genes and mutations causing retinitis pigmentosa. *Clin Genet*. 2013;84(2):132–141.
401. Dratz EA, Hargrave PA. The structure of rhodopsin and the rod outer segment disc membrane. *Trends Biochem Sci*. 1983;8:128–131.
402. Bitensky MW, Wheeler GL, Yamasaki A, et al. Cyclic-nucleotide metabolism in vertebrate photoreceptors: a remarkable analogy and an unraveling enigma. *Curr Topics Membrane Transport*. 1981;15:237–271.
403. McWilliam P, Farrar GJ, Kenna P, et al. Autosomal dominant retinitis pigmentosa (ADRP): localization of an ADRP gene to the long arm of chromosome 3. *Genomics*.

1989;5:619–622.
404. Dryja TP, McGee TL, Reichel E, et al. A point mutation of the rhodopsin gene in one form of retinitis pigmentosa. *Nature*. 1990;343(6256):364–366.
405. Farrar GJ, Findlay JBC, Kumar-Singh R, et al. Autosomal dominant retinitis pigmentosa: a novel mutation in the rhodopsin gene in the original 3q linked family. *Hum Mol Genet*. 1992;1:769–771.
406. Friedman JS, Ray JW, Waseem N, et al. Mutations in a BTB-Kelch protein, KLHL7, cause autosomal-dominant retinitis pigmentosa. *Am J Hum Genet*. 2009;84(6):792–800.
407. Sung C-H, Davenport CM, Hennessey JC, et al. Rhodopsin mutations in autosomal dominant retinitis pigmentosa. *Proc Natl Acad Sci USA*. 1991;88:6481–6485.
408. Marmor MF. Fundus albipunctatus: a clinical study of the fundus lesions, the physiologic deficit, and the vitamin A metabolism. *Adv Ophthalmol*. 1977;43(2):277–302.
409. Kawano H, Hotta Y, Fujiki K, et al. A study on the rhodopsin gene in Japanese retinitis pigmentosa–screening of mutation by restriction endonucreases and frequencies of DNA polymorphisms. *Nippon Ganka Gakkai Zasshi*. 1995;99(10):1151–1157.
410. Chan WM, Yeung KY, Pang CP, et al. Rhodopsin mutations in Chinese patients with retinitis pigmentosa. *Br J Ophthalmol*. 2001;85(9):1046–1048.
411. Gandra M, Anandula V, Authiappan V, et al. Retinitis pigmentosa: mutation analysis of RHO, PRPF31, RP1, and IMPDH1 genes in patients from India. *Mol Vis*. 2008;14:1105–1113.
412. Kim KJ, Kim C, Bok J, et al. Spectrum of rhodopsin mutations in Korean patients with retinitis pigmentosa. *Mol Vis*. 2011;17:844–853.
413. van Soest S, Westerveld A, de Jong PTVM, Bleeker-Wagemakers EM, Bergen AAB. Retinitis pigmentosa: defined from a molecular point of view. *Surv Ophthalmol*. 1999;43(4):321–334.
414. Dryja TP, McGee TL, Hahn LB, et al. Mutations within the rhodopsin gene in patients with autosomal dominant

retinitis pigmentosa. *N Engl J Med*. 1990;323(19):1302–1307.
415. Fishman GA, Stone EM, Gilbert LD, Sheffield VC. Ocular findings associated with a rhodopsin gene codon 106 mutation: glycine-to-arginine change in autosomal dominant retinitis pigmentosa. *Arch Ophthalmol*. 1992;110(5):646–653.
416. Fishman GA, Stone EM, Sheffield VC, Gilbert LD, Kimura AE. Ocular findings associated with rhodopsin gene codon 17 and codon 182 transition mutations in dominant retinitis pigmentosa. *Arch Ophthalmol*. 1992;110(1):54–62.
417. Kranich H, Bartowski S, Denton MJ, et al. Autosomal dominant "sector" retinitis pigmentosa due to a point mutation predicting an Asn-15-Ser substitution of rhodopsin. *Hum Mol Genet*. 1993;2(6):813–814.
418. Berson EL, Rosner B, Sandberg MA, Weigel-DiFranco C, Dryja TP. Ocular findings in patients with autosomal dominant retinitis pigmentosa and rhodopsin, proline-347-leucine. *Am J Ophthalmol*. 1991;111(5):614–623.
419. Restagno G, Maghtheh M, Bhattacharya S, et al. A large deletion at the 3′ end of the rhodopsin gene in an Italian family with a diffuse form of autosomal dominant retinitis pigmentosa. *Hum Mol Genet*. 1993;2(2):207–208.
420. Berson EL, Rosner B, Sandberg MA, Dryja TP. Ocular findings in patients with autosomal dominant retinitis pigmentosa and a rhodopsin gene defect (Pro-23-His). *Arch Ophthalmol*. 1991;109(1):92–101.
421. Oh KT, Longmuir R, Oh DM, et al. Comparison of the clinical expression of retinitis pigmentosa associated with rhodopsin mutations at codon 347 and codon 23. *Am J Ophthalmol*. 2003;136(2):306–313.
422. Sieving PA, Richards JE, Naarendorf F, Bingham EL, Scott K, Alpern M. Dark-light: model for nightblindness from the human rhodopsin Gly-90 Æ Asp mutation. *Proc Natl Acad Sci USA*. 1995;92(3):880–884.
423. Sandberg MA, Weigel-DiFranco C, Dryja TP, Berson EL. Clinical expression correlates with location of rhodopsin mutation in dominant retinitis pigmentosa. *Invest Ophthalmol Vis Sci*. 1995;36(9):1934–1942.

424. Berson EL, Rosner B, Weigel-DiFranco C, Dryja TP, Sandberg MA. Disease progression in patients with dominant retinitis pigmentosa and rhodopsin mutations. *Invest Ophthalmol Vis Sci*. 2002;43(9):3027–3036.
425. Robinson PR, Cohen GB, Zhukovsky EA, Oprian DD. Constitutively active mutants of rhodopsin. *Neuron*. 1992;9(4):719–725.
426. Li T, Franson WK, Gordon JW, Berson EL, Dryja TP. Constitutive activation of phototransduction by K296E opsin is not a cause of photoreceptor degeneration. *Proc Natl Acad Sci USA*. 1995;92(8):3551–3555.
427. Farrar GJ, Kenna P, Jordan SA, et al. A three-base-pair deletion in the peripherin-*RDS* gene in one form of retinitis pigmentosa. *Nature*. 1991;354:478–480.
428. Kajiwara K, Hahn LB, Mukai S, Travis GH, Berson EL, Dryja TP. Mutations in the human retinal degeneration slow gene in autosomal dominant retinitis pigmentosa. *Nature*. 1991;354:480–483.
429. Weleber RG. Phenotypic variation in patients with mutations in the peripherin/RDS gene. *Digit J Ophthalmol*. 1999;5:1–8.
430. Dryja TP, Hahn LB, Kajiwara K, Berson EL. Dominant and digenic mutations in the peripherin/RDS and ROM1 genes in retinitis pigmentosa. *Invest Ophthalmol Vis Sci*. 1997;38:1972–1982.
431. Ma J, Norton JC, Allen AC, et al. Retinal degeneration slow (rds) in mouse results from simple insertion of a t haplotype-specific element into protein-coding exon II. *Genomics*. 1995;28(2):212–219.
432. Arikawa K, Molday LL, Molday RS, Williams DS. Localization of peripherin/rds in the disk membranes of cone and rod photoreceptors: relationship to disk membrane morphogenesis and retinal degeneration. *J Cell Biol*. 1992;116(3):659–667.
433. Bessant DA, Payne AM, Mitton KP, et al. A mutation in NRL is associated with autosomal dominant retinitis pigmentosa. *Nat Genet*. 1999;21(4):355–356.
434. DeAngelis MM, Grimsby JL, Sandberg MA, Berson EL,

Dryja TP. Novel mutations in the NRL gene and associated clinical findings in patients with dominant retinitis pigmentosa. *Arch Ophthalmol*. 2002;120(3):369–375.
435. Keen TJ, Hims MM, McKie AB, et al. Mutations in a protein target of the Pim-1 kinase associated with the RP9 form of autosomal dominant retinitis pigmentosa. *Eur J Hum Genet*. 2002;10(4):245–249.
436. Wada Y, Abe T, Takeshita T, Sato H, Yanashima K, Tamai M. Mutation of human retinal fascin gene (*FSCN2*) causes autosomal dominant retinitis pigmentosa. *Invest Ophthalmol Vis Sci*. 2001;42(10):2395–2400.
437. Farber DB. From mice to men: the cyclic GMP phosphodiesterase gene in vision and disease. The Proctor Lecture. *Invest Ophthalmol Vis Sci*. 1995;36(2):263–275.
438. Gal A, Orth U, Baehr W, Schwinger E, Rosenberg T. Heterozygous missense mutation in the rod cGMP phosphodiesterase beta-subunit gene in autosomal dominant stationary night blindness. *Nat Genet*. 1994;7(4):551.
439. Yau KW. Phototransduction mechanism in retinal rods and cones: the Friedenwald Lecture. *Invest Ophthalmol Vis Sci*. 1994;35(1):9–32.
440. Dryja TP, Finn JT, Peng Y-W, McGee TL, Berson EL, Yau K-W. Mutations in the gene encoding the a subunit of the rod cGMP-gated channel in autosomal recessive retinitis pigmentosa. *Proc Natl Acad Sci USA*. 1995;92(22):10177–10181.
441. Saari JC, Bredberg DL, Noy N. Control of substrate flow at a branch in the visual cycle. *Biochemistry*. 1994;33(10):3106–3112.
442. Maw MA, Kennedy B, Knight A, et al. Mutation of the gene encoding cellular retinaldehyde-binding protein in autosomal recessive retinitis pigmentosa. *Nat Genet*. 1997;17(2):198–200.
443. Morimura H, Berson EL, Dryja TP. Recessive mutations in the RLBP1 gene encoding cellular retinaldehyde- binding protein in a form of retinitis punctata albescens. *Invest Ophthalmol Vis Sci*. 1999;40(5):1000–1004.

444. Burstedt MS, Forsman-Semb K, Golovleva I, Janunger T, Wachtmeister L, Sandgren O. Ocular phenotype of Bothnia dystrophy, an autosomal recessive retinitis pigmentosa associated with an R234W mutation in the RLBP1 gene. *Arch Ophthalmol*. 2001;119(2):260–267.
445. Eichers ER, Green JS, Stockton DW, et al. Newfoundland rod–cone dystrophy, an early-onset retinal dystrophy, is caused by splice-junction mutations in RLBP1. *Am J Hum Genet*. 2002;70(4):955–964.
446. Hagstrom SA, Duyao M, North MA, Li T. Retinal degeneration in *tulp1-/-* mice: vesicular accumulation in the interphotoreceptor matrix. *Invest Ophthalmol Vis Sci*. 1999;40(12):2795–2802.
447. Banerjee P, Kleyn PW, Knowles JA, et al. TULP1 mutation in two extended Dominican kindreds with autosomal recessive retinitis pigmentosa. *Nat Genet*. 1998;18(2):177–179.
448. D'Cruz PM, Yasumura D, Weir J, et al. Mutation of the receptor tyrosine kinase gene Mertk in the retinal dystrophic RCS rat. *Hum Mol Genet*. 2000;9(4):645–651.
449. Gal A, Li Y, Thompson DA, et al. Mutations in MERTK, the human orthologue of the RCS rat retinal dystrophy gene, cause retinitis pigmentosa. *Nat Genet*. 2000;26(3):270–271.
450. Meindl A, Dry K, Herrmann K, et al. A gene (*RPGR*) with homology to the RCC1 guanine nucleotide exchange factor is mutated in X-linked retinitis pigmentosa (RP3). *Nat Genet*. 1996;13:35–42.
451. Fujita R, Buraczynska M, Gieser L, et al. Analysis of the RPGR gene in 11 pedigrees with the retinitis pigmentosa type 3 genotype: paucity of mutations in the coding region but splice defects in two families. *Am J Hum Genet*. 1997;61(3):571–580.
452. Jacobson SG, Buraczynska M, Milam AH, et al. Disease expression in X-linked retinitis pigmentosa caused by a putative null mutation in the RPGR gene. *Invest Ophthalmol Vis Sci*. 1997;38:1983–1997.
453. Comander J, Weigel-DiFranco C, Sandberg MA, Berson EL. Visual function in carriers of X-linked retinitis pigmentosa.

Ophthalmology. 2015;122(9):1899–1906.
454. Andréasson S, Ponjavic V, Abrahamson M, et al. Phenotypes in three Swedish families with X-linked retinitis pigmentosa caused by different mutations in the RPGR gene. *Am J Ophthalmol*. 1997;124:95–102.
455. Buraczynska M, Wu W, Fujita R, et al. Spectrum of mutations in the RPGR gene that are identified in 20% of families with X-linked retinitis pigmentosa. *Am J Hum Genet*. 1997;61(6):1287–1292.
456. Vervoort R, Lennon A, Bird AC, et al. Mutational hot spot within a new RPGR exon in X-linked retinitis pigmentosa. *Nat Genet*. 2000;25(4):462–466.
457. Demirci FY, Rigatti BW, Wen G, et al. X-linked cone-rod dystrophy (locus COD1): identification of mutations in RPGR exon ORF15. *Am J Hum Genet*. 2002;70(4):1049–1053.
458. Yang Z, Peachey NS, Moshfeghi DM, et al. Mutations in the RPGR gene cause X-linked cone dystrophy. *Hum Mol Genet*. 2002;11(5):605–611.
459. Ayyagari R, Mandal MN, Karoukis AJ, et al. Late-onset macular degeneration and long anterior lens zonules result from a CTRP5 gene mutation. *Invest Ophthalmol Vis Sci*. 2005;46(9):3363–3371.
460. Schwahn U, Lenzner S, Dong J, et al. Positional cloning of the gene for X-linked retinitis pigmentosa 2. *Nat Genet*. 1998;19(4):327–332.
461. Rosenberg T, Schwahn U, Feil S, Berger W. Genotype-phenotype correlation in X-linked retinitis pigmentosa 2 (RP2). *Ophthalmic Genet*. 1999;20(3):161–172.
462. Bader I, Brandau O, Achatz H, et al. X-linked retinitis pigmentosa: RPGR mutations in most families with definite X linkage and clustering of mutations in a short sequence stretch of exon ORF15. *Invest Ophthalmol Vis Sci*. 2003;44(4):1458–1463.
463. Fahim AT, Bowne SJ, Sullivan LS, et al. Allelic heterogeneity and genetic modifier loci contribute to clinical variation in males with X-linked retinitis pigmentosa due to RPGR mutations. *PLoS ONE*. 2011;6:e23021.
464. Sharon D, Sandberg MA, Rabe VW, et al. RP2 and RPGR

mutations and clinical correlations in patients with X-linked retinitis pigmentosa. *Am J Hum Genet*. 2003;73:1131–1146.
465. Travis GH, Sutcliffe JG, Bok D. The retinal degeneration slow (rds) gene product is a photoreceptor disc membrane-associated glycoprotein. *Neuron*. 1991;6(1):61–70.
466. Goldberg AF, Loewen CJ, Molday RS. Cysteine residues of photoreceptor peripherin/rds: role in subunit assembly and autosomal dominant retinitis pigmentosa. *Biochemistry*. 1998;37(2):680–685.
467. Moritz OL, Molday RS. Molecular cloning, membrane topology, and localization of bovine rom-1 in rod and cone photoreceptor cells. *Invest Ophthalmol Vis Sci*. 1996;37(2):352–362.
468. Corless JM, Fetter RD. Structural features of the terminal loop region of frog retinal rod outer segment disk membranes: III. Implications of the terminal loop complex for disk morphogenesis, membrane fusion, and cell surface interactions. *J Comp Neurol*. 1987;257(1):24–38.
469. Kajiwara K, Berson EL, Dryja TP. Digenic retinitis pigmentosa due to mutations at the unlinked peripherin/RDS and ROM1 loci. *Science*. 1994;264(5165):1604–1608.
470. Bascom RA, Liu L, Heckenlively JR, Stone EM, McInnes RR. Mutation analysis of the ROM1 gene in retinitis pigmentosa. *Hum Mol Genet*. 1995;4:1895–1902.
471. Abu-Safieh L, Alrashed M, Anazi S, et al. Autozygome-guided exome sequencing in retinal dystrophy patients reveals pathogenetic mutations and novel candidate disease genes. *Genome Res*. 2013;23:236–247.
472. Zelinger L, Banin E, Obolensky A, et al. A missense mutation in DHDDS, encoding dehydrodolichyl diphosphate synthase, is associated with autosomal-recessive retinitis pigmentosa in Ashkenazi Jews. *Am J Hum Genet*. 2011;88(2):207–215.
473. Zhang Q, Zulfiqar F, Xiao X, et al. Severe autosomal recessive retinitis pigmentosa maps to chromosome 1p13.3-p21.2 between D1S2896 and D1S457 but outside ABCA4. *Hum Genet*. 2005;1–10.

474. Martínez-Mir A, Paloma E, Allkimets R, et al. Retinitis pigmentosa caused by a homozygous mutation in the Stargardt disease gene ABCR. *Nat Genet*. 1998;18(1):11–12.
475. Bowne SJ, Humphries MM, Sullivan LS, et al. A dominant mutation in RPE65 identified by whole-exome sequencing causes retinitis pigmentosa with choroidal involvement. *Eur J Hum Genet*. 2011;20:1–8.
476. den Hollander AI, ten Brink JB, de Kok YJ, et al. Mutations in a human homologue of Drosophila crumbs cause retinitis pigmentosa (RP12). *Nat Genet*. 1999;23(2):217–221.
477. Chakarova CF, Hims MM, Bolz H, et al. Mutations in HPRP3, a third member of pre-mRNA splicing factor genes, implicated in autosomal dominant retinitis pigmentosa. *Hum Mol Genet*. 2002;11(1):87–92.
478. Abid A, Ismail M, Mehdi SQ, et al. Identification of novel mutations in *SEMA4A* gene associated with retinal degenerative diseases. *J Med Genet*. 2006;43:378–381.
479. Rajadhyaksha AM, Elemento O, Puffenberger EG, et al. Mutations in FLVCR1 cause posterior column ataxia and retinitis pigmentosa. *Am J Hum Genet*. 2010;87(5):643–654.
480. Nishiguchi KM, Tearle RG, Liu YP, et al. Whole genome sequencing in patients with retinitis pigmentosa reveals pathogenic DNA structural changes and *NEK2* as a new disease gene. *Proc Natl Acad Sci USA*. 2013;110:16139–16144.
481. Seyedahmadi BJ, Rivolta C, Keene JA, et al. Comprehensive screening of the *USH2A* gene in Usher syndrome type II and non-syndromic recessive retinitis pigmentosa. *Exp Eye Res*. 2004;79:167–173.
482. Ma X, Guan L, Wu W, et al. Whole-exome sequencing identifies OR2W3 mutation as a cause of autosomal dominant retinitis pigmentosa. *Sci Rep*. 2015;5:9236.
483. Bujakowska KM, Zhang Q, Siemiatkowska AM, et al. Mutations in IFT172 cause isolated retinal degeneration and Bardet–Biedl syndrome. *Hum Mol Genet*. 2015;24:230–242.
484. Li L, Nakaya N, Chavali VR, et al. A mutation in ZNF513, a putative regulator of photoreceptor development, causes autosomal-recessive retinitis pigmentosa. *Am J Hum Genet*. 2010;87(3):400–409.

485. Collin RW, Safieh C, Littink KW, et al. Mutations in C2ORF71 cause autosomal-recessive retinitis pigmentosa. *Am J Hum Genet*. 2010;86(5):783–788.
486. Bandah-Rozenfeld D, Mizrahi-Meissonnier L, Farhy C, et al. Homozygosity mapping reveals null mutations in FAM161A as a cause of autosomal-recessive retinitis pigmentosa. *Am J Hum Genet*. 2010;87(3):382–391.
487. Zhao C, Bellur DL, Lu S, et al. Autosomal-dominant retinitis pigmentosa caused by a mutation in SNRNP200, a gene required for unwinding of U4/U6 snRNAs. *Am J Hum Genet*. 2009;85(5):617–627.
488. Tuson M, Marfany G, Gonzalez-Duarte R. Mutation of CERKL, a novel human ceramide kinase gene, causes autosomal recessive retinitis pigmentosa (RP26). *Am J Hum Genet*. 2004;74(1):128–138.
489. Wang F, Li H, Xu M, et al. A homozygous missense mutation in NEUROD1 is associated with nonsyndromic autosomal recessive retinitis pigmentosa. *Invest Ophthalmol Vis Sci*. 2015;56:150–155.
490. Nakazawa M, Wada Y, Tamai M. Arrestin gene mutations in autosomal recessive retinitis pigmentosa. *Arch Ophthalmol*. 1998;116:498–501.
491. Aldahmesh MA, Safieh LA, Alkuraya H, et al. Molecular characterization of retinitis pigmentosa in Saudi Arabia. *Mol Vis*. 2009;15:2464–2469.
492. Bandah-Rozenfeld D, Collin RW, Banin E, et al. Mutations in IMPG2, encoding interphotoreceptor matrix proteoglycan 2, cause autosomal-recessive retinitis pigmentosa. *Am J Hum Genet*. 2010;87(2):199–208.
493. Jin Z-B, Huang X-F, Lv J-N, et al. SLC7A14 linked to autosomal recessive retinitis pigmentosa. *Nat Commun*. 2014;5:3517.
494. Rosenfeld PJ, Cowley GS, McGee TL, Sandberg MA, Berson EL, Dryja TP. A null mutation in the rhodopsin gene causes rod photoreceptor dysfunction and autosomal recessive retinitis pigmentosa. *Nat Genet*. 1992;1(3):209–213.
495. Khan MI, Kersten FFJ, Azam M, et al. *CLRN1* mutations cause nonsyndromic retinitis pigmentosa. *Ophthalmology*.

2011;7:1444–1448.
496. McLaughlin ME, Sandberg MA, Berson EL, Dryja TP. Recessive mutations in the gene encoding the ß-subunit of rod phosphodiesterase in patients with retinitis pigmentosa. *Nat Genet*. 1993;4(2):130–134.
497. Maw MA, Corbeil D, Koch J, et al. A frameshift mutation in prominin (mouse)-like 1 causes human retinal degeneration. *Hum Mol Genet*. 2000;9(1):27–34.
498. Ruiz A, Kuehn MH, Andorf JL, Stone E, Hageman GS, Bok D. Genomic organization and mutation analysis of the gene encoding lecithin retinol acyltransferase in human retinal pigment epithelium. *Invest Ophthalmol Vis Sci*. 2001;42(1):31–37.
499. Noor A, Windpassinger C, Patel M, et al. CC2D2A, encoding a coiled-coil and C2 domain protein, causes autosomal-recessive mental retardation with retinitis pigmentosa. *Am J Hum Genet*. 2008;82(4):1011–1018.
500. Wang Y, Guo L, Cai S-P, et al. Exome sequencing identifies compound heterozygous mutations in CYP4V2 in a pedigree with retinitis pigmentosa. *PLoS ONE*. 2012;7:e33673.
501. Huang SH, Pittler SJ, Huang X, Oliveira L, Berson EL, Dryja TP. Autosomal recessive retinitis pigmentosa caused by mutations in the a subunit of rod cGMP phosphodiesterase. *Nat Genet*. 1995;11(4):468–471.
502. Özgül RK, Siemiatkowska AM, Yücel D, et al. Exome sequencing and *cis*-regulatory mapping identify mutations in MAK, a gene encoding a regulator of ciliary length, as a cause of retinitis pigmentosa. *Am J Hum Genet*. 2011;89:253–264.
503. Hagstrom SA, North MA, Nishina PM, Berson EL, Dryja TP. Recessive mutations in the gene encoding the tubby-like protein TULP1 in patients with retinitis pigmentosa. *Nat Genet*. 1998;18:174–176.
504. Sato M, Nakazawa M, Usui T, et al. Mutations in the gene coding for guanylate cyclase-activating protein 2 (GUCA1B gene) in patients with autosomal dominant retinal dystrophies. *Graefes Arch Clin Exp Ophthalmol*. 2004;243:235–

242.
505. Abd El-Aziz MM, Barragan I, O'Driscoll CA, et al. EYS, encoding an ortholog of Drosophila spacemaker, is mutated in autosomal recessive retinitis pigmentosa. *Nat Genet*. 2008;40(11):1285–1287.
506. Kannabiran C, Singh HP, Jalali S. Mapping of locus for autosomal dominant retinitis pigmentosa on chromosome 6q23. *Hum Genet*. 2012;131:717–723.
507. Kennan A, Aherne A, Palfi A, et al. Identification of an IMPDH1 mutation in autosomal dominant retinitis pigmentosa (RP10) revealed following comparative microarray analysis of transcripts derived from retinas of wild-type and $Rho^{(-/-)}$ mice. *Hum Mol Genet*. 2002;11(5):547–558.
508. Davidson AE, Sergouniotis PI, Mackay DS, et al. RP1L1 variants are associated with a spectrum of inherited retinal diseases including retinitis pigmentosa and occult macular dystrophy. *Hum Mutat*. 2013;34:506–514.
509. Pierce EA, Quinn T, Meehan T, McGee TL, Berson EL, Dryja TP. Mutations in a gene encoding a new oxygen-regulated photoreceptor protein cause dominant retinitis pigmentosa. *Nat Genet*. 1999;22(3):248–254.
510. Yokota T, Shiojiri T, Gotoda T, Arai H. Retinitis pigmentosa and ataxia caused by a mutation in the gene for the a-tocopherol-transfer protein. *N Engl J Med*. 1996;335(23):1770–1771.
511. Estrada-Cuzcano A, Neveling K, Kohl S, et al. Mutations in C8orf37, encoding a ciliary protein, are associated with autosomal-recessive retinal dystrophies with early macular involvement. *Am J Hum Genet*. 2012;90:102–109.
512. Chakarova CF, Papaioannou MG, Khanna H, et al. Mutations in TOPORS cause autosomal dominant retinitis pigmentosa with perivascular retinal pigment epithelium atrophy. *Am J Hum Genet*. 2007;81(5):1098–1103.
513. Chen X, Liu Y, Sheng X, et al. PRPF4 mutations cause autosomal dominant retinitis pigmentosa. *Hum Mol Genet*. 2014;23:2926–2939.
514. den Hollander AI, McGee TL, Ziviello C, et al. A

homozygous missense mutation in the IRBP gene (RBP3) associated with autosomal recessive retinitis pigmentosa. *Invest Ophthalmol Vis Sci*. 2009;50(4):1864–1872.
515. Sullivan LS, Koboldt DC, Bowne SJ, et al. A dominant mutation in hexokinase 1 (*HK1*) causes retinitis pigmentosa. *Invest Ophthalmol Vis Sci*. 2014;55:7147–7158.
516. Morimura H, Saindelle-Ribeaudeau F, Berson EL, Dryja TP. Mutations in RGR, encoding a light-sensitive opsin homologue, in patients with retinitis pigmentosa. *Nat Genet*. 1999;23(4):393–394.
517. Avila-Fernandez A, Perez-Carro R, Corton M, et al. Whole-exome sequencing reveals *ZNF408* as a new gene associated with autosomal recessive retinitis pigmentosa with vitreal alterations. *Hum Mol Genet*. 2015;24:4037–4048.
518. Davidson AE, Millar ID, Urquhart JE, et al. Missense mutations in a retinal pigment epithelium protein, bestrophin-1, cause retinitis pigmentosa. *Am J Hum Genet*. 2009;85(5):581–592.
519. Estrada-Cuzcano A, Koenekoop RK, Senechal A, et al. *BBS1* mutations in a wide spectrum of phenotypes ranging from nonsyndromic retinitis pigmentosa to Bardet–Biedl syndrome. *Arch Ophthalmol*. 2012;130:1425–1432.
520. Siemiatkowska AM, van den Born LI, van Hagen MP, et al. Mutations in the mevalonate kinase (*MVK*) gene cause nonsyndromic retinitis pigmentosa. *Ophthalmology*. 2013;120:2697–2705.
521. Fingert JH, Oh K, Chung M, et al. Association of a novel mutation in the retinol dehydrogenase 12 (*RDH12*) gene with autosomal dominant retinitis pigmentosa. *Arch Ophthalmol*. 2008;126:1301–1307.
522. Wang H, den Hollander AI, Moayedi Y, et al. Mutations in *SPATA7* cause Leber congenital amaurosis and juvenile retinitis pigmentosa. *Am J Hum Genet*. 2009;84:380–387.
523. Riazuddin SA, Iqbal M, Wang Y, et al. A splice-site mutation in a retina-specific exon of *BBS8* causes nonsyndromic retinitis pigmentosa. *Am J Hum Genet*. 2010;86:805–812.
524. Finckh U, Xu S, Kumaramanickavel G, et al. Homozygosity

mapping of autosomal recessive retinitis pigmentosa locus (RP22) on chromosome 16p12.1-p12.3. *Genomics*. 1998;48(3):341–345.
525. Burstedt MS, Sandgren O, Holmgren G, Forsman-Semb K. Bothnia dystrophy caused by mutations in the cellular retinaldehyde-binding protein gene (RLBP1) on chromosome 15q26. *Invest Ophthalmol Vis Sci*. 1999;40(5):995–1000.
526. Escher P, Gouras P, Roduit R, et al. Mutations in NR2E3 can cause dominant or recessive retinal degenerations in the same family. *Hum Mutat*. 2009;30:342–351.
527. Xu M, Yang L, Wang F, et al. Mutations in human *IFT140* cause non-syndromic retinal degeneration. *Hum Genet*. 2015;134(10):1069–1078.
528. Shevach E, Ali M, Mizrahi-Meissonnier L, et al. Association between missense mutations in the BBS2 gene and nonsyndromic retinitis pigmentosa. *JAMA Ophthalmol*. 2015;133(3):312–318.
529. Bareil C, Hamel CP, Delague V, Arnaud B, Demaille J, Claustres M. Segregation of a mutation in CNGB1 encoding the beta-subunit of the rod cGMP-gated channel in a family with autosomal recessive retinitis pigmentosa. *Hum Genet*. 2001;108(4):328–334.
530. Davidson AE, Schwarz N, Zelinger L, et al. Mutations in *ARL2BP*, encoding ADP-ribosylation-factor-like 2 binding protein, cause autosomal-recessive retinitis pigmentosa. *Am J Hum Genet*. 2013;93:321–329.
531. Ajmal M, Khan MI, Neveling K, et al. A missense mutation in the splicing factor gene *DHX38* is associated with early-onset retinitis pigmentosa with macular coloboma. *J Med Genet*. 2014;51:444–448.
532. van Lith-Verhoeven JJ, van der Velde-Visser SD, Sohocki MM, et al. Clinical characterization, linkage analysis, and PRPC8 mutation analysis of a family with autosomal dominant retinitis pigmentosa type 13 (RP13). *Ophthalmic Genet*. 2002;23(1):1–12.
533. Dvir L, Srour G, Abu-Ras R, Miller B, Shalev SA, Ben-Yosef T. Autosomal-recessive early-onset retinitis pigmentosa

caused by a mutation in PDE6G, the gene encoding the gamma subunit of rod cGMP phosphodiesterase. *Am J Hum Genet*. 2010;87(2):258–264.
534. Alvarez BV, Vithana EN, Yang Z, et al. Identification and characterization of a novel mutation in the carbonic anhydrase IV gene that causes retinitis pigmentosa. *Invest Ophthalmol Vis Sci*. 2007;48(8):3459–3468.
535. Nevet MJ, Shalev SA, Zlotogora J, Mazzawi N, Ben-Yosef T. Identification of a prevalent founder mutation in an Israeli Muslim Arab village confirms the role of PRCD in the aetiology of retinitis pigmentosa in humans. *J Med Genet*. 2010;47(8):533–537.
536. de Sousa Dias M, Hernan I, Pascual B, et al. Detection of novel mutations that cause autosomal dominant retinitis pigmentosa in candidate genes by long-range PCR amplification and next-generation sequencing. *Mol Vis*. 2013;19:654–664.
537. Vithana EN, Abu-Safieh L, Pelosini L, et al. Expression of PRPF31 mRNA in patients with autosomal dominant retinitis pigmentosa: a molecular clue for incomplete penetrance? *Invest Ophthalmol Vis Sci*. 2003;44(10):4204–4209.
538. Tanackovic G, Ransijn A, Ayuso C, Harper S, Berson EL, Rivolta C. A missense mutation in PRPF6 causes impairment of pre-mRNA splicing and autosomal-dominant retinitis pigmentosa. *Am J Hum Genet*. 2011;88(5):643–649.
539. El Shamieh S, Neuillé M, Terray A, et al. Whole-exome sequencing identifies *KIZ* as a ciliary gene associated with autosomal-recessive rod-cone dystrophy. *Am J Hum Genet*. 2014;94:625–633.
540. Hartong DT, Dange M, McGee TL, Berson EL, Dryja TP, Colman RF. Insights from retinitis pigmentosa into the roles of isocitrate dehydrogenases in the Krebs cycle. *Nat Genet*. 2008;40(10):1230–1234.
541. Hardcastle AJ, Thiselton DL, Zito I, et al. Evidence for a new locus for X-linked retinitis pigmentosa (RP23). *Invest Ophthalmol Vis Sci*. 2000;41(8):2080–2086.

542. Ott J, Bhattacharya S, Chen JD, et al. Localizing multiple X chromosome-linked retinitis pigmentosa loci using multilocus homogeneity tests. *Proc Natl Acad Sci USA*. 1990;87(2):701–704.
543. Gieser L, Fujita R, Göring HH, et al. A novel locus (RP24) for X-linked retinitis pigmentosa maps to Xq26-27. *Am J Hum Genet*. 1998;63(5):1439–1447.
544. Melamud A, Shen G-Q, Chung D, et al. Mapping a new genetic locus for X linked retinitis pigmentosa to Xq28. *J Med Genet*. 2006;43:e27.
545. Weil D, El-Amraoui A, Masmoudi S, et al. Usher syndrome type I G (USH1G) is caused by mutations in the gene encoding SANS, a protein that associates with the USH1C protein, harmonin. *Hum Mol Genet*. 2003;12(5):463–471.
546. Verpy E, Leibovici M, Zwaenepoel I, et al. A defect in harmonin, a PDZ domain-containing protein expressed in the inner ear sensory hair cells, underlies Usher syndrome type 1C. *Nat Genet*. 2000;26(1):51–55.
547. Bolz H, von Brederlow B, Ramirez A, et al. Mutation of CDH23, encoding a new member of the cadherin gene family, causes Usher syndrome type 1D. *Nat Genet*. 2001;27(1):108–112.
548. Chaib H, Kaplan J, Gerber S, et al. A newly identified locus for Usher syndrome type I, USH1E, maps to chromosome 21q21. *Hum Mol Genet*. 1997;6(1):27–31.
549. Ahmed ZM, Riazuddin S, Bernstein SL, et al. Mutations of the protocadherin gene PCDH15 cause Usher syndrome type 1F. *Am J Hum Genet*. 2001;69(1):25–34.
550. Kikkawa Y, Shitara H, Wakana S, et al. Mutations in a new scaffold protein Sans cause deafness in Jackson shaker mice. *Hum Mol Genet*. 2003;12(5):453–461.
551. Astuto LM, Bork JM, Weston MD, et al. CDH23 mutation and phenotype heterogeneity: a profile of 107 diverse families with Usher syndrome and nonsyndromic deafness. *Am J Hum Genet*. 2002;71(2):262–275.
552. Riazuddin IA, Belyantseva APJ, Giese K, et al. Alterations of the CIB2 calcium- and integrin-binding protein cause Usher syndrome type 1J and nonsyndromic deafness DFNB48. *Nat*

Genet. 2012;44:1265–1271.
553. Jaworek R, Bhatti N, Latief SN, et al. *USH1K*, a novel locus for type I Usher syndrome, maps to chromosome 10p11.21-q21.1. *J Hum Genet*. 2012;57:633–637.
554. Eudy JD, Weston MD, Yao S, et al. Mutation of a gene encoding a protein with extracellular matrix motifs in Usher syndrome type IIa. *Science*. 1998;280(5370):1753–1757.
555. Hmani M, Ghorbel A, Boulila-Elgaied A, et al. A novel locus for Usher syndrome type II, USH2B, maps to chromosome 3 at p23-24.2. *Eur J Hum Genet*. 1999;7(3):363–367.
556. Webb TR, Parfitt DA, Gardner JC, et al. Deep intronic mutation in OFD1, identified by targeted genomic next-generation sequencing, causes a severe form of X-linked retinitis pigmentosa (RP23). *Hum Mol Genet*. 2012;21:3647–3654.
557. Ebermann I, Lopez I, Bitner-Glindzicz M, Brown C, Koenekoop RK, Bolz HJ. Deafblindness in French Canadians from Quebec: a predominant founder mutation in the USH1C gene provides the first genetic link with the Acadian population. *Genome Biol*. 2007;8(4):R47.
558. Joensuu T, Hamalainen R, Yuan B, et al. Mutations in a novel gene with transmembrane domains underlie Usher syndrome type 3. *Am J Hum Genet*. 2001;69(4):673–684.
559. Puffenberger EG, Jinks RN, Sougnez C, et al. Genetic mapping and exome sequencing identify variants associated with five novel diseases. *PLoS ONE*. 2012;7:e28936.
560. Eisenberger T, Slim R, Mansour A, et al. Targeted next-generation sequencing identifies a homozygous nonsense mutation in *ABHD12*, the gene underlying PHARC, in a family clinically diagnosed with Usher syndrome type 3. *Orphanet J Rare Dis*. 2012;7:59.
561. Khateb L, Zelinger L, Mizrahi-Meissonnier C, et al. A homozygous nonsense CEP250 mutation combined with a heterozygous nonsense C2orf71 mutation is associated with atypical Usher syndrome. *J Med Genet*. 2014;51:460–469.
562. Crimi M, Galbiati S, Perini MP, et al. A mitochondrial tRNA(His) gene mutation causing pigmentary retinopathy

and neurosensorial deafness. *Neurology*. 2003;60(7):1200–1203.
563. Da Pozzo P, Cardaioli E, Malfatti E, et al. A novel mutation in the mitochondrial tRNA(Pro) gene associated with late-onset ataxia, retinitis pigmentosa, deafness, leukoencephalopathy and complex I deficiency. *Eur J Hum Genet*. 2009;17(8):1092–1096.
564. Adato A, Weil D, Kalinski H, et al. Mutation profile of all 49 exons of the human myosin VIIA gene, and haplotype analysis, in Usher 1B families from diverse origins. *Am J Hum Genet*. 1997;61(4):813–821.
565. Bitner-Glindzicz M, Lindley KJ, Rutland P, et al. A recessive contiguous gene deletion causing infantile hyperinsulinism, enteropathy and deafness identifies the Usher type 1C gene. *Nat Genet*. 2000;26(1):56–60.
566. Ouyang XM, Xia XJ, Verpy E, et al. Mutations in the alternatively spliced exons of USH1C cause non-syndromic recessive deafness. *Hum Genet*. 2002;111(1):26–30.
567. Bork JM, Peters LM, Riazuddin S, et al. Usher syndrome 1D and nonsyndromic autosomal recessive deafness DFNB12 are caused by allelic mutations of the novel cadherin-like gene CDH23. *Am J Hum Genet*. 2001;68(1):26–37.
568. Di Palma F, Holme RH, Bryda EC, et al. Mutations in Cdh23, encoding a new type of cadherin, cause stereocilia disorganization in waltzer, the mouse model for Usher syndrome type 1D. *Nat Genet*. 2001;27(1):103–107.
569. Boeda B, El-Amraoui A, Bahloul A, et al. Myosin VIIa, harmonin and cadherin 23, three Usher I gene products that cooperate to shape the sensory hair cell bundle. *EMBO J*. 2002;21(24):6689–6699.
570. Siemens J, Kazmierczak P, Reynolds A, Sticker M, Littlewood-Evans A, Muller U. The Usher syndrome proteins cadherin 23 and harmonin form a complex by means of PDZ-domain interactions. *Proc Natl Acad Sci USA*. 2002;99(23):14946–14951.
571. Ahmed ZM, Riazuddin S, Ahmad J, et al. PCDH15 is expressed in the neurosensory epithelium of the eye and ear and mutant alleles are responsible for both USH1F and

DFNB23. *Hum Mol Genet*. 2003;12(24):3215–3223.
572. Alagramam KN, Murcia CL, Kwon HY, Pawlowski KS, Wright CG, Woychik RP. The mouse Ames waltzer hearing-loss mutant is caused by mutation of Pcdh15, a novel protocadherin gene. *Nat Genet*. 2001;27(1):99–102.
573. Adato A, Vreugde S, Joensuu T, et al. USH3A transcripts encode clarin-1, a four-transmembrane-domain protein with a possible role in sensory synapses. *Eur J Hum Genet*. 2002;10(6):339–350.
574. Pennings RJ, Fields RR, Huygen PL, Deutman AF, Kimberling WJ, Cremers CW. Usher syndrome type III can mimic other types of Usher syndrome. *Ann Otol Rhinol Laryngol*. 2003;112(6):525–530.
575. Berger W, Kloeckener-Gruissem B, Neidhardt J. The molecular basis of human retinal and vitreoretinal diseases. *Prog Retin Eye Res*. 2010;29(5):335–375.
576. Hosch J, Lorenz B, Stieger K. RPGR: role in the photoreceptor cilium, human retinal disease, and gene therapy. *Ophthalmic Genet*. 2011;32(1):1–11.
577. Rosenfeld PJ, Hahn LB, Sandberg MA, Dryja TP, Berson EL. Low incidence of retinitis pigmentosa among heterozygous carriers of a specific rhodopsin splice site mutation. *Invest Ophthalmol Vis Sci*. 1995;36(11):2186–2192.
578. Liu X, Garriga P, Khorana HG. Structure and function in rhodopsin: correct folding and misfolding in two point mutants in the intradiscal domain of rhodopsin identified in retinitis pigmentosa. *Proc Natl Acad Sci USA*. 1996;93:4554–4559.
579. Garriga P, Liu X, Khorana HG. Structure and function in rhodopsin: correct folding and misfolding in point mutants at and in proximity to the site of the retinitis pigmentosa mutation Leu-125ÆArg in the transmembrane helix C. *Proc Natl Acad Sci USA*. 1996;93:4560–4564.
580. Sung C-H, Schneider BG, Agarwal N, Papermaster DS, Nathans J. Functional heterogeneity of mutant rhodopsins responsible for autosomal dominant retinitis pigmentosa. *Proc Natl Acad Sci USA*. 1991;88(19):8840–8844.
581. Apfelstedt-Sylla E, Kunisch M, Horn M, et al. Ocular

findings in a family with autosomal dominant retinitis pigmentosa and a frameshift mutation altering the carboxyl terminal sequence of rhodopsin. *Br J Ophthalmol*. 1993;77(8):495–501.
582. Hastings ML, Krainer AR. Functions of SR proteins in the U12-dependent AT-AC pre-mRNA splicing pathway. *RNA*. 2001;7(3):471–482.
583. Will CL, Luhrmann R. Spliceosomal UsnRNP biogenesis, structure and function. *Curr Opin Cell Biol*. 2001;13(3):290–301.
584. Brown JD, Beggs JD. Roles of PRP8 protein in the assembly of splicing complexes. *EMBO J*. 1992;11(10):3721–3729.
585. Teigelkamp S, Newman AJ, Beggs JD. Extensive interactions of PRP8 protein with the 5′ and 3′ splice sites during splicing suggest a role in stabilization of exon alignment by U5 snRNA. *EMBO J*. 1995;14(11):2602–2612.
586. Collins CA, Guthrie C. The question remains: is the spliceosome a ribozyme? *Nat Struct Biol*. 2000;7(10):850–854.
587. McKie AB, McHale JC, Keen TJ, et al. Mutations in the pre-mRNA splicing factor gene PRPC8 in autosomal dominant retinitis pigmentosa (RP13). *Hum Mol Genet*. 2001;10(15):1555–1562.
588. Greenberg J, Goliath R, Beighton P, Ramesar R. A new locus for autosomal dominant retinitis pigmentosa on the short arm of chromosome 17. *Hum Mol Genet*. 1994;3(6):915–918.
589. Vithana EN, Abu-Safieh L, Allen MJ, et al. A human homolog of yeast pre-mRNA splicing gene, PRP31, underlies autosomal dominant retinitis pigmentosa on chromosome 19q13.4 (RP11). *Mol Cell*. 2001;8(2):375–381.
590. Makarova OV, Makarov EM, Liu S, Vornlocher HP, Luhrmann R. Protein 61K, encoded by a gene (PRPF31) linked to autosomal dominant retinitis pigmentosa, is required for U4/U6*U5 tri-snRNP formation and pre-mRNA splicing. *EMBO J*. 2002;21(5):1148–1157.
591. Evans K, Al-Maghtheh M, Fitzke FW, et al. Bimodal expressivity in dominant retinitis pigmentosa genetically linked to chromosome 19q. *Br J Ophthalmol*. 1995;79:841–846.

592. Moore AT, Fitzke F, Jay M, et al. Autosomal dominant retinitis pigmentosa with apparent incomplete penetrance: a clinical, electrophysiological, psychophysical, and molecular genetic study. *Br J Ophthalmol*. 1993;77:473–479.
593. McGee TL, Devoto M, Ott J, Berson EL, Dryja TP. Evidence that the penetrance of mutations at the RP11 locus causing dominant retinitis pigmentosa is influenced by a gene linked to the homologous RP11 allele. *Am J Hum Genet*. 1997;61:1059–1066.
594. Horowitz DS, Kobayashi R, Krainer AR. A new cyclophilin and the human homologues of yeast Prp3 and Prp4 form a complex associated with U4/U6 snRNPs. *RNA*. 1997;3(12):1374–1387.
595. Anthony JG, Weidenhammer EM, Woolford JL Jr. The yeast Prp3 protein is a U4/U6 snRNP protein necessary for integrity of the U4/U6 snRNP and the U4/U6.U5 tri-snRNP. *RNA*. 1997;3(10):1143–1152.
596. Baehr W, Chen CK. RP11 and RP13: unexpected gene loci. *Trends Mol Med*. 2001;7(11):484–486.
597. Kuhn AN, Reichl EM, Brow DA. Distinct domains of splicing factor Prp8 mediate different aspects of spliceosome activation. *Proc Natl Acad Sci USA*. 2002;99(14):9145–9149.
598. Murga-Zamalloa C, Swaroop A, Khanna H. Multiprotein complexes of retinitis pigmentosa GTPase regulator (RPGR), a ciliary protein mutated in X-linked retinitis pigmentosa (XLRP). *Adv Exp Med Biol*. 2010;664:105–114.
599. Hong DH, Pawlyk B, Sokolov M, et al. RPGR isoforms in photoreceptor connecting cilia and the transitional zone of motile cilia. *Invest Ophthalmol Vis Sci*. 2003;44(6):2413–2421.
600. Hong DH, Pawlyk BS, Shang J, Sandberg MA, Berson EL, Li T. A retinitis pigmentosa GTPase regulator (RPGR)-deficient mouse model for X-linked retinitis pigmentosa (RP3). *Proc Natl Acad Sci USA*. 2000;97(7):3649–3654.
601. Khanna H, Hurd TW, Lillo C, et al. RPGR-ORF15, which is mutated in retinitis pigmentosa, associates with SMC1, SMC3, and microtubule transport proteins. *J Biol Chem*. 2005;280(39):33580–33587.

602. Mavlyutov TA, Zhao H, Ferreira PA. Species-specific subcellular localization of RPGR and RPGRIP isoforms: implications for the phenotypic variability of congenital retinopathies among species. *Hum Mol Genet*. 2002;11(16):1899–1907.
603. Adato A, Michel V, Kikkawa Y, et al. Interactions in the network of Usher syndrome type 1 proteins. *Hum Mol Genet*. 2005;14(3):347–356.
604. Iannaccone A, Wang X, Jablonski MM, et al. Increasing evidence for syndromic phenotypes associated with RPGR mutations. *Am J Ophthalmol*. 2004;137(4):785–786 [author reply 786].
605. Wright AF, Shu X. X-linked retinal dystrophies and microtubular functions within the retina. *Ophthalmol Res*. 2007;257–267.
606. Saihan Z, Webster AR, Luxon L, Bitner-Glindzicz M. Update on Usher syndrome. *Curr Opin Neurol*. 2009;22(1):19–27.
607. Liu X, Bulgakov OV, Darrow KN, et al. Usherin is required for maintenance of retinal photoreceptors and normal development of cochlear hair cells. *Proc Natl Acad Sci USA*. 2007;104(11):4413–4418.
608. Pan L, Yan J, Wu L, Zhang M. Assembling stable hair cell tip link complex via multidentate interactions between harmonin and cadherin 23. *Proc Natl Acad Sci USA*. 2009;106(14):5575–5580.
609. Yan D, Liu XZ. Genetics and pathological mechanisms of Usher syndrome. *J Hum Genet*. 2010;55(6):327–335.
610. Delprat B, Michel V, Goodyear R, et al. Myosin XVa and whirlin, two deafness gene products required for hair bundle growth, are located at the stereocilia tips and interact directly. *Hum Mol Genet*. 2005;14(3):401–410.
611. Muller U. Cadherins and mechanotransduction by hair cells. *Curr Opin Cell Biol*. 2008;20(5):557–566.
612. Yan D, Li F, Hall ML, et al. An isoform of GTPase regulator DOCK4 localizes to the stereocilia in the inner ear and binds to harmonin (USH1C). *J Mol Biol*. 2006;357(3):755–764.
613. Rhodes CR, Hertzano R, Fuchs H, et al. A Myo7a mutation

cosegregates with stereocilia defects and low-frequency hearing impairment. *Mamm Genome*. 2004;15(9):686–697.
614. Roepman R, Wolfrum U. Protein networks and complexes in photoreceptor cilia. *Subcell Biochem*. 2007;43:209–235.
615. Reiners J, Nagel-Wolfrum K, Jurgens K, Marker T, Wolfrum U. Molecular basis of human Usher syndrome: deciphering the meshes of the Usher protein network provides insights into the pathomechanisms of the Usher disease. *Exp Eye Res*. 2006;83(1):97–119.
616. Jin H, Nachury MV. The BBSome. *Curr Biol*. 2009;19(12):R472–3.
617. Nachury MV, Seeley ES, Jin H. Trafficking to the ciliary membrane: how to get across the periciliary diffusion barrier? *Annu Rev Cell Dev Biol*. 2010;26:59–87.
618. Jin H, White SR, Shida T, et al. The conserved Bardet–Biedl syndrome proteins assemble a coat that traffics membrane proteins to cilia. *Cell*. 2010;141(7):1208–1219.
619. Locke M, Tinsley CL, Benson MA, Blake DJ. TRIM32 is an E3 ubiquitin ligase for dysbindin. *Hum Mol Genet*. 2009;18(13):2344–2358.
620. Schulein R. The early stages of the intracellular transport of membrane proteins: clinical and pharmacological implications. *Rev Physiol Biochem Pharmacol*. 2004;151:45–91.
621. Chinchore Y, Mitra A, Dolph PJ. Accumulation of rhodopsin in late endosomes triggers photoreceptor cell degeneration. *PLoS Genet*. 2009;5(2):e1000377.
622. Deretic D, Williams AH, Ransom N, Morel V, Hargrave PA, Arendt A. Rhodopsin C terminus, the site of mutations causing retinal disease, regulates trafficking by binding to ADP-ribosylation factor 4 (ARF4). *Proc Natl Acad Sci USA*. 2005;102(9):3301–3306.
623. Chen J, Makino CL, Peachey NS, Baylor DA, Simon MI. Mechanisms of rhodopsin inactivation in vivo as revealed by a COOH-terminal truncation mutant. *Science*. 1995;267(5196):374–377.
624. Sung CH, Tai AW. Rhodopsin trafficking and its role in retinal dystrophies. *Int Rev Cytol*. 2000;195:215–267.
625. Luthert PJ, Chong NH. Photoreceptor rescue. *Eye (Lond)*.

1998;12(Pt 3b):591–596.
626. Danesh-Meyer HV, Levin LA. Neuroprotection: extrapolating from neurologic diseases to the eye. *Am J Ophthalmol*. 2009;148(2):186–191.e2.
627. Yoshizawa K, Kiuchi K, Nambu H, et al. Caspase-3 inhibitor transiently delays inherited retinal degeneration in C3H mice carrying the rd gene. *Graefes Arch Clin Exp Ophthalmol*. 2002;240(3):214–219.
628. Murakami Y, Miller JW, Vavvas DG. RIP kinase-mediated necrosis as an alternative mechanisms of photoreceptor death. *Oncotarget*. 2011;2(6):497–509.
629. Sancho-Pelluz J, Arango-Gonzalez B, Kustermann S, et al. Photoreceptor cell death mechanisms in inherited retinal degeneration. *Mol Neurobiol*. 2008;38(3):253–269.
630. Milam AH, Li Z-Y, Fariss RN. Histology of the human retina in retinitis pigmentosa. *Prog Retin Eye Res*. 1998;17(2):175–205.
631. Milam AH, Li Z-Y, Cideciyan AV, Jacobson SG. Clinicopathologic effects of the Q64ter rhodopsin mutation in retinitis pigmentosa. *Invest Ophthalmol Vis Sci*. 1996;37(5):753–765.
632. Naash ML, Peachey NS, Li ZY, et al. Light-induced acceleration of photoreceptor degeneration in transgenic mice expressing mutant rhodopsin. *Invest Ophthalmol Vis Sci*. 1996;37(5):775–782.
633. Roof DJ, Adamian M, Hayes A. Rhodopsin accumulation at abnormal sites in retinas of mice with a human P23H rhodopsin transgene. *Invest Ophthalmol Vis Sci*. 1994;35(12):4049–4062.
634. Milam AH, Jacobson SG. Photoreceptor rosettes with blue cone opsin immunoreactivity in retinitis pigmentosa. *Ophthalmology*. 1990;97(12):1620–1631.
635. Li ZY, Jacobson SG, Milam AH. Autosomal dominant retinitis pigmentosa caused by the threonine-17-methionine rhodopsin mutation: retinal histopathology and immunocytochemistry. *Exp Eye Res*. 1994;58(4):397–408.
636. Daiger SP, Sullivan AS, Rodriguez JA. Correlation of phenotype with genotype in inherited retinal degeneration.

Behav Brain Sci. 1995;18:452–467.
637. Li T, Snyder WK, Olsson JE, Dryja TP. Transgenic mice carrying the dominant rhodopsin mutation P347S: evidence for defective vectorial transport of rhodopsin to the outer segments. *Proc Natl Acad Sci USA*. 1996;93(24):14176–14181.
638. Petters RM, Alexander CA, Wells KD, et al. Genetically engineered large animal model for studying cone photoreceptor survival and degeneration in retinitis pigmentosa. *Nat Biotechnol*. 1997;15(10):965–970.
639. Li ZY, Wong F, Chang JH, et al. Rhodopsin transgenic pigs as a model for human retinitis pigmentosa. *Invest Ophthalmol Vis Sci*. 1998;39(5):808–819.
640. Clarke G, Collins RA, Leavitt BR, et al. A one-hit model of cell death in inherited neuronal degenerations. *Nature*. 2000;406(6792):195–199.
641. Clarke G, Lumsden CJ, McInnes RR. Inherited neurodegenerative diseases: the one-hit model of neurodegeneration. *Hum Mol Genet*. 2001;10(20):2269–2275.
642. Pacione LR, Szego MJ, Ikeda S, Nishina PM, McInnes RR. Progress toward understanding the genetic and biochemical mechanisms of inherited photoreceptor degenerations. *Annu Rev Neurosci*. 2003;26:657–700.
643. Li ZY, Possin DE, Milam AH. Histopathology of bone spicule pigmentation in retinitis pigmentosa. *Ophthalmology*. 1995;102(5):805–816.
644. Meyer KT, Heckenlively JR, Spitznas M, Foos RY. Dominant retinitis pigmentosa: a clinicopathologic correlation. *Ophthalmology*. 1982;89(12):1414–1424.
645. Duvall J, McKechnie NM, Lee WR, Rothery S, Marshall J. Extensive subretinal pigment epithelial deposit in two brothers suffering from dominant retinitis pigmentosa. A histopathological study. *Graefes Arch Clin Exp Ophthalmol*. 1986;224(3):299–309.
646. Brosnahan DM, Kennedy SM, Converse CA, Lee WR, Hammer HM. Pathology of hereditary retinal degeneration associated with hypobetalipoproteinemia. *Ophthalmology*. 1994;101(1):38–45.
647. Del Priore LV, Kaplan HJ, Hornbeck R, Jones Z, Swinn M.

Retinal pigment epithelial debridement as a model for the pathogenesis and treatment of macular degeneration. *Am J Ophthalmol*. 1996;122(5):629–643.
648. Eisenfeld AJ, Bunt-Milam AH, Sarthy PV. Muller cell expression of glial fibrillary acidic protein after genetic and experimental photoreceptor degeneration in the rat retina. *Invest Ophthalmol Vis Sci*. 1984;25(11):1321–1328.
649. Milam AH, De Leeuw AM, Gaur VP, Saari JC. Immunolocalization of cellular retinoic acid binding protein to Müller cells and/or a subpopulation of GABA-positive amacrine cells in retinas of different species. *J Comp Neurol*. 1990;296(1):123–129.
650. Sastry SM, Li ZY, Milam AH. Epiretinal membranes in retinitis pigmentosa. *Invest Ophthalmol Vis Sci*. 1996;37(3):4789.
651. Szamier RB. Ultrastructure of the preretinal membrane in retinitis pigmentosa. *Invest Ophthalmol Vis Sci*. 1981;21(2):227–236.
652. Thanos S, Moore S, Hong Y-M. Retinal microglia. *Prog Retin Eye Res*. 1996;15(2):331–361.
653. Flannery JG, Farber DB, Bird AC, Bok D. Degenerative changes in a retina affected with autosomal dominant retinitis pigmentosa. *Invest Ophthalmol Vis Sci*. 1989;30:191–211.
654. Santos A, Humayun MS, de Juan E Jr, et al. Preservation of the inner retina in retinitis pigmentosa: a morphometric analysis. *Arch Ophthalmol*. 1997;115(4):511–515.
655. Newman NM, Stevens RA, Heckenlively JR. Nerve fibre layer loss in diseases of the outer retinal layer. *Br J Ophthalmol*. 1987;71(1):21–26.
656. Villegas-Perez MP, Vidal-Sanz M, Lund RD. Mechanism of retinal ganglion cell loss in inherited retinal dystrophy. *Neuroreport*. 1996;7(12):1995–1999.
657. Gartner S, Henkind P. Pathology of retinitis pigmentosa. *Ophthalmology*. 1982;89(12):1425–1432.
658. Marc RE, Jones BW, Watt CB, Strettoi E. Neural remodeling in retinal degeneration. *Prog Retin Eye Res*. 2003;22(5):607–655.

659. Jones BW, Watt CB, Frederick JM, et al. Retinal remodeling triggered by photoreceptor degenerations. *J Comp Neurol*. 2003;464(1):1–16.
660. Marc RE, Jones BW, Anderson JR, et al. Neural reprogramming in retinal degeneration. *Invest Ophthalmol Vis Sci*. 2007;48(7):3364–3371.
661. Puthussery T, Taylor WR. Functional changes in inner retinal neurons in animal models of photoreceptor degeneration. *Adv Exp Med Biol*. 2010;664:525–532.
662. Li Z-Y, Kljavin IJ, Milam AH. Rod photoreceptor neurite sprouting in retinitis pigmentosa. *J Neurosci*. 1995;15(8):5429–5438.
663. Gregory-Evans K, Weleber RG. An eye for an eye: new models of genetic ocular disease. *Nat Biotechnol*. 1997;15(10):947–948.
664. Bunt-Milam AH, Saari JC, Klock IB, Garwin GG. Zonulae adherentes pore size in the external limiting membrane of the rabbit retina. *Invest Ophthalmol Vis Sci*. 1985;26(10):1377–1380.
665. Leveillard T, Mohand-Said S, Lorentz O, et al. Identification and characterization of rod-derived cone viability factor. *Nat Genet*. 2004;36(7):755–759.
666. Grunwald JE, Maguire AM, Dupont J. Retinal hemodynamics in retinitis pigmentosa. *Am J Ophthalmol*. 1996;122:502–508.
667. Ward MM, Puthussery T, Vessey KA, Fletcher EL. The role of purinergic receptors in retinal function and disease. *Adv Exp Med Biol*. 2010;664:385–391.
668. Harris HJ. Personal view – genetic counselling – does the terminology matter? *Br Med J*. 1997;315(7117):1241–1242.
669. Korsch BM, Negrete VF. Doctor–patient communication. *Sci Am*. 1972;227(2):66–74.
670. Michie S, Marteau TM, Bobrow M. Genetic counselling: the psychological impact of meeting patients' expectations. *J Med Genet*. 1997;34(3):237–241.
671. Clarke A. Is non-directive counselling possible? *Lancet*. 1991;338:998–1001.
672. Kim RY, Fitzke FW, Moore AT, et al. Autosomal dominant

retinitis pigmentosa mapping to chromosome 7p exhibits variable expression. *Br J Ophthalmol*. 1995;79(1):23–27.
673. Evans K, Fryer A, Inglehearn C, et al. Genetic linkage of cone-rod retinal dystrophy to chromosome 19q and evidence for segregation distortion. *Nat Genet*. 1994;6:210–213.
674. Richards RI, Holman K, Friend K, et al. Evidence of founder chromosomes in fragile X syndrome. *Nat Genet*. 1992;1(4):257–260.
675. Magenis RE, Toth-Fejel S, Allen LJ, et al. Comparison of the 15q deletions in Prader–Willi and Angelman syndromes: specific regions, extent of deletions, parental origin, and clinical consequences. *Am J Med Genet*. 1990;35:333–349.
676. Bird AC. X-linked retinitis pigmentosa. *Br J Ophthalmol*. 1975;59:177–199.
677. Mehta L, Young ID. Attitudes of Asian families to genetic counselling. [Letter] *J Med Genet*. 1985;22(5):413.
678. Pawlowitzki IH, Ruther K, Brunsmann F, Von Gizycki R. Acceptability of prenatal diagnosis for retinitis pigmentosa. [Letter] *Lancet*. 1986;2(8520):1394–1395.
679. Furu T, Kaariainen H, Sankila EM, Norio R. Attitudes towards prenatal diagnosis and selective abortion among patients with retinitis pigmentosa or choroideremia as well as among their relatives. *Clin Genet*. 1993;43(3):160–165.
680. Bothe N, Hetzer R. Ophthalmic disorders and job measures of adults with late onset of visual handicap. *Klin Monatsbl Augenheilkd*. 1992;200(3):237–241.
681. Berson EL, Mehaffey L, Rabin AR. A night vision device as an aid for patients with retinitis pigmentosa. *Arch Ophthalmol*. 1973;90:112–116.
682. Morrissette DL, Marmor MF, Goodrich GL. An evaluation of night vision mobility aids. *Ophthalmology*. 1983;90:1226–1230.
683. Berson EL. Light deprivation for early retinitis pigmentosa: a hypothesis. *Arch Ophthalmol*. 1971;85(5):521–529.
684. Berson EL. Light deprivation and retinitis pigmentosa. *Vision Res*. 1980;20(12):1179–1184.
685. DelBeato P, Tanzilli P, Grenga R, Vingolo EM. It is useful to

perform cataract surgery in retinitis pigmentosa patients? *Invest Ophthalmol Vis Sci*. 1997;38(4):868.
686. Marmor MF. Visual loss in retinitis pigmentosa. *Am J Ophthalmol*. 1980;89:692–698.
687. Kogure S, IIjima H. Preoperative evaluation by laser interferometry in cataractous eyes with retinitis pigmentosa. *Jpn J Ophthalmol*. 1993;37(3):282–286.
688. Newsome DA, Stark WJ Jr, Maumenee IH. Cataract extraction and intraocular lens implantation in patients with retinitis pigmentosa or Usher's syndrome. *Arch Ophthalmol*. 1986;104(6):852–854.
689. Jackson H, Garway-Heath D, Rosen P, Bird AC, Tuft SJ. Outcome of cataract surgery in patients with retinitis pigmentosa. *Br J Ophthalmol*. 2001;85(8):936–938.
690. Hayashi K, Hayashi H, Matsuo K, Nakao F, Hayashi F. Anterior capsule contraction and intraocular lens dislocation after implant surgery in eyes with retinitis pigmentosa. *Ophthalmology*. 1998;105(7):1239–1243.
691. Lee HJ, Min SH, Kim TY. Bilateral spontaneous dislocation of intraocular lenses within the capsular bag in a retinitis pigmentosa patient. *Korean J Ophthalmol*. 2004;18(1):52–57.
692. Davison JA. Capsule contraction syndrome. *J Cataract Refract Surg*. 1993;19(5):582–589.
693. Pierrottet C, Carrara M, Orzalesi N. Cataract surgery in retinitis-pigmentosa. *Invest Ophthalmol Vis Sci*. 1995;36(4):S810.
694. Ozdemir H, Karacorlu M, Karacorlu S. Intravitreal triamcinolone acetonide for treatment of cystoid macular oedema in patients with retinitis pigmentosa. *Acta Ophthalmol Scand*. 2005;83(2):248–251.
695. Oishi A, Otani A, Sasahara M, et al. Photoreceptor integrity and visual acuity in cystoid macular oedema associated with retinitis pigmentosa. *Eye (Lond)*. 2009;23(6):1411–1416.
696. Adackapara CA, Sunness JS, Dibernardo CW, Melia BM, Dagnelie G. Prevalence of cystoid macular edema and stability in oct retinal thickness in eyes with retinitis pigmentosa during a 48-week lutein trial. *Retina*. 2008;28(1):103–110.

697. Hajali M, Fishman GA. The prevalence of cystoid macular oedema on optical coherence tomography in retinitis pigmentosa patients without cystic changes on fundus examination. *Eye (Lond)*. 2009;23(4):915–919.
698. Sandberg MA, Brockhurst RJ, Gaudio AR, Berson EL. Visual acuity is related to parafoveal retinal thickness in patients with retinitis pigmentosa and macular cysts. *Invest Ophthalmol Vis Sci*. 2008;49(10):4568–4572.
699. Grigoropoulos VG, Emfietzoglou J, Nikolaidis P, et al. Optical coherence tomography findings in patients with retinitis pigmentosa and low visual acuity. *Ophthalmic Surg Lasers Imaging*. 2010;41(1):35–39.
700. Walia S, Fishman GA, Hajali M. Prevalence of cystic macular lesions in patients with Usher II syndrome. *Eye (Lond)*. 2009;23(5):1206–1209.
701. Tsilou ET, Rubin BI, Caruso RC, et al. Usher syndrome clinical types I and II: could ocular symptoms and signs differentiate between the two types? *Acta Ophthalmol Scand*. 2002;80(2):196–201.
702. Schwartz SB, Aleman TS, Cideciyan AV, et al. Disease expression in Usher syndrome caused by VLGR1 gene mutation (USH2C) and comparison with USH2A phenotype. *Invest Ophthalmol Vis Sci*. 2005;46(2):734–743.
703. Kuchle M, Nguyen NX, Martus P, Freissler K, Schalnus R. Aqueous flare in retinitis pigmentosa. *Graefes Arch Clin Exp Ophthalmol*. 1998;236(6):426–433.
704. Vinores SA, Kuchle M, Derevjanik NL, et al. Blood–retinal barrier breakdown in retinitis pigmentosa: light and electron microscopic immunolocalization. *Histol Histopathol*. 1995;10(4):913–923.
705. Mallick KS, Zeimer RC, Fishman GA, Blair NP, Anderson RJ. Transport of fluorescein in the ocular posterior segment in retinitis pigmentosa. *Arch Ophthalmol*. 1984;102(5):691–696.
706. Fishman GA, Cunha-Vaz J, Salzano T. Vitreous fluorophotometry in patients with retinitis pigmentosa. *Arch Ophthalmol*. 1981;99(7):1202–1207.
707. Cunha-Vaz JG, Travassos A. Breakdown of the blood–

retinal barriers and cystoid macular edema. *Surv Ophthalmol*. 1984;28(Suppl.):485–492.
708. Cox SN, Hay E, Bird AC. Treatment of chronic macular edema with acetazolamide. *Arch Ophthalmol*. 1988;106(9):1190–1195.
709. Heckenlively JR, Jordan BL, Aptsiauri N. Association of antiretinal antibodies and cystoid macular edema in patients with retinitis pigmentosa. *Am J Ophthalmol*. 1999;127(5):565–573.
710. Wolfensberger TJ, Aptsiauri N, Godley B, Downes S, Bird AC. [Antiretinal antibodies associated with cystoid macular edema]. *Klin Monbl Augenheilkd*. 2000;216(5):283–285.
711. Heckenlively JR, Solish AM, Chant SM, Meyers-Elliott RH. Autoimmunity in hereditary retinal degenerations. II. Clinical studies: antiretinal antibodies and fluorescein angiogram findings. *Br J Ophthalmol*. 1985;69(10):758–764.
712. Chung H, Hwang JU, Kim JG, Yoon YH. Optical coherence tomography in the diagnosis and monitoring of cystoid macular edema in patients with retinitis pigmentosa. *Retina*. 2006;26(8):922–927.
713. Hirakawa H, Iijima H, Gohdo T, Tsukahara S. Optical coherence tomography of cystoid macular edema associated with retinitis pigmentosa. *Am J Ophthalmol*. 1999;128(2):185–191.
714. Stanga PE, Downes SM, Ahuja RM, et al. Comparison of optical coherence tomography and fluorescein angiography in assessing macular edema in retinal dystrophies: preliminary results. *Int Ophthalmol*. 2001;23(4–6):321–325.
715. Oishi A, Nakamura H, Tatsumi I, et al. Optical coherence tomographic pattern and focal electroretinogram in patients with retinitis pigmentosa. *Eye (Lond)*. 2009;23(2):299–303.
716. Sandberg MA, Brockhurst RJ, Gaudio AR, Berson EL. The association between visual acuity and central retinal thickness in retinitis pigmentosa. *Invest Ophthalmol Vis Sci*. 2005;46(9):3349–3354.
717. García-Arumí J, Martinez V, Sararols L, Corcostegui B. Vitreoretinal surgery for cystoid macular edema associated with retinitis pigmentosa. *Ophthalmology*. 2003;110(6):1164–

1169.
718. Newsome DA, Blacharski PA. Grid photocoagulation for macular edema in patients with retinitis pigmentosa. *Am J Ophthalmol*. 1987;103:161–166.
719. Saraiva VS, Sallum JM, Farah ME. Treatment of cystoid macular edema related to retinitis pigmentosa with intravitreal triamcinolone acetonide. *Ophthalmic Surg Lasers Imaging*. 2003;34(5):398–400.
720. Scorolli L, Morara M, Meduri A, et al. Treatment of cystoid macular edema in retinitis pigmentosa with intravitreal triamcinolone. *Arch Ophthalmol*. 2007;125(6):759–764.
721. Forte R, Pannarale L, Iannaccone A, Vingolo EM, Santi G, Pannarale MR. Cystoid macular edema in retinitis pigmentosa – clinical and functional evaluation of patients treated with deflazacort. *Invest Ophthalmol Vis Sci*. 1994;35(4):1958.
722. Artunay O, Yuzbasioglu E, Rasier R, Sengul A, Bahcecioglu H. Intravitreal ranibizumab in the treatment of cystoid macular edema associated with retinitis pigmentosa. *J Ocul Pharmacol Ther*. 2009;25(6):545–550.
723. Melo GB, Farah ME, Aggio FB. Intravitreal injection of bevacizumab for cystoid macular edema in retinitis pigmentosa. *Acta Ophthalmol Scand*. 2007;85(4):461–463.
724. Yuzbasioglu E, Artunay O, Rasier R, Sengul A, Bahcecioglu H. Intravitreal bevacizumab (Avastin) injection in retinitis pigmentosa. *Curr Eye Res*. 2009;34(3):231–237.
725. Fishman GA, Gilbert LD, Fiscella RG, Kimura AE, Jampol LM. Acetazolamide for treatment of chronic macular edema in retinitis pigmentosa. *Arch Ophthalmol*. 1989;107(10):1445–1452.
726. Heckenlively JR. Grid photocoagulation for macular edema in patients with retinitis pigmentosa. *Am J Ophthalmol*. 1987;104:94–95.
727. Grover S, Fishman GA, Fiscella RG, Adelman AE. Efficacy of dorzolamide hydrochloride in the management of chronic cystoid macular edema in patients with retinitis pigmentosa. *Retina*. 1997;17(3):222–231.
728. Grover S, Apushkin MA, Fishman GA. Topical dorzolamide

for the treatment of cystoid macular edema in patients with retinitis pigmentosa. *Am J Ophthalmol*. 2006;141(5):850–858.
729. Apushkin MA, Fishman GA, Grover S, Janowicz MJ. Rebound of cystoid macular edema with continued use of acetazolamide in patients with retinitis pigmentosa. *Retina*. 2007;27(8):1112–1118.
730. Genead MA, Fishman GA. Efficacy of sustained topical dorzolamide therapy for cystic macular lesions in patients with retinitis pigmentosa and Usher syndrome. *Arch Ophthalmol*. 2010;128(9):1146–1150.
731. Thobani A, Fishman GA. The use of carbonic anhydrase inhibitors in the retreatment of cystic macular lesions in retinitis pigmentosa and X-linked retinoschisis. *Retina*. 2011;31(2):312–315.
732. Fishman GA, Gilbert LD, Anderson RJ, Marmor MF, Weleber RG, Viana MAG. Effect of methazolamide on chronic macular edema in patients with retinitis pigmentosa. *Ophthalmology*. 1994;101(4):687–693.
733. Orzalesi N, Pierrottet C, Porta A, Aschero M. Long-term treatment of retinitis pigmentosa with acetazolamide: a pilot study. *Graefes Arch Clin Exp Ophthalmol*. 1993;231(5):254–256.
734. Chen JC, Fitzke FW, Bird AC. Long-term effect of acetazolamide in a patient with retinitis pigmentosa. *Invest Ophthalmol Vis Sci*. 1990;31(9):1914–1918.
735. Kim JE. Intravitreal triamcinolone acetonide for treatment of cystoid macular edema associated with retinitis pigmentosa. *Retina*. 2006;26(9):1094–1096.
736. Querques G, Prascina F, Iaculli C, Noci ND. Intravitreal pegaptanib sodium (Macugen) for refractory cystoid macular edema in pericentral retinitis pigmentosa. *Int Ophthalmol*. 2009;29(2):103–107.
737. Moustafa GA, Moschos MM. Intravitreal aflibercept (Eylea) injection for cystoid macular edema secondary to retinitis pigmentosa – a first case report and short review of the literature. *BMC Ophthalmol*. 2015;15:44.
738. Salom D, Diaz-Llopis M, Garcia-Delpech S, et al. Intravitreal ranibizumab in the treatment of cystoid macular edema

associated with retinitis pigmentosa. *J Ocul Pharmacol Ther*. 2010;26(5):531–532.
739. Foxton RH, Finkelstein A, Vijay S, et al. VEGF-A is necessary and sufficient for retinal neuroprotection in models of experimental glaucoma. *Am J Pathol*. 2013;182(4):1379–1390.
740. Storkebaum E, Lambrechts D, Carmeliet P. VEGF: once regarded as a specific angiogenic factor, now implicated in neuroprotection. *Bioessays*. 2004;26(9):943–954.
741. Gouras P, Carr RE, Gunkel RD. Retinitis pigmentosa in abetalipoproteinaemia: effects of vitamin A. *Invest Ophthalmol*. 1971;10(10):784–793.
742. Berson EL, Rosner B, Sandberg MA, et al. A randomized trial of vitamin A and vitamin E supplementation for retinitis pigmentosa. [Letter] *Arch Ophthalmol*. 1993;111(11):1465–1466.
743. Berson EL, Rosner B, Sandberg MA, et al. A randomized trial of supplemental vitamin A and vitamin E supplementation for retinitis pigmentosa. *Arch Ophthalmol*. 1993;111(6):761–772.
744. Marmor MF. Letter to the editor. *Arch Ophthalmol*. 1993;111:1460–1461.
745. Clowes D. Letter to the editor. *Arch Ophthalmol*. 1993;111:1461–1462.
746. Fielder AR, Marshall J. Letter to the editor. *Arch Ophthalmol*. 1993;111:1463.
747. Bird AC. Retinal photoreceptor dystrophies: LI. Edward Jackson Memorial Lecture. *Am J Ophthalmol*. 1995;119:543–562.
748. Massof RW, Finkelstein D. Editorial: Supplemental vitamin A retards loss of ERG amplitude in retinitis pigmentosa. *Arch Ophthalmol*. 1993;111(6):751–754.
749. Massof RW, Finkelstein D. Vitamin A supplementation for retinitis pigmentosa. [Letter] *Arch Ophthalmol*. 1993;111:1458–1459.
750. Bauernfeind JC. *The safe use of vitamin A: A report of the International vitamin A consultative group*. [Washington, DC: The Nutrition Foundation] 1980.

751. Bendich A, Langseth L. Safety of vitamin A. *Am J Clin Nutr*. 1989;49(2):358–371.
752. Evans K, Hickey-Dwyer MU. Cleft anterior segment with maternal hypervitaminosis A. *Br J Ophthalmol*. 1991;75(11):691–692.
753. Rothman KJ, Moore LL, Singer MR, Nguyen U-SDT, Mannino S, Milunsky A. Teratogenicity of high vitamin A intake. *N Engl J Med*. 1995;333(21):1369–1373.
754. Melhus H, Michaelsson K, Kindmark A, et al. Excessive dietary intake of vitamin A is associated with reduced bone mineral density and increased risk for hip fracture. *Ann Intern Med*. 1998;129(10):770–778.
755. Feskanich D, Singh V, Willett WC, Colditz GA. Vitamin A intake and hip fractures among postmenopausal women. *JAMA*. 2002;287(1):47–54.
756. Michaelsson K, Lithell H, Vessby B, Melhus H. Serum retinol levels and the risk of fracture. *N Engl J Med*. 2003;348(4):287–294.
757. Lips P. Hypervitaminosis A and fractures. *N Engl J Med*. 2003;348(4):347–349.
758. Geubel AP, De Galocsy C, Alves N, Rahier J, Dive C. Liver damage caused by therapeutic vitamin A administration: estimate of dose-related toxicity in 41 cases. *Gastroenterology*. 1991;100:1701–1709.
759. Sibulesky L, Hayes KC, Pronczuk A, Weigel-DiFranco C, Rosner B, Berson EL. Safety of <7500 RE (<25000 IU) vitamin A daily in adults with retinitis pigmentosa. *Am J Clin Nutr*. 1999;69(4):656–663.
760. Fliesler SJ, Anderson RE. Chemistry and metabolism of lipids in the vertebrate retina. *Prog Lipid Res*. 1983;22(2):79–131.
761. Gong J, Rosner B, Rees DG, Berson EL, Weigel-DiFranco CA, Schaefer EJ. Plasma docosahexaenoic acid levels in various genetic forms of retinitis pigmentosa. *Invest Ophthalmol Vis Sci*. 1992;33(9):2596–2602.
762. Schaefer EJ, Robins SJ, Patton GM, et al. Red blood cell membrane phosphatidylethanolamine fatty acid content in various forms of retinitis pigmentosa. *J Lipid Res*.

1995;36(7):1427–1433.
763. Hoffman DR, Uauy R, Birch DG. Red blood cell fatty acid levels in patients with autosomal dominant retinitis pigmentosa. *Exp Eye Res*. 1993;57(3):359–368.
764. Connor WE, Weleber RG, DeFrancesco C, Lin DS, Wolf DP. Sperm abnormalities in retinitis pigmentosa. *Invest Ophthalmol Vis Sci*. 1997;38(12):2619–2628.
765. Hoffman DR, DeMar JC, Heird WC, Birch DG, Anderson RE. Impaired synthesis of DHA in patients with X-linked retinitis pigmentosa. *J Lipid Res*. 2001;42(9):1395–1401.
766. Wheaton DH, Hoffman DR, Locke KG, Watkins RB, Birch DG. Biological safety assessment of docosahexaenoic acid supplementation in a randomized clinical trial for X-linked retinitis pigmentosa. *Arch Ophthalmol*. 2003;121(9):1269–1278.
767. Hoffman DR, Locke KG, Wheaton DH, Fish GE, Spencer R, Birch DG. A randomized, placebo-controlled clinical trial of docosahexaenoic acid supplementation for X-linked retinitis pigmentosa. *Am J Ophthalmol*. 2004;137(4):704–718.
768. Hoffman DR, Hughbanks-Wheaton DK, Pearson NS, et al. Four-year placebo-controlled trial of docosahexaenoic acid in X-linked retinitis pigmentosa (DHAX trial): a randomized clinical trial. *JAMA Ophthalmol*. 2014;132(7):866–873.
769. Berson EL, Rosner B, Sandberg MA, et al. Clinical trial of docosahexaenoic acid in patients with retinitis pigmentosa receiving vitamin A treatment. *Arch Ophthalmol*. 2004;122(9):1297–1305.
770. Berson EL, Rosner B, Sandberg MA, et al. Further evaluation of docosahexaenoic acid in patients with retinitis pigmentosa receiving vitamin A treatment: subgroup analyses. *Arch Ophthalmol*. 2004;122(9):1306–1314.
771. Thomson LR, Toyoda Y, Langner A, et al. Elevated retinal zeaxanthin and prevention of light-induced photoreceptor cell death in quail. *Invest Ophthalmol Vis Sci*. 2002;43(11):3538–3549.
772. Aleman TS, Duncan JL, Bieber ML, et al. Macular pigment and lutein supplementation in retinitis pigmentosa and

Usher syndrome. *Invest Ophthalmol Vis Sci*. 2001;42(8):1873–1881.
773. Berson EL, Rosner B, Sandberg MA, et al. Clinical trial of lutein in patients with retinitis pigmentosa receiving vitamin A. *Arch Ophthalmol*. 2010;128(4):403–411.
774. Massof RW, Fishman GA. How strong is the evidence that nutritional supplements slow the progression of retinitis pigmentosa? *Arch Ophthalmol*. 2010;128(4):493–495.
775. Kiser AK, Dagnelie G. Reported effects of non-traditional treatments and complementary and alternative medicine by retinitis pigmentosa patients. *Clin Exp Optom*. 2008;91(2):166–176.
776. Weleber RG. The Cuban experience. False hope for a cure for retinitis pigmentosa. *Arch Ophthalmol*. 1996;114(5):606–607.
777. Potok A. *Ordinary daylight: portrait of an artist going blind*. Holt, Rinehart and Winston: New York; 1980.
778. Biro I. Therapeutic experiments in cases of retinitis pigmentosa. *Br J Ophthalmol*. 1939;23(5):332–342.
779. Gordon DM. The treatment of retinitis pigmentosa with special reference to the Filatov method. *Am J Ophthalmol*. 1947;30(5):565–580.
780. Katznelson LA, Khoroshilova-Maslova IP, Eliseyeva RF. A new method of treatment of retinitis pigmentosa/pigmentary abiotrophy. *Ann Ophthalmol*. 1990;22(5):167–172.
781. Birch DG, Anderson JL, Fish GE. Longitudinal measures in children receiving ENCAD for hereditary retinal degeneration. *Adv Ophthalmol*. 1991;77(3):185–192.
782. McManus EH, Hartenstine DL, Laties AM, Berson EL. *Summary of Exchange Visit to Helmholtz Institute of Ophthalmology*. [Bethesda, MD: National Eye Institute] 1983.
783. Berson EL, Remulla JF, Rosner B, Sandberg MA, Weigel-DiFranco C. Evaluation of patients with retinitis pigmentosa receiving electric stimulation, ozonated blood, and ocular surgery in Cuba. *Arch Ophthalmol*. 1996;114(5):560–563.
784. Berger RW, Haase W, Gerding H. Original papers: ocular

motility disorders after surgery for retinitis pigmentosa "Cuba-therapy". *Strabismus*. 1995;3(1):13–20.
785. Hetland JG. [Management of retinitis pigmentosa. 8 patients treated for retinitis pigmentosa/Usher syndrome in Cuba]. *Tidsskr Nor Laegeforen*. 1994;114(13):1515–1516.
786. Bacal DA, Rousta S, Hertle RW, Maguire A. Restrictive strabismus after ocular surgery for retinitis pigmentosa in Cuba. *Arch Ophthalmol*. 1997;115:930–931.
787. Reddy NS, Fouzdar NM. Role of acupuncture in the treatment of "incurable" retinal diseases. *Indian J Ophthalmol*. 1983;31(Suppl.):1043–1046.
788. Wu XW, Tang YZ. [Study on treatment of retinitis pigmentosa with traditional Chinese medicine by Flicker electroretinogram]. *Zhongguo Zhong Xi Yi Jie He Za Zhi*. 1996;16(6):336–339.
789. Paskowitz DM, LaVail MM, Duncan JL. Light and inherited retinal degeneration. *Br J Ophthalmol*. 2006;90(8):1060–1066.
790. Cideciyan AV, Hood DC, Huang Y, et al. Disease sequence from mutant rhodopsin allele to rod and cone photoreceptor degeneration in man. *Proc Natl Acad Sci USA*. 1998;95(12):7103–7108.
791. Vaughan DK, Coulibaly SF, Darrow RM, Organisciak DT. A morphometric study of light-induced damage in transgenic rat models of retinitis pigmentosa. *Invest Ophthalmol Vis Sci*. 2003;44(2):848–855.
792. Organisciak DT, Darrow RM, Barsalou L, Kutty RK, Wiggert B. Susceptibility to retinal light damage in transgenic rats with rhodopsin mutations. *Invest Ophthalmol Vis Sci*. 2003;44(2):486–492.
793. Naash MI, Hollyfield JG, Al-Ubaidi MR, Baehr W. Simulation of human autosomal dominant retinitis pigmentosa in transgenic mice expressing a mutated murine opsine gene. *Proc Natl Acad Sci USA*. 1993;90:5499–5503.
794. Walsh N, van Driel D, Lee D, Stone J. Multiple vulnerability of photoreceptors to mesopic ambient light in the P23H transgenic rat. *Brain Res*. 2004;1013(2):194–203.
795. Bicknell IR, Darrow R, Barsalou L, Fliesler SJ, Organisciak

DT. Alterations in retinal rod outer segment fatty acids and light-damage susceptibility in P23H rats. *Mol Vis*. 2002;8:333–340.
796. Eperjesi F, Fowler CW, Evans BJ. Do tinted lenses or filters improve visual performance in low vision? A review of the literature. *Ophthalmic Physiol Opt*. 2002;22(1):68–77.
797. Naash MI, Al-Ubaidi MR, Hollyfield JG, Baehr W. Simulation of autosomal dominant retinitis pigmentosa in transgenic mice. Anderson RE, Hollyfield JG, LaVail MM. *Retinal degenerations*. Plenum Press: New York; 1993:201–210.
798. Humphries MM, Rancourt D, Farrar GJ, et al. Retinopathy induced in mice by targeted disruption of the rhodopsin gene. *Nat Genet*. 1997;15:216–219.
799. Shen J, Yang X, Dong A, et al. Oxidative damage is a potential cause of cone cell death in retinitis pigmentosa. *J Cell Physiol*. 2005;203(3):457–464.
800. Lee SY, Usui S, Zafar AB, et al. N-Acetylcysteine promotes long-term survival of cones in a model of retinitis pigmentosa. *J Cell Physiol*. 2011;226(7):1843–1849.
801. Veske A, Nilsson SE, Narfström K, Gal A. Retinal dystrophy of Swedish Briard/Briard–Beagle dogs is due to a 4-bp deletion in RPE65. *Genomics*. 1999;57(1):57–61.
802. Kijas JW, Cideciyan AV, Aleman TS, et al. Naturally occurring rhodopsin mutation in the dog causes retinal dysfunction and degeneration mimicking human dominant retinitis pigmentosa. *Proc Natl Acad Sci USA*. 2002;99(9):6328–6333.
803. Zhang Q, Acland GM, Wu WX, et al. Different RPGR exon ORF15 mutations in Canids provide insights into photoreceptor cell degeneration. *Hum Mol Genet*. 2002;11(9):993–1003.
804. Farber DB. From mice to men: the cyclic GMP phosphodiesterase gene in vision and disease. *Invest Ophthalmol Vis Sci*. 1995;36:263–275.
805. Ali RR, Reichel MB, Thrasher AJ, et al. Gene transfer into the mouse retina mediate by an adeno-associated viral vector. *Hum Mol Genet*. 1996;5:591–594.

806. Mashhour B, Couton D, Perricaudet M, Briand P. In vivo adenovirus-mediated gene transfer into ocular tissues. *Gene Ther*. 1994;1(2):122–126.
807. Li T, Adamian M, Roof DJ, et al. In-vivo transfer of a reporter gene to the retina mediated by an adenoviral vector. *Invest Ophthalmol Vis Sci*. 1994;35(5):2543–2549.
808. Hoffman LM, Maguire AM, Bennett J. Cell-mediated immune response and stability of intraocular transgene expression after adenovirus-mediated delivery. *Invest Ophthalmol Vis Sci*. 1997;38(11):2224–2233.
809. Bainbridge JW, Smith AJ, Barker SS, et al. Effect of gene therapy on visual function in Leber's congenital amaurosis. *N Engl J Med*. 2008;358(21):2231–2239.
810. Maguire AM, Simonelli F, Pierce EA, et al. Safety and efficacy of gene transfer for Leber's congenital amaurosis. *N Engl J Med*. 2008;358(21):2240–2248.
811. Cideciyan AV, Hauswirth WW, Aleman TS, et al. Human RPE65 gene therapy for Leber congenital amaurosis: persistence of early visual improvements and safety at 1 year. *Hum Gene Ther*. 2009;20(9):999–1004.
812. Simonelli F, Maguire AM, Testa F, et al. Gene therapy for Leber's congenital amaurosis is safe and effective through 1.5 years after vector administration. *Mol Ther*. 2010;18(3):643–650.
813. http://ir.sparktx.com/phoenix.zhtml?c=253900&p=irol-newsArticle&ID=2093863.
814. Haseloff J, Gerlach WL. Simple RNA enzymes with new and highly specific endoribonuclease activities. *Nature*. 1988;334(6183):585–591.
815. Lewin AS, Drenser KA, Hauswirth WW, et al. Ribozyme rescue of photoreceptor cells in a transgenic rat model of autosomal dominant retinitis pigmentosa. *Nat Med*. 1998;4(8):967–971.
816. Georgiadis A, Tschernutter M, Bainbridge JW, et al. AAV-mediated knockdown of peripherin-2 in vivo using miRNA-based hairpins. *Gene Ther*. 2010;17(4):486–493.
817. Stieger K, Lorenz B. Gene therapy for vision loss – recent developments. *Discov Med*. 2010;10(54):425–433.

818. Bok D. Retinal transplantation and gene therapy: present realities and future possibilities. *Invest Ophthalmol Vis Sci*. 1993;34(3):473–476.
819. Li LX, Turner JE. Inherited retinal dystrophy in the RCS rat: prevention of photoreceptor degeneration by pigment epithelial cell transplantation. *Exp Eye Res*. 1988;47(6):911–917.
820. Little CW, Castillo B, DiLoreto DA, et al. Transplantation of human fetal retinal pigment epithelium rescues photoreceptor cells from degeneration in the Royal College of Surgeons rat retina. *Invest Ophthalmol Vis Sci*. 1996;37(1):204–211.
821. Castillo BVJ, del Cerro M, White RM, et al. Efficacy of nonfetal human RPE for photoreceptor rescue: a study in dystrophic RCS rats. *Exp Neurol*. 1997;146(1):1–9.
822. Carr AJ, Vugler AA, Hikita ST, et al. Protective effects of human iPS-derived retinal pigment epithelium cell transplantation in the retinal dystrophic rat. *PLoS ONE*. 2009;4(12):e8152.
823. Algvere PV, Berglin L, Gouras P, Sheng Y. Transplantation of fetal retinal pigment epithelium in age-related macular degeneration with subfoveal neovascularization. *Graefes Arch Clin Exp Ophthalmol*. 1994;232(12):707–716.
824. Du H, Lim SL, Grob S, Zhang K. Induced pluripotent stem cell therapies for geographic atrophy of age-related macular degeneration. *Semin Ophthalmol*. 2011;26(3):216–224.
825. Lu B, Malcuit C, Wang S, et al. Long-term safety and function of RPE from human embryonic stem cells in preclinical models of macular degeneration. *Stem Cells*. 2009;27(9):2126–2135.
826. Wang NK, Tosi J, Kasanuki JM, et al. Transplantation of reprogrammed embryonic stem cells improves visual function in a mouse model for retinitis pigmentosa. *Transplantation*. 2010;89(8):911–919.
827. Lund RD, Wang S, Klimanskaya I, et al. Human embryonic stem cell-derived cells rescue visual function in dystrophic RCS rats. *Cloning Stem Cells*. 2006;8(3):189–199.
828. Kicic A, Shen WY, Wilson AS, Constable IJ, Robertson T,

Rakoczy PE. Differentiation of marrow stromal cells into photoreceptors in the rat eye. *J Neurosci*. 2003;23(21):7742–7749.
829. Pressmar S, Ader M, Richard G, Schachner M, Bartsch U. The fate of heterotopically grafted neural precursor cells in the normal and dystrophic adult mouse retina. *Invest Ophthalmol Vis Sci*. 2001;42(13):3311–3319.
830. Fischer AJ, Reh TA. Potential of Müller glia to become neurogenic retinal progenitor cells. *Glia*. 2003;43(1):70–76.
831. Fischer AJ, Bongini R. Turning Müller glia into neural progenitors in the retina. *Mol Neurobiol*. 2010;42(3):199–209.
832. Tropepe V, Coles BL, Chiasson BJ, et al. Retinal stem cells in the adult mammalian eye. *Science*. 2000;287(5460):2032–2036.
833. Coles BL, Angenieux B, Inoue T, et al. Facile isolation and the characterization of human retinal stem cells. *Proc Natl Acad Sci USA*. 2004;101(44):15772–15777.
834. Cicero SA, Johnson D, Reyntjens S, et al. Cells previously identified as retinal stem cells are pigmented ciliary epithelial cells. *Proc Natl Acad Sci USA*. 2009;106(16):6685–6690.
835. Reh TA, Lamba D, Gust J. Directing human embryonic stem cells to a retinal fate. *Methods Mol Biol*. 2010;636:139–153.
836. Lamba DA, Gust J, Reh TA. Transplantation of human embryonic stem cell-derived photoreceptors restores some visual function in Crx-deficient mice. *Cell Stem Cell*. 2009;4(1):73–79.
837. Eiraku M, Takata N, Ishibashi H, et al. Self-organizing optic-cup morphogenesis in three-dimensional culture. *Nature*. 2011;472(7341):51–56.
838. Nakano T, Ando S, Takata N, et al. Self-formation of optic cups and storable stratified neural retina from human ESCs. *Cell Stem Cell*. 2012;10(6):771–785.
839. Gonzalez-Cordero A, West EL, Pearson RA, et al. Photoreceptor precursors derived from three-dimensional embryonic stem cell cultures integrate and mature within adult degenerate retina. *Nat Biotechnol*. 2013;31(8):741–747.
840. Schwartz SD, Regillo CD, Lam BL, et al. Human embryonic

stem cell-derived retinal pigment epithelium in patients with age-related macular degeneration and Stargardt's macular dystrophy: follow-up of two open-label phase 1/2 studies. *Lancet*. 2015;385(9967):509–516.
841. Takahashi K, Yamanaka S. Induction of pluripotent stem cells from mouse embryonic and adult fibroblast cultures by defined factors. *Cell*. 2006;126(4):663–676.
842. Lamba DA, McUsic A, Hirata RK, Wang PR, Russell D, Reh TA. Generation, purification and transplantation of photoreceptors derived from human induced pluripotent stem cells. *PLoS ONE*. 2010;5(1):e8763.
843. Hirami Y, Osakada F, Takahashi K, et al. Generation of retinal cells from mouse and human induced pluripotent stem cells. *Neurosci Lett*. 2009;458(3):126–131.
844. Zhou L, Wang W, Liu Y, et al. Differentiation of induced pluripotent stem cells of Swine into rod photoreceptors and their integration into the retina. *Stem Cells*. 2011;29(6):972–980.
845. Tucker BA, Mullins RF, Streb LM, et al. Patient-specific iPSC-derived photoreceptor precursor cells as a means to investigate retinitis pigmentosa. *Elife*. 2013;2:e00824.
846. Joe AW, Gregory-Evans K. Mesenchymal stem cells and potential applications in treating ocular disease. *Curr Eye Res*. 2010;35(11):941–952.
847. Lu B, Wang S, Girman S, McGill T, Ragaglia V, Lund R. Human adult bone marrow-derived somatic cells rescue vision in a rodent model of retinal degeneration. *Exp Eye Res*. 2010;91(3):449–455.
848. Wang S, Lu B, Girman S, et al. Non-invasive stem cell therapy in a rat model for retinal degeneration and vascular pathology. *PLoS ONE*. 2010;5(2):e9200.
849. Gregory-Evans K, Chang F, Hodges MD, Gregory-Evans CY. Ex vivo gene therapy using intravitreal injection of GDNF-secreting mouse embryonic stem cells in a rat model of retinal degeneration. *Mol Vis*. 2009;15:962–973.
850. Chang GQ, Hao Y, Wong F. Apoptosis: final common pathway of photoreceptor death in rd, rds, and rhodopsin mutant mice. *Neuron*. 1993;11(4):595–605.

851. Tso MO, Zhang C, Abler AS, et al. Apoptosis leads to photoreceptor degeneration in inherited retinal dystrophy of RCS rats. *Invest Ophthalmol Vis Sci*. 1994;35(6):2693–2699.
852. Portera-Cailliau C, Sung C-H, Nathans J, Adler R. Apoptotic photoreceptor cell death in mouse models of retinitis pigmentosa. *Proc Natl Acad Sci USA*. 1994;91(3):974–978.
853. Cottet S, Schorderet DF. Mechanisms of apoptosis in retinitis pigmentosa. *Curr Mol Med*. 2009;9(3):375–383.
854. Nir I, Kedzierski W, Chen J, Travis GH. Expression of Bcl-2 protects against photoreceptor degeneration in retinal degeneration slow (rds) mice. *J Neurosci*. 2000;20(6):2150–2154.
855. Eversole-Cire P, Concepcion FA, Simon MI, Takayama S, Reed JC, Chen J. Synergistic effect of Bcl-2 and BAG-1 on the prevention of photoreceptor cell death. *Invest Ophthalmol Vis Sci*. 2000;41(7):1953–1961.
856. Hahn P, Lindsten T, Lyubarsky A, et al. Deficiency of Bax and Bak protects photoreceptors from light damage in vivo. *Cell Death Differ*. 2004;11(11):1192–1197.
857. Joseph RM, Li T. Overexpression of Bcl-2 or Bcl-XL transgenes and photoreceptor degeneration. *Invest Ophthalmol Vis Sci*. 1996;37(12):2434–2446.
858. Quiambao AB, Tan E, Chang S, et al. Transgenic Bcl-2 expressed in photoreceptor cells confers both death-sparing and death-inducing effects. *Exp Eye Res*. 2001;73(5):711–721.
859. Frasson M, Sahel JA, Fabre M, Simonutti M, Dreyfus H, Picaud S. Retinitis pigmentosa: rod photoreceptor rescue by a calcium-channel blocker in the rd mouse. *Nat Med*. 1999;5(10):1183–1187.
860. Frasson M, Sahel JA, Fabre M, Simonutti M, Dreyfus H, Picaud S. Retinitis pigmentosa: rod photoreceptor rescue by a calcium-channel blocker in the rd mouse. *Nat Med*. 1999;5(10):1183–1187.
861. Sanges D, Comitato A, Tammaro R, Marigo V. Apoptosis in retinal degeneration involves cross-talk between apoptosis-inducing factor (AIF) and caspase-12 and is blocked by calpain inhibitors. *Proc Natl Acad Sci USA*. 2006;103(46):17366–17371.

862. Vallazza-Deschamps G, Cia D, Gong J, et al. Excessive activation of cyclic nucleotide-gated channels contributes to neuronal degeneration of photoreceptors. *Eur J Neurosci*. 2005;22(5):1013–1022.
863. Pawlyk BS, Li T, Scimeca MS, Sandberg MA, Berson EL. Absence of photoreceptor rescue with D-cis-diltiazem in the rd mouse. *Invest Ophthalmol Vis Sci*. 2002;43(6):1912–1915.
864. Nakazawa M. Effects of calcium ion, calpains, and calcium channel blockers on retinitis pigmentosa. *J Ophthalmol*. 2011;2011:292040.
865. Liu C, Li Y, Peng M, Laties AM, Wen R. Activation of caspase-3 in the retina of transgenic rats with the rhodopsin mutation s334ter during photoreceptor degeneration. *J Neurosci*. 1999;19(12):4778–4785.
866. Bode C, Wolfrum U. Caspase-3 inhibitor reduces apoptotic photoreceptor cell death during inherited retinal degeneration in tubby mice. *Mol Vis*. 2003;9:144–150.
867. Samardzija M, Wenzel A, Thiersch M, Frigg R, Reme C, Grimm C. Caspase-1 ablation protects photoreceptors in a model of autosomal dominant retinitis pigmentosa. *Invest Ophthalmol Vis Sci*. 2006;47(12):5181–5190.
868. Doonan F, Donovan M, Cotter TG. Caspase-independent photoreceptor apoptosis in mouse models of retinal degeneration. *J Neurosci*. 2003;23(13):5723–5731.
869. Faktorovich EG, Steinberg RH, Yasumura D, Matthes MT, LaVail MM. Photoreceptor degeneration in inherited retinal dystrophy delayed by basic fibroblast growth factor. *Nature*. 1990;347(6288):83–86.
870. Sakai T, Kuno N, Takamatsu F, et al. Prolonged protective effect of basic fibroblast growth factor-impregnated nanoparticles in royal college of surgeons rats. *Invest Ophthalmol Vis Sci*. 2007;48(7):3381–3387.
871. Gauthier R, Joly S, Pernet V, Lachapelle P, Di Polo A. Brain-derived neurotrophic factor gene delivery to Müller glia preserves structure and function of light-damaged photoreceptors. *Invest Ophthalmol Vis Sci*. 2005;46(9):3383–3392.
872. Li Y, Tao W, Luo L, et al. CNTF induces regeneration of

cone outer segments in a rat model of retinal degeneration. *PLoS ONE*. 2010;5(3):e9495.
873. Sieving PA, Caruso RC, Tao W, et al. Ciliary neurotrophic factor (CNTF) for human retinal degeneration: phase I trial of CNTF delivered by encapsulated cell intraocular implants. *Proc Natl Acad Sci USA*. 2006;103(10):3896–3901.
874. McGee Sanftner LH, Abel H, Hauswirth WW, Flannery JG. Glial cell line derived neurotrophic factor delays photoreceptor degeneration in a transgenic rat model of retinitis pigmentosa. *Mol Ther*. 2001;4(6):622–629.
875. Wen R, Song Y, Kjellstrom S, et al. Regulation of rod phototransduction machinery by ciliary neurotrophic factor. *J Neurosci*. 2006;26(52):13523–13530.
876. Birch DG, Weleber RG, Duncan JL, Jaffe GJ, Tao W, Ciliary Neurotrophic Factor Retinitis Pigmentosa Study Groups. Randomized trial of ciliary neurotrophic factor delivered by encapsulated cell intraocular implants for retinitis pigmentosa. *Am J Ophthalmol*. 2013;156(2):283–292.
877. Foerster O. Beitriige zur Pathophysiologie der Sehbahn und der Sehsphare. *J Psychol Neuro Lpz*. 1929;39:463–485.
878. Potts AM, Inoue J. The electrically evoked response (EER) of the visual system. II. Effect of adaptation and retinitis pigmentosa. *Invest Ophthalmol*. 1969;8(6):605–612.

43

Hereditary Vitreoretinal Degenerations

Shibo Tang, Xiaoyan Ding, Yan Luo

Hereditary vitreoretinal degeneration, also known as hereditary vitreoretinopathy, is classically characterized by early-onset cataracts, vitreous anomalies, coarse fibrils and membranes, and retinal detachment. Genetic and clinical advances in the last two decades have enabled a reassessment of the essential criteria that define this group of conditions. More recently, these conditions have been defined as the presence of congenital abnormalities of the vitreous, including severe degeneration or maldevelopment, early-

onset progressive cataracts, and an increased predisposition to rhegmatogenous retinal detachment.[1] Additional ocular and systemic features may be present, depending on the underlying cause.

Since many vitreoretinal degenerations are autosomal dominant, high variability in severity and expression is common both within and between families, so examination of more than one family member is often necessary to reach the correct diagnosis. Molecular genetic studies have demonstrated a correlation between the clinical features of the disease and the underlying gene mutation. Thus, the clinician is able to predict which gene is involved within a family and provide appropriate counseling and management. Failure to recognize a syndromic cause of a childhood retinal detachment can lead to vision loss not only in the patient, but also in other siblings, that could have been avoided.

In this chapter, we discuss five main types of vitreoretinopathies: (1) snowflake vitreoretinal degeneration; (2) chondrodysplasias with vitreoretinal degeneration (e.g., Stickler syndrome); (3) X-linked juvenile retinoschisis; (4) the chromosome 5q vitreoretinopathies (e.g., Wagner syndrome); and (5) retinal nuclear receptor (NR2E3)-related diseases (enhanced S-cone syndrome and Goldmann–Favre vitreotapetoretinal degeneration). Several additional vitreoretinal degenerations are also reviewed, including autosomal dominant neovascular inflammatory vitreoretinopathy (ADNIV) and autosomal dominant vitreoretinochoroidopathy (ADVIRC). We identify the common features of vitreoretinal degenerations and highlight those features that can be used to distinguish them from each other clinically. Lattice degeneration and familial exudative vitreoretinopathy are not discussed in this chapter. Table 43.1 summarizes the main features of these disorders. Note that a given patient need not have all of the listed features. The pattern of clinical findings, rather than a specific feature, is the best strategy to make the diagnosis.

TABLE 43.1

Features of Hereditary Vitreoretinal Degenerations

	Snowflake	X-Linked	Wagner	Stickler	Enhance Syndron

	Vitreoretinal Degeneration	X-Linked Retinoschisis	Wagner Syndrome	Stickler Syndrome	Favre Vitreotap Degener
Abbreviation	SVD	XLRS	WGN1	STL1/STL2	ESCS/GF
Inheritance	Autosomal dominant	X-linked recessive	Autosomal dominant	Autosomal dominant or recessive	Autosom
Genetic loci	2q36	Xp22.1	5q13–14	12q13.11,1p21, 6q12-q14,1p33-p32, 20q13.3	15q23
Genes	*KCNJ13*	*RS1*	*CSPG2*	*COL2A1*, *COL11A1*, *COL9A1*, *COL9A2*, *COL9A3*	*NR2E3*
Prevalence	Less than 1 : 10,000	1 : 15, 000–1 : 30, 000	Less than 1 : 1,000,000	1 : 10,000	Less thar
Refraction/motility	Myopic	Axial hyperopia, strabismus	Moderate myopic Pseudostrabismus with positive-angle κ	High myopic Astigmatism	Variable Myopic
Visual acuity	Not usually affected	Vision loss: average visual acuity in young adults is around 20/70	Deteriorates slowly after age of 20 years due to posterior chorioretinal atrophy	Usually good unless affected by retinal detachment or foveal atrophy	Poor cen peripher
Anterior segment	Corneal guttae Presenile cataract	Neovascular glaucoma	Anterior chamber dependent, typical dot-like cortical cataracts, glaucoma	Presenile cataracts with characteristic curved cortical distribution, lentis ectopia	Usually r
Vitreous	Fibrillar vitreous degeneration	Vitreous hemorrhage	Vitreous syneresis, posterior strands and veils in the vitreous cavity	Vitreous syneresis and band formation, membranous vitreous veils in type I, fibrillar vitreous in type II	Usually r be degen
Optic nerve	Dysmorphic optic nerve head, flat appearance, absent cup, waxy pallor	Optic atrophy	Optic atrophy, optic nerve dysmorphism	Usually normal	Usually r
Macula	Usually normal	Foveal schisis, foveal ectopia	Foveal ectopia	Usually normal	Cystoid c of norma lamellae
Retinal vessels	Parapapillary	Lie in either	Abnormal retinal	Sclerosing of	Pigment

Retinal vessels	Parapapillary sheathing, radial perivascular degeneration	Lie in either the outer or inner leaf or cross through the schisis cavity	Abnormal retinal vessel architecture (inverted papilla), perivascular pigmentation, and sheathing	Sclerosing of retinal vessels	Pigmenta degenera arcades
Retinal detachment	20%	5–20%	Infrequent	50–60%	Uncomm
Periphery	Minute inner retinal crystals, focal RPE degeneration, vitreous condensations	Peripheral retinoschisis	Chorioretinal atrophy	Peripheral chorioretinal degeneration	Peripher degenera clumped be prese
Systemic features	None	None	None	Cleft palate Hearing loss Arthritis Midface hypoplasia Epiphyseal dysplasia Osteoarthritis	None
ERG	Reduced in late stages	Selective b-wave reduction	Reduced in late stages, the amplitudes of the b-waves are generally better preserved than those of the a-waves	Usually normal	Enhance Phenoty undetect

ERG, electroretinogram; RPE, retinal pigment epithelium.

Snowflake Vitreoretinal Degeneration

General Features

The term "snowflake vitreoretinal degeneration" (SVD) was originally coined by Hirose et al.[2] in 1974, who described an American family of European extraction with early-onset cataracts, fibrillar vitreous degeneration, vascular sheathing, peripheral minute crystalline-like deposits, and retinal detachment. The condition received its name from the minute crystalline-like deposits that can be seen by contact lens biomicroscopy in some patients.[2] The vitreous degeneration is fibrillar to a variable extent; the bands of condensed vitreous fibrils may obscure fundus details, and peripheral condensations of vitreous on the retinal surface can be observed. Radial or circumferential lattice degeneration,

however, is not seen. The average spherical equivalent is −2.90 D, indicating moderate myopia. Other distinguishing features include a dysmorphic optic nerve head that appears flat and often without a cup. Peripapillary vascular sheathing and atrophy, as well as waxy pallor, may be present.

Clinical Findings

Ocular Features

There were 31 individuals in the Hirose family enrolled in the original study in 1974 (13 affected individuals, 14 unaffected individuals, and 4 unaffected spouses). The 13 subjects diagnosed with SVD ranged from 12 to 85 years of age, with clinical features such as early-onset cataract, fibrillar vitreous degeneration, vascular sheathing, and retinal detachment.[2] The inheritance pattern was autosomal dominant, and no obligatory carriers of the snowflake trait were found to be normal. After about 20 years, Lee et al.[3] restudied 6 of these 13 patients and identified additional clinical features, including corneal guttata (4 out of 5 patients) and optic nerve head dysplasia (the exact number of affected individuals was not recorded). Early-onset cataracts (5 out of 6), fibrillar vitreous degeneration (6 out of 6), and peripheral retinal abnormalities (5 out of 6), including minute crystalline-like deposits called snowflakes (4 out of 6), were common. Compared to other hereditary vitreoretinal degenerations, there was a relatively low rate of retinal detachment, occurring in 1 of the 6 examined family members.[3] Orofacial features, early-onset hearing loss, and arthritis that are typical of Stickler syndrome were absent. Thus, the clinical findings were not typical of Stickler syndrome or chromosome 5q retinopathies, suggesting that SVD may be a distinct form of vitreoretinal degeneration.

According to the dominant features present on fundoscopic examination, SVD has been classified into four stages: (1) extensive white with pressure; (2) snowflake degeneration; (3) sheathing of retinal vessels and fundus pigmentation; and (4) further pigmentation and disappearance of the peripheral retinal vessels. Hejtmancik et al. classified the clinical features of SVD into subgroups of congenital and progressive abnormalities.[4] The

congenital abnormalities include optic nerve head dysmorphism with fibrillar degeneration of the vitreous. Progressive ocular features include corneal guttae, and peripheral retinal degeneration within which minute crystalline deposits, referred to as snowflakes, might be observed. These characteristics distinguish SVD from other vitreoretinal degenerations.

Using Hejtmancik's genetic studies, it is evident that although the term “snowflake” has been used in reports of other families, they do not appear to be the same condition according to the clinical criteria and/or genetic evaluation. Moreover, the proportion of patients diagnosed with nonsyndromic Stickler syndrome that ultimately share a common genetic basis with SVD patients is currently unknown, thus the real prevalence of SVD to date is difficult to estimate. So far, there is only one family reported in the literature with a case history similar to the classic description of SVD. This family was reported by Pollack and colleagues[5,6] and showed an autosomal dominant vitreoretinal degeneration with minute crystalline-like dots, probably similar to the Hirose family. A distinguishing feature of this family, however was the appearance of neovascular tufts in the temporal periphery in 4 of the 9 affected members of the middle generation of the pedigree.[6] Two other reports have described subjects with SVD. Robertson et al.[7] reported familial clustering of granular deposits 100–200 μm in diameter in 10 patients from four families, which was described as snowflake degeneration of the retina in 1982. The deposits were evenly distributed about the circumference of the eye near the equatorial fundus. Smaller crystalline deposits were observed between the granular deposits. However, findings of vitreoretinal degeneration, such as early-onset cataract, severe vitreous degeneration, and retinal detachment, were not observed. The granular deposits are also not similar to those in patients with COL2A1 mutations causing Stickler syndrome.[2,3] Chen and colleagues[8] reported a family with vitreoretinal degeneration in 1986, but they were distinguished from the Hirose family by nyctalopia, poor visual acuity, annular scotomas, and attenuated retinal vessels. They may also have shown different-appearing deposits compared to the classical SVD description.[2] Unfortunately, these two families have not been subject to genetic analysis.

Molecular Genetics of SVD

Jiao et al.[9] reexamined the original family and localized the mutation to chromosome 2q36. Molecular genetic investigation excluded the known locations of genes causing vitreoretinal degeneration,[3] and a novel gene location was subsequently identified. One of the authors (XD) studied the location of Kir7.1 (the protein product of *KCNJ13*) in the retina, and found that it is bound to the inner limiting membrane and the retinal pigment epithelium, which suggests that the mutation could affect development of the vitreous through alteration of Müller cell function.[4] The mutation in *KCNJ13* (MIM #603208) demonstrates that classic vitreoretinal degeneration can arise from gene mutations that are not structural components of the vitreous. Alteration in potassium transport provides a mechanism for the electrophysiologic abnormalities seen in these patients, but further study is required for a precise explanation. The condition is thought to arise from a mutation in *KCNJ13*, disrupting the selective transport of potassium through the channel.[4] Recently, Pattnaik et al, extended the observation that Kir7.1 mutations are associated with not only SVD, but also Leber congenital amaurosis(LCA).[10,11] Thus, SVD can be clinically and genetically confirmed as a unique form of vitreoretinal degeneration.

Visual Psychophysics

Kinetic perimetry shows peripheral defects, which are more pronounced in the superior field.[12] Flicker perimetry reveals abnormalities undetected by kinetic perimetry, and dark adaptation tests show elevated rod thresholds, except during the early stage of the disease.

Electrophysiology

The scotopic b-wave of the electroretinogram (ERG) elicited by dim light is low in amplitude and may be almost extinguished in late stages of the disease. The photopic b-wave and the photopic flicker responses may show decreased amplitudes in some patients. The electro-oculographic light peak–dark trough ratio is abnormal in only a few patients.

Differential Diagnosis

Gene identification in SVD-like families is the gold standard in the diagnosis of SVD. Clinical diagnosis of SVD is difficult, as the clinical manifestation overlaps with other types of vitreoretinal degeneration. The key distinguishing features are fibrillar degeneration of the vitreous, optic nerve dysmorphism, peripheral areas of retinal pigment epithelial degeneration, corneal guttae, and retinal crystalline-like spots. It is unknown if the discrete crystalline-like spots characteristic of the Hirose family are specific indicators of the underlying gene, or a rare manifestation of vitreoretinal degeneration unique to a few families. Severe fibrillar degeneration of the vitreous also can be seen in type II Stickler syndrome (*COL11A1*). Corneal guttae may also be a diagnostic feature of SVD in some pedigrees. Abnormal optic nerve heads and posterior sheathing of the retinal vessels are also suggestive. The optic disc is always flat and without a cup, and nasal deviation of the vessels, waxy pallor, and peripapillary atrophy may also be present.

Stickler Syndrome Type I

This is the most common form of vitreoretinal degeneration. Mutations leading to haploinsufficiency of the collagen 2A1 (*COL2A1*) gene cause Stickler syndrome type I (*STL1*, MIM#108300). These patients have a vitreous degeneration characterized by a unique vitreous appearance with vestigial vitreous gel occupying the immediate retrolental space and no discernible gel in the central vitreous cavity. The expression of syndromic features, including hearing loss, facial dysmorphism, and joint pain, exhibits variability both between and within families.[13]

Stickler Syndrome Type II

Mutations leading to haploinsufficiency of the collagen 11A1 (*COL11A1*) gene cause Stickler syndrome type II (*STL2*, MIM#604841). Unlike *COL2A1* disease, these mutations lead to a fibrillar vitreous degeneration with limited and random fibrils throughout the vitreous cavity.[14–16] In some cases, severe fibrillar degeneration of the vitreous can also be seen.

Marshall Syndrome

Mutations altering intron–exon splicing of the *COL11A1* gene lead to Marshall syndrome (MIM#154780), distinguished from SVD and Stickler syndrome by a more pronounced facial dysmorphism and lower frequency of retinal detachment.[17,18] Membranous vitreous veils and radial lattice have also been noted in patients with Marshall syndrome.[19]

Wagner Syndrome

Wagner syndrome (MIM#143200) is caused by noncoding mutations that are thought to affect the splicing of chondroitin sulfate proteoglycan-2 (CSPG2), the gene encoding versican.[20,21] These mutations may lead to disease through abnormal ratios of versican isoforms. The distinguishing features of Wagner syndrome are pseudostrabismus, thickened and a partially detached posterior hyaloid with an empty vitreous cavity, variable degeneration of the retina and choroid, and the absence of systemic manifestations.[22] The absence of nyctalopia, posterior chorioretinal atrophy, and traction retinal detachment distinguishes Wagner syndrome from other chromosome 5q vitreoretinopathies such as Jansen syndrome and erosive vitreoretinopathy.

Goldmann–Favre Vitreotapetoretinal Degeneration

Patients with Goldmann–Favre vitreotapetoretinal degeneration have nonrecordable ERGs and central and/or peripheral retinoschisis. This is in contrast to patients with snowflake degeneration, who have fairly good ERG responses and absence of central or peripheral retinoschisis.[23]

Management

At this time, no specific management is available, and there are no established guidelines for prophylactic therapy. As the risk of retinal detachment is 20% and cataract surgery of early-onset lens opacification can be difficult due to vitreous liquefaction, family members should be examined to determine if they manifest the condition. Affected patients should be educated about cataract and

retinal detachment and examined regularly. Children should be given special attention because of cataract-induced refractive problems and their frequent failure to recognize and/or report retinal detachment symptoms.

Common issues in the management of hereditary vitreoretinal degenerations are described below:

1. Cataract surgery is difficult in these patients due to lack of vitreous support during surgery, and should be performed by experienced surgeons with specific experience with vitrectomized eyes that behave similarly. Microinvasive 23- or 25-gauge infusion cannulae via the pars plana are beneficial for maintaining the intraocular pressure.

2. Glaucoma can occur, usually after cataract surgery, and should be monitored and treated using established methods.

3. Prophylactic cryopexy is performed by some groups, while peripheral laser retinopexy is favored by others. Although a randomized trial has yet to be published comparing the two methods, a recent report using cryopexy is the most comprehensive study to date.[24] Ang et al. found that, in patients with type I Stickler syndrome, the prevalence of retinal detachment was significantly less in bilateral 360° prophylactic cryotherapy than that in untreated patients, suggesting that prophylactic cryotherapy may be substantially beneficial.[24]

4. Retinal detachments are also common and should be managed using standard vitrectomy-based approaches, including vitrectomy, artificial posterior vitreous detachment, and release of peripheral traction, perfluorocarbon-mediated retinal reattachment, scleral buckle, laser retinopexy, and tamponade with gas or silicone oil.

The Chromosome 5q Retinopathies

Overview

The chromosome 5q retinopathies include **Wagner syndrome**, **erosive vitreoretinopathy (ERVR)**, and **Jansen syndrome**. Jansen

syndrome and ERVR share clinical and allelic features with Wagner syndrome. Knowledge of the chromosome 5q retinopathies has expanded greatly over the past few years, along with the identification of the responsible genes for the allelic syndromes. It is not possible to easily identify a pathologic mutation for the above syndromes due to the difficulties in determining splicing defects in large complex genes. Even so, recent genetic and clinical advances enable a reassessment of the essential criteria that define this group of diseases.

Wagner syndrome is characterized by an optically empty vitreous with avascular vitreous strands and veils, moderate myopia, presenile cataracts, and retinal degeneration with atrophy.[25] Stickler syndrome, in contrast, is also associated with craniofacial abnormalities and a progressive arthropathy.[26] Wagner syndrome and Stickler syndrome were once incorrectly considered as one entity: the Wagner–Stickler syndrome.

Wagner syndrome is an autosomal dominant genetic disorder first mapped to chromosome 5q13–14 in 1995. A mutation in the chondroitin sulfate proteoglycan 2 gene (*CSPG2*), now named *VCAN*, encoding for the versican protein, was found in 2005 and subsequently verified in additional families.[22,27–30] *VCAN* is the only gene currently associated with Wagner syndrome and ERVR.[21,31] Autosomal dominant Stickler syndrome is an inherited progressive disorder of the collagen connective tissues and is associated with the mutation of extracellular matrix collagen genes, such as *COL2A1*, *COL11A*, *COL11A2*, and *COL9A1*.[26,32–34]

Jansen syndrome was described as vitreoretinal and lenticular degeneration associated with retinal detachments in the absence of nonocular findings. However, the disease gene for the original Jansen family was demonstrated to be linked to the same region of chromosome 5q14,[35] where genes for Wagner syndrome and ERVR were located.[27]

ERVR also displays an autosomal dominant inheritance pattern and shares some clinical features with Wagner syndrome. The critical region of the genetic defect underlying ERVR was found to overlap with the critical region for Wagner syndrome, 5q13–q14.[21]

Clinical Findings

Ocular Features

Wagner syndrome is characterized by an optically empty vitreous with equatorial avascular vitreous veils. Additional features include its early-onset, moderate myopia, as well as typical dot-like cortical cataracts, foveal ectopia, abnormal retinal vessels (inverted papilla), perivascular pigmentation and sheathing, retinal thinning, and slowly progressive chorioretinal atrophy. Patients with Wagner syndrome have pseudostrabismus from congenital temporal displacement of the fovea. They also have nyctalopia early in life, and final dark adaptation thresholds are elevated in some patients.[36] Most patients under the age of 20 have normal vision; however, cataract, retinal detachment, optic atrophy, and chorioretinal atrophy may be progressive and cause visual loss with advancing age[23,25,27,28,31] (Fig. 43.1). A recent study showed that most retinal layers were significantly thinner in patients with Wagner syndrome compared to normal controls. Moreover, a thick multilayered membrane adherent to the perifovea but completely detached from the fovea, thus forming a bridge over the foveal pit, was observed in 84% of eyes from patients with Wagner syndrome.[37] In addition to the clinical features of Wagner syndrome, ERVR reveals progressive nyctalopia and visual field constriction. A conspicuous loss of retinal pigment epithelium and choriocapillaries is observed by fluorescein angiography.[21] The vitreous findings are marked syneresis with prominent membranes. Rhegmatogenous retinal detachment is usually described as a feature of ERVR and is less frequent in the original description of Wagner syndrome.[38]

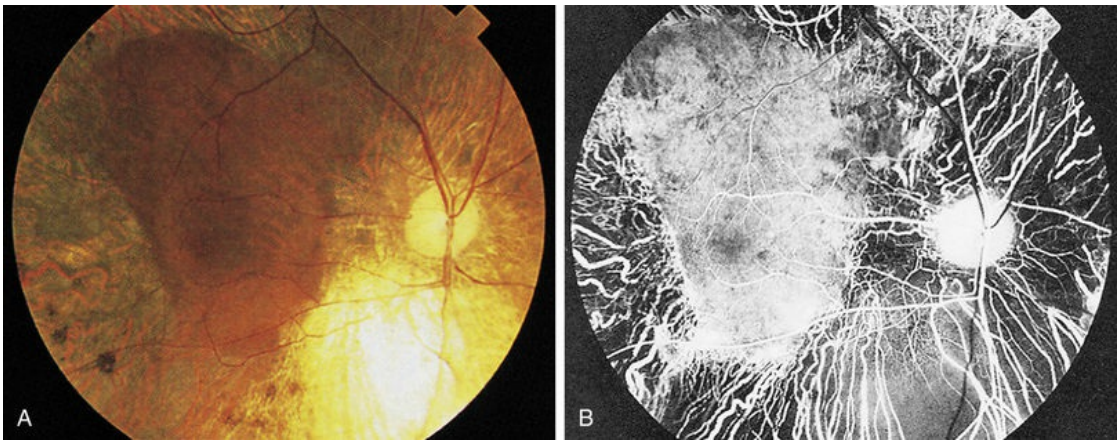

FIG. 43.1 Wagner vitreoretinal degeneration. (A) Marked chorioretinal atrophy with pigment migration into the retina and sparing of the macular area. Visual acuity was 20/25. (B) Fluorescein angiogram of the same eye showing early venous phase. There is extensive atrophy of choriocapillaris, sparing only the macular area. (Reproduced with permission from Graemiger RA, Niemeyer G, Schneeberger SA, et al. Wagner vitreoretinal degeneration. Follow-up of the original pedigree. Ophthalmology 1995;102:1830–1839. Copyright © 1995 American Academy of Ophthalmology.)

Visual Psychophysics

Nyctalopia can be present early in life in some patients. Vision is usually normal as the pathologic process initially involves the retinal periphery, but severe loss of vision will occur in patients when diffuse cone–rod loss ensues as there is progressive chorioretinal atrophy.[1,27]

Electrophysiology

Both the ERG and dark adaptation of patients with the chromosome 5q retinopathies appear to be normal early in life but become progressively abnormal throughout the patient's life. The rod and cone systems are affected to varying degrees but in a family-specific manner. While both a-wave and b-wave amplitudes are reduced, b-wave amplitudes are generally better preserved. Visual field findings can be variable and may include diffuse peripheral loss or partial/complete midperipheral ring scotomas as the chorioretinal atrophy progresses.[39]

Differential Diagnosis

Ophthalmologic examination, an autosomal dominant inheritance pattern of family history, visual field examination, ERG, and orthoptic assessment are critical for definitive diagnosis and timely management. The differential diagnosis includes both autosomal dominant and recessive vitreoretinopathies.

Autosomal Dominant Vitreoretinopathies

Snowflake Vitreoretinal Degeneration.

SVD is a progressive hereditary eye disorder caused by mutations in *KCNJ13*. Diagnostic features of SVD consist of fibrillar vitreous degeneration, early-onset cataract, minute crystalline deposits in the neurosensory retina, and retinal detachment.[4] However, membranous degeneration of the vitreous with avascular strands and veils is not observed in SVD. Retinal defects typically start in the superficial retinal layers and retinal detachment is uncommon.[4,31]

Stickler Syndrome.

Stickler syndrome is genetically distinguished from Wagner syndrome and other chromosome 5q retinopathies. Type I Stickler syndrome is due to *COL2A1* mutation and is associated with retrolental membranous vitreous, while type II Stickler syndrome is due to mutations in *COL11A1* and is associated with a fibrillar or beaded vitreous phenotype. Both type I and II Stickler syndrome have ocular and systemic manifestations, while type III Stickler syndrome, associated with *COL11A2* mutations, has systemic manifestations only. Most, but not all, patients with Stickler syndrome have congenital, nonprogressive, and high-degree myopia. The cataracts may be congenital and nonprogressive, and have an unusual characteristic curved cortical distribution.[40] Retinal detachment is much more common in Stickler syndrome (50%) than in chromosome 5q vitreoretinopathies (15%). Systemic abnormalities are present in Stickler syndrome, such as midface hypoplasia, midline cleft of the palate, bifid uvula, sensorineural hearing loss, and skeletal abnormalities.[26,31–33] Abnormal dark adaptation associated with alterations in the ERG that is common in chromosome 5q retinopathies has not been described in Stickler syndrome.[1,31]

Autosomal Dominant Vitreoretinochoroidopathy.

ADVIRC is caused by mutations in *VMD2* and also has characteristic retinal and vitreous findings, in particular a peripheral retinal circumferential hyperpigmented band, vitreous fibrillar condensation, punctate white opacities in the retina, breakdown of the blood–retinal barrier, and retinal

neovascularization.[41]

Autosomal Recessive Vitreoretinopathies

Goldmann–Favre Syndrome and Enhanced S-Cone Syndrome.

Goldmann–Favre syndrome (GFS) and enhanced S-cone syndrome (ESCS) share common mutations in the *NR2E3* gene and are usually associated with night blindness and visual field abnormalities. ERG typically reveals a severe reduction in rod function and a relatively enhanced function of the short-wavelength-sensitive cones.[31,42] GFS manifests with progressive vitreous changes, hemeralopia, chorioretinal atrophy, and pigmentary retinal degeneration, later resulting in marked visual field loss, retinoschisis in the periphery and/or macula, presenile cataract, and hyperopia rather than myopia.[31,43,44] ESCS lacks the typical marked vitreous changes of GFS.

Knobloch Syndrome.

Knobloch syndrome is an autosomal recessive disorder characterized by pathogenic mutations in the *COL18A1* gene.[45] Characteristic features of Knobloch syndrome are high myopia, vitreoretinal degeneration with retinal detachment, and congenital encephalocele.

Management

Genetic Counseling

Chromosome 5q retinopathies are inherited in an autosomal dominant manner with high penetrance, and prenatal testing may be considered. Children of an affected parent obviously have a 50% chance of inheriting the mutation.

Treatment

Refractive error is corrected by spectacles or contact lenses. Cataract is managed by phacoemulsification and implantation of an intraocular lens. Retinal breaks without retinal detachment are

treated with laser photocoagulation. Vitreoretinal surgery is needed for retinal detachment, vitreoretinal traction involving the macula, or epiretinal membranes involving the macula. Prophylactic cryotherapy has been recently reported to reduce the risk of retinal detachment markedly.[1]

Chondrodysplasias Associated With Vitreoretinal Degeneration

General Features

Chondrodysplasias refer to a group of hereditary and systematic disorders that affect skeletal development and growth. These conditions may also feature ocular, central nervous system, or renal abnormalities. The genes involved in these syndromes affect types II, III, V, X, or XI, collagen molecules that are found mainly in cartilage and vitreous and are essential for the normal development of bones and other connective tissue, thus accounting for the symptoms observed clinically. Antenatal diagnosis, including fetal magnetic resonance imaging, computed tomography, ultrasonography, and genetic testing of fetal DNA obtained from amniocentesis or chorionic villus sampling, is important for the proper management of children and counseling of parents.[46–48]

According to the various "chondrodysplasia genes" and clinical presentations, five syndromes with distinct ocular dysfunctions – **Stickler syndrome**, **Marshall syndrome**, **Kniest dysplasia**, **Knobloch syndrome**, and **Weissenbacher–Zweymuller syndrome** – belong to the family of chondrodysplasias associated with vitreoretinal degeneration.

Stickler syndrome, also known as hereditary progressive arthro-ophthalmopathy, is considered to be the most common chondrodysplasia associated with vitreoretinal degeneration. Types I, II, and III are the three subgroups of Stickler syndrome classified based on genetic heterogeneity. Types I and II Stickler syndrome are caused by mutations in the *COL2A1* gene encoding type II collagen[49] and in the *COL11A1* gene encoding type XI collagen, respectively,[50] and can also be differentiated successfully by vitreous phenotypes. Mutations in *COL2A1* usually result in a

congenital membranous vitreous anomaly, while mutations in *COL11A1* result in an irregular and beaded vitreous.[51,52] Recently, a new subgroup of *COL2A1* mutations was found that can lead to a hypoplastic vitreous which is either optically empty or contains sparse irregular lamellae.[15] Due to the differential splicing, *COL2A1* gene transcription products can be divided into two types: collagen IIA with an exon2-encoded length of 69 (rich in amino acid homocysteine) and collagen IIB without the exon2-encoded peptide. Whereas both collagen IIA and IIB loss results in systemic connective tissues disease, collagen IIA loss also leads to ocular abnormalities. This is because collagen IIA primarily exists in the vitreous.[53,54] Recent studies have indicated that mutations in any collagen IX genes, such as *COL9A1*, *COL9A2*, *COL9A3*, as well as in *LRP2* (lipoprotein receptor-related protein-2) and *LOXL3* (encoding lysyl oxidase-like 3) can cause autosomal recessive Stickler syndrome.[55–60] Thus far, the diagnosis of Stickler syndrome has been based on clinical manifestations without consensus on the minimal clinical diagnostic criteria. The anomalous formation of the vitreous gel structure and its corresponding characteristic abnormalities are essential for the diagnosis of types I and II Stickler syndrome. In addition to these clinical manifestations, a detailed family history should be obtained and the diagnosis can be confirmed by genetic analysis. Recently, the *COL2A1* mutation in peripheral white blood cells has been used to identify patients with type I Stickler syndrome.[56]

Marshall syndrome, an autosomal dominant chondrodysplasia, is caused by a splicing mutation of 54-bp exons in the c-terminal region of the *COL11A1* gene which is located on the short arm of chromosome 1. The mutation in the *COL11A1* gene also causes the recessive form of Marshall syndrome.[61] Although Marshall syndrome and Stickler syndrome are now considered two distinct diseases, a case of a patient with overlapping phenotypes has been described.[62]

Kniest dysplasia, inherited in an autosomal dominant pattern, is a moderately severe collagenopathy. Like type I Stickler syndrome, Kniest dysplasia is associated with heterozygous *COL2A1* mutations that frequently occur de novo.[63] Recently, a novel splice (IVS18+1G>C) mutation in *COL2A1* has been found to be associated

with Kniest dysplasia.[64] As Kniest dysplasia is caused by mutations in *COL2A1* which encodes type II collagen,[65] cartilage and vitreous are mainly involved. It is reported that small deletions or splice site alterations between *COL2A1* gene exons 12 and 24 may cause the inframe deletions of type II collagen.

Knobloch syndrome is a rare and clinically heterogeneous autosomal recessive disorder. Collagen XVIII, which is a basement membrane proteoglycan, distributes in multiple organs of the body and plays an important role in the function and development of the eye, kidney, and nervous system. In most patients with this syndrome, null mutations in the *COL18A1* gene mapped to the long arm of chromosome 21 are thought to induce the abnormalities in collagen XVIII.[66] A novel homozygous *COL18A1* mutation has been revealed to cause Knobloch syndrome by homozygosity mapping and whole exome sequencing.[67,68] There are also case reports of Knobloch syndrome without *COL18A1* gene mutations, such as *ADAMTS18*,[69] and thus immunofluorescent histochemistry of skin biopsy samples has proved to be a useful preliminary and complementary test for the diagnosis of Knobloch syndrome.[70]

Weissenbacher–Zweymuller syndrome, also called Pierre Robin syndrome with fetal chondrodysplasia, is an autosomal recessive disorder characterized by a single-base mutation in the *COL11A2* gene, which substitutes glutamate for glycine.[71] Historically, it was often misdiagnosed as Stickler syndrome. Recently, investigators have differentiated these two syndromes successfully by prenatal ultrasonography.[72]

Clinical Findings

Extraocular Features

Stickler syndrome features a highly variable systemic phenotype, including conductive and sensorineural hearing loss, immunoglobulin deficiency,[22] cleft palate, midfacial underdevelopment, mild spondyloepiphyseal dysplasia, and precocious arthritis[73] (Fig. 43.2). Recently, 3 cases were also reported with associated epilepsy.[74]

FIG. 43.2 Stickler syndrome. Child with facial features including mid-facial hypoplasia and Pierre Robin sequence.

Like Stickler syndrome, Marshall syndrome is characterized by midfacial hypoplasia, sensorineural deafness, and ocular defects (cataract and high myopia). More importantly, it also includes ectodermal dysplasia, absence of frontal sinuses, calcifications of falx and tentorial meninges, as well as distal femoral and proximal tibial epiphyses, and wide tufts of the distal phalanges. Thus neural system, limb, and trunk abnormalities are important features.[75]

Kniest dysplasia has the typical manifestations of short-trunk dwarfism with kyphoscoliosis, enlarged joints with decreased motion, flat midface, cleft palate, and hearing loss.[76]

Extraocular features of Knobloch syndrome are mainly characterized by the occipital encephalocele caused by a midline defect in the occipital bone. Due to its rarity, the spectrum of clinical

variability is not fully understood.

Weissenbacher–Zweymuller syndrome is characterized by midface hypoplasia with a flat nasal bridge, small upturned nasal tip, micrognathia, sensorineural hearing loss, and rhizomelic limb shortening. Radiographic examination may detect dumbbell-shaped femora and humeri and vertebral coronal clefts in these patients.[62] However, some congenital abnormalities, such as dwarfism, developmental delays, and radiologic abnormalities, may return to normality at school age, so it is hypothesized to be dysmaturational rather than syndromic.[77]

Ocular Features

Types I and II Stickler syndrome have a high risk of ocular complications, including congenital high myopia, cataract, glaucoma, and retinal problems,[51,78] including vitreous changes, radial perivascular retinal degeneration, and rhegmatogenous retinal detachment[79] (Fig. 43.3). Recently, giant premacular bursa in posterior vitreous have been described in two patients with Stickler syndrome type 1 using swept-source optical coherence tomography.[80] These findings may manifest at any age and produce vision loss. Unlike Stickler syndrome, rhegmatogenous retinal detachment is unusual in Marshall syndrome and cataracts may be spontaneously absorbed.

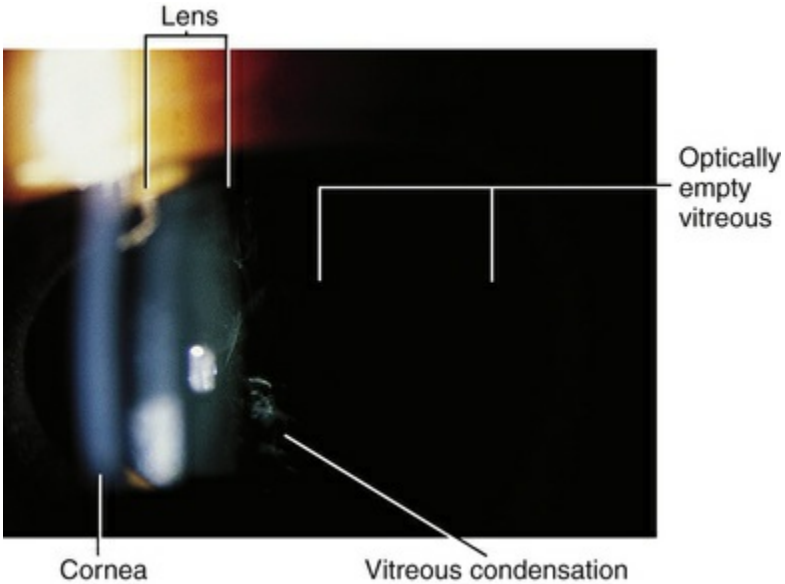

FIG. 43.3 Stickler syndrome. Slit-lamp photograph of

the child shown in Fig. 41.2 showing congenital vitreous abnormality.

The ocular manifestations of Kniest dysplasia mainly consist of high myopia, optically empty vitreous with retrolental and peripheral vitreous membranes, lattice degeneration, and retinal detachment. Ocular manifestations of Knobloch syndrome include high myopia, cataract, vitreoretinal degeneration, and retinal detachment which can lead to progressive and irreversible vision loss. Taken together, smooth irides, ectopia lentis, and characteristic vitreoretinal degeneration may be pathognomonic.[81] Typical characteristics of Weissenbacher–Zweymuller syndrome include strabismus and various refractive errors, which should be treated at an early age to prevent amblyopia.[82]

Differential Diagnosis

Marfan Syndrome

Marfan syndrome is an autosomal dominant disorder characterized by ocular, skeletal, and cardiovascular abnormalities. The ocular manifestations include flat cornea, high myopia, lens subluxation lens, and retinal detachment. It is believed that mutations in *FBN1*, which encodes a component of the extracellular matrix-connective tissue protein fibrillin-1, may result in the pathologic changes of Marfan syndrome.

Wagner Syndrome

As noted above, Wagner syndrome is often confused with Stickler syndrome. Key differentiating features are the typical vitreous abnormalities, higher risk of retinal detachment, and systemic findings of Stickler syndrome versus the characteristic nyctalopia, retinal pigmentary changes, and dark adaption problems of Wagner syndrome.[22,25]

Erosive Vitreoretinopathy

ERVR, as described above, is characterized by an "optically empty vitreous" and avascular vitreous strands and veils, mild or occasionally moderate to severe myopia, presenile cataract, night

blindness of variable degree associated with progressive chorioretinal atrophy, retinal detachment at advanced stages, and reduced visual acuity. Systemic abnormalities are not observed. Rhegmatogenous retinal detachment occurs more frequently in ERVR than in Wagner syndrome.[83]

Management

The most common management strategy is symptomatic treatment for complications such as mandibular distraction osteogenesis for pediatric airway management,[84] mandibular advancement for malocclusion and micrognathia, correction of refractive errors with spectacles, vitrectomy with silicone oil injection for retinal detachment, and symptomatic treatment for arthropathy.

Prevention of secondary complications and surveillance are essential.[85] The rate of retinal detachment has been reported to be as high as 60%,[26] so frequent follow-up and potential interventions, including laser therapy, are of great importance in prevention. In the largest published global cohort of type 1 Stickler syndrome patients, all observations and analyses indicate that the Cambridge prophylactic cryotherapy protocol is safe and markedly reduces the risk of retinal detachment.[86]

Recently, several transgenic mouse models have been developed with mutations in the pro-alpha collagen chain. These animals may serve as useful models for arthro-ophthalmopathies and eventually provide a basis for gene-directed therapy for these conditions.[48,53]

X-Linked Retinoschisis

Overview

X-linked retinoschisis (XLRS) is an inherited retinal degenerative disease caused by mutations of *RS1* on Xp22.1. Haas[87] first described the disease that is now known as retinoschisis in 1898. XLRS was first documented as being X-linked in 1913.[88] The term "X-linked retinoschisis," first used in 1953,[89] is now the generally accepted terminology.[90–92] XLRS is the most common form of juvenile-onset retinal degeneration in males, with a prevalence of

between 1 in 15,000 and 1 in 30,000.[93,94] XLRS is characterized by schisis of the neural retina, including cystic maculopathy, peripheral schisis, and reduced amplitude of the b-wave on the ERG.[95] The common sight-threatening complications of XLRS include retinal detachment, vitreous hemorrhage, and foveal schisis.[96] Females who are heterozygous for the *RS1* mutation commonly have no clinical symptoms of XLRS.[97] To date, no treatment is available to halt the development of schisis in patients with XLRS. Surgical interventions are required for XLRS patients with severe complications, such as retinal detachment and nonclearing vitreous hemorrhage.[98]

Since the causative gene was identified in 1997,[99] approximately 177 mutations of the *RS1* gene responsible for XLRS have been found (http://www.dmd.nl/rs/index.html). *RS1* is exclusively expressed in the photoreceptors and retinal bipolar cells,[100,101] and encodes a 224-amino-acid homo-oligomeric secretory protein complex – retinoschisin. Retinoschisin can be detected throughout the neural retina layers despite its restricted pattern of gene expression.[100–102] A mutant *RS1* gene appears to interfere with the secretion and/or octamerization and function of retinoschisin.[103–105] Wu et al.[103] found that *RS1* exists as a novel octamer in which the eight subunits are joined together by Cys59-Cys223 intermolecular disulfide bonds. Each subunit consists of a 157-amino-acid discoidin domain. Within the discoidin domain, one cysteine (Cys83) exists in its reduced state, and two cysteine pairs (Cys63-Cys219 and Cys110-Cys142) form intramolecular disulfide bonds that are important in protein folding. Mutations of *RS1* disrupt subunit assembly and then cause XLRS. Although insertions, deletions, and splice site mutations have been described, the mutations that encode the discoidin domain are predominantly missense and clustered in exons 4–6. Studies in a Taiwanese family with X-linked retinoschisis revealed that a transition in Exon 4 of the *RS1* gene results in a missense mutation and protein nonsecretion.[106]

Many studies have been focused on understanding the function and role of retinoschisin in retinal cell adhesion. Recently, retinoschisin has been reported to interact with β2 laminin within the extracellular space and αB crystallin intracellularly as it moves

through the secretory pathway.[94,107,108] Molday et al.[109] have confirmed the colocalization of retinoschisin with Na/K-ATPase and SARM1 in photoreceptors and retinal bipolar cells. Gehrig et al.[110] suggested that activation of microglia/glia may trigger the photoreceptor degeneration in retinoschisin-deficient mice and that the Erk1/2-Egr1 pathway may be activated in the pathogenesis of retinoschisis. Also, *RS1* efficiently and reversely binds galactose-agarose and lactose-agarose, indicating the possibility of interaction between *RS1* and glycosylation sites on Na/K ATPase, providing a method for the purification of *RS1*, which may facilitate further functional studies of *RS1*.[111] There may be other influencing factors such as genetic modifiers or environmental influences, since no correlations between mutation type and disease severity or progression exists.[112,113] Certainly, the roles of these potential molecular interactions in XLRS require further investigation.

Clinical Findings

Ocular Features

XLRS has variable disease severity, even when caused by the same *RS1* mutation.[90] Each eye of a patient may have asymmetric progression, but both eyes are invariably involved. Foveal schisis is the characteristic sign of XLRS and is present in 98–100% of cases.[114,115] Although macular changes are present in almost all XLRS patients, the typical foveal schisis, seen as a spokewheel pattern of folds radiating out from the fovea (Fig. 43.4), has been found to appear in only about 70% of XLRS patients. Peripheral retinoschisis is often noted in the inferotemporal region and is present in around 50% of patients[116] (Fig. 43.5). The splitting occurs in the superficial retinal layers, and so retinal vessels may lie in either the outer or inner leaf or cross from one to the other through the schisis cavity. Breaks occur within the inner layer, varying from small holes to large tears,[114] and the fragmentation of the inner leaf can lead to membranous remnants referred to vitreous veils. Other changes, including subretinal linear fibrosis, pigmentation, white retinal flecks, and vascular attenuation or sheathing, often appear in peripheral retina. The common sight-threatening complications of XLRS include traction or rhegmatogenous retinal detachment,

dense vitreous hemorrhage, hemorrhage within a large schisis cavity,[117] and intraretinal splitting involving the macula. Other less common complications include neovascular glaucoma,[118] vitreoretinal traction with secondary macular dragging,[119,120] and optic atrophy.[121] For most retinal detachments associated with XLRS, fluid usually accesses the subretinal space through either outer leaf/layer breaks in the areas of peripheral retinoschisis with inner leaf holes, or full-thickness retinal tears following vitreous detachment. Vitreous hemorrhage and retinal detachment are the most serious complications of XLRS. About 5–20% of XLRS patients may progress to retinal detachment,[114,115] and up to a third of patients develop vitreous hemorrhage,[94,122] which causes severe vision loss.

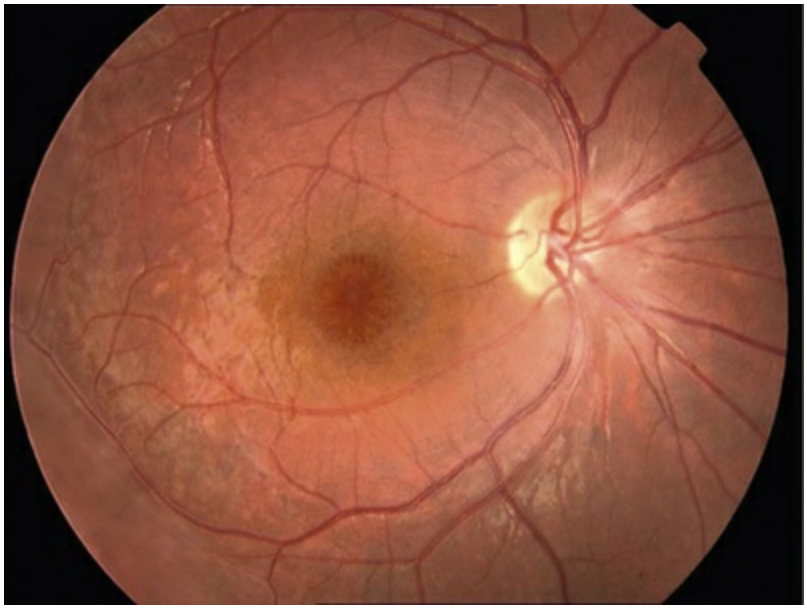

FIG. 43.4 Fundus photograph of X-linked retinoschisis with foveal cysts in a spokewheel pattern.

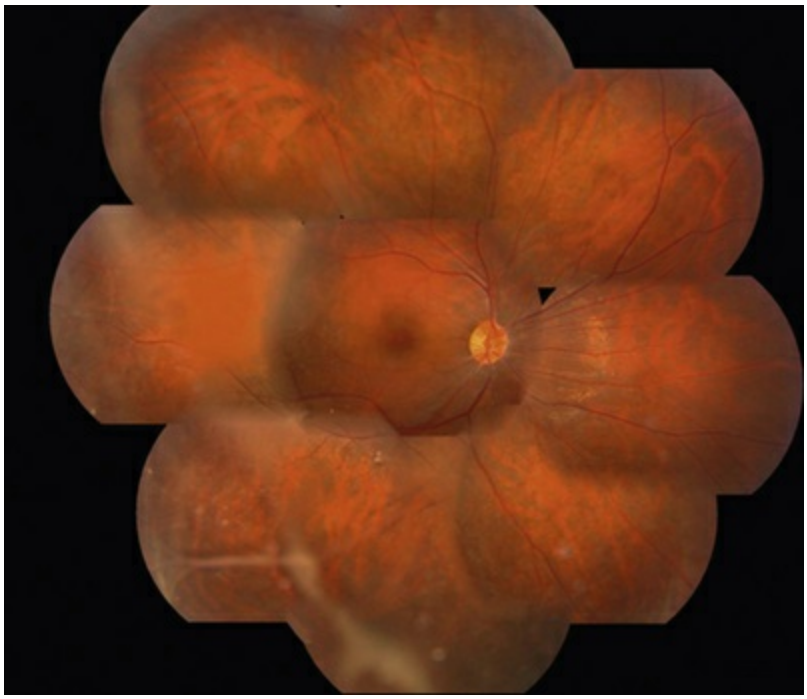

FIG. 43.5 Mosaic fundus photograph of X-linked retinoschisis with peripheral retinoschisis. The retinal vessels can be seen to be elevated from the retina into the vitreous cavity.

Less commonly, the disorder may present in early infancy with strabismus, nystagmus, axial hyperopia, foveal ectopia, or bilateral very large bullous retinoschisis, often with hemorrhage within the schisis cavity or into the vitreous.[122–124]

Visual Psychophysics

Vision loss is the most common clinical presentation in XLRS patients. Visual acuity may deteriorate during the first and second decades of life, presenting as young as 3 months,[98] then remain relatively stable with very slow progression of macular atrophy until the fifth or sixth decade,[125] with eventual progression to legal blindness (acuity <20/200) by the sixth or seventh decade. XLRS patients are often detected when having reading difficulties and poor vision at school age. Visual acuity ranges from 20/20 to less than 20/200. The average visual acuity in young adults is around 20/70. Retinal detachment and vitreous hemorrhage may be the cause of a precipitous drop in visual acuity. Defective color vision (red–green dyschromatopsia) can also be present in XLRS patients.[126] The visual field shows an absolute scotoma in the field

corresponding to the location of the peripheral retinoschisis.

Optical Coherence Tomography

Optical coherence tomography (OCT) helps to enhance the visualization of macular pathologic features in XLRS (Fig. 43.6).[127] The schisis can occur in different layers of the neural retina.[96,128] OCT findings may vary depending on the disease stage.[129,130]

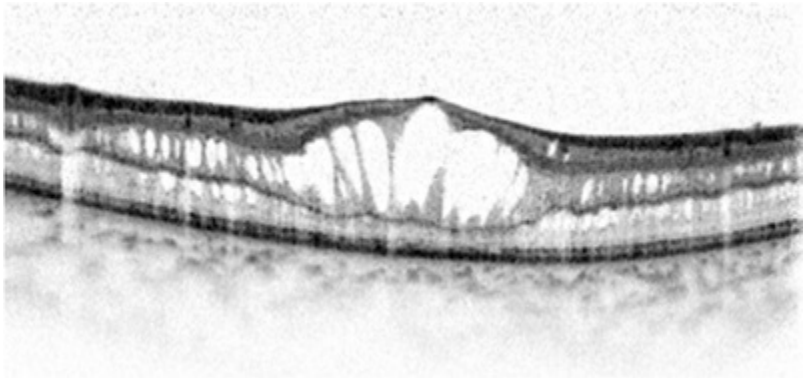

FIG. 43.6 Optical coherence tomography of X-linked retinoschisis demonstrating the splitting of the inner and outer retinal layers.

Electrophysiology

ERG is helpful in the diagnosis of XLRS. There is typically reduced b-wave amplitude with a relatively preserved a-wave amplitude, although a few patients may have a relatively preserved b-wave amplitude.[94] The alteration of the b/ a ratio ("negative" waveform, with a-wave amplitude exceeding the b-wave amplitude) is considered to be an important diagnostic parameter.[131] However, not all individuals with XLRS show the classic electronegative ERG, and b-wave amplitudes may not be significantly different from normal. The a-wave can be normal or near-normal in an XLRS patient, whereas it may also be reduced due to the progressive atrophy of the retinal pigment epithelium.[132] The severity of ERG abnormalities does not appear to correlate with the mutation type.[133] Multifocal ERG can also demonstrate the reduced amplitudes and longer implicit times in the central macula (Fig. 43.7).

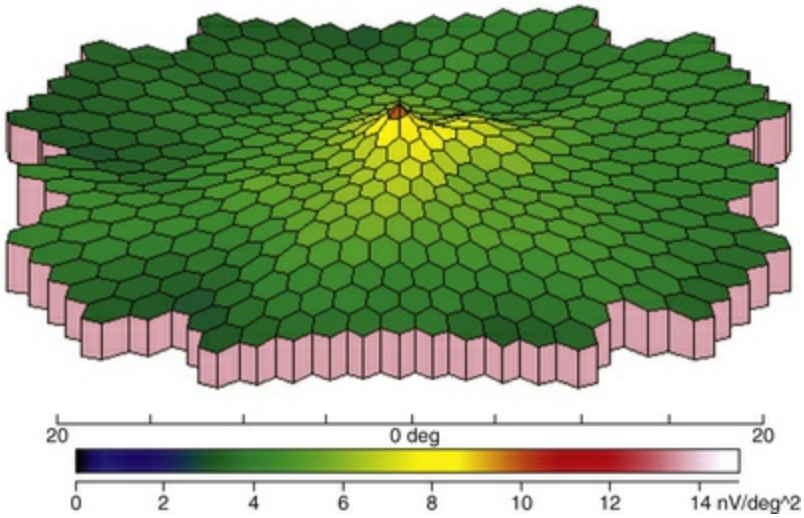

FIG. 43.7 Trace array and three-dimensional response density plot of multifocal electroretinography in X-linked retinoschisis showing reduced response amplitude in the macula.

Differential Diagnosis

The typical foveal schisis in a male with a reduced b-wave on ERG and a family history consistent with X-linked inheritance makes the diagnosis of XLRS very likely.[94] A domelike or slight elevation of a very thin layer of retinal tissue containing blood vessels can be visualized by ophthalmoscopy. Ancillary studies, including OCT and fluorescein angiography, may be useful in supporting the clinical diagnosis when minute foveal schisis is difficult to find by ophthalmoscopy. XLRS patients can be further confirmed with gene diagnosis of the *RS1* gene mutation.

Unlike many full-thickness neurosensory retinal detachments, the very thin and transparent layers of the neural retina in the setting of schisis do not undulate or shift when the position of the eye is changed. Moreover, the retinal abnormalities are always noted in both eyes of patients with XLRS.

In addition to retinal detachment, other disorders, such as cystoid macular edema, degenerative retinoschisis, acquired retinoschisis, amblyopia, Goldmann–Favre vitreoretinal degeneration, ESCS, Eales disease, and VCAN-related vitreoretinopathy, should be considered in the differential diagnosis of XLRS.

Cystoid macular edema is often observed in association with

disorders such as retinal vein occlusion, diabetic retinopathy, uveitis, retinitis pigmentosa, dominantly inherited cystoid macular edema, or intraocular surgery (Irvine–Gass syndrome).[134] Although angiography is not required for diagnosis of XLRS, the absence of leakage in XLRS may aid in differentiating foveal schisis from other causes of cystoid macular edema characterized by late hyperfluorescence in a petaloid pattern (Fig. 43.8).

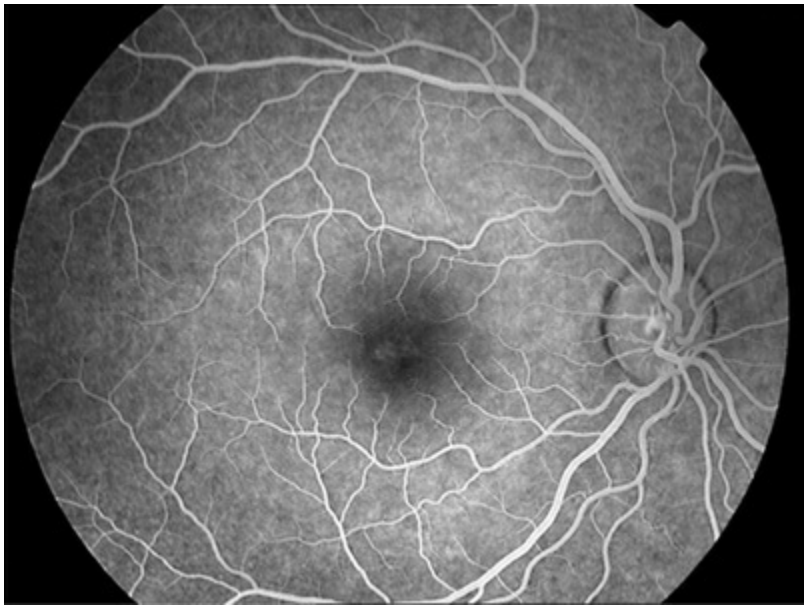

FIG. 43.8 Fluorescein angiogram demonstrating the foveal schisis cavity of X-linked retinoschisis and absence of leakage.

Degenerative retinoschisis is an idiopathic, degenerative splitting of the outer layers of the peripheral retina without ERG abnormalities or *RS1* mutations, occurring in an older age group, typically unilaterally.[94,135]

Goldmann–Favre vitreoretinal degeneration and ESCS caused by mutations in the *NR2E3* gene can also lead to foveal schisis, but the severely impaired vision, including marked visual field loss and nyctalopia, pigmentary clumping, absence of vitreous veils, and markedly reduced a-waves and b-waves with altered timing, should help to differentiate this disease from XLRS.[44]

Management

Genetic Counseling

X-linked inheritance should be explained to XLRS patients. Female carriers have a 50% chance of transmitting the retinoschisis mutation in each pregnancy: males with the mutation will be affected and females with the mutation will be carriers and nearly always have normal visual function. Affected males pass the disease-causing mutation to all of their daughters and none of their sons. Carrier testing for at-risk female relatives and prenatal testing for pregnancy at increased risk are possible if the retinoschisis mutation in the family is known.

Treatment

Pharmacologic Treatment

The successful treatment of schisis cavities with carbonic anhydrase inhibitor has been previously reported.[136] Genead et al.[137] treated 29 eyes of 15 XLRS patients with topical dorzolamide for 4–41 months and noted some positive effects on visual acuity, cystoid macular lesions, and central foveal thickness. Further studies are required to elucidate the true frequency and completeness of the response to dorzolamide, as well as to evaluate for possible recurrence of foveal cystic change.[138] Recently, it has been reported that the effect of acetazolamide in XLRS patients at a dose of 500 mg/day can be observed after one-week treatment with the monitor of AOSLO (adaptive optics scanning laser ophthalmoscopy).[139] More specific pharmacotherapies may become possible as the pathogenetic mechanisms of XLRS are better understood.

Laser

Laser photocoagulation is often considered as an adjuvant or preventive treatment for XLRS.[140,141] However, scatter laser photocoagulation performed in order to flatten peripheral schisis cavities and reduce the likelihood of retinal detachment resulted in retinal detachment in many cases.[142] These potential risks should be considered in discussions with patients. So the timing of administration and effectiveness of laser treatment for XLRS should be carefully considered.

Surgery

Surgical intervention may be required for XLRS patients with severe complications, such as retinal detachment and vitreous hemorrhage. Relevant procedures include scleral buckle,[141] vitrectomy, and perfluorocarbon liquid, perfluorodecalin or sulfur hexafluoride gas tamponade. Vitreous surgery includes core vitrectomy, surgical induction of posterior vitreous detachment, removal of the internal limiting membrane, and gas tamponade.[143] In addition, Wu et al.[144] used autologous plasmin enzyme-assisted vitreoretinal surgery to treat XLRS patients and achieved retinal reattachment in 91% (20/21) of eyes and postoperative visual improvement in 53% (8/15). Researchers have shown an improvement in the severity of foveal schisis after pars plana vitrectomy in some patients with progressive XLRS.[145,146]

Gene Therapy

Gene therapy also holds great promise for the treatment of inherited retinal degenerations.[147] Gene therapy might be an effective treatment for XLRS patients.[148,149] The *RS1* gene delivered intraocularly in RS1-knockout mice was found to restore b-wave amplitude of the treated mice.[150,151] XLRS patients may benefit from the replacement of the *RS1* gene, even at advanced stages, and gene replacement may be a promising treatment for XLRS patients in the near future.[152] However, further work in selection of the appropriate vector and development of cell targeting strategies will be important in the ultimate success of gene therapeutic approaches.[153]

Retina and/or Progenitor Cell Transplantation

Retinal transplantation or replacement also holds promise as a potential future therapy for XLRS disease in conjunction with the development of new surgical techniques and instrumentation. However, due to the limited source of human tissue and ethical considerations, it is important to find an alternative cell source for retinal replacement therapy. Transplantation of stem cells and/or progenitor cells, including retinal progenitor cells, bone marrow-derived cells, and induced pluripotent cells, may eventually

provide an alternative approach to restore vision.[154] Compared to human embryonic stem cells, the use of human bone-marrow-derived cells and induced pluripotent cells does not have significant ethical issues and may eliminate the risk of immunorejection.

Retinal Nuclear Receptor (NR2E3)-Related Diseases

General Features

These vitreoretinopathies include **enhanced S-cone syndrome (ESCS)** and **Goldmann–Favre vitreotapetoretinal degeneration**. *NR2E3* (retinal nuclear receptor subfamily 2, group E, member 3), formerly called photoreceptor-specific nuclear receptor (*PNR*), is a transcription factor of the nuclear hormone receptor superfamily whose expression is uniquely restricted to photoreceptors. Its physiologic activity is essential for proper rod and cone development and maintenance. Mutations in *NR2E3* may suppress cone proliferation during retinal development[155] and lead to an autosomal recessive retinal degeneration of variable severity, encompassing Goldmann–Favre syndrome (GFS),[156,157] ESCS,[158] and clumped pigmentary retinal degeneration.[44,159]

Goldmann–Favre vitreotapetoretinal degeneration (also called Favre microfibrillar vitreoretinal degeneration), a rare condition that affects the retina, vitreous body, and crystalline lens, was first described in 1958.[160,161] The characteristic features are early-onset nyctalopia, fibrillar vitreous degeneration, foveal cysts, peripheral retinoschisis, and retinal degeneration with clumped pigment, and an unusual ERG.[162] An estimated 0.5% of patients with retinitis pigmentosa have clumps of pigment in the midperipheral fundus, referred to as "clumped pigmentation." To and coworkers reviewed the clinical and pathologic findings in patients with clumped pigmentation and found that they had signs and symptoms of NR2E3 disease. Histopathologic study showed that the clinically distinct areas of clumped pigment are due to excessive accumulation of melanin granules in retinal pigment epithelial cells.[159]

ESCS was described in 1990 and named after the enhanced sensitivity of the S-cone system[158,163] due to an increase in the blue cone population with associated variable degeneration of the rod, and red and green cone photoreceptors. Clinical features include early-onset night blindness, cystic maculopathy, and peripheral retinal degeneration characterized by mild visual field loss. The enhanced S-cone ERG shows no response to dim light in the dark-adapted state, but a large, slow response to bright light which persists with light adaptation.[158]

Many psychophysical,[164] histologic,[159,165,166] and animal studies[167,168] have demonstrated that mutations in *NR2E3* lead to an absolute increase in S cones at the expense of M and L cones, decreased rod development, and retinal disorganization and degeneration. Severe loss of rod sensitivity is evident throughout the retina, along with the characteristic enhanced S-cone ERG.

Clinical Findings

Ocular Features

Patients with GFS have progressive loss of vision similar to retinitis pigmentosa, which is caused by retinoschisis, cataract, and pigmentary chorioretinal degeneration. It is the macular retinoschisis that most often accounts for the poor central vision and central scotoma in this disorder (Fig. 43.9). The presenting symptom is frequently night blindness, which is often detected in the first decade of life.[162,169] The intraretinal pigmentation is described as spots of pigment, rather than the bone spicule pattern seen in typical retinitis pigmentosa. The retinoschisis in some patients affects both the central and peripheral retina, and resembles juvenile XLRS. Macular lesions may be isolated from or continuous with the peripheral area of schisis. The peripheral retinoschisis frequently shows oval holes in the inner layer and causes absolute field defects in the peripheral visual field.

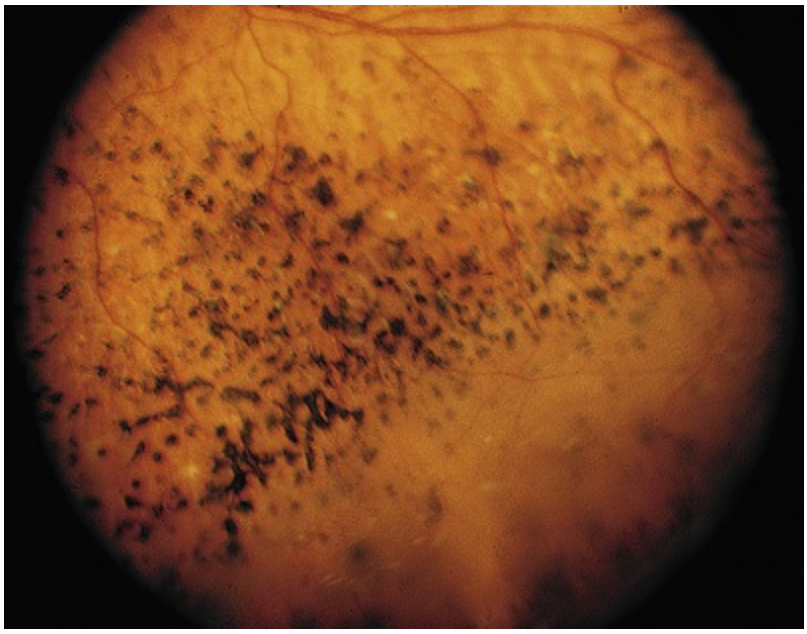

FIG. 43.9 Goldmann–Favre vitreotapetoretinal degeneration, illustrating pigment spots and retinoschisis. (Courtesy of Gerald A. Fishman, MD.)

The most striking vitreous change is liquefaction, which converts a large portion of the vitreous body into an optically empty space, somewhat similar to that found in Wagner syndrome.[169] The space may contain fine fibrous strands and is surrounded by semiliquefied gel containing loose, plated membranes. These membranes have no visible edge and vary in density from one part of the vitreous body to another. The outer layer of the posterior cortex is condensed, resembling a preretinal membrane. When the posterior cortex is detached, it shows depressions that appear to be molded to retinal vessels. The cortex usually adheres to the retinoschisis and to areas with chorioretinal pigmentary proliferation.

Visual Psychophysics

Results of visual field and dark adaptation studies are similar to those from patients with retinitis pigmentosa. The areas of visual field loss correspond to the areas of schisis and pigmentary retinal degeneration. The degree of abnormality of color vision appears to be related to foveal dysfunction.

Electrophysiology

The characteristic ERG shows an undetectable rod-specific response, similar photopic and scotopic responses to a standard single flash, and a 30-Hz lower-amplitude photopic a-wave response. High variability is common and at least partially related to the severity of retinal degeneration.[162] As discussed earlier, the response from the S-cone system accounts for much of the waveform under both scotopic and photopic conditions. The ERG may become undetectable over time.

In addition, ERGs of patients with either ESCS or GFS have greater amplitudes to short-wavelength (e.g., blue) light flashes than to intensity-matched, long-wavelength (e.g., orange) light flashes.[165,170,171] Although rods and S cones are both maximally sensitive to blue light and either might hypothetically mediate this hypersensitivity, the similar ERG amplitudes under scotopic and photopic conditions to single flashes of bright white light indicate that it is mediated predominantly by S cones.[171–173] Evidence from the shape of the ERG a-wave and from psychophysical studies of color sensitivity indicates that the affected retinas have an overabundance of S-cone photoreceptors at birth, a reduced number of L and M cones, and few, if any, functional rod photoreceptors.[173] The relative abundance of S-cone photoreceptors persists even late in the disease, when visual function is severely reduced, as shown by histopathologic examination at autopsy of the eyes of a patient with ESCS.[165]

Differential Diagnosis

Goldmann–Favre vitreotapetoretinal degeneration and ESCS share features with other vitreoretinal degenerations and retinitis pigmentosa.

X-Linked Retinoschisis

Goldmann–Favre vitreotapetoretinal degeneration and ESCS are distinguished from XLRS by autosomal inheritance, presence of severe nyctalopia, and ERG findings. The presence of clumped pigment suggests NR2E3-related disease, whereas vascular attenuation is suggestive of retinitis pigmentosa.

Cystoid Macular Edema

The microcystic changes at the posterior pole have sometimes been confused with those of cystoid macular edema (CME), and fluorescein angiography has been helpful in making this differentiation, showing a characteristic petalloid late leakage in CME that is absent in NR2E3-related disease.

Management

There is no satisfactory treatment for this condition. Standard vitreoretinal approaches are used for rhegmatogenous retinal detachment, and prophylactic treatment of retinal tears using laser photocoagulation should be performed. As discussed in the section on congenital XLRS, prophylactic treatment of breaks in the outer layer of the retinoschisis is generally not recommended. Laser photocoagulation has been used to treat elevated macular retinoschisis.[174]

Other Vitreoretinal Degenerations and Vitreoretinopathies

Autosomal Dominant Vitreoretinochoroidopathy

Kaufman and colleagues described a unique condition with 360° of peripheral chorioretinal atrophy between the ora serrata and a very distinct posterior border near the equator.[175] This feature is not seen in any other disorder to our knowledge. Cataract, moderate fibrillar vitreous degeneration with pigmented cells, cystoid macular edema, neovascularization of the disc, punctate white opacities on the surface of the retina, and retinal detachment may be observed.[176–178] The electro-oculogram may be abnormal,[179] but the ERG is typically normal and nyctalopia is absent.

Autosomal Recessive Inherited Vitreoretinal Dystrophy

Sarra and colleagues reported a family with 4 of 8 siblings affected with early-onset high myopia, vitreous liquefaction, macular staphyloma with chorioretinal atrophy, diffuse peripheral atrophy of the retinal pigment epithelium, and early cataract. There was also a peripheral veil in one subject, but no extraocular manifestations.[180] Monophasic dark adaptation was observed and the ERG showed a severe rod–cone retinal degeneration.[180] Linkage analysis identified chromosome 22q13 with a 2-point lod score of 2.18 as the likely locus.

Hereditary Neovascular Vitreoretinopathies

These conditions are characterized by hereditary peripheral retinal neovascularization with vitreoretinal traction. We discuss here two hereditary conditions without primary vitreous degeneration and unaccompanied by systemic clinical manifestations, such as incontinentia pigmenti, sickle-cell retinopathy, and other peripheral proliferative retinopathies that have been reviewed previously.[181]

Autosomal Dominant Neovascular Inflammatory Vitreoretinopathy

ADNIV is an apparently rare condition characterized by cataract, cystoid macular edema, peripheral retinal scarring and pigmentation, peripheral arteriolar closure, and neovascularization of the peripheral retina at the ora serrata.[152,182] Young adults are asymptomatic, but have vitreous cell and selective b-wave loss on the ERG. Neovascularization may result in traction retinal detachment. About half of patients will develop rubeosis or neovascular glaucoma by age 60 or older. The gene was localized to chromosome 11q13.[183] Vitreous bands and sheets are not observed and the vitreous was not optically empty, enabling differentiation from classical vitreoretinal degenerations such as Stickler, Wagner, and SVD. The peripheral retinal vessels are initially normal in ADNIV, and dragging of the macular vessels as seen in familial exudative vitreoretinopathy is absent.

Dominantly Inherited Peripheral Retinal

Neovascularization

Gitter and colleagues described a family with 7 of 15 members affected with early cataract, uveitis, prominence of the vitreous base, lattice degeneration, and severe peripheral retinal neovascularization leading to vitreous hemorrhage and retinal detachment. The syndrome appears similar to ADNIV, but after reviewing photographs of the ADNIV family, the condition was deemed to be distinct.[184]

References

1. Edwards AO. Clinical features of the congenital vitreoretinopathies. *Eye (Lond)*. 2008;22(10):1233–1242.
2. Hirose T, Lee KY, Schepens CL. Snowflake degeneration in hereditary vitreoretinal degeneration. *Am J Ophthalmol*. 1974;77(2):143–153.
3. Lee MM, Ritter R 3rd, Hirose T, Vu CD, Edwards AO. Snowflake vitreoretinal degeneration: follow-up of the original family. *Ophthalmology*. 2003;110(12):2418–2426.
4. Hejtmancik JF, Jiao X, Li A, et al. Mutations in KCNJ13 cause autosomal-dominant snowflake vitreoretinal degeneration. *Am J Hum Genet*. 2008;82(1):174–180.
5. Gheiler M, Pollack A, Uchenik D, Godel V, Oliver M. Hereditary snowflake vitreoretinal degeneration. *Birth Defects Orig Artic Ser*. 1982;18(6):577–580.
6. Pollack A, Uchenik D, Chemke J, Oliver M. Prophylactic laser photocoagulation in hereditary snowflake vitreoretinal degeneration: a family report. *Arch Ophthalmol*. 1983;101(10):1536–1539.
7. Robertson DM, Link TP, Rostvold JA. Snowflake degeneration of the retina. *Ophthalmology*. 1982;89(12):1513–1517.
8. Chen CJ, Everett TK, Marascalco D. Snowflake degeneration: an independent entity or a variant of retinitis pigmentosa? *South Med J*. 1986;79(10):1216–1223.
9. Jiao X, Ritter R 3rd, Hejtmancik JF, Edwards AO. Genetic linkage of snowflake vitreoretinal degeneration to

chromosome 2q36. *Invest Ophthalmol Vis Sci*. 2004;45(12):4498–4503.
10. Kumar M, Pattnaik BR. Focus on Kir7.1: physiology and channelopathy. *Channels (Austin)*. 2014;8(6):488–495.
11. Pattnaik BR, Shahi PK, Marino MJ, et al. A Novel KCNJ13 Nonsense mutation and loss of Kir7.1 channel function causes Leber congenital amaurosis (LCA16). *Hum Mutat*. 2015;36(7):720–727.
12. Hirose T, Wolf E, Schepens CL. Retinal functions in snowflake degeneration. *Ann Ophthalmol*. 1980;12(10):1135–1146.
13. Aylward B, daCruz L, Ezra E, et al. Stickler syndrome. *Ophthalmology*. 2008;115(9):1636–1637 [author reply 1637-1638].
14. Ang A, Ung T, Puvanachandra N, et al. Vitreous phenotype: a key diagnostic sign in Stickler syndrome types 1 and 2 complicated by double heterozygosity. *Am J Med Genet A*. 2007;143A(6):604–607.
15. Richards AJ, McNinch A, Martin H, et al. Stickler syndrome and the vitreous phenotype: mutations in COL2A1 and COL11A1. *Hum Mutat*. 2010;31(6):E1461–71.
16. Richards AJ, Yates JR, Williams R, et al. A family with Stickler syndrome type 2 has a mutation in the COL11A1 gene resulting in the substitution of glycine 97 by valine in alpha 1 (XI) collagen. *Hum Mol Genet*. 1996;5(9):1339–1343.
17. Annunen S, Korkko J, Czarny M, et al. Splicing mutations of 54-bp exons in the COL11A1 gene cause Marshall syndrome, but other mutations cause overlapping Marshall/Stickler phenotypes. *Am J Hum Genet*. 1999;65(4):974–983.
18. Shanske AL, Bogdanow A, Shprintzen RJ, Marion RW. The Marshall syndrome: report of a new family and review of the literature. *Am J Med Genet*. 1997;70(1):52–57.
19. Brubaker JW, Mohney BG, Pulido JS, Babovic-Vuksanovic D. Vitreous veils and radial lattice in Marshall syndrome. *Ophthalmic Genet*. 2008;29(4):184–185.
20. Kloeckener-Gruissem B, Bartholdi D, Abdou MT, Zimmermann DR, Berger W. Identification of the genetic

defect in the original Wagner syndrome family. *Mol Vis*. 2006;12:350–355.
21. Mukhopadhyay A, Nikopoulos K, Maugeri A, et al. Erosive vitreoretinopathy and Wagner disease are caused by intronic mutations in CSPG2/Versican that result in an imbalance of splice variants. *Invest Ophthalmol Vis Sci*. 2006;47(8):3565–3572.
22. Meredith SP, Richards AJ, Flanagan DW, Scott JD, Poulson AV, Snead MP. Clinical characterisation and molecular analysis of Wagner syndrome. *Br J Ophthalmol*. 2007;91(5):655–659.
23. Batioglu F. Goldmann–Favre vitreoretinal degeneration. *Eur J Ophthalmol*. 2003;13(3):307–310.
24. Ang A, Poulson AV, Goodburn SF, Richards AJ, Scott JD, Snead MP. Retinal detachment and prophylaxis in type 1 Stickler syndrome. *Ophthalmology*. 2008;115(1):164–168.
25. Ronan SM, Tran-Viet KN, Burner EL, Metlapally R, Toth CA, Young TL. Mutational hot spot potential of a novel base pair mutation of the CSPG2 gene in a family with Wagner syndrome. *Arch Ophthalmol*. 2009;127(11):1511–1519.
26. Carroll C, Papaioannou D, Rees A, Kaltenthaler E. The clinical effectiveness and safety of prophylactic retinal interventions to reduce the risk of retinal detachment and subsequent vision loss in adults and children with Stickler syndrome: a systematic review. *Health Technol Assess*. 2011;15(16):iii–xiv [1-62].
27. Brown DM, Graemiger RA, Hergersberg M, et al. Genetic linkage of Wagner disease and erosive vitreoretinopathy to chromosome 5q13-14. *Arch Ophthalmol*. 1995;113(5):671–675.
28. Black GC, Perveen R, Wiszniewski W, Dodd CL, Donnai D, McLeod D. A novel hereditary developmental vitreoretinopathy with multiple ocular abnormalities localizing to a 5-cM region of chromosome 5q13-q14. *Ophthalmology*. 1999;106(11):2074–2081.
29. Kloeckener-Gruissem B, Neidhardt J, Magyar I, et al. Novel VCAN mutations and evidence for unbalanced alternative splicing in the pathogenesis of Wagner syndrome. *Eur J*

Hum Genet. 2013;21(3):352–356.
30. Rothschild PR, Brezin AP, Nedelec B, et al. A family with Wagner syndrome with uveitis and a new versican mutation. *Mol Vis*. 2013;19:2040–2049.
31. Kloeckener-Gruissem B, Amstutz C. VCAN-related vitreoretinopathy. Pagon RA, Adam MP, Ardinger HH, et al. *GeneReviews(R)*. 1993 [Seattle, WA].
32. Fryer AE, Upadhyaya M, Littler M, et al. Exclusion of COL2A1 as a candidate gene in a family with Wagner–Stickler syndrome. *J Med Genet*. 1990;27(2):91–93.
33. Snead MP, Yates JR. Clinical and molecular genetics of Stickler syndrome. *J Med Genet*. 1999;36(5):353–359.
34. McLeod D, Black GC, Bishop PN. Vitreous phenotype: genotype correlation in Stickler syndrome. *Graefes Arch Clin Exp Ophthalmol*. 2002;240(1):63–65 [author reply 66].
35. Perveen R, Hart-Holden N, Dixon MJ, et al. Refined genetic and physical localization of the Wagner disease (WGN1) locus and the genes CRTL1 and CSPG2 to a 2- to 2.5-cM region of chromosome 5q14.3. *Genomics*. 1999;57(2):219–226.
36. Maumenee IH, Stoll HU, Mets MB. The Wagner syndrome versus hereditary arthroophthalmopathy. *Trans Am Ophthalmol Soc*. 1982;80:349–365.
37. Rothschild PR, Burin-des-Roziers C, Audo I, Nedelec B, Valleix S, Brezin AP. Spectral-domain optical coherence tomography in Wagner syndrome: characterization of vitreoretinal interface and foveal changes. *Am J Ophthalmol*. 2015;160(5):1065–1072.
38. Go SL, Maugeri A, Mulder JJ, van Driel MA, Cremers FP, Hoyng CB. Autosomal dominant rhegmatogenous retinal detachment associated with an Arg453Ter mutation in the COL2A1 gene. *Invest Ophthalmol Vis Sci*. 2003;44(9):4035–4043.
39. Graemiger RA, Niemeyer G, Schneeberger SA, Messmer EP. Wagner vitreoretinal degeneration. Follow-up of the original pedigree. *Ophthalmology*. 1995;102(12):1830–1839.
40. Seery CM, Pruett RC, Liberfarb RM, Cohen BZ. Distinctive cataract in the Stickler syndrome. *Am J Ophthalmol*. 1990;110(2):143–148.

41. Yardley J, Leroy BP, Hart-Holden N, et al. Mutations of VMD2 splicing regulators cause nanophthalmos and autosomal dominant vitreoretinochoroidopathy (ADVIRC). *Invest Ophthalmol Vis Sci*. 2004;45(10):3683–3689.
42. Audo I, Michaelides M, Robson AG, et al. Phenotypic variation in enhanced S-cone syndrome. *Invest Ophthalmol Vis Sci*. 2008;49(5):2082–2093.
43. Chavala SH, Sari A, Lewis H, et al. An Arg311Gln NR2E3 mutation in a family with classic Goldmann–Favre syndrome. *Br J Ophthalmol*. 2005;89(8):1065–1066.
44. Sharon D, Sandberg MA, Caruso RC, Berson EL, Dryja TP. Shared mutations in NR2E3 in enhanced S-cone syndrome, Goldmann–Favre syndrome, and many cases of clumped pigmentary retinal degeneration. *Arch Ophthalmol*. 2003;121(9):1316–1323.
45. Menzel O, Bekkeheien RC, Reymond A, et al. Knobloch syndrome: novel mutations in COL18A1, evidence for genetic heterogeneity, and a functionally impaired polymorphism in endostatin. *Hum Mutat*. 2004;23(1):77–84.
46. Cui YX, Xia XY, Bu Y, et al. Rapid molecular prenatal diagnosis of spondyloepiphyseal dysplasia congenita by PCR–SSP assay. *Genet Test*. 2008;12(4):533–536.
47. Wada R, Sawai H, Nishimura G, et al. Prenatal diagnosis of Kniest dysplasia with three-dimensional helical computed tomography. *J Matern Fetal Neonatal Med*. 2011;24(9):1181–1184.
48. Yazici Z, Kline-Fath BM, Laor T, Tinkle BT, Fetal MR. imaging of Kniest dysplasia. *Pediatr Radiol*. 2010;40(3):348–352.
49. Hoornaert KP, Vereecke I, Dewinter C, et al. Stickler syndrome caused by COL2A1 mutations: genotype-phenotype correlation in a series of 100 patients. *Eur J Hum Genet*. 2010;18(8):872–880.
50. Majava M, Hoornaert KP, Bartholdi D, et al. A report on 10 new patients with heterozygous mutations in the COL11A1 gene and a review of genotype-phenotype correlations in type XI collagenopathies. *Am J Med Genet A*. 2007;143A(3):258–264.

51. Vu CD, Brown J Jr, Korkko J, Ritter R 3rd, Edwards AO. Posterior chorioretinal atrophy and vitreous phenotype in a family with Stickler syndrome from a mutation in the COL2A1 gene. *Ophthalmology*. 2003;110(1):70–77.
52. Donoso LA, Edwards AO, Frost AT, et al. Identification of a stop codon mutation in exon 2 of the collagen 2A1 gene in a large stickler syndrome family. *Am J Ophthalmol*. 2002;134(5):720–727.
53. Donoso LA, Edwards AO, Frost AT, et al. Clinical variability of Stickler syndrome: role of exon 2 of the collagen COL2A1 gene. *Surv Ophthalmol*. 2003;48(2):191–203.
54. McAlinden A, Majava M, Bishop PN, et al. Missense and nonsense mutations in the alternatively-spliced exon 2 of COL2A1 cause the ocular variant of Stickler syndrome. *Hum Mutat*. 2008;29(1):83–90.
55. Baker S, Booth C, Fillman C, et al. A loss of function mutation in the COL9A2 gene causes autosomal recessive Stickler syndrome. *Am J Med Genet A*. 2011;155A(7):1668–1672.
56. Nikopoulos K, Schrauwen I, Simon M, et al. Autosomal recessive Stickler syndrome in two families is caused by mutations in the COL9A1 gene. *Invest Ophthalmol Vis Sci*. 2011;52(7):4774–4779.
57. Yaguchi H, Ikeda T, Osada H, Yoshitake Y, Sasaki H, Yonekura H. Identification of the COL2A1 mutation in patients with type I Stickler syndrome using RNA from freshly isolated peripheral white blood cells. *Genet Test Mol Biomarkers*. 2011;15(4):231–237.
58. Schrauwen I, Sommen M, Claes C, et al. Broadening the phenotype of LRP2 mutations: a new mutation in LRP2 causes a predominantly ocular phenotype suggestive of Stickler syndrome. *Clin Genet*. 2014;86(3):282–286.
59. Alzahrani F, Al Hazzaa SA, Tayeb H, Alkuraya FS. LOXL3, encoding lysyl oxidase-like 3, is mutated in a family with autosomal recessive Stickler syndrome. *Hum Genet*. 2015;134(4):451–453.
60. Faletra F, D'Adamo AP, Bruno I, et al. Autosomal recessive Stickler syndrome due to a loss of function mutation in the

COL9A3 gene. *Am J Med Genet A*. 2014;164A(1):42–47.
61. Khalifa O, Imtiaz F, Allam R, et al. A recessive form of Marshall syndrome is caused by a mutation in the COL11A1 gene. *J Med Genet*. 2012;49(4):246–248.
62. Al Kaissi A, Ganger R, Klaushofer K, Grill F. Significant ophthalmoarthropathy associated with ectodermal dysplasia in a child with Marshall-Stickler overlap: a case report. *Cases J*. 2008;1(1):270.
63. Sergouniotis PI, Fincham GS, McNinch AM, et al. Ophthalmic and molecular genetic findings in Kniest dysplasia. *Eye (Lond)*. 2015;29(4):475–482.
64. Al-Hashmi N, Imtiaz F, Ramzan K, et al. Novel splice (IVS18+1G>C) mutation in COL2A1 causing Kniest dysplasia. *Clin Dysmorphol*. 2013;22(1):39–41.
65. Wu M, Liu L, Zhou Z, et al. Kniest dysplasia due to mutation of COL2A1 gene. *Zhonghua Yi Xue Yi Chuan Xue Za Zhi*. 2015;32(3):323–326.
66. Passos-Bueno MR, Suzuki OT, Armelin-Correa LM, et al. Mutations in collagen 18A1 and their relevance to the human phenotype. *An Acad Bras Cienc*. 2006;78(1):123–131.
67. Haghighi A, Tiwari A, Piri N, et al. Homozygosity mapping and whole exome sequencing reveal a novel homozygous COL18A1 mutation causing Knobloch syndrome. *PLoS ONE*. 2014;9(11):e112747.
68. Aldahmesh MA, Khan AO, Mohamed JY, et al. No evidence for locus heterogeneity in Knobloch syndrome. *J Med Genet*. 2013;50(8):565–566.
69. Aldahmesh MA, Khan AO, Mohamed JY, et al. Identification of ADAMTS18 as a gene mutated in Knobloch syndrome. *J Med Genet*. 2011;48(9):597–601.
70. Suzuki O, Kague E, Bagatini K, et al. Novel pathogenic mutations and skin biopsy analysis in Knobloch syndrome. *Mol Vis*. 2009;15:801–809.
71. Pihlajamaa T, Prockop DJ, Faber J, et al. Heterozygous glycine substitution in the COL11A2 gene in the original patient with the Weissenbacher–Zweymuller syndrome demonstrates its identity with heterozygous OSMED (nonocular Stickler syndrome). *Am J Med Genet*.

1998;80(2):115–120.
72. Pacella E, Malvasi A, Tinelli A, et al. Stickler syndrome in Pierre-Robin sequence prenatal ultrasonographic diagnosis and postnatal therapy: two cases report. *Eur Rev Med Pharmacol Sci*. 2010;14(12):1051–1054.
73. Couchouron T, Masson C. Early-onset progressive osteoarthritis with hereditary progressive ophthalmopathy or Stickler syndrome. *Joint Bone Spine*. 2011;78(1):45–49.
74. Savasta S, Salpietro V, Sparta MV, et al. Stickler syndrome associated with epilepsy: report of three cases. *Eur J Pediatr*. 2015;174(5):697–701.
75. Khalifa O, Imtiaz F, Ramzan K, et al. Marshall syndrome: further evidence of a distinct phenotypic entity and report of new findings. *Am J Med Genet A*. 2014;164A(10):2601–2606.
76. Spranger J, Winterpacht A, Zabel B. Kniest dysplasia: Dr. W. Kniest, his patient, the molecular defect. *Am J Med Genet*. 1997;69(1):79–84.
77. Galil A, Carmi R, Goldstein E, Porter B, Bar Ziv J, Chemke J. Weissenbacher-Zweymuller syndrome: long-term follow-up of growth and psychomotor development. *Dev Med Child Neurol*. 1991;33(12):1104–1109.
78. Shenoy BH, Mandal AK. Stickler syndrome associated with congenital glaucoma. *Lancet*. 2013;381(9864):422.
79. Watanabe H, Kohzaki K, Kubo H, Okano K, Watanabe A, Tsuneoka H. [Stickler syndrome with rhegmatogenous retinal detachment.]. *Nippon Ganka Gakkai Zasshi*. 2010;114(5):454–458.
80. Chen KC, Jung JJ, Engelbert M. Giant premacular bursa: a novel finding of the posterior vitreous in two patients with Stickler syndrome type 1 revealed by swept-source optical coherence tomography. Graefes Arch Clin Exp Ophthalmol. 2015. *Graefes Arch Clin Exp Ophthalmol*. 2016;254(3):591–593.
81. Khan AO, Aldahmesh MA, Mohamed JY, Al-Mesfer S, Alkuraya FS. The distinct ophthalmic phenotype of Knobloch syndrome in children. *Br J Ophthalmol*. 2012;96(6):890–895.
82. Rabinowitz R, Gradstein L, Galil A, Levy J, Lifshitz T. The

ocular manifestations of Weissenbacher–Zweymuller syndrome. *Eye (Lond)*. 2004;18(12):1258–1263.
83. Parma ES, Korkko J, Hagler WS, Ala-Kokko L. Radial perivascular retinal degeneration: a key to the clinical diagnosis of an ocular variant of Stickler syndrome with minimal or no systemic manifestations. *Am J Ophthalmol*. 2002;134(5):728–734.
84. Miloro M. Mandibular distraction osteogenesis for pediatric airway management. *J Oral Maxillofac Surg*. 2010;68(7):1512–1523.
85. Ihanamaki T, Metsaranta M, Rintala M, Vuorio E, Sandberg-Lall M. Ocular abnormalities in transgenic mice harboring mutations in the type II collagen gene. *Eur J Ophthalmol*. 1996;6(4):427–435.
86. Fincham GS, Pasea L, Carroll C, et al. Prevention of retinal detachment in Stickler syndrome: the Cambridge prophylactic cryotherapy protocol. *Ophthalmology*. 2014;121(8):1588–1597.
87. Haas J. Ueber das zusammenvorkommen von veraenderungen der retina und choroidea. *Arch Augenheilkd*. 1898;37:343–348.
88. Pagenstecher HE. Über eine unter dem Bilde der Netzhautablösung verlaufende, erbliche Erkrankung der Retina. *Graefes Archiv Ophthalmol*. 1913;86(3):457–462.
89. Jager G. A hereditary retinal disease. *Trans Ophthalmol Soc U K*. 1953;73:617–619.
90. Kim SY, Ko HS, Yu YS, et al. Molecular genetic characteristics of X-linked retinoschisis in Koreans. *Mol Vis*. 2009;15:833–843.
91. Lamey T, Laurin S, Chelva E, De Roach J. Genotypic analysis of X-linked retinoschisis in Western Australia. *Adv Exp Med Biol*. 2010;664:283–291.
92. Teixeira C, Rocha-Sousa A, Trump D, Brandao E, Falcao-Reis F. Identification of XLRS1 gene mutation (608C > T) in a Portuguese family with juvenile retinoschisis. *Eur J Ophthalmol*. 2005;15(5):638–640.
93. Biswas S, Funnell CL, Gray J, Bunting R, Lloyd IC, Stanga PE. Nidek MP-1 microperimetry and Fourier domain

optical coherence tomography (FD-OCT) in X linked retinoschisis. *Br J Ophthalmol*. 2010;94(7):949–950.
94. Sikkink SK, Biswas S, Parry NR, Stanga PE, Trump D. X-linked retinoschisis: an update. *J Med Genet*. 2007;44(4):225–232.
95. Garcia-Arumi J, Corcostegui IA, Navarro R, Zapata MA, Berrocal MH. Vitreoretinal surgery without schisis cavity excision for the management of juvenile X linked retinoschisis. *Br J Ophthalmol*. 2008;92(11):1558–1560.
96. Lesch B, Szabo V, Kanya M, et al. Clinical and genetic findings in Hungarian patients with X-linked juvenile retinoschisis. *Mol Vis*. 2008;14:2321–2332.
97. Vainio-Mattila B, Eriksson AW, Forsius H. X-chromosomal recessive retinoschisis in the Region of Pori. An ophthalmo-genetical analysis of 103 cases. *Acta Ophthalmol (Copenh)*. 1969;47(5):1135–1148.
98. Riveiro-Alvarez R, Trujillo-Tiebas MJ, Gimenez-Pardo A, et al. Correlation of genetic and clinical findings in Spanish patients with X-linked juvenile retinoschisis. *Invest Ophthalmol Vis Sci*. 2009;50(9):4342–4350.
99. Sauer CG, Gehrig A, Warneke-Wittstock R, et al. Positional cloning of the gene associated with X-linked juvenile retinoschisis. *Nat Genet*. 1997;17(2):164–170.
100. Grayson C, Reid SN, Ellis JA, et al. Retinoschisin, the X-linked retinoschisis protein, is a secreted photoreceptor protein, and is expressed and released by Weri-Rb1 cells. *Hum Mol Genet*. 2000;9(12):1873–1879.
101. Molday LL, Hicks D, Sauer CG, Weber BH, Molday RS. Expression of X-linked retinoschisis protein RS1 in photoreceptor and bipolar cells. *Invest Ophthalmol Vis Sci*. 2001;42(3):816–825.
102. Reid SN, Yamashita C, Farber DB. Retinoschisin, a photoreceptor-secreted protein, and its interaction with bipolar and muller cells. *J Neurosci*. 2003;23(14):6030–6040.
103. Wu WW, Wong JP, Kast J, Molday RS. RS1, a discoidin domain-containing retinal cell adhesion protein associated with X-linked retinoschisis, exists as a novel disulfide-linked octamer. *J Biol Chem*. 2005;280(11):10721–10730.

104. Wang T, Zhou A, Waters CT, O'Connor E, Read RJ, Trump D. Molecular pathology of X linked retinoschisis: mutations interfere with retinoschisin secretion and oligomerisation. *Br J Ophthalmol*. 2006;90(1):81–86.
105. Fraternali F, Cavallo L, Musco G. Effects of pathological mutations on the stability of a conserved amino acid triad in retinoschisin. *FEBS Lett*. 2003;544(1–3):21–26.
106. Huang CT, Chen SP, Tsai RK. The gene mutation in a Taiwanese family with X-linked retinoschisis. *Kaohsiung J Med Sci*. 2015;31(6):309–314.
107. Steiner-Champliaud MF, Sahel J, Hicks D. Retinoschisin forms a multi-molecular complex with extracellular matrix and cytoplasmic proteins: interactions with beta2 laminin and alphaB-crystallin. *Mol Vis*. 2006;12:892–901.
108. Horwitz J. Alpha-crystallin can function as a molecular chaperone. *Proc Natl Acad Sci USA*. 1992;89(21):10449–10453.
109. Molday LL, Wu WW, Molday RS. Retinoschisin (RS1), the protein encoded by the X-linked retinoschisis gene, is anchored to the surface of retinal photoreceptor and bipolar cells through its interactions with a Na/K ATPase-SARM1 complex. *J Biol Chem*. 2007;282(45):32792–32801.
110. Gehrig A, Langmann T, Horling F, et al. Genome-wide expression profiling of the retinoschisin-deficient retina in early postnatal mouse development. *Invest Ophthalmol Vis Sci*. 2007;48(2):891–900.
111. Dyka FM, Wu WW, Pfeifer TA, Molday LL, Grigliatti TA, Molday RS. Characterization and purification of the discoidin domain-containing protein retinoschisin and its interaction with galactose. *Biochemistry*. 2008;47(35):9098–9106.
112. Pimenides D, George ND, Yates JR, et al. X-linked retinoschisis: clinical phenotype and RS1 genotype in 86 UK patients. *J Med Genet*. 2005;42(6):e35.
113. Iannaccone A, Mura M, Dyka FM, et al. An unusual X-linked retinoschisis phenotype and biochemical characterization of the W112C RS1 mutation. *Vision Res*. 2006;46(22):3845–3852.
114. Kellner U, Brummer S, Foerster MH, Wessing A. X-linked

congenital retinoschisis. *Graefes Arch Clin Exp Ophthalmol*. 1990;228(5):432–437.
115. Mitamura Y, Miyanishi K, Shizukawa N, et al. A case of X-linked retinoschisis diagnosed in an infant. *Retina*. 2003;23(5):731–732.
116. Peachey NS, Fishman GA, Derlacki DJ, Brigell MG. Psychophysical and electroretinographic findings in X-linked juvenile retinoschisis. *Arch Ophthalmol*. 1987;105(4):513–516.
117. Campbell JP, Skalet AH, Lauer AK. Vitreous veils associated with congenital X-linked retinoschisis. *JAMA Ophthalmol*. 2015;133(8):e151155.
118. Ando A, Takahashi K, Sho K, Matsushima M, Okamura A, Uyama M. Histopathological findings of X-linked retinoschisis with neovascular glaucoma. *Graefes Arch Clin Exp Ophthalmol*. 2000;238(1):1–7.
119. Greven CM, Moreno RJ, Tasman W. Unusual manifestations of X-linked retinoschisis. *Trans Am Ophthalmol Soc*. 1990;88:211–225 [discussion 226-218].
120. Tasman W, Greven C, Moreno R. Nasal retinal dragging in X-linked retinoschisis. *Graefes Arch Clin Exp Ophthalmol*. 1991;229(4):319–322.
121. Sorsby A, Klein M, Gann JH, Siggins G. Unusual retinal detachment possibly sex-linked. *Br J Ophthalmol*. 1951;35(1):1–10.
122. George ND, Yates JR, Moore AT. Clinical features in affected males with X-linked retinoschisis. *Arch Ophthalmol*. 1996;114(3):274–280.
123. George ND, Yates JR, Bradshaw K, Moore AT. Infantile presentation of X linked retinoschisis. *Br J Ophthalmol*. 1995;79(7):653–657.
124. Garg SJ, Lee HC, Grand MG. Bilateral macular detachments in X-linked retinoschisis. *Arch Ophthalmol*. 2006;124(7):1053–1055.
125. Apushkin MA, Fishman GA, Rajagopalan AS. Fundus findings and longitudinal study of visual acuity loss in patients with X-linked retinoschisis. *Retina*. 2005;25(5):612–618.

126. McKibbin M, Booth AP, George ND. Foveal ectopia in X-linked retinoschisis. *Retina*. 2001;21(4):361–366.
127. Muscat S, Fahad B, Parks S, Keating D. Optical coherence tomography and multifocal electroretinography of X-linked juvenile retinoschisis. *Eye (Lond)*. 2001;15(Pt 6):796–799.
128. Yang HS, Lee JB, Yoon YH, Lee JY. Correlation between spectral-domain OCT findings and visual acuity in X-linked retinoschisis. *Invest Ophthalmol Vis Sci*. 2014;55(5):3029–3036.
129. Yu J, Ni Y, Keane PA, Jiang C, Wang W, Xu G. Foveomacular schisis in juvenile X-linked retinoschisis: an optical coherence tomography study. *Am J Ophthalmol*. 2010;149(6):973–978.e2.
130. Andreoli MT, Lim JI. Optical coherence tomography retinal thickness and volume measurements in X-linked retinoschisis. *Am J Ophthalmol*. 2014;158(3):567–573.e2.
131. Tanimoto N, Usui T, Takagi M, et al. Electroretinographic findings in three family members with X-linked juvenile retinoschisis associated with a novel Pro192Thr mutation of the XLRS1 gene. *Jpn J Ophthalmol*. 2002;46(5):568–576.
132. Miyake Y, Shiroyama N, Ota I, Horiguchi M. Focal macular electroretinogram in X-linked congenital retinoschisis. *Invest Ophthalmol Vis Sci*. 1993;34(3):512–515.
133. Bradshaw K, George N, Moore A, Trump D. Mutations of the XLRS1 gene cause abnormalities of photoreceptor as well as inner retinal responses of the ERG. *Doc Ophthalmol*. 1999;98(2):153–173.
134. Deutman AF, Pinckers AJ, Aan de Kerk AL. Dominantly inherited cystoid macular edema. *Am J Ophthalmol*. 1976;82(4):540–548.
135. Gehrig A, White K, Lorenz B, Andrassi M, Clemens S, Weber BH. Assessment of RS1 in X-linked juvenile retinoschisis and sporadic senile retinoschisis. *Clin Genet*. 1999;55(6):461–465.
136. Iannaccone A, Fung KH, Eyestone ME, Stone EM. Treatment of adult-onset acute macular retinoschisis in enhanced S-cone syndrome with oral acetazolamide. *Am J Ophthalmol*. 2009;147(2):307–312.e2.
137. Genead MA, Fishman GA, Walia S. Efficacy of sustained

topical dorzolamide therapy for cystic macular lesions in patients with X-linked retinoschisis. *Arch Ophthalmol*. 2010;128(2):190–197.
138. Bastos AL, Freitas Bde P, Villas Boas O, Ramiro AC. Use of topical dorzolamide for patients with X-linked juvenile retinoschisis: case report. *Arq Bras Oftalmol*. 2008;71(2):286–290.
139. Zhang L, Reyes R, Lee W, et al. Rapid resolution of retinoschisis with acetazolamide. *Doc Ophthalmol*. 2015;131(1):63–70.
140. Gopal L, Shanmugam MP, Battu RR, Shetty NS. Congenital retinoschisis: successful collapse with photocoagulation. *Indian J Ophthalmol*. 2001;49(4):265–266.
141. Avitabile T, Ortisi E, Scott IU, Russo V, Gagliano C, Reibaldi A. Scleral buckle for progressive symptomatic retinal detachment complicating retinoschisis versus primary rhegmatogenous retinal detachment. *Can J Ophthalmol*. 2010;45(2):161–165.
142. Tantri A, Vrabec TR, Cu-Unjieng A, Frost A, Annesley WH Jr, Donoso LA. X-linked retinoschisis: a clinical and molecular genetic review. *Surv Ophthalmol*. 2004;49(2):214–230.
143. Ikeda F, Iida T, Kishi S. Resolution of retinoschisis after vitreous surgery in X-linked retinoschisis. *Ophthalmology*. 2008;115(4):718–722.e1.
144. Wu WC, Drenser KA, Capone A, Williams GA, Trese MT. Plasmin enzyme-assisted vitreoretinal surgery in congenital X-linked retinoschisis: surgical techniques based on a new classification system. *Retina*. 2007;27(8):1079–1085.
145. Gupta MP, Parlitsis G, Tsang S, Chan RV. Resolution of foveal schisis in X-linked retinoschisis in the setting of retinal detachment. *J AAPOS*. 2015;19(2):172–174.
146. Yu H, Li T, Luo Y, et al. Long-term outcomes of vitrectomy for progressive X-linked retinoschisis. *Am J Ophthalmol*. 2012;154(2):394–402.e2.
147. Simonelli F, Maguire AM, Testa F, et al. Gene therapy for Leber's congenital amaurosis is safe and effective through 1.5 years after vector administration. *Mol Ther*.

2010;18(3):643–650.
148. Dyka FM, Molday RS. Coexpression and interaction of wild-type and missense RS1 mutants associated with X-linked retinoschisis: its relevance to gene therapy. *Invest Ophthalmol Vis Sci*. 2007;48(6):2491–2497.
149. Bush RA, Wei LL, Sieving PA. Convergence of human genetics and animal studies: gene therapy for X-linked retinoschisis. *Cold Spring Harb Perspect Med*. 2015;5(8):a017368.
150. Zeng Y, Takada Y, Kjellstrom S, et al. RS-1 gene delivery to an adult Rs1h knockout mouse model restores ERG b-wave with reversal of the electronegative waveform of X-linked retinoschisis. *Invest Ophthalmol Vis Sci*. 2004;45(9):3279–3285.
151. Min SH, Molday LL, Seeliger MW, et al. Prolonged recovery of retinal structure/function after gene therapy in an Rs1h-deficient mouse model of x-linked juvenile retinoschisis. *Mol Ther*. 2005;12(4):644–651.
152. Janssen A, Min SH, Molday LL, et al. Effect of late-stage therapy on disease progression in AAV-mediated rescue of photoreceptor cells in the retinoschisin-deficient mouse. *Mol Ther*. 2008;16(6):1010–1017.
153. Byrne LC, Ozturk BE, Lee T, et al. Retinoschisin gene therapy in photoreceptors, Müller glia or all retinal cells in the Rs1h$^{-/-}$ mouse. *Gene Ther*. 2014;21(6):585–592.
154. Ballios BG, Cooke MJ, van der Kooy D, Shoichet MS. A hydrogel-based stem cell delivery system to treat retinal degenerative diseases. *Biomaterials*. 2010;31(9):2555–2564.
155. Yanagi Y, Takezawa S, Kato S. Distinct functions of photoreceptor cell-specific nuclear receptor, thyroid hormone receptor beta2 and CRX in one photoreceptor development. *Invest Ophthalmol Vis Sci*. 2002;43(11):3489–3494.
156. Schorderet DF, Escher P. NR2E3 mutations in enhanced S-cone sensitivity syndrome (ESCS), Goldmann–Favre syndrome (GFS), clumped pigmentary retinal degeneration (CPRD), and retinitis pigmentosa (RP). *Hum Mutat*. 2009;30(11):1475–1485.
157. Brydak-Godowska J, Makowiec-Tabernacka M. Goldmann–

Favre syndrome - case report. *Klin Oczna*. 2009;111(10–12):346–347.
158. Marmor MF, Jacobson SG, Foerster MH, Kellner U, Weleber RG. Diagnostic clinical findings of a new syndrome with night blindness, maculopathy, and enhanced S cone sensitivity. *Am J Ophthalmol*. 1990;110(2):124–134.
159. To KW, Adamian M, Jakobiec FA, Berson EL. Clinical and histopathologic findings in clumped pigmentary retinal degeneration. *Arch Ophthalmol*. 1996;114(8):950–955.
160. Favre M. Two cases of hyaloid-retinal degeneration. *Ophthalmologica*. 1958;135(5–6):604–609.
161. Francois J, de Rouck A, Cambie E. Goldmann–Favre vitreo-tapeto-retinal degeneration. *Ophthalmologica*. 1974;168(2):81–96.
162. Fishman GA, Jampol LM, Goldberg MF. Diagnostic features of the Favre–Goldmann syndrome. *Br J Ophthalmol*. 1976;60(5):345–353.
163. Marmor MF. A teenager with nightblindness and cystic maculopathy: enhanced S cone syndrome (Goldmann–Favre syndrome). *Doc Ophthalmol*. 2006;113(3):213–215.
164. Hood DC, Cideciyan AV, Roman AJ, Jacobson SG. Enhanced S cone syndrome: evidence for an abnormally large number of S cones. *Vision Res*. 1995;35(10):1473–1481.
165. Milam AH, Rose L, Cideciyan AV, et al. The nuclear receptor NR2E3 plays a role in human retinal photoreceptor differentiation and degeneration. *Proc Natl Acad Sci USA*. 2002;99(1):473–478.
166. Peyman GA, Fishman GA, Sanders DR, Vlchek J. Histopathology of Goldmann–Favre syndrome obtained by full-thickness eye-wall biopsy. *Ann Ophthalmol*. 1977;9(4):479–484.
167. Haider NB, Naggert JK, Nishina PM. Excess cone cell proliferation due to lack of a functional NR2E3 causes retinal dysplasia and degeneration in rd7/rd7 mice. *Hum Mol Genet*. 2001;10(16):1619–1626.
168. Mitton KP, Swain PK, Khanna H, Dowd M, Apel IJ, Swaroop A. Interaction of retinal bZIP transcription factor NRL with Flt3-interacting zinc-finger protein Fiz1: possible

role of Fiz1 as a transcriptional repressor. *Hum Mol Genet*. 2003;12(4):365–373.
169. Feiler-Ofry V, Adam A, Regenbogen L, Godel V, Stein R. Hereditary vitreoretinal degeneration and night blindness. *Am J Ophthalmol*. 1969;67(4):553–558.
170. Jacobson SG, Marmor MF, Kemp CM, Knighton RW. SWS (blue) cone hypersensitivity in a newly identified retinal degeneration. *Invest Ophthalmol Vis Sci*. 1990;31(5):827–838.
171. Jacobson SG, Roman AJ, Roman MI, Gass JD, Parker JA. Relatively enhanced S cone function in the Goldmann–Favre syndrome. *Am J Ophthalmol*. 1991;111(4):446–453.
172. Fishman GA, Peachey NS. Rod–cone dystrophy associated with a rod system electroretinogram obtained under photopic conditions. *Ophthalmology*. 1989;96(6):913–918.
173. Greenstein VC, Zaidi Q, Hood DC, Spehar B, Cideciyan AV, Jacobson SG. The enhanced S cone syndrome: an analysis of receptoral and post-receptoral changes. *Vision Res*. 1996;36(22):3711–3722.
174. Khairallah M, Ladjimi A, Ben Yahia S, Zaouali S, Messaoud R. Boulima K. Elevated macular retinoschisis associated with Goldmann–Favre syndrome successfully treated with grid laser photocoagulation. *Retina*. 2002;22(2):234–237.
175. Kaufman SJ, Goldberg MF, Orth DH, Fishman GA, Tessler H, Mizuno K. Autosomal dominant vitreoretinochoroidopathy. *Arch Ophthalmol*. 1982;100(2):272–278.
176. Lafaut BA, Loeys B, Leroy BP, Spileers W, De Laey JJ, Kestelyn P. Clinical and electrophysiological findings in autosomal dominant vitreoretinochoroidopathy: report of a new pedigree. *Graefes Arch Clin Exp Ophthalmol*. 2001;239(8):575–582.
177. Roider J, Fritsch E, Hoerauf H, Heide W, Laqua H. Autosomal dominant vitreoretinochoroidopathy. *Retina*. 1997;17(4):294–299.
178. Blair NP, Goldberg MF, Fishman GA, Salzano T. Autosomal dominant vitreoretinochoroidopathy (ADVIRC). *Br J Ophthalmol*. 1984;68(1):2–9.
179. Han DP, Lewandowski MF. Electro-oculography in

autosomal dominant vitreoretinochoroidopathy. *Arch Ophthalmol*. 1992;110(11):1563–1567.
180. Sarra GM, Weigell-Weber M, Kotzot D, Niemeyer G, Messmer E, Hergersberg M. Clinical description and exclusion of candidate genes in a novel autosomal recessively inherited vitreoretinal dystrophy. *Arch Ophthalmol*. 2003;121(8):1109–1116.
181. Jampol LM, Ebroon DA, Goldbaum MH. Peripheral proliferative retinopathies: an update on angiogenesis, etiologies and management. *Surv Ophthalmol*. 1994;38(6):519–540.
182. Bennett SR, Folk JC, Kimura AE, Russell SR, Stone EM. Raphtis EM. Autosomal dominant neovascular inflammatory vitreoretinopathy. *Ophthalmology*. 1990;97(9):1125–1135 [discussion 1135-1126].
183. Stone EM, Kimura AE, Folk JC, et al. Genetic linkage of autosomal dominant neovascular inflammatory vitreoretinopathy to chromosome 11q13. *Hum Mol Genet*. 1992;1(9):685–689.
184. Gitter KA, Rothschild H, Waltman DD, Scott B, Azar P. Dominantly inherited peripheral retinal neovascularization. *Arch Ophthalmol*. 1978;96(9):1601–1605.

44

Macular Dystrophies

Elliott H. Sohn, Robert F. Mullins, Edwin M. Stone

Introduction

Historically, the term “macular dystrophy” has been used to refer

to a group of heritable disorders that cause ophthalmoscopically visible abnormalities in the portion of the retina bounded by the temporal vascular arcades. Most medical terms tend to suffer over time because evolving scientific knowledge reveals inconsistencies with their conventional use, and “macular dystrophy” is no exception. For example, age-related macular degeneration (AMD) affects the macula and has a significant genetic component. However, the genes that cause AMD interact with each other and with the environment in a sufficiently non-Mendelian fashion that it is not typically considered one of the macular dystrophies. Achromatopsia, foveal hypoplasia, and albinism are also Mendelian disorders that cause ophthalmoscopically visible abnormalities of the macula, but these, too, are not typically grouped among the macular dystrophies. In the first case, it is probably because the visible macular lesions first appear decades after the visual dysfunction is evident, while in the latter cases, it is probably because the macular abnormalities are developmental, completely stationary, and do not cause any discoloration of the macular structures. The unifying features of the conditions presented in this chapter are that they are inherited in a Mendelian fashion; the associated pathology is limited to the eye; and lesions are biomicroscopically visible in the macula when symptoms first occur (and in some cases, before symptoms occur). For most of the disorders, the mechanism underlying their macular predilection is unclear but may be related to the anatomic differences in density, structure, and composition of the choriocapillaris, Bruch's membrane, retinal pigment epithelium (RPE), and photoreceptor cells; differences in light exposure; regional gene expression patterns; blood flow; or other factors. A better understanding of the development and cell biology of the macular region, and how it differs from the extramacular retina, will be crucial in developing a deeper understanding of macular dystrophies and devising improved therapies for them.

The genes that cause most of the disorders in this chapter have been identified, and at first glance it is tempting to try to eliminate the inconsistencies in the historical clinical nomenclature by abandoning it in favor of a scheme that is solely based on the causative genes. However, there are several serious disadvantages

to such an approach. First, patients present with symptoms and signs – not with genetic test results. In addition, the near-term disease course in a given patient is usually more tightly correlated to their current clinical appearance and visual function than it is to their genotype. Thus, even in the molecular era, clinicians need to think first in terms of clinical patterns and second about the molecular mechanisms underlying these patterns. Prior to 1985 the clinical diagnosis was for all practical purposes the final diagnosis. Today the initial clinical diagnosis is really a hypothesis that has some prognostic weight by itself, and also serves to focus the search for a more precise and definitive molecular understanding of the patient's disease through genetic testing. Clinicians are often bothered by the fact that there is an imperfect correlation between mutations in specific genes and the resulting clinical outcomes. That is, mutations in a single gene (e.g., *PRPH2* and *ABCA4*) can cause quite different clinical appearances in different patients (e.g., retinitis pigmentosa and macular dystrophy) while a single clinical appearance (e.g., retinitis pigmentosa) can be caused by mutations in many different genes. The best way to cope with this imperfect correlation is to simply accept that the clinical diagnosis has greater validity in certain contexts while the molecular diagnosis has greater validity in others – and that the one can often strengthen the other. For example, prior to the discovery of the causative genes, characteristic clinical features were used to select genetically similar patients from heterogeneous clinic populations for the purpose of gene discovery. Now that many of the disease genes are known, genetic testing can be used to select genetically similar cohorts from clinically heterogeneous populations for the purpose of identifying the range of clinical features that can be associated with mutations in each gene. In this chapter we have taken advantage of molecular diagnosis in our patients to illustrate some unusual clinical presentations of these macular dystrophies that would have been difficult to include in such a chapter in the premolecular era. For the most part, we have retained the historical names associated with specific phenotypes and have grouped these whenever they are known to be caused by mutations in a single gene. We have also organized the disorders in the approximate order of their prevalence in the population with the more common diseases first.

Table 44.1 summarizes the genetic characterization for all of the macular dystrophies discussed in this chapter.

TABLE 44.1

Macular Dystrophies

Disease Name	Gene	Chromosome	Inheritance
Best macular dystrophy	*BEST1*	11	AD/AR
Stargardt disease	*ABCA4*	1	AR
Stargardt-like dominant macular dystrophy	*ELOVL4*	6	AD
Prom-1 associated macular dystrophy	*PROM-1*	4	AD
Pattern dystrophy	*PRPH2*	6	AD
Sorsby fundus dystrophy	*TIMP3*	22	AD
Autosomal dominant radial drusen	*EFEMP1*	2	AD
North Carolina macular dystrophy	Unknown	5 and 6	AD
Spotted cystic dystrophy	Unknown	Unknown	AD
Dominant cystoid macular edema	Unknown	7	AD
Fenestrated sheen macular dystrophy	Unknown	Unknown	AD
Glomerulonephritis type II	*CFH*	1	AR

AD, autosomal dominant; AR, autosomal recessive.

The Initial Approach to a Patient With Macular Dystrophy

Perhaps the most important step in managing a patient with a macular dystrophy is to convince oneself that the patient truly has a Mendelian condition and not one of the many toxic, infectious, autoimmune, or multigenic disorders that can mimic them. Except in extraordinary circumstances, macular dystrophies are bilateral, and in the early years of the disease are usually extremely symmetrical in their fundus appearance. Autoimmune disorders like presumed ocular histoplasmosis syndrome and multifocal choroiditis are often bilateral but much less symmetrical in their appearance (Fig. 44.1). Most of the macular dystrophies are inherited in an autosomal dominant fashion and thus one or more living affected relatives often exist. Identification of such a relative is one of the most powerful and most underutilized diagnostic maneuvers the clinician has at his or her disposal. One should always take a careful family history from patients suspected to have a macular dystrophy, realizing that affected individuals over the

age of 50 will often carry the diagnosis of AMD. One should also remember that dominant macular dystrophies often exhibit variable expressivity and incomplete penetrance, such that a patient's parents can be normal by history while more distant relatives can exhibit macular disease. Thus, when taking the history one should be very suspicious of any relative reported to have a macular disease of any kind. One should also examine any first-degree relatives who accompany the patient to the clinic and request fundus photographs and other ophthalmic records from all relatives with a history of macular disease. Not infrequently an affected relative will exhibit the "classic" features of a specific macular dystrophy but carry the diagnosis of AMD while the patient before you will exhibit a more puzzling fundus appearance and/or set of symptoms.

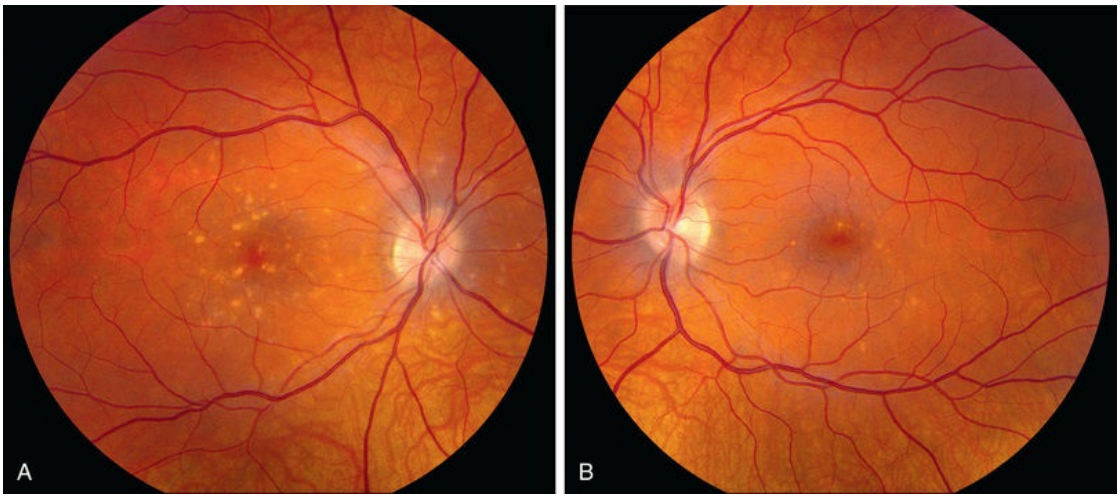

FIG. 44.1 A 33-year-old female with 20/20 visual acuity in both eyes and ovoid-circular fleck-like changes in the macula and around the disc. Although the appearance of either eye could be mistaken for disease due to *ABCA4* or *RDS* mutations, the asymmetry is more suggestive of inflammatory disease. This patient has multifocal choroiditis.

There are two classes of disease one should be especially careful to think about when initially considering a diagnosis of macular dystrophy: neuronal ceroid lipofuscinosis (NCL) and drug toxicity. In children between the ages of 6 and 8 years, NCL (a fatal systemic disease) can present with a Stargardt-like appearance and no

systemic features of any kind (Fig. 44.2). The electroretinogram is usually markedly abnormal in visually symptomatic patients with NCL but is much less likely to be abnormal in a Stargardt patient of that age. The visual dysfunction associated with NCL (both visual field and visual acuity) also tends to progress much more rapidly than Stargardt disease – over months instead of years. The other class of disease to explicitly consider and exclude in every patient suspected to have a macular dystrophy is drug toxicity. One should ask patients whether they are taking or have ever taken any medications over an extended period of time, especially medications for arthritis or skin disease (Fig. 44.3). Table 44.2 provides a list of medications that can cause macular lesions that mimic a macular dystrophy.

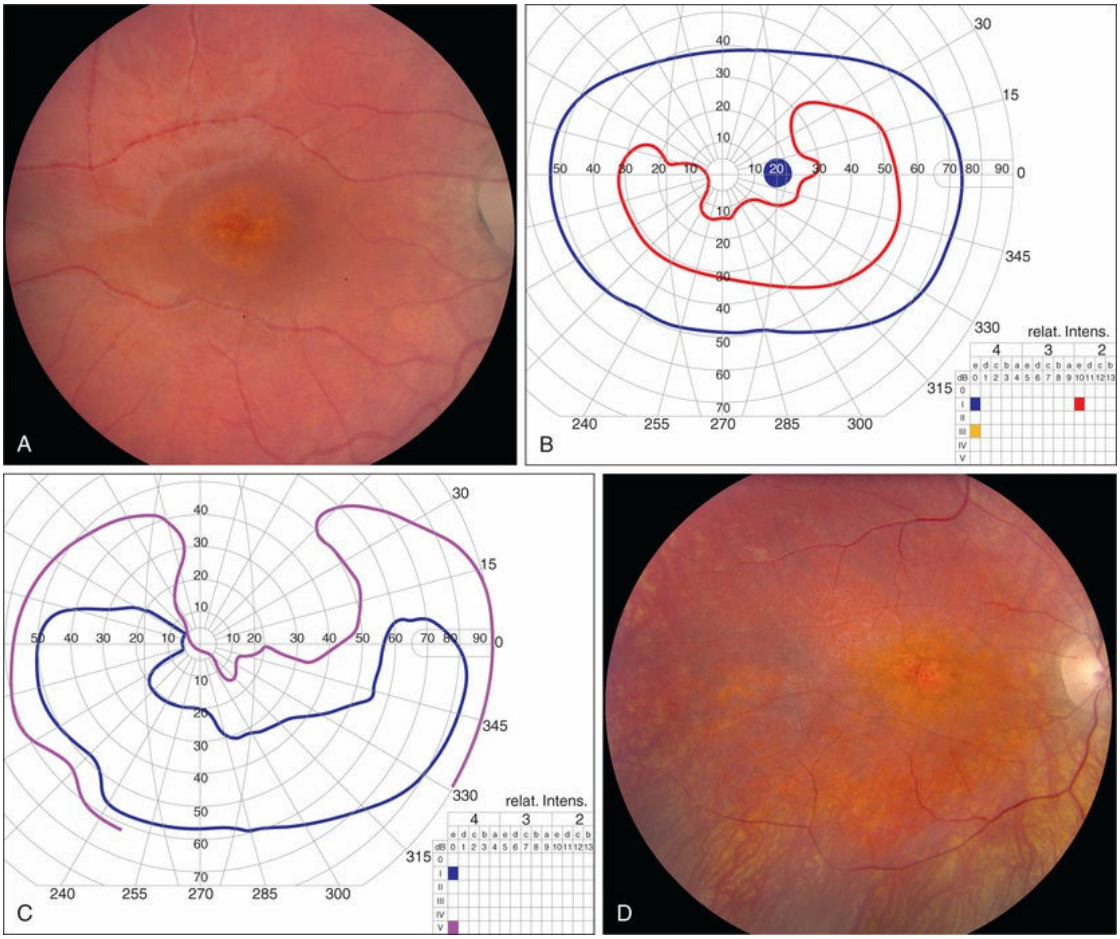

FIG. 44.2 A 5-year-old male with mutations in *PPT1* (Thr75Pro/Arg122Trp) causing neuronal ceroid lipofuscinosis. (A) When first seen he had 20/125 visual acuity and an ovoid area of macular thinning. (B)

On Goldmann perimetry, the I4e isopter is full and the I2e is still detectable. (C) By age 7 years the visual acuity had fallen to counts fingers, and the I2e isopter has been lost and there is a central and superior scotoma to the V4e target. (D) This was accompanied by progressive thinning of the retinal pigment epithelium and narrowing of the retinal vessels throughout the posterior pole.

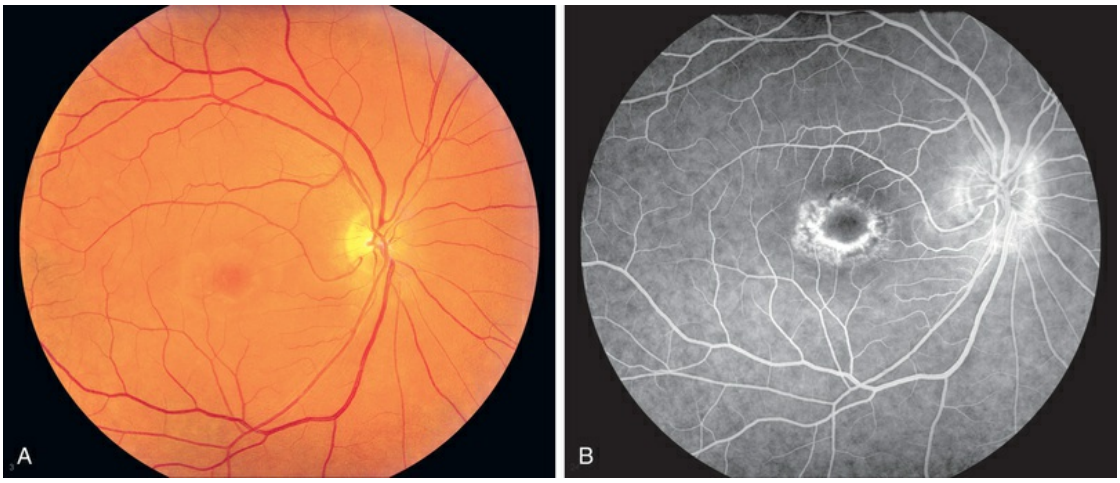

FIG. 44.3 Panels (A) and (B) depict the right eye of a 50-year-old female with plaquenil toxicity and a bull's-eye fundus appearance that could easily be mistaken for Stargardt disease without flecks (compare with Fig. 44.30). Her visual acuity was 20/30.

TABLE 44.2
Drug Toxicities Mimicking Dystrophies

Agent	Reference(s)
Chloroquine	Hobbs et al., 1959; Marmor et al., 2011
Hydroxychloroquine	Shearer et al., 1965; Marmor et al., 2011;
Thioridazine (mellaril)	Weekley et al., 1960
Chlorpromazine (thorazine)	Delong et al., 1965
Clofazimine	Craythorn et al., 1986
Tamoxifen	Kaiser-Kupfer and Lippman, 1978
Oxalosis/methoxyflurane	Bullock and Albert, 1975; Albert et al., 1975
Canthaxanthin	Boudreault et al., 1983; Ros et al., 1985
Nitrofurantoin	Ibanez et al., 1994
Talc	AtLee, 1972
Deferoxamine	Haimovici et al., 2002; Gonzales et al., 2004

Albert DM, Bullock JD, Lahav M, et al. Flecked retina secondary to oxalate crystals from methoxyflurane anesthesia: clinical and experimental studies. Trans Sect Ophthalmol Am Acad Ophthalmol Otolaryngol 1975;79(6):OP817–26.

AtLee WE, Jr. Talc and cornstarch emboli in eyes of drug abusers. JAMA 1972;219(1):49–51.

Boudreault G, Cortin P, Corriveau LA, et al. [Canthaxanthin retinopathy: 1. Clinical study in 51 consumers.] Can J Ophthalmol 1983;18(7):325–8.

Bullock JD, Albert DM. Flecked retina. Appearance secondary to oxalate crystals from methoxyflurane anesthesia. Arch Ophthalmol 1975;93(1):26–31.

Craythorn JM, Swartz M, Creel DJ. Clofazimine-induced bull's-eye retinopathy. Retina 1986;6(1):50–2.

Delong SL, Poley BJ, McFarlane JR, Jr. Ocular changes associated with long-term chlorpromazine therapy. Arch Ophthalmol 1965;73:611–17.

Gonzales CR, Lin AP, Engstrom RE, et al. Bilateral vitelliform maculopathy and deferoxamine toxicity. Retina 2004;24(3):464–7.

Haimovici R, D'Amico DJ, Gragoudas ES, et al. The expanded clinical spectrum of deferoxamine retinopathy. Ophthalmology 2002;109(1):164–71.

Hobbs HE, Sorsby A, Freedman A. Retinopathy following chloroquine therapy. Lancet 1959;2(7101):478–80.

Ibanez HE, Williams DF, Boniuk I. Crystalline retinopathy associated with long-term nitrofurantoin therapy. Arch Ophthalmol 1994;112(3):304–5.

Kaiser-Kupfer MI, Lippman ME. Tamoxifen retinopathy. Cancer Treat Rep 1978;62(3):315–20.

Marmor MF, Kellner U, Lai TY, et al. Revised recommendations on screening for chloroquine and hydroxychloroquine retinopathy. Ophthalmology 2011;118(2):415–22.

Ros AM, Leyon H, Wennersten G. Crystalline retinopathy in patients taking an oral drug containing canthaxanthin. Photodermatol 1985;2(3):183–5.

Shearer RV, Dubois EL. Ocular changes induced by long-term hydroxychloroquine (plaquenil) therapy. Am J Ophthalmol 1967;64(2):245–52.

Weekley RD, Potts AM, Reboton J, et al.. Pigmentary retinopathy in patients receiving high doses of a new phenothiazine. Arch Ophthalmol 1960;64:65–76.

Most macular dystrophies are inherited in an autosomal dominant fashion and the identification of affected individuals in multiple generations make *ABCA4*-associated disease less likely. As a general rule, patients with any of the autosomal dominant macular dystrophies often have visual acuities that are better than one might expect given the striking nature of their fundus findings, while patients with autosomal recessive Stargardt disease caused by mutations in *ABCA4* often have acuities that are poorer than one

might expect given the relatively mild abnormality of their fundus.

Best Macular Dystrophy

Best macular dystrophy (BMD), or Best disease, is an autosomal dominant condition caused by mutations in the *BEST1* gene (OMIM #607854, formerly known as *VMD2*).[1,2] The first family with this dystrophy was described by Friedrich Best in 1905.[3] Other designations for this disease have since been used, including vitelline dystrophy,[4] vitelliruptive degeneration,[5] and vitelliform dystrophy.[6] It is one of the most common Mendelian macular dystrophies, occurring in about 1 in 10,000 individuals. BMD refers to the "classic" form of a single, symmetric egg-yolk-like lesion centered on the fovea of each eye (Figs. 44.4–44.7). However, it is important to realize that *BEST1* mutations are also associated with multiple other phenotypes (multifocal Best dystrophy (Fig. 44.8), autosomal dominant vitreoretinochoroidopathy (Fig. 44.9), and autosomal recessive bestrophinopathy (Fig. 44.10)), which share only a few clinical features, detailed below.

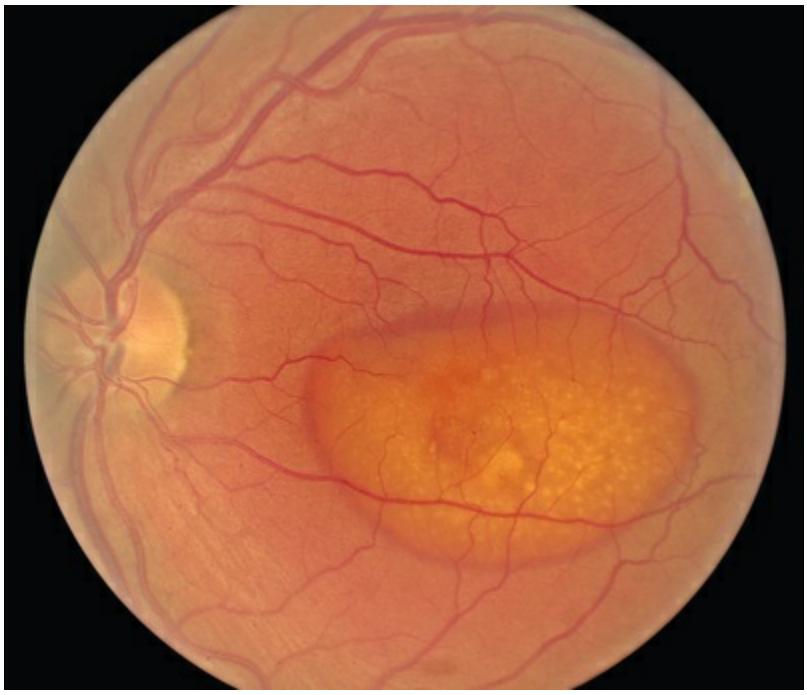

FIG. 44.4 Fundus photograph of the left eye of a 56-year-old male with a Lys30Arg mutation in *BEST1.* This eye has 20/20 visual acuity despite a very large

vitelliform lesion centered on the fovea.

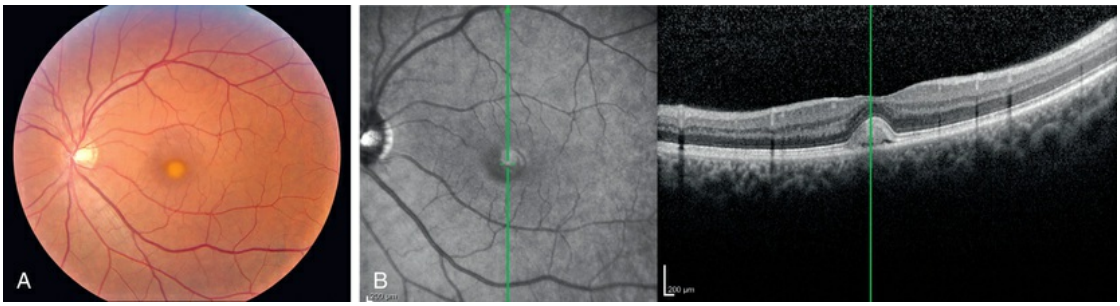

FIG. 44.5 (A) Fundus photograph of the left eye of a 40-year-old male with a Lys30Arg mutation in *BEST1.* There is a small vitelliform lesion in this eye and 20/20 visual acuity. (B) Spectral domain optical coherence tomography demonstrates hyperreflectivity of the vitelliform material in the subretinal space.

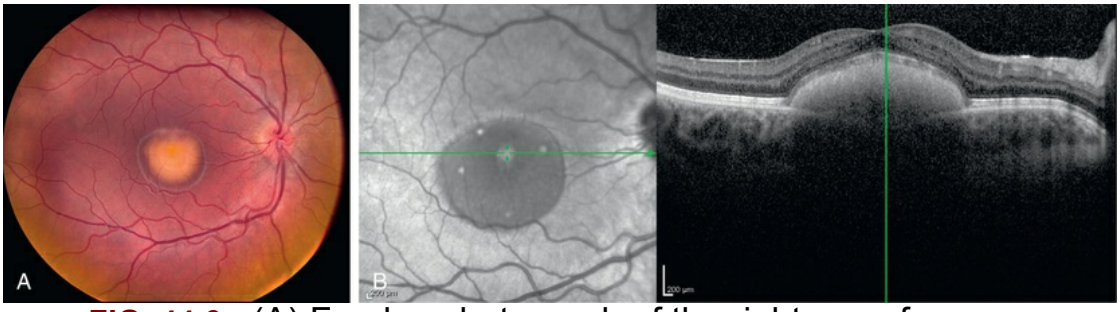

FIG. 44.6 (A) Fundus photograph of the right eye of a 15-year-old male with a Tyr227Asn mutation in *BEST1.* There is a classic vitelliform lesion in this eye and 20/40 visual acuity. (B) Spectral domain optical coherence tomography demonstrates hyperreflectivity of the vitelliform material in the subretinal space.

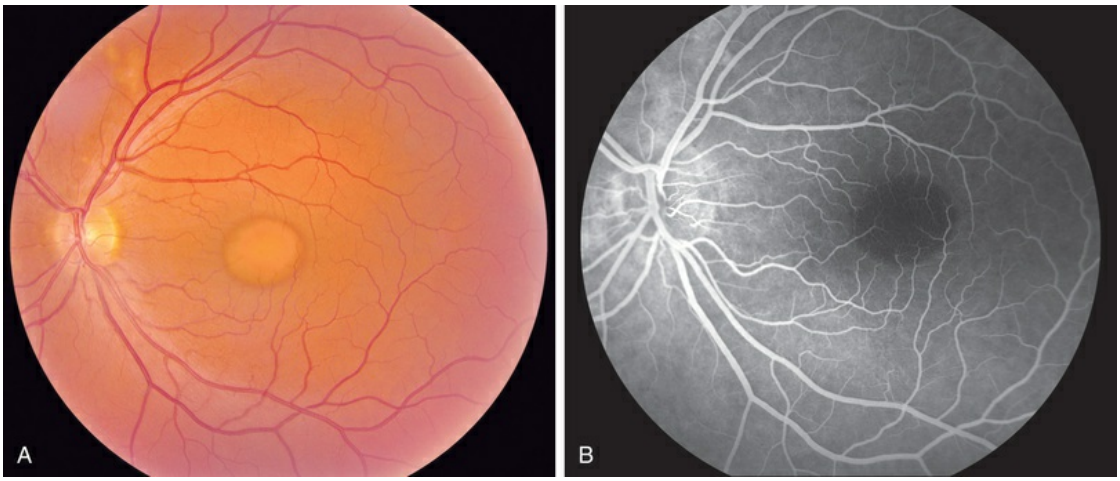

FIG. 44.7 (A) Fundus photograph of the left eye of a 51-year-old male with a 3 nucleotide deletion in *BEST1* (Leu294 del3cTCA). The visual acuity is 20/30 in this eye. The classic vitelliform lesion remains completely homogeneous after more than five decades of life. (B) Fluorescein angiography of this eye reveals almost complete masking of the normal choroidal circulation underlying the lesion.

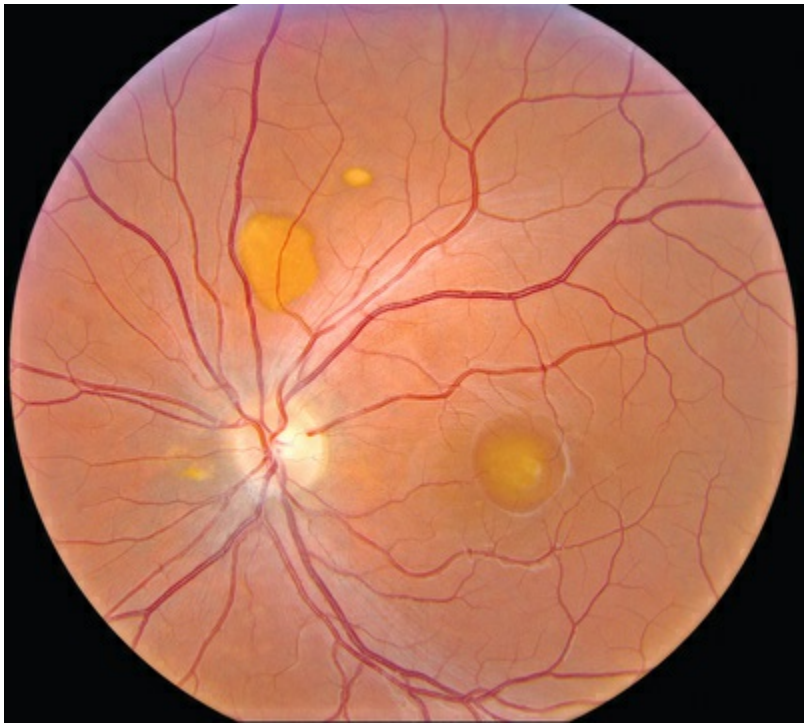

FIG. 44.8 Fundus photograph of the left eye of a 24-year-old male with a Lys30Arg mutation in *BEST1.* There is a vitelliform lesion centered on fixation and a similar lesion superior to the disc. The acuity in this

eye is 20/20.

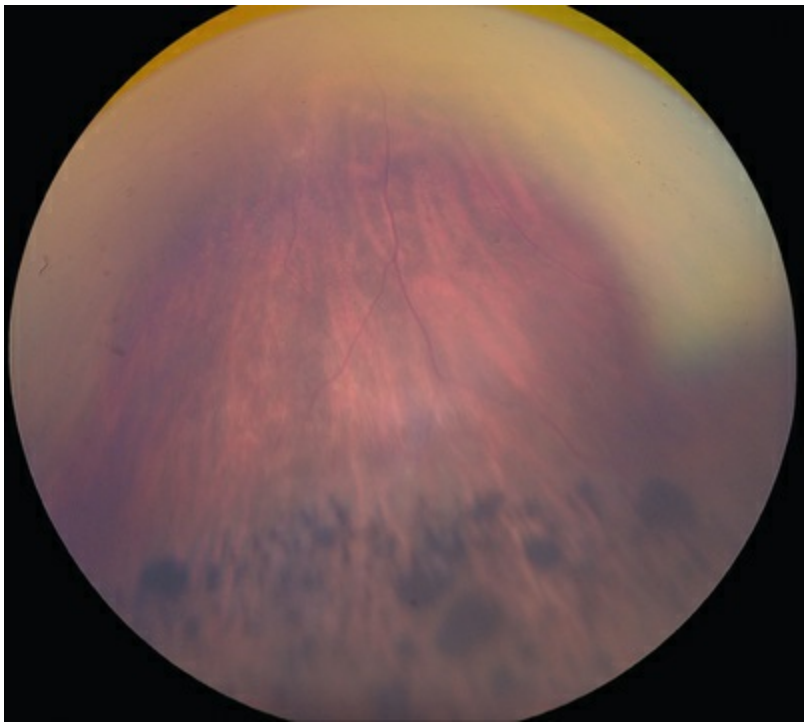

FIG. 44.9 Fundus photograph of the peripheral retina of a 70-year-old woman with ADVIRC caused by an Val239Met mutation in *BEST1*. The visual acuity is 20/100. There is a well-defined border between the normal retinal pigment epithelium and an anterior zone of retinal pigment epithelium clumping and atrophy.
(Photograph courtesy of Dr Kean Oh, Associated Retinal Consultants, Petoskey, Michigan.)

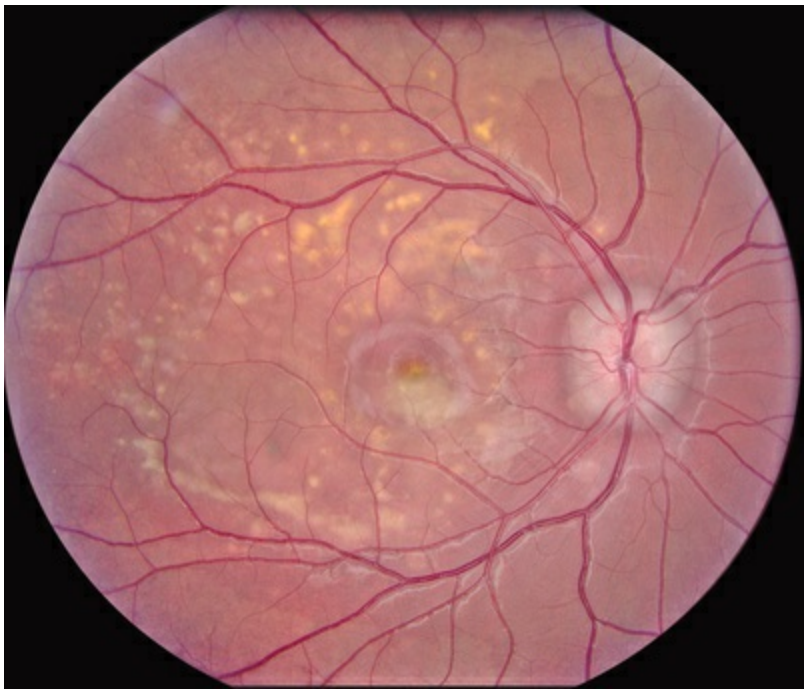

FIG. 44.10 Fundus photograph of an 11-year-old male with two mutations in *BEST1* (Arg141His/Pro152Ala) causing autosomal recessive bestrophinopathy. The visual acuity in this eye is 20/20. There are numerous yellow deposits scattered throughout the posterior pole and a patch of subretinal fibrosis just inferior to the fovea. (Reproduced from Kinnick TR, Mullins RF, Dev S, et al. Autosomal recessive vitelliform macular dystrophy in a large cohort of vitelliform macular dystrophy patients. Retina 2011;31(3):581-95.)

Clinical Features of BMD

The fundus findings associated with BMD are quite varied. The macular lesions that are most characteristic of the disease are known as "vitelliform" because of their egg-yolk-like appearance (Figs. 44.4–44.7). These lesions are typically solitary, round or horizontally oval, yellow, slightly elevated, and are centered on the fovea. Vitelliform lesions in patients with BMD can range in size from a few hundred micrometers (Fig. 44.5) to a few millimeters in diameter (Fig. 44.4). The larger lesions can be seen within the first few years of life, while the smaller lesions typically develop after age 20 and sometimes as late as age 60. As a result, the smaller lesions are sometimes referred to as "adult vitelliform" lesions (Figs. 44.5 and 44.11), a phenotype that also occurs in patients with

mutations in the *PRPH2* gene (discussed more fully below). Some individuals who harbor disease-causing mutations in *BEST1* never develop significant macular lesions.

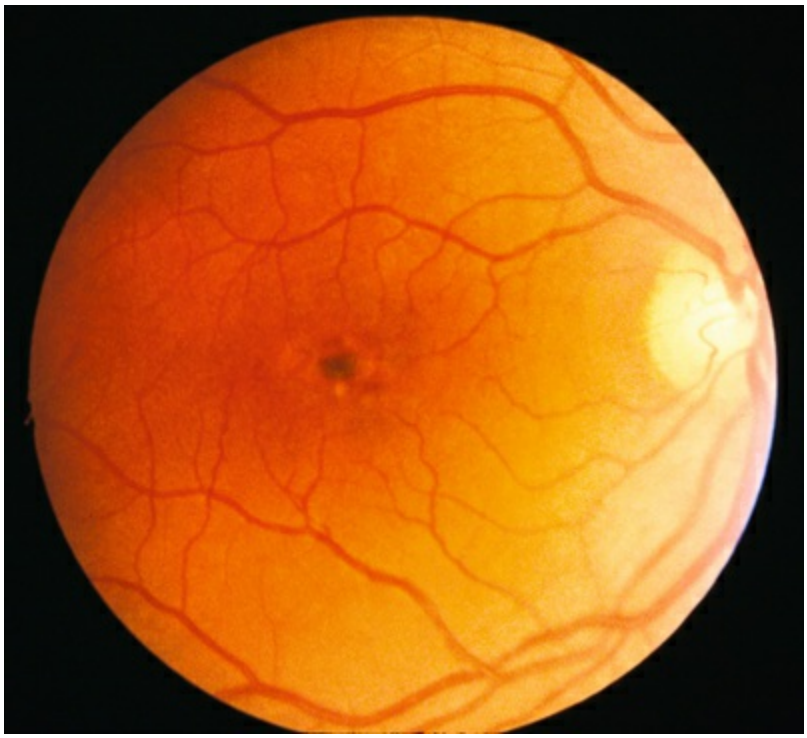

FIG. 44.11 Fundus photograph of the right eye of a 36-year-old female with an Ala243Thr mutation in *BEST1.* The visual acuity in this eye is 20/50. There is a small, oval "dot and halo" lesion centered on the fovea that is reminiscent of pattern dystrophy.

Over time, many vitelliform lesions develop a "pseudohypopyon" appearance in which the yellow material gravitates inferiorly in the subretinal space (Figs. 44.12 and 44.13). Other lesions develop varying amounts of subretinal and sub-RPE fibrosis, RPE atrophy in addition to hyperpigmentation, and atrophy of the RPE. This is sometimes known as a "scrambled-egg lesion" (Fig. 44.14). Many patients develop a single nodule of sub-RPE fibrosis centered very near the fovea (Fig. 44.15). Geographic atrophy is also fairly common after age 60 (Figs. 44.16 and 44.17), but can occur earlier in some patients. As with all diseases that disturb the RPE, true choroidal neovascularization can develop in a few percent of cases (Fig. 44.18).[7] In addition, a few patients with

vitelliform lesions develop subretinal hemorrhage following fairly modest blunt trauma to the head or eye (Fig. 44.19). Fortunately, these hemorrhages usually resolve and good vision returns without treatment. While these many clinical patterns have been described as "stages" by some authors, there is rarely a predictable progression of these fundus changes from one to the other in a given patient. Although the maculas of patients with BMD are usually quite symmetric in the early years of the disease, the two eyes can become quite strikingly different in function and appearance as the disease progresses.

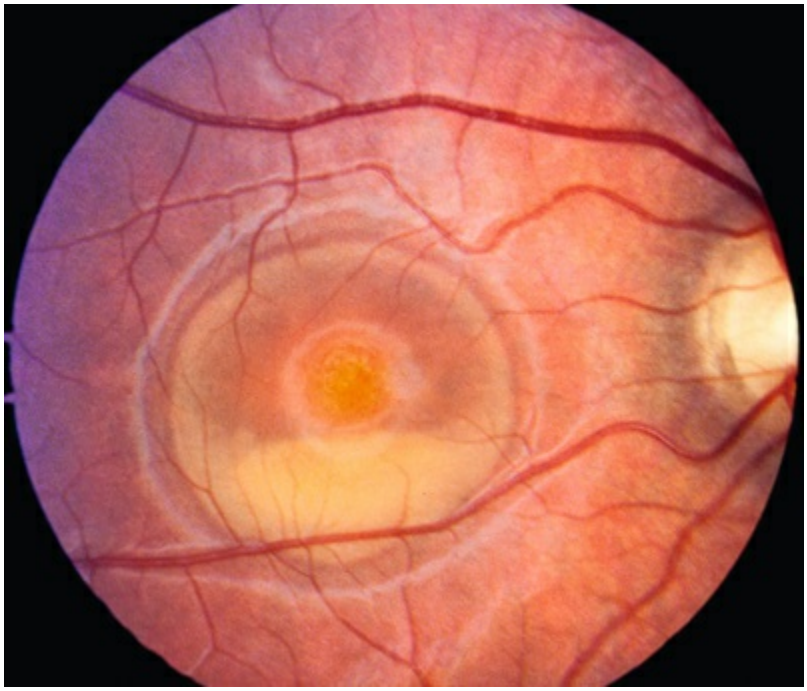

FIG. 44.12 Fundus photograph of the right eye of a 9-year-old male with a Tyr227Asn mutation in *BEST1*. This eye has 20/25 visual acuity. There is a large vitelliform lesion with a pseudohypopyon appearance characterized by layering of the lipofuscin pigment in the inferior aspect of the lesion. Some lipofuscin remains at the very margin of the lesion for its entire circumference.

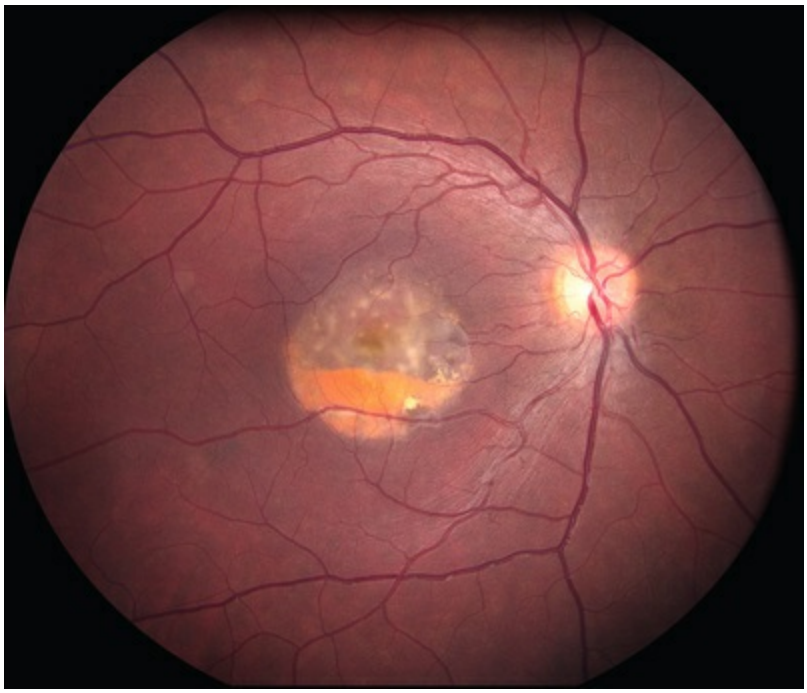

FIG. 44.13 Fundus photograph of the right eye of a 14-year-old male with a Asp302Ala mutation in *BEST1*. This eye has 20/20 visual acuity. The vitelliform lesion has a pseudohypopyon appearance.

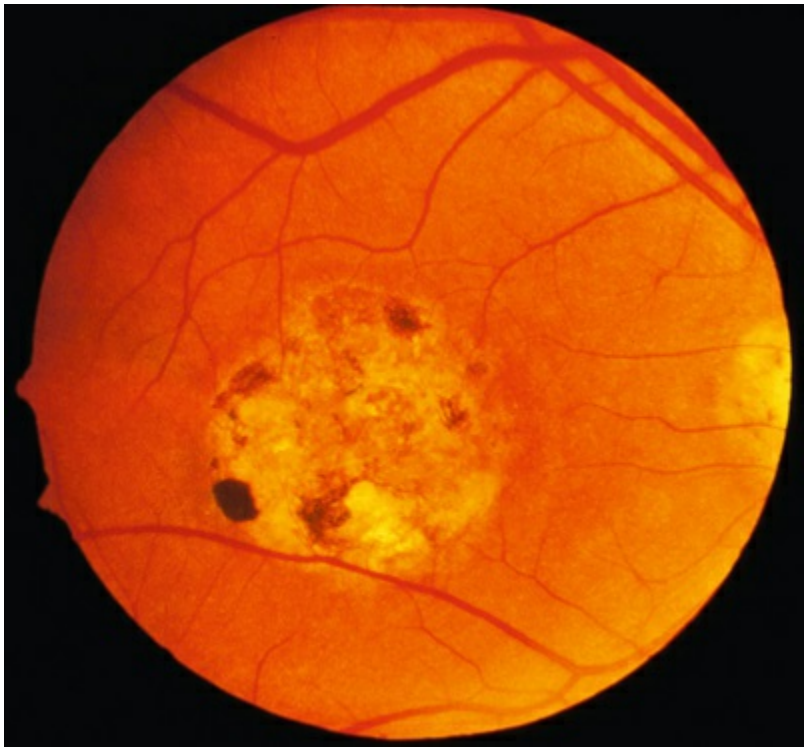

FIG. 44.14 Fundus photograph of the right eye of a 47-year-old male with a Tyr227Asn mutation in *BEST1*.

The acuity in this eye is 20/200. There is a sharply circumscribed area of RPE atrophy and RPE pigment disruption at the site of a previous vitelliform lesion.

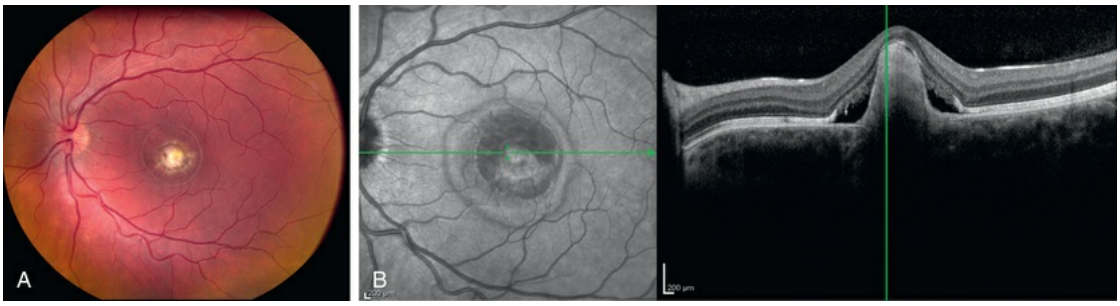

FIG. 44.15 (A) Fundus photograph of the left eye of a 15-year-old male with a Tyr227Asn mutation in *BEST1* and 20/40 visual acuity. There is a fibrotic pillar centered on fixation. (B) Spectral domain optical coherence tomography of this eye reveals the fibrotic pillar to lie beneath the RPE, surrounded by small amounts of subretinal fluid. Long outer segments can be seen extending from the retina into the subretinal fluid.

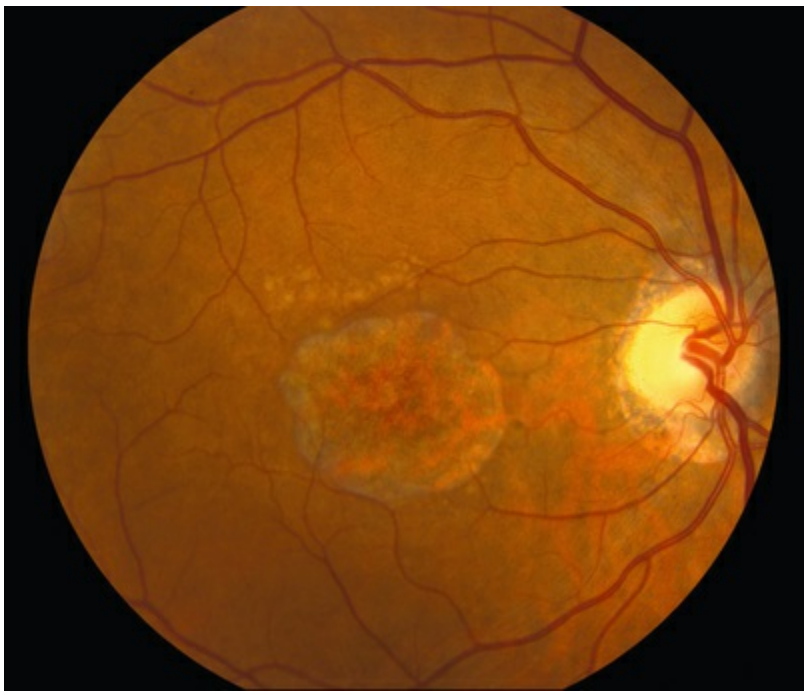

FIG. 44.16 Fundus photograph of the right eye of a 72-

year-old female with a Thr307Ile mutation in *BEST1.* She has 20/80 visual acuity in this eye. There is a circular zone of geographic atrophy centered on fixation, flanked superiorly by a few drusen-like deposits.

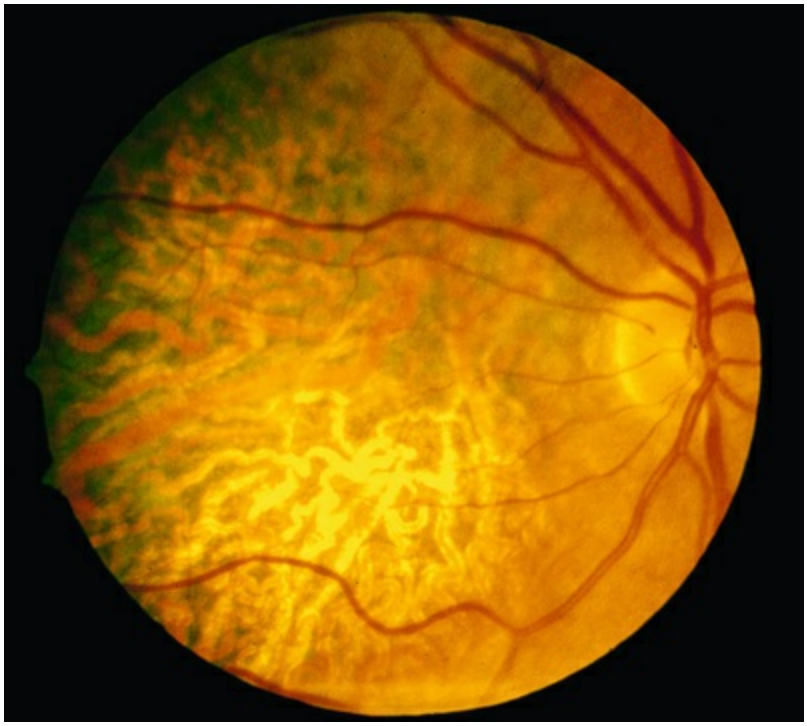

FIG. 44.17 Fundus photograph of the right eye of a 73-year-old female with an Ala243Thr mutation in *BEST1.* She has counts fingers visual acuity in this eye associated with extensive RPE atrophy and depigmentation of the choroidal vessels of the macula.

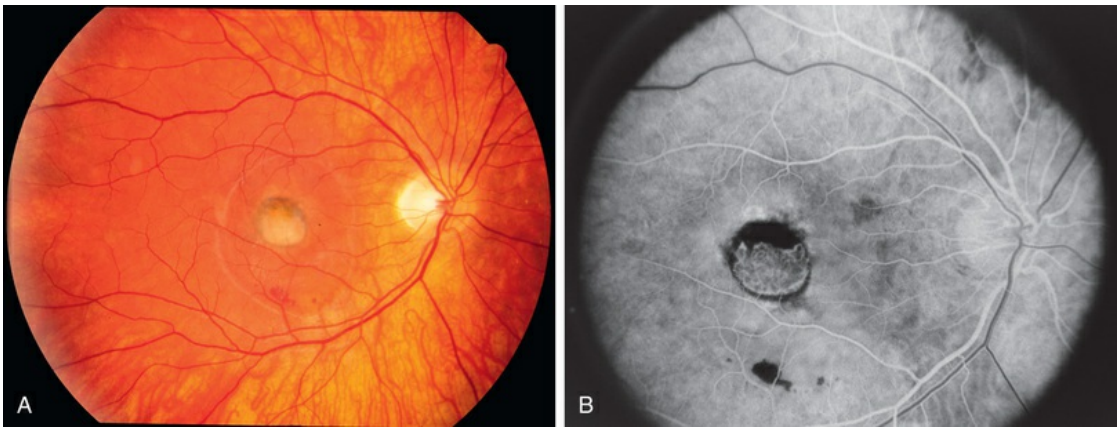

FIG. 44.18 (A) Fundus photograph of the right eye of a 23-year-old female with Best disease and an evolving subretinal fibrotic nodule. A small amount of subretinal blood can be seen at the inferior margin of the associated serous macular detachment. The acuity in this eye is 20/100. (B) The early phase of the fluorescein angiogram of this eye shows a classic choroidal neovascular membrane centered on the fibrotic nodule.

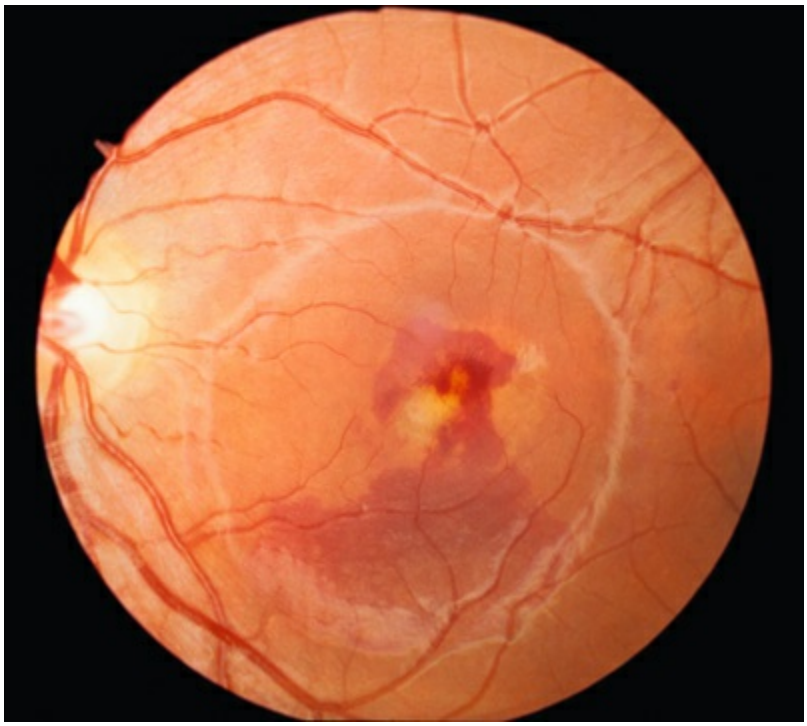

FIG. 44.19 Fundus photograph of the left eye of an 8-year-old male with an Arg218His mutation in *BEST1* and 20/70 visual acuity. The subretinal hemorrhage in the macula was first noted following a moderate blow

to the head not involving the eye. Six months later the acuity in this eye improved to 20/40 and the hemorrhage resolved without treatment.

Although most patients with Best disease exhibit a single lesion centered on the fovea, there have also been numerous reports of patients with multiple vitelliform lesions who also manifest abnormalities on electro-oculography (EOG)[8,9] and mutations in the *BEST1* gene.[10–14] In the most striking form of this multifocal phenotype, sometimes called multifocal Best dystrophy, there are multiple vitelliform lesions scattered throughout the posterior pole of both eyes (see Fig. 44.8). As with typical Best disease, these patients are asymptomatic unless the vitelliform lesions develop fibrotic scarring affecting the center of the macula. Autofluorescence and optical coherence tomography (OCT) imaging of multifocal lesions demonstrate characteristics similar to the solitary lesions seen in typical Best disease. This condition is distinguished from acute exudative polymorphous vitelliform maculopathy[15,16] as patients with the latter disorder have a normal EOG and lack variations in *BEST1*. Notably, the canine model for BMD, which is due to a recessive mutation in the canine *BEST1* gene, is associated with multifocal vitelliform lesions,[17,18] and some human patients with mutations in both alleles of *BEST1* also exhibit multifocal vitelliform lesions.[10,11,13] However, a few individuals with dominantly inherited disease and solitary lesions as children or young adults will also develop additional extramacular lesions later in life (Figs. 44.20 and 44.21).

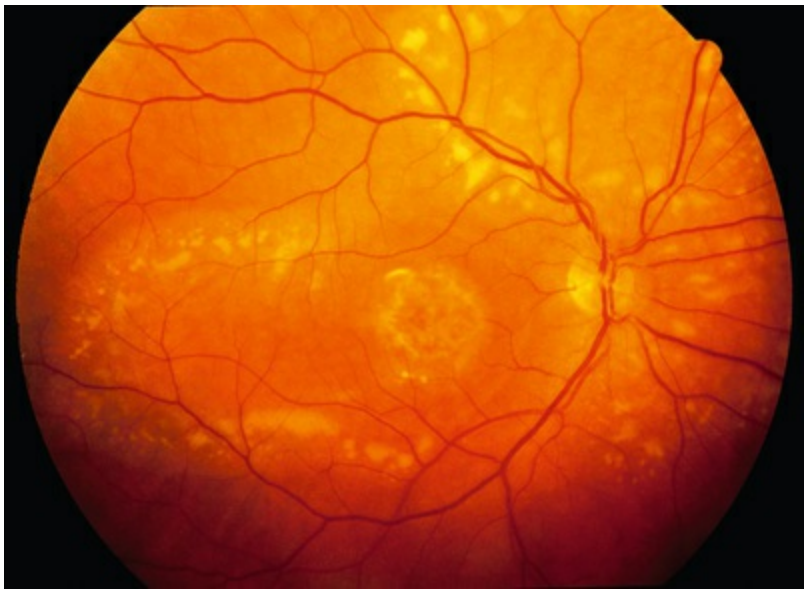

FIG. 44.20 Fundus photograph of the right eye of a 42-year-old male with a Tyr227Asn mutation in *BEST1*. This eye has 20/100 visual acuity and two large areas of subretinal fluid, one involving the entire macula and the other situated superior to the disc There are subretinal deposits of lipofuscin along the edges of both lesions.

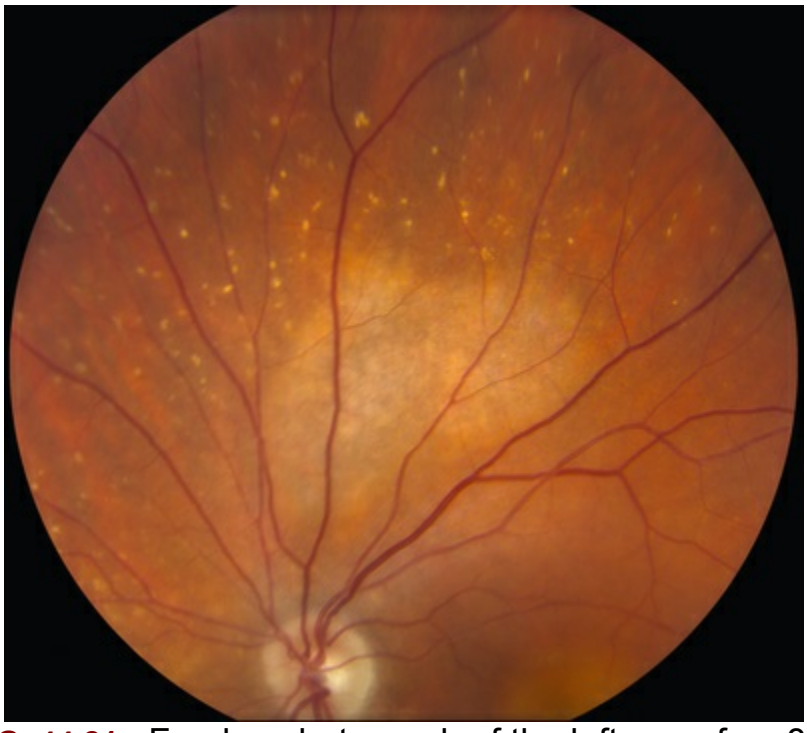

FIG. 44.21 Fundus photograph of the left eye of an 83-year-old female with a Tyr227Asn mutation in *BEST1.*

This eye has 20/80 visual acuity. There is a large vitelliform lesion superior to the disc in addition to a number of more peripheral fleck-like deposits.

Visual Function

Visual acuity (VA) sufficient to drive is usually preserved in at least one eye throughout the first six decades of life, with more substantial visual loss occurring when BMD is complicated by nodular fibrosis, choroidal neovascularization,[19–21] or central geographic atrophy.[22] VA is often 20/20 or better in eyes with undisturbed vitelliform lesions, which is surprising considering the substantial physical separation of the photoreceptor outer segments and the RPE (see Fig. 44.6) that exists for decades in some individuals (see Fig. 44.7). This suggests that the fluid within vitelliform lesions has an ionic composition relatively similar to that of the normal interphotoreceptor matrix and quite distinct from the composition of the subretinal fluid associated with rhegmatogenous retinal detachments. Some vitelliform lesions gradually flatten over time with persistence of good acuity, while others develop nodular sub-RPE scars or RPE atrophy which are associated with poorer visual acuities that are somewhat proportional to the size of the scar. Peripheral visual fields are usually completely normal in BMD, although patients with other *BEST1* phenotypes do exhibit abnormal visual fields in some cases (see below).

Refractive Error

It is common for patients with BMD to have hyperopia,[22,23] which is likely due to shortened axial length.[24] These findings are sometimes associated with narrow angles and/or angle-closure glaucoma[22,24,25] requiring peripheral iridotomy. Hyperopia and angle closure have also been demonstrated in other *BEST1* phenotypes, including autosomal dominant vitreoretinochoroidopathy (ADVIRC)[26,27] and autosomal recessive bestrophinopathy (ARB).[13] Examination of the anterior segment with particular attention to the intraocular pressure and angle is warranted in patients with BMD and other phenotypes associated with *BEST1* mutations.

Optical Coherence Tomography (OCT)

Although there have been no histopathologic studies of eyes with undisturbed vitelliform lesions, spectral domain OCT allows in vivo determination of the anatomy of macular lesions at near histopathologic resolution. The yellow material of a classic vitelliform lesion lies in the subretinal space and appears fairly homogeneous on OCT (see Figs. 44.5B and 44.6B).[28–32] In some patients, over time, some of the yellow pigment disappears and is replaced by clear fluid. The yellow pigment is denser than the clear fluid and settles gravitationally to the bottom of the vitelliform lesion with a fairly sharp horizontal line demarcating the pigment–fluid interface (see Figs. 44.12 and 44.13). This configuration is known as a "pseudohypopyon" and on OCT the yellow pigment appears hyperreflective while the clear subretinal fluid appears hyporeflective (black). Another lesion that is quite common in patients with Best disease and that has a very dramatic appearance on OCT is a fibrotic pillar that develops in the sub-RPE space, usually within 100 μm of the foveal center. These lesions appear hyperreflective on spectral domain OCT and seem to elevate the retina like a circus tent such that they are usually flanked by clear (hyporeflective on OCT) subretinal fluid (see Fig. 44.15B).

The origin of these fibrotic pillars remains obscure. Their sub-RPE location suggests a neovascular origin, but they rarely exhibit a classic neovascular pattern on fluorescein angiography and they tend to become stably fibrotic more rapidly than self-involuting choroidal neovascular membranes (CNVMs) associated with other macular diseases like the presumed ocular histoplasmosis syndrome. Although their height is exaggerated by the normal presentation of spectral domain (SD)-OCT data, they do exhibit an unusual height-to-base ratio compared to involuted CNVMs of other disorders. The development of a fibrotic pillar is associated with a relatively rapid loss of yellow pigment from the vitelliform lesion and a drop in VA, although the acuity typically remains much better than it would if a lesion of similar size and configuration developed in a patient with a different macular disease such as age-related macular degeneration.

Fluorescein Angiography and Autofluorescence

The primary clinical use of fluorescein angiography (FA) in patients with Best disease is to help differentiate non-neovascular alterations in lesion anatomy (e.g., irregular resorption of yellow pigment) from active choroidal neovascularization in patients with a recent decrease in VA. Although the vitelliform lesions of Best disease resemble the pigment epithelial detachments that occur in AMD, their anatomy and composition, however, are quite different and this causes some difficulty when interpreting fluorescein angiograms in patients with Best disease. For example, the yellow pigment filling some vitelliform lesions, especially in very young patients, is extremely hydrophobic and completely excludes fluorescein from the lesion. In such patients the vitelliform lesion blocks the underlying choroidal fluorescence almost as completely as blood would in a patient with AMD (see Fig. 44.7). Over time, the contents of the subretinal vitelliform cavities in some patients become more hydrophilic and in such cases the lesions briskly and completely fill with dye during an angiogram, much as a serous pigment epithelial detachment would in a patient with AMD (Fig. 44.22). In patients with the pseudohypopyon configuration the serous component of the lesion will fill with dye while the yellow pigment in the inferior portion of the lesion will both exclude the fluorescein from the vitelliform cavity and block the underlying choroidal fluorescence. This results in an angiogram that closely resembles a "notched" pigment epithelial detachment, which in AMD patients would suggest the presence of a choroidal neovascular membrane. In patients with Best disease this appearance is much less ominous. Autofluorescence imaging is not typically needed to make the diagnosis of Best disease or to make treatment decisions. From a research perspective, however, it is interesting that undisturbed vitelliform lesions usually exhibit uniform hyperfluorescence, while those that have some amount of sub-RPE fibrosis or atrophy usually exhibit hypofluorescence.[22,33,34] The increased autofluorescence in the undisturbed vitelliform lesions is likely a reflection of the increased amounts of lipofuscin in eyes with Best disease.[35–38]

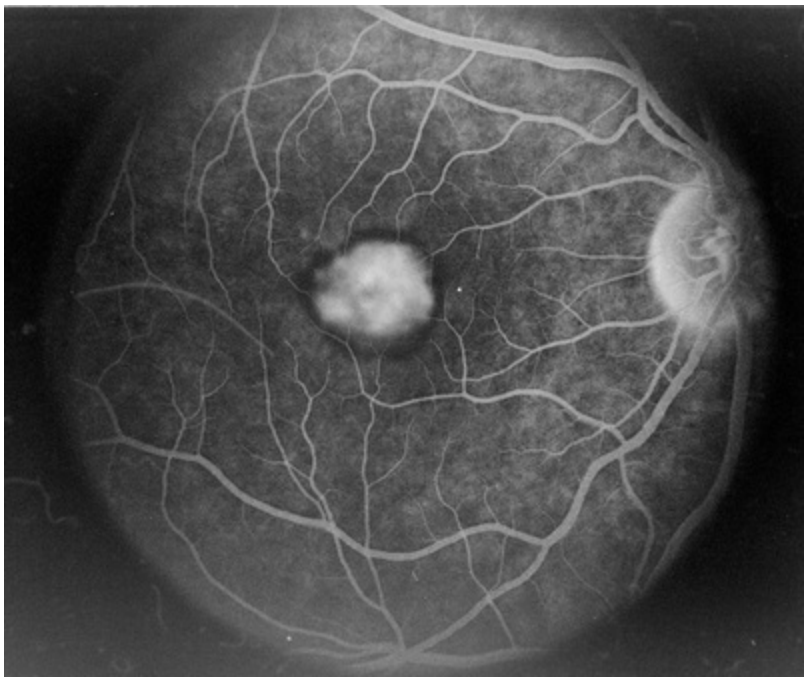

FIG. 44.22 Mid-phase fluorescein angiogram of the right eye of a 31-year-old female with an Ala243Thr mutation in *BEST1*. The acuity in this eye is 20/20. The vitelliform lesion briskly fills with dye simulating a serous pigment epithelial detachment.

Electrophysiology

Before the discovery of the gene responsible for Best disease, electrophysiologic testing played a very prominent role in the diagnosis. The electro-oculogram is usually markedly abnormal in molecularly affected individuals, even when macular lesions are not evident. In normal individuals the cornea positive standing potential of the eye is nearly twofold higher in bright light than it is in darkness, while in patients with Best disease the ratio of the light peak to dark trough (the Arden ratio) is typically less than 1.5. Full-field electroretinography (ERG) cone and rod a- and b-wave amplitudes are usually normal. The advantage of EOG over genetic testing is that diagnostic information can be obtained within an hour or two, while the patient is in the clinic. The disadvantage is that it is usually more expensive and less sensitive than molecular testing. That is, a normal EOG does not exclude the possibility of Best disease,[39–43] as 37.5% of patients in one series had a *BEST1* mutation despite a normal EOG.[39]

Genetics

Best disease was mapped to chromosome 11q13 in 1992,[44] and the causative gene was identified six years later.[1,45,46] Now known as *BEST1*, this gene encodes a 585 amino acid protein known as bestrophin that localizes to the basolateral membrane of the RPE.[47] To date, more than 100 different mutations in *BEST1* have been associated with Best disease.[1,2,22,23,34,41,42,48–62] Most disease-causing mutations are missense variants, and a substantial fraction (about 25%) occur in exon 8, suggesting that the portion of the protein encoded by this exon may be critical to its function.[22] More than 90% of families that have two or more individuals with the clinical diagnosis of Best disease will have a detectable mutation in the coding sequence of *BEST1*. As a result, a negative molecular result is clinically meaningful and suggests that the patient's disease is caused by another gene or that it is a non-Mendelian phenocopy. The gene that most commonly causes macular lesions that are clinically similar to those of Best disease is *PRPH2* (formerly *RDS*), while the most common non-Mendelian phenocopy is a pigment epithelial detachment associated with age-related macular degeneration. Mutations in *IMPG1* have also been associated with bilateral vitelliform macular lesions.[63]

Pathophysiology and Histopathology

Although Best disease is rare, there have been a number of histopathologic reports describing the structural changes that accompany this condition. Histopathologic findings include increased RPE lipofuscin,[37,38,64] loss of photoreceptors[38] (often seen over a relatively intact RPE layer[35,58]), sub-RPE drusenoid material,[35,36] and accumulation of cells and material in the subretinal space (Fig. 44.23). Following the discovery of the Best disease gene, efforts have also been made to identify the relationship between anatomical findings and specific genotypes. For example, eyes have been characterized from patients with Tyr227Asn,[58] Thr6Arg,[64] and a homozygous Trp93Cys donor.[38] From these studies it has been suggested that the eyes of patients with Tyr227Asn mutations are notable for extramacular flecks.[58] A donor eye with this mutation was also found to mislocalize bestrophin.[58]

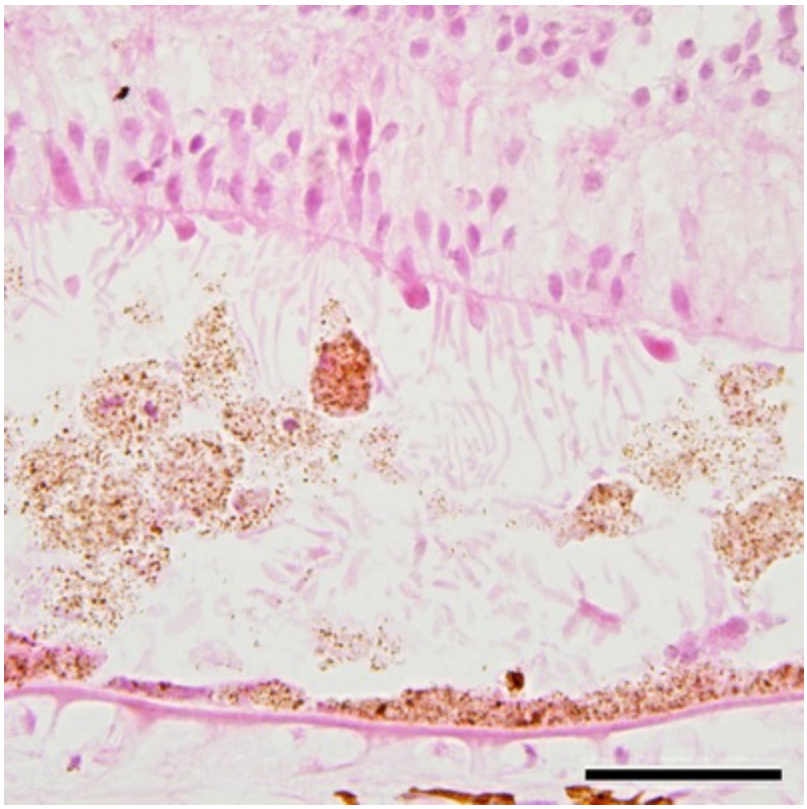

FIG. 44.23 Histologic section of the left eye of an 86-year-old donor with Best disease due to a Thr6Arg mutation in *BEST1*. Note the presence of pigment-laden cells and outer-segment debris in the subretinal space. Scale bar: 50 μm.

The molecular pathophysiology of Best disease is somewhat controversial – owing in part to the difficulty of comparing the behavior of different types of cultured cells with the RPE in vivo – and a thorough discussion of the evidence for the possible functions of the bestrophin-1 protein is beyond the scope of this chapter; it has been well reviewed elsewhere.[65–67] Briefly, the normal function of bestrophin-1 appears to include the regulation of the ionic milieu in the RPE and/or the subretinal space. When overexpressed in some cell types, bestrophin-1 appears to function as a calcium-sensitive chloride channel,[68,69] whereas mice lacking bestrophin-1[70] or harboring a mutant allele (Tryp93Cys)[71] show altered uptake of calcium by the RPE. It has been suggested that impaired ionic flow across the RPE could result in alterations in the adhesiveness between the interphotoreceptor matrix and the RPE or a diminution of outer segment phagocytosis, both of which are sensitive to levels of calcium.[72,73]

Bestrophin-1 is expressed in all RPE cells, not just those underlying the macula. Moreover, the large response of the EOG to changes in light (the Arden ratio) suggests that the entire retina participates in this response, not just the macula. Why then are the most typical Best lesions found in the macula, centered on fixation? The answer may be in part due to differences in bestrophin-1 expression in different regions of the retina.[64] However, it also seems likely that there are regional differences in the adhesion of the photoreceptors to the retinal pigment epithelium. The patient shown in Fig. 44.24 is supportive of this hypothesis. She developed an aggressive epiretinal membrane that created localized traction detachments in her left eye, and she developed yellow vitelliform material in each of these locations. After successful surgery to remove the membrane and relieve the traction, the extramacular vitelliform deposits persisted for years.

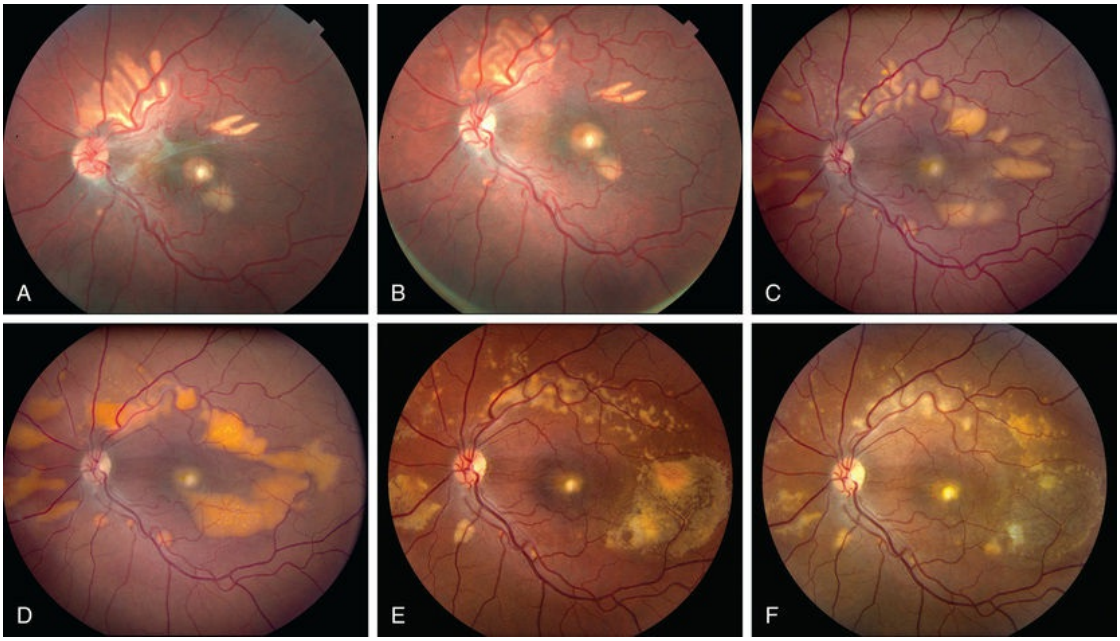

FIG. 44.24 (A) Fundus photograph of the left eye of an 18-year-old female with an Asp302Ala mutation in *BEST1*. This eye has 20/200 visual acuity and a thick epiretinal membrane that has thrown the neurosensory retina into folds. Yellow vitelliform material has formed beneath several of these folds. (B) One week after successful membrane peeling, the visual acuity remains 20/200 but there is little change in the subretinal deposits. (C) Two months after surgery, the

acuity has improved to 20/160, the distortion is much less, and the vitelliform deposits have actually increased in number and extent. (D) Ten months after surgery, at age 19, the acuity has improved to 20/125 and the vitelliform material has coalesced. (E) Four years after surgery, at age 22, the acuity has improved to 20/100 and the vitelliform material has started to disappear. (F) Four and a half years after surgery, the acuity remains 20/100 and the resolution of the vitelliform material is more complete. (Panels A and B courtesy of Dr. Richard Spaide.)

Additional Phenotypes Associated With Mutations in *BEST1*

Autosomal Dominant Vitreoretinochoroidopathy (ADVIRC)

ADVIRC was first described by Kaufman et al. in 1982[74] as a condition with (1) an autosomal dominant inheritance pattern; (2) peripheral pigmentary retinopathy for 360°, with a discrete posterior boundary near the equator (see Fig. 44.9); (3) punctate whitish opacities in the retina; (4) vitreous cells and fibrillar condensation; (5) blood–retinal barrier breakdown; (6) retinal arteriolar narrowing and occlusion; (7) retinal neovascularization; (8) choroidal atrophy; and (9) presenile cataracts (see Fig. 44.9).[75] The EOG is usually abnormal with a relatively normal ERG,[76] but the first electrophysiologic studies of ADVIRC patients[27,76,77] occurred in the premolecular era when genetic testing was not available. It has since been discovered that ADVIRC is caused by splice-altering mutations in *BEST1* and that these patients can also have concomitant developmental abnormalities, including microcornea, hyperopia, and shortened axial length.[26,78,79] Some patients have a severe form of ADVIRC in which both the ERG and EOG are abnormal, thus resembling retinitis pigmentosa.[80,81]

Autosomal Recessive Bestrophinopathy (ARB)

The first description of compound heterozygous *BEST1* mutations causing multifocal yellowish changes in the macula and cystoid

macular edema was published in 2006.[11] Subsequent descriptions of patients with mutation in both *BEST1* alleles have included both compound heterozygous and homozygous mutations and demonstrate a wide spectrum of fundus findings that are not present in their carrier parents.[10,13,82–84] Burgess et al.[13] coined the term "autosomal recessive bestrophinopathy (ARB)" to refer to this unusual presentation of *BEST1*-associated retinal disease. Hyperopia and an abnormal EOG are common. The VA in ARB can be normal but tends to be worse than in autosomal dominant Best disease. Some patients exhibit cystoid macular edema or shallow subretinal fluid that can extend throughout the macula and beyond the arcades. Both solitary and multifocal vitelliform lesions can occur, sometimes associated with flecks within and outside the macula (see Fig. 44.10). OCT can be helpful in detecting the low-lying subretinal fluid, especially in young patients who lack vitelliform lesions. Subretinal fibrosis is more common in ARB than in autosomal dominant disease.

Treatment

Treatment for *BEST1* disease consists primarily of recognizing choroidal neovascularization and hastening its regression with anti-VEGF therapy. Though the natural history of subretinal hemorrhage in BMD is relatively good,[19] preservation of visual function for choroidal neovascularization (CNV) has been reported in retrospective studies using intravitreal bevacizumab and ranibizumab.[82,85–89] In our experience, it is not usually possible to completely eradicate subretinal fluid that exists adjacent to the nodular fibrotic pillars that occur beneath the RPE (see Fig. 44.15B). Thus, when this configuration is seen following treatment of suspected CNV, we would recommend elongating the intervals between anti-VEGF injections, and then discontinuing them altogether, once the VA is stabilized and all subretinal blood has been resorbed. Even in the absence of CNV, subretinal hemorrhage can occur in patients with Best disease following relatively modest head or eye trauma (see Fig. 44.19).[19,90,91] As a result, we usually caution patients against playing sports in which frequent blows to the head are to be expected. Protective eyewear is recommended for

all sports. Many patients with Best disease have poor vision in one eye but retain vision sufficient in the fellow eye to drive for many years. In such individuals we recommend wearing spectacles with safety plastic lenses at all times.

Stargardt Disease

Variations in *ABCA4* (OMIM #601691) are the most common cause of autosomal recessive retinal disease in humans. *ABCA4* mutations were first found in patients with autosomal recessive Stargardt disease[92] and were later shown to also cause cone dystrophy, cone–rod dystrophy, and retinitis pigmentosa.[93–98] As discussed more fully below, a patient's position within this disease spectrum is determined largely by the total amount of residual *ABCA4* function.[98] First described in 1909,[99] Stargardt disease is the mildest of the ABCA4 phenotypes while a form of retinitis pigmentosa is the most severe.

Clinical Features of Stargardt Disease

The clinical presentation of Stargardt disease is quite variable in age of onset, presenting symptoms, and fundus appearance, and this variability is often daunting to ophthalmologists who see the condition infrequently. Most of the differences in clinical findings in patients with *ABCA4* disease can be explained by the interplay of three factors that vary among patients: (1) the severity of their *ABCA4* genotype (and hence the rate at which toxic bisretinoids form in the photoreceptors); (2) the relative sensitivity of the foveal cones to the genotype; and (3) the relative sensitivity of the retinal pigment epithelium to the genotype (Fig. 44.25).[98] The first of these variables can be directly assessed by molecular testing of the *ABCA4* gene while the molecular nature of the latter two remains to be determined.

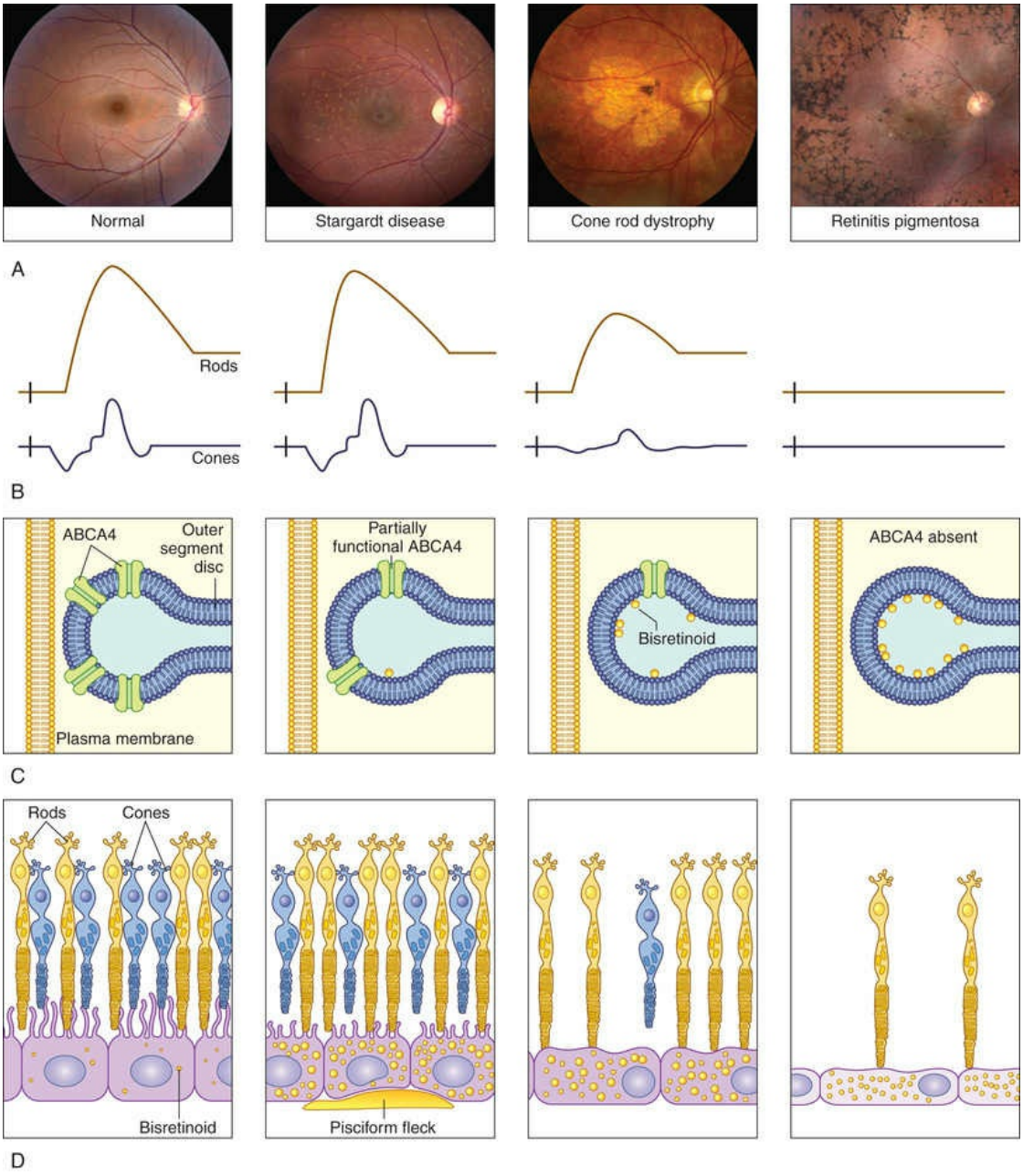

FIG. 44.25 Panel A shows a series of retinal photographs from patients with progressively decreasing amounts of *ABCA4* function (from left to right), ranging from a normal retina to those of patients with Stargardt disease, cone–rod dystrophy, and retinitis pigmentosa. Panel B shows the effects of reduced *ABCA4* function on full-field electroretinograms. The relatively mild reduction in *ABCA4* activity in patients with Stargardt disease has little effect on global photoreceptor function. Moderate loss of *ABCA4* function in patients with cone–rod dystrophy has a greater effect on cone photoreceptors

than it does on rods. Complete loss of *ABCA4* function in some patients with retinitis pigmentosa is associated with extensive loss of both cones and rods and a nonrecordable electroretinogram. Panel C shows the effects of reduced *ABCA4* function on the accumulation of bisretinoid (yellow symbols) on the inner leaflet of the photoreceptor outer-segment disc membranes. Mild reduction in *ABCA4* activity in Stargardt disease is associated with some bisretinoid formation; moderate loss of function in cone–rod dystrophy is associated with intermediate amounts of accumulation; and complete loss of function in retinitis pigmentosa results in maximal accumulation. Panel D shows the histopathologic effects of reduced *ABCA4* activity. In patients with Stargardt disease, the rate of bisretinoid formation in the outer segments is relatively slow and the photoreceptors are not directly injured. Bisretinoids are delivered to the secondary lysosomes of the retinal pigment epithelium (RPE) during the normal phagocytosis of photoreceptor outer segments. Some of this material accumulates beneath the RPE causing pisciform flecks that are visible on ophthalmoscopy. In patients with cone–rod dystrophy, moderate loss of *ABCA4* function results in sufficient accumulation of bisretinoids in photoreceptor outer segments to cause some apoptosis of photoreceptors (in cones more than rods). In patients with retinitis pigmentosa, complete loss of *ABCA4* function causes extensive accumulation of bisretinoids in photoreceptor outer segments, apoptosis of both rod and cone photoreceptors, and associated RPE thinning.

(Reproduced from the New England Journal of Medicine (Sheffield VC, Stone EM. Genomics and the eye. N Engl J Med 2011;364(20):1932-42), with permission.)

The most common presenting complaint is a loss of VA, which can be as mild as 20/30 or as severe as 20/200 depending on the degree to which this drop in acuity is noticeable and troubling to the patient. The age at which the loss of acuity is first recognized can be as early as 5 years or later than 50 years. The very early onset patients usually have a fairly severe *ABCA4* genotype and sensitive foveal cones, while the very late onset patients have a milder *ABCA4* genotype and fairly resistant foveal cones. That is, the

younger onset patients usually have less observable extrafoveal disease, while the very late onset patients have foveal photoreceptors and RPE that are more preserved anatomically than their extrafoveal counterparts. The second most common reason for a patient with Stargardt disease to present to a retina specialist is an abnormal fundus appearance that is incidentally discovered during a routine eye examination. Patients who present in this fashion almost always have fairly resistant foveal cones.

The most characteristic fundus findings in Stargardt disease are light-colored flecks at the level of the retinal pigment epithelium (Fig. 44.26). These flecks differ from drusen in that they are usually more elongated than round and they often contact each other at angles that create a branching or net-like appearance. Occasionally, two adjacent flecks form an obtuse angle that Franceschetti called "pisciform" because of its resemblance to a fish tail.[100] In some patients a cluster of flecks is entirely contained within a one-by-two disc diameter horizontal ellipse centered on fixation (Fig. 44.27), while in other patients the flecks extend well beyond the temporal vascular arcades (Fig. 44.28), almost reaching the equator.

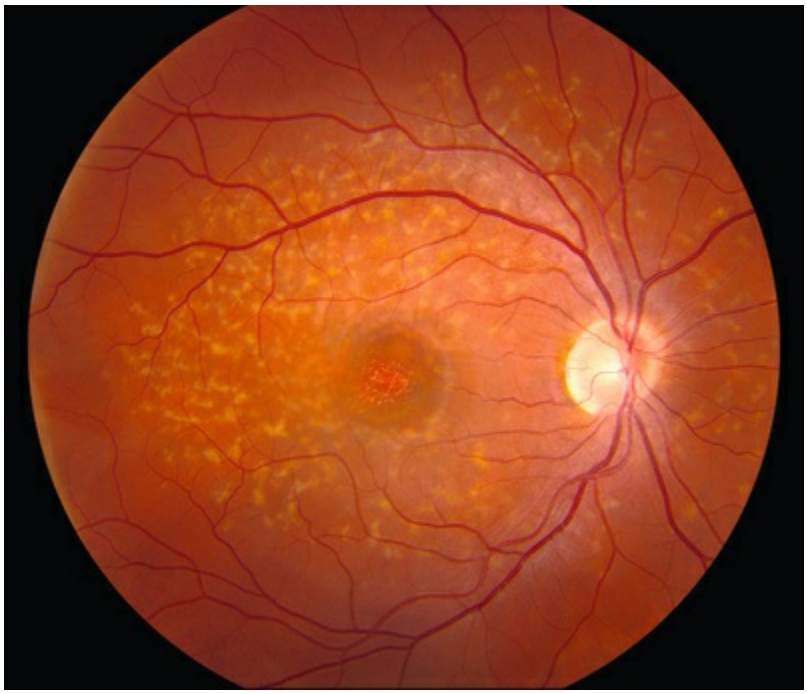

FIG. 44.26 Fundus photograph of the right eye of a 26-year-old female with compound heterozygous mutations in *ABCA4* (IVS40+5 G>A/Val1793Met)

causing Stargardt disease. The visual acuity in this eye is 20/60. There are extensive piscifom flecks throughout the posterior pole and a small circular area of retinal pigment epithelium atrophy centered on the fovea. There are numerous very small crystalline deposits overlying this atrophy.

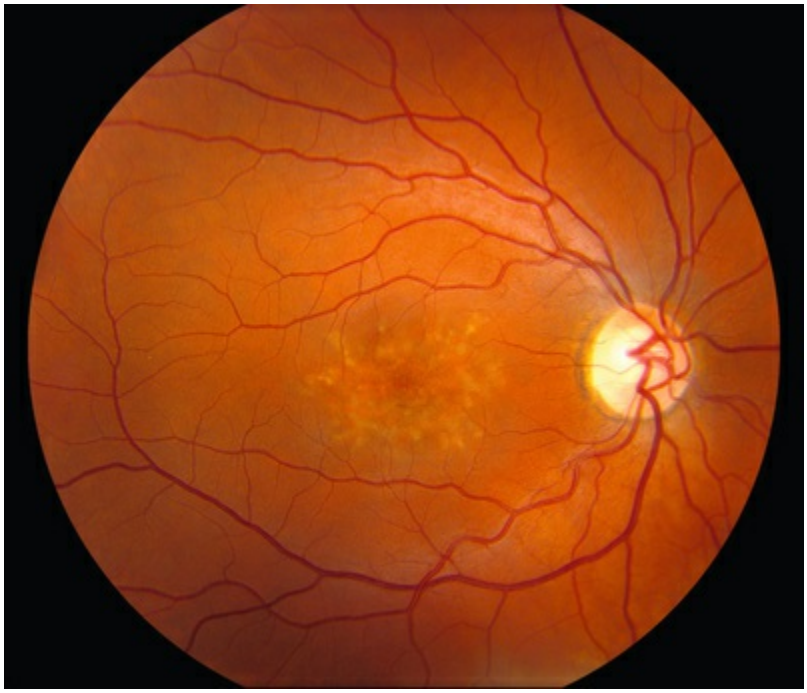

FIG. 44.27 Fundus photograph of the right eye of a 33-year-old female with compound heterozygous mutations in *ABCA4* (Tyr362Stop/Gly1961Glu) causing Stargardt disease. The visual acuity in this eye is 20/125. There is a vermillion appearance to the fundus obscuring the underlying choroidal detail. All of the flecks are confined to an area less than 3 mm in diameter in a pattern that resembles butterfly dystrophy.

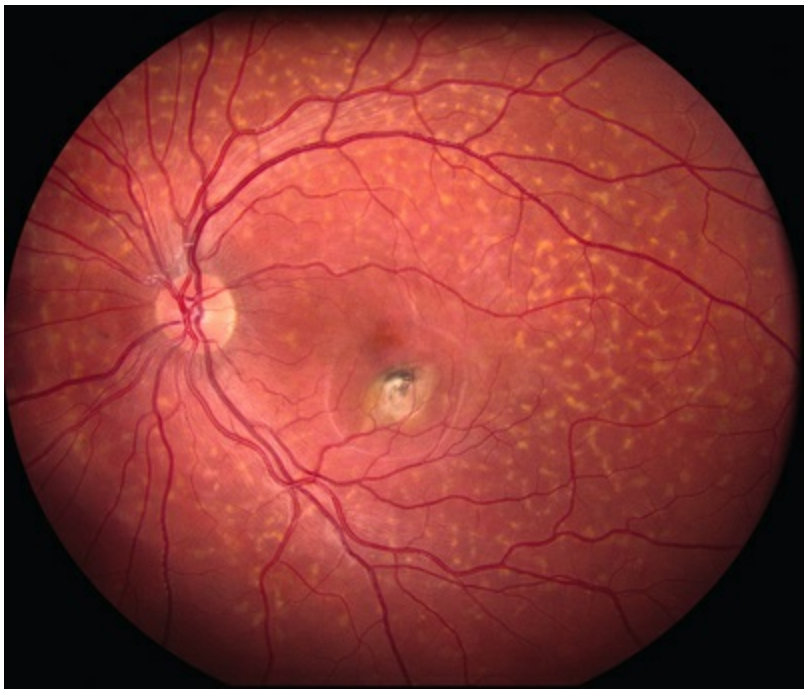

FIG. 44.28 Fundus photograph of the left eye of a 17-year-old male with compound heterozygous mutations in *ABCA4* (IVS40+5 G>A/Val256Val) causing the fundus flavimaculatus variant of Stargardt disease. The visual acuity in this eye is 20/20. There are extensive flecks throughout the posterior pole and a small fibrotic nodule just inferior to the fovea.

In addition to the difference in distribution, Stargardt flecks also differ widely in number, size, color, aspect ratio, and edge definition among different patients. Some patients have no flecks at all (Fig. 44.29), while others have hundreds (see Fig. 44.28). Flecks are most commonly yellow but can range from dirty-white to orange. Some flecks have pigmented edges, and in a few cases this RPE hyperpigmentation can be quite dramatic. Some patients have very small deposits near the fovea that have a crystalline character on biomicroscopy (Fig. 44.30). Flecks outside the central 2 mm of the macula tend to be a bit larger than those nearer the fovea. Some patients have flecks that are almost round, while others have flecks that are several times longer than they are wide. In some individuals with severe *ABCA4* genotypes, the flecks are small and white and are admixed with small patches of subretinal fibrosis that resemble confetti (Fig. 44.31). This is presumably because the widespread photoreceptor injury associated with such genotypes reduces the production of bisretinoids. Some flecks are stable in

position, size, and number for many years, while others grow in number and/or progress to RPE atrophy (Fig. 44.32).

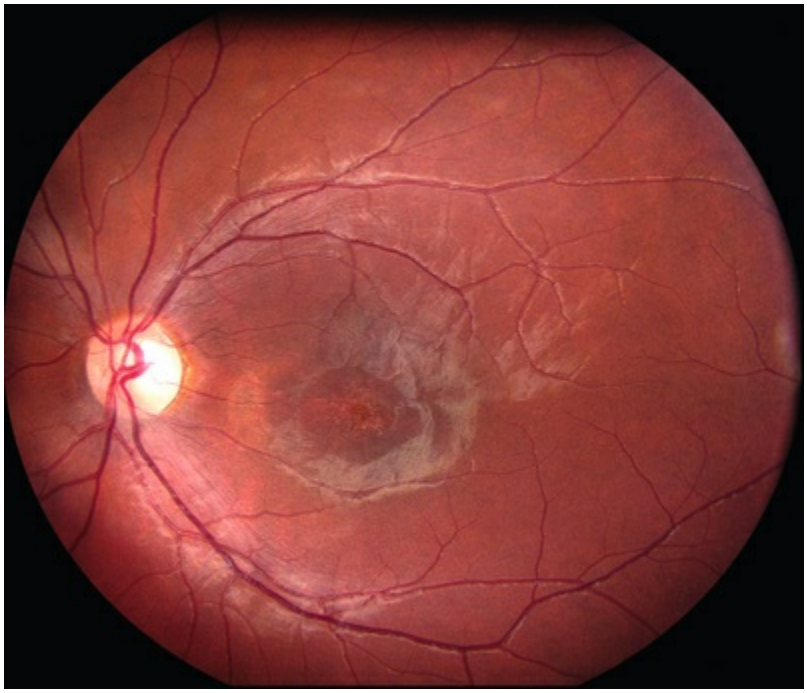

FIG. 44.29 Fundus photograph of the left eye of a 6-year-old male with compound heterozygous mutations in *ABCA4* (IVS9+1 G>A/IVS37+1 G>(A) causing cone–rod dystrophy. The visual acuity is 20/200. The arterioles are slightly narrow for a child of this age and are a clinical sign of a relatively severe *ABCA4* genotype.

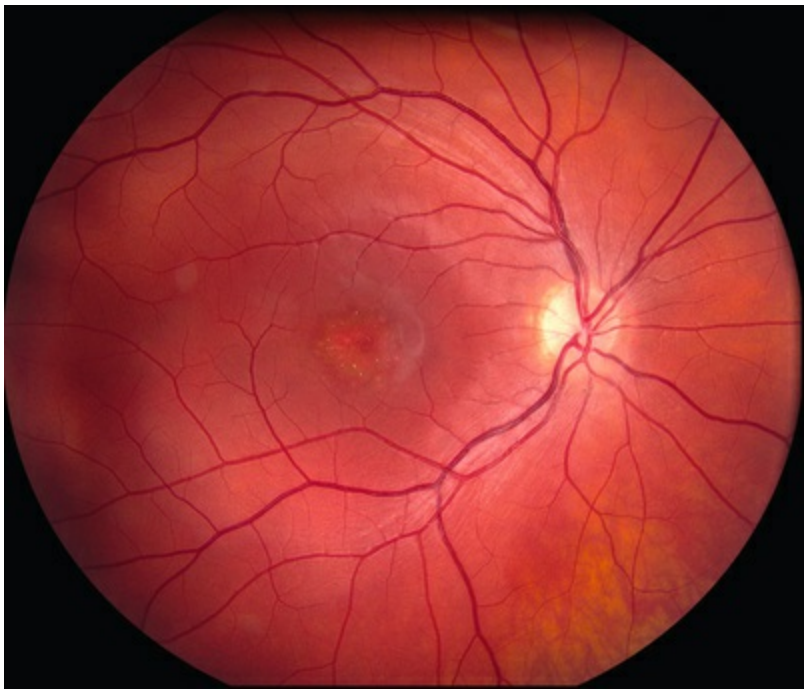

FIG. 44.30 Fundus photograph of the right eye of a 26-year-old male with compound heterozygous mutations in *ABCA4* (Cys2150Tyr/Gly863Ala) causing Stargardt disease. The visual acuity in this eye is 20/80. There is a vermillion appearance to the entire fundus obscuring the underlying choroidal detail. There are no typical flecks. However, there are tiny intraretinal crystals overlying a circular region of RPE atrophy centered on the fovea.

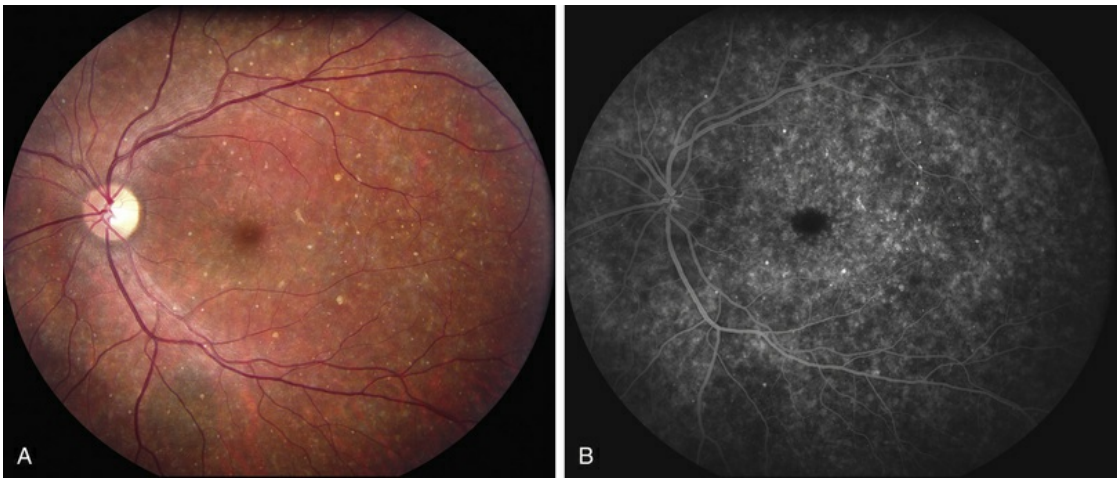

FIG. 44.31 (A) Fundus photograph of the left eye of a 25-year-old female with compound heterozygous mutations in *ABCA4* (Thr1019Met/Lys583Asn) causing

Stargardt disease. The photoreceptors and retinal pigment epithelium (RPE) of the fovea are relatively spared in this patient and the visual acuity remains 20/80 despite extensive injury to the RPE throughout the remainder of the posterior pole. There are numerous superficial confetti-like flecks that seem to represent tiny foci of subretinal fibrosis. (B) Fluorescein angiography of this eye reveals the relative preservation of the foveal and peripapillary retina and RPE. The confetti-like flecks are intensely hyperfluorescent.

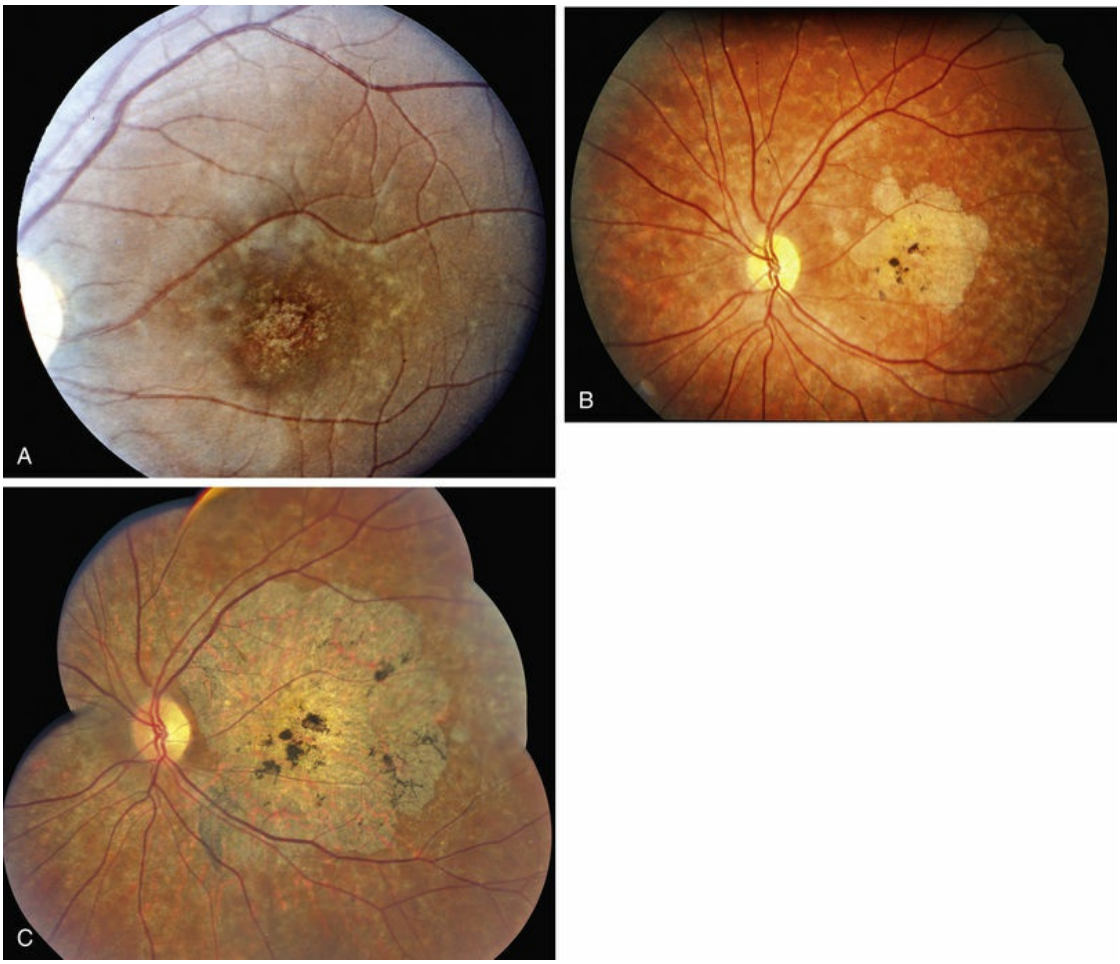

FIG. 44.32 (A) Fundus photograph of the left eye of a 27-year-old female with compound heterozygous mutations in *ABCA4* (Ala1038Val-Ala854Thr/Arg1108Cys) causing Stargardt disease. The visual acuity is 20/200. The small patch of geographic atrophy has a shiny base that glistens in

this photograph. A few small flecks can also be seen ringing the atrophy. (B) At age 30, there has been a modest enlargement of the central atrophy and an increase in the number of peripheral flecks but the acuity remains 20/200. (C) At age 42, the area of central atrophy has continued to enlarge but the acuity has fallen to only 20/250. Some clumps of dark pigment have developed within the atrophic lesion. The peripapillary retina is noticeably spared.

In addition to the many different fleck configurations, the RPE itself responds to *ABCA4* mutations quite differently in different patients depending in part on the severity of the *ABCA4* genotype and in part on the sensitivity of the RPE to the accumulation of bisretinoids. In some patients with relatively mild genotypes, there is little photoreceptor injury, and thus there is a steady supply of bisretinoid to the RPE. In some patients the RPE retains this material intracellularly and as a result becomes somewhat opaque to visible light. On ophthalmoscopy this is recognized as a very uniform vermillion or light-brown color to the fundus with complete obscuration of the underlying choroidal details (see Fig. 44.27, Figs. 44.33 and 44.34). On fluorescein angiography, this is seen as a complete masking of the choroidal circulation. As a result, the dye-filled retinal vessels lie upon a completely hypofluorescent background (Fig. 44.43). In other patients with a very similar bisretinoid load emanating from the photoreceptors, the RPE gradually thins, presumably from apoptotic death of some RPE cells and compensatory stretching of those that survive (Fig. 44.35). Frank RPE atrophy is commonly seen in the center of the macula and the bases of these atrophic lesions have a metallic sheen to them (Fig. 44.32) that is distinctly different from the geographic atrophy that occurs in age-related macular degeneration. In some patients these atrophic lesions become dusted with dark pigment over time (Fig. 44.35). In the later stages of disease, patients with severe genotypes can develop nummular atrophy of the extramacular RPE and choriocapillaris that somewhat resembles choroideremia (Fig. 44.36).

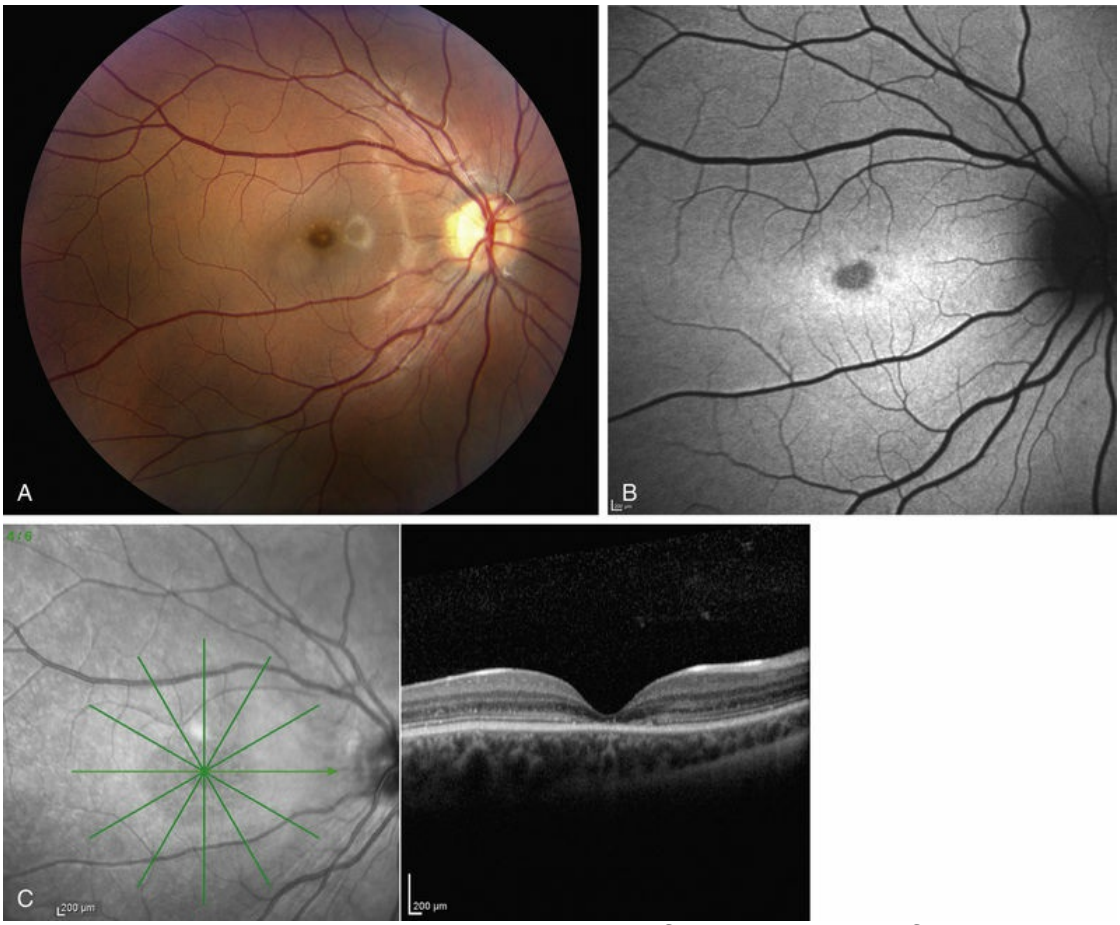

FIG. 44.33 (A) Fundus photograph of the right eye of a 13-year-old female with compound heterozygous mutations in *ABCA4* (IVS38-10 T>C/Gly1961Glu) causing Stargardt disease. The visual acuity in this eye is 20/40. There is a uniform light brown color to the fundus that completely obscures the underlying choroidal detail. This is the ophthalmoscopic equivalent to the “masked choroid” of fluorescein angiography. A few small flecks are visible ringing the atrophic fovea. (B) Autofluorescence imaging reveals a loss of autofluorescence in the atrophic fovea and slightly increased autofluorescence elsewhere. (C) Spectral domain optical coherence tomography reveals selective loss of foveal photoreceptors.

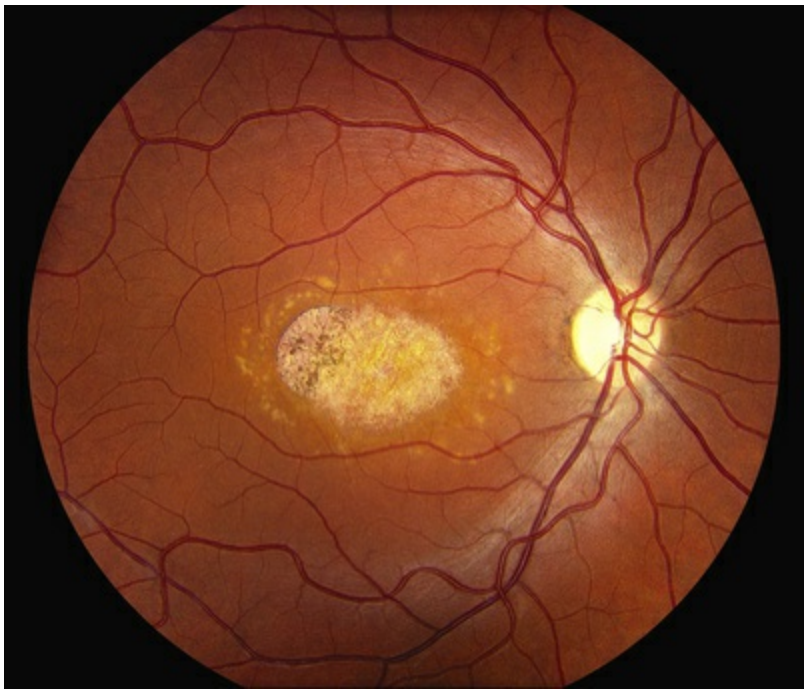

FIG. 44.34 Fundus photograph of the right eye of a 36-year-old female with compound heterozygous mutations in *ABCA4* (Phe608Ile/Gly1961Glu) causing Stargardt disease. The visual acuity in this eye is 20/100. There is a vermillion appearance to the entire fundus obscuring the underlying choroidal detail. The central macular lesion has two distinct components. The temporal third is atrophic with a sharply defined edge and some dark pigment dusting over the atrophy. The nasal two-thirds is more crystalline in appearance. Coarse pisciform flecks ring the central lesion.

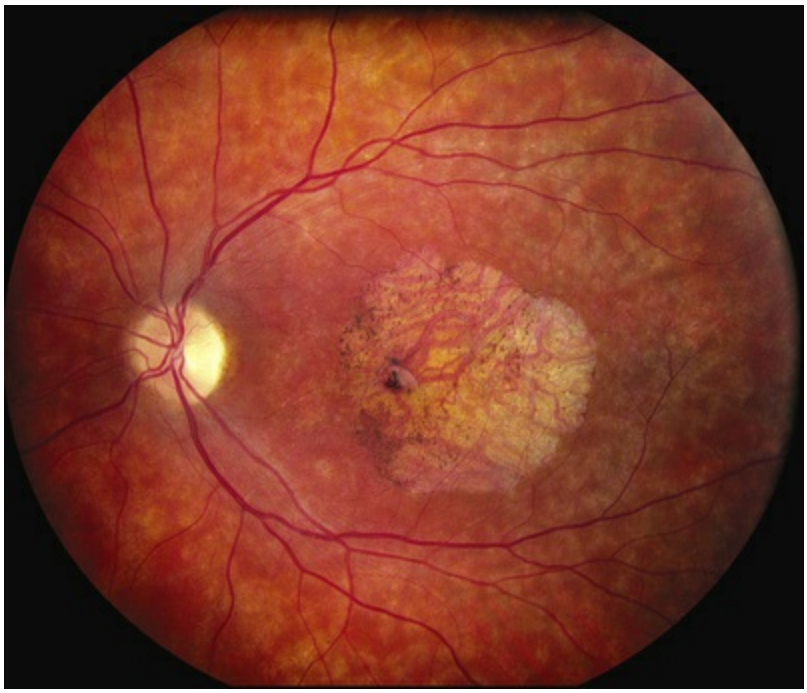

FIG. 44.35 Fundus photograph of the left eye of a 38-year-old female with compound heterozygous mutations in *ABCA4* (Gly863Ala/Leu2109Pro) causing Stargardt disease. The visual acuity in this eye is 5/300. There is a dusting of dark pigment over a sharply demarcated circular area of retinal pigment epithelium (RPE) atrophy centered over the fovea. In addition, there is a reticular network of RPE atrophy throughout the posterior pole. Peripapillary sparing is subtle but present.

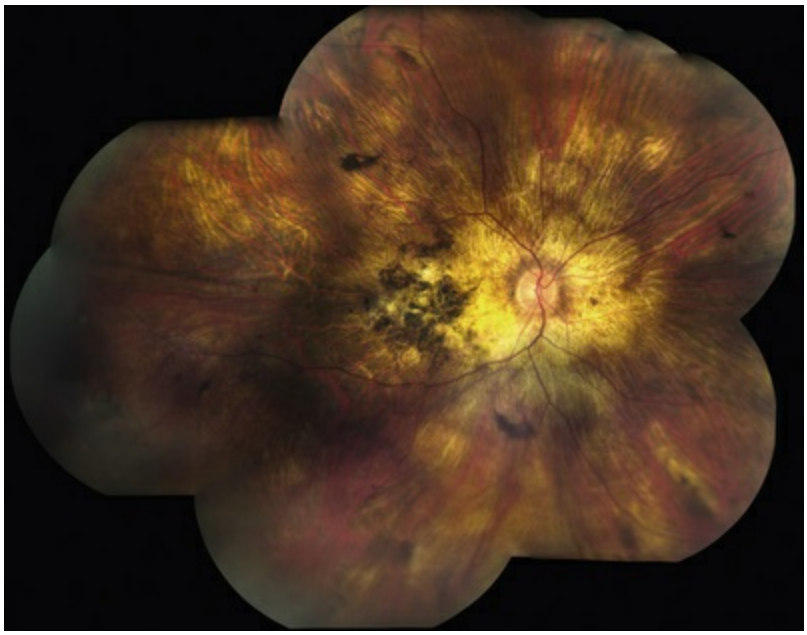

FIG. 44.36 Fundus photograph of the right eye of a 47-year-old male with compound heterozygous mutations in *ABCA4* (Leu2109Pro/IVS38-10 T>C) causing retinitis pigmentosa. The visual acuity is counts fingers at 3 feet. There are nummular areas of retinal pigment epithelium and choroidal atrophy admixed with intraretinal pigmentation, some of which is perivascular. The two clinical features that would suggest mutations in *ABCA4* as the cause of this patient's disease are the extensive macular involvement and the noticeable peripapillary sparing.

A useful diagnostic sign of *ABCA4*-associated retinal disease is a relative sparing of the peripapillary RPE. This sign is often more visible on fluorescein angiography[101] (see Fig. 44.31) or autofluorescence;[102,103] however, it can also be easily observed on ophthalmoscopy alone (Fig. 44.37). The mechanism of this sparing is currently unknown. Patients with *ABCA4*-associated retinal disease are not immune to inflammatory or traumatic retinal injuries, and the coexistence of these disorders can make it difficult to establish the correct diagnoses. Although the frequency with which epiretinal membranes (Figs. 44.38A–D), subretinal fibrosis (Figs. 44.39 and 44.40), and inflammatory nodules (see Fig. 44.38A) occur in Stargardt patients may not be greater than would be expected by chance, the exuberant nature of some of these lesions suggests an adjuvant effect of either the bisretinoids themselves or

the low-grade inflammation that is commonly present in degenerative retinal disease.

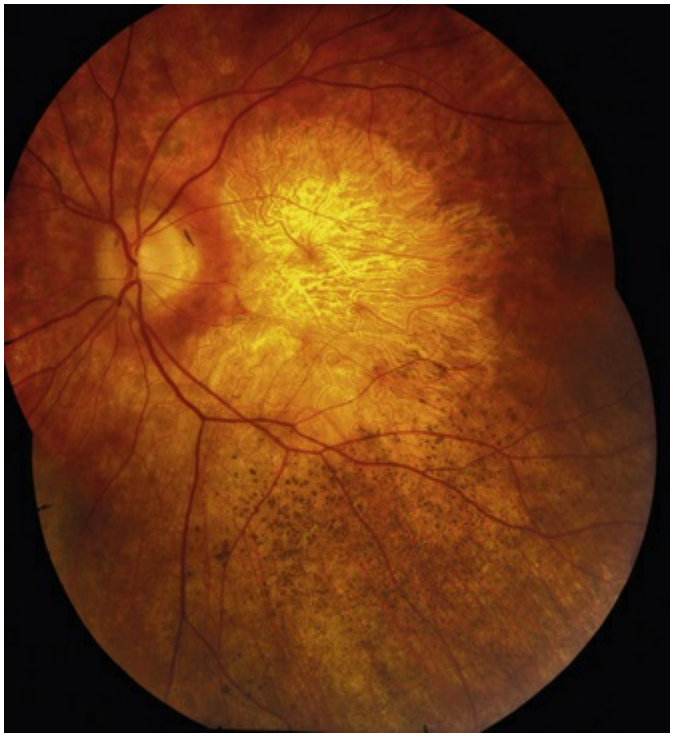

FIG. 44.37 Fundus photograph of the right eye of a 52-year-old male with compound heterozygous mutations in *ABCA4* (Ala1038Val-Leu541Pro/IVS40+5 G>(A) causing cone–rod dystrophy. The visual acuity is 20/50. There is a large area of retinal pigment epithelium and choroidal atrophy in the macula and some fine intraretinal pigmentation inferiorly. The two clinical features that would suggest mutations in *ABCA4* as the cause of this patient's disease are extensive macular involvement and the noticeable peripapillary sparing.

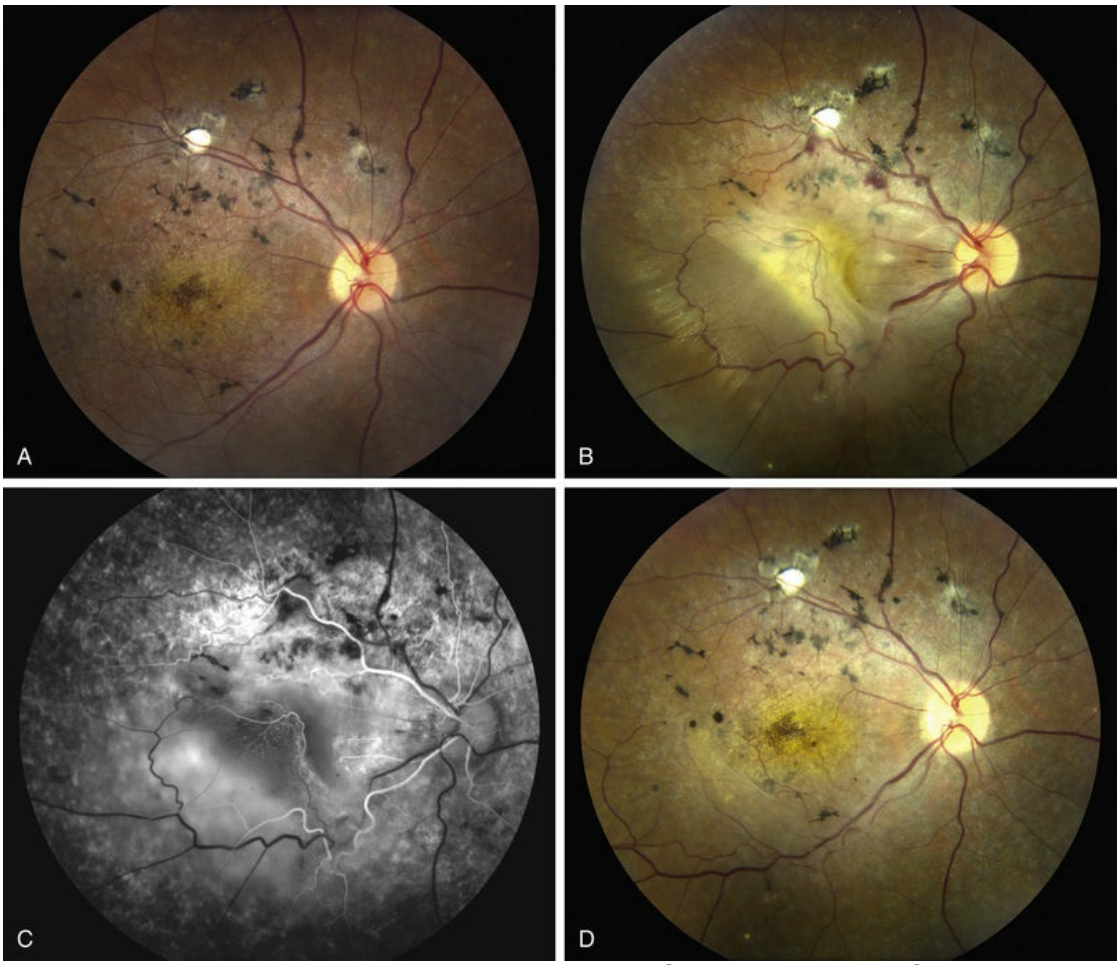

FIG. 44.38 (A) Fundus photograph of the right eye of a 26-year-old female with compound heterozygous mutations in *ABCA4* (Glu1087Lys/ IVS38-10 T>C) causing cone-rod dystrophy. The visual acuity on this visit is 20/400. Narrowed arterioles and bone-spicule like pigmentation are signs of moderate photoreceptor cell loss. The normal xanthophyll pigment gives a golden appearance to the thinned macular RPE. There is an inflammatory nodule along the superotemporal arcade. Five months later, the patient returns, reporting a sudden decrease in vision in the right eye. The acuity is counting fingers and ophthalmoscopy reveals an aggressive epiretinal membrane (B). Fluorescein angiography (C) reveals the retina to be folded on itself with no evidence of a significant choroidal neovascular component despite the small hemorrhages at the superior margin of the lesion. (D) Following vitrectomy and membrane peeling, only a small remnant of the epiretinal membrane persists temporally. The visual acuity has returned to 20/400. (Panels B, C, and D courtesy of Dr. H. Culver Boldt, the University of Iowa.)

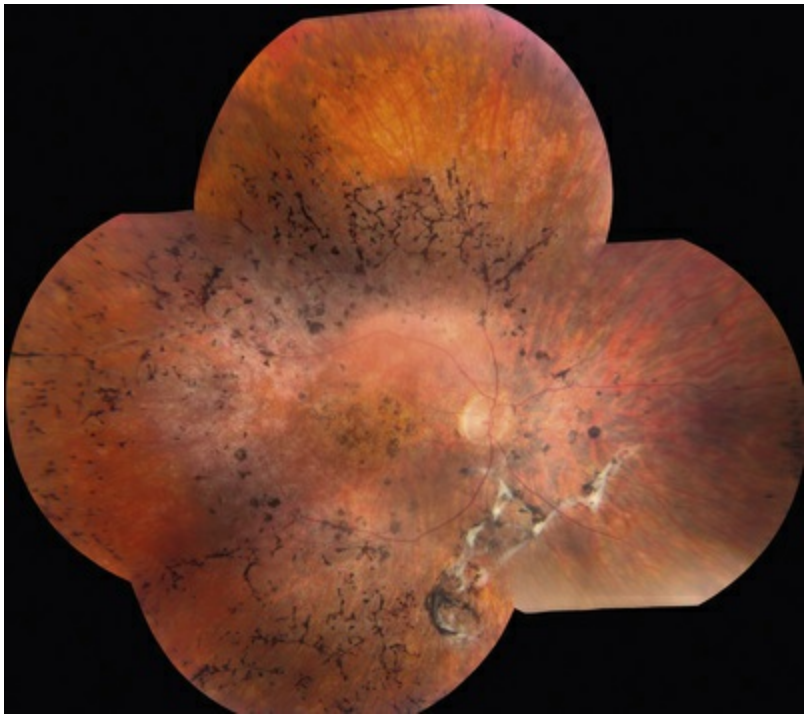

FIG. 44.39 Fundus photograph of the right eye of a 39-year-old female with compound heterozygous mutations in *ABCA4* (Ala1038Val-Leu541Pro/Arg2149Stop) causing retinitis pigmentosa. The visual acuity is 5/300. The two clinical features that would suggest mutations in *ABCA4* as the cause of this patient's disease are the early macular involvement and the extensive subretinal fibrosis inferior to the disc.

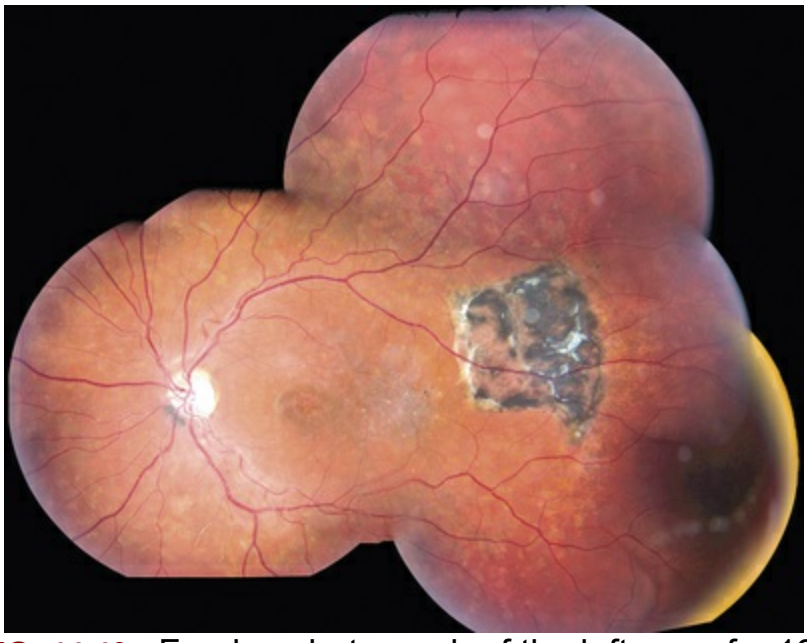

FIG. 44.40 Fundus photograph of the left eye of a 13-year-old female with compound heterozygous mutations in *ABCA4* (Arg653Cys /Pro656Leu) causing Stargardt disease. The visual acuity is 20/125. There is a large plaque of pigmented subretinal fibrosis temporally, possibly related to mild blunt trauma to the eye 5 years earlier. There is some atrophy in the center of the macula and typical flecks are visible along the arcades.

Visual Function

It is important to recognize that the effect of *ABCA4* mutations on VA is frequently at odds with their effect on the visual field. As a result, many patients will have quite full visual fields for many years after their acuity has fallen below the threshold of legal blindness (Fig. 44.41), while a few patients will retain acuity of better than 20/40 despite extensive field loss (Fig. 44.42). Fishman studied 95 patients with Stargardt disease and found that the probability of maintaining a VA of 20/40 in at least one eye was 52% by age 19, 32% by age 29, and 22% by age 39.[104] In a larger cohort of Stargardt disease patients, cross-sectional analysis showed that almost a quarter had VA of 20/40 or better, whereas 4% had VA worse than 20/400.[105] In general, patients with extensive extramacular flecks have a poorer long-term visual prognosis than patients with flecks and/or atrophy that are limited to the

macula.[106,107] Similarly, patients with significant loss of the I2e isopter on Goldmann perimetry have more severe genotypes than those with a more normal I2e response.[98]

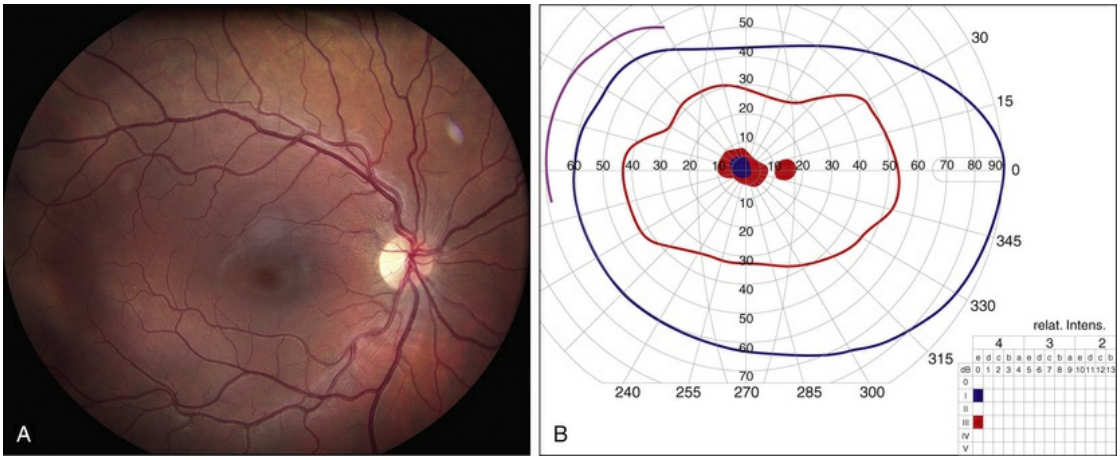

FIG. 44.41 (A) Fundus photograph of the right eye of a 16-year-old female with compound heterozygous mutations in *ABCA4* (Gly1961Glu/Pro1511Arg) causing Stargardt disease. The visual acuity in this eye is 20/70. The fundus is normal except for a very subtle oval area of retinal pigment epithelium granularity beneath the fovea a few hundred micrometers in diameter. (B) Goldmann perimetry is normal except for a small scotoma to the I4e stimulus centered on fixation.

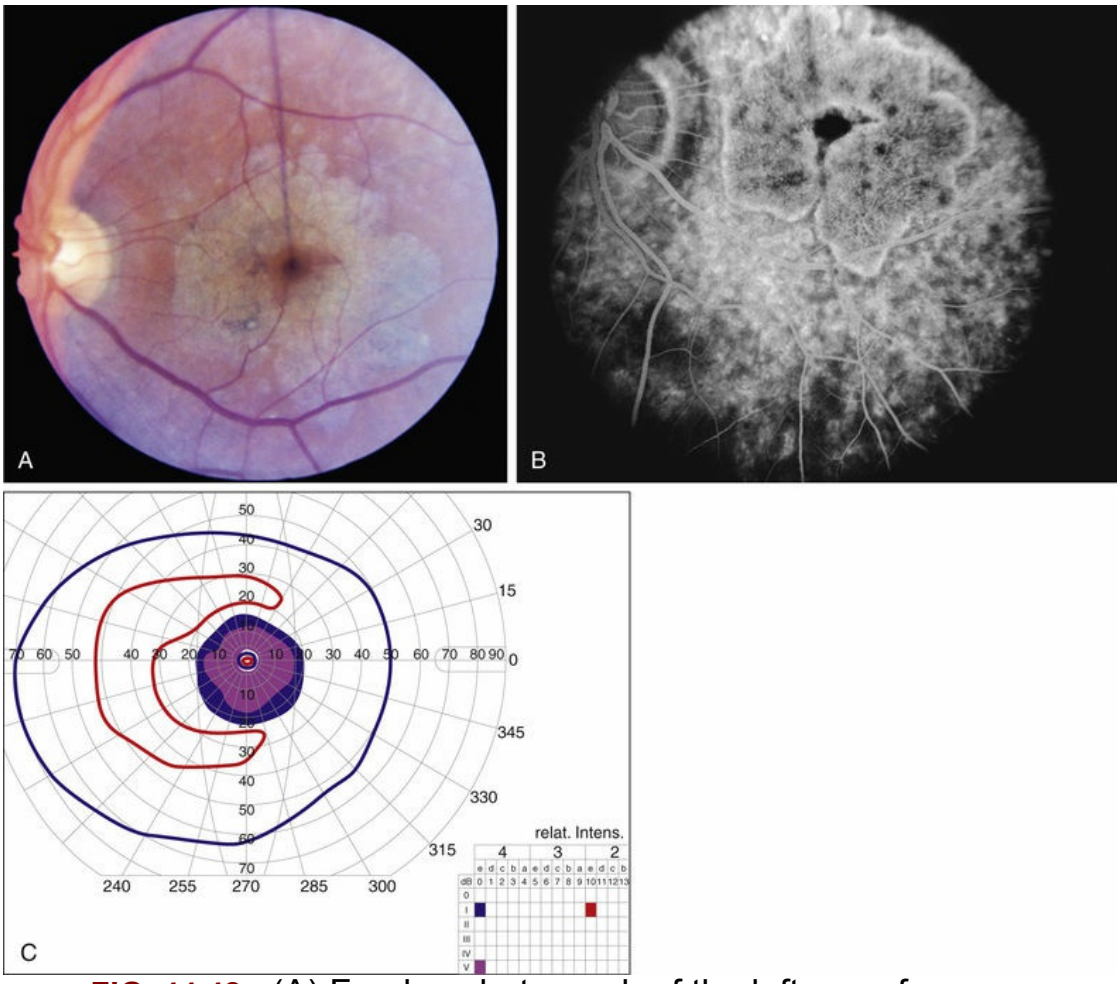

FIG. 44.42 (A) Fundus photograph of the left eye of a 32-year-old male with compound heterozygous mutations in *ABCA4* (Cys1488Arg/Leu2027Phe) causing cone–rod dystrophy. The visual acuity is 20/20. There is an irregular area of complete sparing centered on the fovea, which is surrounded by a large annulus of retinal pigment epithelium (RPE) atrophy. The nasal edge of the atrophic lesion is concave, paralleling the edge of the optic disc. (B) Fluorescein angiography of this eye reveals the completely spared fovea surrounded by RPE atrophy. Relative sparing of the peripapillary retina is also evident. Flecks appear as hyperfluorescent window defects in the otherwise hypofluorescent RPE. (C) Goldmann perimetry of this eye reveals an absolute scotoma corresponding to the perifoveal atrophy. There is a window within this scotoma corresponding to the preserved fovea.

Fluorescein Angiography and Autofluorescence

The accumulation of A2E within the retinal pigment epithelium results in a detectable abnormality on both fluorescein angiography and autofluorescence imaging. With angiography, the A2E blocks the exciting blue light from reaching the dye in the choroidal circulation, resulting in a finding that is variously known as a dark, silent, or masked choroid.[108,109] In these angiograms, the retinal vessels stand out in sharp contrast to the dark background (Fig. 44.43). Flecks and any areas of atrophy are hyperfluorescent, although an annulus of a few hundred microns around the optic disc usually remains hypofluorescent even in the presence of very extensive disease.[101] While FA can be useful in evaluation for a patient with a possible macular dystrophy, if *ABCA4* disease is highly suspected, in our clinic we generally do not perform FA for several reasons. First, there is some evidence that exposure to visible light is a cofactor in the disease (knockout mice reared in darkness do not accumulate A2E,[110] and there is certainly a lot of light exposure associated with a fluorescein angiogram). Second, molecular testing is becoming more sensitive and more widely available (https://www.carverlab.org/) and has the added utility of providing some prognostic information when well-characterized mutations are present.[98] Third, many patients with molecularly proven *ABCA4* disease have a readily visible choroidal circulation on angiography (Fig. 44.44). Thus, as with current molecular tests, the absence of a positive result is not helpful. Fourth, there is a small risk of serious complications from the intravenous dye, and finally, the dynamic range of digital cameras is noticeably less than film, tending to accentuate the contrast between the retinal circulation and the normal choroidal circulation, resulting in a false-positive interpretation of the test in some cases. In patients with Stargardt disease, autofluorescence (AF) imaging can also show areas of RPE atrophy, bull's-eye changes in the macula (see Fig. 44.33B), flecks, and peripapillary sparing.[42,102,103,111–124] We prefer to use reduced-illuminance autofluorescence imaging[125] when needed in patients with suspected *ABCA4* disease.

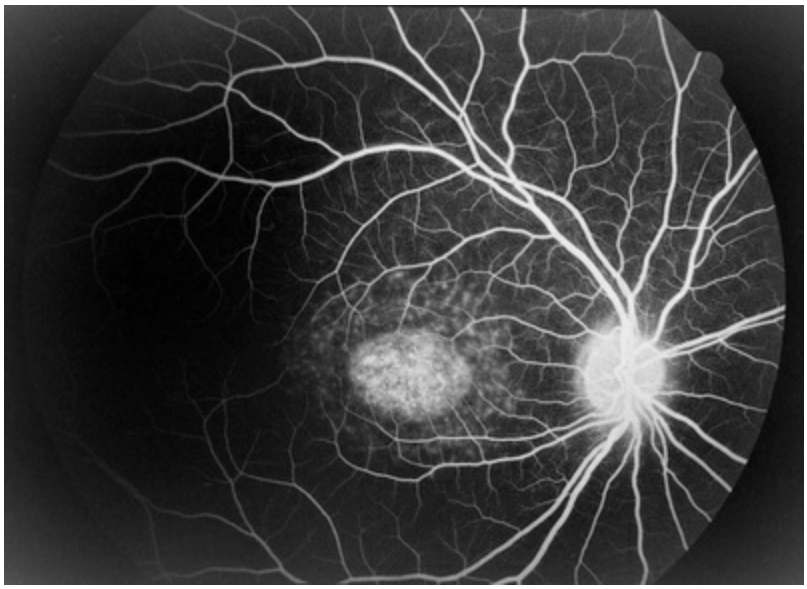

FIG. 44.43 Fluorescein angiogram of the right eye of a 9-year-old female with compound heterozygous mutations in *ABCA4* (Cys54Tyr/Gly550Arg) causing Stargardt disease. The visual acuity in this eye is 20/200. The fluorescence of the choroidal circulation is completely masked by the bisretinoid-containing retinal pigment epithelium except in the center of the macula where flecks and atrophy have created window defects. As a result, the fluorescent retinal vasculature stands out in sharp contrast against the unusually hypofluorescent background.

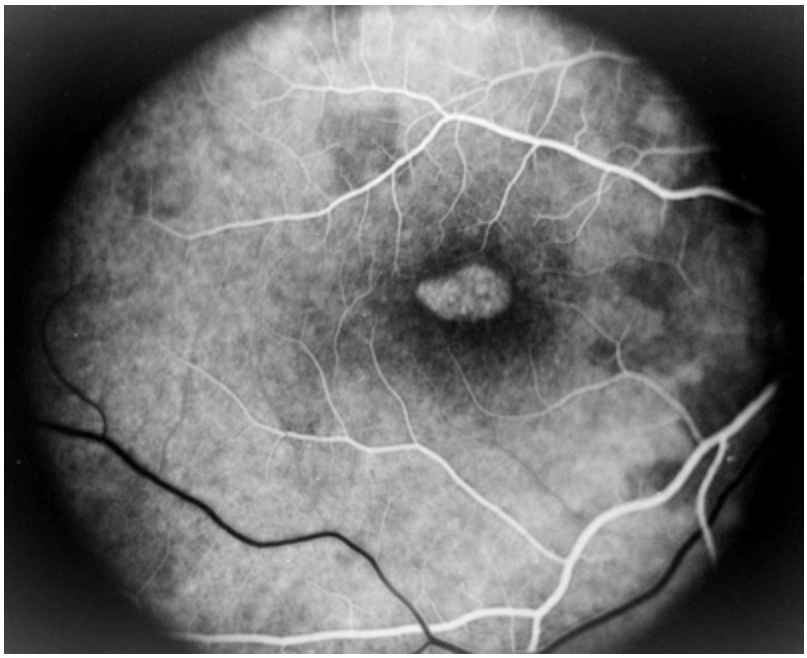

FIG. 44.44 Fluorescein angiogram of the right eye of a 14-year-old male with compound heterozygous mutations in *ABCA4* (Gly1961Glu/Pro1380Leu) causing Stargardt disease. The visual acuity in this eye is 20/250. In this very early frame of the angiogram the choroid is not yet completely filled, making it readily apparent that the choroidal circulation is incompletely masked in this individual.

Optical Coherence Tomography

OCT can reveal the extent of outer retinal loss and RPE atrophy (see Fig. 44.33C), and it can also distinguish the anatomic level of flecks with accuracy.[113,117,126–128] The test is very sensitive to early changes; one study revealed three patients with photoreceptor abnormalities on OCT without an equivalent abnormality on AF.[117] Peripapillary nerve fiber layer thickness can also be altered on OCT but the significance of this is not yet known.[129]

Electrophysiology

Somewhat by definition, the full-field ERG is typically normal in patients with Stargardt disease while cone and cone–rod dysfunction are seen in more severe forms of *ABCA4* disease.[112,130–135] With mild *ABCA4* genotypes, bisretinoids do not seem to accumulate rapidly enough to injure the photoreceptors directly, except for cones in and near the fovea, which seem to be the most sensitive to *ABCA4* dysfunction in most patients. Loss of the latter cells can cause quite a bit of acuity loss without any detectable effect on the full-field ERG. With moderate *ABCA4* genotypes, cones throughout the fundus are directly affected, leading to cone-selective abnormalities in the ERG. With the most severe *ABCA4* genotypes, even rods experience direct injury from A2E accumulation, resulting in effects on all components of the ERG and a fundus appearance that can reasonably be called retinitis pigmentosa (Fig. 44.39).[98,136] It is important to realize that patients with the more severe *ABCA4* genotypes can progress from a clinical pattern consistent with the label "Stargardt disease" to one consistent with "retinitis pigmentosa" over the course of their disease, and it can be very distressing to patients to have their

diagnosis change from one doctor to the next. A few minutes spent explaining that these descriptive labels are used to describe different aspects (e.g., ophthalmoscopic and electrophysiologic) and stages (early and late) of a single disease, and that these descriptions can change over time in an individual patient, can reduce this distress significantly. One of the most valuable uses of the full-field ERG in patients suspected to have *ABCA4*-related retinal disease is in differentiating the earliest onset forms of this condition from juvenile NCL (see Fig. 44.2). In patients with NCL, the ERG is usually severely reduced or extinguished before the age of 10 years. If it is recordable at all, the rod ERG is more severely affected than the cone ERG, and the maximum stimulus intensity scotopic response typically shows an electronegative configuration (greater loss of b-wave than a-wave).[137] In contrast, profound reduction in the full-field scotopic ERG response to the standard maximum stimulus intensity is rare in the first decade of life in patients with *ABCA4* disease, and any reductions that do occur are noticeably cone-selective. Finally, electronegative waveforms have not been reported in *ABCA4*-associated retinal disease. The pattern ERG can be abnormal in patients with Stargardt disease even when the fundus looks relatively normal.[112,128] This led to the proposal of three groups of SD based on electrophysiology: in group 1 there is a severe pattern ERG abnormality with normal scotopic and full-field ERGs; in group 2 there is additional loss of photopic function; and in group 3 there is loss of both photopic and scotopic function.[112] The multifocal ERG is less useful in Stargardt patients than the full-field ERG. Its test–retest reliability and interocular symmetry in SD is significantly lower than in controls.[138]

Genetics

Since the discovery in 1997 that a recessively inherited *ABCA4* mutation causes Stargardt disease,[92] there have been more than 250 different disease-causing alleles identified in *ABCA4* and many nondisease-causing polymorphisms as well. Individuals who counsel patients about their *ABCA4* genotype need to have a thorough understanding of the differences between these two classes of genetic variation. Some laboratories provide a

pathogenicity score for the mutations they identify that can be helpful in this regard.[139,140] Another challenge in counseling patients with *ABCA4*-associated retinal disease is that a significant number of disease-causing mutations lie outside the coding and promoter sequences of the gene, making them difficult to identify. Thus, many patients will have only one of their two disease alleles identified by current testing methods. Mutations in *ABCA4* are thought to be responsible for more than 95% of cases of clinical Stargardt disease, 30–50% of cases of cone–rod dystrophy,[97] and 8% of autosomal recessive retinitis pigmentosa.[98] Most of the remaining 5% of cases with a Stargardt disease phenotype are caused by mutations in *ELOVL4*, *PROM1*, *PRPH2*, or *BEST1*.

The wide range of phenotypes seen in *ABCA4*-associated disease can be attributed to (1) the variable severity of the many disease alleles in the population; (2) the interaction of these alleles with genetic and environmental modifiers (e.g., light exposure, smoking, and diet); and (3) the complex interaction between rods, cones, and RPE cells. Systematic investigation of the clinical findings of large cohorts of patients with known *ABCA4* genotypes has the potential to deduce the specific pathogenic contribution of individual alleles. For example, multiple regression analysis based on an additive model of *ABCA4* function recently enabled the quantification of specific disease-causing power of some of the more common disease-causing *ABCA4* alleles.[98] As additional studies of this kind are performed and combined, it will allow clinicians to better inform patients of their prognosis, help balance enrollment in clinical trials of novel treatments, and facilitate the identification of disease-modifying factors that may form the basis of such treatments.

Pathophysiology and Histopathology

Histologic studies of eyes with Stargardt disease reveal remarkable lipofuscin accumulation in the RPE. For example, an eye from a 9-year-old child with Stargardt, enucleated for retinoblastoma at 16 months of age, showed striking RPE autofluorescence when compared to normal aging.[141] Another unusual finding observed in autopsy tissue from a 62-year-old donor is the presence of

significant lipofuscin accumulation within photoreceptor cell inner segments, suggesting significantly altered processing of retinoids in the outer retina.[142] Attenuation of photoreceptor inner and outer segments over areas of still-organized RPE cells was also noted, consistent with a primary photoreceptor cell defect. In addition, endstage central atrophy of the outer retina, gliosis, and RPE hypertrophy or loss have been seen.[142,143]

The pathophysiology of *ABCA4*-associated disease has been reviewed[136,144,145] and was elucidated in large part through elegant biochemical studies of the *Abca4*$^{-/-}$ mouse.[146] The normal role of ABCA4 is the clearance of a retinoid intermediate of the visual cycle (N-retinylidene phosphatidylethanolamine) from the intradiscal lumen of the outer segments of rods and cones. Condensation of this retinoid with a second vitamin A moiety, which may occur in the photoreceptor cell or in the RPE following outer segment phagocytosis, results in the formation of A2E, a toxic detergent-like compound that can trigger death of RPE cells[147,148] complement activation,[149] and both direct and indirect loss of photoreceptors (see Fig. 44.25).

Treatment

There is currently no proven treatment for *ABCA4* disease. However, there is extensive ongoing research in genetics, disease mechanisms, gene therapy, and cell replacement, and these studies have already identified a number of promising therapeutic strategies that have been tested in animal models and in some cases have progressed to human trials.

Since a primary defect in *ABCA4*-associated retinal disease is an accumulation of toxic bisretinoids in the RPE and photoreceptors, drugs that modulate the visual cycle (e.g., isotretinoin and fenretinide) have been investigated for their potential to slow the formation of these toxic products in *Abca4* knockout mice.[150–152] Similarly, gene replacement therapy has been proposed for *ABCA4* disease and efficacy has been demonstrated in the mouse model.[153–155] Proof of concept, safety, and efficacy for ocular gene therapy in humans has already been shown for *RPE65*-associated Leber's congenital amaurosis,[156,157] and thus gene therapy for

ABCA4-associated disease seems promising for patients who still have substantial visual function (https://clinicaltrials.gov/ct2/show/NCT01367444?term=stargardt&rank=4). Patients who have already experienced extensive loss of RPE and photoreceptors will likely need some type of cell replacement therapy, and one human clinical trial of RPE cell replacement is already completed (https://clinicaltrials.gov/ct2/show/NCT01345006?term=stargardt&rank=7).

As we await the successful demonstration of safety and efficacy of one or more of these interventions, we recommend that our patients wear dark glasses and a hat whenever they are exposed to prolonged bright light (to reduce the rate of formation of all-*trans* retinol in the photoreceptors). We also recommend avoidance of cigarette smoking as our Stargardt patients have anecdotally reported dimming of their vision while smoking. Finally, we recommend avoidance of high-dose vitamin A supplements, including AREDS vitamins, because of their potential to increase the formation of bisretinoids in the retina.

Stargardt-Like Dominant Macular Dystrophy (SLDMD)

In 1994 Stone and coworkers described a large family with a Stargardt-like phenotype and mapped the gene to chromosome 6.[158] In contrast to typical Stargardt disease, this family displayed a clear autosomal dominant pattern of inheritance with high penetrance. Zhang et al. later identified a 5 base pair insertion in the gene *ELOVL4* in the affected members of five families affected with this disease.[159] Although additional disease-causing mutations in *ELOVL4* have been identified,[160,161] the 5 bp deletion is responsible for more than 90% of cases in North America. This condition is characterized by progressive central vision loss; some patients develop symptoms in the first decade of life and the majority have a VA of 20/200 or worse by 30 years of age.[158] The range of fundus findings is almost identical to that of autosomal recessive Stargardt disease and includes pisciform flecks (Figs. 44.45 and 44.46),

peripapillary sparing (Fig. 44.47) and macular atrophy. The bases of the atrophic macular lesions are less likely to have a distinct reflective sheen than those of autosomal recessive Stargardt disease and some patients display a round or cuneiform clump of dark pigment very near fixation (Fig. 44.47). As in *ABCA4*-associated Stargardt disease, a few patients have a severe loss of foveal cones with an otherwise normal fundus (Fig. 44.48). The lipofuscin deposits in SLDMD tend to be a bit larger than those of recessive Stargardt disease and often take on a "butterfly" appearance at some point in the evolution of the macular lesions (Fig. 44.46). For a given degree of fundus abnormality, however, the acuity is usually much more affected in patients with SLDMD than it is in patients with *PRPH2*-associated pattern dystrophy. The ERG is usually normal. These patients are less likely than patients with autosomal recessive Stargardt disease to have a dark choroid on fluorescein angiography, but the flecks are similarly hyperfluorescent in both conditions.

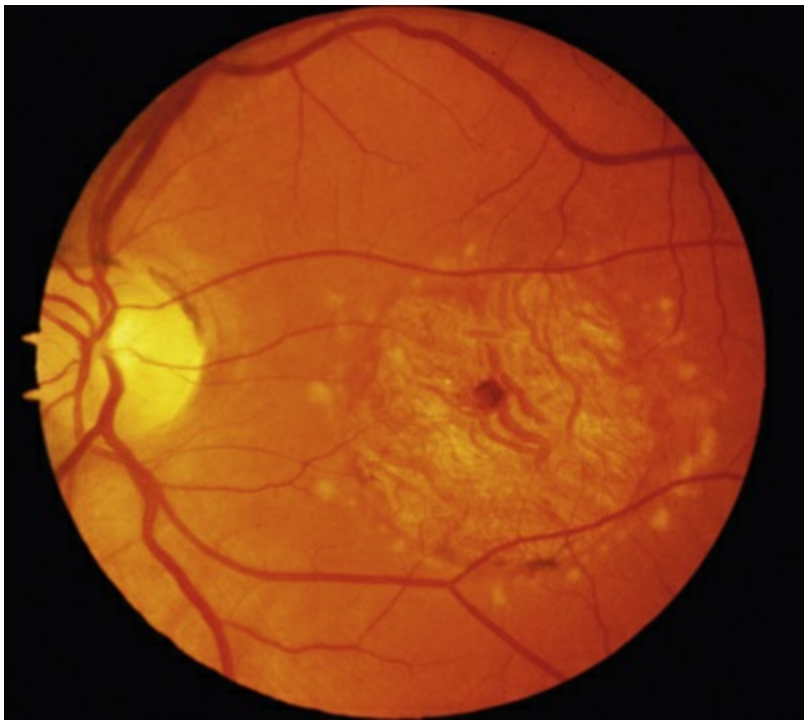

FIG. 44.45 Fundus photograph of the left eye of a 61-year-old male with the common Leu263 del5tttCTTAA mutation in *ELOVL4* causing Stargardt-like dominant macular dystrophy. The visual acuity in this eye is 20/100. All of the most characteristic features of this

disease are present in this patient, including a circular zone of RPE atrophy, a pigmented spot beneath the fovea, and a ring of flecks just beyond the margin of the atrophy.

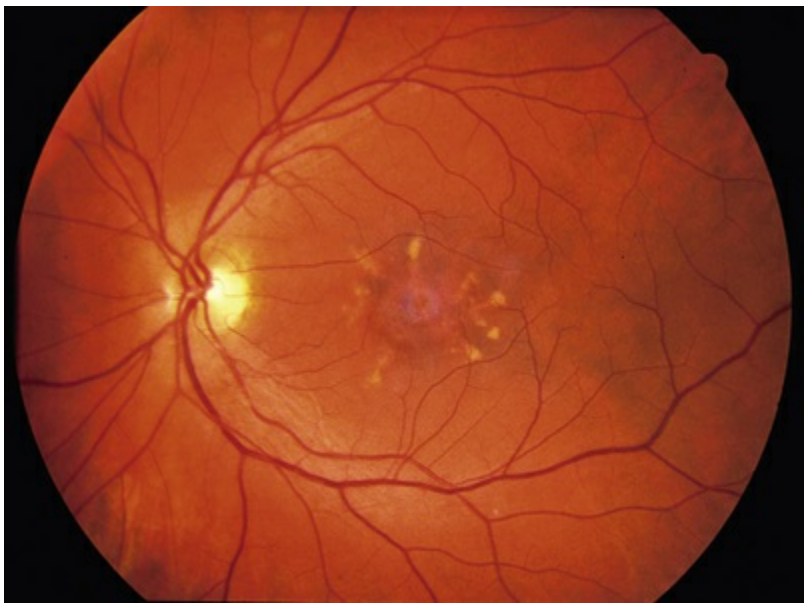

FIG. 44.46 Fundus photograph of the left eye of a 53-year-old male with the common Leu263 del5tttCTTAA mutation in *ELOVL4* causing Stargardt-like dominant macular dystrophy. The visual acuity in this eye is 20/100. There are several branching arms of yellow material at the level of the RPE that extend from a circular area of geographic atrophy centered on fixation. This fundus appearance could easily be confused with *PRPH2*-assocated pattern dystrophy.

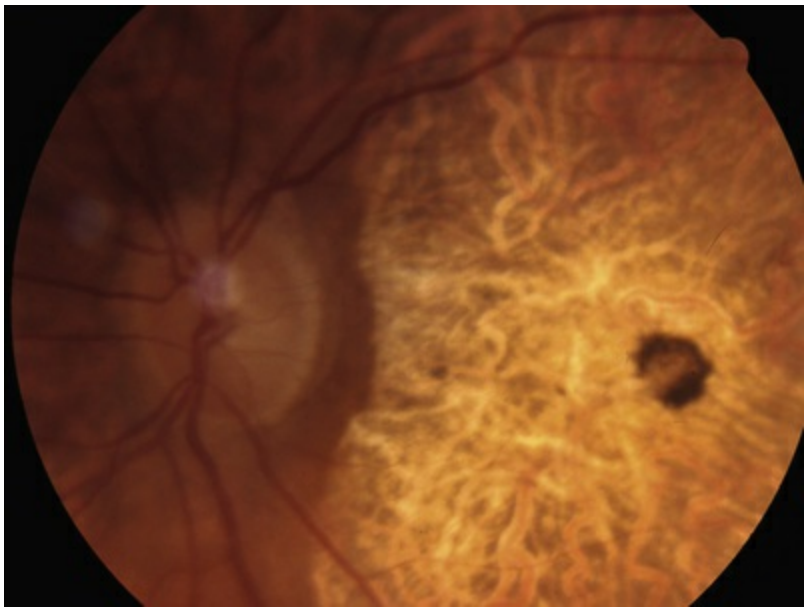

FIG. 44.47 Fundus photograph of the left eye of a 77-year-old female with the common Leu263 del5tttCTTAA mutation in *ELOVL4* causing Stargardt-like dominant macular dystrophy. The visual acuity in this eye is 20/400. At the nasal margin of the large macular lesion there is clear peripapillary sparing.

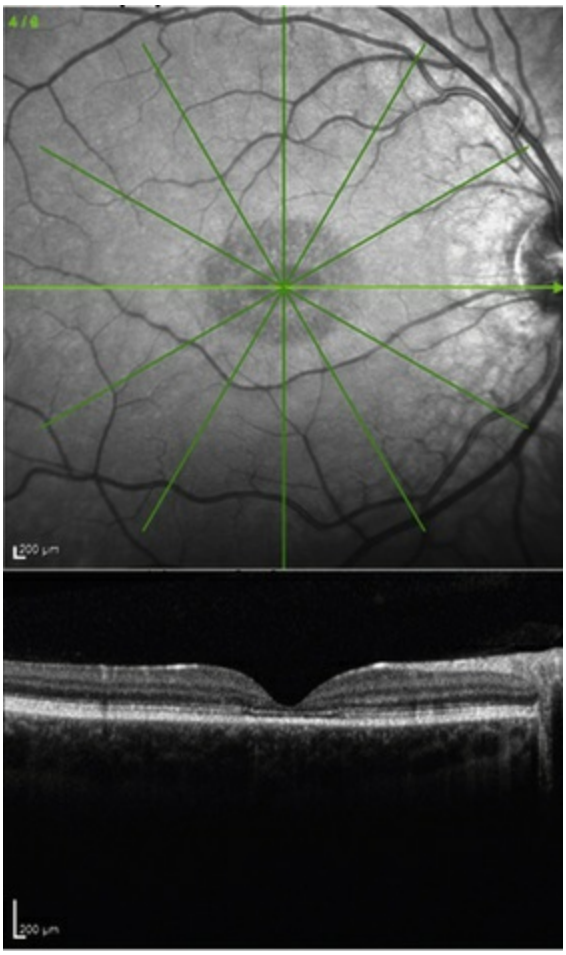

FIG. 44.48 Infrared fundus photograph and spectral domain optical coherence tomogram of the right eye of a 14-year-old male with the common Leu263 del5tttCTTAA mutation in *ELOVL4* causing Stargardt-like dominant macular dystrophy. The visual acuity in this eye is 20/125. Ophthalmoscopically, the fundus is near normal, but spectral domain optical coherence tomography reveals loss of foveal photoreceptors. This selective loss of foveal cones is also seen in a subset of patients with *ABCA4*-associated recessive Stargardt disease (see for example Fig. 44.33).

Pathophysiology

The *ELOVL4* gene encodes the protein "elongation of very long chain fatty acids-4," a biosynthetic enzyme in the endoplasmic reticulum responsible for the synthesis of fatty acids with more than 26 carbons.[162,163] This gene is expressed in brain and retina, where expression is restricted to photoreceptor cells.[159] Mutations

associated with Stargardt-like macular degeneration cause mistrafficking of the mutant protein in vitro,[164] which results in cell death.[165] Mice harboring a single mutant allele of *Elovl4* display mistrafficking of the ELOVL4 protein, show increased lipofuscin formation, and develop peripheral photoreceptor loss.[166,167]

PROM1-Associated Macular Dystrophy

In 2008, Yang et al. showed that an R373C missense mutation in the prominin 1 gene (*PROM1*) caused an autosomal dominant form of macular degeneration[168] in several families with Stargardt-like macular dystrophy and cone-rod degeneration that had been previously mapped to chromosome 4p.[169,170] Mutations in PROM1 were first associated with autosomal recessive retinitis pigmentosa[171,172] but the R373C variant was found to cause an autosomal dominant, highly penetrant bull's-eye maculopathy with little inter- and intrafamilial variability[173] (Fig. 44.49).

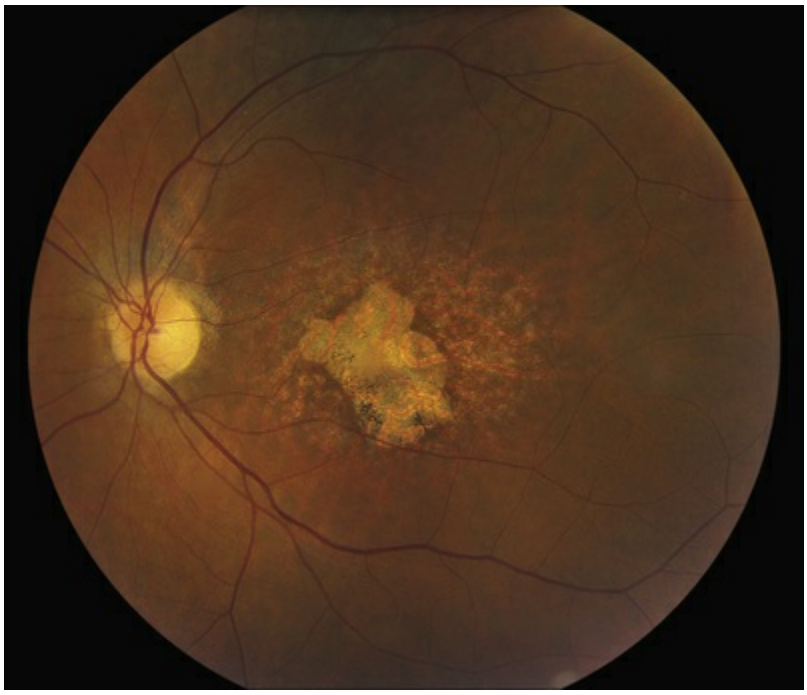

FIG. 44.49 A 48-year-old female with an Arg373Cys mutation in *PROM* causing an area of geographic atrophy in the fovea of the left eye surrounded by

pigmentary alterations. Though the appearance of the macula looks similar to Stargardt disease, there were peripapillary pigment changes in contrast to the peripapillary sparing often seen in Stargardt disease. In addition, the patient's family history is consistent with the autosomal dominant inheritance characteristic of *PROM1*-associated macular dystrophy.

Pattern Dystrophy

Pattern dystrophy (PD) refers to a group of inherited retinal dystrophies characterized by pigment changes at the level of the RPE.[174–176] PD encompasses a broad spectrum of clinical appearances that were originally given names based on the pattern of pigment distribution, such as butterfly-shaped pigment dystrophy (Fig. 44.50),[174] adult-onset vitelliform pattern dystrophy[177,178] (Fig. 44.51), peculiar foveomacular dystrophy[179] (Figs. 44.52A–B), Sjögren's reticular dystrophy of the RPE[179–182] (Figs. 44.52C and 44.53), and fundus pulverulentus.[183,184] The most common causes of all of these different patterns have proven to be mutations in a single gene, *PRPH2* (originally *RDS* – OMIM #179605). Mutations in this gene also cause some cases of central areolar choroidal dystrophy (Fig. 44.54),[185] retinitis pigmentosa,[186–189] and some cases that are nearly identical to the fundus flavimaculatus variant of Stargardt disease (Fig. 44.55). Patients with extensive RPE atrophy will sometimes exhibit peripapillary sparing very similar to that seen in *ABCA4* disease (Fig. 44.56). *PRPH2* mutations usually cause disease in the heterozygous state, and the disorders are thus inherited in an autosomal dominant fashion. Most patients with a *PRPH2*-associated PD will experience macular photostress in their daily life; that is, their central acuity will be slow to recover following exposure to bright light. Thus, a patient who can read 20/30 in a dim clinic lane may be incapable of reading their mail for tens of minutes after walking down a sunlit driveway to retrieve it. Similarly, a waitress with excellent acuity under optimal circumstances may be unable to make change for her customers after walking through a bright kitchen and returning to a dark restaurant. All of the *PRPH2*-associated pattern dystrophies

also share an 18% lifetime risk of choroidal neovascularization.[190]

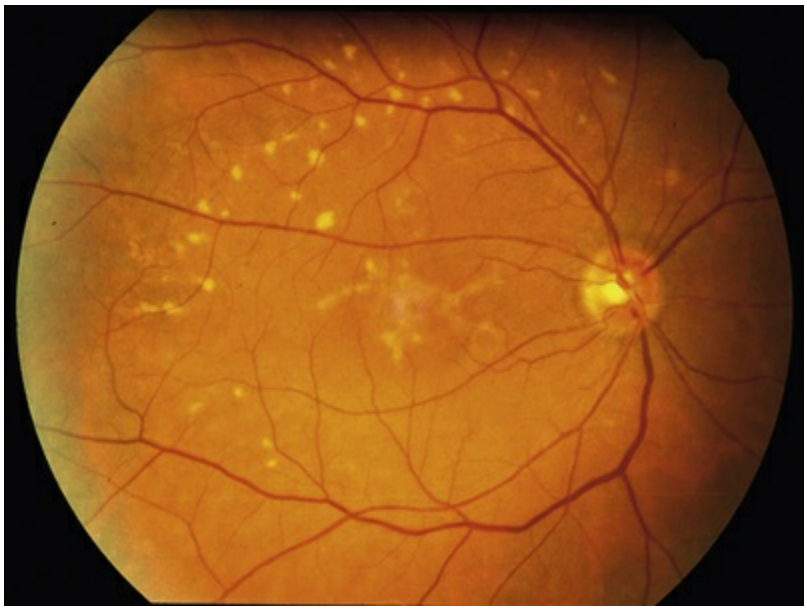

FIG. 44.50 Fundus photograph of the right eye of a 42-year-old female with a Gly167Asp mutation in *PRPH2* causing a butterfly pattern dystrophy. The visual acuity in this eye is 20/20. Although the flecks in the periphery are somewhat reminiscent of Stargardt disease, their globular nature is more consistent with *PRPH2*-associated disease.

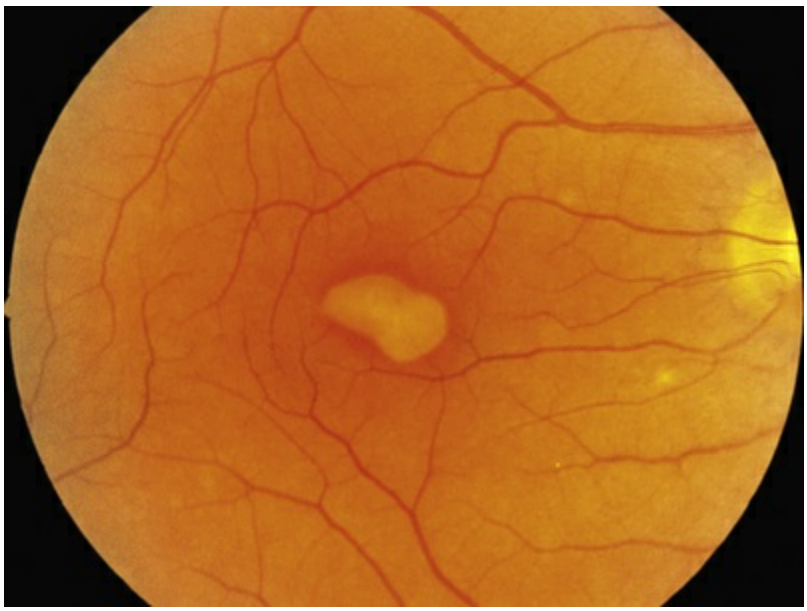

FIG. 44.51 Fundus photograph of the right eye of a 47-

year-old male with a Gly167Asp mutation in *PRPH2* causing an adult vitelliform pattern dystrophy. The visual acuity in this eye is 20/70. Although this lesion is very similar to those caused by *BEST1* mutations, its slightly polygonal shape is more consistent with *PRPH2*-associated disease.

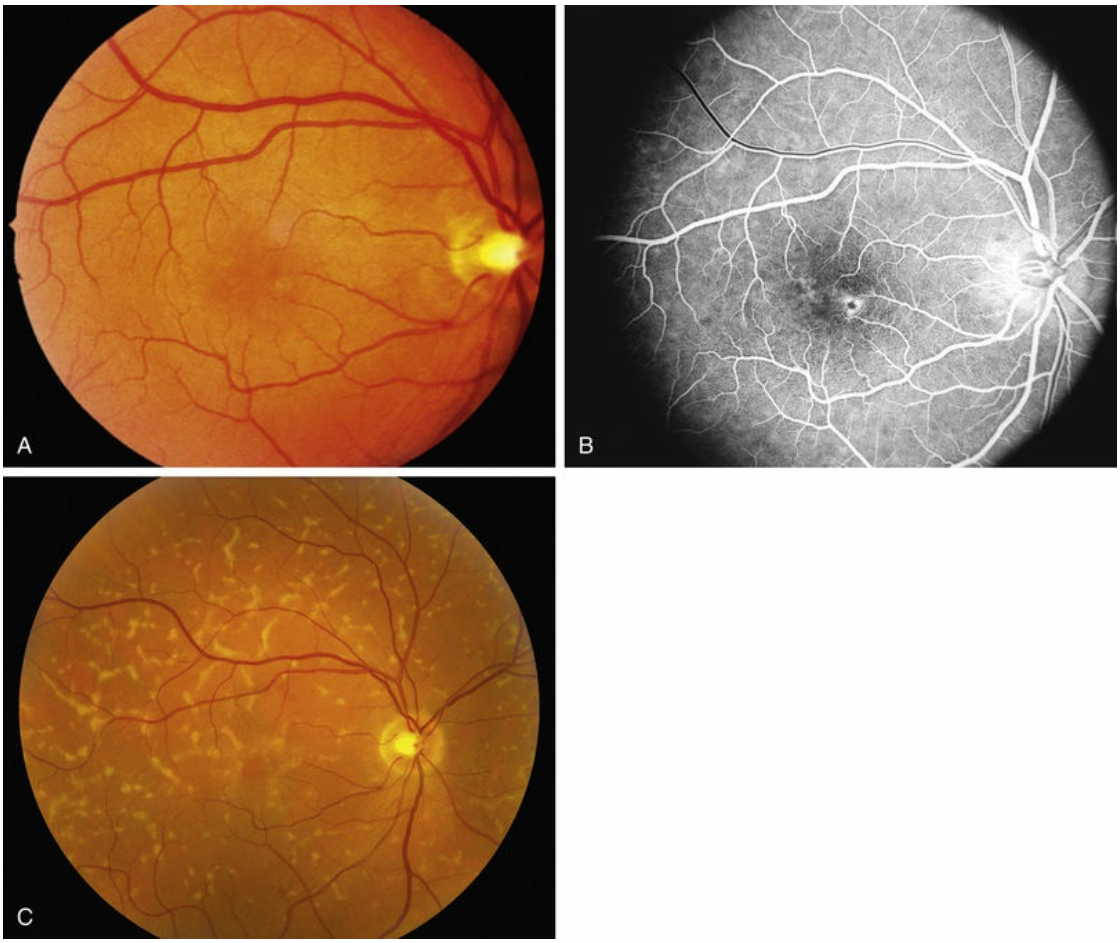

FIG. 44.52 (A) Fundus photograph of the right eye of a 42-year-old female with a Gly167Asp mutation in *PRPH2* causing pattern dystrophy. The visual acuity in this eye is 20/20. With ophthalmoscopy alone there is very little evidence of disease. (B) An early phase fluorescein angiogram of this eye reveals a small dot and halo lesion and a hint of extramacular disease along the superotemporal arcades. (C) This same eye at age 61 exhibits an extensive reticular network of yellow deposits throughout the posterior pole.

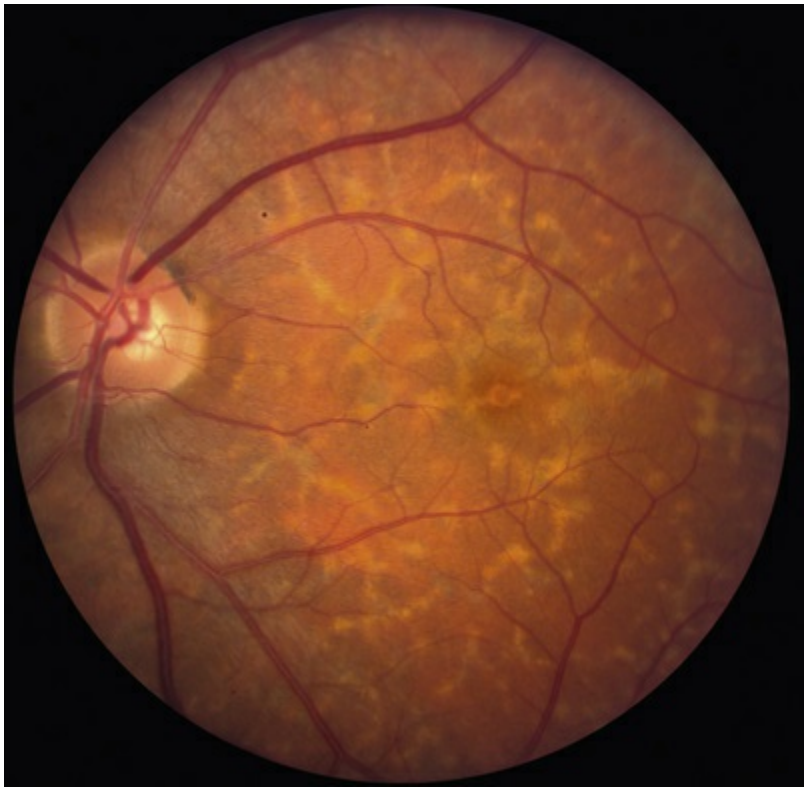

FIG. 44.53 Fundus photograph of the left eye of a 47-year-old male with a Cys82Stop mutation in *PRPH2* causing a reticular pattern dystrophy. The visual acuity in this eye is 20/20. The “knots in the fishnet” described by Sjögren are particularly evident in this patient.

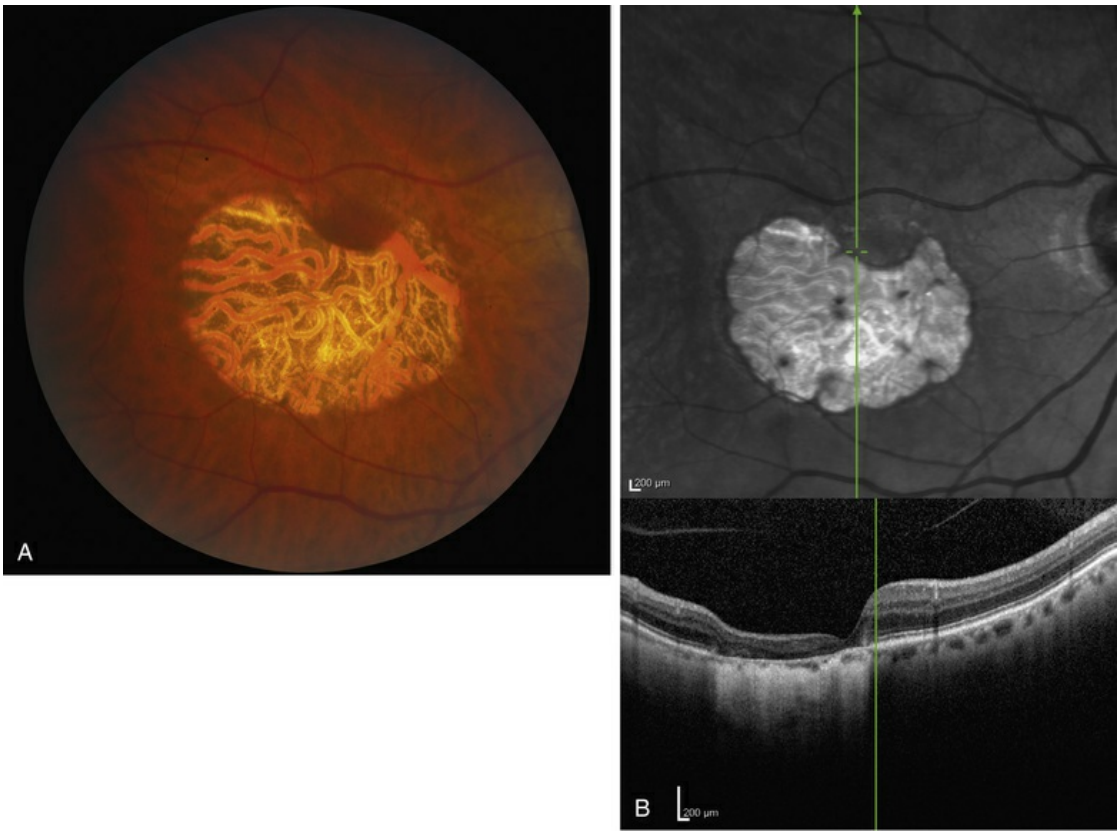

FIG. 44.54 (A) Fundus photograph of the right eye of a 74-year-old male with a Gly108Asp mutation in *PRPH2* causing a central areolar form of pattern dystrophy. The visual acuity in this eye is 20/25. (B) Spectral domain optical coherence tomography reveals a remarkable preservation of photoreceptors and retinal pigment epithelium on the superior edge of the fovea.

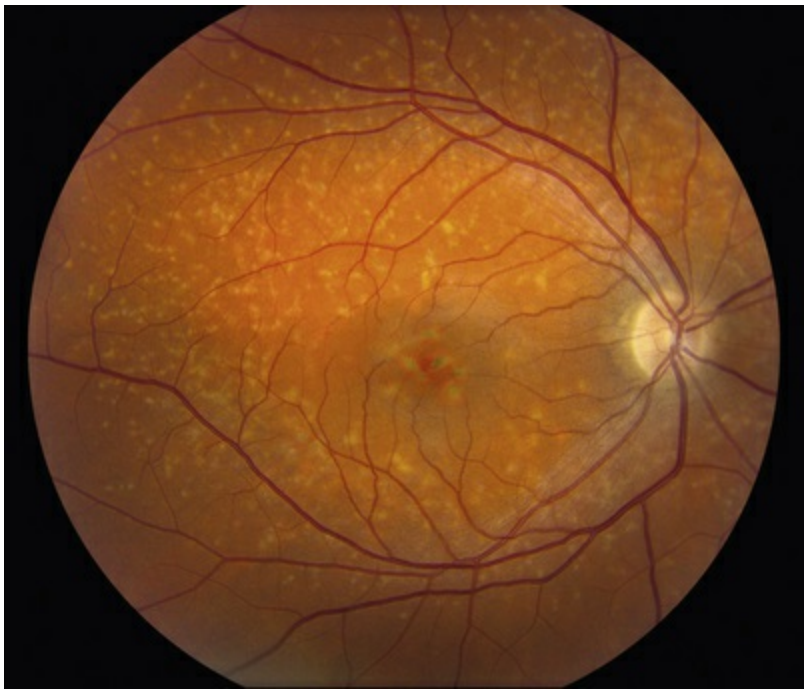

FIG. 44.55 Fundus photograph of the right eye of a 38-year-old female with a IVS2+3 A>T mutation in *PRPH2* causing pattern dystrophy. The visual acuity in this eye is 20/25. The fundus findings are very similar to the fundus flavimaculatus phenotype of *ABCA4*-associated Stargardt disease. However, the dark pigment within the flecks adjacent to the fovea is more characteristic of *PRPH2*-associated disease.

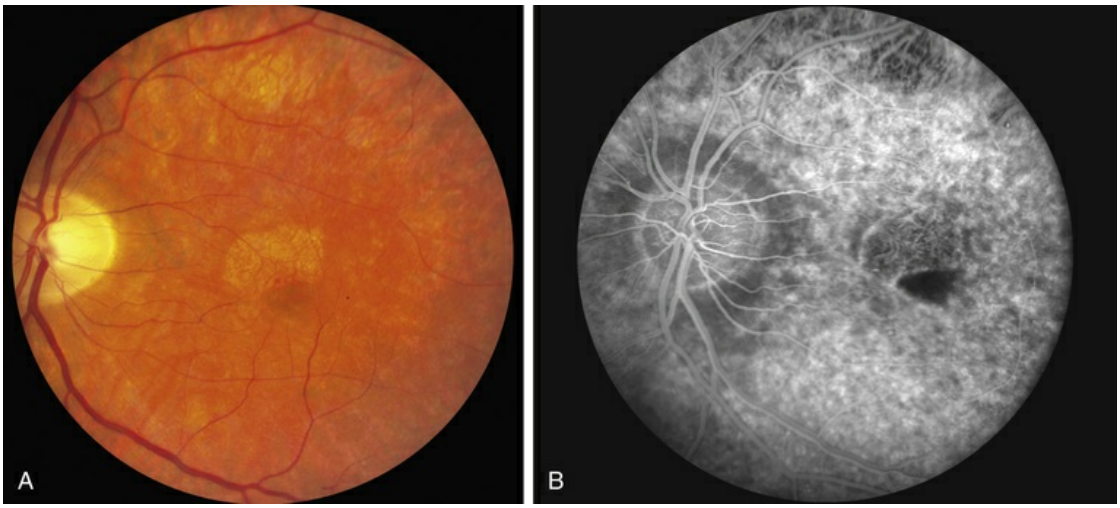

FIG. 44.56 (A) Fundus photograph of the left eye of a 54-year-old male with a Thr146 ins1aC mutation in *PRPH2* causing pattern dystrophy. The visual acuity in this eye is 20/40. There is nummular atrophy in the

macula but relative sparing of the inferior edge of the fovea and the peripapillary retina. (B) On fluorescein angiography, the spared areas of retinal pigment epithelium block the fluorescence from the underlying choroidal vessels.

Like most autosomal dominant disorders, the genetic background plays an important role in the specific clinical manifestations that result from *PRPH2* mutations, and the same point mutation can cause vitelliform lesions in one patient, peculiar foveomacular dystrophy in another, and butterfly-shaped pigment dystrophy in others.[187,191] Gutman described a patient with a vitelliform lesion in one eye and a butterfly-shaped lesion in the other.[192]

Clinical Features and History of Specific Pattern Dystrophies

Butterfly-Shaped Pigment Dystrophy

Deutman described a family with autosomal dominant inheritance that had butterfly-shaped pigmentation located in the RPE.[174] The pigmentation can be yellow, white, or black and accumulate in an unusual configuration of three to five "arms" or "wings" that resemble the wings of a butterfly (see Fig. 44.50). An area of depigmentation often occurs around the pigment. Additional pigment deposits that look like drusen or flecks can be seen peripheral to the central lesion. These changes can occasionally be seen in the 'teens, but symptoms usually do not occur until patients are in their 20s to 30s. Several mutations in *PRPH2* have been shown to be causative of this macular pattern.[191,193–196]

Adult-Onset Foveomacular Vitelliform Pattern Dystrophy

Patients with adult-onset foveomacular vitelliform dystrophy (described by Gass as a "peculiar foveomacular dystrophy"[179]) present asymptomatically or with mild blurring. Fundus examination reveals symmetric, solitary, autofluorescent vitelliform lesions in the macula (usually centered on or just adjacent to the

fovea) that are much smaller in size (less than one-third disc diameter) than the vitelliform lesions of Best disease. These lesions often have a central pigmented spot (see Fig. 44.52B) that is best seen when a narrow beam of a slit lamp is placed just adjacent to the lesion. Partial or complete resorption of the vitelliform material is common and is usually accompanied by outer retinal loss and decreased VA.[197]

Arnold et al. performed histopathologic evaluation of eyes from patients with adult vitelliform lesions. Although genotypes were not determined, the phenotype was consistent with a mutation in *PRPH2* or *BEST1*. These authors noted significant material in the subretinal space beneath the fovea, consisting of outer-segment material and pigment-laden cells. Atrophic changes appeared to be secondary to the accumulation of subretinal material.[198]

Recently, several families exhibiting autosomal dominant inheritance of vitelliform macular lesions have been associated with *IMPG1* and *IMPG2* mutations.[63,199] Patients in this series tended to have moderate visual impairment, drusen-like lesions, normal reflectivity of the RPE line on SD-OCT, and vitelliform deposits between the ellipsoid zone (EZ) and photoreceptor-RPE interdigitation lines on SD-OCT (Fig. 44.57).[199] *IMPG1* and *IMPG2* encode sialoglycoproteins of the interphotoreceptor matrix.[200–202] The patient shown in Fig. 44.49 had normal rod and cone function, consistent with the full-field ERG results observed in previously reported patients with *IMPG1* mutations.[199]

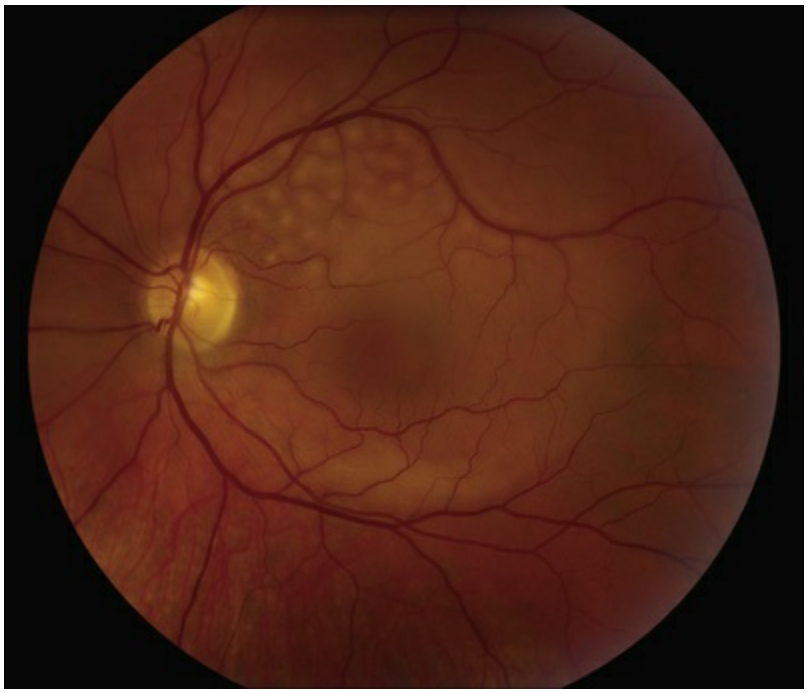

FIG. 44.57 A 58-year-old male with serous macular detachment and yellow subretinal material. Increased autofluorescence correlated to the more discrete yellow areas suggesting high lipofuscin content. Similar findings were present in the right eye (not shown). Genetic testing was positive for a heterozygous *IMPG1* mutation (Thr204Ala) in this patient and his father.

Sjögren's Reticular Dystrophy of the RPE

In reticular dystrophy of the RPE, first reported by Sjögren,[180] the fundus is characterized by a clearly defined network of black-pigmented lines at the level of the RPE that resemble a fishnet with knots or chicken wire. Early cases may have only pigment granules in the fovea but still give the impression of a pigmented network in the process of disintegration. The pigment alterations may be more visible with fluorescein angiography. The network usually starts in the fovea and can extend into the periphery. Some patients in the same family as those with reticular dystrophy also have vitelliform and/or butterfly-shaped pigment changes.[182,203–207] The genotypes of Sjögren's original patients are unknown, but individuals with *PRPH2* mutations can exhibit a pattern very similar to the one he described (see Figs. 44.52C and 44.53).

Central Areolar Choroidal Dystrophy (Central Areolar Retinochoroidal Dystrophy)

Central areolar choroidal dystrophy was, as its name implies, originally thought to be a primarily choroidal disease. However, numerous reports also link this macular pattern to mutations in *PRPH2*.[185,208–216] Thus, the choroidal changes are secondary to a genetic abnormality expressed at the level of the photoreceptors, and a more accurate term might be "central areolar retinochoroidal dystrophy (CARCD)." Visual fields are normal except for central scotomas corresponding to the macular lesions. The earliest change is a fine, mottled depigmentation in the macula of both eyes that appears between the second and fourth decades and gradually evolves into symmetric, sharply outlined, bull's-eye oval or round areas of geographic atrophy of the RPE (see Fig. 44.54). Within the area of RPE atrophy, the reddish-orange color of the large choroidal vessels is replaced by a yellow–white color, sometimes called "choroidal sclerosis" in older literature. VA deteriorates somewhat in the fourth and fifth decades but can remain as good as 20/100 to 20/200 into the seventh and eighth decades.[217–222]

Electrophysiology

Most patients with pattern dystrophy show normal cone and rod amplitudes and implicit times on the full-field ERG,[223] but some reduction can be seen when there are more extensive changes. EOG light-peak to dark-trough ratios are most frequently normal or only modestly subnormal.[223] Genetic testing for variations in *PRPH2* is less expensive than electrophysiology in most institutions and thus we reserve electrophysiologic testing for patients who lack mutations in *PRPH2* and/or who have ophthalmoscopic or perimetric findings suggestive of more widespread photoreceptor disease.

Pathophysiology

PRPH2 encodes a structural protein (peripherin) that plays a critical role in establishing and maintaining the morphology of photoreceptor outer-segment discs.[224,225] Zhang et al.[195] studied eyes from a donor with butterfly dystrophy due to a Cys213Tyr

mutation in *PRPH2* and noted an abrupt transition between healthy and degenerated retina and RPE, with massively lipofuscin-laden RPE cells at the transitions. In another report, surgical samples of retina were collected from a living patient with an Arg172Trp mutation in *PRPH2* and manifested abnormal localization of mutant peripherin protein, as well as ultrastructural alterations in outer-segment disc structure,[226] resembling the whorls observed in mice heterozygous for the *rds* mutation.[227] Thus, the primary defect is both genetically and structurally present in photoreceptor cells, with presumed subsequent injury to the RPE and choriocapillaris. The pathophysiologic interplay between the photoreceptors, the RPE, and the choriocapillaris plays a very important role in *PRPH2*-associated diseases, just as it does in the diseases caused by mutations in *ABCA4*. The most severe mutations in both genes cause direct photoreceptor death, and this in turn leads to bone-spicule-like pigmentation, narrowed arterioles, and clinical symptoms and signs characteristic of retinitis pigmentosa. In such patients, there is very little yellow pigment deposition because the source of the pigment (the photoreceptor outer segments) is lost. In contrast, the milder mutations of both genes, although expressed in the photoreceptors, have their most visible pathologic effects at the level of the retinal pigment epithelium because the normal phagocytic activity of the latter tissue imports the toxic bisretinoid (in the case of *ABCA4*) or misshaped discs (in the case of *PRPH2*). Apoptotic death of the RPE in response to this long-term stress causes death of the underlying choriocapillaris just as it does in age-related macular degeneration.

Treatment

A significant risk for vision loss exists for patients with PD; Francis et al. reported 50% eventually developed poor central acuity due to either geographic atrophy or subretinal neovascularization.[190] However, as in Best disease, many patients can retain driving vision in at least one eye well into their seventh decade of life. Although CNV is slightly less frequent than in age-related macular degeneration, it can be just as devastating to vision, and anti-VEGF injections may result in regression and limitation of vision loss.[228] It

is also helpful to discuss the practical aspects of delayed recovery from exposure to bright light with PD patients because wearing dark glasses and a hat when outside can allow them to adapt more readily when coming inside. Similarly, adjusting the lighting in the patient's home or office to minimize large changes in illumination from one room to the next (e.g., bright kitchen, dim family room) can make a big difference in their activities of daily living.

Sorsby Fundus Dystrophy

In 1949 Sorsby described five families with an autosomal dominantly inherited "fundus dystrophy with unusual features" characterized by macular hemorrhages that usually begin early in the fifth decade of life and pigmentary changes in both maculas.[229] Progressive atrophy of the peripheral choroid and RPE is common and can severely limit ambulatory vision later in life. Now known as Sorsby fundus dystrophy (SFD), this disease is caused by mutations in *TIMP-3* (OMIM #188826).[230]

Clinical Features of SFD

One of the earliest symptoms of the disease is night blindness,[231,232] although this is not typically severe enough to bring a patient to medical attention. When individuals are seen at this early stage, it is often because they are concerned about the severe macular disease in one of their parents. At this point in the disease course ophthalmoscopically visible yellow-to-gray material is present at the level of Bruch's membrane. In some parts of the fundus this material can take the form of drusen (Fig. 44.58), while in other areas the material coalesces into a fairly uniform yellowish-gray sheet that becomes more prominent with increasing age (Fig. 44.59B). Patients most commonly present to an ophthalmologist in the fourth or fifth decade of life,[229] when they develop bilateral subfoveal neovascular membranes (Figs. 44.59A and 44.60) and their VA worsens suddenly. Untreated CNV often results in extensive disciform scarring that severely reduces VA.[233] Marked pigment alterations consisting of atrophy admixed with angular pigment proliferation commonly develop in the macula with or

without CNV. Unlike age-related macular degeneration, which rarely extends beyond the temporal vascular arcades, SFD relentlessly extends peripherally and commonly reduces a patient's acuity to hand motions late in life.

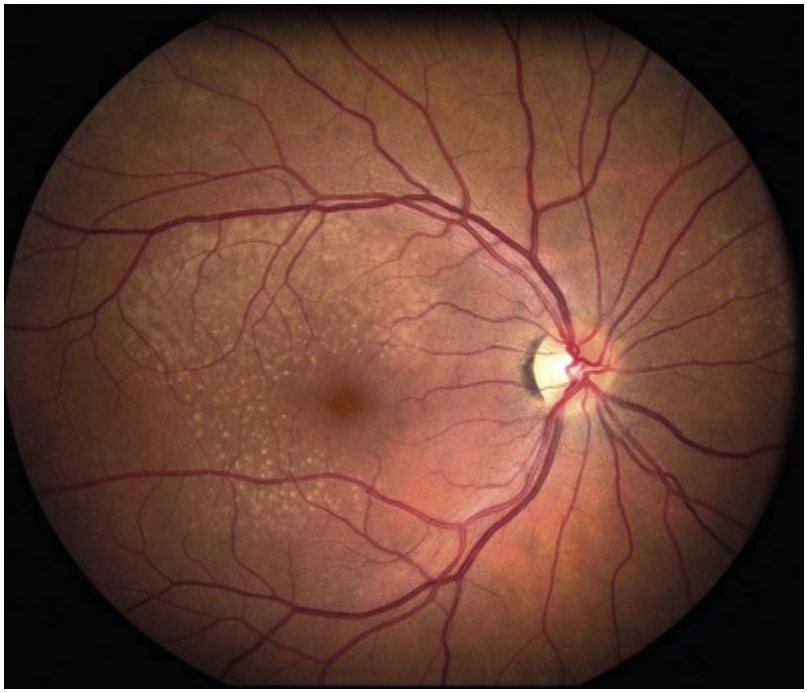

FIG. 44.58 Fundus photograph of the right eye of a 36-year-old female with Ser181Cys mutation in *TIMP-3* causing Sorsby fundus dystrophy. The visual acuity in this eye is 20/15. There are numerous small to medium-sized drusen incompletely ringing the fovea. Superiorly, these drusen merge into a confluent yellow sheet.

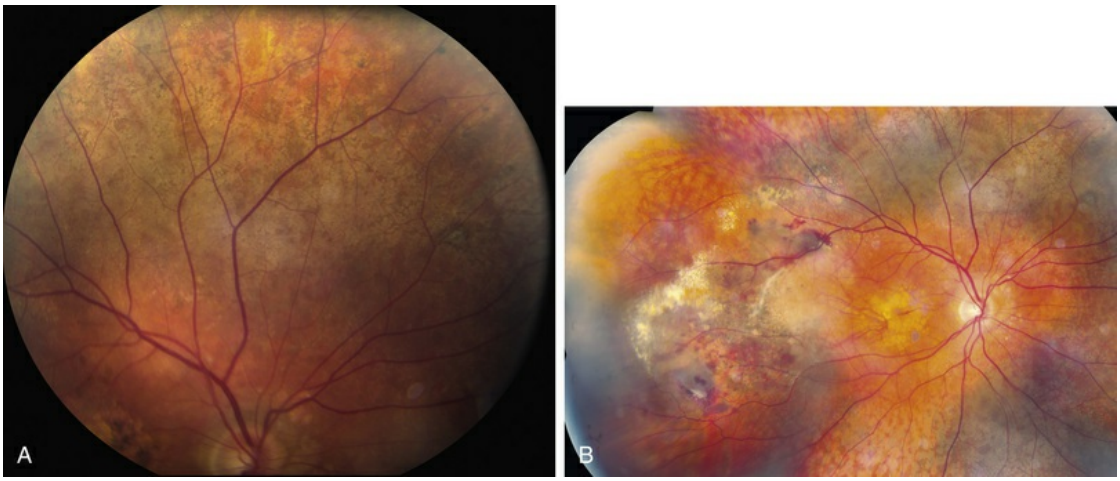

FIG. 44.59 (A) Fundus photograph montage of the right eye of a 55-year-old female with a Ser15Cys mutation in *TIMP-3* causing Sorsby fundus dystrophy. The visual acuity in this eye is 20/125. There is geographic atrophy in the macula and subretinal hemorrhage and exudate temporally indicative of an active choroidal neovascular membrane. (B) A higher magnification view of the retina superior to the disc shows a yellow–gray sheet-like discoloration that corresponds to thickening of Bruch's membrane.

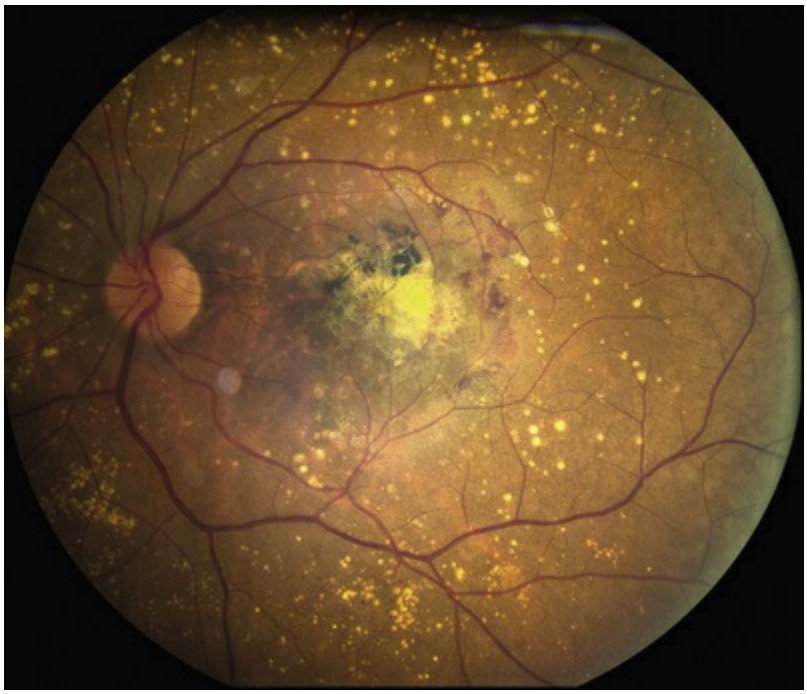

FIG. 44.60 Fundus photograph of the left eye of a 61-year-old female with Trp175Cys mutation in *TIMP-3*

causing Sorsby fundus dystrophy. The visual acuity in this eye is 20/125. There is a central disciform scar and temporal subretinal hemorrhage consistent with an active choroidal neovascular membrane. There are numerous drusen of varying sizes in the periphery.

Genetics

Since its discovery in 1994, at least 14 mutations in *TIMP3* have been identified.[230,234–241] Most people with SFD in the United Kingdom share a common ancestor and thus harbor the same mutation, Ser181Cys.[242,243] A very unusual feature of SFD is that almost all of the reported mutations create a new cysteine residue in the mutant protein, suggesting that a perturbation of tertiary structure through altered disulfide bonding is required for the development of the disease.

Pathophysiology

The *TIMP3* gene encodes a protein, tissue inhibitor of metalloproteinases-3 (TIMP3), which belongs to a family of negative regulators of matrix metalloproteinase activity. TIMP3 physically interacts with several metalloproteinases[244] and regulates their activity in normal tissue homeostasis. Mutations in this gene are likely to cause altered turnover of extracellular matrix. Given that pathologic angiogenesis is a major clinical feature of SFD, it is notable that TIMP3 suppresses angiogenesis by blocking the interaction of VEGF with its receptor KDR.[245]

The most striking characteristic of eyes with SD is the accumulation of lipidic and proteinaceous material between Bruch's membrane and the RPE up to 30 μm in thickness.[246] Histopathologic analyses of eyes from a donor with SFD due to a Ser181Cys mutation in *TIMP3* revealed CNV and thick deposits beneath the RPE that contained TIMP3 and other extracellular matrix components. The presence of basement membrane proteins in the SFD lesions is consistent with the notion that TIMP3 gain-of-function mutations are pathogenic by their dysregulation of matrix turnover. Ultrastructurally, this material contains banded

proteinaceous aggregates with a periodicity suggestive of type VI collagen.[247] Type VI collagen has also been shown to be present at the margins of the lesions by immunohistochemistry.[248]

The TIMP3 protein is a normal component of Bruch's membrane[249] as well as a component of drusen[250] and the abnormal deposits in SFD.[248,251] The accumulation of TIMP3 in SFD may result from the relatively poor turnover of the mutant protein caused by missense mutations.[252]

Dominant mutations in TIMP3 have been recapitulated in mice. Mice harboring a mutant allele of *TIMP3* (Ser156Cys) show abnormalities in the RPE basal infoldings and increased extracellular material between the RPE plasma membrane and its basal lamina.[253] Thus, animal studies and biochemical findings strongly suggest that SFD-causing mutations in TIMP3 cause impaired regulation of metalloproteinases and reduced remodeling of the matrix. Normal synthesis, reduced remodeling of extracellular matrix, and impaired control of angiogenesis would appear sufficient to describe the pathology of SFD. However, when Fogarasi et al. assayed the proteinase inhibitory activity of a TIMP3 protein carrying a common SFD mutation, they found no impairment of proteinase inhibition.[254] Thus, some significant questions about the molecular basis of SFD remain unanswered.

Treatment

Treatment of patients with SFD is aimed at CNV control. Argon laser therapy and PDT are not effective in treating SFD-associated CNVs, possibly due to the thickening of Bruch's membrane.[233,255] However, intravenous bevacizumab has been used in one patient and resulted in CNV regression and improvement in VA.[256]

Autosomal Dominant Radial Drusen (Doyne Honeycomb Retinal Dystrophy, Malattia Leventinese)

A familial macular condition with a honeycomb appearance was described by Doyne in the UK in 1899,[257] and a similar condition

(malattia leventinese, ML) was recognized by Vogt in patients residing in the Leventine Valley of Switzerland in 1925.[258] Surprisingly, it was not until the late 1980s that Gass drew specific attention to one of the most striking clinical features of the condition, the radial distribution of drusen at the temporal periphery of the macular lesions (Fig. 44.61),[259] although at that time he did not explicitly connect this observation to the entities described by Doyne and Vogt. In 1996 Héon and colleagues mapped the disease-causing gene for malattia leventinese to chromosome 2,[260] and in 1999 Stone and coworkers showed that Doyne's honeycomb retinal dystrophy and ML were in fact one disorder caused by a single point mutation (Arg345Trp) in the *EFEMP1* gene.[261] In this chapter, we will use the descriptive term "autosomal dominant radial drusen" (ADRD) to refer to this disease.

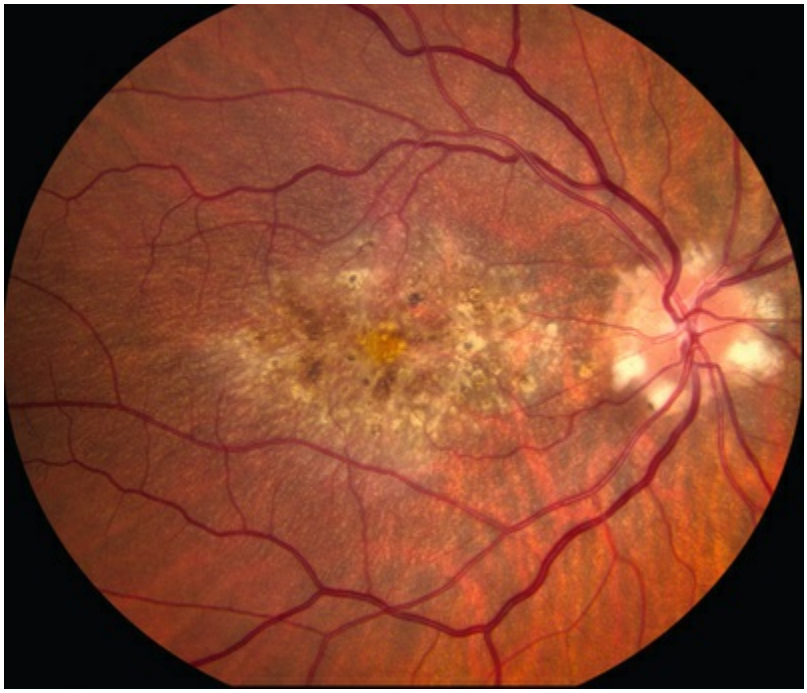

FIG. 44.61 Fundus photograph of the right eye of a 46-year-old female with an Arg345Trp mutation in *EFEMP1* causing autosomal dominant radial drusen. The visual acuity in this eye is 20/40. The large drusen abutting the optic disc are characteristic of this disease as are the delicate radially oriented drusen that are visible along the temporal edge of the macular lesion. A few of the medium-to-large drusen in the central

lesion have fused into a honeycomb configuration.

Clinical Features of ADRD

As with most autosomal dominant conditions, ADRD has a wide range of clinical appearances, presumably due to the variable effect of other genes and environmental factors in different affected individuals. Drusen can be seen in the second decade in some patients while others have barely detectable drusen in the seventh decade. The drusen in the center of the macula and on the nasal edge of the optic disc tend to be large and round (Fig. 44.62), while those at the temporal margin of the macula tend to be smaller, elongated, and radial (see Fig. 44.61). In some patients the small radial drusen can be nearly invisible and reticular pigment changes in the macula can simulate a pattern dystrophy (Fig. 44.63). Most eyes have a group of drusen abutting the nasal aspect of the nerve, even when macular drusen are few or absent.[262] Over time, many eyes develop central atrophy, scarring, and pigment proliferation that can look similar to SFD (Fig. 44.64). However, for a given degree of macular abnormality, the VA in ADRD is typically much better than SFD. Choroidal neovascularization can also complicate ADRD, but this occurs much less frequently than it does in SFD.

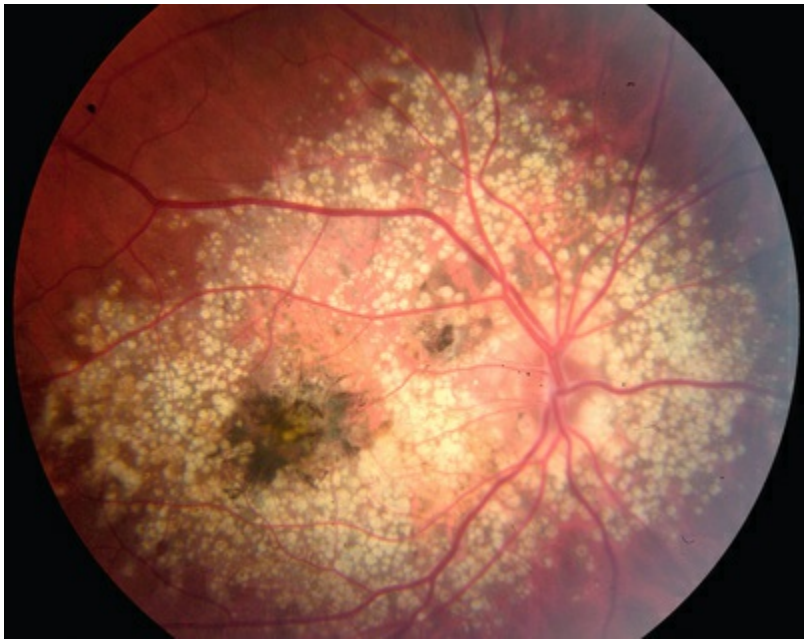

FIG. 44.62 Fundus photograph of the right eye of a 34-year-old male with an Arg345Trp mutation in *EFEMP1* causing autosomal dominant radial drusen. The visual acuity in this eye is 20/80. There is a dense honeycomb of large drusen occupying most of the posterior pole, with dark pigment and RPE atrophy near the center of the macula.

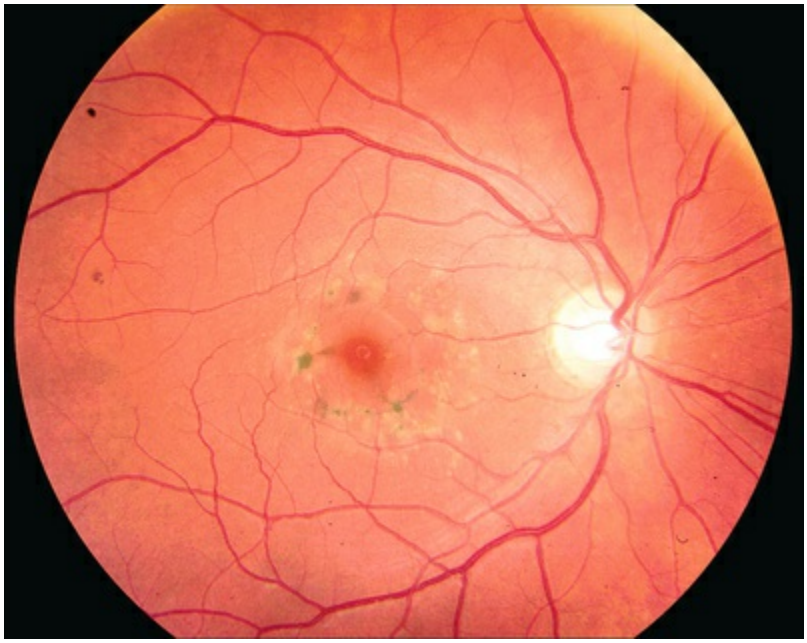

FIG. 44.63 Fundus photograph of the right eye of a 29-year-old female with an Arg345Trp mutation in *EFEMP1* causing autosomal dominant radial drusen. The visual acuity in this eye is 20/20. Reticular pigment changes outline the large central drusen. Fine radial drusen along the temporal and inferior aspects of the macular lesion are nearly invisible.

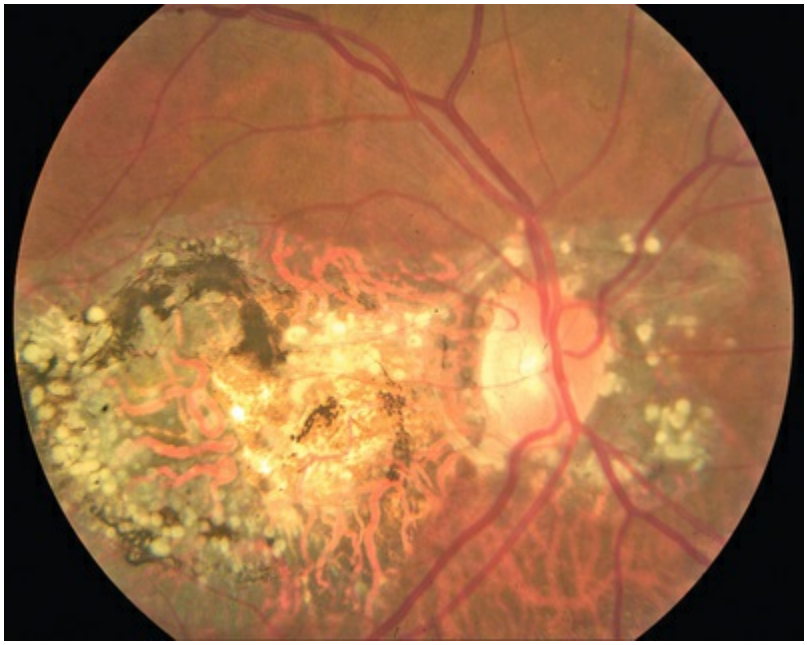

FIG. 44.64 Fundus photograph of the right eye of a 57-year-old female with an Arg345Trp mutation in *EFEMP1* causing autosomal dominant radial drusen. The visual acuity in this eye is counting fingers. There are extensive atrophic changes in the central macula, papillomacular bundle, and peripapillary regions. A few large drusen are present nasal to the nerve head. This eye had a choroidal neovascular membrane treated with photocoagulation 17 years earlier.

Visual Function and Electrophysiology

Even in the presence of extensive drusen, the VA is usually excellent until central atrophy, pigment proliferation, or CNV develop later in life.[262,263] Scotopic sensitivity is reduced and dark-adaptation kinetics are prolonged over confluent macular deposits but are normal elsewhere. The full-field ERG is usually normal, but the pattern ERG is abnormal in most eyes.[264]

Imaging

In contrast to drusen in AMD that tend to be hypoautofluorescent, the drusen in ADRD are hyperautofluorescent.[262,265] Autofluorescence can also be useful to distinguish areas of atrophy that can be challenging to see on clinical examination when there is extensive pathology present. Fluorescein angiography is useful for

the detection of active choroidal neovascularization, while OCT can demonstrate retinal edema, loss of foveal contour, pigment epithelial detachments, and intense sub-RPE reflectivity.[263]

Pathophysiology and Histopathology

The *EFEMP1* gene encodes an extracellular matrix protein known as fibulin-3. Marmorstein et al. studied eyes from an 86-year-old donor with ADRD and found large sub-RPE deposits containing fibulin-3, localized along the apical (i.e., sub-RPE) surface of the deposit, but generally not throughout the druse.[266] Ultrastructural studies have also shown deposition of membranous material in Bruch's membrane.[267] Histologically, drusen in ADRD have a unique onion skin-like lamination that is distinct from age-related drusen (Fig. 44.65).[268] Not only do the drusen show robust fibulin-3 reactivity, they also possess collagen type IV, an extracellular matrix protein absent in age-related drusen. Antibodies directed against the membrane attack complex demonstrate immunoreactivity in ADRD.[268]

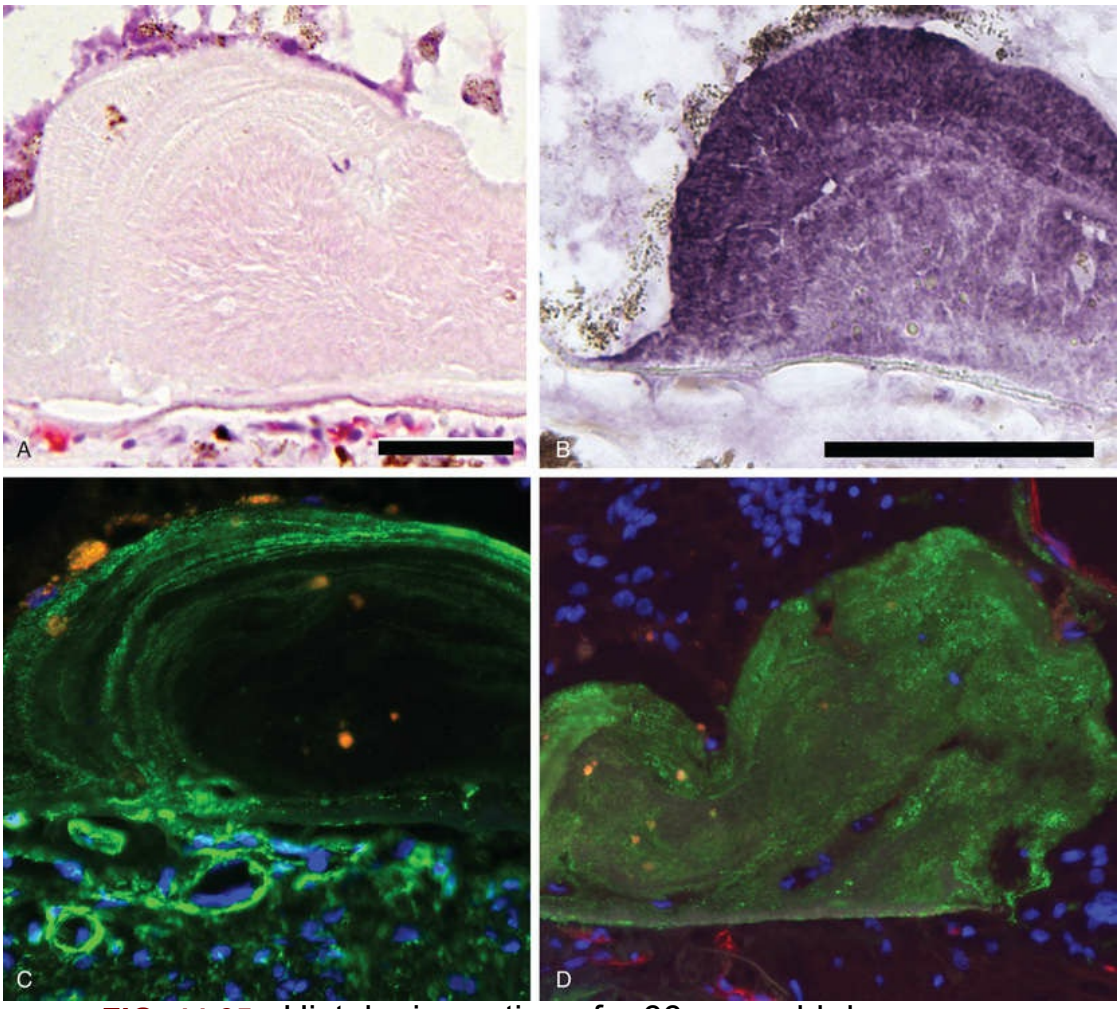

FIG. 44.65 Histologic section of a 66-year-old donor eye with autosomal dominant radial drusen due to an Arg345Trp mutation in the *EFEMP1* gene. The drusen are notable for their size and their unusual onion skin-like lamination (panel A, scale bar: 50 μm); robust fibulin-3 reactivity (panel B, scale bar: 50 μm); anti-collagen IV labeling in green fluorescence (panel C, section also labeled with diamidinophenylindole yielding blue nuclear fluorescence); and anti-C5b-9 complex (aka membrane attack complex) immunoreactivity in green fluorescence (panel D, red vascular labeling, *Ulex europeaeus* agglutinin-I; blue fluorescence, diamidino-phenlindole).

Physiologic studies have provided some insight into the pathogenesis of ADRD. Fibulin-3 bearing the Arg345Trp mutation is poorly secreted by RPE cells in vitro and its accumulation in the endoplasmic reticulum activates the unfolded protein response.[269] Knock-in mice harboring one or more Arg345Trp alleles develop

sub-RPE deposits that, while modest in size compared to the drusen observed in ADRD, share molecular components such as fibulin-3 and TIMP3.[270,271] *EFEMP1* is expressed in both neural retina and RPE/choroid layers[272] and fibulin-3 has been detected in photoreceptor cells, inner retinal neurons, and Bruch's membrane.[266]

Treatment

There is currently no treatment for the underlying disease process of ADRD, but intravitreal anti-VEGF therapy can cause regression of choroidal neovascularization and restore visual function as long as atrophic changes are minimal.[263]

North Carolina Macular Dystrophy

North Carolina Macular Dystrophy (NCMD) was first described as "dominant macular degeneration and aminoaciduria" by Lefler, Wadsworth, and Sidbury,[273] who studied a kindred originating from two Irish brothers who settled in North Carolina in the 1830s.[274] The original North Carolina pedigree now consists of more than 5000 individuals,[275] but families with similar phenotypes have been identified throughout the world.[276–280] It has also been called central areolar pigment epithelial dystrophy[281] and dominant progressive foveal dystrophy.[274] The latter term is a particularly unfortunate misnomer because Small and colleagues clearly demonstrated that NCMD is a developmental abnormality that is almost completely stationary in most individuals.[282] Large lesions are large at birth and do not progress from smaller ones. This complete lack of progression is one of the most reliable diagnostic features of the disease, and accounts to some degree for the amazingly good VA in some patients with very large lesions. That is, because the lesions are present well before maturation of the visual system, patients learn to fixate on the edges of the lesions and develop their visual pathways accordingly. The fundus findings in NCMD tend to be bilateral and quite symmetric. The most characteristic lesion is a circular coloboma centered on fixation with a shiny concave base surrounded by a thick, white fibrotic rim (Fig. 44.66A). Much more difficult to diagnose correctly in the

absence of other family members is the milder manifestation of the disease that can appear as nothing more than a patch of drusen in a young adult with excellent acuity (Figs. 44.66B–C). The VA in NCMD correlates fairly well with the size of the fundus lesions as follows: 20/20 to 20/30 for small (less than 50 μm) lesions; 20/25 to 20/60 for confluent yellow specks in the central macula; and 20/40 to 20/200 when large (500–1000 μm) colobomatous lesions are present (Figs. 44.66A–D).[282,283]

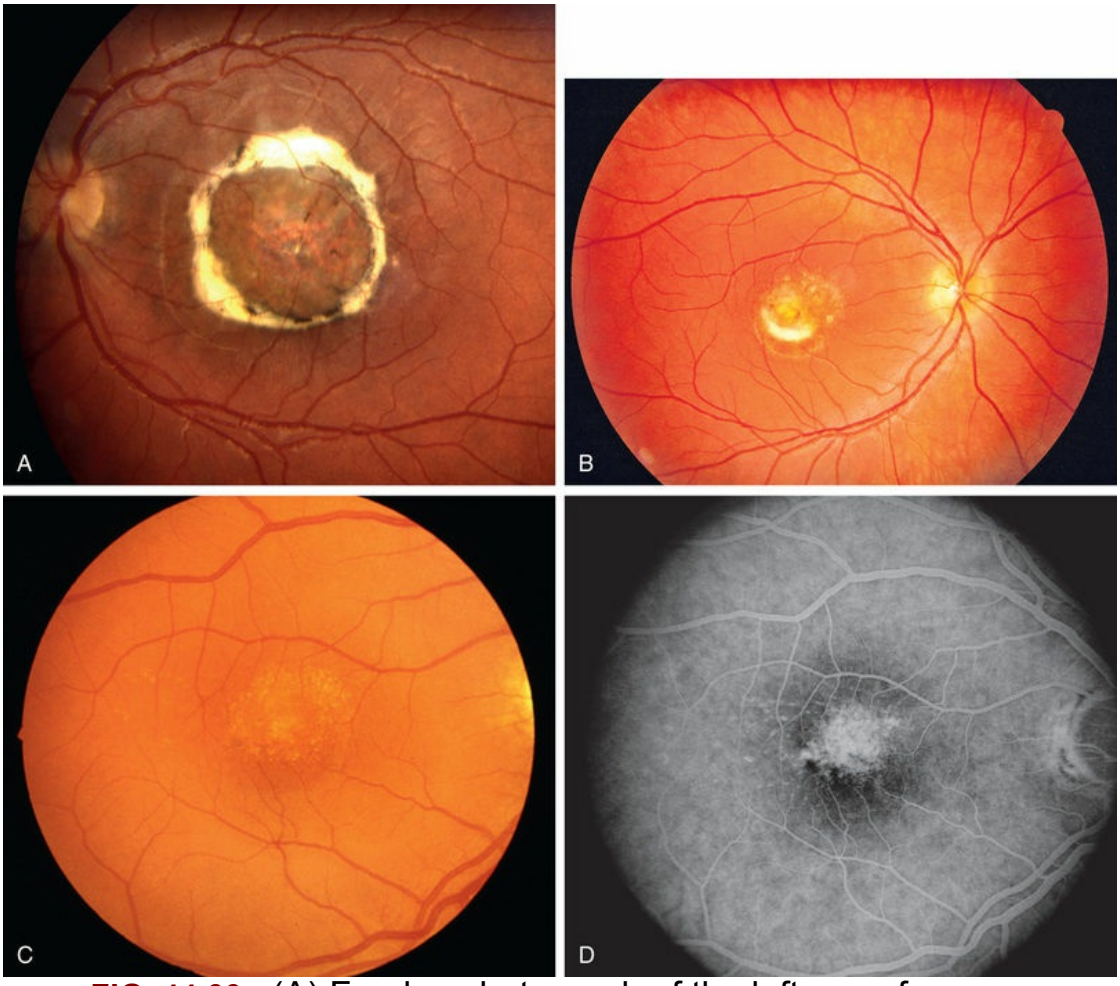

FIG. 44.66 (A) Fundus photograph of the left eye of a 12-year-old female with North Carolina macular dystrophy. The visual acuity in this eye is 20/400 (when fixating on the edge of the lesion). The characteristic fundus findings include a staphylomatous lesion centered in the macula, with a shiny concave base and a thick white fibrotic rim. The disc, vessels, and periphery are all completely normal. (B) The right eye of the 14-year-old sister of the patient

shown in (A). The visual acuity is 20/40. The central concavity is smaller than that of her sister, and the fibrotic rim is incomplete. The retina opposite the fibrotic rim exhibits drusen-like changes. (C) Fundus photograph of the right eye of the 31-year-old mother of the individuals shown in (A) and (B). The visual acuity is 20/20 and the fundus findings are limited to a patch of small drusen-like deposits centered just above the fovea. (D) The extent of these drusen-like deposits is more easily seen in a fluorescein angiogram of the same eye.

NCMD was mapped by Small and coworkers to chromosome 6,[284–286] and another dominant macular dystrophy with clinical features very similar to that of NCMD was mapped to chromosome 5.[287,288] Small and coworkers recently showed that mutations affecting the promoter of the gene *PRDM13* cause the chromosome 6 form of the disease, while a large duplication involving the entire *IRX1* gene was identified in a single family with the chromosome 5 form.[289] In a histopathologic study of one eye from a donor with NCMD, lipofuscin and choriocapillaris atrophy were noted.[290]

Spotted Cystic Dystrophy

Mahajan et al.[291] recently described seven members of a three-generation family with autosomal dominant inheritance of a new dystrophy limited to the macula and characterized by round, flat pigmented spots with or without surrounding hypopigmentation (Fig. 44.67A), cysts in multiple retinal layers on OCT (Fig. 44.67B), and neovascularization. Amblyopia and strabismus were frequently present in affected individuals. VA ranged from 20/20 to 20/200. The pathophysiology and genetic mutation responsible for this condition have not been identified. When active macular neovascularization occurs in affected individuals, it has been responsive to either focal laser or a single injection of bevacizumab.[291]

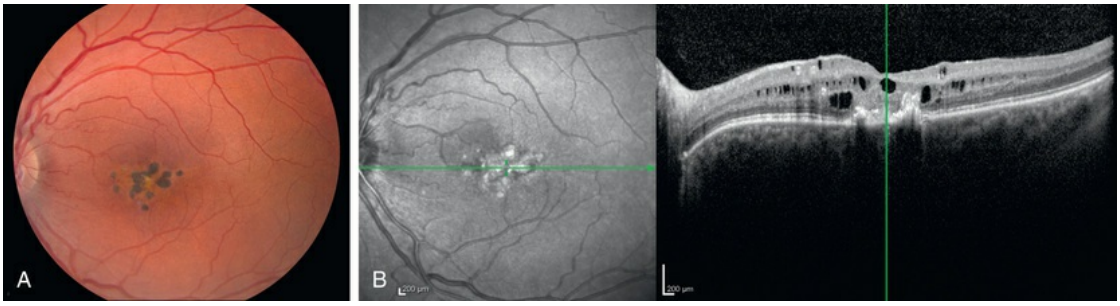

FIG. 44.67 (A) Fundus photograph of the left eye of a 25-year-old female with spotted cystic dystrophy. The visual acuity is 20/70. There are deeply pigmented spots with hypopigmented halos clustered around the fovea. (B) Spectral domain optical coherence tomography reveals intraretinal cysts and hyperreflective lesions that project from the retinal pigment epithelium into the outer retina.

Dominant Cystoid Macular Dystrophy

Dominant cystoid macular dystrophy (DCMD) was described in 1976 by Deutman[292] as an autosomal dominant condition characterized by leaking perimacular capillaries, whitish punctate deposits in the vitreous, a normal ERG, a subnormal EOG, and hyperopia (Fig. 44.68). In the late stages of the disease, an atrophic central "beaten-bronze" macula was common. A second family was identified a few years later,[293] and linkage analysis mapped the chromosomal location of the disease-causing gene to the short arm of chromosome 7.[294] The disease-causing gene for DCMD has not yet been identified. Hogewind and coworkers evaluated intramuscular injections of a somatostatin analog (octreotide acetate) in four patients with DCMD, and seven of the eight eyes showed improvement on fluorescein angiography, with stabilization of VA.[295]

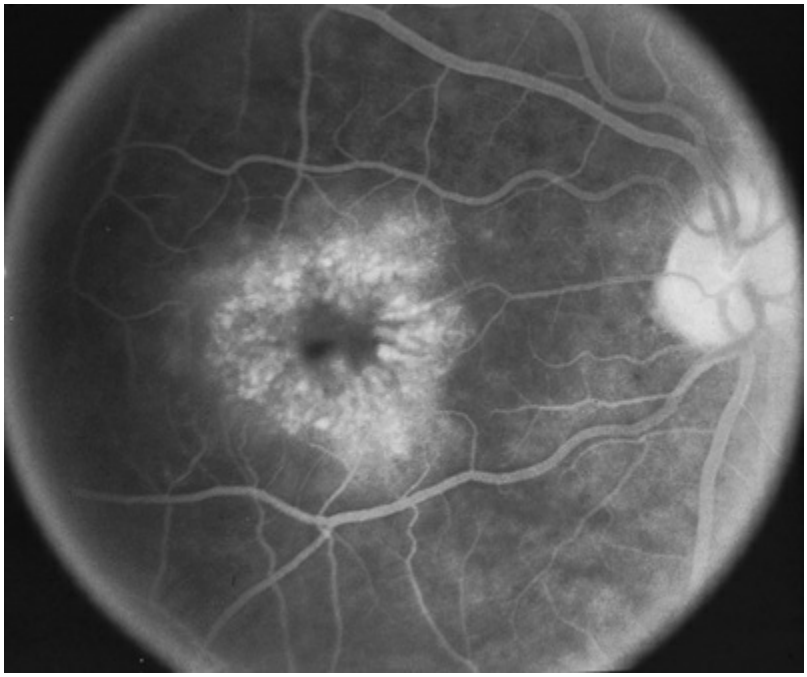

FIG. 44.68 Fluorescein angiogram of the right eye of a patient with dominant cystoid macular edema showing leakage from perifoveal capillaries. (Courtesy of Dr. Gerald Fishman, University of Illinois at Chicago.)

Fenestrated Sheen Macular Dystrophy (FSMD)

Several families have been described with an autosomal dominant macular disorder characterized by central macular sheen with small red fenestrations, occurring as early as the first decade of life and seen as late as the fifth decade (Fig. 44.69). Some middle-aged family members develop a bull's-eye pattern of stippled hypopigmentation in the central macula. Mild functional abnormalities roughly correlate with more advanced age, but patients with the red fenestrations have 20/20 VA. Normal or mildly abnormal ERG findings have been reported.[296–299] The chromosomal location of the disease-causing gene is currently unknown.

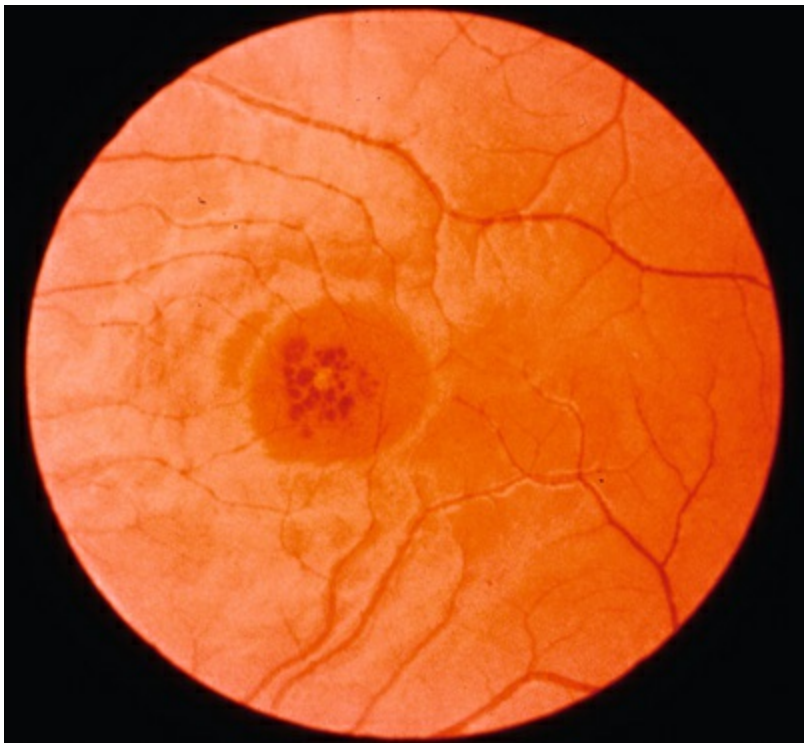

FIG. 44.69 Fundus photograph of the left eye of a 7-year-old patient with fenestrated sheen macular dystrophy. The visual acuity is 20/20. The characteristic lesions are flat red spots clustered about the fovea. (Reproduced from Sneed SR, Sieving PA. Fenestrated sheen macular dystrophy. Am J Ophthalmol 1991;112(1):1-7.)

Glomerulonephritis Type II and Drusen

The majority of patients with membranproliferative glomerulonephritis (MPGN) type II (also known as dense-deposit disease) develop subretinal deposits with the clinical appearance of basal laminar drusen (Fig. 44.70).[300] D'Souza and coworkers followed four MPGN patients with such drusen for 10 years and observed no progression and no vision loss during this interval.[301] In general, VA tends to be preserved unless CNV, exudative drusen, or serous detachment complicate the disease.[302–304] An abnormal EOG with a relatively normal ERG can be seen in some patients, suggesting a more global retinal dysfunction than the visible drusen would suggest.[305,306] Histopathologic studies of the

Bruch's membrane deposits found in MPGN II demonstrate that they are morphologically[307] and compositionally[308] similar to the drusen found in AMD.[309] Abnormal urinalysis in young adults with this phenotype should prompt a referral for work-up of kidney disease.

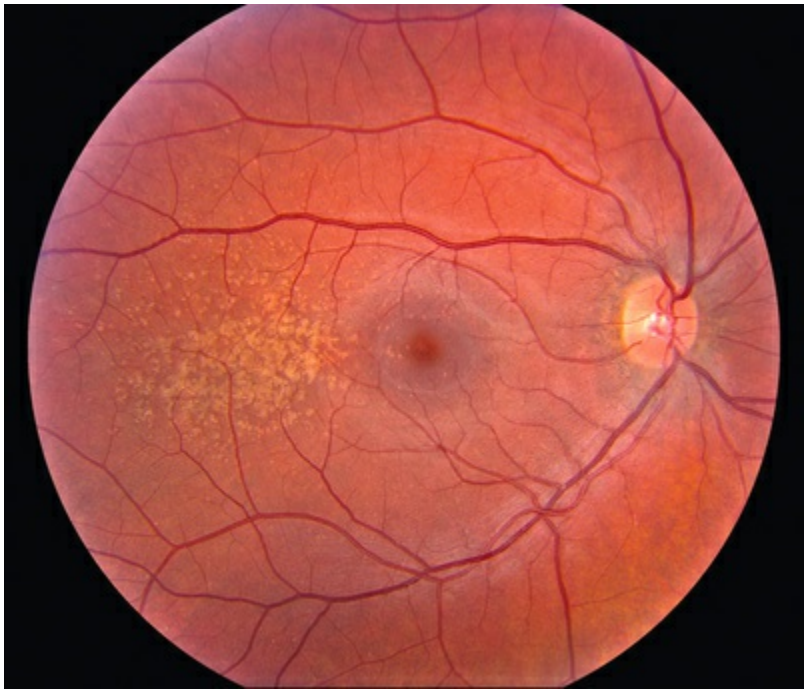

FIG. 44.70 Fundus photograph of the right eye of a 25-year-old female with biopsy-confirmed membranoproliferative glomerulonephritis type II. The visual acuity is 20/20. There are numerous small drusen in the posterior pole, almost all of which are temporal to the fovea.

Maternally Inherited Diabetes and Deafness

Patients with maternally inherited diabetes and deafness (MIDD) often exhibit macular changes that simulate pattern dystrophy (Fig. 44.71). Eighty-five percent of MIDD cases result from an A to G transition at nucleotide 3243 of the mitochondrial DNA. This mutation lies within a mitochondrial tRNA gene and causes a

reduction in function of the respiratory chain.[310,311] Bilateral sensorineural hearing loss is seen in 85–98% of MIDD cases, while pattern macular dystrophy is seen in about 80%.[311] It is estimated that as many as 1% of patients with diabetes mellitus have MIDD.[312] Full-field ERG is typically normal in MIDD with patchy abnormalities in fundus autofluorescence and the multifocal ERG.[313]

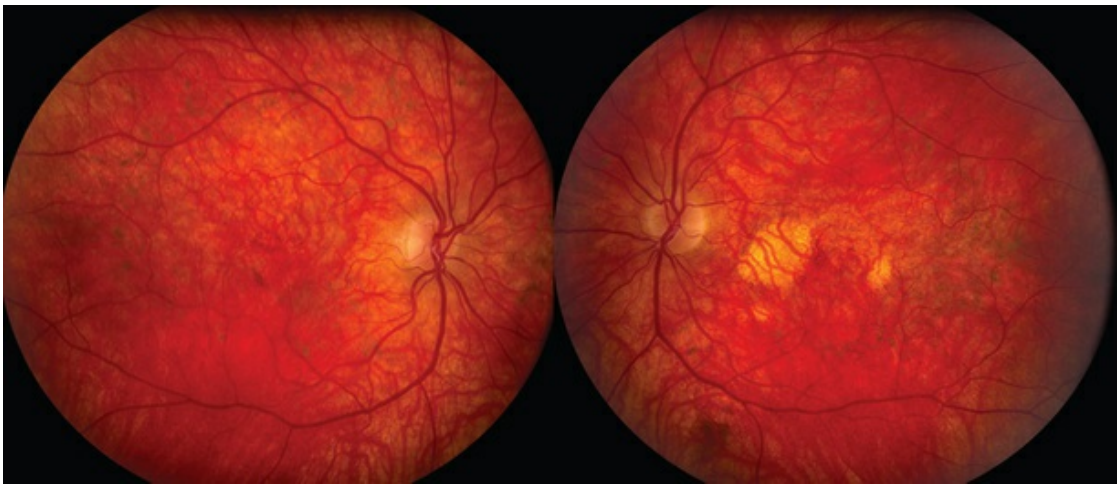

FIG. 44.71 A 36-year-old female with diabetes has pigmentary changes in the extrafoveal macula in both eyes. Left eye has two discrete areas of RPE atrophy, one just nasal to the fovea and a smaller one temporal to the fovea. Visual acuity was 20/15 OD, 20/20 OS. No diabetic retinopathy is present. She is positive for the A3243G variant in mitochondrial DNA causing maternally inherited diabetes and deafness (MIDD).

Acknowledgments

The authors wish to thank Drs Kean Oh (Associated Retinal Consultants, Petoskey, Michigan), Richard Spaide (Vitreous-Retina-Macula Consultants of New York, New York), Gerald A. Fishman (University of Illinois at Chicago), Kent Small (Macula & Retina Institute, Glendale, California), and H. Culver Boldt (the University of Iowa), for generously sharing fundus images with us. We also wish to thank Dr Mina Chung (University of Rochester) for her insights and thoughtful review of the manuscript.

References

1. Petrukhin K, Koisti MJ, Bakall B, et al. Identification of the gene responsible for Best macular dystrophy. *Nat Genet*. 1998;19(3):241–247.
2. Marquardt A, Stohr H, Passmore LA, Kramer F, Rivera A, Weber BH. Mutations in a novel gene, VMD2, encoding a protein of unknown properties cause juvenile-onset vitelliform macular dystrophy (Best's disease). *Hum Mol Genet*. 1998;7(9):1517–1525.
3. Best F. *Ueber eine hereditaere Makulaaffection*. Zeitschr Augenheilkd. 1905:199–212.
4. Braley AE, Spivey BE. Hereditary vitelline macular degeneration: a clinical and functional evaluation of a new pedigree with variable expressivity and dominant inheritance. *Trans Am Ophthalmol Soc*. 1963;61:339–371.
5. Krill AE, Morse PA, Potts AM, Klien BA. Hereditary vitelliruptive macular degeneration. *Am J Ophthalmol*. 1966;61(6):1405–1415.
6. Zanen J, Rausin G. Kyste vitelliforme congenital de la macula. *Bull Soc Belge Ophtalmol*. 1950;96:544.
7. Miller SA, Bresnick GH, Chandra SR. Choroidal neovascular membrane in Best's vitelliform macular dystrophy. *Am J Ophthalmol*. 1976;82(2):252–255.
8. Miller SA. Multifocal Best's vitelliform dystrophy. *Arch Ophthalmol*. 1977;95(6):984–990.
9. Ciulla TA, Frederick AR Jr. Acute progressive multifocal Best's disease in a 61-year-old man. *Am J Ophthalmol*. 1997;123(1):129–131.
10. Kinnick TR, Mullins RF, Dev S, et al. Autosomal recessive vitelliform macular dystrophy in a large cohort of vitelliform macular dystrophy patients. *Retina*. 2011;31(3):581–595.
11. Schatz P, Klar J, Andreasson S, Ponjavic V, Dahl N. Variant phenotype of Best vitelliform macular dystrophy associated with compound heterozygous mutations in VMD2. *Ophthalmic Genet*. 2006;27(2):51–56.
12. Wittstrom E, Ekvall S, Schatz P, Bondeson ML, Ponjavic V,

Andreasson S. Morphological and functional changes in multifocal vitelliform retinopathy and biallelic mutations in BEST1. *Ophthalmic Genet*. 2011;32(2):83–96.
13. Burgess R, Millar ID, Leroy BP, et al. Biallelic mutation of BEST1 causes a distinct retinopathy in humans. *Am J Hum Genet*. 2008;82(1):19–31.
14. Querques G, Zerbib J, Santacroce R, et al. Functional and clinical data of Best vitelliform macular dystrophy patients with mutations in the BEST1 gene. *Mol Vis*. 2009;15:2960–2972.
15. Chan CK, Gass JD, Lin SG. Acute exudative polymorphous vitelliform maculopathy syndrome. *Retina*. 2003;23(4):453–462.
16. Gass JD, Chuang EL, Granek H. Acute exudative polymorphous vitelliform maculopathy. *Trans Am Ophthalmol Soc*. 1988;86:354–366.
17. Guziewicz KE, Zangerl B, Lindauer SJ, et al. Bestrophin gene mutations cause canine multifocal retinopathy: a novel animal model for best disease. *Invest Ophthalmol Vis Sci*. 2007;48(5):1959–1967.
18. Guziewicz KE, Slavik J, Lindauer SJ, Aguirre GD, Zangerl B. Molecular consequences of BEST1 gene mutations in canine multifocal retinopathy predict functional implications for human bestrophinopathies. *Invest Ophthalmol Vis Sci*. 2011;2(7):4497–4505.
19. Chung MM, Oh KT, Streb LM, Kimura AE, Stone EM. Visual outcome following subretinal hemorrhage in Best disease. *Retina*. 2001;21(6):575–580.
20. Mohler CW, Fine SL. Long-term evaluation of patients with Best's vitelliform dystrophy. *Ophthalmology*. 1981;88(7):688–692.
21. Fishman GA, Baca W, Alexander KR, Derlacki DJ, Glenn AM, Viana M. Visual acuity in patients with best vitelliform macular dystrophy. *Ophthalmology*. 1993;100(11):1665–1670.
22. Sohn EH, Francis PJ, Duncan JL, et al. Phenotypic variability due to a novel Glu292Lys variation in exon 8 of the BEST1 gene causing best macular dystrophy. *Arch Ophthalmol*. 2009;127(7):913–920.

23. Renner AB, Tillack H, Kraus H, et al. Late onset is common in best macular dystrophy associated with VMD2 gene mutations. *Ophthalmology*. 2005;112(4):586–592.
24. Wittstrom E, Ponjavic V, Bondeson ML, Andreasson S. Anterior segment abnormalities and angle-closure glaucoma in a family with a mutation in the BEST1 gene and Best vitelliform macular dystrophy. *Ophthalmic Genet*. 2011;32(4):217–227.
25. Wabbels B, Preising MN, Kretschmann U, Demmler A, Lorenz B. Genotype-phenotype correlation and longitudinal course in ten families with Best vitelliform macular dystrophy. *Graefes Arch Clin Exp Ophthalmol*. 2006;244(11):1453–1466.
26. Burgess R, MacLaren RE, Davidson AE, et al. ADVIRC is caused by distinct mutations in BEST1 that alter pre-mRNA splicing. *J Med Genet*. 2009;46(9):620–625.
27. Lafaut BA, Loeys B, Leroy BP, Spileers W, De Laey JJ, Kestelyn P. Clinical and electrophysiological findings in autosomal dominant vitreoretinochoroidopathy: report of a new pedigree. *Graefes Arch Clin Exp Ophthalmol*. 2001;239(8):575–582.
28. Kay CN, Abramoff MD, Mullins RF, et al. Three dimensional distribution of the vitelliform lesion, photoreceptors, and retinal pigment epithelium in the macula of patients with Best vitelliform macular dystrophy. *Retina*. 2012;130(3):357–364.
29. Querques G, Regenbogen M, Quijano C, Delphin N, Soubrane G, Souied EH. High-definition optical coherence tomography features in vitelliform macular dystrophy. *Am J Ophthalmol*. 2008;146(4):501–507.
30. Ferrara DC, Costa RA, Tsang S, Calucci D, Jorge R, Freund KB. Multimodal fundus imaging in Best vitelliform macular dystrophy. *Graefes Arch Clin Exp Ophthalmol*. 2010;248(10):1377–1386.
31. Spaide RF, Noble K, Morgan A, Freund KB. Vitelliform macular dystrophy. *Ophthalmology*. 2006;113(8):1392–1400.
32. Pianta MJ, Aleman TS, Cideciyan AV, et al. In vivo micropathology of Best macular dystrophy with optical

coherence tomography. *Exp Eye Res*. 2003;76(2):203–211.
33. von Ruckmann A, Fitzke FW, Bird AC. In vivo fundus autofluorescence in macular dystrophies. *Arch Ophthalmol*. 1997;115(5):609–615.
34. Boon CJ, Theelen T, Hoefsloot EH, et al. Clinical and molecular genetic analysis of best vitelliform macular dystrophy. *Retina*. 2009;29(6):835–847.
35. Frangieh GT, Green WR, Fine SL. A histopathologic study of Best's macular dystrophy. *Arch Ophthalmol*. 1982;100(7):1115–1121.
36. O'Gorman S, Flaherty WA, Fishman GA, Berson EL. Histopathologic findings in Best's vitelliform macular dystrophy. *Arch Ophthalmol*. 1988;106(9):1261–1268.
37. Weingeist TA, Kobrin JL, Watzke RC. Histopathology of Best's macular dystrophy. *Arch Ophthalmol*. 1982;100(7):1108–1114.
38. Bakall B, Radu RA, Stanton JB, et al. Enhanced accumulation of A2E in individuals homozygous or heterozygous for mutations in BEST1 (VMD2). *Exp Eye Res*. 2007;85(1):34–43.
39. Meunier I, Senechal A, Dhaenens CM, et al. Systematic screening of BEST1 and PRPH2 in juvenile and adult vitelliform macular dystrophies: a rationale for molecular analysis. *Ophthalmology*. 2011;118(6):1130–1136.
40. Pollack K, Kreuz FR, Pillunat LE. [Best's disease with normal EOG. Case report of familial macular dystrophy.]. *Ophthalmologe*. 2005;102(9):891–894.
41. Testa F, Rossi S, Passerini I, et al. A normal electro-oculography in a family affected by best disease with a novel spontaneous mutation of the BEST1 gene. *Br J Ophthalmol*. 2008;92(11):1467–1470.
42. Wabbels B, Demmler A, Paunescu K, Wegscheider E, Preising MN, Lorenz B. Fundus autofluorescence in children and teenagers with hereditary retinal diseases. *Graefes Arch Clin Exp Ophthalmol*. 2006;244(1):36–45.
43. Yu K, Qu Z, Cui Y, Hartzell HC. Chloride channel activity of bestrophin mutants associated with mild or late-onset macular degeneration. *Invest Ophthalmol Vis Sci*. 2007;48(10):4694–4705.

44. Stone EM, Nichols BE, Streb LM, Kimura AE, Sheffield VC. Genetic linkage of vitelliform macular degeneration (Best's disease) to chromosome 11q13. *Nat Genet*. 1992;1(4):246–250.
45. Graff C, Forsman K, Larsson C, et al. Fine mapping of Best's macular dystrophy localizes the gene in close proximity to but distinct from the D11S480/ROM1 loci. *Genomics*. 1994;24(3):425–434.
46. Nichols BE, Bascom R, Litt M, McInnes R, Sheffield VC, Stone EM. Refining the locus for Best vitelliform macular dystrophy and mutation analysis of the candidate gene ROM1. *Am J Hum Genet*. 1994;54(1):95–103.
47. Marmorstein AD, Marmorstein LY, Rayborn M, Wang X, Hollyfield JG, Petrukhin K. Bestrophin, the product of the Best vitelliform macular dystrophy gene (VMD2), localizes to the basolateral plasma membrane of the retinal pigment epithelium. *Proc Natl Acad Sci USA*. 2000;97(23):12758–12763.
48. Allikmets R, Seddon JM, Bernstein PS, et al. Evaluation of the Best disease gene in patients with age-related macular degeneration and other maculopathies. *Hum Genet*. 1999;104(6):449–453.
49. Bakall B, Marknell T, Ingvast S, et al. The mutation spectrum of the bestrophin protein–functional implications. *Hum Genet*. 1999;104(5):383–389.
50. Ponjavic V, Eksandh L, Andreasson S, et al. Clinical expression of Best's vitelliform macular dystrophy in Swedish families with mutations in the bestrophin gene. *Ophthalmic Genet*. 1999;20(4):251–257.
51. Lotery AJ, Munier FL, Fishman GA, et al. Allelic variation in the VMD2 gene in best disease and age-related macular degeneration. *Invest Ophthalmol Vis Sci*. 2000;41(6):1291–1296.
52. White K, Marquardt A, Weber BH. VMD2 mutations in vitelliform macular dystrophy (Best disease) and other maculopathies. *Hum Mutat*. 2000;15(4):301–308.
53. Kramer F, White K, Pauleikhoff D, et al. Mutations in the VMD2 gene are associated with juvenile-onset vitelliform macular dystrophy (Best disease) and adult vitelliform

macular dystrophy but not age-related macular degeneration. *Eur J Hum Genet*. 2000;8(4):286–292.
54. Eksandh L, Bakall B, Bauer B, Wadelius C, Andreasson S. Best's vitelliform macular dystrophy caused by a new mutation (Val89Ala) in the VMD2 gene. *Ophthalmic Genet*. 2001;22(2):107–115.
55. Seddon JM, Afshari MA, Sharma S, et al. Assessment of mutations in the Best macular dystrophy (VMD2) gene in patients with adult-onset foveomacular vitelliform dystrophy, age-related maculopathy, and bull's-eye maculopathy. *Ophthalmology*. 2001;108(11):2060–2067.
56. Stohr H, Marquardt A, Nanda I, Schmid M, Weber BH. Three novel human VMD2-like genes are members of the evolutionary highly conserved RFP-TM family. *Eur J Hum Genet*. 2002;10(4):281–284.
57. Seddon JM, Sharma S, Chong S, Hutchinson A, Allikmets R, Adelman RA. Phenotype and genotype correlations in two best families. *Ophthalmology*. 2003;110(9):1724–1731.
58. Mullins RF, Oh KT, Heffron E, Hageman GS, Stone EM. Late development of vitelliform lesions and flecks in a patient with Best disease: clinicopathologic correlation. *Arch Ophthalmol*. 2005;123(11):1588–1594.
59. Apushkin MA, Fishman GA, Taylor CM, Stone EM. Novel de novo mutation in a patient with Best macular dystrophy. *Arch Ophthalmol*. 2006;124(6):887–889.
60. Marchant D, Yu K, Bigot K, et al. New VMD2 gene mutations identified in patients affected by Best vitelliform macular dystrophy. *J Med Genet*. 2007;44(3):e70.
61. Boon CJ, Klevering BJ, Leroy BP, Hoyng CB, Keunen JE, den Hollander AI. The spectrum of ocular phenotypes caused by mutations in the BEST1 gene. *Prog Retin Eye Res*. 2009;28(3):187–205.
62. Schatz P, Bitner H, Sander B, et al. Evaluation of macular structure and function by OCT and electrophysiology in patients with vitelliform macular dystrophy due to mutations in BEST1. *Invest Ophthalmol Vis Sci*. 2010;51(9):4754–4765.
63. Manes G, Meunier I, Avila-Fernández A, et al. Mutations in

IMPG1 cause vitelliform macular dystrophies. *Am J Hum Genet*. 2013;93(3):571–578.
64. Mullins RF, Kuehn MH, Faidley EA, Syed NA, Stone EM. Differential macular and peripheral expression of bestrophin in human eyes and its implication for Best disease. *Invest Ophthalmol Vis Sci*. 2007;48(7):3372–3380.
65. Marmorstein AD, Cross HE, Peachey NS. Functional roles of bestrophins in ocular epithelia. *Prog Retin Eye Res*. 2009;28(3):206–226.
66. Xiao Q, Hartzell HC, Yu K. Bestrophins and retinopathies. *Pflugers Arch*. 2010;460(2):559–569.
67. Hartzell C, Qu Z, Putzier I, Artinian L, Chien LT, Cui Y. Looking chloride channels straight in the eye: bestrophins, lipofuscinosis, and retinal degeneration. *Physiology (Bethesda)*. 2005;20:292–302.
68. Sun H, Tsunenari T, Yau KW, Nathans J. The vitelliform macular dystrophy protein defines a new family of chloride channels. *Proc Natl Acad Sci USA*. 2002;99(6):4008–4013.
69. Fischmeister R, Hartzell HC. Volume sensitivity of the bestrophin family of chloride channels. *J Physiol*. 2005;562(Pt 2):477–491.
70. Marmorstein LY, Wu J, McLaughlin P, et al. The light peak of the electroretinogram is dependent on voltage-gated calcium channels and antagonized by bestrophin (Best-1). *J Gen Physiol*. 2006;127(5):577–589.
71. Zhang Y, Stanton JB, Wu J, et al. Suppression of Ca2+ signaling in a mouse model of Best disease. *Hum Mol Genet*. 2010;19(6):1108–1118.
72. Marmor MF, Yao XY, Hageman GS. Retinal adhesiveness in surgically enucleated human eyes. *Retina*. 1994;14(2):181–186.
73. Hall MO, Abrams TA, Mittag TW. ROS ingestion by RPE cells is turned off by increased protein kinase C activity and by increased calcium. *Exp Eye Res*. 1991;52(5):591–598.
74. Kaufman SJ, Goldberg MF, Orth DH, Fishman GA, Tessler H, Mizuno K. Autosomal dominant vitreoretinochoroidopathy. *Arch Ophthalmol*. 1982;100(2):272–278.

75. Blair NP, Goldberg MF, Fishman GA, Salzano T. Autosomal dominant vitreoretinochoroidopathy (ADVIRC). *Br J Ophthalmol*. 1984;68(1):2–9.
76. Han DP, Lewandowski MF. Electro-oculography in autosomal dominant vitreoretinochoroidopathy. *Arch Ophthalmol*. 1992;110(11):1563–1567.
77. Kellner U, Jandeck C, Kraus H, Foerster MH. Autosomal dominant vitreoretinochoroidopathy with normal electrooculogram in a German family. *Graefes Arch Clin Exp Ophthalmol*. 1998;236(2):109–114.
78. Vincent A, McAlister C, Vandenhoven C, Heon E. BEST1-related autosomal dominant vitreoretinochoroidopathy: a degenerative disease with a range of developmental ocular anomalies. *Eye (Lond)*. 2011;25(1):113–118.
79. Yardley J, Leroy BP, Hart-Holden N, et al. Mutations of VMD2 splicing regulators cause nanophthalmos and autosomal dominant vitreoretinochoroidopathy (ADVIRC). *Invest Ophthalmol Vis Sci*. 2004;45(10):3683–3689.
80. Oh KT, Vallar C. Central cone dysfunction in autosomal dominant vitreoretino choroidopathy (ADVIRC). *Am J Ophthalmol*. 2006;141(5):940–943.
81. Davidson AE, Millar ID, Urquhart JE, et al. Missense mutations in a retinal pigment epithelium protein, bestrophin-1, cause retinitis pigmentosa. *Am J Hum Genet*. 2009;85(5):581–592.
82. Iannaccone A, Kerr NC, Kinnick TR, Calzada JI, Stone EM. Autosomal recessive Best vitelliform macular dystrophy: report of a family and management of early-onset neovascular complications. *Arch Ophthalmol*. 2011;129(2):211–217.
83. Davidson AE, Sergouniotis PI, Burgess-Mullan R, et al. A synonymous codon variant in two patients with autosomal recessive bestrophinopathy alters in vitro splicing of BEST1. *Mol Vis*. 2010;16:2916–2922.
84. Gerth C, Zawadzki RJ, Werner JS, Heon E. Detailed analysis of retinal function and morphology in a patient with autosomal recessive bestrophinopathy (ARB). *Doc Ophthalmol*. 2009;118(3):239–246.

85. Leu J, Schrage NF, Degenring RF. Choroidal neovascularisation secondary to Best's disease in a 13-year-old boy treated by intravitreal bevacizumab. *Graefes Arch Clin Exp Ophthalmol*. 2007;245(11):1723–1725.
86. Montero JA, Ruiz-Moreno JM, De La Vega C. Intravitreal bevacizumab for adult-onset vitelliform dystrophy: a case report. *Eur J Ophthalmol*. 2007;17(6):983–986.
87. Querques G, Bocco MC, Soubrane G, Souied EH. Intravitreal ranibizumab (Lucentis) for choroidal neovascularization associated with vitelliform macular dystrophy. *Acta Ophthalmol*. 2008;86(6):694–695.
88. Rishi E, Rishi P, Mahajan S. Intravitreal bevacizumab for choroidal neovascular membrane associated with Best's vitelliform dystrophy. *Indian J Ophthalmol*. 2010;58(2):160–162.
89. Heidary F, Hitam WH, Ngah NF, George TM, Hashim H, Shatriah I. Intravitreal ranibizumab for choroidal neovascularization in best's vitelliform macular dystrophy in a 6-year-old boy. *J Pediatr Ophthalmol Strabismus*. 2011;48:e19–22 [Online].
90. Boon CJ, den Hollander AI, Hoyng CB, Cremers FP, Klevering BJ, Keunen JE. The spectrum of retinal dystrophies caused by mutations in the peripherin/RDS gene. *Prog Retin Eye Res*. 2008;27(2):213–235.
91. Chowers I, Zamir E, Banin E, AbdulRazik M, Hemo Y. Blunt trauma in Best's vitelliform macular dystrophy. *Br J Ophthalmol*. 2000;84(11):1330–1331.
92. Allikmets R. A photoreceptor cell-specific ATP-binding transporter gene (ABCR) is mutated in recessive Stargardt macular dystrophy. *Nat Genet*. 1997;17(1):122.
93. Cremers FP, van de Pol DJ, van Driel M, et al. Autosomal recessive retinitis pigmentosa and cone-rod dystrophy caused by splice site mutations in the Stargardt's disease gene ABCR. *Hum Mol Genet*. 1998;7(3):355–362.
94. Martinez-Mir A, Paloma E, Allikmets R, et al. Retinitis pigmentosa caused by a homozygous mutation in the Stargardt disease gene ABCR. *Nat Genet*. 1998;18(1):11–12.
95. Fishman GA, Stone EM, Grover S, Derlacki DJ, Haines HL,

Hockey RR. Variation of clinical expression in patients with Stargardt dystrophy and sequence variations in the ABCR gene. *Arch Ophthalmol*. 1999;117(4):504–510.
96. Maugeri A, Klevering BJ, Rohrschneider K, et al. Mutations in the ABCA4 (ABCR) gene are the major cause of autosomal recessive cone-rod dystrophy. *Am J Hum Genet*. 2000;67(4):960–966.
97. Fishman GA, Stone EM, Eliason DA, Taylor CM, Lindeman M, Derlacki DJ. ABCA4 gene sequence variations in patients with autosomal recessive cone-rod dystrophy. *Arch Ophthalmol*. 2003;121(6):851–855.
98. Schindler EI, Nylen EL, Ko AC, et al. Deducing the pathogenic contribution of recessive ABCA4 alleles in an outbred population. *Hum Mol Genet*. 2010;19(19):3693–3701.
99. Stargardt K. Uber familiare, progressive degeneration in der maculagegend des auges. *Albrecht Von Graefes Arch Ophthalmol*. 1909;71:534–550.
100. Franceschetti A. *La retinopathie ponctuée albescente. Bulletins et memoires de la Société Francaise d'Ophtalmologie*. Masson & Cie: Paris; 1963:14–19.
101. Jayasundera T, Rhoades W, Branham K, Niziol LM, Musch DC, Heckenlively JR. Peripapillary dark choroid ring as a helpful diagnostic sign in advanced stargardt disease. *Am J Ophthalmol*. 2010;149(4):656–660.e2.
102. Cideciyan AV, Swider M, Aleman TS, et al. ABCA4-associated retinal degenerations spare structure and function of the human parapapillary retina. *Invest Ophthalmol Vis Sci*. 2005;46(12):4739–4746.
103. Lois N, Halfyard AS, Bird AC, Holder GE, Fitzke FW. Fundus autofluorescence in Stargardt macular dystrophy-fundus flavimaculatus. *Am J Ophthalmol*. 2004;138(1):55–63.
104. Fishman GA, Farber M, Patel BS, Derlacki DJ. Visual acuity loss in patients with Stargardt's macular dystrophy. *Ophthalmology*. 1987;94(7):809–814.
105. Rotenstreich Y, Fishman GA, Anderson RJ. Visual acuity loss and clinical observations in a large series of patients with Stargardt disease. *Ophthalmology*. 2003;110(6):1151–1158.

106. Oh KT, Weleber RG, Oh DM, Billingslea AM, Rosenow J, Stone EM. Clinical phenotype as a prognostic factor in Stargardt disease. *Retina*. 2004;24(2):254–262.
107. Hadden OB, Gass JD. Fundus flavimaculatus and Stargardt's disease. *Am J Ophthalmol*. 1976;82(4):527–539.
108. Anmarkrud N. Fundus fluorescein angiography in fundus flavimaculatus and Stargardts disease. *Acta Ophthalmol (Copenh)*. 1979;57(2):172–182.
109. Ernest JT, Krill AE. Fluorescein studies in fundus flavimaculatus and drusen. *Am J Ophthalmol*. 1966;62(1):1–6.
110. Radu RA, Mata NL, Bagla A, Travis GH. Light exposure stimulates formation of A2E oxiranes in a mouse model of Stargardt's macular degeneration. *Proc Natl Acad Sci USA*. 2004;101(16):5928–5933.
111. Lois N, Holder GE, Fitzke FW, Plant C, Bird AC. Intrafamilial variation of phenotype in Stargardt macular dystrophy-Fundus flavimaculatus. *Invest Ophthalmol Vis Sci*. 1999;40(11):2668–2675.
112. Lois N, Holder GE, Bunce C, Fitzke FW, Bird AC. Phenotypic subtypes of Stargardt macular dystrophy-fundus flavimaculatus. *Arch Ophthalmol*. 2001;119(3):359–369.
113. Ergun E, Hermann B, Wirtitsch M, et al. Assessment of central visual function in Stargardt's disease/fundus flavimaculatus with ultrahigh-resolution optical coherence tomography. *Invest Ophthalmol Vis Sci*. 2005;46(1):310–316.
114. Sunness JS, Ziegler MD, Applegate CA. Issues in quantifying atrophic macular disease using retinal autofluorescence. *Retina*. 2006;26(6):666–672.
115. Boon CJ, Jeroen Klevering B, Keunen JE, Hoyng CB, Theelen T. Fundus autofluorescence imaging of retinal dystrophies. *Vision Res*. 2008;48(26):2569–2577.
116. Sunness JS, Steiner JN. Retinal function and loss of autofluorescence in stargardt disease. *Retina*. 2008;28(6):794–800.
117. Gomes NL, Greenstein VC, Carlson JN, et al. A comparison of fundus autofluorescence and retinal structure in patients with Stargardt disease. *Invest Ophthalmol Vis Sci*.

2009;50(8):3953–3959.
118. Smith RT, Gomes NL, Barile G, Busuioc M, Lee N, Laine A. Lipofuscin and autofluorescence metrics in progressive STGD. *Invest Ophthalmol Vis Sci*. 2009;50(8):3907–3914.
119. Shah SN, Koozekanani DD, Kim JE. Phenotypic heterogeneity and lesion size measurements in Stargardt macular dystrophy. *Ophthalmic Surg Lasers Imaging*. 2009;40(5):506–512.
120. Sodi A, Bini A, Passerini I, Forconi S, Menchini U, Torricelli F. Different patterns of fundus autofluorescence related to ABCA4 gene mutations in Stargardt disease. *Ophthalmic Surg Lasers Imaging*. 2010;41(1):48–53.
121. Burke TR, Allikmets R, Smith RT, Gouras P, Tsang SH. Loss of peripapillary sparing in non-group I Stargardt disease. *Exp Eye Res*. 2010;91(5):592–600.
122. Anastasakis A, Fishman GA, Lindeman M, Genead MA, Zhou W. Infrared scanning laser ophthalmoscope imaging of the macula and its correlation with functional loss and structural changes in patients with Stargardt disease. *Retina*. 2011;31(5):949–958.
123. Chen Y, Ratnam K, Sundquist SM, et al. Cone photoreceptor abnormalities correlate with vision loss in patients with stargardt disease. *Invest Ophthalmol Vis Sci*. 2011;52(6):3281–3292.
124. Chen B, Tosha C, Gorin MB, Nusinowitz S. Analysis of autofluorescent retinal images and measurement of atrophic lesion growth in Stargardt disease. *Exp Eye Res*. 2010;91(2):143–152.
125. Cideciyan AV, Swider M, Aleman TS, et al. Reduced-illuminance autofluorescence imaging in ABCA4-associated retinal degenerations. *J Opt Soc Am A Opt Image Sci Vis*. 2007;24(5):1457–1467.
126. Cella W, Greenstein VC, Zernant-Rajang J, et al. G1961E mutant allele in the Stargardt disease gene ABCA4 causes bull's eye maculopathy. *Exp Eye Res*. 2009;89(1):16–24.
127. Lim JI, Tan O, Fawzi AA, Hopkins JJ, Gil-Flamer JH, Huang D. A pilot study of Fourier-domain optical coherence tomography of retinal dystrophy patients. *Am J Ophthalmol*.

2008;146(3):417–426.
128. Lenassi E, Jarc-Vidmar M, Glavac D, Hawlina M. Pattern electroretinography of larger stimulus field size and spectral-domain optical coherence tomography in patients with Stargardt disease. *Br J Ophthalmol*. 2009;93(12):1600–1605.
129. Genead MA, Fishman GA, Anastasakis A. Spectral-domain OCT peripapillary retinal nerve fibre layer thickness measurements in patients with Stargardt disease. *Br J Ophthalmol*. 2011;95(5):689–693.
130. Klevering BJ, Deutman AF, Maugeri A, Cremers FP, Hoyng CB. The spectrum of retinal phenotypes caused by mutations in the ABCA4 gene. *Graefes Arch Clin Exp Ophthalmol*. 2005;243(2):90–100.
131. Oh KT, Weleber RG, Stone EM, Oh DM, Rosenow J, Billingslea AM. Electroretinographic findings in patients with Stargardt disease and fundus flavimaculatus. *Retina*. 2004;24(6):920–928.
132. Fukui T, Yamamoto S, Nakano K, et al. ABCA4 gene mutations in Japanese patients with Stargardt disease and retinitis pigmentosa. *Invest Ophthalmol Vis Sci*. 2002;43(9):2819–2824.
133. Gerth C, Andrassi-Darida M, Bock M, Preising MN, Weber BH, Lorenz B. Phenotypes of 16 Stargardt macular dystrophy/fundus flavimaculatus patients with known ABCA4 mutations and evaluation of genotype-phenotype correlation. *Graefes Arch Clin Exp Ophthalmol*. 2002;240(8):628–638.
134. Scholl HP, Besch D, Vonthein R, Weber BH, Apfelstedt-Sylla E. Alterations of slow and fast rod ERG signals in patients with molecularly confirmed Stargardt disease type 1. *Invest Ophthalmol Vis Sci*. 2002;43(4):1248–1256.
135. Birch DG, Peters AY, Locke KL, Spencer R, Megarity CF, Travis GH. Visual function in patients with cone-rod dystrophy (CRD) associated with mutations in the ABCA4(ABCR) gene. *Exp Eye Res*. 2001;73(6):877–886.
136. Sheffield VC, Stone EM. Genomics and the eye. *N Engl J Med*. 2011;364(20):1932–1942.

137. Weleber RG. The dystrophic retina in multisystem disorders: the electroretinogram in neuronal ceroid lipofuscinoses. *Eye (Lond)*. 1998;12(Pt 3b):580–590.
138. Tosha C, Gorin MB, Nusinowitz S. Test–retest reliability and inter-ocular symmetry of multi-focal electroretinography in Stargardt disease. *Curr Eye Res*. 2010;35(1):63–72.
139. Stone EM. Finding and interpreting genetic variations that are important to ophthalmologists. *Trans Am Ophthalmol Soc*. 2003;101:437–484.
140. Philp AR, Jin M, Li S, et al. Predicting the pathogenicity of RPE65 mutations. *Hum Mutat*. 2009;30(8):1183–1188.
141. Steinmetz RL, Garner A, Maguire JI, Bird AC. Histopathology of incipient fundus flavimaculatus. *Ophthalmology*. 1991;98(6):953–956.
142. Birnbach CD, Jarvelainen M, Possin DE, Milam AH. Histopathology and immunocytochemistry of the neurosensory retina in fundus flavimaculatus. *Ophthalmology*. 1994;101(7):1211–1219.
143. Klien BA, Krill AE. Fundus flavimaculatus. Clinical, functional and histopathologic observations. *Am J Ophthalmol*. 1967;64(1):3–23.
144. Tsybovsky Y, Molday RS, Palczewski K. The ATP-binding cassette transporter ABCA4: structural and functional properties and role in retinal disease. *Adv Exp Med Biol*. 2010;703:105–125.
145. Molday RS, Zhang K. Defective lipid transport and biosynthesis in recessive and dominant Stargardt macular degeneration. *Prog Lipid Res*. 2010;49(4):476–492.
146. Weng J, Mata NL, Azarian SM, Tzekov RT, Birch DG, Travis GH. Insights into the function of Rim protein in photoreceptors and etiology of Stargardt's disease from the phenotype in abcr knockout mice. *Cell*. 1999;98(1):13–23.
147. Sparrow JR, Nakanishi K, Parish CA. The lipofuscin fluorophore A2E mediates blue light-induced damage to retinal pigmented epithelial cells. *Invest Ophthalmol Vis Sci*. 2000;41(7):1981–1989.
148. Suter M, Remé C, Grimm C, et al. Age-related macular

degeneration. The lipofusion component N-retinyl-N-retinylidene ethanolamine detaches proapoptotic proteins from mitochondria and induces apoptosis in mammalian retinal pigment epithelial cells. *J Biol Chem*. 2000;275:39625–39630.
149. Zhou J, Kim SR, Westlund BS, Sparrow JR. Complement activation by bisretinoid constituents of RPE lipofuscin. *Invest Ophthalmol Vis Sci*. 2009;50(3):1392–1399.
150. Radu RA, Mata NL, Nusinowitz S, Liu X, Sieving PA, Travis GH. Treatment with isotretinoin inhibits lipofuscin accumulation in a mouse model of recessive Stargardt's macular degeneration. *Proc Natl Acad Sci USA*. 2003;100(8):4742–4747.
151. Radu RA, Han Y, Bui TV, et al. Reductions in serum vitamin A arrest accumulation of toxic retinal fluorophores: a potential therapy for treatment of lipofuscin-based retinal diseases. *Invest Ophthalmol Vis Sci*. 2005;46(12):4393–4401.
152. Ma L, Kaufman Y, Zhang J, Washington I. C20-D3-vitamin A slows lipofuscin accumulation and electrophysiological retinal degeneration in a mouse model of Stargardt disease. *J Biol Chem*. 2011;286(10):7966–7974.
153. Allocca M, Doria M, Petrillo M, et al. Serotype-dependent packaging of large genes in adeno-associated viral vectors results in effective gene delivery in mice. *J Clin Invest*. 2008;118(5):1955–1964.
154. Cideciyan AV, Swider M, Aleman TS, et al. ABCA4 disease progression and a proposed strategy for gene therapy. *Hum Mol Genet*. 2009;18(5):931–941.
155. Kong J, Kim SR, Binley K, et al. Correction of the disease phenotype in the mouse model of Stargardt disease by lentiviral gene therapy. *Gene Ther*. 2008;15(19):1311–1320.
156. Bainbridge JW, Smith AJ, Barker SS, et al. Effect of gene therapy on visual function in Leber's congenital amaurosis. *N Engl J Med*. 2008;358(21):2231–2239.
157. Maguire AM, Simonelli F, Pierce EA, et al. Safety and efficacy of gene transfer for Leber's congenital amaurosis. *N Engl J Med*. 2008;358(21):2240–2248.
158. Stone EM, Nichols BE, Kimura AE, Weingeist TA, Drack A,

Sheffield VC. Clinical features of a Stargardt-like dominant progressive macular dystrophy with genetic linkage to chromosome 6q. *Arch Ophthalmol*. 1994;112(6):765–772.
159. Zhang K, Kniazeva M, Han M, et al. A 5-bp deletion in ELOVL4 is associated with two related forms of autosomal dominant macular dystrophy. *Nat Genet*. 2001;27(1):89–93.
160. Bernstein PS, Tammur J, Singh N, et al. Diverse macular dystrophy phenotype caused by a novel complex mutation in the ELOVL4 gene. *Invest Ophthalmol Vis Sci*. 2001;42(13):3331–3336.
161. Maugeri A, Meire F, Hoyng CB, et al. A novel mutation in the ELOVL4 gene causes autosomal dominant Stargardt-like macular dystrophy. *Invest Ophthalmol Vis Sci*. 2004;45(12):4263–4267.
162. Vasireddy V, Wong P, Ayyagari R. Genetics and molecular pathology of Stargardt-like macular degeneration. *Prog Retin Eye Res*. 2010;29(3):191–207.
163. Agbaga MP, Brush RS, Mandal MN, et al. Role of Stargardt-3 macular dystrophy protein (ELOVL4) in the biosynthesis of very long chain fatty acids. *Proc Natl Acad Sci USA*. 2008;105:12843–12848.
164. Ambasudhan R, Wang X, Jablonski MM, et al. Atrophic macular degeneration mutations in ELOVL4 result in the intracellular misrouting of the protein. *Genomics*. 2004;83(4):615–625.
165. Karan G, Yang Z, Zhang K. Expression of wild type and mutant ELOVL4 in cell culture: subcellular localization and cell viability. *Mol Vis*. 2004;10:248–253.
166. Vasireddy V, Jablonski MM, Khan NW, et al. Elovl4 5-bp deletion knock-in mouse model for Stargardt-like macular degeneration demonstrates accumulation of ELOVL4 and lipofuscin. *Exp Eye Res*. 2009;89(6):905–912.
167. Vasireddy V, Jablonski MM, Mandal MN, et al. Elovl4 5-bp-deletion knock-in mice develop progressive photoreceptor degeneration. *Invest Ophthalmol Vis Sci*. 2006;47(10):4558–4568.
168. Yang Z, Chen Y, Lillo C, et al. Mutant prominin 1 found in patients with macular degeneration disrupts photoreceptor

disk morphogenesis in mice. *J Clin Invest*. 2008;118(8):2908–2916.
169. Kniazeva M, Chiang MF, Morgan B, et al. A new locus for autosomal dominant Stargardt-like disease maps to chromosome 4. *Am J Hum Genet*. 1999;64(5):1394–1399.
170. Michaelides M, Johnson S, Poulson A, et al. An autosomal dominant bull's-eye macular dystrophy (MCDR2) that maps to the short arm of chromosome 4. *Invest Ophthalmol Vis Sci*. 2003;44(4):1657–1662.
171. Maw MA, Corbeil D, Koch J, et al. A frameshift mutation in prominin (mouse)-like 1 causes human retinal degeneration. *Hum Mol Genet*. 2000;9(1):27–34.
172. Zhang Q, Zulfiqar F, Xiao X, et al. Severe retinitis pigmentosa mapped to 4p15 and associated with a novel mutation in the PROM1 gene. *Hum Genet*. 2007;122(3–4):293–299.
173. Michaelides M, Gaillard MC, Escher P, et al. The PROM1 mutation p.R373C causes an autosomal dominant bull's eye maculopathy associated with rod, rod-cone, and macular dystrophy. *Invest Ophthalmol Vis Sci*. 2010;51(9):4771–4780.
174. Deutman AF, van Blommestein JD, Henkes HE, Waardenburg PJ, Solleveld-van Driest E. Butterfly-shaped pigment dystrophy of the fovea. *Arch Ophthalmol*. 1970;83(5):558–569.
175. Hsieh RC, Fine BS, Lyons JS. Patterned dystrophies of the retinal pigment epithelium. *Arch Ophthalmol*. 1977;95(3):429–435.
176. Marmor MF, Byers B. Pattern dystrophy of the pigment epithelium. *Am J Ophthalmol*. 1977;84(1):32–44.
177. Epstein GA, Rabb MF. Adult vitelliform macular degeneration: diagnosis and natural history. *Br J Ophthalmol*. 1980;64(10):733–740.
178. Bloom LH, Swanson DE, Bird AC. Adult vitelliform macular degeneration. *Br J Ophthalmol*. 1981;65(11):800–801.
179. Gass JD. A clinicopathologic study of a peculiar foveomacular dystrophy. *Trans Am Ophthalmol Soc*. 1974;72:139–156.
180. Sjogren H. Dystrophia reticularis laminae pigmentosae

retinae, an earlier not described hereditary eye disease. *Acta Ophthalmol (Copenh)*. 1950;28(3):279–295.
181. Kingham JD, Fenzl RE, Willerson D, Aaberg TM. Reticular dystrophy of the retinal pigment epithelium. A clinical and electrophysiologic study of three generations. *Arch Ophthalmol*. 1978;96(7):1177–1184.
182. Deutman AF, Rumke AM. Reticular dystrophy of the retinal pigment epithelium. Dystrophia reticularis laminae pigmentosa retinae of H. Sjogren. *Arch Ophthalmol*. 1969;82(1):4–9.
183. Slezak H, Hommer K. [Fundus pulverulentus]. *Albrecht Von Graefes Arch Klin Exp Ophthalmol*. 1969;178(2):176–182.
184. de Jong PT, Delleman JW. Pigment epithelial pattern dystrophy. Four different manifestations in a family. *Arch Ophthalmol*. 1982;100(9):1416–1421.
185. Hoyng CB, Heutink P, Testers L, Pinckers A, Deutman AF, Oostra BA. Autosomal dominant central areolar choroidal dystrophy caused by a mutation in codon 142 in the peripherin/RDS gene. *Am J Ophthalmol*. 1996;121(6):623–629.
186. Kajiwara K, Hahn LB, Mukai S, Travis GH, Berson EL, Dryja TP. Mutations in the human retinal degeneration slow gene in autosomal dominant retinitis pigmentosa. *Nature*. 1991;354(6353):480–483.
187. Weleber RG, Carr RE, Murphey WH, Sheffield VC, Stone EM. Phenotypic variation including retinitis pigmentosa, pattern dystrophy, and fundus flavimaculatus in a single family with a deletion of codon 153 or 154 of the peripherin/RDS gene. *Arch Ophthalmol*. 1993;111(11):1531–1542.
188. Farrar GJ, Kenna P, Jordan SA, et al. A three-base-pair deletion in the peripherin-RDS gene in one form of retinitis pigmentosa. *Nature*. 1991;354(6353):478–480.
189. Farrar GJ, Jordan SA, Kenna P, et al. Autosomal dominant retinitis pigmentosa: localization of a disease gene (RP6) to the short arm of chromosome 6. *Genomics*. 1991;11(4):870–874.
190. Francis PJ, Schultz DW, Gregory AM, et al. Genetic and phenotypic heterogeneity in pattern dystrophy. *Br J*

Ophthalmol. 2005;89(9):1115–1119.
191. Nichols BE, Sheffield VC, Vandenburgh K, Drack AV, Kimura AE, Stone EM. Butterfly-shaped pigment dystrophy of the fovea caused by a point mutation in codon 167 of the RDS gene. *Nat Genet*. 1993;3(3):202–207.
192. Gutman I, Walsh JB, Henkind P. Vitelliform macular dystrophy and butterfly-shaped epithelial dystrophy: a continuum? *Br J Ophthalmol*. 1982;66(3):170–173.
193. Nichols BE, Drack AV, Vandenburgh K, Kimura AE, Sheffield VC, Stone EM. A 2 base pair deletion in the RDS gene associated with butterfly-shaped pigment dystrophy of the fovea. *Hum Mol Genet*. 1993;2(8):1347.
194. Fossarello M, Bertini C, Galantuomo M, Cao A, Serra A, Pirastu M. Deletion in the peripherin/RDS gene in two unrelated Sardinian families with autosomal dominant butterfly-shaped macular dystrophy. *Arch Ophthalmol*. 1996;114:448–456.
195. Zhang K, Garibaldi DC, Li Y, Green WR, Zack DJ. Butterfly-shaped pattern dystrophy: a genetic, clinical, and histopathological report. *Arch Ophthalmol*. 2002;120(4):485–490.
196. Yang Z, Li Y, Jiang L, et al. A novel RDS/peripherin gene mutation associated with diverse macular phenotypes. *Ophthalmic Genet*. 2004;25(2):133–145.
197. Querques G, Forte R, Querques L, Massamba N, Souied EH. Natural course of adult-onset foveomacular vitelliform dystrophy: a spectral-domain optical coherence tomography analysis. *Am J Ophthalmol*. 2011;152(2):304–313.
198. Arnold JJ, Sarks JP, Killingsworth MC, Kettle EK, Sarks SH. Adult vitelliform macular degeneration: a clinicopathological study. *Eye (Lond)*. 2003;17(6):717–726.
199. Meunier I, Manes G, Bocquet B, et al. Frequency and clinical pattern of vitelliform macular dystrophy caused by mutations of interphotoreceptor matrix IMPG1 and IMPG2 genes. *Ophthalmology*. 2014;121(12):2406–2414.
200. Kuehn MH, Stone EM, Hageman GS. Organization of the human IMPG2 gene and its evaluation as a candidate gene in age-related macular degeneration and other retinal

degenerative disorders. *Invest Ophthalmol Vis Sci*. 2001;42(13):3123–3129.
201. Kuehn MH, Hageman GS. Molecular characterization and genomic mapping of human IPM 200, a second member of a novel family of proteoglycans. *Mol Cell Biol Res Commun*. 1999;2(2):103–110.
202. Kuehn MH, Hageman GS. Expression and characterization of the IPM 150 gene (IMPG1) product, a novel human photoreceptor cell-associated chondroitin-sulfate proteoglycan. *Matrix Biol*. 1999;18(5):509–518.
203. Fishman GA, Woolf MB, Goldberg MF, Busse B. Reticular tapeto-retinal dystrophy. As a possible late stage of Sjogren's reticular dystrophy. *Br J Ophthalmol*. 1976;60(1):35–40.
204. Chopdar A. Reticular dystrophy of retina. *Br J Ophthalmol*. 1976;60(5):342–344.
205. Kempeneers HP, Dewachter A, Kempeneers GM. Pattern dystrophies of the retinal pigment epithelium. The study of three generations in a family. *Doc Ophthalmol*. 1990;76(3):261–272.
206. Cardillo Piccolino F, Zingirian M. Pattern dystrophy of the retinal pigment epithelium with vitelliform macular lesion: evolution in ten years. *Int Ophthalmol*. 1988;11(4):207–217.
207. Giuffre G, Lodato G. Vitelliform dystrophy and pattern dystrophy of the retinal pigment epithelium: concomitant presence in a family. *Br J Ophthalmol*. 1986;70(7):526–532.
208. Boon CJ, Klevering BJ, Cremers FP, et al. Central areolar choroidal dystrophy. *Ophthalmology*. 2009;116(4):771–782 [782.e1].
209. Yanagihashi S, Nakazawa M, Kurotaki J, Sato M, Miyagawa Y, Ohguro H. Autosomal dominant central areolar choroidal dystrophy and a novel Arg195Leu mutation in the peripherin/RDS gene. *Arch Ophthalmol*. 2003;121(10):1458–1461.
210. Reig C, Serra A, Gean E, et al. A point mutation in the RDS-peripherin gene in a Spanish family with central areolar choroidal dystrophy. *Ophthalmic Genet*. 1995;16(2):39–44.
211. Klevering BJ, van Driel M, van Hogerwou AJ, et al. Central

areolar choroidal dystrophy associated with dominantly inherited drusen. *Br J Ophthalmol*. 2002;86(1):91–96.
212. Keilhauer CN, Meigen T, Weber BH. Clinical findings in a multigeneration family with autosomal dominant central areolar choroidal dystrophy associated with an Arg195Leu mutation in the peripherin/RDS gene. *Arch Ophthalmol*. 2006;124(7):1020–1027.
213. Keilhauer CN, Meigen T, Stohr H, Weber BH. Late-onset central areolar choroidal dystrophy caused by a heterozygous frame-shift mutation affecting codon 307 of the peripherin/RDS gene. *Ophthalmic Genet*. 2006;27(4):139–144.
214. Hoyng CB, van Rijn PM, Deutman AF. Central areolar choroidal dystrophy and slowly progressive sensorineural hearing loss. *Acta Ophthalmol Scand*. 1996;74(6):639–641.
215. Renner AB, Fiebig BS, Weber BH, et al. Phenotypic variability and long-term follow-up of patients with known and novel PRPH2/RDS gene mutations. *Am J Ophthalmol*. 2009;147(3):518–530.e1.
216. Coco RM, Telleria JJ, Sanabria MR, Rodriguez-Rua E, Garcia MT. PRPH2 (Peripherin/RDS) mutations associated with different macular dystrophies in a Spanish population: a new mutation. *Eur J Ophthalmol*. 2010;20(4):724–732.
217. Nettleship E. Central senile areolar choroidal atrophy. *Trans Ophthalmol Soc U K*. 1884;4:165–166.
218. Hoyng CB, Pinckers AJ, Deutman AF. Early findings in central areolar choroidal dystrophy. *Acta Ophthalmol (Copenh)*. 1990;68(3):356–360.
219. Carr RE. Central Areolar Choroidal Dystrophy. *Arch Ophthalmol*. 1965;73:32–35.
220. Mansour AM. Central areolar choroidal dystrophy in a family with pseudoachondroplastic spondyloepiphyseal dysplasia. *Ophthalmic Paediatr Genet*. 1988;9(1):57–65.
221. Noble KG. Central areolar choroidal dystrophy. *Am J Ophthalmol*. 1977;84(3):310–318.
222. Gass J. *Stereoscopic atlas of macular diseases*. 4th ed. Mosby: St. Louis; 2001.
223. Fishman G, Birch D, Holder G, Brigell M. *Electrophysiologic*

testing. 2nd ed. OUP: Oxford; 2001.
224. Farjo R, Naash MI. The role of Rds in outer segment morphogenesis and human retinal disease. *Ophthalmic Genet*. 2006;27(4):117–122.
225. Bok D. Cellular mechanisms of retinal degenerations: RPE65, ABCA4, RDS, and bicarbonate transporter genes as examples. *Retina*. 2005;25(Suppl. 8):S18–20.
226. Wickham L, Chen FK, Lewis GP, et al. Clinicopathological case series of four patients with inherited macular disease. *Invest Ophthalmol Vis Sci*. 2009;50(8):3553–3561.
227. Kedzierski W, Lloyd M, Birch DG, Bok D, Travis GH. Generation and analysis of transgenic mice expressing P216L-substituted rds/peripherin in rod photoreceptors. *Invest Ophthalmol Vis Sci*. 1997;38(2):498–509.
228. Parodi MB, Iacono P, Cascavilla M, Zucchiatti I, Kontadakis DS, Bandello F. Intravitreal bevacizumab for subfoveal choroidal neovascularization associated with pattern dystrophy. *Invest Ophthalmol Vis Sci*. 2010;51(9):4358–4361.
229. Sorsby A, Mason ME. A fundus dystrophy with unusual features. *Br J Ophthalmol*. 1949;33(2):67–97.
230. Weber BH, Vogt G, Pruett RC, Stohr H, Felbor U. Mutations in the tissue inhibitor of metalloproteinases-3 (TIMP3) in patients with Sorsby's fundus dystrophy. *Nat Genet*. 1994;8(4):352–356.
231. Lin RJ, Blumenkranz MS, Binkley J, Wu K, Vollrath D. A novel His158Arg mutation in TIMP3 causes a late-onset form of Sorsby fundus dystrophy. *Am J Ophthalmol*. 2006;142(5):839–848.
232. Lip PL, Good PA, Gibson JM. Sorsby's fundus dystrophy: a case report of 24 years follow-up with electrodiagnostic tests and indocyanine green angiography. *Eye (Lond)*. 1999;13(Pt 1):16–25.
233. Sivaprasad S, Webster AR, Egan CA, Bird AC, Tufail A. Clinical course and treatment outcomes of Sorsby fundus dystrophy. *Am J Ophthalmol*. 2008;146(2):228–234.
234. Tabata Y, Isashiki Y, Kamimura K, Nakao K, Ohba N. A novel splice site mutation in the tissue inhibitor of the metalloproteinases-3 gene in Sorsby's fundus dystrophy

with unusual clinical features. *Hum Genet*. 1998;103(2):179–182.
235. Langton KP, McKie N, Curtis A, et al. A novel tissue inhibitor of metalloproteinases-3 mutation reveals a common molecular phenotype in Sorsby's fundus dystrophy. *J Biol Chem*. 2000;275(35):27027–27031.
236. Barbazetto IA, Hayashi M, Klais CM, Yannuzzi LA, Allikmets R. A novel TIMP3 mutation associated with Sorsby fundus dystrophy. *Arch Ophthalmol*. 2005;123(4):542–543.
237. Jacobson SG, Cideciyan AV, Bennett J, Kingsley RM, Sheffield VC, Stone EM. Novel mutation in the TIMP3 gene causes Sorsby fundus dystrophy. *Arch Ophthalmol*. 2002;120(3):376–379.
238. Jacobson SG, Cideciyan AV, Regunath G, et al. Night blindness in Sorsby's fundus dystrophy reversed by vitamin A. *Nat Genet*. 1995;11(1):27–32.
239. Felbor U, Stohr H, Amann T, Schonherr U, Weber BH. A novel Ser156Cys mutation in the tissue inhibitor of metalloproteinases-3 (TIMP3) in Sorsby's fundus dystrophy with unusual clinical features. *Hum Mol Genet*. 1995;4(12):2415–2416.
240. Felbor U, Benkwitz C, Klein ML, Greenberg J, Gregory CY, Weber BH. Sorsby fundus dystrophy: reevaluation of variable expressivity in patients carrying a TIMP3 founder mutation. *Arch Ophthalmol*. 1997;115(12):1569–1571.
241. Saihan Z, Li Z, Rice J, et al. Clinical and biochemical effects of the E139K missense mutation in the TIMP3 gene, associated with Sorsby fundus dystrophy. *Mol Vis*. 2009;15:1218–1230.
242. Wijesuriya SD, Evans K, Jay MR, et al. Sorsby's fundus dystrophy in the British Isles: demonstration of a striking founder effect by microsatellite-generated haplotypes. *Genome Res*. 1996;6(2):92–101.
243. Gregory-Evans K. What is Sorsby's fundus dystrophy? *Br J Ophthalmol*. 2000;84(7):679–680.
244. Apte SS, Olsen BR, Murphy G. The gene structure of tissue inhibitor of metalloproteinases (TIMP)-3 and its inhibitory

activities define the distinct TIMP gene family. *J Biol Chem*. 1995;270(24):14313–14318.
245. Qi JH, Ebrahem Q, Moore N, et al. A novel function for tissue inhibitor of metalloproteinases-3 (TIMP3): inhibition of angiogenesis by blockage of VEGF binding to VEGF receptor-2. *Nat Med*. 2003;9(4):407–415.
246. Capon MR, Marshall J, Krafft JI, Alexander RA, Hiscott PS, Bird AC. Sorsby's fundus dystrophy. A light and electron microscopic study. *Ophthalmology*. 1989;96(12):1769–1777.
247. Knupp C, Chong NH, Munro PM, Luthert PJ, Squire JM. Analysis of the collagen VI assemblies associated with Sorsby's fundus dystrophy. *J Struct Biol*. 2002;137(1–2):31–40.
248. Chong NH, Alexander RA, Gin T, Bird AC, Luthert PJ. TIMP-3, collagen, and elastin immunohistochemistry and histopathology of Sorsby's fundus dystrophy. *Invest Ophthalmol Vis Sci*. 2000;41(3):898–902.
249. Fariss RN, Apte SS, Olsen BR, Iwata K, Milam AH. Tissue inhibitor of metalloproteinases-3 is a component of Bruch's membrane of the eye. *Am J Pathol*. 1997;150(1):323–328.
250. Kamei M, Apte SS, Rayborn ME, Lewis H, Hollyfield JG. TIMP-3 accumulation in Bruch's membrane and drusen in eyes from normal and age-related macular degeneration donors. La Vail MM, et al. *Degenerative retinal diseases*. Plenum Press: New York; 1997:11–15.
251. Fariss RN, Apte SS, Luthert PJ, Bird AC, Milam AH. Accumulation of tissue inhibitor of metalloproteinases-3 in human eyes with Sorsby's fundus dystrophy or retinitis pigmentosa. *Br J Ophthalmol*. 1998;82(11):1329–1334.
252. Langton KP, McKie N, Smith BM, Brown NJ, Barker MD. Sorsby's fundus dystrophy mutations impair turnover of TIMP-3 by retinal pigment epithelial cells. *Hum Mol Genet*. 2005;14(23):3579–3586.
253. Weber BH, Lin B, White K, et al. A mouse model for Sorsby fundus dystrophy. *Invest Ophthalmol Vis Sci*. 2002;43(8):2732–2740.
254. Fogarasi M, Janssen A, Weber BH, Stohr H. Molecular dissection of TIMP3 mutation S156C associated with Sorsby

fundus dystrophy. *Matrix Biol*. 2008;27(5):381–392.
255. Holz FG, Haimovici R, Wagner DG, Bird AC. Recurrent choroidal neovascularization after laser photocoagulation in Sorsby's fundus dystrophy. *Retina*. 1994;14(4):329–334.
256. Prager F, Michels S, Geitzenauer W, Schmidt-Erfurth U. Choroidal neovascularization secondary to Sorsby fundus dystrophy treated with systemic bevacizumab (Avastin). *Acta Ophthalmol Scand*. 2007;85(8):904–906.
257. Doyne R. A peculiar condition of choroiditis occurring in several members of the same family. *Trans Ophthalmol Soc U K*. 1899;19:71.
258. Vogt A. *Handbuch der gesammten Augenheilkunde. Untersuchungsmethoden. 3rd ed*. 1925.
259. Gass J. Diseases causing choroidal exudative and hemorrhagic localized (disciform) detachment of the retina and pigment epithelium. *Stereoscopic atlas of macular diseases*. Mosby: St. Louis; 1987:96–97.
260. Heon E, Piguet B, Munier F, et al. Linkage of autosomal dominant radial drusen (malattia leventinese) to chromosome 2p16-21. *Arch Ophthalmol*. 1996;114(2):193–198.
261. Stone EM, Lotery AJ, Munier FL, et al. A single EFEMP1 mutation associated with both malattia leventinese and Doyne honeycomb retinal dystrophy. *Nat Genet*. 1999;22(2):199–202.
262. Michaelides M, Jenkins SA, Brantley MA Jr, et al. Maculopathy due to the R345W substitution in fibulin-3: distinct clinical features, disease variability, and extent of retinal dysfunction. *Invest Ophthalmol Vis Sci*. 2006;47(7):3085–3097.
263. Sohn EH, Patel PJ, MacLaren RE, et al. Choroidal neovascular membranes in patients with R345W mutation in fibulin-3 (Doyne honeycomb retinal dystrophy) are responsive to anti-VEGF therapy. *Arch Ophthalmol*. 2011;129(12):1626–1628.
264. Haimovici R, Wroblewski J, Piguet B, et al. Symptomatic abnormalities of dark adaptation in patients with EFEMP1 retinal dystrophy (malattia leventinese/Doyne honeycomb retinal dystrophy). *Eye (Lond)*. 2002;16(1):7–15.

265. Evans K, Gregory CY, Wijesuriya SD, et al. Assessment of the phenotypic range seen in Doyne honeycomb retinal dystrophy. *Arch Ophthalmol*. 1997;115(7):904–910.
266. Marmorstein LY, Munier FL, Arsenijevic Y, et al. Aberrant accumulation of EFEMP1 underlies drusen formation in malattia leventinese and age-related macular degeneration. *Proc Natl Acad Sci USA*. 2002;99(20):13067–13072.
267. Holz FG, Owens SL, Marks J, Haimovici R, Bird AC. Ultrastructural findings in autosomal dominant drusen. *Arch Ophthalmol*. 1997;115(6):788–792.
268. Sohn EH, Wang K, Thompson S, et al. Comparison of drusen and modifying genes in autosomal dominant radial drusen and age-related macular degeneration. *Retina*. 2015;35(1):48–57.
269. Roybal CN, Marmorstein LY, Vander Jagt DL, Abcouwer SF. Aberrant accumulation of fibulin-3 in the endoplasmic reticulum leads to activation of the unfolded protein response and VEGF expression. *Invest Ophthalmol Vis Sci*. 2005;46(11):3973–3979.
270. Fu L, Garland D, Yang Z, et al. The R345W mutation in EFEMP1 is pathogenic and causes AMD-like deposits in mice. *Hum Mol Genet*. 2007;16(20):2411–2422.
271. Marmorstein LY, McLaughlin PJ, Peachey NS, Sasaki T, Marmorstein AD. Formation and progression of sub-retinal pigment epithelium deposits in Efemp1 mutation knock-in mice: a model for the early pathogenic course of macular degeneration. *Hum Mol Genet*. 2007;16(20):2423–2432.
272. Blackburn J, Tarttelin EE, Gregory-Evans CY, Moosajee M, Gregory-Evans K. Transcriptional regulation and expression of the dominant drusen gene FBLN3 (EFEMP1) in mammalian retina. *Invest Ophthalmol Vis Sci*. 2003;44(11):4613–4621.
273. Lefler WH, Wadsworth JA, Sidbury JB Jr. Hereditary macular degeneration and amino-aciduria. *Am J Ophthalmol*. 1971;71(1 Pt 2):224–230.
274. Frank HR, Landers MB 3rd, Williams RJ, Sidbury JB. A new dominant progressive foveal dystrophy. *Am J Ophthalmol*. 1974;8(6):903–916.

275. Small KW. North Carolina macular dystrophy: clinical features, genealogy, and genetic linkage analysis. *Trans Am Ophthalmol Soc*. 1998;96:925–961.
276. Reichel MB, Kelsell RE, Fan J, et al. Phenotype of a British North Carolina macular dystrophy family linked to chromosome 6q. *Br J Ophthalmol*. 1998;82(10):1162–1168.
277. Pauleikhoff D, Sauer CG, Muller CR, Radermacher M, Merz A, Weber BH. Clinical and genetic evidence for autosomal dominant North Carolina macular dystrophy in a German family. *Am J Ophthalmol*. 1997;124(3):412–415.
278. Small KW, Puech B, Mullen L, Yelchits S. North Carolina macular dystrophy phenotype in France maps to the MCDR1 locus. *Mol Vis*. 1997;3:1.
279. Rabb MF, Mullen L, Yelchits S, Udar N, Small KW. A North Carolina macular dystrophy phenotype in a Belizean family maps to the MCDR1 locus. *Am J Ophthalmol*. 1998;125(4):502–508.
280. Kim SJ, Woo SJ, Yu HG. A Korean family with an early-onset autosomal dominant macular dystrophy resembling North Carolina macular dystrophy. *Korean J Ophthalmol*. 2006;20(4):220–224.
281. Fetkenhour CL, Gurney N, Dobbie JG, Choromokos E. Central areolar pigment epithelial dystrophy. *Am J Ophthalmol*. 1976;81(6):745–753.
282. Small KW, Killian J, McLean WC. North Carolina's dominant progressive foveal dystrophy: how progressive is it? *Br J Ophthalmol*. 1991;75(7):401–406.
283. Small KW. North Carolina macular dystrophy, revisited. *Ophthalmology*. 1989;96(12):1747–1754.
284. Small KW, Weber JL, Hung WY, Vance J, Roses A, Pericak-Vance M. North Carolina macular dystrophy: exclusion map using RFLPs and microsatellites. *Genomics*. 1991;11(3):763–766.
285. Small KW, Weber JL, Roses A, Lennon F, Vance JM, Pericak-Vance MA. North Carolina macular dystrophy is assigned to chromosome 6. *Genomics*. 1992;13(3):681–685.
286. Small KW, Udar N, Yelchits S, et al. North Carolina macular dystrophy (MCDR1) locus: a fine resolution genetic map

and haplotype analysis. *Mol Vis*. 1999;5:38.
287. Michaelides M, Johnson S, Tekriwal AK, et al. An early-onset autosomal dominant macular dystrophy (MCDR3) resembling North Carolina macular dystrophy maps to chromosome 5. *Invest Ophthalmol Vis Sci*. 2003;44(5):2178–2183.
288. Rosenberg T, Roos B, Johnsen T, et al. Clinical and genetic characterization of a Danish family with North Carolina macular dystrophy. *Mol Vis*. 2010;16:2659–2668.
289. Small KW, DeLuca AP, Whitmore SS, North Carolina Macular Dystrophy is caused by dysregulation of the retinal transcription factor PRDM13. Ophthalmology 2016;123(1):9–18.
290. Small KW, Voo I, Flannery J, Udar N, Glasgow BJ. North Carolina macular dystrophy: clinicopathologic correlation. *Trans Am Ophthalmol Soc*. 2001;99:233–237 [discussion 7-8].
291. Mahajan VB, Russell SR, Stone EM. A new macular dystrophy with anomalous vascular development, pigment spots, cystic spaces, and neovascularization. *Arch Ophthalmol*. 2009;127(11):1449–1457.
292. Deutman AF, Pinckers AJ, Aan de Kerk AL. Dominantly inherited cystoid macular edema. *Am J Ophthalmol*. 1976;82(4):540–548.
293. Fishman GA, Goldberg MF, Trautmann JC. Dominantly inherited cystoid macular edema. *Ann Ophthalmol*. 1979;11(1):21–27.
294. Kremer H, Pinckers A, van den Helm B, Deutman AF, Ropers HH, Mariman EC. Localization of the gene for dominant cystoid macular dystrophy on chromosome 7p. *Hum Mol Genet*. 1994;3(2):299–302.
295. Hogewind BF, Pieters G, Hoyng CB. Octreotide acetate in dominant cystoid macular dystrophy. *Eur J Ophthalmol*. 2008;18(1):99–103.
296. Sneed SR, Sieving PA. Fenestrated sheen macular dystrophy. *Am J Ophthalmol*. 1991;112(1):1–7.
297. Daily MJ, Mets MB. Fenestrated sheen macular dystrophy. *Arch Ophthalmol*. 1984;102(6):855–856.
298. Slagsvold JE. Fenestrated sheen macular dystrophy. A new

autosomal dominant maculopathy. *Acta Ophthalmol (Copenh)*. 1981;59(5):683–688.
299. O'Donnell FE Jr, Welch RB. Fenestrated sheen macular dystrophy. A new autosomal dominant maculopathy. *Arch Ophthalmol*. 1979;97(7):1292–1296.
300. McAvoy CE, Silvestri G. Retinal changes associated with type 2 glomerulonephritis. *Eye (Lond)*. 2005;19(9):985–989.
301. D'Souza Y, Short CD, McLeod D, Bonshek RE. Long-term follow-up of drusen-like lesions in patients with type II mesangiocapillary glomerulonephritis. *Br J Ophthalmol*. 2008;92(7):950–953.
302. Leys A, Vanrenterghem Y, Van Damme B, Snyers B, Pirson Y, Leys M. Sequential observation of fundus changes in patients with long standing membranoproliferative glomerulonephritis type II (MPGN type II). *Eur J Ophthalmol*. 1991;1(1):17–22.
303. Leys A, Vanrenterghem Y, Van Damme B, Snyers B, Pirson Y, Leys M. Fundus changes in membranoproliferative glomerulonephritis type II. A fluorescein angiographic study of 23 patients. *Graefes Arch Clin Exp Ophthalmol*. 1991;229(5):406–410.
304. Ulbig MR, Riordan-Eva P, Holz FG, Rees HC, Hamilton PA. Membranoproliferative glomerulonephritis type II associated with central serous retinopathy. *Am J Ophthalmol*. 1993;116(4):410–413.
305. Kim RY, Faktorovich EG, Kuo CY, Olson JL. Retinal function abnormalities in membranoproliferative glomerulonephritis type II. *Am J Ophthalmol*. 1997;123(5):619–628.
306. O'Brien C, Duvall-Young J, Brown M, Short C, Bone M. Electrophysiology of type II mesangiocapillary glomerulonephritis with associated fundus abnormalities. *Br J Ophthalmol*. 1993;77(12):778–780.
307. Duvall-Young J, MacDonald MK, McKechnie NM. Fundus changes in (type II) mesangiocapillary glomerulonephritis simulating drusen: a histopathological report. *Br J Ophthalmol*. 1989;73(4):297–302.
308. Mullins RF, Aptsiauri N, Hageman GS. Structure and

composition of drusen associated with glomerulonephritis: implications for the role of complement activation in drusen biogenesis. *Eye (Lond)*. 2001;15(Pt 3):390–395.
309. Mullins RF, Russell SR, Anderson DH, Hageman GS. Drusen associated with aging and age-related macular degeneration contain proteins common to extracellular deposits associated with atherosclerosis, elastosis, amyloidosis, and dense deposit disease. *FASEB J*. 2000;14(7):835–846.
310. van den Ouweland JM, Lemkes HH, Ruitenbeek W, et al. Mutation in mitochondrial tRNA(Leu)(UUR) gene in a large pedigree with maternally transmitted type II diabetes mellitus and deafness. *Nat Genet*. 1992;1(5):368–371.
311. Naing A, Kenchaiah M, Krishnan B, et al. Maternally inherited diabetes and deafness (MIDD): diagnosis and management. *J Diabetes Complications*. 2014;28(4):542–546.
312. Murphy R, Turnbull DM, Walker M, et al. Clinical features, diagnosis and management of maternally inherited diabetes and deafness (MIDD) associated with the 3243A>G mitochondrial point mutation. *Diabet Med*. 2008;25(4):383–399.
313. Bellmann C, Neveu MM, Scholl HP, et al. Localized retinal electrophysiological and fundus autofluorescence imaging abnormalities in maternal inherited diabetes and deafness. *Invest Ophthalmol Vis Sci*. 2004;45(7):2355–2360.

45

Hereditary Choroidal Diseases

Sandeep Grover, Gerald A. Fishman

Introduction

The term “choroidal dystrophy” is likely a misnomer as it implies a primary degenerative process involving the choroidal circulation. However, the current evidence focuses on the retinal pigment epithelium (RPE) as playing an important, if not pivotal, role in the disorders categorized under the rubric of choroidal dystrophy since genetic mutations that affect the RPE can lead to atrophic changes of both the RPE and choriocapillaris.

Nonetheless, the hereditary choroidal dystrophies can be classified in the following manner: (1) choroidal atrophy phenotypes, which can be further subdivided into (a) central areolar choroidal dystrophy (CACD); (b) peripapillary choroidal dystrophy; (c) diffuse choroidal dystrophy; and (d) progressive bifocal chorioretinal atrophy (PBCRA); (2) gyrate atrophy of the choroid and retina; and (3) choroideremia (CHM). While each of the choroidal dystrophies has characteristic fundus features, in certain instances at advanced stages of disease an overlap in fundus appearance may be observed (Box 45.1).

Box 45.1

Brief Classification of Hereditary Choroidal Diseases

1. Choroidal atrophy phenotypes

a. Central areolar choroidal dystrophy

b. Peripapillary choroidal dystrophy

c. Diffuse choroidal dystrophy

d. Progressive bifocal chorioretinal atrophy

2. Gyrate atrophy of the choroid and retina

3. Choroideremia

4. Clinical phenotypes resembling hereditary choroidal diseases

a. Advanced stage of X-linked retinitis pigmentosa

b. Advanced stage of Kearns–Sayre syndrome

c. Bietti crystalline dystrophy

d. Thioridazine (Mellaril) retinal toxicity

e. Advanced stage of Stargardt disease

f. Advanced stage of pattern dystrophy

The common feature of these disorders is degenerative changes of the RPE in the early stages that progress to involve the choriocapillaris, photoreceptor cell layer, and in later stages, the larger choroidal vessels. Whether an abnormality in the choriocapillaris or even photoreceptor cells occurs concurrently with degenerative changes in the RPE has not been conclusively determined. Certain of these dystrophies are generalized and progressive (CHM, gyrate atrophy, and diffuse choroidal dystrophy) whereas others are more localized, either remaining geographically confined (CACD) or progressively expanding (peripapillary choroidal dystrophy and progressive bifocal chorioretinal atrophy) to involve more extensive regions of the fundus. In the advanced stages of certain choroidal dystrophies, the loss of RPE cells, retinal and choroidal tissue, as well as pigment accumulation, may not be easily differentiated from the fundus changes observed in certain other hereditary degenerative or inflammatory retinal disorders.

Choroidal Atrophy Phenotypes

According to Sorsby,[1] this group of disorders can be subdivided into three clinical phenotypes based on their geographical distribution. They include central areolar, peripapillary, and more diffuse or generalized choroidal dystrophy. All can be inherited as either autosomal dominant or autosomal recessive traits. PBCRA is inherited as an autosomal dominant trait.

Central Areolar Choroidal Dystrophy

CACD was first described by Nettleship in 1884. It is inherited primarily as an autosomal dominant trait,[2,3] although autosomal recessive cases have been occasionally reported.[4,5] Yanagihashi and colleagues[6] identified a novel mutation in the peripherin/RDS (retinal degeneration slow) gene in a Japanese family with an autosomal dominant form of CACD.

The initial symptoms of diminished central vision generally begin in the latter part of the second to the early part of the fourth decade. Characteristic bilateral macular lesions are solitary, with well-defined margins, and circular or ovoid in shape (Fig. 45.1). Although they may increase in size and become irregular in shape, they do not involve the peripapillary region or extend beyond the vascular arcades.

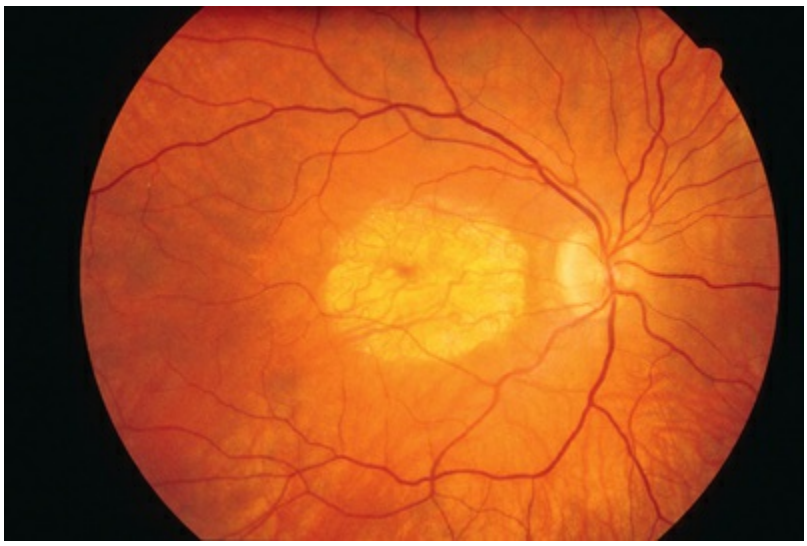

FIG. 45.1 Color fundus photograph from the right eye

of a patient with central areolar choroidal dystrophy shows a well-defined, oval-shaped hypopigmented atrophic macular lesion.

The early fundus changes include a mottling of the RPE in the macula. At this stage, the underlying choroid may appear ophthalmoscopically normal. With the subsequent loss of RPE and choriocapillaris, the underlying choroidal vessels are more readily visualized. With continued loss of RPE and choriocapillaris, the larger choroidal vessels may undergo degeneration. In advanced stages of disease, the sclera is visible as a consequence of choroidal atrophy. Fluorescein angiography at the early stages of the disease shows hyperfluorescence (window defect) due to increased transmission from the underlying normal choriocapillaris. The optic disc and retinal vessels remain normal. Traditionally, full-field electroretinographic (ERG) amplitudes are normal. In some cases, patients diagnosed as having CACD may show reduced cone function. In these instances, consideration should be given to the diagnosis of cone dystrophy.

A few other inherited retinal disorders may show a CACD macular phenotype in their more advanced stages. These, in part, include Stargardt disease, cone dystrophy, North Carolina macular dystrophy, and pattern dystrophy as well as the geographic atrophic macular lesion that can be observed in age-related macular degeneration.

Peripapillary Choroidal Dystrophy

The peripapillary form of choroidal dystrophy is usually inherited as an autosomal recessive trait,[7] although in some instances autosomal dominant transmission may be encountered.

The fundus findings in this form of choroidal dystrophy initially include changes seen in the RPE and later an ophthalmoscopically apparent loss of RPE and choroidal tissue. The important distinction between CACD and the peripapillary phenotype is their location. The peripapillary form begins in the region surrounding the optic disc and slowly enlarges, in finger-like projections, nasally, temporally, and into the macula, eventually occupying the entire posterior pole (Fig. 45.2). In some instances the peripapillary

form can progress to a phenotype similar to the diffuse form.

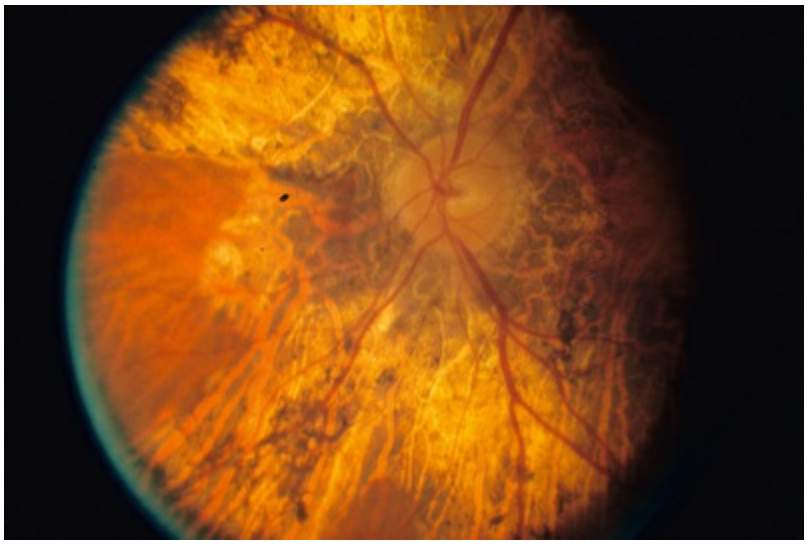

FIG. 45.2 Color fundus photograph from the left eye of a patient with peripapillary choroidal dystrophy shows both retinal pigment epithelium and choroidal atrophy in a region predominantly around the optic disc.

Visual field and dark-adapted final thresholds testing indicate that peripheral to the fundoscopically involved area, retinal function is either normal or mildly impaired. The ERG is either normal or only slightly reduced, reflecting the extent of the disease.[7,8]

The differential diagnosis includes peripapillary pigment epithelial dystrophy in which there are well-defined areas of RPE loss, with direct visualization of the underlying choroidal vasculature. Fluorescein angiography shows an intact choriocapillaris that differentiates it from those with choriocapillaris loss.[7] Another disorder that mimics peripapillary choroidal dystrophy is serpiginous choroiditis, which usually begins in the peripapillary region and then extends into the retina in pseudopod-like extensions, sometimes involving the macula.

Diffuse Choroidal Dystrophy

This diffuse disorder of the RPE and choriocapillaris is most often inherited as an autosomal dominant trait;[9] however, autosomal recessive transmission may occur. The onset of symptoms occurs

most often in the fourth and fifth decade and is usually manifested by poor central vision, impairment of night vision, or both.

The early fundus changes include retinal pigment mottling and hypopigmentation. The disease may initially show a predilection for the posterior pole of the retina before progressing to a more diffuse phenotype. Later there is diffuse atrophy of both the RPE and choriocapillaris while the larger choroid vessels appear sclerotic as yellowish-white bands. Both the posterior pole and the periphery are involved to varying degrees. Even with diffuse involvement in the more advanced stages, the retinal vessels usually remain normal[10] (Fig. 45.3). In the end stages, diffuse choroidal dystrophy cannot be easily differentiated from other diffuse chorioretinal diseases such as thioridazine (Mellaril) retinal toxicity, advanced stages of both pattern dystrophy and Stargardt disease, in addition to the advanced retinopathy seen in the Kearns–Sayre syndrome.

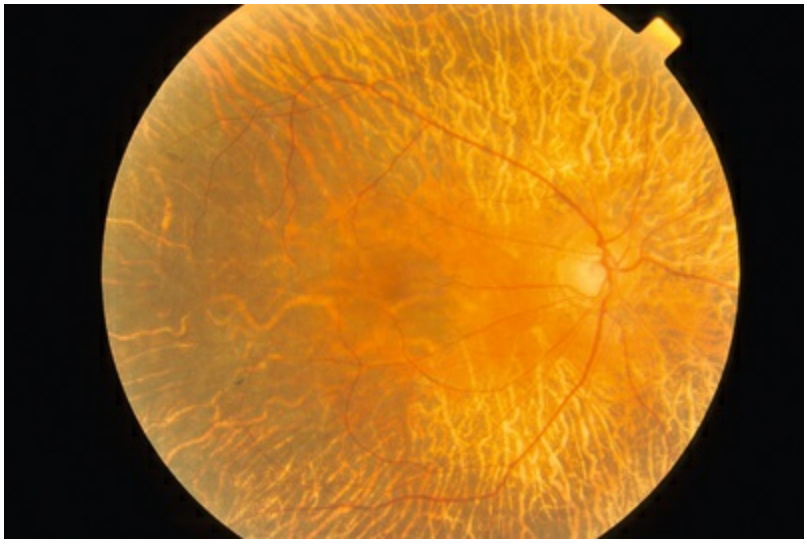

FIG. 45.3 Color fundus photograph from the right eye of a patient with an advanced stage of diffuse choroidal dystrophy shows diffuse retinal pigment epithelium and choroidal atrophy. Both the posterior pole and the retinal periphery are involved to varying degrees.

Psychophysical and electrophysiologic studies reflect the diffuse involvement. Visual fields show a concentric peripheral constriction, while ERG recordings are either subnormal[10] or

undetectable.[7] Fluorescein angiography shows a loss of the choriocapillaris and visualization of the larger choroidal vessels beneath atrophic-appearing RPE.[7,11] A few scattered areas show a patchy choroidal flush pattern indicative of some remnants of the choriocapillaris.

Progressive Bifocal Chorioretinal Atrophy

First described by Douglas et al. in 1968,[12] patients with PBCRA have two foci of chorioretinal atrophy: one a congenital macular lesion and the other that starts nasal to the disc in the first or second decade of life. Both these lesions increase in size until, in the advanced stages, there is only a residual vertical band of normal retina and choroid confluent with the optic nerve. These findings are also associated with myopia, nystagmus and higher incidence of retinal detachments.[13] There is widespread reduction of rod and cone function on electrophysiologic testing. PBCRA is inherited in an autosomal dominant fashion and the gene has been localized to chromosome 6q14 – 16.2.[14]

Gyrate Atrophy of the Choroid and Retina

The first case of this disease was described in 1888 by Jacobsohn[15] as an example of "atypical retinitis pigmentosa." However, Cutler[16] in 1895 and Fuchs[17] in 1896 were the first to recognize the disease as a distinct clinical entity. Gyrate atrophy is a rare choroidal disease with a prevalence of about 1 in 50, 000 in Finland.[18] It is inherited as an autosomal recessive trait, although dominant pedigrees have also been reported.[10] The biochemical abnormalities observed in this disorder were initially described by Simell and Takki[19] in 1973; these included a deficiency of the enzyme ornithine-delta-aminotransferase (OAT), which results in an increase in the plasma ornithine concentration (10–15 times the normal levels). The enzyme OAT is a mitochondrial-encoded enzyme with pyridoxal phosphate (vitamin B_6) enzyme as a cofactor that catalyzes the interconversion of ornithine, glutamate, and proline. This results in

systemic biochemical abnormalities, including hyperornithinemia, and reductions in plasma lysine, glutamine, glutamate, and creatine.[20–22] Either an absence or a marked reduction of OAT in cultured skin fibroblasts and in lymphocytes has been observed.[23] A number of different mutations have been identified within the OAT gene on chromosome 10.[24–26] Kellner and colleagues[27] previously described a gyrate atrophy-like phenotype in six male patients, three of whom were patients of the same family, with normal serum ornithine levels.

The onset of visual symptoms, including poor night vision and constricted peripheral vision, usually begins in the second and third decades. Since both structural and visual functional changes spread from more peripheral to a central location, loss of visual acuity is a later complaint in the disease. Myopia and posterior subcapsular cataracts are frequently observed and vitreous opacities may also be present.[18]

The fundus changes begin in the midperipheral and peripheral retina with a thinning and atrophic appearance of the RPE in which the underlying choroidal vessels may appear either normal or sclerotic. These areas are typically scalloped in shape and are initially separate but tend to become confluent as they slowly progress both centrally and peripherally (Fig. 45.4). Progression of the disease leads to pigment clumping, RPE and choriocapillaris atrophy, and eventual total atrophy of the choroid exposing the white sclera. In the late stages, an annular ring of choroidal atrophy may be seen from the periphery to the posterior pole, usually sparing the macula. The retinal vessels may appear normal initially or attenuated in later stages of the disease when the optic nerve may appear pale.[7,10]

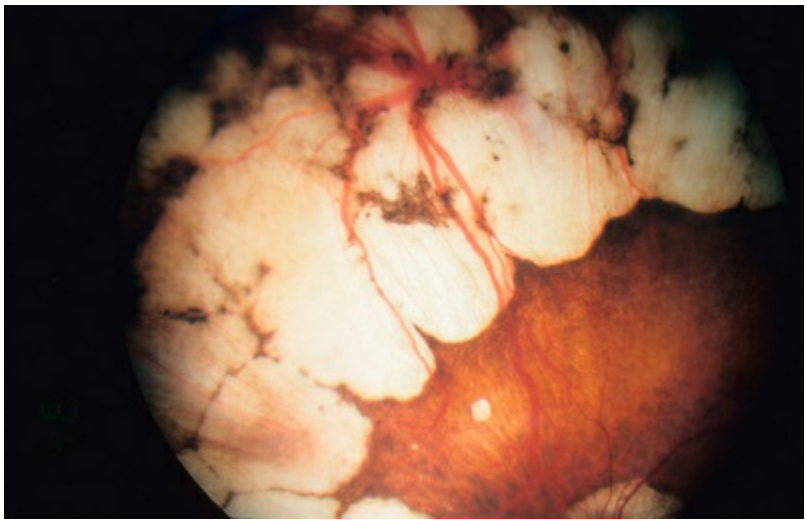

FIG. 45.4 Color fundus photograph from the left eye of a patient with gyrate atrophy of the choroid and retina shows the typical scalloped areas of retinal pigment epithelium and choroidal atrophy.

There are reports on the presence of cystoid macular edema in patients with gyrate atrophy.[28–30] A study by Vasconcelos-Santos et al.[30] showed a short-term therapeutic effect with the use of a 4-mg intravitreal triamcinolone acetonide injection for gyrate atrophy-related macular edema. After drug clearance, the edema recurred, with return of visual acuity to the pretreatment level.

Visual function varies considerably from case to case and seems to be related to the extent of fundus involvement. Visual field testing shows a concentric peripheral constriction of the visual field as the most often observed abnormality. However, an annular ring and paracentral scotomas may develop as the disease progresses. Eventually, if the fovea becomes involved, a central scotoma will be seen.[7,31]

Early in the disease, dark-adaptation testing shows only mild threshold elevations while significant elevation of the final rod thresholds is eventually noted in most patients. In the early stage, full-field ERG recordings may show only a mild abnormality in rod and cone amplitudes, while, as the disease progresses, the ERG responses deteriorate and may eventually become undetectable. The rod responses are affected more severely in the early stages, but later both cone as well as rod function is severely impaired.[32,33] The electro-oculogram (EOG) is normal or only mildly reduced at very early stages. The EOG light-peak to dark-trough ratio becomes

markedly reduced in the later stages. Electromyograms are often abnormal, although only a few patients complain of mild muscle weakness. Muscle biopsy shows atrophic type 2 muscle fibers with tubular aggregates visible on electron microscopy.[34,35] Both electrocardiographic and electroencephalographic abnormalities may be observed in some patients.[36,37] Histopathologic studies show early changes in RPE cells, with subsequent loss of photoreceptors and choriocapillaris, suggesting that these latter changes may be secondary to the loss of RPE cell integrity.[38]

A histopathologic study in the ornithine-deficient mouse model of gyrate atrophy showed earliest changes in the RPE cells in the form of sporadic degeneration of scattered cells. By 6 months, there were more diffuse abnormalities of the RPE with accumulation of large phagosomes and crystalloid inclusions. Although morphologically normal at 2 months, the photoreceptor outer segments became highly disorganized and shortened to 60% of mouse control lengths by 10 months. Additionally, there was a cumulative loss of the photoreceptor cells, which reached 33% by 10 months.[39]

An arginine-restricted diet has been pursued as a form of therapy in patients with gyrate atrophy of the choroid and retina.[20,40–42] Since ornithine is produced from other amino acids, mainly arginine, some investigators advocate that patients be restricted to a rigid low-protein diet, including near-total elimination of arginine with supplementation of essential amino acids. Orally administered pyridoxal phosphate (vitamin B_6), can result in a reduction in plasma ornithine levels in some patients, while others are nonresponsive to B_6.[32] Overall, ERG responses are better maintained by B_6-responsive patients compared to those who are nonresponders.[32,40] While Kaiser-Kupfer et al.[41] concluded that a dietary approach to reducing plasma ornithine was effective in slowing retinal degeneration, this was not similarly observed to occur in patients with gyrate atrophy in studies by Vannas-Sulonen et al.[42] or Berson[40] et al. A study by Katagiri[43] was inconclusive.

Choroideremia

Mauthner in 1872[44] was the first to describe the clinical features of CHM, which is a generalized degeneration of the retina, inherited as an X-linked recessive trait,[45] with an estimated prevalence of 1 in 50, 000.[46] The onset of symptoms occurs in the first and second decades with impairment of night vision and peripheral visual field loss. Central vision is most often preserved until later in life. Males in their 40s generally have useful visual acuity, but typically only a small residual visual field. Later (ages 50–70 years), central vision is more substantially reduced. In a study of 115 males with CHM (mean age 39 years), a slow rate of visual acuity loss with the retention of central visual acuity until the seventh decade was found.[47]

Fundus changes are readily apparent by the second decade of life or earlier. A 22-month-old infant with fundus changes has been described.[45] The clinical diagnosis of affected males is characterized by the following:[47]

- A history of defective dark adaptation, manifesting as poor visual function in dim illumination, is commonly the first symptom. Males may not show this impairment until their early teens.
- The fundus changes in affected males undergo a characteristic progression. The initial appearance is a fine, peppery-like retinal pigment mottling at the midperipheral retina and posterior pole. At this stage, the ERG is abnormal, showing reduced or absent scotopic responses.[10] Focal disturbances in the RPE consisting of pigmentary loss or a metallic sheen follow the "salt and pepper" mottling while the underlying choroid may appear normal or show choriocapillaris atrophy. Occasionally, these areas of focal disturbances assume a shape similar to gyrate atrophy, and the distinction between the two diseases may be difficult on the basis of the fundus appearance (Fig. 45.5). Atrophy of the choroid follows with eventual loss of the entire layer and exposure of bare sclera. The rate of progression will vary from individual to individual and from family to family. These changes are initially most apparent in the midperipheral retina and progress centrally, the macula being the last affected, with central vision preserved until later in the disease. In the final stage, the fundus shows an extensive yellowish-white reflex from the sclera (Fig. 45.6). Cystoid macular edema has also been described by Genead and

Fishman[48] to be present in 63% of patients in a small (*n*=16) cohort.

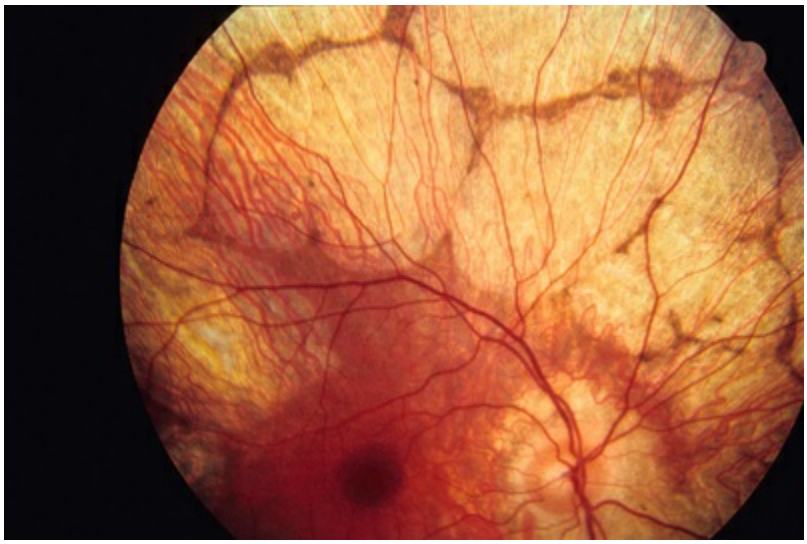

FIG. 45.5 Color fundus photograph from the right eye of a patient with choroideremia shows scalloped areas of retinal pigment epithelium and choroidal atrophy that shows a similarity to lesions observed in patients with gyrate atrophy of the choroid and retina.

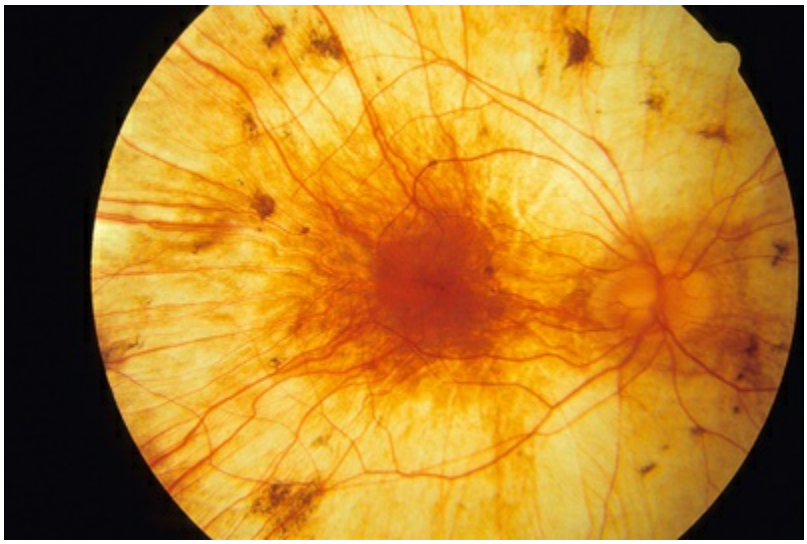

FIG. 45.6 Color fundus photograph from the right eye of a patient with an advanced stage of choroideremia shows a yellowish-white reflex from the sclera due to the extensive atrophy of the retinal pigment epithelium and choroid in the midperipheral retina and posterior pole with scattered pigment clumps. The macula

shows relative sparing.

- Peripheral visual field loss manifests as a ring scotoma that corresponds to areas of chorioretinal degeneration.
- Even in the early stages of the disease, the ERG is most often abnormal under both light- and dark-adapted conditions. The ERG may be normal early in the course of the disease when only a few focal lesions are present,[49] but eventually becomes undetectable in most.[49] Nonetheless, a wide intrafamilial and interfamilial variability in ERG amplitudes with age has been observed.[50] EOG recordings show an abnormally low light-peak to dark-trough ratio.

Visual field testing in affected males is generally normal when only minor pigmentary changes are present at the early stages of the disease. With the occurrence of equatorial and peripapillary choroidal vascular atrophy, there is not infrequently the development of corresponding equatorial diminished retinal sensitivity or ring scotomas and an enlarged blind spot. Gradual deterioration of visual field occurs and ultimately, by the fifth and sixth decades, the patient may show a field of less than 20°. Occasionally, a few peripheral islets of vision remain.

Dark adaptation testing is normal if the patient is seen at an early stage. In general, there is initially an abnormality of the rod portion of the dark adaptation curve. There is progressive deterioration of rod dark adaptation, and eventually the cone portion of the curve becomes involved as well.

Histopathologic examination of a 30-year-old man with CHM showed diffuse abnormalities of the retina, RPE, and choriocapillaris that varied from different areas and appeared to occur independently of each other. In addition, mild T-lymphocyte infiltration was found within the choroid.[51] Prior pathologic specimens[45,52–54] from patients afflicted with CHM showed the following:

1. Extensive atrophy of the choroidal vasculature and Bruch's membrane was found in all subjects. The choroid was most recognizable at the macula.

2. Extensive atrophy of the RPE and photoreceptors was common even in the macula. However, in the eye from the youngest patient, distinct photoreceptor nuclei were seen in the macula.

3. In general, the retinal bipolar, ganglion, and nerve fiber layers were normal.

4. The optic nerve showed an increase in glial tissue within the septa and mild cystoid degeneration among the axons in the neural channels.

The CHM gene was localized to the long arm of the X chromosome (Xq21).[55,56] The gene encodes the Rab escort protein-1 (REP-1) that is involved in the prenylation of Rabs. The REP-1 protein facilitates posttranslational modification of Rab proteins, which regulate intracellular trafficking in the RPE and photoreceptors and is likely involved in the removal of outer-segment disc membranes by the RPE.[57] All currently described mutations in *REP-1*/*CHM*, including deletions, translocations, and mutations, result in protein truncation due to replacement of an arginine residue with a stop codon.[58] In 1998, MacDonald et al.[59] observed the absence of *REP-1* in peripheral lymphocytes of affected individuals that led to the development of an immunoblot assay using anti-REP-1 antibodies to diagnose patients with CHM.

As far as the treatment for CHM is concerned, in a recent phase I/II clinical trial with an adeno-associated viral gene vector encoding REP1 (AAV.REP1), preliminary results after 6 months established the safety and showed a trend for improvement in visual acuity and in rod and cone function.[60] A phase IIb trial is being planned by the same group in the UK. Other phase I/II clinical treatment trials are being planned for enrolment in the United States (ClinicalTrials.gov Identifier:NCT02341807) and Canada (ClinicalTrials.gov Identifier:NCT02077361).

The carrier females of X-linked CHM show the following:

1. With few exceptions, fundus changes are considerably milder than those observed in affected males. Typically there is pigment mottling, best seen in the midperipheral retina, which may also be apparent in the macula. This finding becomes more readily evident

after the second decade and has been described as showing a "moth-eaten appearance." Some of the pigmentary changes in carriers consist of radial bands that course from the midperipheral retina toward the ora serrata (Fig. 45.7). There is no apparent relation between the degree of fundus pigmentary changes and the age of a carrier. The pigmentary changes observed in carriers are due to a skewed X-chromosome inactivation or the presence of an X-chromosome translocation involving Xq21.[61]

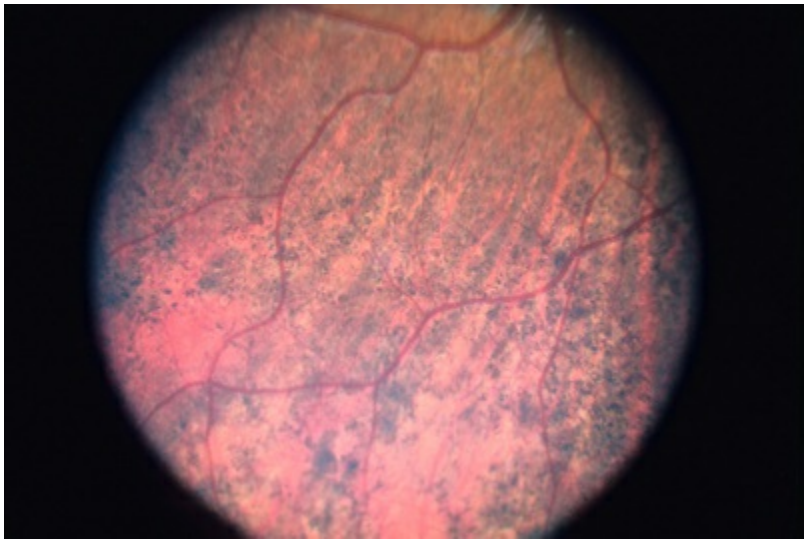

FIG. 45.7 Color fundus photograph from the right eye of a carrier for X-linked choroideremia shows the typical pigment granularity or mottling in the midperipheral retina referred to as a "moth-eaten appearance."

2. In most instances, carrier females do not experience significant visual impairment and in general are asymptomatic. However, carrier females may show changes on ERG, dark adaptation, visual field, and macular microperimetry testing.[62] The ERG may be normal, even in carriers with pigmentary fundus changes. EOG recordings characteristically show no abnormality in the light-peak to dark-trough ratio.[63] Measurement of fundus autofluorescence may demonstrate patchy areas of autofluorescence loss.[64]

3. There are occasional case reports[65,66] in which the carrier female may have retinal and functional changes similar to affected male

patients, but such findings are a rarity.

A histopathologic study[67] of an eye from an 88-year-old carrier of CHM showed a patchy degeneration of photoreceptors and RPE cells that were not strictly concordant. The choriocapillaris was described as normal, except in regions of severe retinal degeneration. Immunofluorescence analysis, with a mouse monoclonal antibody, localized the CHM gene product, *REP-1*, to the rod cytoplasm and amacrine cells but not in cone cells.[67] This observation suggests the possibility that the primary site of this disease may reside in the rods rather than in the RPE or choroid. Labeling observed within small vesicles in the rod cytoplasm is consistent with the association of *REP-1* with intracellular vesicular transport.

Clinical Phenotypes Resembling Hereditary Choroidal Diseases

X-Linked Retinitis Pigmentosa (XLRP)

RP is a group of inherited disorders in which abnormalities of the RPE and photoreceptors lead to progressive visual loss. The initial symptoms of RP include night vision impairment and restriction of the peripheral visual field. A diagnosis of RP includes abnormalities on ERG testing. RP can be inherited in an autosomal dominant, autosomal recessive, or X-linked manner. Mutations in *RPGR* (also called *RP3*) and *RP2* genes are the most common causes of XLRP. Linkage studies suggest that they account for 70–90% and 10–20%, respectively, of XLRP. In the later stages of particularly CHM, when the loss of choroid and retina is significant, the fundus appearance may be confused with end-stage XLRP; however, the degree and appearance of pigment migration into the retina that typifies RP are not characteristically seen in individuals with CHM (Figs. 45.8 and 45.9).

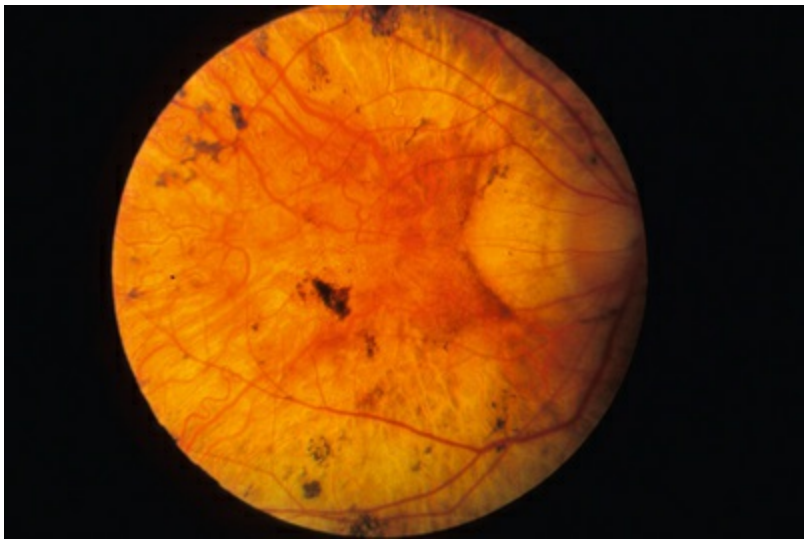

FIG. 45.8 Color fundus photograph from the right eye of a patient with an advanced stage of X-linked retinitis pigmentosa shows extensive atrophy of retinal pigment epithelium and choroid in the posterior pole and midperipheral retina with scattered pigment clumps. The retinal vessels are attenuated.

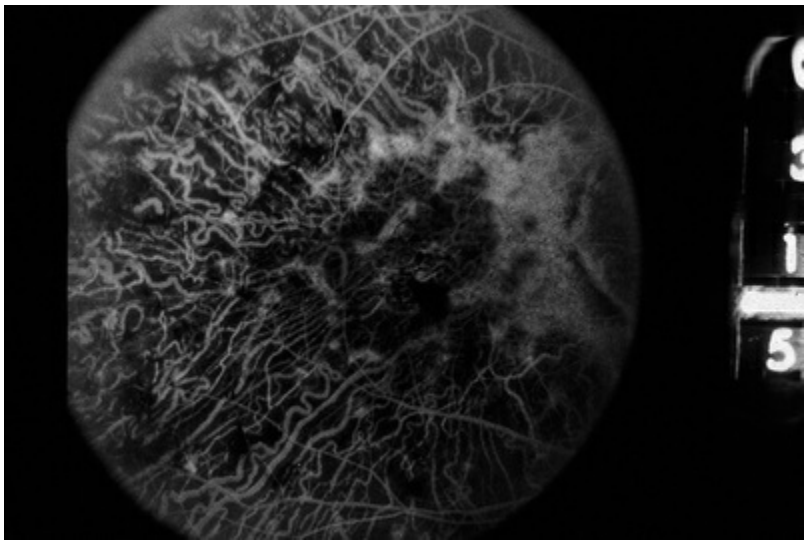

FIG. 45.9 Fluorescein angiogram from the right eye from the same patient depicted in Fig. 45.8 with X-linked retinitis pigmentosa shows extensive atrophy of the retinal pigment epithelium and choriocapillaris corresponding to the pigmentary changes seen ophthalmoscopically.

Kearns–Sayre Syndrome (KSS)

This disease represents a multisystem mitochondrial DNA deletion syndrome that is observed before 20 years of age and consists of a pigmentary retinopathy (Figs. 45.10 and 45.11), progressive external ophthalmoplegia, as well as ptosis. In addition, patients may have at least one of the following: cardiac conduction block, cerebellar ataxia, or cerebrospinal fluid protein concentration greater than 100 mg/dL. Muscle biopsy in such patients shows ragged red fibers by light microscopy and mitochondrial abnormalities by high-resolution microscopy. Three phenotypes were described by Bastiaensen et al.,[68] including infantile, juvenile, and adult-onset forms. In some patients with advanced disease, a generalized atrophy of the RPE and choriocapillaris can be encountered (Fig. 45.11). Subnormal cone and rod a- and b-wave amplitudes are most frequently observed in patients with Kearns–Sayre syndrome.

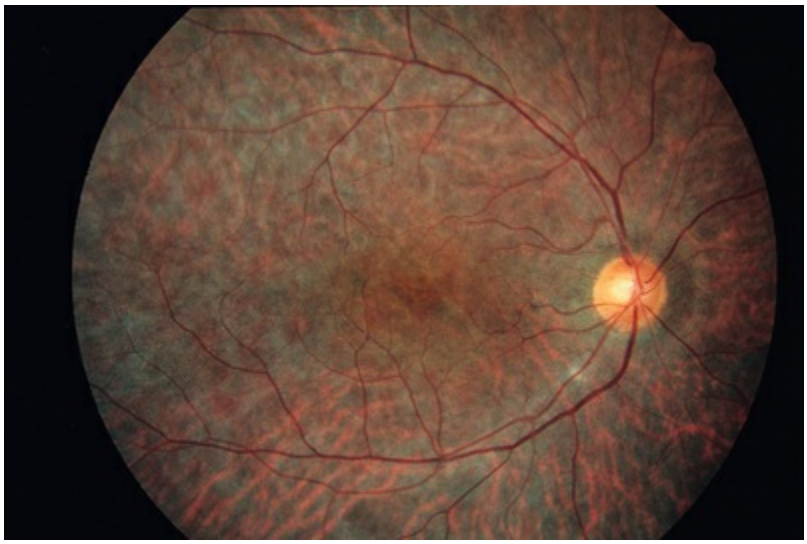

FIG. 45.10 Color fundus photograph from the right eye of a patient with Kearns–Sayre syndrome shows diffuse hypopigmentary changes in the posterior pole and midperipheral retina.

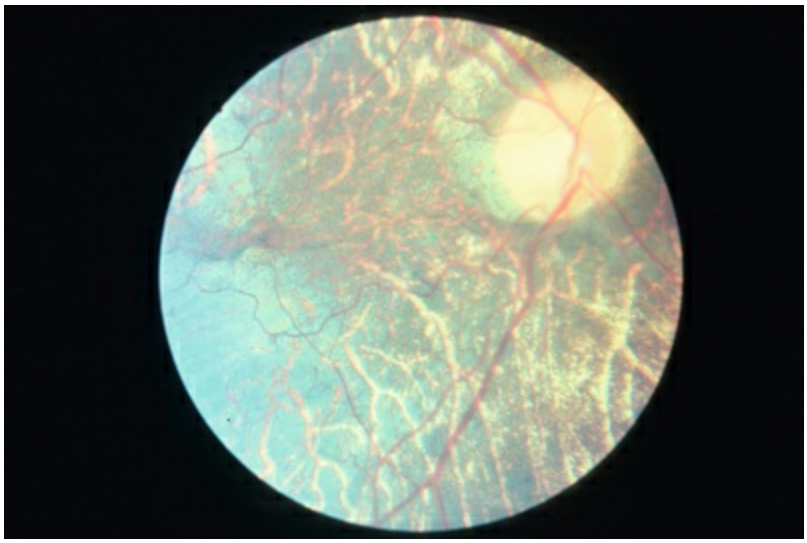

FIG. 45.11 Color fundus photograph from the right eye of a patient with Kearns–Sayre syndrome shows generalized atrophy of the retinal pigment epithelium and choroid that resembles diffuse choroidal dystrophy.

Bietti Crystalline Dystrophy

Patients affected with Bietti crystalline dystrophy most often present within the third decade of life with visual impairment and glistening crystalline-like changes in the posterior pole of the retina. Approximately one-third will also show crystals in the superficial stromal layer of the paralimbal region of the cornea. These cholesterol or cholesterol esters can also be found in fibroblasts as well as circulating lymphocytes, suggesting that this disorder may be a systemic abnormality of lipid metabolism. Both diffuse and more localized forms of retinal degenerative changes may be encountered. These changes involve both RPE and choriocapillaris atrophy and in this sense represent an overlap with the changes observed in choroidal dystrophies. ERG amplitude reduction often parallels the degree of fundus pigmentary changes. The disease is most often transmitted as an autosomal recessive trait. Gekka and colleagues[69] identified a mutation in the *CYP4V2* gene in two Japanese patients with Bietti crystalline dystrophy.

Thioridazine (Mellaril) Retinal Toxicity

Thioridazine was initially introduced in 1959 for the treatment of psychosis. Patients who receive relatively high doses of the drug can experience a decrease in their visual acuity as well as night blindness. Both central and ring scotomas have been observed. In earlier stages, a pigmentary granularity or mottling occurs in the macular or paramacular regions. Subsequently, extensive degenerative changes of the RPE, choriocapillaris, and photoreceptors are seen (Fig. 45.12**)**. A phenotype with geographic, scalloped regions of hypopigmentation and loss of choriocapillaris vessels may become evident. Both this intermediate and a more advanced and more diffuse disease stage can mimic fundus changes seen in CHM, gyrate atrophy, and diffuse choroidal dystrophy phenotypes. ERG recordings show various degrees of diminished photopic and scotopic a- and b-wave responses that parallel in severity the clinically evident fundus changes.

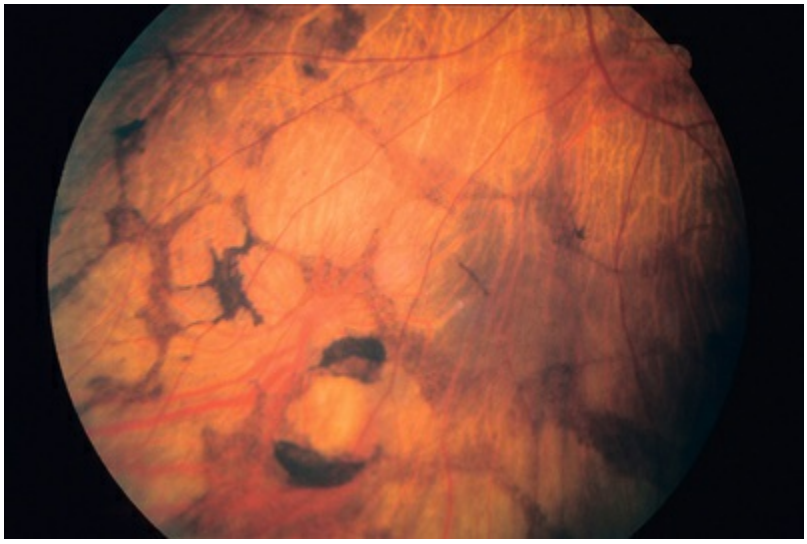

FIG. 45.12 Color fundus photograph from the left eye of a patient with thioridazine (Mellaril) retinal toxicity shows geographic, scalloped regions of hypopigmentation and loss of the retinal pigment epithelium and choroid that are similar to the fundus changes observed in patients with choroideremia and gyrate atrophy of the choroid and retina.

Stargardt Disease

This disease is typically characterized by impairment of central vision within the first 10–20 years of life that often progresses to the level of legal blindness. The peripheral vision is most often preserved. There is a characteristic "beaten bronze" appearance of the macula, with small pisciform yellow–white flecks scattered within the posterior pole and, to a lesser extent, in the midperipheral retina. In the majority of affected patients, fluorescein angiography shows a masking of the fluorescence from the choroidal circulation (dark choroid).[70–73] Although the inheritance is usually autosomal recessive,[74] rare families have been reported with autosomal dominant inheritance.[75–77] The autosomal dominant form has been attributed to mutations in the gene *ELOVL4* (chromosome 6q),[78] whereas the recessive form has been linked to mutations in *ABCA4* (chromosome 1p).[74,79]

The *ABCA4* gene encodes an ATP-binding cassette (ABC) transport protein located in the disc membranes of rod and cone outer segments. The ABCA4 protein is involved in the transport of all *trans*-retinal conjugates across the disc membranes. Mutations in the *ABCA4* gene result in abnormally high levels of lipofuscin pigments to accumulate in the RPE, triggering RPE cell death and causing secondary photoreceptor cell degeneration.

The advanced stages of Stargardt disease[80] may appear as extensive atrophy of the RPE and choroid in the posterior pole and anterior to the vascular arcades (Fig. 45.13). Although the ERG is most often normal to modestly subnormal in the early to middle course of typical autosomal recessive Stargardt disease, it is often more notably abnormal by the advanced stage of disease.

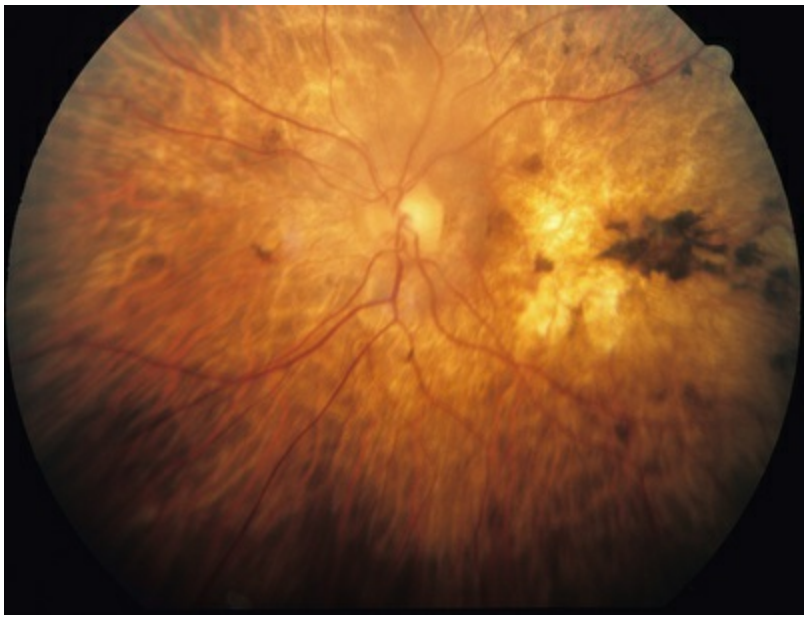

FIG. 45.13 Color fundus photograph from the left eye of a patient with an advanced stage of Stargardt disease shows the extensive atrophy of the retinal pigment epithelium (RPE) and choroid in the posterior pole and anterior to the vascular arcades phenotypically similar to the changes observed in diffuse choroidal dystrophy. Note the relative sparing of the RPE and the choroid in the peripapillary area, not infrequently a feature of Stargardt disease.

Pattern Macular Dystrophy

This disease is an autosomal dominant, fundoscopically variable disorder that involves the accumulation of lipofuscin within RPE cells with subsequent cell degeneration and secondary choriocapillaris loss.[81] The lesions often begin in midlife and can be associated with mild to moderate visual acuity loss.[82,83] Pattern dystrophy can, in late stages, occasionally produce diffusely atrophic changes of the RPE and choroid that resembles CHM or localized RPE and choroidal atrophy resembling CACD.[84]

Conclusion

With the possible exception of gyrate atrophy, there are currently no well-accepted or predictably effective treatments for hereditary

choroidal dystrophies. Nonetheless, periodic ophthalmic examination to monitor progression of these diseases is recommended as affected individuals need counsel regarding their level of visual function loss and prognosis. Ultraviolet and short-wavelength (blue)-blocking sunglasses may have a protective role when an affected individual is outdoors. Low-vision services are designed to benefit those whose ability to function is compromised by clinically significant visual impairment. A low-vision examination may be useful to help optimize the use of remaining visual function. Cataract surgery may be required for individuals with clinically significant lens opacity. Genetic counseling is warranted that can provide patients and families with information on the genetic implications of these disorders, which, in turn, can help them make informed personal decisions.

Treatment trials with gene therapy for individuals with choroideremia are already underway and could possibly become an accepted treatment option in the future. Introduction of recombinant adenovirus containing the full-length *REP-1* CHM coding region has been demonstrated to restore protein levels and *REP-1* activity in enzyme-deficient lymphocytes and fibroblasts in vitro.[85] A report by Genead et al.[86] showed that treatment of cystoid macular edema in CHM patients with a topical dorzolamide 2% ophthalmic formulation can reduce central macular thickness associated with cystoid macular edema on spectral domain optical coherence tomography testing with a potential improvement for visual acuity, while the study by Vasconcelos-Santos et al.[30] showed a short-term beneficial effect on cystoid macular edema in patients with gyrate atrophy and the use of intravitreal triamcinolone acetonide.

With treatment strategies for various inherited retinal diseases emerging, the future looks promising for potentially improving or delaying loss of visual function in patients with inherited choroidal diseases.

References

1. Sorsby A. Choroidal angiosclerosis with special reference to its hereditary character. *Br J Ophthalmol*. 1939;23:433–444.

2. Carr RE. Central areolar choroidal dystrophy. *Arch Ophthalmol*. 1965;73:32–35.
3. Sandvig K. Familial, central, areolar, choroidal atrophy of autosomal dominant inheritance. *Acta Ophthalmol (Copenh)*. 1955;33:71–78.
4. Waardenburg PJ. Familial angiosclerosis of the choroid. *J Genet Hum*. 1952;1:83–90.
5. Sorsby A, Crick RP. Central areolar choroidal sclerosis. *Br J Ophthalmol*. 1953;37:129–139.
6. Yanagihashi S, Nakazawa M, Kurotaki J, et al. Autosomal dominant central areolar choroidal dystrophy and a novel Arg195Leu mutation in the peripherin/RDS gene. *Arch Ophthalmol*. 2003;121:1458–1461.
7. Krill AE, Archer D. Classification of the choroidal atrophies. *Am J Ophthalmol*. 1971;72:562–585.
8. Carr RE, Mittl RN, Noble KG. Choroidal abiotrophies. *Trans Sect Ophthalmol Am Acad Ophthalmol Otolaryngol*. 1975;79:OP796–816.
9. Sorsby A, Davey JB. Generalized choroidal sclerosis; course and mode of inheritance. *Br J Ophthalmol*. 1955;39:257–276.
10. Franceschetti A, Francois J, Babel J. *Chorioretinal heredodegenerations*. Charles C Thomas: Springfield, Ill; 1974.
11. Curry HF Jr, Schonberg SS. Fluorescein photography in choroidal sclerosis. *Arch Ophthalmol*. 1969;81:177–183.
12. Douglas AA, Waheed I, Wyse CT. Progressive bifocal chorio-retinal atrophy: a rare familial disease of the eyes. *Br J Ophthalmol*. 1968;52:742–751.
13. Godley BF, Tiffin PAC, Evans K, et al. Clinical features of progressive bifocal chorioretinal atrophy: a retinal dystrophy linked to chromosome 6q. *Ophthalmology*. 1996;103:893–898.
14. Kelsell RE, Godley BF, Evans K, et al. Localization of the gene for progressive bifocal chorioretinal atrophy (PBCRA) to chromosome 6q. *Hum Mol Genet*. 1995;4:1653–1656.
15. Jacobsohn E. Ein fall von Retinitis pigmentosa atypica. *Klin Monatsbl Augenheilkd*. 1888;26:202–206.
16. Cutler C. Dri ungewohnliche Falle von retino-choroideak Degeneration. *Arch Augenheilkd*. 1895;30:117.

17. Fuchs E. Ueber awei der Retinitis pigmentosa verwandte Krankheiten (retinitis punctate albescens und atrophia gyrate chorioideae et retinae). *Arch Augenheilkd*. 1896;32:111.
18. Takki KK, Milton RC. The natural history of gyrate atrophy of the choroid and retina. *Ophthalmology*. 1981;88:292–301.
19. Simell O, Takki K. Raised plasma-ornithine and gyrate atrophy of the choroid and retina. *Lancet*. 1973;1:1031–1033.
20. Valle D, Walser M, Brusilow SW, et al. Gyrate atrophy of the choroid and retina: amino acid metabolism and correction of hyperornithinemia with an arginine-deficient diet. *J Clin Invest*. 1980;65:371–378.
21. Valle D, Walser M, Brusilow S, et al. Gyrate atrophy of the choroid and retina. Biochemical considerations and experience with an arginine-restricted diet. *Ophthalmology*. 1981;88:325–330.
22. Kaiser-Kupfer MI, de Monasterio FM, Valle D, et al. Gyrate atrophy of the choroid and retina: improved visual function following reduction of plasma ornithine by diet. *Science*. 1980;210:1128–1131.
23. Heinänen K, Näntö-Salonen K, Leino L, et al. Gyrate atrophy of the choroid and retina: lymphocyte ornithine-delta-aminotransferase activity in different mutations and carriers. *Pediatr Res*. 1998;44:381–385.
24. Inana G, Hotta Y, Zintz C, et al. Expression defect of ornithine aminotransferase gene in gyrate atrophy. *Invest Ophthalmol Vis Sci*. 1988;7:1001–1005.
25. Mitchell GA, Brody LC, Siplia I, et al. At least two mutant alleles of ornithine delta-aminotransferase cause gyrate atrophy of the choroid and retina in Finns. *Proc Natl Acad Sci USA*. 1989;86:197–201.
26. McClatchey AI, Kaufman DL, Berson EL, et al. Splicing defect at the ornithine amino-transferase (OAT) locus in gyrate atrophy. *Am J Hum Genet*. 1990;47:790–794.
27. Kellner U, Weleber RG, Kennaway NG, et al. Gyrate atrophy-like phenotype with normal plasma ornithine. *Retina*. 1997;17:403–413.
28. Feldman RB, Mayo SS, Robertson DM, et al. Epiretinal membranes and cystoid macular edema in gyrate atrophy

of the choroid and retina. *Retina*. 1989;9:139–142.
29. Oliveira TL, Andrade RE, Muccioli C, et al. Cystoid macular edema in gyrate atrophy of the choroid and retina: a fluorescein angiography and optical coherence tomography evaluation. *Am J Ophthalmol*. 2005;140:147–149.
30. Vasconcelos-Santos DV, Magalhães EP, Nehemy MB. Macular edema associated with gyrate atrophy managed with intravitreal triamcinolone: a case report. *Arq Bras Oftalmol*. 2007;70:858–861.
31. Kurstjens JH. Choroideremia and gyrate atrophy of the choroid and retina. *Doc Ophthalmol*. 1965;19:1.
32. Weleber RG, Kennaway NG. Clinical trial of vitamin B6 for gyrate atrophy of the choroid and retina. *Ophthalmology*. 1981;88:316–324.
33. Raitta C, Carlson S, Vannas-Sulonen K. Gyrate atrophy of the choroid and retina: ERG of the neural retina and the pigment epithelium. *Br J Ophthalmol*. 1990;74:363–367.
34. Sipilä I, Simell O, Rapola J, et al. Gyrate atrophy of the choroid and retina with hyperornithinemia: tubular aggregates and type 2 fiber atrophy in muscle. *Neurology*. 1979;29:996–1005.
35. Kaiser-Kupfer MI, Kuwabara T, Askanas V, et al. Systemic manifestations of gyrate atrophy of the choroid and retina. *Ophthalmology*. 1981;88:302–306.
36. McCulloch JC, Arshinoff SA, Marliss EB, et al. Hyperornithinemia and gyrate atrophy of the choroid and retina. *Ophthalmology*. 1978;85:918–928.
37. Takki K. Gyrate atrophy of the choroid and retina associated with hyperornithinaemia. *Br J Ophthalmol*. 1974;58:3–23.
38. Wilson DJ, Weleber RG, Green WR. Ocular clinicopathologic study of gyrate atrophy. *Am J Ophthalmol*. 1991;111:24–33.
39. Wang T, Milam AH, Steel G, et al. A mouse model of gyrate atrophy of the choroid and retina: early retinal pigment epithelium damage and progressive retinal degeneration. *J Clin Invest*. 1996;97:2753–2762.
40. Berson EL, Hanson AH 3rd, Rosner B, et al. A two year trial of low protein, low arginine diets or vitamin B6 for patients with gyrate atrophy. *Birth Defects Orig Artic Ser*.

1982;18:209–218.
41. Kaiser-Kupfer MI, Caruso RC, Valle D. Gyrate atrophy of the choroid and retina: long-term reduction of ornithine slows retinal degeneration. *Arch Ophthalmol*. 1991;109:1539–1548.
42. Vannas-Sulonen K, Simell O, Sipilä I. Gyrate atrophy of the choroid and retina: the ocular disease progresses in juvenile patients despite normal or near normal plasma ornithine concentration. *Ophthalmology*. 1987;94:1428–1433.
43. Katagiri S, Gekka T, Hayashi T, et al. OAT mutations and clinical features in two Japanese brothers with gyrate atrophy of choroid and retina. *Doc Ophthalmol*. 2014;128:137–148.
44. Mauthner L. Ein Fall von Chorioideremie. *Berl Natur-Med Ver Innsbruck*. 1872;2:191.
45. McCulloch C, McCulloch RJP. A hereditary and clinical study of choroideremia. *Trans Am Acad Ophthalmol Otolaryngol*. 1948;52:160.
46. MacDonald IM, Sereda C, McTaggart K, et al. Choroideremia gene testing. *Expert Rev Mol Diagn*. 2004;4:478–484.
47. Roberts MF, Fishman GA, Roberts DK, et al. Retrospective, longitudinal, and cross sectional study of visual acuity impairment in choroideraemia. *Br J Ophthalmol*. 2002;86:658–662.
48. Genead MA, Fishman GA. Cystic macular oedema on spectral-domain optical coherence tomography in choroideremia patients without cystic changes on fundus examination. *Eye (Lond)*. 2011;25:84–90.
49. Francis PJ, Fishman GA, Trzupek KM, et al. Stop mutations in exon 6 of the choroideremia gene, CHM, associated with preservation of the electroretinogram. *Arch Ophthalmol*. 2005;123:1146–1149.
50. Ponjavic V, Abrahamson M, Andréasson S, et al. Phenotype variations within a choroideremia family lacking the entire CHM gene. *Ophthalmic Genet*. 1995;16:143–150.
51. MacDonald IM, Russell L, Chan CC. Choroideremia: new findings from ocular pathology and review of recent

literature. *Surv Ophthalmol*. 2009;54:401–407.
52. Rafuse EV, McCulloch C. Choroideremia. A pathological report. *Can J Ophthalmol*. 1968;3:347–352.
53. McCulloch C. Choroideremia: a clinical and pathological review. *Trans Am Ophthalmol Soc*. 1969;67:142–195.
54. McCulloch JC. The pathologic findings in two cases of choroideremia. *Trans Am Acad Ophthalmol Otolaryngol*. 1950;54:565–572.
55. Lewis RA, Nussbaum RL, Ferrell R. Mapping X-linked ophthalmic diseases: provisional assignment of the locus for choroideremia to Xq13-q24. *Ophthalmology*. 1985;92:800–806.
56. Nussbaum RL, Lewis RA, Lesko JG, et al. Choroideremia is linked to the restriction fragment length polymorphism DXYS1 at XQ13–21. *Am J Hum Genet*. 1985;37:473–481.
57. Seabra MC, Brown MS, Slaughter CA, et al. Purification of component A of Rab geranylgeranyl transferase: possible identity with the choroideremia gene product. *Cell*. 1992;70:1049–1057.
58. van den Hurk JA, Schwartz M, van Bokhoven H, et al. Molecular basis of choroideremia (CHM): mutations involving the Rab escort protein-1 (REP-1) gene. *Hum Mutat*. 1997;9:110–117.
59. MacDonald IM, Mah DY, Ho YK, et al. A practical diagnostic test for choroideremia. *Ophthalmology*. 1998;105:1637–1640.
60. MacLaren RE, Groppe M, Barnard AR, et al. Retinal gene therapy in patients with choroideremia: initial findings from a phase 1/2 clinical trial. *Lancet*. 2014;383:1129–1137.
61. Lorda-Sanchez IJ, Ibañez AJ, Sanz RJ, et al. Choroideremia, sensorineural deafness, and primary ovarian failure in a woman with a balanced X-4 translocation. *Ophthalmic Genet*. 2000;21:185–189.
62. Thobani A, Anastasakis A, Fishman GA. Microperimetry and OCT findings in female carriers of choroideremia. *Ophthalmic Genet*. 2010;31:235–239.
63. Yau RJ, Sereda CA, McTaggart KE, et al. Choroideremia carriers maintain a normal electro-oculogram (EOG). *Doc Ophthalmol*. 2007;114:147–151.

64. Preising MN, Wegscheider E, Friedburg C, et al. Fundus autofluorescence in carriers of choroideremia and correlation with electrophysiologic and psychophysical data. *Ophthalmology*. 2009;116:1201–1209.
65. Fraser GR, Friedmann AI. Choroideremia in a female. *Br Med J*. 1968;2:732–734.
66. Harris GS, Miller JR. Choroideremia: visual defects in a heterozygote. *Arch Ophthalmol*. 1968;80:423–429.
67. Syed N, Smith JE, John SK, et al. Evaluation of retinal photoreceptors and pigment epithelium in a female carrier of choroideremia. *Ophthalmology*. 2001;108:711–720.
68. Bastiaensen LA, Notermans SL, Ramaekers CH, et al. Kearns syndrome or Kearns disease: further evidence of a genuine entity in a case with uncommon features. *Ophthalmologica*. 1982;184:40–50.
69. Gekka T, Hayashi T, Takeuchi T, et al. CYP4V2 mutations in two Japanese patients with Bietti's crystalline dystrophy. *Ophthalmic Res*. 2005;37:262–269.
70. Fishman GA, Farber M, Patel BS, et al. Visual acuity loss in patients with Stargardt's macular dystrophy. *Ophthalmology*. 1987;94:809–814.
71. Rotenstreich Y, Fishman GA, Anderson RJ. Visual acuity loss and clinical observations in a large series of patients with Stargardt disease. *Ophthalmology*. 2003;110:1151–1158.
72. Armstrong JD, Meyer D, Xu S, et al. Long-term follow-up of Stargardt's disease and fundus flavimaculatus. *Ophthalmology*. 1998;105:448–457.
73. Aaberg TM. Stargardt's disease and fundus flavimaculatus: evaluation of morphologic progression and intrafamilial co-existence. *Trans Am Ophthalmol Soc*. 1986;84:453–487.
74. Allikmets R, Singh N, Sun H, et al. A photoreceptor cell-specific ATP-binding transporter gene (ABCR) is mutated in recessive Stargardt macular dystrophy. *Nat Genet*. 1997;15:236–246.
75. Cibis GW, Morey M, Harris DJ. Dominantly inherited macular dystrophy with flecks (Stargardt). *Arch Ophthalmol*. 1980;98:1785–1789.
76. Zhang K, Bither PP, Park R, et al. A dominant Stargardt's

macular dystrophy locus maps to chromosome 13q34. *Arch Ophthalmol*. 1994;112:759–764.
77. Stone EM, Nichols BE, Kimura AE, et al. Clinical features of a Stargardt-like dominant progressive macular dystrophy with genetic linkage to chromosome 6q. *Arch Ophthalmol*. 1994;112:765–772.
78. Zhang K, Kniazeva M, Han M, et al. A 5-bp deletion in ELOVL4 is associated with two related forms of autosomal dominant macular dystrophy. *Nat Genet*. 2001;27:89–93.
79. Kaplan J, Gerber S, Larget-Piet D, et al. A gene for Stargardt's disease (fundus flavimaculatus) maps to the short arm of chromosome 1. *Nat Genet*. 1993;5:308–311.
80. Fishman GA. Fundus flavimaculatus: a clinical classification. *Arch Ophthalmol*. 1976;94:2061–2067.
81. Zhang K, Garibaldi DC, Li Y, et al. Butterfly-shaped pattern dystrophy: a genetic, clinical, and histopathological report. *Arch Ophthalmol*. 2002;120:485–490.
82. Marmor MF, Byers B. Pattern dystrophy of the pigment epithelium. *Am J Ophthalmol*. 1977;84:32–44.
83. de Jong PT, Delleman JW. Pigment epithelial pattern dystrophy: four different manifestations in a family. *Arch Ophthalmol*. 1982;100:1416–1421.
84. Watzke RC, Folk JC, Lang RM. Pattern dystrophy of the retinal pigment epithelium. *Ophthalmology*. 1982;89:1400–1406.
85. Anand V, Barral DC, Zeng Y, et al. Gene therapy for choroideremia: in vitro rescue mediated by recombinant adenovirus. *Vision Res*. 2003;43:919–926.
86. Genead MA, McAnany JJ, Fishman GA. Topical dorzolamide for treatment of cystoid macular edema in patients with choroideremia. *Retina*. 2012;32:826–833.

46

Abnormalities of Rod and Cone Function

Angela N. Baldwin, Anthony G. Robson, Anthony T. Moore, Jacque L. Duncan

Introduction

This chapter reviews a genetically heterogeneous group of inherited retinal disorders including stationary conditions such as achromatopsia, blue cone monochromacy and congenital stationary night blindness and progressive cone and cone-rod dystrophies. The clinical findings and diagnostic features including the results of psychophysics and International-standard electrophysiology[1a,1b] are reviewed. Increasingly molecular genetic testing is used to confirm the diagnosis and the chapter highlights how precise phenotyping and electrophysiology are intrinsic to the understanding of gene defects on retinal function. Such knowledge is essential to develop novel treatments, of utmost importance to patients. Congenital color vision deficits and retinitis pigmentosa and related disorders are reviewed in separate chapters.

Disorders of the Cone System

Inherited retinal disorders that primarily affect cone photoreceptors and their postreceptoral pathways can be divided into congenital defects that have early onset and are usually stationary or very slowly progressive over decades, and those with later onset that tend to be more rapidly progressive, leading to degeneration. The stationary disorders include complete and incomplete achromatopsia (forms of rod monochromacy), blue cone monochromacy, and Bornholm eye disease. Progressive dystrophies include those that involve only the cones (cone dystrophies) and those that have a component of rod degeneration (cone–rod dystrophies).

Achromatopsia (Rod Monochromacy)

Achromatopsia is a rare autosomal recessive disorder with an incidence of roughly 1 in 30,000.[1c] In the past, it has been considered stationary[2–6] but cross-sectional and longitudinal studies have demonstrated progressive macular changes[7–12] with no clear relationship between progression and genotype or age.[12–14]

Patients with achromatopsia present in infancy with marked light sensitivity and nystagmus. When old enough to have a formal visual acuity assessment, the vision is reduced to 20/100 or worse and there is very poor color discrimination and photosensitivity with pain in bright light.[12] There may also be paradoxical pupillary responses with constriction when transitioning from light to dark ambient conditions.[15] Hyperopic refractive errors are common. Some patients have an incomplete form of achromatopsia, with slightly better visual acuity in the range of 20/80–20/200 and some residual color vision. Patients with complete achromatopsia may be able to correctly identify primary color by utilizing brightness cues but have abnormal color vision when tested.

Diagnosis

The diagnosis may be suspected on the basis of reduced visual acuity, nystagmus and marked light sensitivity which has been present since birth. On clinical examination, the fundus may be normal or show subtle granularity or atrophy of the macula (Fig. 46.1A). Electrophysiologic testing is crucial to making the diagnosis

and typical findings are shown in Fig. 46.2A.

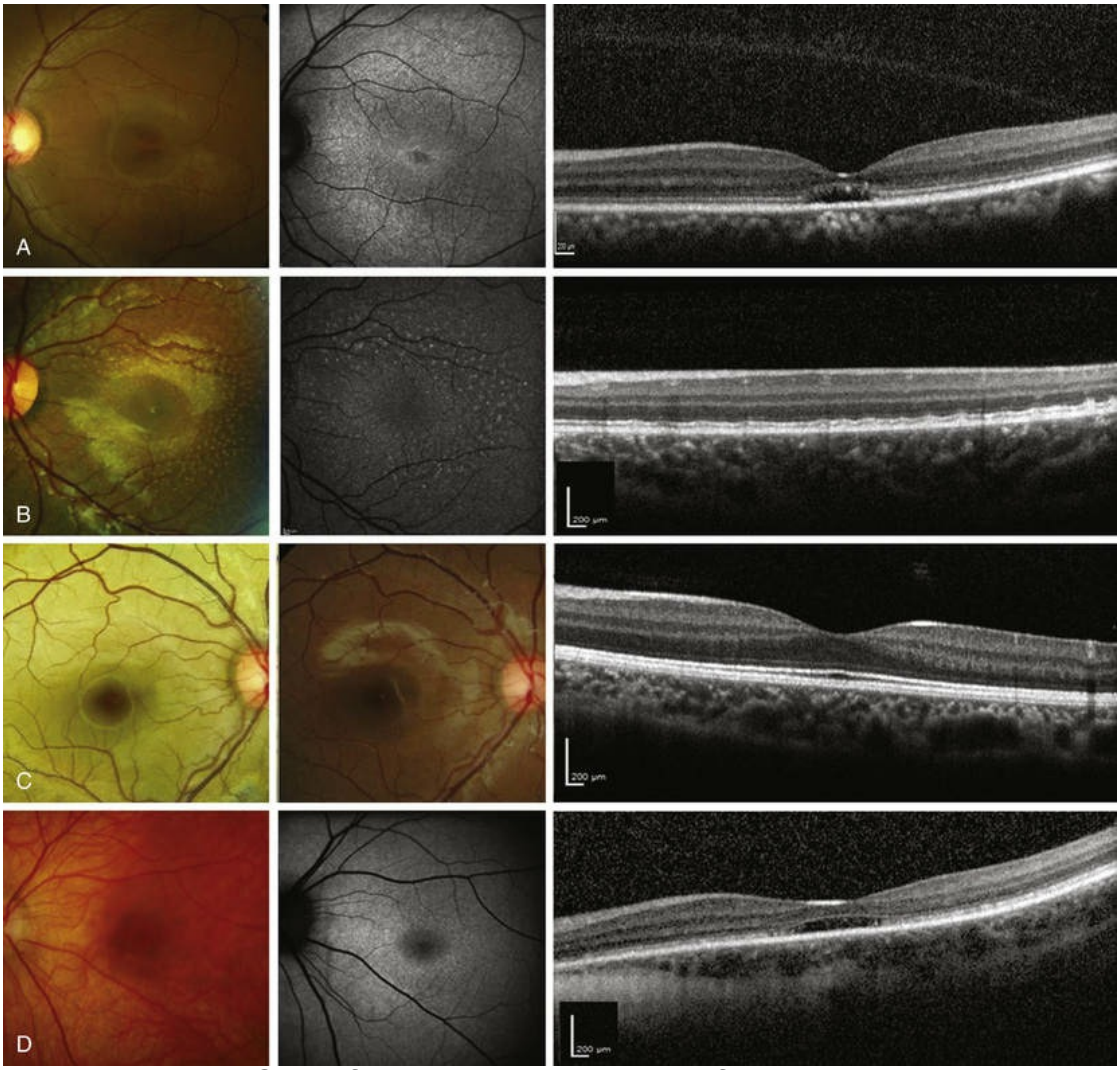

FIG. 46.1 Color fundus photographs (left column A–D and middle column row C), fundus autofluorescence images (middle column, rows A, B, and D) and spectral domain optical coherence tomography (OCT) (right column, A–D) in a patient with rod monochromacy (A), fundus albipunctatus (B), Oguchi disease (C), and cone–rod dystrophy (D). The fundus autofluorescence image in (B) has been enhanced (made brighter) post-acquisition to visualize the low background signal and foci of relatively increased signal surrounding the macula. Fundus photographs in row C are shown under conditions of light adaptation (column 1) and after overnight dark adaptation (middle column), illustrating the Mizuo–Nakamura phenomenon associated with Oguchi disease. Central macular OCT

scans are shown in (A), (C), and (D); in (B) an eccentric scan intersecting several white dot lesions is shown. The electroretinograms corresponding to the same patient are shown in Figs. 46.2 and 46.4.

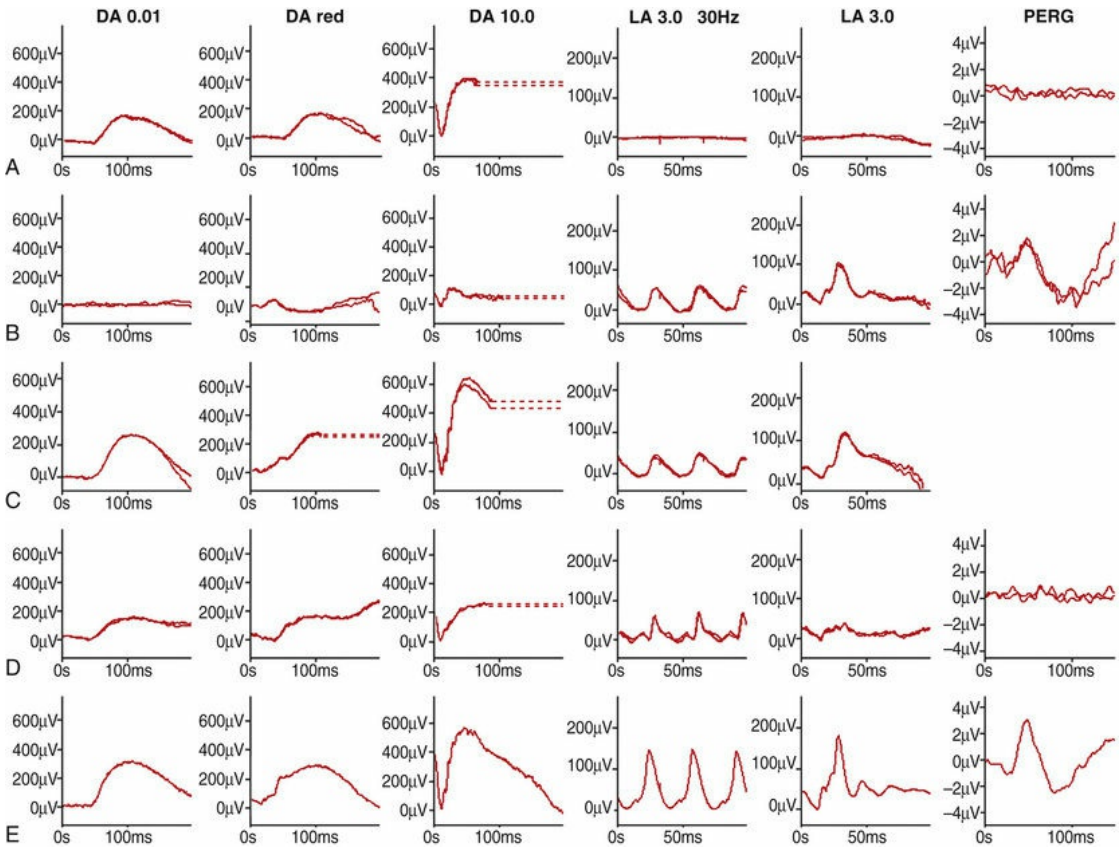

FIG. 46.2 Full-field electroretinograms (ERGs) and pattern ERG (PERG) in a patient with rod monochromacy (A), fundus albipunctatus (B,C), cone–rod dystrophy (D), and in a typical normal subject for comparison (E). Dark-adapted (DA) ERGs are shown for flash strengths of 0.01 and 10.0 cd.s.m^{-2}; light-adapted (LA) ERGs are shown for a flash strength of 3.0 cd.s.m^{-2} (30 Hz and 2 Hz). PERG is recorded to an alternating checkerboard. In the patient with rod monochromacy (A) the DA 0.01 ERG is normal, the DA red ERG lacks the early component, the DA 10.0 ERG shows minimal a-wave reduction and LA ERGs and PERG are undetectable; findings consistent with severe cone system dysfunction. In the case of fundus albipunctatus scotopic recordings (DA 0.01, DA red and DA 10.0 ERGs) are shown after 20 minutes dark

adaptation in the right eye and are severely abnormal (B) consistent with severe rod dysfunction; after overnight (prolonged) dark adaption in the left eye responses are normal (C), consistent with delayed rod dark adaptation. The LA ERGs indicate mild cone system involvement bilaterally but with PERG evidence of spared macular function (shown in right eye only). In the case of cone–rod dystrophy (D) the LA ERGs are more affected than the DA ERGs, with undetectable PERG indicating severe macular involvement. Broken lines in traces replace blink artifacts for clarity. Two traces are superimposed in each response to illustrate consistency.

Under conditions of dark adaptation (DA), the rod (DA 0.01) electroretinogram (ERG) to a dim flash is normal. Scotopic strong flash (DA 10.0) ERG a- and b-waves are often within normal limits but can be mildly subnormal, reflecting loss of the dark-adapted cone system contribution. Light-adapted (LA) cone-mediated ERGs are usually undetectable. It is noted that progressive cone dystrophies are typically characterized by detectable but subnormal and/or delayed photopic ERGs, and the severity of the photopic ERG reduction in rod monochromacy helps make the distinction, particularly in young patients with a relatively short history.

In older individuals other ancillary tests are also helpful in the diagnosis. Farnsworth D-15 color testing may reveal a scotopic axis between the deutan and tritan axes. The Sloan achromatopsia test uses correlation of different shades of gray to various colors in order to distinguish patients with achromatopsia from normal individuals.[16] Dark-adaptation studies show a lack of a cone–rod break, reflecting the lack of cone function. Patients commonly have hypermetropic refractive errors.[17] Visual field testing may reveal a small central scotoma but the peripheral visual fields are either mildly constricted or normal, and, most importantly, remain stable over time.

The severe photopic ERG abnormalities are present from birth and generally precede the less specific and sometimes mild changes seen on optical coherence tomography (OCT); although subtle foveal changes have been detected as early as 0.8 years of age.[18] A recent report calculated the frequency of these findings in a large

series of 77 eyes of achromatopsia patients aged between 4 and 70 years.[7] Disruption of the inner/outer-segment (IS–OS) junction, also known as the ellipsoid zone (EZ) was seen in 70% of eyes, including 42% of those aged 30 years or under. A hyporeflective, optically empty cavity may be seen in the cone layer of the foveola (see Fig. 46.1A), sometimes more visible to the nasal side of the foveal center, where there is a higher density of cone photoreceptors. Foveal hypoplasia is also present in the majority of patients. Disruption of the RPE and outer retinal atrophy can be seen in a minority of patients. Although achromatopsia has traditionally been considered a stationary disorder, it is evident from imaging studies that there is progressive maculopathy in some.[19]

Although the technique is not readily available in most clinics, adaptive optics scanning laser ophthalmoscopy (AOSLO) imaging of the macular photoreceptor mosaic in patients with complete achromatopsia has helped shed light on the pathophysiology.[20] Imaging has revealed residual cone structure in the majority of achromatopsia patients with "gaps" or dark spaces in the photoreceptor mosaic of the macula; a total absence of photoreceptors bearing the characteristics of normal healthy cones has also been observed.[13,21] The remaining photoreceptors appear to have morphologic characteristics typical of rods. However, split detection (non-confocal) AOSLO imaging techniques have been utilized to visualize inner segment structure in the dark spaces seen on confocal AOSLO.[22] These findings suggest that the cone structure is disrupted, resulting in altered wave-guiding characteristics, but that cones are not absent. Furthermore, the amount of residual cone structure varies between patients.[4] AOSLO will likely continue to be valuable as a tool in ensuring the success of emerging human gene therapy trials by identifying patients with retained photoreceptor structure who will benefit the most from intervention, and may demonstrate changes to cone structure in response to therapies.[21,22]

Molecular Basis of Achromatopsia

Achromatopsia is inherited as an autosomal recessive trait and to date six causative genes have been identified; these account for the majority of cases.[23] Most of the reported mutations affect proteins

involved in cone phototransduction, although a recently described gene (*ATF6*) is ubiquitously expressed and encodes a protein that functions as a regulator of the unfolded protein response.[24] It is unclear why the phenotype is confined to the retina. Mutations in two genes, *CNGA3* and *CNGB3*, account for the majority of cases of achromatopsia. These genes encode the alpha- and beta-subunits of cone cyclic-GMP gated (CNG) cation channels. *CNGB3* codes for the beta-subunit and is responsible for approximately 45% the majority of complete achromatopsia cases. *CNGB3* was originally identified in the Pingelapese people in the western Pacific nation of Micronesia where the prevalence of complete achromatopsia was approximately 3000 times greater than that of other general populations.[25,26] The second most-common mutation (25%) is in the *CNGA3* gene, which codes for the alpha-subunit.[27,28] *CNGB3* and *CNGA3* account for at least 70% of all complete achromatopsia cases.[29–32] The most common mutation identified in *CNGB3*, accounting for more than 70% of *CNGB3* disease-causing alleles, is the 1-basepair frameshift deletion c.1148delC (p.Thr383Ile fs*13).[4,19,33] Approximately 40 *CNGB3* variants have been reported, with the majority being nonsense mutations. In contrast, there are over 80 described *CNGA3* disease-causing variants, and most are missense mutations, implying that structural and functional damage to the *CNGA3* alpha-subunits are less well tolerated.[4] The third gene that is associated with complete achromatopsia is *GNAT2*, which codes for the alpha-subunit of cone transducin. Transducin is involved in the phototransduction cascade, and acts to close the cGMP channels. To date 10 *GNAT2* variants have been identified.[34–36] As yet, there have been no differences in phenotype detected between *CNGA3* and *CNGB3* genotypes;[13,37] however, the *GNAT2* genotype may be associated with residual cone function and greater preservation of the outer retinal architecture viewed with SD-OCT and AOSLO imaging.[21] Another phototransduction gene, *PDE6C*, encoding the alpha subunit of cone photoreceptor phosphodiesterase, has also been implicated in achromatopsia.[2,38] Mutations in *PDE6H*, which encodes the inhibitory gamma-subunit of the cone photoreceptor cyclic guanosine monophosphate phosphodiesterase, have also been reported.[39,40] *ATF6*, *GNAT2*, *PDE6C*, and *PDE6H* account for less than 2% of achromatopsia

cases.[35,38,39] The vast majority of incomplete achromatopsia has been linked to missense mutations in *CNGA3*,[2,28] but some patients with this phenotype have been reported to have mutations in *GNAT2* and *CNGB3*.[9,13,41,42]

Treatment and Management

There is currently no treatment for achromatopsia. A phase I/II clinical trial investigating the therapeutic effects and safety of an intraocular implant releasing ciliary neurotrophic factor (CNTF) in patients with *CNGB3*-associated achromatopsia showed reduced rod responses and no evidence of improvement in cone function, but subjects did report decreased light sensitivity and were more tolerant of bright light.[43] Photophobia can also be reduced with low light transmission, orange or red-tinted lenses since rod photoreceptors are less sensitive to orange and red wavelengths of light. Red-tinted soft contact lenses that transmit between 400 and 480 nm can reduce the stigma of wearing dark glasses indoors.[44] Low vision aids may enhance visual acuity and for children with achromatopsia it is important to provide educational support at school. Families with achromatopsia should also be referred for genetic counseling.

Gene replacement with adenoviral-mediated gene transfer has been used to correct the cone dysfunction in animal models of three genetic forms of achromatopsia.[45–47] An observational clinical trial of patients with achromatopsia caused by mutation in *CNGB3* is currently underway (www.clinicaltrials.gov identifiers NCT01846052), and gene replacement therapy trials for patients with achromatopsia caused by mutations in *CNGA3* and *CNGB3* are likely to begin in the future. Electrophysiology is likely to be essential to help identify potential candidates and to objectively monitor safety and efficacy.

Blue-Cone Monochromacy

Blue-cone or S-cone monochromacy (BCM) is a congenital disorder in which two of the three cone systems (long- [L], middle- [M], and short-wavelength [S]) are nonfunctional. BCM affects approximately 1 in 100,000 people, and is characterized by normal

S-cone ("blue-cone") function with absent L ("red")- and M ("green")-cone function. The signs and symptoms resemble congenital achromatopsia, but visual acuity is generally better, in the range of 20/80–20/200 when the affected individuals are old enough to be formally tested. The usual presentation is with reduced vision, light sensitivity and nystagmus in infancy. Family history is a useful clue to distinguish the two entities, since BCM shows X-linked recessive inheritance, compared to autosomal recessive inheritance in congenital achromatopsia. Another distinguishing feature is that the majority of males with BCM are myopic, in contrast to achromatopsia where hyperopia is more common.

Diagnosis

The clinical presentation of BCM and achromatopsia are similar. Fundus examination may be normal, or may reveal progressive pigment irregularities and macular atrophy with ophthalmoscopy and fundus autofluorescence imaging.[32,48,49] There are a number of investigations that help the clinician distinguish between the two disorders. Careful color vision testing can demonstrate preserved short-wavelength sensitivity in BCM. A useful evaluation in the clinic is to use either the Berson plates that have been specifically developed for this purpose[50–52] or the Hardy Rand Rittner (HRR) color plates, which test tritan, deutan, and protan function. Both can be used in young children. New smartphone, tablet, and computer applications (apps) have also been developed for color vision testing. ColorDx by Konan Medical has been validated by, and is routinely used at, the Naval Aerospace Medical Institute to evaluate Navy, Air Force, Coast Guard, Marine, and Army applicants and aviators. At the conclusion of the self-administered test, the app scores the type and severity of the color deficiency. A comprehensive report is generated that can either be printed for the patient's paper chart or sent to the patient's electronic medical record. A Quick Response code (QR code), a barcode that can be scanned and read by a mobile phone, is also included so the patient can obtain additional information about color deficiencies (www.konanmedical.com/colordx). A similar color vision test developed by EnChroma is available both online and as an app. It

also determines the type and extent of color deficiency (http://enchroma.com/test/instructions).

The LA 3.0 30 Hz flicker ERG is normally dominated by the activity of the L- and M-cone systems. In individuals with BCM the 30 Hz flicker ERG is undetectable, consistent with the lower temporal resolution of the S-cone system. Residual or low-amplitude single flash cone (LA 3.0) ERGs may be present,[53] reflecting the normal contribution from the S-cone system. An S-cone ERG, recorded to a blue flash on a yellow or long-wavelength background,[53,54] is preserved and may help distinguish the disorder from rod monochromacy. Scotopic bright-flash ERGs can be normal or mildly attenuated.[32,53,55] in keeping with a loss of the normal cone system contribution, but high myopia may contribute further to attenuation of ERGs. OCT imaging in BCM may show variable macular thinning,[14,56,57] with focal inner-segment disruption observed in an area corresponding to the normal S-cone free zone on SD-OCT.[14] The disorder has been reported to be either stable or progressive, and it is unclear whether this variability is due to the specific mutation, epigenetic influences, and/or environmental factors. However, increased thinning of the foveal outer nuclear layer in older patients with blue cone monochromatism has been reported[56] and there are other reports of progressive loss of S-cone function as patients age, with complete loss of discrimination along the tritan axis.[58–60]

Molecular Basis of Blue Cone Monochromatism

BCM is caused by mutations in the L-cone opsin gene (*OPN1LW)* or M-cone opsin gene (*OPN1MW*), which sit in a tandem array on the X chromosome, or by a deletion of the locus control region (LCR) which controls L- and M- gene expression. The S-opsin gene resides separately on chromosome 7.[58,61] Loss of L- and M-cone function in BCM involves either a one-step or two-step mechanism.[58,59,62] Approximately 40% of patients will have a deletion of the LCR.[48,49,62] Nearly 60% have a two-step mutation process; the first step involves a nonhomologous recombination event between the L- and M-opsin genes, which reduces the number of genes in the opsin array on the X chromosome to one, often a hybrid gene. A second mutation, commonly a missense variant, then occurs in the

remaining opsin gene, rendering it non-functional.[60] The C203R missense mutation in a single L–M hybrid gene is the most frequently reported genotype.[59] Additional rare mechanisms entail either the deletion of an entire exon in a single opsin array gene[59,63] or gene conversion transferring a mutation between *OPN1LW* and *OPN1NM*.[64] Not all cases are explained by mutations in the opsin array or LCR and it is likely that additional mechanisms will be identified.[59,62,65]

Treatment

Patients with BCM may benefit from low vision aids and blue cutoff filters, which reduce light sensitivity and improve contrast.[66] Children with BCM, like those with achromatopsia, will benefit from educational support at school and affected individuals and their families should be offered genetic counseling.

There is currently no treatment for the underlying retinal disease but novel therapies are on the horizon. AOSLO imaging techniques reveal that although there is disruption of the foveal cone mosaic, there may be survival of foveal cones long enough for gene replacement therapy to be effective in restoring foveal cone function. Cone cell losses appear greater in BCM associated with deletion of the LCR.[14,56]

Other technology advances benefitting patients with BCM include a number of smart phone apps designed to help color vision-deficient individuals. Color Naming apps name or speak a color from an image or a live picture, Color Vision Deficiency Compensation apps adjust certain colors on the screen so they are more easily recognized by color-deficient individuals, Matching Color apps locate colors in a picture that match the color chosen by the user and Color Harmonies apps find harmonizing colors, which may prove useful when a color-deficient individual is creating an outfit, or clothing ensemble from his or her wardrobe (http://www.color-blindness.com/2010/12/13/20-iphone-apps-for-the-color-blind).

Bornholm Eye Disease (X-Linked Cone Dysfunction Syndrome With Dichromacy)

This rare X-linked disorder is characterized by myopia, dichromacy, and abnormal or absent cone function on ERG. Fundus examination and retinal imaging is normal and the condition is nonprogressive. In contrast to BCM, there is no nystagmus and visual acuity is better. The two disorders can also be distinguished by careful color vison testing. The original family was reported from the Danish island of Bornholm,[67] but other families have since been reported from Europe[68] and North America.[69] In most families there is a rare variant in the L opsin gene, suggesting that both the dichromacy and cone dysfunction is caused by a dysfunctional cone opsin.[70]

Oligocone Trichromacy

This rare disorder is characterized by reduced visual acuity, mild photophobia, and abnormal cone responses but normal rod responses on ERG, and normal or near normal color vision.[71,72] Nystagmus is a variable feature. The visual loss is of infantile onset and visual fields and fundus examination are normal. AOSLO imaging has demonstrated reduced numbers of healthy cones, suggesting that the disease mechanism is consistent with reduced numbers of foveal cones that function normally.[73] Although the condition is thought to be nonprogressive, long term follow-up has demonstrated mild worsening of central visual function in two subjects with stable visual fields and stable full-field ERGs.[74] Some cases with nystagmus and oligocone trichromacy have been found to have mutations in genes normally associated with achromatopsia.[42,75,76]

Congenital Stationary Night Blindness

Congenital stationary night blindness (CSNB) describes a heterogeneous group of inherited disorders characterized by defective scotopic vision from birth, which is nonprogressive. There is usually symptomatic night blindness, although this may be overlooked especially for individuals living in an urban environment. Some forms of CSNB are associated with visual acuity reduction and nystagmus, and depending on the subtype

there may be color vision impairment and photophobia. The fundus is normal except in two specific forms of CSNB associated with retinal changes that can be helpful in diagnosis. CSNB needs to be distinguished from progressive rod–cone and cone–rod dystrophies and acquired causes of night blindness such as vitamin A deficiency. The full-field ERG is critical for precise diagnosis and phenotyping and to enable focused genetic screening.

CSNB With a Normal Fundus

CSNB with a normal fundus may be subdivided into Schubert–Bornschein[77] CSNB and Riggs-type CSNB[78] according to the full-field ERG findings.

Schubert–Bornschein CSNB

Schubert–Bornschein CSNB is inherited as either an X-linked or an autosomal recessive trait. Patients have a preserved scotopic bright flash ERG a-wave, consistent with normal rod phototransduction, but a reduced b-wave, resulting in an electronegative ERG waveform that indicates dysfunction that is post-phototransduction. This type of CSNB was further subdivided into two phenotypes known as "complete" and "incomplete" CSNB, based on ERG and psychophysical criteria[79] and later shown to be genetically distinct.

Most patients with complete CSNB describe night blindness from infancy and there is often visual acuity reduction (median 20/40), moderate to high myopia, nystagmus that tends to lessen with time, and a small minority have color vision problems.[80,81] Strabismus is common with a risk of amblyopia. The fundus is normal other than myopic changes.[82]

Complete CSNB is characterized by an undetectable dim flash rod (DA 0.01) ERG and a scotopic strong flash (DA 10.0) ERG that is electronegative with normal or largely preserved a-wave (Fig. 46.3A). The LA 3.0 30 Hz flicker ERG may be of normal amplitude but there can be mild delay and/or subtle flattening of the trough between adjacent flicker ERG peaks. The single flash cone (LA 3.0) ERG is of normal or mildly subnormal amplitude but there is usually a broadened bifid a-wave and a sharply rising b-wave

without oscillatory potentials. The ERG findings are consistent with selective ON-bipolar dysfunction, also evident in long-duration ON–OFF ERGs that show attenuation of ON b-waves and preservation of OFF d-waves (Fig. 46.3A). S-cone ERGs are subnormal in keeping with S-cone ON-bipolar dysfunction.

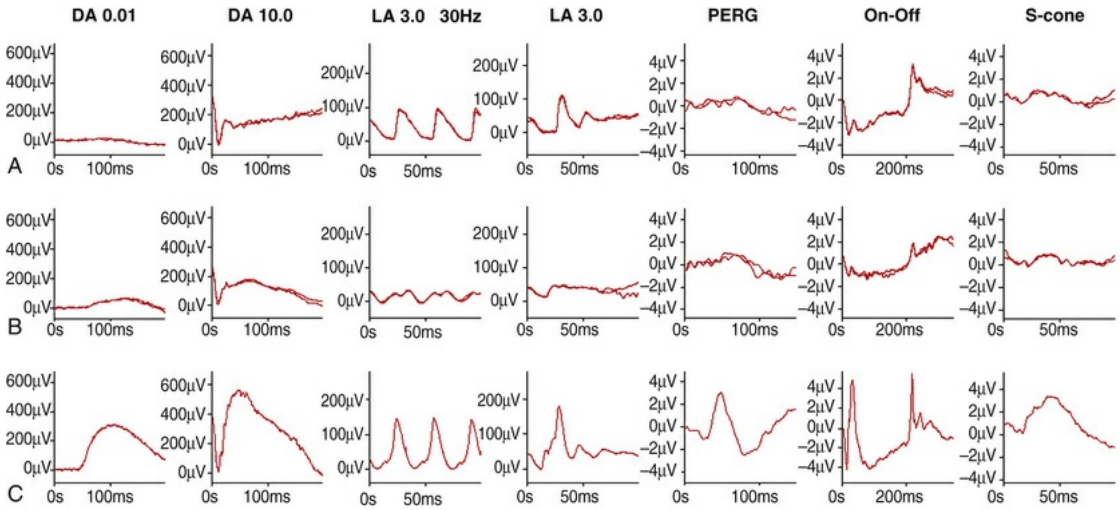

FIG. 46.3 Full-field electroretinograms (ERGs) and pattern ERG (PERG) in complete (A) and incomplete (B) congenital stationary night blindness (CSNB) and in a typical normal subject for comparison (C). Dark-adapted (DA) and light-adapted (LA) ERGs are shown for International-standard flashes (as in Fig. 46.2). Long-duration On–Off ERGs and S cone ERGs are additionally shown (see ref. 82 for stimulus parameters). In the patient with complete CSNB (A) there are ERG abnormalities consistent with generalized retinal dysfunction selectively affecting rod and cone ON-bipolar function. In the case of incomplete CSNB (B) the ERGs indicate generalized rod ON-bipolar and cone ON- and OFF-bipolar cell dysfunction. In these two patients pattern ERG indicate macular dysfunction. Two traces are superimposed in each response to illustrate consistency.

In incomplete CSNB, night blindness has been reported as a presenting symptom in as few as 54% of cases, and photophobia and day vision impairment are common; visual acuity (median about 20/60) tends to be worse than in complete CSNB[80] and patients may be myopic or hyperopic. Some have nystagmus

and/or strabismus.

Incomplete CSNB is associated with a subnormal but detectable scotopic dim flash rod ERG. The strong flash (DA 10.0) ERG is electronegative with normal or largely preserved a-wave, but photopic ERGs are more abnormal than in complete CSNB (Fig. 46.3B). The LA 30 Hz flicker ERG is markedly subnormal and commonly manifests a bifid or twin-peaked waveform shape. The single flash cone ERG is subnormal with a b-wave of similar amplitude to the a-wave (b : a ratio close to 1). Long duration ON–OFF ERGs show both ON b-wave and OFF d-wave reduction (Fig. 46.3B), in keeping with involvement of the cone ON and OFF bipolar systems. The dark-adaptation curve features a rod–cone break, indicating some residual rod system function, but the final threshold is significantly elevated.[83]

Molecular Basis of Schubert–Bornschein CSNB.

X-linked complete CSNB is caused by mutation in *NYX*. Autosomal recessive complete CSNB results from mutation in one of four genes: *GRM6*, *TRPM1*, *GPR179* or *LRIT3*, all implicated genes being expressed in the dendrites of the ON-bipolar cells. X-linked disease accounts for approximately half of genetically confirmed cases.[80,81]

In most cases of incomplete CSNB there is X-linked inheritance and mutation in *CACNA1F*. A few patients have been described with autosomal recessive inheritance and mutations in *CABP4*. Both genes are expressed in the presynaptic photoreceptor membrane and influence glutamate release, in keeping with the ERG evidence of both ON- and OFF-bipolar dysfunction.

Riggs-Type CSNB

Riggs-type CSNB is an autosomal dominant form of the disorder characterized by night blindness with otherwise normal visual function. The initial description of autosomal dominant CSNB was of the Nougaret family by Belgian ophthalmologist Cunier,[84] and was later expanded by Nettleship.[85] The family ultimately encompassed nine generations and 2121 patients, and established that this was indeed a nonprogressive “stationary” form of night blindness. Nougaret's report represents one of the largest pedigrees in ophthalmology and one of the first descriptions of a dominantly

inherited disorder.[86] A similar phenotype was reported in a large Danish family initially described by Rambusch in 1909 and more recently reviewed.[87] In spite of large individual pedigrees, Riggs-type CSNB is rare and accounts for a small minority of documented CSNB cases.[81]

The ERG is consistent with a selective loss of rod photoreceptor function. The DA 0.01 dim flash ERG is undetectable and indicates severe rod system dysfunction. Scotopic red flash ERGs show a preserved cone component (x-wave) but an absent rod system component. Strong flash (DA 10.0) ERG a-waves are markedly subnormal, in keeping with rod photoreceptor dysfunction, and b-waves are subnormal and may be of short peak time with similarities to the preserved cone component in the scotopic red flash ERG. The strong flash ERG may also have a low b : a ratio, but a-wave reduction is an important feature that helps distinguish the disorder from Schubert–Bornschein phenotypes. A similar abnormal strong flash ERG is seen in cases of vitamin A deficiency[88] and after limited (20 minutes) dark adaptation in typical cases of fundus albipunctatus and Oguchi disease.[81,89,90] The detectable but abnormal strong flash ERG likely represents the dark-adapted cone system contribution to the scotopic bright flash ERG, exposed in the absence of a functional rod system. The low b : a ratio in this context (with a-wave reduction) is explained by the saturation of the cone-mediated ERG b-wave to strong flashes; under light-adapted conditions in normal subjects, this well-recognized intensity-response characteristic of cone-mediated ERGs is known as the photopic hill phenomenon.[91,92]

Psychophysical testing shows an absent rod–cone break and elevated final threshold of dark adaptation after a bleach. The lack of rod function measured psychophysically is consistent with a defect at the level of the rod photoreceptors.

The genes implicated in the Riggs-type CSNB were shown to be *GNAT1* (Nougaret family), *PDE6B* ("Rambusch" family) and *RHO*, although in the latter case there are reports of disease progression in some.[93] All genes implicated in autosomal dominant Riggs-type CSNB are involved in rod photoreceptor phototransduction, in keeping with the ERG phenotype. Additionally, an autosomal recessive Riggs-type of CSNB has been reported with a

homozygous frameshift mutation in *SLC24A1*.[94]

CSNB With Abnormal Fundi

There are two forms of CSNB associated with abnormal fundi: fundus albipunctatus and Oguchi disease. Both exhibit autosomal recessive inheritance.

Fundus Albipunctatus

Fundus albipunctatus describes a subgroup of CSNB in which white or yellow dots are typically scattered through the fundus with macular sparing (see Fig. 46.1B). Individuals may complain of night blindness early in childhood without progression or delayed dark adaptation but some remain asymptomatic and the characteristic flecks are detected incidentally on routine fundoscopy. Visual acuity and color vision are usually normal. There are reports of the white dots evolving or disappearing over time[95,96] and maculopathy has been reported in some older individuals,[97] including cases without white dots.[89,96] Fundus albipunctatus needs to be distinguished from other forms of night blindness such as vitamin A deficiency and progressive rod–cone dystrophy including retinitis punctata albescens, and other causes of fleck retina syndrome. The clinical diagnosis is based on history, the retinal appearance, and the results of full-field ERG.

The ISCEV-standard scotopic full-field ERGs, recorded after 20 minutes dark adaptation, are consistent with severe rod photoreceptor dysfunction (see Fig. 46.2B) and have similarities to those associated with vitamin A deficiency and Riggs-type CSNB (see above), but there is variability with subnormal dim flash (DA 0.01) ERGs being detectable in some.[89] Typically the scotopic red flash ERG shows a preserved cone but abnormal rod component, and the bright flash ERG shows a-wave reduction with or without a low b : a ratio. LA ERGs may be normal but in about half of cases there are cone ERG abnormalities,[89,98,99] which tend to be worst in older patients.[97,98] After prolonged dark adaptation the rod-mediated ERGs usually normalize (see Fig. 46.2C),[100,101] but in a minority of cases recovery is incomplete.[89] The ERG abnormalities are consistent with delayed rod dark adaptation, also evident on

psychophysical testing,[102] caused by abnormal retinoid recycling. It is noted that a similar clinical and ERG phenotype may occur in young patients with a form of retinitis punctata albescens known as Bothnia dystrophy. However, in these patients a longer period of dark adaptation (e.g., 24 hours) may be needed to restore the rod-mediated ERGs, and with time there is retinal degeneration and atrophy with ERG evidence of rod–cone dystrophy.

Optical coherence tomography and autofluorescence imaging have recently been used to investigate the flecks in fundus albipunctatus with and without cone dystrophy.[89,103,104] In both reports, OCT demonstrated homogeneous dome-shaped hyperreflective deposits originating from the inner RPE that correlated with the white fundus spots and were noted to project into the outer retina, disrupting the EZ, the external limiting membrane, and the outer nuclear layer (see Fig. 46.1B). Fundus autofluorescence imaging reveals low background fluorescence (Fig. 46.1B), in keeping with life-long disruption of retinoid recycling, with foci of weakly increased signal being associated with only some of the white dots.[89] It is hypothesized that the lesions represent accumulation of retinoids secondary to disrupted production of 11-*cis* retinal.[105]

AOSLO has been used to characterize the cone abnormalities in fundus albipunctatus associated with a mutation in the *RDH5* gene. AOSLO revealed that macular cone density is reduced and the regularity of the macular cone mosaic spatial arrangement is disrupted compared to normal. There are hyperreflective mosaics surrounded by hyporeflective rings in areas corresponding to white fundus spots.[106]

Molecular Basis of Fundus Albipunctatus.

Fundus albipunctatus is associated with mutations in the *RDH5* gene which encodes 11-*cis* retinol dehydrogenase, an enzyme involved in the conversion of 11-*cis*-retinol to 11-*cis* retinal.[107,108] *RDH5* is expressed in the RPE and is involved in production of 11-*cis* retinal that is then transported to photoreceptors for incorporation into rhodopsin. Impaired *RDH5* function would delay retinoid recycling and explains the slowed rod dark adaptation seen in fundus albipunctatus.[103,109] There may be other

pathways involved in the regeneration of 11-*cis* retinal and for cones this may occur in the outer segments,[110] possibly explaining the relative preservation of cone system function.

Oguchi Disease

Oguchi disease is a rare form of night blindness with normal visual acuity, normal color vision, and normal visual fields. The fundus displays a golden sheen that becomes normal after prolonged dark adaptation, a transformation known as the Mizuo–Nakamura phenomenon (Fig. 46.1C).[90,111,112] Subsequent light exposure restores the golden sheen.

The mechanism underlying the Mizuo–Nakamura phenomenon and fundus sheen seen in Oguchi disease remains a subject of speculation. Histopathologic study suggests the presence of an abnormal layer between photoreceptor outer segments and the retinal pigment epithelium (RPE).[113] Recent OCT studies showed that the outer segments appeared shortened in areas with the golden sheen reflex seen in light and suggested that the sheen is related to accumulation of photoactivated rhodopsin in shortened rod outer segments (Fig. 46.1C).[114] Other authors have shown that the EZ was better visualized on OCT following prolonged dark adaptation (and disappearance of the golden sheen), suggesting that reversible changes in the rod photoreceptors related to this mutation may explain the golden sheen reflex. One study utilized AOSLO to assess the integrity of cone and rod mosaics and also concluded that rods, but not cones, change intensity after dark adaptation, indicating that fundus changes in Oguchi disease are the result of changes within the rod photoreceptors.[115]

The ISCEV-standard scotopic ERGs in Oguchi disease, recorded after 20 minutes of dark adaptation, are similar to those seen in Riggs-type CSNB and vitamin A deficiency and are characterized by undetectable rod function (Fig. 46.4A). DA 0.01 ERGs are absent, scotopic red flash ERGs have only the cone component and strong flash ERGs show marked a-wave reduction and may have a low b : a ratio with shortening of b-wave peak time, in keeping with a dark-adapted cone-system origin (see above). LA ERGs are normal. A striking difference from Riggs-type CSNB is that following prolonged dark adaption there is recovery of the rod-mediated ERG

components to dim white and red flashes but to only the first bright flash; subsequent flashes elicit markedly attenuated waveforms (Fig. 46.4B) as obtained after 20 minutes in the dark. Rod-mediated ERG recovery requires further prolonged DA.[116] The dark-adaptation curve shows a normal cone component but the rod–cone break is severely delayed, as the rods exhibit recovery of sensitivity after prolonged dark adaptation of 1–2 hours.

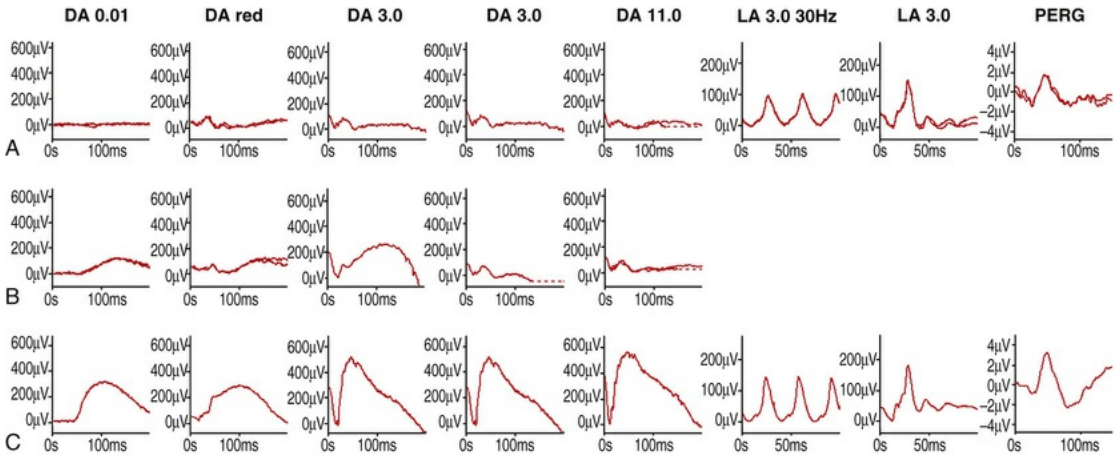

FIG. 46.4 Full-field electroretinograms (ERGs) from the left eye of a child with Oguchi disease (A,B) and from a typical normal subject for comparison (C). Scotopic recordings (DA 0.01, DA red, DA 3.0 and DA 11.0 ERGs) are shown after 25 minutes dark adaptation (DA) (A) and are severely abnormal, consistent with severe rod photoreceptor dysfunction; after overnight (prolonged) dark adaption in the same eye (B) dim flash ERGs (DA 0.01, DA red flash) and the first brighter flash ERG (DA 3.0) show partial recovery of rod-mediated components consistent with delayed rod dark adaptation, but a second bright flash (DA 3.0; interstimulus interval 60 seconds) causes marked DA 3.0 ERG reduction due to desensitization of the rod photoreceptors by the first bright flash. Cone-mediated light-adapted (LA) ERGs and pattern ERG (PERG) are normal. See text for details. Broken lines in traces replace blink artifacts for clarity. Two traces are superimposed to illustrate consistency (except in single flash DA 3.0 ERGs).

Oguchi disease is associated with mutations in two genes, the

rhodopsin kinase gene, *GRK1*, and the arrestin gene, *SAG*.[117,118] Following phototransduction rhodopsin kinase phosphorylates photoactivated rhodopsin and forms a complex with arrestin that prevents interaction with transducin. Mutations in either gene prolong rhodopsin activation leading to continued phototransduction and rod desensitization. Normal sensitivity is restored only when all rhodopsin molecules have been recycled, which takes 4–7 hours. This explains the profoundly delayed kinetics of the dark-adaptation curve[119] and is consistent with the characteristics of the rod-mediated ERGs.

Treatment for CSNB

There is currently no specific treatment available for CSNB. However, new therapeutic approaches are being investigated. A nonrandomized study in which an alternative source of chromophore, 9-*cis* retinal, was given to patients with fundus albipunctatus showed significant improvement in Humphrey visual field mean deviation, rod dark-adaptation recovery rates, and rod ERG responses.[120] It is believed that the 9-*cis* retinal is transported from the liver to the retina, where it combines with opsin to generate isorhodopsin, a visual pigment with a light absorption peak very close to rhodopsin. The 9-*cis* retinal may also reduce the activity of the retinoid cycle and decrease mislocalization of opsin, all of which may potentially stabilize photoreceptors.[121] However, these are preliminary studies and more research is needed before this approach reaches clinical practice.

Progressive Cone Dystrophies

Inherited retinal degenerations that affect cones usually present within the first three decades of life, although there are reports of patients first developing cone dysfunction after the fifth decade.[122–124] Decreased visual acuity and central scotomas, color vision loss, and photophobia are the usual presenting symptoms. The visual defects become worse over time. Rarely the dysfunction is confined to the cone system but in most cases rod dysfunction develops over time. Cone–rod dystrophies are primarily nonsyndromic, but may also form part of a syndromic disorder

such as Bardet–Biedl syndrome, Alstrom syndrome, and spinocerebellar ataxia; as such, the importance of taking a comprehensive medical history is stressed. Cone–rod dystrophy may show autosomal dominant, autosomal recessive or X-linked inheritance and a careful family history will assist with the differential diagnosis, as well as with genetic counseling.

Diagnosis

Patients with cone or early cone-rod dystrophy may present with relatively normal fundi, bilateral decreased acuity, impaired color vision and photosensitivity. Macular changes, when present (see Fig. 46.1D), usually show a high degree of interocular symmetry. In advanced disease peripheral pigmentary deposits, vascular attenuation and optic disc pallor may develop, particularly in those with significant rod involvement. A history of deterioration in visual function and documented progression on repeat examination distinguishes cone degenerations from nonprogressive cone dysfunction syndromes, such as achromatopsia and BCM.

Patients with cone dystrophy show significantly decreased photopic (LA) ERG amplitudes and/or delays in timing. In cone–rod dystrophy the scotopic (DA) ERG responses are also abnormal but are less affected than the LA ERGs (see Fig. 46.2D). If patients are able to adequately fixate there is usually evidence of severe macular dysfunction on PERG (Fig. 46.2D), multifocal ERG or psychophysical testing.[125,126] Visual field examinations are useful for both the diagnostic workup and follow-up evaluations. Early in the course of the disease the fields can show central scotomas with sparing of the periphery. Later, particularly in those patients with cone–rod dystrophies there is progressive peripheral loss over time.

OCT may show thinning of the outer retinal layers, limited mostly to the central retina.[127] Fundus autofluorescence imaging can show central or parafoveal areas of increased or decreased autofluorescence[125,126] (see Fig. 46.1D). The OCT and autofluorescence changes are nonspecific and similar changes may be seen in other retinal degenerations. Electrophysiologic evaluation together with imaging studies and increasingly molecular genetic investigation can help make a definitive diagnosis.[128]

Although not readily available in most clinics, adaptive optics imaging has been used to investigate eyes with cone dystrophy. With this technique the photoreceptor mosaic shows increased cone spacing in cone dystrophy compared to normal subjects or those with retinitis pigmentosa.[129]

Molecular Basis of Cone–Rod Dystrophies

The progressive cone–rod dystrophies are genetically heterogeneous and may be associated with autosomal dominant, autosomal recessive, and X-linked inheritance patterns. At the time of publication, RETNET (http://www.sph.uth.tmc.edu/Retnet/) listed 10 genes with mutations that have been associated with autosomal dominant cone or cone–rod dystrophy, 21 genes associated with autosomal recessive cone or cone–rod dystrophy, and 2 genes associated with X-linked cone–rod dystrophy, which can be viewed in Table 46.1.[130]

TABLE 46.1

Genetic Mutations Associated with Type of Cone and Cone-Rod Dystrophy

Disease Category and Inheritance	Mapped and Identified Genes
Autosomal dominant cone and cone–rod dystrophy	*AIPL1, CRX, GUCA1A, GUCY2D, PITPNM3, PROM1, PRPH2, RIMS1, SEMA4A, UNC119*
Autosomal recessive cone and cone–rod dystrophy	*ABCA4, ADAM9, ATF6, C21orf2, C8orf37, CACNA2D4, CDHR1, CERKL, CNGA3, CNGB3, CNNM4, GNAT2, KCNV2, PDE6C, PDE6H, POC1B, RAB28, RAX2, RDH5, RPGRIP1, TTLL5*
X-linked cone–rod dystrophy	*CACNA1F, RPGR*

Treatment

There are currently no therapies available to reverse the retinal degeneration process in cone dystrophies. Low vision aids, lenses that reduce photosensitivity, and occupational and psychosocial support remain the primary treatment modalities.

Genetic Testing

Genetic diagnosis has become increasingly important for providing optimal care of patients with genetic eye diseases. It is necessary for accurate genetic counseling and provides important information about disease pathogenesis. It will also identify patients that could be recruited to participate in clinical trials of novel therapies.[131] Over 200 identified genes have been linked to inherited retinal disease.[132,133] Clinical molecular genetic testing for a majority of the genes responsible for the diseases covered in this chapter is available at http://www.ncbi.nlm.nih.gov/gtr/tests. Until recently the heterogeneity of these disorders presented a significant challenge for molecular diagnosis, but the advent of next generation sequencing (NGS) has greatly improved the speed and efficiency of molecular diagnosis. Many laboratories now offer NGS sequencing of all genes associated with retinal degeneration in accredited laboratories, and as the costs of such tests fall they should become more widely available in clinical practice.

Conclusions

Inherited retinal degenerations may affect rods or cones primarily, and may be stationary or progressive. Although these conditions are not common, ophthalmologists and retinal specialists must understand the key tests and phenotypic features that distinguish these disorders for appropriate diagnosis, counseling, and management, to guide genetic screening, and to identify potential candidates for future therapeutic interventions. Treatments for photoreceptor degenerations such as gene replacement therapies are in development, and genetic characterization of patients will be increasingly important as treatments are developed for patients with these vision-threatening diseases.

References

1a. McCulloch DL, Marmor MF, Brigell MG, et al. ISCEV Standard for full-field clinical electroretinography (2015 update). *Doc Ophthalmol*. 2015;130(1):1–12.

1b. Bach M, Brigell MG, Hawlina M, et al. ISCEV standard for clinical pattern electroretinography (PERG): 2012 update.

Doc Ophthalmol. 2013;126(1):1–7.

1c. Sharpe LT, Stockman A, Jagle H, et al. Opsin genes, cone photopigments, and colour blindness. Gegenfurtner KS, Sharpe LT. *Color Vision: From Genes to Perception*. Cambridge University Press: Cambridge; 1999.

2. Thiadens AA, den Hollander AI, Roosing S, et al. Homozygosity mapping reveals PDE6C mutations in patients with early-onset cone photoreceptor disorders. *Am J Hum Genet*. 2009;85(2):240–247.

3. Michaelides M, Hunt DM, Moore AT. The cone dysfunction syndromes. *Br J Ophthalmol*. 2004;88(2):291–297.

4. Johnson S, Michaelides M, Aligianis IA, et al. Achromatopsia caused by novel mutations in both CNGA3 and CNGB3. *J Med Genet*. 2004;41(2):e20.

5. Andréasson S, Tornqvist K. Electroretinograms in patients with achromatopsia. *Acta Ophthalmol (Copenh)*. 1991;69(6):711–716.

6. Varsányi B, Wissinger B, Kohl S, et al. Clinical and genetic features of Hungarian achromatopsia patients. *Mol Vis*. 2005;11:996–1001.

7. Thiadens AA, Somervuo V, van den Born LI, et al. Progressive loss of cones in achromatopsia: an imaging study using spectral-domain optical coherence tomography. *Invest Ophthalmol Vis Sci*. 2010;51(11):5952–5957.

8. Thomas MG, Kumar A, Kohl S, et al. High-resolution in vivo imaging in achromatopsia. *Ophthalmology*. 2011;118(5):882–887.

9. Khan NW, Wissinger B, Kohl S, et al. CNGB3 achromatopsia with progressive loss of residual cone function and impaired rod-mediated function. *Invest Ophthalmol Vis Sci*. 2007;48(8):3864–3871.

10. Thomas MG, McLean RJ, Kohl S, et al. Early signs of longitudinal progressive cone photoreceptor degeneration in achromatopsia. *Br J Ophthalmol*. 2012;96(9):1232–1236.

11. Fahim AT, Khan NW, Zahid S, et al. Diagnostic fundus autofluorescence patterns in achromatopsia. *Am J Ophthalmol*. 2013;156(6):1211–1219.e2.

12. Aboshiha J, Dubis AM, Cowing J, et al. A prospective

longitudinal study of retinal structure and function in achromatopsia. *Invest Ophthalmol Vis Sci*. 2014;55(9):5733–5743.
13. Genead MA, Fishman GA, Rha J, et al. Photoreceptor structure and function in patients with congenital achromatopsia. *Invest Ophthalmol Vis Sci*. 2011;52(10):7298–7308.
14. Carroll J, Dubra A, Gardner JC, et al. The effect of cone opsin mutations on retinal structure and the integrity of the photoreceptor mosaic. *Invest Ophthalmol Vis Sci*. 2012;53(13):8006–8015.
15. Ben Simon GJ, Abraham FA, Melamed S. Pingelapese achromatopsia: correlation between paradoxical pupillary response and clinical features. *Br J Ophthalmol*. 2004;88(2):223–225.
16. O'Connor PS, Tredici TJ, Ivan DJ, et al. Achromatopsia: clinical diagnosis and treatment. *J Clin Neuroophthalmol*. 1982;2(4):219–226.
17. Simunovic MP, Moore AT. The cone dystrophies. *Eye (Lond)*. 1998;12(Pt 3b):553–565.
18. Yang P, Michaels KV, Courtney RJ, et al. Retinal morphology of patients with achromatopsia during early childhood: implications for gene therapy. *JAMA Ophthalmol*. 2014;132(7):823–831.
19. Thiadens AA, Slingerland NW, Roosing S, et al. Genetic etiology and clinical consequences of complete and incomplete achromatopsia. *Ophthalmology*. 2009;116(10):1984–1989.e1.
20. Carroll J, Choi SS, Williams DR. In vivo imaging of the photoreceptor mosaic of a rod monochromat. *Vision Res*. 2008;48(26):2564–2568.
21. Dubis AM, Cooper RF, Aboshiha J, et al. Genotype-dependent variability in residual cone structure in achromatopsia: toward developing metrics for assessing cone health. *Invest Ophthalmol Vis Sci*. 2014;55(11):7303–7311.
22. Scoles D, Sulai YN, Langlo CS, et al. In vivo imaging of human cone photoreceptor inner segments. *Invest*

Ophthalmol Vis Sci. 2014;55(7):4244–4251.
23. Mancuso K, Hauswirth WW, Li Q, et al. Gene therapy for red-green colour blindness in adult primates. *Nature*. 2009;461(7265):784–787.
24. Kohl S, Zobor D, Chiang WC, et al. Mutations in the unfolded protein response regulator ATF6 cause the cone dysfunction disorder achromatopsia. *Nat Genet*. 2015;47(7):757–765.
25. Sundin OH, Yang JM, Li Y, et al. Genetic basis of total colourblindness among the Pingelapese islanders. *Nat Genet*. 2000;25(3):289–293.
26. Weale RA. Cone-monochromatism. *J Physiol*. 1953;121(3):548–569.
27. Kohl S, Marx T, Giddings I, et al. Total colourblindness is caused by mutations in the gene encoding the alpha-subunit of the cone photoreceptor cGMP-gated cation channel. *Nat Genet*. 1998;19(3):257–259.
28. Wissinger B, Gamer D, Jägle H, et al. CNGA3 mutations in hereditary cone photoreceptor disorders. *Am J Hum Genet*. 2001;69(4):722–737.
29. Audo I, Kohl S, Leroy BP, et al. TRPM1 is mutated in patients with autosomal-recessive complete congenital stationary night blindness. *Am J Hum Genet*. 2009;85(5):720–729.
30. Weale RA. Photosensitive reactions in foveae of normal and cone-monochromatic observers. *Opt Acta*. 1959;6:17.
31. Gibson IM. Visual mechanisms in a cone-monochromat. *J Physiol*. 1962;161:2.
32. Kellner U, Wissinger B, Tippmann S, et al. Blue cone monochromatism: clinical findings in patients with mutations in the red/green opsin gene cluster. *Graefes Arch Clin Exp Ophthalmol*. 2004;242(9):729–735.
33. Kohl S, Varsanyi B, Antunes GA, et al. CNGB3 mutations account for 50% of all cases with autosomal recessive achromatopsia. *Eur J Hum Genet*. 2005;13(3):302–308.
34. Aligianis IA, Forshew T, Johnson S, et al. Mapping of a novel locus for achromatopsia (ACHM4) to 1p and identification of a germline mutation in the alpha subunit of

cone transducin (GNAT2). *J Med Genet*. 2002;39(9):656–660.
35. Kohl S, Baumann B, Rosenberg T, et al. Mutations in the cone photoreceptor G-protein alpha-subunit gene GNAT2 in patients with achromatopsia. *Am J Hum Genet*. 2002;71(2):422–425.
36. Michaelides M, Aligianis IA, Holder GE, et al. Cone dystrophy phenotype associated with a frameshift mutation (M280fsX291) in the alpha-subunit of cone specific transducin (GNAT2). *Br J Ophthalmol*. 2003;87(11):1317–1320.
37. Sundaram V, Wilde C, Aboshiha J, et al. Retinal structure and function in achromatopsia: implications for gene therapy. *Ophthalmology*. 2014;121(1):234–245.
38. Chang B, Grau T, Dangel S, et al. A homologous genetic basis of the murine cpfl1 mutant and human achromatopsia linked to mutations in the PDE6C gene. *Proc Natl Acad Sci USA*. 2009;106(46):19581–19586.
39. Kohl S, Coppieters F, Meire F, et al. A nonsense mutation in PDE6H causes autosomal-recessive incomplete achromatopsia. *Am J Hum Genet*. 2012;91(3):527–532.
40. Aboshiha J, Dubis AM, Carroll J, et al. The cone dysfunction syndromes. *Br J Ophthalmol*. 2016;100(1):115–121.
41. Stockman A, Smithson HE, Michaelides M, et al. Residual cone vision without alpha-transducin. *J Vis*. 2007;7(4):8.
42. Rosenberg T, Baumann B, Kohl S, et al. Variant phenotypes of incomplete achromatopsia in two cousins with GNAT2 gene mutations. *Invest Ophthalmol Vis Sci*. 2004;45(12):4256–4262.
43. Zein WM, Jeffrey BG, Wiley HE, et al. CNGB3-achromatopsia clinical trial with CNTF: diminished rod pathway responses with no evidence of improvement in cone function. *Invest Ophthalmol Vis Sci*. 2014;55(10):6301–6308.
44. Park WL, Sunness JS. Red contact lenses for alleviation of photophobia in patients with cone disorders. *Am J Ophthalmol*. 2004;137(4):774–775.
45. Alexander JJ, Umino Y, Everhart D, et al. Restoration of cone vision in a mouse model of achromatopsia. *Nat Med*.

2007;13(6):685–687.
46. Michalakis S, Muhlfriedel R, Tanimoto N, et al. Restoration of cone vision in the CNGA3$^{-/-}$ mouse model of congenital complete lack of cone photoreceptor function. *Mol Ther*. 2010;18(12):2057–2063.
47. Komáromy AM, Alexander JJ, Rowlan JS, et al. Gene therapy rescues cone function in congenital achromatopsia. *Hum Mol Genet*. 2010;19(13):2581–2593.
48. Ayyagari R, Kakuk LE, Bingham EL, et al. Spectrum of color gene deletions and phenotype in patients with blue cone monochromacy. *Hum Genet*. 2000;107(1):75–82.
49. Ayyagari R, Kakuk LE, Coats CL, et al. Bilateral macular atrophy in blue cone monochromacy (BCM) with loss of the locus control region (LCR) and part of the red pigment gene. *Mol Vis*. 1999;5:13.
50. Berson EL, Sandberg MA, Rosner B, et al. Color plates to help identify patients with blue cone monochromatism. *Am J Ophthalmol*. 1983;95(6):741–747.
51. Weiss AH, Biersdorf WR. Blue cone monochromatism. *J Pediatr Ophthalmol Strabismus*. 1989;26(5):218–223.
52. Alpern M, Lee GB, Maaseidvaag F, et al. Colour vision in blue-cone 'monochromacy'. *J Physiol*. 1971;212(1):211–233.
53. Gouras P, MacKay CJ. Electroretinographic responses of the short-wavelength-sensitive cones. *Invest Ophthalmol Vis Sci*. 1990;31(7):1203–1209.
54. Arden G, Wolf J, Berninger T, et al. S-cone ERGs elicited by a simple technique in normals and in tritanopes. *Vision Res*. 1999;39(3):641–650.
55. Moskowitz A, Hansen RM, Akula JD, et al. Rod and rod-driven function in achromatopsia and blue cone monochromatism. *Invest Ophthalmol Vis Sci*. 2009;50(2):950–958.
56. Cideciyan AV, Hufnagel RB, Carroll J, et al. Human cone visual pigment deletions spare sufficient photoreceptors to warrant gene therapy. *Hum Gene Ther*. 2013;24(12):993–1006.
57. Barthelmes D, Sutter FK, Kurz-Levin MM, et al. Quantitative analysis of OCT characteristics in patients with achromatopsia and blue-cone monochromatism. *Invest*

Ophthalmol Vis Sci. 2006;47(3):1161–1166.
58. Nathans J, Davenport CM, Maumenee IH, et al. Molecular genetics of human blue cone monochromacy. *Science*. 1989;245(4920):831–838.
59. Gardner JC, Michaelides M, Holder GE, et al. Blue cone monochromacy: causative mutations and associated phenotypes. *Mol Vis*. 2009;15:876–884.
60. Michaelides M, Johnson S, Simunovic MP, et al. Blue cone monochromatism: a phenotype and genotype assessment with evidence of progressive loss of cone function in older individuals. *Eye (Lond)*. 2005;19(1):2–10.
61. Nathans J, Thomas D, Hogness DS. Molecular genetics of human color vision: the genes encoding blue, green, and red pigments. *Science*. 1986;232(4747):193–202.
62. Nathans J, Maumenee IH, Zrenner E, et al. Genetic heterogeneity among blue-cone monochromats. *Am J Hum Genet*. 1993;53(5):987–1000.
63. Ladekjaer-Mikkelsen AS, Rosenberg T, Jørgensen AL. A new mechanism in blue cone monochromatism. *Hum Genet*. 1996;98(4):403–408.
64. Reyniers E, Van Thienen MN, Meire F, et al. Gene conversion between red and defective green opsin gene in blue cone monochromacy. *Genomics*. 1995;29(2):323–328.
65. Greenwald SH, Kuchenbecker JA, Roberson DK, et al. S-opsin knockout mice with the endogenous M-opsin gene replaced by an L-opsin variant. *Vis Neurosci*. 2014;31(1):25–37.
66. Zrenner E, Magnussen S, Lorenz B. [Blue cone monochromasia: diagnosis, genetic counseling and optical aids]. *Klin Monatsbl Augenheilkd*. 1988;193(5):510–517.
67. Haim M, Fledelius HC, Skarsholm. X-linked myopia in Danish family. *Acta Ophthalmol (Copenh)*. 1988;66(4):450–456.
68. Michaelides M, Johnson S, Bradshaw K, et al. X-linked cone dysfunction syndrome with myopia and protanopia. *Ophthalmology*. 2005;112(8):1448–1454.
69. Young TL, Deeb SS, Ronan SM, et al. X-linked high myopia associated with cone dysfunction. *Arch Ophthalmol*.

2004;122(6):897–908.
70. McClements M, Davies WI, Michaelides M, et al. Variations in opsin coding sequences cause X-linked cone dysfunction syndrome with myopia and dichromacy. *Invest Ophthalmol Vis Sci*. 2013;54(2):1361–1369.
71. van Lith G. General cone dysfunction without achromatopsia. [In Pearlman JT, editors. 10th ISCERG Symposium] *Doc Ophthalmol Proc Ser*. 1973;2004b(2):175–180.
72. Michaelides M, Holder GE, Bradshaw K, et al. Oligocone trichromacy: a rare and unusual cone dysfunction syndrome. *Br J Ophthalmol*. 2004;88(4):497–500.
73. Michaelides M, Rha J, Dees EW, et al. Integrity of the cone photoreceptor mosaic in oligocone trichromacy. *Invest Ophthalmol Vis Sci*. 2011;52(7):4757–4764.
74. Smirnov V, Drumare I, Bouacha I, et al. Long-term follow-up of two patients with oligocone trichromacy. *Doc Ophthalmol*. 2015;131(2):149–158.
75. Andersen MK, Christoffersen NL, Sander B, et al. Oligocone trichromacy: clinical and molecular genetic investigations. *Invest Ophthalmol Vis Sci*. 2010;51(1):89–95.
76. Vincent A, Wright T, Billingsley G, et al. Oligocone trichromacy is part of the spectrum of CNGA3-related cone system disorders. *Ophthalmic Genet*. 2011;32(2):107–113.
77. Schubert G, Bornschein H. Analysis of the human electroretinogram. *Ophthalmologica*. 1952;123(6):396–413.
78. Riggs LA. Electroretinography in cases of night blindness. *Am J Ophthalmol*. 1954;38(1:2):70–78.
79. Miyake Y, Yagasaki K, Horiguchi M, et al. Congenital stationary night blindness with negative electroretinogram: a new classification. *Arch Ophthalmol*. 1986;104(7):1013–1020.
80. Bijveld MM, Florijn RJ, Bergen AA, et al. Genotype and phenotype of 101 Dutch patients with congenital stationary night blindness. *Ophthalmology*. 2013;120(10):2072–2081.
81. Zeitz C, Robson AG, Audo I. Congenital stationary night blindness: an analysis and update of genotype-phenotype correlations and pathogenic mechanisms. *Prog Retin Eye Res*. 2015;45:58–110.

82. Sergouniotis PI, Robson AG, Li Z, et al. A phenotypic study of congenital stationary night blindness (CSNB) associated with mutations in the GRM6 gene. *Acta Ophthalmol*. 2011;90(3):e192–7.
83. Miyake Y. [Establishment of the concept of new clinical entities – complete and incomplete form of congenital stationary night blindness]. *Nihon Ganka Gakkai Zasshi*. 2002;106(12):737–755 [discussion 56].
84. Cunier R. Historie d'une hemerolopie, hereditaire depuis siècles dans' un famille de la commune de Vendemian, près Montpellier. *Ann Soc Med de Gand*. 1838;4.
85. Nettleship E. A history of congenital stationary nightblindness in nine consecutive generations. *Trans Ophthalmol Soc U K*. 1907;27:25.
86. Carr RE. Congenital stationary nightblindness. *Trans Am Ophthalmol Soc*. 1974;72:448–487.
87. Rosenberg T, Haim M, Piczenik Y, et al. Autosomal dominant stationary night-blindness: a large family rediscovered. *Acta Ophthalmol (Copenh)*. 1991;69(6):694–702.
88. McBain VA, Egan CA, Pieris SJ, et al. Functional observations in vitamin A deficiency: diagnosis and time course of recovery. *Eye (Lond)*. 2007;21(3):367–376.
89. Sergouniotis PI, Sohn EH, Li Z, et al. Phenotypic variability in RDH5 retinopathy (fundus albipunctatus). *Ophthalmology*. 2011;118(8):1661–1670.
90. Sergouniotis PI, Davidson AE, Sehmi K, et al. Mizuo–Nakamura phenomenon in Oguchi disease due to a homozygous nonsense mutation in the SAG gene. *Eye (Lond)*. 2011;25(8):1098–1101.
91. Wali N, Leguire LE. The photopic hill: a new phenomenon of the light adapted electroretinogram. *Doc Ophthalmol*. 1992;80(4):335–345.
92. Ueno S, Kondo M, Niwa Y, et al. Luminance dependence of neural components that underlies the primate photopic electroretinogram. *Invest Ophthalmol Vis Sci*. 2004;45(3):1033–1040.
93. Dryja TP. Molecular genetics of Oguchi disease, fundus albipunctatus, and other forms of stationary night

blindness: LVII Edward Jackson Memorial Lecture. *Am J Ophthalmol*. 2000;130(5):547–563.
94. Riazuddin SA, Shahzadi A, Zeitz C, et al. A mutation in SLC24A1 implicated in autosomal-recessive congenital stationary night blindness. *Am J Hum Genet*. 2010;87(4):523–531.
95. Sekiya K, Nakazawa M, Ohguro H, et al. Long-term fundus changes due to fundus albipunctatus associated with mutations in the RDH5 gene. *Arch Ophthalmol*. 2003;121(7):1057–1059.
96. Yamamoto H, Yakushijin K, Kusuhara S, et al. A novel RDH5 gene mutation in a patient with fundus albipunctatus presenting with macular atrophy and fading white dots. *Am J Ophthalmol*. 2003;136(3):572–574.
97. Miyake Y, Shiroyama N, Sugita S, et al. Fundus albipunctatus associated with cone dystrophy. *Br J Ophthalmol*. 1992;76(6):375–379.
98. Niwa Y, Kondo M, Ueno S, et al. Cone and rod dysfunction in fundus albipunctatus with RDH5 mutation: an electrophysiological study. *Invest Ophthalmol Vis Sci*. 2005;46(4):1480–1485.
99. Nakamura M, Lin J, Miyake Y. Young monozygotic twin sisters with fundus albipunctatus and cone dystrophy. *Arch Ophthalmol*. 2004;122(8):1203–1207.
100. Cideciyan AV, Haeseleer F, Fariss RN, et al. Rod and cone visual cycle consequences of a null mutation in the 11-*cis*-retinol dehydrogenase gene in man. *Vis Neurosci*. 2000;17(5):667–678.
101. Carr RE, Gouras P. Oguchi's disease. *Arch Ophthalmol*. 1965;73:646–656.
102. Carr RE, Ripps H, Siegel IM. Visual pigment kinetics and adaptation in fundus albipunctatus. *Doc Ophthalmol*. 1974;12.
103. Querques G, Carrillo P, Querques L, et al. High-definition optical coherence tomographic visualization of photoreceptor layer and retinal flecks in fundus albipunctatus associated with cone dystrophy. *Arch Ophthalmol*. 2009;127(5):703–706.

104. Genead MA, Fishman GA, Lindeman M. Spectral-domain optical coherence tomography and fundus autofluorescence characteristics in patients with fundus albipunctatus and retinitis punctata albescens. *Ophthalmic Genet*. 2010;31(2):66–72.
105. Driessen CA, Winkens HJ, Hoffmann K, et al. Disruption of the 11-*cis*-retinol dehydrogenase gene leads to accumulation of cis-retinols and cis-retinyl esters. *Mol Cell Biol*. 2000;20(12):4275–4287.
106. Makiyama Y, Ooto S, Hangai M, et al. Cone abnormalities in fundus albipunctatus associated with RDH5 mutations assessed using adaptive optics scanning laser ophthalmoscopy. *Am J Ophthalmol*. 2014;157(3):558–570.e1-4.
107. Gonzalez-Fernandez F, Kurz D, Bao Y, et al. 11-*cis* retinol dehydrogenase mutations as a major cause of the congenital night-blindness disorder known as fundus albipunctatus. *Mol Vis*. 1999;5:41.
108. Yamamoto H, Simon A, Eriksson U, et al. Mutations in the gene encoding 11-*cis* retinol dehydrogenase cause delayed dark adaptation and fundus albipunctatus. *Nat Genet*. 1999;22(2):188–191.
109. Voigt M, Querques G, Atmani K, et al. Analysis of retinal flecks in fundus flavimaculatus using high-definition spectral-domain optical coherence tomography. *Am J Ophthalmol*. 2010;150(3):330–337.
110. Mata NL, Radu RA, Clemmons RC, et al. Isomerization and oxidation of vitamin a in cone-dominant retinas: a novel pathway for visual-pigment regeneration in daylight. *Neuron*. 2002;36(1):69–80.
111. Oguchi C. Ueber einen Fall von eigenartiger Hemeralopie. *Nippon Ganka Gakkai Zasshi*. 1907;17.
112. Mizuo G. On a new discovery in the dark adaptation on Oguchi's disease. *Acta Soc Ophthalmol*. 1913;17.
113. Kuwakara Y, Ishihara K, Akiya S. Histopathological and electron microscopic studies of the retina of Oguchi's disease. *Acta Soc Ophthalmol Jpn*. 1963;67.
114. Hashimoto H, Kishi S. Shortening of the rod outer segment in Oguchi disease. *Graefes Arch Clin Exp Ophthalmol*.

2009;247(11):1561–1563.
115. Godara P, Cooper RF, Sergouniotis PI, et al. Assessing retinal structure in complete congenital stationary night blindness and Oguchi disease. *Am J Ophthalmol*. 2012;154(6):987–1001.e1.
116. Gouras P. Electroretinography: some basic principles. *Invest Ophthalmol*. 1970;9(8):557–569.
117. Yamamoto S, Sippel KC, Berson EL, et al. Defects in the rhodopsin kinase gene in the Oguchi form of stationary night blindness. *Nat Genet*. 1997;15(2):175–178.
118. Fuchs S, Nakazawa M, Maw M, et al. A homozygous 1-base pair deletion in the arrestin gene is a frequent cause of Oguchi disease in Japanese. *Nat Genet*. 1995;10(3):360–362.
119. Carr RE, Ripps H. Rhodopsin kinetics and rod adaptation in Oguchi's disease. *Invest Ophthalmol Vis Sci*. 1967;6:11.
120. Rotenstreich Y, Harats D, Shaish A, et al. Treatment of a retinal dystrophy, fundus albipunctatus, with oral 9-cis-{beta}-carotene. *Br J Ophthalmol*. 2010;94(5):616–621.
121. Maeda A, Maeda T, Palczewski K. Improvement in rod and cone function in mouse model of fundus albipunctatus after pharmacologic treatment with 9-*cis*-retinal. *Invest Ophthalmol Vis Sci*. 2006;47(10):4540–4546.
122. Krill AE, Deutman AF, Fishman M. The cone degenerations. *Doc Ophthalmol*. 1973;35(1):1–80.
123. Rowe SE, Trobe JD, Sieving PA. Idiopathic photoreceptor dysfunction causes unexplained visual acuity loss in later adulthood. *Ophthalmology*. 1990;97(12):1632–1637.
124. Ladewig M, Kraus H, Foerster MH, et al. Cone dysfunction in patients with late-onset cone dystrophy and age-related macular degeneration. *Arch Ophthalmol*. 2003;121(11):1557–1561.
125. Robson AG, Michaelides M, Saihan Z, et al. Functional characteristics of patients with retinal dystrophy that manifest abnormal parafoveal annuli of high density fundus autofluorescence; a review and update. *Doc Ophthalmol*. 2008;116(2):79–89.
126. Robson AG, Michaelides M, Luong VA, et al. Functional correlates of fundus autofluorescence abnormalities in

patients with RPGR or RIMS1 mutations causing cone or cone rod dystrophy. *Br J Ophthalmol*. 2008;92(1):95–102.
127. Sergouniotis PI, Holder GE, Robson AG, et al. High-resolution optical coherence tomography imaging in KCNV2 retinopathy. *Br J Ophthalmol*. 2012;96(2):213–217.
128. Wang NK, Chou CL, Lima LH, et al. Fundus autofluorescence in cone dystrophy. *Doc Ophthalmol*. 2009;119(2):141–144.
129. Duncan JL, Zhang Y, Gandhi J, et al. High-resolution imaging with adaptive optics in patients with inherited retinal degeneration. *Invest Ophthalmol Vis Sci*. 2007;48(7):3283–3291.
130. Hamel CP. Cone rod dystrophies. *Orphanet J Rare Dis*. 2007;2:7.
131. Daiger SP, Sullivan LS, Bowne SJ. Genes and mutations causing retinitis pigmentosa. *Clin Genet*. 2013;84(2):132–141.
132. Berger W, Kloeckener-Gruissem B, Neidhardt J. The molecular basis of human retinal and vitreoretinal diseases. *Prog Retin Eye Res*. 2010;29(5):335–375.
133. RetNet. *The Retinal Information Network 2013*. http://www.sph.uth.tmc.edu/RetNet; 2013.

SECTION 2

Retinal Vascular Disease

OUTLINE

47

The Epidemiology of Diabetic Retinopathy

Ronald Klein, Barbara E.K. Klein

Introduction

Population-based studies such as the Wisconsin Epidemiologic Study of Diabetic Retinopathy (WESDR)[1–3] that use stereoscopic fundus photographs of seven standard photographic fields and objective grading by standard protocols have provided estimates of the prevalence and severity of diabetic retinopathy. In 1980–82, the WESDR found that 71%, 23%, and 11% of those with type 1 diabetes and 47%, 6%, and 8% of those with type 2 diabetes had retinopathy, proliferative retinopathy, and macular edema, respectively.[3,4] These prevalence estimates, derived from data collected approximately 35 years ago in an 11-county area of southern Wisconsin (99% white), were higher than more recent prevalence data reported in other population-based studies (Table 47.1, Figs. 47.1 and 47.2), in which data from eight such studies were pooled.[5] It is likely that virtually all of the cases of diabetes in these analyses have type 2 diabetes. There were 615 black and 1415 Hispanic individuals included in those studies. The prevalence estimates were limited to persons aged 40 years and older. From these studies, it was estimated that among persons with diabetes, the crude prevalence of diabetic retinopathy was 40% and the crude prevalence of severe vision-threatening retinopathy (preproliferative and proliferative retinopathy or macular edema) was 8%. Prevalence estimates from the pooled studies projected to the diabetic population aged 40 years or older in the United States in the years 2000 and 2030 were 4 and 6.1 million persons with any retinopathy, respectively, of

whom 900,000 and 1.6 million would have signs of vision-threatening retinopathy. Based on grading of fundus images in the more recent 2005–8 National Health and Nutrition Examination Survey (NHANES), 4.2 million people aged 40 years or older with diabetes were estimated to have diabetic retinopathy, of whom 650,000 would have signs of vision-threatening retinopathy.[6] It is expected that the prevalence of diabetes will continue to increase. Without a significant decline in the incidence of diabetic retinopathy, the number of persons with vision-threatening retinopathy may also continue to increase. The estimated prevalences of diabetic retinopathy and diabetic macular edema are also expected to increase due to the development and use of more sensitive detection and assessment modalities such as ultrawide fundus photography[7] and spectral domain optical coherence tomography (SD-OCT).

TABLE 47.1

Studies Included in Estimates of the Prevalence of Diabetic Retinopathy[a]

Variable	Barbados Eye Study, Barbados, West Indies	BDES, Beaver Dam, Wis.	BMES, Blue Mountain, Australia	Melbourne VIP, Melbourne, Australia	Proyecto VER, Nogales and Tucson, Ariz.	SAHS, San Antonio, Tex.[b]	SLVDS, San Luis Valley, Colo.	WESI Southl Wis.
Years study conducted	1988–1992	1988–1990	1992–1994	1991–1998	1999–2000	1985–1987	1984–1988	1980-1982
No. of participants with diabetes mellitus[c]	615	410	252	233	899	351	360	1313
Photographic fields taken[d]	1 and 2	1–7	1–5	1 and 2	1, 2, and 4	1–7	1, 2, and 4	1–7
Age (yr)								
40–49	19.2	6.6	0.0	9.9	17.8	31.22	22.9	7.4
50–64	47.2	36.3	38.9	40.8	44.6	66.7	55.8	35.9
65–74	26.3	34.9	36.5	31.7	25.4	12.5	31.4	33.8
≥75	7.3	22.2	24.6	17.6	12.2	NA	NA	22.8
Gender								
Women	63.4	56.8	47.2	43.8	63.0	58.7	56.4	53.2
Men	36.6	43.2	52.8	56.2	37.0	41.3	33.6	46.8
Race/ethnicity								
Black	100.0	NA	NA	NA	NA	NA	NA	NA
Hispanic	NA	NA	NA	NA	100.0	80.6	64.7	NA
White	NA	100.0	100.0	100.0	NA	19.4	35.3	100.0

Crude prevalence								
Mild NPDR	19.8	22.9	21.0	16.3	36.6	18.2	20.6	36.6
Moderate NPDR	8.0	10.0	4.4	6.9	1.7	13.7	10.3	6.8
Severe NPDR and/or PDR	1.0	2.2	3.6	4.3	6.0	4.3	4.4	6.9
Macular edema	8.6	1.2	4.8	2.2	8.9	2.6	3.3	5.1
DR of any type	28.8	35.1	29.0	27.5	44.3	36.2	35.3	50.3
VTDR	9.1	3.2	6.4	4.3	8.9	5.3	6.4	10.0

[a]Data are given as percentage of persons unless otherwise indicated.

[b]Persons with adult-onset diabetes mellitus only.

[c]The number of persons reported for each study in this table reflects the number contributing to our estimates in the current article [in the published source] and not necessarily the total number of participants in the original study as published.

[d]The photographic fields are described in reference 8 [in the published source the reference is Early Treatment Diabetic Retinopathy Study Research Group. Grading diabetic retinopathy from stereoscopic color fundus photographs – an extension of the modified Airlie House classification. ETDRS report number 10. Ophthalmology 1991;98(5 Suppl):786–806.]

BDES, Beaver Dam Eye Study; BMES, Blue Mountains Eye Study; SAHS, San Antonio Heart Study; SLVDS, San Luis Valley Diabetes Study; VIP, Visual Impairment Project; VER, Vision Evaluation Research; WESDR, Wisconsin Epidemiologic Study of Diabetic Retinopathy. DM, diabetes mellitus; DR, diabetic retinopathy; NA, not applicable; NPDR, nonproliferative diabetic retinopathy; PDR, proliferative diabetic retinopathy; VTDR, vision-threatening diabetic retinopathy.

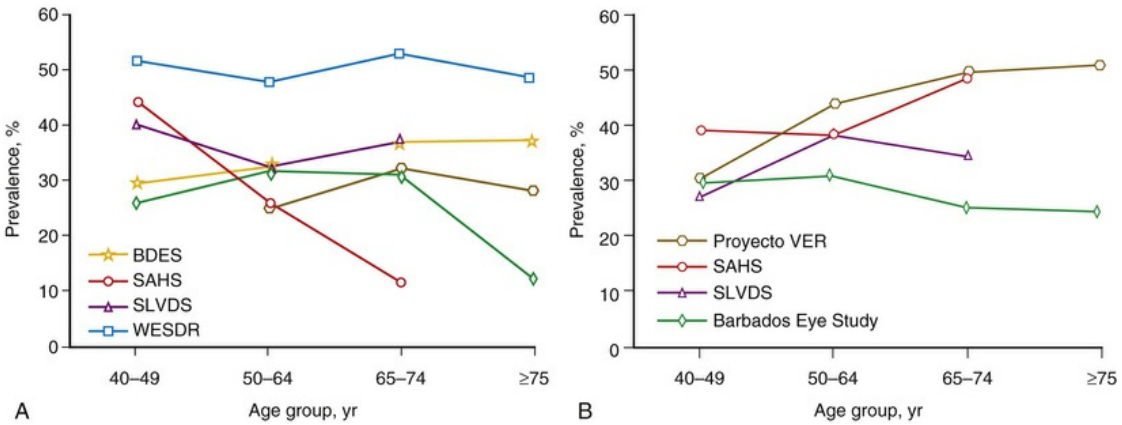

FIG. 47.1 (A) Prevalence of diabetic retinopathy

among white subjects who have diabetes mellitus. (B) Prevalence of diabetic retinopathy among Hispanic and black subjects who have diabetes mellitus. BDES, Beaver Dam Eye Study, Beaver Dam, Wisconsin; SAHS, San Antonio Heart Study, San Antonio, Texas; SLVDS, San Luis Valley Diabetes Study, San Luis Valley, Colorado; VER, Vision Evaluation Research, Nogales and Tucson, Arizona; WESDR, Wisconsin Epidemiologic Study of Diabetic Retinopathy, southern Wisconsin. The Barbados Eye Study was conducted in Barbados, West Indies; all participants were black.

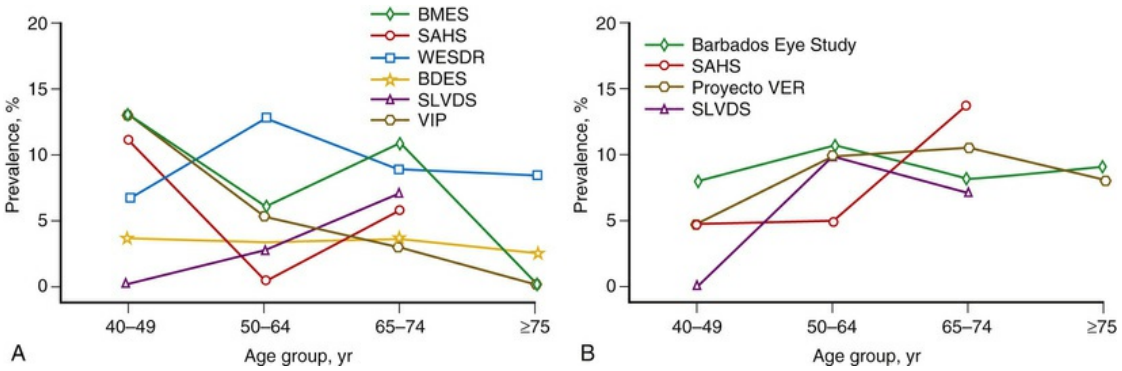

FIG. 47.2 (A) Prevalence of vision-threatening diabetic retinopathy among white subjects who have diabetes mellitus. (B) Prevalence of vision-threatening diabetic retinopathy among Hispanic and black subjects who have diabetes mellitus. BDES, Beaver Dam Eye Study, Beaver Dam, Wisconsin; SAHS, San Antonio Heart Study, San Antonio, Texas; SLVDS, San Luis Valley Diabetes Study, San Luis Valley, Colorado; VIP, Melbourne VIP Study; VER, Vision Evaluation Research, Nogales and Tucson, Arizona; WESDR, Wisconsin Epidemiologic Study of Diabetic Retinopathy, southern Wisconsin. The Barbados Eye Study was conducted in Barbados, West Indies; all participants were black.

The lower prevalence of diabetic retinopathy in more recent studies is thought to be due in part to changes in the management of diabetes.[8–28] In persons with type 1 diabetes in the WESDR there have been dramatic changes in management that include an increase in the use of blood glucose self-monitoring (from 72% in 1984–6 to 91% in 2005–7) and a greater frequency of using three or more injections of insulin per day (from 4% in 1980–2 to 85% in 2005–7). This was associated with a 2.5% decrease in the mean glycosylated hemoglobin A1c (A1c) from 10.1% to 7.6% and a 29% increase in those achieving American Diabetes Association (ADA) guidelines of A1c of <7% from 4% to 33% over the same period.[29]

There have also been changes in the management of glycemia in people with type 2 diabetes. In 1988–94, the use of only one oral hypoglycemic agent was the primary treatment to manage hyperglycemia in people with type 2 diabetes. After the findings from the United Kingdom Prospective Diabetes Study (UKPDS), there was an increase in the use of more than one class of oral hypoglycemic agents over a 5-year period (1999–2004).[30,31] This was associated with a decrease in the mean A1c levels from 7.8% to 7.2%, with a 41% increase (from 41% to 58%) in persons achieving A1c levels of <7.0% in the periods 1999–2000 and 2005–6.

Incidence and Progression of Diabetic Retinopathy and Incidence of Clinically Significant Macular Edema

There are fewer reports of incidence of retinopathy in population-based studies and none in national US samples.[32–47] The incidence of retinopathy in a 4-year interval in the entire WESDR population was 40.3%.[34,35] The 4-year incidence and rates of progression of diabetic retinopathy and macular edema in the WESDR are presented in Table 47.2. Those with type 1 diabetes had a higher incidence of any retinopathy, progression by two or more steps on the Early Treatment Diabetic Retinopathy Study (ETDRS) concatenated severity scale, and progression to proliferative

diabetic retinopathy than those with type 2 diabetes (Table 47.2).[36] The highest 4-year incidence of clinically significant macular edema was in those with type 2 diabetes taking insulin, while the lowest was in those with type 2 diabetes not taking insulin. While the incidence of proliferative diabetic retinopathy was higher in those with type 1 diabetes, the estimate of the number of incident cases in the 4-year period was higher in the group with type 2 diabetes than in the group with type 1 diabetes (120 vs. 83 persons) due to the higher frequency of people with type 2 diabetes.

TABLE 47.2

Four-Year Incidences of Any Retinopathy, Improvement or Progression of Retinopathy, Progression to Proliferative Diabetic Retinopathy (PDR) and Incidence of Clinically Significant Macular Edema (CSME) in Younger-Onset Type 1 Diabetes and Older-Onset Type 2 Diabetes in the Wisconsin Epidemiologic Study of Diabetic Retinopathy, 1980–1986

Retinopathy	Younger-Onset		Older-Onset Taking Insulin		Older-Onset Not Taking Insulin	
	No. at Risk	%	No. at Risk	%	No. at Risk	%
Any retinopathy	271	59.0	154	47.4	320	34.4
Improvement	376	6.9	215	15.3	101	19.8
No change	713	55.1	418	58.1	486	71.0
Progression	713	41.2	418	34.0	486	24.9
Progression to PDR	713	10.5	418	7.4	486	2.3
Incidence of CSME	610	4.3	273	5.1	379	1.3

Note: Number at risk for incidence of any retinopathy refers to group that had no retinopathy (level 10/10) at baseline examination and who were at risk of developing retinopathy at follow-up examination. Number at risk for improvement in retinopathy refers to those with retinopathy levels of 21/21 to 51/51 at baseline examination who could have a decrease in their retinopathy severity by at least two steps or more at follow-up examination. Number at risk for no change, progression or progression to PDR refers to those with retinopathy levels of 10/10 to 51/51 who either did not change by two or more steps or progressed by two or more steps.

Modified from Klein R, Klein BEK, Moss SE, et al: The Wisconsin Epidemiologic Study of Diabetic Retinopathy, IX: four-year incidence and progression of diabetic retinopathy when age at diagnosis is less than 30 years. Arch Ophthalmol 1989;107:237–243; Klein R, Klein BEK, Moss SE et al: [Table 2, page 240] The Wisconsin Epidemiologic Study of Diabetic Retinopathy, X: four-year incidence and progression of diabetic retinopathy when age at diagnosis is 30 years or more. Arch Ophthalmol 1989;107:244–249. Source for the last line comes in part from: Klein R, Moss SE, Klein BEK, et al: The Wisconsin Epidemiologic Study of Diabetic

Retinopathy, XI: the incidence of macular edema. Ophthalmology 1989;96:1501–1510.

There is evidence in more recent studies that the prevalence and incidence of diabetic retinopathy may be decreasing in subjects more recently diagnosed with type 1 diabetes. Hovind and colleagues[48] first showed a declining incidence of proliferative diabetic retinopathy and macular edema in a study of 600 patients with type 1 diabetes diagnosed between 1965 and 1984 in Denmark. In that study, the cumulative incidence of proliferative diabetic retinopathy and macular edema after 20 years of diabetes declined from 31% and 19%, respectively, in those diagnosed from 1965 to 1969, to 13% and 7%, respectively, in those diagnosed from 1979 to 1984. There was also significant improvement in visual acuity and lower prevalence of severe visual impairment in those diagnosed with type 1 diabetes more recently than those diagnosed in earlier periods. These changes were attributed by the authors to improved glycemic control, more aggressive treatment of blood pressure sooner after diagnosis of diabetes, and reduced smoking rates in the more recently diagnosed type 1 diabetic group than in previous years. There was also a decline in the cumulative proportion with severe laser-treated diabetic retinopathy after 25 years of type 1 diabetes from 47% in subjects diagnosed between 1961 and 1965 to 24% in subjects diagnosed between 1971 and 1975 in the Swedish Linköping Diabetes Complications Study.[49,50] However, the Pittsburgh Epidemiology of Diabetic Complications Study did not show a significant decrease in proliferative diabetic retinopathy in those diagnosed more recently.[51] In the WESDR, the annualized estimates for the progression of diabetic retinopathy (4.5% vs. 2.5%) and the incidence of proliferative diabetic retinopathy (3.4% vs. 1.5%), clinically significant macular edema (1.0% vs. 0.4%), and visual impairment (0.7% vs. 0.3%) were higher in the first 12 years of the study (1980–92) than in the subsequent 13 years of the study (1994–2007).[52–55] While adjusting for duration of diabetes, there was also evidence in the WESDR of lower prevalence of proliferative diabetic retinopathy (4% lower in the more recent time period) and visual impairment (9% lower in the more recent time period) but there was no significant change in the prevalence of macular edema. Adjusting for hypertension and A1c somewhat attenuated

the changes.

The Relationship of Race/Ethnicity to Diabetic Retinopathy

In contrast to whites, there are fewer epidemiologic studies regarding the prevalence and incidence of diabetic retinopathy in other racial/ethnic groups in the United States, especially in persons with type 1 diabetes. Data from the New Jersey 725 study cohort, which used similar methods to detect and classify retinopathy severity as in the WESDR cohort, suggest similar changes in the frequency and severity of retinopathy in blacks with type 1 diabetes as found in whites in the WESDR.[27,28,36] At the 6-year follow-up of the same cohort, 56% showed progression of diabetic retinopathy, 15% showed progression to proliferative diabetic retinopathy, and 16% developed macular edema.[46]

In four population-based studies, the NHANES 1988–94 and 2005–8,[19] the Atherosclerosis Risk in Communities (ARIC) study,[56] the Cardiovascular Health Study,[57] and the Multi-Ethnic Study of Atherosclerosis (MESA),[58] retinopathy was more prevalent in blacks than in whites (nearly all with type 2 diabetes). In a cross-sectional analysis of 1038 persons aged 40 years or older and who had type 2 diabetes in the 2005–08 NHANES, the odds ratio (OR) of having diabetic macular edema was 2.6 for non-Hispanic blacks compared to non-Hispanic whites. The presence of macular edema was associated with higher levels of glycosylated hemoglobin and longer duration of diabetes.[59] In the NHANES 1988–94, compared to whites, blacks had a higher frequency of people with poor glycemic control (A1c greater than 8.3%, 37% vs. 30%), high systolic blood pressure (>142 mmHg, 42% vs. 32%), longer duration of diabetes (>14 years, 29% vs. 23%), and on insulin therapy (43% vs. 24%). There was no difference (OR 0.94; 95% confidence interval [CI] 0.54–1.66) in the prevalence of retinopathy between blacks and whites while adjusting for these factors.[19] In addition, there were no statistically significant interactions of race with diabetes severity variables or systolic blood pressure, suggesting that the effect of risk factors was similar in both racial/ethnic groups. Similarly, the

higher prevalence of retinopathy in the ARIC study (28% vs. 17%) and in the MESA (37% vs. 25%) in blacks as compared to whites was no longer statistically significant after adjusting for differences in glycemic and blood pressure control between the races. Higher prevalence of retinopathy in blacks with type 2 diabetes appears to be partially due to poorer glycemic and blood pressure control than in whites. These data suggest that programs designed to better control blood sugar and blood pressure in diabetic blacks might be beneficial.

In most population-based studies, Mexican Americans have been found to have higher frequency and greater severity of diabetic retinopathy than non-Hispanic whites.[5,6,15,16,19,22,58,60] Haffner and colleagues[15] found that after adjusting for all measured risk factors, the frequency of retinopathy in Mexican Americans in San Antonio was 2.4 times the prevalence in non-Hispanic whites studied in the WESDR. Similarly, in the NHANES 1988–94 and 2005–8, the MESA, Proyecto VER, and the Los Angeles Latino Eye Study (LALES), retinopathy was more frequent in Mexican Americans compared to non-Hispanic whites 40 years of age or older.[16,19,58,60] In the NHANES 1988–94, retinopathy was more prevalent in Mexican Americans (OR 2.15; 95% CI 1.15–4.04) than in non-Hispanic whites, adjusting for duration of diabetes, A1c level, blood pressure, and type of hypoglycemic medication used.[5] In the NHANES 2005–8, vision-threatening retinopathy was approximately 3.5 times (95% CI 1.05–12.56) as frequent in Mexican Americans compared to non-Hispanic whites.[6] These variations in prevalence among ethnic groups may be a result of differences in the duration of diabetes prior to diagnosis, definition of diabetes, and levels of glycemia and blood pressure. It may also be due to differences in genetic admixture. Using genetic ancestry data in Mexican Americans participating in the LALES, Gao and colleagues[61] showed that the higher frequency of severe diabetic retinopathy in this group was associated with the degree of gene sharing with Native Americans, independent of duration of diabetes, glycemic control, body mass index, and blood pressure.

Among population-based studies, only the LALES has provided data on the incidence and progression of diabetic retinopathy in Mexican Americans with type 2 diabetes.[47] The 4-year incidence of

diabetic retinopathy and clinically significant macular edema was 34% and 7%, respectively, and progression of retinopathy and progression from nonproliferative to proliferative diabetic retinopathy was 39% and 5%, respectively, over the 4-year period. While these rates are comparable to those found in the WESDR, they are higher than in most other contemporaneous studies of whites with type 2 diabetes.

The prevalence and severity of retinopathy appears to vary among different Native American groups.[10,23,62–64] In studies done in the 1970s, Native Americans were reported to have higher rates of severe retinopathy for a given duration of type 2 diabetes compared to whites.[65,66] However, more recent studies on the incidence and progression of diabetic retinopathy in Pima Indians found a lower 4-year cumulative incidence and progression of diabetic retinopathy (17% and 18% respectively) than reported in non-Hispanic whites in the WESDR with type 2 diabetes (39% and 32% respectively), reflecting possible improvements in glycemic and blood pressure control.[67]

There are few data on the prevalence of retinopathy in other racial/ethnic groups.[25,58,68,69] Asian Americans are estimated to comprise 5.6% of the total American population, and between 2000 and 2010, the total number of people identified as Asian American by the US census was estimated to have grown by 46%.[70,71] In the MESA, the prevalence of any retinopathy in Chinese Americans was similar to that in whites (26% vs. 25%).[58] However, the prevalence of clinically significant macular edema and proliferative diabetic retinopathy was higher (13% vs. 2%) in Chinese Americans than in whites. Patterns of risk factors associated with diabetic retinopathy in Asian Americans were similar to those in non-Hispanic whites. More data on the prevalence and incidence of retinopathy in Chinese and other Asian American groups are needed.

Genetic Factors

Data from studies that examined familial clustering suggest that genetic factors may be involved more strongly in susceptibility to diabetic retinopathy than previously thought.[72,73] In addition, the

time of appearance of retinopathy and its severity are more likely to be similar among diabetic identical twins than dizygotic twins suggests that the tendency to develop diabetic retinopathy, and possibly its progression, may be influenced by genetic factors. However, specific genes have not been found to be strongly or consistently associated with diabetic retinopathy (see Chapter 48, Diabetic retinopathy: Genetics and etiologic mechanisms). The fact that retinopathy is not specific to diabetes in its earliest stages may also contribute to the inability to find and replicate genes associated with diabetic retinopathy.

The reader is referred to a more comprehensive, in-depth discussion of the rapidly evolving field of genetic epidemiology of diabetic retinopathy in Chapter 48. While genes remain relatively permanent characteristics over the course of the lifespan, there is increasing evidence that epigenetic phenomena occur and these may result from exposures as well as influence outcomes.[74–76] This is an expanding area for further research.

Sex

In the WESDR, higher frequencies of proliferative retinopathy were present in men compared to women with type 1 diabetes.[2] However, there were no significant differences in the 4-, 10-, or 14-year incidence or progression of diabetic retinopathy between the sexes.[34,37,42] There were no significant differences in the prevalence or 10-year incidence of retinopathy or rates of progression to proliferative retinopathy between the sexes in people with type 2 diabetes in the WESDR.[3,35,37] In the NHANES 2005–8, compared with women, men aged 40 years or older had a higher prevalence of any retinopathy (32% vs. 26%) but not vision-threatening diabetic retinopathy (4.2% vs. 4.6%).[6]

Age and Puberty

The prevalence and severity of diabetic retinopathy increased with increasing age in persons with type 1 diabetes in the WESDR.[2] In persons under 13 years of age, diabetic retinopathy was infrequent, irrespective of the duration of diabetes. The 4-year incidence of

retinopathy increased with increasing age, with the sharpest increase occurring in persons who were 10–12 years of age at baseline.[34] Four-year rates of progression of retinopathy in younger-onset persons rose steadily with increasing age until 15–19 years of age, after which there was a gradual decline. No child younger than age 13 years at baseline in the WESDR was found to have proliferative retinopathy at the 4-year follow-up. These findings have formed the rationale for guidelines for not screening for retinopathy in children with type 1 diabetes.[77]

In persons with type 1 diabetes in the WESDR, those who were postmenarchal were three times as likely to have retinopathy as those who were premenarchal.[78] Frost-Larsen and Starup[79] found the incidence of retinopathy to be higher after puberty than before, independent of duration or metabolic control of diabetes or type of treatment in 60 children with type 1 diabetes. These findings have been observed in other studies.[80,81] Increases in growth hormone, insulin-like growth factor I, sex hormones, and blood pressure as well as poorer glycemic control (due to increased insulin resistance, poorer compliance, and/or inadequate insulin dosage) have been hypothesized to explain the higher risk of developing retinopathy after puberty.

In persons with type 2 diabetes taking insulin in the WESDR, the 4-year incidence of retinopathy and progression of retinopathy had a tendency to decrease with age.[35] The 4-year incidence of improvement in diabetic retinopathy by two or more steps on the ETDRS severity scale tended to increase with age. For those not taking insulin, the 4-year rate of progression to proliferative retinopathy decreased with age. Few persons aged 75 years or older with type 2 diabetes developed proliferative retinopathy over the 10 years of follow-up. These findings are consistent with data from other population-based studies.[32,33] In one such study of people with type 2 diabetes in Rochester, Minnesota, Ballard and colleagues[11] reported a lower incidence of retinopathy with increasing age in persons with diabetes older than age 60 years. These findings might reflect a less severe disease in those with older-onset diabetes or selective survival.

Type 2 Diabetes in Children and Adolescents

Changes in diet and physical activity in children and adolescents have resulted in a dramatic increase in the frequency of obesity and type 2 diabetes in the United States population. There are relatively few population-based studies which have examined the prevalence of diabetic retinopathy in these individuals. The SEARCH for Diabetes in Youth Cohort reported pilot data based on grading of fundus photographs in 43 persons with a mean age of 21 years and mean duration of type 2 diabetes since diagnosis of 7.2 years, as well as 222 persons with a mean age of 16 years and a mean duration since diagnosis of type 1 diabetes of 6.8 years.[82] The prevalence of any diabetic retinopathy was higher in the group with type 2 diabetes compared to the group with type 1 diabetes (42% vs. 17%). The odds of developing retinopathy were not significantly higher (OR=2.0) in Hispanic and non-Hispanic blacks compared to non-Hispanic whites with type 2 diabetes.

The TODAY study, a clinical trial evaluating the use of metformin in persons with a duration of 2–8 years of type 2 diabetes of youth reported a frequency of diabetic retinopathy of 13.7%.[83] The retinopathy was limited to signs of early nonproliferative disease and was related to the glycosylated hemoglobin level. There is a need for longitudinal data to assess the long-term risk of the incidence and progression of retinopathy and associated risk factors.

Duration of Diabetes

The most consistent relationships of risk factors for complications of diabetes are found between duration of diabetes and the prevalence and severity of diabetic retinopathy and macular edema.[2] The prevalence of retinopathy 3–4 years after diagnosis of diabetes in the WESDR younger-onset group with type 1 diabetes was 14% in men and 24% in women. In persons who had had diabetes for 19–20 years, 50% of men and 33% of women had proliferative retinopathy. Shortly after diagnosis of diabetes, retinopathy was

more frequent in persons with type 2 diabetes compared with those with type 1 diabetes (Figs. 47.3 and 47.4).[3] In the first 3 years after diagnosis of diabetes, 23% of the group with type 2 diabetes not taking insulin had retinopathy, and 2% had proliferative retinopathy.

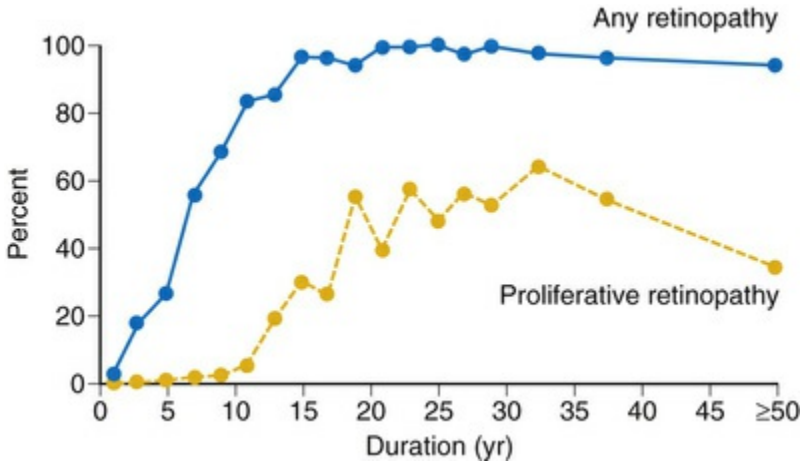

FIG. 47.3 Prevalence of any retinopathy and of proliferative diabetic retinopathy in insulin-taking patients diagnosed with diabetes at age <30 years, by duration of diabetes. Data are from the Wisconsin Epidemiologic Study of Diabetic Retinopathy, 1980–2.

(Reproduced with permission from Klein R, Klein BE, Moss SE. Risk factors for retinopathy. In: Feman SS, editor. Ocular problems in diabetes mellitus. Boston, MA: Blackwell Scientific Publications; 1992. p. 39.)

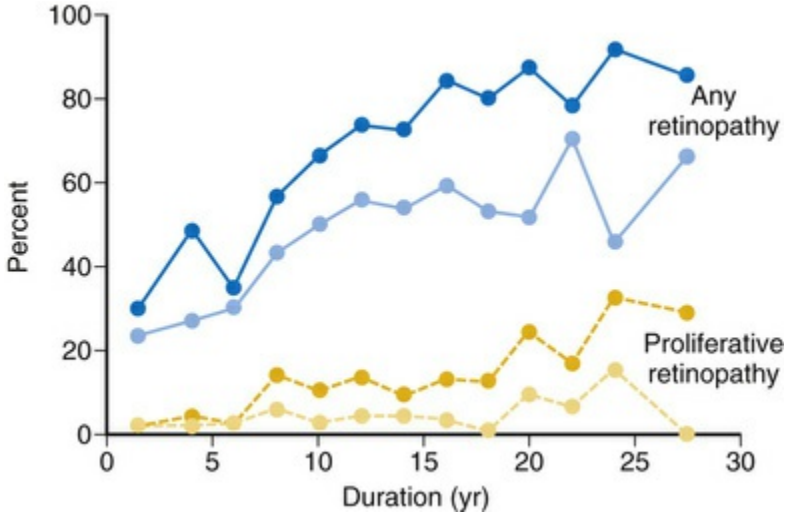

FIG. 47.4 Prevalence of any retinopathy and of

proliferative diabetic retinopathy (%) in participants diagnosed with diabetes at age 30 years or older, by duration of diabetes. Darker colors = on insulin; lighter colors = not on insulin. Data are from the Wisconsin Epidemiologic Study of Diabetic Retinopathy, 1980–2.
(Reproduced with permission from Klein R, Klein BE, Moss SE. Risk factors for retinopathy. In: Feman SS, editor. Ocular problems in diabetes mellitus. Boston, MA: Blackwell Scientific Publications; 1992. p. 39.)

Based on recent follow-up of the WESDR cohort, the prevalence estimates for a given duration likely overestimate the actual prevalence now found in the population.[52] For a specific duration of type 1 diabetes, people diagnosed between 1975 and 1980 had a statistically significantly lower prevalence than persons diagnosed in earlier periods ($P<.001$). This difference remained while adjusting for A1c, systolic and diastolic blood pressure, and presence of proteinuria. Similarly, for specific duration of type 2 diabetes, those diagnosed more recently had a lower prevalence of diabetic retinopathy than those diagnosed in earlier periods.

Harris and colleagues,[84] using retinopathy prevalence data at different durations of diabetes from persons with type 2 diabetes in the WESDR and from a study in Australia, extrapolated to the time when retinopathy prevalence was estimated to be zero. They estimated that the onset of detectable retinopathy occurred approximately 4–7 years after diagnosis of type 2 diabetes in these populations. Using a modification of this approach, a more recent study in an Italian clinic population of persons with older onset diabetes not taking insulin estimated the time between onset and diagnosis of type 2 diabetes to be approximately 6 years.[85]

In the WESDR, the 4- and 10-year incidence of diabetic retinopathy increased with increasing duration of diabetes at baseline.[34,35,37] The risk of developing retinopathy in the younger-onset group was high (74%) after 10 years of diabetes. The 4-year incidence of proliferative diabetic retinopathy varied from 0% during the first 3 years after diagnosis of diabetes to 28% in those with 13–14 years of diabetes. Thereafter, the incidence remained stable.[34] This was shown to be due in part to the competing risk of death in persons with duration of diabetes of 15 or more years.[52] A similar trend was found in a cohort of patients with type 1 diabetes

followed at the Joslin Clinic.[86] In the older-onset WESDR group, 2% of those with less than 5 years and 5% of those with 15 or more years of diabetes who were not taking insulin at baseline developed signs of proliferative diabetic retinopathy at the 4-year follow-up.[35]

Age at Diagnosis

Age at diagnosis was not related to incidence or progression of diabetic retinopathy in any of the diabetes groups followed in the WESDR.[34,35] In contrast, while adjusting for other risk factors, in a cohort with older onset type 2 diabetes in Rochester, Minnesota, the development of retinopathy was significantly associated with younger age at diagnosis.[11]

Glycemia

The Diabetes Control and Complications Trial (DCCT) was "designed to compare intensive with conventional diabetes therapy with regard to their effects on the development and progression of the early vascular and neurologic complications of IDDM."[87] Two of the main questions asked in the study were: "Will intensive therapy prevent the development of diabetic retinopathy in patients with no retinopathy (primary prevention)?" and "Will intensive therapy affect the progression of early retinopathy (secondary intervention)?" In addition, the DCCT examined the magnitude of the effect of intensive insulin treatment on progression of retinopathy, the degree to which this effect changes over time, and the relation of the effect to the level of severity of the retinopathy at baseline.[88–90]

Subjects included persons with type 1 diabetes who were C-peptide-deficient, 13–39 years of age, who were in general good health except for the presence of type 1 diabetes, and did not have hypertension, hypercholesterolemia, or other severe medical conditions. There were two groups. In the primary prevention group, subjects were required to have had type 1 diabetes for 1–5 years, have no retinopathy as detected by stereoscopic fundus photography of seven fields of both eyes, a best corrected visual acuity of 20/25 or better in each eye, and a urinary excretion rate of

<40 mg of albumin in 24 hours. In the secondary prevention group, subjects were required to have had type 1 diabetes for 1–15 years, minimal to moderate nonproliferative retinopathy in at least one eye, best corrected visual acuity of 20/32 or better in each eye, and a urinary excretion rate of <200 mg of albumin per 24 hours.

Randomization was used to assign conventional or intensive insulin therapy.[87] Conventional therapy consisted of one or two injections of insulin per day, daily self-monitoring of urine or blood glucose, and education about exercise and diet. No attempts were made to adjust the insulin dosage on a daily basis. Intensive therapy consisted of administration of insulin three or more times daily by injections or an external pump. In addition, there was adjustment of the insulin dosage under the direction of an expert team, taking into account self-monitoring of blood glucose performed four times per day, dietary intake, and anticipated exercise.[88]

From 1983 through 1989, 1441 patients were randomized. The primary outcome measure was a sustained (at two consecutive 6-month visits) three-step progression of diabetic retinopathy. This was based on an ordinal severity scale based on retinopathy scores in both eyes, determined by grading of stereoscopic color fundus photographs of the seven standard fields. Nonocular outcomes measured in the study were development of urinary albumin excretion of >40 mg per 24 hours (microalbuminuria) or >300 mg per 24 hours (gross proteinuria), and the incidence of clinical neuropathy. Adverse events included mortality, incidence of severe hypoglycemia, weight gain, myocardial infarction, and stroke.

The average follow-up in the study was 6.5 years (range 3–9 years) after randomization. The average difference in A1c between the intensive and conventional treatment groups for both the primary and secondary prevention was nearly 2%. Less than 5% of the cohort in the intensively treated group were able to maintain their A1c level at 6.0% or less over the course of the study.

An important finding of the trial was the statistically significant reduction in risk of sustained progression of retinopathy by three or more steps by 76% (Table 47.3) in the primary prevention group on intensive therapy for glycemic control. In the secondary-intervention cohort, the intensive therapy group had a reduction of

average risk of progression by 54% during the entire study period compared to the patients assigned to the conventional-therapy group. In addition, when both cohorts were combined, the intensive therapy group also had a reduction in risk for development of severe nonproliferative retinopathy or proliferative retinopathy by 47% and of treatment with photocoagulation by 51% (Table 47.3). There was a decrease in the incidence of clinically significant macular edema in the group assigned to intensive therapy compared to those assigned to conventional therapy. However, this difference did not reach statistical significance.

TABLE 47.3

Development and Progression of Long-Term Complications of Diabetes in the Study Cohorts and Reduction in Risk With Intensive as Compared With Conventional Therapy[a]

Complications	Primary Prevention			Secondary Intervention			Bo Co
	Conventional Therapy	Intensive Therapy	Risk Reduction	Conventional Therapy	Intensive Therapy	Risk Reduction	Ri Re
	Rate/100 Patient yr		% (95% CI)	Rate/100 Patient yr		% (95% CI)	% CI
≥3-step sustained retinopathy	4.7	1.2	76 (62–85)[c]	7.8	3.7	54 (39–66)[c]	63 71
Macular edema[d]	–	–	–	3.0	2.0	23 (−13–48)	26
Severe nonproliferative or proliferative retinopathy[d]	–	–	–	2.4	1.1	47 (14–67)[e]	47 67
Laser treatment[f]	–	–	–	2.3	0.9	56 (26–74)[c]	51 70

[a]Rates shown are absolute rates of the development and progression of complications per 100 patient-years. Risk reductions represent the comparison of intensive with conventional treatment, expressed as a percentage and calculated from the proportional-hazards model with adjustment for baseline values as noted, except in the case of neuropathy. CI denotes confidence interval.

[b]Stratified according to the primary-prevention and secondary-prevention cohorts.

[c]$p \leq .002$ by the two-tailed rank-sum test.

[d]Too few events occurred in the primary-prevention cohort to allow meaningful analysis of this variable.

[e]$p < .04$ by the two-tailed rank-sum test.

[f]Denotes the first episode of laser therapy for macular edema or proliferative

retinopathy.

Reprinted with permission from the Diabetes Control and Complications Trial Research Group (DCCT). The effect of intensive treatment of diabetes on the development and progression of long-term complications in insulin-dependent diabetes mellitus. N Engl J Med 1993;329:977–86. Copyright © 1993 Massachusetts Medical Society.

Early worsening of retinopathy in the first year of treatment of the intensive therapy group in the secondary-intervention cohort was observed, as had been reported previously.[91–93] On average, it took about 3 years in this group to demonstrate the beneficial effect of intensive treatment. After 3 years, the beneficial effect of intensive insulin treatment increased over time.

The DCCT investigators also examined whether there was an association of A1c values <8% versus those of ≥8% for progression of retinopathy. When they combined the two groups (conventional and intensive treatment), they found no evidence to support the concept of a glycemic threshold regarding progression of retinopathy, as had been described by others.[94]

Intensive insulin treatment reduced but did not prevent the incidence and progression of retinopathy in persons without signs of retinopathy at the baseline examination. The 9-year cumulative incidence of one microaneurysm or more severe retinopathy in eyes with no retinopathy present at baseline was 70% in persons with <2.5 years of type 1 diabetes and 62% in persons with >2.5 years of type 1 diabetes at baseline. Approximately 40% of these individuals developed a three-step progression of their retinopathy.[89]

The DCCT examined whether intensive therapy was more beneficial when started earlier in the course of type 1 diabetes. They found that the 9-year cumulative incidence of sustained three-step progression in persons without retinopathy with <2.5 years of type 1 diabetes in the intensive therapy group was 7% compared to 20% in those with >2.5 years. The 9-year cumulative incidence of sustained three-step progression in the intensive therapy group was lower in eyes with minimal to early nonproliferative retinopathy at baseline compared to eyes with more severe nonproliferative retinopathy at baseline (11.5–18.2% vs. 43.8%). These data suggested a benefit of beginning intensive treatment earlier in the course of diabetes, prior to the onset of diabetic retinopathy.[89]

The most important adverse event was a two- to threefold

increase in severe hypoglycemia in the intensive insulin treatment group compared to the conventional group. There was a 33% increase in the mean adjusted risk of becoming overweight (body weight more than 120% above the ideal) in persons in the intensive compared to the conventional insulin treatment group, also considered an adverse outcome.

From the trial, it was estimated that intensive therapy would result in a "gain of 920,000 years of sight, 691,000 years free from end-stage renal disease, 678,000 years free from lower extremity amputation, and 611,000 years of life at an additional cost of $4.0 billion over the lifetime" of the 120,000 persons with IDDM in the United States who meet DCCT eligibility criteria.[95] The incremental cost per year of life gained was $28,661, and when adjusted for quality of life, intensive therapy costs $19,987 per quality-of-life year gained. These findings were similar to cost-effectiveness ratios for other medical interventions in the United States.

Fourteen years of additional follow-up of the DCCT cohort after the study was stopped revealed that despite convergence of A1c levels in the intensive and conventional groups, the protective effect of glycemic control was maintained in the intensive group.[96–98] This has been labeled "metabolic memory" and has been found also in persons with type 2 diabetes in the UKPDS (see below).[99] The reason for this finding remains speculative. The 18-year post-DCCT data[100] provide further information on the long-term relationship of the level of glycemia to retinopathy as well as other complications. Those in the former intensive treatment group continue to have a lower cumulative incidence of retinopathy compared to those in the conventional treatment group, but the yearly incidence of the outcomes is now similar, suggesting that risk reduction may essentially be due to a dose effect. That is, the "dose" of glycosylated hemoglobin was lower for an average of 6.5 years in the intensive compared to the conventional treatment group but when the intensive treatment was no longer imposed, the yearly rate of retinopathy endpoints became nearly parallel. This suggests that there may be no "metabolic memory"; what we are observing is the effect of a greater cumulative "dose" of glycosylated hemoglobin in the conventional group. This was implied in the article but not directly stated. In fact, modeled data from a general

population of persons with type 1 diabetes (not participants in a clinical trial) suggest that even persons with relatively tight metabolic control are still not protected from retinopathy or its progression, implying that there is room for improvement in preventive care.[101] Recent data suggest that biochemical pathways involving advanced glycation endproducts and oxidative stress may affect genes and proteins involved in the pathogenesis of diabetic microvascular and macrovascular complications.[98]

The UKPDS was a randomized, controlled clinical trial involving 3867 patients newly diagnosed with type 2 diabetes.[102–104] After 3 months of dietary treatment, patients with a mean of two fasting plasma glucose concentrations of 6.1–15.0 mmol/L were randomly assigned to intensive glycemic control with either a sulfonylurea or insulin or conventional glycemic control. The latter group was further divided into those who were overweight or not. Metformin was included as one of the treatment arms for 1704 overweight patients, and analyses included comparison of the effect of metformin against conventional therapy in overweight patients. After 12 years of follow-up, there was a reduction in rate of progression of diabetic retinopathy of 21% and reduction in need for laser photocoagulation of 29% in the intensive versus the conventional treatment group. In addition, there were no differences in reduction in the incidence of the retinopathy endpoints among the three agents used in the intensive treatment group (chlorpropamide, glibenclamide, and insulin), but the chlorpropamide treatment group failed to show a reduced rate of retinopathy requiring photocoagulation. Furthermore, there was no difference in vision outcomes between conventional and intensive treatments. It was concluded that metformin was preferred as the first-line pharmacologic therapy in newly diagnosed type 2 diabetic patients who were overweight, based on their finding of a significant (39%) reduction in myocardial infarction compared to the conventional treatment group. When metformin was added to sulfonylureas (in both obese and nonobese patients), however, it was associated with increased diabetes-related (96%) and all-cause mortality (60%) when compared to conventional therapy. The intensive treatment group suffered significantly more major hypoglycemic episodes and weight gain than patients in the

conventional group. Economic analyses of the clinical trial data suggested that intensive glucose control increased treatment costs but substantially reduced complication costs and increased the time free of such complications.[104,105]

The development of new treatment modalities for achieving glycemic control has resulted in two randomized clinical trials that permitted evaluation of the effects of near normalization of glycemic level on the incidence of cardiovascular disease and retinopathy. The first trial involved 1791 military veterans with an average age of 60 years and an average duration of 11 years of type 2 diabetes, who had a suboptimal response to therapy for their diabetes. They were randomly assigned to receive either intensive or standard glucose control, with an aim in the intensive therapy group of achieving an absolute reduction of 1.5 percentage points in the A1c level as compared with the standard therapy group. The primary outcome was the time to the first occurrence of a major cardiovascular disease event, and a secondary objective was to evaluate the effect of glycemic control on the incidence and progression of diabetic retinopathy and other microvascular complications.[106,107] The subjects were followed for up to 7.5 years (median: 5.6 years). Despite reaching their glycemic goal (median A1c level at 6 months: 8.4% in the group receiving standard therapy and 6.9% in the intensive therapy group), there were no statistically significant differences in any of the retinopathy outcomes between groups receiving intensive and standard therapy (incidence of retinopathy 42% vs. 49%, p=.27; progression of retinopathy by two or more steps on the ETDRS severity scale 17% vs. 22%, p=.07; progression to proliferative diabetic retinopathy 4% vs. 5%, p=.27) or in progression to clinically significant macular edema (3% vs. 5%, p=.31). While it is possible that a benefit might have been seen if the study was continued, these data lead to the conclusion that decreasing the A1c level from 8.4% to 6.9% in persons with relatively longstanding type 2 diabetes has little benefit in preventing the incidence and progression of retinopathy.

The Action to Control Cardiovascular Risk in Diabetes (ACCORD) trial[108] examined whether intensive treatment with an even lower targeted A1c level (<6.0%) than in the military veteran study versus standard treatment (targeted A1c level 7.0–7.9%)

would reduce the risk of morbidity and mortality from cardiovascular disease (primary endpoint) and microvascular events, such as the incidence of photocoagulation treatment for diabetic retinopathy and incidence of microalbuminuria and macroalbuminuria over a 5-year period (secondary endpoints) in persons with a mean age of 60 years with an average duration of 10 years of type 2 diabetes.[109,110] They reported findings on the same composite microvascular endpoints measured in the UKPDS. The ACCORD Eye examined the incidence and progression of diabetic retinopathy based on grading of fundus photographs in 2856 of the 10,251 ACCORD participants.[109] The authors reported a 33% reduction in the relative risk of progression in persons who received intensive glycemia treatment versus standard therapy (adjusted OR 0.67; 95% CI 0.51–0.87; p=.003) in a relatively short period (4 years). The ACCORD intensive glycemic strategy was prematurely discontinued because of a statistically significant 22% increase in overall mortality in the intensive glycemic group of the study. Median A1c was 6.3% compared with 7.6% in the standard glycemic group. The study closure of the glycemic phase of the trial made it too short and the power too low to observe a protective effect for the severe microvascular endpoints, which usually evolve over a longer period.[37]

An additional clinical trial, the Action in Diabetes and Vascular Disease: Preterax and Diamicron Modified Release Controlled Evaluation (ADVANCE) study of patients with type 2 diabetes, showed no statistically significant effect of glycemic control on severe diabetes related to ocular endpoints.[111]

Based on the results of these studies, it appears that intensive therapy should be the primary public healthcare strategy aimed at reducing the risk of visual loss from diabetic retinopathy in persons with both type 1 and 2 diabetes. The data from the DCCT and UKPDS provided further support for the ADA guidelines of a target goal of A1c level of 7.0% for persons with diabetes, and suggest that this level of control, when achieved earlier after diagnosis of diabetes, may have greater long-term benefit in terms of reducing the incidence and progression of retinopathy.[112] However, data from the NHANES III[113] and the WESDR[114] suggest that few persons with diabetes reach this targeted level of glycemic

control. The data from the military veterans study, the ACCORD, and the ADVANCE suggest that further lowering the level of glycemia does not support applying intensive glycemic control with the current technology to achieve such control in patients with longstanding type 2 diabetes who have or who are at risk of developing cardiovascular disease.[115,116]

C-Peptide Status

The relationship of endogenous insulin secretion to diabetic retinopathy independent of glycemic control is uncertain.[117–120] In the WESDR, the highest prevalence and most severe retinopathy were found in individuals with undetectable or low plasma C-peptide (<0.3 nM), whereas the lowest frequencies and least severe retinopathy were found in older-onset individuals not using insulin who were overweight.[121] Older- and younger-onset individuals who were using insulin and who had no detectable C-peptide had similar frequencies of proliferative retinopathy. While adjusting for other risk factors associated with the incidence and progression of diabetic retinopathy, there was no relationship of C-peptide level to incident or progressed retinopathy in persons with type 1 diabetes in the WESDR.[122] In the DCCT, however, higher C-peptide levels at entry were associated with reduced incidence of retinopathy and lower incidence of hypoglycemic episodes.[123] In the WESDR, while adjusting for characteristics associated with retinopathy in older-onset people who were not taking insulin (type 2 diabetes), there was no protection associated with higher levels of C-peptide.[121,122] These findings suggest that the level of glycemia, and not the level of endogenous insulin secretion as indicated by C-peptide level, is more important in determining the presence and severity of retinopathy in individuals with type 2 diabetes.

Exogenous Insulin

It has been suggested that exogenous insulin may be a possible cause of atherosclerosis and retinopathy in people with type 2 diabetes.[124] In a meta-analysis of seven cohorts with type 2 diabetes, six of which were prospective in design, insulin use was associated

with increased risk of diabetic retinopathy despite adjustment for glycosylated hemoglobin levels. However, the relationship was attenuated and no longer statistically significant after adjustment for duration of type 2 diabetes.[125] In the WESDR, there was no association between the amount or type of exogenous insulin used and the presence, severity, incidence or progression of retinopathy in the older-onset group using insulin whose C-peptide was 0.3 nM or greater.[121,122] These data suggest that exogenous insulin in itself is unlikely to be causally related to retinopathy in diabetic people with normal C-peptide levels. Research aimed at evaluating the possibility of using pluripotent stem cells[126] to endogenously deliver insulin is an exciting area that in the future may allow for better delivery of insulin than currently available. While such research is now confined to the laboratory, the epidemiology of diabetic retinopathy is likely to be influenced by such interventions. Thus, the current management of diabetes supports the notion and scientific evidence that insulin therapy is efficacious for controlling glycemia and for diminishing the likelihood of complications, both micro- and macrovascular complications of diabetes.

Blood Pressure

The UKPDS found that the incidence of retinopathy was associated with systolic blood pressure. For each 10 mmHg decrease in mean systolic blood pressure, a 13% reduction was found for microvascular complications. No threshold was found for any retinopathy endpoint.[127] In the WESDR, a 10 mmHg rise in diastolic blood pressure was found to be associated with a 330% increased 4-year risk of developing macular edema in those with type 1 diabetes and a 210% increased risk in those with type 2 diabetes.[128]

The UKPDS sought to determine whether lowering blood pressure was beneficial in reducing macrovascular and microvascular complications associated with type 2 diabetes.[129] A series of 1048 patients with hypertension (mean blood pressure 160/94 mmHg) were randomized to a regimen of tight control with either captopril (an angiotensin-converting enzyme [ACE] inhibitor) or atenolol (a beta-blocker) and another 390 patients to less tight control of their blood pressure. The aim in the group

randomized to tight control of blood pressure (by the standards at the beginning of the clinical trial) was to achieve blood pressure values <150/<85 mmHg. If these goals were not met with maximal doses of a beta-blocker or ACE inhibitor, additional medications were prescribed, including a loop diuretic, a calcium-channel blocker, and a vasodilator. The aim in the group randomized to less tight control was to achieve blood pressure values <180/<105 mmHg. Tight blood pressure control resulted in a 35% reduction in retinal photocoagulation compared to conventional control, presumably due to a lower incidence of macular edema. After 7.5 years of follow-up, there was a 34% reduction in the rate of progression of retinopathy by two or more steps using the modified ETDRS severity scale and a 47% reduction in the deterioration of visual acuity by 3 lines or more using the ETDRS charts (for example, a reduction in vision from 20/30 to 20/60 or worse on a Snellen chart). Atenolol and captopril were equally effective in reducing the risk of developing these microvascular complications, suggesting that blood pressure reduction itself was more important than the type of medication used to reduce it. The effects of blood pressure control were independent of those of glycemic control. These findings support the recommendations for blood pressure control in patients with type 2 diabetes as a means of preventing visual loss from diabetic retinopathy.

The ACCORD also examined whether in the context of good glycemic control, a "therapeutic strategy that targets a systolic blood pressure of <120 mmHg would reduce cardiovascular disease events compared to a strategy that targets a systolic blood pressure of <140 mmHg in persons with type 2 diabetes."[109] There were 1263 ACCORD-Eye study participants enrolled in the ACCORD blood pressure study. After 1 year, the baseline median systolic blood pressure lowered significantly (from 133 to 117 mmHg) in the intensive blood pressure therapy group compared to the standard blood pressure therapy group and remained stable throughout the remainder of the trial. The rates of progression of diabetic retinopathy were 10% in the group undergoing intensive blood pressure control compared to 9% in the group undergoing standard blood pressure control (adjusted OR 1.23; 95% CI 0.84–1.79; p=.29).

The ADVANCE study also found no beneficial effect of intensive

blood pressure control on progression of diabetic retinopathy.[130] These findings from the ACCORD, ADVANCE, and UKPDS suggest that the benefit in preventing the progression of diabetic retinopathy may be limited to those with type 2 diabetes with uncontrolled high blood pressure.

A number of randomized controlled clinical trials have examined whether specific antihypertensive agents had a protective effect in preventing the progression of retinopathy independent of its effect on blood pressure.[131–137] The Epidemiology and Prevention of Diabetes (EURODIAB) Controlled Trial of Lisinopril in Insulin-Dependent Diabetes Mellitus (EUCLID) study sought to examine the role of an ACE inhibitor in reducing the incidence and progression of retinopathy in a group of largely normotensive type 1 diabetic patients, of whom 85% did not have microalbuminuria at baseline.[131] This study showed a statistically significant 50% reduction in the progression of retinopathy in those taking lisinopril over a two-year period after adjustment for glycemic control. Progression to proliferative retinopathy was also reduced, although the relation was not statistically significant. There was no significant interaction with blood glucose control. It was postulated that ACE inhibitors might have an effect independent of lowering of blood pressure.[132]

The Diabetic Retinopathy Candesartan Trials (DIRECT) were comprised of three randomized double-masked, parallel, placebo-controlled studies, involving 5231 patients with type 1 or type 2 diabetes.[133,134,137] In the DIRECT-Prevent 1, candesartan had a borderline effect (p=.0508) on the primary endpoint, reducing the incidence of retinopathy by two or more steps on the ETDRS severity scale by 18%. In post-hoc analyses, candesartan reduced the incidence of retinopathy by three or more steps by 35% (hazard ratio 0.65; 95% CI 0.48–0.87) in the DIRECT-Prevent 1. In the DIRECT-Protect 1 and 2, candesartan had no statistically significant effect on the progression of retinopathy (defined as three or more steps on the ETDRS severity scale in persons with minimal to moderately severe nonproliferative diabetic retinopathy at baseline). However, in the DIRECT-Protect 2, treatment with candesartan significantly increased a secondary outcome, regression of retinopathy, by 34% (hazard ratio 1.34; 95% CI 1.08–

1.68). The effects were limited to those participants with early retinopathy. Thus, the DIRECT, while suggestive of a beneficial effect of candesartan in reducing the incidence of retinopathy, did not achieve the prespecified primary endpoint in any of the three trials.

The ADVANCE study involved more than 11,000 participants and examined whether lowering of blood pressure via a perindopril–indapamide combination provided additional benefit in preventing diabetic macrovascular and microvascular complications.[130] Although mean systolic and diastolic blood pressure reduction by 5.6 mmHg and 2.2 mmHg, respectively, was achieved, there was no reduction in the 4-year incidence or progression of diabetic retinopathy (5.2% in both treatment and placebo groups).

The Renin-Angiotensin System Study (RASS) was a multicenter controlled trial involving 285 normotensive patients with type 1 diabetes and normoalbuminuria and who were randomly assigned to receive losartan (100 mg daily), enalapril (20 mg daily), or placebo and followed for 5 years.[135] It showed that, as compared with placebo, the odds of retinopathy progression by two or more steps was reduced by 65% with enalapril (OR 0.35; 95% CI 0.14–0.85) and by 70% with losartan (OR 0.30; 95% CI 0.12–0.73), independently of changes in blood pressure.

These clinical trial data show a protective effect on incidence of retinopathy by angiotensin inhibitors or receptor blockers in normotensive, normoalbuminuric persons with no retinopathy, and an inconsistent effect on progression in those with early to moderately severe nonproliferative retinopathy. The reasons for the differences in findings in the RASS, DIRECT, and ADVANCE are not known. Any decision to use these agents to prevent diabetic retinopathy must be tempered by the findings in the RASS and DIRECT of an increase in the albumin excretion rate in those receiving losartan or candesartan compared to those in the placebo group.

Lower systolic blood pressure was associated with a significantly lower risk of retinopathy (relative risk per 10 mmHg decrease 0.87, 95% CI 0.76–0.99) in a meta-analysis of 40 randomized controlled clinical trials in people with diabetes.[138] When the trials were

stratified by mean baseline systolic blood pressure at greater than or less than 140 mmHg, the relative risk for retinopathy was similar regardless of baseline systolic blood pressure status, described as high or low. These findings support the use of medications for lowering of blood pressure in these patients. The investigators of the meta-analysis concluded that in contrast with the recommendations of the Eight Joint National Committee (JNC8) guidelines,[139] for individuals "with mild nonproliferative diabetic retinopathy, the commencement of blood pressure lowering therapy below an initial systolic blood pressure level of 140 mmHg and treatment to a systolic blood pressure level below 130 mmHg should be considered."

In summary, while lacking consistency, the data lean toward a beneficial effect of lower blood pressure to decrease the risk of microvascular complications such as diabetic retinopathy.

Proteinuria and Diabetic Nephropathy

Data from most studies show an association between the prevalence of diabetic nephropathy, as manifest by microalbuminuria or gross proteinuria, and diabetic retinopathy.[2,3,10,13,15,37,140–143] There are anecdotal reports of patients with renal failure having more severe macular edema that improves after dialysis or renal transplantation. Lipid, rheologic, and platelet abnormalities associated with nephropathy may be involved in the pathogenesis of retinopathy. In the WESDR, in those with type 1 diabetes, the relative risk of proliferative retinopathy developing over four years in those with gross proteinuria at baseline was 2.32 (95% CI 1.40–3.83) compared with those without gross proteinuria.[142] However, after adjusting for other relevant risk factors, the relationship was of borderline significance. In persons taking insulin, the relative risk was 2.02 (95% CI 0.91–4.44), and for those not taking insulin it was 1.13 (95% CI 0.15–8.50).

In a cohort study in Pittsburgh of persons with type 1 diabetes, a greater proportion of those with microalbuminuria or overt nephropathy at study entry progressed to proliferative disease over a 2-year follow-up.[144] However, in the same study nephropathy at baseline was not associated with overall progression of retinopathy.

Data from these studies suggest that in those with type 1 diabetes, gross proteinuria is a risk indicator for proliferative retinopathy and they may therefore benefit from regular ophthalmologic evaluation. There have been no clinical trial data to suggest that interventions that prevent or slow diabetic nephropathy will reduce the incidence and progression of retinopathy.

A question that is intriguing but hard to investigate is whether renal disease in persons with type 1 diabetes, regardless of whether it is characteristic diabetic renal disease or nondiabetic renal disease, increases the risk of progression of retinopathy or incidence of macular edema. This is in distinction from the notion of the "common soil hypothesis" described by Stern,[145] Wong and colleagues,[146] and Koenig and Meisinger.[147] The notion for the former hypothesis is that advanced renal disease and its accompanying physiologic derangements (e.g., acidosis, oxidative stress, and mechanisms possibly related to angiotensin II system)[148] in the presence of advanced microvascular disease related to diabetes increase the likelihood of progression of retinopathy. The difficulty in investigating this is that there are few persons with advanced diabetic renal disease who are still at risk of progression of retinopathy. If it is true, then more aggressive treatment of early stages of nephropathy might spare at least some patients from vision loss due to retinopathy, as well as potentially sparing the microvasculature in other organs.[149]

Serum Lipids and Lipid Lowering

Macular edema is an important cause of loss of vision in people with diabetes.[150] Hard exudate, a lipoprotein deposit in the retina, is often associated with macular edema. Data from early clinical studies showed an association of elevated plasma triglycerides and lipids with hard exudate.[151]

In the WESDR, higher serum total cholesterol was associated with higher prevalence of retinal hard exudates in both the younger- and the older-onset groups taking insulin but not in those with type 2 diabetes using oral hypoglycemic agents.[152] In subsequent follow-up, a modest association was found between higher levels of serum high-density lipoprotein (HDL) cholesterol

and decreased prevalence of diabetic retinopathy (OR per 10 mg/dL increase in HDL cholesterol, 0.87) while adjusting for duration of diabetes, glycosylated hemoglobin, statin use, and endstage renal disease status.[153] There were no significant associations between total or HDL cholesterol and incident proliferative diabetic retinopathy or macular edema over successive intervals of follow-up. Statin use was not associated with decreased incidence of proliferative diabetic retinopathy or macular edema. In the ETDRS, higher levels of serum lipids (triglycerides, low-density lipoproteins, and very-low-density lipoproteins) at baseline were associated with increased risk of developing hard exudates in the macula and decreased visual acuity.[154] In a study of Mexican patients with type 2 diabetes, Santos and colleagues[155] showed the frequency of severe retinal hard exudates was higher in those with the epsilon4 allele polymorphism of the apolipoprotein E gene. A large meta-analysis of information obtained from 13 studies indicated that diabetic kidney disease was associated worldwide with higher levels of plasma triglycerides and lower levels of high-density lipoprotein cholesterol among patients with good control of low-density lipoprotein cholesterol.[156] Retinopathy was less robustly associated with these lipids and it may be that the association with retinopathy was secondary to diabetic renal disease.

The ACCORD Lipid study,[109] which enrolled a total of 1593 persons with type 2 diabetes and examined whether fenofibrate and statins to raise the serum HDL cholesterol and lower triglyceride levels in the context of desirable levels of serum LDL cholesterol and good glycemic control would reduce the incidence of macular edema and progression of retinopathy compared to a strategy that only achieves desirable levels of LDL cholesterol and glycemic control using statins alone. Serum triglycerides fell from 162 mg/dL at baseline to 120 mg/dL in the fenofibrate treatment group as compared with a decrease to 147 mg/dL in the placebo group after 1 year (p <.001). The rate of progression of diabetic retinopathy at 4 years was 6.5% in the fenofibrate treatment group compared to 10.2% in the placebo group (adjusted OR 0.60; 95% CI 0.42–0.87; p=.006). These findings are consistent with the findings from the Fenofibrate Intervention and Event Lowering in Diabetes (FIELD)

study, a randomized trial of monotherapy with fenofibrate, which showed a significant reduction in the need for laser therapy for either macular edema or proliferative retinopathy in the fenofibrate treatment group as compared with the placebo group (3.4% vs. 4.9%, $p<.001$).[157] While these findings suggest a beneficial effect of the use of fenofibrate therapy in diabetic patients with elevated triglycerides at risk of progression of diabetic retinopathy and macular edema, a more recent study failed to confirm a significant effect of fenofibrate on macular edema despite an effect on serum triglycerides.[158] This may be explained by relatively low power.

Smoking

Smoking might be expected to be associated with retinopathy because it is associated with vasoconstriction of the small blood vessels.[159] Additionally, smoking may lead to increased platelet aggregation and adhesiveness,[160] which may be thought to predispose to diabetic retinopathy, but most epidemiologic data show no relationship between cigarette smoking and the incidence or progression of that endpoint.[10,11,63,140,141,161–163] In the WESDR, cigarette smoking was not associated with the 4- or 10-year incidence or progression of diabetic retinopathy nor macular edema.[162,163] Despite this, diabetic patients should be advised not to smoke because of an increased risk of cardiovascular and respiratory disease, to which persons with diabetes are already prone, as well as cancer. In the WESDR, after adjusting for other risk factors, younger-onset people who smoked were 2.4 times as likely and older-onset people were 1.6 times as likely to die sooner than people who did not smoke.[164]

Alcohol

Because moderate alcohol consumption is associated with decreased platelet aggregation and adhesiveness, improved glycemic control, and reduction of inflammation, one might anticipate a possible protective effect in reducing the incidence and progression of retinopathy.[165–167] Data from one study suggested such a beneficial effect, while that from another study suggested an

increased risk of proliferative retinopathy.[168,169] No relation between alcohol consumption and diabetic retinopathy was found in a population-based study in Australia.[17] In the UKPDS, a relation of increased alcohol consumption to increased severity of retinopathy was found only in men with newly diagnosed type 2 diabetes.[20] In the EURODIAB Prospective Study of Complications in persons with type 1 diabetes, alcohol consumption was associated with a reduction in progression of diabetic retinopathy.[170] In the ADVANCE Retinopathy Measurements (ADREM), a subset of persons in the ADVANCE with fundus photographs, there was no relation of alcohol consumption to progression of diabetic retinopathy, but for unknown reasons, a decline in the visual acuity at follow-up was seen in those who consumed alcohol when compared with those who abstained from alcohol.[171] In the WESDR, alcohol consumption was associated with a lower frequency of proliferative retinopathy in persons with type 1 diabetes.[172] There was no relationship, however, between alcohol consumption at the 4-year examination and the incidence and progression of retinopathy in either the younger- or older-onset groups at the 10-year follow-up,[173] nor was there a relation to a change in visual acuity. Of interest in the WESDR was an association of reduction in cardiovascular disease mortality in persons with type 1 diabetes who consumed an average of one drink of alcohol per day.[174]

Body Mass Index (BMI)

The relationship between diabetic retinopathy and BMI is inconsistent among various studies.[2,10,11,64,175–179] In the WESDR, body mass was inversely related to the presence or severity of diabetic retinopathy only in persons with type 2 diabetes not using insulin.[178] While adjusting for other risk factors, older-onset persons in the WESDR who were underweight at baseline (BMI <20 kg/m^2 for both men and women) were three times as likely to develop retinopathy as those who were of normal weight (BMI of 20–27.7 kg/m^2 for men and 20–27.2 kg/m^2 for women). It has been speculated that underweight older-onset subjects are more likely to be in a "severe" phase of their type 2 diabetes or have late-onset type 1 diabetes. Persons obese at baseline (BMI >31.0 kg/m^2 for men

and >32.1 kg/m^2 for women) were 35% more likely to have progression of retinopathy and 41% more likely to develop proliferative retinopathy than those who were of normal weight at baseline. However, these associations were not statistically significant.

Physical Activity

Physical activity, through its beneficial effect on glycemic control, would be expected to be associated with decreased prevalence and incidence of diabetic retinopathy.[180] However, few epidemiologic data are available describing the relationship between diabetic retinopathy and physical activity.[176,181–183] One study found no relationship between participating in team sports in high school or college and a history of laser treatment or blindness in people with type 1 diabetes.[176] The same group reported that physical activity in youth did not relate to complications of diabetes.[181,182] In the WESDR, women diagnosed with diabetes before 14 years of age who participated in team sports were less likely to have proliferative diabetic retinopathy than those who did not.[183] There was no association between physical activity or leisure time energy expenditure and the presence and severity of diabetic retinopathy in men. In addition, physical activity was associated with either an increased or decreased risk of progression of retinopathy or the development of proliferative retinopathy over a 6-year interval in people with type 1 diabetes in this study.[184]

Socioeconomic Status

Inconsistent relationships between socioeconomic status and retinopathy severity have been reported.[10,16,185,186] Hanna and colleagues[185] reported a significant correlation between proliferative retinopathy and occupational status (working class) or lower income in a case–control study of 49 people with type 1 diabetes. Haffner and colleagues[186] did not find a relationship between socioeconomic status, measured using a combination of the Duncan Index, educational attainment or income, and severe retinopathy in 343 Mexican Americans and 79 non-Hispanic whites with type 2

diabetes in San Antonio. K. West and colleagues[10] also did not observe a relationship between retinopathy severity and education level in a population of Oklahoma Indians with type 2 diabetes. In the Proyecto VER cohort of Mexican Americans, low income, once adjusted for other factors, was related to proliferative retinopathy (OR 3.93; 95% CI 1.31–11.80).[16]

There are few studies that have examined the relation of socioeconomic factors to incidence and progression of diabetic retinopathy.[46,187] In the New Jersey 725 study, low socioeconomic status was significantly associated with the 6-year incidence of macular edema but not incidence or progression of diabetic retinopathy. In that study, education, income, medical or eye care, and health insurance at baseline were not significantly different between patients with and without macular edema at follow-up. In the WESDR, except for an association of lower incidence of proliferative retinopathy in women with type 1 diabetes of 25 years of age or older with more education, socioeconomic status (education level and Duncan Socioeconomic Index score) was not associated with risk of developing proliferative retinopathy.[187] It may be that the absence of a relationship of socioeconomic status and retinopathy severity in the WESDR and San Antonio Study is related to the lack of an association of glycemia to socioeconomic status in these populations.

Hormone and Reproductive Exposures in Women

In the WESDR, menarchal status at the baseline examination was related to the prevalence and severity of retinopathy[78] as noted previously in the section on puberty. Sex hormones have been hypothesized to explain the higher risk of developing retinopathy after puberty as well.[78] Use of oral contraceptives, which contain estrogens as well as progestins, does not appear to increase the risk of retinopathy[188] nor does use of hormone replacement therapy.[189]

Pregnancy, a condition associated with high levels of estrogens, is associated with more rapid progression of retinopathy. When pregnant women were compared with nonpregnant diabetic

women of similar age and duration of diabetes, the pregnant women were more likely to develop retinopathy if they had not had it before or to have greater likelihood of progression of their retinopathy when the groups were followed for a time interval roughly equal to the length of the pregnancy.[190] This remained true after adjusting for level of glycemia and blood pressure. Similar findings have been reported by others.[191–193]

This may occur in those with type 2 as well as type 1 diabetes.[194] A complementary finding was reported by Lovestam-Adrian and colleagues[195] who found that progression of retinopathy was more likely to occur in diabetic women with preeclampsia than in those without. Similarly, Rosenn and colleagues[196] found that glycemia and blood pressure were important determinants of progression of retinopathy during pregnancy. While these are important factors in nonpregnant women, pregnancy in all likelihood accelerates the process. Other investigators have found that progression of retinopathy was related to prior duration of diabetes.[197,198] Because duration of diabetes is a risk factor for progression of retinopathy irrespective of pregnancy status, this is also not a novel finding. However, it may be useful information in tailoring a follow-up plan for eye care during pregnancy. It has been suggested that laser treatment before pregnancy for women with moderate to severe retinopathy be considered to protect against progression during pregnancy,[199] although a clinical trial of the efficacy of such an approach is lacking. Aside from diabetic retinopathy, diabetic macular edema that occurs during pregnancy poses a threat to vision and this may benefit from laser treatment,[200] although it is unclear how many women with this sight-threatening complication will have remission after parturition.

There are limited data to suggest that serum IGF-1 levels are associated with progression of retinopathy during pregnancy.[201,202] A small study was performed to determine whether the vasoconstrictor endothelin-1 (ET-1), which is elevated in hypertension and diabetes, was associated with severity of retinopathy in pregnancy. While diabetic women had higher levels of ET-1 in pregnancy than nondiabetic women in the same trimester, a relationship to severity of diabetic retinopathy was not found.[203] The study was hampered by its small number of patients

and so must be regarded as inconclusive.

Despite the apparent deleterious effect of pregnancy on retinopathy, however, the number of past pregnancies was unrelated to the severity of diabetic retinopathy in younger-onset women in the WESDR.[189] Similarly, in a study in Oulu, Finland, there appeared to be little influence of second and subsequent pregnancies on retinopathy.[204] These data may be interpreted to suggest that pregnancy imparts a transient increased risk for incidence or progression of retinopathy. However, since there may be decreased fertility that results from more severe or more complicated diabetes, it may be that those who sustain repeated pregnancies are more robust, and this is reflected in relative protection against more severe or more progressive retinopathy.

Another source of exposure to estrogens is hormone replacement therapy. Although this treatment has come under intense scrutiny, there is no evidence to suggest that exposure to these medicines increases the risk of diabetic retinopathy.[189]

Comorbidity and Mortality

In the WESDR, the risk of developing a heart attack, stroke, diabetic nephropathy, and amputation was higher in those with proliferative diabetic retinopathy compared to those with no or minimal nonproliferative retinopathy at baseline (Table 47.4).[205] In persons with type 1 diabetes, while adjusting for age and sex, retinopathy severity was associated with all-cause and ischemic heart disease mortality and in persons with type 2 diabetes with all-cause, ischemic heart disease mortality, and stroke.[206] After adjusting for systemic factors, the relations remained only for all-cause and stroke mortality in persons with type 2 diabetes. These data suggest that the presence of more severe retinopathy in diabetic patients is an indicator for increased risk of ischemic heart disease death, and may identify individuals who should be under care for cardiovascular disease. This had been reported by others.[207–209] The higher risk of cardiovascular disease in persons with more severe retinopathy may be partially due to the association of severe retinopathy with cardiovascular disease risk factors such as increased fibrinogen, increased platelet aggregation,

hyperglycemia, and hypertension.

TABLE 47.4

The Relative Risk for the Prevalence and 4-Year Incidence of Myocardial Infarction, Stroke, and Amputation of Lower Extremities Associated with Presence of Proliferative Retinopathy, Corrected for Age in the Wisconsin Epidemiologic Study of Diabetic Retinopathy

	Myocardial Infarction		Stroke		Amputation of Lower Extremity	
	RR	95% CI	RR	95% CI	RR	95% CI
Younger-onset group						
Prevalence	3.5	1.5–7.9	2.6	0.7–9.7	7.1	2.6–19.7
Incidence	4.5	1.3–15.4	1.6	0.4–5.7	6.0	2.1–16.9
Older-onset group taking insulin						
Prevalence	0.8	0.4–1.4	1.2	0.6–2.4	4.2	2.3–7.9
Incidence	1.2	0.5–3.4	2.9	1.2–6.8	3.4	0.9–13.2
Older-onset group not taking insulin						
Prevalence	0.3	0–2.4	2.9	0.9–9.4	5.2	0.6–45.0
Incidence	1.5	0.2–12.5	6.0	1.1–32.6	7.0	0.8–64.4

CI, confidence interval; RR, relative risk.

New Medical Interventions

Aside from glycemic, blood pressure, and lipid control, no other medical intervention has been demonstrated to reduce the incidence and progression of diabetic retinopathy. Randomized controlled clinical trials of inhibitors of aldose reductase, protein kinase C, and metalloproteinases have not shown efficacy of the intervention in preventing the incidence and progression of retinopathy in people with diabetes.[210] Controlled clinical trials of intravitreally administered vascular endothelial growth factor (VEGF) inhibitors and steroid in the treatment of diabetic macular edema are presented elsewhere.[211]

Public Health Applications of Epidemiologic Data

Based on the observation that many diabetic patients with severe retinopathy were not receiving dilated eye examinations, guidelines for these examinations were developed and implemented using epidemiologic data.[77,212,213] The guidelines recommended that after the initial screening examination, "subsequent examinations for both type 1 and type 2 diabetic patients should be repeated annually by an ophthalmologist or optometrist who is knowledgeable and experienced in diagnosing the presence of diabetic retinopathy, and is aware of its management."[77] However, a number of reports have demonstrated poor compliance with these guidelines.[214–218] In one study, only 16% of diabetic patients who received primary care in upstate New York received an annual ophthalmic examination using funduscopy by an optometrist or ophthalmologist in two consecutive years.[219] Reasons for poor compliance with the recommended ADA guidelines have been provided by others.[214,220,221] Physician factors may explain the reasons that patients may not be receiving optimal care. In one study, 52% of primary care physicians reported that they performed in-office ophthalmoscopic examinations, 90% of which were through undilated pupils, an approach shown to have limited sensitivity to detecting vision-threatening retinopathy in other studies.[220] Moss and colleagues[221] studied persons with type 1 and type 2 diabetes for 10 or more years who were participating in the WESDR. In those not having a dilated eye examination in the previous year, 31% and 35% of those with type 1 diabetes and type 2 diabetes, respectively, reported not having been told by their primary care doctors that they needed one.

Patient factors also explain some of the reasons why guidelines for dilated eye examinations are not being followed. In the WESDR, among those not having a dilated eye examination in the previous year, 79% and 71% of those with type 1 diabetes and type 2 diabetes, respectively, reported not having had one because they had no problems with their eyes, and 32% and 11% said they were too busy. These data suggest the importance of educating patients with diabetes about the asymptomatic nature of diabetic

retinopathy, and the benefits of a dilated eye examination. This has become an important priority of the National Eye Institute (National Eye Health Education Program) and other specialty organizations.[222] Of course, patients may elect not to follow the advice given or deny its importance. Another reason is that of cost. Moss and colleagues[221] found that the ability to afford eye care was also a reason patients gave for not having such care. In that study, 30% of persons with type 1 diabetes and 12% of those with type 2 diabetes said they could not afford an examination.

Reexamination of WESDR data by Batchelder and Barricks[223] led them to conclude that based on the "remarkably low incidence of treatable ocular conditions over 4 years for patients with retinopathy levels 21 or less and over 10 years for patients with no retinopathy at their baseline examination" that "these data do not suggest any difference in effectiveness for screening intervals of 1, 2, 3, or even 4 years for this group of low-risk patients." Others, also using models, have suggested that in those with type 2 diabetes without retinopathy, examinations every 2 years rather than yearly would be adequate to detect vision threatening retinopathy.[224] The National Committee for Quality Assurance[225] released the Health Plan Employer Data and Information Set (HEDIS) 1999 draft which suggested examinations for retinopathy every other year if there was no evidence of retinopathy in the previous year's eye examination, persons were not taking insulin, and if the A1c was less than 8%.[226] However, the WESDR data showed that in individuals with type 2 diabetes with no retinopathy present at baseline, 4 per 1000 developed proliferative retinopathy and 10 per 1000 developed clinically significant macular edema over a 4-year period.[34–36]

There is a need to examine the issue of the sensitivity of the screens in detecting the presence of retinopathy. The epidemiologic data are based on detection of retinopathy by skilled graders using standardized protocols under study conditions to grade stereoscopic color fundus photographs of the Diabetic Retinopathy Study seven standard fields. Studies have demonstrated a variable sensitivity, in practice as low as 33%, in the detection of retinopathy by ophthalmoscopy in people with diabetes.[227] Newer screening approaches, including digital cameras with central reading centers,

are being used for the screening of diabetic patients not under the care of an ophthalmologist. However, a recent meta-analysis showed that retinal photography by a photographer with no specialist medical or eye qualifications (i.e., a health worker or nurse), without using pupil-dilating eye drops (the outreach model), appears unlikely to miss cases of diabetic retinopathy that screening methods using mydriasis or a photographer with specialist medical or eye qualifications would detect.[228] There is a need to conduct further epidemiologic studies and controlled clinical trials to evaluate the interval and type of ophthalmic screening in persons with diabetes and no retinopathy in various healthcare settings to provide better evidence of efficacy of specific approaches to validate new guidelines and screening approaches. There is some evidence that telemedicine programs in England have achieved screening rates of 90%. The success of these screening programs is thought to have contributed, in part, to the finding that diabetic retinopathy is no longer the leading cause of vision loss in English adults aged 25–64 years.[229] The use of telemedicine eye screening in racial minority groups with diabetes living in urban settings has been shown to have potential for prevention of visual loss not only from detection of diabetic retinopathy but also due to detection of other eye conditions such as cataract and glaucoma that are more common in people with diabetes.[230] Cell phone camera applications that detect diabetic retinopathy by taking fundus photographs and transferring them to reading centers are currently being developed for screening purposes.[231,232] At the time of writing, these systems have not yet been validated for screening of diabetic retinopathy. This topic is discussed in detail in Chapter 53, Telescreening for diabetic retinopathy.

Conclusion

Prevention of diabetes remains an important goal in reducing the complications and costs of this disease. Until approaches for primary prevention of diabetes itself become available, clinical trial data have shown that secondary prevention through medical interventions designed to control blood glycemia, blood pressure,

and lipids will reduce the incidence and progression of retinopathy and loss of vision. However, success of these interventions has been limited, in part, due to inability to achieve normalization of blood sugar with current drug delivery systems. While new secondary medical interventions may be of further benefit, tertiary prevention of visual loss (screening examination through a dilated pupil by skilled eye care providers on a regular basis for early detection and subsequent treatment, when indicated, of vision-threatening retinopathy with photocoagulation) remains an important approach to care for diabetic patients.

References

1. Klein R, Klein BE, Moss SE, DeMets DL, Kaufman I, Voss PS. Prevalence of diabetes mellitus in southern Wisconsin. *Am J Epidemiol*. 1984;119(1):54–61.
2. Klein R, Klein BE, Moss SE, Davis MD, DeMets DL. The Wisconsin Epidemiologic Study of Diabetic Retinopathy. II. Prevalence and risk of diabetic retinopathy when age at diagnosis is less than 30 years. *Arch Ophthalmol*. 1984;102(4):520–526.
3. Klein R, Klein BE, Moss SE, Davis MD, DeMets DL. The Wisconsin Epidemiologic Study of Diabetic Retinopathy. III. Prevalence and risk of diabetic retinopathy when age at diagnosis is 30 or more years. *Arch Ophthalmol*. 1984;102(4):527–532.
4. Klein R, Klein BE, Moss SE, Davis MD, DeMets DL. The Wisconsin Epidemiologic Study of Diabetic Retinopathy. IV. Diabetic macular edema. *Ophthalmology*. 1984;91(12):1464–1474.
5. Kempen JH, O'Colmain BJ, Leske MC, et al. The prevalence of diabetic retinopathy among adults in the United States. *Arch Ophthalmol*. 2004;122(4):552–563.
6. Zhang X, Saaddine JB, Chou CF, et al. Prevalence of diabetic retinopathy in the United States, 2005–2008. *JAMA*. 2010;304(6):649–656.
7. Silva PS, Cavallerano JD, Haddad NM, et al. Peripheral lesions identified on ultrawide field imaging predict

increased risk of diabetic retinopathy progression over 4 years. *Ophthalmology*. 2015;122(5):949–956.
8. Antonetti DA, Klein R, Gardner TW. Diabetic retinopathy. *N Engl J Med*. 2012;366(13):1227–1239.
9. Klein R, Klein BE. Vision disorders in diabetes. Harris MI, Cowie CC, Stern MP, et al. *Diabetes in America*. 2nd ed. National Diabetes Data Group: Bethesda, MD; 1995:293–338 [NIH Publication No. 95-1468].
10. West KM, Erdreich LJ, Stober JA. A detailed study of risk factors for retinopathy and nephropathy in diabetes. *Diabetes*. 1980;29(7):501–508.
11. Ballard DJ, Melton LJ III, Dwyer MS, et al. Risk factors for diabetic retinopathy: a population-based study in Rochester, Minnesota. *Diabetes Care*. 1986;9(4):334–342.
12. Danielsen R, Jonasson F, Helgason T. Prevalence of retinopathy and proteinuria in type 1 diabetics in Iceland. *Acta Med Scand*. 1982;212(5):277–280.
13. Knuiman MW, Welborn TA, McCann VJ, Stanton KG, Constable IJ. Prevalence of diabetic complications in relation to risk factors. *Diabetes*. 1986;35(12):1332–1339.
14. Sjolie AK. Ocular complications in insulin treated diabetes mellitus: an epidemiological study. *Acta Ophthalmol Suppl*. 1985;172:1–77.
15. Haffner SM, Fong D, Stern MP, et al. Diabetic retinopathy in Mexican Americans and non-Hispanic whites. *Diabetes*. 1988;37(7):878–884.
16. West SK, Klein R, Rodriguez J, et al. Diabetes and diabetic retinopathy in a Mexican-American population: Proyecto VER. *Diabetes Care*. 2001;24(7):1204–1209.
17. McKay R, McCarty CA, Taylor HR. Diabetic retinopathy in Victoria, Australia: the Visual Impairment Project. *Br J Ophthalmol*. 2000;84(8):865–870.
18. Leske MC, Wu SY, Hyman L, et al. Diabetic retinopathy in a black population: the Barbados Eye Study. *Ophthalmology*. 1999;106(10):1893–1899.
19. Harris MI, Klein R, Cowie CC, Rowland M, Byrd-Holt DD. Is the risk of diabetic retinopathy greater in non-Hispanic blacks and Mexican Americans than in non-Hispanic whites

with type 2 diabetes? A US population study. *Diabetes Care*. 1998;21(8):1230–1235.
20. Kohner EM, Aldington SJ, Stratton IM, et al. United Kingdom Prospective Diabetes Study, 30: diabetic retinopathy at diagnosis of non-insulin-dependent diabetes mellitus and associated risk factors. *Arch Ophthalmol*. 1998;116(3):297–303.
21. Mitchell P, Smith W, Wang JJ, Attebo K. Prevalence of diabetic retinopathy in an older community. The Blue Mountains Eye Study. *Ophthalmology*. 1998;105(3):406–411.
22. Gonzalez Villalpando ME, Gonzalez VC, Arredondo PB, et al. Moderate-to-severe diabetic retinopathy is more prevalent in Mexico City than in San Antonio, Texas. *Diabetes Care*. 1997;20(5):773–777.
23. Berinstein DM, Stahn RM, Welty TK, Leonardson GR, Herlihy JJ. The prevalence of diabetic retinopathy and associated risk factors among Sioux Indians. *Diabetes Care*. 1997;20(5):757–759.
24. Kernell A, Dedorsson I, Johansson B, et al. Prevalence of diabetic retinopathy in children and adolescents with IDDM: a population-based multicentre study. *Diabetologia*. 1997;40(3):307–310.
25. Collins VR, Dowse GK, Plehwe WE, et al. High prevalence of diabetic retinopathy and nephropathy in Polynesians of Western Samoa. *Diabetes Care*. 1995;18(8):1140–1149.
26. Klein R, Klein BE, Moss SE, Linton KL. The Beaver Dam Eye Study: retinopathy in adults with newly discovered and previously diagnosed diabetes mellitus. *Ophthalmology*. 1992;99(1):58–62.
27. Roy MS. Diabetic retinopathy in African Americans with type 1 diabetes: the New Jersey 725. I. Methodology, population, frequency of retinopathy, and visual impairment. *Arch Ophthalmol*. 2000;118(1):97–104.
28. Roy MS, Klein R. Macular edema and retinal hard exudates in African Americans with type 1 diabetes: the New Jersey 725. *Arch Ophthalmol*. 2001;119(2):251–259.
29. Klein R, Klein BE. Are individuals with diabetes seeing better? A long-term epidemiological perspective. *Diabetes*.

2010;59(8):1853–1860.
30. Suh DC, Choi IS, Plauschinat C, Kwon J, Baron M. Impact of comorbid conditions and race/ethnicity on glycemic control among the US population with type 2 diabetes, 1988–1994 to 1999–2004. *J Diabetes Complications*. 2010;24(6):382–391.
31. Ong KL, Cheung BM, Wong LY, Wat NM, Tan KC, Lam KS. Prevalence, treatment, and control of diagnosed diabetes in the U.S. National Health and Nutrition Examination Survey 1999-2004. *Ann Epidemiol*. 2008;18(3):222–229.
32. Dwyer MS, Melton LJ III, Ballard DJ, Palumbo PJ, Trautmann JC, Chu CP. Incidence of diabetic retinopathy and blindness: a population-based study in Rochester, Minnesota. *Diabetes Care*. 1985;8(4):316–322.
33. Teuscher A, Schnell H, Wilson PW. Incidence of diabetic retinopathy and relationship to baseline plasma glucose and blood pressure. *Diabetes Care*. 1988;11(3):246–251.
34. Klein R, Klein BE, Moss SE, Davis MD, DeMets DL. The Wisconsin Epidemiologic Study of Diabetic Retinopathy. IX. Four-year incidence and progression of diabetic retinopathy when age at diagnosis is less than 30 years. *Arch Ophthalmol*. 1989;107(2):237–243.
35. Klein R, Klein BE, Moss SE, Davis MD, DeMets DL. The Wisconsin Epidemiologic Study of Diabetic Retinopathy. X. Four-year incidence and progression of diabetic retinopathy when age at diagnosis is 30 years or more. *Arch Ophthalmol*. 1989;107(2):244–249.
36. Klein R, Moss SE, Klein BE, Davis MD, DeMets DL. The Wisconsin Epidemiologic Study of Diabetic Retinopathy. XI. The incidence of macular edema. *Ophthalmology*. 1989;96(10):1501–1510.
37. Klein R, Klein BE, Moss SE, Cruickshanks KJ. The Wisconsin Epidemiologic Study of Diabetic Retinopathy. XIV. Ten-year incidence and progression of diabetic retinopathy. *Arch Ophthalmol*. 1994;112(9):1217–1228.
38. Henricsson M, Nystrom L, Blohme G, et al. The incidence of retinopathy 10 years after diagnosis in young adult people with diabetes: results from the nationwide population-based Diabetes Incidence Study in Sweden (DISS). *Diabetes*

Care. 2003;26(2):349–354.
39. Lloyd CE, Becker D, Ellis D, Orchard TJ. Incidence of complications in insulin-dependent diabetes mellitus: a survival analysis. *Am J Epidemiol*. 1996;143(5):431–441.
40. Klein R, Palta M, Allen C, Shen G, Han DP, D'Alessio DJ. Incidence of retinopathy and associated risk factors from time of diagnosis of insulin-dependent diabetes. *Arch Ophthalmol*. 1997;115(3):351–356.
41. Tudor SM, Hamman RF, Baron A, Johnson DW, Shetterly SM. Incidence and progression of diabetic retinopathy in Hispanics and non-Hispanic whites with type 2 diabetes. San Luis Valley Diabetes Study, Colorado. *Diabetes Care*. 1998;21(1):53–61.
42. Klein R, Klein BE, Moss SE, Cruickshanks KJ. The Wisconsin Epidemiologic Study of Diabetic Retinopathy. XVII. The 14-year incidence and progression of diabetic retinopathy and associated risk factors in type 1 diabetes. *Ophthalmology*. 1998;105(10):1801–1815.
43. Porta M, Sjoelie AK, Chaturvedi N, et al. Risk factors for progression to proliferative diabetic retinopathy in the EURODIAB Prospective Complications Study. *Diabetologia*. 2001;44(12):2203–2209.
44. Ling R, Ramsewak V, Taylor D, Jacob J. Longitudinal study of a cohort of people with diabetes screened by the Exeter Diabetic Retinopathy Screening Programme. *Eye (Lond)*. 2002;16(2):140–145.
45. Younis N, Broadbent DM, Vora JP, Harding SP. Incidence of sight-threatening retinopathy in patients with type 2 diabetes in the Liverpool Diabetic Eye Study: a cohort study. *Lancet*. 2003;361(9353):195–200.
46. Roy MS, Affouf M. Six-year progression of retinopathy and associated risk factors in African American patients with type 1 diabetes mellitus: the New Jersey 725. *Arch Ophthalmol*. 2006;124(9):1297–1306.
47. Varma R, Choudhury F, Klein R, Chung J, Torres M, Azen SP. Four-year incidence and progression of diabetic retinopathy and macular edema: the Los Angeles Latino Eye Study. *Am J Ophthalmol*. 2010;149(5):752–761.

48. Hovind P, Tarnow L, Rossing K, et al. Decreasing incidence of severe diabetic microangiopathy in type 1 diabetes. *Diabetes Care*. 2003;26(4):1258–1264.
49. Bojestig M, Arnqvist HJ, Karlberg BE, Ludvigsson J. Unchanged incidence of severe retinopathy in a population of type 1 diabetic patients with marked reduction of nephropathy. *Diabet Med*. 1998;15(10):863–869.
50. Nordwall M, Bojestig M, Arnqvist HJ, Ludvigsson J. Declining incidence of severe retinopathy and persisting decrease of nephropathy in an unselected population of Type 1 diabetes: the Linköping Diabetes Complications Study. *Diabetologia*. 2004;47(7):1266–1272.
51. Pambianco G, Costacou T, Ellis D, Becker DJ, Klein R, Orchard TJ. The 30-year natural history of type 1 diabetes complications: the Pittsburgh Epidemiology of Diabetes Complications Study experience. *Diabetes*. 2006;55(5):1463–1469.
52. Klein R, Knudtson MD, Lee KE, Gangnon R, Klein BE. The Wisconsin Epidemiologic Study of Diabetic Retinopathy. XXII. The twenty-five-year progression of retinopathy in persons with type 1 diabetes. *Ophthalmology*. 2008;115(11):1859–1868.
53. Klein R, Knudtson MD, Lee KE, Gangnon R, Klein BE. The Wisconsin Epidemiologic Study of Diabetic Retinopathy. XXIII. The twenty-five-year incidence of macular edema in persons with type 1 diabetes. *Ophthalmology*. 2009;116(3):497–503.
54. Klein R, Lee KE, Knudtson MD, Gangnon RE, Klein BE. Changes in visual impairment prevalence by period of diagnosis of diabetes: the Wisconsin Epidemiologic Study of Diabetic Retinopathy. *Ophthalmology*. 2009;116(10):1937–1942.
55. Klein R, Lee KE, Gangnon RE, Klein BE. The 25-year incidence of visual impairment in type 1 diabetes mellitus: the Wisconsin Epidemiologic Study of Diabetic Retinopathy. *Ophthalmology*. 2010;117(1):63–70.
56. Klein R, Sharrett AR, Klein BE, et al. The association of atherosclerosis, vascular risk factors, and retinopathy in

adults with diabetes: the Atherosclerosis Risk in Communities Study. *Ophthalmology*. 2002;109(7):1225–1234.
57. Klein R, Marino EK, Kuller LH, et al. The relation of atherosclerotic cardiovascular disease to retinopathy in people with diabetes in the Cardiovascular Health Study. *Br J Ophthalmol*. 2002;86(1):84–90.
58. Wong TY, Klein R, Islam FM, et al. Diabetic retinopathy in a multi-ethnic cohort in the United States. *Am J Ophthalmol*. 2006;141(3):446–455.
59. Varma R, Bressler NM, Doan QV, et al. Prevalence of and risk factors for diabetic macular edema in the United States. *JAMA Ophthalmol*. 2014;132(11):1334–1340.
60. Varma R, Torres M, Pena F, Klein R, Azen SP. Prevalence of diabetic retinopathy in adult Latinos: the Los Angeles Latino Eye Study. *Ophthalmology*. 2004;111(7):1298–1306.
61. Gao X, Gauderman WJ, Marjoram P, et al. Native American ancestry is associated with severe diabetic retinopathy in Latinos. *Invest Ophthalmol Vis Sci*. 2014;55(9):6041–6045.
62. Lee ET, Lee VS, Lu M, Russell D. Development of proliferative retinopathy in NIDDM: a follow-up study of American Indians in Oklahoma. *Diabetes*. 1992;41(3):359–367.
63. Lee ET, Lee VS, Kingsley RM, et al. Diabetic retinopathy in Oklahoma Indians with NIDDM: incidence and risk factors. *Diabetes Care*. 1992;15(11):1620–1627.
64. Nelson RG, Newman JM, Knowler WC, et al. Incidence of end-stage renal disease in type 2 (non-insulin-dependent) diabetes mellitus in Pima Indians. *Diabetologia*. 1988;31(10):730–736.
65. Dorf A, Ballintine EJ, Bennett PH, Miller M. Retinopathy in Pima Indians: relationships to glucose level, duration of diabetes, age at diagnosis of diabetes, and age at examination in a population with a high prevalence of diabetes mellitus. *Diabetes*. 1976;25(7):554–560.
66. Bennett PH, Rushforth NB, Miller M, LeCompte PM. Epidemiologic studies of diabetes in the Pima Indians. *Recent Prog Horm Res*. 1976;32:333–376.
67. Looker HC, Krakoff J, Knowler WC, Bennett PH, Klein R,

Hanson RL. Longitudinal studies of incidence and progression of diabetic retinopathy assessed by retinal photography in Pima Indians. *Diabetes Care*. 2003;26(2):320–326.
68. Fujimoto W, Fukuda M. Natural history of diabetic retinopathy and its treatment in Japan. Baba S, Goto Y, Fukui I. *Diabetes mellitus in Asia*. Excerpta Medica: Amsterdam; 1976:225–231.
69. Dowse GK, Humphrey AR, Collins VR, et al. Prevalence and risk factors for diabetic retinopathy in the multiethnic population of Mauritius. *Am J Epidemiol*. 1998;147(5):448–457.
70. Humes KR, Jones NA, Ramirez RR. *Overview of race and Hispanic origin: 2010. 2010 Census Briefs*. US Department of Commerce: Washington, DC; 2011.
71. USCensus Bureau. *Asian/Pacific American Heritage Month: May 2013*. US Department of Commerce: Washington, DC; 2013.
72. The Diabetes Control and Complications Trial Research Group. Clustering of long-term complications in families with diabetes in the Diabetes Control and Complications Trial. The Diabetes Control and Complications Trial Research Group. *Diabetes*. 1997;46(11):1829–1839.
73. Rema M, Saravanan G, Deepa R, Mohan V. Familial clustering of diabetic retinopathy in South Indian Type 2 diabetic patients. *Diabet Med*. 2002;19(11):910–916.
74. Miao F, Chen Z, Genuth S, et al. Evaluating the role of epigenetic histone modifications in the metabolic memory of type 1 diabetes. *Diabetes*. 2014;63(5):1748–1762.
75. Hosseini SM, Boright AP, Sun L, et al. The association of previously reported polymorphisms for microvascular complications in a meta-analysis of diabetic retinopathy. *Hum Genet*. 2015;134(2):247–257.
76. Pirola L. The DCCT/EDIC study: epigenetic clues after three decades. *Diabetes*. 2014;63(5):1460–1462.
77. Fong DS, Aiello L, Gardner TW, et al. Diabetic retinopathy. *Diabetes Care*. 2003;26(Suppl. 1):S99–102.
78. Klein BE, Moss SE, Klein R. Is menarche associated with

diabetic retinopathy? *Diabetes Care*. 1990;13(10):1034–1038.
79. Frost-Larsen K, Starup K. Fluorescein angiography in diabetic children: a follow-up. *Acta Ophthalmol (Copenh)*. 1980;58(3):355–360.
80. Murphy RP, Nanda M, Plotnick L, Enger C, Vitale S, Patz A. The relationship of puberty to diabetic retinopathy. *Arch Ophthalmol*. 1990;108(2):215–218.
81. Kostraba JN, Dorman JS, Orchard TJ, et al. Contribution of diabetes duration before puberty to development of microvascular complications in IDDM subjects. *Diabetes Care*. 1989;12(10):686–693.
82. Mayer-Davis EJ, Davis C, Saadine J, et al. Diabetic retinopathy in the SEARCH for Diabetes in Youth Cohort: a pilot study. *Diabet Med*. 2012;29(9):1148–1152.
83. TODAY Study Group. Retinopathy in youth with type 2 diabetes participating in the TODAY clinical trial. *Diabetes Care*. 2013;36(6):1772–1774.
84. Harris MI, Klein R, Welborn TA, Knuiman MW. Onset of NIDDM occurs at least 4–7 yr before clinical diagnosis. *Diabetes Care*. 1992;15(7):815–819.
85. Porta M, Curletto G, Cipullo D, et al. Estimating the delay between onset and diagnosis of type 2 diabetes from the time course of retinopathy prevalence. *Diabetes Care*. 2014;37(6):1668–1674.
86. Aiello LM, Rand LI, Briones JC, Wafai MZ, Sebestyen JG. Diabetic retinopathy in Joslin Clinic patients with adult-onset diabetes. *Ophthalmology*. 1981;88(7):619–623.
87. Diabetes Control and Complications Trial Research Group. The effect of intensive treatment of diabetes on the development and progression of long-term complications in insulin-dependent diabetes mellitus. *N Engl J Med*. 1993;329(14):977–986.
88. Diabetes Control and Complications Trial Research Group. The effect of intensive diabetes treatment on the progression of diabetic retinopathy in insulin-dependent diabetes mellitus. *Arch Ophthalmol*. 1995;113(1):36–51.
89. Diabetes Control and Complications Trial Research Group. Progression of retinopathy with intensive versus

conventional treatment in the Diabetes Control and Complications Trial. *Ophthalmology*. 1995;102(4):647–661.
90. Diabetes Control and Complications Trial Research Group. The absence of a glycemic threshold for the development of long-term complications: the perspective of the Diabetes Control and Complications Trial. *Diabetes*. 1996;45(10):1289–1298.
91. Kroc Collaborative Study Group. Diabetic retinopathy after two years of intensified insulin treatment. Follow-up of the Kroc Collaborative Study. *JAMA*. 1988;260(1):37–41.
92. Lauritzen T, Frost-Larsen K, Larsen HW, Deckert T. Two-year experience with continuous subcutaneous insulin infusion in relation to retinopathy and neuropathy. *Diabetes*. 1985;34(Suppl. 3):74–79.
93. Dahl-Jørgensen K, Brinchmann-Hansen O, Hanssen KF, Sandvik L, Aagenaes O. Rapid tightening of blood glucose control leads to transient deterioration of retinopathy in insulin dependent diabetes mellitus: the Oslo study. *Br Med J (Clin Res Ed)*. 1985;290(6471):811–815.
94. Warram JH, Manson JE, Krolewski AS. Glycosylated hemoglobin and the risk of retinopathy in insulin-dependent diabetes mellitus. *N Engl J Med*. 1995;332(19):1305–1306.
95. Diabetes Control and Complications Trial Research Group. Lifetime benefits and costs of intensive therapy as practiced in the diabetes control and complications trial. *JAMA*. 1996;276(17):1409–1415.
96. The Diabetes Control and Complications Trial/Epidemiology of Diabetes Interventions and Complications Research Group. Retinopathy and nephropathy in patients with type 1 diabetes four years after a trial of intensive therapy. *N Engl J Med*. 2000;342(6):381–389.
97. The Epidemiology of Diabetes Interventions and Complications (EDIC) Study Group. Sustained effect of intensive treatment of type 1 diabetes mellitus on development and progression of diabetic nephropathy. *JAMA*. 2003;290(16):2159–2167.

98. Cooper ME. Metabolic memory: implications for diabetic vascular complications. *Pediatr Diabetes*. 2009;10(5):343–346.
99. Holman RR, Paul SK, Bethel MA, Matthews DR, Neil HA. 10-year follow-up of intensive glucose control in type 2 diabetes. *N Engl J Med*. 2008;359(15):1577–1589.
100. Lachin JM, White NH, Hainsworth DP, Sun W, Cleary PA, Nathan DM. Effect of intensive diabetes therapy on the progression of diabetic retinopathy in patients with type 1 diabetes: 18 years of follow-up in the DCCT/EDIC. *Diabetes*. 2015;64(2):631–642.
101. Klein BE, Klein R. Further insight on the limits of success of glycemic control in type 1 diabetes. *Diabetes*. 2015;64(2):341–343.
102. United Kingdom Prospective Diabetes Study (UKPDS) Group. Intensive blood-glucose control with sulphonylureas or insulin compared with conventional treatment and risk of complications in patients with type 2 diabetes (UKPDS 33). *Lancet*. 1998;352(9131):837–853.
103. United Kingdom Prospective Diabetes Study (UKPDS) Group. Effect of intensive blood-glucose control with metformin on complications in overweight patients with type 2 diabetes (UKPDS 34). *Lancet*. 1998;352(9131):854–865.
104. Gray A, Raikou M, McGuire A, et al. Cost effectiveness of an intensive blood glucose control policy in patients with type 2 diabetes: economic analysis alongside randomised controlled trial (UKPDS 41). United Kingdom Prospective Diabetes Study Group. *BMJ*. 2000;320(7246):1373–1378.
105. Hermann JM, Hammes HP, Rami-Merhar B, et al. HbA1c variability as an independent risk factor for diabetic retinopathy in type 1 diabetes: a German/Austrian multicenter analysis on 35,891 patients. *PLoS ONE*. 2014;9(3):e91137.
106. Duckworth WC, McCarren M, Abraira C. Glucose control and cardiovascular complications: the VA Diabetes Trial. *Diabetes Care*. 2001;24(5):942–945.
107. Duckworth WC, Abraira C, Moritz T, et al. Glucose control and vascular complications in veterans with type 2 diabetes. *N Engl J Med*. 2009;360(2):129–139.

108. Chew EY, Davis MD, Danis RP, et al. The effects of medical management on the progression of diabetic retinopathy in persons with type 2 diabetes: the Action to Control Cardiovascular Risk in Diabetes (ACCORD) Eye Study. *Ophthalmology*. 2014;121(12):2443–2451.
109. Chew EY, Ambrosius WT, Davis MD, et al. Effects of medical therapies on retinopathy progression in type 2 diabetes. *N Engl J Med*. 2010;363(3):233–244.
110. Ismail-Beigi F, Craven T, Banerji MA, et al. Effect of intensive treatment of hyperglycaemia on microvascular outcomes in type 2 diabetes: an analysis of the ACCORD randomised trial. *Lancet*. 2010;376(9739):419–430.
111. Patel A, MacMahon S, Chalmers J, et al. Intensive blood glucose control and vascular outcomes in patients with type 2 diabetes. *N Engl J Med*. 2008;358(24):2560–2572.
112. American Diabetes Association. Standards of medical care for patients with diabetes mellitus. *Diabetes Care*. 1994;17(6):616–623.
113. Harris MI. Health care and health status and outcomes for patients with type 2 diabetes. *Diabetes Care*. 2000;23(6):754–758.
114. Klein R, Klein BE, Moss SE, Cruickshanks KJ. The medical management of hyperglycemia over a 10-year period in people with diabetes. *Diabetes Care*. 1996;19(7):744–750.
115. Klein BE. Reduction in risk of progression of diabetic retinopathy. *N Engl J Med*. 2010;363(3):287–288.
116. Klein R. Intensive treatment of hyperglycaemia: ACCORD. *Lancet*. 2010;376(9739):391–392.
117. Smith RB, Pyke DA, Watkins PJ, Binder C, Faber OK. C-peptide response to glucagon in diabetics with and without complications. *N Z Med J*. 1979;89(634):304–306.
118. Sjoberg S, Gunnarsson R, Gjotterberg M, Lefvert AK, Persson A, Ostman J. Residual insulin production, glycaemic control and prevalence of microvascular lesions and polyneuropathy in long-term type 1 (insulin-dependent) diabetes mellitus. *Diabetologia*. 1987;30(4):208–213.
119. Sjoberg S, Gjotterberg M, Lefvert AK, Gunnarsson R,

Ostman J. Significance of residual insulin production in long-term type I diabetes mellitus. *Transplant Proc*. 1986;18:1498–1499.
120. Madsbad S, Lauritzen E, Faber OK, Binder C. The effect of residual beta-cell function on the development of diabetic retinopathy. *Diabet Med*. 1986;3(1):42–45.
121. Klein R, Moss SE, Klein BE, Davis MD, DeMets DL. Wisconsin Epidemiologic Study of Diabetic Retinopathy. XII. Relationship of C-peptide and diabetic retinopathy. *Diabetes*. 1990;39(11):1445–1450.
122. Klein R, Klein BE, Moss SE. The Wisconsin Epidemiologic Study of Diabetic Retinopathy. XVI. The relationship of C-peptide to the incidence and progression of diabetic retinopathy. *Diabetes*. 1995;44(7):796–801.
123. Steffes MW, Sibley S, Jackson M, Thomas W. Beta-cell function and the development of diabetes-related complications in the diabetes control and complications trial. *Diabetes Care*. 2003;26(3):832–836.
124. Serghieri G, Bartolomei G, Pettenello C, Mammini P, DeGiorgio LA. Raised retinopathy prevalence rate in insulin-treated patients: a feature of obese type II diabetes. *Transplant Proc*. 1986;18:1576–1577.
125. Zhao C, Wang W, Xu D, Li H, Li M, Wang F. Insulin and risk of diabetic retinopathy in patients with type 2 diabetes mellitus: data from a meta-analysis of seven cohort studies. *Diagn Pathol*. 2014;9:130.
126. Muir KR, Lima MJ, Docherty HM, Docherty K. Cell therapy for type 1 diabetes. *QJM*. 2014;107(4):253–259.
127. Adler AI, Stratton IM, Neil HA, et al. Association of systolic blood pressure with macrovascular and microvascular complications of type 2 diabetes (UKPDS 36): prospective observational study. *BMJ*. 2000;321(7258):412–419.
128. Klein R, Klein BE, Moss SE, Cruickshanks KJ. The Wisconsin Epidemiologic Study of Diabetic Retinopathy. XV. The long-term incidence of macular edema. *Ophthalmology*. 1995;102(1):7–16.
129. United Kingdom Prospective Diabetes Study (UKPDS) Group. Tight blood pressure control and risk of

macrovascular and microvascular complications in type 2 diabetes: UKPDS 38. *BMJ*. 1998;317(7160):703–713.
130. Patel A, MacMahon S, Chalmers J, et al. Effects of a fixed combination of perindopril and indapamide on macrovascular and microvascular outcomes in patients with type 2 diabetes mellitus (the ADVANCE trial): a randomised controlled trial. *Lancet*. 2007;370(9590):829–840.
131. Chaturvedi N, Sjolie AK, Stephenson JM, et al. Effect of lisinopril on progression of retinopathy in normotensive people with type 1 diabetes. The EUCLID Study Group. EURODIAB controlled trial of lisinopril in insulin-dependent diabetes mellitus. *Lancet*. 1998;351(9095):28–31.
132. Chaturvedi N. Modulation of the renin-angiotensin system and retinopathy. *Heart*. 2000;84(Suppl. 1):i29–31.
133. Chaturvedi N, Sjoelie AK, Svensson A. The DIabetic Retinopathy Candesartan Trials (DIRECT) Programme, rationale and study design. *J Renin Angiotensin Aldosterone Syst*. 2002;3(4):255–261.
134. Chaturvedi N, Porta M, Klein R, et al. Effect of candesartan on prevention (DIRECT-Prevent 1) and progression (DIRECT-Protect 1) of retinopathy in type 1 diabetes: randomised, placebo-controlled trials. *Lancet*. 2008;372(9647):1394–1402.
135. Mauer M, Zinman B, Gardiner R, et al. Renal and retinal effects of enalapril and losartan in type 1 diabetes. *N Engl J Med*. 2009;361(1):40–51.
136. Mitchell P, Wong TY. DIRECT new treatments for diabetic retinopathy. *Lancet*. 2008;372(9647):1361–1363.
137. Sjølie AK, Klein R, Porta M, et al. Effect of candesartan on progression and regression of retinopathy in type 2 diabetes (DIRECT-Protect 2): a randomised placebo-controlled trial. *Lancet*. 2008;372(9647):1385–1393.
138. Emdin CA, Rahimi K, Neal B, Callender T, Perkovic V, Patel A. Blood pressure lowering in type 2 diabetes: a systematic review and meta-analysis. *JAMA*. 2015;313(6):603–615.
139. James PA, Oparil S, Carter BL, et al. 2014 evidence-based guideline for the management of high blood pressure in adults: report from the panel members appointed to the

Eighth Joint National Committee (JNC 8). *JAMA*. 2014;311(5):507–520.
140. Jerneld B. Prevalence of diabetic retinopathy: a population study from the Swedish island of Gotland. *Acta Ophthalmol Suppl*. 1988;188:3–32.
141. Kostraba JN, Klein R, Dorman JS, et al. The Epidemiology of Diabetes Complications Study. IV. Correlates of diabetic background and proliferative retinopathy. *Am J Epidemiol*. 1991;133(4):381–391.
142. Klein R, Moss SE, Klein BE. Is gross proteinuria a risk factor for the incidence of proliferative diabetic retinopathy? *Ophthalmology*. 1993;100(8):1140–1146.
143. Cruickshanks KJ, Ritter LL, Klein R, Moss SE. The association of microalbuminuria with diabetic retinopathy. The Wisconsin Epidemiologic Study of Diabetic Retinopathy. *Ophthalmology*. 1993;100(6):862–867.
144. Lloyd CE, Klein R, Maser RE, Kuller LH, Becker DJ, Orchard TJ. The progression of retinopathy over 2 years: the Pittsburgh Epidemiology of Diabetes Complications (EDC) Study. *J Diabetes Complications*. 1995;9(3):140–148.
145. Stern MP. Diabetes and cardiovascular disease. The "common soil" hypothesis. *Diabetes*. 1995;44(4):369–374.
146. Wong CW, Wong TY, Cheng CY, Sabanayagam C. Kidney and eye diseases: common risk factors, etiological mechanisms, and pathways. *Kidney Int*. 2014;85(6):1290–1302.
147. Koenig W, Meisinger C. Uric acid, type 2 diabetes, and cardiovascular diseases: fueling the common soil hypothesis? *Clin Chem*. 2008;54(2):231–233.
148. Benigni A, Cassis P, Remuzzi G. Angiotensin II revisited: new roles in inflammation, immunology and aging. *EMBO Mol Med*. 2010;2(7):247–257.
149. Lim LS, Cheung CY, Sabanayagam C, et al. Structural changes in the retinal microvasculature and renal function. *Invest Ophthalmol Vis Sci*. 2013;54(4):2970–2976.
150. Moss SE, Klein R, Klein BE. The incidence of vision loss in a diabetic population. *Ophthalmology*. 1988;95(10):1340–1348.
151. Duncan LJ, Cullen JF, Ireland JT, Nolan J, Clarke BF, Oliver

MF. A three-year trial of atromid therapy in exudative diabetic retinopathy. *Diabetes*. 1968;17(7):458–467.
152. Klein BE, Moss SE, Klein R, Surawicz TS. The Wisconsin Epidemiologic Study of Diabetic Retinopathy. XIII. Relationship of serum cholesterol to retinopathy and hard exudate. *Ophthalmology*. 1991;98(8):1261–1265.
153. Klein BE, Myers CE, Howard KP, Klein R. Serum lipids and proliferative diabetic retinopathy and macular edema in persons with long-term type 1 diabetes mellitus: the Wisconsin Epidemiologic Study of Diabetic Retinopathy. *JAMA Ophthalmol*. 2015;133(5):503–510.
154. Chew EY, Klein ML, Ferris FL III, et al. Association of elevated serum lipid levels with retinal hard exudate in diabetic retinopathy. Early Treatment Diabetic Retinopathy Study (ETDRS) Report 22. *Arch Ophthalmol*. 1996;114(9):1079–1084.
155. Santos A, Salguero ML, Gurrola C, Munoz F, Roig-Melo E, Panduro A. The epsilon4 allele of apolipoprotein E gene is a potential risk factor for the severity of macular edema in type 2 diabetic Mexican patients. *Ophthalmic Genet*. 2002;23(1):13–19.
156. Sacks FM, Hermans MP, Fioretto P, et al. Association between plasma triglycerides and high-density lipoprotein cholesterol and microvascular kidney disease and retinopathy in type 2 diabetes mellitus: a global case-control study in 13 countries. *Circulation*. 2014;129(9):999–1008.
157. Keech AC, Mitchell P, Summanen PA, et al. Effect of fenofibrate on the need for laser treatment for diabetic retinopathy (FIELD study): a randomised controlled trial. *Lancet*. 2007;370(9600):1687–1697.
158. Massin P, Peto T, Ansquer JC, et al. MacuFEN Study Investigators FT. Effects of fenofibric acid on diabetic macular edema: the MacuFen study. *Ophthalmic Epidemiol*. 2014;21(5):307–317.
159. Goldsmith JR, Landaw SA. Carbon monoxide and human health. *Science*. 1968;162(860):1352–1359.
160. Hawkins RI. Smoking, platelets and thrombosis. *Nature*. 1972;236(5348):450–452.

161. Klein R, Klein BE, Davis MD. Is cigarette smoking associated with diabetic retinopathy? *Am J Epidemiol*. 1983;118(2):228–238.
162. Moss SE, Klein R, Klein BE. Association of cigarette smoking with diabetic retinopathy. *Diabetes Care*. 1991;14(2):119–126.
163. Moss SE, Klein R, Klein BE. Cigarette smoking and ten-year progression of diabetic retinopathy. *Ophthalmology*. 1996;103(9):1438–1442.
164. Klein R, Moss SE, Klein BE, DeMets DL. Relation of ocular and systemic factors to survival in diabetes. *Arch Intern Med*. 1989;149(2):266–272.
165. Jakubowski JA, Vaillancourt R, Deykin D. Interaction of ethanol, prostacyclin, and aspirin in determining human platelet reactivity in vitro. *Arteriosclerosis*. 1988;8(4):436–441.
166. Albert MA, Glynn RJ, Ridker PM. Alcohol consumption and plasma concentration of C-reactive protein. *Circulation*. 2003;107(3):443–447.
167. Greenfield JR, Samaras K, Jenkins AB, Kelly PJ, Spector TD, Campbell LV. Moderate alcohol consumption, estrogen replacement therapy, and physical activity are associated with increased insulin sensitivity: is abdominal adiposity the mediator? *Diabetes Care*. 2003;26(10):2734–2740.
168. Kingsley LA, Dorman JS, Doft BH, et al. An epidemiologic approach to the study of retinopathy: the Pittsburgh diabetic morbidity and retinopathy studies. *Diabetes Res Clin Pract*. 1988;4(2):99–109.
169. Young RJ, McCulloch DK, Prescott RJ, Clarke BF. Alcohol: another risk factor for diabetic retinopathy? *Br Med J (Clin Res Ed)*. 1984;288(6423):1035–1037.
170. Beulens JW, Kruidhof JS, Grobbee DE, Chaturvedi N, Fuller JH, Soedamah-Muthu SS. Alcohol consumption and risk of microvascular complications in type 1 diabetes patients: the EURODIAB Prospective Complications Study. *Diabetologia*. 2008;51(9):1631–1638.
171. Lee CC, Stolk RP, Adler AI, et al. Association between alcohol consumption and diabetic retinopathy and visual acuity – the AdRem Study. *Diabet Med*. 2010;27(10):1130–

1137.
172. Moss SE, Klein R, Klein BE. Alcohol consumption and the prevalence of diabetic retinopathy. *Ophthalmology*. 1992;99(6):926–932.
173. Moss SE, Klein R, Klein BE. The association of alcohol consumption with the incidence and progression of diabetic retinopathy. *Ophthalmology*. 1994;101(12):1962–1968.
174. Valmadrid CT, Klein R, Moss SE, Klein BE, Cruickshanks KJ. Alcohol intake and the risk of coronary heart disease mortality in persons with older-onset diabetes mellitus. *JAMA*. 1999;282(3):239–246.
175. Diabetes Drafting Group. Prevalence of small vessel and large vessel disease in diabetic patients from 14 centres. The World Health Organisation Multinational Study of Vascular Disease in Diabetics. *Diabetologia*. 1985;28(Suppl.):615–640.
176. LaPorte RE, Dorman JS, Tajima N, et al. Pittsburgh Insulin-Dependent Diabetes Mellitus Morbidity and Mortality Study: physical activity and diabetic complications. *Pediatrics*. 1986;78(6):1027–1033.
177. van Leiden HA, Dekker JM, Moll AC, et al. Risk factors for incident retinopathy in a diabetic and nondiabetic population: the Hoorn study. *Arch Ophthalmol*. 2003;121(2):245–251.
178. Klein R, Klein BE, Moss SE. Is obesity related to microvascular and macrovascular complications in diabetes? The Wisconsin Epidemiologic Study of Diabetic Retinopathy. *Arch Intern Med*. 1997;157(6):650–656.
179. Lu J, Hou X, Zhang L, et al. Association between body mass index and diabetic retinopathy in Chinese patients with type 2 diabetes. *Acta Diabetol*. 2015;52(4):701–708.
180. Wadén J, Tikkanen H, Forsblom C, et al. Leisure time physical activity is associated with poor glycemic control in type 1 diabetic women: the FinnDiane study. *Diabetes Care*. 2005;28(4):777–782.
181. Orchard TJ, Dorman JS, Maser RE, et al. Factors associated with avoidance of severe complications after 25 yr of IDDM. Pittsburgh Epidemiology of Diabetes Complications Study I. *Diabetes Care*. 1990;13(7):741–747.

182. Kriska AM, LaPorte RE, Patrick SL, Kuller LH, Orchard TJ. The association of physical activity and diabetic complications in individuals with insulin-dependent diabetes mellitus: the Epidemiology of Diabetes Complications Study – VII. *J Clin Epidemiol*. 1991;44(11):1207–1214.
183. Cruickshanks KJ, Moss SE, Klein R, Klein BE. Physical activity and proliferative retinopathy in people diagnosed with diabetes before age 30 yr. *Diabetes Care*. 1992;15(10):1267–1272.
184. Cruickshanks KJ, Moss SE, Klein R, Klein BE. Physical activity and the risk of progression of retinopathy or the development of proliferative retinopathy. *Ophthalmology*. 1995;102(8):1177–1182.
185. Hanna AK, Roy M, Zinman B, et al. An evaluation of factors associated with proliferative diabetic retinopathy. *Clin Invest Med*. 1985;8(2):109–116.
186. Haffner SM, Hazuda HP, Stern MP, Patterson JK, van Heuven WA, Fong D. Effects of socioeconomic status on hyperglycemia and retinopathy levels in Mexican Americans with NIDDM. *Diabetes Care*. 1989;12(2):128–134.
187. Klein R, Klein BE, Jensen SC, Moss SE. The relation of socioeconomic factors to the incidence of proliferative diabetic retinopathy and loss of vision. *Ophthalmology*. 1994;101(1):68–76.
188. Klein BE, Moss SE, Klein R. Oral contraceptives in women with diabetes. *Diabetes Care*. 1990;13(8):895–898.
189. Klein BE, Klein R, Moss SE. Exogenous estrogen exposures and changes in diabetic retinopathy. The Wisconsin Epidemiologic Study of Diabetic Retinopathy. *Diabetes Care*. 1999;22(12):1984–1987.
190. Klein BE, Moss SE, Klein R. Effect of pregnancy on progression of diabetic retinopathy. *Diabetes Care*. 1990;13(1):34–40.
191. Chew EY, Mills JL, Metzger BE, et al. Metabolic control and progression of retinopathy. The Diabetes in Early Pregnancy Study. National Institute of Child Health and Human Development Diabetes in Early Pregnancy Study.

Diabetes Care. 1995;18(5):631–637.
192. Hemachandra A, Ellis D, Lloyd CE, Orchard TJ. The influence of pregnancy on IDDM complications. *Diabetes Care*. 1995;18(7):950–954.
193. The Diabetes Control and Complications Trial Research Group. Effect of pregnancy on microvascular complications in the Diabetes Control and Complications Trial. *Diabetes Care*. 2000;23(8):1084–1091.
194. Rasmussen KL, Laugesen CS, Ringholm L, Vestgaard M, Damm P, Mathiesen ER. Progression of diabetic retinopathy during pregnancy in women with type 2 diabetes. *Diabetologia*. 2010;53(6):1076–1083.
195. Lovestam-Adrian M, Agardh CD, Aberg A, Agardh E. Pre-eclampsia is a potent risk factor for deterioration of retinopathy during pregnancy in type 1 diabetic patients. *Diabet Med*. 1997;14(12):1059–1065.
196. Rosenn B, Miodovnik M, Kranias G, et al. Progression of diabetic retinopathy in pregnancy: association with hypertension in pregnancy. *Am J Obstet Gynecol*. 1992;166(4):1214–1218.
197. Temple RC, Aldridge VA, Sampson MJ, Greenwood RH, Heyburn PJ, Glenn A. Impact of pregnancy on the progression of diabetic retinopathy in type 1 diabetes. *Diabet Med*. 2001;18(7):573–577.
198. Lauszus F, Klebe JG, Bek T. Diabetic retinopathy in pregnancy during tight metabolic control. *Acta Obstet Gynecol Scand*. 2000;79(5):367–370.
199. Rahman W, Rahman FZ, Yassin S, Al-Suleiman SA, Rahman J. Progression of retinopathy during pregnancy in type 1 diabetes mellitus. *Clin Experiment Ophthalmol*. 2007;35(3):231–236.
200. Vestgaard M, Ringholm L, Laugesen CS, Rasmussen KL, Damm P, Mathiesen ER. Pregnancy-induced sight-threatening diabetic retinopathy in women with type 1 diabetes. *Diabet Med*. 2010;27(4):431–435.
201. Lauszus FF, Klebe JG, Bek T, Flyvbjerg A. Increased serum IGF-I during pregnancy is associated with progression of diabetic retinopathy. *Diabetes*. 2003;52(3):852–856.

202. Ringholm L, Vestgaard M, Laugesen CS, Juul A, Damm P, Mathiesen ER. Pregnancy-induced increase in circulating IGF-I is associated with progression of diabetic retinopathy in women with type 1 diabetes. *Growth Horm IGF Res*. 2011;21(1):25–30.
203. Best RM, Hayes R, Hadden DR, Chakravarthy U, Archer DB. Plasma levels of endothelin-1 in diabetic retinopathy in pregnancy. *Eye (Lond)*. 1999;13(Pt 2):179–182.
204. Vääräsmäki M, Anttila M, Pirttiaho H, Hartikainen AL. Are recurrent pregnancies a risk in type 1 diabetes? *Acta Obstet Gynecol Scand*. 2002;81(12):1110–1115.
205. Klein R, Klein BE, Moss SE. Epidemiology of proliferative diabetic retinopathy. *Diabetes Care*. 1992;15(12):1875–1891.
206. Klein R, Klein BE, Moss SE, Cruickshanks KJ. Association of ocular disease and mortality in a diabetic population. *Arch Ophthalmol*. 1999;117(11):1487–1495.
207. Davis MD, Hiller R, Magli YL, et al. Prognosis for life in patients with diabetes: relation to severity of retinopathy. *Trans Am Ophthalmol Soc*. 1979;77:144–170.
208. Hanis CL, Chu HH, Lawson K, et al. Mortality of Mexican Americans with NIDDM. Retinopathy and other predictors in Starr County, Texas. *Diabetes Care*. 1993;16(1):82–89.
209. Neil A, Hawkins M, Potok M, Thorogood M, Cohen D, Mann J. A prospective population-based study of microalbuminuria as a predictor of mortality in NIDDM. *Diabetes Care*. 1993;16(7):996–1003.
210. Sorbinil Retinopathy Trial Research Group. A randomized trial of sorbinil, an aldose reductase inhibitor, in diabetic retinopathy. *Arch Ophthalmol*. 1990;108(9):1234–1244.
211. Elman MJ, Aiello LP, Beck RW, et al. Randomized trial evaluating ranibizumab plus prompt or deferred laser or triamcinolone plus prompt laser for diabetic macular edema. *Ophthalmology*. 2010;117(6):1064–1077.
212. Witkin SR, Klein R. Ophthalmologic care for persons with diabetes. *JAMA*. 1984;251(19):2534–2537.
213. Singer DE, Nathan DM, Fogel HA, Schachat AP. Screening for diabetic retinopathy. *Ann Intern Med*. 1992;116(8):660–671.

214. Sprafka JM, Fritsche TL, Baker R, Kurth D, Whipple D. Prevalence of undiagnosed eye disease in high-risk diabetic individuals. *Arch Intern Med*. 1990;150(4):857–861.
215. Brechner RJ, Cowie CC, Howie LJ, Herman WH, Will JC, Harris MI. Ophthalmic examination among adults with diagnosed diabetes mellitus. *JAMA*. 1993;270(14):1714–1718.
216. Weiner JP, Parente ST, Garnick DW, Fowles J, Lawthers AG, Palmer RH. Variation in office-based quality: a claims-based profile of care provided to Medicare patients with diabetes. *JAMA*. 1995;273(19):1503–1508.
217. Bressler NM, Varma R, Doan QV, et al. Underuse of the health care system by persons with diabetes mellitus and diabetic macular edema in the United States. *JAMA Ophthalmol*. 2014;132(2):168–173.
218. Healthcare Effectiveness Data and Information Set (HEDIS®) 2015. National Committee for Quality Assurance: Washington, DC; 2014.
219. Kraft SK, Marrero DG, Lazaridis EN, Fineberg N, Qiu C, Clark CM Jr. Primary care physicians' practice patterns and diabetic retinopathy: current levels of care. *Arch Fam Med*. 1997;6(1):29–37.
220. Bresnick GH, Mukamel DB, Dickinson JC, Cole DR. A screening approach to the surveillance of patients with diabetes for the presence of vision-threatening retinopathy. *Ophthalmology*. 2000;107(1):19–24.
221. Moss SE, Klein R, Klein BE. Factors associated with having eye examinations in persons with diabetes. *Arch Fam Med*. 1995;4(6):529–534.
222. National Institutes of Health. *The National Eye Health Education Program. From Vision to Research to Health Educations: Planning the Partnership*. National Institutes of Health: Bethesda, MD; 1990.
223. Batchelder T, Barricks M. The Wisconsin Epidemiologic Study of Diabetic Retinopathy. *Arch Ophthalmol*. 1995;113(6):702–703.
224. Vijan S, Hofer TP, Hayward RA. Cost-utility analysis of screening intervals for diabetic retinopathy in patients with type 2 diabetes mellitus. *JAMA*. 2000;283(7):889–896.

225. National Committee for Quality Assurance. *Health Plan Employers Data and Information Set (HEDIS®), Version 2.5*. National Committee for Quality Assurance: Washington, DC; 1996.
226. Klein R, Klein BE. The epidemiology of diabetic retinopathy. Ryan SJ, Schachat AP, Wilkinson WP, Glaser B. *Retina*. 4th ed. Mosby: St. Louis; 2005:1503–1521.
227. Velez R, Haffner SM, Stern MP, van Heuven WA. Ophthalmologist versus retinal photographs in screening for diabetic retinopathy [abstract]. *Clin Res*. 1987;35:363A.
228. Bragge P, Gruen RL, Chau M, Forbes A, Taylor HR. Screening for presence or absence of diabetic retinopathy: a meta-analysis. *Arch Ophthalmol*. 2011;129(4):435–444.
229. Liew G, Michaelides M, Bunce C. A comparison of the causes of blindness certifications in England and Wales in working age adults (16–64 years), 1999–2000 with 2009–2010. *BMJ Open*. 2014;4(2):e004015.
230. Owsley C, McGwin G Jr, Lee DJ, et al. Diabetes eye screening in urban settings serving minority populations: detection of diabetic retinopathy and other ocular findings using telemedicine. *JAMA Ophthalmol*. 2015;133(2):174–181.
231. Solanki K. *EyeArt [computer program]*. http://www.eyenuk.com/eyeart.html.
232. Solanki K. *EyeMark [computer program]*. http://www.eyenuk.com/eyemark.html.

48

Diabetic Retinopathy

Genetics and Etiologic Mechanisms

Nickisa M. Hodgson, Jie Zhu, Frances Wu, Henry A. Ferreyra, Kang Zhang

Introduction

Diabetic retinopathy is the leading cause of blindness among individuals between 25 and 74 years of age in the industrialized world. It affects three out of four diabetic patients after 15 years of disease duration. Chronic hyperglycemia is the primary factor leading to the development of diabetic retinopathy and other complications of the disease. The importance of long-term glycemic control has been conclusively established in the landmark clinical trials including the Diabetes Control and Complications Trial (DCCT),[1] and the UK Prospective Diabetes Study (UKPDS).[2,3] Duration of diabetes diagnosis, hypertension, elevated hemoglobin A1C, and male sex are strong risk factors for the development of diabetic retinopathy.[4–6]

However, the mechanisms by which elevated blood sugar levels lead to the development of diabetic retinopathy and the anatomic changes visible histopathologically remain to be fully elucidated. This chapter will review the biochemical and molecular pathways believed to be responsible for the development of diabetic retinopathy and will highlight recent developments in genetics and epigenetics that provide insight into the influential role of genetic susceptibility.

Anatomic Lesions

Loss of Pericytes

Loss of pericytes is one of the earliest and most specific signs of diabetic retinopathy. This finding was first described by Cogan,

Kuwabara, and coworkers after examining trypsin-digested retinal vasculature flat mounts from diabetic human subjects.[7–9] Since their initial report, their findings have been confirmed by various investigators.[2,10,11] In humans and canines, trypsin digestion of retinal vasculature flat mounts reveals the loss of pericytes as evidenced by the development of pericyte ghosts, empty aneurysmal spaces bulging from the capillary walls that lack the darkly staining nucleus of a viable pericyte (Fig. 48.1A). Pericytes are normally identifiable in these spaces by their nuclei, which stain darkly and are spaced regularly along the capillary wall, producing the appearance of "bumps on a log" (Fig. 48.1B).

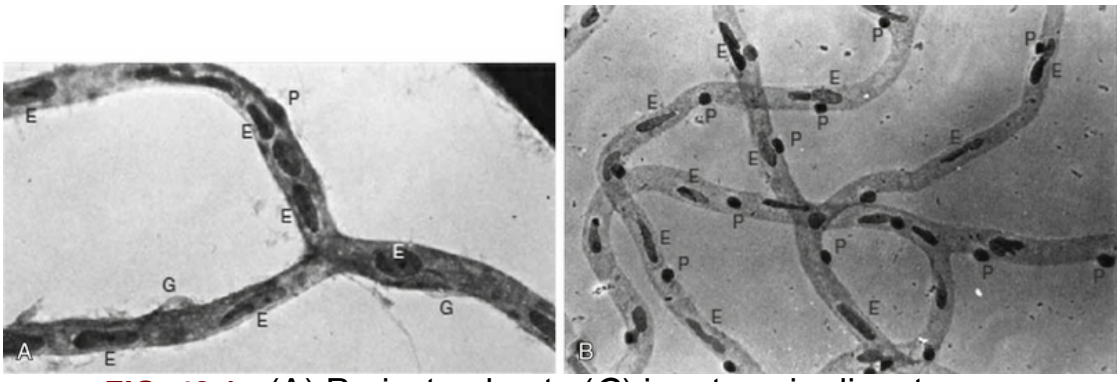

FIG. 48.1 (A) Pericyte ghosts (*G*) in a trypsin digest preparation from a 42-year-old woman with background diabetic retinopathy who died of a dissecting aneurysm of the aorta. The ghost represents the vacant space in the capillary basement membrane, formerly occupied by an intramural pericyte nucleus that has degenerated. Normal pericyte (*P*) and endothelial cell (*E*) nuclei are also shown. The preparation was stained with periodic acid–Schiff (PAS) reagent and hematoxylin. Magnification ×575. (B) A trypsin digest preparation from the retina of a nondiabetic, 55-year-old man who died of a myocardial infarction. Note the regular array of pericyte (*P*) and endothelial cell (*E*) nuclei. The preparation was stained with PAS reagent and hematoxylin. (Magnification ×450.)

Pericytes are contractile cells that play an important role in microvascular autoregulation.[12] Loss of pericytes leads to

alterations of vascular intercellular contacts and impairment of the inner blood–retina barrier. These effects result in the venous dilation and beading that is visible clinically. Loss of intercellular contacts also appears to promote endothelial cell proliferation resulting in the development of microaneurysms.[13] Loss of pericytes appears to be especially significant in the development of diabetic retinopathy, although pericyte loss has also been reported in diabetic peripheral neuropathy leading to neuronal ischemia.[14] The mechanism by which hyperglycemia leads to pericyte degeneration remains largely unknown. The two leading hypotheses implicate the aldose reductase pathway and platelet-derived growth factor-beta (PDGF-β).

Akagi et al. reported the localization of the enzyme aldose reductase in retinal capillary pericytes but not in endothelial cells in human specimens using immunohistochemistry techniques.[15] These findings would be consistent with the specific loss of capillary pericytes observed in diabetic retinopathy and other microvascular complications of diabetes.[16] Two other groups, however, were unable to identify the presence of aldose reductase in rodent and canine retinal capillaries using immunohistochemistry techniques.[17,18] In addition, a third group reported the presence of aldose reductase activity in cultured bovine retinal capillary pericytes as well as retinal capillary endothelial cells. They also found aldose reductase activity in cultured monkey retinal pericytes.[19] These conflicting reports probably result from species-specific differences in aldose reductase expression and highlight the need to use caution when interpreting animal models of disease.

PDGF-β has been found to be critical in the recruitment of pericytes in the vasculature of various tissues and organs.[20] It is well documented that endothelial cells express PDGF-β,[21–24] and in vitro pericytes are known to express PDGF-β receptors and respond to PDGF-β.[25,26] Lindahl et al. reported that in the PDGF-β-deficient mouse model, pericytes fail to develop in developing capillaries during angiogenesis.[27] Subsequent studies using PDGF-β- and PDGF receptor-β (PDGFR-β)-deficient mice found that while PDGF-β/PDGFR-β-independent induction of pericyte precursors may occur, the expansion of pericytes is dependent on an intact PDGF-β/PDGFR-β paracrine signaling pathway.[28] Ablation of either

PDGF-β or PDGFR-β led to identical phenotypes in these mice.[29] These studies suggest that endothelial cell-derived PDGF-β promotes the comigration of PDGFR-β-expressing pericytes along sprouting new vessels, and the interruption of the PDGF-β/PDGFR-β results in the observed deficiency of pericytes in capillaries. Since PDGF-β has been found to be critical in the recruitment of pericytes during angiogenesis, it has been suggested that PDGF-β may play an important role in maintaining pericyte viability in mature vasculature, although no studies have confirmed this hypothesis.

Capillary Basement Membrane Thickening

Thickening of capillary basement membranes is a well-documented lesion of diabetic retinopathy, visible on electron microscopy. Additional electron microscopic findings include deposition of fibrillar collagen and "Swiss cheese" vacuolization of the otherwise homogenous pattern of basement membrane collagen. The biochemical mechanism leading to basement membrane thickening remains unknown but studies suggest a role for the aldose reductase and the sorbitol pathway.[30–33] Nondiabetic rats fed a galactose-rich diet for prolonged periods of time develop retinal capillary basement membrane thickening, fibrillar collagen deposition, and Swiss cheese vacuolization. By contrast, rats fed a control diet or a galactose-rich diet along with the aldose reductase inhibitor sorbinil do not develop basement membrane thickening.[30,33] However, the observation that basement membrane thickening of renal glomeruli in diabetic and galactosemic rats is not inhibited by aldose reductase inhibitors casts doubt that the aldose reductase pathway is the primary pathway and suggests that basement membrane thickening may be a secondary nonspecific response.[34]

Glycation of basement membrane collagen by enzymatic[35] and nonenzymatic processes[36] may be another mechanism that plays a role in basement membrane thickening. Besides type IV collagen, the predominant type of collagen present in the basement membrane, other collagen types and noncollagen macromolecules, such as laminin,[37] entactin, heparan sulfate proteoglycan,[38,39] and basement membrane-bound growth factors, are also present.[38]

Glycation appears to alter the structure of the basement membrane by changing the chemical composition and relative amounts of these components. For example, Shimomura/Spiro and Spiro/Spiro reported decreased heparan sulfate proteoglycan in renal glomeruli from diabetic human subjects.[40,41] Quantitative electron microscopic immunocytochemical studies have found that retinal and renal glomeruli basement membrane thickening in galactosemic rats is associated with a relative increase in the levels of type IV collagen and laminin, while the relative levels of heparan sulfate proteoglycan remain unchanged.[32,34]

Microaneurysms

Although pericyte loss is the earliest sign of diabetic retinopathy, it is only observable histologically. The earliest clinically visible sign of diabetic retinopathy is the microaneurysm.[42] Microaneurysms appear as grape-like or spindle-shaped dilations of retinal capillaries on light microscopy.[7] They can be either hypercellular or acellular. By ophthalmoscopic examination, microaneurysms appear as tiny, intraretinal red dots located in the inner retina. By fluorescein angiography, they appear as punctate hyperfluorescent dots with variable amounts of fluorescein leakage.

Pericyte cell death and loss of vascular intercellular contacts may lead to endothelial cell proliferation and microaneurysm development.[27,43,44] Pericytes appear to exert an antiproliferative effect and pericyte loss may explain the development of hypercellular microaneurysms. However, this mechanism does not account for acellular microaneurysms. Acellular microaneurysms may develop from hypercellular microaneurysms that become acellular from endothelial cell and pericyte apoptosis.[45]

Pericyte loss may also result in weakening of the capillary wall, promoting the development of microaneurysms at the structural weak points. Pericytes contain myofibrils with contractile properties and may act as smooth muscle cells of larger vessels, exerting tone to the vessel wall in order to counteract the transmural pressure. Loss of pericyte tone may result in focal dilation of the vessel wall leading to the development of a microaneurysm. However, the transmural pressure of the capillary

bed is low relative to the arterial circulation, and retinal capillary microaneurysms can develop in other diseases in which pericyte loss is not observed.[46,47]

Capillary Acellularity

Complete loss of the cellular elements of the retinal capillary network can be seen as a more advanced microvascular lesion in diabetic retinopathy and other microvascular retinopathies. In clinicopathologic correlations with fluorescein angiograms on enucleated and autopsied eyes, the retinal vascular digests of the enucleated eye showed that acellular capillaries are nonfunctional since they appeared as regions of nonperfusion on angiography.[48] The mechanism by which capillaries become acellular is unknown and can be seen in diabetes or in experimental diabetes or galactosemia in animal models.

Breakdown of Blood–Retina Barrier

Breakdown of the blood–retina barrier is an important pathophysiologic feature of diabetic retinopathy that leads to the development of macular edema, the leading cause of vision loss in diabetic patients. One mechanism by which the function of this barrier becomes altered involves opening of the tight junctions between vascular endothelial cell processes.[49,50] These tight junctions, also known as zonula occludens, appear as a pentalaminar structure on electron microscopy, consisting of two outer and one central electron-dense layer sandwiching two electron-lucent layers, giving the appearance of two "fused" plasma membranes. Using tracers such as lanthanum chloride or horseradish peroxidase, electron microscopy can be used to demonstrate that these molecules cannot pass in the presence of an intact tight junction. However, when the tight junctions are open, they become permeable to these tracer molecules.[50] Several important proteins are involved with the formation and function of tight junctions, with ZO-1 (zonula occludens) and occludin being the best characterized. In the presence of histamine, the expression of ZO-1 in cultured retinal endothelial cells is reduced in a dose-dependent manner.[51] Culturing in astrocyte-conditioned medium

increases expression of ZO-1 while high glucose decreases expression of ZO-1.[52] These in vitro results have also been supported by in vivo studies. Reduced expression and anatomic distribution of occludin was found in experimental diabetes.[53] Likewise, in experimentally diabetic rats and in diabetic humans, antihistamines reduce leakage of fluorescein into the vitreous.[54,55]

Vascular endothelial growth factor (VEGF) has been found to be an important mediator leading to the breakdown of the inner blood–retina barrier. Before the discovery of its well-documented role in promoting neovascularization, VEGF was found to increase the permeability of vessels, leading to its alternative name "vascular permeability factor."[56] The mechanism by which VEGF leads to the breakdown of the inner blood–retina barrier appears to involve alteration of endothelial cell tight junctions. Intravitreal injection of VEGF in rats increased the production of the free radical nitric oxide and led to phosphorylation of ZO-1.[57,58]

Another important factor promoting retinal vascular permeability involves the kallikrein–kinin system. Proteonomic studies of the vitreous from patients with advanced diabetic retinopathy have identified components of the kallikrein-kinin system, including plasma kallikrein, factor XII, and kininogen.[59,60] In rodent models, activation of plasma kallikrein in the vitreous has been found to increase retinal vascular permeability.[61] Likewise, inhibition of the kallikrein-kinin system reduces retinal vascular leakage caused by diabetes and hypertension.[61,62] The mechanism by which the kallikrein-kinin system promotes vascular permeability probably involves bradykinin. Bradykinin, via nitric oxide, induces vasorelaxation of retinal arterioles.[63] Intravenous infusion of bradykinin results in dilation of retinal arterioles and venules, an effect that is reduced by indomethacin and the cyclooxygenase-2 selective inhibitor nimesulide.[64] Bradykinin is also a neuropeptide with a direct effect on glia and neurons, which can release vasoactive factors that affect blood flow and vascular permeability.[65]

Biochemical Mechanisms in the Pathogenesis of Diabetic Retinopathy

Chronic hyperglycemia is known to be the major etiologic factor leading to all of the microvascular complications of diabetes, including diabetic retinopathy. However, the biochemical mechanisms by which hyperglycemia acts currently remain unclear. Proposed theories will be discussed in detail in the subsequent sections of this chapter.

Although diabetic retinopathy does not manifest the classic "rubor, tumor, calor, and dolor" features of an inflammatory disease and lacks a prominent infiltration of inflammatory cells, there are characteristics that imply a chronic low-grade inflammatory component. In the retinas of diabetic rats, increased activation of leukocytes with increased amounts of inflammatory cytokines and adhesion molecules have been observed. The upregulation of these molecules enhances leukocyte adhesion to retinal capillary walls, leading to increased capillary stasis, occlusion, and ultimately hypoxia as seen in diabetic retinopathy.[66–68] Clinically, it has been observed that intravitreal corticosteroid injections decrease diabetic macular edema, often with improvement of visual acuity.[69,70] The mechanism by which intravitreal corticosteroids reduce macular edema in diabetes and other etiologies, like retinal vein occlusions, is unclear, but the antiinflammatory effects of corticosteroids support an inflammatory component to the development of at least diabetic macular edema. Likewise, there is growing evidence that the kinin–kallikrein system, which plays an important role in the inflammatory cascade by acting on phospholipase and promoting the release of arachidonic acid and the production of prostaglandins, contributes to the development of diabetic macular edema.[71]

The tetracycline class of antibiotics has been demonstrated to have antiinflammatory effects in animal models in addition to antibiotic properties. Further, low-dose tetracyclines have been shown to inhibit retinal cell apoptosis and microglial changes. An open label phase I/II trial of patients on daily minocycline demonstrated an improvement in visual acuity and decreased foveal thickness compared to historical controls.[72–74] In a randomized control trial of subjects with nonproliferative diabetic retinopathy (NPDR) and proliferative diabetic retinopathy (PDR),

Scott et al. demonstrated that taking 100 mg of doxycycline daily was associated with a statistically significant increased mean frequency doubling perimetry (FDP) foveal sensitivity, a marker of inner retinal function, compared to placebo at 6, 12, and 24 months.[75] Further studies will be needed to validate these results and determine if tetracyclines are a viable treatment for diabetic retinopathy.

The Aldose Reductase Theory

Elevation of intracellular glucose levels can cause increased activation of the aldose reductase pathway. Aldose reductase uses the reduced form of nicotinamide adenine dinucleotide phosphate (NADPH) as a cofactor to reduce many aldose sugars into their respective sugar alcohols. Glucose is reduced to sorbitol, which is then oxidized into fructose by sorbitol dehydrogenase. However, sorbitol may build up to high intracellular levels because the sorbitol dehydrogenase reaction is slow and the accumulating sorbitol does not easily cross the plasma membrane into the extracellular space. In normoglycemic conditions, the aldose reductase pathway is nonoperative because glucose is a poor substrate for aldose reductase due to its high binding constant (kM). However, in the setting of hyperglycemia, the aldose reductase pathway becomes activated once the other enzymatic pathways of glucose metabolism become saturated. Lens epithelium expresses high levels of aldose reductase, and accumulation of sorbitol is believed to lead to the development of a cataract in diabetes.[76] Osmotic stress has been proposed as the mechanism by which elevated intracellular sorbitol leads to the pathologic changes seen in diabetes.[77] However, the levels of sorbitol in vascular cells are in the nanomolar range, which is orders of magnitude less than other glucose metabolites, which have ranges in the micromolar and millimolar range.[78]

A different mechanism that may account for the role of aldose reductase involves the cellular redox balance. Increases in the utilization of aldose reductase in the hyperglycemic state of diabetes will result in a decline in intracellular NADPH that alters the cellular redox balance and may decrease the production of nitric

oxide in endothelial cells.[79] Similarly, the increased use of sorbitol dehydrogenase can lead to an increase in the NADH/NAD^+ ratio that alters the cellular redox balance and may lead to oxidative stress and cellular damage.[80]

Of interest to animal models of diabetes, galactose is reduced by aldose reductase into galactitol. However, sorbitol dehydrogenase cannot oxidize galactitol, resulting in the rapid intracellular accumulation of galactitol. In the setting of chronic galactosemia, diabetic-like vascular basement membrane changes,[30,31] and pericyte loss, development of microaneurysms and capillary acellularity[81] have been reported. When these experiments were repeated and the animals were also treated with aldose reductase inhibitors, it was reported that the development of diabetic-like retinopathy changes was slowed, although most animals developed some degree of changes.[33,82–84] While aldose reductase inhibitors were reported to slow or prevent some of the pathologic changes in animal models of diabetes, the aldose reductase inhibitor sorbinil was found not to be effective in humans in the Sorbinil Retinopathy trial.[85] The lack of efficacy of aldose reductase inhibitors in human trials may, however, reflect dose-limiting side-effects of the drug that may have precluded it from achieving therapeutic levels in the tissues of interest.

Advanced Glycation Endproduct (AGE) Theory

Accelerated aging by nonenzymatic glycation and crosslinking of proteins has been proposed as a mechanism to explain the complications of diabetes.[86] Advanced glycation endproducts (AGEs) is the collective name given to proteins, lipids, and nucleic acids that undergo irreversible modification by reducing sugars or sugar-derived products. The series of chemical reactions that lead to the formation of AGEs is called the Maillard reaction. The Maillard reaction is responsible for the "browning" of tissue seen with aging as well as the "browning" of food during cooking. The initial chemical reaction is known as early glycation and involves reversible nonenzymatic binding of a sugar to amino acid groups on proteins, lipids, or nucleic acids. They form Schiff bases which

can undergo rearrangement to form more stable Amadori products. Glycosylated hemoglobin (HbA1c) and fructosamine are well-known examples of Amadori products used clinically as markers of glycemic control. Although they are not AGEs, they can undergo further reactions to eventually lead to the formation of AGEs. Formation of AGEs may directly damage cells by impairing the function of a variety of proteins,[87] including both extracellular proteins like collagen[88] and intracellular proteins.[89,90] AGE has been shown to activate apoptosis of RPE cells and induce mitochondrial dysfunction.[91]

The cellular effect of AGEs is also mediated by its binding to receptors, namely receptor for AGE (RAGE). RAGE is a multiligand transmembrane receptor that is part of the immunoglobulin superfamily of proteins and is upregulated in diabetic retinas.[92,93] When bound to AGEs, it initiates a cascade of signal transduction involving at least $p21^{ras}$, p44/p42 mitogen-activated protein kinase (MAPK), nuclear factor-kappa B (NF-κB), and protein kinase C (PKC).[94–99] Activation of these intracellular kinases can subsequently lead to cell dysfunction.[100]

Aminoguanidine is an inhibitor of AGE formation and has been reported to block the development of many of the microvascular complications of diabetes in animal models.[101–105] The effects of aminoguanidine cannot be automatically attributed to the blockade of the AGE pathway, however, since aminoguanidine also has parallel action as an inhibitor of inducible nitric oxide synthase and oxidants.[106] Studies also suggest aminoguanidine protects against apoptosis of retinal ganglion cells in diabetic rats via inhibition of AGE formation and downregulation of NF-κB.[107] Owing to limits secondary to toxicity, clinical trials in humans have been inconclusive; in animal models, however, the use of soluble RAGE to block binding of AGEs to RAGE has been found to prevent many of the effects of hyperglycemia.

Photoreceptor Metabolism Theory

Rods expend more energy in darkness, requiring up to four times as much adenosine triphosphate (ATP) in darkness compared to light. Reports have theorized that dark-adapted rods may be

implicated in the development of retinal degenerative disease, including diabetic retinopathy.[108] In the dark-adapted state, rods consume high levels of oxygen thus reducing the PO_2 of the inner retina. Hyperglycemia results in pseudohypoxia of the retina and coupled with anoxia of the inner retina during the dark-adapted state, VEGF production is increased.[108–110] Further support of this theory is the proposed mechanism that panretinal photocoagulation is effective by reducing retinal PO_2. In a small pilot study, Nguyen et al. demonstrated that supplemental oxygen therapy over 3 months improves visual acuity and diabetic macular edema as measured by foveal thickness on OCT.[111] Arden et al. performed a clinical trial of 12 patients with diabetes and NPDR in which eyes were randomized to illumination via a "glow patch" versus control to test this theory. Preliminary results demonstrated that after treatment, eyes randomized to illumination had fewer microaneurysms and dot–blot hemorrhages whereas untreated eyes developed more microaneurysms and dot–blot hemorrhages.[112] Further studies are required to elucidate the role of hypoxia in the development and progression of DR and whether oxygen therapy or light adaptation may mitigate disease.

Reactive Oxygen Intermediates (ROI) Theory

One of the oldest theories proposes that chronic hyperglycemia leads to the complications of diabetes by increasing oxidative stress. The usual metabolic pathway of glucose is through glycolysis and the tricarboxylic acid cycle, which takes place in the mitochondria and yields reducing equivalents used to drive the synthesis of adenosine triphosphate via oxidative phosphorylation. However, byproducts of oxidative phosphorylation include free radicals, such as superoxide anion, whose production is increased by high levels of glucose.[113] Free radicals can damage mitochondrial DNA[114] as well as cellular proteins[115] and are also produced by the autoxidation of glucose. Elevated oxidative stress also reduces nitric oxide levels,[116,117] promotes leukocyte adhesion to the endothelium and decreases the barrier function of endothelial cells,[118] and damages cellular proteins.[119] Diabetic mice that overexpress Cu^{2+}/Zn^{2+} superoxide dismutase develop less mesangial expansion

compared to wild-type diabetic mice, suggesting that oxidative stress promotes at least some complications of diabetes.[120] Oxidative stress can also activate PKC by increasing the formation of diacylglycerol (DAG).[121]

There is some evidence of increased oxidative stress in diabetic patients. It has been reported that diabetic patients have lower levels of antioxidants, such as vitamin C, vitamin E, and glutathione,[122–124] although these results have not been unequivocally reproduced by other researchers.[125] However, other markers of oxidative stress, such as oxidized low-density lipoprotein[126] and urinary isoprostanes, are elevated in diabetic patients.[127] In animal models of diabetes, the use of antioxidants has blocked the development of some of the microvascular complications of diabetes.[128–132] One clinical trial reported that high doses of vitamin E (>1000 IU/day) and lipoic acid improved retinal blood flow and creatinine clearance in diabetic patients.[133] However, most studies evaluating antioxidants to prevent the complications of diabetes in people have been unsuccessful.[134]

Protein Kinase C (PKC) Theory

PKC is a ubiquitous enzyme that appears to promote the development of many of the complications of diabetes without the involvement of the aldose reductase pathway. It has been observed that diabetes and galactosemia can produce elevation of DAG within cells of the retina and aorta in dogs despite treatment with the aldose reductase inhibitor sorbinil.[135,136] Activation of PKC occurs through the activation of phospholipase C, which leads to an increase in intracellular Ca^{2+} and DAG, which in turn results in the activation of PKC.[137] Hyperglycemia can result in pathologic activation of PKC. Elevated glucose levels result in activation of the glycolytic pathway and lead to increased levels of intracellular glyceraldehyde-3-phosphate. Glyceraldehyde-3-phosphate can promote the de novo synthesis of DAG through glycerol-3-phosphate, which in turn activates PKC.[138] Activation of PKC can also be mediated by AGE[98] and ROI.[121]

Elevated levels of DAG and PKC activity have been detected in the tissues of animals with diabetes.[139] The pathologic effects of

PKC activation that cause vascular damage are mediated through increased vascular permeability,[140] disruption of nitric oxide regulation,[141,142] increased leukocyte adhesion to vessel walls,[143] and changes in blood flow.[144] Overactivation of PKC leads to overexpression of VEGF causing changes in retinal vascularity. In fact, the effects of PKC on retinal blood flow as measured by fluorescein video angiography, as well as glomerular filtration rate and albumin excretion rate, were improved in a dose-dependent fashion with ruboxistaurin (LY333531), a PKC-β inhibitor.[145] VEGF[146] and endothelin[147] can also activate PKC, which in turn can promote the expression of growth factors like VEGF[148] and transforming growth factor-beta (TGF-β).[149] PKC activation can influence other signally pathways, such as MAPK or NF-κB.[150] A novel B adrenergic receptor agonist, compound 49b, reduces VEGF in diabetic rat models and reduced PKC phosphorylation in the diabetic retina.[151] Further, insulin-like growth factor binding protein-3 (IGFBP3) is protective to the retina by inhibiting the eNOS and the PKCzeta pathway, inhibiting VEGF production.[152]

PKC inhibition by ruboxistaurin has been reported to block many of the vascular abnormalities in endothelial cells and contractile cells from the retina, arteries, and renal glomeruli.[153] In animal models of diabetes, ruboxistaurin protected against or reversed many of the early vascular changes seen with retinopathy, nephropathy, and neuropathy.[145,146,154,155] However, a prospective clinical trial of ruboxistaurin did not meet its primary outcome (progression to sight-threatening diabetic macular edema or application of focal/grid photocoagulation for diabetic macular edema) at 30 months although there was a significant reduction of progression to sight-threatening diabetic macular edema when considered alone.[156] An open-label extension of the Protein Kinase C Diabetic Retinopathy Study 2 (PKCDRS-2) reported that over a 6-year study period patients with the greatest ruboxistaurin exposure (~5 years) had less sustained moderate vision loss (>15-letter decline) compared to those in the original placebo group (~2 years of ruboxistaurin use).[157] A prospective combined analysis of the two phase III trials revealed no statistical significant difference between ruboxistaurin use and standard care.[158]

Insulin Receptors and Glucose Transporters

In certain types of cells, such as adipocytes and skeletal muscle cells, insulin is required to transport glucose from the extracellular fluid across the plasma membrane into the cytoplasm. This action requires a specific receptor for insulin on the plasma membrane. Although it has been commonly stated that the microvascular complications of diabetes do not occur in tissues in which insulin is required for the transport of glucose into cells, insulin receptors have been reported on the pericytes and endothelial cells of the retinal microvessels.[159] There is no evidence, however, that the retinal microvascular insulin receptors are required for glucose transport, although insulin does enhance glycogen synthesis from radiolabeled glucose in retinal microvascular pericytes and endothelial cells and aortic smooth-muscle cells, but not in aortic endothelial cells.[159] Insulin in physiologic concentrations (as low as 10 ng/ml) stimulated [3H]-thymidine incorporation into retinal microvascular pericytes and endothelial cells and aortic smooth-muscle cells but not aortic endothelial cells.[159] It is noteworthy that, in these experiments, such low concentrations of insulin produced an effect, because unphysiologically high (e.g., 1 mg/ml) concentrations of insulin will stimulate proliferation of many types of cultured cells. However, since microvascular endothelial cells and pericytes do not normally proliferate in the mature retina,[160] the importance of these results for normal retinal vascular physiology is unclear. Additionally, these results indicate that there are metabolic differences between microvascular endothelial cells and the endothelial cells of larger vessels, so that translation of results from one type of vascular endothelial cell to another must be done with great caution. Insulin receptors (IR) from retinal neurons and blood vessels share many similar properties with insulin receptors from other peripheral tissues, and retinal neurons express numerous proteins that are attributed to the insulin signaling cascade as in other tissues.[161] The retinal IR, when stimulated with insulin, possesses tyrosine kinase activity towards an exogenous substrate. These similarities among IRs in vitro suggest that retinal IRs may function in a cell-specific manner in vivo. The IR in retina behaves similarly to liver IR in vitro, while retinal IR activity is more similar to brain IR activity in vivo where the IR is maintained

in a tonic state of activity. This difference may result from how circulating insulin is delivered to tissues of the body, and suggests that the blood–retinal barrier (BRB) stabilizes insulin access to the retina.[162] It was also observed that the retinal vascular cells were more sensitive to the growth promoting effect of insulin than aortic endothelial and smooth muscle cells. Furthermore, the IR in RPE cells localized exclusively to the basolateral surface of the cell, suggesting a possible role in unidirectional insulin transport from the choroidal circulation to the photoreceptors.[163]

There are at least five different types of facilitated cell membrane glucose transporters, designated GLUT1, GLUT2, GLUT3, GLUT4, and GLUT5, that appear to be most important for the intracellular transport of glucose in tissues like the retina that do not require insulin. Of these, GLUT1 appears to be the most prevalent in the retina,[164–166] occurring in microvascular and macrovascular endothelial cells and on RPE cells, as well as in the Müller cells. GLUT2 localization has been reported by immunocytochemistry at the apical ends of the Müller cells of the rat retina, facing the interphotoreceptor matrix,[167] while GLUT3 has been reported by similar techniques to be localized to the plexiform layers of the rat[168] and human[166] retina. An initial report using light microscopic immunocytochemistry in human eyes[164,165] also reported GLUT1 in the nerve fiber layer of the retina and in photoreceptor cell bodies, but GLUT1 was absent from retinal neovascular proliferations in the eyes of diabetic subjects.

The factors mediating glucose transport and glucose transporter expression are not as well defined in the retina as they are in the brain. Expression of GLUT1 in the various cell types within the retina is preserved during development and is evident as early as 8 weeks of gestation.[12] In contrast, GLUT3 is not detected in the neuroretina in the fetus and localizes to the inner synaptic layer only in the adult retina.[12] As in other tissues, glucose transport and/or GLUT1 expression is modulated by hypoxia, growth factors and glucose in primary cultures of retinal endothelial cells, a cell culture model of the inner BRB.[169,170] In cultured human retinal pigment epithelial cells, 2-deoxyglucose uptake and GLUT1 transcript have been shown to be upregulated in response to serum, insulin-like growth factor-1 (IGF-1), basic fibroblast growth factor

(bFGF), platelet-derived growth factor (PDGF), and epidermal growth factor (EGF). Because GLUT1 represents a unique portal of entry of glucose into the endothelial cells of the inner BRB, changes in retinal endothelial cell GLUT1 expression and glucose transport may have a major impact in providing substrate to the various pathogenic processes thought to underlie the development of diabetic retinopathy.[171]

Whether galactose also enters cells by one or more of these facilitated glucose transporters has not been directly tested. However, the fact that rats fed a 50% galactose diet – which also contains the normal amount of glucose – double their food intake by comparison with normal rats, but nevertheless gain weight at only 60–70% of the rate of the normal animals,[172] suggests that the excessive amount of galactose competes with glucose for the transport sites, thereby limiting the entry of glucose into cells and diminishing glucose-requiring cellular energy metabolism. However, galactose can participate in other cellular pathways along with glucose, including protein glycation/advanced glycation endproduct formation and synthesis of DAG to activate PKC.[136] Whether glucose or galactose can upregulate the mRNAs governing synthesis of any of the GLUT proteins in a fashion such that this upregulation persists long after cessation of the hyperglycemic or galactosemic state has not yet been explored.

Genetic Factors in the Pathogenesis of Diabetic Retinopathy

There is good evidence that diabetic retinopathy has a genetic predisposition.[173] Diabetic Retinopathy Study (DRS) data indicated that only 50% of nonproliferative diabetic retinopathy (NPDR) patients developed PDR, and many diabetic patients never developed diabetic retinopathy (DR). Twin studies of DR also lend support to this notion.[174] Some investigators have also suggested that aldose reductase gene polymorphisms may be associated with risk of DR.[175–181] A meta-analysis, however, showed no significant relationship between aldose reductase C106T polymorphism and risk of DR.[182] There appears to be considerable value in further

investigation of genetic factors related to the pathogenesis of the more severe forms of DR: severe nonproliferative and proliferative retinopathy, as well as macular edema. Nearly all individuals with type 1 diabetes, and most with type 2 disease, will demonstrate some of the lesions of early retinopathy with sufficient disease duration, but only 50% or less will develop proliferative disease.[183,184] Like clinically evident diabetic nephropathy, which similarly affects fewer than 50% of all diabetic subjects regardless of the duration of their diabetes, this suggests genetic factors are likely involved in the development of these severe forms of retinopathy.

Several studies have explored the relationship between human leukocyte antigen (HLA) antigens, expressed on cell surfaces and the presence, or severity, of DR. Rand et al.,[185] used a case–control design and found subjects who had HLA-DR phenotypes 3/4, 3/X, and 4/X had no increased risk of proliferative retinopathy as compared with "control" diabetic subjects, matched for age, sex, and diabetes duration, but without retinopathy. This question was also investigated in a group of 425 subjects with insulin-dependent diabetes who were randomly selected from a much larger population-based study,[186] and these authors found a significantly increased risk of PDR in subjects with the HLA $DR4^{+}$ DR3 phenotype.

More recent studies have investigated other aspects of the genetics of diabetic retinopathy. Of particular note is a report from the DCCT research group,[187] which examined familial clustering of severe DR (Early Treatment Diabetic Retinopathy Study (ETDRS) score >47, i.e., severe preproliferative disease) among families of DCCT subjects with multiple diabetic members. Significant associations were found when the correlation of retinopathy severity among family members was investigated. However, a less strong familial clustering of diabetic nephropathy was found. This is surprising since evidence from other studies has demonstrated considerable familial clustering of diabetic nephropathy, a complication of diabetes that is now considered to have a strong genetic component.[188–191]

Although many genes and proteins of vascular growth have been studied in association with PDR, few if any definitive predisposing genes for PDR have been identified. One of the best-known and

most well studied genes is the vascular endothelial growth factor gene, *VEGF*.[192–194] VEGF refers to two families of proteins created by alternate splicing of exon 8 in the *VEGF* gene[195] and is an important mediator of ischemia-induced vascularization and neovascularization. Current research of VEGF has focused on the role that certain single nucleotide polymorphisms (SNP) may play in contributing either a risk or protective effect in patients.[195–197] Recently, three SNPs in the promoter and 5′UTR regions of the gene (C(-7)T, C(-634)G, T(-1498), and G(-1190)A) were studied for frequency differences between patients with and without PDR.[196] These studies have looked at different genetic populations, focusing on Japanese and Indian patients. The results of these genetic studies are at times confusing, as a disease-associated SNP in one population may not confer a risk in another population. For example, in the Japanese population, the CC genotype at the C(-634)G region was significantly associated with PDR, whereas CG genotype at the same site was found to be risk-associated in the Indian population. In addition, disease duration, age, and sex must also be taken into account.

Ramprasad and coworkers in 2007 described work evaluating the role of SNPs within the receptor for advanced glycation endproducts (RAGE) in PDR.[198] At least 20 different polymorphisms have been studied within the *RAGE* gene. Interaction between the receptor RAGE and its associated glycation ligands plays a role in initiating a proinflammatory cascade, and this interaction has been studied in many disorders of chronic inflammation, including peripheral vascular disease and PDR. Research in these SNPs has shown disease association with the NPDR disease phenotype, yet this association needs to be replicated in other independent cohorts. More recently, Balasubbu et al.[199] analyzed the association of nine candidate genes (*RAGE*, *PEDF*, *AKR1B1*, *EPO*, *HTRA1*, *ICAM*, *HFE*, *CFH*, and *ARMS2*) but only found a significant association with diabetic retinopathy in one locus (rs2070600 in *RAGE* → reduces risk).

PDR and endstage renal disease (ESRD) are two of the most common and severe microvascular complications of diabetes. There is a high concordance in the development of PDR and ESRD in diabetic patients, as well as strong familial aggregation of these

complications, suggesting a common underlying genetic mechanism. However, the precise gene(s) and genetic variant(s) involved remain largely unknown. Erythropoietin (EPO) is a potent angiogenic factor observed in the diabetic human and mouse eye. By a combination of case–control association and functional studies, Tong et al.[200] demonstrated that the T allele of SNP rs1617640 in the promoter of the *EPO* gene is significantly associated with PDR and ESRD. The study was performed in three European-American cohorts (Utah: $P = 1.91\times10^{-3}$; GoKinD: $P = 2.66\times10^{-8}$; Boston: $P = 2.1\times10^{-2}$). The EPO concentration in human vitreous was 7.5-fold higher in normal subjects with the TT risk genotype than in those with the GG genotype. Computational analysis suggests that the risk allele (T) of rs1617640 creates a matrix match with the EVI1/MEL1 or AP1 binding site, accounting for an observed 25-fold enhancement of luciferase reporter expression as compared to the G allele. These results suggest that rs1617640 in the *EPO* promoter is significantly associated with PDR and ESRD and suggest EPO as a potential pathway mediating severe diabetic microvascular complications.[200]

Genome-wide association studies (GWAS) of diabetic retinopathy have also been pursued. In a Taiwanese population, Huang et al. found genetic associations for susceptibility for development of diabetic retinopathy in five loci, including *PLXDC2* and *ARHGAP22*, which are genes implicated in endothelial cell proliferation and capillary permeability.[201] In addition, a GWAS on a small (286 total) Mexican-American diabetic cohort identified 32 SNPs (in 11 regions) with a nominal association for severe diabetic retinopathy, though none was located in traditional candidate genes for diabetes or diabetic retinopathy.[202] A meta-analysis of GWAS studies in this study group and the Diabetes Genetic Replication and Meta Analysis Consortium (DIAGRAM), identified signals in HNF1A and CDKN2A/CDKN2B.[203]

In two large type I diabetes cohorts, several novel genetic loci associated with sight-threatening complications due to diabetic retinopathy, were identified, including rs10521145 in the intron of CCDC101, a histone acetyltransferase.[204]

Catalyzed by the rapid advances in whole-genome SNP genotyping technologies and the construction of reference

haplotype maps, genetic variants associated with ~300 traits have successfully been mapped by GWAS in the past few years, using a *P*-value threshold of 10^{-5}. GWAS is based on the hypothesis that common diseases are mainly caused by common genetic variants in the population (Common Disease Common Variants, CD-CV), each having relatively weak effects.[205] This assumption appears to be generally true for many genetic traits such as age-related macular degeneration.[206–208] Another hypothesis is Common Disease Rare Variants (CD-RV), or that common diseases are due to the presence of many rare variants in the same genes or pathways, each having relative strong effects. There is mounting evidence suggesting that CD-RV is also true for many diseases.[209–212] In diseases such as cancer, coronary atherosclerosis, and Parkinson's disease, nonsynonymous variants in the disease genes were found more frequently in the disease samples compared to the controls and a higher proportion of these are predicted to be damaging.[209,213,214] Causal variants under the CD-RV hypothesis are difficult to detect in GWAS, because they are in very weak linkage disequilibrium with the tagging SNPs included in genotyping assays. Deep resequencing in the case and control population is required to uncover such variants.[215] Due to the high cost of large-scale resequencing, only a very limited number of candidate genes have been screened.

Genome-wide methylation technologies have been applied to study human aging and disease.[216] Epigenetic variants may play a role in the development of diabetic retinopathy. Epigenetics involves alterations in gene expression via DNA methylation, histone modification, and microRNA. Agardh et al. reported a significant difference in methylation of 349 CpG sites of 233 genes including *TNF*, *CHN2*, *GIPR*, *GLRA1*, *GPX1*, *AHRR*, and *BCOR* associated with PDR in type 1 diabetics versus controls.[217] Further, the authors concluded that *BCOR* had the most significant methylation differences and may be used as a biomarker to predict PDR. A large Finnish Study[218] found an association with diabetic retinopathy and the polymorphism SUV39H2 which encodes histone methyltransferase, indicating histone modification may be involved in the development of DR. Further, Kadiyala et al.[219] determined there is an increase in histone acetyltransferase in

diabetes that may increase inflammatory proteins leading to microvascular complications. Changes in MiRNA expression also occur in diabetic eyes. These alterations include downregulation of miR200 which regulates VEGF.[220] Upregulation of miR-29b has been determined to be protective against retinal ganglion cell apoptosis in early stages of diabetes.[221] Epigenetic markers may provide a role in determining which patients are susceptible to DR, and for developing targeted therapies.

Other Ocular Factors

Becker[222] reported in 1967 that glaucoma was associated with a decreased prevalence and severity of diabetic retinopathy in affected eyes. Other studies have reported similar results. This has never been confirmed in a methodologically precise epidemiologic study, although Becker's claim seems to be correct based on other clinical observations (Fig. 48.2). This is an important point that should be evaluated in a proper case–control study. If it is true, the explanation is unclear. If the effect is observable only in true glaucoma and not in ocular hypertension, in which the intraocular pressure is chronically elevated without damage to the retinal ganglion cell or optic nerve fiber layers, then it may be related in some way to loss of metabolic activity in the retina with degeneration of ganglion cells. If the effect is related simply to elevated intraocular pressure, the explanation for this observation would be less obvious.

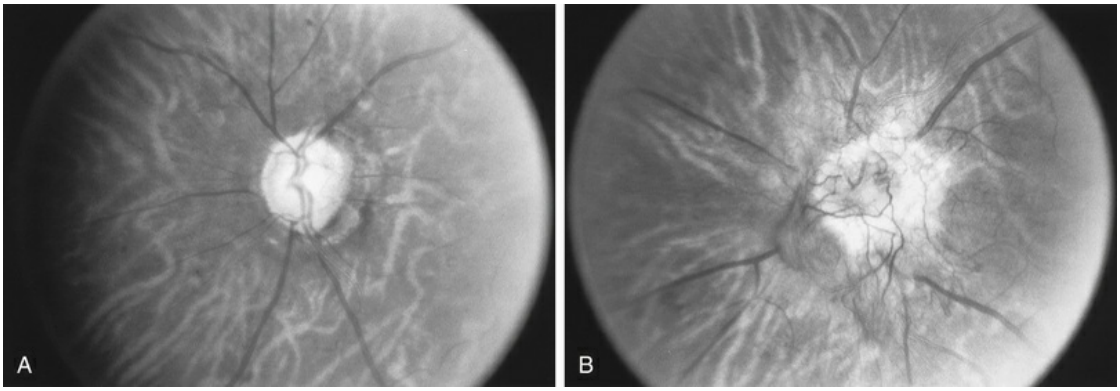

FIG. 48.2 This 64-year-old man presented with asymmetric, chronic open angle glaucoma and

markedly asymmetric diabetic retinopathy. Intraocular pressure in the right eye was 32 mmHg, visual acuity was 20/80, and there was a glaucomatous visual field defect and pronounced glaucomatous cupping of the optic nerve head. In the left eye, the pressure was 16 mmHg, visual acuity was 20/20, and there was only physiologic cupping. The patient had had diabetes mellitus for 15 years. (A) Photograph of the right optic nerve head shows extensive cupping of the optic nerve, though without nasal displacement of the vessels. (B) Photograph of the left optic nerve shows extensive neovascularization.

It has also been reported that myopia is associated with a decreased prevalence and severity of diabetic retinopathy.[223] This effect of myopia on the prevalence of proliferative diabetic retinopathy has been confirmed by Rand et al.[185] who found an interesting interaction between myopia of greater than 2 diopters and HLA-D-group antigens. Fewer subjects in their "case" group with proliferative retinopathy had myopia of this degree than did subjects in the control group, who had diabetes of 15 years' or more duration and minimal or no retinopathy. Subjects with 2 D or more of myopia and HLA-D group phenotypes 3/0, 4/0, or X/X had a relative risk for proliferative disease of 1.0 as compared with the control group (i.e., their risk was no different from that of the controls), while the overall risk for all subjects, regardless of refractive error, with these HLA-D group phenotypes was 3.[79]

The initial observations leading to the development of panretinal photocoagulation (or scatter) treatment for proliferative diabetic retinopathy were made by Aiello and colleagues at the Symposium on the Treatment of Diabetic Retinopathy,[224] who noted that eyes with a great deal of retinochoroidal scarring from trauma, inflammatory disease, etc. had markedly reduced prevalence and severity of diabetic retinopathy. The effect is unexplained, but the most widespread current hypothesis is that it results from decreased retinal metabolism – in particular, a decreased need for oxygen, with a resultant diminished production of a vasoproliferative (angiogenic) factor.[225,226] The immediate practical application of this observation was the attempt, through extensive photocoagulation of the midperipheral retina (panretinal or scatter

photocoagulation), to produce the same effect iatrogenically, a technique that significantly reduces the rate of progression to severe visual loss in PDR.[227]

Retinopathy in Different Forms of Diabetes

There is no evidence that retinopathy differs in different forms of diabetes. Proliferative retinopathy is more prevalent at any given duration of the systemic disease in type 1 than in type 2 diabetes,[183,184] but, as noted earlier, it is not clear whether this is due to different metabolic factors in the two types of diabetes, to differences in the ages of the patients (type 1 patients are, on average, much younger), or to the higher mean blood glucose levels in type 1 patients. Macular edema probably occurs with equal prevalence as a function of disease duration in both type 1 and type 2 diabetes.[228] Type 2 diabetes is more common after the age of 30[184] (although "type 2 diabetes of youth" is becoming increasingly frequently recognized[229]), but, despite the apparently mild metabolic defect, proliferative retinopathy can occur as well in this form of the disease (Fig. 48.3). Similarly, vision-threatening retinopathy can occur in patients with "secondary" diabetes – that which occurs, for example, following pancreatitis, hemochromatosis, or acromegaly. The patient whose retinal photographs are shown in Figs. 48.4A–B had acromegaly secondary to a pituitary adenoma and also developed background diabetic retinopathy with macular edema. Since the acromegaly had been treated and the patient had normal levels of circulating growth hormone, the retinopathy may have been related to diabetes secondary to the acromegaly, or to a type 2 diabetes that would have developed regardless of the presence of acromegaly.

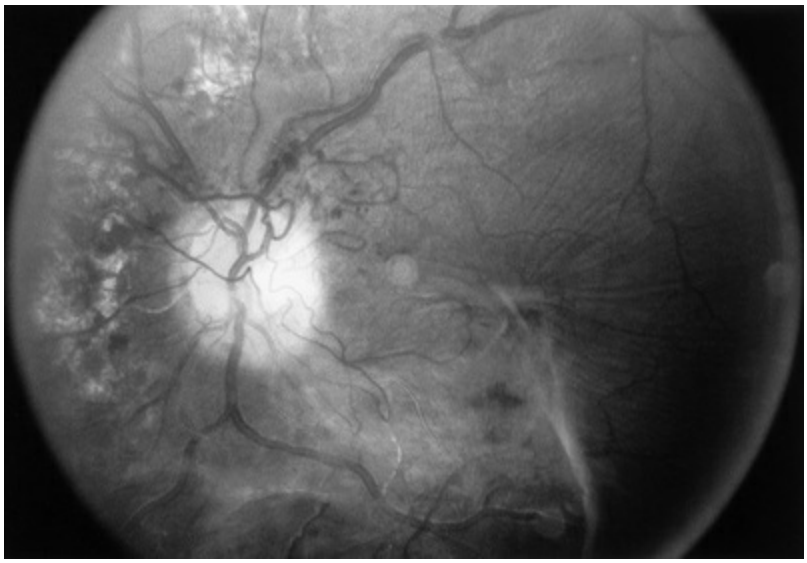

FIG. 48.3 Photograph showing the fundus of the left eye of a 32-year-old woman who had had diabetes mellitus since the age of 12 but had never required insulin. At the time of this photograph she was being maintained on dietary management and sulfonylurea medication. She therefore has the diagnosis of “type 2 diabetes of youth.” As the photograph demonstrates, she has developed substantial proliferative diabetic retinopathy with extensive optic nerve head neovascularization and fibroglial proliferation producing traction on the macula. The right eye had been lost because of proliferative diabetic retinopathy with neovascular glaucoma.

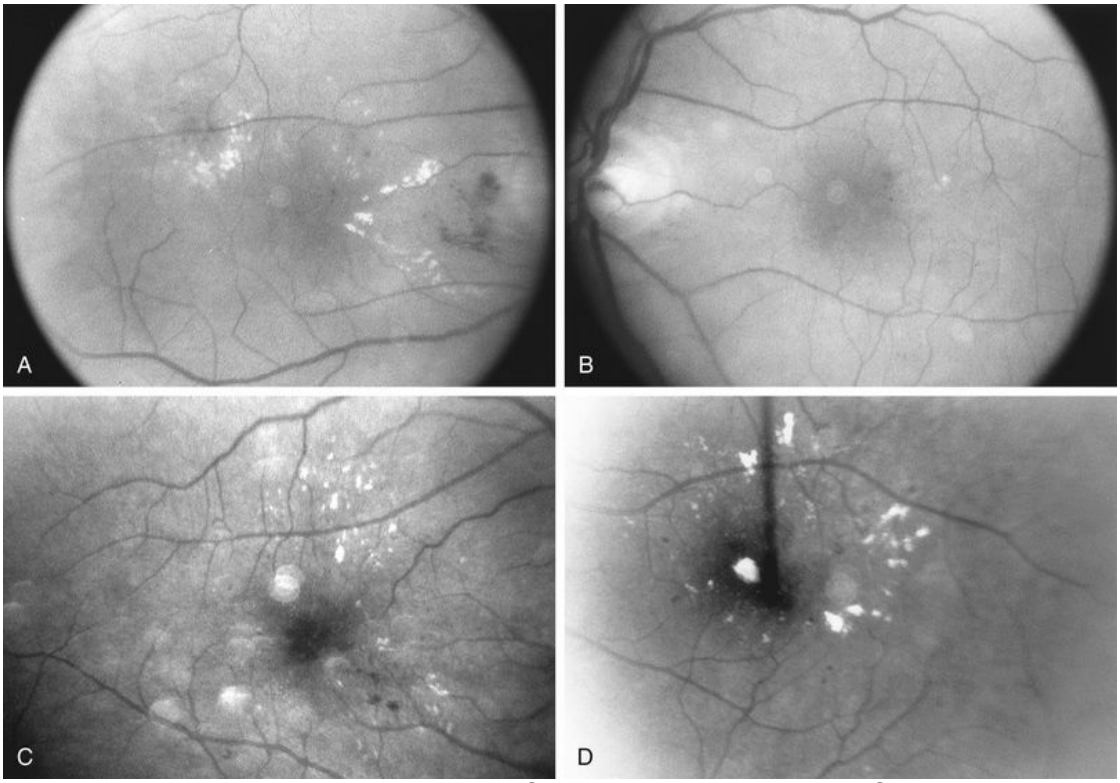

FIG. 48.4 (A) Photograph of the macular region of the right eye of an 84-year-old man who had developed acromegaly 12 years previously. Treatment with bromocriptine has maintained serum growth hormone levels in the normal range. Subsequent to his development of acromegaly, he was found to have type 2 diabetes mellitus, and he developed background diabetic retinopathy with macular edema, for which he received focal argon laser photocoagulation. Subsequently, he developed a central retinal vein occlusion in his right eye, for which he received panretinal argon laser photocoagulation. Nevertheless, neovascular glaucoma ensued, requiring cyclocryotherapy and medical therapy to manage the intraocular pressure and maintain at least some visual acuity. (B) The left eye of the same patient shows a few microaneurysms and minimal lipid deposition. (C) Photograph of the right eye of a 52-year-old man with acromegaly and type 2 diabetes mellitus. Bromocriptine treatment brought serum growth hormone levels to the normal range. Background diabetic retinopathy and macular edema are present. (D) The left macular region of the same patient, also showing background diabetic retinopathy with macular edema.

Animal Models in the Study of Diabetic Retinopathy

Studies of the pathogenesis and treatment of human disease can be facilitated by the development of models of the disease in animals. There have been numerous attempts to reproduce the lesions of diabetic retinopathy in animals. Although several authors have claimed positive results, there are only a few animal models in which one or more of the lesions of diabetic retinopathy have been produced with unquestioned validity. Foremost among these are dogs, with spontaneous[230] or induced[231] diabetes of 3–5 years' duration. These animals develop loss of capillary pericytes and ultimately also of endothelial cells with nonfunctional, acellular capillaries; capillary basement membrane thickening, and microaneurysm formation. Early intraretinal neovascularization has also been observed. However, more advanced lesions, including retinal edema (dogs do not have a macula, so true macular edema cannot develop) and neovascularization into the vitreous, have not been reported.

Because of the ease of working with small animals, there have been many attempts to develop diabetic retinopathy in rodents, including mice and, in particular, rats. Claims of producing lesions such as microaneurysms[101] and pericyte dropout[101] in rats with experimental diabetes of less than 1 year have not been validated by Engerman et al.[231] or Tilton et al.[232] However, rats with diabetes or galactosemia[30,31] develop retinal capillary basement membrane thickening, a lesion that has been widely observed in many microvascular systems in the body in human and animal diabetes.[233] In addition, rats that have been galactosemic for 18 months or more develop pericyte loss and, eventually, capillary acellularity,[84,172,234,235] and some rats that have been fed a 30–50% galactose diet for up to 24 months develop a halo of dilated, hypercellular vessels surrounding the optic nerve.[84,172,234,235] Whether these represent intraretinal neovascularization or simply dilated preexisting vascular channels is uncertain. Of particular interest is a report that pericyte and endothelial cell nuclei in short-term

diabetic or galactosemic rats, and in retinal capillaries from donor eyes of humans with diabetes, undergo apoptosis as demonstrated by appropriate nuclear labeling techniques.[45] It is unknown what stimulus is induced by prolonged hyperglycemia, or galactosemia, that causes programmed death of retinal capillary cells to a greater extent than capillary cells elsewhere in the body.

Because of the similarity of their retinal anatomy to that of humans, one might expect that nonhuman primates with diabetes of sufficient duration would be good models for human diabetic retinopathy. However, studies of rhesus monkeys with diabetes for as long as 10 years have revealed occasional microaneurysms but no other lesions.[231,236]

Doubtless a major reason for the difficulty in producing lesions of diabetic retinopathy in animals with diabetes is the factor of disease duration. In diabetic dogs a minimum disease duration of 3–5 years is necessary for the development of the earliest lesions of retinopathy, and this is identical to the duration required for retinopathy to develop in humans with type 1 diabetes.[184,237,238] Rats and mice normally have a lifespan of under 3 years, and after the onset of diabetes it is difficult to maintain these animals for much more than 1 year. Several investigators have reported the development of lesions resembling diabetic retinopathy in rats fed a 50% galactose diet for 28 months.[84,172,234] These lesions include pericyte "ghosts," acellular capillaries, and vascular dilation and tortuosity. Whether microaneurysms develop in galactosemic rats is controversial.[45,84,172,234–236] The use of a high-galactose diet to produce a model of diabetic retinopathy originated from the hypothesis that the enzyme sequence known as the "sorbitol pathway" is responsible for the earliest lesions of diabetic retinopathy. Since galactose, along with glucose, is a substrate for this pathway, its use in producing models of retinopathy is a good test of the hypothesis. Previously, Kern and Engerman,[104] as well as Kador and associates,[82,83] have produced a diabetic-like retinopathy in dogs fed a 50% galactose diet for 3–4 years. Kern and Engerman have also reported a diabetic-like retinopathy in mice fed a 30% galactose diet for 21–26 months.[239] They reported that, unlike galactosemic rats, galactosemic mice developed true microaneurysms. These findings raise two important questions. First, why might mice, dogs, and

humans develop microaneurysms after chronic diabetes, or galactosemia, and rats do not? Second, how might the presence of retinopathy in chronically galactosemic mice be relevant to the hypothesis that the "sorbitol pathway" is an important causal mechanism for diabetic retinopathy? Both these questions will be considered in more detail in later sections of this chapter.

Species- and organ-specific variations in anatomy and in metabolic pathways may be important considerations in the development of microvascular lesions in the retina or other organs. Pericyte dropout and microaneurysm formation have not been found either in the brains of diabetic human subjects,[240] or in those of diabetic or galactosemic dogs,[241] even though these lesions are common in the retina and were present in the retinas of the same human or animal subjects in whose cerebral cortexes they could not be found. It might be argued that, in these studies, retinas were examined by the trypsin digest procedure in which the entire, intact retinal vasculature can be spread on a microscope slide and examined in detail. This cannot be done with cerebral cortical vasculature, which must be examined histologically following homogenization and sieving through a nylon mesh that retains only vascular fragments. Capillaries that have lost cells or are otherwise abnormal may be sufficiently fragile that they are broken into smaller pieces by this technique and are lost in the sieving process. Although the retina is derived embryologically from the brain, and both retina and brain have a microvasculature featuring thick endothelial cell cytoplasm and tight junctions between endothelial cells that produce a blood–tissue barrier to many molecules, pericyte coverage of the endothelial cell tube of capillaries of the retina is substantially greater in the two species that have been studied (rat and monkey) than it is in the brains of these species.[242,243] The same is probably true in humans, where the data from retina closely resemble data from the retinas of monkeys, but it has not been possible to obtain retinal and brain tissue from the same human donors adequate to perform these morphometric studies. Although galactosemic rats develop a diabetic-like retinopathy, rats have a much smaller ratio of pericytes to endothelial cells in their retinal microcirculations than do humans.[232,242,244] Comparisons of the retinal and cerebral pericyte :

endothelial cell ratios in retinas and brains of rats with those of dogs, mice, and humans have not been carried out, but would be of interest because dogs, humans, and (at least according to one group of investigators) mice develop true capillary microaneurysms with long-term diabetes (dogs and humans) and galactosemia (dogs and mice), while rats do not.

Two useful animal models of neovascularization exist, both in nondiabetic animals. The first, originally described by Ashton[222] and by Patz,[245] is produced by exposing neonatal kittens or puppies to an atmosphere high in oxygen for up to a few days just after birth. This produces at least a peripheral, or in more severe cases a generalized,[246] vasoconstriction, followed by the development of retinal new vessels. These vessels are transient, however, and regress spontaneously after a few weeks. This model was initially developed to simulate retinopathy of prematurity, a condition that may develop following exposure of premature human infants to a high-oxygen atmosphere. The development of the new vessels, according to the hypothesis that has been favored for a number of years,[226] presumably resulted from production by the hypoxic retina cells (hypoxic because of the profound vasoconstriction that followed the hyperoxia) of an "angiogenesis factor."[247] More recently, hyperoxygenation during the neonatal period has been applied to mice and rats, producing a model of peripheral retinal neovascularization similar to that of retinopathy of prematurity in human infants (Fig. 48.5), that has been exploited for studies of the production, and inhibition, of angiogenesis factors.[248–250] A second model of intraretinal and subretinal (beneath the neural retina, but arising from the retinal and not the choroidal circulation) neovascularization has recently been described, using transgenic mice that overexpress the gene for VEGF.[251] This model is additional evidence that VEGF is capable of producing retinal neovascularization, although in a quite artificial situation that may not be relevant to human ocular diseases associated with neovascularization. The new vessels in these transgenic mice extend from the retinal circulation to beneath the photoreceptor layer of the neural retina but do not enter the RPE. The reason for this outward growth, rather than inward into the vitreous, is that the promoter used to carry the VEGF gene into the retina is the

rhodopsin gene, which is localized to the photoreceptor cells.

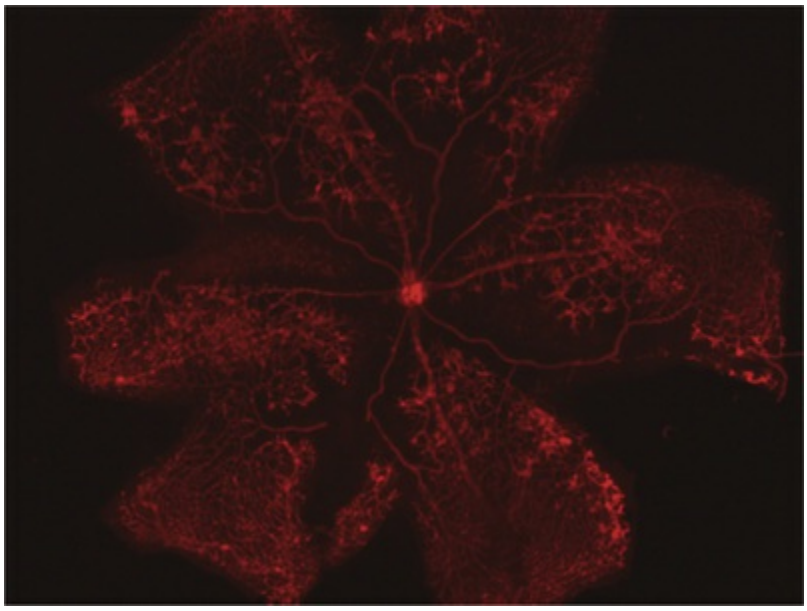

FIG. 48.5 Flat mount of the retinal vessels from an eye of a neonatal albino rat that had been exposed with its mother to an atmosphere in which the oxygen level was varied in stepwise fashion between 50% and 10% every 24 h over the first 14 days after birth. The animal was then returned to room air for the next 6 days and then euthanized, the eyes enucleated, and the retinal vessels visualized using a histochemical technique with isolectin. This demonstrates an area of nonperfusion in the peripheral retinal vasculature, similar to those that develop in human diabetic retinopathy. (Magnifications: ×15.)

Cell Culture Studies

The intact human or experimental animal is a complex organism, in which the study of the intricate metabolic pathways that ultimately lead to diabetic retinopathy may be difficult.

Since the mid-1970s, techniques have been developed to isolate and grow in culture the component cells of both large and small blood vessels, including those from the retina. In 1975, Buzney et al. described the culture of retinal microvascular pericytes from bovine and monkey eyes.[252] Subsequently Frank et al.[253] and several

others[254–256] described the culture of retinal microvascular endothelial cells. More recent evidence indicates that glial cells of the retina and optic nerve may also be important in the development, at least in the later stages of diabetic retinopathy, of neovascularization and, perhaps, macular edema. Methods are available for retinal glial cell culture. These techniques add an extra tool for research in diabetic retinopathy, but one that must be used with caution. One can use cell culture studies to investigate certain biochemical processes, but with great caution that the processes being studied have not been greatly modified in culture from those that occur in vivo. The same can be said for the investigation of physiologic function, e.g., phagocytosis, cell contraction, or cell motility. Diabetic retinopathy requires years to develop in the intact human or experimental animal. It has not yet been possible to maintain cultures of retinal cells for that duration, and there is no way of ascertaining that alterations produced in cells by exposure to high glucose or galactose over a short time in culture are truly related to the development of the anatomic and functional lesions of diabetic retinopathy over a very long time in the intact retina. Finally, although capillary tube-like structures composed of micro- and macrovascular endothelial cells have been produced under certain conditions in culture,[257–259] these may not be truly analogous either to normal vessels or to abnormal new vessels in the intact retina.

Despite these caveats, there are several results using cultured retinal microvascular cells that appear to be relevant to the physiology of the intact retinal microcirculation. These include the elegant studies of D'Amore and associates,[43,44] in which microvascular endothelial cells were cocultured with a variety of other cell types that had been growth-arrested with an antibiotic and were then plated together with endothelial cells in different proportions. Most of the cells used for the cocultures, including bovine RPE cells, human skin fibroblasts, mouse 3T3 fibroblasts, and Madin–Darby canine kidney cells, greatly stimulated endothelial cell proliferation. By contrast, pericytes and vascular smooth-muscle cells dramatically inhibited endothelial cell proliferation, even when the pericytes or smooth-muscle cells were added in ratios as low as 1 : 10 with the endothelial cells.[43] For the

coculture to be effective in retarding endothelial cell proliferation, pericyte or smooth-muscle cell processes had to make contact with the endothelial cells. Transfer of "conditioned media" from pericyte or smooth-muscle cell cultures was ineffective in producing growth inhibition. In studying the mechanism of the inhibition, these authors found that it was produced by the release, and activation, of TGF-β.[44] Pericytes or smooth-muscle cells alone produce this polypeptide in an inactive form. The cocultured cells, in physical contact with one another, both produce and activate TGF-β. This finding suggests that one function of pericytes in the retina is to inhibit the proliferation of endothelial cells. Thus, the loss of pericytes that occurs early in the course of diabetic retinopathy may facilitate the later development of microaneurysms (clusters of newly formed endothelial cells) and of frank neovascularization. In fact, just this result has been reported in an experiment using mice with a targeted disruption ("knockout") of the gene for the PDGF-β.[27] This genetic defect is lethal, but histopathologic examination of the fetal PDGF-β-deficient animals shows an absence of capillary pericytes – whose antenatal development is evidently controlled by this growth factor – and the frequent appearance of microaneurysms throughout the microcirculation of the retina and brain.

Pericytes are considered to be contractile cells, regulating flow through the capillaries analogous to the function of the smooth-muscle cells of the larger vessels. Cultured pericytes are immunocytochemically positive for smooth-muscle actin,[260] and in culture they contract either spontaneously[261] or in response to a variety of agents.[262–264] Thus, loss of pericytes from the retinal microcirculation may produce alterations in retinal blood flow. However, direct evidence for pericyte contraction in the circulation of the intact retina has never been obtained. Tilton et al.[265] performed a morphometric study of capillaries in rats following infusion of various vasoconstrictor agents and found evidence of contraction of pericytes in skeletal muscle capillaries but not of those in cardiac muscle. Butryn and coworkers conducted a similar study in the retinal vessels of rats following intravitreal infusion of ET-1, an extremely powerful vasoconstrictor.[266] Although they found evidence of contraction of arteriolar smooth muscle, they

could not demonstrate contraction of retinal capillary pericytes.

Conclusion

Considerable progress has been made in our understanding of the genetic susceptibility factors and etiologic mechanisms underlying the development of diabetic retinopathy. Considerable additional work is necessary, however, to fully elucidate the sequence of events that lead to this increasingly common blinding disorder.

Acknowledgments

Kang Zhang, MD, PhD, was supported by grants from the Chinese National 985 Project to Sichuan University and West China Hospital, NIH/NEI, VA Merit Award, Research to Prevent Blindness, and BWF Clinical Scientist Award in Translational Research.

References

1. The Diabetes Control and Complications Trial Research Group. The effect of intensive treatment of diabetes on the development and progression of long-term complications in insulin-dependent diabetes mellitus. *N Engl J Med*. 1993;329:977–986.
2. UK Prospective Diabetes Study (UKPDS) Group. Intensive blood-glucose control with sulphonylureas or insulin compared with conventional treatment and risk of complications in patients with type 2 diabetes (UKPDS 33). *Lancet*. 1998;352:837–853.
3. UK Prospective Diabetes Study Group. Tight blood pressure control and risk of macrovascular and microvascular complications in type 2 diabetes (UKPDS 38). *Br Med J*. 1998;317:703–713.
4. Nittala MG, Keane PA, Zhang K, et al. Risk factors for proliferative diabetic retinopathy in a Latino American population. *Retina*. 2014;24(8):1594–1599.

5. Davis MD, Fisher MR, Gangnon RE, et al. Risk factors for high-risk proliferative diabetic retinopathy and severe visual loss: Early Treatment Diabetic Retinopathy Study Report #18. *Invest Ophthalmol Vis Sci*. 1998;39(2):233–252.
6. Porta M, Sjoelie AK, Chaturvedi N, et al. Risk factors for progression to proliferative diabetic retinopathy in the EURODIAB Prospective Complications Study. *Diabetologia*. 2001;44:2203–2209.
7. Cogan DG, Toussaint D, Kuwabara T. Retinal vascular patterns. IV. Diabetic retinopathy. *Arch Ophthalmol*. 1961;66:366–378.
8. Kuwabara T, Cogan DG. Studies of retinal vascular patterns. I. Normal architecture. *Arch Ophthalmol*. 1960;64:904–911.
9. Kuwabara T, Cogan DG. Retinal vascular patterns. VI. Mural cells of the retinal capillaries. *Arch Ophthalmol*. 1963;69:492–502.
10. Speiser P, Gittelsohn AM, Patz A. Studies on diabetic retinopathy. 3. Influence of diabetes on intramural pericytes. *Arch Ophthalmol*. 1968;80:332–337.
11. Yanoff M. Diabetic retinopathy. *N Engl J Med*. 1966;274:1344–1349.
12. Shepro D, Morel NM. Pericyte physiology. *FASEB J*. 1993;7:1031–1038.
13. Aiello LP, Cavallerano J, Bursell SE. Diabetic eye disease. *Endocrinol Metab Clin North Am*. 1996;25:271–291.
14. Cameron NE, Eaton SE, Cotter MA, et al. Vascular factors and metabolic interactions in the pathogenesis of diabetic neuropathy. *Diabetologia*. 2001;44:1973–1988.
15. Akagi Y, Kador PF, Kuwabara T, et al. Aldose reductase localization in human retinal mural cells. *Invest Ophthalmol Vis Sci*. 1983;24:1516–1519.
16. Tilton RG, Hoffmann PL, Kilo C, et al. Pericyte degeneration and basement membrane thickening in skeletal muscle capillaries of human diabetics. *Diabetes*. 1981;30:326–334.
17. Kern TS, Engerman RL. Distribution of aldose reductase in ocular tissues. *Exp Eye Res*. 1981;33:175–182.
18. Ludvigson MA, Sorenson RL. Immunohistochemical

localization of aldose reductase. II. Rat eye and kidney. *Diabetes*. 1980;29:450–459.
19. Buzney SM, Frank RN, Varma SD, et al. Aldose reductase in retinal mural cells. *Invest Ophthalmol Vis Sci*. 1977;16:392–396.
20. Brownlee M. Biochemistry and molecular cell biology of diabetic complications. *Nature*. 2001;414:813–820.
21. Barrett TB, Gajdusek CM, Schwartz SM, et al. Expression of the sis gene by endothelial cells in culture and in vivo. *Proc Natl Acad Sci USA*. 1984;81:6772–6774.
22. Collins T, Ginsburg D, Boss JM, et al. Cultured human endothelial cells express platelet-derived growth factor B chain: cDNA cloning and structural analysis. *Nature*. 1985;316:748–750.
23. Collins T, Pober JS, Gimbrone MA Jr, et al. Cultured human endothelial cells express platelet-derived growth factor A chain. *Am J Pathol*. 1987;126:7–12.
24. DiCorleto PE, Bowen-Pope DF. Cultured endothelial cells produce a platelet-derived growth factor-like protein. *Proc Natl Acad Sci USA*. 1983;80:1919–1923.
25. Bernstein LR, Antoniades H, Zetter BR. Migration of cultured vascular cells in response to plasma and platelet-derived factors. *J Cell Sci*. 1982;56:71–82.
26. D'Amore PA, Smith SR. Growth factor effects on cells of the vascular wall: a survey. *Growth Factors*. 1993;8:61–75.
27. Lindahl P, Johansson BR, Leveen P, et al. Pericyte loss and microaneurysm formation in PDGF-B-deficient mice. *Science*. 1997;277:242–245.
28. Hellstrom M, Kalen M, Lindahl P, et al. Role of PDGF-B and PDGFR-beta in recruitment of vascular smooth muscle cells and pericytes during embryonic blood vessel formation in the mouse. *Development*. 1999;126:3047–3055.
29. Leveen P, Pekny M, Gebre-Medhin S, et al. Mice deficient for PDGF B show renal, cardiovascular, hematological abnormalities. *Genes Dev*. 1994;8:1875–1887.
30. Robison WG Jr, Kador PF, Kinoshita JH. Retinal capillaries: basement membrane thickening by galactosemia prevented with aldose reductase inhibitor. *Science*. 1983;221:1177–1179.

31. Frank RN, Keirn RJ, Kennedy A, et al. Galactose-induced retinal capillary basement membrane thickening: prevention by Sorbinil. *Invest Ophthalmol Vis Sci*. 1983;24:1519–1524.
32. Das A, Frank RN, Zhang NL, et al. Increases in collagen type IV and laminin in galactose-induced retinal capillary basement membrane thickening – prevention by an aldose reductase inhibitor. *Exp Eye Res*. 1990;50:269–280.
33. Robison WG Jr, Kador PF, Akagi Y, et al. Prevention of basement membrane thickening in retinal capillaries by a novel inhibitor of aldose reductase, tolrestat. *Diabetes*. 1986;35:295–299.
34. Das A, Frank RN, Zhang NL. Sorbinil does not prevent galactose-induced glomerular capillary basement membrane thickening in the rat. *Diabetologia*. 1990;33:515–521.
35. Nishio Y, Warren CE, Buczek-Thomas JA, et al. Identification and characterization of a gene regulating enzymatic glycosylation which is induced by diabetes and hyperglycemia specifically in rat cardiac tissue. *J Clin Invest*. 1995;96:1759–1767.
36. Brownlee M, Cerami A. The biochemistry of the complications of diabetes mellitus. *Annu Rev Biochem*. 1981;50:385–432.
37. Timpl R, Rohde H, Robey PG, et al. Laminin – a glycoprotein from basement membranes. *J Biol Chem*. 1979;254:9933–9937.
38. Grant DS, Kleinman HK. Regulation of capillary formation by laminin and other components of the extracellular matrix. *EXS*. 1997;79:317–333.
39. Kennedy A, Frank RN, Mancini MA. In vitro production of glycosaminoglycans by retinal microvessel cells and lens epithelium. *Invest Ophthalmol Vis Sci*. 1986;27:746–754.
40. Shimomura H, Spiro RG. Studies on macromolecular components of human glomerular basement membrane and alterations in diabetes: decreased levels of heparan sulfate proteoglycan and laminin. *Diabetes*. 1987;36:374–381.
41. Spiro RG, Spiro MJ. Effect of diabetes on the biosynthesis of

the renal glomerular basement membrane: studies on the glucosyltransferase. *Diabetes*. 1971;20:641–648.
42. Friedenwald JS. Diabetic retinopathy. *Am J Ophthalmol*. 1950;33:1187–1199.
43. Orlidge A, D'Amore PA. Inhibition of capillary endothelial cell growth by pericytes and smooth muscle cells. *J Cell Biol*. 1987;105:1455–1462.
44. Antonelli-Orlidge A, Saunders KB, Smith SR, et al. An activated form of transforming growth factor beta is produced by cocultures of endothelial cells and pericytes. *Proc Natl Acad Sci USA*. 1989;86:4544–4548.
45. Mizutani M, Kern TS, Lorenzi M. Accelerated death of retinal microvascular cells in human and experimental diabetic retinopathy. *J Clin Invest*. 1996;97:2883–2890.
46. Ashton N, Kok DA, Foulds WS. Ocular pathology in macroglobulinaemia. *J Pathol Bacteriol*. 1963;86:453–461.
47. Duke JR, Wilkinson CP, Sigelman S. Retinal microaneurysms in leukaemia. *Br J Ophthalmol*. 1968;52:368–374.
48. Kohner EM, Henkind P. Correlation of fluorescein angiogram and retinal digest in diabetic retinopathy. *Am J Ophthalmol*. 1970;69:403–414.
49. Daneman D, Drash AL, Lobes LA, et al. Progressive retinopathy with improved control in diabetic dwarfism (Mauriac's syndrome). *Diabetes Care*. 1981;4:360–365.
50. Wallow IH, Engerman RL. Permeability and patency of retinal blood vessels in experimental diabetes. *Invest Ophthalmol Vis Sci*. 1977;16:447–461.
51. Gardner TW, Lesher T, Khin S, et al. Histamine reduces ZO-1 tight-junction protein expression in cultured retinal microvascular endothelial cells. *Biochem J*. 1996;320(Pt 3):717–721.
52. Gardner TW. Histamine, ZO-1 and increased blood-retinal barrier permeability in diabetic retinopathy. *Trans Am Ophthalmol Soc*. 1995;93:583–621.
53. Barber AJ, Antonetti DA, Gardner TW. Altered expression of retinal occludin and glial fibrillary acidic protein in experimental diabetes. The Penn State Retina Research

Group. *Invest Ophthalmol Vis Sci*. 2000;41:3561–3568.
54. Enea NA, Hollis TM, Kern JA, et al. Histamine H1 receptors mediate increased blood–retinal barrier permeability in experimental diabetes. *Arch Ophthalmol*. 1989;107:270–274.
55. Gardner TW, Eller AW, Friberg TR, et al. Antihistamines reduce blood–retinal barrier permeability in type I (insulin-dependent) diabetic patients with nonproliferative retinopathy: a pilot study. *Retina*. 1995;15:134–140.
56. Keck PJ, Hauser SD, Krivi G, et al. Vascular permeability factor, an endothelial cell mitogen related to PDGF. *Science*. 1989;246:1309–1312.
57. Antonetti DA, Barber AJ, Hollinger LA, et al. Vascular endothelial growth factor induces rapid phosphorylation of tight junction proteins occludin and zonula occluden 1: a potential mechanism for vascular permeability in diabetic retinopathy and tumors. *J Biol Chem*. 1999;274:23463–23467.
58. Lakshminarayanan S, Antonetti DA, Gardner TW, et al. Effect of VEGF on retinal microvascular endothelial hydraulic conductivity: the role of NO. *Invest Ophthalmol Vis Sci*. 2000;41:4256–4261.
59. Gao BB, Clermont A, Rook S, et al. Extracellular carbonic anhydrase mediates hemorrhagic retinal and cerebral vascular permeability through prekallikrein activation. *Nat Med*. 2007;13:181–188.
60. Gao BB, Chen X, Timothy N, et al. Characterization of the vitreous proteome in diabetes without diabetic retinopathy and diabetes with proliferative diabetic retinopathy. *J Proteome Res*. 2008;7:2516–2525.
61. Phipps JA, Clermont AC, Sinha S, et al. Plasma kallikrein mediates angiotensin II type 1 receptor-stimulated retinal vascular permeability. *Hypertension*. 2009;53:175–181.
62. Abdouh M, Talbot S, Couture R, et al. Retinal plasma extravasation in streptozotocin-diabetic rats mediated by kinin B(1) and B(2) receptors. *Br J Pharmacol*. 2008;154:136–143.
63. Jeppesen P, Aalkjaer C, Bek T. Bradykinin relaxation in small porcine retinal arterioles. *Invest Ophthalmol Vis Sci*. 2002;43:1891–1896.

64. Kojima N, Saito M, Mori A, et al. Role of cyclooxygenase in vasodilation of retinal blood vessels induced by bradykinin in Brown Norway rats. *Vascul Pharmacol*. 2009;51:119–124.
65. Parpura V, Basarsky TA, Liu F, et al. Glutamate-mediated astrocyte-neuron signalling. *Nature*. 1994;369:744–747.
66. Adamis AP. Is diabetic retinopathy an inflammatory disease? *Br J Ophthalmol*. 2002;86:363–365.
67. Joussen AM, Murata T, Tsujikawa A, et al. Leukocyte-mediated endothelial cell injury and death in the diabetic retina. *Am J Pathol*. 2001;158:147–152.
68. Joussen AM, Poulaki V, Mitsiades N, et al. Nonsteroidal anti-inflammatory drugs prevent early diabetic retinopathy via TNF-alpha suppression. *FASEB J*. 2002;16:438–440.
69. Martidis A, Duker JS, Greenberg PB, et al. Intravitreal triamcinolone for refractory diabetic macular edema. *Ophthalmology*. 2002;109:920–927.
70. Yilmaz T, Weaver CD, Gallagher MJ, et al. Intravitreal triamcinolone acetonide injection for treatment of refractory diabetic macular edema: a systematic review. *Ophthalmology*. 2009;116:902–911 [quiz 912–903].
71. Feener EP. Plasma kallikrein and diabetic macular edema. *Curr Diab Rep*. 2010;10:270–275.
72. Wang AL, Yu AC, Lau LT, et al. Minocycline inhibits LPS-induced retinal microglia activation. *Neurochem Int*. 2005;47(1–2):152–158.
73. Federici TJ. The non-antibiotic properties of tetracyclines: clinical potential in ophthalmic disease. *Pharmacol Res*. 2011;64(6):614–623.
74. Baptiste DC, Powell KJ, Jollimore CAB, et al. Effects of minocycline and tetracycline on retinal ganglion cell survival after axotomy. *Neuroscience*. 2005;134(2):575–582.
75. Scott IU, Jackson GR, Quillen DA, et al. Effect of doxycycline vs placebo on retinal function and diabetic retinopathy progression in mild to moderate nonproliferative diabetic retinopathy: a randomized proof-of-concept clinical trial. *JAMA Ophthalmol*. 2014;132(9):1137–1142.
76. Kinoshita JH. Mechanisms initiating cataract formation. Proctor Lecture. *Invest Ophthalmol*. 1974;13:713–724.

77. Gabbay KH. Hyperglycemia, polyol metabolism, complications of diabetes mellitus. *Annu Rev Med*. 1975;26:521–536.
78. Van den Enden MK, Nyengaard JR, Ostrow E, et al. Elevated glucose levels increase retinal glycolysis and sorbitol pathway metabolism: implications for diabetic retinopathy. *Invest Ophthalmol Vis Sci*. 1995;36:1675–1685.
79. Tesfamariam B. Free radicals in diabetic endothelial cell dysfunction. *Free Radic Biol Med*. 1994;16:383–391.
80. Williamson JR, Chang K, Frangos M, et al. Hyperglycemic pseudohypoxia and diabetic complications. *Diabetes*. 1993;42:801–813.
81. Engerman RL, Kern TS. Experimental galactosemia produces diabetic-like retinopathy. *Diabetes*. 1984;33:97–100.
82. Kador PF, Akagi Y, Takahashi Y, et al. Prevention of retinal vessel changes associated with diabetic retinopathy in galactose-fed dogs by aldose reductase inhibitors. *Arch Ophthalmol*. 1990;108:1301–1309.
83. Kador PF, Akagi Y, Terubayashi H, et al. Prevention of pericyte ghost formation in retinal capillaries of galactose-fed dogs by aldose reductase inhibitors. *Arch Ophthalmol*. 1988;106:1099–1102.
84. Robinson WG Jr, Laver NM, Jacot JL, et al. Diabetic-like retinopathy ameliorated with the aldose reductase inhibitor WAY-121,509. *Invest Ophthalmol Vis Sci*. 1996;37:1149–1156.
85. Sorbinil Retinopathy Trial Research Group. A randomized trial of sorbinil, an aldose reductase inhibitor, in diabetic retinopathy. *Arch Ophthalmol*. 1990;108:1234–1244.
86. Monnier VM, Kohn RR, Cerami A. Accelerated age-related browning of human collagen in diabetes mellitus. *Proc Natl Acad Sci USA*. 1984;81:583–587.
87. Brownlee M, Vlassara H, Cerami A. Nonenzymatic glycosylation and the pathogenesis of diabetic complications. *Ann Intern Med*. 1984;101:527–537.
88. Brownlee M. Advanced protein glycosylation in diabetes and aging. *Annu Rev Med*. 1995;46:223–234.
89. Chibber R, Molinatti PA, Kohner EM. Intracellular protein glycation in cultured retinal capillary pericytes and

endothelial cells exposed to high-glucose concentration. *Cell Mol Biol*. 1999;45:47–57.
90. Giardino I, Edelstein D, Brownlee M. Nonenzymatic glycosylation in vitro and in bovine endothelial cells alters basic fibroblast growth factor activity: a model for intracellular glycosylation in diabetes. *J Clin Invest*. 1994;94:110–117.
91. Wang XL, Yu T, Yan QC, et al. AGEs promote oxidative stress and induce apoptosis in retinal pigmented epithelium cells RAGE-dependently. *J Mol Neurosci*. 2015;56(2):449–460.
92. Neeper M, Schmidt AM, Brett J, et al. Cloning and expression of a cell surface receptor for advanced glycosylation end products of proteins. *J Biol Chem*. 1992;267:14998–15004.
93. Schmidt AM, Vianna M, Gerlach M, et al. Isolation and characterization of two binding proteins for advanced glycosylation end products from bovine lung which are present on the endothelial cell surface. *J Biol Chem*. 1992;267:14987–14997.
94. Lander HM, Tauras JM, Ogiste JS, et al. Activation of the receptor for advanced glycation end products triggers a p21(ras)-dependent mitogen-activated protein kinase pathway regulated by oxidant stress. *J Biol Chem*. 1997;272:17810–17814.
95. Hofmann MA, Drury S, Fu C, et al. RAGE mediates a novel proinflammatory axis: a central cell surface receptor for S100/calgranulin polypeptides. *Cell*. 1999;97:889–901.
96. Huttunen HJ, Fages C, Rauvala H. Receptor for advanced glycation end products (RAGE)-mediated neurite outgrowth and activation of NF-kappaB require the cytoplasmic domain of the receptor but different downstream signaling pathways. *J Biol Chem*. 1999;274:19919–19924.
97. Taguchi A, Blood DC, del Toro G, et al. Blockade of RAGE-amphotericin signalling suppresses tumour growth and metastases. *Nature*. 2000;405:354–360.
98. Beauchamp MC, Michaud SE, Li L, et al. Advanced glycation end products potentiate the stimulatory effect of

glucose on macrophage lipoprotein lipase expression. *J Lipid Res*. 2004;45:1749–1757.
99. Yan SD, Schmidt AM, Anderson GM, et al. Enhanced cellular oxidant stress by the interaction of advanced glycation end products with their receptors/binding proteins. *J Biol Chem*. 1994;269:9889–9897.
100. Schmidt AM, Stern DM. RAGE: a new target for the prevention and treatment of the vascular and inflammatory complications of diabetes. *Trends Endocrinol Metab*. 2000;11:368–375.
101. Hammes HP, Martin S, Federlin K, et al. Aminoguanidine treatment inhibits the development of experimental diabetic retinopathy. *Proc Natl Acad Sci USA*. 1991;88:11555–11558.
102. Brownlee M, Vlassara H, Kooney A, et al. Aminoguanidine prevents diabetes-induced arterial wall protein cross-linking. *Science*. 1986;232:1629–1632.
103. Friedman EA. Advanced glycosylated end products and hyperglycemia in the pathogenesis of diabetic complications. *Diabetes Care*. 1999;22(Suppl. 2):B65–71.
104. Kern TS, Engerman RL. Pharmacological inhibition of diabetic retinopathy: aminoguanidine and aspirin. *Diabetes*. 2001;50:1636–1642.
105. Wautier JL, Zoukourian C, Chappey O, et al. Receptor-mediated endothelial cell dysfunction in diabetic vasculopathy: soluble receptor for advanced glycation end products blocks hyperpermeability in diabetic rats. *J Clin Invest*. 1996;97:238–243.
106. Nilsson BO. Biological effects of aminoguanidine: an update. *Inflamm Res*. 1999;48:509–515.
107. Kim J, Kim CS, Sohn E, et al. Aminoguanidine protects against apoptosis of retinal ganglion cells in Zucker diabetic fatty rats. *Eur Rev Med Pharmacol Sci*. 2014;18(11):1573–1578.
108. Arden GB, Sidman RL, Arap W, et al. Rod driven hypoxia. *Br J Ophthalmol*. 2005;89:764–769.
109. Lin MK, Kim SH, Zhang L, et al. Rod metabolic demand drives progression in retinopathies. *Taiwan J Ophthal*. 2015;1–4.
110. Williamson JR, Chang K, Frangos M, et al. Hyperglycemic

pseudohypoxia and diabetic complications. *Diabetes*. 1993;42:801–813.
111. Nguyen QD, Shah SM, Van Anden E, et al. Supplemental oxygen improves macular edema: a pilot study. *Invest Ophthalmol Vis Sci*. 2004;45(2):617–624.
112. Arden GB, Gunduz MK, Kurtenbach A, et al. A preliminary trial to determine whether prevention of dark adaptions affects the course of early diabetic retinopathy. *Eye*. 2010;24:1149–1155.
113. Nishikawa T, Edelstein D, Du XL, et al. Normalizing mitochondrial superoxide production blocks three pathways of hyperglycaemic damage. *Nature*. 2000;404:787–790.
114. Suzuki S, Hinokio Y, Komatu K, et al. Oxidative damage to mitochondrial DNA and its relationship to diabetic complications. *Diabetes Res Clin Pract*. 1999;45:161–168.
115. Hunt JV, Dean RT, Wolff SP. Hydroxyl radical production and autoxidative glycosylation: glucose autoxidation as the cause of protein damage in the experimental glycation model of diabetes mellitus and ageing. *Biochem J*. 1988;256:205–212.
116. Giugliano D, Ceriello A, Paolisso G. Oxidative stress and diabetic vascular complications. *Diabetes Care*. 1996;19:257–267.
117. Tesfamariam B. Selective impairment of endothelium-dependent relaxations by prostaglandin endoperoxide. *J Hypertens*. 1994;12:41–47.
118. Lum H, Roebuck KA. Oxidant stress and endothelial cell dysfunction. *Am J Physiol Cell Physiol*. 2001;280:C719–41.
119. Baynes JW. Role of oxidative stress in development of complications in diabetes. *Diabetes*. 1991;40:405–412.
120. Craven PA, Melhem MF, Phillips SL, et al. Overexpression of Cu2+/Zn2+ superoxide dismutase protects against early diabetic glomerular injury in transgenic mice. *Diabetes*. 2001;50:2114–2125.
121. Taher MM, Garcia JG, Natarajan V. Hydroperoxide-induced diacylglycerol formation and protein kinase C activation in vascular endothelial cells. *Arch Biochem Biophys*.

1993;303:260–266.
122. Jain SK, McVie R. Effect of glycemic control, race (white versus black), duration of diabetes on reduced glutathione content in erythrocytes of diabetic patients. *Metabolism*. 1994;43:306–309.
123. Jennings PE, Chirico S, Jones AF, et al. Vitamin C metabolites and microangiopathy in diabetes mellitus. *Diabetes Res*. 1987;6:151–154.
124. Karpen CW, Cataland S, O'Dorisio TM, et al. Production of 12-hydroxyeicosatetraenoic acid and vitamin E status in platelets from type I human diabetic subjects. *Diabetes*. 1985;34:526–531.
125. Oberley LW. Free radicals and diabetes. *Free Radic Biol Med*. 1988;5:113–124.
126. Hayden JM, Reaven PD. Cardiovascular disease in diabetes mellitus type 2: a potential role for novel cardiovascular risk factors. *Curr Opin Lipidol*. 2000;11:519–528.
127. Devaraj S, Hirany SV, Burk RF, et al. Divergence between LDL oxidative susceptibility and urinary F(2)-isoprostanes as measures of oxidative stress in type 2 diabetes. *Clin Chem*. 2001;47:1974–1979.
128. Cameron NE, Cotter MA. Neurovascular dysfunction in diabetic rats. Potential contribution of autoxidation and free radicals examined using transition metal chelating agents. *J Clin Invest*. 1995;96:1159–1163.
129. Cameron NE, Cotter MA, Archibald V, et al. Anti-oxidant and pro-oxidant effects on nerve conduction velocity, endoneurial blood flow and oxygen tension in non-diabetic and streptozotocin-diabetic rats. *Diabetologia*. 1994;37:449–459.
130. Nagamatsu M, Nickander KK, Schmelzer JD, et al. Lipoic acid improves nerve blood flow, reduces oxidative stress, improves distal nerve conduction in experimental diabetic neuropathy. *Diabetes Care*. 1995;18:1160–1167.
131. Lal MA, Korner A, Matsuo Y, et al. Combined antioxidant and COMT inhibitor treatment reverses renal abnormalities in diabetic rats. *Diabetes*. 2000;49:1381–1389.
132. Kowluru RA, Tang J, Kern TS. Abnormalities of retinal

metabolism in diabetes and experimental galactosemia. VII. Effect of long-term administration of antioxidants on the development of retinopathy. *Diabetes*. 2001;50:1938–1942.
133. Bursell SE, Clermont AC, Aiello LP, et al. High-dose vitamin E supplementation normalizes retinal blood flow and creatinine clearance in patients with type 1 diabetes. *Diabetes Care*. 1999;22:1245–1251.
134. Yusuf S, Dagenais G, Pogue J, et al. Vitamin E supplementation and cardiovascular events in high-risk patients. The Heart Outcomes Prevention Evaluation Study Investigators. *N Engl J Med*. 2000;342:154–160.
135. Xia P, Aiello LP, Ishii H, et al. Characterization of vascular endothelial growth factor's effect on the activation of protein kinase C, its isoforms, endothelial cell growth. *J Clin Invest*. 1996;98:2018–2026.
136. Xia P, Inoguchi T, Kern TS, et al. Characterization of the mechanism for the chronic activation of diacylglycerol-protein kinase C pathway in diabetes and hypergalactosemia. *Diabetes*. 1994;43:1122–1129.
137. Nishizuka Y. Intracellular signaling by hydrolysis of phospholipids and activation of protein kinase C. *Science*. 1992;258:607–614.
138. Inoguchi T, Battan R, Handler E, et al. Preferential elevation of protein kinase C isoform beta II and diacylglycerol levels in the aorta and heart of diabetic rats: differential reversibility to glycemic control by islet cell transplantation. *Proc Natl Acad Sci USA*. 1992;89:11059–11063.
139. Ishii H, Koya D, King GL. Protein kinase C activation and its role in the development of vascular complications in diabetes mellitus. *J Mol Med*. 1998;76:21–31.
140. Nagpala PG, Malik AB, Vuong PT, et al. Protein kinase C beta 1 overexpression augments phorbol ester-induced increase in endothelial permeability. *J Cell Physiol*. 1996;166:249–255.
141. Kuboki K, Jiang ZY, Takahara N, et al. Regulation of endothelial constitutive nitric oxide synthase gene expression in endothelial cells and in vivo: a specific vascular action of insulin. *Circulation*. 2000;101:676–681.

142. Bohlen HG, Nase GP. Arteriolar nitric oxide concentration is decreased during hyperglycemia-induced betaII PKC activation. *Am J Physiol Heart Circ Physiol*. 2001;280:H621–7.
143. Nonaka A, Kiryu J, Tsujikawa A, et al. PKC-beta inhibitor (LY333531) attenuates leukocyte entrapment in retinal microcirculation of diabetic rats. *Invest Ophthalmol Vis Sci*. 2000;41:2702–2706.
144. Shiba T, Inoguchi T, Sportsman JR, et al. Correlation of diacylglycerol level and protein kinase C activity in rat retina to retinal circulation. *Am J Physiol*. 1993;265:E783–93.
145. Ishii H, Jirousek MR, Koya D, et al. Amelioration of vascular dysfunctions in diabetic rats by an oral PKC beta inhibitor. *Science*. 1996;272:728–731.
146. Aiello LP, Bursell SE, Clermont A, et al. Vascular endothelial growth factor-induced retinal permeability is mediated by protein kinase C in vivo and suppressed by an orally effective beta-isoform-selective inhibitor. *Diabetes*. 1997;46:1473–1480.
147. Schiffrin EL, Touyz RM. Vascular biology of endothelin. *J Cardiovasc Pharmacol*. 1998;32(Suppl. 3):S2–13.
148. Williams B, Gallacher B, Patel H, et al. Glucose-induced protein kinase C activation regulates vascular permeability factor mRNA expression and peptide production by human vascular smooth muscle cells in vitro. *Diabetes*. 1997;46:1497–1503.
149. Koya D, Jirousek MR, Lin YW, et al. Characterization of protein kinase C beta isoform activation on the gene expression of transforming growth factor-beta, extracellular matrix components, prostanoids in the glomeruli of diabetic rats. *J Clin Invest*. 1997;100:115–126.
150. Tomlinson DR. Mitogen-activated protein kinases as glucose transducers for diabetic complications. *Diabetologia*. 1999;42:1271–1281.
151. Jiang Y, Zhang Q, Steinle JJ. Beta-adrenergic receptor agonist decreases VEGF levels through altered eNOS and PKC signaling in diabetic retina. *Growth Factors*. 2015;26:1–8.
152. Zhang Q, Jiang Y, Steinle JJ. IGFBP-3 reduces eNOS and

PKCzeta phosphorylation, leading to lowered VEGF levels. *Mol Vis*. 2015;21:604–611.
153. Meier M, King GL. Protein kinase C activation and its pharmacological inhibition in vascular disease. *Vasc Med*. 2000;5:173–185.
154. Danis RP, Bingaman DP, Jirousek M, et al. Inhibition of intraocular neovascularization caused by retinal ischemia in pigs by PKCbeta inhibition with LY333531. *Invest Ophthalmol Vis Sci*. 1998;39:171–179.
155. Nakamura J, Kato K, Hamada Y, et al. A protein kinase C-beta-selective inhibitor ameliorates neural dysfunction in streptozotocin-induced diabetic rats. *Diabetes*. 1999;48:2090–2095.
156. Effect of ruboxistaurin in patients with diabetic macular edema: thirty-month results of the randomized PKC-DMES clinical trial. *Arch Ophthalmol*. 2007;125:318–324.
157. Sheetz MJ, Aiello LP, Shahri N. Effect of ruboxistaurin (RBX) on visual acuity decline over a 6-year period with cessation and reinstitution of therapy: results of an open-label extension of the Protein Kinase C Diabetic Retinopathy Study 2 (PKC-DRS2). *Retina*. 2011;31:1053–1059.
158. Sheetz MJ, Aiello LP, Davis MD, MBDL and MBCU Study Groups, et al. The effect of the oral PKC β inhibitor ruboxistaurin on vision loss in two phase 3 studies. *Invest Ophthalmol Vis Sci*. 2013;54(3):1750–1757.
159. King GL, Buzney SM, Kahn CR, et al. Differential responsiveness to insulin of endothelial and support cells from micro- and macrovessels. *J Clin Invest*. 1983;71:974–979.
160. Engerman RL, Pfaffenb D, Davis MD. Cell turnover of capillaries. *Lab Invest*. 1967;17:738–743.
161. Reiter CE, Gardner TW. Functions of insulin and insulin receptor signaling in retina: possible implications for diabetic retinopathy. *Progr Retinal Eye Res*. 2003;22:545–562.
162. Reiter CE, et al. Characterization of insulin signaling in rat retina in vivo and ex vivo. *Am J Physiol Endocrinol Metabol*. 2003;285:E763–74.

163. Sugasawa K, et al. Immunocytochemical analyses of distributions of Na, K-ATPase and GLUT1, insulin and transferrin receptors in the developing retinal pigment epithelial cells. *Cell Structure Function*. 1994;19:21–28.
164. Kumagai AK, Glasgow BJ, Pardridge WM. GLUT1 glucose transporter expression in the diabetic and nondiabetic human eye. *Invest Ophthalmol Vis Sci*. 1994;35:2887–2894.
165. Kumagai AK, Vinores SA, Pardridge WM. Pathological upregulation of inner blood–retinal barrier Glut1 glucose transporter expression in diabetes mellitus. *Brain Res*. 1996;706:313–317.
166. Mantych GJ, Hageman GS, Devaskar SU. Characterization of glucose transporter isoforms in the adult and developing human eye. *Endocrinology*. 1993;133:600–607.
167. Watanabe T, Mio Y, Hoshino FB, et al. GLUT2 expression in the rat retina: localization at the apical ends of Müller cells. *Brain Res*. 1994;655:128–134.
168. Watanabe T, Matsushima S, Okazaki M, et al. Localization and ontogeny of GLUT3 expression in the rat retina. *Brain Res Dev Brain Res*. 1996;94:60–66.
169. Mandarino LJ, Finlayson J, Hassell JR. High glucose downregulates glucose transport activity in retinal capillary pericytes but not endothelial cells. *Invest Ophthalmol Vis Sci*. 1994;35:964–972.
170. Takagi H, King GL, Aiello LP. Hypoxia upregulates glucose transport activity through an adenosine-mediated increase of GLUT1 expression in retinal capillary endothelial cells. *Diabetes*. 1998;47:1480–1488.
171. Kumagai AK. Glucose transport in brain and retina: implications in the management and complications of diabetes. *Diabetes/Metabol Res Rev*. 1999;15:261–273.
172. Frank RN, Amin R, Kennedy A, et al. An aldose reductase inhibitor and aminoguanidine prevent vascular endothelial growth factor expression in rats with long-term galactosemia. *Arch Ophthalmol*. 1997;115:1036–1047.
173. Warpeha KM, Chakravarthy U. Molecular genetics of microvascular disease in diabetic retinopathy. *Eye (Lond)*. 2003;17:305–311.

174. Field LL. Genetic linkage and association studies of type I diabetes: challenges and rewards. *Diabetologia*. 2002;45:21–35.
175. Kao YL, Donaghue K, Chan A, et al. An aldose reductase intragenic polymorphism associated with diabetic retinopathy. *Diabetes Res Clin Pract*. 1999;46:155–160.
176. Demaine A, Cross D, Millward A. Polymorphisms of the aldose reductase gene and susceptibility to retinopathy in type 1 diabetes mellitus. *Invest Ophthalmol Vis Sci*. 2000;41:4064–4068.
177. Demaine AG. Polymorphisms of the aldose reductase gene and susceptibility to diabetic microvascular complications. *Curr Med Chem*. 2003;10:1389–1398.
178. Wang Y, Ng MC, Lee SC, et al. Phenotypic heterogeneity and associations of two aldose reductase gene polymorphisms with nephropathy and retinopathy in type 2 diabetes. *Diabetes Care*. 2003;26:2410–2415.
179. Sivenius K, Niskanen L, Voutilainen-Kaunisto R, et al. Aldose reductase gene polymorphisms and susceptibility to microvascular complications in type 2 diabetes. *Diabet Med*. 2004;21:1325–1333.
180. Petrovic MG, Peterlin B, Hawlina M, et al. Aldose reductase (AC)n gene polymorphism and susceptibility to diabetic retinopathy in type 2 diabetes in Caucasians. *J Diabetes Complications*. 2005;19:70–73.
181. Richeti F, Noronha RM, Waetge RT, et al. Evaluation of AC(n) and C(-106)T polymorphisms of the aldose reductase gene in Brazilian patients with DM1 and susceptibility to diabetic retinopathy. *Mol Vis*. 2007;13:740–745.
182. Zhou M, Zhang P, Xu X, et al. The relationship between aldose reductase c106t polymorphism and diabetic retinopathy: an updated meta-analysis. *Invest Ophthalmol Vis Sci*. 2015;56(4):2279–2289.
183. Klein R, Klein BE, Moss SE, et al. The Wisconsin epidemiologic study of diabetic retinopathy. III. Prevalence and risk of diabetic retinopathy when age at diagnosis is 30 or more years. *Arch Ophthalmol*. 1984;102:527–532.
184. Klein R, Klein BE, Moss SE, et al. The Wisconsin

epidemiologic study of diabetic retinopathy. II. Prevalence and risk of diabetic retinopathy when age at diagnosis is less than 30 years. *Arch Ophthalmol*. 1984;102:520–526.
185. Rand LI, Krolewski AS, Aiello LM, et al. Multiple factors in the prediction of risk of proliferative diabetic retinopathy. *N Engl J Med*. 1985;313:1433–1438.
186. Cruickshanks KJ, Vadheim CM, Moss SE, et al. Genetic marker associations with proliferative retinopathy in persons diagnosed with diabetes before 30 years of age. *Diabetes*. 1992;41:879–885.
187. The Diabetes Control and Complications Trial Research Group. Clustering of long-term complications in families with diabetes in the diabetes control and complications trial. *Diabetes*. 1997;46:1829–1839.
188. Krolewski AS, Canessa M, Warram JH, et al. Predisposition to hypertension and susceptibility to renal disease in insulin-dependent diabetes mellitus. *N Engl J Med*. 1988;318:140–145.
189. Krolewski AS, Doria A, Magre J, et al. Molecular genetic approaches to the identification of genes involved in the development of nephropathy in insulin-dependent diabetes mellitus. *J Am Soc Nephrol*. 1992;3:S9–17.
190. Pettitt DJ, Saad MF, Bennett PH, et al. Familial predisposition to renal disease in two generations of Pima Indians with type 2 (non-insulin-dependent) diabetes mellitus. *Diabetologia*. 1990;33:438–443.
191. Seaquist ER, Goetz FC, Rich S, et al. Familial clustering of diabetic kidney disease: evidence for genetic susceptibility to diabetic nephropathy. *N Engl J Med*. 1989;320:1161–1165.
192. Aiello LP, Avery RL, Arrigg PG, et al. Vascular endothelial growth factor in ocular fluid of patients with diabetic retinopathy and other retinal disorders. *N Engl J Med*. 1994;331:1480–1487.
193. Aiello LP. Angiogenic pathways in diabetic retinopathy. *N Engl J Med*. 2005;353:839–841.
194. Miller JW, Adamis AP, Aiello LP. Vascular endothelial growth factor in ocular neovascularization and proliferative diabetic retinopathy. *Diabetes Metab Rev*. 1997;13:37–50.

195. Robinson CJ, Stringer SE. The splice variants of vascular endothelial growth factor (VEGF) and their receptors. *J Cell Sci*. 2001;114:853–865.
196. Suganthalakshmi B, Anand R, Kim R, et al. Association of VEGF and eNOS gene polymorphisms in type 2 diabetic retinopathy. *Mol Vis*. 2006;12:336–341.
197. Buraczynska M, Ksiazek P, Baranowicz-Gaszczyk I, et al. Association of the VEGF gene polymorphism with diabetic retinopathy in type 2 diabetes patients. *Nephrol Dial Transplant*. 2007;22:827–832.
198. Ramprasad S, Radha V, Mathias RA, et al. RAGE gene promoter polymorphisms and diabetic retinopathy in a clinic-based population from South India. *Eye (Lond)*. 2007;21:395–401.
199. Balasubbu S, Sundaresan P, Rajendran A, et al. Association analysis of nine candidate gene polymorphisms in Indian patients with type 2 diabetic retinopathy. *BMC Med Genet*. 2010;11:158.
200. Tong Z, Yang Z, Patel S, et al. Promoter polymorphism of the erythropoietin gene in severe diabetic eye and kidney complications. *Proc Natl Acad Sci USA*. 2008;105:6998–7003.
201. Huang YC, Lin JM, Lin HJ, et al. Genome-wide association study of diabetic retinopathy in a Taiwanese population. *Ophthalmology*. 2011;118:642–648.
202. Fu YP, Hallman DM, Gonzalez VH, et al. Identification of diabetic retinopathy genes through a genome-wide association study among Mexican-Americans from Starr County, Texas. *J Ophthalmol*. 2010;2010 [pii: 861291].
203. Parra EJ, Below JE, Krithika S, et al. Genome-wide association study of type 2 diabetes in a sample from Mexico City and a meta-analysis of a Mexican-American sample from Starr County, Texas. *Diabetologia*. 2011;54(8):2038–2046.
204. Grassi MA, Tikhomirov A, Ramalingam S, et al. Genome-wide meta-analysis for severe diabetic retinopathy. *Hum Mol Genet*. 2011;20:2472–2481.
205. Reich DE, Lander ES. On the allelic spectrum of human disease. *Trends Genet*. 2001;17:502–510.

206. Klein RJ, Zeiss C, Chew EY, et al. Complement factor H polymorphism in age-related macular degeneration. *Science*. 2005;308:385–389.
207. Dewan A, Liu M, Hartman S, et al. HTRA1 promoter polymorphism in wet age-related macular degeneration. *Science*. 2006;314:989–992.
208. Yang Z, Camp NJ, Sun H, et al. A variant of the HTRA1 gene increases susceptibility to age-related macular degeneration. *Science*. 2006;314:992–993.
209. Cohen JC, Kiss RS, Pertsemlidis A, et al. Multiple rare alleles contribute to low plasma levels of HDL cholesterol. *Science*. 2004;305:869–872.
210. Kotowski IK, Pertsemlidis A, Luke A, et al. A spectrum of PCSK9 alleles contributes to plasma levels of low-density lipoprotein cholesterol. *Am J Hum Genet*. 2006;78:410–422.
211. Ahituv N, Kavaslar N, Schackwitz W, et al. Medical sequencing at the extremes of human body mass. *Am J Hum Genet*. 2007;80:779–791.
212. Romeo S, Pennacchio LA, Fu Y, et al. Population-based resequencing of ANGPTL4 uncovers variations that reduce triglycerides and increase HDL. *Nat Genet*. 2007;39:513–516.
213. Smigrodzki R, Parks J, Parker WD. High frequency of mitochondrial complex I mutations in Parkinson's disease and aging. *Neurobiol Aging*. 2004;25:1273–1281.
214. Bielas JH, Loeb KR, Rubin BP, et al. Human cancers express a mutator phenotype. *Proc Natl Acad Sci USA*. 2006;103:18238–18242.
215. Altshuler D, Daly MJ, Lander ES. Genetic mapping in human disease. *Science*. 2008;322:881–888.
216. Hannum G, Guinney J, Zhao L, et al. Genome-wide methylation profiles reveal quantitative views of human aging rates. *Mol Cell*. 2013;49(2):359–367.
217. Agardh E, Lundstig A, Perfilyev A, et al. Genome-wide analysis of DNA methylation in subjects with type 1 diabetes identifies epigenetic modifications associated with proliferative diabetic retinopathy. *BMC Med*. 2015;13:182.
218. Syreeni A, El-Osta A, Forsblom C, FinnDiane Study Group, et al. Genetic examination of SETD7 and SUV39H1/H2

methyltransferases and the risk of diabetes complications in patients with type 1 diabetes. *Diabetes*. 2011;60(11):3073–3080.
219. Kadiyala CS, Zheng L, Du Y, et al. Acetylation of retinal histones in diabetes increases inflammatory proteins: effects of minocycline and manipulation of histone acetyltransferase (HAT) and histone deacetylase (HDAC). *J Biol Chem*. 2012;287(31):25869–25880.
220. McArthur K, Feng B, Wu Y, et al. MicroRNA-200b regulates vascular endothelial growth factor-mediated alterations in diabetic retinopathy. *Diabetes*. 2011;60(4):1314–1323.
221. Silva VA, Polesskaya A, Sousa TA, et al. Expression and cellular localization of microRNA-29b and RAX, an activator of the RNA-dependent protein kinase (PKR), in the retina of streptozotocin-induced diabetic rats. *Mol Vis*. 2011;17:2228–2240.
222. Becker B. Diabetes and glaucoma; and Ashton N. Oxygen and the growth and development of retinal vessels: in vivo and in vitro studies. Kimura SJ, Caygill WM. *Vascular complications of diabetes mellitus, with special emphasis on microangiopathy of the eye*. Mosby: St. Louis; 1967.
223. Jain IS, Luthra CL, Das T. Diabetic retinopathy and its relation to errors of refraction. *Arch Ophthalmol*. 1967;77:59–60.
224. Goldberg MF, Fine SL, United States Public Health Service. *Symposium on the Treatment of Diabetic Retinopathy*. US Neurological and Sensory Disease Control Program: Arlington, VA; 1969 [Washington, DC: US Government Printing Office].
225. Patz A. Studies on retinal neovascularization. Friedenwald Lecture. *Invest Ophthalmol Vis Sci*. 1980;19:1133–1138.
226. Weiter JJ, Zuckerman R. The influence of the photoreceptor-RPE complex on the inner retina: an explanation for the beneficial effects of photocoagulation. *Ophthalmology*. 1980;87:1133–1139.
227. The Diabetic Retinopathy Study Research Group. Photocoagulation treatment of proliferative diabetic retinopathy. Clinical application of Diabetic Retinopathy

Study (DRS) findings, DRS Report number 8. *Ophthalmology*. 1981;88:583–600.
228. Klein R, Klein BE, Moss SE, et al. The Wisconsin epidemiologic study of diabetic retinopathy. IV. Diabetic macular edema. *Ophthalmology*. 1984;91:1464–1474.
229. Tattersall RB, Fajans SS. A difference between the inheritance of classical juvenile-onset and maturity-onset type diabetes of young people. *Diabetes*. 1975;24:44–53.
230. Patz A, Maumenee AE. Studies on diabetic retinopathy. I. Retinopathy in a dog with spontaneous diabetes mellitus. *Am J Ophthalmol*. 1962;54:532–541.
231. Engerman R, Finkelstein D, Aguirre G, et al. Ocular complications. *Diabetes*. 1982;31:82–88.
232. Tilton RG, LaRose LS, Kilo C, et al. Absence of degenerative changes in retinal and uveal capillary pericytes in diabetic rats. *Invest Ophthalmol Vis Sci*. 1986;27:716–721.
233. Engerman RL, Colquhoun PJ. Epithelial and mesothelial basement membranes in diabetic patients and dogs. *Diabetologia*. 1982;23:521–524.
234. Kern TS, Engerman RL. Galactose-induced retinal microangiopathy in rats. *Invest Ophthalmol Vis Sci*. 1995;36:490–496.
235. Robison WG Jr, McCaleb ML, Feld LG, et al. Degenerated intramural pericytes ('ghost cells') in the retinal capillaries of diabetic rats. *Curr Eye Res*. 1991;10:339–350.
236. Bloodworth JM Jr, Engerman RL, Anderson PJ. Microangiopathy in the experimentally diabetic animal. *Adv Metab Disord*. 1973;2(Suppl. 2):245–250.
237. Frank RN, Hoffman WH, Podgor MJ, et al. Retinopathy in juvenile-onset diabetes of short duration. *Ophthalmology*. 1980;87:1–9.
238. Palmberg P, Smith M, Waltman S, et al. The natural history of retinopathy in insulin-dependent juvenile-onset diabetes. *Ophthalmology*. 1981;88:613–618.
239. Kern TS, Engerman RL. A mouse model of diabetic retinopathy. *Arch Ophthalmol*. 1996;114:986–990.
240. de Oliveira F. Pericytes in diabetic retinopathy. *Br J Ophthalmol*. 1966;50:134–143.

241. Kern TS, Engerman RL. Capillary lesions develop in retina rather than cerebral cortex in diabetes and experimental galactosemia. *Arch Ophthalmol*. 1996;114:306–310.
242. Frank RN, Dutta S, Mancini MA. Pericyte coverage is greater in the retinal than in the cerebral capillaries of the rat. *Invest Ophthalmol Vis Sci*. 1987;28:1086–1091.
243. Frank RN, Turczyn TJ, Das A. Pericyte coverage of retinal and cerebral capillaries. *Invest Ophthalmol Vis Sci*. 1990;31:999–1007.
244. Tilton RG, Miller EJ, Kilo C, et al. Pericyte form and distribution in rat retinal and uveal capillaries. *Invest Ophthalmol Vis Sci*. 1985;26:68–73.
245. Patz A. The role of oxygen in retrolental fibroplasia. *Trans Am Ophthalmol Soc*. 1968;66:940–985.
246. Kremer I, Kissun R, Nissenkorn I, et al. Oxygen-induced retinopathy in newborn kittens: a model for ischemic vasoproliferative retinopathy. *Invest Ophthalmol Vis Sci*. 1987;28:126–130.
247. Wise GN, Dollery CT, Henkind P. *The retinal circulation*. Harper & Row: New York; 1971.
248. Smith LE, Kopchick JJ, Chen W, et al. Essential role of growth hormone in ischemia-induced retinal neovascularization. *Science*. 1997;276:1706–1709.
249. Aiello LP, Pierce EA, Foley ED, et al. Suppression of retinal neovascularization in vivo by inhibition of vascular endothelial growth factor (VEGF) using soluble VEGF-receptor chimeric proteins. *Proc Natl Acad Sci USA*. 1995;92:10457–10461.
250. Penn JS, Rajaratnam VS, Collier RJ, et al. The effect of an angiostatic steroid on neovascularization in a rat model of retinopathy of prematurity. *Invest Ophthalmol Vis Sci*. 2001;42:283–290.
251. Okamoto N, Tobe T, Hackett SF, et al. Transgenic mice with increased expression of vascular endothelial growth factor in the retina: a new model of intraretinal and subretinal neovascularization. *Am J Pathol*. 1997;151:281–291.
252. Buzney SM, Frank RN, Robison WG Jr. Retinal capillaries: proliferation of mural cells in vitro. *Science*. 1975;190:985–

986.
253. Frank RN, Kinsey VE, Frank KW, et al. In vitro proliferation of endothelial cells from kitten retinal capillaries. *Invest Ophthalmol Vis Sci*. 1979;18:1195–1200.
254. Bowman PD, Betz AL, Goldstein GW. Primary culture of microvascular endothelial cells from bovine retina: selective growth using fibronectin coated substrate and plasma derived serum. *In Vitro*. 1982;18:626–632.
255. Buzney SM, Massicotte SJ. Retinal vessels: proliferation of endothelium in vitro. *Invest Ophthalmol Vis Sci*. 1979;18:1191–1195.
256. Gitlin JD, D'Amore PA. Culture of retinal capillary cells using selective growth media. *Microvasc Res*. 1983;26:74–80.
257. Madri JA, Williams SK. Capillary endothelial cell cultures: phenotypic modulation by matrix components. *J Cell Biol*. 1983;97:153–165.
258. Montesano R, Orci L, Vassalli P. In vitro rapid organization of endothelial cells into capillary-like networks is promoted by collagen matrices. *J Cell Biol*. 1983;97:1648–1652.
259. Goto F, Goto K, Weindel K, et al. Synergistic effects of vascular endothelial growth factor and basic fibroblast growth factor on the proliferation and cord formation of bovine capillary endothelial cells within collagen gels. *Lab Invest*. 1993;69:508–517.
260. Herman IM, D'Amore PA. Microvascular pericytes contain muscle and nonmuscle actins. *J Cell Biol*. 1985;101:43–52.
261. Kelley C, D'Amore P, Hechtman HB, et al. Microvascular pericyte contractility in vitro: comparison with other cells of the vascular wall. *J Cell Biol*. 1987;104:483–490.
262. Das A, Frank RN, Weber ML, et al. ATP causes retinal pericytes to contract in vitro. *Exp Eye Res*. 1988;46:349–362.
263. Kelley C, D'Amore P, Hechtman HB, et al. Vasoactive hormones and cAMP affect pericyte contraction and stress fibres in vitro. *J Muscle Res Cell Motil*. 1988;9:184–194.
264. Chakravarthy U, Gardiner TA, Anderson P, et al. The effect of endothelin 1 on the retinal microvascular pericyte. *Microvasc Res*. 1992;43:241–254.
265. Tilton RG, Kilo C, Williamson JR, et al. Differences in

pericyte contractile function in rat cardiac and skeletal muscle microvasculatures. *Microvasc Res*. 1979;18:336–352.
266. Butryn RK, Ruan H, Hull CM, et al. Vasoactive agonists do not change the caliber of retinal capillaries of the rat. *Microvasc Res*. 1995;50:80–93.

49

Diabetes Mellitus

Mario Skugor

Introduction

Diabetes mellitus is the most common disorder of energy metabolism. Type 2 diabetes mellitus comprises about 90% of all patients, and most of the rest have type 1 diabetes mellitus. Glycemic control is critical for these patients because poor control, over time, leads to development of microvascular complications.

The microvascular complications affect small blood vessels and include nephropathy, neuropathy, and retinopathy. In the United States, 57.9% of diabetic patients have one or more diabetes complications, and 14.3% have three or more.[1]

Diabetic nephropathy is defined as the presence of persistent proteinuria >0.5 g/day. Overt nephropathy is characterized by progressive decline in renal function resulting in endstage renal disease.

Neuropathy is a group of conditions characterized by nerve dysfunction. The condition is classified according to the nerves affected. The classification of neuropathy includes focal, diffuse, sensory, motor, and autonomic neuropathy.

Retinopathy is divided into nonproliferative retinopathy and proliferative retinopathy. Nonproliferative retinopathy is characterized by development of microaneurysms, venous loops, retinal hemorrhages, hard exudates, and soft exudates (see Chapter

50, Nonproliferative diabetic retinopathy and diabetic macular edema). Proliferative retinopathy is defined as presence of new blood vessels with or without vitreous hemorrhage (see Chapter 51, Proliferative diabetic retinopathy).

Prevalence of Retinopathy

With type 1 diabetes, 13% of patients have retinopathy at 5 years, and 90% after 10–15 years. The proliferative retinopathy develops in 25% of type 1 diabetics after 15 years.[1] Insulin-treated patients with type 2 diabetes have a 40% prevalence of retinopathy after 5 years, and 24% if treated with oral hypoglycemic agents. After 15–19 years of diabetes, the prevalence increases to 84% and 53% respectively. Proliferative retinopathy is present in 2% of type 2 patients within the 5 years of diagnosis and in 25% after 25 years or more.[2]

Glycemic Control and Retinopathy

In the Wisconsin Epidemiologic Study[3] in diabetics younger than 30 years and those who were older and treated with oral hypoglycemic agents or insulin, baseline HbA1C correlated with the incidence and progression of retinopathy, and progression of proliferative retinopathy.

In the Diabetes Control and Complications Trial[4] (DCCT) of 1441 people with type 1 diabetes, 726 had no retinopathy, and normal albumin excretion, while 715 had mild-to-moderate background retinopathy with normal albumin excretion or microalbuminuria at baseline.

The subjects received intensive therapy or conventional treatment. The intensive treatment consisted of insulin delivered by insulin pumps or multiple daily injections (three or more injections per day). The participants were seen every month.

The conventional group received no more than two daily insulin injections. The clinic visits were every 2 or 3 months. Follow-up was an average of 6.5 years. The mean hemoglobin A1C was 9.1% in the conventional group and 7.2% in the intensively treated group throughout the study. Risk reduction was 70% for clinically

important sustained retinopathy, 56% for laser photocoagulation, and 60% for sustained microalbuminuria. Similar benefits were seen for nephropathy, too. Even more importantly, four years after DCCT was closed, hemoglobin A1C was 8.2% in the conventional treatment group and 7.9% in the intensive treatment group, but retinopathy events including proliferative retinopathy, macular edema, and need for laser therapy were still 74%, 77%, and 77% lower respectively in the intensively treated group.[5]

The Kumamato Trial[6] studied 102 patients with type 2 diabetes. The intensive therapy with multiple daily insulin injections was compared against once- or twice-daily insulin injections and resulted in hemoglobin A1C levels of 7.1% and 9.4%. Two-step progression of retinopathy decreased 69%, nephropathy progression decreased 70%, and nerve conduction velocities improved.

The United Kingdom Prospective Diabetes Study[7,8] achieved an average hemoglobin A1C of 7.9% in the conventional treatment group and 7% in the intensive treatment group in 5102 patients with type 2 diabetes. There was a 27% risk reduction for retinal photo coagulation at 12 years in intensive group.

The Hypertension and Diabetes Study[9,10] was part of the UKPDS Study. There were 1148 patients with type 2 diabetes and coexisting hypertension that were studied. On average, the tight control group averaged 144/82 mmHg and the control group averaged 154/87 mmHg. Tight control experienced 35% reduction in retinal photocoagulation, 34% reduction in two-step deterioration of retinopathy, and 47% risk reduction in 3-line deterioration in the ETDRS chart over 7.5 years.

The Euclid Trial[11] demonstrated in 354 type 1 diabetics aged 20–59 who were normotensive that lisinopril treatment resulted in a 50% reduction in retinopathy progression, 73% reduction in two-grade retinopathy progression, and an 82% reduction in development of proliferative retinopathy.

These studies are discussed in greater detail in Chapter 47 (Epidemiology of diabetic retinopathy).

Goals of Treatment

Based on the above described studies, the American Diabetes Association (ADA) recommends[12] a goal for preprandial capillary glucose of 70–130 mg/dL. The postprandial glucose goal is <180 mg/dL with a hemoglobin (Hb) A1C goal of less than 7%. The ADA target for blood pressure is <140/90 mmHg. The American Association of Clinical Endocrinology recommends preprandial glucose targets of <110, postprandial <140, and HbA1C <6.5%.[13] The recommended blood pressure goal is <130/80 mmHg. In hypertensive patients with microalbuminuria or albuminuria, ACE inhibitors or angiotensin II receptor blockers should be strongly considered.

Patients with type 1 diabetes should have an initial dilated and comprehensive eye exam within 3–5 years of the diagnosis, and those with type 2 diabetes should have an eye exam shortly after diagnosis. All diabetics should have subsequent eye exams annually. Exams should be performed by an ophthalmologist or optometrist knowledgeable and experienced in diagnosing retinopathy.

Patients with diabetes should be referred to an endocrinologist if targets for glycemic control cannot be achieved, or patients are experiencing significant hypoglycemia. Patients who have complications of diabetes should, also, be referred to an endocrinologist.

All patients should be advised to adhere to a healthy lifestyle consisting of attention to diet, regular physical activity, and smoking cessation. However, most will still require pharmacologic treatment.

Glycemic Control: Pharmacologic Treatment

Treatment options for noninsulin therapy are summarized in Table 49.1. Insulin and insulin analogs are summarized in Table 49.2.

TABLE 49.1

Noninsulin Therapies

Subgroup	Generic Name	Class	Route	Comments
Biguanides	Glucophage (Metformin)	Sensitizer	Oral	Weight loss No hypoglycemia GI upset
Thiazolidinediones	Rosiglitazone (Avandia)	Sensitizer	Oral	Weight gain Peripheral edema
	Pioglitazone (Actos)			
Alpha-glucosidase inhibitors	Acarbose (Precose) Miglitol (Glyset)		Oral	GI upset No hypoglycemia
Sulfonylureas	Chlorpropamide (Diabinese)	Secretagogue	Oral	Hypoglycemia Weight gain
	Glibenclamide (Glyburide)			
	Glimepiride (Amaryl)			
	Glipizide (Glucotrol)			
	Tolazamide (Tolinase)			
	Tolbutamide (Orinase)			
Glinides	Nateglinide (Starlix)	Secretagogue	Oral	Weight gain
	Repaglinide (Prandin)			
Exenatide	Byetta	GLP-1 analog	SC	Weight loss GI upset
Liraglutide	Victoza	GLP-1 analog	SC	Weight loss Nausea
Albiglutide	Tenzeum	GLP-1 analog	SC	Nausea and vomiting
Dulaglutide	Trulicity	GLP-1 analog	SC	Nausea and vomiting
Extended release exenatide	Bydureon	GLP-1 analog	SC	Weight loss nausea
Pramlintide	Symlin	Incretin	SC	Weight loss GI upset Adjunctive therapy with insulin
Dipeptidyl peptidase-4 inhibitors (DPP-4s)	Sitagliptin (Januvia)	DPP-4 ihibitors	Oral	No hypoglycemia Nasopharyngitis Weight neutral
	Saxagliptin (Onglyza)			
	Linagliptin (Trajenta)			
Rapid release bromocriptine	Cycloset	Other	Oral	Taken within 2 hours of awakening
SGLT-2 Inhibitors	Dapagliflozin Empagliflozin Canagliflozin	SGLT-2	Oral	Lowers blood pressure Causes weight loss Used once a day

GI, gastrointestinal; SC, subcutaneous.

TABLE 49.2

Forms of Insulin

Insulin (Brand)	Onset	Peak	Effective Duration
RAPID-ACTING			
Aspart (NovoLog)	5–15 min	30–90 min	<5 h
Lispro (Humalog)	5–15 min	30–90 min	<5 h
Glulisine (Apidra)	5–15 min	30–90 min	<5 h
Inhaled Insulin (Afrezza)	5–15 min	30–90 min	<5 h
SHORT-ACTING			
Regular	30–60 min	2–3 h	5–8 h
INTERMEDIATE, BASAL			
Neutral protamine Hagedorn (NPH)	2–4 h	4–10 h	10–16 h
LONG-ACTING, BASAL			
Insulin glargine (Lantus)	2–4 h	No peak	20–24 h
Insulin detemir (Levemir)	3–8 h	No peak	17–24 h
Insulin degludec (Tresiba)	3–4 h	No peak	36–42 h
PREMIXED			
75% Insulin lispro protamine/25% insulin lispro (Humalog Mix 75/25)	5–15 min	Dual	10–16 h
50% Insulin lispro protamine/50% insulin lispro (Humalog Mix 50/50)	5–15 min	Dual	10–16 h
70% Insulin lispro protamine/30% insulin aspart (Novolog Mix 70/30)	5–15 min	Dual	10–16 h
70% NPH/ 30% regular	30–60 min	Dual	10–16 h

Data from Rodbard HW, Blonde L, Braithwaite SS, et al. American Association of Clinical Endocrinologists medical guidelines for clinical practice for the management of diabetes mellitus. Endocr Pract 2008;14(6):802-803.

Insulin Sensitizers

Biguanides (Metformin)

Available since the late 1950s, metformin was developed from the French lilac biguanides, which was used in folk medicine for centuries. Metformin suppresses the hepatic glucose output, but it also enhances insulin sensitivity of muscle and fat. It affects primarily fasting glucose levels.

The most common side-effects of metformin are gastrointestinal complaints: diarrhea, nausea, abdominal discomfort, and a metallic taste. All of these improve over time or with dose reduction. Metformin also has a potential to produce very rare, but life-threatening lactic acidosis (<1 in 100,000). The use of metformin is contraindicated in patients with a serum creatinine 1.5 mg/dL or

higher in male patients or 1.4 mg/dL or higher in female patients. It is best to avoid use in patients with hepatic impairment and it should be stopped 48 hours prior to procedures that carry risk of acute renal failure, and can be resumed when stable renal function is demonstrated.

Metformin does not cause hypoglycemia when used as monotherapy. It can lead to weight loss (3–5% of body weight), and it has been shown to decrease plasma triglycerides concentration (10–20%).

Dosing is typically twice daily; however, it can be dosed three times daily (with meals) or once daily (extended release). The typical starting dose is 500 mg daily. The maximum dose is 2550 mg per day but most practitioners use up to 2000 mg per day. Gradual titration of metformin, starting at 500 mg with breakfast and increasing by 500 mg in weekly intervals until a dose of 1000 mg with breakfast and dinner is reached helps to prevent GI side effects.[14,15]

Thiazolidinediones

Thiazolidinediones (TZDs) are agonists of peroxisome proliferator-activated receptor-gamma (PPARg) and primarily enhance insulin sensitivity of muscle and fat, and mildly of the liver. TZDs lower fasting and postprandial blood glucose levels.

The side-effects include weight gain, with an increase in subcutaneous adiposity, and fluid retention which typically manifests as peripheral edema, but heart failure has been observed to occur on occasion. As such, these agents should be avoided in patients with functional class III or IV heart failure. TZDs have been shown to have an association with an increased risk of fractures, particularly in women. In June 2011 the US Food and Drug Administration (FDA) added a warning to the pioglitazone label about the possibility that use of pioglitazone for longer than a year may be associated with increased risk of bladder cancer. The TZDs do not cause hypoglycemia when used as monotherapy. Use of pioglitazone but not rosiglitazone leads to lowering triglycerides, increasing high-density lipoprotein cholesterol (HDL), and increasing the low-density lipoprotein cholesterol (LDL) particle size.

Dosing is once a day. It takes 2–12 weeks for TZDs to become fully effective. For rosiglitazone, the starting dose is 4 mg/day and maximum dose is 8 mg/day. For pioglitazone, the starting dose is 15 mg/day and the maximum dose is 45 mg/day.[16,17]

Insulin Secretagogues

Insulin secretagogues stimulate secretion of insulin from the pancreas, thereby decreasing hepatic glucose production and enhancing glucose uptake by muscles and fat.

Sulfonylureas

Sulfonylureas lower fasting and postprandial glucose levels. Main adverse effects include weight gain (about 2 kg upon initiation) and hypoglycemia. The hypoglycemia episodes can be significant (leading to need for assistance, coma, or seizure) and are seen more often in the elderly and in patients with liver or kidney dysfunction or patients who often skip meals. Dosing is typically once daily. Newer, second-generation, sulfonylureas (glipizide and glimepiride) may have less risk of hypoglycemia than older ones (glibenclamide) because their action is somewhat glucose-dependent.[18,19]

Glinides

Glinides work in a manner similar to sulfonylureas; however, they have a more-rapid onset of action and a short duration of action, so they are a good option for patients with erratic timing of meals. They have a lower risk of hypoglycemia than sulfonylureas; they have a similar to lower risk of weight gain with initiation of therapy. Caution must be used in patients with liver dysfunction. Dosing is immediately before meals.[19]

Alpha-Glucosidase Inhibitors

Alpha-glucosidase inhibitors block the enzyme alpha-glucosidase in the brush borders of the small intestine, which delays absorption of carbohydrates (absorbed in the mid and distal portions of the small intestine instead). They primarily target postprandial

hyperglycemia without causing hypoglycemia. Gastrointestinal complaints, such as bloating, abdominal cramps, flatulence and diarrhea, are the main side-effects. Use should be avoided in patients with severe hepatic or renal impairment. Dosing must be prior to carbohydrate-containing meals.[19,20]

Incretin-Based Therapies

Incretin based therapies enhance insulin secretion and suppress glucagon secretion in a glucose-dependent manner, and thus, do not increase risk of hypoglycemia when used as monotherapy or in combination with metformin, TZD-s or SGLT-2 inhibitors. The DPP-4 inhibitors are given orally and increase endogenous levels of glucagon-like-peptide-1 (GLP-1) after the meal. The GLP-1 analogs are given as injections and increase its level throughout the day. The GLP-1 analogs also delay gastric emptying and suppress appetite through central action which causes some weight loss with use of these medications. The major side-effects are gastrointestinal complaints: nausea, vomiting, and diarrhea. All incretin-based therapies may cause slight increase in risk of acute pancreatitis and patients have to be warned to stop it if they develop abdominal pain.

Exenatide

Exenatide is a GLP-1 analog derived from the saliva of the Gila monster.

Dosing is twice-daily by subcutaneous injection and it has to be taken with meals. The starting dose is 5 mg. If this dose is tolerated, 10 mg is used after 1 month.[19]

The extended action preparation of exenatide, which was released in the spring of 2012, is used as a weekly subcutaneous injection. Side-effects and indications are the same as for short-acting exenatide.

Liraglutide

Liraglutide is another GLP-1 analog that is derived from the native human GLP-1 and maintains 97% homology with it.

Liraglutide is taken once a day, any time of the day and with no

need to take it with meals. Side-effects are nausea, vomiting, and diarrhea, but only small percentage of patients will have to stop therapy because of side-effects.

Initial dose is 0.6 mg per day, which is increased to 1.2 mg/day after one week. This dose is considered therapeutic but it can be increased to 1.8 mg/day after another week if glycemic goals are not achieved.[21] The Albiglutide and Dulagutide are two new GLP-1 analogs which are given weekly recently came on market. Both seem to be as effective as older ones.

Dipeptidyl Peptidase 4 Inhibitors

Dipeptidyl peptidase 4 (DPP 4) is a cell membrane protein that rapidly degrades GLP-1 and glucose-dependent insulinotropic polypeptide (GIP). Its inhibitors increase endogenous levels of these peptides and act primarily on postprandial blood glucose levels, but reductions in fasting glucose are also seen. These medications are weight-neutral. It is generally well tolerated, and the most common side-effect is nausea. An increase in nasopharyngitis and headache has also been seen.

Dosing is orally once daily. Dose reduction is needed with renal impairment for most of these medications.[22]

Pramlintide

Pramlintide is a synthetic form of amylin, a hormone secreted by beta-cells that acts to suppress glucagon secretion, slow gastric emptying, and suppress appetite through central pathways. It acts primarily on postprandial blood glucose levels.

The side-effects are gastrointestinal complaints, especially nausea, and hypoglycemia. Benefits of therapy include some weight loss.

In the United States it is currently approved only as an adjunctive therapy with insulin, but it can be used for both type 1 and type 2 diabetes mellitus. Patients can see up to a 50% reduction in their insulin requirements with the addition of pramlintide. Starting dose for type 2 diabetes mellitus is generally 60 mg subcutaneously before meals and for type 1 it is 15 mg before each meal. It can be used in patients taking insulin, metformin, or sulfonylureas.[19]

Bromocriptine

The exact mechanism of action by which bromocriptine improves glycemic control is not known. Bromocriptine is a central dopamine agonist and when given in rapid release form in the morning within the 2 hours of awakening it improves glycemic control for patients with type 2 diabetes.

Side-effects include hypotension, somnolence and nausea. Individuals with psychiatric disorders may experience exacerbation while taking bromocriptine.

The initial dose is 0.8 mg, which is increased in weekly increments by 0.8 mg until a therapeutic dose of 1.6–4.8 mg is achieved. Bromocriptine is taken with food to diminish nausea.[23]

SGLT-2 Inhibitors

The newest group of medications, SGLT-2 inhibitors, block the resorption of the glucose from the urine back into the circulation (by inhibiting the glucose/sodium cotransporter 2). This leads to increased glycosuria leading to lowering of the serum glucose levels and also to some weight loss and lowering of the blood pressure. The FDA has approved dapagliflozin, canagliflozin, and empagliflozin for use in the United States. Side-effects include increase in genital yeast infections and, of more concern, development of euglycemic ketoacidosis. This side-effect is only observed in postmarketing studies and the risk is small and not yet well defined.[24]

Insulin and Insulin Analogs

Insulin was discovered in 1921, and clinical testing in humans started in 1922. To this date it remains the most direct method of reducing hyperglycemia. There is no upper limit in dosing for therapeutic effect.

Hypoglycemia is the main concern. Studies have shown that episodes where the patient required assistance due to hypoglycemia occurred between 1 and 3 per 100,000 patient-years. Weight gain can occur after initiation and is typically about 2 to 4 kg.

Most brands are available in both vial and pen form for delivery.

Long-acting insulin analogs (degludec, detemir and levemir) have a very even action profile throughout the day and are the best options for providing the basal insulin. The NPH insulin has a peak after injection and patients need to eat after injection to prevent hypoglycemia. Short-acting insulin analogs (apidra, glulisine, and aspart) have very fast onset of action and duration of action independent of the dose. The regular human insulin has slower onset of action and duration of action is proportional to the dose. Table 49.2 summarizes the different formulations of insulin and insulin analogs available.[19,25]

The latest addition to the arsenal is inhaled insulin. It is used for prandial coverage. It requires spirometry before starting the therapy, and cannot be used in smokers and individuals with lung diseases. Dosing is in increments of four units which may prevent fine tuning of the meal dose. It is too early to know how well this product will be accepted by patients and healthcare providers.

Initiation and Titration of Therapy

There are several different regimens for insulin therapy. These are summarized in Table 49.3. All patients with type 1 diabetes mellitus require use of insulin products. Patients with type 2 disease also often require insulin, which can be combined with oral hypoglycemic agents. Insulin can be delivered by subcutaneous (SC) injection, intravenous drip, subcutaneous insulin pump therapy and as inhaled insulin.

TABLE 49.3

Regimens for Insulin Therapy

Insulin Regimen	Hba_{1c} (%)	Medication	Pattern	Diet History	Lifestyle	Monitoring
Basal only	>7.5-10	Oral medications adequately control postprandial glucose excursions	High fasting glucose with minimal glucose rise during the day	Small, regular meals; large meals will result in postprandial hyperglycemia	Reluctance to do MDI; requires oral agents	Fasting
Basal–bolus	>7.5	—	Regimen	Regimen can	Erratic	Frequent

(MDI)			can be matched to any pattern to achieve glycemic control	be matched to any diet to achieve glycemic control	schedule, motivated to achieve tight glycemic control	blood glucose monitoring (minimum before meals and bedtime)
ONCE- OR TWICE-DAILY PREMIXED						
Rapid-acting analog and intermediate-acting	>7.5	Oral agent failure (maximum tolerated dosages, contraindications, cost issues)	Any fasting glucose; glucose rises during the day	Large suppers, small lunches	Consistent daily routine, reluctance to do MDI	Fasting and presupper (if insulin is administered twice daily)
Regular and NPH	>7.5%	Oral agent failure (maximum tolerated dosages, contraindications, cost issues)	Any fasting glucose; glucose rises during the day	Isocaloric meals or larger lunches	Consistent daily routine, reluctance to do MDI	Fasting and presupper (if insulin is administered twice daily)

HbA_{1c}, glycated hemoglobin; MDI, multiple daily injections.

Type I Diabetes

Multiple SC Injections

This regimen combines a long-acting agent that is used once or twice daily and provides basal insulin needs, and a rapid-acting agent for prandial coverage used with meals. When initiating therapy with glargine or detemir as the basal insulin, traditionally 50% of the total daily dose is given as basal insulin and the rest as prandial insulin divided equally before meals. Meal dose of insulin can be fixed, but it is better to determine the dose based on carbohydrate content of the meal. This requires learning carbohydrate counting and knowing the dose of insulin required to cover counted carbohydrates. The help of a diabetic educator is needed for this to be achieved. Patients are also provided with a sliding scale (correction insulin) to use as a third component of therapy at times when blood glucose is higher than desired.

Safe starting daily insulin dose is typically 0.3 U/kg total (divided between long-acting and rapid-acting) daily for the patients with type 1 diabetes mellitus and 0.5 U/kg for those with type 2 disease. Key to good control is blood glucose self-monitoring by the patient and frequent adjustment of the regimen until control is achieved.[26]

Insulin Pump Therapy

The insulin pump delivers insulin continuously by the SC route and allows use of varying basal insulin rates in different periods of day and administration of the meal bolus as a single discrete bolus or as an extended bolus (square bolus) over a certain amount of time, which allows a better match between insulin delivery and glucose absorption from the meal in patients with abnormalities of gastric emptying. Use of pumps is becoming more popular, improves glycemic control and quality of life[27,28] and should particularly be considered in the following patients:

- Those unable to achieve target goals with basal–bolus regimens.
- Patients with frequent hypoglycemia or brittle diabetes.
- Patients with dawn phenomenon. (Dawn phenomenon is increase in the morning blood glucose level under the influence of morning [5–8 a.m.] surge of hormone secretion, especially cortisol, but also growth hormone, glucagon and epinephrine, and it is a different from Somogyi phenomenon which pertains to morning hyperglycemia caused by hormonal response to nocturnal hypoglycemia.)
- Pregnant patients.
- Patients with hypoglycemic unawareness or requiring more intense monitoring due to complications.
- Patients who are able to monitor blood glucose several times daily and make insulin dosage adjustments.

Recently, continuous glucose monitors have been developed that measure interstitial glucose levels every few minutes and are used in conjunction with insulin pumps. Their use improves HbA1c and decreases the number of hypoglycemic episodes.[29]

Type 2 Diabetes

About 85% patients with type 2 diabetes will require insulin at one time. Insulin is started once multiple oral medications cannot control glucose anymore. The exact moment to start insulin will vary and decisions are individualized. Adding basal coverage is the first step and prandial coverage is added later (either at all meals or at the largest meal first). Premixed insulin combination can be used

twice a day (before breakfast and dinner) with success in some patients, especially if lunch is skipped.

Gestational Diabetes

In patients with gestational diabetes, insulin therapy is indicated when exercise and nutritional therapy are ineffective in controlling prandial and fasting blood glucose levels. Basal therapy alone may be sufficient, but often multiple daily injections are required.

References

1. Mitka M. Report quantifies diabetes complications. *JAMA*. 2007;297(21):2337–2338.
2. Klein R, Klein BEK, Moss SE, et al. The Wisconsin Epidemiologic Study of Diabetic retinopathy: II. Prevalence and risk of diabetic retinopathy when age at diagnosis is less than 30 years. *Arch Ophthalmol*. 1984;102:527–532.
3. Klein R, Klein BEK, Moss SE. Relation of glycemic control to diabetic microvascular complications in diabetes mellitus. *Ann Intern Med*. 1996;124:90–96.
4. Diabetes Control and Complications Trial Research Group. The effect of intensive treatment of diabetes on the development and progression of long-term complications in insulin-dependent diabetes mellitus. *N Engl J Med*. 1993;329:977–986.
5. Diabetes Control and Complications Trial/Epidemiology of Diabetes Interventions and Complications Research Group. Retinopathy and nephropathy in patients with type 1 diabetes four years after a trial of intensive therapy. *N Engl J Med*. 2000;342:381–389.
6. Ohkubo Y, Kishikawa H, Araki E, et al. Intensive insulin therapy prevents the progression of diabetic microvascular complications in Japanese patients with non-insulin-dependent diabetes mellitus: a randomized prospective 6-year study. *Diabetes Res Clin Pract*. 1995;28:103–117.
7. UK Prospective Diabetes Study (UKPDS) Group. Effect of intensive blood-glucose control with metformin on

complications in overweight patients with type 2 diabetes (UKPDS 34). *Lancet*. 1998;352:854–865 [erratum 1998;352:1557].
8. UK Prospective Diabetes Study Group. Intensive blood-glucose control with sulphonylureas or insulin compared with conventional treatment and risk of complications in patients with type 2 diabetes (UKPDS 33). *Lancet*. 1998;352:837–853 [erratum 1999;354:602].
9. UK Prospective Diabetes Study Group. Efficacy of atenolol and captopril in reducing risk of macrovascular and microvascular complications in type 2 diabetes: UKPDS 39. *BMJ*. 1998;317:713–720.
10. UK Prospective Diabetes Study Group. Tight blood pressure control and risk of macrovascular and microvascular complications in type 2 diabetes: UKPDS 38. *BMJ*. 1998;317:703–713 [erratum 1999;38:29].
11. Chautervedi N, Sjolie AK, Stephenson JM, et al. and the EUCLID Study Group. Effect of lisinopril on progression of retinopathy in normotensive people with type 1 diabetes. EURODIAB Controlled Trial of Lisinopril in Insulin-Dependent Diabetes Mellitus. *Lancet*. 1998;351:28–31.
12. Standards of Medical Care in Diabetes – 2015: American Diabetes Association. *Diabetes Care*. 2015;38(Suppl. 1).
13. Handelsman J, et al. American Association of Clinical Endocrinologists and the American College of Endocrinology. Clinical practice guidelines for developing a diabetes mellitus comprehensive care plan – 2015. *Endo Pract*. 2015;(Suppl. 1).
14. Bailey CJ, Turner RC. Metformin. *N Engl J Med*. 1998;339(25):1860–1861.
15. Bailey CJ. Biguanides and NIDDM. *Diabetes Care*. 1992;15(6):755–772.
16. Dormandy JA, Charbonnel C, Eckland DJ, et al. Secondary prevention of macrovascular events in patients with type 2 diabetes in the PROactive Study (PROspective pioglitAzone Clinical Trial In macroVascular Events): a randomised controlled trial. *Lancet*. 2005;8:1279–1289.
17. Nathan DM, Buse JB, Davidson MB, et al. Management of

hyperglycemia in type 2 diabetes: a consensus algorithm for the initiation and adjustment of therapy: update regarding thiazolidinediones. *Diabetes Care*. 2008;31(1):173–175.
18. UK Prospective Diabetes Study (UKPDS) Group. Intensive blood-glucose control with sulphonylureas or insulin compared with conventional treatment and risk of complications in patients with type 2 diabetes (UKPDS 33). UK Prospective Diabetes Study (UKPDS) Group. *Lancet*. 1998;352(9131):837–853.
19. Fonseca V, Kulkarni K. Management of type 2 diabetes: oral agents, insulin, and injectables. *J Am Dietetic Assoc*. 2008;108(4):S29–33.
20. Chiasson JL, Josse RG, Gomis R, et al. Acarbose treatment and the risk of cardiovascular disease and hypertension in patients with impaired glucose tolerance: The STOP–NIDDM Trial. *JAMA*. 2003;290:486–494.
21. Victoza (liraglutide). www.accessdata.fda.gov/drugsatfda_docs/label/…/022341s004lbl.pdf.
22. Dicker D. DPP-4 inhibitors – impact on glycemic control and cardiovascular risk factors. *Diabetes Care*. 2011;34(S2):376–378.
23. Cycloset (bromocriptine mesylate). www.accessdata.fda.gov/drugsatfda_docs/label/2009/02086
24. Abdul-Ghani MA, Norton L, DeFronzo RA. Efficacy and safety of SGLT2 inhibitors in the treatment of type 2 diabetes mellitus. *Curr Diab Rep*. 2012;12(3):230–238.
25. Hirsch IB, Bergenstal RM, Parkin CG, et al. A real-world approach to insulin therapy in primary care practice. *Clinical Diabetes*. 2005;23:78–86.
26. Rodbard HW, Blonde L, Braithwaite SS, et al. American Association of Clinical Endocrinologists medical guidelines for clinical practice for the management of diabetes mellitus. *Endocr Pract*. 2008;14(6):802–803.
27. Pickup JC. Insulin-pump therapy for type 1 diabetes mellitus. *N Engl J Med*. 2012;366:1616–1624.
28. Nicolucci A, Maione A, Franciosi M, et al. Quality of life and treatment satisfaction in adults with Type 1 diabetes: a

comparison between continuous subcutaneous insulin infusion and multiple daily injections. *Diabet Med*. 2008;25:213–220.
29. Greene C, Brown D, Wallace J, et al. Comparative accuracy of 3 blood glucose monitoring systems that communicate with an insulin pump. *Endocrine Pract*. 2014;20:1016–1021.

50

Nonproliferative Diabetic Retinopathy and Diabetic Macular Edema

Henry E. Wiley, Emily Y. Chew, Frederick L. Ferris III

Diabetes mellitus (DM) comprises a heterogeneous group of disorders of carbohydrate, protein, and fat metabolism manifesting hyperglycemia. Diabetic retinopathy is a microangiopathy resulting from the chronic effects of the disease, and shares similarities with the microvascular alterations that occur in other tissues vulnerable to DM such as the kidneys and the peripheral nerves. Although the

metabolic derangement has direct effects on the neurons and support cells of the retina, the retinal vascular changes dominate the clinical manifestations of disease and are directly implicated in the macular edema and neovascularization that represent the principal causes of vision loss. Diabetic retinopathy is classified into nonproliferative and proliferative stages. Nonproliferative diabetic retinopathy (NPDR) involves progressive intraretinal microvascular alterations that can lead to a more advanced proliferative stage defined by extraretinal neovascularization.

This chapter discusses the clinical manifestations and management of NPDR and diabetic macular edema (DME). Proliferative diabetic retinopathy (PDR) is reviewed in Chapter 51 (Proliferative diabetic retinopathy).

Natural Course of Nonproliferative Diabetic Retinopathy

Diabetes Mellitus Without Retinopathy

Retinal microvascular alterations visible on ophthalmoscopy typically develop years following the onset of DM. Chapter 48 (Diabetic retinopathy: Genetics and etiologic mechanisms) reviews what we know about the early biochemical and cellular alterations leading to diabetic retinopathy, while Chapter 47 (The epidemiology of diabetic retinopathy) discusses the incidence and prevalence of retinopathy. Experimental models of diabetic retinopathy in dogs and rats, and studies of human autopsy eyes, indicate that early alterations in retinal blood vessels include the loss of capillary pericytes (Fig. 50.1) and thickening of the capillary basement membrane.[1–21]

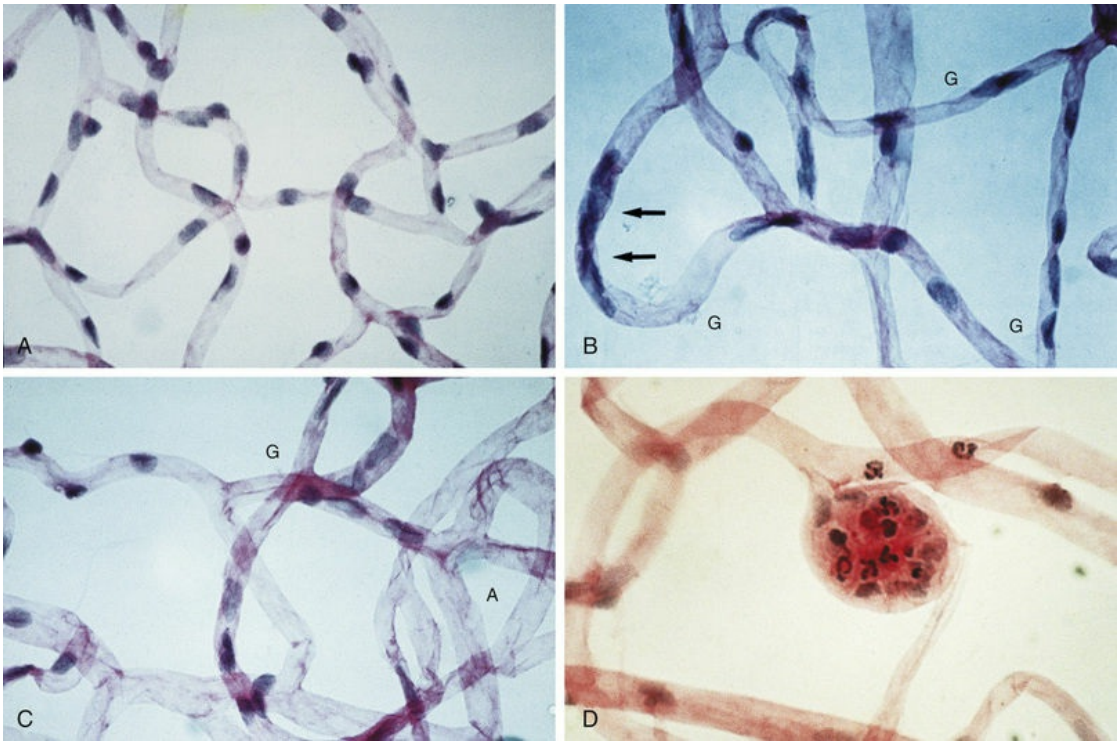

FIG. 50.1 Photomicrographs of mounted retinal capillaries following trypsin digestion and staining with periodic acid-Schiff–hematoxylin, demonstrating retinal capillary alterations in a canine model for diabetic retinopathy. (A) Normal capillaries showing a typical distribution of endothelial cells and pericytes from a control dog fed normal chow (original magnification, ×825). (B,C) Pericyte ghosts (*G*), focal proliferation of endothelial cells (*arrows*), and acellular capillaries (*A*) are visible in a dog fed a galactose diet for 24 months (original magnification, ×825 and ×925, respectively). (D) A microaneurysm is present in a dog fed a galactose diet for 27 months (original magnification, ×570). (Courtesy of Dr. Peter Kador.)

There is preliminary evidence that parenchymal cells of the retina exhibit changes in the early stages of disease, including glial cell reactivity, alterations in glutamate metabolism, and neuron cell death.[22–28] Several studies have documented subtle changes in contrast sensitivity and color perception in people with DM in the absence of visible retinopathy,[29–34] but it remains unclear whether these effects result from deficits in retinal function, or from other diabetic alterations such as cataractogenesis. Central vision (measured by visual acuity) and peripheral vision (measured by

common perimetric tests) typically remain normal in DM prior to onset of clinically evident retinopathy, in the absence of other factors such as cataract.

Microaneurysms

Microaneurysms, identified clinically by ophthalmoscopy as deep-red dots varying from 25 to 100 μm in diameter, are usually the first visible sign of diabetic retinopathy. Although microaneurysms are occasionally seen in normal aging adults and also occur in other retinal vascular diseases, such as retinal vein occlusion and radiation retinopathy, they are a hallmark of NPDR.

Microaneurysms arise as hypercellular saccular outpouchings of the capillary wall that can be well visualized in trypsin-digest retinal mounts (see Fig. 50.1D).[1] Their lumina are sometimes occluded by agglutinated erythrocytes or thrombus. Over time they sometimes become acellular, just as damaged retinal capillaries can evolve into "ghost" vessels devoid of endothelial cells and pericytes. The mechanism for microaneurysm formation is unknown. Possible contributing factors may include alterations in the retinal microenvironment from metabolic effects on neurons, glial cells, and endothelial cells; endothelial cell injury secondary to leukostasis from altered interaction between endothelial cells and leukocytes; response of endothelial cells to altered balance between proliferative and antiproliferative factors; structural changes in the capillary wall (such as from loss of pericytes); or increase in intraluminal pressure.

Microaneurysms visualized by ophthalmoscopy or angiography commonly appear and disappear over time, though some retain a stable appearance for years. The presence of microaneurysms alone, in the absence of other features of diabetic retinopathy, remains compatible with normal vision. However, as the number of microaneurysms increases, there is a greater risk of retinopathy progression.[35–37]

Retinal Vascular Hyperpermeability

Subtle compromise of the blood–retinal barrier may begin at an early stage of disease, even preceding the appearance of

retinopathy, but clinically appreciable retinal vascular hyperpermeability typically follows the appearance of microaneurysms. Visualized clinically by angiography, leakage may arise from microaneurysms, retinal capillaries, or other microvascular abnormalities, and can be highly variable in magnitude and extent. Retinal vascular incompetence may or may not result in localized areas of thickening of the retina. Hard exudates, extravascular deposits of lipid-rich material that result from spillage and incomplete resorption of plasma lipoproteins, may accumulate. Intraretinal hemorrhages appear in the posterior pole and in the retinal periphery. The vascular alterations responsible for hyperpermeability in NPDR remain incompletely understood, but may involve dysfunction of the tight junctions between retinal capillary endothelial cells. Possible mechanisms for breakdown of the blood–retinal barrier are discussed in Chapter 29 (Blood–retinal barrier, immune privilege, and autoimmunity).

Diabetic Macular Edema

DME, defined as macular thickening resulting from diabetic retinopathy, results from retinal vascular hyperpermeability and other alterations in the retinal microenvironment, and represents a common cause of vision loss among people with DM. DME can occur in eyes with a wide spectrum of underlying retinopathy, from mild NPDR to PDR. It can occur in areas of demonstrable retinal vascular incompetence, as visualized by angiography, and also in regions of retinal ischemia. In areas of vascular incompetence, DME may result from leakage of microaneurysms, or it may evolve from diffuse leakage of hyperpermeable capillaries. In areas of capillary nonperfusion on angiography, retinal thickening may result from ischemia in the absence of prominent vascular leakage, though hyperpermeable microvascular abnormalities at the borders of such regions may contribute to swelling. Macular edema may or may not be characterized by intraretinal cyst formation. In some cases, usually in the setting of severe thickening involving the fovea, subretinal fluid may also be present. However, presence of subretinal fluid occurring in the absence of associated severe intraretinal thickening (or recent history of severe intraretinal

thickening), eccentric to the foveal center, or associated with any RPE abnormality (such as retinal pigment epithelial detachment), should prompt consideration of other conditions.

The pathogenesis of DME remains poorly understood, partly because of the absence of a good animal model. Chapter 48 (Diabetic retinopathy: Genetics and etiologic mechanisms) reviews what we know about the early biochemical and cellular alterations leading to DME, while Chapter 30(Mechanism of macular edema) discusses factors involved in the pathogenesis of macular edema of different causes.

Extrafoveal foci of retinal thickening and hard exudates may not cause symptoms or affect visual acuity, but DME that involves or threatens the center of the macula carries a significant risk of vision loss. In the Early Treatment of Diabetic Retinopathy Study (ETDRS), the 3-year risk of moderate visual loss (a decrease of three lines or more on a logarithmic visual acuity chart, corresponding to a doubling of the initial visual angle) among untreated eyes with DME involving or threatening the center of the macula was 32%.[38] The natural history of DME is variable. In some eyes, it can persist for years, while in others it may spontaneously resolve. Chapter 47 (The epidemiology of diabetic retinopathy) discusses the incidence and prevalence of DME and consequent vision loss.

Capillary Closure, Microvascular Remodeling, and Retinal Ischemia

One of the most serious consequences of diabetic retinopathy is progressive loss of functional retinal capillaries. Trypsin-digest preparations of the retina show areas of acellular capillaries, or "ghost" vessels, which have lost the endothelial cells and pericytes that once lined them (see Fig. 50.1C). When patches of such acellular capillaries, first seen early in the course of NPDR, increase and become confluent, the terminal arterioles that supply these capillaries often become occluded. Regions of acellular capillaries in histologic sections have been shown to correspond to areas of capillary nonperfusion visualized by fluorescein angiography.[39] Adjacent to these areas of retinal ischemia, clusters of microaneurysms and hypercellular vessels often develop. It has

been difficult to determine whether such vessels represent altered preexisting capillaries or neovascularization within the retina. Such vessels are described clinically as intraretinal microvascular abnormalities (IRMA), a term intended to accommodate both possibilities.

Progressive capillary closure and resulting retinal ischemia are commonly associated with increasing IRMA, intraretinal hemorrhages, and venous abnormalities such as segmental dilation (venous beading). Occasionally, in cases of extensive capillary nonperfusion, the retina acquires a featureless appearance with a relative dearth of visible vessels, hemorrhages, or microvascular abnormalities. Retinal ischemia represents another cause for vision loss in NPDR, and also plays a central role in the pathogenesis of PDR by stimulating elaboration of vascular endothelial growth factor A (VEGF-A) and other angiogenic factors.[40,41] Chapter 51 (Proliferative diabetic retinopathy) discusses the natural course of PDR.

Alterations of the Vitreous Gel and Vitreoretinal Interface

The vitreous gel plays a key role in the fibrovascular proliferation of PDR, but it may also exert important effects at earlier stages of retinopathy. Epiretinal membrane formation, arising from liquefaction of the vitreous gel and consequent effects at the vitreoretinal interface, can occur with advancing age in otherwise healthy eyes but is more common in diabetic eyes.[42–46] It has been hypothesized that liquefaction of the vitreous gel out of proportion to diminution of posterior vitreoretinal adhesion may underlie the pathophysiology of many vitreoretinal diseases,[47] and observations at vitrectomy suggest that the posterior cortical vitreous is frequently more adherent to the retina in the setting of diabetic retinopathy. Studies have documented a number of biochemical changes to the vitreous gel in the setting of DM, including increased collagen fibril cross-linking, accumulation of advanced glycation end products that may augment vitreoretinal adhesion and incite retinal glial cell reactivity, and alterations in the concentration of various soluble proteins.[48–52]

The role of the vitreous gel in the pathophysiology of diabetic retinopathy may extend beyond its capacity to exert mechanical effects on the retina. For example, there is evidence that the vitreous may function as an important regulator of intraocular oxygen tension, a finding that could have important implications for diabetic retinopathy and other diseases involving retinal hypoxia.[53,54]

Clinical Evaluation of Nonproliferative Diabetic Retinopathy

Comprehensive evaluation of a patient with DM begins with identification of extraocular factors associated with risk of diabetic retinopathy and its progression. Such factors are presented briefly here and discussed in greater detail in Chapter 47 (The epidemiology of diabetic retinopathy). Pertinent medical history is sought from the patient, and supplemented by records from his or her primary care physician or endocrinologist as warranted.

Duration of Diabetes Mellitus

The duration of DM is strongly associated with risk of retinopathy. Cross-sectional and longitudinal analyses from population-based epidemiologic studies have established the association between prevalence of retinopathy and duration of disease.[55–64] The Wisconsin Epidemiologic Study of Diabetic Retinopathy (WESDR) examined prevalence and severity of diabetic retinopathy in a younger-onset group consisting of those diagnosed with DM prior to 30 years of age who were taking insulin at the time of the evaluation (predominantly type 1 DM) and an older-onset group consisting of those diagnosed with DM at 30 years of age or older (predominantly type 2 DM), the latter subdivided according to whether insulin was being used at the time of evaluation. The prevalence of retinopathy may have changed somewhat since the 1980s when WESDR data was collected, given interim advances and evolving standards of care in management of DM, but the WESDR remains one of our most definitive sources of information about the

epidemiology of diabetic retinopathy in the United States. In the younger-onset group, retinopathy (consisting of NPDR or PDR) was seen in 13% of those with less than a 5-year duration of DM and in 90% of those with a duration of 10–15 years.[59] In the older-onset group using insulin, retinopathy was seen in 40% of those with less than a 5-year duration of disease and in 84% of those with a duration of 15–19 years, while the corresponding rates in the older-onset group not taking insulin were 24% and 53%, respectively.[58]

Among those with type 2 DM, in which disease onset is often more insidious than in type 1 DM and in which hyperglycemia can remain asymptomatic for years, age at diagnosis may not always accurately reflect disease duration. The Centers for Disease Control and Prevention estimate that 29.1 million people in the United States have DM, of whom 8.1 million do not know they have it.[65] The prevalence of undiagnosed type 2 DM is felt to be the key factor explaining the higher rates of retinopathy noted soon after diagnosis among people with type 2 DM (24% in the older-onset group not taking insulin with less than a 5-year duration of disease in the WESDR) compared with those with type 1 DM (13% in the younger-onset group with less than a 5-year duration of disease).

Hyperglycemia

The relationship between the degree of hyperglycemia and the presence and severity of diabetic retinopathy has been extensively studied in observational studies and clinical trials. The observational studies have demonstrated that greater hyperglycemia is associated with increased prevalence and severity of diabetic retinopathy.[56,58–61,63,64] Several key randomized controlled clinical trials have demonstrated that better glycemic control is associated with a decreased risk of secondary complications of DM, including diabetic retinopathy.[66–73]

In the Diabetes Control and Complications Trial (DCCT), 1441 participants with type 1 DM were randomly assigned to either conventional or more intensive insulin treatment and followed for a period of 4–9 years.[66,67,70,73] The average difference in glycosylated hemoglobin (hemoglobin A1C [HbA1C]) between the two groups

was almost 2%. Intensive insulin treatment, as defined by the DCCT, was associated with a decreased risk of both the development and progression of diabetic retinopathy. In patients without retinopathy at enrollment, the 3-year risk of developing retinopathy was reduced by 75% in the intensive insulin treatment group compared with the conventional treatment group. The benefit of better glycemic control was also evident in patients with existing retinopathy at baseline, as shown by a 50% reduction in the rate of progression of retinopathy compared with controls. At the 6- and 12-month visits, more intensive insulin treatment exerted a small adverse effect on retinopathy progression, similar to that described in other trials of glycemic control. However, among eyes with little or no retinopathy at the time of initiating better control of hyperglycemia, it was found that such "early worsening" of retinopathy was unlikely to threaten vision. When the DCCT results were stratified by levels of glycosylated hemoglobin, there was a 35–40% reduction in the risk of retinopathy progression for every 10% decrease in HbA1C (e.g., from 8% to 7.2%). This represented a fivefold increase in risk of progression for patients with HbA1C around 10% compared with those with HbA1C around 7%. Notably, there was also a statistically significant reduction in other microvascular complications of DM, including nephropathy and peripheral neuropathy, with more intensive glycemic control in the DCCT.

When the randomized controlled clinical trial was completed, DCCT participants were informed of the results and enrolled in a follow-up phase of the study, known as the Epidemiology of Diabetes Intervention and Complications (EDIC) study.[70] After an additional 7 years of follow-up, during which the HbA1C values in both treatment groups did not differ significantly (8.1% vs. 8.2%, p=.09), the rate of retinopathy progression remained significantly lower in those who had received more intensive treatment in the DCCT than in those who had received conventional therapy. Thus, more intensive glycemic control over a period of 6.5 years conferred benefits well beyond the period of differential glycemic control between the two groups.

In the United Kingdom Prospective Diabetes Study (UKPDS), 3867 patients with newly diagnosed type 2 DM were randomly

assigned to conventional therapy or to more intensive glycemic control with either insulin or a sulfonylurea.[68,69] Among participants treated with conventional therapy, those who were overweight were given metformin and those who were not overweight did not receive this medication. After 12 years, the rate of retinopathy progression was reduced by 21% and the use of laser photocoagulation was reduced by 29% in those getting intensive glycemic control compared with those getting conventional treatment. For every percentage point decrease in HbA1C (e.g., 9% to 8%), there was a 35% reduction in the risk of microvascular complications of disease.

The results of the UKPDS have recently been corroborated by those of another large randomized controlled clinical trial, the Action to Control Cardiovascular Risk in Diabetes (ACCORD) study. The ACCORD study randomly assigned 10, 251 patients with type 2 DM to very intensive glycemic control (targeting HbA1C less than 6%), or to standard treatment (targeting HbA1C between 7% and 7.9%). A subset including 2856 participants was evaluated for progression of retinopathy by comparison of fundus photographs taken at baseline and at 4 years.[72] In this subset at one year, median HbA1C in the intensive treatment cohort was 6.4% compared with 7.5% in the cohort getting conventional therapy. In the intensive treatment group, the rate of retinopathy progression was 7.3% at 4 years, compared with 10.4% in the standard therapy group (adjusted odds ratio, 0.67; 95% confidence interval [CI] 0.51–0.87; p=.003). The glycemia trial, performed alongside other studies evaluating control of blood pressure and plasma lipids, was halted early at a median of 3.7 years because of an increased rate of death from all causes in participants treated with intensive control compared with those managed with standard control (5% vs. 4%, respectively), and the very intensive control approach was abandoned.

Hypertension

In addition to assessing the effects of differential glycemic control, the UKPDS provided a randomized comparison between more intensive blood pressure control (targeting a systolic blood pressure

less than 150 mmHg) and less intensive blood pressure control (targeting a systolic blood pressure less than 180 mmHg) in a large cohort of participants with newly diagnosed type 2 DM.[74] Study results demonstrated that intensive blood pressure control was associated with a decreased risk of retinopathy progression. Of 1148 hypertensive participants in the UKPDS, 758 were allocated to more intensive control of blood pressure and 390 to less intensive control with a median follow-up of 8.4 years. More intensive blood pressure control resulted in a 37% reduction in microvascular complications of DM, predominantly a reduced risk of retinal photocoagulation, compared with less intensive control. An earlier report assessing the effects of various blood pressure medications on diabetic retinopathy had suggested that there might be a specific benefit of angiotensin-converting enzyme (ACE) inhibition, even in normotensive persons. The UKPDS included a randomized comparison of beta blockers and ACE inhibitors within the more intensive blood pressure control arm. Benefit from more intensive blood pressure control was noted in both the beta blocker and ACE inhibitor treatment groups, with no statistically significant difference between them, suggesting that the treatment effect was probably attributable to blood pressure reduction and not to a specific effect of ACE inhibition.

The ACCORD study attempted to extend the results of the UKPDS by assessing the effect of very tight blood pressure control on retinopathy. In this study, 4733 of the 10 ,251 participants with type 2 DM were randomly assigned to very intensive control of blood pressure (targeting a systolic blood pressure less than 120 mmHg) or standard blood pressure control (targeting a systolic blood pressure less than 140 mmHg). A subset of 1263 participants in the blood pressure trial was evaluated for progression of retinopathy just as in the glycemia arm of the study, with comparison of fundus photographs at baseline and 4 years.[72] Rate of progression of retinopathy at 4 years was not significantly different in the two groups (10.4% of those treated intensively compared with 8.8% of those treated with standard care, with an adjusted odds ratio of 1.23; 95% CI 0.84–1.79; p=.29). The results of the UKPDS and ACCORD study are not necessarily contradictory in this regard, given the very different targets used for more and less

intensive control of blood pressure between the two trials.

Dyslipidemia

Elevated levels of plasma cholesterol were associated with greater severity of retinal hard exudates in the WESDR and in the ETRDS.[75,76] Independent of coincident retinal thickening, the severity of retinal hard exudates at baseline was associated with decreased visual acuity in the ETDRS. The severity of retinal hard exudates was also a significant risk factor for moderate visual loss during the course of the study. Elevated levels of plasma triglycerides were associated with a greater risk of developing high-risk PDR in the ETDRS patients.[77] Two recent randomized controlled clinical trials evaluating the plasma lipid-modulatory agent fenofibrate in combination with statins in individuals with elevated plasma lipids have demonstrated that fenofibrate reduces the risk of diabetic retinopathy progression while only providing modest alterations in the plasma lipid profile.[72,78] It is presently uncertain whether the effects of fenofibrate on diabetic retinopathy are secondary to its plasma lipid-modulatory activity or to some other mechanism.

Other Extraocular Factors

Diabetic retinopathy can worsen precipitously in the setting of pregnancy. Chapter 95 (Pregnancy-related diseases) reviews the natural history of retinopathy in pregnancy. Diabetic nephropathy, as measured by albuminuria, proteinuria, or manifestations of renal failure, has been inconsistently associated with progression of retinopathy.[77,79,80] Anemia has been associated with progression of diabetic retinopathy in two small case series and two epidemiologic studies.[77,81–83] The ETDRS found association between decrease in hematocrit and increase in the incidence of high-risk PDR in an adjusted multivariate model. A few reports have suggested an association between diabetic neuropathy or cardiovascular autonomic neuropathy and progression of retinopathy.[77,84,85] Significant progress has been made in understanding the heritable contributions to the development of DM, particularly the type 1 form and certain familial and syndromic variants of the disease, but

the identification of genetic risk factors for development and progression of diabetic retinopathy has been challenging. Chapter 48 (Diabetic retinopathy: Genetics and etiologic mechanisms) reviews our present knowledge about the genetics of diabetic retinopathy.

Ophthalmic Evaluation

Ophthalmic evaluation of a patient with DM begins with identification of pertinent features of ocular history, including previous diagnosis of diabetic retinopathy or DME, comorbid ophthalmic conditions, and previous medical or surgical treatment. The severity of existing retinopathy is a powerful predictor of risk of retinopathy progression and vision loss, as discussed below in the section "Classification of diabetic retinopathy." Knowledge of any previous treatment has recently become more relevant for management of NPDR and DME. A proliferating array of therapeutic options and the variability of treatment efficacy among individuals have made management algorithms more complex and clinical decision-making more contingent on assessment of the success of previous treatment strategies. Most pharmacologic therapies leave no lasting marks like the telltale scars of laser photocoagulation, making clinicians more reliant on history-taking and review of records for evidence of prior treatment.

A comprehensive eye examination in a person with DM includes measurement of visual acuity and intraocular pressure (IOP); evaluation of the anterior segment by slit-lamp biomicroscopy; gonioscopy when warranted (such as in the setting of elevated IOP, neovascularization of the iris, or glaucoma); and dilated funduscopic examination.[86] Evaluation of the anterior segment prior to dilation of the pupil may allow visualization of neovascularization of the iris or anterior chamber angle not possible following mydriasis. Dilation of the pupil is important for adequate assessment of the posterior segment. In the absence of pupil dilation, only 50% of eyes are correctly diagnosed for the presence and severity of retinopathy.[87]

Ophthalmoscopy, including stereoscopic evaluation of the posterior pole and visualization of the vitreous gel and peripheral

retina, remains the standard for clinical diagnosis and characterization of NPDR and DME. Examination of the posterior pole is best achieved using slit-lamp biomicroscopy with accessory lenses. A handheld accessory lens may provide sufficient visualization of the posterior pole and midperipheral retina, but in cases where superior stereopsis and discrimination are desired, an examination contact lens coupled to the eye surface after application of topical anesthetic drops can be used. The peripheral retina is typically surveyed using indirect ophthalmoscopy, but slit-lamp biomicroscopy with an accessory lens may serve as a supplement or substitute when visualization with high magnification is warranted. A three- or four-mirror contact lens coupled to the eye surface can also be used to examine peripheral lesions under high magnification. Red-free illumination can be useful at highlighting retinal vessels and associated lesions of NPDR such as microaneurysms, hemorrhages, and IRMA.

Ancillary Ocular Imaging

Imaging modalities in common clinical use for management of NPDR and DME include fundus photography, fluorescein angiography (FA), and optical coherence tomography (OCT).

Fundus Photography

Fundus photography is a valuable clinical tool for evaluating progression of retinopathy in individual patients and in participants in clinical trials. Photography is used in clinical practice to document the status of retinopathy and effects of treatment. Though not always as sensitive as ophthalmoscopy at detecting subtle features of diabetic retinopathy such as IRMA and early extraretinal neovascularization, photography can be useful in documenting certain findings in select patients. For example, it can be used to record the extent and distribution of hard exudates in DME, the extent of retinal alterations in severe NPDR, and the appearance of laser photocoagulation burns. Chapter 51 (Proliferative diabetic retinopathy) discusses its role in documenting the extent and characteristics of neovascularization, fibrous proliferation, and retinal traction. The development of

digital systems capable of high-resolution images immediately accessible to the clinician has expanded the role of fundus photography in clinical practice, facilitating record-keeping, information-sharing among providers, and use of images as a teaching tool with patients.

Fluorescein Angiography

Fluorescein angiography (FA), consisting of photography or videography of the fundus using cameras equipped with appropriate filters following intravenous injection of the hydrocarbon dye fluorescein sodium, has been used clinically in ophthalmology for over 50 years and is described in detail in Chapter 1 (Fluorescein angiography: Basic principles and interpretation). FA has multiple uses in the clinical evaluation of diabetic retinopathy. Because intravenous injection of fluorescein sodium can be associated with life-threatening adverse reactions (with risk of death estimated at approximately 1/200, 000),[88] FA for evaluation of diabetic retinopathy is largely confined to settings in which important aspects of management hinge on the results of the test. FA has been used extensively for evaluation of diabetic retinopathy, and is not known to pose any special hazards in DM. Nephropathy or renal failure is not a contraindication to testing.[89] In NPDR, FA is most commonly indicated for further characterization of DME diagnosed on ophthalmoscopy (Fig. 50.2), and its utility in this setting is discussed below in the section "Clinical evaluation of diabetic macular edema."

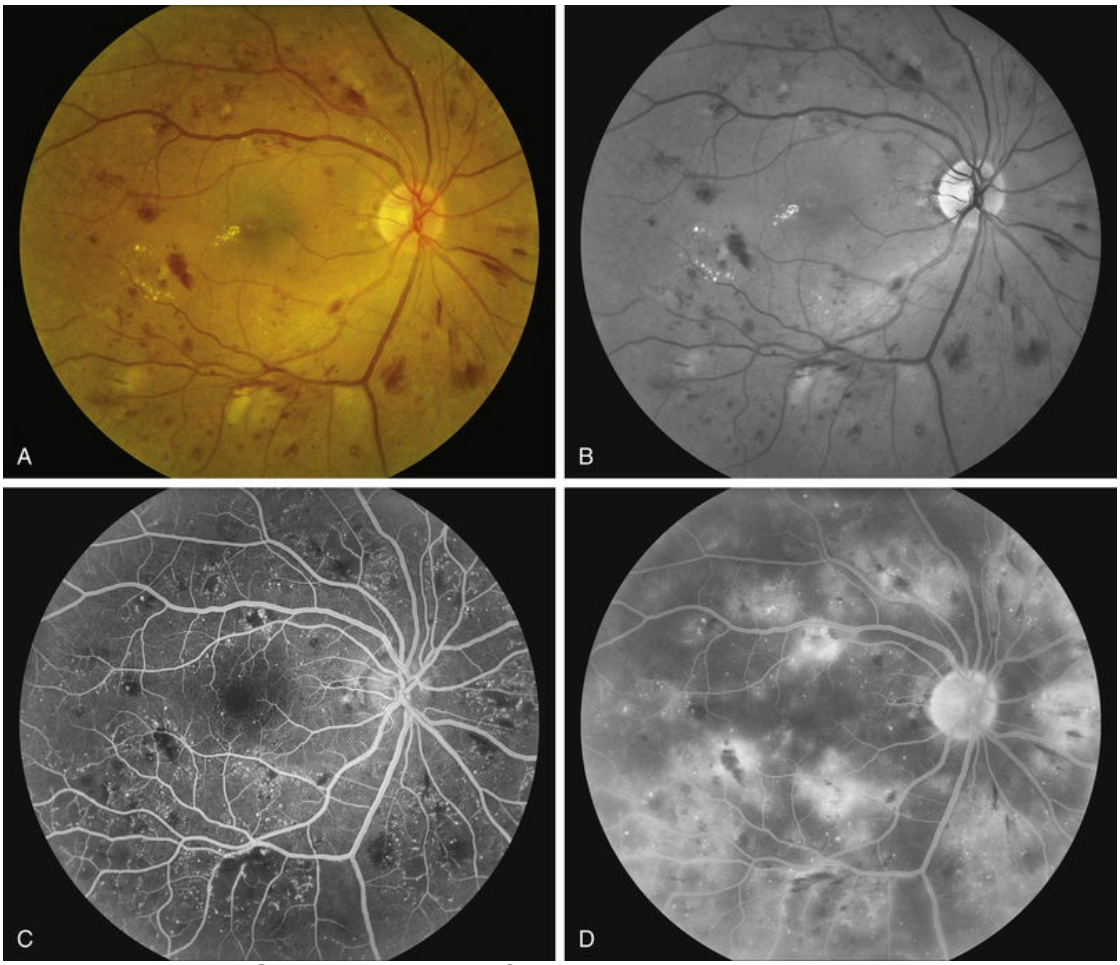

FIG. 50.2 Severe nonproliferative diabetic retinopathy and diabetic macular edema. (A) Color photograph illustrating microaneurysms, intraretinal hemorrhages, cotton-wool spots, and hard exudates. Diffuse, severe retinal thickening, visible with stereoscopic viewing on biomicroscopy, is present. Microaneurysms appear as variably-sized small red dots. Many dot-blot and flame hemorrhages are present, and most can be readily distinguished from microaneurysms by their size and less sharply demarcated borders. Punctate and larger foci of hard exudates appear as yellow-white intraretinal deposits with sharply demarcated borders, most prominent temporal to the fovea. (B) Red-free photograph provides contrast highlighting the abnormalities seen in the color image. (C) Fluorescein angiogram, early frame. Microaneurysms are visible as variably-sized hyperfluorescent dots. Note that angiography allows visualization of microaneurysms not readily seen in the color or red-free photographs. Hemorrhages and hard exudates are hypofluorescent. Significant regions of capillary nonperfusion, visible as

areas where normal, faint, diffuse hyperfluorescence from capillaries is absent, are present outside the macula, bordered in many areas by leaking microvascular abnormalities. (D) Fluorescein angiogram, late frame. Multifocal late leakage is visible as poorly demarcated hyperfluorescence emanating from incompetent retinal capillaries, microaneurysms, and microvascular abnormalities. (National Eye Institute, Bethesda, MD.)

FA can also be used to investigate vision loss incompletely explained by ophthalmoscopy and other less-invasive testing. In some cases, significant capillary nonperfusion involving the fovea and parafovea, best visualized during the arteriovenous transit phase of the angiogram, implicates macular ischemia as a cause for vision loss. In other cases, FA may suggest other causes for vision loss unrelated to diabetic retinopathy.

FA is occasionally used in eyes with presumed NPDR to search for early lesions of extraretinal neovascularization not detected by ophthalmoscopy or fundus photography, such as in cases where preretinal or vitreous hemorrhage suggests PDR, but no cause for bleeding is seen by ophthalmoscopy. The technique in this setting requires a view of the fundus not overly obscured by hemorrhage, and use of either wide-angle lenses or "sweep" fields to image as much of the retina as possible. Its success depends on the prominent leakage of fluorescein dye characteristic of extraretinal neovascularization, typically readily visible against the background of other vascular alterations, but it is important to note that intraretinal alterations such as IRMA can exhibit similar leakage. Sometimes stereoscopic images or further ophthalmoscopy may clarify the extraretinal nature of neovascularization and associated leakage.

Commonly used grading systems for severity of diabetic retinopathy do not consider findings on FA, and FA is not indicated for classification of disease. While FA is a sensitive means for detection of early features of NPDR such as microaneurysms and retinal capillary hyperpermeability, it is not clinically indicated to screen for mild retinopathy.[86]

Optical Coherence Tomography

OCT, which utilizes low-coherence interferometry involving near-infrared light for cross-sectional imaging of intraocular structures, has emerged over the last two decades as a fast, noninvasive means of imaging the retina, vitreoretinal interface, and the retinal pigment epithelium (RPE) in NPDR and other macular diseases. The basic principles of OCT and the applications of this technology to evaluation of the retina are discussed in Chapter 3 (Optical coherence tomography). In NPDR, OCT is commonly used to characterize DME (Fig. 50.3) and abnormalities of the vitreoretinal interface.

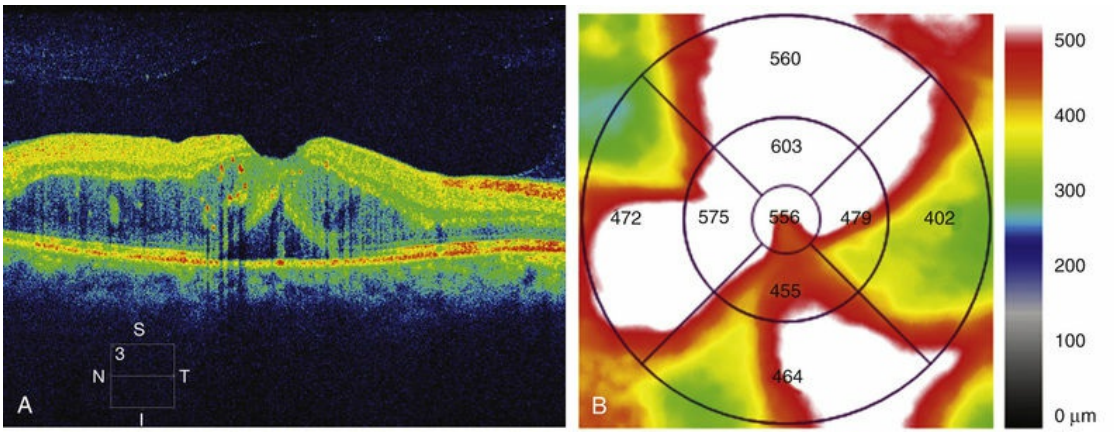

FIG. 50.3 Optical coherence tomography (OCT) characterization of macular thickening in nonproliferative diabetic retinopathy and diabetic macular edema. (A) A 6-mm horizontal line scan obtained with a spectral domain OCT system (Cirrus, Carl Zeiss Meditec) imaging the macula of the eye illustrated in Fig. 50.2 shows severe retinal thickening, with presence of subfoveal subretinal fluid. Punctate juxtafoveal lipid visible in Fig. 50.2 appears as small intraretinal hyperreflective foci just temporal to the fovea. (B) The false-color retinal thickness map generated by automated segmentation of a 6×6 mm 512×128 Macular Cube scan (Cirrus, Carl Zeiss Meditec), with overlay of the standard nine-field grid showing mean thickness values for each subfield. Mean thickness is greater than in 99% of normal eyes in all subfields, based on a comparison to data in the Cirrus normative database. (National Eye Institute, Bethesda, MD.)

The rapid pace of technologic progress, resulting in improvements such as spectral domain imaging and image-registration capability in many systems, makes for substantial variability in image acquisition, processing, and output metrics among presently available OCT platforms. For example, the spectral domain Cirrus OCT (Carl Zeiss Meditec, Dublin, CA), though its output is similar in many ways to that of the time domain Stratus OCT (Carl Zeiss Meditec), uses a distinct automated segmentation algorithm that results in retinal thickness values that are approximately 30–55 μm greater than those reported by the Stratus OCT in eyes with DME.[90] Meaningful interpretation of an OCT scan requires familiarity with the system utilized, including understanding of scan acquisition, indicators of scan quality, processing of raw data, algorithms for automated segmentation, and format of output metrics, as well as knowledge of any normative database used by system software to compare a given set of measurements to a normal range. Caution is warranted in comparing OCT scans obtained using different systems, and clinical researchers using OCT must grapple with such issues in planning studies that require standardization of data among clinical sites.

Techniques being developed for volumetric analysis of blood flow using spectral domain and swept source OCT machines and specialized processing software allow for high-resolution noninvasive imaging of the retinal and choroidal vasculature.[91,92] Preliminary reports testing OCT angiography in eyes with diabetic retinopathy demonstrate the ability to image a subset of microaneurysms, microvascular abnormalities, capillary nonperfusion, and extraretinal neovascularization.[91-93] OCT angiographic images differ in key ways from those obtained using fluorescein angiography (for example, OCT angiography does not assess the vascular incompetence seen as staining and leakage on fluorescein angiography), and current technology is limited by susceptibility to motion artifact, but the techniques offer great promise as a future research and clinical tool for evaluation of diabetic retinopathy.

Investigators of the Diabetic Retinopathy Clinical Research Network (DRCR.net),[94] a collaborative network of over 100 sites in the United States and Canada dedicated to multicenter clinical

research of diabetic retinopathy, have rigorously evaluated OCT as a test yielding measures of macular thickness in diabetic eyes. Most DRCR.net trials to date have been performed using the time domain Stratus OCT and its scanning algorithm known as the fast macular thickness map, which obtains 128 axial scans (A scans) along each of six radial lines (each 6 mm in length) intersecting at a common center, with a total scan time of 1.9 seconds. Recent DRCR.net trials have made use more of the newer spectral domain OCT platforms offering much greater density of A scans with comparable acquisition times. Concurrent use of time domain and spectral domain systems has made it necessary to develop conversion algorithms for comparison of thickness values generated on different OCT platforms,[95] and a recent DRCR.net trial on comparative efficacy of three VEGF antagonists for treatment of DME used conversion of all thickness measurements to time domain-equivalent values for analysis and reporting.[96]

DRCR.net investigators compared thickness of the central subfield of the standard nine-field thickness grid in 97 patients with minimal or no retinopathy and no central macular thickening on examination to normal values in the Stratus OCT database.[97] Results showed no significant difference between central subfield mean thickness of diabetic eyes with minimal or no retinopathy and normal values imputed from nondiabetic individuals in the database, suggesting that the presence of DM is not associated with clinically important changes in central subfield mean thickness in the absence of retinopathy. The study noted a statistically significant difference between central subfield mean thickness in men and women, similar to findings in other reports.

DRCR.net investigators evaluated the reproducibility of OCT in eyes with DME, and established thresholds indicative of meaningful change in retinal thickness. In a prospective multicenter one-day study evaluating diurnal variation of DME, 212 eyes of 107 participants with DME involving the foveal center on biomicroscopy and central subfield mean thickness of 225 μm or greater were imaged multiple times on Stratus OCT and the scans were evaluated by a reading center.[98] Both eyes were imaged six times during the day, and at each of these six sittings a pair of scans was generated, with repeat imaging done for scans of suboptimal

quality. Of a possible 1284 pairs, 1223 were analyzed. Reproducibility was better for central subfield mean thickness than for center-point thickness, not surprising considering that the former incorporates more data points. The median absolute difference between replicate measurements of central subfield mean thickness was 7 μm. Expressed as a percentage difference between the two measurements, the half-width of the 95% CI for a change in central retinal thickness was 10% for eyes with central subfield mean thickness less than 400 μm, and 13% for eyes with central subfield mean thickness equal to or greater than 400 μm. The authors concluded that a change in central subfield mean thickness greater than 11% using the Stratus OCT for DME is likely to be real.

Funduscopic Lesions of Nonproliferative Diabetic Retinopathy

Small or nonperfused microaneurysms may not be discernible on ophthalmoscopy, but those that are visible appear as small deep-red dots between 25 and 100 μm in diameter within the retina (Figs. 50.2A–B and 50.4). Microaneurysms in NPDR typically arise in the posterior pole, but they can also be present in the midperipheral and peripheral retina, particularly in more severe retinopathy. They may be solitary or may appear in clusters. They may remain stable across months or even years, but many eventually disappear. On FA, microaneurysms are visible during arteriovenous transit as hyperfluorescent dots within the retina (Fig. 50.2C). This hyperfluorescence typically persists in later phases of the angiogram, and may or may not be associated with leakage in mid- and late frames (Fig. 50.2D). FA is a sensitive means of detecting microaneurysms and may reveal lesions that were poorly visible or not visible on ophthalmoscopy.

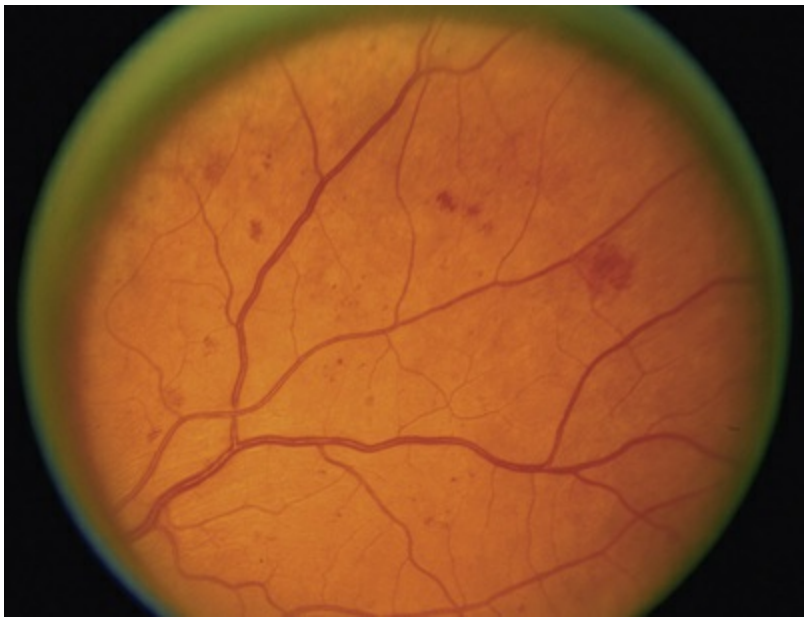

FIG. 50.4 Standard photograph 2A, intermediate standard for hemorrhages/microaneurysms. ETDRS extension of the Modified Airlie House classification of diabetic retinopathy. (Courtesy of the Diabetic Retinopathy Study Research Group.)

Intraretinal hemorrhages in NPDR are variable in appearance, just as in other retinal diseases (Figs. 50.2A–B and 50.4). Dot-blot hemorrhages are typically small with sharply demarcated borders, and are sometimes indistinguishable from microaneurysms on ophthalmoscopy. Flame hemorrhages can be larger and manifest wispy margins as a consequence of their location in the nerve fiber layer. Intraretinal hemorrhages appear hypofluorescent on FA, blocking normal fluorescence from the underlying choroid, and consequently FA offers ready distinction between microaneurysms and hemorrhages (Fig. 50.2C). Intraretinal hemorrhages can be present in the posterior pole and in more peripheral retina, and frequently appear and disappear over weeks or months. Hemorrhages on the optic disc are not typical for diabetic retinopathy and should raise suspicion for neovascularization or a comorbid condition affecting the optic nerve head. Variability in the density of hemorrhages between one sector of the retina and another is common, but striking asymmetry sometimes suggests a superimposed process such as a branch retinal vein occlusion.

Hard exudates are visible on ophthalmoscopy as sharply demarcated yellow–white deposits within the retina (Figs. 50.2A–B

and 50.5). They are visible on OCT line scans as hyperreflective foci within the retina (Fig. 50.3A). With stereoscopic viewing they are readily distinguishable from drusen, which reside external to the retina. Hard exudates are often distributed at the border between edematous and nonedematous retina. They may form a circinate ring around areas of prominent vascular hyperpermeability such as a cluster of microaneurysms. They tend to form in the posterior pole in association with macular thickening, but small collections are sometimes present in more peripheral retina. They are hypofluorescent on FA, blocking underlying choroidal fluorescence (Fig. 50.2C). Hard exudates may appear and disappear over months or years. When severe, they may undergo organization and may cause subretinal fibrosis.

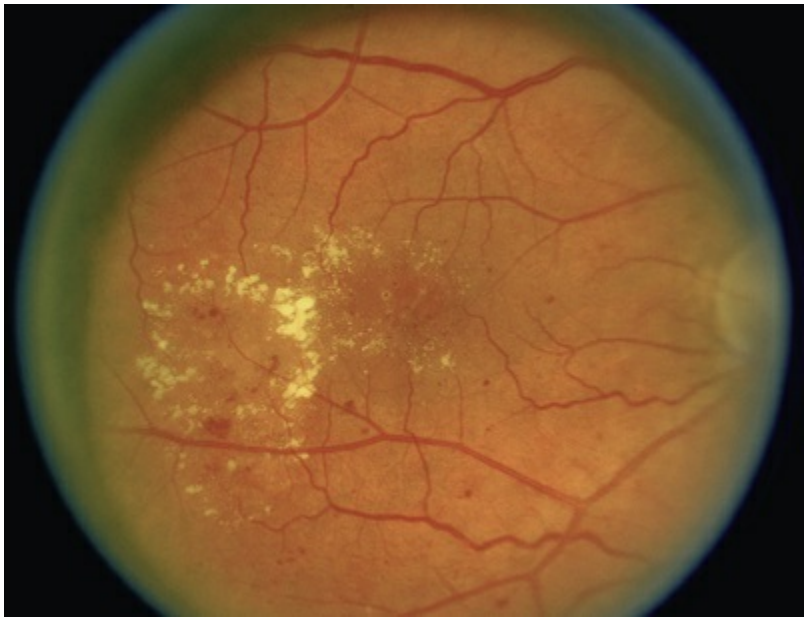

FIG. 50.5 Standard photograph 4, severe standard for hard exudates. ETDRS extension of the Modified Airlie House classification of diabetic retinopathy. Hard exudates in the temporal macula form a circinate ring.
(Courtesy of the Diabetic Retinopathy Study Research Group.)

Cotton-wool spots, patches of relative ischemia affecting the nerve fiber layer of the retina, are visible on ophthalmoscopy as small white patches with wispy borders situated in the inner retina (Figs. 50.2A–B and 50.6). They are hypofluorescent on FA, blocking underlying choroidal fluorescence (Figs. 50.2C–D). They commonly

appear and disappear over weeks or months.

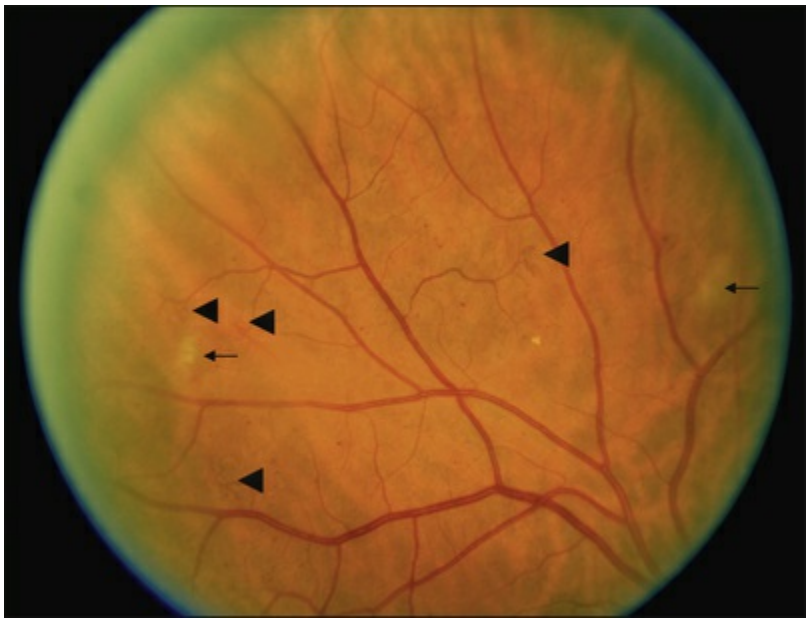

FIG. 50.6 Standard photograph 8A, less severe of two standards for cotton-wool spots and intraretinal microvascular abnormalities (IRMA). ETDRS extension of the Modified Airlie House classification of diabetic retinopathy. Cotton-wool spots are visible in two areas as subtle white patches with wispy borders (*arrows*). Several areas of IRMA are visible as abnormal, tortuous, dilated retinal vessels (*arrowheads*). (Courtesy of the Diabetic Retinopathy Study Research Group.)

The major retinal vessels can exhibit changes in appearance in the setting of advanced retinopathy. Arterioles may appear thin or white. Venules may appear dilated and tortuous. Venous loops are occasionally present. Venous beading consists of localized areas of change in vessel caliber, visible as alternating regions of relative dilation and constriction (Fig. 50.7).

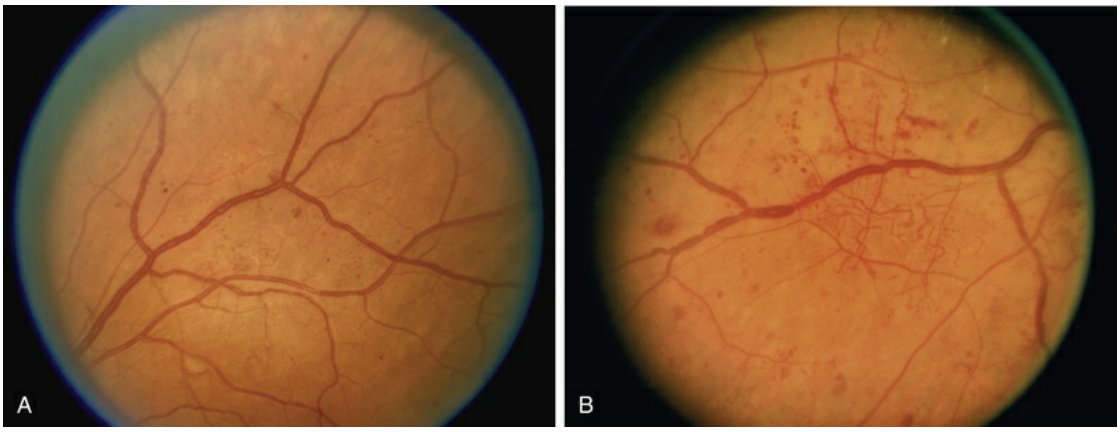

FIG. 50.7 Standard photographs 6A and 6B, less and more severe standards for venous beading. ETDRS extension of the Modified Airlie House classification of diabetic retinopathy. (A) Less severe standard (6A). Two branches of the superior temporal venule show beading that is definite but not severe. (B) More severe standard (6B). Most large and small venule branches show severe beading. (Courtesy of the Diabetic Retinopathy Study Research Group.)

IRMA appear as segments of dilated and tortuous retinal vasculature amidst retinal vessels that are normally too small to be visible on ophthalmoscopy (Fig. 50.6). They are usually readily distinguishable from extraretinal neovascularization on careful biomicroscopy. On FA they appear hyperfluorescent during the arteriovenous transit phase, may leak in later phases, and are often situated at the borders of areas of capillary nonperfusion. They may persist for months or years.

In occasional cases, typical lesions of severe NPDR, such as intraretinal hemorrhages, venous abnormalities, and IRMA, may be sparse or absent in regions of the retina despite profound underlying microvascular alterations poorly visible on ophthalmoscopy. When such areas of "featureless" retina are widespread, the bland appearance may belie the severity of disease. Careful ophthalmoscopy usually reveals manifestations of severe retinal ischemia such as arteriolar narrowing and sheathing, absence of normal vessel markings, and retinal thinning in the setting of an eye at high risk for advanced retinopathy. FA can be used to confirm clinical suspicion when necessary, characteristically revealing widespread capillary nonperfusion in areas of featureless

retina.

Classification of Diabetic Retinopathy

The Diabetic Retinopathy Study, a landmark clinical trial that established the efficacy of scatter laser photocoagulation for reduction of severe vision loss secondary to PDR, used an adaptation of the Airlie House classification of diabetic retinopathy originally developed in 1968.[99] This modified Airlie House system was extended for grading severity of retinopathy in the ETDRS.[100] Grading of retinopathy in the ETDRS involved evaluation of seven-field 30-degree nonsimultaneous stereo color fundus photographs by trained readers. Over 30 characteristics were separately graded, using standard photographs to define thresholds for scoring (see Figs. 50.4–50.7 for some of the standard photographs utilized in the system), and a summary grade was assigned. The ETDRS diabetic retinopathy severity scale was evaluated for its reproducibility as part of the study and was validated as a grading system with prognostic power.[100–102] ETDRS investigators assigned thresholds to define mild NPDR, moderate NPDR, severe NPDR, early PDR, and high-risk PDR (Box 50.1). The 5-year rates of development of high-risk PDR in eyes randomly assigned to deferral of photocoagulation (no laser treatment unless features of high-risk PDR developed) for eyes with mild, moderate, and severe NPDR at baseline were 15.5%, 26.5%, and 56%, respectively.

Box 50.1

Classification of Diabetic Retinopathy in the Early Treatment of Diabetic Retinopathy Study (ETDRS)

Mild NPDR

At least one microaneurysm, AND criteria not met for more severe retinopathy.

Moderate NPDR

Hemorrhages/microaneurysms ≥ standard photograph 2A (Fig. 50.4); AND/OR cotton-wool spots, venous beading, or IRMA

definitely present; AND criteria not met for more severe retinopathy

Severe NPDR

Cotton-wool spots, venous beading, and IRMA definitely present in at least two of photographic fields 4–7; OR two of the three preceding features present in at least two of fields 4–7 and hemorrhages/microaneurysms present in fields 4–7 ≥ standard photograph 2A (Fig. 50.4) in at least one of them; OR IRMA present in each of fields 4–7 and ≥ standard photograph 8A (Fig. 50.6) in at least two of them; AND criteria not met for more severe retinopathy.

Early PDR

New vessels; AND criteria not met for high-risk PDR.

High-risk PDR

New vessels on or within one disc diameter of the optic disc (neovascularization of the disc [NVD]) ≥ standard photograph 10A (approximately $\frac{1}{4}$–$\frac{1}{3}$ disc area) with or without vitreous or preretinal hemorrhage; OR vitreous and/or preretinal hemorrhage accompanied by new vessels, either NVD < standard photograph 10A or new vessels elsewhere (NVE) ≥ $\frac{1}{4}$ disc area.

IRMA, intraretinal microvascular abnormalities;; NPDR, nonproliferative diabetic retinopathy; PDR, proliferative diabetic retinopathy.

Grading and classification of retinopathy in the ETDRS involved evaluation of modified Airlie House seven-field 30° nonsimultaneous stereo color fundus photographs by trained readers. Photographic fields 4 and 6 image superior retina and are tangential to both a vertical line through the center of the optic disc and a horizontal line crossing its superior border. Photographic fields 5 and 7 image inferior retina and are tangential to both a vertical line through the center of the optic disc and a horizontal line crossing its inferior border. A set of standard photographs was

used to define thresholds for grading and classification (see Figs. 50.4–50.7 for some of the standard photographs utilized in the system).

The prognostic utility of a 1-step or a 2-or-greater-step progression in the ETDRS diabetic retinopathy severity scale has been evaluated using data from the WESDR.[103] Findings indicated that 1-step or 2-or-greater-step worsening in level of retinopathy over 4 years strongly predicted the development of PDR during the subsequent 6 years. The ETDRS diabetic retinopathy severity scale remains the standard for photographic grading of retinopathy in clinical trials. The schema is impractical for routine clinical use because of its complexity and its basis in photographic – not ophthalmoscopic – assessment of the fundus, but the ETDRS definitions for mild, moderate, and severe NPDR and early and high-risk PDR were incorporated into clinical practice. A 4–2–1 rule was popularized to simplify the definition of severe NPDR.[104] Upon examination of the four midperipheral quadrants of the retina, the presence of any one of the following features was considered sufficient for diagnosis of severe NPDR (in the absence of evidence for PDR): (1) severe intraretinal hemorrhages and microaneurysms in all *four* quadrants (≥ standard photograph 2A; Fig. 50.4); (2) venous beading in *two* or more quadrants; or (3) moderate IRMA in at least *one* quadrant (≥ standard photograph 8A; Fig. 50.6). If any two of these features were present, the retinopathy was considered very severe. It is worth pointing out that the 4–2–1 rule uses a threshold for definition of severe NPDR inclusive of milder retinopathy than the definition of severe NPDR used in the ETDRS.

In answer to the need for a simplified classification of diabetic retinopathy to facilitate communication among clinicians worldwide, the Global Diabetic Retinopathy Project Group published proposed International Clinical Diabetic Retinopathy and Diabetic Macular Edema Severity Scales in 2003 (Table 50.1).[105] The classification was developed using evidence from studies such as the ETDRS and WESDR to draw distinctions in retinopathy severity most important for prognosis and management, and approximates the definitions used in the ETDRS.

TABLE 50.1

Disease Severity Scales for Diabetic Retinopathy and Diabetic Macular Edema

Proposed Disease Severity Level	Findings Observable on Dilated Ophthalmoscopy
No apparent retinopathy	No abnormalities
Mild NPDR	Microaneurysms only
Moderate NPDR	More than just microaneurysms but less than severe NPDR
Severe NPDR	One or more of the following, in the absence of PDR: More than 20 intraretinal hemorrhages in each of four quadrants Definite venous beading in two or more quadrants Prominent IRMA in one or more quadrants
PDR	One or more of the following: Extraretinal neovascularization Vitreous or preretinal hemorrhage Extraretinal neovascularization
No apparent DME	No retinal thickening or hard exudates in the posterior pole
Mild DME	Some retinal thickening or hard exudates in the posterior pole, distant from the center of the macula
Moderate DME	Retinal thickening or hard exudates near the center of the macula but not involving the center
Severe DME	Retinal thickening or hard exudates involving the center of the macula

DME, diabetic macular edema; IRMA, intraretinal microvascular abnormalities; NPDR, nonproliferative diabetic retinopathy; PDR, proliferative diabetic retinopathy.

DME is defined as retinal thickening, assessed by stereoscopic evaluation of the fundus by slit-lamp biomicroscopy or assessment of photographs. Hard exudates are a sign of present or past retinal thickening.

Adapted with permission from Wilkinson CP, Ferris FL 3rd, Klein RE, et al. Proposed international clinical diabetic retinopathy and diabetic macular edema disease severity scales. Ophthalmology 2003;110:1677–82.

Clinical Evaluation of Diabetic Macular Edema

Clinical evaluation of DME involves consideration of a number of features relevant to prognosis and treatment. Careful assessment of pertinent systemic factors, underlying retinopathy severity, and coexisting ocular conditions (cataract, glaucoma, history of intraocular surgery, etc.), as previously outlined above, supplements the characterization of DME discussed below.

Distribution of Retinal Thickening and Hard Exudates

The ETDRS defined clinically significant macular edema (CSME) as any of the following noted on biomicroscopy: (1) thickening of the retina at or within 500 μm of the center of the macula; (2) hard exudates at or within 500 μm of the center of the macula, if associated with thickening of the adjacent retina (not residual hard exudates remaining after the disappearance of retinal thickening); or (3) a zone or zones of retinal thickening one disc area or larger, any part of which is within one disc diameter of the center of the macula.[38]

The definition for CSME was based on observation that retinal thickening or hard exudation involving or threatening the fovea frequently leads to vision loss. Careful assessment of the distribution of retinal thickening and hard exudates and their relation to the center of the macula remains paramount to management of DME. Severity of DME in the International Clinical Diabetic Macular Edema Disease Severity Scale is based solely on whether retinal thickening and hard exudates involve or threaten the center of the macula, reflecting the importance of foveal involvement for prognosis and management.[105]

While diagnosis on biomicroscopic examination remains the clinical standard for detection of DME, OCT is now routinely used as a fast and noninvasive tool to quantitatively map areas of macular thickening (Fig. 50.3). Subtle changes in distribution of thickening over time and relationship to the fovea can be documented with good-quality scans that serially image the same region of the macula. The standardization afforded by OCT has proven valuable in clinical practice and in research. Hard exudates can be visualized on OCT as hyperreflective foci within the retina (Fig. 50.3A), but biomicroscopic examination and fundus photography remain important to document their extent and proximity to the fovea (Figs. 50.2A–B).

Magnitude of Retinal Thickening

The degree of thickening at any given point in the retina has

traditionally been estimated on biomicroscopy and stereoscopic photographs, but OCT has emerged as a superior means of quantifying retinal thickness. The sensitivity of OCT for retinal thickening exceeds that of contact lens-assisted biomicroscopy performed by experienced examiners.[106] Correlation between the estimated degree of retinal thickening at the center of the macula on stereoscopic photographs and the center point thickness measured on time domain OCT is modest, reflecting the limitations of grading retinal thickness on photographs.[107]

OCT processing yields several metrics useful in characterizing the thickness of the retina in DME. Central subfield mean thickness, inner and outer subfield mean thicknesses, and macular volume for the standard nine-field thickness grid are readily generated from the scanning and segmentation algorithms available on various OCT machines. A DRCR.net study concluded that central subfield mean thickness is well-suited as a metric for central macular thickness in clinical research, with high reproducibility and good correlation to other measures in the setting of DME.[108] Mean thickness in other subfields and total macular volume are useful in assessing extrafoveal macular edema.

OCT is capable of detecting areas of subtle macular edema that are sometimes not suspected on ophthalmoscopy. Easy detection of such "subclinical" thickening has added a new and provocative facet to management of DME, challenging clinicians to incorporate knowledge of more mild pathology into clinical decision-making. Conversely, OCT can illustrate areas of retinal thinning that sometimes result from advanced retinopathy, and the possibility of such underlying tissue loss should be kept in mind when assessing the magnitude of any superimposed DME.

Retinal Microvascular Alterations and Vascular Hyperpermeability

Findings on ophthalmoscopy may suggest areas of vascular incompetence or retinal ischemia responsible for macular edema. For example, a circinate lipid ring may imply leakage from a particular cluster of microaneurysms, or intraretinal microvascular abnormalities may highlight the borders of a region of capillary

closure. But more definitive information about the extent of microvascular alterations and any associated vascular hyperpermeability can be gained using FA. Stereoscopic images are sometimes helpful, allowing visualization of areas of retinal thickening and localization of angiographic features to various depths within or external to the retina.

The retinal microvasculature and any areas of capillary nonperfusion are best imaged in the arteriovenous transit phase of the angiogram. Microaneurysms and microvascular abnormalities, sometimes unsuspected on ophthalmoscopy, are readily visualized (Figs. 50.2C–D). The absence of normal hyperfluorescence from capillaries in a region where they should usually exist indicates capillary nonperfusion on an angiogram of sufficient image quality (Fig. 50.2C). Areas of foveal capillary nonperfusion manifest as an abnormally large foveal avascular zone or as irregularity in the borders of this region. Unfortunately, visualization of capillary nonperfusion requires resolution near the limit of present camera systems, and even slight decreases in image quality (such as from poor focus or cataract) can impair assessment. The retina in areas of capillary nonperfusion may be edematous, normal thickness, or thin.

FA is useful in evaluating retinal vascular competence, illustrating areas of hyperpermeability where dye leaks into the extravascular space (Fig. 50.2D). Fluorescein leakage may emanate from discrete microaneurysms or microvascular abnormalities visible on the angiogram, or it may accumulate in areas of diffuse retinal capillary incompetence. Microaneurysms, microvascular abnormalities, and capillary telangiectasis visualized in the early phase of the angiogram can exhibit progressive leakage best appreciated in later phases, between 5 and 10 minutes after injection of dye. Fluorescein leakage may be present in a region of the retina that is edematous, normal thickness, or thin, and is therefore not synonymous with macular edema. However, ETDRS investigators and others have demonstrated correlation between area of fluorescein leakage and extent of retinal thickening on stereoscopic photographs and OCT.[109–111]

Traction by Vitreous Gel and Epiretinal

Proliferation

Macular edema can occur secondary to traction exerted by cortical vitreous gel and epiretinal membranes at points of attachment to the retina. In some cases retinal thickening may result solely from the mechanical forces transmitted to the retina, without significant secondary alterations in vascular permeability. Macular edema in such cases can result from traction even in the absence of retinal vascular leakage demonstrable by FA. In other cases, mechanical traction may exert an effect on the competence of retinal capillaries. Macular edema in these cases results from the combined effects of mechanical distortion and retinal microvascular leakage. Complicating clinical assessment of the role of mechanical traction in diabetic eyes is the backdrop of microvascular alterations present as a consequence of the metabolic disease. The clinician is faced with presence of macular edema, a visible hyaloid or epiretinal membrane with attachment to the retina, and a pattern of retinal vascular leakage on FA, and must judge how significant a role the membrane plays in the retinal thickening and vascular leakage.

In some cases, findings on biomicroscopy, OCT, and FA strongly suggest a tractional component to macular edema (Fig. 50.8). A thickened posterior hyaloid membrane or epiretinal membrane with attachment in the area of macular edema, with or without retinal striae, may be visible on biomicroscopic examination. OCT may show a hyaloid or epiretinal membrane stretched taut over an area of retinal thickening. This membrane may appear uniformly attached to the retina or may show multiple points of focal attachment, the latter frequently associated with focal corrugations of the inner aspect of the retina. The region of macular edema may correspond closely with the area in which the membrane has attachment to the retina, and retina outside this area of attachment may be uninvolved, with an appreciable step-off in thickness at the borders of membrane attachment. Fluorescein leakage, if present, may arise diffusely from telangiectatic retinal capillaries in the region of macular edema. These features are similar to those seen in vitreomacular traction in the setting of incomplete posterior vitreous separation or epiretinal membrane formation with macular edema in nondiabetic eyes.

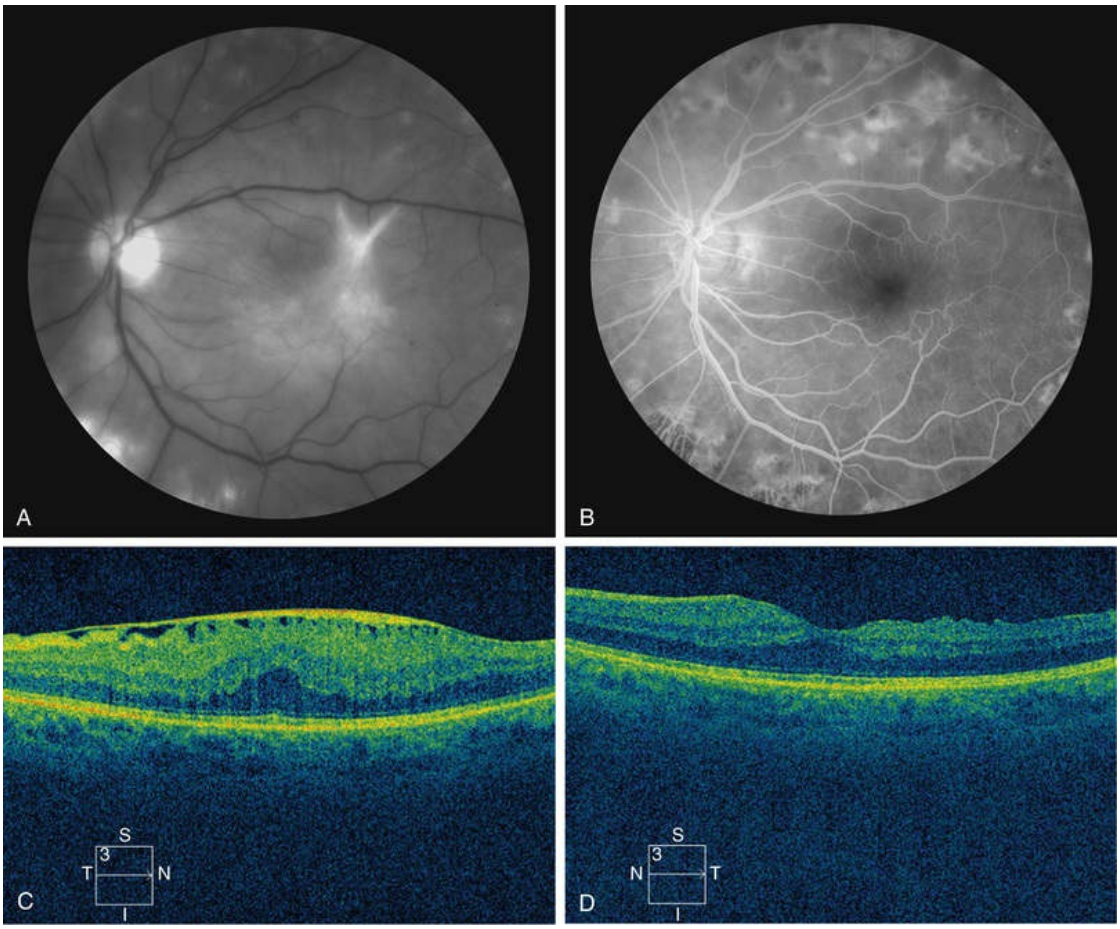

FIG. 50.8 Macular edema predominantly secondary to vitreomacular traction and epiretinal proliferation. (A) A photograph of the left macula shows a thick epiretinal membrane in a 61-year-old woman with history of proliferative diabetic retinopathy treated with scatter laser photocoagulation. Retinal striae are visible in the nasal macula. There was no visible separation of the posterior hyaloid on biomicroscopy. Visual acuity measured 20/80. (B) An early frame of the fluorescein angiogram shows relatively mild microvascular alterations with only occasional microaneurysms. Later frames (not pictured) showed only very mild diffuse leakage from capillaries. (C) An optical coherence tomography (OCT) 6-mm horizontal line scan through the foveal center shows presence of a thick epiretinal membrane with multiple focal attachments to the retina, resulting in a corrugated appearance to the inner retinal surface. Severe noncystic central thickening is present. (D) A corresponding OCT line scan following vitrectomy with membrane peeling shows relief of traction and near-resolution of retinal thickening. Intraoperative medications included

subconjunctival dexamethasone and cefazolin and postoperative medications included topical prednisolone acetate 1% and moxifloxacin. No laser photocoagulation was performed. Visual acuity improved to 20/40. (National Eye Institute, Bethesda, MD.)

In other cases, a posterior hyaloid or epiretinal membrane visible on ophthalmoscopy or OCT may not appear to exert a predominant mechanical effect on the retina, and findings may suggest that retinal microvascular alterations from the metabolic disease are responsible for macular edema (Fig. 50.9). A subtle glistening of the vitreoretinal interface on biomicroscopy may reveal the presence of the membrane, or the membrane may only be visible on OCT. A membrane visible on OCT may parallel the contour of the inner aspect of the retina with areas of attachment, but without any corrugated distortion of the inner retina or retinal striae visible on biomicroscopy. The area of macular edema may exhibit a gradually tapering convexity, with or without presence of cysts, without any abrupt step-off to noninvolved areas at its borders. Biomicroscopy may show discrete microaneurysms in the area of macular edema, and FA may show areas of focal leakage from such microaneurysms or other microvascular abnormalities. Incomplete posterior vitreous separation or epiretinal membrane formation in the absence of retinal distortion or thickening in nondiabetic eyes is often compatible with normal vision. Such membranes, when present in eyes with DME, may be incidental to the macular edema associated with the retinopathy.

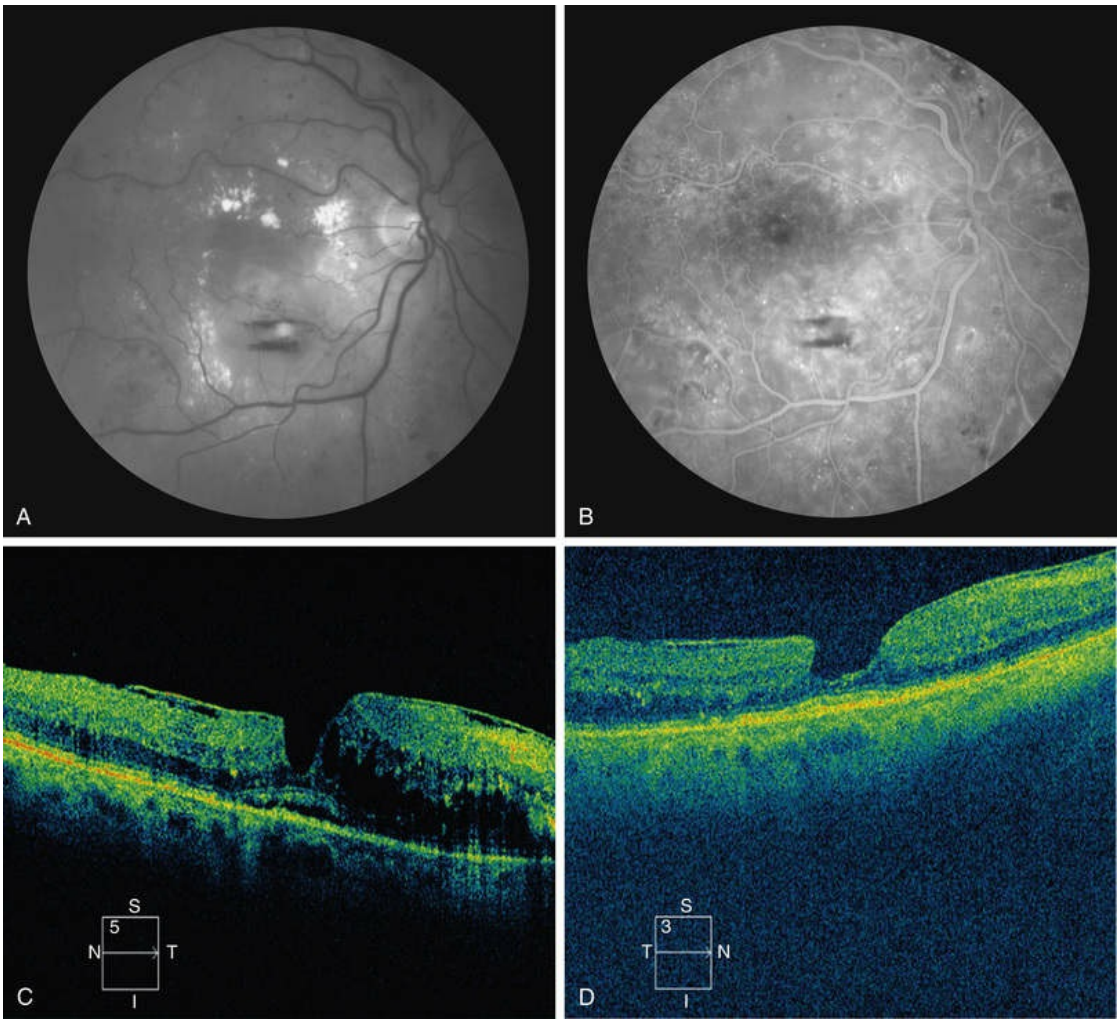

FIG. 50.9 Macular edema predominantly secondary to retinal vascular alterations from diabetes mellitus, with presence of an epiretinal or posterior hyaloid membrane exerting only mild mechanical effects. (A) A photograph of the right macula shows microaneurysms, intraretinal hemorrhages, cotton-wool spots, and hard exudates in a 74-year-old woman with severe nonproliferative diabetic retinopathy. There is no visible epiretinal membrane or retinal striae formation. Visual acuity measured 20/50. (B) An early frame of the fluorescein angiogram shows extensive vascular alterations, including presence of microaneurysms, patches of capillary nonperfusion, and microvascular abnormalities. Later frames (not pictured) showed severe leakage, most prominent in the areas of greatest retinal thickening inferonasal to the fovea. (C) An optical coherence tomography (OCT) 6-mm horizontal line scan through the foveal center shows presence of severe retinal thickening nasal to the fovea and mild retinal thickening temporal to the

fovea, with presence of intraretinal cysts and scant subfoveal fluid. A thin epiretinal or posterior hyaloid membrane is present nasal and temporal to the foveal center. There is minimal distortion of the inner retinal surface, except at the temporal margin of the foveal depression, where an abrupt step-off in thickness suggests a local mechanical effect. (D) A corresponding OCT line scan 2 years later following treatment with multiple sessions of focal/grid laser photocoagulation, one bevacizumab injection, and one subtenon triamcinolone acetonide injection shows significant improvement in retinal thickening, with resolution of intraretinal cysts and subretinal fluid. Persistence of an abrupt step-off of the inner retinal surface at the temporal margin of the foveal depression suggests a mild local mechanical effect. No vitrectomy was performed. (National Eye Institute, Bethesda, MD.)

In many eyes with a visible membrane and at least some evidence for mechanical distortion of the retina, macular edema may result from a combination of tractional effects and microvascular alterations associated with the diabetic retinopathy. It may be unclear which factor predominates, and in such cases, evaluation across time can be helpful. In clinical practice, this often involves treatment of macular edema, starting with less-invasive nonsurgical approaches, with careful assessment of the response to treatment.

Alterations in the Retinal Pigment Epithelium

In most eyes with untreated DME, the RPE appears normal on ophthalmoscopy, OCT, and FA. Longstanding macular edema is occasionally accompanied by pigmentary alterations or atrophy of RPE. More commonly, RPE changes reflect stigmata of previous laser photocoagulation in eyes previously treated for DME (Fig. 50.10A). Visualization of discrete laser scars on FA, not always visible on ophthalmoscopy, allows assessment of the adequacy and extent of past treatment and can be helpful in planning further therapy (Fig. 50.10B). Autofluorescence imaging has recently emerged as a less invasive means of evaluating such RPE alterations and may largely supplant angiography for this application in DME (Fig. 50.10C).[112,113]

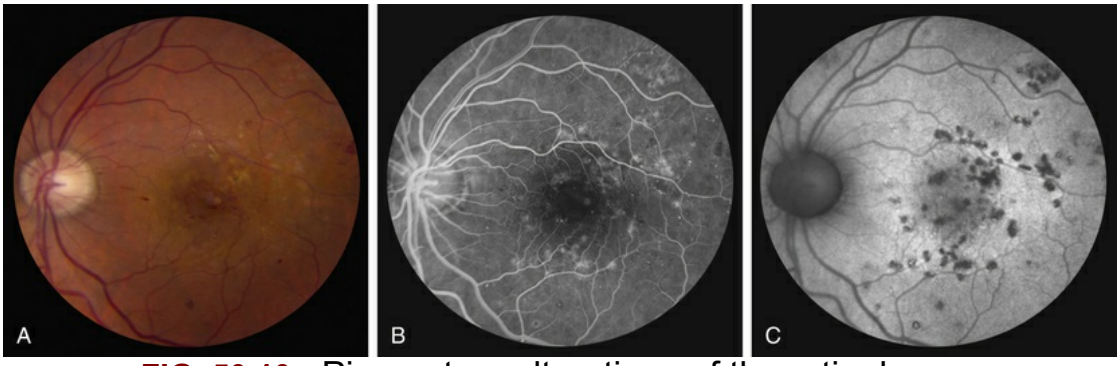

FIG. 50.10 Pigmentary alterations of the retinal pigment epithelium (RPE) secondary to laser photocoagulation. (A) Color photograph showing scattered microaneurysms and intraretinal hemorrhages in the setting of nonproliferative diabetic retinopathy and diabetic macular edema previously treated with focal/grid laser photocoagulation, with focal hypo- and hyperpigmented alterations of the RPE most prominent superotemporal to the fovea. (B) An early frame of the fluorescein angiogram (FA) shows multiple circular spots of hyperfluorescence, some with hypofluorescent centers, corresponding to laser scars. Note that more laser scars are visible on the FA than on the color photograph. (C) A fundus autofluorescence photograph (modified fundus camera, single-flash, 580/700 nm) demonstrates circular spots of hypofluorescence, some with hyperfluorescent centers, corresponding to the same laser scars visualized by FA. Intraretinal hemorrhages also appear hypofluorescent. (National Eye Institute, Bethesda, MD.)

Subretinal Fibrosis

Subretinal fibrosis is an uncommon feature of DME associated with severe hard exudates or disruption of the RPE by overaggressive laser treatment. In the ETDRS, investigators identified 109 eyes with subretinal fibrosis, defined as a mound or sheet of gray-to-white tissue beneath the retina at or near the center of the macula.[114] Very severe hard exudates were present in the macula of 74% of these eyes prior to appearance of subretinal fibrosis; by comparison, exudates this severe were seen only in 2.5% of eyes with CSME that did not develop subretinal fibrosis ($p<.001$). Among 264 eyes with

very severe hard exudates in the macula at any time during the ETDRS, subretinal fibrosis developed in 31%, while among 5498 eyes with CSME and lesser levels of hard exudation, such fibrosis developed in only 0.05%. In the 4823 eyes that underwent laser photocoagulation for treatment of DME, only 9 eyes developed subretinal fibrosis adjacent to a laser photocoagulation scar, making this at worst a rare complication of such treatment.

Visual Acuity and Its Correlation to Retinal Thickening and Fluorescein Leakage

Retinal thickening that involves or threatens the fovea frequently leads to vision loss. In the ETDRS, the 3-year risk of moderate vision loss was 32% among eyes observed with CSME.[38] However, studies have shown variable but generally modest correlation between central retinal thickness and concurrently measured visual acuity.[115–122] In one study of 251 eyes of 210 participants in a randomized clinical trial evaluating laser techniques, in which vision was tested with an electronic ETDRS protocol following standardized refraction and central retinal thickening was measured using time domain OCT and evaluated by a reading center, the correlation between visual acuity and center-point thickness was 0.52 at the baseline time point (Fig. 50.11).[123] The slope of the corresponding best-fit line was 4.4 letters (95% CI 3.5–5.3) of better visual acuity for every 100 μm decrease in center point thickness.

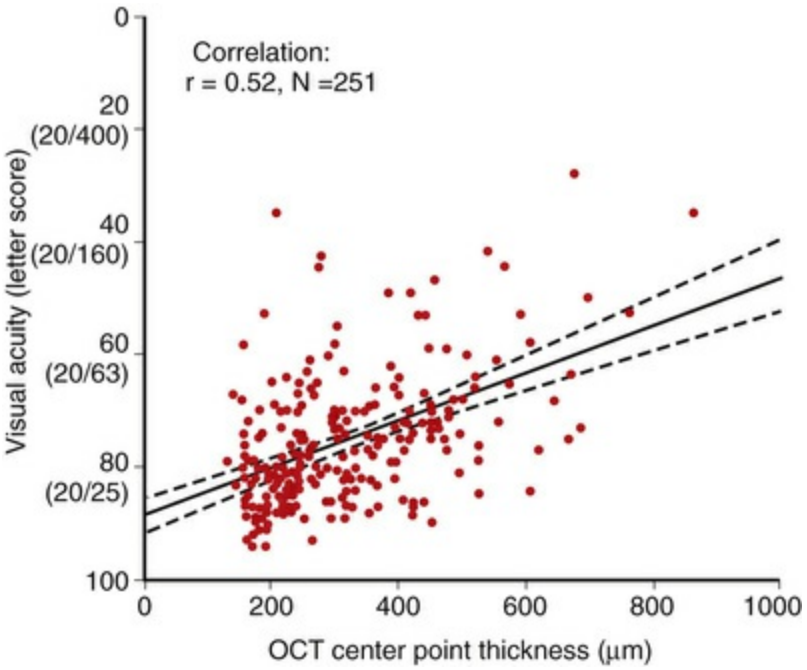

FIG. 50.11 Scatterplot comparing concurrently measured optical coherence tomography center point thickness and visual acuity at a single timepoint (baseline) in 251 eyes (210 participants) with diabetic macular edema in a randomized clinical trial evaluating laser techniques. The solid line represents the regression line and the dotted lines represent the 95% CI for the mean. (Adapted with permission from Diabetic Retinopathy Clinical Research Network. Relationship between optical coherence tomography-measured central retinal thickness and visual acuity in diabetic macular edema. Ophthalmology 2007;114:525–36.)

Fluorescein leakage on FA has low correlation with concurrently measured visual acuity. Among 422 eyes (a mix of study and nonstudy eyes) of participants in the randomized clinical trial evaluating laser techniques mentioned previously, the area of fluorescein leakage within an ETDRS macular grid was graded at baseline and correlated to several other baseline measures.[110] Correlation of the area of fluorescein leakage with visual acuity was 0.33, compared with a value of 0.38 for OCT central subfield mean thickness and 0.58 for OCT total macular volume.

Diurnal Variation of DME

On average, retinal thickness in DME decreases slightly during the day, but the proportion of eyes with DME exhibiting clinically

meaningful changes is small. In the largest study to date, 156 eyes of 96 participants with center-involved DME on ophthalmoscopy and central subfield mean thickness of 225 μm or greater were evaluated at six time points between 8 am and 4 pm using the Stratus OCT.[124] Two scans of adequate quality were obtained at each time point and sent to a reading center. The mean change in relative central subfield thickening, defined to represent the change in excess retinal thickness, was a decrease of 6% (95% CI −9% to −3%) between the 8 am and 4 pm time points. The mean absolute change was a decrease in 13 μm (95% CI −17 to −8 μm). Three percent (5 of 156) of eyes met a composite endpoint of 25% or greater decrease in relative central subfield thickening and 50 μm or greater decrease in central subfield mean thickness at two consecutive time points, and 1% (2 of 156) of eyes exhibited increases in both measures by at least these amounts.

Management of Nonproliferative Diabetic Retinopathy and Diabetic Macular Edema

Modification of Systemic Risk Factors

Control of hyperglycemia is critical to minimizing risk of onset and progression of diabetic retinopathy. The benefits of better glycemic control for reducing risk of retinopathy progression have been demonstrated in multiple randomized controlled clinical trials, including the DCCT, EDIC study, UKPDS, and ACCORD study mentioned previously and further discussed in Chapter 47 (The epidemiology of diabetic retinopathy).[66,67,69,70,72,73] The American Diabetes Association recommends glycemic control targeting a hemoglobin A1C of 7.0% or lower for most people with DM.[125] Not only does such a target lower risk of retinopathy onset and progression, it also lowers risk of other microvascular complications of disease, such as neuropathy and nephropathy. The ACCORD study has provoked debate about whether more aggressive targeting of near-normal hemoglobin A1C values is desirable.[126,127] As discussed earlier, the ACCORD study included a

trial that randomly assigned 10,251 patients with type 2 DM to intensive glycemic control targeting HbA1C of less than 6% or to standard treatment targeting HbA1C between 7% and 7.9%. The glycemia trial was stopped after a median of 3.7 years because of an increase in all-cause mortality in the intensive treatment group (5% in the intensive treatment group versus 4% in the standard treatment group; hazard ratio 1.21; 95% CI 1.02–1.44).[128] Rates of hypoglycemia requiring assistance were significantly higher in the intensive treatment group than in the standard treatment group (10.5% vs. 3.5%; *p*=.001), corroborating similar findings among intensively treated participants in other clinical trials of glycemic control, but the higher mortality rate noted in participants in the ACCORD study could not be readily attributed to complications of hypoglycemia. Despite evidence that aggressive targeting of near-normal glycosylated hemoglobin levels may offer benefit in reducing microvascular complications of DM, there is consensus that such an approach should be pursued cautiously based on the mortality findings of the ACCORD study.[125]

Control of hypertension is also beneficial in lowering risk of progression of diabetic retinopathy, as demonstrated in the UKPDS.[68,74] Hypertensive participants with newly diagnosed type 2 DM in the UKPDS were randomly assigned to more intensive blood pressure control (targeting a systolic blood pressure less than 150 mmHg) and less intensive blood pressure control (targeting a systolic blood pressure less than 180 mmHg) and also randomly assigned to treatment with beta blockers or ACE inhibitors. The UKPDS showed benefit of better control of blood pressure, as discussed previously. The ACCORD study, which included a blood pressure trial that randomly assigned participants to more or less intensive control of blood pressure (targeting a systolic blood pressure less than 120 mmHg or less than 140 mmHg, respectively), did not show benefit in reducing risk of retinopathy progression in a subset of participants evaluated for eye disease.[72] While provocative, the results of the ACCORD study do not necessarily contradict the findings of the UKPDS, given the very different targets used for more and less intensive control of blood pressure between the two trials. It is possible that modest control of severe hypertension (as done in the UKPDS) lowers retinopathy

progression, while very aggressive lowering of blood pressure below present standard of care (as done in the ACCORD study) lends no additional benefit. Alternatively, the disparity in findings could be attributable to differences in the study populations.

Treatment of dyslipidemia may be beneficial to retinopathy, based on consideration of observational data from studies like the WESDR and the ETDRS.[75,76] However, there is no evidence from randomized controlled clinical trials that plasma lipid-lowering reduces risk of retinopathy onset or progression, largely because persons with dyslipidemia need to lower their lipid levels to reduce the risk of cardiovascular disease, making such trials difficult or impossible. The ACCORD study, together with another randomized controlled clinical trial called the Fenofibrate Intervention and Event Lowering in Diabetes (FIELD) study, suggests a possible role for fenofibrate in reducing risk of retinopathy progression, but it is unclear whether the mechanism of action involves alteration of the plasma lipid profile.[72,78] Fenofibrate is discussed further below as a potential systemic treatment for diabetic retinopathy.

Retinopathy Screening and Surveillance

Sight-threatening retinopathy may not cause symptoms prompting evaluation until disease is advanced. Treatment to reduce risk of vision loss in eyes with sight-threatening complications of diabetic retinopathy is most effective when initiated before severe vision loss has occurred. These facts underpin the importance of screening and surveillance for retinopathy, but reports suggest that many people with DM do not receive eye examination on the schedule recommended by organizations such as the American Diabetes Association and the American Academy of Ophthalmology.[86,129–133] For example, an analysis of Medicare claims data for beneficiaries with DM 65 years of age and older revealed that only between 50% and 60% received annual eye examinations over a 15-month period.[131] In many less-developed countries the situation is much worse, with only a small fraction receiving any eye evaluation at all.

The recommended schedule for screening and surveillance for NPDR reflects knowledge about the epidemiology and natural

history of disease. Initial eye examination is recommended 5 years following diagnosis of type 1 DM, and at time of diagnosis for those with type 2 DM.[86] Recommended follow-up examination for persons with type 1 and type 2 DM with no retinopathy is yearly. In the absence of DME, those with mild to moderate NPDR should be evaluated every 6–12 months, and those with severe NPDR should be seen every 2–4 months. Patients with DME merit frequent follow-up, generally at least every 2–4 months, and sometimes monthly depending on treatment. Any new ocular symptoms should prompt timely evaluation tailored to the circumstances.

In the setting of pregnancy, eye examinations are recommended prior to conception and early during the first trimester.[86] Follow-up for pregnant patients with no retinopathy, mild NPDR, or moderate NPDR should be individualized based on the severity and recent changes in retinopathy. Pregnant patients with severe NPDR should be evaluated every 1–3 months. Specific circumstances, such as presence of DME, may dictate need for more frequent follow-up.

A comprehensive eye evaluation, including dilated funduscopic examination by an ophthalmologist experienced in management of diabetic eye disease, remains the standard of care for retinopathy screening in areas with adequate access to ophthalmic care. However, as imaging and information-sharing technologies continue to improve, remote screening for diabetic retinopathy, such as review of digital fundus photographs acquired outside the ophthalmologist's office, may offer a cost-effective alternative. In such a model, patients manifesting findings indicative of a certain level of retinopathy and patients for whom adequate images cannot be obtained are referred to an ophthalmologist for full evaluation.[134] A number of large telemedicine initiatives for assessment of diabetic retinopathy, including a project in the Department of Veterans Affairs medical system in the United States and programs carried out on a nationwide scale in Great Britain, have demonstrated improved screening rates in targeted populations, and have provided preliminary evidence for feasibility, benefit, and cost-effectiveness.[134–138] A number of studies have reported the sensitivity and specificity of various remote screening platforms compared with the standard of dilated funduscopic examination by an ophthalmologist or expert evaluation of seven-field fundus

photographs obtained by an ophthalmic photographer.[139–145] Ultra-wide field scanning laser ophthalmoscopic imaging and improved OCT technologies show particular promise for sensitive detection of retinopathy and DME with nonmydriatic testing.[138,146,147] The ultimate success of the telemedicine approach hinges not only on a suitable imaging platform, but on a host of elements such as validated systems for data acquisition and analysis, appropriate quality metrics and controls, a sustainable economic model for implementation, and a referral system with resources adequate for management of identified cases.[138]

Ocular Treatment for Diabetic Macular Edema

Treatment paradigms for DME have evolved considerably over the last several years, in the setting of a number of pivotal clinical trials demonstrating safety and efficacy of several locally administered drugs for this indication. Intravitreous injection of medications inhibiting the activity of vascular endothelial growth factor A (VEGF-A) isoforms has recently supplanted focal/grid laser photocoagulation as first-line treatment for many eyes with DME involving the foveal center.[86] The results of clinical trials testing bevacizumab (Avastin, Genentech), ranibizumab (Lucentis, Genentech), and aflibercept (Eylea, Regeneron Pharmaceuticals) demonstrate visual acuity gains superior to those achieved with focal/grid laser photocoagulation, with low rates of treatment complications.[96,148–152] In 2012, the US Food and Drug Administration (FDA) approved ranibizumab (0.3 mg) administered by monthly intravitreous injection for treatment of DME.[153] In 2014, aflibercept (2 mg) administered by monthly intravitreous injection for five injections, followed by injection every 4–8 weeks thereafter, was approved for treatment of DME.[154]

Intravitreous injection of various corticosteroid formulations has shown efficacy for treatment of DME in several clinical trials,[148,155,156] but the well-characterized adverse effects of cataract, ocular hypertension, and glaucoma have somewhat limited use of these agents. In 2014, the fluocinolone acetonide (0.19 mg) intravitreal implant (Iluvien, Alimera Sciences) and the dexamethasone (0.7

mg) intravitreal implant (Ozurdex, Allergan) both received FDA approval for treatment of DME,[157,158] and triamcinolone acetonide suspension for intravitreous injection is used off-label for this indication.

Focal/grid laser photocoagulation, first proven effective for treatment of DME in the ETDRS, remains helpful in a number of settings, particularly for management of extrafoveal clinically significant macular edema, fovea-involving edema not severe enough to warrant injection pharmacotherapy, instances in which there is contraindication for intravitreous injection, and as an adjunct to treatment in select cases. Much remains to be clarified regarding the optimal use of focal/grid laser photocoagulation and intravitreous pharmacotherapy in various circumstances. A DRCR.net trial described below comparing intravitreous ranibizumab plus prompt focal/grid laser photocoagulation, ranibizumab with deferral of laser treatment for at least 24 weeks, intravitreous triamcinolone acetonide plus prompt laser treatment, and focal/grid laser photocoagulation alone showed superiority of ranibizumab arms, and did not show added benefit of combining ranibizumab with prompt laser treatment in the first 24 weeks.[148] But while this and other recent trials support a strategy of initiating treatment with VEGF antagonist monotherapy in the setting of significant fovea-involving DME, they do not provide guidance for eyes not meeting study entry criteria, or for adjunct use of focal/grid laser photocoagulation in a variety of situations later during a course of injections. Focal/grid laser photocoagulation continues to be employed alongside intravitreous pharmacotherapy in clinical trials and in practice, and future studies will hopefully provide valuable guidance on the optimal use of these two effective treatment modalities. Vitrectomy can be useful for management of DME in certain situations, particularly with evidence of vitreomacular traction, but has not been proven effective in any randomized controlled clinical trial, and involves surgical risks that must be carefully considered.

Despite important progress in treatment, DME remains a significant cause of vision loss. This reflects shortcomings in diagnosis and treatment of DM, inadequacies in screening and surveillance of diabetic retinopathy, and limitations of present

treatments for DME. Current treatment options for DME offer a better chance for visual improvement than ever before, but even optimal therapy does not always restore normal macular function or structure. In a randomized controlled clinical trial demonstrating treatment benefits similar to those in other recent studies, groups gaining most vision (those treated with intravitreous injections of ranibizumab plus prompt or deferred focal/grid laser photocoagulation) demonstrated an 8- or 9-letter mean gain in visual acuity at the 2-year visit compared with a baseline mean visual acuity of 63 letters.[148] Such results indicate that on average vision in these eyes improved from approximately 20/50− to 20/40+. At 2 years, the percentage of eyes with central subfield mean thickness equal to or greater than 250 μm (using a time domain system for which normal thickness measures approximately 200 μm) was 43% in the ranibizumab plus prompt laser group and 42% in the ranibizumab plus deferred laser group, reflecting a significant number of eyes with residual macular edema despite treatment.

The ETDRS concept of CSME, discussed earlier in this chapter, remains relevant to management of DME, but recognition of edema warranting treatment is tempered by consideration of the various inclusion and exclusion criteria used in recent clinical trials and by recognition of the sensitivity of OCT for detection of more subtle thickening than was possible in the ETDRS era. Eyes with clinically significant macular edema that threatens but does not involve the macular center are at high risk of vision loss,[38] but have been excluded from most recent clinical trials, leaving uncertainty about the best treatment options in these cases. Such eyes received focal/grid laser photocoagulation in the ETDRS, but it is not known how laser treatment compares to other therapeutic options. Likewise, recent trials have frequently excluded eyes with very good and very poor visual acuity, making evidence-based decision-making more difficult in these cases. The sensitivity of OCT for retinal thickening allows identification of very mild disease, often termed “subclinical” macular edema because it is not easily visible on biomicroscopy. OCT thickness values specified in eligibility criteria and in retreatment algorithms in clinical trials indicate what threshold of thickening was considered significant enough to treat

and retreat in a given study; however, such information provides no guidance on whether outcomes would have differed if other thickness thresholds had been used instead. Areas of macular thickening and hard exudate not meeting criteria for CSME can usually be observed vigilantly, with institution of treatment if CSME evolves.[38] One recent study evaluated the natural history of subclinical DME in 43 eyes in 39 subjects with a center point thickness of 225–299 μm, measured on a time domain OCT system, and absence of visible foveal thickening on biomicroscopic exam.[159] The cumulative probability of either treatment for DME (performed at the discretion of the investigator), or increase in center point thickness of 50 μm or greater from baseline, with a center point thickness value of 300 μm or greater, was 27% (95% CI: 14–38%) at 1 year, and 38% (95% CI: 23–50%) at 2 years, indicating the need for surveillance of these eyes for progression to CSME.

Attention to the context of DME is important for management. The principles of treatment of DME remain the same regardless of the underlying severity of diabetic retinopathy, but management may differ depending on the circumstances. There are special considerations for treatment of DME in the context of PDR, given the imperative to administer any necessary treatment to lower risk of vision loss from the complications of proliferative disease. Chapter 51 (Proliferative diabetic retinopathy) discusses considerations for management of DME in the setting of PDR. Other ocular conditions may impact DME or the choice of treatment. For example, postoperative cystoid macular edema may complicate DME following intraocular surgery and may warrant different treatment. Presence of glaucoma may contraindicate use of local corticosteroids. Some such considerations are included in the following discussion, but an exhaustive review is beyond the scope of this chapter.

Pharmacotherapy With Vascular Endothelial Growth Factor (VEGF) Antagonists

VEGF-A exerts potent effects on retinal vascular permeability, and concentrations of certain VEGF-A isoforms in the retina and vitreous are elevated in diabetic retinopathy.[42,43,160] Various VEGF antagonists have been developed for ophthalmic and

nonophthalmic uses, including bevacizumab, a humanized murine monoclonal antibody binding VEGF-A; ranibizumab, a humanized murine monoclonal antibody fragment, also binding VEGF-A; pegaptanib sodium, an aptamer specifically inhibiting the VEGF-A 165 isoform; and aflibercept, a human fusion protein incorporating ligand-binding elements from VEGF receptors and the Fc region of an IgG1 molecule. Intravenous administration for ophthalmic disease has been studied for some agents,[161–163] but intravitreous injection has become the standard route of delivery to the eye. Following demonstration of efficacy in neovascular age-related macular degeneration, choroidal neovascularization from other causes, and macular edema following retinal vein occlusion, various VEGF antagonists have been evaluated for treatment of DME in a number of pivotal clinical trials.

The first major clinical trial to report results was designed by DRCR.net investigators to compare four strategies for treatment of DME, including focal/grid laser photocoagulation alone, intravitreous injection of ranibizumab (0.5 mg) with deferral of early laser for at least 24 weeks, intravitreous injection of ranibizumab (0.5 mg) with early laser within 10 days of first injection, and intravitreous injection of triamcinolone acetonide (4 mg) with early laser.[148,164] A total of 854 eyes of 691 participants with DME involving the center of the fovea and visual acuity of 20/32 to 20/320 were randomly assigned to one of four treatments. The main outcome measure, mean change in visual acuity, was evaluated at one year. Retreatment algorithms were generally intended to require further therapy in eyes with residual disease in order to maximize treatment effects in the first year. Focal/grid laser photocoagulation was repeated as often as every 13 weeks, ranibizumab was readministered as frequently as every 4 weeks, and triamcinolone acetonide was reinjected as often as every 16 weeks. At one year, mean change in visual acuity was significantly better in the ranibizumab plus prompt laser (+9 letters) and ranibizumab and deferred laser (+9 letters) groups compared with the prompt laser plus sham injection group (+3 letters; both $p<.001$). Mean change in visual acuity in the triamcinolone plus prompt laser group (+4 letters) was not significantly different from that in the prompt laser plus sham injection group (+3 letters; $p=.31$).

Reductions in retinal thickness measured by OCT were similar in the ranibizumab and triamcinolone groups, and these improvements were greater than that measured in the prompt laser plus sham injection group at one year, but it is important to note that at two years, reductions in retinal thickness were similar in all groups.

FDA approval of ranibizumab (0.3 mg) for treatment of DME was based on safety and efficacy demonstrated in the DRCR.net study and in two other large randomized clinical trials.[148,164,151] In the RISE and RIDE studies, 759 patients contributing a single eye with fovea-involving DME and visual acuity of 20/40 to 20/320 were randomly assigned to receive monthly injections of ranibizumab (0.3 mg or 0.5 mg) or sham injections during the first 24 months, with focal/grid laser photocoagulation administered starting at 3 months for eyes meeting certain criteria. The main outcome measure for both studies was the proportion of patients gaining ≥15 letters on best corrected visual acuity at 24 months. In RISE, 18% of sham-treated patients gained ≥15 letters, compared with 45% of 0.3-mg (p<.0001) and 39% of 0.5-mg (p<.001) ranibizumab-treated patients. In RIDE, 12% of sham-treated patients gained ≥15 letters, compared with 33% of 0.3-mg (p<.0001) and 46% of 0.5-mg (p<.0001) ranibizumab-treated patients. Significant decreases in macular edema as measured by OCT were documented in patients treated with ranibizumab compared with sham. No significant additional benefit was measured in patients receiving the 0.5-mg dose compared with the 0.3-mg dose, leading to approval of the 0.3-mg dose.

Approval of aflibercept (2 mg) for treatment of DME was based on the results of two large randomized clinical trials.[152] In the VIVID and VISTA studies, 872 patients contributing a single eye with fovea-involving DME and visual acuity of 20/40 to 20/320 were randomly assigned to aflibercept (2 mg) every 4 weeks; aflibercept (2 mg) every 4 weeks for five injections, then every 8 weeks thereafter; or focal/grid laser photocoagulation and sham injection. The main outcome measure was the mean change in visual acuity at one year. In VIVID, the mean change in visual acuity was 10.5 letters in the group receiving aflibercept every 4 weeks and 10.7 letters in the group receiving aflibercept every 8 weeks after five

monthly treatments, compared with 1.2 letters in the group getting laser (p<.0001 for both). In VISTA the corresponding changes were 12.5 and 10.7 letters, compared with 0.2 letters in the laser group (p<.0001 for both).

Most recently, the DRCR.net compared bevacizumab (1.25 mg), which remains a popular off-label option, ranibizumab (0.3 mg), and aflibercept (2 mg) for treatment of fovea-involving DME in eyes with visual acuity of 20/32 to 20/320.[96] The retreatment algorithm was generally intended to require monthly injection in eyes with residual disease in order to maximize treatment effects, particularly in the first 24 weeks of the study, and involved focal/grid laser photocoagulation for eyes meeting criteria for residual disease starting at 24 weeks. Analysis of the primary outcome, mean change in visual acuity at one year, showed that there was an overall relative benefit of aflibercept compared with the other two drugs. However, there was a statistically significant interaction between baseline visual acuity and the treatment effect for aflibercept, warranting stratification of the results by baseline visual acuity. The treatment effect was similar among the three drugs for eyes with baseline visual acuity letter score ≥69 (approximately 20/40 or better), and demonstrated superiority of aflibercept for eyes with baseline visual acuity letter score <69 (20/50 or worse) (Fig. 50.12). Corresponding improvements in retinal thickness mirror the changes in visual acuity (Fig. 50.13).

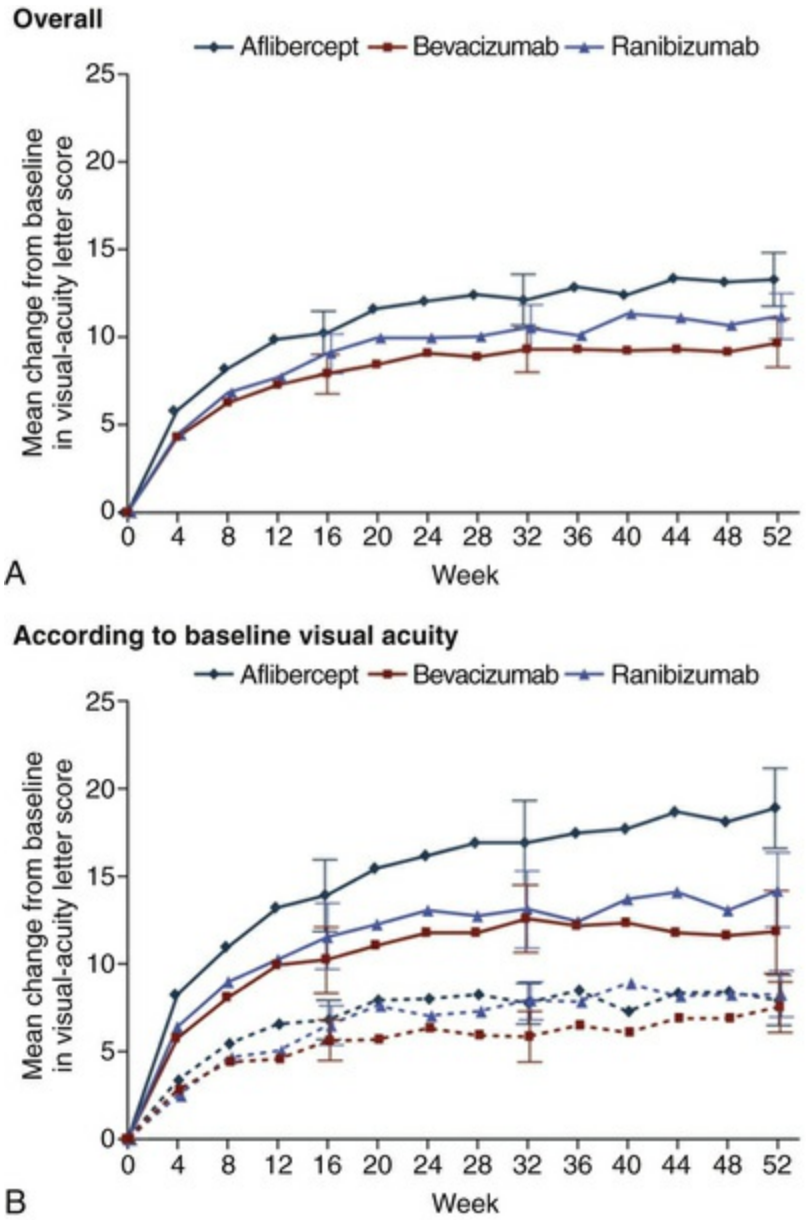

FIG. 50.12 Change in visual acuity at one year (primary outcome measure) for eyes randomly assigned to aflibercept (2 mg), bevacizumab (1.25 mg), or ranibizumab (0.3 mg) in a large clinical trial (660 participants) testing comparative efficacy for fovea-involving diabetic macular edema. Shown are the changes in visual acuity overall (A) and according to baseline visual acuity (B). In panel B, solid lines indicate baseline visual acuity of 20/50 or worse, and dashed lines indicate baseline visual acuity of 20/32 to 20/40. Outlying values were truncated to 3 standard deviations from the mean. Whiskers indicate 95% confidence intervals. (From Diabetic Retinopathy Clinical Research Network et al. Aflibercept, bevacizumab, or ranibizumab for diabetic macular edema. New England Journal of Medicine 2015;372:1193-203. Copyright © 2015

Massachusetts Medical Society. Reprinted with permission from Massachusetts Medical Society.)

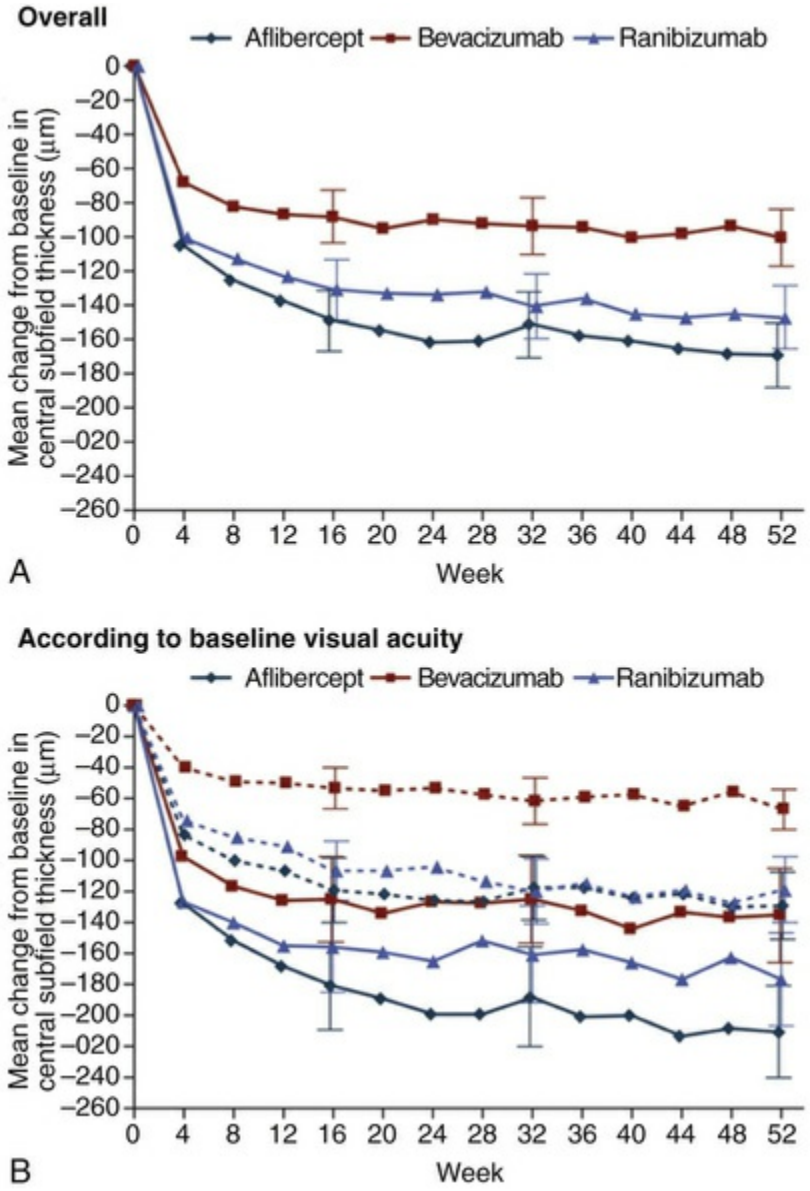

FIG. 50.13 Change in retinal thickness, measured as central subfield mean thickness on optical coherence tomography (OCT), at one year for eyes randomly assigned to aflibercept (2 mg), bevacizumab (1.25 mg), or ranibizumab (0.3 mg) in a large clinical trial (660 participants) testing comparative efficacy for fovea-involving diabetic macular edema. Shown are the changes in central subfield thickness overall (A) and according to baseline visual acuity (B). In B, solid lines indicate baseline visual acuity of 20/50 or worse,

and dashed lines indicate baseline visual acuity of 20/32 to 20/40. Whiskers indicate 95% confidence intervals. (From Diabetic Retinopathy Clinical Research Network et al. Aflibercept, bevacizumab, or ranibizumab for diabetic macular edema. New England Journal of Medicine 2015;372:1193-203. Copyright © 2015 Massachusetts Medical Society. Reprinted with permission from Massachusetts Medical Society.)

Three- and five-year follow up in a few of these trials demonstrates continued benefit of VEGF antagonist therapy in the setting of further treatment when warranted, and has not revealed any new safety concerns.[165,166] The frequency of treatment appears to decrease with time. In the DRCR.net trial described above comparing ranibizumab with prompt focal/grid laser photocoagulation, ranibizumab with deferred laser, triamcinolone with prompt laser, and sham injection with laser, the median number of injections over five years was 13 in the ranibizumab with prompt laser group and 17 in the ranibizumab with deferred laser group, with the majority occurring in the first year. Only a few injections were given during the second year, and approximately half of participants in the ranibizumab-treated groups did not need any injections in the fifth year.[166]

A meta-analysis of eight DRCR.net trials using VEGF antagonists and saline (as a control) in diabetic eyes showed a rate of endophthalmitis around 1 per 2700 injections.[167] Eleven cases of endophthalmitis were reported among 28,786 injections, using a technique involving use of povidone iodine, a lid speculum, and topical anesthesia. Only two participants among the eight trials received a series of injections without pre-application of povidone iodine, in violation of study protocol, and both developed endophthalmitis, underscoring the critical importance of this agent for minimizing infection risk. Among injections performed with use of povidone iodine, six cases of endophthalmitis among 11,565 injections (0.05%) occurred with use of topical antibiotics (used at the discretion of the investigator), while three among 17,208 injections (0.02%) occurred without use of topical antibiotics (p=.17). While not a statistically significant difference, this and other data have suggested that topical antibiotics are at least unlikely to lower infection risk.[168] An exploratory analysis by the DRCR.net suggests

that serial VEGF antagonist injection may increase risk of ocular hypertension or glaucoma.[169] The cumulative probability of sustained IOP elevation, defined as a measurement of 22 mmHg or greater representing an increase of at least 6 mmHg from baseline at two consecutive visits, was measured in eyes with no history of open angle glaucoma in the DRCR.net trial comparing ranibizumab with prompt or deferred focal/grid laser photocoagulation, triamcinolone with prompt laser, and laser with sham injection. Three hundred twenty-two eyes in the ranibizumab groups were compared with 260 eyes in the laser with sham injection group. The cumulative probability of sustained IOP elevation over 3 years was 9.5% for eyes in the ranibizumab-treated groups, compared with 3.4% for eyes in the laser and sham injection group (difference of 6.1%; 99% CI −0.2–12.3%; hazard ratio for ranibizumab group versus sham group, 2.9; 99% CI –1.0–7.9; p=.01). A recent Cochrane meta-analysis of studies evaluating VEGF antagonists for DME showed no increase in rates of systemic serious adverse events or arterial thromboembolic events for subjects treated with VEGF antagonists compared with controls,[170] corroborating similar findings from a Cochrane review of bevacizumab and ranibizumab use for exudative age-related macular degeneration.[171]

Pharmacotherapy With Corticosteroids

Corticosteroids have immune modulatory and antiangiogenic properties and have been utilized for treatment of ophthalmic disease since the 1950s.[172–177] Common adverse effects, including hyperglycemia and other metabolic alterations difficult to manage in the setting of DM, limit their long-term systemic use, but a number of formulations allowing local delivery to the eye have been developed. The limited intraocular penetration of existing topical preparations makes them unsuitable for treatment of most retinal diseases, but injectable corticosteroids and sustained-release formulations for intraocular use have been evaluated for efficacy in DME.

The first corticosteroid to be tested in large clinical trials for treatment of DME was triamcinolone acetonide, administered by intravitreous injection.[148,164,178,179] A study by the DRCR.net enrolled 840 eyes of 693 participants with DME involving the foveal center

and visual acuity of 20/32 to 20/320, with a primary outcome measure of mean change in visual acuity at two years.[178,179] Eyes were randomly assigned to receive focal/grid laser photocoagulation, intravitreous injection of triamcinolone acetonide (1 mg), or intravitreous injection of triamcinolone acetonide (4 mg), both corticosteroid arms utilizing a preservative-free formulation of the drug. Persistent or new macular edema was retreated every 4 months. Mean change in visual acuity at two years was significantly better in laser-treated eyes (+1 letter) than in eyes receiving 1 mg triamcinolone (−2 letters; p=.02) and 4 mg triamcinolone (−3 letters; p=.002). The mean number of treatments over two years was 2.9 in the laser group, 3.5 in the 1 mg triamcinolone group, and 3.1 in the 4 mg triamcinolone group. Corticosteroids are well known to promote cataract and to elevate IOP in some eyes, and such effects were carefully documented in this study. Cataract surgery was performed in 13% of eyes in the laser group, 23% of eyes in the 1 mg triamcinolone group, and 51% of eyes in the 4 mg triamcinolone group by two years. Intraocular pressure elevation of 10 mmHg or more from baseline at any study visit was noted in 4%, 16%, and 33% of eyes in the three groups, respectively, by 2 years. There were no cases of endophthalmitis or inflammatory pseudoendophthalmitis among 1649 intravitreous injections. Addressing whether cataract formation obscured benefit of treatment of DME in eyes receiving corticosteroids, subgroup analysis of 145 eyes pseudophakic at baseline showed mean change in visual acuity of +2 letters in the laser group, +2 letters in the 1-mg triamcinolone group, and −1 in the 4-mg triamcinolone group at 2 years. Investigators judged that the superiority of focal/grid laser photocoagulation could not be explained solely by cataract progression in triamcinolone-injected groups. This conclusion was supported by data on change in retinal thickness. At 2 years, mean improvement in OCT central subfield mean thickness was significantly greater in the laser group (139 μm) compared with the 1 mg triamcinolone group (86 μm; p<.001) and the 4 mg triamcinolone group (77 μm; p<.001).

A second trial, discussed above in the section "Pharmacotherapy with VEGF antagonists," compared a combination of intravitreous injection of preservative-free triamcinolone (4 mg) and focal/grid

laser photocoagulation to three other strategies, including focal/grid laser photocoagulation with sham injection, intravitreous injection of ranibizumab plus prompt focal/grid laser photocoagulation, and intravitreous injection of ranibizumab and deferral of early laser.[148,164] At the primary endpoint of 1 year, mean change in visual acuity was not significantly different in the triamcinolone plus laser group (+4 letters) compared with the prompt laser plus sham injection group (+3 letters; p=.31). However, subgroup analysis of eyes pseudophakic at baseline showed a trend toward benefit in the triamcinolone plus laser group comparable to that seen in ranibizumab groups and superior to that seen in the laser group. Investigators judged that cataract formation, cataract surgery, or both may have adversely impacted benefit of combination therapy with intravitreous injection of triamcinolone and focal/grid laser photocoagulation in phakic eyes. Taken together, the results of these two trials suggest that while monotherapy with intravitreous injection of triamcinolone acetonide is inferior to monotherapy with focal/grid laser photocoagulation, the combination of the two treatments in pseudophakic eyes might possibly be superior to laser alone.

Sustained-release inserts designed for intraocular delivery of fluocinolone acetonide and dexamethasone have been developed and tested for various ophthalmic applications, and two such formulations have been recently approved for treatment of DME. An intravitreous insert releasing stable quantities of fluocinolone acetonide for three years (Iluvien, Alimera Sciences), consisting of a nonbiodegradable cylinder (3.5×0.37 mm) introduced into the vitreous cavity via injection by 25-gauge needle, was recently approved for treatment of DME in patients previously treated with corticosteroids without a clinically significant increase in IOP.[157] In the FAME trial, 956 patients contributing a single eye with fovea-involving DME after at least one prior session of focal/grid laser photocoagulation; visual acuity of 20/50 to 20/400 Snellen equivalent; and no glaucoma, ocular hypertension, or use of IOP-lowering medications, were randomly assigned to fluocinolone acetonide insert releasing 0.2 μg/day, fluocinolone acetonide insert releasing 0.5 μg/day, or sham injection, with "rescue" focal/grid laser photocoagulation performed for persistent macular edema in

all three groups.[155] The proportion of participants with improvement in visual acuity of 15 letters or more from baseline at 2 years, the main outcome measure for the trial, was 29% in both groups receiving the fluocinolone acetonide insert, compared with 16% for the sham group (p=.002 for both). At 2 years, among study eyes that were phakic at baseline, cataract surgery had been performed in 75% of eyes in the low-dose group and 85% of eyes in the high-dose group, compared with 23% of eyes in the sham group. At 2 years, incisional glaucoma surgery had been performed in 3.7% of eyes in the low-dose group and 8.1% of eyes in the high-dose group, compared with 0.5% of eyes in the sham group. Visual gain in eyes receiving inserts was greater in those that were pseudophakic at baseline and similar in magnitude to benefit seen in eyes treated with intravitreous triamcinolone and prompt focal/grid laser photocoagulation in the DRCR.net trial.

A dexamethasone intravitreous insert (Ozurdex, Allergan) consisting of a biodegradable pellet releasing high levels of drug for approximately 60 days and delivered via surgical sclerotomy or 22-gauge needle-injector system was recently approved for treatment of DME.[158] In the MEAD studies, two randomized clinical trials pooled for analysis, 1048 patients contributing a single eye with fovea-involving DME, visual acuity of 20/50 to 20/200, and no glaucoma or ocular hypertension, were randomly assigned to the dexamethasone 350-μg insert, dexamethasone 700-μg insert, or sham injection, and were retreated every 6 months for residual disease, without any focal/grid laser photocoagulation.[156] The proportion of participants with improvement in visual acuity of 15 letters or more from baseline at 3 years, the main outcome measure for the study, was 18% for the low-dose insert and 22% for the high-dose insert, compared with 12% for the sham group (p<.02 for both). However, these results must be interpreted with caution, because only 607 (58%) of 1048 participants completed 3-year follow-up, and the primary efficacy analysis was performed by carrying last observations forward for a substantial number of participants withdrawing early. Cataract progression requiring surgery and IOP elevation were common in both groups receiving insert, but rates are difficult to compare to other studies in the setting of the substantial dropout rate for all participants. At 3 years, among

study eyes that were phakic at baseline, cataract surgery had been performed in 52% of eyes in the low-dose group and 59% of eyes in the high-dose group, compared with 7% of eyes in the sham group. Intraocular pressure of 25 mmHg or greater measured at any visit during the study was present in 27% of eyes in the low-dose group and 32% of eyes in the high-dose group, compared with 4% in the sham group.

There is ample evidence for efficacy of various corticosteroids in treatment of DME, but none has shown superiority to intravitreous injection of VEGF antagonists or focal/grid laser photocoagulation when used as monotherapy. However, these medications can be very useful in select circumstances, particularly for DME refractory to other therapies in pseudophakic eyes without glaucoma or ocular hypertension. The need for less frequent administration is a present advantage over existing VEGF antagonists, but frequent follow-up is still necessary to monitor for intraocular pressure elevation and glaucoma.

Focal/Grid Laser Photocoagulation

The efficacy of focal/grid laser photocoagulation for treatment of DME was established in the ETDRS,[38] though its mechanisms of action continue to be debated even three decades later. Chapter 41 (Retinal laser therapy: Biophysical basis and applications) describes the principles of ophthalmic laser therapy and discusses hypotheses about its mechanisms. The ETDRS was a landmark randomized controlled trial with a complex study design enrolling 3711 participants to test the effect of different strategies of focal/grid and scatter laser photocoagulation and the use of daily aspirin on retinopathy progression and vision loss in eyes with disease ranging from mild NPDR to early (non-high-risk) PDR.[180] At 3 years, eyes with mild or moderate NPDR plus macular edema at baseline treated with immediate focal/grid laser photocoagulation showed an approximately 50% decrease in the rate of moderate vision loss (defined as a decrease of three lines or more on a logarithmic visual acuity chart, corresponding to a doubling of the initial visual angle) compared with similar eyes randomly assigned to deferral of photocoagulation (11.2% vs. 21.1%; $p<.001$). Eyes with severe NPDR or early PDR and macular edema at baseline treated

with immediate focal/grid laser photocoagulation were concomitantly treated with immediate full or mild scatter laser, and showed reduction in moderate vision loss apparent at time points later than 3 years, reflecting an early detrimental effect of immediate scatter photocoagulation.

Treatment of eyes assigned to immediate focal/grid laser photocoagulation in the ETDRS involved argon laser application to areas of retinal thickening identified on biomicroscopy and characterized by FA.[181] The procedure involved "direct" treatment of all microaneurysms exhibiting leakage of fluorescein dye in regions of retinal thickening between 500 and 3000 μm from the foveal center. Burn characteristics for direct treatment included size 50–100 μm, exposure 0.05–0.10 seconds, and intensity sufficient to whiten or darken large microaneurysms. The study treatment technique also included "grid" laser application to areas of diffuse leakage of fluorescein dye and areas of capillary nonperfusion in regions of retinal thickening between 500 and 3000 μm from the foveal center, with spacing between spots of at least one burn-width. Burn characteristics for grid treatment included size up to 200 μm, exposure 0.05–0.10 seconds, and intensity described as "mild." Eyes were assessed every 4 months, and retreatment was performed for CSME exhibiting any treatable areas. Minor effects on visual field were attributed to focal/grid laser photocoagulation, but at 4 months the occurrence of scotomas within 20 degrees of fixation identified by kinetic perimetry among eyes with mild or moderate NPDR and macular edema was similar between eyes assigned to immediate focal/grid laser photocoagulation and eyes assigned to deferral of photocoagulation.[102] More significant effects on visual field were attributed to full and mild scatter laser. Additional adverse effects of laser treatment included choroidal neovascularization and subsequent fibrosis that can occur in areas of disruption of the RPE caused by laser photocoagulation, sometimes years following the procedure, but this complication was infrequent and often self-limited. Subretinal fibrosis was noted in proximity to a laser scar in only 9 of 4823 eyes treated with focal/grid laser photocoagulation in the ETDRS.[114]

The technique for focal/grid laser photocoagulation has evolved since the ETDRS, trending toward application of smaller, less

intense burns, and less frequently making use of a fluorescein angiogram to guide treatment. Present standard technique is well summarized by parameters for "modified-ETDRS" focal/grid laser photocoagulation specified by the DRCR.net for use in its protocols (Table 50.2).[182] The development and availability of novel ophthalmic laser systems has led to extrapolation of the argon green laser parameters to other platforms. One randomized prospective study treating 171 eyes (91 participants) with modified grid laser for treatment of DME found no significant difference in visual acuity or other measures comparing the argon green laser to the diode (810 nm) laser.[183] Some uncertainty persists regarding whether other systems and techniques vary in clinically important ways from focal/grid laser photocoagulation using the argon laser.[119,184–193] The value of applying laser photocoagulation in ETDRS-style to areas of retinal thickening and fluorescein leakage was tested in a randomized DRCR.net study comparing standard modified-ETDRS technique to a novel procedure consisting of milder but more extensive burns applied throughout the macula in 323 eyes with DME involving the foveal center.[194] Standard modified-ETDRS laser resulted in significantly greater reduction in retinal thickening in central subfield mean thickness on OCT compared with the modified grid treatment (adjusted mean difference, 33 μm; 95% CI 5–61 μm; p=.02). Mean change in visual acuity was similar (0 and −2 letters, respectively, 95% CI −0.5 to 5 letters; p=.10) at 12 months.

TABLE 50.2

Modified-ETDRS Focal/Grid Laser Photocoagulation Technique Used by the Diabetic Retinopathy Clinical Research Network (DRCR.net)

Treatment Parameter	DRCR.net Technique for Modified-ETDRS Focal/Grid Laser Photocoagulation
Direct treatment	Directly treat all leaking microaneurysms in areas of retinal thickening between 500 and 3000 μm from the center of the macula (although may treat between 300 and 500 μm of center if center-involved edema persists after initial focal photocoagulation, but generally not if the visual acuity is better than 20/40)
Change in microaneurysm color with direct	Not required, but at least a mild gray–white burn should be evident beneath all microaneurysms

treatment	
Spot size for direct treatment	50 μm
Burn duration for direct treatment	0.05–0.1 seconds
Grid treatment	Apply to all areas with edema not associated with microaneurysms; if fluorescein angiography is obtained, grid is applied to areas of edema with angiographic nonperfusion when judged indicated by the investigator
Area considered for grid treatment	500–3000 μm superiorly, nasally, and inferiorly from center of macula; 500–3500 μm temporally from macular center; no burns placed within 500 μm of disc
Burn size for grid treatment	50 μm
Burn duration for grid treatment	0.05–0.1 seconds
Burn intensity for grid treatment	Barely visible (light gray)
Burn separation for grid treatment	Two visible burn widths apart
Wavelength (grid and direct treatment)	Green to yellow wavelengths

[a]The DRCR.net provides separate guidelines for the PASCAL photocoagulation system.

Use of fluorescein angiography to direct the treatment is at the discretion of the physician. Laser treatment following an injection, if needed, is based on the preinjection macular appearance. Any laser wavelength for photocoagulation within the green to yellow spectrum may be chosen.[a] Lenses used for treatment cannot increase or reduce the burn size by more than 10%.

Adapted with permission. Modified-ETDRS Focal Photocoagulation Technique accessed at http://publicfiles.jaeb.org/drcrnet/Misc/FocalGridProcedure42711.pdf.

The benefits of focal/grid laser photocoagulation have been highlighted by more recent clinical trials following the ETDRS. Many of the eyes treated in the ETDRS had good visual acuity at baseline, limiting the amount of potential vision gain from any intervention; accordingly, the efficacy of laser in the treated ETDRS cohort as a whole consisted chiefly of a reduction of vision loss. However, in an ETDRS subgroup of 114 eyes with thickening of the foveal center, visual acuity worse than 20/32, and mild or moderate NPDR treated with immediate focal/grid laser photocoagulation in the ETDRS, change in mean visual acuity from baseline at two years was +4 letters, with 29% of eyes improving 10 letters or more. By

comparison, in a subset of 235 eyes meeting the same baseline criteria for which laser was deferred, change in mean visual acuity from baseline at two years was −6 letters, with 12% improving 10 letters or more (Ferris FL, unpublished data, 2008). Results of recent trials enrolling eyes with more advanced disease support the suggestion that the benefits of focal/grid laser photocoagulation may exceed those demonstrated in the treated ETDRS cohort as a whole. In the previously mentioned study comparing focal/grid laser photocoagulation to injection of intravitreous triamcinolone, which enrolled 840 eyes with visual acuity of 20/40 to 20/320 with retinal thickening involving the center of the fovea and a range of underlying diabetic retinopathy, the 330 eyes randomly assigned to laser treatment showed a change in mean visual acuity of +1 letter (standard deviation, ±17 letters) at 2 years, with improvement of 15 letters or more in 18% of laser-treated eyes.[178] In another study discussed above comparing focal/grid laser photocoagulation alone to intravitreous injection of ranibizumab or triamcinolone acetonide combined with laser treatment in eyes with center-involved DME and baseline visual acuity of 20/32 to 20/320, the change in mean visual acuity at 2 years was +3 letters (standard deviation, ±15 letters) in 211 eyes treated with focal/grid laser photocoagulation alone.[164]

Although focal/grid laser photocoagulation mitigates the morbidity of DME, it is often insufficient to restore normal vision or completely resolve macular edema. Requirement for multiple treatments is common. Even with retreatment, a significant proportion of eyes continue to manifest residual DME. In the aforementioned DRCR.net trial testing focal/grid laser photocoagulation alone versus intravitreous injection of ranibizumab or triamcinolone acetonide plus laser, eyes treated with laser alone manifested a median central subfield mean thickness of 266 μm at 2 years, representing a median improvement of 113 μm.[164] However, this represents an appreciable amount of residual thickening compared with normal central subfield mean thickness (approximately 200 μm). Only 39% of eyes in the laser group achieved a central subfield mean thickness of less than 250 μm with at least a 25 μm decrease in thickness from baseline. Ten percent of eyes treated with laser alone lost 15 or more letters of

visual acuity at 2 years from baseline.

Vitrectomy

A number of small case series have reported benefit of vitrectomy in the setting of demonstrable vitreomacular traction and epiretinal proliferation in DME.[195–198] Differences in patient populations, definition of clinically significant vitreoretinal traction, surgical approach, use of laser and medications as adjunct treatment, outcome measures, and follow-up, alongside the customary limitations and biases of retrospective studies, make it difficult to assess the efficacy of surgery. A noncontrolled prospective study representing one of the largest series published to date evaluated vitrectomy for 87 eyes with DME and evidence for vitreomacular traction as judged by the investigator.[199] Intervention was nonstandardized, with vitrectomy variably accompanied by epiretinal membrane peeling, internal limiting membrane peeling, use of scatter laser, and injection of corticosteroids. At the primary endpoint at 6 months, visual acuity improved by 10 letters or more in 38% (95% CI 28–49%) and worsened by 10 letters or more in 22% (95% CI 13–31%). Adverse events included endophthalmitis in one eye, retinal detachment in 3 eyes, vitreous hemorrhage in 5 eyes, and elevated IOP necessitating treatment in 7 eyes.

Results of case series evaluating vitrectomy for DME even in the absence of any visible vitreoretinal traction have been mixed, with some reports suggesting efficacy and others not.[200–208] Two very small randomized trials showed no evidence for significant benefit.[209,210] In the absence of any data from large, well-designed clinical trials, efficacy remains uncertain at best and, weighed against well-known risks of surgery, does not typically warrant vitrectomy for this indication alone. The possibility of benefit is presently most relevant to surgical decision-making in PDR, in which treatment of DME is undertaken simultaneously with surgical management of fibrovascular proliferation, vitreous hemorrhage, and retinal detachment. The role for surgery in management of PDR is discussed in Chapter 115 (Surgery for proliferative diabetic retinopathy).

Ocular Treatment for Nonproliferative Diabetic Retinopathy

Various local therapies have been evaluated for their effects on altering the course of NPDR. The efficacy of scatter laser photocoagulation for reduction of severe vision loss among eyes with advanced retinopathy (severe NPDR and PDR) was established in the Diabetic Retinopathy Study.[211] The ETDRS was designed partly to clarify the optimal point during the course of retinopathy for administration of scatter laser photocoagulation. In the ETDRS, eyes were randomly assigned to early laser photocoagulation or deferral of laser treatment. Eyes were categorized according to presence or absence of macular edema and according to severity of retinopathy, and further randomly assigned to various laser strategies in a complex study design. In addition to testing the effects of focal/grid laser photocoagulation for macular edema, the ETDRS also evaluated the effects of immediate "mild" and "full" scatter photocoagulation in eyes with more severe retinopathy (severe NPDR and non-high-risk PDR) with and without macular edema and delayed mild and full scatter photocoagulation in eyes with less severe retinopathy and macular edema. At 5 years, the rate of severe vision loss (defined as visual acuity less than 5/200 at two consecutive visits) was low in eyes receiving early laser treatment (2.6%) and in those with deferral of laser (3.7%) (Fig. 50.14).[102] Rates of severe vision loss in the subset of eyes with mild or moderate NPDR were even lower. On the basis of these findings, ETDRS investigators recommended against scatter laser photocoagulation for mild and moderate NPDR, provided that adequate follow-up could be anticipated. They suggested consideration of scatter laser photocoagulation for severe NPDR and non-high-risk PDR, with potential benefit balanced against adverse effects of laser on visual acuity and visual fields. The use of scatter laser photocoagulation in diabetic retinopathy is further discussed in Chapter 51 (Proliferative diabetic retinopathy).

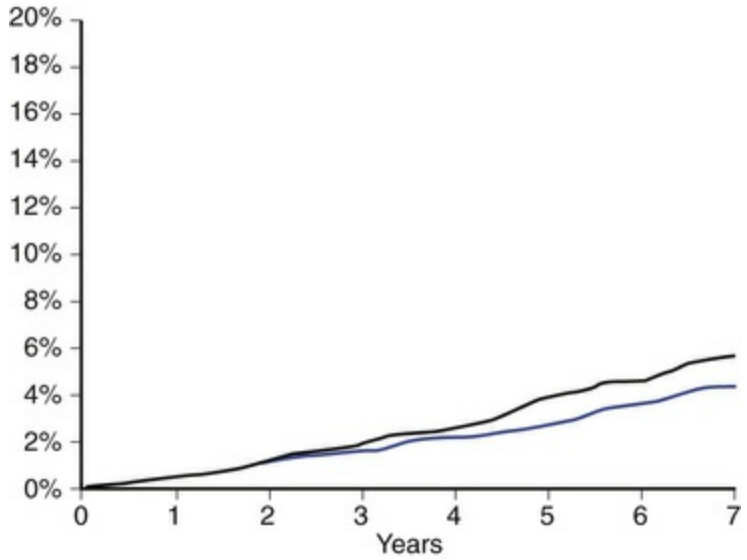

FIG. 50.14 Life table cumulative event rates of severe vision loss in all eyes assigned to immediate laser photocoagulation (blue) or deferral of laser photocoagulation (black) in the ETDRS. (Adapted with permission from Early Treatment Diabetic Retinopathy Study Research Group. ETDRS report number 9. Early photocoagulation for diabetic retinopathy. Ophthalmology 1991;98:766–85.)

There is good evidence indicating that local administration of VEGF antagonists for treatment of DME mitigates the severity of retinopathy (Fig. 50.15), and ranibizumab and aflibercept have recently been approved by the FDA for treatment of diabetic retinopathy in patients with DME.[153,154] In the RISE and RIDE trials, discussed above in "Pharmacotherapy with vascular endothelial growth factor (VEGF) antagonists," analysis of secondary outcome measures demonstrated that ranibizumab-treated eyes were significantly less likely to exhibit worsening of retinopathy, less likely to progress to PDR, and more likely to show improvement in retinopathy.[212] At 2 years, worsening of 3 steps or greater on the ETDRS diabetic retinopathy severity scale was present in 5% of sham-treated eyes, compared with 1.3% of eyes assigned to ranibizumab 0.3 mg (p=.04) and 0.9% of eyes assigned to ranibizumab 0.5 mg (p=.007); improvement of 3 steps or greater was present in 1.3% of sham-treated eyes, compared with 13.2% of eyes assigned to ranibizumab 0.3 mg (p<.001) and 14.5% of eyes assigned to ranibizumab 0.5 mg (p<.001). Progression of retinopathy, measured using a composite index including cases of progression to

PDR or vitreous hemorrhage, and cases undergoing panretinal photocoagulation or vitrectomy, occurred in 34% of sham-treated eyes, compared with 11% of eyes in each of the ranibizumab groups (p<.001 for both). In the VIVID and VISTA trials, also mentioned above in "Pharmacotherapy with vascular endothelial growth factor (VEGF) antagonists," analysis of secondary outcome measures demonstrated that aflibercept-treated eyes were significantly more likely to show improvement in retinopathy.[152] In VIVID at one year, an improvement of 2 steps or greater on the ETDRS diabetic retinopathy severity scale was present in 8% of sham-treated eyes, compared with 28% of eyes assigned to aflibercept 2 mg every 8 weeks after 5 monthly injections and 33% of eyes assigned to aflibercept 2 mg every 4 weeks (p<.001 for both). In VISTA, the corresponding rates were 14% in sham-treated eyes, compared with 29% and 34% in aflibercept groups, respectively (p<.01 for both).

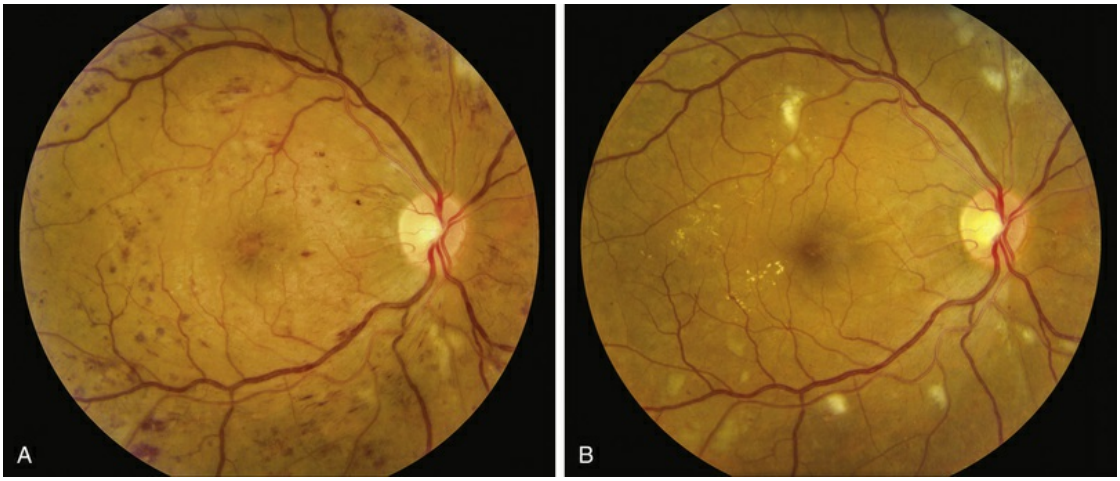

FIG. 50.15 Improvement of retinopathy in an eye receiving intravitreous injections of vascular endothelial growth factor antagonists for diabetic macular edema (DME) in the setting of nonproliferative diabetic retinopathy (NPDR). (A) A photograph of the right eye shows severe NPDR and severe fovea-involving DME in a 39-year-old man. Visual acuity tested 20/40, and optical coherence tomography (OCT) central subfield mean thickness measured 557 μm on Cirrus OCT. The patient enrolled in a crossover study in which the eye received injection of bevacizumab (1.25 mg) or ranibizumab (0.3 mg) every 4 weeks according to a

randomly-assigned treatment schedule. (B) A photograph of the same eye 36 weeks later, after 9 injections. Note the decrease in number of visible intraretinal hemorrhages and microaneurysms, and the new hard exudates temporally that represent the vestige of previous retinal thickening. Visual acuity improved to 20/20, and OCT central subfield mean thickness measured 240 μm. (National Eye Institute, Bethesda, MD.)

It is possible that corticosteroids may also exert beneficial effects on retinopathy.[148,164,213] An exploratory analysis in a DRCR.net study comparing focal/grid laser photocoagulation to intravitreous injection of triamcinolone acetonide (1 mg or 4 mg) evaluated progression of retinopathy, measured using a composite index including cases of progression to PDR or vitreous hemorrhage and cases undergoing panretinal photocoagulation or vitrectomy.[213] At 2 years, the cumulative probability of retinopathy progression was significantly lower in the 4 mg triamcinolone group (21%) but not in the 1 mg triamcinolone group (29%) compared with the laser group (31%; p=.005 and p=.64, respectively). Further investigation is necessary to better understand the risks and benefits of local pharmacotherapy for management of diabetic retinopathy, particularly in the absence of DME. A recent DRCR.net trial showed that serial intravitreous ranibizumab is comparable to panretinal photocoagulation for treatment of proliferative diabetic retinopathy at 2 years,[214] and another study testing VEGF antagonists for management of severe NPDR is being launched. For the moment, the effects on retinopathy at least weigh among the benefits for eyes receiving these drugs for treatment of DME.

Other Systemic Treatment for Nonproliferative Diabetic Retinopathy

Antiplatelet agents have been evaluated for treatment of diabetic retinopathy in a few randomized controlled clinical trials. In a 3-year study, 475 participants with early retinopathy were randomly assigned to daily aspirin, aspirin plus dipyridamole, or placebo, and progression of retinopathy was measured as the change in the

number of microaneurysms visualized on FA.[215] The annual increase in microaneurysms was significantly greater in the placebo group than in the treatment groups, but the growth rate was low (less than two microaneurysms per year) in all groups. In an analogous 3-year study involving 435 participants randomly assigned to daily ticlopidine or placebo, the annual increase in microaneurysms was greater in the placebo group than in the treatment group in an analysis that showed low appearance rates and borderline statistical significance.[216] Neither study showed a change in severity level of retinopathy, and the clinical significance of differences in microaneurysm counts remains uncertain.

The most definitive evidence for effects of antiplatelet therapy comes from the ETDRS, in which 3711 participants were randomly assigned to aspirin (650 mg per day) or placebo. Eyes assigned to deferral of laser photocoagulation were assessed for the effects of aspirin on progression of diabetic retinopathy. Aspirin use did not affect the severity of retinopathy or the risk of visual loss over 7 years.[217] Aspirin use did not increase the incidence, severity, or duration of preretinal or vitreous hemorrhage in eyes with deferral of photocoagulation or in eyes randomly assigned to early laser treatment.[217,218] Participants randomly assigned to aspirin exhibited a 17% reduction in morbidity and mortality from cardiovascular disease compared with participants receiving placebo, corroborating benefits seen in other studies. Aspirin remains an important therapy for control of cardiovascular risk, which is often high in persons with DM, and no level of retinopathy severity, including PDR, should contraindicate its use. The ETDRS results apply to persons with significant diabetic retinopathy, and some uncertainty remains about any effects of antiplatelet agents in very mild NPDR.

Sorbinil, an inhibitor of the enzyme aldose reductase, which catalyzes the conversion of glucose to sorbitol, was evaluated in a randomized controlled clinical trial following animal studies suggesting that these drugs might slow the development of diabetic retinopathy.[7,11,12] The Sorbinil Retinopathy Trial randomized 497 participants with type 1 DM and mild or no retinopathy to sorbinil or placebo.[219] The percentage of participants showing significant progression of diabetic retinopathy, defined as a two-step or greater

worsening on the ETDRS diabetic retinopathy severity scale on fundus photographs, was not significantly different between the two groups after 3–4 years of follow-up.

Inhibitors targeting the protein kinase C family, which is implicated in VEGF-mediated vasopermeability and endothelin-mediated vasoconstriction in animal models of diabetic retinopathy,[220–223] have been developed and evaluated for effects on diabetic retinopathy. Ruboxistaurin, an inhibitor of beta-isoforms of protein kinase C, has been evaluated in two randomized controlled clinical trials. In the first, which randomly assigned 252 participants with moderate to very severe NPDR to receive ruboxistaurin or placebo for 36–46 months, rates of retinopathy progression were not significantly different between groups, but participants taking ruboxistaurin (32 mg/day) showed a significant delay in time to moderate vision loss (doubling of the visual angle) compared with those taking placebo (p=.038).[224] In a second larger study, 685 participants with moderate to very severe NPDR were randomly assigned to ruboxistaurin or placebo and evaluated at 3 years for rates of sustained moderate vision loss, defined as decrease in ETDRS visual acuity score of 15 letters or more (doubling of the visual angle) for 6 months or longer.[225] The rate of sustained moderate vision loss was significantly lower in the ruboxistaurin group (5.5%) than in the placebo group (9.1%), representing a 40% risk reduction (p=.034). Focal/grid laser photocoagulation was initiated 26% less frequently among those treated with ruboxistaurin than among those receiving placebo (p=.008). There was no significant difference between rates of retinopathy progression between the two groups. Despite intriguing results, further clinical testing necessary for regulatory approval in the United States and in Europe has not been pursued and the drug remains unavailable.

Fenofibrate, a peroxisome proliferator-activated receptor (PPAR) alpha agonist, has been evaluated for efficacy in treatment of diabetic retinopathy in combination with statin therapy as a plasma lipid-modulating agent capable of lowering triglyceride levels and raising high-density lipoprotein (HDL) cholesterol levels. Two randomized controlled clinical trials have suggested benefit of fenofibrate for diabetic retinopathy. The Fenofibrate Intervention

and Event Lowering in Diabetes (FIELD) study was a large trial randomizing 9795 participants with type 2 DM to fenofibrate (200 mg/day) or placebo.[78] The cumulative percentage of participants receiving initiation of laser treatment for retinopathy (including focal/grid and scatter laser photocoagulation), a prespecified tertiary endpoint in the main study, was significantly lower in the fenofibrate group (3.4%) than in the placebo group (4.9%; hazard ratio, 0.69; 95% CI 0.56–0.84; *p*=.0002) over six years. Progression by two steps or greater on an adapted ETDRS diabetic retinopathy severity scale, the primary endpoint of a substudy involving analysis of two-field 45° fundus photographs for 1012 participants, did not differ significantly between fenofibrate and placebo groups. Investigators commented on a significantly higher rate of retinopathy progression in the placebo group compared with the fenofibrate group among participants with retinopathy at baseline, but the number of incident cases was small in both groups. The ACCORD study, discussed above, was a complex trial that included a lipid study randomizing 5518 participants with type 2 DM and dyslipidemia to receive simvastatin plus fenofibrate (160 mg/day) or simvastatin plus placebo. In the lipid study, 1593 participants were evaluated for effects of fenofibrate on retinopathy.[72] At 4 years, the rate of progression of retinopathy, defined as a composite measure of three-step or greater progression on the ETDRS diabetic retinopathy severity scale or worsening requiring laser photocoagulation or vitrectomy, was significantly lower in the fenofibrate group (6.5%) compared with the placebo group (10.2%; adjusted odds ratio 0.60; 95% CI 0.42–0.87; *p*=.006).

The results of the FIELD and ACCORD studies are intriguing, particularly in the setting of some uncertainty about whether or not the benefit of fenofibrate on retinopathy is secondary to its effects on plasma lipid alterations, given relatively modest effects on plasma HDL cholesterol and triglyceride levels among fenofibrate-treated participants in both trials.

A number of other agents have been evaluated for benefit in treatment of diabetic retinopathy, including ACE inhibitors, inhibitors of advanced glycation endproduct formation, growth hormone antagonists, antioxidants, and others. At the present time, the systemic strategies with a definite role in the management of

diabetic retinopathy involve those interventions effective in controlling underlying hyperglycemia, hypertension, and dyslipidemia.

Conclusion

Diabetic retinopathy is a leading cause of vision loss in working-age Americans and a significant cause of blindness worldwide.[226,227] Its impact is expected to grow in the setting of profound increases in prevalence of DM projected in coming decades. At the present time, one in 9 American adults has DM. The Centers for Disease Control and Prevention predict prevalence among Americans will increase to between one in 5 and one in 3 by 2050.[65] The International Diabetes Federation estimates that as many as 592 million people worldwide will have DM in 2035, an increase from the approximately 387 million people estimated to have the disease in 2014.[228]

We have made tremendous progress in managing diabetic retinopathy. Large well-designed clinical trials have provided important information about the benefits of controlling hyperglycemia and hypertension to lower risk of retinopathy and its complications. Landmark studies in the 1970s and 1980s established the efficacy of laser photocoagulation, which reduces risk of moderate vision loss from DME by 50% and risk of blindness from PDR by 90%. Recent clinical trials have established the superiority of VEGF antagonists delivered by intravitreous injection compared with focal/grid laser photocoagulation for DME involving the center of the macula. Present treatment strategies offer vision gain in a significant proportion of patients.

Significant challenges remain, however. To combat the increasing burden of disease, we must develop better preventive strategies. To realize the benefits of existing treatments, we must greatly improve our success at screening and surveillance for diabetic retinopathy and facilitate access to timely therapy. To develop more effective treatments, we must better understand the biochemical and cellular basis for disease and rationally target key pathways. The recent success of intravitreous pharmacotherapy for treatment of DME represents a significant milestone in rational design of therapy, and

will hopefully galvanize development of better methods for sustained drug delivery to the retina. If the achievements of the last several decades are predictive of further progress, we stand to make significant further strides in eliminating vision loss secondary to diabetic retinopathy in the near future.

References

1. Cogan DG, Toussaint D, Kuwabara T. Retinal vascular patterns. IV. Diabetic retinopathy. *Arch Ophthalmol*. 1961;66:366–378.
2. Cogan DG, Kuwabara T. Capillary shunts in the pathogenesis of diabetic retinopathy. *Diabetes*. 1963;12:293–300.
3. Kuwabara T, Cogan DG. Retinal vascular patterns. VI. Mural cells of the retinal capillaries. *Arch Ophthalmol*. 1963;69:492–502.
4. Toussaint D, Dustin P. Electron microscopy of normal and diabetic retinal capillaries. *Arch Ophthalmol*. 1963;70:96–108.
5. Speiser P, Gittelsohn AM, Patz A. Studies on diabetic retinopathy. 3. Influence of diabetes on intramural pericytes. *Arch Ophthalmol*. 1968;80:332–337.
6. Babel J, Leuenberger P. A long term study on the ocular lesions in streptozotocin diabetic rats. *Albrecht Von Graefes Arch Klin Exp Ophthalmol*. 1974;189:191–209.
7. Robison WG Jr, Kador PF, Kinoshita JH. Retinal capillaries: basement membrane thickening by galactosemia prevented with aldose reductase inhibitor. *Science*. 1983;221:1177–1179.
8. Sima AA, Garcia-Salinas R, Basu PK. The BB Wistar rat: an experimental model for the study of diabetic retinopathy. *Metabolism*. 1983;32:136–140.
9. Engerman RL, Kern TS. Experimental galactosemia produces diabetic-like retinopathy. *Diabetes*. 1984;33:97–100.
10. Kozak WM, Marker NA, Elmer KK. Effects of aldose reductase inhibition on the retina and health indices of streptozotocin-diabetic rats. *Doc Ophthalmol*. 1986;64:355–377.
11. Kador PF, Akagi Y, Terubayashi H, et al. Prevention of

pericyte ghost formation in retinal capillaries of galactose-fed dogs by aldose reductase inhibitors. *Arch Ophthalmol*. 1988;106:1099–1102.
12. Kador PF, Akagi Y, Takahashi Y, et al. Prevention of retinal vessel changes associated with diabetic retinopathy in galactose-fed dogs by aldose reductase inhibitors. *Arch Ophthalmol*. 1990;108:1301–1309.
13. Takahashi Y, Wyman M, Ferris F 3rd, et al. Diabetes like preproliferative retinal changes in galactose-fed dogs. *Arch Ophthalmol*. 1992;110:1295–1302.
14. Kern TS, Engerman RL. Comparison of retinal lesions in alloxan-diabetic rats and galactose-fed rats. *Curr Eye Res*. 1994;13:863–867.
15. Engerman RL, Kern TS. Retinopathy in animal models of diabetes. *Diabetes Metab Rev*. 1995;11:109–120.
16. Kador PF, Takahashi Y, Wyman M, et al. Diabetes like proliferative retinal changes in galactose-fed dogs. *Arch Ophthalmol*. 1995;113:352–354.
17. Kern TS, Engerman RL. Galactose-induced retinal microangiopathy in rats. *Invest Ophthalmol Vis Sci*. 1995;36:490–496.
18. Robison WG Jr. Diabetic retinopathy: galactose-fed rat model. *Invest Ophthalmol Vis Sci*. 1995;36(4A):1743–1744.
19. Kobayashi T, Kubo E, Takahashi Y, et al. Retinal vessel changes in galactose-fed dogs. *Arch Ophthalmol*. 1998;116:785–789.
20. Kador PF, Takahashi Y, Akagi Y, et al. Age-dependent retinal capillary pericyte degeneration in galactose-fed dogs. *J Ocul Pharmacol Ther*. 2007;23:63–69.
21. Roy S, Ha J, Trudeau K, et al. Vascular basement membrane thickening in diabetic retinopathy. *Curr Eye Res*. 2010;35:1045–1056.
22. Barber AJ. A new view of diabetic retinopathy: a neurodegenerative disease of the eye. *Prog Neuropsychopharmacol Biol Psychiatry*. 2003;27:283–290.
23. Barber AJ, Lieth E, Khin SA, et al. Neural apoptosis in the retina during experimental and human diabetes. Early onset and effect of insulin. *J Clin Invest*. 1998;102:783–791.

24. Lieth E, Barber AJ, Xu B, et al. Glial reactivity and impaired glutamate metabolism in short-term experimental diabetic retinopathy. Penn State Retina Research Group. *Diabetes*. 1998;47:815–820.
25. Lieth E, Gardner TW, Barber AJ, et al. Retinal neurodegeneration: early pathology in diabetes. *Clin Experiment Ophthalmol*. 2000;28:3–8.
26. Martin PM, Roon P, Van Ells TK, et al. Death of retinal neurons in streptozotocin-induced diabetic mice. *Invest Ophthalmol Vis Sci*. 2004;45:3330–3336.
27. Mizutani M, Gerhardinger C, Lorenzi M. Muller cell changes in human diabetic retinopathy. *Diabetes*. 1998;47:445–449.
28. Whitmire W, Al-Gayyar MM, Abdelsaid M, et al. Alteration of growth factors and neuronal death in diabetic retinopathy: what we have learned so far. *Mol Vis*. 2011;17:300–308.
29. Della Sala S, Bertoni G, Somazzi L, et al. Impaired contrast sensitivity in diabetic patients with and without retinopathy: a new technique for rapid assessment. *Br J Ophthalmol*. 1985;69:136–142.
30. Greenstein V, Sarter B, Hood D, et al. Hue discrimination and S cone pathway sensitivity in early diabetic retinopathy. *Invest Ophthalmol Vis Sci*. 1990;31:1008–1014.
31. Kurtenbach A, Wagner U, Neu A, et al. Brightness matching and colour discrimination in young diabetics without retinopathy. *Vision Res*. 1994;34:115–122.
32. Sokol S, Moskowitz A, Skarf B, et al. Contrast sensitivity in diabetics with and without background retinopathy. *Arch Ophthalmol*. 1985;103:51–54.
33. Tregear SJ, Knowles PJ, Ripley LG, et al. Chromatic-contrast threshold impairment in diabetes. *Eye (Lond)*. 1997;11(Pt 4):537–546.
34. Trick GL, Burde RM, Gordon MO, et al. The relationship between hue discrimination and contrast sensitivity deficits in patients with diabetes mellitus. *Ophthalmology*. 1988;95:693–698.
35. Klein R, Meuer SM, Moss SE, et al. The relationship of retinal microaneurysm counts to the 4-year progression of

diabetic retinopathy. *Arch Ophthalmol*. 1989;107:1780–1785.
36. Klein R, Meuer SM, Moss SE, et al. Retinal microaneurysm counts and 10-year progression of diabetic retinopathy. *Arch Ophthalmol*. 1995;113:1386–1391.
37. Kohner EM, Sleightholm M. Does microaneurysm count reflect severity of early diabetic retinopathy? *Ophthalmology*. 1986;93:586–589.
38. Early Treatment Diabetic Retinopathy Study Research Group. Photocoagulation for diabetic macular edema. Early Treatment Diabetic Retinopathy Study report number 1. *Arch Ophthalmol*. 1985;103:1796–1806.
39. Kohner EM, Henkind P. Correlation of fluorescein angiogram and retinal digest in diabetic retinopathy. *Am J Ophthalmol*. 1970;69:403–414.
40. Adamis AP, Miller JW, Bernal MT, et al. Increased vascular endothelial growth factor levels in the vitreous of eyes with proliferative diabetic retinopathy. *Am J Ophthalmol*. 1994;118:445–450.
41. Aiello LP, Avery RL, Arrigg PG, et al. Vascular endothelial growth factor in ocular fluid of patients with diabetic retinopathy and other retinal disorders. *N Engl J Med*. 1994;331:1480–1487.
42. Fraser-Bell S, Ying-Lai M, Klein R, et al. Prevalence and associations of epiretinal membranes in Latinos: the Los Angeles Latino Eye Study. *Invest Ophthalmol Vis Sci*. 2004;45:1732–1736.
43. Kawasaki R, Wang JJ, Sato H, et al. Prevalence and associations of epiretinal membranes in an adult Japanese population: the Funagata study. *Eye (Lond)*. 2009;23:1045–1051.
44. Klein R, Klein BE, Wang Q, et al. The epidemiology of epiretinal membranes. *Trans Am Ophthalmol Soc*. 1994;92:403–425 [discussion 25–30].
45. Mitchell P, Smith W, Chey T, et al. Prevalence and associations of epiretinal membranes. The Blue Mountains Eye Study, Australia. *Ophthalmology*. 1997;104:1033–1040.
46. Ng CH, Cheung N, Wang JJ, et al. Prevalence and risk factors for epiretinal membranes in a multi-ethnic United

States population. *Ophthalmology*. 2011;118:694–699.
47. Sebag J. Anomalous posterior vitreous detachment: a unifying concept in vitreo-retinal disease. *Graefes Arch Clin Exp Ophthalmol*. 2004;242:690–698.
48. Barile GR, Pachydaki SI, Tari SR, et al. The RAGE axis in early diabetic retinopathy. *Invest Ophthalmol Vis Sci*. 2005;46:2916–2924.
49. Gao BB, Chen X, Timothy N, et al. Characterization of the vitreous proteome in diabetes without diabetic retinopathy and diabetes with proliferative diabetic retinopathy. *J Proteome Res*. 2008;7:2516–2525.
50. Kim T, Kim SJ, Kim K, et al. Profiling of vitreous proteomes from proliferative diabetic retinopathy and nondiabetic patients. *Proteomics*. 2007;7:4203–4215.
51. Sebag J, Buckingham B, Charles MA, et al. Biochemical abnormalities in vitreous of humans with proliferative diabetic retinopathy. *Arch Ophthalmol*. 1992;110:1472–1476.
52. Shitama T, Hayashi H, Noge S, et al. Proteome profiling of vitreoretinal diseases by cluster analysis. *Proteomics Clin Appl*. 2008;2:1265–1280.
53. Holekamp NM. The vitreous gel: more than meets the eye. *Am J Ophthalmol*. 2010;149:32–36.
54. Shui YB, Holekamp NM, Kramer BC, et al. The gel state of the vitreous and ascorbate-dependent oxygen consumption: relationship to the etiology of nuclear cataracts. *Arch Ophthalmol*. 2009;127:475–482.
55. Chen MS, Kao CS, Chang CJ, et al. Prevalence and risk factors of diabetic retinopathy among noninsulin-dependent diabetic subjects. *Am J Ophthalmol*. 1992;114:723–730.
56. Cikamatana L, Mitchell P, Rochtchina E, et al. Five-year incidence and progression of diabetic retinopathy in a defined older population: the Blue Mountains Eye Study. *Eye (Lond)*. 2007;21:465–471.
57. Klein R, Klein BE, Moss SE, et al. The Wisconsin Epidemiologic Study of diabetic retinopathy. XIV. Ten-year incidence and progression of diabetic retinopathy. *Arch Ophthalmol*. 1994;112:1217–1228.

58. Klein R, Klein BE, Moss SE, et al. The Wisconsin Epidemiologic Study of diabetic retinopathy. III. Prevalence and risk of diabetic retinopathy when age at diagnosis is 30 or more years. *Arch Ophthalmol*. 1984;102:527–532.
59. Klein R, Klein BE, Moss SE, et al. The Wisconsin Epidemiologic Study of diabetic retinopathy. II. Prevalence and risk of diabetic retinopathy when age at diagnosis is less than 30 years. *Arch Ophthalmol*. 1984;102:520–526.
60. Leske MC, Wu SY, Hennis A, et al. Hyperglycemia, blood pressure, and the 9-year incidence of diabetic retinopathy: the Barbados Eye Studies. *Ophthalmology*. 2005;112:799–805.
61. Svensson M, Eriksson JW, Dahlquist G. Early glycemic control, age at onset, and development of microvascular complications in childhood-onset type 1 diabetes: a population-based study in northern Sweden. *Diabetes Care*. 2004;27:955–962.
62. Varma R, Choudhury F, Klein R, et al. Four-year incidence and progression of diabetic retinopathy and macular edema: the Los Angeles Latino Eye Study. *Am J Ophthalmol*. 2010;149:752–761 e1–3.
63. Wong TY, Cheung N, Tay WT, et al. Prevalence and risk factors for diabetic retinopathy: the Singapore Malay Eye Study. *Ophthalmology*. 2008;115:1869–1875.
64. Zhang X, Saaddine JB, Chou CF, et al. Prevalence of diabetic retinopathy in the United States, 2005–2008. *JAMA*. 2010;304:649–656.
65. Centers for Disease Control and Prevention. *National Diabetes Statistics Report: Estimates of diabetes and its burden in the United States*. [Atlanta, GA: CDC; Update 2015, May 15. Online] http://www.cdc.gov/diabetes/data/statistics/2014StatisticsRe 2014.
66. The Diabetes Control and Complications Trial Research Group. The effect of intensive treatment of diabetes on the development and progression of long-term complications in insulin-dependent diabetes mellitus. *N Engl J Med*. 1993;329:977–986.
67. Diabetes Control and Complications Trial Research Group.

The relationship of glycemic exposure (HbA1c) to the risk of development and progression of retinopathy in the diabetes control and complications trial. *Diabetes*. 1995;44:968–983.
68. UK Prospective Diabetes Study (UKPDS) Group. Intensive blood-glucose control with sulphonylureas or insulin compared with conventional treatment and risk of complications in patients with type 2 diabetes (UKPDS 33). *Lancet*. 1998;352:837–853.
69. UK Prospective Diabetes Study (UKPDS) Group. Effect of intensive blood-glucose control with metformin on complications in overweight patients with type 2 diabetes (UKPDS 34). *Lancet*. 1998;352:854–865.
70. The Diabetes Control and Complications Trial/Epidemiology of Diabetes Intervention and Complications Study Research Group. Effect of intensive therapy on the microvascular complications of type 1 diabetes mellitus. *JAMA*. 2002;287:2563–2569.
71. Holman RR, Paul SK, Bethel MA, et al. 10-year follow-up of intensive glucose control in type 2 diabetes. *N Engl J Med*. 2008;359:1577–1589.
72. Chew EY, Ambrosius WT, Davis MD, et al. Effects of medical therapies on retinopathy progression in type 2 diabetes. *N Engl J Med*. 2010;363:233–244.
73. The effect of intensive diabetes treatment on the progression of diabetic retinopathy in insulin-dependent diabetes mellitus. The Diabetes Control and Complications Trial. *Arch Ophthalmol*. 1995;113:36–51.
74. UK Prospective Diabetes Study Group. Tight blood pressure control and risk of macrovascular and microvascular complications in type 2 diabetes: UKPDS 38. *BMJ*. 1998;317:703–713.
75. Klein BE, Moss SE, Klein R, et al. The Wisconsin Epidemiologic Study of Diabetic Retinopathy. XIII. Relationship of serum cholesterol to retinopathy and hard exudate. *Ophthalmology*. 1991;98:1261–1265.
76. Chew EY, Klein ML, Ferris FL 3rd, et al. Association of elevated serum lipid levels with retinal hard exudate in

diabetic retinopathy. Early Treatment Diabetic Retinopathy Study (ETDRS) Report 22. *Arch Ophthalmol*. 1996;114:1079–1084.
77. Davis MD, Fisher MR, Gangnon RE, et al. Risk factors for high-risk proliferative diabetic retinopathy and severe visual loss: Early Treatment Diabetic Retinopathy Study Report no. 18. *Invest Ophthalmol Vis Sci*. 1998;39:233–252.
78. Keech AC, Mitchell P, Summanen PA, et al. Effect of fenofibrate on the need for laser treatment for diabetic retinopathy (FIELD study): a randomised controlled trial. *Lancet*. 2007;370:1687–1697.
79. Janka HU, Warram JH, Rand LI, et al. Risk factors for progression of background retinopathy in long-standing IDDM. *Diabetes*. 1989;38:460–464.
80. Rand LI, Prud'homme GJ, Ederer F, et al. Factors influencing the development of visual loss in advanced diabetic retinopathy. Diabetic Retinopathy Study (DRS) Report no. 10. *Invest Ophthalmol Vis Sci*. 1985;26:983–991.
81. Berman DH, Friedman EA. Partial absorption of hard exudates in patients with diabetic end-stage renal disease and severe anemia after treatment with erythropoietin. *Retina*. 1994;14:1–5.
82. Qiao Q, Keinanen-Kiukaanniemi S, Laara E. The relationship between hemoglobin levels and diabetic retinopathy. *J Clin Epidemiol*. 1997;50:153–158.
83. Shorb SR. Anemia and diabetic retinopathy. *Am J Ophthalmol*. 1985;100:434–436.
84. Krolewski AS, Barzilay J, Warram JH, et al. Risk of early-onset proliferative retinopathy in IDDM is closely related to cardiovascular autonomic neuropathy. *Diabetes*. 1992;41:430–437.
85. Tesfaye S, Stevens LK, Stephenson JM, et al. Prevalence of diabetic peripheral neuropathy and its relation to glycaemic control and potential risk factors: the EURODIAB IDDM Complications Study. *Diabetologia*. 1996;39:1377–1384.
86. American Academy of Ophthalmology Retina Panel. *Preferred Practice Pattern® guidelines: Diabetic retinopathy*. [San Francisco, CA: AAO] http://www.aao.org/preferred-

practice-pattern/diabetic-retinopathy-ppp--2014; 2014.
87. Klein R, Klein BE, Neider MW, et al. Diabetic retinopathy as detected using ophthalmoscopy, a nonmydriatic camera and a standard fundus camera. *Ophthalmology*. 1985;92:485–491.
88. Yannuzzi LA, Rohrer KT, Tindel LJ, et al. Fluorescein angiography complication survey. *Ophthalmology*. 1986;93:611–617.
89. *AK-FLUOR (fluorescein sodium) injection for intravenous use*. [Full prescribing information. Package insert. Revised 7/] 2008.
90. Forooghian F, Cukras C, Meyerle CB, et al. Evaluation of time domain and spectral domain optical coherence tomography in the measurement of diabetic macular edema. *Invest Ophthalmol Vis Sci*. 2008;49:4290–4296.
91. Jia Y, Bailey ST, Hwang TS, et al. Quantitative optical coherence tomography angiography of vascular abnormalities in the living human eye. *Proc Natl Acad Sci USA*. 2015;112:E2395–402.
92. Schwartz DM, Fingler J, Kim DY, et al. Phase-variance optical coherence tomography: a technique for noninvasive angiography. *Ophthalmology*. 2014;121:180–187.
93. Ishibazawa A, Nagaoka T, Takahashi A, et al. Optical coherence tomography angiography in diabetic retinopathy: a prospective pilot study. *Am J Ophthalmol*. 2015;160:35–44.
94. *Diabetic Retinopathy Clinical Research Network*. http://drcrnet.jaeb.org/; 2007–15.
95. Bressler SB, Edwards AR, Chalam KV, et al. Reproducibility of spectral-domain optical coherence tomography retinal thickness measurements and conversion to equivalent time-domain metrics in diabetic macular edema. *JAMA Ophthalmol*. 2014;132:1113–1122.
96. Diabetic Retinopathy Clinical Research Network. Aflibercept, bevacizumab, or ranibizumab for diabetic macular edema. *N Engl J Med*. 2015;372:1193–1203.
97. Bressler NM, Edwards AR, Antoszyk AN, et al. Retinal thickness on Stratus optical coherence tomography in

people with diabetes and minimal or no diabetic retinopathy. *Am J Ophthalmol*. 2008;145:894–901.
98. Krzystolik MG, Strauber SF, Aiello LP, et al. Reproducibility of macular thickness and volume using Zeiss optical coherence tomography in patients with diabetic macular edema. *Ophthalmology*. 2007;114:1520–1525.
99. Diabetic Retinopathy Study Research Group. A modification of the Airlie House classification of diabetic retinopathy. Report no. 7. *Invest Ophthalmol Vis Sci*. 1981;21:210–226.
100. Grading diabetic retinopathy from stereoscopic color fundus photographs – an extension of the modified Airlie House classification. ETDRS report number 10. Early Treatment Diabetic Retinopathy Study Research Group. *Ophthalmology*. 1991;98:786–806.
101. Fundus photographic risk factors for progression of diabetic retinopathy. ETDRS report no. 12. Early Treatment Diabetic Retinopathy Study Research Group. *Ophthalmology*. 1991;98:823–833.
102. Early photocoagulation for diabetic retinopathy. ETDRS report no. 9. Early Treatment Diabetic Retinopathy Study Research Group. *Ophthalmology*. 1991;98:766–785.
103. Klein R, Klein BE, Moss SE. How many steps of progression of diabetic retinopathy are meaningful? The Wisconsin Epidemiologic Study of diabetic retinopathy. *Arch Ophthalmol*. 2001;119:547–553.
104. Murphy RP. Management of diabetic retinopathy. *Am Fam Physician*. 1995;51:785–796.
105. Wilkinson CP, Ferris FL 3rd, Klein RE, et al. Proposed international clinical diabetic retinopathy and diabetic macular edema disease severity scales. *Ophthalmology*. 2003;110:1677–1682.
106. Brown JC, Solomon SD, Bressler SB, et al. Detection of diabetic foveal edema: contact lens biomicroscopy compared with optical coherence tomography. *Arch Ophthalmol*. 2004;122:330–335.
107. Davis MD, Bressler SB, Aiello LP, et al. Comparison of time-domain OCT and fundus photographic assessments of retinal thickening in eyes with diabetic macular edema.

Invest Ophthalmol Vis Sci. 2008;49:1745–1752.
108. Browning DJ, Glassman AR, Aiello LP, et al. Optical coherence tomography measurements and analysis methods in optical coherence tomography studies of diabetic macular edema. *Ophthalmology*. 2008;115:1366–1371 [1371.e1].
109. Fluorescein angiographic risk factors for progression of diabetic retinopathy. ETDRS report number 13. Early Treatment Diabetic Retinopathy Study Research Group. *Ophthalmology*. 1991;98:834–840.
110. Danis RP, Scott IU, Qin H, et al. Association of fluorescein angiographic features with visual acuity and with optical coherence tomographic and stereoscopic color fundus photographic features of diabetic macular edema in a randomized clinical trial. *Retina*. 2010;30:1627–1637.
111. Neubauer AS, Chryssafis C, Priglinger SG, et al. Topography of diabetic macular oedema compared with fluorescein angiography. *Acta Ophthalmol Scand*. 2007;85:32–39.
112. Framme C, Roider J. Immediate and long-term changes of fundus autofluorescence in continuous wave laser lesions of the retina. *Ophthalmic Surg Lasers Imaging*. 2004;35:131–138.
113. Muqit MM, Gray JC, Marcellino GR, et al. Fundus autofluorescence and Fourier-domain optical coherence tomography imaging of 10 and 20 millisecond Pascal retinal photocoagulation treatment. *Br J Ophthalmol*. 2009;93:518–525.
114. Fong DS, Segal PP, Myers F, et al. Subretinal fibrosis in diabetic macular edema. ETDRS report 23. Early Treatment Diabetic Retinopathy Study Research Group. *Arch Ophthalmol*. 1997;115:873–877.
115. Bandello F, Polito A, Del Borrello M, et al. "Light" versus "classic" laser treatment for clinically significant diabetic macular oedema. *Br J Ophthalmol*. 2005;89:864–870.
116. Catier A, Tadayoni R, Paques M, et al. Characterization of macular edema from various etiologies by optical coherence tomography. *Am J Ophthalmol*. 2005;140:200–206.
117. Goebel W, Kretzchmar-Gross T. Retinal thickness in diabetic

retinopathy: a study using optical coherence tomography (OCT). *Retina*. 2002;22:759–767.
118. Hee MR, Puliafito CA, Wong C, et al. Quantitative assessment of macular edema with optical coherence tomography. *Arch Ophthalmol*. 1995;113:1019–1029.
119. Laursen ML, Moeller F, Sander B, et al. Subthreshold micropulse diode laser treatment in diabetic macular oedema. *Br J Ophthalmol*. 2004;88:1173–1179.
120. Massin P, Duguid G, Erginay A, et al. Optical coherence tomography for evaluating diabetic macular edema before and after vitrectomy. *Am J Ophthalmol*. 2003;135:169–177.
121. Otani T, Kishi S. Tomographic findings of foveal hard exudates in diabetic macular edema. *Am J Ophthalmol*. 2001;131:50–54.
122. Ozdemir H, Karacorlu M, Karacorlu SA. Regression of serous macular detachment after intravitreal triamcinolone acetonide in patients with diabetic macular edema. *Am J Ophthalmol*. 2005;140:251–255.
123. Browning DJ, Glassman AR, Aiello LP, et al. Relationship between optical coherence tomography-measured central retinal thickness and visual acuity in diabetic macular edema. *Ophthalmology*. 2007;114:525–536.
124. Danis RP, Glassman AR, Aiello LP, et al. Diurnal variation in retinal thickening measurement by optical coherence tomography in center-involved diabetic macular edema. *Arch Ophthalmol*. 2006;124:1701–1707.
125. American Diabetes Association. Standards of medical care in diabetes – 2015. *Diabetes Care*. 2015;38(Suppl. 1):S1–93.
126. Lachin JM. Point: Intensive glycemic control and mortality in ACCORD – a chance finding? *Diabetes Care*. 2010;33:2719–2721.
127. Riddle MC. Counterpoint: Intensive glucose control and mortality in ACCORD – still looking for clues. *Diabetes Care*. 2010;33:2722–2724.
128. Gerstein HC, Miller ME, Genuth S, et al. Long-term effects of intensive glucose lowering on cardiovascular outcomes. *N Engl J Med*. 2011;364:818–828.
129. Fong DS, Sharza M, Chen W, et al. Vision loss among

diabetics in a group model Health Maintenance Organization (HMO). *Am J Ophthalmol*. 2002;133:236–241.
130. Kraft SK, Marrero DG, Lazaridis EN, et al. Primary care physicians' practice patterns and diabetic retinopathy. Current levels of care. *Arch Fam Med*. 1997;6:29–37.
131. Lee PP, Feldman ZW, Ostermann J, et al. Longitudinal rates of annual eye examinations of persons with diabetes and chronic eye diseases. *Ophthalmology*. 2003;110:1952–1959.
132. Paz SH, Varma R, Klein R, et al. Noncompliance with vision care guidelines in Latinos with type 2 diabetes mellitus: the Los Angeles Latino Eye Study. *Ophthalmology*. 2006;113:1372–1377.
133. Schoenfeld ER, Greene JM, Wu SY, et al. Patterns of adherence to diabetes vision care guidelines: baseline findings from the Diabetic Retinopathy Awareness Program. *Ophthalmology*. 2001;108:563–571.
134. Zimmer-Galler IE, Kimura AE, Gupta S. Diabetic retinopathy screening and the use of telemedicine. *Curr Opin Ophthalmol*. 2015;26:167–172.
135. Kirkizlar E, Serban N, Sisson JA, et al. Evaluation of telemedicine for screening of diabetic retinopathy in the Veterans Health Administration. *Ophthalmology*. 2013;120:2604–2610.
136. Liew G, Michaelides M, Bunce C. A comparison of the causes of blindness certifications in England and Wales in working age adults (16–64 years), 1999–2000 with 2009–2010. *BMJ Open*. 2014;4:e004015.
137. Looker HC, Nyangoma SO, Cromie DT, et al. Rates of referable eye disease in the Scottish National Diabetic Retinopathy Screening Programme. *Br J Ophthalmol*. 2014;98:790–795.
138. Silva PS, Aiello LP. Telemedicine and eye examinations for diabetic retinopathy: a time to maximize real-world outcomes. *JAMA Ophthalmol*. 2015;133:525–526.
139. Ahmed J, Ward TP, Bursell SE, et al. The sensitivity and specificity of nonmydriatic digital stereoscopic retinal imaging in detecting diabetic retinopathy. *Diabetes Care*. 2006;29:2205–2209.

140. Bursell SE, Cavallerano JD, Cavallerano AA, et al. Stereo nonmydriatic digital-video color retinal imaging compared with Early Treatment Diabetic Retinopathy Study seven standard field 35-mm stereo color photos for determining level of diabetic retinopathy. *Ophthalmology*. 2001;108:572–585.
141. Fransen SR, Leonard-Martin TC, Feuer WJ, et al. Clinical evaluation of patients with diabetic retinopathy: accuracy of the Inoveon diabetic retinopathy-3DT system. *Ophthalmology*. 2002;109:595–601.
142. Lin DY, Blumenkranz MS, Brothers RJ, et al. The sensitivity and specificity of single-field nonmydriatic monochromatic digital fundus photography with remote image interpretation for diabetic retinopathy screening: a comparison with ophthalmoscopy and standardized mydriatic color photography. *Am J Ophthalmol*. 2002;134:204–213.
143. Schiffman RM, Jacobsen G, Nussbaum JJ, et al. Comparison of a digital retinal imaging system and seven-field stereo color fundus photography to detect diabetic retinopathy in the primary care environment. *Ophthalmic Surg Lasers Imaging*. 2005;36:46–56.
144. Tennant MT, Greve MD, Rudnisky CJ, et al. Identification of diabetic retinopathy by stereoscopic digital imaging via teleophthalmology: a comparison to slide film. *Can J Ophthalmol*. 2001;36:187–196.
145. Whited JD. Accuracy and reliability of teleophthalmology for diagnosing diabetic retinopathy and macular edema: a review of the literature. *Diabetes Technol Ther*. 2006;8:102–111.
146. Kernt M, Hadi I, Pinter F, et al. Assessment of diabetic retinopathy using nonmydriatic ultra-widefield scanning laser ophthalmoscopy (Optomap) compared with ETDRS 7-field stereo photography. *Diabetes Care*. 2012;35:2459–2463.
147. Silva PS, Cavallerano JD, Sun JK, et al. Nonmydriatic ultrawide field retinal imaging compared with dilated standard 7-field 35-mm photography and retinal specialist examination for evaluation of diabetic retinopathy. *Am J*

Ophthalmol. 2012;154:549–559.
148. Elman MJ, Aiello LP, Beck RW, et al. Randomized trial evaluating ranibizumab plus prompt or deferred laser or triamcinolone plus prompt laser for diabetic macular edema. *Ophthalmology*. 2010;117:1064–1077.e35.
149. Mitchell P, Bandello F, Schmidt-Erfurth U, et al. The RESTORE study: ranibizumab monotherapy or combined with laser versus laser monotherapy for diabetic macular edema. *Ophthalmology*. 2011;118:615–625.
150. Michaelides M, Kaines A, Hamilton RD, et al. A prospective randomized trial of intravitreal bevacizumab or laser therapy in the management of diabetic macular edema (BOLT study) 12-month data: report 2. *Ophthalmology*. 2010;117:1078–1086.e2.
151. Nguyen QD, Brown DM, Marcus DM, et al. Ranibizumab for diabetic macular edema: results from 2 phase III randomized trials: RISE and RIDE. *Ophthalmology*. 2012;119:789–801.
152. Korobelnik JF, Do DV, Schmidt-Erfurth U, et al. Intravitreal aflibercept for diabetic macular edema. *Ophthalmology*. 2014;121:2247–2254.
153. *LUCENTIS – ranibizumab injection, solution (Genentech, Inc)*. [Full prescribing information. Package insert. Updated 2/] 2015.
154. *EYLEA – aflibercept injection, solution (Regeneron Pharmaceuticals, Inc)*. [Full prescribing information. Package insert. Updated 8/] 2015.
155. Campochiaro PA, Brown DM, Pearson A, et al. Long-term benefit of sustained-delivery fluocinolone acetonide vitreous inserts for diabetic macular edema. *Ophthalmology*. 2011;118:626–635.
156. Boyer DS, Yoon YH, Belfort R Jr, et al. Three-year, randomized, sham-controlled trial of dexamethasone intravitreal implant in patients with diabetic macular edema. *Ophthalmology*. 2014;121:1904–1914.
157. *ILUVIEN – Fluocinolone acetonide implant*. [Package insert. Full prescribing information. Updated 12/] 2014.
158. *OZURDEX – dexamethasone implant*. [Package insert. Full

prescribing information. Updated 9/] 2014.
159. Diabetic Retinopathy Clinical Research Network, et al. Observational study of subclinical diabetic macular edema. *Eye (Lond)*. 2012;26:833–840.
160. Hofman P, Blaauwgeers HG, Tolentino MJ, et al. VEGF-A induced hyperpermeability of blood–retinal barrier endothelium in vivo is predominantly associated with pinocytotic vesicular transport and not with formation of fenestrations. Vascular endothelial growth factor-A. *Curr Eye Res*. 2000;21:637–645.
161. Michels S, Rosenfeld PJ, Puliafito CA, et al. Systemic bevacizumab (Avastin) therapy for neovascular age-related macular degeneration twelve-week results of an uncontrolled open-label clinical study. *Ophthalmology*. 2005;112:1035–1047.
162. Moshfeghi AA, Rosenfeld PJ, Puliafito CA, et al. Systemic bevacizumab (Avastin) therapy for neovascular age-related macular degeneration: twenty-four-week results of an uncontrolled open-label clinical study. *Ophthalmology*. 2006;113:2002.e1–2002.e12.
163. Nguyen QD, Shah SM, Hafiz G, et al. A phase I trial of an IV-administered vascular endothelial growth factor trap for treatment in patients with choroidal neovascularization due to age-related macular degeneration. *Ophthalmology*. 2006;113:1522.e1–1522.e14.
164. Elman MJ, Bressler NM, Qin H, et al. Expanded 2-year follow-up of ranibizumab plus prompt or deferred laser or triamcinolone plus prompt laser for diabetic macular edema. *Ophthalmology*. 2011;118:609–614.
165. Brown DM, Nguyen QD, Marcus DM, et al. Long-term outcomes of ranibizumab therapy for diabetic macular edema: the 36-month results from two phase III trials: RISE and RIDE. *Ophthalmology*. 2013;120:2013–2022.
166. Elman MJ, Ayala A, Bressler NM, et al. Intravitreal Ranibizumab for diabetic macular edema with prompt versus deferred laser treatment: 5-year randomized trial results. *Ophthalmology*. 2015;122:375–381.
167. Bhavsar AR, Glassman AR, Stockdale CR, et al. Elimination

of topical antibiotics for intravitreous injections and the importance of using povidone-iodine; Update from the Diabetic Retinopathy Clinical Research Network. *JAMA Ophthalmol*. 2016;134:1181–1183.
168. Chen RW, Rachitskaya A, Scott IU, et al. Is the use of topical antibiotics for intravitreal injections the standard of care or are we better off without antibiotics? *JAMA Ophthalmol*. 2013;131:840–842.
169. Bressler SB, Almukhtar T, Bhorade A, et al. Repeated intravitreous ranibizumab injections for diabetic macular edema and the risk of sustained elevation of intraocular pressure or the need for ocular hypotensive treatment. *JAMA Ophthalmol*. 2015;133:589–597.
170. Virgili G, Parravano M, Menchini F, et al. Antivascular endothelial growth factor for diabetic macular oedema. *Cochrane Database Syst Rev*. 2014;(10) [CD007419].
171. Moja L, Lucenteforte E, Kwag KH, et al. Systemic safety of bevacizumab versus ranibizumab for neovascular age-related macular degeneration. *Cochrane Database Syst Rev*. 2014;(9) [CD011230].
172. Crum R, Szabo S, Folkman J. A new class of steroids inhibits angiogenesis in the presence of heparin or a heparin fragment. *Science*. 1985;230:1375–1378.
173. Folkman J, Ingber DE. Angiostatic steroids. Method of discovery and mechanism of action. *Ann Surg*. 1987;206:374–383.
174. Gordon DM. Prednisone and prednisolone in ocular disease. *Am J Ophthalmol*. 1956;41:593–600.
175. Ingber DE, Madri JA, Folkman J. A possible mechanism for inhibition of angiogenesis by angiostatic steroids: induction of capillary basement membrane dissolution. *Endocrinology*. 1986;119:1768–1775.
176. Fauci A. Clinical aspects of immunosuppression: use of cytotoxic agents and corticosteroids. Bellanti JA. *Immunology II*. WB Saunders: Philadelphia; 1978.
177. Nussenblatt R, Whitcup S, Palestine A. *Uveitis: fundamentals and clinical practice*. Mosby: St. Louis; 1996.
178. Diabetic Retinopathy Clinical Research Network. A

randomized trial comparing intravitreal triamcinolone acetonide and focal/grid photocoagulation for diabetic macular edema. *Ophthalmology*. 2008;115:1447–1449 [1449.e1–10].
179. Beck RW, Edwards AR, Aiello LP, et al. Three-year follow-up of a randomized trial comparing focal/grid photocoagulation and intravitreal triamcinolone for diabetic macular edema. *Arch Ophthalmol*. 2009;127:245–251.
180. Early Treatment Diabetic Retinopathy Study design and baseline patient characteristics. ETDRS report number 7. *Ophthalmology*. 1991;98:741–756.
181. Treatment techniques and clinical guidelines for photocoagulation of diabetic macular edema. Early Treatment Diabetic Retinopathy Study Report no. 2. Early Treatment Diabetic Retinopathy Study Research Group. *Ophthalmology*. 1987;94:761–774.
182. Diabetic Retinopathy Clinical Research Network. *Focal/grid photocoagulation (modified-ETDRS) technique*. [2013, Oct 25. Online] http://publicfiles.jaeb.org/FocalGridPhotocoagulation10_25_
183. Akduman L, Olk RJ. Diode laser (810 nm) versus argon green (514 nm) modified grid photocoagulation for diffuse diabetic macular edema. *Ophthalmology*. 1997;104:1433–1441.
184. Bolz M, Kriechbaum K, Simader C, et al. In vivo retinal morphology after grid laser treatment in diabetic macular edema. *Ophthalmology*. 2010;117:538–544.
185. Kumar V, Ghosh B, Mehta DK, et al. Functional outcome of subthreshold versus threshold diode laser photocoagulation in diabetic macular oedema. *Eye (Lond)*. 2010;24:1459–1465.
186. Lavinsky D, Cardillo JA, Melo LA Jr, et al. Randomized clinical trial evaluating mETDRS versus normal or high-density micropulse photocoagulation for diabetic macular edema. *Invest Ophthalmol Vis Sci*. 2011;52:4314–4323.
187. Muqit MM, Gray JC, Marcellino GR, et al. Barely visible 10-millisecond pascal laser photocoagulation for diabetic macular edema: observations of clinical effect and burn localization. *Am J Ophthalmol*. 2010;149:979–986.e2.
188. Nakamura Y, Mitamura Y, Ogata K, et al. Functional and

morphological changes of macula after subthreshold micropulse diode laser photocoagulation for diabetic macular oedema. *Eye (Lond)*. 2010;24:784–788.
189. Ohkoshi K, Yamaguchi T. Subthreshold micropulse diode laser photocoagulation for diabetic macular edema in Japanese patients. *Am J Ophthalmol*. 2010;149:133–139.
190. Venkatesh P, Ramanjulu R, Azad R, et al. Subthreshold micropulse diode laser and double frequency neodymium: YAG laser in treatment of diabetic macular edema: a prospective, randomized study using multifocal electroretinography. *Photomed Laser Surg*. 2011;29:727–733.
191. Figueira J, Khan J, Nunes S, et al. Prospective randomised controlled trial comparing sub-threshold micropulse diode laser photocoagulation and conventional green laser for clinically significant diabetic macular oedema. *Br J Ophthalmol*. 2009;93:1341–1344.
192. Jain A, Collen J, Kaines A, et al. Short-duration focal pattern grid macular photocoagulation for diabetic macular edema: four-month outcomes. *Retina*. 2010;30:1622–1626.
193. Luttrull JK, Musch DC, Mainster MA. Subthreshold diode micropulse photocoagulation for the treatment of clinically significant diabetic macular oedema. *Br J Ophthalmol*. 2005;89:74–80.
194. Fong DS, Strauber SF, Aiello LP, et al. Comparison of the modified Early Treatment Diabetic Retinopathy Study and mild macular grid laser photocoagulation strategies for diabetic macular edema. *Arch Ophthalmol*. 2007;125:469–480.
195. Harbour JW, Smiddy WE, Flynn HW Jr, et al. Vitrectomy for diabetic macular edema associated with a thickened and taut posterior hyaloid membrane. *Am J Ophthalmol*. 1996;121:405–413.
196. Kaiser PK, Riemann CD, Sears JE, et al. Macular traction detachment and diabetic macular edema associated with posterior hyaloidal traction. *Am J Ophthalmol*. 2001;131:44–49.
197. Lewis H, Abrams GW, Blumenkranz MS, et al. Vitrectomy for diabetic macular traction and edema associated with posterior hyaloidal traction. *Ophthalmology*. 1992;99:753–759.

198. Pendergast SD, Hassan TS, Williams GA, et al. Vitrectomy for diffuse diabetic macular edema associated with a taut premacular posterior hyaloid. *Am J Ophthalmol*. 2000;130:178–186.
199. Haller JA, Qin H, Apte RS, et al. Vitrectomy outcomes in eyes with diabetic macular edema and vitreomacular traction. *Ophthalmology*. 2010;117:1087–1093.e3.
200. Dillinger P, Mester U. Vitrectomy with removal of the internal limiting membrane in chronic diabetic macular oedema. *Graefes Arch Clin Exp Ophthalmol*. 2004;242:630–637.
201. Figueroa MS, Contreras I, Noval S. Surgical and anatomical outcomes of pars plana vitrectomy for diffuse nontractional diabetic macular edema. *Retina*. 2008;28:420–426.
202. Hartley KL, Smiddy WE, Flynn HW Jr, et al. Pars plana vitrectomy with internal limiting membrane peeling for diabetic macular edema. *Retina*. 2008;28:410–419.
203. Higuchi A, Ogata N, Jo N, et al. Pars plana vitrectomy with removal of posterior hyaloid face in treatment of refractory diabetic macular edema resistant to triamcinolone acetonide. *Jpn J Ophthalmol*. 2006;50:529–531.
204. Ikeda T, Sato K, Katano T, et al. Vitrectomy for cystoid macular oedema with attached posterior hyaloid membrane in patients with diabetes. *Br J Ophthalmol*. 1999;83:12–14.
205. La Heij EC, Hendrikse F, Kessels AG, et al. Vitrectomy results in diabetic macular oedema without evident vitreomacular traction. *Graefes Arch Clin Exp Ophthalmol*. 2001;239:264–270.
206. Recchia FM, Ruby AJ, Carvalho Recchia CA. Pars plana vitrectomy with removal of the internal limiting membrane in the treatment of persistent diabetic macular edema. *Am J Ophthalmol*. 2005;139:447–454.
207. Rosenblatt BJ, Shah GK, Sharma S, et al. Pars plana vitrectomy with internal limiting membranectomy for refractory diabetic macular edema without a taut posterior hyaloid. *Graefes Arch Clin Exp Ophthalmol*. 2005;243:20–25.
208. Yanyali A, Horozoglu F, Celik E, et al. Long-term outcomes of pars plana vitrectomy with internal limiting membrane removal in diabetic macular edema. *Retina*. 2007;27:557–566.

209. Patel JI, Hykin PG, Schadt M, et al. Diabetic macular oedema: pilot randomised trial of pars plana vitrectomy vs macular argon photocoagulation. *Eye (Lond)*. 2006;20:873–881.
210. Thomas D, Bunce C, Moorman C, et al. A randomised controlled feasibility trial of vitrectomy versus laser for diabetic macular oedema. *Br J Ophthalmol*. 2005;89:81–86.
211. The Diabetic Retinopathy Study Research Group. Photocoagulation treatment of proliferative diabetic retinopathy. Clinical application of Diabetic Retinopathy Study (DRS) findings, DRS Report no. 8. *Ophthalmology*. 1981;88:583–600.
212. Ip MS, Domalpally A, Hopkins JJ, et al. Long-term effects of ranibizumab on diabetic retinopathy severity and progression. *Arch Ophthalmol*. 2012;130:1145–1152.
213. Bressler NM, Edwards AR, Beck RW, et al. Exploratory analysis of diabetic retinopathy progression through 3 years in a randomized clinical trial that compares intravitreal triamcinolone acetonide with focal/grid photocoagulation. *Arch Ophthalmol*. 2009;127:1566–1571.
214. Diabetic Retinopathy Clinical Research Network. Panretinal photocoagulation vs intravitreous ranibizumab for proliferative diabetic retinopathy: a randomized clinical trial. *JAMA*. 2015;314:2137–2146.
215. The DAMAD Study Group. Effect of aspirin alone and aspirin plus dipyridamole in early diabetic retinopathy: a multicenter randomized controlled clinical trial. *Diabetes*. 1989;38:491–498.
216. The TIMAD Study Group. Ticlopidine treatment reduces the progression of nonproliferative diabetic retinopathy. *Arch Ophthalmol*. 1990;108:1577–1583.
217. Effects of aspirin treatment on diabetic retinopathy. ETDRS report number 8. Early Treatment Diabetic Retinopathy Study Research Group. *Ophthalmology*. 1991;98:757–765.
218. Chew EY, Klein ML, Murphy RP, et al. Effects of aspirin on vitreous/preretinal hemorrhage in patients with diabetes mellitus. Early Treatment Diabetic Retinopathy Study report no. 20. *Arch Ophthalmol*. 1995;113:52–55.

219. Sorbinil Retinopathy Trial Research Group. A randomized trial of sorbinil, an aldose reductase inhibitor, in diabetic retinopathy. *Arch Ophthalmol*. 1990;108:1234–1244.
220. Aiello LP, Bursell SE, Clermont A, et al. Vascular endothelial growth factor-induced retinal permeability is mediated by protein kinase C in vivo and suppressed by an orally effective beta-isoform-selective inhibitor. *Diabetes*. 1997;46:1473–1480.
221. Xu X, Zhu Q, Xia X, et al. Blood–retinal barrier breakdown induced by activation of protein kinase C via vascular endothelial growth factor in streptozotocin-induced diabetic rats. *Curr Eye Res*. 2004;28:251–256.
222. Yokota T, Ma RC, Park JY, et al. Role of protein kinase C on the expression of platelet-derived growth factor and endothelin-1 in the retina of diabetic rats and cultured retinal capillary pericytes. *Diabetes*. 2003;52:838–845.
223. Zhu Q, Xu X, Xia X, et al. Role of protein kinase C on the alteration of retinal endothelin-1 in streptozotocin-induced diabetic rats. *Exp Eye Res*. 2005;81:200–206.
224. PKC-DRS Study Group. The effect of ruboxistaurin on visual loss in patients with moderately severe to very severe nonproliferative diabetic retinopathy: initial results of the Protein Kinase C beta Inhibitor Diabetic Retinopathy Study (PKC-DRS) multicenter randomized clinical trial. *Diabetes*. 2005;54:2188–2197.
225. Aiello LP, Davis MD, Girach A, et al. Effect of ruboxistaurin on visual loss in patients with diabetic retinopathy. *Ophthalmology*. 2006;113:2221–2230.
226. Congdon N, O'Colmain B, Klaver CC, et al. Causes and prevalence of visual impairment among adults in the United States. *Arch Ophthalmol*. 2004;122:477–485.
227. World Health Organization. *Fact sheet no. 312: Diabetes*. [Geneva: WHO] http://www.who.int/mediacentre/factsheets/fs312/en/; 2015.
228. International Diabetes Federation. *IDF Diabetes Atlas*. 6th ed. IDF: Brussels; 2014 [Key Findings] https://www.idf.org/diabetesatlas/update-2014.

51

Proliferative Diabetic Retinopathy

Jennifer K. Sun, Paolo S. Silva, Jerry D. Cavallerano, Barbara A. Blodi, Matthew D. Davis, Lloyd M. Aiello, Lloyd Paul Aiello

Since we are not yet able to prevent retinal changes in diabetic patients we must be content to accept, lessen, or slow the progress of these degenerative retinal vascular changes.

(William Parkes Beetham, MD. Visual prognosis of proliferating diabetic retinopathy. Br J Ophthalmol, 1963.)

The earliest diabetes-induced changes in the retina are biochemical, hemodynamic, and cellular in nature. Often these changes are initially imperceptible clinically and may have no or minimal effect on vision. In contrast, proliferative diabetic retinopathy (PDR) represents an advanced stage of diabetic eye disease characterized by the growth of newly formed retinal vessels on the retina or optic disc that extend along the retinal surface or into the vitreous cavity, significantly increasing the risk for vision loss.[1,2] Among patients with diabetes, nearly 25% with type 1 and 15.5% with type 2 will develop PDR after 15 years of diabetes.[3,4] The rate of progression to PDR is highest among type 1 patients, with a 42% cumulative risk over 25 years.[5] Furthermore, there is a strong association between PDR and uncontrolled systemic disease.[6,7] The publication of landmark clinical trials establishing the importance of intensive glycemic control in preventing the onset and progression of retinopathy and other diabetic complications in both type 1 and type 2 diabetes has led to marked improvement in the medical care of patients with diabetes over the past two decades. With these improvements there has been a corresponding decline in the incidence of PDR.[8–11] Nevertheless, the ocular complications arising from development of PDR remain a leading cause of severe vision loss in many developed countries worldwide.[10]

This chapter begins with a brief discussion of the pathogenesis of PDR and the circumstances under which preretinal new vessels appear and are recognized clinically. A detailed description of the natural course of PDR follows, emphasizing four fundamental processes: (1) the cycle of proliferation and regression typical of new vessels; (2) proliferation of fibrous tissue accompanying new vessels; (3) formation of adhesions between fibrovascular proliferations and the posterior vitreous surface; and (4) contraction of the posterior vitreous surface and associated proliferations. Other sections of this chapter consider the relationship of PDR to duration and type of diabetes, glycemic control, and other factors. The treatment of PDR is reviewed with emphasis on findings of clinical trials and guidelines for management, including recent data on the use of vascular endothelial growth factor inhibitors. Rapidly evolving novel treatment strategies that hold promise as less invasive primary interventions or as adjunctive therapy when photocoagulation response is inadequate are also presented.

Pathogenesis of Proliferative Diabetic Retinopathy

Hyperglycemia and metabolic changes from diabetes lead to alterations in the retinal vasculature that result in reduced perfusion of the retinal tissue.[12] This state of relative retinal ischemia is thought to be the primary angiogenic stimulus that plays a central role in the pathogenesis of PDR. Various angiogenic factors such as angiopoietin, erythropoietin, basic fibroblast growth factor (bFGF), insulin-like growth factor (IGF), protein kinase C (PKC), tumor growth factor (TGF), and platelet-derived growth factor (PDGF) have stimulatory or modulating activities during the development of PDR. However, based on in vivo and in vitro studies, the protein vascular endothelial growth factor (VEGF) appears to be primarily responsible for the ischemia-driven angiogenic pathology in PDR.[13–15] The role of VEGF in PDR is well supported by studies demonstrating high concentrations of VEGF in the vitreous of patients with PDR which are closely correlated with extent of disease activity.[13,16] Following successful laser

treatment or in patients with naturally quiescent PDR, VEGF vitreous concentrations are low or undetectable.[13] Furthermore, the direct role for VEGF mediation of the neovascular response in PDR was demonstrated by showing that vitreous fluids from patients with active PDR were angiogenic in vitro, and this angiogenic stimulus could be blocked using a VEGF-specific inhibitor. Intraocular vessels from PDR and diabetes-induced iris neovascularization are exquisitely sensitive to VEGF inhibitors, often showing initial regression within one day of treatment.[17]

Although VEGF appears to be the primary direct causative angiogenic factor in PDR, the complex mechanisms regulating in vivo angiogenesis likely involve factors other than VEGF as well. Angiogenic pathways such as the angiopoietin/Tie-2 system modulate the effect of VEGF and directly affect retinal pericytes and endothelial cells, which are the principal cell types thought to be involved in the pathologic processes of PDR.[18,19] In addition, hyperglycemia reduces PDGF survival-promoting activity, thus leading to pericyte apoptosis and diabetic vasculopathy. This mechanism is driven by hyperglycemia-induced activation of protein kinase C-δ (PKC-δ), which leads to increased expression of a protein tyrosine phosphatase called Src homology-2 domain-containing phosphatase-1 (SHP-1). SHP-1 activation in turn mediates resistance to PDGF, resulting in loss of cellular survival mechanisms and increased pericyte apoptosis.[20] Inhibition of SHP-1 is being investigated as a possible protective mechanism against initial retinal changes that underlie subsequent development of PDR.[20] VEGF-independent pathways such as that mediated by erythropoietin (EPO) have also been implicated in the development of PDR.[21] Single nucleotide polymorphisms (SNPs) that increase EPO expression have been associated with development of PDR and severe renal disease in a small genetic study of three independent patient populations.[22,23] Antiangiogenic mediators such as pigment epithelium-derived factor (PEDF) are reportedly lower in patients with diabetes and in patients with active PDR compared to other retinopathies.[24] An interplay between both angiogenic and antiangiogenic pathways may be important in the eye at various stages of retinopathy.[25] A more detailed discussion regarding the pathologic angiogenesis of PDR is presented in

Chapter 28 (Basic mechanisms of pathologic retinal and choroidal angiogenesis).

Origin and Early Recognition of Preretinal New Vessels

The risk of PDR is greatest in eyes with severe and very severe nonproliferative diabetic retinopathy (NPDR), characterized by the presence and severity of intraretinal microvascular abnormalities (IRMA), venous beading, extensive retinal hemorrhages or microaneurysms (H/Ma), and, to a lesser extent, soft exudates (cotton-wool spots) (Fig. 51.1). In the Diabetic Retinopathy Study (DRS), severe NPDR was defined as the presence of at least three of the above four characteristics, each generally involving at least two quadrants of the fundus. Approximately 50% of such eyes assigned to the untreated control group developed PDR within 15 months.[26] Today a quick assessment of severe or very severe NPDR can be derived from determining the extent and severity of H/MA (moderately severe in 4 quadrants), VB (definitely present in 2 or more quadrants), and IRMA (obvious in 1 or more quadrant) – the 4-2-1 rule (Box 51.1). Any one of these findings indicates severe NPDR and two or more represent very severe NPDR. As noted above, these advanced levels of NPDR are associated with a high likelihood of developing PDR.

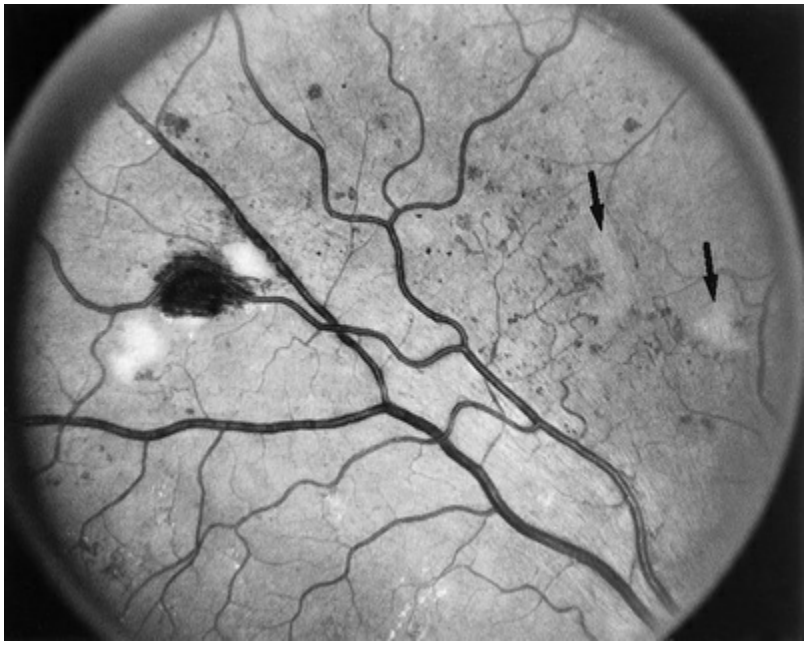

FIG. 51.1 Severe nonproliferative diabetic retinopathy (NPDR). On the left are two prominent soft exudates with a large blot hemorrhage between them. Venous beading is present where the superior branch of the superotemporal vein passes by the upper exudate. On the right are two faint soft exudates (*arrows*) and many intraretinal microvascular abnormalities. (Courtesy of Early Treatment Diabetic Retinopathy Study Research Group.)

Box 51.1

The 4-2-1 Rule

Severe NPDR (any one of the following)

- H/MA ≥ Standard 2A (Fig. 51.20) in four quadrants
- VB definitely present in two or more quadrants
- IRMA ≥ Standard 8A (Fig. 51.21) in one or more quadrants

Very severe NPDR (two or more of the above)

H/MA, hemorrhage/microaneurysms; IRMA, intraretinal microvascular abnormalities; NPDR, nonproliferative vitreoretinopathy; VB, venous bleeding.

The lesions characterizing severe NPDR are related to retinal capillary closure, and their frequent presence in eyes that are about to develop preretinal new vessels is one important observation

linking these processes. Further evidence has been provided by the fluorescein angiographic montages of Shimizu and coworkers,[27] who found that the extent of capillary closure observed using angiography increased as the severity of new vessels increased on the following four-step scale: (1) none, (2) new vessels involving the retina but sparing the disc, (3) new vessels involving the disc, and (4) neovascularization of the anterior chamber angle with neovascular glaucoma. Muraoka and Shimizu[28] have provided serial fluorescein angiographic observations supporting the view that some lesions designated as IRMA or reduplication of small venules are in fact intraretinal new vessels revascularizing areas of capillary loss.

Although there is little doubt that the presence of severe NPDR is predictive of subsequent neovascularization, characteristic intraretinal lesions are not always extensively present when preretinal new vessels are first recognized. A possible explanation for this dichotomy is the relatively transient nature of some of these lesions. Cotton-wool spots usually disappear within 6–12 months.[29] H/MA have a half-life of approximately 3 months.[30] Blot hemorrhages and IRMA tend to disappear after extensive capillary closure, when the number of small vascular branches decreases and small arterioles become sclerosed, taking on a white thread-like appearance. This condition is sometimes described as "featureless fundus" (Fig. 51.2B) and can lead to a mistaken impression that the degree of retinal pathology is less severe than is actually present.

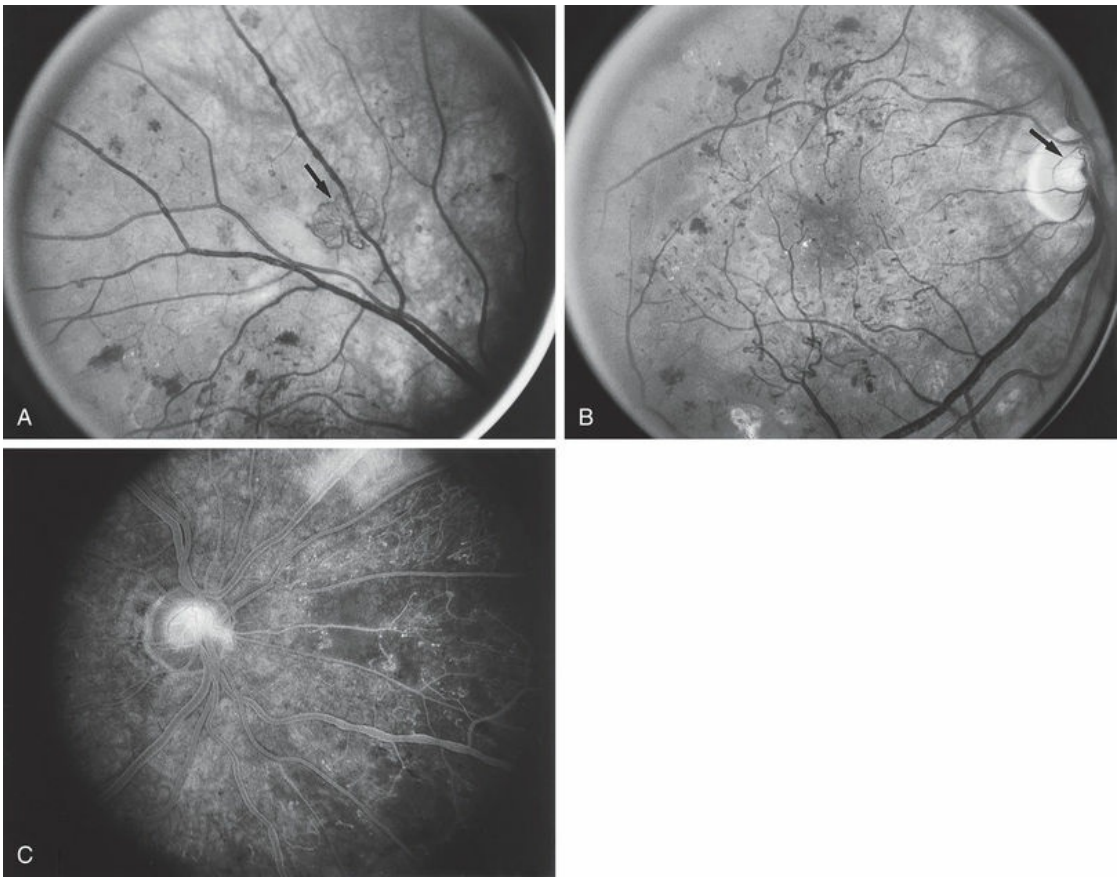

FIG. 51.2 Early proliferative diabetic retinopathy (PDR). (A) New vessels form a small wheel-like network (*arrow*) in the superotemporal quadrant of an eye with venous beading, soft exudates, intraretinal microvascular abnormalities (IRMAs), and blot hemorrhages. (B) Posterior pole of the same eye, showing IRMAs and retinal hemorrhages centrally and a featureless retina near the left edge of the figure. With stereoscopic examination, the vascular loop on the disc (*arrow*) could be seen to bridge the physiologic cup and was clearly a new vessel. (C) In the late-stage angiogram, new vessels on the disc are no longer filled with fluorescent blood; they stand out in contrast to the pool of fluorescein that has leaked from them. Prominent fluorescein leakage along the superonasal vein at the upper edge of the figure is from new vessels there. An area of capillary dropout is located nasal to the disc. (Courtesy of Early Treatment Diabetic Retinopathy Study Research Group.)

New vessels may arise anywhere in the retina; however, they are most frequently seen posteriorly, within about 45 degrees of the

optic disc. They are particularly common on the disc itself (Davis reported 69% of 155 eyes with PDR;[31] Taylor and Dobree, 73% of 86 eyes[32]). In the DRS, among 1377 control-group eyes with new vessels present in baseline photographs, 15% had new vessels only on or within 1 disc diameter (DD) of the disc or in the vitreous cavity anterior to this area (new vessels on disc, or NVD), 40% had new vessels only outside this zone (new vessels elsewhere, or NVE), and 45% had new vessels in both zones.[33] In the DRS, NVE occurred most frequently in the superotemporal quadrant (field 4, 27%), followed in frequency by the inferonasal (field 7, 21%) quadrant.[34] Although less common, the appearance of neovascularization arising from the perifoveal capillaries has also been reported.[35]

NVD (defined as NV at or within 1 DD of the disc[36]) begins as fine loops or networks of vessels lying on the surface of the disc or bridging across the physiologic cup. They are usually easily identified once established, but in their earliest stages they may be overlooked, especially with the low magnification of binocular indirect ophthalmoscopy. They also may be difficult to distinguish from normal vessels in nonstereoscopic photographs or with monocular direct ophthalmoscopy. The most satisfactory examination methods are those that provide a magnified stereoscopic view, using either biomicroscopy with contact or precorneal lens or stereoscopic 30-degree photography. New vessels can readily be identified using fluorescein angiography during which they will leak profusely, unlike normal physiologic vasculature (Fig. 51.2).

Evaluation of early NVE requires identification of the lesion and differentiation from IRMA. Binocular indirect ophthalmoscopy of the retina combined with a biomicroscopic or direct ophthalmoscopic examination of any suspicious lesions and careful review within 5 or 6 DD of the disc is a useful approach. Indirect ophthalmoscopy alone is not adequate.

Although ETDRS seven standard field stereoscopic photographs remain the gold standard for photographic documentation of diabetic retinal pathology[35,37] (Fig. 51.3A) these images only cover approximately 30% of the retinal surface. Recent advances in ophthalmic imaging now show up to 82% of the retinal surface in a

single ultrawide-field fundus or fluorescein angiography image (Fig. 51.3B). Multiple studies have demonstrated that 200-degree ultrawide-field images detect more diabetic retinopathy lesions than evident using routine standard 30-degree photography, and that these lesions suggest a more severe level of retinopathy in nearly 10% of eyes.[37–40] Furthermore, ultrawide-field fluorescein angiography enhances the detection of areas of peripheral vessel leakage and nonperfusion in diabetic eyes.[41] Extent of peripheral nonperfusion is highly correlated with the presence of peripheral lesions and diabetic retinopathy severity level.[41] Additional advanced retinal imaging techniques such as optical coherence tomography-angiography (OCT-A) allow visualization of the retinal vessels in three dimensions without contrast agent. Adaptive optics scanning laser ophthalmoscopy (AOSLO) provides a smaller retinal field of view, but ultrahigh resolution to a theoretical limit of 2 μm, thus allowing the identification of new retinal vessels well before they are detectable clinically

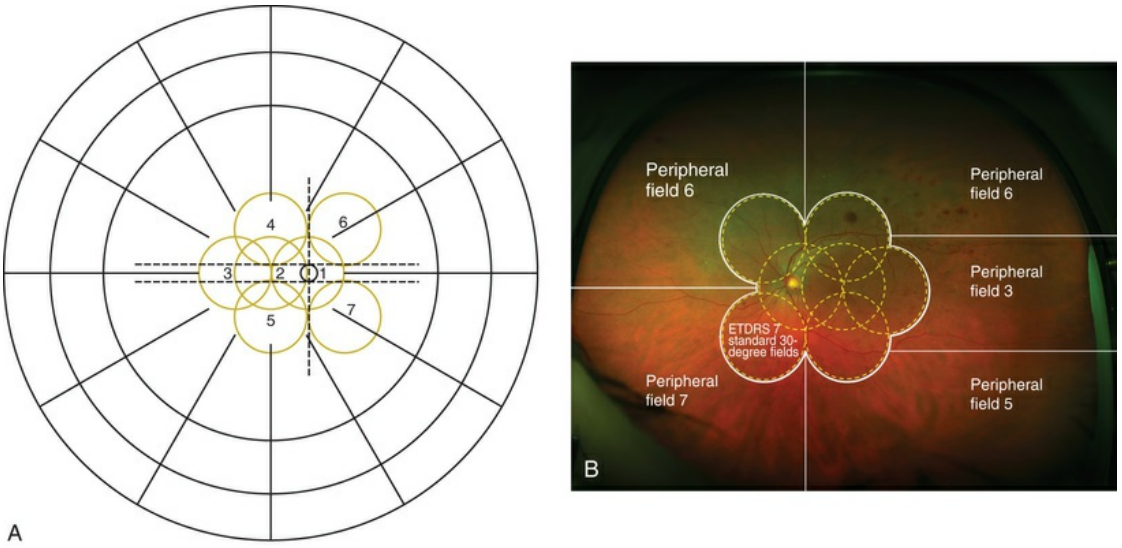

FIG. 51.3 (A) Modified Airlie House classification. Seven standard photographic fields are shown for the right eye. Field 1 is centered on the disc, field 2 on the macula, and field 3 temporal to the macula so that its nasal edge passes through the center of the macula. Fields 4 to 7 are tangential to a vertical line passing through the center of the disc and to horizontal lines passing through its upper and lower poles, as shown. (B) Mydriatic ultrawide-field 200° image with overlay of

the Early Treatment Diabetic Retinopathy Study 7 standard photographic fields and the proposed extended peripheral fields. (Panel A reproduced with permission from Diabetic Retinopathy Study Research Group. A modification of the Airlie House classification of diabetic retinopathy. DRS report number 7. Invest Ophthalmol Vis Sci 1981;21:210–226. Panel B reproduced with permission from Silva PS, et al. Peripheral lesions identified by mydriatic ultrawide field imaging: distribution and potential impact on diabetic retinopathy severity. Ophthalmology 2013;120:2587-95.)

When new vessels are not discovered by any of these techniques but are strongly suspected because of recent vitreous hemorrhage, examination of the more peripheral retina with biomicroscopy and a Goldmann three-mirror lens may be helpful. The possibility that the vitreous hemorrhage may come from a peripheral retinal tear, unrelated to DR, should be kept in mind, and a careful examination of the peripheral fundus with scleral depression should be performed.

More difficult than finding NVE may be distinguishing between early NVE and IRMA. This differentiation is particularly difficult if IRMA are extensive and NVE do not yet show any of their unique features – more superficial location, formation of wheel-like networks, extension across both arterial and venous branches of the underlying retinal vascular network, and accompanying fibrous proliferation. In unusual borderline cases, fluorescein angiography can distinguish between the profuse leakiness of preretinal new vessels and the less leaky IRMA.

Natural Course of Proliferative Diabetic Retinopathy

The natural course of PDR involves the development of new vessels on the retina and optic disc that extend along the retinal surface and the vitreous. These new vascular growths commonly develop progressively, increasing fibrous proliferation. The subsequent contraction of the fibrous tissue can lead to traction retinal detachment and vitreous hemorrhage – the two most common complications associated with severe visual loss in PDR. Invariably,

treated or untreated, PDR will eventually progress to an involutional quiescent stage that may remain stable for decades. Visual outcome is dependent on the degree of damage to critical visual structures that has occurred by that point. Panretinal laser photocoagulation or intravitreous therapy with anti-vascular endothelial growth factor agents (anti-VEGF) induce this quiescent state earlier, usually with less associated retinal damage and visual loss.

Development and Proliferation of New Vessels

Initially, new vessels may be barely visible. Later, their caliber is commonly one-eighth to one-quarter that of a major retinal vein at the disc margin, and occasionally they are as large as such veins (Fig. 51.4). New vessels frequently form networks that often resemble part or all of a carriage wheel. The vessels radiate like spokes from the center of the complex to a circumferential vessel bounding its periphery (see Figs. 51.2A and 51.4). New vessel networks may also be irregular in shape, without a distinct radial pattern. New vessel patches often lie over retinal veins and appear to drain into them. The superotemporal vein is involved somewhat more frequently than others.[40,41] In the 1158 DRS control-group eyes that had NVE in at least one of the five photographic fields in which they were graded (fields 3 to 7 in Fig. 51.3), the number of times each field was involved was assessed. In each eye a count of one was divided equally among all fields containing NVE, and the counts for each field were totaled for all eyes. Field 4, which usually includes a major portion of the superotemporal vein, had a score of 308 (27% of 1158), whereas other scores ranged from 194 (17%) for field 5 to 242 (21%) for field 7.[2]

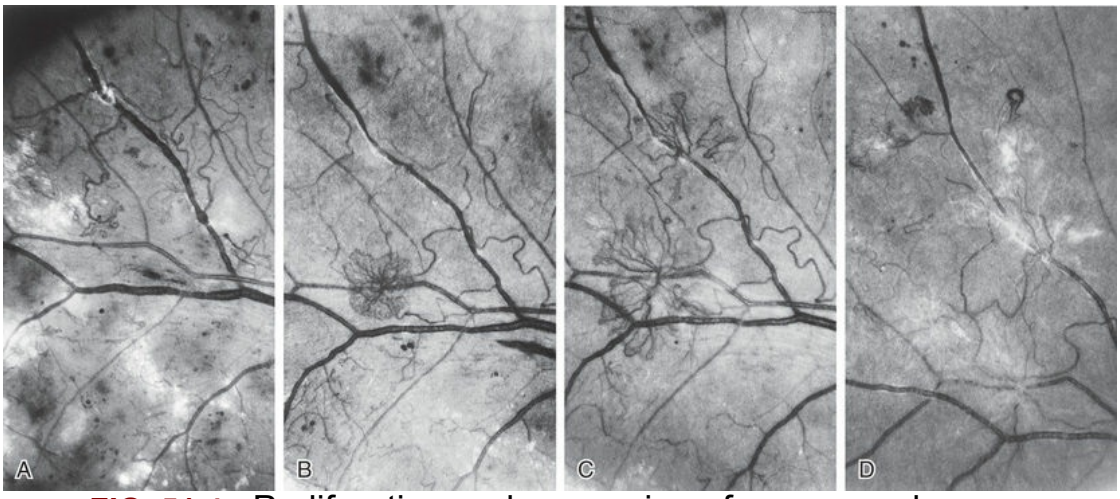

FIG. 51.4 Proliferation and regression of new vessels elsewhere (NVE). (A) Severe nonproliferative diabetic retinopathy in a patient with newly diagnosed type 2 diabetes (superotemporal quadrant of the right eye). Present were many microaneurysms, hemorrhages, and hard exudates, as well as extensive retinal edema and venous beading. Most of the tortuous small vessels appeared to be within the retina (large intraretinal microvascular abnormalities), but some may have been on its surface. (B) Eight months later, marked improvement in the intraretinal abnormalities was noted, but a wheel-like network of new vessels had appeared on the surface of the retina. Venous beading had decreased, and venous sheathing had increased. (C) Three months later, the new vessel patch had enlarged, and a second patch had developed above it. During the next 2 years the new vessels continued to grow slowly at the edges of the patches, while regressing at their centers. (D) Three years after they had appeared, most of the new vessels had regressed, although there was still one dilated loop at the upper edge of the upper patch. No contraction of fibrous proliferation or vitreous had occurred, no vitreous hemorrhage was present, and vision remained good.

At times new vessels grow for several disc diameters across the retina without forming prominent networks. The new vessels appear much like normal retinal vessels but are easily recognized as new vessels because of their unique capability of crossing both arterioles and veins in the underlying retina (Figs. 51.5 and 51.6).

New vessels of this type commonly arise on the disc and are often accompanied during their actively growing phase by mild-to-moderate thickening of the disc and surrounding retina (Fig. 51.7). This appearance is similar to typical cases of diabetic papillopathy,[42] in which all or most of the dilated small vessels on and adjacent to the disc are intraretinal and characteristically do not leak on fluorescein angiography.

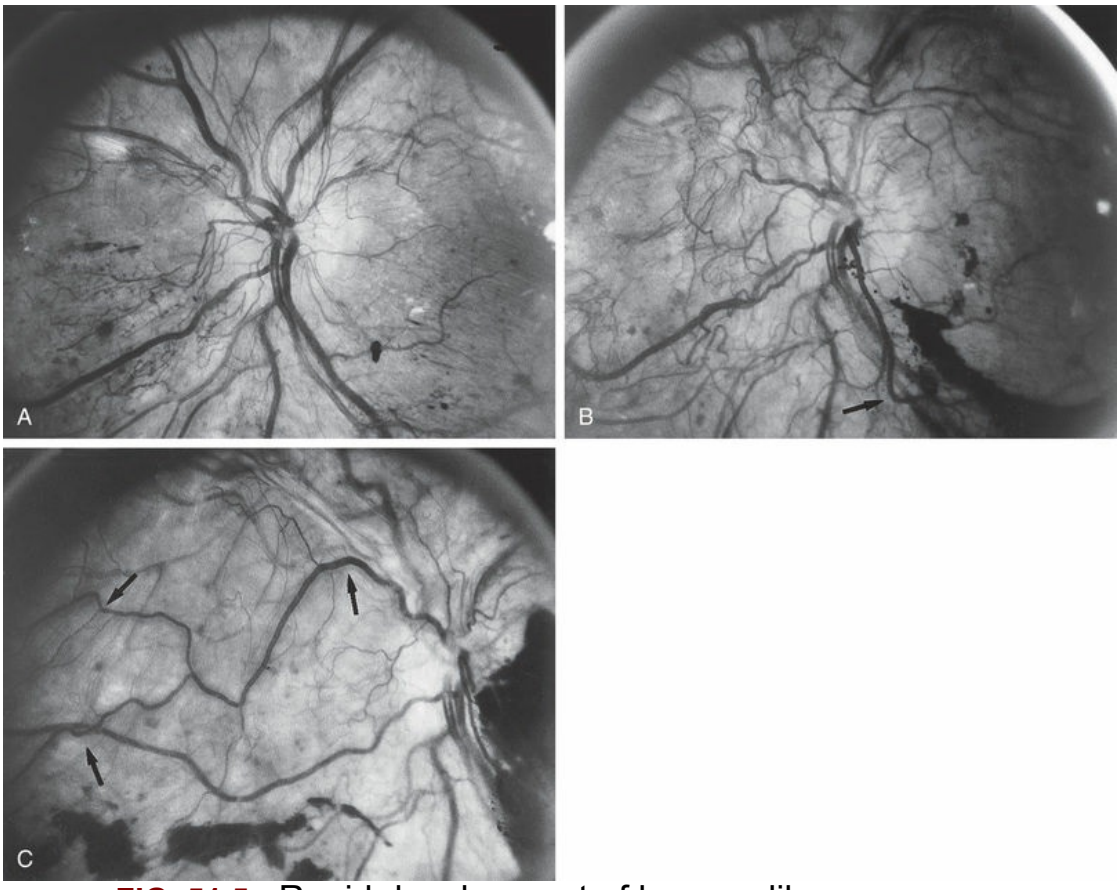

FIG. 51.5 Rapid development of large-caliber new vessels from the disc. (A) In the left eye of this 21-year-old white woman, whose age at diagnosis of diabetes was 7 years, new vessels arose on the disc and extended across its margins in all quadrants. The disc margins were blurred. There were soft and hard exudates, intraretinal microvascular abnormalities, and hemorrhages in the retina and on its surface. Blood pressure was 126/96 mmHg. (B) Two months later, new vessels had grown remarkably, and preretinal hemorrhage had increased. *Arrow* indicates large new vessel that crosses the inferotemporal artery and vein.

(C) Three months later, one of the new vessels (*arrows*) had become as large as a major retinal vein and extended nasally beyond the edge of the figure. The new vessels on and adjacent to the disc had regressed partially. Two months later, the patient died suddenly of a myocardial infarction.

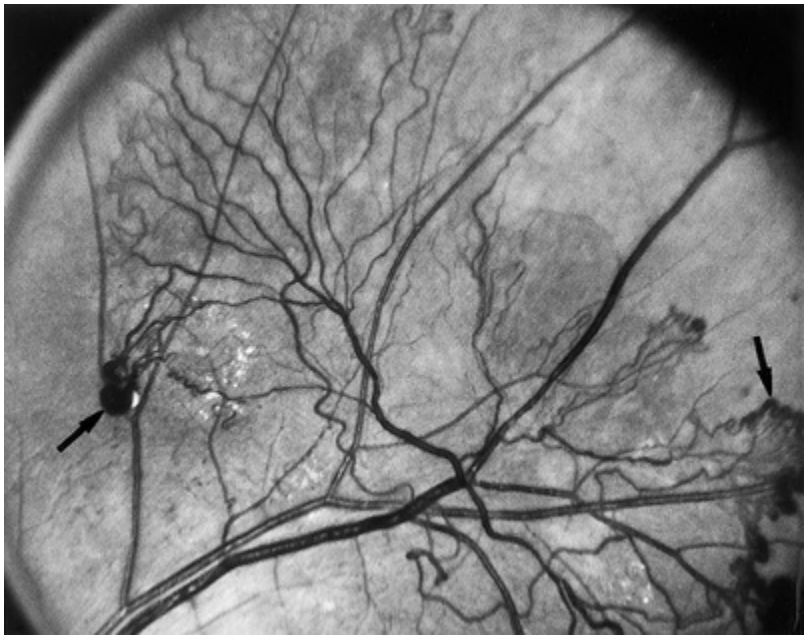

FIG. 51.6 New vessels elsewhere (NVE) without prominent network formation. Over much of their course, these new vessels did not form networks. Large aneurysmal dilations were present at the end of a long new-vessel loop (*left arrow*) and at the circumference of a partial wheel-like network (*right arrow*). (Courtesy of Diabetic Retinopathy Study Research Group.)

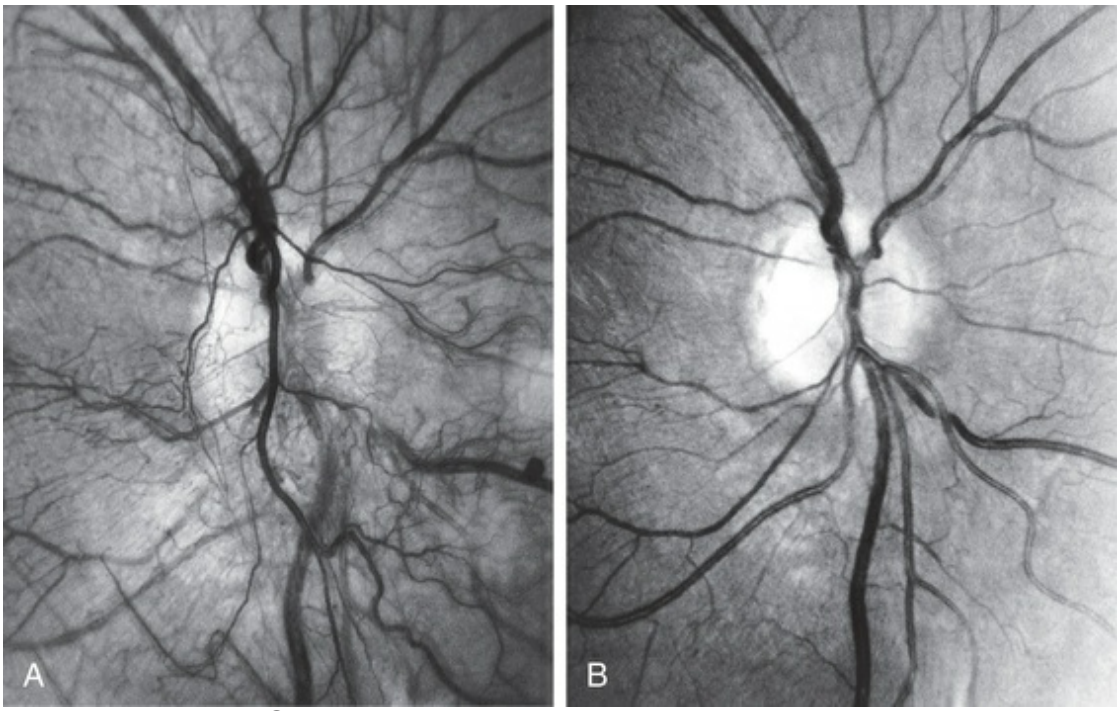

FIG. 51.7 Optic disc swelling. This 20-year-old man, whose diabetes had been diagnosed at age 14, sought ophthalmologic attention because of the sudden onset of floaters, first in the left eye and several days later in the right eye. (A) The disc was swollen, had blurred margins, and was partially obscured by extensive new vessels arising on it and extending on to the retina in all quadrants. (B) Five months later, disc swelling had resolved, and all new vessels had regressed spontaneously. Vision remained 20/15. (Courtesy of Diabetic Retinopathy Study Research Group.)

The growth rate of new vessels is extremely variable. In some patients a patch of vessels may show little change over many months, whereas in others a definite increase may be seen in 1–2 weeks. Early in their evolution, new vessels appear bare, but later, delicate white fibrous tissue usually becomes visible adjacent to them. The common clinical convention of referring to such tissue as "fibrous" is adhered to in this chapter, even though it has been shown to contain both fibrocytes and glial cells.[43,44] New vessels characteristically follow a course of proliferation followed by partial or complete regression.[40,45] Regression of a wheel-shaped net of new vessels typically begins with a decrease in the number and caliber of the vessels at the center of the patch, followed by their partial replacement with fibrous tissue. Simultaneously, the peripheral

vessels tend to become narrower, although they may still be growing in length and the patch may still be enlarging (Fig. 51.4). At times, regressing new vessels appear to become sheathed. The width of the sheath, which presumably represents opacification and thickening of the vessel wall, increases until only a network of white lines without visible blood columns remains (Fig. 51.8). At times certain new vessels seem to become preferential channels, enlarging while adjacent vessels regress and disappear. Fresh, active new vessels are commonly seen emerging from the edges of partially regressed patches, and new vessels are frequently seen at different stages of development in different areas of the same eye. Early in their evolution, the fibrous components of fibrovascular proliferations tend to be translucent and are easily underestimated. Subsequently, with increasing growth, contraction, or separation from the retina, they become more prominent. If contraction of the vitreous and fibrovascular proliferations does not occur, new vessels may pass through all the stages described here without causing any visual symptoms. Concurrently, a decrease in intraretinal lesions and in the caliber of major retinal vessels may occur as retinopathy enters the quiescent stage. Occasionally, new vessels appear to regress completely, leaving no trace of their previous presence.[46]

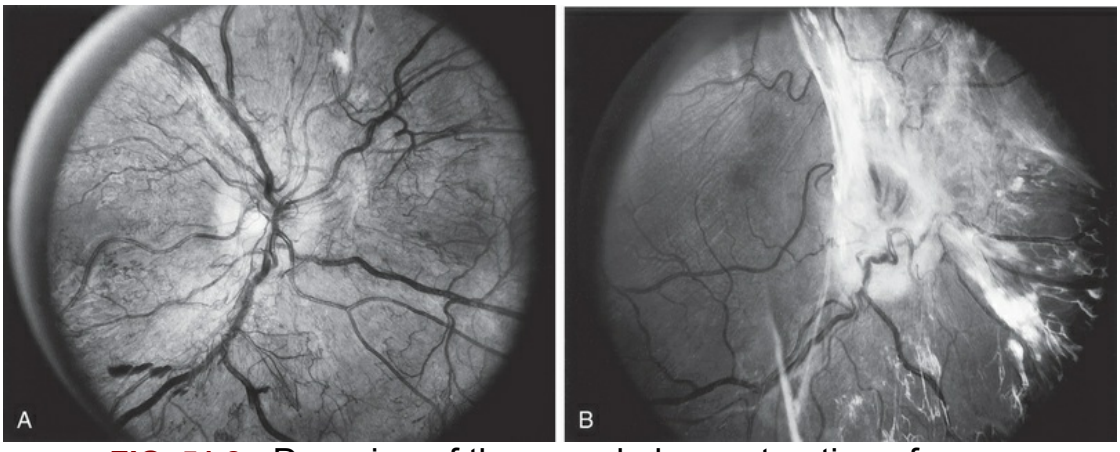

FIG. 51.8 Dragging of the macula by contraction of fibrovascular proliferations; regression of new vessels. (A) In the right eye of this 21-year-old woman, whose age at diagnosis of diabetes was 10 years, extensive new vessels were present on the surface of the disc and retina, as well as many dilated intraretinal vessels

(intraretinal microvascular abnormalities). A soft exudate was noted about 1 disc diameter (DD) superonasally to the disc, and several small preretinal hemorrhages were found (near bottom left). The macula was in its normal position, centered at or just temporal to the left edge of the figure. Fibrous tissue accompanying the new vessels was visible adjacent to the temporal vascular arcades and nasal to the disc. Fibrous proliferations were actually much more extensive but were transparent and difficult to detect. Visual acuity was 20/20. Contraction of the proliferations occurred within the next several months, dragging the retina nasally and superiorly, and new vessels regressed. (B) Four years later, the center of the macula was above the disc and about 1 DD temporal to it. The central dark retinal pigment epithelial pigmentation appeared to coincide with the neurosensory macula. The first major bifurcation of the inferotemporal vein had been pulled upward to the disc margin from its previous position. New vessels had regressed completely, some of them now appearing as networks of white lines. Visual acuity was 20/30.
(Courtesy of Diabetic Retinopathy Vitrectomy Study Research Group.)

Based on the findings of the DRS, the development of PDR with high-risk characteristics places the patient at an increased risk for visual loss and generally requires prompt laser treatment. Recently, as discussed later in this chapter, treatment with anti-VEGF agents is showing promise for treatment of PDR as well. PDR with high-risk characteristics is defined by one or more of the following lesions: (1) NVD that is approximately one-quarter to one-third disc area or more in size (i.e., greater than or equal to NVD in standard photograph No. 10A); (2) any amount of NVD if fresh vitreous or preretinal hemorrhage is present; or (3) NVE greater than or equal to one-half disc area in size if fresh vitreous or preretinal hemorrhage is present. Therefore, attention must be paid to the presence, location, and severity of new vessels, as well as the presence or absence of preretinal or vitreous hemorrhages.[2]

Contraction of the Vitreous and

Fibrovascular Proliferation

Before the onset of posterior vitreous detachment, neovascular networks appear to propagate primarily on or slightly anterior to the retina. At this stage, slit-lamp examination of new vessel patches that appear to be slightly elevated shows no change in the vitreous adjacent to them nor any separation between them and the retina. This finding suggests that mild thickening of the retina may be responsible for the slightly elevated appearance of the new vessels. Typically, the edges of such a new vessel patch are tightly apposed to the retina, and its center appears slightly elevated, giving the patch as a whole a mildly convex curvature. Nearly all new-vessel patches are adherent to the posterior vitreous surface. This adhesion becomes apparent when posterior vitreous detachment occurs adjacent to the patch, pulling its edge forward. If vitreous detachment surrounds the patch, all its edges become more elevated than its center, giving its anterior surface a concave appearance.

Before the beginning of posterior vitreous detachment, new vessels are usually asymptomatic.[31,45] Small hemorrhages in the posterior vitreous are occasionally seen near the growing ends of the new vessels, but they usually remain subhyaloid or hang suspended in the most posterior portion of the vitreous without becoming apparent to the patient. When symptomatic vitreous hemorrhages occur, some evidence of localized posterior vitreous detachment can usually be found. When only a small area of the posterior vitreous surface is detached, the hemorrhage appears flat and very close to the retina, but as detachment becomes more extensive, this surface moves forward and assumes a curved contour more or less parallel to the retina and about 0.5–2 DD anterior to it. This otherwise smoothly curved surface is held posteriorly by vitreoretinal adhesions at the sites of new vessels. The new vessels in turn tend to be pulled forward in these same areas (Fig. 51.9). Vitreous strands and opacities can usually be seen anterior to the posterior vitreous surface, whereas posteriorly the vitreous cavity is optically empty or contains red blood cells.[31,47] The principal force pulling the posterior vitreous surface forward usually appears to be the forward vector resulting from contraction of this surface and the fibrovascular proliferation growing along it.

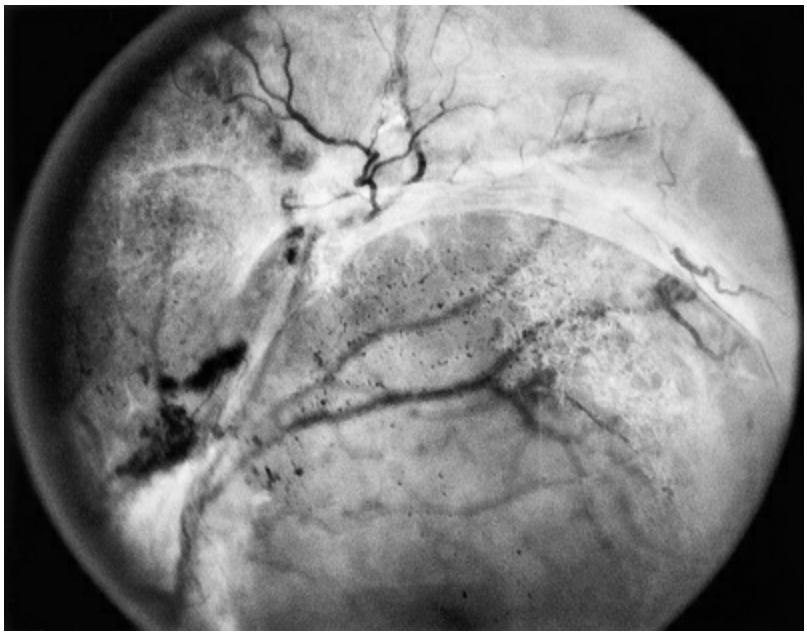

FIG. 51.9 The posterior vitreous surface. In this left eye fibrovascular proliferations were present at the disc and above the superotemporal vascular arcade. The posterior vitreous surface was adherent to these proliferations but was detached elsewhere. In the center of the figure the posterior vitreous surface was thin (visible only with slit illumination), but its position is marked by fine dots of hemorrhage deposited on it. Temporal to this area, the posterior vitreous surface has the typical "Swiss cheese" appearance, that is, the surface can be seen as a semiopaque sheet in which there are round and oval clear areas. This same appearance is present 1–2 disc diameters above the disc, near the left edge of the figure. The retina was attached but is blurred, in part because the camera was focused on the elevated proliferations and also because of blood present in the posterior fluid vitreous.
(Courtesy of Diabetic Retinopathy Vitrectomy Study Research Group.)

Posterior vitreous detachment usually begins near the posterior pole, the most common locations being the region of the superotemporal vessels, temporal to the macula, and above or below the disc.[31] Detachment of the vitreous from the disc can be prevented by adhesions between the vitreous and fibrovascular proliferations arising there. Vitreous detachment is not a smoothly progressive process. It occurs in abrupt steps, usually halting whenever its advancing edge meets a patch of active or regressed

new vessels. If contraction continues, the NV patch is pulled forward, with or without the underlying retina, and vitreous detachment spreads beyond it. At times, the peripheral spread of posterior vitreous detachment is halted temporarily by invisible adhesions to the retina in areas where no new vessels are present. These adhesions are indicated by a subtle linear elevation of the inner surface of the retina at the junction of posteriorly detached and anteriorly attached vitreous. After several weeks or months, vitreous detachment usually spreads farther peripherally, and the subtle retinal fold flattens. Extension of the detachment throughout the periphery can sometimes require months to years to reach completion.

Traction exerted on new vessels appears to be a factor contributing to the recurrent vitreous hemorrhages that often coincide with extension of vitreous detachment. Hemorrhages also occur independently, sometimes in relation to bouts of severe coughing or vomiting and occasionally at the time of insulin reactions. More often they occur during sleep or are unrelated to any obvious factor.[48,49] Blood in the fluid vitreous posterior to the detached vitreous framework usually absorbs within weeks or several months, retaining its red color until absorbed. Hemorrhage in the formed vitreous tends to lose its red color and become white before absorption is complete. Absorption of a large hemorrhage from the formed vitreous is usually slow, requiring many months, or in some cases may never resorb completely.

The arrangement and movement of blood in the posterior fluid vitreous often make it possible to define the limits of posterior vitreous detachment ophthalmoscopically.[40,50] In areas of vitreous detachment, the presence of fresh blood in the posterior fluid vitreous obscures fundus details, distinguishing these areas from adjacent areas in which the vitreous remains attached and details of the retina are clear. In the upper quadrants of the fundus, blood tends to become deposited in thin meridional streaks on the detached posterior vitreous surface, identifying its position. Inferiorly, blood pools between the detached vitreous and attached retina, outlining the inferior extent of vitreous detachment and often forming a fluid-level or “boat-shaped” hemorrhage. At times, even when posterior vitreous detachment cannot definitely be

identified with slit lamp and contact lens, a thin, curving line of subhyaloid hemorrhage parallel to and behind the inferior equator can be seen, presumably marking the lower edge of an area of vitreous detachment. Occasionally, the posterior vitreous surface can be traced across the macula on slit-lamp examination, but usually its continuity is lost in this region. In some of these cases a round or oval hole with sharp edges can be detected in the posterior vitreous surface, occupying an area 2–4 DD wide in the posterior pole. The posterior vitreous surface in this area appears broken, with solid vitreous protruding back through the hole and coming into contact with the retina. At times the surface of a bulging mushroom of vitreous can be seen extending posteriorly through such a hole, occasionally with hemorrhage suspended within its lower part (Fig. 51.10).

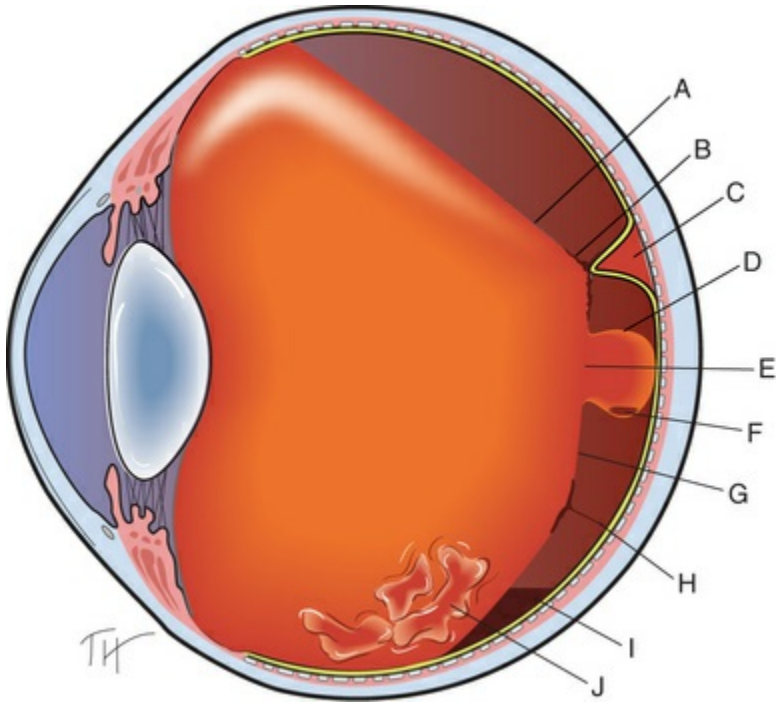

FIG. 51.10 Vitreous detachment in proliferative diabetic retinopathy. (A) Blood deposited on the detached posterior surface of the formed vitreous after hemorrhage into the posterior fluid vitreous. (B) Neovascular and fibrous proliferations creating a tight vitreoretinal adhesion, which pulls the retina forward and holds the formed vitreous posteriorly. (C) Localized collection of subretinal fluid. (D) Curved upper surface of a “mushroom” of formed vitreous

extending posteriorly to reach the retina through a "hole" in the posterior vitreous surface. (E) Hole in the posterior vitreous surface. (F) Blood collected in the dependent portion of the mushroom of vitreous after hemorrhage into the formed vitreous. (G) Posterior vitreous surface. (H) A single new vessel stretching between the retina and proliferations on the detached posterior vitreous surface without traction retinal detachment. (I) Blood with fluid level pooling between the retina and the posterior vitreous surface above the inferior limit of vitreous detachment after hemorrhage into the posterior fluid vitreous. (J) Blood settled out in the inferior part of the formed vitreous.

Retinal Distortion and Traction Detachment

With contraction of an extensive sheet of fibrovascular proliferation, distortion or displacement ("dragging") of the macula may occur.[51] In some cases the central, more intensely pigmented area of the retinal pigment epithelium (RPE) appears to be dragged with the neurosensory macula toward the major focus of contracted tissue, whereas in other cases only the neurosensory macula appears displaced. Since the most common site of extensive fibrovascular proliferations is on and near the disc, the macula is usually dragged nasally and often also somewhat vertically (Figs. 51.11 and 51.12).

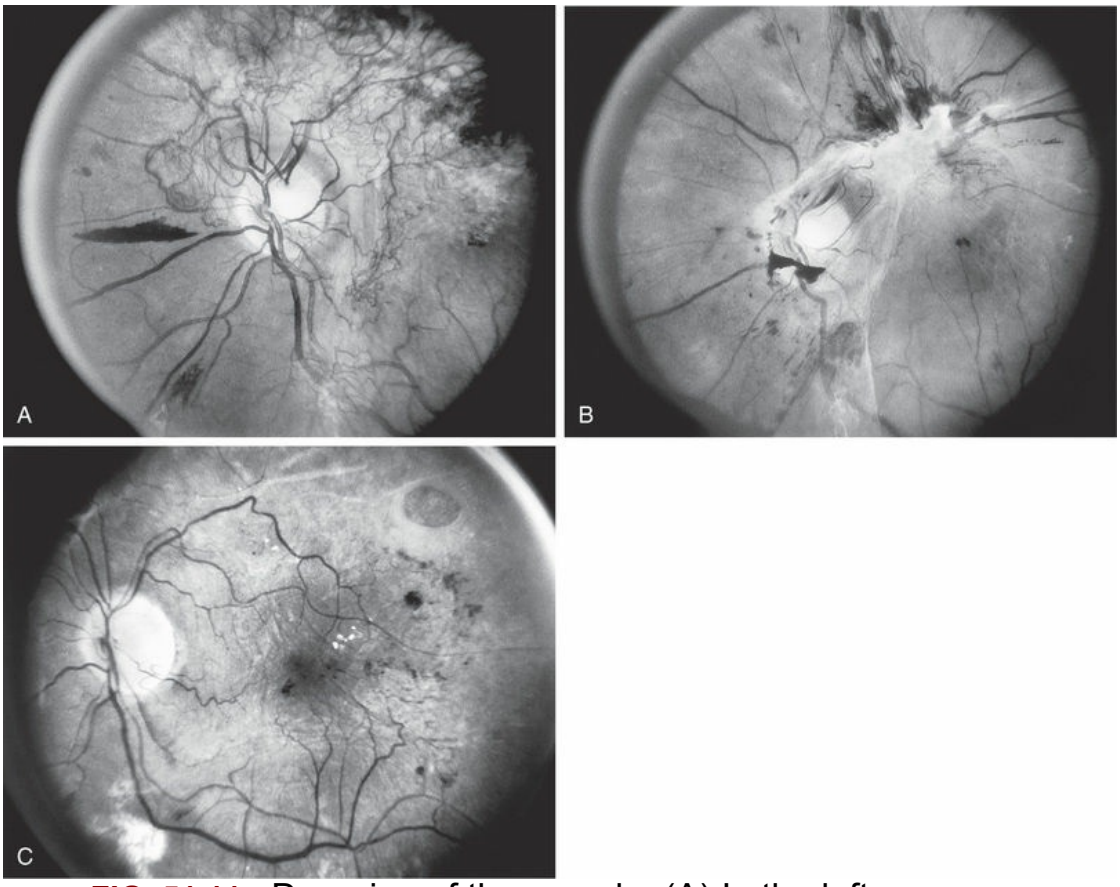

FIG. 51.11 Dragging of the macula. (A) In the left eye of this 39-year-old white woman, whose age at diagnosis of diabetes was 10 years, extensive fibrovascular proliferations were present on and adjacent to the disc, centered superotemporally. The temporal edge of the patch of proliferations was tightly apposed to the retina, and the nasal edge was elevated about one-third of a disc diameter by localized posterior vitreous detachment, the lower edge of which was marked by a preretinal hemorrhage. Visual acuity was 20/60. Scatter photocoagulation was initiated. (B) Three weeks after photocoagulation, the patient noted a marked decrease in visual acuity and returned for examination. There had been marked regression of the new vessels. Contraction of the proliferations had pulled the neurosensory macula (but not the corresponding, more deeply pigmented retinal pigment epithelium) up and nasally. Vitrectomy was carried out. (C) Two months later, visual acuity had improved to 20/30, and the neurosensory macula had returned to near-normal position. There appeared to be a rather large, full-thickness retinal break (near upper right corner), but this did not lead to retinal detachment

during the remaining 3 years of follow-up. At 4-year follow-up, vision had improved to 20/20. (Courtesy of Diabetic Retinopathy Vitrectomy Study Research Group.)

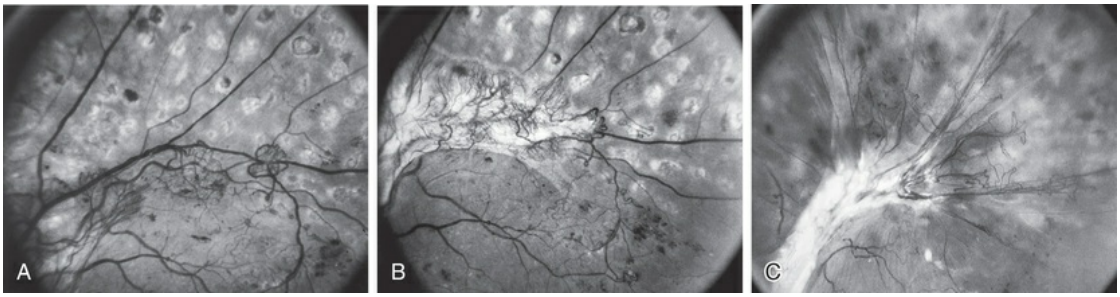

FIG. 51.12 Contraction of fibrovascular proliferations leading to extensive retinal detachment. (A) In the left eye of this 35-year-old man, whose age at diagnosis of diabetes was 14 years, networks of new vessels extended over the surface of the retina along the superotemporal vein. Scars were typical of initial scatter photocoagulation, with space between scars available for additional treatment. (B) Four months later, new vessels had increased, and dense fibrous tissue had appeared. (C) Seven months later, fibrous proliferations had contracted. Broad adhesions prevented them from pulling away from the retina. Instead, the retina was pulled forward (detached) throughout the area shown in the figure. The photocoagulation scars were blurred by the overlying detached retina (and are out of focus). (Courtesy of Diabetic Retinopathy Vitrectomy Study Research Group.)

Contraction of vitreous or areas of fibrovascular proliferation may also lead to retinal detachment. This retinal detachment may be limited to avulsion of a retinal vessel, usually a vein, sometimes accompanied by vitreous hemorrhage. Alternatively, a relatively thin fold of retina may become elevated, with only a narrow zone of retinal detachment adjacent to its base, sometimes outlined by a pigmented demarcation line. In other cases retinal detachment may be more extensive, but the concave shape that is typical of traction detachment is generally maintained. At times, small, apparently full-thickness retinal holes may be seen near the proliferation. These

sometimes, but not always, lead to rhegmatogenous detachment. When such detachment does occur, it tends to have a flat or convex anterior surface and be more extensive, often reaching the ora serrata. The occurrence and severity of retinal detachment are influenced by the timing and degree of shrinkage of the vitreous and fibrovascular proliferations and by the type, extent, and location of the new vessels responsible for vitreoretinal adhesions. Extensive nets of large-caliber new vessels accompanied by heavy fibrous tissue produce broad, tight vitreoretinal adhesions. Contraction of such proliferations is often followed by extensive retinal detachment (Fig. 51.12). New vessels with little accompanying fibrous tissue tend to produce less extensive vitreoretinal adhesions and less risk of retinal detachment, particularly when posterior vitreous detachment begins soon after the onset of neovascularization (Fig. 51.13). At times, new vessels that extend for a considerable distance along the surface of the retina appear to be adherent to the retina only at their sites of origin and to the vitreous only near their distal ends. In this case, the posterior vitreous surface can pull away from the retina by a distance equal to the length of the vessels before exerting traction on the retina. When new vessels are confined to the surface of the disc, vitreous detachment can reach completion without producing traction on the retina, since there are no vitreoretinal adhesions. Retinal detachment does not occur in such eyes, but recurrent vitreous hemorrhage from the new vessels is common.

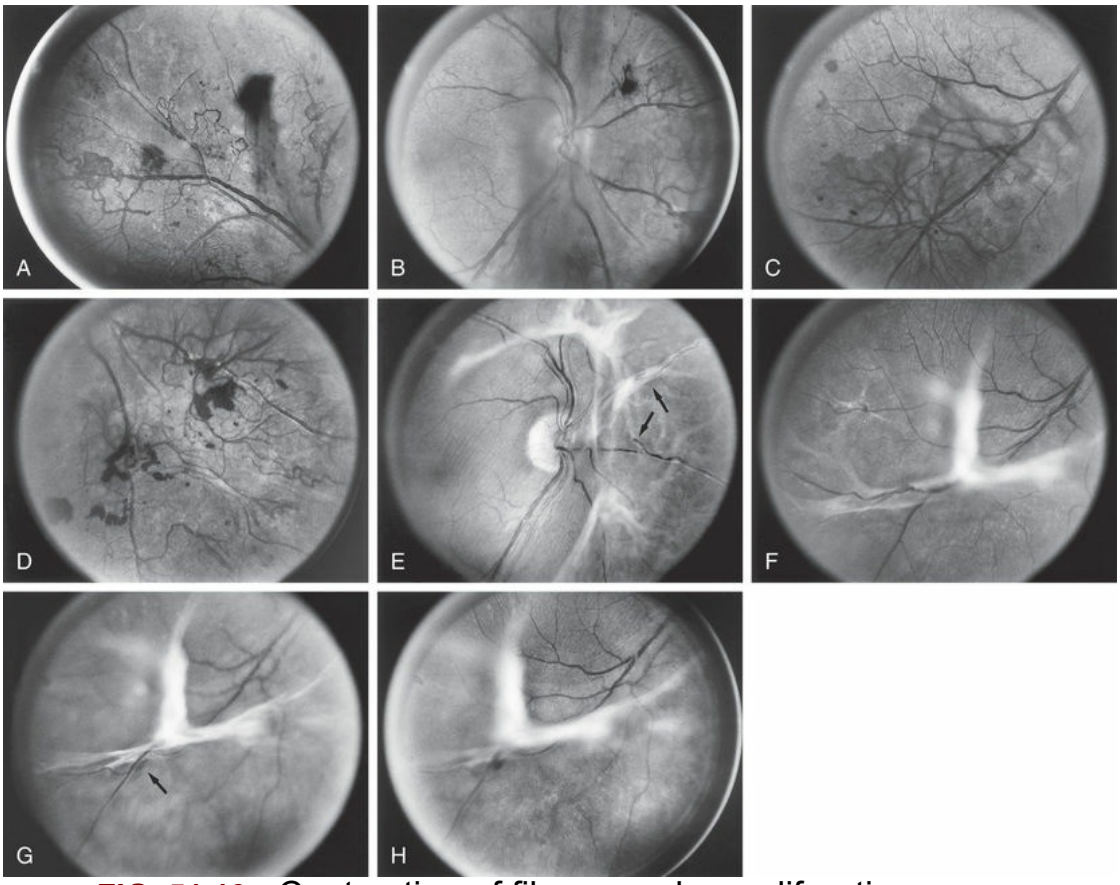

FIG. 51.13 Contraction of fibrovascular proliferations with limited vitreoretinal adhesions, leading to pulled-up retinal vessels and localized retinal detachment, and spontaneous regression of new vessels. (A) In the superotemporal quadrant of the right eye of this 25-year-old man, whose age at diagnosis of diabetes was 8 years, several small, wheel-shaped networks of new vessels on the surface of the retina, venous beading, intraretinal microvascular abnormalities, and localized hemorrhage far anterior to the retina in the formed vitreous were noted. Several small, white, threadlike arterioles were present superiorly, where the retina appeared featureless, indicating loss of much of the retinal capillary bed. (B) The disc and new vessels nasal to it are blurred by vitreous hemorrhage. The macula is visible in its normal position at the left edge of the figure. (C) New vessels along the inferior temporal vein were in focus inferiorly, where they were on the surface of the retina, but were out of focus above the vein, where they were about a half-disc diameter (DD) anterior to the retina, growing along the detached posterior vitreous surface. (D) New vessels and thin fibrous proliferations inferonasal to the disc.

Inferiorly, the new vessels were flat on the surface of the retina; superiorly, they were elevated about a half-DD in front of the retina, on the detached posterior vitreous surface. Preretinal hemorrhages marked the inferior extent of posterior vitreous detachment. Visual acuity was 20/20. (E) One year later, following spontaneous regression of the new vessels and completion of posterior vitreous detachment, most of the proliferations were far anterior to the retina and out of focus. The inferonasal vein had been pulled upward to the horizontal meridian, and a loop of it had been pulled forward (*lower arrow*) without adjacent retinal detachment. The superonasal vein was also pulled forward, together with a narrow fold of retina (*upper arrow*). Tension lines ran through the macula, which had been displaced somewhat downward. (F) The inferotemporal vein had been pulled forward, together with a narrow fold of retina, but the adjacent retina was flat. Visual acuity was 20/30. (G) (focused on the elevated inferotemporal vein) Three years later, a small oval retinal hole (*arrow*) could be seen just below the point where the inferotemporal vein was most highly elevated. Retinal detachment extended inferotemporally past the edge of the figure. (H) (focused on the attached posterior retina) The retina above the superotemporal vein remained flat, and visual acuity had improved to 20/20. Panels (G) and (H) may be viewed stereoscopically by relaxing convergence (or using a base-out prism). (Courtesy of Diabetic Retinopathy Vitrectomy Study Research Group.)

Involutional or "Quiescent" Proliferative Diabetic Retinopathy

Diabetic retinopathy ultimately reaches an involutional stage wherein the retinopathy has "burned-out" and is termed "quiescent." At this stage, vitreous contraction has reached completion and the vitreous is detached from all areas of the retina except where vitreoretinal adhesions associated with new vessels prevent such detachment.[40,45,52,53] Vitreous hemorrhages decrease in frequency and severity and may stop entirely, although many

months may elapse before substantial vitreous clearing occurs. Some degree of retinal detachment may be present at this stage. If the detachment is localized and the macula remains intact, visual acuity may be good. However, dragging or distortion of the macula or longstanding macular edema can lead to substantial reduction in vision. In some cases, retinal detachment involves the entire posterior pole, with resultant severe loss of vision. Although spontaneous partial reattachment occasionally occurs, if the macula has been detached for months or years, significant return of vision is unusual.

A marked reduction in the caliber of retinal vessels is characteristic of this stage. Previously dilated or beaded veins return to normal caliber or become narrower and often appear sheathed. Fewer small venous branches are visible. Changes in the arterioles are often even more striking, with decreased caliber and reduction of the number of visible branches. Some small arterioles can appear to be white threads without visible blood columns. Characteristically, only occasional retinal hemorrhages and microaneurysms are present. New vessels are usually reduced in caliber and number, and at times no patent new vessels can be seen. Fibrous tissue may become thinner and more transparent, allowing the retina to be observed more clearly. Vision loss at this stage is related to macular detachment, macular ischemia, chronic macular edema, optic nerve disease or media opacity. Marked vision loss may be due to severe retinal ischemia.

Relationship of Proliferative Diabetic Retinopathy to Type and Duration of Diabetes

In a population-based stereophotographic study carried out by Klein and coworkers,[54] the prevalence of PDR in insulin-taking patients younger than 30 at diagnosis (exclusively or mainly type 1) was near zero when duration of diabetes was less than 10 years and then rose rapidly to about 50% in persons with 20 years or more of diabetes. Subsequent reports from the Joslin 50-Year Medalist Study suggest that the prevalence of PDR remains approximately 50% in

patients who have survived with insulin-dependent diabetes for 50 years or more.[55] In an older-onset (30 years or more) insulin-taking group, which included both diabetes types, prevalence of PDR rose fairly steadily, from 2% in persons with less than 5 years of diabetes to about 25% in those with 20 years or more. In the older-onset, noninsulin-taking (type 2) group, prevalence of PDR increased only slightly with duration, from less than 5% before 20 years to about 5% thereafter (Fig. 51.14).[56] Among patients with PDR, its severity did not appear to differ between the younger-onset and the combined older-onset groups. In each case, in the worse eye about 25% of patients had DRS high-risk characteristics and 15% had retinopathy severity ungradable because of extensive vitreous hemorrhage, phthisis bulbi, or enucleation secondary to complications of DR.[7] In patients with PDR, macular edema was more common in the combined older-onset group with retinal thickening or scars of previous focal photocoagulation present in at least one eye in about 45% (versus 30% in the younger-onset group).[57]

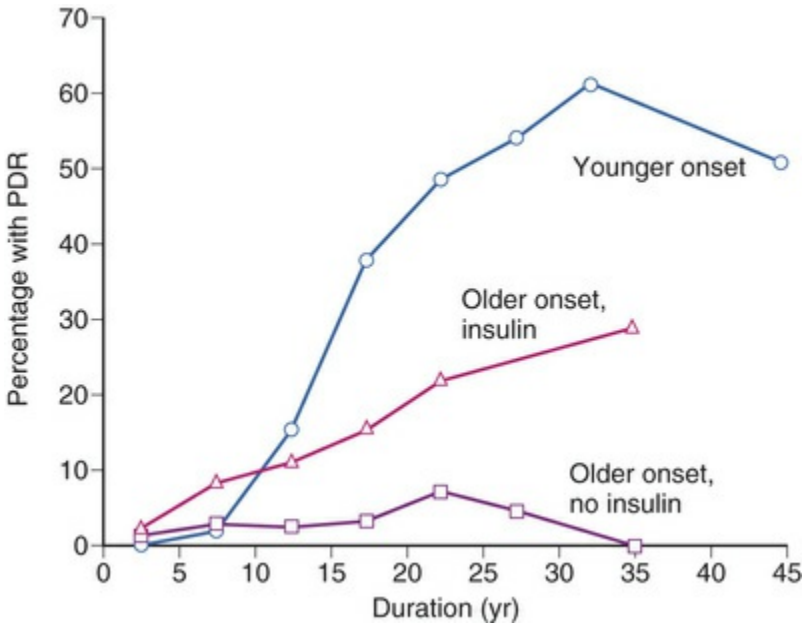

FIG. 51.14 Percentage of people with proliferative diabetic retinopathy (PDR) by duration of diabetes in each of the three groups. (Reproduced with permission from Klein R, Davis M, Moss S, et al. The Wisconsin Epidemiologic Study of Diabetic Retinopathy: a comparison of retinopathy in younger and older onset diabetic persons. In: Vranic M, Hollenberg C, Steiner G, eds. Comparison of type I and II

diabetes. New York: Plenum Press; 1985.)

The Diabetic Retinopathy Vitrectomy Study (DRVS) found a substantial variation in severity of PDR by diabetes type among persons with vitreous hemorrhage severe enough to reduce visual acuity to 5/200 or less for a period of at least 1 month.[58–61] In this study the severity of new vessels, fibrous proliferation, and vitreoretinal adhesions was significantly less with type 2 diabetes (Table 51.1).

TABLE 51.1

Percentage of Diabetic Retinopathy Vitrectomy Study (DRVS) Group H Eyes Assigned to Early Vitrectomy With Specified Severity Level of New Vessels, Fibrous Proliferations, and Vitreoretinal Adhesions, by Diabetes Type

Fundus Abnormality	Diabetes Type[a]		
	Type 1	Mixed	Type 2
New vessels ≥1 disc area	81.1 %	58.2 %	42.2 %
Fibrous proliferations ≥2 disc areas	68.2 %	47.7 %	44.5%
Vitreoretinal adhesions ≥4 disc areas	47.8 %	34.5 %	23.6 %

[a]Type 1, age at diagnosis 20 years or younger and taking insulin at study entry. Mixed, age at diagnosis 21–39 years and taking insulin at study entry. Type 2, age at diagnosis 40 years or older, or not taking insulin at study entry.

Diabetes with onset after age 30 (typically type 2 diabetes) is 8–10 times more common than the younger-onset type (typically type 1), and in clinical practice PDR is seen with about equal frequency in the younger- and older-onset groups. Klein et al.[54,56] estimated that in the population they surveyed, 43% of patients with PDR were in the younger-onset group, 42% were in the older-onset insulin-taking group, and 15% were in the noninsulin-taking group. In the DRS, in which more than 90% of the 1742 patients examined had PDR in at least one eye, 44% were classified as juvenile-onset (younger than 20 years at diagnosis and taking insulin at entry into the study); 28% as adult-onset, possibly insulin-dependent (age 20 years or older at diagnosis, not overweight, and taking insulin); and

26% as classic adult-onset (mild symptomatic or asymptomatic onset at age 20 years or older and either overweight or not taking insulin at study entry). The remaining 2% were not classifiable.[33] Aiello and coworkers[62] described the distribution of age at diabetes diagnosis among 244 patients with PDR at the Joslin Clinic during a 5-month period: diagnosis age less than 20 years, 53%; 20–39 years, 25%; and 40 years or older, 22%.

In a comprehensive meta-analysis including 28 prospective interventional or observational studies comprising 27,120 diabetic patients with at least 10 years of follow-up, lower rates of progression to PDR and severe visual loss were observed in those more recently diagnosed with diabetes.[10] The 4-year risk of progression to PDR and severe visual loss was substantially lower among participants in 1986–2008 (2.6% and 3.2%) than in 1975–1985 (19.5% and 9.7%). At 10 years, similar patterns were observed with participants in 1986–2008 studies having lower proportions of PDR and NPDR at all time points than participants in 1975–1985 studies. National population-based estimates have reflected this trend of a reduction in the prevalence of PDR, presumably reflecting improved glycemic and systemic control as well as earlier detection of retinal complications.[63] These trends in the reduction of PDR and visual loss are discussed in greater detail in Chapter 47 (The epidemiology of diabetic retinopathy).

Proliferative Diabetic Retinopathy and Blood Glucose Control

The results from the Diabetes Control and Complications Trial (DCCT)/Epidemiology of Diabetes Interventions and Complications (EDIC) and the United Kingdom Prospective Diabetes Study (UKPDS) have established the benefit of intensive blood glucose control in reducing the risk for DR in both type 1 and type 2 patients.[64–73] These large multicenter trials demonstrated conclusively that the long-term risks for the development and progression of DR can be reduced dramatically by improving blood glucose control with intensive treatment.[64–73]

Additional evidence that better glycemic control in patients with

severe NPDR or early PDR reduces their risk of further progression is provided by Early Treatment Diabetic Retinopathy Study (ETDRS) multivariable analyses of risk factors for progression to high-risk PDR. HbA1c at baseline was a strong risk factor. Patients with HbA1c >12% had the highest risk of progression and patients with HbA1c <8.3% had the lowest risk of progression (OR 1.59 vs. 1.00, P <0.0001).[74] Even in the lowest A1c category, the 5-year rate of developing high-risk PDR from severe NPDR was high (50%). These data suggest that the benefits of better control continue to be manifest even once severe NPDR or PDR has developed.

Early Worsening of Retinopathy With Improved Glycemic Control

Soon after HbA1c assays, home blood glucose monitoring and continuous subcutaneous insulin infusion became widely available, several small clinical trials and case series reported the frequent occurrence of unexpected worsening of DR[75] in the first 3–12 months following the initiation of intensive insulin therapy (termed "early worsening").[76–79] In most of these early trials the patients enrolled had no more than mild-to-moderate NPDR at baseline and the early worsening, when it occurred, was usually mild (development of cotton-wool spots and/or IRMA) and transient. In some reports, however, when glycemic control was very poor and/or retinopathy more severe at baseline, some eyes developed severe PDR and/or macular edema and substantial visual loss.[75,80]

In the DCCT, cotton-wool spots or IRMA, or both, developed in only 1% of 348 patients entering the trial with no retinopathy. This proportion increased to 48% in the 60 patients with mild nonproliferative retinopathy, defined as the presence of microaneurysms plus mild retinal hemorrhages and/or hard exudates. Recovery was frequent and at the 4-year follow-up visit progression from baseline on the ETDRS scale was about the same in intensive treatment group eyes that had experienced early worsening as in conventional treatment group eyes that had not (1.3 vs. 1.0 steps). Clinically important early worsening (defined as development of PDR, severe NPDR, or clinically significant

macular edema) was not observed in patients with no retinopathy or with microaneurysms involving only one eye, but it occurred in 6 of the 32 patients with moderate NPDR. DCCT patients were followed closely, and early worsening did not lead to serious visual loss, but DCCT findings support the conclusion that early worsening may be more common and more sight-threatening in patients with more severe retinopathy and/or very poor glycemic control. For this reason, patients with advanced nonproliferative or active proliferative DR should be monitored closely before and for several months after initiation of intensive insulin treatment.[70,75,80,81] Panretinal photocoagulation prior to initiation of such treatment may be considered when factors suggest a particular need to protect against advancing severe retinopathy. Such considerations include very severe NPDR or active PDR, longstanding very poor glycemic control and high likelihood of suboptimal follow-up.[75] The most important risk factors for early worsening were higher baseline HbA1c and greater reduction of HbA1c after enrollment. Possible mechanisms include[75,80] alterations in retinal blood flow, decreased autoregulation of the retinal circulation, transient ischemia owing to a decrease in nutrient substrate, and insulin-induced changes in retinal homeostasis that lead to an increase in growth factors such as VEGF.[82–84] Because the short- and long-term benefits of improved glycemic control in reducing the risk of retinopathy progression are remarkable[67] and because treatments for sight-threatening retinopathy are highly effective in preventing visual loss, intensive glycemic control should not be discouraged for fear of retinopathy progression.[72]

Absence of Proliferative Diabetic Retinopathy in Individuals With Diabetes of Extreme Duration

Despite the nearly universal development of some degree of retinopathy in people with diabetes given sufficient time, the development of PDR plateaus at approximately 60%. This observation has generated significant research interest, as it suggests that there may be protective mechanisms that may delay

or prevent the progression to PDR. There are published reports on two unique cohorts of type 1 patients with more than 50 years of type 1 diabetes. The Golden Years cohort from the United Kingdom was noted to have characteristic normal body mass, low insulin dose, a favorable lipid profile, and a positive family history of longevity consistent with possibly genetically determined favorable outcomes.[85] The Joslin 50-year Medalist cohort has been characterized for all four major diabetic vascular complications of retinopathy, nephropathy, neuropathy, and cardiovascular disease. The 50-Year Medalist Study[84,85] has demonstrated that substantial proportions of individuals may survive diabetes duration of 50 years or more and remain free of advanced diabetic vasculopathy including PDR (49.4%). Longitudinal data from a subgroup of 97 Medalists followed for an average of 20.6 years and 39.4 visits suggests that retinopathy worsening occurs almost entirely within the first two decades of follow-up and eyes that do not develop PDR have a slower rate of retinopathy progression. These findings strongly suggest the existence of a subgroup of individuals who develop early protection against the long-term adverse effects of hyperglycemia. Furthermore, despite multiple studies that have strongly associated worse glycemic control, hypertension, and hyperlipidemia with more severe diabetic retinopathy or diabetic macular edema (DME) in patients with shorter duration diabetes, no relationship has been found between these factors and PDR status in the Medalists. Instead, initial findings suggest that specific combinations of advanced glycation endproducts may be associated with increased risk for (carboxyethyl-lysine and pentosidine) or protection from (carboxymethyl-lysine and fructose-lysine) PDR in this unique cohort. Ongoing studies in the Medalists and other populations with extremely long duration of diabetes may yield additional insights into protective mechanisms against PDR development, including novel genetic, biochemical, and physiologic factors.

Systemic Medications and Proliferative Diabetic Retinopathy

Systemic medications are often used in the setting of diabetes mellitus to attain optimal glycemic control and treat coexisting conditions. These drugs can have beneficial or deleterious effects on the onset or progression of diabetic eye disease. There is mounting evidence that oral systemic medications can reduce microvascular complications possibly through mechanisms other than their effect on glycemic control, blood pressure, and lipid lowering. The results of clinical trials on glycemic control (DCCT,[64,68] EDIC,[72,73] UKPDS,[65,70,71] ACCORD,[86] ADVANCE,[87] lipid-lowering medications (ACCORD-EYE,[88] FIELD,[89]) and angiotensin-converting enzyme inhibitors (EURODIAB,[90] EUCLID,[90] ADVANCE[86]), angiotensin II type 1-receptor blockers (DIRECT[90,91] RASS[92]) on retinopathy progression are discussed in detail in Chapter 47 (The epidemiology of diabetic retinopathy) and Chapter 50 (Nonproliferative diabetic retinopathy and diabetic macular edema).

Evidence to support the rationale of using systemically active therapeutic agents to prevent or limit local microvascular complications such as PDR is also growing. Thiazolidinediones are a class of oral hypoglycemic agents used in the treatment of type 2 diabetes that activate the peroxisome proliferator-activated receptor-gamma (PPAR-γ) – a transcription factor known to regulate the expression of genes primarily located in adipose tissue, but also present in other tissues such as the retina.[93] The thiazolidinedione rosiglitazone has been reported to delay the onset of PDR, possibly because of antiangiogenic effects mediated by PPAR-γ agonist activity.[94,95] Shen and colleagues[94] performed a longitudinal medical record review of 124 patients treated with rosiglitazone and 158 patients not receiving rosiglitazone as controls, who were matched by baseline characteristics including level of HbA1c. Among patients with severe NPDR receiving rosiglitazone, the relative risk of progression to PDR at 3 years was reduced by 59% (p=.045), and this effect continued over 5 years of follow-up. Furthermore, at 5 years of follow-up, a significantly smaller proportion of patients in the rosiglitazone group experienced a decline of 3 or more lines in visual acuity (0.5% vs. 38.0%; p=.03). No difference was found in the incidence of diabetic macular edema or clinically significant macular edema (CSME)

between the groups (p=.28). Initial case series and more a prospective cohort-based electronic medical record-based review have reported the association of thiazolidinedione use and DME (OR 2.6; 95% CI 2.4–3.0). However, data from the largest clinical trial study to date to evaluate an association between thiazolidinedione exposure and DME in patients with type 2 diabetes demonstrated no such association. Thus, it appears that that DME can occur at least sporadically with thiazolidinedione use, although this is relatively rare.

Peripheral Diabetic Retinal Lesions and the Risk of Retinopathy Progression

Multiple independent groups have reported that the presence of peripheral retinal lesions as seen on ultrawide-field imaging may suggest an increased DR severity in 9–15% of eyes.[37,38,96] Predominantly peripheral lesions (PPL), defined as the presence of more than 50% of a specific DR lesion located outside standard ETDRS fields, may be present in up to 50% of eyes. Prospective longitudinal 4-year data has shown that the presence of PPL is associated with a 3.2-fold increased risk for 2 or more step DR progression and a 4.7-fold increased risk of developing PDR.[97] The appearance of DR lesions in the peripheral retina is hypothesized to result from underlying capillary nonperfusion and be potentially associated with the progression of DR. Furthermore, the extent of capillary nonperfusion in the midperiphery has been reported to increase in parallel with DR severity.[27,96] The extent of capillary nonperfusion is thought to correlate with tissue hypoxia and is generally regarded as an irreversible process driving overall ischemia in an eye.[27] The attendant appearance of diabetic PPL with capillary nonperfusion could potentially explain the link between these lesions and the increased risk for retinopathy progression.[41]

Other Risk Factors for Proliferative

Most studies seeking to identify risk factors for the development of PDR begin with patients who have various levels of NPDR or no visible retinopathy at all, and make comparisons of baseline factors between those who do and do not develop PDR. As expected, the significant risk factors for the development of PDR include increasing NPDR severity, decreased visual acuity, and elevated HbAlc. Additional risk factors included the presence of diabetic neuropathy, decreased hematocrit, increased serum triglyceride, and decreased plasma albumin.[74] However, it should be noted that if the risk factors for progression from severe NPDR to PDR differ substantially from those mediating onset or progression of earlier NPDR, previous studies may not have readily identified these differences.

The association of elevated serum lipids with increased risk of progression to high-risk PDR and their association with increased hard exudates and decreased visual acuity,[98] provide additional motivation for lowering the frequently elevated lipid levels observed in diabetic patients. Data from the ACCORD-EYE study show that DR progression rates were reduced from 10.2% with placebo to 6.5% with fenofibrate therapy for dyslipidemia (adjusted OR 0.60; 95% CI 0.42–0.87; p=.006), although the benefit from fenofibrate treatment appeared to be independent of its effects on lipid levels in this study.[88] Severe anemia is a less frequently encountered problem in diabetic patients, but its association with increased risk of severe retinopathy has been suggested by ETDRS analyses and three other reports.[74] Hypertension was not identified as a risk factor for development of high-risk PDR in the ETDRS, while findings in previous studies have been variable.[7,74] In the UKPDS, patients with hypertension were randomized between more- and less-intensive regimens of blood pressure control, and retinopathy progression was significantly less common in the former, as was the incidence of photocoagulation and of a 3 or more line decrease in visual acuity. Risk reductions after 7.5 years ranged from 35% to 45% for these outcomes. Progression to PDR was too infrequent for meaningful analysis. A more detailed discussion of the epidemiology and risk factors for DR is presented in Chapter 47

(The epidemiology of diabetic retinopathy).

Management of Proliferative Diabetic Retinopathy

Familiarity with the natural course of PDR suggests two principal therapeutic approaches: first, to prevent or regress the proliferation of new vessels, and, second, to prevent or relieve the effects of contraction of the posterior vitreous surface and fibrovascular proliferation. This section deals mainly with the first aim, as the second is discussed in Chapter 115 (Surgery for proliferative diabetic retinopathy). The cornerstone of diabetes eye care is the maintenance of intensive glycemic control, which is remarkably effective in reducing the risk of onset and progression of DR and the development of PDR.[64–73] Once active proliferative changes have begun, glycemic control alone is usually insufficient. A variety of other approaches have been attempted including pituitary ablation in the 1960s, which was rapidly supplanted by laser photocoagulation as the treatment of choice for more than four decades now. Recently, the use of anti-VEGF therapy has been shown to be a safe and effective alternative to laser for the treatment of PDR. In addition, new therapeutic interventions are now on the horizon. The following section discusses these past, present, and future approaches.

Pituitary Ablation

Building on the fundamental discovery of Biasotti and Houssay[99] that hypophysectomy reduced the severity of diabetes in pancreatectomized dogs, Luft and coworkers[100] carried out hypophysectomy in the hope of ameliorating the vascular complications of diabetes. Further impetus was provided by Poulsen's report[100,101] of remission of DR in a woman with postpartum anterior pituitary insufficiency (Sheehan syndrome). Over the next 25 years, various types of pituitary suppression were used, ranging from external irradiation to transfrontal hypophysectomy. A consensus developed among advocates of

these procedures that complete or nearly complete suppression of anterior pituitary function (pituitary ablation) produced rapid improvement in eyes with severe NPDR and actively growing new vessels not yet accompanied by extensive fibrous proliferations. Although only two randomized trials have been reported,[101] both small and neither in itself compelling, the weight of evidence supports the belief that it had some beneficial effect. Particularly persuasive are comparisons between patients in whom trans-sphenoidal implantation of radioactive yttrium was followed by complete or nearly complete anterior pituitary suppression and similar patients in whom little or no suppression was achieved. Substantially better outcome was observed in the former group.[102] Additional support is provided by a nonrandomized comparison of eyes with very extensive new vessels and IRMA, in which outcome was better in the eyes of patients undergoing pituitary ablation than in similar eyes receiving photocoagulation or no treatment.[103] Pituitary ablation is now only of historical interest because laser photocoagulation and anti-VEGF therapy are both far more effective and also free of the many substantial disadvantages of inducing and living in the hypopituitary state with concomitant diabetes (e.g., operative and immediate postoperative risks, increased susceptibility to severe insulin reactions, need for continuing replacement of adrenal corticosteroids, sterility).

The favorable effect of pituitary ablation on retinopathy is thought to be mediated by suppression of growth hormone activity and effects on insulin-like growth factor 1 (IGF-1).[104] Daily subcutaneous injections of a genetically engineered growth hormone receptor antagonist, pegvisomant, have been given for 3 months in 25 patients with non-high-risk PDR. Regression of new vessels did not occur in any patient, although the serum level of IGF-1, a growth factor whose secretion is stimulated by growth hormone, did decrease an average of 55% compared to baseline levels.[105] In a small randomized clinical trial, multiple daily subcutaneous injections of octreotide, a somatostatin analog that inhibits both growth hormone and insulin-like growth factor, were given to 11 patients with severe NPDR or non-high-risk PDR. During 15 months' follow-up, 1 out of 22 of these patients' eyes required scatter laser photocoagulation compared to 9 out of 24

eyes of 12 patients randomly assigned to an untreated control group.[106] However, larger clinical trials of somatostatin analogs were not found to be effective.

Early Laser Trials

Early observations noted that certain ocular conditions seemed to prevent severe diabetic retinopathy. In addition, as many as 10% of patients experienced spontaneous resolution of PDR.[53] In these eyes the retinopathy becomes stable, the hemorrhages resolve, the retinal vasculature becomes quiescent, the proliferating tissue thins, the retinal veins lose their distended appearance, the retinal arteries become small and attenuated and many obliterated vessel branches are observed. This appearance of the retina is strikingly similar to eyes that have undergone chorioretinal scarring, optic atrophy, high myopia, retinitis pigmentosa, and the endstage of the desired outcome following pituitary ablation.[107,108] The initial use of the xenon arc photocoagulator developed by Meyer–Schwickerath[109] in the treatment of PDR involved direct treatment of new vessels on the surface of the retina, particularly those that appeared to be the source of vitreous hemorrhage.[110–112] Large, slow, moderately intense burns were used, turning the retina white adjacent to the new vessels and sometimes causing them to narrow and the flow within them to slow. These effects were the result of heat generated when light was absorbed by the RPE or by hemorrhage within the retina or on its surface. Direct destruction of new vessels required heavy burns, which usually involved the full thickness of the retina and often led to nerve fiber bundle field defects, particularly if hemorrhages were present in or on the retina. When new vessels were located some distance from the RPE, either in the vitreous or on the optic disc, they could not be treated directly with the xenon arc photocoagulator because it was not possible to concentrate enough energy in a short enough time to coagulate the rapidly flowing blood within them. The hope that this effect would be possible with the narrow, intense, blue–green beam of the argon laser was part of the rationale for its development.

Before the argon laser became widely available, and before recognition of the tendency for NVD and elevated NVE to regrow

after apparently successful direct treatment, the novel concept of panretinal photocoagulation described above began to evolve. Based on observations of remarkable asymmetry of retinopathy favoring the involved eye in diabetic patients who had unilateral disseminated chorioretinal scarring, high myopia, or optic atrophy, Beetham and Aiello began a study in which ruby laser burns were scattered across the retina from the posterior pole to the midperiphery.[108,113,114] The hope was that the induced scarring might have a distant effect across the retina and promote regression of new vessels and diminution of retinal edema and vascular congestion.[108,115,116] The long wavelength and very brief exposure time of the ruby laser limited burns mainly to the outer layers of the retina, without immediately visible effects in new vessels on its surface.

The mechanisms by which panretinal photocoagulation mediates its remarkable benefit were then not fully understood. A theoretical possibility was that retinal cells may produce growth-inhibiting factors in response to photocoagulation injury. Such factors have not been shown to be of importance in vivo to date.[117,118] However, several mechanisms now appear to contribute toward the beneficial effect. Ischemic retina, which produces neovascularization-inducing growth factors (e.g., VEGF), is destroyed, thus reducing the angiogenic stimulus. It is thought that a primary mediating factor is an increase in oxygenation from the choroid to the inner retina that occurs through the laser scars due to the thinning of the retina in the treated area.[119–123] Indeed, retinal blood flow decreases and the autoregulatory response to breathing pure oxygen improves following scatter photocoagulation, as might be expected if more oxygen reached the inner retina from the choroid.[124,125] Furthermore, direct measurements of increased vitreous oxygen have been made using intraocular microelectrodes.[126] The oxygen concentration of the vitreous is much higher overlying the areas of laser burns than over the untreated retina. Regardless of the relative contributions of these mechanisms, the remarkable efficacy of panretinal photocoagulation in the treatment of PDR has been thoroughly documented in multiple randomized clinical trials.

Panretinal Photocoagulation

The initial reports concerning photocoagulation were limited by small numbers of patients, brief periods of follow-up, or lack of a randomly selected control group.[118] Randomized clinical trials were needed to fully evaluate the possible benefits and risks of this treatment. Two collaborative studies were initiated in the early 1970s: the British multicenter trial using xenon arc photocoagulation[127] and the National Eye Institute's Diabetic Retinopathy Study (DRS), which compared xenon arc and argon laser photocoagulation to no photocoagulation in patients with PDR.[128] The DRS provided the initial evidence to establish the safety and efficacy of modern panretinal (scatter) photocoagulation (PRP).

The DRS conclusively demonstrated that PRP significantly reduces the risk of severe visual loss (SVL) from PDR, particularly when high-risk PDR is present.[1,26,129] Patients entering the DRS had PDR in at least one eye or severe NPDR in both eyes. Visual acuity of 20/100 or better was present in each eye. Each patient was randomly assigned to either the argon or xenon treatment group. One eye was randomly assigned to photocoagulation treatment and the other to indefinite deferral of treatment (i.e., no treatment ever), unless evidence that treatment was beneficial resulted in a change of study protocol. Patients were followed at 4-month intervals according to a protocol that provided for measurement of best-corrected visual acuity under standard lighting conditions, with separate charts for each eye. The visual acuity examiners did not know the identity of the treated eye or type of treatment and attempted to reduce patient bias by urging the patient to read as far down the chart as possible with each eye, guessing at letters until more than one in a line was missed.[1]

DRS treatment techniques are summarized in Table 51.2. Both techniques included scatter treatment with burns spaced about one-half to one burn-width apart, extending from the posterior pole to the equator and often completed in a single sitting. The argon treatment technique specified 800–1600 500-μm scatter burns of 0.1 second duration and direct treatment of new vessels on the disc (later excluded from direct treatment) and elsewhere, whether flat or elevated. Direct treatment was also applied to microaneurysms or other lesions thought to be causing macular edema. Follow-up treatment was applied as needed at 4-month intervals. The xenon

technique was similar, but burns were fewer, of longer duration, and stronger. Direct treatment was not applied to elevated new vessels or those on the surface of the disc in the xenon-treated group.

TABLE 51.2
Diabetic Retinopathy Study Photocoagulation Techniques

	Argon Laser	Xenon Arc
Scatter treatment		
No. of burns	800–1600 (500 μm)	400–800 (3 degrees)
	or 500–1000	or 200–400
	(1000 μm)	(4.5 degrees)
Exposure time	0.1 s	Not specified
Direct treatment[a]		
Surface NVE	+	+
Elevated NVE	+	–
NVD	+	–
Macular edema	+	+
Follow-up treatment	+	+

[a]NVD, new vessels on or within 1 disc diameter (DD) of the disc; NVE, new vessels elsewhere (more than 1 DD from the disc).

Reproduced with permission from Diabetic Retinopathy Study Research Group. Photocoagulation treatment of proliferative diabetic retinopathy: clinical application of Diabetic Retinopathy Study (DRS) findings. DRS report number 8. Ophthalmology 1981; 88:583–600. Copyright 1981, with permission from the American Academy of Ophthalmology.

The principal outcome of the DRS was visual acuity of <5/200 at each of two consecutively completed follow-up visits, scheduled at least 4 months apart (termed severe visual loss). Visual acuity of <5/200 was chosen as the level at which vision becomes too poor to be useful for walking about or for other self-care activities. The requirement of two consecutive visits was included because the rate of recovery to better visual acuity after a single visit at the <5/200 level was 29% in the control group and 49% in the treated group whereas after two visits it was 12% and 29%, respectively, and after three visits, 8% and 21%.[1] Because recovery was somewhat more common in treated eyes, the chosen endpoint tends to underestimate the treatment benefit.

Table 51.3 presents 2-year cumulative rates of severe visual loss in eyes grouped by baseline retinopathy severity and treatment assignment.[2] For severe visual loss to be present at the 2-year visit,

visual acuity had to be <5/200 no later than the 20-month visit. For all eyes in the untreated control group, the risk of severe visual loss within 2 years was 15.9%, and this risk was reduced to 6.4% by treatment. The risk was greatest in group J (36.9% in the control group). These eyes had preretinal or vitreous hemorrhage and NVD exceeding those in standard photograph 10A of the modified Airlie House classification (Fig. 51.15). The risk appeared somewhat lower for eyes with NVD of this severity without hemorrhage (group I, 26.2% in the control group). Similar risks (25.6% and 29.7%, respectively) were observed for untreated eyes in groups H and F, eyes with vitreous or preretinal hemorrhage, and less severe new vessels. Eyes in these four groups were referred to in the DRS as eyes with high-risk characteristics or, alternatively, eyes with three or four new vessel-vitreous hemorrhage (NV-VH) risk factors, these factors being (1) new vessels present; (2) new vessels located on or within 1 DD of the disc (NVD); (3) new vessels moderate to severe (NVD equaling or exceeding those in standard photograph 10A or, for eyes without NVD, NVE equaling or exceeding one-half disc area in at least one photographic field); and (4) vitreous or preretinal hemorrhage (or both) present. In counting risk factors, the presence and severity of NVE were considered only in eyes without NVD because a subgroup analysis indicated that in eyes with NVD the presence of moderate or severe NVE did not further increase the risk of severe visual loss.[2] In the remaining groups (A through E and G), the risk without treatment varied from 3.6 to 10.5%. Treatment reduced the rate of severe visual loss in each group, most impressively in groups F through J. Since it appeared that a small permanent reduction in visual acuity might occur in 10–20% of treated eyes, the DRS investigators concluded in 1976 that prompt photocoagulation treatment was usually desirable for eyes with high-risk characteristics. The protocol was therefore modified to allow treatment of eyes originally assigned to the untreated control group, if they had high-risk characteristics at the time or developed them subsequently.[1]

TABLE 51.3

Cumulative 2-Year Rates of Severe Visual Loss in Eyes Grouped by Baseline Retinopathy Severity and Treatment Assignment

Retinopathy Severity Group	NVE	NVD	VH/PRH	No. of NV–VH Risk Factors	Control		Treated		Z-Value
					SVL (%)	No. at Risk[a]	SVL (%)	No. at Risk[a]	
A	0	0	0	0	3.6	195	3.0	182	0.4
B	0	0	+	1	4.2	11	0.0	16	1.0
C	<1/2 DA	0	0	1	6.8	120	2.0	96	1.8
D	<1/2 DA	0	+	2	6.4	18	0.0	19	1.1
E	≥1/2 DA	0	0	2	6.9	125	4.3	141	1.0
F	≥1/2 DA	0	+	3	29.7	40	7.2	41	3.0
G	+ or 0	<10A	0	2	10.5	114	3.1	126	2.4
H	+ or 0	<10A	+	3	25.6	39	4.3	35	2.9
I	+ or 0	≥10A	0	3	26.2	150	8.5	174	4.7
J	+ or 0	≥10A	+	4	36.9	76	20.1	107	3.2
All eyes					15.9	897	6.4	946	7.2

[a]In the 20- to 24-month interval.

DA, disc area (NVE <1/2 DA indicates that NVE do not equal or exceed one-half the area of the disc in any of the standard photographic fields, NVE ≥1/2 DA indicates that NVE equal or exceed this area in at least one of these fields); NVD, New vessels on or within 1 disc diameter of the optic disc; NVE, new vessels elsewhere (i.e., outside the area defined as NVD); NV–VH risk factors, new vessel–vitreous hemorrhage risk factors (see text); SVL, severe visual loss (visual acuity <5/200 at two or more consecutively completed follow-up visits scheduled at 4-month intervals); VH/PRH, vitreous/preretinal hemorrhage; 10A, standard photograph 10A of the modified Airlie House classification (Fig. 51.15).

Reproduced with permission from the Diabetic Retinopathy Study Research Group. Indications for photocoagulation treatment of diabetic retinopathy. DRS report number 14. Int Ophthalmol Clin 1987;27:239–253.

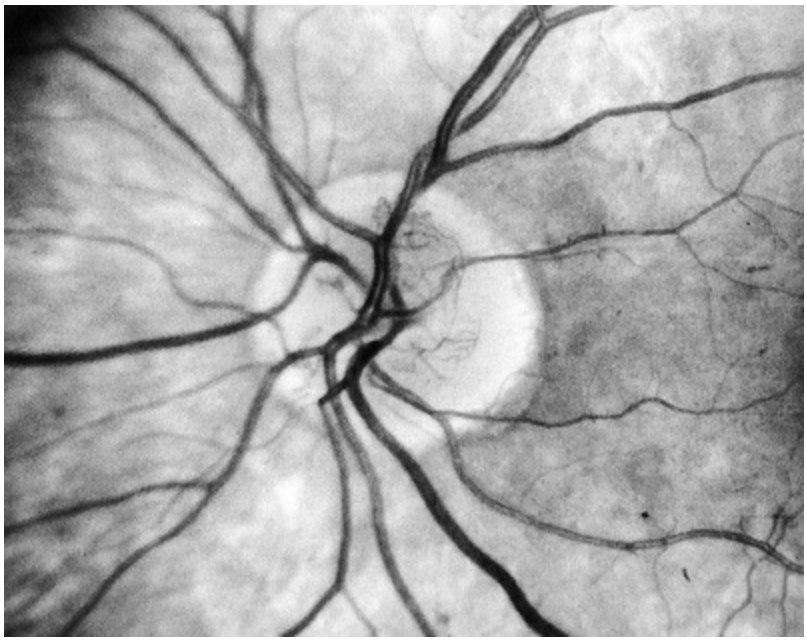

FIG. 51.15 Standard photograph 10A of the modified Airlie House classification, defining the lower limit of moderate new vessels on or within 1 disc diameter of the disc. (Reproduced with permission from Diabetic Retinopathy Study Research Group. A modification of the Airlie House classification of diabetic retinopathy. DRS report number 7. Invest Ophthalmol Vis Sci 1981;21:210–226.)

In Table 51.4, the retinopathy severity groups presented in Table 51.3 have been combined, and observations from follow-up visits completed after the 1976 protocol change have been included.[1] Forty-three percent of the 2-year visits and all the 4-year visits included in this analysis were carried out after the 1976 protocol change. At the 2-year visit, 12% of control-group eyes had been treated, and by the 4-year visit 35% had been treated. All eyes were classified in the group to which they were originally randomly assigned, without reference to treatment of control-group eyes. In the control group the 2-year risk of severe visual loss increased from 3.2% in eyes with NPDR to 7% in eyes with PDR without high-risk characteristics, and to 26.2% in eyes with high-risk characteristics. The 4-year rates in these groups were, respectively, 12.8, 20.9, and 44.0%. Treatment reduced the risk of severe visual loss by 50% to 65% in all three groups at both 2 and 4 years, except for the NPDR group at 2 years.

TABLE 51.4

Cumulative 2- and 4-Year Rates of Severe Visual loss in Eyes

Grouped by Baseline Retinopathy Severity and Treatment Assignment[a]

Retinopathy Severity	Groups[b]	No. of NV–VH Risk Factors	Follow-Up	Control		Treated		Z-Value
				SVL (%)	No. at Risk[c]	SVL (%)	No. at Risk[c]	
NPDR	A	0	2-year	3.2	297	2.8	303	0.3
			4-year	12.8	183	4.3	188	3.6
PDR without HRC	B–E, G	1 or 2	2-year	7.0	603	3.2	615	3.1
			4-year	20.9	332	7.4	390	6.5
PDR with HRC	F, H–J	3 or 4	2-year	26.2	473	10.9	570	7.1
			4-year	44.0	238	20.4	324	8.5
All eyes			2-year	14.0	1278	6.2	1489	7.4
			4-year	28.5	754	12.0	903	11.0

[a]As in Table 51.3.

[b]NV–VH risk factors, new vessel–vitreous hemorrhage risk factors (see text); SVL, severe visual loss (visual acuity <5/200 at two or more consecutively completed follow-up visits scheduled at 4-month intervals).

[c]In the 20- to 24-month interval for the 2-year rates, at the 44- to 48-month interval for the 4-year rates.

HRC, high-risk characteristics; NPDR, nonproliferative diabetic retinopathy; PDR, proliferative diabetic retinopathy.

Reproduced with permission from Diabetic Retinopathy Study Research Group. Indications for photocoagulation treatment of diabetic retinopathy. DRS report number 14. Int Ophthalmol Clin 1987;27:239–253.

Fig. 51.16 depicts cumulative rates of severe visual loss by treatment assignment (argon and xenon groups combined) for up to 6 years. Two separate analyses are summarized, one excluding and the other including visits made after the 1976 protocol change. The curves for control-group eyes are very similar over the first 20 months of follow-up, and those for treated eyes are similar over at least the first 28 months. The difference between the two control-group curves is probably due, at least in part, to the beneficial effect of treatment experienced by some of these eyes after the protocol change, and the long-term analysis probably underestimates treatment effect. In each of these analyses, treatment reduced the risk of severe visual loss by 50% or more at and after the 16-month visit.[129] In Fig. 51.17, the Fig. 51.16 plots including all visits are presented separately for the argon and xenon groups. The treatment effect (i.e., the difference between treatment and control groups) appeared somewhat greater in the xenon group, but this

difference was small, its statistical significance was borderline, and its clinical importance was outweighed by the greater harmful effects of DRS xenon treatment.

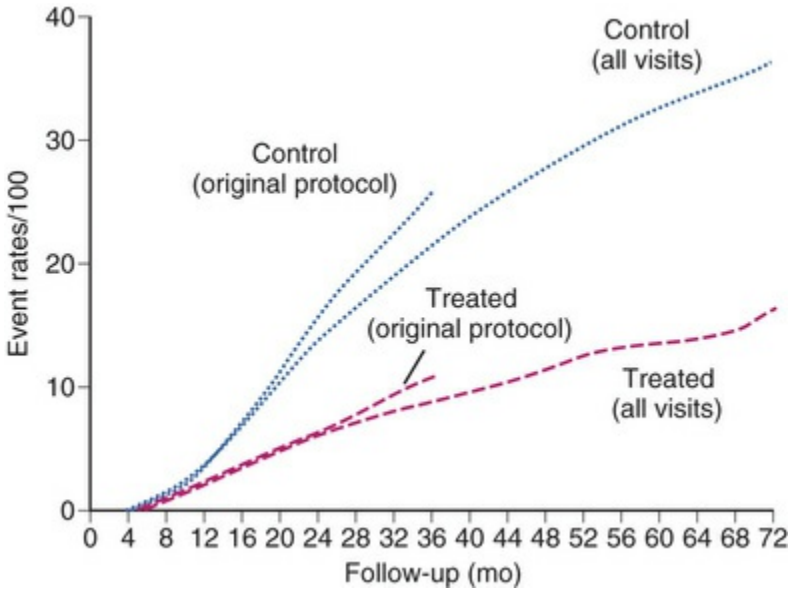

FIG. 51.16 Cumulative rates of severe visual loss, including and excluding observations made after the 1976 protocol change, for argon and xenon groups combined. (Reprinted from Diabetic Retinopathy Study Research Group. Photocoagulation treatment of proliferative diabetic retinopathy: clinical application of Diabetic Retinopathy Study (DRS) findings. DRS report number 8. Ophthalmology 1981;88:583–600. Copyright 1981, with permission from the American Academy of Ophthalmology.)

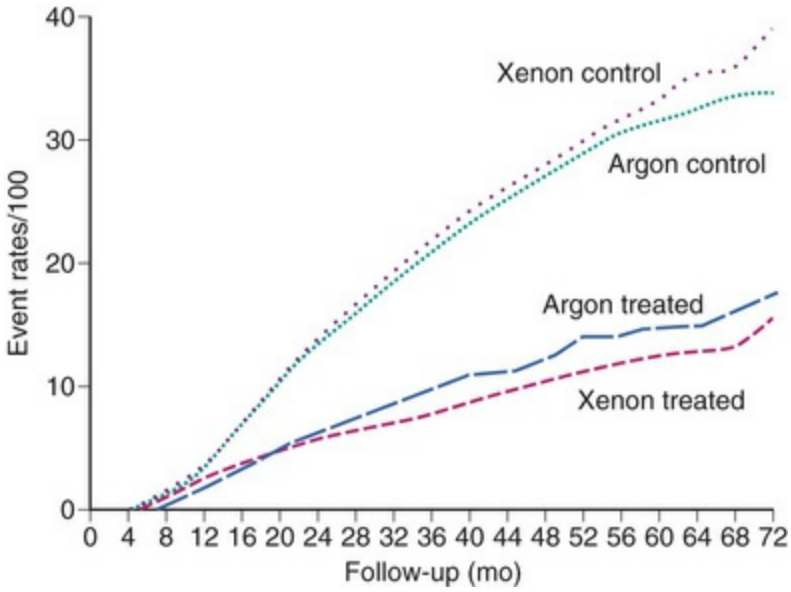

FIG. 51.17 Cumulative rates of severe visual loss by treatment group. (Reprinted from Diabetic Retinopathy Study Research Group. Photocoagulation treatment of proliferative diabetic retinopathy: clinical application of Diabetic Retinopathy Study (DRS) findings. DRS report number 8. Ophthalmology 1981;88:583–600. Copyright 1981, with permission from the American Academy of Ophthalmology.)

A temporary decrease in visual acuity is frequently noted after extensive scatter photocoagulation, with recovery to the pretreatment level in most cases within several weeks. In the DRS, visual acuity decreases of one or more lines from which recovery did not occur were attributed to treatment in 14% of argon-treated and 30% of xenon-treated eyes. Visual field losses were also more common in the xenon group[129,130] (Table 51.4). In a small subgroup of eyes with severe fibrous proliferations or localized traction retinal detachment, or both, visual acuity decreases of 5 lines or more were attributed to xenon treatment in 18% of eyes but were not significantly more frequent in argon-treated than in control eyes.[130]

In Fig. 51.18, the Fig. 51.16 plots including all visits are presented separately for the three subgroups shown in Table 51.4. In each subgroup treatment reduced the risk of severe visual loss to about one-half of that observed in control-group eyes, but this effect became apparent later, and the percentage of eyes treated that benefited (the arithmetic difference between treated and control groups) was smaller as retinopathy severity decreased. On the basis of this analysis and the estimates of the harmful effects of treatment

summarized in Table 51.5, the DRS confirmed its previous conclusion that, for eyes with high-risk characteristics, the chance of benefit from treatment clearly outweighed its risk and recommended prompt photocoagulation for most such eyes.[129]

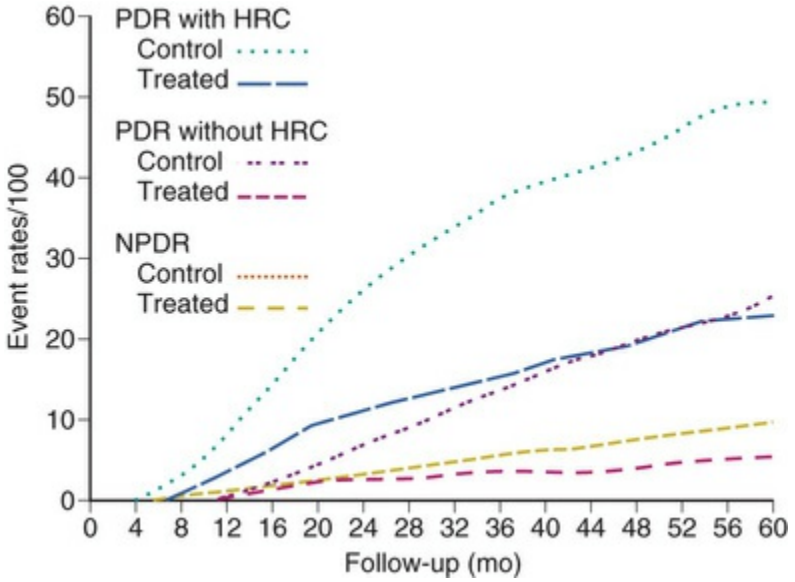

FIG. 51.18 Cumulative rates of severe visual loss for eyes classified by the presence of proliferative retinopathy (PDR) and high-risk characteristics (HRC) in baseline fundus photographs, argon, and xenon groups combined. NPDR, Nonproliferative diabetic retinopathy. (Reprinted from Diabetic Retinopathy Study Research Group. Photocoagulation treatment of proliferative diabetic retinopathy: clinical application of Diabetic Retinopathy Study (DRS) findings. DRS report number 8. Ophthalmology 1981;88:583–600. Copyright 1981, with permission from the American Academy of Ophthalmology.)

TABLE 51.5

Estimated Percentages of Eyes With Harmful Effects Attributable to Diabetic Retinopathy Study Treatment

	Argon (%)	Xenon (%)
Constriction of visual field (Goldmann IVe4 test object) to an average of		
≤45°, >30° per meridian	5	25
≤30° per meridian	0	25
Decrease in visual acuity		
1 line	11	19
≥ 2 lines	3	11

Reproduced with permission from Diabetic Retinopathy Study Research Group. Photocoagulation treatment of proliferative diabetic retinopathy: clinical application of Diabetic Retinopathy Study (DRS) findings. DRS report number 8. Ophthalmology 1981;88:583–600.

For eyes with severe NPDR or PDR without high-risk characteristics, the DRS concluded that either prompt treatment or careful follow-up with prompt treatment if high-risk characteristics developed was satisfactory and that DRS results were not helpful in choosing between these strategies. In unadjusted analyses of DRS control-group eyes that had PDR without high-risk characteristics, the severity of each of three retinopathy characteristics was associated with risk of visual loss: retinal hemorrhages or microaneurysms, arteriolar abnormalities, and venous caliber abnormalities. These lesions – and soft exudates and IRMAs – were also risk factors for visual loss in control-group eyes with NPDR.[33] A multivariable analysis that included all DRS control-group eyes found baseline visual acuity, extent of NVD, elevation of NVD (a measure of contraction of vitreous and fibrous proliferations), and severity of hemorrhages or microaneurysms, arteriolar abnormalities, venous caliber abnormalities, and vitreous or preretinal hemorrhage all to be risk factors for visual loss. Neither in this analysis, nor in a similar one confined to DRS control-group eyes that were free of NVD, was the extent of NVE found to be a risk factor.[131] These findings support clinical impressions that NVE on the surface of the retina often proliferate and regress over a period of years, remaining asymptomatic unless contraction of vitreous and fibrous proliferations begins, and that the severity of intraretinal lesions may be of greater prognostic importance than the extent of NVE.

When the DRS first reported evidence of a beneficial treatment effect and modified its protocol to encourage treatment of control-group eyes with high-risk characteristics, it also modified its treatment protocol. Because the harmful effects of the DRS argon treatment were less than those observed with the xenon treatment used in the DRS, argon was given preference and, in the hope of further reducing harmful side-effects, scatter treatment was more often divided between two or more episodes several days apart. However, because the beneficial treatment effect in the xenon group, in which no focal treatment had been applied to NVD or

elevated NVE, had been at least as great as that in the argon group, these technically difficult parts of the argon protocol were dropped. Two large case series[132,133] and two smaller randomized trials reported beneficial treatment effects similar to those found in the DRS.[134,135]

Early Treatment Diabetic Retinopathy Study and the Timing of Treatment

As mentioned previously, for eyes with severe NPDR or early (not high-risk) PDR, DRS results were not helpful in determining which of two treatment strategies would be attended by a more favorable visual outcome: (1) immediate photocoagulation or (2) frequent follow-up and prompt initiation of photocoagulation only if high-risk PDR developed. One of the goals of the Early Treatment Diabetic Retinopathy Study (ETDRS), a randomized clinical trial sponsored by the National Eye Institute, was to compare these alternatives (designated "early photocoagulation" and "deferral of photocoagulation," respectively) in patients with mild to severe NPDR or early PDR, with or without macular edema.[136] Other goals were to evaluate photocoagulation for diabetic macular edema[137] and to determine the possible effects of aspirin on DR.[138] Between 1980 and 1985, 3711 patients were enrolled and assigned randomly to aspirin 650 mg/day or placebo. One eye of each patient was randomly assigned to early photocoagulation and the other to deferral. Follow-up ranged from 3 to 8 years. Eyes assigned to early photocoagulation were randomly assigned to either of two scatter treatment protocols, full or mild. The full scatter protocol called for 500 μm, 0.1 sec argon blue–green or green laser burns of moderate intensity, placed one-half burn apart, extending from the posterior pole to the equator. Between 1200 and 1600 burns were applied, divided between two or more sittings. The mild scatter protocol was the same, except that 400–650 more widely spaced burns were applied to the same area in a single sitting. Direct (local) treatment was specified for patches of flat surface NVE that were two disc areas or less in extent (the area of a circle about 1.4 times the diameter of the disc), using confluent, moderately intense burns that extended 500 μm beyond the edges of the patch. For larger

patches or several small ones close together, full scatter alone to this area was an acceptable alternative. No direct treatment was carried out for NVD.[139]

One important outcome measure used in the ETDRS was the first occurrence of either severe visual loss, as defined in the DRS, or vitrectomy.[136] These events were combined because progression to a stage requiring vitrectomy may rightly be considered an undesirable outcome for ETDRS-eligible eyes and since presumably most eyes selected for vitrectomy before the occurrence of severe visual loss (68% of the 243 ETDRS eyes undergoing vitrectomy) would have developed severe visual loss within several months if vitrectomy had not been performed. Five-year life-table rates of severe visual loss or vitrectomy, and relative risks for early photocoagulation compared to deferral over the entire follow-up period, are shown in Table 51.6. The first two rows include eyes with macular edema, subdivided by retinopathy severity. As anticipated, the poor outcome was more frequent in eyes with more severe retinopathy (in the deferral group, 10% in eyes with severe NPDR or early PDR versus 4% in eyes with mild to moderate NPDR). In both of these retinopathy subgroups, early treatment reduced the event rate to about one-half that of the deferral group, but the percentage of eyes treated that benefited was only 2–4%. The third row of the table includes all eyes without macular edema regardless of retinopathy severity (eyes with mild NPDR were not eligible unless macular edema was present), and outcome here was intermediate between that in rows 1 and 2. Some harmful effects of scatter photocoagulation were also observed in the ETDRS, including an early decrease in visual acuity (a doubling or more of the visual angle at the 4-month visit in about 10% of eyes assigned to early full scatter, compared to about 5% of eyes assigned to deferral) and some decrease in visual field. Both beneficial and harmful effects were somewhat greater with full than with mild scatter.

TABLE 51.6

Cumulative 5-Year Rates of Severe Visual Loss or Vitrectomy, and Relative Risks for the Entire Period of Follow-Up, by Baseline Retinopathy Status and Treatment Group

Baseline Retinopathy	Treatment Group				Relative Risk (99% CI)
	Early Photocoagulation		Deferral		
	NO. AT BASELINE	5-YEAR RATE (%)	NO. AT BASELINE	5-YEAR RATE (%)	
Mild to moderate NPDR with macular edema (0.33–0.94)	1448	2	1429	4	0.55
Severe NPDR or early PDR with macular edema (0.47–0.99)	1090	6	1103	10	0.68
Moderate to severe NPDR or early PDR without macular edema	1173	4	1179	5	0.78 (0.47–1.29)

CI, confidence interval; NPDR, nonproliferative diabetic retinopathy; PDR, proliferative diabetic retinopathy.

Reprinted from early photocoagulation for diabetic retinopathy. Early Treatment of Diabetic Retinopathy Study report number 9. Early Treatment of Diabetic Retinopathy Study Group. Ophthalmology 1991;98:766–785. Copyright 1991, with permission from the American Academy of Ophthalmology.

Fig. 51.19 presents cumulative incidence rates of high-risk PDR in ETDRS eyes assigned to deferral of photocoagulation, by severity of retinopathy at baseline. It is of interest that high-risk PDR developed at about equal rates in eyes with moderate PDR or very severe NPDR, with rates of about 50% after 18 months. Figs. 51.15, 51.20 and 51.21 present the standard photographs used in the definitions of high-risk PDR and very severe NPDR, the most important severity levels for application to clinical practice. It is convenient to express the approximate definitions of severe and very severe NPDR with the 4-2-1 rule described earlier (see Box 51.1).

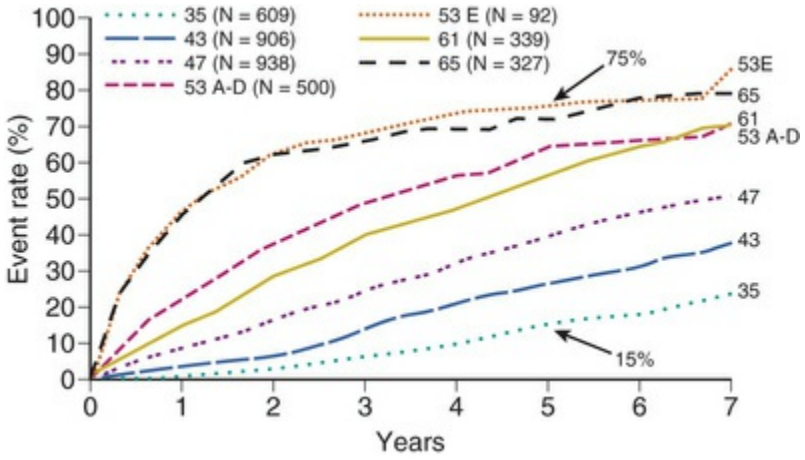

FIG. 51.19 Cumulative incidence of high-risk

proliferative diabetic retinopathy in the eyes of Early Treatment Diabetic Retinopathy Study (ETDRS) patients assigned to deferral of photocoagulation. The 5-year rate for eyes with mild nonproliferative diabetic retinopathy (NPDR: level 35) was 15%. For eyes with very severe NPDR (level 53E) or moderate PDR (level 65), the 5-year rate was about 75% and the 1-year rate was almost 50%. Levels 43 and 47 represent moderate NPDR; level 53A–D, severe NPDR; and level 61, mild PDR (NVE less than half-disc area or fibrous proliferation only). (Reprinted from Early Treatment of Diabetic Retinopathy Study Group. Early photocoagulation for diabetic retinopathy. ETDRS report no. 9. Ophthalmology 1991;98:766–785. Copyright 1991, with permission from the American Academy of Ophthalmology.)

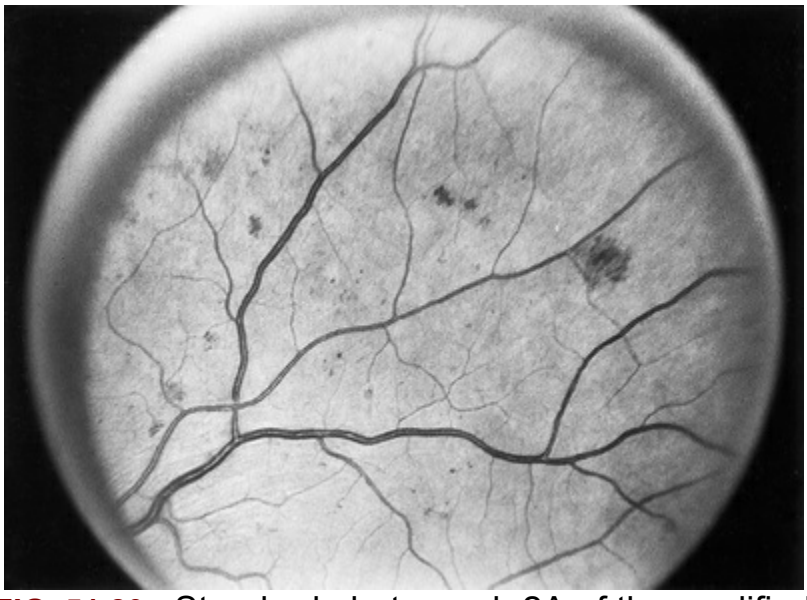

FIG. 51.20 Standard photograph 2A of the modified Airlie House classification, defining lower margin of the "severe" category for retinal hemorrhages and microaneurysms. (Reproduced with permission from Diabetic Retinopathy Study Research Group. A modification of the Airlie House classification of diabetic retinopathy. DRS report number 7. Invest Ophthalmol Vis Sci 1981;21:210–226.)

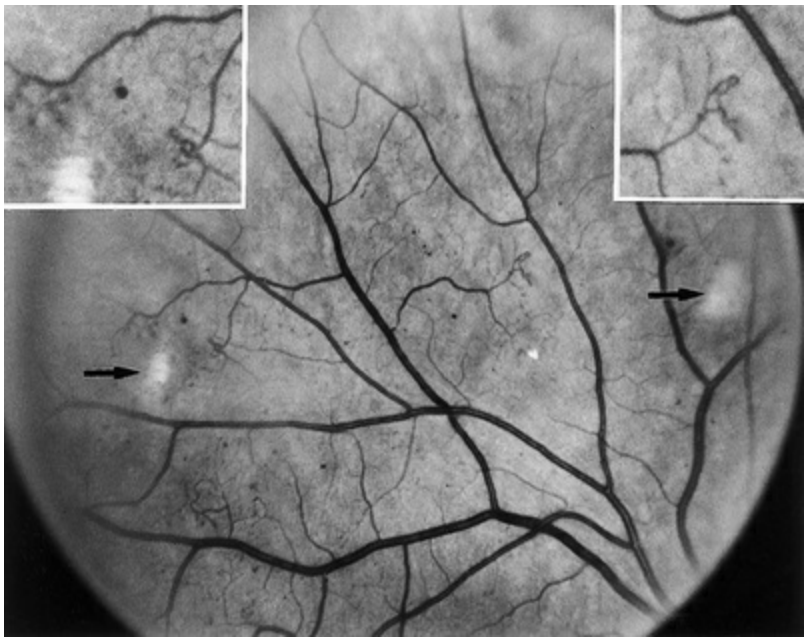

FIG. 51.21 Standard photograph 8A of the modified Airlie House classification, defining the lower margin of the "moderate" category for intraretinal microvascular abnormalities (IRMAs) (and for soft exudates, indicated by *arrows*). IRMAs are prominent in three areas, two of which are shown in insets. Additional IRMAs can be seen when the color transparencies used in grading are viewed stereoscopically with 5× magnification.

(Reproduced with permission from Diabetic Retinopathy Study Research Group. A modification of the Airlie House classification of diabetic retinopathy. DRS report number 7. Invest Ophthalmol Vis Sci 1981;21:210–226.)

The ETDRS recommended that scatter treatment not be used in eyes with mild to moderate NPDR but that it be considered for eyes approaching the high-risk stage (i.e., eyes with very severe NPDR or moderate PDR) and that it usually should not be delayed when the high-risk stage is present. The recommendation to consider photocoagulation for eyes approaching the high-risk stage was made because, although both the benefits and risks of treatment were small and roughly in balance, the risk–benefit ratio was approaching a clearly favorable range. A policy of continued observation would be expected to spare only a minority of eyes from the risks of treatment, while increasing the risk that rapid progression might occur between follow-up visits and that entry into the high-risk stage might be marked by occurrence of a large vitreous hemorrhage, making satisfactory treatment difficult. In

choosing between prompt treatment and deferral, the commitment of the patient to careful follow-up and the state of the fellow eye were important factors. If visual function decreased in the fellow eye after scatter photocoagulation, deferral of treatment in the second eye may be desirable. On the other hand, in a patient whose first eye had an unfortunate outcome without photocoagulation or one with photocoagulation only after PDR was advanced, prompt treatment may be preferable, particularly if close follow-up will be difficult.

These initial ETDRS recommendations were made without regard to patient age or type of diabetes. Subsequent analyses of ETDRS data suggest that, among patients whose retinopathy is in the severe NPDR to non-high-risk PDR range, the benefit of prompt treatment is greater in those who have type 2 diabetes or are older than 40 years of age (these characteristics are highly correlated, and analyses using either gave almost identical results)[140] (Fig. 51.22). In the type 2 group, the 5-year rate of severe visual loss or vitrectomy was about 5% in eyes assigned to early photocoagulation versus 13% in eyes assigned to deferral, whereas in the type 1 group the rates were about 8% in both treatment groups (Fig. 51.19). In eyes assigned to deferral, severe visual loss or vitrectomy developed over the first 3 years at about the same rate in both diabetes types; apparently the greater treatment effect in type 2 diabetes resulted mainly from greater responsiveness to early treatment. The DRS also found greater photocoagulation treatment benefit in patients with type 2 diabetes.[140] Greater responsiveness to photocoagulation in older versus younger patients has also been observed in other studies.[141,142] These studies are consistent with the clinical impression that, in patients with type 2 diabetes, high-risk PDR is often first detected on the basis of a symptomatic vitreous hemorrhage in an eye in which new vessels had not been observed on previous visits, whereas in patients with type 1 diabetes, NVD is more often the first sign of high-risk PDR, an occurrence more easily managed with photocoagulation.

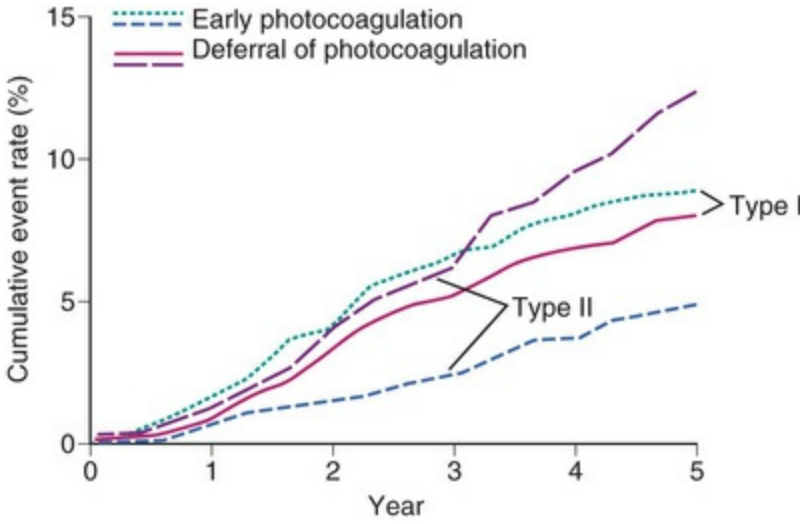

FIG. 51.22 Development of severe visual loss or vitrectomy in eyes with severe nonproliferative or early proliferative retinopathy at baseline. Early treated eyes compared with deferred eyes, for those with type 1 (p=.43) and type 2 (p=.0001) diabetes. Test for interaction of treatment and type (p=.0002). (Reproduced with permission from Ferris F. Early photocoagulation in patients with either type 1 or type 2 diabetes. Trans Am Ophthalmol Soc 1996;94:505–537.)

Thus, in older patients with type 2 diabetes who have very severe NPDR or early PDR, ETDRS results and clinical impression suggest that prompt photocoagulation is probably safer than deferral. In younger patients with type 1 diabetes, ETDRS results suggest that there is little to lose from deferring scatter photocoagulation until high-risk PDR develops assuming appropriate compliance with follow-up. However, even in younger patients, when early NVD (less than shown in Fig. 51.15) is accompanied by the intraretinal signs of severe or very severe NPDR (see Fig. 51.2), prompt treatment is generally recommended. On the other hand, when younger patients have only mild intraretinal lesions and NVE (only) that appears stable, an initial period of observation is generally recommended. If new vessels are demonstrated to be growing, photocoagulation is usually recommended. However, these eyes often remain asymptomatic for many years, with little new vessel growth and often demonstrate spontaneous regression of the new vessels. In such eyes vitreoretinal adhesions tend to be delicate, and when posterior vitreous detachment occurs, there is less tendency for traction retinal detachment. When the process of

posterior vitreous detachment has reached completion in such an eye, new vessels are likely to be few, narrow, elevated, and partially replaced by fibrous proliferations, and there may be little to be gained from photocoagulation at this stage unless vitreous hemorrhages are occurring. Presumably the reduced aggressiveness of new vessels in the setting of posterior vitreous detachment results from the lack of the posterior vitreous face scaffold for proliferation and less possibility for retinal traction.

Systemic factors should also be considered when deciding whether to initiate treatment in patients with very severe NPDR or moderate PDR. The progression of retinopathy may accelerate during pregnancy,[143,144] development of renal failure,[145] extreme illness, and poor glycemic control. If photocoagulation is deferred until high-risk characteristics develop in these situations, these more pressing problems may make it difficult to provide prompt and complete photocoagulation.

Panretinal Photocoagulation and Advanced Proliferative Diabetic Retinopathy

There is widespread agreement that PRP should be performed promptly in most eyes with PDR and high-risk characteristics. However, progressive contraction of fibrous proliferations leading to displacement or detachment of the macula sometimes follows PRP in eyes with extensive fibrous proliferations (see Fig. 51.11). Such cases have led to some reluctance to advise photocoagulation in this situation. Few such eyes were included in the DRS, but analyses of such cases indicated that outcome was better with photocoagulation than without it and suggested that it is only excessively heavy treatment that should be avoided. The adverse treatment effect was only evident in the xenon group, and even there the benefit of treatment outweighed its risks.[130] When high-risk characteristics are definitely present, PRP should usually be carried out, despite the presence of fibrous proliferation or localized traction retinal detachment. Treatment directly over areas of fibrous proliferation and retinal detachment should be avoided, and treatment strength should be mild to moderate. Extensive neovascularization in the anterior chamber angle is a strong

indication for PRP (and anti-VEGF treatment) regardless of the presence of high-risk characteristics as regression of these new vessels before extensive closure of the angle has occurred can prevent neovascular glaucoma.[132,146]

Current Techniques of Panretinal Photocoagulation

The DRS and ETDRS validated the effectiveness of PRP and established the indications and parameters for the treatment of PDR several decades ago.[129,139] These concepts persist mostly unchanged to this day as a result of their remarkable efficacy. A summary of the current protocol for PRP is presented in Table 51.7.

TABLE 51.7

Current Treatment Protocol for Panretinal (PRP) Laser Photocoagulation

Burn Characteristic	Recommendations
CONVENTIONAL SLITLAMP LASER DELIVERY SYSTEMS	
Size (on retina)	500 μm (e.g., argon laser using 200-μm spot size with Rodenstock lens, or equivalent), 400 μm (e.g., 200-μm spot size with Mainster 165, Volk Quadraspheric or SuperQuad 160) or 500-μm spot size with 3-mirror contact lens
Exposure	0.1 seconds recommended, 0.05–0.2 allowed
Intensity	Mild white retinal burns (i.e., 2+ to 3+ burns)
Distribution	Edges 1 burn width apart
No. of sessions/sittings	1 to 3
Nasal proximity to disc	No closer than 500 μm
Temp. proximity to center	No closer than 3000 μm
Superior/inferior limit	No further posterior than 1 row within the temporal arcades
Extent	Arcades (~3000 μm from the macular center) to at least the equator
Number of final burns:	1200–1600
Wavelength	Green or yellow (red can be used if vitreous hemorrhage is present precluding use of green or yellow)
AUTOMATED PATTERN SCANNING LASER DELIVERY SYSTEMS	
Size (on retina)	400 μm (e.g., 200 μm spot size with Mainster 165, Volk Quadraspheric or SuperQuad 160)
Exposure	0.02 seconds
Intensity	Mild white retinal burns

Distribution	Edges 0.5 burn width apart
No. of sessions/sittings	Unrestricted (generally should be completed in <6)
Nasal proximity to disc	No closer than 500 μm
Temp. proximity to center	No closer than 3000 μm
Superior/inferior limit	No further posterior than 1 row within the temporal arcades
Extent	Arcades (~3000 μm from the macular center) to at least the equator
Number of final burns	1800-2400
Wavelength	Green (532 nm) only
Patterns	2×2, 3×3, 4×4, 5×5 as needed for uniform focus/uptake
INDIRECT LASER DELIVERY SYSTEMS	
Size (on retina)	400 to 500 μm spot size with 20 D, 28 D, or 30 D indirect lens (depending on diopter of indirect lens)
Exposure	0.050–0.10 seconds
Intensity	Mild white retinal burns
Distribution	Edges 1 burn width apart
No. of sessions/sittings	Unrestricted (generally should be completed in <6)
Nasal proximity to disc	No closer than 500 μm
Temp. proximity to center	No closer than 3000 μm
Superior/inferior limit	No further posterior than 1 row within the temporal arcades
Extent	Arcades (~3000 μm from the macular center) to at least the equator
Number of final burns	1200–2000
Wavelength	Green (532 nm) only

Adapted from the Diabetic Clinical Research Network Procedure Manuals.

Direct (Local) Treatment of NVE

In the ETDRS, investigators had the option of applying direct photocoagulation (referred to as "local treatment") to flat new vessels on the retina. Confluent argon laser burns of 200–1000-μm spot size and a 0.1–0.5-sec duration were specified with a resulting appearance (Fig. 51.23A) very similar to that obtained with mild xenon arc photocoagulation. Local treatment was limited to patches of NVE <2 disc areas in size in order to avoid large scotomas or nerve fiber bundle field defects. Most retina specialists today do not perform local treatment; the efficacy of PRP without it, although clearly good, is not precisely known.

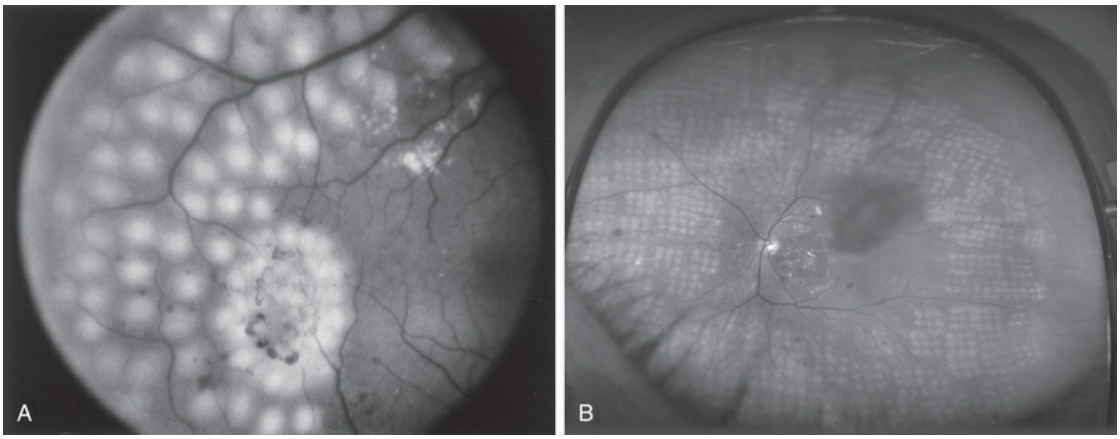

FIG. 51.23 (A) Immediate posttreatment photograph illustrating Early Treatment Diabetic Retinopathy Study full-scatter treatment and local confluent treatment of a patch of new vessels everywhere (NVE). (B) Appearance of pattern scanning laser burns 1 week after treatment. (Panel A reproduced with permission from Early Treatment of Diabetic Retinopathy Study Research Group. Techniques for scatter and local photocoagulation treatment of diabetic retinopathy: the ETDRS report no. 3. Int Ophthalmol Clin 1987;27:254–264; panel B courtesy of the Beetham Eye Institute Library.)

Distribution and Strength of Panretinal Photocoagulation

A common feature of most scatter laser treatment protocols is the location of burns beginning about 2–3 DD from the center of the macula and extending peripherally to the equator. It is important to realize that the size of the burn produced depends not only on the spot-size setting used, but also on the lens, power, and duration, so it is difficult to compare techniques precisely, even those using the same wavelength and spot-size setting, on the basis of number and theoretical size of burns. It is also difficult to describe burn strength. Reporting power level is not particularly helpful, since the required power for a burn of given strength, even if spot-size setting and duration are kept constant, depends on the clarity of the media and the pigmentation of the fundus. The ETDRS protocol for full scatter treatment provides useful guidelines for initial treatment,[139] calling for a total of 1200–1600 500-μm 0.1-sec argon laser burns of moderate intensity placed one-half to one burn apart and divided

between two or more sittings (at least 2 weeks apart if two sittings and at least 4 days apart if three or more sittings). Burns appear to enlarge slightly within several minutes after their application, resulting in the closer spacing of the scatter burns shown in Fig. 51.23A. As discussed below, recent studies, however, have shown that completing an entire ETDRS style PRP in one setting is not associated with major drawbacks and is a viable treatment option.[147]

Pattern Scanning Laser Delivery Systems

The development of scanning laser delivery systems (PAtterned SCAnning Laser [PASCAL®, Topcon Medical Systems, Paramus, NJ; Visulas 532s VITE, Carl Zeiss Meditec, Dublin, CA; Vitra Multispot Laser, Quantel Medical, Bozeman, MT; MC-500 Vixi, Nidek, Fremont, CA]) has given ophthalmologists the ability to deliver various semi-automated operator-selected multispot burn patterns. These systems utilize a 532-nm frequency-doubled neodymium-doped yttrium aluminum garnet (Nd : YAG) solid-state laser and typically have a 20-ms pulse duration for each laser burn that is 5–10 times shorter as compared with conventional lasers. This allows defined multispot patterns to be delivered nearly simultaneously with a single application of the foot pedal. The shorter duration results in less thermal damage, less burn spread, and potentially improves patient comfort and safety without apparently compromising efficacy.

Preclinical animal experiments on the effects of various pulse durations demonstrated that laser burns of pulse durations greater than 20 ms resulted in significant diffusion of heat with a less homogeneous lesion on histologic examination.[148] Pulse durations of approximately 20 ms have been shown to represent an optimal compromise between the favorable impact of speed, spatial localization, and reduced collateral damage with a sufficient therapeutic window.[149] The 10–30-ms pulse of the pattern laser systems is associated clinically with a more uniform and predictable burn dimension with minimal thermal spread compared with conventional photocoagulation.[148,150,151] Clinically, pattern scanning laser burns are typically lighter in intensity and

more uniform, as confirmed by clinical retinal morphologic studies that demonstrated pattern scanning laser burns to be nearly identical in size and sharply delineated from the surrounding untreated retina.[152] Furthermore, the area of tissue destruction was confined to the outer retinal layers, from the outer nuclear layer to the RPE, reflecting less energy spread and less damage to the inner retinal layers and choroid[152] (Fig. 51.23).

Number of Episodes Used for Scatter Treatment

Among the techniques in use for PDR alone, the number of sittings in which initial scatter treatment is carried out varies from one to four or more. Those techniques using a smaller number of larger burns tend toward a single sitting, rarely with retrobulbar anesthesia, whereas those using a larger number of smaller burns have generally been divided into two or more sittings without such anesthesia. In general, multiple sittings may reduce discomfort, but may cause delays and inconvenience for patients. Angle-closure glaucoma secondary to serous detachment of the peripheral choroid and ciliary body is reportedly less common when treatment is carried out in two or more sessions over a period of 1 or 2 weeks.[153]

The DRCR.net conducted an observational study to compare the effects of 1-sitting vs. 4-sitting PRP on DME in subjects with severe NPDR or early PDR with relatively good visual acuity and no or mild center-involved macular edema.[154] Patients enrolled in the study were treated with 1 sitting or 4 sittings of PRP in a nonrandomized, prospective, multicenter clinical trial. The median change in central subfield thickness was slightly greater in the 1-sitting group (n=84) than in the 4-sitting group (n=71) at the 3-day (+9 μm vs. +5 μm, p=.01) and 4-week visits (+ 13 μm vs. +5 μm, p=.003). At the 34-week primary outcome visit, the slight differences had reversed, with the thickness being slightly greater in the 4-sitting group than in the 1-sitting group (+14 μm vs. +22 μm, p=.06). Visual acuity changes paralleled OCT changes: 1 vs. 4 sittings at 3 days (−3 vs. −1 letters, p=.005), 4 weeks (−1 vs. −1 letters, p=.37) and 34 weeks (0 vs. −2 letters, p=.006). The results of the study suggest that clinically meaningful differences are unlikely in OCT thickness

or visual acuity following application of PRP in a single sitting compared with 4 sittings in patients without center-involved macular edema and good vision.

Wavelength

The Krypton-Argon Regression of Neovascularization Study (KARNS) randomly assigned 907 eyes (of 696 patients) that had NVD equaling or exceeding those in Fig. 51.15 to scatter photocoagulation (1600–2000 moderate-intensity 500-mm burns) with either blue–green argon or red krypton wavelengths.[141] If, after the initial treatment, NVD increased by more than 0.5 disc area, retreatment was recommended (and could also be applied for other reasons, such as increasing NVE or vitreous hemorrhage). Retreatment was carried out in 36% and 33%, respectively, of the argon and krypton groups. Worsening NVD was the reason for the retreatment in ~40% of retreated eyes in each group. Regression of NVD to less than that shown in Fig. 51.15 was observed in almost identical proportions of the two groups (41.4% and 41.8%, respectively, at 3 months and 55.0% and 52.8%, respectively, at 1 year). No differences were found in the effectiveness of argon versus krypton treatment, although retrobulbar anesthesia was used more frequently with krypton treatment. In two small randomized trials, diode (810 nm) and double-frequency Nd : YAG (532 nm) lasers gave results similar to those of the argon green laser.[155,156]

Regression of New Vessels After Initial Photocoagulation and Indications for Retreatment

There is general agreement that substantial regression of new vessels usually occurs within days or weeks after the initial application of scatter photocoagulation and that eyes in which new vessels continue to grow despite initial treatment or recur after partial or complete regression may respond well to additional treatment. However, data documenting the rapidity and

completeness of regression are sparse, and many reports do not clearly separate results after initial treatment and results after initial treatment plus retreatment as needed. Table 51.8 summarizes much of the available information. From these studies it appears that, on average, about two-thirds of eyes have a satisfactory response to initial scatter treatment. This ratio tends to be more favorable in patients with type 2 diabetes. Patients with severe intraretinal lesions and actively growing new vessels, who typically have type 1 diabetes, often need multiple treatments.[161]

TABLE 51.8
Regression of Neovascularization After Scatter Photocoagulation

Author (Publication Year)	Initial Photocoagulation				
	No. of Eyes	Pretreatment Retinopathy Severity (No. of Burns)	Response Criterion	Time to Evaluation	No. (%) With Favorable Response
Doft and Blankenship, 1984[157]	50	High-risk PDR (1200 one episode)	Absence of high-risk PDR	3 days	10 (20%)
				2 weeks	25 (50%)
				3 weeks	36 (72%)
				6 month	31 (62%)
Blankenship. 1988[158]	31	NVD≥1/4 disc area	NVD< 1/4 disc area	1 month	30 (97%)
				6 months	24 (77%)
Vander et al., 1991[159]	59	High-risk PDR (“full-scatter”)	Absence of high-risk PDR	3 months	35 (59%)
KARNS, 1993[141]	907	NVD ≥ standard 10A (1600–2	NVD < 50% of baseline	3 months	490 (54%)
		NVD ≥ standard 10A (1600–2000)	NVD 50–99% of baseline	3 months	172 (19%)
DRS, 1978[26]	188	NVD ≥ standard 10A	No NVD or NVE	1 year	38 (20%)
		Argon (800–1000)	NVD < standard 10A	1 year	64 (34%)
	163	Xenon arc (200–800)	No NVD or NVE	1 year	36 (22%)
			NVD < standard 10A	1 year	62 (38%)
Rogell, 1983[160]	55	PDR (1100–1500 total in two episodes)	“Substantial regression”	1 month	21 (38%)
	34	Retreatment (300–400)	“Substantial regression”	1 month	30 (88%)

NVD, neovascularization of disc; NVE, neovascularization elsewhere; PDR, proliferative diabetic retinopathy.

The ETDRS protocol contains guidelines for follow-up treatment that seem suitable for general use. Six factors are considered: (1) change in new vessels since the last visit or last photocoagulation treatment; (2) appearance of the new vessels (caliber, degree of network formation, extent of accompanying fibrous tissue); (3) frequency and extent of vitreous hemorrhage since the last visit or last photocoagulation treatment; (4) status of vitreous detachment; (5) extent of photocoagulation scars; and (6) extent of traction retinal detachment and fibrous proliferations.[139] If new vessels appear to be active, as suggested by formation of tight networks, paucity of accompanying fibrous tissue, and increase in extent in comparison to the previous visit, additional photocoagulation is considered. The case for additional treatment is stronger if the extent of new vessels is substantially greater than it was at the time of initial treatment for high-risk characteristics or if vitreous or preretinal hemorrhages are occurring repeatedly (Fig. 51.6). Decreased caliber of new vessels and fibrous proliferation development suggest that retinopathy is entering a quiescent stage in which additional treatment may not be needed. A single episode of vitreous hemorrhage coincident with the occurrence of extensive posterior vitreous detachment, particularly if the only vitreoretinal adhesion remaining is at the disc, argues less for additional photocoagulation than do recurrent hemorrhages unrelated to such an occurrence. Additional photocoagulation may be needed less frequently in the setting of extensive posterior vitreous detachment because additional growth of new vessels is limited as is the extent of vitreoretinal adhesions. The extent and location of photocoagulation scars may also influence the decision regarding additional photocoagulation treatment. If the scars are widely spaced, or if there are areas where treatment was omitted, benefit from additional photocoagulation is more likely. In the presence of extensive scars where additional treatment would be placed over old scars, additional treatment may be less beneficial and be associated with increased risk of side-effects such as loss of visual field or nyctalopia. In such cases indefinite deferral of photocoagulation with or without anti-VEGF therapy may sometimes be the best alternative, even though there are extensive new vessels on the detached posterior vitreous surface and/or small

vitreous hemorrhages are occurring occasionally. If severe vitreous hemorrhage or vision-threatening proliferation occurs, vitrectomy, with endolaser if untreated peripheral retina is present, may be the best treatment option.

Complications of PRP

Although remarkably effective, visually threatening complications from PRP may arise (Box 51.2). It is important that such complications are identified and treated promptly to prevent further vision loss. Diabetes affects most ocular structures and may increase risks of potential complications following PRP. Diabetes-related corneal neuropathy may predispose eyes to corneal epithelial trauma possibly leading to secondary infection or recurrent corneal erosions if undetected.[162] The use of the appropriate coupling solution, proper placement, and minimal manipulation of the contact lens during laser treatment may minimize shearing and friction of the corneal surface. Iritis or iris burns and lenticular burns may occur with poorly dilated pupils, cataractous lenses or improper laser focus.[163] Careful focusing and optimizing papillary dilation can help avoid these complications, particularly when high-power, long-duration laser treatment is used. Some degree of discomfort is reported in most patients undergoing PRP. Carefully titrating burn intensity, shortening exposure time, and avoiding the ciliary nerves at the horizontal meridian will minimize patient discomfort. Judicious use of retrobulbar, peribulbar, sub-Ttenon or subconjunctival anesthesia may increase patient comfort and effectively complete treatment in some patients. Such procedures are usually not required, however, for the vast majority of individuals.

Box 51.2

Complications of Scatter (PRP) Photocoagulation

Loss of visual function

- Moderate visual loss
- Diminished or loss of visual field

- Diminished contrast sensitivity
- Diminished color vision
- Reduced or loss of dark adaptation

Damage to posterior ocular structures

- Inadvertent foveal or optic disc damage
- Retinal nerve fiber thinning
- Retinal tear
- Choriodal hemorrhage
- Choriodal neovascularization
- Vitreous, preretinal or subhyaloid hemorrhage

Complication related to blood retinal barrier breakdown

- Macular edema
- Choriodal detachment/effusion and secondary angle closure
- Iritis and increased intraocular pressure
- Exudative retinal detachment

Complications related to the destructive nature of the procedure

- Pain during treatment and shortly after treatment
- Corneal epithelial defects and recurrent erosions
- Mydriasis and paresis of accommodation
- Iris burns and damage
- Lenticular burns or opacification

Complications related to contraction of fibrovascular tissue

- Progressive traction retinal detachment
- Vitreous, preretinal or subhyaloid hemorrhage

The inherent destructive nature of PRP may also lead to adverse effects on the retina, including macular edema, serous macular/retinal detachment, contraction of preretinal membranes, choroidal detachment and angle closure glaucoma.[164] Choroidal effusion is commonly observed after PRP within the first week. These effusions are usually asymptomatic but may cause angle closure, especially in predisposed hyperopic eyes with shallow chambers. Inadvertent direct photocoagulation of the central macula is a potential and obviously detrimental complication that can result in permanent scotoma and substantial visual loss. Careful attention to anatomic landmarks and adherence to a strict standardized treatment regimen for each patient can reduce this risk. Intense, small spot-size burns, especially in the red light spectrum, may predispose to the rupture of Bruch's membrane. Clinically, Bruch's membrane rupture is associated with risk of hemorrhage and secondary choroidal neovascularization. Intermittent direct pressure on the globe with the contact lens often stops any associated hemorrhaging and low intensity, confluent large laser burns may be applied to the bleeding area to help control hemorrhaging. Inadvertent photocoagulation of the long posterior ciliary nerve may result in permanent mydriasis and loss of accommodation.[165] Substantial visual field loss may be caused by high-density, high-intensity PRP, and a sudden decrease in central vision may occur with occlusion of limited remaining arterioles supplying the macula.[131] Even with uncomplicated PRP, some decline in visual function has been reported, including moderate visual loss, impaired night vision, diminished visual field, reduced color vision, and reduced contrast sensitivity.[166]

Macular edema sometimes increases, at least temporarily, after scatter photocoagulation, and this edema may be followed by transient or persistent reduction of visual acuity.[167–169] In the ETDRS, 18% of eyes had center-involved DME and less severe retinopathy

without center involvement at baseline at 4 months.[136] The DRS also found early harmful effects, which were greater in the xenon group.[130] At the 6-week posttreatment visit, 21% of argon-treated and 46% of xenon-treated eyes that had DME and were free of high-risk characteristics at baseline had a decrease in visual acuity of 2 or more lines, compared with 9% of untreated eyes. Comparable percentages for eyes with neither DME nor high-risk characteristics were 9% argon, 18% xenon, and 3% untreated. After one year of follow-up in the group with DME at baseline, the greater progression of retinopathy in untreated eyes had led them to catch up with treated eyes; the percentages with a decrease in visual acuity of 2 or more lines were 32% argon, 33% xenon, and 34% untreated.[129,170]

Antiangiogenic Therapies for Proliferative Diabetic Retinopathy

Intravitreous antiangiogenic agents can induce rapid and extensive regression of ischemia-related ocular neovascularization. Multiple types of VEGF inhibitors have shown a beneficial activity in PDR. Mendrinos and coworkers published a case report demonstrating rapid regression of neovascularization after a single injection of pegaptanib which was sustained for more than 15 months.[171] Bevacizumab has been shown by Avery et al. to induce regression of new vessels in PDR as early as 24 hours after injection, but with a variable sustained effect ranging between 2 and 11 weeks.[172] Jorge et al. demonstrated short-term resolution of leakage from retinal neovascularization at 6 weeks after a single intravitreous injection of bevacizumab in 15 patients with persistent new vessels despite panretinal laser photocoagulation. At 12 weeks, 14 out of 15 patients had recurrent leakage but to a lesser extent than at baseline.[173] Other studies have reported similar short-term efficacy of bevacizumab in inducing regression of retinal neovascularization.[174–176]

Results from a recent DRCR.net study comparing the safety and efficacy of intravitreous anti-VEGF therapy (ranibizumab) with deferred PRP to prompt PRP demonstrate that visual acuity after 2

years of treatment is noninferior in eyes treated with anti-VEGF for PDR (DRCR.net Protocol S).[147] Moreover, this trial found that eyes treated with anti-VEGF had less visual acuity loss, less visual field loss, less need for vitrectomy and less frequent development of DME than eyes that received PRP. These findings suggest that anti-VEGF may be a reasonable alternative to PRP in eyes with PDR, especially those eyes with concurrent central involved DME.

The study enrolled 394 eyes with PDR from 305 participants who were randomly assigned to initial treatment with either ranibizumab (0.5 mg) or PRP. The PRP group received laser photocoagulation at baseline. The ranibizumab group received a baseline intravitreous injection of ranibizumab that was repeated monthly through the first 5 months unless all neovascularization was absent in the eye, in which case injections could be deferred after month 3. At 6 months, treatment in the ranibizumab group was given on a prn basis based on neovascular status. Eyes both with and without central-involved DME at baseline could be enrolled in the study, but were required to be treated with ranibizumab at the baseline visit if center-involved DME was present.

Over the course of 2 years, eyes without baseline DME randomized to ranibizumab received a median of 10 injections while eyes with baseline DME received a median of 14 injections. Relatively few eyes in the ranibizumab group needed PRP (12 eyes, 6% received PRP), but multiple eyes in the PRP group (92 eyes, 45%) received retreatment with additional PRP after the baseline laser session.

At 2 years, mean improvement in visual acuity was +2.8 in the ranibizumab group as compared to +0.2 in the PRP group (difference +2.2, 95% CI −0.5 to +5.0, noninferiority $p<.001$). Area under the curve for visual acuity outcomes suggested a greater benefit in the ranibizumab group, with a mean difference between groups of +4.2 (95% CI +3.0 to +5.4, $p<.001$). Multiple secondary outcomes favored the anti-VEGF-treated eyes, including visual field sensitivity loss (mean difference 372 dB, 95 % CI 213 to 531, $p<.001$), vitrectomy rates (4% vs. 15%, $p<.001$), and DME onset (10% vs. 27%, $p<.001$). There were no major differences in rates of major cardiovascular or thromboembolic events between the treatment

arms. A single eye of the eyes randomized to ranibizumab developed endophthalmitis (0.5%).

Given the excellent visual and anatomic results obtained with ranibizumab therapy in this study, many clinicians may choose to consider anti-VEGF as an alternative first-line therapy to PRP in eyes with PDR. Eyes that present with PDR accompanied by central-involved DME are likely to initiate anti-VEGF treatment as therapy for the DME. In these eyes, there is no need to additionally perform PRP given the good control of ocular neovascularization achievable with anti-VEGF and the adverse effects on peripheral visual fields associated with laser treatment. Although only the 2-year primary results have been reported to date, this study will continue for a total of 5 years' follow-up. Further results from this trial will help better define the role of VEGF inhibitors in the management of diabetic ocular neovascular complications and provide additional important safety data for long-term exposure.

Indications for Vitrectomy

When vitrectomy was initially introduced in 1970 by Machemer et al.,[177] the major indications in eyes with PDR were severe vitreous hemorrhage that had failed to clear spontaneously after a year and traction retinal detachment involving the center of the macula. As this procedure came into widespread use, it was recognized that it can be of value earlier in the course of severe PDR and its indications have broadened[59,60] (Box 51.3). A more extensive discussion of vitrectomy and surgical interventions for the proliferative complications of diabetic retinopathy is presented in Chapter 15 (Surgery for proliferative diabetic retinopathy).

Box 51.3

Indications for Vitrectomy

1. To permit visualization of the retinal and adequate photocoagulation of active retinopathy

a. Severe nonclearing vitreous hemorrhage

b. Dense subhyaloid or premacular hemorrhage

c. Anterior segment neovascularization with an associated media opacity

2. To relieve traction of the retina that is threatening or causing visual impairment

a. Traction retinal detachment involving or threatening the fovea

b. Vitreomacular traction , macular striae or distortion causing visual loss

c. Combined traction–rhegmatogenous retinal detachment

d. Epiretinal membranes or opacified posterior vitreous face causing visual loss

3. To control progressive retinopathy or complications despite adequate retinal photocoagulation

a. Progressive fibrovascular proliferation

b. Anterior hyloidal fibrovascular proliferation

c. Ghost cell/hemolytic glaucoma

Telemedicine Approaches for the Detection of Proliferative Diabetic Retinopathy

The current strategies in the management of PDR are highly effective and reduce the risk of severe loss by over 95%. However,

more than half of the diabetes population does not receive appropriate care and advanced stages of PDR remain one of the leading causes of severe visual loss in the working age population. The current challenge lies in appropriately identifying patients at risk and enhancing the ability to deliver eye care that ultimately leads to preservation of vision and prevention of diabetes-related blindness. Telemedicine approaches have the potential to address these needs and expand the scope of eye care to virtually any location across different barriers to care. In the Indian Health Service, the use of telemedicine programs for diabetic retinopathy increased the rate of examination and treatment for DR resulting in a significant increase in the rate of DR surveillance and a proportional increase in the rate of laser treatment for DR. The rate of annual retinal examinations increased from 50% (95% CI 44–56%) to 75% (70–80%; $p<.000001$), representing a 50% increase in the retinal examination rate. The rate of laser therapy increased from 19.6 per 1000 patients with diabetes in 1999 to 29.5 per 1000 in 2003 for a 51% increase in the laser treatment rate.[178] Teleophthalmology programs using validated means of retinal imaging are both less costly and more effective due to its accurate assessment of DR severity allowing identification of eyes with PDR and treatment with PRP.[179] Maximizing telemedicine-based outcomes by utilizing technical enhancements to optimize image acquisition and automate image analysis as well as identification of predictive novel retinal lesions can potentially transform the way diabetes eye care is delivered while significantly expanding its reach.

Conclusion

Proliferative diabetic retinopathy is a severe sight-threatening complication of diabetes. While PDR cannot be fully prevented, scatter (panretinal) laser photocoagulation is effective in preserving vision and preventing vision loss. Increased understanding of the biochemical mechanisms underlying PDR are providing new therapeutic approaches with the promise to be both effective and less destructive than current photocoagulation techniques. Strong data now demonstrates that anti-VEGF therapy for PDR is not inferior to PRP in terms of visual outcome at 2 years and indeed is

associated with less visual field loss, lower vitrectomy rates, and less frequent development of DME. Need for PRP is rare in eyes with PDR that are treated with anti-VEGF.

It is important to keep in mind that a comprehensive approach to diabetes care is particularly critical for patients with advanced retinopathy. Only with the coordinated care between eyecare providers and the many other members of the diabetic patient's medical care team can optimal ophthalmic outcomes be achieved. The development of PDR is strongly associated with the presence of significant systemic disease. Progressive retinal ischemia and the release of local growth factors are the main pathogenic mechanisms underlying the development of PDR. The natural course of PDR involves highly active phases of retinal neovascularization and fibrous proliferation, potentially leading to visual loss if left untreated. Timely panretinal laser photocoagulation can reduce the risk of severe visual loss by 96%, with long-term preservation of vision. Recent data suggest that anti-VEGF therapy is also a safe and effective treatment alternative for eyes with PDR. This is especially pertinent for eyes with PDR that are initiating treatment with anti-VEGF for DME, as PRP can usually be safely deferred until the DME is resolved, at which time their neovascular status can be reevaluated. Multiple studies have suggested that systemic and intravitreal pharmacologic therapies may induce regression of retinal neovascularization and prevent the onset or slow the progression to PDR. These approaches, if adequately sustained and proven safe and efficacious in rigorous clinical trials, will represent a major treatment advance. Fortunately, with timely and appropriate care, the vast majority of severe visual loss from PDR can already be prevented, albeit with potential attendant side-effects and complications. Given the advances underway in the systemic and ocular management of diabetes, it is likely that the future of PDR therapy will be marked by even greater benefit, reduced risk, and fewer side effects.

References

1. Preliminary report on effects of photocoagulation therapy. The Diabetic Retinopathy Study Research Group. *Am J*

Ophthalmol. 1976;81(4):383–396.
2. Four risk factors for severe visual loss in diabetic retinopathy. The third report from the Diabetic Retinopathy Study. The Diabetic Retinopathy Study Research Group. *Arch Ophthalmol*. 1979;97(4):654–655.
3. Klein R, Klein BE, Moss SE, et al. The Wisconsin Epidemiologic Study of Diabetic Retinopathy. IX. Four-year incidence and progression of diabetic retinopathy when age at diagnosis is less than 30 years. *Arch Ophthalmol*. 1989;107(2):237–243.
4. Klein R, Klein BE, Moss SE, et al. The Wisconsin Epidemiologic Study of Diabetic Retinopathy. X. Four-year incidence and progression of diabetic retinopathy when age at diagnosis is 30 years or more. *Arch Ophthalmol*. 1989;107(2):244–249.
5. Hovind P, Klein R, Lee KE, et al. The Wisconsin Epidemiologic Study of Diabetic Retinopathy XXII. The twenty-five-year progression of retinopathy in persons with type 1 diabetes. *Ophthalmology*. 2008;115(11):1859–1868.
6. Aiello LP, Cahill MT, Wong JS. Systemic considerations in the management of diabetic retinopathy. *Am J Ophthalmol*. 2001;132:760–766.
7. Klein R, Klein BE, Moss SE. Epidemiology of proliferative diabetic retinopathy. *Diabetes Care*. 1992;15(12):1875–1891.
8. Hovind P, Tarnow L, Rossing K, et al. Decreasing incidence of severe diabetic microangiopathy in type 1 diabetes. *Diabetes Care*. 2003;26(4):1258–1264.
9. Klein R, Klein BE, Moss SE, et al. The medical management of hyperglycemia over a 10-year period in people with diabetes. *Diabetes Care*. 1996;19(7):744–750.
10. Wong TY, Mwamburi M, Klein R, et al. Rates of progression in diabetic retinopathy during different time periods: a systematic review and meta-analysis. *Diabetes Care*. 2009;32(12):2307–2313.
11. Klein R, Klein BE. Are individuals with diabetes seeing better? A long-term epidemiological perspective. *Diabetes*. 2010;59(8):1853–1860.
12. Stefansson E. Ocular oxygenation and the treatment of

diabetic retinopathy. *Surv Ophthalmol*. 2006;51(4):364–380.
13. Aiello LP, Avery RL, Arrigg PG, et al. Vascular endothelial growth factor in ocular fluid of patients with diabetic retinopathy and other retinal disorders. *N Engl J Med*. 1994;331(22):1480–1487.
14. Miller JW, Adamis AP, Shima DT, et al. Vascular endothelial growth factor/vascular permeability factor is temporally and spatially correlated with ocular angiogenesis in a primate model. *Am J Pathol*. 1994;145(3):574–584.
15. Pierce EA, Avery RL, Foley ED, et al. Vascular endothelial growth factor/vascular permeability factor expression in a mouse model of retinal neovascularization. *Proc Natl Acad Sci USA*. 1995;92(3):905–909.
16. Adamis AP, Miller JW, Bernal MT, et al. Increased vascular endothelial growth factor levels in the vitreous of eyes with proliferative diabetic retinopathy. *Am J Ophthalmol*. 1994;118(4):445–450.
17. Avery RL. Regression of retinal and iris neovascularization after intravitreal bevacizumab (Avastin) treatment. *Retina*. 2006;26(3):352–354.
18. Cai J, Kehoe O, Smith GM, et al. The angiopoietin/Tie-2 system regulates pericyte survival and recruitment in diabetic retinopathy. *Invest Ophthalmol Vis Sci*. 2008;49(5):2163–2171.
19. Takagi H, Koyama S, Seike H, et al. Potential role of the angiopoietin/tie2 system in ischemia-induced retinal neovascularization. *Invest Ophthalmol Vis Sci*. 2003;44(1):393–402.
20. Geraldes P, Hiraoka-Yamamoto J, Matsumoto M, et al. Activation of PKC-delta and SHP-1 by hyperglycemia causes vascular cell apoptosis and diabetic retinopathy. *Nat Med*. 2009;15(11):1298–1306.
21. Watanabe D, Suzuma K, Matsui S, et al. Erythropoietin as a retinal angiogenic factor in proliferative diabetic retinopathy. *N Engl J Med*. 2005;353(8):782–792.
22. Tong Z, Yang Z, Patel S, et al. Promoter polymorphism of the erythropoietin gene in severe diabetic eye and kidney complications. *Proc Natl Acad Sci USA*. 2008;105(19):6998–

7003.
23. Abhary S, Burdon KP, Casson RJ, et al. Association between erythropoietin gene polymorphisms and diabetic retinopathy. *Arch Ophthalmol*. 2010;128(1):102–106.
24. Ogata N, Tombran-Tink J, Nishikawa M, et al. Pigment epithelium-derived factor in the vitreous is low in diabetic retinopathy and high in rhegmatogenous retinal detachment. *Am J Ophthalmol*. 2001;132(3):378–382.
25. Praidou A, Androudi S, Brazitikos P, et al. Angiogenic growth factors and their inhibitors in diabetic retinopathy. *Curr Diabetes Rev*. 2010;6(5):304–312.
26. Photocoagulation treatment of proliferative diabetic retinopathy: the second report of Diabetic Retinopathy Study findings. *Ophthalmology*. 1978;85(1):82–106.
27. Shimizu K, Kobayashi Y, Muraoka K. Midperipheral fundus involvement in diabetic retinopathy. *Ophthalmology*. 1981;88(7):601–612.
28. Muraoka K, Shimizu K. Intraretinal neovascularization in diabetic retinopathy. *Ophthalmology*. 1984;91(12):1440–1446.
29. Kohner EM, Dollery CT, Bulpitt CJ. Cotton-wool spots in diabetic retinopathy. *Diabetes*. 1969;18(10):691–704.
30. Kohner EM, Dollery CT. The rate of formation and disappearance of microaneurysms in diabetic retinopathy. *Trans Ophthalmol Soc U K*. 1970;90:369–374.
31. Davis MD. Vitreous contraction in proliferative diabetic retinopathy. *Arch Ophthalmol*. 1965;74(6):741–751.
32. Taylor E, Dobree JH. Proliferative diabetic retinopathy. Site and size of initial lesions. *Br J Ophthalmol*. 1970;54(1):11–18.
33. Diabetic retinopathy study. Report number 6. Design, methods, and baseline results. Report number 7. A modification of the Airlie House classification of diabetic retinopathy. Prepared by the Diabetic Retinopathy. *Invest Ophthalmol Vis Sci*. 1981;21(1 Pt 2):1–226.
34. Prud'homme G, Rand L. The Diabetic Retinopathy Study Research Group: distribution of maximum grade of lesion in proliferative diabetic retinopathy. *Invest Ophthalm Vis Sci*. 1981;20(Suppl.):59.
35. Joondeph BC, Joondeph HC, Flood TP. Foveal

neovascularization in diabetic retinopathy. *Arch Ophthalmol*. 1987;105(12):1672–1675.
36. Grading diabetic retinopathy from stereoscopic color fundus photographs – an extension of the modified Airlie House classification. ETDRS report number 10. Early Treatment Diabetic Retinopathy Study Research Group. *Ophthalmology*. 1991;98(Suppl. 5):786–806.
37. Silva PS, Cavallerano JD, Sun JK, et al. Peripheral lesions identified by mydriatic ultrawide field imaging: distribution and potential impact on diabetic retinopathy severity. *Ophthalmology*. 2013;120(12):2587–2595.
38. Price LD, Au S, Chong NV. Optomap ultrawide field imaging identifies additional retinal abnormalities in patients with diabetic retinopathy. *Clin Ophthalmol*. 2015;9:527–531.
39. Kernt M, Hadi I, Pinter F, et al. Assessment of diabetic retinopathy using nonmydriatic ultra-widefield scanning laser ophthalmoscopy (Optomap) compared with ETDRS 7-field stereo photography. *Diabetes Care*. 2012;35(12):2459–2463.
40. Talks SJ, Manjunath V, Steel DH, et al. New vessels detected on wide-field imaging compared to two-field and seven-field imaging: implications for diabetic retinopathy screening image analysis. *Br J Ophthalmol*. 2015;99(12):1606–1609.
41. Silva PS, Dela Cruz AJ, Ledesma MG, et al. Diabetic retinopathy severity and peripheral lesions are associated with nonperfusion on ultrawide field angiography. *Ophthalmology*. 2015;122(12):2465–2472.
42. Schwartz JS, Pavan PR. Optic disc edema. *Int Ophthalmol Clin*. 1984;24(4):83–91.
43. Kampik A, Kenyon KR, Michels RG, et al. Epiretinal and vitreous membranes. Comparative study of 56 cases. *Arch Ophthalmol*. 1981;99(8):1445–1454.
44. Nork TM, Wallow IH, Sramek SJ, et al. Muller's cell involvement in proliferative diabetic retinopathy. *Arch Ophthalmol*. 1987;105(10):1424–1429.
45. Dobree JH. Proliferative diabetic retinopathy: evolution of

the retinal lesions. *Br J Ophthalmol*. 1964;48:637–649.
46. Bandello F, Gass JD, Lattanzio R, et al. Spontaneous regression of neovascularization at the disk and elsewhere in diabetic retinopathy. *Am J Ophthalmol*. 1996;122(4):494–501.
47. Tolentino FI, Lee PF, Schepens CL. Biomicroscopic study of vitreous cavity in diabetic retinopathy. *Arch Ophthalmol*. 1966;75(2):238–246.
48. Anderson B Jr. Activity and diabetic vitreous hemorrhages. *Ophthalmology*. 1980;87(3):173–175.
49. Tasman W. Diabetic vitreous hemorrhage and its relationship to hypoglycemia. *Mod Probl Ophthalmol*. 1979;20:413–414.
50. Larsen HW. Diabetic retinopathy. An ophthalmoscopic study with a discussion of the morphologic changes and the pathogenetic factors in this disease. *Acta Ophthalmol Suppl*. 1960;(Suppl. 60):1–89.
51. Bresnick GH, Haight B, De Venecia G. Retinal wrinkling and macular heterotopia in diabetic retinopathy. *Arch Ophthalmol*. 1979;97(10):1890–1895.
52. Ramsay WJ, Ramsay RC, Purple RL, et al. Involutional diabetic retinopathy. *Am J Ophthalmol*. 1977;84(6):851–858.
53. Beetham WP. Visual prognosis of proliferating diabetic retinopathy. *Br J Ophthalmol*. 1963;47:611–619.
54. Klein R, Klein BE, Moss SE, et al. The Wisconsin epidemiologic study of diabetic retinopathy. II. Prevalence and risk of diabetic retinopathy when age at diagnosis is less than 30 years. *Arch Ophthalmol*. 1984;102(4):520–526.
55. Sun JK, Keenan HA, Cavallerano JD, et al. Protection from retinopathy and other complications in patients with type 1 diabetes of extreme duration: the joslin 50-year medalist study. *Diabetes Care*. 2011;34(4):968–974.
56. Klein R, Klein BE, Moss SE, et al. The Wisconsin epidemiologic study of diabetic retinopathy. III. Prevalence and risk of diabetic retinopathy when age at diagnosis is 30 or more years. *Arch Ophthalmol*. 1984;102(4):527–532.
57. Klein R, Klein BE, Moss SE, et al. The Wisconsin Epidemiologic Study of Diabetic Retinopathy. XV. The

long-term incidence of macular edema. *Ophthalmology*. 1995;102(1):7–16.
58. Early vitrectomy for severe vitreous hemorrhage in diabetic retinopathy. Two-year results of a randomized trial. Diabetic Retinopathy Vitrectomy Study report 2. The Diabetic Retinopathy Vitrectomy Study Research Group. *Arch Ophthalmol*. 1985;103(11):1644–1652.
59. Early vitrectomy for severe proliferative diabetic retinopathy in eyes with useful vision. Clinical application of results of a randomized trial – Diabetic Retinopathy Vitrectomy Study Report 4. The Diabetic Retinopathy Vitrectomy Study Research Group. *Ophthalmology*. 1988;95(10):1321–1334.
60. Early vitrectomy for severe proliferative diabetic retinopathy in eyes with useful vision. Results of a randomized trial – Diabetic Retinopathy Vitrectomy Study Report 3. The Diabetic Retinopathy Vitrectomy Study Research Group. *Ophthalmology*. 1988;95(10):1307–1320.
61. Early vitrectomy for severe vitreous hemorrhage in diabetic retinopathy. Four-year results of a randomized trial: Diabetic Retinopathy Vitrectomy Study Report 5. *Arch Ophthalmol*. 1990;108(7):958–964.
62. Aiello LM, Rand LI, Briones JC, et al. Diabetic retinopathy in Joslin Clinic patients with adult-onset diabetes. *Ophthalmology*. 1981;88(7):619–623.
63. Zhang X, Saaddine JB, Chou CF, et al. Prevalence of diabetic retinopathy in the United States, 2005-2008. *JAMA*. 2010;304(6):649–656.
64. The effect of intensive treatment of diabetes on the development and progression of long-term complications in insulin-dependent diabetes mellitus. The Diabetes Control and Complications Trial Research Group. *N Engl J Med*. 1993;329(14):977–986.
65. Intensive blood-glucose control with sulphonylureas or insulin compared with conventional treatment and risk of complications in patients with type 2 diabetes (UKPDS 33). UK Prospective Diabetes Study (UKPDS) Group. *Lancet*. 1998;352(9131):837–853.

66. Progression of retinopathy with intensive versus conventional treatment in the Diabetes Control and Complications Trial. Diabetes Control and Complications Trial Research Group. *Ophthalmology*. 1995;102(4):647–661.
67. The effect of intensive diabetes treatment on the progression of diabetic retinopathy in insulin-dependent diabetes mellitus. The Diabetes Control and Complications Trial. *Arch Ophthalmol*. 1995;113(1):36–51.
68. Effect of intensive therapy on the microvascular complications of type 1 diabetes mellitus. *JAMA*. 2002;287(19):2563–2569.
69. Sustained effect of intensive treatment of type 1 diabetes mellitus on development and progression of diabetic nephropathy: the Epidemiology of Diabetes Interventions and Complications (EDIC) study. *JAMA*. 2003;290(16):2159–2167.
70. Gerstein HC, Miller ME, Byington RP, et al. Effects of intensive glucose lowering in type 2 diabetes. *N Engl J Med*. 2008;358(24):2545–2559.
71. Holman RR, Paul SK, Bethel MA, et al. 10-year follow-up of intensive glucose control in type 2 diabetes. *N Engl J Med*. 2008;359(15):1577–1589.
72. White NH, Sun W, Cleary PA, et al. Prolonged effect of intensive therapy on the risk of retinopathy complications in patients with type 1 diabetes mellitus: 10 years after the Diabetes Control and Complications Trial. *Arch Ophthalmol*. 2008;126(12):1707–1715.
73. White NH, Cleary PA, Dahms W, et al. Beneficial effects of intensive therapy of diabetes during adolescence: outcomes after the conclusion of the Diabetes Control and Complications Trial (DCCT). *J Pediatr*. 2001;139(6):804–812.
74. Davis MD, Fisher MR, Gangnon RE, et al. Risk factors for high-risk proliferative diabetic retinopathy and severe visual loss: Early Treatment Diabetic Retinopathy Study Report #18. *Invest Ophthalmol Vis Sci*. 1998;39(2):233–252.
75. Early worsening of diabetic retinopathy in the Diabetes Control and Complications Trial. *Arch Ophthalmol*. 1998;116(7):874–886.

76. Dahl-Jorgensen K, Brinchmann-Hansen O, Hanssen KF, et al. Rapid tightening of blood glucose control leads to transient deterioration of retinopathy in insulin dependent diabetes mellitus: the Oslo study. *Br Med J (Clin Res Ed)*. 1985;290(6471):811–815.
77. Lauritzen T, Frost-Larsen K, Larsen HW, et al. Two-year experience with continuous subcutaneous insulin infusion in relation to retinopathy and neuropathy. *Diabetes*. 1985;34(Suppl. 3):74–79.
78. Brinchmann-Hansen O, Dahl-Jorgensen K, Hanssen KF, et al. The response of diabetic retinopathy to 41 months of multiple insulin injections, insulin pumps, and conventional insulin therapy. *Arch Ophthalmol*. 1988;106(9):1242–1246.
79. Blood glucose control and the evolution of diabetic retinopathy and albuminuria: a preliminary multicenter trial. The Kroc Collaborative Study Group. *N Engl J Med*. 1984;311(6):365–372.
80. Funatsu H, Yamashita H, Ohashi Y, et al. Effect of rapid glycemic control on progression of diabetic retinopathy. *Jpn J Ophthalmol*. 1992;36(3):356–367.
81. Agardh CD, Eckert B, Agardh E. Irreversible progression of severe retinopathy in young type I insulin-dependent diabetes mellitus patients after improved metabolic control. *J Diabetes Complications*. 1992;6(2):96–100.
82. Ernest JT, Goldstick TK, Engerman RL. Hyperglycemia impairs retinal oxygen autoregulation in normal and diabetic dogs. *Invest Ophthalmol Vis Sci*. 1983;24(7):985–989.
83. Grunwald JE, Brucker AJ, Braunstein SN, et al. Strict metabolic control and retinal blood flow in diabetes mellitus. *Br J Ophthalmol*. 1994;78(8):598–604.
84. Grunwald JE, Brucker AJ, Schwartz SS, et al. Diabetic glycemic control and retinal blood flow. *Diabetes*. 1990;39(5):602–607.
85. Bain SC, Gill GV, Dyer PH, et al. Characteristics of type 1 diabetes of over 50 years duration (the Golden Years Cohort). *Diabet Med*. 2003;20(10):808–811.
86. Ismail-Beigi F, Craven T, Banerji MA, et al. Effect of

intensive treatment of hyperglycaemia on microvascular outcomes in type 2 diabetes: an analysis of the ACCORD randomised trial. *Lancet*. 2010;376(9739):419–430.
87. Patel A, MacMahon S, Chalmers J, et al. Effects of a fixed combination of perindopril and indapamide on macrovascular and microvascular outcomes in patients with type 2 diabetes mellitus (the ADVANCE trial): a randomised controlled trial. *Lancet*. 2007;370(9590):829–840.
88. Chew EY, Ambrosius WT, Davis MD, et al. Effects of medical therapies on retinopathy progression in type 2 diabetes. *N Engl J Med*. 2010;363(3):233–244.
89. Keech AC, Mitchell P, Summanen PA, et al. Effect of fenofibrate on the need for laser treatment for diabetic retinopathy (FIELD study): a randomised controlled trial. *Lancet*. 2007;370(9600):1687–1697.
90. Chaturvedi N, Porta M, Klein R, et al. Effect of candesartan on prevention (DIRECT-Prevent 1) and progression (DIRECT-Protect 1) of retinopathy in type 1 diabetes: randomised, placebo-controlled trials. *Lancet*. 2008;372(9647):1394–1402.
91. Sjolie AK, Klein R, Porta M, et al. Effect of candesartan on progression and regression of retinopathy in type 2 diabetes (DIRECT-Protect 2): a randomised placebo-controlled trial. *Lancet*. 2008;372(9647):1385–1393.
92. Mauer M, Zinman B, Gardiner R, et al. Renal and retinal effects of enalapril and losartan in type 1 diabetes. *N Engl J Med*. 2009;361(1):40–51.
93. Pershadsingh HA, Moore DM. PPARgamma agonists: potential as therapeutics for neovascular retinopathies. *PPAR Res*. 2008;2008:164273.
94. Shen LQ, Child A, Weber GM, et al. Rosiglitazone and delayed onset of proliferative diabetic retinopathy. *Arch Ophthalmol*. 2008;126(6):793–799.
95. Panigrahy D, Singer S, Shen LQ, et al. PPARgamma ligands inhibit primary tumor growth and metastasis by inhibiting angiogenesis. *J Clin Invest*. 2002;110(7):923–932.
96. Wessel MM, Aaker GD, Parlitsis G, et al. Ultra-wide-field angiography improves the detection and classification of

diabetic retinopathy. *Retina*. 2012;32(4):785–791.
97. Silva PS, Cavallerano JD, Haddad NM, et al. Peripheral lesions identified on ultrawide field imaging predict increased risk of diabetic retinopathy progression over 4 years. *Ophthalmology*. 2015;122(5):949–956.
98. Chew EY, Klein ML, Ferris FL 3rd, et al. Association of elevated serum lipid levels with retinal hard exudate in diabetic retinopathy. Early Treatment Diabetic Retinopathy Study (ETDRS) report 22. *Arch Ophthalmol*. 1996;114(9):1079–1084.
99. Biasotti A, Houssay BA. Phlorrhizin diabetes in fasting or fed hypophysectomized dogs. *J Physiol*. 1932;77(1):81–91.
100. Luft R, Olivecrona H, Sjogren B. [Hypophysectomy in man]. *Nord Med*. 1952;47(11):351–354.
101. Kohner EM, Joplin GF, Blach RK, et al. Pituitary ablation in the treatment of diabetic retinopathy. (A randomized trial). *Trans Ophthalmol Soc U K*. 1972;92:79–90.
102. Panisset A, Kohner EM, Cheng H, et al. Diabetic retinopathy: new vessels arising from the optic disc. II. Response to pituitary ablation by yttrium 90 implant. *Diabetes*. 1971;20(12):824–833.
103. Kohner EM, Hamilton AM, Joplin GF, et al. Florid diabetic retinopathy and its response to treatment by photocoagulation or pituitary ablation. *Diabetes*. 1976;25(2):104–110.
104. Smith LE, Shen W, Perruzzi C, et al. Regulation of vascular endothelial growth factor-dependent retinal neovascularization by insulin-like growth factor-1 receptor. *Nat Med*. 1999;5(12):1390–1395.
105. The effect of a growth hormone receptor antagonist drug on proliferative diabetic retinopathy. *Ophthalmology*. 2001;108(12):2266–2272.
106. Boehm BO, Lang GK, Jehle PM, et al. Octreotide reduces vitreous hemorrhage and loss of visual acuity risk in patients with high-risk proliferative diabetic retinopathy. *Horm Metab Res*. 2001;33(5):300–306.
107. Beetham WP. Visual Prognosis of Proliferating Diabetic Retinopathy. *Br J Ophthalmol*. 1963;47:611–619.

108. Aiello LM, Beetham WP, Balodimos MC, et al. Ruby laser photocoagulation in treatment of diabetic proliferating retinopathy: Preliminary report. Goldberg MF, Fine SL. *Symposium on the Treatment of Diabetic Retinopathy. Publication no.1890 ed*. U.S. Department of Health, Education, and Welfare: Arlington, VA; 1968:437–463.
109. Meyer-Schwickerath G. Light coagulation; a method for treatment and prevention of the retinal detachment. *Albrecht Von Graefes Arch Ophthalmol*. 1954;156(1):2–34.
110. Okun E, Cibis PA. The role of photocoagulation in the therapy of proliferative diabetic retinopathy. *Arch Ophthalmol*. 1966;75(3):337–352.
111. Wetzig PC, Jepson CN. Treatment of diabetic retinopathy by light coagulation. *Am J Ophthalmol*. 1966;62(3):459–465.
112. Wetzig PC, Worlton JT. Treatment of diabetic retinopathy by light-coagulation: a preliminary study. *Br J Ophthalmol*. 1963;47:539–541.
113. Beetham WP, Aiello LM, Balodimos MC, et al. Ruby-laser photocoagulation of early diabetic neovascular retinopathy: preliminary report of a long-term controlled study. *Trans Am Ophthalmol Soc*. 1969;67:39–67.
114. Beetham WP, Aiello LM, Balodimos MC, et al. Ruby laser photocoagulation of early diabetic neovascular retinopathy. Preliminary report of a long-term controlled study. *Arch Ophthalmol*. 1970;83(3):261–272.
115. Meyer-Schwickerath RE, Schott K. Diabetic retinopathy and photocoagulation. *Am J Ophthalmol*. 1968;66(4):597–603.
116. Okun E. The effectiveness of photocoagulation in the therapy of proliferative diabetic retinopathy (PDR). (A controlled study in 50 patients). *Trans Am Acad Ophthalmol Otolaryngol*. 1968;72(2):246–252.
117. Glaser BM, Campochiaro PA, Davis JL Jr, et al. Retinal pigment epithelial cells release an inhibitor of neovascularization. *Arch Ophthalmol*. 1985;103(12):1870–1875.
118. Ederer F, Hiller R. Clinical trials, diabetic retinopathy and photocoagulation. A reanalysis of five studies. *Surv Ophthalmol*. 1975;19(5):267–286.

119. Stefansson E, Hatchell DL, Fisher BL, et al. Panretinal photocoagulation and retinal oxygenation in normal and diabetic cats. *Am J Ophthalmol*. 1986;101(6):657–664.
120. Gerstein DD, Dantzker DR. Retinal vascular changes in hereditary visual cell degeneration. *Arch Ophthalmol*. 1969;81(1):99–105.
121. Molnar I, Poitry S, Tsacopoulos M, et al. Effect of laser photocoagulation on oxygenation of the retina in miniature pigs. *Invest Ophthalmol Vis Sci*. 1985;26(10):1410–1414.
122. Weiter JJ, Zuckerman R. The influence of the photoreceptor-RPE complex on the inner retina. An explanation for the beneficial effects of photocoagulation. *Ophthalmology*. 1980;87(11):1133–1139.
123. Wolbarsht ML, Landers MB III. The rationale of photocoagulation therapy for proliferative diabetic retinopathy: a review and a model. *Ophthalmic Surg*. 1980;11(4):235–245.
124. Grunwald JE, Riva CE, Brucker AJ, et al. Altered retinal vascular response to 100% oxygen breathing in diabetes mellitus. *Ophthalmology*. 1984;91(12):1447–1452.
125. Patel V, Rassam S, Newsom R, et al. Retinal blood flow in diabetic retinopathy. *BMJ*. 1992;305(6855):678–683.
126. Stefansson E, Machemer R, de Juan E Jr, et al. Retinal oxygenation and laser treatment in patients with diabetic retinopathy. *Am J Ophthalmol*. 1992;113(1):36–38.
127. Cheng H. Multicentre trial of xenon-arc photocoagulation in the treatment of diabetic retinopathy. A randomized controlled study. Interim report. *Trans Ophthalmol Soc U K*. 1975;95(2):351–357.
128. Editorial: The Diabetic Retinopathy Study. *Arch Ophthalmol*. 1973;90(5):347–348.
129. Photocoagulation treatment of proliferative diabetic retinopathy. Clinical application of Diabetic Retinopathy Study (DRS) findings, DRS report number 8. The Diabetic Retinopathy Study Research Group. *Ophthalmology*. 1981;88(7):583–600.
130. Photocoagulation treatment of proliferative diabetic retinopathy: relationship of adverse treatment effects to

retinopathy severity. Diabetic retinopathy study report no. 5. *Dev Ophthalmol*. 1981;2:248–261.
131. Rand LI, Prud'homme GJ, Ederer F, et al. Factors influencing the development of visual loss in advanced diabetic retinopathy. Diabetic Retinopathy Study (DRS) report no. 10. *Invest Ophthalmol Vis Sci*. 1985;26(7):983–991.
132. Little HL, Rosenthal AR, Dellaporta A, et al. The effect of pan-retinal photo-coagulation on rubeosis iridis. *Am J Ophthalmol*. 1976;81(6):804–809.
133. Okun E, Johnston GP, Boniuk I, et al. Xenon arc photocoagulation of proliferative diabetic retinopathy. A review of 2688 consecutive eyes in the format of the Diabetic Retinopathy Study. *Ophthalmology*. 1984;91(12):1458–1463.
134. Photocoagulation for proliferative diabetic retinopathy: a randomised controlled clinical trial using the xenon-arc. *Diabetologia*. 1984;26(2):109–115.
135. Hercules BL, Gayed II, Lucas SB, et al. Peripheral retinal ablation in the treatment of proliferative diabetic retinopathy: a three-year interim report of a randomised, controlled study using the argon laser. *Br J Ophthalmol*. 1977;61(9):555–563.
136. Early photocoagulation for diabetic retinopathy. ETDRS report number 9. Early Treatment Diabetic Retinopathy Study Research Group. *Ophthalmology*. 1991;98(Suppl. 5):766–785.
137. Photocoagulation for diabetic macular edema. Early Treatment Diabetic Retinopathy Study report number 1. Early Treatment Diabetic Retinopathy Study research group. *Arch Ophthalmol*. 1985;103(12):1796–1806.
138. Effects of aspirin treatment on diabetic retinopathy. ETDRS report number 8. Early Treatment Diabetic Retinopathy Study Research Group. *Ophthalmology*. 1991;98(Suppl. 5):757–765.
139. Techniques for scatter and local photocoagulation treatment of diabetic retinopathy: Early Treatment Diabetic Retinopathy Study report no. 3. The Early Treatment Diabetic Retinopathy Study Research Group. *Int Ophthalmol*

Clin. 1987;27(4):254–264.
140. Ferris F. Early photocoagulation in patients with either type I or type II diabetes. *Trans Am Ophthalmol Soc*. 1996;94:505–537.
141. Randomized comparison of krypton versus argon scatter photocoagulation for diabetic disc neovascularization. The Krypton Argon Regression Neovascularization Study report number 1. *Ophthalmology*. 1993;100(11):1655–1664.
142. Meyer-Schwickerath G, Gerke E. Bjerrum Lecture. Treatment of diabetic retinopathy with photocoagulation. Results of photocoagulation therapy of proliferative retinopathy in childhood-onset and maturity-onset diabetes and an approach to the dosage in photocoagulation. *Acta Ophthalmol (Copenh)*. 1983;61(5):756–768.
143. Chew EY, Mills JL, Metzger BE, et al. Metabolic control and progression of retinopathy. The Diabetes in Early Pregnancy Study. National Institute of Child Health and Human Development Diabetes in Early Pregnancy Study. *Diabetes Care*. 1995;18(5):631–637.
144. Klein BE, Moss SE, Klein R. Effect of pregnancy on progression of diabetic retinopathy. *Diabetes Care*. 1990;13(1):34–40.
145. Mathiesen ER, Ronn B, Storm B, et al. The natural course of microalbuminuria in insulin-dependent diabetes: a 10-year prospective study. *Diabet Med*. 1995;12(6):482–487.
146. Pavan PR, Folk JC, Weingeist TA, et al. Diabetic rubeosis and panretinal photocoagulation. *Arch Ophthalmol*. 1983;101(6):882–884.
147. Gross JG, Glassman AR, Jampol LM, et al. Panretinal photocoagulation vs intravitreous ranibizumab for proliferative diabetic retinopathy: a randomized clinical trial. *JAMA*. 2015;314(20):2137–2146.
148. Blumenkranz MS, Yellachich D, Andersen DE, et al. Semiautomated patterned scanning laser for retinal photocoagulation. *Retina*. 2006;26(3):370–376.
149. Jain A, Blumenkranz MS, Paulus Y, et al. Effect of pulse duration on size and character of the lesion in retinal photocoagulation. *Arch Ophthalmol*. 2008;126(1):78–85.

150. Muqit MM, Sanghvi C, McLauchlan R, et al. Study of clinical applications and safety for Pascal(R) laser photocoagulation in retinal vascular disorders. *Acta Ophthalmol*. 2012;90(2):155–161.
151. Velez-Montoya R, Guerrero-Naranjo JL, Gonzalez-Mijares CC, et al. Pattern scan laser photocoagulation: safety and complications, experience after 1301 consecutive cases. *Br J Ophthalmol*. 2010;94(6):720–724.
152. Kriechbaum K, Bolz M, Deak GG, et al. High-resolution imaging of the human retina in vivo after scatter photocoagulation treatment using a semiautomated laser system. *Ophthalmology*. 2010;117(3):545–551.
153. Liang JC, Huamonte FU. Reduction of immediate complications after panretinal photocoagulation. *Retina*. 1984;4(3):166–170.
154. Diabetic Retinopathy Clinical Research Network, Brucker AJ, Qin H, et al. Observational study of the development of diabetic macular edema following panretinal (scatter) photocoagulation given in 1 or 4 sittings. *Arch Ophthalmol*. 2009;127(2):132–140.
155. Bandello F, Brancato R, Lattanzio R, et al. Double-frequency Nd:YAG laser vs. argon-green laser in the treatment of proliferative diabetic retinopathy: randomized study with long-term follow-up. *Lasers Surg Med*. 1996;19(2):173–176.
156. Bandello F, Brancato R, Trabucchi G, et al. Diode versus argon-green laser panretinal photocoagulation in proliferative diabetic retinopathy: a randomized study in 44 eyes with a long follow-up time. *Graefes Arch Clin Exp Ophthalmol*. 1993;231(9):491–494.
157. Doft BH, Blankenship G. Retinopathy risk factor regression after laser panretinal photocoagulation for proliferative diabetic retinopathy. *Ophthalmology*. 1984;91:1453–1457.
158. Blankenship GW. A clinical comparison of central and peripheral argon laser panretinal photocoagulation for proliferative diabetic retinopathy. *Ophthalmology*. 1988;95:170–177.
159. Vander JF, Duker JS, Benson WE, et al. Long-term stability and visual outcome after favorable initial response of

proliferative diabetic retinopathy to panretinal photocoagulation. *Ophthalmology*. 1991;98:1575–1579.
160. Rogell GD. Incremental panretinal photocoagulation. Results in treating proliferative diabetic retinopathy. *Retina*. 1983;3:308–311.
161. Case reports to accompany Early Treatment Diabetic Retinopathy Study Reports 3 and 4. The Early Treatment Diabetic Retinopathy Study Research Group. *Int Ophthalmol Clin*. 1987;27(4):273–333.
162. Dogru M, Kaderli B, Gelisken O, et al. Ocular surface changes with applanation contact lens and coupling fluid use after argon laser photocoagulation in noninsulin-dependent diabetes mellitus. *Am J Ophthalmol*. 2004;138(3):381–388.
163. Bloom SM, Mahl CF, Schiller SB. Lenticular burns following argon panretinal photocoagulation. *Br J Ophthalmol*. 1992;76(10):630–631.
164. Moriarty AP, Spalton DJ, Shilling JS, et al. Breakdown of the blood-aqueous barrier after argon laser panretinal photocoagulation for proliferative diabetic retinopathy. *Ophthalmology*. 1996;103(5):833–838.
165. Patel JI, Jenkins L, Benjamin L, et al. Dilated pupils and loss of accommodation following diode panretinal photocoagulation with sub-tenon local anaesthetic in four cases. *Eye (Lond)*. 2002;16(5):628–632.
166. Fong DS, Girach A, Boney A. Visual side effects of successful scatter laser photocoagulation surgery for proliferative diabetic retinopathy: a literature review. *Retina*. 2007;27(7):816–824.
167. McDonald HR, Schatz H. Macular edema following panretinal photocoagulation. *Retina*. 1985;5(1):5–10.
168. McDonald HR, Schatz H. Visual loss following panretinal photocoagulation for proliferative diabetic retinopathy. *Ophthalmology*. 1985;92(3):388–393.
169. Meyers SM. Macular edema after scatter laser photocoagulation for proliferative diabetic retinopathy. *Am J Ophthalmol*. 1980;90(2):210–216.
170. Ferris FL 3rd, Podgor MJ, Davis MD. Macular edema in

Diabetic Retinopathy Study patients. Diabetic Retinopathy Study Report number 12. *Ophthalmology*. 1987;94(7):754–760.
171. Mendrinos E, Donati G, Pournaras CJ. Rapid and persistent regression of severe new vessels on the disc in proliferative diabetic retinopathy after a single intravitreal injection of pegaptanib. *Acta Ophthalmol*. 2009;87(6):683–684.
172. Avery RL, Pearlman J, Pieramici DJ, et al. Intravitreal bevacizumab (Avastin) in the treatment of proliferative diabetic retinopathy. *Ophthalmology*. 2006;113(10):1695.e1–1695.e15.
173. Jorge R, Costa RA, Calucci D, et al. Intravitreal bevacizumab (Avastin) for persistent new vessels in diabetic retinopathy (IBEPE study). *Retina*. 2006;26(9):1006–1013.
174. Erdol H, Turk A, Akyol N, et al. The results of intravitreal bevacizumab injections for persistent neovascularizations in proliferative diabetic retinopathy after photocoagulation therapy. *Retina*. 2010;30(4):570–577.
175. Mirshahi A, Roohipoor R, Lashay A, et al. Bevacizumab-augmented retinal laser photocoagulation in proliferative diabetic retinopathy: a randomized double-masked clinical trial. *Eur J Ophthalmol*. 2008;18(2):263–269.
176. Tonello M, Costa RA, Almeida FP, et al. Panretinal photocoagulation versus PRP plus intravitreal bevacizumab for high-risk proliferative diabetic retinopathy (IBeHi study). *Acta Ophthalmol*. 2008;86(4):385–389.
177. Machemer R, Buettner H, Norton EW, et al. Vitrectomy: a pars plana approach. *Trans Am Acad Ophthalmol Otolaryngol*. 1971;75(4):813–820.
178. Wilson C, Horton M, Cavallerano J, et al. Addition of primary care-based retinal imaging technology to an existing eye care professional referral program increased the rate of surveillance and treatment of diabetic retinopathy. *Diabetes Care*. 2005;28(2):318–322.
179. Whited JD, Datta SK, Aiello LM, et al. A modeled economic analysis of a digital tele-ophthalmology system as used by three federal health care agencies for detecting proliferative diabetic retinopathy. *Telemed J E Health*. 2005;11(6):641–651.

52

Hypertension

Carol Yim-lui Cheung, Tien Y. Wong

Introduction

Hypertension is the leading risk factor for cardiovascular disease (CVD) and mortality worldwide,[1] with a projected number of 1.56 billion individuals with hypertension by 2025.[2]

Hypertension has profound effects on both the structure and function of the vasculature in the eye. The retinal, choroidal, and optic nerve circulations undergo a range of pathophysiologic changes in response to elevated blood pressure resulting in a spectrum of clinical signs known as hypertensive retinopathy, choroidopathy, and optic neuropathy, respectively.[3] Hypertension is also a major risk factor for many other eye diseases, including the development and progression of diabetic retinopathy,[4] retinal vein occlusion,[5] retinal arterial macroaneurysm,[6] and possibly age-related macular degeneration and glaucoma.[3,7]

Hypertensive Retinopathy

Definition and Classification

Retinopathy is the most common manifestation of hypertension, which develops due to acute and/or chronic elevations in blood pressure. Hypertensive retinopathy is broadly divided into different stages.[8] The initial response to elevated blood pressure is vasospasm and an increase in vasomotor tone, with consequent narrowing of retinal arterioles to control for optimal blood volume ("vasoconstrictive" phase). This stage is seen clinically as generalized or diffuse retinal arteriolar narrowing.

Persistently elevated blood pressure leads to the "sclerotic" phase, which manifests pathologically as intimal thickening, media wall hyperplasia, and hyaline degeneration. This stage accords with diffused and localized (focal) retinal arteriolar narrowing, arteriolar wall opacification ("silver" or "copper wiring"), and compression of the venules by structural changes in the arterioles (arteriovenous "nicking" or "nipping").

With chronically sustained blood pressure elevation, the blood–retinal barrier is disrupted. Pathologic changes at this stage ("exudative" phase) include necrosis of the smooth muscles and endothelial cells, exudation of blood and lipids, and retinal nerve fiber layer ischemia, which results in microaneurysms, retinal hemorrhages, hard exudates, and cotton-wool spots seen in the retina.

Very severe hypertension (i.e., "malignant hypertension" phase)

may lead to optic disc swelling which may reflect underlying hypertensive encephalopathy with raised intracranial pressure.[3,7–9]

The above phases of hypertensive retinopathy are not always sequential. For example, in patients with acutely raised blood pressure, signs of retinopathy reflecting the "exudative" stage (e.g., retinal hemorrhage) may be present without features of the "sclerotic" stage (e.g., arteriovenous nicking). Furthermore, elevated blood pressure does not fully explain all the pathophysiologic mechanisms of hypertensive retinopathy. Other processes involved in the pathogenesis of hypertensive retinopathy signs include inflammation,[10] endothelial dysfunction,[11] abnormal angiogenesis,[12] and oxidative stress.[13] In fact, hypertensive retinopathy signs are detected frequently in persons without a known history of hypertension.[14]

There have been many different classifications for hypertensive retinopathy. Traditionally, the Keith–Wagener–Baker system classifies patients with hypertension into four groups of increasing severity.[15] However, it is difficult to distinguish early retinopathy grades (e.g., group 1 signs are not easily distinguished from group 2 signs).[9,16] A simplified classification of hypertensive retinopathy based on prognosis of different signs from recent population-based data has been proposed and has been shown to have high reliability[9,17]:

1. **None**: no detectable signs.

2. **Mild**: Generalized arteriolar narrowing, focal arteriolar narrowing, arteriovenous nicking, arteriolar wall opacification (silver or copper wiring), or a combination of these signs (Fig. 52.1).

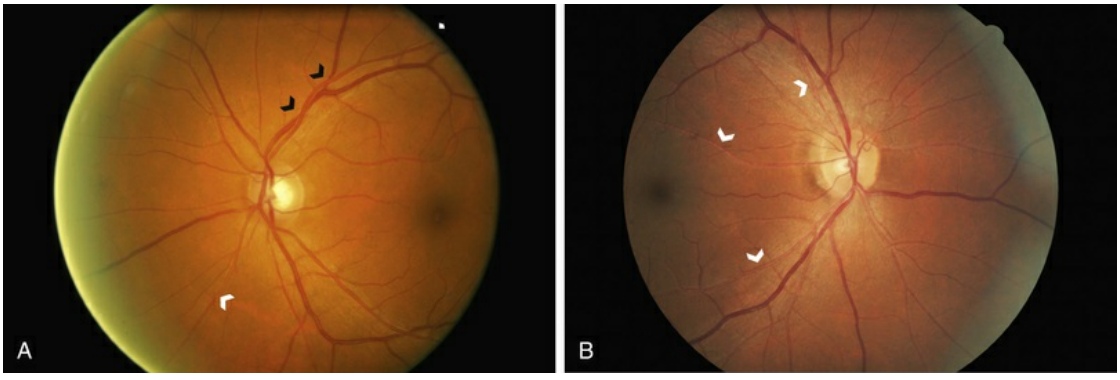

FIG. 52.1 Examples of mild hypertensive retinopathy. Panel A shows arteriovenous nicking (*black arrows*) and focal narrowing (*white arrow*). Panel B shows opacification (silver or copper wiring) of arteriolar wall (*white arrows*).

3. **Moderate**: Hemorrhages (blot, dot, or flame-shaped), microaneurysms, cotton-wool spots, hard exudates, or a combination of these signs (Fig. 52.2).

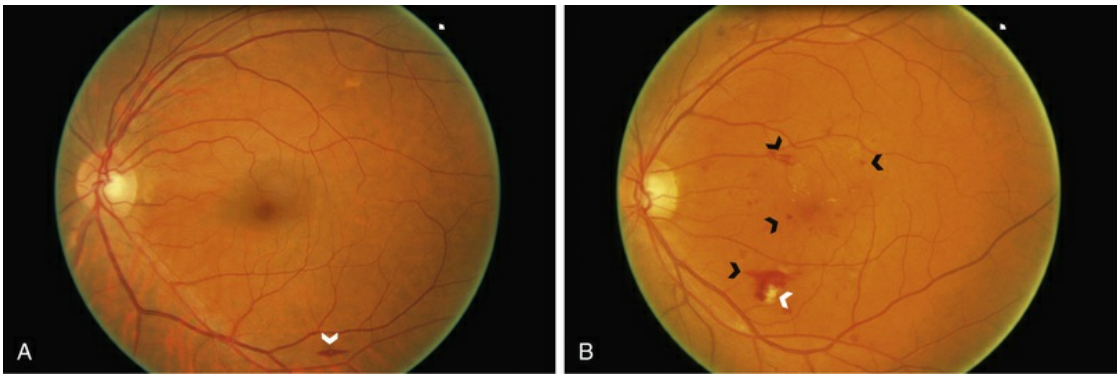

FIG. 52.2 Examples of moderate hypertensive retinopathy. Panel A shows a flame-shaped retinal hemorrhage (*white arrow*). Panel B shows a cotton-wool spot (*white arrow*), retinal hemorrhages and microaneurysms (*black arrows*).

4. **Malignant**: Signs of moderate retinopathy in combination with optic disc swelling, in the presence of severely elevated blood pressure (Fig. 52.3).

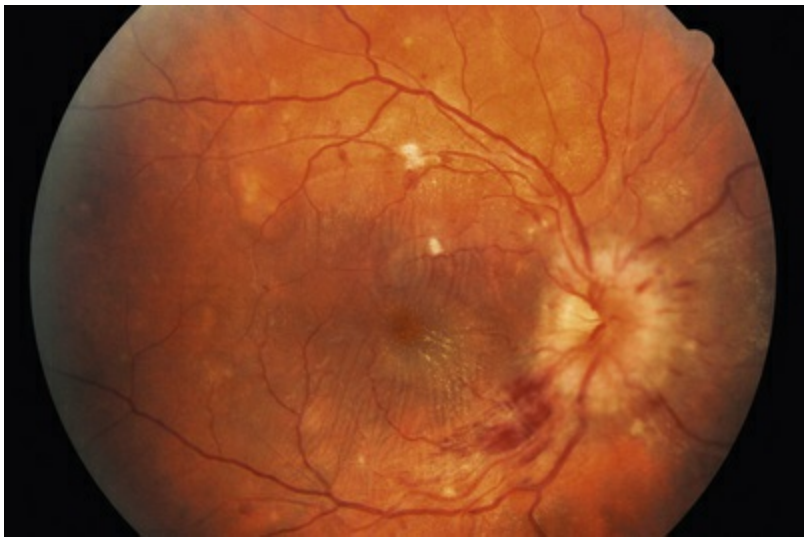

FIG. 52.3 Example of malignant hypertensive retinopathy. Retinal hemorrhages, cotton-wool spots, hard exudates, and swelling of the optic disc are present.

The application of digital retinal photography and imaging software has allowed measurements of retinal vessel widths to quantify generalized arteriolar narrowing objectively.[18,19] Studies using such methods show that generalized retinal arteriolar narrowing is strongly related to blood pressure and risk of hypertension.[20,21] There is also evidence that retinal venular diameter may convey independent prognostic information.[22] However, the measurement of retinal vessel width from photographs largely reflects the width of the red blood cell column (i.e., internal lumen diameter), and it does not capture the vessel wall, as the wall is transparent to the light. Furthermore, the measurement of retinal vessel width using these methods requires specialized computer software and trained technicians and is thus not yet widely available for clinical use.

It has been argued that the clinical assessment of hypertensive retinopathy signs is of limited additional value in the management of patients with hypertension.[23] Most international hypertension management guidelines, however, including those of the US Joint National Committee on Prevention, Detection, Evaluation, and Treatment of High Blood Pressure (JNC), the British Society of Hypertension and the European Society of Hypertension (ESH), the European Society of Cardiology (ESC), and National Institute of Health and Clinical Excellence (NICE)[24–27] still emphasize that

hypertensive retinopathy, with left ventricular hypertrophy and renal impairment, is an indicator of target organ damage, and that its presence should be an indication for a more aggressive approach in managing these hypertensive patients.[25] Whether the retinal examinations should be performed by physicians using the direct ophthalmoscope, by ophthalmologists, or via standardized assessment using digital retinal photography remains unclear.

Epidemiology

In the past 30 years, epidemiologic studies that have used retinal photography and standardized assessment methods to document and define hypertensive retinopathy have contributed to a greater understanding of the epidemiology, risk factors, and systemic associations of hypertensive retinopathy signs in the general population with different racial samples.[28]

With the exception of optic disc swelling, hypertensive retinopathy signs are generally common in persons 40 years of age or older, even in the absence of diabetes mellitus, with prevalence ranges from 2% to 17%.[29–36] These studies also demonstrate that hypertensive retinopathy signs increase with age, and may vary by race/ethnicity (Chinese have a higher prevalence of hypertensive retinopathy than Caucasian whites) and possibly gender (men have higher rates than women).

While it is well established that hypertensive retinopathy signs are strongly correlated with blood pressure levels,[28,37,38] new epidemiologic studies show three particularly interesting features. First, there is now good evidence that some signs, particularly generalized retinal arteriolar narrowing, may precede the development of hypertension.[20,21,39] The association between retinal arteriolar narrowing and incident hypertension has been confirmed in a recent meta-analysis of 10,229 participants without prevalent hypertension, diabetes, or cardiovascular disease.[40] In some studies, normotensive persons with this sign were more likely to develop hypertension and, among those with mild hypertension, were more likely to develop the severe stages of hypertension.[41] Thus, generalized retinal arteriolar narrowing, possibly reflecting more widespread systemic peripheral vasoconstriction, may be an early

preclinical marker of hypertension.

Second, new studies in children have demonstrated that the association between retinal arteriolar narrowing and elevated blood pressure can be observed even in children as young as 4–5 years of age. These findings suggest that the impact of elevated blood pressure on the retinal microcirculation occurs in early life,[42–44] which may then "track" through to adulthood, even before the onset of overt hypertension.

Third, there is now evidence to show that hypertensive retinopathy signs are associated with past blood pressure levels and other parameters of blood pressure. Generalized retinal arteriolar narrowing and arteriovenous nicking, for example, are related not only to current blood pressure levels, but also to blood pressure levels measured in the past, suggesting these two retinal signs reflect the cumulative effects of longstanding hypertension and are persistent markers of chronic hypertensive damage. In contrast, focal arteriolar narrowing, retinal hemorrhages, microaneurysms, and cotton-wool spots are related only to concurrently measured blood pressure, mirroring the effects of short-term blood pressure changes.[38] Furthermore, central blood pressure, directly reflecting the blood pressure load on target organs, is more closely associated with retinal arteriolar narrowing than brachial blood pressure.[45] In regard to other common clinical hypertension phenotypes, retinal arteriolar narrowing is also associated with masked hypertension and white coat hypertension, similar to sustained hypertension.[46]

Finally, retinal venular diameter, not traditionally considered part of the spectrum of hypertensive retinopathy signs, may convey additional information regarding the state of the retinal vasculature and systemic health. Studies found that retinal venular widening or dilation is also related to elevated blood pressure levels and incident hypertension,[21,22,37,40,47] suggesting that the venule may exhibit different optimal flow characteristics across the vascular network compared with arterioles in the presence of hypertension.[48] This may also suggest that venules are not merely passive conductance vessels but represent a dynamic component responsive to changes in the microcirculation.[49] Whether retinal venular dilation should be included as part of the classification of hypertensive retinopathy remains unclear at this time.

Relationship With Stroke

Retinal and cerebral small vessels share similar embryologic origin, anatomical features, and physiologic properties. There are now numerous studies that have reported the strong link between the presence of hypertensive retinopathy and both subclinical and clinical stroke as well as other cerebrovascular conditions.

In one large multicenter US study, middle-aged, generally healthy persons with moderate hypertensive retinopathy signs were more likely to have subclinical MRI-defined cerebral infarction, cerebral white matter lesions, cerebral atrophy, and cerebral microbleeds than those without these signs.[50–54] Furthermore, persons with moderate hypertensive signs at baseline were more likely to develop an incident clinical stroke,[55–58] and incident lacunar stroke,[59] than persons without these signs, even controlling for traditional risk factors. Another large cohort study based in Rotterdam, The Netherlands, has further reported associations of larger retinal venular diameter with incidence of hemorrhagic stroke.[60]

Some recent studies further demonstrated that hypertensive retinopathy may allow further refinement and subtyping of stroke. In a multicenter study of patients with acute stroke, different hypertensive retinopathy signs were associated with specific stroke subtypes.[61] For example, retinal arteriolar narrowing was associated with lacunar stroke, while retinal hemorrhages were linked with cerebral hemorrhages. These findings suggest that hypertensive signs reflect specific cerebral microvasculopathy and may further help to understand the underlying pathologic mechanisms.[59,61–63]

Relationship With Coronary Heart Disease

The presence of hypertensive retinopathy signs is associated with multiple markers of subclinical atherosclerotic diseases, including coronary artery calcification,[64] aortic stiffness,[65–66] left ventricular hypertrophy,[67] and carotid intima-media thickness.[68] There is also evidence that hypertensive retinopathy signs are predictive of clinical coronary artery disease events and congestive heart failure; however, the results of these studies show less consistent associations than with stroke.[69–71] In one study, persons with

moderate hypertensive retinopathy were three times more likely to develop congestive heart failure than those without retinopathy, while controlling for the presence of other cardiovascular risk factors.[72]

Hypertensive retinopathy has also been associated with increased risk of CVD mortality, stroke mortality, and coronary heart disease mortality.[14,73,74] In one study, persons with moderate hypertensive retinopathy were more likely to die from coronary heart disease than persons without this sign, with an equivalent risk similar to that of diabetes.[73] These data suggest that hypertensive retinopathy may convey additional prognostic information than other risk measures of CVD.

Relationship With Other End-Organ Damage of Hypertension

The significance of hypertensive retinopathy signs as risk indicators has long been recognized in patients with renal disease.[75] Retinopathy signs have also been associated with other indicators of hypertensive target organ damage, such as microalbuminuria and renal impairment.[76–78] Such association was independent of blood pressure, diabetes, and other risk factors, and was also seen in persons without diabetes or hypertension. Furthermore, hypertensive retinopathy was correlated with left ventricular hypertrophy, even in patients with mild-to-moderate hypertensive retinopathy, suggesting that its presence is an indicator of other target organ damage.[79–81]

Taken in totality, these data suggest hypertensive retinopathy signs are markers of systemic vascular disease, which may mirror preclinical structural changes in the cerebral and coronary microcirculations, and represent a greater burden of cardiovascular risk factors that predispose people to develop CVD. The presence of hypertensive retinopathy may therefore convey additional prognostic information than other risk measures of CVD.

Relationship With Dementia

Hypertension is also a risk factor for cognitive impairment and

dementia.[82] A number of studies have now demonstrated that hypertensive signs are associated with poorer cognitive performance and dementia, even controlling for age, blood pressure levels, and traditional risk factors.[83–84] For example, retinopathy signs were associated with decline in standardized cognitive test scores in a multicenter US study and with decline in the Modified Mini-Mental State Examination (3MSE) in a cohort of older women.[85–86] Another large population-based prospective study also reported associations of retinopathy with prevalent dementia, and of retinal venular widening with development of dementia.[87–88] However, not all studies are consistent, and in one, retinopathy was not associated with either incident dementia or incident Alzheimer's disease and vascular dementia. Recent studies also showed that more quantitative changes in the retinal vascular network parameters (e.g., sparser retinal vasculature) were associated with Alzheimer's disease.[89–91] These studies may provide insight into mechanisms underlying the relationship between hypertension and cognitive impairment.

Hypertensive Choroidopathy

Hypertensive choroidopathy is less well recognized compared with hypertensive retinopathy. The underlying mechanism of hypertensive choroidopathy is related to choroidal ischemia which has effects on the retinal pigment epithelium and retina. Like the retinal vessels, the choroidal vessels may also undergo fibrinoid necrosis at the level of the choroidal capillaries in the presence of elevated blood pressure, leading to hypertensive choroidopathy signs that include Elschnig spots (round, deep, and gray–yellow patches at the level of the retinal pigment epithelium) and Siegrist streaks (linear hyperpigmented streaks along choroidal arteries). In severe cases, there may also be serous retinal detachment which can lead to vision loss.[92–94]

Hypertensive Optic Neuropathy

Bilateral optic disc swelling or papilledema is commonly caused by accelerated or malignant hypertension, representing the “malignant

hypertensive retinopathy" stage in the above classification. The pathogenesis of optic disc swelling secondary to accelerated hypertension remains controversial. Ischemia, raised intracranial pressure, and hypertensive encephalopathy are all possible mechanisms that can result in papilledema.[94] Bilateral disc swelling is strongly correlated with CVD risk and mortality,[14,15,74] and these patients need urgent antihypertensive management.[9]

Future Directions

There are several areas of research in the field of hypertensive retinopathy. First, widespread use of digital fundus photography and new computer software analysis have provided the opportunity to quantify and monitor hypertensive retinopathy signs in a more objective manner in larger populations and in clinical settings. In addition to the measurement of retinal vascular caliber used in previous studies, new research has identified a number of other retinal vascular features, such as branching angles, bifurcation, fractal dimension, tortuosity, vascular length-to-diameter ratio, and wall-to-lumen ratio, that may also be related to hypertension.[95–100] These newer, quantitatively measured retinal vascular changes may offer increasingly accurate and reliable parameters reflecting early and subtle retinal vascular abnormalities, which potentially provide additional predictive value of CVD risk outcomes.

Second, other ocular imaging technologies, such as cellular-level retinal imaging using adaptive optics, retinal vessel oxygen saturation using retinal oximetry, flicker light-induced vasodilation using dynamic retinal vessel analysis, retinal blood flow using Doppler optical coherence tomography (OCT), choroidal vasculature imaging using enhanced depth imaging with spectral domain OCT and swept source OCT, and capillary-level non-dye-based mapping of retinal vasculature using OCT angiography have been recently developed. These technologies hold promise for more detailed analysis of hypertensive changes in the eye and correlations with systemic end-organ damage.

Third, genetic epidemiology studies have provided clues to new vascular pathophysiologic processes linked to hypertensive

retinopathy signs.[47] For example, a population-based genome-wide association study demonstrated four novel loci associated with retinal venular caliber, an endophenotype of the microcirculation associated with clinical CVD.[101] Other studies have reported genetic loci associated with retinal arteriolar caliber and hypertensive retinopathy signs.[102–103] These genetic studies may allow understanding of the contribution and biological mechanisms of microcirculatory changes that underlie CVD.

Finally, assessment of hypertensive retinopathy signs also allows the study of new therapies for hypertension. Studies have demonstrated regression of hypertensive retinopathy signs in response to blood pressure reduction and that regression patterns are different in response to different antihypertensive regimens (e.g., angiotensin-converting enzyme inhibitors appear to have a more favorable effect on the retinal vasculature).[104–106] Regression of hypertensive retinopathy signs has been shown to be associated with significantly better outcomes in terms of left ventricular hypertrophy and extent of target organ damage.[107] Further prospective controlled trials are required to clarify whether specific reduction of hypertensive retinopathy also reduces the morbidity and mortality associated with CVD.

Conclusion

Hypertension has widespread effects on the ocular vasculature. Hypertensive retinopathy signs are commonly seen in the general adult population and are associated with both subclinical and clinical measures of CVD. Patients with hypertensive retinopathy may therefore benefit from a careful assessment of blood pressure and other vascular factors, and appropriate CVD risk management.

References

1. Lawes CM, Vander HS, Rodgers A. Global burden of blood-pressure-related disease, 2001. *Lancet*. 2008;371(9623):1513–1518.
2. Kearney PM, Whelton M, Reynolds K, et al. Global burden of hypertension: analysis of worldwide data. *Lancet*.

2005;365(9455):217–223.
3. Wong TY, Mitchell P. The eye in hypertension. *Lancet*. 2007;369(9559):425–435.
4. Cheung N, Mitchell P, Wong TY. Diabetic retinopathy. *Lancet*. 2010;376(9735):124–136.
5. Wong TY, Scott IU. Clinical practice. Retinal-vein occlusion. *N Engl J Med*. 2010;363(22):2135–2144.
6. Panton RW, Goldberg MF, Farber MD. Retinal arterial macroaneurysms: risk factors and natural history. *Br J Ophthalmol*. 1990;74:595–600.
7. Bhargava M, Ikram MK, Wong TY. How does hypertension affect your eyes? *J Hum Hypertens*. 2011;26(2):71–83.
8. Tso MO, Jampol LM. Pathophysiology of hypertensive retinopathy. *Ophthalmology*. 1982;89(10):1132–1145.
9. Wong TY, Mitchell P. Hypertensive retinopathy. *N Engl J Med*. 2004;351(22):2310–2317.
10. Klein R, Sharrett AR, Klein BE, et al. Are retinal arteriolar abnormalities related to atherosclerosis?: The Atherosclerosis Risk in Communities Study. *Arterioscler Thromb Vasc Biol*. 2000;20(6):1644–1650.
11. Delles C, Michelson G, Harazny J, et al. Impaired endothelial function of the retinal vasculature in hypertensive patients. *Stroke*. 2004;35(6):1289–1293.
12. Tsai WC, Li YH, Huang YY, et al. Plasma vascular endothelial growth factor as a marker for early vascular damage in hypertension. *Clin Sci*. 2005;109(1):39–43.
13. Coban E, Alkan E, Altuntas S, et al. Serum ferritin levels correlate with hypertensive retinopathy. *Med Sci Monit*. 2010;16(2):CR92–5.
14. Wong TY, Klein R, Klein BE, et al. Retinal microvascular abnormalities and their relationship with hypertension, cardiovascular disease, and mortality. *Surv Ophthalmol*. 2001;46(1):59–80.
15. Keith NM, Wagener HP, Barker NW. Some different types of essential hypertension: their course and prognosis. *Am J Med Sci*. 1939;197(3):332–343.
16. Dodson PM, Lip GY, Eames SM, et al. Hypertensive retinopathy: a review of existing classification systems and

a suggestion for a simplified grading system. *J Hum Hypertens*. 1996;10(2):93–98.
17. Downie LE, Hodgson LA, Dsylva C, et al. Hypertensive retinopathy: comparing the Keith-Wagener-Barker to a simplified classification. *J Hypertens*. 2013;31(5):960–965.
18. Wong TY, Knudtson MD, Klein R, et al. Computer-assisted measurement of retinal vessel diameters in the Beaver Dam Eye Study: methodology, correlation between eyes, and effect of refractive errors. *Ophthalmology*. 2004;111(6):1183–1190.
19. Cheung CY, Hsu W, Lee ML, et al. A new method to measure peripheral retinal vascular caliber over an extended area. *Microcirculation*. 2010;17(7):495–503.
20. Wong TY, Klein R, Sharrett AR, et al. Retinal arteriolar diameter and risk for hypertension. *Ann Intern Med*. 2004;140(4):248–255.
21. Ikram MK, Witteman JC, Vingerling JR, et al. Retinal vessel diameters and risk of hypertension: the Rotterdam Study. *Hypertension*. 2006;47(2):189–194.
22. Wong TY, Kamineni A, Klein R, et al. Quantitative retinal venular caliber and risk of cardiovascular disease in older persons: the cardiovascular health study. *Arch Intern Med*. 2006;166(21):2388–2394.
23. van den Born BJ, Hulsman CA, Hoekstra JB, et al. Value of routine funduscopy in patients with hypertension: systematic review. *BMJ*. 2005;331(7508):73.
24. Williams B, Poulter NR, Brown MJ, et al. British Hypertension Society guidelines for hypertension management 2004 (BHS-IV): summary. *Br Med J*. 2004;328(7440):634–640.
25. Chobanian AV, Bakris GL, Black HR, et al. The Seventh Report of the Joint National Committee on Prevention, Detection, Evaluation, and Treatment of High Blood Pressure: the JNC 7 report. *JAMA*. 2003;289(19):2560–2572.
26. Mansia G, De Backer G, Dominiczak A, et al. 2007 ESH-ESC Guidelines for the management of arterial hypertension: the task force for the management of arterial hypertension of the European Society of Hypertension (ESH) and of the

European Society of Cardiology (ESC). *Blood Press*. 2007;16(3):135–232.
27. National Institute of Health and Clinical Excellence. *Hypertension: clinical management of primary hypertension in adults*. [NICE Clinical Guideline 127] https://www.nice.org.uk/guidance/cg127/chapter/1-Guidance; 2011.
28. Hubbard LD, Brothers RJ, King WN, et al. Methods for evaluation of retinal microvascular abnormalities associated with hypertension/sclerosis in the Atherosclerosis Risk in Communities Study. *Ophthalmology*. 1999;106(12):2269–2280.
29. Klein R. Retinopathy in a population-based study. *Trans Am Ophthalmol Soc*. 1992;90:561–594.
30. Jeganathan VS, Cheung N, Tay WT, et al. Prevalence and risk factors of retinopathy in an Asian population without diabetes: the Singapore Malay Eye Study. *Arch Ophthalmol*. 2010;128(1):40–45.
31. Peng XY, Wang FH, Liang YB, et al. Retinopathy in persons without diabetes: the Handan Eye Study. *Ophthalmology*. 2010;117(3):531–537 [537.e1-2].
32. Chao JR, Lai MY, Azen SP, et al. Retinopathy in persons without diabetes: the Los Angeles Latino Eye Study. *Invest Ophthalmol Vis Sci*. 2007;48(9):4019–4025.
33. Wong TY, Liew G, Tapp RJ, et al. Relation between fasting glucose and retinopathy for diagnosis of diabetes: three population-based cross-sectional studies. *Lancet*. 2008;371(9614):736–743.
34. Ojaimi E, Nguyen TT, Klein R, et al. Retinopathy signs in people without diabetes: the multi-ethnic study of atherosclerosis. *Ophthalmology*. 2011;118(4):656–662.
35. Wong TY, Klein R, Duncan BB, et al. Racial differences in the prevalence of hypertensive retinopathy. *Hypertension*. 2003;41(5):1086–1091.
36. Bhargava M, Cheung CY, Sabanayagam C, et al. Prevalence and risk factors for retinopathy in persons without diabetes: the Singapore Indian Eye Study. *Acta Ophthalmol*. 2014;92(8):e602–9.
37. Cheung CY, Tay WT, Mitchell P, et al. Quantitative and

qualitative retinal microvascular characteristics and blood pressure. *J Hypertens*. 2011;29(7):1380–1391.
38. Wong TY, Hubbard LD, Klein R, et al. Retinal microvascular abnormalities and blood pressure in older people: the Cardiovascular Health Study. *Br J Ophthalmol*. 2002;86(9):1007–1013.
39. Klein R, Klein BE, Moss SE, et al. The relationship of retinopathy in persons without diabetes to the 15-year incidence of diabetes and hypertension: Beaver Dam Eye Study. *Trans Am Ophthalmol Soc*. 2006;104:98–107.
40. Ding J, Wai KL, McGeechan K, et al. Retinal vascular caliber and the development of hypertension: a meta-analysis of individual participant data. *J Hypertens*. 2014;32(2):207–215.
41. Smith W, Wang JJ, Wong TY, et al. Retinal arteriolar narrowing is associated with 5-year incident severe hypertension: the Blue Mountains Eye Study. *Hypertension*. 2004;44(4):442–447.
42. Mitchell P, Cheung N, de Haseth K, et al. Blood pressure and retinal arteriolar narrowing in children. *Hypertension*. 2007;49(5):1156–1162.
43. Li LJ, Cheung CY, Liu Y, et al. Influence of blood pressure on retinal vascular caliber in young children. *Ophthalmology*. 2011;118(7):1459–1465.
44. Gishti O, Jaddoe VW, Felix JF, et al. Retinal microvasculature and cardiovascular health in childhood. *Pediatrics*. 2015;135(4):678–685.
45. Kumagai K, Tabara Y, Yamashiro K, et al. Central blood pressure relates more strongly to retinal arteriolar narrowing than brachial blood pressure: the Nagahama Study. *J Hypertens*. 2015;33(2):323–329.
46. Triantafyllou A, Doumas M, Anyfanti P, et al. Divergent retinal vascular abnormalities in normotensive persons and patients with never-treated, masked, white coat hypertension. *Am J Hypertens*. 2013;26(3):318–325.
47. Sun C, Wang JJ, Mackey DA, et al. Retinal vascular caliber: systemic, environmental, and genetic associations. *Surv Ophthalmol*. 2009;54(1):74–95.
48. Patton N, Aslam T, Macgillivray T, et al. Asymmetry of

retinal arteriolar branch widths at junctions affects ability of formulae to predict trunk arteriolar widths. *Invest Ophthalmol Vis Sci*. 2006;47(4):1329–1333.
49. Liew G, Wang JJ, Mitchell P, et al. Retinal vascular imaging: a new tool in microvascular disease research. *Circ Cardiovasc Imaging*. 2008;1(2):156–161.
50. Kawasaki R, Cheung N, Mosley T, et al. Retinal microvascular signs and 10-year risk of cerebral atrophy: the Atherosclerosis Risk in Communities (ARIC) Study. *Stroke*. 2010;41(8):1826–1828.
51. Wong TY, Klein R, Sharrett AR, et al. Cerebral white matter lesions, retinopathy, and incident clinical stroke. *JAMA*. 2002;288(1):67–74.
52. Cooper LS, Wong TY, Klein R, et al. Retinal microvascular abnormalities and MRI-defined subclinical cerebral infarction: the Atherosclerosis Risk in Communities Study. *Stroke*. 2006;37(1):82–86.
53. Cheung N, Mosley T, Islam A, et al. Retinal microvascular abnormalities and subclinical magnetic resonance imaging brain infarct: a prospective study. *Brain*. 2010;133(Pt 7):1987–1993.
54. Hilal S, Ong YT, Cheung CY, et al. Microvascular network alterations in retina of subjects with cerebral small vessel disease. *Neurosci Lett*. 2014;577:95–100.
55. Wong TY, Klein R, Couper DJ, et al. Retinal microvascular abnormalities and incident stroke: the Atherosclerosis Risk in Communities Study. *Lancet*. 2001;358(9288):1134–1140.
56. Ong YT, Wong TY, Klein R, et al. Hypertensive retinopathy and risk of stroke. *Hypertension*. 2013;62(4):706–711.
57. Cheung CY, Tay WT, Ikram MK, et al. Retinal microvascular changes and risk of stroke: the Singapore Malay Eye Study. *Stroke*. 2013;44(9):2402–2408.
58. Kawasaki R, Xie J, Cheung N, et al. Retinal microvascular signs and risk of stroke: the Multi-Ethnic Study of Atherosclerosis (MESA). *Stroke*. 2012;43(12):3245–3251.
59. Yatsuya H, Folsom AR, Wong TY, et al. Retinal microvascular abnormalities and risk of lacunar stroke: Atherosclerosis Risk in Communities Study. *Stroke*.

2010;41(7):1349–1355.
60. Wieberdink RG, Ikram MK, Koudstaal PJ, et al. Retinal vascular calibers and the risk of intracerebral hemorrhage and cerebral infarction: the Rotterdam Study. *Stroke*. 2010;41(12):2757–2761.
61. Lindley RI, Wang JJ, Wong MC, et al. Retinal microvasculature in acute lacunar stroke: a cross-sectional study. *Lancet Neurol*. 2009;8(7):628–634.
62. Baker ML, Hand PJ, Wong TY, et al. Retinopathy and lobar intracerebral hemorrhage: insights into pathogenesis. *Arch Neurol*. 2010;67(10):1224–1230.
63. Baker ML, Hand PJ, Liew G, et al. Retinal microvascular signs may provide clues to the underlying vasculopathy in patients with deep intracerebral hemorrhage. *Stroke*. 2010;41(4):618–623.
64. Wong TY, Cheung N, Islam FM, et al. Relation of retinopathy to coronary artery calcification: the multi-ethnic study of atherosclerosis. *Am J Epidemiol*. 2008;167(1):51–58.
65. Cheung N, Sharrett AR, Klein R, et al. Aortic distensibility and retinal arteriolar narrowing: the multi-ethnic study of atherosclerosis. *Hypertension*. 2007;50(4):617–622.
66. Triantafyllou A, Anyfanti P, Gavriilaki E, et al. Association between retinal vessel caliber and arterial stiffness in a population comprised of normotensive to early-stage hypertensive individuals. *Am J Hypertens*. 2014;27(12):1472–1478.
67. Cheung N, Bluemke DA, Klein R, et al. Retinal arteriolar narrowing and left ventricular remodeling: the multi-ethnic study of atherosclerosis. *J Am Coll Cardiol*. 2007;50(1):48–55.
68. Kawasaki R, Cheung N, Islam FM, et al. Is diabetic retinopathy related to subclinical cardiovascular disease? *Ophthalmology*. 2011;118(5):860–865.
69. Michelson EL, Morganroth J, Nichols CW, et al. Retinal arteriolar changes as an indicator of coronary artery disease. *Arch Intern Med*. 1979;139(10):1139–1141.
70. Wong TY, Klein R, Sharrett AR, et al. Retinal arteriolar narrowing and risk of coronary heart disease in men and women. The Atherosclerosis Risk in Communities Study.

JAMA. 2002;287(9):1153–1159.
71. Duncan BB, Wong TY, Tyroler HA, et al. Hypertensive retinopathy and incident coronary heart disease in high risk men. *Br J Ophthalmol*. 2002;86(9):1002–1006.
72. Wong TY, Rosamond W, Chang PP, et al. Retinopathy and risk of congestive heart failure. *JAMA*. 2005;293(1):63–69.
73. Liew G, Wong TY, Mitchell P, et al. Retinopathy predicts coronary heart disease mortality. *Heart*. 2009;95(5):391–394.
74. Wong TY, Klein R, Nieto FJ, et al. Retinal microvascular abnormalities and 10-year cardiovascular mortality: a population-based case–control study. *Ophthalmology*. 2003;110(5):933–940.
75. Gunn RM. Ophthalmoscopic evidence of (1) arterial changes associated with chronic renal diseases and (2) of increased arterial tension. *Trans Ophthalmol Soc U K*. 1982;12:124–125.
76. Saitoh M, Matsuo K, Nomoto S, et al. Relationship between left ventricular hypertrophy and renal and retinal damage in untreated patients with essential hypertension. *Intern Med*. 1998;37(7):576–580.
77. Wong TY, Coresh J, Klein R, et al. Retinal microvascular abnormalities and renal dysfunction: the atherosclerosis risk in communities study. *J Am Soc Nephrol*. 2004;15(9):2469–2476.
78. Yip W, Sabanayagam C, Teo BW, et al. Retinal microvascular abnormalities and risk of renal failure in Asian populations. *PLoS ONE*. 2015;10(2):e0118076.
79. Kim GH, Youn HJ, Kang S, et al. Relation between grade II hypertensive retinopathy and coronary artery disease in treated essential hypertensives. *Clin Exp Hypertens*. 2010;32(7):469–473.
80. Cuspidi C, Meani S, Valerio C, et al. Prevalence and correlates of advanced retinopathy in a large selected hypertensive population. The Evaluation of Target Organ Damage in Hypertension (ETODH) study. *Blood Press*. 2005;14(1):25–31.
81. Tikellis G, Arnett DK, Skelton TN, et al. Retinal arteriolar narrowing and left ventricular hypertrophy in African Americans: the Atherosclerosis Risk in Communities

(ARIC) study. *Am J Hypertens*. 2008;21(3):352–359.
82. Nagai M, Hoshide S, Kario K. Hypertension and dementia. *Am J Hypertens*. 2010;23(2):116–124.
83. Cheung CY, Ong YT, Ikram MK, et al. Retinal microvasculature in Alzheimer's disease. *J Alzheimers Dis*. 2014;42(Suppl. 4):S339–52.
84. Heringa SM, Bouvy WH, van den Berg E, et al. Associations between retinal microvascular changes and dementia, cognitive functioning, and brain imaging abnormalities: a systematic review. *J Cereb Blood Flow Metab*. 2013;33(7):983–989.
85. Lesage SR, Mosley TH, Wong TY, et al. Retinal microvascular abnormalities and cognitive decline: the ARIC 14-year follow-up study. *Neurology*. 2009;73(11):862–868.
86. Haan M, Espeland MA, Klein BE, et al. Cognitive function and retinal and ischemic brain changes: the Women's Health Initiative. *Neurology*. 2012;78(13):942–949.
87. de Jong FJ, Schrijvers EM, Ikram MK, et al. Retinal vascular caliber and risk of dementia: the Rotterdam study. *Neurology*. 2011;76(9):816–821.
88. Schrijvers EM, Buitendijk GH, Ikram MK, et al. Retinopathy and risk of dementia: the Rotterdam Study. *Neurology*. 2012;79(4):365–370.
89. Cheung CY, Ong YT, Ikram MK, et al. Microvascular network alterations in the retina of patients with Alzheimer's disease. *Alzheimers Dement*. 2014;10(2):135–142.
90. Williams MA, McGowan AJ, Cardwell CR, et al. Retinal microvascular network attenuation in Alzheimer's disease. *Alzheimers Dement*. 2015;1(2):229–235.
91. Frost S, Kanagasingam Y, Sohrabi H, et al. Retinal vascular biomarkers for early detection and monitoring of Alzheimer's disease. *Transl Psychiatry*. 2013;3:e233.
92. Luo BP, Brown GC. Update on the ocular manifestations of systemic arterial hypertension. *Curr Opin Ophthalmol*. 2004;15(3):203–210.
93. Bourke K, Patel MR, Prisant LM, et al. Hypertensive choroidopathy. *J Clin Hypertens (Greenwich)*. 2004;6(8):471–

472.
94. Chatterjee S, Chattopadhyay S, Hope-Ross M, et al. Hypertension and the eye: changing perspectives. *J Hum Hypertens*. 2002;16(10):667–675.
95. Witt N, Wong TY, Hughes AD, et al. Abnormalities of retinal microvascular structure and risk of mortality from ischemic heart disease and stroke. *Hypertension*. 2006;47(5):975–981.
96. Cheung CY, Zheng Y, Hsu W, et al. Retinal vascular tortuosity, blood pressure, and cardiovascular risk factors. *Ophthalmology*. 2011;118(5):812–818.
97. Liew G, Wang JJ, Cheung N, et al. The retinal vasculature as a fractal: methodology, reliability, and relationship to blood pressure. *Ophthalmology*. 2008;115(11):1951–1956.
98. Hughes AD, Martinez-Perez E, Jabbar AS, et al. Quantification of topological changes in retinal vascular architecture in essential and malignant hypertension. *J Hypertens*. 2006;24(5):889–894.
99. Ritt M, Schmieder RE. Wall-to-lumen ratio of retinal arterioles as a tool to assess vascular changes. *Hypertension*. 2009;54(2):384–387.
100. Muraoka Y, Tsujikawa A, Kumagai K, et al. Age- and hypertension-dependent changes in retinal vessel diameter and wall thickness: an optical coherence tomography study. *Am J Ophthalmol*. 2013;156(4):706–714.
101. Ikram MK, Sim X, Jensen RA, et al. Four novel loci (19q13, 6q24, 12q24, and 5q14) influence the microcirculation in vivo. *PLoS Genet*. 2010;6(10):e1001184.
102. Sim X, Jensen RA, Ikram MK, et al. Genetic loci for retinal arteriolar microcirculation. *PLoS ONE*. 2013;8(6):e65804.
103. Jensen RA, Sim X, Li X, et al. Genome-wide association study of retinopathy in individuals without diabetes. *PLoS ONE*. 2013;8(2):e54232.
104. Hughes AD, Stanton AV, Jabbar AS, et al. Effect of antihypertensive treatment on retinal microvascular changes in hypertension. *J Hypertens*. 2008;26(8):1703–1707.
105. Dahlof B, Stenkula S, Hansson L. Hypertensive retinal vascular changes: relationship to left ventricular

hypertrophy and arteriolar changes before and after treatment. *Blood Press*. 1992;1(1):35–44.
106. Thom S, Stettler C, Stanton A, et al. Differential effects of antihypertensive treatment on the retinal microcirculation: an Anglo-Scandinavian cardiac outcomes trial substudy. *Hypertension*. 2009;54(2):405–408.
107. Coll-de-Tuero G, González-Vázquez S, Rodríguez-Poncelas A, et al. Retinal arteriole-to-venule ratio changes and target organ disease evolution in newly diagnosed hypertensive patients at 1-year follow-up. *J Am Soc Hypertens*. 2014;8(2):83–93.

53

Telescreening for Diabetic Retinopathy

Rajiv Raman, Tarun Sharma

Introduction

The criteria for human diseases amenable to screening approaches were defined by the World Health Organization in 1968[1] and diabetic retinopathy fulfills all of these. Visual impairment due to diabetic retinopathy is a significant health problem; however, it has a recognizable presymptomatic stage.[2] The Diabetes Control and Complications Trial (DCCT) and the UK Prospective Diabetes Study (UKPDS) established that intensive diabetes management to obtain near-euglycemic control can prevent and delay the progression of diabetic retinopathy in patients with diabetes.[3,4] Timely laser photocoagulation therapy can also prevent loss of vision in a large proportion of patients with sight-threatening diabetic retinopathy.[5] Screening for diabetic retinopathy saves vision at a relatively low cost, which has been demonstrated in various studies.[6,7] The American Academy of Ophthalmology

recommends annual dilated eye examinations, beginning at the time of diagnosis for patients with type II diabetes.[2] For those with type I diabetes, the recommendation is retinal examination 3–5 years after diagnosis, with annual exams thereafter.[2] The barriers for successful screening are numerous and include the high cost of care, poor awareness levels, lack of symptoms in the early stages of disease, socioeconomic factors, and poor geographic access to care.[8] Current screening programs for diabetic retinopathy are either ophthalmologist-based (with actual presence of the ophthalmologist at the site of screening) or ophthalmologist-led (no ophthalmologist at the site of screening). Table 53.1 summarizes the key differences between the two models. Telemedicine for retinopathy screening is an ophthalmologist-led screening model, which may be a logical potential alternative for patients who have been noncompliant with the traditional face-to-face examination by an ophthalmologist. Telemedicine is the exchange of medical data by electronic telecommunications technology allowing a patient's medical problems to be evaluated, monitored, and possibly treated while the patient and physician are located at sites physically remote from each other.[9]

TABLE 53.1

Differences Between the Ophthalmologist-Led and Ophthalmologist-Based Models for Screening for Diabetic Retinopathy

	Ophthalmologist-Led Model (Telescreening)	Ophthalmologist-Based Model
Brief description	Paramedical staff acquire data/images, which are then transferred for interpretation by ophthalmologist	Screening is performed by ophthalmologist
Feasibility	Yes, with less human resources	Needs trained expert
Maintenance	Required	Not required
Capital expenditure	More	Less
Revenue expenditure	Less	More
Interobserver bias	Less	More
Digital photo archiving	Yes	No
Acceptance by community	Yes	Yes

Guidelines for Telescreening Program

American Telemedicine Association Telehealth Practice Recommendations for Diabetic Retinopathy

The American Telemedicine Association (ATA), Ocular Telehealth Special Interest Group, and the National Institutes of Standards and Technology Working Group established the telescreening guidelines for diabetic retinopathy (DR).[10] The ATA recommends that telehealth programs for DR should demonstrate an ability to compare favorably with Early Treatment Diabetic Retinopathy Study (ETDRS) film or digital photography. For screening programs with low thresholds for referral, the International Clinical Diabetic Retinopathy Disease Severity Scale may be used in place of ETDRS scales; however, protocols should state the reference standard used for validation and relevant datasets used for comparison.

The ATA recognizes four categories of telescreening programs, of which higher categories (3 and 4) are generally not necessary for screening programs that do not involve actual management of diabetic eye disease:

Category 1: The program allows identification of patients who have no or minimal DR and distinguishes them from those who have more than minimal DR.

Category 2: The program allows identification of patients who do not have sight-threatening DR and distinguishes them from those who have potentially sight-threatening DR.

Category 3: The program can identify ETDRS-defined levels of nonproliferative DR (mild, moderate, or severe), proliferative DR (early, high-risk), and diabetic macular edema with accuracy sufficient to determine appropriate follow-up and treatment strategies.

Category 4: The program matches or exceeds the ability of ETDRS photographs to identify DR lesions to determine levels of DR and

macular edema. Functionally, category 4 validation indicates that a program can replace ETDRS photographs in any clinical or research program.

These levels of validation as described by the American Telemedicine Association affect the cost of implementing the system, as well as the expected benefits and savings from the information and recommendations that they generate.

Steps of Telescreening

The flow of steps of the telescreening process is diagrammed in Fig. 53.1. In brief, patient enrollment is performed after defining the data to be collected. Since ocular telescreening services for diabetic retinopathy satisfy the criteria of low-risk telehealth procedures and are within commonly accepted standards of practice, signature consent may not be required. However, practitioners should provide patients with information about the telescreening program they would reasonably want to know, including differences between care delivered using ocular telehealth approaches versus traditional face-to-face encounters, and a description of what is to be done at the patient's site and the remote site. The data collected include fundus images, along with patient examination findings (identification, demographic, and medical information) and some morphologic information that is used to make a clinical decision. Fundus images of both eyes of the patient are acquired under a fixed, predetermined imaging protocol. These images are taken by a trained technician using a fundus camera. Due to various factors, the quality of the acquired images may be below the grading standard, thus not providing any meaningful information for examination by the reader. This can be addressed by employing an automatic image quality assessment module. An automatic image quality assessment module will ensure that the images transmitted for diagnosis conform to prescribed gradability standards. During the quality assurance process, the gradable images are selected for compression, whereas the identification of poor quality images can trigger reimaging by the technician. The patient data comprising the clinical data and the fundus images are compressed to make

them suitable for low-bandwidth network connectivity. The patient data are transmitted to the servers via the Internet or satellite. At the reading center, the images are graded for presence of retinal lesions and the determination of a diabetic retinopathy level; referred to "next level" graders if necessary; and a retinopathy structured report is generated. Only qualified readers should perform retinal image grading and interpretation. If a reader is not a licensed eye care provider, specific training is required. A licensed, qualified eye care provider with expertise in diabetic retinopathy and familiarity with telescreening program technology should supervise the readers. An adjudicating reader (an ophthalmologist with special qualifications in diabetic retinopathy by training or experience) may resolve discrepant interpretations. Image processing algorithms should undergo rigorous clinical validation. A report comprising the findings, the results and the medical advice given by the expert is made available to the patient and the care team at the remote site through an accessible interface.

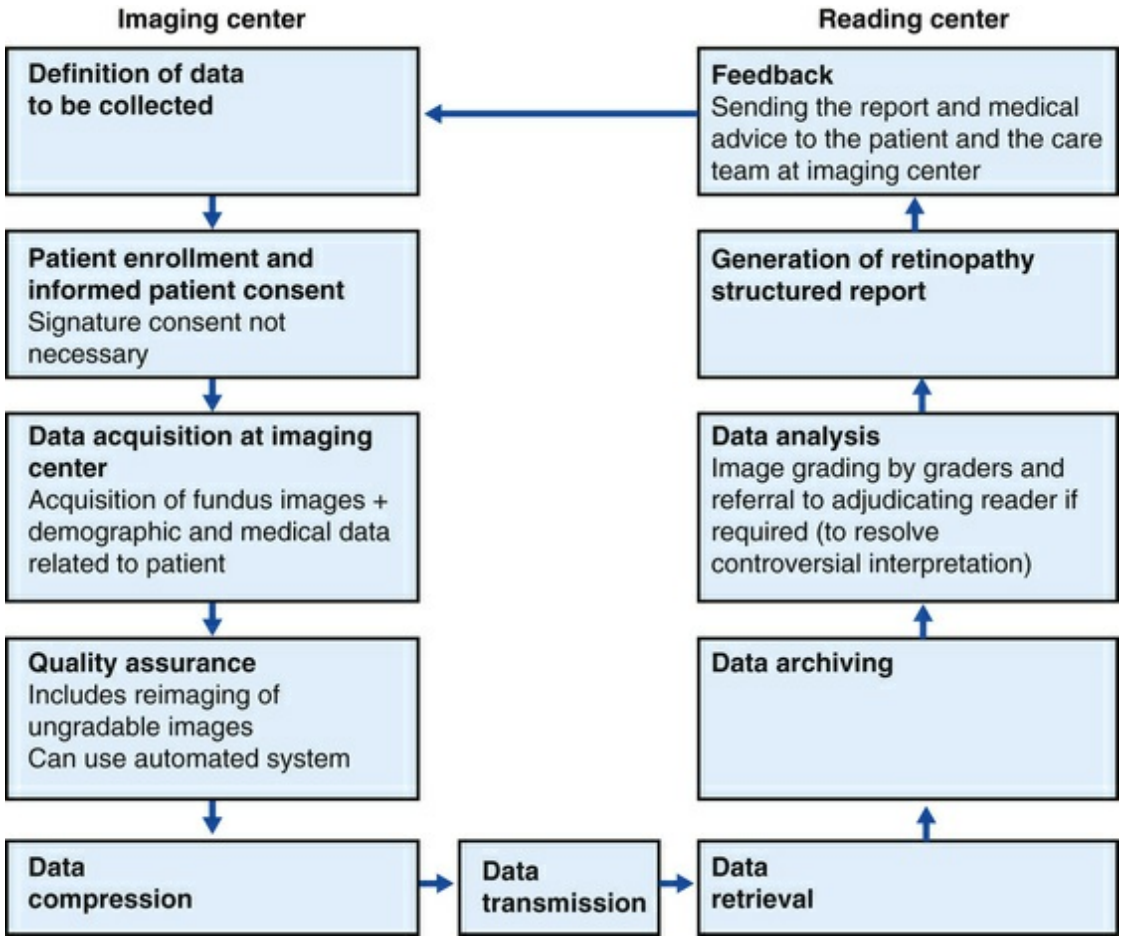

FIG. 53.1 Flowchart representing the steps of telescreening. This figure shows the sequential steps of telescreening carried out at the imaging center and the reading center.

Technical Considerations

Image Acquisition

The gold standard for telescreening is the ETDRS 7 mydriatic standard field 35 mm stereoscopic color fundus photographs.[11] However, more practical alternatives, such as digital fundus photography[12,13] and nonmydriatic fundus photography,[14,15] have been evaluated. Digital imaging has the advantage of faster and easier acquisition, transmission, and storage. Several investigators have reported a high level of correlation between stereoscopic digital imaging and slide film for the identification of most features of diabetic retinopathy.[12,13]

Regarding nonmydriatic fundus photography, a higher rate of unreadable photographs has been reported through undilated versus dilated pupils.[14,15] Diabetic persons often have smaller pupils and a greater incidence of cataracts, which may limit image quality if the procedure is performed through an undilated pupil. Pupil dilation using 0.5% tropicamide is associated with a minimal risk of angle closure glaucoma. Programs using pupil dilation should have a defined protocol to recognize and address this potential complication.

The unsatisfactory performance of nonmydriatic photography has led to the concept of "targeted mydriasis," offering mydriasis only to a preselected group of patients, in whom undilated photography is known to produce dismal results.[15] However, the exact "target" remains to be defined. Based on ROC curve analysis, Raman et al.[16] predetermined the cutoff values for "target mydriasis" groups as vision <6/12 (20/40 Snellen equivalent) and age >59 years. Staged mydriasis is another option.[17] In this model, a nonmydriatic single digital photograph for screening is taken. If an unsatisfactory nonmydriatic photograph is obtained, the patient undergoes immediate pupillary dilation with 1% tropicamide and

the photograph is then repeated. Using this protocol, 75–80% of patients do not require mydriasis.

According to ATA recommendations, image acquisition personnel ("imagers") should possess the knowledge and skills for independent imaging or with assistance and consultation by telephone, since a licensed eye care professional may not be physically available at all times during a telehealth session.

After acquisition, the transfer of the images can be "real-time" or by a "store-and-forward" technique. In real-time transfer, the captured images and associated data are immediately ("simultaneously") seen by the remote ophthalmologist. In a store-and-forward technique, captured images and data are compressed, stored, and then forwarded for retrieval by a remote ophthalmologist later.

Silva and colleagues[18] evaluated real-time ultrawide-field (UWF) image evaluation of DR in a Diabetes Telemedicine programme and found that point-of-care evaluation of UWF images by nonphysician imagers had good sensitivity and specificity for identification of DR and referable DR. Only 0.1% of referable DR cases were missed; but it reduced the load of the reading center by 60%.

Compression

Data and image compression facilitates transmission and storage of retinal images. The time needed for transmission can also be dramatically reduced by image compression.

Compression may be used if algorithms have undergone clinical validation. Image data can be compressed using a variety of standards, including JPEG, JPEG Lossless, JPEG 2000, and Run-length encoding (RLE). The International Standards Organization (ISO/IEC JTC1/SC2/WG10) has prepared an International Standard, ISO/IS-15444–1 (JPEG 2000 Part 1), for the digital compression and coding of continuous-tone still images. This standard is known as the JPEG 2000 Standard. Digital Imaging and Communication in Medicine (DICOM) recognizes JPEG and JPEG 2000 for lossy compression of medical images.[19] ATA recommends that the compression types and ratios should be periodically reviewed to

ensure appropriate clinical image quality and diagnostic accuracy. Some studies have attempted to look at the effect of various levels of compression on the quality of the image with both subjective and objective parameters.[20,21] The level of acceptable compression ranges from 1 : 28 to 1 : 52.[20,21]

Data Transfer, Archiving, and Retrieval

The described telemedicine models reported earlier used the Internet to transmit images.[22,23] In rural areas and mobile clinics, satellite transmission is a more preferred option because of poor infrastructure. A variety of technologies are available for data communication and transfer. Telescreening programs should determine specifications for transmission technologies best suited to their needs.

The images and reports are transmitted digitally via electronic picture archiving and communication systems (PACS); this eliminates the need for manual file transfer or retrieval. A PACS consists of four major components: the imaging instrumentation, a secured network for the transmission of patient information, workstations for interpreting and reviewing images, and archives for the storage and retrieval of images and reports. The universal format for PACS image storage and transfer is DICOM. To minimize errors, data communications should be compliant with DICOM standards.

Telescreening systems should provide storage capacities in compliance with facility, state, and federal medical record retention regulations. Digital images obtained by telescreening are typically stored locally on a PACS for rapid retrieval. Past images and reports should also be available for retrieval. It is important and is required in the United States by the Security Rule's Administrative Safeguards section of the Health Insurance Portability and Accountability Act (HIPAA) that facilities have a means of recovering images in the event of an error or disaster.

Security and Documentation

Transmission of retinal imaging studies and study results should conform to HIPAA privacy and security requirements. Ocular

telehealth systems should have defined network and software security protocols so as to protect patient confidentiality and identification of image data. Protective measures should be taken to safeguard data integrity against intentional or unintentional data corruption. If using the Internet, the Security Rule's Technical Safeguards section of HIPAA requires that the images be encrypted during transmission. Privacy should be ensured through a minimum 128-bit encryption and two-factor authentication technology.

The ATA recommends that reports should be based on Health Level 7 (HL7) and DICOM standards software forms and should meet interoperability standards. Medical nomenclature should conform to Systematized Nomenclature of Medicine Clinical Terms (SNOMED CT®) standards.

Operational Considerations

Detection of Diabetic Retinopathy and Macular Edema

As per ATA recommendation, both the ETDRS and International Clinical Diabetic Retinopathy Disease Severity Scales may be used for classifying diabetic retinopathy and macular edema. Nonstereo imaging methods can detect diabetic retinopathy quite well, but diabetic macular thickening cannot be detected as reliably. Hence, all nonstereo imaging methods need additional information about retinal thickness for an accurate assessment of macular edema.

Role of the Reading Center to Grade Retinal Images

Pathways of Grading

At the reading center, the grader examines the retinal images for evidence of diabetic change in the eye and assesses those images for disease against the minimum dataset. There are two possible routes for a grading pathway.

Pathway 1: Disease/No Disease Grading.

This involves three stages of grading prior to any referral to an arbitration-level grader:

Stage 1: The grader assesses patient image sets to classify into disease and no disease without grading the level of disease. Urgent referrals should be passed for immediate assessment by an ophthalmologist.

Stage 2: A random 10% of the patient's no disease image sets, together with all the disease image sets are reviewed for an initial full disease grade by a different grader accredited to carry out that level of grading. That second grader should not see the result of the first grader prior to grading.

Stage 3: This is carried out in all cases where an initial full disease grade indicates evidence of diabetic retinopathy in the eye. All referable image sets are reassessed by a different grader who carries out a second full disease grade on these images masked to the initial grading.

Pathway 2: Full Disease Grading.

This involves two stages of grading prior to any referral to an arbitration grader:

Stage 1: A grader carries out a full disease grade on all image sets. Urgent referrals should be passed to the grading center for immediate assessment by an ophthalmologist.

Stage 2: A different masked grader will assess a random 10% of the images where no diabetic retinopathy is evident and carry out a second full grade on all the disease image sets from the stage 1 grade.

Arbitration Grade

An arbitration grading procedure is carried out in both the pathways, if there is a difference of opinion between the first full disease grader and the second full disease grader on the level of

disease or whether or not there should be a referral. Usually this will be done by an ophthalmologist or an experienced screener, accredited for this level of work. Most grading centers find it helpful if arbitration grading is carried out on all referable retinopathy diagnoses in advance of a referral to an ophthalmologist for treatment in order to reduce the burden of avoidable referrals to eye clinics.

To make best use of limited resources, it has been proposed that the assessment of image quality and the presence or absence of any diabetic retinopathy could be performed by relatively inexperienced "disease/no disease" graders after a short period of training. Experienced "full disease" graders would then identify patients, deemed to have retinopathy, for referral to an ophthalmologist.[24]

Reading Personnel

The gold standard of image reading by ophthalmologists is impractical in rural areas. Ruamviboonsuk et al.[25] evaluated the interobserver differences among the nonphysician personnel (local ophthalmic photographers and certified ophthalmic nurses, who attended an intensive instruction course for this screening program) and ophthalmologists (retina specialists and general ophthalmologists without additional training), in the interpretation of single-field digital fundus images for diabetic retinopathy screening. Retinal specialists had the best agreement among the groups. Photographers were more reliable than the nurses. The authors concluded that the retina specialists should be effective interpreters without additional training, general ophthalmologists may need more training, but nonphysician personnel must have comprehensive training.

Recently, the concept of crowdsourcing has been explored in DR grading. Crowdsourcing is an online, distributed problem-solving and production model that leverages the collective intelligence of online communities to serve a specific goal. Brady et al.[26] explored whether a crowdsourcing interface could be used to train workers to classify fundus photos as normal or abnormal and subsequently perform grading of DR. They compared the performance of the trainees to expert graders. They observed that with minimum

training, the previously untrained workforce recruited through a public crowdsourcing platform could rapidly and correctly classify images as normal or abnormal with good accuracy. Crowdsourcing may prove to be potential solution to having adequate and available graders for community screening.

Handling of Ungradable Images

ATA guidelines recommend that the inability to obtain or read images should be considered a positive finding and patients with unobtainable or unreadable images should be promptly reimaged or referred for evaluation by an eye care specialist. Authors from the Joslin Vision Network (JVN) reported that of those images that were judged ungradable, a large proportion had pathology that required referral for comprehensive examination.[27] In the Gloucestershire Study, 3.7% of patients had unassessable images (including those with cataract), of whom 10.3% had referable retinopathy.[14]

The United Kingdom National Screening Committee (UKNSC) recommends that arrangements should be made for patients with ungradable images to be examined either by an ophthalmologist or by a trained and accredited person supervised by an ophthalmologist (as in the Scottish scheme). It may still not be possible to assess a very small number of patients due to a range of disabilities (for example, it may not be possible for a patient to hold still in one position either for assessment or for treatment). It should be noted that some patients with ungradable images may be unsuitable for treatment due to a condition that is not going to be improved with treatment in either eye. Clearly great care must be taken before such a decision is made.

While nonmydriatic photography screening is being successfully used, several factors have been reported to result in ungradable images in nonmydriatic retinal photography. Increasing age is an important factor.[28] Media opacity such as cataract and small pupil are other major factors. Scanlon et al.[28] suggested that a 20% failure rate for nonmydriatic photography might be acceptable. They also supported the use of nonmydriatic photography for the group of individuals <50 years of age who are at the lowest risk of ungradable images, if the screening programs are directed towards

the detection of sight-threatening diabetic retinopathy.

Quality Assurance

In 2000, the UKNSC stressed the integration of quality assurance as a core feature of telescreening programs for diabetic retinopathy and proposed the criteria and minimal/achievable standards for each quality assurance objective.[29] Since then, other ongoing quality assurance programs have published their methods and outcomes.[30,31] Different screening programs have different criteria for image regrading, resulting in different numbers of retinal photographs that need to be regraded for quality assurance (6–46%).[32]

There are two categories of quality assurance:[33]

(a) Internal quality assurance that is integrated as part of the day-to-day workflow in a screening program measured against national standards.

(b) External quality assurance which has three main functions: the monitoring of ongoing program performance against the quality standards, the organization of peer-review visits, and the administration of an external proficiency testing system for all graders.

There is international consensus that screening programs for diabetic retinopathy should achieve at least 80% sensitivity, 95% specificity, and <5% technical failure rates.[34] The quality assurance group of the National Screening Committee has recommended that quality assurance should involve the second examination of all images initially reported to have any diabetic retinopathy, together with 10% of the negative images, independently as part of the internal quality assurance system.[35]

The ATA and UKNSC have established the national standards for quality assurance for a diabetic retinopathy screening program. ATA has specified major categories of performance to be evaluated, as applicable to the program, at the level of the originating site and at the reading center. The UKNSC has provided 19 standards or parameters for quality assurance. Several authors have suggested further measures. Leese et al.[32] recommended the use of automated

grading systems running in parallel with manual grading; and concentrating quality assurance in the smaller number of patients with high-risk nonproliferative disease.

Evaluating Telescreening Programs

Efficacy

Telescreening has been shown to detect diabetic retinopathy and macular edema with a reasonably high sensitivity and specificity.[9,36] Whited et al.[36] reviewed the available literature and noted that the sensitivity and specificity values ranged from 50% to 93% for detection of diabetic retinopathy. Similar high efficacy was reported on comparing teleophthalmology for macular edema detection to both gold standards, i.e., slit-lamp biomicroscopy and stereoscopic photography.[36]

Lili Shi et al.[37] recently reported, in a meta-analysis of 20 studies involving 1960 participants, the accuracy of telescreening. Pooled sensitivity was >80% to detect no DR and PDR, >70% to detect mild and moderate NPDR and macular edema and 53% for detecting severe NPDR. Pooled specificity was >90% except in detecting mild NPDR which was 89%. Accuracy was higher in digital images obtained through mydriasis than nonmydriasitic and was highest for wide-angle (100–200°) images, especially for detection of No DR and mild DR.

Patient Satisfaction

Since telescreening involves remote care without evaluation by the doctor in person, there are concerns regarding lack of satisfaction among patients. Studies have shown, however, that telescreening has equal, if not better, satisfaction than in-person evaluation by a doctor.[38,39] Paul et al. assessed patient satisfaction levels and factors influencing satisfaction during teleophthalmology consultation in India using a patient satisfaction questionnaire. He found that 37.34% of the patients felt that telescreening is more satisfying than an in-person evaluation, and 60% felt that both models are equally satisfying. It was also noted that patients who asked questions

during the screening were 2.18 times more likely to be satisfied with teleophthalmology than those who did not. Mansberger et al.[40] showed that a telemedicine program using a nonmydriatic camera increased participation for diabetic retinopathy screening. Telemedicine could be used to triage patients with diabetes for further evaluation with an eye care provider, especially in minority and low-access settings.

Cost-Effectiveness

Bjorvig et al.,[41] in an economic analysis, concluded that telemedicine was a less costly option for screening in places with higher patient workloads. Telemedicine was also proven to be cost-effective in the prison populations by Aoki et al.,[42] where it may have special utility due to costs and safety issues associated with transporting prisoners.

Gomez-Ulla et al.[6] did a comparative cost analysis of diabetic retinopathy telescreening versus standard ophthalmoscopy, from both Public Healthcare System (PHS) and patient perspectives. The authors concluded that from the PHS perspective, direct fundus examination is less costly than telescreening owing to the higher capital costs required for the purchase of digital imaging equipment. From a global perspective, however, the digital imaging alternative is more convenient because the travel cost and loss of income for the patient are lower.

Jones et al.[7] reviewed the evidence available on cost-effectiveness. They concluded that telemedicine is cost-effective for retinopathy screening in remote and rural communities and other groups with travel difficulties and the cost-effectiveness increases with an increase in patient workload. Rachanapalle and colleagues[43] evaluated the cost-utility of telescreening for DR in India and found that by using the WHO threshold of cost-effectiveness, the rural teleophthalmology was cost effective ($1320 per QALY) compared to no screening from a health provider perspective. The study found that screening once in two years was more cost-effective in these rural settings.

Advances in Telescreening

Recent advances resulting in better and faster telecommunication, miniaturization of diagnostic equipment including digital cameras, and automation of retinal image analysis, offer excellent opportunities to expand telescreening services in more remote areas.

Smartphones for Diabetic Retinopathy Screening

The latest generations of smartphones feature faster processors, enhanced memory, smaller batteries, and efficient operating systems that are capable of advanced functions, and have paved the way for numerous applications (apps) that are affecting our personal and work environments. The newer generation of portable eye cameras can be configured with smartphone-based attachments and integrated lens adapters.[44–47] They use the smartphone-inbuilt camera for image acquisition, and some later versions have also attempted to utilize apps designed for screening of preliminary abnormalities based on artificial intelligence-driven algorithms. These camera systems and apps offer the prospect of a low-cost retinal screening solution for diabetic retinopathy.

The Welch Allyn iExaminer is a type of adapter that turns the PanOptic Ophthalmoscope into a mobile digital imaging device. It aligns the optical access of the PanOptic Ophthalmoscope to the visual axis of the iPhone 4 or 4S (Apple, Cupertino, CA) camera to capture high resolution (5/8 megapixel; depending upon the iPhone model) pictures of the posterior pole including the macula and optic nerve. Another mobile phone-based retinal camera is the Ocular CellScope.[45] It is comprised of a mobile phone, a housing that contains the illumination and collection optics, and an integrated phone holder that ensures alignment of the illuminating and collecting optics with the phone's camera. It uses a single 54D ophthalmic lens for focusing and capturing reflected light, in turn utilizing the autofocus mechanism of the iPhone's camera to correct for variability in axial length and refractive error in the subject's eye.

Portable eye examination kit (PEEK) is a mobile app and clip-on hardware that can be used for imaging the retina. This system stores GPS data for each patient screened for later reference. The device uses a 20 D or 28 D lens in front of the phone's camera and utilizes the phone's inbuilt flash system as a powerful light source.

Recently, Ryan et al.[47] described the results of comparison of smartphone-based, nonmydriatic and mydriatic photography in DR (CAMARA study). They used a 20 D lens-assisted smartphone photography system and concluded that smartphone and nonmydriatic photography were able to detect DR and sight-threatening DR. However, the nonmydriatic camera was more sensitive at detecting DR than the smart phone.

Automated Retinal Image Analysis

The shortage of manpower imposes a limitation on the screening capability of telehealth programs serving a steadily growing diabetic population. Therefore, an automated image analysis system able to detect diabetic retinopathy is a vital necessity, especially in the coming years.

Over the past decade several attempts have been made to either semiautomate or fully automate retinal image analysis. Tools have been developed for analyzing and enhancing the image quality (correction of illumination, increasing image contrast, histogram equalization, vessel segmentation, edge sharpening, and image deconvolution), and for providing automated identification of pathologic retinal lesions (neural networks, region growing, morphologic analysis, and classification algorithms).[48] Automated identification of retinal lesions can identify the absence or presence of diabetic retinopathy based on the detection of microaneurysms and dot hemorrhages (dark lesions),[49] or can detect referable retinopathy based on the detection of exudates (bright lesions) and blot hemorrhages (dark lesions).[50]

Winder et al.[48] conducted a structured survey of algorithms for the automatic detection of retinopathy in digital color retinal images. The authors pointed out the need for clear guidelines and goals in image processing research in order to avoid producing results that are difficult to compare in terms of the success of the

algorithms or techniques.

Image reading algorithms must be tested against images that are acquired in actual screening settings, since lower image quality can greatly diminish their performance. Validation against the standard retinal image databases, such as STARE, DRIVE, or MESSIDOR, show sensitivity and specificity above 90% for most algorithms;[51] however, they may not reflect performance in "real-world" settings. Image quality in actual screening settings is often less than optimal due to many factors such as variability of photographer quality, patient cooperation, and media opacity and small pupils, which are frequent with diabetes and advanced age. Future validation studies in actual screening settings are needed.

Conclusion

Telescreening has the enormous potential to offer remote care to patients with diabetes without compromising the quality of care. However, to maximize the chance for success, it is essential that all telescreening programs should define clear goals, establish appropriate quality control measures, and adhere to regulatory and statutory requirements. Prospective studies demonstrating a reduction in vision loss from diabetic retinopathy as a result of telescreening programs will be of critical importance, before telescreening strategies can be adopted as the standard for routine clinical management of patients with diabetes.

References

1. Wilson JMG, Jungner G. Principles and practice of screening for disease. *WHO Chron*. 1968;22:473.
2. American Diabetes Association. Standards of medical care in diabetes – 2008. *Diabetes Care*. 2008;31(Suppl. 1):S12–54.
3. The DCCT Research Group. The effect of intensive diabetes treatment on the progression of diabetic retinopathy in insulin-dependent diabetes mellitus. *Arch Ophthalmol*. 1995;113:36–51.
4. UK Prospective Diabetes Study (UKPDS) Group. Intensive blood-glucose control with sulphonylureas or insulin

compared with conventional treatment and risk of complications in patients with type 2 diabetes (UKPDS 33). *Lancet*. 1998;352:837–853.
5. Early Treatment Diabetic Retinopathy Study Research Group. Early photocoagulation treatment for diabetic retinopathy, ETDRS report number 9. *Ophthalmology*. 1991;98:766–785.
6. Gomez-Ulla F, Alonso F, Aibar B, et al. A comparative cost analysis of digital fundus imaging and direct fundus examination for assessment of diabetic retinopathy. *Telemed J E Health*. 2008;14:912–918.
7. Jones S, Edwards RT. Diabetic retinopathy screening: a systematic review of the economic evidence. *Diabet Med*. 2010;27:249–256.
8. Hazin R, Barazi MK, Summerfield M. Challenges to establishing nationwide diabetic retinopathy screening programs. *Curr Opin Ophthalmol*. 2011;22:174–179.
9. Zimmer-Galler IE, Zeimer R. Telemedicine in diabetic retinopathy screening. *Ophthalmol Clin*. 2009;49:75–86 [(Spring)].
10. Cavallerano J, Lawrence MG, Zimmer-Galler I, et al. American Telemedicine Association, Ocular Telehealth Special Interest Group; National Institute of Standards and Technology Working Group. Telehealth practice recommendations for diabetic retinopathy. *Telemed J E Health*. 2004;10:469–482.
11. Early Treatment Diabetic Retinopathy Study Research Group. Grading diabetic retinopathy from stereoscopic color fundus photographs: an extension of the modified Airlie House classification. ETDRS report number 10. *Ophthalmology*. 1991;98:786–806.
12. Tennant MT, Greve MD, Rudnisky CJ, et al. Identification of diabetic retinopathy by stereoscopic digital imaging via teleophthalmology: a comparison to slide film. *Can J Ophthalmol*. 2001;36:187–196.
13. Liesenfeld B, Kohner E, Piehlmeier W, et al. A telemedical approach to the screening of diabetic retinopathy: digital fundus photography. *Diabetes Care*. 2000;23:345–348.

14. Scanlon PH, Malhotra R, Thomas G, et al. The effectiveness of screening for diabetic retinopathy by digital imaging photography and technician ophthalmoscopy. *Diabet Med*. 2003;20:467–474.
15. Murgatroyd H, Ellingford A, Cox A, et al. Effect of mydriasis and different field strategies on digital image screening of diabetic eye disease. *Br J Ophthalmol*. 2004;88:920–924.
16. Raman R, Rani PK, Mahajan S, et al. The tele-screening model for diabetic retinopathy: evaluating the influence of mydriasis on the gradability of a single-field 45 degrees digital fundus image. *Telemed J E Health*. 2007;13:597–602.
17. Murgatroyd H, Cox A, Ellingford A, et al. Can we predict which patients are at risk of having an ungradeable digital image for screening for diabetic retinopathy? *Eye (Lond)*. 2008;22:344–348.
18. Silva PS, Cavallerano JD, Tolls D, et al. Potential efficiency benefits of nonmydriatic ultrawide field retinal imaging in an ocular telehealth diabetic retinopathy program. *Diabetes Care*. 2014;37(1):50–55.
19. *Digital Imaging and Communications in Medicine (DICOM) Supplement 61:JPEG 2000 Transfer Syntaxes*. ftp://medical.nema.org/medical/dicom/final/sup61_ft.pdf.
20. Eikelboom RH, Yogesan K, Barry CJ, et al. Methods and limits of digital image compression of retinal images for telemedicine. *Invest Ophthalmol Vis Sci*. 2000;41:1916–1924.
21. Newsom RSB, Clover A, Costen MTJ, et al. Effect of digital image compression on screening for diabetic retinopathy. *Br J Ophthalmol*. 2001;85:799–802.
22. Luzio S, Hatcher S, Zahlmann G, et al. Feasibility of using the TOSCA telescreening procedures for diabetic retinopathy. *Diabet Med*. 2004;21:1121–1128.
23. Aiello LM, Bursell SE, Cavallerano J, et al. Joslin Vision Network Validation Study: pilot image stabilization phase. *J Am Optom Assoc*. 1998;69:699–710.
24. Harding S, Greenwood R, Aldington S, et al. Grading and disease management in national screening for diabetic retinopathy in England and Wales. *Diabet Med*. 2003;20:965–

971.
25. Ruamviboonsuk P, Teerasuwanajak K, Tiensuwan M, Thai Screening for Diabetic Retinopathy Study Group, et al. Interobserver agreement in the interpretation of single-field digital fundus images for diabetic retinopathy screening. *Ophthalmology*. 2006;113:826–832.
26. Brady CJ, Villanti AC, Pearson JL, et al. Rapid grading of fundus photographs for diabetic retinopathy using crowdsourcing. *J Med Internet Res*. 2014;16(10):e233.
27. Cavallerano AA, Cavallerano JD, Katalinic P, et al. Use of Joslin Vision Network digital-video nonmydriatic retinal imaging to assess diabetic retinopathy in a clinical program. *Retina*. 2003;23:215–223.
28. Scanlon PH, Foy C, Malhotra R, et al. The influence of age, duration of diabetes, cataract, and pupil size on image quality in digital photographic retinal screening. *Diabetes Care*. 2005;28:2448–2453.
29. Garvican L, Clowes J, Gillow T. Preservation of sight in diabetes: developing a national risk reduction programme. *Diabet Med*. 2000;17:627–634.
30. Arun CS, Young D, Batey D, et al. Establishing ongoing quality assurance in a retinal screening programme. *Diabet Med*. 2006;23:629–634.
31. Schneider S, Aldington SJ, Kohner EM, et al. Quality assurance for diabetic retinopathy telescreening. *Diabet Med*. 2005;22:794–802.
32. Leese GP, Ellis JD. Quality assurance for diabetic retinal screening. *Diabet Med*. 2007;24:579–581.
33. UK National Screening Committee [Internet]. *Gloucester, UK: NHS Diabetic Eye Screening Programme*. [January; cited 2012 4 Feb; Workbook 4.4. Essential elements in developing a diabetic retinopathy screening programme] http://diabeticeye.screening.nhs.uk/workbook; 2012.
34. Taylor R, Broadbent DM, Greenwood R, et al. Mobile retinal screening in Britain. *Diabet Med*. 1998;15:344–347.
35. Garvican L, Scanlon PH. A pilot quality assurance scheme for diabetic retinopathy risk reduction programmes. *Diabet Med*. 2004;21:1066–1074.

36. Whited JD. Accuracy and reliability of teleophthalmology for diagnosing diabetic retinopathy and macular edema: a review of the literature. *Diabetes Technol Ther*. 2006;8:102–111.
37. Shi L, Wu H, Dong J, Jiang K, Lu X, Shi J. Telemedicine for detecting diabetic retinopathy: a systematic review and meta-analysis. *Br J Ophthalmol*. 2015;99(6):823–831.
38. Luzio S, Hatcher S, Zahlmann G, et al. Feasibility of using the TOSCA telescreening procedures for diabetic retinopathy. *Diabet Med*. 2004;21:1121–1128.
39. Paul PG, Raman R, Rani PK, et al. Patient satisfaction levels during teleophthalmology consultation in rural South India. *Telemed J E Health*. 2006;12:571–578.
40. Mansberger SL, Gleitsmann K, Gardiner S, et al. Comparing the effectiveness of telemedicine and traditional surveillance in providing diabetic retinopathy screening examinations: a randomized controlled trial. *Telemed J E Health*. 2013;19(12):942–948.
41. Bjorvig S, Johansen MA, Fossen K. An economic analysis of screening for diabetic retinopathy. *J Telemed Telecare*. 2002;8:32–35.
42. Aoki N, Dunn K, Fukui T, et al. Costeffectiveness analysis of telemedicine to evaluate diabetic retinopathy in a prison population. *Diabetes Care*. 2004;27:1095–1101.
43. Rachapelle S, Legood R, Alavi Y, et al. The cost-utility of telemedicine to screen for diabetic retinopathy in India. *Ophthalmology*. 2013;120(3):566–573.
44. Haddock LJ, Kim DY, Mukai S. Simple, inexpensive technique for high-quality smartphone fundus photography in human and animal eyes. *J Ophthalmol*. 2013;2013:518479.
45. Maamari R, Keenan J, Fletcher D, et al. A mobile phone-based retinal camera for portable wide field imaging. *Br J Ophthalmol*. 2014;98:438–441.
46. Myung D, Jais A, He L, et al. 3D printed smartphone indirect lens adapter for rapid, high quality retinal imaging. *J MTM*. 2014;3:9–15.
47. Ryan ME, Rajalakshmi R, Prathiba V, et al. Comparison Among Methods of Retinopathy Assessment (CAMRA)

Study: smartphone, nonmydriatic, and mydriatic photography. *Ophthalmology*. 2015;122(10):2038–2043.
48. Winder RJ, Morrow PJ, McRitchie IN, et al. Algorithms for digital image processing in diabetic retinopathy. *Comput Med Imaging Graph*. 2009;33:608–622.
49. Philip S, Fleming AD, Goatman KA, et al. The efficacy of automated "disease/no disease" grading for diabetic retinopathy in a systematic screening programme. *Br J Ophthalmol*. 2007;91:1512–1517.
50. Fleming AD, Goatman KA, Philip S, et al. The role of haemorrhage and exudate detection in automated grading of diabetic retinopathy. *Br J Ophthalmol*. 2010;94:706–711.
51. Kauppi T, Kämäräinen JK, Lensu L, et al. Constructing benchmark databases and protocols for medical image analysis: diabetic retinopathy. *Comput Math Methods Med*. 2013;2013:368514.

54

Retinal Artery Occlusions

Purnima S. Patel, SriniVas R. Sadda

Central retinal artery occlusion was first described in 1859 in von Graefe's report of multiple systemic emboli in the setting of endocarditis causing obstruction of the central retinal artery.[1] Since

then significant literature has accumulated on retinal artery occlusions. Below, we use an arbitrary classification, including the new finding of paracentral acute middle maculopathy, to discuss these disorders in sequence:

- Central retinal artery occlusion (CRAO)
- Branch retinal artery occlusion (BRAO)
- Cilioretinal artery occlusion (CLRAO)
- Combined retinal artery and vein occlusion
- Cotton-wool spots
- Paracentral acute middle maculopathy (PAMM).

Central Retinal Artery Occlusion

Epidemiology

The true incidence of CRAO is unknown. The estimated incidence of CRAO is reported to be roughly 1 in 10 ,000 cases at tertiary referral centers,[2,3] being even lower for the general population, at approximately 8.5 cases per 100,000.[3] Similar to other vascular disorders, CRAOs are largely seen in older adults, but cases in children and young adults have been reported.[4,5] Average age at presentation is in the early sixties with greater than 90% presenting at over 40 years. Men are affected more frequently. No predilection for one eye over the other has been reported; however, 1–2% of cases may manifest bilateral involvement.[6]

Clinical Features

Typically, patients with acute CRAO present with sudden, monocular, painless, severe vision loss. In some cases, premonitory amaurosis fugax may be reported. Amaurosis fugax represents transient acute retinal ischemia and typically suggests an embolic source of occlusion. Presence of amaurosis fugax also has a higher correlation with stroke compared with retinal emboli alone.[7] The risk of CRAO after amaurosis fugax is estimated to be only 1% per year.[8] Although CRAO rarely presents simultaneously in both eyes, it may occur sequentially.[9]

Presenting visual acuity ranges from counting fingers to light perception in 74–90% of eyes.[6–10] Central visual acuity may be near normal in patients who have a transient CRAO or a cilioretinal artery perfusing the fovea. Connolly et al. reported a trend toward better visual acuities in patients with CRAO secondary to giant cell arteritis as compared with those due to other, largely embolic causes.[11] The presence of an embolus is usually associated with poorer vision. In Hayreh's prospective natural history study of 260 eyes with CRAO, eyes with counting fingers or worse visual acuity presenting within 7 days of onset had the best potential for improved vision.[10] The absence of light perception is rare. In such cases, concomitant choroidal circulation deficit (e.g., due to ophthalmic artery occlusion) or optic nerve involvement should be considered.[6] Visual acuity tends to improve only within the first week of onset with minimal chance for appreciable improvement subsequently.[11] Visual recovery has shown to correlate with presenting visual acuity and the duration of visual impairment.[12] Although visual acuity may spontaneously improve in up to 22% of patients with nonarteritic CRAO,[11] less than 10% of patients report a meaningful recovery.[13]

Typically an afferent pupillary defect develops within seconds following obstruction of the central retinal artery regardless of macular sparing.[4] Intraocular pressure is often normal at presentation but may become elevated in the setting of rubeosis iridis.

In a majority of cases of acute CRAO, the anterior-segment exam is normal initially. If rubeosis iridis is present acutely, presence of concomitant carotid artery obstruction should be considered. The incidence of rubeosis in CRAO is 16.6–18.8%.[14–16] As compared to central retinal vein occlusions (CRVO), iris rubeosis tends to occur earlier after CRAO – at a mean of 4–5 weeks after onset compared to 5 months after onset in CRVO. Not surprisingly, rubeosis is more common in more severe and complete obstructions with extensive nonperfusion. The risk of developing iris neovascularization is greater for obstructions lasting more than 1 week versus those lasting only a few days after onset.[14–16] With carotid obstruction, rubeosis iridis can cause elevated intraocular pressure above perfusion pressure in the central retinal artery leading to an

obstruction via this mechanism. Laser panretinal photocoagulation induces successful regression in approximately 65% of cases.[17]

In his 1891 report, Nettleship described in detail the ophthalmoscopic appearance of CRAO. "The classic dense, white haze of the central region in the retina with a well-marked clear patch at the yellow-spot was very well shown; there were no hemorrhages; the arteries and veins were of about normal size, but no pulsation could be produced in any of them by pressure with the finger upon the globe."[18] Hayreh investigated fundus changes in CRAOs in a large retrospective review in 2007 of 248 eyes of 240 patients. In the acute phase, his group noted a cherry-red spot (90%), posterior pole retinal opacity or whitening (58%), box-carring of retinal arteries and veins (19% and 20% respectively), retinal arterial attenuation (32%), optic disc edema (22%), and optic nerve pallor (39%). The retinal findings were predominantly located in the posterior pole with a normal-appearing periphery.[19]

Typically, retinal whitening in the posterior pole and a cherry-red spot are the earliest characteristic changes in CRAO. Retinal whitening corresponds to ischemic damage to the inner half of the retina with opacification of the retinal nerve fiber and ganglion cell layers from cessation of axoplasmic transport. The opacification is visible ophthalmoscopically where the ganglion cell layer is more than one cell thick, i.e., the macula, except in the foveal region, where a cherry-red spot is seen (Fig. 54.1). The outer nuclear and plexiform layers and photoreceptors remain intact, as demonstrated in histologic studies (Fig. 54.2).[20,21] The size of the cherry-red spot varies depending on width of the foveola. The cherry-red spot is actually normal-appearing retina being observed in high contrast against the surrounding opacified retina. The thin retina in this location is nourished by the underlying choroidal circulation and as a result does not become hypoxic or opacified, permitting visualization of the normal underlying retinal pigment epithelium (RPE) and choroid.[22] Similarly, the retinal periphery in CRAO appears normal because the retina is also thinner with a single layer of ganglion cells, such that the nutrition of the inner retinal layers can be maintained by the choroidal circulation alone. The probability of a cherry-red spot still being present decreases with increasing duration from the onset of CRAO: 88% after 1 week, 59%

after 2 weeks, 47% after 3 weeks, and 19% after 4 weeks after onset. Typically, the retinal opacification resolves over 4–6 weeks, although at least some retinal whitening is noted in 17% of patients with complete, nontransient CRAO after 1 month.[19] Pathologically, this evolution corresponds to a resolution of initial acute ischemia-induced intracellular edema with subsequent loss of neuronal cells and the development of an acellular scar of the inner retinal cell layers (Fig. 54.2).[23]

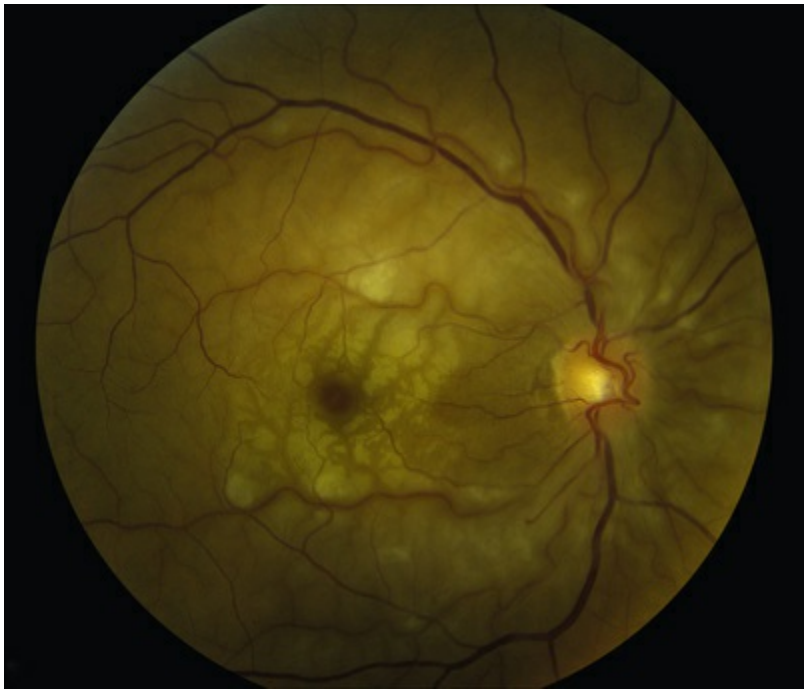

FIG. 54.1 Acute central retinal artery obstruction. Color fundus photo demonstrating superficial retinal whitening or opacification in the posterior pole with evidence of a central cherry-red spot. The opacification is most prominent in the perifoveal area. (Courtesy of Dr. Steven Yeh, Emory Eye Center, Atlanta.)

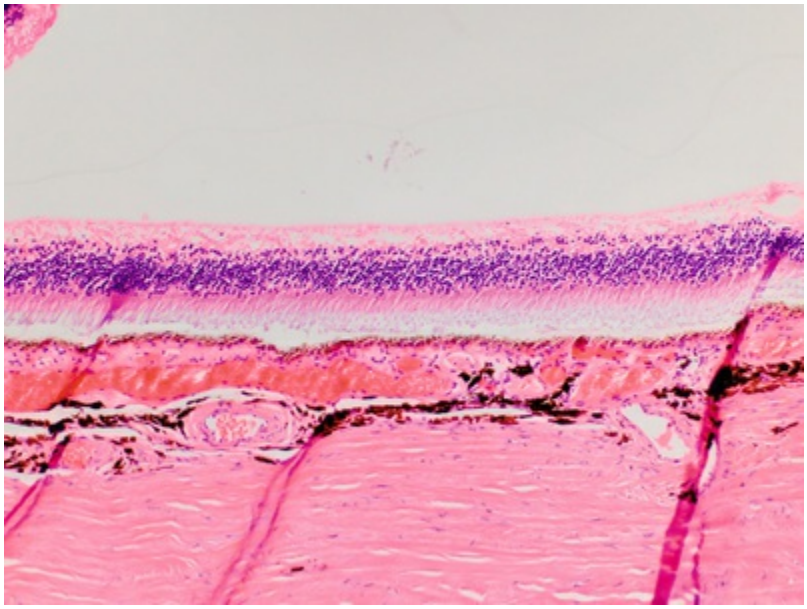

FIG. 54.2 Histopathologic findings in central retinal artery obstruction. In the chronic stage of the disease, the inner retinal layers show significant atrophy (hematoxylin and eosin, ×25). (Courtesy of Dr.Hans Grossniklaus, Emory Eye Center, Atlanta.)

A patent cilioretinal artery supplying some or all of the papillomacular bundle is seen in approximately one-third of cases. Retinal whitening will be clearly demarcated around the area of preserved macula perfused by the cilioretinal circulation (Fig. 54.3A). In these cases, the visual acuity will be dictated by the location and extent of the papillomacular bundle perfused.[10,24–26] Sparing of the fovea may be associated with excellent visual acuity, albeit with a significant visual field deficit corresponding to the topography of the occlusion.

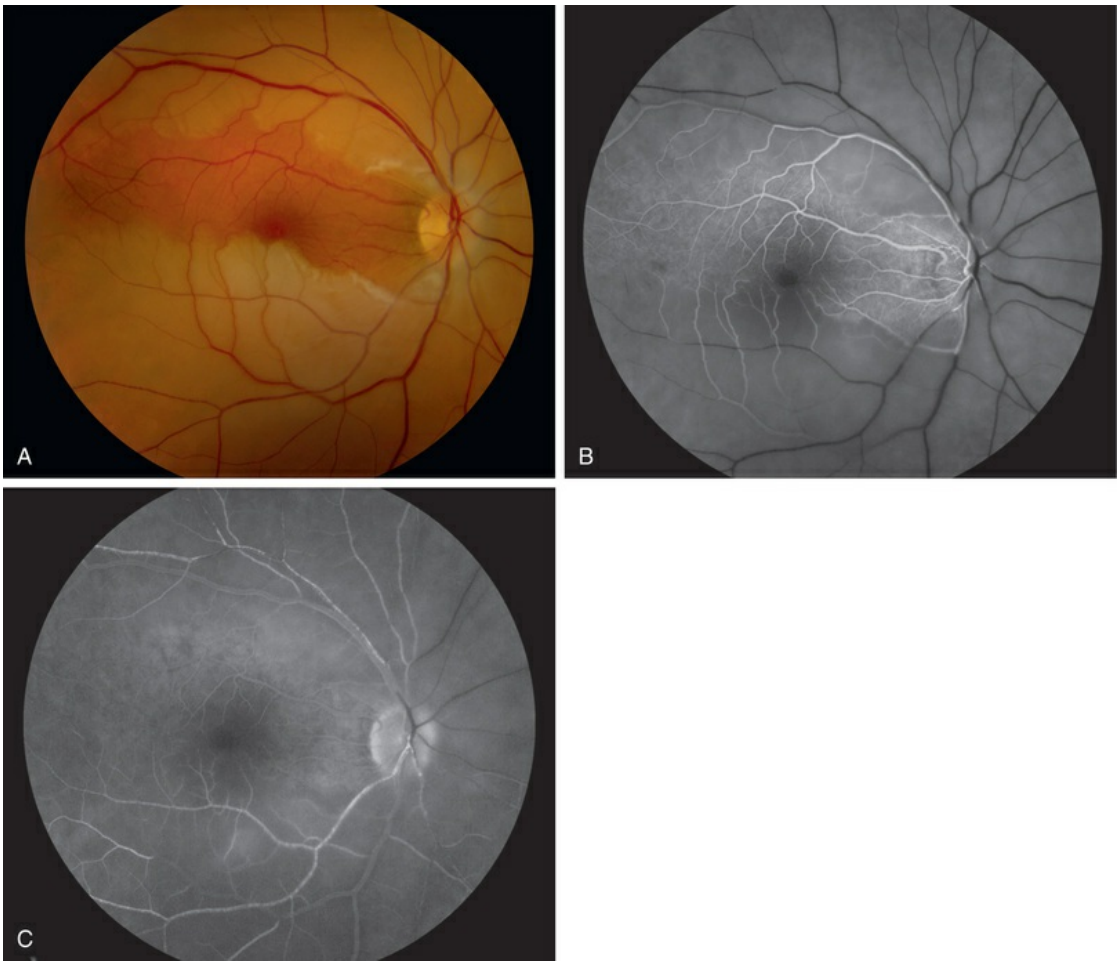

FIG. 54.3 Acute central retinal artery occlusion with cilioretinal artery sparing. (A) Retinal opacification is clearly demarcated around the preserved macula perfused by the patent cilioretinal artery. The perfused area includes the fovea; therefore the patient's presenting visual acuity was good. (B) At 25 seconds the cilioretinal artery is perfused with retrograde flow into the retinal veins. (C) At 9 minutes the arterial circulation is still not completely filled, demonstrating a severely delayed arteriovenous transit time (Courtesy of Dr. John Payne, Emory Eye Center, Atlanta.)

The appearance of the retinal vasculature can be quite variable soon after the onset of CRAO; therefore, the presence of a normal-appearing vasculature should not exclude the diagnosis. In Nettleship's 19th-century description of CRAO, he noted the appearance of the retinal vasculature to have a stagnated arterial blood column without attenuation.[19] In Hayreh's natural history study,[19] only 15% of acute CRAO had normal-appearing retinal arteries. Box-carring or segmentation of the blood column of both

the arteries and veins can occur secondary to separation of blood serum from erythrocytes in a rouleaux formation.

Retinal emboli are visible in 20–40% of eyes with CRAO.[4,27] Retinal emboli are the most common cause of nonarteritic CRAO and BRAO.[28] The most common variant is a yellow, refractile cholesterol embolus (Hollenhorst plaque) (Fig. 54.4). According to a study by Arruga and Sanders, retinal emboli consist of cholesterol in 74% of cases, calcified material in 15.5%, and platelet and fibrin in 15.5%.[29] These cholesterol emboli typically originate from the carotid arteries in the setting of atherosclerotic disease, but can also arise from the aortic arch, ophthalmic artery, or proximal central retinal artery. Cholesterol emboli are often small, do not completely obstruct retinal arterial blood flow, and are frequently found at bifurcation sites (Fig. 54.4). Emboli can often be asymptomatic. Migration with disappearance of retinal emboli is common.[19] Calcific emboli are less common than cholesterol emboli but are typically larger and cause more severe or complete obstruction. They most commonly originate from the cardiac valves.[22,30]

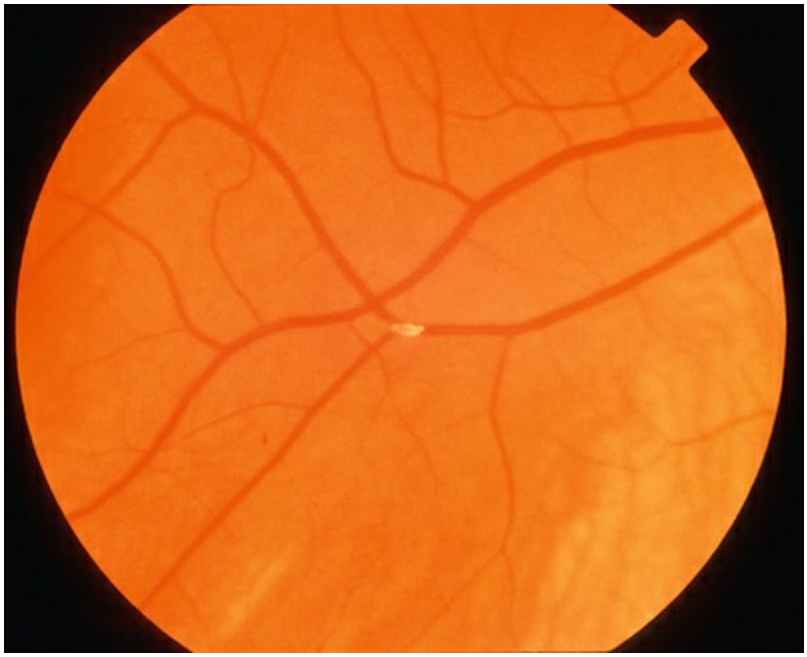

FIG. 54.4 Cholesterol embolus at an arterial bifurcation along the superotemporal arcade.

The optic nerve is acutely edematous in nearly all cases of arteritic CRAO as a result of associated anterior ischemic optic

neuropathy. In the acute phase of nonarteritic CRAO, the disc may be normal, hyperemic, edematous, and, rarely, pale. Acute-phase optic nerve pallor is due to ischemic opacification of the surface nerve fiber layer since this layer is supplied by retinal circulation.[31] Neovascularization of the disc in acute CRAO is rare but has been reported, typically in association with a chronically hypoxic retina (e.g., concomitant diabetic retinopathy, ischemic CRVO, or ocular ischemia).[18,19]

The most frequent findings in the chronic stage of eyes with CRAO are optic atrophy (91%), retinal arterial attenuation (58%), cilioretinal collaterals (18%), macular RPE changes (11%), and cotton-wool spots (3%) (Fig. 54.5). Chronic-phase optic nerve pallor is due to optic atrophy and nerve fiber loss (see Figs. 54.2 and 54.10). In arteritic CRAO, the associated anterior ischemic optic neuropathy also contributes to the development of pallor.[19] In chronic CRAO, neovascularization of the optic disc rarely occurs, presumably because nonviable tissue is less likely to elaborate angiogenic factors compared with chronically ischemic but viable retinal tissue seen in cases of diabetic retinopathy or retinal vein occlusion.[32] Incidence of neovascularization of the disc in one retrospective study was only 1.8%.[33] Concomitant rubeosis iridis may also occur in the setting of chronic CRAO. Retinal arterial attenuation is more common in the chronic phase than in the acute phase.[19] Months after an acute CRAO, cilioretinal collaterals may develop as a result of a compensatory enlargement of capillary anastomoses between retinal capillaries on the surface of the disc and ciliary capillaries deeper in the optic nerve head. The probability of developing cilioretinal disc collaterals was 4% at 1 month and 18% at 3 months from onset of CRAO in one study.[20] Macular RPE changes are seen with CRAO but are much less common than in ophthalmic artery obstruction, where the choroidal circulation is also involved.

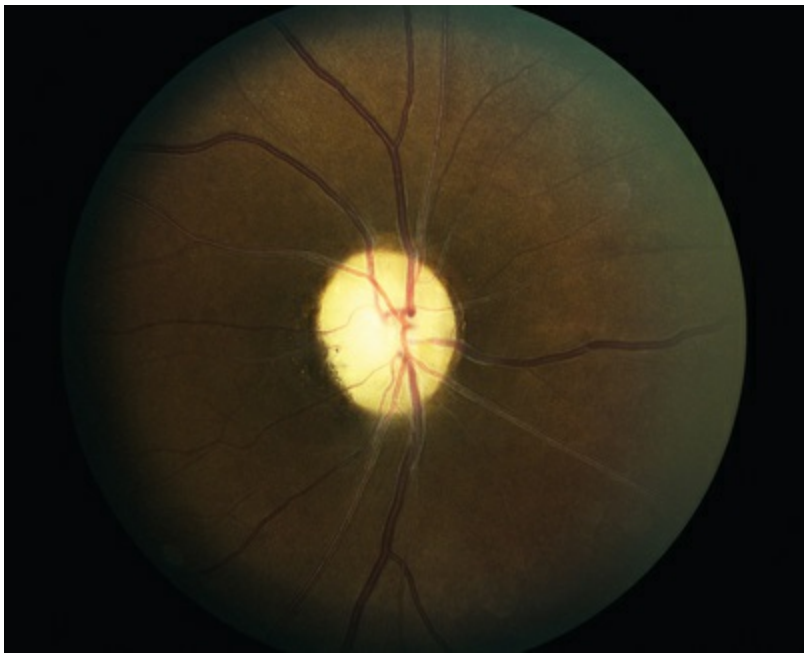

FIG. 54.5 Chronic central retinal artery occlusion. Optic nerve pallor from atrophy and severe arterial attenuation is seen in this patient with a remote central artery occlusion.

Ancillary Studies

Initially, fluorescein angiography in CRAO almost always shows some variable residual retinal circulation with delayed and sluggish filling of the retinal vasculature. Complete absence of retinal filling is rare. Appearance of dye in the central retinal artery is typically delayed by 5–20 seconds. However, the delay in retinal arterial branches is even more substantial. The fluorescein dye lines the arterial walls in a pattern similar to the laminar flow filling of normal retinal veins. In cases with visible intraarterial emboli, the arteriovenous transit time can be even further delayed (Figs. 54.3B–C).[34] The severity of obstruction and retinal ischemia correlates with less favorable initial visual acuities. Staining of the optic disc can be variable; however, staining of the retinal vessels is rare. Typically, the retinal circulation is reestablished after an acute CRAO, but the inner retinal tissue has generally already infarcted by then. Therefore, although the fluorescein angiogram may return to relatively normal appearance, the vision loss, optic nerve atrophy, and arterial narrowing persist.[22] For patients with a normalized

fluorescein angiogram who do not go on to develop optic atrophy, the diagnosis of a true CRAO should be called into question, though it is possible that some individuals may have reperfusion before the irreversible damage has occurred.

In the acute stage, optical coherence tomography (OCT) shows increased reflectivity of the inner retina. This corresponds to intracellular edema and explains the lack of intraretinal, hyporeflective fluid spaces in cases of CRAO or BRAO. The reflectivity of the outer retinal layers and RPE is blocked by the highly reflective inner retinal layer. No retinal thickening secondary to the accumulation of serous fluid escaping from retinal capillaries into the extracellular space is seen (Fig. 54.6). OCT images of chronic CRAO show thinning and atrophy of the inner retina. OCT can be helpful in cases of chronic CRAO where the fundus appears featureless but the OCT shows inner retinal atrophy (not just nerve fiber layer atrophy) with preservation of the outer retina.[35,36]

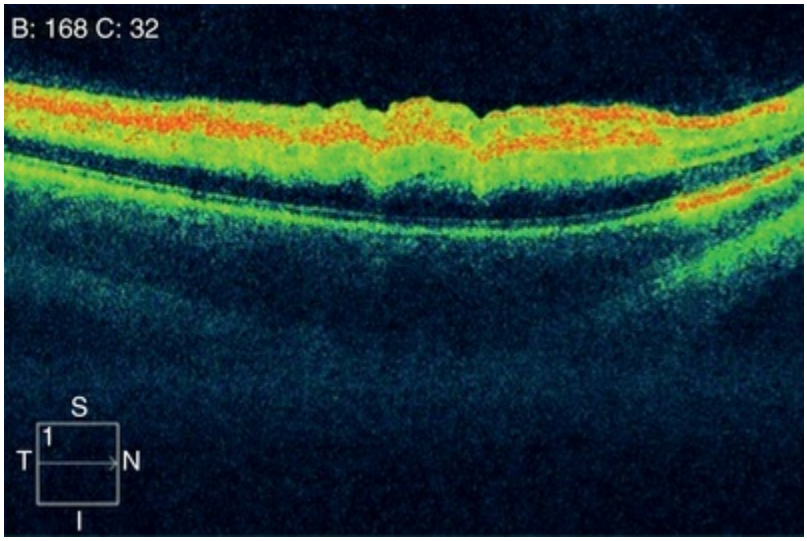

FIG. 54.6 Spectral-domain optical coherence tomography (SD-OCT) of acute central retinal artery occlusion (CRAO). An irregular foveal contour is seen with a highly reflective, thickened inner retina. The outer retina is relatively hyporeflective because of blocking from the thickened inner retina. The external limiting membrane, ellipsoid zone, and retinal pigment epithelium are intact, as would be expected with acute CRAO.

Central scotoma is the most common defect observed on visual field testing followed by paracentral scotoma. Patients with cilioretinal sparing show a preserved central island of vision corresponding to the area perfused by the patent cilioretinal artery. Peripheral constriction is the most common visual field deficit noted in these patients.[10] A preserved temporal island may be seen in some patients, presumably secondary to choroid-derived perfusion of the nasal retina.[24] Visual field defects improve in approximately 28% of patients, remain stable in 57%, and worsen in 7%.[10]

Electroretinography typically demonstrates more severe attenuation of the b-wave than the a-wave since the inner retinal layers are more affected – this produces a characteristic negative waveform with the scotopic white stimulus (Fig. 54.7). Diminution of the a-wave and b-wave may suggest outer retinal damage secondary to choroidal vascular hypoperfusion in the setting of an ophthalmic artery occlusion in addition to a CRAO.[37]

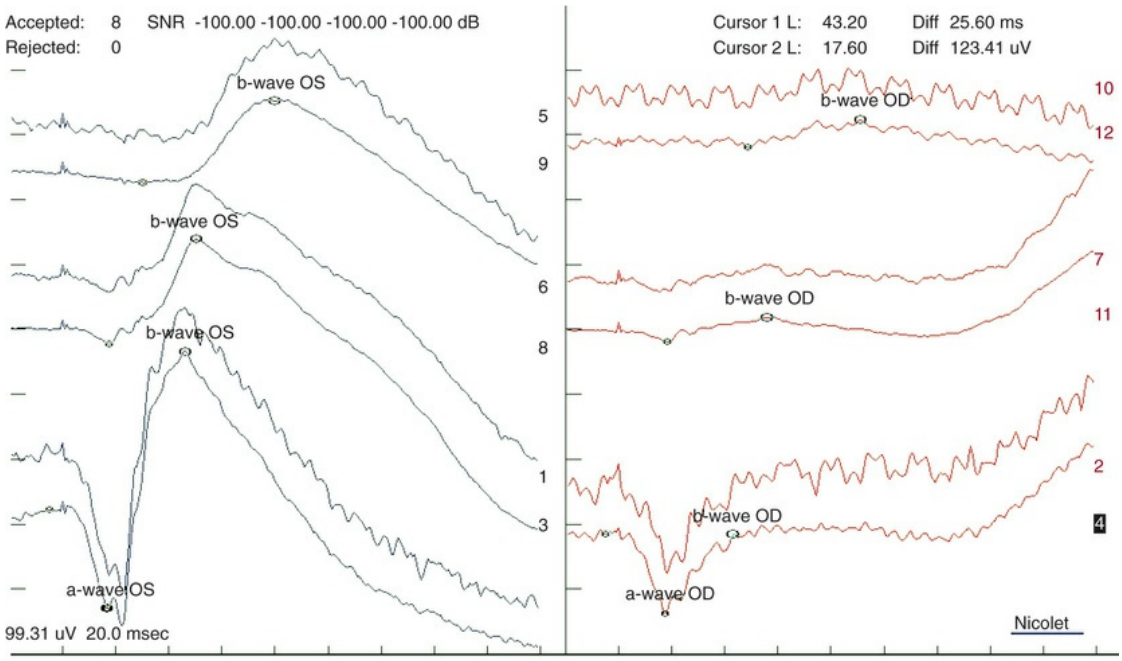

FIG. 54.7 Electroretinogram. The responses from a normal eye are seen on the left. The tracings on the right are from an eye with a central retinal artery occlusion (CRAO). The bottom right tracing shows the maximum response to the scotopic white stimulus. The a-wave is of normal amplitude; however, the b-wave

does not reach the baseline, yielding a negative waveform, as is typically seen with a CRAO.

Systemic Associations

The distribution of systemic associations for CRAO varies depending on age. Overall, embolism from carotid artery atherosclerosis is the most common etiology; however, carotid disease is relatively rare in patients under the age of 40 in whom cardiac embolism is the most common etiology.[4,5,38] The systemic and ocular abnormalities that have been associated with retinal arterial occlusions are summarized in Box 54.1.

Box 54.1

Systemic and Ocular Abnormalities Associated With Retinal Arterial Occlusion

Embolic Sources

- Systemic arterial hypertension (via atherosclerotic plaque formation)[6,22]
- Carotid atherosclerosis[7,98,99]
- Cardiac valvular disease (rheumatic,[45] mitral valve prolapse,[45,46] aortic stenosis,[45] mitral annular calcification[56])
- Left ventricular hypertrophy and segmental wall motion abnormalities[56]
- Thrombus after myocardial infarction[56]
- Cardiac myxoma[41–43]
- Tumors[47,100]
- Carotid artery dissection[101]
- Intravenous drug use[102]
- Lipid emboli (pancreatitis)[103]

- Purtscher retinopathy (trauma)[104]
- Loiasis[105]
- Radiologic studies (carotid angiography,[101] cerebral angiography,[35] cardiac catheterization,[60] lymphography,[61] hysterosalpingography[106])
- Carotid endarterectomy[107]
- Deep vein thrombosis (via paradoxical embolus through a cardiac wall defect)[108]

Trauma

- Retrobulbar injection[67]
- Orbital floor fracture repair[68]
- Anesthesia[69]
- Penetrating injury[71]
- Nasal surgery[109]

Coagulopathies

- Sickle-cell disease[110]
- Homocystinuria[111]
- Lupus anticoagulant[112]
- Protein C and/or S deficiency[113]
- Antithrombin III deficiency[113]
- Activated protein C resistance[114]
- Factor V Leiden[115]

- Platelet abnormalities[4]
- Oral contraceptives[116]
- Pregnancy[4]
- Leukemia/lymphoma[85]

Ocular Conditions

- Prepapillary arterial loops[117]
- Optic disc drusen[118]
- Increased intraocular pressure (from intravitreal injection,[87] gas expansion after vitrectomy,[119] prone intraoperative positioning,[120] retrobulbar hemorrhage,[121] orbital emphysema[122]
- Optic neuritis[123]

Collagen Vascular Disease

- Giant cell arteritis[124]
- Systemic lupus erythematosus[125]
- Polyarteritis nodosa[126]
- Wegener's granulomatosis[127]
- Fibromuscular dysplasia[128]

Other Vasculitides and Inflammatory Conditions

- Orbital mucormycosis[129]
- Toxoplasmosis[130]
- Toxocaraisis[131]
- Lyme disease[132]

- Behçet disease[133]
- Cat-scratch disease[134]
- Herpes simplex associated acute retinal necrosis[135]

Miscellaneous Associations

- Susac syndrome[136]
- Cosmetic facial fillers[137]
- Migraine[138]
- Hypotension[22]

Ryan SJ. Retina, 4th edn. Philadelphia: Elsevier/Mosby; 2006.

The Beaver Dam Eye Study, a large population-based study in Wisconsin, found a 10-year cumulative incidence of retinal emboli of 1.5%. The incidence of retinal emboli varied with age; those 65 years of age or older at baseline were 2.4 times as likely to develop a retinal embolus compared with persons 43–54 years old at baseline. Retinal emboli were more likely in men than in women. Incidence of bilateral emboli was rare; however, multiple emboli in the same eye may be seen in up to one-third of cases. Persons with retinal emboli in Beaver Dam were 2.4 times as likely to have a diagnosis of stroke on their death certificate over an 11-year period compared with those without retinal emboli.[39] The large population-based studies, the Atherosclerosis Risk in Communities (North Carolina) and the Cardiovascular Health Study (Australia), both looked at a biracial population and showed that retinal arteriolar emboli were associated with hypertension, higher systolic blood pressure, carotid artery plaque, increased plasma fibrinogen levels, coronary heart disease, increased plasma lipoprotein levels, and current cigarette smoking. In multivariable models, significant independent predictors were carotid artery plaque, hypertension status, and current cigarette smoking.[40] In the heart, sources of emboli are aortic or mitral valve lesions, patent foramen ovale, left atrial tumor, and myxoma.[41–43]

The presence of a Hollenhorst plaque or retinal artery occlusion is associated with a low prevalence of carotid atherosclerosis requiring carotid endarterectomy. Furthermore, in contrast to amaurosis fugax, these ocular findings are not associated with a high risk for hemispheric neurologic events.[44] However, patients with retinal emboli do have an associated higher mortality rate.[39,41,45,46] Pooled data from the Beaver Dam Eye Study and the Blue Mountain Eye study of two older populations suggest that retinal emboli predict a modest increase in all-cause and stroke-related mortality independent of cardiovascular risk factors.[47] The prevalence of diabetes, hypertension, ischemic heart disease, cerebrovascular accidents, and smoking is significantly higher in patients with retinal arterial occlusions.[6,38–40,44,48–50]

Evaluation

Patients with CRAO typically present to a physician several days after the acute onset; therefore, the etiologic workup is generally recommended on an outpatient basis along with a primary care physician. However, ruling out giant cell arteritis in patients older than 50 years with a positive review of systems does represent a true emergency. Evaluation for giant cell arteritis includes compete blood count with platelets, erythrocyte sedimentation rate, and C-reactive protein. If suspicion is high, the patient should be started on steroid therapy and scheduled for a temporal artery biopsy to prevent vision loss in the fellow eye.[51]

Rarely, a patient with acute CRAO may present within the first few hours of visual deficit. These patients should be admitted for observation, treatment, and immediate workup as their risk is higher for cerebral infarction.[13,52] Patients presenting with transient CRAO or retinal transient ischemic attacks (TIA), or amaurosis fugax, should also be treated as a medical emergency. These patients should undergo immediate evaluation by an ophthalmologist to rule out other causes of transient monocular vision loss and giant cell arteritis before emergent referral to a center with 24/7 stroke treatment teams and the ability to perform emergent brain magnetic resonance imaging.[53] Following the most recent guidelines form the American Heart Association, a Boston

study found the probability of an abnormal MRI was higher in embolic versus nonembolic retinal ischemia (28% vs. 8%) and in permanent vision loss patients versus retinal TIA patients (13% vs. 18%).[54]

The evaluation of an embolic source includes carotid Doppler imaging and echocardiography since the most common sources of retinal emboli are from the carotid artery or the heart. As most retinal emboli are relatively small, when evaluating the results of carotid Doppler ultrasonography, the presence or absence of plaque is more important than whether a hemodynamically significant stenosis is present; the latter is more important in determining the need for carotid endarterectomy. Carotid Doppler is limited by the lack of imaging of the thoracic and intracranial portion of the carotid artery and poor resolution for detection of microemboli.[55]

Although a cardiogenic cause is less common, identification is important as chronic anticoagulation may be indicated to prevent more serious adverse events. A cardiac evaluation is especially important in young patients and those with calcific emboli. In patients with acute retinal arterial obstruction at low cardioembolic risk, transthoracic echocardiography (TTE) results in anticoagulation or cardiac surgery in only 1.5% of patients.[56] Transesophageal echocardiography (TEE) has a higher yield than the transthoracic approach in the cardiovascular evaluation of patients with retinal artery occlusion. In patients without a cardiac history and a normal TTE examination (including normal size and function of cardiac chambers and normal valves with no calcification, along with the absence of atrial fibrillation), the yield of subsequent TEE for identifying intracardiac pathology is low. However, in patients in whom clinical and TTE findings are suggestive of possible intracardiac or aortic thrombus, TEE should be considered as an adjunct to the systemic workup.[57] A computed tomography (CT) angiogram or magnetic resonance imaging angiogram should be considered in special cases such as suspected carotid or aortic dissection. Since the cardiac morbidity and mortality are significant in patients with retinal artery occlusion, a baseline electrocardiogram is recommended.[9,11]

A hypercoagulability evaluation should be considered for patients less than 50 years of age with a suggestive history (e.g.,

prior thrombosis, miscarriage, or family history) or unknown embolic source. Workup includes blood tests for factor V Leiden mutation; protein C, protein S, and antithrombin III deficiencies; homocysteine levels; sickle-cell disease; and antiphospholipid antibodies. Other tests for monoclonal gammopathy, cancer, infection, and disseminated intravascular coagulation may be ordered depending on the clinical circumstance.[13]

Treatment

CRAO continues to be a challenging disease entity to treat. Typically treatment is either conservative or invasive. Most reports of treatment outcome are anecdotal as a result of low incidence.[58] Spontaneous resolution can occur in up to 22% of patients[11] and has been reported to occur up to 3 days after initial onset.[59] However, less than 10% of patients report meaningful visual recovery.[60,61] Rarely do patients have complete spontaneous recovery.[62]

Based on experimental models of CRAO in rhesus monkeys, the retina suffers no damage up to 97 minutes after an acute CRAO, but after 4 hours the retina suffers massive irreversible damage. Therefore, no treatment instituted after about 4 hours from onset can logically restore any vision in the setting of complete obstruction. Additionally, this model showed the longer the ischemia, the longer the time to recovery.[10] Humans rarely have complete obstruction, unlike the animal model; therefore, treatment for CRAO has been recommended within 24 hours of symptom onset. Given the relative rarity of CRAO and variability in time to presentation, therapeutic trials have been limited in sample size, thus reducing the power to detect small treatment benefits. For a new therapy to have a major impact on the management of this disease, it would need to double or triple the success rate of current conventional therapy yet still maintain a low risk for morbidity and mortality.

Current conventional therapy consists of dislodging emboli, reducing intraocular pressure and increasing retinal blood flow, vasodilating the ocular blood supply, improving retinal circulation, decreasing retinal edema, maintaining retinal oxygenation until spontaneous reperfusion, and acting on the thrombus.[13] None of

these treatments have proven effective. Their use is largely based on anecdotal reports and small case series. In a small study of 11 patients, Rumelt et al. found that a systematic regimen involving multiple, sequential treatment steps had better visual outcomes than arbitrary treatment with conservative measures. The protocol included ocular massage, sublingual isosorbide dinitrate, intravenous acetazolamide, intravenous mannitol or oral glycerol, anterior-chamber paracentesis, intravenous methylprednisolone, streptokinase, and retrobulbar tolazine. Treatment with one or two conservative modalities was usually insufficient.[3,63] In a Cochrane Controlled Trials Register comparing any treatment for CRAO with another treatment, Fraser and Siriwardena found no randomized controlled trials meeting their inclusion criteria. They concluded that insufficient data existed to decide if any beneficial treatments existed for CRAO.[64]

Ocular massage is performed using either a Goldmann contact lens or digital massage to apply ocular pressure with an in-and-out movement to dislodge a possibly obstructing embolus. Repeated massage with 10–15 seconds of pressure followed by a sudden release is recommended. This maneuver can produce retinal arterial vasodilation, thereby improving retinal blood flow.[65] A mixture of 95% oxygen and 5% carbon dioxide (carbogen) can be provided to induce vasodilation and improve oxygenation, but efficacy has not been proven.[66] Hyperbaric oxygen provides oxygen at levels of atmospheric pressure. The purpose of hyperbaric oxygen is to preserve the retina in an oxygenated state until recanalization and reperfusion occur, typically at 72 hours. The hyperbaric oxygen increases the arterial oxygen pressure and thereby increases nitric oxide synthesis, leading to vasodilation. Case reports of successful treatment have been published.[67–69] Anterior-chamber paracentesis causes a sudden decrease in intraocular pressure, possibly causing the arterial perfusion pressure behind the obstruction to force an obstructing embolus downstream. This treatment has shown some success in retrospective analyses;[70,71] however, a study by Atebara et al. compared anterior-chamber paracentesis and carbogen therapy with no intervention and found no significant difference in visual outcome.[66] Vasodilating medications that have been utilized to increase retinal blood flow in retinal arterial occlusion include

pentoxifylline, nitroglycerin, and isosorbide dinitrate.[3,72,73] Isovolemic hemodilution is used to increase oxygen supply to retinal tissue by replacing 500 mL of blood with the same volume of hydroxy-ethyl starch. In vascular disease, the limiting factor in tissue oxygenation is blood flow and not oxygen-carrying capacity. In this situation lowering blood viscosity by decreasing the hematocrit and plasma viscosity will improve tissue oxygen levels.[64,74]

Various surgical techniques have also been explored for treatment of CRAO. Neodymium : yttrium aluminum garnet (Nd-YAG) laser arteriotomy in patients with CRAO has been reported for extrusion of an embolus, reopening of the central retinal artery, and return of vision. A fundus contact lens is used with the laser in single-burst mode. The laser is focused slightly deep to the vessel wall at the site of the embolus to avoid photodisruption and opacification of the overlying nerve fiber layer. In patients with small emboli, the laser is focused on the center of the plaque. In patients with elongated emboli, the laser is focused slightly on the distal or downstream end to reduce the chance of hemorrhage. Pulses are delivered directly to the emboli, beginning with the lowest power setting and then with increasing energy until either (1) achieving photofragmentation of the embolus within the arteriole without creating an opening in the vessel wall and without vitreous hemorrhage or (2) creating visible removal of the embolus from within arteriole into the vitreous cavity, typically associated with a limited vitreous hemorrhage. Digital pressure can be applied to the globe to help stop bleeding, if it occurs.[75]

Corticosteroids should be used only when arteritic CRAO from giant cell arteritis is suspected. Anticoagulants should be reserved for secondary prevention of cerebral and ocular infarction in those rare patients who have an underlying systemic disease such as atrial fibrillation, acute internal carotid artery dissection, or a hypercoagulable condition.[13]

With the common use of thrombolytics for acute cerebrovascular accidents, their potential application in the setting of acute CRAO has been considered. Intravenously or intraarterially administered thrombolytics currently in use include streptokinase, urokinase, and tissue plasminogen activator (t-PA). Intravenous

administration is relatively easy and workup prior to treatment is minimal, including blood tests and a brain CT; however, intravenous thrombolytics do increase the risk of systemic hemorrhage. Because of the increased systemic risks, most thrombolysis strategies currently in use are intraarterial.[13] In 2010 the European Assessment Group for Lysis in the Eye (EAGLE) study group published the results of the first prospective, randomized clinical trial evaluating the effect of intraarterial t-PA compared with conservative treatment. Of note, no true placebo arm was included in the study. At 1 month, the mean best-corrected visual acuity improved significantly in both groups but no significant difference was noted between groups. Clinically significant visual improvement (0.3 logMAR) was noted in 60.0% of patients in the conventional therapy group and 57.1% of patients in the thrombolysis group. The trial was stopped early because of apparent similarity in efficacy between groups and the higher rate of adverse events, namely cerebral hemorrhage, in the intraarterial t-PA group.[74] The EAGLE study highlights the importance of careful randomized controlled trials, as the rate of visual improvement in the conventional therapy group was higher than one might expect from prior retrospective studies.

Branch Retinal Artery Occlusion

BRAOs are thought to represent 38% of all acute retinal artery obstructions.[24] Patients generally present with monocular vision loss, which may be restricted to one part of the visual field. Initial visual acuity is better than 20/40 in approximately three-fourths of patients.[76,77] Presenting visual field defects include a central scotoma in 20%, a central altitudinal defect in 13%, and sector defects in 49%.[77]

Fundoscopically, a sectoral pattern of retinal opacification is seen. The whitening is most prominent in the posterior pole along the distribution of the obstructed vessel. Areas of more intense whitening are often seen at the borders of the ischemic area (Fig. 54.8). These probably occur secondary to blocked axoplasmic flow in the nerve fiber layer as it reaches the hypoxic retina. BRAOs typically occur at vessel bifurcations, and 98% of the time the

temporal vessels are affected – this may, however, be due to a presentation bias, as nasal occlusions may be asymptomatic and undetected. Emboli are visible 58–62% of the time.[76,78]

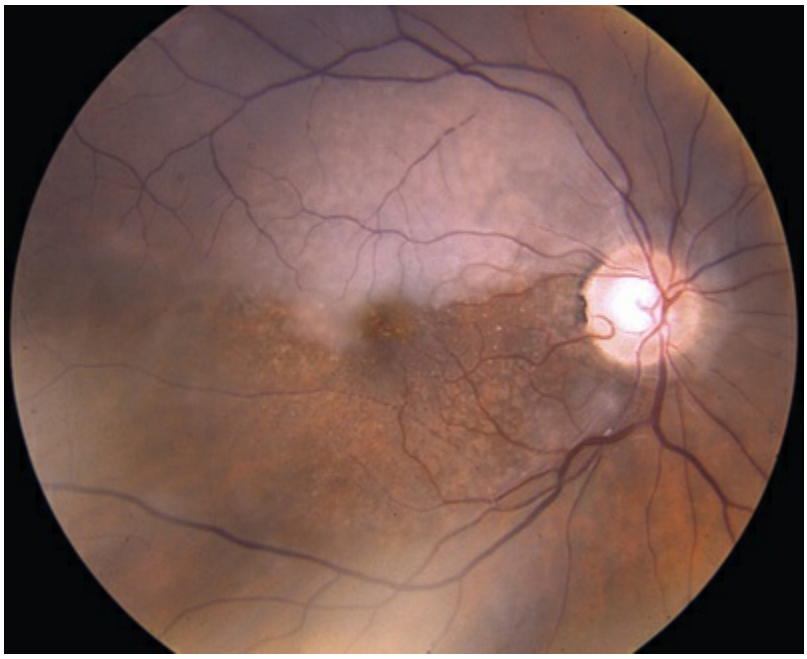

FIG. 54.8 Branch retinal artery occlusion of the superotemporal arcade. Retinal opacification of the superior macula is seen with segmentation within the superior temporal arterioles.

In the chronic stage of BRAO, sectoral nerve fiber layer loss and arterial attenuation may be seen (Fig. 54.9). Rarely in the chronic phase, posterior-segment and/or iris neovascularization will be seen after BRAO, particularly in patients with diabetes.[79] Artery-to-artery collaterals may also be seen and are pathognomonic for BRAO.[80]

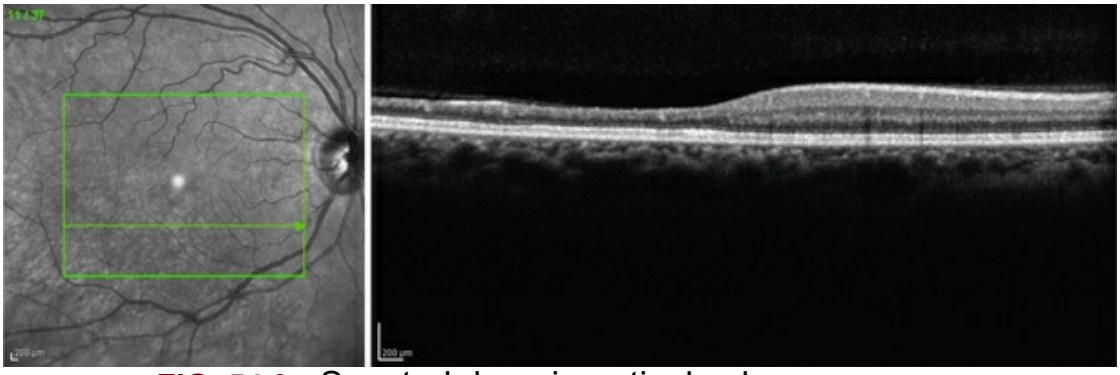

FIG. 54.9 Spectral domain optical coherence tomography of a chronic branch retinal artery occlusion shows sectoral inner retinal atrophy down to the inner nuclear layer in the inferotemporal macula.

The visual prognosis in eyes with symptomatic BRAO is generally good with acuity usually improving to 20/40 or better in 80% of eyes.[4] Hayreh et al., in their natural history study of 133 eyes, reported visual acuity to correlate with foveal involvement and the extent of irreversible ischemic damage to the retina.[77] Ros et al. showed an improvement in visual field deficit by Goldmann perimetry in 80% of 201 eyes surveyed.[76]

Risk factors for BRAO are similar to CRAO; therefore a similar evaluation is generally recommended.[76] Giant cell arteritis tends to present much less often with a BRAO than a CRAO. In cases of an obstruction at a bifurcation, the etiology is more often embolic.

Since the visual prognosis is typically good for BRAO, aggressive therapy is generally not pursued unless significant foveal involvement is seen. Additionally, the good prognosis makes the positive effect of treatment more difficult to discern from natural history.

Cilioretinal Artery Occlusion

CLRAOs account for 5% of retinal arterial obstructions.[81] Cilioretinal arteries enter the retina from the temporal optic disc, separate from the central retinal artery, and can be seen on exam in 20% of eyes. On fluorescein angiography, they are seen 32% of the time and fill concomitantly with the choroidal circulation.[25] Fundoscopically, an area of superficial retinal whitening is seen along the course of the cilioretinal artery.

When evaluating CLRAO, typically three distinct groups are found: (1) isolated CLRAO; (2) CLRAO associated with CRVO; and (3) CLRAO in conjunction with anterior ischemic optic neuropathy. Brown et al. found 90%, 70%, and 0% of eyes achieved 20/40 or better vision in each group, respectively.[82] Initial visual field defects include cecocentral scotoma, central scotoma, and central superior or inferior altitudinal defect.[77]

Isolated CLRAOs typically have a good prognosis, with nearly 90% achieving 20/40 or better vision and 60% returning to 20/20. Even with severe damage to the papillomacular bundle, potential visual acuity can be quite good, presumably secondary to intact superior and inferior nerve fiber layer bundles supplying the fovea.

CLRAO in conjunction with a CRVO comprises 40% of CLRAO.[82] Approximately 5% of eyes with CRVO also have a CLRAO.[83] Visual acuity correlates with the degree of venous obstruction. The venous obstructions are usually nonischemic and tend not to cause iris neovascularization or neovascular glaucoma.[82] Reduced hydrostatic pressure in the cilioretinal artery may predispose the cilioretinal artery to stasis and thrombosis in the setting of increased hydrostatic pressure within the retinal venous system. Optic disc edema may also contribute by decreasing the area of the cilioretinal artery and thereby the flow.[83]

CLRAO in association with anterior ischemic optic neuropathy is seen in 15% of eyes with CLRAO and has a poor visual prognosis, ranging from 20/400 to no light perception secondary to optic nerve damage. Typically a hyperemic or pale edematous optic disc is seen with superficial retinal whitening along the course of the cilioretinal artery.[82] Acute pale swelling is more suggestive of giant cell arteritis and is usually associated with more severe vision loss. Giant cell arteritis has a selective tendency to involve the posterior ciliary artery, resulting in its occlusion, which in turn results in simultaneous development of both arteritic anterior ischemic optic neuropathy and CLRAO.[77]

Systemic evaluation is similar to CRAO except investigation for embolic sources is likely not indicated for cases associated with CRVO. Ocular treatment is generally not pursued unless concern for underlying giant cell arteritis exists.

Combined Retinal Artery and Vein Occlusion

CRVO can be seen in association with CRAO,[84] BRAO,[85] and CLRAO.[86,87] Patients with combined CRAO/BRAO and CRVO generally present with sudden decreased vision. The fundus exam shows superficial retinal whitening with a cherry-red spot and signs of venous obstruction, such as dilated, tortuous veins, intraretinal hemorrhages, optic disc edema, cotton-wool spots, and marked thickening of the retina (Figs. 54.10A and 54.11).[84] The CRAO seen with a CRVO may not be a true CRAO but may be secondary to the occlusion of the central retinal vein in the region of the lamina cribrosa. The blood cannot exit out of the retinal vascular bed as a result of complete blockage of the central retinal vein, and secondarily compromises entry of blood into the eye.[55] Fluorescein angiography shows severe widespread retinal capillary nonperfusion with sudden termination or pruning of the mid-sized retinal vessels. Minimal macular leakage is seen as a result of closure of these vessels despite the clinical appearance.[88]

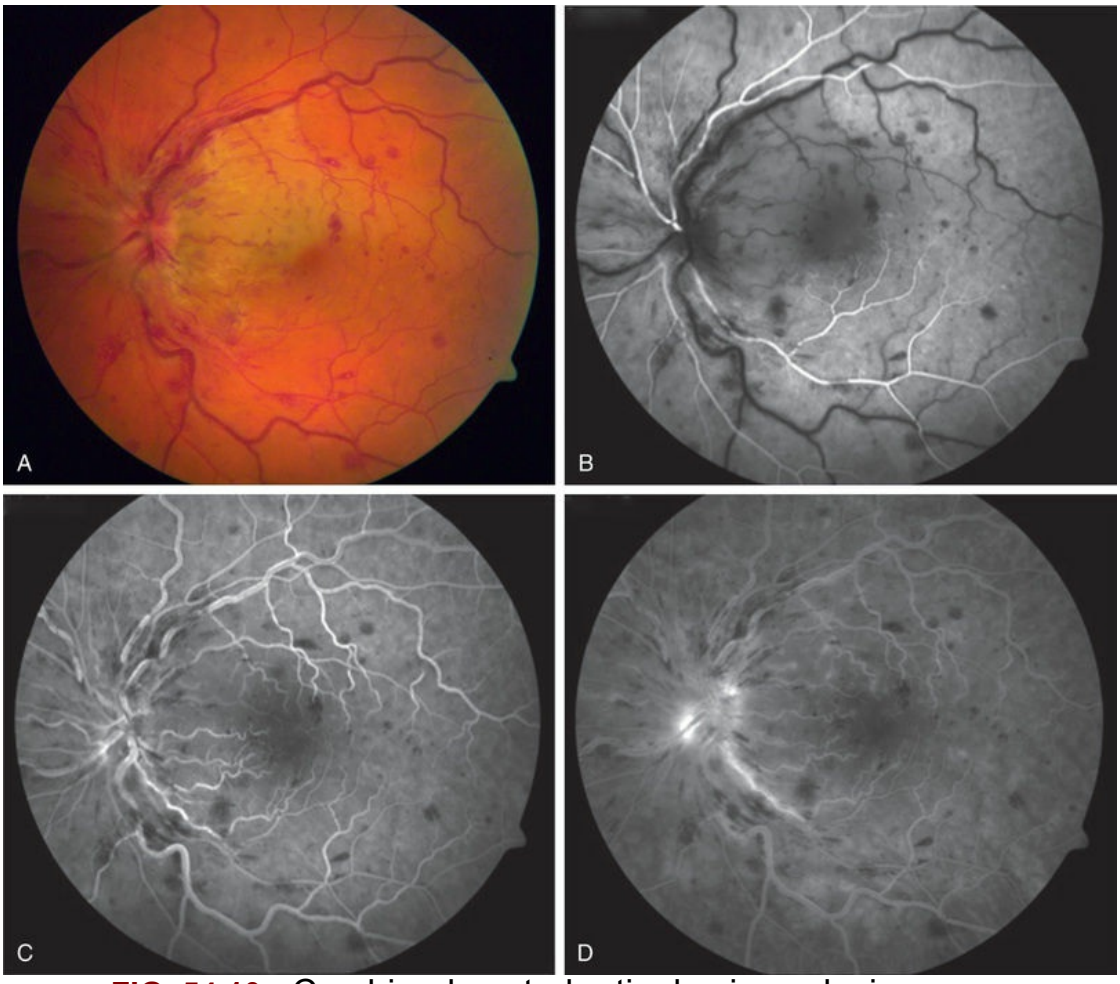

FIG. 54.10 Combined central retinal vein occlusion with branch retinal artery occlusion. (A) Fundus photograph of an acute central retinal venous occlusion (CRVO) with a branch retinal artery occlusion (BRAO) in a patient with the factor V Leiden mutation. Optic disc hyperemia and edema, dilated and tortuous veins, intraretinal hemorrhages, and cotton-wool spots are seen, consistent with a CRVO. Superotemporal to the disc, retinal opacification is seen consistent with a BRAO. (B) Fluorescein angiography shows initial nonperfusion of the branch retinal artery superior to the fovea. (C) Marked delay in transit consistent with the occlusive process is seen. The arteriole occlusion is not complete as the dye eventually does get into the artery. (D) In the late frames, disc leakage is seen consistent with the CRVO.

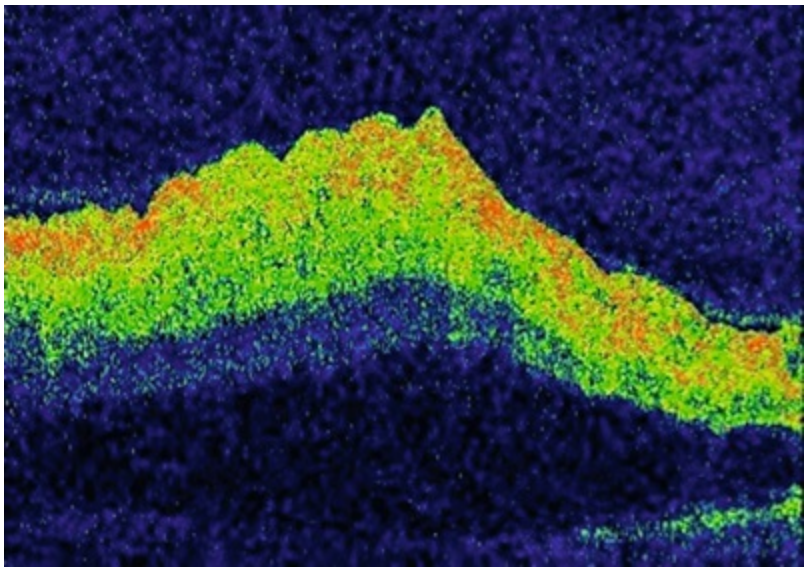

FIG. 54.11 Spectral domain optical coherence tomography of the patient shown in Fig. 54.10. Inner and outer retinal edema can be seen consistent with the combined central retinal venous occlusion and branch retinal artery occlusion. The dense hyperreflectivity of the inner retinal edema from the BRAO induce a shadow effect on the inner retina.

The visual prognosis is generally poor, with visual acuity in the hand motions range.[88] After 6–8 weeks, optic nerve pallor is seen with severe arterial attenuation. Histopathology of the chronic phase shows hemorrhagic retinal necrosis and inner retinal atrophy consistent with a CRVO and CRAO. The macula shows typical cystoid changes. Rubeosis iridis develops in about 80% of eyes, leading to neovascular glaucoma as the end result.[84] This can be seen as early as 1–2 weeks but is seen on average at about 6 weeks. Aggressive treatment with panretinal photocoagulation is recommended.[88]

Combined CRAO and CRVO has been associated with many diverse entities, including syphilis, optic neuritis, leukemia, lymphoma, temporal arteritis, orbital inflammatory disease, posterior scleritis, systemic lupus erythematosus, trauma, retrobulbar injections, and superior ophthalmic vein thrombosis.[85] Intravitreal gentamicin injection may cause a similar appearance; however, angiography would show normal filling of the choroid, retinal arteries, and veins.[89]

Cotton-Wool Spots

Cotton-wool spots are often referred to using the misnomer "soft exudates" and are described as slightly elevated, small, yellow-white or gray-white, cloud-like lesions with fimbriated borders in the superficial retina (Figs. 54.12A–B). They are usually restricted to the posterior segment of the fundus and they rarely exceed one-third of the area of the optic disc.[90] Cotton-wool spots rarely cause vision loss unless they involve the fovea and typically resolve within 6–12 weeks,[90] though they may last longer in diabetics.[91]

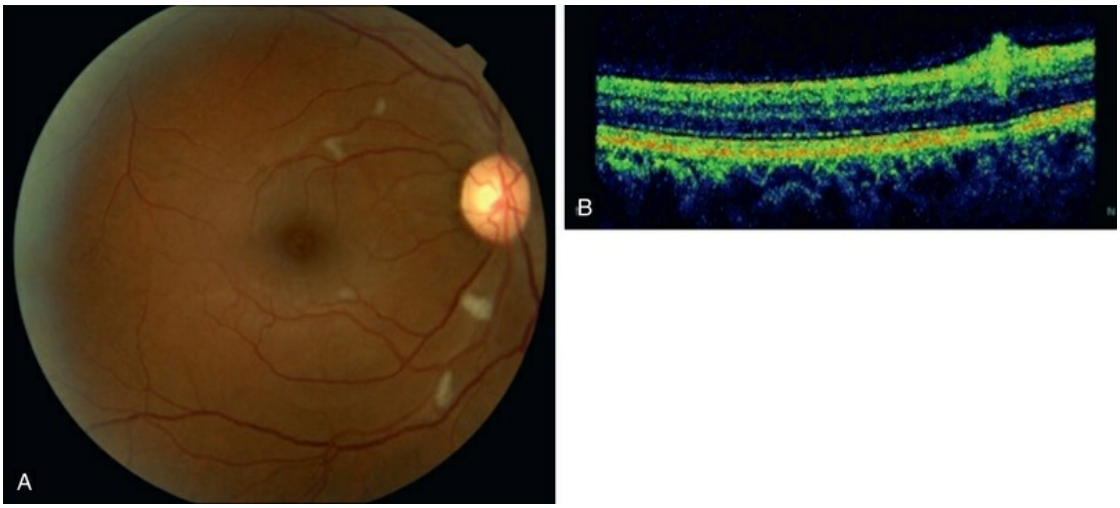

FIG. 54.12 Cotton-wool spots. (A) Fundus photo showing multiple cotton-wool spots in a patient with interferon-β1a retinopathy. (B) Spectral domain optical coherence tomography through one of the cotton-wool spots shows focal thickening and elevation of the nerve fiber layer.

A cotton-wool spot is hypothesized to develop secondary to obstruction of a retinal arteriole with resultant ischemia. The focal hypoxia causes blockage of axoplasmic flow within the nerve fiber layer with subsequent deposition of intraaxonal organelles.[92] Early light microscopy of cotton-wool spots in the retina revealed the presence of a cytoid body, a round, dark-staining "pseudonucleus" within a grossly swollen nerve fiber layer (Fig. 54.13). The application of electron microscopic techniques revealed the composition of cytoid bodies to be an accumulation of

intracytoplasmic organelles, largely mitochondria, with a major lipid component.[93]

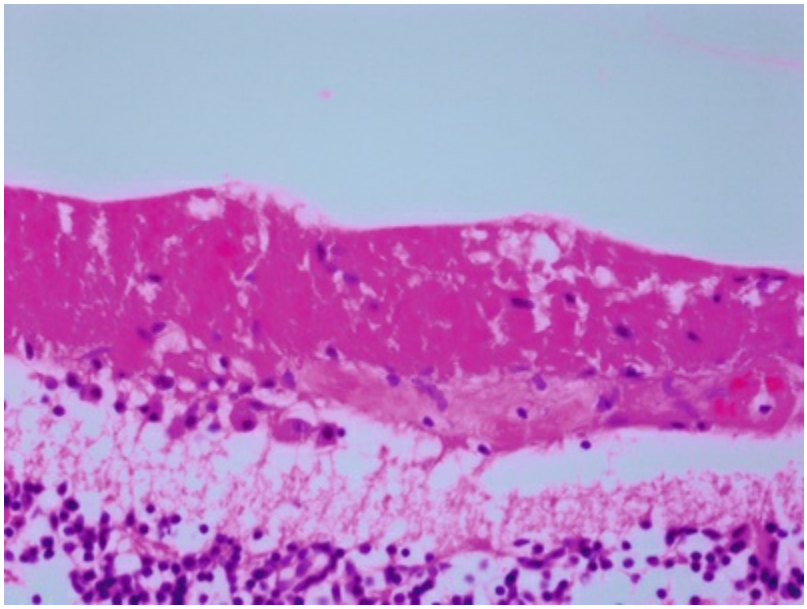

FIG. 54.13 Light microscopic section of a cotton-wool spot in the retina showing swelling of the nerve fiber layer with the presence of cytoid bodies (hematoxylin and eosin, ×100). (Courtesy of Dr. Hans Grossniklaus, Emory Eye Center, Atlanta.)

Diabetes mellitus and systemic hypertension are by far the most common etiologies of cotton-wool spots, followed by undiagnosed diabetes and hypertension. In patients who have a cotton-wool spot and no known history of diabetes, an elevated blood sugar level is identified in 20% of patients and an elevated blood pressure (diastolic blood pressure of 90 mmHg or greater) in 50% of patients. Cotton-wool spots, however, may be observed in association with numerous other diseases (Box 54.2). Fortunately, most patients who present with cotton-wool spots have other systemic or ocular findings that help narrow down their specific etiology. The presence of even one cotton-wool spot in an otherwise normal fundus necessitates an investigation for systemic etiologic factors. A giant cell arteritis workup is not necessary unless a positive review of systems is noted. In approximately 95% of cases, a systemic underlying condition can be found. Almost any etiology that can cause a CRAO or BRAO can potentially also produce cotton-wool

Box 54.2

Etiologies for Cotton-Wool Spots

Ischemic

Diabetes

Hypertension

Retinal vein occlusion

Ocular ischemic syndrome

Severe anemia

Hyperviscosity/hypercoagulable state/dysproteinemia

Radiation

Acute blood loss

Embolic

Carotid emboli

Cardiac emboli

- Cardiac valvular disease
- Endocarditis
- Rheumatic heart disease

Deep venous emboli

White cell emboli/Purtscher and Purtscher-like retinopathy (head trauma, long bone fractures, acute pancreatitis, chest compression injury, amniotic fluid emboli, fat emboli)

Foreign-body emboli (intravenous drug abuse, talc)

Collagen Vascular Disease

Systemic lupus erythematosus

Dermatomyositis

Scleroderma

Polyarteritis nodosa

Giant cell arteritis

Infectious

HIV retinopathy

Fungemia

Bacteremia

Rocky Mountain spotted fever (*Rickettsia rickettsii*)

Cat-scratch disease (*Bartonella henselae*)

Leptospirosis

Onchocerciasis (*Onchocerca volvulus*)

Toxic

Interferon (α_{2a}, β_{1a})

Neoplastic

Leukemia

Lymphoma

Metastatic carcinoma

Miscellaneous

Traumatic

Tractional (epiretinal membrane)

High-altitude retinopathy

Papilledema/papillitis

Reproduced with permission from Brown GC, Brown MM, Hiller T, et al. Cotton-wool spots. Retina 1985;5:206–14.

Paracentral Acute Middle Maculopathy

PAMM was first described in 2013 as a band-like hyperreflectivity seen on spectral domain optical coherence tomography (SD-OCT) at the level of the inner nuclear layer (INL) correlating with a paracentral area of deep retinal whitening on biomicroscopy or color photography (Fig. 54.14B).[95] As compared to cotton-wool spots, PAMM lesions are deeper, grayer, and smother (Fig. 54.14A). PAMM is thought to be a result of intermediate capillary plexus (ICP) and/or deep capillary plexus (DCP) ischemia. Therefore, PAMM is difficult to visualize with traditional fluorescein angiography. To date, near-infrared reflectance and SD-OCT imaging are the most sensitive modalities for imaging PAMM. The recent advent of OCT angiography has demonstrated preferential disruption of the ICP and DCP (Fig. 54.15) in these cases. PAMM may complicate other retinal vascular diseases including diabetic retinopathy, hypertensive retinopathy, sickle-cell retinopathy, Purtscher retinopathy, central retinal vein occlusion, and retinal arterial occlusion.[96,97] PAMM may also be idiopathic even developing in young healthy patients and in the context of migraine. Nevertheless, presence of PAMM should prompt a search for contributing systemic or extrinsic vascular risk factors.[96]

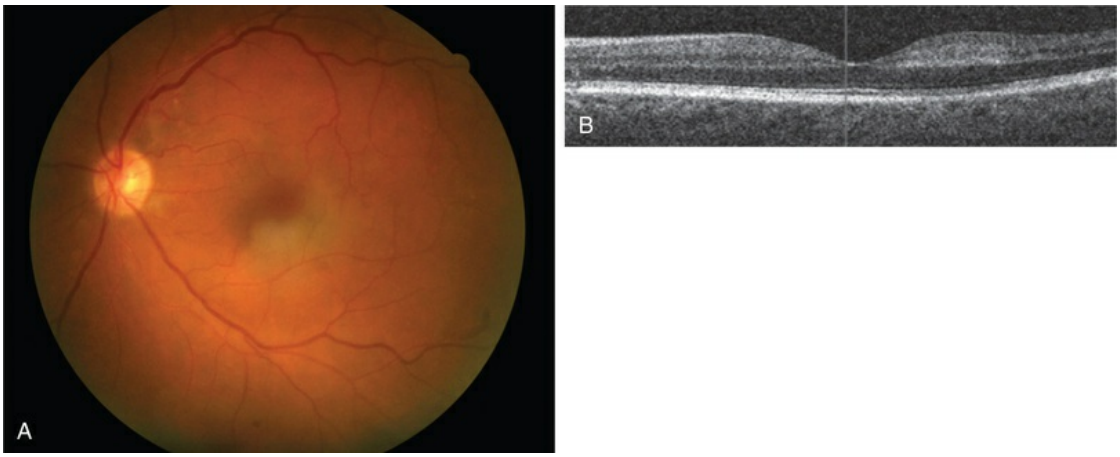

FIG 54.14 Paracentral acute middle maculopathy. (A) Color fundus photo showing inferotemporal parafoveal deep retinal whitening. (B) Spectral domain optical coherence tomography at presentation exhibiting temporal parafoveal band-like hypereflectivity of the inner nuclear layer corresponding to the area of retinal whitening seen in the fundus photo. (Courtesy of Dr. David Sarraf, David Geffen School of Medicine, UCLA.)

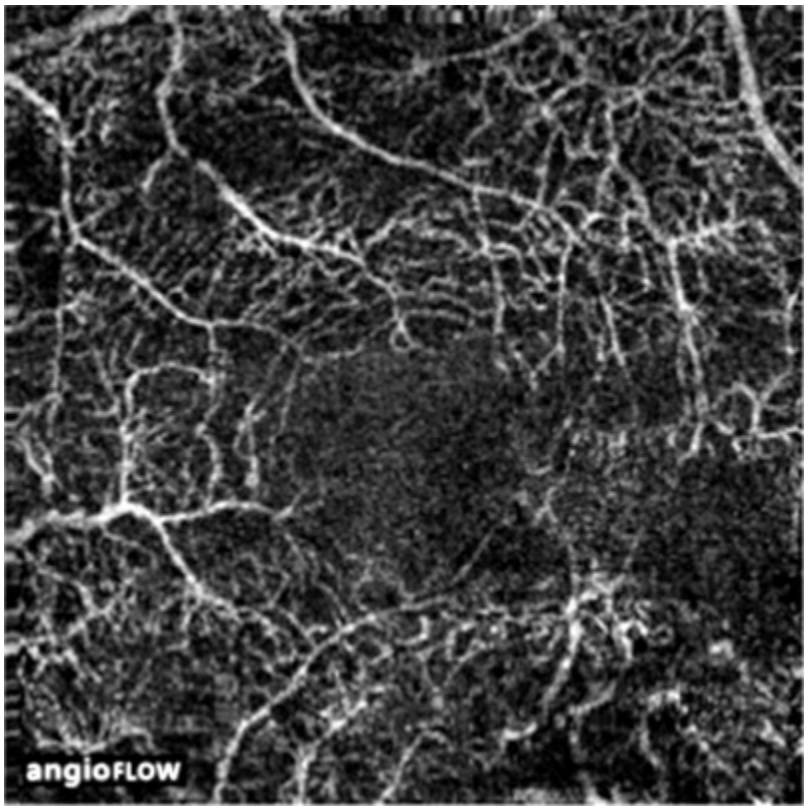

FIG. 54.15 Paracentral acute middle maculopathy. Optical coherence tomography angiography. 3 × 3 mm

macular cube with enface imaging of the deep capillary shows a profound loss of the deep capillary plexus.
(Courtesy of Dr. David Sarraf, David Geffen School of Medicine, UCLA.)

References

1. Graefe AV. Ueber Embolie der arteria centralis retinae als Urscahe plotzlicher Erblingdung. *Arch fur Ophthalmol*. 1859;5:136–157.
2. Ryan SJ. *Retina*. 4th ed. Elsevier/Mosby: Philadelphia; 2006.
3. Rumelt S, Dorenboim Y, Rehany U. Aggressive systematic treatment for central retinal artery occlusion. *Am J Ophthalmol*. 1999;128(6):733–738.
4. Brown GC, Magargal LE, Shields JA, et al. Retinal arterial obstruction in children and young adults. *Ophthalmology*. 1981;88(1):18–25.
5. Greven CM, Slusher MM, Weaver RG. Retinal arterial occlusions in young adults. *Am J Ophthalmol*. 1995;120(6):776–783.
6. Brown GC, Magargal LE. Central retinal artery obstruction and visual acuity. *Ophthalmology*. 1982;89(1):14–19.
7. Breen LA. Atherosclerotic carotid disease and the eye. *Neurol Clin*. 1991;9(1):131–145.
8. Kline L. The natural history of patients with amaurosis fugax. *Ophthalmol Clin North Am*. 1996;9:351–357.
9. Appen RE, Wray SH, Cogan DG. Central retinal artery occlusion. *Am J Ophthalmol*. 1975;79(3):374–381.
10. Hayreh SS, Zimmerman MB. Central retinal artery occlusion: visual outcome. *Am J Ophthalmol*. 2005;140(3):376–391.
11. Connolly BP, Krishnan A, Shah GK, et al. Characteristics of patients presenting with central retinal artery occlusion with and without giant cell arteritis. *Can J Ophthalmol*. 2000;35(7):379–384.
12. Augsburger JJ, Magargal LE. Visual prognosis following treatment of acute central retinal artery obstruction. *Br J Ophthalmol*. 1980;64(12):913–917.

13. Biousse V, Calvetti O, Bruce BB, et al. Thrombolysis for central retinal artery occlusion. *J Neuroophthalmol*. 2007;27(3):215–230.
14. Duker JS, Brown GC. Iris neovascularization associated with obstruction of the central retinal artery. *Ophthalmology*. 1988;95(9):1244–1250.
15. Duker JS, Sivalingam A, Brown GC, et al. A prospective study of acute central retinal artery obstruction: the incidence of secondary ocular neovascularization. *Arch Ophthalmol*. 1991;109(3):339–342.
16. Hayreh SS, Rojas P, Podhajsky P, et al. Ocular neovascularization with retinal vascular occlusion-III. Incidence of ocular neovascularization with retinal vein occlusion. *Ophthalmology*. 1983;90(5):488–506.
17. Duker JS, Brown GC. The efficacy of panretinal photocoagulation for neovascularization of the iris after central retinal artery obstruction. *Ophthalmology*. 1989;96(1):92–95.
18. Nettleship E. *Unusual appearance in a case of retinal embolism about 30 hours after its occurrence*. [Stuttgardt] 1891.
19. Hayreh SS, Zimmerman MB. Fundus changes in central retinal artery occlusion. *Retina (Philadelphia, Pa.)*. 2007;27(3):276–289.
20. Hayreh SS, Kolder HE, Weingeist TA. Central retinal artery occlusion and retinal tolerance time. *Ophthalmology*. 1980;87(1):75–78.
21. Hayreh SS, Zimmerman MB, Kimura A, et al. Central retinal artery occlusion: retinal survival time. *Exp Eye Res*. 2004;78(3):723–736.
22. Gold D. Retinal arterial occlusion. *Trans Sect Ophthalmol Am Acad Ophthalmol Otolaryngol*. 1977;83(3 Pt 1):OP392–408.
23. Yanoff MFB. Retinal ischemia. *Ocular pathology – a text and atlas*. J.B. Lippincott Co: Philadelphia; 1989.
24. Brown GC, Shields JA. Cilioretinal arteries and retinal arterial occlusion. *Arch Ophthalmol*. 1979;97(1):84–92.
25. Justice J Jr, Lehmann RP. Cilioretinal arteries: a study based on review of stereo fundus photographs and fluorescein angiographic findings. *Arch Ophthalmol*. 1976;94(8):1355–

1358.
26. Singh S, Dass R. The central artery of the retina. II. A study of its distribution and anastomoses. *Br J Ophthalmol*. 1960;44:280–299.
27. Sharma S, ten Hove MW, Pinkerton RM, et al. Interobserver agreement in the evaluation of acute retinal artery occlusion. *Can J Ophthalmol*. 1997;32(7):441–444.
28. Hayreh SS. Acute retinal arterial occlusive disorders. *Prog Retin Eye Res*. 2011;30(5):359–394.
29. Arruga J, Sanders MD. Ophthalmologic findings in 70 patients with evidence of retinal embolism. *Ophthalmology*. 1982;89(12):1336–1347.
30. Ramakrishna G, Malouf JF, Younge BR, et al. Calcific retinal embolism as an indicator of severe unrecognised cardiovascular disease. *Heart*. 2005;91(9):1154–1157.
31. Hayreh SS. Blood supply of the optic nerve head and its role in optic atrophy, glaucoma, and oedema of the optic disc. *Br J Ophthalmol*. 1969;53(11):721–748.
32. Hayreh SS, Podhajsky P. Ocular neovascularization with retinal vascular occlusion. II. Occurrence in central and branch retinal artery occlusion. *Arch Ophthalmol*. 1982;100(10):1585–1596.
33. Duker JS, Brown GC. Neovascularization of the optic disc associated with obstruction of the central retinal artery. *Ophthalmology*. 1989;96(1):87–91.
34. David NJ, Norton EW, Gass JD, et al. Fluorescein angiography in central retinal artery occlusion. *Arch Ophthalmol*. 1967;77(5):619–629.
35. Chen SN, Hwang JF, Chen YT. Macular thickness measurements in central retinal artery occlusion by optical coherence tomography. *Retina (Philadelphia, Pa.)*. 2011;31(4):730–737.
36. Schuman JS, Puliafito CA, Fujimoto JG. *Optical coherence tomography of ocular diseases*. 2nd ed. Slack Inc.: Thorofare, NJ; 2004.
37. Henkes HE. Electroretinography in circulatory disturbances of the retina. II: The electroretinogram in cases of occlusion of the central retinal artery or of its branches. *Arch*

Ophthalmol. 1954;51(1):42–53.
38. Hayreh SS, Podhajsky PA, Zimmerman MB. Retinal artery occlusion: associated systemic and ophthalmic abnormalities. *Ophthalmology*. 2009;116(10):1928–1936.
39. Klein R, Klein BE, Moss SE, et al. Retinal emboli and cardiovascular disease: the Beaver Dam Eye Study. *Trans Am Ophthalmol Soc*. 2003;101:173–180 [discussion 80-2].
40. Wong TY, Larsen EK, Klein R, et al. Cardiovascular risk factors for retinal vein occlusion and arteriolar emboli: the Atherosclerosis Risk in Communities & Cardiovascular Health studies. *Ophthalmology*. 2005;112(4):540–547.
41. Jampol LM, Wong AS, Albert DM. Atrial myxoma and central retinal artery occlusion. *Am J Ophthalmol*. 1973;75(2):242–249.
42. Campbell JK. Early diagnosis of an atrial myxoma with central retinal artery occlusion. *Ann Ophthalmol*. 1974;6(11):1207–1208 [10-1].
43. Cogan DG, Wray SH. Vascular occlusions in the eye from cardiac myxomas. *Am J Ophthalmol*. 1975;80(3 Pt 1):396–403.
44. Dunlap AB, Kosmorsky GS, Kashyap VS. The fate of patients with retinal artery occlusion and Hollenhorst plaque. *J Vasc Surg*. 2007;46(6):1125–1129.
45. Wilson LA, Warlow CP, Russell RW. Cardiovascular disease in patients with retinal arterial occlusion. *Lancet*. 1979;1(8111):292–294.
46. Greven CM, Weaver RG, Harris WR, et al. Transesophageal echocardiography for detecting mitral valve prolapse with retinal artery occlusions. *Am J Ophthalmol*. 1991;111(1):103–104.
47. Tarkkanen A, Merenmies L, Makinen J. Embolism of the central retinal artery secondary to metastatic carcinoma. *Acta Ophthalmol (Copenh)*. 1973;51(1):25–33.
48. Klein R, Klein BE, Jensen SC, et al. Retinal emboli and stroke: the Beaver Dam Eye Study. *Arch Ophthalmol*. 1999;117(8):1063–1068.
49. Wong TY, Klein R. Retinal arteriolar emboli: epidemiology and risk of stroke. *Curr Opin Ophthalmol*. 2002;13(3):142–146.
50. Cheung N, Lim L, Wang JJ, et al. Prevalence and risk factors

of retinal arteriolar emboli: the Singapore Malay Eye Study. *Am J Ophthalmol*. 2008;146(4):620–624.
51. Biousse V, Newman NJ. Ischemic optic neuropathies. *N Engl J Med*. 2015;372(25):2428–2436.
52. Park SJ, Choi NK, Yang BR, et al. Risk and risk periods for stroke and acute myocardial infarction in patients with central retinal artery occlusion. *Ophthalmology*. 2015;122(11):2336–2343.
53. Biousse V. Acute retinal arterial ischemia: an emergency often ignored. *Am J Ophthalmol*. 2014;157(6):1119–1121.
54. Helenius J, Arsava EM, Goldstein JN, et al. Concurrent acute brain infarcts in patients with monocular visual loss. *Ann Neurol*. 2012;72(2):286–293.
55. Hayreh SS. Prevalent misconceptions about acute retinal vascular occlusive disorders. *Prog Retin Eye Res*. 2005;24(4):493–519.
56. Sharma S, Naqvi A, Sharma SM, et al. Transthoracic echocardiographic findings in patients with acute retinal arterial obstruction: a retrospective review. Retinal Emboli of Cardiac Origin Group. *Arch Ophthalmol*. 1996;114(10):1189–1192.
57. Kramer M, Goldenberg-Cohen N, Shapira Y, et al. Role of transesophageal echocardiography in the evaluation of patients with retinal artery occlusion. *Ophthalmology*. 2001;108(8):1461–1464.
58. Rumelt S, Brown GC. Update on treatment of retinal arterial occlusions. *Curr Opin Ophthalmol*. 2003;14(3):139–141.
59. Duker JS, Brown GC. Recovery following acute obstruction of the retinal and choroidal circulations: a case history. *Retina (Philadelphia, Pa.)*. 1988;8(4):257–260.
60. Meyer CH, Holz FG. Images in clinical medicine: blurred vision after cardiac catheterization. *N Engl J Med*. 2009;361(24):2366.
61. Rasmussen KE. Retinal and cerebral fat emboli following lymphography with oily contrast media. *Acta Radiol Diagn (Stockh)*. 1970;10(3):199–202.
62. Perkins SA, Magargal LE, Augsburger JJ, et al. The idling retina: reversible visual loss in central retinal artery

obstruction. *Ann Ophthalmol*. 1987;19(1):3–6.
63. Kim RW, Juzych MS, Eliott D. Ocular manifestations of injection drug use. *Infect Dis Clin North Am*. 2002;16(3):607–622.
64. Fraser S, Siriwardena D. Interventions for acute non-arteritic central retinal artery occlusion. *Cochrane Database Syst Rev*. 2002;(1) [CD001989].
65. Ffytche TJ. A rationalization of treatment of central retinal artery occlusion. *Trans Ophthalmol Soc U K*. 1974;94(2):468–479.
66. Atebara NH, Brown GC, Cater J. Efficacy of anterior chamber paracentesis and Carbogen in treating acute nonarteritic central retinal artery occlusion. *Ophthalmology*. 1995;102(12):2029–2034 [discussion 34-5].
67. Morgan CM, Schatz H, Vine AK, et al. Ocular complications associated with retrobulbar injections. *Ophthalmology*. 1988;95(5):660–665.
68. Emery JM, Huff JD, Justice J Jr. Central retinal artery occlusion after blow-out fracture repair. *Am J Ophthalmol*. 1974;78(3):538–540.
69. Hollenhorst RW, Svien HJ, Benoit CF. Unilateral blindness occurring during anesthesia for neurosurgical operations. *Arch Ophthalmol*. 1954;52(6):819–830.
70. Johnson LN, Krohel GB, Hong YK, et al. Central retinal artery occlusion following transfemoral cerebral angiography. *Ann Ophthalmol*. 1985;17(6):359–362.
71. Brown GC, Magargal LE. Sudden occlusion of the retinal and posterior choroidal circulations in a youth. *Am J Ophthalmol*. 1979;88(4):690–693.
72. Incandela L, Cesarone MR, Belcaro G, et al. Treatment of vascular retinal disease with pentoxifylline: a controlled, randomized trial. *Angiology*. 2002;53(Suppl. 1):S31–4.
73. Kuritzky S. Nitroglycerin to treat acute loss of vision. *N Engl J Med*. 1990;323(20):1428.
74. Schumacher M, Schmidt D, Jurklies B, et al. Central retinal artery occlusion: local intra-arterial fibrinolysis versus conservative treatment, a multicenter randomized trial. *Ophthalmology*. 2010;117(7):1367–1375.e1.

75. Opremcak E, Rehmar AJ, Ridenour CD, et al. Restoration of retinal blood flow via translumenal Nd:YAG embolysis/embolectomy (TYL/E) for central and branch retinal artery occlusion. *Retina (Philadelphia, Pa.)*. 2008;28(2):226–235.
76. Ros MA, Magargal LE, Uram M. Branch retinal-artery obstruction: a review of 201 eyes. *Ann Ophthalmol*. 1989;21(3):103–107.
77. Hayreh SS, Podhajsky PA, Zimmerman MB. Branch retinal artery occlusion: natural history of visual outcome. *Ophthalmology*. 2009;116(6):1188–1194.e1–4.
78. Hayreh SS, Zimmerman MB. Fundus changes in branch retinal arteriolar occlusion. *Retina (Philadelphia, Pa.)*. 2015;35(10):2060–2066.
79. Shah GK, Sharma S, Brown GC. Iris neovascularization following branch retinal artery occlusion. *Can J Ophthalmol*. 1998;33(7):389–390.
80. Sharma MC, Volpe NJ. Collaterals in branch retinal artery occlusion. *Ophthalmic Surg Lasers*. 1999;30(4):324–325.
81. Brown GC, Magargal LE, Sergott R. Acute obstruction of the retinal and choroidal circulations. *Ophthalmology*. 1986;93(11):1373–1382.
82. Brown GC, Moffat K, Cruess A, et al. Cilioretinal artery obstruction. *Retina (Philadelphia, Pa.)*. 1983;3(3):182–187.
83. Fong AC, Schatz H, McDonald HR, et al. Central retinal vein occlusion in young adults (papillophlebitis). *Retina (Philadelphia, Pa.)*. 1992;12(1):3–11.
84. Richards RD. Simultaneous occlusion of the central retinal artery and vein. *Trans Am Ophthalmol Soc*. 1979;77:191–209.
85. Duker JS, Cohen MS, Brown GC, et al. Combined branch retinal artery and central retinal vein obstruction. *Retina (Philadelphia, Pa.)*. 1990;10(2):105–112.
86. McLeod D. Cilio-retinal arterial circulation in central retinal vein occlusion. *Br J Ophthalmol*. 1975;59(9):486–492.
87. Hayreh SS, Fraterrigo L, Jonas J. Central retinal vein occlusion associated with cilioretinal artery occlusion. *Retina (Philadelphia, Pa.)*. 2008;28(4):581–594.
88. Brown GC, Duker JS, Lehman R, et al. Combined central

retinal artery-central vein obstruction. *Int Ophthalmol*. 1993;17(1):9–17.
89. Brown GC, Eagle RC, Shakin EP, et al. Retinal toxicity of intravitreal gentamicin. *Arch Ophthalmol*. 1990;108(12):1740–1744.
90. Cotton-wool spots. *Br Med J*. 1966;2(5528):1474.
91. Hodge JV, Dollery CT. Retinal soft exudates: a clinical study by colour and fluorescence photography. *Q J Med*. 1964;33:117–131.
92. McLeod D, Marshall J, Kohner EM, et al. The role of axoplasmic transport in the pathogenesis of retinal cotton-wool spots. *Br J Ophthalmol*. 1977;61(3):177–191.
93. Ashton N. Pathophysiology of retinal cotton-wool spots. *Br Med Bull*. 1970;26(2):143–150.
94. Brown GC, Brown MM, Hiller T, et al. Cotton-wool spots. *Retina (Philadelphia, Pa.)*. 1985;5(4):206–214.
95. Sarraf D, Rahimy E, Fawzi AA, et al. Paracentral acute middle maculopathy: a new variant of acute macular neuroretinopathy associated with retinal capillary ischemia. *JAMA Ophthalmol*. 2013;131(10):1275–1287.
96. Rahimy E, Kuehlewein L, Sadda SR, et al. Paracentral acute middle maculopathy: what we knew then and what we know now. *Retina (Philadelphia, Pa.)*. 2015;35(10):1921–1930.
97. Chen X, Rahimy E, Sergott RC, et al. Spectrum of Retinal vascular diseases associated with paracentral acute middle maculopathy. *Am J Ophthalmol*. 2015;160(1):26–34.e1.
98. Sharma S, Brown GC, Pater JL, et al. Does a visible retinal embolus increase the likelihood of hemodynamically significant carotid artery stenosis in patients with acute retinal arterial occlusion? *Arch Ophthalmol*. 1998;116(12):1602–1606.
99. Kollarits CR, Lubow M, Hissong SL. Retinal strokes. I. Incidence of carotid atheromata. *JAMA*. 1972;222(10):1273–1275.
100. Masuda H, Ohira A, Shibuya Y, et al. Branch retinal artery occlusion caused by an embolus of metastatic gastric adenocarcinoma. *Arch Ophthalmol*. 2002;120(9):1209–1211.
101. Hwang JF, Chen SN, Chiu SL, et al. Embolic cilioretinal

artery occlusion due to carotid artery dissection. *Am J Ophthalmol*. 2004;138(3):496–498.
102. AtLee WE Jr. Talc and cornstarch emboli in eyes of drug abusers. *JAMA*. 1972;219(1):49–51.
103. Inkeles DM, Walsh JB. Retinal fat emboli as sequela to acute pancreatitis. *Am J Ophthalmol*. 1975;80(5):935–938.
104. Madsen PH. Traumatic retinal angiopathy (Purtscher). *Ophthalmologica*. 1972;165(5):453–458.
105. Toussaint D, Danis P. Retinopathy in generalized loa-loa filariasis: a clinicopathological study. *Arch Ophthalmol*. 1965;74(4):470–476.
106. Charawanamuttu AM, Hughes-Nurse J, Hamlett JD. Retinal embolism after hysterosalpingography. *Br J Ophthalmol*. 1973;57(3):166–169.
107. Treiman RL, Bloemendal LC, Foran RF, et al. Ipsilateral blindness: a complication of carotid endarterectomy. *Arch Surg*. 1977;112(8):928–932.
108. Nakagawa T, Hirata A, Inoue N, et al. A case of bilateral central retinal artery obstruction with patent foramen ovale. *Acta Ophthalmol Scand*. 2004;82(1):111–112.
109. Lee DH, Yang HN, Kim JC, et al. Sudden unilateral visual loss and brain infarction after autologous fat injection into nasolabial groove. *Br J Ophthalmol*. 1996;80(11):1026–1027.
110. Goldberg MF. Retinal vaso-occlusion in sickling hemoglobinopathies. *Birth Defects Orig Artic Ser*. 1976;12(3):475–515.
111. Wilson RS, Ruiz RS. Bilateral central retinal artery occlusion in homocystinuria: a case report. *Arch Ophthalmol*. 1969;82(2):267–268.
112. Kleiner RC, Najarian LV, Schatten S, et al. Vaso-occlusive retinopathy associated with antiphospholipid antibodies (lupus anticoagulant retinopathy). *Ophthalmology*. 1989;96(6):896–904.
113. Bertram B, Remky A, Arend O, et al. Protein C, protein S, and antithrombin III in acute ocular occlusive diseases. *Ger J Ophthalmol*. 1995;4(6):332–335.
114. Vignes S, Wechsler B, Elmaleh C, et al. Retinal arterial occlusion associated with resistance to activated protein C.

Br J Ophthalmol. 1996;80(12):1111.
115. Talmon T, Scharf J, Mayer E, et al. Retinal arterial occlusion in a child with factor V Leiden and thermolabile methylene tetrahydrofolate reductase mutations. *Am J Ophthalmol*. 1997;124(5):689–691.
116. Friedman S, Golan A, Shoenfeld A, et al. Acute ophthalmologic complications during the use of oral contraceptives. *Contraception*. 1974;10(6):685–692.
117. Brown GC, Magargal L, Augsburger JJ, et al. Preretinal arterial loops and retinal arterial occlusion. *Am J Ophthalmol*. 1979;87(5):646–651.
118. Purcell JJ Jr, Goldberg RE. Hyaline bodies of the optic papilla and bilateral acute vascular occlusions. *Ann Ophthalmol*. 1974;6(10):1069–1072 [1074].
119. Fang IM, Huang JS. Central retinal artery occlusion caused by expansion of intraocular gas at high altitude. *Am J Ophthalmol*. 2002;134(4):603–605.
120. Stambough JL, Dolan D, Werner R, et al. Ophthalmologic complications associated with prone positioning in spine surgery. *J Am Acad Orthop Surg*. 2007;15(3):156–165.
121. Goldsmith MO. Occlusion of the central retinal artery following retrobulbar hemorrhage. *Ophthalmologica*. 1967;153(3):191–196.
122. Linberg JV. Orbital emphysema complicated by acute central retinal artery occlusion: case report and treatment. *Ann Ophthalmol*. 1982;14(8):747–749.
123. Abrams JD. Papillitis complicated by central retinal artery occlusion. *Br J Ophthalmol*. 1963;47:53.
124. Alwitry A, Holden R. One hundred transient monocular central retinal artery occlusions secondary to giant cell arteritis. *Arch Ophthalmol*. 2003;121(12):1802–1803.
125. Gold DH, Morris DA, Henkind P. Ocular findings in systemic lupus erythematosus. *Br J Ophthalmol*. 1972;56(11):800–804.
126. Solomon SM, Solomon JH. Bilateral central retinal artery occlusions in polyarteritis nodosa. *Ann Ophthalmol*. 1978;10(5):567–569.
127. Haynes BF, Fishman ML, Fauci AS, et al. The ocular

manifestations of Wegener's granulomatosis: fifteen years experience and review of the literature. *Am J Med*. 1977;63(1):131–141.
128. Sawada T, Harino S, Ikeda T. Central retinal artery occlusion in a patient with fibromuscular dysplasia. *Retina (Philadelphia, Pa.)*. 2004;24(3):461–464.
129. Luo QL, Orcutt JC, Seifter LS. Orbital mucormycosis with retinal and ciliary artery occlusions. *Br J Ophthalmol*. 1989;73(8):680–683.
130. Willerson D Jr, Aaberg TM, Reeser F, et al. Unusual ocular presentation of acute toxoplasmosis. *Br J Ophthalmol*. 1977;61(11):693–698.
131. Brown GC, Tasman WS. Retinal arterial obstruction in association with presumed *Toxocara canis* neuroretinitis. *Ann Ophthalmol*. 1981;13(12):1385–1387.
132. Lightman DA, Brod RD. Branch retinal artery occlusion associated with Lyme disease. *Arch Ophthalmol*. 1991;109(9):1198–1199.
133. Colvard DM, Robertson DM, O'Duffy JD. The ocular manifestations of Behçet's disease. *Arch Ophthalmol*. 1977;95(10):1813–1817.
134. Solley WA, Martin DF, Newman NJ, et al. Cat scratch disease: posterior segment manifestations. *Ophthalmology*. 1999;106(8):1546–1553.
135. Weissman HM, Biousse V, Schechter MC, et al. Bilateral central retinal artery occlusion associated with herpes simplex virus-associated acute retinal necrosis and meningitis: case report and literature review. *Ophthalmic Surg Lasers Imaging Retina*. 2015;46(2):279–283.
136. Susac JO, Hardman JM, Selhorst JB. Microangiopathy of the brain and retina. *Neurology*. 1979;29(3):313–316.
137. Park SW, Woo SJ, Park KH, et al. Iatrogenic retinal artery occlusion caused by cosmetic facial filler injections. *Am J Ophthalmol*. 2012;154(4):653–662.e1.
138. Beversdorf D, Stommel E, Allen C, et al. Recurrent branch retinal infarcts in association with migraine. *Headache*. 1997;37(6):396–399.

55

Acquired Retinal Macroaneurysms

Emily Y. Chew, Robert P. Murphy

Clinical Description

Acquired retinal macroaneurysms are fusiform or round dilations of the retinal arterioles that occur in the posterior fundus within the first three orders of arteriolar bifurcation.[1]

Often they are located at the site of an arteriolar bifurcation or an arteriovenous crossing (Fig. 55.1). The supratemporal artery is the most commonly reported site of involvement because patients with such involvement are more likely to have visual impairment. Women make up the majority of reported cases. Most cases are unilateral, while 10% may be bilateral. Retinal macroaneurysm was estimated to occur in 1 in 9000 in the Beijing Eye Study.[2]

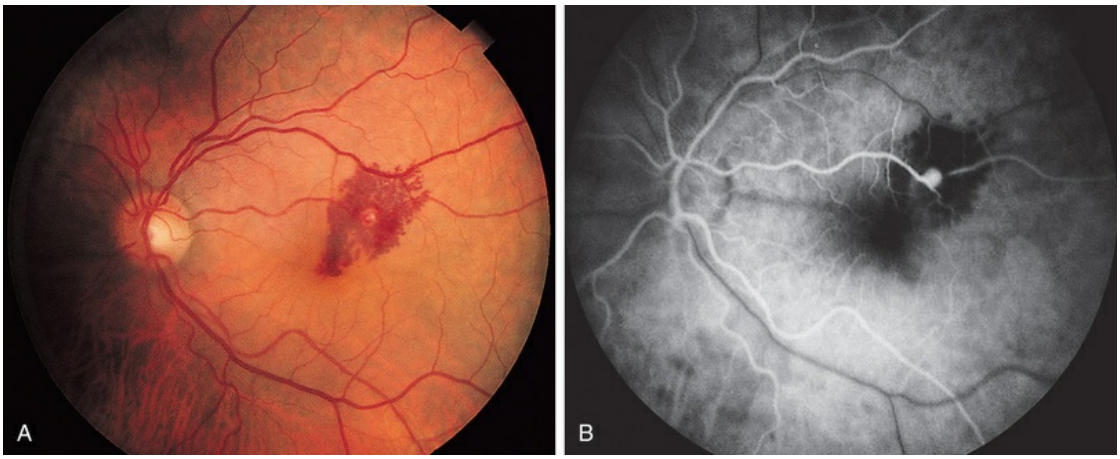

FIG. 55.1 (A) A 62-year-old woman with hypertension had a subretinal hemorrhage associated with a macroaneurysm in her left supratemporal artery. (B) The fluorescein angiogram demonstrated hypofluorescence from blockage from the retinal hemorrhage and hyperfluorescence of the retinal macroaneurysm itself, apparent as a round dilation located at the arteriolar bifurcation.

Most commonly, retinal macroaneurysm affects patients in the sixth and seventh decades of life. Often associated are vascular problems such as hypertension and general arteriosclerotic cardiovascular disease, as noted by Robertson,[3] who first coined the term *retinal macroaneurysm.* Uncontrolled hypertension can present with a retinal artery macroaneurysm and its accompanying vitreous hemorrhage.[4] Other investigators have confirmed this association with hypertension.[5] Serum lipid and lipoprotein abnormalities have also been reported in patients with this condition.[6] Systemic investigations for hypertension and cardiovascular disease should be conducted in patients who have a retinal arteriolar macroaneurysm.

Although a patient with a retinal arteriolar macroaneurysm may be asymptomatic if the macula is not involved (Fig. 55.2), the most common clinical symptom is decline in central visual acuity as a result of retinal edema, exudation, or hemorrhage.[7] Bleeding from macroaneurysms can occur in the subretinal space, into the retina, beneath the internal limiting membrane, or into the vitreous. So-called hourglass hemorrhages are typical. Hemorrhage in the space beneath the retinal pigment epithelium may produce a dark lesion simulating an ocular tumor such as malignant melanoma,[8] or a

lesion associated with age-related macular degeneration. A complication of the vitreous hemorrhage also includes the development of angle closure glaucoma.[9]

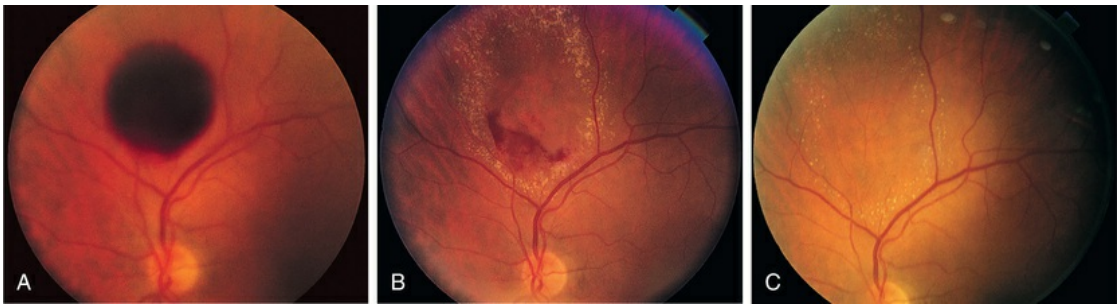

FIG. 55.2 (A) The retinal hemorrhage superior to the optic disc, associated with a retinal macroaneurysm, caused no ocular symptoms. (B) Six months later, the retinal macroaneurysm is partially obstructed by the resolving retinal hemorrhage, with a surrounding ring of lipid. (C) Eight months later, the macroaneurysm has spontaneously involuted, with complete resolution of the hemorrhage and a decrease in the lipid.

The hemorrhage may also partially or completely obscure the aneurysm (Fig. 55.3). Occasionally, multiple macroaneurysms occur. Other retinal microvascular changes associated with macroaneurysms include widening of the periarterial capillary-free zone around the area of the aneurysm, capillary dilation and nonperfusion, microaneurysms, and artery-to-artery collaterals.

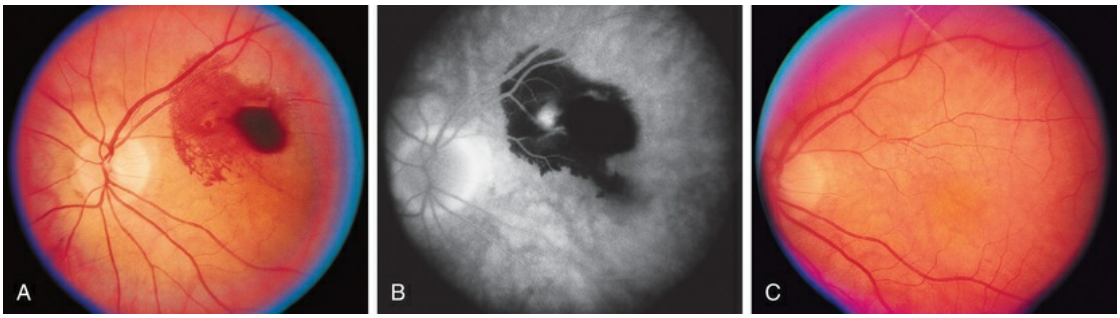

FIG. 55.3 (A) A preretinal hemorrhage partially obscures the retinal macroaneurysm. (B) The fluorescein angiogram shows the hyperfluorescence that corresponds to the hemorrhage and the hyperfluorescence of the retinal macroaneurysm. (C)

At 20 months later, there is spontaneous resolution of the hemorrhage and the retinal macroaneurysm.

Diagnosis of Retinal Macroaneurysm

Fluorescein angiography initially may fail to demonstrate the macroaneurysm because of blockage by the surrounding hemorrhage. Dense hemorrhage in the retina can cause marked hypofluorescence. In such cases of dense hemorrhage, indocyanine green angiography may be useful because its absorption and emission peak in the near-infrared range allow the light to penetrate the hemorrhage to a greater extent than fluorescein angiography.[10] A small case series using indocyanine green angiography has demonstrated these lesions to be pulsatile and contiguous with the arterial wall, pathognomonic of an insolated retinal artery macroaneurysm.[11] The macroaneurysm typically fills in the early arterial phase of the angiogram. The appearance of the late phase of the fluorescein angiogram varies, ranging from little staining of the vessel wall to marked leakage. Leakage of surrounding dilated capillaries also may be seen. The lipid often present in the macular area fails to block fluorescein unless the amount of lipid is massive. Macular hole formation following rupture of a retinal arterial macroaneurysm has been reported.[12,13]

Histopathologic studies of macroaneurysms have shown gross distension of the involved retinal arteriole. Surrounding this are fibroglial proliferation, dilated capillaries, extravasated blood, lipoidal exudates, and hemosiderin deposits.

Evaluation of the retinal structure with optical coherence tomography was conducted in a series of patients with retinal macroaneurysm.[14] Although most of the retinal structure was intact at the initial exam, subretinal hemorrhage or extensive exudative changes from retinal macroaneurysm can cause the deterioration of the foveal outer photoreceptor layer with a poor visual outcome. In a study of exudative macular diseases, including retinal macroaneurysms and other pathologic processes, the “pearl necklace” sign was seen as hyperreflective dots in a contiguous ring around the inner wall of cystoid spaces in the outer plexiform layer

of the retina.[15] This is not specific for retinal macroaneurysms but may alert the clinician to the several causes associated with such exudative disease.

Natural Course and Treatment of Retinal Macroaneurysms

Several series have reported on the natural history and treatment response of macroaneurysms.[6,16,17] Some investigators believe the visual prognosis is excellent in most patients who have macroaneurysms and do not have treatment because the lesions can thrombose and undergo spontaneous involution with clearing of the macular exudate.[2] However, the exudative process may progress in some patients and cause structural damage to the macula with loss of vision (Fig. 55.4).[18] Moderate visual loss also may occur if bleeding causes secondary morphologic changes in the macula. No clear indication for treatment with laser photocoagulation has been established, and the beneficial effects of such treatments have not been proven.

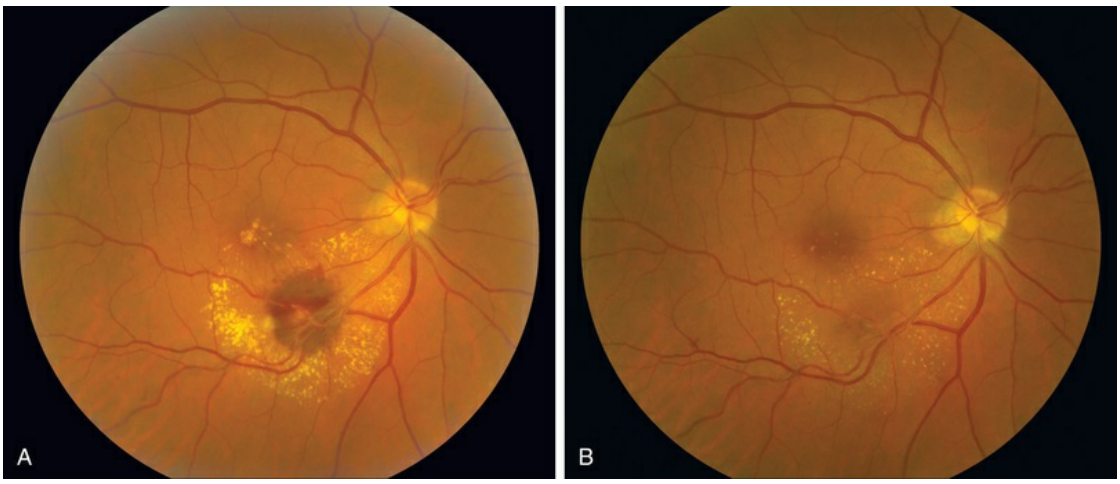

FIG. 55.4 A 65-year-old man noted decreased vision in his right eye to 20/32. He had a history of hypertension and was borderline diabetic. (A) The macroaneurysm is located along the inferior temporal retinal artery with evidence of subretinal hemorrhage as well as marked hard exudate, extending into the center of the macula. (B) Observation over 9 months demonstrated a

gradual clearing of the retinal hard exudate. Visual acuity was 20/25.

More recently, 37 patients with macroaneurysms and symptoms for at least 2 months were treated with a course of three doses of intravitreal bevacizumab.[19] Improvement in visual acuity at week 12 was documented with an accompanying decrease in central retinal thickness that appeared clinically and statistically significant. A retrospective case–control study evaluating the use of intravitreal bevacizumab found that treated eyes tended to have a more rapid resolution of the hemorrhage and macular edema.[20]

Vitrectomy was performed for clearing the macular hemorrhage associated with the rupture of a macroaneurysm.[21] The results of vitrectomy are variable depending on the location of the hemorrhage from the retinal macroaneurysms. The vision is particularly poor in those patients who have dense submacular hemorrhage.[22]

Pneumatic displacement with or without tissue plasminogen activator has also been used for the therapy of submacular hemorrhage associated with a macroaneurysm.[23] Yag laser has also been used to treat such premacular hemorrhage.[24] The surgical excision of the retinal macroaneurysm with scissors and diathermy followed by the drainage of the submacular hemorrhage was also explored in two cases, with some improvement in vision.[25]

Many investigators consider direct laser photocoagulation of the macroaneurysm if the lipid exudate coming from it threatens the fovea. Treatment when hemorrhage is present is fraught with difficulties. There is also the danger of occluding the retinal arteriole during treatment. This potential complication must always be considered when the distal portion of the arteriole being considered for treatment supplies the macula.

A recent retrospective review of patients treated and untreated found that visual acuity results in the long term were comparable, whether they were observed or treated with laser photocoagulation or vitrectomy.[26]

The investigators concluded from this case series that at longer follow-up, most had reasonably good vision with or without treatment. When macular holes occur as a consequence of the disease, the visual acuity is not likely to improve.

The differential diagnoses of retinal macroaneurysms include other retinal vascular abnormalities, including diabetic retinopathy, retinal telangiectasia, retinal capillary angioma, cavernous hemangioma, malignant melanoma,[8] and the hemorrhagic pigment epithelial detachment of age-related macular degeneration.[27]

References

1. Pitkänen L, Tommila P, Kaarniranta K, et al. Retinal arterial macroaneurysms. *Acta Ophthalmol*. 2014;92(2):101–104.
2. Xu L, Wang Y, Jonas JB. Frequency of retinal macroaneurysm in adult Chinese, Beijing Eye Study. *Br J Ophthalmol*. 2007;91:840–841.
3. Robertson DM. Macroaneurysms of the retinal arteries. *Trans Am Acad Ophthalmol Otolaryngol*. 1973;77:55–67.
4. Sekuri C, Kayikcioglu M, Kaykcioglu O. Retinal artery macroaneurysm as initial presentation of hypertension. *Int J Cardiol*. 2004;93:87–88.
5. Moosavi RA, Fong KCS, Chopdar A. Retinal artery macroaneurysms: clinical and fluorescein angiographic features in 34 patients. *Eye (Lond)*. 2006;20:1011–1020.
6. Cleary PE, Kohner EM, Hamilton AM, et al. Retinal macroaneurysms. *Br J Ophthalmol*. 1975;59:355–361.
7. Rabb MF, Gagliano DA, Teske MP. Retinal arterial macroaneurysms. *Surv Ophthalmol*. 1988;33:73–96.
8. Fritsche PL, Flipsen E, Polak BC. Subretinal hemorrhage from retinal arterial macroaneurysm simulating malignancy. *Arch Ophthalmol*. 2000;118:1704–1705.
9. Arthur SN, Mason J, Roberts B, et al. Secondary acute angle-closure glaucoma associated with vitreous hemorrhage after ruptured retinal arterial macroaneurysm. *Am J Ophthalmol*. 2004;138:682–683.
10. Townsend-Pico WA, Meyers SM, Lewis H. Indocyanine green angiography in the diagnosis of retinal arterial macroaneurysms associated with submacular and preretinal hemorrhages: a case series. *Am J Ophthalmol*. 2000;129:33–37.
11. Schneider U, Wagner AL, Kreissig I. Indocyanine green

videoangiography of hemorrhagic retinal arterial macroaneurysms. *Ophthalmologica*. 1997;211:115–118.
12. Mitamura Y, Terashima H, Takeuchi S. Macular hole formation following rupture of retinal arterial macroaneurysm. *Retina*. 2002;22:113–115.
13. Sato R, Yasukawa T, Hirano Y, et al. Early-onset macular holes following ruptured retinal arterial macroaneurysms. *Graefes Arch Clin Exp Ophthalmol*. 2008;246:1779–1782.
14. Tsujikawa A, Sakamoto A, Ota M, et al. Retinal structural changes associated with retinal arterial macroaneurysm examined with optical coherence tomography. *Retina*. 2009;29:782–792.
15. Gelman SK, Freund KB, Shah VP, et al. The pearl necklace sign: a novel spectral domain optical coherence tomography finding in exudative macular disease. *Retina*. 2014;34(10):2088–2095.
16. Abdel-Khalek MN, Richardson J. Retinal macroaneurysm: natural history and guidelines for treatment. *Br J Ophthalmol*. 1986;70:2–11.
17. Lewis RA, Norton EWD, Gass JDM. Acquired arterial macro-aneurysms of the retina. *Br J Ophthalmol*. 1976;60:21–30.
18. Yang CS, Tsai DC, Lee FL, et al. Retinal arterial macroaneurysms: risk factors of poor visual outcome. *Ophthalmologica*. 2005;219:366–372.
19. Pichi F, Morara M, Torrazza C, et al. Intravitreal bevacizumab for macular complications from retinal arterial macroaneurysms. *Am J Ophthalmol*. 2013;155:287–294.
20. Cho HJ, Rhee TK, Kim HS, et al. Intravitreal bevacizumab for symptomatic retinal arterial macroaneurysm. *Am J Ophthalmol*. 2013;155:898–904.
21. Zhao P, Hayashi H, Oshima K, et al. Vitrectomy for macular hemorhage associated with retinal arterial macroaneurysm. *Ophthalmology*. 2000;107:613–617.
22. Nakamura H, Hayakawa K, Sawguchi S, et al. Visual outcome after vitreous, sub-internal limiting membrane, and/or submacular hemorrhage removal associated with

ruptured retinal arterial macroaneurysms. *Graefes Arch Clin Exp Ophthalmol*. 2008;246:661–669.
23. Mizutani T, Yasukawa T, Ito Y, et al. Pneumatic displacement of submacular hemorrhage with or without tissue plasminogen activator. *Graefes Arch Clin Exp Ophthalmol*. 2011;249:1153–1157.
24. Dahreddine M, Eldirani H, Mutsinzi E. Retinal macroaneurysm complicated by premacular hemorrhage: treatment by YAG laser disruption. *J Fr Ophtalmol*. 2011;34:131.
25. Oie Y, Emi K. Surgical excision of retinal macroaneurysms with submacular hemorrhage. *Jpn J Ophthalmol*. 2006;50:550–553.
26. Koinzer S, Heckmann J, Tode J, et al. Long-term, therapy-related visual outcome of 49 cases with retinal arterial macroaneurysm: a case series and literature review. *Br J Ophthalmol*. 2015;99(10):1345–1353.
27. Hochman MA, Seery CM, Zarbin MA. Pathophysiology and management of subretinal hemorrhage. *Surv Ophthalmol*. 1997;42:195–213.

56

Branch Retinal Vein Occlusion

Angela Bessette, Peter K. Kaiser

Introduction

Branch retinal vein occlusion (BRVO) is a common cause of retinal vascular disease.[1] A recent meta-analysis of 50,000 participants from 11 studies found a prevalence of 4.42 per 1000 adults and estimated that 13.9 million adults worldwide are affected by BRVO.[2]

Systemic vascular diseases such as hypertension and arteriosclerosis are risk factors for BRVO. Age is also a strong risk factor for BRVO, and many epidemiologic studies have confirmed that the prevalence increases with increasing age. It occurs most frequently between the ages of 60 and 70 years. Men and women are affected equally, and additional studies are needed to determine

whether racial/ethnic variations exist or are secondary to a higher prevalence of uncontrolled risk factors in at-risk populations.[2–4] The pathologic interruption of venous flow in these eyes almost always occurs at a retinal arteriovenous intersection, where a retinal artery crosses over a retinal vein. This section discusses the pathophysiology, clinical features, evaluation, and treatment of patients with BRVO.

Risk Factors

In addition to age, systemic hypertension and the retinal arteriolar changes associated with it, including arteriovenous nicking and retinal arteriolar narrowing, are well-established risk factors for BRVO.[3–7] Other cardiovascular risk factors, such as diabetes, smoking, hyperlipidemia, atrial fibrillation, renal dysfunction, and atherosclerosis, have also been associated with an increased risk of BRVO.[3–8] The role of hypercoagulability in the pathogenesis of BRVO is controversial and studies have shown conflicting results. Rehak and associates reported an increased prevalence of Factor V Leiden mutation in patients with RVO; however, a meta-analysis of thrombophilic risk factors by Janssen and colleagues found an association with hyperhomocysteinemia and anticardiolipin antibodies, but not with Factor V Leiden mutation.[9,10] Another meta-analysis identified elevated plasma homocysteine and lower serum folate as risk factors.[11] Thus, while hypercoagulability may play a role in younger patients and in patients without typical cardiovascular risk factors,[10] more studies are needed to provide a more definitive link. In contrast, higher serum levels of high-density lipoprotein and light to moderate alcohol consumption may be protective.[8] Studies have also suggested a correlation between certain ocular risk factors and BRVO, including shorter axial length and a history of glaucoma.[3,8,12–15] Retinal and systemic vasculitides have been associated with the development of BRVO.[16–18]

Pathogenesis

The pathologic interruption of venous flow in eyes with BRVO almost always occurs at an arteriovenous crossing.[19–22] In 99% of 106

eyes with BRVO, the artery was found to cross over the obstructed vein.[20] This observation coupled with the strong association of BRVO with systemic hypertension and arteriosclerosis support the theory that mechanical compression plays a role in the pathogenesis of BRVO.[20,21] Histopathologically, the retinal artery and vein share a common adventitial sheath, and in some cases, a common medium.[23] The lumen of the vein may be compressed up to 33% at a normal arteriovenous crossing site, and this may be further exacerbated by increased rigidity and thickening of the arterial wall due to arterioscelerosis.[22–24] The vitreous may also play a role in compression of susceptible arteriovenous crossing sites, as evidenced by studies demonstrating that eyes with decreased axial length and higher likelihood of vitreomacular attachment at the arteriovenous crossing are at increased risk of BRVO.[12,15,22]

Some have postulated that turbulent blood flow at the crossing site causes focal swelling of the endothelium and thicker vein wall tissue, leading to venous obstruction.[22,23,25] Based on histopathologic studies, others have suggested that venous thrombus formation at the point of occlusion is the primary pathologic event.[26]

It is likely that the pathogenesis of BRVO is multifactorial with contributions from mechanical obstruction, degeneration of the vessel wall, and hematologic abnormalities, such as inflammatory disorders and thrombophilia, in at-risk individuals.[24,27]

The resulting venous obstruction leads to elevation of venous pressure upstream of the crossing that may overload the collateral drainage capacity resulting in intraretinal hemorrhages, macular edema, and ischemia.[22,28]

Clinical Features

Symptoms

Patients with BRVO present with sudden painless loss of vision or a visual field defect. Subclinical presentations may occur if a tributary distal to the macula or a nasal retinal vein is involved. Rarely, patients with BRVO will present with floaters from a vitreous hemorrhage if the initial vein occlusion was unrecognized and retinal neovascularization has occurred.

Signs

Patients typically present with a wedge-shaped distribution of intraretinal hemorrhage that is less marked if the occlusion is perfused (or nonischemic), and more extensive if the occlusion is nonperfused (or ischemic) and associated with retinal capillary nonperfusion. The Branch Vein Occlusion Study Group (BVOS) defined ischemic BRVO as those with greater than a total of five disc diameters of nonperfusion on fluorescein angiography (FA).[1] The location of the venous blockage determines the distribution of the intraretinal hemorrhage; if the venous obstruction is at the optic nerve head, two quadrants of the fundus may be involved, whereas if the occlusion is peripheral to the disc, one quadrant or less may be involved. If the venous blockage is peripheral to tributary veins draining the macula, there may be no macular involvement and consequently minimal to no decrease in visual acuity.

The most common location for BRVOs is in the superotemporal quadrant.[20,29] This favored location may be attributed to a larger number of arteriovenous crossings in the superotemporal quadrant.[20] Fig. 56.1 demonstrates the typical acute appearance of a BRVO involving the superotemporal quadrant of the right eye. A narrowed branch retinal vein passing under a retinal artery can sometimes be identified proximal to the hemorrhage. Rarely, a patient may present initially with very little intraretinal hemorrhage, which then becomes more extensive in the succeeding weeks to months. In these instances, it is presumed that an incomplete block at the arteriovenous crossing has progressed to more complete occlusion.

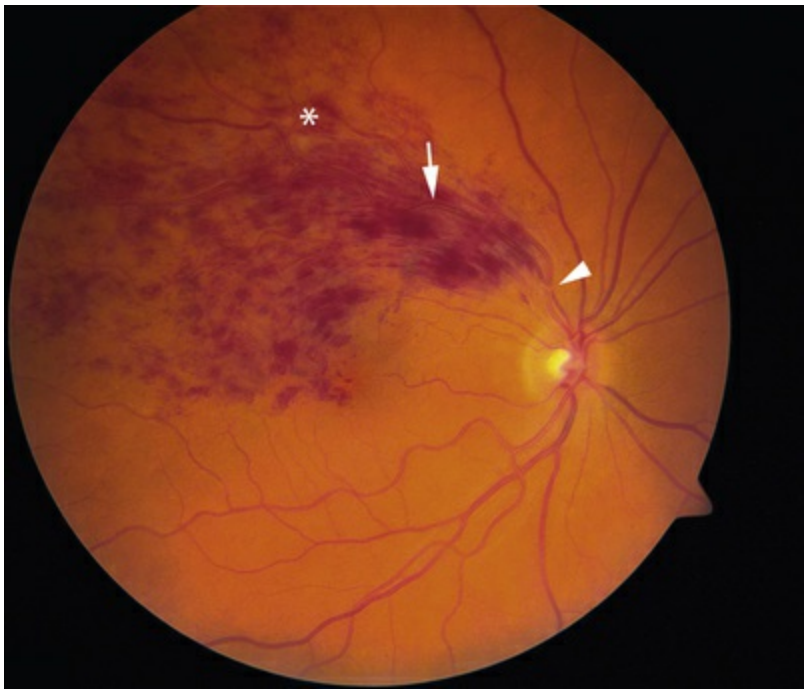

FIG. 56.1 Acute branch retinal vein occlusion. Intraretinal hemorrhages in a wedge-shaped pattern delineating the area drained by the occluded vein. The occluded vessel is often seen passing underneath a retinal artery (*arrowhead*). Cotton-wool spots (*asterisk*) are sometimes seen. Note the dilated and tortuous occluded vein (*arrow*) compared to the normal retinal vein in the inferior arcade.

Over time the intraretinal hemorrhage may completely resorb. Without the characteristic segmental distribution of intraretinal hemorrhage, the ophthalmoscopic diagnosis may be more difficult in this situation, but the segmental distribution of retinal vascular abnormalities that occurred during the acute phase will persist and be apparent on FA. In many cases, macular edema can be detected by optical coherence tomography (OCT). The presence of intraretinal fluid, subretinal fluid, or cystoid macular edema is visible on OCT B-scans, and three-dimensional (3D) views or retinal thickness maps can reveal areas of localized increased retinal thickening. In the chronic phase of the disease, after intraretinal hemorrhage absorption, the diagnosis may depend on detecting a segmental distribution of retinal vascular abnormalities that may include capillary nonperfusion, dilation of capillaries, microaneurysms, telangiectatic vessels, and collateral vessel formation (Fig. 56.2).

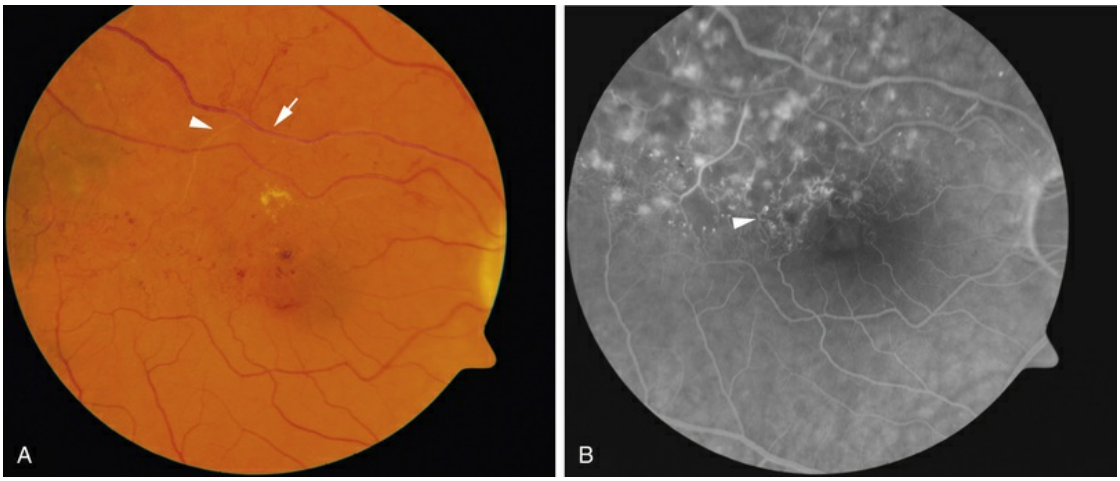

FIG. 56.2 Chronic branch retinal vein occlusion. (A) Color fundus photograph showing microaneurysms, exudates, and a sclerosed retinal vein (*arrowhead*) draining into a sheathed vessel (*arrow*). (B) Corresponding mid- to late-phase fluorescein angiogram shows abundant collaterals (arrowhead) and highlights the microvascular abnormalities.

Complications

There are three common vision-limiting complications of BRVO: (1) macular edema; (2) macular ischemia; and (3) sequelae of neovascularization.

During the acute phase, extensive intraretinal hemorrhages may block the view of macular ischemia and leakage on the FA. Under these circumstances it is impossible to evaluate the perfusion status because the hemorrhage itself blocks the view of the vasculature. In addition, the hemorrhage in the foveal center may reduce visual acuity independently of any macular edema or ischemia. Since this reduction in visual acuity may completely recover if there is no other cause for the visual loss, such as macular edema or macular capillary nonperfusion, observation in these cases can be considered. When there is extensive foveal hemorrhage, OCT is an important ancillary test to look for macular edema.

Retinal and iris neovascularization, vitreous hemorrhage, traction retinal detachment, and neovascular glaucoma are complications that manifest late in the course of the disease due to ischemia. With the exception of macular ischemia, these complications can largely

be treated or prevented. Thus, it is important that patients with BRVO be closely followed.

Natural History

In order to accurately counsel patients on prognosis and weigh the effectiveness of different treatment options, it is important to understand the natural history of BRVO. To this end, Rogers and associates performed a systematic review of all BRVO articles published through 2008 and found that, in 1608 eyes, visual acuity generally improved without treatment although improvement beyond 20/40 was uncommon. Macular edema developed in 5–15% of eyes over a period of 1 year and of those presenting with macular edema, 18–41% resolved by 1 year.[2]

BRVO is a broad classification of one type of retinal vascular disease which may be subtyped to better predict visual prognosis and the development of vision-limiting complications. In the Branch Vein Occlusion Study, 31–41% of patients with ischemic BRVO (defined as >5 disc diameters of nonperfusion on FA) developed neovascularization or vitreous hemorrhage compared with 11% of patients with nonischemic BRVO.[1] Thus, eyes with ischemic BRVO may need to be followed more closely.

BRVO may also be subtyped as a major BRVO where one of the four major branch retinal veins is affected or macular BRVO where only a smaller, macular vein is occluded. Hayreh et al. found that retinal and optic disc neovascularization occurred only in major BRVO. Although time to resolution of macular edema was similar in both major and macular BRVO (20.8 months vs. 18.2, respectively), eyes with macular BRVO did not show the same improvement in visual acuity with resolution of macular edema as eyes with major BRVO (58% vs. 76% improved, respectively).[30,31]

Clinical Evaluation

Clinical Examination

A complete ophthalmic examination should be performed, paying particular attention to the history of glaucoma and signs of

intraocular inflammation, since these may be risk factors for BRVO. Careful examination of the iris and angle should be performed in appropriate cases to monitor for early signs of rubeosis or neovascular glaucoma. Initially, when the risk of macular edema and neovascularization is higher, patients should be followed every month. Once stable, and if visually significant macular edema and other complications are not present, follow-up can be extended.

Fluorescein Angiography

To help verify the diagnosis and evaluate for complications, FA should be obtained to delineate the retinal vascular characteristics that may have prognostic significance: macular leakage and edema, macular ischemia, and large segments of capillary nonperfusion that may portend eventual neovascularization. FA is the only technique that will accurately define the capillary abnormalities in BRVO; it is therefore particularly important that high-quality angiography be obtained (Fig. 56.3).

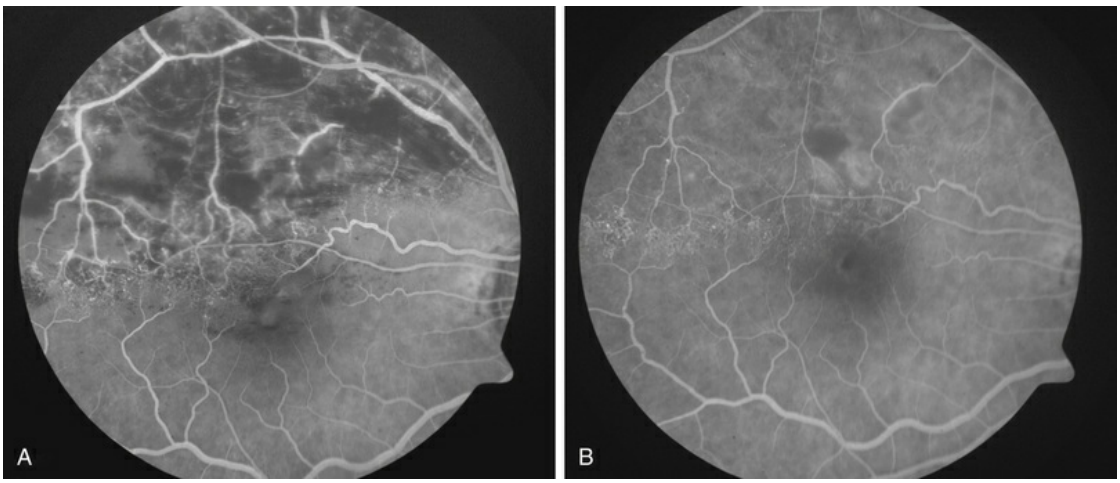

FIG. 56.3 Fluorescein angiogram of branch retinal vein occlusion. (A) Blocked fluorescence from intraretinal hemorrhage is common in acute branch retinal vein occlusion. Note the telangiectatic vessels forming collaterals across the horizontal raphe. The hemorrhages obscure underlying areas of capillary nonperfusion and edema. (B) Six months later, the hemorrhages have cleared, revealing small patches of nonperfusion and macular edema.

The characteristic finding on FA is delayed filling of the occluded retinal vein. Varying amounts of capillary nonperfusion, blockage from intraretinal hemorrhages, microaneurysms, telangiectatic collateral vessels, and dye extravasation from macular edema or retinal neovascularization are other features encountered. In chronic cases, when the hemorrhages have resolved, microvascular changes on FA may provide the only clues of a previous BRVO.

When FA demonstrates macular leakage and edema with cystoid involvement of the fovea, but no capillary nonperfusion, it is presumed that the macular edema is the cause of vision loss. When macular edema is present ophthalmoscopically within the first 6 months after a BRVO and there is little or no leakage on FA, macular ischemia may be the cause of the macular edema. In such circumstances, the edema almost always spontaneously resorbs in the first year after the occlusion, often with improvement in visual acuity.[32] Studies have shown conflicting results as to whether the severity of capillary nonperfusion in the macular region is associated with the degree of improvement in visual acuity. Finkelstein showed that eyes with a broken foveal capillary ring had greater improvement in visual acuity than those with intact capillary perfusion, while a retrospective study by Hayreh failed to demonstrate any such correlation.[31,32]

Unfortunately, acute BRVOs with dense intraretinal hemorrhages may make FA interpretation challenging due to blockage of fluorescence by the hemorrhages. Thus, it is advisable to obtain FA only after the intraretinal hemorrhages have cleared significantly from the macula. Other diagnostic tests, such as OCT, can be obtained in the acute phase to aid in the diagnosis of macular edema.

Wide-Field Angiography

Ultrawide-field fluorescein angiography (UWFA) is not yet a commonly used imaging modality for patients with BRVO; however, it may help elucidate the role of peripheral retinal vascular pathology in the pathogenesis of vision loss in eyes with RVOs. It is very useful to delineate areas of peripheral nonperfusion and help categorize a patient based on perfusion status. A retrospective study of patients with branch and

hemiretinal vein occlusions using the Optos C200MA ultrawide-field imaging system revealed that peripheral retinal nonperfusion (Fig. 56.4) is correlated with both macular edema and retinal neovascularization.[33] Future studies are needed to determine whether laser photocoagulation targeted to areas of peripheral retinal nonperfusion decreases macular edema, reduces treatment burden, and regresses neovascularization in patients with BRVOs.

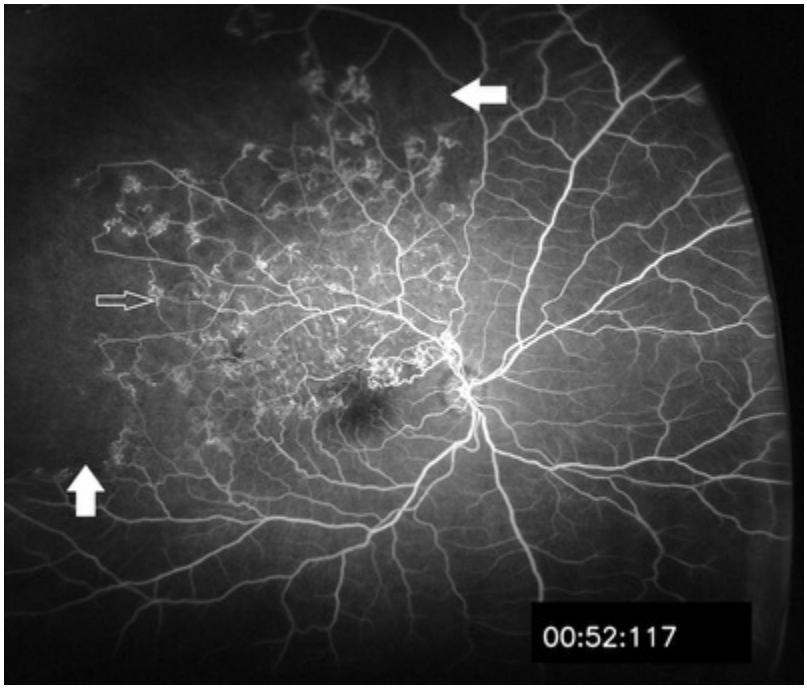

FIG. 56.4 Wide-field fluorescein angiogram using the Optos200TX ultrawide-field imaging system demonstrating extensive area of peripheral nonperfusion (*outlined by solid arrows*) and collateral formation (*hollow arrow*) in a patient with a superotemporal BRVO and chronic macular edema.

Optical Coherence Tomography

OCT has arguably become the most important imaging modality in the treatment of patients with BRVO and macular edema. OCT offers a noninvasive and rapid method of quantitatively measuring macular edema and its response to treatment. The characteristic findings of BRVO on OCT B-scans are cystoid macular edema, intraretinal hyperreflectivity from hemorrhages or exudates,

shadowing from edema and hemorrhages, and occasionally subretinal fluid[34,35] (Fig. 56.5A). Cube or 3D scans are also useful to delineate the areas of retinal thickening and to monitor for changes with treatment. OCT has been shown to be more sensitive in detecting macular edema and subretinal fluid in patients with BRVO than clinical examination or FA, and may be especially helpful in the acute setting when blockage from intraretinal hemorrhages limits the interpretation of FA.[34] In chronic cases, photoreceptor ellipsoid zone and external limiting membrane abnormalities from longstanding macular ischemia and macula edema may also be seen (Fig. 56.5B). Integrity of the ellipsoid zone on baseline OCT in patients with macular edema from BRVO has been associated with better visual outcome after treatment of the macular edema.[36] When these structures are disrupted or absent, visual improvement is less likely.

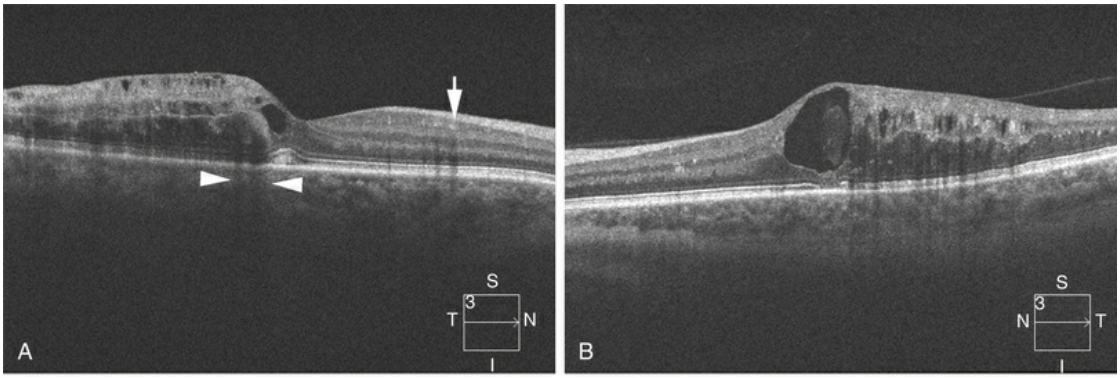

FIG. 56.5 Spectral-domain optical coherence tomography (OCT) of an eye with a branch retinal vein occlusion (BRVO). (A) Raster scan of the BRVO in Fig. 56.1 reveals cystoid macular edema, intraretinal fluid, and shadowing (*between arrowheads*). Intraretinal heme (*arrow*) appears hyperreflective and produces a shadow on OCT. (B) Raster scan of a chronic BRVO with inner/outer-segment abnormalities and a large cyst.

Diagnostic Workup

Young Patient

BRVO typically occurs in patients beyond their sixth decade of life.[2] Younger patients with BRVO may have a higher prevalence of cardiovascular risk factors than their age-matched counterparts, including hypertension, hyperlipidemia, and an increased body mass index.[37] However, if no cardiovascular risk factors are identified, it is important to rule out any other predisposing condition. Although the role of thrombophilic risk factors in retinal vein occlusion is still controversial, there have been case series that suggest a higher risk of thrombophilic disorders, such as Factor V Leiden mutation, in younger patients presenting with RVO.[38,39] A detailed history should be taken focusing on personal or family history of venous thromboembolism or underlying hypercoagulable condition. A thorough ophthalmologic history and examination should evaluate for ocular diseases such as glaucoma or uveitis that may predispose to RVO.

Based upon the results of the history and examination, workup should be tailored to the patient and performed in consultation with an internist. Systemic blood pressure should be checked and the patient should be screened for undiagnosed cardiovascular risk factors, including hyperlipidemia and diabetes.

In young patients without cardiovascular risk factors or with systemic symptoms suggestive of a coagulopathy, workup should include a complete blood count, prothrombin time/partial thromboplastin time/international normalized ratio, lipid panel, serum homocysteine, anticardiolipin antibodies, antinuclear antibodies with lupus anticoagulant, protein C/S, antithrombin III, activated protein C resistance, and factor V Leiden.[10,40]

Older Patient

In patients older than 60 years, additional workup is usually not necessary since the majority of these cases are idiopathic or due to hypertension or atherosclerosis.

Bilateral or Numerous BRVO Patients

In bilateral cases and cases with a history of multiple BRVOs, searching for an infectious or inflammatory disorder or hypercoagulopathy may be warranted. Although the vast majority of these cases can be attributed to systemic hypertension, there are

numerous case reports of patients with bilateral vein occlusions and systemic inflammatory disorders or hypercoagulopathies.[41–43] The workup should proceed in the manner described for young patients.

Treatment Options

Treatment of Underlying Etiology

Systemic Anticoagulation

In cases where a hypercoagulopathy has been identified, anticoagulation may be considered in consultation with an internist. In most cases, however, anticoagulant therapy has not been shown to be beneficial in either the prevention or the management of BRVO. Since the systemic administration of anticoagulants can be associated with systemic complications, and could, in theory, increase the severity of intraretinal hemorrhage occurring in the acute phase, such therapy is generally not recommended.

Vitrectomy With Sheathotomy

The majority of the venous lesions in BRVO occur downstream from the arteriovenous crossing site. In a retrospective review of color photographs and FAs of patients with BRVO, Kumar and associates[22] identified venous narrowing at the crossing site, and in the majority of cases, evidence of downstream hemodynamic changes on angiogram, including venous-phase leakage, abnormal flow, and presumed thrombi. The authors suggested that removal of the compressive factor by sectioning the adventitial sheath (sheathotomy) was a potentially effective treatment for BRVO.

In the first report of sheathotomy for BRVO, Osterloh and Charles[44] reported significant visual improvement in the one case (20/200 to 20/25+ over 8 months). In the second report, Opremcak and Bruce[45] reported equal or improved visual acuity in 12 of 15 patients (80%). Ten of those patients (67%) had improved postoperative visual acuities, with an average gain of four lines of vision. Three patients had a decline in visual acuity, with an average of two lines of vision lost. All patients had marked resolution of the intraretinal hemorrhage and edema. Mester and

Dillinger reported 43 cases of BRVO treated with sheathotomy with similar results. In 16 of the cases, removal of the internal limiting membrane in the area of the arteriovenous crossing was also performed.[46] Despite these promising results, there have been many case series and retrospective reviews of patients treated with vitrectomy and sheathotomy that have not shown a statistically significant improvement in postoperative median visual acuity.[47–48] Some authors have experienced difficulty in separating the artery from the vein at the crossing site. Han and colleagues reported 20 cases of vitrectomy and attempted sheathotomy. While the visual outcome results were similar to those reported by Opremcak and Bruce, in 19 of the 20 cases, the authors were unable to separate the artery from the vein.[49] No randomized, controlled study evaluating the benefit of sheathotomy has been published. Given the potential complications of the procedure, including retinal tear, retinal detachment, vascular bleeding, nerve fiber layer defects with associated scotoma, vitreous hemorrhage, and postoperative cataract,[50] vitrectomy with sheathotomy is currently not employed as first-line therapy.

Treatment of Vision-Limiting Complications

Treatment of Neovascularization and Vitreous Hemorrhage

Laser Treatment.

The collaborative BVOS,[1] a multicenter randomized clinical trial supported by the National Eye Institute, randomized patients with BRVO to receive panretinal scatter photocoagulation to prevent neovascular complications.[1] They reported that eyes with ischemic BRVO that show large areas (>5 disc diameters) of retinal capillary nonperfusion have approximately a 40% chance of developing neovascularization (NV) and that about 60% of those eyes with NV will experience periodic vitreous hemorrhage. If peripheral scatter laser photocoagulation is applied in eyes with large areas of nonperfusion, the incidence of neovascularization can be reduced from about 40% to 20%. However, if one were to treat prophylactically, many eyes (60%) that would never develop

neovascularization would receive peripheral scatter laser photocoagulation and the subsequent side-effects of such treatment. The BVOS data also strongly suggest that photocoagulation after the development of neovascularization is as effective in preventing vitreous hemorrhage as is photocoagulation before the development of neovascularization.[1] For these reasons, it is recommended that laser photocoagulation be applied only after neovascularization is observed.

Iris neovascularization is a rare complication of BRVO; it appears, however, that diabetes (with or without retinopathy) may increase this risk. Retinal neovascularization is particularly difficult to recognize in BRVO because the collaterals that develop frequently may mimic neovascularization. Arising presumably from preexisting capillaries, these collaterals occur as vein-to-vein channels around the blockage site, across the temporal raphe, and in other locations to bypass the blocked retinal segment. These collaterals frequently become quite tortuous, mimicking the appearance of neovascularization if they are evaluated by ophthalmoscopy alone. When it is unclear whether an abnormal vascular pattern represents collateral formation or true neovascularization, FA (Fig. 56.6) can be helpful because leakage from neovascularization is more prominent than from collateral vessels.

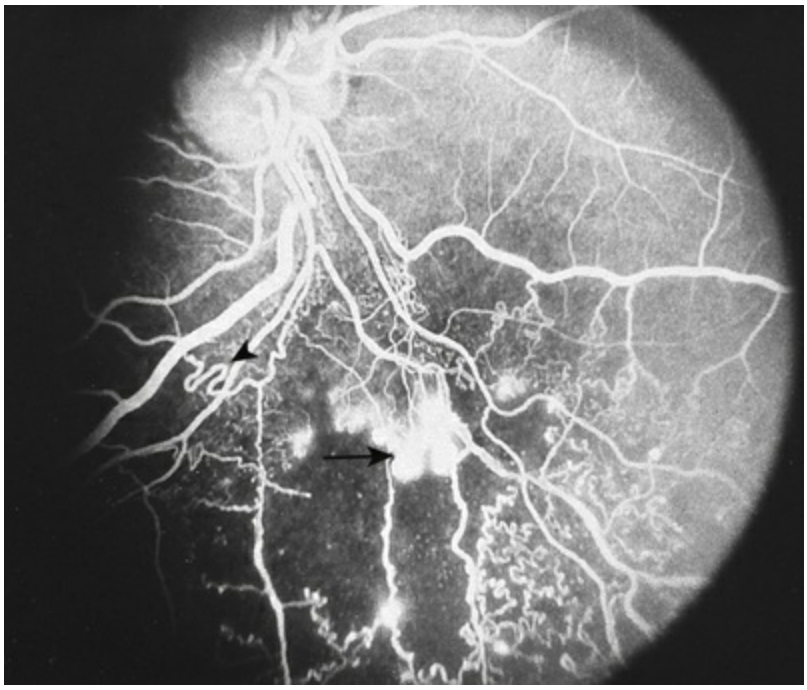

FIG. 56.6 Retinal neovascularization with leakage (*arrow*) can be differentiated from collaterals that are not leaking (*arrowhead*).

When neovascularization is unequivocally confirmed by FA or UWFA, peripheral scatter laser photocoagulation can reduce the likelihood of vitreous hemorrhage from about 60% to 30%.[1] As demonstrated in Fig. 56.7, the scatter laser photocoagulation can be applied with argon blue–green laser to achieve "medium" white burns (200–500 μm in diameter) spaced one burn width apart and covering the entire area of capillary nonperfusion, as defined by FA, but extending no closer than two disc diameters from the center of the fovea and extending peripherally at least to the equator. Retrobulbar anesthesia can be used as needed for discomfort associated with the scatter photocoagulation, but generally is not required.

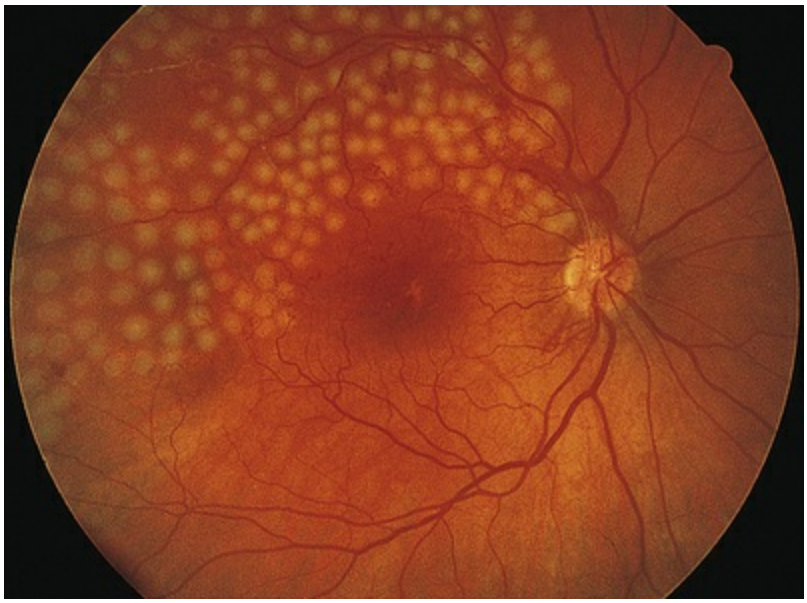

FIG. 56.7 Immediate posttreatment fundus photograph showing pattern of peripheral scatter photocoagulation.

Familiarity with the laser treatment technique is required to individualize the treatment. Important variables, such as residual intraretinal hemorrhage, thickness of the retina from edema, location of collaterals, and presence of retinal traction, influence the exact mode of therapy within the above general treatment guidelines. There are numerous complications of laser photocoagulation; however, it is generally recognized that with proper attention to detail, complications are infrequent. Side-effects of treatment, including generation of scotoma, merit careful consideration and discussion with the patient before initiation of treatment. It is particularly important to recognize that laser photocoagulation should never be placed over extensive intraretinal hemorrhage in the acute phase of branch vein occlusion because the laser energy will be absorbed by the intraretinal hemorrhage rather than at the level of the pigment epithelium, likely damaging the nerve fiber layer and possibly enhancing the development of preretinal fibrosis.

Of patients who develop neovascularization, approximately 60% experience episodes of vitreous hemorrhage if the condition is left untreated. The short- and long-term visual consequences of vitreous hemorrhage in BRVO have not been carefully studied. In some cases, the hemorrhage may be mild or may clear spontaneously without causing permanent visual impairment.

However, in some patients, vitreous hemorrhage from neovascularization can lead to prolonged visual disability in the affected eye. When the hemorrhage is dense, B-scan ultrasonography may help rule out an associated traction retinal detachment. Most eyes can be observed. If the vitreous hemorrhage does not spontaneously clear in a few months, a pars plana vitrectomy with sector endolaser photocoagulation can be considered.

Treatment of Macular Edema

Laser Treatment

A separate group of patients in the BVOS were randomized to determine whether argon laser photocoagulation may reduce visual loss from macular edema. Important eligibility criteria included fluorescein-proven, perfused macular edema involving the foveal center, clearing of intraretinal hemorrhage from the foveal center, recent BRVO (usually 3–18 months' duration), no diabetic retinopathy, and vision reduced to 20/40 or worse after best corrected refraction.[51] Argon laser photocoagulation was applied in a grid pattern throughout the leaking area demonstrated by FA (Fig. 56.8). Laser treatment extended no closer to the fovea than the edge of the capillary-free zone and no further into the periphery than the major vascular arcade. Recommended treatment parameters included a duration of 0.1 second, a 100-μm diameter spot size, and a power setting sufficient to produce a “medium” white burn. FA was repeated 2–4 months after the treatment, and additional photocoagulation was applied to residual areas of leakage if reduced visual acuity persisted.

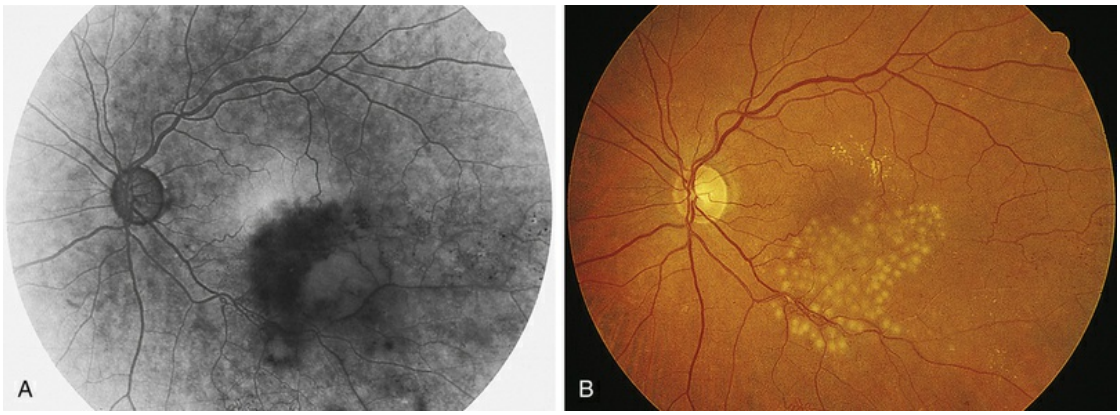

FIG. 56.8 Grid macular laser for macular edema. (A) Fluorescein angiogram, late phase, demonstrating macular edema with foveal involvement. (B) Immediate posttreatment fundus photograph showing grid pattern of laser photocoagulation.

Improvement in visual acuity was assessed in several ways.[51] When improvement was defined as reading two or more Snellen lines better than baseline at two consecutive visits, treated eyes showed visual improvement more often than untreated eyes. After 3 years of follow-up, 63% of treated eyes gained two or more lines of vision, compared to 36% of untreated eyes. The average gain in visual acuity for treated eyes was one more Snellen line than in untreated eyes.

Before laser photocoagulation is performed, it is important to obtain high-quality FAs of the macula; the FA must demonstrate that the macular edema involves the center of the fovea and that there is not a large amount of capillary nonperfusion adjacent to the capillary-free zone that could explain the visual loss. In addition, it is important to follow patients for a length of time sufficient to ascertain that macular edema is not resolving spontaneously. During this period of follow-up, it should be demonstrated that there is clearing of intraretinal hemorrhage and that there is no hemorrhage in the center of the fovea that could account for a spontaneously reversible cause of visual loss. In the application of the grid photocoagulation, laser absorption occurs at the level of the pigment epithelium; photocoagulation is not applied to close the leaking and dilated capillary vasculature directly and immediately. Although it is not understood how the laser treatment may act in lessening edema, it is interesting to note that preliminary

experimental studies in the normal primate have shown a decrease in capillary diameter when this form of therapy is used and when laser absorption occurs at the level of the pigment epithelium.[52] One explanation for the effect of grid pattern photocoagulation is that it results in a thinning of the retina (in particular the outer retina), reducing oxygen consumption and increasing choroidal delivery of oxygen to the inner retina, producing a consequent autoregulatory constriction of the retinal vasculature in the leaking area and thereby decreasing the edema.

In the application of grid pattern laser photocoagulation, it is crucial to obtain good definition of landmarks so that the center of the fovea can be identified and avoided. Since landmarks frequently may be obscured in the macula after BRVO, such cases can be managed more effectively and safely by treating well peripheral to the capillary-free zone in the first sitting. When the patient returns in 2 months for follow-up evaluation, a repeat FA may identify more clearly the amount of further treatment that needs to be applied closer to the edge of the capillary-free zone, because the pigmentation of the previous treatment is then visible. Consequently, treatment in this next sitting may be advanced closer to the edge of the capillary-free zone, if that is deemed necessary because of persistent foveal edema and vision loss. The placement of grid laser treatment in this repetitively staged fashion may be safer and appears to be just as effective as a single treatment.

For the grid treatment used in the BVOS, the argon blue–green wavelength was employed.[51] This is the only wavelength that has been proven effective and it is unknown whether argon green and krypton red photocoagulation are equally effective. In other diseases, when laser treatment is applied inside the capillary-free zone, it is recognized that krypton red and argon green laser photocoagulation are absorbed less than blue–green by the xanthophyll pigment of the inner retina that is present in increasing concentrations close to the foveal center. However, because the grid treatment never comes closer to the fovea than the capillary-free zone, the BVOS did not encounter any problems with the argon blue–green laser in this region; consequently, this laser continues to be recommended.

In the past, the summary recommendations for management of

acute branch vein occlusion from the BVOS emphasize waiting for several months before considering laser therapy. If the vision is reduced to 20/40 or worse, clinicians were advised to wait 3–6 months for sufficient clearing of retinal hemorrhage to permit high-quality FA and then evaluate for macular edema and macular ischemia. If perfused macular edema accounts for the visual loss, and vision continues to be 20/40 or worse without spontaneous improvement, grid macular photocoagulation was considered. However, the BVOS conclusions need to be balanced against the improvements in vision seen with anti-vascular endothelial growth factor (VEGF) agents. In general, laser therapy is a second- or even third-line therapy, as the anti-VEGF agents have considerably better efficacy. It should also be noted that if macular ischemia accounts for the visual loss, no laser treatment is recommended.

Steroid Treatment

Macular edema in BRVO results from increased vascular permeability mediated at least in part by upregulation of VEGF.[53] Intravitreal steroids have been shown in animal models to inhibit the expression of VEGF and thus reduce macular edema in retinal vascular disease.[54,55] In addition, inflammatory cells around the site of the occlusion are often present. Although intraocular corticosteroids are generally well tolerated, they can have significant side-effects, including cataract formation and glaucoma. Several trials have evaluated the use of corticosteroids in the treatment of macular edema in BRVO.

Triamcinolone.

In the Standard Care vs. Corticosteroid for Retinal Vein Occlusion (SCORE) BRVO study, the effectiveness and safety of intravitreal triamcinolone acetate (IVTA) for the treatment of macular edema from BRVO were evaluated.[56] In this multicenter, randomized controlled study, 411 patients were randomized to receive macular grid laser, 1 mg IVTA, or 4 mg IVTA. Retreatment was allowed every 4 months for each group unless the treatment was successful, futile, or contraindicated. There was no significant difference in vision or the reduction of macular edema measured by OCT at the end of 12 months between each group. Respectively, 29%, 26%, and

27% of eyes in the laser, 1-mg IVTA, and 4-mg IVTA groups gained a visual acuity score of ≥15 ETDRS letters. Subgroup analysis of pseudophakic eyes also failed to demonstrate a significant difference in vision. Three-year results from 128 patients suggested that the laser group maintained a significantly greater average increase in vision (12.9 letters) compared with the two IVTA groups (4.4 letters, 1-mg and 8.0 letters, 4-mg). Significant side-effects from IVTA included cataract formation and elevation of intraocular pressure (IOP) requiring treatment. Both side-effects were dose-dependent.[56]

As a result of this study, IVTA is not recommended as first-line therapy for macular edema in BRVO. However, it can be considered in patients where anti-VEGF injections or macular grid laser are ineffective, as the treatment was found to be relatively safe, especially in pseudophakic eyes.

Dexamethasone Implant.

The Global Evaluation of Implantable Dexamethasone in Retinal Vein Occlusion with Macular Edema (GENEVA) study evaluated a sustained-release, biodegradable, dexamethasone intravitreal implant (Ozurdex, Allergan, Irvine, CA) for the treatment of macular edema in central retinal vein occlusion (CRVO) and BRVO patients.[57] Ozurdex is a biodegradable copolymer of poly (d,l-lactide-co-glycolide) acid (PLGA) containing micronized dexamethasone. It is injected intravitreally through a pars plana route using a 23-gauge custom injector, and it gradually releases the total dose of dexamethasone over several months via Krebs cycle breakdown of the PLGA into lactic and glycolic acid, and finally into water and carbon dioxide. In this multicenter, randomized controlled study, the primary outcome of an increase in best corrected visual acuity (BCVA) of ≥15 ETDRS letters was achieved in 30% of the Ozurdex 0.7-mg group (n=291), 26% of the 0.35-mg group (n=260), and 13% of the sham group (n=279) 60 days after injection (peak response) in patients with BRVO (p<.001 for each group versus sham). A statistically significant difference between both Ozurdex groups and sham was seen up to 90 days after injection. At 90 days after injection, there was a significant improvement (p<.001) in central retinal thickness measured by OCT

in both Ozurdex groups, compared with the sham group. The mean SD decrease in central retinal thickness at 90 days was 208±201 μm, 177±197 μm, and 85±173 μm in the 0.7-mg, 0.35-mg and sham groups, respectively. The OCT results are from pooled data including both BRVO and CRVO patients. The only complications that were significantly greater in the Ozurdex groups compared with sham were elevated IOP and anterior-chamber cell. Most eyes with elevated IOP were successfully managed with topical therapy, but five eyes required a procedure to lower the pressure adequately.

The study was followed by a 6-month open-label extension in which all groups, including sham, were eligible for a 0.7-mg Ozurdex injection at Day 180 on an as-needed basis. The results demonstrated that there is no increase in the risk of serious adverse effects, including IOP rise, with a second treatment; however, there was a statistically significant increase in the development of cataract with repeated injection. The improvement in BCVA after the second treatment was similar to that achieved after the first treatment; however, the improvements in BCVA in the delayed-treatment group (initial sham group) never matched those who received earlier treatment.[58]

A major difference between the GENEVA study and other recent BRVO studies is the absence of a macular grid laser group, or rescue laser treatment for the sham group. The GENEVA study showed that the dexamethasone implant is an alternative treatment to macular grid laser in the appropriate patient population (i.e., no glaucoma, pseudophakic) and is approved by the Food and Drug Administration (FDA) for this indication. Future studies are needed to determine the optimum interval and criteria for retreatment.

Anti-VEGF Treatment

In patients with BRVO, retinal ischemia leads to the secretion of VEGF, which leads to increased vascular permeability, vasodilation, migration of endothelial cells, and neovascularization.[53,59,60] Increased vascular permeability and perhaps vasodilation lead to retinal edema. Thus, inhibition of VEGF is an attractive treatment for macular edema from BRVO. There are several anti-VEGF agents currently used in the treatment of RVOs. We will discuss the use of

ranibizumab (Lucentis), bevacizumab (Avastin), and aflibercept (Eylea). Ranibizumab is an affinity-matured, humanized monoclonal antibody fragment (Fab) that binds all VEGF-A isoforms. Aflibercept is a fusion protein composed of key binding domains from VEGF receptors 1 and 2 fused to the Fc portion of human immunoglobulin G that binds all isoforms of VEGF-A, VEGF-B, VEGF-C, and placental growth factor (PlGF). Bevacizumab is a full-length, humanized monoclonal antibody that binds all VEGF-A isoforms and is FDA-approved for colorectal cancer, but is used off-label in the eye. At this time, ranibizumab and aflibercept are both FDA-approved for the treatment of macular edema secondary to RVO.

Ranibizumab.

The Branch Retinal Vein Occlusion (BRAVO) study was a prospective, multicenter, randomized controlled study to evaluate the efficacy and safety of ranibizumab in the treatment of macular edema from BRVO.[61] Patients were randomized into three groups: (1) sham injection (n=132); (2) 0.3-mg ranibizumab (n=134); and (3) 0.5-mg ranibizumab (n=131). In the first 6 months, injections were given monthly. A 28-day screening period excluded patients with spontaneous and rapid improvement in vision of >10 ETDRS letters. At month 3, a patient was eligible for rescue laser if a gain of <5 ETDRS letters, or improvement of <50 μm in central subfield thickness, was observed compared with the visit 3 months prior. If rescue laser was not applied at month 3, the same criteria were used to determine eligibility for rescue laser at each subsequent monthly visit. At 6 months, both ranibizumab groups gained +16.6 and +18.3 ETDRS letters (0.3-mg and 0.5-mg groups, respectively) compared with a gain of +7.3 letters in the control group (p<.0001 for each group versus sham). The percentage of patients who improved greater than 15 ETDRS letters was 55.2% and 61.1% (0.3-mg and 0.5-mg groups, respectively) compared with 28.8% in the control group (p<.0001 for each group versus sham). During the first 6 months, 54.5% of the control group required rescue laser therapy compared with 18.7% in the 0.3-mg and 19.8% in the 0.5-mg ranibizumab groups.[61]

After the first 6 months, all three groups were allowed to receive

"as needed" (PRN) intravitreal ranibizumab (0.5 mg for sham group, ranibizumab groups continued to receive their respective doses) at monthly intervals if they had vision ≤20/40 or mean central foveal thickness ≥250 μm. Despite receiving only PRN treatments, patients in both ranibizumab groups maintained their vision gain at 12 months. Although the control group showed a benefit from the PRN treatment regimen, the final vision gained at 12 months was not equivalent to that achieved in the eyes started on prompt ranibizumab treatment.[62]

The HORIZON Trial was an open-label extension of BRAVO in which patients were seen at least every 3 months and given 0.5 mg ranibizumab if mean central foveal thickness was ≥250 μm or if there was persistent macular edema deemed to be affecting the patient's visual acuity. Patients received significantly fewer injections than during the first year of the trial averaging 2.4 injections (0.3/0.5-mg group), 2.1 injections (0.5/0.5-mg group), and 2.0 injections (sham/0.5-mg group); however, visual acuity gains were still maintained. The mean change in BCVA letter score at 12 months from the HORIZON baseline was −2.3, −0.7, and 0.9 in the 0.3/0.5-mg, 0.5/0.5-mg, and sham/0.5-mg treatment groups, respectively. No additional adverse events were identified.[63]

Aflibercept.

The VIBRANT study was a double-masked, active-controlled, randomized, multicenter phase III trial comparing the safety and efficacy of intravitreal aflibercept versus macular grid laser in the treatment of macular edema from BRVO. Eyes were randomized to 2 mg intravitreal aflibercept (IAI) every 4 weeks (for a series of 6 injections, n=91) or grid laser (with rescue if needed, n=92). The primary outcome was percentage of eyes which gained ≥15 ETDRS letters at week 24. In the IAI group, 52.7% of eyes achieved the primary outcome versus 26.7% of eyes in the laser group. The IAI group gained an average of 17.0 ETDRS letters compared to 6.9 letters (p=.0003) in the laser group and achieved a mean reduction of 280.5 μm in central retinal thickness compared to 128 μm in the laser group (p<.0001). VIBRANT was the first trial to compare anti-VEGF therapy directly with laser and the results were strongly in favor of aflibercept with similar side-effect profiles in both groups.[64]

Bevacizumab.

Bevacizumab is currently used off-label for the treatment of macular edema related to BRVO and is an attractive therapeutic option due to its relatively low cost compared to other anti-VEGF agents. Although there have been no multicenter, randomized-controlled trials evaluating the safety and efficacy of bevacizumab in treating macular edema from BRVO, there have been numerous case series and small prospective studies showing that bevacizumab is effective at improving visual acuity and decreasing macular edema, as measured by OCT.[65–69] Recently, the MARVEL study group published a prospective, randomized, noninferiority trial comparing PRN bevacizumab to ranibizumab for the treatment of macular edema secondary to BRVO. Although the study was underpowered to show noninferiority, it did show a similar increase in BCVA (15.6 vs. 18.1 ETDRS letters) and decrease in central retinal thickness (−201.7 vs. −177.1 μm) in the bevacizumab and ranibizumab groups, respectively.[70] A retrospective study comparing bevacizumab to ranibizumab for macular edema secondary to RVO (CRVO and BRVO) also showed similar efficacy with regard to anatomic and visual outcomes.[71] Thus, bevacizumab is a viable treatment option for macular edema secondary to BRVO. The National Eye Institute is currently conducting the Study of COmparative Treatments for REtinal Vein Occlusion 2 (SCORE2) study. SCORE2 is a multicenter, prospective, randomized noninferiority trial of eyes with macular edema secondary to central retinal vein occlusion, comparing intravitreal bevacizumab every 4 weeks with intravitreal aflibercept every 4 weeks. Eligible participants will be followed for 12 months.

Vitrectomy Without Sheathotomy

There is evidence that vitreomacular attachment itself may contribute to the development of macular edema in BRVO.[72] Saika and coworkers reported reduction in macular edema and restoration of normal foveal contour in 10 of 19 eyes after vitrectomy, posterior hyaloid separation, and intraocular gas tamponade.[73] In a prospective comparison study, vitrectomy with separation of the posterior hyaloid without sheathotomy was found to be as effective in reducing macular edema and improving visual

acuity as combined vitrectomy with posterior hyaloid removal and sheathotomy.[74] Possible explanations for the clinical improvements in these studies include removal of vitreous traction, increased oxygenation of the macula, and tamponade of the macula by intraocular gas.

Due to the risk of intraoperative complications and the availability of less invasive alternatives, vitrectomy with or without sheathotomy has limited clinical use as a first-line therapy.

Follow-Up

The major complications that can lead to vision loss in patients with BRVO include macular edema, macular ischemia, and neovascularization. Treatment is available for macular edema and neovascularization and follow-up should be tailored to monitor the development of these complications adequately. Initially, patients should be followed closely every month for the development of macular edema and/or neovascularization. Anti-VEGF therapy should be initiated for patients with macular edema without spontaneous improvement. Grid laser and/or steroids may be considered in patients when anti-VEGF therapy is not showing sufficient therapeutic efficacy. Once macular edema has stabilized or has resolved, the follow-up interval can be extended to 3–6 months or even longer for stable chronic cases. Patients with previously untreated retinal nonperfusion measuring >5 disc diameters should be followed at closer intervals (3 months) due to the increased risk for neovascular complications. Only after failure of medical therapy, should surgery be considered.

Conclusions

BRVO is a common cause of vision loss, but many treatment options are available and emerging therapies are under investigation. With the advent of so many new treatment options over the past decade, future studies are needed to establish evidence-based guidelines for the treatment of the vision-limiting complications of BRVO. The BRAVO and VIBRANT trials established that intravitreal anti-VEGF therapy results in better

visual and anatomical outcomes than macular grid laser, which had been the standard of care for macular edema associated with BRVO for over 25 years.[64] Currently, there are three available anti-VEGF therapies used in clinical practice. While there have been several studies showing similar efficacy between ranibizumab and bevacizumab,[70–71] there has been no multicenter, randomized trial comparing the efficacy of the three agents for the treatment of macular edema associated with BRVO. The SCORE2 is evaluating aflibercept and bevacizumab head to head. Future studies are also needed to establish the appropriate treatment regimen. In both the VIBRANT and BRAVO trials, patients received monthly injections for the first 6 months.[61,64] It is unknown if patients can maintain the same treatment benefits with PRN injections or a longer duration between injections. PRN treatment does appear to be an effective long-term treatment regimen in extension studies of the clinical trials. The SHORE study randomized patients with macular edema from BRVO to monthly versus PRN ranibizumab after receiving monthly injections for 7 months. The investigators found similar visual acuity outcomes in both groups.[75] Currently, steroid injections are second-line therapy owing to side-effects including increased IOP and cataract. Finally, pilot studies suggest that combination therapy may have a synergistic treatment effect as well as reduce treatment burden. Maturi et al. showed that the combination of intravitreal bevacizumab and dexamethasone resulted in fewer injections and better anatomic outcomes than bevacizumab alone.[76] Another group found that dexamethasone implant and grid laser resulted in better anatomic and visual outcomes than dexamethasone alone.[77] Randomized controlled trials are needed to establish the role and timing of combination therapy with regards to the currently available treatment modalities.

References

1. Branch Vein Occlusion Study Group. Argon laser scatter photocoagulation for prevention of neovascularization and vitreous hemorrhage in branch vein occlusion. A randomized clinical trial. *Arch Ophthalmol*. 1986;104:34–41.

2. Rogers SL, McIntosh RL, Lim L, et al. Natural history of branch retinal vein occlusion: an evidence-based systematic review. *Ophthalmology*. 2010;117:1094–1101.
3. Klein R, Moss SE, Meuer SM, et al. The 15-year cumulative incidence of retinal vein occlusion: the Beaver Dam Eye Study. *Arch Ophthalmol*. 2008;126:513–518.
4. Cheung N, et al. Traditional and novel cardiovascular risk factors for retinal vein occlusion: the multiethnic study of atherosclerosis. *Invest Ophthalmol Vis Sci*. 2008;49:4297–4302.
5. Wong TY, Marino Larsen EK, Klein R, et al. Cardiovascular risk factors for retinal vein occlusion and arteriolar emboli: the Atherosclerosis Risk in Communities and Cardiovascular Health Studies. *Ophthalmology*. 2005;112:540–547.
6. Mitchell P, Smith W, Chang A. Prevalence and associations of retinal vein occlusion in Australia: the Blue Mountains Eye Study. *Arch Ophthalmol*. 1996;114:1243–1247.
7. Ponto KA, Elbaz H, Peto T, et al. Prevalence and risk factors of retinal vein occlusion: the Gutenberg Health Study. *J Thromb Haemost*. 2015;13:1–10.
8. Eye Disease Case-control Study Group. Risk factors for branch retinal vein occlusion. *Am J Ophthalmol*. 1993;116:286–296.
9. Janssen MCH, den Heijer M, Cruysberg JRM, et al. Retinal vein occlusion: a form of venous thrombosis or a complication of atherosclerosis? A meta-analysis of thrombophilic factors. *Thromb Haemost*. 2005;93:1021–1026.
10. Rehak M, Rehak J, Muller M, et al. The prevalence of activated protein C (APC) resistance and factor V Leiden is significantly higher in patients with retinal vein occlusion without general risk factors: case–control study and meta-analysis. *Thromb Haemost*. 2008;99:925–929.
11. Cahill MT, Stinnett SS, Fekrat S. Meta-analysis of plasma homocysteine, serum folate, serum vitamin B(12), and thermolabile MTHFR genotype as risk factors for retinal vascular occlusive disease. *Am J Ophthalmol*. 2003;136:1136–1150.
12. Ariturk N, Oge Y, Erkan D, et al. Relation between retinal

vein occlusions and axial length. *Br J Ophthalmol*. 1996;80:633–636.
13. Majji AB, Janarthanan M, Naduvilath TJ. Significance of refractive status in branch retinal vein occlusion. A case-control study. *Retina*. 1997;17:200–204.
14. Simons BD, Brucker AJ. Branch retinal vein occlusion. Axial length and other risk factors. *Retina*. 1997;17:191–195.
15. Timmerman EA, de Lavalette VW, van den Brom HJ. Axial length as a risk factor to branch retinal vein occlusion. *Retina*. 1997;17:196–199.
16. Jaulim A, Ahmed B, Khanam T, et al. Branch retinal vein occlusion: epidemiology, pathogenesis, risk factors, clinical features, diagnosis, and complications. an update of the literature. *Retina*. 2013;33:901–910.
17. Sungur G, Hazirolan D, Hekimoglu E, et al. Late-onset Behcet's disease: demographic, clinical, and ocular features. *Graefes Arch Clin Exp Ophthalmol*. 2010;248:1325–1330.
18. Salvo G, Li Calzi C, Anastasi M, et al. Branch retinal vein occlusion followed by central retinal artery occlusion in Churg–Strauss syndrome: unusual ocular manifestations in allergic granulomatous angiitis. *Eur J Ophthalmol*. 2009;19:314–317.
19. Weinberg D, Dodwell DG, Fern SA. Anatomy of arteriovenous crossings in branch retinal vein occlusion. *Am J Ophthalmol*. 1990;109:298–302.
20. Zhao J, Sastry SM, Sperduto RD, et al. Arteriovenous crossing patterns in branch retinal vein occlusion. The Eye Disease Case–Control Study Group. *Ophthalmology*. 1993;100:423–428.
21. Duker JS, Brown GC. Anterior location of the crossing artery in branch retinal vein obstruction. *Arch Ophthalmol*. 1989;107:998–107:9.
22. Kumar B, Yu DY, Morgan WH, et al. The distribution of angioarchitectural changes within the vicinity of the arteriovenous crossing in branch retinal vein occlusion. *Ophthalmology*. 1998;105:424–427.
23. Seitz R. *The retinal vessels*. CV Mosby: St. Louis; 1964:20–74.
24. Rehak J, Rehak M. Branch retinal vein occlusion:

pathogenesis, visual prognosis, and treatment modalities. *Curr Eye Res*. 2008;33:111–131.
25. Clemett RS. Retinal branch vein occlusion: changes at the site of obstruction. *Br J Ophthalmol*. 1974;58:548–554.
26. Frangieh GT, Green WR, Barraquer-Somers E, et al. Histopathologic study of nine branch retinal vein occlusions. *Arch Ophthalmol*. 1982;100:1132–1140.
27. Ehlers JP, Fekrat S. Retinal vein occlusion: beyond the acute event. *Surv Ophthalmol*. 2011;56:281–299.
28. Cristoffersen NL, Larsen M. Pathophysiology and hemodynamics of branch retinal vein occlusion. *Opthalmology*. 1999;106:2054–2062.
29. Klein R, Klein BE, Moss SE, et al. The epidemiology of retinal vein occlusion: the Beaver Dam Eye Study. *Trans Am Ophthalmol Soc*. 2000;98:133–141 [discussion 141–3].
30. Hayreh SS, Zimmerman MB. Fundus changes in branch retinal vein occlusion. *Retina*. 2015;35:1016–1027.
31. Hayreh SS, Zimmerman MB. Branch retinal vein occlusion natural history of visual outcome. *JAMA Ophthalmol*. 2014;132:13–22.
32. Finkelstein D. Ischemic macular edema: recognition and favorable natural history in branch vein occlusion. *Arch Ophthalmol*. 1992;11:1427–1434.
33. Prasad PS, Oliver SC, Coffee RE, et al. Ultra wide-field angiographic characteristics of branch retinal and hemicentral retinal vein occlusion. *Ophthalmology*. 2010;117:780–784.
34. Spaide RF, Lee JK, Klancnik JK Jr, et al. Optical coherence tomography of branch retinal vein occlusion. *Retina*. 2003;23:343–347.
35. Lerche RC, Schaudig U, Scholz F, et al. Structural changes of the retina in retinal vein occlusion – imaging and quantification with optical coherence tomography. *Ophthalmic Surg Lasers*. 2001;32:272–280.
36. Kang HM, Chung EJ, Kim YM, et al. Spectral-domain optical coherence tomography (SD-OCT) patterns and response to intravitreal bevacizumab therapy in macular edema associated with branch retinal veinocclusion. *Graefes Arch*

Clin Exp Ophthalmol. 2013;251:501–508.
37. Lam HD, Lahey JM, Kearney JJ, et al. Young patients with branch retinal vein occlusion: a review of 60 cases. *Retina*. 2010;30:1520–1523.
38. Arsene S, Delahousse B, Regina S, et al. Increased prevalence of factor V Leiden in patients with retinal vein occlusion and under 60 years of age. *Thromb Haemost*. 2005;94:101–106.
39. Kuhli C, Hattenbach LO, Scharrer I, et al. High prevalence of resistance to APC in young patients with retinal vein occlusion. *Graefes Arch Clin Exp Ophthalmol*. 2002;240:163–168.
40. Lahey M, Tunc M, Kearney J, et al. Laboratory evaluation of hypercoagulable states in patients with central retinal vein occlusion who are less than 56 years of age. *Ophthalmology*. 2002;109:126–131.
41. Chai SM, Mathur R, Ong SG. Retinal vasculopathy in Fanconi anemia. *Ophthalmic Surg Lasers Imaging*. 2009;40:498–40:4.
42. Patricio MS, Portelinha J, Passarinho MP, et al. Tubercular retinal vasculitis. *BMJ Case Rep*. 2013;2013 [pii: bcr2013008924].
43. Tewari HK, Khosla A, Khosla PK, et al. Bilateral branch vein occlusion. *Acta Ophthalmol*. 1992;70:278–280.
44. Osterloh MD, Charles S. Surgical decompression of branch retinal vein occlusions. *Arch Ophthalmol*. 1988;106:1469–1471.
45. Opremcak EM, Bruce RA. Surgical decompression of branch retinal vein occlusion via arteriovenous crossing sheathotomy: a prospective review of 15 cases. *Retina*. 1999;19:1–19.
46. Mester U, Dillinger P. Vitrectomy with arteriovenous decompression and internal limiting membrane dissection in branch retinal vein occlusion. *Retina*. 2002;22:740–746.
47. Cahill MT, Kaiser PK, Sears JE, et al. The effect of arteriovenous sheathotomy on cystoid macular oedema secondary to branch retinal vein occlusion. *Br J Ophthalmol*. 2003;87:1329–1332.

48. Le Rouic JF, Bejjani RA, Rumen F, et al. Adventitial sheathotomy for decompression of recent onset branch retinal vein occlusion. *Graefes Arch Clin Exp Ophthalmol*. 2001;239(10):747–751.
49. Han DP, Bennett SR, Williams DF, et al. Arteriovenous crossing dissection without separation of the retina vessels for treatment of branch retinal vein occlusion. *Retina*. 2003;23:145–151.
50. Chung EJ, Lee H, Koh HJ. Arteriovenous crossing sheathotomy versus intravitreal triamcinolone acetonide injection for treatment of macular edema associated with branch retinal vein occlusion. *Graefes Arch Clin Exp Ophthalmol*. 2008;246(7):967–974.
51. Branch Vein Occlusion Study Group. Argon laser photocoagulation for macular edema in branch vein occlusion. *Am J Ophthalmol*. 1984;98:271–298.
52. Wilson DJ, Finkelstein D, Quigley HA, et al. Macular grid photocoagulation: an experimental study on the primate retina. *Arch Ophthalmol*. 1988;106:100–110.
53. Noma H, Minamoto A, Funatsu H, et al. Intravitreal levels of vascular endothelial growth factor and interleukin-6 are correlated with macular edema in branch retinal vein occlusion. *Graefes Arch Clin Exp Ophthalmol*. 2006;244:309–315.
54. Zhang X, Bao S, Lai D, et al. Intravitreal triamcinolone acetonide inhibits breakdown of the blood–retinal barrier through differential regulation of VEGF-A and its receptors in early diabetic rat retinas. *Diabetes*. 2008;57:1026–1033.
55. McAllister IL, Vijayasekaran S, Chen SD, et al. Effect of triamcinolone acetonide on vascular endothelial growth factor and occludin levels in branch retinal vein occlusion. *Am J Ophthalmol*. 2009;147:838–846.
56. Scott IU, Ip MS, VanVeldhuisen PC, et al. A randomized trial comparing the efficacy and safety of intravitreal triamcinolone with standard care to treat vision loss associated with macular edema secondary to branch retinal vein occlusion: the Standard Care vs Corticosteroid for Retinal Vein Occlusion (SCORE) study report 6. *Arch*

Ophthalmol. 2009;127:1115–1127.
57. Haller JA, Bandello F, Belfort R Jr, et al. Randomized, sham-controlled trial of dexamethasone intravitreal implant in patients with macular edema due to retinal vein occlusion. *Ophthalmology*. 2010;117:1134–1146.
58. Haller JA, Bandello F, Belfort R Jr, et al. Dexamethasone intravitreal implant in patients with macular edema related to branch or central retinal vein occlusion: twelve-month study results. *Ophthalmology*. 2011;118:2453–2460.
59. Aiello LP, Avery RL, Arrigg PG, et al. Vascular endothelial growth factor in ocular fluid of patients with diabetic retinopathy and other retinal disorders. *N Engl J Med*. 1994;331:1480–1487.
60. Bates DO. Vascular endothelial growth factors and vascular permeability. *Cardiovasc Res*. 2010;87:262–287.
61. Campochiaro PA, Heier JS, Feiner L, et al. Ranibizumab for macular edema following branch retinal vein occlusion: six-month primary end point results of a phase III study. *Ophthalmology*. 2010;117:1102–1112.
62. Brown DM, Campochiaro PA, Bhisitkul RB, et al. Sustained benefits from Ranibizumab for macular edema following branch retinal vein occlusion: 12-month outcomes of a Phase III study. *Ophthalmology*. 2011;118:1594–1602.
63. Heier JS, Campochiaro PA, Yau L, et al. Ranibizumab for macular edema due to retinal vein occlusion: long-term follow-up in the HORIZON Trial. *Ophthalmology*. 2012;119:802–809.
64. Campochiaro PA, Clark WL, Boyer DS, et al. Intravitreal aflibercept for macular edema following branch retinal vein occlusion: the 24-week results of the VIBRANT study. *Ophthalmology*. 2015;122:538–544.
65. Jaissle GB, Leitritz M, Gelisken F, et al. One-year results after intravitreal bevacizumab therapy for macular edema secondary to branch retinal vein occlusion. *Graefes Arch Clin Exp Ophthalmol*. 2009;247:27–33.
66. Gregori NZ, Rattan GH, Rosenfeld PJ, et al. Safety and efficacy of intravitreal bevacizumab (avastin) for the management of branch and hemiretinal vein occlusion.

Retina. 2009;29:913–925.
67. Ehlers JP, Decroos FC, Fekrat S. Intravitreal bevacizumab for macular edema secondary to branch retinal vein occlusion. *Retina*. 2011;31:1856–1862.
68. Hikichi T, Higuchi M, Matsushita T, et al. Two-year outcomes of intravitreal bevacizumab therapy for macular oedema secondary to branch retinal vein occlusion. *Br J Ophthalmol*. 2014;98:195–199.
69. Prager F, Michels S, Kriechbaum K, et al. Intravitreal bevacizumab (Avastin) for macular oedema secondary to retinal vein occlusion: 12-month results of a prospective clinical trial. *Br J Ophthalmol*. 2009;93:452–456.
70. Narayanan R, Panchal B, Das T, et al. A randomized, double-masked, controlled study of the efficacy and safety of intravitreal bevacizumab versus ranibizumab in the treatment of macular oedema due to branch retinal vein occlusion: MARVEL Report No. 1. *Br J Ophthalmol*. 2015;99:954–959.
71. Yuan A, Ahmad BU, Xu D, et al. Comparison of intravitreal ranibizumab and bevacizumab for the treatment of macular edema secondary to retinal vein occlusion. *Int J Ophthalmol*. 2014;7(1):86–91.
72. Takahashi MK, Hikichi T, Akiba J, et al. Role of the vitreous and macular edema in branch retinal vein occlusion. *Ophthalmic Surg Lasers*. 1997;28:294–299.
73. Saika S, Tanaka T, Miyamoto T, et al. Surgical posterior vitreous detachment combined with gas/air tamponade for treating macular edema associated with branch retinal vein occlusion: retinal tomography and visual outcome. *Graefes Arch Clin Exp Ophthalmol*. 2001;239:729–732.
74. Figueroa MS, Torres R, Alvarez MT. Comparative study of vitrectomy with and without vein decompression for branch retinal vein occlusion: a pilot study. *Eur J Ophthalmol*. 2004;14(1):40–47.
75. Campochiaro PA, Wykoff CC, Singer M, et al. Monthly versus as-needed ranibizumab injections in patients with retinal vein occlusion: The SHORE Study. *Ophthalmology*. 2014;121:2432–2442.

76. Maturi RK, Chen V, Raghinaru D, et al. A 6-month, subject-masked, randomized controlled study to assess efficacy of dexamethasone as an adjunct to bevacizumab compared with bevacizumab alone in the treatment of patients with macular edema due to central or branch retinal vein occlusion. *Clin Ophthalmol*. 2014;8:1057–1064.
77. Pichi F, Specchia C, Vitale L, et al. Combination therapy with dexamethasone intravitreal implant and macular grid laser in patients with branch retinal vein occlusion. *Am J Ophthalmol*. 2014;157:607–615.

57

Central Retinal Vein Occlusion

Patrick Oellers, Paul Hahn, Sharon Fekrat

Introduction

Central retinal vein occlusion (CRVO) is a retinal vascular condition that may cause significant ocular morbidity. It commonly affects men and women equally and occurs predominantly in persons over the age of 65 years.[1–3] In this population, there may be associated systemic vascular disease, including hypertension and diabetes.[4] Younger individuals who present with a clinical picture of CRVO may have an underlying hypercoagulable or inflammatory etiology.[5,6] Population-based studies report the prevalence of CRVO at <0.1 to 0.4%.[2,7,8] CRVO is usually a unilateral disease; however, the annual risk of developing a CRVO in the fellow eye is approximately 1% per year, and it is estimated that up to 7% of persons with CRVO may develop CRVO in the fellow eye within 5 years of onset in the first eye.[1,9] Individuals with CRVO demonstrate a significant decrease in vision-related quality of life as

well as increased illness burden with increased healthcare costs and resource use as compared to a reference group.[10–12] CRVO may impact a person's ability to perform activities of daily living, especially in cases of bilateral CRVO or when concurrent ocular disease limits vision in the fellow eye.

Clinical Features

CRVO usually presents with sudden painless loss of vision, but it may also present with a history of gradual visual decline. The typical clinical constellation in CRVO includes intraretinal hemorrhages (both superficial flame-shaped and deep blot type) in all four quadrants of the fundus with a dilated, tortuous retinal venous system. The hemorrhages radiate from the optic nerve head, are variable in quantity, and may result in the classic "blood and thunder" appearance (Fig. 57.1). Optic nerve head swelling, splinter hemorrhages, cotton-wool spots, and macular edema (ME) are present to varying degrees (Figs. 57.2 and 57.3). Breakthrough vitreous hemorrhage may also be observed.

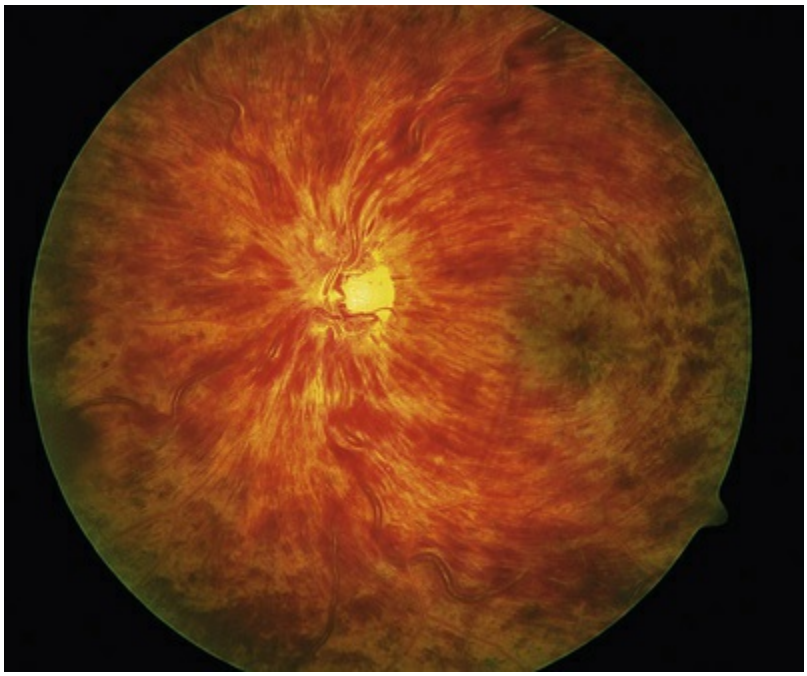

FIG. 57.1 Fundus photograph of a central retinal vein occlusion with extensive intraretinal hemorrhage. Extensive blocking on fluorescein angiography

precludes accurate determination of perfusion status.

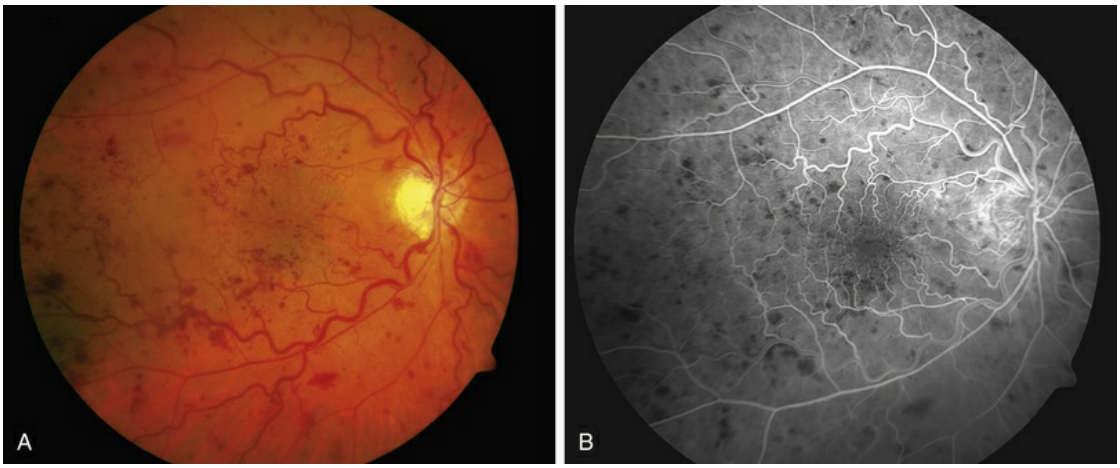

FIG. 57.2 (A) Fundus photograph of a central retinal vein occlusion demonstrating typical features of venous tortuosity, macular thickening, and intraretinal hemorrhage in all four quadrants of the fundus. (B) Early-phase angiogram of the fundus depicted in (A), demonstrating an intact parafoveal capillary network in this perfused central retinal vein occlusion.

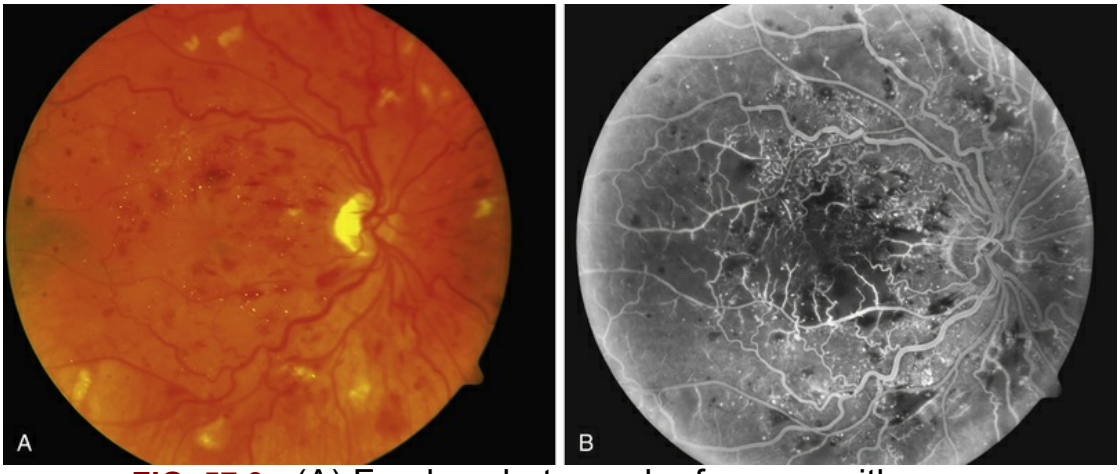

FIG. 57.3 (A) Fundus photograph of an eye with central retinal vein occlusion demonstrating scattered intraretinal hemorrhage, venous engorgement, and cotton-wool spots. (B) Midphase fluorescein angiogram of the eye shown in (A), demonstrating capillary nonperfusion involving the foveal center. This eye also had extensive peripheral nonperfusion and is an

example of the nonperfused form of central retinal vein occlusion.

A cilioretinal artery occlusion rarely occurs in association with CRVO. Together, these occlusions have been hypothesized to constitute a distinct clinical entity arising from a sudden increase in the intraluminal capillary pressure due to CRVO, inducing relative occlusion of the cilioretinal artery whose perfusion pressure is lower than the central retinal artery.[13,14] Rarely, a central retinal arterial occlusion may also accompany a CRVO.[15]

With time, the extent of intraretinal hemorrhage may decrease or resolve completely with variable degrees of secondary retinal pigment epithelium alterations. The time course for resolution of the hemorrhages varies and is dependent on the amount of hemorrhage produced by the occlusion. In the natural history of CRVO, ME often chronically persists despite resolution of intraretinal hemorrhage (Fig. 57.4). An epiretinal membrane and foveal pigmentary alterations may develop.[16] Optociliary "shunt" vessels can form on the optic nerve head, a sign of newly formed collateral channels with the choroidal circulation (Fig. 57.5). Neovascularization of the optic disc (NVD) or retinal neovascularization elsewhere (NVE) may develop as a response to secondary retinal ischemia. The vessels that comprise NVD are typically of smaller caliber than optociliary shunt vessels, branch into a vascular network resembling a net, and leak on fluorescein angiography. Fibrovascular proliferation from NV may result in vitreous hemorrhage or traction retinal detachment.

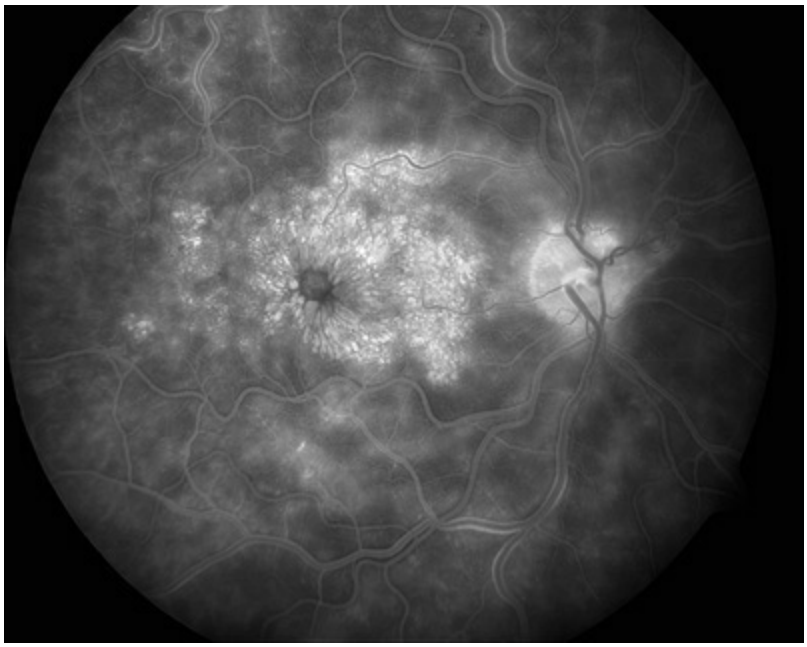

FIG. 57.4 Fluorescein angiogram of a chronic central retinal vein occlusion with resolution of intraretinal hemorrhage but persistence of cystoid macular edema demonstrated by petaloid leakage.

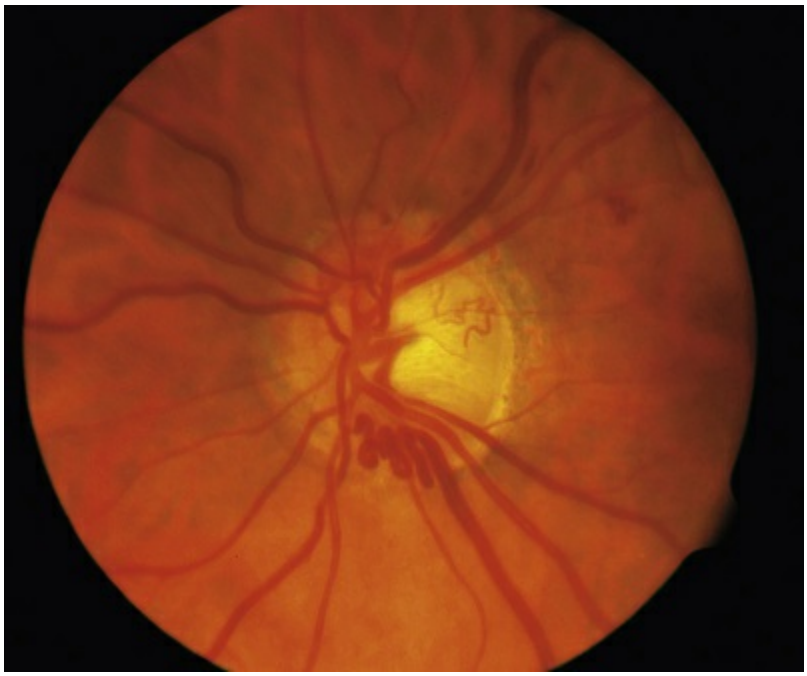

FIG. 57.5 Fundus photograph demonstrating optociliary shunt vessels (aka collaterals) at the inferior border of the optic nerve head in this patient with a chronic central retinal vein occlusion. These vessels do not leak on fluorescein angiography.

Much of our knowledge on the natural history of CRVO stems from the results of the Central Vein Occlusion Study (CVOS), a randomized, multicenter clinical trial of 728 eyes with CRVO. In this study, visual acuity at the time of presentation was variable but an important prognostic indicator of final visual outcome. Baseline visual acuity was 20/40 or better in 29% of affected eyes, 20/50 to 20/200 in 43%, and 20/250 or worse in 28%; median baseline acuity was 20/80.[3,17] Of those with initial visual acuity of 20/40 or better, the majority maintained this acuity. Individuals with intermediate visual acuity (20/50 to 20/200) had a variable outcome: 21% improved to better than 20/50, 41% stayed in the intermediate group, and 38% were worse than 20/200. Persons with poor visual acuity at onset (less than 20/200) had only a 20% chance of improvement.[9]

Anterior segment findings may include iris and/or angle neovascularization (NVI/NVA). NVI typically begins at the pupillary border but may extend across the iris surface. NVA is detected during undilated gonioscopy as fine branching vessels bridging the scleral spur and may develop without any NVI in 6–12% of eyes with ischemic CRVO.[3,9,18] The CVOS used an index of any two clock hours of NVI or any NVA as significant anterior segment NV, which was found in 16% of eyes with 10 to 29 disc areas of angiographic nonperfusion and 52% with 75 disc areas or more of angiographic nonperfusion.[9] In the CVOS, worse initial visual acuity correlated with the development of NVI/NVA: 5% in eyes ≥20/40 or better, 14.8% in eyes 20/50 to 20/200, and 30.8% in eyes with <20/200 acuity.[9] Longstanding NVA may lead to secondary angle closure from peripheral anterior synechiae formation. Elevated intraocular pressure associated with NVI/NVA is the hallmark of neovascular glaucoma.

Perfusion Status

The CVOS classified the perfusion status of a CRVO as perfused, nonperfused, or indeterminate based on fluorescein angiographic characteristics. Angiographic assessment of perfusion status is based on the CVOS photographic protocol, which used a

conventional wide-angle fundus camera with sweeps of the midperiphery 30 seconds after intravenous injection of fluorescein.

A perfused CRVO (aka nonischemic, incomplete, or partial) demonstrates <10 disc areas of retinal capillary nonperfusion on angiography (Fig. 57.2). These eyes typically have a lesser degree of intraretinal hemorrhage on presentation. Generally, eyes with perfused CRVO have better initial and final visual acuity. A nonperfused CRVO (aka ischemic, hemorrhagic, or complete) demonstrates ≥10 disc areas of retinal capillary nonperfusion on angiography (Fig. 57.3). Acutely, these eyes often demonstrate a greater degree of intraretinal hemorrhage, macular and disc edema, and capillary nonperfusion than eyes with perfused CRVO. A CRVO is categorized as indeterminate when there is sufficient intraretinal hemorrhage to prevent angiographic determination of the perfusion status. Other examination features that may help in determining the perfusion status include baseline visual acuity, presence of an afferent pupillary defect, electroretinography (a negative waveform may be seen), and Goldmann perimetry.[5,9,19,20]

The CVOS classification of initial perfusion status was important for determining the natural history of the disease.[9] Poor visual acuity and large areas of retinal capillary nonperfusion were significant factors associated with an increased risk of NVI/NVA. In eyes initially categorized as perfused, 10% (56/538) developed NVI/NVA compared to 35% (61/176) of eyes initially characterized as nonperfused or indeterminate. At 3 years, there was a 45% chance of developing neovascular glaucoma after onset of ischemic CRVO.[1] Overall, 34% of initially perfused eyes converted to nonperfused status after 3 years, which has been associated with worsening visual acuity.[9,21] In the CVOS, 38 eyes (83%) with an indeterminate CRVO at baseline were ultimately determined to be nonperfused. Initial visual acuity was highly correlated with degree of nonperfusion – eyes with nonperfused CRVO were much more likely than those with perfused CRVO to have poor visual acuity at initial presentation and final visit.[9,16] Hayreh and Zimmerman have retrospectively studied a large patient cohort and found that the risk for ocular neovascularization is much greater in ischemic than in perfused CRVO and greatest within the first 6 months of onset. In ischemic CRVO, the cumulative probability of development of

NVI in this series was 49%, NVA 37%, NVG 29%, NVE 9%, and NVD 6% within 6 months of CRVO onset. In perfused CRVO, neovascular complications occurred in 1.3% during available follow-up.[20,22]

Ultrawide-field angiography has enabled mapping of peripheral retinal nonperfusion not easily visualized with a conventional camera. Adjusted protocols for grading extent of nonperfusion are being developed from photographs taken with ultrawide-field angiography, which may prove important in redefining characteristics of perfused vs. nonperfused CRVO.[21,23–26]

Pathogenesis

The pathophysiology of CRVO is not clearly understood. Histopathologic studies of eyes enucleated for CRVO demonstrated a thrombus occluding the lumen of the central retinal vein at or just proximal to the lamina cribrosa,[27] suggesting that the anatomic variations at the level of the lamina cribrosa may be important in the development of a CRVO. Within the retrolaminar portion of the optic nerve, the central retinal artery and vein are aligned parallel to each other in a common tissue sheath where they are naturally compressed as they cross through the rigid sieve-like openings in the lamina cribrosa but typically give off branching collateral vessels just before piercing the lamina. These vessels may be subject to compression from mechanical stretching of the lamina, as with increases in intraocular pressure, which may cause a posterior bowing of the lamina and subsequent impingement on the central retinal vein. Furthermore, local factors may predispose to occlusion of the central retinal vein, including compression by an atherosclerotic central retinal artery or primary occlusion of the central retinal vein from inflammation.

Hemodynamic alterations may produce stagnant flow and subsequent thrombus formation in the central retinal vein, including diminished blood flow, increased blood viscosity, and an altered lumen wall (Virchow triad). Experimentally, occlusion of both the retrolaminar central retinal artery and central retinal vein, posterior to the lamina cribrosa and prior to the branching of collateral channels from the main trunk, was required to produce

the clinical appearance of a hemorrhagic (ischemic) CRVO.[16] This implies that concurrent retinal artery insufficiency or occlusion may play a role in an ischemic CRVO. It is hypothesized that a less hemorrhagic, more likely nonischemic, CRVO may be due to occlusion of the central retinal vein at a site further posterior, allowing normal collateral channels to provide alternative routes of venous drainage.

In the largest histopathologic study of eyes with CRVO, 29 eyes enucleated for acute (within 6 hours) and chronic (up to 10 years) occlusions were reviewed,[27] some of which had concurrent neovascular glaucoma. In acute occlusions, a thrombus at the level of the lamina cribrosa was adherent to a portion of the vein wall devoid of an endothelial lining. Subsequently, there was endothelial cell proliferation within the vein and secondary inflammatory cell infiltrates. Recanalization of the thrombus was demonstrated in eyes 1–5 years after the documented occlusion.

Neovascularization of the anterior and posterior segment and severity of ME are modulated by growth factors released from the ischemic retina. Green and colleagues demonstrated inner retinal ischemic changes in 25% of eyes enucleated for CRVO.[27] In a study of enucleated eyes with CRVO and neovascular glaucoma, intraretinal vascular endothelial growth factor (VEGF) production from areas of ischemic retina was demonstrated.[28] Analysis of vitreous fluid from patients with CRVO demonstrated increased levels of VEGF along with other cytokines and growth factors.[29–31] Intraocular VEGF levels correlate with severity of ocular findings including neovascularization and vascular permeability,[32] prompting the development of anti-VEGF agents for the treatment of CRVO.

Risk Factors and Associations

Concurrent systemic vascular disease is a risk factor for CRVO (Box 57.1). The Eye Disease Case–Control Study found an increased risk of any type of CRVO in persons with systemic hypertension and diabetes mellitus.[4] Similar associations with systemic hypertension were found in other studies.[36–40] Diabetes mellitus was more prevalent in individuals with nonperfused CRVO than in matched

controls from large population databases.[36,37] Diabetes with end-organ damage in particular may carry an increased risk.[33] Hyperlipidemia, arteriosclerosis, and smoking have also been linked to the development of vein occlusions.[2,34,39] A recent large longitudinal cohort study based on insurance billing codes linked African American race to a higher risk for CRVO.[33]

Box 57.1

Risk Factors and Associations With CRVO

- **Ethnicity:** African race
- **Systemic vascular diseases:** Diabetes mellitus, hypertension, carotid insufficiency
- **Ocular diseases:** Open angle glaucoma, ischemic optic neuropathy, pseudotumor cerebri, tilted optic nerve heads, optic nerve head drusen
- **Hematologic alterations:** Hyperviscosity syndromes: dysproteinemias (multiple myeloma), blood dyscrasias (polycythemia vera, lymphoma, leukemia, sickle-cell disease or trait), anemia, elevated plasma homocysteine, factor XII deficiency, antiphospholipid antibody syndrome, activated protein C resistance, protein C deficiency, protein S deficiency
- **Inflammatory/autoimmune vasculitis:** Systemic lupus erythematosus
- **Medications:** Oral contraceptives, diuretics, hepatitis B vaccine
- **Infectious vasculitis:** HIV, syphilis, herpes zoster, sarcoidosis
- **Other:** After retrobulbar block, dehydration, Valsalva, pregnancy

HIV, human immunodeficiency virus.

Data from references 5, 33, 34, 35.

Hematologic abnormalities, particularly conditions that predispose to a hypercoagulable state, have been identified in persons with CRVO. Individuals less than 60 years of age may have

a greater association with hypercoagulable states and inflammatory conditions compared to older persons with a higher incidence of systemic vascular disease risk factors.[5,6] Lahey and colleagues found one abnormal laboratory value suggesting systemic hypercoagulability in 27% of 55 patients younger than 56 years of age.[41] Studies have demonstrated an increased incidence of coagulation cascade abnormalities, including protein C deficiency, protein S deficiency, activated protein C resistance, presence of factor V Leiden, presence of antiphospholipid antibodies, hyperhomocysteinemia, antithrombin III deficiency, prothrombin gene mutations, and abnormal fibrinogen levels.[42–49] Hyperviscosity from blood dyscrasias, dysproteinemias, and dehydration have also been reported with CRVO.[50–53] In addition, abrupt changes in venous or intracranial pressure such as from Valsalva maneuvers have been implicated in the pathogenesis of CRVO.[54,55]

An increased risk of CRVO is present in eyes with open angle glaucoma.[4,56] Other ocular conditions causing deformation or mechanical pressure on the optic nerve head and lamina cribrosa, including ischemic optic neuropathy, tilted optic nerve head, optic nerve head drusen, optic disc traction syndrome, and pseudotumor cerebri,[50,57] have also been associated with CRVO. External compression of the globe and optic nerve from thyroid-related ophthalmopathy, mass lesions, or head trauma with orbital fracture may also result in CRVO.[5]

Clinical Evaluation

At the time of initial presentation, a careful assessment of the CRVO duration and the degree of ME and retinal ischemia will determine treatment options and the follow-up schedule. An ocular history may determine the onset of the occlusion, although individuals may not have noted vision loss if the fellow eye has maintained good acuity. A history of systemic diseases, such as hypertension, diabetes, and heart disease, and a personal or family history of thrombosis or hypercoagulable state should be determined.

The ophthalmic examination should be performed on both eyes and include visual acuity, pupillary reaction, and intraocular pressure. Undilated slit-lamp examination is performed to detect

NVI. Undilated gonioscopy is essential to determine the presence of NVA or evidence of angle closure from peripheral anterior synechiae, since NVA may be present without any NVI in up to 12% of eyes.[18] Ophthalmoscopic examination will help differentiate a CRVO from intraretinal hemorrhage associated with carotid occlusive disease, in which dot–blot hemorrhage is classically confined to the temporal midperiphery.[58] Adjunctive imaging studies, including optical coherence tomography (OCT) and fluorescein angiography, are helpful in evaluating and following presence of ME and perfusion status.

In general, a systemic workup is not indicated in persons older than 60 years of age with known systemic risk factors for CRVO as above. Younger patients are more likely to have predisposing conditions resulting in thrombotic disease.[6,41] A systemic workup may be considered in younger individuals without risk factors as noted above, and in those with a prior occlusion in the fellow eye, bilateral simultaneous CRVO, mixed type vascular occlusion, severe worsening nonperfusion, prior systemic thrombotic disease, family history of thrombosis, or other symptoms suggestive of a hematologic or rheumatologic condition (Box 57.2).[9,46]

Box 57.2

Suggested Laboratory Workup for CRVO in Appropriate Cases

- **Blood dyscrasias:** CBC with differential, serum protein electrophoresis
- Hypercoagulable conditions: serum viscosity, lupus anticoagulant, antiphospholipid antibody, fasting plasma homocysteine, factor V Leiden, antithrombin III, prothrombin gene mutation, protein C, protein S
- Cardiovascular/diabetes: fasting lipid profile, hemoglobin A1C, blood pressure

Therapeutic Options

Treatment for central retinal vein occlusion is directed at treating

the sequelae of CRVO, particularly ME and neovascularization, and not the underlying etiology. The recent development of intravitreal pharmacotherapy has revolutionized the treatment of CRVO-associated ME (Table 57.1; Fig. 57.6).[59–67] While these intravitreal agents can also improve secondary neovascularization, panretinal laser photocoagulation (PRP) remains the definitive treatment. Alternative experimental therapies have sought to modify the anatomic alterations believed to be responsible for CRVO. Of course, appropriate management of blood pressure and other systemic factors is always of paramount importance.

TABLE 57.1

Randomized, Sham-Controlled Trials Investigating Intravitreal Pharmacologic Agents for CRVO-Associated Macular Edema

Study	Drug	Intervention	Eyes	Duration	Mean Letter Gain	Percentage of ≥15 Letter Gain
Ip et al. 2009[60] (SCORE)	Intravitreal triamcinolone	IVT 4, 1 mg every 4 months PRN vs. observation	271	12 mth	−1 to 2 (1 and 4 mg) vs. −12 (observation)	26% (4 mg), 27% (1 mg), 7% (sham)
Haller et al. 2010[61] (GENEVA)	Intravitreal dexamethasone implant	IVDEX 0.7 and 0.35 mg for CRVO and BRVO vs. sham	437	6 mth	N/A	30 days: 21%, 20%, 7% 60 days: 29%, 33%, 9% in 0.7 mg, 0.35 mg and sham groups, respectively 90 days: 24% (0.35) vs. 10% (sham) No significant difference between 0.7 mg and sham 180 days: No differences
Brown et al. 2010[62] (CRUISE)	Intravitreal ranibizumab	Monthly IVR 0.3 and 0.5 mg vs.	392	6 mth	14.9, 12.7 and 0.8 in 0.5, 0.3 mg and sham	47%, 46%, 17% in 0.5, 0.3 mg

		sham				ranibizumab and sham
Wroblewski et al. 2009[63]	Intravitreal pegaptanib sodium	Monthly IVP 0.3, 1 mg vs. sham	98	6 mth	+7.1, +9.9 and −3.2 for 0.3, 1 mg and sham. Only 1 mg statistically significant	No difference between groups
Boyer et al. 2012[64] (COPERNICUS)	Intravitreal aflibercept	Monthly IVA 2 mg vs. sham	189	6 mth	+17.3 (IVA) vs. −4.0 (sham)	56% (IVA) vs. 12% (sham)
Epstein et al.[65] 2012	Intravitreal bevacizumab	IVB 1.25 mg every 6 weeks vs. sham	60	6 mth	+14.1 (bevacizumab) vs −2.0 (sham)	60% (IVB) vs. 20% (sham)
Holz et al. 2013[66] (GALILEO)	Intravitreal aflibercept	Monthly IVA 2 mg vs. sham	177	6 mth	+18.0 (IVA) vs. +3.3 (sham)	60% (IVA) vs. 22% (sham)
Korobelnik et al. 2014[67] (GALILEO)	Intravitreal aflibercept	IVA q8 weeks PRN vs. sham		12 mth	+16.9 (aflibercept) vs. +3.8 (sham)	60% (IVA) vs. 32% (sham)

IVA, intravitreal aflibercept; IVB, intravitreal bevacizumab; IVDEX, intravitreal dexamethasone implant; IVP, intravitreal pegaptanib; IVR, intravitreal ranibizumab; IVT, intravitreal triamcinolone.

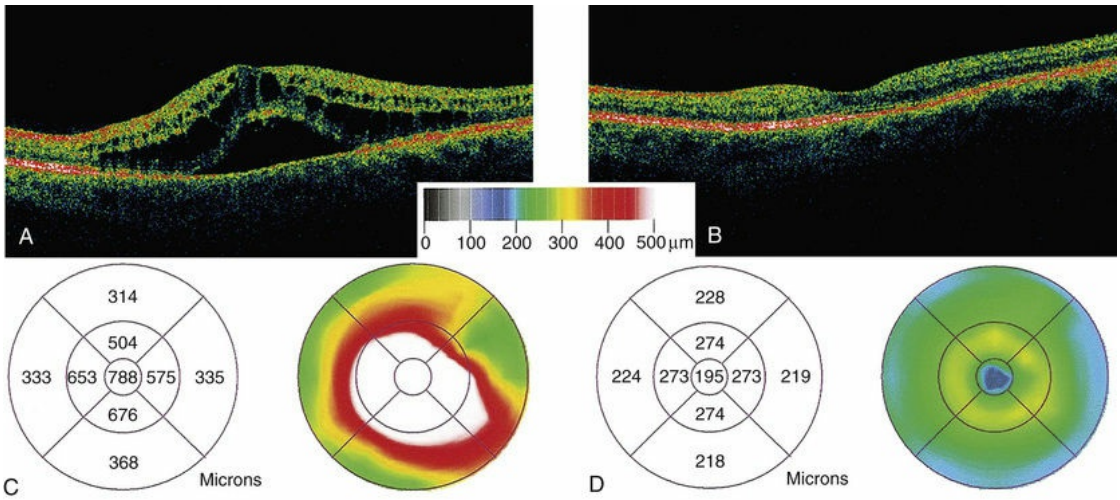

FIG. 57.6 A 67-year-old male with 5-month history of vision loss from a central retinal vein occlusion who received a single intravitreal injection of triamcinolone

acetonide (4 mg) to treat persistent cystoid macular edema. (A) Preinjection optical coherence tomography (OCT) demonstrating prominent retinal thickening in the macular region with inner and outer retinal cysts and subretinal fluid accumulation. (B) 4-month postinjection OCT demonstrating dramatic resolution of retinal thickening and return of normal foveal contour. (C) Retinal thickness map and corresponding color map from (A) with marked macular thickening. (D) Retinal thickness map and corresponding color map from (B) with normal retinal thickness measurements.

Treatment of Macular Edema

Observation

The CVOS Group M report studied the effect of grid pattern argon laser photocoagulation to improve visual acuity in 155 eyes with perfused CRVO-associated ME and 20/50 acuity or worse.[68] Laser treatment involved a grid pattern in the area of leaking capillaries within 2 disc diameters of the foveal center but not within the foveal avascular zone. At 36 months, there was no significant difference in mean visual acuity between treated (20/200) and untreated (20/160) eyes despite reduction of angiographic ME. Widespread damage to the perifoveal capillary network has been hypothesized to contribute to the lack of visual recovery. Therefore, the CVOS did not recommend grid laser photocoagulation for CRVO-associated ME. In the absence of robust treatment options before the recent advent of intravitreal pharmacotherapy for retinal diseases,[69] standard of care for CRVO-associated ME was observation.

Corticosteroid Therapy

The exact mechanism of action of corticosteroids in modulating retinal edema is unknown. It is believed that corticosteroids maintain antiinflammatory effects with modulation of production of cytokines and growth factors, including VEGF. Corticosteroids are also thought to stabilize the blood–retinal barrier with reduction in vascular permeability.[70,71] There is little evidence for systemic

administration of corticosteroids to treat ME from CRVO, unless the vein occlusion is associated with underlying systemic inflammatory disease.[72] Intravitreal delivery of corticosteroids provides targeted delivery of the drug to the retinal vessels and macular tissue while limiting potential systemic toxicity.

Following case reports on the use of intravitreal triamcinolone (IVTA) for the treatment of CRVO-associated ME,[73–76] the **S**tandard of Care vs. Corticosteroid for Retinal Vein Occlusion (SCORE) study compared the efficacy and safety of two doses of preservative-free IVTA (1 mg and 4 mg) vs. standard of care (observation per CVOS) for the treatment of ME in 271 eyes with CRVO.[60] In this randomized, multicenter clinical trial, eyes were retreated with IVTA every 4 months for 1 year unless certain criteria were met.

The SCORE study showed significant improvement in visual acuity with IVTA compared to observation.[60] At 1 year, 26% of eyes in the 4 mg group and 27% of eyes in the 1 mg group gained ≥15 letters compared to 7% of untreated eyes.

Primary ocular adverse events included cataract formation and elevated IOP.[60] Cataract formation was observed in 26% and 33% in the 1-mg and 4-mg IVTA groups, respectively, compared to 18% in the observation group. Over 2 years, 27% of eyes from the 4-mg group and 3% in the 1-mg group required cataract surgery, but no eyes from the observation group did. Elevated IOP was observed in 20% and 35% of eyes in the 1-mg and 4-mg IVTA groups, respectively, compared to 8% in the observation group.

The limited duration of the response to IVTA therapy has prompted the development of sustained-release corticosteroids for the treatment of CRVO-associated ME. In a prospective series of 24 eyes with vision loss from chronic ME secondary to CRVO, improvements in visual acuity and ME after 3 years were observed in eyes surgically implanted with a sustained-release intravitreal fluocinolone acetonide implant (Retisert; Bausch & Lomb). In this series, all phakic eyes developed visually significant cataracts, 33% required surgical intervention for increased intraocular pressure, and an additional 38% received intraocular pressure-lowering medications.[77]

In 2009, a sustained-release intravitreal dexamethasone delivery

system, Ozurdex (Allergan), was FDA-approved for the treatment of ME secondary to CRVO. A multicenter, international study at 167 sites in 24 countries reported the 6-month outcomes of a 0.35 mg and 0.7 mg Ozurdex dose for ME in eyes with retinal vein occlusion, a group consisting of both branch retinal vein occlusion and CRVO, compared to sham-injected eyes.[61] The Ozurdex implant resulted in improved mean visual acuity, increased rate of ≥15 letter gain and lower rate of ≤15 letter loss. Subgroup analysis was performed on 136 CRVO eyes injected with Ozurdex. The 0.7-mg group demonstrated significant gains of ≥15 letters compared to sham control at 30 days and at 60 days, but not at 90 or 180 days. The 0.35-mg group demonstrated significant gains of ≥15 letters compared to sham at 30–90 days, but not at 180 days. No significant difference in cataract formation or cataract surgery was identified between the treated and untreated groups. Ocular hypertension occurred in 4% of eyes receiving the drug delivery system, and most were able to be managed with topical medications. Two retinal detachments occurred in the study, one in the sham group and one in the 0.7-mg group.[61] The study was followed by an open-label 6-month extension phase in which all patients received Ozurdex 0.7 mg at day 180 after baseline, which yielded similar results in visual acuity. Cataract progression was reported in 30% and medical treatment for increased intraocular pressure was initiated in 36% in 0.7/0.7 mg Ozurdex group.[78]

Intravitreal Anti-VEGF Therapy

VEGF plays a key role in the pathophysiology of CRVO and its sequelae. Markedly elevated levels of VEGF have been demonstrated in the vitreous of eyes with ischemic CRVO.[29] It has been hypothesized that VEGF may cause capillary endothelial cell proliferation that leads to progressive vascular closure, promoting nonperfusion in CRVO.[79,80] Anti-VEGF therapy may result in enhanced retinal perfusion, lowered intravenous pressure, and the normalization of venous diameter and tortuosity.[22,79] Several intravitreal anti-VEGF treatments are available, including ranibizumab (Lucentis, Genentech), aflibercept (Eylea, Regeneron), bevacizumab (Avastin, Genentech), and pegaptanib (Macugen, Bausch & Lomb).

Ranibizumab

The double-masked, multicenter, randomized phase III Central Retinal Vein OcclUsIon (CRUISE) trial prospectively compared monthly intravitreal injections of 0.3 mg or 0.5 mg ranibizumab to sham-injected controls in the treatment of 392 patients with CRVO and ME.[62] Eyes treated with 0.3 mg and 0.5 mg ranibizumab gained 12.7 and 14.9 letters, respectively, at 6 months compared to a 0.8 letter gain in the sham group. Additionally 46% (0.3 mg) and 48% (0.5 mg) of eyes treated with intravitreal ranibizumab gained ≥15 letters from baseline compared to only 17% in the sham group, with significant reductions in central retinal thickness in the treatment groups. Systemic and ocular adverse events were rare (Table 57.1).

Following the 6-month endpoint, all groups, including the sham group, were treated with monthly ranibizumab on an as-needed basis, limiting further information on the natural history of CRVO and any long-term comparison.[17,81] Overall, ranibizumab groups maintained visual acuity gains, and there was also visual and anatomic improvement in the sham/0.5-mg ranibizumab group.[81,82] The results of the CRUISE study prompted FDA-approval of ranibizumab for the treatment of CRVO.

Long-term effects of ranibizumab therapy and associated burden of treatment have been investigated in two follow-up studies. A prospective, open-label extension trial HORIZON enrolled 304 patients who completed CRUISE.[83] Patients were seen at least every 3 months for 12 months and were eligible for an intravitreal injection if OCT central subfield thickness exceeded 250 μm or if there was recurrent or persistent edema limiting visual acuity. Interestingly, this dosing scheme resulted in reductions in percent of patients who gained ≥15 letters from initial study baseline compared to the CRUISE 12-month endpoint in the ranibizumab 0.5-mg (45% compared to 59%) and 0.3/0.5-mg group (39% vs. 47%), while the sham/0.5-mg group remained stable (38% vs. 38%). Following this, a prospective open-label extension trial named The Extended follow-up of patients with ME due to bRanch rETinal vein occlusion or centrAl retinal veIn occlusioN previously treated with intravitreal ranibizumab (RETAIN) investigated a subset who completed HORIZON for 2 additional years.[84] Patients were seen monthly in the first year and at least every 3 months (up to every

month) in the second year. Intravitreal injections of 0.5 mg ranibizumab were given if any intraretinal fluid was identified. At the final visit 53% gained ≥15 letters. Median letter improvement of 14.0 was not statistically different compared to the CRUISE endpoint. Notably, a small number of patients lost vision 4 years after enrollment into CRUISE compared to baseline. This was associated with recalcitrant ME, pigmentary changes believed to represent photoreceptor damage that was often related to foveal ischemia and epiretinal membrane formation. This study gave insight into long-term treatment burden. The investigators noted great heterogeneity in number of injections and required length of treatment until stabilization of ME. Within year 4 of follow-up, 56% required six injections on average, whereas 44% were stable without any injections. Attempts to reduce injection frequency by adding sector PRP to nonperfused retina thus far have not been promising.[85]

Aflibercept

Two double-masked, randomized, prospective phase III trials named COPERNICUS and GALILEO were carried out to investigate intravitreal aflibercept for CRVO-associated ME.[64,66] COPERNICUS enrolled 189 eyes with ME secondary to CRVO in the United States, and GALILEO enrolled 177 eyes in Europe and the Asia/Pacific region. Both trials evaluated 2.0 mg intravitreal aflibercept given monthly vs. sham injections for 6 months. In COPERNICUS, 56% gained ≥15 letters in the aflibercept group vs. 12% in the sham group. Mean letter gain was 17.3 in aflibercept eyes, whereas sham eyes lost a mean of 4.0 letters. In GALILEO, 60% gained ≥15 letters in the treatment group compared to 22% in the sham group, with mean letter gains of 18.0 vs. 3.3. Neither GALILEO nor COPERNICUS reported systemic thromboembolic events in the treatment groups in the first 6 months, and ocular events were rare (Table 57.1). Based on these studies, aflibercept received FDA-approval for ME secondary to CRVO.

Following the initial 6 months, all eyes enrolled in COPERNICUS switched to monthly PRN (as needed) aflibercept, while in GALILEO only the treatment group became eligible for monthly PRN injections, but the control group was maintained on sham

injections.[67,86] The 1-year data from these studies demonstrated that the treatment groups maintained visual acuity gains. Additionally, 2-year results have been published from COPERNICUS and 18-month results from GALILEO, providing further information on long-term visual outcomes as well as associated treatment burden.[87,88] In COPERNICUS, from week 52 forward, all patients were evaluated at least quarterly (but up to every 4 weeks) and were treated on a PRN basis. Results indicated that visual acuity gains slightly diminished during less frequent follow-up.[87] In GALILEO, from week 52 to 76, all eyes received intravitreal aflibercept as needed every 8 weeks. At the last follow-up, visual acuity gains were largely maintained in the treatment group.[88] Both studies demonstrated significant range and heterogeneity in terms of number of needed injections during the PRN treatment period.

Pegaptanib

Pegaptanib (Macugen) is currently the third FDA-approved intravitreal anti-VEGF agent, which received approval for the treatment of neovascular age-related macular degeneration, but not for CRVO. In a phase II double-masked, multicenter, randomized trial, patients with CRVO receiving off-label 0.3 mg or 1 mg pegaptanib every 6 weeks for 24 weeks were prospectively compared to sham-injected controls.[63] There was no significant difference in gain of ≥15 letters among groups, 0.3 mg and 1 mg. Only the 1 mg group showed slightly statistically significant mean letter improvement compared to sham. Given the enhanced efficacy of other anti-VEGF agents, pegaptanib use for CRVO remains low.

Bevacizumab

Much of our understanding of the role of anti-VEGF agents in the treatment of retinal disease comes from studies with bevacizumab. While bevacizumab is not FDA-approved for intravitreal use, its ophthalmic use quickly grew due to its low cost, reported efficacy, and availability prior to the approval of ranibizumab. Epstein and coworkers evaluated bevacizumab vs sham injection in a prospective, randomized, double-masked study of 60 eyes with ME secondary to CRVO. In the initial 6 months, injections were given every 6 weeks. After 6 months, the percentage of ≥15 letter gainers

was 60% in the bevacizumab group vs. 20% in the sham group.[65] In the following 6 months, all eyes received intravitreal bevacizumab every 6 weeks. One year after baseline, the percentage gaining ≥15 letters was 60% in the bevacizumab group and 33% in the sham/bevacizumab group.[89] No cases of endophthalmitis or retinal detachment were reported; likewise no serious nonocular events were reported.

The extensive international intravitreal use of bevacizumab remains off-label. A prospective, randomized study marginally failed to demonstrate noninferiority of bevacizumab against ranibizumab for branch retinal vein occlusion-associated ME, while noninferiority was established by two large trials on neovascular age-related macular degeneration.[90–92] It is unclear if these results are applicable to the treatment of CRVO. The SCORE2 trial is currently evaluating whether bevacizumab is noninferior to aflibercept.

Intravitreal pharmacologic therapeutics including the anti-VEGF agents ranibizumab, aflibercept, and bevacizumab as well as an intravitreal long-term release dexamethasone implant and intravitreal preservative-free triamcinolone have significantly expanded our treatment options. Given the efficacy of intravitreal pharmacologic agents in the treatment of CRVO, and given their favorable side-effect profile, the use of intravitreal pharmacotherapy has replaced observation as the previous standard of care established by the CVOS for treatment of CRVO-associated ME.[59,93] There is good evidence to suggest that earlier treatment with anti-VEGF agents is preferable to delayed treatment and that many eyes will continue to require frequent long-term injections. Reduced follow-up frequencies as well as PRN dosing schemas after initial visual acuity gains may result in visual acuity losses.[93] No sophisticated evidence-based information exists on the relative efficacies of the different anti-VEGF options.[94] Little information is known about the efficacies of intravitreal anti-VEGF vs. corticosteroids. A small prospectively randomized study suggested reduced need for injections with corticosteroids, but these were associated with significantly more adverse events, particularly increases in intraocular pressure and visually significant premacular membranes.[95] Another small prospective

trial tested monotherapy with intravitreal Ozurdex vs. combination therapy with bevacizumab and demonstrated no significant differences.[96]

In the authors' clinical practice, CRVO-associated ME is usually treated with serial anti-VEGF injections. Corticosteroid agents are reserved for severe or refractory cases, particularly in pseudophakic eyes without glaucoma. Further understanding of differences in treatment choices as well as development of sophisticated dosing schemes will likely improve management of our patients.

Neovascularization During Anti-VEGF Therapy

While anti-VEGF treatment alters the natural history of CRVO, neovascular events are reduced but not eliminated. Even under clinical study conditions among CRUISE, COPERNICUS, and GALILEO patients, neovascularization occurred in between 5.3% and 7.8%. Neovascular events in CRVO during anti-VEGF therapy may often be delayed, especially during times of decreased follow-up frequency or after discontinuation of anti-VEGF treatment when the disease was thought to be less active and also to occur to a higher extent in eyes with ischemic rather than perfused CRVO. DeCroos and colleagues retrospectively analyzed 32 patients who developed neovascularization during anti-VEGF therapy.[97] Neovascular events occurred after a mean treatment interval of 17.2 months (standard deviation, 10.3 months) with a mean treatment-free interval of 6.3 months (standard deviation, 7.3 months). Notably, CRUISE excluded patients with a brisk relative afferent pupillary defect or visual acuity worse than 20/320, thereby limiting information on severe nonperfusion. Addressing this, Brown and coworkers prospectively investigated a CRVO cohort of 20 eyes with severe nonperfusion.[98] They found that 50% of eyes developed neovascular complications during concurrent treatment with ranibizumab after a mean follow-up of 24 months (range, 3–44 months).

Definitive Treatment of Ocular Neovascularization

Laser Photocoagulation

The CVOS Group N report compared the efficacy of PRP at the time of study entry in eyes with nonperfused CRVO that did not have evidence of NVI/NVA (early treatment group, *n*=90) with delayed, but prompt, PRP application only when NVI/NVA was detected (no early treatment group, *n*=91).[99] NVI/NVA developed in 20% of early treatment and 34% of no early treatment eyes. There was greater resolution of NVI/NVA by 1 month after PRP in 56% of no early treatment eyes compared with 22% of early treatment eyes. The CVOS therefore recommended that PRP be delivered promptly after the development of NVI/NVA but not prophylactically in eyes with nonperfused CRVO. In approximately 90% of cases, the regression of NVI/NVA occurs within 1–2 months of PRP. Persistent neovascularization after PRP should be followed closely, and additional PRP may be applied in attempts to halt its progression. Persons presenting with NVD/NVE without NVI/NVA should be treated with PRP, as performed in eyes with proliferative diabetic retinopathy or branch retinal vein occlusion, to prevent anterior segment neovascularization. Prophylactic placement of PRP may be considered in eyes with nonperfused CRVO and risk factors for developing NVI/NVA (male gender, short duration of CRVO, extensive retinal nonperfusion, and extensive retinal hemorrhage) or in cases where frequent ophthalmologic follow-up is not possible.

Medical Therapy

Topical or systemic antiglaucoma agents may be required to reduce elevated intraocular pressure due to NVA. Topical corticosteroids can reduce anterior segment inflammation by stabilizing tight junctions in neovascular tissue, thereby reducing vascular exudation. Cycloplegic agents prevent posterior synechiae formation between the iris and lens. Anti-VEGF agents may result in rapid regression of any intraocular neovascularization, but these agents should be used as a temporizing adjunctive measure with subsequent placement of PRP for definitive treatment of NVI/NVA/NVD/NVE.[100] Failure of medical therapy to control intraocular pressure may require surgical intervention (e.g., trabeculectomy or tube placement).

Treatment of Systemic Medical Conditions

Identification and treatment of systemic vascular risk factors, such as systemic hypertension and diabetes mellitus, is of paramount importance in individuals with CRVO. Coordination with the internist is strongly recommended. The role of systemic anticoagulation is unclear as there is no evidence that agents such as aspirin or heparin can prevent or alter the natural history of CRVO; patients taking warfarin sodium (Coumadin) can still develop CRVO despite maintaining therapeutic levels of anticoagulation.[101] Prophylactic use of these medications, however, may help prevent nonocular thrombotic events, especially in individuals with known systemic vascular disease, and may be considered in coordination with the patient's internist.

Oral pentoxifylline is a vasodilator and enhancer of red blood cell deformability used in systemic vascular diseases to improve perfusion to occluded vessels and enhance the development of collateral circulation. A retrospective series of 11 patients treated with oral pentoxifylline (400 mg three times a day) for an average of 5 months demonstrated a 10% mean reduction in macular thickening by volumetric OCT but did not demonstrate a change in visual acuity or perfusion status.[102]

The reported increased plasma viscosity in persons with CRVO has prompted interest in systemic hemodilution to increase oxygen supply to the retina. Prospective, randomized controlled clinical trial of selected CRVO patients demonstrated significant visual acuity gains, reduced conversion to nonperfusion,[103] and reduced the need for intravitreal bevacizumab injections when used in combination.[104] Hemodilution is likely not appropriate for patients with anemia, renal insufficiency, or pulmonary insufficiency, which may limit its clinical use.[103,105]

Alternative Treatments Aimed at Underlying Etiology

Chorioretinal Venous Anastomosis

In eyes with perfused CRVO, investigators have bypassed the occluded central retinal vein by creating a chorioretinal

anastomosis (CRA) between a nasal branch retinal vein and the choroidal circulation. Successful creation of an anastomosis may allow transretinal retrograde flow of venous blood from the eye and prevent the development of retinal ischemia or allow reduction of ME. CRAs have been created through a surgical transretinal venipuncture technique[106,107] or, more commonly, through argon or Nd-YAG laser delivery directly at a branch retinal vein to rupture the posterior vein wall and Bruch's membrane.[108,109] McAllister and colleagues prospectively randomized 113 patients with nonischemic CRVO to laser-induced CRA or sham treatment.[110] Treated eyes demonstrated significant visual acuity gains, but this was counteracted by significant side-effects.

Immediate complications from this technique may include intraretinal, subretinal, or vitreous hemorrhage, while long-term complications include nonclearing vitreous hemorrhage, epiretinal avascular proliferation, fibrovascular proliferation, secondary neovascularization (choroidal, retinal, choroidovitreal, anterior segment), and traction retinal detachment.[106,111,112] Visual recovery may be limited in spite of successful anastomosis creation due to thrombosis of the treated vein with progressive distal retinal ischemia.

Tissue Plasminogen Activator

Thrombolytic agents have been proposed as a treatment of a suspected thrombus in the central retinal vein. If a thrombus is indeed etiologic, lysis is recommended within 21 days of its formation. Recombinant tissue plasminogen activator (r-tPA) is a synthetic fibrinolytic agent that converts plasminogen to plasmin and destabilizes intravascular thrombi. Reduction in clot size may facilitate dislodging of the entire thrombus or recanalization of the occluded retinal vein. Recombinant tissue plasminogen activator has been administered by several routes: systemic, intravitreal, and by endovascular cannulation of retinal vessels.

Systemic administration of low-dose (50 μg) front-loaded r-tPA has been attempted in two pilot studies with visual acuity improvement in 30–73% of patients.[113,114] In a prospective, multicenter randomized trial of 41 patients with CRVO, Hattenbach and colleagues demonstrated significant 1-year improvement of 3

lines in 45% of patients undergoing low dose r-tPA compared to 21% of patients undergoing hemodilution.[115] Another study examining high-dose (<100 μg) systemic tPA for the treatment of 96 patients reported development of intraocular hemorrhage in three patients and a fatal stroke in one patient.[116] While Hattenbach did not observe any serious adverse events in his trial of low-dose r-tPA, these complications highlight the importance of approaching systemic administration of r-tPA with caution.

Intravitreal delivery of r-tPA has potential advantages, including decreased risk of systemic complications, directed delivery to the vitreous cavity, and subsequent access to the retinal vessels with low risk of ocular morbidity from the procedure. Of 47 persons in three noncontrolled studies of intravitreal r-tPA for both ischemic and nonischemic CRVO of less than 21 days' duration, 28–44% had 3 lines of visual acuity improvement with 6 months follow-up.[117–119] Administration of r-tPA did not significantly alter final perfusion status, especially in pretreatment ischemic eyes.[120] Although there were no significant treatment-related complications, differences in inclusion criteria and dosage of r-tPA used (between 66 and 100 μg) limits generalizations from these studies.

Endovascular delivery of r-tPA involves cannulation of retinal vessels, either through a neuroradiologic or a vitreoretinal approach, with delivery of minute quantities of r-tPA directly into the occluded vein to dissolve the suspected thrombus.[121,122] Weiss and Bynoe reported their technique of vitrectomy followed by cannulation of a branch vein and infusion of r-tPA towards the optic nerve head.[123] In their uncontrolled study, 50% of 28 eyes with CRVO of greater than 1-month duration and worse than 20/400 preoperative acuity recovered more than 3 lines by a mean follow-up of 12 months. Complications included vitreous hemorrhage in seven eyes and treated retinal detachment in one eye. In another prospective study of 13 patients undergoing endovascular r-tPA delivery, visual recovery did not correspond with successful thrombolysis, and complications including retinal detachment, phthisis, neovascular glaucoma, and cataract were considered unacceptably high.[124]

Surgical Treatments

Vitrectomy

Vitreous surgery may be useful to address complications of CRVO and even to attempt to alter the natural course of the disease. Eyes with nonclearing vitreous hemorrhage from secondary retinal neovascularization may benefit from surgical evacuation. At the time of vitrectomy, clearing of the hemorrhage can be combined with removal of epiretinal membranes and removal of fibrovascular proliferations, if present, and the placement of complete PRP.[125] Although this technique may prevent or aid in regression of anterior segment neovascularization, visual outcomes may be limited due to the extent of underlying retinal nonperfusion.[126] In eyes with extensive anterior segment neovascularization and neovascular glaucoma, vitrectomy and endolaser PRP may be combined with pars plana placement of a glaucoma drainage device to avoid anterior chamber hemorrhage at the time of tube placement.

The potential role of vitrectomy with peeling of the internal limiting membrane has also been investigated for treatment of ME secondary to CRVO. Small studies have demonstrated an improvement in ME accompanied by improvement in acuity.[127–129] In contrast, one study showed no significant improvement in vision despite improvement of central foveal thickness.[130]

The use of vitrectomy with membrane peel in the treatment of CRVO-associated ME requires further investigation with randomized trials to establish its efficacy, particularly given the development of effective and less invasive intravitreal pharmacologic agents. Vitrectomy alters the pharmacokinetics of these intravitreal agents, which may reduce duration of effect and as such, the use of vitrectomy in the treatment of CRVO may result in decreased efficacy of further intravitreal pharmacotherapy.[131] This should be carefully balanced against the expected benefits of vitrectomy.

Radial Optic Neurotomy

Opremcak and colleagues first reported combining vitrectomy with radial optic neurotomy (RON) involving transvitreal incision of the nasal scleral ring to release pressure on the central retinal vein at the level of the scleral outlet. In a nonrandomized study of 117

consecutive eyes undergoing RON, Opremcak reported anatomic resolution of ME in 95% and visual improvement in 71% of eyes.[132] Interpretation of these impressive results must consider the nonrandomized nature of the study and the absence of a control group. While subsequent reports, including a prospective randomized trial, on radial optic neurotomy have also demonstrated visual improvement,[133–136] no study has replicated the reported 71% improvement, and some studies have reported that visual improvement following RON is comparable to natural history.[135] In contrast, other studies have not demonstrated improvement in visual acuity[137] or in central retinal hemodynamics,[138,139] questioning the role for RON in CRVO treatment. Importantly, RON has been associated with significant risks, including postoperative visual field defects, laceration of central retinal vessels, globe perforation, choroidal neovascularization, subretinal hemorrhage, and retinal detachment.[133,135–137,140] Evidence of the efficacy of RON in the management of CRVO is limited but currently does not clearly demonstrate a beneficial role. With the availability of effective intravitreal pharmacologic agents, the use of RON for CRVO has largely been abandoned.

Follow-Up

Prior to the availability of intravitreal pharmacotherapy for the treatment of CRVO-associated ME, follow-up for eyes with CRVO to detect neovascular complications was typically guided by visual acuity at initial presentation. Eyes with initial acuity of ≥20/40 were generally examined every 1–2 months for 6 months, then annually if stable. Eyes with initial acuity <20/200 were seen monthly for the initial 6-months, then bimonthly for the next 6 months, as these eyes have a greater degree of nonperfusion and a higher risk of developing NVI/NVA. Eyes with acuity between 20/50 and 20/200 have an intermediate risk of developing NVI/NVA and were also typically examined monthly for the first 6 months. Eyes that experienced a drop in visual acuity below the 20/200 level during follow-up were reevaluated with assessment of perfusion status and presence of neovascularization, and monthly follow-up for an

additional 6 months was recommended for these eyes.[9] With the development of intravitreal pharmacologic agents, this paradigm has changed. Follow-up intervals for patients undergoing treatment with intravitreal pharmacotherapy should currently be based on clinical response to treatment. Close monitoring and frequent treatment for several years may be required for prevent recurrent ME and neovascular complications.

Conclusion

CRVO is a sight-threatening disease with significant ocular morbidity including ME and intraocular neovascularization. Before the recent advent of intravitreal pharmacotherapy in its management, the standard of care was guided by results from the Central Vein Occlusion Study, which recommended observation of ME and retinal ischemia with management of neovascular sequelae using PRP. In the absence of robust treatment options for CRVO,[69] other approaches including the administration of r-tPA, creation of chorioretinal anastomosis, and various surgical interventions had been reported with variable success and often unacceptable side effects. More recently, intravitreal corticosteroids and then anti-VEGF agents have demonstrated improvements in ME, visual acuity, and even neovascular complications with a favorable side effect profile. The use of ranibizumab (Lucentis), aflibercept (Eylea), and a sustained-release dexamethasone implant (Ozurdex) have been FDA-approved for the treatment of CRVO. Intravitreal pharmacotherapy has now replaced observation as the standard of care for the management of CRVO.

References

1. Hayreh SS, Zimmerman MB, Podhajsky P. Incidence of various types of retinal vein occlusion and their recurrence and demographic characteristics. *Am J Ophthalmol*. 1994;117(4):429–441.
2. Mitchell P, Smith W, Chang A. Prevalence and associations of retinal vein occlusion in Australia. The Blue Mountains Eye Study. *Arch Ophthalmol*. 1996;114(10):1243–1247.

3. Baseline and early natural history report. The Central Vein Occlusion Study. *Arch Ophthalmol*. 1993;111(8):1087–1095.
4. Risk factors for central retinal vein occlusion. The Eye Disease Case–Control Study Group. *Arch Ophthalmol*. 1996;114(5):545–554.
5. Gutman FA. Evaluation of a patient with central retinal vein occlusion. *Ophthalmology*. 1983;90(5):481–483.
6. Fong AC, Schatz H. Central retinal vein occlusion in young adults. *Surv Ophthalmol*. 1993;37(6):393–417.
7. Klein R, Klein BE, Moss SE, et al. The epidemiology of retinal vein occlusion: the Beaver Dam Eye Study. *Trans Am Ophthalmol Soc*. 2000;98:133–141 [discussion 41-3].
8. Rogers S, McIntosh RL, Cheung N, et al. The prevalence of retinal vein occlusion: pooled data from population studies from the United States, Europe, Asia, and Australia. *Ophthalmology*. 2010;117(2):313–319.e1.
9. Natural history and clinical management of central retinal vein occlusion. The Central Vein Occlusion Study Group. *Arch Ophthalmol*. 1997;115(4):486–491.
10. Deramo VA, Cox TA, Syed AB, et al. Vision-related quality of life in people with central retinal vein occlusion using the 25-item National Eye Institute Visual Function Questionnaire. *Arch Ophthalmol*. 2003;121(9):1297–1302.
11. Fekrat S, Shea AM, Hammill BG, et al. Resource use and costs of branch and central retinal vein occlusion in the elderly. *Curr Med Res Opin*. 2010;26(1):223–230.
12. Suner IJ, Margolis J, Ruiz K, et al. Direct medical costs and resource use for treating central and branch retinal vein occlusion in commercially insured working-age and Medicare populations. *Retina*. 2014;34(11):2250–2258.
13. Schatz H, Fong AC, McDonald HR, et al. Cilioretinal artery occlusion in young adults with central retinal vein occlusion. *Ophthalmology*. 1991;98(5):594–601.
14. Hayreh SS, Fraterrigo L, Jonas J. Central retinal vein occlusion associated with cilioretinal artery occlusion. *Retina*. 2008;28(4):581–594.
15. Brown GC, Duker JS, Lehman R, et al. Combined central retinal artery–central vein obstruction. *Int Ophthalmol*.

1993;17(1):9–17.
16. Hayreh SS, Podhajsky PA, Zimmerman MB. Natural history of visual outcome in central retinal vein occlusion. *Ophthalmology*. 2011;118(1):119–133.e1-2.
17. Decroos FC, Fekrat S. The natural history of retinal vein occlusion: what do we really know? *Am J Ophthalmol*. 2011;151(5):739–741.e2.
18. Browning DJ, Scott AQ, Peterson CB, et al. The risk of missing angle neovascularization by omitting screening gonioscopy in acute central retinal vein occlusion. *Ophthalmology*. 1998;105(5):776–784.
19. Hayreh SS, Klugman MR, Beri M, et al. Differentiation of ischemic from nonischemic central retinal vein occlusion during the early acute phase. *Graefes Arch Clin Exp Ophthalmol*. 1990;228(3):201–217.
20. Hayreh SS, Zimmerman MB. Ocular neovascularization associated with central and hemicentral retinal vein occlusion. *Retina*. 2012;32(8):1553–1565.
21. Wykoff CC, Brown DM, Croft DE, et al. Progressive retinal nonperfusion in ischemic central retinal vein occlusion. *Retina*. 2015;35(1):43–47.
22. Sophie R, Hafiz G, Scott AW, et al. Long-term outcomes in ranibizumab-treated patients with retinal vein occlusion; the role of progression of retinal nonperfusion. *Am J Ophthalmol*. 2013;156(4):693–705.
23. Tsui I, Franco-Cardenas V, Hubschman JP, et al. Ultrawide-field fluorescein angiography can detect macular pathology in central retinal vein occlusion. *Ophthalmic Surg Lasers Imaging*. 2012;43(3):257–262.
24. Tsui I, Kaines A, Havunjian MA, et al. Ischemic index and neovascularization in central retinal vein occlusion. *Retina*. 2011;31(1):105–110.
25. Spaide RF. Peripheral areas of nonperfusion in treated central retinal vein occlusion as imaged by wide-field fluorescein angiography. *Retina*. 2011;31(5):829–837.
26. Spaide RF. Prospective study of peripheral panretinal photocoagulation of areas of nonperfusion in central retinal vein occlusion. *Retina*. 2013;33(1):56–62.

27. Green WR, Chan CC, Hutchins GM, et al. Central retinal vein occlusion: a prospective histopathologic study of 29 eyes in 28 cases. *Retina*. 1981;1(1):27–55.
28. Pe'er J, Folberg R, Itin A, et al. Vascular endothelial growth factor upregulation in human central retinal vein occlusion. *Ophthalmology*. 1998;105(3):412–416.
29. Aiello LP, Avery RL, Arrigg PG, et al. Vascular endothelial growth factor in ocular fluid of patients with diabetic retinopathy and other retinal disorders. *N Engl J Med*. 1994;331(22):1480–1487.
30. Funk M, Kriechbaum K, Prager F, et al. Intraocular concentrations of growth factors and cytokines in retinal vein occlusion and the effect of therapy with bevacizumab. *Invest Ophthalmol Vis Sci*. 2009;50(3):1025–1032.
31. Noma H, Funatsu H, Mimura T, et al. Vitreous levels of interleukin-6 and vascular endothelial growth factor in macular edema with central retinal vein occlusion. *Ophthalmology*. 2009;116(1):87–93.
32. Boyd SR, Zachary I, Chakravarthy U, et al. Correlation of increased vascular endothelial growth factor with neovascularization and permeability in ischemic central vein occlusion. *Arch Ophthalmol*. 2002;120(12):1644–1650.
33. Stem MS, Talwar N, Comer GM, et al. A longitudinal analysis of risk factors associated with central retinal vein occlusion. *Ophthalmology*. 2013;120(2):362–370.
34. O'Mahoney PR, Wong DT, Ray JG. Retinal vein occlusion and traditional risk factors for atherosclerosis. *Arch Ophthalmol*. 2008;126(5):692–699.
35. The Eye Disease Case–Control Study Group. Risk factors for branch retinal vein occlusion. *Am J Ophthalmol*. 1993;116(3):286–296.
36. Elman MJ, Bhatt AK, Quinlan PM, et al. The risk for systemic vascular diseases and mortality in patients with central retinal vein occlusion. *Ophthalmology*. 1990;97(11):1543–1548.
37. Hayreh SS, Zimmerman B, McCarthy MJ, et al. Systemic diseases associated with various types of retinal vein occlusion. *Am J Ophthalmol*. 2001;131(1):61–77.

38. Koizumi H, Ferrara DC, Brue C, et al. Central retinal vein occlusion case-control study. *Am J Ophthalmol*. 2007;144(6):858–863.
39. Cheung N, Klein R, Wang JJ, et al. Traditional and novel cardiovascular risk factors for retinal vein occlusion: the multiethnic study of atherosclerosis. *Invest Ophthalmol Vis Sci*. 2008;49(10):4297–4302.
40. Di Capua M, Coppola A, Albisinni R, et al. Cardiovascular risk factors and outcome in patients with retinal vein occlusion. *J Thromb Thrombolysis*. 2010;30(1):16–22.
41. Lahey JM, Tunc M, Kearney J, et al. Laboratory evaluation of hypercoagulable states in patients with central retinal vein occlusion who are less than 56 years of age. *Ophthalmology*. 2002;109(1):126–131.
42. Williamson TH, Rumley A, Lowe GD. Blood viscosity, coagulation, and activated protein C resistance in central retinal vein occlusion: a population controlled study. *Br J Ophthalmol*. 1996;80(3):203–208.
43. Gottlieb JL, Blice JP, Mestichelli B, et al. Activated protein C resistance, factor V Leiden, and central retinal vein occlusion in young adults. *Arch Ophthalmol*. 1998;116(5):577–579.
44. Hayreh SS, Zimmerman MB, Podhajsky P. Hematologic abnormalities associated with various types of retinal vein occlusion. *Graefes Arch Clin Exp Ophthalmol*. 2002;240(3):180–196.
45. Hvarfner C, Hillarp A, Larsson J. Influence of factor V Leiden on the development of neovascularisation secondary to central retinal vein occlusion. *Br J Ophthalmol*. 2003;87(3):305–306.
46. Cahill MT, Stinnett SS, Fekrat S. Meta-analysis of plasma homocysteine, serum folate, serum vitamin B(12), and thermolabile MTHFR genotype as risk factors for retinal vascular occlusive disease. *Am J Ophthalmol*. 2003;136(6):1136–1150.
47. Yap YC, Barampouti F. Central retinal vein occlusion secondary to protein S deficiency. *Ann Ophthalmol (Skokie)*. 2007;39(4):343–344.

48. Rehak M, Rehak J, Muller M, et al. The prevalence of activated protein C (APC) resistance and factor V Leiden is significantly higher in patients with retinal vein occlusion without general risk factors. Case–control study and meta-analysis. *Thromb Haemost*. 2008;99(5):925–929.
49. Incorvaia C, Parmeggiani F, Costagliola C, et al. The heterozygous 20210 G/A genotype prevalence in patients affected by central and branch retinal vein occlusion: a pilot study. *Graefes Arch Clin Exp Ophthalmol*. 2001;239(4):251–256.
50. Ciardella AP, Clarkson JG, Guyer DR, et al. Central retinal vein occlusion: a primer and review. Guyer DR, Yannuzzi LA, Chang S, et al. *Retina–Vitreous–Macula*. W.B. Saunders: New York; 1999.
51. Francis PJ, Stanford MR, Graham EM. Dehydration is a risk factor for central retinal vein occlusion in young patients. *Acta Ophthalmol Scand*. 2003;81(4):415–416.
52. Alexander P, Flanagan D, Rege K, et al. Bilateral simultaneous central retinal vein occlusion secondary to hyperviscosity in Waldenstrom's macroglobulinaemia. *Eye (Lond)*. 2008;22(8):1089–1092.
53. Al-Abdulla NA, Thompson JT, LaBorwit SE. Simultaneous bilateral central retinal vein occlusion associated with anticardiolipin antibodies in leukemia. *Am J Ophthalmol*. 2001;132(2):266–268.
54. Sbeity ZH, Mansour AM. Recurrent retinal vein occlusion after playing a wind instrument. *Graefes Arch Clin Exp Ophthalmol*. 2004;242(5):428–431.
55. Weiss KD, Kuriyan AE, Flynn HW Jr. Central retinal vein occlusion after prolonged vomiting and repeated Valsalva maneuvers associated with gastroenteritis and dehydration. *Ophthalmic Surg Lasers Imaging Retina*. 2014;45:e23–5 [Online].
56. Dev S, Herndon L, Shields MB. Retinal vein occlusion after trabeculectomy with mitomycin C. *Am J Ophthalmol*. 1996;122(4):574–575.
57. Rumelt S, Karatas M, Pikkel J, et al. Optic disc traction syndrome associated with central retinal vein occlusion.

Arch Ophthalmol. 2003;121(8):1093–1097.
58. Kearns TP. Differential diagnosis of central retinal vein obstruction. *Ophthalmology*. 1983;90(5):475–480.
59. Hahn P, Fekrat S. Best practices for treatment of retinal vein occlusion. *Curr Opin Ophthalmol*. 2012;23(3):175–181.
60. Ip MS, Scott IU, VanVeldhuisen PC, et al. A randomized trial comparing the efficacy and safety of intravitreal triamcinolone with observation to treat vision loss associated with macular edema secondary to central retinal vein occlusion: the Standard Care vs Corticosteroid for Retinal Vein Occlusion (SCORE) study report 5. *Arch Ophthalmol*. 2009;127(9):1101–1114.
61. Haller JA, Bandello F, Belfort R Jr, et al. Randomized, sham-controlled trial of dexamethasone intravitreal implant in patients with macular edema due to retinal vein occlusion. *Ophthalmology*. 2010;117(6):1134–1146.e3.
62. Brown DM, Campochiaro PA, Singh RP, et al. Ranibizumab for macular edema following central retinal vein occlusion: six-month primary end point results of a phase III study. *Ophthalmology*. 2010;117(6):1124–1133.e1.
63. Wroblewski JJ, Wells JA 3rd, Adamis AP, et al. Pegaptanib sodium for macular edema secondary to central retinal vein occlusion. *Arch Ophthalmol*. 2009;127(4):374–380.
64. Boyer D, Heier J, Brown DM, et al. Vascular endothelial growth factor trap-eye for macular edema secondary to central retinal vein occlusion: six-month results of the phase 3 COPERNICUS Study. *Ophthalmology*. 2012;119(5):1024–1032.
65. Epstein DL, Algvere PV, von Wendt G, et al. Bevacizumab for macular edema in central retinal vein occlusion: a prospective, randomized, double-masked clinical study. *Ophthalmology*. 2012;119(6):1184–1189.
66. Holz FG, Roider J, Ogura Y, et al. VEGF trap-eye for macular oedema secondary to central retinal vein occlusion: 6-month results of the phase III GALILEO study. *Br J Ophthalmol*. 2013;97(3):278–284.
67. Korobelnik JF, Holz FG, Roider J, et al. Intravitreal Aflibercept injection for macular edema resulting from

central retinal vein occlusion: one-year results of the phase 3 GALILEO Study. *Ophthalmology*. 2014;121(1):202–208.
68. Evaluation of grid pattern photocoagulation for macular edema in central vein occlusion. The Central Vein Occlusion Study Group M report. *Ophthalmology*. 1995;102(10):1425–1433.
69. Hayreh SS. Management of central retinal vein occlusion. *Ophthalmologica*. 2003;217(3):167–188.
70. Nauck M, Karakiulakis G, Perruchoud AP, et al. Corticosteroids inhibit the expression of the vascular endothelial growth factor gene in human vascular smooth muscle cells. *Eur J Pharmacol*. 1998;341(2–3):309–315.
71. Felinski EA, Antonetti DA. Glucocorticoid regulation of endothelial cell tight junction gene expression: novel treatments for diabetic retinopathy. *Curr Eye Res*. 2005;30(11):949–957.
72. Shaikh S, Blumenkranz MS. Transient improvement in visual acuity and macular edema in central retinal vein occlusion accompanied by inflammatory features after pulse steroid and anti-inflammatory therapy. *Retina*. 2001;21(2):176–178.
73. Jonas JB, Kreissig I, Degenring RF. Intravitreal triamcinolone acetonide as treatment of macular edema in central retinal vein occlusion. *Graefes Arch Clin Exp Ophthalmol*. 2002;240(9):782–783.
74. Ip MS, Kumar KS. Intravitreous triamcinolone acetonide as treatment for macular edema from central retinal vein occlusion. *Arch Ophthalmol*. 2002;120(9):1217–1219.
75. Greenberg PB, Martidis A, Rogers AH, et al. Intravitreal triamcinolone acetonide for macular oedema due to central retinal vein occlusion. *Br J Ophthalmol*. 2002;86(2):247–248.
76. Park CH, Jaffe GJ, Fekrat S. Intravitreal triamcinolone acetonide in eyes with cystoid macular edema associated with central retinal vein occlusion. *Am J Ophthalmol*. 2003;136(3):419–425.
77. Jain N, Stinnett SS, Jaffe GJ. Prospective study of a fluocinolone acetonide implant for chronic macular edema from central retinal vein occlusion: thirty-six-month results.

Ophthalmology. 2012;119(1):132–137.
78. Haller JA, Bandello F, Belfort R Jr, et al. Dexamethasone intravitreal implant in patients with macular edema related to branch or central retinal vein occlusion twelve-month study results. *Ophthalmology*. 2011;118(12):2453–2460.
79. Ferrara DC, Koizumi H, Spaide RF. Early bevacizumab treatment of central retinal vein occlusion. *Am J Ophthalmol*. 2007;144(6):864–871.
80. Campochiaro PA, Bhisitkul RB, Shapiro H, et al. Vascular endothelial growth factor promotes progressive retinal nonperfusion in patients with retinal vein occlusion. *Ophthalmology*. 2013;120(4):795–802.
81. Campochiaro PA, Brown DM, Awh CC, et al. Sustained benefits from ranibizumab for macular edema following central retinal vein occlusion: twelve-month outcomes of a phase III study. *Ophthalmology*. 2011;118(10):2041–2049.
82. Varma R, Bressler NM, Suner I, et al. Improved vision-related function after ranibizumab for macular edema after retinal vein occlusion: results from the BRAVO and CRUISE trials. *Ophthalmology*. 2012;119(10):2108–2118.
83. Heier JS, Campochiaro PA, Yau L, et al. Ranibizumab for macular edema due to retinal vein occlusions: long-term follow-up in the HORIZON trial. *Ophthalmology*. 2012;119(4):802–809.
84. Campochiaro PA, Sophie R, Pearlman J, et al. Long-term outcomes in patients with retinal vein occlusion treated with ranibizumab: the RETAIN study. *Ophthalmology*. 2014;121(1):209–219.
85. Campochiaro PA, Hafiz G, Mir TA, et al. Scatter photocoagulation does not reduce macular edema or treatment burden in patients with retinal vein occlusion: the RELATE Trial. *Ophthalmology*. 2015;122(7):1426–1437.
86. Brown DM, Heier JS, Clark WL, et al. Intravitreal aflibercept injection for macular edema secondary to central retinal vein occlusion: 1-year results from the phase 3 COPERNICUS study. *Am J Ophthalmol*. 2013;155(3):429–437.e7.
87. Heier JS, Clark WL, Boyer DS, et al. Intravitreal aflibercept

injection for macular edema due to central retinal vein occlusion: two-year results from the COPERNICUS study. *Ophthalmology*. 2014;121(7):1414–1420.e1.
88. Ogura Y, Roider J, Korobelnik JF, et al. Intravitreal aflibercept for macular edema secondary to central retinal vein occlusion: 18-month results of the phase 3 GALILEO study. *Am J Ophthalmol*. 2014;158(5):1032–1038.
89. Epstein DL, Algvere PV, von Wendt G, et al. Benefit from bevacizumab for macular edema in central retinal vein occlusion: twelve-month results of a prospective, randomized study. *Ophthalmology*. 2012;119(12):2587–2591.
90. Narayanan R, Panchal B, Das T, et al. A randomised, double-masked, controlled study of the efficacy and safety of intravitreal bevacizumab vs ranibizumab in the treatment of macular oedema due to branch retinal vein occlusion: MARVEL report no. 1. *Br J Ophthalmol*. 2015;99(7):954–959.
91. Chakravarthy U, Harding SP, Rogers CA, et al. Alternative treatments to inhibit VEGF in age-related choroidal neovascularisation: 2-year findings of the IVAN randomised controlled trial. *Lancet*. 2013;382(9900):1258–1267.
92. Martin DF, Maguire MG, Ying GS, et al. Ranibizumab and bevacizumab for neovascular age-related macular degeneration. *N Engl J Med*. 2011;364(20):1897–1908.
93. Yeh S, Kim SJ, Ho AC, et al. Therapies for macular edema associated with central retinal vein occlusion: a report by the American Academy of Ophthalmology. *Ophthalmology*. 2015;122(4):769–778.
94. Hahn P, Fekrat S. Aflibercept for central retinal vein occlusion: an ongoing revolution or are we spinning in place? *Am J Ophthalmol*. 2013;155(3):415–417.e2.
95. Ding X, Li J, Hu X, et al. Prospective study of intravitreal triamcinolone acetonide vs bevacizumab for macular edema secondary to central retinal vein occlusion. *Retina*. 2011;31(5):838–845.
96. Mayer WJ, Wolf A, Kernt M, et al. Twelve-month experience with Ozurdex for the treatment of macular edema associated with retinal vein occlusion. *Eye (Lond)*.

2013;27(7):816–822.
97. DeCroos FC, Todorich B, Alshareef R, et al. Neovascular events in eyes with central retinal vein occlusion undergoing serial bevacizumab or ranibizumab intravitreal injections: a retrospective review. *J Ophthalmic Vis Res*. 2014;9(4):461–468.
98. Brown DM, Wykoff CC, Wong TP, et al. Ranibizumab in preproliferative (ischemic) central retinal vein occlusion: the rubeosis anti-VEGF (RAVE) trial. *Retina*. 2014;34(9):1728–1735.
99. A randomized clinical trial of early panretinal photocoagulation for ischemic central vein occlusion. The Central Vein Occlusion Study Group N report. *Ophthalmology*. 1995;102(10):1434–1444.
100. Iliev ME, Domig D, Wolf-Schnurrbursch U, et al. Intravitreal bevacizumab (Avastin) in the treatment of neovascular glaucoma. *Am J Ophthalmol*. 2006;142(6):1054–1056.
101. Mruthyunjaya P, Wirostko WJ, Chandrashekhar R, et al. Central retinal vein occlusion in patients treated with long-term warfarin sodium (Coumadin) for anticoagulation. *Retina*. 2006;26(3):285–291.
102. Park CH, Scott AW, Fekrat S. Effect of oral pentoxifylline on cystoid macular edema associated with central retinal vein occlusion. *Retina*. 2007;27(8):1020–1025.
103. Glacet-Bernard A, Atassi M, Fardeau C, et al. Hemodilution therapy using automated erythrocytapheresis in central retinal vein occlusion: results of a multicenter randomized controlled study. *Graefes Arch Clin Exp Ophthalmol*. 2011;249:505–512.
104. Kreutzer TC, Wolf A, Dirisamer M, et al. Intravitreal ranibizumab vs isovolemic hemodilution in the treatment of macular edema secondary to central retinal vein occlusion: twelve-month results of a prospective, randomized, multicenter trial. *Ophthalmologica*. 2015;233(1):8–17.
105. Chen HC, Wiek J, Gupta A, et al. Effect of isovolaemic haemodilution on visual outcome in branch retinal vein

occlusion. *Br J Ophthalmol*. 1998;82(2):162–167.
106. Fekrat S, de Juan E Jr. Chorioretinal venous anastomosis for central retinal vein occlusion: transvitreal venipuncture. *Ophthalmic Surg Lasers*. 1999;30(1):52–55.
107. Peyman GA, Kishore K, Conway MD. Surgical chorioretinal venous anastomosis for ischemic central retinal vein occlusion. *Ophthalmic Surg Lasers*. 1999;30(8):605–614.
108. McAllister IL, Constable IJ. Laser-induced chorioretinal venous anastomosis for treatment of nonischemic central retinal vein occlusion. *Arch Ophthalmol*. 1995;113(4):456–462.
109. Fekrat S, Goldberg MF, Finkelstein D. Laser-induced chorioretinal venous anastomosis for nonischemic central or branch retinal vein occlusion. *Arch Ophthalmol*. 1998;116(1):43–52.
110. McAllister IL, Gillies ME, Smithies LA, et al. The Central Retinal Vein Bypass Study: a trial of laser-induced chorioretinal venous anastomosis for central retinal vein occlusion. *Ophthalmology*. 2010;117(5):954–965.
111. McAllister IL, Douglas JP, Constable IJ, et al. Laser-induced chorioretinal venous anastomosis for nonischemic central retinal vein occlusion: evaluation of the complications and their risk factors. *Am J Ophthalmol*. 1998;126(2):219–229.
112. Bavbek T, Yenice O, Toygar O. Problems with attempted chorioretinal venous anastomosis by laser for nonischemic CRVO and BRVO. *Ophthalmologica*. 2005;219(5):267–271.
113. Hattenbach LO, Steinkamp G, Scharrer I, et al. Fibrinolytic therapy with low-dose recombinant tissue plasminogen activator in retinal vein occlusion. *Ophthalmologica*. 1998;212(6):394–398.
114. Hattenbach LO, Wellermann G, Steinkamp GW, et al. Visual outcome after treatment with low-dose recombinant tissue plasminogen activator or hemodilution in ischemic central retinal vein occlusion. *Ophthalmologica*. 1999;213(6):360–366.
115. Hattenbach LO, Friedrich Arndt C, Lerche R, et al. Retinal vein occlusion and low-dose fibrinolytic therapy (R.O.L.F.): a prospective, randomized, controlled multicenter study of low-dose recombinant tissue plasminogen activator vs hemodilution in retinal vein occlusion. *Retina*.

2009;29(7):932–940.
116. Elman MJ. Thrombolytic therapy for central retinal vein occlusion: results of a pilot study. *Trans Am Ophthalmol Soc*. 1996;94:471–504.
117. Lahey JM, Fong DS, Kearney J. Intravitreal tissue plasminogen activator for acute central retinal vein occlusion. *Ophthalmic Surg Lasers*. 1999;30(6):427–434.
118. Glacet-Bernard A, Kuhn D, Vine AK, et al. Treatment of recent onset central retinal vein occlusion with intravitreal tissue plasminogen activator: a pilot study. *Br J Ophthalmol*. 2000;84(6):609–613.
119. Elman MJ, Raden RZ, Carrigan A. Intravitreal injection of tissue plasminogen activator for central retinal vein occlusion. *Trans Am Ophthalmol Soc*. 2001;99:219–221 [discussion 22-3].
120. Ghazi NG, Noureddine B, Haddad RS, et al. Intravitreal tissue plasminogen activator in the management of central retinal vein occlusion. *Retina*. 2003;23(6):780–784.
121. Paques M, Vallee JN, Herbreteau D, et al. Superselective ophthalmic artery fibrinolytic therapy for the treatment of central retinal vein occlusion. *Br J Ophthalmol*. 2000;84(12):1387–1391.
122. Weiss JN. Treatment of central retinal vein occlusion by injection of tissue plasminogen activator into a retinal vein. *Am J Ophthalmol*. 1998;126(1):142–144.
123. Weiss JN, Bynoe LA. Injection of tissue plasminogen activator into a branch retinal vein in eyes with central retinal vein occlusion. *Ophthalmology*. 2001;108(12):2249–2257.
124. Feltgen N, Junker B, Agostini H, et al. Retinal endovascular lysis in ischemic central retinal vein occlusion: one-year results of a pilot study. *Ophthalmology*. 2007;114(4):716–723.
125. Lam HD, Blumenkranz MS. Treatment of central retinal vein occlusion by vitrectomy with lysis of vitreopapillary and epipapillary adhesions, subretinal peripapillary tissue plasminogen activator injection, and photocoagulation. *Am J Ophthalmol*. 2002;134(4):609–611.
126. Yeshaya A, Treister G. Pars plana vitrectomy for vitreous

hemorrhage and retinal vein occlusion. *Ann Ophthalmol*. 1983;15(7):615–617.
127. Liang XL, Chen HY, Huang YS, et al. Pars plana vitrectomy and internal limiting membrane peeling for macular oedema secondary to retinal vein occlusion: a pilot study. *Ann Acad Med Singapore*. 2007;36(4):293–297.
128. Raszewska-Steglinska M, Gozdek P, Cisiecki S, et al. Pars plana vitrectomy with ILM peeling for macular edema secondary to retinal vein occlusion. *Eur J Ophthalmol*. 2009;19(6):1055–1062.
129. Park DH, Kim IT. Long-term effects of vitrectomy and internal limiting membrane peeling for macular edema secondary to central retinal vein occlusion and hemiretinal vein occlusion. *Retina*. 2010;30(1):117–124.
130. DeCroos FC, Shuler RK Jr, Stinnett S, et al. Pars plana vitrectomy, internal limiting membrane peeling, and panretinal endophotocoagulation for macular edema secondary to central retinal vein occlusion. *Am J Ophthalmol*. 2009;147(4):627–633.e1.
131. Hahn P. Successful treatment of neovascular age-related macular degeneration following single bevacizumab failure using aflibercept in a vitrectomized eye. *Clin Ophthalmol*. 2014;8:2129–2131.
132. Opremcak EM, Rehmar AJ, Ridenour CD, et al. Radial optic neurotomy for central retinal vein occlusion: 117 consecutive cases. *Retina*. 2006;26(3):297–305.
133. Weizer JS, Stinnett SS, Fekrat S. Radial optic neurotomy as treatment for central retinal vein occlusion. *Am J Ophthalmol*. 2003;136(5):814–819.
134. Hasselbach HC, Ruefer F, Feltgen N, et al. Treatment of central retinal vein occlusion by radial optic neurotomy in 107 cases. *Graefes Arch Clin Exp Ophthalmol*. 2007;245(8):1145–1156.
135. Arevalo JF, Garcia RA, Wu L, et al. Radial optic neurotomy for central retinal vein occlusion: results of the Pan-American Collaborative Retina Study Group (PACORES). *Retina*. 2008;28(8):1044–1052.
136. Aggermann T, Brunner S, Krebs I, et al. A prospective,

randomised, multicenter trial for surgical treatment of central retinal vein occlusion: results of the Radial Optic Neurotomy for Central Vein Occlusion (ROVO) study group. *Graefes Arch Clin Exp Ophthalmol*. 2013;251(4):1065–1072.
137. Martinez-Jardon CS, Meza-de Regil A, Dalma-Weiszhausz J, et al. Radial optic neurotomy for ischaemic central vein occlusion. *Br J Ophthalmol*. 2005;89(5):558–561.
138. Crama N, Gualino V, Restori M, et al. Central retinal vessel blood flow after surgical treatment for central retinal vein occlusion. *Retina*. 2010;30(10):1692–1697.
139. Skevas C, Wagenfeld L, Feucht M, et al. Radial optic neurotomy in central retinal vein occlusion does not influence ocular hemodynamics. *Ophthalmologica*. 2011;225(1):41–46.
140. Opremcak EM, Bruce RA, Lomeo MD, et al. Radial optic neurotomy for central retinal vein occlusion: a retrospective pilot study of 11 consecutive cases. *Retina*. 2001;21(5):408–415.

58

Macular Telangiectasia

Emily Y. Chew, Lawrence A. Yannuzzi

Introduction

Macular telangiectasia (mac tel), or idiopathic perifoveal or juxtafoveal telangiectasia, includes several, different vascular diseases affecting the capillaries of the posterior pole. While complex classifications have been used, there are essentially two basic and distinct forms: (1) a developmental or congenital, usually unilateral vascular anomaly, which may be part of the larger spectrum of Coats disease and now often called mac tel type 1; and (2) a presumably acquired bilateral form found in middle-aged and older persons, which has been termed macular, juxtafoveal, or perifoveal telangiectasia and is now known as mac tel type 2. This chapter will focus on mac tel type 2, the bilateral, acquired form of perifoveal telangiectasia from unknown cause with characteristic alterations of the macular capillaries and neurosensory degeneration.

Classification of Macular Telangiectasia

In 1968, Gass recognized that Coats disease was a developmental vascular disease and he also introduced a new distinct entity, which

was called idiopathic juxtafoveolar retinal telangiectasis.[1] This resulted in an extensive, detailed classification in 1993.[2] However, this classification was further refined by Yanuzzi in 2006, using the new diagnostic, adjunctive imaging systems such as optical coherence tomography and high-speed stereoscopic angiography in a cohort of 36 patients with mac tel of various types. He introduced the name "idiopathic macular telangiectasia."[3] He proposed mac tel type 1 for "aneurysmal" telangiectasia, which was formerly known as Coats disease or Leber miliary aneurysm. The former condition, coined as juxtafoveal telangiectasia by Gass, became idiopathic macular telangiectasia or mac tel type 2. Other existing types of juxtafoveal telangiectasia that were associated with other systemic disease were eliminated in this new classification, because of the lack of subjects in the other categories.

Epidemiology

Prevalence of Disease: Estimates From Population-Based Studies

Beaver Dam Eye Study

The Beaver Dam Eye Study[4] regraded the stereoscopic fundus photographs of the eyes of 4926 subjects aged 43–84, 99% of whom were white, for mac tel type 2. Five individuals, one woman and four men, were identified to have mac tel type 2, which translates into a prevalence of 0.1% (95% confidence interval [CI] 0.09–0.1). The average age was 63 years, with a range from 52 to 68 years. Bilateral manifestations were found in two patients.

Melbourne Collaborative Cohort Study

This Australian study[5] analyzed 22, 415 Caucasians for the presence of typical features of mac tel type 2 on nonmydriatic color fundus photographs in a population study. Twelve patients with "possible" unilateral mac tel type 2 and five patients with signs of bilateral mac tel type 2 were identified. The average age amongst bilateral cases was 63 and ranged from 53 to 72 years. Three of the five bilateral cases were female. Only one "very convincing case

with early gray sheen and telangiectatic vessels temporal to the fovea" was reported. The authors concluded that the incidence in their studied population ranged from 0.0045% to 0.022%, a prevalence which is significantly lower than the one found in the Beaver Dam Eye Study.

Study in Africa

An additional study was conducted in two populations in African countries.[6] Of the 8599 participants, the prevalence of mac tel type 2 was 0.06% (95% CI 0.02–0.21%) and 0.06% (95% CI 0.01–0.17%) in Kenya and Nigeria, respectively. These were again assessed on color fundus photographs.

The techniques used to evaluate each of these studies were different, likely accounting for the varying rates. It is possible that all three studies may have underestimated the true prevalence because only color fundus images were available. Other imaging technologies such as fluorescein angiography (FA), optical coherence tomography (OCT), or fundus autofluorescence (FAF) have been demonstrated to be sensitive in detecting early and asymptomatic disease stages of mac tel type 2.[7]

The Macular Telangiectasia (MacTel) Project

The Macular Telangiectasia (MacTel) Project, which consists of an international consortium of investigators evaluating the natural history of this ocular condition with the goal of conducting clinical trials to assess potential therapies, also enrolled a mostly white population. The involvement of other ethnicities is not well studied.

Although Gass and Blodi did not find gender differences in their cohort of 140 patients (94 with mac tel type 2),[8] the proportions of women reported by the MacTel Project (n=310) and by Yannuzzi were about 64% and 58%, respectively.[9] On average, the MacTel Project participants (mean age 61 ± 9 years) had their disease diagnosed at age 57 (± 9 years).

Clinical Presentation

Fundus Appearance

The disease is usually bilateral, but one eye may be more advanced than the other. All lesions tend to begin temporal to the foveal center but may subsequently involve the entire parafoveolar area. The earliest fundoscopic manifestation of mac tel type 2 is a subtle loss of retinal transparency in the perifoveal region (Fig. 58.1).[3] This becomes more pronounced over time, and dilation of the parafoveal capillaries in the temporal parafoveal area ensues, and may extend to surround the fovea. These mildly ectatic capillaries were described to affect mainly the deeper capillary network (Fig. 58.2).[2] However, others have identified involvement of both the inner and outer retinal circulation.[3,9] In contrast to mac tel type 1, retinal hard exudate is not seen unless there is evidence of neovascularization. Crystalline deposits at the vitreoretinal interface may be seen throughout the course of the disease (Fig. 58.3).[2,10]

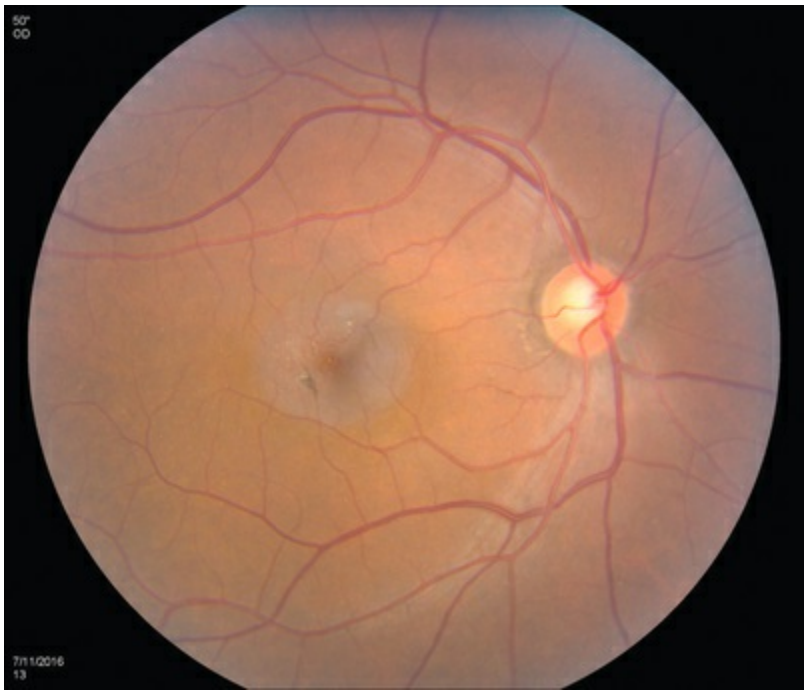

FIG. 58.1 Loss of retinal transparency, resulting in grayish discoloration of the retina can be seen centered around the fovea.

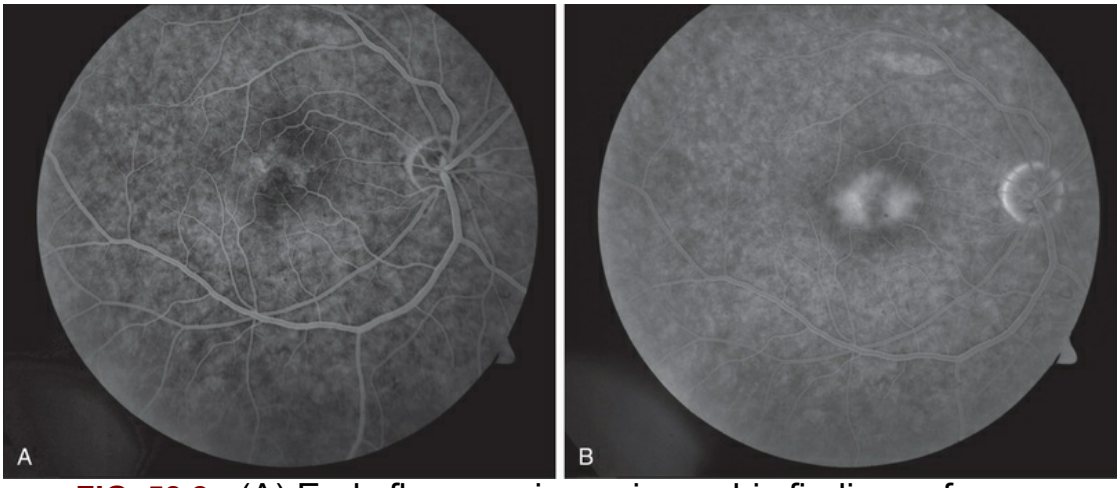

FIG. 58.2 (A) Early fluorescein angiographic findings of macular telangiectasia type 2 and (B) late leakage.

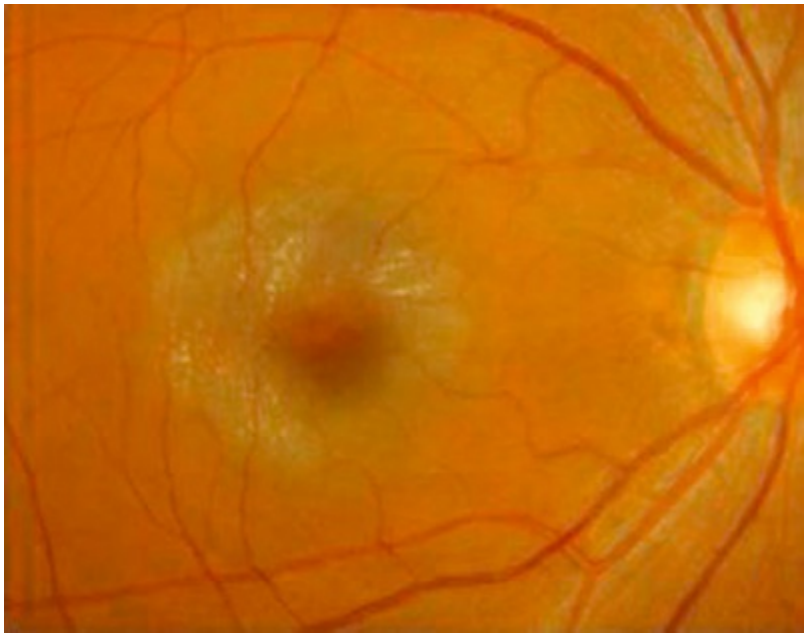

FIG. 58.3 Crystalline dots can be seen at the vitreoretinal interface.

Blunted, dilated venules, either as single or multiple vessels, are often associated with ectatic capillaries. As vessels course towards the fovea, they usually decrease in diameter but, in mac tel type 2, they dilate and may make a right-angle turn, diving into the deeper retinal layers (Fig. 58.4). Eventually, intraretinal pigment migration and RPE hyperplasia along these diving dilated venules may occur[3] (Fig. 58.5). In addition to RPE cell migration, atrophic changes in

the neurosensory retina are another frequent finding.

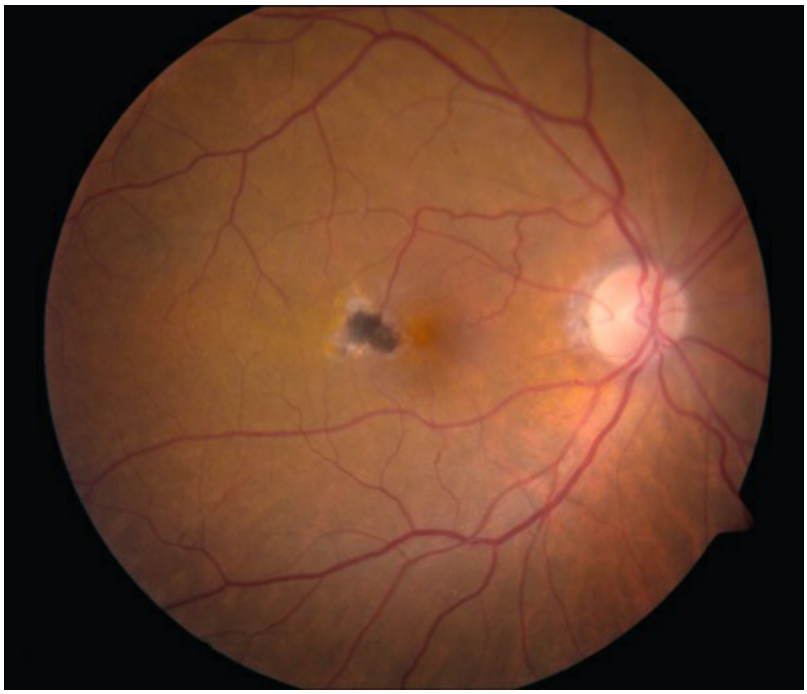

FIG. 58.4 Right-angle retinal vessels, manifested as blunted arterioles or venules that connect the superficial and deeper retinal plexus, are typical fundoscopic features of macular telangiectasia type 2. The right-angle vessels may be difficult to appreciate without stereoscopy. A pigment plaque is also seen in this patient's eye.

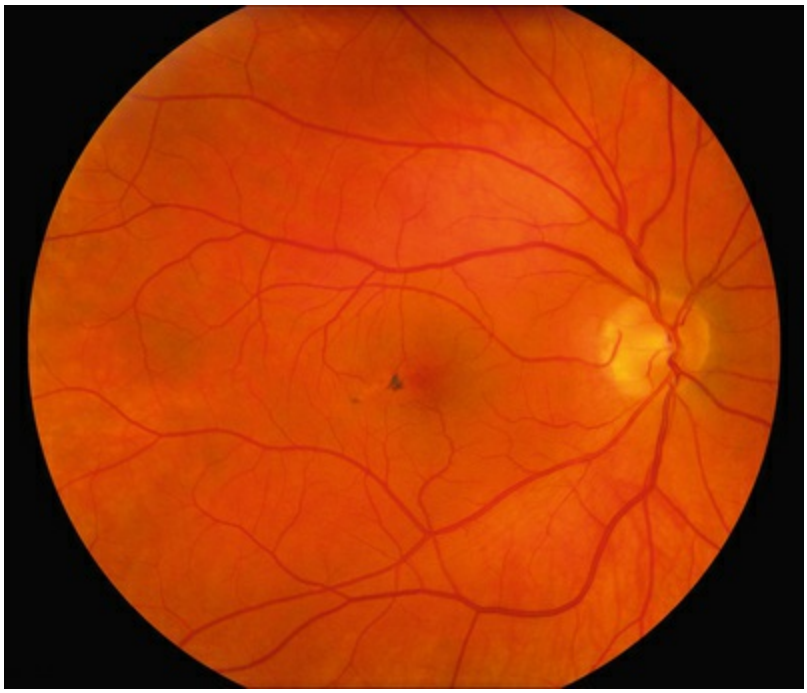

FIG. 58.5 Retinal pigment epithelial hyperplasia surrounds the right-angle venule.

A yellow spot, or vitelliform lesion, in the center of the fovea with slight loss of the foveal depression may become apparent in some eyes.[3] Other foveal changes include lamellar or full-thickness macular holes that have been detected on clinical exams and some confirmed by OCT imaging.[3,11–15] The degeneration and atrophy associated with this disease contribute to the formation of such holes. Surgical repair may not necessarily result in either structural or functional improvement.[9]

The development of neovascularization is often, but not always, preceded by the right-angle venule and the intraretinal pigment hyperplasia that is often temporal to the fovea.[2,3] The neovascularization is most commonly seen temporal to the fovea.[16] Retinal hard exudates, intraretinal edema, and subretinal or intraretinal hemorrhage may occur (Fig. 58.6). These neovascular complexes are retinal in origin, as seen by the feeder vessel from the retinal arteries and the drainage into venules (Fig. 58.7). This may be indistinguishable from choroidal neovascularization with chorioretinal anastomosis. A disciform scar may be the advanced stage of this process (Fig. 58.8).

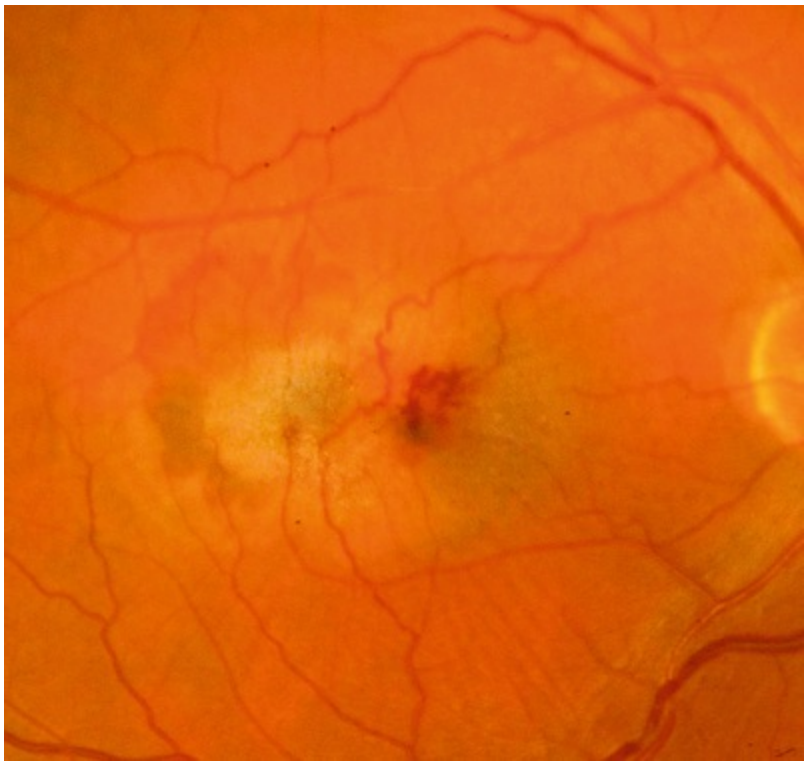

FIG. 58.6 Subretinal neovascularization is a rare complication of macular telangiectasia type 2. Intra- and subretinal hemorrhage, as shown here, are features of neovascular macular telangiectasia type 2.

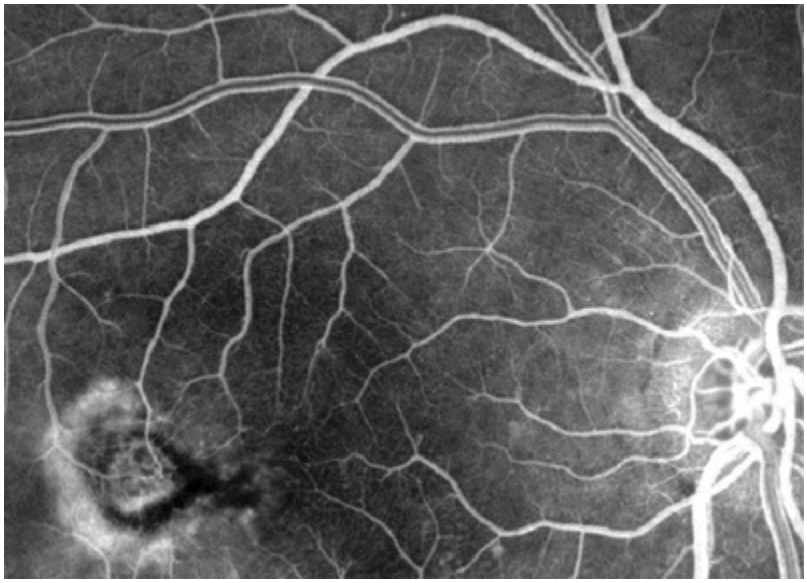

FIG. 58.7 Neovascular macular telangiectasia type 2 shows a subretinal neovascular membrane, which is fed by a retinal arteriole and in turn drained by a retinal venule.

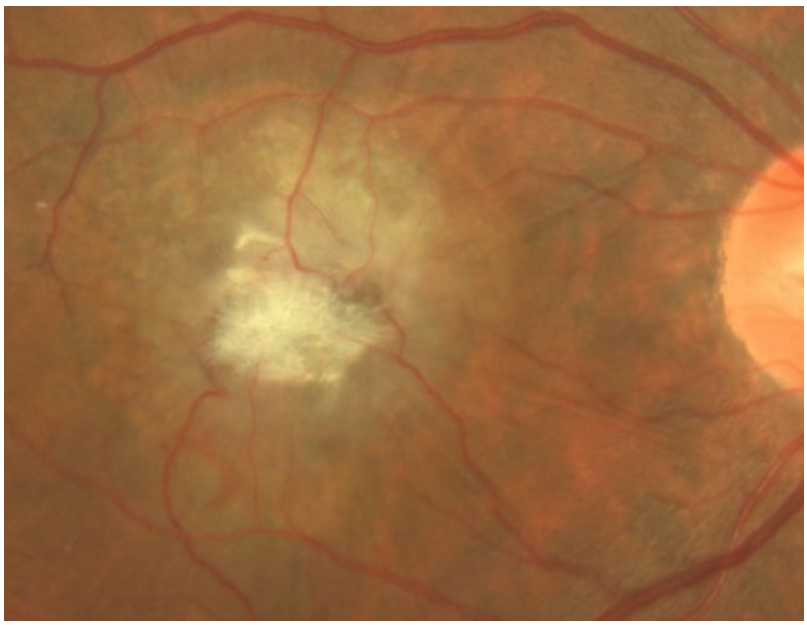

FIG. 58.8 A fibrovascular scar with chorioretinal anastomosis can be the endpoint of the pathogenic process of macular telangiectasia type 2, and is indistinguishable from disciform scarring in wet age-related macular degeneration. However, there is a lack of drusen, and usually the retinal pigment hyperplasia is prominent.

Retinal Imaging

Fundus Autofluorescence

One of the earliest signs of mac tel type 2 is the loss of the hypofluorescent center seen normally on blue-light FAF due to the depletion of macular pigment in this condition (Fig. 58.9). Even in the absence of any fluorescein leakage or any other signs, especially in patients with asymmetric mac tel type 2,[7] this is diagnostic of the ocular condition. The area of retinal pigment hyperplasia will appear hypofluorescent on the FAF (Fig. 58.9).

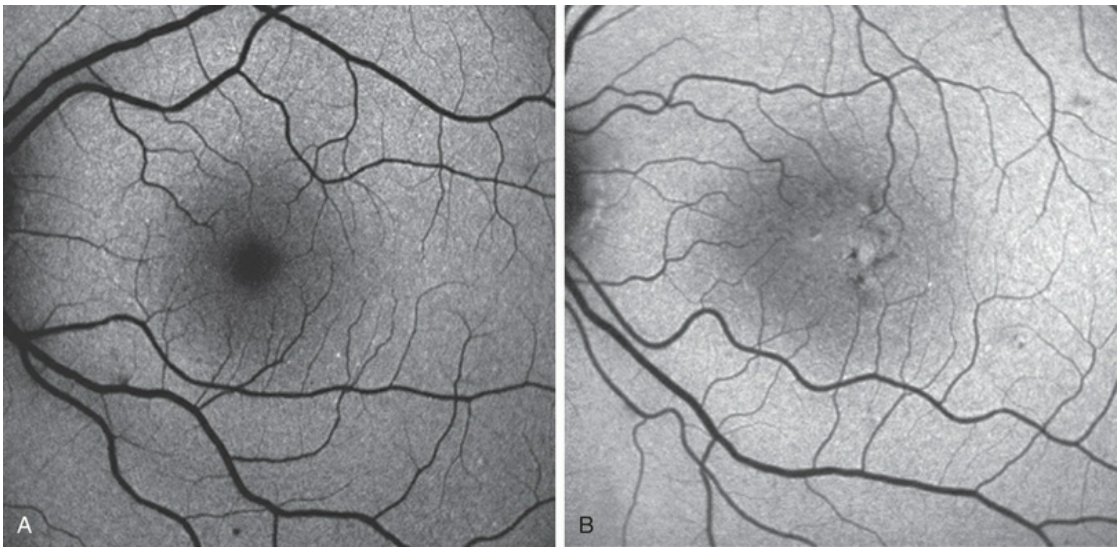

FIG. 58.9 A loss of foveal luteopigment is an early finding in macular telangiectasia type 2. (A) Blocking of autofluorescence in the central macula by healthy luteopigment. (B) Unmasking of hyperautofluorescence as well as spotty blocking from intraretinal pigment.

Fluorescein Angiography

The hallmark finding in mac tel type 2 has been the characteristic telangiectactic capillaries on FA, again starting predominantly temporal to the fovea (Fig. 58.10). Eventually, the entire parafoveal area is involved (Fig. 5.2). Stereoscopic angiography has demonstrated that the deeper vasculature is involved but more superficial capillaries may also contribute to the fluorescein leakage.[2] Traditionally, the use of FA was essential in the diagnosis of mac tel type 2. However, OCT changes, as described below, may precede the development of any FA findings. Imaging with spectral domain OCT angiography has also provided insight into the three-dimensional aspects of the vascular abnormalities in mac tel type 2.[17,18]

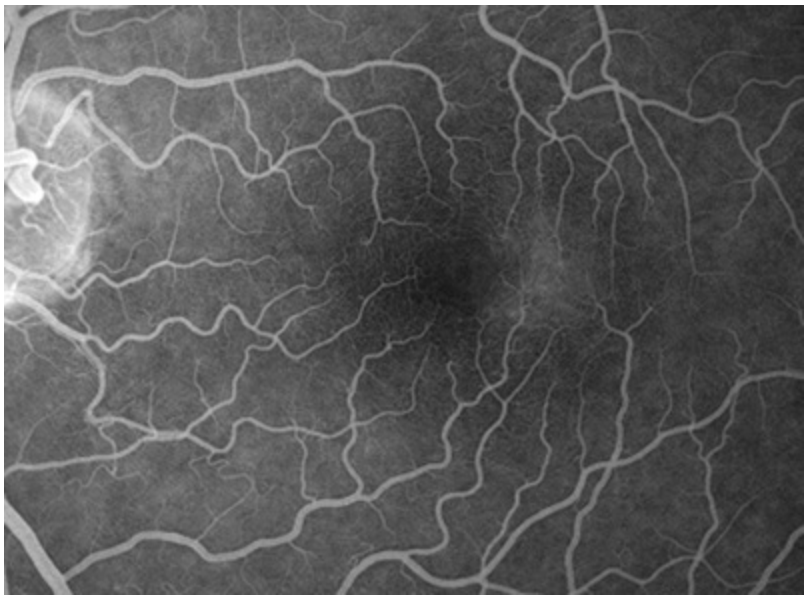

FIG. 58.10 Late staining in the temporal perifoveal area is an early angiographic feature of macular telangiectasia type 2.

Optical Coherence Tomography

OCT provides valuable information as to the diagnosis and natural course of mac tel type 2. The most subtle and earliest change may be the temporal enlargement of the foveal pit, resulting in an asymmetric pit with the temporal area being thinner than the nasal.[7] There are corresponding changes to the outer nuclear and/or photoreceptor layer. With time, the disruption of the photoreceptor inner/outer-segment (IS/OS) junction (now termed the ellipsoid zone) is seen,[19] again temporal to the fovea. With progression, there will be hyporeflective cavities in the inner retina, and these may clinically be described as "pseudolamellar macular holes." There are no pockets of leakage from the FA that correspond to these hyporeflective cavities. The disease progresses with increasing hyporeflective cavities in the outer neurosensory retina leading eventually to atrophy (Fig. 58.11). The foci of retinal pigment hyperplasia manifest as hyperreflective intraretinal lesions that appear to migrate into the inner retinal layers, with associated posterior shadowing. The "en face" view rendered from the OCT illustrates the ellipsoid or IS/OS junction loss that may be useful for an outcome measurement in clinical studies of mac tel type 2.

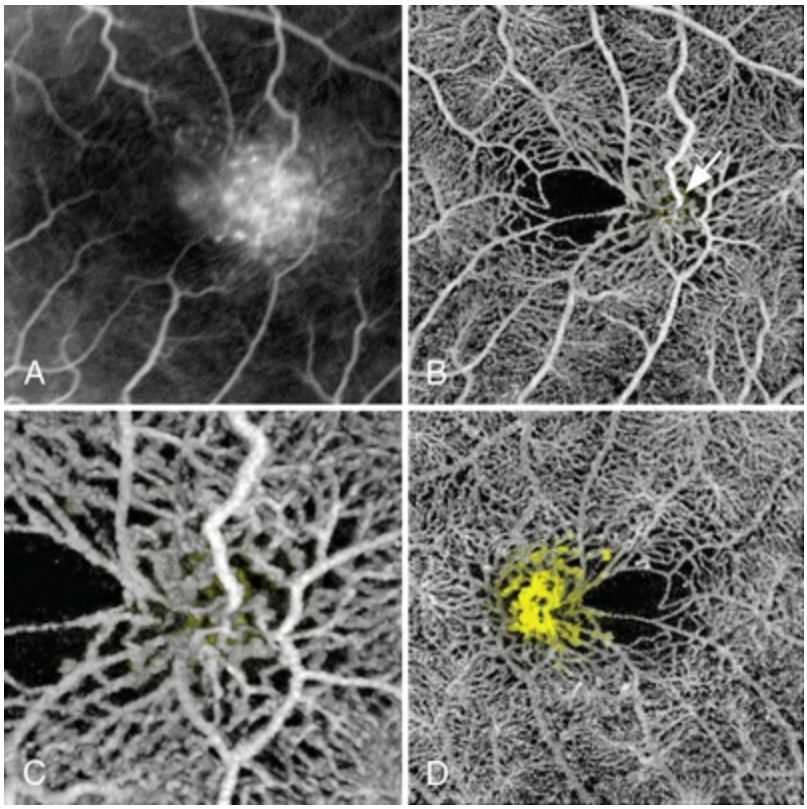

FIG. 58.11 (A) Midphase fluorescein angiogram showing temporal macular staining secondary to macular telangiectasia type 2. (B) Volume-rendered optical coherence tomography angiography of the same location. The abnormally deep vessels are largely masked from view by the overlying retinal vessels. Note how the retinal vessels seem to be drawn toward a locus in the temporal macula, at the site where the right-angle vein enters the deeper retina (*arrow*). (C) Close-up of (B) showing the vascular anatomy where the retina vein dives down. Note the clarity of the visualization of the vessels provided by the volume-rendering process. (D) When the retina is viewed from behind, the vascular invasion, shown in yellow, is readily seen. (Courtesy of Rick Spaide, MD.)

Adaptive Optics Imaging

Adaptive optics imaging, a technique that corrects for the optical aberrations of the eye and usually utilizes a scanning laser ophthalmoscope, allows evaluation of the cone photoreceptor mosaic.[20] Cone density evaluations in individuals with mac tel have

identified areas of paracentral cone loss despite the absence of capillary abnormalities seen on FA.[21]

Other investigators have compared the results of the photoreceptor assessment from "en face" views from the spectral domain OCT with those obtained on adaptive optics scanning laser ophthalmoscopy (AO-SLO) using a split detector.[22] Interesting discrepancies have been observed in which the AO-SLO demonstrated a substantial number of photoreceptors in areas of low or missing ellipsoid zone reflectivity on "en face" OCT. However, this was not demonstrated in another study that was conducted using a flood-illumination adaptive optics camera.[23] Additional studies with the AO-SLO using microperimetry showed a remarkable visual sensitivity and recovery of visibility of the cones with adaptive optics in areas previously considered to have loss of cones in two eyes with mac tel lesions.[24] The investigators suggest that such lesions with a preserved external limiting membrane may contain cones that are functional but have abnormal scattering and/or wave guiding characteristics, making them difficult to image by conventional AO-SLO. These studies highlight the need for multimodal imaging in the future to fully evaluate the natural course of this condition in regards to the health of the cones in the so-called "mac tel area."

Visual Function

Impaired reading vision is the most common presentation (79%), followed by the presence of metamorphopsia (12%) in the early stages of the disease.[11,25] Visual impairment may be mild; however, loss of vision in one eye is frequently reported.[2] Vision may decrease gradually with the progression of the disease. Visual acuity less than 20/200 (legal blindness) is rare but may be seen in the advanced stages with marked atrophy of the central photoreceptors or secondary to a large area affected by neovascularization.[2,3,16,26] In the MacTel Project, the mean visual acuity at baseline was 20/40 in 522 eyes that had not previously received therapy.[8] Visual acuity was 20/20 or better in 16% and 20/32 or better in approximately 50%. The most common risk factors associated with lower visual acuity in this cohort were characteristics found in more advanced disease, namely retinal

pigment hyperplasia and the right-angle venules. Similar visual acuity results were reported by Gass and Blodi.[2] In a retrospective study, 25% of eyes (6/24) remained stable during a follow-up period of 10–17 years.[26]

Despite the mild visual impairment, the vision-related quality of life is impacted markedly. In the MacTel Project, the National Eye Institute Visual Functioning Questionnaire (NEI-VFQ-25) was administered to all participants.[27] They reported significantly lower vision-related function in all domains compared to a group of participants in a study of age-related macular degeneration and who had similar visual acuities. A subset of these participants, enrolled in the MacTel Project, was tested using the Impact of Vision Impairment questionnaire.[28] Similar results were seen in this second study.

Microperimetry

Another method of evaluating function is the use of microperimetry, which may help to correlate the structural changes with the functional changes.[29–33] Retinal sensitivity defects appear to correlate with the outer retinal atrophy seen on OCT imaging.[34] In areas of retinal pigment hyperplasia, there is often a dense scotoma. The use of microperimetry to correlate with changes seen on OCT may result in a reasonable outcome measurement for measuring changes over time, which may be especially useful for clinical trials that will be designed to test various therapies.

Staging and Prognostic Factors

From their extensive clinical experience and review of fundus photographs, Gass and Blodi concluded that various mac tel type 2 lesions appear in an orderly fashion over time.[2] Some lesions, such as retinal opacification, may be easily missed because of image quality. There was no availability of noninvasive tools such as OCT or FAF to assist in their classification of this condition. Nevertheless, the authors had remarkable clinical acumen and developed a scale that has been part of this landmark study. However, the present usefulness of this scale is somewhat limited, as it does not incorporate OCT. With further research into the

natural history of mac tel type 2, another scale incorporating newer technologies may be of value. A major challenge for studying therapies for mac tel type 2 is the development of reproducible and clinically meaningful outcome measurements. When structural and functional correlations can be made, such outcome measurements may become more evident.

Genetics

The occurrence of this condition in monozygotic twins,[7,35–37] siblings, and families[2,7,38–41] suggests a genetic association in mac tel type 2. A vertical transmission pattern would also suggest an autosomal dominant pattern, but there may be variable expressivity or penetrance with monozygotic twins showing different disease severities.[7] Environmental influences or gene-to-gene interaction might account for this variation. The ataxia telangiectasia mutated gene (*ATM*), responsible for the ataxia telangiectasia syndrome, has been implicated in the pathogenesis of mac tel type 2.[42,43] A number of candidate genes known to cause other retinal diseases, such as those causing familial exudative vitreoretinopathy and Norrie disease, or those with a role in retinal neovascularization or macular pigment metabolism, have recently been excluded to play a role in the pathogenesis of mac tel type 2.[44] Evaluation of a gene that might be involved with xanthophyll transport also demonstrated no statistically significant association.[45]

Association of Systemic Diseases

Early reports have implicated an increased risk of diabetes in patients with mac tel type 2.[38,46] The MacTel Project, the largest population of mac tel type 2 patients to date, found a high prevalence of diabetes mellitus (28%) and also hypertension (52%).[8] Strikingly similar numbers were reported for diabetes and hypertension in another series.[43] Further follow-up of the MacTel Project has demonstrated the important associations with diabetes, obesity, and cardiovascular disease.[47] These risk factors may further our understanding of the pathogenesis of this condition.

Differential Diagnosis

Retinal capillary telangiectasia may result from a multitude of retinal vascular inflammatory or occlusive conditions. However, mac tel type 2 is quite distinct from other conditions where retinal telangiectasia is a prominent feature. Branch retinal vein occlusions can give rise to segmental capillary changes, but this can be readily distinguished since it involves an area of distribution distal to an arteriolar-venular crossing, and does not cross the horizontal raphe, unless there is already collateral formation. Radiation retinopathy usually involves a larger retinal area, and is accompanied by cotton-wool spots and preretinal neovascularization, both features that are not characteristic of mac tel type 2. A history of radiation to the eye, orbit, or head can be readily elicited. Neovascular mac tel type 2 may masquerade as neovascular age-related macular degeneration, and vice versa. Since digital angiography (often monoscopic) has largely replaced stereo-film FA, precise localization of the retinal layer displaying the hyperfluorescence may be more difficult. However, in neovascular age-related macular degeneration, drusen and RPE changes are usually present and retinal capillary disease is uncommon. OCT imaging will help localize the lesion and demonstrate other typical features, either in the same, or in the contralateral eye. Late stages of neovascular mac tel type 2 may, however, be indistinguishable from a disciform scar with chorioretinal anastomosis in age-related macular degeneration. Another entity to consider in the differential diagnosis would be tamoxifen retinopathy.[48] A recent report demonstrated that tamoxifen retinopathy may have pseudocystic foveal cavitation that mimics cavities seen in eyes with mac tel type 2.

Clinicopathologic Correlation

It is curious that vascular changes are not prominent features of early mac tel type 2, but blunting of the foveal reflex is typical. Based on the staining of the retina with fluorescein in eyes with minimal edema, Gass has postulated that it is possible that the primary abnormality may be found in the parafoveal retinal neural or Müller cells.[49] This is illustrated in a case where OCT and ERG

changes in the form of inner-lamellar holes and reduced cone responses manifested before the development of typical vascular changes.[50] Xanthophyll is probably primarily stored in Müller cells, and this could be a surrogate measure of the health and concentration of Müller cells in that region. Xanthophyll concentration is already diminished in early mac tel.[51] Histopathologic examination of the eyes of a 58-year-old woman with mac tel type 2 did not demonstrate telangiectatic capillaries, but did show narrowing of the vessel diameter. Instead, pericyte degeneration and lipid accumulation within the capillary walls, as well as multilaminated basement membrane, were found[52] – all similar to those seen in diabetics and prediabetics. Another histopathologic study[53] demonstrated dilation and proliferation of retinal capillaries into the outer retinal, subretinal, and preretinal spaces. Perivascular pigment migration along the telangiectatic vessels was also seen. A sharp demarcation between the edematous and nonedematous retina was present and involved all layers of the retina, including the nerve fiber layer and the ganglion cell layer. The most detailed histopathologic study to date examined the eye of a 65-year-old patient with mac tel type 2 and found reduced expression of Müller cell-specific markers in the fovea, which correlated with macroscopically visible pigment depletion in this area.[54] These investigators confirmed these findings in another pair of autopsy eyes.[55] The Müller cell loss in MacTel type 2 matches the area of macular pigment depletion. In this example, the loss of the IS/OS junction seen on OCT corresponded to the region where rods were depleted but cones were still present.

Therapeutic Options

There are no generally accepted therapies for lesions of mac tel type 2 not associated with neovascularization. There are anecdotal case reports, but no randomized controlled clinical trials conducted in this ocular condition. Laser photocoagulation[56] or photodynamic therapy[57] does not appear to improve or stabilize visual acuity in non-neovascular mac tel type 2. Antiangiogenic agents seem to be equally ineffective in most reported series despite angiographic and tomographic effects,[58,59] although individual patients may

experience a functional benefit[60] However, antiangiogenic therapy has been reported to result in potentially deleterious effects in eyes with the non-neovascular form of the disease.[61]

For neovascular complications of mac tel type 2, transpupillary therapy[62,63] and photodynamic therapy[64] have been reported to be somewhat efficacious, but have recently been replaced by antiangiogenic agents, which may be able to stabilize neovascular complications of mac tel type 2 and even improve vision.[65,66] Mac tel type 2 may be complicated by the development of a full-thickness macular hole. The success rate after surgical repair appears to be lower than for idiopathic macular holes, probably depending on the relative contribution of tangential traction versus the neurodegeneration that is part of mac tel type 2.[14,67,68]

To treat the purported neurodegenerative component, a safety trial of implants of ciliary neurotrophic factor was conducted.[69] Seven participants demonstrated no safety concerns 36 months following implantation. Other neuroprotective agents are under consideration for the future.

Summary and Future Research Directions

Despite a marked increase in our knowledge of mac tel type 2, the pathogenesis remains unknown. It has been well established that it is a bilateral disease that affects patients in the sixth decade of life. Most individuals progress from an asymptomatic, but clinically identifiable state, through a well-characterized pathogenic sequence eventually to develop significant visual disability, despite pharmacologic, laser, and surgical attempts at treatment. Future research will hopefully unravel the molecular basis and identify more specific targets for a cure.

References

1. Gass JD. A fluorescein angiographic study of macular dysfunction secondary to retinal vascular disease. V. Retinal telangiectasis. *Arch Ophthalmol*. 1968;80:592–605.

2. Gass JD, Blodi BA. Idiopathic juxtafoveolar retinal telangiectasis. Update of classification and follow-up study. *Ophthalmology*. 1993;100:1536–1546.
3. Yannuzzi LA, Bardal AM, Freund KB, et al. Idiopathic macular telangiectasia. *Arch Ophthalmol*. 2006;124:450–460.
4. Klein R, Blodi BA, Meuer SM, et al. The prevalence of macular telangiectasia type 2 in the Beaver Dam eye study. *Am J Ophthalmol*. 2010;150:55–62.
5. Aung KZ, Wickremasinghe SS, Makeyeva G, et al. The prevalence estimates of macular telangiectasia type 2. *Retina*. 2010;30:473–478.
6. Sallo FB, Leung I, Mathenge W, et al. The prevalence of type 2 idiopathic macular telangiectasia in two African populations. *Ophthalmic Epidemiol*. 2012;19:185–189.
7. Gillies MC, Zhu M, Chew EY, et al. Familial asymptomatic macular telangiectasia type 2. *Ophthalmology*. 2009;116:2422–2429.
8. Clemons TE, Gillies MC, Chew EY, et al. Baseline characteristics of participants in the natural history study of macular telangiectasia (MacTel) MacTel Project Report No. 2. *Ophthalmic Epidemiol*. 2010;17:66–73.
9. Karth PA, Raja SC, Brown DM, Kim JE. Outcomes of macular hole surgeries for macular telangiectasia type 2. *Retina*. 2014;34:907–915.
10. Moisseiev J, Lewis H, Bartov E, et al. Superficial retinal refractile deposits in juxtafoveal telangiectasis. *Am J Ophthalmol*. 1990;109:604–605.
11. Heeren TF, Holz FG, Charbel Issa P. First symptoms and their age of onset in macular telangiectasia type 2. *Retina*. 2014;34:916–919.
12. Patel B, Duvall J, Tullo AB. Lamellar macular hole associated with idiopathic juxtafoveolar telangiectasia. *Br J Ophthalmol*. 1988;72:550–551.
13. Koizumi H, Iida T, Maruko I. Morphologic features of group 2A idiopathic juxtafoveolar retinal telangiectasis in three-dimensional optical coherence tomography. *Am J Ophthalmol*. 2006;142:340–343.
14. Charbel Issa P, Scholl HP, Gaudric A, et al. Macular full-

thickness and lamellar holes in association with type 2 idiopathic macular telangiectasia. *Eye (Lond)*. 2009;23:435–441.
15. Shukla D. Evolution and management of macular hole secondary to type 2 idiopathic macular telangiectasia. *Eye (Lond)*. 2011;25:532–533.
16. Engelbrecht NE, Aaberg TM Jr, Sung J, et al. Neovascular membranes associated with idiopathic juxtafoveolar telangiectasis. *Arch Ophthalmol*. 2002;120:320–324.
17. Spaide RF, Klancnik JM Jr, Cooney MJ, et al. Volume-rendering optical coherence tomography angiography of macular telangiectasia type 2. *Ophthalmology*. 2015;122(11):2261–2269.
18. Thorell MR, Zhang Q, Huang Y, et al. Swept-source OCT angiography of macular telangiectasia type 2. *Ophthalmic Surg Lasers Imaging Retina*. 2014;45:369–380.
19. Sallo FB, Peto T, Egan C, et al. The IS/OS junction layer in the natural history of type 2 idiopathic macular telangiectasia. *Invest Ophthalmol Vis Sci*. 2012;53:7889–7895.
20. Roorda A, Romero-Borja F, Donnelly Iii W, et al. Adaptive optics scanning laser ophthalmoscopy. *Opt Express*. 2002;10:405–412.
21. Ooto S, Hangai M, Takayama K, et al. High-resolution photoreceptor imaging in idiopathic macular telangiectasia type 2 using adaptive optics scanning laser ophthalmoscopy. *Invest Ophthalmol Vis Sci*. 2011;52:5541–5550.
22. Scoles D, Flatter JA, Cooper RF, et al. Assessing photoreceptor structure associated with ellipsoid zone disruptions visualized with optical coherence tomography. *Retina*. 2016;36(1):91–103.
23. Jacob J, Paques M, Krivosic V, et al. Meaning of visualizing retinal cone mosaic on adaptive optics images. *Am J Ophthalmol*. 2015;159:118–123.
24. Wang Q, Tuten WS, Lujan BJ, et al. Adaptive optics microperimetry and OCT images show preserved function and recovery of cone visibility in macular telangiectasia type 2 retinal lesions. *Invest Ophthalmol Vis Sci*. 2015;56:778–

786.
25. Charbel Issa P, Holz FG, Scholl HPN. Metamorphopsia in patients with macular telangiectasia type 2. *Doc Ophthalmol*. 2009;119:133–140.
26. Watzke RC, Klein ML, Folk JC, et al. Long-term juxtafoveal retinal telangiectasia. *Retina*. 2005;25:727–735.
27. Clemons TE, Gillies MC, Chew EY, et al. The National Eye Institute visual function questionnaire in the Macular Telangiectasia (MacTel) project. *Invest Ophthalmol Vis Sci*. 2008;49:4340–4346.
28. Lamoureux EL, Maxwell RM, Marella M, et al. The longitudinal impact of macular telangiectasia (MacTel) type 2 on vision-related quality of life. *Invest Ophthalmol Vis Sci*. 2011;52:2520–2524.
29. Charbel Issa P, Helb HM, Rohrschneider K, et al. Microperimetric assessment of patients with type II macular telangiectasia. *Invest Ophthalmol Vis Sci*. 2007;48:3788–3795.
30. Charbel Issa P, Helb HM, Holz FG, et al. Correlation of macular function with retinal thickness in nonproliferative type 2 idiopathic macular telangiectasia. *Am J Ophthalmol*. 2008;245:169–175.
31. Maruko I, Iida T, Sekiryu T, et al. Early morphological changes and functional abnormalities in group 2A idiopathic juxtafoveolar retinal telangiectasis using spectral domain optical coherence tomography and microperimetry. *Br J Ophthalmol*. 2008;92:1488–1491.
32. Schmitz-Valckenberg S, Ong EE, Rubin GS, et al. Structural and functional changes over time in MacTel patients. *Retina*. 2009;29:1314–1320.
33. Wong WT, Forooghian F, Majumdar Z, et al. Fundus autofluorescence in type 2 idiopathic macular telangiectasia: correlation with optical coherence tomography and microperimetry. *Am J Ophthalmol*. 2009;148:573–583.
34. Sallo FB, Peto T, Egan C, et al. The IS/OS junction layer in the natural history of type 2 idiopathic macular telangiectasia. *Invest Ophthalmol Vis Sci*. 2012;53:7889–7895.
35. Hannan SR, Madhusudhana KC, Rennie C, et al. Idiopathic

juxtafoveolar retinal telangiectasis in monozygotic twins. *Br J Ophthalmol*. 2007;91:1729–1730.
36. Menchini U, Virgili G, Bandello F, et al. Bilateral juxtafoveolar telangiectasis in monozygotic twins. *Am J Ophthalmol*. 2000;129:401–403.
37. Siddiqui N, Fekrat S. Group 2A idiopathic juxtafoveolar retinal telangiectasia in monozygotic twins. *Am J Ophthalmol*. 2005;139:568–570.
38. Chew EY, Murphy RP, Newsome DA, et al. Parafoveal telangiectasis and diabetic retinopathy. *Arch Ophthalmol*. 1986;104:71–75.
39. Hutton WL, Snyder WB, Fuller D, et al. Focal parafoveal retinal telangiectasis. *Arch Ophthalmol*. 1978;96:1362–1367.
40. Isaacs TW, McAllister IL. Familial idiopathic juxtafoveolar retinal telangiectasis. *Eye (Lond)*. 1996;10(5):639–642.
41. Oh KT, Park DW. Bilateral juxtafoveal telangiectasis in a family. *Retina*. 1999;19:246–247.
42. Mauget-Faÿsse M, Vuillaume M, Quaranta M, et al. Idiopathic and radiation-induced ocular telangiectasia: the involvement of the ATM gene. *Invest Ophthalmol Vis Sci*. 2003;44:3257–3262.
43. Barbazetto IA, Room M, Yannuzzi NA, et al. ATM gene variants in patients with idiopathic perifoveal telangiectasia. *Invest Ophthalmol Vis Sci*. 2008;49:3806–3811.
44. Parmalee NL, Schubert C, Merriam JE, et al. Analysis of candidate genes for macular telangiectasia type 2. *Mol Vis*. 2010;16:2718–2726.
45. Szental JA, Baird PN, Richardson AJ, et al. Analysis of glutathione S-transferase Pi isoform (GSTP1) single-nucleotide polymorphisms and macular telangiectasia type 2. *Int Ophthalmol*. 2010;30:645–650.
46. Millay RH, Klein ML, Handelman IL, et al. Abnormal glucose metabolism and parafoveal telangiectasia. *Am J Ophthalmol*. 1986;102:363–370.
47. Clemons TE, Gillies MC, Chew EY, et al. Medical characteristics of patients with macular telangiectasia type 2 (MacTel Type 2) MacTel Project Report number 3. *Ophthalmic Epidemiol*. 2013;20:109–113.

48. Doshi RR, Fortun JA, Kim BT, et al. Pseudocystic foveal cavitation in tamoxifen retinopathy. *Am J Ophthalmol*. 2014;157:1291–1298.
49. Gass JDM. Histological study of presumed parafoveal telangiectasia. *Retina*. 2000;20:226–227.
50. Barthelmes D, Gillies MC, Fleischhauer JC, et al. A case of idiopathic perifoveal telangiectasia preceded by features of cone dystrophy. *Eye (Lond)*. 2007;21:1534–1535.
51. Helb HM, Charbel Issa P, Van der Veen RL, et al. Abnormal macular pigment distribution in type 2 idiopathic macular telangiectasia. *Retina*. 2008;28:808–816.
52. Green WR, Quigley HA, de la Cruz Z, et al. Parafoveal retinal telangiectasis: light and electron microscopy studies. *Trans Ophthalmol Soc U K*. 1980;100:162–170.
53. Eliassi-Rad B, Green WR. Histologic study of presumed parafoveal telangiectasis. *Retina*. 1999;19:332–335.
54. Powner MB, Gillies MC, Tretiach M, et al. Perifoveal Müller cell depletion in a case of macular telangiectasia type 2. *Ophthalmology*. 2010;117:2407–2416.
55. Power MB, Gillies MC, Zhu M, et al. Loss of müller's cells and photoreceptors in macular telangiectasia type 2. *Ophthalmology*. 2013;120:2344–2352.
56. Park DW, Schatz H, McDonald HR, et al. Grid laser photocoagulation for macular edema in bilateral juxtafoveal telangiectasis. *Ophthalmology*. 1997;104:1838–1846.
57. De Lahitte GD, Cohen SY, Gaudric A. Lack of apparent short-term benefit of photodynamic therapy in bilateral, acquired, parafoveal telangiectasis without subretinal neovascularization. *Am J Ophthalmol*. 2004;138:892–894.
58. Gamulescu MA, Walter A, Sachs H, et al. Bevacizumab in the treatment of idiopathic macular telangiectasia. *Graefes Arch Clin Exp Ophthalmol*. 2008;246:1189–1193.
59. Charbel Issa P, Finger RP, Kruse K, et al. Monthly ranibizumab for nonproliferative macular telangiectasia type 2: a 12-month prospective study. *Am J Ophthalmol*. 2011;151:876–886.
60. Matt G, Sacu S, Ahlers C, et al. Thirty-month follow-up after intravitreal bevacizumab in progressive idiopathic macular

telangiectasia type 2. *Eye (Lond)*. 2010;24:1535–1541.
61. Kupitz EH, Heeren TF, Holz FG, et al. Poor long-term outcome of anti-vascular endothelial growth factor therapy in nonproliferative macular telangiectasia type 2. *Retina*. 2015;35(12):2619–2626.
62. Shukla D, Singh J, Kolluru CM, et al. Transpupillary thermotherapy for subfoveal neovascularization secondary to group 2A idiopathic juxtafoveolar telangiectasis. *Am J Ophthalmol*. 2004;138:147–149.
63. Nachiappan K, Shanmugam MP. Treatment of CNVM secondary to idiopathic juxtafoveal retinal telangiectasis by transpupillary thermotherapy. *Am J Ophthalmol*. 2005;139:577–578.
64. Snyers B, Verougstraete C, Postelmans L, et al. Photodynamic therapy of subfoveal neovascular membrane in type 2A idiopathic juxtafoveolar retinal telangiectasis. *Am J Ophthalmol*. 2004;137:812–819.
65. Kovach JL, Rosenfeld PJ. Bevacizumab (avastin) therapy for idiopathic macular telangiectasia type II. *Retina*. 2009;29:27–32.
66. Narayanan R, Chhablani J, Sinha M, et al. Efficacy of anti-vascular endothelial growth factor therapy in subretinal neovascularization secondary to macular telangiectasia type 2. *Retina*. 2012;32:2001–2005.
67. Gregori N, Flynn HW Jr. Surgery for full-thickness macular hole in patients with idiopathic macular telangiectasia type 2. *Ophthalmic Surg Lasers Imaging*. 2010;41:1–4.
68. Shukla D. Evolution and management of macular hole secondary to type 2 idiopathic macular telangiectasia. *Eye (Lond)*. 2011;25:532–533.
69. Chew EY, Clemons TE, Peto T, et al. Ciliary neurotrophic factor for macular telangiectasia type 2: results from a phase 1 safety trial. *Am J Ophthalmol*. 2015;159:659–666.

59

Coats Disease

Nikolas J.S. London, Carol L. Shields, Julia A. Haller

History

Coats disease is an idiopathic condition characterized by telangiectatic and aneurysmal retinal vessels with intraretinal and subretinal exudation and fluid.[1] Coats disease was first described by Scottish ophthalmologist George Coats in 1908.[2] In his initial classification Coats separated this new entity into three distinct groups. Group I included eyes with massive subretinal exudation and no demonstrable vascular abnormalities. Group II consisted of eyes with massive subretinal exudation and multiple retinal vascular abnormalities with intraretinal hemorrhage. Group III included eyes with massive subretinal exudation and frank retinal arteriovenous malformations.[2] Eugen von Hippel later demonstrated that group III represented the distinctly separate entity of angiomatosis retinae (later retermed retinal capillary hemangioma or retinal hemangioblastoma), prompting Coats to drop this group from his classification. In 1912, and again in 1915, Theodor von Leber described a disease with similar telangiectatic and aneurysmal retinal vessels that lacked the massive subretinal exudation described by Coats.[3,4] This condition was later named Leber multiple miliary aneurysms. In a 1916 paper Leber concluded that what he had described was merely an earlier stage of the disease process identified by Coats.[5,6] This conclusion was later reinforced by Reese, who described an eye with Leber miliary aneurysms that progressed into a classic case of Coats disease during long-term follow-up.[7] Although some authors have disagreed, most authorities today classify Leber disease as an early or nonprogressive form of Coats disease.[5,8,9]

Histopathology, Etiology, and Pathogenesis

Early descriptions of Coats disease focused primarily on the morphology of the disease and attempted to explain the disease process solely on the basis of fundoscopic and histopathologic changes.[10,11] The first observations published by Coats focused on histopathologic examination of six eyes enucleated for this

condition that he received from various colleagues.[2] From these histopathologic specimens, Coats described subretinal masses of fibrous tissue intimately adherent to the outer retina. Most of the eyes had associated retinal thickening, degeneration, and detachment, as well as diffuse vascular abnormalities. Four of the six eyes had associated retinal hemorrhages, and most had cholesterol crystals. One eye had evidence of bone formation. Coats believed the vascular changes represented secondary manifestations of the underlying disease and that the exudation was secondary to organization and partial resorption of retinal hemorrhages, as he often found hemorrhages in association with the exudation.[2] Coats also postulated that the primary process might be infectious in light of the mononuclear infiltrate found on histopathologic examination. This infectious theory of Coats disease was supported by a number of other reports, including those of Evens,[12] Straub,[13] and Müller,[13] who suspected toxoplasmosis as the underlying cause. Subsequent investigations and the failure of antiinflammatory adrenocorticotropic hormone and steroid therapies have refuted early theories of a primary infectious or inflammatory etiology.[13,14]

Pathologic samples of eyes with Coats disease were once abundant owing to enucleations for suspected intraocular tumor.[15] Moreover, most histopathologic reports describe findings in eyes with advanced stages of the disease. Gross examination of enucleated eyes typically reveals bullous retinal detachment.[16] Subretinal fluid has a viscous, lipid-rich, yellow appearance with glistening crystals.[16] Microscopically, the subretinal exudation contains collections of foamy histiocytes and cholesterol clefts.[16] The outer retina is thickened by exudation, with variable penetration of inner retinal layers.[16] Areas of the inner retina also contain numerous, large, dilated, and telangiectatic vessels.[16] Other vascular abnormalities include degenerated and hypocellular walls, narrowed lumen with or without thrombi, capillary dropout, neovascularization, as well as perivascular sheathing and/or pigmentation.[1,9,17–23] Thickened vessel walls show characteristic heavy periodic acid–Schiff-positive deposits.[1] Flat preparations prepared by trypsin digestion reveal vascular aneurysms measuring 50–350 μm, often forming large sausage-like

outpouchings and located on shunt vessels.[1] Advanced cases may have intraocular bone formation, with evidence of calcification on echography and computed tomography (CT) scanning that potentially confuses the diagnosis with retinoblastoma.[24,25] Electron microscopy confirms diffuse structural abnormalities of the retinal vasculature. Tripathi and Ashton described prominent structural alterations of retinal vessels in areas of retinal thickening, with thickened walls mostly replaced by a laminated fibrous coating of basement membrane-like material.[18] Most affected vessels were completely devoid of endothelium and pericytes, with red blood cells, plasma, and fibrin filling the lumina. There was patchy thinning or even absence of the vessel wall in some areas, with the vessel lumen extending to the basement membrane of adjacent glial cells.[18] More recently, Kase and associates noted the presence of VEGF immunoreactivity in both subretinal macrophages as well as in the detached retina and blood vessels, with significantly higher VEGF levels in eyes with vascular abnormalities compared to those without. Further, they noted immunoreactivity for VEGF receptor-2 in the endothelia of abnormal vessels.[26] Levels of VEGF in aqueous humor are also significantly elevated in eyes with Coats disease and appear to increase with higher disease severity.[27] These findings support the widely held view that Coats disease is a disorder of vascular integrity as well as point to a potential therapeutic option in anti-VEGF medications.

Indeed, work in molecular genetics suggests that Coats disease may be part of a spectrum of related genetic disorders known as "retinal hypovasculopathies,"[28,29] which includes Norrie disease, familial exudative vitreoretinopathy (FEVR), fascioscapulohumeral muscular dystrophy (FSHD), and the osteoporosis pseudoglioma syndrome.[29–37] These diseases share a similar ocular phenotype, characterized by a failure to vascularize fully the retinal periphery and associated telangiectatic, incompetent remnant vasculature. Each of these conditions can be related to abnormalities in the Wnt signaling pathway during retinal angiogenesis.[28,29,38]

Several reports have implicated a deficiency of Norrin, a retinal protein, in the pathogenesis of Coats disease.[39,40] In one case report, a female with unilateral Coats disease gave birth to a son affected by Norrie disease.[39] Both carried a missense mutation within the

Norrie disease pseudoglioma gene, *NDP*, on chromosome Xp11.2. Further analysis on archival tissue from nine enucleated eyes from males with unilateral Coats disease revealed a mutation in *NDP* in one subject. Knockout mouse models of Norrie disease model demonstrate abnormalities of the retinal vessels, including telangiectasia, bulb-like dilations, and underdevelopment of the capillary bed.[41,42] Elevated levels of hypoxia-inducible factor-1α and vascular endothelial growth factor (VEGF), as well as characteristic electroretinogram patterns in these mice, confirmed inner retinal hypoxia.[42] Moreover, ectopic lens expression of Norrin in knockout mice induces the formation of normal deep retinal capillaries and completely prevents abnormalities in retinal angiogenesis.[43] These observations suggest a genetic basis for Coats disease and that a *NDP* mutation may be responsible.

Although FEVR and Coats disease share certain clinical features, they likely do not share a common genetic basis. Robataille and associates studied DNA expression of the frizzled-4 gene, *FZD4*, in 68 cases of FEVR and 16 cases of Coats disease.[44] They found 11 *FZD4* mutations in FEVR cases and no mutations in Coats disease cases. They concluded that germline mutations in *FZD4* do not appear to be a common cause of Coats disease, implying that Coats disease does not likely represent asymmetric FEVR and is a distinct ocular condition.

Other genetic pathways have been explored. Cremers and associates found that 55% of eyes with retinitis pigmentosa and Coats-like secondary exudative vasculopathy contained a mutation in the *CRB1* gene.[45] This suggests that *CRB1* could be involved in primary Coats disease as well as other retinal diseases and dystrophies. Recently, "Coats plus" disease was discovered to be the result of mutations in the *CTC1* gene, which encodes telomere maintenance component 1, believed to be necessary for telomere integrity.[46]

Clinical Presentation

Coats disease is classically a painless ophthalmic condition. The disease affects males three times as often as females and has no reported racial or ethnic predilection.[47] Coats disease is unilateral in

80–95% of cases.[5,47,48] Some of the bilateral cases in older reports could represent secondary bilateral Coats-like retinopathy with systemic conditions and not true primary Coats disease. Any patient with bilateral presumed Coats disease should be evaluated for conditions that cause Coats-like exudative retinopathy, such as retinitis pigmentosa, pars planitis, FSHD, FEVR, or other diseases.[49] Based on a study of 150 consecutive cases, the mean age at diagnosis is 5 years with a range of 1 month to 63 years.[47] Some speculate that the disease could be present at birth.[13,50]

In an analysis of 150 consecutive cases of Coats disease, presenting symptoms included decreased visual acuity (43%), strabismus (23%: Fig. 59.1), leukocoria/xanthocoria (20%: Fig. 59.1), pain (3%), heterochromia (1%), nystagmus (1%), and no symptom (8%).[47] Visual acuity was 20/20 to 20/50 in 12% of all eyes, 20/60 to 20/100 in 11%, 20/200 to counting fingers in 18%, and hand motions to no light perception in 58%. Nearly 90% of eyes had a normal anterior-segment examination. Those with findings included cataract (8%), iris neovascularization (8%), shallow anterior chamber (4%), corneal edema (3%), cholesterol in the anterior chamber (3%: Fig. 59.1),[51,52] and megalocornea (2%). Retinal findings included telangiectasia (100%), intraretinal exudation (99%), exudative retinal detachment (81% with 42% demonstrating partial retinal detachment and 58% with total retinal detachment), retinal hemorrhage (13%), retinal macrocyst (11%), vasoproliferative tumor (6%), and optic disc neovascularization (1%). No eyes in this cohort presented with vitreous hemorrhage. Other studies have described macular fibrosis in up to 23% of patients, developing in an area of previous dense exudation and involving the fovea in all cases.[53]

FIG. 59.1 Unique clinical features occasionally seen in Coats disease. (A) Young boy who presented with leukocoria and esotropia of the left eye. He had stage 5 disease, including total retinal detachment, cataract, and prephthisis. The decision was made to observe. (B) Young girl with xanthocoria of the right eye. (C) Young girl who presented with a total retinal detachment abutting the posterior surface of the lens. (D) Young girl with anterior-chamber cholesterolosis of the right eye.

Adult cases of Coats disease are similar in clinical presentation and disease course, but generally have a smaller area of involvement, slower disease progression, more frequent hemorrhage near larger aneurysmal dilated vessels, and typically do not present with strabismus.[54] Although the adult form of the disease has been described as frequently associated with hypercholesterolemia, such an association does not appear to occur in the juvenile form.[14,55]

The typical ophthalmoscopic picture in Coats disease is that of localized, yellow, subretinal exudation associated with adjacent vascular anomalies, including sheathing, telangiectasia, tortuosity, aneurysmal dilation, zones of capillary dropout, and occasionally neovascularization.[13,47] There is variability in this clinical picture.[47]

Exudation, hemorrhage, or a combination appears minimal during less active stages of the disease and can progress to massive findings, obscuring the retinal vasculature in more aggressive stages. The vascular abnormalities can be subtle and clinically undetectable or can be obvious as a dominant feature. The clinical course is also variable, but is generally slowly progressive. Spontaneous remission has been observed but is exceptional.[56] Subretinal choroidal neovascularization rarely occurs in areas of lipid deposition. As subretinal fluid and exudation increase, the retinal detachment progresses and can reach a highly elevated state, visible behind the lens (Fig. 59.1). Hemorrhagic and nonhemorrhagic retinal macrocysts can occur as a result of chronic coalescent intraretinal cystoid edema.[57] Secondary complications such as iridocyclitis, cataract, and secondary neovascular glaucoma can lead to phthisis bulbi in severe cases.[2,15,58]

Several staging systems for Coats disease have been proposed.[2,59] The most recent and widely used was introduced by Shields and associates in 2000 (Table 59.1).[60] Stage 1 is characterized by retinal telangiectasia. Stage 2 has telangiectasia and intraretinal exudation, extrafoveal exudation defines stage 2A (Fig. 59.2), whereas foveal involvement defines stage 2B. Stage 3 is defined by exudative retinal detachment; 3A is a subtotal detachment, with 1 and 2 designating extrafoveal and foveal involvement, respectively (Fig. 59.3); and 3B is a total retinal detachment (Fig. 59.4). Stage 4 has total retinal detachment plus elevated intraocular pressure (Fig. 59.3), and stage 5 is endstage disease, occasionally with phthisis bulbi (Fig. 59.1). Using this classification for grouping of 124 cases, Shields and associates found stage 1 in 1%, stage 2 in 14% (2A in 8%, 2B in 6%), stage 3 in 69% (3A1 in 19%, 3A2 in 19%, 3B in 30%), stage 4 in 15%, and stage 5 in 2%.[60] Based on classification and treatment, visual acuity strongly depended on stage at diagnosis.[47,61] At the time of Coats disease control, poor visual acuity (20/200 or worse) was found in 0% of stage 1, 53% of stage 2, 74% of stage 3, and 100% of stage 4 and stage 5.[60]

TABLE 59.1

Staging System for Coats Disease With Prevalence on Presentation

Stage	Simplified Format	Criteria	Prevalence[60]
1	T	Retinal telangiectasia (T) only	1%
2	T+E	Telangiectasia and exudation (E)	14%
2A		Extrafoveal	8%
2B		Foveal	6%
3	T+E+D	Exudative retinal detachment (D)	69%
3A		Subtotal	38%
3A1		Extrafoveal	19%
3A2		Foveal	19%
3B		Total	30%
4	T+E+D+G	Total retinal detachment and glaucoma (G)	15%
5	T+E+D+G+P	Advanced endstage disease often with phthisis (P) bulbi	2%

Adapted from Shields et al.[60]

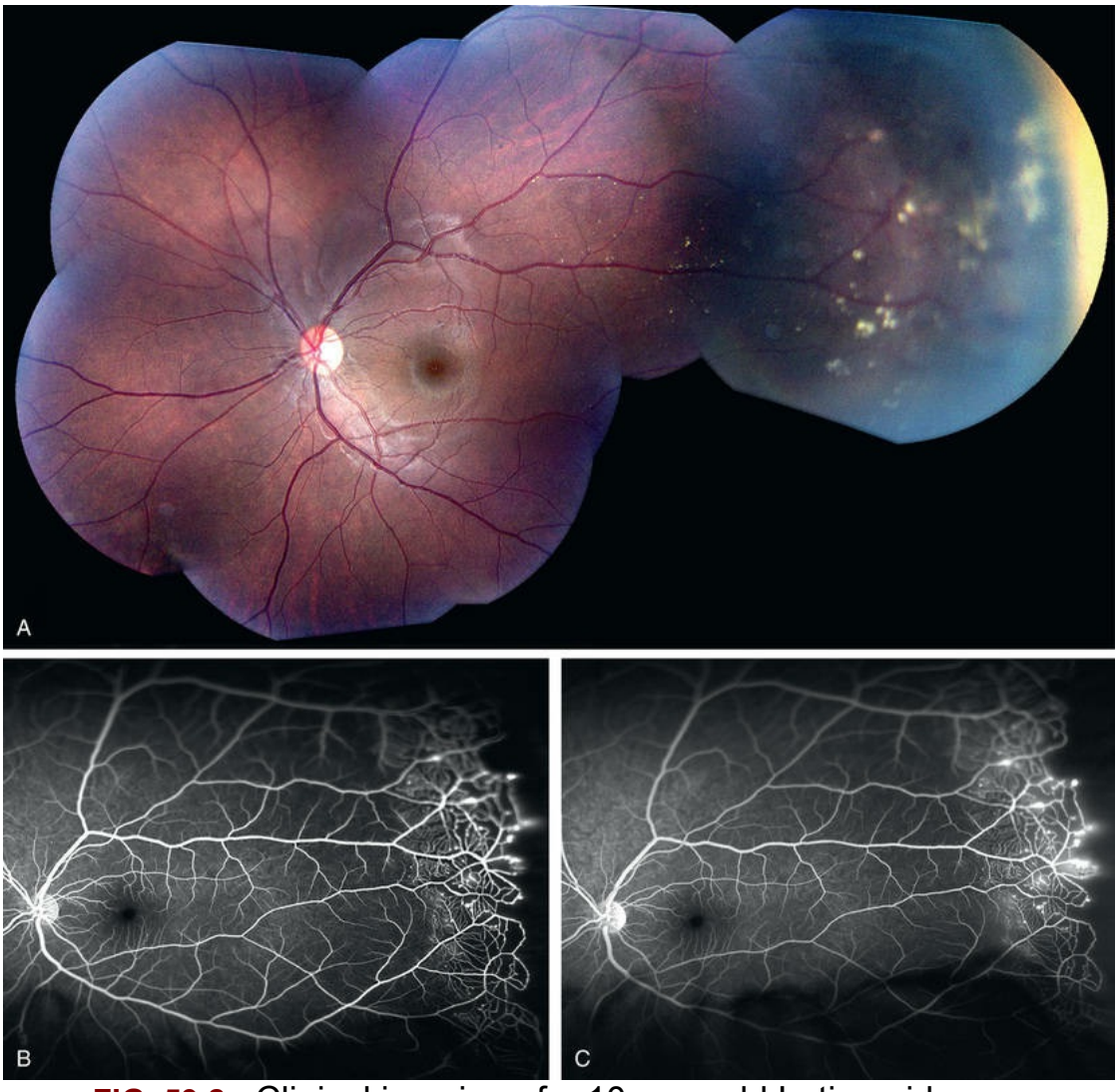

FIG. 59.2 Clinical imaging of a 10-year-old Latina girl with stage 2A Coats disease in the left eye. (A)

Montage color photograph. Note the exudation and vascular telangiectasia in the far temporal periphery. (B) Midphase wide-field fluorescein angiogram of the same patient. Note the far peripheral avascularity and adjacent telangiectatic vasculature. (C) Late-phase wide-field fluorescein angiogram of the same patient. Note the mild dye leakage from telangiectasia.

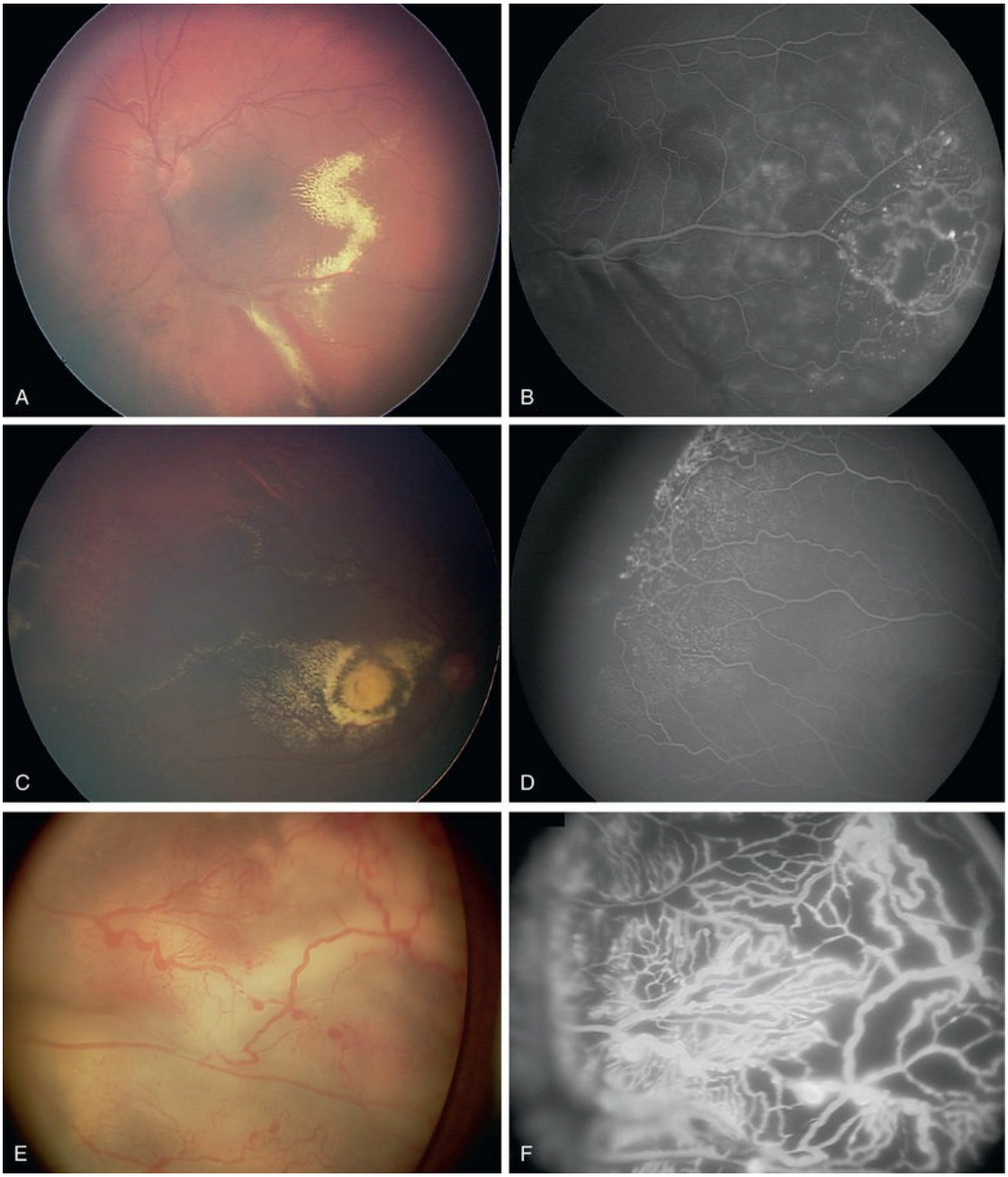

FIG. 59.3 Clinical images of various stages of Coats disease, including 3A1, 3A2, and 4. (A) Color fundus photograph of a patient with stage 3A1 Coats disease. Note the temporal extrafoveal exudation. (B) Recirculation-phase fluorescein angiogram of the same patient as in (A). Note the temporal vascular abnormalities, areas of capillary nonperfusion, and perivascular dye leakage. (C) Color fundus photograph of a patient with stage 3A2 Coats disease with prominent foveal exudation. Also note the subtle temporal vascular telangiectasia and aneurysmal

vessels. (D) The extent of vascular abnormalities is more apparent in this midphase fluorescein angiogram. Note the telangiectasia adjacent to a wide zone of peripheral avascularity. (E) Color fundus photograph of a patient with stage 4 disease who presented with a total exudative retinal detachment and elevated intraocular pressure. (F) Fluorescein angiography revealed prominent capillary nonperfusion between dilated, abnormal vasculature.

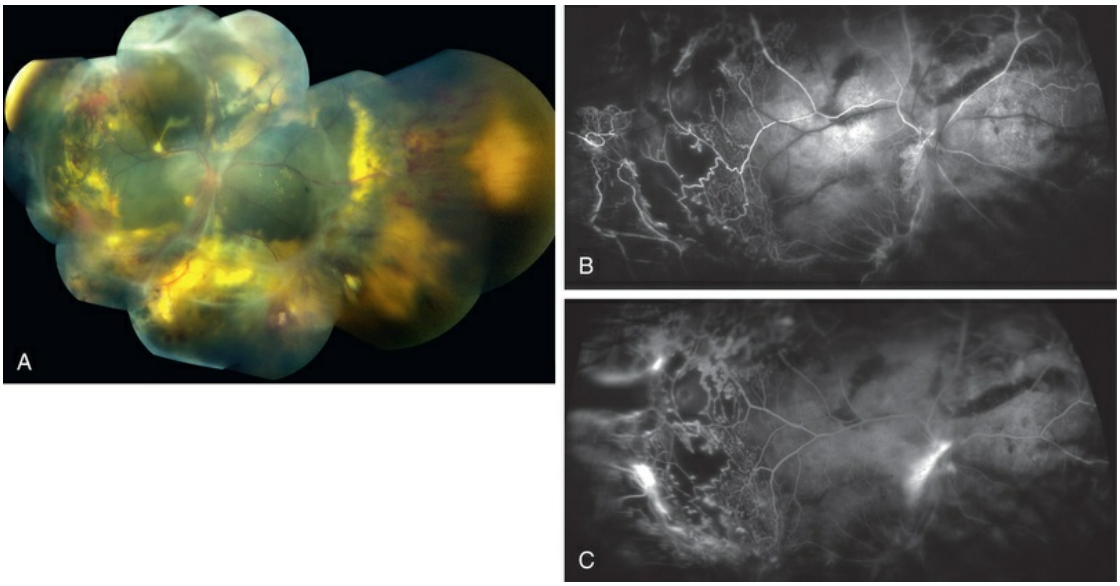

FIG. 59.4 Clinical imaging of a 17-year-old African American man with stage 3B Coats disease in the right eye. (A) Montage color fundus photograph depicting extensive subretinal exudation, a total retinal detachment, diffuse midperipheral vascular abnormalities, and optic nerve head neovascularization. (B) Early-phase fluorescein angiogram, centered more temporally than the color photo, demonstrating filling of telangiectatic and aneurysmal vascular channels, most prominent in the temporal periphery. Adjacent to telangiectatic vessels are large areas of retinal capillary nonperfusion. (C) In the later phase of the angiogram, leakage of dye from telangiectatic vessels and disc neovascularization are seen. (Courtesy of Carl Regillo, MD, Wills Eye Institute.)

Diagnostic Testing

Ancillary testing may be useful when the diagnosis of Coats disease is suspected, but other clinical entities must be ruled out, most notably retinoblastoma.[62] Particularly when retinal detachment with subretinal exudation and dilated retinal vessels coexist, even an experienced clinician may have difficulty differentiating these entities ophthalmoscopically. Fluorescein angiography is critical to document classic findings to establish the diagnosis. Echography may enable differentiation between Coats disease and retinoblastoma on the basis of features such as the character of the retinal detachment and the presence or absence of subretinal calcifications. Echography is less useful when the retinoblastoma is poorly calcified and also has shortcomings in detecting optic nerve or extraocular extension of retinoblastoma when heavy calcification exists.[63]

Fluorescein Angiography

The typical fluorescein angiographic picture of Coats disease is one of numerous localized anomalies of the retinal vasculature with peripheral retinal nonperfusion (Figs. 59.2–59.6). Telangiectasia, aneurysms, beading of vessel walls, and various vascular communicating channels are found with larger vessels. These vessels show early and persistent leakage, which verifies their role as the source of exudation and hemorrhage. This leakage represents breakdown of the blood–retinal barrier, which can further be detected by vitreous fluorophotometry.[64] Microvascular involvement is demonstrated with areas of diffuse loss of the capillary bed or areas of complete capillary nonperfusion on angiography. Geographic zones of microvascular involvement are typically surrounded by areas of arteriolar and venular anomalies. Although some early authors described cases of massive exudation or hemorrhage without areas of obvious vascular involvement, fluorescein angiography and histopathologic specimens invariably show unsuspected anomalous vessels. The ability to identify all anomalous vessels, especially those with the greatest degree of leakage, has made adequate treatment of Coats disease a

possibility.[5,60,65,66]

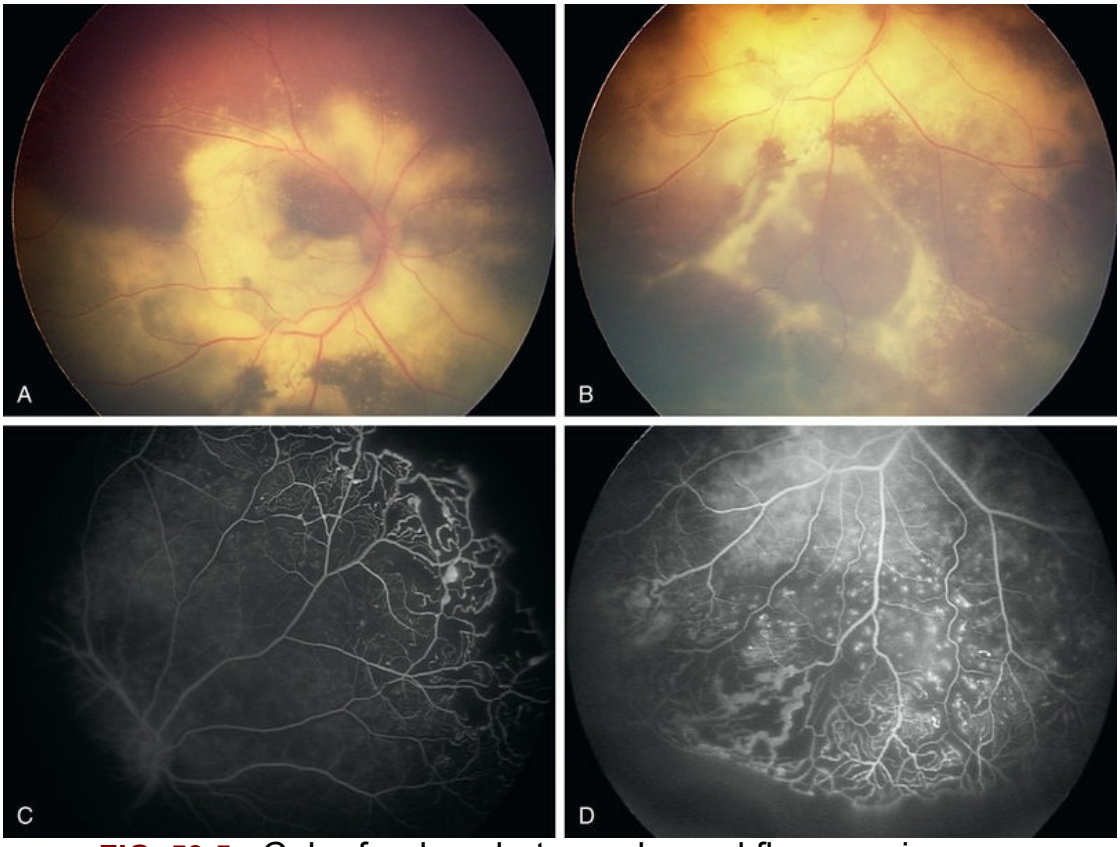

FIG. 59.5 Color fundus photography and fluorescein angiography of a patient with stage 4 Coats disease. Macular (A) and inferior (B) color photographs depicting extensive subretinal exudate. Note the elevated retinal detachment in (B). (C) Early-phase fluorescein angiogram of the superonasal retinal periphery. Note the blunted, telangiectatic, and aneurysmal vasculature just posterior to a zone of avascular retina. (D) Midphase fluorescein angiogram of the inferior retina corresponding to (B), depicting similar angiographic findings as well as prominent sausage-like vascular dilations.

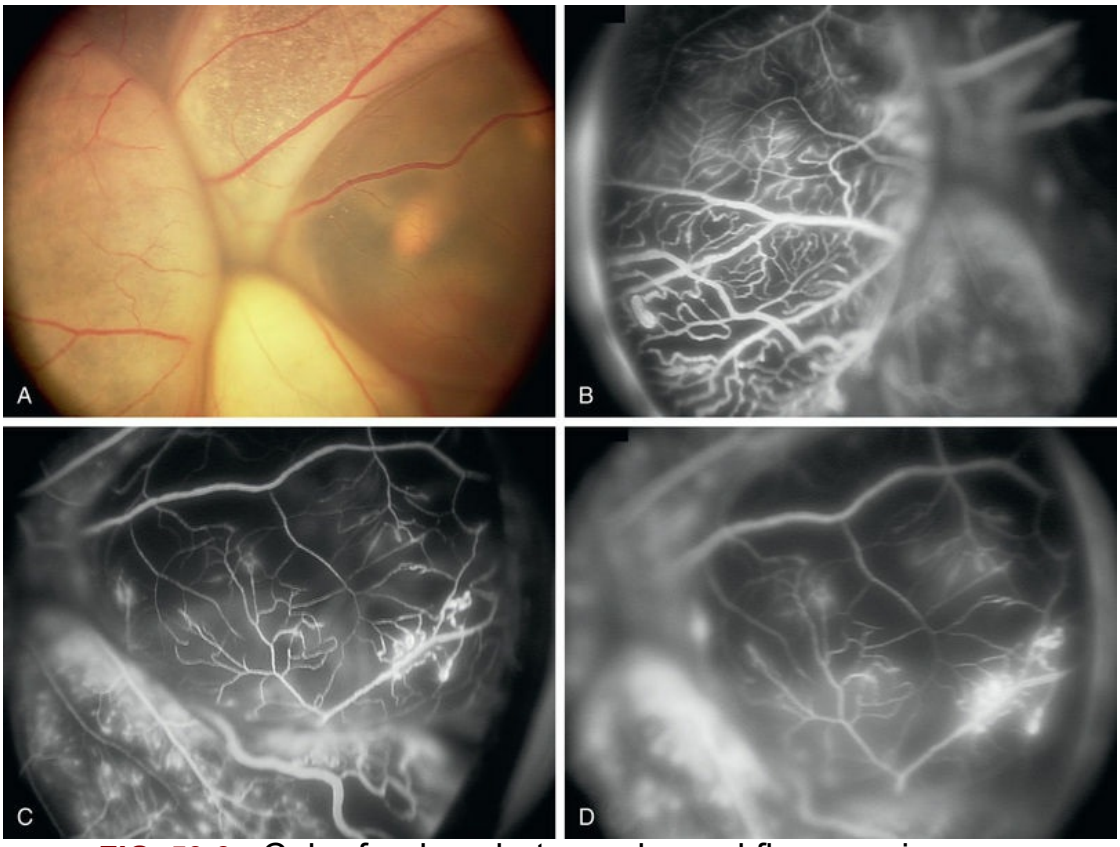

FIG. 59.6 Color fundus photography and fluorescein angiogram of a patient with a total bullous retinal detachment associated with Coats disease. (A) Color fundus photograph depicting the very bullous retinal detachment. (B–D) Fluorescein angiogram images of the same patient depicting typical angiographic features of Coats disease.

Newer techniques have enabled imaging of the retinal periphery using RetCam and Optos cameras. Wide-field angiography enables images of the peripheral vasculature that can aid in the diagnosis of subtle cases as well as facilitate targeted laser treatment and monitoring of disease progression (Figs. 59.2 and 59.5). RetCam photography is particularly important in peripheral imaging in pediatric patients.[67]

Computed Tomography

Computed tomography (CT) is valuable because of its ability to characterize intraocular morphology, quantify subretinal densities, identify vascularities within the subretinal space through the use of contrast enhancement, and detect other abnormalities that may be

associated in the orbital or intracranial space. Spiral CT has the advantage of reducing anesthesia risk in small children and also decreases acquisition time, and staff and equipment monitoring requirements.[68]

Magnetic Resonance Imaging

Magnetic resonance imaging (MRI) as an auxiliary test is useful because it permits multiplanar imaging and superior contrast resolution and yields biochemical insight into the structure and composition of tissues.[69,70] It is less useful in detecting calcium than either ultrasound or CT scanning.[63,71] An MRI study of 28 patients with leukocoria or intraocular mass, or both, found that retinoblastomas could be reliably distinguished from Coats disease, toxocariasis, and persistent hyperplastic primary vitreous.[71] Calcification could not be reliably detected on MRI scanning.

Doppler Ultrasonography

High-resolution Doppler ultrasound has been suggested as a diagnostic adjunct, providing unique information with real-time imaging and duplex pulse Doppler evaluation.[72] This technique may delineate structural abnormalities not shown by CT or MRI.

Optical Coherence Tomography

Optical coherence tomography (OCT) allows for quantitative documentation of retinal thickening and is particularly useful in monitoring macular involvement over the course of treatment. Typical findings include (1) prominent intraretinal hyperreflective material that corresponds to hard exudate seen on examination and on color fundus photography; (2) intraretinal cystoid edema; and (3) less commonly, subretinal fluid. Hard exudates and cystoid edema are most prominent in the outer retina (Fig. 57.7A). Hard exudates commonly cause a shadowing defect of deeper structures and may form a “string of pearls” configuration with a row of hyperreflective dots along the inner wall of cystoid spaces in the outer plexiform layer.[73]

OCT angiography (OCTA) is an emerging technology with

potential applicability for a variety of retinal vascular diseases, including Coats disease. By comparing backscattered OCT signal intensity across a series of B-scans at the same location, OCTA enables visualization of erythrocyte movement, and as such, blood flow. Volumetric angiographic information is provided that can be evaluated as individual vascular networks from the internal limiting membrane to the choroid. As a noninvasive imaging modality, this is particularly attractive in a disease that affects a large number of pediatric patients. To date, however, there is little published information on the utility of OCTA in Coats disease. Fig. 59.7 shows an OCTA macular scan of a young male patient with Coats disease and associated macular edema affecting the right eye. There is artifact due to poor fixation, which is a common problem with the current technology, but there is evidence of mild reduction in the perifoveal capillary density. As the technology improves and more data are obtained, OCTA may prove useful in the evaluation of patients with Coats disease.

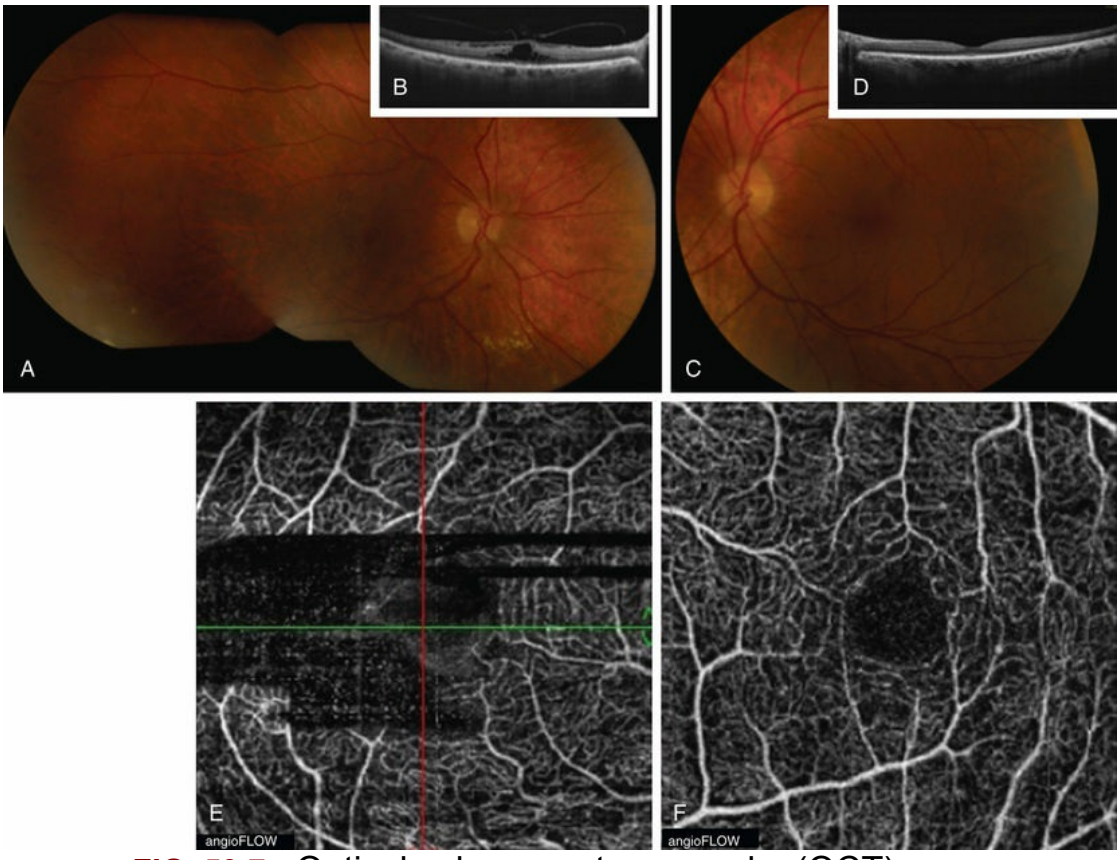

FIG. 59.7 Optical coherence tomography (OCT) angiography in Coats disease. (A) Montage color

fundus photography of the involved right eye showing subtle evidence of vascular abnormalities in the temporal and inferotemporal periphery as well as mild hard exudates in the central macula. (B) Horizontal OCT B-scan of the central macula demonstrating vitreomacular traction, an epiretinal membrane, and cystoid macular edema. (C,D) Color fundus photograph and macular OCT of the left eye showing normal anatomy. (E) OCT angiogram of the right eye showing fixation artifact and mild reduction of the perifoveal capillary density. (F) Normal OCT angiogram of the left eye showing a healthy superficial capillary plexus.

Blood Testing

Aqueous lactic dehydrogenase and isoenzyme levels have not proved valuable in distinguishing between Coats disease and retinoblastoma. Examination of subretinal fluid, although rarely used, is accurate in confirming the diagnosis of Coats disease on the basis of cholesterol crystal and pigment-laden macrophages in the absence of tumor cells.[63]

Differential Diagnosis

The differential diagnosis of Coats disease includes other conditions that produce leukocoria or strabismus,[19] including retinoblastoma,[15,74] retinal detachment, persistent hyperplastic primary vitreous, congenital cataract, Norrie disease, and FEVR,[75] among other diagnoses. Shields and associates reviewed 150 cases of Coats disease and found that the diagnosis was correct in 64 cases (41%).[47] The mistaken referring diagnoses included retinoblastoma in 43 cases (27%), retinal detachment in 12 (8%), retinal hemorrhage in 7 (4%), toxocariasis in 4 (3%), choroidal melanoma in 2 (1%), choroidal hemangioma in 2 (1%), coloboma in 2 (1%), endophthalmitis in 2 (1%), and single cases of cytomegalovirus retinitis, retinopathy of prematurity, traumatic retinopathy, and toxoplasmosis. In 18 cases (11%) there was no submitted diagnosis.

Numerous entities have been described as presenting with a Coats-like picture, including several systemic conditions, and Coats disease can also simulate other exudative retinal conditions such as FEVR, peripheral vasculitis, Eales disease, and FSHD (Table 59.2). FEVR is an important consideration and can present with peripheral avascularity with telangiectasia and exudation. FEVR can be differentiated based on the typical presence of retinal dragging, a positive family history, and bilaterality, all of which are rare in Coats disease. A Coats-like picture of bilateral retinal telangiectasia and exudation has been described in patients with deafness and FSHD.[76,105,106] It is believed that the retinal vascular abnormalities, muscular dystrophy, and deafness in FSHD may all be a consequence of a common mechanism based on abnormal Wnt signaling.[37]

TABLE 59.2

Clinical Conditions That Can Present With Coats-Like Retinal Findings

SYSTEMIC CONDITIONS	Muscular dystrophy[76–79] Turner syndrome[80] Epidermal nevus syndrome[81] Cornelia de Lange syndrome[82] Alport syndrome[83] Senior–Loken syndrome (familial renal-retinal dystrophy)[84] 13q deletion syndrome[85] Renal transplantation[86] Ch 3 inversion[87] Hallermann–Streiff syndrome[88] Aplastic anemia[89] Multiple glomus tumors[90] Telangiectasia of the nasal mucosa[91] Osteoporosis pseudoglioma syndrome[92] Focal segmental glomerulosclerosis[93]
OCULAR CONDITIONS THAT CAN SIMULATE JUVENILE COATS DISEASE	Retinoblastoma[48] Retinal detachment Congenital cataract Norrie disease[39] Persistent hyperplastic primary vitreous Ocular toxocariasis Retinal capillary hemangiomatosis Retinal cavernous hemangiomatosis Vasoproliferative tumor Familial exudative vitreoretinopathy
OCULAR CONDITIONS THAT CAN SIMULATE COATS DISEASE AT ANY AGE	Branch retinal vein occlusion[94] Eales disease Vasculitis

	Tumor accompanied by exudation Diabetic vasculopathies with lipid exudation Ocular toxoplasmosis[95] Morning-glory disc anomaly[96] Idiopathic retinal gliosis[97] Retinal dysplasia[98] Type 1 idiopathic juxtafoveolar telangiectasis Retinitis pigmentosa[99–104] Retinal macroaneurysm Retinal capillary hemangiomatosis Familial exudative vitreoretinopathy Any vasculopathy producing exudation Epiretinal membrane with secondary exudation

A Coats-like picture associated with varied skeletal defects, cerebellar and extrapyramidal movement disorder, epileptic seizures, leukodystrophic changes, and postnatal growth failure has been referred to as "Coats plus syndrome."[107] In order to avoid confusion, the term "Coats disease" should be reserved for cases of idiopathic retinal telangiectasia associated with intraretinal exudation with or without exudative retinal detachment, without evidence of vitreoretinal traction.[7,47]

Isolated case reports have described a number of other disorders occurring concurrently with Coats disease, including retinitis pigmentosa,[99,108] Senior–Loken syndrome,[84] the ichthyosis hystrix variant of epidermal nevus syndrome,[81] Turner syndrome,[109] diffuse central nervous system venous abnormality,[110] and Hallermann–Streiff syndrome[88] (see Table 59.2). Small, in 1968, reported the combination of mental retardation, muscular dystrophy, and an exudative vasculopathy in four siblings.[76] Egerer and associates noted histologic evidence of rosettes characteristic of retinal dysplasia in a series of nine enucleated eyes carrying the diagnosis of Coats disease.[98] Fogle and colleagues noted an exudative vasculopathy with a clinical picture similar to that of Coats disease arising from abnormal choroidal vessels in both eyes of a patient with retinitis pigmentosa.[100] Despite these reports, no definite connection has been made between other systemic or ocular conditions and Coats disease.

Treatment

Treatment for Coats disease depends on the stage of disease. Mild cases with only retinal telangiectasia (stage 1) should be documented with color fundus photography and wide-field fluorescein angiography and followed conservatively. If subretinal fluid or exudation develop, then intervention is necessary. For more advanced stages (2 through 4), treatment involves ablation with photocoagulation or cryotherapy to areas of telangiectatic vasculature and retinal nonperfusion. Surgical intervention to repair traction, hemorrhage, or rhegmatogenous retinal detachment is rarely necessary.

Ablative Therapies – Laser Photocoagulation and Cryotherapy

In less severe cases of exudation due to Coats disease, with or without retinal detachment, argon or diode laser photocoagulation is the treatment of choice (Fig. 59.8).[111–113] Fluorescein angiographic guidance assists directed treatment of vascular leakage.[67,114] Most wavelengths of laser light are adequate for treatment, although those near the yellow portion of the spectrum have better absorption by blood in the target vascular channels and may be particularly useful if the vessels are in detached retina. Leaking lesions are treated directly with moderate to large (100–500 μm, depending on size and location of the target lesions) applications of moderate-intensity light. Scatter photocoagulation to areas of extensive nonperfusion is of unproven value but could decrease the risk of later neovascularization. If lesions are too peripheral to be reached with the slit-lamp delivery system, the indirect ophthalmoscope-mounted laser, transscleral laser, or cryotherapy can be used.[115] These methods may be particularly useful in small children, who usually require general anesthesia for treatment. Of note, extensive laser photocoagulation can result in transient disruption of the blood–retinal barrier, paradoxically increasing retinal exudation. Several sessions of therapy, approximately every 3 months, are often necessary to produce complete resolution of exudation or detachment.[60,111,116] Complications of photocoagulation in Coats disease include inflammation, choroidal detachment, progressive exudation, creation of chorioretinal and vitreochoroidal

anastomoses, epiretinal membrane formation, sympathetic ophthalmia, rhegmatogenous retinal detachment, and hemorrhage.

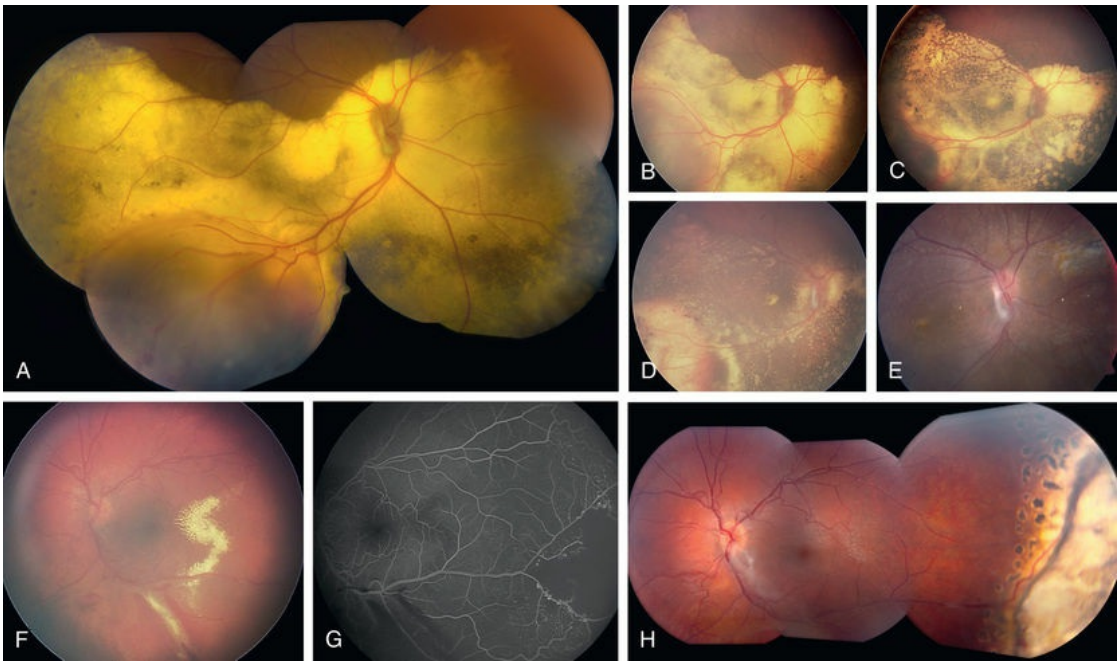

FIG. 59.8 Color fundus photographs from two patients demonstrating the effect of laser photocoagulation. Laser photocoagulation was used to treat focal areas of leakage in the peripheral retina with a modified scatter pattern to zones of capillary nonperfusion. Burns were 100–500 μm and of moderate intensity applied through a fundus contact lens. (A) Montage color fundus photograph of a separate patient with stage 4 Coats disease. Note the extensive exudation. (B–E) Sequential color fundus photographs following treatment with laser photocoagulation; the exudation and retinal detachment were noted to be slowly improving. (F) Color fundus photograph of the left macula in a patient with stage 3A1 Coats disease. (G) Fluorescein angiogram of the same patient delineating areas of retinal nonperfusion and vascular abnormalities that are used to guide laser photocoagulation. (H) Montage color photograph of the same patient following treatment with laser photocoagulation. Note the laser scars in the far temporal periphery as well as the total resolution of retinal exudation. The visual acuity following treatment improved to 20/20.

Double freeze–thaw cryotherapy is also useful in ablating affected areas of the retina and is particularly helpful in cases where laser is ineffective, such as extensive subretinal exudation or retinal detachment. In some cases it may be necessary to drain subretinal fluid to obtain sufficient retinal vascular freezing. As with laser photocoagulation, many more advanced cases require multiple sessions.[60] To minimize side-effects in eyes with extensive vascular abnormalities, selective treatment with cryotherapy to two or fewer quadrants per session may be advised, as well as avoidance of the ciliary body. In some cases with advanced disease and imminent glaucoma, treatment of the entire four quadrants of the retina is necessary. Compared to laser, cryotherapy is associated with more inflammation and patient discomfort as well as potential complications, which include subcapsular cataract, proliferative vitreoretinopathy, and total retinal detachment.[66]

The use of photodynamic therapy in combination with intravitreal bevacizumab for adult Coats disease was reported in a single case report, with apparent success.[117]

Pharmacologic Therapies

Intravitreal corticosteroids, including triamcinolone acetonide (IVTA) and sustained-release dexamethasone, are effective in reducing macular edema and subretinal exudation.[118–121] Othman and colleagues recently described their experience in 15 eyes treated with 4 mg IVTA in combination with traditional treatment modalities and followed for at least 1 year. All patients experienced an improvement in visual acuity, although 40% required cataract surgery and one patient required intraocular pressure-lowering drops.[118] IVTA has been combined with cryotherapy in cases of severe exudative detachments.[122]

Intravitreal anti-VEGF agents have been reported to be effective in reducing subretinal fluid and macular exudation in children with Coats if given alone[123–127] or in combination with IVTA,[128] laser photocoagulation, or cryotherapy.[125,126,128–134]

Intraocular VEGF levels are known to be substantially elevated in eyes with Coats disease, with dramatic decline following intravitreal anti-VEGF injection.[135,136] In a study of four eyes with

Coats disease, the intraocular VEGF levels were nearly 2400 pg/mL, compared to 15 pg/mL in five eyes with rhegmatogenous retinal detachment.[136] In one eye with stage 2B disease in that report, the intraocular VEGF level decreased from 1247 pg/mL to 20.4 pg/mL 1 month after a single injection of intravitreal bevacizumab, with a corresponding improvement in visual acuity. VEGF levels may be elevated secondary to retinal ischemia associated with the abnormal vasculature.

Although in most of the available reports anti-VEGF agents appeared to be well tolerated, the case numbers are small, with limited follow-up. There is some evidence that anti-VEGF injections may accelerate the formation of vitreous fibrosis.[127,137] In the largest published series to date of eight eyes, Ramasubramanian and Shields noted the development of vitreous fibrosis in four eyes after a mean of 1.75 injections and 5 months of follow-up. In three of these patients, this progressed to traction retinal detachment.[137] It is also important to note that anti-VEGF injections are not a definitive treatment regimen and may not reduce the overall treatment burden for patients. Ray et al. compared 10 patients who received anti-VEGF injections plus ablative treatments versus 10 patients who received ablative treatment alone and noted more treatment in the anti-VEGF group with no difference in the time to disease control. Notably, however, there were two treatment failures in the ablative group compared to none in the combined group.[133] It is important to consider that we have no data on the long-term consequences of repeated anti-VEGF injections in children. Larger studies with longer follow-up will be necessary to establish the safety of anti-VEGF in juvenile Coats disease.

In contrast, the safety profile of anti-VEGF injections in adults is well established, and several small studies have shown the efficacy of anti-VEGF agents in adult-onset Coats with macular involvement.[138,139]

Surgery

Less invasive measures are usually effective in treating exudative retinal detachment with Coats disease;[140] however, eyes with advanced retinal detachment abutting the crystalline lens or those

with a rhegmatogenous component to the detachment may benefit from surgical repair.

Machemer and Williams reported improvement in the clinical course of selected cases of Coats disease with vitreous surgery consisting of removal of vitreal and preretinal membranes to eliminate traction detachment, combined with destruction of leaking vessels.[141] Other authors have advocated the use of vitrectomy with internal drainage of subretinal fluid to flatten the retina, before vasoablative procedures, and intraocular tamponade with gas or silicone oil.[142–144] Silodor and associates have used intraocular infusion, drainage of subretinal fluid, and cryotherapy with success in eyes with advanced bullous retinal detachment.[145] In their series of 13 children with blindness from Coats disease, six that were followed without surgery developed painful neovascular glaucoma necessitating enucleation and seven that were surgically repaired avoided glaucoma and the eyes remained cosmetically acceptable. When transscleral drainage of extensive subretinal fluid is necessary, a pediatric infusion cannula placed in the anterior chamber works well for maintaining the globe (Fig. 59.9).

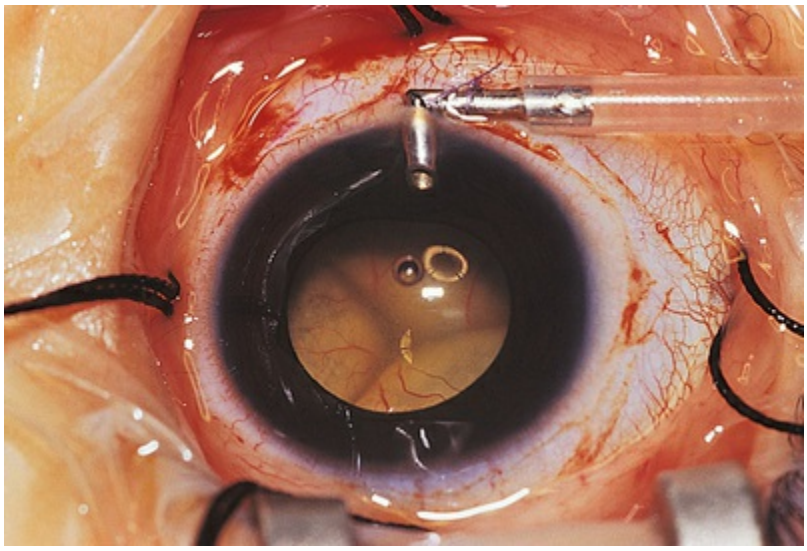

FIG. 59.9 In this eye of an 18-month-old boy with total exudative retinal detachment, anatomic stability was achieved by infusion into the anterior chamber, posterior drainage of subretinal fluid, and cryotherapy to 11 clock-hours of peripheral vascular anomalies.

(Reproduced with permission from Haller JA. Coats' disease and retinal telangiectasia. In: Yanoff M, Duker JS, editors. Ophthalmology. London: Mosby;

1999.)

Endstage cases associated with neovascular or angle closure glaucoma, or a blind painful eye may require enucleation.[60,146] Alternatively, eyes with neovascular glaucoma may respond to transscleral diode laser cyclophotocoagulation.[147]

Outcomes

In a series of 103 eyes, published by Shields and associates in 2001, telangiectasia resolved completely (47%) or partially (53%) over a mean interval of 15 months following treatment.[60] Following treatment, inactive telangiectasia and old exudation were found in 45% of cases at 17 months.[60] Residual telangiectatic areas are often left untreated, especially if there is no fresh exudation or subretinal fluid. The goal of treatment is to close telangiectasia so that further leakage is halted. In 7% of cases by 10 years, recurrence of leakage from residual or new telangiectasia can occur.[60]

Anatomically, most cases (76%) stabilize or improve following treatment, with the minority (8%) progressively worsening.[60] Approximately 20% require enucleation for neovascular glaucoma or painful phthisis bulbi.[60] In the large series by Shields and colleagues on 150 patients, 117 individuals (124 eyes) were managed and followed for a median of 23 months and outcomes were determined. Management included observation in 22 eyes (18%), photocoagulation in 16 (13%), cryotherapy in 52 (42%), retinal detachment repair with drainage of subretinal fluid and cryotherapy or photocoagulation in 20 (17%), and enucleation in 14 (11%). Often multiple sessions were required. The median interval from initial treatment to complete resolution of telangiectasia was 10 months (range 2–123 months). Exudation resolved completely in 46 cases (45%) over a median of 12 months. Of the 88 eyes with retinal detachment prior to treatment, 50 (57%) had complete resolution of the detachment. Unfortunately, visual outcome with this condition is generally poor as foveal exudation and retinal detachment often destroy macular function. In that series, final visual acuity was 20/50 or better in 16%, 20/60 to 20/100 in 8%, 20/200 to finger counting in 29%, and hand motions to no light

perception in 47%.[60] Severe vision loss was due to persistent foveal exudation, retinal detachment, and/or subfoveal fibrosis. Risk factors predictive of poor visual outcome (20/200 or worse) included noncaucasian race, postequatorial (p=.01), diffuse (p=.01), or superior (p=.04) location of telangiectasia and exudation, failed resolution of subretinal fluid after treatment (p=.02), and presence of retinal macrocysts (p=.02). Significant risk factors for enucleation included elevated intraocular pressure (greater than 22 mmHg; p<.001) and iris neovascularization (p<.001) at presentation.

Following resolution of exudation, extensive subretinal fibrosis and pigmentation, particularly in the fovea, can limit visual recovery. Intraocular surgical intervention carries the added risks of endophthalmitis, retinal tear formation, rhegmatogenous retinal detachment, and proliferative vitreoretinopathy.[5,109,148–151] Patients should be followed lifelong for recurrence (Fig. 59.10).[60,152–154]

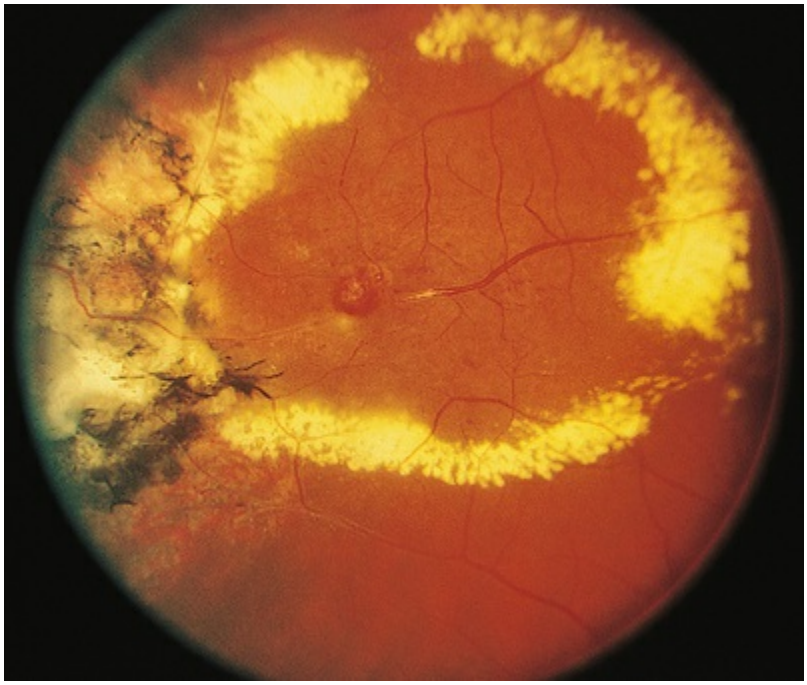

FIG. 59.10 This patient, previously treated successfully for Coats-type exudative retinopathy (see old scarring and fibrosis to the left of the photograph), has now developed a new adjacent area of vascular malformation and aneurysmal dilation, with a circinate lipid exudate.

References

1. Egbert PR, Chan CC, Winter FC. Flat preparations of the retinal vessels in Coats' disease. *J Pediatr Ophthalmol*. 1976;13:336–339.
2. Coats G. Forms of retinal disease with massive exudation. *R Lond Ophthalm Hosp Rep*. 1908;525:440–525.
3. Leber TH. Über eine durch Vorkommen multipler Miliaraneurysmen charakterisierte Form von Retinaldegeneration. *Albrecht Von Graefes Arch Ophthalmol*. 1912;81:1–14.
4. Leber TH. Retinitis exudativa (Coats), retinitis und chorioretinitis serofibrinosa degenerans. *Graefe-Saemisch Augenheilk*. 1915;7:1267–1319.
5. Egerer I, Tasman W, Tomer T. Coats disease. *Arch Ophthalmol*. 1974;92:109–112.
6. Leber T. Die Krankheiten der Netzhaut. *Handbuch der gesamten Augenheilkunde*. Engelmann, Graefe und Saemisch: Leipzig; 1916.
7. Reese AB. Telangiectasis of the retina and Coats' disease. *Am J Ophthalmol*. 1956;42:1–8.
8. Bonnet M. Le syndrome de Coats. *J Fr Ophtalmol*. 1980;3:57–66.
9. Theodossiadis GP, Bairaktaris-Kouris E, Kouris T. Evolution of Leber's miliary aneurysms: a clinicopathological study. *J Pediatr Ophthalmol Strabismus*. 1979;16:364–370.
10. Sugar HS. Coats' disease: telangiectatic or multiple vascular origin. *Am J Ophthalmol*. 1958;45:508–517.
11. Wise GN. Coats' disease. *AMA Arch Ophthalmol*. 1957;58:735–746.
12. Evens L, Francois J, Rabaey M, et al. Etude histo-pathologique d'une rétinite de coats probablement toxoplasmique. *Ophthalmologica*. 1956;132:1–12.
13. Imre G. Coats' disease. *Am J Ophthalmol*. 1962;54:175.
14. Woods AC, Duke JR. Coats's disease. I. Review of the literature, diagnostic criteria, clinical findings, and plasma lipid studies. *Br J Ophthalmol*. 1963;47:385–412.

15. Naumann GD, Portwich E. Etiology and final clinical cause for 1000 enucleations. (A clinico-pathologic study.) (author's transl.). *Klin Monbl Augenheilkd*. 1976;168:622–630.
16. Eagle RC Jr. *Eye pathology*. Lippincott Williams & Wilkins: Philadelphia; 2011:221–222.
17. Hogan M, Zimmerman L. *Ophthalmic pathology: an atlas and textbook*. WB Saunders: Philadelphia; 1962.
18. Tripathi R, Ashton N. Electron microscopical study of Coats' disease. *Br J Ophthalmol*. 1971;55:289–301.
19. Chang MM, McLean IW, Merritt JC. Coats' disease: a study of 62 histologically confirmed cases. *J Pediatr Ophthalmol Strabismus*. 1984;21:163–168.
20. Duke JR, Woods AC. Coats's disease. II. Studies on the identity of the lipids concerned, and the probable role of mucopolysaccharides in its pathogenesis. *Br J Ophthalmol*. 1963;47:413–434.
21. Farkas TG, Potts AM, Boone C. Some pathologic and biochemical aspects of Coats' disease. *Am J Ophthalmol*. 1973;75:289–301.
22. Takei Y. Origin of ghost cell in Coats' disease. *Invest Ophthalmol*. 1976;15:677–681.
23. Yannuzzi L, Gitter K, Schatz H. *The macula: a comprehensive text and atlas*. Williams & Wilkins: Baltimore, MD; 1979.
24. Senft SH, Hidayat AA, Cavender JC. Atypical presentation of Coats disease. *Retina*. 1994;14:36–38.
25. Pe'er J. Calcifications in Coats' disease. *Am J Ophthalmol*. 1988;106:742–743.
26. Kase S, Rao N, Yoshikawa H, et al. Expression of vascular endothelial growth factor in eyes with Coats' disease. *Invest Ophthalmol Vis Sci*. 2013;54(1):57–62.
27. Zhao Q, Peng X, Chen F, et al. Vascular endothelial growth factor in Coats' disease. *Acta Ophthalmol*. 2014;92:e225–8.
28. Ye X, Wang Y, Cahill H, et al. Norrin, Frizzled-4, and Lrp5 signaling in endothelial cells controls a genetic program for retinal vascularization. *Cell*. 2009;139:285–298.
29. Clevers H. Eyeing up new Wnt pathway players. *Cell*. 2009;139:227–229.
30. Lin P, Shankar SP, Duncan J, et al. Retinal vascular

abnormalities and dragged maculae in a carrier with a new NDP mutation (c. 268delC) that caused severe Norrie disease in the proband. *J AAPOS*. 2010;14:93–96.
31. Dickinson JL, Sale MM, Passmore A, et al. Mutations in the NDP gene: contribution to Norrie disease, familial exudative vitreoretinopathy and retinopathy of prematurity. *Clin Experiment Ophthalmol*. 2006;34:682–688.
32. Warden SM, Andreoli CM, Mukai S. The Wnt signaling pathway in familial exudative vitreoretinopathy and Norrie disease. *Semin Ophthalmol*. 2007;22:211–217.
33. Qin M, Hayashi H, Oshima K, et al. Complexity of the genotype–phenotype correlation in familial exudative vitreoretinopathy with mutations in the LRP5 and/or FZD4 genes. *Hum Mutat*. 2005;26:104–112.
34. Jiao X, Ventruto V, Trese MT, et al. Autosomal recessive familial exudative vitreoretinopathy is associated with mutations in LRP5. *Am J Hum Genet*. 2004;75:878–884.
35. Chen ZY, Battinelli EM, Fielder A, et al. A mutation in the Norrie disease gene (NDP) associated with X-linked familial exudative vitreoretinopathy. *Nat Genet*. 1993;5:180–183.
36. Chung BD, Kayserili H, Ai M, et al. A mutation in the signal sequence of LRP5 in a family with an osteoporosis-pseudoglioma syndrome (OPPG)-like phenotype indicates a novel disease mechanism for trinucleotide repeats. *Hum Mutat*. 2009;30:641–648.
37. Fitzsimons RB. Retinal vascular disease and the pathogenesis of facioscapulohumeral muscular dystrophy. A signalling message from Wnt? *Neuromuscul Disord*. 2011;214:263–271.
38. Xu Q, Wang Y, Dabdoub A, et al. Vascular development in the retina and inner ear: control by Norrin and Frizzled-4, a high-affinity ligand-receptor pair. *Cell*. 2004;116:883–895.
39. Black GC, Perveen R, Bonshek R, et al. Coats' disease of the retina (unilateral retinal telangiectasis) caused by somatic mutation in the NDP gene: a role for norrin in retinal angiogenesis. *Hum Mol Genet*. 1999;8:2031–2035.
40. Shastry BS, Trese MT. Overproduction and partial

purification of the Norrie disease gene product, norrin, from a recombinant baculovirus. *Biochem Biophys Res Commun*. 2003;312:229–234.
41. Berger W, van de Pol D, Bachner D, et al. An animal model for Norrie disease (ND): gene targeting of the mouse ND gene. *Hum Mol Genet*. 1996;5:51–59.
42. Luhmann UF, Lin J, Acar N, et al. Role of the Norrie disease pseudoglioma gene in sprouting angiogenesis during development of the retinal vasculature. *Invest Ophthalmol Vis Sci*. 2005;46:3372–3382.
43. Ohlmann A, Scholz M, Goldwich A, et al. Ectopic norrin induces growth of ocular capillaries and restores normal retinal angiogenesis in Norrie disease mutant mice. *J Neurosci*. 2005;25:1701–1710.
44. Robitaille JM, Zheng B, Wallace K, et al. The role of Frizzled-4 mutations in familial exudative vitreoretinopathy and Coats disease. *Br J Ophthalmol*. 2011;95:574–579.
45. Cremers FP, Maugeri A, den Hollander AI, et al. The expanding roles of ABCA4 and CRB1 in inherited blindness. *Novartis Found Symp*. 2004;255:68–79 [discussion 79–84, 177–8].
46. Anderson B, Kasher P, Mayer J, et al. Mutations in CTC1, encoding conserved telomere maintenance component 1, cause Coats plus. *Nat Genet*. 2012;44(3):338–343.
47. Shields JA, Shields CL, Honavar SG, et al. Clinical variations and complications of Coats disease in 150 cases: the 2000 Sanford Gifford Memorial Lecture. *Am J Ophthalmol*. 2001;131:561–571.
48. Shields JA, Shields CL. Differentiation of Coats' disease and retinoblastoma. *J Pediatr Ophthalmol Strabismus*. 2001;38:262–266 [quiz 302–263].
49. Vance SK, Wald KJ, Sherman J, et al. Subclinical facioscapulohumeral muscular dystrophy masquerading as bilateral Coats disease in a woman. *Arch Ophthalmol*. 2011;129:807–809.
50. Campbell FP. Coats' disease and congenital vascular retinopathy. *Trans Am Ophthalmol Soc*. 1976;74:365–424.
51. Gupta N, Beri S, D'Souza P. Cholesterolosis bulbi of the

anterior chamber in Coats disease. *J Pediatr Ophthalmol Strabismus*. 2009;1–3.
52. Shields JA, Eagle RC Jr, Fammartino J, et al. Coats' disease as a cause of anterior chamber cholesterolosis. *Arch Ophthalmol*. 1995;113:975–977.
53. Jumper JM, Pomerleau D, McDonald HR, et al. Macular fibrosis in Coats disease. *Retina*. 2010;30(Suppl.):S9–14.
54. Smithen LM, Brown GC, Brucker AJ, et al. Coats' disease diagnosed in adulthood. *Ophthalmology*. 2005;112:1072–1078.
55. Yeung J, Harris GS. Coats' disease: A study of cholesterol transport in the eye. *Can J Ophthalmol*. 1976;11:61–68.
56. Deutsch TA, Rabb MF, Jampol LM. Spontaneous regression of retinal lesions in Coats' disease. *Can J Ophthalmol*. 1982;17:169–172.
57. Goel SD, Augsburger JJ. Hemorrhagic retinal macrocysts in advanced Coats disease. *Retina*. 1991;11:437–440.
58. Friedenwald H, Friedenwald JS. Terminal stage in a case of retinitis with massive exudation. *Trans Am Ophthalmol Soc*. 1929;27:188–194.
59. Cahill M, O'Keefe M, Acheson R, et al. Classification of the spectrum of Coats' disease as subtypes of idiopathic retinal telangiectasis with exudation. *Acta Ophthalmol Scand*. 2001;79:596–602.
60. Shields JA, Shields CL, Honavar SG, et al. Classification and management of Coats disease: the 2000 Proctor Lecture. *Am J Ophthalmol*. 2001;131:572–583.
61. Lai CH, Kuo HK, Wu PC, et al. Manifestation of Coats' disease by age in Taiwan. *Clin Experiment Ophthalmol*. 2007;35:361–365.
62. Smirniotopoulos JG, Bargallo N, Mafee MF. Differential diagnosis of leukokoria: radiologic-pathologic correlation. *Radiographics*. 1994;14:1059–1079 [quiz 1052–81].
63. Haik BG. Advanced Coats' disease. *Trans Am Ophthalmol Soc*. 1991;89:371–476.
64. Cunha-Vaz JG. The blood–retinal barriers. *Doc Ophthalmol*. 1976;41:287–327.
65. Ridley ME, Shields JA, Brown GC, et al. Coats' disease.

Evaluation of management. *Ophthalmology*. 1982;89:1381–1387.
66. Tarkkanen A, Laatikainen L. Coat's disease: clinical, angiographic, histopathological findings and clinical management. *Br J Ophthalmol*. 1983;67:766–776.
67. Kang K, Wessel M, Tong J, et al. Ultra-widefield imaging for the management of pediatric retinal diseases. *J Pediatr Ophthalmol Strabismus*. 2013;50(5):282–288.
68. O'Brien JM, Char DH, Tucker N, et al. Efficacy of unanesthetized spiral computed tomography scanning in initial evaluation of childhood leukocoria. *Ophthalmology*. 1995;102:1345–1350.
69. Beets-Tan RG, Hendriks MJ, Ramos LM, et al. Retinoblastoma: CT and MRI. *Neuroradiology*. 1994;36:59–62.
70. Lai WW, Edward DP, Weiss RA, et al. Magnetic resonance imaging findings in a case of advanced Coats' disease. *Ophthalmic Surg Lasers*. 1996;27:234–238.
71. Mafee MF, Goldberg MF, Cohen SB, et al. Magnetic resonance imaging versus computed tomography of leukocoric eyes and use of in vitro proton magnetic resonance spectroscopy of retinoblastoma. *Ophthalmology*. 1989;96:965–975 [discussion 966–75].
72. Glasier CM, Brodsky MC, Leithiser RE Jr, et al. High resolution ultrasound with Doppler: a diagnostic adjunct in orbital and ocular lesions in children. *Pediatr Radiol*. 1992;22:174–178.
73. Gelman S, Freund KB, Shah V, et al. The pearl necklace sign. a novel spectral domain optical coherence tomography finding in exudative macular disease. *Retina*. 2014;34:2088–2095.
74. Lam HD, Samuel MA, Rao NA, et al. Retinoblastoma presenting as Coats' disease. *Eye (Lond)*. 2008;22:1196–1197.
75. Plager DA, Orgel IK, Ellis FD, et al. X-linked recessive familial exudative vitreoretinopathy. *Am J Ophthalmol*. 1992;114:145–148.
76. Small RG. Coats' disease and muscular dystrophy. *Trans Am Acad Ophthalmol Otolaryngol*. 1968;72:225–231.
77. Matsuzaka T, Sakuragawa N, Terasawa K, et al.

Facioscapulohumeral dystrophy associated with mental retardation, hearing loss, and tortuosity of retinal arterioles. *J Child Neurol*. 1986;1:218–223.
78. Desai UR, Sabates FN. Long-term follow-up of facioscapulohumeral muscular dystrophy and Coats' disease. *Am J Ophthalmol*. 1990;110:568–569.
79. Gurwin EB, Fitzsimons RB, Sehmi KS, et al. Retinal telangiectasis in facioscapulohumeral muscular dystrophy with deafness. *Arch Ophthalmol*. 1985;103:1695–1700.
80. Cameron JD, Yanoff M, Frayer WC. Coats' disease and Turner's syndrome. *Am J Ophthalmol*. 1974;78:852–854.
81. Burch JV, Leveille AS, Morse PH. Ichthyosis hystrix (epidermal nevus syndrome) and Coats' disease. *Am J Ophthalmol*. 1980;89:25–30.
82. Folk JC, Genovese FN, Biglan AW. Coats' disease in a patient with Cornelia de Lange syndrome. *Am J Ophthalmol*. 1981;91:607–610.
83. Kondra L, Cangemi FE, Pitta CG. Alport's syndrome and retinal telangiectasia. *Ann Ophthalmol*. 1983;15:550–551.
84. Schuman JS, Lieberman KV, Friedman AH, et al. Senior–Loken syndrome (familial renal-retinal dystrophy) and Coats' disease. *Am J Ophthalmol*. 1985;100:822–827.
85. Genkova P, Toncheva D, Tzoneva M, et al. Deletion of 13q12. 1 in a child with Coats disease. *Acta Paediatr Hung*. 1986;27:141–143.
86. Berger M, Lieberman KV, Schoeneman MJ, et al. Coats' disease in a renal transplant recipient. *Nephrol Dial Transplant*. 1987;2:120–123.
87. Skuta GL, France TD, Stevens TS, et al. Apparent Coats' disease and pericentric inversion of chromosome 3. *Am J Ophthalmol*. 1987;104:84–86.
88. Newell SW, Hall BD, Anderson CW, et al. Hallermann–Streiff syndrome with Coats disease. *J Pediatr Ophthalmol Strabismus*. 1994;31:123–125.
89. Kajtar P, Mehes K. Bilateral Coats' retinopathy associated with aplastic anaemia and mild dyskeratotic signs. *Am J Med Genet*. 1994;49:374–377.
90. Bhushan M, Kumar S, Griffiths CE. Multiple glomus

tumours, Coats' disease and basic fibroblast growth factor. *Br J Dermatol*. 1997;137:454–456.
91. Gärtner J, Draf W. Leber's miliary aneurysms associated with telangiectasia of the nasal mucosa. *Am J Ophthalmol*. 1975;79:56–58.
92. Frontali M, Stomeo C, Dallapiccola B. Osteoporosis-pseudoglioma syndrome: report of three affected sibs and an overview. *Am J Med Genet*. 1985;22:35–47.
93. Reynolds BC, Lemmers RJ, Tolmie J, et al. Focal segmental glomerulosclerosis, Coats'-like retinopathy, sensorineural deafness and chromosome 4 duplication: a new association. *Pediatr Nephrol*. 2010;25:1551–1554.
94. Luckie AP, Hamilton AM. Adult Coats' disease in branch retinal vein occlusion. *Aust N Z J Ophthalmol*. 1994;22:203–206.
95. Frezzotti R, Berengo A, Guerra R, et al. Toxoplasmic Coats' retinitis: a parasitologically proved case. *Am J Ophthalmol*. 1965;59:1099–1102.
96. Kremer I, Cohen S, Izhak RB, et al. An unusual case of congenital unilateral Coats's disease associated with morning glory optic disc anomaly. *Br J Ophthalmol*. 1985;69:32–37.
97. Green WR. Bilateral Coats' disease: massive gliosis of the retina. *Arch Ophthalmol*. 1967;77:378–383.
98. Egerer I, Rodrigues MM, Tasman WS. Retinal dysplasia in Coat's disease. *Can J Ophthalmol*. 1975;10:79–85.
99. Khan JA, Ide CH, Strickland MP. Coats'-type retinitis pigmentosa. *Surv Ophthalmol*. 1988;32:317–332.
100. Fogle JA, Welch RB, Green WR. Retinitis pigmentosa and exudative vasculopathy. *Arch Ophthalmol*. 1978;96:696–702.
101. Lanier JD, McCrary JA 3rd, Justice J. Autosomal recessive retinitis pigmentosa and Coats disease: a presumed familial incidence. *Arch Ophthalmol*. 1976;94:1737–1742.
102. Spallone A, Carlevaro G, Ridling P. Autosomal dominant retinitis pigmentosa and Coats'-like disease. *Int Ophthalmol*. 1985;8:147–151.
103. Arrigg PG, Lahav M, Hutchins RK, et al. Pigmentary retinal degeneration and Coats' disease: a case study. *Ophthalmic*

Surg. 1988;19:432–436.
104. Kim RY, Kearney JJ. Coats-type retinitis pigmentosa in a 4-year-old child. *Am J Ophthalmol*. 1997;124:846–848.
105. Padberg GW, Brouwer OF, de Keizer RJ, et al. On the significance of retinal vascular disease and hearing loss in facioscapulohumeral muscular dystrophy. *Muscle Nerve*. 1995;2:S73–80.
106. Shields CL, Zahler J, Falk N, et al. Neovascular glaucoma from advanced Coats disease as the initial manifestation of facioscapulohumeral dystrophy in a 2-year-old child. *Arch Ophthalmol*. 2007;125:840–842.
107. Crow YJ, McMenamin J, Haenggeli CA, et al. Coats' plus: a progressive familial syndrome of bilateral Coats' disease, characteristic cerebral calcification, leukoencephalopathy, slow pre- and post-natal linear growth and defects of bone marrow and integument. *Neuropediatrics*. 2004;35:10–19.
108. Pruett RC. Retinitis pigmentosa: clinical observations and correlations. *Trans Am Ophthalmol Soc*. 1983;81:693–735.
109. Asdourian G. Vascular anomalies of the retina. Peyman G, Sanders D, Goldberg M. *Principles and practices of ophthalmology*. Saunders: Philadelphia; 1980.
110. Robitaille JM, Monsein L, Traboulsi EI. Coats' disease and central nervous system venous malformation. *Ophthalmic Genet*. 1996;17:215–218.
111. Schefler AC, Berrocal AM, Murray TG. Advanced Coats' disease: management with repetitive aggressive laser ablation therapy. *Retina*. 2008;28(Suppl.):S38–41.
112. Spitznas M, Joussen F, Wessing A. Treatment of Coats' disease with photocoagulation. *Albrecht Von Graefes Arch Klin Exp Ophthalmol*. 1976;199:31–37.
113. Shapiro MJ, Chow CC, Karth PA, et al. Effects of green diode laser in the treatment of pediatric Coats disease. *Am J Ophthalmol*. 2011;151:725–731.e2.
114. Suzani M, Moore AT. Intraoperative fluorescein angiography-guided treatment in children with early Coats' disease. *Ophthalmology*. 2015;122(6):1195–1202.
115. Sneed SR, Blodi CF, Pulido JS. Treatment of Coats' disease with the binocular indirect argon laser photocoagulator.

Arch Ophthalmol. 1989;107:789–790.
116. Couvillion SS, Margolis R, Mavrofjides E, et al. Laser treatment of Coats' disease. *J Pediatr Ophthalmol Strabismus*. 2005;42:367–368.
117. Kim J, Park KH, Woo SJ. Combined photodynamic therapy and intravitreal bevacizumab injection for the treatment of adult Coats' disease: a case report. *Korean J Ophthalmol*. 2010;24:374–376.
118. Othman IS, Moussa M, Bouhaimed M. Management of lipid exudates in Coats disease by adjuvant intravitreal triamcinolone: effects and complications. *Br J Ophthalmol*. 2010;94:606–610.
119. Jarin RR, Teoh SC, Lim TH. Resolution of severe macular oedema in adult Coat's syndrome with high-dose intravitreal triamcinolone acetonide. *Eye (Lond)*. 2006;20:163–165.
120. Lei S, Lam WC. Efficacy and safety of dexamethasone intravitreal implant for refractory macular edema in children. *Can J Ophthalmol*. 2015;50(3):236–241.
121. Ghazi N, Al Shamsi H, Larsson J, et al. Intravitreal triamcinolone in Coats' disease. *Ophthalmology*. 2012;119(3):648–649.
122. Bergstrom CS, Hubbard GB 3rd. Combination intravitreal triamcinolone injection and cryotherapy for exudative retinal detachments in severe Coats disease. *Retina*. 2008;28(Suppl.):S33–7.
123. Entezari M, Ramezani A, Safavizadeh L, et al. Resolution of macular edema in Coats' disease with intravitreal bevacizumab. *Indian J Ophthalmol*. 2010;58:80–82.
124. Alvarez-Rivera LG, Abraham-Marin ML, Flores-Orta HJ, et al. Coat's disease treated with bevacizumab (Avastin). *Arch Soc Esp Oftalmol*. 2008;83:329–331.
125. Lin CJ, Hwang JF, Chen YT, et al. The effect of intravitreal bevacizumab in the treatment of Coats disease in children. *Retina*. 2010;30:617–622.
126. Gaillard M, Mataftsi A, Balmer A, et al. Ranibizumab in the management of advanced Coats disease stages 3B and 4. *Retina*. 2014;34(11):2275–2281.

127. Zheng X, Jiang Y. The effect of intravitreal bevacizumab injection as the initial treatment for Coats' disease. *Graefes Arch Clin Exp Ophthalmol*. 2014;252:35–42.
128. Cakir M, Cekic O, Yilmaz OF. Combined intravitreal bevacizumab and triamcinolone injection in a child with Coats disease. *J AAPOS*. 2008;12:309–311.
129. Venkatesh P, Mandal S, Garg S. Management of Coats disease with bevacizumab in 2 patients. *Can J Ophthalmol*. 2008;43:245–246.
130. Cackett P, Wong D, Cheung CM. Combined intravitreal bevacizumab and argon laser treatment for Coats' disease. *Acta Ophthalmol*. 2010;88:e48–9.
131. Kaul S, Uparkar M, Mody K, et al. Intravitreal anti-vascular endothelial growth factor agents as an adjunct in the management of Coats' disease in children. *Indian J Ophthalmol*. 2010;58:76–78.
132. Kodama A, Sugioka K, Kusaka S, et al. Combined treatment for Coats' disease: retinal laser photocoagulation combined with intravitreal bevacizumab injection was effective in two cases. *BMC Ophthalmol*. 2014;14:36.
133. Ray R, Barañano D, Hubbard G. Treatment of Coats' disease with intravitreal bevacizumab. *Br J Ophthalmol*. 2013;97:272–277.
134. Villegas V, Gold A, Berrocal A, et al. Advanced Coats' disease treated with intravitreal bevacizumab combined with laser vascular ablation. *Clin Ophthalmol*. 2014;8:973–976.
135. Sun Y, Jain A, Moshfeghi DM. Elevated vascular endothelial growth factor levels in Coats disease: rapid response to pegaptanib sodium. *Graefes Arch Clin Exp Ophthalmol*. 2007;45:1387–1388.
136. He YG, Wang H, Zhao B, et al. Elevated vascular endothelial growth factor level in Coats' disease and possible therapeutic role of bevacizumab. *Graefes Arch Clin Exp Ophthalmol*. 2010;248:1519–1521.
137. Ramasubramanian A, Shields CL. Bevacizumab for Coats' disease with exudative retinal detachment and risk of vitreoretinal traction. *Br J Ophthalmol*. 2012;96:356–359.

138. Goel N, Kumar V, Seth A, et al. Role of intravitreal bevacizumab in adult onset Coats' disease. *Int Ophthalmol*. 2011;31:183–190.
139. Jun JH, Kim YC, Kim KS. Resolution of severe macular edema in adult Coats' disease with intravitreal triamcinolone and bevacizumab injection. *Korean J Ophthalmol*. 2008;22:190–193.
140. Zhao T, Wang K, Ma Y, et al. Resolution of total retinal detachment in Coats' disease with intravitreal injection of bevacizumab. *Graefes Arch Clin Exp Ophthalmol*. 2011;249:1745–1746.
141. Machemer R, Williams JM Sr. Pathogenesis and therapy of traction detachment in various retinal vascular diseases. *Am J Ophthalmol*. 1988;105:170–181.
142. Yoshizumi MO, Kreiger AE, Lewis H, et al. Vitrectomy techniques in late-stage Coats'-like exudative retinal detachment. *Doc Ophthalmol*. 1995;90:387–394.
143. Muftuoglu G, Gulkilik G. Pars plana vitrectomy in advanced Coats' disease. *Case Rep Ophthalmol*. 2011;2:15–22.
144. Peyman GA, Dellacroce JT, Ebrahim SA. Removal of submacular exudates in a patient with Coats disease: a case report. *Retina*. 2006;26:836–839.
145. Silodor SW, Augsburger JJ, Shields JA, et al. Natural history and management of advanced Coats' disease. *Ophthalmic Surg*. 1988;19:89–93.
146. Shields JA, Shields CL. Review: Coats disease: the 2001 LuEsther T. Mertz lecture. *Retina*. 2002;22:80–91.
147. de Silva DJ, Brookes JL. Cyclodiode treatment of neovascular glaucoma secondary to Coats' disease. *Br J Ophthalmol*. 2007;91:690–691.
148. Harris GS. Coats' disease, diagnosis and treatment. *Can J Ophthalmol*. 1970;5:311–320.
149. Schatz H, Burton T, Yanuzzi L, et al. Abnormal retinal and disc vessels and retinal leak. Schatz H. *Interpretation of fundus fluorescein angiography*. Mosby: St. Louis; 1978.
150. Mondon H, Hamard H, Girard P, et al. [Retinal gliosis associated with Coats' disease]. *Bull Soc Ophtalmol Fr*. 1970;70:881–883.

151. Theodossiadis GP. Some clinical, fluorescein-angiographic, and therapeutic-aspects of Coats' disease. *J Pediatr Ophthalmol Strabismus*. 1979;16:257–262.
152. Shienbaum G, Tasman WS. Coats disease: a lifetime disease. *Retina*. 2006;26:422–424.
153. Tasman W. Coats' disease. *Am Fam Physician*. 1977;15:107.
154. Egerer I, Tasman W, Tomer TT. Coats disease. *Arch Ophthalmol*. 1974;92:109–112.

60

Hemoglobinopathies

Adrienne W. Scott, Morton F. Goldberg, Gerard A. Lutty

In a landmark 1910 *Archives of Internal Medicine* article,[1] Dr James Herrick described "peculiar, elongated, sickle-shaped red blood corpuscles" from a peripheral blood smear of a Grenadian dental student with recurring medical illnesses. He reported the first written description of sickle-cell disease (SCD).[1–3] Linus Pauling and colleagues in 1949 were the first to implicate a defective hemoglobin molecule within the erythrocyte as the cause of the disease.[4,5]

The term "sickle-cell disease" encompasses the group of hemoglobinopathies characterized by intravascular hemolysis and by defective oxygen transport. In a normal red blood cell, two α-globin subunits, two β-globin subunits, and a central heme molecule combine to form adult hemoglobin (Hb A). The β-globin gene, an oxygen transport gene, is found on the short arm of chromosome 11.[6,7] Hemoglobin S (Hb S) results from a single amino acid point mutation in which a valine molecule substitutes for a glutamic acid at the sixth position within the β-globin chain.

Hemoglobin C (Hb C) is caused by a glutamic acid to lysine change in the β-globin molecule.

SCD is transmitted through the autosomal recessive mode of inheritance. Two copies of Hb S may combine with one another (SS disease), or one copy of Hb S and another β-globin variant, such as Hb C, may combine (compound heterozygous SC disease).[7] Individuals with one copy of Hb A and one copy of Hb S are described as having the sickle-cell trait, the typically, but not invariably, symptom-free carrier state for SCD. β-thalassemia occurs when a reduced amount of β-globin is present. This condition is called beta-plus (β^+) thalassemia, whereas the absence of β-globin is called beta-zero (β^0). Either of these conditions may combine with Hb S, leading to a compound heterozygous state.[7]

Prevalence

To date, SCD remains the most common inherited blood disorder, which occurs in 1/500 African American births.[8–10] Approximately 250,000 children are born worldwide with SCD each year.[7] SCD causes about 5% of deaths in children under 5 years in Africa, more than 9% of such deaths in West Africa, and up to 16% of under-5 deaths in individual West African countries.[11] Approximately 8% (or 1 in 12) of black Americans possess sickle-cell trait, which is usually not associated with increased mortality or morbidity (except in hyphema), and is thought to confer protection against malarial infection.[10] The hemoglobin concentration in sickle-cell trait is typically 35–40% Hb S and 55–60% Hb A.[7] Although sickle-cell trait subjects are generally asymptomatic, they may encounter systemic complications of SCD under conditions of extreme hypoxia.[12] Populations of African descent possess the highest frequency of Hb S. At-risk genotypes for SCD are also observed in people of Mediterranean, Caribbean, South and Central American, Arab, and East Indian descent.[7] HbSS disease occurs in approximately 0.15% of African descendants in North America.[7,13] Those with SS disease do not typically become symptomatic until after 6 months of age, when fetal hemoglobin (Hb F) is replaced with Hb S. These individuals have a decreased life expectancy, as they are prone to developing severe anemia and are highly

susceptible to recurrent infections.[14] Individuals with HbSC disease, the compound heterozygotes, typically exhibit 50% Hb S and 50% Hb C hemoglobin and typically have less systemic morbidity from the systemic complications of SCD, and have an approximately normal life expectancy.[7] Sickle β-thalassemia patients are typically encountered in central African and Mediterranean countries and normally have hemoglobin composition of 60–90% Hb S and 10–30% Hb F.[7,15]

Genetic Modifiers

Phenotypic expression of SCD is quite variable, even among those with the same genotype. Environmental effects and multiple gene interactions are thought to be at play. Further, the ability of an individual to generate Hb F may lead to reduced disease severity. Different β-globin cluster haplotypes may result in different levels of Hb F.[7,16] Levels of Hb F have been shown to inversely correlate with the clinical manifestations of SCD.[17] The higher the Hb F, the milder the manifestations of sickle-cell disease. Hydroxyurea therapy works to increase the amount of Hb F in circulation in individuals with SCD.

Pathophysiology

The interplay among abnormal erythrocytes and hypoxic, hyperosmolar, or acidotic conditions leads to the abnormal rheology and hemolysis that are characteristic of SCD. In Hb S, a strongly hydrophobic nonpolar valine takes the place of a polar strongly hydrophilic glutamic acid residue.[5] Upon deoxygenation in the microcirculation, hydrophobic residues within Hb S are exposed and associate with hydrophobic regions of adjacent molecules. This polymerization results in the generation of rigid fibers of Hb S, which damage the red blood cell membrane and cytoskeleton and cause the cell to assume an elongated sickle shape. This polymerization process is reversible as oxygenation increases, and the cell may resume its native more pliable discoid shape. However, the repeated cycle of sickling and unsickling of the red blood cell may lead to permanent damage to the erythrocyte

membrane, irreversible sickling, and hemolysis. The mean corpuscular hemoglobin concentration (MCHC) may be the most important factor contributing to the rate of Hb S polymerization.[5] The higher the MCHC, the more hemoglobin molecules that are available to participate in polymerization, and the closer these molecules are to one another, further promoting a favorable environment for Hb S polymerization.[18,19]

The erythrocyte's original state of oxygenation also impacts the extent and rate of polymerization.[15,16] An intrinsic property of the normal erythrocyte is the ability to deform easily in order to pass through capillaries with smaller diameters than its own. Decreased erythrocyte deformability and increased rigidity can cause increased capillary transit time, leading to deoxygenation and sickling. These events promote increased permeability of the cell membrane to potassium, sodium, and calcium cations, which leads to efflux of water from the cell, contraction of cellular volume, and resultant increase in Hb S concentration.[5,19,20,21]

In addition to mechanical obstruction of blood vessels by dense, sickled erythrocytes, these sickled erythrocytes display increased adhesion to matrix proteins of the vascular endothelium, such as laminin,[22,23] and thus cause direct damage to the endothelium. Integrin α4β1, integrin-associated protein, sulfated glycolipid, lutheran protein, phosphatidylserine, band 3 protein, and CD36 are adhesion molecules expressed in sickled erythrocytes and have been implicated in the cellular adhesion and red blood cell aggregation.[24–26] Immature erythrocytes and reticulocytes increase in SCD following intravascular hemolysis. These cells also have increased adhesion molecules, such as integrin α4β1,[27–29] which promote pathologic adhesion to the vascular endothelium, specifically to vascular cell adhesion molecule-1 (VCAM-1). Direct activation of endothelial cells occurs in response to elevated circulating cytokines, such as tumor necrosis factor-alpha (TNF-α) and interleukin-1β (IL-1β),[30,31] which upregulate expression of endothelial adhesion molecules like intercellular adhesion molecule-1 (ICAM-1), VCAM-1, E-selectin, and P-selectin.[32,33]

Inflammation likely plays a role in the vaso-occlusive process in SCD. Lutty and colleagues demonstrated retention of irreversibly sickled SS red cells and adherence of red cells in reticulocyte-rich

fractions in the retina and choroid of rat eyes under hypoxic conditions or following TNF-α stimulation.[34–36] TNF-α and IL-1 may contribute to vaso-occlusion by accelerating the production of adhesion molecules on the vascular endothelium and by activating polymorphonuclear leukocytes.[30] Additional evidence implicates inflammatory mediators in sickle-cell disease, as TNF-α and IL-1 have been shown to be upregulated in the sera of individuals with SCD at baseline.[31,37,38]

Nitric oxide (NO) is a potent vasodilator and regulator of vascular tone; it is derived from the vascular endothelial NO synthase. SCD has been associated with elevated reactive oxygen species, which scavenge NO and metabolize arginine, its precursor.[7] L-arginine as an oral supplement has been given to induce NO production in transgenic sickle-cell mice; therefore, oral arginine supplementation may be a potential therapy to improve vasodilation, thus facilitating blood flow in sickle-cell disease.[38,39]

Vascular endothelial growth factor (VEGF), which is upregulated by hypoxia, is present in the serum of SCD patients at baseline and is elevated during vaso-occlusive crises.[40] Elevated VEGF has been demonstrated in eyes with sickle-cell retinopathy.[41,42] VEGF has also been shown to increase levels of cell adhesion molecules, such as ICAM-1 and VCAM-1.[43,44] Angiopoietin-1 (Ang-1) and angiopoietin-2 (Ang-2) interact with the Tie-2 receptor on endothelial cells, regulating angiogenesis. Ang-1 is responsible for the maintenance and stabilization of mature blood vessels, while Ang-2 leads to vessel destabilization and dissociation of pericytes and is upregulated by hypoxia and VEGF.[45] Interaction among these proteins may be important in the pathophysiology of neovascularization in SCD.

Systemic Manifestations

Over recent years, as the life expectancy of those affected by SCD has increased, so have the number of chronic complications that these individuals experience.[12,46] Sickling of the erythrocytes, with resultant intravascular hemolysis, thrombosis, ischemia, and tissue necrosis, causes a myriad of systemic complications, including cerebrovascular accident, acute chest syndrome, pulmonary

hypertension, splenic sequestration, priapism, osteonecrosis, cholelithiasis, pneumonia, leg ulcers, aplastic crisis, renal disease, need for recurrent transfusions, episodic, painful vaso-occlusive crises, and premature death.[7]

Severe visual impairment and blindness from complications of proliferative sickle-cell retinopathy (PSR) may also occur. For reasons that are as yet unclear, subjects with HbSC disease typically display less systemic morbidity from their hemoglobinopathy than do subjects with HbSS disease, but they have a higher likelihood of experiencing vasoproliferative retinal complications than their homozygous HbSS counterparts.[47] In one study, retinopathy was detected in 33% of patients with HbSC disease compared to 3% of patients with HbSS disease.[37]

Several theories have been proposed to explain this difference. One explanation could be that HbSS patients typically have a shorter life expectancy than HbSC patients and may not live long enough to manifest the retinal disease. Alternatively, the difference in retinopathy among sickle-cell genotypes may be due to the higher hematocrit and cell density, and the lower Hb F, of individuals with HbSC as compared to HbSS individuals.[7] The overall lower hematocrit in HbSS patients, and the resultant lowered viscosity of blood, may confer a relative protection from vaso-occlusion in the retinal circulation.[48] Another theory is that the retinal vaso-occlusions in SS disease may be so complete that no viable tissue remains to produce the growth factors necessary to mount a proliferative response. In HbSC disease, the vascular occlusions may be less complete, and they may occur in the setting of a chronic hypoxic, rather than a totally anoxic, state. HbSS patients are possibly more likely to have complete vascular occlusions, whereas HbSC patients may show a chronic state of incomplete vascular ischemia rather than complete vascular occlusions. Thus, in HbSC, a steady-state release of angiogenic growth factors from the remaining viable tissue may occur, leading to vasoproliferation.[49] Finally, Lutty and colleagues showed that irreversibly sickled HbSS erythrocytes are easily trapped in retinal capillaries and precapillary arterioles in hypoxic conditions in a rat model.[16,35] HbSC cells, however, regardless of oxygen levels, were less easily trapped in the retinal microvasculature. When the

vascular endothelium was stimulated with cytokines, retention of HbSC cells did occur. The authors suggested that vaso-occlusion in HbSC disease may be the result of the complex interaction among cytokines, the fibrinolytic cascade, leukocyte interactions, and activation of the vascular endothelium with induction of adhesion molecules.[13,35] These data suggest that retention of sickled cells in the retina is not primarily mechanical (rigid cells retained in a small lumen) but rather is due to hypoxia-initiated cytokines and their receptors.

Alterations in potassium-chloride (K-Cl) cotransport have also been shown to be different in HbSC and HbSS, and this difference has been shown to be clinically significant.[50] One study demonstrated that K-Cl transport correlated with the formation of sickle cells, and K-Cl transport was higher in blood samples in HbSC patients. Increased K-Cl cotransport activity was also correlated with retinopathy.[50]

Ophthalmic Clinical Features

Retrobulbar and Orbital Involvement

Orbital involvement of SCD is uncommon, but is clinically important to recognize when it occurs. One study reported periorbital swelling during vaso-occlusive crisis.[51] Infarction of orbital bones and orbital hematomas occur and may lead to the orbital compression syndrome. These patients typically have lid edema, fever, facial pain, proptosis, restriction of motility, and resultant diplopia. These syndromes usually resolve with treatment of the underlying crisis, antibiotics, and steroids. Orbital involvement in SCD may cause sudden permanent unilateral loss of vision without detectable retinal arterial changes due to retrobulbar ischemic optic neuropathy.[7,52] Urgent decompression of the orbit may be required. Recurrent bilateral lacrimal gland swelling has also been reported.[53]

Anterior Segment Involvement

Anterior segment involvement may be present in SCD. One

characteristic finding is the saccular and sausage-like or linear dilations of the smallest conjunctival vessels,[54] most easily seen with high magnification (Fig. 60.1). Paton described these comma-shaped and isolated linear capillary segments in the inferior bulbar conjunctival vessels and coined the term "conjunctival sign." It is uncommon in those with high Hb F levels.[55] Local heat from the slit lamp induces vasodilation and causes normalization of these abnormalities,[56,57] whereas topical vasoconstricting drops increase the abnormal vascular pattern.[58,59] These conjunctival vascular changes vary with oxygenation status and are more prevalent in HbSS disease than in HbSC disease.[55] Biomicroscopic inspection shows constriction of these conjunctival vessels during painful crises, with normal blood flow returning on recovery.[59]

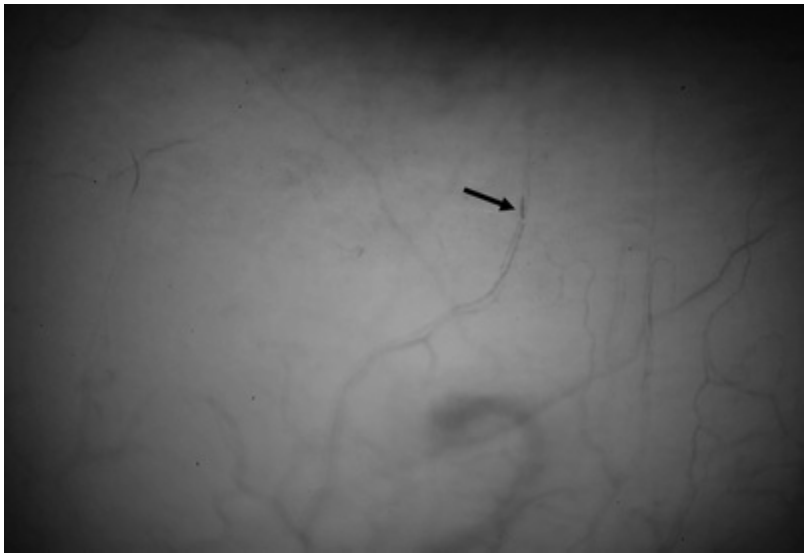

FIG. 60.1 The bulbar conjunctiva of an HbSS patient demonstrates abnormal linear dilations (*black arrow*) that appear to be disconnected from the adjacent vascular network.

Segmental iris atrophy can be seen in individuals with SCD (Fig. 60.2).[60,61] Iris atrophy may result from sectoral ischemic necrosis involving radial iris arteries. Secondary neovascularization of the iris stroma has also been described and documented with intravenous fluorescein angiography. In one instance this neovascular frond resembled that classically seen as the "sea fan" in PSR.[13,62] Neovascular glaucoma rarely occurs.[7,63]

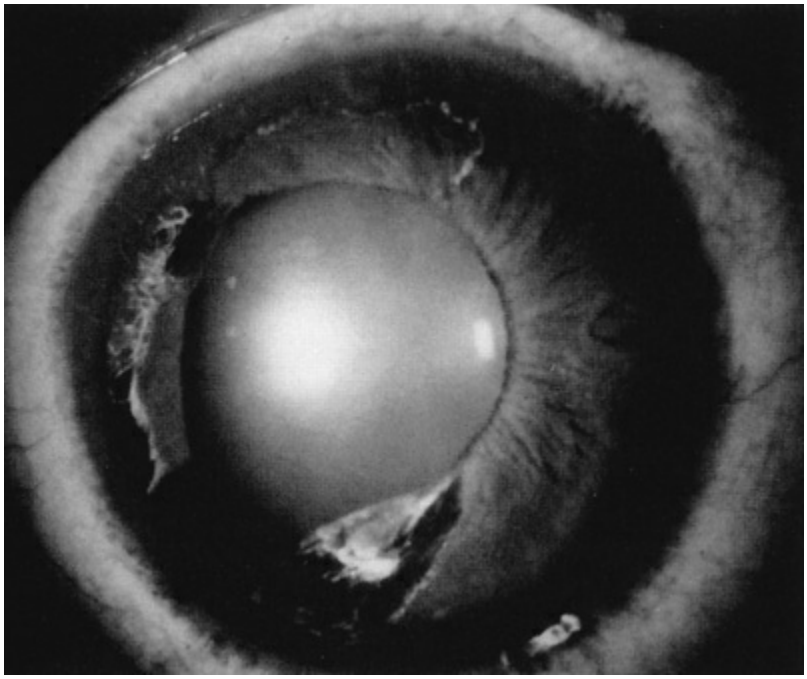

FIG. 60.2 Atrophy and irregularity of the iris at the pupillary border are seen as a result of sectoral ischemic necrosis in a patient with sickle-cell disease.

Hyphema in a patient with SCD and in those with sickle-cell trait represents a sight-threatening emergency, as even modest elevations of intraocular pressure (IOP) have resulted in permanent loss of vision from retinal artery occlusion.[63–66] Sickled erythrocytes may clog the trabecular meshwork,[62] causing elevation in IOP. Although intensive medical management to lower IOP in SCD patients with hyphema is recommended, IOP-lowering medications must be used cautiously. Repetitive use of carbonic anhydrase inhibitors, for example, is contraindicated in SCD patients with hyphema, as some of these medications cause intracameral acidotic conditions that may worsen erythrocyte sickling. Early surgical intervention for IOP control should be considered, typically by paracentesis of the anterior chamber.[67] Intracameral tissue plasminogen activator may be a potentially useful agent in the treatment of large posttraumatic hyphema in some cases.[68] Hyperoxygenation of the patient may also be helpful.

Posterior Segment Involvement

Vitreoretinal Interface

The pathologic retinal neovascularization caused by retinal ischemia in SCD can result in loss of vision from vitreous hemorrhage.[69,70] Other abnormalities of the fundus have been described, such as peripheral retinal whitening. This has been described in 93% of HbSS patients,[71] 83% of HbSC patients,[72] and 82% of Hb S Thal patients.[73]

Flat, brown, ovoid lesions in the retinal periphery have also been noted in SCD and termed "dark without pressure." The underlying choroid appears normal on ophthalmoscopy, and the corresponding fluorescein angiogram is also normal.[13,74,75]

Optic Nerve

The optic nerve in patients with SCD may show dilated capillaries at the optic nerve head that appear as small red dots and represent precapillary arterioles plugged with sickled erythrocytes.[13,58,71,76] These changes are not visually significant, because the vascular occlusions are transient. Optic disc neovascularization is rare, but has been reported in four HbSC patients[13,77–80] and one HbSS patient.[13,71]

Macula

Though the hallmark of ocular SCD is the peripheral retinopathy, the macula is also susceptible to infarction from vaso-occlusive disease. The "macular depression sign" has been described as an oval depression of the bright foveal reflex as a result of macular thinning due to ischemic atrophy.[81] This finding is best detected using red-free illumination. The extent of macular vascular changes has not been shown to correlate with visual acuity. In one study, an enlarged foveal avascular zone (FAZ) was identified in patients with SCD on fluorescein angiography as compared to healthy, age-matched controls.[82] Within the SCD group, visual acuity did not correlate with FAZ size.

OCT provides in vivo images of abnormalities of macular morphology, even in asymptomatic patients.[83] Hoang and coworkers[84] described macular retinal thinning using spectral domain optical coherence tomography (SD-OCT), most notably in the deeper retinal layers in the central macula and parafoveal retina. Additionally, the authors noted "splaying," or blunting of

the foveal contour on SD-OCT in asymptomatic SCD patients with areas of focal parafoveal thinning (Fig. 60.3). Paracentral acute middle maculopathy has also been described in SCD.[85,86] This condition may be seen in patients with unexplained acute vision loss and is diagnosed by hyperreflectivity of the parafoveal inner nuclear layer on SD-OCT. Another study also described thinning of the temporal macula in patients with PSR on SD-OCT and suggested that this finding should lead clinicians to perform peripheral wide-field angiography to evaluate the retinal periphery for ischemia.[87] Mathew and colleagues detected macular splaying on SD-OCT in 40% of patients and noted a higher prevalence of proliferative sickle-cell retinopathy in eyes of patients with areas of temporal macular thinning on SD-OCT. No significant differences in choroidal thickness were noted in eyes with and without retinal thinning.[88] Macular hole,[89] epiretinal membranes,[90] macular schisis,[91] and posterior pole neovascularization[92] have all been reported as complications of SCD (Fig. 60.4).

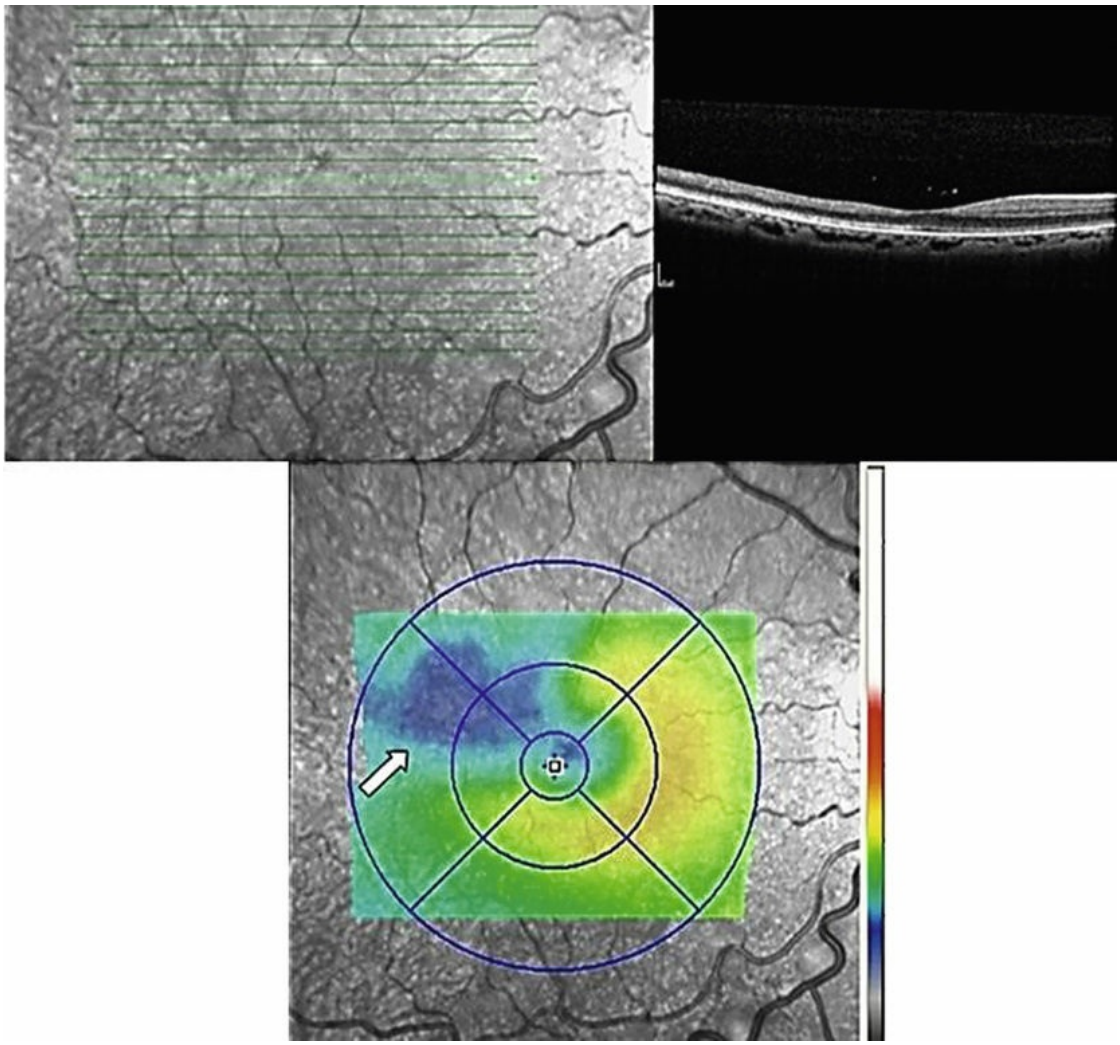

FIG. 60.3 Spectral domain optical coherence tomography demonstrates “foveal splaying” (saucerization of the foveal pit) and focal thinning (*white arrow*) within the temporal foveal region in a patient with HbSS disease.

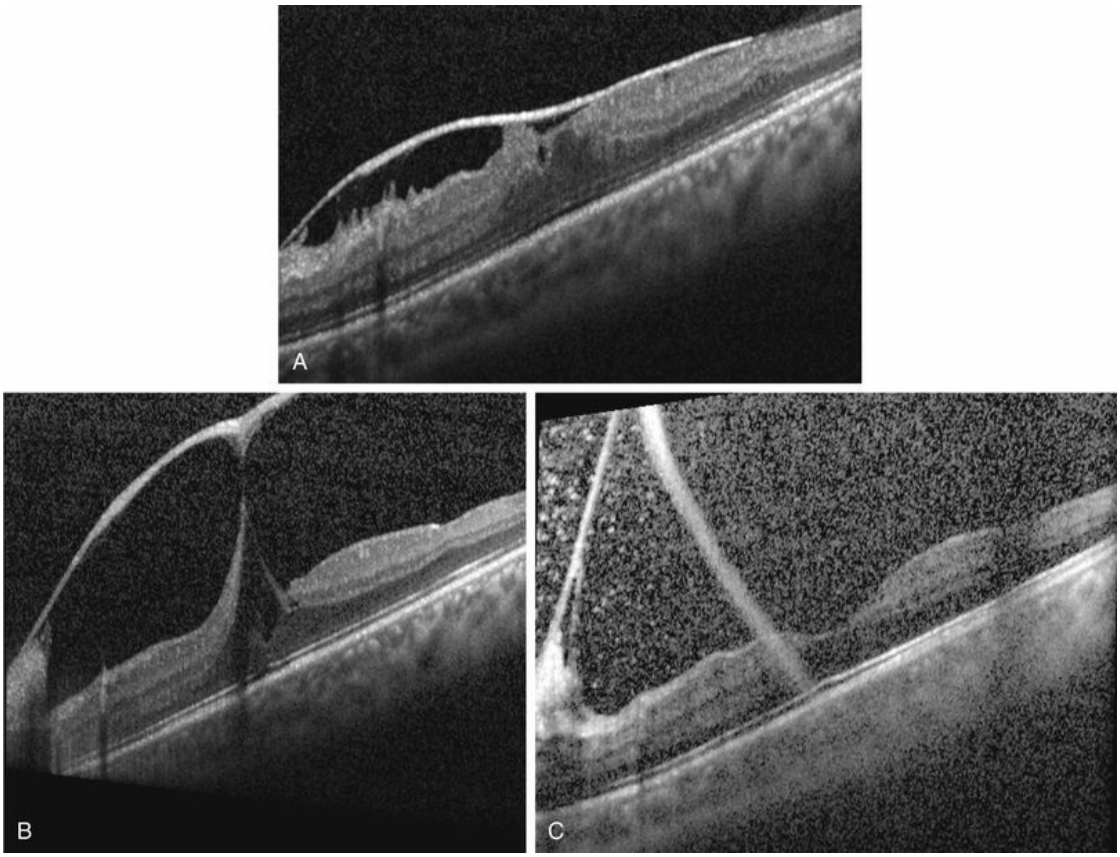

FIG. 60.4 (A) An HbSC patient, with a history of PSR with a macular epiretinal membrane. (B) Development of vitreomacular traction (VMT) one month following supplemental scatter laser photocoagulation to the peripheral retina. (C) Release of the VMT 2 months following laser photocoagulation with return to normal foveal contour. Image quality is degraded because of vitreous hemorrhage.

Angioid Streaks

Angioid streaks, associated with linear breaks in Bruch's membrane, have a well-documented association with SCD, occurring in 1–2% of patients.[13,71,93] These irregular, reddish subretinal bands are most commonly found in patients with the HbSS genotype.[71,94] The incidence of angioid streaks in these eyes increases with age.[95] Angioid streaks in SCD may occur as the result of hypoxia, inflammatory cytokine release, and tissue damage.[7,96] Heavy calcification and breaks in Bruch's membrane have been demonstrated in cadaver eyes of an HbSS patient with angioid streaks.[97] Angioid streaks in SCD usually have a benign course, and

resultant choroidal neovascularization (CNV) is rare in SCD patients.[13]

Retinal Vasculature

Peripheral vascular tortuosity may be more commonly observed in HbSS patients.[7] One study reported increased retinal vascular tortuosity in 47% of HbSS patients and 32% of HbSC patients,[98] although another reported 11% with vascular tortuosity in both HbSS and HbSC patients.[71,72] This discrepancy could be due to an imprecise definition of vascular tortuosity.[7]

Retinal vascular occlusions frequently occur in the peripheral retina in patients with SCD, and peripheral retinal nonperfusion is a common finding. Arteriovenous anastomoses may occur (Fig. 60.5). "Silver-wiring" of retinal arterioles represents permanently occluded arterioles (Fig. 60.6).

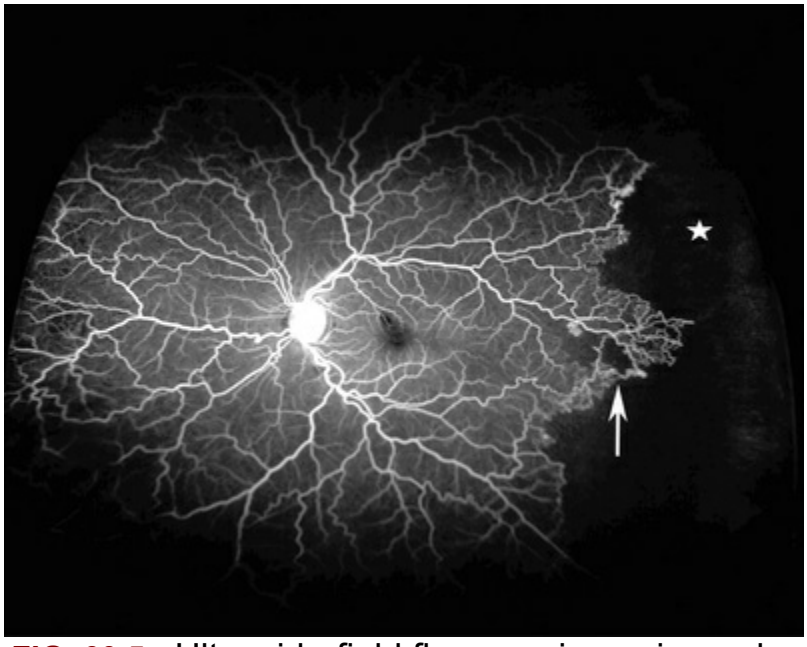

FIG. 60.5 Ultrawide-field fluorescein angiography demonstrates striking peripheral nonperfusion at the temporal border of the retina (*star*) with arteriovenous anastomoses (*arrow*).

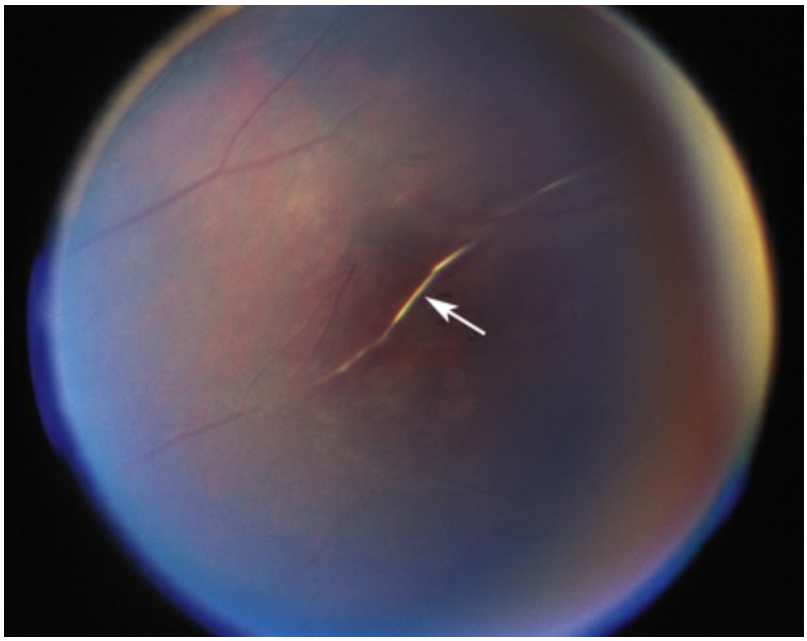

FIG. 60.6 Silver-wiring and occlusion of a peripheral retinal arteriole (*arrow*).

Depending on its location, vascular occlusion may cause temporary or permanent loss of vision, or no loss of vision at all. The cause of these occlusions may be multifactorial, potentially involving sickled erythrocytes attaching to vascular endothelium, or the activation of the coagulation cascade, with secondary intimal injury.[2,99] In the peripheral temporal retina, where vessels become markedly narrow, arteriolar occlusions are common. Although the occlusions clinically appear to be inside precapillary arterioles, the vaso-occlusions may actually start in the capillary bed downstream, where sickled erythrocytes have difficulty traversing the narrow lumens due to their nondeformability.

Vaso-occlusion arising from the posterior ciliary arterial circulation may potentially cause choroidal infarction in SCD. Histopathologic studies show impacted red blood cells, increased fibrin, and platelet fibrin thrombi in cases of choroidal occlusion.[100,101] CNV may rarely occur spontaneously[102] or result from high-energy laser burns.[103]

Nonproliferative Sickle Retinopathy

Salmon Patch Hemorrhages

Salmon patch lesions are pinkish-orange hemorrhages located between the retina and its internal limiting membrane (Fig. 60.7). They may arise from areas of bleeding into the retina adjacent to areas of nonperfusion and have been described as a "blowout" of an occluded arteriole.[104,105] Although the hemorrhage is initially red, it may turn a salmon color over time because of progressive hemolysis. The localized collection of blood may remain under the internal limiting membrane, travel into the subretinal space, or spread into the vitreous.[13,104,105]

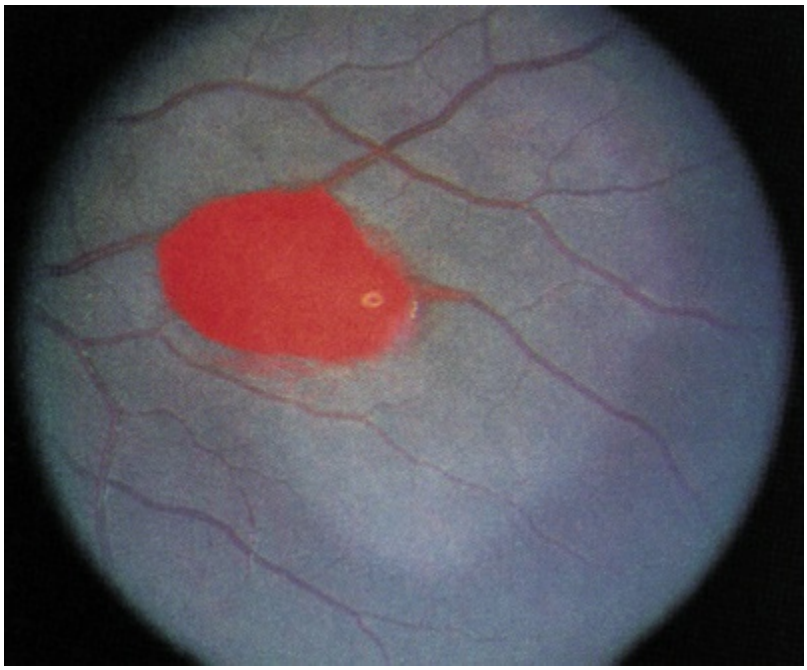

FIG. 60.7 A salmon patch hemorrhage results from "blowout" of blood from an occluded retinal arteriole.

Iridescent Spots

If arteriolar occlusion causes retinal hemorrhage, a small schisis cavity may develop after the intraretinal portion of the hemorrhage resolves.[13] The cavity may contain hemosiderin-laden macrophages, which can appear as multiple refractile or iridescent spots (Fig. 60.8).

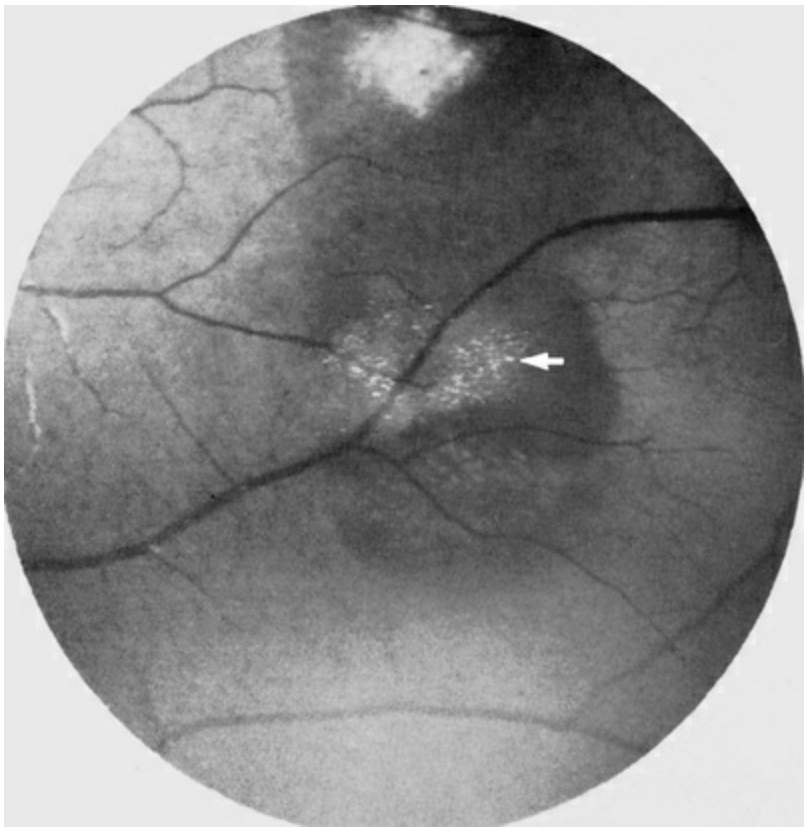

FIG. 60.8 Iridescent spots (*arrow*) are shown within a retinoschisis cavity and may represent hemosiderin-laden macrophages.

Black Sunbursts

Black sunbursts are flat, stellate, or round areas of hyperpigmentation and result when intraretinal hemorrhage tracks into the subretinal space (Fig. 60.9).[104,106] On histopathologic study, black sunbursts can show focal hypertrophy of the retinal pigment epithelium (RPE).[104] This "sunburst sign" may also represent localized choroidal ischemic damage to the overlying RPE.[107] Another hypothesis is that the black sunburst may be the RPE response to an area of underlying CNV.[102,108]

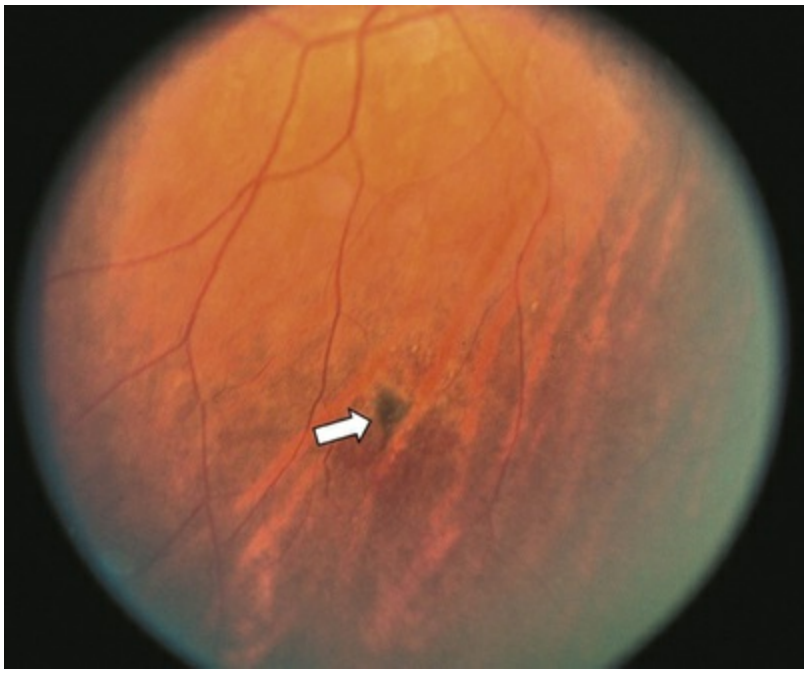

FIG. 60.9 A small black sunburst (*arrow*) may represent focal hypertrophy or hyperplasia of the retinal pigment epithelium.

Proliferative Sickle Retinopathy

A critical event in the development of PSR is the formation of the sea fan, so named for its close resemblance to the marine invertebrate *Gorgonia flabellum* (Fig. 60.10). Peripheral retinal arteriolar occlusions are the inciting events in sea fan formations. Occlusion of the vasculature causes release of growth factors, resulting in formation of these neovascular fronds. Complications of PSR are the major contributor to vision loss in SCD. Sea fans are predisposed to hemorrhage into the vitreous, and to cause vitreous membrane formation, tractional retinoschisis, and tractional or combined rhegmatogenous-tractional retinal detachment.[48] Sea fans often form at arteriovenous crossings and may have multiple feeding arterioles and draining venules (Fig. 60.11).[109]

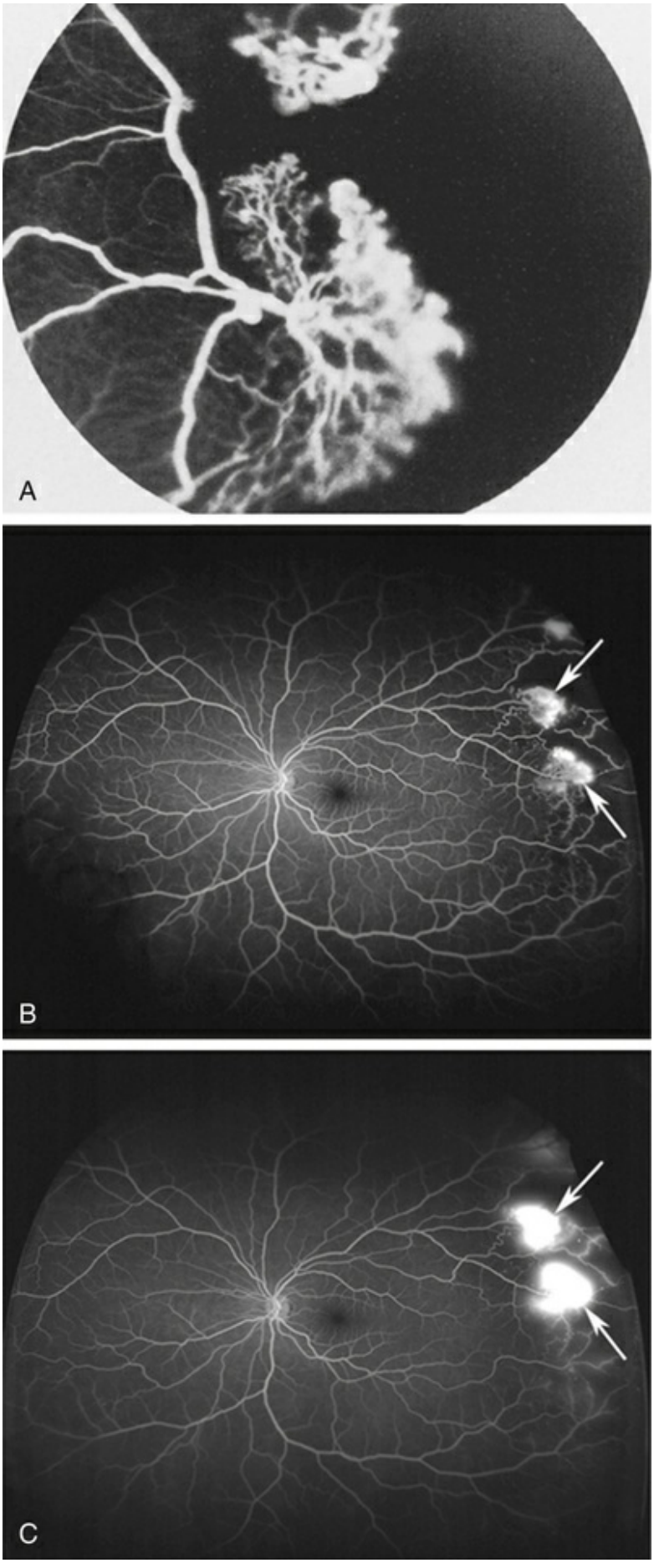
A
B
C

FIG. 60.10 Sea fan lesions are shown in the peripheral fundus in a patient with HbSC disease. The frond-like vascular structures are typically present at the border of perfused and nonperfused peripheral retina. (A) A 30° image shows details of a sea fan. (B) Ultrawide-field fluorescein angiography demonstrates bright hyperfluorescence of the sea fan lesions in another patient. (C) The later phase of the angiogram from the patient in (B) shows diffuse leakage from the neovascular fronds (*arrows*).

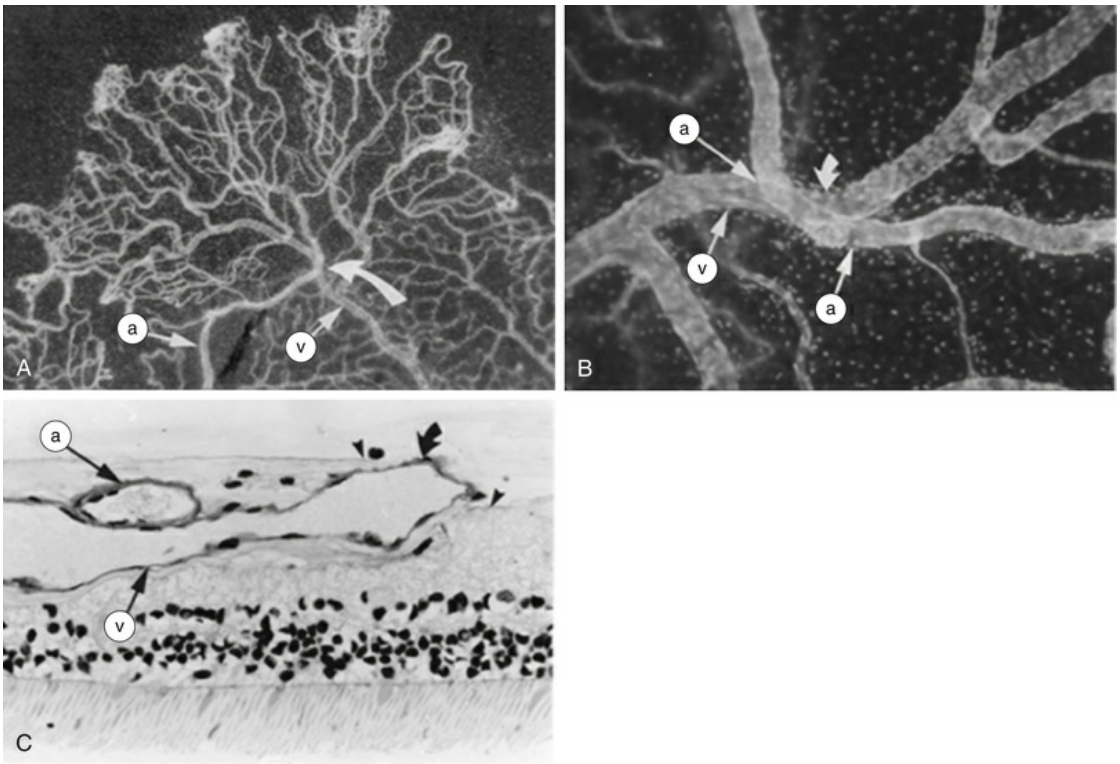

FIG. 60.11 Flat-embedded ADPase retina from a 40-year-old HbSS subject. (A) A sea fan formation is shown with dark-field illumination of the retina en bloc before sectioning. This formation occurred at the crossing (*curved arrow*) of an artery (*a*) and vein (*v*) and had five connections to the arterial circulation and four connections to venous channels. (B) Higher magnification of the arteriovenous crossing. (C) Cross-section of the arteriovenous crossing shows the retina is very thin in this region at the border of perfused and

nonperfused retina. (Reproduced with permission from McLeod DS, Fukushima A, Goldberg MF, et al. Histopathologic features of neovascularization in sickle-cell retinopathy. Am J Ophthalmol 1997;124:455–72.)

In 1971, Goldberg devised the widely utilized classification system for PSR (Table 60.1).[110]

TABLE 60.1
Goldberg Classification of Proliferative Sickle-Cell Retinopathy

Stage I	Peripheral arterial occlusions
Stage II	Peripheral arteriovenous anastomoses
Stage III	Neovascular and fibrous proliferations
Stage IV	Vitreous hemorrhage
Stage V	Retinal detachment

Goldberg Stages

Stage I

Stage I retinopathy is defined by peripheral vascular occlusion.[58] The peripheral retina may show multiple simultaneous arteriolar occlusions, and silver-wiring of the arterioles may be present. Vaso-occlusion occurs primarily in the peripheral temporal retina due to longer arteriovenous transit times (with deoxygenation), an increased number of occludable bifurcation sites, and decreased perfusion.

Stage II

In this stage, vascular remodeling at the border of perfused and nonperfused retina occurs. Arteriovenous anastomoses form connections between occluded arterioles and adjacent terminal venules by way of preexisting capillaries (Fig. 60.5). The anastomoses do not leak on fluorescein angiography (FA), confirming that these early vascular lesions are derived from preexisting mature blood vessels with an intact blood–retinal barrier, as opposed to being truly neovascular.

Stage III

Sea fan fronds are the hallmark of stage III PSR and are perhaps the

trademark lesion of sickle-cell retinopathy (Fig. 60.10). These lesions are most commonly found in the superotemporal retina, followed by the inferotemporal, superonasal, and inferonasal quadrants. Sea fans represent true neovascularization, and thus display diffuse leakage on fluorescein angiography (Fig. 60.10). Sea fan neovascularization causes chronic transudation into the vitreous, which in turn leads to vitreous degeneration and retinal traction, with possible vitreous hemorrhage and retinal detachment.[13,48,58]

Most sea fans are found at the border of perfused and nonperfused retina, and they grow toward the ora serrata.[48,80] Sea fan neovascular complexes often arise from the venous aspect of the arteriovenous anastomoses, and develop approximately 18 months following the formation of these arteriovenous connections[13,48] (Fig. 60.11). Chronic ischemia within the peripheral retina leads to an increase in angiogenic factors, such as VEGF and basic fibroblastic growth factor.[13,41,100] Pigment epithelial growth factor/VEGF balance may play a role in the angiogenesis of these lesions as well as the subsequent, spontaneous regression of some (but not all) neovascular complexes.[42]

Another potential mechanism for sea fan development has been proposed.[101] Arteriolar occlusive events may create hydrostatic back-pressure, causing extrusion of the upstream segment of the blocked vessel into the preretinal space. The rise in intraluminal pressure may cause expansion of the extruded vessel, with resultant stretching of the pericytes and endothelial cells. This process may stimulate endothelial cells, leading to endothelial cell proliferation[111] and subsequent neovascularization.[101,112]

Sea fans typically possess at least one feeding arteriole and one draining venule and are most commonly found at the sites of arteriovenous anastomoses and arteriovenous crossings.[109,110] A network of these lesions with multiple anastomoses may develop with multiple feeding and draining vessels, and they may form tractional vitreous bands.

Stage IV

Vitreous hemorrhage represents Goldberg stage IV. Sea fans grow or are pulled into the vitreous chamber, and vitreous traction on the delicate neovascular fronds may cause bleeding into the vitreous.

Vitreous hemorrhage may be localized over the sea fan, and an individual may remain visually asymptomatic. However, dramatic, sudden loss of vision may occur as the hemorrhage disseminates into the vitreous. Vitreous hemorrhage occurs more commonly in HbSC than in HbSS.[71,93,98] The risk of recurrent vitreous hemorrhage also increases if an eye has more than 60° of circumferential retinal neovascularization, or if a patient initially presents with vitreous hemorrhage.[113] Chronic vitreous hemorrhage may give rise to fibroglial membranes and vitreous strands, which may produce traction and resultant retinal detachment.[48,58]

Stage V

Presence of tractional and/or rhegmatogenous retinal detachment (TRD) defines Goldberg stage V (Fig. 60.12). TRD develops as the result of chronic vitreous hemorrhage or chronic transudation from neovascular tissue and resultant vitreous membrane formation. Retinal breaks may also occur due to localized retinal atrophy and thinning from chronic vaso-occlusion and ischemia.[48] Traction may also induce retinal breaks. In contrast to the TRD commonly seen in proliferative diabetic retinopathy, the TRD in SCD most commonly involves the peripheral retina as opposed to the posterior pole. Alternative classification schemes for PSR have been proposed, but are not widely utilized.[114,115]

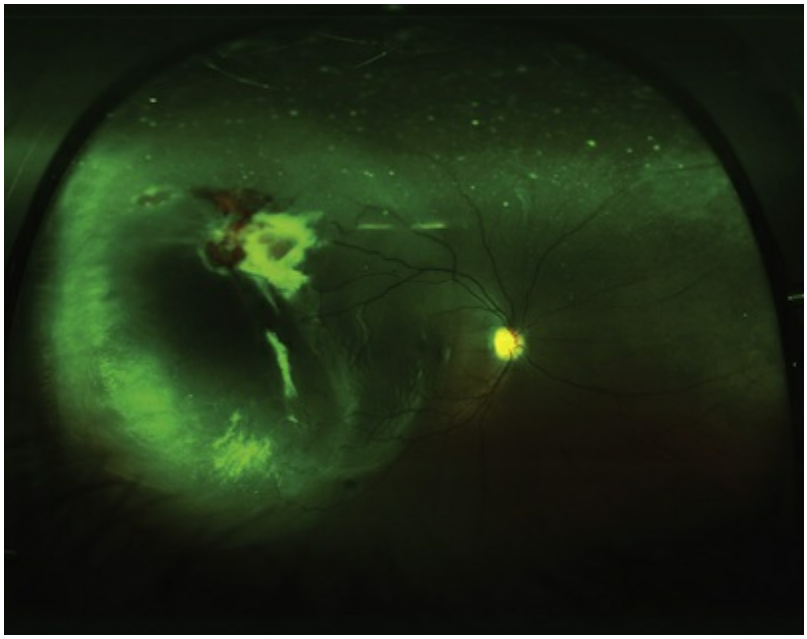

FIG. 60.12 A combined tractional-rhegmatogenous retinal detachment from sea fan neovascularization is demonstrated with bullous subretinal fluid throughout the macula in a patient with HbSC and PSR. (Reproduced with permission from Moshiri A, Ha NK, Ko FS, Scott AW. Bevacizumab presurgical treatment for proliferative sickle-cell retinopathy-related retinal detachment. Retin Cases Brief Rep 2013;7:204-5).

Incidence/Prevalence

The incidence of PSR is higher in those individuals with HbSC disease and S-β thalassemia than in individuals with HbSS disease. In one natural history study of SCD patients followed longitudinally over 20 years, prevalence of PSR was greater in those with HbSC disease, and by the ages of 24–26 years, PSR had occurred in 43% of subjects with HbSC disease and in only 14% of subjects with HbSS disease.[116]

Risk Factors

Fox and colleagues described risk factors that increase an individual's likelihood of developing PSR.[117] In the HbSS genotype, high total hemoglobin in males and a low Hb F in both males and females were associated with the development of PSR. In the HbSC

genotype, increased mean cell volume and low Hb F increased the risk in men and women. High total hemoglobin and high MCHC caused a higher PSR risk of PSR in men with the HbSC genotype.[7,117]

Natural History

Autoinfarction of the proliferative sickle lesions occurs frequently, and, as a result, spontaneous regression of PSR may occur in about 32% of eyes.[116] The mechanism of autoinfarction is not completely understood. This process may be due to chronic and repetitive vaso-occlusion within the vascular channels of the sea fan neovascular complexes. In a cohort of 120 patients with HbSS disease and 222 patients with HbSC disease followed for 10 years, loss of visual acuity occurred in 10% of untreated eyes.[118] Loss of vision most commonly resulted from PSR, specifically vitreous hemorrhage, TRD, and epiretinal membranes. Patients with nonproliferative disease had a lower incidence of loss of vision over the 10-year period than did their counterparts with PSR.[118]

Ophthalmic Treatments

No intervention is indicated for small, flat, asymptomatic peripheral lesions, given the relatively low risk of spontaneous hemorrhage and the relatively high probability of autoinfarction.[119,120a] Treatment may be required in cases of rapid growth of a sea fan, presence of large, elevated sea fans, spontaneous hemorrhage, or bilateral proliferative disease.[13] The goal of intervention in these cases is to prevent the progression of stage III PSR to stages IV or V.

Scatter laser photocoagulation is the current mainstay of treatment in PSR (Fig. 60.13). The objective of scatter laser treatment is similar to that traditionally employed in the management of proliferative diabetic retinopathy, in which ischemic retina is ablated by laser photocoagulation, thus decreasing the stimulus for secretion of pathologic growth factors. Laser photocoagulation of ischemic retina may also help to decrease the overall oxygen requirement of the retina. Through laser destruction of ischemic,

damaged peripheral retina, intravascular oxygen may be shunted to healthier, more viable retinal tissue. Hypoxia inducible factor 1 alpha and VEGF are strongly expressed eyes with PSR in areas of avascular retina, areas anterior to the boundary between perfused and non perfused retina, and in posterior ischemic retina.[120b]

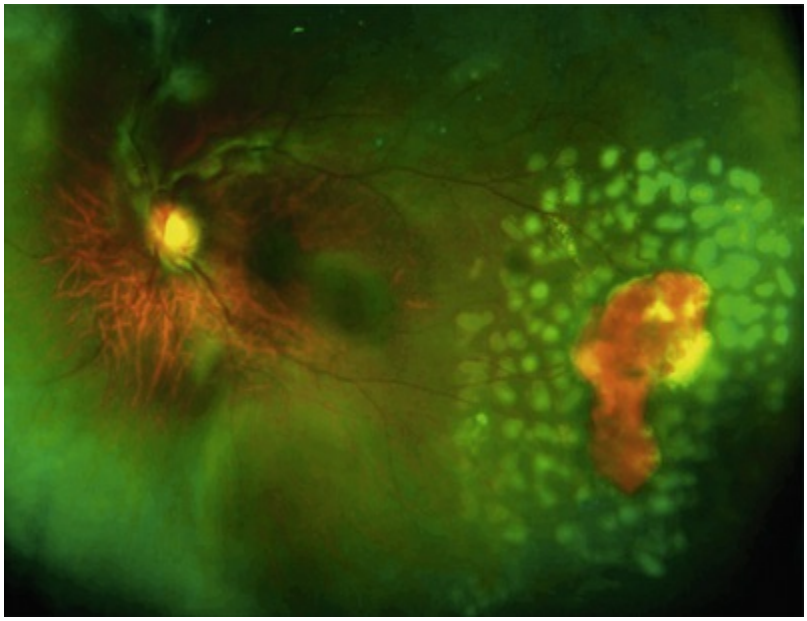

FIG. 60.13 A sea fan lesion with localized hemorrhage is depicted on ultrawide-field fundus photography immediately after scatter laser treatment in a patient with HbSC disease.

Anti-VEGF agents have been successful in the management of PSR. Intravitreal bevacizumab has been reported to cause complete regression of retinal neovascularization and resolution of vitreous hemorrhage in eyes with PSR.[121,122] One group noted complete regression of neovascularization and resolution of vitreous hemorrhage after a single intravitreal ranibizumab injection in a patient with PSR, with no recurrence after 9 months of follow-up.[123] Intravitreal bevacizumab has also been used as a preoperative surgical adjunct for retinal detachment associated with proliferative sickle-cell retinopathy. Moshiri and our group observed that administering preoperative intravitreal bevacizumab caused regression of sea fan neovascularization, facilitating surgical dissection and removal of retinal traction bands, and decreased intraoperative bleeding (Fig. 60.12).[124] Further study is warranted to

assess the role of anti-VEGF therapy in PSR.

Vitrectomy may be considered for nonclearing vitreous hemorrhage, and may be indicated to improve visualization of retinal pathology to facilitate treatment such as photocoagulation. A possible therapeutic approach is combining vitrectomy with scatter laser photocoagulation, with consideration of an anti-VEGF injection in an eye with active PSR.

Exchange transfusion, erythropheresis, and hyperbaric oxygen have been utilized in the past to minimize complications from surgically induced anterior-segment ischemia. These methods showed no clear benefit and were associated with systemic complications.[125] Vitrectomy in an eye with PSR can be reasonably safe with today's modern vitrectomy techniques without these extra measures. The vitreoretinal surgeon should take special care to maximize perfusion in the eye by avoiding elevations in intraocular pressure (IOP) throughout the procedure and thereafter. In routine vitrectomy surgery, intraoperative bleeding is often managed by the surgeon's temporarily raising IOP by elevating the height of the infusion bottle until hemostasis is achieved. Eyes with PSR may be particularly sensitive to ischemic insult from even transient IOP elevations. It follows that measures to reduce the likelihood of intraoperative hemorrhage during vitrectomy surgery, such as pretreatment with intravitreal anti-VEGF, should be considered. It is also critical that the surgeon coordinate with the anesthesiologist to ensure that the patient is well oxygenated throughout and after the procedure.

Given the propensity for peripheral retinal breaks and other peripheral vitreoretinal pathology to develop, scleral buckling may be considered in SCD to relieve traction from peripheral vasoproliferative lesions. Though anterior segment ischemia is a feared complication of scleral buckling in eyes with sickle-cell retinopathy, scleral buckles have safely been utilized in sickle-cell retinal detachment surgery.[126]

Williamson and colleagues reported their experience with management of vitreoretinal complications of sickle-cell retinopathy.[127] A high rate of iatrogenic retinal tears was noted while peeling membranes from the atrophic, ischemic peripheral retina using delamination (i.e., tangential peeling of preretinal

fibrous tissue from the retinal surface). Therefore, these authors recommended segmentation (removal of anterior–posterior traction) techniques instead of delamination.

Imaging

Selected imaging modalities facilitate diagnosis, monitoring, and assessment of responses to treatment in sickle-cell retinopathy. Indocyanine green angiography (ICGA) has been studied as a way to assess choroidal perfusion, but the utility of ICGA in sickle-cell retinopathy is unclear.[128] The use of ultrawide-field (UWF) imaging is helpful to detect and monitor peripheral lesions (Fig. 60.12). Wide field fundus photography and FA are best for detecting early retinal changes since the vaso-occlusions are in the far periphery, which many photographers can not visualize with standard cameras. FA remains the gold-standard imaging tool for assessment of retinal perfusion and neovascularization. A potential limitation of conventional FA is the difficulty in imaging the pathology of the far peripheral retina in some eyes with sickle retinopathy.[114] Accordingly, UWF imaging has become useful in the evaluation of the retinal periphery in such eyes. As previously mentioned, SD-OCT provides important details about foveal anatomy, which may aid in the diagnosis and management of sickle retinopathy,[81,83–87] even in asymptomatic patients.

A drawback of FA is that it is invasive and time-consuming, and lacks an ability to capture the peripapillary and deep capillary networks. OCT angiography (OCTA) is a nascent noninvasive imaging modality. Motion contrast is used to create detailed volumetric scans by which the retinal microvasculature is visualized. OCTA provides both structural and functional information regarding retinal blood flow.[129] Imaging studies have shown that patients with sickle-cell disease may suffer ischemia in the deep capillary networks, even with an apparently intact FAZ on FA (Figs. 60.14 and 60.15). Our group performed OCTA on consecutive patients with sickle-cell disease.[130] Five out of 10 eyes had retinal thinning identified on SD-OCT, each of which had corresponding loss of vascular density on OCTA. These OCTA images support the concept that nonperfusion of the deep capillary

plexus may be responsible for some of the areas of macular thinning seen on SD-OCT, as each patient with macular thinning had corresponding loss of vascular flow on OCTA that was more apparent in the deep plexus than in the superficial plexus.[130] OCTA may detect abnormalities present in the retinal microvasculature that may not be detected on FA (Fig. 60.14),[129] and though its utility is yet unclear, OCTA may, therefore, play a role in understanding retinal vascular pathology in patients with SCD.

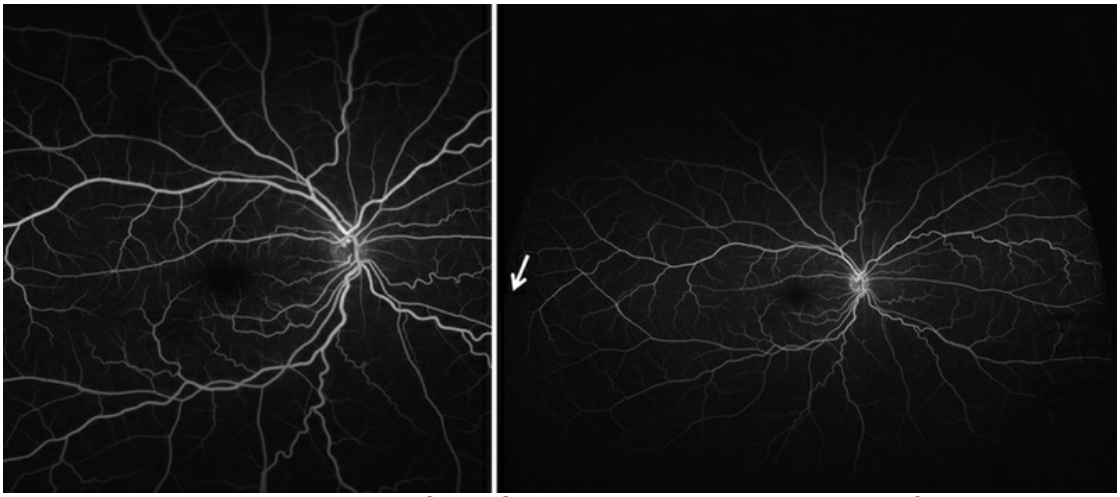

FIG. 60.14 Ultrawide-field fluorescein angiography of a patient with HbSS disease shows normal macular perfusion and very subtle peripheral nonperfusion in the temporal retinal periphery (*arrow*).

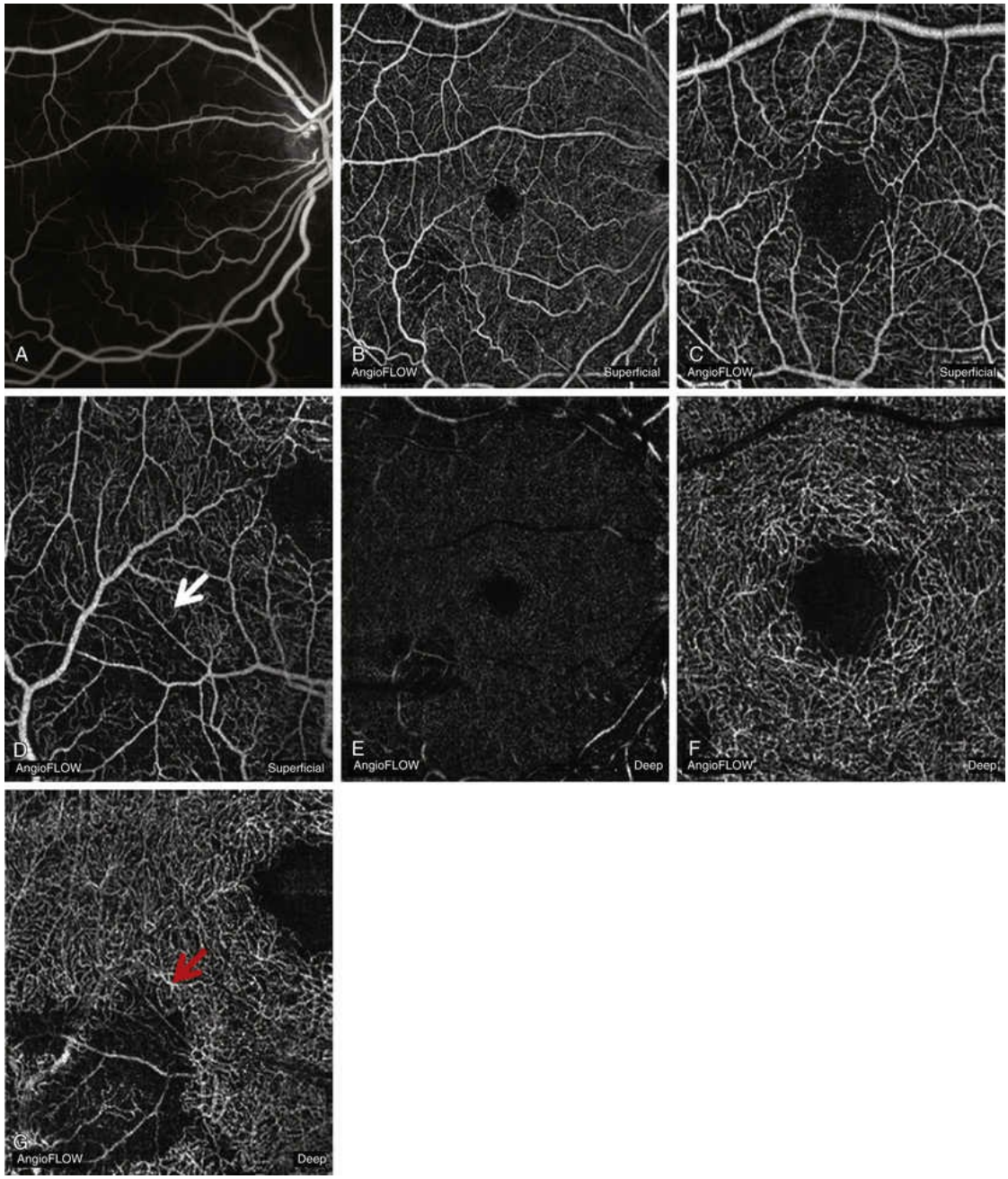

FIG. 60.15 Optical coherence tomography angiography (OCTA) of the same patient from Fig. 60.14. (A) Fluorescein angiography shows an intact foveal avascular zone and normal macular perfusion. (B–D) OCTA shows mild capillary dropout in the superficial capillary layer (*white arrow*). (E–G) OCTA shows significant capillary dropout in the deep capillary plexus (*red arrow*).

Health Maintenance and Retinopathy Screening

Large clinical trials providing guidelines for screening, monitoring, and management in order to minimize the complications of sickle-cell disease are limited. Expert consensus recommendations do exist for health maintenance,[131] including supportive management of painful sickle-cell crises (Table 60.2). Strong recommendations exist for referral of SCD patients to a retinal specialist beginning at about age 10 years for retinopathy screening, with reexamination in 1–2 years for those who have "normal" screening exams. However, although a "strong" recommendation is based on expert consensus, high-quality evidence-based data on which to base screening recommendations are lacking. Teleretinal screening has shown promise in diseases such as diabetic retinopathy and retinopathy of prematurity. Nonphysicians may acquire high-quality fundus images, which can then be transmitted to remote reading centers for interpretation by experts. Telemedicine may be a potential future strategy to determine which patients with SCD would benefit from referral for detailed ophthalmic examination.

TABLE 60.2

Evidence-Based Recommendations for Health Maintenance in Sickle-Cell Disease

Evidence-Based Health Maintenance Recommendations for SCD[a]	Strength of Recommendation	Quality of Evidence
PREVENTION OF INVASIVE PNEUMOCOCCAL INFECTION		
Administer oral penicillin prophylaxis (125 mg for those aged <3 yr and 250 mg for those aged ≥3 yr) twice daily until age 5 yr in all children with HBSS	Strong	Moderate
Discontinue prophylactic penicillin in children with HbSS at age 5 yr unless they have had a splenectomy or invasive pneumococcal infection; ensure completion of pneumococcal vaccination series before discontinuation	Moderate	Moderate
Ensure that persons of all ages with SCD have been vaccinated against *Streptococcus pneumoniae*	Strong	Moderate
IMMUNIZATIONS		
Children aged 6–18 yr with functional or anatomic asplenia should receive 1 dose of PCV13 (conjugate 130-valent vaccine)	Consensus	Adapted[b]
Adults aged ≥19 yr who have not received pneumococcal vaccine but have functional or anatomic asplenia and who have not previously received PCV13 or PPSV23 (23-valent polysaccharide		

vaccine) should receive 1 dose of PCV13 first, followed by a dose of PPSV23 at least 8 wk later, with subsequent doses of PPSV23 to follow current PPSV23 recommendations for adults at high risk		
A second PPSV23 dose is recommended 5 yr after the first PPSV23 dose for persons ages 19–64 with functional or anatomic asplenia		
In addition, those who received PPSV23 before age 65 yr for any indication should receive another dose of the vaccine at age 65 yr or later if at least 5 yr have elapsed since their previous PPSV23 dose		
Adults aged ≥19 yr with previous PPSV23 vaccination and functional or anatomic asplenia who received ≥1 doses of PPSV23 should be given a PCV13 dose ≥1 yr after the last PPSV23 dose		
For those who require additional doses of PPSV23, the first doses should be given no sooner than 8 wk after PCV13 dose and at least 5 yr after the most recent dose of PPSV23		
Screening for hepatitis C: screen for HCV infection in persons at higher risk for infection (e.g., those with multiple transfusions) and offer 1-time screening for HCV infection to all adults born between 1945 and 1965	Consensus	Adapted[c]
Electrocardiogram screening: do not screen asymptomatic children or adults with SCD with electrocardiograms	Weak	Low
SCREENING FOR RETINOPATHY		
Refer to an ophthalmologist for a dilated eye examination to evaluate for retinopathy beginning at age 10 yr	Strong	Low
For persons having a normal dilated retinal examination, rescreen at 1- to 2-yr intervals	Consensus	Panel expertise[d]
SCREENING FOR RISK OF STROKE USING NEUROIMAGING		
In children with SCA, screen annually (beginning at age 2 yr and continuing until at least age 16 yr) with transcranial Doppler, according to the methods used in the STOP studies	Strong	Moderate
In children with conditional (170–199 cm/s) or elevated (≥200 cm/s) transcranial Doppler results, refer to a specialist with expertise in long-term transfusion therapy aimed at preventing stroke	Strong	High
In children with genotypes other than SCA (e.g., HbSβ*-thalassemia or HbSC), do not perform screening with transcranial Doppler	Strong	Low
In asymptomatic children with SCD, do not perform screening with MRI or CT	Moderate	Low
In asymptomatic adults with SCD, do not perform screening with neuroimaging (transcranial Doppler, MRI, or CT)	Moderate	Very low
Screening for pulmonary disease: do not screen asymptomatic children and adults with pulmonary function tests	Moderate	Low
Contraception, reproductive counseling and opioid use during pregnancy	Consensus	Adapted[e]

[a]The order of the recommendations was chosen to reflect the frequency with which they will likely need to be implemented. For example, immunization recommendations apply to all individuals with SCD, whereas pulmonary function assessment or contraceptive information may be needed for only a portion of those with SCD.

[b]Consensus adapted from 2014 recommendations of Advisory Committee on

Immunization Practices (ACIP).

[c]Consensus-adapted recommendations from the US Preventative Services Task Force (USPSTF). Box 1 contains criteria for consensus-adapted recommendations.[131]

[d]Box 1 contains criteria for panel expertise consensus.[131]

[e]Consensus-adapted recommendations from the World Health Organization (WHO) and the US Centers for Disease Control and Prevention (CDC). Box 1 contains criteria for consensus-adapted recommendations.[131]

CT, computed tomography; HCV, hepatitis C virus; MRI, magnetic resonance imaging; SCA, sickle cell-anemia; SCD, sickle-cell disease; STOP, Stroke Prevention Trial in Sickle Cell Anemia.

Potential Therapeutic Options for the Future

SCD remains a devastating disease associated with multiorgan dysfunction and premature death. The only known curative therapy for sickle-cell disease is myeloablative conditioning and allo-stem cell therapy from HLA-matched sibling donors.[132] Treatment strategies that decrease Hb S and increase Hb F have been shown to decrease the systemic morbidity of SCD, in that higher Hb F may interfere with polymerization of Hb S. Agents to increase Hb F include hydroxyurea, omega-3 fatty acids, and erythropoietin. Hydroxyurea is the only approved oral medication for SCD.[133] The burden of Hb S cells may be reduced through transfusion or hemapheresis. Warfarin, heparin, and ticlopidine may also be utilized as adjunctive therapies in patients with SCD because these medicines work as antithrombotic agents. Additional future areas of investigation include hematopoietic stem cell transplantation, gene therapy, and autologous gene correction stem cell designs.[7,133,134]

References

1. Herrick JB. Peculiar elongated and sickle-shaped red blood

corpuscles in a case of severe anemia. *Arch Intern Med*. 1910;6:517–521.
2. Savitt TL. Tracking down the first recorded sickle cell patient in western medicine. *J Natl Med Assoc*. 2010;102:981–992.
3. Savitt TL, Goldberg MF. Herrick's 1910 case report of sickle cell anemia: the rest of the story. *JAMA*. 1989;261:266–271.
4. Pauling L, Itano HA, Singer SJ, et al. Sickle cell anemia, a molecular disease. *Science*. 1949;110:543–548.
5. Barabino GA, Platt NO, Kaul DK. Sickle cell biomechanics. *Annu Rev Biomed Eng*. 2010;12:345–367.
6. Ashley-Koch A, Yang Q, Olney RS. Sickle hemoglobin (HbS) allele and sickle cell disease: a HuGE review. *Am J Epidemiol*. 2000;151:839–845.
7. Elagouz M, Jyothi S, Gupta B, et al. Sickle cell disease and the eye: old and new concepts. *Surv Ophthalmol*. 2010;55:359–377.
8. Neumayr L, Pringle S, Giles S, et al. Chart card: feasibility of a tool for improving emergency department care in sickle cell disease. *J Natl Med Assoc*. 2010;102:1017–1023.
9. Rosenberg JB, Hutcheson K. Pediatric sickle retinopathy: correlation with clinical factors. *J AAPOS*. 2011;15:49–53.
10. National Heart, Lung and Blood Institute. *Who is at risk for sickle cell anemia?*. [Online; Available] http://www.nhlbi.nih.gov/health/dci/Diseases/Sca/SCA_Wh 2008.
11. World Health Organization. *Sickle-cell anaemia: report by the Secretariat*. http://apps.who.int/iris/handle/10665/20659; 2008.
12. Serjeant G. *Sickle cell disease*. Oxford University Press: Oxford; 1985.
13. Emerson GG, Harlan JB, Fekrat S, et al. Hemoglobinopathies. Ryan SJ. *Retina*. 4th ed. Elsevier: Edinburgh; 2006:1429–1445.
14. Gill FM, Sleeper LA, Weiner SJ, et al. Clinical events in the first decade in a cohort of infants with sickle cell disease: Cooperative Study of Sickle Cell Disease. *Blood*. 1995;86:776–783.

15. Bunn HF. Disorders of hemoglobin. Braunwald E, Isselbacher KJ, Petersdorf RG, et al. *Harrison's principles of internal medicine*. 11th ed. McGraw-Hill: New York; 1987:1518–1523.
16. Powara D, Hiti A. Sickle cell anemia: beta S gene cluster haplotypes as genetic markers for severe disease expression. *Am J Dis Child*. 1993;147:1197–1202.
17. Thomas PW, Higgs DR, Serjeant GR. Benign clinical course in homozygous sickle cell disease: a search for predictors. *J Clin Epidemiol*. 1997;50:121–126.
18. Ferrone FA. Polymerization and sickle cell disease: a molecular review. *Microcirculation*. 2004;11:115–128.
19. Bunn HF. Pathogenesis and treatment of sickle cell disease. *N Engl J Med*. 1997;337:762–769.
20. Mohandas N, Rossi ME, Clark MR. Association between morphologic distortion of sickle cells and deoxygenation-induced cation permeability increase. *Blood*. 1986;68:450–454.
21. Brugnara C, Bunn HF, Tosteson DC. Regulation of erythrocyte cation and water content in sickle cell anemia. *Science*. 1986;232:388–390.
22. Fabry ME, Kaul DK. Sickle cell vasocclusion. *Hematol Oncol Clin North Am*. 1991;5:375–398.
23. Hebbel RP. Adhesive interactions of sickle erythrocytes with endothelium. *J Clin Invest*. 1997;100:S83–6.
24. Sugihara K, Sugihara T, Mohandas N, et al. Thrombospondin mediates adherence of CD36+ sickle erythrocytes to endothelial cells. *Blood*. 1992;80:2634–2642.
25. Swerlick RA, Eckman JR, Kumar A, et al. Alpha 4 beta 1 expression on sickle reticulocytes; vascular cell adhesion molecule 1 dependent binding to the endothelium. *Blood*. 1993;82:1891–1899.
26. Wun T, Paglieroni T, Field CL, et al. Platelet-erythrocyte adhesion in sickle cell disease. *J Investig Med*. 1999;47:121–127.
27. Kaul DK, Fabry ME, Nagel RL. The pathophysiology of vascular obstruction in the sickle syndromes. *Blood Rev*. 1996;10:29–44.

28. Joneckis CC, Ackley RL, Orringer EP, et al. Integrin alpha 4 beta 1 and glycoprotein IV (CD36) are expressed on circulating reticulocytes in sickle cell anemia. *Blood*. 1993;82:3548–3555.
29. Setty BN, Stuart MJ. Vascular cell adhesion molecule 1 is involved in mediating hypoxia-induced sickle red blood cell adherence to endothelium; potential role in sickle cell disease. *Blood*. 1996;88:2311–2320.
30. Francis RB Jr, Haywood LJ. Elevated immunoreactive tumor necrosis factor and interleukin-1 in sickle cell disease. *J Natl Med Assoc*. 1992;84:611–615.
31. Malave I, Perdomo Y, Escalona E, et al. Levels of tumor necrosis factor α/cachectin (TNFα) in sera from patients with sickle cell disease. *Acta Haematol*. 1993;90:172–176.
32. Solovey A, Lin Y, Browne P, et al. Circulating activated endothelial cells in sickle cell anemia. *N Engl J Med*. 1997;337:1584–1590.
33. Kunz Mathews M, McLeod DS, Merges C, et al. Neutrophils and leukocyte adhesion molecules in sickle cell retinopathy. *Br J Ophthalmol*. 2002;86:684–690.
34. Lutty GA, Otsuji T, Taomoto M, et al. Mechanisms for sickle red blood cell retention in choroid. *Curr Eye Res*. 2002;25:163–171.
35. Lutty GA, Phelan A, McLeod DS, et al. A rat model for sickle-cell mediated vaso-occlusion in retina. *Microvasc Res*. 1996;52:270–280.
36. Lutty GA, Taomoto M, Cao J, et al. Inhibition of TNF-alpha-induced sickle RBC retention in retina with a VLA-4 antagonist. *Invest Ophthalmol Vis Sci*. 2001;42:1349–1355.
37. Lutty GA, Goldberg MF. Ophthalmological complications. Embury SH, Hebbel RP, Mohandas N, et al. *Sickle cell disease: basic principles and clinical practice*. Raven Press: New York; 1992:703–724.
38. Vichinsky E. New therapies in sickle cell disease. *Lancet*. 2002;360:629–631.
39. Wood KC, Hsu LL, Gladwin MT. Sickle cell disease vasculopathy; a state of nitric oxide resistance. *Free Radic Biol Med*. 2008;44:1506–1528.

40. Gurkan E, Tanriverdi K, Baslamish F. Clinical relevance of vascular endothelial growth factor levels in sickle cell disease. *Ann Hematol*. 2005;84:71–75.
41. Cao J, Kunz Mathews MK, McLeod DS, et al. Angiogenic factors in human proliferative sickle cell retinopathy. *Br J Ophthalmol*. 1999;83:838–846.
42. Kim DY, Mocanu V, McLeod DS, et al. Expression of pigment epithelium-derived factor (PEDF) and vascular endothelial growth factor (VEGF) in sickle cell retina and choroid. *Exp Eye Res*. 2003;7:433–445.
43. Lu M, Perez VL, Ma N. VEGF increases retinal vascular ICAM-1 expression in vivo. *Invest Ophthalmol Vis Sci*. 1999;40:1808–1812.
44. Perlman N, Selvaraj SK, Batra S, et al. Placenta growth factor activates monocytes and correlates with sickle cell disease severity. *Blood*. 2003;102:1506–1514.
45. Oh H, Takagi H, Suzuma K, et al. Hypoxia and vascular endothelial growth factor selectively upregulate angiopoietin-2 in bovine microvascular endothelial cells. *J Biol Chem*. 1999;274:15732–15739.
46. Fadugbagbe AO, Gurgel RQ, Mendonca CQ, et al. Ocular manifestations of sickle cell disease. *Ann Trop Paediatr*. 2010;30:19–26.
47. Ballas SK, Lewis CN, Noone AM, et al. Clinical, hematological, and biochemical features of Hb SC disease. *Am J Hematol*. 1982;13:37–51.
48. Goldberg MF. Retinal neovascularization in sickle cell retinopathy. *Trans Am Acad Ophthalmol Otolaryngol*. 1977;83:Op409–31.
49. Gagliano DA, Jampol L, Rabb M. Sickle cell disease. Lippincott Raven: Philadelphia; 1996:1–40. Tasman WS, Jaeger E. *Duane's clinical ophthalmology*. vol. 3.
50. Rees DC, Thein SL, Oseil A, et al. The clinical significance of K-Cl cotransport activity in red cells of patients with HbSC disease. *Haematologica*. 2015;100:595–600.
51. Ganesh A, William RR, Mitra S, et al. Orbital involvement in sickle cell disease: a report of 5 cases and review of literature. *Eye (Lond)*. 2001;15:774–780.

52. Perlman JI, Forman S, Gonzalez ER. Retrobulbar ischemic optic neuropathy associated with sickle cell disease. *J Neuroophthalmol*. 1994;14:45–48.
53. Adewoye AH, Ramsey J, McMahon L, et al. Lacrimal gland enlargement in sickle cell disease. *Am J Hematol*. 2006;81:888–889.
54. Condon PI, Sergeant GR. Ocular findings in elderly cases of homozygous sickle cell disease in Jamaica. *Br J Ophthalmol*. 1976;60:361–364.
55. Paton D. The conjunctival sign of sickle cell disease. *Arch Ophthalmol*. 1961;66:90–94.
56. Fink AI, Funahashi T, Robinson M, et al. Conjunctival blood flow in sickle cell disease: preliminary report. *Arch Ophthalmol*. 1961;66:824–829.
57. Paton D. The conjunctival sign of sickle-cell disease. Further observations. *Arch Ophthalmol*. 1962;68:627–632.
58. Nagpal KC, Goldberg MF, Rabb MF. Ocular manifestations of sickle hemoglobinopathies. *Surv Ophthalmol*. 1977;21:391–411.
59. Funahashi T, Fink A, Robinson M, et al. Pathology of conjunctival vessels in sickle-cell disease: a preliminary report. *Am J Ophthalmol*. 1964;57:713–718.
60. Chambers J, Puglisi J, Kernitsky R, et al. Iris atrophy in hemoglobin SC disease. *Am J Ophthalmol*. 1974;77:247–249.
61. Galinos S, Rabb MF, Goldberg MF, et al. Hemoglobin SC disease and iris atrophy. *Am J Ophthalmol*. 1973;75:421–425.
62. Bergren RL, Brown GC. Neovascular glaucoma secondary to sickle cell retinopathy. *Am J Ophthalmol*. 1992;113:718–719.
63. Goldberg MF. The diagnosis and treatment of secondary glaucoma after hyphema in sickle cell patients. *Am J Ophthalmol*. 1979;87:43–49.
64. Goldberg MF. Sickled erythrocytes, hyphema, and secondary glaucoma IV. The rate and percentage of sickling of erythrocytes in rabbit aqueous humor, in vitro and in vivo. *Ophthalmic Surg*. 1979;10:62–69.
65. Goldberg MF. Sickled erythrocytes, hyphema, and secondary glaucoma I. The diagnosis and treatment of sickled erythrocytes in human hyphemas. *Ophthalmic Surg*.

1979;10:17–31.
66. Goldberg MF, Dizon R, Raichand M. Sickled erythrocytes, hyphema, and secondary glaucoma II. Injected sickle cell erythrocytes into human, monkey, and guinea pig anterior chambers: the introduction of sickling and secondary glaucoma. *Ophthalmic Surg*. 1979;10:32–51.
67. Deutsch TA, Weinreb RN, Goldberg MF. Indications for surgical management of hyphema in patients with sickle cell trait. *Arch Ophthalmol*. 1984;102:566–569.
68. Karaman K, Culic S, Erceg I, et al. Treatment of post-traumatic trabecular meshwork thrombosis and secondary glaucoma with intracameral tissue plasminogen activator in previously unrecognized sickle cell anemia. *Coll Antropol*. 2005;29(Suppl. 1):123–126.
69. Henry MD, Chapman AZ. Vitreous hemorrhage and retinopathy associated with sickle cell disease. *Am J Ophthalmol*. 1954;38:204–209.
70. Hannon JF. Vitreous hemorrhages associated with sickle cell-hemoglobin C disease. *Am J Ophthalmol*. 1956;42:707–712.
71. Condon PI, Serjeant GR. Ocular findings in homozygous sickle cell anemia in Jamaica. *Am J Ophthalmol*. 1972;73:533–543.
72. Condon PI, Serjeant GR. Ocular findings in hemoglobin SC disease in Jamaica. *Am J Ophthalmol*. 1972;74:921–931.
73. Condon PI, Serjeant GR. Ocular findings in sickle cell thalassemia in Jamaica. *Am J Ophthalmol*. 1972;74:1105–1109.
74. Nagpal KC, Goldberg MF, Asdourian G, et al. Dark-without-pressure fundus lesions. *Br J Ophthalmol*. 1975;59:476–479.
75. Fawzi AA, Nielsen JS, Mateo-Montoya A, et al. Multimodal imaging of white and dark without pressure fundus lesions. *Retina*. 2014;34:2376–2387.
76. Goldberg MF. Retinal vaso-occlusion in sickling hemoglobinopathies. *Birth Defects Orig Artic Ser*. 1976;12:475–515.
77. Condon PI, Serjeant GR. Behaviour of untreated proliferative sickle retinopathy. *Br J Ophthalmol*. 1980;64:404–411.

78. Kimmel AS, Magargal LE, Tasman WS. Proliferative sickle retinopathy and neovascularization at the disc: regression following treatment with peripheral scatter laser photocoagulation. *Ophthalmic Surg*. 1986;17:20–22.
79. Ober RR, Michels RG. Optic disk neovascularization in hemoglobin SC disease. *Am J Ophthalmol*. 1978;85:711–714.
80. Raichand M, Goldberg MF, Nagpal KC, et al. Evolution of neovascularization in sickle cell retinopathy: a prospective fluorescein angiographic study. *Trans Am Ophthalmol Soc*. 1992;90:481–504.
81. Goldbaum MH. Retinal depression sign indicating a small retinal infarct. *Am J Ophthalmol*. 1978;86:45–55.
82. Sanders RJ, Brown GC, Rosenstein RB, et al. Foveal avascular zone diameter and sickle cell disease. *Arch Ophthalmol*. 1991;109:812–815.
83. Witkin AJ, Rogers AH, Ko TH, et al. Optical coherence tomography demonstration of macular infarction in sickle cell retinopathy. *Arch Ophthalmol*. 2006;124:746–747.
84. Hoang QV, Chau FY, Shahidi M, et al. Central macular splaying and outer retinal thinning in asymptomatic sickle cell patients by spectral-domain optical coherence tomography. *Am J Ophthalmol*. 2011;151:990–994.
85. Chen X, Rahimi E, Sergott R, et al. Spectrum of retinal vascular diseases associated with paracentral acute middle maculopathy. *Am J Ophthalmol*. 2015;160:26–34e.1.
86. Ilginis T, Keane PA, Tufail A. Paracentral acute middle maculopathy in sickle cell disease. *JAMA Ophthalmol*. 2015;133:614–616.
87. Murthy RK, Grover S, Chalam K. Temporal macular thinning on spectral-domain optical coherence tomography in proliferative sickle cell retinopathy. *Arch Ophthalmol*. 2011;129:247–249.
88. Mathew R, Bafiq R, Ramu J, et al. Spectral domain optical coherence tomography in patients with sickle cell disease. *Br J Ophthalmol*. 2015;99:967–972.
89. Raichand M, Dizon RV, Nagpal KC, et al. Macular holes associated with proliferative sickle cell retinopathy. *Arch Ophthalmol*. 1987;96:1592–1596.

90. Moriarty BJ, Acheson RW, Serjeant GR. Epiretinal membranes in sickle cell disease. *Br J Ophthalmol*. 1987;71:466–469.
91. Schubert HD. Schisis in sickle cell retinopathy. *Arch Ophthalmol*. 2005;123:1607–1609.
92. Frank RN, Cronin MA. Posterior pole neovascularization in a patient with hemoglobin SC disease. *Am J Ophthalmol*. 1979;88:680–682.
93. Clarkson JG. The ocular manifestations of sickle cell disease: a prevalence and natural history study. *Trans Am Ophthalmol Soc*. 1992;90:481–504.
94. Clarkson JG, Altman RD. Angioid streaks. *Surv Ophthalmol*. 1982;26:235–246.
95. Condon PI, Serjeant GR. Ocular findings in elderly cases of homozygous sickle cell disease in Jamaica. *Br J Ophthalmol*. 1976;60:361–364.
96. Aessopos A, Farmakis D, Loukopoulos D. Elastic tissue abnormalities resembling pseudoxanthoma elasticum in beta thalassemia and the sickling syndromes. *Blood*. 2002;99:30–35.
97. Jampol LM, Acheson R, Eagle RC, et al. Calcification of Bruch's membrane in angioid streaks with homozygous sickle cell disease. *Arch Ophthalmol*. 1987;105:93–98.
98. Welch RB, Goldberg MF. Sickle-cell hemoglobin and its relation to fundus abnormality. *Arch Ophthalmol*. 1966;75:353–362.
99. Fine LC, Petrovic V, Irvine AR, et al. Spontaneous central retinal artery occlusion in hemoglobin SC disease. *Am J Ophthalmol*. 2000;130:680–681.
100. Lutty GA, Merges C, Crone S, et al. Immunohistochemical insights into sickle cell retinopathy. *Curr Eye Res*. 1994;13:125–138.
101. McLeod DS, Goldberg MF, Lutty GA. Dual-perspective analysis of vascular formations in sickle cell retinopathy. *Arch Ophthalmol*. 1993;111:1234–1245.
102. Liang JC, Jampol LM. Spontaneous peripheral chorioretinal neovascularization in association with sickle cell anemia. *Br J Ophthalmol*. 1983;67:107–110.

103. Condon PI, Jampol LM, Ford SM, et al. Choroidal neovascularization induced by photocoagulation in sickle cell disease. *Br J Ophthalmol*. 1981;65:192–197.
104. Romayananda N, Goldberg MF, Green WR. Histopathology of sickle cell retinopathy. *Trans Am Acad Ophthalmol Otolaryngol*. 1973;77:652–676.
105. Gagliano DA, Goldberg MF. The evolution of salmon-patch hemorrhages in sickle cell retinopathy. *Arch Ophthalmol*. 1989;107:1814–1815.
106. Serjeant GR, Serjeant BE. The eyes. Serjeant GR, Serjeant BE. *Sickle cell disease*. 3rd ed. Oxford University Press: Oxford; 2001:366–392.
107. Emerson GG, Lutty GA. Effects of sickle cell disease on the eye: clinical features and treatment. *Hematol Oncol Clin North Am*. 2005;19:957–963.
108. Lutty GA, McLeod DS, Pachinis A, et al. Retinal and choroidal neovascularization in a transgenic mouse model of sickle cell disease. *Am J Pathol*. 1994;145:490–497.
109. McLeod DS, Merges C, Fukushima A, et al. Histopathologic features of neovascularization in sickle cell retinopathy. *Am J Ophthalmol*. 1997;124:455–472.
110. Goldberg MF. Natural history of untreated proliferative sickle retinopathy. *Arch Ophthalmol*. 1971;85:428–437.
111. Curtis AS, Seehar GM. The control of cell division by tension or diffusion. *Nature*. 1978;274:52–53.
112. van Meurs JC. Evolution of a retinal hemorrhage in a patient with sickle-cell hemoglobin C disease. *Arch Ophthalmol*. 1995;113:1074–1075.
113. Condon PI, Whitelocke RA, Bird AC, et al. Recurrent visual loss in homozygous sickle cell disease. *Br J Ophthalmol*. 1985;69:700–706.
114. Penman AD, Talbot JF, Chuang EL, et al. New classification of peripheral retinal vascular changes in sickle cell disease. *Br J Ophthalmol*. 1994;78:681–689.
115. Sayag D, Binaghi M, Souied EH, et al. Retinal photocoagulation for proliferative sickle cell retinopathy: a prospective clinical trial with new sea fan classification. *Eur J Ophthalmol*. 2008;18:248–254.

116. Downes SM, Hambleton IR, Chuang EL, et al. Incidence and natural history of proliferative sickle cell retinopathy: observations from a cohort study. *Ophthalmology*. 2005;112:1869–1875.
117. Fox PD, Dunn DT, Morris JS, et al. Risk factors for proliferative sickle retinopathy. *Br J Ophthalmol*. 1990;74:172–176.
118. Moriarty BJ, Acheson RW, Condon PI, et al. Patterns of visual loss in untreated sickle cell retinopathy. *Eye (Lond)*. 1988;2:330–335.
119. Condon P, Jampol LM, Farber MD, et al. A randomized clinical trial of feeder vessel photocoagulation of proliferative sickle cell retinopathy. II. Update and analysis of risk factors. *Ophthalmology*. 1984;91:1496–1498.
120a. Rednam KR, Jampol LM, Goldberg MF. Scatter retinal photocoagulation for proliferative sickle cell retinopathy. *Am J Ophthalmol*. 1982;93:594–599.
120b. Rodrigues M, Kashiwabuchi F, Deshpande M, et al. Expression pattern of H1 alpha supports circumferential application of scatter laser for proliferative sickle retinopathy. *IOVS*. 2016;57:6739–6746.
121. Shaikh S. Intravitreal bevacizumab (Avastin) for the treatment of proliferative sickle retinopathy. *Indian J Ophthalmol*. 2008;56:259.
122. Siquiera RC, Costa RA, Scott IU, et al. Intravitreal bevacizumab (Avastin) injection associated with regression of retinal neovascularization caused by sickle cell retinopathy. *Acta Ophthalmol Scand*. 2006;84:834–835.
123. Mitropoulos PG, Chatziralli IP, Parikakis EA, et al. Intravitreal ranibizumab for stage IV proliferative sickle cell retinopathy: a first case report. *Case Rep Ophthalmol Med*. 2014; 10.1155/2014/682583 [published online; Nov 23].
124. Moshiri A, Ha NK, Ko FS, et al. Bevacizumab presurgical treatment for proliferative sickle-cell retinopathy-related retinal detachment. *Retin Cases Brief Rep*. 2013;7:204–205.
125. Bove JR. Transfusion-transmitted diseases: current problems and challenges. *Prog Hematol*. 1986;14:123–147.
126. Pulido JS, Flynn HW, Clarkson JG, et al. Pars plana

vitrectomy in the management of the complications of proliferative sickle retinopathy. *Arch Ophthalmol*. 1988;106:1553–1557.
127. Williamson TH, Rajput R, Laidlaw DAH, et al. Vitreoretinal management of the complications of sickle cell retinopathy by observation or pars plana vitrectomy. *Eye (Lond)*. 2009;23:1314–1320.
128. Diallo JW, Kuhn D, Hayman-Gawrilow P, et al. Contribution of indocyanine green angiography in sickle cell retinopathy. *J Fr Ophtalmol*. 2009;32:430–435.
129. de Carlo TE, Romano A, Waheed NK, Duker JS. A review of optical coherence tomography angiography (OCTA). *Int J Retina Vitreous*. 2015;1:1–15.
130. Han I, Tadarati M, Scott AW. Macular vascular abnormalities identified by optical coherence tomography angiography in patients with sickle cell disease. *JAMA Ophthalmol*. 2015;133(11):1337–1340.
131. Yawn BP, Buchanan GR, Afenyi-Annan AN, et al. Management of sickle cell disease: summary of the 2014 evidence-based report by expert panel members. *JAMA*. 2014;312:1033–1048.
132. Freed J, Talano J, Small T, et al. Allogeneic cellular and autologous stem cell therapy for sickle cell disease: 'whom, when and how'. *Bone Marrow Transplant*. 2011;47:1489–1498.
133. Green NS, Barral S. Emerging science of hydroxyurea therapy for pediatric sickle cell disease. *Pediatr Res*. 2014;75:196–204.
134. Ribeil J, Hacein-Bey-Abina S, Paye E, et al. Gene therapy in a patient with sickle cell disease. *N Engl J Med*. 2017;376(9):848–855.

61

Radiation Retinopathy

Leigh Spielberg, Patrick De Potter, Anita Leys

Introduction

Radiation retinopathy (RR) is a slowly progressive, delayed-onset occlusive microangiopathy of the retinal vasculature that occurs with variable latency after exposure of the retina to ionizing radiation. First described by Stallard in 1933,[1] the term encompasses all retinal vascular changes, including ischemic and proliferative RR (PRR) and radiation maculopathy. It is a potentially devastating sequela of exposure of the eye to any source of radiation, including local plaque radiation treatment (brachytherapy), external-beam radiation treatment (ERBT), proton beam radiation, helium ion radiotherapy, and gamma knife radiotherapy of the eye, ocular adnexa, orbit, and head and neck structures.[2–6] Radiotherapy offers an alternative to enucleation for patients with retinoblastoma, choroidal melanoma, and ocular metastases,[7–9] as well as life-saving treatment of orbital, sinus, and intracranial tumors. Since the Collaborative Ocular Melanoma Study showed similar survival rates after radiotherapy and enucleation, the shift towards globe-salvaging therapeutic strategies has increased the use of radiation and consequently increased its complications, with reports of the incidence of RR ranging from 3% to over 20%.[10,11] The current interest in use of radiation in the treatment of neovascular age-related macular degeneration (AMD) might further increase the risk of this complication.[12–15]

The risk of RR is related to characteristics of the radiation treatment itself, the presence of systemic disease, and exposure to radiation sensitizers such as chemotherapy. Fundoscopic findings can be highly variable, ranging from scattered retinal hemorrhages, microaneurysms, and cotton-wool spots to macular edema, large-vessel occlusion, extensive ischemic retinopathy and maculopathy, and consequent retinal and ocular neovascularization. Within the retina, the posterior pole is particularly sensitive to this pathology,[16] with grave implications for visual prognosis. Indeed, macular edema involving the fovea is a major source of visual morbidity in patients with radiation retinopathy. Further, RR has a long latency and may not be clinically detectable for 8 years or more.[17]

Although RR has a variable course, it is frequently fulminant, with a tendency for the vasculopathy to progressively decrease

vision by affecting the macular microvasculature. Further, the structural damage is often irreversible, particularly in cases with macular nonperfusion and ischemia.

Etiology, Pathogenesis, and Histopathology

RR can be described as a progressive obliterative arteritis that initiates a characteristic pattern of degenerative and proliferative vascular changes and microvascular dysfunction. The therapeutic, tumoricidal effects of radiotherapy are generated both directly, via injury to the DNA of rapidly dividing cells, and indirectly, via the production of free radicals. However, these processes damage not only the tumor itself but also the vascular and interstitial support structures of healthy tissue. This induces an acute transudative as well as a slowly progressive occlusive vasculopathy.[18] The initial pathologic change, and the fundamental abnormality, is retinal vascular endothelial cell injury and loss[18–21] and associated inflammation,[22] which occur primarily in capillaries, followed by capillary closure, clearly visible with fluorescein angiography (FA),[17,23–25] leading to retinal ischemia, nerve tissue necrosis, and fibrovascular proliferation.[16,21,24,26,27]

The loss of capillary cellularity leads to the development of microaneurysms, and hemodynamic alterations produce fenestrated telangiectatic retinal vessels. Larger retinal vessels become involved later in the course of the retinopathy; diameter reduction of major retinal arteries and veins of up to 75% has been demonstrated in animal models.[22] Closure of blood vessels is the single most characteristic finding on FA, although other abnormalities, such as retinal angiomatous proliferation, have been described.[28] Ghost vessels are later visible ophthalmoscopically. Both central retinal artery occlusion[29] and interruption of the choroidal circulation[30,31] have been described as a consequence of high-dose irradiation. Choriocapillary hypoperfusion is detectable several months after treatment,[31] leading to choroidopathy and chorioretinal atrophy. The widespread vascular occlusion induces the production of vascular endothelial growth factor (VEGF),[21]

leading to neovascularization and increased vascular permeability, both of which result in vascular leakage and tissue edema.[32] Uveal effusion can also be present.[33]

The disappearance of choriocapillaris, retinal pigment epithelium (RPE), photoreceptors, and retinal nerve fibers, along with leukocyte invasion, has been demonstrated histologically.[34] Areas devoid of photoreceptor cells correspond with areas of pigment dispersion with reduced numbers of melanocytes. There is a thickening of arteriolar and capillary walls and endothelial cell loss. In contrast to diabetic retinopathy, in which pericytes are initially affected, RR exhibits an early loss of endothelial cells. However, pericytes can be affected in severely damaged capillaries.

Optical coherence tomography (OCT) demonstrates significant thinning of the inner plexiform, inner nuclear, and outer plexiform layers, suggesting that primary radiation-induced damage is initially confined to the inner layers of the retina.[35] However, secondary functional changes may occur in the outer retina.[36]

Natural History and Clinical Features

RR displays clinical and angiographic features that are virtually identical to those seen in diabetic retinopathy.[37] This is unsurprising, as both radiation and diabetes primarily damage the retinal capillaries. Ophthalmoscopically, microaneurysms are the first to appear. They are near-universally present[38] and are closely followed by intraretinal hemorrhages, macular capillary dilation and nonperfusion, and nerve fiber layer infarcts (cotton-wool spots; Figs. 61.1 and 61.2).[17] Retinal edema, hard exudates, telangiectasia, and perivascular sheathing may follow in variable sequence and latency. Hard exudates have been found to be more prevalent after brachytherapy (Fig. 61.3), whereas retinal hemorrhages and microaneurysms are more commonly found after EBRT.[16] The telangiectatic-like vessels are a feature of established retinopathy and are likely to represent collateral vasculature at the edges of capillary occlusion.[17] Confluent areas of capillary closure lead to the development of large areas of retinal capillary nonperfusion.

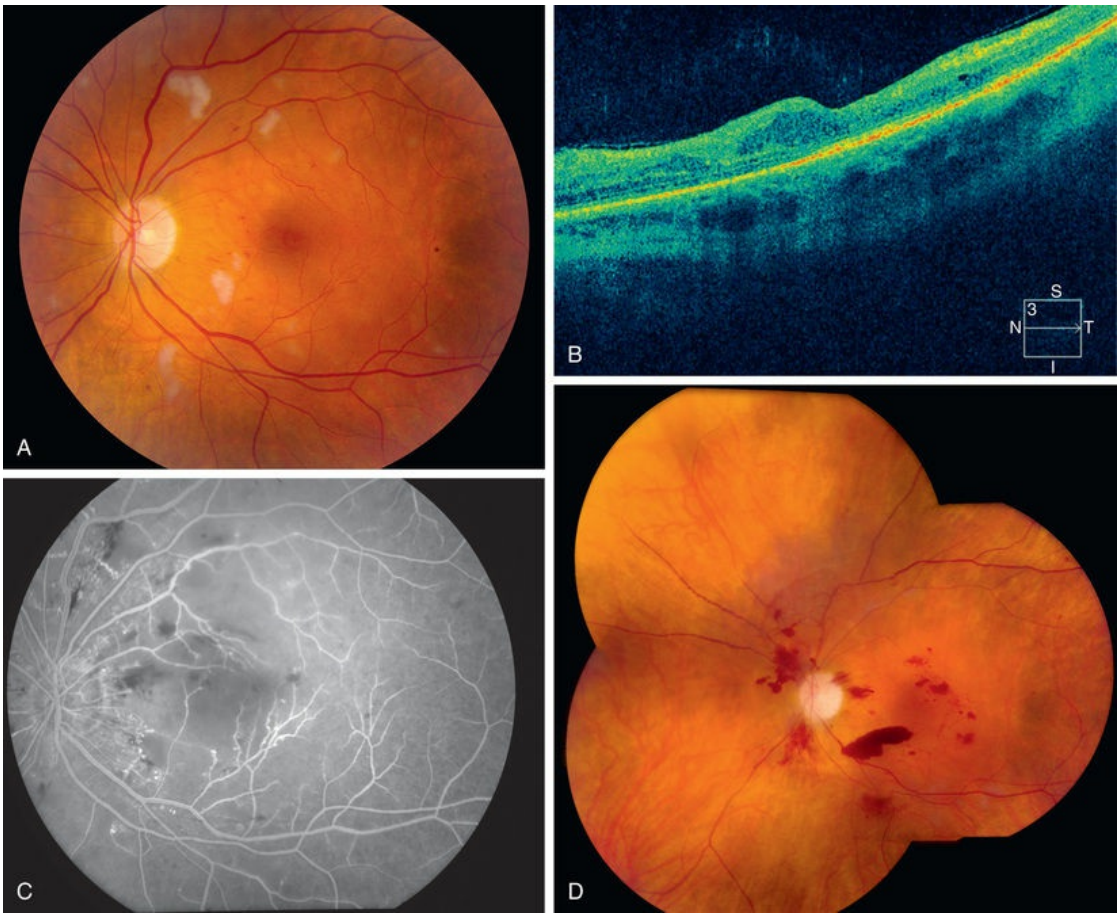

FIG. 61.1 A 32-year-old woman was treated with four cycles of rituximab and fractionated external-beam radiation therapy (20×2 Gy) for a non-Hodgkin lymphoma of the left maxillary sinus. Swelling of lids, ptosis, conjunctival redness, and dry-eye symptoms were the first ocular complications. Shortly thereafter, loss of visual acuity was noted due to radiation retinopathy and optic neuropathy with numerous cotton-wool spots, retinal hemorrhages, and pallor of the optic disc (A). Macular edema (B) as well as progressive capillary nonperfusion (C) were noted subsequently. A single intravitreal steroid injection was administered. Two years after radiotherapy, and 15 months after diagnosis of the radiation retinopathy, subhyaloidal and vitreous hemorrhages due to optic disc neovascularization and widespread retinal nonperfusion (D) were observed. Neither rubeosis iridis nor increased intraocular pressure was observed. However, final visual acuity was reduced to counting fingers.

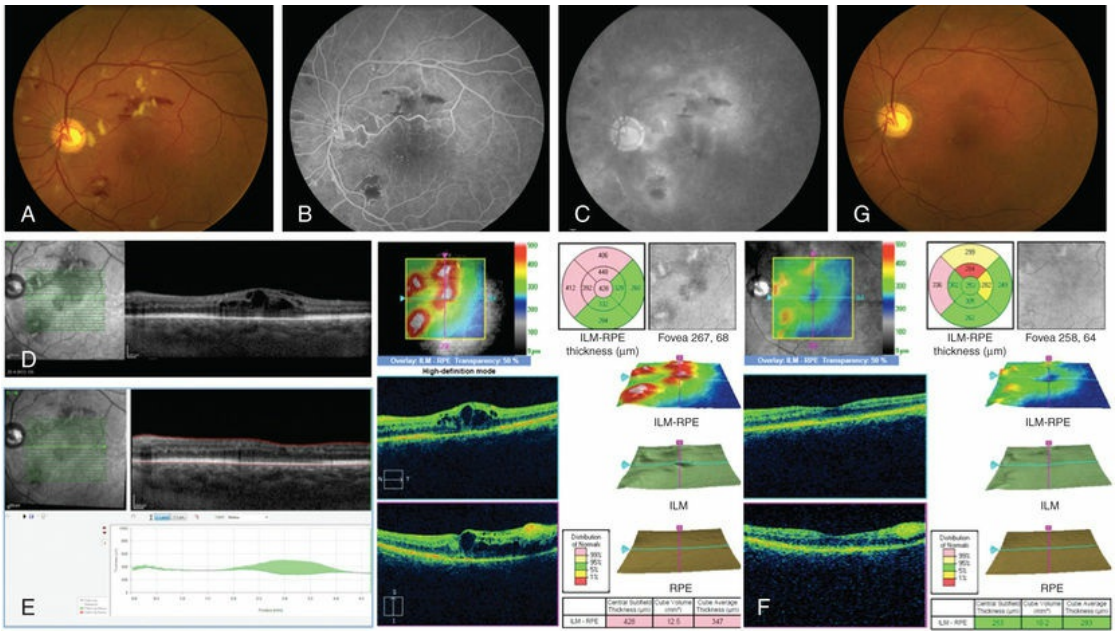

FIG. 61.2 A 63-year-old male noticed visual loss in his left eye 3 years after resection and subsequent radiotherapy (60 Gray in 2-Gray fractions) of a temporal anterior meningioma. At presentation, visual acuity was 20/40. Radiation retinopathy was diagnosed, with macular edema and numerous cotton-wool spots and hemorrhages in the posterior pole (A). Fluorescein angiography demonstrated capillary dropout (B) and leakage (C). Optical coherence tomography (OCT) showed marked cystoid edema (D). Four days after intravitreal bevacizumab injection, the edema had resolved, as demonstrated on Spectralis (E) and Cirrus (F) OCT. The radiation retinopathy remained mild during the 27 months follow-up, and visual acuity was 20/32 at last visit (G).

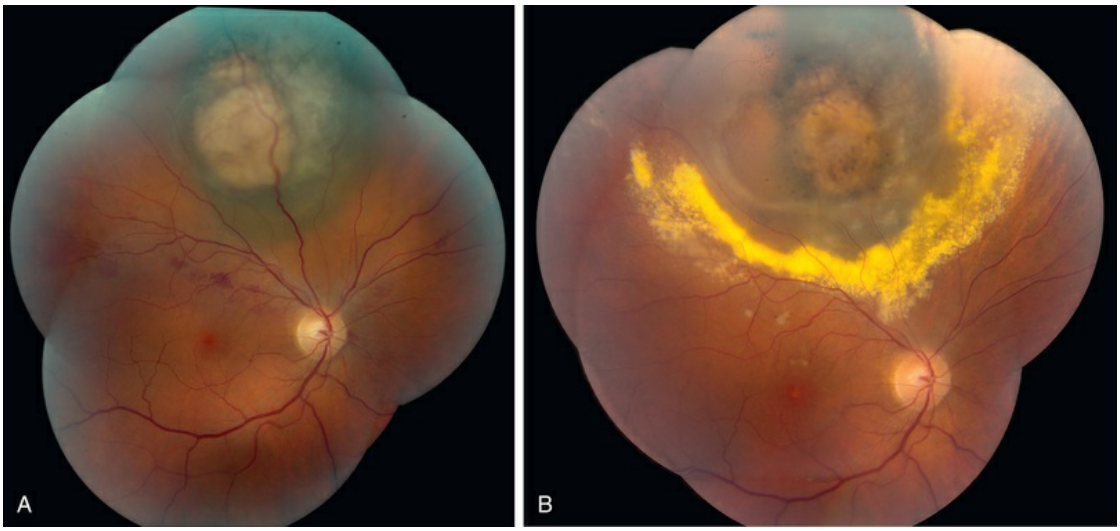

FIG. 61.3 (A) Large mushroom-shaped choroidal melanoma before I^{125} plaque radiotherapy. (B) Radiation retinopathy is documented 14 months after treatment with supramacular cotton-wool spots, exudative retinal detachment, and hard exudates threatening the macula.

The fluorescein angiographic hallmarks of the condition are the presence of severe retinal capillary nonperfusion, capillary dilation, and microaneurysms, frequently combined with macular edema or ischemia.[16] Central macular chorioretinal anastomosis has also been described.[39] Neovascularization may develop later (Fig. 61.1), and does so in approximately 32% of eyes with RR.[40] This development is referred to as proliferative radiation retinopathy (PRR), and its presence is ominous. Analogous to proliferative diabetic retinopathy, it suggests profound ischemia and carries a worse prognosis for long-term visual acuity. If left untreated, it can lead to neovascular glaucoma, vitreous hemorrhage, and traction retinal detachment caused by fibrovascular proliferation similar to that seen in diabetic retinopathy. However, in contrast to diabetic retinopathy and other retinal vasculopathies, neovascularization does not typically extend through the internal limiting membrane into the vitreous.[21] Nevertheless, vitreous hemorrhage can occur, and its presence is associated with a poor prognosis for both vision and globe salvage, as well as for ghost cell or neovascular glaucoma. It also impedes the clinician's ability to monitor the retinopathy and to employ laser photocoagulation to treat progression (Table 61.1).

TABLE 61.1

Findings in 87 Eyes With Radiation Retinopathy

Complication	Incidence
Macular ischemia	76%
Clinically significant macular edema	76%
Nonproliferative radiation retinopathy	68%
Radiation optic neuropathy	55%
Cataract	52%
Proliferative radiation retinopathy	32%
Vitreous hemorrhage	24%
Glaucoma	12%
Radiation keratopathy	10%
Traction retinal detachment	5%

Adapted from Kinyoun JL. Long-term visual acuity results of treated and untreated radiation retinopathy (an AOS thesis). Trans Am Ophthalmol Soc 2008;106:325–35.

Classification

There is currently no standard method of classification for RR, although several methods have been developed. These can be categorized as clinical/ophthalmoscopic; fluorescein angiographic; or OCT-based. Finger and Kurli proposed a four-stage, prognosis-related classification that uses ophthalmoscopic and fluorescein angiographic findings to classify macular and extramacular changes.[41] In this system, Stage 1 includes extramacular ischemic changes; Stage 2 includes macular ischemic changes; Stage 3 indicates (extra)macula ischemic changes and the presence of macular edema and retinal neovascularization; and Stage 4 encompasses vitreous hemorrhage and at least 5 disc areas of retinal ischemia, whether macular or extramacular.

FA allows the clinician to determine the condition of the macula, allowing maculopathy to be subdivided into ischemic and nonischemic variants, which is of significant prognostic importance. FA also allows for the classification of macular edema, which is useful if grid or focal laser photocoagulation is to be administered. The Early Treatment Diabetic Retinopathy Study (ETDRS) definition of clinically significant macular edema has been applied to macular edema associated with radiation damage. In these cases, it is referred to as clinically significant radiation macular edema,

which follows the ETDRS definitions: retinal thickening within 500 mm of the fovea; edema-associated hard exudates within 500 mm of the fovea; and one or more zones of retinal thickening ≥1 disc area, any part of which is within 1 disc diameter of the fovea.[42]

As in the management of diabetic retinopathy, OCT is indispensable. Macular edema is visible on OCT approximately 5 months earlier than clinically detectable radiation maculopathy.[43] Horgan et al. proposed a five-point OCT-based grading scale based on standard reference OCT images: Grade 1 is extrafoveolar, noncystoid edema; Grade 2 is extrafoveolar cystoid edema; Grade 3 is foveolar noncystoid edema; Grade 4 is mild-to-moderate foveolar cystoid edema; and Grade 5 is severe foveolar cystoid edema.[43] This study demonstrated OCT evidence of macular edema as early as 4 months after plaque radiotherapy for uveal melanoma, with a peak incidence at 12–18 months, and that it is associated with significant vision loss.

The introduction of OCT-angiography (OCT-A) has allowed visualization of vascular changes prior to their detection on OCT. A recent study suggests that OCT-A can benefit diagnosis and follow-up of patients with RR, allowing earlier detection and more precise management.[44]

The classification of RR into proliferative (PRR) and nonproliferative (NPRR) subtypes is also of great prognostic importance. A retrospective study using Kaplan–Meier analysis reported a PRR rate of 5.8% at 5 years and 7% at 10 and 15 years in 3841 eyes treated with plaque radiotherapy for uveal melanoma.[45]

Risk Factors

Risk factors for the development of RR can be divided into internal (inherent/patient) and external (iatrogenic) factors. The primary patient factor is concomitant vascular disease such as diabetes mellitus.[46] Since both diabetes and radiation primarily damage the retinal capillaries, this synergistic effect is to be expected, as the capillaries experience an early loss of pericytes due to diabetes and endothelial cell loss due to radiation. Destruction of these two cell types leaves little cellular structural support for capillaries and thus results in capillary closure, aneurysms, vessel leakage, and

hemorrhage. Concomitant diabetes mellitus is also a poor prognostic indicator for visual acuity, increasing the risk of visual loss by nearly 300%.[47] This is in part due to the association of diabetes mellitus with an increased incidence and severity of neovascular complications, including neovascular glaucoma[48] and radiation papillopathy[49] following radiotherapy.[50] Other vascular disorders predisposing to RR are arterial hypertension and coronary artery disease.[51] Tumor characteristics likely to lead to a worse prognosis include large tumors and close proximity to the macula and optic disc.[52] Multivariate analysis of a large retrospective study indicates three primary risk factors for proliferative RR after plaque radiotherapy for uveal melanoma: young age, diabetes mellitus, and shorter tumor distance to the optic disc.[53]

Chemotherapy, whether or not concurrent/concomitant with the radiation therapy, also increases the risk of RR,[16,54] as may pregnancy.[55] Chemotherapy increases the vulnerability of the retinal vasculature to radiation damage, possibly via an increase in oxygen-derived free radicals.[26] It also increases the risk of PRR, which carries a worse prognosis than NPRR.[56] The concomitant administration of chemotherapy increases the risk of visual complications,[16,26,54,57–59] potentiates the development of RR at lower radiation doses,[16] and may shorten the latent period between exposure and retinopathy.[54,58,60]

Incidence and Dosimetry

The most important external or iatrogenic risk factors relate to the radiation itself. These are radiation type, treatment modality (external beam vs. brachytherapy or plaque), total radiation dose and the fractionation schedule of that dosage, the total elapsed time in the course of irradiation treatment, and errors in treatment technique and/or dosage calculations.[59,61,62]

Radiation Type

If a large enough dose is applied, any type of radiation can result in retinopathy and its associated complications. RR is found in 87% of

patients after plaque radiotherapy for juxtapapillary melanomas, and radiation maculopathy in 89% after proton beam irradiation. However, neither of these radiation types is as highly associated with severe sight-limiting complications (such as rubeosis and neovascular glaucoma) as gamma knife treatment, which may lead to complete loss of vision in nearly 50%.[5]

Treatment Modality

An important factor to be considered is the surveillance of patients whose eyes are exposed to EBRT. In contrast to patients treated with retinal plaques for choroidal melanoma, who are periodically evaluated by retinal specialists and ocular oncologists, patients treated with EBRT are less likely to be regularly evaluated with dilated ophthalmoscopic examinations several years after treatment. Considering the progressive pathophysiology and latency of RR, early posttreatment checkups might be insufficient, and subsequent delays in ophthalmic diagnosis and treatment can result in long-term macular edema leading to ischemia, fibrosis, and irreversible vision loss.

Total Radiation Dose

The association between dose and RR is well established.[29] However, a precise threshold has been difficult to determine. The condition does not usually occur at total doses <45 Gy unless an additional risk factor such as diabetes is present.[62,63] In a study of 68 eyes that underwent EBRT for primary extracranial head and neck tumors, the dose–response curve for retinopathy was characterized by a dramatic increase in incidence between 45 and 55 Gy.[63] Nearly all patients receiving higher doses developed retinopathy. A more recent retrospective review suggests that the incidence can be significantly reduced by hyperfractionated (twice-daily doses of 1.1–1.2 Gy) EBRT.[62] However, above 70 Gy, the overall incidence of retinopathy approaches 40%.

Fractionation Schedule

During EBRT, increased fraction size correlates with an increased

incidence of retinal complications.[16,26,59,64,65] A dose per fraction below 1.9 Gy/fraction has been shown to decrease the incidence of retinopathy.[63] This is referred to as hyperfractionation, which theoretically allows the retina enough time to repair single-strand DNA breaks before a second nearby insult can occur.[62] This reduces late toxicity to the retina. However, for brachytherapy, which is primarily used for the treatment of choroidal melanoma, fractionation is not possible, since the radiation is delivered continuously at a predetermined dose for a certain period of time.

Volume of Retina Irradiated

The volume of retina irradiated has also been shown to be a significant predictor of retinopathy. Eyes receiving more than 50 Gy to greater than 60% of the retina have been shown to be more likely to develop RR.[29]

Total Elapsed Time

The latency between radiotherapy and the onset of clinically significant retinopathy can range from 1 month to 15 years, but it most commonly occurs between 6 months and 3 years. High-dose, single-fraction treatment regimens are associated with a more rapid onset.[66]

Differential Diagnosis and Diagnostic Evaluation

RR can occur many years after radiation therapy. Because of this potential delay, RR may not be recognized as the cause of visual loss. Further, due to the ophthalmoscopic and angiographic similarities, RR may be misdiagnosed as diabetic or hypertensive retinopathy. However, a dilated ophthalmic examination combined with a careful history, including questioning of the patient and a thorough review of the treatment records to determine whether the eyes were included in the field of radiation, will usually lead to the diagnosis. The diagnosis should be considered following cephalic radiation for any reason, including treatment for orbital

inflammatory disease such as thyroid disease[67] and orbital pseudotumor,[68] sinus malignancies, and periocular cutaneous lesions. Two features of RR that distinguish it from diabetic retinopathy is the atrophy of the RPE sometimes seen after radiation treatment and the possibility of unilateral disease.

Bone marrow transplant retinopathy can mimic RR, and it can be very difficult to distinguish the two unless affected patients have a history of exposure to one (e.g., radiation) and not the other (e.g., bone marrow transplantation).[69] Other potential causes of the observed retinal abnormalities include multiple branch retinal artery occlusions, multiple retinal venous occlusive episodes, or retinal telangiectasia from other causes. Severe anemia, leukemia, and human immunodeficiency virus (HIV)/acquired immunodeficiency syndrome (AIDS) must be excluded before the diagnosis of RR can be definitively made.

Although the diagnosis can usually be made clinically, further evaluation should be considered. Fluorescein and indocyanine green angiography can be useful to define the extent of retinal ischemia and vascular anomalies.[70,71] If macular pathology is suspected, OCT should be carried out to determine the degree of macular edema, since macular thickness on OCT correlates with visual acuity for up to 2 years after plaque treatment.[43]

Prevention and Treatment

There is no widely accepted treatment protocol for RR. Treatment has until now been based on its clinical, histopathologic, and angiographic similarities with diabetic retinopathy and retinal vein occlusion, diseases for which large randomized controlled studies have already been successfully conducted.[24,72,73]

Retinal laser photocoagulation of the ischemic retina has been shown to be beneficial in the prevention of retinal and iris neovascularization.[74,75] The rationale is that the destruction of oxygen-consuming photoreceptor cells and RPE decreases the intraocular VEGF concentrations, thereby inhibiting active retinal neovascularization.[76] However, the visual acuity results of laser treatment have been disappointing. Attempts to improve visual acuity results following plaque brachytherapy have included

prophylactic treatment with sector laser photocoagulation and/or sub-Tenon triamcinolone injection and/or repeated intravitreal anti-VEGF injections.[77,78] In other conditions with established RR, anti-VEGF injection is currently the gold standard treatment of the macular edema and ischemic complications.

Finger et al. reported the use of laser photocoagulation to obliterate the ischemic zone caused by ophthalmic plaque brachytherapy.[41] They observed regression of early-stage RR in 64% of treated eyes and found that only 18.75% of the "high-risk" patients who were treated prophylactically with sector scatter laser later developed RR. Laser photocoagulation has also been used for the treatment of macular edema secondary to RR. Although macular ischemia is currently not treatable, the frequently associated macular edema may respond to photocoagulation. Hykin et al. reported a visual acuity improvement of at least one line on the Snellen chart in 42% of affected eyes at 6 months, although the difference between treated patients and controls was not significant at 12 and 24 months.[79]

Corticosteroids have both angiostatic and vascular antipermeability properties that have been harnessed in the treatment of neovascular AMD, diabetic retinopathy, and macular edema due to various conditions.[80] Intravitreal triamcinolone has been reported to be of both visual and anatomic benefit in the treatment of both radiation maculopathy[81,82] and optic neuropathy.[83] However, when compared with intravitreal injection, periocular triamcinolone is associated with lower rates of steroid-induced glaucoma,[84] cataracts, retinal detachment, and endophthalmitis.[85–87] More recently, the beneficial effects of intravitreal dexamethasone 0.7-mg implants have been demonstrated.[88–90]

During the past several years, the focus has shifted to anti-VEGF agents for the treatment of intraocular neovascularization and vascular permeability. Finger et al. first reported the efficacy of intravitreal bevacizumab therapy for the treatment of radiation maculopathy and optic neuropathy.[91] This led to the regression of retinal edema, hemorrhages, exudates, and neovascularization after ophthalmic plaque radiation therapy. Since this early report, many reports have been published, suggesting the crucial role of intravitreal injection of both bevacizumab[92] and ranibizumab,[93] in

the treatment of radiation maculopathy[94] and optic neuropathy[95] due to plaque brachytherapy[96] and EBRT.[97] High-dose (2.0 mg) ranibizumab has also been successfully used in patients who were failing standard dose (0.5 mg) anti-VEGF therapy.[98] Anti-VEGF agents have also been used to treat the secondary complications of RR, namely neovascular glaucoma and exudative retinal detachment.[99] Whether it is most effective to administer anti-VEGF agents prophylactically or only upon development of pathology has not yet been conclusively determined. However, a small study by Gupta et al. suggested that patients with shorter duration of macular edema benefited more than those with long-standing retinal disease.[94] Further, the optimal administration schedule has not yet been determined.

Of course, prevention would be ideal. Reduced risk of human error in dosage calculations, improved shielding techniques, and increased surveillance of patients at risk for developing RR are desirable goals. Further, patients should be thoroughly informed of the possible consequences of radiation therapy, particularly in cases in which the treatment is being administered for nonlethal pathology such as Graves orbitopathy.

Prognosis

The visual prognosis is largely dependent on the extent and location of capillary nonperfusion[100] as well as the presence of neovascularization. If the perifoveal capillary net is involved, the prognosis for central vision is grave, due to either retinal atrophy or persistent macular edema, as well as from neovascularization, which occurs at the interface of perfused and nonperfused retina, as well as on the optic nerve head. PRR, present in approximately one-third of eyes with RR, is likely to carry an inferior long-term visual prognosis (mean visual acuity 20/440) than the nonproliferative type (mean visual acuity 20/100), although this retrospective study had a very different follow-up duration for PRR (109 months) and NPRR (27 months).[101] The same study reported macular edema to be more common in PRR (85.7%) than in NPRR (71.2%). Shields et al. found predictors of poor visual acuity at long-term follow-up following plaque radiotherapy included patient age ≥60 years,

tumor base ≥10 mm, tumor thickness >8 mm, radiation dose to the tumor base of ≥33, 300 cGy, and increasing radiation dose to the optic disc.[102] Tumor location is also of great importance, with tumors located posterior to the equator at increased risk for radiation maculopathy and loss of central vision.[103]

Conclusion

There are two quite distinct situations that should be considered by ophthalmologists treating patients at risk for RR. In the first situation, patients will have been treated with plaque brachytherapy. They may develop capillary nonperfusion in the retinal sector containing the plaque, as well as exudative lesions that can threaten the macula. Patients must thus be followed up closely and potentially treated prophylactically with sector laser if indicated. In these cases, the patients will likely be closely followed and the developing RR will be identified and managed shortly thereafter.

The second situation involves patients who will have been treated by nonophthalmologists for extraocular tumors with techniques besides brachytherapy. These patients are at great risk for remaining undiagnosed or diagnosed late because they are less likely to have been followed as closely as patients treated for intraocular disease. A nonophthalmologist is likely to take action only when the patient complains of visual loss, which often means that the retinopathy has progressed to an advanced stage. Moreover, many patients will only develop retinopathy years after the radiation therapy, long after they have been discharged from the care of the physician who administered the radiation. Indeed, an ophthalmologist may not be consulted until vision loss has been detected by patients.

The ophthalmologist must consider this diagnosis when confronted with a patient with retinovascular disease with cotton-wool spots, microaneurysms, exudative changes, and capillary dropout that looks like more common conditions, particularly diabetic retinopathy, but with a medical history that includes radiation therapy which may have damaged the posterior segment of the eye.

References

1. Stallard HB. Radiant energy as (a) a pathogenic and (b) a therapeutic agent in ophthalmic disorders. *Br J Ophthalmol*. 1933;6:1–126 [Suppl].
2. Finger PT, Chin KJ, Duvall G, Palladium-103 for Choroidal Melanoma Study Group. Palladium-103 ophthalmic plaque radiation therapy for choroidal melanoma: 400 treated patients. *Ophthalmology*. 2009;116:790–796.
3. Krema H, Somani S, Sahgal A, et al. Stereotactic radiotherapy for treatment of juxtapapillary choroidal melanoma: 3-year follow-up. *Br J Ophthalmol*. 2009;93:1172–1176.
4. Gragoudas ES, Seddon JM, Egan K, et al. Long-term results of proton beam irradiated uveal melanomas. *Ophthalmology*. 1987;94:349–353.
5. Haas A, Pinter O, Papaefthymiou G, et al. Incidence of radiation retinopathy after high-dosage single-fraction gamma knife radiosurgery for choroidal melanoma. *Ophthalmology*. 2002;109:909–913.
6. Levy RP, Fabrikant JI, Frankel KA, et al. Heavy-charged-particle radiosurgery of the pituitary gland: clinical results of 840 patients. *Stereotact Funct Neurosurg*. 1991;57:22–35.
7. Finger PT, Chin KJ, Duvall G. Palladium-103 ophthalmic plaque radiation therapy for choroidal melanoma: 400 treated patients. *Ophthalmology*. 2009;116:790–796.
8. Finger PT. Radiation therapy for orbital tumors: concepts, current use, and ophthalmic radiation side effects. *Surv Ophthalmol*. 2009;54:545–568.
9. Finger PT, Pro MJ, Schneider S, et al. Visual recovery after radiation therapy for bilateral subfoveal acute myelogenous leukemia (AML). *Am J Ophthalmol*. 2004;138:659–662.
10. Shields CL, Naseripour M, Cater J, et al. Plaque radiotherapy for large posterior uveal melanomas (> or = 8 mm thick) in 354 consecutive patients. *Ophthalmology*. 2002;109:1838–1849.
11. Gunduz K, Shields CL, Shields JA, et al. Radiation retinopathy following plaque radiotherapy for posterior

uveal melanoma. *Arch Ophthalmol*. 1999;117:609–614.
12. Evans JR, Sivagnanavel V, Chong V. Radiotherapy for neovascular age-related macular degeneration. *Cochrane Database Syst Rev*. 2010;(5) [CD004004].
13. Petrarca R, Dugel PU, Bennett M, et al. Macular epiretinal brachytherapy in treated age-related macular degeneration (MERITAGE): month 24 safety and efficacy results. *Retina*. 2014;34(5):874–879.
14. Morales-Canton V, Quiroz-Mercado H, Velez-Montoya R, et al. 16 and 24 Gy low-voltage X-ray irradiation with ranibizumab therapy for neovascular age-related macular degeneration: 12-month outcomes. *Am J Ophthalmol*. 2013;155(6):1000–1008.
15. Dugel PU, Bebchuk JD, Nau J, CABERNET Study Group, et al. Epimacular brachytherapy for neovascular age-related macular degeneration: a randomized, controlled trial (CABERNET). *Ophthalmology*. 2013;120(2):317–327.
16. Brown GC, Shields JA, Sanborn G, et al. Radiation retinopathy. *Ophthalmology*. 1982;89:1494–1501.
17. Amoaku WM, Archer DB. Cephalic radiation and retinal vasculopathy. *Eye (Lond)*. 1990;4:195–203.
18. Archer DB, Amoaku WMK, Gardinar TA. Radiation retinopathy: clinical, histopathological, ultrastructural and experimental correlations. *Eye (Lond)*. 1991;5:239–251.
19. Irvine AR, Alvarado JA, Wara WM, et al. Radiation retinopathy: an experimental model for the ischemic-proliferative retinopathies. *Trans Am Ophthalmol Soc*. 1981;79:103–122.
20. Egbert PR, Fajarado LF, Donaldson SS, et al. Posterior ocular abnormalities after irradiation for retinoblastoma: a histopathological study. *Br J Ophthalmol*. 1980;64:660–665.
21. Irvine RA, Wood IS. Radiation retinopathy as an experimental model for ischemic proliferative retinopathy and rubeosis iridis. *Am J Ophthalmol*. 1987;103:790–797.
22. Hiroshiba N, Ogura Y, Sasai K, et al. Radiation-induced leukocyte entrapment in the rat retinal microcirculation. *Invest Ophthalmol Vis Sci*. 1999;40:1217–1222.
23. Hayreh SS. Post-radiation retinopathy: a fluorescence

fundus angiographic study. *Br J Ophthalmol*. 1970;54:705–714.
24. Kinyoun JL, Chittum ME, Wells CG. Photocoagulation treatment of radiation retinopathy. *Am J Ophthalmol*. 1988;105:470–478.
25. Archer DB, Amoaku WM, Gardiner TA. Radiation retinopathy – clinical, histopathological, ultrastructural and experimental correlations. *Eye (Lond)*. 1991;5:239–251.
26. Wara WM, Irvine AR, Neger RE, et al. Radiation retinopathy. *Int J Radiat Oncol Biol Phys*. 1979;5:81–83.
27. Irvine AR, Alvarado JA, Wara WM, et al. Radiation retinopathy: an experimental model for the ischemic-proliferative retinopathies. *Trans Am Ophthalmol Soc*. 1981;79:103–122.
28. De Salvo G, Hannan SR, James N, et al. Retinal angiomatous proliferation occurring after radiotherapy. *Eye (Lond)*. 2013;27(3):447–449.
29. Takeda A, Shigematsu N, Suzuki S, et al. Late retinal complications of radiation therapy for nasal and paranasal malignancies: relationship between irradiated-dose area and severity. *Int J Radiat Oncol Biol Phys*. 1999;44:599–605.
30. Archer DB, Gardiner TA. Ionizing radiation and the retina. *Curr Opin Ophthalmol*. 1994;5:59–65.
31. Midena E, Segato T, Valenti M, et al. The effect of external eye irradiation on choroidal circulation. *Ophthalmology*. 1996;103:1651–1660.
32. Ferrara N. Vascular endothelial growth factor: basic science and clinical progress. *Endocr Rev*. 2004;25:581–611.
33. Finger PT. Radiation retinopathy is treatable with anti-vascular endothelial growth factor bevacizumab (Avastin). *Int J Radiat Oncol Biol Phys*. 2008;70:974–977.
34. Krebs IP, Krebs W, Merriam JC, et al. Radiation retinopathy: electron microscopy of retina and optic nerve. *Histol Histopathol*. 1992;7:101–110.
35. Raman R, Pal SS, Krishnan T, et al. High-resolution optical coherence tomography correlates in ischemic radiation retinopathy. *Cutan Ocul Toxicol*. 2010;29:57–61.
36. Levitz LM. The use of optical coherence tomography to

determine the severity of radiation retinopathy. *Ophthalmic Surg Lasers Imaging*. 2005;36:410–411.
37. Gass J. *Stereoscopic atlas of macular diseases, diagnosis and treatment*. 3rd ed. Mosby: St. Louis; 1987:404–405.
38. Li M, Qiu G, Luo W, et al. Clinical investigation of radiation retinopathy fundus and fluorescein angiographic features. *Yan Ke Xue Bao*. 1999;15:183–186.
39. Berker N, Aslan O, Batman C, et al. Choroidal neovascular membrane in radiation retinopathy. *Clin Experiment Ophthalmol*. 2006;34:625–626.
40. Kinyoun JL. Long-term visual acuity results of treated and untreated radiation retinopathy (an AOS thesis). *Trans Am Ophthalmol Soc*. 2008;106:325–335.
41. Finger PT, Kurli M. Laser photocoagulation for radiation retinopathy after ophthalmic plaque radiation therapy. *Br J Ophthalmol*. 2005;89:730–738.
42. Early Treatment of Diabetic Retinopathy Study Group. Photocoagulation for macular edema. Early Treatment Diabetic Retinopathy Study Report Number 1. *Arch Ophthalmol*. 1985;103:1796–1806.
43. Horgan N, Shields CL, Mashayekhi A, et al. Early macular morphological changes following plaque radiotherapy for uveal melanoma. *Retina*. 2008;28:263–273.
44. Veverka KK, AbouChehade JE, Iezzi R Jr, et al. Noninvasive grading of radiation retinopathy: the use of optical coherence tomography angiography. *Retina*. 2015;35(11):2400–2410.
45. Bianciotto C, Shields CL, Pirondini C, et al. Proliferative radiation retinopathy after plaque radiotherapy for uveal melanoma. *Ophthalmology*. 2010;117:1005–1012.
46. Viebahn M, Barricks ME, Osterloh MD. Synergism between diabetic and radiation retinopathy: case report and review. *Br J Ophthalmol*. 1991;75:629–632.
47. Packer S, Rotman M. Radiotherapy of choroidal melanoma with iodine 125. *Int Ophthalmol Clin*. 1980;20:135–142.
48. Conway R, Poothullil A, Daftari I, et al. Estimates of ocular and visual retention following treatment of extra-large uveal melanomas by proton beam radiotherapy. *Arch*

Ophthalmol. 2006;124:839–843.
49. Rudoler SB, Corn BW, Shields CL, et al. External beam irradiation for choroid metastases: identification of factors predisposing to long-term sequelae. *Int J Radiat Oncol Biol Phys*. 1997;38:251–256.
50. Gunduz K, Shields CL, Shields JA, et al. Plaque radiotherapy of uveal melanoma with predominant ciliary body involvement. *Arch Ophthalmol*. 1999;117:170–177.
51. Wakelkamp IM, Tan H, Saeed P, et al. Orbital irradiation for Graves' ophthalmopathy: is it safe? A long-term follow-up study. *Ophthalmology*. 2004;111:1557–1562.
52. Stack R, Elder M, Abdelaal A, et al. New Zealand experience of I^{125} brachytherapy for choroidal melanoma. *Clin Experiment Ophthalmol*. 2005;33:490–494.
53. Bianciotto C, Shields CL, Pirondini C, et al. Proliferative radiation retinopathy after plaque radiotherapy for uveal melanoma. *Ophthalmology*. 2010;117:1005–1012.
54. Chan RC, Shukovsky LJ. Effects of irradiation on the eye. *Radiology*. 1976;120:673–675.
55. Kumar B, Palimar P. Accelerated radiation retinopathy in diabetes and pregnancy. *Eye (Lond)*. 2004;14:107–108.
56. Kinyoun JL, Lawrence BS, Barlow WE. Proliferative radiation retinopathy. *Arch Ophthalmol*. 1996;114:1097–1100.
57. Bagan SM, Hollenhorst RW. Radiation retinopathy after irradiation of intracranial lesions. *Am J Ophthalmol*. 1979;88:694–697.
58. Lopez PF, Steinberg P, Dabbs CK, et al. Bone marrow transplant retinopathy. *Am J Ophthalmol*. 1991;112:635–646.
59. Chacko DC. Considerations in the diagnosis of radiation injury. *JAMA*. 1981;245:1255–1258.
60. Bagan SM, Hollenhorst RW. Radiation retinopathy after irradiation of intracranial lesions. *Am J Ophthalmol*. 1979;88:694–697.
61. Dunavoelgyi R, Georg D, Zehetmayer M, et al. Dose-response of critical structures in the posterior eye segment to hypofractioned stereotactic photon radiotherapy of choroidal melanoma. *Radiother Oncol*. 2013;108(2):348–353.
62. Monroe AT, Bhandare N, Morris CG, et al. Preventing

radiation retinopathy with hyperfractionation. *Int J Radiat Oncol Biol Phys*. 2005;61:856–864.
63. Parsons JT, Bova FJ, Fitzgerald CR, et al. Radiation retinopathy after external-beam irradiation: analysis of time–dose factors. *Int J Radiat Oncol Biol Phys*. 1994;30:765–773.
64. Nikoskelainen E, Joensuu H. Retinopathy after irradiation for Graves' ophthalmopathy (Letter). *Lancet*. 1989;2:690–691.
65. Miller M, Goldberg S, Bullock J. Radiation retinopathy after standard radiotherapy for thyroid-related ophthalmopathy. *Am J Ophthalmol*. 1991;112:600–601.
66. Durkin SR, Roos D, Higgs B, et al. Ophthalmic and adnexal complications of radiotherapy. *Acta Ophthalmol Scand*. 2007;85:240–250.
67. Bradley EA, Gower EW, Bradley DJ, et al. Orbital radiation for graves ophthalmopathy: a report by the American Academy of Ophthalmology. *Ophthalmology*. 2008;115:398–409.
68. Eng TY, Boersma MK, Fuller CD, et al. The role of radiation therapy in benign diseases. *Hematol Oncol Clin North Am*. 2006;20:523–557.
69. Viebahn M, Barricks ME, Osterloh MD. Synergism between diabetic and radiation retinopathy: case report and review. *Br J Ophthalmol*. 1991;75:629–632.
70. Spaide RF, Borodoker N, Shah V. Atypical choroidal neovascularization in radiation retinopathy. *Am J Ophthalmol*. 2002;133:709–711.
71. Spaide RF, Leys A, Hermann-Delamazure B, et al. Radiation-associated choroidal neovasculopathy. *Ophthalmology*. 1999;106:2254–2260.
72. Kinyoun JL, Zamber RW, Lawrence BS, et al. Photocoagulation treatment for clinically significant radiation macular oedema. *Br J Ophthalmol*. 1995;70:144–149.
73. Branch Vein Occlusion Study Group. Argon laser scatter photocoagulation for prevention of neovascularization and vitreous hemorrhage in branch vein occlusion: a randomized clinical trial. *Arch Ophthalmol*. 1986;104:34–41.
74. Augsburger JJ, Roth SE, Magargal LE, et al. Panretinal

photocoagulation for radiation-induced ocular ischemia. *Ophthalmic Surg*. 1987;18:589–593.
75. Finger PT. Radiation therapy for choroidal melanoma. *Surv Ophthalmol*. 1997;42:215–232.
76. Barnstable CJ, Tombran-Tink J. Neuroprotective and anti-angiogenic actions of PEDF in the eye: molecular targets and therapeutic potential. *Prog Retin Eye Res*. 2004;23:561–577.
77. Materin MA, Bianciotto CG, Wu C, et al. Sector laser photocoagulation for the prevention of macular edema after plaque radiotherapy for uveal melanoma: a pilot study. *Retina*. 2012;32:1601–1607.
78. Shah SU, Shields CL, Bianciotto CG, et al. Intravitreal bevacizumab at 4-month intervals for prevention of macular edema after plaque radiotherapy of uveal melanoma. *Ophthalmology*. 2014;121:269–275.
79. Hykin PG, Shields CL, Shields JA, et al. The efficacy of focal laser therapy in radiation-induced macular edema. *Ophthalmology*. 1998;105:1425–1429.
80. Ciulla TA, Walker JD, Fong DS, et al. Corticosteroids in posterior segment disease: an update on new delivery systems and new indications. *Curr Opin Ophthalmol*. 2004;15:211–220.
81. Sutter FK, Gillies MC. Intravitreal triamcinolone for radiation-induced macular edema. *Arch Ophthalmol*. 2003;121:1491–1493.
82. Shields CL, Demirci H, Dai V, et al. Intravitreal triamcinolone acetonide for radiation maculopathy after plaque radiotherapy for choroidal melanoma. *Retina*. 2005;25:868–874.
83. Shields CL, Demirci H, Marr BP, et al. Intravitreal triamcinolone acetonide for acute radiation papillopathy. *Retina*. 2006;26:537–544.
84. Iwao K, Inatani M, Kawaji T, et al. Frequency and risk factors for intraocular pressure elevation after posterior sub-Tenon capsule triamcinolone acetonide injection. *J Glaucoma*. 2007;16:251–256.
85. Gillies MC, Sutter FK, Simpson JM, et al. Intravitreal

triamcinolone for refractory diabetic macular edema: two-year results of a double-masked, placebo-controlled, randomized clinical trial. *Ophthalmology*. 2006;113:1533–1538.
86. Conti SM, Kertes PJ. The use of intravitreal corticosteroids, evidence-based and otherwise. *Curr Opin Ophthalmol*. 2006;17:235–244.
87. Horgan N, Shields CL, Mashayekhi A, et al. Periocular triamcinolone for prevention of macular edema after plaque radiotherapy of uveal melanoma: a randomized controlled trial. *Ophthalmology*. 2009;116:1383–1390.
88. Russo A, Avitabile T, Uva M, et al. Radiation macular edema after Ru-106 plaque brachytherapy for choroidal melanoma resolved by an intravitreal dexamethasone 0.7-mg implant. *Case Rep Ophthalmol*. 2012;3:71–76.
89. Baillif S, Maschi C, Gastaud P, et al. Intravitreal dexamethasone 0.7-mg implant for radiation macular edema after proton beam therapy for choroidal melanoma. *Retina*. 2013;33:1784–1790.
90. Tarmann L, Langmann G, Mayer C, et al. Ozurdex reduces the retinal thickness in radiation maculopathy refractory to bevacizumab. *Acta Ophthalmol*. 2014;92:e694–6.
91. Finger PT, Chin K. Anti-vascular endothelial growth factor bevacizumab (Avastin) for radiation retinopathy. *Arch Ophthalmol*. 2007;125:751–756.
92. Bakri SJ, Larson TA. The variable efficacy of intravitreal bevacizumab and triamcinolone acetonide for cystoid macular edema due to radiation retinopathy. *Semin Ophthalmol*. 2015;30(4):276–280.
93. Jutley G, Shona OA, Leen RC, et al. Response to ranibizumab following tachyphylaxis to bevacizumab in a patient with radiation maculopathy following stereotactic fractionated radiotherapy for optic nerve meningioma. *Arch Ophthalmol*. 2012;130:1466–1470.
94. Gupta A, Muecke JS. Treatment of radiation maculopathy with intravitreal injection of bevacizumab (Avastin). *Retina*. 2008;28:964–968.
95. Finger PT, Chin KJ. Antivascular endothelial growth factor

bevacizumab for radiation optic neuropathy: secondary to plaque radiotherapy. *Int J Radiat Oncol Biol Phys*. 2012;82:789–798.
96. Mashayekhi A, Rojanaporn D, Al-Dahmash S, et al. Monthly intravitreal bevacizumab for macular edema after iodine-125 plaque radiotherapy of uveal melanoma. *Eur J Ophthalmol*. 2014;24:228–234.
97. Subrayan V, Khaw KW, Peyman M, et al. Intravitreal bevacizumab for radiation-induced cystoid macular oedema in patients with nasopharyngeal carcinoma: a clinical series. *Ophthalmologica*. 2013;229:208–211.
98. Finger PT, Chin KJ. High-dose (2.0 mg) intravitreal ranibizumab for recalcitrant radiation retinopathy. *Eur J Ophthalmol*. 2013;23:850–856.
99. Vasquez LM, Somani S, Altomare F, et al. Intracameral bevacizumab in the treatment of neovascular glaucoma and exudative retinal detachment after brachytherapy in choroidal melanoma. *Can J Ophthalmol*. 2009;44:106–107.
100. Noble KG, Kupersmith MJ. Retinal vascular remodelling in radiation retinopathy. *Br J Ophthalmol*. 1984;68:475–478.
101. Kinyoun JL. Long-term visual acuity results of treated and untreated radiation retinopathy (an AOS thesis). *Trans Am Ophthalmol Soc*. 2008;106:325–335.
102. Shields CL, Shields JA, Cater J, et al. Plaque radiotherapy for uveal melanoma: long-term visual outcome in 1106 consecutive patients. *Arch Ophthalmol*. 2000;118:1219–1228.
103. Finger PT. Tumour location affects the incidence of cataract and retinopathy after ophthalmic plaque radiation therapy. *Br J Ophthalmol*. 2000;84:1068–1070.

62

Ocular Ischemic Syndrome

Gary C. Brown, Sanjay Sharma, Melissa M. Brown

In 1963, Kearns and Hollenhorst[1] reported on the ocular symptoms and signs occurring secondary to severe carotid artery obstructive disease. They called the entity "venous stasis retinopathy" and noted that it occurred in approximately 5% of patients with severe carotid artery insufficiency or thrombosis. Some confusion has since arisen with this term because it has also been used to designate mild central retinal venous occlusion.[2] A number of additional alternative names have been proposed, including ischemic ocular inflammation,[3] ischemic oculopathy,[4] and the ocular ischemic syndrome.[5,6] Histopathologic examination of eyes with the entity generally does not reveal inflammation,[7,8] and therefore the descriptive term the present authors and Dr. Larry Magargal originated was the ocular ischemic syndrome.[5,6]

Demographics and Incidence

The mean age of patients with the ocular ischemic syndrome (OIS) is about 65 years, with a range generally from the fifties to the eighties. No racial predilection has been identified, and males are affected more than females by a ratio of about 2 : 1. Either eye can

be affected, and in approximately 20% of patients, ocular involvement is bilateral.[5] The incidence of the disease has not been extensively studied, but from the work of Sturrock and Mueller[9] an annual estimate of 7.5 cases/million persons can be made. This number may be falsely low, since it is possible that a number of cases are misdiagnosed.

Etiology

In general, a 90% or greater stenosis of the ipsilateral carotid arterial system is present in eyes with the OIS.[5] It has been shown that a 90% carotid stenosis reduces the ipsilateral central retinal artery perfusion pressure by about 50%.[10,11] The obstruction can occur within the common carotid or internal carotid artery. In about 50% of cases, the affected vessel is 100% occluded, while in 10% there is bilateral 100% carotid artery obstruction in association with collateral vessels.[5] Atherosclerotic obstructions are more common at arterial bifurcations.

Occasionally, obstruction of the ipsilateral ophthalmic artery can also be responsible.[5,12,13] Rarely, an isolated obstruction of the central retinal artery alone can mimic the dilated (but not tortuous) retinal veins and retinal hemorrhages seen in eyes with the OIS.[14]

Atherosclerosis within the carotid artery is the cause of the great majority of cases of the OIS.[5] Dissecting aneurysm of the carotid artery has been reported as a cause,[15] as has giant cell arteritis,[16] radiation damage,[17] Moyamoya syndrome,[18] melanoma of the optic disc,[19] and Takayasu arteritis.[20] Hypothetically, entities such as fibromuscular dysplasia,[21] Behçet disease,[22] trauma,[23] and other inflammatory entities that cause carotid artery obstruction could lead to the OIS. Increased levels of homocysteine and C-reactive protein have been associated with the OIS.[24]

Symptoms

Visual Loss

Greater than 90% of patients with the OIS relate a history of visual loss in the affected eye(s).[5] In two-thirds of cases, it occurs over a

period of weeks, but it is abrupt in approximately 12%. In this latter group, with sudden visual loss, there is often a cherry-red spot present on funduscopic examination (Fig. 62.1).

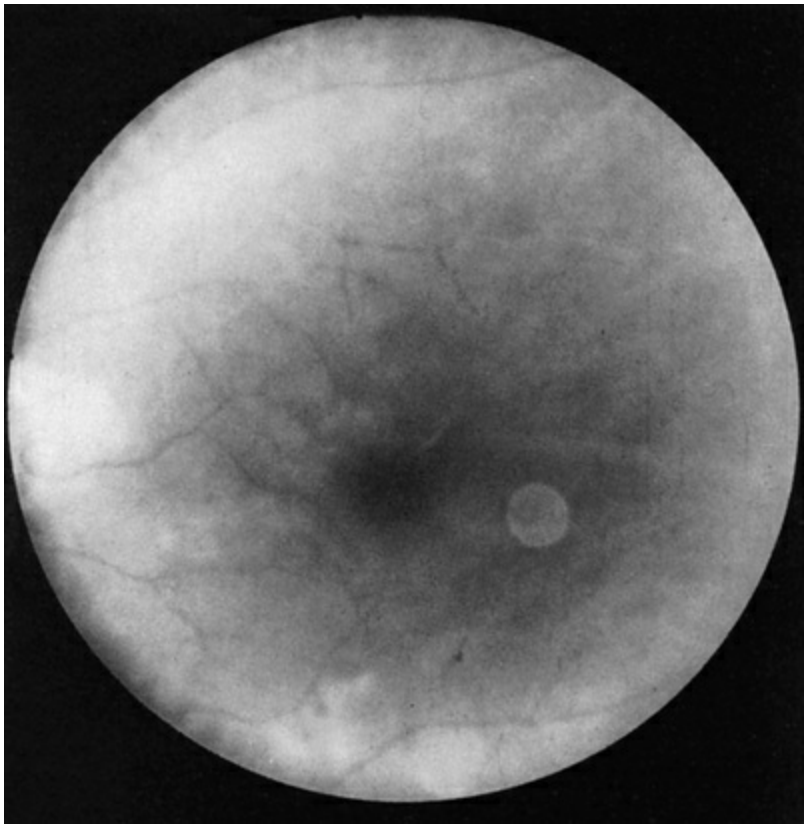

FIG. 62.1 Cherry-red spot in the left eye of a 66-year-old man with rubeosis iridis, a 100% ipsilateral common carotid artery obstruction, and a history of rapid visual loss.

Prolonged Light Recovery

Prolonged recovery following exposure to a bright light has been described in patients with severe carotid artery obstruction.[25] Concurrent attenuation of the visual evoked response has also been observed in these cases after light exposure. The phenomenon has been attributed to ischemia of the macular retina. In cases of bilateral, severe carotid artery obstruction, the visual loss after exposure to bright light occurs in both eyes, mimicking occipital lobe ischemia due to vertebrobasilar disease.[26]

Scintillating Scotomas

Dissection of the internal carotid artery has been reported to cause scintillating scotomas that resemble a migraine aura.[27] While these could theoretically be associated with the classic OIS, they have not been observed by the authors. Pulsating lights can be seen, however, in association with vertebrobasilar insufficiency.[28] In this latter instance, vertigo, syncope, and/or headache are often present. Photopsias secondary to the OIS are unusual.[28]

Amaurosis Fugax

A history of amaurosis fugax is elicited in about 10–15% of OIS patients.[5,29] Amaurosis fugax, or fleeting loss of vision for seconds to minutes, is thought to most commonly be caused by emboli to the central retinal arterial system, although vasospasm may also play a role.[30] Although the majority of people with amaurosis fugax alone do not have the OIS, it can be an indicator of concomitant, ipsilateral carotid artery obstructive disease. About one-third of patients with amaurosis fugax have an ipsilateral carotid artery obstruction of 75% or greater.[31] Rarely, it has been associated with a stenosis of the ophthalmic artery.[31]

Pain

Pain is present in the affected eye or orbital region in about 40% of cases,[5] and we refer to it as "ocular angina." Most often, it is described as a dull ache. It can occur secondary to neovascular glaucoma, but in those cases in which the intraocular pressure is normal, the cause may be ischemia to the globe and/or ipsilateral dura.

Signs

Visual Acuity

The presenting visual acuities of patients with the OIS are bimodally distributed, with 43% of affected eyes having vision ranging from 20/20 to 20/50, and 37% having counting fingers or

worse vision.[32] Absence of light perception is generally not seen early but can develop in the later stages of the disease, usually secondary to neovascular glaucoma. Among all eyes with the OIS after one year of follow-up, including those with and without treatment, approximately 24% remain in the 20/20–20/50 group and 58% have counting fingers vision or worse. The visual prognosis is often poor unless carotid surgical intervention can be undertaken,[33–35] although we have seen one case of spontaneous resolution.

External Collaterals

Prominent collateral vessels are occasionally seen on the forehead (Fig. 62.2). These vessels connect the external carotid system on one side of the head to that on the other. These vascular collaterals should not be mistaken for the enlarged tender vessels seen with giant cell arteritis, since temporal artery biopsy may shut down this important source of collateral blood flow to the brain.

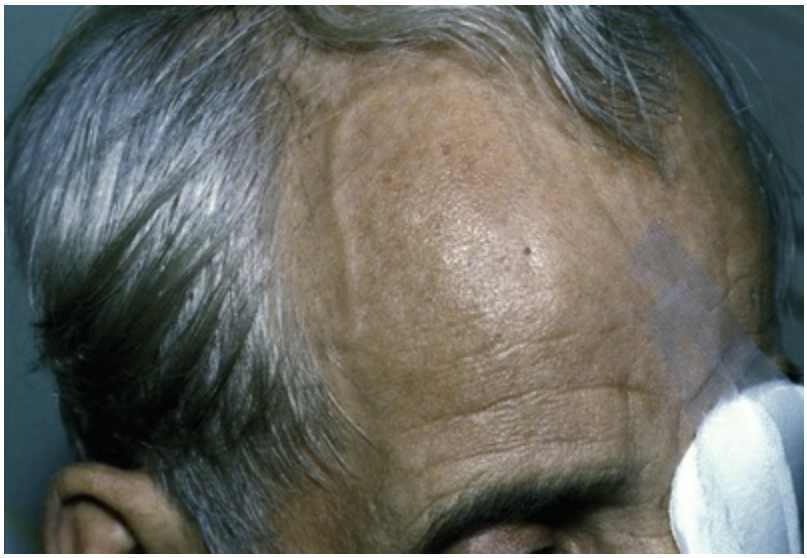

FIG. 62.2 Prominent collateral arteries from the right external carotid arterial system to the left external arterial system in a patient with a 100% common left carotid artery stenosis.

Anterior Segment Changes

Neovascularization of the iris is encountered in approximately two-thirds of eyes with the OIS at the time of presentation[5] (Fig. 62.3). Nevertheless, only slightly over half of these eyes have or develop an increase in intraocular pressure, even if the anterior chamber angle is closed by fibrovascular tissue. Impaired ciliary body perfusion, with a subsequent decrease in aqueous production, likely accounts for this phenomenon.

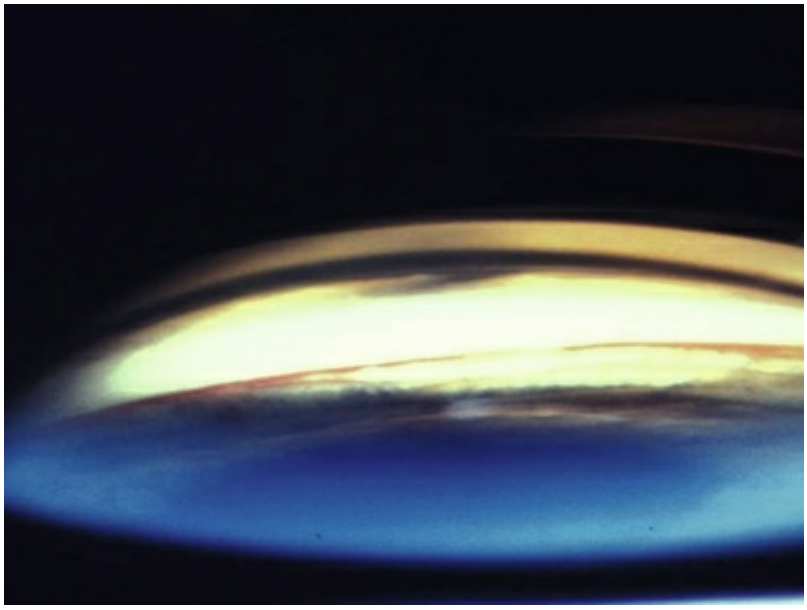

FIG. 62.3 Gonioscopy of neovascularization of the iris and angle in an eye with the ocular ischemic syndrome. A red arc of fibrovascular tissue is present, closing the anterior chamber angle.

Flare in the anterior chamber is usually present in eyes with rubeosis iridis (iris neovascularization). An anterior chamber cellular response is seen in almost one-fifth of eyes with the OIS,[5] but it rarely exceeds grade 2^+, on a 0 to 4^+ range, as per the Schlaegel classification.[36] Keratic precipitates can be present but are typically small.

In unilateral cases, there is generally little difference between the degree of lens opacification in each eye. As the disease advances, however, cataractous lens changes can develop. In advanced cases, the lens may become mature.

Posterior Segment Findings

The retinal arteries are usually narrowed, and the retinal veins are most often dilated, but not tortuous (Fig. 62.4). The venous dilation may be accompanied by beading, but usually not to the extent seen in eyes with marked preproliferative or proliferative diabetic retinopathy. Dilation of the veins is probably a nonspecific response to the ischemia from the inflow obstruction. Nevertheless, in some eyes both the retinal arteries and veins are narrowed. In contrast, eyes with central retinal vein obstruction usually also have dilated retinal veins, but they are typically tortuous.[5] The fact that the OIS occurs secondary to impaired inflow, while central retinal vein obstruction is usually associated with compromised outflow resulting from thrombus formation at or near the lamina cribrosa,[37] probably accounts for this difference.

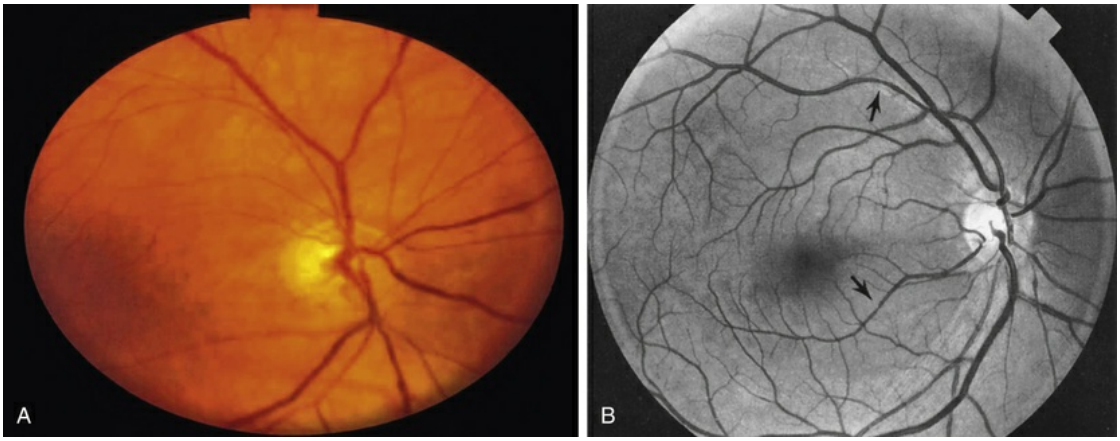

FIG. 62.4 (A) Narrowed, beaded retinal arteries and dilated, beaded, but not tortuous, retinal veins in an ocular ischemic syndrome eye. (B) Focal narrowing of the retinal arteries (*arrows*) in the right eye of a 55-year-old man with ocular ischemic syndrome and bilateral internal carotid artery obstructions. (Panel B reproduced with permission from Brown GC, Magargal LE. The ocular ischemic syndrome. Clinical, fluorescein angiographic and carotid angiographic features. Int Ophthalmol 1988;11:239–51.)

Retinal hemorrhages are seen in about 80% of affected eyes. They are most commonly present in the midperiphery but can also extend into the posterior pole (Figs. 62.5 and 62.6 online). While

dot and blot hemorrhages are the most common variant, superficial retinal hemorrhages in the nerve fiber layer are occasionally seen. The hemorrhages probably arise secondary to leakage from the smaller retinal vessels, which have sustained endothelial damage as a result of the ischemia. Similar to the case with diabetic retinopathy, they may also result from the rupture of microaneurysms. In general, the hemorrhages seen with the OIS are less numerous than those accompanying central retinal vein obstruction. They are almost never confluent.

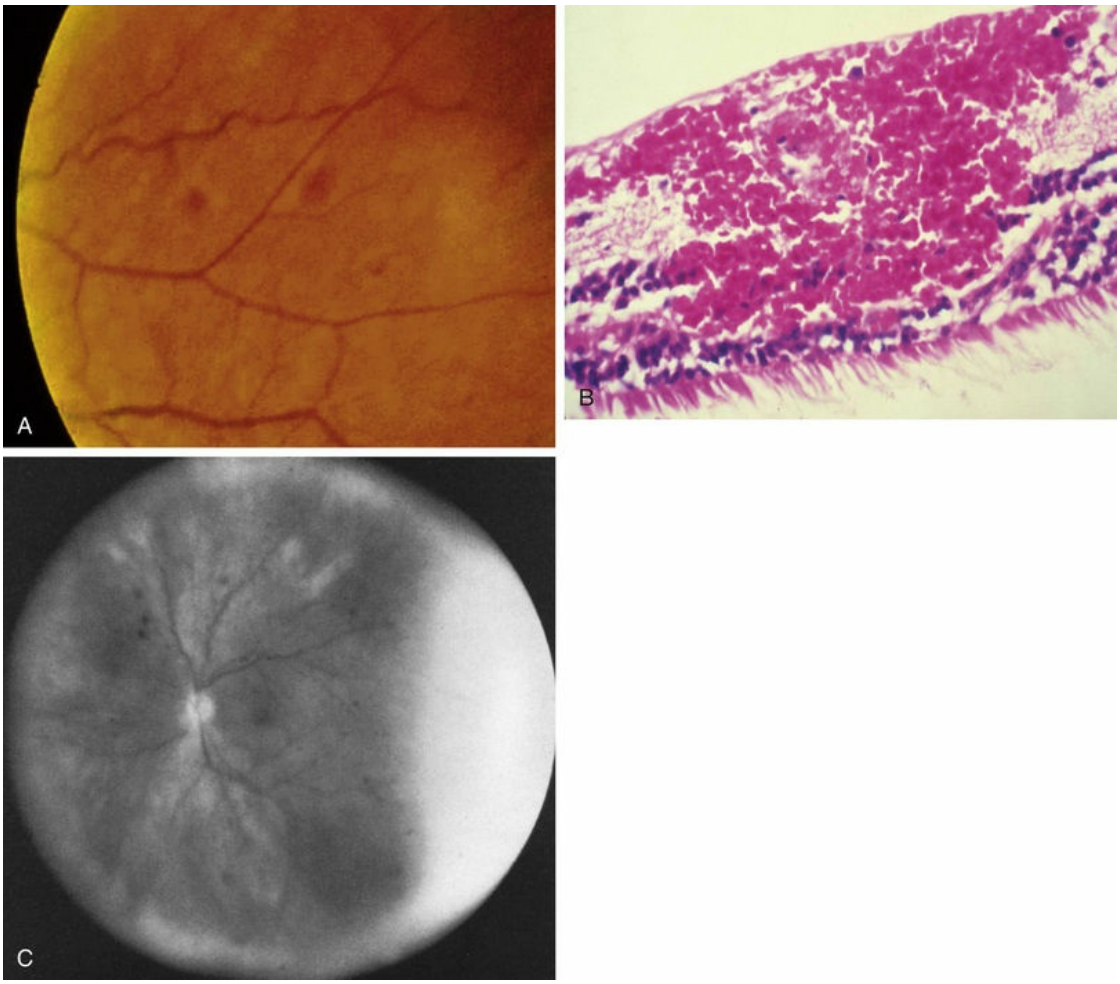

FIG. 62.5 (A) Round retinal hemorrhages in the midperiphery of an eye with the ocular ischemic syndrome. (B) Histopathologic correlate of a retinal hemorrhage in an ocular ischemic syndrome eye demonstrates blood throughout the retina (hematoxylin and eosin, ×60). (C) Wide-angle photograph demonstrating retinal hemorrhages in the midperiphery in an eye with the ocular ischemic syndrome. (Panel B,

photograph courtesy of Dr. W. Richard Green.)

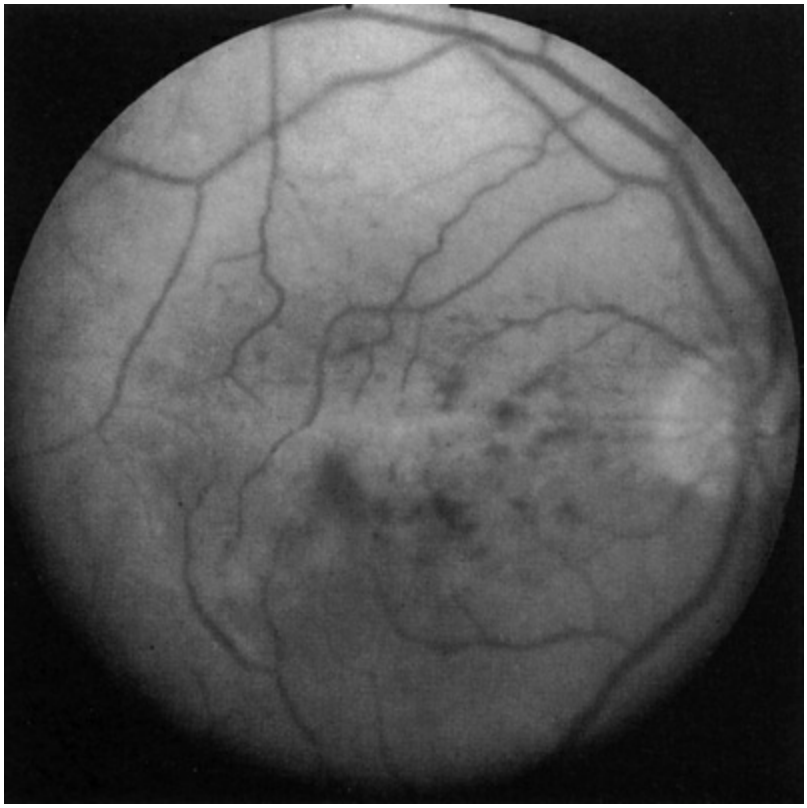

FIG. 62.6 Right fundus of a 35-year-old man with a cherry-red spot, rubeosis iridis, and retinal hemorrhages in the macula. A 95% right internal carotid artery obstruction was present.

Microaneurysms are frequently observed outside the posterior pole, but can be seen in the macular region also. Hyperfluorescence with fluorescein angiography (Fig. 62.7) differentiates these abnormalities from hypofluorescent retinal hemorrhages. Retinal telangiectasia has also been described.[38]

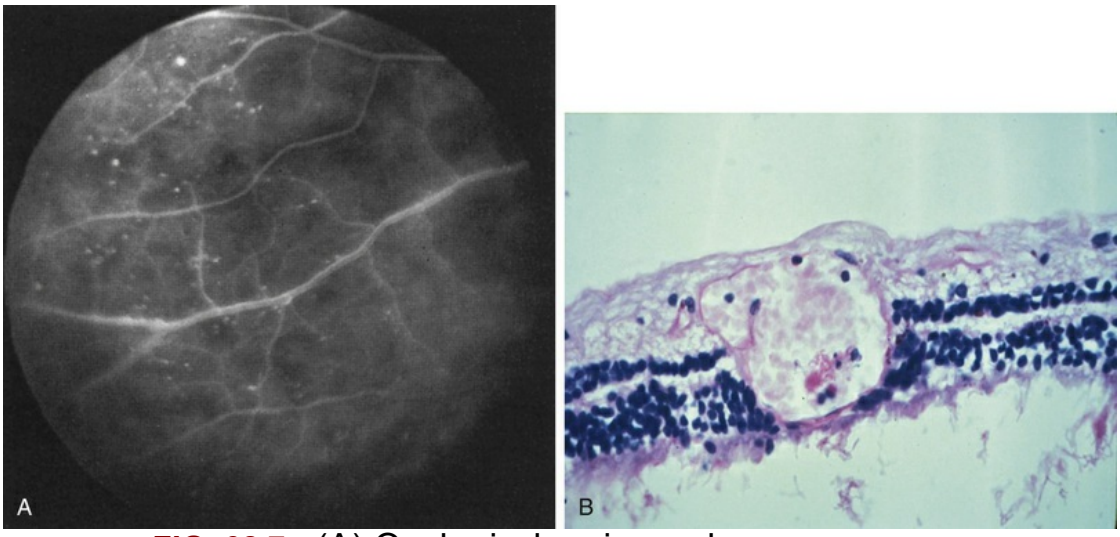

FIG. 62.7 (A) Ocular ischemic syndrome eye: fluorescein angiogram demonstrating numerous hyperfluorescent microaneurysms in the midperipheral retina. (B) Histopathologic correlation of a microaneurysm in an eye with the ocular ischemic syndrome discloses that the anomaly traverses the entire retina (periodic-acid Schiff, ×60). (Panel A reproduced with permission from Brown GC, Magargal LE. The ocular ischemic syndrome. Clinical, fluorescein angiographic and carotid angiographic features. Int Ophthalmol 1988;11:239–51. Panel B courtesy of Dr. W. Richard Green.)

Posterior segment neovascularization can occur at the optic disc or on the retina. Neovascularization of the disc (Fig. 62.8) is encountered in about 35% of eyes, while neovascularization of the retina is seen in about 8%.[5] Vitreous hemorrhage arising from traction upon the neovascularization by the vitreous gel has been reported to occur in 4% of eyes with the OIS in a retrospective study.[5] Rarely, the neovascularization can progress to severe preretinal fibrovascular proliferation (Fig. 62.9 online). Neovascularization of the retina (Fig. 62.10 online) is encountered in 8% of eyes with ocular ischemia. It is usually present concomitant with neovascularization of the disc.

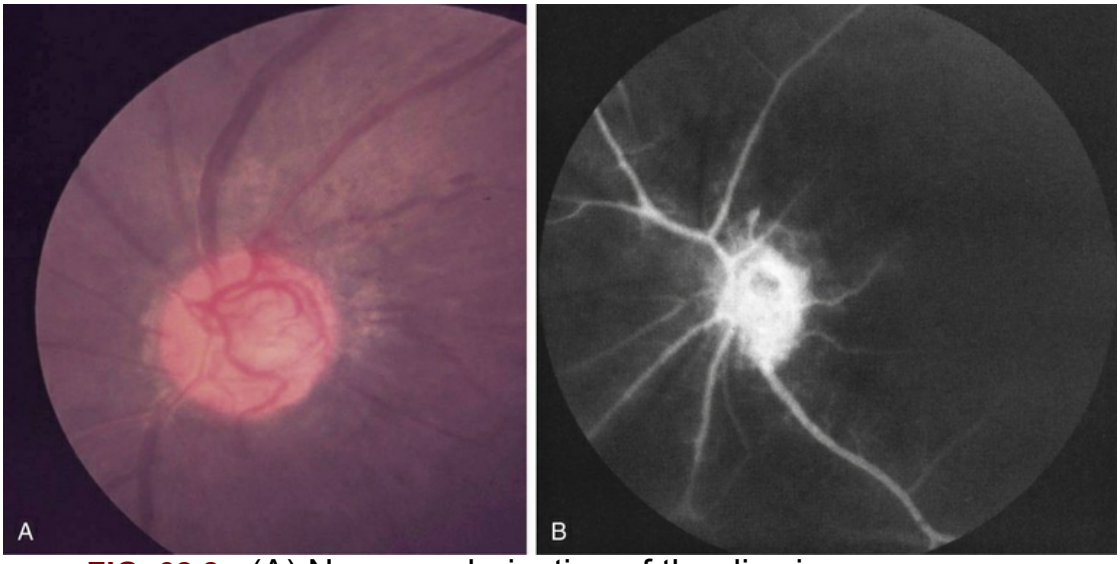

FIG. 62.8 (A) Neovascularization of the disc in an eye with the ocular ischemic syndrome. (B) Fluorescein angiogram of the eye in panel (A) reveals marked hyperfluorescence resulting from leakage of dye from new vessels. (Reproduced with permission from Brown GC, Magargal LE, Simeone FA, et al. Arterial obstruction and ocular neovascularization. Ophthalmology 1982;89:139–46. Copyright © 1982 American Academy of Ophthalmology.)

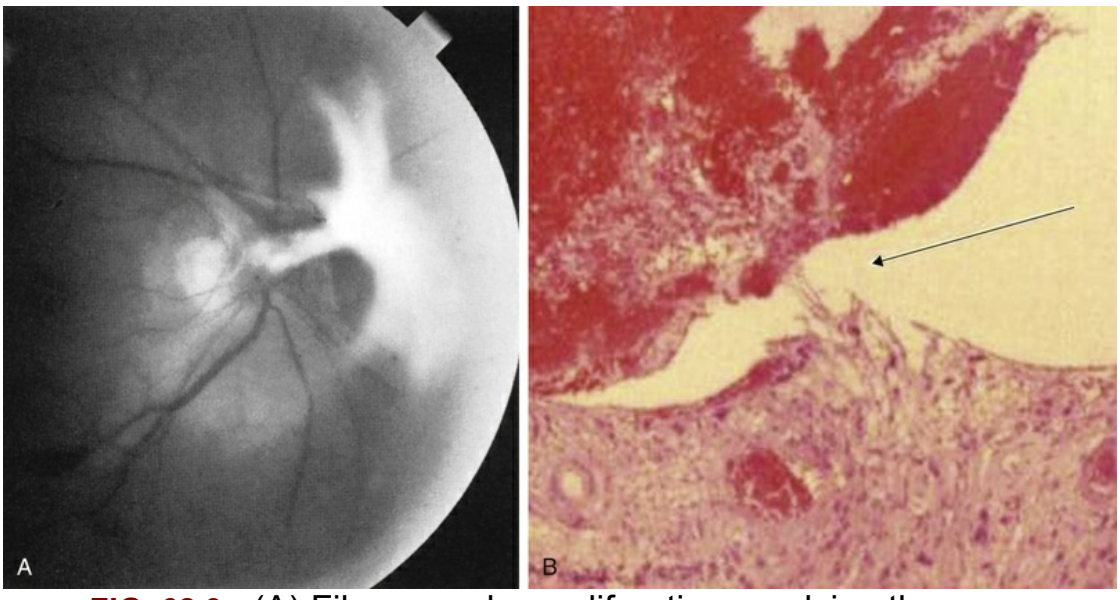

FIG. 62.9 (A) Fibrovascular proliferation overlying the optic disc and causing retinal traction in an eye with the ocular ischemic syndrome. (B) Histopathology of an eye with ischemic retinopathy demonstrates a connection of neovascularization of the optic disc on

stretch (*arrow*) between the inferior disc and the superior vitreous gel filled with blood. Presumably, the intravitreal blood occurred as a result of rupture of the thin-walled vessels on stretch (hematoxylin and eosin, ×60). (Panel A reproduced with permission from Brown GC, Magargal LE. The ocular ischemic syndrome. Clinical, fluorescein angiographic and carotid angiographic features. Int Ophthalmol 1988;11:239–51.)

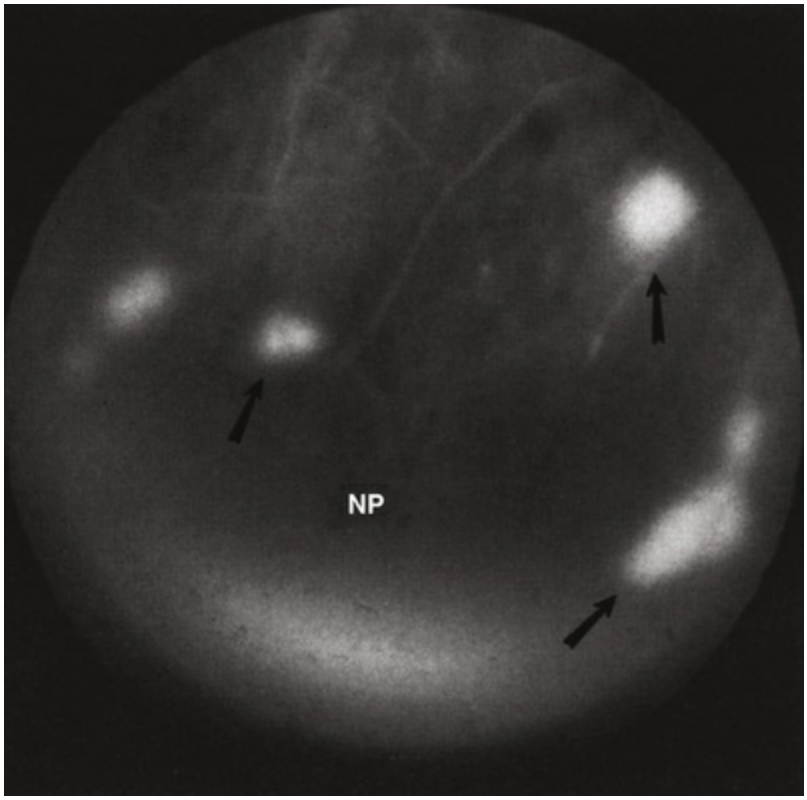

FIG. 62.10 Neovascularization of the retina (*arrows*) with fluorescein angiography in a nondiabetic person affected by the ocular ischemic syndrome. Retinal capillary nonperfusion (*NP*) can be seen. (Reproduced with permission from Brown GC, Magargal LE, Simeone FA, et al. Arterial obstruction and ocular neovascularization. Ophthalmology 1982;89:139–46. Copyright © 1982 American Academy of Ophthalmology.)

A cherry-red spot is seen in approximately 12% of eyes with the OIS (see Fig. 62.1).[5] It can occur secondary to inner layer retinal ischemia from embolic obstruction of the central retinal artery, but may also develop when the intraocular pressure exceeds the perfusion pressure within the central retinal artery, particularly in

eyes with neovascular glaucoma.

Additional posterior segment signs[5] include cotton-wool spots (Fig. 62.11 online) in 6% of eyes, spontaneous retinal arterial pulsations in 4% (Fig. 62.12), and cholesterol emboli within the retinal arteries in 2%. In contrast to spontaneous retinal venous pulsations, which are a normal variant and located at the base of the large veins on the optic disc, the arterial pulsations are usually more pronounced and may extend a disc diameter or more out from the optic disc into the surrounding retina. Anterior ischemic optic neuropathy (Fig. 62.13) has also been reported in OIS eyes.[39,40] Acquired arteriovenous communications of the retina have been reported.[41]

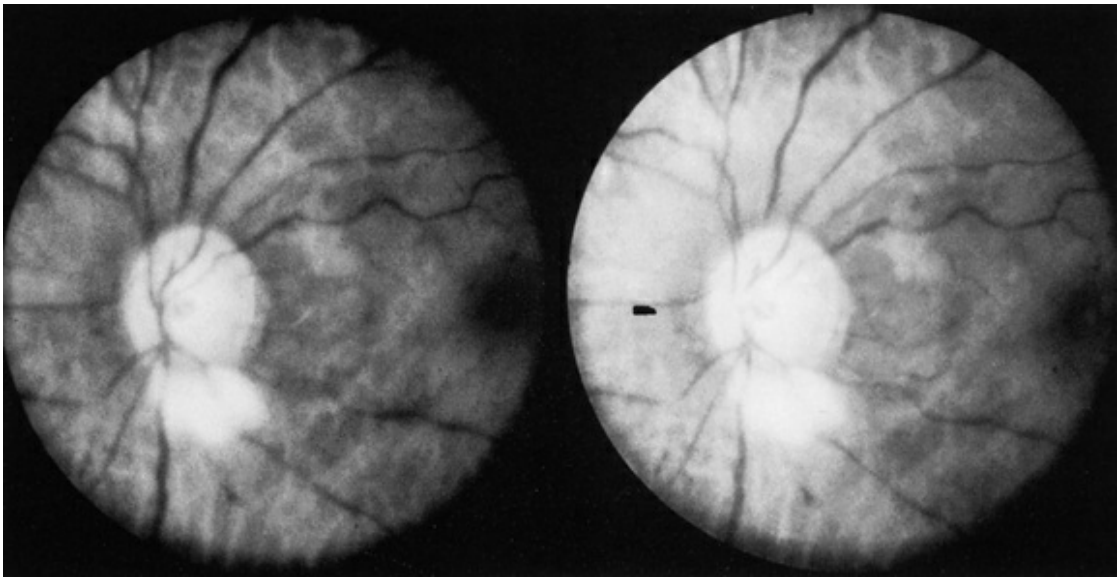

FIG. 62.12 Photographs taken several seconds apart in a fundus affected by the ocular ischemic syndrome. Closure of the retinal arteries can be seen on the right.
(Reproduced with permission from Brown GC, Magargal LE. The ocular ischemic syndrome. Clinical, fluorescein angiographic and carotid angiographic features. Int Ophthalmol 1988;11:239–51.)

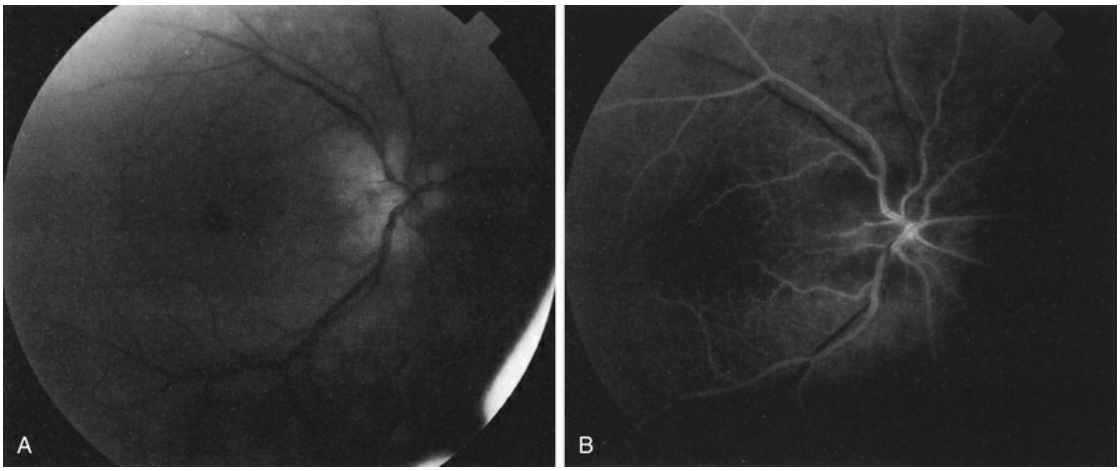

FIG. 62.13 (A) Pale optic disc resulting from ischemic optic neuropathy in a 67-year-old man with a 100% right internal carotid artery obstruction. Midperipheral retinal hemorrhages and iris neovascularization were also present. (B) Fluorescein angiogram of the eye in panel (A) at 81 seconds after injection. The nerve head is hypofluorescent. (Reproduced with permission from Brown GC. Anterior ischemic optic neuropathy occurring in association with carotid artery obstruction. J Clin Neuroophthalmol 1986;6:39–42.)

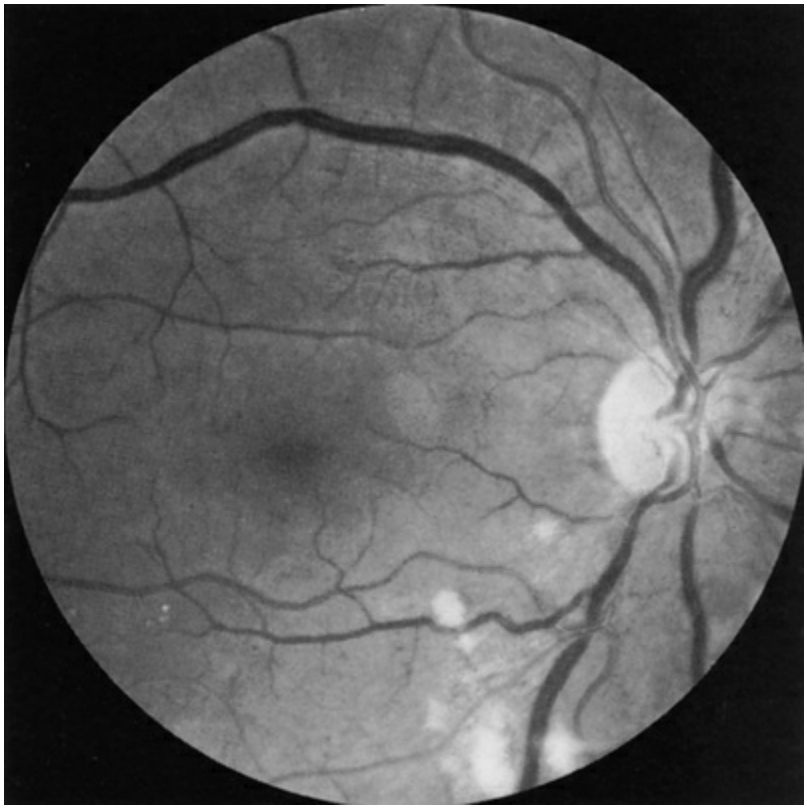

FIG. 62.11 Cotton-wool spots in the fundus of a man

with the ocular ischemic syndrome. Irregularly dilated retinal veins are also evident.

A list of the symptoms and anterior and posterior segment signs found with the ocular ischemic syndrome is shown in Table 62.1.[1–5,9]

TABLE 62.1

Symptoms and Anterior and Posterior Segment Signs Seen in Eyes With the Ocular Ischemic Syndrome

	Prevalence
OIS SYMPTOMS	
Vision loss, typically gradual	90%
Periorbital pain (ocular angina)	495
Amaurosis fugax	10–15%
Prolonged light recovery	Uncertain
ANTERIOR SEGMENT SIGNS	
Rubeosis iridis	67%
Neovascular glaucoma	35%
Uveitis (cells and flare)	18%
POSTERIOR SEGMENT SIGNS	
Narrowed retinal arteries	Most
Dilated retinal veins	Most
Retinal hemorrhages	80%
Neovascularization	37%
Optic disc	35%
Retina	8%
Cherry-red spot	12%
Cotton-wool spot(s)	6%
Spontaneous retinal arterial pulsations	4%
Vitreous hemorrhage	4%
Cholesterol emboli	2%
Ischemic optic neuropathy	2%

OIS, ocular ischemic syndrome.

Adapted from Brown GC, Magargal LE. The ocular ischemic syndrome. Clinical, fluorescein angiographic and carotid angiographic features. Int Ophthalmol 1988;11:239–51.

Ancillary Studies

Fluorescein Angiography

The intravenous fluorescein angiographic signs[5] associated with the ocular ischemic syndrome are listed in Table 62.2.

TABLE 62.2

Fluorescein Angiographic Signs Seen in Eyes With the Ocular Ischemic Syndrome

Sign	Prevalence
Delayed and/or patchy choroidal filling	60%[5]
Prolonged retinal arteriovenous transit time	95%[5]
Retinal vascular staining	85%[5]
Macular edema	17%[42]
Other signs	
Retinal capillary nonperfusion	Common
Optic nerve head hyperfluorescence	If macular edema present
Microaneurysmal hyperfluorescence	Most cases

Delayed arm-to-choroid and arm-to-retina circulation times are frequently observed in the OIS. However, these measurements may be difficult to assess, since they depend upon whether the dye was injected in the antecubital fossa or hand, and also on the rate of injection. The observation of a well-demarcated, leading edge of fluorescein dye within a retinal artery after an intravenous injection is a distinctly unusual finding. It can be seen in eyes with the OIS, secondary to hypoperfusion (Fig. 62.14).

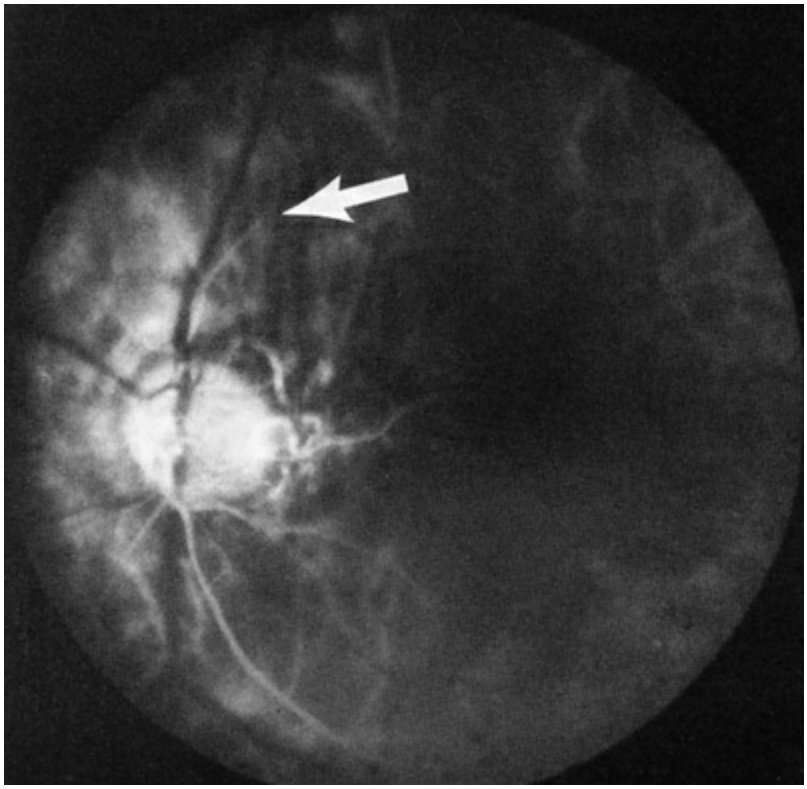

FIG. 62.14 Fluorescein angiogram of an eye with the

ocular ischemic syndrome at 38 seconds after injection. A leading edge of the dye (*arrow*) is present within a retinal artery. (Reproduced with permission from Brown GC, Magargal LE, Simeone FA, et al. Arterial obstruction and ocular neovascularization. Ophthalmology 1982;89:139–46. Copyright © 1982 American Academy of Ophthalmology.)

Normally, the choroidal filling is completed within 5 seconds after the first appearance of dye. Sixty percent of eyes with the OIS demonstrate patchy and/or delayed choroidal filling (Fig. 62.15).[5] In some instances, the filling is delayed for a minute or longer. Although not the most sensitive sign, an abnormality in choroidal filling is the most specific fluorescein angiographic sign in ocular ischemic eyes.

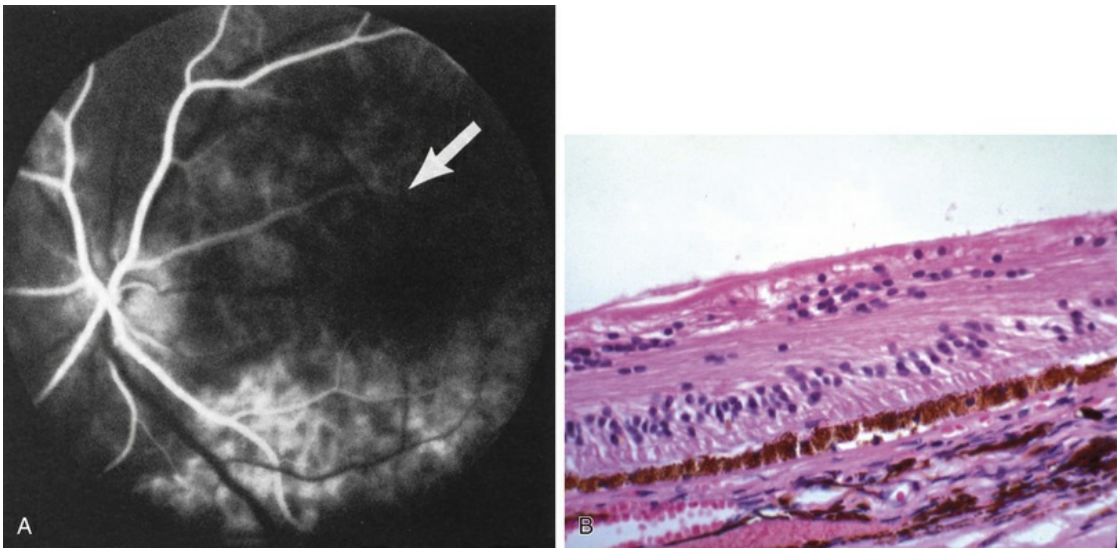

FIG. 62.15 (A) Fluorescein angiogram of an ocular ischemic syndrome eye at 44 seconds after injection shows patchy choroidal filling. A leading edge of dye (*arrow*) can again be seen within a retinal artery. (B) Histopathology of an ocular ischemic syndrome retina reveals a paucity of retinal ganglion cells, as well as cells in both the inner nuclear and outer nuclear layers, the latter the cell bodies for the rods and cones. These features occur secondary to panretinal ischemia from both retinal and choroidal hypoperfusion. The retinal pigment epithelial cells appear to be intact, correlating with the clinical picture that retinal pigment epithelial dropout and hyperplasia do not appear to be prominent

funduscopic features associated with the ocular ischemic syndrome (hematoxylin and eosin, ×60). (Panel A reproduced with permission from Brown GC, Magargal LE. The ocular ischemic syndrome. Clinical, fluorescein angiographic and carotid angiographic features. Int Ophthalmol 1988;11:239–51. Panel B courtesy of Dr. W. Richard Green.)

Prolongation of the retinal arteriovenous transit time is seen in 95% of eyes with the OIS (high sensitivity) but can also be seen in eyes with central retinal artery obstruction and central retinal vein obstruction (low specificity).[5] Normally, the major retinal veins in the temporal vascular arcade are completely filled within 10–11 seconds after the first appearance of dye within the corresponding retinal arteries. In extreme cases of the OIS, the retinal veins fail to fill throughout the study. Staining of the retinal vessels in the later phases of the study is seen in approximately 85% of eyes (Figs. 62.16 online and 62.17).[5] Both larger and smaller vessels can be involved, the arteries generally more so than the veins. Chronic hypoxic damage to endothelial cells may account for the staining. In contrast, staining of the retinal vessels is uncommon, with central retinal artery obstruction alone. With central retinal vein obstruction, the veins can demonstrate late staining, but the retinal arteries are generally not affected.

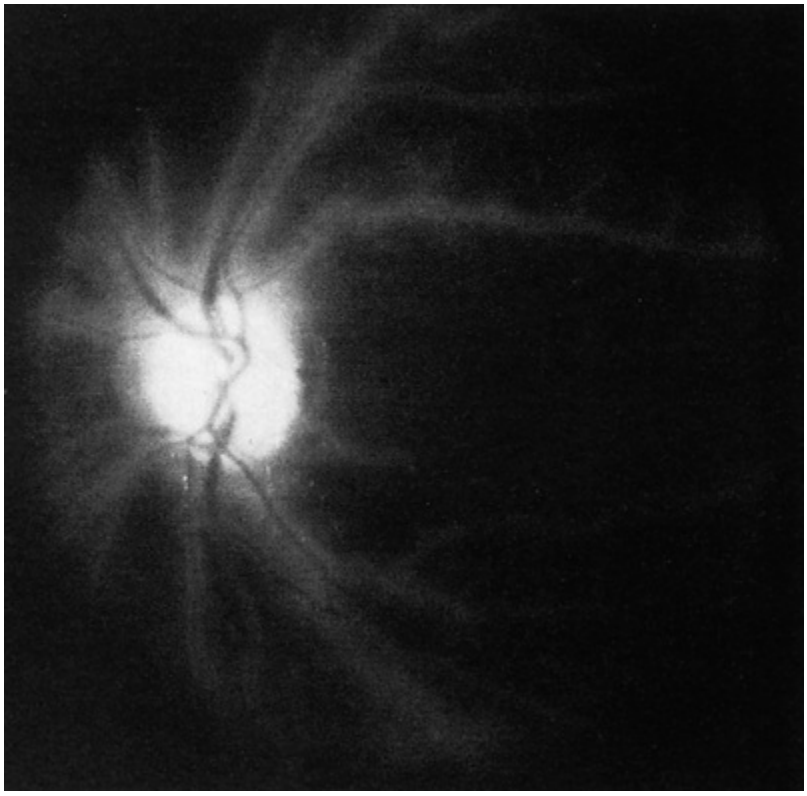

FIG. 62.17 Prominent staining of the retinal arteries in the later phases of fluorescein angiography in an eye with the ocular ischemic syndrome.

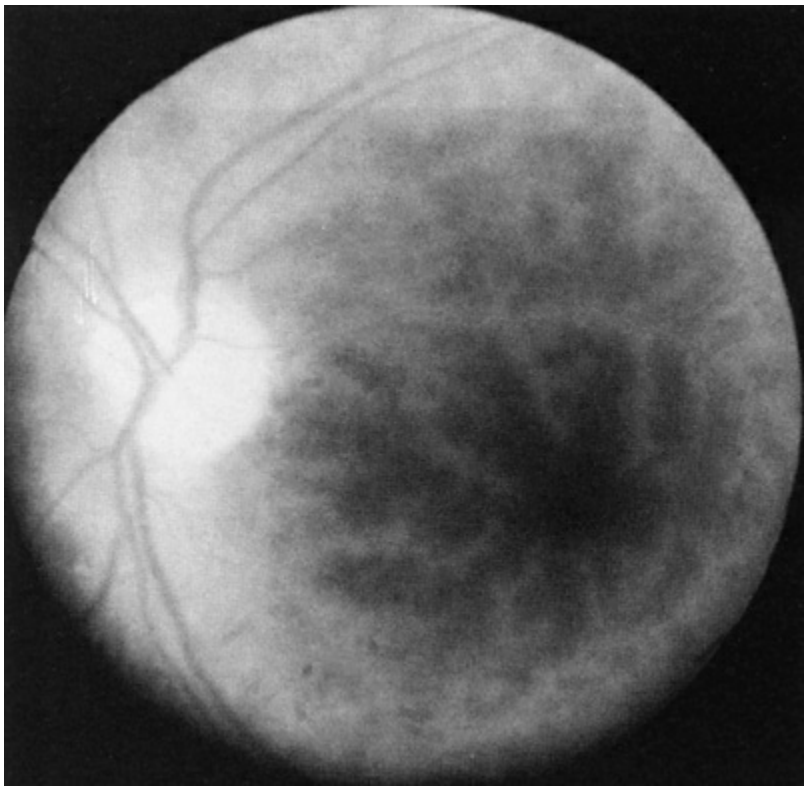

FIG. 62.16 Staining of the macular vessels in the ocular ischemic syndrome. (Reproduced with permission from Brown GC, Magargal LE. The ocular ischemic syndrome. Clinical, fluorescein angiographic and carotid angiographic features. Int Ophthalmol 1988;11:239–51.)

Macular leakage and edema evident on fluorescein angiography is seen in about one-sixth of eyes with the OIS[42] (Fig. 62.18). Hypoxia, and subsequent endothelial damage, within the smaller retinal vessels, as well as leakage from microaneurysms, may account for this phenomenon (Fig. 62.19). Dye accumulation may be mild or severe, and is usually associated with hyperfluorescence of the optic disc. The disc, however, is typically not swollen. Despite the prominent leakage with fluorescein angiography, the ophthalmoscopic cystic changes of macular edema are generally not as pronounced as those seen after ocular surgery or those associated with diabetic retinopathy.

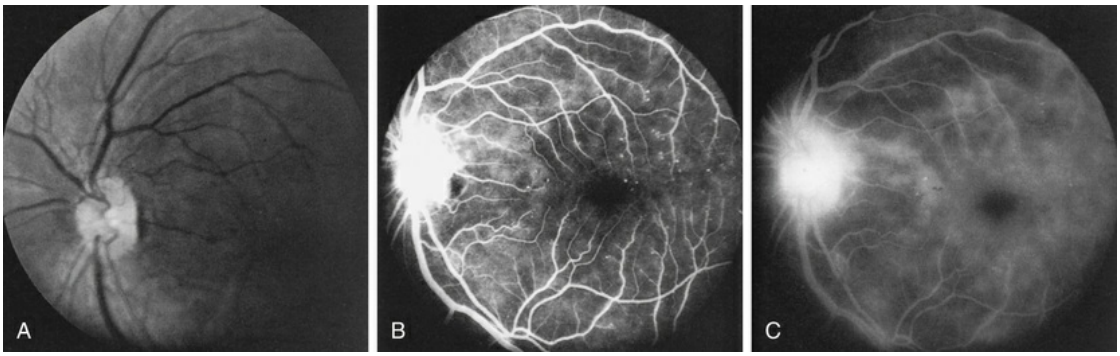

FIG. 62.18 (A) Left fundus of a 60-year-old woman with a 100% left internal carotid artery obstruction. The retinal veins are dilated, but not tortuous. (B) Fluorescein angiogram of the eye in panel (A) at more than 60 seconds after injection. A number of microaneurysms are present, and the optic disc is hyperfluorescent. (C) At several minutes after injection, prominent leakage of dye is evident. (Reproduced with permission from Brown GC. Macular edema in association with severe carotid artery obstruction. Am J Ophthalmol 1986;102:442; American Journal of Ophthalmology. Copyright © Ophthalmic Publishing Group.)

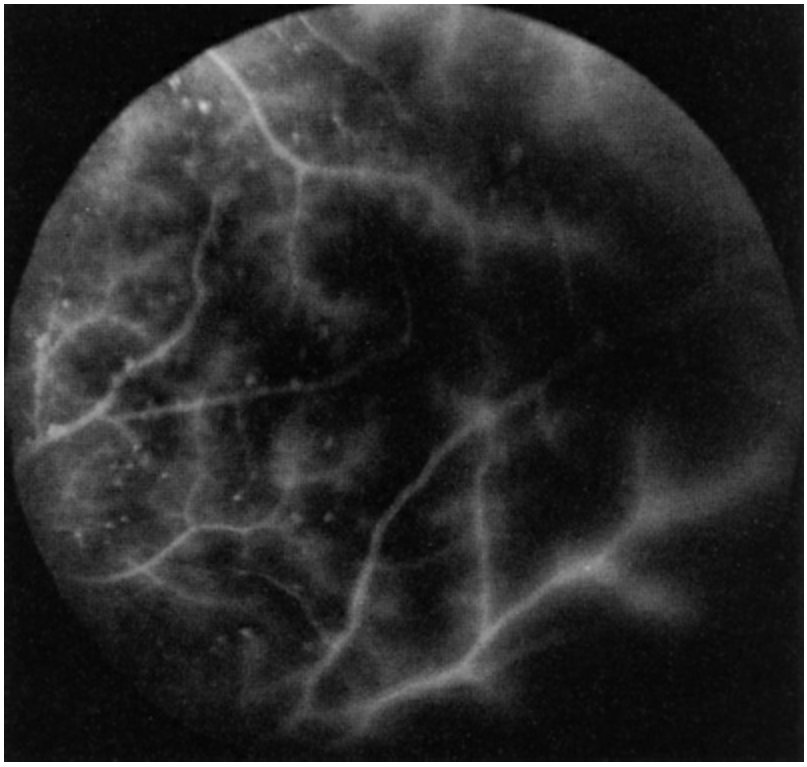

FIG. 62.19 Peripheral fluorescein angiogram of the same eye shown in Fig. 62.18. Many hyperfluorescent microaneurysms are seen, as is staining of the retinal vessels. (Reproduced with permission from Brown GC. Macular edema in association with severe carotid artery obstruction. Am J Ophthalmol 1986;102:442; American Journal of Ophthalmology. Copyright © Ophthalmic Publishing Group.)

Retinal capillary nonperfusion can be seen in some eyes (Fig. 62.20 online). The histopathologically observed absence of endothelial cells and pericytes within the retinal capillaries most likely corresponds to the areas of nonperfusion seen with fluorescein angiography.[7,8,43]

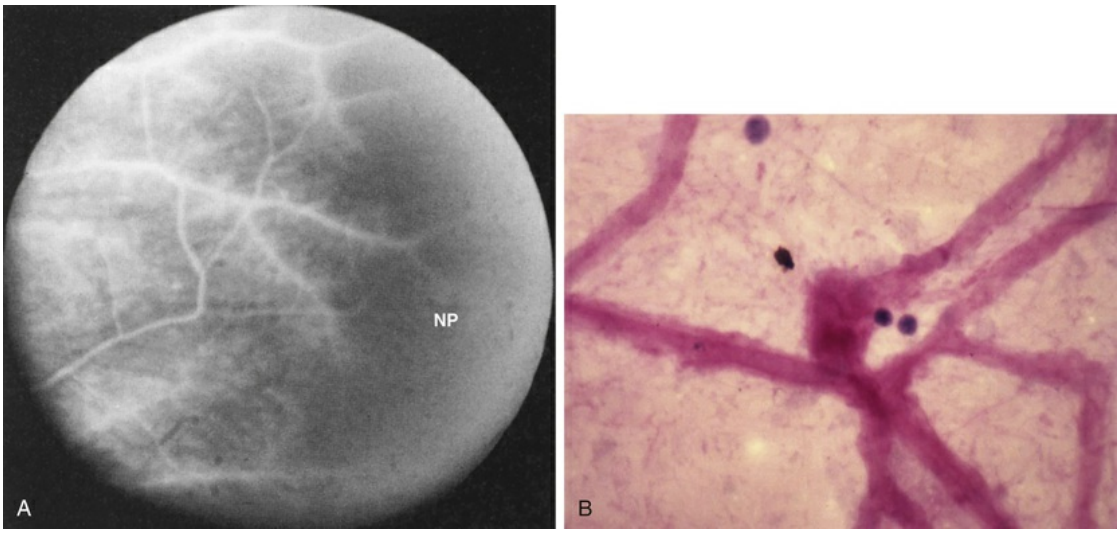

FIG. 62.20 (A) Fluorescein angiography reveals retinal capillary nonperfusion (NP) in an ocular ischemic syndrome eye. (B) Trypsin digest of the retinal vessels of an ocular ischemic syndrome eye reveals loss of both the endothelial cells and pericytes (hematoxylin and eosin, ×200). (Panel A reproduced with permission from Brown GC, Magargal LE. The ocular ischemic syndrome. Clinical, fluorescein angiographic and carotid angiographic features. Int Ophthalmol. 1988;11:239–51. Panel B courtesy of Dr. W. Richard Green.)

Bilateral, simultaneous, intravenous fluorescein angiography is a technique that has been reported to be helpful diagnostically in patients with a unilateral OIS.[44] However, the technique requires specialized equipment and is not generally available.

Electroretinography

The electroretinogram typically discloses a diminution of the amplitude, or absence, of both the a- and b-waves in eyes with the OIS[5,6] (Fig. 62.21). The b-wave corresponds to activity of the Müller and/or bipolar cells, and therefore to inner layer retinal function, while the a-wave correlates with activity of the photoreceptors in the outer retina.[45–47] Therefore, with central retinal artery obstruction, in which there is essentially inner layer retinal ischemia, the b-wave amplitude is characteristically decreased. With the OIS there is both retinal vascular and choroidal compromise, leading to ischemia of the inner and outer retina, respectively. Thus, both the b-wave and a-waves are affected.

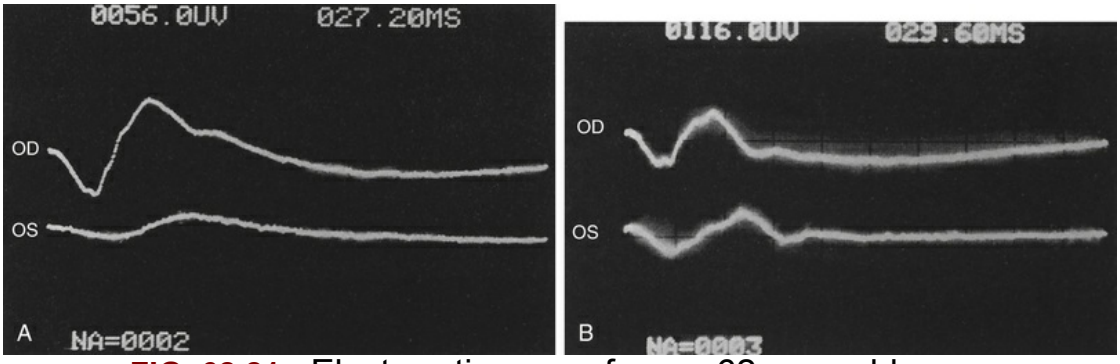

FIG. 62.21 Electroretinogram from a 62-year-old woman with ocular ischemic syndrome and a severe left carotid artery stenosis. The tracing of the right eye *(OD)* is seen above, and that of the left eye *(OS)* is seen below. (A) The a- and the b-waves are markedly diminished in the left eye before endarterectomy. (B) After left endarterectomy the amplitudes of the a- and b-waves have increased in the left eye. The vision correspondingly improved from counting fingers to 20/70.

Reduction in the amplitude of the oscillatory potential of the b-wave has been noted in eyes with retinal ischemia secondary to carotid artery stenosis.[47] This can be seen in patients with proven carotid artery disease, even in the presence of a normal fluorescein angiogram.

Carotid Artery Imaging

Carotid angiography typically discloses a 90% or greater obstruction of the ipsilateral internal or common carotid artery in persons with the OIS (Fig. 62.22).[5] Noninvasive tests, such as duplex ultrasonography and oculoplethysmography, have an accuracy of approximately between 88 and 95% in detecting carotid stenosis of 75% or greater.[48–50] Nonetheless, magnetic resonance angiography and imaging (MRA/MRI) are the gold standard in this arena, especially since MRI/MRA identifies the degree of occlusion, as well as intraplaque hemorrhage, plaque ulceration, plaque neovascularization, fibrous cap thickness, and a lipid-rich necrotic core. These factors seem to play a role in risk stratification in regard to plaque enlargement and rupture.[51] Computerized tomography angiography and imaging can very effectively delineate plaque and

the degree of obstruction, but is not as effective as magnetic imaging techniques for identifying plaque composition. Identification of plaque composition and prognosis is an area of great interest at this time.

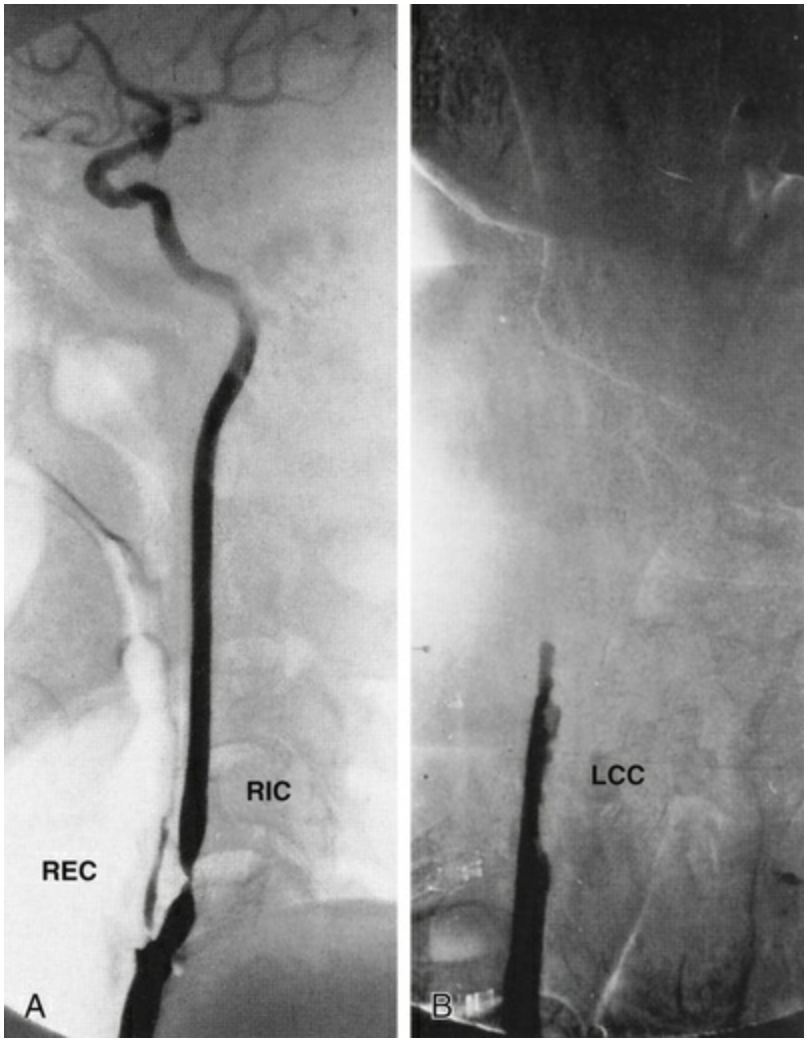

FIG. 62.22 Carotid angiography in a patient with bilateral ocular ischemic syndrome. (A) A marked stenosis is visible within the right internal carotid artery (*RIC*), as well as in the right external carotid artery (*REC*). (B) A 100% obstruction of the left common carotid artery (*LCC*) is present. (Reproduced with permission from Brown GC, Magargal LE. The ocular ischemic syndrome. Clinical, fluorescein angiographic and carotid angiographic features. Int Ophthalmol 1988;11:239–51.)

Others

Visual evoked potentials have been used to study eyes with severe carotid artery stenosis. The recovery time of the amplitude of the major positive peak after photostress has been shown to improve in patients with severe stenosis after endarterectomy.[52]

Ophthalmodynamometry can be of benefit in detecting decreased ocular perfusion in cases of unilateral OIS.[10,53] In the absence of an ophthalmodynamometer, Kearns[53] has advocated light digital pressure on the upper lid of the affected eye during ophthalmoscopy. Retinal arterial pulsations can usually be readily induced in eyes with the OIS. This is generally not the case in eyes with central retinal vein obstruction, an entity that can be confused with the OIS.

Optical coherence tomography (OCT) has shown decreased thickness of the choroid in OIS eyes.[54] It is possible that future studies utilizing OCT angiography may disclose additional abnormalities in the setting of OIS.

Systemic Associations

Diseases associated in one way or another with atherosclerosis are frequently seen in conjunction with the OIS. Systemic arterial hypertension has been reported in 73% of OIS patients, and concomitant diabetes mellitus has been observed in 56%.[55] In an age-matched historical control population from the Framingham Study,[56] the corresponding prevalences for systemic arterial hypertension and diabetes mellitus were 26% and 6%.

At the time of presentation, almost one-fifth of patients relate a history of having peripheral vascular disease for which previous bypass surgery was required.[55] The stroke rate for patients for people with the OIS is approximately 4% per year.[55]

A rare but serious cause of OIS is giant cell arteritis.[57] This condition has been reported to cause bilateral loss of vision, which may occur despite treatment with steroids.[58]

Mortality data[55] have shown that the 5-year death rate for patients with the OIS is 40%. The leading cause of death is cardiovascular disease, which accounts for about two-thirds of

cases. Stroke is the second leading cause of death. Thus, most patients with the OIS should be considered for cardiac evaluation, in addition to a carotid artery workup. It is also important to note that Mizener et al.[59] noted that in 69% of their patients, the OIS was the first clinical manifestation of carotid occlusive disease, a fact that only further underscores the importance of timely systemic evaluation in these patients.

Differential Diagnosis

The entities that are most commonly confused with the ocular ischemic syndrome include mild central retinal vein obstruction and diabetic retinopathy. Features that differentiate these abnormalities are listed in Table 62.3. In contrast to the OIS, the veins in eyes with mild, or nonischemic, central retinal vein obstruction are often dilated and tortuous. Additionally, it is difficult with light digital pressure on the lid to induce retinal arterial pulsations in eyes with central retinal vein obstruction. Not so with the OIS. While both entities usually have a prolonged retinal arteriovenous transit time, choroidal filling defects and prominent retinal arterial staining are usually absent on fluorescein angiography in eyes with central retinal vein obstruction.

TABLE 62.3

Features That Differentiate the Ocular Ischemic Syndrome, Central Retinal Vein Obstruction, and Diabetic Retinopathy

Clinical Features	OIS	CRVO	Diabetic Retinopathy
Laterality	80% unilateral	Usually unilateral	Bilateral
Age	50s–80s	50s–80s	Variable
Fundus signs			
Venous status	Dilated (not tortuous), beaded	Dilated and tortuous	Dilated and beaded
Hemorrhages	Peripheral, dot, and blot	Nerve fiber layer, posterior pole	Posterior pole, dot, and blot
Microaneurysms	In midperiphery	Variable	Present in posterior pole
Exudate	Absent	Rare	Common
Optic disc	Normal	Swollen	Affected in papillopathy
Retinal arterial perfusion pressure	Decreased	Normal	Normal

Fluorescein angiography			
Choroidal filling	Delayed, patchy	Normal	Normal
Arteriovenous transit time	Prolonged	Prolonged	May be prolonged
Late retinal vessel staining	Arterial	Venous	Usually absent

CRVO, central retinal vein obstruction; OIS, ocular ischemic syndrome.

Diabetic retinopathy can exist concomitantly with the OIS. The presence of hard exudate in the posterior pole usually suggests diabetic retinopathy, rather than the OIS.[5] As is the case with central retinal vein obstruction, choroidal filling defects and retinal arterial staining are generally absent on fluorescein angiography in eyes with diabetic retinopathy.

In some cases of diabetic retinopathy, the OIS can exacerbate the proliferative changes. It has not been definitively proven that carotid stenosis is protective against the development of proliferative diabetic retinopathy.[60]

Treatment

With regard to vision, the natural course of the ocular ischemic syndrome is uncertain. Nonetheless, most eyes with the fully developed entity probably have a poor long-term outcome. When iris neovascularization is present, well over 90% of eyes become legally blind within a year of discovery.[32]

Total Carotid Artery Obstruction

When a carotid artery is 100% obstructed, endarterectomy is usually ineffective since a thrombus often propagates distally to the next major vessel. In these cases, extracranial to intracranial bypass surgery, usually from the superficial temporal artery to the middle cerebral artery, has been attempted to alleviate the obstruction. Although reports suggest that this procedure can be of benefit initially in salvaging vision in eyes with the OIS,[61–66] we found the visual prognosis at one year after the surgery to be universally poor, despite the fact that 20% of patients had visual improvement within the first 3 months of surgery.[32] Additionally, the procedure has not been shown in a large randomized study to be of benefit in

preventing the risk of ischemic stroke.[67]

That said, some authors have offered objective support of improvement in perfusion following endarterectomy. Costa et al.[68] were able to demonstrate increased mean peak systolic flow velocities and end diastolic velocities in the orbital vessels following surgery, with a significant reduction of the mean resistance indices in the central retinal and posterior ciliary arteries.[7]

Kawaguchi et al.[69] evaluated the effects of superficial temporal to middle cerebral artery (STA–MCA) bypass in a series of patients with the OIS. These authors compared a number of clinical parameters including carotid Doppler flow imaging in 32 patients who received STA–MCA as compared to nine patients with OIS who did not have STA–MCA. Prior to surgery all 32 patients had reversal of flow in their ophthalmic arteries. The mean peak systolic flow improved to 0.15 m/s at 3 months as compared to −0.26 at baseline. In addition, whereas all patients had reversal of flow in the ophthalmic artery preoperatively, 56% developed antegrade flow at the 3-month period. In the final analysis, 47% had visual improvement following surgery.

Less-Than-Total Carotid Artery Obstruction

Although there are no randomized studies that compare the natural history of the disease to the course after carotid endarterectomy, this surgery may also stabilize or improve vision in the eyes of patients who undergo successful endarterectomy prior to the development of iris neovascularization.[32,70] Not withstanding, the visual results associated with this treatment are fair at best. In the series of Sivalingam et al.,[32] at the end of one year 7% of eyes with the OIS that underwent endarterectomy had visual improvement, 33% were unchanged, and 60% had worse vision. Among the 60 total OIS eyes in the group, an endarterectomy was performed for only three without iris neovascularization. At the end of one-year follow-up the vision was better in one, stable in one, and worse in the third. Endarterectomy appears to rarely cause regression of iris neovascularization in eyes with the OIS.[71]

More recent data demonstrated that carotid revascularization

surgery results in improved retinal blood in 80% of cases, although the long-term visual implications are unclear.[72] Stenting can also be undertaken in select cases to successfully restore blood flow within the carotid artery.[73,74] Rarely, bilateral external carotid obstruction can cause the OIS.[75] In this instance, external carotid endarterectomy can be considered. In cases of the OIS with ipsilateral internal carotid and external carotid obstructions, it would seem that reversal of both would yield the best ocular prognosis, but this is not known with certainty at the current time.

It should be noted that eyes with the OIS will occasionally develop a severe increase in intraocular pressure after ipsilateral carotid endarterectomy.[76,77] This is most likely to occur in eyes with iris neovascularization and anterior chamber angle compromise from fibrovascular tissue formation. Although aqueous outflow is impaired in such eyes, ciliary body perfusion and aqueous humor formation are also decreased secondary to the carotid stenosis. When the carotid obstruction is suddenly reversed, ciliary body perfusion and aqueous humor formation increase, but the outflow obstruction in the anterior chamber angle is still present. Thus, the intraocular pressure rises dramatically. Ciliary body destructive procedures or glaucoma filtering surgery may be required in these cases.

Carotid Endarterectomy in General

Several large randomized studies have been published concerning the indications for carotid endarterectomy in general.[78-81] Carotid endarterectomy has been proven to be efficacious in both symptomatic patients with high-grade (70–99%) symptomatic carotid stenosis,[79] and in asymptomatic patients with greater than (or equal to) 60% stenosis.[80] Specifically, the investigators of the North American Symptomatic Carotid Endarterectomy Trial[79] noted a 17% absolute risk reduction from 26% to 9% in the cumulative 2-year risk of ipsilateral stroke, and a 10% absolute risk reduction in fatal ipsilateral stroke when those randomized to endarterectomy were compared to those who were treated medically. The European Carotid Surgery Trialists' Collaborative Group[78] also were able to demonstrate a similar treatment effect of

carotid endarterectomy for patients with 70–99% stenosis (sixfold reduction in 3-year risk of ipsilateral stroke), but also found that in the 0–29% stenosis group, the early risks of surgery (2.3% died or had a disabling stroke within 30 days of surgery) outweighed the 3-year benefit when compared to medical therapy. The investigators of the Asymptomatic Carotid Atherosclerosis Study[65] were able to demonstrate an aggregate risk reduction of 53% in the incidence of death or stroke, when those randomized to surgery were compared to those who received medical treatment. Asymptomatic patients with carotid artery stenosis of 60% or greater reduction in diameter were eligible to benefit.

A Cochrane Database Systematic Review[82] incorporating 35 ,000 years of patient follow-up recently demonstrated that carotid surgery: (1) increased the 5-year risk of ipsilateral ischemic stroke in patients with less than 30% stenosis (n = 1746, absolute risk reduction (ARR) −2.2%, p=.05); (2) had no significant effect in patients with 30–49% stenosis (n=1429, ARR 3.2%, p=.6), was of marginal benefit in patients with 50–69% stenosis (n=1549, ARR 4.6%, p= .04), and was highly beneficial in patients with 70% to 99% stenosis (n=1095, ARR 16.0%, p<.001). Accordingly, any patient with the OIS and severe carotid artery stenosis should be evaluated for carotid endarterectomy or stenting.[74] The implications of plaque composition and surgery should become clearer with time.[51]

Medical Therapy

Since atherosclerosis is, by far, the most common cause of the OIS, medical therapy should be directed toward treating atherogenic disease by controlling risk factors such as systemic arterial hypertension, smoking, diabetes mellitus, and hyperlipidemia. Of considerable importance is the fact that high-dose (40 mg per os daily) rosuvastatin therapy[83,84] and high-dose (80 mg per os daily) atorvastatin therapy[84] have been shown to decrease the volume of coronary artery atherosclerotic lesions, an event likely generalizable to atherosclerosis elsewhere in the body. Since cardiac disease is the leading cause of death associated with the OIS, evaluation by a cardiologist should be considered.[55]

Direct Ocular Therapeutic Modalities

Full scatter panretinal laser photocoagulation has been advocated for ocular ischemic eyes with iris neovascularization and/or posterior segment neovascularization.[70,85,86] This generally consists of 1500–2000 500 μm burns with the argon green laser. Unlike the situation when iris neovascularization occurs secondary to diabetic retinopathy, in which there is regression in a majority of cases with full scatter panretinal photocoagulation, approximately 36% of OIS eyes will demonstrate regression of the iris neovascularization after full scatter treatment. If the anterior chamber angle is completely closed by fibrovascular tissue and there is no posterior segment neovascularization, panretinal photocoagulation is probably not indicated unless a glaucoma filtering procedure is being considered, as higher success rates of filtration surgery have been reported when PRP has been performed.[87]

While there is little in the reported literature regarding the management of macular edema secondary to this condition, Klais and Spaide reported excellent clinical resolution of fluid and dramatic improvement in vision in a patient treated with intravitreal triamcinolone acetonide.[88] Intravitreal bevacizumab has been used for the treatment of the iris neovascularization and macular edema associated with the OIS.[89] Nonetheless, intravitreal bevacizumab has been shown to cause vision loss due to a circulatory disturbance in OIS eyes.[90] Any intraocular injection into an OIS eye could raise the intraocular pressure to above that in the choroidal and central retinal arterial circulations, both of which have similar perfusion pressures. Thus, such eyes should be monitored very carefully after injection, with a consideration of anterior chamber paracentesis if these circulations appear shut down (very narrowed retinal arteries, a pale optic disc, and a lightened fundus).

References

1. Kearns TP, Hollenhorst RW. Venous stasis retinopathy of occlusive disease of the carotid artery. *Proc Mayo Clin*. 1963;38:304–312.

2. Hayreh SS. So-called "central retinal vein occlusion." Venous-stasis retinopathy. *Ophthalmologica*. 1976;172:14–37.
3. Knox DL. Ischemic ocular inflammation. *Am J Ophthalmol*. 1965;60:995–1002.
4. Young LHY, Appen RE. Ischemic oculopathy, a manifestation of carotid artery disease. *Arch Neurol*. 1981;38:358–361.
5. Brown GC, Magargal LE. The ocular ischemic syndrome. Clinical, fluorescein angiographic and carotid angiographic features. *Int Ophthalmol*. 1988;11:239–251.
6. Brown GC, Magargal LE, Simeone FA, et al. Arterial obstruction and ocular neovascularization. *Ophthalmology*. 1982;89:139–146.
7. Kahn M, Green WR, Knox DL, et al. Ocular features of carotid occlusive disease. *Retina*. 1986;6:239–252.
8. Michelson PE, Knox DL, Green WR. Ischemic ocular inflammation. A clinicopathologic case report. *Arch Ophthalmol*. 1971;86:274–280.
9. Sturrock GD, Mueller HR. Chronic ocular ischaemia. *Br J Ophthalmol*. 1984;68:716–723.
10. Kearns TP. Ophthalmology and the carotid artery. *Am J Ophthalmol*. 1979;88:714–722.
11. Kobayashi S, Hollenhorst RW, Sundt TM Jr. Retinal arterial pressure before and after surgery for carotid artery stenosis. *Stroke*. 1971;2:569–575.
12. Bullock J, Falter RT, Downing JE, et al. Ischemic ophthalmia secondary to an ophthalmic artery occlusion. *Am J Ophthalmol*. 1972;74:486–493.
13. Madsen PH. Venous-stasis insufficiency of the ophthalmic artery. *Acta Ophthalmol*. 1965;40:940–947.
14. Magargal LE, Sanborn GE, Zimmerman A. Venous stasis retinopathy associated with embolic obstruction of the central retinal artery. *J Clin Neuroophthalmol*. 1982;2:113–118.
15. Duker JS, Belmont JB. Ocular ischemic syndrome secondary to carotid artery dissection. *Am J Ophthalmol*. 1988;106:750–752.
16. Hamed LM, Guy JR, Moster ML, et al. Giant cell arteritis in the ocular ischemic syndrome. *Am J Ophthalmol*.

1992;113:702–705.
17. Tang Y, Luo D, Peng W, et al. Ocular ischemic syndrome secondary to carotid artery occlusion as a late complication of radiotherapy of nasopharyngeal carcinoma. *J Neuroophthalmol*. 2010;30:315–320.
18. Papavasileiou E, Sobrin L, Papaliodis GN. Ocular ischemic syndrome presenting as retinal vasculitis in a patient with moyamoya syndrome. *Retin Cases Brief Rep*. 2015;9(2):170–172.
19. Salinas-La Rosa CM. Malignant transformation of optic nerve melanocytoma into melanoma associated with ocular ischemic syndrome and oculocardiac reflex: Case report and review of the literature. *Semin Ophthalmol*. 2015;19:1–4.
20. Sakthiswary R, Syazarina SO, Shaharir SS, et al. Blindness in a pulseless young woman: lessons learned. *Ocul Immunol Inflamm*. 2012;20(4):309–311.
21. Effeney DJ, Krupski WC, Stoney RJ, et al. Fibromuscular dysplasia of the carotid artery. *Aust NZ J Surg*. 1983;53:527–531.
22. Dhobb M, Ammar F, Bensaid Y, et al. Arterial manifestations in Behçet's disease: four new cases. *Ann Vasc Surg*. 1986;1:249–252.
23. Sadun AA, Sebag J, Bienfang DC. Complete bilateral internal carotid artery occlusion in a young man. *J Clin Neuroophthalmol*. 1983;3:63–66.
24. Hong IH, Ahn JK, Chang S, et al. Diagnostic efficacy of total homocysteine and C-reactive protein for ocular ischemic syndrome. *Eye (Lond)*. 2011;25:1650–1654.
25. Donnan GA, Sharbrough FW. Carotid occlusive disease. Effect of bright light on visual evoked response. *Arch Neurol*. 1982;39:687–689.
26. Wiebers DO, Swanson JW, Cascino TL, et al. Bilateral loss of vision in bright light. *Stroke*. 1989;20:554–558.
27. Ramadan NM, Tietjen GE, Levine SR, et al. Scintillating scotomata associated with internal carotid artery dissection: report of three cases. *Neurology*. 1991;41:1084–1087.
28. Brown GC, Brown MM, Fischer DH. Photopsias: A key to diagnosis. *Ophthalmology*. 2015;122:2084–2094.

29. Hayreh SS, Zimmerman MB. Amaurosis fugax in ocular vascular occlusive disorders: prevalence and pathogeneses. *Retina*. 2014;34(1):115–122.
30. Winterkorn JM, Teman AJ. Recurrent attacks of amaurosis fugax treated with calcium channel blocker. *Ann Neurol*. 1991;30:423–425.
31. Aasen J, Kerty E, Russell D, et al. Amaurosis fugax: clinical, Doppler and angiographic findings. *Acta Neurol Scand*. 1988;77:450–455.
32. Sivalingam A, Brown GC, Magargal LE. The ocular ischemic syndrome. III. Visual prognosis and the effect of treatment. *Int Ophthalmol*. 1991;15:15–20.
33. Kawaguchi S, Okuno S, Sakaki T, et al. Effect of carotid endarterectomy on chronic ocular ischemic syndrome due to internal carotid artery stenosis. *Neurosurgery*. 2001;48(2):328–332 [discussion 322-3].
34. Kawaguchi S, Iida J, Uchiyama Y. Ocular circulation and chronic ocular ischemic syndrome before and after carotid treatment. *Int Ophthalmol*. 1991;15:15–20.
35. Kawaguchi S, Iida J, Uchiyama Y. Ocular circulation and chronic ocular ischemic syndrome before and after carotid artery revascularization surgery. *J Ophthalmol*. 2012;2012:350475.
36. Schlaegel T. Symptoms and signs of uveitis. Harper and Row: Hagerstown; 1983:1–7. Duane TD. *Clinical ophthalmology*. vol. 4.
37. Green WR, Chan CC, Hutchins GM, et al. Central retinal vein occlusion. A prospective histopathologic study of 29 eyes in 28 cases. *Retina*. 1981;1:27–55.
38. Campo RV, Reeser FH. Retinal telangiectasia secondary to bilateral carotid artery occlusion. *Arch Ophthalmol*. 1983;101:1211–1213.
39. Brown GC. Anterior ischemic optic neuropathy occurring in association with carotid artery obstruction. *J Clin Neuroophthalmol*. 1986;6:39–42.
40. Waybright EA, Selhorst JB, Combs J. Anterior ischemic optic neuropathy with internal carotid artery occlusion. *Am J Ophthalmol*. 1982;93:42–47.

41. Bolling JP, Buettner H. Acquired retinal arteriovenous communications in occlusive disease of the carotid artery. *Ophthalmology*. 1990;97:1148–1152.
42. Brown GC. Macular edema in association with severe carotid artery obstruction. *Am J Ophthalmol*. 1986;102:442–448.
43. Dugan JD, Green WR. Ophthalmic manifestations of carotid occlusive disease. *Eye*. 1991;5:226–238.
44. Choromokos EA, Raymond LA, Sacks JG. Recognition of carotid stenosis with bilateral simultaneous retinal fluorescein angiography. *Ophthalmology*. 1982;89:1146–1148.
45. Carr RE, Siegel JM. Electrophysiologic aspects of several retinal diseases. *Am J Ophthalmol*. 1964;58:95–107.
46. Henkes HE. Electroretinography in circulatory disturbances of the retina. II. The electroretinogram in cases of occlusion of the central retinal artery or one of its branches. *Arch Ophthalmol*. 1954;51:42–53.
47. Coleman K, Fitzgerald D, Eustace P, et al. Electroretinography, retinal ischaemia and carotid artery disease. *Eur J Vasc Surg*. 1990;4:569–573.
48. Bosley TM. The role of carotid noninvasive tests in stroke prevention. *Semin Neurol*. 1986;6:194–203.
49. Castaldo JE, Nicholas GG, Gee W, et al. Duplex ultrasound and ocular pneumoplethysmography concordance in detecting severe carotid stenosis. *Arch Neurol*. 1989;46:518–522.
50. Neale ML, Chambers JL, Kelly AT, et al. Reappraisal of duplex criteria to assess significant carotid artery stenosis with special reference to reports of the North American Symptomatic Carotid Endarterectomy Trial and the European Carotid Surgery Trial. *J Vasc Surg*. 1994;20:642–649.
51. Brinjikji W, Huston J 3rd, Rabinstein AA, et al. Contemporary carotid imaging: from degree of stenosis to plaque vulnerability. *J Neurosurg*. 2015;31:1–16.
52. Banchini E, Franchi A, Magni R, et al. Carotid occlusive disease. An electrophysiological investigation. *J Cardiovasc Surg*. 1987;28:524–527.

53. Kearns TP. Differential diagnosis of central retinal vein obstruction. *Ophthalmology*. 1983;90:475–480.
54. Kang HM, Lee CS, Lee SC. Thinner subfoveal choroidal thickness in eyes with ocular ischemic syndrome than in unaffected contralateral eyes. *Graefes Arch Clin Exp Ophthalmol*. 2014;252(5):851–852.
55. Sivalingham A, Brown GC, Magargal LE, et al. The ocular ischemic syndrome II. Mortality and systemic morbidity. *Int Ophthalmol*. 1989;13:187–191.
56. Kannel WB, Gordon T, editors. The Framingham Study. Public Health Service Publication No. NIH 77–1247, Section 6, Tables 6–9, Section 29, Tables A-22 and A-23, Section 32. p. 84–5.
57. Casson RJ, Fleming FK, Shaikh A, et al. Bilateral ocular ischemic syndrome secondary to giant cell arteritis. *Arch Ophthalmol*. 2001;119:306–307.
58. Hwang JM, Girkin CA, Perry JD, et al. Bilateral ocular ischemic syndrome secondary to giant cell arteritis progressing despite corticosteroid treatment. *Am J Ophthalmol*. 1999;127:102–104.
59. DMizener JB, Podhajsky P, Hayreh SS. Ocular ischemic syndrome. *Ophthalmology*. 1997;104:859–864.
60. Duker J, Brown GC, Bosley TM, et al. Asymmetric proliferative diabetic retinopathy and carotid artery disease. *Ophthalmology*. 1990;97:869–874.
61. Edwards MS, Chater NL, Stanley JA. Reversal of chronic ischaemia by extracranial–intracranial arterial by-pass. *Neurosurgery*. 1980;7:480–483.
62. Katz B, Weinstein PR. Improvement of photostress recovery testing after extracranial–intracranial bypass surgery. *Br J Ophthalmol*. 1986;70:277–280.
63. Kearns TP, Younge BR, Peipgras PG. Resolution of venous stasis retinopathy after carotid artery bypass surgery. *Proc Mayo Clin*. 1980;55:342–346.
64. Kiser WD, Gonder J, Magargal LE, et al. Recovery of vision following treatment of the ocular ischemic syndrome. *Ann Ophthalmol*. 1983;15:305–310.
65. Shibuya M, Suzuki Y, Takayasu M, et al. Effects of STA–

MCA anastomosis for ischaemic oculopathy due to occlusion of the internal carotid artery. *Acta Neurochir*. 1990;103:71–75.
66. Kearns TP, Siebert RG. The ocular aspects of carotid artery surgery. *Trans Am Ophthalmol Soc*. 1978;76:247–265.
67. The EC/IC Bypass Study Group. Failure of extracranial–intracranial arterial bypass to reduce the risk of ischemic stroke. Results of an international randomized trial. *N Engl J Med*. 1985;313:1191–1200.
68. Costa VP, Kuzniec S, Molnar LJ, et al. The effects of carotid endarterectomy on the retrobulbar circulation of patients with severe occlusive carotid artery disease. An investigation by color Doppler imaging. *Ophthalmology*. 1999;106:306–310.
69. Kawaguchi S, Sakaki T, Kamada K, et al. Effects of superficial temporal to middle cerebral artery bypass for ischaemic retinopathy due to internal carotid artery occlusion/stenosis. *Acta Neurochir (Wien)*. 1994;129:166–170.
70. Johnston ME, Gonder JR, Canny CL. Successful treatment of the ocular ischemic syndrome with panretinal photocoagulation and cerebrovascular surgery. *Can J Ophthalmol*. 1988;23:114–119.
71. Hauch TL, Busuttil RW, Yoshizumi MO. A report of iris neovascularization. An indication for carotid endarterectomy. *Surgery*. 1984;95:358–362.
72. Cardia G, Porfido D, Guerriero S, et al. Retinal circulation after carotid artery revascularization. *Angiology*. 2011;62:372–375.
73. Fintelman R, Rosenwasser RH, Jabbour P, et al. An old problem, a new solution. *Surv Ophthalmol*. 2010;55:85–88.
74. Marx JL, Hreib K, Choi IS, et al. Percutaneous carotid artery angioplasty and stenting for ocular ischemic syndrome. *Ophthalmology*. 2004;111:2284–2291.
75. Alizai AM, Trobe JD, Thompson BG, et al. Ocular ischemic syndrome after occlusion of both external carotid arteries. *J Neuroophthalmol*. 2005;25:268–272.
76. Coppeto JR, Wand M, Bear L, et al. Neovascular glaucoma and carotid artery obstructive disease. *Am J Ophthalmol*.

1985;99:567–570.
77. Melamed S, Irvine J, Lee DA. Increased intraocular pressure following endarterectomy. *Ann Ophthalmol*. 1987;19:304–306.
78. European Carotid Surgery Trialists' Collaborative Group. MRC European Carotid Surgery Trial: interim results for symptomatic patients with severe (70–99%) or with mild carotid stenosis. *Lancet*. 1991;337:1235–1243.
79. North American Symptomatic Carotid Endarterectomy Trial Collaborators. Beneficial effect of carotid endarterectomy in symptomatic patients with high-grade carotid stenosis. *N Engl J Med*. 1991;325:445–453.
80. Asymptomatic Carotid Atherosclerosis Study Group. Carotid endarterectomy for patients with asymptomatic internal carotid artery stenosis. *JAMA*. 1995;273:1421–1428.
81. Mayberg MR, Wilson SE, Yatsu F, et al. Carotid endarterectomy and prevention of cerebral ischemia in symptomatic carotid stenosis. [for the; Veterans Affairs Cooperative Studies Program 309 Trialist Group] *JAMA*. 1991;266:3289–3294.
82. Rerkasem K, Rothwell PM. Carotid endarterectomy for symptomatic carotid stenosis. *Cochrane Database Syst Rev*. 2011;(4) [CD001081].
83. Nissen SE, Nicholls SJ, Sipahi I, et al. Effect of very high-intensity statin therapy on regression of coronary atherosclerosis: the ASTEROID trial. [for the; ASTEROID Investigators] *JAMA*. 2006;295:1556–1565.
84. Puri R, Libby P, Nissen SE, et al. Long-term effects of maximally intensive statin therapy on changes in coronary atheroma composition: insights from SATURN. *Heart J Cardiovasc Imaging*. 2014;15:380–388.
85. Carter JE. Panretinal photocoagulation for progressive ocular neovascularization secondary to occlusion of the common carotid artery. *Ann Ophthalmol*. 1984;16:572–576.
86. Eggleston TF, Bohling CA, Eggleston HC, et al. Photocoagulation for ocular ischemia associated with carotid artery occlusion. *Ann Ophthalmol*. 1980;12:84–87.
87. Allen RC, Bellows AR, Hutchinson BT, et al. Filtration

surgery in the treatment of neovascular glaucoma. *Ophthalmology*. 1982;89:1181–1187.
88. Klais CM, Spaide RF. Intravitreal triamcinolone acetonide injection in ocular ischemic syndrome. *Retina*. 2004;24:459–461.
89. Amselem L, Montero J, Diaz-Llopis M, et al. Intravitreal bevacizumab (Avastin) injection in ocular ischemic syndrome. *Am J Ophthalmol*. 2007;144:122–124.
90. Jo YJ, Min JK, Woo JM, et al. Acute vision loss associated with retinal circulatory disturbances after intravitreal injection of bevacizumab. *J Ocul Pharmacol Ther*. 2013;29:79–83.

63

Coagulopathies

Sandra Liakopoulos, Florian M.A. Heussen, SriniVas R. Sadda

Introduction

A variety of hereditary as well as acquired diseases belong to the group of coagulopathies – diseases that affect the blood clotting system, causing hypercoagulability and susceptibility to bleeding. Important coagulopathies include disseminated intravascular coagulation (DIC), primary immune thrombocytopenia (ITP, also known as idiopathic thrombocytopenic purpura), thrombotic thrombocytopenic purpura (TTP), and the HELLP syndrome (hemolytic anemia (H), elevated liver enzymes (EL), and low platelet count (LP)). Since coagulopathies are multiorgan disease processes, ocular involvement may occur and show characteristic

changes that should be recognized by ophthalmologists and retina specialists.

General Considerations

Disseminated Intravascular Coagulation

Disseminated intravascular coagulation (DIC) is often described as a secondary disease process typically associated with other disease entities.[1] The presence of DIC increases the risk of mortality beyond that associated with the primary disease.[2] A cascading activation of both procoagulants and fibrinolysis leads to simultaneous, uncontrolled hemorrhages and diffuse thrombosis of small and large vessels affecting virtually all mucocutaneous tissues and various organs, ultimately resulting in end-organ failure (see Box 63.1). As such, DIC is regarded as one of the most common causes of death. But not all presentations of DIC are lethal; it may also manifest as low-grade disease with a chronic or compensated

Box 63.1

Clinical Manifestations of Disseminated Intravascular Coagulation

Hemorrhagic Events

- Petechiae
- Purpura
- Hemorrhagic bullae
- Hematoma
- Wound bleeding

Peripheral Thrombotic Events

- Acral cyanosis
- Gangrene

Central/Organ Dysfunction

- Fever
- Hypotension
- Acidosis
- Proteinuria
- Hypoxia
- CNS dysfunction

Triggering events for DIC are manifold and range from trauma to malignancies, septicemia, obstetric complications, cardiovascular disease, inflammatory disorders, and renal disease, only to name a few. Whether DIC will pursue a fulminant or compensated course is loosely related to the disease entity with which it is associated. Chronic conditions such as cardiovascular disease, autoimmune diseases, or hematologic disorders tend to be associated with a low-grade DIC, whereas more acutely presenting entities such as crush injuries are more likely to trigger a fulminant DIC with poor prognosis. Furthermore, DIC is not restricted to a particular age range and may occur in neonates as well as elderly individuals.

The currently established theory of pathogenesis is an initial activation of the coagulation cascade following inflammation or damage to tissue and vascular endothelial cells.[3] Fibrin formation leads to microvascular or macrovascular thrombosis. Soon thereafter, fibrinolysis is upregulated and the consumption of platelets in the obstructed microcirculation causes a systemic thrombocytopenia (cell count $<100 \times 10^9$/L), thereby generating an environment of simultaneous clotting and extrusion of hemorrhages. Despite a common pathophysiologic pathway, clinical manifestations of the disease may vary widely (see Box 63.1), complicating diagnosis and treatment management.

The onset of DIC is usually marked by fever, shock, acidosis and, more specifically, widespread hemorrhaging, acral cyanosis, gangrene, and end-organ failure. Bleeding from more than three

unrelated sites at once and a recent medical history compatible with known causes of DIC can direct the clinician towards the diagnosis. Definite diagnosis is heavily based on positive laboratory test results for platelet count, D-dimer (fibrin degradation product or FDP), antithrombin-III, protein C, prothrombin time, partial thromboplastin time, and fibrinogen.[4]

Treatment of DIC is difficult and should primarily address the underlying cause. DIC spontaneously resolves in many cases when the underlying causative disorder is effectively treated; however, removal of its cause does not necessarily alleviate the process in all cases. Replacement treatment such as frozen plasma transfusion or infusion of antithrombin-III, fibrinogen, and platelet-concentrates can help to limit hemorrhages. If features of thrombosis predominate, anticoagulant treatment may be required. Activated protein C has been suggested to treat this condition;[5] however, most recent studies did not show any advantage over placebo, and thus this agent has been removed from the market and relevant guidelines have been revised.[6,7] A new promising adjunctive agent that is currently under evaluation is human soluble thrombomodulin.[6,8] Thrombin binds to this molecule, which will then convert protein C into active protein C.

Thrombotic Thrombocytopenic Purpura and Primary Immune Thrombocytopenia

Thrombotic thrombocytopenic purpura (TTP) is a severe thrombotic microangiopathy caused by platelet adhesion and aggregation mediated by endothelial cell-attached ultra-large von Willebrand factor multimers (ULvWF). The underlying cause is a congenital or acquired (autoimmune) deficiency of the von Willebrand factor-cleaving protease ADAMTS-13[9] TTP is more frequent in young female adults than in males or older individuals. Most presentations of the disease are idiopathic, although familial and secondary TTP have been described. Pregnancy, treatment with certain drugs (clopidogrel, cyclosporine, tacrolimus), and malignancies are associated with a higher incidence of TTP. Of note, systemic (not intravitreal) treatment with bevacizumab, a monoclonal antibody to VEGF that is commonly used intravitreally

for management of ocular neovascular disorders, can induce a TTP-like microangiopathy.[10]

TTP is accompanied by profound thrombocytopenia, erythrocyte fragmentation, and increased serum levels of lactate dehydrogenase (LDH).[11] Partial vessel occlusion by platelet-rich thrombi may result in organ ischemia. Clinically, TTP manifests with fever, renal failure, neurologic symptoms, purpura, and signs of hemolytic anemia. There is often a prodromal phase that may consist of headache, dizziness, nausea, and abdominal pain, presumably caused by microinfarction of the viscera. Though there are chronic smoldering patterns of the disease, an acute and fulminant course is not uncommon and, if left untreated, can be lethal. In some cases, ocular manifestations as described below may present as the first signs of the disease; thus, prompt referral to a hematologist may be life-saving.[12] Plasmapheresis is the principal treatment for this condition and can be supplemented by immunosuppressive therapy (corticosteroids and rituximab), although relapses are generally the rule.[13]

Although primary immune thrombocytopenia (ITP, also known as idiopathic thrombocytopenic purpura) also features thrombocytopenia and purpura, the underlying pathophysiology is distinctly different from TTP. ITP is an acquired autoimmune disorder characterized by isolated thrombocytopenia often occurring in the absence of any identifiable precipitants.[14,15] Current concepts in the pathogenesis of thrombocytopenia in ITP include immunologic destruction of platelets and impaired platelet production.[14] Fortunately, ITP is self-limiting in most cases and responds well to treatment with corticosteroids, intravenous immunoglobulin (IVIg), anti-D immunoglobulin (anti-D), rituximab, or the thrombopoietin-receptor agonists (TPO-RAs). Splenectomy may be considered in selected cases for children and adolescents with chronic or persistent ITP who have significant or persistent bleeding, and lack of responsiveness or intolerance of other therapies.[15] Rarely, the extremely low platelet counts seen in ITP can cause severe, life-threatening complications.

HELLP Syndrome

The incidence of the HELLP syndrome (toxemia of pregnancy) is reported as being between 0.2 and 0.6% of all pregnancies.[16] "HELLP" is an abbreviation of the three main features of the syndrom: hemolytic anemia (H), elevated liver enzymes (EL), and low platelet count (LP). While being regarded as a microangiopathy much like TTP, it can also convert into a fulminant DIC in 20% of cases. The mortality rate is around 1.1% with adequate management, yet other serious complications such as abruptio placentae (16%), acute renal failure (7.7%), or pulmonary edema (6%) can occur more frequently.[17]

Ophthalmic Involvement

Although there are many differences regarding the underlying etiology or management of the various coagulopathies discussed in this chapter, they all may present with similar ophthalmic manifestations (see Figs. 63.1–63.3). The precise frequency of ocular complications, however, is unknown, as many cases may remain unrecognized due to the life-threatening nature of those systemic diseases. Relatively few reports are available regarding ocular complications of DIC as most cases are diagnosed and reported after the patients have died.[18] By comparison, many more reports can be found in the literature describing ophthalmic findings in TTP, ITP, or HELLP syndrome.[19-37] Some groups have reported that ocular signs and symptoms occur in up to 14% of patients with TTP.[22]

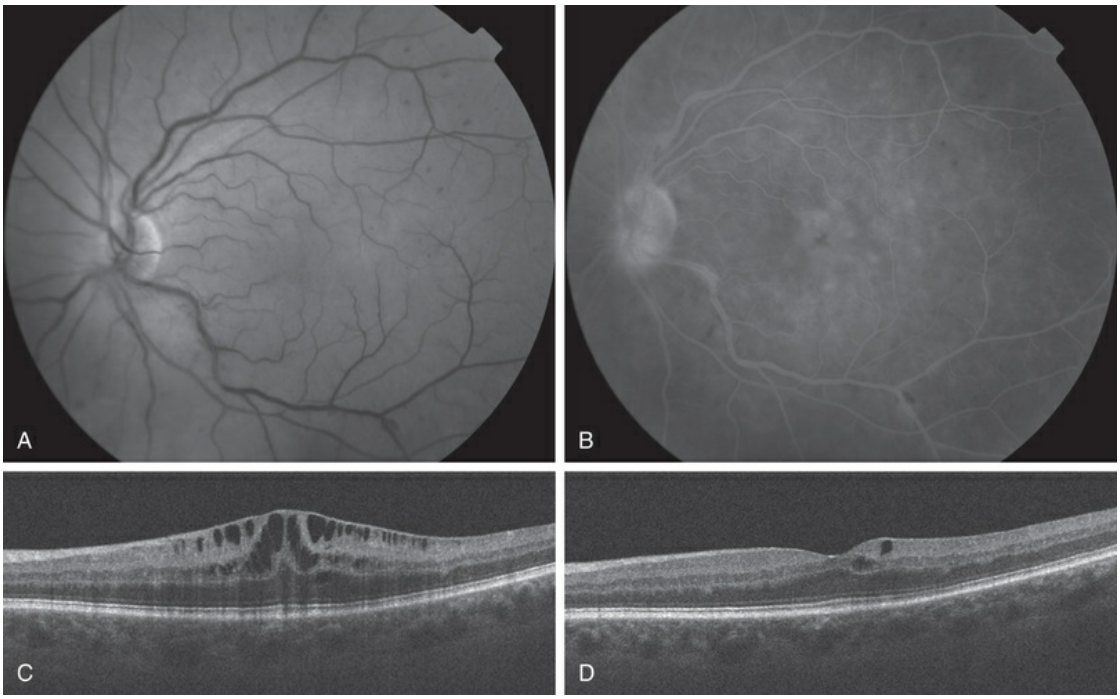

FIG. 63.1 A 75-year-old woman presented with a recent diagnosis of primary immune thrombocytopenia (ITP) and acute blurring of vision in her left eye with a visual acuity of 20/60. (A) Red-free photograph of the left eye illustrates a few scattered intraretinal hemorrhages in all quadrants with blurring of the inferior disc margin and loss of the foveal reflex. (B) Late-phase fluorescein angiogram demonstrates leakage from parafoveal capillaries with accumulation of dye in cystoid spaces as well as disc hyperfluorescence and focal staining of some vessels. (C) Spectral domain optical coherence tomography (SD-OCT) B-scan through the foveal center shows cystoid macular edema involving multiple retinal layers. (D) SD-OCT B-scan 2 weeks following treatment with a single injection of intravitreal ranibizumab 0.5 mg. Note significant reduction in edema.

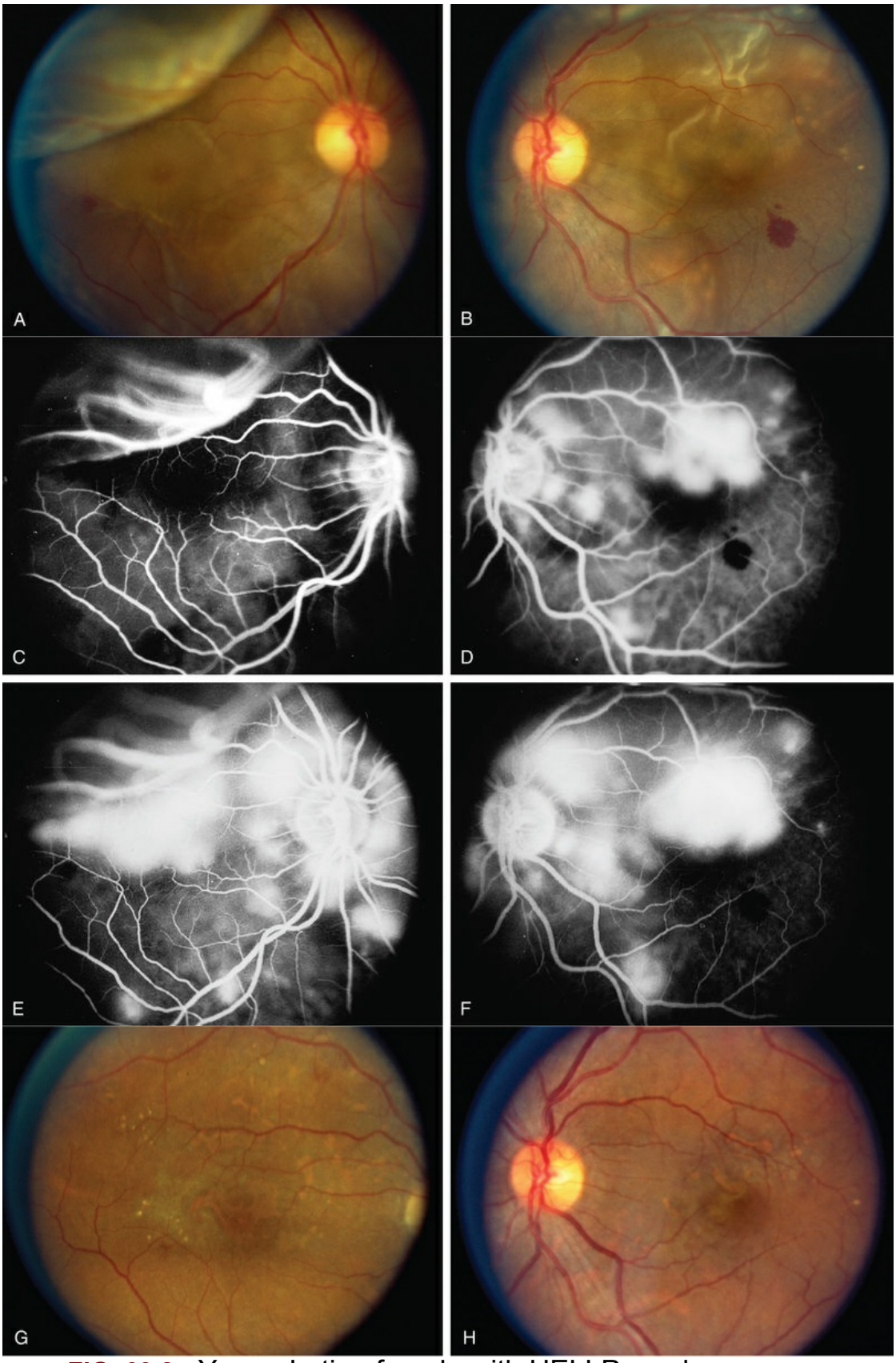

FIG. 63.2 Young Latino female with HELLP syndrome (toxemia of pregnancy). (A,B) Severe serous retinal detachments involving the macula as well as the

periphery and Elschnig spots can be seen in both eyes on color fundus photography. (C,D) Early phase and (E,F) late phase fluorescein angiogram demonstrates multiple areas of leakage originating from the choroid. (G,H) During follow-up, resolution of fluid and hemorrhages was noted, though pigment epithelial alterations were still evident. (Images courtesy of David Sarraf, Stein Eye Institute, University of California - Los Angeles.)

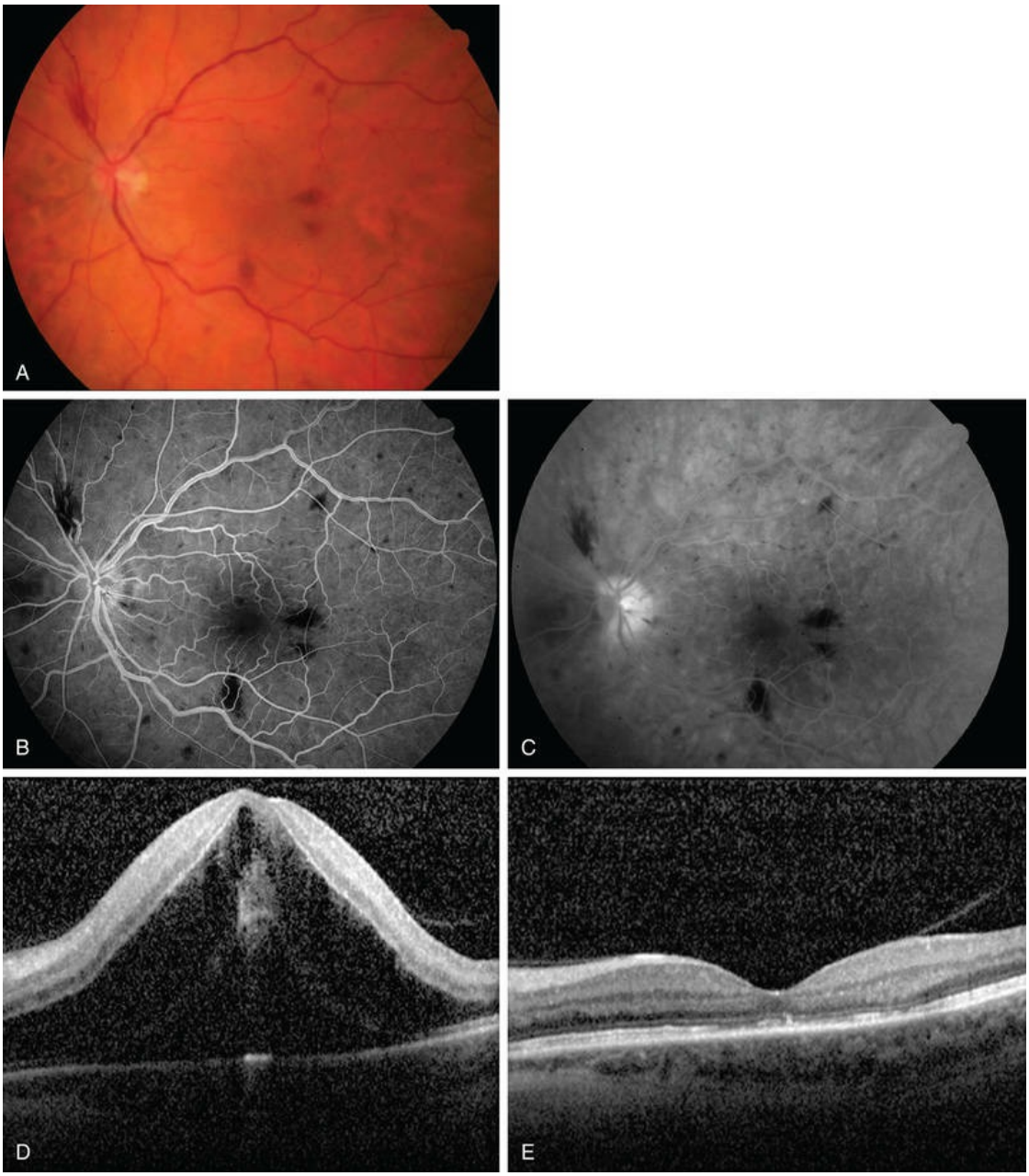

FIG. 63.3 Forty-five-year-old female with suspected disseminated intravascular coagulation (DIC) after

arteriovenous shunt surgery due to kidney transplant failure. (A) Color fundus photography illustrates many retinal hemorrhages. (B) Early and (C) late phase fluorescein angiogram demonstrates only mild leakage from smaller retinal vessels with disc hyperfluorescence and some late-appearing hyperfluorescence at the level of the choroid (especially superiorly). (D) Spectral domain optical coherence tomography (OCT) shows severe accumulation of intra- and subretinal fluid. One month later, there was spontaneous resolution of the fluid on OCT, though alterations at the level of the ellipsoid zone were still observed (E).

The hypercoagulable state in these individuals typically leads to choriocapillaris occlusion by fibrin-platelet clots, whereas subcutanenous or subconjunctival,[23] choroidal, retinal, or vitreous hemorrhages[19,21,24] are thought to be indicative of thrombocytopenia and anemia. A patchy delay in filling of the choroidal vessels on fluorescein angiography can be an early sign of ophthalmic complications. Pathophysiologically, microthrombi in the choriocapillaris cause localized ischemic injury to the retinal pigment epithelium (RPE), resulting in a dysfunction of the outer blood–retinal barrier as well as a decreased ability of the RPE to transport fluid out of the subretinal space.[25] Fluid extravasation from choroidal vessels can then pass through small disruptions of the RPE, extending into the subretinal space and manifesting as serous retinal detachments.[26] Intraretinal, subretinal, and sub-RPE fluid accumulations have been reported.[12,33–35] Fluid accumulation may resolve spontaneously when systemic conditions improve; however, macular pigmentary changes may persist after resolution of fluid. Intravitreal anti-VEGF therapy has been tried, but the benefits are uncertain (Fig. 63.1).

Hemorrhage in the posterior segment may vary from subclinical small intraretinal dot hemorrhages to widespread sub-RPE, subretinal, or intravitreal hemorrhage resulting in dramatic decrease in vision.[19,21,24] Some groups have reported large tears of the RPE leading to acute vision loss.[27] Choroidal hemorrhage seems to be more specific and has rarely been described in conditions other than the coagulopathic disorders described in this chapter.

Cotton-wool spots, typically located around the optic disc, are generally related to a secondary cause such as hypertension or other systemic disease.[28] Whereas the decrease in vision from fluid accumulation and hemorrhage may recover following resolution and resorption,[20] visual impairment due to choroidal infarction is frequently permanent.[29]

The preferential localization of fibrin-formation and occlusion in the choroidal bed at the posterior pole has not yet been fully explained. Cogan proposed the hypothesis that a sudden deceleration of the blood flow between the short posterior ciliary arteries and the choriocapillaris sinusoids greatly facilitates clot precipitation in this region.[18] Involvement of the retinal vasculature has been rarely reported, with findings including impaired retinal circulation, retinal artery or retinal vein occlusion, and purtscher-like retinopathy.[30,36–38] In these cases, the authors have speculated that the underlying diseases may have been the cause of the retinal vascular changes instead of a direct effect of DIC. More recently, ultra-widefield fluorescein angiography revealed the presence of peripheral retinal vascular leakage in a patient with HELLP syndrom.[35] Lin et al. concluded that in addition to a choroidal etiology for the serous retinal detachment, breakdown of the blood–retinal barrier manifest in retinal vasculature may have also contributed to the observed findings.[35]

There are also reports describing ocular involvement of DIC and TTP in neonates.[39] Common causes of mechanisms in this setting include placenta previa, sepsis, trauma, hepatocellular failure, or infant respiratory distress syndrome (IRDS). The ocular fundi show extensive hemorrhages in the retina or the vitreous, usually with concomitant focal retinal detachments. In selected neonatal cases, anterior segment manifestations were also observed with hyphema, thrombi in the iris and the ciliary body, and subconjunctival hemorrhage.[40]

Ocular manifestations of toxemia of pregnancy are discussed in detail in Chapter 95 (Pregnancy-related diseases). As the HELLP syndrome may be associated with DIC, all of the above-mentioned complications may occur in this condition. Additionally, hypertensive retinal vascular changes are not uncommon. Mere presence of serous retinal detachments should not be used as an

indicator of DIC, as these may also occur in pregnancy independent of the presence or absence of DIC and pregnancy-associated hypertension.[31,32]

Conclusion

DIC and related coagulopathies generally exhibit very similar ocular manifestations, which include widespread retinal or vitreous hemorrhage, subretinal or intraretinal fluid accumulation, and choroidal infarction. The anterior segment is rarely involved in these disease processes. While visual loss related to these conditions is usually not the chief driver in the treatment of the underlying potentially life-threatening systemic diseases, ocular findings may be the initial presentation that enables the diagnosis of these disorders.

References

1. Bick RL. Disseminated intravascular coagulation: current concepts of etiology, pathophysiology, diagnosis, and treatment. *Hematol Oncol Clin North Am*. 2003;17:149–176.
2. Gando S, Kameue T, Nanzaki S, et al. Disseminated intravascular coagulation is a frequent complication of systemic inflammatory response syndrom. *Thromb Haemost*. 1996;75:224–228.
3. Levi M, Nieuwdorp M, vander Poll T, et al. Metabolic modulation of inflammation-induced activation of coagulation. *Semin Thromb Hemost*. 2008;34:26–32.
4. Favaloro EJ. Laboratory testing in disseminated intravascular coagulation. *Semin Thromb Hemost*. 2010;36:458–468.
5. Bernard GR, Vincent AL, Laterre PF, et al. Efficiacy and safety of recombinant human activated protein C for severe sepsis. *N Engl J Med*. 2001;344:699–709.
6. Levi M. Diagnosis and treatment of disseminated intravascular coagulation. *Int J Lab Hematol*. 2014;36:228–236 [Review].
7. Thachil J, Toh CH, Levi M, et al. The withdrawal of

Activated Protein C from the use in patients with severe sepsis and DIC [Amendment to the BCSH guideline on disseminated intravascular coagulation]. *Br J Haematol*. 2012;157:493–494.
8. Yamakawa K, Aihara M, Ogura H, et al. Recombinant human soluble thrombomodulin in severe sepsis: a systematic review and meta-analysis. *J Thromb Haemost*. 2015;13(4):508–519.
9. Tsai HM. Platelet activation and the formation of the platelet plug: deficiency of ADAMTS13 causes thrombotic thrombocytopenic purpura. *Arterioscler Thromb Vasc Biol*. 2003;23:388–396.
10. Lim W, Vesely SK, George JN. The role of rituximab in the management of patients with acquired thrombotic thrombocytopenic purpura. *Blood*. 2015;125:1526–1531.
11. Moake JL. Thrombotic microangiopathies. *N Engl J Med*. 2002;347:589–600.
12. Hay-Smith G, Sagoo MS, Raina J. Fatal thrombotic thrombocytopenic pupura presenting with choroidal vasculopathy and serous retinal detachment. *Eye (Lond)*. 2006;20:982–984.
13. Blombery P, Scully M. Management of thrombotic thrombocytopenic purpura: current perspectives. *J Blood Med*. 2014;5:15–23 [Review].
14. Neunert C, Lim W, Crowther M, et al. American Society of Hematology. The American Society of Hematology 2011 evidence-based practice guideline for immune thrombocytopenia. *Blood*. 2011;117:4190–4207 [Review].
15. Neunert CE. Current management of immune thrombocytopenia. *Hematology Am Soc Hematol Educ Program*. 2013;2013:276–282 [Review].
16. Stella C, Malik K, Sibai B. HELLP syndrome: an atypical presentation. *Am J Obstet Gynecol*. 2008;198:e6–8.
17. Sibai BM, Ramadan MK, Usta I, et al. Maternal morbidity and mortality in 442 pregnancies with hemolysis, elevated liver enzymes, and low platelets (HELLP syndrome). *Am J Obstet Gynecol*. 1993;169:1000–1006.
18. Cogan DG. Ocular involvement in disseminated

intravascular coagulopathy. *Arch Ophthalmol*. 1975;93:1–8.
19. Majji A, Bhatia K, Mathai A. Spontaneous bilateral peripapillay, subhyalid and vitreous hemorrhage with severe anemia secondary to idiopathic thrombocytopenic purpura. *Indian J Ophthalmol*. 2010;58:234–236.
20. Meyer CH, Callizo J, Mennel S, et al. Complete resorption of retinal hemorrhages in idiopathic thrombocytopenic purpura. *Eur J Ophthalmol*. 2007;17:128–129.
21. Karagiannis D, Gregor Z. Valsalva retinopathy associated with idiopathic thrombocytopenic purpura and positive antiphospholipid antibodies. *Eye (Lond)*. 2006;20:1447–1449.
22. Wyszynski RE, Fran KE, Grossniklaus HE. Bilateral retinal detachments in thrombotic thrombocytopenic purpura. *Graefes Arch Clin Exp Ophthalmol*. 1988;226:501–504.
23. Sodhi PK, Jose R. Subconjunctival hemorrhage: the first presenting clinical feature of idiopathic thrombocytopenic purpura. *Jpn J Ophthalmol*. 2003;47:316–318.
24. Okuda A, Inoue M, Shinoda K, et al. Massive bilateral vitreoretinal hemorrhage in patient with chronic refractory idiopathic thrombocytopenic purpura. *Graefes Arch Clin Exp Ophthalmol*. 2005;243:1190–1193.
25. Nanayakkara P, Gans RO, Reichert-Thoen J, et al. Serous retinal detachment as an early presentation of thrombotic thrombocytopenic purpura. *Eur J Intern Med*. 2000;11:286–288.
26. Jellie HG, Gonder JR, Canny CL, et al. Ocular involvement in thrombotic thrombocytopenic purpura: the angiographic and histopathological features. *Can J Ophthalmol*. 1984;19:279–283.
27. Hartley KL, Benz MS. Retinal pigment epithelium tear associated with a serous detachment in a patient with thrombotic thrombocytopenic purpura and hypertension. *Retina*. 2004;24:806–808.
28. Matsuo T, Matsuura S, Nakagawa H. Retinopathy in a patient with thrombotic thrombocytopenic purpura complicated by polymyositis. *Jpn J Ophthalmol*. 2000;44:161–164.
29. Patel N, Riordan-Eva P, Chong V. Persistent visual loss after

retinochoroidal infarction in pregnancy-induced hypertension and disseminated intravascular coagulation. *J Neuroophthalmol*. 2005;25:128–130.
30. Schwartz SG, Hickey M, Puliafito CA. Bilateral CRAO and CRVO from thrombotic thrombocytopenic purpura: OCT findings and treatment with triamcinolone acetonide and bevacizumab. *Ophthalmic Surg Lasers Imaging*. 2006;37:420–422.
31. Brismar G, Schimmelpfennig W. Bilateral exudative retinal detachment in pregnancy. *Acta Ophthalmol (Copenh)*. 1989;67:699–702.
32. Mayo GL, Tolentino MJ. Images in clinical medicine. Central serous chorioretinopathy in pregnancy. *N Engl J Med*. 2005;353:e6.
33. Dewilde E, Huygens M, Cools G, et al. Hypertensive choroidopathy in pre-eclampsia: two consecutive cases. *Ophthalmic Surg Lasers Imaging Retina*. 2014;45:343–346.
34. Gundlach E, Junker B, Gross N, et al. Bilateral serous retinal detachment. *Br J Ophthalmol*. 2013;97:939–940 [949].
35. Lin P, Hahn P, Fekrat S. Peripheral retinal vascular leakage demonstrated by ultra-widefield fluorescein angiography in preeclampsia with HELLP syndrome. *Retina*. 2012;32:1689–1690.
36. Viola F, Vezzola D, Villani E, et al. Purtscher-like retinopathy in septicemic disseminated intravascular coagulation associated with nephrotic syndrome. *Eur J Ophthalmol*. 2013;23:601–603.
37. Hill ML, Skelley JP, Pomerleau D, et al. Diagnostic and therapeutic challenges. *Retina*. 2013;33:1989–1992.
38. Lewis K, Herbert EN, Williamson TH. Severe ocular involvement in disseminated intravascular coagulation complicating meningococcaemia. *Graefes Arch Clin Exp Ophthalmol*. 2005;243:1069–1070.
39. Schaffer DB. Eye findings in intrauterine infections. *Clin Perinatol*. 1981;8:415–443.
40. Ortiz JM, Yanoff M, Cameron JD, et al. Disseminated intravascular coagulation in infancy and in the neonate: ocular findings. *Arch Ophthalmol*. 1982;100:1413–1415.

64

Pediatric Retinal Vascular Diseases

Thomas C. Lee, Michael F. Chiang

Retinopathy of Prematurity

Retinopathy of prematurity (ROP) is a disease affecting the retinas of premature infants. Its key pathologic feature, local ischemia with subsequent retinal neovascularization, has common features with other proliferative disorders such as diabetic and sickle-cell retinopathy. ROP is unique in that the vascular disease is found only in infants with incompletely vascularized retinas. The spectrum of ROP disease ranges from mild cases without visual sequelae to advanced cases with bilateral irreversible blindness.

Historical Perspective

Early History

ROP was first described in 1942[1,2] and quickly became recognized as the primary cause of childhood blindness throughout the developed world.[3] Terry's original reports designated the condition retrolental fibroplasia (RLF), based on his impression that it involved a proliferation of the embryonic hyaloid system, but Owens and Owens[4] found that the hyaloid system was normal at birth and that RLF developed postnatally. As the pathogenesis and clinical manifestations became better understood, the term "retinopathy of prematurity" was adopted.

The discovery of the relationship between supplementary oxygen and ROP in the 1950s[5–9] led to rigid curtailment of oxygen supplementation in the nursery, and a dramatic decrease in ROP incidence followed. Unfortunately, this had an adverse effect on infant morbidity and mortality (e.g., respiratory distress syndrome, cerebral palsy, neurologic disorders).[10–12]

Retinopathy of Prematurity and Contemporary Nursery Practices

By the early 1970s, arterial blood gas analysis had come into general use, and the oxygen requirements of premature infants with respiratory distress syndrome were better documented.[13] This enabled pediatricians to titrate the incubator oxygen concentration to more nearly meet the individual premature infant's oxygen needs.

Modern transcutaneous oxygen monitoring and continuous pulse oximetry have provided additional noninvasive tools, allowing neonatologists to monitor babies in real time more closely. These have stimulated studies, including large multicenter oxygen restriction trials, which have found that lower target oxygen saturation levels (e.g., 85–89%) correlate with significantly improved rates of severe ROP but are also associated with increased mortality rates.[14–16] At this time, general consensus regarding target oxygen saturation levels that balance ROP risk and mortality has not been reached.

With improvements in neonatology practice, more of the smallest premature infants are now surviving. Eight percent of low-birthweight infants survived in 1950, but with ventilators, surfactant, intravenous nutrition, and other gains in knowledge,

survival has risen to 37–72%.[17–19] Clearly, infants are surviving today with more immature retinal vasculature and therefore higher ROP risk. For this reason, and because of common pathophysiology with other proliferative vascular diseases such as diabetic retinopathy, there has been mounting interest in ROP.[20–22]

The Role of Oxygen

Clinical Findings

Results of controlled nursery studies[5,8] that suggested supplementary oxygen to be the principal cause of ROP in the epidemic of the early 1950s were confirmed, and the role of prolonged oxygen was documented in a collaborative randomized controlled trial.[9]

Since that time, attempts to delineate the critical blood oxygen levels producing ROP have not resulted in definitive conclusions. In a prospective study of 589 infants monitored by intermittent blood gas measurements, and where clinical goals were to avoid elevated arterial oxygen, the occurrence of ROP was not related to arterial oxygen levels.[23] Only the duration of oxygen exposure was a risk factor. Somewhat unexpectedly, continuous transcutaneous monitoring of blood oxygen levels was found in one study to be of no more value than intermittent monitoring in preventing visual disability.[24]

Recent studies, including large multicenter oxygen restriction trials, have found that lower target oxygen saturation levels (e.g., 85–89%) correlate with significantly improved rates of severe ROP, but are associated with increased mortality rates.[14–16] At this time, a consensus about optimal target oxygen saturation levels has not been reached.

Experimental Findings

In the early 1950s the laboratory kitten model, which produced lesions resembling the early stages of human ROP, was used extensively because it demonstrated selective response to oxygen by the immature retinal vessels.[6,7] In the full-term newborn kitten, the immature retinal vascularization is comparable to that of a human fetus at 6 months' gestation, thus providing the unique

opportunity to study the response to oxygen of the immature retina, albeit in a full-term, healthy animal.[3] When hyperoxia studies were extended to other animal models, such as the young mouse and puppy,[6] the general concept of oxygen toxicity to immature retinal vessels was reinforced.

Investigators[26,27] have pointed out the histologic differences in the retinas of these animal models from the human but were unable to explain why progression to retinal detachment did not occur. It is noteworthy that McLeod et al. reported the production of intravitreal neovascularization with traction retinal folds in young dogs exposed to hyperoxia.[28] These findings add to the potential application of the canine model to investigate these stages of ROP (Figs. 64.1 and 64.2 online).

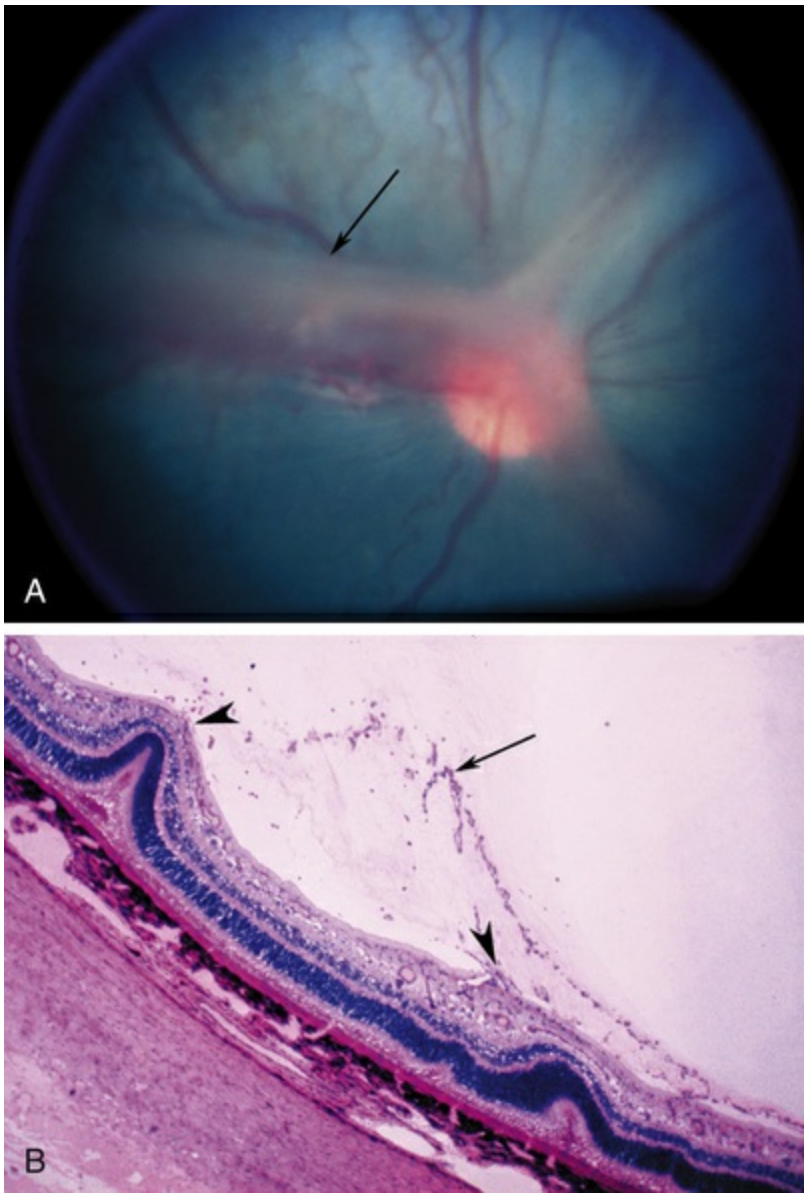

FIG. 64.1 (A) Ophthalmoscopic examination of a 45-day-old dog exposed to 100% oxygen for the first 4 days of life disclosed a 2-mm-wide area of retinal neovascularization (*arrow*) extending from the disc to the temporal midperiphery. Two similar structures are present at the 2- and 5-o'clock positions. (B) Area of temporal retinal neovascularization (*arrow*) indicated by arrow in A shows mild folds in the retina (*arrowheads*) (periodic acid–Schiff and hematoxylin, ×50).

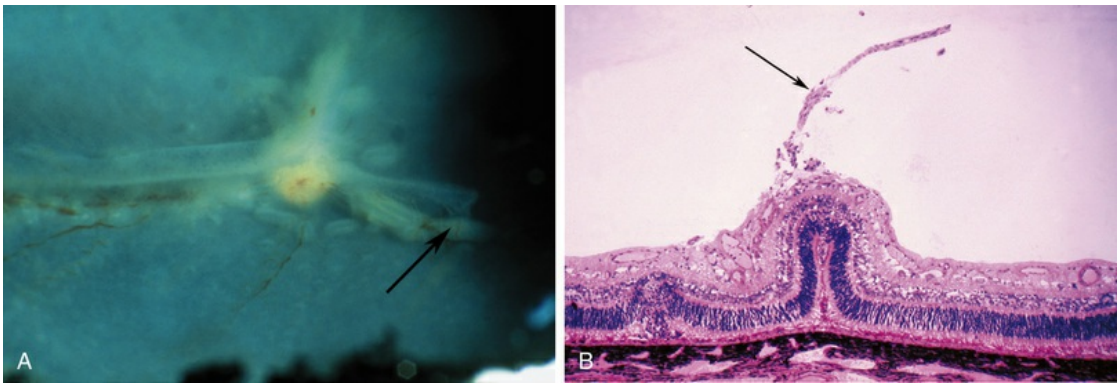

FIG. 64.2 (A) Gross appearance of the areas of neovascularization extending temporally and two smaller areas in the same 45-day-old dog shown in Fig. 64.1. A denser 2 × 0.5-mm area is present inferior nasally (*arrow*). (B) Area from A (marked by *arrow*) discloses retinal neovascularization (*arrow*) attached to the apex of a retinal fold (periodic acid–Schiff and hematoxylin, ×125).

The hyperoxic animal models demonstrated that only the incompletely vascularized retina was susceptible to oxygen's adverse effect, and that the more immature the vascularization, the greater the pathologic response to oxygen.[29] These findings supported the clinical observation that the infant with a less mature retina has greater ROP susceptibility, and that the infant with a fully vascularized retina has no risk. Accordingly, the temporal retina, the last part to vascularize, remains susceptible to ROP the longest (Fig. 64.3 online).

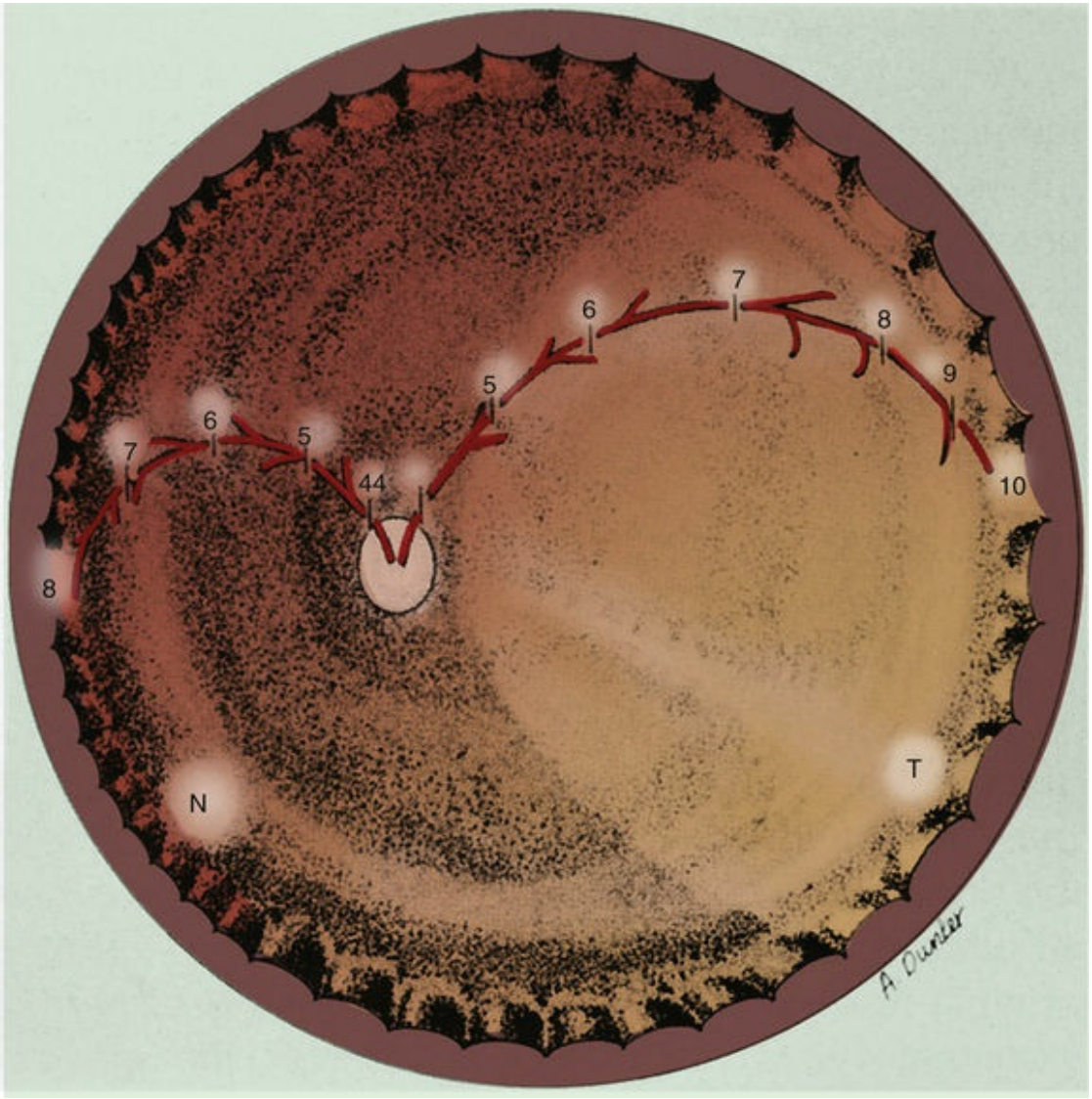

FIG. 64.3 Schematic diagram of retinal vessel development in humans. At 4 months' gestation, vessels grow from the disc to reach the ora serrata nasally at 8 months and the ora temporally shortly after term. The vascularization of the newborn kitten corresponds to the 6½-month-gestation human fetus. *N*, nasal retina; *T*, temporal retina; numbers refer to months' gestational age.

Mechanism of Oxygen's Effects on the Immature Retina

Primary Stage of Retinal Vasoconstriction and Vascular Occlusion

The primary effect of elevated blood oxygen in any retina is vasoconstriction, which, if sustained, is followed by some degree of vascular closure. In young kittens, initial vasoconstriction occurs within several minutes after oxygen exposure. Vascular caliber is reduced by approximately 50% initially, but then rebounds to its original dimensions. Continued oxygen exposure results in gradual vasospasm during the next 4–6 hours, until the vessels are approximately 80% constricted.[30] At this stage, constriction is still reversible. However, if significantly elevated arterial oxygen partial pressure levels persist for an additional period (e.g., 10–15 hours), some immature peripheral vessels are permanently occluded.[7,23]

This occlusion progresses as the duration of hyperoxia increases, and local vascular obliteration is complete after 2–3 days of exposure. In the dog, after 4 days of exposure to hyperoxia, most capillaries are lost and only major blood vessels survive.[31]

Electron microscopic observations demonstrate selective hyperoxic injury to the endothelial cells of the most immature vessels, without obvious changes in the neuronal elements of the retina.[32]

Secondary Stage of Retinal Neovascularization

After removal of the laboratory animal to ambient air following sustained hyperoxia, marked endothelial proliferation arises from the residual vascular complexes adjacent to retinal capillaries ablated during hyperoxia (Fig. 64.4 online). This can be demonstrated on fluorescein angiography (Fig. 64.5). Nodules of proliferating endothelial cells canalize to form new vessels that not only grow within the retina but also erupt through the internal limiting membrane to grow on its surface, similar to the neovascularization in other proliferative retinopathies (Figs. 64.6–64.9). In the dog and cat, the initial preretinal neovascular formations are like angioblastic masses with few lumens (formations sometimes called “popcorn”), which mature into neovascular formations that include vessels invested with pericytes.[33,34] Although the neovascularization may be extensive, this is generally the maximum response to oxygen in the kitten model and is followed by progressive vascular remodeling and involution of abnormalities. The preretinal neovascularization in

the dog persists and can develop into tented membranes that create traction retinal folds in the retina (Figs. 64.1 and 64.2 online).[28] The mouse and rat preretinal neovascular formations, however, will regress after 5 days.[30–37] Although regression is rapid and spontaneous in mice, the mouse model has been useful in evaluating topical[38] and systemic drugs,[39,40] experimental gene therapy strategies,[41,42] and endogenous inhibitors like pigment epithelial growth factor.[43]

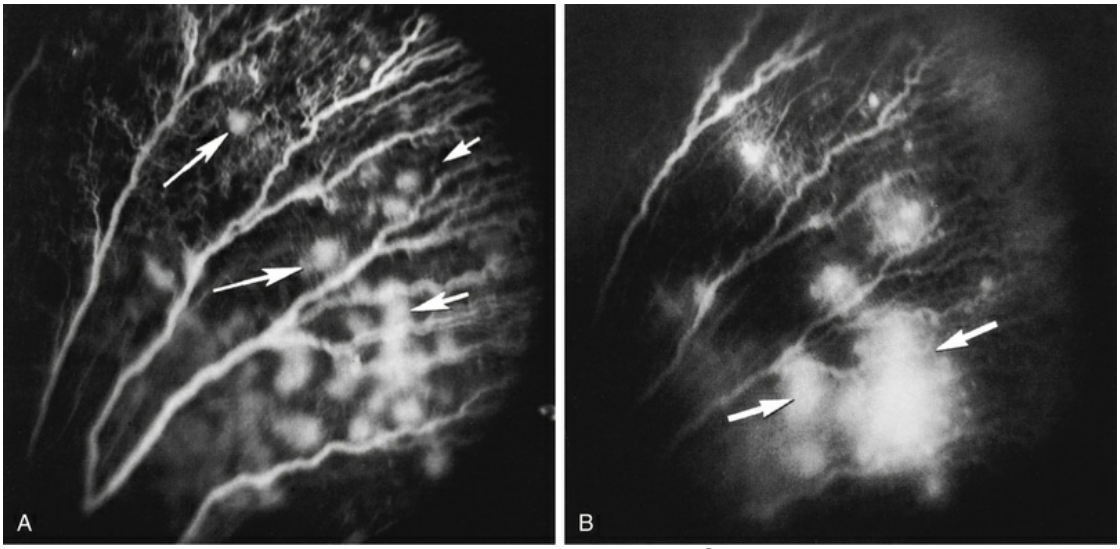

FIG. 64.5 (A) Fluorescein angiogram of a young kitten with oxygen-induced retinal neovascularization (*arrows*); midtransit phase of angiogram. (B) Late phase of angiogram of young kitten in (A). Note dye leakage from neovascularization (*arrows*).

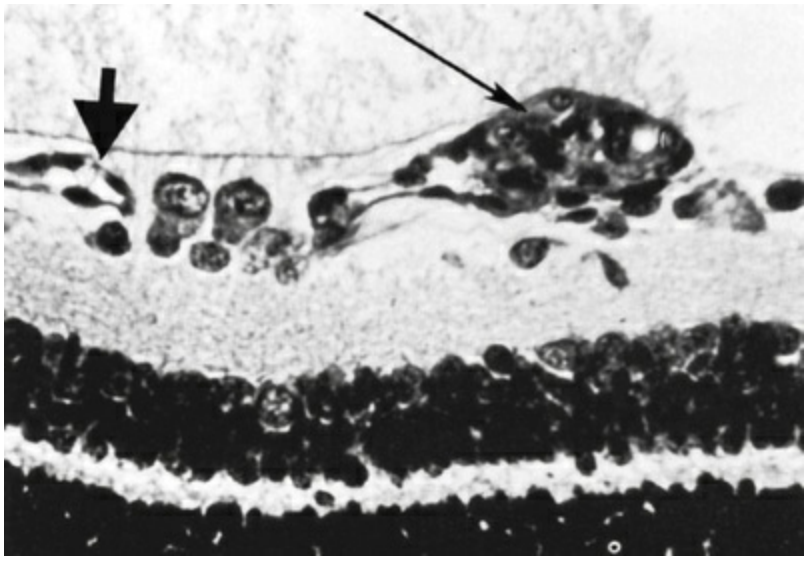

FIG. 64.6 Cross-section of the eye of a 21-day-old mouse exposed to hyperoxia. Normal capillary is seen just posterior to the area of vascular closure (*short arrow*); an endothelial nodule proliferating from the most anterior part of the vascularized retina is erupting through the internal limiting membrane (*long arrow*).

(Reproduced with permission from Patz A, Eastham A, Higginbotham DH, et al. Oxygen studies in retrolental fibroplasia. II. The production of the microscopic changes of retrolental fibroplasia in experimental animals. Am J Ophthalmol 1953;36:1511–22.)

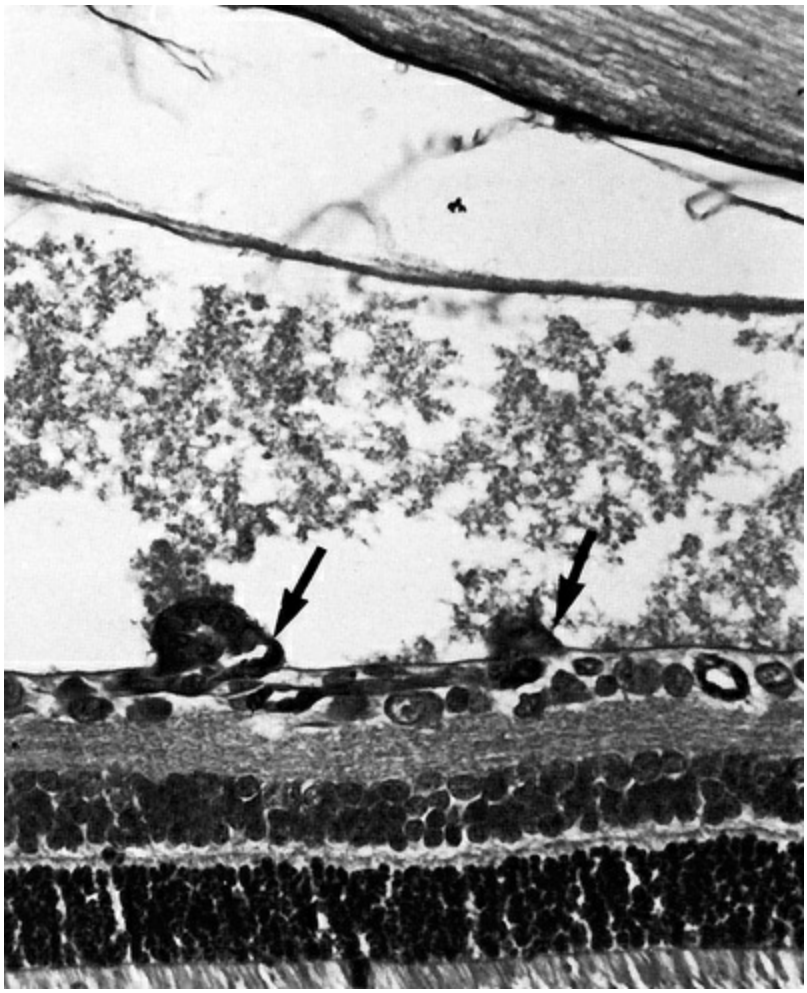

FIG. 64.7 Cross-section of the eye of a young mouse exposed to hyperoxia showing neovascularization on the surface of the retina just posterior to the zone of capillary closure (*arrows*). *R*, anterior retina; *L*, lens.

(Reproduced with permission from Patz A. Clinical and experimental studies on retinal neovascularization. Am J Ophthalmol 1982;94:715.)

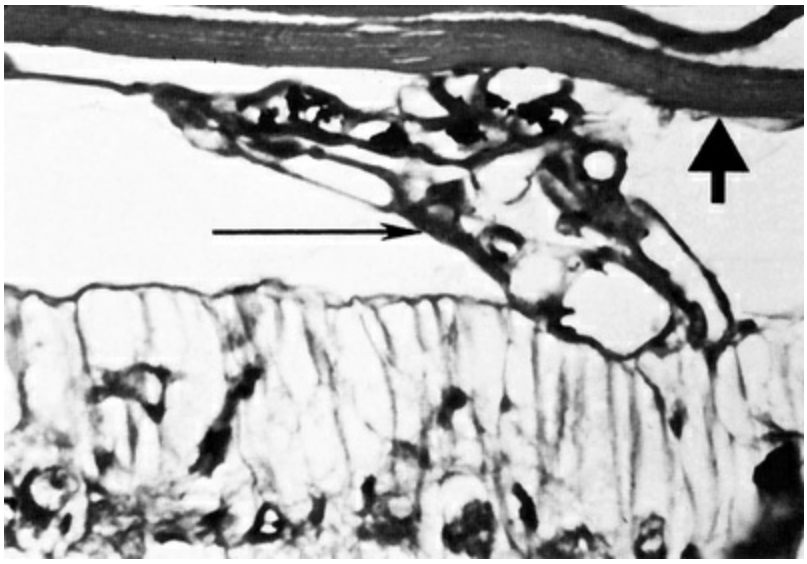

FIG. 64.8 Cross-section of the retina of a young kitten exposed to hyperoxia. Intravitreal neovascularization is seen just posterior to the zone of capillary closure (*long arrow*). *Short arrow*, lens capsule. (Reproduced with permission from Patz A. Oxygen studies in retrolental fibroplasia. IV. Clinical and experimental observations. Am J Ophthalmol 1954;38:291.)

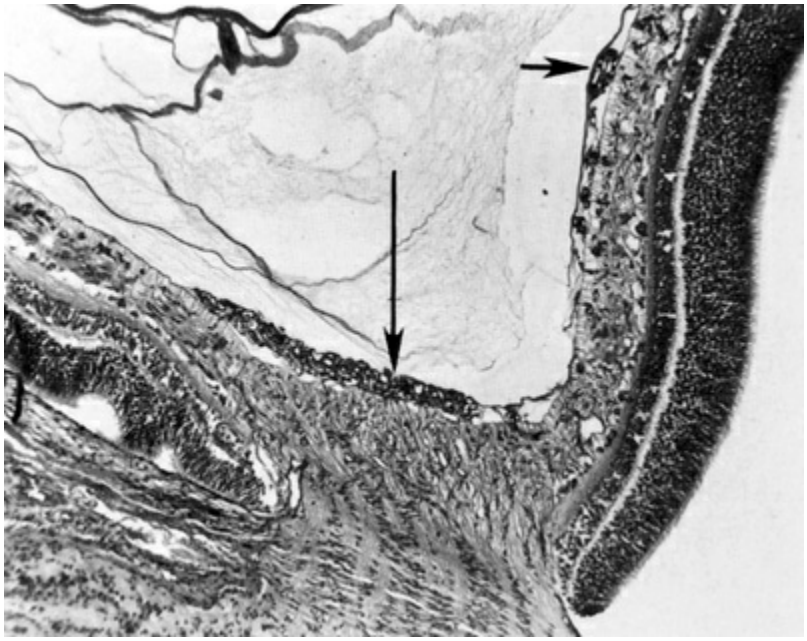

FIG. 64.9 Section of the retina of a young kitten exposed to hyperoxia. Neovascularization is seen over the surface of the disc (*long arrow*). *Short arrow* indicates small nodules of surface neovascularization. (Reproduced with permission from Patz A. Oxygen studies in retrolental fibroplasia. IV. Clinical and experimental observations. Am J Ophthalmol

1954;38:291.)

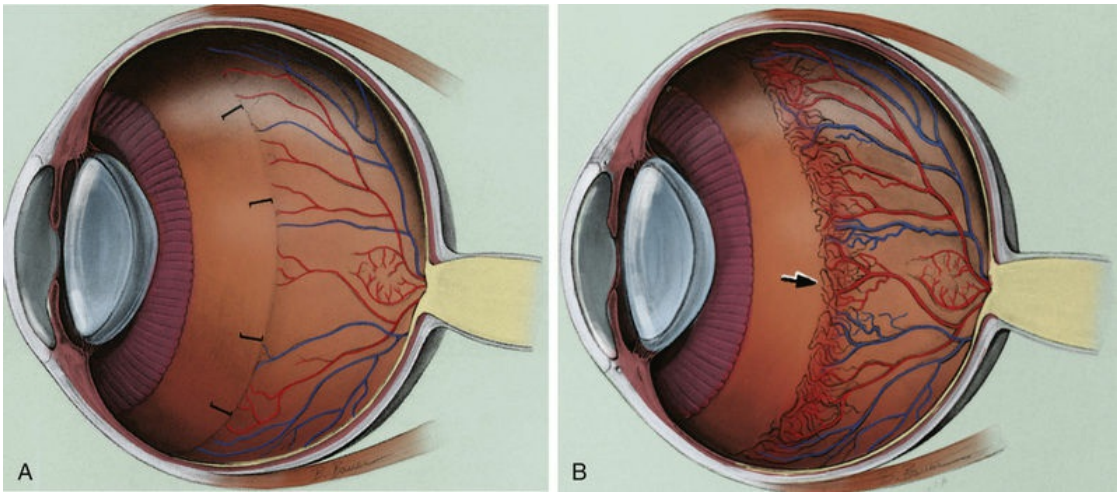

FIG. 64.4 (A) Schematic diagram of vascular closure of the most anterior and immature retinal vascular bed (indicated by brackets) of a young kitten exposed to hyperoxia for a relatively short period. The posterior, more mature vessels are unaffected. (B) Three weeks after removal of the subject in (A) to ambient air, neovascularization has developed immediately posterior to the area of capillary closure (*arrow*). (Panel B, reproduced with permission from Patz A. Oxygen studies in retrolental fibroplasia. IV. Clinical and experimental observations. Am J Ophthalmol 1954;38:291.)

Oxygen exerts an important effect on the remodeling of the original primitive capillary network that develops in the retina.[44] Capillaries regress from areas of higher oxygen concentration and grow toward areas of lower oxygen. Penn et al.[45] used experimentally alternating periods of high and low oxygen in the rat pup model to produce a more proliferative form of retinopathy. Pierce and colleagues[21] used hyperoxia and hypoxia in a mouse pup model to demonstrate the correlation of vascular endothelial growth factor (VEGF) protein production with periods of low oxygen and its disappearance during oxygenation.

Pathogenesis

Normal Retinal Vasculogenesis

It is appropriate to review normal retinal vascular development as background for understanding ROP pathogenesis. Michaelson[33] originally suggested that retinal capillaries arise by budding from preexistent arteries and veins that originate from the hyaloid vessels at the optic nerve head. Cogan[34] proposed a similar mechanism, except for the hypothesis of budding of solid endothelial cords from hyaloid vessels. Ashton[37] suggested that mesenchyme, the blood vessel precursor, grows from the optic disc through the nerve fiber layer to the periphery of the retina. Mesenchymal precursors have recently been observed far in advance of formed blood vessels in human fetal retinas.[46] On the posterior edge of the advancing mesenchyme, a "chicken-wire" meshwork of capillaries develops and undergoes absorption and remodeling to produce mature retinal arteries and veins that are surrounded by the capillary meshwork.[37,44] Variations in capillary development may be species-specific. However, across all species studied to date, VEGF appears to be a key factor guiding vascular growth, which most closely fits the identity of Michaelson's proposed "factor X."[33] In the kitten, Chan-Ling and Stone demonstrated the role of astrocytes leading to growth of the capillary network.[47–49] Provis et al.[50] demonstrated the expression of VEGF message in the predicted location in the developing normal human retina, just anterior to the developing vessels (Fig. 64.10).

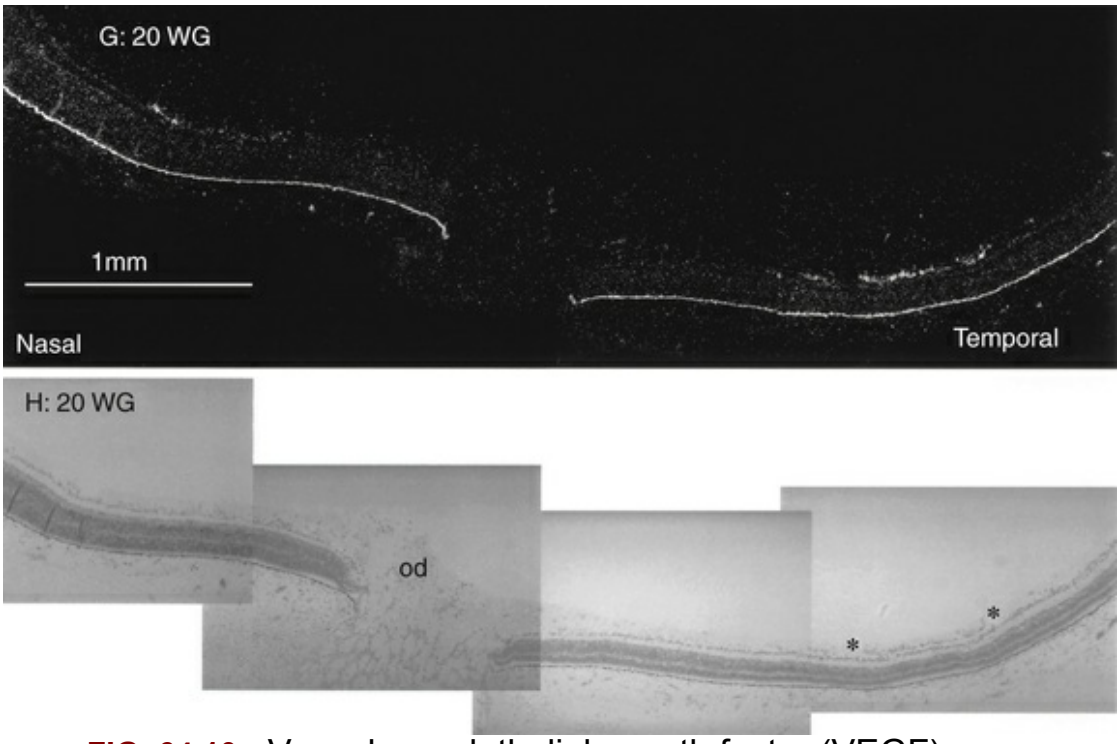

FIG. 64.10 Vascular endothelial growth factor (VEGF) mRNA expression in the human fetal retina. Bright (*H*) and dark-field (*G*) views of the retina in cross-section from a 20-week gestation human fetus. In dark-field illumination the retinal pigment epithelium is prominent. Note the greater differentiation of the retinal layers in the section to the right (temporal) of the optic disc. The vascular layer lies superficially, VEGF mRNA expression being limited to the most distal portion of that vasculature (*G*), indicated in the light-field image (*H*) by asterisks. (Reproduced with permission from Provis JM, Leech J, Diaz CM, et al. Development of the human retinal vasculature – cellular relations and VEGF expression. Exp Eye Res 1997;65:555–68.)

Fig. 64.11 shows the normal rate of progression of the retinal vessels into the far retinal periphery in human premature infants without ROP according to their postconceptional age (gestational age at birth plus chronologic age). More than 80% of prematurely born infants have been observed to develop this relatively mature retinal vasculature by the time they reach full term.

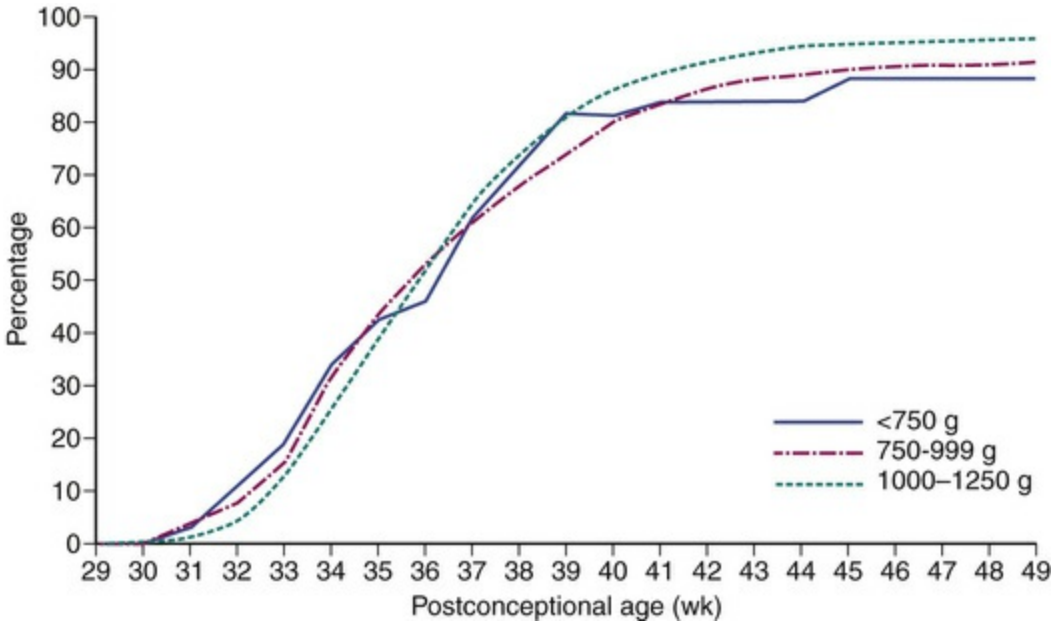

FIG. 64.11 Cumulative proportion of infants with no retinopathy of prematurity whose vessels end in zone III, by postconceptional age. (With permission from Palmer EA, Flynn JT, Hardy RJ, et al. Incidence and early course of retinopathy of prematurity. Ophthalmology 1991;98:1628–40.)

Pathogenesis of Retinopathy of Prematurity

Initial changes in the developing vessels are described above, and historically this was believed to be an injury initiated by "excess" oxygen. Alon et al. demonstrated that hyperoxia caused downregulation of VEGF and death of endothelial cells, suggesting that VEGF is an endothelial survival factor.[51] In the time that follows closure of these growing vessels, the differentiating retina becomes increasingly ischemic and hypoxic and VEGF is upregulated,[52,53] driving the neovascularization.[48]

Theoretically, the provision of increased oxygen should downregulate the release of such growth factor(s) and permit neovascularization to remodel and regress in an orderly fashion. Szewczyk[54] proposed this and treated infants with significant ROP by returning them to oxygen. With no controls, it is difficult to know from his report if this success was simply due to spontaneous involution of ROP. This hypothesis was tested in the kitten model of oxygen-induced retinopathy. Systemic mild hypoxia was found to worsen the retinopathy,[55] whereas mild hyperoxia improved it.[56]

With National Institutes of Health sponsorship, the multicenter Supplemental Therapeutic Oxygen for Prethreshold ROP (STOP-ROP) trial, chaired by Dale L. Phelps, found that, once the ROP was established, raising the oxygen saturation mildly did not harm the ROP, but neither was it of clear benefit.[57]

The clinical and histopathologic observations of Flynn and coworkers[58–62] led them to postulate the following sequence of events in human ROP pathogenesis:

1. Endothelial injury occurs where it has just differentiated from mesenchyme to form the primitive capillary meshwork. This is reminiscent of animal studies in which a short duration of hyperoxia resulted in capillary damage limited to the most recently differentiated vascular complexes (see Fig. 64.4A online). It is currently believed that environmental factors other than oxygen also are involved. For example, Brooks and associates found that nitric oxide may contribute to the vaso-obliterative stage of ROP,[63] while Alon et al. found that reduced VEGF may result in death of endothelial cells[51] because of its role as a survival factor.

2. After this injury to the vascular endothelium, the mesenchyme and mature arteries and veins survive and merge via the few remaining vascular channels to form a mesenchymal arteriovenous shunt which replaces the destroyed or damaged capillary bed.

3. The mesenchymal arteriovenous shunt is located at the demarcation between the avascular and vascularized retina. It consists of a nest of primitive mesenchymal and maturing endothelial cells that are fed by mature arteries and veins. No capillaries are found in the region of the shunt. Flynn[60] suggested that this structure represents the pathognomonic lesion of acute ROP.

Flynn described a dormant period after the injury (days to months), during which retinal findings are relatively stable. The tissues comprising the shunt may thicken, and the gray-white initial color of the structure turns from pink to salmon to red. He stated: "during this period when vasculogenic activity resumes in the retina, the fate of the eye is decided."[60] Flynn pointed out that when

the cells inside the shunt divide and differentiate into normal capillary endothelium, they form primitive endothelial tubes that send forth a brush border of capillaries that grows anteriorly into the avascular retina. This represents ROP involution, which he observed to occur in more than 90% of cases at this early stage. In progressive disease, however, the primitive cells inside the shunt proliferate and erupt through the internal limiting membrane, growing on the surface of the retina and into the vitreous body. Flynn stated: "it is this lack of differentiation and destructive proliferation of cells and their invasion into spaces and tissues where they do not belong that is the chief event in the process of membrane proliferation leading to traction detachment."[60]

Foos[64–66] suggested a pathogenesis of ROP based on examination of histopathologic material. He used the terms "vanguard" and "rearguard" to describe cellular components of the developing retina. The vanguard (anterior) component contains spindle-shaped cells thought to be glia, which play a role in nourishing the immature retina during development.[67] The rearguard contains primitive endothelial cells. As the retina matures, the endothelial cells aggregate into cords that, according to Foos,[66] subsequently lumenize and become the primordial capillaries of the retina. It is from the rearguard and primitive endothelial cells that neovascularization of ROP develops (Figs. 64.12 and 64.13). Foos noted that, as the developing vasculature reaches its most anterior extent and matures, the spindle cells of the vanguard disappear. The work of Chan-Ling et al.,[46] McLeod et al.,[68] and Provis et al.[50] showed that spindle cells are endothelial precursors and, in fetal human and neonatal dog retina,[68] the precursors organize and differentiate to form the initial retinal vasculature.[46]

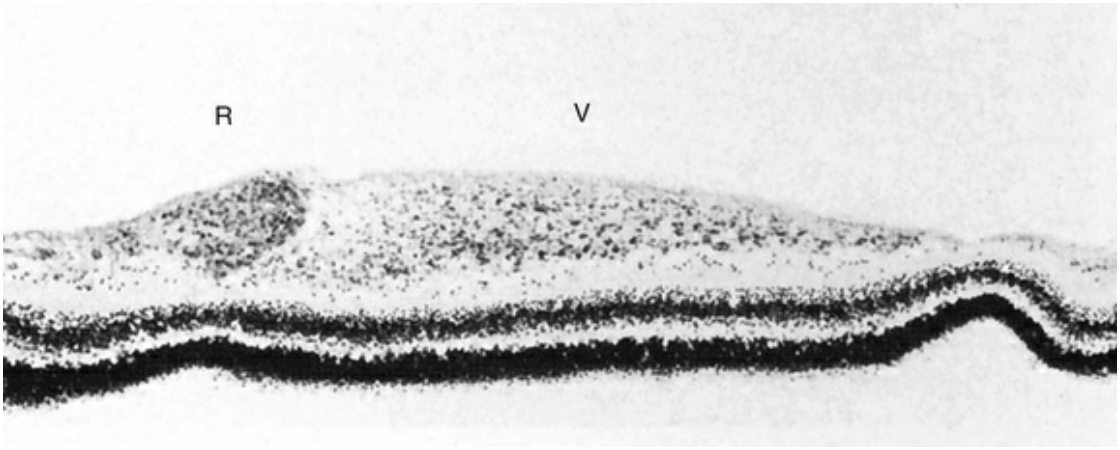

FIG. 64.12 Retinopathy of prematurity, stage 2, in a 27-week stillborn infant, showing a meridional section through the retinal ridge, with a thick layer of spindle cells that tapers anteriorly (to the right), representing the proliferative vanguard zone. Nodule of proliferating endothelial cells is seen in the rearguard zone. *R*, rearguard zone; *V*, vanguard zone. (Reproduced with permission from Foos RY. Retinopathy of prematurity – pathologic correlation of clinical stages. Retina 1987;7:260–76.)

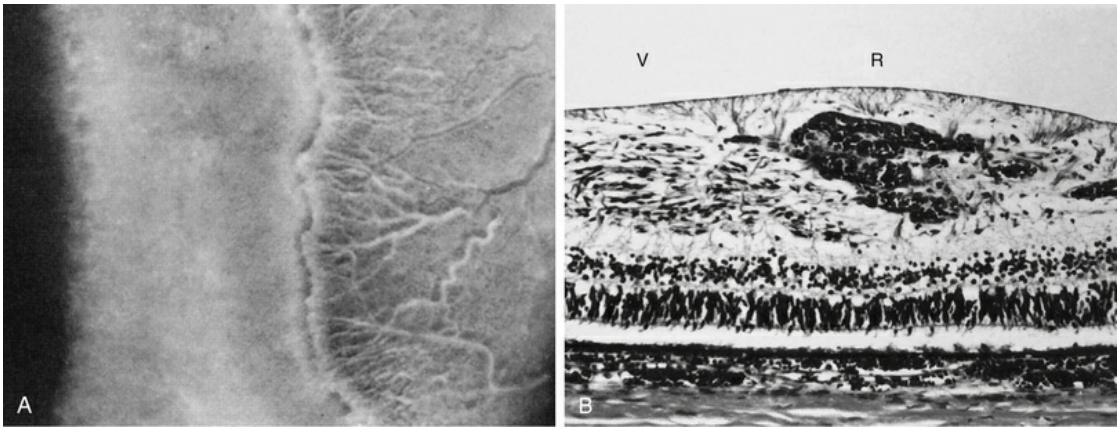

FIG. 64.13 (A) Retinopathy of prematurity, stage 2 specimen from a 29-week-old infant. Photomicrograph shows moderately elevated ridge, with tortuosity of retinal vessels posterior to ridge. (B) Photomicrograph of ridge in eye from (A) with posterior aspect of a thickened vanguard zone (*V*) and conspicuous vasodilation of rearguard zone (*R*), which has been characterized clinically as an arteriovenous shunt. (Reproduced with permission from Foos RY. Retinopathy of prematurity – pathologic correlation of clinical stages. Retina 1987;7:260–76.)

International Classification

The international classification of ROP divided the retina into three anteroposterior zones and describes the extent of disease by the 30° meridians (clock-hours) involved (Fig. 64.14). Retinal changes are divided into stages of severity, based on descriptive and photographic standards.[69]

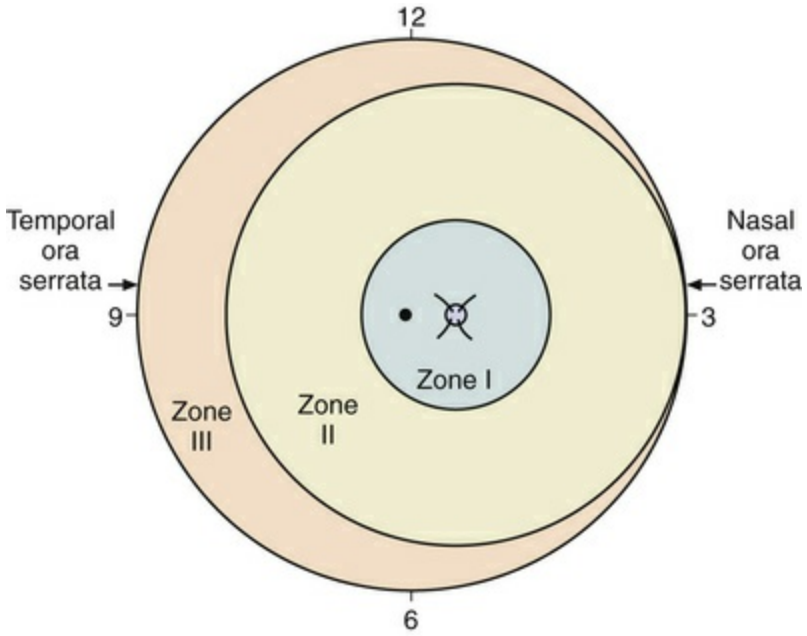

FIG. 64.14 Schematic diagram of a right eye, showing zones of the retina and clock-hours used to describe the location and extent of retinopathy of prematurity.

Zones of Involved Retina

Each of the three zones of the retina is centered on the optic disc (Fig. 64.14). Zone I includes the posterior pole and is defined as a circle, centered on the disc, whose radius is twice the distance from the disc to the center of the macula. It subtends an arc of about 60° (Fig. 64.15). Zone II extends from the peripheral border of zone I to a concentric circle tangential to the nasal ora serrata. Temporally, this boundary corresponds approximately to the anatomic equator. Once the nasal vessels have reached the ora serrata, zone III is the

remaining temporal crescent of retina anterior to zone II. Zone III, which is the farthest from the disc, is the last zone to become vascularized. It is clinically important to continue classifying ROP as zone II if there remains any active ROP or immature vessels in the nasal retina.

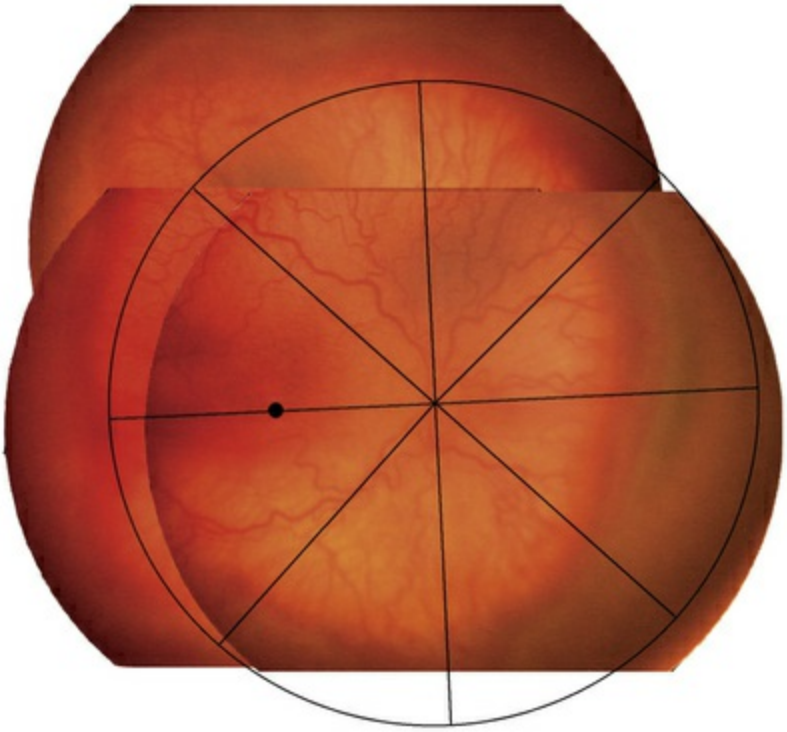

FIG. 64.15 Zone 1 grid overlaid on a montage of RetCam photos: black dot represents foveal center. Radius of circle is twice the distance from the disc to the fovea. This illustration demonstrates how retinopathy of prematurity may involve both zones I and II in the same eye.

Although the definition of the different zones is fairly explicit, the actual diagnosis at the bedside can be subjective, especially with respect to zone I. Because the fovea remains poorly defined in premature infants, the center of the macula is an estimation. Work by Chiang et al. showed that when 10 experts reviewed digital fundus images, there was disagreement regarding which examinations displayed zone I ROP in 33% of the cases.[70]

Extent of Retinopathy of Prematurity

The extent of the ROP changes is described according to the twelve 30° sectors involved, labeled as hours of the clock (see Fig. 64.14): the nasal side of the right eye is at 3:00, and the nasal side of the left eye is at 9:00.

Staging

Abnormal peripheral changes are divided into three stages, which may progress to retinal detachment (stages 4–5) (Figs. 64.16 and 64.17).

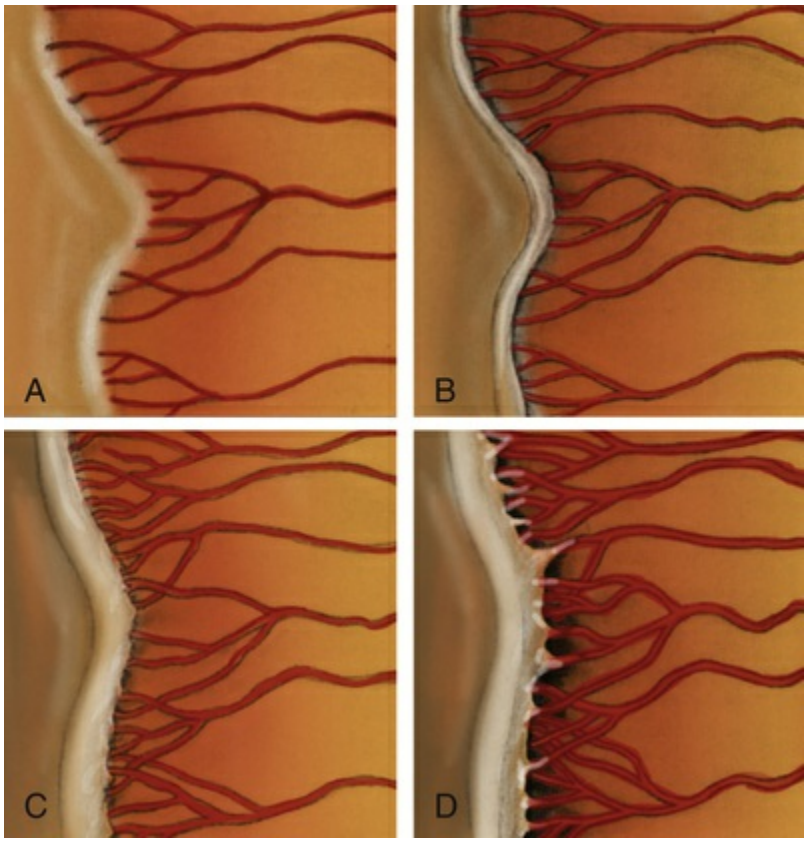

FIG. 64.16 Diagrams modified from color photographs of the international classification of retinopathy of prematurity. Vascularized, more mature retina is seen to the right and avascular retina to the left. (A) The demarcation line of stage 1. (B) The characteristic ridge of stage 2 is noted. (C) Extraretinal fibrovascular proliferative tissue of "mild" stage 3. (D) "Moderate" proliferation of extraretinal fibrovascular tissue from the ridge in more advanced stage 3. (Modified with permission from Committee for the Classification of Retinopathy of Prematurity. An international

classification of retinopathy of prematurity. Arch Ophthalmol 1984;102:1130–4.)

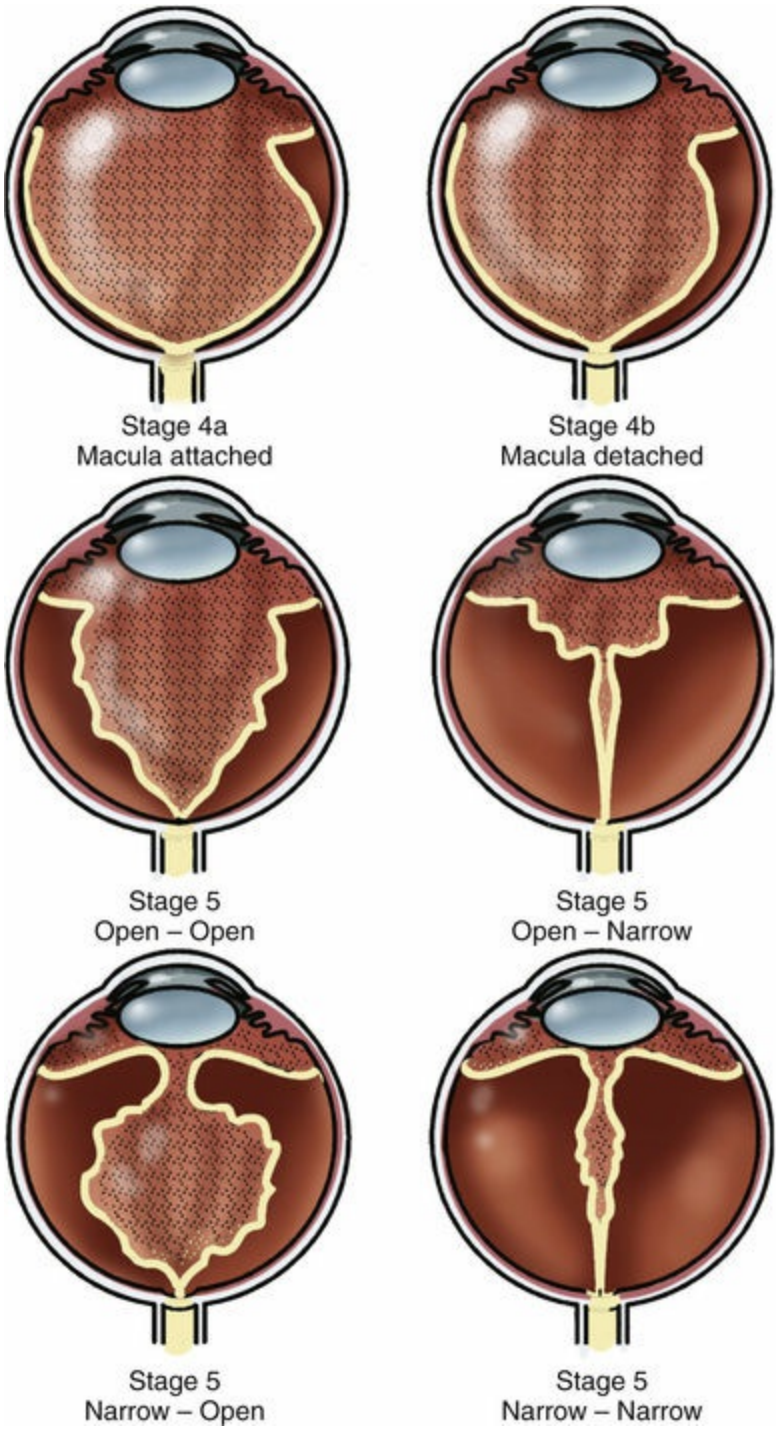

FIG. 64.17 Retinopathy of prematurity detachment configurations. Top two, stage 4a and b detachments; bottom four, stage 5. (Courtesy of Rand Spencer, MD.)

Stage 1: Demarcation Line

Stage 1 is characterized by the presence of a demarcation line, the first ophthalmoscopic sign of ROP (Fig. 64.16A). This represents a structure separating the anterior, avascular retina from the posterior, vascularized retina. It appears flat and white, and lies within the plane of the retina. Abnormal branching or arcading of vessels leads up to the line. Stage 1 is relatively evanescent, generally either progressing to stage 2 or involuting to normal vascularization within several weeks. According to Garner,[71] the stage 1 demarcation line morphologically comprises two relatively distinct zones. The more anterior vanguard zone is formed by a mass of spindle-shaped cells, which are the progenitors of the differentiated vascular endothelium. As such, it corresponds to the primitive mesenchyme (spindle cells) seen in normal fetal development but with a considerable increase in the number of cells. It is this hyperplasia, involving both thickening and widening, that makes the demarcation line visible.[71]

Stage 2: Ridge

In stage 2, the demarcation line has grown into a ridge with height and width, which extends centripetally within the globe (Fig. 64.16B). The ridge may be white or pink and, rarely, vessels may even leave the surface of the retina to enter it. Small tufts of new vessels ("popcorn" lesions) may be seen located posterior to the ridge structure but not attached to it. The absence of fibrovascular growth from the surface of the ridge separates this stage from stage 3. According to Garner, the stage 2 retinal ridge results from the proliferation of endothelial cells "with some evidence of organization into recognizable vascular channels."[71] Flynn et al.[61] demonstrated that in this stage these channels leak fluorescein on angiographic examination.

Stage 3: Ridge With Extraretinal Fibrovascular Proliferation

Stage 3 is characterized by the addition of extraretinal, fibrovascular tissue proliferating from the former ridge (Figs. 64.16C–D). This proliferating tissue is localized continuous with the posterior and

interior aspect of the ridge, causing a ragged appearance of the ridge as proliferation increases into the vitreous. As in stage 2, vessels may leave the surface of the retina to enter the ridge and could be mistaken for retinoschisis or even detachment. The presence of elevated retinal vessels coursing from the retinal surface to the height of the ridge does not alone constitute a retinal detachment;[69] however, this may signify presence of vitreous traction. According to Foos,[66] the stage 3 "extraretinal vascularization" may appear placoid, polypoid, or pedunculated on histologic examination. The placoid pattern is the most common and also the most important because it correlates with subsequent development of retinal detachment. Foos demonstrated that these extraretinal vessels are apparently derived from proliferating endothelial cells and not from the vasoformative mesenchymal "spindle" cells based on his factor VIII preparations. He also observed significant synchysis and condensation of the vitreous body in stage 3. Foos suggested that a condensation of the vitreous body over the ridge is related to depolymerization of hyaluronic acid and collapse of the collagenous framework into optically visible structures.[66]

"Plus" and "Pre-Plus" Disease.

Plus disease signifies a more florid form of ROP. Increasing dilation and tortuosity of the retinal vessels, iris vascular engorgement, pupillary rigidity, and vitreous haze indicate progressive vascular incompetence. When vascular changes are so marked that the posterior veins are enlarged and the arterioles tortuous, this represents plus disease, and a plus sign is added to the ROP stage number. This finding is a key sign of worse prognosis.[72] A published standard photograph selected by expert consensus, which has been used in four multicenter clinical trials and represents the minimum arteriolar tortuosity and venous dilation required for plus disease, is shown in Fig. 64.18A. There has been increasing recognition of a spectrum of retinal vascular abnormalities in ROP. In 2005, the revised international classification defined an intermediate "pre-plus" categorization as abnormal arteriolar tortuosity and venous dilation of the posterior pole, which is insufficient for diagnosis of plus disease.[73] Studies

have shown that up to 70% of patients with pre-plus ROP will go on to require laser treatment.[74] Studies have shown that the diagnosis of plus disease may be subjective and qualitative, even among experts, and future definitions may be based on more quantitative measures.[75–77]

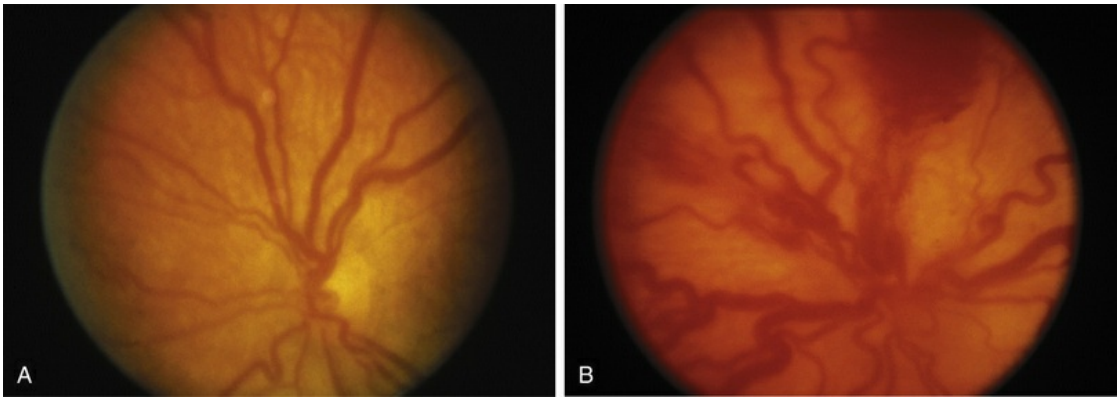

FIG. 64.18 Plus disease examples. (A) Fundus photograph of minimum dilation and tortuosity of retinal vessels considered as plus disease in National Institutes of Health studies of retinopathy of prematurity. (B) Fundus appearance of an extremely severe degree of posterior pole plus disease in an eye that soon developed total retinal detachment. (Panel A reproduced with permission from Cryotherapy for Retinopathy of Prematurity Cooperative Group. Multicenter trial of cryotherapy for retinopathy of prematurity: preliminary results. Arch Ophthalmol 1988;106:471–9. Panel B courtesy of Ophthalmic Photography, Oregon Health & Science University, Portland.)

Zone I Retinopathy of Prematurity.

ROP located in zone I can be dangerously deceptive, in that the proliferation signifying stage 3 can appear spread out "flat" on the retina posterior to the ridge, rather than elevated.[36] In severe plus disease cases inside zone I, centripetal proliferation from the ridge may occur virtually simultaneously with detachment of the retina. Flynn and Chan-Ling examined the distinction between vasculogenesis (de novo formation of new vessels by transformation of vascular precursor cells) and angiogenesis (budding from existing vessels) with regard to the distinction of zone I and zone II ROP. They proposed that zone I ROP correlates

with vasculogenesis and is therefore less sensitive to treatment by laser or cryotherapy because the disease mechanism is not VEGF-mediated. They proposed that zone II ROP correlates with angiogenesis, is mediated by hypoxia-induced VEGF-165, and is therefore more sensitive to treatment by laser or cryotherapy.[78]

Aggressive Posterior Retinopathy of Prematurity.

The 2005 revised international classification of ROP designated an uncommon, severe form of disease as "aggressive posterior ROP." This rapidly progressive disease variant had been previously termed "rush disease" and is characterized by its location in zone I or posterior zone II, ill-defined nature of the peripheral retinopathy, and prominent plus disease out of proportion to the peripheral findings.[73] This diagnosis can be made by a single examination without serial evaluation and may not progress through the class stages 1–3. In fact, the peripheral disease may appear as a flat area of neovascularization at the junction of vascular and avascular retina.

Classification of Retinal Detachment

In 1987, ophthalmologists and pathologists established a second international committee, which expanded the original 1984 international classification to describe the morphology, location, and extent of retinal detachment (Fig. 64.17).[79] This classification was based on an understanding of the development of severe ROP gained from surgical experience[80] and pathology.[66] Stage 4 (subtotal) retinal detachment is usually tractional elevation added to findings in stage 3, although there may also be exudative effusion from adjacent active stage 3 neovascularization.

Stage 4A: Extrafoveal Retinal Detachment

Typically this is a concave traction detachment in the peripheral retina without involvement of the central macula (Fig. 64.19). Generally, these detachments are located at the sites of extraretinal fibrovascular proliferation with associated vitreous traction. Elevation may start in any zone where there was stage 3 disease that incompletely involuted following ablative treatment with laser

photocoagulation or cryotherapy, and they may become circumferential. They may extend for 360° in the periphery without elevation of the macula, or they may be segmental, occupying only a portion of the periphery. The prognosis anatomically and visually is relatively good in the absence of posterior extension.

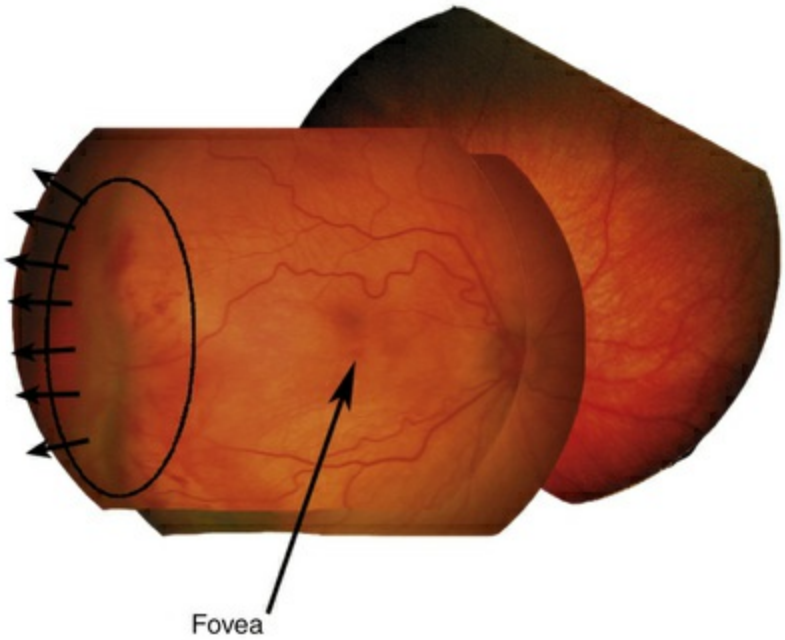

FIG. 64.19 Stage 4A retinopathy of prematurity (ROP). Fundus photo montage of right eye showing elevation of retina posterior to incompletely regressed stage 3 ROP with vitreous traction (*arrows*). Oval approximates area of retinal detachment.

Stage 4B: Partial Retinal Detachment Including the Fovea

This can follow extension of stage 4A, or may appear as a fold from the disc through zone I to zones II and III (Fig. 64.20). Once a stage 4 detachment involves the fovea, the prognosis for recovery of good visual acuity is poor.

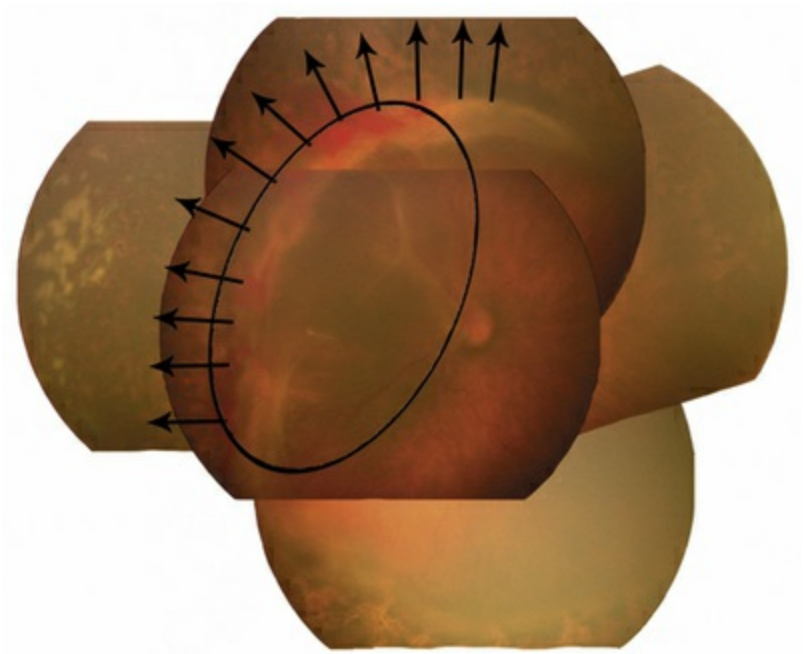

FIG. 64.20 Stage 4B retinopathy of prematurity (ROP). Fundus photo montage of right eye showing elevation of retina posterior to fibrotic ridge of incompletely regressed stage 3 ROP. *Arrows* away from ridge indicate vectors of vitreous traction elevating ridge and adjacent retina, including the macula. Oval outline approximates area of retinal detachment.

Stage 5: Total Retinal Detachment

This is virtually always funnel-shaped. The classification of stage 5 detachments divides the funnel into an anterior and a posterior part (Fig. 64.17). When open both anteriorly and posteriorly, the detachment has a concave configuration and extends to the optic disc. An alternative configuration is one in which the funnel is narrow both anteriorly and posteriorly, and the detached retina is located just behind the lens. A third, less common type is one in which the funnel is open anteriorly but narrowed posteriorly. Least common is a funnel that is narrow anteriorly and open posteriorly.

Other Factors Related to Retinal Detachment

The classification of retinal detachment in ROP focuses attention on certain physical findings in stages 4 and 5:

1. Appearance of the retrolenticular space. This space may be occupied by heavily vascularized translucent tissue, which represents disease activity. As the disease subsides, the tissue occupying this space becomes white, with a scarcity of blood vessels. This is the appearance that gave rise to the original term "retrolental fibroplasia."

2. Peripheral trough. The presence of a peripheral red reflex in combination with apparent narrow funnel stage 5 retinal detachment indicates the presence of attached or shallowly detached avascular, stretched, and nonfunctioning peripheral retina.

3. Anterior segment. In more severe cases of ROP, the anterior segment may become involved as follows:

a) Shallow anterior chamber and corneal edema. A relatively shallow anterior chamber may be a normal early finding in a premature infant's eye; however, when a progressively shallow anterior chamber develops along with a retinal detachment in ROP, it has serious implications. Some cases progress to acute angle closure glaucoma or to a flat chamber and corneal decompensation. (See later section on glaucoma.)

b) Iris abnormalities. Posterior synechiae, iris atrophy, and ectropion uveae are common formations in eyes with stage 4 or 5 ROP. Particularly in eyes with stage 5 disease, the iris may become rigid and the pupil difficult to dilate because of adhesions to the anterior lens capsule and persistence of the pupillary membrane with retention of its vascular network. Rarely, the pupil can seclude, leading to

iris bombé and angle closure. (See later section on glaucoma.)

4. Other tissues. Subretinal blood and exudate may be identifiable by ultrasonography or optical coherence tomography, but it may be difficult to distinguish one from another. Subretinal fibrotic membranes may be present but usually are recognized only during surgery.

Involution of Retinopathy of Prematurity

Involution of ROP typically begins after 38 weeks' postconceptional/postmenstrual age and may be characterized by a downgrading of staging and/or growth of retinal vessels into a more peripheral zone.[81]

Regressed ROP: Retinal Detachment, Strabismus, and Amblyopia

Although active ROP usually involutes without progressing to retinal detachment, cicatricial sequelae can remain even in those cases.[82,83] The relatively stable state of the eye after retinopathy has run its course is referred to as regressed ROP. In Box 64.1 the residual changes have been classified into those affecting the retinal periphery and those affecting the posterior fundus. Retinal pigmentary changes may be mistaken for side-effects of treatment.[84]

Box 64.1

Regressed Retinopathy of Prematurity

Peripheral Changes

Vascular

Failure to vascularize peripheral retina

Abnormal, nondichotomous branching of retinal vessels

Vascular arcades with circumferential interconnection

Telangiectatic vessels

Retinal

Pigmentary changes

Vitreoretinal interface changes

Thin retina

Peripheral folds

Vitreous membranes with or without attachment to retina

Lattice-like degeneration

Retinal breaks

Traction or rhegmatogenous retinal detachment

Posterior Changes

Vascular

Vascular tortuosity

Straightening of blood vessels in temporal arcade

Abnormal narrowing or widening in the angle of insertion of major temporal arcade

Retinal

Pigmentary changes

Distortion and ectopia of macula

Stretching and folding of retina in macular region leading to periphery

Vitreoretinal interface changes

Vitreous membrane

Dragging of retina over disc

The most serious complications of regressed ROP are late development of retinal detachment and angle closure glaucoma. At almost any age after the neonatal period, but especially several years after birth, retinal detachment remains a risk in eyes with sequelae from ROP. Eyes with high myopia, peripheral retinal pigmentary changes or lattice-like degeneration, vitreoretinal interface changes, vitreous condensation, and stretching and folding of the retina are at special risk of developing retinal breaks and detachment. Eyes with partial retinal detachment present at about 3 months after threshold retinopathy remain at risk for progression of the detachment.[85] Overall visual outcomes for 61 eyes studied were poor: only six eyes had better than 20/200 visual acuity.[85] These patients and their parents should be alert to the symptoms of retinal detachment as soon as the child is old enough to appreciate and report them.

Patients with regressed ROP are at risk for developing strabismus and amblyopia.[86–90] In the Cryotherapy for Retinopathy of Prematurity (CRYO-ROP) study, 200 (6.6%) of 3030 infants who had weighed <1251 g at birth were strabismic at the 3-month examination. Presence of ROP was found to be a significant predictor of strabismus at 3 months. Subgroup analysis determined that the risk for strabismus increased as the zone of ROP became more posterior and the stage more severe.[91] Regular examinations and attention to refractive, visual, and extraocular muscle status are indicated for all infants who have had ROP until about age 18 months, and thereafter as clinically indicated.

In the multicenter Early Treatment for ROP (ETROP) study, the prevalence of strabismus at 6 months corrected age was 20% among

infants with high-risk prethreshold ROP and 10% among infants with low-risk prethreshold ROP. At 9 months corrected age, 30% of infants with high-risk prethreshold ROP had strabismus, and risk factors associated with development of strabismus included abnormal fixation behavior, presence of amblyopia, and outborn birth status (i.e., birth outside a study-affiliated hospital).[92] Overall, ophthalmologists should be aware of significant variability in ocular alignment early in life among infants with a history of severe ROP.

History of Prematurity

In patients with a history of prematurity, particularly when there is significant myopia dating back to early childhood, careful examination is recommended to rule out any evidence of regressed ROP. This should be done regardless of the presenting age of the patient. Particular attention should be given to the temporal periphery of the retina in view of its relatively greater potential effects on macular vision.

Ocular Findings of Regressed Retinopathy of Prematurity

Myopia

In the CRYO-ROP study, 20% of infants with birthweight <1251 g were found to develop myopia in the first 2 years of life. The lower the birthweight, the higher the chance of myopia. Among infants with ROP, the incidence of myopia increased in direct relationship to the severity of ROP. For example, in patients who developed zone II, stage 3 ROP (without plus disease), 44–45% were myopic at 12 and 24 months postterm. In contrast, infants of this same birthweight group who never developed ROP had a 13% incidence of myopia.[93]

In the ETROP study, infants treated for high-risk prethreshold ROP were found to have 58% prevalence of myopia (defined as spherical equivalent ≥0.25 D) at age 6 months postterm, 68% prevalence of myopia at 9 months postterm, and little change thereafter until 3 years postnatal age. The prevalence of high

myopia increased steadily between ages 6 months and 3 years. There was little difference in prevalence of myopia or high myopia between eyes with zone I versus zone II ROP, or between eyes with plus disease versus without plus disease. However, prevalence of myopia and high myopia was higher in eyes with retinal residual of ROP such as straightened temporal vessels or macular heterotopia.[94] The exact mechanism of the myopia remains unclear. Fletcher and Brandon[95] suggested that it might be due to an elongation of the globe, alteration of the lens or the corneal curvature, or a combination of these factors.

Other Refractive and Binocular Defects

Astigmatism and anisometropia are relatively common in patients with regressed ROP. In the CRYO-ROP study, 2518 infants born weighing <1251 g were refracted at 12 months postterm, and 3.3% had anisometropia. Of the 1548 who had ROP of some degree, 4.8% had anisometropia.[93] In the ETROP study, 401 infants with prethreshold ROP in one or both eyes were randomized to early treatment (laser photocoagulation at high-risk prethreshold ROP) versus conventional treatment only if threshold ROP developed. All infants were refracted at 6 and 9 months correct age, and at 2 and 3 years postnatal age. The prevalence of astigmatism was similar at each test age in the early treatment and conventional management groups. For both groups, there was an increase in prevalence of astigmatism (defined as >1.00 D) from 32% at 6 months to 42% at 3 years.[96]

Approximately 20% of ROP cases are asymmetric at the time they reach threshold for treatment, and this asymmetry may well contribute to anisometropia. Amblyopia, nystagmus, and strabismus are also common after ROP has regressed.[86,87,91,97] Taken together, these findings highlight the importance of follow-up ophthalmology examinations in infants with a history of severe ROP.

Lens and Corneal Changes

At the 12-month examination of the CRYO-ROP study, there was an overall incidence of cataract of 0.3% in the natural history population. The incidence of cataract among eyes with a history of

zone I ROP or zone II stage 3+ ROP was approximately 2.5%.[98] At the final 6-year examination of the ETROP study, cataract or aphakia was found in 4.9% of early-treated eyes and in 7.2% of conventionally managed eyes in 271 children with symmetric ROP.[99] Kushner[97] pointed out that early development of cataract may seriously compromise vision in the presence of retinal abnormalities. Results can be satisfactory from cataract surgery in adults with a history of ROP.[100] Patients with ROP also have an increased risk of developing irregularities of corneal curvature, band keratopathy, and acute hydrops.[72]

Glaucoma in Retinopathy of Prematurity

Patients with retinopathy can develop acute or subacute glaucoma later in life. In the ETROP Study, 1.67% of enrolled eyes went on to develop glaucoma during the first six years of life. This was associated with a shallow chamber and stage 4B or worse retinal detachments.[101] This complication, which does not always look typical of iris bombé, may occur at any time: in the nursery, shortly after discharge, and throughout childhood. Where feasible, parents should be instructed to recognize the appearance of corneal haze and episcleral injection, and to seek ophthalmic consultation for these concerns. A trial of topical steroids and cycloplegic agents is recommended in suitable cases of glaucoma in the setting of ocular damage from ROP,[102] and further glaucoma management may be required.

Angle Closure Glaucoma in Regressed Retinopathy of Prematurity

Eyes with regressed ROP are at increased risk of developing acute angle closure glaucoma, even in adulthood.[103,104] Kushner[102] pointed out that certain patients with mild degrees of regressed ROP have a predilection for developing ciliary block glaucoma. Because these forms of glaucoma may be treatable by surgery in selected cases, ophthalmologists and patients should be aware of these potential complications, their associated signs and symptoms, and their management.

Differential Diagnosis

Although the differential diagnosis in a premature infant in a neonatal intensive care unit (NICU) is almost exclusively limited to ROP, there are several conditions that can mimic ROP out of that context in older children. Familial exudative retinopathy, incontinentia pigmenti (IP), and Norrie disease can all present with peripheral ischemic retina resulting in a traction retinal detachment secondary to retinal neovascularization. ROP can be excluded in these cases if there is no history of prematurity. Retinoblastoma can simulate a retinal detachment, although it is exudative and has a convex as opposed to concave surface. The tumors associated with exudative detachments are typically quite large and would be seen on ultrasound. Persistent fetal vasculature (PFV) can have a similar appearance to ROP, but is usually unilateral. Coats disease is also generally unilateral and has substantial lipid exudates which are not typically seen in ROP.

Risk Factors

In general, prematurity, low birthweight, a complex hospital course, and prolonged supplemental oxygen are today's established risk factors for the development of ROP.[10,73,105,106] Supplemental oxygen given for a period of weeks, without specific indication, was abundantly documented to be a major cause of ROP during the epidemic of the 1950s but is no longer the predominant factor in cases of ROP seen since the mid-1970s. Now, neonatal advances have resulted in improved survival rates of extremely low-birthweight children. The risk of developing treatment-requiring ROP is higher in this group, with as many as 25% of children born at 750 g or less developing plus disease.[107]

The role of blood carbon dioxide levels in the development of ROP is controversial. Bauer and Widmayer,[108] following Flower's observation[109] that carbon dioxide enhanced the oxygen-induced retinal changes in Beagles, conducted a retrospective analysis of infants with low birthweights. They reported that higher arterial carbon dioxide values were the most important variable in separating those infants of equal gestation who developed ROP from those without disease. Biglan et al.[110] and Brown et al.[105,111]

failed to confirm this association and, indeed, found that infants with "scarring retinopathy of prematurity" had lower carbon dioxide blood levels. It is likely that this parameter, like many others, is associated with an unstable clinical course – as is ROP – but not necessarily linked with it causally.

Numerous other neonatal health factors have been reported to be associated with ROP, including cyanosis, apnea, mechanical ventilation, intraventricular hemorrhages, seizures, transfusions, septicemia, in utero hypoxia, anemia, patent ductus arteriosus, and vitamin E deficiency.[13,25,89,106,108–117] These associations require further investigation to identify causal relationships. In the CRYO-ROP natural history cohort of 4099 infants born weighing less than 1251 g, significant additional factors were identified, including white race, multiple birth, and being transported elsewhere for intensive care. Once ROP develops, greater risk is associated with ROP located in zone I, the presence of plus disease, the severity of stage, and the extent of circumferential involvement.[118,119] The risk factors studied during the CRYO-ROP study were consolidated into a mathematical model that can predict the risk of an unfavorable outcome for a particular eye that reaches prethreshold severity.[120]

Examination Procedures in the Nursery

General Aspects and Timing of the Examination

The nursery surveillance carried out in the CRYO-ROP study produced definitive information concerning the early course of ROP. The "natural history" portion of this study recorded data from 4099 infants born weighing less than 1251 g. The study showed that ROP occurs on a schedule according to the infant's corrected age (postmenstrual age since mother's last menstrual period, or postconceptional age), rather than the time since birth, the so-called chronologic age (Fig. 64.21).[118] For infants in the birthweight category studied, it was found that those who develop stage 1 ROP (and no worse) do so at a median of 34.3 postmenstrual weeks. The median time for onset of stage 2 ROP that progresses no further is 35.4 weeks, and 95% of these cases have onset at 32 weeks or later. For patients with eyes that reached the treatment randomization "threshold" severity of stage 3+ ROP (at least five

contiguous or eight interrupted clock-hours in zones I or II), the threshold was reached at a median of 36.9 weeks (90% of cases were in the range of 33.6–42.0 weeks) (Table 64.1).

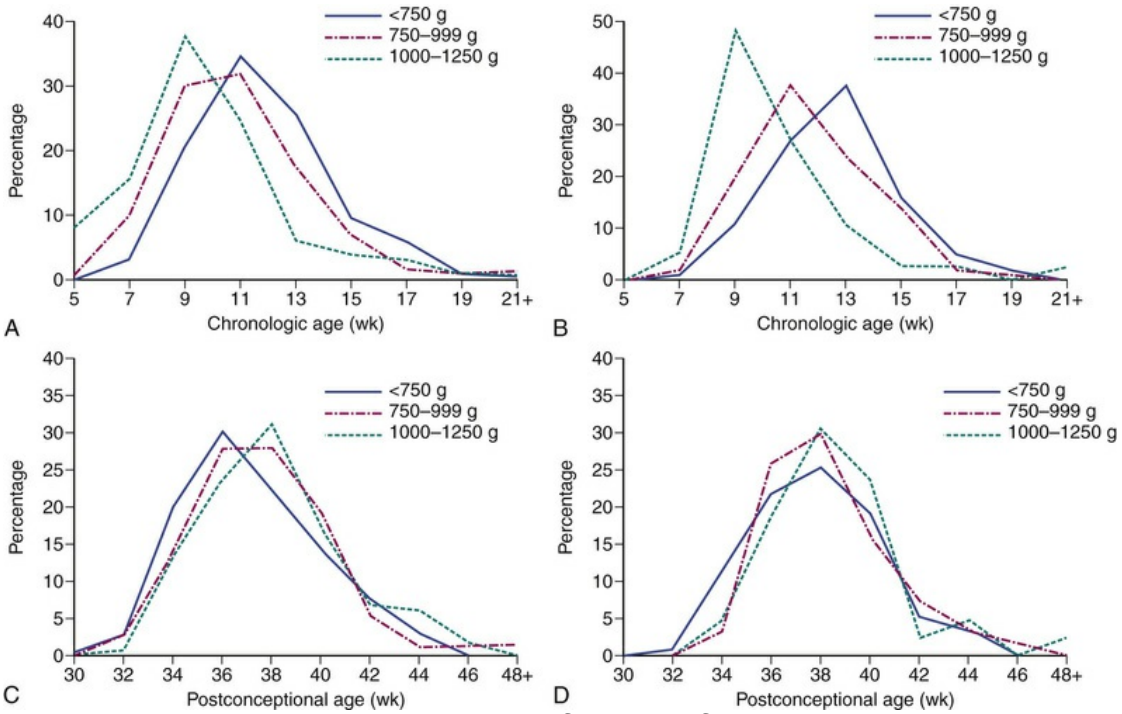

FIG. 64.21 (A) Distribution of onset of prethreshold retinopathy of prematurity (ROP) by chronologic age and by birthweight. (B) Comparable data for threshold ROP. (C) Prethreshold data by postconceptional age, for comparison with A (by chronologic age). (D) Threshold data by postconceptional age, for comparison with B (by chronologic age). (Reproduced with permission from Palmer EA, Flynn JT, Hardy RJ, et al. Incidence and early course of retinopathy of prematurity. Ophthalmology 1991;98:1628–40.)

TABLE 64.1

Onset of Retinopathy of Prematurity Events in Postconceptional Age (Weeks)

Stage	5th Percentile	Median	95th Percentile
1	—[a]	34.3	39.1
2	32	35.4	40.7
Threshold	33.6	36.9	42

[a]Not available; 17% of infants had stage 1 retinopathy of prematurity on the first

examination.

Reproduced with permission from Palmer EA, Flynn JT, Hardy RJ, et al. Incidence and early course of retinopathy of prematurity. Ophthalmology 1991;98:1628–1640.

Screening Guidelines

Because ROP can progress to blindness during the first 3 months of life[121] and treatment is available to arrest it in many cases, a protocol has been recommended for examining the eyes of premature infants during that time span to detect the onset of advancing ROP and specifically the development of prethreshold ROP defined as ROP of less severity than the threshold severity in the CRYO-ROP trial: specifically as any ROP in zone I, or zone II ROP of stage 2+ or stage 3 with or without plus disease. The current recommendations from the American Academies of Ophthalmology and Pediatrics are that children born at 30 weeks or less, or at less than 1500 g, should be screened for ROP. Specifically those born at a gestational age of 27 weeks or less should have their first examination at 31 weeks and children born from 28 to 32 weeks should have their first examination 4 weeks after birth. The subsequent examination schedule is determined by findings on the initial examination, as discussed at the end of this chapter.[122] If the infant reaches 45 weeks' gestational age without developing prethreshold ROP or worse, the risk of visual loss from ROP is minimal.[76] It should also be noted that these are data from the United States and the natural history of ROP may be different in other parts of the world.

Side-Effects of the Examination

Very-low-birthweight infants, while they are still in a precarious general condition, must be managed with care. The stress of an indirect ophthalmoscopic examination is necessary whenever the risk of treatable disease capable of progressing to blindness exists or when information is needed to assist in the general medical evaluation.[123] Screening programs must be designed around the consideration that the procedure may be stressful for the infant.

Techniques of Eye Examination

Eye examinations should be performed at the request of, or with the

approval of, an attending neonatologist. Pupils may be effectively dilated in most infants with Cyclomydril eye drops (cyclopentolate 0.2% and phenylephrine 1%), with the excess drops immediately blotted from the lids to minimize systemic side-effects such as hypertension and intestinal ileus.[123] The examination is performed about 25–30 minutes later using a binocular indirect ophthalmoscope and condensing lens. More heavily pigmented infants sometimes fail to respond adequately to the mydriatic drops, in which case 0.5% cyclopentolate or 1% tropicamide, or both, and 2.5% phenylephrine may be substituted and instilled twice. Most examiners generally use a lid speculum, and there are now a variety of designs suitable for premature infants (e.g., Barraquer, Sauer, Alfonso specula). The infant's hands should be physically restrained, and a nurse ordinarily assists with the examination. As a precaution against viral or chlamydial transfer, the lid speculum must be sterile for each infant and the examination lens should be wiped with an alcohol sponge between cases whenever it has touched the infant's face. The universal precaution of wearing gloves during examination is recommended.

In general, ROP severe enough to cause serious concern will be visible far enough posteriorly in the fundus to bring it into view without scleral indentation. However, to determine the final maturity of retinal vascularization requires either serial examinations past full term or, preferably, examination of the nasal retina to the ends of the growing vessels to determine whether vascularization has advanced into zone III.[79,118] For this far-nasal peripheral retinal examination, scleral indentation or eye positioning is generally needed. An aluminum-wired Calgiswab nasopharyngeal culture swab can be used as an inexpensive, sterile, and relatively gentle tool for this. The tip can be bent to any desired angle, even to resemble a fine muscle hook. Scleral depressors designed for infant examinations (e.g., Flynn depressor) are also commercially available. For scleral depression, topical anesthetic, such as proparacaine, is typically used. It is recommended that a member of the nursery staff be present during the entire examination to monitor the infant's airway, vital signs, and behavior and to deal with apnea or other adverse reactions that may occur.

Informing the Patient's Family

Often ROP becomes severe just as the infant is achieving medical stability, making it especially difficult on parents who have already experienced much anxiety. The ophthalmologist or neonatologist should keep families informed of the results of eye examinations. The ophthalmologist should contact the parents at the time it is first realized that the ROP is becoming severe, for example, when it develops in zone I or when zone II ROP reaches stage 3. If the parents are kept apprised of the eye condition as it develops, it may soften the emotional impact if the ROP ultimately causes vision damage, and it helps pave the way for discussion of possible surgical intervention.

Prophylaxis and Therapy

The Role of Vitamin E

Vitamin E was considered as a potential agent to prevent ROP due to its antioxidant properties. It was evaluated by Johnson et al.[124,125] with subsequent controlled clinical trials having tested the role of large doses of vitamin E.[126–133] The results were equivocal and a report from the Institute of Medicine published in 1986 concluded: "Vitamin E as prophylaxis for retinopathy of prematurity was subject to a detailed analysis. This committee found no conclusive evidence either of benefit or harm from vitamin E administration. Risks from vitamin E appear to be minimal for premature infants provided that doses are kept moderate to achieve a blood level no higher than 3 mg/dl."[134] Currently, there is no formal recommendation on the use of vitamin E in the management of ROP.

The Role of Light

Historically there has been interest in a possible relationship between light and ROP. In his original descriptions of RLF, Terry[135] considered premature exposure of the eye to light as an important etiologic possibility.

Before the importance of the role of inspired oxygen levels was recognized in ROP, two studies addressed the question of the effect

of light. In the late 1940s, Hepner et al.[136] patched the eyes of five premature infants from birth until they weighed 2000 g. They found that four of the five infants developed ROP, and they concluded that light was not a factor in its development. In 1952, Locke and Reese[137] reported on a series of 22 premature infants (birthweight less than 2000 g) in which they had patched one eye of each baby. Both found that there was no difference in the incidence of ROP between the patched eyes and the unpatched eyes.[136,137]

To examine the relationship between light exposure and ROP more definitively, a feasibility trial of light-reducing goggles (LIGHT-ROP study), chaired by James D. Reynolds, was sponsored by the National Eye Institute in 1995 at three nurseries in the United States. Half of 409 infants with birthweights of less than 1250 g were randomly selected either to wear goggles containing 97% near-neutral density filters until 31 weeks' postconceptional age or to undergo no extraordinary light reduction. The study concluded that there is no clinically important effect of light on the occurrence or severity of ROP.[138] Neither the American Academy of Ophthalmology nor the American Academy of Pediatrics has made any recommendations about restricting ambient light from the eyes of premature infants.

Cryotherapy

From 1968, reports suggested that ablative treatment of the peripheral retina of premature infants with ROP may ameliorate the course of the disease. Those early reports suggested that photocoagulation[139,140] or cryotherapy[141,142] may accomplish this goal. Throughout the early 1980s, studies produced conflicting results and opinions regarding the efficacy and role of cryotherapy for severe ROP.[143–148] The need for a large-scale clinical trial was apparent.

The Multicenter Trial of Cryotherapy.

The CRYO-ROP study was organized in 1985 under the chairmanship of Earl A. Palmer. Supported by the National Eye Institute, the study began enrolling premature infants weighing 1250 g or less at birth in 1986. Infants eligible for the cryotherapy trial had stage 3 ROP, involving five or more clock-hours of retina

posterior to zone III in the presence of a standardized plus disease.[69,107] The results of the CRYO-ROP study were evaluated through a masked comparison by fundus photographs of the incidence of objectively visible macular fold, retinal detachment, or retrolental mass in the eyes that received cryotherapy, with those eyes not receiving it.[149] Cryotherapy was found to reduce the listed unfavorable fundus outcomes over the serial examination visits. At the 10-year outcome assessment, unfavorable fundus outcomes were present in 27% of treated eyes versus 48% of control eyes, and visual acuity was 20/200 or worse in 44% of treated eyes versus 62% of control eyes.[149]

Current Concepts in Management of Retinopathy of Prematurity

Treatment Techniques

Cryotherapy – Special Considerations.

The average number of individual freezes used in the CRYO-ROP study was 50. As with other forms of eye surgery, a number of factors are considered in determining the method of analgesia or anesthesia, including the physical arrangement of the nursery, proximity to operating or procedure rooms, experience of the anesthesiologist, current medical stability of the infant, "track record" of the infant in tolerating previous stressful procedures, experience of the cryosurgeon, and posterior extent of retinopathy.

Laser – Special Considerations.

During the early 1990s laser ablation gained acceptance as an alternative to cryotherapy. In general, ophthalmologists have found that the LIO delivery system is technically easier than cryotherapy and creates fewer postoperative sequelae, such as inflammation and swelling. Furthermore, it seemed apparent that the outcomes of treatment of threshold disease in zone I and posterior zone II were superior to cryotherapy, and at least equivalent to cryotherapy results for zone II disease.[150–159]

When LIO delivery systems became available around 1990, the only laser offered was an argon photocoagulator (488–532 nm).

Subsequently, the diode laser (810 nm) photocoagulator was introduced. Although circumstances may require taking patients to the operating suite for ROP laser therapy, it can also be done in the NICU, with the patient under local anesthesia and with or without the aid of conscious sedation. Subsequently, large spot laser indirect headsets became available which offered threefold increase in area covered by an individual spot.

A technique of laser treatment in the NICU is to place the infant swaddled in a blanket in an open warmer. Mydriatic drops are instilled, and treatment is performed with the aid of a neonatal nurse. A neonatologist must always be available in the nursery should resuscitation be necessary. A heart rate monitor, apnea monitor, and pulse oximeter are used throughout the procedure. Topical anesthesia is instilled in the eye(s) to be treated, and a lid speculum is placed. Lidocaine 2% is injected subconjunctivally in each quadrant (0.25–0.3 ml) for local anesthesia. Approximately 10 minutes is allowed for the anesthetic to take effect. Treatment is then begun with the LIO delivery system, generally with a 28-D-condensing lens. Appropriate laser safety precautions must be taken for the protection of all personnel involved.

Photocoagulation burns are distributed in a confluent pattern to minimize skip areas. The objective of the treatment is to apply burns throughout the entire peripheral nonvascularized retina. Treatment is generally started at the anterior edge of the vascularized retina and applied out to the ora serrata utilizing a Calgiswab or similar instrument for eye positioning and scleral depression. Initial settings for the diode laser are a power of 0.2 W and a pulse duration of 0.3–0.4 seconds. This power setting is usually subthreshold for photocoagulation, and power is titrated up until a yellowish-gray reaction is observed in the retina. The power and/or pulse duration often needs to be varied from one area to another in the avascular retina.

The total number of laser applications necessary to treat a given eye will depend primarily on the size of the avascular zone in the eye. In the authors' experience, if the ROP is in mid to peripheral zone II, then 1000 laser spots may be sufficient to cover the entire nonvascularized retina. However, if the eye to be treated has vessel growth only in zone I, then it is not unusual to apply 1500–3000

laser spots for adequate coverage. Laser is usually performed during a single session in the event there is a postlaser hyphema or vitreous hemorrhage that would prevent subsequent treatment. However, circumstances such as reduced visibility or patient distress may necessitate more than one treatment session. Occasionally, inadvertently skipped areas near the ROP ridge require supplementary laser treatment, in the absence of involution.

The Early Treatment for Retinopathy of Prematurity Trial

In 1999, the National Eye Institute funded a clinical trial, under the chairmanship of William V. Good, to study optimal ROP treatment indications. In this trial, called the ETROP study, eyes were randomized to early peripheral retinal ablation or conventional management (observation until threshold criteria developed) once they achieved a high-risk level of prethreshold ROP. The ETROP study showed a significant benefit of earlier treatment intervention as measured by visual acuity outcome at a corrected age of 9 months and in the structural outcome of the retina at corrected ages of 6 and 9 months.[160] In the selected high-risk eyes that were studied, unfavorable acuity results were reduced by earlier treatment intervention to 14.5%, from 19.5% in the conventionally treated control group (p=.01). Unfavorable structural outcomes were reduced from 15.6% in the control group to 9.1% in the early treatment eyes (p<.001).

The ETROP study results, published in December 2003, produced a new clinical algorithm as a guide for treatment intervention in eyes with severe ROP.[160] Prompt treatment is indicated for eyes with type 1 ROP, and continued serial observations without treatment are recommended for eyes with type 2 ROP, as shown in Table 64.2. The ETROP group cautions that plus disease should involve at least two quadrants (usually six or more clock-hour segments) with dilation and tortuosity of the posterior retinal blood vessels as they exit the optic nerve, meeting the published standard (Fig. 64.18A).

TABLE 64.2

Type 1 ROP ("New Threshold")	Type 2 ROP
Administer peripheral ablation treatment	Wait and watch for progression
Zone II:	Zone II:
Plus disease with stage 2 or 3	Stage 3 without plus disease
Zone I:	Zone I:
Plus disease with stage 1, 2, or 3	Stage 1 or 2 without plus disease
Stage 3 without plus disease	

ETROP, Early Treatment for ROP; ROP, retinopathy of prematurity.

At the final study outcome examinations performed at age 6 years, unfavorable visual acuity outcomes in eyes with type 1 ROP were reduced by early treatment to 25.1% from 32.8% in the conventionally treated control group (p=.02). Interestingly, unfavorable visual acuity outcomes in eyes with type 2 ROP increased in the early treatment group to 23.6% from 19.4% in the conventionally treated group, although this difference was not statistically significant (p=.37).[99]

Retinal Detachment

There is a need for randomized trials of treatment approaches for retinal detachment from ROP. Current clinical thinking about the treatment of retinal detachment from ROP is discussed in Chapter 118 (Surgical management of retinopathy of prematurity).

The ETROP Study: Better Outcomes, Changing Clinical Strategy

In the ETROP trial, only 66% of the high-risk eyes selected at random to be treated conventionally went on to receive laser therapy (cryotherapy was rarely used). Secondary analysis of the large database produced a simplified revision of the indications for treatment, which was a great practical improvement over the computer-generated algorithm used to select the research subjects for the study[120] (Table 64.2).

Some of the advantages of an earlier treatment policy may be lost if newborn eye examinations do not occur, as in the ETROP study. Careful reading of the methods used in the trial[161] reveals a real

impact on an intensive care unit's policy for serial ROP examinations. Therefore, consider the following schedule for infants who do not meet criteria for treatment:[122]

- 1-week or less follow-up for type 2 ROP (Table 64.2):
  - Zone II stage 3 and no plus
  - Zone I stage 1 or 2 and no plus
- 1–2-week follow-up:
  - Zone II, no plus, stage 2
  - Zone I, immature, no ROP
  - Zone I, regressing ROP
- 2-week follow-up:
  - Zone II, no plus, stage 1
  - Zone II, regressing ROP
- 2–3-week follow-up:
  - Zone III, no plus, stage 1 or 2
  - Zone II, immature, no ROP
  - Zone III, regressing ROP.

Favorable signs, with respect to progression or involution of ROP, include attainment of postmenstrual age of 45 weeks without developing at least type 2 (as defined above) ROP, and either the completion of full retinal vascularization or progression of retinal

vascularization into zone III without previous zone II ROP.[76]

Anti-VEGF Therapy for Posterior Retinopathy of Prematurity

There have been numerous trials demonstrating the benefits of bevacizumab in adult patients suffering from choroidal neovascular membranes in the setting of wet age-related macular degeneration. Based on this experience, many investigators have been interested in using a similar approach for the treatment of aggressive ROP. A number of recent case series have reported that intravitreal injections of anti-VEGF antibodies (e.g., bevacizumab) are a very promising approach for the treatment of aggressive ROP, with the possibility of easier administration and improved preservation of peripheral retina compared to laser.[162–167] The BEAT-ROP study was a prospective multicenter trial which included 150 infants with bilateral stage 3+ disease in zone I or posterior zone II were randomized to intravitreal bevacizumab (0.625 mg) versus conventional laser treatment. This showed that infants treated with bevacizumab for stage 3+ disease in zone I had significantly fewer disease recurrences and better structural outcomes at 54 weeks' postmenstrual age, although there was no difference for infants with ROP in posterior zone II.[168] Specifically, 6% of the children with zone 1 treatment-requiring ROP needed additional therapy. In contrast, 42% of the eyes treated with laser required additional therapy. It should be noted that in the ETROP study the unfavorable structural outcome was only 29.6% for zone I with stage 3 and/or plus and 22.2% for zone II with plus and no stage 3.

Although there is the possibility of improved treatment efficacy with bevacizumab, ROP recurrences have been reported several months postinjection.[168] Unlike laser treatment, where the regression is often durable and permanent, the potential for recurrence after bevacizumab injection emphasizes the need for prolonged follow-up examinations. In the BEAT-ROP study the recurrences often occurred many months after initial injection with a mean onset of 16 weeks post injection.[168] This places a special burden on both the family and the screening physician to continue frequent follow-up often beyond 50 weeks of gestational age. Early

reports of recurrence from Hu et al. identified children who had initial response to bevacizumab treatment but then recurred aggressively and in some cases went on to stage 4 or 5 detachments.[169] This emphasized the need for close follow-up especially for those children who remained in zone I or posterior zone II despite advancing gestational age. More recently, ranibizumab has been used as initial monotherapy with most reporting an initial response similar to that seen with bevacizumab.[170] With increasing use, some centers report much higher recurrence rates after ranibizumab with some as high as 83% within 6 weeks of injection.[170,171]

Until ROP can be prevented, it behooves physicians caring for premature infants to detect treatment-requiring cases through coordinated and timely methods. Neonatologists, ophthalmologists, discharge coordinators, and ROP coordinators must collaborate in adhering to local policies developed to benefit these infants.

Other Pediatric Retinal Vascular Diseases

Coats Disease

Coats disease arises from abnormal telangiectatic retinal vessels that result in profuse leakage, leading to retinal edema and exudative detachments. It was originally described in 1908 by George Coats, who noted that patients with this condition had unilateral telangiectatic vessels with associated lipid deposits.[172] Interestingly, none of the patients described in the original paper were children, and it was not until subsequent observations that its incidence in the pediatric population was appreciated.

Children often present initially with leukocoria. This is increasingly identified by parents who notice a glow in the setting of a flash photograph, which results from either an exudative detachment or subfoveal lipid exudate as a consequence of distant telangiectasias in the peripheral retina. The differential diagnosis includes retinoblastoma, familial exudative retinopathy, and PFV. In those cases where there are only telangiectatic vessels and subretinal lipid deposits, the diagnosis is relatively straightforward,

especially if wide-angle fluorescein angiography is performed (Fig. 64.22). In those cases where there is a prominent exudative detachment, discriminating between retinoblastoma and Coats disease can be challenging. One useful feature is the color of the subretinal material: an exudative detachment from retinoblastoma will often have tumor visible underneath the retina with a whitish color and a mayonnaise-like appearance. In contrast, the subretinal material in Coats disease will often appear more yellow-green with a mustard-like appearance. In addition, an eye with retinoblastoma will often have a substantial dome-shaped mass on ultrasound. The presence of telangiectatic vessels, however, is not limited to Coats disease, and many exudative detachments from retinoblastoma will have similar vessels.

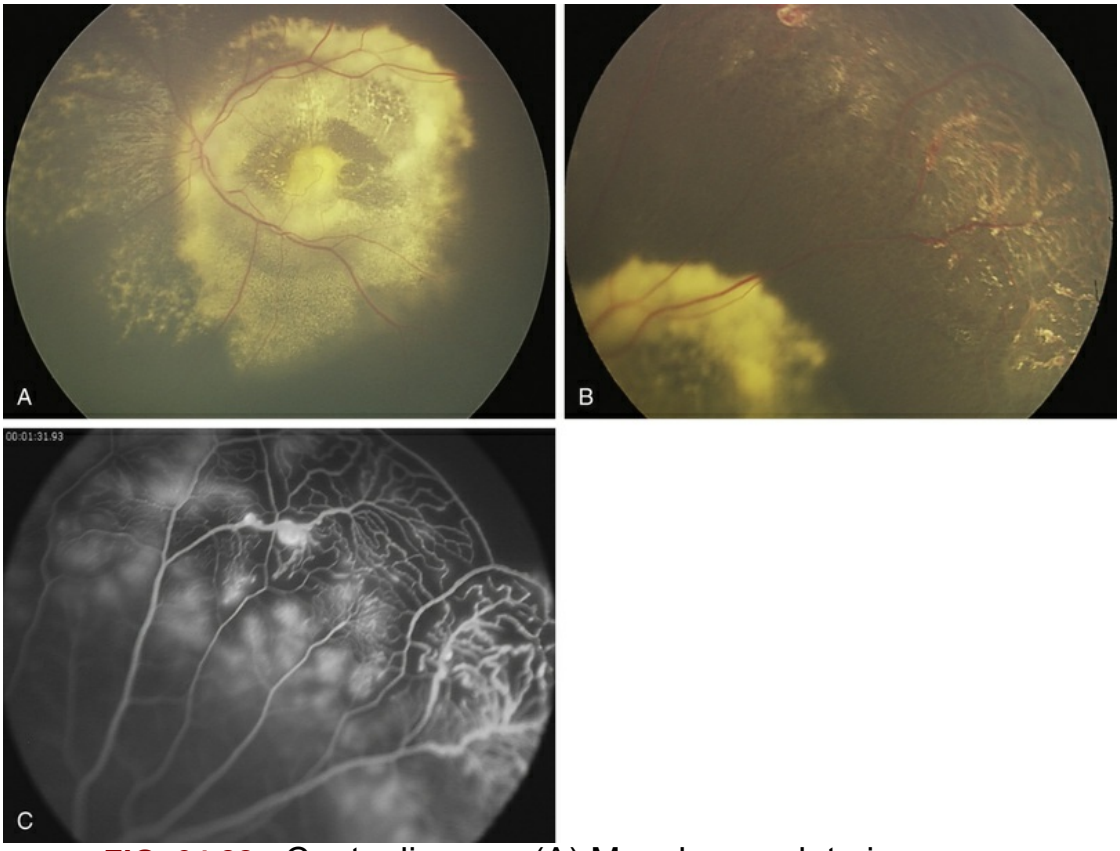

FIG. 64.22 Coats disease. (A) Macular exudate in a child with Coats disease. (B) Telangiectatic vessels are seen in the temporal periphery. (C) Fluorescein angiography reveals capillary dropout and vascular dilation.

In 2001, Shields et al. proposed a classification system based on response to treatment. Stage 1 eyes have telangiectasias only. Stage 2 eyes have in addition exudation in either extrafoveal (2a) or subfoveal (2b) locations. Stage 3 eyes have an exudative detachment that is subtotal (3a) or total (3b). Of the stage 3a eyes, if it involves the fovea, then it is stage 3a1, and if it remains outside the fovea, it is stage 3a2. Stage 4 is a detachment with glaucoma, and stage 5 is endstage disease.[173]

The primary treatment of Coats disease involves laser photocoagulation directly to telangiectatic vessels. It is helpful to have wide-angle fluorescein angiography to identify the full extent of the disease. By using a green 532-nm frequency-doubled yttrium aluminum garnet (YAG) laser indirect, it is possible to coagulate the vessels even in areas where the retina is fully detached.[174] This often requires multiple treatment sessions under anesthesia over successive months. In more recalcitrant cases, subretinal fluid drainage can help expose more retina that may be hidden anteriorly due to the extent of the detachment. In severe cases, vitrectomy with external drainage may be necessary. Prior to considering any invasive treatment, retinoblastoma must be clearly ruled out.

Bevacizumab has been used by some centers with the rationale that it may decrease the vascular permeability and amount of subretinal fluid.[175] Recent work by Ray et al. showed that in a retrospective review, bevacizumab in conjunction with conventional laser therapy did not impact overall resolution of the disease.[176] In addition, Ramasubramanian et al. showed that of the eight patients who received injections, half developed vitreous fibrosis with some developing traction detachments requiring vitrectomy.[177] In the absence of randomized trials, the benefit of bevacizumab for Coats disease remains unclear.

Little is known regarding the etiology of Coats disease. There is no clear hereditary component, and it is rarely bilateral. Although there is a mild sex predisposition toward males and it can be more common in the Asian population, there is little else that would point to an underlying cause. Interestingly, although there is often widespread ischemia due to capillary dropout, there is rarely any retinal neovascularization or vitreous hemorrhage. This is despite the high rate of neovascular glaucoma in advanced cases.

Persistent Fetal Vasculature

Originally labeled as persistent hyperplastic primary vitreous (PHPV), PFV is a result of incomplete regression of the vascular primary vitreous leaving a stalk of fibrovascular tissue extending from the optic nerve to the posterior lens capsule.[178] This often leads to a white opaque membrane behind the lens, resulting in dense amblyopia. The ciliary processes are often drawn towards the center and are associated with some degree of microphthalmia. The retina around the optic nerve can be drawn up into the stalk and in some cases can involve the entire length of the stalk, making surgical amputation of the stalk a risk.

There are a number of conditions that can present with a traction detachment, including familial exudative vitreoretinopathy (FEVR), Norrie disease, incontinentia pigmenti, and retinoblastoma. PFV is almost always unilateral and can be distinguished from the hereditary conditions based on bilaterality. Also the implantation of the stalk is generally to the central posterior lens capsule, whereas in FEVR, Norrie, and incontinentia pigmenti, there is not a stalk but rather a fold that usually runs to the temporal ora serrata. Eyes with retinoblastoma are rarely microphthalmic and will have a mass with possible calcifications on ultrasound.

Treatment for PFV can vary from observation to surgical amputation of the stalk. In some cases, the stalk is mild and the macula can be visualized. If the retina is intact and there are macular structures, a surgical approach to clear the visual access can be helpful. In some cases, the posterior plaque is quite dense and upon removal the stalk ends up being less severe with relatively normal retinal architecture. Some have advocated surgical treatment in the setting of significantly deformed retina, even when the vision is at light perception. Amputation of the stalk is thought in these cases to prevent phthisis and allow for continued eye growth.[179]

Little is known about the pathogenesis of PFV. The primary vitreous undergoes a well-described programmed involution, and in patients with PFV, it is believed that this process is altered. Recent work suggests that astrocytes may play a role in altering how this process happens and may prevent the hyaloid artery from underdoing a macrophage-mediated involution.[180]

Incontinentia Pigmenti

Previously called Bloch–Sulzberger syndrome, after the two dermatologists who first recognized the condition, IP is an X-linked dominant disease with ocular, central nervous system, dermatologic, and dental abnormalities. It is associated with a mutation in the *NEMO* gene located on Xq28. The resulting protein regulates the activity of NF-κB, increasing a cell's sensitivity to apoptotic signals and resulting in increase endothelial cell death.[181]

Ocular findings include retinal ischemia with neovascularization that can lead to vitreous hemorrhage and traction detachment. The differential diagnosis based solely on the ocular findings includes ROP, FEVR, and Norrie disease. However, unlike these diseases, the ischemia in IP does not mimic a developmental vascular pattern with distinct areas of vascularized retina posteriorly and avascular retina anteriorly. Instead, the peripheral ischemia is often accompanied by ischemia in posterior vascularized retina and in some cases the macula as well (Fig. 64.23A). Usually, the diagnosis of IP is made soon after birth based on the presence of the skin blisters (Fig. 64.23B). Approximately one in three children with IP have obvious retinal abnormalities on examination, and one in four have traction retinal detachments.[182]

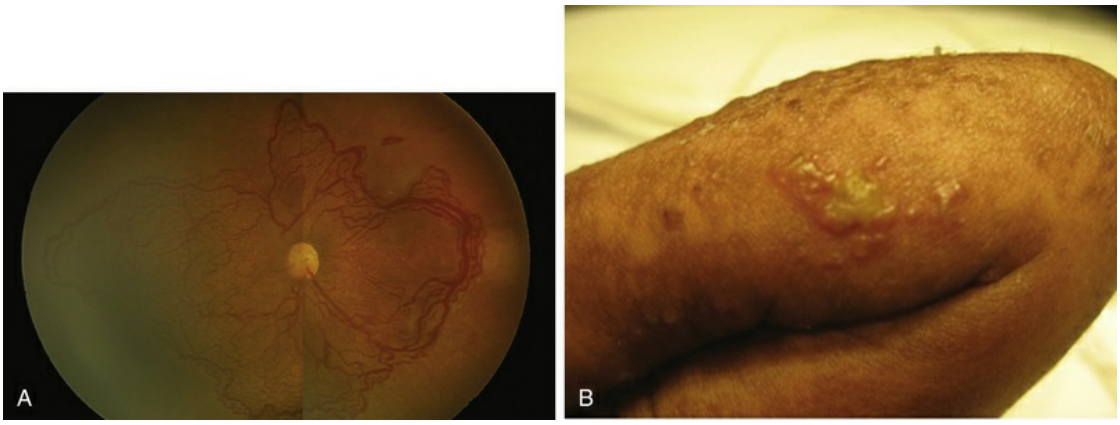

FIG. 64.23 Incontinentia pigmenti (IP). (A) Widespread retinal ischemia both peripherally and in the macula. (B) Skin pustules in a newborn with IP.

Ocular management for IP includes regular examinations, including those done under anesthesia. Some have recommended

monthly examinations from birth to 4 months of age and then every 3 months until the patient is 1 year old. Examinations can then be performed every 6 months until 3 years of age and then every 6 months after that. Fluorescein angiography can be helpful in identifying the area and extent of ischemia. The managing physician should be careful about the presence of any ischemia, since this potentially can be progressive and may result in neovascularization and subsequent detachment. Eyes at risk for traction detachments can be treated with laser to ischemic areas.

Familial Exudative Vitreoretinopathy and Norrie Disease

FEVR and Norrie disease are both conditions that may result from genetic mutations affecting the Wnt pathway. They can present with similar retinal findings. These mutations result in incomplete development of the retinal vessels similar to what is seen in ROP. Patients can have peripheral avascular retina, neovascular membranes, and traction retinal detachments. In addition to the retinal findings, Norrie disease, which is X-linked recessive, can also be associated with hearing loss and mental retardation. The differential diagnosis for both includes ROP, PFV/PHPV, and IP.

Management of any patient where FEVR or Norrie disease is being considered should include careful examination under anesthesia and, when possible, fluorescein angiography. Both conditions can have an asymmetric presentation and can mimic PFV. In these cases the presumed unaffected eye may have subtle fundoscopic abnormalities that can be overlooked in an outpatient clinic setting and even under anesthesia. Wide-angle fluorescein angiography can provide a very definitive assessment of the vasculature in both eyes and may demonstrate premature termination of the peripheral vessels and subclinical neovascularization. In eyes with ischemia and neovascularization but no detachment, laser photocoagulation to the avascular retina can induce regression and prevent a detachment. When traction retinal detachment is present, some have advocated vitrectomy to release stress on the retina and ciliary body to reduce the likelihood of hypotony and maintain light perception vision when present.[183]

In the case of FEVR, the mutation occurs in the *FZD4* gene that encodes the frizzled-4 receptor. This receptor binds Wnt ligands 3, 5a, and 8a as well as Norrin and triggers the translocation of β-catenin to the nucleus where it can activate transcription of genes involved in cell proliferation. In Norrie disease, the mutation occurs in the *NDP* gene that produces norrin, a secreted protein that can bind frizzled-4.[184,185] Recently, another gene, *TSPAN12*, was found to facilitate norrin binding to frizzled-4 and loss of *TSPAN12* was found in some patients with FEVR.[186] There is currently ongoing investigation as to whether mutations in these genes may also increase the risk of developing aggressive ROP.

Newborn Screening for Retinal Disease

With the exception of ROP, pediatric retinal disease is often diagnosed very late and is usually initially detected by the parents. A large study by Abramson et al. showed that 80% of the time, parents were the first to identify leukocoria in children with retinoblastoma while the pediatrician was the initial source of diagnosis in only 8% of the cases.[187] This raises the argument of using photoscreening for early detection of pediatric retinal diseases before the condition becomes symptomatic. A large prospective study by Li et al. of digital fundus exams of 3573 newborn children showed that 0.5% of had retinal pathologies and that an additional 6% had macular hemorrhages.[188]

Although the instrument used (RetCam, Clarity MSI) in this study was appropriate in a newborn nursery setting, it would be impractical to perform in an outpatient pediatric examination office. More recently, several smartphone-based applications have been developed to assess nonverbal children for amblyopia, as well as cataracts and retinal diseases.[189] Although still in the early stages of evaluation, these platforms have the potential to reduce the time to diagnosis for retinal diseases with the hope that earlier detection will lead to a reduction in visual loss in this vulnerable population.

References

1. Terry TL. Extreme prematurity and fibroblastic overgrowth of persistent vascular sheath behind each crystalline lens. I. Preliminary report. *Am J Ophthalmol*. 1942;25:203–204.
2. Terry TL. Fibroblastic overgrowth of persistent tunica vasculosa lentis in premature infants. II. Report of cases – clinical aspects. *Arch Ophthalmol*. 1943;29:36–53.
3. Patz A. The role of oxygen in retrolental fibroplasias. *Trans Am Ophthalmol Soc*. 1968;66:940–985.
4. Owens WC, Owens EU. Retrolental fibroplasia in premature infants. *Am J Ophthalmol*. 1949;32:1–29.
5. Patz A, Hoeck LE, De La Cruz E. Studies on the effect of high oxygen administration in retrolental fibroplasia. I. Nursery observations. *Am J Ophthalmol*. 1952;35:1248–1253.
6. Patz A, Eastham A, Higginbotham DH, et al. Oxygen studies in retrolental fibroplasia. II. The production of the microscopic changes of retrolental fibroplasia in experimental animals. *Am J Ophthalmol*. 1953;36:1511–1522.
7. Ashton N, Ward B, Serpell G. Role of oxygen in the genesis of retrolental fibroplasia: a preliminary report. *Br J Ophthalmol*. 1953;37:513–520.
8. Lanman JT, Guy LP, Dancis J. Retrolental fibroplasia and oxygen therapy. *JAMA*. 1954;55:223–226.
9. Kinsey VE. Retrolental fibroplasia: cooperative study of retrolental fibroplasia and the use of oxygen. *Arch Ophthalmol*. 1956;56:481–543.
10. Bolton DPG, Cross KW. Further observations on cost of preventing retrolental fibroplasias. *Lancet*. 1974;1:445–448.
11. Avery ME, Oppenheimer EH. Recent increase in mortality from hyaline membrane disease. *J Pediatr*. 1960;57:553–559.
12. McDonald AD. Cerebral palsy in children of very low birth weight. *Arch Dis Child*. 1963;38:579–588.
13. Strang LB, MacLeish MH. Ventilatory failure and right-to-left shunt in newborn infants with respiratory distress. *Pediatrics*. 1961;28:17–27.
14. Chow LC, Wright KW, Sola A, et al. Can changes in clinical practice decrease the incidence of severe retinopathy of

prematurity in very low birth weight infants? *Pediatrics*. 2003;111:339–345.
15. SUPPORT Study Group of the Eunice Kennedy Shriver NICHD Neonatal Research Network. Target ranges of oxygen saturation in extremely preterm infants. *N Engl J Med*. 2010;362:1959–1969.
16. Stenson B, Brocklehurst P, Tarnow-Mordi W, et al. Increased 36-week survival with high oxygen saturation target in extremely premature infants. *N Engl J Med*. 2001;364:1680–1682.
17. Finnstrom O, Olausson PO, Sedin G, et al. The Swedish national prospective study on extremely low birth weight (ELBW) infants – incidence, mortality, morbidity and survival in relation to level of care. *Acta Paediatr*. 1998;86:503–511.
18. National NeoKnowledge Network. *Multi-institutional comparative analysis for births in 1996. Based on 1810 liveborn infants <1000 g birth weight*. MDS: Wayne, PA; 1997.
19. Strebel R, Bucher HU. Improved chance of survival for very small premature infants in Switzerland. *Schweiz Med Wochenschr*. 1994;124:1653–1659.
20. Smith LE. Through the eyes of a child: understanding retinopathy through ROP. The Friedenwald lecture. *Invest Ophthalmol Vis Sci*. 2008;49:5177–5182.
21. Pierce EA, Foley ED, Smith LEH. Regulation of vascular endothelial growth factor by oxygen in a model of retinopathy of prematurity. *Arch Ophthalmol*. 1996;114:1219–1228 [(note: see correction of errata in Arch Ophthalmol 115:427, 1997.)].
22. Stone J, Maslim J. Mechanisms of retinal angiogenesis. *Prog Ret Eye Res*. 1996;16:157–181.
23. Patz A. Current concepts of the effect of oxygen on the developing retina. *Curr Eye Res*. 1984;3:159–163.
24. Flynn JT, Bancalari E, Bawol R, et al. Retinopathy of prematurity: a randomized, prospective trial of transcutaneous oxygen monitoring. *Ophthalmology*. 1987;94:630–638.
25. Lucey JF, Dangman B. A reexamination of the role of oxygen

in retrolental fibroplasias. *Pediatrics*. 1984;73:82–96.
26. Gole GA. Animal models of retinopathy of prematurity. Silverman WA, Flynn JT. *Retinopathy of prematurity*. Blackwell: Boston, MA; 1985:53–96.
27. Kretzer FL, Hittner HM. Initiating events in the development of retinopathy of prematurity. Silverman WA, Flynn JT. *Retinopathy of prematurity*. Blackwell: Boston, MA; 1985:121–152.
28. McLeod DS, D'Anna SA, Lutty GA. Clinical and histopathologic features of canine oxygen-induced proliferative retinopathy. *Invest Ophthalmol Vis Sci*. 1998;39:1918–1932.
29. Ashton N, Ward B, Serpell G. Effect of oxygen on developing retinal vessels with particular reference to the problem of retrolental fibroplasias. *Br J Ophthalmol*. 1954;38:397–432.
30. Ashton N, Cook C. Direct observation of the effect of oxygen on developing vessels: a preliminary report. *Br J Ophthalmol*. 1954;38:433–440.
31. McLeod DS, Brownstein R, Lutty GA. Vaso-obliteration in the canine model of oxygen-induced retinopathy. *Invest Ophthalmol Vis Sci*. 1996;37:300–311.
32. Ashton N, Pedler C. Studies on developing retinal vessels. IX. Reaction of endothelial cells to oxygen. *Br J Ophthalmol*. 1962;16:257–276.
33. Michaelson IC. The mode of development of the vascular system of the retina with some observations on its significance for certain retinal diseases. *Trans Ophthalmol Soc U K*. 1948;68:137–180.
34. Cogan DG. Development and senescence of the human retinal vasculature. *Trans Ophthalmol Soc U K*. 1963;83:465–489.
35. Penn JS, Henry MM, Tolman BL. Exposure to alternating hypoxia and hyperoxia causes severe proliferative retinopathy in the newborn rat. *Pediatric Res*. 1994;36:724–731.
36. Smith LEH, Wesolowski E, McLellan A, et al. Oxygen-induced retinopathy in the mouse. *Invest Ophthalmol Vis Sci*.

1994;35:101–111.
37. Ashton N. Oxygen and the growth and development of retinal vessels: in vivo and in vitro studies. *Am J Ophthalmol*. 1966;62:412–435.
38. Riecke B, Chavakis E, Bretzel R, et al. Topical application of integrin antagonists inhibits proliferative retinopathy. *Horm Metab Res*. 2001;33:307–311.
39. Wilkinson-Berka J, Alousis N, Kelly D, et al. COX-2 inhibition and retinal angiogenesis in a mouse model of retinopathy of prematurity. *Invest Ophthalmol Vis Sci*. 2003;44:974–979.
40. Higgins RD, Hendricks-Munoz KD, Caines VV, et al. Hyperoxia stimulates endothelin-1 secretion from endothelial cells; modulation by captopril and nifedipine. *Curr Eye Res*. 1998;17:487–493.
41. Raisler BJ, Berns KI, Grant MB, et al. Adeno-associated virus type-2 expression of pigmented epithelium-derived factor or Kringles 1–3 of angiostatin reduce retinal neovascularization. *Proc Natl Acad Sci USA*. 2001;99:8909–8914.
42. Aurricchio A, Behling KC, Maguire A, et al. Inhibition of retinal neovascularization by intraocular viral-mediated delivery of anti-angiogenic agents. *Mol Ther*. 2002;6:490–494.
43. Stellmach V, Crawford SE, Zhou W, et al. Prevention of ischemia-induced retinopathy by the natural ocular antiangiogenic agent pigment epithelium-derived factor. *Proc Natl Acad Sci USA*. 2001;98:2593–2597.
44. Phelps DL. Oxygen and developmental retinal capillary remodeling in the kitten. *Invest Ophthalmol Vis Sci*. 1990;31:2194–2200.
45. Penn JS, Tolman BAL, Henry MM. Oxygen-induced retinopathy in the rat: relationship of retinal nonperfusion to subsequent neovascularization. *Invest Ophthalmol Vis Sci*. 1994;35:3429–3435.
46. Chan-Ling T, McLeod DS, Hughes S, et al. Astrocyte–endothelial cell relationships during human retinal vascular development. *Invest Ophthalmol Vis Sci*. 2004;45:2020–2032.
47. Chan-Ling T, Tout S, Hollander H, et al. Vascular changes

and their mechanisms in the feline model of retinopathy of prematurity. *Invest Ophthalmol Vis Sci*. 1992;33:2128–2147.
48. Stone J, Itin A, Chan-Ling T, et al. The roles of endothelial growth factor (VEGF) and neuroglia in retinal vascularization during normal development and in retinopathy of prematurity. *J Neurochem*. 1995;65:121.
49. Stone J, Chan-Ling T, Pe'er J, et al. Roles of vascular endothelial growth factor and astrocyte degeneration in the genesis of retinopathy of prematurity. *Invest Ophthalmol Vis Sci*. 1996;37:290–299.
50. Provis JM, Leech J, Diaz CM, et al. Development of the human retinal vasculature – cellular relations and VEGF expression. *Exp Eye Res*. 1997;65:555–568.
51. Alon T, Hemo I, Itin A, et al. Vascular endothelial growth factor acts as a survival factor for newly formed retinal vessels and has implications for retinopathy of prematurity. *Nature Med*. 1995;1:1024–1028.
52. Donahue ML, Phelps DL, Watkins RH, et al. Retinal vascular endothelial growth factor (VEGF) mRNA expression is altered in relation to neovascularization in oxygen-induced retinopathy. *Curr Eye Res*. 1996;15:175–184.
53. Dorey CK, Aouididi S, Reynaud X, et al. Correlation of vascular permeability factor/vascular endothelial growth factor with extraretinal neovascularization in rat. *Arch Ophthalmol*. 1996;114:1210–1217.
54. Szewczyk TS. Retrolental fibroplasia and related ocular diseases: classification, etiology, and prophylaxis. *Am J Ophthalmol*. 1953;36:1333–1361.
55. Phelps DL, Rosenbaum A. Effects of marginal hypoxemia on recovery from oxygen-induced retinopathy in the kitten model. *Pediatrics*. 1984;73:1–10.
56. Phelps DL. Reduced severity of oxygen-induced retinopathy in kittens recovered in 28% oxygen. *Pediatr Res*. 1988;24:106–109.
57. STOP-ROP Multicenter Study Group. Supplemental therapeutic oxygen for prethreshold retinopathy of prematurity (STOP-ROP), a randomized, controlled trial. I. Primary outcomes. *Pediatrics*. 2000;105:295–310.

58. Cantolino SJ, O'Grady GE, Herrera JA, et al. Ophthalmoscopic monitoring of oxygen therapy in premature infants: fluorescein angiography in acute retrolental fibroplasias. *Am J Ophthalmol*. 1971;72:322–331.
59. Flynn JT. Acute proliferative retrolental fibroplasia: evolution of the lesion. *Graefes Arch Klin Exp Ophthalmol*. 1975;195:101–111.
60. Flynn JT. Retinopathy of prematurity. *Pediatr Clin North Am*. 1987;34:1487–1515.
61. Flynn JT, Cassady J, Essner D, et al. Fluorescein angiography in retrolental fibroplasia: experience from 1969–1977. *Ophthalmology*. 1979;86:1700–1723.
62. Flynn JT, O'Grady GE, Herrera J. Retrolental fibroplasia: I. Clinical observations. *Arch Ophthalmol*. 1977;95:217–223.
63. Brooks SE, Gu X, Samuel S, et al. Reduced severity of oxygen-induced retinopathy in eNOS-deficient mice. *Invest Ophthalmol Vis Sci*. 2001;42:222–228.
64. Foos RY. Acute retrolental fibroplasias. *Graefes Arch Klin Exp Ophthalmol*. 1975;95:87–100.
65. Foos RY. Chronic retinopathy of prematurity. *Ophthalmology*. 1985;92:563–574.
66. Foos RY. Retinopathy of prematurity – pathologic correlation of clinical stages. *Retina*. 1987;7:260–276.
67. Cogan DG, Kuwabara T. Accessory cells in vessels of the perinatal human retina. *Arch Ophthalmol*. 1986;104:747–752.
68. McLeod DS, Lutty GA, Wajer SD, et al. Visualization of a developing vasculature. *Microvasc Res*. 1987;33:257–269.
69. Committee for the Classification of Retinopathy of Prematurity. An international classification of retinopathy of prematurity. *Arch Ophthalmol*. 1984;102:1130–1134.
70. Chiang MF, Thyparampil PJ, Rabinowitz D. Interexpert agreement in the identification of macular location in infants at risk for retinopathy of prematurity. *Arch Ophthalmol*. 2010;128(9):1153–1159.
71. Garner A. The pathology of retinopathy of prematurity. Silverman WA, Flynn JT. *Retinopathy of prematurity*. Blackwell: Boston, MA; 1985:19–52.
72. Hittner HM, Rhodes LM, McPherson AR. Anterior segment

abnormalities in cicatricial retinopathy of prematurity. *Ophthalmology*. 1979;86:803–816.
73. International Committee for the Classification of Retinopathy of Prematurity. The International Classification of Retinopathy of Prematurity revisited. *Arch Ophthalmol*. 2005;123:991–999.
74. Wallace DK, Freedman SF, Hartnett ME, et al. Predictive value of pre-plus disease in retinopathy of prematurity. *Arch Ophthalmol*. 2011;129(5):591–596.
75. Chiang MF, Jiang L, Gelman R, et al. Interexpert agreement of plus disease diagnosis in retinopathy of prematurity. *Arch Ophthalmol*. 2007;125:875–880.
76. Reynolds JD, Dobson V, Quinn GE, et al. Evidence-based screening criteria for retinopathy of prematurity: natural history data from the CRYO-ROP and LIGHT-ROP studies. *Arch Ophthalmol*. 2002;120:1470–1476.
77. Wallace DK, Quinn GE, Freedman SF, et al. Agreement among pediatric ophthalmologists in diagnosing plus and pre-plus disease in retinopathy of prematurity. *J AAPOS*. 2008;12:352–356.
78. Flynn JT, Chan-Ling T. Retinopathy of prematurity: two distinct mechanisms that underlie zone 1 and zone 2 disease. *Am J Ophthalmol*. 2006;142:46–59.
79. International Committee for Classification of the Late Stages of Retinopathy of Prematurity. An international classification of retinopathy of prematurity: II. The classification of retinal detachment. *Arch Ophthalmol*. 1987;105:906–912.
80. Machemer R. Description and pathogenesis of late stages of retinopathy of prematurity. *Ophthalmology*. 1985;92:1000–1004.
81. Repka MX, Palmer EA. Involution of retinopathy of prematurity. *Arch Ophthalmol*. 2000;118:645–649.
82. Cryotherapy for Retinopathy of Prematurity Cooperative Group. The natural ocular outcome of premature birth and retinopathy: status at one year. *Arch Ophthalmol*. 1994;112:903–912.
83. Cryotherapy for Retinopathy of Prematurity Cooperative

Group. Multicenter trial of cryotherapy for retinopathy of prematurity: Snellen acuity and structural outcome at 5½ years. *Arch Ophthalmol*. 1996;114:417–424.
84. Fishburne BC, Winthrop KL, Robertson JE. Atrophic fundus lesions associated with untreated retinopathy of prematurity. *Am J Ophthalmol*. 1997;124:247–249.
85. Gilbert WS, Quinn GE, Dobson V, et al. Partial retinal detachment at 3 months after threshhold retinopathy of prematurity. *Arch Ophthalmol*. 1996;114:1085–1091.
86. Kushner BJ. Strabismus and amblyopia associated with regressed retinopathy of prematurity. *Arch Ophthalmol*. 1982;100:256–261.
87. Schaffer DB, Quinn GE, Johnson L. Sequelae of arrested mild retinopathy of prematurity. *Arch Ophthalmol*. 1984;102:373–376.
88. Cats BP, Tan KEWP. Prematures with and without regressed retinopathy of prematurity: comparison of long-term (6–10 years) ophthalmological morbidity. *J Pediatr Ophthalmol Strabismus*. 1989;26:271–275.
89. Robinson R, O'Keefe M. Follow-up study on premature infants with and without retinopathy of prematurity. *Br J Ophthalmol*. 1993;77:91–94.
90. Snir M, Nissenkorn I, Sherf I, et al. Visual acuity, strabismus, and amblyopia in premature babies with and without retinopathy of prematurity. *Ann Ophthalmol*. 1988;20:256–258.
91. Bremer D, Fellows RR, Palmer EA, et al. Strabismus in premature infants in the first year of life. *Arch Ophthalmol*. 1998;116:329–333.
92. Vanderveen DK, Coats DK, Dobson V, et al. Prevalence and course of strabismus in the first year of life for infants with prethreshold retinopathy of prematurity: findings from the Early Treatment for Retinopathy of Prematurity Study. *Arch Ophthalmol*. 2006;124:766–773.
93. Quinn GE, Dobson V, Repka MX, et al. Development of myopia in infants with birth weights less than 1251 grams. *Ophthalmology*. 1992;99:329–340.
94. Quinn GE, Dobson V, Davitt BV, et al. Progression of

myopia and high myopia in the Early Treatment for Retinopathy of Prematurity Study: findings to 3 years of age. *Ophthalmology*. 2008;115:1058–1064.
95. Fletcher MC, Brandon S. Myopia of prematurity. *Am J Ophthalmol*. 1955;40:474–481.
96. Davitt BV, Dobson V, Quinn GE, et al. Astigmatism in the Early Treatment for Retinopathy of Prematurity Study. *Ophthalmology*. 2009;116:332–339.
97. Kushner BJ. The sequelae of regressed retinopathy of prematurity. Silverman WA, Flynn JT. *Retinopathy of prematurity*. Blackwell: Boston, MA; 1985:239–248.
98. Summers GC, Phelps DL, Tung B, et al. Ocular cosmesis in retinopathy of prematurity. *Arch Ophthalmol*. 1992;110:1092–1097.
99. Early Treatment for Retinopathy of Prematurity Cooperative Group. Final visual acuity results in the Early Treatment for Retinopathy Study. *Arch Ophthalmol*. 2010;128:663–671.
100. Krolicki TJ, Tasman W. Cataract extraction in adults with retinopathy of prematurity. *Arch Ophthalmol*. 1995;113:173–177.
101. Bremer DL, Rogers DL, Good WV, et al. Glaucoma in the Early Treatment for Retinopathy of Prematurity (ETROP) study. *J AAPOS*. 2012;16(5):449–452.
102. Kushner BJ. Ciliary block glaucoma in retinopathy of prematurity. *Arch Ophthalmol*. 1982;100:1078–1079.
103. Pollard ZF. Secondary angle-closure glaucoma in cicatricial retrolental fibroplasia. *Am J Ophthalmol*. 1980;89:651–653.
104. Smith J, Shivitz I. Angle-closure glaucoma in adults with cicatricial retinopathy of prematurity. *Arch Ophthalmol*. 1984;102:371–372.
105. Brown DR, Biglan AW, Stretavsky MAM. Screening criteria for the detection of retinopathy of prematurity in patients in a neonatal intensive care unit. *J Pediatr Ophthalmol Strabismus*. 1987;24:212–214.
106. Clark C, Gibbs JAH, Maniello R, et al. Blood transfusions: a possible risk factor in retrolental fibroplasias. *Acta Paediatr Scand*. 1981;70:535–539.
107. Cryotherapy for Retinopathy of Prematurity Cooperative

Group. Multicenter trial of cryotherapy for retinopathy of prematurity: preliminary results. *Arch Ophthalmol*. 1988;106:471–479.
108. Bauer CR, Widmayer SM. A relationship between $PaCO_2$ and retrolental fibroplasia (RLF). *Pediatr Res*. 1981;15:649.
109. Flower RW. *A new perspective on the pathogenesis of retrolental fibroplasia: the influence of elevated arterial CO_2*. [Retinopathy of Prematurity Conference] 1981 [Dec. 4–6].
110. Biglan AW, Brown DR, Reynolds JD, et al. Risk factors associated with retrolental fibroplasias. *Ophthalmology*. 1981;91:1504–1511.
111. Brown DR, Milley JR, Ripepi U, et al. Retinopathy of prematurity – risk factors in a five-year cohort of critically ill premature neonates. *Am J Dis Child*. 1987;141:154–160.
112. Kretzer FL, Hittner HM, Johnson AT, et al. Vitamin E and retrolental fibroplasia: ultrastructural support of clinical efficacy. *Ann NY Acad Sci*. 1982;393:145–166.
113. Aranda JV, Clark TE, Maniello R, et al. Blood transfusions (BT): possible potentiating risk factor in retrolental fibroplasia (RLF). *Pediatr Res*. 1975;9:362.
114. Bossi E, Koerner F, Zulauf M. *Retinopathy of prematurity (ROP): risk factors – a statistical analysis with matched pairs*. [Retinopathy of Prematurity Conference] 1981 [Dec. 4–6].
115. Procianoy RS, Garcia-Prats JA, Hittner HM, et al. An association between retinopathy of prematurity and interventricular hemorrhage in very low birth weight infants. *Acta Paediatr Scand*. 1981;70:473–477.
116. Sacks M, Schaffer DB, Anday EK, et al. Retrolental fibroplasia and blood transfusion in very low birth-weight infants. *Pediatrics*. 1981;68:770–774.
117. Hammer ME, Mullen PW, Ferguson JG, et al. Logistic analysis of risk factors in acute retinopathy of prematurity. *Am J Ophthalmol*. 1986;102:1–6.
118. Palmer EA, Flynn JT, Hardy RJ, et al. Incidence and early course of retinopathy of prematurity. *Ophthalmology*. 1991;98:1628–1640.
119. Schaffer DB, Palmer EA, Plotsky DF, et al. Prognostic factors in the natural course of retinopathy of prematurity.

Ophthalmology. 1993;100:230–236.
120. Hardy RJ, Palmer EA, Dobson V, et al. Risk analysis of prethreshold retinopathy of prematurity. *Arch Ophthalmol*. 2003;121:1697–1701.
121. Palmer EA. Optimal timing of examination for acute retrolental fibroplasia. *Ophthalmology*. 1981;88:662–668.
122. Section on Ophthalmology American Academy of Pediatrics, American Academy of Ophthalmology, American Association for Pediatric Ophthalmology and Strabismus. Screening examination of prematurity infants for retinopathy of prematurity. *Pediatrics*. 2006;117:572–576 [Erratum in: Pediatrics 2006;118:1324].
123. Palmer EA. Risks of dilating a child's pupils. *Trans Pac Coast Oto Ophthalmol Soc*. 1982;63:141–145.
124. Johnson L, Schaffer D, Boggs TR. The premature infant, vitamin E deficiency, and retrolental fibroplasia. *Am J Clin Nutr*. 1974;27:1158–1171.
125. Johnson LH, Schaffer DB, Goldstein DE, et al. Influence of vitamin E treatment (Rx) and adult blood transfusions on mean severity of retrolental fibroplasia (MS-RLF) in premature infants. *Pediatr Res*. 1977;11:535.
126. Hittner HM, Godio LB, Rudolph AJ, et al. Retrolental fibroplasia: efficacy of vitamin E in a double-blind clinical study of preterm infants. *N Engl J Med*. 1981;305:1365–1371.
127. Phelps DL. Vitamin E and retinopathy of prematurity. Silverman WA, Flynn JT. *Retinopathy of prematurity*. Blackwell: Boston, MA; 1985:181–206.
128. Phelps DL, Rosenbaum AL, Isenberg SJ, et al. Tocopherol efficacy and safety for preventing retinopathy of prematurity: a randomized, controlled, double-masked trial. *Pediatrics*. 1987;79:489–500.
129. Finer NN, Schindler RF, Peters KL, et al. Vitamin E and retrolental fibroplasia: improved visual outcome with early vitamin E. *Ophthalmology*. 1983;90:428–435.
130. Puklin JE, Simon RM, Ehrenkranz RA. Influence on retrolental fibroplasia of intramuscular vitamin E administration during respiratory distress syndrome. *Ophthalmology*. 1982;89:96–103.

131. Milner RA, Watts JL, Paes B, et al. *Retrolental fibroplasia in 1500 gram neonates: part of a randomized clinical trial of the effectiveness of vitamin E*. [Retinopathy of Prematurity Conference] 1981 [Dec. 4–6].
132. Johnson L, Bowen F, Herman N, et al. The relationship of prolonged elevation of serum vitamin E levels to neonatal bacterial sepsis (SEP) and necrotizing enterocolitis (NEC). *Pediatr Res*. 1983;17:319.
133. Schaffer DB, Johnson L, Quinn GE, et al. Vitamin E and retinopathy of prematurity: follow-up at one year. *Ophthalmology*. 1985;92:1005–1011.
134. Institute of Medicine. *Report of a study: vitamin E and retinopathy of prematurity*. National Academy: Washington, DC; 1986.
135. Terry TL. Fibroplastic overgrowth of the persistent tunica vasculosa lentis in premature infants. IV. Etiologic factors. *Arch Ophthalmol*. 1943;29:54–65.
136. Hepner WR, Krause AC, Davis ME. Retrolental fibroplasia and light. *Pediatrics*. 1949;3:824–828.
137. Locke JC, Reese AB. Retrolental fibroplasia: the negative role of light, mydriatics, and the ophthalmoscopic examinations in its etiology. *Arch Ophthalmol*. 1952;48:44–47.
138. Reynolds JD, Hardy RJ, Kennedy KA, et al. Lack of efficacy of light reduction in preventing retinopathy of prematurity. *N Engl J Med*. 1998;338:1572–1576.
139. Nagata M, Kobayashi Y, Fukuda H. Photocoagulation for the treatment of the retinopathy of prematurity (first report). *J Clin Ophthalmol*. 1968;22:419.
140. Oshima K, Ikui H, Kano M, et al. Clinical study and photocoagulation of retinopathy of prematurity. *Folia Ophthalmol Jpn*. 1971;22:700–707.
141. Payne JW, Patz A. Treatment of acute proliferative retrolental fibroplasia. *Trans Am Acad Ophthalmol Otolaryngol*. 1972;76:1234–1246.
142. Yamashita Y. Studies on retinopathy of prematurity. III. Cryocautery for retinopathy of prematurity. *Rinsho Ganka*. 1972;26:385–393.
143. Palmer EA, Biglan AW, Hardy RJ. Retinal ablative therapy

for active proliferative retinopathy of prematurity: history, current status, and prospects. Silverman WA, Flynn JT. *Retinopathy of prematurity*. Blackwell: Boston, MA; 1985:207–228.
144. Kingham JD. Acute retrolental fibroplasia. II. Treatment by cryosurgery. *Arch Ophthalmol*. 1978;96:2049–2053.
145. Kalina RE. Treatment of retrolental fibroplasia. *Surv Ophthalmol*. 1980;24:229–236.
146. Hindle NW. Cryotherapy for retinopathy of prematurity to prevent retrolental fibroplasias. *Can J Ophthalmol*. 1982;17:207–212.
147. Mousel DK. Cryotherapy for retinopathy of prematurity: a personal retrospective. *Ophthalmology*. 1985;92:375–378.
148. Tasman W, Brown GC, Schaffer DB, et al. Cryotherapy for active retinopathy of prematurity. *Ophthalmology*. 1986;93:580–585.
149. Cryotherapy for Retinopathy of Prematurity Cooperative Group. Multicenter trial of cryotherapy for retinopathy of prematurity: ophthalmological outcomes at 10 years. *Arch Ophthalmol*. 2001;119:1110–1118.
150. Landers MB III, Toth CA, Semple CS, et al. Treatment of retinopathy of prematurity with argon laser photocoagulation. *Arch Ophthalmol*. 1992;110:44–47.
151. McNamara JA, Tasman WS, Brown GC, et al. Laser photocoagulation for retinopathy of prematurity. *Ophthalmology*. 1991;98:576–580.
152. O'Keefe M, Burke J, Algawi K, et al. Diode laser photocoagulation to the vascular retina for progressively advancing retinopathy of prematurity. *Br J Ophthalmol*. 1995;79:1012–1014.
153. Hammer ME, Pusateri TJ, Hess JB, et al. Threshold retinopathy of prematurity. Transition from cryopexy to laser treatment. *Retina*. 1995;15:486–489.
154. Capone A Jr, Diaz-Rohena R, Sternberg P Jr, et al. Diode-laser photocoagulation for zone 1 threshold retinopathy of prematurity. *Am J Ophthalmol*. 1993;116:444–450.
155. Hunter DG, Repka MX. Diode laser photocoagulation for threshold retinopathy of prematurity: a randomized study.

Ophthalmology. 1993;100:238–244.
156. McNamara JA, Tasman W, Vander JF, et al. Diode laser photocoagulation for retinopathy of prematurity: preliminary results. *Arch Ophthalmol*. 1992;110:1714–1716.
157. Fleming TN, Runge PE, Charles ST. Diode laser photocoagulation for prethreshold, posterior retinopathy of prematurity. *Am J Ophthalmol*. 1992;114:589–592.
158. DeJoyce MH, Ferrone PJ, Trese MT. Diode laser ablation for threshold retinopathy of prematurity. *Arch Ophthalmol*. 2000;118:365–367.
159. White JE, Repka MX. Randomized comparison of diode laser photocoagulation versus cryotherapy for threshold retinopathy of prematurity: three-year outcome. *J Pediatr Ophthalmol Strabismus*. 1997;34:83–87.
160. Early Treatment for Retinopathy of Prematurity Cooperative Group. Revised indications for treatment of retinopathy of prematurity: results of the early treatment for retinopathy of prematurity randomized trial. *Arch Ophthalmol*. 2003;121:1684–1696.
161. Early Treatment for Retinopathy of Prematurity Cooperative Group. Multicenter trial of early treatment for retinopathy of prematurity: study design. *Controlled Clin Trials*. 2004;25:311–325.
162. Quiroz-Mercado H, Martinez-Castellanos MA, Hernandez-Rojas ML, et al. Antiangiogenic therapy with intravitreal bevacizumab for retinopathy of prematurity. *Retina*. 2008;28(3 Suppl.):S19–25 [Erratum in: Retina 2009; 29:127].
163. Travassos A, Teixeira S, Ferreira P, et al. Intravitreal bevacizumab in aggressive posterior retinopathy of prematurity. *Ophthalmic Surg Lasers Imaging*. 2007;38:233–237.
164. Lalwani GA, Berroca AM, Murray TG, et al. Off-label use of intravitreal bevacizumab (Avastin) for salvage treatment in progressive threshold retinopathy of prematurity. *Retina*. 2008;28(Suppl.):S13–18.
165. Kusaka S, Shima C, Wada K, et al. Efficacy of intravitreal injection of bevacizumab for severe retinopathy of prematurity: a pilot study. *Br J Ophthalmol*. 2008;92:1450–

1455.
166. Law JC, Recchia FM, Morrison DG, et al. Intravitreal bevacizumab as adjunctive treatment for retinopathy of prematurity. *J AAPOS*. 2010;14:6–10.
167. Wu WC, Yeh PT, Chen SN, et al. Effects and complications of bevacizumab use in patients with retinopathy of prematurity: a multicenter study in Taiwan. *Ophthalmology*. 2011;118:176–183.
168. Mintz-Hittner HA, Kennedy KA, Chuang AZ, et al. Efficacy of intravitreal bevacizumab for stage 3+ retinopathy of prematurity. *N Engl J Med*. 2011;364:603–615.
169. Hu J, Blair MP, Shapiro MJ, et al. Reactivation of retinopathy of prematurity after bevacizumab injection. *Arch Ophthalmol*. 2012;130(8):1000–1006.
170. Chen SN, Lian I, Hwang YC, et al. Intravitreal anti-vascular endothelial growth factor treatment for retinopathy of prematurity: comparison between ranibizumab and bevacizumab. *Retina*. 2015;35(4):667–674.
171. Wong RK, Hubschman S, Tsui I. Reactivation of retinopathy of prematurity after ranibizumab treatment. *Retina*. 2015;35(4):675–680.
172. Coats G. Forms of retinal disease with massive exudation. *R Lond Ophthalmic Hosp Rep*. 1908;17:440–525.
173. Shields JA, Shields CL, Honavar SG, et al. Clinical variations and complications of Coats disease in 150 cases: the 2000 Sanford Gifford memorial lecture. *Am J Ophthalmol*. 2001;131:561–571.
174. Shapiro MJ, Chow CC, Karth PA, et al. Effects of green diode laser in the treatment of pediatric Coats disease. *Am J Ophthalmol*. 2011;151:725–731.e2.
175. Lin CJ, Hwang JF, Chen YT, et al. The effect of intravitreal bevacizumab in the treatment of Coats disease in children. *Retina*. 2010;30(4):617–622.
176. Ray R, Barañano DE, Hubbard GB. Treatment of Coats' disease with intravitreal bevacizumab. *Br J Ophthalmol*. 2013;97(3):272–277.
177. Ramasubramanian A, Shields CL. Bevacizumab for Coats' disease with exudative retinal detachment and risk of

vitreoretinal traction. *Br J Ophthalmol*. 2012;96(3):356–359.
178. Goldberg MF. Persistent fetal vasculature (PFV): an integrated interpretation of signs and symptoms associated with persistent hyperplastic primary vitreous (PHPV). LIV Edward Jackson memorial lecture. *Am J Ophthalmol*. 1997;124:587–626.
179. Shaikh S, Trese MT. Lens-sparing vitrectomy in predominantly posterior persistent fetal vasculature syndrome in eyes with nonaxial lens opacification. *Retina*. 2003;23:330–334.
180. Zhang C, Asnaghi L, Gongora C, et al. A developmental defect in astrocytes inhibits programmed regression of the hyaloid vasculature in the mammalian eye. *Eur J Cell Biol*. 2011;90:440–448.
181. Jin DY, Jeang KT. Isolation of full-length cDNA and chromosomal localization of human NF-κB modulator NEMO to Xq28. *J Biomed Sci*. 1999;6:115–120.
182. O'Doherty M, McCreery K, Green AJ, et al. Incontinentia pigmenti – ophthalmological observation of a series of cases and review of the literature. *Br J Ophthalmol*. 2011;95:11–16.
183. Walsh MK, Drenser KA, Capone A Jr, et al. Early vitrectomy effective for Norrie disease. *Arch Ophthalmol*. 2010;128:456–460.
184. Chen ZY, Battinelli EM, Fielder A, et al. A mutation in the Norrie disease gene (NDP) associated with X-linked familial exudative vitreoretinopathy. *Nat Genet*. 1993;5:180–183.
185. Xu Q, Wang Y, Dabdoub A, et al. Vascular development in the retina and inner ear: control by norrin and frizzled-4, a high-affinity ligand-receptor pair. *Cell*. 2004;116:883–895.
186. Junge HJ, Yang S, Burton JB, et al. TSPAN12 regulates retinal vascular development by promoting Norrin- but not Wnt-induced FZD4/beta-catenin signaling. *Cell*. 2009;139:299–311.
187. Abramson DH, Beaverson K, Sangani P, et al. Screening for retinoblastoma: presenting signs as prognosticators of patient and ocular survival. *Pediatrics*. 2003;112(6 Pt 1):1248–1255.

188. Li LH, Li N, Zhao JY, et al. Findings of perinatal ocular examination performed on 3573, healthy full-term newborns. *Br J Ophthalmol*. 2013;97(5):588–591.
189. Arnold RW, Armitage MD. Performance of four new photoscreeners on pediatric patients with high risk amblyopia. *J Pediatr Ophthalmol Strabismus*. 2014;51(1):46–52.

65

Telescreening for Retinopathy of Prematurity

Michael F. Chiang

Limitations of Traditional Care

Traditional screening for retinopathy of prematurity (ROP) involves indirect ophthalmoscopy at the neonatal intensive care unit (NICU)

bedside. Although this has been effective at identifying infants with severe treatment-requiring disease,[1–3] there are important limitations. Ophthalmoscopic examinations are logistically difficult and require significant travel time and coordination. Findings are documented using hand-drawn sketches, which are subjective and qualitative (Fig. 65.1). There may be variability in diagnosis of critical features such as zone I and plus disease,[4,5] and there is enormous medicolegal liability. Surveys have found that the number of retinal specialists and pediatric ophthalmologists willing to manage ROP is decreasing for these reasons.[6] Meanwhile, more infants are at risk for disease because of increasing premature birth rates and improved neonatal survival throughout the world.

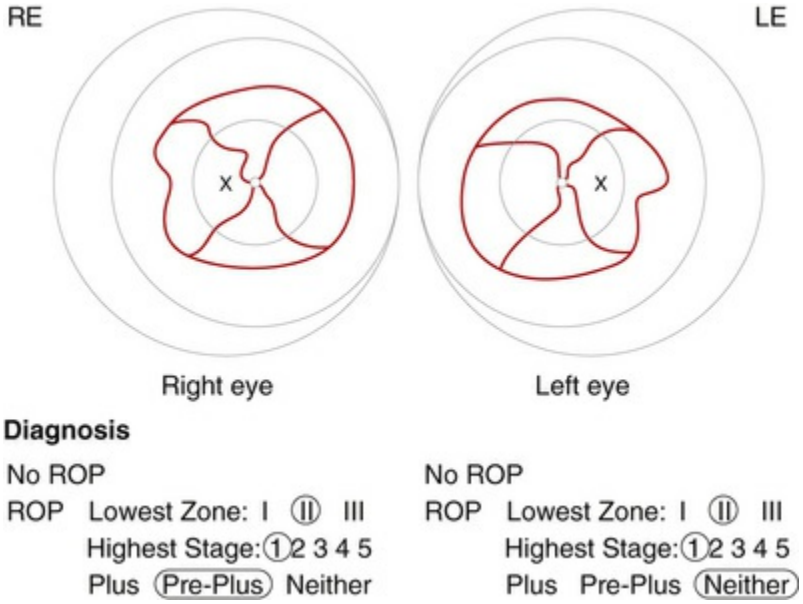

FIG. 65.1 Documentation of traditional indirect ophthalmoscopy using annotated examination template. Limitations include subjective and qualitative documentation, and difficulty identifying change during serial examinations.

Telemedicine as an Emerging Approach

Telemedicine is an emerging approach with potential to improve

the quality, delivery, and cost of care. This may be particularly important in areas with limited accessibility to care. In this approach, clinical data and images are captured from the infant's eyes by trained personnel in the NICU. Data are transmitted for review by a remote ophthalmologist, who communicates management recommendations. Examples of wide-angle images taken with a commercially available camera (RetCam; Clarity Medical Systems, Pleasanton, CA) are shown in Fig. 65.2. It has been shown that trained neonatal nurses can capture high-quality retinal images,[7,8] and that imaging may cause less physiologic stress to infants than ophthalmoscopy with scleral depression.[9]

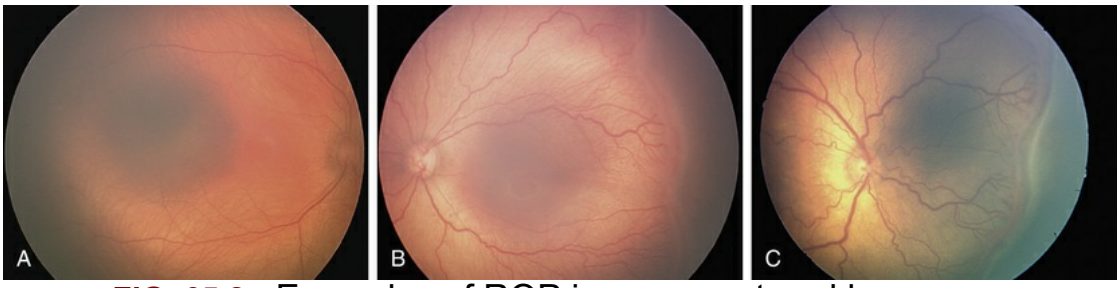

FIG. 65.2 Examples of ROP images captured by a trained neonatal nurse during routine screening using a wide-angle camera (RetCam; Clarity Medical Systems, Pleasanton, CA). Images demonstrate retinas with (A) no ROP, (B) type 2 ROP based on the presence of stage 3 disease in zone II, and (C) type 1 treatment-requiring ROP based on the presence of plus disease as well as posterior stage 3 disease.

In a telemedicine approach, the availability of archived retinal images would provide other advantages. Infant photographs could be directly compared to reference images,[1] and may be transmitted securely to experts for second opinions. Images provide objective documentation of clinical findings, improve recognition of disease progression, enhance communication, and create infrastructure for education and research.[10]

Evaluation Studies

Accuracy

Diagnostic accuracy of telemedicine for ROP has been evaluated since the late 1990s. Virtually all studies have used wide-angle digital images captured by a neonatal nurse, ophthalmologist, or ophthalmic photographer. Although these studies have varied in design and outcome measure, most have compared the diagnostic performance of telemedicine to a reference standard of dilated ophthalmoscopy. Schwartz et al. (19 eyes from 10 infants) examined accuracy of telemedicine in a selected group of infants at 30–32 weeks postmenstrual age (PMA), all of whom had moderate or severe ROP. The sensitivity and specificity of telemedicine for detecting prethreshold or worse ROP were 89% and 100%, respectively.[11]

Since then, research has involved larger and broader cohorts of consecutively-enrolled infants. For diagnosis of any ROP, studies have demonstrated sensitivity of 46–97% and specificity of 49–100% compared to a reference standard of indirect ophthalmoscopy[7,12,13] (Table 65.1). Generally, lower accuracy has been found while examining infants at lower PMA, and when detecting presence of mild ROP (e.g., stage 1). This is presumably because younger infants have milder disease with more subtle diagnostic features, and because it may be technically more difficult to image smaller eyes with increased media opacities.[14]

TABLE 65.1

Diagnostic Accuracy of Telescreening for Detection of Any ROP Using Images Captured by Wide-Angle Camera[a]

Study	Outcome Measures	Sensitivity/Specificity
Roth et al., 2001[13]	Any ROP	0.82/0.94
Yen et al., 2002[14]	Any ROP at 32–34 wk PMA	0.46/1.00
	Any ROP at 38–40 wk PMA	0.76/1.00
Chiang et al., 2006[12]	Any ROP	0.82–0.86/0.49–0.96
Shah et al., 2006[15]	Any ROP	0.86/0.92
Chiang et al., 2007[7]	Any ROP at 31–33 wk PMA	0.73–0.94/0.89–0.97
	Any ROP at 35–37 wk PMA	0.91–0.97/0.98–1.00
Dhaliwal et al., 2009[16]	Any ROP at 34 wk PMA or 4–6 wk CA	0.60/0.91

[a]RetCam; Clarity Medical Systems, Pleasanton, CA. For definition of "clinically significant ROP", see text. Reference standard was standard indirect ophthalmoscopy.

CA, chronologic age; PMA, postmenstrual age; ROP, retinopathy of prematurity; wk, weeks.

Other studies have examined the accuracy of telemedicine for detecting clinically significant ROP (Table 65.2). Ells et al. (371 exams from 36 infants) found sensitivity 100% and specificity 96% for diagnosis of "referral-warranted ROP"* during serial examinations throughout an infant's hospital course.[17] Wu et al. (serial exams from 43 infants) performed telemedicine screening for prethreshold or worse ROP and found sensitivity 100% and specificity 98%.[18] Chiang et al. (163 exams from 64 infants) reported sensitivity 72–83% and specificity 90–99% for detection of type 2 or worse ROP, and sensitivity 85–90% and specificity 95–97% for detection of treatment-requiring ROP.[12] The multicenter prospective Photo-ROP Study (300 exams from 51 infants) found sensitivity 92% and specificity 37% for detection of "clinically significant ROP"† during weekly examinations throughout an infant's hospital course.[19]

TABLE 65.2

Diagnostic Accuracy of Telescreening for Detection of Clinically Significant ROP Using Images Captured by Wide-Angle Camera[a]

Study	Outcome Measures	Sensitivity/Specificity
Ells et al., 2003[17]	Any ROP zone I, presence of plus disease, or presence of any stage 3 ROP at any time during hospital course	1.00/0.96
Chiang et al., 2006[12]	Type 2 or worse ROP	0.72–0.83/0.90–0.99
	Treatment-requiring ROP	0.85–0.90/0.95–0.97
Wu et al., 2006[18]	Prethreshold or worse ROP	1.00/0.98
Chiang et al., 2007[7]	Type 2 or worse ROP at 31–33 wk PMA	0.71–0.86/0.93–0.97
	Type 2 or worse ROP at 35–37 wk PMA	1.00/0.85–0.94
	Treatment requiring ROP at 31–33 wk PMA	NA/0.94–1.00
	Treatment requiring ROP at 35–37 wk PMA	1.00/0.81–0.94
Photo-ROP Cooperative Group, 2008[19]	"Clinically significant ROP"	0.92/0.37
Dhaliwal et al., 2009[16]	Stage 3 ROP at 34 wk PMA or 4–6 wk CA	0.57/0.98
	Presence of plus disease	0.80/0.98
Lorenz et al., 2009[20]	Suspected treatment-requiring ROP: threshold ROP in zone II, prethreshold in zone I, or disease possibly requiring treatment but not reliably classified from images	1.00/NA
Dai et al., 2011[21]	Treatment-requiring ROP	1.00/0.98
Wang et al., 2015[8]	Treatment-requiring ROP	1.00/1.00
Quinn et al., 2015[22]	Any ROP zone I, presence of plus disease, or presence of stage 3 ROP	0.82/0.90 (individual eyes), 0.90/0.87 (both

		eyes)

[a]RetCam; Clarity Medical Systems, Pleasanton, CA. For definition of "clinically significant ROP," see text. Reference standard was standard indirect ophthalmoscopy.

CA, chronologic age; NA, not applicable; PMA, postmenstrual age; ROP, retinopathy of prematurity; wk, weeks.

In a prospective study, Chiang et al. (248 exams from 67 infants) examined the effect of PMA and disease severity on telemedicine accuracy. At 31–33 weeks PMA, the sensitivity and specificity was 71–86% and 93–97%, respectively, for detection of type 2 or worse ROP, and the specificity for detection of treatment-requiring ROP was 94–100%. At 35–37 weeks PMA, sensitivity and specificity were 91–97% and 98–100%, respectively, for detection of any ROP, 100–100% and 85–94%, respectively, for detection of type 2 or worse ROP, and 100–100% and 81–94%, respectively, for detection of treatment-requiring ROP.[7] The finding of higher accuracy in older infants was in agreement with previous studies.[14]

Dhaliwal et al. (245 exams from 81 infants) conducted a masked, double-observer prospective longitudinal cohort study. Two pediatric ophthalmologists were randomized to perform examinations using either telemedicine or ophthalmoscopy. Absolute agreement between ophthalmoscopy and telemedicine was 96% for detection of stage 3, and 97% for detection of plus disease.[16] Dai et al. (422 exams from 108 infants) conducted a study in which all infants received telemedicine imaging and ophthalmoscopy by a pediatric ophthalmologist. Images were reviewed independently by a masked grader. Using ophthalmoscopy as the reference standard, sensitivity of telemedicine for detecting treatment-requiring ROP (i.e., type 1 or worse) was 100% and specificity was 98%. The positive predictive value of telemedicine for detecting treatment-requiring ROP was 86%, and the negative predictive value was 100%.[21]

Scott et al. compared the accuracy of telemedicine vs. ophthalmoscopy using a study design in which these two methods were performed by the *same* experts in 67 consecutive infants. There was absolute intragrader agreement of 86% (178/206 eyes) and kappa 0.66–0.85 between ophthalmoscopy and telemedicine. Among the 14% (28/206 eyes) intra-expert discrepancies, some cases

provided photographic evidence that ophthalmoscopy failed to recognize mild ROP that was detected by telemedicine. There were also discrepancies involving presence of zone I and plus disease, in which telemedicine may have provided theoretic advantages by allowing examiners to review their diagnoses or make more exact measurements of anatomic landmarks.[23]

The multicenter e-ROP study (5520 exams analyzed from 1257 infants) implemented a system in which images were captured by trained nonphysician imagers and interpreted by trained nonphysician graders. When comparing the image-set grading of each eye to indirect ophthalmoscopy as a reference standard, the sensitivity for detecting "referral-warranted ROP"* was 82% and specificity was 90%. When both eyes of an infant were considered, the sensitivity was 90% and specificity was 87%.[22]

Image Quality

Several studies have examined the quality of images captured by nurses, ophthalmic photographers, or ophthalmologists. Ells et al. found that wide-angle images were captured successfully in 96% of examinations, and that 94% of image sets could be graded remotely.[17] Wu et al. found that 79% of initial retinal images and 78% of repeated images were acceptable.[18] The Photo-ROP cooperative group found that 92% of image sets were acceptable.[19] Chiang et al. reported that telemedicine graders reported an "unknown" diagnosis because of inadequate image quality or insufficient retinal coverage in 0–41% of exams at 31–33 weeks PMA and in 0–7% of exams at 35–37 weeks PMA.[7] Lorenz et al. reported that, among 6460 telemedicine imaging sessions conducted at five NICUs over a six-year period, nearly 98% were of adequate quality.[20] Heavy fundus pigmentation, corneal and vitreous haze, smaller palpebral fissures, and limited dilation may be associated with decreased image quality.[7,12,15,18] Quinn et al. reported in a multicenter study that among 5520 image sets captured by nonphysician study-certified personnel, 91% of images were of adequate quality, 6% were of poor quality, and 3% were missing.[22]

Cost-Effectiveness, Speed, and Satisfaction

Economic and practical factors must be considered for long-term viability of telemedicine systems. Two studies have compared cost-effectiveness of telemedicine versus ophthalmoscopy for ROP management. One study, performed in the United States, found that telemedicine is more cost-effective than traditional ophthalmoscopy ($3193 per quality-adjusted life year [QALY] compared to $5617/QALY).[24] The second study, performed in the United Kingdom, modeled five possible strategies for ROP surveillance using telemedicine and ophthalmoscopy, and found that telemedicine using image capture and grading by visiting nurses (£175 per infant examined) and telemedicine using image capture by visiting nurses and image grading by remote ophthalmologists (£201/infant examined) were more cost-effective than traditional ophthalmoscopy at the NICU bedside (£321/infant examined).[25]

Other studies have examined logistical factors such as examination time and acceptability to patients. Richter et al. found that telemedicine examinations required significantly less physician time than ophthalmoscopy (1.02–1.75 minutes per telemedicine exam versus 4.17–6.63 minutes per ophthalmoscopic exam).[26] Lee et al. developed and validated a survey instrument to assess attitudes toward digital imaging and telemedicine by parents, and found high acceptance of these technologies. Families did, however, report that face-to-face contact with physicians was important.[27]

Evaluation of Operational ROP Telemedicine Programs

Real-world telemedicine programs have been implemented in several centers, typically relying on trained neonatal technicians or nurses to capture images and transfer data for interpretation by remote ophthalmologists. Infants identified with clinically significant disease are either examined locally by an ophthalmologist or transferred for further evaluation.

A telemedicine program involving five German NICUs has been operational since 2001. In this program all premature infants at risk

for ROP are screened with imaging and also examined by local ophthalmologists. All suspected treatment-requiring ROP stages were detected with 100% sensitivity, and the overall positive predictive value for treatment-requiring ROP was 88.2% after 6460 examinations in 1222 infants.[20]

A similar program involving six NICUs, in which nurses are trained to capture serial images, has been used for routine telemedicine management at Stanford University since 2005.[8] Infants felt to have referral-warranted (i.e., type 2 or worse) or treatment-requiring (i.e., type 1 or worse) ROP were referred for complete ophthalmoscopic evaluation. Within one week of NICU discharge, all infants in this program received a mandatory ophthalmoscopic examination by the same retinal specialist. The sensitivity of telemedicine for identifying referral-warranted and treatment-requiring ROP was reported to be 100%, the positive predictive value of telemedicine for identifying treatment-requiring ROP was 96%, and the negative predictive value was 100%. No known cases of treatment-requiring ROP were missed, and there were no adverse anatomic outcomes.[8]

Weaver and Murdock reported a real-world telemedicine system in rural Montana, in which 582 telemedicine exams were performed on 137 infants from 2007 to 2011. Infants with referral-warranted ROP (defined as type 2 or worse; zone II, stage 2 with pre-plus disease, or poorly imaged eyes) were transferred within 24 hours. Thirteen infants were transferred for referral-warranted ROP, of whom 9 ultimately required laser treatment. Prompt transfer of all infants was feasible, and there were no poor anatomic outcomes during the study period.[28]

Vinekar et al. implemented a public–private partnership program in India, which has provided telemedicine ROP screening by nonphysicians, which may become a model for outreach screening in middle-income countries. During a 77-month period, 20,214 imaging sessions were captured from 7106 infants at 36 rural centers.[29]

Barriers and Challenges

Despite technologic advances to support telemedicine for ROP

management, its widespread adoption has been limited by factors such as medical licensure and lack of consistent insurance coverage and reimbursement policies. The level of diagnostic accuracy required for implementation of real-world ROP telemedicine systems is unclear, given concerns about medicolegal liability. Furthermore, it is difficult to rigorously assess accuracy because there may be variability in the reference standard of indirect ophthalmoscopy. Capturing images with sufficient diagnostic quality may not always be practical, particularly in the peripheral retinas of younger infants, warranting reevaluation either by repeat imaging or ophthalmoscopy. Finally, implementation of telemedicine for ROP requires approval of physicians and financial investments for new equipment and information technologies.

Future Directions

Telemedicine has potential benefits for ROP management, education, and research. Studies have demonstrated that it has very high accuracy for detection of clinically significant ROP. Attention should be given to training protocols and to the assignment of roles and responsibilities for neonatology and ophthalmology personnel. Rules must be defined for cases in which image quality is inadequate, and when digital imaging is impractical because of systemic illness, infection contact precautions, or other reasons. Development of image capture protocols will help standardize the process of ROP telemedicine diagnosis. Reading software, which helps optimize workflow and mitigate risk, should be accessible for ophthalmologists and hospitals.[30] The success from operational programs suggests this is practical, but maintenance of sustainable ROP telemedicine programs will require generalizable solutions to these challenges.

Disclosure

MFC is an unpaid member of the Scientific Advisory Board for Clarity Medical Systems (Pleasanton, CA) and a Consultant for Novartis (Basel, Switzerland).

References

1. International Committee for the Classification of Retinopathy of Prematurity. The International Classification of Retinopathy of Prematurity revisited. *Arch Ophthalmol*. 2005;123:991–999.
2. Early Treatment for Retinopathy of Prematurity Cooperative Group. Revised indications for the treatment of retinopathy of prematurity: results of the early treatment for retinopathy of prematurity randomized trial. *Arch Ophthalmol*. 2003;121:1684–1694.
3. Fierson WM, American Academy of Pediatrics Section on Ophthalmology; American Academy of Ophthalmology; American Association for Pediatric Ophthalmology and Strabismus; American Association of Certified Orthoptists. Screening examination of premature infants for retinopathy of prematurity. *Pediatrics*. 2013;131:189–195.
4. Chiang MF, Jiang L, Gelman R, et al. Interexpert agreement of plus disease diagnosis in retinopathy of prematurity diagnosis. *Arch Ophthalmol*. 2007;125:875–880.
5. Chiang MF, Thyparampil PJ, Rabinowitz D. Interexpert agreement in identification of macular location in infants at risk for retinopathy of prematurity. *Arch Ophthalmol*. 2010;128:1153–1159.
6. Ocular Surgery News U.S. Edition. *Survey: Physicians being driven away from ROP treatment*. http://www.healio.com/ophthalmology/retina-vitreous/news/print/ocular-surgery-news/%7Bedfa784c-a2ac-4f93-b473-5be5d07d82ca%7D/survey-physicians-being-driven-away-from-rop-treatment; 2006.
7. Chiang MF, Wang L, Busuioc M, et al. Telemedical retinopathy of prematurity diagnosis: accuracy, reliability, and image quality. *Arch Ophthalmol*. 2007;125:1531–1538.
8. Wang SK, Callaway NF, Wallenstein MB, et al. SUNDROP: six years of screening for retinopathy of prematurity with telemedicine. *Can J Ophthalmol*. 2015;50:101–106.
9. Mukherjee AN, Watts P, Al-Madfai H, et al. Impact of retinopathy of prematurity screening examination on

cardiorespiratory indices: a comparison of indirect ophthalmoscopy and RetCam imaging. *Ophthalmology*. 2006;113:1547–1552.
10. Chiang MF, Gelman R, Martinez-Perez ME, et al. Image analysis for retinopathy of prematurity diagnosis. *J AAPOS*. 2009;13:438–445.
11. Schwartz SD, Harrison SA, Ferrone PJ, et al. Telemedical evaluation and management of retinopathy of prematurity using a fiberoptic digital fundus camera. *Ophthalmology*. 2000;107:25–28.
12. Chiang MF, Keenan JD, Starren J, et al. Accuracy and reliability of remote retinopathy of prematurity diagnosis. *Arch Ophthalmol*. 2006;124:322–327.
13. Roth DB, Morales D, Feuer WJ, et al. Screening for retinopathy of prematurity employing the RetCam 120: sensitivity and specificity. *Arch Ophthalmol*. 2001;119:268–272.
14. Yen KG, Hess D, Burke B, et al. Telephotoscreening to detect retinopathy of prematurity: preliminary study of the optimum time to employ digital fundus camera imaging to detect ROP. *J AAPOS*. 2002;6:64–70.
15. Shah PK, Narendran V, Saravanan VR, et al. Screening for retinopathy of prematurity: a comparison between binocular indirect ophthalmoscopy and RetCam 120. *Indian J Ophthalmol*. 2006;54:35–38.
16. Dhaliwal C, Wright E, Graham C, et al. Wide-field digital retinal imaging versus binocular indirect ophthalmoscopy for retinopathy of prematurity screening: a two-observer prospective, randomised comparison. *Br J Ophthalmol*. 2009;93:355–359.
17. Ells AL, Holmes JM, Astle WF, et al. Telemedicine approach to screening for severe retinopathy of prematurity: a pilot study. *Ophthalmology*. 2003;110:2113–2117.
18. Wu C, Petersen RA, VanderVeen DK. RetCam imaging for retinopathy of prematurity screening. *J AAPOS*. 2006;10:107–111.
19. Photographic Screening for Retinopathy of Prematurity (PHOTO-ROP) Cooperative Group. The photographic

screening for retinopathy of prematurity study (PHOTO-ROP): primary outcomes. *Retina*. 2008;28:S47–54.
20. Lorenz B, Spasovska K, Elflein H, et al. Wide-field digital imaging based telemedicine for screening for acute retinopathy of prematurity (ROP). Six-year results of a multicentre field study. *Graefes Arch Clin Exp Ophthalmol*. 2009;247:1251–1262.
21. Dai S, Chow K, Vincent A. Efficacy of wide-field digital retinal imaging for retinopathy of prematurity screening. *Clin Exp Ophthalmol*. 2011;39:23–29.
22. Quinn GE, Ying GS, Daniel E, et al. Validity of a telemedicine system for the evaluation of acute-phase retinopathy of prematurity. *JAMA Ophthalmol*. 2014;132:1178–1184.
23. Scott KA, Kim DY, Wang L, et al. Telemedical diagnosis of retinopathy of prematurity: intraphysician and agreement between ophthalmoscopic examination and image-based interpretation. *Ophthalmology*. 2008;115:1222–1228.
24. Jackson KM, Scott KE, Graff-Zivin J, et al. Cost-utility analysis of telemedicine and ophthalmoscopy for retinopathy of prematurity management. *Arch Ophthalmol*. 2008;126:493–499.
25. Castillo-Riquelme MC, Lord J, Moseley MJ, et al. Cost-effectiveness of digital photographic screening for retinopathy of prematurity in the United Kingdom. *Int J Technol Assess Health Care*. 2004;20:201–213.
26. Richter GM, Sun G, Lee TC, et al. Speed of telemedicine vs. ophthalmoscopy for retinopathy of prematurity diagnosis. *Am J Ophthalmol*. 2009;148:136–142.
27. Lee JY, Du YE, Coki O, et al. Parental perceptions toward digital imaging and telemedicine for retinopathy of prematurity management. *Graefes Arch Clin Exp Ophthalmol*. 2010;248:141–147.
28. Weaver DT, Murdock TJ. Telemedicine detection of type 1 ROP in a distant neonatal intensive care unit. *J AAPOS*. 2012;16:229–233.
29. Vinekar A, Jayadev C, Mangalesh S, et al. Role of tele-medicine in retinopathy of prematurity screening in rural

outreach centers in India – a report of 20,214 imaging sessions in the KIDROP program. *Semin Fetal Neonatal Med*. 2015;20:335–345.

30. Fierson WM, Capone A Jr, American Academy of Pediatrics Section on Ophthalmology; American Academy of Ophthalmology, American Association of Certified Orthoptists. Telemedicine for evaluation of retinopathy of prematurity. *Pediatrics*. 2015;135:e238–54.

[*]"Referral-warranted ROP" was defined as any ROP in zone I, plus disease, or stage 3 ROP.

[†]Clinically significant ROP was defined as (a) zone I, any ROP, without vascular dilation or tortuosity; (b) zone II, stage 2, with up to one quadrant of vascular dilation and tortuosity; (c) zone II, stage 3, with up to one quadrant of vascular dilation and tortuosity; (d) any vascular dilation and tortuosity noted in eyes for which ridge characteristics were not interpretable (not imaged or poor image quality); or (e) any ROP noted in eyes for which disc features (plus disease) were not interpretable (not imaged or poor image quality).

[*]"Referral-warranted ROP" was defined as any ROP in zone I, plus disease, or stage 3 ROP.

SECTION 3

Choroidal Vascular/Bruch's Membrane Disease

OUTLINE

76 Uveal Effusion Syndrome and Hypotony Maculopathy

66

Epidemiology and Risk Factors for Age-Related Macular Degeneration

Johanna M. Seddon, Lucia Sobrin, Durga S. Borkar

Introduction

Age-related macular degeneration (AMD) is a complex disease with genetic and environmental etiology and is the leading cause of irreversible blindness.[1,2] AMD is estimated to affect more than 8 million individuals in the United States. The advanced form of the disease impacts more than 1.75 million individuals,[1] adversely affecting quality of life and activities of daily living, and causing many individuals to lose their independence in their retirement years. Despite the introduction of new therapies for prevention and treatment of AMD, the prevalence of AMD is expected to increase by 97% by the year 2050.[3]

Although some treatments are available for AMD, including

specific nutritional intake and dietary supplements for dry AMD[4–12] and anti-VEGF therapies for neovascular disease (NV),[13–15] preventive measures are needed to reduce the burden of this disease. Smoking is the most consistently identified modifiable risk factor.[16,17] Obesity may also affect AMD incidence and progression to advanced disease.[18] There has also been great progress in identifying the genetic variants that impact AMD risk.[19–36] The knowledge of genetic risk variants for the disease coupled with knowledge of nongenetic risk factors has improved the ability to predict which patients will develop advanced forms of this disease.[2] Although much progress has been made over the past two decades, identifying the causes and mechanisms underlying AMD remains a challenge.

Classification

It is important for investigators to standardize definitions of a disease and its subtypes in order to enhance comparability and to promote collaborative efforts. Toward this goal, an international classification and grading system for AMD was recommended, although it is not universally applied.[37] In this system, drusen and RPE irregularities are called age-related maculopathy and only geographic atrophy (GA) and NV are called AMD. Clinical manifestations of AMD can be subcategorized according to the specific type of AMD.[10,38] For example, the Age-Related Eye Disease Study (AREDS) has a 4-step scale that combines noncentral GA into stage 3 and both central GA and NV into one stage, 4. Individuals with visual loss presumed to be due to AMD are also classified as stage 4. The Clinical Age-Related Maculopathy Staging system (CARMS) separates GA and NV into two distinct subtypes and classifies individuals solely on their phenotype.[38] Both central and noncentral GA are classified as stage 4, and NV is classified as stage 5. The CARMS system has been useful for clinical management and genetic epidemiologic research and has been used in numerous studies.[9,18,27,28–36,39,40] More detailed systems have been used in some of the population-based studies described below,[41,42] and an updated classification developed under the auspices of the Beckman Initiative for Macular Research may be useful for future

studies.[43] New subcategories of AMD will evolve as genetic and epidemiologic studies provide further insight into disease pathogenesis.

Incidence and Prevalence

Population-based studies have provided information on the prevalence of AMD within the United States, and include the National Health and Nutrition Examination Survey (NHANES),[44,45] the Framingham Eye Study (FES),[46] the Chesapeake Bay Watermen Study,[41] the Beaver Dam Eye Study (BDES),[47] the Baltimore Eye Survey,[48] and the Salisbury Eye Evaluation Project.[49] Population-based studies outside the United States include the Rotterdam Study in the Netherlands,[50] the Blue Mountains Eye Study (BMES) in Australia,[51] and the Barbados Eye Study.[52] Prevalence is quite variable for all types of AMD due to differences in definitions of AMD, but rates are more consistent for "advanced AMD."

The total prevalence of AMD in the United States was estimated in 2004 using pooled findings from seven large population-based studies both inside and outside the United States and applying those prevalence rates to the US population.[1] This meta-analysis by the Eye Diseases Prevalence Group calculated the overall prevalence of NV and/or GA to be 1.47% of the US population aged 40 years or older. The most recent NHANES, conducted from 2005 to 2008, sampled approximately 5500 persons.[45] The total prevalence of any AMD in this civilian noninstitutionalized US population aged 40 years or older was 6.5%, and 809 ,000 persons in the United States were estimated to have late AMD.[45]

Studies conducted outside the United States have found similar or lower rates of AMD. In the Rotterdam Study, the prevalence of AMD was observed to be slightly lower compared with the BDES in Wisconsin.[50] In the BMES in Australia, the authors also found lower prevalence of all lesions related to AMD in each age stratum.[51] Methodologic differences between studies may exist, but the lower prevalence rates found in these countries may also reflect genetic or environmental differences compared with the US population.

A few studies have been done to evaluate the incidence of AMD. The FES used the age-specific prevalence data to estimate 5-year

incidence rates of AMD, according to the definition of AMD in that study. These estimates were 2.5%, 6.7%, and 10.8% for individuals who were 65, 70, and 75 years of age, respectively.[53] The BDES found that the 5-year cumulative incidence of early AMD increased from 3.9% in individuals aged 43–54 years to 22.8% in persons 75 years and older. The overall 5-year incidence of late AMD was 0.9%. Persons 75 years of age or older had a 5.4% incidence rate of late AMD. The Visual Impairment Project of Melbourne, Australia, found the overall 5-year incidence of AMD to be 0.49%.[54] The overall incidence of early AMD was 17.3% in this population of participants 40 years and older. As with the BDES, incidence of AMD increased with age – up to 6.3% for people aged 80 years and older at baseline. The Barbados Eye Study described a 5.2% 4-year incidence of early macular changes in a black population, with an extremely low incidence of exudative AMD, which may be attributable in part to differences in the racial/ethnic composition of this population[55] (discussed below in the "Race/ethnicity" section).

Quality of Life

The psychologic costs associated with AMD underscore the growing importance of this disease on the expanding older adult population. For this reason it is important to incorporate a functional component into studies of AMD. An early study found that patients with visual loss resulting from AMD often report this disease as their worst medical problem and have a diminished quality of life.[56] Similarly, in one study of wellbeing, patients with AMD had comparable scores to patients with chronic obstructive pulmonary disease and acquired immunodeficiency syndrome (AIDS); the poor quality of life in patients with AMD was related to greater emotional distress, worse self-reported general health, and greater difficulty carrying out daily activities.[57] More recently, the National Eye Institute Visual Function Questionnaire and the Macular Disease Dependent Quality of Life Questionnaire have been used in AMD studies.[58,59]

Sociodemographic Risk Factors

Age

All studies demonstrate that the prevalence, incidence, and progression of all forms of AMD rise steeply with increasing age. There was a 17-fold increased risk of AMD comparing the oldest to the youngest age group in the Framingham Study.[46] In the Watermen Study, the prevalence of moderate to advanced AMD doubled with each decade after age 60.[41] In the BDES, approximately 30% of individuals 75 years of age or older had early AMD; of the remainder, 23% developed early AMD within 5 years.[47,60] By age 75 years and older in that study, 7.1% had late AMD, compared with 0.1% in the age group 43–54 years and 0.6% among persons aged 55–64 years. Pooled data in a prevalence paper showed similar rates, with dramatic increases in rates for both men and women over age 80.[1]

Gender

Several studies[1,46,47,50] have shown no overall difference in the frequency of AMD between men and women, after controlling for age. However, in NHANES III, men, regardless of race and age, had a lower prevalence of AMD than women.[44] Incidence rates in the Beaver Dam population also suggest a gender difference. After adjusting for age, women aged 75 years or older had approximately twice the incidence of early AMD compared to men.[60] A study using reported incidence of exudative AMD in the United States among Medicare beneficiaries supported the Beaver Dam results.[61] In the BMES, there were consistent, although not significant, gender differences in prevalence for most AMD lesions, with women having higher rates for soft, indistinct drusen, but not for retinal pigmentary abnormalities.[51] A case–control study in AREDS also found women had a higher risk for intermediate drusen.[62] Residual confounding by age in the broad age category "75 and older" may partially explain the differences between studies as there are more women than men in that age group. Additional research is needed to assess these associations.

Race/Ethnicity

Ophthalmologists observe visual loss caused by NV less frequently among US ethnic minority groups compared with Caucasians. In the Baltimore Eye Survey, AMD accounted for 30% of bilateral blindness among whites and for 0% among African Americans.[63] Data from a population-based study of blacks in Barbados, West Indies,[52,55] revealed that incidence of AMD and signs of AMD changes occurred commonly but at a lower frequency than in predominantly white populations in other studies. Hispanics also have a lower prevalence of advanced AMD compared to non-Hispanics. Late-stage AMD was significantly less frequent among Hispanics vs. non-Hispanic whites in the BDES (odds ratio [OR] 0.07; 95% confidence interval (CI) 0.01–0.49).[64] The Los Angeles Latino Eye Study indicates Latinos have a relatively high rate of early AMD but not late AMD.[65] Among persons aged 40–79 years, the age-specific prevalence of late AMD in Asians was comparable with that reported from white populations, but early AMD signs were less common among Asians.[66] It is also important to consider that approximately half of Asian patients with AMD may actually have the polypoidal variant of AMD, which may respond differently to therapies for standard management of NV.[67] These variations suggest that both race and ethnicity are important determinants of AMD.

Socioeconomic Status

Lower levels of education and lower income have been shown to be related to increased morbidity and mortality from a number of diseases,[68] and there are mixed findings for AMD. The Eye Disease Case Control Study (EDCCS), a National Eye Institute-sponsored multicenter study, was designed to study risk factors for several types of maculopathy, including NV.[69] Persons with higher levels of education had a slightly reduced risk of NV, but the association did not remain statistically significant after adjustment for other risk factors.[69] Education was also inversely related to AMD in case–control and prospective studies based on the AREDS population even in multivariate analyses.[62,70] Similarly, a more recent study in Singapore found that lower education level was associated with a significantly higher prevalence of early AMD, when controlling for

age, cardiovascular risk factors, and cigarette smoking, although no association was found with income.[71] In the BDES, no association was found between maculopathy and education, income, employment status, or marital status.[72] Furthermore, no association was found in the FES,[46] although different definitions of AMD were used in this report, compared with the more recent studies. It is possible that education is a surrogate marker for other behaviors and lifestyles that are related to AMD, and it is important to consider this variable in analyses of AMD risk factors.

Ocular Risk Factors

Several studies have shown an association between AMD and hyperopia, which has been supported by meta-analyses of these results.[73,74] The results of some studies, including the BMES, suggest that the association may only apply to early AMD.[74,75] A potential limitation is the clinical setting in which they were conducted. As ophthalmology practices tend to contain a disproportionate number of myopic patients, controls selected from such practices tend to have a higher prevalence of myopia than the general population. However, two population-based studies that reduce this bias, the BMES and Rotterdam Study, have also demonstrated similar results.[75,76] This association, therefore, might implicate structural and mechanical differences that render some eyes predisposed to maculopathy.[77]

Consistent with the association between AMD and hyperopic refractive error, the EDCCS demonstrated that eyes with larger cup-to-disc ratios had a reduced risk of exudative AMD. This effect persisted even after multivariate modeling,[69] adjusting for known and potential confounding factors. While this association has been demonstrated in another population-based study in India,[78] whether this finding is meaningful in terms of the mechanisms associated with the development of AMD awaits further study.

Higher levels of ocular melanin may be protective against light-induced oxidative damage to the retina, as melanin can act as a free radical scavenger and may have an antiangiogenesis function. To date, the literature is inconclusive about the relationship between iris color and AMD. Darker irides have been found to be protective

in some studies but not in others.[79] Differences between studies may be partly related to the use of different definitions of disease, different number and types of other factors evaluated simultaneously, and residual confounding by ethnicity in some studies.

Data regarding the relationship between cataracts and AMD are also inconsistent. FES investigators found no relationship,[80] whereas data from the NHANES did support a relationship between AMD and lens opacities.[81] In the BDES, in which photographs of the lens and macula were graded, nuclear sclerosis was associated with increased odds of early AMD (OR 1.96; 95% CI 1.3–3.0) but not of late AMD. Neither cortical nor posterior subcapsular cataracts were related to AMD.[82] A case–control study of 1844 cases and 1844 controls indicated that lens opacities or cataract surgery were associated with an increased risk of AMD.[83]

Although AMD-affected individuals reported better visual function and quality of life after cataract surgery,[84] a history of cataract surgery has been found to be associated with an increased risk for advanced AMD in some studies.[85,86] Investigators have postulated that this association might arise because the cataractous lens can block damaging ultraviolet light. Inflammatory changes after cataract surgery may also cause progression from early to late AMD. In the BDES, previous cataract surgery at baseline was associated with a statistically significant increased risk for progression of AMD (OR 2.7) and for development of late AMD (OR 2.8; 95% CI 1.03–7.6).[87] A more recent analysis from the BDES examining this question over a 20-year interval supports this association for late AMD;[88] however, in other recent prospective studies, including the large AREDS study cohort, there was no evidence to support a higher rate of progression of AMD in patients who underwent cataract surgery.[89,90]

Behavioral and Lifestyle Factors

Smoking

The preponderance of epidemiologic evidence indicates a strong positive association between both wet and dry AMD and smoking.

Seddon et al. in a prospective cohort study reported that women in the Nurses' Health Study who currently smoked 25 or more cigarettes per day had a relative risk (RR) of 2.4 (95% CI 1.4–4), and women who were past smokers had an RR of 2.0 (95% CI 1.2–3.4) for developing incident AMD compared with women who never smoked.[16] There was a dose–response relationship between AMD and pack-years of smoking, and risk remained elevated for many years after smoking cessation. Results were consistent for various definitions of AMD, including non-exudative and exudative AMD, with different levels of visual loss, and for different definitions of smoking. It was estimated that 29% of the AMD cases in that study could be attributable to smoking.[16] These results were supported by a study among men participating in the Physicians' Health Study.[91] Several other studies have also shown an increased risk of AMD among smokers.[62,92–95] Smoking is an important, independent, modifiable risk factor for AMD.

Mechanisms by which smoking may increase the risk of developing AMD include its adverse effect on blood lipids by decreasing levels of high-density lipoprotein (HDL) and increasing platelet aggregability and fibrinogen, increasing oxidative stress and lipid peroxidation, and reducing plasma levels of antioxidants.[16] In animal models, nicotine has been shown to increase the size and severity of experimental NV, suggesting that non-neuronal nicotinic receptors may also play a part in the effect of smoking on advanced AMD.[96] Smoking is independently associated with AMD even after adjusting for the genes complement factor H (*CFH*) Y402H or *ARMS2*/*HTRA1* genotypes[97–99] (see "Genetic factors" below).

Diet

Diets high in antioxidant-rich fruits and vegetables are related to a lower risk of AMD. The first study launched to evaluate diet and AMD, the Dietary Intake Study ancillary to the EDCCS, showed an inverse association between exudative AMD and dietary intake of carotenoids.[5] In that study reported in 1994, a diet rich in green leafy vegetables containing the carotenoids lutein and zeaxanthin was associated with a reduction in the risk of exudative AMD, and

they are also associated with macular pigment.[100–102] Intake of 6 mg of lutein per day was significantly associated with a 43% reduction in risk of AMD.[17] A prospective double-masked study involving lutein and antioxidant supplementation in a group of 90 individuals showed that visual function was improved with 10 mg of lutein or a lutein/antioxidant formula.[103] In a British study of 380 men and women, lower plasma levels of zeaxanthin were also found to be associated with an increased risk of AMD.[104] A prospective follow-up study has shown that fruit intake is inversely associated with exudative AMD. Participants who consumed three or more servings of fresh fruit per day have a RR of 0.64 (95% CI 0.44–0.93) compared to those who consumed less than 1.5 servings per day.[4] Evidence regarding the beneficial effect of lutein on risk of AMD was also supported by analyses of diet data from AREDS.[105]

The role of antioxidant vitamins in the pathogenesis of AMD has received a great deal of attention. Antioxidants, including vitamin C (ascorbic acid), vitamin E (alpha-tocopherol), and the carotenoids (including alpha-carotene, beta-carotene, cryptoxanthin, lutein, and zeaxanthin), may be relevant to AMD as a result of their physiologic functions and the location of some of these nutrients in the retina. Trace minerals such as zinc, selenium, copper, and manganese may also be involved in antioxidant functions of the retina. Antioxidants could prevent oxidative damage to the retina, which could in turn prevent development of AMD.[5,106] Damage to retinal photoreceptor cells could be caused by photo-oxidation or by free radical-induced lipid peroxidation,[107,108] leading to impaired function of the RPE and eventually to degeneration involving the macula. The deposit of oxidized compounds in healthy tissue may result in cell death because they are indigestible by cellular enzymes.[108,109] Antioxidants may scavenge, decompose, or reduce the formation of harmful compounds. These early studies evaluating dietary impact on the pathogenesis of AMD provided background for subsequent clinical trials investigating the impact of dietary supplementation on the disease course in dry AMD.

An association between dietary fat intake, omega-3 fatty acids, and AMD was first reported in 1994 and published in 2001.[7,8] This association was primarily due to vegetable fat rather than animal fat. An inverse, protective association was found for higher

consumption of docosahexaenoic acid (DHA) and eicosapentaenoic acid (EPA) omega-3 fatty acids in the multivariate model.[8] Associations were also shown between risk of AMD and total fat, vegetable, monounsaturated, and polyunsaturated fats as well as linoleic acid.[8] These relationships were strengthened in a prospective longitudinal study of progression to advanced forms of AMD in an independent cohort.[9] A high intake of fish and omega-3 fatty acids reduced this risk when linoleic acid intake was low.[9,18] Later studies using data from the Women's Health Initiative, the Women's Health Study, and Australia confirmed that regular consumption of omega-3 fatty acids and fish were beneficial and they were associated with significantly decreased risk of early AMD.[110–112] Nuts have also been shown to decrease the risk of AMD progression.[9] In the BDES, individuals with greater saturated fat and cholesterol intake also had increased risk for early AMD.[113] Analyses of dietary data from AREDS support the previous observations of a beneficial effect of higher intake of omega-3 fatty acids.[114] One a study using data from this population suggested that not only can a higher intake of omega-3 fatty acids reduce the risk of GA, but the relationship may also be modified by genetic susceptibility.[115]

Dietary Supplements

The AREDS confirmed that antioxidant and zinc supplementation can decrease the risk of AMD progression and vision loss.[10] This study included a double-blind clinical trial in 11 centers around the United States, randomly assigning 3640 participants to take daily oral supplements of antioxidants, zinc, antioxidants and zinc, or placebo. Both zinc alone and antioxidants and zinc together significantly reduced the odds of developing advanced AMD in participants with intermediate signs of AMD (see Chapter 68, Age-related macular degeneration: Non-neovascular early AMD, intermediate AMD, and geographic atrophy) in at least one eye. The zinc supplement included zinc (80 mg) as zinc oxide and copper (2 mg) as cupric oxide; the antioxidant supplement included vitamin C (500 mg), vitamin E (400 IU), and beta-carotene (15 mg).

The AREDS2 expanded on the use of antioxidant vitamins for the

prevention of AMD progression.[11] The primary goal of AREDS2 was to evaluate the efficacy and safety of supplements containing lutein plus zeaxanthin and/or omega-3 fatty acids in reducing the risk of developing advanced AMD, as suggested in previous observational studies of dietary intake as described above. The use of much lower doses of zinc than the original AREDS formulation and the omission of beta-carotene was also investigated. Notably, the dietary study published in 1994 showed a benefit of dietary lutein and zeaxanthin but no benefit of dietary beta-carotene on risk of developing NV.[5] AREDS2 enrolled 4203 participants, aged 50–85 years, who were considered at risk of developing advanced AMD. Participants were randomized to placebo, lutein/zeaxanthin (10 mg/2 mg), omega-3 fatty acids DHA (350 mg) and EPA (650 mg), or lutein/zeaxanthin and DHA/EPA, in addition to taking the original first-generation AREDS supplements described above. A second randomization was performed in approximately three-quarters (72%) of participants to investigate the effect of eliminating beta-carotene and reducing the zinc level from 80 mg in the original AREDS supplement to 25 mg.

In the initial analysis, additional supplementation with lutein/zeaxanthin and/or DHA/EPA was not shown to reduce the risk of progression to advanced AMD.[11] However, secondary analyses showed that lutein/zeaxanthin could be helpful in reducing the risk of AMD progression, particularly in patients with bilateral large drusen at baseline.[12] The overall results of the secondary analyses and the potential increased lung cancer risk in current and former smokers taking beta-carotene supplements led to the recommendation of supplementing with lutein/zeaxanthin rather than beta-carotene. Comparison of low-dose zinc supplementation to the higher dose in the original AREDS formulation did not reveal a statistically significant difference. While AREDS2 provided valuable information, several issues have been raised including the generalizability of the study results to a less well-nourished population, the complex randomization design, the lack of a true placebo group, and the relatively short duration of the trial.

Alcohol Intake

Studies that have examined the relationship between AMD and alcohol consumption yield mixed results. In the EDCCS, no significant relationship between alcohol intake and exudative AMD was noted in univariate analyses,[69] but an inverse association could not be ruled out in multivariate analyses. A study using data from the Nurses' Health Study found no significant relationship between moderate alcohol consumption and risk of AMD; however, there was a modestly increased risk of early, dry AMD in drinkers consuming 30 g/d or more of alcohol.[116] In a case–control study using NHANES I data, moderate wine consumption was associated with a decreased risk of developing AMD, although the analysis did not control for the potential confounding effects of smoking.[117] The BDES found heavy drinkers were more likely to develop late AMD,[93] whereas the BMES found an increased risk of early AMD only in current spirits drinkers.[118] A prospective cohort study using data from the Melbourne Collaborative Cohort Study showed that drinking more than 20 g of alcohol per day was associated with an approximately 20% increase in the odds of early AMD, but did not replicate these findings for late AMD.[119] The evidence to date does not provide consistent support that alcohol intake has a large effect on the development of AMD.

Obesity and Physical Activity

There is an association between progression to advanced stages of AMD and overall obesity, abdominal adiposity, and higher waist–hip ratio AMD.[18] Early stages of AMD have been associated with body mass index.[120–125] In a prospective cohort study of AMD progression, 261 individuals with some sign of nonadvanced AMD in at least one eye and a body mass index (BMI) between 25 and 29 had a RR of 2.32 (95% CI 1.32–4.07) for progression to advanced AMD when compared to those with a BMI of less than 25.[18] Those with a BMI of 30 or higher had a RR of 2.35 (95% CI 1.27–4.34) compared to the lowest category (BMI <25), after controlling for other factors. Similarly, increased waist circumference and higher waist-to-hip ratio were associated with increased risk of AMD progression. In the BMES, obesity was associated with higher incidence of AMD during the 10-year follow-up,[124] and the BDES

showed a similar association of increased risk of early AMD with increasing measures of obesity.[125] Vigorous physical activity three times a week reduced the risk of AMD progression by 25% compared to no physical activity.[18] Obesity and physical activity are modifiable factors that may alter an individual's risk of AMD and progression over time to advanced stages of the disease. In one study, the susceptibility to advanced AMD associated with *CFH* Y402H was modified by BMI, and both higher BMI and current and past smoking increased risk of advanced AMD within the same genotype category[97] (see "Genetic factors" below).

Sunlight Exposure

Literature to date regarding the association between sunlight exposure and AMD is conflicting. Overall, the data do not support a strong association between ultraviolet radiation exposure and risk of AMD, although a small effect cannot be excluded. In the BDES,[126] increased time spent outdoors in the summer was associated with a twofold increased risk of advanced AMD. The 5-year[127] and 10-year[128] incidence of early AMD in the BDES confirmed this association, although the 10-year incidence study showed few significant associations between environmental light and incidence and progression of early AMD. The EDCCS[69] and the Pathologies Oculaires Liées à l'Age (POLA) study in France[129] showed no significant association between advanced AMD and sunlight exposure. Sensitivity to sunburn may also be a risk factor. An Australian case–control study noted an association between sun-sensitive skin and risk of neovascular AMD.[130] The European Eye Study found no association between overall sunlight exposure and neovascular or early AMD; however, a subgroup analysis suggested a positive association between lifetime sunlight exposure and NV among individuals in the quartile of lowest antioxidant level intake (vitamin C, zeaxanthin, vitamin E, and dietary zinc).[131] Conflicting results from these studies exemplify the difficulties encountered when studying this complex exposure. These difficulties include challenges in measuring short-term and lifetime exposure and the effect of potential confounding variables, such as sun sensitivity and sun avoidance behaviors or even dietary

composition. Furthermore, studies have evaluated different populations with different stages of AMD and people with varying intensity of exposures.

Medications

The use of certain medications may be associated with AMD, although studies yield mixed results. Some studies have shown borderline statistically significant associations between increased risk of early AMD with use of antihypertensive medication, especially beta blockers.[132] Other studies have shown a decreased rate of NV among AMD patients taking aspirin, but the results have been inconsistent.[133] Similarly, a possible protective association between statins and AMD has been investigated in numerous studies with varied findings.[134] The use of statins may be associated with decreased NV due to their antiinflammatory and antioxidant properties.[135] Increased levels of C-reactive protein in patients with AMD underscore the role of inflammation in the pathophysiology of the disease,[136] and it may be the antiinflammatory effects of statins that affect risk, rather than the cholesterol-lowering effect of the medication. The potential link between anticholesterol medications is more intriguing given the finding that the lipase C (*LIPC)* gene, a gene that influences high-density lipoprotein (HDL) level, and other genes involved in cholesterol pathways, including cholesteryl ester transfer protein (*CETP*), are associated with AMD.[30,31]

Cardiovascular-Related Factors

Cardiovascular Diseases

It is important to study possible cardiovascular risk factors not only to understand the etiology of AMD, but also because anti-VEGF therapies may have cardiovascular risk. Some studies have suggested an association between AMD and clinical manifestations of cardiovascular disease (CVD). These studies suggested that many of the same risk factors for CVD were also associated with AMD. It was hypothesized that the pathogenesis of these two

disease spectrums may share causal pathways, and this could be helpful in identifying susceptible individuals who may benefit most from disease prevention measures as well as related mechanisms.[137]

The presence of atherosclerotic lesions, determined by ultrasound, was examined in relation to risk of macular degeneration in a large population-based study conducted in the Netherlands.[138] Results obtained from this cross-sectional study showed a 4.5-fold increased risk of late AMD (defined as GA or NV) associated with plaques in the carotid bifurcation, and a twofold increased risk associated with plaques in the common carotid artery. Lower-extremity arterial disease (as measured by the ratio of the systolic blood pressure [SBP] level of the ankle to the SBP of the arm) was also associated with a 2.5-times increased risk of AMD.

In addition, a case–control study found a relationship between AMD and a history of one or more CVDs.[139] The NHANES I study reported a positive association between AMD and cerebrovascular disease, but positive associations with other vascular diseases did not reach statistical significance.[140] A Finnish study reported a significant correlation between occurrence of AMD and the severity of retinal arteriosclerosis;[141] however, other studies found that individuals who reported a history of cardiovascular disease did not have a significantly greater risk of AMD.[69,92,142,143] At the same time, many CVD risk factors are associated with AMD.[2,137]

Blood Pressure and Hypertension

The role of blood pressure in the etiology of AMD remains unclear. There was a small and consistent statistically significant relationship between AMD and systemic hypertension in three cross-sectional population-based studies.[140,144,145] The BDES reported that SBP was associated with incidence of RPE depigmentation,[146] 10-year incidence of advanced AMD lesions, and progression of AMD.[135] That study has also shown that arteriovenous nicking, a retinal vascular characteristic associated with hypertension, is associated with an increased incidence of AMD.[147] The Rotterdam Study also showed a relationship between elevated SBP and incidence of AMD.[148] In the Macular Photocoagulation Study, there

was an associated between hypertension and increased incidence of exudative AMD in the fellow eye of individuals with exudative AMD in one eye at baseline (RR 1.7; 95% CI 1.2–2.4).[149] In another case–control study, dry AMD was not associated with hypertension, but exudative AMD was significantly associated with both hypertension and antihypertensive medication use.[132] Other cross-sectional[92,138,150] and case–control studies,[69] as well as a prospective study[142] did not show an increased risk of AMD associated with current hypertension or systolic or diastolic blood pressure. Overall evidence suggests a possible mild to moderate association between elevated blood pressure and AMD. Assessment of this relationship could be enhanced by evaluating the duration of hypertension and its effects on onset and progression of maculopathy in large study populations with a sufficient number of participants with advanced stages of AMD.

Cholesterol Levels

There is some evidence linking cholesterol level to AMD, but results are not consistent. The EDCCS reported a statistically significant fourfold increased risk of exudative AMD associated with the highest serum cholesterol level (>4.88 mmol/L) and twofold increased risk in the middle-cholesterol-level group, compared with the lowest-cholesterol-level group, controlling for other factors.[69] A positive association was found between risk of AMD and increasing HDL levels in the population-based POLA study,[121] the Rotterdam Study,[151] and the EPIC–Norfolk Eye Study.[152] A case–control study showed that higher HDL cholesterol levels tended to reduce the risk of AMD.[153] The BDES found that early AMD was related to low total serum cholesterol levels in women and men older than 75. Furthermore, men with early AMD had higher HDL and lower total cholesterol-to-HDL ratios.[92,146] A small, not significant increased risk of wet AMD was seen with increasing triglyceride level in the EDCCS.[69] This trend was not seen in the Rotterdam Study[142] or the BDES[97] but both studies had small numbers of exudative AMD cases.

The genes involved in the HDL cholesterol pathway that have been associated with AMD have had discordant effects between the

HDL-increasing alleles and the protective or risk effects for AMD. An HDL-raising allele of the *LIPC* gene was associated with a reduced risk of AMD, whereas an HDL-increasing allele of *CETP* increased risk for AMD.[30,31] Furthermore, mean HDL level was lower in advanced AMD cases compared with controls in one study, and this association was independent of the *LIPC* genotype.[153] In turn, *LIPC* genotype was associated with advanced AMD independent of HDL level and other factors including dietary lutein, smoking, BMI, and other AMD-related genetic variants.[154] The mechanisms through which genetic variants in the HDL cholesterol pathway exert their effect on AMD risk require further investigation.

In summary, serum cholesterol levels may be related to exudative AMD, but there is a more consistent relationship with dietary fat intake (see section on "Diet"). The mechanisms through which variants in HDL-related genes affect AMD risk is not simply through their influence on serum HDL level. Dissection of the mechanisms by which HDL mediates AMD risk may illuminate additional treatment strategies. This possible association with cholesterol intake may indicate a relationship with atherosclerosis.[137]

Diabetes

Many studies have investigated the relationship between diabetes and AMD, and most have found no significant relationships. Only a few studies suggested a possible positive association.[155] One difficulty related to these studies is the uncertainty of diagnosing AMD in the presence of diabetic retinopathy involving the macula. In addition, many studies of AMD exclude persons with diabetic retinopathy. This could result in attenuated relationships between AMD and diabetes in published studies.

Hormonal and Reproductive Factors

There is evidence to support a small protective effect of hormone therapy on AMD,[156,157] but associations with pregnancies[158] or menopause[158,159] are more mixed. The EDCCS showed a marked

decrease in the risk of NV among postmenopausal women who used estrogen therapy,[69] as did a cross-sectional study.[156] No relationship was found in the BDES between years of estrogen therapy and exudative AMD (OR 0.9 [per 1 year of therapy]; 95% CI 0.8–1.1) or any of the less severe forms of AMD among women;[158] however, this study had limited power to detect a potential effect of estrogen therapy on advanced AMD. Some studies,[160,161] including the BMES,[159] reported no relationship between AMD and hormone replacement therapy or early menopause. However, the BMES did describe a small but significant decrease in risk of early AMD with increasing number of years between menarche and menopause. A study of 799 female participants found a protective association between estrogen therapy, either hormone replacement therapy or birth control pills, and NV.[162] The Women's Health Initiative Sight Exam study demonstrated a protective association between combined estrogen and progestin hormone therapy and NV as well as soft drusen, but not early-stage AMD.[163] The evidence is sparse with varying results, but a protective effect of estrogen on AMD is possible.

Inflammatory Factors

Studies have suggested that inflammation plays a role in the pathogenesis of drusen and AMD.[136,137,164–166] Examination of tissue samples has shown that "cellular debris" from RPE cells becomes trapped in the RPE basal lamina and Bruch's membrane, potentially causing a chronic inflammatory response that could prompt drusen formation.[164] Drusen contain proteins that are associated with chronic and acute inflammatory responses[165] and other age-related diseases, including amyloid P component and complement proteins.[166] Inflammation is also associated with angiogenesis, and may play a role in the neovascularization seen in the advanced exudative form of AMD.

A study of 930 individuals showed that serum levels of the systemic inflammatory marker, high sensitivity C-reactive protein, are significantly elevated in individuals with advanced AMD.[136] This study showed that, after adjusting for variables including age, gender, BMI, and smoking, the OR for AMD comparing the highest

and lowest quartiles of C-reactive protein was 1.65 (95% CI 1.07–2.55, *p* for trend = .02). Higher levels of high-sensitivity CRP and single nucleotide polymorphisms (SNPs) in the *CFH* and *ARMS2* genes were found to be independently associated with greater risk of AMD within most genotype groups.[167] These elevated levels suggest that reducing inflammation may slow the progression of AMD. Some studies raise the possibility that medications with anti-inflammatory properties, such as statins[134] and triamcinolone,[168] may be beneficial.

The existence of multiple, complement-related AMD risk alleles has provided further support for the inflammatory pathogenesis theory for AMD and sheds light on the role of uncontrolled alternative complement pathway activation in this disease (see "Genetic factors" below). *CFH* inhibits the alternative complement pathway by blocking formation of and accelerating the decay of alternative pathway C3 convertases; it also serves as a cofactor for the Factor-1-mediated cleavage and inactivation of C3b.[169] The *CFH* Y402H variant is within the *CFH* binding site for heparin and C-reactive protein. Binding to these sites increases the affinity of factor H (FH) for C3b, which in turn increases the ability of FH to inhibit complement's effects.[170]

As a result of the complement-related genetic discoveries, various complement-modulating agents are currently in clinical trials for the treatment of AMD.[171] Systemic administration of the anti-C5 antibody, eculizumab, was investigated for geographic atrophy and the phase II study failed to show efficacy of this therapeutic agent.[172] Other agents in various phases of clinical trials include intravitreal compstatin/POT-4 (C3 inhibitor), intravitreal ARC1905 (a C5 inhibitor), and intravitreal lampalizumab (an antibody against Complement Factor D).

Genetic Factors

AMD is a complex, polygenic disease in which multiple common genetic variants each add a small to moderate amount of increased risk, while rare variants have higher risk, and all contribute to disease in addition to environmental factors.[2,173] The risk of developing the disease is threefold higher in people who have a

family member with AMD than in those without an affected first-degree relative.[174,175] Since 2005, several genetic variants have been consistently associated with AMD, including common and rare variants in the *CFH* gene and variants in several other genes in the alternative complement cascade,[27,33,176,177,178] including Factor B (*BF*)/Complement Component 2 (*C2*),[26,27] Complement Component 3 (*C3*),[28] and Complement Factor I (*CFI*).[29] Rare genotypic variants in the *CFH* gene, such as the R1210C rare variant, are associated with higher risk of disease, extensive drusen accumulation and earlier onset of advanced disease.[40,177]

Several genes not involved in the complement cascade have also been implicated as AMD risk factors. Variation in the *ARMS2/HTRA1* locus on chromosome 10 has been convincingly associated with AMD with an effect size similar to or greater than that of *CFH*.[23–25,179] The function of this gene is not completely elucidated, but there is evidence that it confers a somewhat greater risk for wet AMD compared to GA.[33,35] *LIPC* and tissue inhibitor of metalloproteinase 3 (*TIMP3*) were associated with AMD in two large genome-wide association studies.[30,31] *LIPC* is involved in HDL cholesterol metabolism and *TIMP3* is implicated in a Mendelian, early-onset form of macular degeneration, Sorsby fundus dystrophy.[180] More recently, new variants near the collagen type X alpha 1 precursor/fyn related kinase (*COL10A1/FRK)* genes and in *VEGFA* were discovered to be associated with advanced AMD,[34] supporting the association noted with the gene *COL8A1*[30,34] and emphasizing the importance of extracellular matrix biology and angiogenesis in AMD. The genetic variants discovered to date explain about half of the classical sibling risk of AMD, and commercial genetic testing for some AMD risk variants is currently available. Knowledge of genetic variation at risk loci increases the ability to predict AMD progression above and beyond knowledge of demographics, ocular factors, smoking history, and BMI.[176,178,181–183] Although there is not yet a consensus on how genetic testing should be integrated into clinical practice, genotyping may become a useful tool for identifying individuals who have a higher risk for disease onset and progression. These patients may benefit from more intense monitoring and/or preventive treatment strategies, and may help with designing

clinical trials.[176,178,181–183]

Pharmacogenetics

Pharmacogenetic studies have explored the association of the *CFH* and/or *ARMS2/HTRA1* polymorphisms with patients' responses to anti-VEGF therapy and antioxidant supplementations. One retrospective cohort study found that patients with the *CFH* Y204H CC genotype had worse visual outcomes with intravitreal bevacizumab than did those with the *CFH* TC and TT genotypes; they found no pharmacogenetic relationship with *ARMS2/HTRA1*.[184] This relationship between *CFH* genotype and poorer visual acuity outcomes with intravitreal bevacizumab was corroborated by a prospective study.[185] Another retrospective study evaluating only the *CFH* locus found that patients who were homozygous for the Y402H risk allele have a 37% significantly higher risk of requiring additional intravitreal ranibizumab injections.[186] There were no significant treatment interactions with *ARMS2/HTRA1*. A recent study, that evaluated more AMD genes as well as nongenetic factors as predictors of response to anti-VEGF treatment, showed significant improvement in visual acuity after one year for the low-risk *CFH* genotypes and among subjects with a low *CFH* risk score.[187] In analyses of data derived from two large clinical trials comparing anti-VEGF treatments, no significant differences regarding genotypes were reported.[188,189]

Results from pharmacogenetic analyses to assess whether genetic susceptibility may influence response to antioxidant/mineral supplements have been conflicting. In a retrospective analysis of the AREDS data, an interaction between *CFH* Y402H genotype and supplementation with antioxidants plus zinc and zinc alone was observed.[181,190] Two studies using data from the AREDS study established risk prediction models for progression to AMD and showed a benefit of antioxidant-mineral supplementation for *CFH* homozygous low-risk genotypes but little benefit for the *CFH* homozygous risk genotype.[181,182] These studies did not identify any interactions between antioxidant/mineral supplements and other genetic variants. Further studies suggested that certain genotypic subgroups had neutral or even unfavorable responses to AREDS

supplements, and some genotypic subgroups had a greater reduction in disease progression rate with zinc only or antioxidants only, compared with the combined AREDS formulation.[191,192] However, a separate analysis of a subgroup of the same data suggested that there is no interaction between genotype and response to AREDS supplements.[193,194] Differences in definitions and sample sizes for subgroups and analytic methods may explain some of the variation in the results. Another study using a larger AREDS cohort and applying a different analysis found no beneficial AREDS treatment effect among subjects with the *CFH* high risk genotype, and a significant interaction was observed for the NV subtype.[195] On the other hand, the higher risk genotype group for *ARMS2* appeared to benefit more from the supplements, with a significant interaction.[195] There is currently no formal recommendation for genetic testing in determining the appropriateness of antioxidant/mineral supplementation.

Conclusion

AMD is a multifactorial disease that affects a large proportion of the population. Research to date has yielded some preventive measures and a few effective treatments for the advanced exudative form of the disease, and there are ongoing studies investigating possible therapeutics for advanced dry AMD. Several factors that could modify individual risk have been identified, including smoking, dietary intake of omega-3 fatty acids, green leafy vegetables, and fruit with antioxidants including lutein and zeaxanthin, as well as exercise and maintaining a healthy overall and abdominal weight. Studies have shown mixed effects of sunlight exposure, medication use, and alcohol intake. The understanding of the genetic architecture of AMD has increased significantly over the past decade and those pathways underscore the roles of inflammation, immune mechanisms, HDL cholesterol metabolism, angiogenesis, and dysfunction of extracellular matrix proteins, in the etiology of this disease. A combination of these genetic and nongenetic factors can predict rates of progression to advanced AMD subtypes over time. Ongoing studies of therapies targeting these mechanisms of disease may potentially change treatment paradigms for the

advanced forms of the disease, and may reduce rates of transition to stages of AMD that cause visual loss among high-risk individuals.

References

1. Friedman DS, O'Colmain BJ, Munoz B, et al. Prevalence of age-related macular degeneration in the United States. *Arch Ophthalmol*. 2004;122(4):564–572.
2. Sobrin L, Seddon JM. Nature and nurture- genes and environment- predict onset and progression of macular degeneration. *Prog Retin Eye Res*. 2014;40:1–15.
3. Rein DB, Wittenborn JS, Zhang X, et al. Forecasting age-related macular degeneration through the year 2050: the potential impact of new treatments. *Arch Ophthalmol*. 2009;127(4):533–540.
4. Cho E, Seddon JM, Rosner B, et al. Prospective study of intake of fruits, vegetables, vitamins, and carotenoids and risk of age-related maculopathy. *Arch Ophthalmol*. 2004;122(6):883–892.
5. Seddon JM, Ajani UA, Sperduto RD, et al. Dietary carotenoids, vitamins A, C, and E, and advanced age-related macular degeneration. Eye Disease Case–Control Study Group. *JAMA*. 1994;272(18):1413–1420.
6. Mares-Perlman JA, Brady WE, Klein R, et al. Serum antioxidants and age-related macular degeneration in a population-based case–control study. *Arch Ophthalmol*. 1995;113(12):1518–1523.
7. Seddon J, et al. Dietary fat intake and age-related macular degeneration. *Invest Ophthalmol Vis Sci*. 1994;35 [ARVO abstract 2003].
8. Seddon JM, Rosner B, Sperduto RD, et al. Dietary fat and risk for advanced age-related macular degeneration. *Arch Ophthalmol*. 2001;119(8):1191–1199.
9. Seddon JM, Cote J, Rosner B. Progression of age-related macular degeneration: association with dietary fat, transunsaturated fat, nuts, and fish intake. *Arch Ophthalmol*. 2003;121(12):1728–1737.

10. Age-Related Eye Disease Study Group. A randomized, placebo-controlled, clinical trial of high-dose supplementation with vitamins C and E, beta carotene, and zinc for age-related macular degeneration and vision loss: AREDS report no. 8. *Arch Ophthalmol*. 2001;119(10):1417–1436.
11. Lutein + zeaxanthin and omega-3 fatty acids for age-related macular degeneration: the Age-Related Eye Disease Study 2 (AREDS2) randomized clinical trial. *JAMA*. 2013;309(19):2005–2015.
12. Chew EY, Clemons TE, Sangiovanni JP, et al. Secondary analyses of the effects of lutein/zeaxanthin on age-related macular degeneration progression: AREDS2 report no. 3. *JAMA Ophthalmol*. 2014;132(2):142–149.
13. Rosenfeld PJ, Brown DM, Heier JS, et al. Ranibizumab for neovascular age-related macular degeneration. *N Engl J Med*. 2006;355(14):1419–1431.
14. Regillo CD, Brown DM, Abraham P, et al. Randomized, double-masked, sham-controlled trial of ranibizumab for neovascular age-related macular degeneration: PIER Study year 1. *Am J Ophthalmol*. 2008;145(2):239–248.
15. Spaide RF, Laud K, Fine HF, et al. Intravitreal bevacizumab treatment of choroidal neovascularization secondary to age-related macular degeneration. *Retina*. 2006;26(4):383–390.
16. Seddon JM, Willett WC, Speizer FE, et al. A prospective study of cigarette smoking and age-related macular degeneration in women. *JAMA*. 1996;276(14):1141–1146.
17. Tomany SC, Wang JJ, Van Leeuwen R, et al. Risk factors for incident age-related macular degeneration: pooled findings from 3 continents. *Ophthalmology*. 2004;111(7):1280–1287.
18. Seddon JM, Cote J, Davis N, et al. Progression of age-related macular degeneration: association with body mass index, waist circumference, and waist-hip ratio. *Arch Ophthalmol*. 2003;121(6):785–792.
19. Klein RJ, Zeiss C, Chew EY, et al. Complement factor H polymorphism in age-related macular degeneration. *Science*. 2005;308(5720):385–389.
20. Edwards AO, Ritter R 3rd, Abel KJ, et al. Complement factor

H polymorphism and age-related macular degeneration. *Science*. 2005;308(5720):421–424.
21. Haines JL, Hauser MA, Schmidt S, et al. Complement factor H variant increases the risk of age-related macular degeneration. *Science*. 2005;308(5720):419–421.
22. Hageman GS, Anderson DH, Johnson LV, et al. A common haplotype in the complement regulatory gene factor H (HF1/CFH) predisposes individuals to age-related macular degeneration. *Proc Natl Acad Sci USA*. 2005;102(20):7227–7232.
23. Rivera A, Fisher SA, Fritsche LG, et al. Hypothetical LOC387715 is a second major susceptibility gene for age-related macular degeneration, contributing independently of complement factor H to disease risk. *Hum Mol Genet*. 2005;14(21):3227–3236.
24. Dewan A, Liu M, Hartman S, et al. HTRA1 promoter polymorphism in wet age-related macular degeneration. *Science*. 2006;314(5801):989–992.
25. Yang Z, Camp NJ, Sun H, et al. A variant of the HTRA1 gene increases susceptibility to age-related macular degeneration. *Science*. 2006;314(5801):992–993.
26. Gold B, Merriam JE, Zernant J, et al. Variation in factor B (BF) and complement component 2 (C2) genes is associated with age-related macular degeneration. *Nat Genet*. 2006;38(4):458–462.
27. Maller J, George S, Purcell S, et al. Common variation in three genes, including a noncoding variant in CFH, strongly influences risk of age-related macular degeneration. *Nat Genet*. 2006;38(9):1055–1059.
28. Maller JB, Fagerness JA, Reynolds RC, et al. Variation in complement factor 3 is associated with risk of age-related macular degeneration. *Nat Genet*. 2007;39(10):1200–1201.
29. Fagerness JA, Maller JB, Neale BM, et al. Variation near complement factor I is associated with risk of advanced AMD. *Eur J Hum Genet*. 2009;17(1):100–104.
30. Neale BM, Fagerness J, Reynolds R, et al. Genome-wide association study of advanced age-related macular degeneration identifies a role of the hepatic lipase gene

(LIPC). *Proc Natl Acad Sci USA*. 2010;107(16):7395–7400.
31. Chen W, Stambolian D, Edwards AO, et al. Genetic variants near TIMP3 and high-density lipoprotein-associated loci influence susceptibility to age-related macular degeneration. *Proc Natl Acad Sci USA*. 2010;107(16):7401–7406.
32. Sobrin L, Maller JB, Neale BM, et al. Genetic profile for five common variants associated with age-related macular degeneration in densely affected families: a novel analytic approach. *Eur J Hum Genet*. 2010;18(4):496–501.
33. Sobrin L, Reynolds R, Yu Y, et al. ARMS2/HTRA1 Locus can confer differential susceptibility to the advanced subtypes of age-related macular degeneration. *Am J Ophthalmol*. 2010;151:345–352.
34. Yu Y, Bhangale TR, Fagerness J, et al. Common variants near FRK/COL10A1 and VEGFA are associated with advanced age-related macular degeneration. *Hum Mol Genet*. 2011;20(18):3699–3709.
35. Sobrin L, Ripke S, Yu Y, et al. Heritability and genome-wide association study to assess genetic differences between advanced age-related macular degeneration subtypes. *Ophthalmology*. 2012;119(9):1874–1885.
36. Fritsche LG, Chen W, Schu M, et al. Seven new loci associated with age-related macular degeneration. *Nat Genet*. 2013;45(4):433–439.
37. Bird AC, Bressler NM, Bressler SB, et al. An international classification and grading system for age-related maculopathy and age-related macular degeneration. The International ARM Epidemiological Study Group. *Surv Ophthalmol*. 1995;39(5):367–374.
38. Seddon JM, Sharma S, Adelman RA. Evaluation of the clinical age-related maculopathy staging system. *Ophthalmology*. 2006;113(2):260–266.
39. Seddon JM, Santangelo SL, Book K, et al. A genomewide scan for age-related macular degeneration provides evidence for linkage to several chromosomal regions. *Am J Hum Genet*. 2003;73(4):780–790.
40. Raychaudhuri S, Ripke S, Li M, et al. Associations of

CFHR1-CFHR3 deletion and a CFH SNP to age-related macular degeneration are not independent. *Nat Genet*. 2010;42(7):553–555 [author reply 555-556].
41. Bressler NM, Bressler SB, West SK, et al. The grading and prevalence of macular degeneration in Chesapeake Bay watermen. *Arch Ophthalmol*. 1989;107(6):847–852.
42. Klein R, Davis MD, Magli YL, et al. The Wisconsin age-related maculopathy grading system. *Ophthalmology*. 1991;98(7):1128–1134.
43. Ferris FL III, Wilkinson CP, Bird A, et al. Clinical classification of age-related macular degeneration. *Ophthalmology*. 2013;120(4):844–851.
44. Klein R, Rowland ML, Harris MI. Racial/ethnic differences in age-related maculopathy. Third National Health and Nutrition Examination Survey. *Ophthalmology*. 1995;102(3):371–381.
45. Klein R, Chou CF, Klein BE, et al. Prevalence of age-related macular degeneration in the US population. *Arch Ophthalmol*. 2011;129(1):75–80.
46. Leibowitz HM, Krueger DE, Maunder LR, et al. The Framingham Eye Study monograph: an ophthalmological and epidemiological study of cataract, glaucoma, diabetic retinopathy, macular degeneration, and visual acuity in a general population of 2631 adults, 1973-1975. *Surv Ophthalmol*. 1980;24(Suppl.):335–610.
47. Klein R, Klein BE, Linton KL. Prevalence of age-related maculopathy. The Beaver Dam Eye Study. *Ophthalmology*. 1992;99(6):933–943.
48. Friedman DS, Katz J, Bressler NM, et al. Racial differences in the prevalence of age-related macular degeneration: the Baltimore Eye Survey. *Ophthalmology*. 1999;106(6):1049–1055.
49. West SK, Munoz B, Rubin GS, et al. Function and visual impairment in a population-based study of older adults. The SEE project. Salisbury Eye Evaluation. *Invest Ophthalmol Vis Sci*. 1997;38(1):72–82.
50. Vingerling JR, Dielemans I, Hofman A, et al. The prevalence of age-related maculopathy in the Rotterdam Study.

Ophthalmology. 1995;102(2):205–210.
51. Mitchell P, Smith W, Attebo K, et al. Prevalence of age-related maculopathy in Australia. The Blue Mountains Eye Study. *Ophthalmology*. 1995;102(10):1450–1460.
52. Schachat AP, Hyman L, Leske MC, et al. Features of age-related macular degeneration in a black population. The Barbados Eye Study Group. *Arch Ophthalmol*. 1995;113(6):728–735.
53. Podgor MJ, Leske MC, Ederer F. Incidence estimates for lens changes, macular changes, open-angle glaucoma and diabetic retinopathy. *Am J Epidemiol*. 1983;118(2):206–212.
54. Mukesh BN, Dimitrov PN, Leikin S, et al. Five-year incidence of age-related maculopathy: the Visual Impairment Project. *Ophthalmology*. 2004;111(6):1176–1182.
55. Leske MC, Wu SY, Hyman L, et al. Four-year incidence of macular changes in the Barbados Eye Studies. *Ophthalmology*. 2004;111(4):706–711.
56. Mangione CM, Gutierrez PR, Lowe G, et al. Influence of age-related maculopathy on visual functioning and health-related quality of life. *Am J Ophthalmol*. 1999;128(1):45–53.
57. Williams RA, Brody BL, Thomas RG, et al. The psychosocial impact of macular degeneration. *Arch Ophthalmol*. 1998;116(4):514–520.
58. Clemons TE, Chew EY, Bressler SB, et al. National Eye Institute Visual Function Questionnaire in the Age-Related Eye Disease Study (AREDS): AREDS report no. 10. *Arch Ophthalmol*. 2003;121(2):211–217.
59. Mitchell J, Wolffsohn J, Woodcock A, et al. The MacDQoL individualized measure of the impact of macular degeneration on quality of life: reliability and responsiveness. *Am J Ophthalmol*. 2008;146(3):447–454.
60. Klein R, Klein BE, Jensen SC, et al. The five-year incidence and progression of age-related maculopathy: the Beaver Dam Eye Study. *Ophthalmology*. 1997;104(1):7–21.
61. Javitt JC, Zhou Z, Maguire MG, et al. Incidence of exudative age-related macular degeneration among elderly Am. *Ophthalmology*. 2003;110(8):1534–1539.
62. Age-Related Eye Disease Study Group. Risk factors

associated with age-related macular degeneration. A case–control study in the age-related eye disease study: Age-Related Eye Disease Study report number 3. *Ophthalmology*. 2000;107(12):2224–2232.
63. Sommer A, Tielsch JM, Katz J, et al. Racial differences in the cause-specific prevalence of blindness in east Baltimore. *N Engl J Med*. 1991;325(20):1412–1417.
64. Cruickshanks KJ, Hamman RF, Klein R, et al. The prevalence of age-related maculopathy by geographic region and ethnicity. The Colorado–Wisconsin Study of Age-Related Maculopathy. *Arch Ophthalmol*. 1997;115(2):242–250.
65. Varma R, Fraser-Bell S, Tan S, et al. Prevalence of age-related macular degeneration in Latinos: the Los Angeles Latino eye study. *Ophthalmology*. 2004;111(7):1288–1297.
66. Kawasaki R, Yasuda M, Song SJ, et al. The prevalence of age-related macular degeneration in Asians: a systematic review and meta-analysis. *Ophthalmology*. 2010;117(5):921–927.
67. Lim LS, Mitchell P, Seddon JM, et al. Age-related macular degeneration. *Lancet*. 2012;379(9827):1728–1738.
68. Adler NE, Boyce WT, Chesney MA, et al. Socioeconomic inequalities in health. No easy solution. *JAMA*. 1993;269(24):3140–3145.
69. Eye Disease Case–Control Study Group. Risk factors for neovascular age-related macular degeneration. The Eye Disease Case–Control Study Group. *Arch Ophthalmol*. 1992;110(12):1701–1708.
70. Seddon JM, Francis PJ, George S, et al. Association of CFH Y402H and LOC387715 A69S with progression of age-related macular degeneration. *JAMA*. 2007;297(16):1793–1800.
71. Cackett P, Tay WT, Aung T, et al. Education, socio-economic status and age-related macular degeneration in Asians: the Singapore Malay Eye Study. *Br J Ophthalmol*. 2008;92(10):1312–1315.
72. Klein R, Klein BE, Jensen SC, et al. The relation of socioeconomic factors to age-related cataract, maculopathy, and impaired vision. The Beaver Dam Eye Study. *Ophthalmology*. 1994;101(12):1969–1979.

73. Pan CW, Ikram MK, Cheung CY, et al. Refractive errors and age-related macular degeneration: a systematic review and meta-analysis. *Ophthalmology*. 2013;120(10):2058–2065.
74. Li Y, Wang J, Zhong X, et al. Refractive error and risk of early or late age-related macular degeneration: a systematic review and meta-analysis. *PLoS ONE*. 2014;9(3):e90897.
75. Wang JJ, Mitchell P, Smith W. Refractive error and age-related maculopathy: the Blue Mountains Eye Study. *Invest Ophthalmol Vis Sci*. 1998;39(11):2167–2171.
76. Ikram MK, van Leeuwen R, Vingerling JR, et al. Relationship between refraction and prevalent as well as incident age-related maculopathy: the Rotterdam Study. *Invest Ophthalmol Vis Sci*. 2003;44(9):3778–3782.
77. Friedman E, Ivry M, Ebert E, et al. Increased scleral rigidity and age-related macular degeneration. *Ophthalmology*. 1989;96(1):104–108.
78. Krishnaiah S, Das TP, Kovai V, et al. Associated factors for age-related maculopathy in the adult population in southern India: the Andhra Pradesh Eye Disease Study. *Br J Ophthalmol*. 2009;93(9):1146–1150.
79. Sun HP, Lin Y, Pan CW. Iris color and associated pathological ocular complications: a review of epidemiologic studies. *Int J Ophthalmol*. 2014;7(5):872–878.
80. Sperduto RD, Hiller R, Seigel D. Lens opacities and senile maculopathy. *Arch Ophthalmol*. 1981;99(6):1004–1008.
81. Liu IY, White L, LaCroix AZ. The association of age-related macular degeneration and lens opacities in the aged. *Am J Public Health*. 1989;79(6):765–769.
82. Klein R, Klein BE, Wang Q, et al. Is age-related maculopathy associated with cataracts? *Arch Ophthalmol*. 1994;112(2):191–196.
83. Chaine G, Hullo A, Sahel J, et al. Case–control study of the risk factors for age related macular degeneration. France-DMLA Study Group. *Br J Ophthalmol*. 1998;82(9):996–1002.
84. Lundstrom M, Brege KG, Floren I, et al. Cataract surgery and quality of life in patients with age related macular degeneration. *Br J Ophthalmol*. 2002;86(12):1330–1335.
85. Freeman EE, Munoz B, West SK, et al. Is there an association

between cataract surgery and age-related macular degeneration? Data from three population-based studies. *Am J Ophthalmol*. 2003;135(6):849–856.
86. Fraser-Bell S, Choudhury F, Klein R, et al. Ocular risk factors for age-related macular degeneration: the Los Angeles Latino Eye Study. *Am J Ophthalmol*. 2010;149(5):735–740.
87. Klein R, Klein BE, Jensen SC, et al. The relationship of ocular factors to the incidence and progression of age-related maculopathy. *Arch Ophthalmol*. 1998;116(4):506–513.
88. Klein BE, Howard KP, Lee KE, et al. The relationship of cataract and cataract extraction to age-related macular degeneration: the Beaver Dam Eye Study. *Ophthalmology*. 2012;119(8):1628–1633.
89. Chew EY, Sperduto RD, Milton RC, et al. Risk of advanced age-related macular degeneration after cataract surgery in the Age-Related Eye Disease Study: AREDS report no. 25. *Ophthalmology*. 2009;116(2):297–303.
90. Dong LM, Stark WJ, Jefferys JL, et al. Progression of age-related macular degeneration after cataract surgery. *Arch Ophthalmol*. 2009;127(11):1412–1419.
91. Christen WG, Glynn RJ, Manson JE, et al. A prospective study of cigarette smoking and risk of age-related macular degeneration in men. *JAMA*. 1996;276(14):1147–1151.
92. Klein R, Klein BE, Franke T. The relationship of cardiovascular disease and its risk factors to age-related maculopathy: the Beaver Dam Eye Study. *Ophthalmology*. 1993;100(3):406–414.
93. Klein R, Klein BE, Tomany SC, et al. Ten-year incidence of age-related maculopathy and smoking and drinking: the Beaver Dam Eye Study. *Am J Epidemiol*. 2002;156(7):589–598.
94. Delcourt C, Diaz JL, Ponton-Sanchez A, et al. Smoking and age-related macular degeneration. The POLA Study. Pathologies Oculaires Liées à l'Age. *Arch Ophthalmol*. 1998;116(8):1031–1035.
95. Myers CE, Klein BE, Gangnon R, et al. Cigarette smoking and the natural history of age-related macular degeneration: the Beaver Dam Eye Study. *Ophthalmology*. 2014;121(10):1949–1955.

96. Suner IJ, Espinosa-Heidmann DG, Marin-Castano ME, et al. Nicotine increases size and severity of experimental choroidal neovascularization. *Invest Ophthalmol Vis Sci*. 2004;45(1):311–317.
97. Seddon JM, George S, Rosner B, et al. CFH gene variant, Y402H, and smoking, body mass index, environmental associations with advanced age-related macular degeneration. *Hum Hered*. 2006;61(3):157–165.
98. Francis PJ, George S, Schultz DW, et al. The LOC387715 gene, smoking, body mass index, environmental associations with advanced age-related macular degeneration. *Hum Hered*. 2007;63(3–4):212–218.
99. Lechanteur YT, van de Camp PL, Smailhodzic D, et al. Association of smoking and CFH and ARMS2 risk variants with younger age at onset of neovascular age-related macular degeneration. *JAMA Ophthalmol*. 2015;133(5):533–541.
100. Bone RA, Landrum JT, Guerra LH, et al. Lutein and zeaxanthin dietary supplements raise macular pigment density and serum concentrations of these carotenoids in humans. *J Nutr*. 2003;133(4):992–998.
101. Krinsky NI, Landrum JT, Bone RA. Biologic mechanisms of the protective role of lutein and zeaxanthin in the eye. *Annu Rev Nutr*. 2003;23:171–201.
102. Bernstein PS, Delori FC, Richer S, et al. The value of measurement of macular carotenoid pigment optical densities and distributions in age-related macular degeneration and other retinal disorders. *Vision Res*. 2010;50(7):716–728.
103. Richer S, Stiles W, Statkute L, et al. Double-masked, placebo-controlled, randomized trial of lutein and antioxidant supplementation in the intervention of atrophic age-related macular degeneration: the Veterans LAST study (Lutein Antioxidant Supplementation Trial). *Optometry*. 2004;75(4):216–230.
104. Gale CR, Hall NF, Phillips DI, et al. Lutein and zeaxanthin status and risk of age-related macular degeneration. *Invest Ophthalmol Vis Sci*. 2003;44(6):2461–2465.

105. SanGiovanni JP, Chew EY, Clemons TE, et al. The relationship of dietary carotenoid and vitamin A, E, and C intake with age-related macular degeneration in a case-control study: AREDS report no. 22. *Arch Ophthalmol*. 2007;125(9):1225–1232.
106. Evereklioglu C, Er H, Doganay S, et al. Nitric oxide and lipid peroxidation are increased and associated with decreased antioxidant enzyme activities in patients with age-related macular degeneration. *Doc Ophthalmol*. 2003;106(2):129–136.
107. Anderson RE, Kretzer FL, Rapp LM. Free radicals and ocular disease. *Adv Exp Med Biol*. 1994;366:73–86.
108. Anderson RE, Rapp LM, Wiegand RD. Lipid peroxidation and retinal degeneration. *Curr Eye Res*. 1984;3(1):223–227.
109. Young RW. Pathophysiology of age-related macular degeneration. *Surv Ophthalmol*. 1987;31(5):291–306.
110. Parekh N, Voland RP, Moeller SM, et al. Association between dietary fat intake and age-related macular degeneration in the Carotenoids in Age-Related Eye Disease Study (CAREDS): an ancillary study of the Women's Health Initiative. *Arch Ophthalmol*. 2009;127(11):1483–1493.
111. Christen WG, Schaumberg DA, Glynn RJ, et al. Dietary Ω-3 fatty acid and fish intake and incident age-related macular degeneration in women. *Arch Ophthalmol*. 2011;129(7):921–929.
112. Chong EW, Robman LD, Simpson JA, et al. Fat consumption and its association with age-related macular degeneration. *Arch Ophthalmol*. 2009;127(5):674–680.
113. Mares-Perlman JA, Brady WE, Klein R, et al. Dietary fat and age-related maculopathy. *Arch Ophthalmol*. 1995;113(6):743–748.
114. SanGiovanni JP, Chew EY, Agron E, et al. The relationship of dietary omega-3 long-chain polyunsaturated fatty acid intake with incident age-related macular degeneration: AREDS report no. 23. *Arch Ophthalmol*. 2008;126(9):1274–1279.
115. Reynolds R, Rosner B, Seddon JM. Dietary omega-3 fatty

acids, other fat intake, genetic susceptibility, and progression to incident geographic atrophy. *Ophthalmology*. 2013;120(5):1020–1028.
116. Cho E, Hankinson SE, Willet WC, et al. Prospective study of alcohol consumption and the risk of age-related macular degeneration. *Arch Ophthalmol*. 2000;118(5):681–688.
117. Obisesan TO, Hirsch R, Kosoko O, et al. Moderate wine consumption is associated with decreased odds of developing age-related macular degeneration in NHANES-1. *J Am Geriatr Soc*. 1998;46(1):1–7.
118. Smith W, Mitchell P. Alcohol intake and age-related maculopathy. *Am J Ophthalmol*. 1996;122(5):743–745.
119. Adams MK, Chong EW, Williamson E, et al. 20/20 – Alcohol and age-related macular degeneration: the Melbourne Collaborative Cohort Study. *Am J Epidemiol*. 2012;176(4):289–298.
120. Klein BE, Klein R, Lee KE, et al. Measures of obesity and age-related eye diseases. *Ophthalmic Epidemiol*. 2001;8(4):251–262.
121. Delcourt C, Michel F, Colvez A, et al. Associations of cardiovascular disease and its risk factors with age-related macular degeneration: the POLA study. *Ophthalmic Epidemiol*. 2001;8(4):237–249.
122. Schaumberg DA, Christen WG, Hankinson SE, et al. Body mass index and the incidence of visually significant age-related maculopathy in men. *Arch Ophthalmol*. 2001;119(9):1259–1265.
123. Smith W, Mitchell P, Leeder SR, et al. Plasma fibrinogen levels, other cardiovascular risk factors, and age-related maculopathy: the Blue Mountains Eye Study. *Arch Ophthalmol*. 1998;116(5):583–587.
124. Maralani HG, Tai BC, Wong TY, et al. Metabolic syndrome and risk of age-related macular degeneration. *Retina*. 2015;35(3):459–466.
125. Howard KP, Klein BE, Lee KE, et al. Measures of body shape and adiposity as related to incidence of age-related eye diseases: observations from the Beaver Dam Eye Study. *Invest Ophthalmol Vis Sci*. 2014;55(4):2592–2598.

126. Cruickshanks KJ, Klein R, Klein BE. Sunlight and age-related macular degeneration. The Beaver Dam Eye Study. *Arch Ophthalmol*. 1993;111(4):514–518.
127. Cruickshanks KJ, Klein R, Klein BE, et al. Sunlight and the 5-year incidence of early age-related maculopathy: the Beaver Dam Eye Study. *Arch Ophthalmol*. 2001;119(2):246–250.
128. Tomany SC, Cruickshanks KJ, Klein R, et al. Sunlight and the 10-year incidence of age-related maculopathy: the Beaver Dam Eye Study. *Arch Ophthalmol*. 2004;122(5):750–757.
129. Delcourt C, Carriere I, Ponton-Sanchez A, et al. Light exposure and the risk of age-related macular degeneration: the Pathologies Oculaires Liées à l'Age (POLA) study. *Arch Ophthalmol*. 2001;119(10):1463–1468.
130. Darzins P, Mitchell P, Heller RF. Sun exposure and age-related macular degeneration. An Australian case–control study. *Ophthalmology*. 1997;104(5):770–776.
131. Fletcher AE, Bentham GC, Agnew M, et al. Sunlight exposure, antioxidants, and age-related macular degeneration. *Arch Ophthalmol*. 2008;126(10):1396–1403.
132. Hyman L, Schachat AP, He Q, et al. Hypertension, cardiovascular disease, and age-related macular degeneration. Age-Related Macular Degeneration Risk Factors Study Group. *Arch Ophthalmol*. 2000;118(3):351–358.
133. Sobrin L, Seddon JM. Regular aspirin use and risk of age-related macular degeneration. *Am J Ophthalmol*. 2013;156(2):213–217.e2.
134. Gehlbach P, Li T, Hatef E. Statins for age-related macular degeneration. *Cochrane Database Syst Rev*. 2015;(2) [CD006927].
135. Hall NF, Martyn CN. Could statins prevent age-related macular degeneration? *Expert Opin Pharmacother*. 2002;3(7):803–807.
136. Seddon JM, Gensler G, Milton RC, et al. Association between C-reactive protein and age-related macular degeneration. *JAMA*. 2004;291(6):704–710.
137. Snow KK, Seddon JM. Do age-related macular degeneration

and cardiovascular disease share common antecedents? *Ophthalmic Epidemiol*. 1999;6(2):125–143.
138. Vingerling JR, Dielemans I, Bots ML, et al. Age-related macular degeneration is associated with atherosclerosis. The Rotterdam Study. *Am J Epidemiol*. 1995;142(4):404–409.
139. Hyman LG, Lilienfeld AM, Ferris FL III, et al. Senile macular degeneration: a case–control study. *Am J Epidemiol*. 1983;118(2):213–227.
140. Goldberg J, Flowerdew G, Smith E, et al. Factors associated with age-related macular degeneration. An analysis of data from the first National Health and Nutrition Examination Survey. *Am J Epidemiol*. 1988;128(4):700–710.
141. Hirvela H, Luukinen H, Laara E, et al. Risk factors of age-related maculopathy in a population 70 years of age or older. *Ophthalmology*. 1996;103(6):871–877.
142. Vinding T. Age-related macular degeneration: an epidemiological study of 1000 elderly individuals. With reference to prevalence, funduscopic findings, visual impairment and risk factors. *Acta Ophthalmol Scand Suppl*. 1995;217:1–32.
143. Fernandez AB, Wong TY, Klein R, et al. Age-related macular degeneration and incident cardiovascular disease: the Multi-Ethnic Study of Atherosclerosis. *Ophthalmology*. 2012;119(4):765–770.
144. Sperduto RD, Hiller R. Systemic hypertension and age-related maculopathy in the Framingham Study. *Arch Ophthalmol*. 1986;104(2):216–219.
145. La TY, Cho E, Kim EC, et al. Prevalence and risk factors for age-related macular degeneration: Korean National Health and Nutrition Examination Survey 2008–2011. *Curr Eye Res*. 2014;39(12):1232–1239.
146. Klein R, Klein BE, Jensen SC. The relation of cardiovascular disease and its risk factors to the 5-year incidence of age-related maculopathy: the Beaver Dam Eye Study. *Ophthalmol*. 1997;104(11):1804–1812.
147. Klein R, Klein BE, Tomany SC, et al. The relation of retinal microvascular characteristics to age-related eye disease: the Beaver Dam eye study. *Am J Ophthalmol*. 2004;137(3):435–

444.
148. van Leeuwen R, Ikram MK, Vingerling JR, et al. Blood pressure, atherosclerosis, and the incidence of age-related maculopathy: the Rotterdam Study. *Invest Ophthalmol Vis Sci*. 2003;44(9):3771–3777.
149. Macular Photocoagulation Study Group. Risk factors for choroidal neovascularization in the second eye of patients with juxtafoveal or subfoveal choroidal neovascularization secondary to age-related macular degeneration. *Arch Ophthalmol*. 1997;115(6):741–747.
150. Klein R, Klein BE, Marino EK, et al. Early age-related maculopathy in the cardiovascular health study. *Ophthalmology*. 2003;110(1):25–33.
151. van Leeuwen R, Klaver CC, Vingerling JR, et al. Cholesterol and age-related macular degeneration: is there a link? *Am J Ophthalmol*. 2004;137(4):750–752.
152. Yip JL, Khawaja AP, Chan MP, et al. Cross-sectional and longitudinal associations between cardiovascular risk factors and age related macular degeneration in the EPIC–Norfolk Eye Study. *PLoS ONE*. 2015;10(7):e0132565.
153. Reynolds R, Rosner B, Seddon JM. Serum lipid biomarkers and hepatic lipase gene associations with age-related macular degeneration. *Ophthalmology*. 2010;117(10):1989–1995.
154. Seddon JM, Reynolds R, Rosner B. Associations of smoking, body mass index, dietary lutein, and the LIPC gene variant rs10468017 with advanced age-related macular degeneration. *Mol Vis*. 2010;16:2412–2424.
155. Chen X, Rong SS, Xu Q, et al. Diabetes mellitus and risk of age-related macular degeneration: a systematic review and meta-analysis. *PLoS ONE*. 2014;9(9):e108196.
156. Snow KK, Cote J, Yang W, et al. Association between reproductive and hormonal factors and age-related maculopathy in postmenopausal women. *Am J Ophthalmol*. 2002;134(6):842–848.
157. Snow KK, Seddon JM. Age-related eye diseases: impact of hormone replacement therapy, and reproductive and other risk factors. *Int J Fertil Womens Med*. 2000;45(5):301–313.

158. Klein BE, Klein R, Jensen SC, et al. Are sex hormones associated with age-related maculopathy in women? The Beaver Dam Eye Study. *Trans Am Ophthalmol Soc*. 1994;92:289–295 [discussion 295-287].
159. Smith W, Mitchell P, Wang JJ. Gender, oestrogen, hormone replacement and age-related macular degeneration: results from the Blue Mountains Eye Study. *Aust N Z J Ophthalmol*. 1997;25(Suppl. 1):S13–15.
160. Abramov Y, Borik S, Yahalom C, et al. The effect of hormone therapy on the risk for age-related maculopathy in postmenopausal women. *Menopause*. 2004;11(1):62–68.
161. Klein R, Deng Y, Klein BE, et al. Cardiovascular disease, its risk factors and treatment, and age-related macular degeneration: Women's Health Initiative Sight Exam ancillary study. *Am J Ophthalmol*. 2007;143(3):473–483.
162. Edwards DR, Gallins P, Polk M, et al. Inverse association of female hormone replacement therapy with age-related macular degeneration and interactions with ARMS2 polymorphisms. *Invest Ophthalmol Vis Sci*. 2010;51(4):1873–1879.
163. Haan MN, Klein R, Klein BE, et al. Hormone therapy and age-related macular degeneration: the Women's Health Initiative Sight Exam Study. *Arch Ophthalmol*. 2006;124(7):988–992.
164. Anderson DH, Mullins RF, Hageman GS, et al. A role for local inflammation in the formation of drusen in the aging eye. *Am J Ophthalmol*. 2002;134(3):411–431.
165. Johnson LV, Leitner WP, Staples MK, et al. Complement activation and inflammatory processes in Drusen formation and age related macular degeneration. *Exp Eye Res*. 2001;73(6):887–896.
166. Mullins RF, Russell SR, Anderson DH, et al. Drusen associated with aging and age-related macular degeneration contain proteins common to extracellular deposits associated with atherosclerosis, elastosis, amyloidosis, and dense deposit disease. *FASEB J*. 2000;14(7):835–846.
167. Seddon JM, Gensler G, Rosner B. C-reactive protein and

CFH, ARMS2/HTRA1 gene variants are independently associated with risk of macular degeneration. *Ophthalmology*. 2010;117(8):1560–1566.
168. Becerra EM, Morescalchi F, Gandolfo F, et al. Clinical evidence of intravitreal triamcinolone acetonide in the management of age-related macular degeneration. *Curr Drug Targets*. 2011;12(2):149–172.
169. Soames CJ, Sim RB. Interactions between human complement components factor H, factor I and C3b. *Biochem J*. 1997;326(Pt 2):553–561.
170. Schramm EC, Clark SJ, Triebwasser MP, et al. Genetic variants in the complement system predisposing to age-related macular degeneration: a review. *Mol Immunol*. 2014;61(2):118–125.
171. Gehrs KM, Jackson JR, Brown EN, et al. Complement, age-related macular degeneration and a vision of the future. *Arch Ophthalmol*. 2010;128(3):349–358.
172. Holz FG, Strauss EC, Schmitz-Valckenberg S, et al. Geographic atrophy: clinical features and potential therapeutic approaches. *Ophthalmology*. 2014;121(5):1079–1091.
173. Seddon JM, Sobrin L. Epidemiology of age-related macular degeneration. Albert D, Miller J, Azar D, et al. *Albert & Jakobiec's Principles and practice of ophthalmology*. W.B. Saunders: Philadelphia; 2007:413–422.
174. Seddon JM, Ajani UA, Mitchell BD. Familial aggregation of age-related maculopathy. *Am J Ophthalmol*. 1997;123(2):199–206.
175. Klaver CC, Wolfs RC, Assink JJ, et al. Genetic risk of age-related maculopathy. Population-based familial aggregation study. *Arch Ophthalmol*. 1998;116(12):1646–1651.
176. Seddon JM, Reynolds R, Yu Y, et al. Three new genetic loci (R1210C in CFH, variants in COL8A1 and RAD51B) are independently related to progression to advanced macular degeneration. *PLoS ONE*. 2014;9(1):e87047.
177. Ferrara D, Seddon JM. Phenotypic characterization of complement factor H R1210C rare genetic variant in age-related macular degeneration. *JAMA Ophthalmol*.

2015;133(7):785–791.
178. Seddon JM, Silver RE, Kwong M, et al. Risk prediction for progression of macular degeneration: 10 common and rare genetic variants, demographic, environmental, and macular covariates. *Invest Ophthalmol Vis Sci*. 2015;56(4):2192–2202.
179. Jakobsdottir J, Conley YP, Weeks DE, et al. Susceptibility genes for age-related maculopathy on chromosome 10q26. *Am J Hum Genet*. 2005;77(3):389–407.
180. Weber BH, Vogt G, Pruett RC, et al. Mutations in the tissue inhibitor of metalloproteinases-3 (TIMP3) in patients with Sorsby's fundus dystrophy. *Nat Genet*. 1994;8(4):352–356.
181. Seddon JM, Reynolds R, Maller J, et al. Prediction model for prevalence and incidence of advanced age-related macular degeneration based on genetic, demographic, and environmental variables. *Invest Ophthalmol Vis Sci*. 2009;50(5):2044–2053.
182. Seddon JM, Reynolds R, Yu Y, et al. Risk models for progression to advanced age-related macular degeneration using demographic, environmental, genetic, and ocular factors. *Ophthalmology*. 2011;118(11):2203–2211.
183. Seddon JM, Silver RE, Kwong M, et al. Risk prediction for progression of macular degeneration: 10 common and rare genetic variants, demographic, environmental, and macular covariates. *Invest Ophthalmol Vis Sci*. 2015;56(4):2192–2202.
184. Brantley MA Jr, Fang AM, King JM, et al. Association of complement factor H and LOC387715 genotypes with response of exudative age-related macular degeneration to intravitreal bevacizumab. *Ophthalmology*. 2007;114(12):2168–2173.
185. Nischler C, Oberkofler H, Ortner C, et al. Complement factor H Y402H gene polymorphism and response to intravitreal bevacizumab in exudative age-related macular degeneration. *Acta Ophthalmol*. 2011;89(4):e344–9.
186. Lee AY, Raya AK, Kymes SM, et al. Pharmacogenetics of complement factor H (Y402H) and treatment of exudative age-related macular degeneration with ranibizumab. *Br J Ophthalmol*. 2009;93(5):610–613.
187. Shah AR, Williams S, Baumal CR, et al. Predictors of

response to intravitreal anti-vascular endothelial growth factor treatment of age-related macular degeneration. *Am J Ophthalmol*. 2016;163:154–166.e8.
188. Hagstrom SA, Ying GS, Pauer GJ, et al. Pharmacogenetics for genes associated with age-related macular degeneration in the Comparison of AMD Treatments Trials (CATT). *Ophthalmology*. 2013;120(3):593–599.
189. Lotery AJ, Gibson J, Cree AJ, et al. Pharmacogenetic associations with vascular endothelial growth factor inhibition in participants with neovascular age-related macular degeneration in the IVAN Study. *Ophthalmology*. 2013;120(12):2637–2643.
190. Klein ML, Francis PJ, Rosner B, et al. CFH and LOC387715/ARMS2 genotypes and treatment with antioxidants and zinc for age-related macular degeneration. *Ophthalmology*. 2008;115(6):1019–1025.
191. Awh CC, Hawken S, Zanke BW. Treatment response to antioxidants and zinc based on CFH and ARMS2 genetic risk allele number in the Age-Related Eye Disease Study. *Ophthalmology*. 2015;122(1):162–169.
192. Awh CC, Lane AM, Hawken S, et al. CFH and ARMS2 genetic polymorphisms predict response to antioxidants and zinc in patients with age-related macular degeneration. *Ophthalmology*. 2013;120(11):2317–2323.
193. Chew EY, Klein ML, Clemons TE, et al. Genetic testing in persons with age-related macular degeneration and the use of the AREDS supplements: to test or not to test? *Ophthalmology*. 2015;122(1):212–215.
194. Chew EY, Klein ML, Clemons TE, et al. No clinically significant association between CFH and ARMS2 genotypes and response to nutritional supplements: AREDS report number 38. *Ophthalmology*. 2014;121(11):2173–2180.
195. Seddon JM, Silver ES, Rosner B. Response to AREDS supplements according to genetic factors: survival analysis approach using the eye as the unit of analysis. *Br J Ophthalmol*. 2016;100:1731–1737.

67

Pathogenetic Mechanisms in Early Age-Related Macular Degeneration

Alan Bird

Introduction

Age-related macular degeneration (AMD) can be divided into early and late stages. In early disease, visual acuity is good, and in the fundus, focal deposits, called drusen, are seen in Bruch's membrane. The distribution and size of drusen varies from one patient to another, although their attributes are highly concordant between eyes of an individual implying that their morphology reflects the risk factors of disease in that individual. There may also be pigmentary changes at the level of the retinal pigment epithelium (RPE).

The three forms of late AMD cause loss of central vision. With few exceptions[1] the most common form is choroidal neovascularization (CNV), in which blood vessels grow inwards from the choroid into or through Bruch's membrane. Detachment of the retinal pigment epithelium (PED), in which there is accumulation of fluid between the RPE and Bruch's membrane, is relatively uncommon. In geographic atrophy (GA) there is well-defined loss of RPE and photoreceptor cells.

It is generally considered that GA is the default pathway of the disease process of early AMD, and that CNV occurs as a reactive event during the evolution of early changes. The treatment of CNV is well established and is described elsewhere in this book. If the default pathway of early AMD to GA is correct, it would be expected that GA would follow at some stage following successful treatment of CNV, and there is evidence to support this conclusion.[2,3] There is no well-recognized treatment whereby the disease mechanisms inducing transition from early AMD to GA can be modified.

The structures involved in the early AMD are the photoreceptor cells in the outer retina, the RPE, Bruch's membrane, and the capillary bed in the inner choroid (choriocapillaris). In early AMD changes occur in all these tissues throughout the eye, although they are most marked at the macula that subserves central vision in which there is a high density of cones. The changes in each of these

tissues represent a potential target for treatment based on the current understanding of the relevant pathogenic mechanisms. In this chapter changes in each tissue will be described and the logic of the various therapeutic approaches will be discussed.

Structural Changes

Choroid

In the young, the choroidal capillary bed is formed of a sinusoidal complex in which the capillary bed is fenestrated and lacks tight junctions. It is believed that the nature of the choriocapillaris is determined largely by the constitutive expression of vascular endothelial growth factor (VEGF) outwards by the RPE toward the choroid.[4–8] In one morphometric study it was found that the density of the choriocapillaris decreases with age in eyes without AMD[9] and choroidal casts have shown that the capillary bed may become tubular.[10] With advanced AMD, loss or narrowing of the choriocapillaris may become more marked.[11–16]

A clue as to possible clinical detection of change in the choriocapillaris came from studies of Sorsby fundus dystrophy, a monogenic disorder characterized by major thickening of Bruch's membrane and a prolonged choroidal filling phase on fluorescein angiography.[17] It was thought that the diffusely thickened Bruch's membrane represented a barrier to diffusion of VEGF towards the choroid resulting in changes in the capillary bed to a tubular state and with loss of fenestrae such that acquisition of fluorescence of the inner choroid is irregular and delayed.[18,19] This angiographic sign has also been identified in patients with AMD.[20] It is not known whether this sign indicates only change in circulation, or if slow egress of dye into the extravascular space is due largely to loss of fenestrae; poor diffusion through lipid-laden tissues may also contribute to this angiographic abnormality. The potential significance of this clinical sign has been established by demonstrating discrete areas of scotopic threshold elevation of up to 3.4 log units and slow dark adaptation, which corresponded closely to regions of choroidal perfusion abnormality.[21,22] Loss of photopic function was less marked. Subsequent studies have also

shown that the recovery from bleaching is prolonged[23] and the functional loss has an impact on daily tasks.[24]

Therapeutic Implications

It is most likely that modification of the choroid in AMD is a response to alteration of neighboring tissues rather representing an intrinsic change, although the consequent reduction of metabolic supply to the outer retina may play a contributory role in the generating of disease. However, the possibility that choroidal changes occur independently of changes in other tissues cannot be excluded. This is not seen as a good target for therapy currently.

Bruch's Membrane

A direct relationship between aging and thickness of Bruch's membrane has been established both by electron and light microscopy,[25,26] and in one study the correlation coefficients (R^2) were only 0.57 and 0.32, respectively, with great variation in the elderly.[27] Thus about half of the change in thickness must be explained by factors other than age, such as genetic or environmental influences. In AMD the thickening is greater than with aging alone due to accumulation of material internal to the inner collagenous layer that has been termed the basal laminar deposit.[28]

Several studies on the nature of the deposits have been undertaken. Consequent upon discussion of the pathogenesis of PEDs, it was hypothesized that reduction of the hydraulic conductivity of Bruch's membrane would hamper movement of water towards the choroid, thus causing it to accumulate in the sub-RPE space.[29] This demands that Bruch's membrane contains a high lipid content that would increase the resistance of fluid flow. A series of investigations followed to test this hypothesis and support was derived from both histopathologic, biochemical, biophysical, and clinical observations. A study of frozen tissue undertaken using histochemical staining on human eyes with an age range between 1 and 95 years showed accumulation of lipids with age that varied greatly both in the quantity and form of lipids in the elderly.[30] Some eyes stained for neutral lipids alone, some stained predominantly

for phospholipids, and others stained equally for both neutral lipids and phospholipids. To confirm these conclusions, material extracted by universal lipid solvents from tissue of eye-bank fresh eyes was analyzed by thin layer and gas chromatography.[31,32] After separation, the chemical species were identified by mass spectroscopy, which included fatty acids, cholesterol esters, triglycerides, and phospholipids. This study confirmed the conclusion that the quantity of total lipid in Bruch's membrane increases with age. Little or no lipid was extracted from specimens from donors younger than 50 years of age. In specimens from donors older than 50 years, the increase was exponential. Eyes from donors over the age of 60 years showed wide variation of total lipid extracted from donors of similar age, and that the ratio of phospholipids to neutral fats was different from one specimen to another. The ratio of neutral lipids to phospholipids did not correlate with the total quantity of lipid. The finding that the major lipid species were phospholipids and fatty acids rather than cholesterol and cholesterol esters, and that only 50% of the phospholipids was phosphatidylcholine, led to the conclusion that the lipids were of a cellular (presumably RPE) rather than plasma origin.[32] Curcio and coworkers, using different extraction methods, reported that cholesterol and cholesterol esters were the major lipids rather than phospholipids.[33] As in the previous study, however, it was concluded that the lipids were of RPE origin on the basis of the nature of the cholesterol. Unlike atheroma, there was little free cholesterol.

Finally, measurements of hydraulic conductivity of Bruch's membrane showed that it becomes reduced with age,[34,35] and after the age of 50 years there is a close direct linear relationship between resistance of fluid flow and lipid content.

Clinical observations were sought to support the concept that the biochemical content as well as thickness of Bruch's membrane influenced subsequent clinical behavior. It was hypothesized that drusen that are hyperfluorescent on fluorescein angiography must be hydrophilic allowing free diffusion of water-soluble sodium fluorescein into the abnormal deposit and that there would be binding of dye to polar molecules. By contrast, if the drusen were hypofluorescent it would imply that they are hydrophobic due to

the presence of neutral lipids. This conclusion was supported by histologic observations in which it was shown that in vitro binding of sodium fluorescein correlated well with the biochemical contents of drusen as shown by histochemistry.[36] Drusen rich in neutral lipids did not bind fluorescein, whereas those with little lipid content bound fluorescein strongly.

It would be predicted that the highest resistance to water flow and diffusion in Bruch's membrane would be found in eyes destined to suffer tears of the detached RPE, in which there is sufficient tangential stress in the detached tissues to cause them to rupture. The slow accumulation of fluorescein in the sub-RPE space in those destined to tear supports this concept. The determination that a tear in one eye implied high risk of a similar event occurring in the fellow eye[37] provided the opportunity to test the concept further. A comparison was made of the drusen in the fellow eye of a tear with those of the fellow eye of one with visual loss due to subretinal neovascularization. It was shown that the drusen were larger, more confluent, and less fluorescent on angiography in the former group than in the latter.[38] Thus, there is good reason to believe that thickening and lipid accumulation in Bruch's membrane would hamper movement of metabolites and water between the RPE and choroid.

There is considerable lipid trafficking through Bruch's membrane, and lipids are believed to accumulate as they fail to pass freely through a thickened Bruch's membrane. This demands that Bruch's membrane becomes thicker as a prerequisite for this lipid accumulation. Analysis has been undertaken of proteins in aging Bruch's membrane since this is likely to initiate the thickening. Recent studies have shown that several of the proteins associated with the immune system, such as C3, C5b–C9, and complement factor H (CFH), are present in high quantity in Bruch's membrane in AMD.[39] These observations serve to underline the potential significance of a disordered immune system to AMD. However, unlike inflammation elsewhere there is no infiltration by inflammatory cells in the absence of CNV. Beta-amyloid has also been identified.[40] In the inner part of Bruch's membrane there are high levels of vitronectin.[41–43] The origin of the proteins is in doubt given that there is RPE expression of some of the constituents

although a major contribution may come from plasma. Furthermore, there is no certainty as to the mechanisms causing accumulation and stabilization of the proteins. The state of the proteins is unknown, but circumstantial evidence suggests that they are oligomerized[44] and that oligomerization may be generated by high levels of zinc or other metallic ions. In Bruch's membrane the levels of zinc are very high.[45] The levels of bioavailable zinc are many times that necessary to cause oligomerization of CFH in vitro, and oligomerization occurs at even lower levels if CFH is mixed with C3.[46] Thus the proteins may not have the biological properties of the monomers. Withdrawal of zinc reverses the polarization.

A recent report describes the presence of spherules of hydroxyapatite round cholesterol-rich cores in Bruch's membrane that may be an additional factor inducing protein accumulation.[47] These spherules had been described previously, but their nature had not been established. It has been shown that these spherules become covered by proteins that may be different from one spherule to another, and it was argued that these spherules may act as an initiator of oligomerization.

Further insight into the possible mechanisms of accumulation of material in Bruch's membrane was derived from observation in the $CFH^{-/-}$ mouse.[48] It is acknowledged that a gene knockout is not necessarily homologous with a polymorphism, that the immune system in mouse is dissimilar from human and mouse does not have a macula. However, if reduction of CFH activity is important, as has been concluded from genetic studies, the observations may help in understanding AMD. In this mouse there is thickening of the renal glomerulus basement membrane, but surprisingly, Bruch's membrane was thinner than in age-matched mice. This implies that dysregulation of the immune system alone may not explain thickening of Bruch's membrane and that the presence of the CFH protein itself may be important to the process.

Therapeutic Implications

If thickening of Bruch's membrane and impedance of metabolic exchange and fluid movement is important to the pathogenesis of AMD, several therapeutic approaches might be considered. Reduction of the availability of the constituent proteins may slow

the disease process, such as might be achieved with the chronic use of antiinflammatory agents. Once thickening is established, mobilizing lipids or breaking down the oligomers may be achieved with the use of antibodies or possibly zinc buffers, as has been suggested in Alzheimer's disease.[49] There might be potential risks in rapid generation of monomers.[50] Alternatively, the lipids might be mobilized. All these approaches would increase hydraulic conductivity and improve metabolic exchange between the RPE and choriocapillaris. In addition, it may induce an increase in choroidal circulation and in the density of fenestrae.

The Retinal Pigment Epithelium

Accumulation of residual bodies that fluoresce can be used as an index of age change in the RPE. A quadratic relationship exists in donor eyes between age, and both autofluorescence and residual body quantity as measured by autofluorescence imaging as seen by light microscopy and electron microscopy, respectively.[27] The slowing of accumulation in the elderly was not surprising since the population of photoreceptors decreases in late life.[51] The relationship between age and autofluorescence, however, is not close, with an adjusted R^2 of only 0.45, and for residual bodies the R^2 was 0.50,[27] reflecting the wide variation in the eyes from elderly donors. Thus 50% of the variation in either autofluorescence or residual bodies is not explained by aging, the suspicion being that genetic or environmental factors would play a role in determining the variance. Most surprising was the relationship between autofluorescence and residual body volume. The relationship was direct, which would have been expected since it is from the residual bodies that the autofluorescence is derived. However, the R^2 was only 0.26. In retrospect, the variation between specimens should not have been surprising since only a small proportion of the material in residual bodies fluoresces, and this proportion may be influenced by circumstances such as vitamin A content in diet. If rodents are given a diet low in vitamin A the residual bodies do not fluoresce, whereas in littermates given a diet high in vitamin A the residual content of the RPE is similar but they fluoresce brightly.[52] From this observation it might be concluded that those with high

autofluorescence levels had a diet high in vitamin A.

The clinical relevance of these findings is underlined by the ability now to image RPE autofluorescence in vivo through the efforts of Fitzke and von Rückmann.[53] This was achieved initially using a confocal scanning laser ophthalmoscope with an excitation wavelength of 488 nm. Emission is recorded above 514 nm by inserting a barrier filter. The evidence that the signal originates from lipofuscin in the RPE is derived from the work of Delori and coworkers.[54] The spectral nature of the signal is characteristic of lipofuscin and is derived from internal to the choroid and external to the neurosensory retina. It has been shown that in early AMD the distribution of autofluorescence varies from one patient to another. In about half of eyes with early AMD, autofluorescence is homogeneous, whereas in the remainder, diffusely irregular or focally increased autofluorescence is seen.[55,56] Drusen do not appear to explain the differences, since apart from serogranular drusen at the fovea, drusen in AMD do not influence autofluorescence significantly. It has been shown that in bilateral early AMD the pattern of autofluorescence is symmetric, implying that the autofluorescence characteristics reflect the form of disease in an individual that may be determined by the genetic or environmental influences. In patients with unilateral visual loss from AMD, focal increased autofluorescence in the good eye is associated with GA in the other eye and predicts the development of GA in the good eye.[56] This impression was reinforced by the observation that if a high level of autofluorescence is found around the perimeter of GA, this area becomes atrophic within one year,[57] whereas cases without marginal hyperautofluorescence tend not to have progression of their GA.

The underlying molecular mechanisms by which changes in the RPE result in the development of GA have been subject to debate. It has been argued that the cytoplasmic volume occupied by the residual bodies may interfere with cell metabolism.[58] It has been shown that lipofuscin is a free radical generator and that may cause cell damage.[59] In addition, there is evidence for toxic effects of individual lipofuscin compounds. A2-E, a Schiff-base product of retinaldehyde and ethanolamine, has surfactant-like properties on biomembranes that have been shown in one study to increase

intralysosomal pH by inhibition of the ATP-dependent lysosomal proton pump that in turn would inhibit activity of lysosomal hydrolases.[60] Furthermore, A2-E has been shown to cause leakage of lysosomes in vitro.[61] Release of lysosomal content may cause further RPE cell dysfunction and cell death. Another study failed to confirm a rise in lysosomal pH, possibly because lower quantities of lipofuscin were used, but it did show that lipid degradation was reduced.[62] Thus, both studies imply that lipofuscin reduces the activity of phagolysosomal enzymes.

The possible consequences of reduced RPE lysosomal degradation have been investigated in vivo. Interference with degradation of lysosomes was achieved in 11-week-old Sprague–Dawley rats by injection of 5 μL of a lysosomal protease inhibitor, E-64 (2.22 μM), intravitreally.[63] A single injection of E-64 caused a transient accumulation of phagolysosome-like inclusion bodies in the RPE. Furthermore, two or three injections on alternate days caused greater accumulation of these inclusions associated with changes in intracellular organelles such as loss of smooth endoplasmic reticulum and of RPE cell conformation. This was accompanied by shortening and loss of photoreceptor outer segments without prior dysmorphic changes, photoreceptor loss, reduction of fenestrae in the choroidal capillaries, and invasion of Bruch's membrane by fibroblasts and pericytes. Intravitreal injection of vehicle for comparison induced no such structural changes.

It was considered likely that the changes in the RPE reflected reduced metabolism of lipids and reduction of basolateral VEGF expression caused the loss of fenestrae. The shortening and loss of the outer segments was thought to be due to impaired morphogenesis of disc membranes rather than a direct effect of E-64 on photoreceptor cells, because there was no vesiculation of disc membranes. The shortening of the OS could be explained by the lack of available lipids due to the inability of the RPE to break down and recycle the contents of the phagosome. The findings imply greater dependence upon the availability of products of phagosomal degradation for OS renewal than was previously considered, and that acquisition of plasma-derived material is insufficient to sustain this process fully. The ability of the RPE to

recycle lipids has been well illustrated.[64,65] The observed changes in rats are similar in many respects to age changes in RPE, photoreceptor, and choroid in humans, although there are major differences between such an acute experiment and the consequences of lifelong metabolic activity, and species differences between rat and human.

Thus, both experimental evidence and clinical observations illustrate a potential pathogenetic mechanism of GA and explain the association of GA with focal increased autofluorescence if the latter is witness to the inability to recycle phagosomal contents.

Another potential intriguing consequence of the presence of lipofuscin is the demonstration that photodegradation products of the fluorophore induce the complement cascade that may be relevant to Bruch's membrane thickening.[66]

Measurement of visual function over areas of increased autofluorescence showed loss of scotopic function that was much greater than photopic, and that the loss was as great as 3.5 log units.[67] The question as to whether the loss is due to cell loss or cell dysfunction was not addressed.

In addition it has been shown that RPE mitochondrial damage is severe in some eyes from elderly donors,[68, 69] although the relevance of this finding to RPE and photoreceptor cell loss has not been investigated to date.

Therapeutic Implications

If increased lipofuscin is important to genesis of GA, it would argue against dietary supplementation with vitamin A or its precursors. Efforts are now underway to reduce the accumulation of lipofuscin therapeutically by restricting the availability of vitamin A to the retina. Initial results have shown the potential benefits of this approach in the ABCA4 knockout mouse[70,71] and trials in humans have been initiated.[72] Agents that increase lysosomal activity or lower phagolysosomal pH might also be effective. On theoretic grounds light restriction might also be helpful. In addition illumination with near infrared light may improve mitochondrial function that would address the RPE deficit in those in whom this is a problem.[73]

Outer Retina

Relative to other structures there has been little attention paid to physical changes in the neurosensory-retina in AMD. This is surprising since in early histologic studies it was concluded that photoreceptor cell loss occurs progressively in early AMD, although it was thought that this may occur as a consequence of RPE dysfunction.[74,75] Considerable evidence exists to support the conclusion that photoreceptor loss occurs early in the course of disease in some and that disease mechanisms internal to the RPE are important in early AMD.

Three papers report findings from ocular coherence tomography in patients with GA.[76–78] Areas of the fundus beyond the edge of atrophy in which the retina appeared unexceptional by ophthalmoscopy were imaged to determine the thickness of the photoreceptor layer. In some subjects there was an abrupt change from the lack of photoreceptor cells in the area of atrophy, to a normal thickness outer nuclear layer. However, in others there was evidence of major photoreceptor loss for a considerable distance beyond the edge of GA.

Several studies have been undertaken on functional attributes in early AMD. All report that there is a major loss of scotopic sensitivity and less profound loss of photopic sensitivity in a proportion.[21,23,67,79–88] In none of these studies was the question addressed as whether the loss was due to photoreceptor loss or photoreceptor dysfunction.

Observations in the CFH knockout mouse may also be relevant to photoreceptor cell loss in AMD.[48] It had been shown that visual function was reduced when compared with age-matched mice despite the lack of expected Bruch's membrane thickening. In these mice, the photoreceptor outer segments were dysmorphic and there was increased C3 expression in the outer retina. The relevance of C3 to outer segment morphology or of disease mechanism inducing high levels of C3 is unknown. As a result of these observations it was concluded that the consequences of the high-risk CFH polymorphism might not be restricted to its influence upon Bruch's membrane. Of possible relevance is that RPE expression of CFH in vitro appears to be apically into the outer retina rather than through the basolateral domain into the choroid.[89] These observations raise

the possibility that there is a role played by the immune system in photoreceptor health, and that disturbance of the immune system may cause demise of photoreceptor cells that is unrelated to changes in Bruch's membrane or the RPE. It is also of interest that some have failed to reproduce the findings in the knockout mouse. There is a suspicion that the changes may not occur in a pathogen-free animal house.

Further evidence of a pathogenetic component of AMD internal to the RPE was originally described in 1990 as an irregular appearance on blue light reflection.[90] It is believed that this is associated with deposits internal to the RPE termed reticular pseudodrusen.[91] The material has not been fully characterized but is stated not to be lipid-rich, and to contain cholesterol but not cholesterol esters; in these respects they differ from deposits external to the RPE.[92]

A recent histopathologic study has been undertaken on donor eyes with GA[93] examining the same question as had been addressed with optical coherence tomography (OCT). It was shown that for a considerable distance beyond the edge of GA there was major photoreceptor loss in a majority of eyes (Figs. 67.1 and 67.2). The only photoreceptors were cones, there were no outer segments, and a few cones had inner segments. In addition, in three donor eyes with early AMD the outer nuclear layer was reduced to 2–3 layers. As a consequence it was concluded that the visual loss in early AMD is due to photoreceptor loss at least in part. In addition, measuring the area of GA is not a good measure of photoreceptor survival.

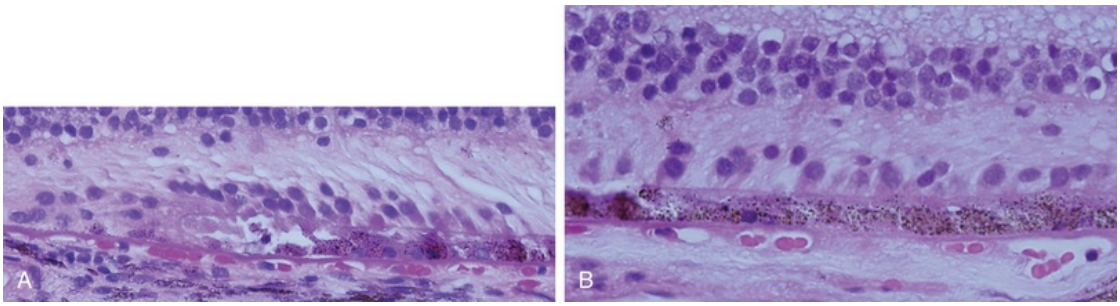

FIG. 67.1 Light micrograph of a 70-year-old donor with geographic atrophy (GA) showing that photoreceptor cells are restricted to a few cones with inner segments

only beyond the edge of GA (*arrow*) (A). Over a distance of 1400 µm only cones with few inner segments are seen (B). There is little Bruch's membrane thickening, the choriocapillaris is well perfused throughout, and the RPE is unexceptional physically.

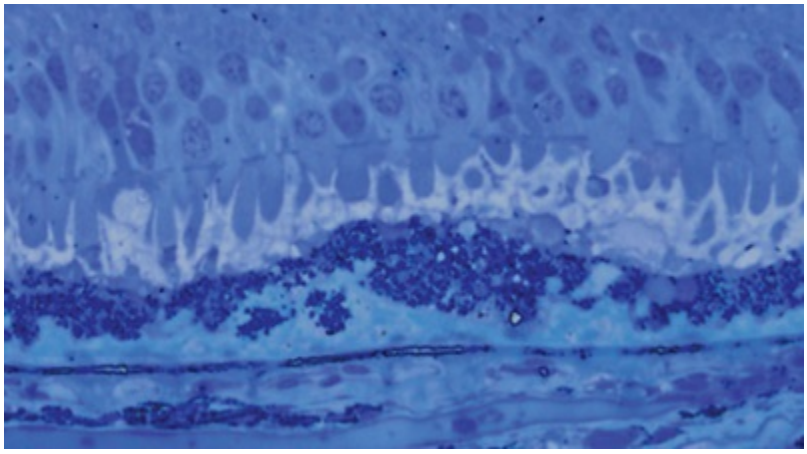

FIG. 67.2 Light micrograph of a 78-year-old female donor in whom geographic atrophy (GA) had been diagnosed. Some distance from the edge of GA, there is marked loss of photoreceptor cells, Bruch's membrane is very thick due largely to the presence basal laminar deposits, and the choriocapillaris is not perfused.

Therapeutic Implications

Preservation of the photoreceptor cells might be best achieved by improving RPE function by reduction of accumulation of lipofuscin that may be achieved through manipulation of bisretinoid formation in the photoreceptor outer segment. Restriction of vitamin A availability presumably would achieve this end. Neuroprotective agents might be of benefit as has been hypothesized in the treatment of glaucoma.[94] Such an approach might slow or prevent photoreceptor cell loss, and this has been attempted with the use of a slow-release device that uses cells embedded in a matrix that express ciliary neurotrophic factor (CNTF).[95] There is early indication that this may be successful in the

management of retinitis pigmentosa.[96] The relevance of the immune system to retinal health and immune dysfunction to generation of AMD are unknown but may represent a target for therapy in future.

Balance of Tissue Change in Early AMD

In the histopathology study,[93] great variation was shown in changes in the various tissues involved in AMD pathogenesis (Figs. 67.1 and 67.2). When a comparison was made between autofluorescence derived from the RPE and basal laminar thickness, an inverse relationship was found between the two. This is understandable since thickening of Bruch's membrane would represent a barrier to diffusion from choroid to the RPE and restrict availability of vitamin-A to the retina, although other explanations may account for this. It was also the case that some of the eyes examined had profound photoreceptor cells loss without manifest physical change in either Bruch's membrane or the RPE (Fig. 67.1). This implies that in some cases photoreceptor loss may occur due disease mechanisms internal to the RPE.

Conclusion

In age-related macular degeneration, changes occur in the choroid, Bruch's membrane, the RPE, and outer retina. Both genetic and environmental influences have been identified as conferring risk of disease and presumably initiate disease through their cumulative effect. However, there is doubt as to tissues primarily affected by these factors. It is clear that the balance of changes in the various tissues varies from one case to another, which is not surprising given that the factors conferring risk vary from one case to another. Thus in some individuals Bruch's membrane thickening may be the most threatening change, whereas it may be the RPE alterations in others. It is also possible that photoreceptor loss may not be due to structural or functional change of either the RPE or Bruch's membrane in some cases but is a consequence of an abnormality

limited to the outer retina. If correct, therapy directed to one aspect of the disorder should be reserved to those in whom the specific tissue is the primary threat to photoreceptor survival. To achieve this goal it would be necessary to have knowledge of changes in the various tissues involved. If it is shown that the phenotype correlates well with genetic risk variants, genetic testing may be used to select cases for a specific therapeutic approach.

The photoreceptor population could be assessed using imaging such as OCT, or visualization of the photoreceptor cells with adaptive optics. The same objective could be achieved using psychophysics means such as visual field recording, microperimetry, or fine matrix mapping. Assessment of the concentration of bleachable rhodopsin using reflectometry might be the most effective method of determining the population of viable photoreceptor cells.[97,98] Whatever testing device is used, it would be important to assess the scotopic, as well as the photopic, system. The health of the RPE might be assessed by measuring absolute levels of autofluorescence. Such measurements are aided by the use of an internal standard in the imaging device.[99] An external standard would be ideal, although it is not clear how this could be achieved. There is some doubt as to whether or not the thickness of Bruch's membrane could be measured in vivo, but it is likely that the state of the choroid is determined by access of VEGF expressed outward by the RPE. Thus choroidal thickness and choriocapillaris flow would be influenced by the biophysical properties of Bruch's membrane. Both these have been measured recently, although variation in normal subjects has yet to be fully established. Characterization of disease in this way would be important in selecting patients for a specific therapeutic approach and in monitoring the response to treatment. Without segregation of cases on the basis of phenotype, effective treatment of a component may not be evident in treatment trials since the treatment would only be appropriate to a proportion of cases recruited to the trial. It is true that the tissues are metabolically interdependent and modulation of age change in one tissue may have secondary benefits on its neighbors.

Some treatments may modify progress of disease in a large proportion of cases. The main purpose of any treatment is

preservation of function such that neuroprotection may be appropriate whatever the nature of disease. Similarly, modulation of the immune system may be of benefit in a wide range of AMD although systemic treatment may not influence complement-induced changes internal to the RPE.

The presence of drusen has been used to recruit patients to all the clinical studies to date. This ignores diffuse thickening of Bruch's membrane, abnormal autofluorescence from the RPE, and photoreceptor loss. In particular, reticular pseudodrusen, which is undoubtedly a part of AMD, may occur in the absence of drusen such that this form of disease would be underrepresented in studies. Recently, a functional study of subjects over the age of 60 years with normal ocular fundi revealed abnormal recovery from bleach in a proportion of subjects.[100] Whether or not they are manifesting AMD is open to debate, but if OCT shows photoreceptor loss, it would be reasonable to conclude that they do so. Thus studies of AMD are incomplete, and it would be good to see the entry criteria being enlarged in future research projects.

References

1. Jonasson F, Arnarsson A, Sasaki H, et al. The prevalence of age-related maculopathy in Iceland: Reykjavik eye study. *Arch Ophthalmol*. 2003;121:379–385.
2. Grunwald JE, Daniel E, Huang J, et al. Risk of geographic atrophy in the comparison of age-related macular degeneration treatments trials. *Ophthalmology*. 2014;121:150–161.
3. Kurihara T, Westenskow PD, Bravo S, et al. Targeted deletion of Vegfa in adult mice induces vision loss. *J Clin Invest*. 2012;122:4213–4217.
4. Korte GE, Repucci V, Henkind P. RPE destruction causes choriocapillary atrophy. *Invest Ophthalmol Vis Sci*. 1984;25:1135–1145.
5. Blaauwgeers HG, Holtkamp GM, Rutten H, et al. Polarized vascular endothelial growth factor secretion by human retinal pigment epithelium and localization of vascular endothelial growth factor receptors on the inner

choriocapillaris: evidence for a trophic paracrine relation. *Am J Pathol*. 1999;155:421–428.
6. Kannan R, Zhang N, Sreekumar PG, et al. Stimulation of apical and basolateral VEGF-A and VEGF-C secretion by oxidative stress in polarized retinal pigment epithelial cells. *Mol Vis*. 2006;12:1649–1659.
7. Saint-Geniez M, Kurihara T, Sekiyama E, et al. An essential role for RPE-derived soluble VEGF in the maintenance of the choriocapillaris. *Proc Natl Acad Sci USA*. 2009;106:18751–18756.
8. McLeod DS, Grebe R, Bhutto I, et al. Relationship between RPE and choriocapillaris in age-related macular degeneration. *Invest Ophthalmol Vis Sci*. 2009;50:4982–4991.
9. Ramrattan RS, van der Schaft TL, Mooy CM, et al. Morphometric analysis of Bruch's membrane, the choriocapillaris, and the choroid in aging. *Invest Ophthalmol Vis Sci*. 1994;35:2857–2864.
10. Olver J. Quoted by AC Bird in: Therapeutic targets in age-related macular disease. *J Clin Invest*. 2010;120:3033–3041.
11. Hogan MJ. Macular diseases, pathogenesis: electron microscopy of Bruch's membrane. *Trans Am Acad Ophthalmol Otolaryngol*. 1965;69:683–690.
12. Green WR, Key SN. Senile macular degeneration: a histopathol study. *Trans Am Ophthalmol Soc*. 1977;75:180–250.
13. Sarks SH. *Changes in the region of the choriocapillaris in aging and degeneration. 23rd Concilium on Ophthalmology*. [Kyoto] 1978:228–238.
14. Lindner M, Bezatis A, Czauderna J, et al. Choroidal thickness in geographic atrophy secondary to age-related macular degeneration. *Invest Ophthalmol Vis Sci*. 2015;56:875–882.
15. Yiu G, Chiu SJ, Petrou PA, et al. Relationship of central choroidal thickness with age-related macular degeneration status. *Am J Ophthalmol*. 2015;159:617–626.
16. Tso MOM. Pathogenetic factors of aging macular degeneration. *Ophthalmology*. 1985;92:628–635.
17. Polkinghorne PJ, Capon MR, Berninger TA, et al. Sorsby's

fundus dystrophy: a clinical study. *Ophthalmology*. 1989;96:1763–1768.
18. Meves H. Die pathologisch-anatomischen gefassveranderungen des Auges bei der beningen und malingen Nephrosklerose. *Albrecht Von Graefes Arch Ophthalmol*. 1948;168:287.
19. Friedman E, Smith TR, Kuwabara T, et al. Choroidal vascular patterns in hypertension. *Arch Ophthalmol*. 1964;71:842.
20. Pauleikhoff D, Chen JC, Chisholm IH, et al. Choroidal perfusion abnormalities in age related macular disease. *Am J Ophthalmol*. 1990;109:211–217.
21. Chen JC, Fitzke FW, Pauleikhoff D, et al. Functional loss in age-related Bruch's membrane change with choroidal perfusion defect. *Invest Ophthalmol Vis Sci*. 1992;33:334–340.
22. Steinmetz RL, Haimovici R, Jubb C, et al. Symptomatic abnormalities of dark adaptation in patients with age-related Bruch's membrane change. *Br J Ophthalmol*. 1993;77:549–554.
23. Owsley C, Jackson GR, White M, et al. Delays in rod-mediated dark adaptation in early age-related maculopathy. *Ophthalmology*. 2001;108:1196–1202.
24. Scilley K, Jackson GR, Cideciyan AV, et al. Early age-related maculopathy and self-reported visual difficulty in daily life. *Ophthalmology*. 2002;109:1235–1242.
25. Green WR, Key SN. Senile macular degeneration: a histopathol study. *Trans Am Ophthalmol Soc*. 1977;75:180–250.
26. Ramrattan RS, van der Schaft TL, Mooy CM, et al. Morphometric analysis of Bruch's membrane, the choriocapillaris, and the choroid in aging. *Invest Ophthalmol Vis Sci*. 1994;35:2857–2864.
27. Okubo A, Rosa RH, Bunce KV, et al. The relationships between age changes in retinal pigment epithelium and Bruch's membrane. *Invest Ophthalmol Vis Sci*. 1999;40:443–449.
28. Curcio CA, Millican CL. Basal linear deposit and large drusen are specific for early age-related maculopathy. *Arch*

Ophthalmol. 1999;117:329–339.
29. Bird AC, Marshall J. Retinal pigment epithelial detachments in the elderly. *Trans Ophthalmol Soc U K*. 1986;105:674–682.
30. Pauleikhoff D, Harper CA, Marshall J, et al. Aging changes in Bruch's membrane: a histochemical and morphol study. *Ophthalmology*. 1990;97:171–178.
31. Holz FG, Sheraidah G, Pauleikhoff D, et al. Analysis of lipid deposits extracted from macular and peripheral Bruch's membrane. *Arch Ophthalmol*. 1994;112:402–406.
32. Sheraidah G, Steinmetz R, Maguire J, et al. Correlation between lipids extracted from Bruch's membrane and age. *Ophthalmology*. 1993;100:47–51.
33. Li CM, Chung BH, Presley JB, et al. Lipoprotein-like particles and cholesteryl esters in human Bruch's membrane: initial characterization. *Invest Ophthalmol Vis Sci*. 2005;46:2576–2586.
34. Moore DJ, Hussain AA, Marshall J. Age related variation in the hydraulic conductivity of Bruch's membrane. *Invest Ophthalmol Vis Sci*. 1995;36:1290–1297.
35. Starita C, Hussain AA, Patmore A, et al. Localization of the site of major resistance to fluid transport in Bruch's membrane. *Invest Ophthalmol Vis Sci*. 1997;38:762–767.
36. Pauleikhoff D, Zuels S, Sheraidah G, et al. Correlation between biochemical composition and fluorescein binding of deposits in Bruch's membrane. *Ophthalmology*. 1992;99:1548–1553.
37. Chuang EL, Bird AC. Bilaterality of tears of the retinal pigment epithelium. *Br J Ophthalmol*. 1988;72:918–920.
38. Chuang EL, Bird AC. The pathogenesis of tears of the retinal pigment epithelium. *Am J Ophthalmol*. 1988;105:185–190.
39. Hageman GS, Luthert PJ, Victor Chong NH, et al. An integrated hypothesis that considers drusen as biomarkers of immune-mediated processes at the RPE–Bruch's membrane interface in aging and age-related macular degeneration. *Prog Retin Eye Res*. 2001;20:705–732.
40. Yoshida T, Ohno-Matsui K, Ichinose S, et al. The potential role of amyloid beta in the pathogenesis of age-related macular degeneration. *J Clin Invest*. 2005;115:2793–2800.

41. Hageman GS, Mullins RF, Russell SR, et al. Vitronectin is a constituent of ocular drusen and the vitronectin gene is expressed in human retinal pigmented epithelial cells. *FASEB J*. 1999;13:477–484.
42. Lommatzsch A, Hermans P, Weber B, et al. Complement factor H variant Y402H and basal laminar deposits in exudative age-related macular degeneration. *Graefes Arch Clin Exp Ophthalmol*. 2007;245:1713–1716.
43. Wasmuth S, Lueck K, Baehler H, et al. Increased vitronectin production by complement-stimulated human retinal pigment epithelial cells. *Invest Ophthalmol Vis Sci*. 2009;50:5304–5309.
44. Nan R, Gor R, Gor J, et al. Uncontrolled zinc- and copper-induced oligomerisation of the human complement regulator factor H and its possible implications for function and disease. *J Mol Biol*. 2008 Dec;384:1341–1352.
45. Lengyel I, Flinn JM, Peto T, et al. High concentration of zinc in sub-retinal pigment epithelial deposits. *Exp Eye Res*. 2007;84:772–780.
46. Nan R, Tetchner S, Rodriguez E, et al. Zinc-induced self-association of complement C3b and Factor H: implications for inflammation and age-related macular degeneration. *J Biol Chem*. 2013;288:19197–19210.
47. Thompson RB, Valentina Reffatto V, Bundy JG, et al. Identification of hydroxyapatite spherules provides new insight into subretinal pigment epithelial deposit formation in the aging eye. *Proc Natl Acad Sci USA*. 2015;112:1565–1570.
48. Coffey PJ, Gias C, McDermott CJ, et al. Complement factor H deficiency in aged mice causes retinal abnormalities and visual dysfunction. *Proc Natl Acad Sci USA*. 2007;104:16651–16656.
49. Lovell MA. A potential role for alterations of zinc and zinc transport proteins in the progression of Alzheimer's disease. *J Alzheimers Dis*. 2009;16:471–483.
50. Li W, Chen S, Ma M, et al. Complement 5b-9 complex-induced alterations in human RPE cell physiology. *Med Sci Monit*. 2010;16:17–23.

51. Curcio CA, Medeiros NE, Millican CL. Photoreceptor loss in age-related macular degeneration. *Invest Ophthalmol Vis Sci*. 1996;37:1236–1249.
52. Katz ML, Norberg M. Influence of dietary vitamin A on autofluorescence of leupeptin-induced inclusions in the retinal pigment epithelium. *Exp Eye Res*. 1992;54:239–246.
53. von Rückmann A, Fitzke FW, Bird AC. Distribution of fundus autofluorescence with a scanning laser ophthalmoscope. *Br J Ophthalmol*. 1995;79:407–412.
54. Delori FC, Dorey CK, Staurenghi G, et al. In vivo fluorescence of the ocular fundus exhibits retinal pigment epithelial lipofuscin characteristics. *Invest Ophthalmol Vis Sci*. 1995;36:718–729.
55. von Rückmann A, Fitzke FW, Bird AC. In vivo fundus autofluorescence in age related macular degeneration. *Invest Ophthalmol Vis Sci*. 1997;38:478–486.
56. Lois N, Coco R, Hopkins J, et al. Fundus autofluorescence in patients with age-related macular degeneration and high risk characteristics. *Am J Ophthalmol*. 2002;133:341–349.
57. Holz FG, Bellman C, Staudt S, et al. Fundus autofluorescence and development of geographic atrophy in age-related macular degeneration. *Invest Ophthalmol Vis Sci*. 2001;42:1051–1056.
58. Feeney-Burns L, Eldred GE. The fate of the phagosome: conversion to "age-pigment" and impact in human retinal pigment epithelium. *Trans Ophthalmol Soc U K*. 1984;103:416–421.
59. Rozanowska M, Korytowski W, Rozanowski B, et al. Photoreactivity of aged human RPE melanosomes: a comparison with lipofuscin. *Invest Ophthalmol Vis Sci*. 2002;43:2088–2096.
60. Holz FG, Schutt F, Kopitz J, et al. Inhibition of lysosomal degradative functions in RPE cells by a retinoid component of lipofuscin. *Invest Ophthalmol Vis Sci*. 1999;40:737–743.
61. Schutt F, Bergmann M, Holz FG, et al. Isolation of intact lysosomes from human RPE cells and effects of A2-E on the integrity of the lysosomal and other cellular membranes. *Graefes Arch Clin Exp Ophthalmol*. 2002;240:983–988.

62. Lakkaraju A, Finnemann SC, Rodriguez-Boulan E. The lipofuscin fluorophore A2E perturbs cholesterol metabolism in retinal pigment epithelial cells. *Proc Natl Acad Sci USA*. 2007;104:11026–11031.
63. Okubo A, Sameshima M, Unoki K, et al. Ultrastructural changes associated with accumulation of inclusion bodies in rat retinal pigment epithelium. *Invest Ophthalmol Vis Sci*. 2000;41:4305–4312.
64. Wiegand RD, Koutz CA, Stinson AM, et al. Conservation of docosahexaenoic acid in rod outer segments of rat retina during n-3 and n-6 fatty acid deficiency. *J Neurochem*. 1991;57:1690–1699.
65. Stinson AM, Wiegand RD, Anderson RE. Recycling of docosahexaenoic acid in rat retinas during n-3 fatty acid deficiency. *J Lipid Res*. 1991;32:2009–2017.
66. Zhou J, Kim SR, Westlund BS, et al. Complement activation by bisretinoid constituents of RPE lipofuscin. *Invest Ophthalmol Vis Sci*. 2009;50:1392–1399.
67. Scholl HPN, Bellmann C, Dandekar SS, et al. Photopic and scotopic fine matrix mapping of retinal areas of increased fundus autofluorescence in patients with age related macular degeneration. *Invest Ophthalmol Vis Sci*. 2004;45:574–583.
68. Brennan LA, Kantorow M. Mitochondrial function and redox control in the aging eye: role of MsrA and other repair systems in cataract and macular degenerations. *Exp Eye Res*. 2009;88:195–203.
69. Terluk MR, Kapphahn RJ, Soukup LM, et al. Investigating mitochondria as a target for treating age-related macular degeneration. *J Neurosci*. 2015;35:7304–7311.
70. Radu RA, Mata NL, Nusinowitz S, et al. Treatment with isotretinoin inhibits lipofuscin accumulation in a mouse model of recessive Stargardt's macular degeneration. *Proc Natl Acad Sci USA*. 2003;100:4742–4747.
71. Charbel I, Barnard AR, Hermann P, et al. Rescue of the Stargardt phenotype in Abca4 knockout mice through inhibition of vitamin A dimerization. *Proc Natl Acad Sci USA*. 2015;112:8415–8420.

72. Mata NL, Kichter JB, Vogel R, et al. Investigation of oral fenretinide for treatment of geographic atrophy in age-related macular degeneration. *Retina*. 2013;33:498–507.
73. Gkotsi D, Begum R, Salt T, et al. Recharging mitochondrial batteries in old eyes. Near infra-red increases ATP. *Exp Eye Res*. 2014;122:50–53.
74. Hogan MJ. Role of the retinal pigment epithelium in macular disease. *Trans Am Acad Ophthalmol Otolaryngol*. 1972;76:64–80.
75. Sarks SH. Ageing and degeneration in the macular region: a clinico-pathol study. *Br J Ophthalmol*. 1976;60:324–341.
76. Wolf-Schnurrbusch UEK, Enzmann V, Brinkmann CK, et al. Morphol changes in patients with geographic atrophy assessed with a novel spectral OCT-SLO combination. *Invest Ophthalmol Vis Sci*. 2008;49:3095–3099.
77. Fleckenstein M, Issa PC, Helb HM, et al. High-resolution spectral domain-OCT imaging in geographic atrophy associated with age-related macular degeneration. *Invest Ophthalmol Vis Sci*. 2008;49:4137–4144.
78. Bearelly S, Chau FY, Koreishi A, et al. Spectral domain optical coherence tomography imaging of geographic atrophy margins. *Ophthalmology*. 2009;116:1762–1769.
79. Owsley C, Jackson GR, Cidecyan AV, et al. Psychophysical evidence for rod vulnerability in age-related macular degeneration. *Invest Ophthalmol Vis Sci*. 2000;41:267–273.
80. Jackson GR, Owsley C, Curdio CA. Photoreceptor degeneration and dysfunction in aging and age-related maculopathy. *Ageing Res Rev*. 2002;1:381–396.
81. Owsley C, McGwin G Jr, Jackson GR, et al. Cone- and rod-mediated dark adaptation impairment in age-related maculopathy. *Ophthalmology*. 2007;114:1728–1735.
82. Dimitrov PN, Guymer RH, Zele AJ, et al. Measuring rod and cone dynamics in age-related maculopathy. *Invest Ophthalmol Vis Sci*. 2008;49:55–65.
83. Dimitrov PN, Robman LD, Varsamidis M, et al. Visual function tests as potential biomarkers in age-related macular degeneration. *Invest Ophthalmol Vis Sci*. 2011;52:9457–9469.

84. Clark ME, McGwin G Jr, Neely D, et al. Association between retinal thickness measured by spectral-domain optical coherence tomography (OCT) and rod-mediated dark adaptation in non-exudative age-related maculopathy. *Br J Ophthalmol*. 2011;95:1427–1432.
85. Dimitrov P, Roban LD, Varsamadis M, et al. et al. Relationship between clinical macular changes and retinal function in age-related macular degeneration. *Invest Ophthalmol Vis Sci*. 2012;53:5213–5220.
86. Dimopoulos IS, Tennent M, Johnson A, et al. Subjects with unilateral neovascular AMD have bilateral delays in rod-mediated phototransduction activation kinetics and in dark adaptation recovery. *Invest Ophthalmol Vis Sci*. 2013;54:5186–5195.
87. Jackson GR, Scott IU, Kim IK, et al. Diagnostic sensitivity and specificity of dark adaptometry for detection of age-related macular degeneration. *Invest Ophthalmol Vis Sci*. 2014;55:1427–1431.
88. Steinberg JS, Fitzke FW, Flimmer R, et al. Scotopic and photopic microperimetry in patients with reticular drusen and age-related macular degeneration. *JAMA Ophthalmol*. 2015;133:690–697.
89. Kim YH, He S, Kase S, et al. Regulated secretion of complement factor H by RPE and its role in RPE migration. *Graefes Arch Clin Exp Ophthalmol*. 2009;247:651–659.
90. Mimoun G, Soubrane G, Coscas G. Macular drusen. *J Fr Ophtalmol*. 1990;13:511–530.
91. Zweifel SA, Spaide RF, Curcio CA, et al. Reticular pseudodrusen are subretinal drusenoid deposits. *Ophthalmology*. 2010;117:303–312.
92. Oak AS, Messinger JD, Curcio CA. Subretinal drusenoid deposits: further characterization by lipid histochemistry. *Retina*. 2014;34:825–826.
93. Bird AC, Phillips RL, Hageman GS. Geographic atrophy: a histopathol assessment. *JAMA Ophthalmol*. 2014;132:338–345.
94. Fu QL, Li X, Yip HK, et al. Combined effect of brain-derived neurotrophic factor and LINGO-1 fusion protein on long-

term survival of retinal ganglion cells in chronic glaucoma. *Neuroscience*. 2009;162:375–382.
95. Zhang K, Hopkins JJ, Heier JS, et al. Ciliary neurotrophic factor delivered by encapsulated cell intraocular implants for treatment of geographic atrophy in age-related macular degeneration. *Proc Natl Acad Sci USA*. 2011;108:6241–6245.
96. Talcott KE, Ratnam K, Sundquist SM, et al. Longitudinal study of cone photoreceptors during retinal degeneration and in response to ciliary neurotrophic factor treatment. *Invest Ophthalmol Vis Sci*. 2011;52:2219–2226.
97. Kemp CM, Jacobson SG, Faulkner DJ. Two types of visual dysfunction in autosomal dominant retinitis pigmentosa. *Invest Ophthalmol Vis Sci*. 1988;29:1235–1241.
98. Chuang EL, Sharp DM, Fitzke FW, et al. Retinal dysfunction in central serous retinopathy. *Eye (Lond)*. 1987;1:20–25.
99. Burke TR, Duncker T, Woods RL, et al. Quantitative fundus autofluorescence in recessive Stargardt disease. *Invest Ophthalmol Vis Sci*. 2014;55:2841–2852.
100. Owsley C, Huisingh C, Clark ME, et al. Comparison of visual function in older eyes in the earliest stages of age-related macular degeneration to those in normal macular health. *Curr Eye Res*. 2015;1–7.

68

Age-Related Macular Degeneration

Non-Neovascular Early AMD, Intermediate AMD, and Geographic Atrophy

Adam S. Wenick, Neil M. Bressler, Susan B. Bressler

Introduction

Age-related macular degeneration (AMD) has been the leading cause of legal blindness in patients aged 65 and over,[1] and in 2010 it remained the most common overall cause of blindness in the developed world.[2] Using data from the 2000 census, it has been estimated that in the United States more than 8 million people have specific AMD features that put them at risk for progression to advanced AMD and vision loss.[3,4] Over a 5-year period about 1.3 million of these individuals are predicted to develop the advanced forms of AMD, namely neovascular (NVAMD) or foveal geographic atrophy (FGA).[3] The relative contribution of AMD to the prevalence of visual impairment and blindness in the developed world continues to rise as a direct result of the increasing percentage of elderly persons in the United States and other industrialized countries and due to the improved management of other eye diseases.[2,4–6] Hundreds of thousands of people aged 75 and over in the United States are anticipated to join the pool of people at increased risk of developing advanced AMD over subsequent 5-year periods.[7] Without new treatments or prevention strategies, rates of vision impairment associated with AMD are expected to rise further. By 2020, it has been estimated that 196 million people worldwide will be affected by AMD, increasing to 288 million people by 2040.[8]

Prevalence estimates for the proportion of cases of late AMD due to NVAMD compared to geographic atrophy (GA) (considering GA in any posterior pole location) among Western populations range from almost a 1 : 1 ratio to a 2 : 1 ratio.[4–6] In contrast to earlier studies,[4,9] the most recent comprehensive meta-analysis of population-based data among individuals of European ancestry did not find age-specific differences in the prevalence of NVAMD compared to GA.[10] Prevalence of late AMD (NVAMD or GA) roughly quadruples with each decade beyond age 50.[10] As an example, the predicted prevalence of late AMD rises from 5.2% (95% confidence interval [CI] 3.8–7.1%) to 13.2% (95% CI 9.5–17.6%) for people age ≥60 years as compared to those ≥80 years.[10]

Within the past 10 years novel and improved treatments for the neovascular form of advanced AMD have been adopted throughout the developed world. As such, in the years ahead, the percentage of AMD patients with vision impairment or legal blindness associated

with neovascular AMD is anticipated to decline substantially.[11,12] This effect has already been reported in several recent small population studies citing declining rates of individuals registered as blind from AMD, coinciding with the widespread clinical use of intravitreal anti-vascular endothelial growth factor (VEGF) therapy to manage NVAMD.[13–15] However, despite our current best treatments, due to aging populations, the overall burden of vision loss from both NVAMD and non-neovascular AMD (NNVAMD) is expected to increase.[5,6] The same therapeutic progress has not been made for management of advanced non-neovascular AMD (NNVAMD), namely FGA or GA (located anywhere within the posterior pole). As such, the importance of the later forms of NNVAMD, also known as atrophic AMD, as a leading cause of vision impairment is expected to increase.

A major step toward a better understanding of AMD was taken when Gass[16] clarified that drusen, senile macular degeneration, and senile disciform macular degeneration represented a single disease. Since this time, there has been a lack of consensus regarding terminology used to define AMD and different classification systems have been proposed.[17–20] In 1995, the International Age-Related Maculopathy Study Group devised a classification and grading system for standardizing the terminology and grading used in epidemiologic studies.[18] This classification system has been widely employed and uses the term age-related maculopathy (ARM) for the earlier changes that are presently associated with AMD (drusen and retinal pigment epithelial abnormalities other than GA) and reserves the term AMD for NVAMD or any GA. More recent clinical studies such as the Age-Related Eye Disease Study (AREDS) considered all of these clinical manifestations to be various stages of AMD, omitting the term ARM, while classifying NVAMD and FGA as the advanced forms of AMD. More recent efforts to standardize terminology and classification of AMD have continued in order to assist clinicians and researchers in managing this disease.[19,20] In these more contemporary classification systems, there is early, intermediate, and late AMD. “Late” AMD encompasses NVAMD and GA, that is GA found anywhere within two disc diameters of the foveal center (“any” GA),[19,20] in contrast to the terminology used in AREDS, which restricted inclusion of GA

to FGA when describing advanced AMD.[17]

This chapter is devoted to description of the clinical and histopathologic changes that can occur in the aging macula, which range from what is considered normal aging to the development of more significant drusen and retinal pigment epithelium (RPE) changes that may impair visual function and are considered risk factors for the development of either form of advanced AMD, as well as descriptions of advanced non-neovascular AMD itself. In addition this chapter focuses on the clinical management of this spectrum of macular pathology. Neovascular AMD will be the subject of another chapter (Chapter 69, Neovascular (exudative or "wet") age-related macular degeneration). The term *AMD* will be used to describe alterations that are considered pathologic and distinct from normal aging and that confer risk for the development of late AMD. The term *non-neovascular AMD* (NNVAMD) encompasses any AMD feature(s) in the absence of choroidal neovascularization (CNV) or its sequelae, and the term "dry" AMD will be avoided as it has been variably used to describe any AMD feature in the absence of choroidal neovascularization, has been used as a synonym for GA specifically,[18] or has been used to describe atrophic appearing disciform scars.

Normal Aging of the Macula

One of the difficulties in establishing a classification system for AMD is separating the manifestations of normal aging from those of disease. Aging is a fundamental biologic phenomenon that occurs even in the absence of disease, each cell having a genetically programmed lifespan. Tissues that are comprised of cell types that do not undergo renewal with mitotic division, such as those in the central nervous system and the retina, are more likely to demonstrate changes with age.

Macular Examination Findings

With age there is loss of the foveal and foveolar reflexes. This may be due to disappearance of cells from the inner retinal layers, shallowing of the walls of the foveal pit, and enlargement of the

capillary-free zone.[21] A few small, hard drusen are practically ubiquitous among people of all ages.[22–26] Irregularity of the RPE pigmentation may give rise to a fine granularity in the macula, and the fundus commonly demonstrates a tigroid background. This senile tigroid fundus (Fig. 68.3A) is increasingly apparent with advancing age but remains compatible with normal vision. It is unrelated to skin pigmentation and differs from the tigroid fundus in youth in that the choroidal vessels become visible beneath the macula as part of aging. Commonly there is a peripapillary halo of RPE atrophy in which the exposed vessels may be sheathed and the intervascular spaces appear pale. A lower number of perifoveal arterioles and venules have also been reported.[27]

Histopathologic and Compositional Changes of the Aging Macula

The RPE, Bruch's membrane, and choriocapillaris have integrated functions to provide support for the photoreceptors. Prior to aging (Fig. 68.1A), there is a large number of photoreceptors, the RPE is a monolayer of single cells, Bruch's membrane is not thickened, and the choroid consists of three layers of vessels. As each of these tissues has at one time been regarded as primarily at fault in fostering the development of AMD, it is necessary to consider the changes developing in these structures during life in the absence of AMD (Fig. 68.1B).

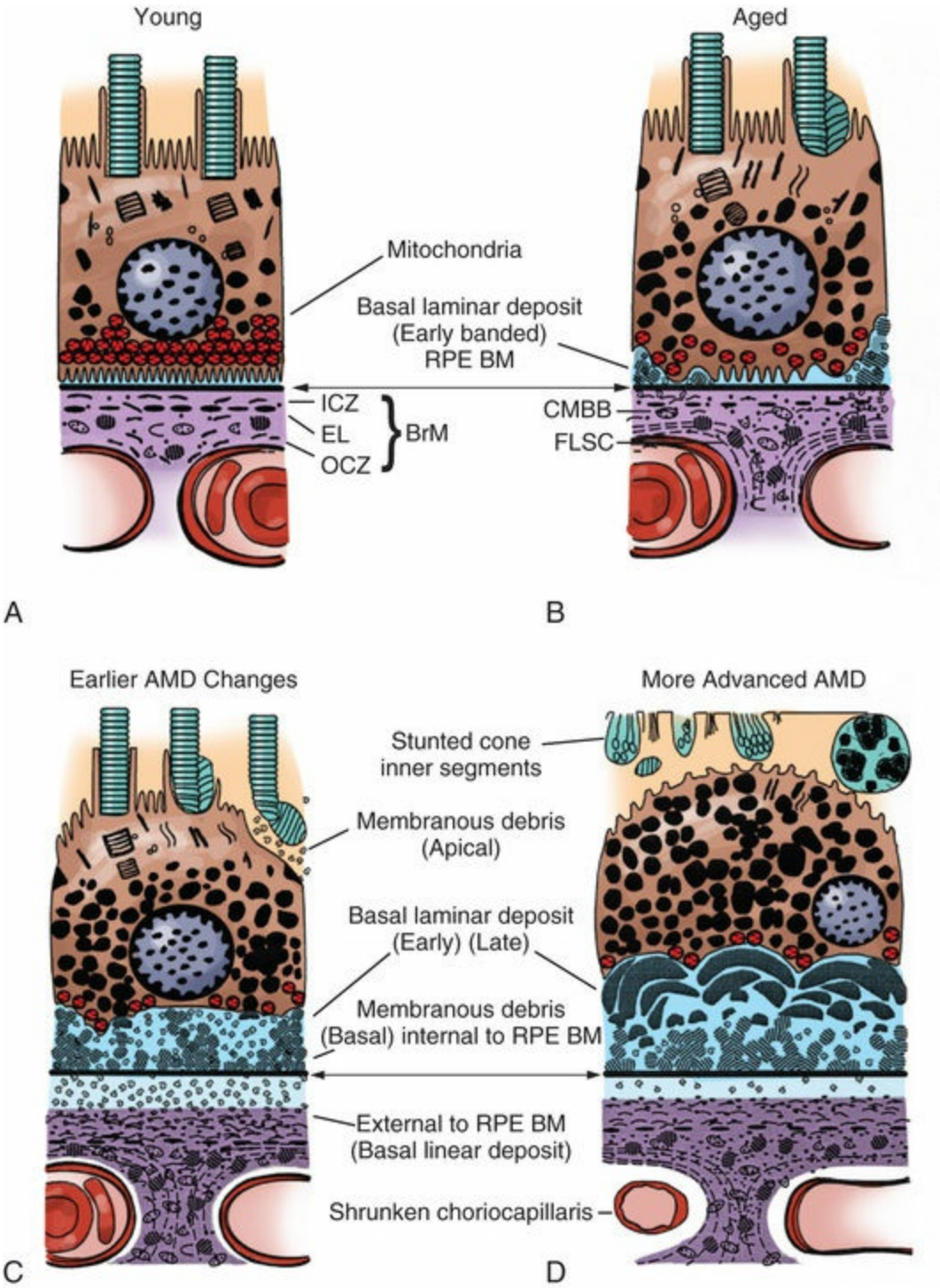

FIG. 68.1 Diagram depicting the ultrastructural features of aging and the evolution of age-related macular degeneration (AMD). Bruch's membrane (BrM) is defined as an inner and outer collagenous zone (ICZ and OCZ) separated by an elastic layer (EL) but excluding the basement membranes of the retinal pigment epithelium (RPE BM) and choriocapillaris. The principal distinguishing feature of each stage is the quantity and type of basal laminar deposit (BlamD)

present at the base of the RPE. (A) Young. The BlamD is absent. Mitochondria lie at the base of the cell. The pigment granules comprise elliptical melanin granules in the apical part of the cell and the incompletely degraded products of phagolysosomal digestion, or lipofuscin, toward the base. (B) Aged. Patches of the early, or striated, type of BlamD appear on the inner aspect of the RPE basement membrane, where the basal infoldings of the cells are reduced. Also, fewer apical microvilli are present. Elongated rod outer segments attest to impaired phagocytosis. Progressive accumulation of lipofuscin causes the RPE cells to enlarge. Coated membrane-bound bodies (CMBB) accumulate in Bruch's membrane and, together with an increase in fibrous long-spacing collagen *(FLSC)*, cause thickening of the OCZ. (C) Early histologic changes seen in AMD. The early type of BlamD now forms a continuous layer. Membranous debris in the form of coiled lipid membranes is found (1) at the apex of the RPE as subretinal drusenoid deposits, where there is more distortion of outer segments; (2) at the base of the RPE interspersed among the strands of BlamD, where it may form basal mounds; (3) as a layer between the RPE basement membrane and the ICZ (basal linear deposit (BlinD)), where it may build up into soft drusen; and (4) within the collagenous zones. Coated membrane-bound bodies and fibrous long-spacing collagen accumulating in Bruch's membrane can be seen in the intercapillary pillars extending to the level of the outer surface of the choroidal capillaries. (D) More advanced changes in AMD. A thick layer of late BlamD is present, predominantly of the amorphous type. Being a later development, the amorphous layer lies on the internal aspect of the early type and appears to be formed in waves. The retinal pigment cells are engorged with lipofuscin and become rounder, with loss of both apical microvilli and basal infoldings. Cell fallout occurs, and necrotic portions of cells containing membrane-bound granules are liberated into the subretinal space. The photoreceptor outer segments disappear, leaving stunted cone inner segments. The membranous debris disappears, resulting in “empty spaces” between the strands of early BlamD internal to the basement membrane and

the regression of any soft drusen present external to the basement membrane. The choroidal capillaries undergo atrophy.

Photoreceptors and Ganglion Cells

Cone density and number at the foveal center does not significantly change during the first eight decades of life,[28–30] which argues against foveal cone vulnerability during normal aging. A significant loss of foveal cones may occur beyond age 90, but this loss variably occurs.[31] In contrast to the stability of foveal cone density with age, age-related loss of centrally located and peripheral rods, equatorial cones, and ganglion cells has been described to be common.[28,30] With aging, rod and cone outer segments become disorganized and convoluted, possibly as an expression of impaired phagocytosis by the RPE.[28,32] This may lead to the accumulation of outer-segment material external to the apical surface of the RPE[31] and lipofuscin deposition within cone inner segments.[33,34] Loss of rods generally begins between the second and fourth decades of life with continued, but potentially slower rate of loss noted, with each successive decade.[30] The centrally located ganglion cell layer shows a similar rate of cell loss with age such that the rod and ganglion cell layer densities maintain a constant ratio.[28,30] The pattern of the central photoreceptor mosaic appears unchanged with age as the remaining rods enlarge to occupy space vacated by the rod loss.[28] It is unknown whether the age-associated central rod loss is due to a primary defect within the rods themselves or whether it is due to RPE dysfunction that affects renewal of rod and not cone outer segments.[28]

Retinal Pigment Epithelium

Throughout life, each RPE cell is responsible for a diurnal cycle of engulfing photoreceptor outer segments that have been shed; the rod outer segments being digested by day and the cone outer segments by night.[35] Over a lifetime, this represents a heavy burden as 10–15% of rod outer segments are phagocytized each day.[36] Rod outer segments have a unique composition of approximately 50% phospholipid and 50% protein with most of the protein being

rhodopsin.[37] Damage to photoreceptor outer segment molecules, namely peroxidation of phospholipid molecules that comprise the outer-segment membranes and free-radical damage to rhodopsin and other outer-segment proteins, may occur as a result of free-radical chain reactions initiated by radiation, light, or oxygen metabolism.[38,39] After phagocytosis by the RPE, the lysosomal degradation enzymes may fail to "recognize" these abnormal molecules, causing molecular degradation to fail with accumulation of lipofuscin in the RPE lysosomes. Over time the RPE accumulates lipofuscin granules.[38,39] Free radicals may also damage the RPE cells' own molecules, and there is evidence that enzymatic inactivation may occur within aged RPE cells. Such inactivation has been demonstrated with cathepsin D, the main lysosomal protease responsible for rhodopsin degradation.[40] In addition to processing shed photoreceptor outer segments, the RPE must also remove material that accumulates from the death of individual photoreceptors and RPE cells. Finally, as the RPE is a nondividing tissue, autophagy, the process by which cells degrade dysfunctional cellular components, also may lead to further accumulation of lipofuscin within the RPE.

Accumulation of lipofuscin in the RPE has been demonstrated to increase with age, with the largest accumulation occurring in the second decade of life followed by progressive accumulation at a slower rate throughout the remainder of life.[38,41] With age, and more prominently in the macula than in the periphery, the RPE also shows an increase in melanolysosomes and melanolipofuscin granules.[41] These complex granules are thought to be melanin granules undergoing repair or degradation.[41] Due to the increase in lipofuscin granules, melanolysosomes, and melanolipofuscin with age, the volume of RPE cytoplasm not occupied by pigments decreases with age.[41] This may reduce RPE cell function and lead to cell death.[29]

In addition to the accumulation of pigmented granules, other morphologic changes occur within the RPE with age. The normal, young RPE is composed of a single layer of hexagonal cells of equal size and degree of pigmentation.[42] With advancing age, increased pleomorphism is noted with regards to cell size, shape, and pigmentation.[42] RPE cells in the macula are also noted to become

taller and narrower with aging.[42] Prominent histologic changes may also occur with aging at the base, or underside, of the RPE cell in the absence of any clinical findings to suggest AMD.[43,44] These changes include loss of basal infoldings and early, patchy deposition of material termed basal laminar deposits (BlamD), termed "basal linear deposits" in the older literature, which lie anterior to the basement membrane of the RPE and posterior to the basal surface of the RPE (Fig. 68.1B).[43,44] Pathologic progressive accumulation of these BlamD is discussed in the section below under "Pathologic changes seen in NNVAMD" (see footnote regarding nomenclature in this section below).

In addition, RPE cell number decreases with age, particularly in the peripheral retina.[29,30,45] There is less consistent data on age-related macular RPE cell loss.[29–31,41,45] The ratio of foveal photoreceptors to RPE cells remains stable with age,[30,31] with an approximated average cone-to-RPE ratio of 24 : 1.

Bruch's Membrane

Although anatomists regard Bruch's membrane as a five-layered structure, alterations are more readily understood by simplifying Bruch's membrane, essentially excluding the basement membranes of the RPE and choriocapillaris, as proposed by Gass.[46] Bruch's membrane can then be thought of as a 3-layer, sheet-like condensation of the innermost portion of the choroidal stroma that consists of an inner (ICZ) and outer collagenous zone (OCZ) separated by an elastic layer. A linear relationship exists between age and thickness of these three internal layers within Bruch's membrane,[44,47–49] with an average thickness of 2 μm in the first decade of life increasing to 4.7 μm by the 10th decade.[48] Changes to the ICZ account for a small proportion of the age-related increased thickness to Bruch's membrane, with a majority of the increased thickness occurring within the OCZ,[49] while no significant change in thickness occurs in the elastic layer.[47] The normal age-related changes that occur within Bruch's membrane can be identified early in life with transmission electron microscopy (TEM)[47,49,50] and through biochemical assays[51–53] prior to becoming visible with light microscopy.[43]

Three types of changes that contribute to this age-related Bruch's

membrane thickening have been described on TEM within the collagen and elastic layers. These changes include the deposition of coated, membrane-bound bodies; the deposition of collagen that appears as banded material; and the formation of mineralized deposits.[44,47–50,54–56] In addition, with normal aging, the presence of a small number of drusen can also be identified by light microscopy or TEM between the ICZ and the basement membrane of the RPE.[43,44,50,54] These drusen, as they relate to normal aging, will be described later in this section.

Coated, Membrane-Bound Bodies.

The majority of the normal age-related thickening of Bruch's membrane is due to accumulation of rounded, coated, membrane-bound bodies[49] (Figs. 68.1B and 68.2). This material may result from the shedding of unwanted RPE basal cytoplasm through the basement membrane of the RPE.[49,50] These membrane-bound bodies have been identified in the process of spilling their contents of coated vesicles and granular material into Bruch's membrane.[49] Membrane-bound bodies have been identified in first and second decades of life within the ICZ,[49,50] while absent within the first 2 years of life.[47,49] Membrane-bound bodies subsequently occur, even in greater amounts, in the OCZ.[49,50] In a study of 68 eyes, among the 20 eyes from donors, aged 20–60, 90% had this type of deposit in Bruch's membrane specimens from the macula in both the ICZ and OCZ; the remaining few in this age range did not have these deposits in either location. Each of the 38 eyes older than 60 years had this type of change in both the ICZ and OCZ, with more prominent changes in the OCZ compared to younger eyes. Only 2 of the 10 eyes from donors younger than 20 (aged 17 and 18) had these types of deposits, one in the ICZ only and the other in the ICZ and OCZ.[50]

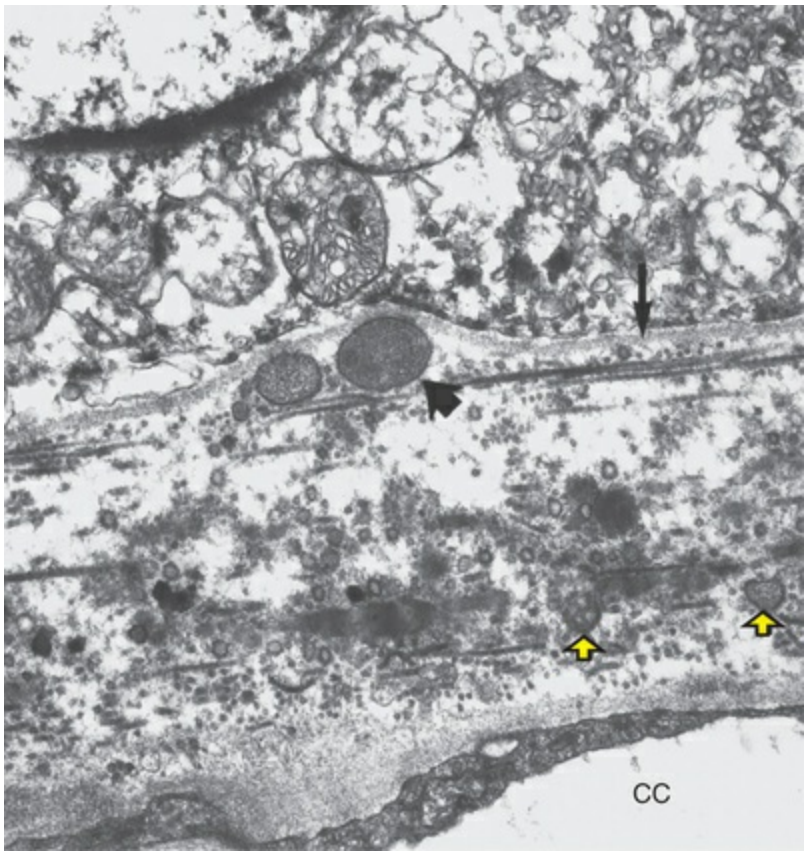

FIG. 68.2 Electron micrograph (x11800) shows accumulation of debris in Bruch's membrane. The patient was 62 years of age and had 20/20 vision; however, this process can be detected as early as the second decade. Coated membrane-bound bodies (*short arrow*) are apparently trapped between the basement membrane of the retinal pigment epithelium (RPE) (*long arrow*) and the inner collagenous zone (entrapment sites). Others lie in the outer collagenous layer (*yellow arrows*). Some have ruptured, releasing vesicular and granular material and fragments of the coated membrane. (Courtesy of MC Killingsworth.)

Collagen.

A general increase in collagen deposition occurs within both the ICZ[47] and OCZ. The 64-nanometer (nm) banded fibers are found in increasing numbers within both of these layers with age and are believed to be fibrillar type I collagen.[51] Clumps of fibrous long-spacing collagen with band periodicity ranging from 100 to 133 nm also accumulate.[47,49,51,57] The molecular composition of the long spacing collagen is uncertain, but it appears similar to banded

material that is also present in BlamD.[43,44,50] These longer spaced collagen deposits are found primarily in the OCZ or embedded in the basement membrane of the choriocapillaris[47,57] (Fig. 68.1B). These deposits have been found as early as age 19, and their prevalence progressively increases with age[57] such that they are present in all eyes age 40 and older.[49] There is a significant linear decline in Bruch's membrane solubility with age, and this may be due to increase in collagen crosslinking.[51] Other components that have been identified in Bruch's membrane with age by biochemical or by immunoelectron microscopy (EM) analysis include collagen types III, IV, and V, fibronectin, chondroitin sulfate, dermatan sulfate, and proteoglycans.[51,55]

Mineralized Deposits.

Mineralized deposits accumulate less frequently than the above changes[47,49,50] and have been described as fine granules on collagen fibers in the ICZ in younger eyes. However, they are more commonly seen in the elastic layer in eyes from middle-aged persons.[47,49,50]

Other than the thickening of Bruch's membrane, described above, the most significant other histologic findings in Bruch's membrane, visible by light microscopy, do not become evident until the fifth decade.[43] These changes are comprised of hyalinization and patchy basophilia.[43] With increasing age, diffuse deposition of hyalinized material occurs in the collagenous zones and can also extend down the intercapillary pillars,[43] the spaces between the capillaries of the choriocapillaris. Using special stains with light microscopy calcium deposits may be noted within Bruch's membrane in about 60% of eyes over age 30.[43,44]

As determined both biochemically and with light and electron microscopic study, the lipid content of Bruch's membrane also increases after the fourth decade.[52,53,56] Lipid increases exponentially with age[52] and consists largely of phospholipids, triglycerides, fatty acids, and free cholesterol.[52,53] The lack of cholesterol ester in Bruch's membrane indicates that the source of lipid in Bruch's membrane is likely independent of the bloodstream.[52] Likewise, peroxidized lipids in Bruch's membrane increase exponentially with age.[58] The peroxidized lipids are derived from long-chain

polyunsaturated fatty acids, particularly docosahexaenoic acid (DHA) and linolenic acid, which are polyunsaturated fatty acids found in photoreceptor outer segments.[58] Lipid peroxides have been shown to induce neovascularization of the retina and choroid by inducing expression of a cascade of angiogenic cytokines.[59,60]

The presence of small, hard drusen are common in eyes with normal gross fundus appearance.[43,44] These appear mostly as hyalinized globular material between the ICZ and RPE basement membrane on light microscopy,[43] and they frequently contain calcium in eyes from older individuals (beyond age 60).[44,54] Ultrastructurally, the smallest ones are composed of material resembling cytoplasm or of cell fragments with organelles, including mitochondria and coated vesicles, and are present as early as the fourth decade of life.[54] Small drusen that are somewhat larger (spanning the width of 2–4 RPE cells) in young eyes contain fine granular particles, many "bent fibers," and masses of basophilic material, resembling nucleoplasm.[54]

The structural and ultrastructural changes described in Bruch's membrane above may be expected to decrease the rate at which fluid can pass through Bruch's membrane. Hydraulic conductivity is the measurement of the bulk flow of fluid through a test membrane in response to applied pressure. Studies have shown a decrease in hydraulic conductivity through Bruch's membrane with age. The decrease in conductivity is greatest in the first four decades of life,[61,62] and then it continues to decline at a slower rate with increasing age. This raises questions about the mechanisms through which this decline occurs as the linear increase in thickness of Bruch's membrane[48] and the exponential increase in lipid with advancing age[52] would suggest that the rate of loss of hydraulic conductivity would more closely parallel these changes.

Using excimer laser to produce ultrathin shavings of Bruch's membrane, the greatest resistance to water flow through Bruch's membrane throughout life resides within the ICZ.[62] Serial ultrathin sections have led to estimates of the porosity at sequential levels of Bruch's membrane and have confirmed that the ICZ has the lowest porosity. Calculations based on the pore radii and length further confirm that the ICZ also has the lowest flow rate. This, too, is at odds with histologic studies, noted above, that show that greater

increases in thickening of Bruch's membrane occur in the OCZ. Clearly, further studies are required, as only a limited number of younger eyes have been examined. Reductions in permeability of Bruch's membrane with age, brought about through structural and/or biochemical changes, may in turn compromise RPE structure and function.

Choroid

Progressive histologic changes are also noted to occur in the choroid with age. Comparing the macula of normal eyes in the first and 10th decades of life, the density of the choroidal capillaries decreases in a linear fashion by 45%, the diameter of the choriocapillaris decreases by 34%, and average choroidal thickness decreases from 200 μm to 80 μm.[48] The reduction in choriocapillaris permits the larger choroidal vessels to be seen more readily on clinical examination, accounting for the senile tigroid fundus (Fig. 68.3A).

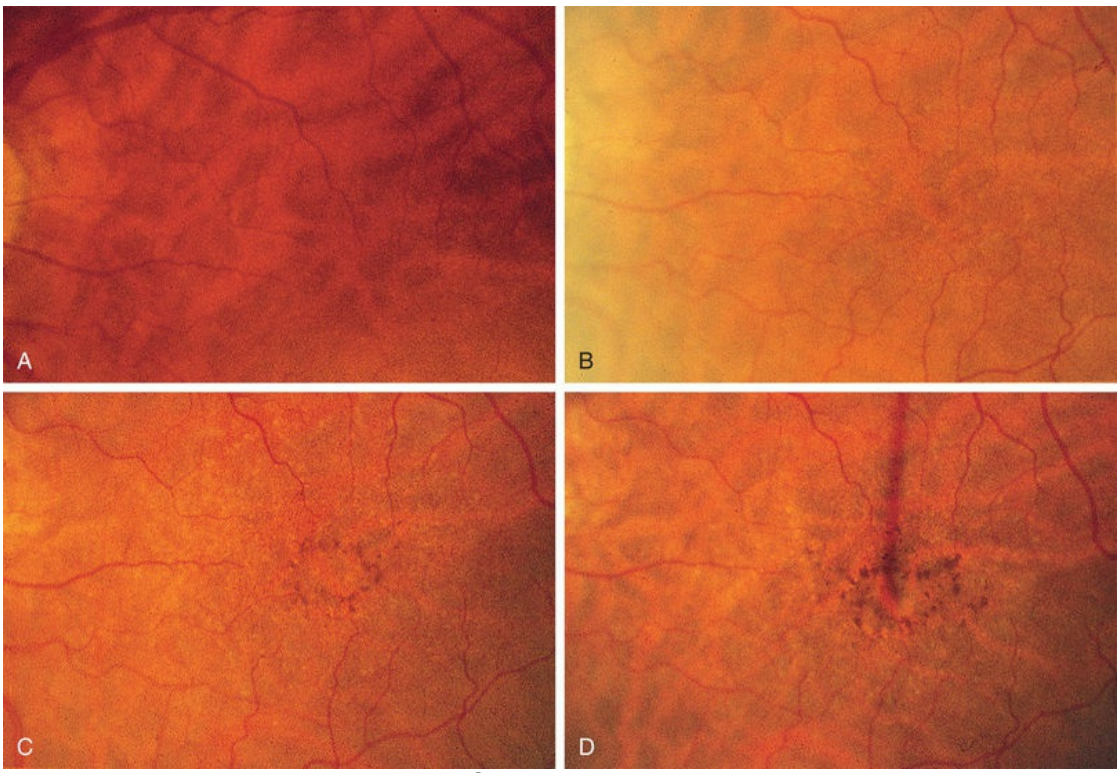

FIG. 68.3 Evolution of retinal pigment epithelium abnormalities developing into geographic atrophy over 16 years (continues in Fig. 68.38). (A) At age 68, the

patient has a normal left fundus with senile tigroid pattern (vision 20/15). (B) At age 73, small drusen-like dots are present centrally, ≤63 μm in size (vision 20/20). (C) At age 77, a ring of pigment clumps developed around the foveal center. (D) At age 79, pigment clumping around fixation has increased; vision is still 20/20. The choroidal vascular pattern has become more prominent in the fovea consistent with nongeographic atrophy. (Reproduced from Sarks JP, Sarks SH, Killingsworth M. Evolution of geographic atrophy of the retinal pigment epithelium. Eye 1988; 2:552–577.)

Age-Related Macular Changes as Seen on Fundus Imaging

The structural changes noted with normal aging, as described in the previous sections, do correlate with observations made on clinical imaging performed in living persons. Fluorescein angiography demonstrates an increase in the area occupied by the foveal avascular zone (FAZ) with age; mean area of the FAZ is estimated at 0.53 mm^2 among individuals younger than 40 years as compared with 0.61 mm^2 for individuals over age 40.[21] Studies using blue-field stimulation[63] and scanning laser Doppler flowmetry[64] have also shown a decrease in blood flow in the retinal macular capillaries of older individuals. Each of these observations may correlate with loss of centrally located ganglion cells that occur with age.

Enhanced-depth imaging optical coherence tomography (EDI-OCT) of the choroid (performed with spectral domain OCT (SD-OCT) and 1050-nm wavelength light source) corroborates the histologic findings of decreased density of macular choroidal capillaries and decreased choroidal thickness that occurs with age. Despite significant variability of choroidal thickness measurements among normal individuals, the mean central subfield thickness measurements of the choroid decrease by about 2 μm per year of age among subjects between the ages of 20 and 68.[65] A larger study that included patients between age 50 and 93 reported an annual decrease in central choroidal thickness of 4 μm for each successive year.[66] Enface swept-source OCT images in individuals age 24–66

years has confirmed age-related thinning of the choroid and specifically the choriocapillaris, with no significant change in the deeper layers of the choroid.[67] As might be anticipated, choroidal blood flow also decreases with age among normal subjects as assessed by laser Doppler flowmetry.[68] Indocyanine green angiography (ICGA) shows age-related alterations in filling patterns. Young subjects demonstrate early arteriolar filling in the fovea with rapid expansion peripherally within fine, tortuous, and multibranching arterioles, whereas in older subjects the choroidal arterioles are more sparse, thicker, straighter, and have fewer branches[69] (Fig. 68.4).

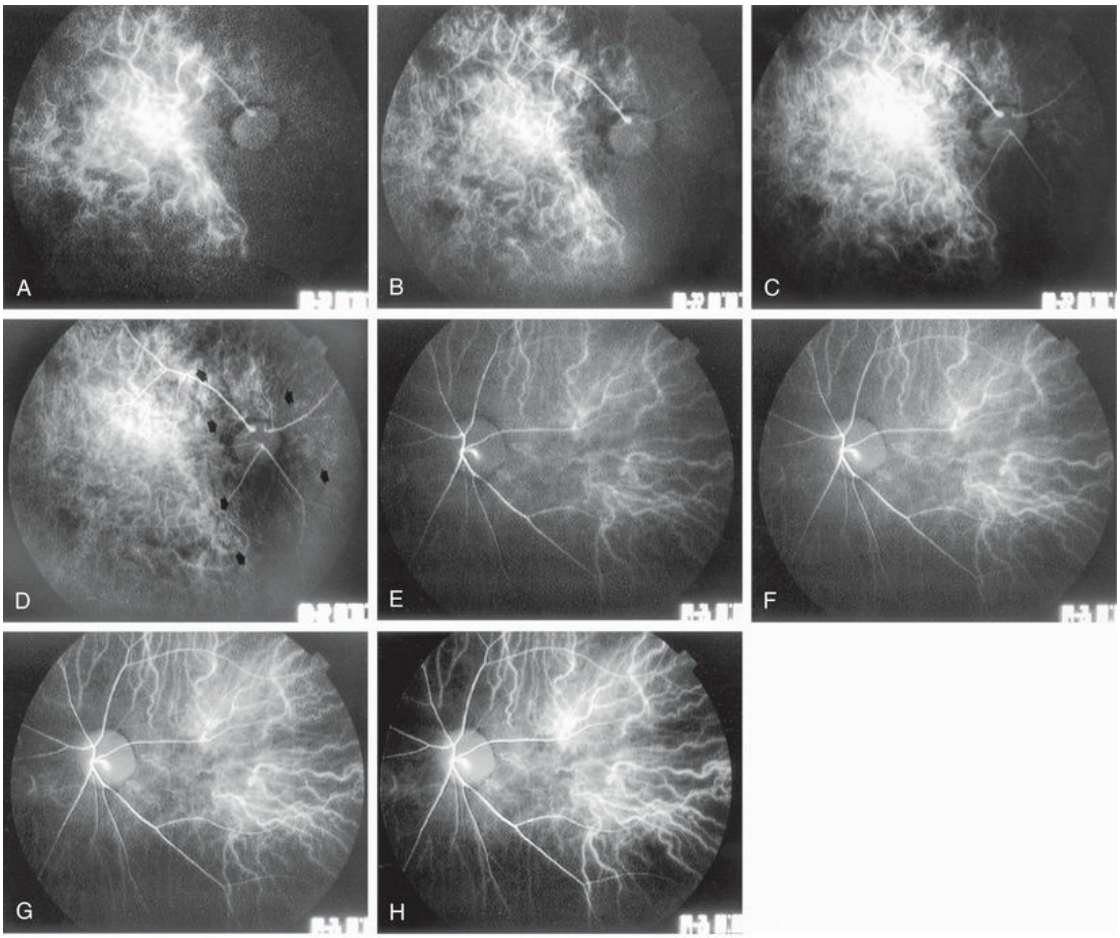

FIG. 68.4 The initial arterial filling pattern during indocyanine green angiography of normal subjects. (A–D) 22-year-old man. The arteriolar filling begins in the subfoveal region in radial fashion toward the peripheral fundus. The dye fills rapidly, and the arterioles run in a fine, tortuous, and multibranching

fashion throughout the time course. The vertical watershed zone through the optic disc is clearly observed (*arrow*). (E–H) 62-year-old man. The choroidal arterioles are scanty in the posterior fundus. The vessels are thickened and run a straight course with reduced branching. The watershed zone is blurred. (Reproduced with permission from Ito YN, Mori K, Young-Duvall J, et al. Aging changes of the choroidal dye filling pattern in indocyanine green angiography of normal subjects. Retina. 2001;21(3):237-42.)

Fundus autofluorescence imaging (FAF) also corroborates histologic findings associated with aging. Lipofuscin is the predominant fluorophore responsible for in vivo FAF, and quantification of in vivo FAF demonstrates an age-related increase in macular FAF that would be expected based on the increased accumulation of lipofuscin within the RPE with age.[70]

Pathology of Non-Neovascular AMD

A clinical diagnosis of AMD is appropriate when extensive small drusen[17] or any medium or large-sized druse or drusen,[19] with or without RPE abnormalities, are found during examination of the posterior pole. The clinical parameters describing drusen size and extent (area involved) and presence of pigmentary abnormalities are critical as they are the strongest predictors of progression to the late stages of AMD.[71,72] Studies evaluating the histopathology of aged eyes, including those with AMD, have typically failed to focus on the gross fundus appearance to describe the size and extent of drusen. In addition, drusen components are often lost during tissue processing. Therefore, separate histopathologic definitions of AMD have been described[43,73–75] that are difficult to correlate to clinical grading scales that focus largely on the extent of drusen. Histopathologic studies are critical to advance our understanding of the disease processes, while clinical studies provide more limited information about mechanisms of the disease processes but are essential to the understanding of clinical disease evolution. It is challenging to correlate clinical findings with those seen histopathologically, as some of the best described histopathologic features of AMD, such as pathologic basal deposits (described

below), are not visible with ophthalmoscopy and presently do not have correlate findings with in vivo retinal imaging of the posterior pole. The advent of high-resolution OCT, which provides images with resolution that is analogous to histologic cross-sections, has improved our ability to correlate clinical findings to the well-described histologic findings that occur in AMD. However, at present there is limited availability of histologic specimens from eyes that were imaged in vivo with these instruments to provide direct clinical (OCT)-pathologic comparisons. This section describes the range of histopathologic alterations that are found in eyes with NNVAMD and summarizes our best current understanding of the clinical exam features and retinal imaging correlates of these various findings.

Histologic Alterations of Non-Neovascular AMD that May Not Be Apparent on Ophthalmoscopy

Basal Deposits* and Membranous Debris

On histopathologic examination, degeneration of the RPE[74] along with the presence of membranous debris, basal linear deposits (BlinD), and extensive basal laminar deposits (BlamD) (the latter two are collectively referred to as basal deposits)[43,75,77] are the hallmarks of AMD. BlamD are located between the RPE cells and the basement membrane of the RPE, and BlinD form external to the basement membrane of the RPE and internal to Bruch's membrane[76] (Figs. 68.1C–D). Neither deposit is visible in the fundus on examination, and TEM is needed to definitively differentiate one from the other.[78] Along with membranous debris, these basal deposits, as defined in this paragraph, are described in greater detail below.

Basal Laminar Deposits: Early and Late Forms.

Basal laminar deposits (BlamD) lie posterior to the RPE, between the RPE cell plasma membrane and the basement membrane of the cell (see Figs. 68.1C–D and 68.5–68.9). This is in contrast to drusen, which lie external to the basement membrane of the RPE. BlamD

can be demonstrated consistently by the seventh decade[43] but has been found even in the fifth decade.[44] Initially the deposit occurs in a patchy distribution anterior to thickened or basophilic segments of Bruch's membrane, anterior to intercapillary pillars, or anterior to small drusen.[43] The deposit can be classified histologically as class 1 (occurring in small, solitary patches), class 2 (a thin continuous layer on a histologic section), or class 3 (a thick layer, at least half the height of the RPE cell).[44] As noted in the "Normal aging" section above, this deposit can be a part of normal aging, but only class I deposits are consistent with normal aging, whereas class 2 and 3 deposits are strongly associated with the presence of AMD, by clinical or by histopathologic definitions.[43,44,75,77]

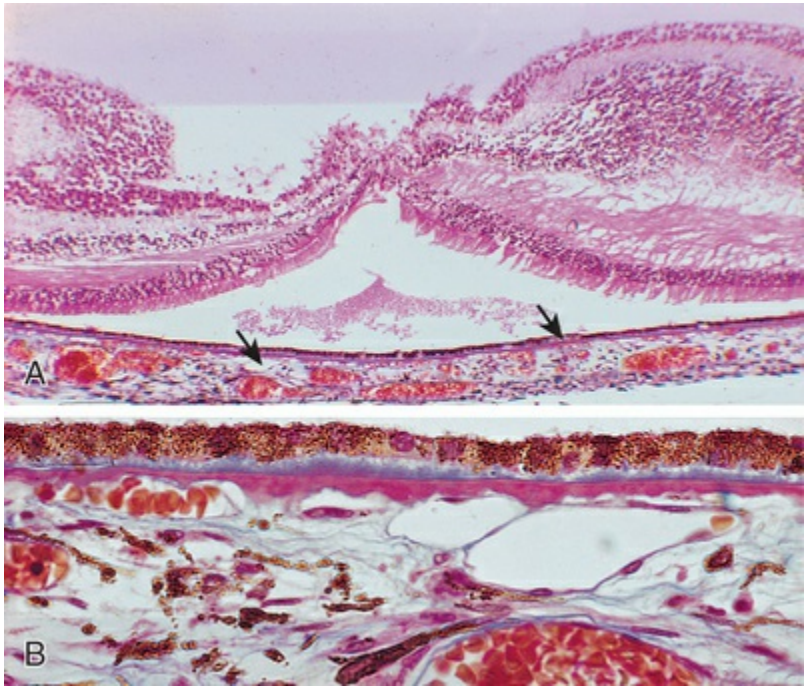

FIG. 68.5 (A) Section through the macula of a 79-year-old man. Fundus appeared normal, and vision was 20/30. Early form of basal laminar deposit is seen as continuous, blue-staining layer beneath the retinal pigment epithelium. Unstained spaces (*right arrow*) would correspond to membranous debris on electron microscopy. *Arrow* at left indicates area magnified in panel B (×75). (B) Basal laminar deposit is most developed over a thicker segment of Bruch's membrane. Hyalinization of Bruch's membrane extends down intercapillary pillars (picro-Mallory stain;

×500). (Reproduced with permission from Sarks SH. Aging and degeneration in the macular region: a clinico-pathological study. Br J Ophthalmol 1976;60:324–41.)

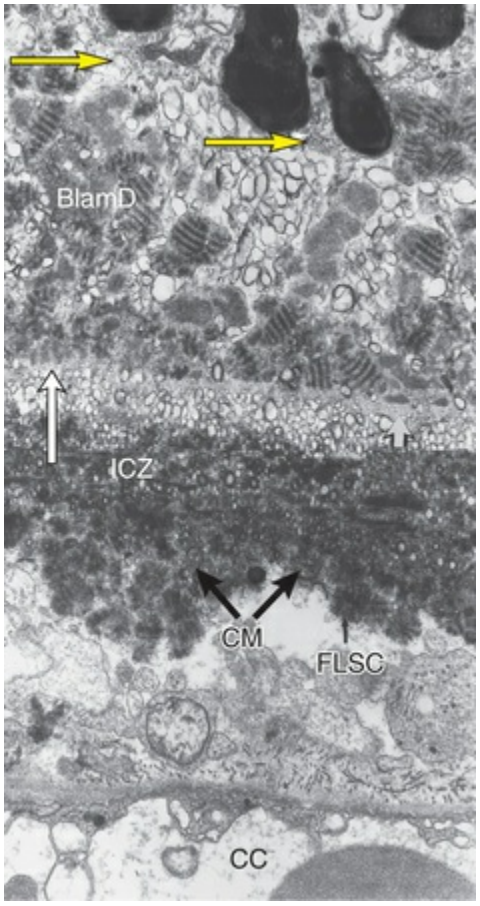

FIG. 68.6 Electron micrograph illustrating diffuse basal laminar deposit (BlamD) and diffuse basal linear deposit (BlinD) that develop in age-related macular degeneration, corresponding to Fig. 68.1C. Horizontal *yellow arrows* indicate the basal plasma membrane of the retinal pigment epithelium (RPE). Early-type BlamD (*BlamD*) projects inward from the RPE basement membrane (*white arrows*) and comprises mainly banded material resembling fibrous long-spacing collagen. Coiled membranes with a bilayered structure of lipids lie among the clumps of BlamD and appear to pass through the basement membrane to lie between it and the inner collagenous zone (*ICZ*) as a component of BlinD, as well as filtering into the membrane itself. Identifiable structures within Bruch's membrane include fragments of coated membrane (*CM*) and fibrous long-

spacing collagen (*FLSC*). *CC*, choriocapillaris. (x11,780.) (Reproduced with permission from Killingsworth MC, Sarks JP, Sarks SH. Macrophages related to Bruch's membrane in age-related macular degeneration. Eye 1990; 4:613–621.)

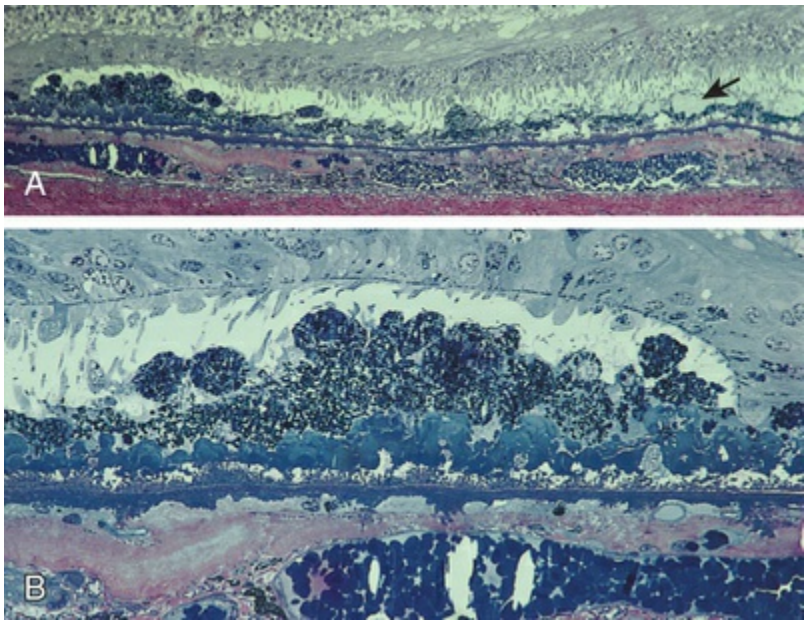

FIG. 68.7 Same eye as in Figs. 68.3 and 68.38. Section passes through the temporal margin of the area of geographic atrophy. (A) Photoreceptors become fewer and outer segments wider and stunted as they approach the edge. Vacuolated appearance under the retinal pigment epithelium (RPE) is due to disappearance of membranous debris. Collections of membranous debris can be seen on the internal (apical) surface of RPE (*arrow*), possibly due to failure of phagocytosis (x150). (B) Hyperpigmented edge noted clinically corresponds to a double layer of RPE, the inner layer representing necrotic hyperpigmented cells in the process of being eliminated. Late amorphous form of basal laminar deposit (BlamD) lies internal to striated form and has a multilaminar appearance, suggesting formation in successive waves according to the level of RPE (see Fig. 68.1D). Photoreceptors disappear, and external limiting membrane terminates on BlamD (methylene blue and basic fuscin; x500). (Reproduced with permission from Sarks JP, Sarks SH, Killingsworth M. Evolution of geographic atrophy of the retinal pigment

epithelium. Eye 1988; 2:552–577.)

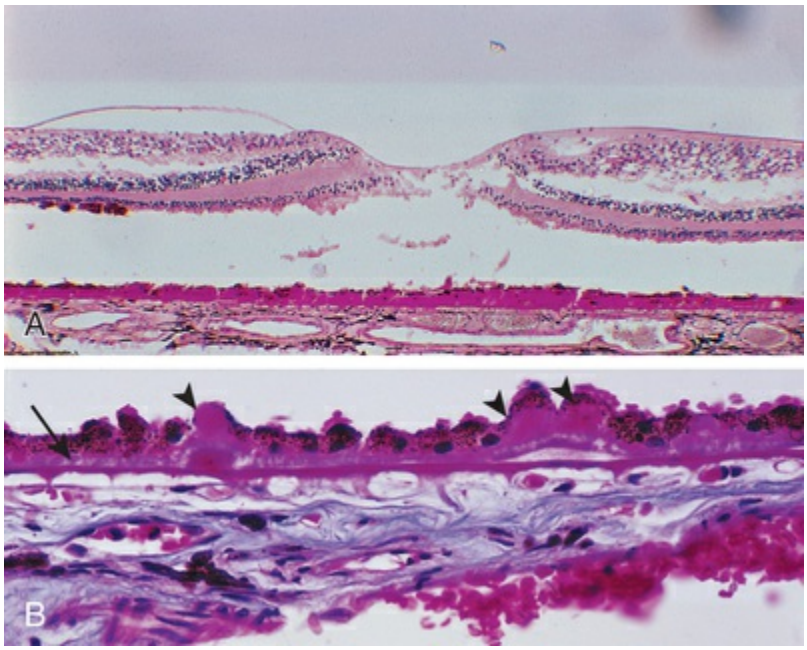

FIG. 68.8 (A) Incipient atrophy, showing an unusually thick layer of late BlamD. This material is hyalinized and periodic acid–Schiff-positive; on electron microscopy it would have a corresponding amorphous appearance. The retinal pigment epithelium forms a very attenuated layer over the surface and seems about to disappear (periodic acid–Schiff; ×45). (B) Parafoveal area from the same eye shows the different deposits. The two forms of the BlamD are seen: the blue-staining, early form (*long arrow*) and, on its inner surface, nodular collections of the late hyalinized form (*arrowheads*). External to the BlamD lie two typical drusen; beneath the *short arrow at left* is a small hard druse; beneath the two *short arrows at right* is a soft druse (picro-Mallory stain; ×500). (Reproduced with permission from Sarks SH. Aging and degeneration in the macular region: a clinico-pathological study. Br J Ophthalmol 1976;60:324–41.)

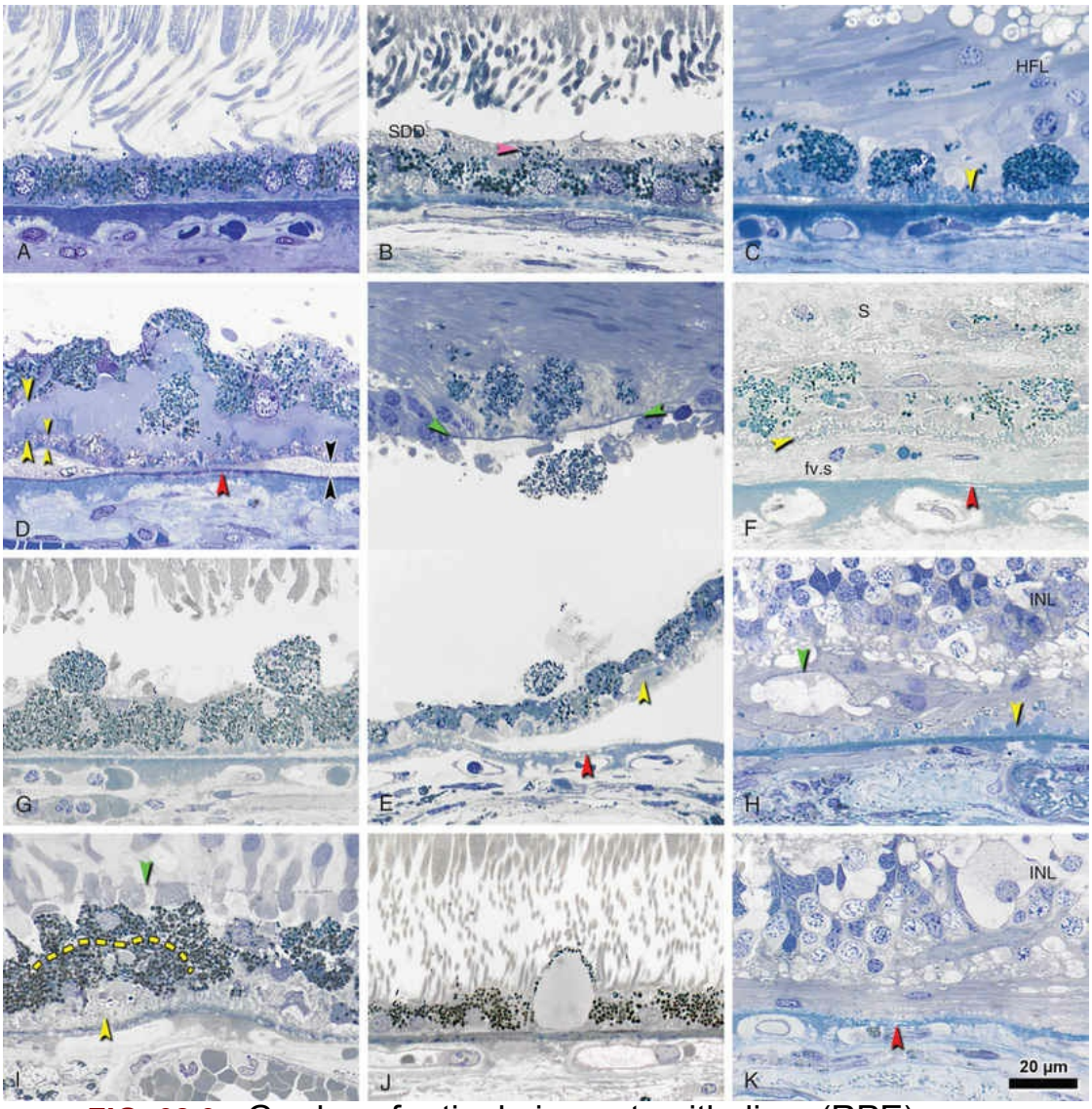

FIG. 68.9 Grades of retinal pigment epithelium (RPE) morphology in late age-related macular degeneration (AMD). Submicrometer epoxy resin sections were stained with toluidine blue. Epithelial RPE and RPE morphologies with epithelial components (A,B,D,E,G,I,J); nonepithelial (noncontinuous) morphologies (C,F); atrophic RPE (H,K). (A) "Nonuniform" RPE: slightly "Nonuniform" morphology and pigmentation with small patches of early basal laminar deposit (BLamD). (B) "Very Nonuniform" RPE: more nonuniformity in shape and pigmentation; melanosomes within apical processes (*pink arrowhead*). Subretinal drusenoid deposits (*SDD*) localize to RPE apical aspect. (C) "Dissociated" RPE: individual RPE cells with or without nuclei in atrophic area, adherent to early BlamD. Some RPE granules are translocated among HFL fibers. (D) "Shedding"

RPE: basal translocation of shed RPE fragments into a thick continuous layer of BlamD (late and early forms shown by large and small *yellow arrowheads*, respectively); BlinD (*black arrowheads*). (E) "Intraretinal" RPE: anterior migration through ELM. Epithelial component remains atop BlamD (bottom), which in turn overlies an artifactually empty soft druse. Photoreceptors have degenerated. Retina is artifactually detached. (F) Cells "entombed" by a subretinal scar(s) together with nonpigmented cells. Persistent BlamD divides subretinal fibrocellular scar in the subretinal space from fibrovascular scar (*fv.s*) in sub-RPE space. This histologic phenotype occurs only in neovascular AMD and is therefore not describe further in the text. (G) "Sloughed" RPE: release of spherical cells into the subretinal space; the epithelial component overlies BlamD (blue) and BlinD (gray). (H) "Atrophy with BlamD": absent RPE and persistent BlamD. Photoreceptors have atrophied. ELM delimits endstage outer retinal tubulation. (I) "Bilaminar": double layers of epithelial RPE (delimited by *dotted line*) adherent to BlamD. (J) "Vacuolated" RPE: cells with a single large vacuole delimited apically by extremely effaced cytoplasm. (K) "Atrophy without BlamD": absent RPE, absent BlamD. Photoreceptors have atrophied. *Yellow arrowheads*, BlamD; *red arrowheads*, calcification in BrM; *green arrowheads*, ELM. *HFL*, Henle fiber layer; *INL*, inner nuclear layer.

(Reproduced with permission from Zanzottera EC, Messinger JD, Ach T, et al. The Project MACULA retinal pigment epithelium grading system for histology and optical coherence tomography in age-related macular degeneration. Invest Ophthalmol Vis Sci. 2015;56(5):3253-68.)

The deposit has two different appearances that are termed "early" and "late" BlamD. The early form is seen in normal aging as well as in eyes with early or late stages of AMD, while the late form is present with increasing frequency in eyes with late AMD manifestations (GA and CNV).[43,75] Early BlamD appear on light microscopy as pale-staining eosinophilic material that stains blue with picro-Mallory and shows faint anteroposterior striations (Fig. 68.5). In contrast, the light microscopic appearance of late BlamD is a thick, hyalinized layer that stains red with picro-Mallory, similar

to hyalinized Bruch's membrane, and is more periodic acid–Schiff-positive than the earlier, banded form (Figs. 68.7 and 68.8). Being a later development, it forms a distinct layer on the anterior surface of the earlier form (Figs. 68.2D, 68.7 and 68.8) and may approximate the thickness of the normal RPE, occasionally displaying nodular elevations on its internal surface[43,75,78] (Fig. 68.8).

With electron microscopy the BlamD is seen to consist of three phenotypes: fibrillar, polymerized, and amorphous. The fibrillar and polymerized phenotypes are present in early BlamD, and the fibrillar form may only be detected as irregular nodules lying on the anterior surface of the original RPE basement membrane. The polymerized form resembles the fibrous long-spacing collagen seen within Bruch's membrane and is also found in the cornea, trabecular meshwork, and other tissues in the body with aging.[57] It projects anteriorly from the original RPE basement membrane[79] (Fig. 68.6) and accounts for the striations, or bush-like appearance, seen histologically in the early forms. The amorphous form of the BlamD is seen in late BlamD. It has a flocculent appearance and consists mainly of amorphous material that forms anterior to early BlamD[75] (Figs. 68.7 and 68.8). It is often associated with attenuation of the overlying RPE (see Fig. 68.10).

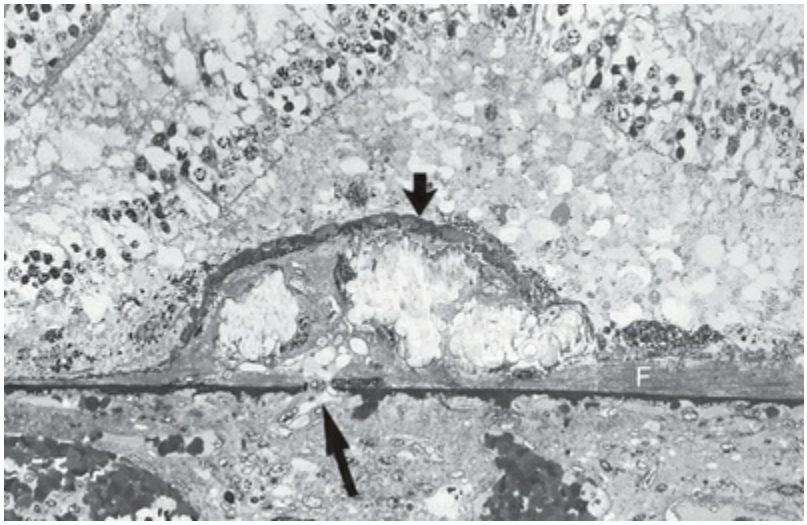

FIG. 68.10 Example of regressing druse in an area of geographic atrophy. The druse is covered by late, amorphous BlamD (*short arrow*) and has dystrophic calcification. A clinically unsuspected small vessel passes through a gap in Bruch's membrane beneath

the druse (*long arrow*). A layer of fibrous tissue (F) lies on the anterior surface of Bruch's membrane. (Methylene blue and basic fuchsin, x240.) (Reproduced from Sarks JP, Sarks SH, Killingsworth M. Evolution of geographic atrophy of the retinal pigment epithelium. Eye 1988; 2:552–577.)

The similarity of the BlamD to basement membrane and its proximity to rough endoplasmic reticulum at the base of the RPE cells suggest that it is a secretory product of the RPE.[79,80] It reacts with antibodies against type IV collagen, heparan sulfate proteoglycans, and laminin,[80] but the BlamD is biochemically distinct from the RPE basement membrane, and a faulty, degradative process rather than enhanced synthesis may account for its accumulation in aged maculas.[50,55]

On examination, BlamD have not been identified in the fundus with any certainty, but the histopathologic presence of late BlamD may be presumed when significant pigment alterations are present on clinical examination.[75]

Basal Linear Deposits.

Basal linear deposits (BlinD) form a thin layer between the RPE basement membrane and the ICZ of Bruch's membrane (Fig. 68.6, see Fig. 68.9D). These deposits are difficult to distinguish with light microscopy; however, they are well visualized with TEM. BlinD can become continuous with soft drusen, soft drusen may form within this layer (discussed in a later section)[75–77,81] (see Fig. 68.11) and the deposit itself is sometimes referred to as diffuse drusen.[77,78] These deposits are comprised largely of membranous debris while the other major component of BlinD are non-membrane-bound electron-lucent droplets.[77] The BlinD appear to disturb the normal attachment of the RPE to Bruch's membrane, creating a cleavage plane, in which RPE detachments may develop due to blood or serous fluid and into which early choroidal new vessels may grow.[82]

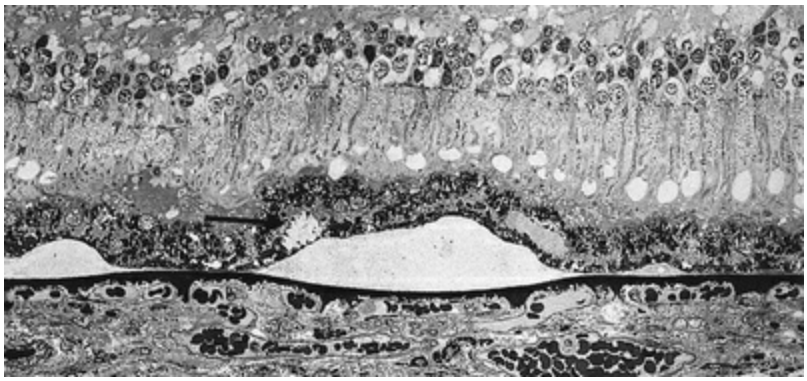

FIG. 68.11 Semithin section showing medium-sized soft drusen from the left eye of the patient illustrated in Fig. 68.22. Since these deposits are focal accentuations of a continuous layer of debris, their margins are ill defined and they readily become confluent. It is into this plane that choroidal new vessels grow; a neovascular membrane was present nearby. Drusen appear empty or very finely granular at this magnification. The arrow points to a small basal mound of similar appearance, lying above the druse. Higher magnification is shown in Fig. 68.27 (methylene blue and basic fuchsin, x240). (Reproduced from Sarks JP, Sarks SH, Killingsworth MC. Evolution of soft drusen in age-related macular degeneration. Eye 1994;8:269–283.)

Membranous Debris.

Membranous debris is identified with TEM and accumulates in three locations in eyes with AMD: anterior to the RPE basement membrane (along with BlamD) (Fig. 68.12), immediately posterior to the RPE basement membrane (as a component of BlinD and within soft drusen that develop in this plane), and in the subretinal space at the apex of the RPE (see Fig. 68.13).[73,75] When samples are processed to preserve lipid, membranous debris does not resemble surrounding cells or vesicles as it is composed of solid lipid particles rather than having an aqueous interior.[83]

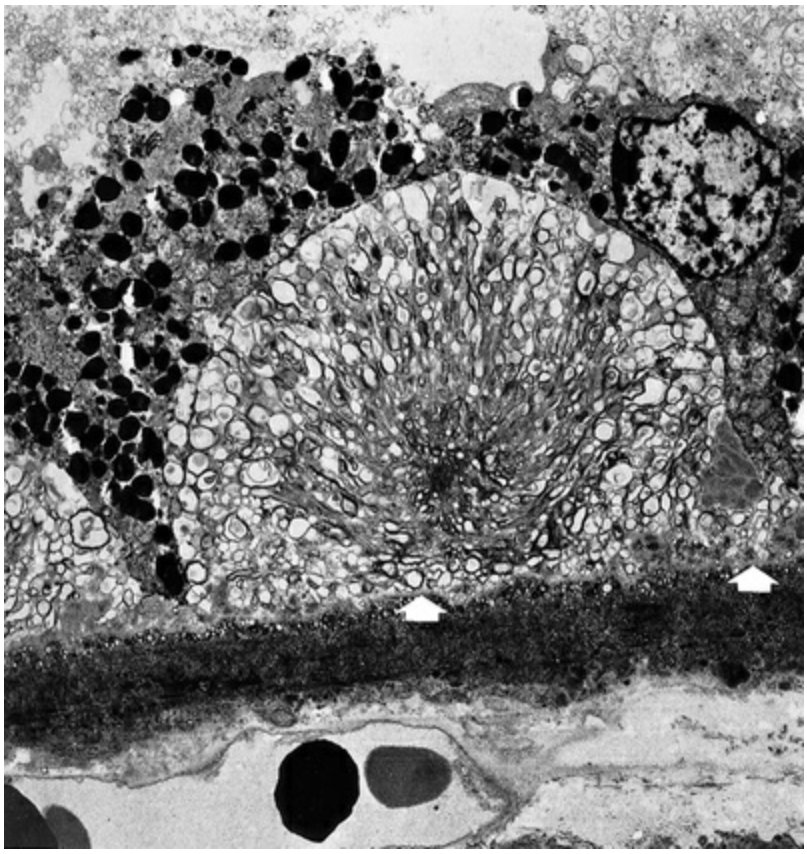

FIG. 68.12 Basal mound lying internal to retinal pigment epithelium (RPE) basement membrane. Electron micrograph shows buildup of coiled membranous debris separating the grossly abnormal RPE from its basement membrane. These collections are referred to as “basal mounds” and may account for the drusen-like dots noted clinically. Only a very thin layer of membranous debris lies external to the basement membrane (*arrows*), so there are no soft drusen (×1680). (Courtesy of M.C. Killingsworth.)

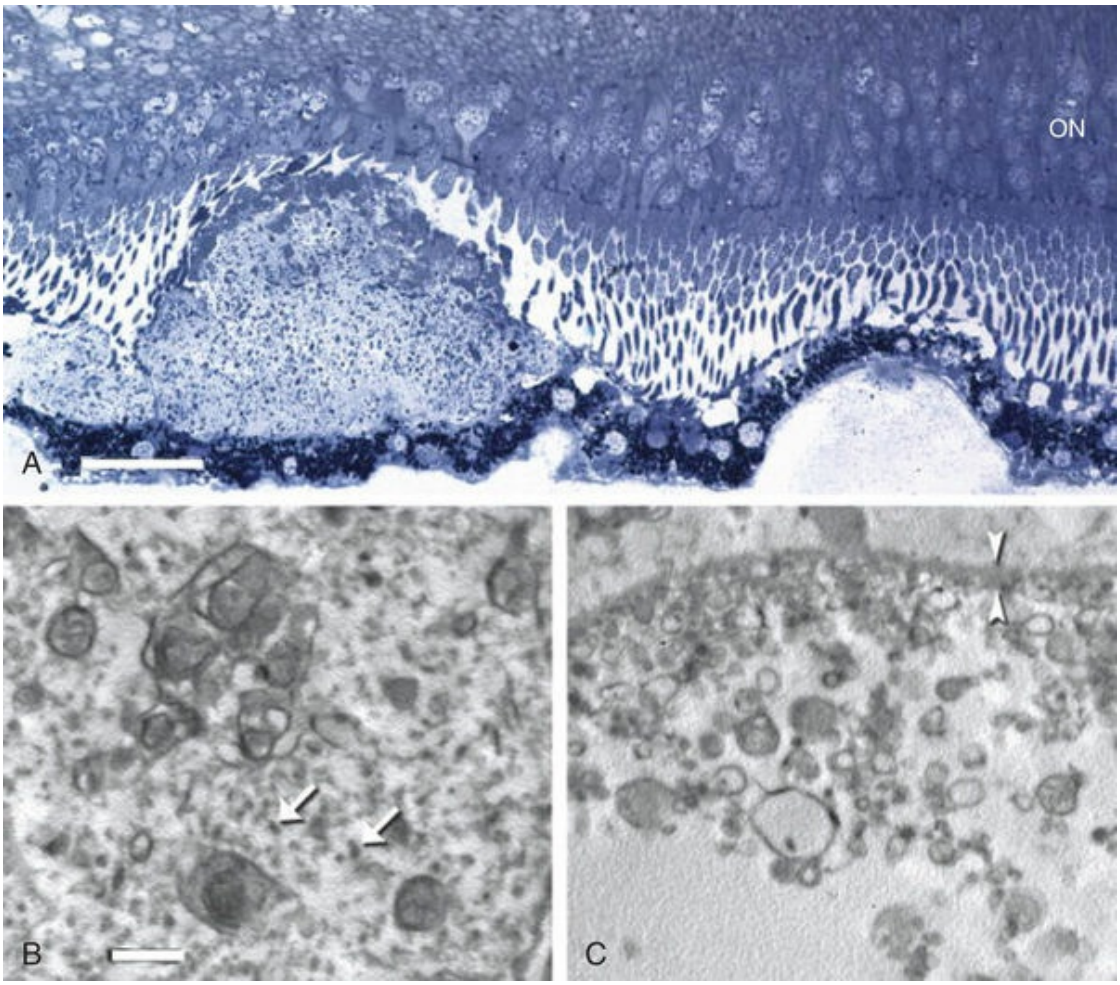

FIG. 68.13 Disposition and ultrastructure of subretinal drusenoid deposits and soft drusen. Sections were postfixed by the osmium-tannic acid-paraphenylenediamine method for neutral lipid and sectioned at 1 μm for staining with toluidine blue (A) or sectioned for transmission electron microscopy (B,C). (A) Adjacent subretinal drusenoid deposit (at left) and soft druse (at right) that is attached to the retinal pigment epithelium. The subretinal drusenoid deposit is well formed, with overlying photoreceptors that are deflected or shortened. It includes an apical cap of material, distinct from outer segments in both staining density and size. The soft druse has partial contents that bind little stain. Both retinal pigment epithelia underlying the deposit and overlying the druse are minimally disturbed. Scale bar: 25 μm. *ON*, outer nuclear layer. (B,C) The interior of the subretinal drusenoid deposit has complex membranous whorls with neutral lipid interiors dispersed throughout a ground substance with globular proteins (*arrows*). In

contrast, the soft druse has membranous debris of simpler shapes, mostly spheres, and heterogeneous sizes. Much of the druse contents are missing, consistent with the known physical fragility of these lesions. Globular proteins present in (B) are absent in (C). Scale bar: 1 μm. *Arrowheads* indicate retinal pigment epithelium basal lamina. (Reproduced with permission from Spaide RF, Curcio CA. Drusen characterization with multimodal imaging. Retina. 2010;30(9):1441-54.)

When membranous debris is present anterior to the RPE basement membrane, it is in conjunction with continuous early or late BlamD. It is not found in this tissue plane in the absence of BlamD[74,75] (Fig. 68.6). In this particular location the membranous debris forms layers and then basal mounds internal to the RPE basement membrane (Figs. 68.1C and 68.12). Membranous debris in this location is not demonstrated well in conventional light microscopic histologic sections, since the mounds manifest only as small, unstained spaces within the BlamD (Fig. 68.14). As the mounds of membranous debris associated with BlamD enlarge and fuse, the RPE overlying it shows more derangement and cell dropout.[75]

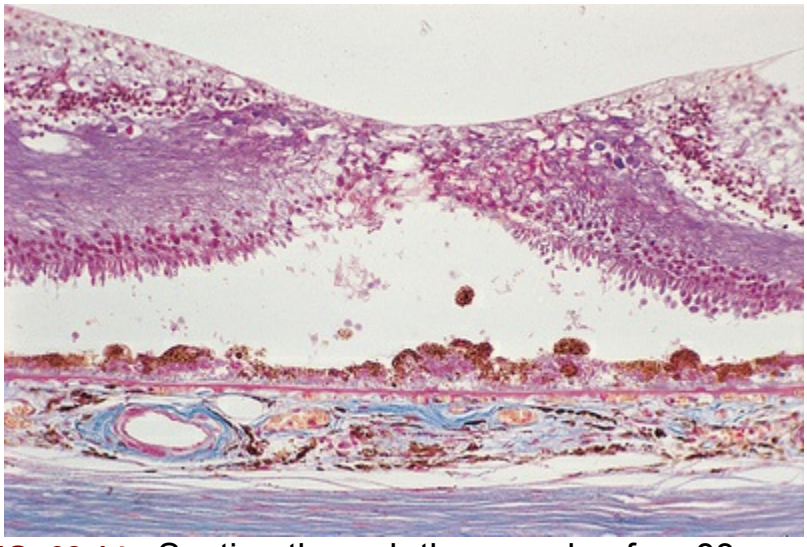

FIG. 68.14 Section through the macula of an 83-year-old man in whom pigment changes were evident clinically. Stretches of attenuated, hypopigmented retinal pigment epithelium (RPE) alternate with clumps from which hyperpigmented cells are shed into the

subretinal space. Basal laminar deposit is thicker and comprises both early and late forms. Small, unstained patches beneath the RPE would correspond to mounds of membranous debris on electron microscopy (×525). (Reproduced with permission from Sarks SH. Aging and degeneration in the macular region: a clinico-pathological study. Br J Ophthalmol 1976;60:324–41.)

Membranous debris posterior to the RPE basement are a major component of BlinD (discussed above), and membranous debris in the subretinal space has been correlated with the clinical appearance of subretinal drusenoid deposits (reticular pseudodrusen), which are described further below.[73,84]

Significance of Basal Deposits and Membranous Debris.

By light microscopy, the finding of continuous BlamD is regarded as the hallmark of AMD. However, by TEM, it is membranous debris that correlates more closely with clinical signs of AMD. In particular, increased accumulations are associated with late stage AMD.[75,77] This association had been noted by Sarks and coworkers[75,81] and was studied in a more formal way by Curcio and Millican.[77] In the latter study, TEM findings from eyes with and without AMD based on histopathologic evidence of drusen and RPE changes were evaluated to determine the sensitivity and specificity of various TEM features for diagnosing AMD. Identification of BlinD or large drusen (both features consisting of membranous debris external to the RPE basement membrane) had a specificity of 0.73 and a sensitivity of 0.9 for an AMD diagnosis, whereas continuous BlamD with membranous debris had a specificity of 0.68 and sensitivity of 0.7. The specificity of BlinD and continuous BlamD was similar, meaning that most eyes with either feature had AMD; however, the lower sensitivity of continuous BlamD as compared to BlinD means that many eyes with AMD do not have continuous BlamD while they are likely to have BlinD. When any BlamD, as opposed to continuous BlamD, was evaluated, sensitivity increased but specificity decreased, meaning that most eyes with AMD had some BlamD, but many eyes with BlamD do not necessarily have typical clinical features of AMD.[77] This is consistent with the concept that some BlamD is consistent with

normal aging and the presence of any form of membranous debris (within BlinD, within large drusen, associated with BlamD) signifies the pathologic state of AMD.

Retinal Pigment Epithelium and Photoreceptors

During normal aging, lipofuscin and complex melanolipofuscin granules accumulate in RPE cells and the cells become pleomorphic in size, shape, and degree of pigmentation. Pathologic changes within the RPE that have been described in AMD include the continued accumulation of these materials while the cells enlarge and lose their regular shape.[75] The posterior or basal surface of the cells shows loss of the basal infoldings and a consequent reduction in surface area. The RPE becomes increasingly separated from its basement membrane by thickening of the BlamD and more membranous debris.[75] Occasional cells undergo lipoidal degeneration or become vacuolated.[75,85,86] Finally, the hyperpigmented cells resulting from this phagocytic overload round off and lose all but a few apical microvilli.[75] This may indicate a loss of their ability to phagocytose.[75] Lipofuscin becomes packed into large degenerate retinal pigment cells or membrane-bound bodies and can be shed into the subretinal or sub-RPE space (Fig. 68.1D; see Figs. 68.9G–E and 68.14).[75]

The changes described above may appear visible on macular examination as small focal areas of hyper- or hypopigmentation. Focal hyperpigmentation correlates histologically with localized areas of RPE cell hypertrophy, which may be accompanied by clumps of hyperpigmented cells in the sub-RPE space, the subretinal space (see Fig. 68.14), and migrating to the outer nuclear layer (ONL) of the neurosensory retina.[75,86] Using SD-OCT[87] and ultrahigh resolution (UHR) OCT,[88,89] moderate to intense hyperreflective deposits have been demonstrated, in vivo, within these various planes. These findings have corresponded to foci of hyperpigmentation on clinical examination or on fundus photographs. It is common for eyes with drusen to have these intraretinal deposits recognized on histopathology or OCT directly anterior to the drusen, primarily in the subretinal space or ONL, but migration can occur into more anterior retinal layers.[43,86,88] Focal hypopigmentation correlates with attenuated, depigmented RPE

cells surrounding the hyperpigmented cells.[78]

Based on histologic examination of RPE cells from eyes with various stages of AMD, Sarks, et al. proposed the following sequence of events occur for the evolution of progressive RPE atrophy.[75] When a RPE cell dies, the products are phagocytosed by its neighbors. These cells in turn become filled with lipofuscin and round off, losing their ability to phagocytose. As the dead cells are discarded, nearby viable cells migrate and increase in surface area. This results in thinned, hypopigmented cells adjacent to focal hyperpigmentation. Finally, neighboring cells can no longer stretch to fill the gap and atrophy results. Hyperpigmentation therefore precedes hypopigmentation, and this in turn is the prelude to the development of patches of atrophy.[75]

Progressive derangement of the RPE is accompanied by dropout of photoreceptors, with a reduction in the number of nuclei in the ONL. The inner segments tend to become shorter and more bulbous, and the outer segments may terminate in collections of membranes over the apical surface of the RPE[75] (Fig. 68.7). More advanced progressive changes that occur in the RPE and photoreceptors in eyes with GA are discussed further in a later section on this topic.

Bruch's Membrane and Choroid

In eyes with AMD, hyalinization and densification of Bruch's membrane extends posteriorly along the intercapillary pillars and may even surround the choriocapillaris[43] (Fig. 68.5, see Fig. 68.9). Some segments of Bruch's membrane thin, and small breaks within it develop.[79] Non-membrane-bound electron-lucent droplets of the type found in BlinD can also be identified in the ICZ and OCZ.[77]

The density of veins in the macular choroid is significantly reduced.[74] Away from regions of atrophy, the percent vascular area of the choriocapillaris and diameter of capillaries are not significantly different compared to control eyes.[90] However, fewer fenestrations per capillary are noted in eyes with GA compared to control eyes even in regions with overlying intact RPE.[90]

In addition to the structural changes identified within the choroid and Bruch's membrane, macrophages, giant cells, fibroblasts, and occasional lymphocytes are found in proximity to the outer surface

of Bruch's membrane in the space formerly occupied by the choroidal capillaries.[79,91] This chronic, low-grade inflammatory reaction, which possibly develops in response to the membranous debris liberated by degenerating RPE, is often found in the choroid near breaks in Bruch's membrane[79,92] and may be a link in the chain of events leading to CNV and progressive atrophy.

Drusen

As noted above, the clinical hallmark of AMD is the presence of at least one medium-size druse[19] or extensive small drusen,[17] with or without RPE abnormalities. The spectrum of drusen, how drusen evolve, and the histopathologic and imaging characteristics of drusen will be detailed in this section. Descriptions of clinical grading systems for AMD that highlight drusen features and the prognostic implications of these variables are discussed further in the section on management of NNVAMD.

Drusen Characteristics Identified With Ophthalmoscopy or Fundus Photography

Drusen can be described in terms of size, color, morphology,[81,93] and extent. Drusen size is estimated by comparing the shortest diameter of a druse to the width of a major retinal vein as it crosses the edge of the optic disc.[72,94] At this location the retinal vein has an approximate diameter of 125 μm. Drusen are labeled *small* when they are less than half the width of the reference vein (<63 μm), m*edium or intermediate* when judged at least equal to half the vein width but less than the full width (63 μm to <125 μm), and *large* when they are at least as big as the full retinal vein width (≥125 μm). For research studies, more precise estimates of drusen size are made by overlaying circles of known diameter to fundus images and selecting the smallest circle diameter that contains the shortest drusen diameter within it (Fig. 68.15) or by using digital software to measure individual drusen diameter on digital fundus images.[95] Drusen color varies from white, to pale yellow, to bright yellow. Concentrating on the morphology of drusen, both its borders and its central substance, drusen can be broadly divided into hard and

soft categories, with soft drusen being further subdivided into soft indistinct or soft distinct based on further characterization of the sharpness of the drusen borders.[17] Soft drusen are generally medium size or larger and have an amorphous appearance centrally and along the border. Viewed stereoscopically they appear to have an inherent thickness. Soft drusen may converge or become confluent with one another and demonstrate heterogeneity in size and shape. Hard drusen tend to be small and have a sharp or distinct appearance throughout the deposit, and they tend to exist individually from one another. As drusen size and morphology are highly correlated with one another, current drusen descriptions have largely shifted to inclusion of size alone, as this can be derived with more objectivity than describing drusen morphology.

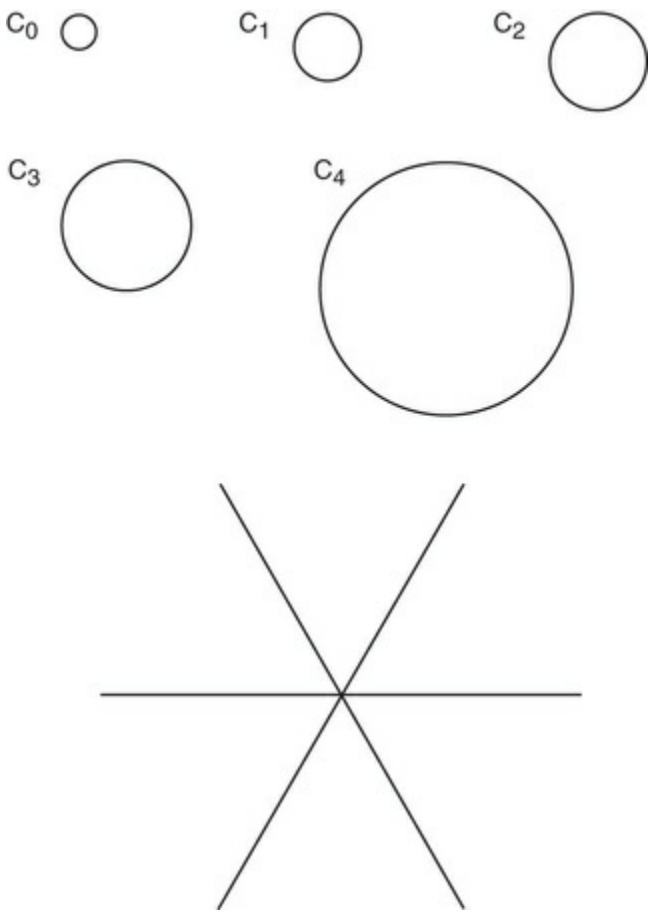

FIG. 68.15 Standard circles C0, C1, C2, C3, and C4 that are used to grade the size of specified lesions. They are reduced on a transparent sheet to range from 1/24 to 1/3 disc diameter, thereby representing 63 μm, 125 μm, 175 μm, 250 μm, and 500 μm, respectively.

Circle C0 is used to differentiate small from medium drusen, circle C1 is used to differentiate medium from large drusen, and circle C2 indicates the minimum area on which to base a definition of geographic atrophy. The diagonal lines facilitate locating the central point and estimating size of lesions. (Reproduced with permission from Bird AC, Bressler NB, Bressler SB, et al. An international classification and grading system for age-related maculopathy and age-related macular degeneration. Surv Ophthalmol 1995;39:367–374.)

The extent or severity of macular involvement may be assessed by noting drusen number or the total macular area occupied by drusen.[17,71,93] Drusen number may be simpler to categorize on clinical exam than mentally sweeping all drusen into an area and estimating the size of the area occupied by the "condensed" drusen. Drusen number may be described as *minimal* or *nonextensive* under the following conditions: when there are fewer than five and the largest druse present is small; when there are fewer than 20 and the most advanced druse present is soft, indistinct, and extensive soft distinct drusen are not present; or when there are fewer than 65 soft distinct drusen in the absence of extensive soft indistinct drusen on macular examination. Moderate or extensive drusen are present when the number of drusen within these drusen subtypes is exceeded. Area occupied by drusen is largely reserved for research purposes, as it requires study of fundus photographs with the assistance of templates that depict a spectrum of area sizes to estimate the total drusen area. Alternatively, software programs for use with human operators or automated programs may be used to identify and outline each druse present within the macula on digital color images of the fundus[95] or from OCT images[96] and then sum these areas to derive total macular area occupied by drusen. The total area occupied by drusen is the single most important prognostic feature for AMD worsening and is discussed in the section on management of NNVAMD.

Different patterns of age-related drusen distribution have been reported.[97] The superior and temporal quadrants of the posterior pole are typically associated with the largest area of soft indistinct drusen involvement. However, after adjusting for the differences in absolute area mapped by the nine subfields illustrated in the

ETDRS 6 mm diameter grid (Fig. 68.16), it is the central subfield that has the highest percent area occupied by drusen.[97] Subretinal drusenoid deposits (reticular drusen) are most commonly found in the superior and temporal subfields and are sparser centrally.[73,98] Comparisons between the two eyes of an individual with bilateral NNVAMD may demonstrate a fair degree of symmetry in drusen number, type, and distribution.[97,99]

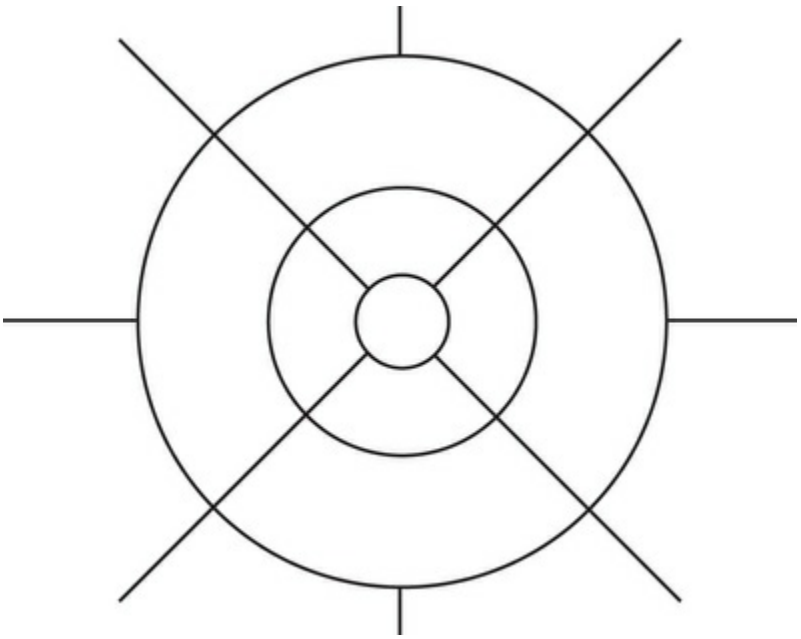

FIG. 68.16 Standard grid for classification of age-related macular degeneration. For a 30° fundus camera the diameters of the central, middle, and outer circles are 1000 μm, 3000 μm, and 6000 μm, respectively. These circles represent the central, inner, and outer subfields. The diagonal lines help to center the grid on the macula. (Reproduced with permission from Klein R, Davis MD, Magli YL, et al. The Wisconsin age-related maculopathy grading system. Ophthalmology 1991;98:1128–34.)

Drusen may have a life cycle, as drusen number may increase or decrease over time while size and morphology can also evolve. Some drusen may grow larger in diameter, taller in height, and coalesce while others may spontaneously regress. Drusen regression is characterized by reduction in yellow color, decrease in thickness, greater definition of drusen borders, potential appearance of glistening calcification, and the emergence of RPE

atrophy or depigmentation (see Fig. 68.17).[81,100,101] This is discussed further later in this section.

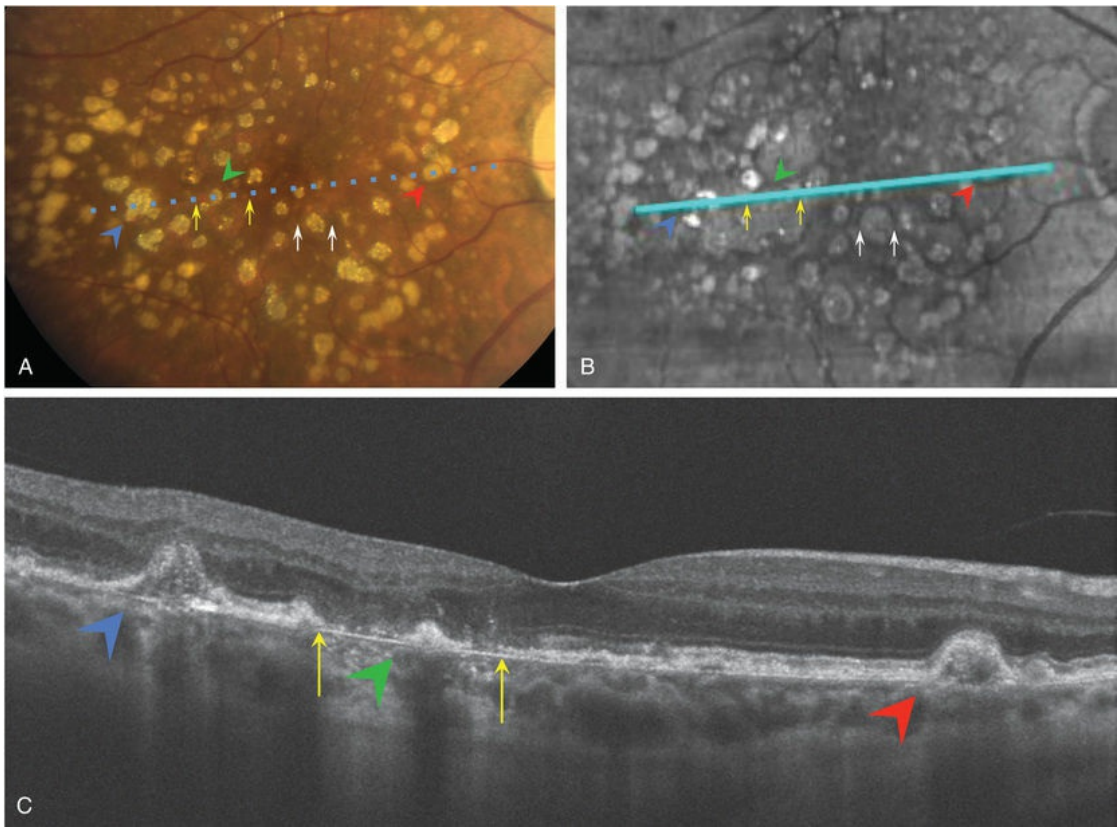

FIG. 68.17 Images of the right eye of a 76-year-old Caucasian woman with non-neovascular age-related macular degeneration (AMD) in the right eye and neovascular AMD in the left eye. Images show calcified drusen and multifocal, fovea-sparing geographic atrophy (GA) in the right eye in various stages of regression of drusen and progression of GA. (A) Color fundus photograph, (B) near infrared reflectance (NIR) image from Zeiss Cirrus spectral domain optical coherence tomography (SD-OCT), (C) high resolution SD-OCT scan through area shown as dashed blue line on color photography and as solid blue line on NIR image. *Blue arrowheads* show regressing calcified druse with developing GA. On OCT image, retinal pigment epithelium, ellipsoid layer, and external limiting membrane (ELM) overlying this druse is not visible. Highly reflective material is present. *Green arrowhead* shows regressed, calcified druse within area of GA (area of GA is between *yellow*

arrows). *Red arrowheads* show large druse with no apparent calcification on color photographs and examination. On SD-OCT imaging, this druse has internal hyper- and hyporeflective characteristics. Overlying ellipsoid layer and ELM is intact. *White arrows* denote a small focus of GA surrounding a regressed calcified druse. Extent of GA is more evident on NIR image compared to color photographs. This region is not captured in the SD-OCT B-scan image that is shown.

Clinicopathologic Characteristics of Drusen

Typical age-related drusen are deposits of extracellular material, which lie between the basement membrane of the RPE cells and the ICZ of Bruch's membrane (Fig. 68.18), the same tissue plane in which BlinD are found.[81] The clinical description of drusen mentioned at the beginning of this section pertains to the ophthalmoscopic appearance at a fixed point in time. Different histologic classification systems for drusen have been described,[76,78,81,102] with some relying solely on ultrastructural classification of the drusen,[102] others combining clinicopathologic correlations and more global assessments of the histologic features of the maculas,[76,78] and others combining historical changes on clinical exam and imaging with histopathologic assessment.[81] As these studies each have their own focus and different methods, it has been difficult to unify these classification systems.[102] Furthermore, there is relatively scant information describing drusen composition and structure and a relatively limited number of eyes that have been available for direct clinicopathologic correlation. In addition, the contents of soft drusen are easily lost during histopathologic processing, and thus all the constituents of these drusen may not have been identified. Discordance between the descriptions of ultrastructure of drusen and assumptions about drusen composition based on clinical descriptions also exists. For example, drusen of each of the four ultrastructural phenotypes described by Hageman could occur clinically in a range of drusen sizes that would appear small to large with ophthalmoscopy.[102] As clinically apparent small drusen correlate with hard morphology

and large drusen correlate with soft morphology, it would follow that the different ultrastructural phenotypes may exist in both hard and soft appearance on clinical exam. One can argue that any existing classification system may not be widely generalizable to clinical findings. Additionally, while limited clinicopathologic correlation studies focusing on drusen exist in this era of modern retinal imaging,[103] no studies have tried to relate the histologic description of drusen from older publications to observations made with FAF and SD-OCT images. Therefore, in the following sections, these prior classification schemes may be referenced, but the distinction, especially between differing soft drusen types under these classification systems,[76,78,81] will be deemphasized in this discussion.

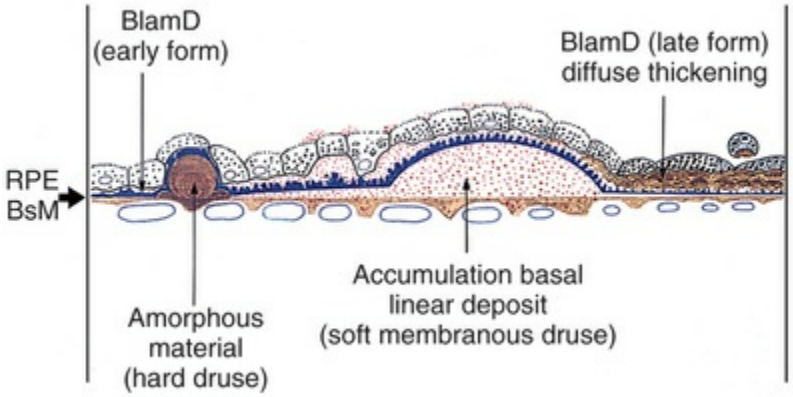

FIG. 68.18 Diagram showing the relationship to the retinal pigment epithelium (RPE) basement membrane (BsM) of the deposits accumulating under the RPE during the evolution of age-related macular degeneration. The basal laminar deposit (BlamD) lies internal to the BsM, and typical drusen lie external. The BlamD exists in an early, striated form (shown in blue) and late amorphous form (shown in brown). Membrane coils are found both internal to the BsM, as mounds at the base of the RPE, and external to the BsM, as the BlinD, where it may form soft, membranous drusen. Hard drusen consist predominantly of amorphous material.

Small, Hard Drusen

Small, hard drusen are not visible in the fundus until they have a diameter of 30–50 μm, equivalent to the width of two to three RPE cells. They are difficult to see in lightly pigmented fundi, but use of red-free light may facilitate identification. Small, hard drusen may first be noted within 1500 μm of the fovea,[97] but when numerous they are most common on the temporal side of the fovea. They tend to occur in clusters. Another common pattern for this type of drusen is a wide band outside the vascular arcades that continues nasal to the disc, with sparing of the posterior pole. Toward the equator they assume a linear arrangement in relation to a polygonal pattern of hyperpigmented lines, giving rise to reticular (honeycomb) degeneration of the pigment epithelium.

By following a number of patients with small, hard drusen over time, Sarks and coworkers described the process by which these drusen may fuse to form large drusen, which they termed "pseudosoft" drusen. Initially small, hard drusen that form in a cluster may remain as discrete deposits on ophthalmoscopy, even if they appear to touch one another. As the drusen become more closely packed, the cluster morphs into a single larger deposit that clinically appears soft; however, the small drusen can usually still be made out in red-free light[81] (Fig. 68.19). These fused drusen are up to 250 μm in diameter, depending on the number of drusen in the cluster. If sufficiently elevated, they may tent up the RPE and retina, which may cause a reddish halo around the base of the deposit[81] (Fig. 68.20). These clusters of fused, small, hard drusen can be found in middle age. Some of these drusen slowly regress over many years leaving a focal patch of RPE atrophy or GA (Fig. 68.20). This cycle may be completed in younger persons before the BlinD and membranous debris characteristic of AMD have developed. As such these cluster-derived large drusen can occur independently of the intermediate or advanced stages of AMD.

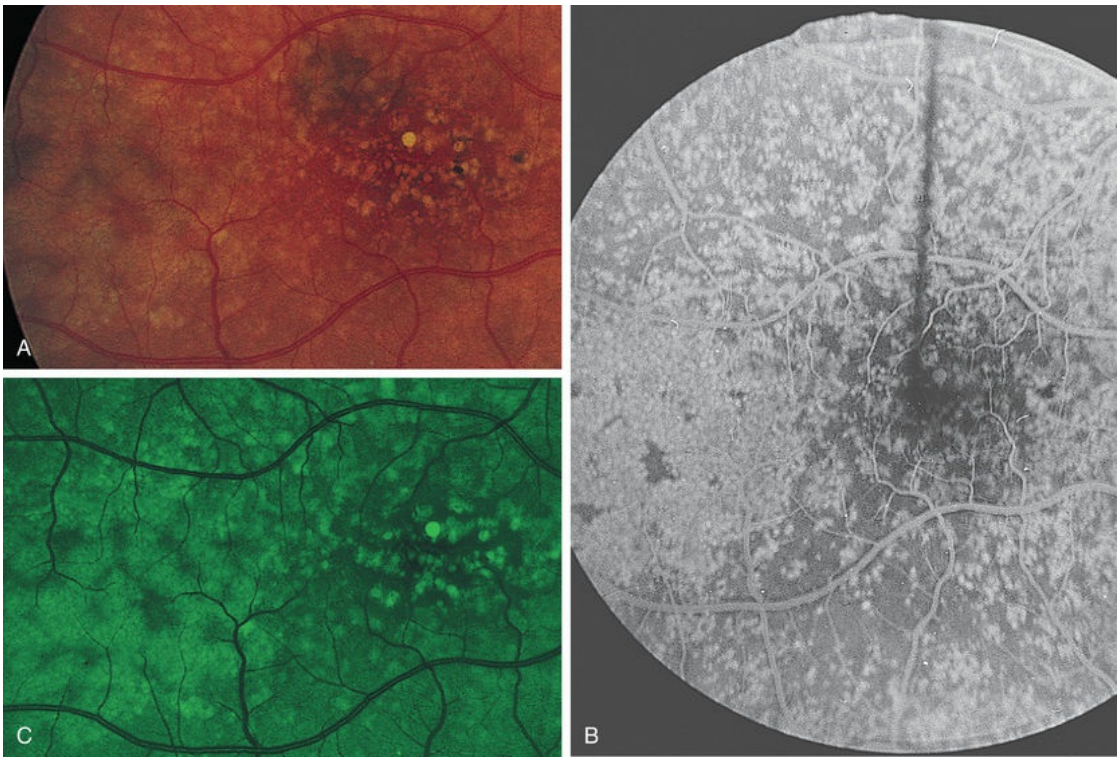

FIG. 68.19 Soft, cluster-derived drusen (pseudosoft drusen). Right fundus of a 50-year-old man with 20/20 vision (A). Groups of mainly small, hard drusen associated with hyperpigmentation are seen at the fovea. Large, soft, confluent drusen appear to be located temporal to the fovea, but in red-free light (C), and particularly on fluorescein angiography (B), the soft drusen can be seen to consist of closely packed clusters of small, hard drusen.

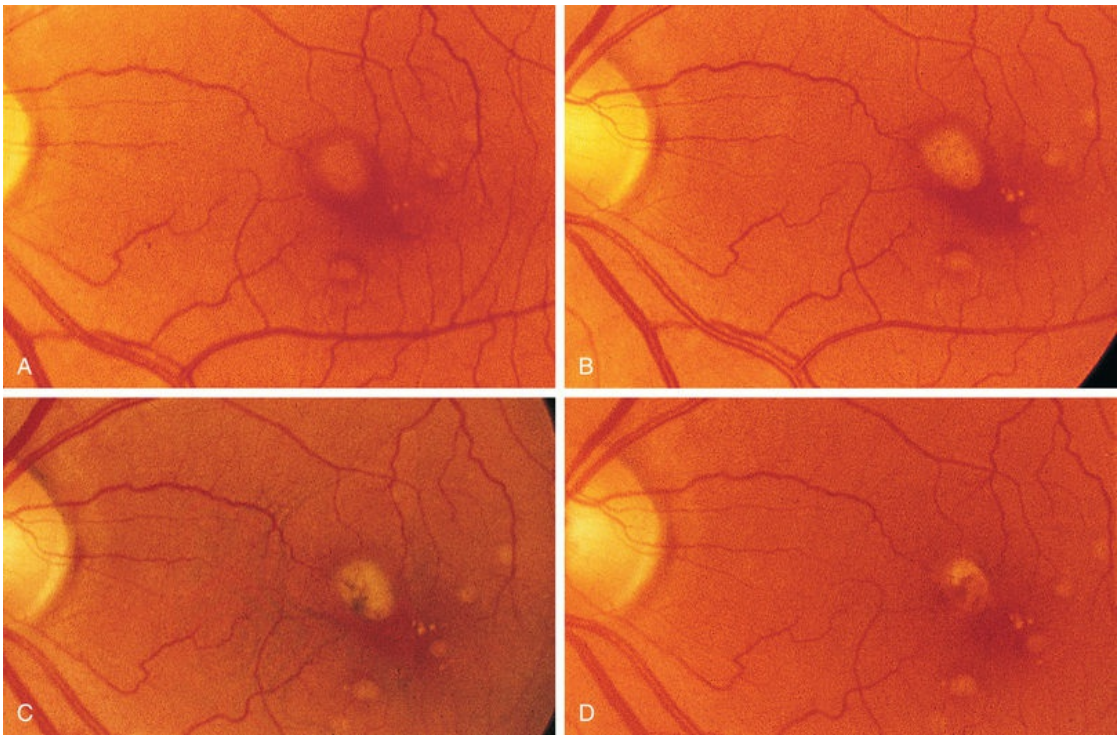

FIG. 68.20 Patient illustrating large pseudosoft druse with halo around base, apparently derived from a fused cluster of small, hard drusen. Photographs trace the regression of the druse over 9 years. The druse was located just superior to the foveal center and vision remained unaffected. (A) At age 48, the druse is surrounded by a red halo. (B) At age 52, the druse appears whiter, and pigment stippling is present over the surface. (C) At age 54, the halo fades as the druse becomes shallower and clumps of hyperpigmentation are preceding the formation of a patch of geographic atrophy (GA). (D) At age 57, the drusen material is resorbing and a patch of GA is emerging. This appearance may be called incipient GA. (Reproduced from Sarks SH. Drusen patterns predisposing to geographic atrophy of the retinal pigment epithelium. Aust J Ophthalmol 1982;10:91–97.)

Large, Soft Drusen

For drusen that they considered to be associated with AMD, Sarks et al. made the distinction between larger, more distinct soft-appearing drusen that they termed "granular soft" drusen (Fig. 68.21) and paler, shallower medium-size drusen with more indistinct borders that they termed "soft membranous" drusen[81] (Fig. 68.22). This nomenclature was based on clinicopathologic data

(detailed below) from a limited number of eyes with these features that had been followed for many years. The former are about 250 μm in diameter and have a yellow, solid appearance, their confluence resulting in crescentic or sinuous shapes (Fig. 68.21). The latter are usually smaller than 250 μm, most commonly 63–175 μm in diameter. Their margins are usually indistinct, and they readily become confluent (Fig. 68.22). They described these drusen as common in eyes with intermediate or advanced AMD.[81]

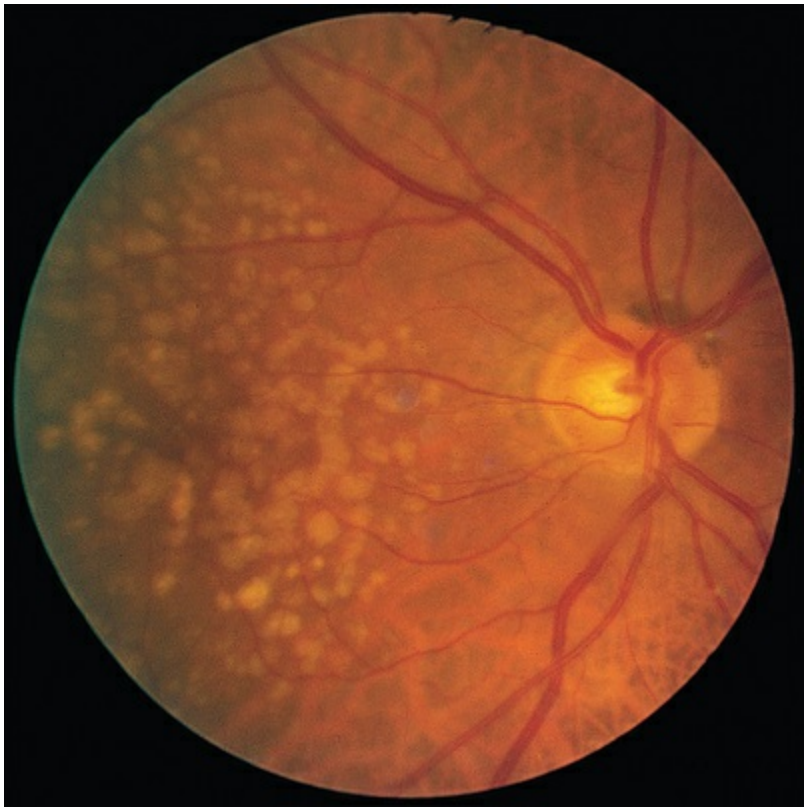

FIG. 68.21 Soft drusen of granular structure. Numerous soft, yellow drusen of solid appearance in the right eye of a 72-year-old man. Confluence of soft drusen results in a sinuous pattern. Patient died 3 years later, and corresponding histopathology (see Fig. 68.26) demonstrated a granular structure derived from broken down small, hard drusen. (Reproduced with permission from Sarks SH. Drusen and their relationship to senile macular degeneration. Aust J Ophthalmol 1980; 8:117–130.)

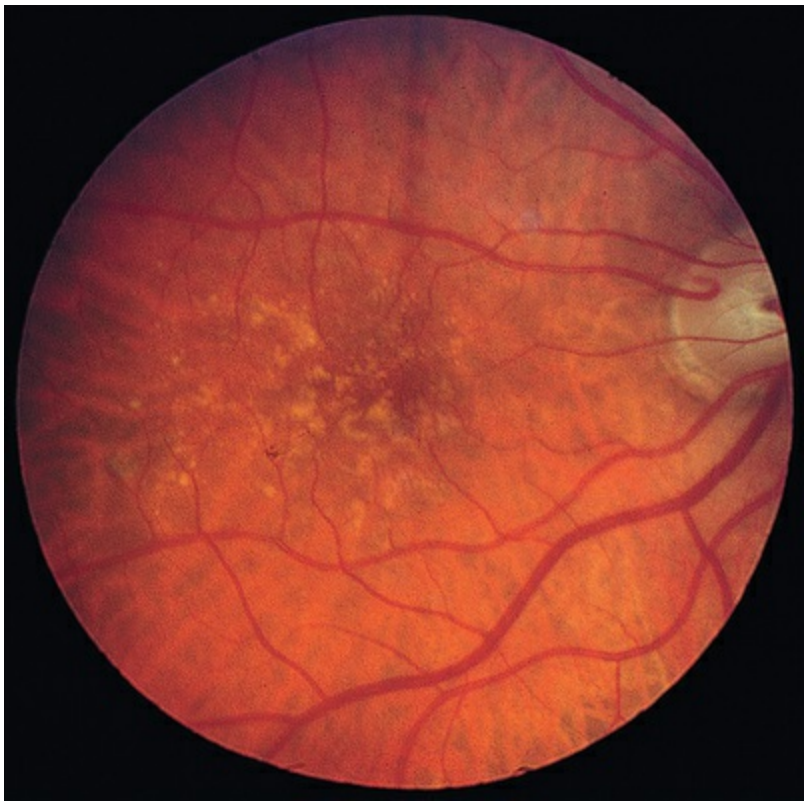

FIG. 68.22 Color photograph of the right eye of a 71-year-old man showing soft, indistinct drusen composed of membranous debris. This eye developed a hemorrhagic disciform lesion shortly before the patient died at age 75. The left eye had similar drusen and also proved to contain an early active neovascular membrane. The morphology of the drusen in the left eye is illustrated in Figs. 68.11, 68.27, and 68.28.

(Reproduced with permission from Sarks JP, Sarks SH, Killingsworth MC. Evolution of soft drusen in age-related macular degeneration. Eye 1994;8:269–283.)

Soft drusen that are larger than 250 μm, but more so those larger than 500 μm, may have an accumulation of serous fluid, may be translucent on retroillumination, and may be referred to as drusenoid PEDs[104–107] (Figs. 68.23 and 68.24). A fluid component is presumed due to their appearance on retroillumination and their sometimes rapid resolution following laser photocoagulation performed at the border of the drusenoid PED.[108] These drusen were described as a separate clinicopathologic category by Sarks et al.,[81] but they likely represent a continuum of progression from other drusen types. They appear to evolve from progressive confluence of existing soft drusen often retaining a scalloped

outline representing the borders of the original individual druse before they merged.[81,107] They often grow to larger than one disc diameter (DD) (2.54 mm^2) in size with one prospective study showing an average size of 4.19 mm^2 at initial presentation with 14 of 16 drusenoid PEDs larger than 1 DD.[105] In another retrospective report one-third of the 61 drusenoid PEDs were greater than 1 DD at the presenting visit.[107] Drusenoid PEDs have variable elevation or thickening but tend to be shallower than serous PEDs and have less variable topography than fibrovascular PEDs. Drusenoid PEDs may enlarge over time, both in height and extent, and ultimately regress, with or without the development of NGA and GA. As overlying hyperpigmentation and hypopigmentation develop, often in the form of a radiating pigment figure, the contents become whiter and more inspissated. Once heavy pigment clumping has appeared, the drusenoid PED generally begins to collapse and may be replaced by GA[75,104] (Fig. 68.23). Relative to other types of PEDs, drusenoid PEDs have unique ophthalmoscopic and angiographic features (described below).

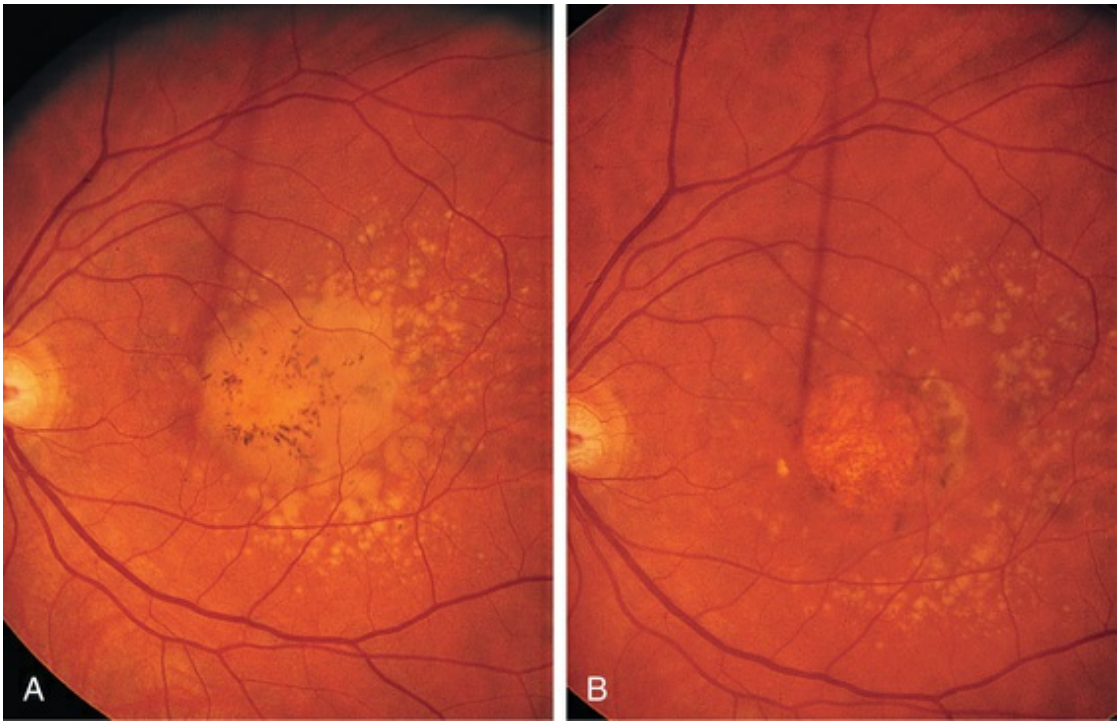

FIG. 68.23 Development of geographic atrophy following the collapse of a drusenoid pigment epithelial detachment (PED). (A) Left eye of a 65-year-old woman with a drusenoid PED that had been observed

to develop from the confluence of soft drusen. Clumps of focal hyperpigmentation developed on the surface of the PED (vision 20/50). Choroidal neovascularization (CNV) was never identified on fluorescein angiography (FA), rather the PED was brightly fluorescent. (B) Three years later the PED had collapsed, with an area of geographic atrophy replacing much of the same area. Many of the surrounding soft drusen have spontaneously resolved as well, many without overt signs of nongeographic atrophy in their place.

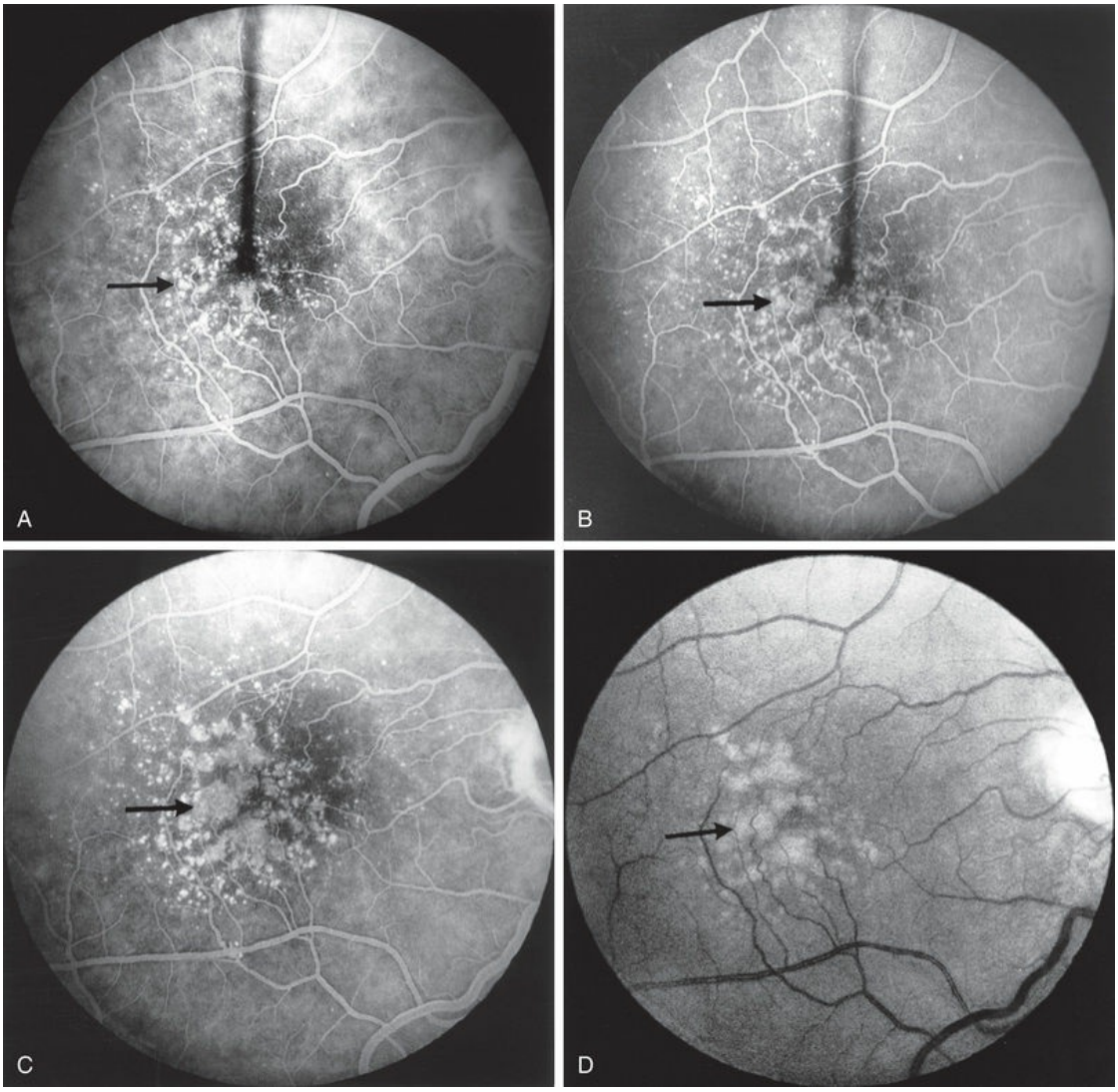

FIG. 68.24 Patient showing evolution of clusters of small, hard drusen into larger, soft, confluent drusen (*arrows*), presumably due to the addition of serous fluid. Fluorescein angiograms of the right eye of a man

at age 55 (A), 58 (B), and 61 (C). The drusen farthest from the fovea remain discrete. In the inner macula they form clusters in which the individual drusen are more difficult to distinguish owing to confluence and breakdown. The more central clusters have become completely homogeneous on fluorescein angiography. (D) Red-free photograph at age 61 shows corresponding clinical picture. Homogenized clusters have a soft, yellow appearance. Visual acuity remained 20/20, although the patient had been aware of some deterioration.

All drusen types may in time disappear,[7,26,109] but this does not necessarily signify a return to a more normal state, since areas of drusen may be replaced by other subtle or more severe manifestations of AMD. When drusen fade some eyes appear "improved," but whether this is associated with a decreased risk of the late stages of AMD remains to be seen. It is doubtful that the RPE remains unaffected at these locations as fluorescein angiography (FA) may show increased transmission of fluorescence where drusen have faded.

Drusen often begin to regress in conjunction with failure of overlying RPE, frequently assuming a whiter and harder appearance as the contents of the druse become inspissated (see Fig. 68.20). Hyperpigmentation and hypopigmentation often develop over the surface of the druse. Later the margins become irregular and foci of calcification may appear, especially after the age of 60 years. Ultimately the drusen fade and may leave multifocal patches of nongeographic atrophy (NGA) and GA that reflect their original distribution. Glistening calcium deposits may remain in these atrophic areas for many years (Fig. 68.17).

Histopathology of Drusen

Small, Hard (Hyalinized, Nodular) Drusen

Small, hard drusen histologically are focal globular deposits of hyalinized material along the inner aspect of Bruch's membrane with staining properties similar to hyalinized Bruch's membrane (see Fig. 68.8).[81] They have also been called nodular drusen.[78] Histopathologic specimens have shown that within an area of

clinically apparent hard drusen clusters there are often numerous intervening drusen too small ("microdrusen") to be seen on clinical examination.[81] This is the predominant drusen type found in postmortem specimens from younger persons, and they are ubiquitous, present in 83% of donors between age 36 and 94 (mean 67 years).[110] Certain changes in Bruch's membrane may precede formation of these drusen.[111] In eyes with only a few drusen, small, hyalinized plaques of densification in Bruch's membrane are observed, sometimes with extensions into the OCZ and even on to the anterior surface of the choroid.

These drusen have an amorphous appearance on electron microscopy (Fig. 68.25).[81] Another early change, seen only by electron microscopy, is that of coated membrane-bound bodies, both ruptured and intact (see Fig. 68.2), that are trapped between the basement membrane of the RPE and the inner collagenous zone (entrapment sites) as well as in the OCZ.[111] Entrapment sites are found in specimens from all ages and probably indicate a normal aging phenomenon.

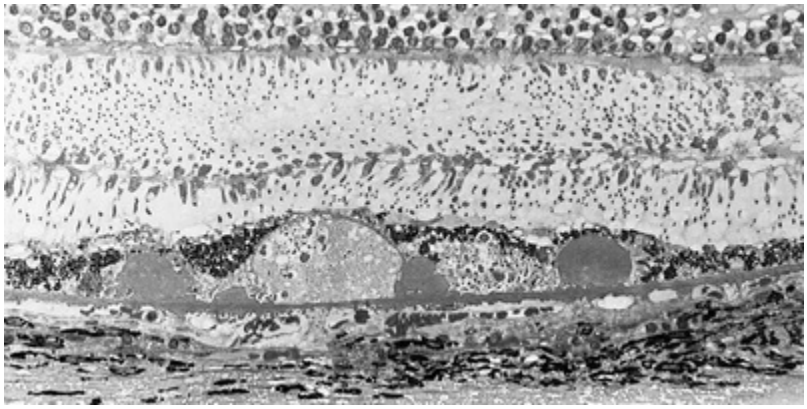

FIG. 68.25 Electron micrograph shows a parafoveal cluster of small, hard drusen measuring 250 μm in diameter with the drusen touching and fusing. Larger drusen inside the cluster are breaking down into globules of hyaline material, leaving small, hyalinized drusen around the perimeter. The smallest drusen would not be seen clinically, but they can be assumed to be present around the larger, visible drusen. Retinal pigment epithelium over the larger drusen is thinned. Fundus had shown only a few drusen clusters. Vision was 20/20 2 years before death at age 81; lens

opacities and dementia precluded further documentation. The cluster would appear as a single deposit, and fluorescein angiography (not performed) would be expected to demonstrate brightly staining, small drusen around a more homogeneous center (methylene blue and basic fuchsin, ×290).

In eyes with many small, hard drusen the Bruch's membrane findings noted above become more extensive. Hyalinized drusen form anterior to these changes, and as they grow they become hemispherical or almost globular. When small, hard drusen grow larger than about 63 μm, the amorphous contents become less compact and paler-staining, a process that begins in the posterior part of the druse. On electron microscopy, greater electron density is noted at the borders and less in the center.[81] Microdrusen, or rounded elevations 2 μm in diameter, and composed of very dense amorphous material, may be seen in the intervening space between drusen.[81] Single hard drusen rarely exceed 125 μm, and further enlargement is the result of the fusion of several drusen, which have been termed "cluster-derived drusen."[81] As the RPE anterior to the drusen degenerates, the contents of the drusen become increasingly dispersed (Fig. 68.25) or, especially in older patients, coarsely granular (Fig. 68.26). Softening of the margins of hard drusen correlates with spreading of the base of the druse along Bruch's membrane (Figs. 68.25 and 68.26).

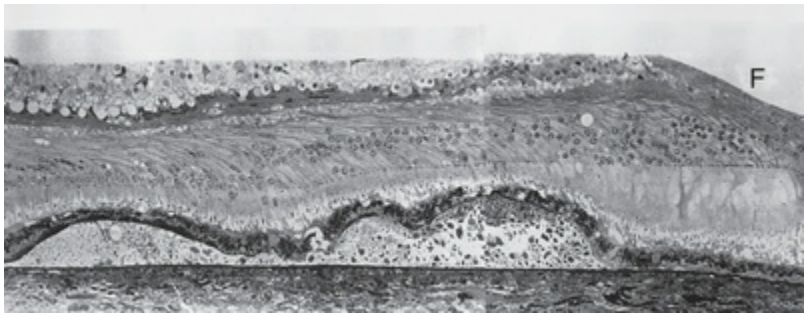

FIG. 68.26 Semithin section through edge of fovea (*F*) of eye shown in Fig. 68.21 demonstrates confluence of three soft drusen. Drusen have a granular structure, comprising variably sized globules of amorphous material, some membrane-bound. This material may be derived from the breakdown of small hard drusen,

several of which were still present around the edge of these drusen. Note that, as the contents break down, drusen tend to lose sharp margins and nodular surface elevations present in fused clusters (see Figs. 68.8 and 68.18). The fellow eye demonstrated similar drusen, but many were regressing (methylene blue and basic fuchsin, ×115). (Reproduced with permission from Sarks JP, Sarks SH, Killingsworth MC. Evolution of soft drusen in age-related macular degeneration. Eye 1994;8:269–83.)

In addition to the above findings, note there is an alternate hypothesis as to the generation of hard drusen, which is that some hard drusen are actually lipoidal degeneration of RPE cells.[78,85]

Soft Drusen

While distinct clinicopathologic categories of soft drusen have been described, these drusen types may differ only in their relative proportion of component material. Granular soft drusen have a coarsely granular structure on transmission electron microscopy (Fig. 68.26), consisting of membrane-bound globules of amorphous material, small membrane fragments, and other cellular debris. The presence of microdrusen and the proximity of some of these drusen to hyalinized (hard) drusen (Fig. 68.25) may indicate that the granular contents represent, in part, cluster-derived drusen in which the original hard drusen have broken down. In fact, it is the drusen in the center of a hard derived drusen cluster that appear to be initially affected (Fig. 68.25), as small, hard drusen may remain identifiable around the perimeter of the cluster. The detection of this heterogeneous composition, either on FA (Fig. 68.24) or in histologic sections, led to the designation semisolid.[112] A thin layer of this granular material would appear to resemble the soft drusen described by Green[76,78] as localized detachment of the RPE and BlamD deposit, in an eye with diffuse BlamD (Fig. 68.26).

Other drusen contain mostly membranous debris and can be thought of as localized accumulations of the same or similar material to that of which BlinD are comprised. Sarks et al. termed these “membranous” drusen, and Green referred to them either as “localized detachment of RPE and basal linear material in an eye with diffuse BlamD and BlinD” or a “localized detachment due to

localized accumulation of basal linear material in an eye with diffuse BlamD but not diffuse BlinD." As such Green created two categories from what Sarks described as "membranous" drusen, these two categories being differentiated based on whether or not diffuse BlinD were present.[78] On light microscopy, these drusen are pale-staining and faintly periodic acid–Schiff-positive, with a finely granular or ground-glass appearance; they may even appear optically empty. However, on electron microscopy they contain tightly packed membrane coils (Figs. 68.11 and 68.27; see also Fig. 68.13). A small amount of amorphous material may be present within the coils, so their contents have also been described as vesicular and granular electron-dense, lipid-rich material.[76,78] This membranous debris is morphologically similar to that which forms basal mounds internal to the RPE basement membrane, and continuity between the mounds and drusen through the basement membrane can at times be observed (Fig. 68.27).

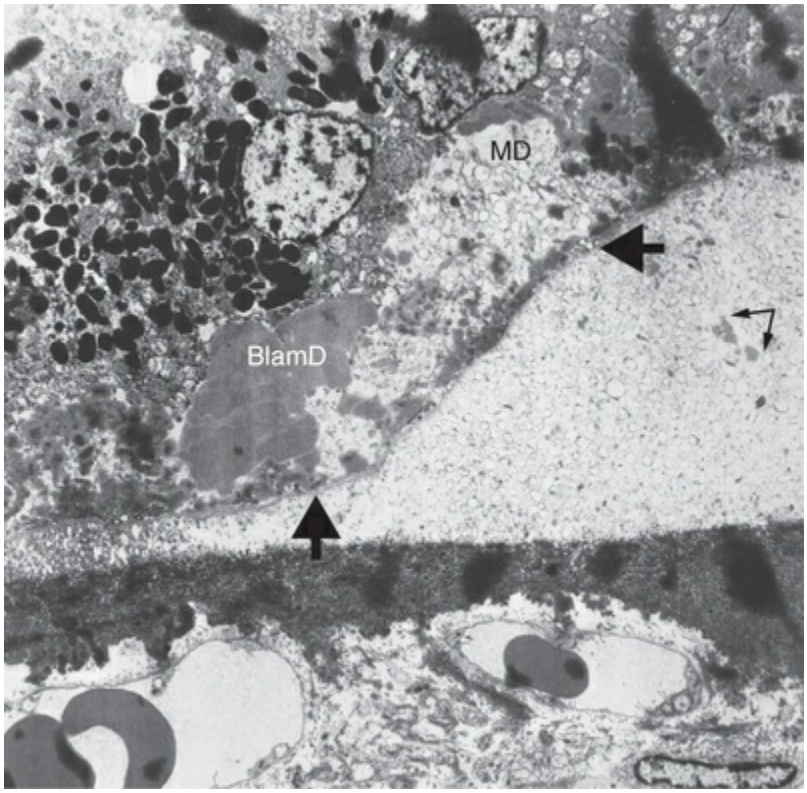

FIG. 68.27 Electron micrograph corresponding to the area indicated in Fig. 68.11 shows formation of a soft druse made up of coiled lipid membranes lying external to the basement membrane of the retinal

pigment epithelium (RPE) (*arrows*). The membranes appear first at the base of the RPE, where they may form basal mounds (*MD*). At the site of the right-hand arrow, some membranes can be seen within the basement membrane of the RPE and appear to be entering the soft druse from the basal mound. Some of the coils appear empty, and others contain amorphous material (*double arrow*). These drusen are specific for age-related macular degeneration, since they are only found after membranous debris develops. *BlamD*, Basal laminar deposit (x2210). (Reproduced with permission from Sarks JP, Sarks SH, Killingsworth MC. Evolution of soft drusen in age-related macular degeneration. Eye 1994;8:269–283.)

The BlamD anterior to these drusen is usually the early type because membranous material declines as late BlamD appears. Although these soft drusen are believed to develop de novo, small, hard drusen are commonly also present and then become incorporated into the membranous drusen; the amorphous contents of the hard drusen break down (Fig. 68.28).

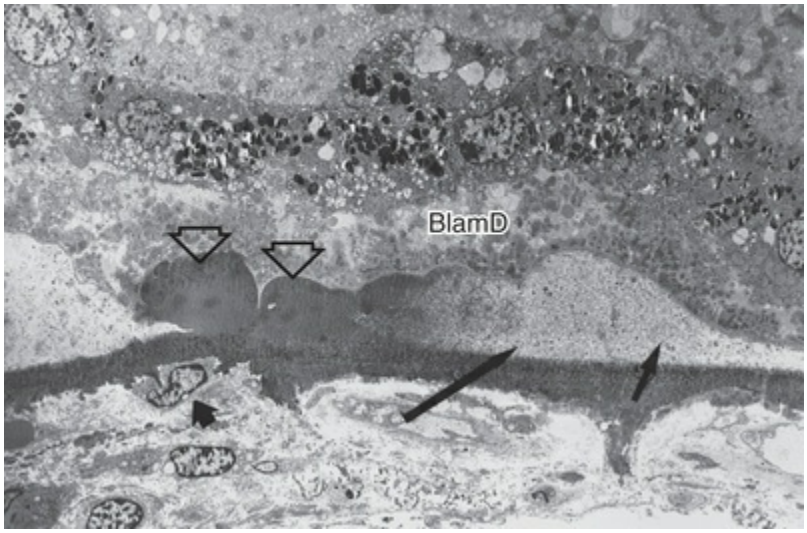

FIG. 68.28 Electron micrograph of the same eye in Figs. 68.11, 68.22 and 68.27 shows a cluster of subclinical, small, hard drusen (*open arrowhead*) apparently becoming eroded by membranous debris and breaking down into small membrane-bound particles (*central arrow*). At right (*shorter arrow*), druse consists of more characteristic membranous debris. This scenario suggests that small, hard drusen

become incorporated into soft drusen once membranous debris develops. Early-type basal laminar deposit (*BlamD*) lies over drusen. Note that the basal laminar deposit and retinal pigment epithelium remain anchored at the site of hard drusen but are separated from Bruch's membrane on either side by soft drusen. *Solid arrowhead* at left points to macrophage-type cell adjacent to outer surface of Bruch's membrane, where retina remains attached (x1260). (Courtesy of MC Killingsworth.)

Drusenoid PEDs, in some cases, represent large accumulations of membranous debris between the basement membrane of the RPE and the ICZ of Bruch's membrane.[78] It has been hypothesized that fluid my become trapped within drusenoid PEDs due to a failure of the RPE to pump water from this area due to lipoidal debris in Bruch's membrane creating a hydrophobic barrier.[113]

Regressing Drusen

On histopathologic examination both the RPE and the photoreceptors anterior to regressing drusen disappear, leaving a thick layer of late-type amorphous BlamD over the apex of the druse (Fig. 68.10). Macrophage invasion of regressing drusen has led to the hypothesis that they are instrumental in removing membranous debris. Material that is not removed becomes invaded by glial cells or collagen fibers or undergoes dystrophic calcification.

Imaging of Drusen

Angiography: Fluorescein and Indocyanine Green

Small Drusen.

Small, hard drusen may be visible with FA, even when as small as 25 μm, fluorescing brightly in the midvenous phase and fading soon after the background choroidal fluorescence does so[81] (Fig. 68.24). With coalescence of small, hard drusen, FA continues to show bright nonuniform fluorescence of these drusen through the midphase followed by late fading. The edges remain distinct initially but can become indistinct with softening of the margins of

the drusen. However, the presence of individual small drusen can usually still be discerned on FA (Fig. 68.19). In contrast to FA, with ICGA, small, hard drusen in aged individuals cannot be visualized in the early or the late phases of the ICG study.[114]

Medium and Larger Drusen including Drusenoid PEDs.

As opposed to small and hard drusen, soft drusen are not generally hyperfluorescent in the early phases of FA (Fig. 68.29). They hyperfluorescence in later stages with less intensity than hard drusen and with some inherent variability in intensity[103,114] (Fig. 68.29). In late phases of the FA, some soft drusen fade while others stain.

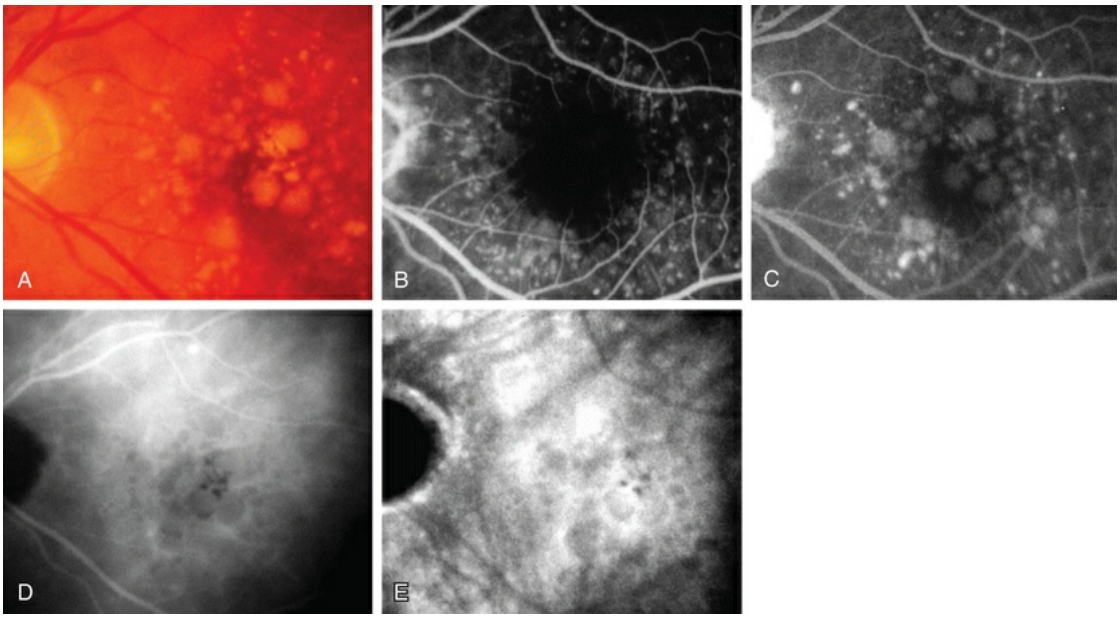

FIG. 68.29 Retina of 73-year-old subject with soft drusen and surrounding hard drusen. (A) Color photograph of retina. (B) Early phase fundus fluorescein angiogram showing early hyperfluorescence of hard drusen. (C) Late phase fundus fluorescein angiogram showing later staining of soft drusen. (D) Early phase indocyanine green angiogram (ICGA) showing hypofluorescence of the soft drusen centrally. Hard drusen are unable to be discerned. (E) Late phase ICGA showing persisting hypofluorescence of soft drusen. Note the surrounding relative hyperfluorescence of the margin of drusen. Hard drusen are isofluorescent. (Reproduced with permission from

Chang AA, Guyer DR, Orlock DR, et al. Age-dependent variations in the drusen fluorescence on indocyanine green angiography. Clin Exp Ophthalmol. 2003;31(4):300-4.)

The evolution of changes to drusen seen over a 6-year period in Fig. 68.24 suggests that small drusen may become incorporated into larger drusen. In the more peripheral macula the brightly fluorescent small drusen remain discrete. In the more central macula they form clusters in which the individual druse become progressively more difficult to distinguish. These drusen fill more slowly with fluorescein than the peripheral drusen but often show a few brightly fluorescent highlights around the edge of the deposits. The drusen clusters closest to the fovea may become completely homogeneous in intensity and filling characteristics during FA.

Drusenoid PEDs appear shallowly elevated and manifest faint late fluorescence similar to the filling of the surrounding soft fluid drusen.[104] Hyperpigmentation overlying the drusen create hypofluorescent figures on the anterior surface of the drusenoid PEDs.

With ICGA, soft drusen in individuals age 55 and older tend to be hypofluorescent (darker) relative to the background choroidal fluorescence pattern throughout the study with a thin hyperfluorescent margin on the outside of the druse appearing in the late phase[114] (Fig. 68.29). ICG is also a water-soluble dye and may not accumulate within the substance of the central druse where hydrophobic neutral lipids may be present. The hypofluorescence with ICGA is even more prominent with drusenoid PEDs in early, mid, and late phases, with masking of the underlying choroidal vessels due to thick overlying drusen material.[107]

Fundus Autofluorescence

Unless associated with overlying RPE changes, small drusen are not usually visible on FAF imaging. FAF imaging of soft drusen may show slight (mild intensity) hyperautofluorescence at the edges of the druse or throughout the druse (Fig. 68.30). Areas of hypoautofluorescence may indicate incipient atrophy over soft drusen.[115]

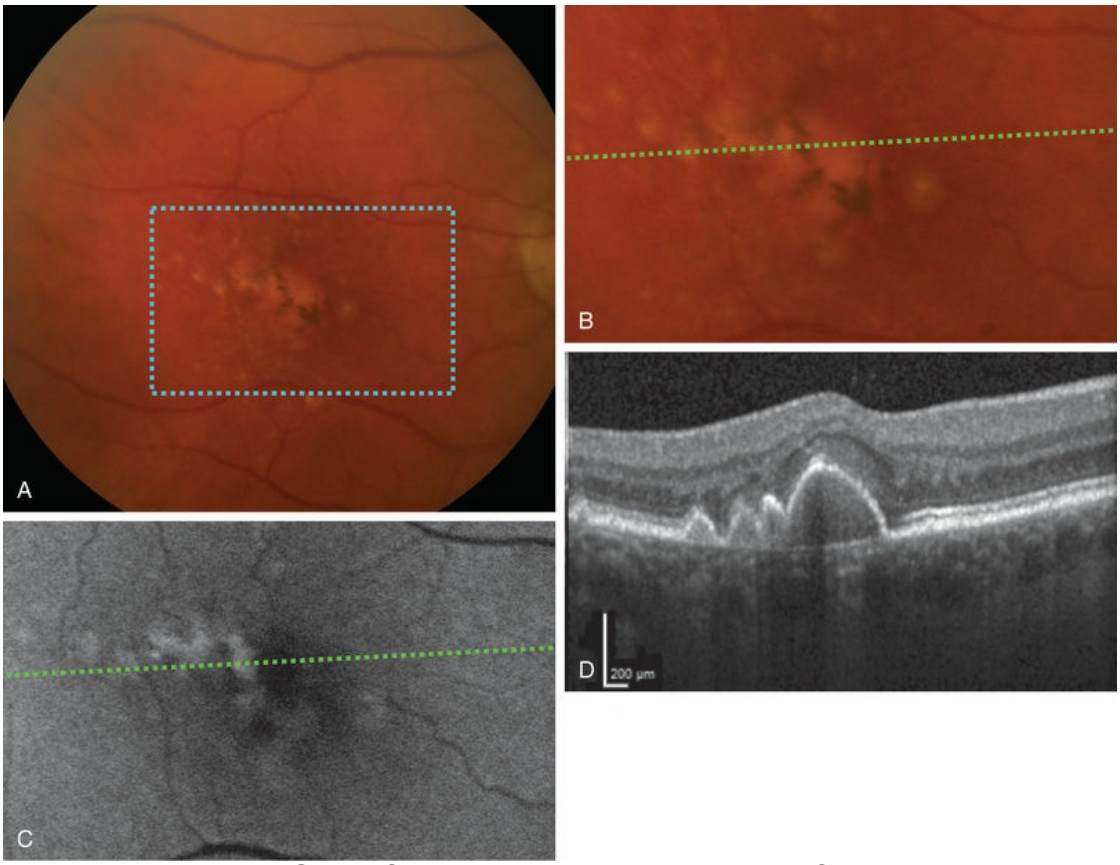

FIG. 68.30 Color fundus photographs (A,B), fundus autofluorescence (FAF) image (C), and Heidelberg spectral domain optical coherence tomography (SD-OCT) (D) image of the right eye of a 72-year-old Caucasian woman with intermediate non-neovascular age-related macular degeneration with large drusen and retinal pigment epithelium (RPE) changes. (B–D) Magnification of region in blue box in (A). Areas of hyperautofluorescence on FAF imaging (C) correspond to some of the soft drusen and RPE changes on color photograph (A,B). Corresponding drusen are present in this area on SD-OCT image (D). Ellipsoid zone disruption is also noted over these drusen.

Spectral Domain OCT

Small or hard drusen appear as slight elevations of the RPE using SD-OCT imaging, while soft drusen appear as 63–1000 µm wide deposits posterior to the RPE (Fig. 68.30D). Although soft drusen throughout the posterior pole of an individual eye may appear similar on clinical examination, they often manifest a variety of OCT appearances (Figs. 68.17C and 68.30D). The most common

appearance is convex-shaped deposits with homogenous medium internal reflectivity[116] (Fig. 68.30D). This pattern was seen in nearly all eyes (99%) with intermediate AMD in an ancillary study performed within the Age-Related Eye Disease Study 2 (AREDS2). The SD-OCT findings identified in this study among 314 eyes (314 participants) with intermediate AMD are shown in Fig. 68.31.[117] Drusen with high and low internal reflectivity were less common, present in 43% and 61% of eyes, respectively. Drusen with hypo- or hyperreflective cores (see Fig. 68.25C) were present in approximately 25% of eyes.[117] Anterior to the drusen more than 90% of eyes had thinning of the photoreceptor layer over some drusen with variable alterations in the ellipsoid zone (Figs. 68.17C and 68.30D). Foci of hyperreflectivity in the neurosensory retina anterior to the drusen was present in half[117] and may correlate with pigment or RPE cell migration into the retina[86] (Fig. 68.30D).

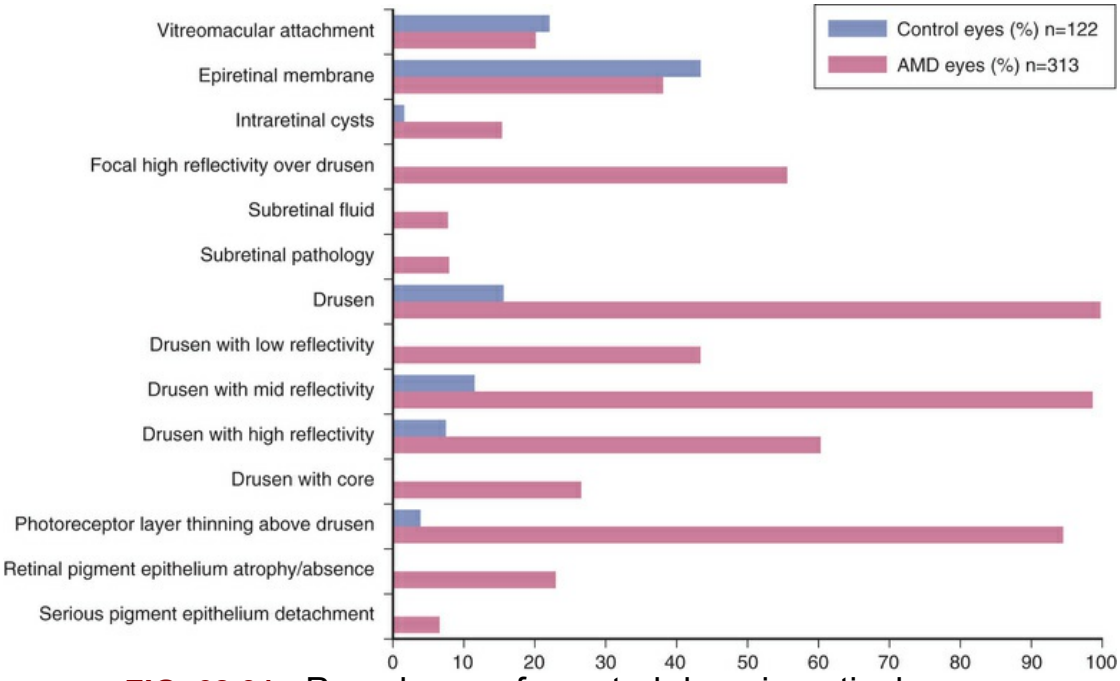

FIG. 68.31 Prevalence of spectral domain optical coherence tomography (SD-OCT) retinal changes and drusen characteristics among 313 AREDS category 3 age-related macular degeneration study eyes in the AREDS2 ancillary SD-OCT study. (Reproduced with permission from Leuschen JN, Schuman SG, Winter KP, et al. Spectral-domain optical coherence tomography characteristics of intermediate age-related macular degeneration. Ophthalmology. 2013;120(1):140-50.)

Automated algorithms have been developed that are applied to SD-OCT images to quantitate the two-dimensional area and three-dimensional volume occupied by drusen[96] and drusenoid PEDs[105] in the macula. These software programs are likely to become commercially available. Measurements using these algorithms are highly reproducible with an intraclass correlation coefficient of >0.99 for drusen area and volume.[96] Serial imaging over time using these programs has confirmed the dynamic evolution of macular drusen. In a prospective study of 143 eyes of 100 patients, mean drusen volume and area increased over time. However, at 12 months drusen volume had increased in 48%, remained stable in 40%, and decreased in 12% of eyes. Drusen volume measurements were defined as stable if the value at follow-up was within the 95% test–retest tolerance limits for the baseline measurement and as increased or decreased if the measurements fell outside of this range. Decreases in drusen volume were more common in eyes with larger baseline drusen volume.[118] In a prospective natural history study of 130 patients (186 eyes with non-advanced AMD), 16 eyes of 11 patients with drusenoid PEDs were identified during the study. Eight of these eyes continued to have a drusenoid PED till the end of follow-up (mean 18.5 months). Among the remaining 8 eyes, 7 had an increase in drusenoid PED volume before regression of the drusenoid PED was associated with progression to GA (5 eyes) or development of CNV (2 eyes). One eye had at least a 50% reduction in drusenoid PED volume without progressing to GA or CNV.[105]

On near infrared reflectance (NIR) imaging obtained with scanning laser ophthalmoscopy, often while obtaining SD-OCT, soft drusen may show decreased brightness relative to the surrounding background.[103]

Histochemistry of Drusen

Five substructural phenotypes of drusen have been described, but they do not correlate well with clinical drusen phenotypes as varying clinical phenotypes are comprised of similar molecules.[102] Drusen contain neutral fats and phospholipids,[119] as well as glycoconjugates containing specific carbohydrate residues.[120,121] The

latter were found in all classes of drusen, suggesting that both hard and soft drusen may have a similar origin.[121] Many hard and soft drusen contain specific cores with a carbohydrate-rich composition confined to distinct domains. These cores are positioned centrally within the drusen and are typically juxtapositioned to Bruch's membrane.[120] Some researchers have suggested that they may represent an early nucleation site around which other drusen-associated molecules including lipid are subsequently deposited.[92,120]

Other distinct components common to all phenotypes of hard and soft drusen include apolipoprotein E, immunoglobulins, factor X, amyloid P component, complement C5 and C5b-9 terminal complexes, fibrinogen, and thrombospondin.[121] Vitronectin is a major constituent of both hard and soft drusen, and vitronectin mRNA is expressed locally in the RPE, suggesting that vitronectin may participate in the pathogenesis of AMD.[122] A number of these drusen-associated constituents are participants in humoral and cellular immunity, including a number of acute-phase reactants, plasma proteins that rapidly elevate in response to inflammatory stimuli.

Other Patterns of Drusen and RPE Abnormalities that May be Found in Eyes With NNVAMD

Subretinal Drusenoid Deposits

Clinical Appearance.

Subretinal drusenoid deposits[73,84,123] (reticular pseudodrusen,[124] reticular drusen[25,93]) appear as a pale yellowish interlacing network of individual deposits, each about 250 μm in diameter (range 25–1000 μm) that resemble soft confluent drusen.[93,103] They are more readily visible when the fundus is examined with blue light.[84,103,125,126] Initially they appear most prominent in the superior macula (Fig. 68.32) although the network may slowly extend into other quadrants while sparing the fovea.[73,98]

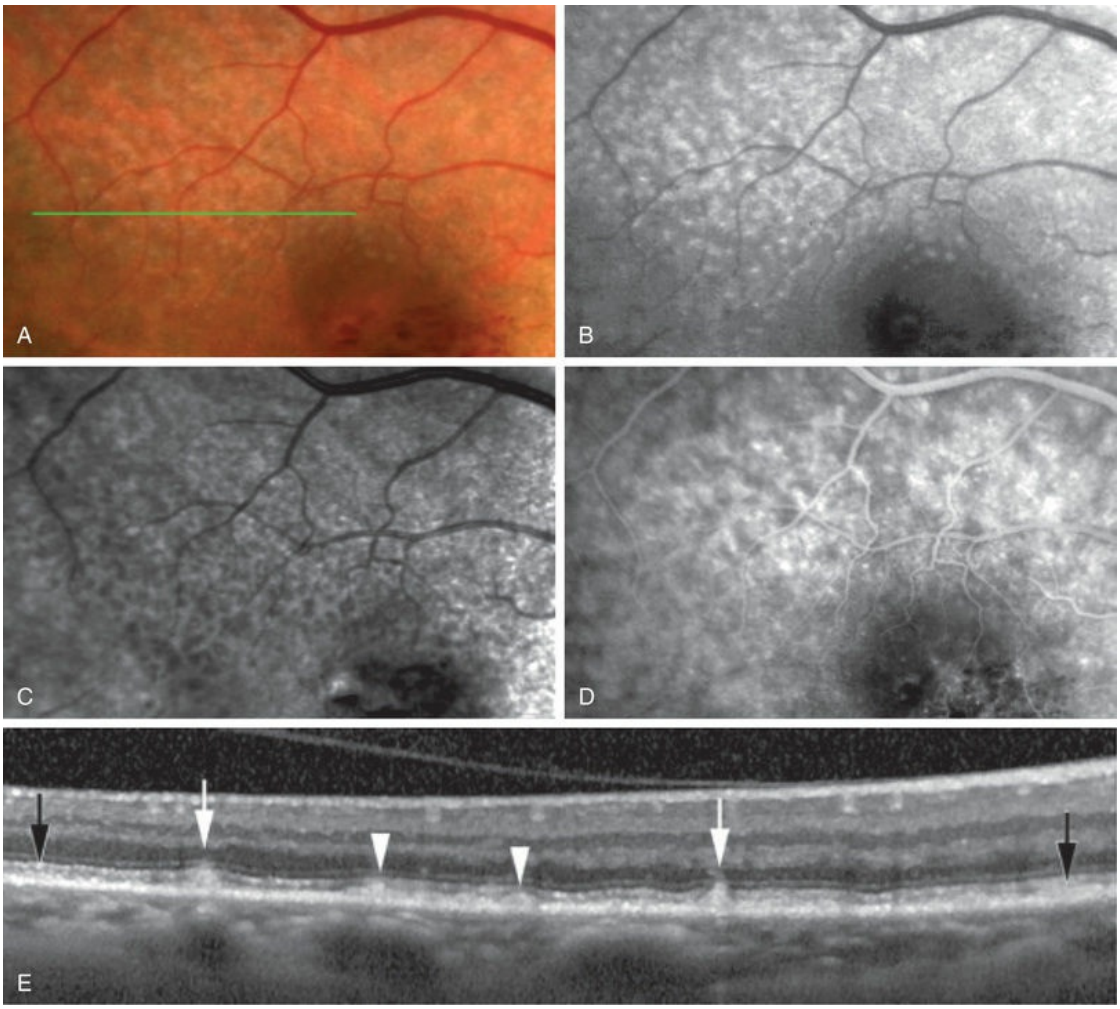

FIG. 68.32 (A) The color photograph shows a lacy arrangement of subtle whitish accumulations in a 78-year-old patient. The spectral domain optical coherence tomography (SD-OCT) slice location is shown as a green line. (B) The accumulated material is evident in the blue channel of the color photograph. (C) Near infrared imaging shows a denser array of dark material. (D) Late-phase fluorescein angiogram shows subtle variation in the background fluorescence. (E) An OCT scan shows drusenoid deposits in the subretinal space (stage 1: diffuse material between retinal pigment epithelium (RPE) and ellipsoid zone, *black arrows*; stage 2: sufficient material to alter contour of ellipsoid layer, *arrowhead*; stage 3: material breaks through ellipsoid layer, *white arrows*). Note the lack of sub-RPE drusen in this section. (Reproduced with permission from Zweifel SA, Spaide RF, Curcio CA, et al. Reticular pseudodrusen are subretinal drusenoid deposits. Ophthalmology. 2010;117(2):303-12 e1.)

Histology.

By light microscopy, the bases of reticular pseudodrusen appear to consist of flocculent material that lies in the subretinal space. This material has a dense cap that contains refractile material.[84,127] The photoreceptors anterior to these deposits show shortening or loss of outer segments and inner segment deflection or loss,[73] and the material can extend past the inner/outer-segment junction[127] (Fig. 68.33 and see Fig. 68.13). They can be present in isolation or in confluent drusenoid mounds and may be conical or flat in shape.[73,103] On TEM evaluation, subretinal drusenoid deposits have been shown to correspond to membranous debris in the subretinal space as had been described by Sarks et al.[73,75,84,103] They are comprised of accumulations of membranous debris, as well as flocculent material (Fig. 68.13B), similar in appearance to that seen in BlinD and BlamD and soft drusen (Fig. 68.13C).[73,75,103,127] By immunohistochemistry, these deposits have been shown to contain unesterified cholesterol, apoE, complement factor H, and vitronectin components that are also present in soft drusen.[127]

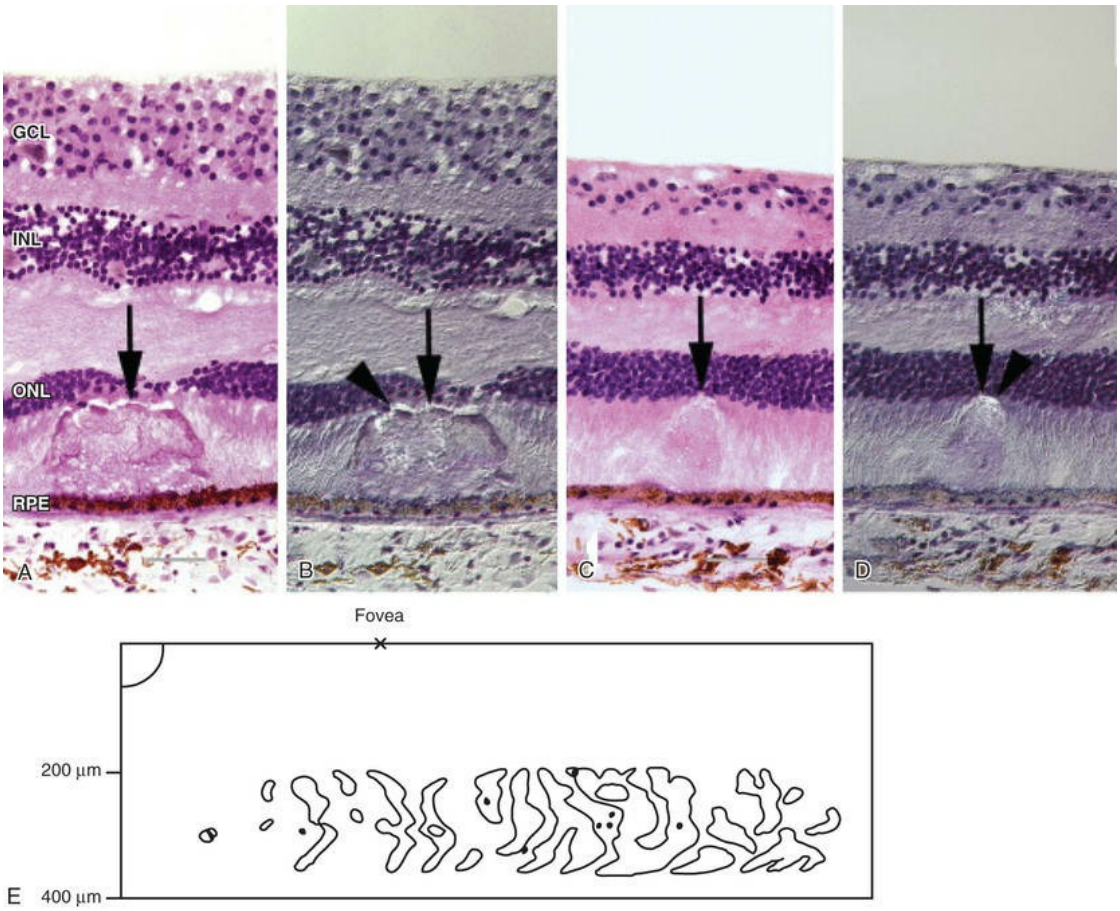

FIG. 68.33 Histologic analysis of subretinal drusenoid debris; 10-µm-thick cryosections were stained with hematoxylin and viewed with bright field (A,C) and differential interference contrast (B,D) microscopy. Scale bar: 50 µm. (A) Note the accumulation of material above the retinal pigment epithelium (RPE) (*arrow*). This subretinal drusenoid deposit (*arrow*) had a loosely packed flocculent base with dense cap. Note the decrease in the number of overlying photoreceptor nuclei. (B) The cap had refractile material (*arrowhead*). (C) In a separate section, a subretinal drusenoid deposit (*arrow*) extended from the RPE up to the outer nuclear layer. (D) There is refractile material on the upper surface of the deposit. (E) The distribution of subretinal drusenoid deposits (all >20 µm wide) was evaluated by examining 100 cryosections, each approximately 11 mm in length, that were obtained starting 200 µm inferior to the fovea, which is marked by an *X*. Typical drusen (all <45 µm) are shown as *black dots*. The subretinal drusenoid deposits formed an interconnected branching pattern. *GCL*, ganglion cell layer; *INL*, inner nuclear layer; *ONL*, outer nuclear

layer; *RPE*, retinal pigment epithelium. (Reproduced with permission from Zweifel SA, Spaide RF, Curcio CA, et al. Reticular pseudodrusen are subretinal drusenoid deposits. Ophthalmology. 2010;117(2):303-12 e1.)

Imaging.

With en face viewing, subretinal drusenoid deposits are best visualized using the blue channel of color photographs (Figs. 68.32A–B) or best captured using red-free photographs or NIR images obtained with the scanning laser ophthalmoscope. With the latter, they appear darker than the uninvolved surrounding areas (Fig. 68.32C).[103] Likewise, on autofluorescence imaging they appear darker than the surrounding areas.[103] With FA, these deposits have either no visible appearance or display minimal hypofluorescence (Fig. 68.32D).[103] SD-OCT images show deposits of material anterior to the RPE, in the subretinal space (Fig. 68.32E).[84,103] The material can be configured as relatively flat aggregates to conical mounds that extend to the region between the inner and outer photoreceptor segments. The deposits appear to be smaller in size on NIR scanning laser ophthalmoscope images compared to color photographs or OCT images[103] and appear to be far more extensive when visualized with OCT as compared to color photographs.[123] Outer retinal atrophy in the absence of frank GA has been demonstrated by SD-OCT following regression of subretinal drusenoid deposits.[128]

Vitelliform Lesions in Eyes With Non-neovascular AMD

The presence of yellowish, subretinal material in the central macula has been associated with cuticular drusen[129] (discussed below) or as part of a spectrum of changes that are now termed pattern dystrophy.[130] This material can also accumulate in the macula of eyes with typical AMD (defined either by histopathology or by presence of large drusen clinically) (Fig. 68.34).[131,132] Vitelliform lesions are not a common manifestation of AMD,[131,132] and its presence has not been correlated with any particular histologic stage of AMD.[131] As such, it is unclear if this material accumulates as part of the pathogenesis of AMD or whether it is a concomitant finding related to the simultaneous presence of a second disease

process.[131,132]

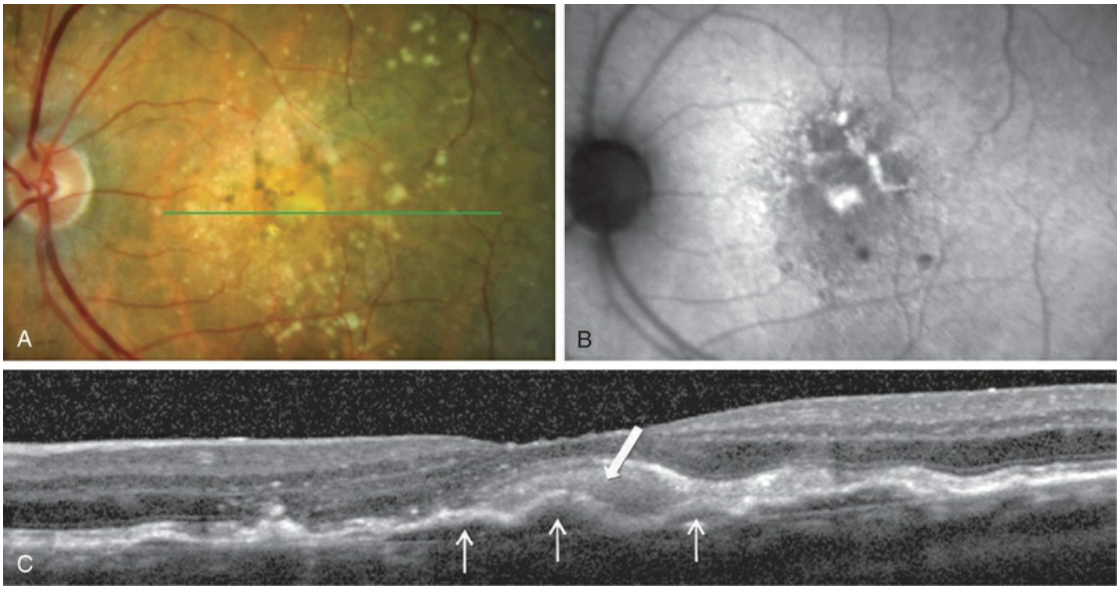

FIG. 68.34 (A) Color fundus photograph of the left eye of an 83-year-old woman diagnosed with non-neovascular age-related macular degeneration showing a vitelliform lesion surrounded by several large drusen in the central macula. (B) Fundus autofluorescence revealing hyperautofluorescence in the macular area corresponding to the vitelliform lesion and areas of increased pigmentation seen on fundus photograph. (C) Spectral domain optical coherence tomography demonstrating hyperreflective material in the subretinal space corresponding to the vitelliform material (*wide arrow*). Large drusen are also present underneath the vitelliform material (*arrows*). (Reproduced with permission from Lima LH, Laud K, Freund KB, et al. Acquired vitelliform lesion associated with large drusen. Retina. 2012;32(4):647-51.)

On examination and color photographs (Fig. 68.34A), these lesions appears as yellow, semiopaque, slightly thickened deposits with indistinct borders through which areas of hyperpigmentation can sometimes be seen within or posterior to the yellow lesion. When present, they usually occur as a single lesion in the fovea, but can occur in multiple and noncentral macular locations.[133] In eyes with AMD, these lesions range from 350 to 1760 μm in greatest linear diameter.[132] With time this material may enlarge or spontaneously resolve with development of outer retinal and RPE

atrophy in its place.

These lesions are invariably hyperautofluorescent in FAF imaging (Fig. 68.34B), with the pattern of hyperautofluorescence correlating well with the extent of the yellowish material.[132,133] During FA, these lesions are hypofluorescent in the early phase as the vitelliform material blocks background choroidal fluorescence. However, in the late phase of the study there is intense hyperfluorescence as the dye stains the vitelliform material.[133] The intense late hyperfluorescence of a vitelliform lesion can mimic that of choroidal neovascularization, making study of the early phase angiogram critical to differentiating the two processes. Less intense late staining on FA can also result in the face of RPE atrophy that may follow spontaneous resolution of the vitelliform lesion. On SD-OCT imaging, the vitelliform material is identified in the subretinal space as a fairly uniform hyperreflective deposit (Fig. 68.34C) that ranges from 32 to 580 μm in thickness.[132] These lesions may also have within them or contiguous to them hyporeflective subretinal spaces, which are thought to reflect a component of subretinal fluid that can occur in the absence of CNV.[133] Vitelliform lesions may lie anterior to drusen or retinal pigment epithelial detachments (PEDs). The ellipsoid layer anterior to the vitelliform lesion may range from completely intact to having complete disruption or absence.[133] In eyes in which the vitelliform lesion resolves with time, OCT has shown atrophy of the ellipsoid layer and RPE.

On histologic examination, this extracellular material appears as debris in the subretinal space that exhibits pale-staining rounded bodies with picro-Mallory, consistent with photoreceptor material.[131] The initiating mechanism is believed to be impaired phagocytosis of photoreceptor outer segments. Overlying photoreceptor loss and underlying central loss of RPE pigmentation with release of pigment granules into the material can be seen. Increased pigmentation and reduplication of the RPE can be seen at the edges of the lesion.[131] Ultrastructural analysis confirms the disorganization of photoreceptor outer segments and the presence of debris derived from photoreceptor outer segments and pigment from the RPE.[131]

Basal Laminar Drusen/Cuticular Drusen

Gass first described the syndrome referred to as basal laminar or cuticular drusen in 1977.[134] This condition is distinct from AMD and most commonly is diagnosed in individuals who are in their 40s or 50s with a great degree of symmetry between their two eyes. On examination, innumerable, uniform, round, densely packed and transparent 50–75-μm diameter sub-RPE deposits are present (Fig. 68.35A) that are best seen with retroillumination. Subretinal yellowish vitelliform material may also be present within the posterior pole.

Basal laminar drusen were initially attributed to internal nodularity of the RPE basement membrane[129] but with time have been more accurately recognized as nodularity due to diffuse drusen.[135,136] Histologic specimens are sparse but show that this material accumulates between the basement membrane of the RPE and the ICZ of Bruch's membrane, in the same location as typical drusen.[136] Green categorized this entity as "diffuse drusen with internal nodularity"[78] and considered the material to represent thickening of the internal portion of Bruch's membrane rather than lying anterior to the ICZ.[78,135] These deposits appear to protrude into the RPE, and the overlying RPE cells have been noted to be thinned at the apex of the deposit and show signs of degeneration.[103,136] At the ultrastructural level, two different compositions have been described that can be present side-by-side in the same eye, one type being comprised of a uniformly homogenous material, mostly of 20-nm "granules."[136] The other type is heterogeneous and consists of electron-dense and electron-lucent inclusions, spherical profiles of various diameters, fibrin-like profiles, curvilinear profiles, and material that may represent cellular debris. This second type is further distinguished by calcium-containing inclusions.[135,136] Their composition also appears to be similar to that of "typical" drusen.[136]

During FA, basal laminar drusen show early and late pinpoint dots of hyperfluorescence and appear more numerous than can be appreciated on clinical exam. They produce a "starry-sky" appearance on FA, as the myriads of small, hard drusen fluoresce (Fig. 68.35B). Unlike the small, hard drusen seen in eyes with early AMD, basal laminar drusen appear slightly hyperfluorescent in early phase with increased hyperfluorescence on late phase with ICGA.[137,138] If vitelliform material is also present, this material

appears hypofluorescent throughout the time course of ICGA.[138] Using autofluorescence imaging these drusen are hypoautofluorescent, possibly due to thinning of the RPE at the apex of the deposit.[103] On SD-OCT, they appear to have a blunted triangular shape and their close proximity to one another and their marked numbers create a sawtooth pattern (Fig. 68.35C).[103]

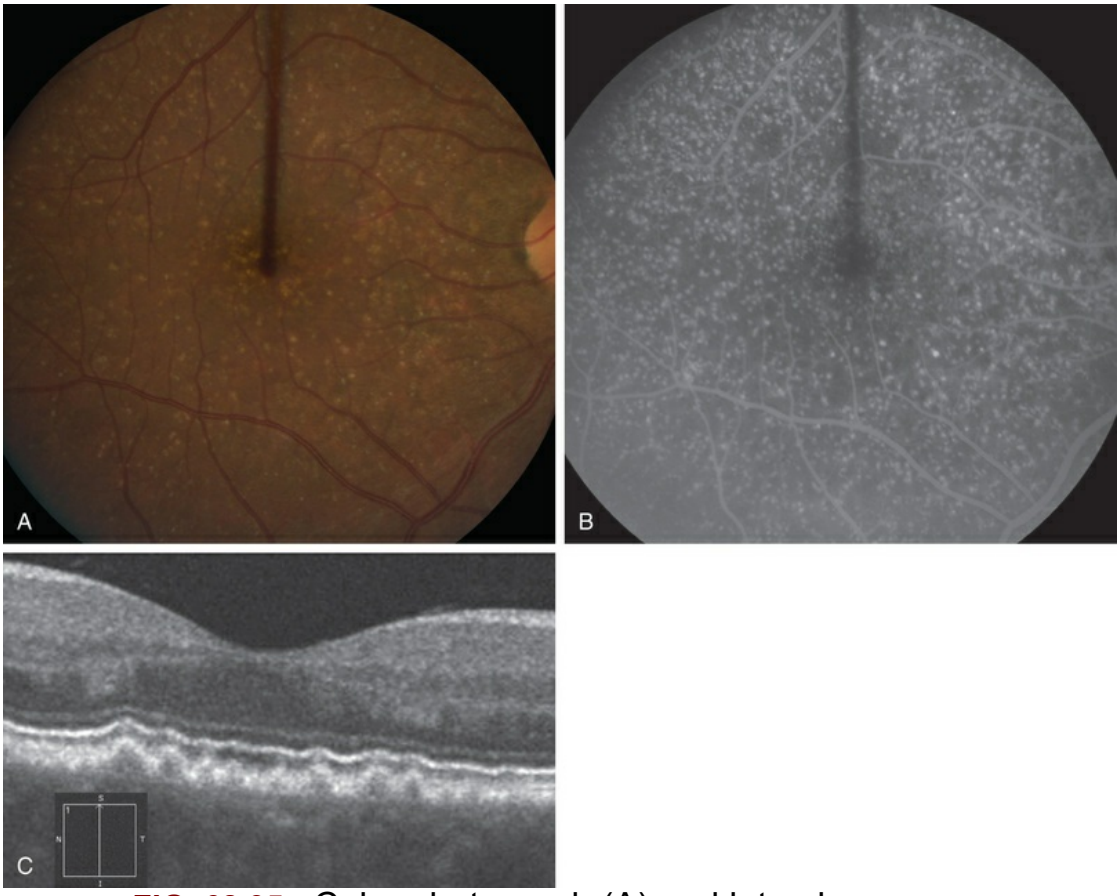

FIG. 68.35 Color photograph (A) and late phase fluorescein angiography (FA) image (B) of the right eye of a 62-year-old African American woman with basal laminar/cuticular drusen. Note that hyperfluorescent drusen on FA appear more numerous ("starry-sky appearance") than can be appreciated on the color photograph. Vertical high-resolution spectral domain optical coherence tomography image (C) of the left eye of a 51-year-old Caucasian woman with basal laminar/cuticular drusen demonstrates a characteristic "saw-tooth" pattern of elevation of the retinal pigment epithelium (RPE). Increased transmission of signal through the RPE, posterior to the apex of the drusen

compared to the edges of the drusen, subtly visible in this image, has been described and has been attributed to relative thinning of the RPE at the apex and thickening of the RPE at the edges of this type of drusen.[103]

Retinal Pigment Epithelial Abnormalities: Nongeographic Atrophy, Focal Hyperpigmentation, and GA

Along with drusen, the other hallmark features of AMD are noted to be RPE abnormalities. This is a collective term that includes a range of alterations from focal hyper- and hypopigmentation to geographic atrophy. This category of abnormalities increases the risk that an eye will have subsequent disease progression, independent of the drusen features that may be simultaneously present. The most extreme form of RPE abnormality, GA, is recognized clinically as sharply circumscribed areas of RPE loss through which the underlying choroidal vessels become visible.[93] Histopathologic examination of eyes with GA have identified well-demarcated regions of attenuated or absent RPE with associated loss of the overlying photoreceptors and underlying choriocapillaris. A continuum of pigment abnormalities that may culminate in GA have been described clinically, and this is complemented by histologic studies that suggest that progressive RPE abnormalities are markers for progression of NNVAMD.[75,86] Through clinicopathologic assessment, including use of SD-OCT, some correlation has been drawn between clinically apparent changes and those described with histology. As noted in the normal aging section, some loss and dysfunction/irregularity of RPE cells is considered a component of normal aging. However, more significant RPE changes occur as part of NNVAMD that may culminate in widespread RPE cell death and the formation of GA.

Clinical Findings in the Progression of RPE Abnormalities to GA

Nongeographic Atrophy (Incipient Atrophy, RPE Degeneration, RPE Depigmentation, Hypopigmentation)

Nongeographic atrophy (NGA)[22] may be thought of as incipient atrophy as it may immediately precede geographic atrophy in the same location. These alterations do not have distinct borders but are recognized as patches of RPE thinning or depigmentation or hypopigmentation, which may have associated clumps of pigment within them or along the border of the region. The affected region may appear more yellow or pink than the normal fundus background, due to attenuation of the RPE and partial visualization of choroidal blood flow.

Focal Hyperpigmentation

Focal hyperpigmentation can develop in areas without drusen (Figs. 68.3C–D), but more commonly is noted surrounding the border of a druse or anterior to drusen or drusenoid PEDs (Figs. 68.23A and 68.30). On stereoscopic examination, focal hyperpigmentation may appear at the level of the RPE or it may be intraretinal. Focal hyperpigmentation is a more common finding than hypopigmentation or depigmentation. Of 3212 eyes within AREDS examined to construct the 9-step severity scale, 25% (800 eyes) were noted to have pigment changes by the AREDS centralized reading center. While 419 eyes were graded as containing macular depigmentation, 748 eyes had hyperpigmentation. It is possible that focal hyperpigmentation precedes depigmentation, or increases the likelihood of identifying depigmentation (which may be subtle) as only 52 eyes with depigmentation did not have focal hyperpigmentation.[71]

Development of GA

Many eyes that progress to GA have large drusen that undergo regression[75,82,139] (Fig. 68.17). In fact, the total macular area occupied by drusen is an established risk factor for progression to GA.[71,140] RPE degeneration is usually more advanced immediately anterior to drusen, which may be appreciated clinically as RPE clumps or RPE depigmentation on the anterior surface of drusen (Figs. 68.20,

68.23 and 68.30). As this RPE alteration on the surface of the druse progresses, the drusen material may regress and the pattern of GA may initially reflect the distribution of past drusen (Fig. 68.17). In younger patients such foci of GA that form in this manner may remain as discrete lobules for many years (see Fig. 68.20), but when progressive AMD manifestations affect the RPE in between discrete areas, patches of GA may enlarge and coalesce in an irregular manner (Figs. 68.17 and 68.36). In eyes with more advanced GA, the only evidence that it evolved via a multifocal distribution in relation to drusen may be scattered calcified deposits within the GA as well as a few small outlying islands of GA.[100,101] Some eyes may show a continuum of all of these manifestations of NNVAMD simultaneously. Fig. 68.37 illustrates an eye with many large and confluent drusen remaining in the macular periphery surrounding a large central region of NGA. Within the NGA there is a focal area of hyperpigmentation and at least one area of extrafoveal GA is present in the superotemporal macula and another suspected superiorly. Areas of both NGA and GA may be more apparent on FA, in which the contrast of black, white, and grey changes is more striking than the varying shades of red, orange, pink, and yellow that are noted on clinical examination.

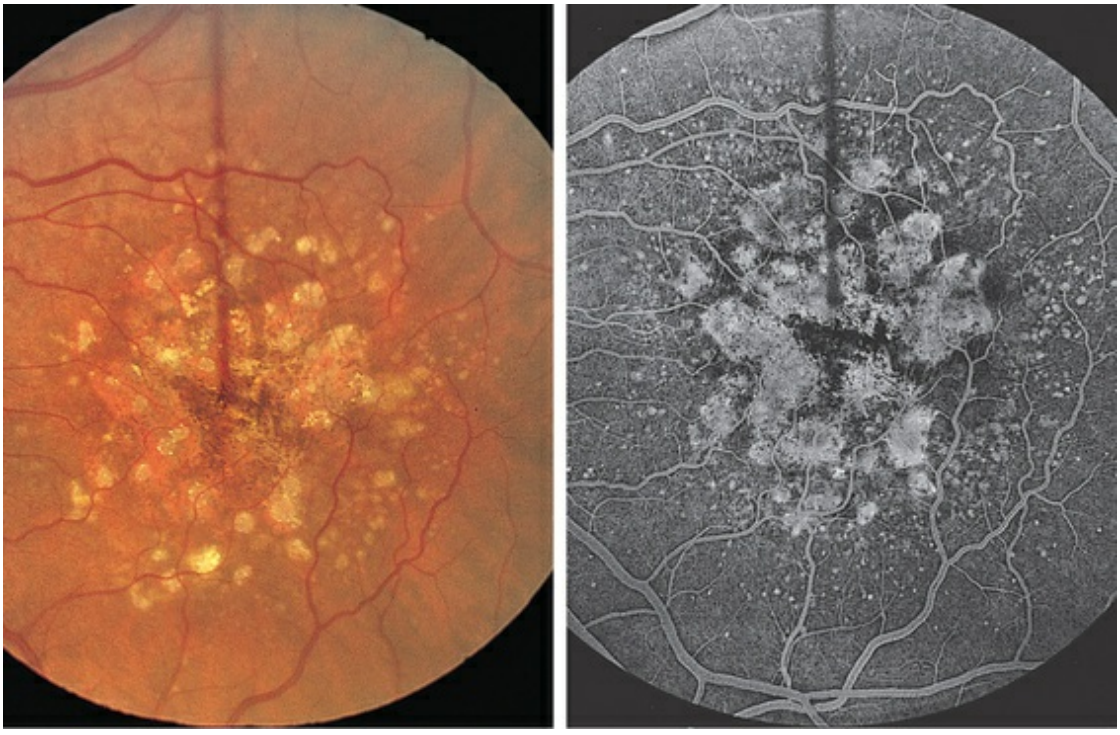

FIG. 68.36 Regressing drusen, showing multifocal pattern of geographic atrophy (GA), in a patient 69 years of age. The separate patches of GA have spread into the surrounding retina, and many have coalesced to produce this pattern. The drusen within these areas have disappeared, and only calcified particles remain. Vision was 20/40, with partial preservation of an island of foveal retinal pigment epithelial, but the patient was unable to read along a line.

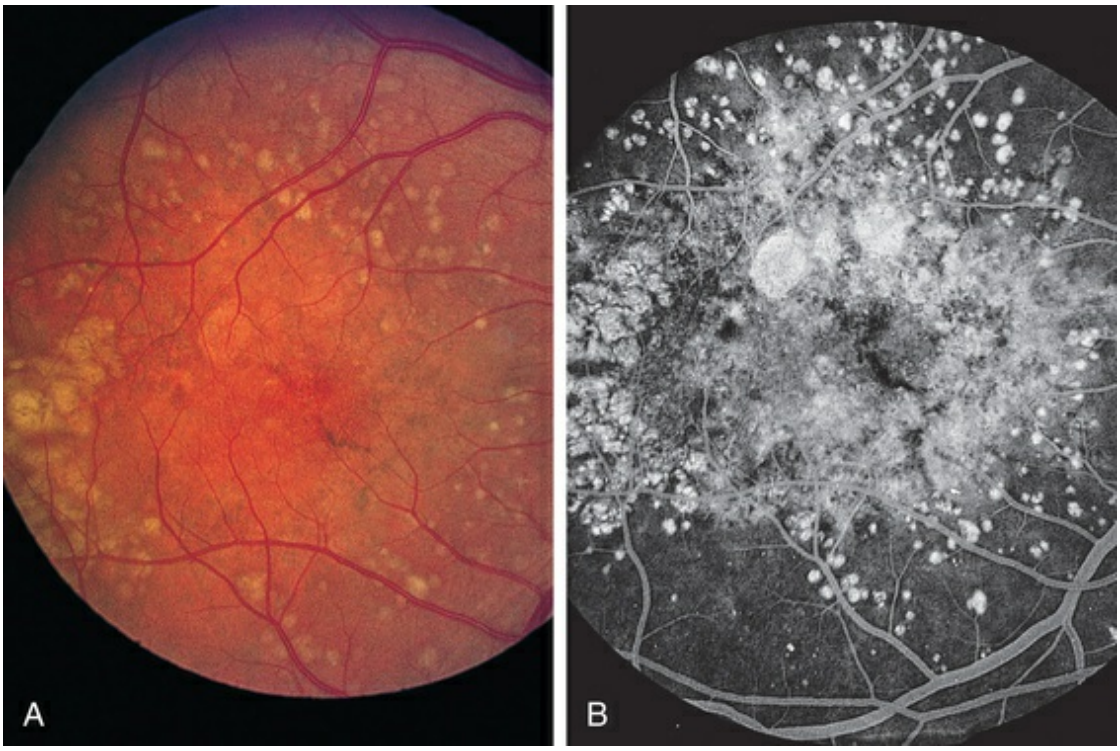

FIG. 68.37 Color photograph (A) and midphase angiogram (B) of eye with nongeographic atrophy and geographic atrophy. Fluorescein angiogram revealed numerous, mostly small, hard drusen, although many aggregated into clusters. Drusen are fading centrally in an area of incipient atrophy of the retinal pigment epithelium, which appears as a pinker area of the fundus (A), showing diffuse hyperfluorescence (B). Geographic atrophy commences as rounded, more circumscribed, brighter window defects within the incipient atrophy (B). Vision was still 20/15.

In the AREDS, 95 eyes developed GA during the initial 4 years of

follow-up. A retrospective review of the annual fundus photographs that preceded the development of GA identified the following features present at the site that eventually developed GA: drusen >125 μm in 96%, confluent drusen in 94%, hyperpigmentation in 96%, drusen >250 μm in 83%, hypopigmentation in 82%, and refractile deposits presumed to be calcification in 23%.[101] The time between the documentation of each of these features and the incident GA varied by specific feature, ranging from 6 years for confluent drusen to 2.5 years for hypopigmentation or refractile deposits. In addition, an orderly sequence of these features was cataloged as drusen progressed to include sites of hyperpigmentation and then exhibit regression of the drusen material. These areas evolved into sites of RPE hypopigmentation and eventually GA.[101] Some of these observations were corroborated in the Complications of Age-Related Macular Degeneration Prevention Trial (CAPT), as among the 114 eyes in the observation arm that developed incident GA, 84% did so in areas previously occupied by drusen.[100]

This evolution of RPE alterations progressing to GA often begins in the perifoveal area, but the contiguous slow expansion of GA lobules becomes an increasing threat to foveal function with time. When GA is first noted to be present, it may exist as a single or as multifocal lobules that spare the foveal center. However, some eyes do present with GA affecting the foveal center. In the CAPT the location of GA among the incident cases was noted to be as follows: 20% involved the fovea, 18% were within 250 μm of the fovea, 61% were 250–1500 μm from the foveal center, and 1% were greater than 1500 μm from the foveal center.

It should be noted that GA may also form independent of the location of drusen. This may occur in eyes in which large drusen are not captured in significant numbers at any point in time. Stippling of the RPE pigmentation and small or medium drusen may coexist, but GA does not begin in relation to individual drusen.[75] Rather the atrophy may begin around the perimeter of the fovea in a band of microreticular hyperpigmentation[75] (Fig. 68.38), although this is not always the case (Fig. 68.39 and see Fig. 68.3). Spread continues into retina affected by NGA and can be rapid when the ring of pigment clumps is pronounced. This pattern of

GA tends to expand in a horseshoe-like configuration around the central fovea, or it develops simultaneously in several areas around the foveal perimeter that eventually merge.[75,141] The nasal or temporal side of the horseshoe eventually becomes involved such that a complete bull's-eye pattern surrounds the fovea. The preserved foveal island eventually succumbs as the GA slowly expands concentrically.

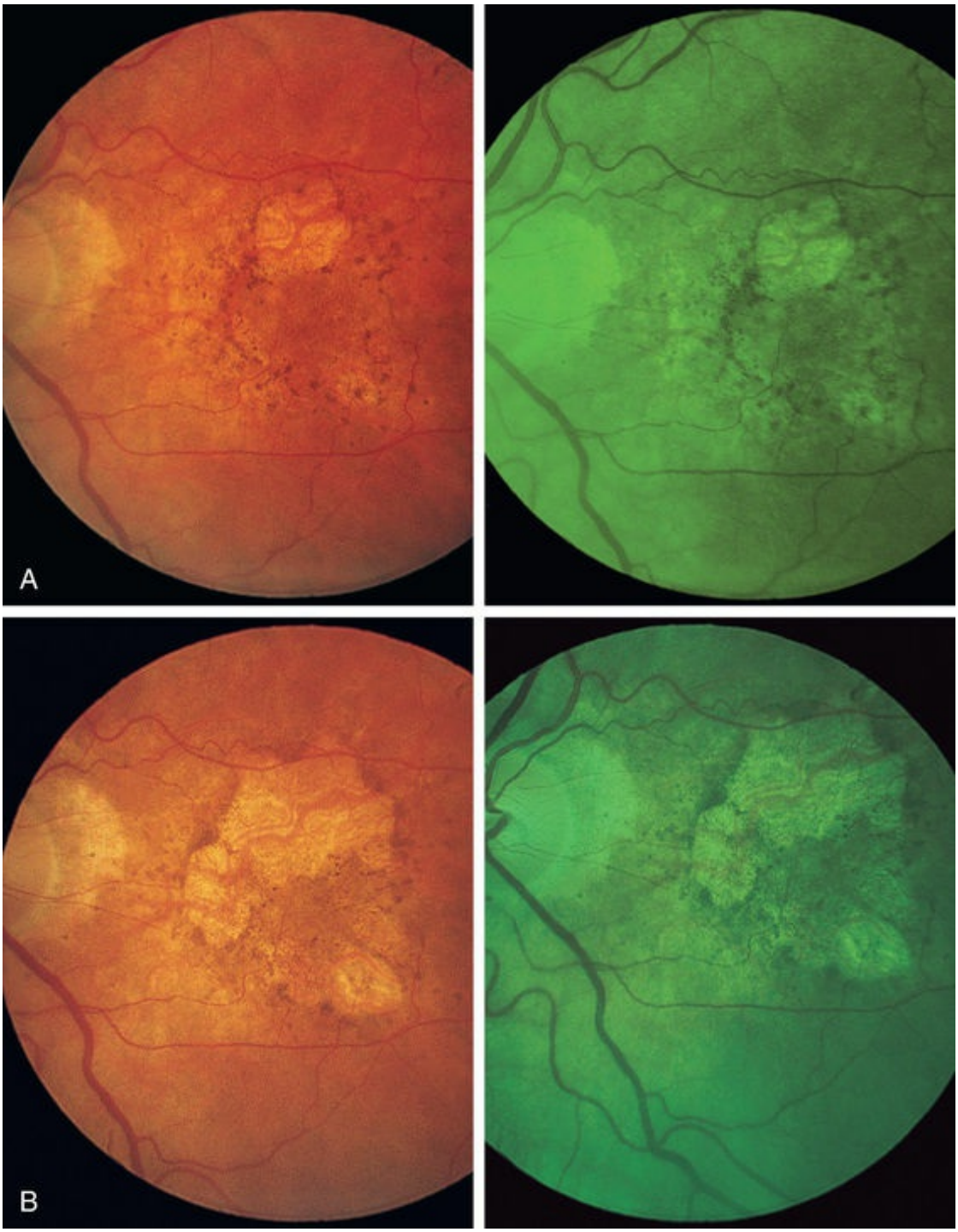

FIG. 68.38 An eye illustrating the spread of geographic atrophy (GA) unrelated to drusen. (A) At age 68, GA was developing in relation to a ring of nongeographic atrophy, which also contained reticular hyperpigmentation, located around the perimeter of the fovea. (B) As the GA expanded, 1 year later, in a horseshoe fashion, it replaced the nongeographic atrophy (incipient atrophy).

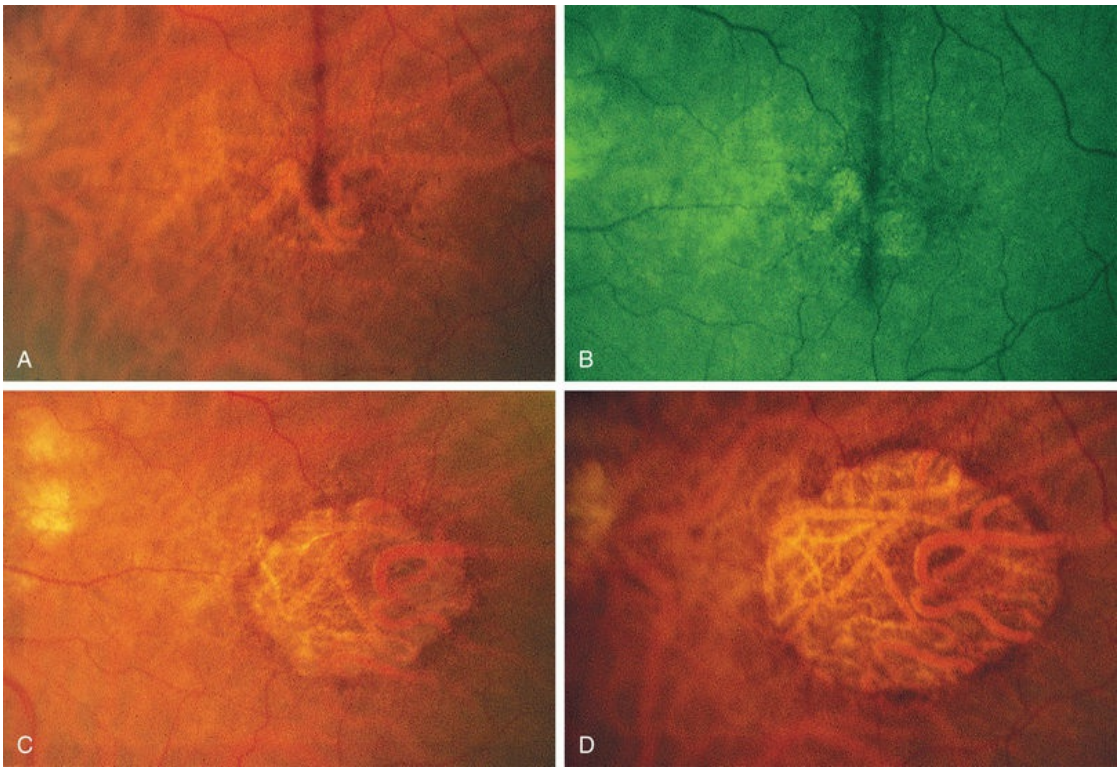

FIG. 68.39 This is the same patient shown in Fig. 68.3. (A) Color and (B) red-free images at age 81. The patient is fixing between two small areas of geographic atrophy (GA) that occupy the site where previous focal pigmentation was seen. Pigment clumping and small drusen-like dots surround the GA. This surrounding nongeographic atrophy corresponds to the site at which GA developed subsequently in (C) and (D); vision is still 20/30. (C) At age 82, GA has expanded to involve the fovea and dots have faded. Vision has dropped to 20/200. (D) At age 84, the GA has almost doubled in size; vision is 20/400. Choroidal atrophy causes exposed vessels to appear white. Patient died at age 85. Pathology of this eye is shown in Fig. 68.7.
(Reproduced from Sarks JP, Sarks SH, Killingsworth M. Evolution of geographic atrophy of the retinal pigment epithelium. Eye 1988;2:552–577.)

GA may also arise following collapse of an RPE detachment (see Fig. 68.23), particularly drusenoid RPE detachments that are formed by the confluence of large soft drusen.[104,106] The emergence of GA in this scenario is consistent with the mechanism of drusen-related GA described above; however, it should be differentiated from atrophy that is caused by resolution of a fibrovascular PED (FVPED). The latter is more appropriately considered atrophic scarring rather

than true GA given the presence of CNV. Also in the setting of CNV and FVPED, RPE rips may occur. The resulting retraction of the pigment epithelium leaves a sharply demarcated area of denuded RPE in which there is increased visualization of the choroidal vessels. Such an area may mimic an area of GA. Features that help distinguish an RPE rip from GA include the following: marked subretinal and intraretinal fluid overlying the area in the acute phase, visible scrolling or bunching of the RPE at the edge of the denuded RPE, and intense early fluorescence on a fluorescein angiogram with relative blockage in a linear configuration along the margin of the hyperfluorescent area from the scrolled RPE.

Histopathologic Alterations Associated With RPE Abnormalities With Progression to GA

RPE Alterations

Many of the histologic changes that occur to the RPE during the progression to GA are discussed in the "Histologic alterations of non-neovascular AMD which may not be apparent on ophthalmoscopy" section above. Zanzoterra et al. more recently described changes that occur in the RPE in late AMD, including eyes with GA, and proposed a morphologic grading system that introduced new nomenclature.[86] The earliest RPE changes they describe are a "nonuniform" morphology and pigmentation of RPE cells that is associated with patches of early BlamD (Fig. 68.9A). This may progress to "very nonuniform" appearance in shape and pigmentation of RPE cells that contain melanosomes in the apical processes (Fig. 68.9B). This is associated with increased BlamD as well as subretinal drusenoid deposits. Later changes include "shedding" of RPE cells (Fig. 68.9D), which is described as basal translocation of RPE cells or fragments into a continuous thick layer of BlamD, and the presence of "sloughed" RPE into the subretinal space (Fig. 68.9G). "Sloughed" RPE is felt to be a precursor to "intraretinal" RPE that has migrated past the external limiting membrane (ELM) (Fig. 68.9E). The presence of ELM indicates an area that is not considered to have GA. Further progression leads to "dissociated" RPE, cells that lack epithelial characteristics and are found in areas of GA (Fig. 68.9C). These cells were found associated

with BlamD in regions lacking ELM within degenerated ONL 34% of the time, within Henle fiber layer 60% of the time, and in the foveal inner nuclear layer 6% of the time. "Atrophy with BlamD" (Fig. 68.9H) and "atrophy without BlamD" (Fig. 68.9K) were used to described areas with no remaining RPE cells. Further categories of "bilaminar" RPE (Fig. 68.9I and see Fig. 68.7), with double layers of epithelial RPE, "vacuolated" RPE (Fig. 68.9J), and "entombed" RPE (within scar from CNV) (Fig. 68.9F) were described. All but the last category were present in eyes with GA, and "bilaminar" RPE was much more common in eyes with CNV compared to GA. The later changes ("dissociated" and "atrophy with and without BlamD") were more prominent in central locations, with the earlier changes noted in sections taken from both the central and superior macula.[86] Clinical imaging correlates to many of these changes outlined above are discussed below in the imaging section.

Photoreceptor Changes

As noted earlier, progressive derangement of the RPE is accompanied by dropout of photoreceptors, a reduction in the number of nuclei in the ONL, shorter and more bulbous inner segments, and termination of outer segments in collections of membranes over the apical surface of the RPE[75] (Figs. 68.7 and 68.9B). By histopathology, only a minority of cases of GA show sharply demarcated areas of photoreceptor loss at the perimeter of the GA.[142] It is more common to find a broad transition zone that shows loss of rods and altered cones. The cones lose their outer segments, and some lose their inner segments as well.[142] In the transition zone, the ONL progressively thins as it approaches the GA.[142]

Changes to Choroid and Bruch's Membrane

In eyes that exhibit GA, within the portions of the macula that retain RPE, the choriocapillaris remains relatively normal. However, in areas with progressive RPE loss there is progressive loss of choriocapillaris.[90] In the macular regions that are not affected by GA, the choriocapillaris has a vascular area (defined as the percentage of the choriocapillaris layer occupied by blood vessels) of 72%, which is not significantly different from that of age-

matched eyes without AMD. In the regions that border GA this drops to 52%, and in the GA area itself it is reduced to 38%.[90] Likewise, mean capillary diameters were 13.9 μm in areas unaffected by GA (not significantly different from age-matched eyes without AMD), 10.3 μm in border regions, and 7.9 μm in regions of GA.[90]

In the setting of GA, obliteration of the choriocapillaris is accompanied by erosion of the intercapillary pillars of Bruch's membrane, and in longstanding cases Bruch's membrane becomes thinner. Fibroblasts and macrophage processes are found in contact with the outer surface of Bruch's membrane, commonly splitting off fragments or even passing through small breaks in Bruch's membrane.[92] Pigmented cells, likely of RPE origin, described as "subducted" cells may also become associated with Bruch's membrane.[143]

In longstanding GA, there are fewer large choroidal vessels and the exposed choroidal arteries may display white sheathing of their walls or even appear bloodless (Fig. 68.39D). This appearance was formerly called senile choroidal sclerosis, but on histologic examination the white fibrotic appearance does not result from sclerosis; the majority of arteries show only fibrous replacement of the media without thickening of the walls and with retention of wide lumina. This appearance is instead an expression of choroidal atrophy,[82] as loss of the choriocapillaris and the middle layer of vessels throws the remaining larger vessels into greater prominence. The white sheathing is due to the disproportionate thickening of the vessel walls by becoming flattened in the thinned choroid, but in many cases it also reflects a reduced blood column.

Imaging of Nongeographic Atrophy and Geographic Atrophy

Fluorescein Angiography

With FA, areas of NGA demonstrate diffuse hyperfluorescence; however, the intensity of the fluorescence is not as bright as that associated with GA (Fig. 68.37). The reticular or punctate pattern of hyperpigmentation that is often associated with NGA (Fig. 68.37) is responsible for areas of blocked fluorescence that appear

hypofluorescent. GA is recognized as lobules of hyperfluorescence that appear during the transit phase of the angiogram, sometimes with visualization of the choroidal vessels passing through the region (Figs. 68.36 and 68.40A).[144] There may be a surrounding rim of blocked fluorescence from pigment at the border of GA. In late-phase images the areas may decrease in intensity, but some staining may persist (Fig. 68.40B). These sharply demarcated areas are bright but never as intensely fluorescent as an RPE rip. Small areas of GA, particularly in an environment of diffuse NGA, are more apparent and can be recognized as GA more readily using FA compared to traditional color fundus photography (Fig. 68.36).[100]

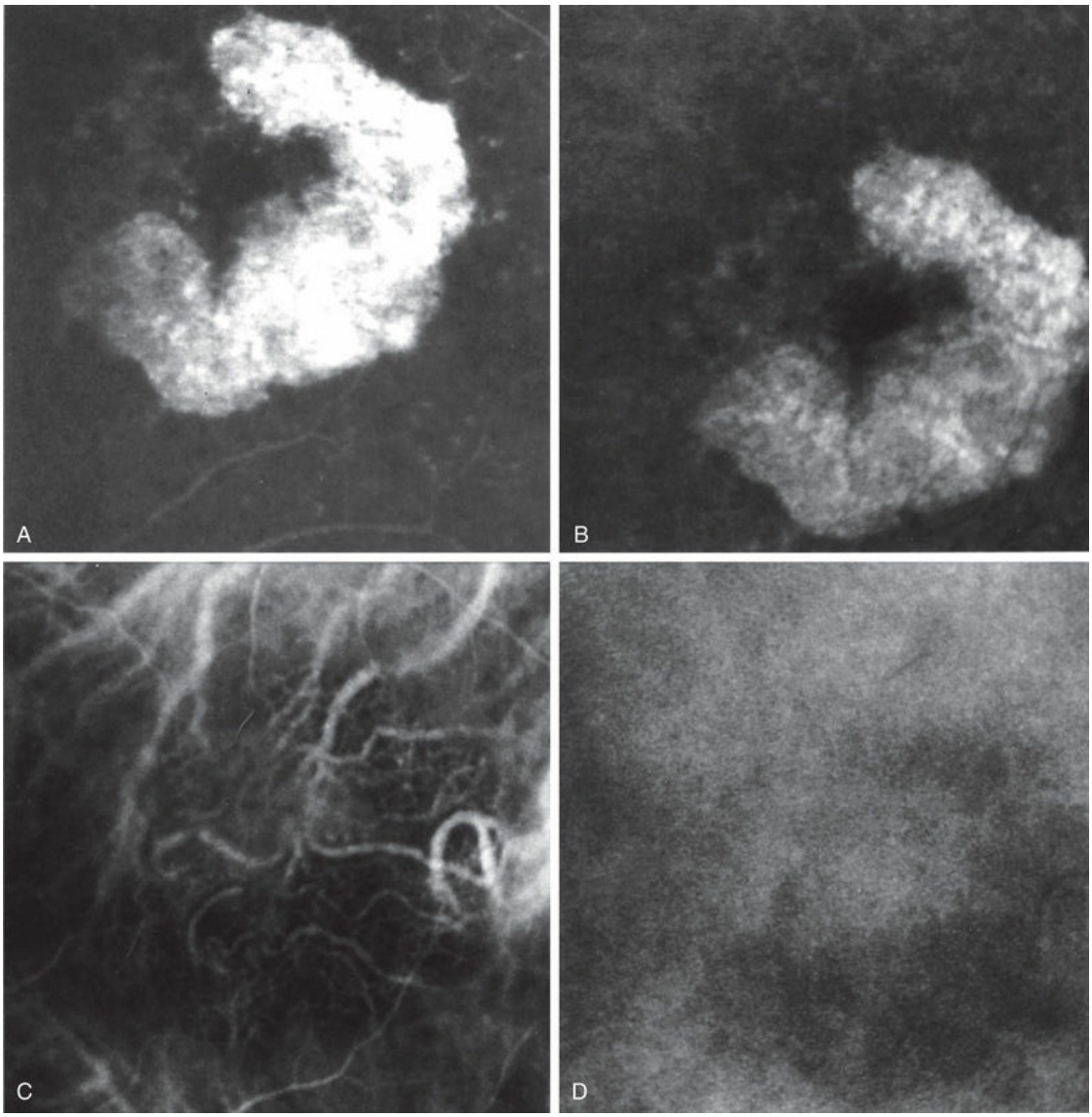

FIG. 68.40 A 73-year-old man with geographic atrophy (GA) secondary to age-related macular degeneration

without any signs or history of choroidal neovascularization. (A) Early fluorescein angiogram (FA) demonstrates hyperfluorescence in the area of the transmission defect. (B) Late hyperfluorescence or staining of the choroid and sclera is visible in the area of the GA. (C) Early indocyanine green angiogram (ICGA) reveals a better visibility or accentuation of the choroidal vessels in the area of the transmission defect evident on FA. The gray veil-like fluorescence from the choriocapillaris is not evident. (D) Late ICGA reveals homogeneous hypofluorescence in the area of the transmission defect with no evidence of late hyperfluorescence. (Reproduced with permission from Schneider U, Sherif-Adel S, Gelisken F, et al. Indocyanine green angiography and transmission defects. Acta Ophthalmol Scand. 1997;75(6):653-6.)

Indocyanine Green Angiography

Findings on ICGA of NGA are much more subtle than those seen on FA. Either no apparent change may be visible or a loss of the uniform background fluorescence, contributed by choriocapillaris, may be noted. However, changes on ICGA are more apparent when GA is present. In early phase ICGA images, GA appears as a well-defined area with increased visibility of the larger choroidal vessels (Fig. 68.40C). These regions correspond to the area of window defect that GA creates on FA. Loss of the uniform gray hyperfluorescence of the normal choriocapillaris and varying degrees of closure of the small and medium-size choroidal vessels are also noted on early phase images in the region of GA. In contrast to FA, late phase findings on ICGA are that of hypofluorescence in the area of GA, with an identical lesion size on these two types of fluorescent imaging (Fig. 68.40D).[144]

Fundus Autofluorescence

The associated hyperpigmentation in NGA may be more easily delineated on autofluorescence images as areas lacking FAF due to absorption of the exciting light by melanin granules. Alternatively, the associated hyperpigmentation may appear as increased foci of FAF if melanolipofuscin has accumulated in the pigmented sites.[145] The areas of hypopigmentation generally are associated with

decreased FAF, suggesting the absence of RPE cells or degenerated RPE cells with reduced lipofuscin content.[145]

Actual lesions of GA appear as sharply defined and homogeneous areas of hypoautofluorescence on FAF imaging due to RPE loss with corresponding loss of lipofuscin accumulation (Figs. 68.41 and 68.42). The FAF pattern in the "junctional" area of the atrophic and nonatrophic tissue has a more varied appearance. In the junctional area, three patterns of high-intensity FAF have been noted including "banded," "focal," and "patchy." Five additional patterns of hyperautofluorescence that appear more diffuse have also been described in AMD (Fig. 68.42). In these diffuse patterns, increased FAF is present at the margin of the GA and elsewhere in the posterior pole. The pattern of increased FAF may provide prognostic information for rates and location of GA enlargement. Eyes with GA and no hyperautofluorescence and eyes with a focal pattern have been noted to progress slowly, while eyes with the banded pattern or any of the diffuse patterns have been noted to progress more rapidly.[145] When diffuse patterns of FAF are identified, as existing GA enlarges, or as new areas of GA form, they do so at the sites that previously manifested increased FAF. In contrast to the high degree of variation in FAF patterns seen between individuals with GA, a high degree of symmetry has been noted for the pattern of increased FAF in patients with bilateral GA. As there is some evidence that specific patterns of increased FAF in the junctional zone are associated with GA growth rates, some clinical trials evaluating interventions to limit the growth of GA are presently requiring that these "high-risk" patterns, notably the banded or diffuse patterns, be present upon study entry.[145]

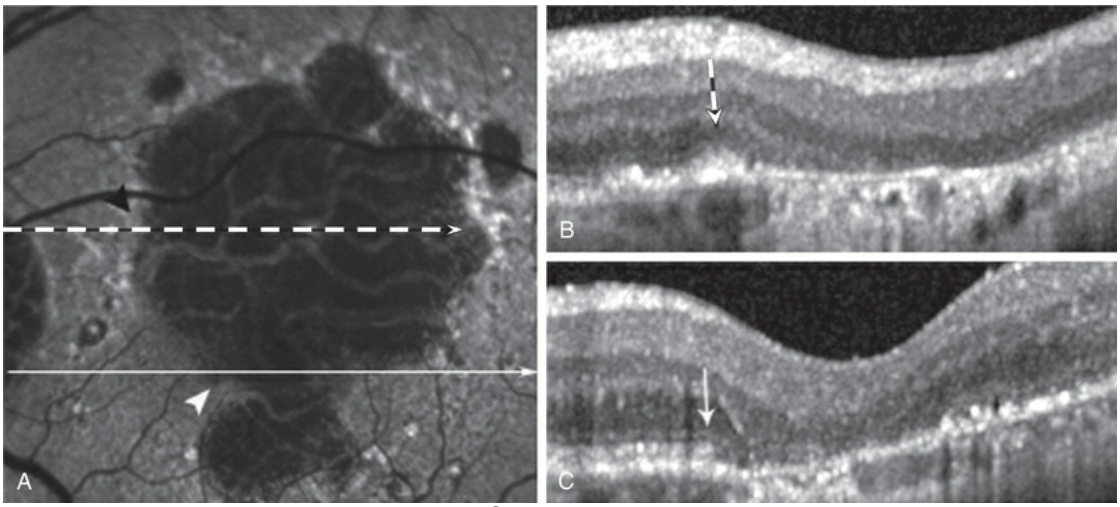

FIG. 68.41 Fundus autofluorescence (FAF) (A) and spectral domain optical coherence tomography (SD-OCT) images (B,C) with horizontal scans at two different levels in a patient with geographic atrophy. (B) SD-OCT image showing irregular margins with structural alterations at the outer retina (*black and white dashed arrow*) corresponding to increased FAF (*black arrowhead*) at the nasal margin. (C) Horizontal scans through the area of no abnormal FAF (*white arrowhead*) showing smooth margins on the SD-OCT (*white arrow*). In B and C, enhanced signal from the choroid corresponds to the area of GA. In panel B, progressive thinning of the outer nuclear layer is present over the more central (older) portions of geographic atrophy. (Reproduced with permission from Brar M, Kozak I, Cheng L, et al. Correlation between spectral-domain optical coherence tomography and fundus autofluorescence at the margins of geographic atrophy. Am J Ophthalmol. 2009;148(3):439-44.)

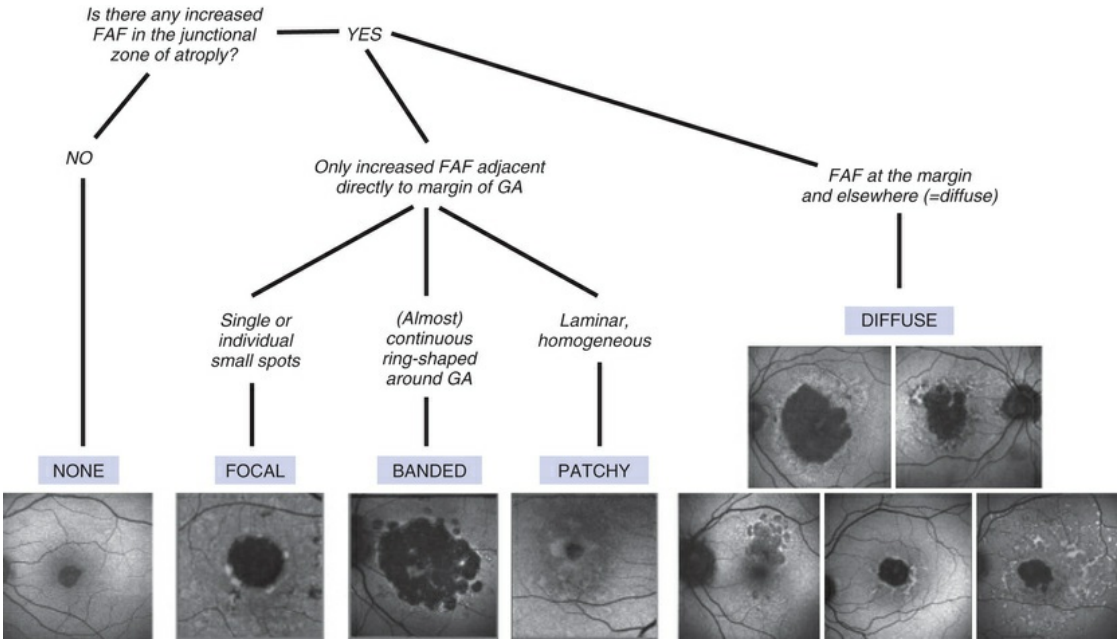

FIG. 68.42 Classification of fundus autofluorescence (FAF) patterns in the junctional zone in patients with geographic atrophy due to age-related macular degeneration. Eyes with no increased FAF intensity at all are graded as "None" (= slow progressor). The eyes with increased FAF are divided into two groups depending on the configuration of increased FAF surrounding atrophy. Eyes showing areas with increased FAF directly adjacent to the margin of the atrophic patch(es) and elsewhere are called "Diffuse" (= rapid progressors) and are subdivided in five groups. From left to right: (top row) fine granular, branching, (bottom row) trickling, reticular, and fine granular with punctuated spots. Eyes with increased FAF only at the margin of geographic atrophy (GA) are split into three subtypes ("Focal" [= slow progressor], "Banded" [= rapid progressor], and "Patchy" [= unclear progression rate, occurs rarely]) according to their typical FAF pattern around atrophy. (Reproduced with permission from Schmitz-Valckenberg S, Fleckenstein M, Scholl HP, et al. Fundus autofluorescence and progression of age-related macular degeneration. Surv Ophthalmol. 2009;54(1):96-117.)

One particular pattern of FAF in GA termed the "diffuse-trickling" phenotype (Fig. 68.42) has been associated with the fastest growth rate of GA. Eyes with this FAF pattern exhibit on clinical examination dense granular hyperpigmentary changes in the central macula, as well as hyperpigmentation at the borders of

the GA. Typically, large or soft drusen are not present in these eyes.[146] This rapidly progressive form of GA likely comprises at least some of the cases of GA that have been described to occur in locations independent of drusen.[75,100]

Spectral Domain Optical Coherence Tomography

As noted previously, one of the earliest findings of RPE abnormalities that can be appreciated with SD-OCT[87] and ultrahigh resolution (UHR) OCT[88,89] is moderate to intense hyperreflective foci within various planes of the retina that correspond to foci of hyperpigmentation on clinical examination or on fundus photographs. It is common for eyes with drusen to have these intraretinal deposits recognized on histopathology or OCT directly anterior to the drusen, primarily in the subretinal space or ONL, but migration can occur into more anterior retinal layers.[43,86,88] Their histopathologic correlates are believed to be the "sloughed" and "intraretinal" grades of RPE that are commonly seen in nonatrophic area of eyes with GA (see Fig. 68.9E,G).[86] In the AREDS2, an ancillary study of SD-OCT findings in a sample of participants suggested that the number of these hyperreflective foci on SD-OCT progressively increased during a 2-year observation period and, with time, were increasingly common within more anterior layers of the retina.[147] In this ancillary study, hyperreflective foci in eyes with drusen increase the odds that an eye will progress to GA within 2 years by a factor of 4.7.[147] Furthermore, the magnitude of the increased risk of progression to GA is modulated by the number of baseline hyperreflective foci and the more anterior location of the hyperreflective foci.[147]

In the AREDS2 ancillary SD-OCT study referred to above, RPE atrophy or loss was noted in 23% of eyes identified to have intermediate AMD clinically while 2.5% were noted to have a patch of RPE atrophy exceeding a diameter of 360 μm extending beneath the fovea. Had these regions of foveal GA been clinically apparent, the eyes would have been graded as advanced AMD rather than intermediate AMD, but neither the clinical examination nor the stereoscopic color photographs disclosed the presence of foveal GA.[117] SD-OCT may thus be a more sensitive means of detecting small areas of GA compared to fundus photography. Drusen with

high reflectivity, low reflectivity, and drusen with cores were less commonly seen than the ubiquitous drusen of medium reflectivity (see Fig. 68.30). However, eyes that contained drusen with these former characteristics, rather than eyes only with drusen with medium, homogenous reflectivity, were more likely to have areas of RPE atrophy or absence.[117]

In the setting of clinically apparent GA, SD-OCT images show the absence of several structures, including the ONL, ELM, and the ellipsoid layer, and either absence or marked attenuation of the RPE and Bruch's membrane complex (Figs. 68.17, 68.41 and 68.43).[148,149] As a result of these alterations, there is choroidal signal enhancement or relative choroidal hyperreflectivity (Figs. 68.17, 68.41 and 68.43). This group of OCT alterations corresponds to the same area with severe reduction of FAF signal on FAF images.[149] Junctional regions between GA and the surrounding macula show abrupt breaks in the ellipsoid layer and RPE/Bruch's membrane complex and curved endings of the ELM as it merges with the atrophic region. Areas of increased FAF on FAF images in eyes with GA have been shown to correspond to highly reflective material and thickening at the level of the RPE and increased outer retinal alterations compared to borders of GA that do not demonstrate increased FAF[150] (Figs. 68.41 and 68.43). Over areas of existing GA, progressive thinning of the ONL occurs with time, and the outer plexiform layer (OPL) becomes progressively closer to the level of the RPE (Fig. 68.41).[148]

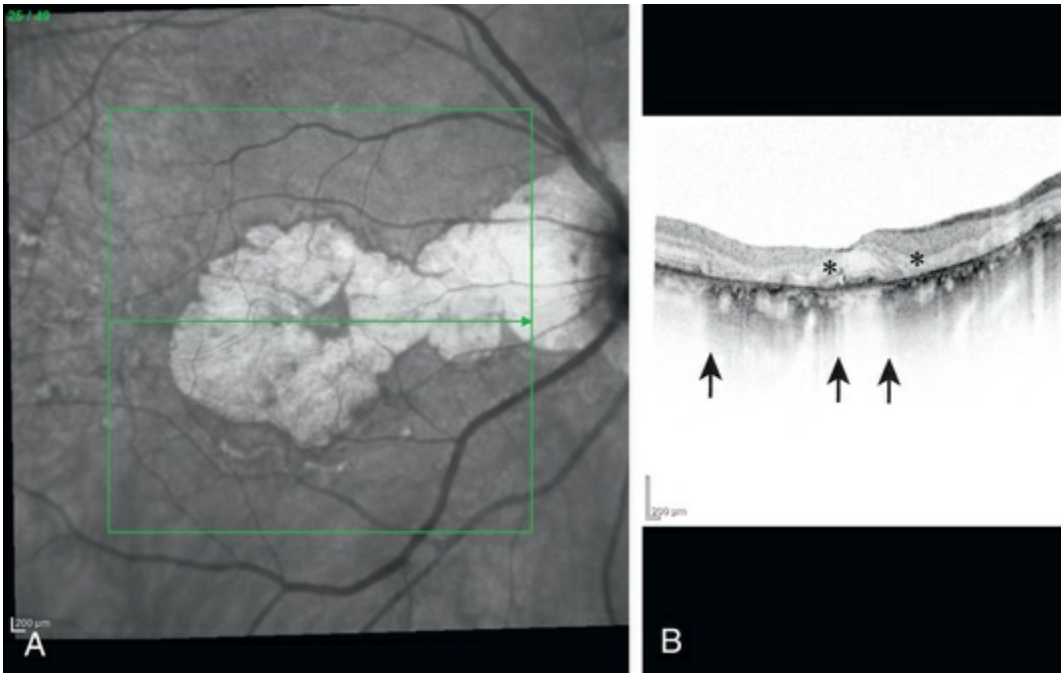

FIG. 68.43 Heidelberg Spectralis optical coherence tomography image in an eye with a large ring of geographic atrophy (GA) sparing the foveal center. (A) Near infrared image. (B) B-scan through the foveal center. The B-scan image shows two areas of GA on either side of a preserved island of tissue in the fovea. *Black arrows* denote enhanced signal from the choroid, which corresponds to the area of GA (*black arrows* mark where this begins and ends). Immediately anterior to the zone of enhanced choroidal signal there is attenuation or loss of the following layers: Bruch's membrane, retinal pigment epithelium, ellipsoid zone, and the external limiting membrane (ELM). Note the curved endings of the ELM at the lateral margins of the preserved foveal island as it merges with the atrophic region (*asterisks*).

Comparison of SD-OCT and FAF imaging in one prospective observational study of 81 eyes of 42 patients with GA demonstrated that delineation of GA borders using an OCT software algorithm that takes into account characteristics of the OPL, ELM, RPE, and choroidal signal enhancement, correlated with areas of lost FAF. Multivariate analysis showed that complete choroidal signal enhancement, OPL shifting, and loss of the ELM had a strong correlation to the hypoautofluorescent regions on FAF.[151] In this study, there was better intergrader agreement for identification of

foveal sparing GA with SD-OCT compared with FAF images and the findings on OCT had a higher correlation with visual acuity (VA) measurements compared to FAF.[151] NIR can also be used to more easily identify areas of GA compared to color photographs (Figs. 68.17A–B, see also Fig. 68.43). Within the Fundus Autofluorescence in Age-Related Macular Degeneration (FAM) study, a semi-automated software tool was used to combine NIR and FAF images to reliably monitor progression of GA in the subset of 47 eyes of 36 patients with foveal sparing of GA.[152] These results are discussed further in the following section.

An additional SD-OCT finding that has been described in eyes with late AMD, in the setting of either GA or CNV, is outer retinal tubulation (ORT).[153,154] ORT is a thick reflective line surrounding a sometimes extensive and branching tubular hyporeflective cavity within the ONL[153] (Figs. 68.44C–D). ORT can be differentiated from cystoid abnormalities, as only ORT has a hyperreflective border surrounding the hyporeflective space. (Figs. 68.44C–D).[153] ORT has recently been shown to correlate to a histopathologic finding that had been described earlier in eyes with AMD.[153,155] Histopathologically, ORT consists of degenerate red–green cones and Müller cells that surround these structures (Figs. 68.44A–B).[155] The hyperreflective border is thought to be due to mitochondria within the inner segments of the degenerate photoreceptors. When hyperreflective material is present within the cavity of ORT on SD-OCT images, this corresponds to RPE cells or macrophages on histopathologic sections within the cavities of ORTs.[153]

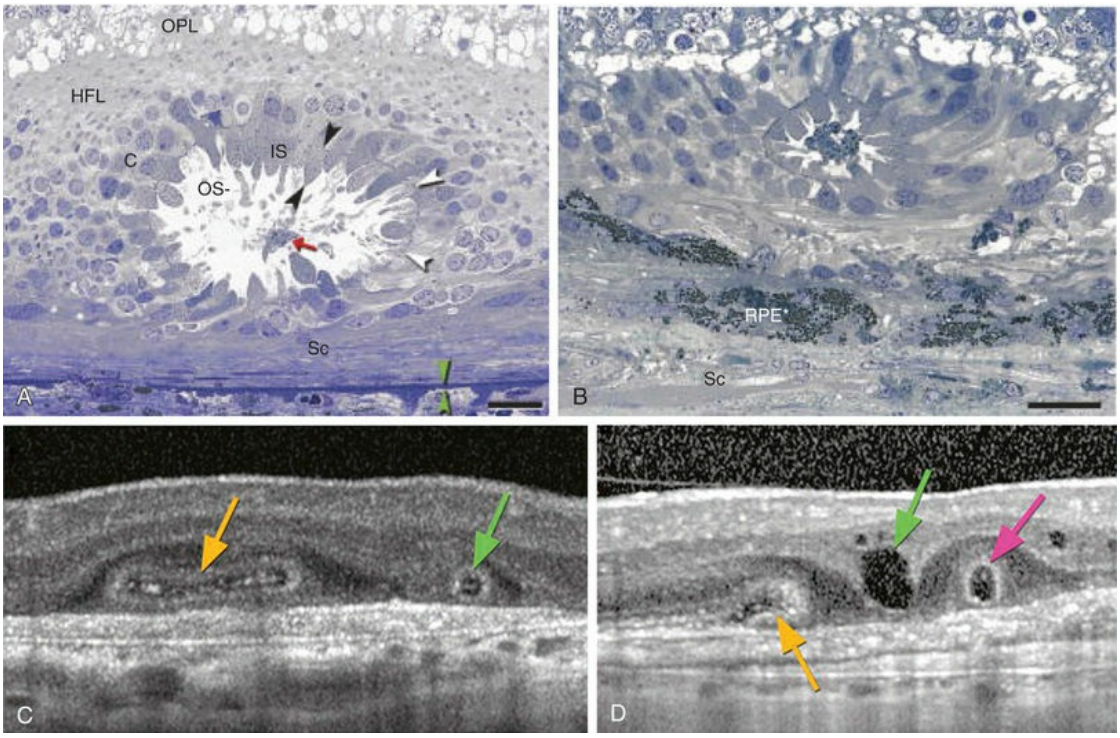

FIG. 68.44 Histologic (A,B) and spectral domain optical coherence tomography (OCT) (C,D) appearance of outer retina tubulation (ORT). Images are from patients with neovascular age-related macular degeneration, but this finding is also present in eyes with geographic atrophy and no choroidal neovascularization. (A,B) Toluidine blue-stained 0.8-μm thick sections of maculas postfixed by osmium-tannic acid-paraphenylenediamine method. Scale bars: 25 μm. (A) Closed ORT: cone nuclei (*C*) surround a lumen delimited by the external limiting membrane (ELM) (*white arrowheads*). Cone inner segments, some with outer segments, protrude into the lumen, maintaining a radial organization with respect to the lumen center. Inner segments have mitochondria-containing ellipsoids, and less frequently, myoids (one cell containing both indicated by *black arrowheads*). One cell with green-staining lipofuscin granules is in the lumen (*red arrow*). Henle fiber layer (*HFL*) contains darkly stained cone fibers in cross-section. *Sc*, fibrocellular scar. *Green arrowheads*, Bruch's membrane, which is breached in this panel (79-year-old-man). (B) Nucleated retinal pigment epithelium (RPE) cell within an ORT lumen; *RPE**, RPE-derived cells with spherical melanosomes; *Sc*, fibrovascular scar (87-year-old man). (C,D) Heidelberg Spectralis

OCT imaging (with signal averaging). (C) A flat and ovoid cross-section with a hyperreflective border (*orange arrow*) has internal hyperreflective material in the lumen. A circular cross-section has a hyperreflective border (*green arrow*). (D) A cross-section showing a forming tubulation (forme fruste ORT) with a free edge to scroll (*orange arrow*) next to an ovoid cross-section with internal hyporeflectivity lacking a hyperreflective border, located in the outer plexiform layer (cystoid space, *green arrow*). Also present is a circular cross-section of an ORT with a thick hyperreflective border (*pink arrow*) in the outer nuclear layer. (Adapted with permission from Schaal KB, Freund KB, Litts KM, et al. Outer retinal tubulation in advanced age-related macular degeneration: optical coherence tomographic findings correspond to histology. Retina. 2015;35(7):1339-50.)

SD-OCT has also been used to quantitate the degree of choroidal thinning that occurs in the presence of GA, and these findings parallel those seen with histopathologic examination.[74,90,156,157] Significant thinning of all of the choroidal layers has been demonstrated by SD-OCT.[156,157]

Growth of Geographic Atrophy

In various clinical research studies the progression of GA has been monitored reliably using sequential color fundus photographs,[158] SD-OCT,[148,159,160] FAF images,[152,161] and NIR images.[152] The annual growth rate of GA has been associated with the total area of GA present at baseline, with larger lesions expanding at a faster annual rate.[158,160–162] However, this association is no longer present when areas are analyzed after applying a square root transformation, which adjusts growth rates to account for differences in baseline lesion size.[160] In AREDS the average change in GA area (across the spectrum of lesion sizes) was 1.78 mm^2 per year based on review of sequential color fundus photographs. Although the growth rate of GA is correlated between eyes of individuals with bilateral GA at the group level, there is a moderate degree of variation between right and left eyes at the individual level.[158] One prospective, longitudinal natural history study of 86 eyes from 64 participants

showed a mean annual enlargement rate of 1.2 mm^2 using sequential SD-OCT images; and a smaller baseline size of GA was hypothesized as the explanation for the slower rate of progression compared to other studies.[160] In a natural history cohort study of eyes with GA, the FAM study, the annual GA growth rate was 1.52 mm^2 using sequential FAF images with a range of progression rates from 0.38 to 3.02 mm^2 per year depending on the FAF phenotype.[161] The median baseline area of GA in this study was noted to be larger at 7.04 mm^2 as compared with 3.15 mm^2 in the SD-OCT study noted above.

In the subset of 47 eyes of 36 patients (mean age 73.8±7.5 years) with foveal sparing GA in the FAM study, FAF and NIR was used to monitor GA growth towards the periphery versus towards the fovea, with mean follow-up time of 25.2 ±16.9 months. The mean annual progression of GA was 2.27±0.22 mm^2 towards the periphery and 0.25 ± 0.03 mm^2 toward the fovea. This represented a 2.8-fold faster rate of atrophy progression toward the periphery than toward the fovea when square root-transformation analysis was performed.[152] This corresponds to the clinical observation that some foveal tissue often remains intact until very late in progression of GA. Sarks had previously noted that total GA area averaged 13.5 mm^2, or more than 5 DD, when there was complete foveal involvement.[75]

There is also some evidence that the presence of outer retinal tubulation in the area of GA is associated with a slower GA growth rate.[159] This association warrants further study, as it may be a potential confounding variable that needs to be considered in intervention trials aiming to limit GA growth.

Prognosis and Management of Non-Neovascular AMD

This section focuses on the clinical care of patients with NNVAMD and details data regarding the risk of future vision loss conferred by the presence of the changes noted in the prior sections. The impact that these alterations have on visual function, and the specific management of patients with NNVAMD, will be reviewed. The latter includes discussion of the role of micronutrient supplements on disease progression, use of patient self-monitoring devices, and standard care monitoring strategies, including discussion of recommended frequency of office visits, considerations regarding cataract surgery, the use of the implantable miniature telescope in eyes with endstage NNVAMD, and current phase 3 clinical trials for treatment of GA.

Risk of AMD Anatomic Progression

The AREDS trial provides natural history data describing the natural course of AMD through at least 5 years for participants who were assigned to placebo. Eyes with early AMD, those with extensive (total area involved ≥125-μm diameter circle) small drusen or nonextensive (total area ≤360-μm diameter soft indistinct or ≤660-μm diameter soft distinct) medium drusen, were shown to have an approximately 1% chance of progression to advanced AMD over 5 years. An individual who has intermediate AMD (extensive medium drusen, i.e., greater than the areas of medium drusen noted above; at least 1 large druse; or nonfoveal GA) in their most advanced eye had an 18% chance of progression to advanced AMD over 5 years. Of the patients with intermediate AMD in their most advanced eye, those who had large drusen in each eye or noncentral GA in at least one eye had a 27% chance of progression to advanced AMD in this time period compared with a 6% chance among those with intermediate AMD without these characteristics. The highest risk group was identified as the fellow eye of individuals with unilateral advanced AMD, or vision loss to below 20/32 from AMD in their first eye. The healthier fellow eyes among

these participants had a 43% probability to progress to advanced AMD by 5 years[163] (Fig. 68.45A).

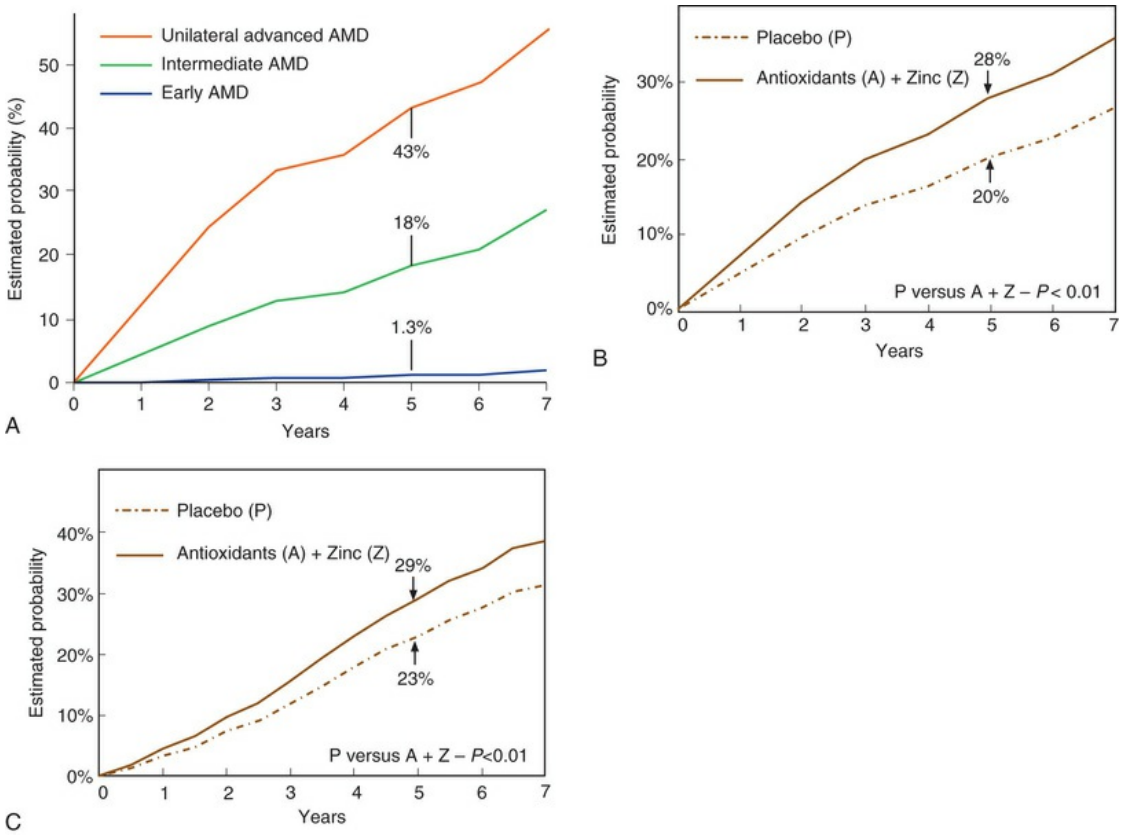

FIG. 68.45 Results of the Age-Related Eye Disease Study (AREDS) clinical trial. Risk of progressing to advanced age-related macular degeneration (AMD) within 5 years for patients with (A) early AMD, intermediate AMD, and unilateral advanced AMD assigned to placebo. (B) The effect of treatment with antioxidants and zinc for eyes with intermediate AMD or unilateral advanced AMD. (C) Effect of antioxidants and zinc on ≥15 letter vision loss in patients with intermediate or monocular advanced AMD.

The AREDS investigators also developed a detailed severity scale for AMD, largely for research purposes, as it is based on careful qualitative and quantitative review of stereoscopic color fundus photographs.[71] Photographs at study entry and annual photographs beginning at year 2 from AREDS participants were graded for drusen characteristics (size, type, and area), RPE abnormalities (increased pigment, depigmentation, and GA), and presence of

abnormalities consistent with neovascular AMD. Relationships between various combinations of baseline characteristics and development of advanced AMD (NVAMD or foveal GA) by the 5-year examination were explored to develop a 9-step severity scale that sorts the 5-year risk of progression to advanced AMD from less than 1% in step 1 to about 50% in step 9.[71] About half the eyes that had at least a 3-step progression between baseline, and the 5-year examination showed stepwise progression through intervening severity levels at intervening visits.[71]

Based on the fundus features that had the greatest prognostic value in the 9-step severity scale, the AREDS group developed a simple grading scale that lends itself to quantifying patient risk in clinical practice. Each eye of a person is scored individually, assigning one point for the presence of large drusen and one point for the presence of RPE abnormalities. A cumulative person score ranging from 0 to 4 is calculated. To apply this simplified scale to an individual with unilateral advanced AMD to calculate the risk for the fellow eye, the eye with foveal GA or NVAMD receives a score of 2, such that the person score would range from 2 to 4. Individuals who do not have large drusen in either eye but manifest bilateral medium drusen receive 1 total point and earn additional points if RPE abnormalities are present. Each person score has been associated with an escalating estimated 5-year risk that ranges from 0.5% to 50%[72] and 10-year risk that ranges from 1.5% to 71%[164] that at least 1 eye will progress to advanced AMD (Table 68.1).

TABLE 68.1

Risk of Development of Advanced AMD in at Least 1 Eye Per Year Based Upon Simple Scale Person Score at Baseline

Simple Scale Score	Year									
	1	2	3	4	5	6	7	8	9	10
0	0.1	0.1	0.4	0.5	0.5	0.6	0.8	0.8	1.2	1.5
1	0.5	1.7	2.4	3.1	4.1	4.7	5.1	6.3	7.2	8.4
2	1.1	3.2	5.8	7.5	9.4	14.0	17.1	21.5	23.6	27.6
3	2.7	8.8	15.8	21.9	26.2	30.4	36.2	42.1	46.9	52.7
4	2.8	14.2	27.6	35.6	44.5	49.3	54.1	62.0	67.5	71.4

AMD, Age-related macular degeneration.

Data from Chew EY, Clemons TE, Agron E, et al. Ten-year follow-up of age-related

macular degeneration in the age-related eye disease study: AREDS report no. 36. JAMA Ophthalmol. 2014;132(3):272-7.

This simplified severity scale served as the basis of a more elaborate multivariate analysis to create a model that predicted risk of progression to advanced AMD (CNV or any GA) among AREDS participants. The final risk assessment model included additional factors (individual age, family history, smoking status, presence of very large (≥250 μm) drusen, and complement factor H (CFH)) and ARMS2 gene polymorphisms that modify rates of AMD progression.[94] The variable with the strongest predictive value in this model remains the AREDS simple scale score, with hazard ratio (HR) of 50.65 for AMD progression comparing simple scale score of 4 to a score of 0. Although other person or ocular characteristics remained significant in this multivariate analysis, the magnitude of their effects was substantially less with hazard ratios ranging from 1.03 for each year of age greater than 55 to 2.00 for an ARMS2 genotype of TT compared to GG (Table 68.2). The final model did not incorporate polymorphisms in the C2, C3, complement factor I (CFI), and APOE genes as these did not modify risk of progression in this multivariate analysis. The validity of this model was confirmed by applying it to a subset of CAPT study participants in whom genetic testing was available.[94] This model can be accessed online via website and permits the user to enter patient data (optional inclusion of genotype) to calculate patient-specific probabilities of disease progression.

TABLE 68.2

Hazard Ratios for Development of Advanced AMD Based on Multivariate Analysis in Risk Assessment Model developed by Klein et al.

Variable	Total (%)	HR (95% CI)	*p* value
Simple Scale Score			
0	1006 (39)		
1	444 (17)	6.38 (3.48–11.69)	<.001
2	444 (17)	14.12 (8.06–24.75)	<.001
3	329 (13)	34.53 (19.79–60.26)	<.001
4	376 (14)	50.65 (28.86–88.89)	<.001
CFH, rs1061170			
TT	789 (30)		
CT	1177 (45)	1.28 (1.02–1.61)	.03

CC	636 (24)	1.44 (1.14–1.83)	.003
ARMS2, rs10490924			
GG	1324 (51)		
GT	1005 (39)	1.56 (1.30–1.86)	<.001
TT	273 (10)	2.00 (1.59–2.50)	<.001
Very Large Drusen[a]			
No	2105 (81)		
Yes	497 (19)	1.79 (1.50–2.14)	<.001
Smoking			
No	2448 (94)		
Yes	154 (6)	1.78 (1.37–2.31)	<.001
Family History[b]			
No	2178 (84)		
Yes	424 (16)	1.40 (1.16–1.70)	<.001
Advanced AMD in One Eye			
No	2229 (86)		
Yes	373 (14)	1.21 (1.02–1.45)	.03
Age Mean (SD), yr	68.12 (4.96)	1.03 (1.01–1.05)	<.001

[a]Drusen 250 μm or larger.

[b]First-degree family member with any AMD.

Data from Klein ML, Francis PJ, Ferris FL, 3rd, et al. Risk assessment model for development of advanced age-related macular degeneration. Arch Ophthalmol. 2011;129(12):1543-50.)

Since the fundus AMD features identified on clinical examination – those that are reflected in the AREDS simple scale assessment – are the most powerful predictors of disease progression, genetic testing even in combination with other demographic information in the absence of fundus phenotype is not recommended. For example, using this model, for a 70-year-old patient with simple scale score of 0, the risk assessment for advanced AMD within 5 years falls between 0% if no other risk factors (those other than phenotype) are present and only 3% in the presence of the highest risk genotype and all other predictive factors being present. However, this 3% risk would soar to 53% if the simple scale value were 2 and drusen ≥250 μm were present. While genetic testing and the factors other than fundus phenotype should not be utilized in isolation, they can modify the risk and add significant predictive power for any given patient. Using the simple scale alone, a 70-year-old patient with a score of 4 would be assessed a 50% probability of progressing to advanced AMD within 5-years. However, using the full risk assessment model, the risk for this patient would be refined and may actually range from 19% to 93%. Additionally, this model provides predictions for development of

each of the two subtypes of advanced AMD, GA or CNV.

Risk of AMD Progression Based on Specific AMD Manifestations

Small Drusen

Population-based studies[22,24–26,109] have reported that one or more small drusen are commonly present in the macula. Small drusen were identified in 95.5% of a population-based survey among men aged 43–86 (mean 62.3)[24] and in 98.8% of individuals over age 49 participating in an Australian-based population survey.[25] Pathologic studies support the conclusion that the presence of a few small, hard drusen is not a risk factor for AMD as they appear to be ubiquitous in histologic specimens from individuals age 50 and older.[110] However, several studies[7,109,165] have found that with increased numbers of (or area occupied by) small drusen, an eye is more likely to develop larger drusen with time. In the Beaver Dam Eye Study, among participants with only small hard drusen at baseline the 5-year incidence of intermediate-size drusen varied according to the area occupied by small drusen at baseline. Eyes with baseline small drusen area >9086 μm^2 had 17% progress to intermediate drusen, whereas those with area <2596 μm^2 area had 8% progression.[165] The AREDS study confirmed eyes with small drusen may progress to large drusen. The 10-year probability that AREDS participants with only small drusen at baseline would progress to large drusen was 12.8%.[9]

Longitudinal clinical studies of at least 5 years' duration suggest advanced AMD rarely develops in eyes with only small drusen at presentation, regardless of the total area involved.[7,94,163] Within AREDS the 10-year rate of advanced AMD was 1.5% for eyes with only small drusen at baseline; even lower rates were observed among participants without advanced AMD in the fellow eye.[164]

Intermediate or Large Drusen and RPE Changes

Eyes that present with intermediate-size drusen are at risk of progressing to large drusen and advanced AMD. In AREDS, 37% and 4.6% of participants who had medium-sized drusen (as their

largest size) in their most advanced eye developed large drusen and advanced AMD, respectively, within 10 years of follow-up. The prevalence of these events is greater, at 71% and 14%, respectively, when the participant has medium-size drusen in each eye at baseline.[164]

Eyes with large drusen remain at even higher risk of developing advanced AMD compared with those with medium drusen. AREDS participants with bilateral large drusen in the absence of baseline RPE abnormalities had 36% progress to advanced AMD by 10 years, while rates climbed to 66% when RPE abnormalities accompanied bilateral large drusen at baseline.[164] This highlights the fact that RPE abnormalities, independent of drusen, impart risk for AMD progression.

As AREDS was a prospective study, eyes that initially developed large drusen and RPE abnormalities during follow-up were identified. There were 570 eyes, all in participants without advanced AMD in the fellow eye at entry, in which temporal relationships were explored between development of these fundus features and further AMD progression. Nine percent developed advanced AMD within 5 years of the detection of large drusen and RPE abnormalities, with about a 3 : 1 ratio of NVAMD : FGA.

The location that large drusen occupy also modulates the risk of disease progression. When large drusen were present solely within 1 DD of the foveal center (the central zone), in the absence of advanced AMD in either eye, 22% progressed to advanced AMD within 10 years as compared to 4% among eyes with large drusen located within 1 and 2 DD (the outer zone) from the foveal center. Rates were higher (38%) when drusen occupied both areas, and even more substantial if RPE abnormalities were present. By year 10 nearly 60% of eyes with large drusen in the central and outer zones, in association with RPE abnormalities, progressed to advanced AMD.[164]

Population-based studies have also demonstrated that risk of progression to late forms of AMD is related to the size and extent of drusen, as well as the presence or absence of RPE abnormalities. In the Beaver Dam Eye Study, the 15-year cumulative incidence rate for late AMD (any GA or CNV) was nearly 40% among eyes of participants with large drusen and total drusen area >700 μm

diameter circle at baseline. In contrast, the 15-year cumulative incidence of late AMD was only 8% when the largest druse was medium size and the cumulative drusen area was >320 μm diameter circle and 2% when only small drusen were present.[166] For participants whose baseline drusen area was in the largest quartile, simultaneous presence of RPE abnormalities increased the 15-year risk for late AMD from about 30% (eyes without RPE abnormalities) to >50%. Application of the AREDS AMD severity scale to fundus photographs of Beaver Dam Eye Study participants generated an OR of 2.7 (95% CI 2.3–3.1) for each step increase AMD level at baseline and the 15-year progression rates to late AMD.[166]

Risk of Geographic Atrophy

The 15-year cumulative incidence of any GA in the Beaver Dam Eye Study was approximately 1% in eyes with medium drusen and 7% in eyes with large drusen at baseline. When baseline drusen area was greater than a 700 μm diameter circle in eyes with large drusen, 24% developed GA.

The greater the severity of presenting levels of RPE abnormalities coexisting with large drusen, the greater likelihood that incident advanced AMD will be either FGA or NVAMD as compared to primarily NVAMD. When baseline bilateral large drusen and at least unilateral RPE abnormalities coexist, progression to FGA is common, occurring in 44% of AREDS participants within 10 years.[164] In the absence of pigment changes at baseline, even with baseline bilateral large drusen <1% of AREDS participants developed FGA at 5 years and only 10% did so at 10 years, compared with 32% who developed NVAMD at 10 years.[164]

Risk of NVAMD

The 15-year cumulative incidence of NVAMD in the Beaver Dam Eye Study was approximately 2% in eyes with medium drusen and 10% among those with large drusen at baseline. When baseline drusen area was >700-μm diameter circle in eyes with large drusen, this risk rose to 20%.

When bilateral large drusen are present, progression to NVAMD is common, occurring in 32% of AREDS participants without RPE abnormalities and 45% with at least unilateral baseline RPE

abnormalities within 10 years.[164] The development of GA does not protect an eye from also developing NVAMD; in fact, the risk of neovascular AMD is quite high in the presence of GA. Among 981 eyes with incident GA during AREDS follow-up, 16% progressed to NVAMD when the fellow eye did not have NVAMD at baseline, while 36% did so when the fellow eye had neovascular AMD.

Drusenoid PEDs.

Within AREDS, 282 eyes with drusenoid PEDS (diagnosed in the absence of advanced AMD) were followed prospectively for at least 5 years. Within 5 years 42% developed advanced AMD with approximately 1 : 1 ratio of FGA : NVAMD.[106] Earlier progression to advanced AMD was more likely to manifest as NVAMD; however, Kaplan–Meier analysis showed the cumulative percentage of eyes developing FGA surpassed the number of eyes with NVAMD at 7 years. Five-year progression rates to advanced AMD (42% vs. 25%, $p<.001$) and specifically rates of FGA (18% vs. 7%, $p<.001$) were higher in this group of participants than those with large drusen and pigmentary abnormalities. Those that did not develop advanced AMD still tended to show evidence of disease progression with development of calcification, pigmentary changes (typically hypopigmentation), and noncentral GA.[106] By 10 years, 55% of eyes with drusenoid PEDs are expected to develop FGA and 40% NVAMD.

In a retrospective study, with 61 eyes of 32 patients with drusenoid PEDs (defined as 0.5 DD of soft, confluent drusen under the center of the macula), followed for median 2 years (range 1–17 years), Kaplan–Meier survival analysis suggested these eyes had a 50% chance of developing GA within 7 years.[107] Eyes with larger-size drusenoid PEDs and metamorphopsia were more apt to develop GA sooner than other eyes and remained at highest risk for incident CNV.[107]

Advanced AMD in Fellow Eye.

Annual incidence rates of 5–14% were estimated for the development of advanced AMD in the fellow eye of individuals with unilateral NVAMD in a retrospective review of 101 patients followed for up to 9 years.[167] Drusen number, size, and confluence

were important predictive factors for progression among these fellow eyes.[167] In a prospective study of 670 individuals with unilateral CNV participating in the Macular Photocoagulation Study, risk factors for fellow eye progression to NVAMD included five or more drusen (any size) or ≥1 druse >63 μm.[168]

Actual 5-year progression rates to advanced AMD using the AREDS simple scale scoring system are slightly higher for each respective person score, when an individual has unilateral advanced AMD.[72] The risk assessment model that is based on AREDS data showed a hazard ratio of 1.21 (95% CI 1.02–1.45) for incident advanced AMD among individuals with unilateral advanced AMD compared with those without advanced AMD in either eye (Table 68.2).[94] Individuals with unilateral advanced AMD who had no drusen or only small drusen in AREDS had 10-year progression rates to advanced AMD of 8.6% in their fellow eye compared with 0.7% among individuals without any advanced AMD.[164] Similarly, advanced AMD in the first eye modulated the risk for progression to advanced AMD in a fellow eye with medium drusen with 10-year progression rates of 26% compared with 4% in the absence of first-eye advanced AMD. Among eyes with large drusen and RPE abnormalities, 10-year rates of progression to advanced AMD increased from 50% in the absence of first-eye advanced AMD to 77% in the presence of unilateral advanced AMD.[164]

Subretinal Drusenoid Deposits.

Although eyes with soft drusen may also contain subretinal drusenoid deposits, the subretinal drusenoid deposits are an independent predictive factor for progression to advanced AMD. However, the magnitude of risk associated with soft drusen is far in excess of that associated with reticular drusen. In a prospective case–control study, the OR for development of any GA or CNV in eyes with soft drusen was 16.6 (95% CI 7.5–14.9), whereas the OR for subretinal drusenoid deposits was 2.6 (95% CI 1.1–6.5).[123]

Impact of NNVAMD on Vision Function

Early and Intermediate NNVAMD

Visual Acuity.

Minimal, if any, deficits in VA are commonly associated with early and intermediate AMD. Within the Macular Photocoagulation Study (MPS) of extrafoveal CNV, 128 participants had a fellow eye with NNVAMD at baseline. At the 5-year examination, 76 of these eyes remained free of neovascular AMD. Median VA among these eyes was 20/20 at baseline and at the 5-year examination.[169] AREDS study eyes were required to have VA of ≥20/32 at enrollment, and the actual median baseline acuity was 83 letters (Snellen equivalent $20/20^{-}$) among eyes that entered with large drusen. At the 10-year examination, median VA was 81 letters (Snellen equivalent $20/25^{+}$) among this subset of large drusen eyes that had not progressed to advanced AMD.[164]

Drusenoid PEDs may exist in the setting of 20/40 or better VA with or without metamorphopsia.[107] Within AREDS, there were 282 eyes that had drusenoid PEDs in the absence of advanced AMD at baseline. Initial mean VA was about 80 letters (Snellen equivalent 20/25), and this fell to 72 letters (Snellen equivalent 20/40) at 5 years among the 57% that did not progress to advanced AMD. The rate of moderate vision loss (≥3 lines) was 21% in this subset, which was higher than that seen among eyes that had large drusen and focal hyperpigmentation at entry and did not progress to advanced AMD (21% vs. 13%, p=.01). Vision decline appeared related to development of incipient RPE atrophy (nongeographic atrophy) with functional loss of photoreceptors that lie anterior to the drusenoid PED. Among the eyes with drusenoid PED that progressed to FGA, much larger decreases in VA occurred.[106]

Other Measures of Vision Function.

While VA often remains normal or close to normal in eyes with early or intermediate AMD, other measures of visual function may reflect pathology. A recent study assessed VA, low luminance acuity, dark adaptation, macular light sensitivity via 24-2 HVF testing, and spatial contrast sensitivity in 1260 eyes of 640 participants. This study included participants with minimum age of 60 without fundus lesions of AMD (1007 eyes) and with "early" AMD (253 eyes) identified on color fundus photographs.[170] Eyes were classified as normal (no AMD) if total drusen area was <125

μm in the absence of RPE abnormalities, whereas "early" AMD reflected steps 2, 3, or 4 on the AREDS AMD 9-step severity scale, which corresponds to a maximum drusen area (DA) of ≤0.2 DA without RPE changes or <0.028 DA if definite RPE changes were also present.[71,170] Mean (± SD) VA was logMAR 0.043±0.13 (Snellen equivalent 20/22) in the normal eyes and logMAR 0.069±0.13 (Snellen equivalent 20/23) in the AMD eyes. Rod-mediated dark adaptation was significantly reduced in the AMD eyes compared to controls, but the other vision function tests showed no significant difference.[170]

Midena et al. evaluated macular function among individuals with minimum age of 50, VA >20/25, and >10 medium or large drusen within 1500 μm of the fovea.[171] Each of 47 participants contributed one study eye. Thirty-four participants had NNVAMD in each eye (eye with better acuity chosen or randomly selected eye if acuity was the same in each eye), and in 13, the fellow eye had CNV. Thirty-six age-matched controls each contributed one study eye. Of note, noncentral GA was present in 10% and focal hyperpigmentation in one-third of the NNVAMD eyes. Both static and dynamic contrast sensitivity functions (sinusoidal spatial frequency gratings were static or modulated with time), macular recovery function following bright light stimuli, and central visual field sensitivity as measured by 10–2 Humphrey visual field, were impaired, to clinically relevant degrees, in the eyes with NNVAMD compared to age-matched control eyes (*p* values ranged from <.001 to .008). The only type of testing performed in this study with no significant difference between AMD and control subjects was Farnsworth–Munsell 100 hue testing.

Microperimetry testing has also identified deficits in eyes with NNVAMD. When retinal sensitivity in the macula of AMD eyes classified as AREDS category 2 (164 eyes) or AREDS category 3 (155 eyes) was compared with 200 age-matched controls, mean sensitivity was decreased among the AMD eyes relative to controls in each of 5 rings of test points around the fovea.[172] This test covered the central 10°, and greater decreases were seen among the AREDS category 3 eyes compared to category 2 eyes.[172] Mean sensitivities (dB) were 29.8±1.7 in age-matched controls, 24.9±3.9 in category 2 eyes, and 21.8±5.34 in category 3 eyes (*p*<.001 for each

individual pairwise comparison).[172] While some studies have shown a relative decrease in sensitivity when testing is performed directly over large drusen,[173] other studies have been unable to confirm this while making similar observations only when testing is located in areas without clinical signs of drusen.[174] This conflicting data likely reflects the variable degree to which RPE and photoreceptors may become anatomically and functionally affected overlying drusen. In support of this concept it has been demonstrated that areas of decreased sensitivity in eyes with confluent soft drusen correspond to regions with ellipsoid band loss or RPE irregularity on OCT.[175]

Eyes with subretinal drusenoid deposits have been reported to manifest abnormalities in contrast sensitivity thresholds and microperimetry.[176,177] Using Pelli–Robson contrast sensitivity testing in 51 eyes of 36 patients with NNVAMD, the presence of subretinal drusenoid deposits was noted to be inversely correlated with contrast sensitivity score (p=.012).[176] In a prospective case series of 22 eyes from 18 patients with well-demarcated subretinal drusenoid deposits, scotopic or rod-mediated function was compromised with a relatively sharp demarcation of reduced scotopic threshold noted in the areas with visible subretinal drusenoid deposits compared to areas without the deposits.[177]

Geographic Atrophy

When GA affects the foveal center, VA compromise may be moderate to severe; however, prior to definitive foveal involvement eyes with GA may have a more insidious loss of acuity. In the CAPT, 91 fellow eyes developed GA at or beyond 2 years following study entry in the absence of other retinal disease or CNV.[100] For assessment of the effect incident GA had on VA, 87 of these eyes were each matched to a control eye that did not develop GA or CNV. The mean best corrected acuity was 81 letters ($20/25^{+2}$) at baseline for cases and control eyes. One year prior to the date at which GA was recognized on fundus photographs in the GA cases, VA letter score had fallen on average (±SD) by 5(±9) letters relative to baseline. Among control eyes letter score had decreased an average of 0.7(±6) at the same time point. Among the GA cases, when GA was initially detected (located anywhere in the macula),

mean change in VA was −7(±12) letters from baseline; however, the magnitude of vision loss at first detection of GA was directly related to the incident GA location. There was a mean loss of 24 letters for incident FGA, 5 letters for GA extending to the FAZ, and 2 letters when the proximal edge of GA was ≥250 μm from the foveal center.[100]

These observations were corroborated in AREDS, as the median VA was 77 letters (Snellen equivalent 20/32^{+}) at the visit one year prior to identification of FGA among 685 eyes with incident FGA during follow-up.[164] The median acuity fell by 12 letters from one year prior to identification of FGA to a score of 65 (Snellen equivalent 20/50) at the visit in which FGA was documented.[164] By 10 years following development of FGA the median acuity had fallen further to 27 letters (~20/320).[164] Among the incident cases of GA in AREDS, 35% presented with FGA. Among the remaining 65% that progressed to FGA from noncentral GA, the median time from noncentral GA to FGA was 2.5 years.[158] Within AREDS, 895 eyes of 686 participants who did not have any GA or CNV in either eye at baseline developed GA within 1500 μm of the fovea. In 209 participants, incident GA developed in both eyes with median time of 7 years for second eye incident GA.[158]

The time course of progressive VA impairment from GA is highly dependent upon the initial location of GA and its growth rate (see previous section on "Growth of GA"). Prognostication therefore requires each case to be assessed individually. Several case series have provided natural history data.[75,141,162,178–180] In a longitudinal cohort study of 74 eyes with at least one area (≥500 μm in diameter) of GA within 1 DD of the fovea and VA of ≥20/50 at entry, at 2 years 50% lost ≥3 lines of acuity and 25% lost ≥6 lines.[180]

VA alone may not accurately represent the depth of vision impairment for many individuals with GA. Large single or multiple areas of atrophy may spare the foveal center and greatly impact near vision activities such as reading. Reading rate is slowed by paracentral scotomas, and some eyes with geographic atrophy also demonstrate abnormal foveal dark-adapted sensitivity, reduced VA in dim illumination, and reduced contrast sensitivity.[180] Even when the central fovea becomes involved with GA, vision function may vary depending on the patient's ability to find a surviving island of

retina within the atrophic area, or the least affected portion of retina outside the area.[179] There seems to be a preference to fixate with the scotoma to the right of the object of interest,[181] favoring the ability to see the beginning of a line when reading rather than the end of text. Visual retraining may enable a patient to use the closest viable area of retina. However, magnifying aids often do not help these individuals to read as the magnified image is projected into the sites of GA. The combination of reduced VA with progressive enlargement of atrophy, occurring bilaterally in most patients, can lead to significant impairment of visual function.[162,179]

The Role for Micronutrient Supplements in Management of Non-Neovascular AMD: AREDS and AREDS2

The AREDS demonstrated that micronutrient supplements consisting of specific antioxidants (500 mg vitamin C, 400 IU vitamin E, and 15 mg beta-carotene) and minerals (80 mg zinc oxide with 2 mg cupric oxide to reduce the risk of zinc-induced, copper-deficiency anemia) reduce progression to advanced AMD. However, these benefits are only apparent among individuals with intermediate AMD or unilateral advanced AMD[163] (Fig. 68.45A). The treatment benefit was confirmed through 10 years of follow-up (Fig. 68.46), even though all participants were counseled to use the combination supplements when the randomized component of the trial ended.[164] The clinical trial ended when 90% of participants had completed 5 years of follow-up. The results were driven by a risk reduction for NVAMD as there was no definitive evidence to suggest that GA development or progression to FGA was affected (Fig. 68.46A).[163,164]

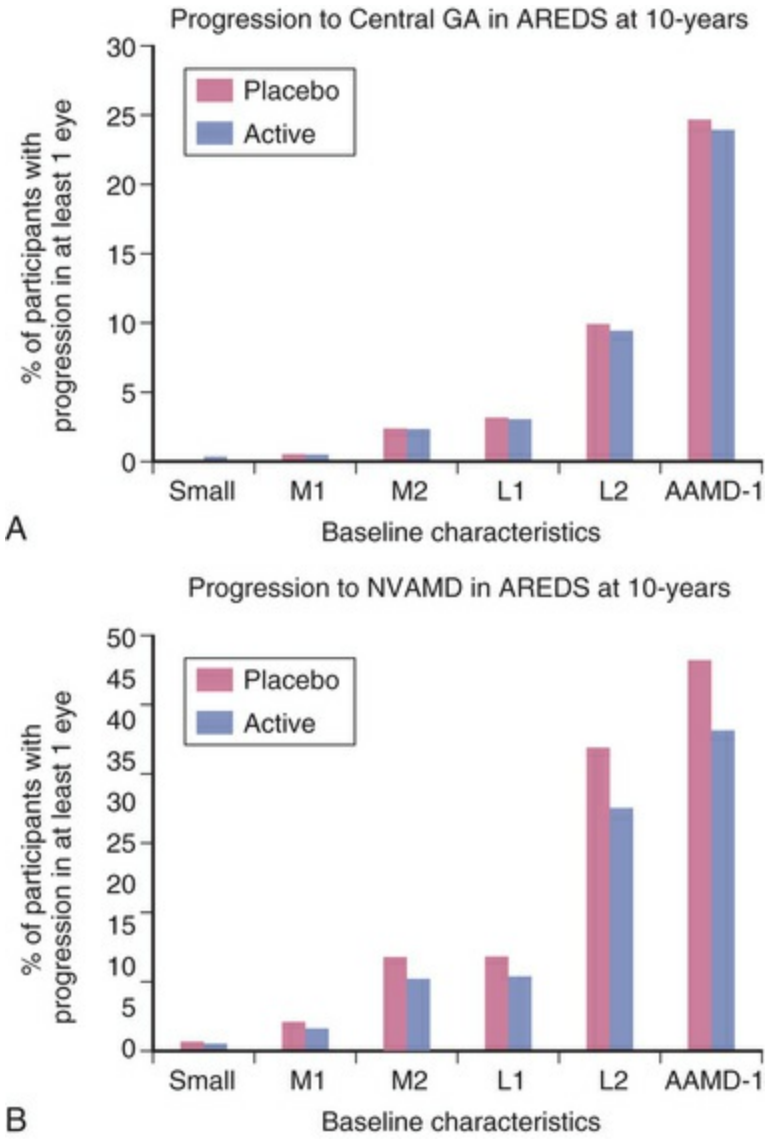

FIG. 68.46 Rates of progression to advanced age-related macular degeneration (AMD) at 10-years within the Age-Related Eye Disease Study (AREDS), related to baseline characteristics in active versus placebo groups. (A) Rates of progression to central geographic atrophy *(GA)* correlate to baseline severity but are unaffected by use of supplements. (B) Rates of progression to neovascular AMD *(NVAMD)* correlate to baseline severity and are reduced by use of supplements. *AAMD-1*, advanced AMD in fellow eye at baseline; *L1*, large drusen as most advanced feature in one eye; *L2*, large drusen as most advanced feature in both eyes; *M1*, medium drusen as most advanced feature in 1 eye; *M2*, medium drusen as most advanced feature in both eyes; *Small*, small drusen only at baseline. (Adapted with permission from Chew EY, Clemons TE, Agron E, et al. Ten-year follow-up of age-related macular degeneration in the age-

related eye disease study: AREDS report no. 36. JAMA Ophthalmol. 2014;132(3):272-7.)

Klein et al. first reported a possible differential response to supplements within the AREDS study depending upon CFH genotype.[182] Using AREDS data, Awh reported analyses that indicated that participants with only some CFH and ARMS2 genotypes benefited from supplements and that AREDS participants with some genotypes at these loci showed an unfavorable response to supplements.[183,184] Chew and coworkers have also analyzed data from AREDS in this regard and did not find a differential effect of supplements based on genotype and have argued that Awh and colleagues analyses are biased as they were a post hoc analysis of the data.[185] The American Academy of Ophthalmology addressed these reports in its Preferred Practice Pattern for AMD that was updated in 2015 and did not recommend genetic testing when considering recommendations for use of supplements. A randomized, prospective trial would be needed to show the utility of genetic testing in this setting.

The objective of AREDS2 was to determine if a combination of lutein/zeaxanthin (L/Z 10 mg/2 mg) and/or omega-3 long-chain polyunsaturated fatty acids in the form of eicosapentaenoic acid (EPA) (650 mg) and DHA (350 mg) could further reduce progression to advanced AMD when added to the AREDS supplements.[186,187] A secondary objective was to explore whether modifications to the original AREDS formulation could maintain the benefits and improve the safety of the micronutrient supplements when compared with the original formulation. These modifications included reducing the zinc dose to 25 mg and eliminating beta-carotene completely.[187] The obligatory primary and voluntary secondary randomization of this prospective clinical trial is shown in Fig. 68.47. At entry participants were to be at least 50 years of age and have bilateral evidence of large drusen (contributing 2 study eyes) in the absence of advanced AMD or large drusen in one eye (contributing 1 study eye) and advanced AMD in the fellow eye. In the primary analysis, with median follow-up of 5 years, there was no significant reduction in progression to advanced AMD when comparing the lutein/zeaxanthin and/or DHA/EPA arms to control.[186] Progression

rates to advanced AMD were about 30% in each of the four treatment assignments at 5 years. Exploratory secondary analyses referred to as the "main effects" grouped all participants receiving L/Z and compared them to those assigned to supplements without L/Z, essentially doubling the number of eyes in the analysis and increasing the power of the analysis to find a statistically significant difference. This analysis suggested that L/Z may reduce progression to advanced AMD with a hazard ratio (HR) of 0.90 (95% CI 0.82–0.99, p=.04).[188] Analysis of the secondary randomization showed that elimination of beta-carotene or reducing the zinc dosage had no significant effect on progression to advanced AMD.[186] Another exploratory secondary subgroup analysis utilized about one-third of the entire cohort to identify participants assigned to control in the primary randomization and the original AREDS formulation in the secondary randomization and compare them to those assigned to the L/Z only arm in the primary randomization and an AREDS supplement without any beta-carotene in the secondary randomization. This explores the efficacy associated with an AREDS supplement in which L/Z essentially would replace beta-carotene. This analysis provided HR 0.82 (95% CI 0.69–0.96) for advanced AMD, primarily due to a reduction in NVAMD (HR 0.78, 95% CI 0.64–0.94).[188] None of the analyses identified a difference between groups or subgroups for rates of at least moderate vision loss. The study did not incorporate a prespecified noninferiority analysis for any alterations to the original formulation in comparison to the original formulation for anatomic or functional outcomes. Therefore, questions remain as to whether an AREDS2 recommended formulation that substitutes L/Z for beta-carotene can achieve similar anatomic and functional outcomes relative to the original formula. No difference was seen in the rates of serious adverse events in any of the four primary treatment arms; however, more lung cancer cases were identified in the beta-carotene vs. no beta-carotene subgroups (2% vs. 0.9%, p=.04), occurring mostly in former smokers.[186]

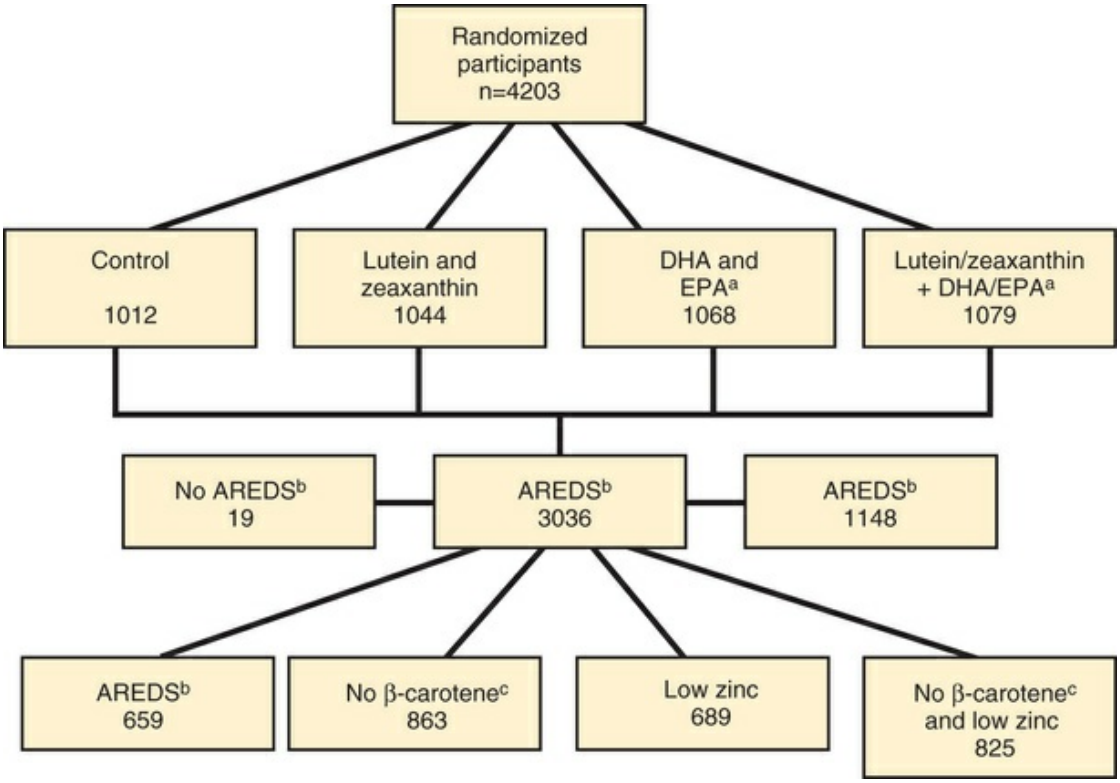

FIG. 68.47 Age-Related Eye Disease Study 2 Study Design. Primary randomization was 1 : 1 : 1 : 1 into four groups: control (no lutein/zeaxanthin or DHA/EPA), lutein/zeaxanthin only, DHA/EPA only, or lutein/zeaxanthin and DHA/EPA. Participants were given the option of continuing the original AREDS formula (*n*=1148) or undergoing secondary randomization into four groups: the original AREDS formula, the original formula with no beta-carotene, the original formula with reduced zinc, or the original formula with no beta-carotene and reduced zinc. Nineteen individuals declined the secondary randomization and use of the AREDS supplement. [a] DHA and EPA = docosahexaenoic acid and eicosapentaenoic acid; [b] AREDS supplements: vitamins C (500 mg) and E (400 international units), beta-carotene (15 mg), zinc (oxide 80 mg), and copper (cupric oxide 2 mg); [c] Smokers were randomly assigned to one of the two no beta-carotene arms; low zinc = 25 mg daily. (Reproduced with permission from Chew EY, Clemons T, SanGiovanni JP, et al. The Age-Related Eye Disease Study 2 (AREDS2): study design and baseline characteristics (AREDS2 report number 1). Ophthalmology. 2012;119(11):2282-9.)

Clinical Application of the AREDS and AREDS2 Results

The management of non-neovascular AMD begins with screening individuals at risk of the disease for its presence, essentially anyone that is age 50 and older. Applying disease prevalence rates from population-based studies to the US census report of 2000, it is estimated that 8 million Americans age ≥55 years have large drusen (≥125 μm) in at least one eye.[4,163] By 2020 an estimated 6.4 million additional people in the United States are expected to have large drusen in at least one eye.[4,163] It is presumed that the majority of these individuals are asymptomatic and may present for care in the context of routine ophthalmologic examination or for an ophthalmic condition other than AMD. During such examinations, practitioners should consider screening for AMD. If on examination there is subretinal or intraretinal fluid, hemorrhage, lipid, or RPE elevation, then neovascular AMD may be present. A fluorescein angiogram and OCT would be indicated to confirm a diagnosis of NVAMD and to assist with management options, as outlined in Chapter 69 (Neovascular (exudative or "wet") age-related macular degeneration).

Assuming there are no overt signs of neovascular AMD, then the practitioner should be assessing RPE abnormalities and drusen. If there is no evidence of AMD, or if the clinical evaluation is consistent with early AMD (as the most advanced AMD feature in both eyes), then no supplements are indicated. This is based on the absence of any benefit when these individuals received active treatment within AREDS. Supplements did not reduce progression to intermediate or advanced AMD in these eyes. These individuals may be counseled that they are at very low risk of visually significant disease within the next 5 years. It is reasonable to suggest they undergo annual reassessments to look for intermediate AMD as generally one-third of AREDS participants with early AMD progressed to intermediate AMD during the first 5 years of follow-up.[163]

If intermediate AMD is noted in at least one eye, then consideration of a dietary supplement such as that used in AREDS or AREDS2 is reasonable providing the individual's physician knows of no contraindication to using these high-dose supplements

long term. Individuals with at least unilateral intermediate AMD or unilateral advanced AMD who were assigned to the original AREDS formulation of antioxidants plus zinc had lower rates of AMD progression (Fig. 68.45B) and of moderate vision loss (Fig. 68.45C) through at least 10 years of follow-up.

Although there is minimal risk associated with the use of these supplements (Tables 68.3 and 68.4), a discussion of the modest treatment benefit and the minimal risks is appropriate. The magnitude of the treatment benefit is affected by the AMD status at treatment initiation with those that have already lost function in one with AMD having the largest benefit. Individuals who are currently cigarette smokers should be advised that beta-carotene supplements have been associated with a small but definite increase in lung cancer and mortality in the context of randomized trials assessing beta-carotene in cohorts at risk of lung cancer.[189,190] For these patients, use of an AREDS-like supplement that omits beta-carotene and includes L/Z (a formulation recommended for consideration by the AREDS2 group) may achieve the desired reduction in AMD progression while avoiding a heightened risk of lung cancer. A similar discussion is reasonable for individuals who are former smokers, so they can make an informed decision as to which supplement they feel is most appropriate to maximize their protection from AMD progression and vision loss and minimize their risk of morbidity and mortality.

Table 68.3
Safety – Antioxidants

Condition	No Antioxidants (%)	Antioxidants (%)
Hospitalization for mild/moderate symptoms	10.1	7.4
Hospitalization for infections	0.8	1.6
Circulatory	0.8	0.3
Skin, subcutaneous tissue	1.0	2.2
Change in skin color	6.0	8.3
Chest pain	23.1	20.2

TABLE 68.4
Safety – Zinc Oxide

Condition	No Zinc (%)	Zinc (%)

Hospitalization for mild/moderate symptoms	7.8	9.7
Hospitalization for genitourinary	4.9	7.5
Hospitalization for genitourinary problems in men	4.4	8.6
Circulatory	0.3	0.9
Anemia	10.2	13.2
Difficulty swallowing pills	15.3	17.8

If a person has unilateral advanced AMD (either central GA or neovascular AMD/disciform scar), the fellow eye is in the highest risk category, particularly if the fellow eye has large drusen and RPE abnormalities. These individuals (irrespective of specific non-neovascular AMD manifestations in this fellow eye) should be encouraged to use an AREDS supplement, with the smoking history caveats as discussed above.

If an individual has advanced AMD in both eyes, then the practitioner may consider recommending an AREDS-type supplement if visual acuity is relatively good (20/100 or better) in at least one eye in the presence of CNV. This consideration is based on AREDS data, which showed a decreased risk of further moderate vision loss in this NVAMD eye. However, this observation applied only to eyes with CNV and acuity of ≥20/100 at baseline (Table 68.5). The potential role of micronutrient supplements in patients with bilateral CNV undergoing management with anti-VEGF therapy is unknown, as this was not evaluated during AREDS or AREDS2.

TABLE 68.5

Effect of Treatment on Risk of Moderate Vision Loss From Baseline in Eyes With Neovascular Age-Related Macular Degeneration at Baseline

	Odds Ratio	99% CI	p value
Baseline VA 20/100 or Better (*n* = 260)[a]			
Antioxidant vs. no antioxidant	0.54	0.30–0.95	0.005
Zinc vs. no zinc	0.99	0.56–1.74	0.96
Antioxidant vs placebo	0.35	0.15–0.81	0.001
Zinc vs placebo	0.65	0.28–1.50	0.18
Antioxidant + zinc vs. placebo	0.53	0.23–1.24	0.05
Baseline VA 20/200 or Better (*n* = 352)[b]			
Antioxidant vs. no antioxidant	0.66	0.40–1.07	0.03
Zinc vs. no zinc	1.10	0.67–1.79	0.62
Antioxidant vs. placebo	0.56	0.27–1.13	0.03
Zinc vs. placebo	0.93	0.46–1.89	0.79
Antioxidant + zinc vs. placebo	0.72	0.36–1.46	0.24

[a]167 participants had moderate vision loss.

[b]206 participants had moderate vision loss.

CI, confidence interval; VA, visual acuity.

Modeling of data from AREDS and epidemiologic surveys of the US population reporting prevalence rates of AMD have suggested that approximately 300,000 individuals would avoid development of advanced AMD in at least one eye during a 5-year period if all 8 million people at risk of AMD progression were identified, educated in regards to supplement use, and were compliant in their use of an AREDS-type supplement. Nevertheless, an additional 1 million people will still develop advanced AMD over the same time period, of whom approximately two-thirds will develop NVAMD. With the availability of our current substantially effective anti-VEGF treatments for neovascular AMD, early diagnosis of neovascular AMD has become increasingly important. As anti-VEGF therapy is most effective at preventing further vision loss, as compared to vision improvement, initiation of treatment before vision is moderately compromised is critical to maximizing vision outcome for NVAMD patients. Therefore, individuals with intermediate AMD or unilateral advanced AMD are typically asked to return to their ophthalmologist on a regular basis for the following reasons: (1) to update staging of their AMD and update them on current AMD management practices; (2) to reassess functional needs related to any increased visual impairment related to progression of atrophic changes; (3) to identify any asymptomatic neovascular AMD for which prompt treatment may favorably affect final vision outcome; (4) to review the regular need and methods for periodic self-monitoring to increase the chance that the individual will identify progression to NVAMD should it occur in the setting of minimal vision loss; and (5) to be reminded to promptly contact their ophthalmologist if symptoms of progression are suspected. The frequency of regular visits for patients with unilateral or bilateral NNVAMD (or frequency of examination of eyes with NNVAMD in patients undergoing treatment for unilateral NVAMD) should be dictated by the projected risk for development of NVAMD based on the drusen and RPE abnormalities present in the eye(s).

Home Monitoring for Progression to NVAMD

Amsler grid testing has been shown to have limited sensitivity for detection of incident NVAMD in eyes with previously documented NNVAMD,[191–195] for example, sensitivity 0.42 (95% CI, 0.15–0.72) for detection of incident CNV[194] and 0.526 for detection of any CNV when Amsler grid testing is administered in an office setting.[195] Despite these observations many eye care providers recommend its use to individuals at risk of AMD progression. More recently, a perimetry device, the Preferential Hyperacuity Perimeter (PreView PHP, Carl Zeiss Meditec, Dublin, CA) was shown, in an office setting, to have greater sensitivity for detection of NVAMD when compared to an Amsler grid test when evaluated in 19 individuals with neovascular AMD: sensitivity 100% with PHP vs. 53% with Amsler grid, p=.004 (191). Additional in-office studies demonstrated that the device could differentiate eyes with recent-onset neovascular AMD from those with intermediate AMD with both a high sensitivity (85%) and high specificity (85%).[196] A similar device (ForeseePHP 2.05 Notal Vision, Ltd, Tel Aviv, Israel) was evaluated within a nested case–control study as part of the Carotenoids and coantioxidants in patients with Age-Related Maculopathy (CARMA) clinical trial. Eyes that progressed to CNV before the device was incorporated into the follow-up clinic visits had larger magnitude losses in visual acuity from baseline and larger choroidal neovascular lesion size at time of CNV detection than eyes that progressed to CNV after the device was adopted as part of the follow-up visit protocol. In this study, following the incorporation of the PHP device, 10 participants developed CNV, 9 of which were tested with the PHP device, and all 9 were detected with the device.[197]

The same technology has been developed into a home monitoring device (ForeseeHome, Notal Vision, Ltd, Tel Aviv, Israel) and was evaluated in a large-scale clinical trial performed at AREDS2 clinical trial sites, the HOME Study.[198] A total of 1520 participants (age 53 to 90 years) were randomly assigned to standard care home monitoring plus the home monitoring device versus standard care monitoring alone (with or without an Amsler grid). The primary outcome was the change in best corrected visual acuity letter score between baseline and CNV detection. Participants had bilateral

large drusen (2 potential study eyes) or large drusen in one eye (study eye) and advanced AMD in the fellow eye and at least 20/60 visual acuity in the study eye(s). Individuals assigned to the device were asked to test a minimum of twice/week but encouraged to test daily. Among the 51 eyes in the device group that progressed to CNV the median loss of acuity was 4 letters as compared with the 31 CNV events detected in the standard care arm, which suffered a median loss of 9 letters p=.021). Since the median acuity was 20/25 at study entry, this equated to 87% of the device group retaining vision of at least 20/40 at CNV detection compared with 62% in the standard care arm (p=.014). A reasonably low false-positive rate was noted in the device arm, mean 0.24 false-positive device initiated alerts per patient per year, which equates to 1 false-positive visit per device user for every 4.2 monitoring years. Incorporating a home monitoring strategy as was evaluated in the HOME study ought to identify a larger proportion of patients with incident CNV who retain better levels of vision at diagnosis of CNV. This in turn should translate into superior vision outcomes when these eyes are managed with anti-VEGF therapy for their NVAMD. Even with the potential for devices such as this to improve our ability to detect disease progression, including progression in the setting of better vision preservation, it is unlikely that all incident CNV cases will be detected by this method. A sizeable minority of NNVAMD patients will not be able to use the device, compliance may wane among users, and sensitivity for CNV events is not 100%. Periodic office examinations to identify progression among individuals who have failed to recognize or act upon new symptoms and to reinforce the need for regular self-vision checks is therefore still indicated.

Intermediate Stage of Age-Related Macular Degeneration and Cataract Surgery

In an aged population, the question of cataract extraction commonly arises, requiring an estimation of the postoperative visual acuity and the duration of the anticipated vision benefits. Despite coexistence of AMD, most individuals can derive vision benefits following cataract surgery when lens opacity is assessed to be a component of the preexisting visual impairment. During the

AREDS, 1939 eyes underwent cataract surgery. Although eyes without AMD (*n*=626) had the largest change in visual acuity at 8.4 letters between the two study visits that immediately straddled the time of cataract surgery, those with mild (early) AMD (*n*=406) gained 6.1 letters, intermediate AMD (*n*=712) eyes gained 3.9 letters, and even those with advanced AMD (*n*=195) gained 1.9 letters.[199] In each AMD subgroup these improvements represented a statistically significant change from baseline and were associated with 10 or more letter improvements in each AMD subgroup as follows: no AMD 41%, mild AMD 32%, intermediate AMD 29%, and advanced AMD 24%. Analysis of the eyes with longer-term follow-up of at least 1 year following cataract surgery suggested the early improvements in visual acuity were sustained in all AMD subgroups.[199]

Favorable outcomes following cataract surgery were corroborated in 1232 eyes that covered the spectrum of AMD severity and underwent cataract surgery during participation in AREDS2. Eyes that underwent cataract surgery during AREDS2 were categorized using the AREDS AMD severity scale.[71] Eyes with mild AMD (severity scale 1–3, *n*=30) gained 11.2 letters, moderate AMD (severity scale 4–6, *n*=346) gained 11.1 letters, severe AMD (severity scale 7–8, *n*=462) gained 8.7 letters, noncentral GA (severity scale 9, *n*=70) gained 8.9 letters, and central GA and/or neovascular disease (severity scale 10–11, *n*=324) gained 6.8 letters when comparing visual acuity changes between the two study visits that immediately straddled the cataract surgery.[71] This did represent a statistically significant mean gain in visual acuity from preoperative levels for each of the AMD subgroups. The proportion of patients that improved by 10 or more letters was highest at 37% among the mild AMD subgroup, and successively decreased along the AMD spectrum, but remained 24% among those with advanced AMD. Between 12 and 20% improved by 15 or more letters with cataract surgery, with minimal variations between the AMD subgroups.[71]

The findings of AREDS and AREDS2 provide evidence that argues against a harmful effect of cataract surgery on acceleration of AMD progression, a concern that has been raised by findings from epidemiologic studies. The biologic argument has been that

photic injury at or following cataract surgery and inflammation associated with the surgery may trigger AMD progression. A combined analysis of two population-based surveys (the Beaver Dam and Blue Mountains Eye Studies) suggested that cataract surgery increased the risk of incident neovascular AMD by a factor of 5 within 5 years of surgery.[200] These observations may have been due to easier visualization of the fundus after surgery and postoperative identification of neovascular AMD that was actually preexisting before cataract surgery. AREDS has the advantage of regular prospective data collection as compared to population-based surveys, which evaluate cross-sectional outcomes at different points in time. In the AREDS a variety of analytic methods were used to explore development of neovascular AMD or central GA following cataract surgery and no clear deleterious effect of any concerning magnitude was identified.[201]

The best evidence at this time suggests that patients with AMD can derive vision benefit from cataract surgery and that cataract surgery does not appear to increase the risk of AMD progression. These patients should not be discouraged from undergoing cataract surgery if there is concurrent cataract. Ophthalmologists should be aware of the possibility that eyes with advanced AMD (especially geographic atrophy in a blonde fundus or CNV with minimal subretinal fluid, hemorrhage, lipid, or scarring) might not be readily apparent through a cataract, despite preoperative imaging. Preexisting advanced AMD may explain the vision loss experienced by the patient, which may be mistakenly attributed to a cataract. When this is the case the vision outcomes following cataract surgery are more modest than what would be expected in the absence of advanced AMD. When and if vision continues to deteriorate following cataract surgery from progression of AMD that had not been identified prior to cataract surgery despite its preexistence, patients may inappropriately associate progression of their AMD and vision loss with the cataract surgery itself due to the temporal relationships of cataract surgery and making the more appropriate diagnosis of the AMD stage. As such, careful examination of the fundus for signs of advanced AMD, immediately before cataract surgery in any individual at risk for AMD, is important. Potential clues that advanced AMD may exist

posterior to a cataract include the presence of advanced AMD in the contralateral eye, pigmentary abnormalities in the macula (which may be associated with less visible atrophy or CNV), or glistening from calcification (which is usually associated with geographic atrophy). Performance of fluorescein angiography and OCT prior to cataract surgery can potentially identify areas of visually significant atrophy or raise suspicion of preexisting NVAMD. The presence of either of these may affect decisions to proceed with cataract surgery, as well as assist in formulating prognosis and AMD treatment plan. Even when atrophy is suspected on examination, angiography, or OCT, the indistinct landmarks and poor image quality can make it difficult to tell where the center of the fovea lies in relationship to preexisting RPE abnormalities and whether various layers of the neurosensory retina are intact.

Management of Visual Impairment From NNVAMD

Among patients with unilateral or bilateral advanced non-neovascular AMD, as well as those with vision impairment attributed to nongeographic atrophy, noncentral GA, or confluent foveal drusen or drusenoid PED, rehabilitation with a low-vision service should be considered. Experienced eye care and social service professionals can determine what services or devices might help the individual optimize the vision function and simultaneously adapt and cope with their vision impairment. Issues specific to driving may need to be considered.

In phakic patients with bilateral advanced and endstage untreatable AMD (central GA or stable disciform scar from NVAMD), consideration can be given for implanting a visual prosthetic device, also referred to as an implantable miniature telescope (IMT; VisionCare Ophthalmic Technologies, Saratoge, CA) (Fig. 68.48).[202] This device provides 2.2 to 3 times magnification of the central visual field and affords approximately 2 times the field of view of that associated with a similar strength external telescope. A prospective, open-label, multicenter clinical trial of 217 participants (age 55–93) with bilateral central visual acuity loss (20/80-20/800) related to central GA or stable disciform scars

evaluated the device, limiting inclusion to individuals that prior to enrollment demonstrated at least a 5-letter improvement with an external telescope. Furthermore, study participants may have experimented with an external telescope for several days at home to evaluate the loss of binocularity and peripheral vision that comes with use of a telescope. The fellow eyes of these individuals were used as the control groups, they did not receive the implant, and the fellow eye was expected to provide peripheral vision for the participant. A total of 206 (95%) of 217 eyes were implanted with the device, as 11 procedures were aborted at the time of surgery. Two devices (1%) required removal one month after placement due to condensation within the telescopic cylinder due to device damage at the time of implantation.[202] Postoperatively, the patients were asked to participate in six visual rehabilitation sessions to learn how to adapt to use of the telescope in daily life. These visits included training in learning to use alternate viewing between eyes for peripheral and central tasks. Among the 192 implanted eyes for which 1-year follow-up information was reported, 67% of implanted eyes gained at least 3 lines of distance visual acuity as compared to 13% of the fellow eyes. An improvement of at least 3 lines at both distance and near occurred in 53% with the IMT vs. 10% of fellow eyes.[202] Safety concerns at 1 year included the observation that 5% experienced at least a 2-line visual acuity loss at distance or near. In addition, mean endothelial cell death following implantation of the device was 20% at 3 months and 25% at 12 months.[202] A potential limitation of this study was the lack of a control group that received intensive vision rehabilitation in the absence of the IMT, so the extent to which a placebo effect is associated with the device and the intensive rehabilitation are responsible for the study results is unknown.

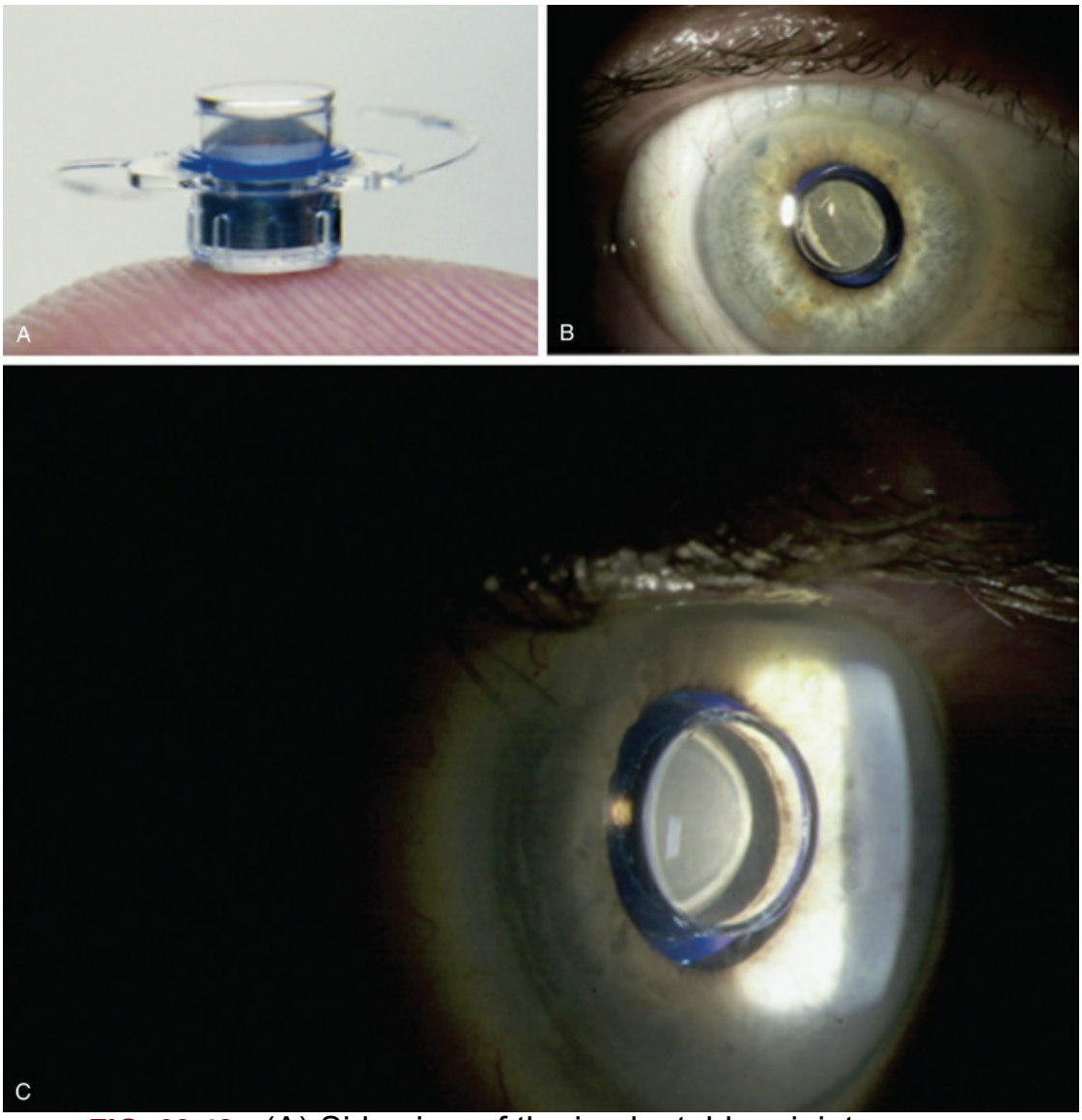

FIG. 68.48 (A) Side view of the implantable miniature telescope (top is anterior aspect of the device). The anterior quartz high-plus wide-angle microoptic is positioned behind the front window and a refractive air space. The posterior wide-angle microoptic is not visible because it is hidden inside the bushing that prevents light scatter in the posterior portion of the device cylinder. (B) Implanted study eye 6 weeks after surgery. The blue-light restrictor can be seen behind the iris. Photograph credit: James P. Gilman. (C) The anterior microoptical element can be seen illuminated behind the front window of the device. The front window protrudes marginally through the iris plane. Photograph credit: James P. Gilman. (Photograph credits panels B and C: James P. Gilman. Reproduced with permission from Hudson HL, Lane SS, Heier JS, et al. Implantable miniature telescope for the treatment of

visual acuity loss resulting from end-stage age-related macular degeneration: 1-year results. Ophthalmology. 2006;113(11):1987-2001.)

This device has been FDA approved for patients 75 and older with bilateral central vision loss related to advanced AMD. Postoperative visual rehabilitation is critical in managing patients undergoing implantation of this device, as is thorough preoperative evaluation in conjunction with low vision specialists. In addition, the facility with which the retina can be examined and treated for new pathology following the surgery remains a potential concern, though successful imaging has been described in a patient with the IMT using scanning laser ultrawide-field autofluorescence and fluorescein angiography.[203] Therefore, consideration of candidates who are truly endstage and not AMD treatment candidates is important.

Future Directions for Management of NNVAMD

Future research in AMD will likely focus on pathophysiology, new interventions, and enhanced means of preventing development and progression of the disease. On the horizon are the results of two phase III clinical trials evaluating treatments to limit vision impairment from progressive GA. The interventions under investigation will not reverse atrophy but may limit progressive enlargement of GA.

Emixustat hydrochloride (ACU-4429; Acucela, Inc., Tokyo, Japan) is an orally available small molecule that has been designed to inhibit the visual cycle isomerase (RPE-specific 65-kDa protein, RPE65) as a means of reducing the accumulation of vitamin A-based toxins, such as N-retinylidene-N-retinylethanolamine (A2E).[204] Reducing the concentration of such toxins within the RPE may slow GA progression. Based on its mechanism of action, it is expected to suppress rod photoreceptor activity, which may have adverse clinical side-effects. In a phase II, randomized, placebo-controlled study of 72 subjects with any GA, 54 patients were randomized to emixustat (2 mg, 5 mg, 7 mg, or 10 mg orally once daily) and 18 were randomized to placebo. The primary objective

was to explore the safety and tolerability over a 3-month period and evaluate the drug pharmacodynamics.[204] Chromatopsia (54% vs. 17%), described as a dark or colored tint to vision, as well as dark adaptation deficits (48% vs. 6%), were frequently reported by participants taking the drug when compared to placebo.[204] Rates were highest (83%) in the 10-mg treatment arm. Other adverse events were more prevalent in the combined emixustat groups compared with placebo and included the following subjective complaints: visual impairment (26% vs. 6%), blurred vision (15% vs. 6%), and visual field defect (15% vs. 0%). The objective measurement of reduced best corrected visual acuity was also more prevalent with the study drug (11% vs. 0%). Study drug was prematurely discontinued in the 7-mg and 10-mg arms (at a median of 25 days) due to the rate of adverse ocular events. Eighty-five percent of ocular adverse events resolved during the study or within 2 weeks of drug discontinuation and about half of the cases of chromatopsia resolved while still on study drug.[204] Suppression of rod photoreceptor activity as measured by ERG followed a dose response and recovered to baseline levels 7–14 days following drug discontinuation. No change in cone photoreceptor function was noted.[204] Emixustat is currently being evaluated in a 2-year, phase IIb/III (NCT01802866), randomized, placebo-controlled clinical trial of patients with GA. Active treatment arms are assigned to 2-mg, 5-mg, or the 10-mg dose. The study completion date was July of 2016.[205]

The other active intervention for GA that is in late phase development is lampalizumab (FCFD4514S; F. Hoffmann-La Roche, Ltd, Basel, Switzerland). This biologic product is an anticomplement factor D monoclonal antibody fragment.[206] As part of the alternative complement pathway, factor D acts upstream of complement factor H and is a rate-limiting step in the activation of the cascade and is present in lower levels than other complement factors.[206,207] The activation of complement pathways has been implicated in the pathogenesis of GA, both by demonstration of complement molecules in higher levels in pathologic specimens of eyes with AMD and GA and by genetic associations demonstrating that complement gene polymorphisms, and specifically complement factor H, are associated with increased risk of GA.[208]

The safety and tolerability of a single intravitreal injection of lampalizumab ranging from 0.1 to 10 mg was deemed acceptable in a phase Ia trial of 18 participants.[206]

The MAHALO study (NCT01229215), a phase II trial of intravitreal lampalizumab, 10 mg dosed monthly (*n*=43) or every other month (*n*=44) versus sham injection monthly (*n*=21) or every other month (*n*=21), reported 18-month, primary outcome findings in patients with GA at study entry at the 2013 American Society of Retina Specialist meeting in Toronto, Canada.[205] The study outcomes have not appeared in peer-reviewed literature at this time; however, further development of this drug is ongoing in the hopes that it will slow progression of GA, particularly in a subgroup of individuals who have the complement factor I (CFI) polymorphism. CFI also acts in the alternative complement cascade, and individuals with this polymorphism appeared to have larger areas of GA at baseline or faster GA expansion rates and possibly a larger treatment benefit was observed in this subgroup. Two identically designed parallel, double-masked, randomized, international phase III trials evaluating the safety and efficacy of lampalizumab (10 mg administered intravitreally every 4 or 6 weeks versus sham injection) are presently enrolling participants with GA: SPECTRI (NCT02247531) and CHROMA (NCT02247479). One eye of approximately 1879 patients with bilateral GA will be included in these studies, and the primary outcome will be the change in GA area at 48 weeks, while measures of visual function, including visual function questionnaire scores and high contrast and low-luminance visual acuity at 1 and 2 years, will provide important secondary outcomes.[205] Each treatment arm will include patients that are CFI biomarker positive or negative.

In parallel to these randomized clinical trials, there are two separate parallel, prospective observational studies of patients with GA that are presently enrolling participants. Between the two studies there is a combined goal of 560 participants to be followed for 48 months, with interim analysis at 24 months. These studies seek to better characterize the relationships between visual function and the progression of GA and to generate new information on the relationship between genotype and GA progression.[205] One of these studies, Proxima A (NCT02479386), will enroll participants with

bilateral GA, and the other study, Proxima B (NCT02399072), will enroll participants with unilateral GA in two cohorts, one with and one without CNV in the fellow eye.[205] The findings from these observational studies may aid in the design of future clinical trials for treatments of GA and could identify potential new targets for treatment.

References

1. Ferris FL 3rd. Senile macular degeneration: review of epidemiologic features. *Am J Epidemiol*. 1983;118(2):132–151.
2. Bourne RR, Stevens GA, White RA, et al. Causes of vision loss worldwide, 1990-2010: a systematic analysis. *Lancet Glob Health*. 2013;1(6):e339–49.
3. Bressler NM, Bressler SB, Congdon NG, et al. Potential public health impact of Age-Related Eye Disease Study results: AREDS report no. 11. *Arch Ophthalmol*. 2003;121(11):1621–1624.
4. Friedman DS, O'Colmain BJ, Munoz B, et al. Prevalence of age-related macular degeneration in the United States. *Arch Ophthalmol*. 2004;122(4):564–572.
5. Owen CG, Jarrar Z, Wormald R, et al. The estimated prevalence and incidence of late stage age related macular degeneration in the UK. *Br J Ophthalmol*. 2012;96(5):752–756.
6. Minassian DC, Reidy A, Lightstone A, et al. Modelling the prevalence of age-related macular degeneration (2010–2020) in the UK: expected impact of anti-vascular endothelial growth factor (VEGF) therapy. *Br J Ophthalmol*. 2011;95(10):1433–1436.
7. Klein R, Klein BE, Jensen SC, et al. The five-year incidence and progression of age-related maculopathy: the Beaver Dam Eye Study. *Ophthalmology*. 1997;104(1):7–21.
8. Wong WL, Su X, Li X, et al. Global prevalence of age-related macular degeneration and disease burden projection for 2020 and 2040: a systematic review and meta-analysis. *Lancet Glob Health*. 2014;2(2):e106–16.
9. Owen CG, Fletcher AE, Donoghue M, et al. How big is the burden of visual loss caused by age related macular

degeneration in the United Kingdom? *Br J Ophthalmol*. 2003;87(3):312–317.
10. Rudnicka AR, Jarrar Z, Wormald R, et al. Age and gender variations in age-related macular degeneration prevalence in populations of European ancestry: a meta-analysis. *Ophthalmology*. 2012;119(3):571–580.
11. Bressler NM, Doan QV, Varma R, et al. Estimated cases of legal blindness and visual impairment avoided using ranibizumab for choroidal neovascularization: non-Hispanic white population in the United States with age-related macular degeneration. *Arch Ophthalmol*. 2011;129(6):709–717.
12. Campbell JP, Bressler SB, Bressler NM. Impact of availability of anti-vascular endothelial growth factor therapy on visual impairment and blindness due to neovascular age-related macular degeneration. *Arch Ophthalmol*. 2012;130(6):794–795.
13. Borooah S, Jeganathan VS, Ambrecht AM, et al. Long-term visual outcomes of intravitreal ranibizumab treatment for wet age-related macular degeneration and effect on blindness rates in south-east Scotland. *Eye (Lond)*. 2015;29:1156–1161.
14. Bloch SB, Larsen M, Munch IC. Incidence of legal blindness from age-related macular degeneration in Denmark: year 2000 to 2010. *Am J Ophthalmol*. 2012;153(2):209–213.e2.
15. Skaat A, Chetrit A, Belkin M, et al. Time trends in the incidence and causes of blindness in Israel. *Am J Ophthalmol*. 2012;153(2):214–221.e1.
16. Gass JD. Pathogenesis of disciform detachment of the neuroepithelium. *Am J Ophthalmol*. 1967;63(3):1–139.
17. Age-Related Eye Disease Study Research Group. The Age-Related Eye Disease Study system for classifying age-related macular degeneration from stereoscopic color fundus photographs: the Age-Related Eye Disease Study Report Number 6. *Am J Ophthalmol*. 2001;132(5):668–681.
18. Bird AC, Bressler NM, Bressler SB, et al. An international classification and grading system for age-related maculopathy and age-related macular degeneration. The

International ARM Epidemiological Study Group. *Surv Ophthalmol*. 1995;39(5):367–374.
19. Ferris FL 3rd, Wilkinson CP, Bird A, et al. Clinical classification of age-related macular degeneration. *Ophthalmology*. 2013;120(4):844–851.
20. Klein R, Meuer SM, Myers CE, et al. Harmonizing the classification of age-related macular degeneration in the three-continent AMD consortium. *Ophthalmic Epidemiol*. 2014;21(1):14–23.
21. Laatikainen L, Larinkari J. Capillary-free area of the fovea with advancing age. *Invest Ophthalmol Vis Sci*. 1977;16(12):1154–1157.
22. Bressler NM, Bressler SB, West SK, et al. The grading and prevalence of macular degeneration in Chesapeake Bay watermen. *Arch Ophthalmol*. 1989;107(6):847–852.
23. Klein R, Cruickshanks KJ, Nash SD, et al. The prevalence of age-related macular degeneration and associated risk factors. *Arch Ophthalmol*. 2010;128(6):750–758.
24. Klein R, Klein BE, Linton KL. Prevalence of age-related maculopathy. The Beaver Dam Eye Study. *Ophthalmology*. 1992;99(6):933–943.
25. Mitchell P, Smith W, Attebo K, et al. Prevalence of age-related maculopathy in Australia. The Blue Mountains Eye Study. *Ophthalmology*. 1995;102(10):1450–1460.
26. Vingerling JR, Dielemans I, Hofman A, et al. The prevalence of age-related maculopathy in the Rotterdam Study. *Ophthalmology*. 1995;102(2):205–210.
27. Ibrahim YW, Bots ML, Mulder PG, et al. Number of perifoveal vessels in aging, hypertension, and atherosclerosis: the Rotterdam Study. *Invest Ophthalmol Vis Sci*. 1998;39(6):1049–1053.
28. Curcio CA, Millican CL, Allen KA, et al. Aging of the human photoreceptor mosaic: evidence for selective vulnerability of rods in central retina. *Invest Ophthalmol Vis Sci*. 1993;34(12):3278–3296.
29. Dorey CK, Wu G, Ebenstein D, et al. Cell loss in the aging retina. Relationship to lipofuscin accumulation and macular degeneration. *Invest Ophthalmol Vis Sci*. 1989;30(8):1691–

1699.
30. Gao H, Hollyfield JG. Aging of the human retina: differential loss of neurons and retinal pigment epithelial cells. *Invest Ophthalmol Vis Sci*. 1992;33(1):1–17.
31. Feeney-Burns L, Burns RP, Gao CL. Age-related macular changes in humans over 90 years old. *Am J Ophthalmol*. 1990;109(3):265–278.
32. Marshall J, Grindle J, Ansell PL, et al. Convolution in human rods: an ageing process. *Br J Ophthalmol*. 1979;63(3):181–187.
33. Iwasaki M, Inomata H. Lipofuscin granules in human photoreceptor cells. *Invest Ophthalmol Vis Sci*. 1988;29(5):671–679.
34. Tucker GS. Refractile bodies in the inner segments of cones in the aging human retina. *Invest Ophthalmol Vis Sci*. 1986;27(5):708–715.
35. Young RW. The Bowman lecture, 1982. Biological renewal. Applications to the eye. *Trans Ophthalmol Soc U K*. 1982;102(Pt 1):42–75.
36. Young RW. Visual cells and the concept of renewal. *Invest Ophthalmol Vis Sci*. 1976;15(9):700–725.
37. Daemen FJ. Vertebrate rod outer segment membranes. *Biochim Biophys Acta*. 1973;300(3):255–288.
38. Feeney-Burns L, Berman ER, Rothman H. Lipofuscin of human retinal pigment epithelium. *Am J Ophthalmol*. 1980;90(6):783–791.
39. Young RW. Pathophysiology of age-related macular degeneration. *Surv Ophthalmol*. 1987;31(5):291–306.
40. Rakoczy PE, Baines M, Kennedy CJ, et al. Correlation between autofluorescent debris accumulation and the presence of partially processed forms of cathepsin D in cultured retinal pigment epithelial cells challenged with rod outer segments. *Exp Eye Res*. 1996;63(2):159–167.
41. Feeney-Burns L, Hilderbrand ES, Eldridge S. Aging human RPE: morphometric analysis of macular, equatorial, and peripheral cells. *Invest Ophthalmol Vis Sci*. 1984;25(2):195–200.
42. Friedman E, Ts'o MO. The retinal pigment epithelium. II. Histologic changes associated with age. *Arch Ophthalmol*.

1968;79(3):315–320.
43. Sarks SH. Ageing and degeneration in the macular region: a clinico-pathological study. *Br J Ophthalmol*. 1976;60(5):324–341.
44. van der Schaft TL, Mooy CM, de Bruijn WC, et al. Histologic features of the early stages of age-related macular degeneration: a statistical analysis. *Ophthalmology*. 1992;99(2):278–286.
45. Panda-Jonas S, Jonas JB, Jakobczyk-Zmija M. Retinal pigment epithelial cell count, distribution, and correlations in normal human eyes. *Am J Ophthalmol*. 1996;121(2):181–189.
46. Gass JD. *Stereoscopic atlas of macular diseases: diagnosis and treatment*. 4th ed. Mosby: St Louis; 1997.
47. Hogan MJ, Alvarado J. Studies on the human macula. IV. Aging changes in Bruch's membrane. *Arch Ophthalmol*. 1967;77(3):410–420.
48. Ramrattan RS, van der Schaft TL, Mooy CM, et al. Morphometric analysis of Bruch's membrane, the choriocapillaris, and the choroid in aging. *Invest Ophthalmol Vis Sci*. 1994;35(6):2857–2864.
49. Killingsworth MC. Age-related components of Bruch's membrane in the human eye. *Graefes Arch Clin Exp Ophthalmol*. 1987;225(6):406–412.
50. Feeney-Burns L, Ellersieck MR. Age-related changes in the ultrastructure of Bruch's membrane. *Am J Ophthalmol*. 1985;100(5):686–697.
51. Karwatowski WS, Jeffries TE, Duance VC, et al. Preparation of Bruch's membrane and analysis of the age-related changes in the structural collagens. *Br J Ophthalmol*. 1995;79(10):944–952.
52. Holz FG, Sheraidah G, Pauleikhoff D, et al. Analysis of lipid deposits extracted from human macular and peripheral Bruch's membrane. *Arch Ophthalmol*. 1994;112(3):402–406.
53. Sheraidah G, Steinmetz R, Maguire J, et al. Correlation between lipids extracted from Bruch's membrane and age. *Ophthalmology*. 1993;100(1):47–51.
54. Burns RP, Feeney-Burns L. Clinico-morphologic correlations

of drusen of Bruch's membrane. *Trans Am Ophthalmol Soc*. 1980;78:206–225.
55. Marshall GE, Konstas AG, Reid GG, et al. Type IV collagen and laminin in Bruch's membrane and basal linear deposit in the human macula. *Br J Ophthalmol*. 1992;76(10):607–614.
56. Pauleikhoff D, Harper CA, Marshall J, et al. Aging changes in Bruch's membrane: a histochemical and morphologic study. *Ophthalmology*. 1990;97(2):171–178.
57. van der Schaft TL, de Bruijn WC, Mooy CM, et al. Is basal laminar deposit unique for age-related macular degeneration? *Arch Ophthalmol*. 1991;109(3):420–425.
58. Spaide RF, Ho-Spaide WC, Browne RW, et al. Characterization of peroxidized lipids in Bruch's membrane. *Retina*. 1999;19(2):141–147.
59. Armstrong D, Ueda T, Ueda T, et al. Lipid hydroperoxide stimulates retinal neovascularization in rabbit retina through expression of tumor necrosis factor-α, vascular endothelial growth factor and platelet-derived growth factor. *Angiogenesis*. 1998;2(1):93–104.
60. Tamai K, Spaide RF, Ellis EA, et al. Lipid hydroperoxide stimulates subretinal choroidal neovascularization in the rabbit. *Exp Eye Res*. 2002;74(2):301–308.
61. Moore DJ, Hussain AA, Marshall J. Age-related variation in the hydraulic conductivity of Bruch's membrane. *Invest Ophthalmol Vis Sci*. 1995;36(7):1290–1297.
62. Starita C, Hussain AA, Patmore A, et al. Localization of the site of major resistance to fluid transport in Bruch's membrane. *Invest Ophthalmol Vis Sci*. 1997;38(3):762–767.
63. Grunwald JE, Piltz J, Patel N, et al. Effect of aging on retinal macular microcirculation: a blue field simulation study. *Invest Ophthalmol Vis Sci*. 1993;34(13):3609–3613.
64. Groh MJ, Michelson G, Langhans MJ, et al. Influence of age on retinal and optic nerve head blood circulation. *Ophthalmology*. 1996;103(3):529–534.
65. Ouyang Y, Heussen FM, Mokwa N, et al. Spatial distribution of posterior pole choroidal thickness by spectral domain optical coherence tomography. *Invest Ophthalmol Vis Sci*. 2011;52(9):7019–7026.

66. Wei WB, Xu L, Jonas JB, et al. Subfoveal choroidal thickness: the Beijing Eye Study. *Ophthalmology*. 2013;120(1):175–180.
67. Adhi M, Ferrara D, Mullins RF, et al. Characterization of choroidal layers in normal aging eyes using enface swept-source optical coherence tomography. *PLoS ONE*. 2015;10(7):e0133080.
68. Grunwald JE, Hariprasad SM, DuPont J. Effect of aging on foveolar choroidal circulation. *Arch Ophthalmol*. 1998;116(2):150–154.
69. Ito YN, Mori K, Young-Duvall J, Yoneya S. Aging changes of the choroidal dye filling pattern in indocyanine green angiography of normal subjects. *Retina*. 2001;21(3):237–242.
70. Delori FC, Dorey CK, Staurenghi G, et al. In vivo fluorescence of the ocular fundus exhibits retinal pigment epithelium lipofuscin characteristics. *Invest Ophthalmol Vis Sci*. 1995;36(3):718–729.
71. Davis MD, Gangnon RE, Lee LY, et al. The Age-Related Eye Disease Study severity scale for age-related macular degeneration: AREDS Report No. 17. *Arch Ophthalmol*. 2005;123(11):1484–1498.
72. Ferris FL, Davis MD, Clemons TE, et al. A simplified severity scale for age-related macular degeneration: AREDS report no. 18. *Arch Ophthalmol*. 2005;123(11):1570–1574.
73. Curcio CA, Messinger JD, Sloan KR, et al. Subretinal drusenoid deposits in non-neovascular age-related macular degeneration: morphology, prevalence, topography, and biogenesis model. *Retina*. 2013;33(2):265–276.
74. Spraul CW, Lang GE, Grossniklaus HE. Morphometric analysis of the choroid, Bruch's membrane, and retinal pigment epithelium in eyes with age-related macular degeneration. *Invest Ophthalmol Vis Sci*. 1996;37(13):2724–2735.
75. Sarks JP, Sarks SH, Killingsworth MC. Evolution of geographic atrophy of the retinal pigment epithelium. *Eye (Lond)*. 1988;2(Pt 5):552–577.
76. Green WR, Enger C. Age-related macular degeneration histopathologic studies. The 1992 Lorenz E. Zimmerman Lecture. *Ophthalmology*. 1993;100(10):1519–1535.

77. Curcio CA, Millican CL. Basal linear deposit and large drusen are specific for early age-related maculopathy. *Arch Ophthalmol*. 1999;117(3):329–339.
78. Bressler NM, Silva JC, Bressler SB, et al. Clinicopathologic correlation of drusen and retinal pigment epithelial abnormalities in age-related macular degeneration. *Retina*. 1994;14(2):130–142.
79. Loffler KU, Lee WR. Basal linear deposit in the human macula. *Graefes Arch Klin Exp Ophthalmol*. 1986;224(6):493–501.
80. van der Schaft TL, Mooy CM, de Bruijn WC, et al. Immunohistochemical light and electron microscopy of basal laminar deposit. *Graefes Arch Clin Exp Ophthalmol*. 1994;232(1):40–46.
81. Sarks JP, Sarks SH, Killingsworth MC. Evolution of soft drusen in age-related macular degeneration. *Eye (Lond)*. 1994;8(Pt 3):269–283.
82. Green WR, Key SN 3rd. Senile macular degeneration: a histopathologic study. *Trans Am Ophthalmol Soc*. 1977;75:180–254.
83. Curcio CA, Presley JB, Millican CL, et al. Basal deposits and drusen in eyes with age-related maculopathy: evidence for solid lipid particles. *Exp Eye Res*. 2005;80(6):761–775.
84. Zweifel SA, Spaide RF, Curcio CA, et al. Reticular pseudodrusen are subretinal drusenoid deposits. *Ophthalmology*. 2010;117(2):303–312.e1.
85. el Baba F, Green WR, Fleischmann J, et al. Clinicopathologic correlation of lipidization and detachment of the retinal pigment epithelium. *Am J Ophthalmol*. 1986;101(5):576–583.
86. Zanzottera EC, Messinger JD, Ach T, et al. The Project MACULA Retinal Pigment Epithelium Grading System for Histology and Optical Coherence Tomography in Age-Related Macular Degeneration. *Invest Ophthalmol Vis Sci*. 2015;56(5):3253–3268.
87. Schuman SG, Koreishi AF, Farsiu S, et al. Photoreceptor layer thinning over drusen in eyes with age-related macular degeneration imaged in vivo with spectral-domain optical coherence tomography. *Ophthalmology*. 2009;116(3):488–

496.e2.
88. Ho J, Witkin AJ, Liu J, et al. Documentation of intraretinal retinal pigment epithelium migration via high-speed ultrahigh-resolution optical coherence tomography. *Ophthalmology*. 2011;118(4):687–693.
89. Pieroni CG, Witkin AJ, Ko TH, et al. Ultrahigh resolution optical coherence tomography in non-exudative age related macular degeneration. *Br J Ophthalmol*. 2006;90(2):191–197.
90. McLeod DS, Grebe R, Bhutto I, et al. Relationship between RPE and choriocapillaris in age-related macular degeneration. *Invest Ophthalmol Vis Sci*. 2009;50(10):4982–4991.
91. Penfold PL, Killingsworth MC, Sarks SH. Senile macular degeneration: the involvement of immunocompetent cells. *Graefes Arch Klin Exp Ophthalmol*. 1985;223(2):69–76.
92. Killingsworth MC, Sarks JP, Sarks SH. Macrophages related to Bruch's membrane in age-related macular degeneration. *Eye (Lond)*. 1990;4(Pt 4):613–621.
93. Klein R, Davis MD, Magli YL, et al. The Wisconsin age-related maculopathy grading system. *Ophthalmology*. 1991;98(7):1128–1134.
94. Klein ML, Francis PJ, Ferris FL 3rd, et al. Risk assessment model for development of advanced age-related macular degeneration. *Arch Ophthalmol*. 2011;129(12):1543–1550.
95. Shin DS, Javornik NB, Berger JW. Computer-assisted, interactive fundus image processing for macular drusen quantitation. *Ophthalmology*. 1999;106(6):1119–1125.
96. Gregori G, Wang F, Rosenfeld PJ, et al. Spectral domain optical coherence tomography imaging of drusen in nonexudative age-related macular degeneration. *Ophthalmology*. 2011;118(7):1373–1379.
97. Wang Q, Chappell RJ, Klein R, et al. Pattern of age-related maculopathy in the macular area. The Beaver Dam Eye Study. *Invest Ophthalmol Vis Sci*. 1996;37(11):2234–2242.
98. Steinberg JS, Fleckenstein M, Holz FG, et al. Foveal sparing of reticular drusen in eyes with early and intermediate age-related macular degeneration. *Invest Ophthalmol Vis Sci*. 2015;56(8):4267–4274.

99. Wang JJ, Mitchell P, Smith W, et al. Bilateral involvement by age related maculopathy lesions in a population. *Br J Ophthalmol*. 1998;82(7):743–747.
100. Brader HS, Ying GS, Martin ER, et al. Complications of Age-Related Macular Degeneration Prevention Trial Research G. Characteristics of incident geographic atrophy in the complications of age-related macular degeneration prevention trial. *Ophthalmology*. 2013;120(9):1871–1879.
101. Klein ML, Ferris FL 3rd, Armstrong J, et al. Retinal precursors and the development of geographic atrophy in age-related macular degeneration. *Ophthalmology*. 2008;115(6):1026–1031.
102. Hageman GS, Mullins RF. Molecular composition of drusen as related to substructural phenotype. *Mol Vis*. 1999;5:28.
103. Spaide RF, Curcio CA. Drusen characterization with multimodal imaging. *Retina*. 2010;30(9):1441–1454.
104. Casswell AG, Kohen D, Bird AC. Retinal pigment epithelial detachments in the elderly: classification and outcome. *Br J Ophthalmol*. 1985;69(6):397–403.
105. Alexandre de Amorim Garcia Filho C, Yehoshua Z, Gregori G, et al. Spectral-domain optical coherence tomography imaging of drusenoid pigment epithelial detachments. *Retina*. 2013;33(8):1558–1566.
106. Cukras C, Agron E, Klein ML, et al. Natural history of drusenoid pigment epithelial detachment in age-related macular degeneration: Age-Related Eye Disease Study report no. 28. *Ophthalmology*. 2010;117(3):489–499.
107. Roquet W, Roudot-Thoraval F, Coscas G, et al. Clinical features of drusenoid pigment epithelial detachment in age related macular degeneration. *Br J Ophthalmol*. 2004;88(5):638–642.
108. Complications of Age-Related Macular Degeneration Prevention Trial Research G. Laser treatment in patients with bilateral large drusen: the complications of age-related macular degeneration prevention trial. *Ophthalmology*. 2006;113(11):1974–1986.
109. Bressler NM, Munoz B, Maguire MG, et al. Five-year incidence and disappearance of drusen and retinal pigment

epithelial abnormalities. Waterman study. *Arch Ophthalmol*. 1995;113(3):301–308.
110. Coffey AJ, Brownstein S. The prevalence of macular drusen in postmortem eyes. *Am J Ophthalmol*. 1986;102(2):164–171.
111. Sarks SH, Arnold JJ, Killingsworth MC, et al. Early drusen formation in the normal and aging eye and their relation to age related maculopathy: a clinicopathological study. *Br J Ophthalmol*. 1999;83(3):358–368.
112. Sarks SH. Council lecture. Drusen and their relationship to senile macular degeneration. *Aust J Ophthalmol*. 1980;8(2):117–130.
113. Bird AC. Doyne lecture. Pathogenesis of retinal pigment epithelial detachment in the elderly; the relevance of Bruch's membrane change. *Eye (Lond)*. 1991;5(Pt 1):1–12.
114. Chang AA, Guyer DR, Orlock DR, et al. Age-dependent variations in the drusen fluorescence on indocyanine green angiography. *Clin Experiment Ophthalmol*. 2003;31(4):300–304.
115. Wu Z, Luu CD, Ayton LN, et al. Fundus autofluorescence characteristics of nascent geographic atrophy in age-related macular degeneration. *Invest Ophthalmol Vis Sci*. 2015;56(3):1546–1552.
116. Khanifar AA, Koreishi AF, Izatt JA, et al. Drusen ultrastructure imaging with spectral domain optical coherence tomography in age-related macular degeneration. *Ophthalmology*. 2008;115(11):1883–1890.
117. Leuschen JN, Schuman SG, Winter KP, et al. Spectral-domain optical coherence tomography characteristics of intermediate age-related macular degeneration. *Ophthalmology*. 2013;120(1):140–150.
118. Yehoshua Z, Wang F, Rosenfeld PJ, et al. Natural history of drusen morphology in age-related macular degeneration using spectral domain optical coherence tomography. *Ophthalmology*. 2011;118(12):2434–2441.
119. Pauleikhoff D, Zuels S, Sheraidah GS, et al. Correlation between biochemical composition and fluorescein binding of deposits in Bruch's membrane. *Ophthalmology*. 1992;99(10):1548–1553.

120. Mullins RF, Hageman GS. Human ocular drusen possess novel core domains with a distinct carbohydrate composition. *J Histochem Cytochem*. 1999;47(12):1533–1540.
121. Mullins RF, Johnson LV, Anderson DH, et al. Characterization of drusen-associated glycoconjugates. *Ophthalmology*. 1997;104(2):288–294.
122. Hageman GS, Mullins RF, Russell SR, et al. Vitronectin is a constituent of ocular drusen and the vitronectin gene is expressed in human retinal pigmented epithelial cells. *FASEB J*. 1999;13(3):477–484.
123. Zweifel SA, Imamura Y, Spaide TC, et al. Prevalence and significance of subretinal drusenoid deposits (reticular pseudodrusen) in age-related macular degeneration. *Ophthalmology*. 2010;117(9):1775–1781.
124. Arnold JJ, Sarks SH, Killingsworth MC, et al. Reticular pseudodrusen: a risk factor in age-related maculopathy. *Retina*. 1995;15(3):183–191.
125. Mimoun G, Soubrane G, Coscas G. [Macular drusen]. *J Fr Ophtalmol*. 1990;13(10):511–530.
126. Cohen SY, Dubois L, Tadayoni R, et al. Prevalence of reticular pseudodrusen in age-related macular degeneration with newly diagnosed choroidal neovascularisation. *Br J Ophthalmol*. 2007;91(3):354–359.
127. Rudolf M, Malek G, Messinger JD, et al. Sub-retinal drusenoid deposits in human retina: organization and composition. *Exp Eye Res*. 2008;87(5):402–408.
128. Spaide RF. Outer retinal atrophy after regression of subretinal drusenoid deposits as a newly recognized form of late age-related macular degeneration. *Retina*. 2013;33(9):1800–1808.
129. Gass JD, Jallow S, Davis B. Adult vitelliform macular detachment occurring in patients with basal laminar drusen. *Am J Ophthalmol*. 1985;99(4):445–459.
130. Gass JD. A clinicopathologic study of a peculiar foveomacular dystrophy. *Trans Am Ophthalmol Soc*. 1974;72:139–156.
131. Arnold JJ, Sarks JP, Killingsworth MC, et al. Adult vitelliform macular degeneration: a clinicopathological

study. *Eye (Lond)*. 2003;17(6):717–726.
132. Lima LH, Laud K, Freund KB, et al. Acquired vitelliform lesion associated with large drusen. *Retina*. 2012;32(4):647–651.
133. Freund KB, Laud K, Lima LH, et al. Acquired vitelliform lesions: correlation of clinical findings and multiple imaging analyses. *Retina*. 2011;31(1):13–25.
134. Gass JD. *Stereoscopic atlas of macular disease: diagnosis and treatment*. 2nd ed. Mosby: St. Louis; 1977.
135. Kenyon KR, Maumenee AE, Ryan SJ, et al. Diffuse drusen and associated complications. *Am J Ophthalmol*. 1985;100(1):119–128.
136. Russell SR, Mullins RF, Schneider BL, et al. Location, substructure, and composition of basal laminar drusen compared with drusen associated with aging and age-related macular degeneration. *Am J Ophthalmol*. 2000;129(2):205–214.
137. Guigui B, Leveziel N, Martinet V, et al. Angiography features of early onset drusen. *Br J Ophthalmol*. 2011;95(2):238–244.
138. Quaranta M, Buglione M, Lo Schiavo Elia R, et al. [Indocyanine green angiography of basal laminar drusen in the retinal pigment epithelium associated with vitelliform macular degeneration]. *J Fr Ophtalmol*. 1998;21(3):185–190.
139. Gass JD. Drusen and disciform macular detachment and degeneration. *Arch Ophthalmol*. 1973;90(3):206–217.
140. Complications of Age-Related Macular Degeneration Prevention Trial Research G. Risk factors for choroidal neovascularization and geographic atrophy in the complications of age-related macular degeneration prevention trial. *Ophthalmology*. 2008;115(9):1474–1479 [1479.e1-6].
141. Maguire P, Vine AK. Geographic atrophy of the retinal pigment epithelium. *Am J Ophthalmol*. 1986;102(5):621–625.
142. Bird AC, Phillips RL, Hageman GS. Geographic atrophy: a histopathological assessment. *JAMA Ophthalmol*. 2014;132(3):338–345.
143. Zanzottera EC, Messinger JD, Ach T, et al. Subducted and

melanotic cells in advanced age-related macular degeneration are derived from retinal pigment epithelium. *Invest Ophthalmol Vis Sci*. 2015;56(5):3269–3278.
144. Schneider U, Sherif-Adel S, Gelisken F, et al. Indocyanine green angiography and transmission defects. *Acta Ophthalmol Scand*. 1997;75(6):653–656.
145. Schmitz-Valckenberg S, Fleckenstein M, Scholl HP, et al. Fundus autofluorescence and progression of age-related macular degeneration. *Surv Ophthalmol*. 2009;54(1):96–117.
146. Fleckenstein M, Schmitz-Valckenberg S, Martens C, et al. Fundus autofluorescence and spectral-domain optical coherence tomography characteristics in a rapidly progressing form of geographic atrophy. *Invest Ophthalmol Vis Sci*. 2011;52(6):3761–3766.
147. Christenbury JG, Folgar FA, O'Connell RV, et al. Progression of intermediate age-related macular degeneration with proliferation and inner retinal migration of hyperreflective foci. *Ophthalmology*. 2013;120(5):1038–1045.
148. Fleckenstein M, Schmitz-Valckenberg S, Adrion C, et al. Tracking progression with spectral-domain optical coherence tomography in geographic atrophy caused by age-related macular degeneration. *Invest Ophthalmol Vis Sci*. 2010;51(8):3846–3852.
149. Schmitz-Valckenberg S, Fleckenstein M, Gobel AP, et al. Optical coherence tomography and autofluorescence findings in areas with geographic atrophy due to age-related macular degeneration. *Invest Ophthalmol Vis Sci*. 2011;52(1):1–6.
150. Brar M, Kozak I, Cheng L, et al. Correlation between spectral-domain optical coherence tomography and fundus autofluorescence at the margins of geographic atrophy. *Am J Ophthalmol*. 2009;148(3):439–444.
151. Sayegh RG, Simader C, Scheschy U, et al. A systematic comparison of spectral-domain optical coherence tomography and fundus autofluorescence in patients with geographic atrophy. *Ophthalmology*. 2011;118(9):1844–1851.
152. Lindner M, Boker A, Mauschitz MM, et al. Directional

kinetics of geographic atrophy progression in age-related macular degeneration with foveal sparing. *Ophthalmology*. 2015;122(7):1356–1365.
153. Schaal KB, Freund KB, Litts KM, et al. Outer retinal tubulation in advanced age-related macular degeneration: optical coherence tomographic findings correspond to histology. *Retina*. 2015;35(7):1339–1350.
154. Zweifel SA, Engelbert M, Laud K, et al. Outer retinal tubulation: a novel optical coherence tomography finding. *Arch Ophthalmol*. 2009;127(12):1596–1602.
155. Curcio CA, Medeiros NE, Millican CL. Photoreceptor loss in age-related macular degeneration. *Invest Ophthalmol Vis Sci*. 1996;37(7):1236–1249.
156. Adhi M, Lau M, Liang MC, et al. Analysis of the thickness and vascular layers of the choroid in eyes with geographic atrophy using spectral-domain optical coherence tomography. *Retina*. 2014;34(2):306–312.
157. Lindner M, Bezatis A, Czauderna J, et al. Choroidal thickness in geographic atrophy secondary to age-related macular degeneration. *Invest Ophthalmol Vis Sci*. 2015;56(2):875–882.
158. Lindblad AS, Lloyd PC, Clemons TE, et al. Change in area of geographic atrophy in the Age-Related Eye Disease Study: AREDS report number 26. *Arch Ophthalmol*. 2009;127(9):1168–1174.
159. Hariri A, Nittala MG, Sadda SR. Outer retinal tubulation as a predictor of the enlargement amount of geographic atrophy in age-related macular degeneration. *Ophthalmology*. 2015;122(2):407–413.
160. Yehoshua Z, Rosenfeld PJ, Gregori G, et al. Progression of geographic atrophy in age-related macular degeneration imaged with spectral domain optical coherence tomography. *Ophthalmology*. 2011;118(4):679–686.
161. Holz FG, Bindewald-Wittich A, Fleckenstein M, et al. Progression of geographic atrophy and impact of fundus autofluorescence patterns in age-related macular degeneration. *Am J Ophthalmol*. 2007;143(3):463–472.
162. Sunness JS, Margalit E, Srikumaran D, et al. The long-term

natural history of geographic atrophy from age-related macular degeneration: enlargement of atrophy and implications for interventional clinical trials. *Ophthalmology*. 2007;114(2):271–277.
163. Age-Related Eye Disease Study Research G. A randomized, placebo-controlled, clinical trial of high-dose supplementation with vitamins C and E, beta carotene, and zinc for age-related macular degeneration and vision loss: AREDS report no. 8. *Arch Ophthalmol*. 2001;119(10):1417–1436.
164. Chew EY, Clemons TE, Agron E, et al. Ten-year follow-up of age-related macular degeneration in the age-related eye disease study: AREDS report no. 36. *JAMA Ophthalmol*. 2014;132(3):272–277.
165. Klein R, Myers CE, Lee KE, et al. Small drusen and age-related macular degeneration: the Beaver Dam Eye Study. *J Clin Med*. 2015;4(3):424–440.
166. Klein R, Klein BE, Knudtson MD, et al. Fifteen-year cumulative incidence of age-related macular degeneration: the Beaver Dam Eye Study. *Ophthalmology*. 2007;114(2):253–262.
167. Sarraf D, Gin T, Yu F, et al. Long-term drusen study. *Retina*. 1999;19(6):513–519.
168. Macular Photocoagulation Study Group. Risk factors for choroidal neovascularization in the second eye of patients with juxtafoveal or subfoveal choroidal neovascularization secondary to age-related macular degeneration. *Arch Ophthalmol*. 1997;115(6):741–747.
169. Macular Photocoagulation Study Group. Five-year follow-up of fellow eyes of patients with age-related macular degeneration and unilateral extrafoveal choroidal neovascularization. *Arch Ophthalmol*. 1993;111(9):1189–1199.
170. Owsley C, Huisingh C, Clark ME, et al. Comparison of visual function in older eyes in the earliest stages of age-related macular degeneration to those in normal macular health. *Curr Eye Res*. 2015;1–7.
171. Midena E, Degli Angeli C, Blarzino MC, et al. Macular function impairment in eyes with early age-related macular

degeneration. *Invest Ophthalmol Vis Sci*. 1997;38(2):469–477.
172. Vujosevic S, Smolek MK, Lebow KA, et al. Detection of macular function changes in early (AREDS 2) and intermediate (AREDS 3) age-related macular degeneration. *Ophthalmologica*. 2011;225(3):155–160.
173. Midena E, Vujosevic S, Convento E, et al. Microperimetry and fundus autofluorescence in patients with early age-related macular degeneration. *Br J Ophthalmol*. 2007;91(11):1499–1503.
174. Sunness JS, Johnson MA, Massof RW, et al. Retinal sensitivity over drusen and nondrusen areas: a study using fundus perimetry. *Arch Ophthalmol*. 1988;106(8):1081–1084.
175. Iwama D, Tsujikawa A, Ojima Y, et al. Relationship between retinal sensitivity and morphologic changes in eyes with confluent soft drusen. *Clin Exp Ophthalmol*. 2010;38(5):483–488.
176. Ooto S, Suzuki M, Vongkulsiri S, et al. Multimodal visual function testing in eyes with nonexudative age-related macular degeneration. *Retina*. 2015;35(9):1726–1734.
177. Steinberg JS, Fitzke FW, Fimmers R, et al. Scotopic and photopic microperimetry in patients with reticular drusen and age-related macular degeneration. *JAMA Ophthalmol*. 2015;133(6):690–697.
178. Schatz H, McDonald HR. Atrophic macular degeneration: rate of spread of geographic atrophy and visual loss. *Ophthalmology*. 1989;96(10):1541–1551.
179. Sunness JS, Gonzalez-Baron J, Applegate CA, et al. Enlargement of atrophy and visual acuity loss in the geographic atrophy form of age-related macular degeneration. *Ophthalmology*. 1999;106(9):1768–1779.
180. Sunness JS, Rubin GS, Applegate CA, et al. Visual function abnormalities and prognosis in eyes with age-related geographic atrophy of the macula and good visual acuity. *Ophthalmology*. 1997;104(10):1677–1691.
181. Sunness JS, Applegate CA, Haselwood D, et al. Fixation patterns and reading rates in eyes with central scotomas from advanced atrophic age-related macular degeneration and Stargardt disease. *Ophthalmology*. 1996;103(9):1458–

1466.
182. Klein ML, Francis PJ, Rosner B, et al. CFH and LOC387715/ARMS2 genotypes and treatment with antioxidants and zinc for age-related macular degeneration. *Ophthalmology*. 2008;115(6):1019–1025.
183. Awh CC, Hawken S, Zanke BW. Treatment response to antioxidants and zinc based on CFH and ARMS2 genetic risk allele number in the Age-Related Eye Disease Study. *Ophthalmology*. 2015;122(1):162–169.
184. Awh CC, Lane AM, Hawken S, et al. CFH and ARMS2 genetic polymorphisms predict response to antioxidants and zinc in patients with age-related macular degeneration. *Ophthalmology*. 2013;120(11):2317–2323.
185. Chew EY, Klein ML, Clemons TE, et al. No clinically significant association between CFH and ARMS2 genotypes and response to nutritional supplements: AREDS report number 38. *Ophthalmology*. 2014;121(11):2173–2180.
186. Age-Related Eye Disease Study 2 Research G. Lutein + zeaxanthin and omega-3 fatty acids for age-related macular degeneration: the Age-Related Eye Disease Study 2 (AREDS2) randomized clinical trial. *JAMA*. 2013;309(19):2005–2015.
187. Group AR, Chew EY, Clemons T, et al. The Age-Related Eye Disease Study 2 (AREDS2): study design and baseline characteristics (AREDS2 report number 1). *Ophthalmology*. 2012;119(11):2282–2289.
188. Age-Related Eye Disease Study 2 Research G, Chew EY, Clemons TE, et al. Secondary analyses of the effects of lutein/zeaxanthin on age-related macular degeneration progression: AREDS2 report No. 3. *JAMA Ophthalmol*. 2014;132(2):142–149.
189. The Alpha-Tocopherol, Beta Carotene Cancer Prevention Study Group. The effect of vitamin E and beta carotene on the incidence of lung cancer and other cancers in male smokers. *N Engl J Med*. 1994;330(15):1029–1035.
190. Omenn GS, Goodman GE, Thornquist MD, et al. Risk factors for lung cancer and for intervention effects in CARET, the Beta-Carotene and Retinol Efficacy Trial. *J Natl*

Cancer Inst. 1996;88(21):1550–1559.
191. Achard OA, Safran AB, Duret FC, et al. Role of the completion phenomenon in the evaluation of Amsler grid results. *Am J Ophthalmol*. 1995;120(3):322–329.
192. Fine AM, Elman MJ, Ebert JE, et al. Earliest symptoms caused by neovascular membranes in the macula. *Arch Ophthalmol*. 1986;104(4):513–514.
193. Schuchard RA. Validity and interpretation of Amsler grid reports. *Arch Ophthalmol*. 1993;111(6):776–780.
194. Do DV, Gower EW, Cassard SD, et al. Detection of new-onset choroidal neovascularization using optical coherence tomography: the AMD DOC Study. *Ophthalmology*. 2012;119(4):771–778.
195. Goldstein M, Loewenstein A, Barak A, et al. Results of a multicenter clinical trial to evaluate the preferential hyperacuity perimeter for detection of age-related macular degeneration. *Retina*. 2005;25(3):296–303.
196. Loewenstein A, Ferencz JR, Lang Y, et al. Toward earlier detection of choroidal neovascularization secondary to age-related macular degeneration: multicenter evaluation of a preferential hyperacuity perimeter designed as a home device. *Retina*. 2010;30(7):1058–1064.
197. Lai Y, Grattan J, Shi Y, et al. Functional and morphologic benefits in early detection of neovascular age-related macular degeneration using the preferential hyperacuity perimeter. *Retina*. 2011;31(8):1620–1626.
198. Group AHSR, Chew EY, Clemons TE, et al. Randomized trial of a home monitoring system for early detection of choroidal neovascularization home monitoring of the Eye (HOME) study. *Ophthalmology*. 2014;121(2):535–544.
199. Forooghian F, Agron E, Clemons TE, et al. Age-Related Eye Disease Study Research G. Visual acuity outcomes after cataract surgery in patients with age-related macular degeneration: age-related eye disease study report no. 27. *Ophthalmology*. 2009;116(11):2093–2100.
200. Wang JJ, Klein R, Smith W, et al. Cataract surgery and the 5-year incidence of late-stage age-related maculopathy: pooled findings from the Beaver Dam and Blue Mountains

eye studies. *Ophthalmology*. 2003;110(10):1960–1967.
201. Chew EY, Sperduto RD, Milton RC, et al. Risk of advanced age-related macular degeneration after cataract surgery in the Age-Related Eye Disease Study: AREDS report 25. *Ophthalmology*. 2009;116(2):297–303.
202. Hudson HL, Lane SS, Heier JS, et al. Implantable miniature telescope for the treatment of visual acuity loss resulting from end-stage age-related macular degeneration: 1-year results. *Ophthalmology*. 2006;113(11):1987–2001.
203. Yonekawa Y, Wolfe JD. Monitoring age-related macular degeneration through an implantable miniature telescope using ultra-wide-field imaging. *JAMA Ophthalmol*. 2015;133(6):e1588.
204. Dugel PU, Novack RL, Csaky KG, et al. Phase II, randomized, placebo-controlled, 90-day study of emixustat hydrochloride in geographic atrophy associated with dry age-related macular degeneration. *Retina*. 2015;35(6):1173–1183.
205. *ClinicalTrials.gov: National Institutes of Health*. https://www.clinicaltrials.gov.
206. Do DV, Pieramici DJ, van Lookeren Campagne M, et al. A phase Ia dose-escalation study of the anti-factor D monoclonal antibody fragment FCFD4514S in patients with geographic atrophy. *Retina*. 2014;34(2):313–320.
207. Serruto D, Rappuoli R, Scarselli M, et al. Molecular mechanisms of complement evasion: learning from staphylococci and meningococci. *Nat Rev Microbiol*. 2010;8(6):393–399.
208. McHarg S, Clark SJ, Day AJ, et al. Age-related macular degeneration and the role of the complement system. *Mol Immunol*. 2015;67(1):43–50.

*The original observations by light microscopy distinguished only one deposit. This was referred to as the basal linear deposit, and it proved a useful histologic marker for the stage of the disease.[43] Subsequent electron microscopic studies showed that the deposit, originally via light microscopy, lies internal to the RPE basement membrane. Thus the name of this deposit was changed to basal laminar deposit. However, another layer could also be demonstrated, lying external to the basement membrane. Green and Enger[76] suggested retaining the term basal laminar deposit for the material internal to the basement membrane, but resurrecting the term basal

linear deposit for the diffuse layer of vesicular and granular material on the external aspect. The acronym BLD that has previously been used, however, could be used to represent either of these types of deposits. This chapter will use the acronyms BlamD for basal laminar deposit and BlinD for basal linear deposit and refer to both of them generically as basal deposits, as proposed by Curcio and Millican.[77]

69

Neovascular (Exudative or "Wet") Age-Related Macular Degeneration

Christopher J. Brady, Neil M. Bressler, Susan B. Bressler

Epidemiology

Age-related macular degeneration (AMD), left untreated, is the major cause of severe visual loss in older adults.[1,2] Most AMD patients have macular drusen or retinal pigment epithelial abnormalities, or both.[3] Approximately 10% of AMD patients manifest the neovascular form of the disease.[4] Neovascular AMD includes choroidal neovascularization (CNV) and associated manifestations such as retinal pigment epithelial detachment (PED), retinal pigment epithelial tears, fibrovascular disciform scarring, and vitreous hemorrhage.[3] In the absence of anti-vascular endothelial growth factor (anti-VEGF) therapy, the vast majority of people with severe vision loss (20/200 or worse in either eye) from AMD have the neovascular form.[4]

Risk Factors

The prevalence of AMD-associated vision loss in at least one eye increases with age. For example, AMD was the leading cause of blindness in white (prevalence 2.7 per 1000; 95% CI 1.2–5.4) but not black subjects randomly selected to participate in the Baltimore Eye Survey. In this study, AMD resulting in blindness affected 3% of all white subjects 80 years of age or older.[5]

AMD may be a multifactorial syndrome with different causative factors damaging the macula and resulting in common clinical manifestations that are recognized clinically as AMD. Risk factors implicated in clinical and laboratory studies include drusen, visible (but not ultraviolet) light injury, micronutrient deficiency as measured in blood serum levels or by dietary history, cigarette smoking, family history (genetic predisposition[6,7]), and cardiovascular risk factors (including systemic hypertension).[8–10] Recent epidemiologic studies have found an association with aspirin use and neovascular AMD,[11] but many authors have

suggested that a causative relationship needs to be proven before any widespread change in clinical practice relative to aspirin use is undertaken.[12–15] Likewise, a suggestion that cataract extraction may lead to neovascular AMD was not borne out in a prospective study.[16] More detailed information regarding the epidemiology of AMD is reviewed in Chapter 66 (Epidemiology and risk factors for age-related macular degeneration).

Clinical Presentation

Overview

Blurred vision and distortion, especially distorted near vision, are the symptoms most patients with CNV notice first.[3,17] Patients also may complain of decreased vision, micropsia, metamorphopsia, or a scotoma; however, many times they volunteer no symptoms or report only vague visual complaints.[18] Symptoms generally arise from sub-RPE or subretinal fluid, intraretinal fluid, blood, or destruction of photoreceptors and the retinal pigment epithelium (RPE) by fibrocellular or fibrovascular tissue proliferating in the subretinal or sub-RPE space.[19–22] In some but not all cases, areas of distortion or scotoma can be mapped out on an Amsler grid. Visual acuity, although frequently decreased and often involving both eyes, may not always be affected or may affect only one eye. Functional vision generally declines in accordance with Snellen visual acuity, especially based on the better-seeing eye. Thus patients with poor Snellen acuity in the better-seeing eye generally report decreased ability to perform functional tasks (e.g., face recognition, telling time) with the affected eye.[23]

Biomicroscopic Features

In some patients with AMD, CNV may appear as a gray–green elevation of tissue deep to the retina with overlying detachment of the neurosensory retina (Fig. 69.1). The gray–green color may arise from hyperplastic RPE in response to the CNV, as has typically been seen in patients, usually younger individuals, with the ocular histoplasmosis syndrome (OHS),[24] pathologic myopia, and other

conditions complicated by CNV. This gray–green appearance is not always present in older individuals with AMD. Often, the presence of blood or lipid or a sensory retinal detachment in an older patient with vision loss indicates the presence of CNV. The CNV capillary network may become more apparent when the overlying RPE has atrophied. Occasionally, a shallow neurosensory detachment may be the only presenting sign of underlying CNV. Elevated RPE, also termed a pigment epithelial detachment (PED), even without overlying subretinal fluid, may also suggest the presence of CNV to be identified subsequently by a fluorescein angiogram. RPE folds associated with a shallow RPE elevation usually indicate the presence of CNV.[25] These subtle clinical findings can be missed easily without careful stereoscopic slit-lamp biomicroscopic examination, facilitated with a contact lens.

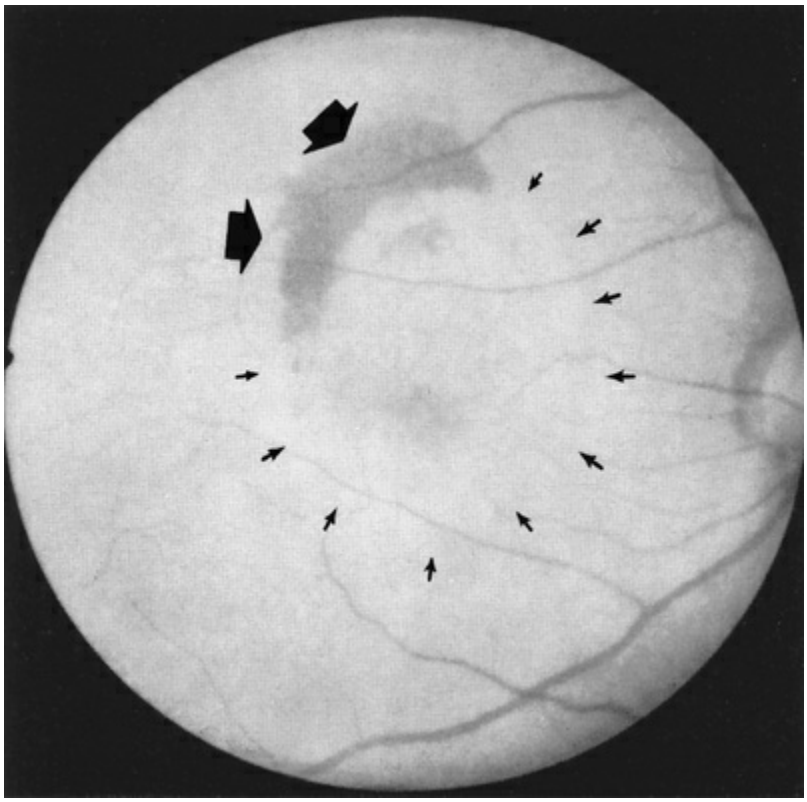

FIG. 69.1 Fundus photograph of choroidal neovascularization. Note area of hemorrhage (*large arrows*), as well as neurosensory retinal detachment (*small arrows*). (Reproduced with permission from Elman MJ. Age-related macular degeneration. Int Ophthalmol Clin 1986;26:117–44.)

Retinal Pigment Epithelial Detachments

Retinal PEDs appear clinically as sharply demarcated, dome-shaped elevations of the RPE (Fig. 69.2). They usually transilluminate if they are filled predominantly with serous fluid. Often, there is accompanying RPE atrophy and "pigment figure" formation. Pigment figures, a reticulated pattern of increased pigmentation extending radially over the PED, likely due to migration of RPE cells into the outer retinal space, indicate chronicity of disease and probably have no prognostic significance. The presence of a PED may or may not be a feature of CNV, depending on whether neovascularization is present beneath or above the PED. The fluorescein angiographic pattern (see subsequent discussion) can differentiate a drusenoid PED,[26] which does not have CNV, from a fibrovascular PED, which is a form of occult CNV,[27] as well as from a serous PED, which may or may not overlie an area with CNV.[27] Several clinical signs suggest the presence of CNV underlying an area of PED identified biomicroscopically, including overlying sensory retinal detachment and lipid, blood, and chorioretinal folds radiating from the PED.[3] Although an overlying sensory retinal detachment on optical coherence tomography (OCT) may be a clue to the presence of CNV beneath a PED,[28] sometimes a shallow neurosensory detachment may occur as a result of breakdown of the physiologic RPE pump or from disruption of the tight junctions between adjacent RPE cells in the absence of CNV identified on fluorescein angiography (FA). Unlike a PED, the borders of a neurosensory detachment are not sharply demarcated. Blood within or surrounding a PED implies the presence of CNV (Fig. 69.3). When confined to the sub-RPE space, the blood may appear as a discretely elevated, green or dark-red mound. The hemorrhage can dissect through the RPE into the subsensory retinal space or into the retina. Rarely, blood may pass through the retina into the vitreous cavity, causing extensive vitreous hemorrhage. The Submacular Surgery Trials (SST) Research Group suggested that this event was more likely in predominantly hemorrhagic lesions that were large (>12 disc areas) or associated with very poor visual acuity (worse than 20/1280 Snellen equivalent) on presentation to a retina specialist.[29]

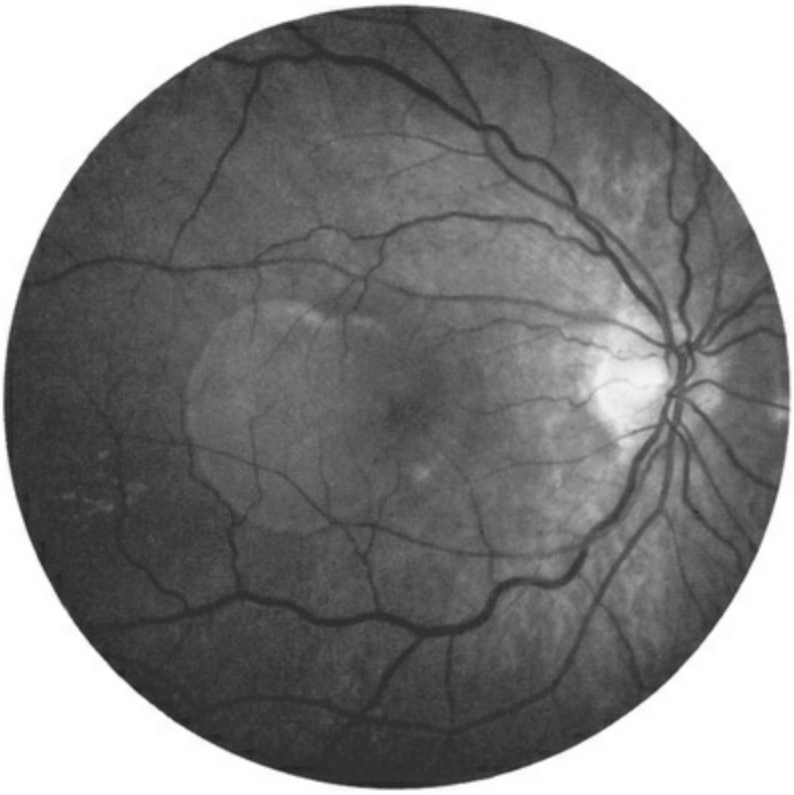

FIG. 69.2 Fundus photograph in which a round, sharply demarcated mound indicates the detached retinal pigment epithelium. (Reproduced with permission from Bressler NM, Bressler SB, Fine SL. Age-related macular degeneration. Surv Ophthalmol 1988;32:375–413.)

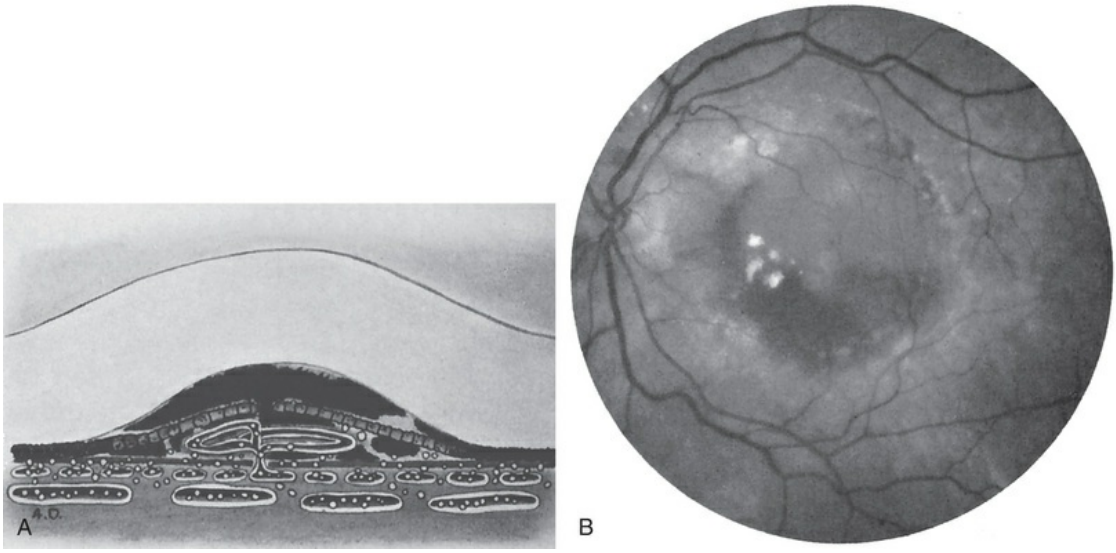

FIG. 69.3 Hemorrhagic retinal pigment epithelial detachment. (A) Sketch of hemorrhagic detachment in which the blood has also dissected underneath the

sensory retina. (B) Fundus photograph of hemorrhagic pigment epithelial detachment. (Reproduced with permission from Bressler NM, Bressler SB, Fine SL. Age-related macular degeneration. Surv Ophthalmol 1988;32:375–413.)

Massive Subretinal Hemorrhage

Massive subretinal hemorrhage is an unusual complication of neovascular AMD. If – extremely rarely – total hemorrhagic retinal detachment occurs, secondary angle closure glaucoma may develop. These patients may report sudden visual loss followed by pain.[30] Anticoagulation therapy may contribute to massive subretinal hemorrhage. In one report,[31] 19% of AMD patients with massive subretinal hemorrhage were taking sodium warfarin or aspirin, though in the Comparison of Age-Related Macular Degeneration Treatments Trial, an association with anticoagulant or antiplatelet therapy and subretinal hemorrhage was found only in patients with hypertension.[32] Although sodium warfarin therapy may contribute to massive subretinal hemorrhages in neovascular AMD, antiplatelet therapy (aspirin) likely is a chance association because several Macular Photocoagulation Study (MPS) reports did not observe any increased risk of hemorrhage associated with the use of aspirin.[33–35] Furthermore, comparing baseline characteristics in study participants with predominantly choroidal neovascular lesions in the SST Group N Trial[36] with participants with predominantly hemorrhagic lesions,[29] no difference in use of aspirin was detected. Epidemiology studies found an association of aspirin use with neovascular AMD as mentioned above,[11] but this finding does not necessarily confirm or refute a cause and effect relationship of aspirin with the development of predominantly hemorrhagic lesions or massive subretinal hemorrhages.[37]

The strongest evidence suggests that patients with AMD who need to follow a regimen of aspirin therapy should continue to do so without unnecessary fear they will increase their risk of subretinal hemorrhage.

Breakthrough Vitreous Hemorrhage

In most cases of neovascular AMD, the peripheral visual field remains unaffected. If bleeding breaks through the retina into the vitreous cavity, however, patients may complain of severe and sudden visual loss involving the peripheral visual field, as well as the central field.

Retinal Pigment Epithelial Tears

RPE dehiscence or tears of the RPE have been described as a complication associated with CNV, often in an eye with a serous or fibrovascular PED.[38–41] Tears occur at the junction of attached and detached RPE, perhaps when the PED no longer can resist the stretching forces from the fluid in the sub-RPE space emanating from the underlying occult CNV (Fig. 69.4) or from the contractile forces of the underlying fibrovascular tissue that may be associated intimately or entwined with the overlying RPE. When the RPE tears, the free edge of the RPE retracts and rolls toward the mound of fibrovascular tissue. Acutely, a serous detachment of the sensory retina may be caused by the leaking of fluid from the exposed choriocapillaris.[26] This is rarely seen after a few days following the tear. Though some ophthalmologists have suggested that RPE tears occur as a result of anti-VEGF therapy, data from 1298 patients in the three ranibizumab phase III trials showed no difference in the rate of RPE tear formation in the active ranibizumab arms compared with the control arms.[42]

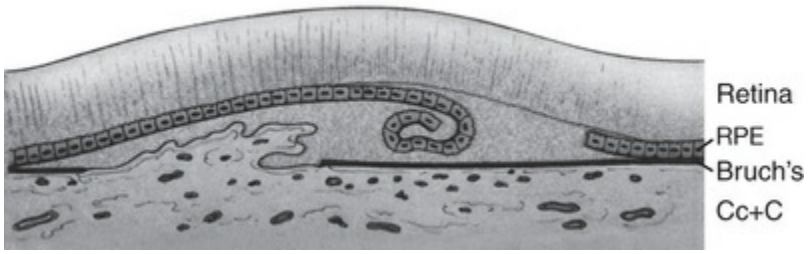

FIG. 69.4 Sketch of tear or rip of the retinal pigment epithelium (RPE), showing contracted RPE tear. Cc + C, choriocapillaris and choroid. (Reproduced with permission from Bressler NM, Bressler SB, Fine SL. Age-related macular degeneration. Surv Ophthalmol 1988;32:375–413.)

Disciform Scars

Histologically, CNV usually is accompanied by fibrous tissue, even when no fibrous tissue is readily apparent on initial presentation to an ophthalmologist.[21,43,44] This fibrous tissue may be accompanied by CNV (fibrovascular tissue) or not (fibroglial tissue).[21] The fibrous tissue complex may be beneath the RPE (usually proliferating within the inner aspect of an abnormally thickened Bruch's membrane) and has been termed type I, or between the RPE and the photoreceptors, termed type II.[45] While some authors speculate that these histopathologic types correspond to occult CNV and classic CNV respectively,[46,47] there is little evidence to support the universality of this histopathologic correlation.[48] Often, over time, the plane of the RPE is destroyed by the fibrovascular or fibroglial tissue, so the location of the CNV with respect to the RPE no longer can be identified readily. When the fibrous tissue becomes apparent clinically, the CNV and fibrous tissue complex may be termed a disciform scar.

Clinically, disciform lesions may vary in color, although typically they appear white to yellow. Hyperpigmented areas may be present depending on the degree of RPE hyperplasia within the scar tissue. Disciform fibrovascular scars may continue to grow, with new areas of neovascularization proliferating along the edge, invading previously unaffected areas of retina (Fig. 69.5). Varying degrees of subretinal hemorrhage and lipid may overlie or surround the scar. Occasionally, fibrovascular scars may precipitate massive transudation of fluid, mimicking a retinal detachment. The scars may be accompanied by massive lipid, as might be seen in retinal telangiectasis from Coats disease, and hence, historically sometimes were called a “senile Coats response” in AMD.[19] Disciform scars occasionally masquerade as choroidal tumors when substantial pigment is seen.[49] Not infrequently, anastomoses are observed between the retina and the fibrovascular tissue.[20] As a rule, most fibrovascular scars involve the fovea and cause severe visual loss. However, in some scars, surviving islands of intact photoreceptor cells noted histologically may explain the better visual performance than would be predicted from the morphologic appearance alone. Reading vision, rarely better than 20/200, becomes severely compromised in most cases with extensive scars.

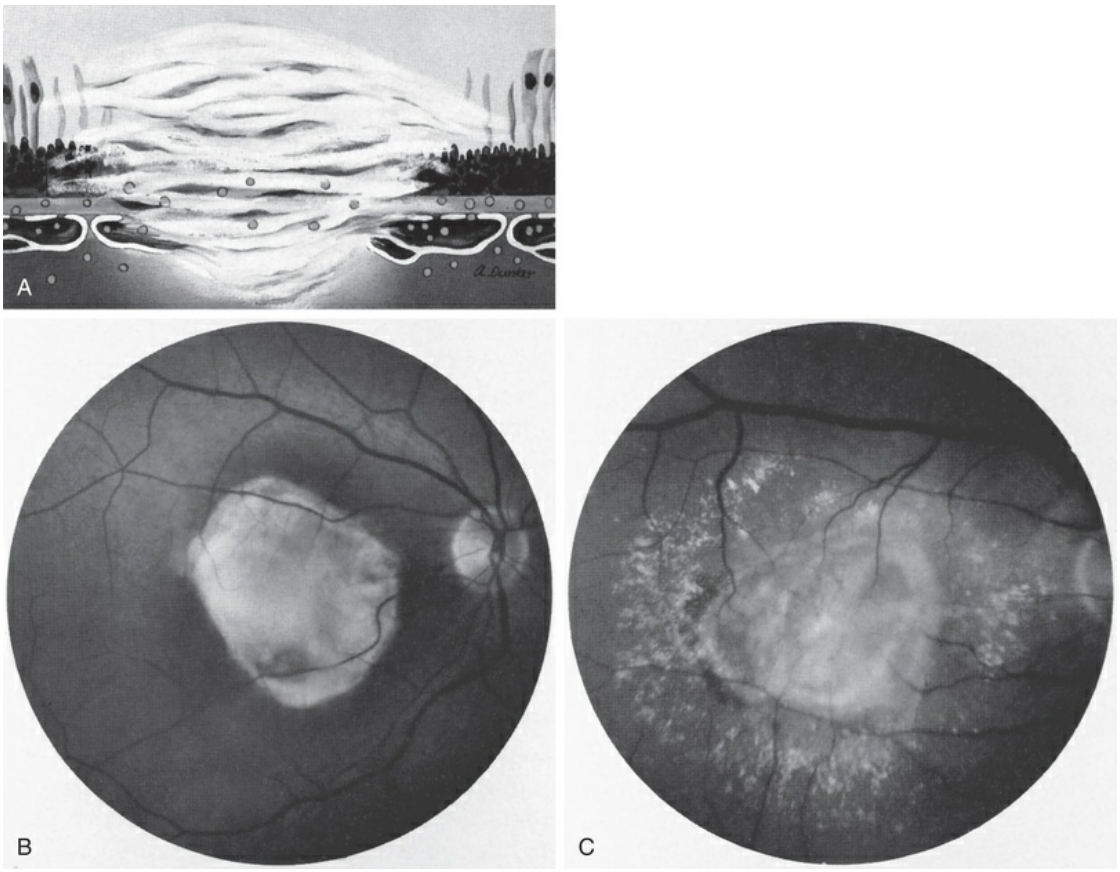

FIG. 69.5 Disciform scar. (A) Sketch demonstrating that most of the sensory retina, pigment epithelium, and inner choroid has been replaced by a fibrovascular scar. (B) Fundus photograph of a disciform scar after choroidal neovascularization. (C) Fundus photograph of a disciform scar in which continued subretinal fluid and lipid from persistent choroidal neovascularization at the periphery of the fibrous tissue can be seen.

(Reproduced with permission from Bressler NM, Bressler SB, Fine SL. Age-related macular degeneration. Surv Ophthalmol 1988;32:375–413.)

Ancillary Testing

Optical Coherence Tomography

The development of anti-VEGF medicines developed alongside developments in retinal imaging, allowing clinicians to observe and record objective, relatively small changes in retinal thickness over time. While clinical examination, color fundus photography, and FA have been the standard means of retinal evaluation prior to the

development of optical coherence tomography (OCT), in recent studies, such as the Comparison of AMD Treatments Trial (CATT), in which investigators had discretion to use OCT or FA to make retreatment decisions, more than 95% of such decisions were based on OCT findings.[50–52] The technology underlying OCT and its clinical applications are discussed in detail in Chapter 3 (Optical coherence tomography), with a detailed section discussing neovascular AMD.

In contrast to standard OCT for evaluating CNV in AMD, OCT angiography is a new technology, recently approved by the FDA for diagnostic use in the United States. By using differential measurements of blood cell flow, images of the retinal and choroidal vascular networks can be obtained without the administration of a contrast agent such as fluorescein. Utility in the management of patients with neovascular AMD has yet to be demonstrated but may provide helpful information without the additional discomfort and risk of parenteral injection of fluorescein.[53] Additionally, if the technology can reliably identify CNV, OCT angiography may prove particularly helpful in ascertaining the absence or presence of CNV in lesions that can be challenging to interpret on traditional FA, such as in the presence of vitelliform lesions or in the presence of underlying central serous chorioretinopathy.

Fluorescein Angiography

Overview

Whenever one suspects CNV for which treatment might be indicated, one should consider obtaining stereoscopic FA promptly, even in an era of ubiquitous spectral domain OCT. The treating ophthalmologist is about to embark on a recommendation for treatment involving medications that carry risks, potentially large expenses, and many years of follow-up. Although the clinical picture may be "obviously" CNV, other lesions masquerading as CNV can exist (see below). Having a fluorescein angiogram at the time of diagnosis reduces the possibility that an error in diagnosis will be made. In a systematic review of trials in which multiple

imaging modalities were used, OCT was found to be 85% sensitive for active neovascular AMD, but only 48% specific,[54] suggesting that a regimen using OCT alone to decide on treatment or retreatment might result in overtreatment. This is particularly relevant as regimens such as "as needed" and "treat and extend" are designed to minimize the burden of treatment but often based on OCT evaluations in the absence of FA. It is important to consider that no comparison of outcomes of treatment decisions based on results of using either or both tests has been published.

In addition, FA frequently allows one to determine the pattern of fluorescence (classic or occult), boundaries (well defined or poorly defined), composition (e.g., predominantly CNV, predominantly classic CNV, predominantly CNV with a minimally classic composition, predominantly CNV with an occult with no classic composition, predominantly hemorrhagic), and location of the neovascular lesions with respect to the geometric center of the foveal avascular zone (FAZ). Although many physicians no longer refer to CNV composition, entry criteria for most of the treatment trials cited later in this chapter relied in part on lesion composition. If one chooses to treat only patients who would have been eligible for, e.g., the MARINA trial, baseline angiography is necessary. Since eligibility for current clinical trials (e.g., https://clinicaltrials.gov/show/NCT02462486, https://clinicaltrials.gov/show/NCT02418754) continues to hinge upon lesion composition, clinician scientists who enroll subjects in clinical trials for neovascular AMD still should consider understanding the angiographic features of the disease. Finally, it is possible that some treatments may perform differently on different lesion subtypes, and knowledge of composition may allow for better outcomes in these subgroups.[55] Additional technical details about FA can be found in Chapter 1 (Fluorescein angiography: Basic principles and interpretation).

High-quality stereoscopic fluorescein angiograms, together with meticulous slit-lamp biomicroscopic examination (ideally with a contact lens examination using topical anesthesia and hard contact lens wetting solution to avoid degradation of any subsequent image acquisition that might occur if an ophthalmic demulcent is used), facilitate detecting obvious and subtle features of CNV on

angiography.[27,56,57] It should be noted that the descriptive terms below refer to patterns of fluorescence on FA that have been shown to be reliable and reproducible in multicenter clinical trials,[27,58,59] and in practice, and are not related to terms based on other imaging such as OCT, indocyanine green angiography, histopathology, or immunohistochemistry. A comprehensive review of FA remains highly relevant to clinicians and researchers interested in neovascular AMD.

Classic Choroidal Neovascularization

The fluorescein angiographic appearance of classic CNV consists of a discrete, well-demarcated focal area of hyperfluorescence that can be discerned in the early phases of the angiogram, sometimes before dye has completely filled the retinal vessels during choroidal filling.[27,58,59] Although fluorescein can occasionally be observed within the actual capillary network of CNV in the early phase of the angiogram (Fig. 69.6A), the ability to visualize the appearance of actual new vessels is not needed to diagnose classic CNV and is not a specific feature of classic versus occult CNV.[27,58–60] As the angiogram is evaluated within the area of classic CNV, hyperfluorescence increases in intensity and extends beyond the boundaries of the hyperfluorescent area identified in earlier phases of the angiogram through mid- and late-phase frames. Fluorescein may also pool in subsensory retinal fluid overlying the classic CNV (Fig. 69.6B), best seen when visualizing early- and late-phase frames of classic CNV on stereoscopic images. This presentation of classic CNV is in contrast to the appearance of an area of RPE atrophy on FA, which, like classic CNV, is hyperfluorescent during the early phase of the angiogram (Fig. 69.7A). The increased fluorescence through the atrophic patch results from increased transmission of fluorescein through an overlying RPE with a reduced amount of pigment that normally obscures the choroidal blush (sometimes termed a window, or transmission, defect). Unlike the increase in extent and intensity of hyperfluorescence due to leakage from the fluorescence of classic CNV, RPE atrophy does not show leakage of fluorescein at its boundaries through the mid- and late-phase frames. The fluorescence fades after several minutes (Fig. 69.7B),

without leakage of fluorescein beyond the boundaries of hyperfluorescence defined in the early stages. Two other lesions in AMD that may show an area of discrete hyperfluorescence in the early phase of the angiogram include a serous PED and a rip or tear of the RPE (angiographic features that differentiate these abnormalities from classic CNV are discussed later). Neither one of these latter abnormalities should show fluorescein leakage in later phases of the angiogram at the boundary of the hyperfluorescence noted in earlier phases.

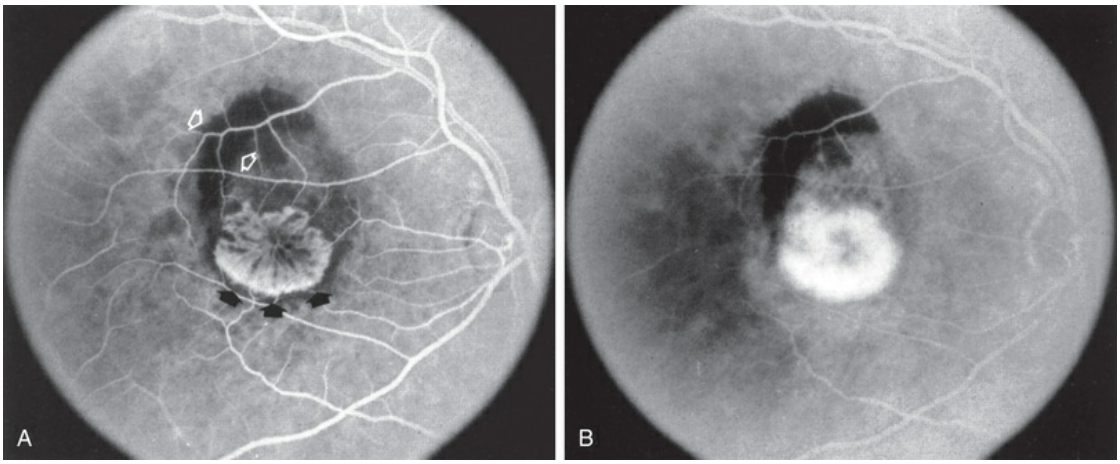

FIG. 69.6 (A) Early transit phase of fluorescein angiogram showing fine net of vessels corresponding to part of choroidal neovascular lesion (black arrows). (B) Late phase of the fluorescein angiogram, demonstrating an increase in the degree and size of fluorescence. In both panels (A) and (B) there is blocked fluorescence resulting from overlying hemorrhage (*white arrows*). (Reproduced with permission from Elman MJ. Age-related macular degeneration. Int Ophthalmol Clin 1986;26:117–44.)

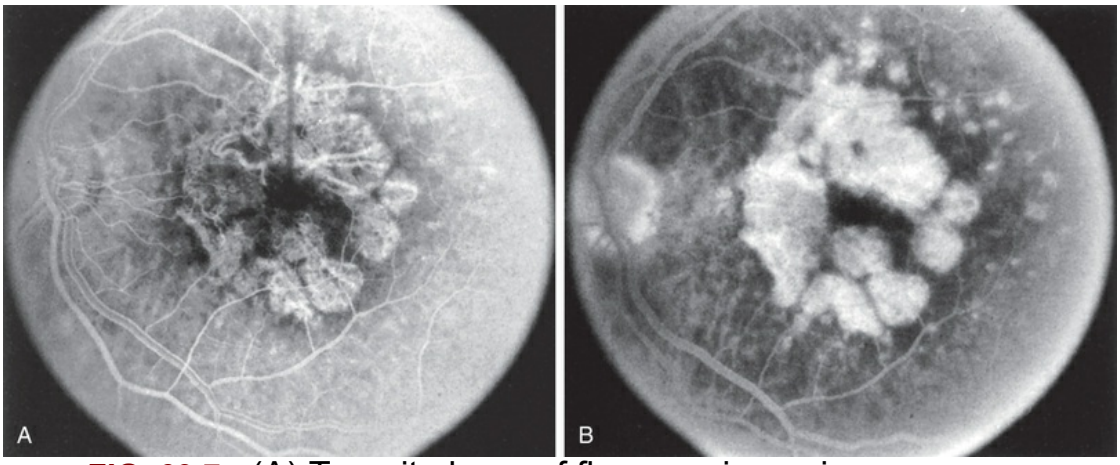

FIG. 69.7 (A) Transit phase of fluorescein angiogram, showing hyperfluorescence corresponding to atrophic zones of the retinal pigment epithelium (transmission, or window, defect) and easily visualized choroidal vessels (too large to be vessels of choroidal neovascularization). (B) Hypofluorescence does not increase in size and fades with the later phases of the angiogram. This is in contrast to the pattern seen in choroidal neovascularization (Fig. 69.5). (Reproduced with permission from Elman MJ. Age-related macular degeneration. Int Ophthalmol Clin 1986;26:117–44.)

Occult Choroidal Neovascularization

Occult CNV refers to two hyperfluorescent patterns on FA.[27,58,59] The first pattern, termed a fibrovascular pigment epithelial detachment (FVPED), is best appreciated with stereoscopic views, usually at approximately 1–2 min after dye injection. It appears as an irregular elevation of the RPE, often stippled with hyperfluorescent dots (Fig. 69.8). The boundaries may or may not show leakage in the late-phase frames as fluorescein collects within the fibrous tissue or pools in the subretinal space overlying the FVPED. The exact boundaries of a FVPED can usually be determined most accurately only when fluorescence sharply outlines the elevated RPE. The amount of elevation depends on the quality of the stereoscopic photographs and the thickness of the fibrovascular tissue. Stereoscopic pairs of fluorescein angiogram frames can sometimes facilitate identification of the boundaries of the elevated RPE, although not always, as the elevation can slope

gradually down to the normal level of the RPE. The second pattern, late leakage of an undetermined source (Fig. 69.9), refers to late choroidal-based leakage in which there is no clearly identifiable classic CNV or FVPED in the early or mid-phase of the angiogram to account for an area of leakage in the late phase. Often this pattern of occult CNV can appear as speckled hyperfluorescence with pooling of dye in the subretinal space overlying the speckles. Usually the boundaries of this type of CNV cannot be determined precisely.

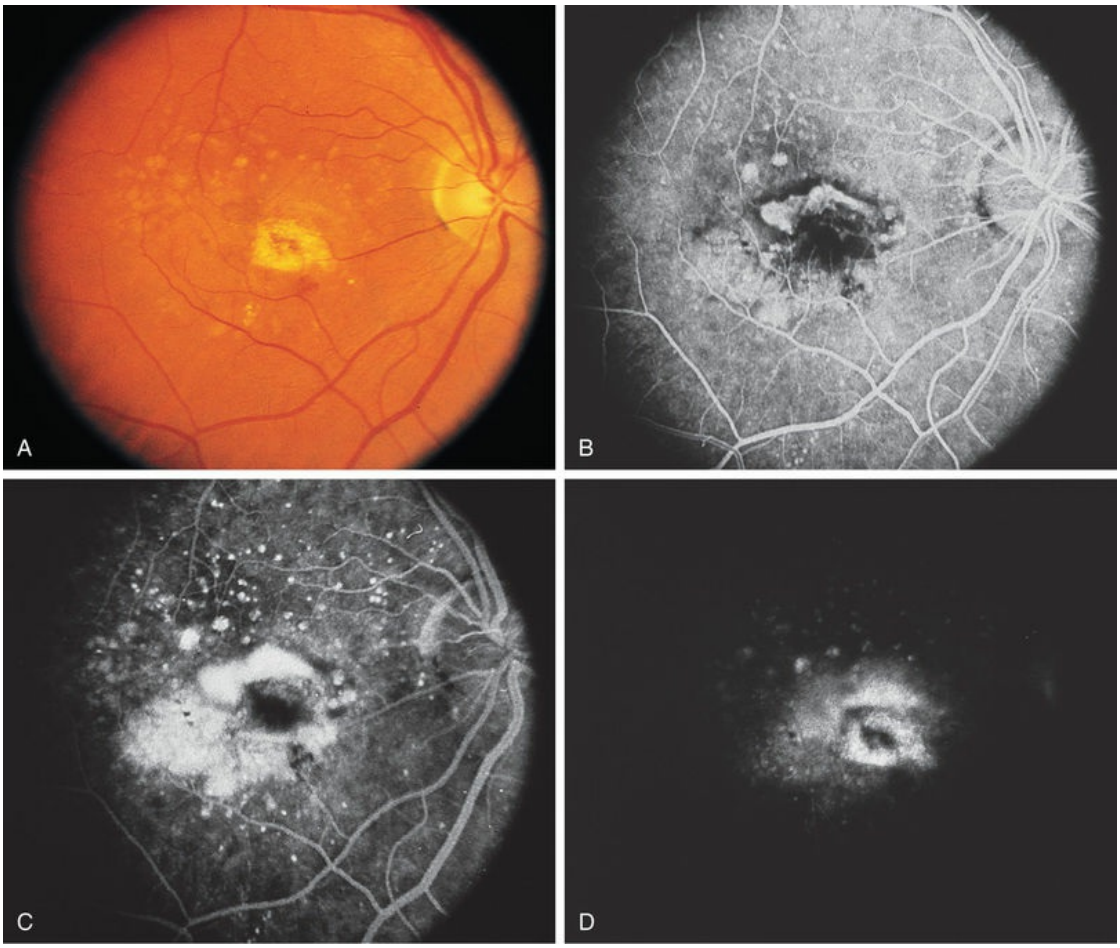

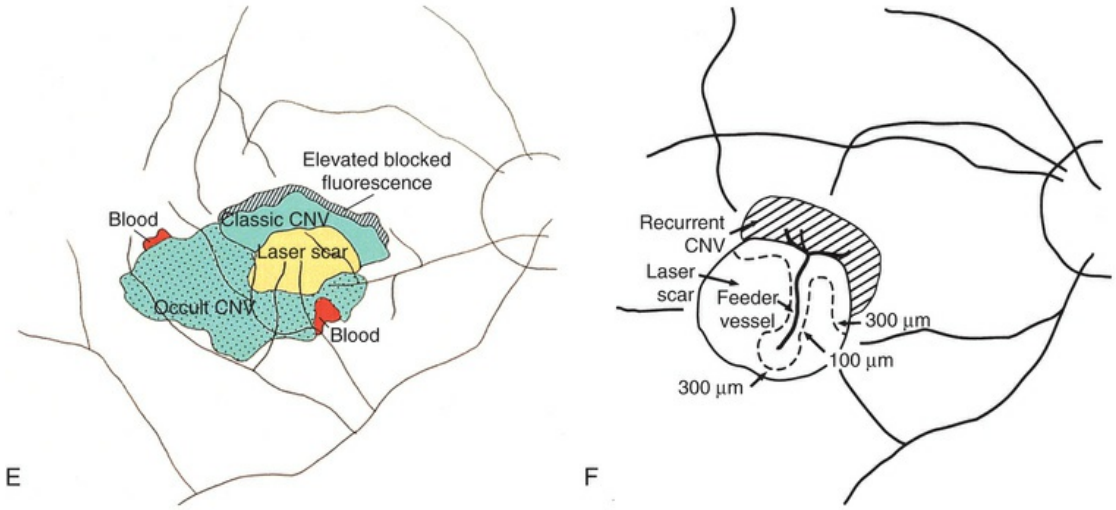

FIG. 69.8 Classic and occult choroidal neovascularization (CNV) with well-demarcated borders. (A) Color photograph shows scar from prior photocoagulation surrounded by several clues to suggest recurrent CNV, including subretinal hemorrhage, subretinal lipid, irregular elevation of retinal pigment epithelium (RPE) below the area of prior laser treatment, and overlying subretinal fluid. (B) Early phase of fluorescein angiogram shows area of classic CNV, scar from prior laser treatment, and irregular elevation of RPE with stippled hyperfluorescence representing fibrovascular pigment epithelial detachment (PED) inferior and temporal to the scar. (C) Photograph of the same eye 1 min after fluorescein injection. Note fluorescein leakage already apparent from classic CNV and increased intensity of stippled hyperfluorescence corresponding to fibrovascular PED. The boundaries of the fibrovascular PED remain well demarcated. (D) Angiogram taken 10 min after fluorescein injection shows persistence of fluorescein staining and leakage within a sensory retinal detachment overlying the lesion. It is difficult to determine the precise demarcation of fluorescence outlining the elevated RPE from these photographs alone. Although a fairly well-demarcated border can be seen in (C), the intensity of fluorescence at the boundary of elevated RPE is quite irregular in these late-phase photographs, with some areas fading relative to fluorescence of remaining areas of elevated RPE (D). (E,F) Composite drawings using multiple stereoscopic photographs from angiogram show

interpretation of the boundaries of the lesion. At each clock-hour, the boundary of the lesion is clearly demarcated; the lesion included classic CNV, which occupies the foveal center. (Reproduced with permission from Macular Photocoagulation Study Group. Subfoveal neovascular lesions in age-related macular degeneration: guidelines for evaluation and treatment in the Macular Photocoagulation Study. Arch Ophthalmol 1991;109:1242–57.)

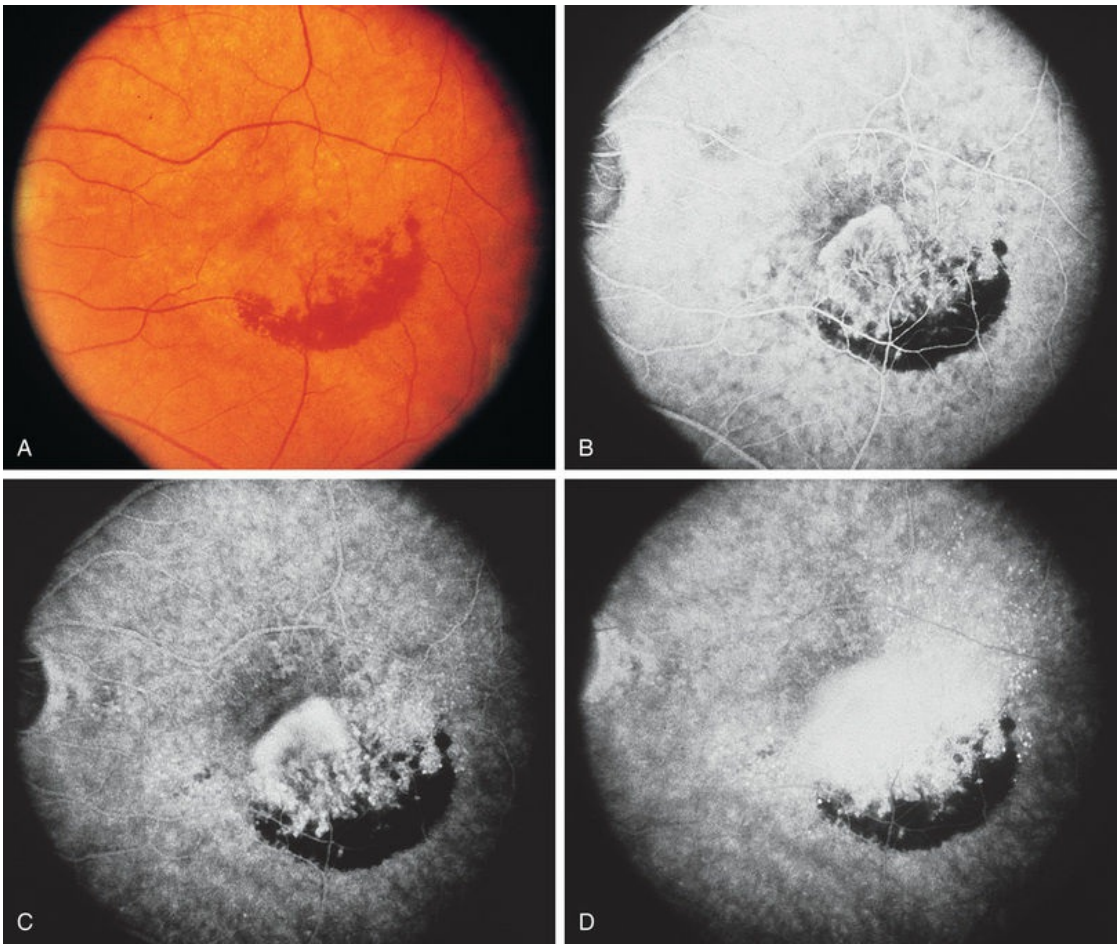

FIG. 69.9 Occult choroidal neovascularization (CNV) accompanied by classic CNV. (A) Subretinal fluid and hemorrhage in eye with drusen. (B) Early phase of fluorescein angiogram shows both feeder vessels to classic CNV and fibrovascular pigment epithelial detachment (PED). Blocked fluorescence due to thick blood obscures inferior boundary of occult CNV. (C) Mid-phase stereoscopic photographs of angiogram show leakage from classic CNV. (D) Late phase of angiogram shows other areas of late leakage of undetermined source with no discernible, discrete,

well-demarcated area of hyperfluorescence from classic CNV or fibrovascular PED detectable in early or mid-phase frames of angiogram that might be considered a source of late leakage. This lesion is considered poorly demarcated. (Reproduced with permission from Macular Photocoagulation Study Group. Subfoveal neovascular lesions in age-related macular degeneration: guidelines for evaluation and treatment in the Macular Photocoagulation Study. Arch Ophthalmol 1991;109:1242–57.)

Other Terms Relevant to Interpreting Fluorescein Angiography of Choroidal Neovascularization

It is important to distinguish between what are termed the "lesion" and the various "lesion components" of which the lesion is composed when discussing fluorescein interpretation and treatment of CNV.[27,58,59] A lesion component may be described as classic or occult CNV or any of four angiographic features that could obscure the boundaries of classic or occult CNV. These four features include (1) blood that is visible on color fundus photographs and thick enough to obscure the normal choroidal fluorescence; (2) hypofluorescence due to hyperplastic pigment or fibrous tissue, or blood not visible on color fundus photographs; (3) a serous detachment of the RPE (Fig. 69.10); and (4) scar from CNV which either stains or blocks fluorescence (depending on the extent of RPE within the scar). The first two of these four features block the angiographic view of the choroid, making it impossible to determine whether CNV is located in the area of this component. The bright, reasonably uniform, early hyperfluorescence associated with a serous detachment of the RPE (described later) may obscure hyperfluorescence from classic or occult CNV and therefore interfere with the ability to judge whether CNV extends under the area of the serous detachment. The term "lesion," again, refers to the entire complex of lesion components.

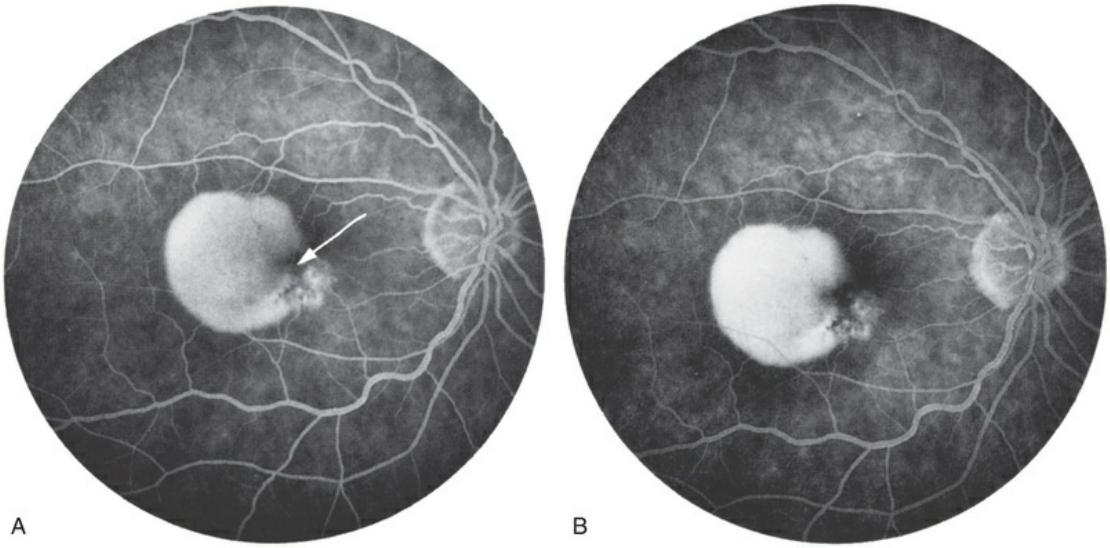

FIG. 69.10 Fluorescein angiogram of serous retinal pigment epithelial detachment. (A) Early transit phase of a fluorescein angiogram demonstrates uniform fluorescence under the dome of the detachment. Note the deformation of the otherwise round detachment by a notch of the hyperfluorescence (*arrow*). (B) Later phase of the fluorescein angiogram demonstrates persistent hyperfluorescence that does not extend beyond the margins of the hyperfluorescence seen in the early transit phase. (Reproduced with permission from Bressler NM, Bressler SB, Fine SL. Age-related macular degeneration. Surv Ophthalmol 1988;32:375–413.)

The terms "well-defined" (synonymous with well-demarcated) and "poorly defined" (synonymous with poorly demarcated or ill-defined) refer to a description of the boundaries of the entire lesion (not of individual lesion components). In a well-defined lesion, the entire boundary for 360° is well demarcated (for example, Figs. 69.6, 69.11 and 69.12). If the entire boundary is not well demarcated for 360°, then the lesion is poorly defined (for example, Fig. 69.9). Thus the terms well-defined and classic should not be used interchangeably, nor should poorly defined and occult.

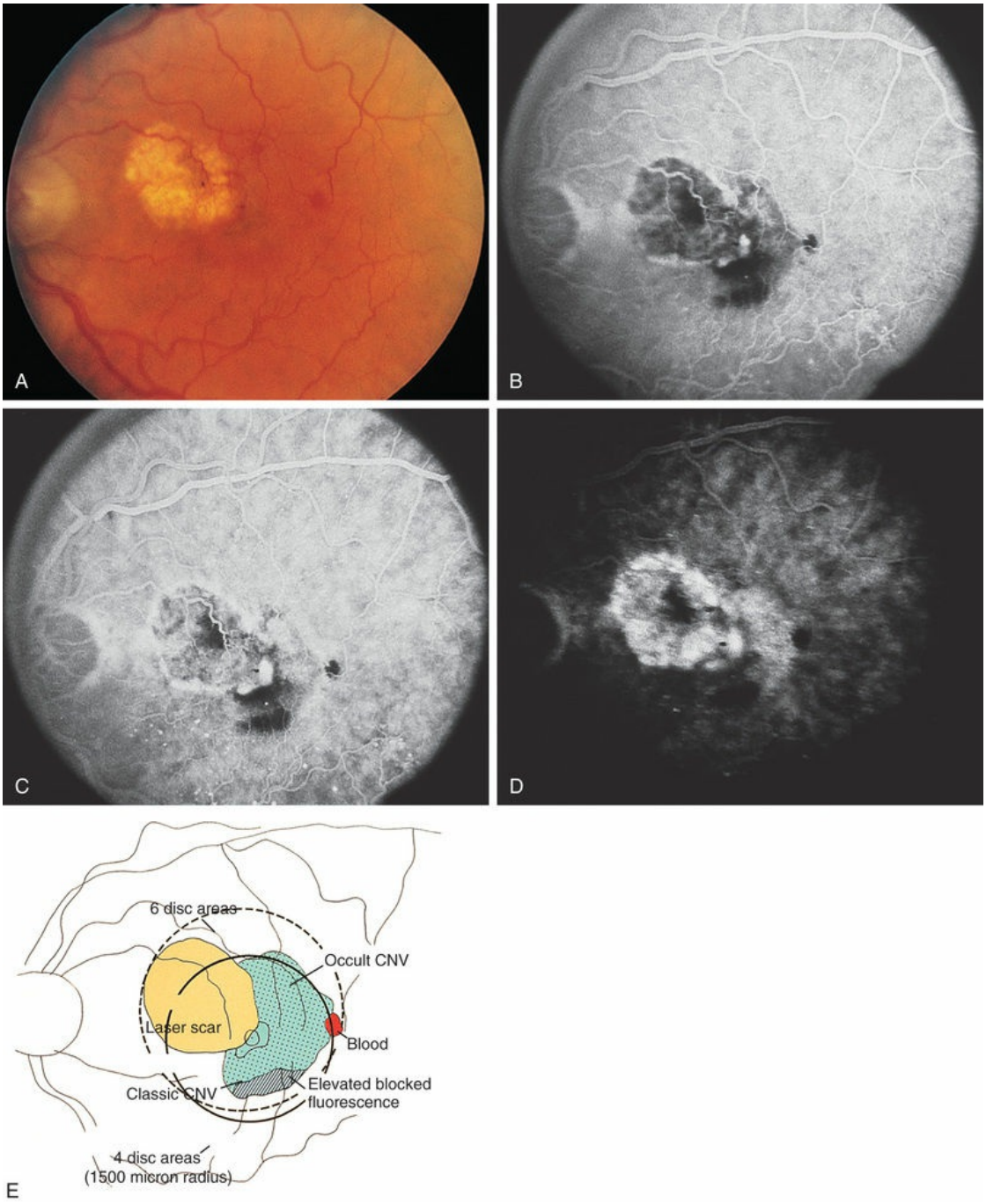

FIG. 69.11 Classic and occult choroidal neovascularization (CNV) and elevated blocked fluorescence (EBF) with well-demarcated borders. (A) Recurrent subfoveal CNV. Note small area of hemorrhage temporal to recurrence. (B) Early phase of fluorescein angiogram shows sharp demarcation of hyperfluorescence of classic CNV. (C) Mid-phase photograph of angiogram with fluorescein leakage from classic CNV and sharply demarcated hyperfluorescence of elevated retinal pigment

epithelium due to fibrovascular pigment epithelial detachment and indicative of occult CNV. EBF still obscures choroidal fluorescence and possibly the inferior boundary of CNV. (D) Late phase of angiogram demonstrates fluorescein leakage from both classic and occult neovascularization. Note hardly discernible EBF. (E) Composite drawing using multiple stereoscopic photographs of angiogram shows interpretation of boundaries of lesion. Since each lesion component (classic CNV, occult CNV, blood, and EBF) has well-demarcated boundaries, boundaries of entire lesion are considered well demarcated. (Reproduced with permission from Macular Photocoagulation Study Group. Subfoveal neovascular lesions in age-related macular degeneration: guidelines for evaluation and treatment in the Macular Photocoagulation Study. Arch Ophthalmol 1991;109:1242–57.)

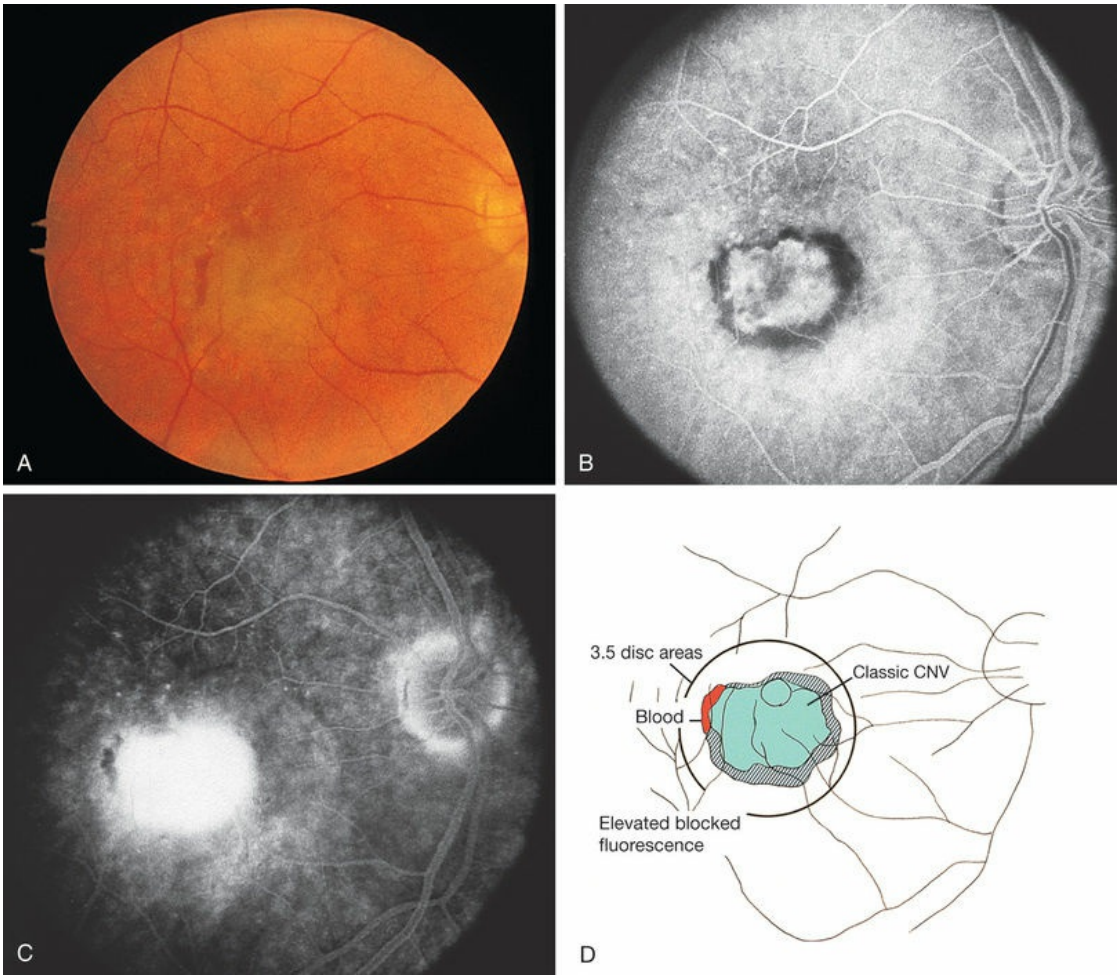

FIG. 69.12 (A) Subfoveal choroidal neovascularization

(CNV) and contiguous blood. (B) Early phase of fluorescein angiogram shows classic CNV with blocked fluorescence corresponding to contiguous blood that obscures boundaries of CNV along temporal border. Remaining blocked fluorescein surrounding CNV (elevated when viewed stereoscopically) was probably due to the fibrous component of CNV. (C) Late phase of fluorescein angiogram demonstrates that borders of CNV, blood, and elevated blocked fluorescence (green, red, and blue, respectively) in (D) were derived from viewing the entire stereoscopic fluorescein angiogram taken according to study protocol. (D) Drawing demonstrates that combined areas of blood and elevated blocked fluorescence that obscured borders of CNV did not exceed area of visible CNV.

(Reproduced with permission from Macular Photocoagulation Study Group. Subfoveal neovascular lesions in age-related macular degeneration: guidelines for evaluation and treatment in the Macular Photocoagulation Study. Arch Ophthalmol 1991;109:1242–57.)

The term “predominantly CNV” indicates that at least 50% of the lesion is composed of either classic CNV or occult CNV, or both, while the term “predominantly hemorrhagic” indicates that at least 50% of the lesion is composed of hemorrhage.[58,59]These terms remain critical in the management of AMD, since treatments for CNV with anti-VEGF therapy, or less frequently, with laser photocoagulation, photodynamic therapy (PDT), or surgery, have been tested only in lesions that are predominantly CNV or predominantly hemorrhagic. After determining whether a lesion's composition is predominantly CNV, it should be determined whether the lesion is predominantly classic, rather than minimally classic or occult with no classic. If predominantly classic, then treatment could be considered with or without evidence of presumed recent disease progression (formally defined as evidence of blood associated with CNV, or definite visual acuity loss within 3 months, or definite growth of the lesion within 3 months). Treatment of minimally classic or occult with not classic lesions has only been demonstrated formally to be beneficial compared with no treatment with evidence of presumed recent disease progression. A therapeutic trial of anti-VEGF therapy might be considered in the setting of visual acuity loss and intraretinal or subretinal fluid

judged to be contributing to this visual acuity loss and judged likely to resolve following initiation of anti-VEGF therapy.

Retinal Pigment Epithelium Detachments in Age-Related Macular Degeneration

Various changes in an eye with AMD may result in elevation or detachment of the RPE, as seen on stereoscopic biomicroscopic or angiographic evaluation. The term RPE detachment or retinal pigment epithelial detachment (retinal PED) secondary to AMD in the ophthalmic literature remains confusing because various RPE detachments may have quite different compositions, fluorescein angiographic appearances, prognoses, and management. Fortunately, these various RPE detachments can usually be differentiated on the basis of fluorescein angiographic patterns of fluorescence. The patterns include the following: (1) fibrovascular PEDs,[27] a subset of occult CNV (see Figs. 69.8 and 69.9); (2) serous detachments of the RPE[61] (see Fig. 69.10); (3) hemorrhagic detachments of the RPE, in which blood from a choroidal neovascular lesion is noted beneath or exterior to the RPE (see Fig. 69.3); and (4) drusenoid RPE detachments,[28] in which large areas of confluent, soft drusen are noted. Fibrovascular PEDs show a stippled fluorescence along the surface of the RPE by the middle phase of the angiogram and may show pooling of dye in the overlying subsensory retinal space in the late phase (see Fig. 69.8). Serous PEDs in contrast, show uniform, bright hyperfluorescence in the early phase, with a smooth contour to the RPE by the middle phase, and little, if any, leakage at the borders of the PED by the late phase (see Fig. 69.10). The fluorescent pattern of a serous PED obscures the ability to determine whether classic or occult CNV exists within or beneath the area of the serous PED.

A hemorrhagic detachment of the RPE will block choroidal fluorescence because of the mound-like collection of blood beneath the RPE (see Fig. 69.3). Occasionally a hemorrhagic detachment of the RPE may be mistaken for a choroidal melanoma, but usually hemorrhagic detachments of the RPE do not demonstrate the low internal reflectivity on A-scan ultrasonography characteristically seen in choroidal melanomas. Finally, a drusenoid RPE

detachment[26] represents extensive areas of large, confluent drusen. Drusenoid RPE detachments can be distinguished from serous detachments of the RPE since the former fluoresce faintly during the transit and do not progress to bright hyperfluorescence in the late phase of the angiogram. In addition, drusenoid RPE detachments will usually have a less smooth, less distinct boundary compared with serous RPE detachments. Drusenoid RPE detachments can be distinguished from fibrovascular PEDs by their lack of stippled hyperfluorescence and lack of persistent staining or leakage in the late phase of the angiogram. RPE detachments due to large, soft, confluent drusen are usually smaller, shallower, and more irregular in outline than are fibrovascular PEDs. In addition, the drusenoid RPE detachments often have reticulated pigment clumping overlying the large, soft, confluent drusen, a scalloped border, and have less fluorescence in late-phase frames as compared with earlier-phase frames.

Other Angiographic Features

Speckled Hyperfluorescence

Speckled fluorescence (Fig. 69.13A) in the absence of fluorescein leakage consists of several punctuate spots of hyperfluorescence, usually within 500 μm of each other that are apparent between 2 and 5 minutes after fluorescein injection and cannot be detected in early phase frames in contrast to drusen.[56] The fluorescence of these spots persists or increases in intensity by the late phase of the angiogram (Fig. 69.13B), in contrast to drusen or atrophy of the retinal pigment epithelium, which do not remain brightly hyperfluorescent by the late phase of the angiogram. Typically, clusters of speckles appear at the edge of the CNV lesion, rather than the typical distribution of drusen throughout the macular area. This angiographic feature was previously reported to be associated with recurrent CNV.[56] If speckled hyperfluorescence is noted in the presence of fluorescein leakage in the late phase frames in the absence of elevation of the RPE, this would be considered occult CNV.

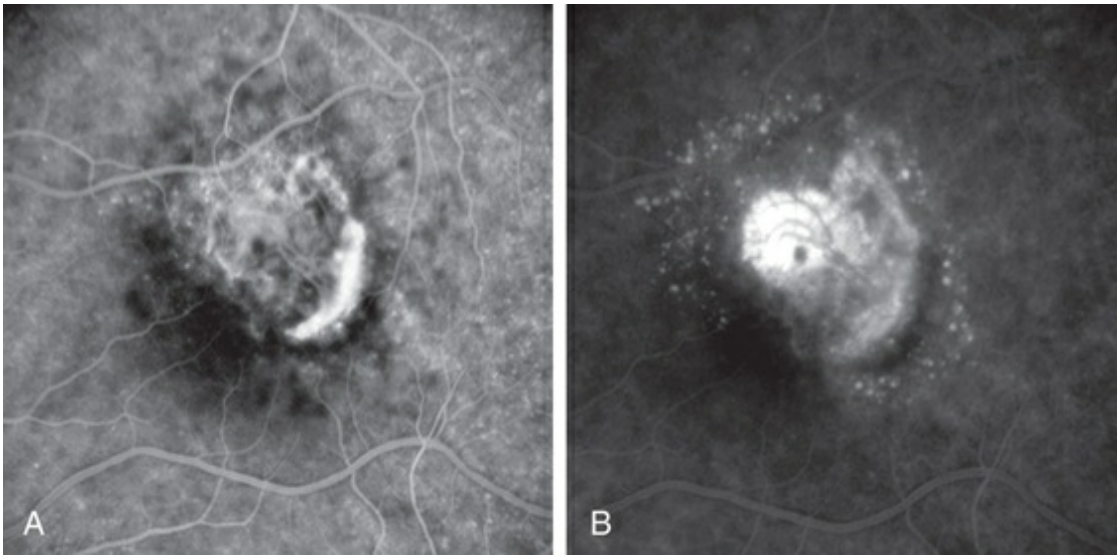

FIG. 69.13 (A,B) Example of speckled fluorescence noted in an eye with choroidal neovascularization. Multiple punctuate spots of hyperfluorescence within 500 μm of each other are apparent in a late phase frame (B) but cannot be detected in early phase frame (A). Note the typical appearance of clusters of speckles at the edge of the CNV lesion. (© Neil M. Bressler, MD, Johns Hopkins University, 2011.)

Retinal Lesion Anastomosis ("Retinal Angiomatous Proliferans," "RAP Lesion," or "Chorioretinal Anastomosis")

Retinal vessels can anastomose with CNV from AMD.[62] The vessels can be seen dividing at right angles from the surface of the retina to the neovascular lesion (as may be seen with idiopathic parafoveal telangiectasis). These vessels may also be seen in the setting of disciform scarring. Some descriptions of these vessels have suggested that they can develop prior to the development of CNV (as is seen in the subretinal neovascularization that can develop in an individual with idiopathic parafoveal telangiectasis). Theoretically, these descriptions seem plausible if sufficient VEGF production, which typically would be involved in the development of CNV, first led to the development of proliferation of retinal capillaries. However, there is no evidence that these vessels develop in the absence of CNV from AMD on histopathology. Furthermore, most cases show evidence of CNV in the presence of these

anastomoses of retinal vessels with the neovascular lesion, and those cases that do not show obvious CNV often have difficult angiograms to interpret to state with certainty that CNV is not present. The area of anastomosis, when noted before development of extensive visible scar tissue, often shows a bright area of fluorescence in the early phase, occasionally accompanied by a small area of intraretinal hemorrhage. While some reports have suggested that the natural history of lesions with these anastomoses is worse than the natural history without these anastomoses, there is no strong evidence to support this impression at this time.

Loculated Fluid

This fluid consists of a well-demarcated area of hyperfluorescence that appears to represent pooling of fluorescein in a compartmentalized space anterior to the choroidal neovascular leakage, usually seen in the late phase of the angiogram.[63] Although the loculated fluid may conform to a pattern of typical cystoid macular edema, it can also pool within an area deep to the sensory retina in a shape that does not bear any resemblance to cystoid macular edema.

Retinal Pigment Epithelial Tears

RPE tears have a characteristic fluorescein angiographic appearance.[64] The denuded RPE displays marked early hyperfluorescence. Later, staining of the choroid and sclera may be observed, but fluorescein generally does not leak from the denuded area. The folded pigment epithelial mound blocks fluorescence; however, this area may leak later during the angiogram, presumably from underlying CNV. Tears may occur following development of a serous PED in the absence of CNV. In addition, tears may occur following development of CNV, sometimes accompanied by large areas of hemorrhage. Tears in any of these situations may occur without any antecedent treatment or may occur soon after treatment, and need not preclude further therapy out of concern for worsening the tear.[42]

Disciform Scars

Fibrovascular scars frequently hyperfluoresce from both fluorescein leakage and staining. Hypofluorescence due to blocking may also be observed if there is an RPE pigmentary reaction.

Indocyanine Green Angiography

Indocyanine green (ICG) is a dye that is more highly protein-bound than sodium fluorescein and that fluoresces in the near-infrared wavelength. These properties have been suggested to be useful in the evaluation and management of CNV (see Chapter 2, Indocyanine green angiography). Three basic patterns of fluorescence have been reported in ICG angiography (ICGA) of CNV judged to be occult on FA: a small, focal "hot spot" (a bright area of fluorescence more than one disc area that usually shows by the mid-phase of the angiogram), a plaque (a well-demarcated area of fluorescence more than one disc area in size that emerges relatively late in the angiogram), and ill-defined fluorescence.[65,66] Several types of lesions defined by the EVEREST study group as indicative of polypoidal choroidal vasculopathy (a pattern of CNV, just as classic and occult CNV are patterns of CNV on fluorescein angiography) including nodular polyps on stereo viewing, hypofluorescent halo around nodules, abnormal vascular channel supplying polyps, pulsatile filling of polyps, and orange subretinal nodules corresponding to hyperfluorescent polyps on angiogram.[67] PCV also typically is accompanied by multifocal areas of RPE abnormalities, similar to, or perhaps sometimes due to, underlying features of central serous choroidopathy.[68] PCV also shows multifocal areas of CNV, often outside of the posterior pole, accompanied by multifocal areas of PED, sometimes with breakthrough vitreous hemorrhage.[69] However, to date, it has not been demonstrated that detection or characterization of these lesions by ICG has a beneficial effect on patient outcomes in EVEREST, and additional studies such as PLANET (https://clinicaltrials.gov/ct2/show/NCT02120950) and EVEREST 2 (https://clinicaltrials.gov/ct2/show/NCT01846273) are awaited. Until carefully designed, randomized clinical trials are conducted that show that ICG-guided therapy of AMD-related CNV (that escaped detection by clinical examination, FA, and OCT), with or without

patterns of PCV, result in a better visual outcome than no treatment, one cannot know for sure if this particular diagnostic intervention or recognition of this pattern of CNV with or without ICGA is beneficial.[70] The role of ICGA in the setting of polypoidal choroidal vasculopathy patterns of CNV also is discussed further in Chapter 74 (Polypoidal choroidal vasculopathy).

Pathogenesis

Choroidal Neovascularization

Histopathology

CNV appears as a neovascular sprout growing under or through the RPE via breaks in Bruch's membrane[20] (Figs. 69.14 and 69.15). Usually this occurs in association with evidence of fibroblasts, myofibroblasts, lymphocytes, and macrophages.[71] Various growth factors are suspected to be involved in the development of this CNV, such as vascular endothelial growth factor (VEGF).[72] It is clear, though, there are other factors involved, since diseases such as diabetic macular edema and macular edema due to retinal vein occlusion respond to VEGF blockade, but do not develop CNV. Following penetration of the inner aspect of Bruch's membrane, the new vessels proliferate laterally between the RPE and Bruch's membrane.[20] As these neovascular twigs mature, they develop a more organized vascular system stemming from a trunk of feeder vessels off the choroid, as well as proliferation of fibrous tissue. The endothelial cells in the arborizing neovascular tufts lack the barrier function of more mature endothelial cells. Hence these new vessels can leak fluid (and fluorescein) in the neurosensory, subsensory, and RPE layers of the retina. Proteins and lipids may accompany this process and precipitate in any layer of the retina. In addition, the fragile vessels are prone to hemorrhage. Occasionally, blood may extend through all the layers of the retina, breaking through into the vitreous cavity. Ultimately, in the absence of treatment, a fibrovascular scar results, usually causing disruption and death of the overlying sensory retinal tissue accompanied by severe visual loss.

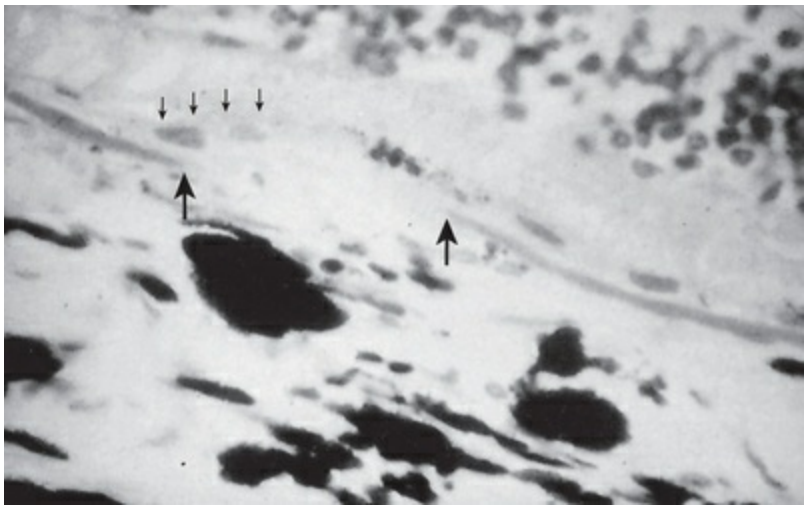

FIG. 69.14 Photomicrograph of choroidal neovascularization (*outlined by small arrows*) beneath the retinal pigment epithelium growing through a break in Bruch's membrane (*large arrows*). (Reproduced with permission from Elman MJ. Age-related macular degeneration. Int Ophthalmol Clin 1986;26:117–44.)

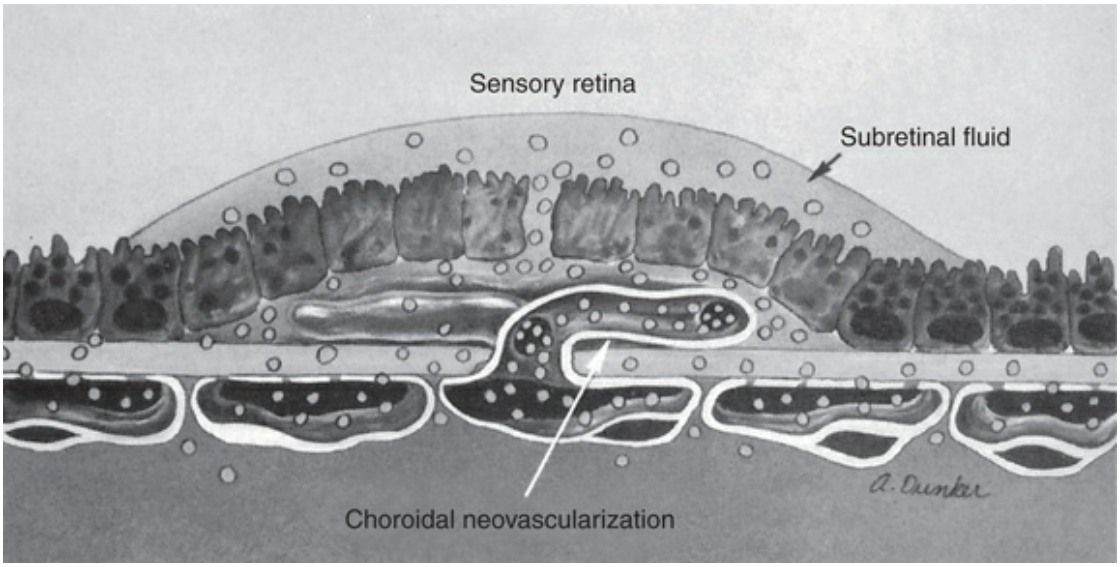

FIG. 69.15 Sketch of choroidal neovascularization showing ingrowth of vessels from the choriocapillaris, through a break in Bruch's membrane, into the subretinal pigment epithelial space. (Reproduced with permission from Bressler NM, Bressler SB, Fine SL. Age-related macular degeneration. Surv Ophthalmol 1988;32:375–413.)

Associated Factors

The stimulus for vascular ingrowth of choroidal vessels remains unknown, but several theories have been advanced. Soft drusen have been associated histopathologically with CNV. The soft drusen represent focal accumulation of membranous debris (ultrastructurally termed basal linear deposits) accumulated as a diffuse, shallow layer between the RPE basement membrane and the inner aspect of Bruch's membrane.[19,20,22,73–78] This material should not be confused with basal laminar deposit, which is material that collects between the RPE plasma membrane and the basement membrane of the RPE and accumulates with age but may not lead to vision loss from CNV or geographic atrophy and therefore may not be part of AMD.[73,74] The term should also not be confused with basal laminar drusen, also called cuticular drusen, which usually present in midlife with a myriad of small, translucent drusen that appear like a starry sky on a fluorescein angiogram and may be associated with vitelliform macular detachments, as discussed below.[3,79] Some investigators believe that soft drusen represent extracellular matrix material produced by the RPE.[73,80] Deposition of this material may suggest a widespread RPE abnormality.[73] The diffusely thickened area is weakly attached, allowing the development of localized detachments seen clinically as soft drusen. These localized detachments can coalesce into larger drusenoid or serous RPE detachments.[22] Alternatively, drusen may act as an indirect angiogenic factor by attracting macrophages from the choroid.[71]

Breaks in Bruch's membrane permit ingrowth of new vessels from the choriocapillaris. However, these breaks can also be seen without ingrowth of choroidal new vessels. Some investigators have suggested that endothelial cells of growing CNV may actually produce the break in Bruch's membrane rather than grow through preexisting breaks in Bruch's membrane.[81] An inflammatory component seen in association with AMD may play a role in the development of CNV.[82] Eyes with AMD show an increased prevalence of lymphocytes, fibroblasts, and macrophages within Bruch's membrane as compared with control eyes without AMD. However, these findings are not specific to eyes with neovascular AMD.[82,83] The presence of macrophages and lymphocytes near

breaks in Bruch's membrane suggests that leukocytes may be involved in the induction of CNV growth and the release of collagenases from endothelial cells. It is postulated that leukocytes may initially stimulate neovascular proliferation, promote the release of factors leading to breakdown of Bruch's membrane, and even affect (with pericytes) the dilation of new vessels.[84] Whether these inflammatory cells act as mediators of the degenerative changes seen in Bruch's membrane or directly stimulate new vessel growth remains unknown. Finally, as mentioned above, other angiogenic factors, such as VEGF or a platelet-derived growth factor (PDGF),[72,85,86] may contribute to the ingrowth of new vessels from the choroid through Bruch's membrane into the sub-RPE space. Growth factors leading to neovascular formation may arise from an imbalance between stimulating and inhibiting chemical modulators. The RPE has been implicated as the source of these factors, but RPE cells may also act indirectly through the attraction of macrophages.[87]

Differential Diagnosis by Clinical Presentation

Choroidal Neovascularization

CNV may arise in association with a number of conditions other than AMD, such as presumed ocular histoplasmosis syndrome, pathologic myopia, angioid streaks (especially when associated with pseudoxanthoma elasticum), choroidal ruptures, and idiopathic causes. Whether AMD is present when CNV arises in patients older than 50 years without drusen is controversial.

CNV may masquerade as central serous chorioretinopathy (CSR). Although the classic case of CSR shows a “smokestack” configuration on FA, the more common presentation is a dot of hyperfluorescence that merely increases in size and intensity of fluorescence, much like a small area of CNV. One must strongly consider CNV in patients aged 50 and older who have even otherwise typical-appearing CSR, since the latter condition is most often seen prior to the fifth decade of life.

Basal laminar, or cuticular, drusen may be complicated by foveal

detachments of vitelliform material in one or both eyes that may mimic neovascular AMD. Contact lens examination with transillumination of the fundus in these cases reveals an appearance similar to that of pigskin, with a myriad of small drusen. Angiographically, literally hundreds of bright spots appear very early during the angiogram, an appearance that has been described as a "starry sky." These patients are usually asymptomatic until they accumulate vitelliform lesions in the fovea. The ensuing foveal detachment by this material, which can be unilateral or bilateral, simulates the foveal detachment that occurs with subfoveal CNV. The hyperfluorescence usually progressively fills the area of vitelliform material, rather than showing one area of bright fluorescence early that leaks late in classic CNV. Unlike subfoveal CNV, which most often progresses to a disciform scar with visual acuity of 20/200 or worse, eyes with a foveal detachment secondary to cuticular drusen resolve without scarring. While the retina then may have an area of RPE atrophy about one to two disc areas in size, acuity is more often in the range of 20/80 to 20/125.

When one identifies any condition with a vitelliform detachment, it is critical to determine if the late-phase bright fluorescence is progressive fluorescein staining of the vitelliform material or leakage of fluorescein from CNV, which might benefit from initiating therapy. Pattern dystrophies of the RPE may also cause vitelliform detachments in which the angiographic pattern can mimic CNV. It is important to recognize that patients with cuticular drusen or pattern dystrophy can still develop typical drusen associated with AMD or actual CNV.

Vitreous Hemorrhage

If a new patient has vitreous hemorrhage (VH) in one eye and signs of AMD in the other eye, other causes of vitreous hemorrhage must first be ruled out. Common causes of VH include retinal tear formation and retinal vascular diseases such as diabetic retinopathy or branch vein occlusion. Ultrasonography can often differentiate breakthrough VH secondary to neovascular AMD or retinal vascular causes from VH caused by a tumor (Fig. 69.16).

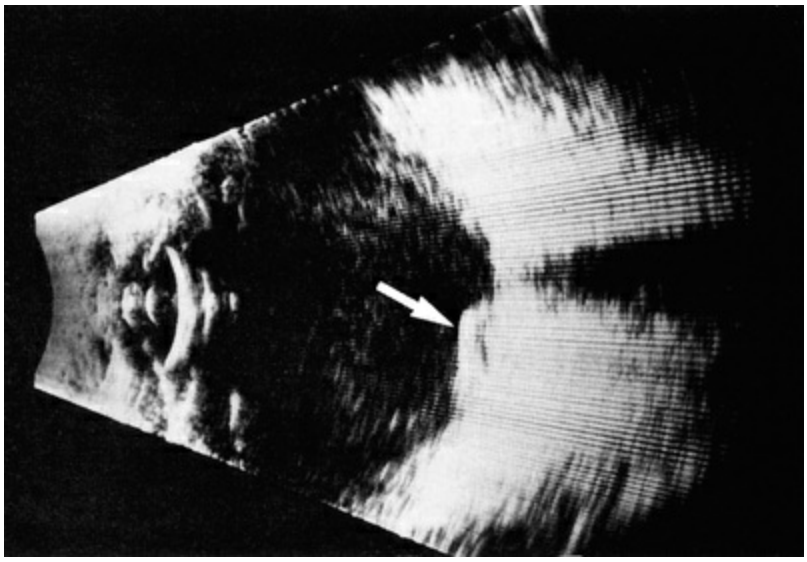

FIG. 69.16 Ultrasound image of a vitreous hemorrhage associated with neovascular age-related macular degeneration in which a relatively flat and broad-based posterior pole lesion (*arrow*) with a fairly homogeneous pattern and with no choroidal excavation seen.

(Reproduced with permission from Bressler NM, Bressler SB, Fine SL. Age-related macular degeneration. Surv Ophthalmol 1988;32:375–413.)

Natural History

Most prospective natural history data of CNV comes from control (untreated) groups of individuals participating in randomized clinical trials conducted prior to the anti-VEGF era. As such, the natural-history information is specific to the eligibility criteria of those trials and not reflective of the natural history of the universe of choroidal neovascular lesions in the population. With this caveat in mind, the natural history from these trials is reviewed to provide some evidence regarding the outcome of these lesions without treatment. In the Macular Photocoagulation Study (MPS), approximately 50–60% of untreated eyes lost 6 or more lines of vision over 2–3 years.[34,35,88–91]

A broader group of subfoveal lesions in the Treatment of Age-related macular degeneration with Photodynamic therapy (TAP) investigation described a slightly better prognosis with approximately 50–60% losing 3 or more lines after 2 years and 20–30% losing 6 or more lines of visual acuity.[83,92] With increasing size

of predominantly classic lesions on presentation, the average visual acuity is more likely to be worse by 2 years.[93]

A variety of studies have shown that cases of predominantly CNV with a composition that is occult with no classic CNV, or minimally classic CNV, have a more heterogeneous outcome.[93–99] Most of this information is from series in clinical trials with presumed recent disease progression. Some cases may remain stable for years without visual loss, whereas other cases may develop severe visual loss at a rate similar to the deterioration noted for cases of classic CNV only. Furthermore, increasing size of minimally classic or occult with no classic lesions is not associated with a worse natural history outcome.[93]

Up to 50% of the cases with no classic CNV may develop classic CNV within a year of presentation.[94–96,100] Cases that develop some classic CNV may be more likely to have severe visual acuity loss.[95,96,100] Results from several clinical trials suggest that the natural history of lesions with classic CNV but no occult CNV is worse than the natural history of lesions with classic and occult CNV or occult with no classic CNV.[96,98,101] It is likely that the natural history of lesions with classic and occult CNV may lie somewhere between the natural course of lesions with classic CNV only and occult CNV only.[96]

Natural Course of Large Subfoveal Subretinal Hemorrhage in AMD

Some eyes with subfoveal subretinal hemorrhage associated with AMD have poor outcomes. However, the visual acuity of other eyes does not deteriorate or may improve spontaneously.[102–104] Such findings underscore the importance of carefully evaluating the risks of therapeutic interventions for these cases, such as surgery[105,106] to remove subretinal hemorrhage and associated CNV, in randomized clinical trials.[107] The SST Group B Trial of relatively large, predominantly hemorrhagic subfoveal lesions demonstrated that although 36% of untreated eyes had severe visual loss, 41% of untreated eyes remained stable or improved over the course of 24 months of follow-up in the study.[29] Furthermore, this trial noted that 18% of large subfoveal subretinal hemorrhages progressed to a

vitreous hemorrhage as blood dissected from the subretinal space through the retina and into the vitreous cavity.[36]

Retinal Pigment Epithelial Tears

Patients with RPE tears involving the foveal center may initially maintain good vision but usually develop severe visual loss. However, cases with RPE tears through the fovea and preservation of good visual acuity have been reported.[108] Unfortunately, there is a substantial risk of AMD-related visual loss in the fellow eye. Schoeppner and associates[109] reported a cumulative risk of visual loss in the fellow eye of patients who had an RPE tear in the eye as 37% at 1 year, 59% at 2 years, and 80% at 3 years of follow-up. Visual loss usually arose from development of a PED, RPE tear, or CNV.

Treatment

Pharmacologic Therapy With Anti-VEGF Products and Overall Management Approach to CNV in AMD

A current approach to neovascular AMD is summarized in Fig. 69.17.[113] Based on the results from several clinical trials evaluating anti-VEGF therapies for CNV in AMD,[50,51,86,110,111] and a Cochrane systematic review of the literature,[112] a current approach to management of subfoveal CNV in AMD in which the CNV is the predominant component (that is, the area of any classic CNV plus any occult CNV is at least 50% of the area of the lesion) is summarized in Fig. 69.18. The retreatment criteria used in trials of discontinuous therapy are reviewed in Table 69.1. The closer the lesion features resemble those of the cases enrolled in these trials, the more likely the results of those trials apply to those cases. The more the treatment regimen resembles the regimen followed in these trials, the more likely the results for patients will follow the results noted in the trials. For lesions that are predominantly scar or predominantly a serous PED, it is unknown if any treatment is beneficial. For lesions that are predominantly hemorrhagic (area of

blood at least 50% of the area of the lesion), anti-VEGF therapy might be considered to reduce the risk of additional severe visual acuity loss, although it is not known if such therapy might increase the chance of visual acuity improvement compared with no treatment.[114,115] The results of prospective case series[114] have suggested that the risk of substantial visual loss or breakthrough of hemorrhage into the vitreous is reduced with anti-VEGF therapy for these lesions, and the CATT investigation included some lesions in which the lesion was predominantly hemorrhagic.[50]

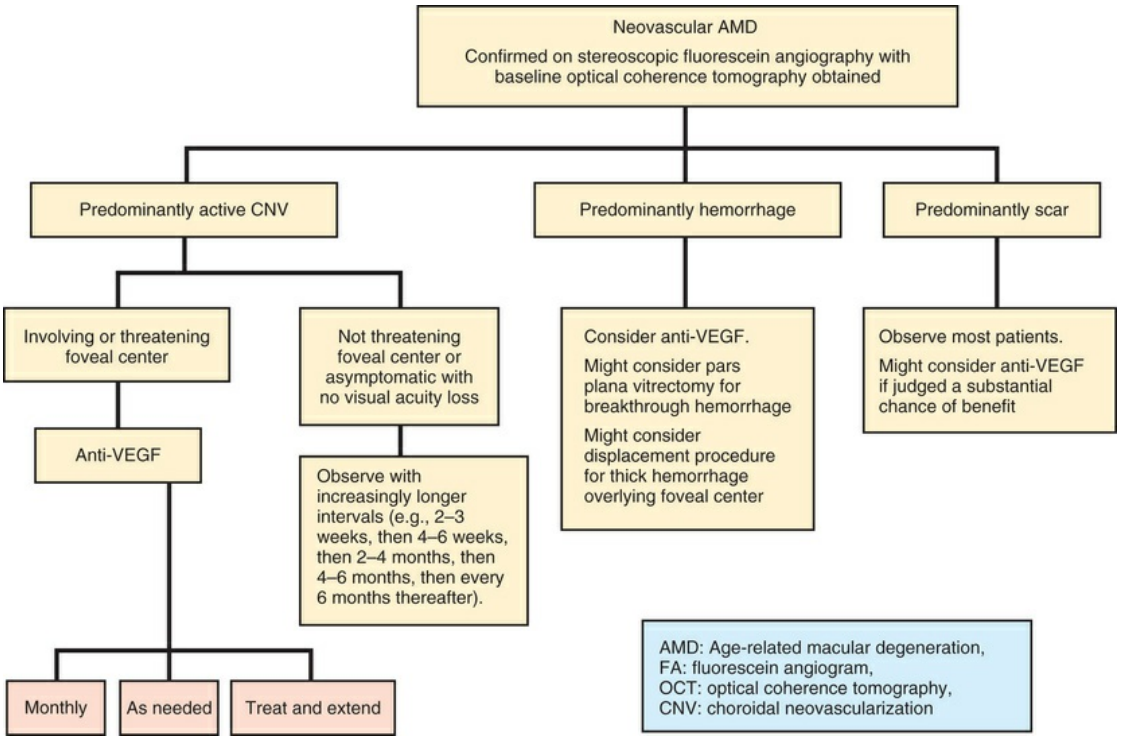

FIG. 69.17 Decision to initiate therapy based on the clinical presentation of neovascular age-related macular degeneration. *AMD,* age-related macular degeneration; *CNV,* choroidal neovascular membrane; *OCT,* optical coherence tomography; *PCV,* polypoidal choroidal vasculopathy; *PDT,* photodynamic therapy; *PRN,* "pro re nata"/"as needed"; *VEGF,* vascular endothelial growth factor.

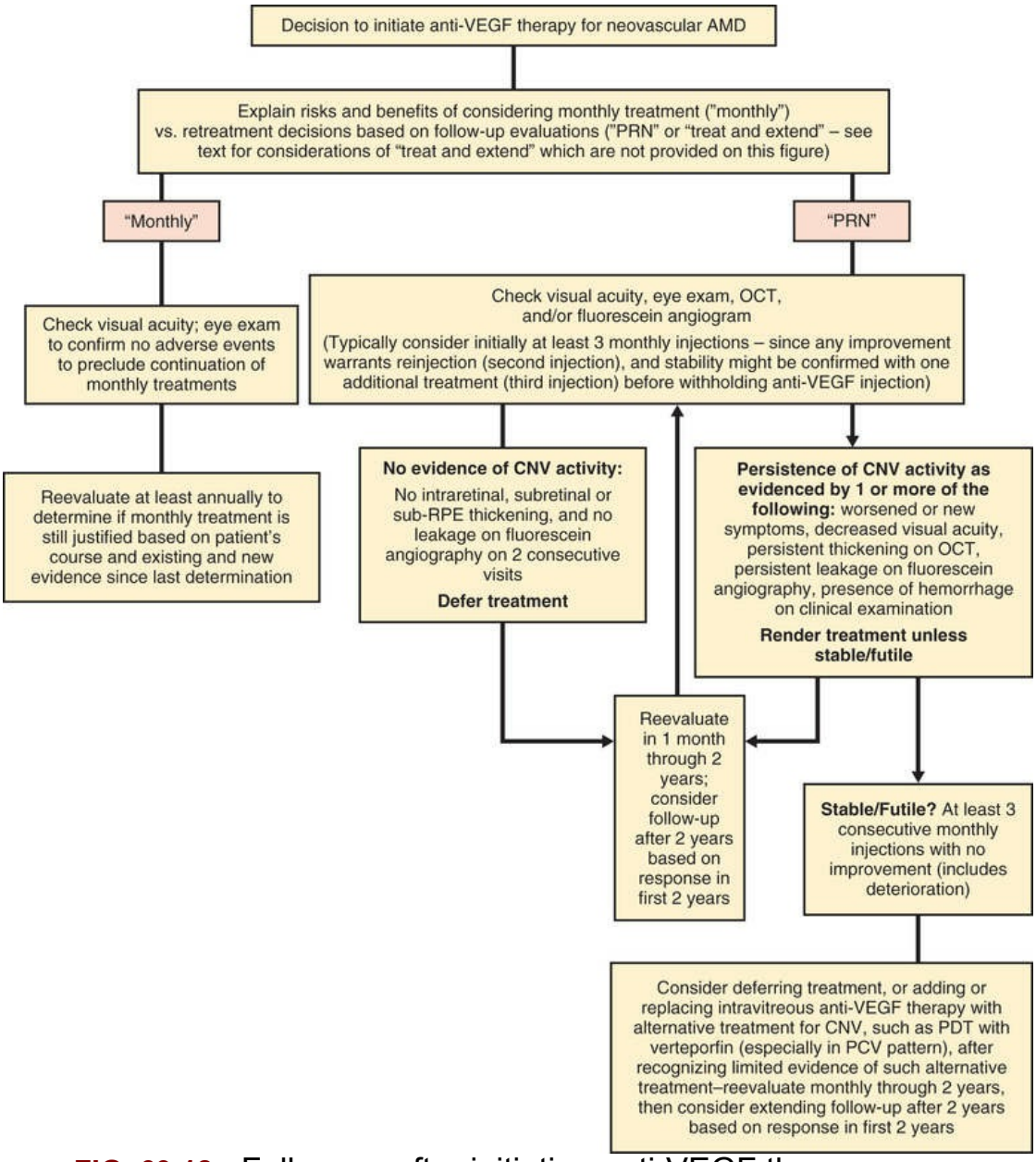

FIG. 69.18 Follow-up after initiating anti-VEGF therapy for neovascular age-related macular degeneration. *AMD,* age-related macular degeneration; *CNV,* choroidal neovascularization; *OCT,* optical coherence tomography; *PDT,* photodynamic therapy; *PRN,* "pro re nata"/"as needed"; *VEGF,* vascular endothelial growth factor. (© Neil M. Bressler, MD, Johns Hopkins University, 2011.)

TABLE 69.1

Retreatment Criteria Used in Trials of "As Needed" Therapy[a]

IVAN	*Requires 3 consecutive treatments every time treatment is resumed.*

	Increasing intraretinal fluid on OCT or Fresh blood or Persistent intraretinal fluid *and* a drop in visual acuity ≥10 letters over the past 3 months If there was uncertainty, then FA was obtained and retreatment given if: Fluorescein leakage >25% of the lesion circumference or Expansion of CNV
CATT	Fluid on time domain or spectral domain OCT ("with the exception of eyes in which there has been no decrease in fluid after three consecutive monthly injections"), or New or persistent hemorrhage or Decreased visual acuity as compared with previous examination or Fluorescein dye leakage or increased lesion size on fluorescein angiogram
VIEW1 and VIEW 2 (Year 2)	Twelve weeks since previous injection or New or persistent fluid on OCT or Increase in central retinal thickness of ≥100 μm compared to lowest previous value or New onset of classic neovascularization or New or persistent leakage on fluorescein angiogram or New macular hemorrhage
HARBOR	≥5-letter decrease in vision from the previous visit Any evidence of disease activity on spectral domain OCT (e.g., intraretinal fluid, subretinal fluid, or subretinal pigment epithelial fluid)

[a]Retreatment criteria used in several clinical trials including discontinuous therapy.

CNV, choroidal neovascular membrane; FA, fluorescein angiogram; OCT, optical coherence tomography.

Pegaptanib sodium (Macugen®) was the first FDA-approved intravitreous anti-VEGF injection for neovascular AMD. While the initial trial results showed decreased loss of vision compared with PDT, this anti-VEGF therapy largely has been replaced based on the more favorable results utilizing 0.5-mg ranibizumab (Lucentis®),[86,110] repackaged or compounded 1.25-mg bevacizumab (Avastin®),[50,51] and aflibercept (EYLEA®).[111]

Efficacy of Ranibizumab vs. PDT With Verteporfin for Predominantly Classic Subfoveal CNV Lesions

Trial participants in the ANCHOR study had CNV lesions that were predominantly classic CNV (at least 50% of the total area of the lesion was classic CNV).[110] Unlike eligibility requirements for the MARINA study (see following section), participants were not required to have presumed recent disease progression (usually defined as presence of blood, documented recent loss of visual

acuity, or documented recent growth of the CNV lesion). Participants in the experimental group received ranibizumab monthly for 24 months.

Mean visual acuity letter score at baseline was 47.1 (approximate Snellen equivalent of 20/125^{+2}) in the 0.5-mg ranibizumab group. For the primary outcome (visual acuity decline of fewer than 15 letters from baseline at 12 months, an amount judged clinically relevant for a patient who might present with an average visual acuity of 20/80 to 20/100 from neovascular AMD), 96.4% of the 0.5-mg group (n=140) and 64.3% of the verteporfin group (n=143) avoided this loss (p<.001).[110] These outcomes were maintained at 24 months for most subjects, with 89.9% of the 0.5-mg group and 65.7% of the verteporfin group avoiding a loss of 3 lines or greater. Investigators also reported that visual acuity improved by 15 letters or more in 40.3% of the 0.5-mg group, as compared with 5.6% of the verteporfin group (p<.001) at 12 months,[110] and 41.0% of the 0.5-mg group gained 3 or more lines of visual acuity versus only 6.3% of the verteporfin group at 24 months. Differences in the mean visual acuity from baseline visual acuity were noted as early as 1 month, when 8.4 letters of improvement occurred in the 0.5-mg ranibizumab group compared with 0.5 letters in the PDT group (p<.001).[110] At 12 months, mean visual acuity improved by 11.3 letters in the 0.5-mg ranibizumab group but decreased by a mean of 9.5 letters in the verteporfin group (p<.001).[110] At 24 months, mean visual acuity improved by 10.7 letters in the 0.5-mg ranibizumab group but decreased by 9.8 letters in the verteporfin group.

Although PDT produced outcomes that likely were better than the natural course of the disease, the 24-month data reinforced the conclusions of the 12-month data previously published and indicated that the increased chance of avoiding 15 or more letter loss and of gaining 15 or more letters with monthly intravitreous ranibizumab persisted through at least 2 years compared with standard applications of PDT.

Efficacy of Ranibizumab vs. Sham Treatment for Minimally Classic or Occult With No Classic Subfoveal Choroidal Neovascular

Lesions and Presumed Recent Disease Progression

In a phase III, double-blind, sham-controlled, randomized clinical trial, eligibility criteria included subfoveal CNV with lesion composition on FA that was minimally classic or occult with no classic component accompanied by presumed recent disease progression.[86] Mean visual acuity letter score at baseline was 53.7 ($20/80^{-1}$) in the 0.5-mg ranibizumab group.[86] Using the primary outcome of visual acuity decline of fewer than 15 letters from baseline as a measure of efficacy, 94.6% of those in the 0.5-mg ranibizumab group and 62.2% of those in the sham-injection group met the primary goal ($p<.001$) after 12 months of treatment.[86] At 24 months, 90.0% of those in the 0.5-mg ranibizumab group and 52.9% of those in the sham-injection group met the primary goal ($p<.001$).[55]

At 12 months, visual acuity improved by 15 or more letters in 33.8% of the 0.5-mg ranibizumab group, as compared with 5% of the sham-injection group ($p<.001$).[86] Participants in the 0.5-mg ranibizumab group achieved mean increases in visual acuity of 7.2 letters, whereas the sham-injection group lost an average of 10.4 letters ($p<.001$).[86] At 24 months, participants in the 0.5-mg ranibizumab group gained a mean of 6.6 letters of visual acuity, compared with a mean loss of 14.9 letters in the sham-injection group ($p<.001$).[86]

In addition to experiencing improvements in objectively measurable visual outcomes, at 12 and 24 months, patients treated with ranibizumab were more likely to improve with respect to self-reported vision-related quality of life (QOL),[23,116,117] regardless of whether the better- or worse-seeing eye was treated. This information is complementary to the visual acuity outcomes described above because although most physicians and patients make decisions based on functional parameters such as a patient's ability to read, watch television, and avoid dependence on others because of vision, the primary outcome measure in most recent trials evaluating treatments for neovascular AMD has been visual acuity in the treated eye.[86,110] Although changes in visual acuity on an eye chart are important in understanding treatment effects, measures of visual acuity do not always completely capture the

degree of visual function. Clinicians may assume that visual function or patient's perception of visual function improves along with visual acuity; however, this is not always the case.[118] Among MARINA participants, scores on the National Eye Institute Visual Function Questionnaire-25 (NEI VFQ-25) relating to activities that require both near vision (such as sewing) and distance vision (such as watching television) were more likely to improve by 10 or more points, a clinically relevant amount, in the ranibizumab group than in the sham-injection group ($p<0.001$).[116] In addition, ranibizumab-treated patients were less likely to perceive themselves as being dependent on others because of their vision.[116] Similar results were confirmed in the ANCHOR trial.

Impact of Noninferiority Results on the Role of Aflibercept or Bevacizumab and on Frequency of Treatment

The Comparison of Age-related Macular Degeneration Treatments Trial (CATT) protocol[50,51] was designed to answer two important questions relevant to treatment of CNV in AMD: (1) does bevacizumab injected every 4 weeks provide visual acuity results which are not worse (strictly speaking, which are noninferior) to ranibizumab injected every 4 weeks with an acceptable safety profile; and (2) does either bevacizumab or ranibizumab when provided "as needed" result in visual acuity outcomes equivalent to those following ranibizumab provided every 4 weeks? Here, "as needed" means that an initial injection is given with subsequent examinations of the eye every 4 weeks through 2 years; reinjection is given at the time of any examination at which any disease activity is noted. Activity includes subretinal or intraretinal fluid or thickening on OCT, new or persistent hemorrhage from CNV, persistent fluorescein leakage from CNV or growth of CNV on fluorescein angiography, or visual acuity loss since the most recent injection.

The major outcomes during the first year which are relevant to these important questions included the following: (1) visual acuity outcomes when using bevacizumab every 4 weeks were not worse (noninferior) to those when using ranibizumab every 4 weeks; (2)

visual acuity outcomes when using ranibizumab as needed, based on examinations every 4 weeks, were equivalent to those when ranibizumab was given every 4 weeks; (3) visual acuity outcomes when bevacizumab as needed was compared with ranibizumab every 4 weeks were inconclusive, i.e., possibly not worse but also possibly inferior; (4) CATT participants assigned to ranibizumab as needed received an average of approximately seven treatments in the first year and those assigned to bevacizumab as needed received an average of approximately eight treatments, a difference that likely was real but likely not clinically relevant given the total number of injections given over 2 years; (5) although no difference between ranibizumab and bevacizumab participants was identified with respect to proportions of participants who had myocardial infarction, cerebrovascular accidents, or endophthalmitis, the combined bevacizumab groups had a higher rate of systemic serious adverse events (AEs) than the combined ranibizumab groups (24% for bevacizumab, 19% for ranibizumab) – of note, the point estimates for these systemic serious AEs was higher in the bevacizumab as-needed group than the bevacizumab every-4-weeks group, and the bevacizumab group might have been at greater risk based on slight imbalances in baseline characteristics in the bevacizumab group that favored the development of these serious systemic AES; and (6) the average cost of drug per patient for the first year was $23, 400 in the ranibizumab every-4-weeks group, $13 ,800 in the ranibizumab as-needed group, and $595 in the bevacizumab every-4-weeks group. Two-year data confirmed that every-4-week bevacizumab was equivalent to ranibizumab, the increased risk of serious systemic AEs with bevacizumab was sustained, and the average visual acuity in both the bevacizumab-as-needed and ranibizumab-as-needed groups continued to decline from year 1 to year 2.[49] In summary, there were some efficacy and safety differences favoring ranibizumab over bevacizumab if costs are not a consideration for the individual patient, although the large cost differences make bevacizumab the more cost-effective regimen from a societal perspective or from the business perspective of an insurance company.

The HARBOR trial confirmed the validity of using an “as needed” approach with monthly monitoring, but considered

mainly OCT in the decision process regarding retreatment ("≥ 5-letter decrease in vision from the previous visit or any evidence of disease activity on SD-OCT (e.g., intraretinal fluid, subretinal fluid, or subretinal pigment epithelial fluid)").[119] In this study, subjects received ranibizumab monthly or "as needed" following a 3-month loading period. After 24 months, the mean gain in visual acuity was 9.1 letters in the monthly group, compared with 7.9 in the "as needed" group. HARBOR also explored the use of 2.0 mg ranibizumab for neovascular AMD, but found slightly lower mean visual acuity gains at this higher does, and therefore no justification for going above the standard approved 0.5-mg dose.

The 1-year results from the IVAN trial comparing bevacizumab and ranibizumab, and continuous and discontinuous treatment[120] confirmed that the bevacizumab group appeared to have a slightly smaller mean gain in visual acuity at 1 year compared with the ranibizumab group (when combining both continuous and discontinuous treatment groups), and the discontinuous group (which required three consecutive monthly injections whenever treatment was resumed) appeared to have only a slightly smaller gain in mean visual acuity when compared with the continuous group (combining the ranibizumab and bevacizumab groups). Analysis of the 2-year follow-up data was likewise inconclusive with respect to noninferiority or inferiority of bevacizumab versus ranibizumab groups, and was also inconclusive with respect to continuous versus discontinuous therapy (equivalent after year 1).[121] Two important differences between this trial were that a noninferiority limit of 3.5 letters was used (in contrast with 5 letters in CATT), and comparisons between bevacizumab and ranibizumab regimens were pooled, such that comparisons of the "as needed" regimens of each agent were not made. Likewise, bevacizumab as needed was not compared with monthly ranibizumab, so the failure to confidently demonstrate noninferiority of as needed bevacizumab with monthly ranibizumab, observed in CATT, could not be confirmed or disproven in IVAN.

With the publication of the VIEW 1 and VIEW 2 results, another anti-VEGF agent, aflibercept, became available for the treatment of neovascular AMD. These trials confirmed that aflibercept given

every 4 weeks for three doses followed by every 8 weeks through 48 weeks gave equivalent outcomes to ranibizumab every 4 weeks.[111] Unlike ANCHOR and MARINA trials, the second year of these trials tested discontinuous therapy of each agent. Either aflibercept or ranibizumab was given at least every 12 weeks, as well as when retreatment was judged to be indicated based on clinical parameters, including OCT, as evaluated every 4 weeks. In the second year, a small decline in the average visual acuity for each group was seen. Because no head-to-head comparison with bevacizumab was done, prospective trial data cannot be used to comment on relative efficacy of bevacizumab with aflibercept in neovascular AMD. This question is of relevance since aflibercept, on average, has been shown to be superior to bevacizumab in a randomized clinical trial comparing them for diabetic macular edema involving the center of the macula when visual acuity was relatively impaired (20/50 or worse).[122] The treatment of diabetic macular edema is discussed in detail in Chapter 50 (Nonproliferative diabetic retinopathy and diabetic macular edema).

Safety of Anti-VEGF Therapy

Safety issues with anti-VEGF intravitreous injections include local ocular AEs from the drug or the injection, as well as potential systemic AEs of the drug. Ocular AEs may be categorized as common but not serious, and rare but potentially serious. AEs that are common but not serious include subconjunctival hemorrhage, vitreous floaters from medication or vitreous hemorrhage, and discomfort from antiseptic used to prepare the ocular surface before the injection. Endophthalmitis is a rare but potentially serious ocular AE that may develop after any intravitreous injection, regardless of what is being injected. Just how much preparation is necessary to minimize the development of postinjection infections is controversial. Based on data from the Diabetic Retinopathy Clinical Research Network, there is little evidence to support the need for pretreatment or posttreatment topical antibiotics.[123] Some clinicians use sterile gloves and drapes. All clinicians seem to agree that retraction of the eyelids with either a lid speculum or manual

retraction, and povidone iodine treatment for at least 30 seconds overlying the area to receive the injection, are recommended to minimize endophthalmitis risks. Other rare but serious ocular AEs include sterile inflammation, vitreous hemorrhage, retinal tear or detachment, and increased intraocular pressure, which in the ANCHOR and MARINA trials was listed as a serious AE (SAE) but might not always be considered an SAE by a treating ophthalmologist.

Systemic AEs from intravitreous anti-VEGF agents can be a theoretic, if not real, concern; VEGF inhibitors that cross into the general circulation can compromise functions that rely on VEGF outside of the eye, such as wound healing and the formation of new blood vessels around the heart or brain in cases of ischemia. Patients with AMD already are at higher risk of cardiovascular disease than the general population by virtue of their age, and patients with such risk were not systematically excluded from participating in these clinical trials. Consequently, participants in clinical trials of VEGF inhibitors were carefully monitored for possible increases in blood pressure, occurrence of myocardial infarction/stroke, and nonocular hemorrhages.

There was no evidence that ranibizumab 0.5 mg was associated with increases in either diastolic or systolic blood pressure in ANCHOR. In fact, treatment-related hypertension emerged in a larger proportion of PDT patients (12 of 143, or 8.4%) than among 0.5-mg ranibizumab patients (9 of 140, or 6.4%).[110] Among participants in the MARINA trial, approximately 16% in both the 0.5-mg ranibizumab and sham-injection groups developed hypertension.[86]

Nonocular hemorrhages include events such as cerebral or gastrointestinal bleeding. In the ANCHOR trial, nonocular hemorrhage was more frequent in the 0.5-mg ranibizumab group (6.4%) than in the PDT group (2.1%). In the MARINA trial, the cumulative frequency of nonocular hemorrhage by month 24 was 5.5% (13 of 236) in the sham-injection group, compared with 8.8% (21 of 239) in the 0.5-mg ranibizumab group.

With respect to cardiovascular or cerebrovascular events, during the ANCHOR trial, 1 subject in the PDT group (0.7%) and 3 subjects in the ranibizumab 0.5 mg group (2.1%) developed nonfatal

myocardial infarctions, although the events occurred at times that were unrelated to treatment. The frequency of stroke (1 in each group) and cerebral infarction (0 in each group) in the ANCHOR trial were too low to draw meaningful conclusions.

At 24 months, the overall frequency of cardiovascular systemic events in the MARINA trial was similar in the 0.5-mg ranibizumab and sham-injection groups. There were only small differences in the frequency of thromboembolic events between the sham-injection group (3.8%) and the ranibizumab 0.5-mg group (4.6%). The frequency of death (2.5%) was the same in the ranibizumab 0.5-mg and sham-injection groups. Two individuals in each group died of stroke. A pooled analysis of five of the ranibizumab clinical trials showed a trend for increasing risk of cerebrovascular accident (CVA) over 2 years, although a definitive risk could not be identified. The odds ratio for 0.5 mg ranibizumab versus control was 2.2 (95% confidence interval: 0.8–7.1), though among patients at high risk for CVA, the odds ratio was higher (7.7; 95% confidence interval 1.2–177, although if controlling for multiple analyses, or using a 99% CI because of the multiple analyses performed in this study, the confidence interval would cross 1.0, precluding one from determining with certainty if there was an increased risk among patients at high risk for CVA).[124]

A Cochrane systematic review on the systematic safety of ranibizumab and bevacizumab analyzed data from nine non-industry-sponsored studies (which included CATT and IVAN), including 3665 subjects.[125] The authors were not able to determine a difference between the agents for deaths, all serious systemic adverse events, or specific subsets of adverse events in the first 24 months of therapy, with the exception of gastrointestinal disorders. The authors did note heterogeneity of subjects across the included trials but concluded there was inadequate evidence to suggest that systemic safety should be used as a justification of policies mandating one anti-VEGF agent over another.[125] Although event rates for these cerebrovascular or cardiovascular events appear to be low with anti-VEGF agents, ophthalmologists should discuss the theoretic potential for these risks, since only a moderate or large difference in event rates, not a small difference, has been ruled out from the current literature.

Since ranibizumab is a recombinant monoclonal antibody (mAb) that contains both mouse- and human-derived segments, the human segments are engineered into the monoclonal antibody to minimize the chance that the patient's immune system will react against the mAb. Nevertheless, some patients treated with ranibizumab may develop antibodies to it. Thus, ranibizumab trials included routine testing of participants for antiranibizumab antibodies using an electrochemiluminescent assay.

In the ANCHOR trial, 8% of 0.5-mg ranibizumab subjects and 1.5% of subjects with PDT had low levels of antibodies to ranibizumab at baseline. At trial conclusion, 3.9% of 0.5-mg ranibizumab subjects had developed antibodies to ranibizumab, compared with 0% in the PDT group. In the MARINA trial, none of the subjects in the 0.5-mg ranibizumab group and 0.5% of those in the sham-injection group had antibodies to ranibizumab at baseline. After 24 months, 6.3% of subjects treated with ranibizumab 0.5 mg and 1.1% of those in the sham-injection group developed antibodies to ranibizumab.

The clinical implications of baseline and postexposure immunoreactivity to ranibizumab remain unclear. Although the numbers were small, subjects in the ANCHOR trial who were immunoreactive were more likely to develop inflammation than those who were not. In the HORIZON open-label extension study of both ANCHOR and MARINA in which subjects were treated "as needed," antiranibizumab antibodies were detected in <2.8% of subjects at months 36, 48, 60, or at an early termination visit in the subjects initially treated with ranibizumab and in none of the ranibizumab-untreated subjects, though this was a much smaller group (n=63 samples). Of 15 subjects who experienced intraocular inflammation for whom antibody status was obtained, 1 subject was antibody-positive and another's antibody data were missing.[126]

Evidence-Based Recommendations for Clinical Practice

Based on the information summarized above and published from other randomized clinical trials, the following implications should be considered.

If treatment with bevacizumab is to be initiated in an eye with CNV due to AMD, the patient should be informed that using bevacizumab, treatment every 4 weeks for at least the next year, without dependence on OCT or other imaging, has been shown by CATT to be equivalent to ranibizumab every 4 weeks. The ophthalmologist should keep in mind that comparison of visual acuity outcomes when bevacizumab or ranibizumab from treatment initiation, or aflibercept starting 1 year after treatment initiation, was given "as needed," with examinations every 4 weeks, visual acuity outcomes appeared, on average, to be slightly worse. While a slightly worse outcome may not be clinically relevant one year after treatment initiation, it becomes relevant if the decline in the average visual acuity continues 2 years or more after initiating treatment, as it appears to do at least from 1–2 years after treatment initiation. Also, the ophthalmologist and patient must keep the following in mind: There are potentially slightly better visual acuity outcomes with ranibizumab as needed or aflibercept as needed or aflibercept every other month after several monthly injections when compared with outcomes using bevacizumab as needed but not necessarily bevacizumab monthly. However, from the societal perspective or perspective of the business of the insurance company, the knowledge that the use of bevacizumab leads to a very cost-effective management of this condition compared with use of ranibizumab or aflibercept should be considered.

Ranibizumab given as needed with examinations every 4 weeks, including OCT, to detect features that suggest the need for retreatment, provides equivalent visual acuity outcomes to ranibizumab every 4 weeks at 1 year and 2 years, but the regimen has not been evaluated beyond 2 years, when physicians must base their management on the individual patient's response for the previous two years. Aflibercept every-4 weeks for three doses followed by every-8-weeks to 1 year also provides equivalent results to every-4-weeks ranibizumab; when the group given this regimen received an as-needed regimen starting at 1 year, the average visual acuity declined by 2 years, although not by a clinically relevant amount. However, if this decline were to continue during treatment 3 or 5 years after initiating therapy, the

decline could be clinically relevant.

Follow-Up After Deciding to Initiate Anti-VEGF Therapy for Neovascular AMD

Fig. 69.18 provides one approach[113] to consider if monthly anti-VEGF therapy with bevacizumab or ranibizumab, or three monthly doses of aflibercept followed by every-2-months aflibercept, is not employed. The approach considers repeating therapy as long as improvement is noted on subjective symptoms, visual acuity, biomicroscopic examination, OCT, or fluorescein angiography. The approach errs on the side of treatment since failure to treat when VEGF is present could result in irreversible visual acuity loss from fibrosis involving the retina or RPE.

Another approach, known as "treat and extend," is widely used in the United States.[127] In this regimen, monthly therapy is administered until the macular OCT is free of fluid, and then the treatment interval is extended, typically by 1–2 weeks.[128] Several retrospective studies[129–131] and noncomparative prospective trials[132,133] have demonstrated improvement in visual acuity using treat and extend approaches. Limitations in the current retrospective studies include losses to follow-up which can bias the results, retrospective data collection, which also can bias the results, and an inability to know whether the cases might have done even better (or worse) if followed monthly with an "as needed" regimen for 2 years. The 1-year results of a prospective trial comparing monthly ranibizumab to a treat-and-extend regimen using ranibizumab showed change in vision in the treat-and-extend arm was no worse than (not inferior to) the monthly arm with a noninferiority margin (lower bounds of the 95% confidence interval in the difference in the outcomes between the arms) of 5 letters. However, the formal noninferiority results were not presented in the publication, nor were details of baseline characteristics for each treatment group. Differences in baseline characteristics in this relatively small study could have biased the results provided.[134] Additional prospective trials are underway or being planned,[128] which may help clarify any efficacy hierarchy among these three alternatives.

Long-Term Results of Anti-VEGF Therapy

Most of the previously mentioned clinical trials of anti-VEGF agents followed subjects monthly for 24 months. There have been several reports of longer-term follow-up with large losses to follow-up that can bias the results to look better than the real results may be using treatment of anti-VEGF therapy for neovascular AMD,[126,135,136] all of which reveal a decline of visual acuity back to near baseline over 5–7 years. None of the studies continued monthly treatment or evaluation, and all were subject to high loss to follow-up rates. Several investigators have noted increased prevalence or growth of geographic atrophy with long-term anti-VEGF therapy[137] including an apparent "dose-response" in CATT with monthly ranibizumab causing more atrophy than bevacizumab and more in the continuous arms versus the "as needed" arms,[138,139] though it is not clear if such lesions are a result of the underlying disease (drusen going on to geographic atrophy because CNV and scar were avoided with anti-VEGF treatment), an alternative to fibrotic scar (a thin atrophic scar mimicking geographic atrophy), or an actual side-effect of VEGF blockade increasing the chance of drusen to progress to geographic atrophy compared with whether no anti-VEGF is given.[140–142] Since some of these studies[141] have shown progression of geographic atrophy in an eye receiving anti-VEGF therapy to be similar to the progression of geographic atrophy in the fellow eye in the absence of anti-VEGF therapy, at least some of the progressive geographic atrophy likely is due to the natural history of drusen progressing to geographic atrophy in the absence of CNV and scar avoided by the anti-VEGF treatment.

Previously Employed Therapies

Prior to the advent of anti-VEGF therapy, several methods of treatment were employed in the treatment of neovascular AMD that are rarely in use today. These are fully discussed in the previous edition of this volume[143] and are summarized only briefly below.

Laser Treatment of Well-Defined Choroidal

Neovascular Lesions

Laser photocoagulation was shown to be beneficial[33–35] for well-defined lesions not involving the foveal center or very small lesions involving the foveal center with a component of classic CNV. Failure to cover the entire lesion increases the likelihood of recurrent CNV[144–146] and additional visual acuity loss.[144,146,147] Since treatment destroys retinal tissue (and corresponding function),[146] such treatment generally is reserved only for cases that are extrafoveal and in which it is judged that a scotoma from the laser is preferred over proceeding with anti-VEGF therapy.

Photodynamic Therapy

Until 1999, no treatment other than laser photocoagulation had been shown to reduce the risk of vision loss in patients with CNV from AMD in large-scale, randomized clinical trials. The TAP Study Group[92,148] reported that PDT with verteporfin (Visudyne) can reduce the risk of moderate and severe visual acuity loss for at least 2 years in patients with predominantly classic subfoveal lesions.[101] For occult with no classic lesions, the Verteporfin In Photodynamic therapy (VIP) Trial in AMD showed that PDT could reduce the risk of moderate and severe visual acuity loss at 2 years, though the primary outcome was not met.[99]

PDT involves the use of an intravenously injected photosensitizing drug combined with a low-intensity laser light to cause damage of choroidal neovascular tissue through a photochemical reaction by the light-activated drug that appears to result in direct cellular injury, including damage to vascular endothelial cells and vessel thrombosis.[149,150] While most individuals lose some vision after PDT, this may not apply for patients with the polypoidal choroidal vasculopathy pattern of CNV, as suggested in small studies within an Asian population.[151] PCV is discussed further in Chapter 74 (Polypoidal choroidal vasculopathy).

Submacular Surgery

Studies, including a Cochrane systematic review,[152] have shown

that visual acuity outcomes with submacular surgery are no different compared with observation for subfoveal CNV in patients with AMD in which a majority of the lesion is CNV and there is evidence of classic CNV.[36] Alternative surgical approaches have also been explored for managing CNV and its neovascular complications, including macular translocation[153] and mechanical displacement of relatively large submacular hemorrhages using intraocular gas injection. A 2008 Cochrane systematic review identified only one randomized controlled trial comparing macular translocation to PDT and found the evidence was insufficient to recommend this intervention,[154,155] a conclusion that must recognize even greater differences likely would be seen if compared to anti-VEGF therapy. In a 5-year retrospective review of results from the 56 cases out of 255 cases whose complete records were available, there was a mean gain of 1.5 lines of vision from baseline. This led the authors to recommend consideration of macular translocation only to patients with bilateral disease unlikely to respond to anti-VEGF therapy,[156] and even then, the large bias of the results when almost 80% of the cases were missing from the 5-year follow-up suggests extreme caution with this conclusion.

When AMD-related CNV is associated with a large submacular hemorrhage, intraocular injection of gas with or without pars plana vitrectomy and face-forward or face-down positioning may allow for mechanical displacement of the blood and the potential for at least temporary recovery of visual acuity.[157–160] The improvement may not have long-term benefit if the underlying neovascular lesion and its accompanying destruction of the retina, not the blood, determines the ultimate visual outcome. For this reason, anti-VEGF therapy alone may be sufficient for some of these lesions.[115] Pars plana vitrectomy for clearing of hemorrhage that has broken through into the vitreous cavity also may be considered and may be lower risk than surgeries that involve mechanical manipulation of the retina itself.

Radiation Therapy

The use of radiation therapy for CNV in AMD is based on the possibility that radiation can damage rapidly proliferating

neovascular tissue. Several early studies were inconsistent in documenting a benefit to this approach, either using external beam, plaques, or use of a probe with local irradiation.[161–163] A 2010 Cochrane systematic review of 13 trials of various design likewise concluded that the body of literature does not provide support for this approach and urged consideration of some form of masking in future trials.[164] A more recent randomized controlled trial comparing epiretinal macular brachytherapy in 494 treatment-naive patients demonstrated that the radiation plus ranibizumab was inferior to quarterly plus "as needed" ranibizumab.[165,166] Studies that have evaluated the potential of these therapies to reduce the number of intravitreous injections have not provided concomitant evidence of similar or improved visual acuity outcomes in association with a decreased number of intravitreous injections.[167]

Other Pharmacologic Therapies and Combination Therapies

A variety of other pharmacologic therapies are under investigation for the treatment of neovascular AMD, including inhibitors of platelet-derived growth factor,[168] complement,[169] and inflammatory modulators.[170] In addition, novel delivery devices for pharmacologic therapies,[171] and combinations of therapies, are under investigation,[172,173] as are viral vector-based gene therapy to deliver anti-VEGF[174] and other inhibitors of angiogenesis.[175] Given the public health importance and biologic variability of visual acuity outcomes with CNV in AMD, changes in the management of CNV in AMD should be influenced strongly by large-scale, appropriately designed randomized clinical trials with adequate follow-up that show benefit before new therapies are incorporated into standard practice.

Early Identification of Choroidal Neovascularization

It has become critically important to identify, while potentially still at a treatable stage, those eyes at high risk for visual loss soon after

developing CNV. Unfortunately, the likelihood of finding a case that will benefit from treatment appears to be time-dependent. FA studies have suggested growth of CNV lesions at an average rate of 10–18 μm per day.[176,177] Grey and colleagues[178] reported that patients with acute visual loss from AMD are more likely to still have extrafoveal CNV if they are examined within the first month after the onset of symptoms.

Clearly, identifying lesions before they extend under the foveal center, or more often, when visual acuity loss may be minimal even if the lesion extends under the foveal center, is worthwhile. Furthermore, identifying lesions while visual acuity is relatively good might result in better levels of final visual acuity since most cases treated with anti-VEGF therapy avoid substantial visual acuity loss but fewer than 50% have substantial visual acuity gain. A substudy of the Age-Related Eye Disease Study 2 that randomized patients at high risk for CNV to home testing with a hyperacuity visual field device versus conventional monitoring evaluated the decrease in visual acuity at the time of CNV detection. The study was terminated early by the Data and Safety Monitoring Committee at a prespecified interim analysis due to achievement of statistical significance with an average of fewer letters lost from baseline in the device arm (4 letters) compared with standard care monitoring (9 letters).[179] Similar technology also may prove helpful in monitoring patients already under treatment for neovascular AMD.[180] Whether other devices, such as those that can be used on smartphones, will be able to provide similar or better results remains to be proven in further studies.

Prevention of Choroidal Neovascularization

The Age-Related Eye Disease Study (AREDS) suggested that dietary supplements of vitamins C, E, beta-carotene, and zinc can reduce the chance of CNV developing in eyes with large drusen, especially when retinal pigment epithelial abnormalities were present and when these features were in both eyes.[181] Likewise the AREDS 2 study demonstrated that while the substitution of lutein

and zeaxanthin for beta-carotene did not reduce progression to CNV compared with the beta-carotene formulation, this substitution may reduce the risk of lung cancer in current or recently former smokers.[182] The Complications of Age-related Macular Degeneration Prevention Trial (CAPT) was not able to demonstrate that light laser photocoagulation, which has been associated with a decreased visualization of drusen,[183] can prevent the development of complications of AMD associated with visual loss, including CNV and geographic atrophy.

Risk of Fellow-Eye Involvement

When one eye has developed CNV, it is important to monitor the other eye for CNV.[184] Development of CNV in the second eye can be devastating, since patients may have functioned quite well with good vision in their remaining eye but would be abruptly confronted for the first time with severe lifestyle impairment with development of CNV in both eyes. It is therefore paramount to discover and treat CNV as soon as possible to maximize the possibility of detecting treatable lesions. Because patients may be aware of symptoms only when the fovea has become involved, it would be useful to stratify risk based on fundus appearance and perhaps employ more aggressive monitoring strategies in those deemed at high risk.

The investigators of the MPS Group studied the eyes of 670 patients enrolled in the trials of laser therapy for extrafoveal, juxtafoveal, and subfoveal CNV to identify fundus characteristics that might be predictive of CNV development in the uninvolved fellow eyes.[185–187] Follow-up ranged from 3 to 5 years and revealed an overall incidence of 35%, which is consistent with previously reported figures. Application of life table estimation methods to this data yielded cumulative incidence rates of 10%, 28%, and 42% at 1, 3, and 5 years respectively. Three characteristics of the central macula and one systemic factor were associated independently with increased risk of developing CNV: the presence of five or more drusen, one or more large drusen, focal hyperpigmentation, and systemic hypertension. A substantial difference in prognosis was seen depending on the number of risk factors present. Estimated 5-

year incidence rates ranged from 7% for the subgroup with no risk factors to 87% for the subgroup with all four risk factors. Similarly, in AREDS, subjects enrolled with advanced AMD (either neovascular AMD or central atrophy of the RPE) in one eye only at study entry had a 43% chance of developing advanced AMD in the fellow eye by 5 years.[181] The type of CNV present in the affected eye, classic versus occult, appeared to have no effect on the rate of CNV development in the fellow eye. It must be stressed that these figures do not apply to patients with non-neovascular abnormalities only in both eyes. They are, however, very important in counseling the AMD patient who has just experienced the initial development of CNV in one eye with respect to prognosis and frequency of follow-up to try to protect the vision in the other eye.

Patient Education and Rehabilitation

Patient education is an extremely important part of the management of patients with AMD. All patients over the age of 50 who have drusen should be made aware of the importance of regular central visual acuity testing in each eye to facilitate early detection of CNV. Although the Amsler grid is often recommended, it is not particularly sensitive or specific; frequently, changes in near or distance vision herald underlying neovascularization not detected by the patient on an Amsler grid.[17] Therefore, patients experiencing any change in vision in eyes at risk for neovascularization should be encouraged to contact their ophthalmologist promptly. Although patients should be counseled about the risk of severe central visual loss, they should also be reassured that AMD almost never leads to total blindness. Patients at risk should be informed that, in its more severe neovascular form, central visual tasks can be severely and permanently impaired. In light of the therapeutic implications of prompt anti-VEGF therapy when indicated, the importance of quickly reporting new visual symptoms must be stressed to all patients. At the same time, they should be reassured that no harm will come by continuing to read or perform routine visual tasks. On the contrary, patients should be encouraged to continue reading and to pursue vigorously any visual activity that they enjoy.

Treatment does not end in the physician's office when the diagnosis is established or when anti-VEGF therapy is applied. Visual rehabilitation forms an integral part of patient care in AMD. Patients with central visual impairment should be evaluated and educated in the use of visual aids such as magnifiers. Magnification and improved contrast sensitivity through bright illumination are particularly helpful. To arrive at the best magnifying aid, one starts with a complete low visual evaluation. In addition, the patient should be counseled on available low-vision materials such as large-print newspapers, magazines, and books, as well as tablets and e-readers with high contrast screens and enlargeable fonts. Large-print materials or electronically magnified text permit many people who are unable to read normal print to continue reading for a considerable period of time. Many newspapers and periodicals are currently published in large-print editions or electronically as available through the internet. The local library can assist with the selection of magazines and books available in large print. The Library of Congress in Washington, DC, maintains a list of books and magazines available on loan without cost on virtually every subject. The combination of bright illumination, powerful magnification, high contrast, and large type allows all but the most severely impaired patients to continue reading, albeit on a more limited scale. Reading skills frequently need to be re-learned in a painstakingly slow process. Nevertheless, the ability to continue reading, even on a limited basis, may provide tremendous psychological benefit to these patients. Some patients with AMD may find the use of a closed-circuit television viewer helpful for reading. This machine uses a projection device to magnify one or several words on to a television screen. Unfortunately, this instrument is large and fairly expensive; thus it is generally purchased by people with sufficient economic means for use in primarily one location such as at work or at home. However, the nearly ubiquitous availability of electronic tablets, with their ability to magnify, has proven beneficial in place of more cumbersome closed-circuit television systems. For those patients who are unable to take advantage of large-print materials or who cannot use magnification devices, talking books or recordings are available. These may be borrowed through local libraries or from the Library

of Congress. Audio recordings of popular books are also sold at many bookstores and through web services such as Audible.com.

Patients with severe visual loss require early referral to an appropriate agency for low vision so that they can take advantage of community support services. Information can be obtained from the Directory of Agencies serving the visually handicapped in the United States through the American Foundation for the Blind. The American Foundation for the Blind also provides information regarding other aids such as talking books and clocks and watches that audibly tell time.

Because AMD can place severe restrictions on many activities such as driving and rapid reading of small print, visual rehabilitation efforts are directed toward preserving the patient's independence as much as possible. Toward this end, social service consultations are invaluable. In addition, in-house evaluations by agencies designed to assist the visually impaired are useful in helping with activities of daily living. Simple recommendations, such as using brightly colored utensils on a white or black background in the kitchen, as well as suggestions on improving existing lighting, can be of tremendous benefit. Similar ideas aimed at increasing contrast may improve the quality of life for these patients. Patients often become frustrated because of their inability to perform certain fine visual tasks, such as reading and sewing. Unable to recognize faces from across the room, patients with visual loss from AMD may feel isolated and withdraw from social contact. In the absence of any external tell-tale signs of blindness, friends and relatives may attribute the lack of recognition to a sudden “snobbishness” rather than to visual impairment. Patient and family alike should be educated about these problems. In particular, patients should be encouraged to become more outgoing, which in turn fosters recognition of others through speech rather than vision. Discussion of the patient's problems by the physician often helps to relieve patients of much of their burdens.

Ophthalmologists must recognize that older patients can have difficulty coping with the new onset of severe visual loss. Patients may resist efforts to use magnifying devices for a variety of reasons, including denial and secondary gain. Often tremulousness

interferes with the patient's ability to use certain aids. All these conditions may increase the tendency to depression or anxiety that many patients with visual loss have, including patients with AMD.[188,189] In addition to caring for the eye, the ophthalmologist should serve as the patient's advocate, marshaling his or her resources for the patient's benefit. This includes compassionate support, educating the patient and family, and making appropriate referrals to maintain the patient's quality of life. With complete care of the patient, many individuals at risk for, or suffering severe visual loss from, neovascular AMD can continue to enjoy fulfilling lives.

Disclosure

The Johns Hopkins University School of Medicine receives research grants from Bayer, Genentech/Roche, Lumenis, Novartis, Optovue, Regeneron, for N.M.B.'s or S.B.B.'s effort in research activities with those industries.

References

1. Friedman DS, O'Colmain BJ, Munoz B, et al. Prevalence of age-related macular degeneration in the United States. *Arch Ophthalmol*. 2004;122(4):564–572.
2. Bressler NM, Doan QV, Varma R, et al. Estimated cases of legal blindness and visual impairment avoided using ranibizumab for choroidal neovascularization: non-Hispanic white population in the United States with age-related macular degeneration. *Arch Ophthalmol*. 2011;129(6):709–717.
3. Bressler NM, Bressler SB, Fine SL. Age-related macular degeneration. *Surv Ophthalmol*. 1988;32(6):375–413.
4. Ferris FL, Fine SL, Hyman L. Age-related macular degeneration and blindness due to neovascular maculopathy. *Arch Ophthalmol*. 1984;102(11):1640–1642.
5. Sommer A, Tielsch JM, Katz J, et al. Racial differences in the cause-specific prevalence of blindness in east Baltimore. *N Engl J Med*. 1991;325(20):1412–1417.

6. Schultz DW, Klein ML, Humpert AJ, et al. Analysis of the ARMD1 locus: evidence that a mutation in HEMICENTIN-1 is associated with age-related macular degeneration in a large family. *Hum Mol Genet*. 2003;12(24):3315–3323.
7. Black JR, Clark SJ. Age-related macular degeneration: genome-wide association studies to translation. *Genet Med*. 2016;18(4):283–289.
8. Katsi VK, Marketou ME, Vrachatis DA, et al. Essential hypertension in the pathogenesis of age-related macular degeneration: a review of the current evidence. *J Hypertens*. 2015;33(12):2382–2388.
9. Hyman L, Schachat AP, He Q, Leske MC. Hypertension, cardiovascular disease, and age-related macular degeneration. Age-Related Macular Degeneration Risk Factors Study Group. *Arch Ophthalmol*. 2000;118(3):351–358.
10. Taylor HR, West S, Munoz B, Rosenthal FS, Bressler SB, Bressler NM. The long-term effects of visible light on the eye. *Arch Ophthalmol*. 1992;110(1):99–104.
11. Liew G, Mitchell P, Wong TY, Rochtchina E, Wang JJ. The association of aspirin use with age-related macular degeneration. *JAMA Intern Med*. 2013;173(4):258–264.
12. Christen WG, Chew EY. Does long-term aspirin use increase the risk of neovascular age-related macular degeneration? *Expert Opin Drug Safety*. 2014;13(4):421–429.
13. Sobrin L, Seddon JM. Regular aspirin use and risk of age-related macular degeneration. *Am J Ophthalmol*. 2013;156(2):213–217.e2.
14. Kaul S, Diamond GA. Relationship of aspirin use with age-related macular degeneration: association or causation? Comment on "The association of aspirin use with age-related macular degeneration". *JAMA Intern Med*. 2013;173(4):264–266.
15. Covinsky KE. The incremental nature of clinical research: Comment on "The association of aspirin use with age-related macular degeneration". *JAMA Intern Med*. 2013;173(4):266.
16. Dong LM, Stark WJ, Jefferys JL, et al. Progression of age-related macular degeneration after cataract surgery. *Arch*

Ophthalmol. 2009;127(11):1412–1419.
17. Fine AM, Elman MJ, Ebert JE, Prestia PA, Starr JS, Fine SL. Earliest symptoms caused by neovascular membranes in the macula. *Arch Ophthalmol*. 1986;104(4):513–514.
18. Loewenstein A, Bressler N, Bressler S. *Epidemiology of RPE disease. Retinal pigment epithelium: current aspects of function and disease*. Oxford University Press: New York; 1999.
19. Green WR, Key SN 3rd. Senile macular degeneration: a histopathologic study. *Trans Am Ophthalmol Soc*. 1977;75:180–254.
20. Green WR, Enger C. Age-related macular degeneration histopathologic studies. The 1992 Lorenz E. Zimmerman Lecture. *Ophthalmology*. 1993;100(10):1519–1535.
21. Bressler SB, Silva JC, Bressler NM, Alexander J, Green WR. Clinicopathologic correlation of occult choroidal neovascularization in age-related macular degeneration. *Arch Ophthalmol*. 1992;110(6):827–832.
22. Green WR, McDonnell PJ, Yeo JH. Pathologic features of senile macular degeneration. *Ophthalmology*. 1985;92(5):615–627.
23. Bressler NM, Chang TS, Suner IJ, et al. Vision-related function after ranibizumab treatment by better- or worse-seeing eye: clinical trial results from MARINA and ANCHOR. *Ophthalmology*. 2010;117(4):747–756.e4.
24. Doyle W, Davidof F, Makley T, et al. Histopathology of an active lesion of ocular histoplasmosis. *Ophthal Forum*. 1984;2:105–111.
25. Schatz H, McDonald HR, Johnson RN. Retinal pigment epithelial folds associated with retinal pigment epithelial detachment in macular degeneration. *Ophthalmology*. 1990;97(5):658–665.
26. Bird AC, Marshall J. Retinal pigment epithelial detachments in the elderly. *Trans Ophthalmol Soc U K*. 1986;105(Pt 6):674–682.
27. Macular Photocoagulation Study Group. Subfoveal neovascular lesions in age-related macular degeneration. Guidelines for evaluation and treatment in the macular photocoagulation study. *Arch Ophthalmol*. 1991;109(9):1242–

1257.
28. Elman MJ, Fine SL, Murphy RP, Patz A, Auer C. The natural history of serous retinal pigment epithelium detachment in patients with age-related macular degeneration. *Ophthalmology*. 1986;93(2):224–230.
29. Bressler NM, Bressler SB, Childs AL, et al. Surgery for hemorrhagic choroidal neovascular lesions of age-related macular degeneration: ophthalmic findings: SST report no. 13. *Ophthalmology*. 2004;111(11):1993–2006.
30. Wood WJ, Smith TR. Senile disciform macular degeneration complicated by massive hemorrhagic retinal detachment and angle closure glaucoma. *Retina*. 1983;3(4):296–303.
31. el Baba F, Jarrett WH 2nd, Harbin TS Jr, et al. Massive hemorrhage complicating age-related macular degeneration. Clinicopathologic correlation and role of anticoagulants. *Ophthalmology*. 1986;93(12):1581–1592.
32. Ying GS, Maguire MG, Daniel E, Grunwald JE, Ahmed O, Martin DF. Association between antiplatelet or anticoagulant drugs and retinal or subretinal hemorrhage in the comparison of age-related macular degeneration treatments trials. *Ophthalmology*. 2016;123(2):352–360.
33. Macular Photocoagulation Study Group. Laser photocoagulation of subfoveal recurrent neovascular lesions in age-related macular degeneration. Results of a randomized clinical trial. *Arch Ophthalmol*. 1991;109(9):1232–1241.
34. Macular Photocoagulation Study Group. Laser photocoagulation of subfoveal neovascular lesions in age-related macular degeneration. *Arch Ophthalmol*. 1991;109(9):1220.
35. Macular Photocoagulation Study Group. Laser photocoagulation for juxtafoveal choroidal neovascularization. Five-year results from randomized clinical trials. Macular Photocoagulation Study Group. *Arch Ophthalmol*. 1994;112(4):500–509.
36. Hawkins BS, Bressler NM, Miskala PH, et al. Surgery for subfoveal choroidal neovascularization in age-related macular degeneration: ophthalmic findings: SST report no.

11. *Ophthalmology*. 2004;111(11):1967–1980.
37. de Jong PT, Chakravarthy U, Rahu M, et al. Associations between aspirin use and aging macula disorder: the European Eye Study. *Ophthalmology*. 2012;119(1):112–118.
38. Haller Yeo J, Marcus S, Murphy RP. Retinal pigment epithelial tears. *Ophthalmology*. 1988;95(1):8–13.
39. Cantrill HL, Ramsay RC, Knobloch WH. Rips in the pigment epithelium. *Arch Ophthalmol*. 1983;101(7):1074–1079.
40. Decker WL, Sanborn GE, Ridley M, Annesley WH Jr, Sorr EM. Retinal pigment epithelial tears. *Ophthalmology*. 1983;90(5):507–512.
41. Green SN, Yarian D. Acute tear of the retinal pigment epithelium. *Retina*. 1983;3(1):16–20.
42. Cunningham ET Jr, Feiner L, Chung C, Tuomi L, Ehrlich JS. Incidence of retinal pigment epithelial tears after intravitreal ranibizumab injection for neovascular age-related macular degeneration. *Ophthalmology*. 2011;118(12):2447–2452.
43. Grossniklaus HE, Green WR. Histopathologic and ultrastructural findings of surgically excised choroidal neovascularization. Submacular Surgery Trials Research Group. *Arch Ophthalmol*. 1998;116(6):745–749.
44. Grossniklaus HE, Miskala PH, Green WR, et al. Histopathologic and ultrastructural features of surgically excised subfoveal choroidal neovascular lesions: submacular surgery trials report no. 7. *Arch Ophthalmol*. 2005;123(7):914–921.
45. Gass JDM. *Stereoscopic atlas of macular diseases: diagnosis and treatment*. 4th ed. Mosby Inc: St. Louis; 1997.
46. Grossniklaus HE, Green WR. Choroidal neovascularization. *Am J Ophthalmol*. 2004;137(3):496–503.
47. Lafaut BA. Clinicopathological correlation in exudative age related macular degeneration: histological differentiation between classic and occult choroidal neovascularisation. *Br J Ophthalmol*. 2000;84(3):239–243.
48. Submacular Surgery Trials Research Group. Comparison of 2D reconstructions of surgically excised subfoveal choroidal neovascularization with fluorescein angiographic features:

SST report no. 15. *Ophthalmology*. 2006;113(2):279.e1–279.e5.
49. Margalit E, Bressler NM. Retinal pigment epithelium tumorlike lesion arising from an area treated with laser photocoagulation. *Arch Ophthalmol*. 2003;121(1):130–132.
50. Comparison of Age-related Macular Degeneration Treatments Trials Research Group. Ranibizumab and bevacizumab for treatment of neovascular age-related macular degeneration: two-year results. *Ophthalmology*. 2012;119(7):1388–1398.
51. The CATT Research Group. Ranibizumab and bevacizumab for neovascular age-related macular degeneration. *N Engl J Med*. 2011;364(20):1897–1908.
52. Schachat AP, Thompson JT. Optical coherence tomography, fluorescein angiography, and the management of neovascular age-related macular degeneration. *Ophthalmology*. 2015;122(2):222–223.
53. Kuehlewein L, Bansal M, Lenis TL, et al. Optical coherence tomography angiography of type 1 neovascularization in age-related macular degeneration. *Am J Ophthalmol*. 2015;160(4):739–748.e2.
54. Castillo MM, Mowatt G, Elders A, et al. Optical coherence tomography for the monitoring of neovascular age-related macular degeneration: a systematic review. *Ophthalmology*. 2015;122(2):399–406.
55. Heier J. *Final Results from a phase 2 study of squalamine lactate ophthalmic solution 0.2% (OHR-102) in neovascular age-related macular degeneration (AMD)*. American Society of Retina Specialists: Vienna, Austria; 2015.
56. Dyer DS, Brant AM, Schachat AP, Bressler SB, Bressler NM. Angiographic features and outcome of questionable recurrent choroidal neovascularization. *Am J Ophthalmol*. 1995;120(4):497–505.
57. Sykes SO, Bressler NM, Maguire MG, Schachat AP, Bressler SB. Detecting recurrent choroidal neovascularization. Comparison of clinical examination with and without fluorescein angiography. *Arch Ophthalmol*. 1994;112(12):1561–1566.
58. Barbazetto I, Burdan A, Bressler NM, et al. Photodynamic

therapy of subfoveal choroidal neovascularization with verteporfin: fluorescein angiographic guidelines for evaluation and treatment – TAP and VIP report no. 2. *Arch Ophthalmol*. 2003;121(9):1253–1268.
59. Submacular Surgery Trials Research Group. Guidelines for interpreting retinal photographs and coding findings in the Submacular Surgery Trials (SST): SST report no. 8. *Retina*. 2005;25(3):253–268.
60. Koenig F, Soubrane G, Coscas G. [Angiographic aspects of senile macular degeneration: spontaneous course.]. *J Fr Ophtalmol*. 1984;7(2):93–98.
61. Hyman LG, Lilienfeld AM, Ferris FL 3rd, Fine SL. Senile macular degeneration: a case–control study. *Am J Epidemiol*. 1983;118(2):213–227.
62. Yannuzzi LA, Negrao S, Iida T, et al. Retinal angiomatous proliferation in age-related macular degeneration. *Retina*. 2001;21(5):416–434.
63. Bressler NM, Bressler SB, Alexander J, et al. Loculated fluid: a previously undescribed angiographic finding in macular degeneration. *Arch Ophthalmol*. 1991;109:211–215.
64. Chuang EL, Bird AC. The pathogenesis of tears of the retinal pigment epithelium. *Am J Ophthalmol*. 1988;105(3):285–290.
65. Regillo CD, Benson WE, Maguire JI, Annesley WH Jr. Indocyanine green angiography and occult choroidal neovascularization. *Ophthalmology*. 1994;101(2):280–288.
66. Yannuzzi LA, Slakter JS, Sorenson JA, Guyer DR, Orlock DA. Digital indocyanine green videoangiography and choroidal neovascularization. *Retina*. 1992;12(3):191–223.
67. Tan CS, Ngo WK, Chen JP, Tan NW, Lim TH. EVEREST study report 2: imaging and grading protocol, and baseline characteristics of a randomised controlled trial of polypoidal choroidal vasculopathy. *Br J Ophthalmol*. 2015;99(5):624–628.
68. Pang CE, Freund KB. Pachychoroid neovasculopathy. *Retina*. 2015;35(1):1–9.
69. MacCumber MW, Dastgheib K, Bressler NM, et al. Clinicopathologic correlation of the multiple recurrent serosanguineous retinal pigment epithelial detachments

syndrome. *Retina*. 1994;14(2):143–152.
70. Bressler NM, Bressler SB. Indocyanine green angiography. Can it help preserve the vision of our patients? *Arch Ophthalmol*. 1996;114(6):747–749.
71. Killingsworth MC, Sarks JP, Sarks SH. Macrophages related to Bruch's membrane in age-related macular degeneration. *Eye (Lond)*. 1990;4(4 Pt 4):613–621.
72. Ambati J, Ambati BK, Yoo SH, Ianchulev S, Adamis AP. Age-related macular degeneration: etiology, pathogenesis, and therapeutic strategies. *Surv Ophthalmol*. 2003;48(3):257–293.
73. Bressler NM, Silva JC, Bressler SB, Fine SL, Green WR. Clinicopathologic correlation of drusen and retinal pigment epithelial abnormalities in age-related macular degeneration. *Retina*. 1994;14(2):130–142.
74. Curcio CA, Millican CL. Basal linear deposit and large drusen are specific for early age-related maculopathy. *Arch Ophthalmol*. 1999;117(3):329–339.
75. Sarks SH. Drusen and their relationship to senile macular degeneration. *Aust N Z J Ophthalmol*. 1980;8(2):117–130.
76. Sarks SH, Van Driel D, Maxwell L, Killingsworth M. Softening of drusen and subretinal neovascularization. *Trans Ophthalmol Soc U K*. 1980;100(3):414–422.
77. Sarks SH. Ageing and degeneration in the macular region: a clinico-pathological study. *Br J Ophthalmol*. 1976;60(5):324–341.
78. Sarks S, Penfold P, Killingsworth M, Van Driel D. Patterns in macular degeneration. *Retinal Dis*. 1985;87–93.
79. Kenyon KR, Maumenee AE, Ryan SJ, Whitmore PV, Green WR. Diffuse drusen and associated complications. *Am J Ophthalmol*. 1985;100(1):119–128.
80. Eagle RC Jr. Mechanisms of maculopathy. *Ophthalmology*. 1984;91(6):613–625.
81. Heriot WJ, Henkind P, Bellhorn RW, Burns MS. Choroidal neovascularization can digest Bruch's membrane. *Ophthalmology*. 1984;91(12):1603–1608.
82. Loffler KU, Lee WR. Basal linear deposit in the human macula. *Graefes Arch Clin Exp Ophthalmol*. 1986;224(6):493–

501.
83. Penfold PL, Killingsworth MC, Sarks SH. Senile macular degeneration: the involvement of immunocompetent cells. *Graefes Arch Clin Exp Ophthalmol*. 1985;223(2):69–76.
84. Penfold PL, Provis JM, Billson FA. Age-related macular degeneration: ultrastructural studies of the relationship of leucocytes to angiogenesis. *Graefes Arch Clin Exp Ophthalmol*. 1987;225(1):70–76.
85. Campochiaro PA, Hackett SF, Vinores SA, et al. Platelet-derived growth factor is an autocrine growth stimulator in retinal pigmented epithelial cells. *J Cell Sci*. 1994;107(Pt 9):2459–2469.
86. Rosenfeld PJ, Brown DM, Heier JS, et al. Ranibizumab for neovascular age-related macular degeneration. *N Engl J Med*. 2006;355(14):1419–1431.
87. Glaser BM. Extracellular modulating factors and the control of intraocular neovascularization: an overview. *Arch Ophthalmol*. 1988;106(5):603–607.
88. Macular Photocoagulation Study Group. Argon laser photocoagulation for neovascular maculopathy: 3-year results from randomized clinical trials. *Arch Ophthal*. 1986;104(5):694.
89. Macular Photocoagulation Study Group. Argon laser photocoagulation for neovascular maculopathy. Five-year results from randomized clinical trials. *Arch Ophthalmol*. 1991;109(8):1109–1114.
90. Macular Photocoagulation Study Group. Argon laser photocoagulation for senile macular degeneration. *Arch Ophthal*. 1982;100(6):912.
91. Macular Photocoagulation Study Group. Laser photocoagulation of subfoveal neovascular lesions of age-related macular degeneration. *Arch Ophthal*. 1993;111(9):1200.
92. Treatment of Age-Related Macular Degeneration with Photodynamic Therapy (TAP) Study Group. Photodynamic therapy of subfoveal choroidal neovascularization in age-related macular degeneration with verteporfin: two-year results of 2 randomized clinical trials – TAP report 2. *Arch*

Ophthalmol. 2001;119(2):198–207.
93. Treatment of Age-Related Macular Degeneration with Photodynamic Therapy (TAP) Study Group. Effect of lesion size, visual acuity, and lesion composition on visual acuity change with and without verteporfin therapy for choroidal neovascularization secondary to age-related macular degeneration: TAP and VIP report no. 1. *Am J Ophthalmol*. 2003;136(3):407–418.
94. Bressler NM, Frost LA, Bressler SB, Murphy RP, Fine SL. Natural course of poorly defined choroidal neovascularization associated with macular degeneration. *Arch Ophthalmol*. 1988;106(11):1537–1542.
95. Bressler NM, Maguire MG, Murphy PL, et al. Macular scatter ("grid") laser treatment of poorly demarcated subfoveal choroidal neovascularization in age-related macular degeneration. *Arch Ophthalmol*. 1996;114(12):1456–1464.
96. Macular Photocoagulation Study Group. Occult Choroidal Neovascularization: Influence on visual outcome in patients with age-related macular degeneration. *Arch Ophthalmol*. 1996;114(4):400.
97. Soubrane G, Coscas G, Francais C, Koenig F. Occult subretinal new vessels in age-related macular degeneration. Natural history and early laser treatment. *Ophthalmology*. 1990;97(5):649–657.
98. Tani PM, Buettner H, Robertson DM. Massive vitreous hemorrhage and senile macular choroidal degeneration. *Am J Ophthalmol*. 1980;90(4):525–533.
99. Visudyne® In Minimally Classic Choroidal Neovascularization Study Group. Verteporfin therapy of subfoveal choroidal neovascularization in age-related macular degeneration: two-year results of a randomized clinical trial including lesions with occult with no classic choroidal neovascularization –verteporfin in photodynamic therapy report 2. *Am J Ophthalmol*. 2001;131(5):541–560.
100. Treatment of Age-Related Macular Degeneration with Photodynamic Therapy (TAP) Study Group. Natural history of minimally classic subfoveal choroidal

neovascular lesions in the treatment of age-related macular degeneration with photodynamic therapy (TAP) investigation: outcomes potentially relevant to management – TAP report no. 6. *Arch Ophthalmol*. 2004;122(3):325–329.
101. Treatment of Age-Related Macular Degeneration with Photodynamic Therapy (TAP) Study Group. Verteporfin therapy of subfoveal choroidal neovascularization in patients with age-related macular degeneration: additional information regarding baseline lesion composition's impact on vision outcomes – TAP report no. 3. *Arch Ophthalmol*. 2002;120(11):1443–1454.
102. Avery RL, Fekrat S, Hawkins BS, Bressler NM. Natural history of subfoveal subretinal hemorrhage in age-related macular degeneration. *Retina*. 1996;16(3):183–189.
103. Bennett SR, Folk JC, Blodi CF, Klugman M. Factors prognostic of visual outcome in patients with subretinal hemorrhage. *Am J Ophthalmol*. 1990;109(1):33–37.
104. Berrocal MH, Lewis ML, Flynn HW Jr. Variations in the clinical course of submacular hemorrhage. *Am J Ophthalmol*. 1996;122(4):486–493.
105. Hanscom TA. Diddie KR. Early surgical drainage of macular subretinal hemorrhage. *Arch Ophthalmol*. 1987;105(12):1722–1723.
106. Lewis H. Intraoperative fibrinolysis of submacular hemorrhage with tissue plasminogen activator and surgical drainage. *Am J Ophthalmol*. 1994;118(5):559–568.
107. Bressler NM. Submacular surgery. Are randomized trials necessary? *Arch Ophthalmol*. 1995;113(12):1557–1560.
108. Bressler NM, Finklestein D, Sunness JS, Maguire AM, Yarian D. Retinal pigment epithelial tears through the fovea with preservation of good visual acuity. *Arch Ophthalmol*. 1990;108(12):1694–1697.
109. Schoeppner G, Chuang EL, Bird AC. The risk of fellow eye visual loss with unilateral retinal pigment epithelial tears. *Am J Ophthalmol*. 1989;108(6):683–685.
110. Brown DM, Kaiser PK, Michels M, et al. Ranibizumab versus verteporfin for neovascular age-related macular degeneration. *N Engl J Med*. 2006;355(14):1432–1444.

111. Heier JS, Brown DM, Chong V, et al. Intravitreal aflibercept (VEGF trap-eye) in wet age-related macular degeneration. *Ophthalmology*. 2012;119(12):2537–2548.
112. Solomon SD, Lindsley K, Vedula SS, Krzystolik MG, Hawkins BS. Anti-vascular endothelial growth factor for neovascular age-related macular degeneration. *Cochrane Database Syst Rev*. 2014;(8) [CD005139].
113. Bressler NM. Antiangiogenic approaches to age-related macular degeneration today. *Ophthalmology*. 2009;116(10 Suppl.):S15–23.
114. Chang MA, Do DV, Bressler SB, Cassard SD, Gower EW, Bressler NM. Prospective one-year study of ranibizumab for predominantly hemorrhagic choroidal neovascular lesions in age-related macular degeneration. *Retina*. 2010;30(8):1171–1176.
115. Shienbaum G, Garcia Filho CA, Flynn HW Jr, Nunes RP, Smiddy WE, Rosenfeld PJ. Management of submacular hemorrhage secondary to neovascular age-related macular degeneration with anti-vascular endothelial growth factor monotherapy. *Am J Ophthalmol*. 2013;155(6):1009–1013.
116. Chang TS, Bressler NM, Fine JT, et al. Improved vision-related function after ranibizumab treatment of neovascular age-related macular degeneration: results of a randomized clinical trial. *Arch Ophthalmol*. 2007;125(11):1460–1469.
117. Bressler NM, Chang TS, Fine JT, Dolan CM, Ward J. Improved vision-related function after ranibizumab vs photodynamic therapy: a randomized clinical trial. *Arch Ophthalmol*. 2009;127(1):13–21.
118. Miskala PH, Bressler NM, Meinert CL. Relative contributions of reduced vision and general health to NEI-VFQ scores in patients with neovascular age-related macular degeneration. *Arch Ophthalmol*. 2004;122(5):758–766.
119. Ho AC, Busbee BG, Regillo CD, et al. Twenty-four-month efficacy and safety of 0.5 mg or 2.0 mg ranibizumab in patients with subfoveal neovascular age-related macular degeneration. *Ophthalmology*. 2014;121(11):2181–2192.
120. IVAN Study Investigators. Ranibizumab versus

bevacizumab to treat neovascular age-related macular degeneration: one-year findings from the IVAN randomized trial. *Ophthalmology*. 2012;119(7):1399–1411.
121. Chakravarthy U, Harding SP, Rogers CA, et al. Alternative treatments to inhibit VEGF in age-related choroidal neovascularisation: 2-year findings of the IVAN randomised controlled trial. *Lancet*. 2013;382(9900):1258–1267.
122. Wells JA, Glassman AR, Ayala AR, et al. Aflibercept, bevacizumab, or ranibizumab for diabetic macular edema. *N Engl J Med*. 2015;372(13):1193–1203.
123. Bhavsar AR, Googe JM Jr, Stockdale CR, et al. Risk of endophthalmitis after intravitreal drug injection when topical antibiotics are not required: the diabetic retinopathy clinical research network laser–ranibizumab–triamcinolone clinical trials. *Arch Ophthalmol*. 2009;127(12):1581–1583.
124. Bressler NM, Boyer DS, Williams DF, et al. Cerebrovascular accidents in patients treated for choroidal neovascularization with ranibizumab in randomized controlled trials. *Retina*. 2012;32(9):1821–1828.
125. Moja L, Lucenteforte E, Kwag KH, et al. Systemic safety of bevacizumab versus ranibizumab for neovascular age-related macular degeneration. *Cochrane Database Syst Rev*. 2014;(9) [CD011230].
126. Singer MA, Awh CC, Sadda S, et al. HORIZON: an open-label extension trial of ranibizumab for choroidal neovascularization secondary to age-related macular degeneration. *Ophthalmology*. 2012;119(6):1175–1183.
127. Rezaei KA. *2015 Global trends in retina survey*. American Society of Retina Specialists: Vienna, Austria; 2015.
128. Freund KB, Korobelnik JF, Devenyi R, et al. Treat-and-extend regimens with anti-VEGF agents in retinal diseases: a literature review and consensus recommendations. *Retina*. 2015;35(8):1489–1506.
129. Gupta OP, Shienbaum G, Patel AH, Fecarotta C, Kaiser RS, Regillo CD. A treat and extend regimen using ranibizumab for neovascular age-related macular degeneration clinical and economic impact. *Ophthalmology*. 2010;117(11):2134–

2140.
130. Shienbaum G, Gupta OP, Fecarotta C, Patel AH, Kaiser RS, Regillo CD. Bevacizumab for neovascular age-related macular degeneration using a treat-and-extend regimen: clinical and economic impact. *Am J Ophthalmol*. 2012;153(3):468–473.e1.
131. Oubraham H, Cohen SY, Samimi S, et al. Inject and extend dosing versus dosing as needed: a comparative retrospective study of ranibizumab in exudative age-related macular degeneration. *Retina*. 2011;31(1):26–30.
132. Fung AT, Kumar N, Vance SK, et al. Pilot study to evaluate the role of high-dose ranibizumab 2.0 mg in the management of neovascular age-related macular degeneration in patients with persistent/recurrent macular fluid <30 days following treatment with intravitreal anti-VEGF therapy (the LAST Study). *Eye (Lond)*. 2012;26(9):1181–1187.
133. Berg K, Pedersen TR, Sandvik L, Bragadottir R. Comparison of ranibizumab and bevacizumab for neovascular age-related macular degeneration according to LUCAS treat-and-extend protocol. *Ophthalmology*. 2015;122(1):146–152.
134. Wykoff CC, Croft DE, Brown DM, et al. Prospective trial of treat-and-extend versus monthly dosing for neovascular age-related macular degeneration: TREX-AMD 1-year results. *Ophthalmology*. 2015;122(12):2514–2522.
135. Gillies MC, Campain A, Barthelmes D, et al. Long-term outcomes of treatment of neovascular age-related macular degeneration: data from an observational study. *Ophthalmology*. 2015;122(9):1837–1845.
136. Rofagha S, Bhisitkul RB, Boyer DS, Sadda SR, Zhang K. Seven-year outcomes in ranibizumab-treated patients in ANCHOR, MARINA, and HORIZON: a multicenter cohort study (SEVEN-UP). *Ophthalmology*. 2013;120(11):2292–2299.
137. Bhisitkul RB, Mendes TS, Rofagha S, et al. Macular atrophy progression and 7-year vision outcomes in subjects from the ANCHOR, MARINA, and HORIZON studies: the SEVEN-UP study. *Am J Ophthalmol*. 2015;159(5):915–924.e2.
138. Grunwald JE. Author reply: To PMID 24084496.

Ophthalmology. 2014;121(7):e35.
139. Grunwald JE, Pistilli M, Ying GS, et al. Growth of geographic atrophy in the comparison of age-related macular degeneration treatments trials. *Ophthalmology*. 2015;122(4):809–816.
140. Channa R, Sophie R, Bagheri S, et al. Regression of choroidal neovascularization results in macular atrophy in anti-vascular endothelial growth factor-treated eyes. *Am J Ophthalmol*. 2015;159(1):9–19.e1-2.
141. Tanaka E, Chaikitmongkol V, Bressler SB, Bressler NM. Vision-threatening lesions developing with longer-term follow-up after treatment of neovascular age-related macular degeneration. *Ophthalmology*. 2015;122(1):153–161.
142. Sophie R, Wang J, Campochiaro PA. Re: Grunwald et al.: Risk of geographic atrophy in the comparison of age-related macular degeneration treatments trials. *Ophthalmology*. 2014;121(7):150–161.
143. Ryan SJ. *Retina*. 5th ed. Saunders: St. Louis; 2013.
144. Macular Photocoagulation Study Group. Persistent and recurrent neovascularization after krypton laser photocoagulation for neovascular lesions of age-related macular degeneration. *Arch Ophthalmol*. 1990;108(6):825–831.
145. Macular Photocoagulation Study Group. Persistent and recurrent neovascularization after laser photocoagulation for subfoveal choroidal neovascularization of age-related macular degeneration. *Arch Ophthalmol*. 1994;112(4):489–499.
146. Macular Photocoagulation Study Group. The influence of treatment extent on the visual acuity of eyes treated with Krypton laser for juxtafoveal choroidal neovascularization. *Ophthalmol*. 1995;113(2):190–194.
147. Macular Photocoagulation Study Group. Recurrent choroidal neovascularization after argon laser photocoagulation for neovascular maculopathy. *Arch Ophthalmol*. 1986;104(4):503–512.
148. Photodynamic therapy of subfoveal choroidal neovascularization in age-related macular degeneration

with verteporfin: one-year results of 2 randomized clinical trials – TAP report. Treatment of age-related macular degeneration with photodynamic therapy (TAP) Study Group. *Arch Ophthalmol*. 1999;117(10):1329–1345.
149. Miller JW, Schmidt-Erfurth U, Sickenberg M, et al. Photodynamic therapy with verteporfin for choroidal neovascularization caused by age-related macular degeneration: results of a single treatment in a phase 1 and 2 study. *Arch Ophthalmol*. 1999;117(9):1161–1173.
150. Schmidt-Erfurth U, Miller JW, Sickenberg M, et al. Photodynamic therapy with verteporfin for choroidal neovascularization caused by age-related macular degeneration: results of retreatments in a phase 1 and 2 study. *Arch Ophthalmol*. 1999;117(9):1177–1187.
151. Koh A, Lee WK, Chen LJ, et al. EVEREST study: efficacy and safety of verteporfin photodynamic therapy in combination with ranibizumab or alone versus ranibizumab monotherapy in patients with symptomatic macular polypoidal choroidal vasculopathy. *Retina*. 2012;32(8):1453–1464.
152. Giansanti F, Eandi CM, Virgili G. Submacular surgery for choroidal neovascularisation secondary to age-related macular degeneration. *Cochrane Database Syst Rev*. 2009;(2) [CD006931].
153. de Juan E Jr, Loewenstein A, Bressler NM, Alexander J. Translocation of the retina for management of subfoveal choroidal neovascularization II: a preliminary report in humans. *Am J Ophthalmol*. 1998;125(5):635–646.
154. Eandi CM, Giansanti F, Virgili G. Macular translocation for neovascular age-related macular degeneration. *Cochrane Database Syst Rev*. 2008;(4) [CD006928].
155. Gelisken F, Voelker M, Schwabe R, et al. Full macular translocation versus photodynamic therapy with verteporfin in the treatment of neovascular age-related macular degeneration: 1-year results of a prospective, controlled, randomised pilot trial (FMT-PDT). *Graefes Arch Clin Exp Ophthalmol*. 2007;245(8):1085–1095.
156. van Romunde SH, Polito A, Bertazzi L, Guerriero M, Pertile

G. Long-term results of full macular translocation for choroidal neovascularization in age-related macular degeneration. *Ophthalmology*. 2015;122(7):1366–1374.
157. Hassan AS, Johnson MW, Schneiderman TE, et al. Management of submacular hemorrhage with intravitreous tissue plasminogen activator injection and pneumatic displacement. *Ophthalmology*. 1999;106(10):1900–1906 [discussion 6–7].
158. Kadonosono K, Arakawa A, Yamane S, et al. Displacement of submacular hemorrhages in age-related macular degeneration with subretinal tissue plasminogen activator and air. *Ophthalmology*. 2015;122(1):123–128.
159. Chang W, Garg SJ, Maturi R, et al. Management of thick submacular hemorrhage with subretinal tissue plasminogen activator and pneumatic displacement for age-related macular degeneration. *Am J Ophthalmol*. 2014;157(6):1250–1257.
160. Martel JN, Mahmoud TH. Subretinal pneumatic displacement of subretinal hemorrhage. *JAMA Ophthalmol*. 2013;131(12):1632–1635.
161. Bergink GJ, Hoyng CB, van der Maazen RW, Vingerling JR, van Daal WA, Deutman AF. A randomized controlled clinical trial on the efficacy of radiation therapy in the control of subfoveal choroidal neovascularization in age-related macular degeneration: radiation versus observation. *Graefes Arch Clin Exp Ophthalmol*. 1998;236(5):321–325.
162. Spaide RF, Guyer DR, McCormick B, et al. External beam radiation therapy for choroidal neovascularization. *Ophthalmology*. 1998;105(1):24–30.
163. A prospective, randomized, double-masked trial on radiation therapy for neovascular age-related macular degeneration (RAD Study). Radiation therapy for age-related macular degeneration. *Ophthalmology*. 1999;106(12):2239–2247.
164. Evans JR, Sivagnanavel V, Chong V. Radiotherapy for neovascular age-related macular degeneration. *Cochrane Database Syst Rev*. 2010;(5) [CD004004].
165. Jackson TL, Dugel PU, Bebchuk JD, et al. Epimacular

brachytherapy for neovascular age-related macular degeneration (CABERNET): fluorescein angiography and optical coherence tomography. *Ophthalmology*. 2013;120(8):1597–1603.
166. Dugel PU, Bebchuk JD, Nau J, et al. Epimacular brachytherapy for neovascular age-related macular degeneration: a randomized, controlled trial (CABERNET). *Ophthalmology*. 2013;120(2):317–327.
167. Jackson TL, Chakravarthy U, Slakter JS, et al. Stereotactic radiotherapy for neovascular age-related macular degeneration: year 2 results of the INTREPID study. *Ophthalmology*. 2015;122(1):138–145.
168. Dong A, Seidel C, Snell D, et al. Antagonism of PDGF-BB suppresses subretinal neovascularization and enhances the effects of blocking VEGF-A. *Angiogenesis*. 2014;17(3):553–562.
169. Weismann D, Hartvigsen K, Lauer N, et al. Complement factor H binds malondialdehyde epitopes and protects from oxidative stress. *Nature*. 2011;478(7367):76–81.
170. Xie B, Shen J, Dong A, Rashid A, Stoller G, Campochiaro PA. Blockade of sphingosine-1-phosphate reduces macrophage influx and retinal and choroidal neovascularization. *J Cell Physiol*. 2009;218(1):192–198.
171. Kim AJ, Boylan NJ, Suk JS, Lai SK, Hanes J. Non-degradative intracellular trafficking of highly compacted polymeric DNA nanoparticles. *J Control Release*. 2012;158(1):102–107.
172. Kaiser PK, Boyer DS, Cruess AF, et al. Verteporfin plus ranibizumab for choroidal neovascularization in age-related macular degeneration: twelve-month results of the DENALI study. *Ophthalmology*. 2012;119(5):1001–1010.
173. Larsen M, Schmidt-Erfurth U, Lanzetta P, et al. Verteporfin plus ranibizumab for choroidal neovascularization in age-related macular degeneration: twelve-month MONT BLANC study results. *Ophthalmology*. 2012;119(5):992–1000.
174. Pechan P, Rubin H, Lukason M, et al. Novel anti-VEGF chimeric molecules delivered by AAV vectors for inhibition of retinal neovascularization. *Gene Ther*. 2009;16(1):10–16.

175. Prea SM, Chan EC, Dusting GJ, Vingrys AJ, Bui BV, Liu GS. Gene Therapy with endogenous inhibitors of angiogenesis for neovascular age-related macular degeneration: beyond anti-VEGF therapy. *J Ophthalmol*. 2015;2015:201726.
176. Klein ML, Jorizzo PA, Watzke RC. Growth features of choroidal neovascular membranes in age-related macular degeneration. *Ophthalmology*. 1989;96(9):1416–1419 [discussion 20–1].
177. Vander JF, Morgan CM, Schatz H. Growth rate of subretinal neovascularization in age-related macular degeneration. *Ophthalmology*. 1989;96(9):1422–1426 [discussion 6–9].
178. Grey RH, Bird AC, Chisholm IH. Senile disciform macular degeneration: features indicating suitability for photocoagulation. *Br J Ophthalmol*. 1979;63(2):85–89.
179. Chew EY, Clemons TE, Bressler SB, et al. Randomized trial of a home monitoring system for early detection of choroidal neovascularization home monitoring of the Eye (HOME) study. *Ophthalmology*. 2014;121(2):535–544.
180. Querques G, Querques L, Rafaeli O, Canoui-Poitrine F, Bandello F, Souied EH. Preferential hyperacuity perimeter as a functional tool for monitoring exudative age-related macular degeneration in patients treated by intravitreal ranibizumab. *Invest Ophthalmol Vis Sci*. 2011;52(9):7012–7018.
181. Age-Related Eye Disease Study Research Group. A randomized, placebo-controlled, clinical trial of high-dose supplementation with vitamins C and E, beta carotene, and zinc for age-related macular degeneration and vision loss: AREDS report no. 8. *Arch Ophthalmol*. 2001;119(10):1417–1436.
182. Lutein + zeaxanthin and omega-3 fatty acids for age-related macular degeneration: the Age-Related Eye Disease Study 2 (AREDS2) randomized clinical trial. *JAMA*. 2013;309(19):2005–2015.
183. Choroidal Neovascularization Prevention Trial Research Group. Laser treatment in eyes with large drusen. Short-term effects seen in a pilot randomized clinical trial. *Ophthalmology*. 1998;105(1):11–23.

184. Thomas MA, Grand MG, Williams DF, Lee CM, Pesin SR, Lowe MA. Surgical management of subfoveal choroidal neovascularization. *Ophthalmology*. 1992;99(6):952–968 [discussion 75–6].
185. The Macular Photocoagulation Study Group. Relationship of drusen and abnormalities of the retinal pigment epithelium to the prognosis of neovascular macular degeneration. *Arch Ophthalmol*. 1990;108(10):1442–1447.
186. Macular Photocoagulation Study Group. Five-year follow-up of fellow eyes of patients with age-related macular degeneration and unilateral extrafoveal choroidal neovascularization. *Arch Ophthalmol*. 1993;111(9):1189–1199.
187. Macular Photocoagulation Study Group. Risk factors for choroidal neovascularization in the second eye of patients with juxtafoveal or subfoveal choroidal neovascularization secondary to age-related macular degeneration. *Arch Ophthalmol*. 1997;115(6):741–747.
188. Rovner BW, Casten RJ, Hegel MT, et al. Low vision depression prevention trial in age-related macular degeneration: a randomized clinical trial. *Ophthalmology*. 2014;121(11):2204–2211.
189. Casten R, Rovner BW, Leiby BE, Tasman W. Depression despite anti-vascular endothelial growth factor treatment of age-related macular degeneration. *Arch Ophthalmol*. 2010;128(4):506–508.

70

Pharmacotherapy of Age-Related Macular Degeneration

Loh-Shan B. Leung, Marco A. Zarbin, Philip J. Rosenfeld, Brian Toy, Daniel F. Martin, Mark S. Blumenkranz

Introduction

Age-related macular degeneration (AMD) is a spectrum of related diseases that have in common the progressive decline of vision as a

consequence of dysfunction of the central retina and its underlying supporting elements, principally the retinal pigment epithelium (RPE) and choroid in older adults.[1] Although the disease is seen in all racial and ethnic groups, it is more commonly encountered in females and light-skinned individuals and typically presents after the 7th decade.[2–5] The disease has been traditionally classified into early, intermediate, and late stages.[1]

The early stages consist of alterations in the coloration of the macular pigment epithelium, both hypo- and hyperpigmentation, and the presence of drusen of greater than 125 μm in diameter. The early phases have been variously referred to as nonexudative, preangiogenic, or dry AMD (Fig. 70.1). The intermediate stage of the disease consists of more extensive medium sized or large sized drusen. In contrast, exudative or neovascular AMD is a late onset phenomenon, occurring in eyes with high risk characteristics including the presence of extensive soft drusen, Bruch's membrane thickening, and focal hyperpigmentation. This phase of the disease is characteristically accompanied by rapid loss of vision over a period of 6–12 months and the development of a central disciform fibrotic scar. Without intervention, the visual acuity generally decreases to the range 20/200 or worse, over the 12 months following the onset of this phase.[3,5] In light of major improvements in therapy for this condition in the past 5–10 years, previously employed forms of treatment, including thermal laser photocoagulation and surgery, are now viewed to have limited benefit for this condition, particularly when it presents with involvement of the center of the fovea.[6–10] In recent years, AMD therapy has become increasingly targeted toward specific molecular pathways. The discovery of multiple genes and markers for AMD and neovascularization has identified a significant number of new targets for pharmacotherapy.

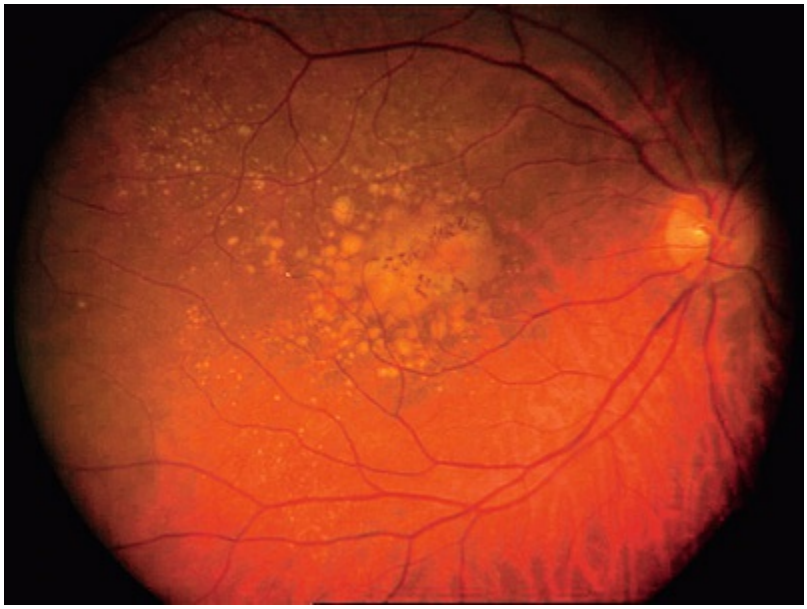

FIG. 70.1 Color fundus photograph of right eye patient with early age-related macular degeneration. Note the extensive drusen throughout the posterior pole, some of which appear calcific and others large and soft. The patient has not yet progressed to the stage of either geographic atrophy, or choroidal neovascularization.

Relevant to the purpose of this chapter, it is important to understand that the mechanisms of vision loss in AMD differ according to the stage, and that different stages may be amenable to different points of attack.[2,5] Importantly, at least two separate and distinct mechanisms for vision loss occur in exudative AMD: (1) Proliferation of new vessels accompanied by secondary fibrosis and disorganization of the pigment epithelium and outer retina, which is a somewhat gradual process; (2) secondary alterations in the permeability of retinal and choroidal vessels accompanied by retinal pigment epithelial dysfunction leading to the accumulation of serous or serosanguinous fluid beneath the RPE, neurosensory retina, or within the retina itself, and are associated with more acute visual dysfunction. Preventing the vision loss associated with advanced forms of nonexudative disease has proved more challenging. In recent years an increased understanding of the mechanisms underlying drusen formation, pigment epithelial senescence, and loss of photoreceptors and choriocapillaris has made it more feasible to address therapeutically, visual dysfunction arising from the atrophic form of the disease (Fig. 70.2).

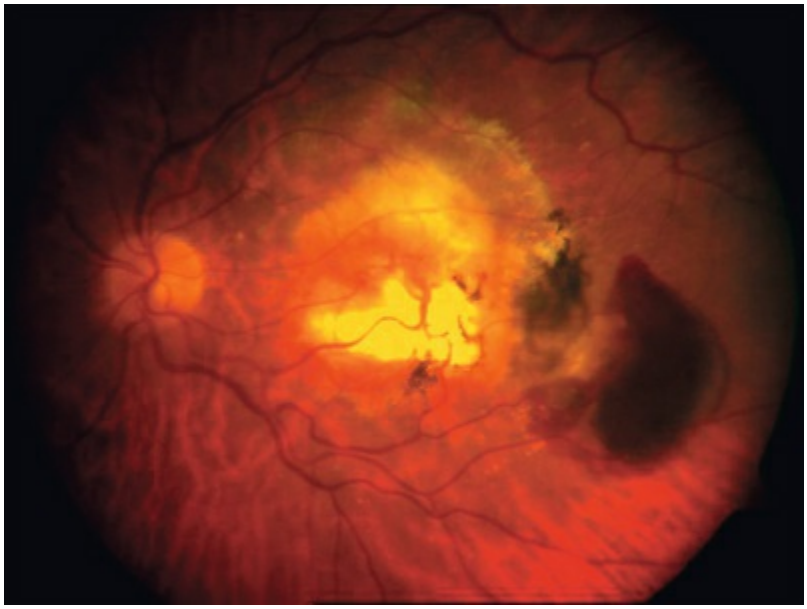

FIG. 70.2 Color photograph of the left eye of another patient with the severe form of late exudative age-related macular degeneration. Note the extensive scarring beneath the sensory retina, hemorrhage, and lipid exudation.

Etiologic Factors

A variety of factors are thought to play a role in the development of AMD, including genetic susceptibility, a localized inflammatory state, and a host of potentially modifiable environmental factors, including smoking, comorbidities, diet, medications, and light exposure.[11]

The Genetics of Complement in AMD

Over the last decade high-resolution genome scans for susceptibility loci in populations enriched for either choroidal neovascularization (CNV), geographic atrophy (GA), or both suggest susceptibility loci on numerous chromosomes. A number of candidate genes and their functions are listed in Table 70.1. An exhaustive discussion of the genetics and postulated mechanisms of AMD is beyond the scope of this chapter; however, several genes deserve mention.

TABLE 70.1
Candidate Genes for Age-Related Macular Degeneration

Location	Gene	Function	Strength of Association
1p22.1	*ABCA4*	ATP binding/ATPase	Possible
1q25–1q32	*HMCN1*	Extracellular matrix	Possible
1q31.3	*CFH*	Complement component	Established
3p21.3	*CX3CR1*	Chemokine receptor regulator of immune response	Probable
4q35.1	*TLR3*	Toll-like receptor: activator of inflammatory cytokine response to viral dsRNA	Possible
6p12	*VEGFA*	Regulator of angiogenesis and vascular permeability	Possible
6p21.3	*C2*	Complement component (classical pathway)	Probable
6p21.3	*CFB*	Complement component (alternate pathway)	Probable
6q24–q14	*ELOVL4*	Photoreceptor-specific elongation enzyme of long-chain fatty acids	Possible
9p24	*VLDLR*	VLDL transporter	Possible
9q32–q33	*TLR4*	Activates inflammatory immunity in response to bacterial lipopolysaccharide	Possible
10q26.13	*HTRA1*	Serine protease	Locus established, individual gene contributions unknown
10q26.13	*PLEKHA1*	Phospholipid-binding protein	
10q26.13	*ARMS2*	Unknown	
12p11–p13	*LRP6*	Wnt signaling protein	Possible
14q32.12	*FBLN5*	ECM protein, promotes endothelial cell adhesion	Possible
19p13.3	*C3*	Complement component	Probable
19q13.2	*APOE*	Lipoprotein binding, internalization, metabolism	Established
22q12.3	*TIMP3*	Metalloproteinase inhibitor (extracellular matrix protein)	Possible

A significant breakthrough in the study of AMD genetics came in 2005, when it was discovered that single nucleotide polymorphisms (SNPs) in the regulation of the complement activation locus (RCA) of chromosome 1q31.3 increased the risk of AMD. The RCA locus contains the gene encoding complement factor H (*CFH*). The tyr402his protein polymorphism increased the risk of AMD between 2.7- and 7.4-fold and appeared to account for between 43% and 50% of the attributable risk of AMD. Additionally, it has been suggested that CFH genotypes may influence an individual's response to certain treatment modalities and medications, including bevacizumab, photodynamic therapy with verteporfin, and AREDS nutritional supplementation.[12–16] *CFH* is responsible for

downregulating activation of the complement system, including c5b-9, known as the membrane attack complex (MAC). MAC is thought to be important in the immune-mediated damage to the choriocapillaris and the RPE and an important pathogenic component of drusen.[17,18]

Two recent studies found protective associations against the development of advanced AMD in those with genetic polymorphisms of the complement components C2 (Odds ratio 0.35–0.46) and complement factor B (CFB) (OR 0.35–0.44). The complement component C3 is the central part of the complement cascade, and its gene, located on chromosome 19, is a candidate for involvement in AMD, in part because its cleavage component C3a has been identified in drusen.[19,20a,20b] Additionally, C3 has also been associated with the development of GA (OR 2.66–3.9). Fig. 70.3 illustrates other complement components implicated in the pathogenesis of AMD.

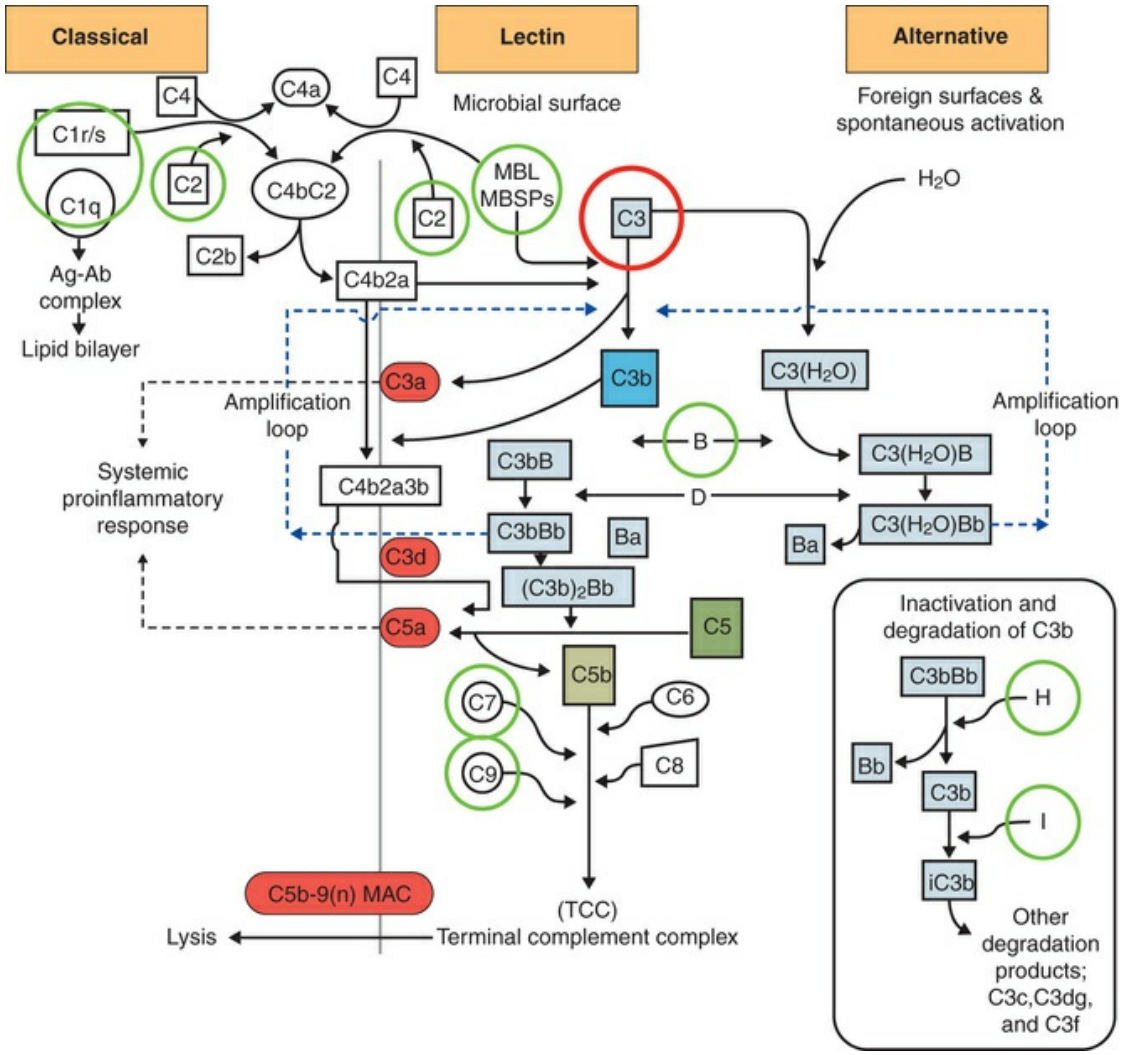

FIG. 70.3 AMD-associated mutations in the complement cascade. Four major activation pathways for the complement system are known, and three of these are illustrated. (The fibrinolytic-activated Intrinsic pathway is not shown.) Activation of the complement system plays an important role in immunity. Inappropriate complement activation can damage tissue. Multiple complement components have been linked to AMD (green circles), including drusen, geographic atrophy, and choroidal neovascularizations. Complement C3 (red circle) is the key point of convergence of all activation pathways.

(Reproduced with permission from Zarbin M, Rosenfeld, PJ. Review of emerging treatments for age-related macular degeneration. In: Stratton RD, Hauswirth WW, Gardner TW, editors. Oxidative stress in applied basic research and clinical practice: Studies in retinal and choroidal disorders. New York: Humana Press; 2012.)

Other Associated Genes

The genetic locus on chromosome 10q26 is the home to three genes, PLEKHA1, ARMS2, and HTRA1, which have been associated with AMD. Among these, ARMS2 has been the most consistent association, but its function is as yet unknown. HTRA1, in contrast, has been localized to drusen, but its association with AMD is inconsistent.[20c] The gene products of tissue inhibitor of metalloproteinase 3 (TIMP-3, chromosome 22) and endothelial growth factor (EGF) containing fibulin-like extracellular matrix protein 1 (EFEMP-1, chromosome 2), which act to inhibit the stimulatory effects of vascular endothelial growth factor (VEGF) on vascular cells, have been independently associated with advanced AMD in genome scans mentioned previously.[21,22] Multiple distinct alleles in exon5 of the gene encoding TIMP-3 have been causally linked to Sorsby fundus dystrophy, an autosomal dominant form of exudative macular degeneration with phenotypic similarities to exudative AMD,[23–25] although it is not thought to account for the majority of patients with exudative AMD.[26] TIMP-3 is also found in increasing quantities and associated with thickening of Bruch's membrane during aging, including within drusen and the RPE.[27–29] An Arg to Trp mutation in EFEMP-1 is thought to cause the abnormal accumulation of extensive drusen in malattia leventinese, an inherited macular degenerative disease with phenotypic characteristics closely correlated with advanced nonexudative AMD.[27,30]

Early onset macular retinal degenerations such as Stargardt disease, characterized by the accumulation of lipofuscin within the RPE, have shed light on both the pathophysiology of RPE apoptosis and potential therapeutic avenues.[31,32] While initial reports also suggested that the *ABCR* gene linked to Stargardt disease might also be a dominant susceptibility locus for AMD, subsequent investigators have been unable to confirm this apparent increased frequency.[33,34] Nonetheless, increased amounts of lipofuscin are present in both Stargardt disease and in the earlier stages of the nonexudative AMD, and both diseases are characterized by GA in their later stages, suggesting that an understanding of the common pathways expressed by these two different diseases may provide some pharmacologic insights. Biochemical studies on the lipofuscin

found in both Stargardt disease and AMD confirm that the principal component is A2E, which accumulates in cells of the RPE and results in RPE apoptosis, photoreceptor death, and vision loss.[18,35,36] This process is thought to be initiated by light activation of rhodopsin in the course of normal visual transduction as the first reactant in A2E biosynthesis. Isotretinoin, which slows the synthesis of 11-*cis* retinaldehyde and regeneration of rhodopsin, is able to slow the accumulation of lipofuscin in ABCR knock-out mice and also aged wild-type mice.[35] This suggests that compounds with mechanisms of action similar to isotretinoin, which is structurally related to vitamin A, may represent another therapeutic avenue for the slowing or prevention of AMD.[18,32,34–36]

Environmental Factors

Diet

The principal environmental factors thought to be associated with age-related macular degeneration include diet, history of smoking, light exposure, and use of supplemental medications. Earlier AREDS reports have established a relationship between dietary intake of omega-3 long-chain polyunsaturated fatty acids and reduced risk of neovascular AMD (Odds ratio 0.61), as well as progression from drusen to GA.[37–39] A large case control study has suggested that higher dietary intake of carotenoids, particularly lutein and zeaxanthin, was associated with a lower risk of AMD with the highest quintile having a 43% reduction compared with those in the lowest quintile. In that study no reduction could be found with the use of oral vitamin A, vitamin E, or vitamin C.[40] Subsequent studies suggest that the use of foods, particularly fruits rich in antioxidants and carotenoids, when consumed at the level of three servings or more per day result in a pooled multivariate reduced relative risk of 0.64 compared with persons who consumed less than 1.5 servings per day.[2] However, there have been a number of studies that have demonstrated little to no benefit with dietary regimens.[21,41–43,44] The AREDS2 has studied supplementation with lutein and zeaxanthin and omega-3 fatty acids (see below).

Smoking[a]

Most studies have consistently implicated smoking as a statistically significant risk factor for the development of late-stage AMD.[2,47] In a meta-analysis of three pooled studies from the United States, The Netherlands, and Australia, smoking was one of only two significant associations identified with incident AMD along with total serum cholesterol. Current smoking is associated with a 4.55-fold increased risk of neovascular AMD (vs. "never" smokers) and a 2.54-fold increased risk of atrophic AMD (vs. "never" smokers).[48] Based on a pooled analysis of data, the risks of both neovascular and atrophic AMD seem to decrease once one stops smoking.[48]

Light Exposure

Although there is a considerable body of compelling experimental data to suggest that increased retinal irradiance is positively correlated with an increased likelihood of advanced AMD, the epidemiologic evidence supporting this hypothesis is modest.[3,49,50] In the Beaver Dam Eye Study, participants exposed to summer sun for more than 5 hours a day during selected periods of time were at increased risk for increased retinal pigment (relative risk 3.17) and early AMD (relative risk 2.14) after 10 years of follow-up compared with those exposed to less than 2 hours per day.[50]

The underlying rationale for the hypothesis that increased light stress predisposes to AMD rests on the role of oxidative stress inherent with photo bleaching of the photoreceptors and to a lesser extent pigment epithelium. In particular, reactive oxygen intermediates (ROI) including hydrogen peroxide, singlet oxygen, and other short-lived species, which arise as the byproducts of cellular metabolism, are known to have a toxic effect on cellular membranes.[41] It is felt that the cumulative effects of chronic low levels of these species result in profound damage to the retina and pigment epithelium through lipid peroxidation, mitochondrial DNA damage, and induction of apoptosis.[2,41] Experimental studies have confirmed the deleterious effect of chronic light and in particular blue and ultraviolet light on the RPE in part through the creation of A2E oxiranes, a major component of lipofuscin. The presence of natural antioxidants derived from dietary sources

including lutein, zeaxanthin, lycopene, and ascorbate are thought to mitigate the effects of photo-oxidation by quenching free radicals and other intermediate species.[41] It has been hypothesized that this represents one, but not the only mechanism of action, of the antioxidants in the AREDS study.[51]

Use of Medications

Meta-analyses of pooled prospective studies suggest that certain medications may be associated with an increased or decreased risk of age-related macular degeneration. Antihypertensive medications, particularly beta blockers, are associated with modest increased risk, whereas hormone replacement therapy in women, and tricyclic antidepressants, confer some relative protection.[52a] The potential effect of statins on AMD progression has been studied as a preplanned cohort of the Age-Related Eye Disease Study 2 (AREDS2), with no significant association with progression to late AMD (HR 1.08, 0.83–1.41). However, a more recent interventional pilot study in which 26 patients with many large, soft drusenoid deposits were adminstered 80 mg of atorvastatin demonstrated regression of drusen in 10 patients, with an average gain of 3 letters of vision in these patients.[52b] These observations may be able to be further exploited in the development of new classes of drugs in addition to avoiding potentially harmful drug interactions.

The Pathophysiology of Exudative AMD: the Crucial Role of Cytokines

Definition and Steps in Angiogenesis

Angiogenesis refers to the creation of new blood vessels from existing blood vessels, and therefore is contrasted from the process of vasculogenesis seen characteristically in utero in which vessels are created de novo. The process of angiogenesis has been characterized as occurring in a series of orderly events (adapted from The Angiogenesis Foundation, https://www.angio.org/learn/angiogenesis/). (1) To monitor and supply sufficient amounts of oxygen to surrounding tissues, blood

vessels have oxygen and hypoxia-induced sensors, or receptors, which allow vessel remodeling to adjust the blood flow accordingly. (2) Hypoxia or other endogenous signals activate cells and induce the release signaling factors (such as VEGF, Ang-2, fibroblast growth factor, and chemokines) to promote the growth of new blood capillaries from preexisting vessels. (3) Pericytes detach from the vessel, and endothelial cells are activated and lose their close contact as the vessel dilates. (4) In sprout formation, a tip cell is selected which releases matrix metalloproteases to degrade the basement membrane and remodel the extracellular matrix. (5) Tip cells are polarized and extend numerous filopodia to guide sprout migration toward angiogenic stimuli. (6) Stalk cells follow the tip cell and proliferate, extending the sprout. Proliferating stalk cells establish junctions with neighboring endothelial cells and release signals that bind to extracellular membrane components and regulate vascular lumen formation. (7) Fusion of neighboring branches occurs when two tip cells encounter each other, establish EC–EC junctions, and form a continuous lumen. Extracellular matrix is deposited to establish a new basement membrane, endothelial cell proliferation ceases, and pericytes are recruited to stabilize the new vessel. (8) Once blood flow is established, the perfusion of oxygen and nutrient reduces angiogenic stimuli and inactivates endothelial cell oxygen sensors, reestablishing the quiescent state of the blood vessel. Antiangiogenic therapies currently under investigation are thought to inhibit angiogenesis at various steps in this process.

VEGF and Other Modulators of Angiogenesis

Regardless of the inciting stimulus involved in the development of pathologic neovascularization, it is now well established that VEGF plays a principal role including not only the neovascular forms of AMD, but also diabetic retinopathy, iris neovascularization, and retinopathy of prematurity. Additionally other cytokines may play an important role as well, including fibroblast growth factor (FGF), pigment epithelium-derived factor (PEDF), the integrins, angiopoietins, and matrix metalloproteinase (MMP) inhibitors.[2,23,53–56]

VEGF undoubtedly represents the putative factor X first postulated by Michaelson associated with pathologic neovascularization.[2] First described as a vasopermeability factor associated with tumors, the molecule has since been cloned and well characterized.[57,58] VEGF has two important characteristics relevant to its role in the pathogenesis of the neovascular forms of AMD: (1) induction of angiogenesis through endothelial proliferation, migration, and new capillary formation and (2) enhancement of vascular permeability.

Vascular Permeability

VEGF produces important increases in hydraulic conductivity of isolated microvessels that are mediated by increased calcium influx and likely changes in levels of nitric oxide caused by induction of nitric oxide synthetase (NOS). While VEGF is both necessary and sufficient when administered exogenously to induce both these effects in vitro and in vivo, it is also well known that a number of other growth factors participate in this process. Some represent steps in a cascade initiated by VEGF while others act upstream.[59,60] The chemical structure of VEGF is that of a heparin-binding homodimeric glycoprotein of 45 kilodaltons.[57] VEGF has significant homology to PDGF. The human VEGF gene is organized into 8 exons separated by 7 introns and is localized in chromosome 6p21.3. Although there is only a single gene for VEGF-A, alternate posttranslational exon splicing results in the generation of between four and six different isoforms having 121, 145, 165, 183, 189, and 206 amino acids respectively after signal sequence cleavage[56,57] (Fig. 70.4). $VEGF_{165}$ exists in both soluble and bound forms[57] (Fig. 70.5) and is thought to be predominantly responsible for pathologic neovascularization.

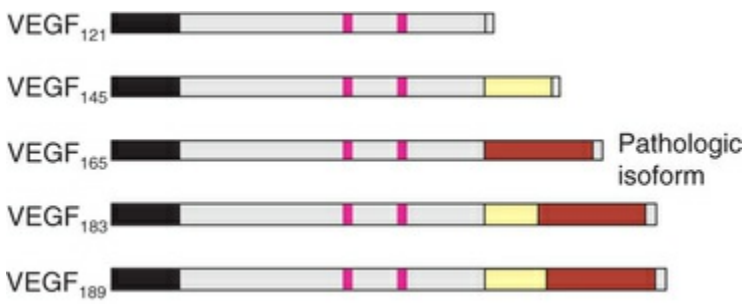

FIG. 70.4 Multiple isoforms of VEGF exist in nature and appear to participate to a differential degree in the normal events of vasculogenesis, as well as the pathologic events of angiogenesis occurring in response to local stimuli. Although there is only a single gene for VEGF, alternate splicing as well as posttranscriptional modification by plasminogen in the extracellular matrix accounts for a variety of isoforms that determine the relative balance between normal vascular homeostasis and pathologic neovascularization. The shorter amino acid length isoforms VEGF121 and VEGF145 are principally found in soluble form, whereas the longer spliced lengths 183, 189, and 206 are principally tissue fixed and bound by heparin. VEGF165 is thought to stimulate pathologic neovascularization and exists both in soluble and tissue fixed configurations.

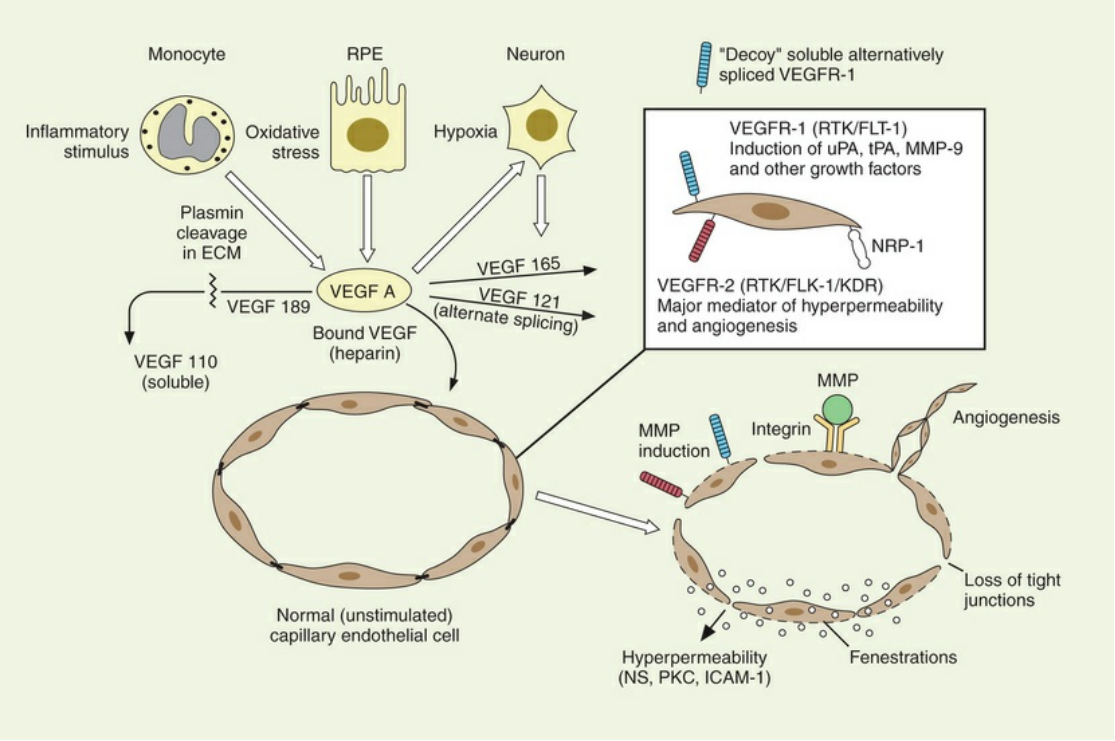

FIG. 70.5 Pathways of VEGF expression and effects on vascular cells are demonstrated schematically. A variety of cells contribute to VEGF release, including monocytes, retinal pigment epithelial cells, and neurons responding to inflammation, oxidative stress, and hypoxia respectively. These and other cell types produce predominantly VEGF-A which is expressed in various isoforms through transcriptional and post-translational steps. VEGF165 and VEGF121 are the predominant forms, with VEGF 189 being cleaved in the extracellular matrix to VEGF110, a soluble form by activated plasmin. Each of these molecules, but principally VEGF165, bind to endothelial cells through specific receptors VEGFR-1 and VEGFR-2. A sequence of events is set in motion through subsequent intracellular messaging systems as well as extracellular events that result in the loss of tight junctions between individual endothelial cells, the formation of fenestrations within endothelial cells and calcium-mediated permeability channels resulting in loss of the normal inner and outer blood–retinal barriers. Additionally matrix metalloproteinase activation occurs through its interaction with integrin receptors alpha v beta 3 and alpha v beta 5, which are found on the surface of endothelial cells exclusively following induction of the cell through activation with

the VEGFR-1.

Although VEGF inhibitors share in common an attempt to mitigate the proliferative and permeability effects of VEGF on normal and neovascular tissue, there are likely to be differences in both efficacy and safety related to the choice of agents for several reasons. From a theoretical standpoint, since $VEGF_{165}$ is the principal isoform involved in pathologic neovascularization, it has been argued that leaving the other three principal isoforms intact (121, which is principally diffusible in soluble form, and 189 and 206, which are principally matrix-bound through high affinity heparin binding sites) avoids the possibility of interference with normal homeostatic mechanisms associated with constitutive VEGF expression. Indeed, previous animal studies suggested that blockade of $VEGF_{164}$ in the mouse (equivalent to $VEGF_{165}$ in humans) is as effective as nonselective antibody-mediated VEGF blockade in preventing pathologic neovascularization in a hypoxia-induced angiogenesis model, while not interfering with normal physiologic development of retinal vasculature.[61,62] However, it has become apparent with widespread use of bevacizumab and ranibizumab (monoclonal antibodies against multiple VEGF isoforms) that nonselective blockade has few untoward effects on normal retinal vascular physiology.

VEGF Receptors

VEGF exerts its effects on cells through two highly related receptor tyrosine kinases (RTKs) VEGFR-1 and VEGFR-2.[57] VEGFR-1 also termed FLT-1 (FMS-like tyrosine kinase) was described first, but its role remains open to debate. Like VEGF, VEGFR-1 is upregulated by a hypoxia-inducing factor (HIF)-dependent mechanism. The receptor undergoes weak tyrosine autophosphorylation in response to VEGF. It is thought not to be primarily a mitogenic stimulus but rather a "decoy" receptor, which downregulates the activity of VEGF by sequestering and rendering the factor less available to VEGFR-2 (Figs. 70.5–70.6). This factor may be most important during embryogenesis rather than during pathologic neovascularization as well as in hematopoietic bone marrow-

derived cells and neural signaling.[57,63]

VEGFR-2 (KDR in Humans or FLK-1 in Mice)

VEGFR-2 binds VEGF with lower affinity relative to VEGFR-1, but is felt to be the major mediator of the mitogenic, angiogenic, and permeability enhancing effects of VEGF. The binding site for VEGF on VEGFR-2 has been mapped to the second and third IgG-like domains, and it undergoes dimerization and strong ligand-dependent tyrosine phosphorylation resulting in a mitogenic chemotactic and pro-survival signal. It appears to have at least two separate tyrosine phosphorylation sites. VEGFR-2 is thought to be critical as a survival factor with apoptosis occurring in its absence.

A large body of evidence exists to support the critical and probably rate-limiting role of VEGF in neovascular forms of AMD. High messenger RNA levels and increased VEGF receptor levels are observed in areas of CNV in primates as well as in the extracted neovascular membranes of patients removed at surgery and following autopsy.[2,64] Additionally there are strong indications that elevated levels of VEGF are the proximal cause for the hyperpermeability seen not only in diabetic macular edema, but in patients with subsensory and intraretinal fluid associated with CNV as well. The permeability changes resulting from VEGFR-2 are thought to be mediated to a large extent by endothelial nitric oxide synthetase-based generation of increased nitric oxide levels and associated changes in calcium flux (Fig. 70.6). These alterations can be reversed either by direct blockade of VEGF, the receptor, or NOS using a knock-out model.[2,58,59] Inactivation of soluble VEGF by monoclonal antibodies directed against it or inhibition of ICAM also appear to be effective as well. Other methods of direct inhibition of VEGF include inhibition of its tyrosine kinase receptors (VEGFR-1 and -2), either by systemic administration or gene transfer.[65] Indirect inhibition of VEGF effects can be attained through modulation of intracellular adhesion molecule (ICAM), or indirect effects on nitric oxide phosphorylase, nitric oxide synthetase, or protein kinase C, another modulator of permeability.

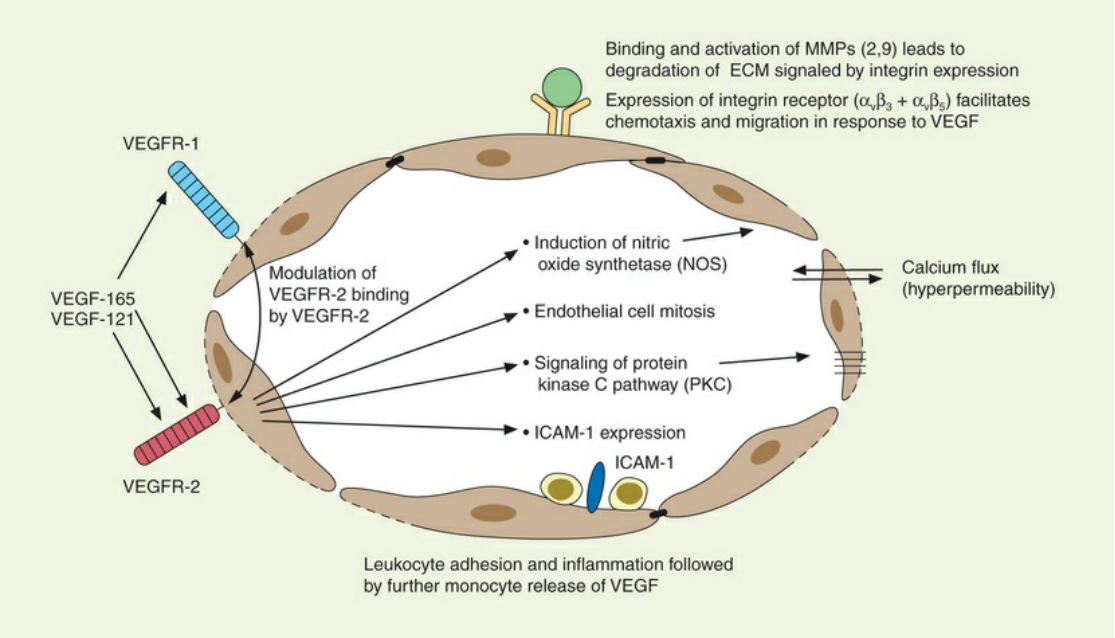

FIG. 70.6 Intracellular signaling including induction of nitric oxide synthetase (NOS), protein kinase C activation (PKC) and expression of ICAM-1 leading to leukocyte adherence and further changes in permeability mediated by calcium flux and protein kinase C.

A number of other cytokines and factors have been identified that influence VEGF or VEGF-associated effects in the process of angiogenesis.[2,66–74] Selected factors of interest are described in more detail below and represent possible targets for intervention.

Platelet-Derived Growth Factor

PDGF is a homo- or heterodimeric glycoprotein that stimulates pericyte and vascular smooth muscle cell recruitment in angiogenesis, which are essential in the maintenance and survival of new vessels. The PDGF receptors (PDGFR-A and PDGFR-B) are tyrosine kinases and are expressed differentially on different cell types, with PDGFR-B being more extensively expressed in endothelial cells, vascular smooth muscle cells, and fibroblasts, among others.[75,76] In the absence of PDGFR-B signaling, vascular pericytes detach, and the integrity of vessels is lost. Immature vessels are highly sensitive to the withdrawal of VEGF prior to pericyte recruitment and coverage; conversely, when pericyte coverage is complete, new vessels are resistant to VEGF

withdrawal. This is the so-called plasticity window, during which time vessels can regress rapidly with changes in exposure to growth factors.[77,78] PDGF blockade in animal models of corneal neovascularization has resulted in prevention and regression of new vessels.[79,80] PDGF blockade alone or combined with VEGF inhibition (taking advantage of the plasticity window) may thus serve as a potent inhibitor of neovascular AMD.

Matrix Metalloproteinases and Tissue Inhibitors of Metalloproteinases

Expression of matrix metalloproteinases (MMPs) and their associated RNA, particularly MMP-2 and MMP-9, have been associated with pathologic neovascularization. Both matrix metalloproteinases are activated by VEGF and other regulatory cytokines and act to digest the extracellular matrix and thereby facilitate the spreading and chemotaxis of actively proliferating endothelial cells as they aggregate to form new capillaries.[2] Matrix metalloproteinases appear to be modulated and principally downregulated by naturally occurring tissue inhibitors of metalloproteinases (TIMPs) of which TIMP-1, TIMP-2, and TIMP-4 are thought to be soluble, and TIMP-3 principally extracellular matrix-bound. TIMP-3 is thought to play an important and possibly critical role in the natural modulation of matrix metalloproteinase regulation in Bruch's membrane, and is found in increased amounts in drusen and thickened basement membranes associated with AMD.[24,25,28,29,81] An experimental model that either delivers increased amounts of TIMP-3 or induces over expression of TIMP-3 by gene therapy demonstrate potent antiangiogenic effects for this molecule.[82,83]

Tissue Factor

Tissue factor (TF) is a transmembrane receptor for the coagulation factor VII/VIIa.[84] Upon vascular injury, TF forms a complex with factor VII, initiating the coagulation cascade. Constitutively expressed within vascular endothelium, the secondary activities of TF (and the TF/VIIa complex) include the promotion of inflammation and angiogenesis. In cancer biology, a link between

TF and VEGF expression has been established in a number of cancers, and TF is believed to induce angiogenesis in part through VEGF induction.[85,86] Relevant to AMD, in addition to the amyloid, apolipoprotein E, and complement factors that are found in drusen, factor X, and fibrinogen have also been identified, which are closely related to TF activity.[87,88] Tissue factor itself has been identified by immunostaining in RPE cells and macrophages in post-mortem eyes with CNV and in surgically excised CNV lesions, as well as in animal models of AMD.[64,88] Tissue factor inhibition through antibody targeting of factor VII has been demonstrated to obliterate lesions in laser-induced animal models of CNV.[89,90]

Angiopoietins

Angiopoietins, which are also highly specific for endothelial cells, perform a variety of other regulatory activities related to supporting cells and the extracellular matrix. A laboratory study suggests that two different isoforms, Angiopoietin 1 and Angiopoietin 2, appear to have differential and counter-acting effects on the vasculature. Angiopoietin 2, which is upregulated by both hypoxia and VEGF, binds to an endothelial cell receptor TIE2 and enhances VEGF-mediated retinal neovascularization, but does not by itself stimulate endothelial cells or proliferation in vitro.[2,91] Angiopoietin 1 appears to play a maturation role and is associated with non-leaky behavior and may have potential therapeutic benefit through its inhibition of inflammatory pathways.[2] Another protein, angiopoietin-like protein 4 (ANGPTL4), has recently been found in elevated levels within the aqueous humor of eyes with proliferative diabetic retinopathy, and is upregulated by hypoxia and HIF and is both necessary and sufficient to promote retinal angiogenesis.[92] It is as yet unknown if this may also play a role in CNV.

Pigment Epithelium-Derived Factor

A variety of naturally occurring cytokines are known to have a downregulatory effect on angiogenesis and VEGF-mediated effect on cells. Notably, pigment epithelium-derived factor (PEDF), which is secreted by the pigment epithelium in vivo as well as in cell culture, has been shown to be biochemically identical to the product

of the wild type of retinoblastoma tumor suppressor gene (*RB*) and is thought to induce differentiation of retinoblastoma cells, inhibit microglial growth, and other important regulatory functions in addition to its effects on angiogenesis.[49] Its relevance to AMD is likely related to its role in counterbalancing VEGF. In a study of donor human eyes with and without AMD, relative VEGF and PEDF levels were measured using immunoreactivity assays. Interestingly, VEGF levels were not significantly different between the two groups of eyes, even in the presence of advanced exudative change. In contrast, PEDF levels were much lower in the RPE and choroid of eyes with AMD, suggesting that it is lower levels of PEDF in the ocular milieu that may contribute to the formation of CNV.[93] Results from in vitro studies have suggested that the role of PEDF is regulation or inhibition of VEGF receptor signaling, rather than direct VEGF antagonism.[94]

Pathogenic Factors in Atrophic AMD

The factors that result in the progression of mild or moderate AMD to advanced atrophic AMD (geographic atrophy) are poorly understood. It is clear that immune dysregulation, inflammation, and oxidative stress play key roles in the development and progression of AMD, with angiogenesis as one late-stage outcome of the chronic local inflammatory state. The genetics of the complement system and their associations with AMD have been discussed above, although it is still unclear how genotypic variations in complement lead to the AMD phenotype. Clinicopathologic specimens demonstrate the presence of inflammatory cells in Bruch's membrane, and bioactive fragments of C3 (C3a) and C5 (C5a) in drusen of AMD eyes and elevated vascular endothelial growth factor (VEGF) expression in RPE cells.[95,96] Inflammatory foci and white cells are also commonly seen in the choroid in autopsy specimens of patients with CNV.[64,95–100] Geographic atrophy has been associated with loss of a regulatory enzyme *DICER1*, and subsequent upregulation of an inflammatory complex called the NRLP3 inflammasome, leading to secretion of multiple inflammatory cytokines, including IL-6, TNF-α, IL-1β, and IL-18.[101,102] This process may be triggered by N-retinylidene-N-

retinylethanolamine (A2E), and associated free radicals and reactive oxygen intermediates related to the formation of this component of lipofuscin, ultimately stimulating both apoptotic and angiogenic signals[18,41,103] (Fig. 70.7). The inflammatory cascade is further characterized by retinal microglial activation and choroidal macrophage infiltration.[104,105] Given the compelling evidence that inflammation has a causative effect on the development and progression of AMD, therapy aimed at reducing inflammation through complement inhibition or regulation; immunomodulation; or stabilization of intracellular organelles, such as lysosomes and resultant proteolysis, may be successful pharmacologic strategies.[104,105]

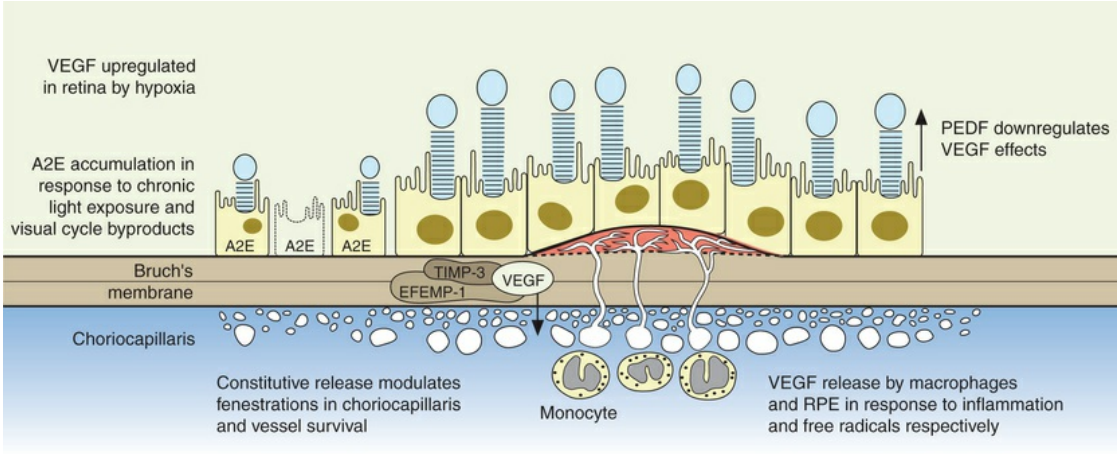

FIG. 70.7 Schematic diagram of pathogenic mechanisms associated with atrophic and exudative age-related macular degeneration. Normal constitutive release of VEGF, which is responsible for maintenance of fenestrations and other desirable permeability effects on the normal choriocapillaris through basal lateral secretion in an outward direction, appears to be effectively counterbalanced by the apical secretion of cytokines inhibitory for angiogenesis, including pigment epithelial derived (PEDF). This results in the relative avascularity of the outer retina as seen in the diagram on the right. In response to chronic light exposure and oxidation of phospholipids associated with the visual cycle, A2E and other oxidative byproducts accumulate in the retinal pigment epithelium, accounting for the characteristic autofluorescence seen on fundus photography. They also result in senescence of the

pigment epithelium and apoptotic death associated with secondary atrophic effects on the overlying photoreceptors and underlying choriocapillaris, seen on the left in the diagram. The accumulation of increased lipoproteins as well as other glycoproteins including TIMP-3 and EFEMP-1 contribute to the thickening of Bruch's membrane, characteristically seen in patients with more advanced forms of the disease (seen centrally). Low-grade inflammation, chemoattraction of monocytes, and proangiogenic signals both from the pigment epithelium and inflammatory cells lead to vascular ingrowth from the choroid through defects in calcific and fragmented Bruch's membrane.

Among the components of drusen is fibrillar amyloid, and specifically amyloid-β, which has been associated with Alzheimer's disease, Huntington disease, Downs syndrome, and other neurodegenerative conditions.[106] Within the retina, amyloid is localized within vesicles in drusen, and chronic exposure of the retina to amyloid is postulated to lead to overexpression of proinflammatory cytokines such as IL-1β and IL-8, which play roles in generating reactive oxygen species and in chemotaxis. Amyloid-β has also been demonstrated in degenerating brains to induce chronic inflammation via the complement system, and may play a similar role in the retina. Indeed, amyloid has been found to colocalize with the complement factor C3 in drusen.[107,108] As a component of drusen, amyloid deposition may contribute to RPE dysfunction and ultimately atrophy.

Choroidal ischemia may be another factor contributing to atrophic macular degeneration. Studies have demonstrated that eyes with age-related macular degeneration have decreased arterial blood flow on indocyanine green angiography.[109] Additionally, newer imaging technologies such as high-resolution ultrasound, as well as spectral domain optical coherence tomography (OCT) with enhanced depth imaging, have revealed characteristics consistent with choroidal ischemia in eyes with AMD.[110,111a] Additionally, histopathologic study of postmortem eyes demonstrated remodeling and loss of the choriocapillaris even in intermediate AMD.[111b]

Agents Currently in Use or Under Investigation: Neovascular AMD

VEGF Inhibition: Monotherapy

A variety of methods are now available to directly inhibit the $VEGF_{165}$ molecule and its various other isoforms. These include the use of monoclonal antibodies directed at one or more isoforms, antibody fragments, and molecules directed at one or more of the VEGF receptors including native decoys, tyrosine kinase inhibitors, fusion proteins, and modified naturally occurring proteins. Additionally, because VEGF is thought to initiate a cascade of intracellular signals initially, and subsequently extracellular events, it is possible to inhibit VEGF effects either through prevention of secretion of the molecule, direct inhibition of the molecule in the extracellular space, blockade of the receptors, or through interruption in the downstream intracellular signaling pathways leading to both intra- and extracellular events.[112] Finally, new technologies for sustained drug delivery are being explored.

Monoclonal Antibody: Bevacizumab

Bevacizumab (Avastin; Genentech/Roche, South San Francisco, CA, USA) is a humanized monoclonal antibody (IgG1) against human VEGF-A that selectively inhibits all isoforms and bioactive proteolytic breakdown products of VEGF-A. Bevacizumab is an immunoglobulin G molecule comprised of amino acid sequences which are about 93% human and 7% murine. Preclinical studies in animal models of various tumor cell lines, as well as different forms of ocular neovascularization, indicated that the fully sized antibody had excellent efficacy against the primary permeability and proliferative effects of VEGF isoforms. Following extensive clinical testing, it was found to be effective in slowing tumor growth through its effects on angiogenesis.[57] Bevacizumab was FDA-approved in 2004 as a treatment for metastatic colorectal cancer when given intravenously at a dose of 5 mg/kg and infused every 2 weeks in combination with 5-fluorouracil. Bevacizumab was shown

to increase survival, response rate, and duration of response compared with conventional therapy consisting of irinotecan, fluorouracil, and leucovorin for metastatic colorectal cancer.[113] Additional phase III clinical trials with bevacizumab have since resulted in FDA-approval for the treatment of lung, kidney, and brain cancers.

In 2004, a study investigating the use of systemic bevacizumab in patients with exudative AMD (Systemic Avastin for Neovascular AMD – SANA) was initiated at the Bascom Palmer Eye Institute. This study was the first demonstration that bevacizumab was effective for this disease. In this open-label, uncontrolled study, 18 patients underwent two to three intravenous infusions of bevacizumab (5 mg/kg) to evaluate the potential safety and efficacy of systemic bevacizumab over 6 months.[114,115] Although clinical trials using intravitreal pegaptanib and ranibizumab for CNV were underway, the prior use of bevacizumab for ocular disease in humans using any route had previously been untested. While no serious adverse events were observed, and only a mild transient increase in blood pressure was identified, the SANA study was too small to establish the safety of bevacizumab. However, significant improvements in visual acuity and OCT central retinal thickness (CRT) measurements were observed comparable to the changes observed in the early phase ranibizumab trials.

While systemic bevacizumab (5 mg/kg) was shown to reduce leakage from CNV, decrease OCT central retinal thickness measurements, and significantly improve vision in exudative AMD, the intravenous use of bevacizumab for exudative AMD was never widely adopted, because the intravitreal approach uses up to 500-fold less drug, is much less expensive, and is perceived to be safer due to the smaller dose of drug. In the first-reported case of intravitreal bevacizumab,[116] a patient with recurrent CNV secondary to AMD, who had previously been treated with verteporfin photodynamic therapy (PDT) in combination with triamcinolone acetonide followed by treatment with pegaptanib injections, was shown to improve with a decrease in OCT central retinal thickness and subretinal fluid, as well as improvement of subjective visual distortion, within 1 week of a single injection of 1.0 mg bevacizumab.

The bevacizumab used for this injection was the commercially available form available as 100 mg and 400 mg preservative-free, single-use vials in volumes of 4 mL or 16 mL (25 mg/mL). The 100 mg product is formulated in 240 mg α(alpha),α(alpha)-trehalose dihydrate, 23.2 mg sodium phosphate (monobasic, monohydrate), 4.8 mg sodium phosphate (dibasic, anhydrous), 1.6 mg polysorbate 20, and was diluted in water prior to intravenous infusion. For off-label intravitreal use, bevacizumab was not diluted, but rather dispensed into individual syringes for intravitreal injection and the volume (dose) of injection ranged from 0.05 mL (1.25 mg) to 0.1 mL (2.5 mg).

Initially, there was concern that a molecule as large as the 149-kilodalton bevacizumab could penetrate the retina and effectively treat CNV compared with ranibizumab, which is one-third the size. However, it became apparent that bevacizumab could penetrate the retina based upon the empiric observations of decreased subretinal fluid on OCT examination and improved visual acuities in treated patients. Subsequently, Han et al. were the first to show that a full-length immunoglobulin the size of bevacizumab was capable of penetrating the rabbit retina after an intravitreal injection.[117] Sharar et al. used qualitative immunofluorescence to confirm that intravitreal bevacizumab was able to completely penetrate the retina by 24 hours and was essentially absent at 4 weeks after an injection.[118] Moreover, Dib et al. demonstrated bevacizumab molecules in the subretinal space of all six eyes studied 2 hours after an intravitreal bevacizumab injection of 0.05 mL (1.25 mg), confirming the initial observations that the molecule could rapidly diffuse through the retina.[119]

The ocular pharmacokinetics of various other monoclonal antibodies injected into the vitreous cavity of monkeys and rabbits demonstrated a half-life of about 5.6 days.[120,121] Studies of bevacizumab in rabbits and monkeys suggest a half-life in the range of 4–6 days.[122–124] A human study reported that a single dose of intravitreal bevacizumab had a half-life of 3 days and was likely to provide complete intravitreal VEGF blockade for a minimum of 4 weeks.[125] One human study suggested a half-life of 6.7 days, and yet another study has reported a half-life of as long as 9.8 days.[126,127] It is likely that human ocular pharmacokinetics of bevacizumab varies

from patient to patient, depending on factors such as the extent of vitreous liquefaction and the phakic status of the eye.

Since the first case of intravitreal bevacizumab for the treatment of exudative AMD was reported, numerous retrospective studies and a few small prospective studies using a dose range between 1.0 and 2.5 mg have been published, all demonstrating clinically significant improvement in mean visual acuity, reduction in fluorescein angiographic leakage, and resolution of OCT-visualized edema in up to 90% of bevacizumab-treated patients. These reports also supported the apparent clinical safety of bevacizumab. As of the time of writing (2015), despite the subsequent approval of ranibizumab in 2006, the off-label use of intravitreal bevacizumab has become the most common treatment for exudative AMD in the United States.[128,129] In addition, it has also become frequently used for a wide range of other forms of macular new vessels including pathologic high myopia, multifocal choroiditis, and ocular histoplasmosis; it has also been used successfully for treatment of clinically significant macular edema from diabetic retinopathy, retinal venous occlusions, and retinopathy of prematurity.[130–138] Its efficacy relative to the FDA-approved ranibizumab was demonstrated in the CATT study (described later).

Antigen Binding Fragment: Ranibizumab

Ranibizumab (Lucentis; Genentech/Roche, South San Francisco, CA, USA) is a humanized anti-VEGF-A recombinant Fab fragment that has been affinity-matured to increase its binding affinity for VEGF-A. Ranibizumab binds within the VEGFR binding domain of all biologically active isoforms of VEGF-A. Two randomized, double-masked, pivotal phase 3 clinical trials have demonstrated that monthly intravitreal injections of ranibizumab are an effective and safe treatment for subfoveal CNV in AMD patients.[139,140]

The MARINA study assessed the response of minimally classic or occult CNV to ranibizumab.[139] Patients (n=716) were assigned randomly to receive sham injection (n=238), 0.3 mg (n=238), or 0.5 mg (n=240) ranibizumab. After 4 months of follow-up, approximately 90% of ranibizumab-treated patients had lost fewer than 15 letters on the Bailey-Lovie (ETDRS) chart as compared to 53% of the sham-injected patients. This treatment response was

independent of lesion size, initial visual acuity, or whether the lesion was classified as minimally classic or occult with no classic CNV on fluorescein angiography. Vision improved by at least 15 letters in approximately 33% of patients receiving 0.5 mg ranibizumab at 24 months of follow-up vs. 4% in the sham-injected patients (Fig. 70.8). Approximately 1% of patients receiving intravitreal ranibizumab developed endophthalmitis. The risk of cataract was approximately 0.2%. There were no cases of retinal detachment among patients receiving intravitreal therapy. Despite the theoretical risk of systemic vascular complications, there was no imbalance among treated and control groups regarding hypertension, and the risk of myocardial infarction among sham-injected, 0.3-mg, and 0.5-mg cohorts was 1.7%, 2.5%, and 1.3%, respectively. The risk of stroke among the three groups was 0.8%, 1.3%, and 2.5%, respectively. The risk of nonocular hemorrhage was 5.5%, 9.2%, and 8.8% in each of the three cohorts, respectively. None of these differences was statistically significant, although the authors recognized that the study was not powered to detect small differences.

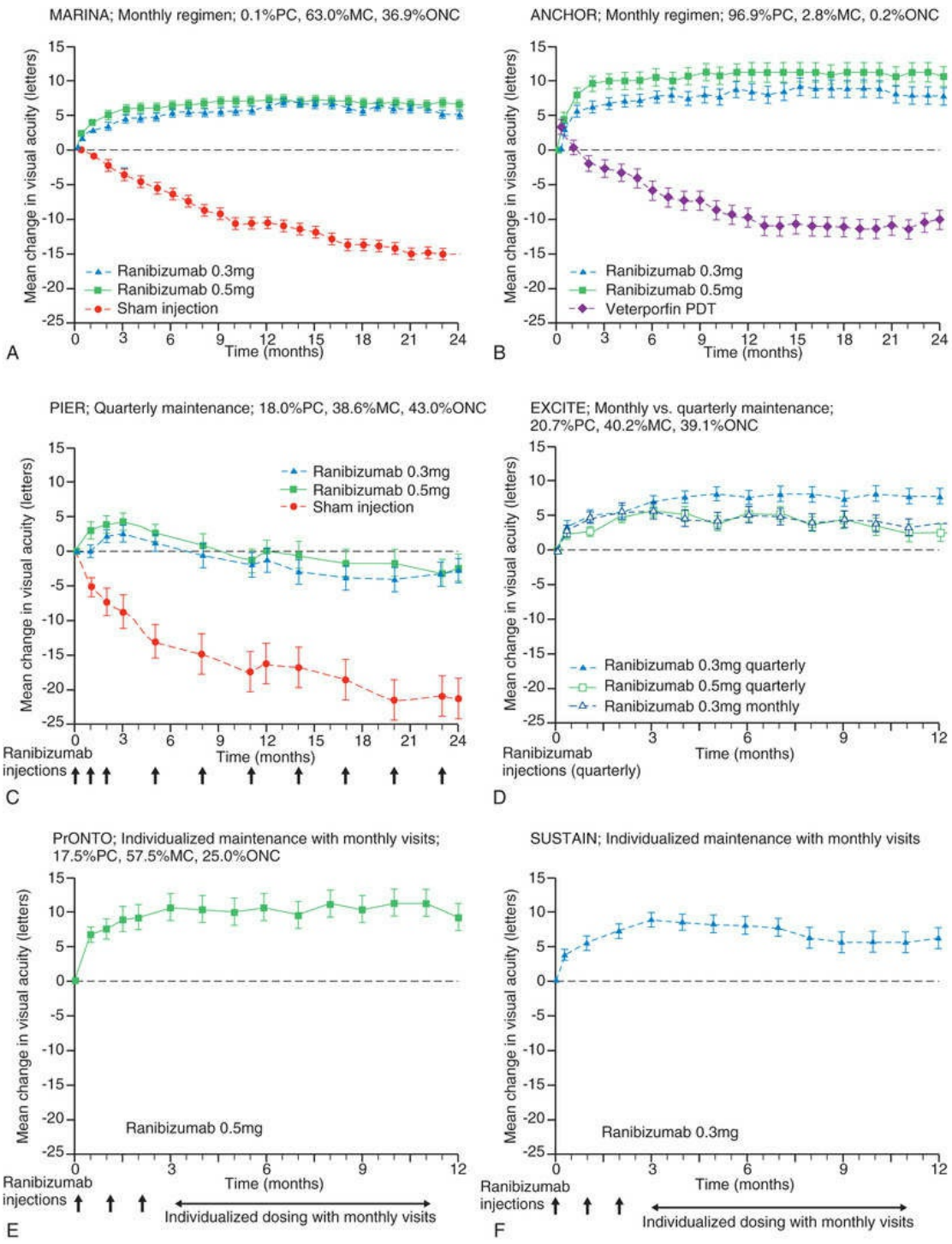

FIG. 70.8 Mean change from baseline in best corrected visual acuity by month for (A) MARINA, (B) ANCHOR, (C) PIER, (D) EXCITE, (E) PrONTO, (F) SUSTAIN.

Panel C reproduced with permission from Regillo, et al. Ranibizumab (Lucentis) in treatment of neovascular age-related macular degeneration (AMD): 2-year results of PIER study, poster PO459 presented at the AAO 2007. Panel E reproduced with permission from Fung AE, Lalwani GA, Rosenfeld PJ, et al. An optical coherence tomography-guided, variable dosing regimen with intravitreal ranibizumab (Lucentis) for neovascular age-related macular degeneration. Am J Ophthalmol 2007;143:566–83, Copyright 2007, with permission from Elsevier. Compilation reproduced with permission from Mitchell P, Korobelnik JF, Lanzetta P, et al. Ranibizumab (Lucentis) in neovascular age-related macular degeneration: evidence from clinical trials. Br J Ophthalmol 2010;94(1):2–13.)

The ANCHOR study assessed the response of patients with predominantly classic CNV as determined by fluorescein angiography.[140] Patients (n=423) were randomly assigned to receive verteporfin-PDT plus sham injection (n=143) or sham PDT plus injection of either 0.3 mg (n=140) or 0.5 mg (n=140) ranibizumab. At 12 months follow-up, approximately 95% of ranibizumab-treated patients lost less than 15 letters of vision vs. 64% in the verteporfin active treatment control group. Forty percent of patients treated with 0.5 mg ranibizumab gained at least 15 letters vision vs. 6% in the verteporfin treatment cohort. At month 24, the visual benefit from ranibizumab remained statistically (p<.0001 vs. PDT) and clinically significant: 89.9% to 90.0% of ranibizumab-treated patients had lost <15 letters from baseline (vs. 65.7% of PDT patients); 34% to 41.0% had gained ≥15 letters (vs. 6.3% of PDT group); and, on average, visual acuity was improved from baseline by 8.1 to 10.7 letters (vs. a mean decline of 9.8 letters in the PDT groups).[141] Changes in lesion anatomic characteristics on fluorescein angiography also favored ranibizumab (all comparisons p<.0001 vs. PDT). Overall, there was no imbalance among groups in rates of serious ocular and nonocular adverse events. In the pooled ranibizumab groups, 3 (1.1%) of 277 patients developed presumed endophthalmitis in the study eye (rate per injection = 3/5921, or 0.05%). Retinal detachment was observed in one patient in both the verteporfin (0.7%) and 0.3-mg ranibizumab (0.7%) cohorts. There were no cases of lens injury. The risk of hypertension was the same in all cohorts. The risk of myocardial infarction among verteporfin, 0.3-mg ranibizumab, and 0.5-mg ranibizumab cohorts was 0.7%, 0.7%, and 2.1%, respectively. The risk of stroke or cerebral infarction was 0.7% in each of the three cohorts. The risk of

nonocular hemorrhage was 2.1%, 5.1%, and 6.4% in each of the three cohorts. Immunoreactivity to ranibizumab before treatment was 1.5%, 3.2%, and 0.8% among the verteporfin, 0.3-mg ranibizumab, and 0.5-mg ranibizumab cohorts, respectively. Immunoreactivity was present in 1.6%, 1.6%, and 3.9% of patients in each of these cohorts, respectively, after 12 months of treatment. The concern regarding immunoreactivity is that patients who develop an immune response might exhibit increased intraocular inflammation following intravitreal injection and consequently might not respond to the medication as well as patients who do not exhibit such a response. In practice, most retina surgeons have not observed this phenomenon and the drug has been minimally immunogenic in the doses tested.[142]

In both the MARINA and ANCHOR trials, visual acuity improvement seemed to reach a plateau by the 4-month time point (Fig. 70.8). Because monthly injections were considered inconvenient and daunting for some patients and their family members, and entailed risk as well as considerable expense, studies were undertaken to evaluate alternative treatment regimens. The PIER and EXCITE studies provided useful information in this regard.[143,144] In PIER, a phase IIIb multicenter, randomized, double-masked trial, patients with subfoveal CNV were randomly assigned to sham injection (n=63), 0.3 mg ranibizumab (n=60), or 0.5 mg ranibizumab (n=61). Patients received sham or ranibizumab injections every 4 weeks for three doses followed by additional treatment every 3 months. By month 12, mean changes from baseline visual acuity were −16.3, −1.6, and −0.2 letters for the sham, 0.3-mg, and 0.5-mg groups, respectively ($p \leq .0001$, each ranibizumab dose vs. sham). Ranibizumab arrested CNV growth and reduced leakage from CNV. The treatment effect declined, however, in the ranibizumab groups during quarterly dosing. At month 3, for example, the mean changes from baseline vision had been gains of +2.9 and +4.3 letters for the 0.3-mg and 0.5-mg doses, respectively. During study year 2, eligible sham-group patients crossed over to 0.5 mg ranibizumab quarterly. Later in year 2, all eligible randomized patients rolled over to 0.5 mg ranibizumab monthly dosing. The ranibizumab-treated patients showed an improvement in mean visual acuity during the first 3 months of the study, but

this improvement was not sustained. Nonetheless, the 0.5-mg ranibizumab cohort had a mean visual acuity change that was 16 letters better than that of the sham cohort by month 12 ($p<.0001$). By month 24, visual acuity had decreased an average of 21.4, 2.2, and 2.3 letters from baseline in the sham, 0.3-mg, and 0.5-mg groups ($p<.0001$ for each ranibizumab group vs. sham). The visual acuity of sham patients who crossed over to ranibizumab decreased over time, with an average loss of 3.5 letters 10 months after crossover. The visual acuity of patients in the 0.3-mg and 0.5-mg cohorts who rolled over to monthly ranibizumab injections increased for an average gain of 2.2 and 4.1 letters, respectively, 4 months after transition. These data indicate that injecting patients with ranibizumab every 3 months (after an induction phase of three monthly injections) does not produce the same chance for visual benefit as monthly injection, at least during the first 12 months of therapy. Ranibizumab appeared to provide additional visual benefit to treated patients who rolled over to monthly dosing, but not to patients who began receiving ranibizumab after >14 months of sham injections.

The EXCITE study was a 12-month, multicenter, randomized, double-masked, active-controlled, phase IIIb study designed to demonstrate the noninferiority of a quarterly treatment vs. monthly intravitreal ranibizumab treatment regimen in patients with AMD-associated CNV.[145] Patients with primary or recurrent subfoveal CNV secondary to AMD (353 patients), including those with predominantly classic, minimally classic, or occult (no classic component) lesions, were enrolled. Patients were randomized (1:1:1) to 0.3 mg quarterly, 0.5 mg quarterly, or 0.3 mg monthly doses of ranibizumab. Treatment comprised three consecutive monthly injections followed by a 9-month maintenance phase (either monthly or quarterly injection). In the per-protocol population (293 patients), visual acuity increased from baseline to month 12 by 4.9, 3.8, and 8.3 letters in the 0.3-mg-quarterly (104 patients), 0.5-mg-quarterly (88 patients), and 0.3-mg-monthly (101 patients) dosing groups, respectively. Similar results were observed in the intent-to-treat (ITT) population (353 patients). The mean decrease in CRT from baseline to month 12 in the ITT population was −96.0 μm in 0.3-mg-quarterly, −105.6 μm in 0.5-mg-quarterly,

and −105.3 μm in 0.3-mg-monthly group. At month 12, the visual acuity gain in the monthly treatment cohort was higher than that of the quarterly regimens. The noninferiority of a quarterly regimen was not achieved with reference to 5.0 letters.

The SUSTAIN study is a 12-month, phase III, multicenter, open-label, single-arm study involving 513 ranibizumab-naive patients with AMD-associated CNV.[146] In this study, patients received three initial monthly injections of ranibizumab (0.3 mg) and thereafter as-needed (pro re nata, PRN) retreatment for 9 months based on prespecified retreatment criteria. Patients switched to 0.5 mg ranibizumab after approval in Europe. The average number of retreatments from months 3 to 11 was 2.7. Mean best corrected visual acuity (BCVA) increased steadily from baseline to month 3 to reach +5.8 letters, decreased slightly from month 3 to 6, and remained stable from month 6 to 12, reaching +3.6 at month 12. The mean change in CRT was −101.1 μm from baseline to month 3 and −91.5 μm from baseline to month 12.

In summary, data from the ANCHOR, MARINA, PIER, EXCITE, and SUSTAIN studies indicated that after a loading dose period of three monthly injections, subsequently monthly ranibizumab injections give superior visual acuity outcomes compared to quarterly or PRN injections (Fig. 70.9).

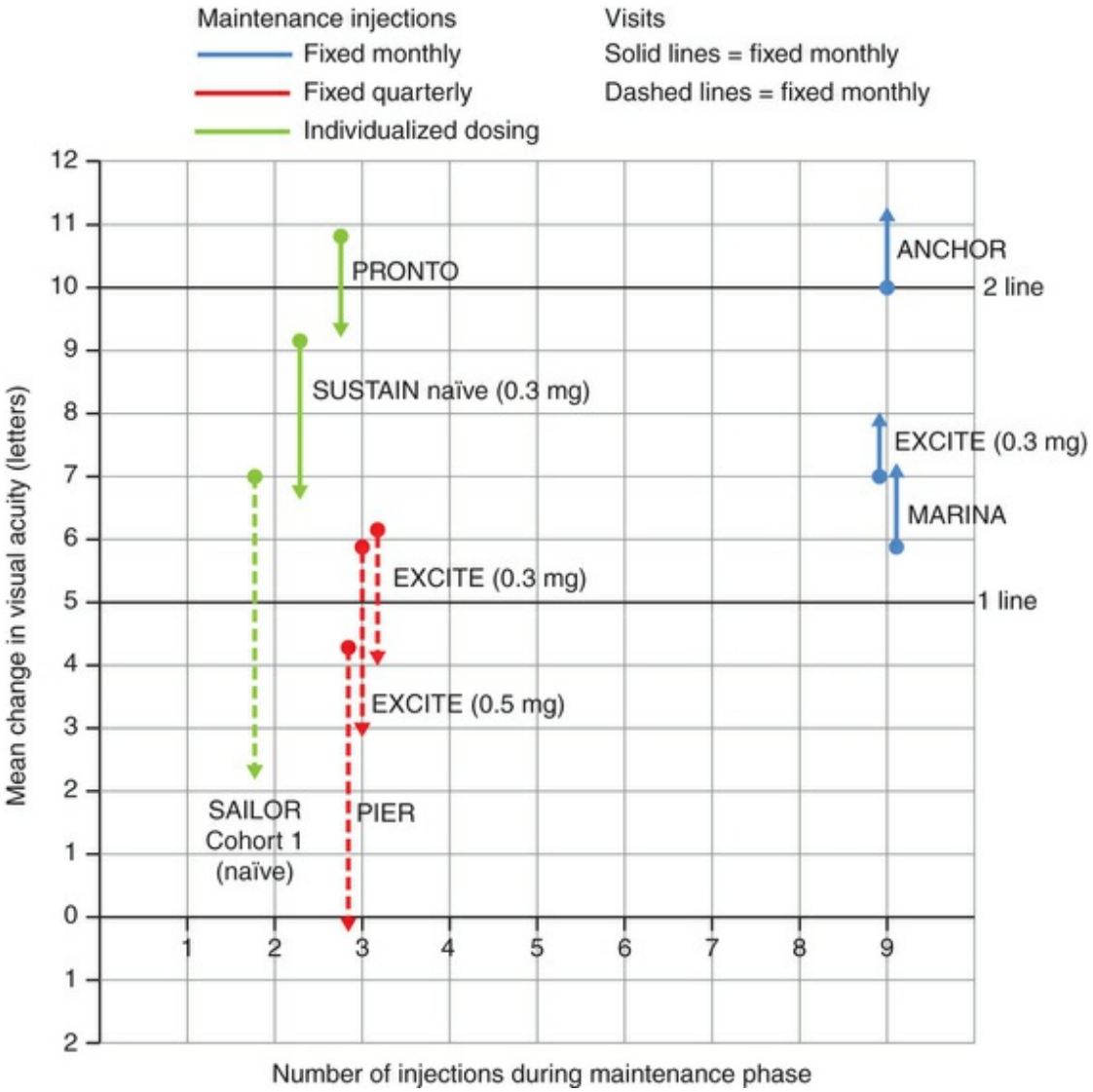

FIG. 70.9 Mean change in visual acuity from baseline at the end of the loading phase (●) and at 12 months (*arrowhead*) against the number of injections during 9 months of the maintenance phase (ranibizumab 0.5 mg data unless indicated). (Reproduced with permission from Mitchell P, Korobelnik JF, Lanzetta P, et al. Ranibizumab (Lucentis) in neovascular age-related macular degeneration: evidence from clinical trials. Br J Ophthalmol 2010;94:2–13.)

In the PrONTO (Prospective OCT Imaging of Patients with Neovascular AMD Treated with Intraocular Lucentis) study, patients (n=40) received 0.5 mg ranibizumab at entry, month 1, and month 2.[147] OCT measurements were obtained at baseline and at least monthly after injection (more frequently during the first two months after entry). Fluorescein angiograms were obtained at baseline and every 3 months thereafter. Retreatment with

ranibizumab was done only if one or more of the following conditions was observed: (1) OCT central retinal thickness increased 100 μm; (2) ≥5 letter visual loss associated with subretinal fluid (as judged with OCT); (3) new onset classic CNV; (4) new macular hemorrhage; (5) persistent subretinal or intraretinal fluid was present one month after the previous injection. One day after the first injection, there was a decrease in the mean OCT thickness of 47 μm. By month 12, the mean visual acuity improved by 9.3 letters (p<.001), and the mean central thickness decreased by 178 μm compared with baseline (p<.001). Mean visual acuity improvement was 9.3 letters, and the mean RCT had decreased by 178 μm. The average number of injections over the first year was 5.6. Visual acuity improved ≥15 letters in 35% of patients, and once macular fluid resorbed completely, the mean interval before another injection was 4.5 months. During the second year, the retreatment criteria were amended to include retreatment if any qualitative increase in the amount of fluid was detected using OCT.[148] Forty patients were enrolled and 37 completed the 2-year study. At month 24, the mean visual acuity improved by 11.1 letters (p<.001), and CRT decreased by 212 μm (p<.001). Visual acuity improved by 15 letters or more in 43% of patients. These visual acuity and OCT outcomes were achieved with an average of 9.9 injections over 24 months. The PrONTO Study data suggested that OCT-guided variable-dosing regimens with intravitreal ranibizumab were capable of achieving visual acuity outcomes comparable to those from the phase III clinical studies, but with fewer intravitreal injections.

Although the risk of arterial thromboembolic events was not increased to a statistically significant degree among ranibizumab-treated patients in these phase III studies (overall risk ~2.1% in ranibizumab-treated patients during year 1 vs. ~1.1% among controls), some concerns were expressed about relative safety compared with alternative therapies, efficacy aside, as the studies were not powered for statistical significance between the two different ranibizumab doses. Year-2 data from the MARINA study indicate the overall rate of antiplatelet trialists' collaboration (APTC)-defined arterial thromboembolic events, which includes nonfatal myocardial infarction, nonfatal stroke, and death from a

vascular or unknown cause,[149] was 4.6%, 4.6%, and 3.8% among the 0.5-mg ranibizumab, 0.3-mg ranibizumab, and control cohorts, respectively. Year-2 data from the ANCHOR study indicate the overall rate of APTC arterial thromboembolic events was 5%, 4.4%, and 4.2% in the 0.5-mg, 0.3-mg, and verteporfin-PDT cohorts, respectively. The PIER[143,144] and EXCITE[145] studies had similar results in this regard.

The SAILOR study was a phase IIIb study whose objectives were to evaluate the safety of 0.3 mg and 0.5 mg Lucentis in patients with AMD-associated subfoveal CNV. In cohort 1 of this study, the dose was randomly assigned and administered once a month for 3 months and thereafter as needed based on retreatment criteria. In SAILOR, there was a numerically higher rate of cerebrovascular stroke with 0.5 mg ranibizumab compared with 0.3 mg ranibizumab (1.2 vs. 0.7%), which was not statistically significant in patients with a history of stroke.[150] In the SUSTAIN study, a total of 249 patients (48.5%) reported ocular adverse events, 5 patients (1.2%) with ocular serious adverse events involving the study eye (retinal hemorrhage, cataract, retinal pigment epithelial tear, reduced visual acuity, vitreous hemorrhage), 19 patients (3.7%) with arteriothromboembolic events were observed, with 8 deaths (1.5%).[146] The most frequent adverse events in the study eye were reduced visual acuity (18.5%), retinal hemorrhage (7.2%), increased intraocular pressure (7.0%), and conjunctival hemorrhage (5.5%). Overall, the ocular and systemic risks associated with ranibizumab use appear to be low and within a reasonable range when taking into account the associated likelihood of visual improvement in properly selected patients (Table 70.2).

TABLE 70.2

Summary of Key Ocular and Nonocular Adverse Events in Ranibizumab Clinical Trials

	MARINA (24-Month Data)			ANCHOR (12-Month Data)		
	Ranibizumab 0.3 mg (*n* = 238)	Ranibizumab 0.5 mg (*n* = 240)	Sham control (*n* = 238)	Ranibizumab 0.3 mg (*n* = 137)	Ranibizumab 0.5 mg (*n* = 140)	Verteporfin control (*n* = 143)
KEY SERIOUS OCULAR ADVERSE EVENTS						

Presumed endophthalmitis	2 (0.8)	3 (1.3)	0	0	2 (1.4)	0
Culture-positive	0	0	0	0	1 (0.7)	0
Culture-negative	1 (0.4)	3 (1.3)	0	0	0	0
Culture not done	1 (0.4)	0	0	0	1 (0.7)	0
Uveitis	3 (1.3)	3 (1.3)	0	0	1 (0.7)	0
Retinal detachments	0	0	1 (0.4)	1 (0.7)	0	1 (0.7)
Retinal tear	1 (0.4)	1 (0.4)	0	0	0	0
Retinal hemorrhage	NA	NA	NA	NA	NA	NA
Detachment of RPE	NA	NA	NA	NA	NA	NA
Vitreous hemorrhage	1 (0.4)	1 (0.4)	2 (0.8)	1 (0.7)	0	0
KEY NONOCULAR ADVERSE EVENTS						
Hypertension	41 (17.2)	39 (16.3)	18 (16.1)	3 (2.2)	9 (6.4)	12 (8.4)
KEY ARTERIAL THROMBOEMBOLIC EVENTS (NONFATAL)						
Myocardial infarction	6 (2.5)[a]	3 (1.3)[b]	4 (1.7)	1 (0.7)	3 (2.1)	1 (0.7)
Stroke	3 (1.3)[c]	6 (2.5)[b,d]	2 (0.8)[e,f]	0	1 (0.7)	1 (0.7)
Cerebral infarction	NA	NA	NA	1 (0.7)	0	0
DEATH						
Vascular cause	3 (1.3)[c,g]	3 (1.3)[h]	4 (1.7)[i]	1 (0.7)[j]	2 (1.4)[k]	1 (0.7)[j]
Nonvascular cause	2 (0.8)	3 (1.3)	2 (0.8)	2 (1.5)	0	1 (0.7)
Nonocular hemorrhage	22 (9.2)	21 (8.8)	13 (5.5)	7 (5.1)	9 (6.4)	3 (2.1)

[a]One patient had two episodes.

[b]One patient had a myocardial infarction and a hemorrhagic stroke, both nonfatal.

[c]One patient had a nonfatal ischemic stroke and died of an unknown cause.

[d]One patient had a cerebral ischemic incident that was categorized as an ischemic stroke.

[e]One patient in the sham group received a single ranibizumab 0.5-mg dose in error approximately 8 months before the onset of stroke.

[f]One patient had a second episode of stroke, which resulted in death.

[g]Two patients died from myocardial infarction and one from an unknown cause.

[h]One patient died from a small- bowel infarct and two from stroke.

[i]Two patients died from stroke, one from congestive heart failure, and one from an unknown cause.

[j]One patient died from cardiac arrest.

[k]One patient died from cardiac failure and one from worsening of chronic heart failure.

[l]One patient died from cerebral hemorrhage.

[m]One patient died from cardiorespiratory arrest.

AE, adverse event; NA, not available; RPE, retinal pigment epithelium.

Reproduced with permission from Mitchell P, Korobelnik JF, Lanzetta P, et al. Ranibizumab (Lucentis) in neovascular age-related macular degeneration: evidence from clinical trials. Br J Ophthalmol 2010;94(1):2–13.

HARBOR

HARBOR is a 24-month duration phase III randomized clinical trial in which patients with active subfoveal CNV were randomized 1:1:1:1 to receive intravitreal ranibizumab 0.5 mg monthly, 0.5 mg × 3 loading doses with monthly follow-up and additional injections as needed, 2.0 mg monthly, or 2.0 mg × 3 loading doses with monthly follow-up and additional injections as needed (Fig. 70.10).[151,152] Patients in the PRN cohorts received additional injections if there was ≥5 ETDRS letter decrease from the previous visit or any evidence of disease activity on SD-OCT. The primary endpoint was the mean change from baseline in BCVA at month 12. Secondary endpoints included the mean change from baseline in BCVA at month 24, the mean number of ranibizumab injections, the mean change from baseline in central foveal thickness by SD-OCT over time, and the proportion of patients who gained ≥15 ETDRS letters in BCVA. There was no significant difference in visual outcome between the 0.5-mg-monthly and 2.0-mg-monthly cohorts (approximately 9 ETDRS letter gain), and there was no significant difference in outcome between the 0.5-mg-PRN and 2.0-mg-PRN cohorts (8 ETDRS letter gain) (Fig. 70.11). There was no clinically important difference in BCVA outcome between the monthly and PRN cohorts for each ranibizumab dose. Of note, the 0.5-mg-PRN cohort received a mean of 13.3 injections during the 24-month follow-up (vs. 21.4 in the monthly cohort), and the 2.0-mg-PRN cohort received a mean of 11.2 injections during the 24-month follow-up (vs. 21.6 in the monthly cohort). Thus, PRN injection posology (which includes 3 monthly loading doses) results in a 40–50% reduction in the number of injections without compromising BCVA outcome during the 24-month follow-up period. In fact, only 7% of the patients in the 0.5-mg-PRN cohort and only 2% in the 2-mg-PRN cohort required monthly injections during the 24-month

follow-up. Mean change in central foveal thickness at 24-month follow-up was comparable for all cohorts (~175 μm reduction from baseline), with the majority of the reduction having occurred by month 3. The proportion of patients gaining ≥15 ETDRS letters was comparable in all cohorts (~30–35%). Higher dosing of ranibizumab was not associated with an increase risk of systemic complications such as antiplatelet trialists collaboration arterial thromboembolic events, death, nonfatal myocardial infarction, or nonfatal cerebrovascular accident.

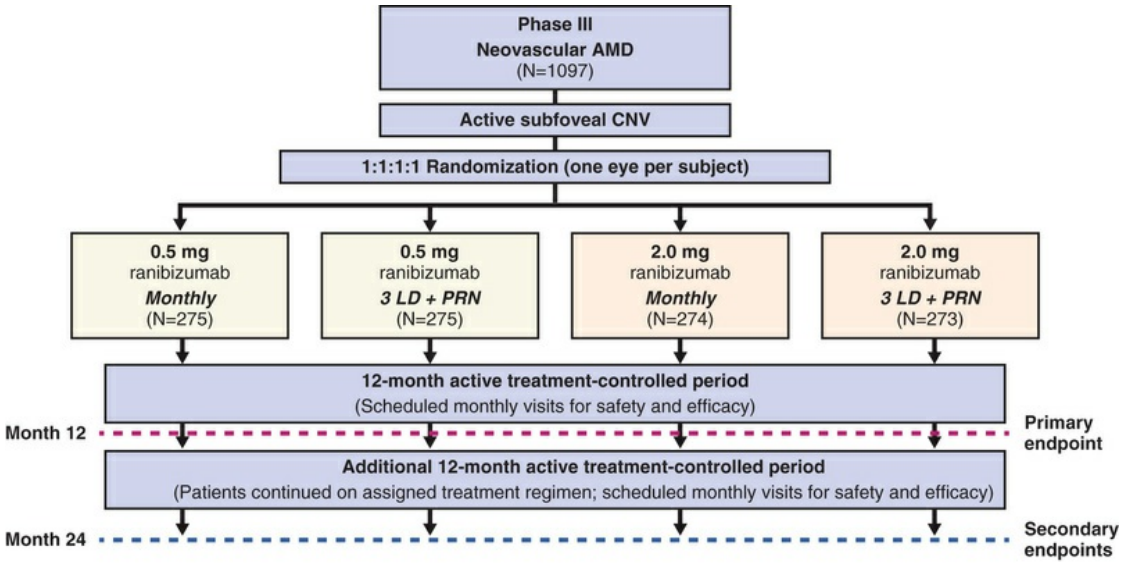

AMD = age related macular degeneration; CNV = choroidal neovascularization; LD = Loading dose; PRN = as needed.

FIG. 70.10 HARBOR phase III study design. (Reproduced with permission from Busbee et al. Ophthalmology. 2013;120(5):1046-1056; Ho et al. Ophthalmology. 2014;121(11):2181-9.)

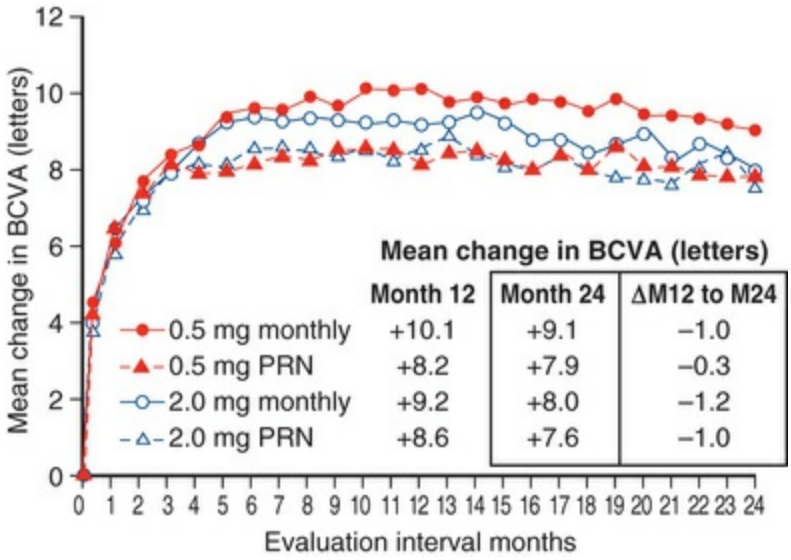

FIG. 70.11 HARBOR phase 3 study visual outcomes.

(Reproduced with permission from Busbee et al. Ophthalmology. 2013;120(5):1046-1056; Ho et al. Ophthalmology. 2014;121(11):2181-92.)

The development of GA was assessed in the HARBOR trial using fluorescein angiography and color fundus photographs. Atrophy was defined as well-defined areas of depigmentation with increased visibility of choroidal vessels at least 250 μm in diameter that correspond to flat areas of well-demarcated staining on fluorescein angiography. Atrophy associated without RPE-tears was not included. Rates of atrophy in ranibizumab-treated eyes were 9% at month 3, 21% at month 12, and 29% at month 24. These rates are similar to those reported in the CATT (20%, month 24) and IVAN (28%, month 24) trials. Visual outcome was similar among patients with vs. without GA at baseline, indicating that even if GA is present at baseline and even if treatment increases the risk of developing GA (still an unproved hypothesis), BCVA outcome at month 24 in the setting of active subfoveal CNV is still far better with 0.5 mg ranibizumab therapy than without it. In the HARBOR trial, risk factors for developing GA included the presence of intraretinal cysts (by OCT) at baseline and presence of GA in the fellow eye. The presence of subretinal fluid at baseline seemed to be associated with a reduced risk of developing GA. It is important to note that patients with subretinal fluid were treated according to their preassigned protocol throughout the HARBOR trial to achieve the observed visual outcomes. There was a trend for the 2.0-mg-monthly cohort to have an increased risk of GA compared to the

0.5-mg-PRN cohort, but the difference in risk was not statistically significant. Patients receiving 0.5 mg ranibizumab monthly had a statistically significant increased risk of developing GA compared to patients receiving 0.5 mg as needed. Thus, monthly treatment may be associated with a higher risk of developing GA. Data with regard to GA from the HARBOR study should be interpreted with caution because (1) this analysis was done post-hoc; (2) there was no natural history control group; (3) detection methods for GA were not optimal (e.g., fundus autofluorescence was not obtained); and (4) quantitative data on progression were not obtained.

Comparison of Age-Related Macular Degeneration Treatments Trial (CATT)

Despite a relative lack of level 1 evidence prior to 2011, bevacizumab had become the most widely used agent for AMD in the world due to a number of factors, including its low cost compared to ranibizumab, similarity in therapeutic mechanism, and its availability to physicians prior to the FDA approval of ranibizumab. A large amount of data from retrospective reviews, interventional case series, and anecdotal reports has provided physicians with evidence to support the continued off-label use of bevacizumab. However, in the absence of a large, randomized clinical controlled trial comparing bevacizumab to ranibizumab, the gold standard treatment, several questions have arisen: (1) Does one treatment offer superior visual outcomes to another? (2) What is the optimal treatment regimen and interval? (3) Is the safety profile of bevacizumab comparable to that of ranibizumab, which has been subjected to rigorous phase 1–phase 4 evaluation? The CATT was designed to address these questions.[129]

The CATT is a multicenter, randomized clinical trial, that enrolled 1,208 patients with previously untreated subfoveal CNV due to AMD, as determined by leakage on fluorescein angiogram and fluid on time-domain OCT. The primary outcome measure in the study was visual acuity change. The study designers also elected to examine the proportion of patients with a 15-letter difference in vision, number of injections, fluid and thickness on OCT, lesion size on fluorescein angiography, incidence of ocular and systemic adverse events, and annual treatment cost as

secondary treatment endpoints. Patients were randomized to one of four groups: (1) ranibizumab 0.5 mg monthly (every 28 days); (2) bevacizumab 1.25 mg monthly; (3) ranibizumab as needed (when signs of active neovascularization were present); (4) bevacizumab as needed (with the same indications for retreatment as in group 3). The study was designed to determine noninferiority of one treatment group with respect to each of the remaining three groups, using a statistically robust 99.2% confidence interval and a noninferiority limit of 5 ETDRS letters.

Visual acuity data were available for 1,105 patients at one year. The six pairwise comparisons showed the following: (1) bevacizumab monthly injections (8.0 letters gained) and ranibizumab monthly injections (+8.5 letters) yielded equivalent visual outcomes; (2) bevacizumab given as needed (+5.9 letters) was also equivalent to ranibizumab similarly given as needed (+6.8 letters); (3) ranibizumab given as needed was equivalent to ranibizumab given monthly; (4) ranibizumab given was also equivalent to bevacizumab given monthly; (5) bevacizumab given as needed when compared to bevacizumab given monthly or (6) ranibizumab given monthly, was not noninferior (inconclusive). Detailed visual and anatomic outcome data are shown in Fig. 70.12 and Table 70.3.

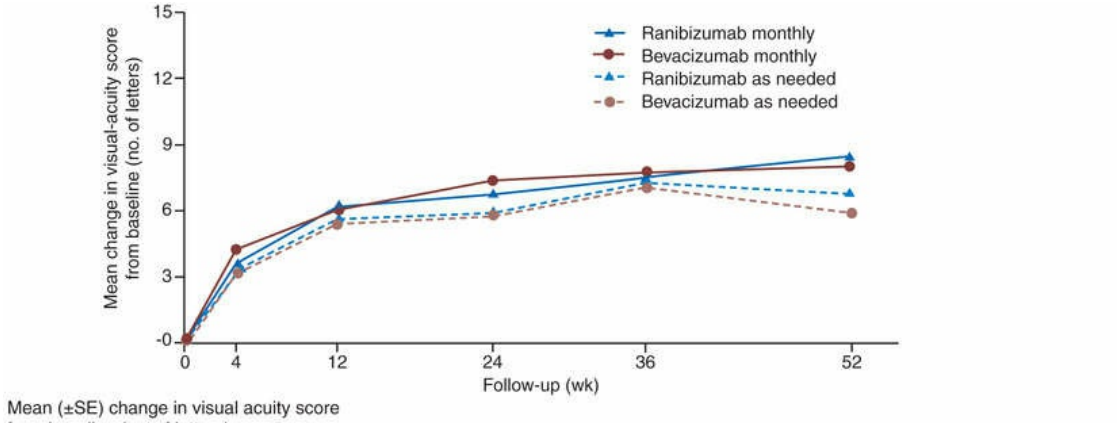

Mean (±SE) change in visual acuity score from baseline (no. of letters)

Ranibizumab monthly	+3.6±0.5	+6.1±0.7	+6.6±0.8	+7.5±0.9	+8.5±0.8
Bevacizumab monthly	+4.3±0.6	+6.1±0.7	+7.3±0.9	+7.7±1.0	+8.0±1.0
Ranibizumab as needed	+3.3±0.6	+5.6±0.7	+5.8±0.7	+7.2±0.7	+6.8±0.8
Bevacizumab as needed	+3.2±0.5	+5.6±0.7	+5.8±0.8	+7.1±0.9	+5.9±1.0

A

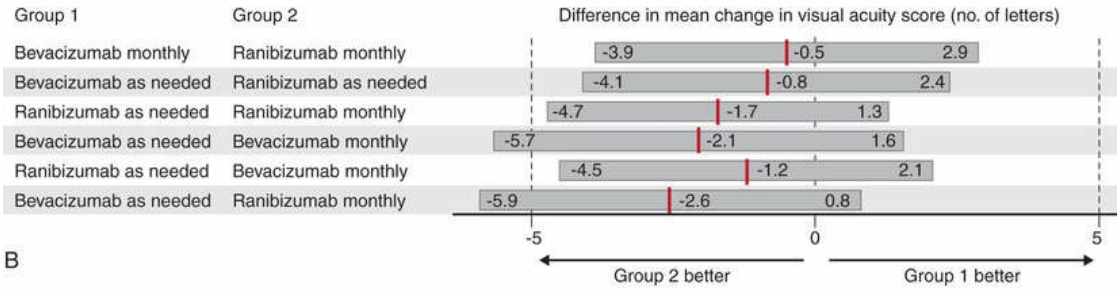

B

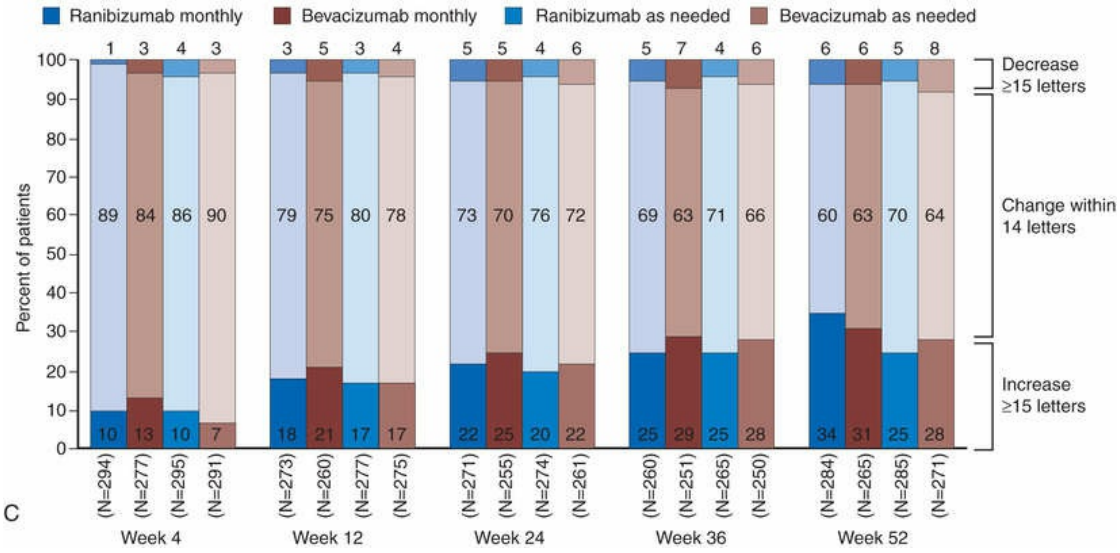

C

FIG. 70.12 Comparison of Age-Related Macular Degeneration Treatments Trials Research, first-year study results. (A) Mean change in the visual-acuity score during the first year of follow-up. (B) Differences between pairs of study groups in the mean change from baseline to 1 year in the visual-acuity score. The red vertical lines indicate means, and the gray bars 99.2% confidence intervals. Negative values reflect a

greater mean increase in group 2. Confidence intervals within −5 and +5 letters (dashed vertical lines) indicate that the two groups are equivalent. Confidence intervals extending beyond the noninferiority limit of −5 letters indicate that the comparison of the two groups is inconclusive with respect to noninferiority. (C) Proportions of patients in each group with a decrease of 15 letters or more, a change within 14 letters, or an increase of 15 letters or more from baseline values during the first study year. (Reproduced with permission from Martin DF, Maguire MG, Ying GS, et al. Ranibizumab and bevacizumab for neovascular age-related macular degeneration. N Engl J Med 2011;364:1897–1908.)

TABLE 70.3

CATT One-Year Outcomes: Primary Outcome (Visual Acuity) and Additional Outcomes

Outcome	Ranibizumab		Bevacizumab		*p* value
	Monthly *n* = 284	As needed *n* = 285	Monthly *n* = 265	As needed *n* = 271	
ETDRS Letter Score (Snellen Equivalent), No. (%)					
83–97 (20/12–20/20)	42 (14.8)	38 (13.3)	45 (17.0)	40 (14.8)	
68–82 (20/25–20/40)	149 (52.5)	141 (49.5)	134 (50.6)	127 (46.9)	
53–67 (20/50–20/80)	52 (18.3)	66 (23.2)	47 (17.7)	57 (21.0)	
38–52 (20/100–20/160)	23 (8.1)	23 (8.1)	21 (7.9)	24 (8.9)	
≤37 (≤20/200)	18 (6.3)	17 (6.0)	18 (6.8)	23 (8.5)	
Mean letter score (±SD)	68.8 ± 17.7	68.4 ± 16.4	68.4 ± 18.2	66.5 ± 19.0	.45
Change from Baseline Vision, no. (%)					
≥15 letter increase	97 (34.2)	71 (24.9)	83 (31.3)	76 (28.0)	
5–14 letter increase	90 (31.7)	103 (36.1)	98 (37.0)	90 (33.2)	
≤4 letter change	62 (21.8)	75 (26.3)	50 (18.9)	59 (21.8)	
5–14 letter decrease	19 (6.7)	23 (8.1)	18 (6.8)	23 (8.5)	
≥15 letter decrease	16 (5.6)	13 (4.6)	16 (6.0)	23 (23.8)	
Mean change (letters ±SD)	8.5 ± 14.1	6.8 ± 13.1	8.0 ± 15.8	5.9 ± 15.7	.16
OCT Foveal Thickness (μm)[a]					
Mean total thickness[b]	266 ± 125	294 ± 139	300 ± 149	308 ± 127	.002
Mean change from baseline[c]	−196 ± 176	−168 ± 186	−164 ± 181	−152 ± 178	.03
Mean number of injections	11.7 ± 1.5	6.9 ± 3.0	11.9 ± 1.2	7.7 ± 3.5	<.001
Average annual cost/patient	$23 400	$13 800	$595	$385	

[a]The total foveal thickness includes the retina, subretinal fluid, choroidal neovascularization, and retinal pigment epithelial elevation.

[b]Data were missing for 4 patients in the ranibizumab-monthly group, 4 patients in the

ranibizumab-as-needed group, 4 patients in the bevacizumab-monthly group, and 5 patients in the bevacizumab-as-needed group.

[c]Data were missing for 4 patients in the ranibizumab-monthly group, 7 patients in the ranibizumab-as-needed group, 5 patients in the bevacizumab-monthly group, and 6 patients in the bevacizumab-as-needed group.

Reproduced with permission from Martin DF, Maguire MG, Ying GS, et al. Ranibizumab and bevacizumab for neovascular age-related macular degeneration. N Engl J Med 2011;364:1897–908.

Secondary visual outcomes were similarly equivalent, with 91.5% (bevacizumab PRN) to 95.4% (ranibizumab PRN) of patients not having a decrease in vision of 15 letters or more from baseline, and 24.9% (ranibizumab PRN) to 34.2% (ranibizumab monthly) experiencing a gain of at least 15 letters. Anatomic outcomes showed that all groups had substantial decreases in retinal thickness as measured by OCT at 1 year, although the monthly ranibizumab group experienced a greater decrease in thickness (196±176 μm) than those patients receiving bevacizumab as needed (152±178 μm, p=.03). The mean number of injections given in the PRN groups was 7.7±3.5 (bevacizumab) and 6.9±3.0 (ranibizumab) out of 13 possible, translating to an average yearly cost of $385 vs. $13,800, respectively. The average cost to patients given monthly injections was $595 for bevacizumab and $23,400 for ranibizumab (Table 70.3).

Deaths occurred in 2.0% of the entire study group over the one-year period, with no significant difference among any of the groups. The occurrence of arteriothrombotic events was 2–3% for each group, also without significant differences. Venous thrombotic events occurred in 4 out of 286 patients receiving bevacizumab monthly (p=.08 difference between all groups) but occurred infrequently in all groups. When serious systemic adverse events were pooled among drug-specific groups, they occurred in 24.1% of patients receiving bevacizumab vs. 19.0% of those receiving ranibizumab (p=.04). Endophthalmitis occurred in 0.05% of the total number of injections, without a significant difference between medication groups. All other serious ocular adverse events occurred with rare frequency (Table 70.4).

TABLE 70.4

CATT First-Year Serious Adverse Events[a]

Event Type	Ranibizumab		Bevacizumab		*p* value	
	Monthly *n* = 301	As needed *n* = 298	Monthly *n* = 286	As needed *n* = 300	By Group	By Drug
SYSTEMIC EVENTS						
Death (all causes)	4 (1.3)	5 (1.7)	4 (1.4)	11 (3.7)	.18	.22
Arteriothrombotic event	7 (2.3)	6 (2.0)	6 (2.1)	8 (2.7)	.97	.85
Nonfatal myocardial infarction[b]	2 (0.7)	3 (1.0)	2 (0.7)	1 (0.3)	.78	.73
Nonfatal stroke	3 (1.0)	1 (0.3)	2 (0.7)	2 (0.7)	.88	1
Death from vascular causes	2 (0.7)	2 (0.7)	2 (0.7)	5 (1.7)	.57	.38
Venous thrombotic event	0	2 (0.7)	4 (1.4)	1 (0.3)	.08	.28
Transient ischemic attack	1 (0.3)	2 (0.7)	0	3 (1.0)	.48	1
Hypertension	0	0	2 (0.7)	0	.06	.24
One or more systemic event	53 (17.6)	61 (20.5)	64 (22.4)	77 (25.7)	.11	.04
OCULAR EVENTS						
Endophthalmitis	2 (0.7)	0	4 (1.4)	0	.03	.45
Pseudoendophthalmitis	1 (0.3)	0	0	0	1	1

[a]Multiple events in the same category counted only once.

[b]Includes deaths following myocardial infarction, stroke, or cardiac arrest.

Reproduced with permission from Martin DF, Maguire MG, Ying GS, et al. Ranibizumab and bevacizumab for neovascular age-related macular degeneration. N Engl J Med 2011;364:1897–908.

The impact of the one-year CATT study results was significant, establishing the equivalent visual outcomes of ranibizumab and bevacizumab when given monthly. Although bevacizumab as needed, when compared to ranibizumab or bevacizumab monthly, yielded inconclusive results, all other groups showed similar efficacy. Rosenfeld proposed in explanation that the treatment effect for bevacizumab may be less durable in some patients; thus, giving more frequent injections might improve visual outcomes in that subgroup.[153a] Importantly, the first-year study results also appeared to establish that as-needed ranibizumab (as well as monthly bevacizumab) was as effective as monthly ranibizumab, which not only has significant implications for treatment cost, but also for the cumulative risk of injection-associated adverse events, as well as patient anxiety surrounding treatment administration. Interestingly, although the effect of the medication on retinal thickness was more prominent for ranibizumab, this did not

translate to better vision as compared to bevacizumab. Finally, the study authors recognized that the CATT was insufficiently powered to determine a difference in infrequently occurring systemic and ocular adverse events, and although bevacizumab was associated with a higher overall rate of systemic adverse events, these events involved organ systems not typically associated with systemic anti-VEGF therapy. In particular, the rate of arteriothrombotic and venous thrombotic events was no different between the two medications, and was low in all groups. Additionally, the risk of adverse events was not noted to correlate with increased exposure to medication, with a higher rate of occurrence in patients receiving injections on an as-needed basis.

The second year results of CATT, published in mid-2012, described the visual impact of switching from monthly to PRN treatment after the first year, as well as any differences in disease activity or progression, as demonstrated by fluid on OCT, leakage on fluorescein angiography, and lesion size. In addition, the use of high-resolution spectral-domain OCT in year 2 allowed for comparison between standard and high-resolution imaging in the detection of disease activity.

At week 52 of the study, the study groups were modified such that monthly treatment groups were reassigned at random to either maintain monthly dosing or switch to as-needed dosing of the same medication. The existing PRN groups maintained the same dosing regimen. Comparisons in the second year were not made between each drug regimen group, as the reassignment resulted in a larger number of groups, and consequently reduced group size and statistical power. Rather, the analysis compared bevacizumab with ranibizumab, and monthly with as-needed dosing groups.

In patients maintaining the same dosing regimen (either monthly or as needed) through the 2-year study period, vision change remained similar, with monthly ranibizumab showing the greatest visual improvement (+8.8 letters), followed by monthly bevacizumab (+7.8), as-needed ranibizumab (+6.7), and as-needed bevacizumab (+5.0). There was no significant difference when comparing all ranibizumab groups with all bevacizumab groups (which showed 1.4 letters less gain relative to ranibizumab), but PRN therapy showed less vision improvement by 2.4 letters relative

to monthly therapy (p=.046). Secondary visual outcomes were also similar, including the final mean acuity (Snellen equivalent about 20/40 in all groups), the proportion gaining or losing 15 letters, and the proportion with 20/20 or better or 20/200 or worse final vision. Of note, those receiving bevacizumab as needed required more injections over the course of the study (14.1 total injections) than those receiving ranibizumab as needed (12.6), a significant difference consistent with the higher proportion of visits with detectable fluid.

Anatomic outcomes showed improved retinal thickness in patients treated monthly as compared to those treated as needed (29 μm difference, p=.005). Additionally, the proportion of patients without fluid as detected by OCT was lower in both the ranibizumab group and the monthly group (up to 45.5% in the monthly ranibizumab group); similarly, the proportion of patients with no fluorescein leakage was higher in patients treated monthly, and lesion area remained stable in these patients while growing in the as-needed group. However, the study also found that the proportion of monthly patients developing GA was significantly higher in patients receiving monthly treatment as compared to the as-needed group, with the highest rate in those receiving ranibizumab monthly. (Vision and anatomic outcomes are detailed in Fig. 70.13 and Table 70.5).

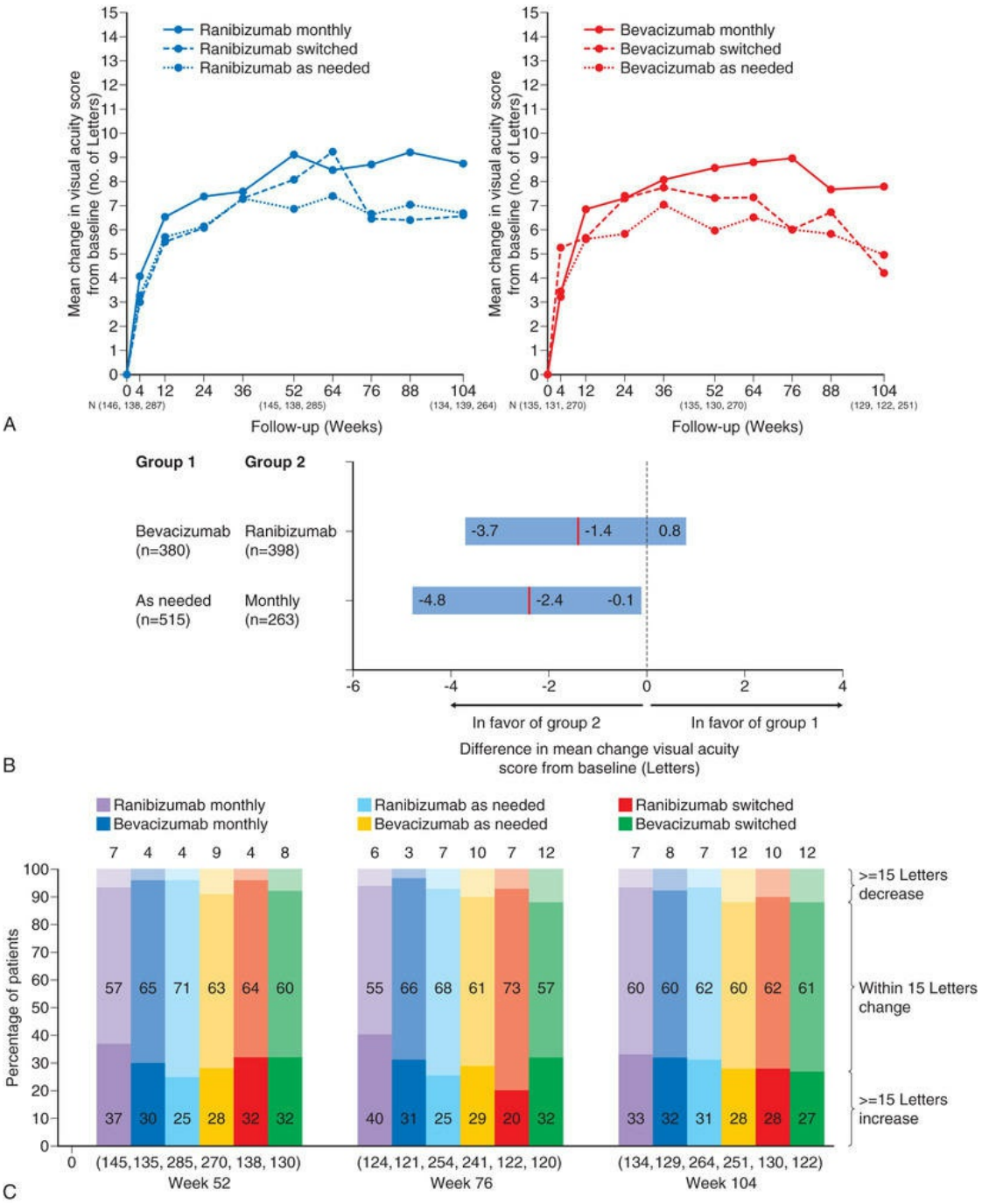

FIG. 70.13 (A) The mean change in visual acuity from enrollment over time by dosing regimen within drug group ranibizumab (left) and bevacizumab (right). (B) Differences in mean change in visual acuity at 2 years and 95% confidence intervals in patients treated with the same dosing regimen for 2 years. (C) The 3-line change in visual acuity from enrollment by treatment group and follow-up time. (Reproduced with permission from Martin DF, Maguire MG, Fine SL, et al. Ranibizumab and bevacizumab for treatment of neovascular age-related macular degeneration: two-year results. Ophthalmology.

TABLE 70.5

CATT 2-Year Outcomes: Patients Treated With the Same Dosing Regimen for 2 Years

Outcome	Ranibizumab		Bevacizumab		*p* value	
	Monthly *n* = 134	As Needed *n* = 264	Monthly *n* = 129	As Needed *n* = 251	By Drug	By Regimen
Visual Acuity Score (Letters) (Snellen Equivalent), no. (%)						
83–97 (20/12–20)	24 (17.9)	44 (16.7)	17 (13.2)	35 (13.9)		
68–82, (20/25–40)	67 (50.0)	123 (46.6)	61 (47.3)	121 (48.2)		
53–67 (20/50–80)	23 (17.2)	59 (22.3)	31 (24.0)	46 (18.3)		
38–52 (20/100–160)	11 (8.2)	23 (8.7)	14 (10.9)	28 (11.2)		
≤37 (≤20/200)	9 (6.7)	15 (5.7)	6 (4.7)	21 (8.4)		
Mean letters (SD)	68.5 (18.9)	68.5 (15.3)	68.2 (16.1)	66.0 (19.9)	.17	.41
Change in Visual Acuity Score from Baseline (Letters), no. (%)						
≥15 increase	44 (32.8)	81 (30.7)	41 (31.8)	71 (28.3)		
5–14 increase	49 (36.6)	78 (29.5)	36 (27.9)	79 (31.5)		
≤4 change	22 (16.4)	62 (23.5)	31 (24.0)	49 (19.5)		
5–14 decrease	10 (7.5)	24 (9.1)	11 (8.5)	23 (9.2)		
≥15 decrease	9 (6.7)	19 (7.2)	10 (7.8)	29 (11.6)		
Mean (SD)	8.8 (15.9)	6.7 (14.6)	7.8 (15.5)	5.0 (17.9)	.21	.046
No. Treatments, 2 yr mean (SD)	22.4 (3.9)	12.6 (6.6)	23.4 (2.8)	14.1 (7.0)	.01[a]	—
Mean Cost of Drug/Patient	$44,800	$25,200	$1170	$705		
Total Thickness at Fovea (μm)						
Mean (SD)[b]	267 (143)	293 (129)	274 (137)	306 (134)	.26	.005
Mean change (SD) from baseline[c]	−190 (172)	−166 (190)	−180 (196)	−153 (189)	.38	.08
Retinal Thickness and Subfoveal Fluid Thickness (μm)						
Mean (SD)[b]	162 (81)	167 (75)	166 (79)	169 (83)	.63	.53
Mean change (SD) from baseline[c]	−91 (152)	−78 (131)	−84 (133)	−84 (145)	.86	.54
Fluid on OCT, no. (%)						
None	61 (45.5)	59 (22.3)	39 (30.2)	35 (13.9)	.0003	<.0001
Present	69 (51.5)	198 (75.0)	87 (67.4)	212 (84.5)		
Unknown/missing	4 (3.0)	7 (2.7)	3 (2.3)	4 (1.6)		
Dye Leakage on Angiogram, no. (%)						
None	102 (76.1)	183 (69.3)	97 (75.2)	161 (64.1)	0.24	0.002
Present	24 (17.9)	75 (28.4)	27 (20.9)	81 (32.3)		
Unknown/missing	8 (6.0)	6 (2.3)	5 (3.9)	9 (3.6)		
Area of Lesion, mm^2						
Mean (SD)[d]	6.7 (7.8)	8.5 (7.4)	7.8 (8.5)	8.6 (8.3)	.44	.04
Mean change (SD) from baseline[e]	−0.4 (6.8)	1.9 (6.5)	1.6 (5.9)	3.0 (7.0)	.006	.0003
Geographic Atrophy, no. (%)[f]						
None	90 (70.3)	205 (84.0)	99 (80.5)	200 (85.8)	.13	.007
Nonfoveal	27 (21.1)	28 (11.5)	17 (13.8)	20 (8.6)		

Foveal	6 (4.7)	9 (3.7)	5 (4.1)	10 (4.3)		
Unknown/missing	5 (3.9)	2 (0.8)	2 (1.6)	3 (1.3)		

[a]Comparison restricted to as-needed groups.

[b]Number of unknown in each group unknown or missing: 3, 3, 3, 1.

[c]Number in each group unknown or missing: 3, 3, 6, 2.

[d]Includes choroidal neovascularization, hemorrhage, blocked fluorescence, serous pigment epithelium detachment, scar, geographic atrophy, nongeographic atrophy or tear of the retinal pigment epithelium, adjacent to the location of choroidal neovascularization at baseline. Number in each group unknown or missing: 12, 8, 16, 18.

[e]Number in each group unknown or missing: 16, 12, 22, 27.

[f]Areas of hypopigmentation or hyperfluorescence of ≥250 μm diameter having ≥2 of the following characteristics: circular shape, sharp borders, visible choroidal vessels. Areas meeting this definition surrounding a scar were not considered geographic atrophy. Excluded those with geographic atrophy at enrollment: 6 (4.4%), 6 (4.7%), 20 (7.8%), 18 (7.2%).

OCT, optical coherence tomography; SD, standard deviation. The dashes indicate that calculation of a *p* value is not appropriate. The treatment groups are defined by dosing regimen; therefore, the role of random variation in producing a difference by regimen is not relevant because by definition they are different.

Reproduced with permission from Martin DF, Maguire MG, Fine SL, et al. Ranibizumab and bevacizumab for treatment of neovascular age-related macular degeneration: two-year results. Ophthalmology 2012;119(7):1388-98.

In contrast to patients maintaining monthly therapy through 2 years, those switching to as-needed therapy at week 52 lost from 1.8 (ranibizumab) to 3.6 (bevacizumab) letters after year 1 (p=.03 when comparing monthly to PRN), resulting in very similar visual outcomes to patients maintained on as-needed therapy since study enrollment for both medications. Final visual acuity was similar for all groups, without significant differences between bevacizumab and ranibizumab, or between monthly and as-needed therapy. Anatomically, retinal thickness increased significantly, from 19 μm (ranibizumab) to 31 μm (bevacizumab) in patients who were reassigned to as-needed therapy. The proportion of patients without fluid on OCT was significantly lower in patients who switched regimens, as well as in patients receiving bevacizumab. As in patients receiving the same regimen through year 2, the proportion demonstrating dye leakage was higher in switched patients. Although the lesion area was not significantly different in either group, the rate of development of GA was higher in

ranibizumab patients as well as those receiving monthly dosing (Table 70.6).

TABLE 70.6

CATT 2-Year Outcomes: Patients Whose Dosing Regimen was Reassigned at 1 Year

Outcome	Ranibizumab		Bevacizumab		*p* value	
	Monthly *n* = 134	Switched *n* = 130	Monthly *n* = 129	Switched *n* = 122	Drug	Regimen
Visual Acuity Score (Letters) (Snellen Equivalent), no. (%)						
83–97 (20/12–20)	24 (17.9)	22 (16.9)	17 (13.2)	23 (18.9)		
68–82 (20/25–40)	67 (50.0)	61 (46.9)	61 (47.3)	54 (44.3)		
53–67 (20/50–80)	23 (17.2)	23 (17.7)	31 (24.0)	19 (15.6)		
38–52 (20/100–160)	11 (8.2)	13 (10.0)	14 (10.9)	11 (9.0)		
≤37, ≤20/200	9 (6.7)	11 (8.5)	6 (4.7)	15 (12.3)		
Mean letters (SD)	68.5 (18.9)	67.7 (18.5)	68.2 (16.1)	65.0 (21.8)	.39	.23
Change in Visual Acuity Score from 1 Year (Letters), no. (%)[a]						
≥15 increase	4 (3.0)	6 (4.6)	8 (6.2)	2 (1.7)		
5–14 increase	34 (25.6)	19 (14.6)	21 (16.3)	17 (14.0)		
≤4 change	58 (43.6)	66 (50.8)	63 (48.8)	61 (50.4)		
5–14 decrease	28 (21.1)	27 (20.8)	27 (20.9)	26 (21.5)		
≥15 decrease	9 (6.8)	12 (9.2)	10 (7.8)	15 (12.4)		
Mean (SD)	−0.3 (11.1)	−1.8 (11.2)	−0.6 (10.3)	−3.6 (12.1)	.29	.03
No. of Treatments, Year 2, mean (SD)	10.5 (3.1)	5.0 (3.8)	11.3 (2.3)	5.8 (4.4)	.11[b]	—
Cost of Drug/Patient	$21,000	$10,000	$565	$290		
Total Thickness at Fovea, μm						
Mean (SD)[c]	267 (143)	295 (135)	274 (137)	334 (190)	.09	.001
Mean change (SD) from1 yr[d]	1 (78)	31 (78)	−9 (94)	19 (114)	.18	.0004
Retinal Thickness and Subfoveal Fluid Thickness, μm						
Mean (SD)[c]	162 (81)	162 (63)	166 (79)	189 (116)	.04	.14
Mean change (SD) from 1 yr[d]	12 (51)	10 (46)	−5 (61)	16 (92)	.35	.12
Fluid on OCT						
None	61 (45.5)	25 (19.2)	39 (30.2)	22 (18.0)	.03	<.0001
Present	69 (51.5)	100 (76.9)	87 (67.4)	97 (79.5)		
Unknown/missing	4 (3.0)	5 (3.8)	3 (2.3)	3 (2.5)		
Dye Leakage on Angiogram						
None	102 (76.1)	88 (67.7)	97 (75.2)	80 (65.6)	0.59	0.01
Present	24 (17.9)	37 (28.5)	27 (20.9)	36 (29.5)		
Unknown/missing	8 (6.0)	5 (3.8)	5 (3.9)	6 (4.9)		
Area of Lesion, mm^2						
Mean (SD)[e]	6.7 (7.8)	9.0 (8.1)	7.8 (8.5)	8.2 (7.8)	0.80	0.06
Mean change (SD) from 1 year[f]	0.7 (4.5)	1.7 (5.3)	1.1 (4.0)	1.8 (5.7)	0.63	0.08
Geographic Atrophy, no. (%)[g]						
None	90 (70.3)	97 (80.8)	99 (80.5)	97 (86.7)	0.05	0.02
Nonfoveal	27 (21.1)	16 (13.3)	17 (13.8)	6 (5.4)		
Foveal	6 (4.7)	4 (3.3)	5 (4.1)	6 (5.4)		

Unknown/missing	5 (3.9)	3 (2.5)	2 (1.6)	3 (2.7)		

[a]Number in each group unknown or missing: 1, 0, 0, 1.

[b]Comparison restricted to as-needed groups.

[c]Number in each group unknown or missing: 3, 3, 3, 1.

[d]Number in each group unknown or missing: 5, 3, 4, 5.

[e]See Table 70.5 for definition. Number in each group unknown or missing: 12, 8, 8, 6.

[f]Number in each group unknown or missing: 22, 17, 15, 14.

[g]See Table 70.5 for definition. Excluded those with geographic atrophy at baseline: 6, 10, 6, 10.

OCT, optical coherence tomography; SD, standard deviation. The dashes indicate that calculation of a *p* value is not appropriate. The treatment groups are defined by dosing regimen; therefore, the role of random variation in producing a difference by regimen is not relevant because by definition they are different.

Reproduced with permission from Martin DF, Maguire MG, Fine SL, et al. Ranibizumab and bevacizumab for treatment of neovascular age-related macular degeneration: two-year results. Ophthalmology 2012;119(7):1388-98.

In contrast to the first year of the study, when all study patients underwent testing with time domain OCT only, in year 2 22.6% of scans were performed on high-resolution spectral domain OCT. Treatment decisions in the second year were consistent with reading center interpretation of OCT fluid in 68.5% of the ranibizumab group and 69.6% of the bevacizumab group; 95% of these cases resulted in undertreatment (the reading center interpreted fluid, yet the patient did not receive injection). The use of spectral domain OCT did not appear to increase the consistency between treating physicians and the reading center, with 70.1% agreement in the spectral domain group versus 68.7% in the time domain group.

As reported in the first year of results, the rate of systemic adverse events was significantly higher in the bevacizumab group than in the ranibizumab group, at 39.9% as compared to 31.7% overall, and 24.4% vs. 18.0% in the second year alone. Interestingly, this difference persisted even after excluding vascular events previously associated with systemic anti-VEGF drugs. In addition, as noted in the first year, over the course of 2 years patients treated as needed had a higher rate of systemic serious adverse events than those treated monthly (risk ratio of 1.30, p=.009), although this

difference in the second year alone was not significant. There was no difference between drugs in the proportion of patients who died (6.1% vs. 5.3%) or in the number of arteriothrombotic (5.0% vs. 4.7%) or venous thrombotic events (1.7% vs. 0.5%). Endophthalmitis occurred in 7 patients receiving bevacizumab and 4 patients receiving ranibizumab (p=.38), with 10 of these 11 cases occurring in patients receiving monthly therapy (Table 70.7).

TABLE 70.7
CATT Adverse Events Within 2 Years of Enrollment

Event Type	Ranibizumab (n = 599), no. (%)	Bevacizumab (n = 586), no. (%)	p value[a]
SYSTEMIC SERIOUS			
Death, all causes	32 (5.3)	36 (6.1)	.62
Arteriothrombotic events	28[b] (4.7)	29 (5.0)	.89
Nonfatal stroke	8 (1.3)	8 (1.4)	1
Nonfatal myocardial infarction	9 (1.5)	7 (1.2)	.80
Vascular death	12 (2.0)	14 (2.4)	.70
Venous thrombotic events	3 (0.5)	10 (1.7)	.054
Hypertension	3 (0.5)	4 (0.7)	.72
One or more serious event	190 (31.7)	234 (39.9)	.004
PREVIOUSLY ASSOCIATED WITH ANTI-VEGF TREATMENT[c]			
Yes	45 (7.5)	62 (10.6)	.07
No	170 (28.4)	202 (34.5)	.02
MEDDRA SYSTEM ORGAN CLASS[d]			
Cardiac disorders	47 (7.8)	62 (10.6)	.11
Infections	41 (6.8)	54 (9.2)	.14
Nervous system disorders	34 (5.7)	36 (6.1)	.81
Injury and procedural complications	23 (3.8)	35 (6.0)	.11
Neoplasms benign and malignant	27 (4.5)	22 (3.8)	.56
Gastrointestinal disorders	11 (1.8)	28 (4.8)	.005
Any other system organ class	81 (13.5)	104 (17.8)	.046
OCULAR EVENT, STUDY EYE			
Endophthalmitis	4 (0.7)	7 (1.2)	.38
Pseudoendophthalmitis	1 (0.2)	1 (0.2)	1

[a]Fisher exact test.

[b]One patient had both a nonfatal stroke and a nonfatal myocardial infarction.

[c]Arteriothrombotic events, systemic hemorrhage, congestive heart failure, venous thrombotic events, hypertension, and vascular death.

[d]Data are listed only for system organ classes with 35 or more events.

MedDRA, *Medical Dictionary for Regulatory Activities*; VEGF, vascular endothelial growth factor.

Reproduced with permission from Martin DF, Maguire MG, Fine SL, et al.

Ranibizumab and bevacizumab for treatment of neovascular age-related macular degeneration: two-year results. Ophthalmology. 2012;119(7):1388-98.

The second year of the CATT was not designed to determine the relative efficacy of each dosing regimen for each medication. However, the following conclusions may be drawn:

1. In contrast to the first-year results, longer-term follow-up suggests that as-needed therapy is less effective than monthly therapy overall in terms of visual gain.

2. Visual acuity and visual gain are associated with, but do not closely mirror, retinal thickness or presence of fluid.

3. One year of monthly therapy does not appear to confer lesion stability when subsequently changing to as-needed therapy.

4. When given as needed, bevacizumab is required more frequently than ranibizumab, on average 1.5 more injections over the 2-year period.

5. Geographic atrophy appears to occur with greater frequency in patients receiving monthly therapy.

6. Spectral domain OCT does not appear to increase the accuracy of identifying retinal fluid by the treating physician.

7. Endophthalmitis occurs at similar rates in ranibizumab- and bevacizumab-treated patients, although (as one may expect) it appears to be associated with an increased rate of injections, occurring most often in patients treated monthly.

8. The increased rate of systemic serious adverse events in bevacizumab persisted in the second year. The authors remained unsure of the reason for the increased risk ratio of systemic adverse events. As in the first year, the rate of vascular events previously associated with anti-VEGF therapy was similar in both groups.

The two-year CATT results certainly supported the continued off-label use of bevacizumab for exudative AMD. In addition, it appears that monthly dosing for any anti-VEGF therapy results in

better and more sustained visual outcomes than as-needed dosing. However, the decision of which treatment regimen should be made with careful consideration, given the cost of monthly therapy (roughly twice that of as-needed therapy for each drug respectively), as well as the possible (although unproven) increased risk of GA, which over a treatment course of years may lead to significant visual loss. Five-year outcomes of the CATT were published in 2016. Follow up visual acuity was available from 647 of the 914 living patients, with results demonstrating that visual gains attained in the first two years were lost in the subsequent 3 years after the conclusion of the study (−3 letters from baseline, −11 letters from the second year). Fifty percent of patients had at least 20/40 vision, with 10% maintaining 20/20 vision and 20% with 20/200 or worse. The primary cited reasons for decreased vision over the 3 years following study completion were increase in patients with retinal thinning (<120 microns); increase in prevalence of geographic atrophy; and increase in lesion size. Although conclusions cannot be drawn regarding particular treatment regimens or medications, the five-year outcomes confirmed the role of anti-VEGF therapy for AMD.[153b]

IVAN and Other Trials

Similar to the CATT, the IVAN (alternative treatments to Inhibit VEGF in Age-related choroidal Neovascularization) trial also compared administration of ranibizumab and bevacizumab in a continuous or regimen. The trial randomized 628 patients (with 610 receiving treatment) to one of the four groups (ranibizumab monthly or PRN, bevacizumab monthly or PRN), with the primary outcome measure of best corrected distance visual acuity (as measured by ETDRS letters). Secondary outcome measures included safety/adverse events, quality of life assessment, cost and resource use, and notably, serum VEGF levels. The trial specified a noninferiority limit of 3.5 letters. In contrast to CATT, eyes that met retreatment criteria (any subretinal or increasing intraretinal fluid or fresh blood, drop in vision, or specified criteria on fluorescein angiography in the absence of vision or OCT changes) required an additional cycle of 3 monthly injections.

Five hundred twenty-five patients completed 2-year follow-up in

the IVAN study. Visual acuity results were similar for each group (ranibizumab group: 67.8 letters; bevacizumab group: 66.1; continuous regimen: 66.6; discontinuous regimen: 67.3, see Fig. 70.14). Bevacizumab was neither noninferior nor inferior to ranibizumab, and the discontinuous regimen was neither noninferior nor inferior to the continuous regimen (inconclusive). As in the 1-year results, neurosensory retinal thickness and lesion thickness were lower in those receiving continuous therapy (314.7 μm vs. 338.5 μm). Discontinuous therapy was also associated with significantly higher rates of fluid on OCT and active neovascularization, compared with continuous administration. No drug differences existed for these indices. Similar to the CATT, there was a significantly higher rate of new GA occurring in the continuous regimen group, although there were no drug differences with respect to this condition.

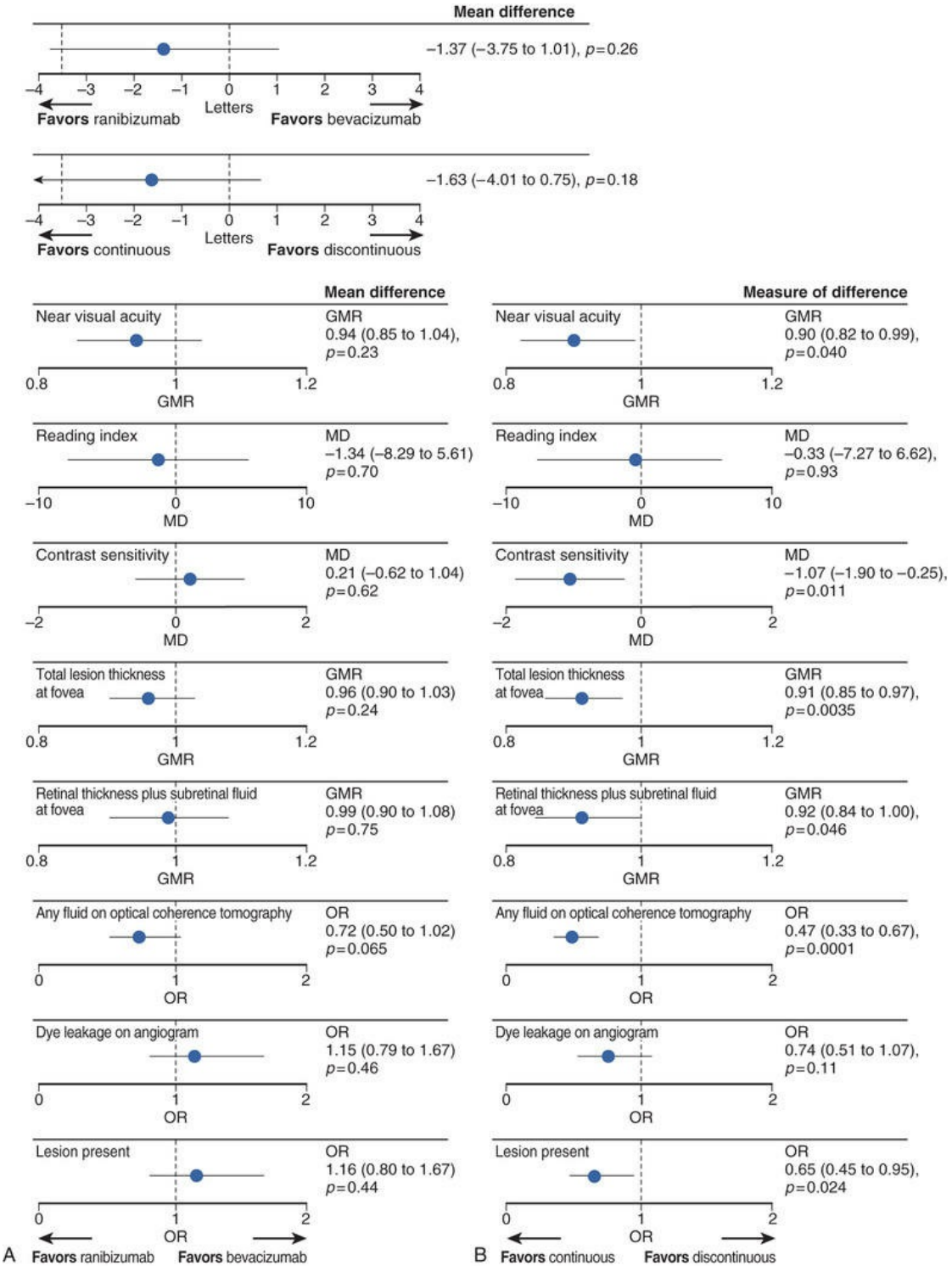

FIG. 70.14 IVAN results. Upper panel: Mean differences in best corrected distance visual acuity at 2 years. By drug (top) and by regimen (bottom). Black dashed line shows non-inferiority limit of –3.5 letters. Mean differences estimated with data from visits 0, 3, 6, 9, 12, 15, 18, 21, and 24, adjusted for center size. 95% CIs given in parentheses and shown by bars.

Lower panel: Secondary outcomes at 2 years: (A) by drug; (B) by regimen. 95% CIs given in parentheses and shown by bars. GMR, geometric mean ratio; IVAN, Inhibition of VEGF in Age-related choroidal Neovascularization trial; MD, mean difference; OR, odds ratio. (Reproduced with permission from Chakravarthy U, Harding SP, Rogers CA, et al. Alternative treatments to inhibit VEGF in age-related choroidal neovascularisation: 2-year findings of the IVAN randomised controlled trial. Lancet. 2013;382(9900):1258-67, Figs. 1,2.)

The rate of death was similar for each drug group, although more patients died in the discontinuous group than the continuous group. The rates of arteriothrombotic events or heart failure were similar in all groups, as were the rates of developing at least one systemic serious adverse event.

The authors of the IVAN pooled data from both the IVAN and CATT studies, confirming that bevacizumab was noninferior to ranibizumab, but also showing that discontinuous treatment was inferior to continuous treatment in terms of best corrected distance visual acuity (Fig. 70.15). Importantly, the finding from the CATT that continuous therapy led to higher rates of GA than discontinuous therapy was confirmed in the IVAN trial as well. The meta-analysis also showed that both mortality and the risk of serious adverse events were higher with discontinuous treatment, leading the authors to speculate that immunologic sensitization with intermittent dosing may play a role; there was no difference in mortality, serious adverse events, or vascular/arteriothrombotic events when comparing the two drugs (Fig. 70.16). As with the CATT, the IVAN trial suggests that bevacizumab and ranibizumab, and continuous and discontinuous, have similar efficacy (or at least very little clinically significant difference). However, the authors concluded that choosing a single optimal treatment strategy remains challenging, particularly in light of the mortality difference favoring continuous therapy, in contrast to the increased rate of GA (as well as the difference in cost) favoring discontinuous therapy.

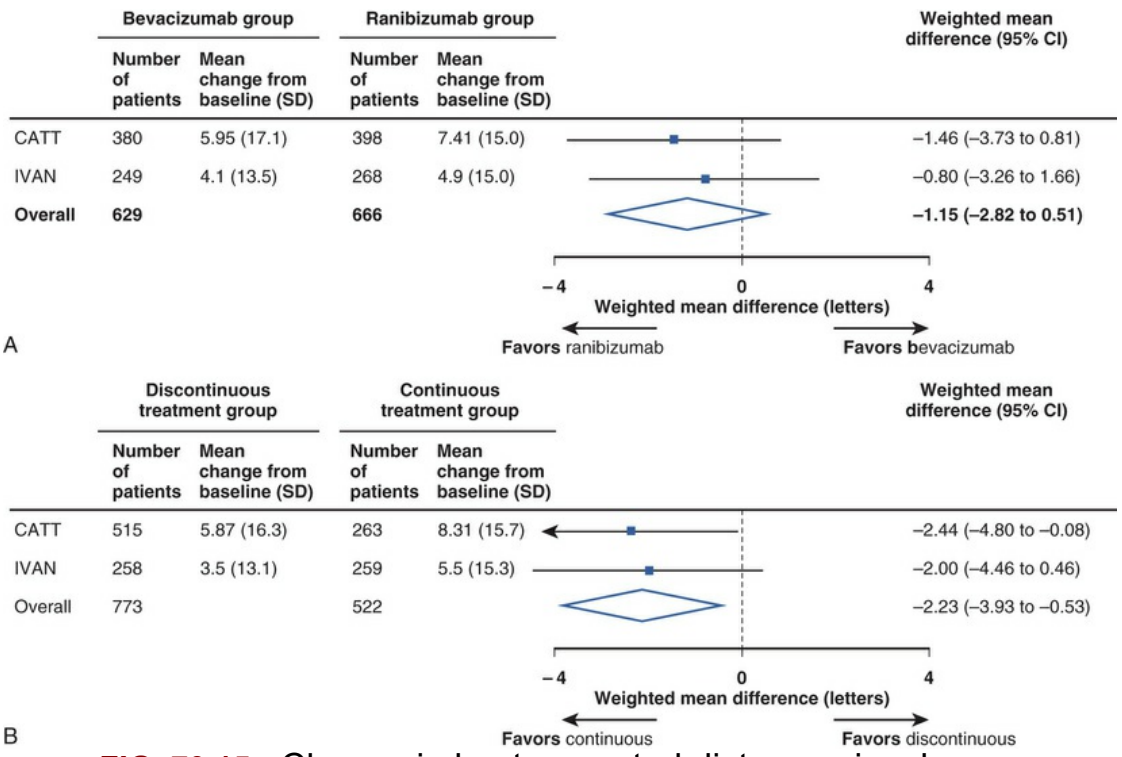

FIG. 70.15 Change in best corrected distance visual acuity in CATT and IVAN at 2 years: (A) by drug; (B) by regimen. 95% CIs shown by bars. CATT, Comparison of Age-related macula degeneration Treatment Trials; IVAN, Inhibition of VEGF in Age-related choroidal Neovascularization trial. (Reproduced with permission from Chakravarthy U, Harding SP, Rogers CA, et al. Alternative treatments to inhibit VEGF in age-related choroidal neovascularisation: 2-year findings of the IVAN randomised controlled trial. Lancet. 2013;382(9900):1258-67, Figs. 1,2.)

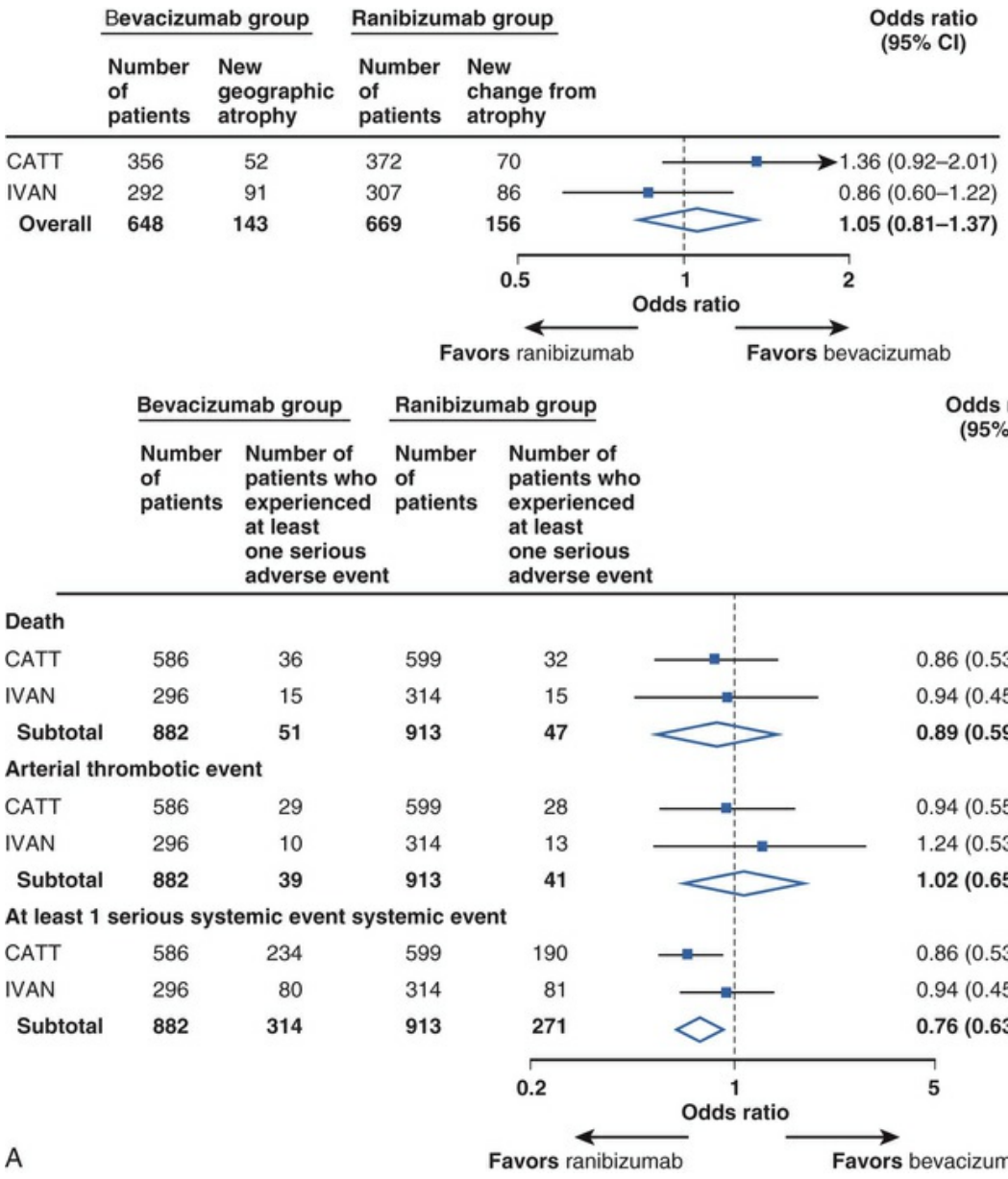
Bevacizumab group
Ranibizumab group
Odds ratio (95% CI)
Number of patients
New geographic atrophy
Number of patients
New change from atrophy
CATT 356 52 372 70 1.36 (0.92–2.01)
IVAN 292 91 307 86 0.86 (0.60–1.22)
Overall 648 143 669 156 1.05 (0.81–1.37)
0.5
1
2
Odds ratio
Favors ranibizumab
Favors bevacizumab
Bevacizumab group
Ranibizumab group
Odds ratio (95%CI)
Number of patients
Number of patients who experienced at least one serious adverse event
Number of patients
Number of patients who experienced at least one serious adverse event
Death
CATT 586 36 599 32 0.86 (0.53–1.41)
IVAN 296 15 314 15 0.94 (0.45–1.96)
Subtotal 882 51 913 47 0.89 (0.59–1.33)
Arterial thrombotic event
CATT 586 29 599 28 0.94 (0.55–1.60)
IVAN 296 10 314 13 1.24 (0.53–2.86)
Subtotal 882 39 913 41 1.02 (0.65–1.50)
At least 1 serious systemic event systemic event
CATT 586 234 599 190 0.86 (0.53–1.41)
IVAN 296 80 314 81 0.94 (0.45–1.96)
Subtotal 882 314 913 271 0.76 (0.63–0.93)
0.2
1
5
Odds ratio
Favors ranibizumab
Favors bevacizumab
A

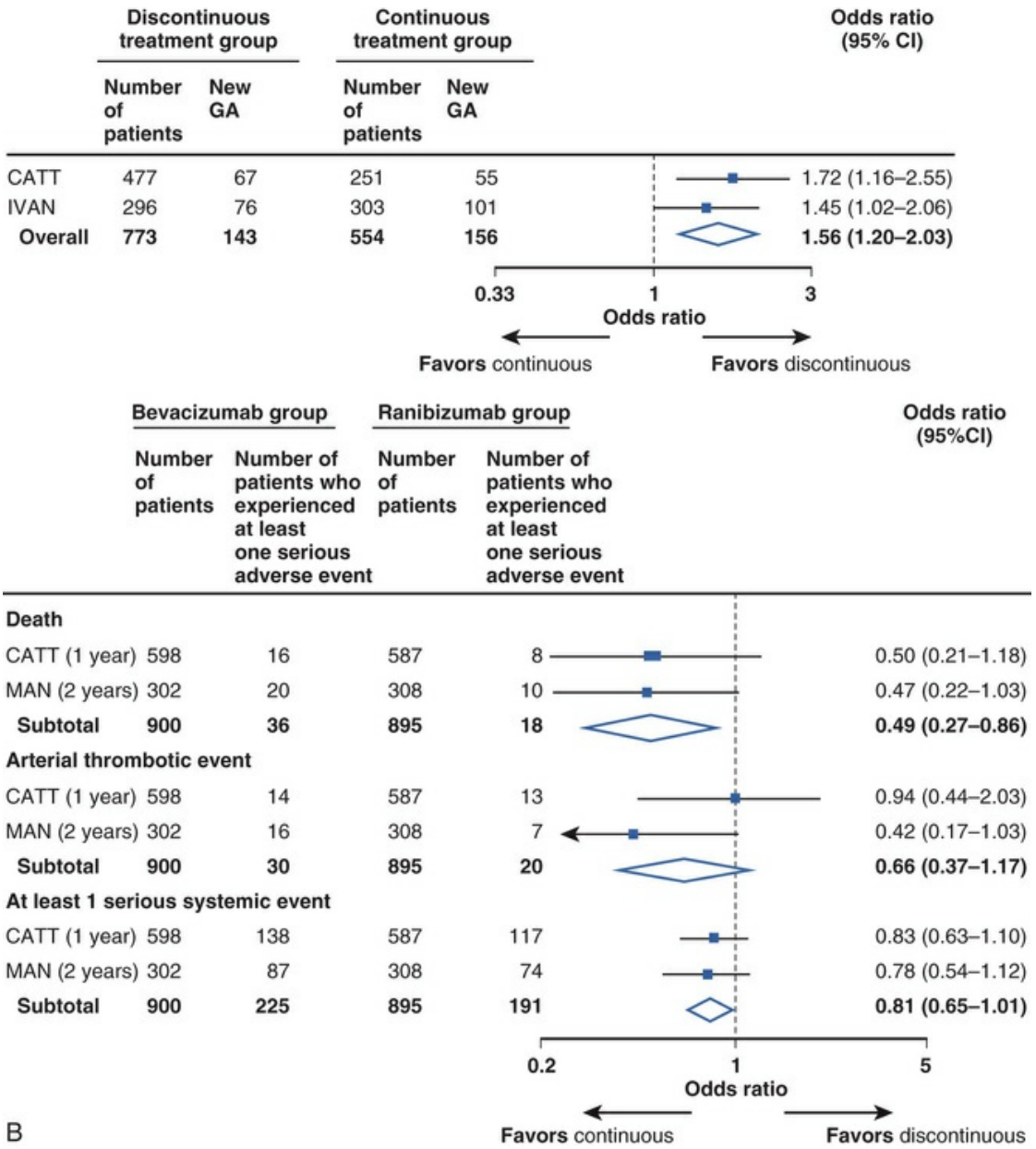

FIG. 70.16 Upper panel: Geographic atrophy in CATT and IVAN at 2 years. Lower panel: Safety outcomes in CATT and IVAN at 2 years. (A) By drug. (B) By regimen. 95% CIs shown by bars. CATT, Comparison of Age-related macular degeneration Treatment Trials; GA, geographic atrophy; IVAN, Inhibition of VEGF in Age-related choroidal Neovascularization trial.

(Reproduced with permission from Chakravarthy U, Harding SP, Rogers CA, et al. Alternative treatments to inhibit VEGF in age-related choroidal neovascularisation: 2-year findings of the IVAN randomised controlled trial. Lancet. 2013;382(9900):1258-67, Figs. 1,2.)

Since the CATT, several other studies have also compared ranibizumab and bevacizumab with various treatment strategies.

The Groupe d'Evaluation Français Avastin vs. Lucentis (GEFAL) study was a noninferiority trial performed in France, enrolling and randomizing 501 patients to bevacizumab and ranibizumab, given PRN with monthly follow-up, after an initial loading-dose period of three monthly injections. Bevacizumab and ranibizumab showed equivalent changes in BCVA (5.4 vs. 3.6 letters, respectively), and in the percentages of patients gaining or losing either 5 or 15 letters, with a similar number of injections required (6.8 vs. 6.5). There were no differences in the rate of adverse events. These results were felt to be consistent with the CATT results, although the visual gains were less than in the CATT due to a larger percentage of patients with poor vision (<20/200) at baseline in GEFAL, and hence fewer letters gained in this subgroup.[154] Similarly, the Multicenter Anti-VEGF Trial in Austria (MANTA) randomized 321 patients 1 : 1 to either bevacizumab or ranibizumab, given PRN (with monthly follow-up) after three monthly loading injections. The primary outcome (gain in BCVA at one year) was similar in each group, with a gain of 4.9 vs. 4.1 letters for bevacizumab and ranibizumab, respectively, requiring a mean of 6.1 vs. 5.8 injections. As in previous studies, the proportions of patients gaining or losing 5 or 15 letters were similar in both groups, as were the rates of significant adverse events.[155] In contrast to GEFAL and MANTA, the Comparison of Bevacizumab (Avastin) and Ranibizumab (Lucentis) in exudative Age-related Macular Degeneration (BRAMD) study randomized 327 patients to bevacizumab or ranibizumab, given monthly. Although the gain in BCVA was similar between the two groups (5.1 vs. 6.4 letters for bevacizumab and ranibizumab, respectively), a higher percentage of patients receiving bevacizumab experienced a gain (24% vs. 19%) or a loss (11% vs. 5%) of at least 15 letters when compared to ranibizumab. As in previous studies, anatomic outcomes revealed a higher percentage of patients receiving bevacizumab had fluid on OCT. Safety outcomes were similar in both groups.[156]

Many physicians have adopted the so-called "treat-and-extend" therapy as a strategy to reduce injection burden while maintaining regular surveillance for active exudative disease. The Lucentis Compared to Avastin Study (LUCAS) in Norway was first to address this regimen in a randomized controlled trial. Enrolling 441

patients, the trial randomized patients to receive either ranibizumab or bevacizumab to be given every 4 weeks until no active exudative disease was present as determined by OCT and fundus biomicroscopy.[157] The next follow-up and injection was then extended by 2 weeks at a time (6-week interval, followed by 8-week interval, and so on) until active neovascular disease was detected, to a maximum of 12 weeks. If a study examiner determined that there was disease recurrence or persistent activity, the interval was then shortened by 2 weeks at a time until the disease became inactive again, with subsequent extension to a maximum of 2 weeks shorter than the interval at the previous recurrence. Nonresponders (patients with no change or increase in central retinal thickness after the first three injections) were allowed to withdraw from the study (20 patients). The study was designed as a noninferiority trial with a limit of 5 letters. In the 86% of study patients who completed one year of follow-up, the change in BCVA was equivalent in both the bevacizumab (+7.9 letters) and ranibizumab (+8.2 letters) groups, and the proportions of patients gaining or losing 5 or 15 letters were also similar. Anatomic outcomes revealed a similar decrease in CRT in both groups (−112 μm vs. −120 μm for bevacizumab and ranibizumab, respectively). The mean number of treatments required, however, was significantly higher in the bevacizumab group (8.9 injections vs. 8.0 injections, p=.001). The incidence of arteriothrombotic events, and specifically nonfatal myocardial infarction (MI), was higher in the ranibizumab group (although at baseline, more patients in this group had history of MI). The study authors concluded that bevacizumab and ranibizumab were equivalent when administered in a treat-and-extend protocol.[157]

The results of the above studies comparing bevacizumab and ranibizumab seem to support the same conclusions: although ranibizumab may result in slightly better anatomic outcomes, this does not necessarily translate to better vision. Additionally, the higher rate of systemic adverse events experienced by the patients treated with bevacizumab in the CATT has not been confirmed in other studies.

Soluble Receptor: Aflibercept

Aflibercept (VEGF-TRAP EYE, Eylea™; Regeneron

Pharmaceuticals, Tarrytown, NY, USA) is a soluble fusion protein that combines ligand-binding elements taken from the extracellular components of VEGF receptors 1 and 2 fused to the Fc portion of IgG1.[158] As with ranibizumab, it has a high affinity for VEGF,[159] and aflibercept is thought penetrate all layers of the retina.[160] Unlike bevacizumab and ranibizumab that inhibit just VEGF-A, aflibercept also binds VEGF-B and PlGF.[159,161] The phase 1 study of aflibercept, known as CLEAR-IT 1 (CLinical Evaluation of Anti-angiogenesis in the Retina Intravitreal Trial), showed safety and a functional and anatomical improvement with a dose of 0.5 and 2 mg.[162] The phase II trial, known as CLEAR-IT 2, evaluated the biologic effects and safety of aflibercept during a 12-week fixed-dosing period in patients with exudative AMD followed by PRN dosing out to 1 year.[163,164] Patients were randomized 1:1:1:1:1 to aflibercept during the fixed-dosing phase (day 1 to week 12): 0.5 or 2 mg every 4 weeks on day 1 and at weeks 4, 8, and 12; or 0.5, 2, or 4 mg every 12 weeks on day 1 and at week 12. At week 12, treatment with aflibercept resulted in a significant mean decrease in CRT from baseline in all groups combined ($p<.0001$). The reduction with the 2 mg every 4 week and 0.5 mg every 4 week regimens was significantly greater than each of the quarterly dosing regimens. Visual acuity increased significantly by a mean of 5.7 letters at 12 weeks in the combined group ($p<.0001$), with the greatest mean gain of >8 letters in the monthly dosing groups.

In the PRN dosing phase of the study out to week 52, the decrease in CRT observed at week 12 versus baseline remained significant at weeks 12 to 52 (−130 μm from baseline at week 52), and CNV size regressed from baseline. After achieving a significant improvement in visual acuity during the 12 weeks, PRN dosing for 40 weeks maintained improvements in visual acuity out to 52 weeks (5.3-letter gain; $p<.0001$). The most robust improvements and consistent maintenance of visual acuity generally occurred in patients initially dosed with 2 mg every 4 weeks for 12 weeks. These patients demonstrated a gain of 9 letters at 52 weeks. Overall, a mean of 2 injections was administered after the 12-week fixed-dosing phase, and the mean time to first reinjection was 129 days. Nineteen percent of patients received no injections and 45% received 1 or 2 injections. During the year long study, PRN dosing

at weeks 16–52 maintained the significant anatomic and vision improvements established during the 12-week fixed-dosing phase with a low frequency of reinjection, and the drug was generally safe and well tolerated.

Based on the phase 2 results, aflibercept appeared to be a new anti-VEGF treatment requiring fewer intravitreal injections compared with ranibizumab and bevacizumab. This hypothesis was tested in the phase III VIEW 1 and VIEW 2 studies (VEGF Trap-Eye: Investigation of Efficacy and Safety in Wet AMD) in which aflibercept was compared with the standard monthly dosing regimen of 0.5 mg ranibizumab (NCT00509795). In these two parallel phase III studies (VIEW 1 in the United States and Canada, VIEW 2 in Europe, the Middle East, Asia-Pacific, and Latin America), patients with exudative AMD were randomized 1:1:1:1 to aflibercept 0.5 mg monthly (0.5q4), aflibercept 2 mg monthly (2q4), aflibercept 2 mg every 2 months (following three monthly loading doses – 2q8), or ranibizumab administered 0.5 mg every month during the first year of the studies (Rq4). Over 1,200 patients were randomized in each study. The studies were designed as noninferiority trials with the primary endpoint as the proportion of patients who maintained vision over 52 weeks compared to ranibizumab.

After 1 year, at least 94% of all groups achieved the primary endpoint of <15 ETDRS letters lost. There was no difference in the outcomes when the three aflibercept groups were compared with the ranibizumab group.[165–167] When comparing secondary outcomes, the VIEW 1 study demonstrated that the mean change in BCVA was significantly higher in the 2q4 group than the ranibizumab group (10.9 vs. 8.1 letters), although VIEW 2 seemed to demonstrate an opposite effect, with mean improvement 2.1 letters greater in the ranibizumab group (not statistically significant). All other groups in VIEW 1 and 2, and when the data were integrated, showed no significant differences. Most notably, there was no difference between intravitreal aflibercept dosed every 2 months, and ranibizumab dosed monthly. This was true with respect to visual acuity improvement, OCT central retinal thickness, and safety outcomes. Similar to the paradoxical dose-response seen in the IVAN trial, the group with the highest exposure to aflibercept (2q4)

experienced the lowest rate of systemic adverse events. Specifically, there were no differences in the rates of arterial thromboembolic events or death between ranibizumab and aflibercept. When the 1-year data were presented to the FDA in 2011, the panel unanimously recommended approval.

After the 52-week endpoint, all regimen groups switched from a fixed monthly or bimonthly injection schedule to a variable dosing schedule, with injections given at least quarterly.[168] Follow-up was monthly with reinjection allowed according to visual and anatomic criteria. At 96 weeks, 91.5–92.4% of patients maintained vision, with average gains of 7.9, 7.6, 6.6, and 7.6 letters in the Rq4, 2q4, 0.5q4, and 2q8 groups, with similar numbers of patients attaining 15 letters of improvement or more in the second phase of the study as in the first (Fig. 70.17). During this phase, there was also an average increase in OCT central retinal thickness and a modest decline in the percentage of patients with no fluid on OCT in all treatment groups. The mean number of injections administered was similar (about 16 over the 96 week study period) in each group with the exception of the 2q8 group, which received about 11 injections on average. As in the 52-week data, safety was comparable and revealed no significant differences between the groups in all serious adverse events or in arterial thrombotic events. The authors concluded that over the 96-week study period, aflibercept offered similar visual and anatomic outcomes as ranibizumab, and could be given less frequently, with an average of five fewer injections.[169]

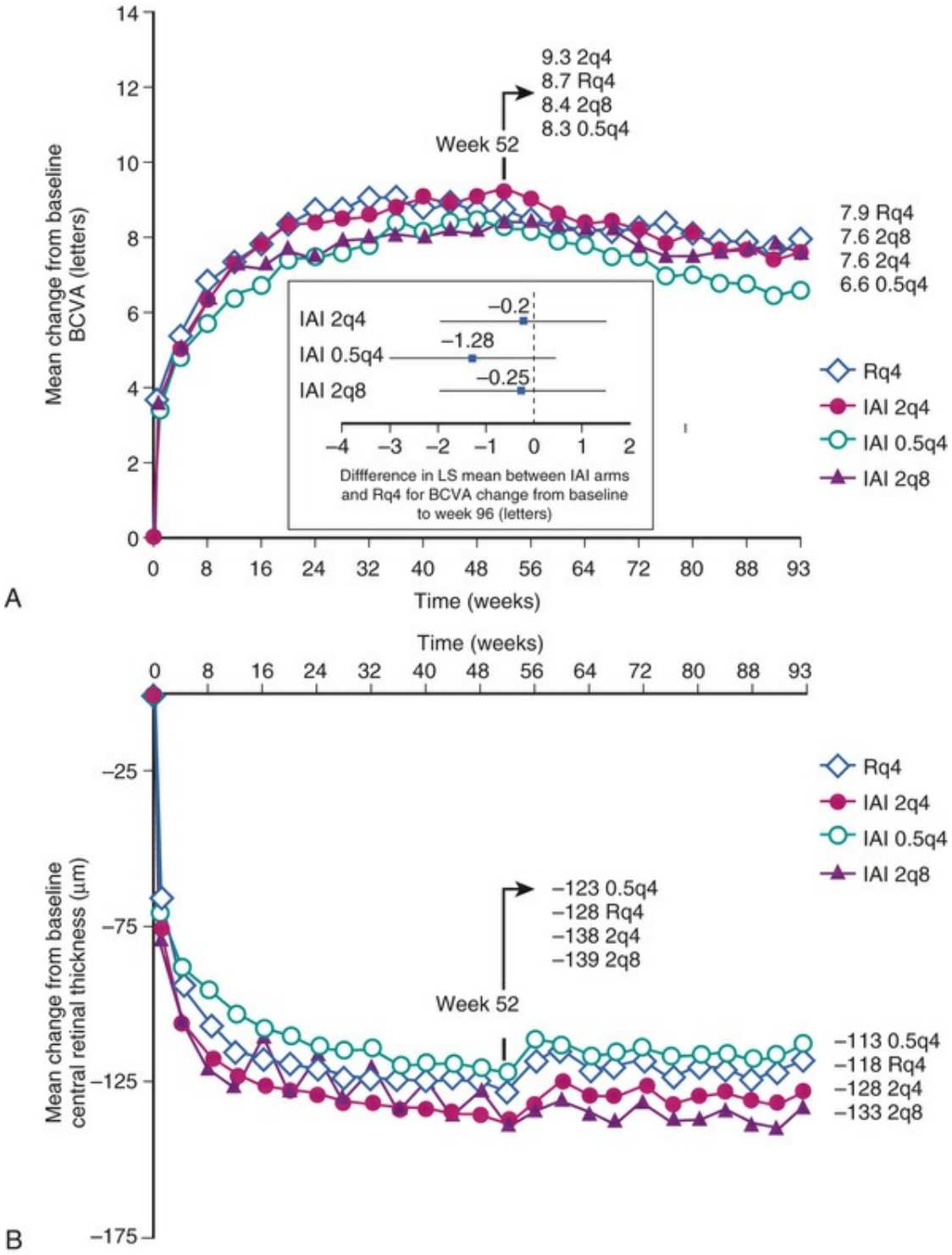

FIG. 70.17 VIEW 1/2 study cohort visual acuity and anatomic outcomes. (A) Mean change from baseline best corrected visual acuity (BCVA). The inset shows the difference in least square (LS) mean (with 95% confidence interval) between intravitreal aflibercept arms and ranibizumab (aflibercept minus ranibizumab) for BCVA change from baseline to week 96, full analysis set. (B) Mean change from baseline central

retinal thickness, full analysis set. Missing values were imputed using the last-observation-carried-forward method. The outcomes for the aflibercept and ranibizumab groups were similar at both weeks 52 and 96. (Reproduced with permission from Schmidt-Erfurth et al., Ophthalmology 2014;121(1):193-201, Figs. 1B and 2A.)

Conbercept (Previously KH902)

Conbercept (Chengdu Kanghong Biotechnology Ltd, Sichuan, People's Republic of China) is a fusion protein that combines ligand-binding elements taken from the second extracellular domain of VEGF receptor 1(Flt-1) and the third and fourth binding domain of VEGF receptor 2 (KDR) to the Fc portion of IgG1.[170] Compared with aflibercept, the inclusion of the additional extracellular domain 4 of VEGF receptor 2(KDRd4) may stabilize the three-dimensional structure and increase the efficiency of dimerization.[171] Conbercept has a much higher affinity for VEGF due to this extra extracellular domain and may have a longer half-life in the vitreous.[170,172] Additionally, conbercept has affinity for placental growth factor (PlGF), another member of the VEGF family implicated in the development of CNV.[173,174] Preclinical in vivo experiments have shown that intravitreal conbercept is able to inhibit leakage and growth of CNV in rhesus monkeys without signs of toxicity at doses of 300 and 500 μg.[170] In a phase 1, dose escalation study, intravitreal injections of conbercept up to a dose of 3.0 mg were well tolerated in 28 patients. On day 42 after a single injection, the mean change in visual acuity from baseline was +19.6 letters with no subjects losing 1 letter or more and 57% of patients gaining 15 letters or more from baseline. The mean change in center point retinal thickness from baseline was −77.2 μm and the mean decrease in CNV area was 12.6%. No safety concerns were detected after a single intravitreal injection.

A phase 2 study performed in China (AURORA) randomized 122 patients to 0.5 mg or 2 mg doses, administered for three monthly loading doses, followed by a secondary randomization to either monthly (Q1M) or PRN administration at the same dose for the remaining 9 months of the 12-month study. At 3 months, the 0.5-mg group experienced almost 9 letters of visual improvement,

compared with 10.4 letters of improvement in the 2-mg group. At 12 months, the visual gains were similar in each of the four groups: 9.3 (0.5 mg Q1M); 14.3 (0.5 mg PRN); 15.4 (2 mg Q1M); 12.4 (2 mg PRN). The proportion of patients with a 15-letter gain was similar, with 31%, 50%, 46.7%, and 42.3% of eyes reaching this threshold in the 0.5-mg Q1M, 0.5-mg PRN, 2-mg Q1M, and 2-mg PRN groups, respectively. At least 96% of all eyes lost fewer than 15 letters in all groups (Fig. 70.18). Central retinal thickness on OCT showed significant decrease, as did CNV size and leakage area on fluorescein angiography at 12 months without significant differences among the groups. Less than five injections over the 12-month period were administered in each PRN group, while, as expected, each monthly group received more than eight injections in the maintenance phase.

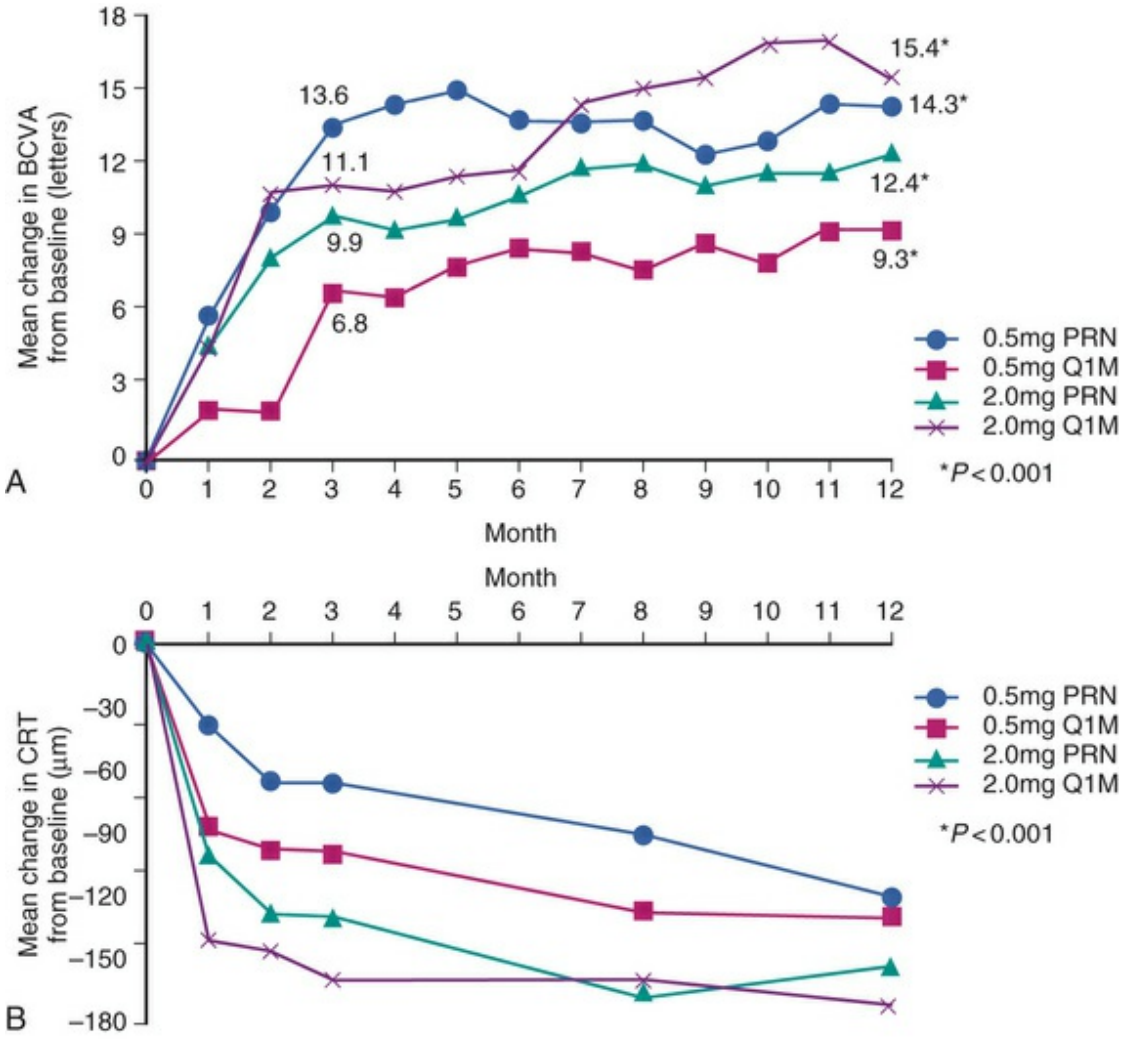

FIG. 70.18 AURORA study visual and anatomic outcomes. Upper panel: The mean change in best corrected visual acuity (BCVA) from baseline over time in patients in the four dosing regimen treatment groups through 12 months. Lower panel: The mean change in central retinal thickness (CRT) from baseline over time using the four dosing regimens through 12 months. The CRT reduced rapidly during the first 3-month loading phase and then continued to decrease through month 12. (Reproduced with permission from Li X, Xu G, Wang Y, et al. Safety and efficacy of conbercept in neovascular age-related macular degeneration: results from a 12-month randomized phase 2 study: AURORA study. Ophthalmology. 2014;121(9):1740-7.)

Adverse events were reported in the majority of patients in the study, although most were mild or moderate and self-limited. Serious adverse events related to the study intervention included

cataract progression in one eye, which necessitated cataract extraction, and a patient with post-injection culture-negative endophthalmitis, treated with antibiotics. There were no systemic adverse events, including arteriothrombotic, cardiovascular, or cerebrovascular complications, during the study.

Based on the promising phase II results, the phase 3 PHOENIX trial was initiated, assigning 125 patients in a 2 : 1 randomization to the treatment group with three monthly injections of conbercept 0.5 mg, followed by two monthly sham injections and a trimonthly injection with conbercept until month 12 (treatment at months 0, 1, 2, 5, 8, and 11); or the sham group, which received three sham injections at months 0, 1, and 2, followed by crossover into the treatment group. Twelve-month results showed a 10-letter improvement in the treatment group. There was a decrease in OCT central macular thickness of 79 μm at 3 months. No additional safety data were available at the time of publication.[175] Based on phase III results, the potential for quarterly dosing of conbercept compares favorably with ranibizumab (dosed monthly) and aflibercept (dosed bimonthly) in terms of treatment burden and cost, particularly in China, where at the time of publication, the off-label use of bevacizumab is still prohibited. Conbercept was approved by the China State Food and Drug Administration for use in exudative macular degeneration in 2013.

Anti-VEGF Agents Under Investigation

RTH258 (Formerly ESBA1008).

RTH258 (Alcon/Novartis, Fort Worth, TX, USA) is single-chain antibody fragment that targets all isoforms of VEGF-A. With a molecular weight 26 kDa, it is considerably smaller than other VEGF inhibitors, which may theoretically increase retinal penetration, allow for higher concentration of drug at the target tissue, and reduce systemic exposure, all of which have been supported in animal studies. After encouraging phase I results, showing favorable visual acuity improvement when compared to ranibizumab, a recent dose escalation, randomized phase II trial compared a single injection of the medication, with ranibizumab 0.5 mg in 194 patients. The primary endpoint was change in OCT

central retinal thickness at 1 month, with the noninferiority endpoint met at the two highest dosing groups (4.5 and 6 mg).[176] Additionally, after the single injection, the OCT thickness remained relatively stable over months 1 and 2 compared to a relative increase in the ranibizumab group, implying a longer duration of action of the study medication. Visual acuity results were similar, with the highest-dose group attaining 10.4 letters, versus 6.5 letters gained for ranibizumab. The study was not powered to detect differences in adverse events, but there were no significant concerns. In a second phase II study, the OSPREY trial compared RTH258 6 mg to aflibercept 2 mg at weeks 12 and 16 of a 56-week study. Treatment was dosed every 8 weeks through week 32, then every 12 weeks until the end of the study, with rescue treatments given as frequently as every month in between scheduled injections. The 89 patient study demonstrated noninferiority, with no significant adverse events. Importantly, fewer rescue treatments were required in the RTH258 group through both phases of the study, with about half of patients maintained on q12week injections.[177] These results support the further investigation of this medication for the treatment of neovascular AMD in phase III trials, and in particular, the potential use in sustained drug delivery devices, where a high localized concentration and long duration of action are of particular value.

DARPins and Abicipar Pegol.

The designed ankyrin repeat proteins (DARPin) are a family of small (14–21 kDa) single-domain proteins that are genetically engineered to bind to a target with high affinity and specificity. Derived from natural ankyrin repeat proteins, the DARPin consists of a repeat protein domain, whose purpose in nature is to bind a target with any number of consequent actions. As a therapeutic agent, DARPins address many of the shortcomings of antibodies: at one-tenth the size of an IgG antibody, they demonstrate excellent tissue penetration; they demonstrate exceptional thermal stability, with half-lives of more than 60 days in some cases; they have very low risk of immunogenicity due to the absence of an Fc antibody portion; they can be purified and concentrated to high levels; and importantly, they are easily produced.[178]

The DARPin abicipar pegol (formerly MP0112; Molecular Partners, Zurich-Schlieren, Switzerland) is a potent antagonist to all VEGF-A isoforms and binds with high affinity (Kd 1-4 pM). Additionally, the intravitreal half-life is at least 2 weeks. Ranibizumab, in contrast, has a Kd of ≤192 pM for the active isoforms of VEGF-A, and has a half-life of about 7 days.[179] Similar to the currently used VEGF antagonists, abicipar inhibits VEGF-A activity through direct binding.

A phase I/II trial (NCT01086761) examining the safety and dosing of abicipar was performed in France, Switzerland, and the Czech Republic.[180] The nonrandomized study enrolled 32 patients, injecting one eye with a single dose of abicipar. The primary aim of the study was to assess safety and tolerability, with efficacy as a secondary outcome measure. The medication was administered in a dose-escalation design, with six dosing cohorts (0.04 mg, 0.15 mg, 0.4 mg, 1 mg, 2 mg, and 3.6 mg). There was no control group, although rescue therapy was allowed, with the specific criteria varying by region. One patient in the 2-mg cohort developed endophthalmitis, which was believed to be sterile; thus, 1 mg was determined to be the maximum tolerated dose, and no patients were enrolled in the highest-dosing cohort. Milder inflammatory responses, both anterior and posterior, were also seen and resolved either with steroid therapy or without any intervention. Other adverse events included conjunctival hemorrhage, vitreous hemorrhage, and hypertension, each occurring in one patient. Notably, serum antidrug antibodies were detected in eight patients. In all dosing cohorts, there was decrease in CRT after the first week, with further reduction at week 4 in the higher-dosing cohorts. Fluorescein angiography also showed a decrease in lesion size and leakage area at week 4. Vision remained stable in all cohorts over the duration of the study, with no significant gain or loss at 16 weeks. Over the course of the 16-week study, rescue therapy was required in 20 of 22 patients in the 0.04–0.4 mg cohorts, and 4 of the 10 patients receiving 1 or 2 mg, with a longer time to rescue therapy in the higher-dose cohorts (up to 10 weeks, vs. 5–7 weeks in the lower dose cohorts). The drug was detectable in the serum up to 2 weeks only in the highest-dosing cohort.

The study authors concluded that abicipar/MP0112 had no

systemic safety concerns, and that the dose-limiting intraocular inflammation was likely related to impurities in drug processing; a new purification process was initiated as a result. Although they acknowledged that the study was small and uncontrolled, the preliminary efficacy results suggested that DARPins indeed offer improved duration of action over antibody therapy, and that further study would be warranted.

Sustained Drug Delivery

Although VEGF inhibitors are the mainstay of AMD therapy, their effectiveness is limited by the half-life of the molecules within the eye. After intravitreal injection with bevacizumab, the elimination half-life can range from 8 to 11 days, with detectable antibody for up to 2 months.[181] The half-life of ranibizumab is slightly shorter, at just over 7 days,[179] with monthly dosing recommended by the manufacturer. Many studies have demonstrated comparable visual outcomes using PRN or treat-and-extend strategies; however, PRN dosing requires monthly follow-up, and many clinicians still favor dosing at least quarterly for maintenance. Additionally, as the intravitreal concentration of the drug declines over time, the risk of reactivation and breakthrough bleeding increases toward the end of the treatment interval. These limitations of the current treatments may lead to considerable treatment burden for patients; pharmaceutical and device manufacturers have consequently investigated various ways to increase the duration of effect of anti-VEGF therapy.

Encapsulated Cell Technology

Encapsulated cell technology (ECT) involves the insertion of living cells into a tissue to produce and secrete a recombinant gene product. These cells are encapsulated within a semipermeable polymer,[182] which prevents immune response from the host antibodies and immune cells while allowing for diffusion of oxygen and nutrients to nourish the cells contained within. The technology is flexible, allowing for any number of gene products to be secreted, and allowing for dose modification or removal if treatment is no longer desired, unlike gene therapy. The constitutive secretion from

the implant may also allow for lower concentrations necessary for therapeutic effect, compared with bolus intravitreal injection therapy.

Neurotech (Lincoln, RI, USA) has developed an ECT implant specifically for use in the eye. It is 6–8 mm long and designed to be placed through a pars plana incision 2–3 mm in length. The NT-503 implant consists of an encapsulated human RPE cell line transfected to secrete a soluble VEGF-receptor-Fc fusion protein (VEGF-R). Preclinical data suggested that the intravitreal concentration of VEGF antagonist could be maintained at a level comparable to or exceeding that of bevacizumab injections.[183] Human studies showed that implant was well tolerated,[184] and the VEGF-R produced by the cell lines binds with high affinity to its target. The second generation of device showed safety and efficacy when two devices were implanted in the same eye, with improvements in vision (5 of 7 patients) and decreases in OCT fluid (5 of 6 patients) in preliminary results.[185] The latest generation of implant, the NT-503-3, contains multiple chambers, allowing for the release of higher doses of the therapeutic agent at rates of up to 12 μg/day, as well as the possibility of combination therapies, with the use of multiple cell lines within the same device (Fig. 70.19). A phase I/II study was terminated in 2016 after failing to meet its primary endpoint. An implant that releases both anti-PDGF and anti-VEGF (NT-506) is currently in preclinical development (see below for discussion on PDGF). The NT-501 implant that secretes ciliary neurotrophic factor (CNTF) was evaluated in a phase II study for GA,[186] although the company has not pursued this avenue further.

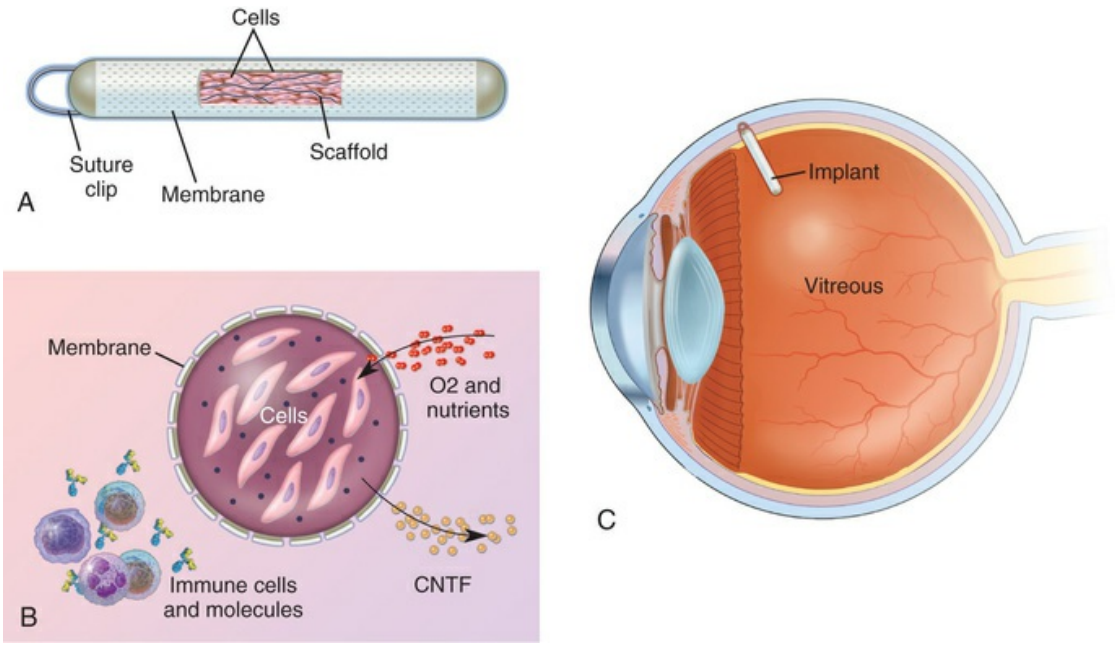

FIG. 70.19 Schematic illustration of implant using encapsulated cell technology. The implant (panel A) is composed of a section of semipermeable membrane capsule which contains cells and scaffold. The membrane capsule is sealed at both ends with a suture clip at one end for anchoring on the sclera. The membrane allows oxygen and nutrients to diffuse in and therapeutic agent (CNTF in this case) to diffuse out. It also keeps components of the immune system out (panel B). The implant is 6 mm in length and 1 mm in diameter. It is outside the visual axis of the eye when anchored to the sclera (panel C). (Reproduced with permission from Wen R, Tao W, Li Y, et al. CNTF and retina. Prog Retin Eye Res. 2012;31(2):136-51.)

Port Delivery System

ForSight VISION4 (Menlo Park, CA, USA) has developed a refillable port drug delivery system (PDS), and in 2010 entered into a collaboration agreement with Genentech/Roche to develop anti-VEGF therapies using this modality. The PDS is an implantable device, placed surgically through the pars plana with a 3.2-mm sutureless incision. Ranibizumab solution is preloaded into the device, which controls the continuous release of the medication between refill procedures, which can be performed in the office. A phase I study implanted the PDS in 20 patients, following them

monthly, using OCT and visual acuity to determine when to refill the device. The PDS was refilled with 500 μg, of which 250 μg was given in a bolus and 250 μg released over time.

There was significant visual and anatomic improvement at 12 months, with an average of 12 letters gained. Fifty percent of patients gained 3 lines or more. Patients required a mean of 4.2 refills over the 12 months. Four of the 20 patients suffered adverse events associated with the implant: one developed endophthalmitis, two suffered vitreous hemorrhage, and one developed traumatic cataract associated with the implantation procedure.

As the study was designed to test the proof of concept and evaluate safety, efficacy was not the primary goal. As such, six implants were removed after 12 months to examine for integrity over the course of the study and were found to have similar performance to new implants. The phase II LADDER study is underway, testing three doses of ranibizumab, compared to monthly therapy over 9 months.[187]

Replenish MicroPump

The MicroPump (Replenish, Inc., Pasadena, CA, USA) is an microelectromechanical systems (MEMS) device designed to release medication from a refillable reservoir into the eye at a controlled rate. Implanted in a similar manner as a glaucoma drainage device, the pump system is sutured to the sclera under the conjunctiva and the Tenon capsule, with a cannula inserted transclerally through the pars plana. Medication is contained in a drug reservoir and is pumped through the cannula and into the eye via a one-way check valve. Although the first generation device was actuated manually, there was significant variation in drug delivery according to the duration and pressure applied to the device.[188] In the second generation of device, the drug reservoir contains a current-regulated electrolysis pump, which induces a phase change of water to hydrogen and oxygen gas, generating positive pressure in the reservoir that pumps the medication into the eye (Fig. 70.20).[189] Precise control of drug delivery and communication with the device is performed wirelessly through a proprietary telemetry system. The reservoir can be refilled via a 31-gauge needle.

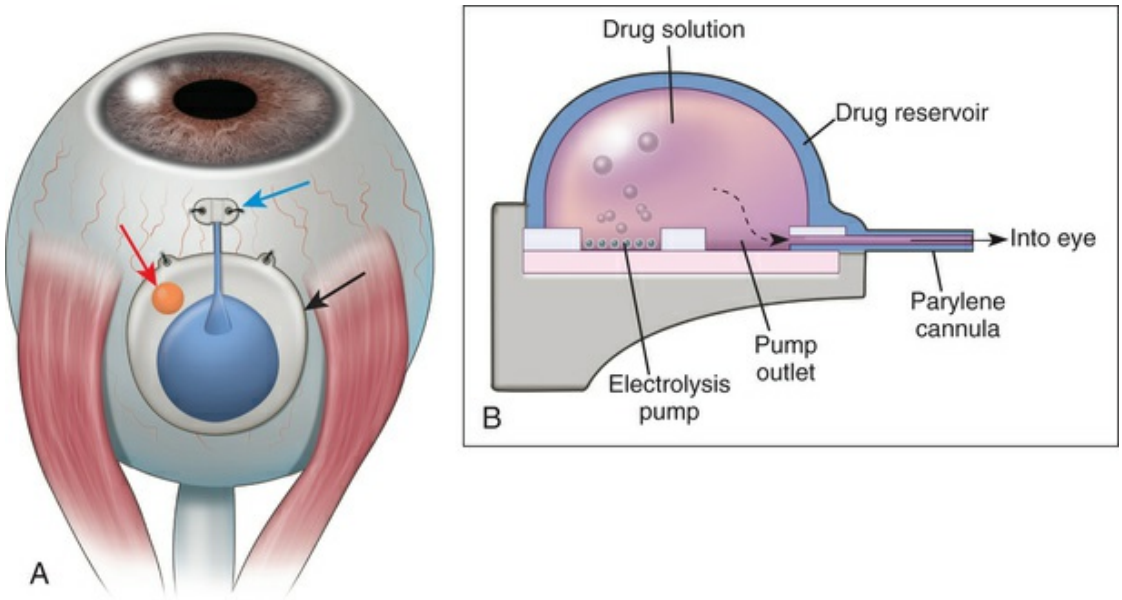

FIG. 70.20 (A) Schematic representation of the Posterior MicroPump Drug Delivery System (PMP; Replenish, Inc) implanted into the subconjunctival space between the superior and lateral rectus muscles. *Blue arrow* indicates the intraocular cannula at the pars plana location. *Red arrow* indicates the refill port. *Black arrow* indicates the body of the PMP that contains the hermetic sealing package with all electronics, the drug reservoir, and the check valve. (B) Gas bubble evolution resulting from electrolysis in drug reservoir of packaged electrically controlled device. (Panel A reproduced with permission from Humayun et al., Transl Vis Sci Technol. 2014;3(6):5; panel B reproduced with permission from Saati et al., Trans Am Ophthalmol Soc. 2009;107:60-70.)

Preclinical studies demonstrated good biocompatibility, with only minimal chronic external inflammation and capsular formation around the implant in animal studies, and no extrusion of the device or evidence of fibrous ingrowth through the cannula tract on histopathology.[190] The implant device is expected to remain functional within the eye for more than 5 years. A feasibility study in patients with diabetic macular edema demonstrated proper functioning of the pump in delivering the preprogrammed dosage of 0.085 mg ranibizumab within 90 minutes of filling the reservoir in 7 of the 11 study patients. The surgical implantation procedure was tolerated well without complications, and there were no serious ocular adverse events during the 90-day study period.[191]

This study represented the first implantation of an electronic drug delivery pump within the eye for retinal disease, and demonstrated its feasibility as a potential future avenue for treatment of macular degeneration.

Adeno-Associated Viral Vector (AAV) Gene Transduction

Another important strategy for sustained drug delivery is gene therapy via viral vector genetic transduction. Several targets have been explored, including VEGFR-1 and PEDF.

As previously discussed, the angiogenic effects of VEGF are mediated through the endothelial receptor tyrosine kinases, VEGFR-1 (also called Flt-1) and VEGFR-2 (Flk-1/KDR), with Flt-1 having a tenfold-higher affinity for VEGF.[192] A naturally existing soluble form of Flt-1 (sFlt-1) has no transmembrane domains, and thus has no signal transduction properties, instead forming a heterodimer with Flt-1 and Flk-1 extracellular domains.[193] This molecule has provided a unique target for gene therapy using an adeno-associated viral (AAV) vector.

AAV vectors are particular suited for gene therapy in part because of their low immunogenicity and pathogenicity, and ability to induce long-term gene expression in the eye. They have been used with success for gene transduction of PEDF for animal models of CNV,[194] and have been tested in human trials for RPE65-associated Leber congenital amaurosis.[195–197] Moreover, for a soluble gene product such as sFlt-1, gene therapy may be especially effective, as transduction need not be cell-specific.[192]

AAV-mediated sFlt-1 (and related fusion protein) gene therapy has been successful in a number of animal models, including rodent and primate.[192,198–201] Lai et al. tested gene transfer using an injected AAV vector with full-length sFlt-1 on both mice and monkeys.[192] In the mouse, they found a marked decrease in hyperfluorescence on fluorescein angiography in sFlt-1 transduced eyes when compared to noninjected and control AAV-Green Fluorescent Protein (GFP)-injected eyes. Morphologically, they found that more extensive CNV-induced photoreceptor loss occurred in the noninjected and control eyes when compared to sFlt-1 eyes. Electroretinographic studies showed no significant loss of function as a result of sFlt-1

transduction. Primate studies showed similarly encouraging results, including prevention of CNV induced by laser, without evidence of toxicity on histology. Importantly, long-term expression of transduced gene products, with detection of sFlt-1 mRNA at up to 17 months after injection. A similar recent primate study tested an AAV vector tied to a gene for a novel fusion protein of a single domain of sFlt-1 and a human IgG1 heavy chain Fc fragment (termed sFLT01), finding both long-term expression over 5 months, as well as inhibition of CNV in a dose-dependent fashion.[200]

Results from a recent phase I trial of recombinant AAV vector (rAAV) encoding sFLT-1 were published in 2015.[202] The study randomized eight patients in a 3 : 1 fashion to either low-dose (1×10^{10} vector genomes) or high-dose (1×10^{11} vector genomes) gene therapy via subretinal injection, or to no gene therapy. After an initial 8-week safety evaluation period of the patients randomized to the low-dose group, a second group was randomized to the high-dose group. Notably, patients previously treated with anti-VEGF therapy were not excluded, with no washout period prior to baseline visit. All patients received an injection of ranibizumab at baseline and at week 4. Additional ranibizumab was given according to rescue criteria suggesting active progression of CNV. Among the six patients receiving treatment, BCVA improved in five compared with baseline, with three gaining at least 10 letters, and one patient improving by 15 letters. A single rescue injection with ranibizumab was required in two patients over the course of 52 weeks. One patient had an increase in anti-AAV2 antibodies over the course of the study, but was not deemed to be associated with safety or efficacy. The authors concluded that the rAAV2.sFLT-1 was safe and well tolerated, with potential as a long-term treatment option for AMD. Readers are referred to Chapter 36, Gene therapy for retinal disease, for more information on this developing technology.

Other Targets

hI-con1.

hI-con1 (ICON-1; Iconic Therapeutics, Inc., South San Francisco, CA, USA) is a recombinant protein targeting TF, consisting of two

identical chains of mutant human factor VII (fVII), fused to human IgG1 Fc. In order to minimize the risk of inducing disseminated intravascular coagulation through fVII binding to TF, an amino acid substitution is introduced into the hI-con1 fVII domain, inhibiting the initiation of the coagulation pathway. A 24-week phase 1 trial (NCT01485588) established safety and tolerability of a single intravitreal injection of hI-con1 in patients with exudative AMD in a dose-escalating fashion. In results presented at the American Academy of Ophthalmology Retina Subspecialty Day in November 2012, the compound was found to be well tolerated without ocular or systemic safety concerns, with gains in visual acuity, improvement in OCT thickness, and reduction in angiographic lesion size. The phase II randomized, double-masked controlled EMERGE trial (NCT02358889) was initiated in February 2015, and will compare hI-con1 as monotherapy to combination therapy using both hI-con1 and ranibizumab, versus monthly ranibizumab as control.

Regorafenib.

Regorafenib (Bayer, Wuppertal, Germany) is a multikinase inhibitor developed for oncology, targeting a number of intracellular and membrane-bound receptor tyrosine kinases involved in tumor angiogenesis, oncogenesis, and maintenance. Among its targets are VEGF receptors 1–3 and platelet-derived growth factor receptor β (PDGFR-β). Originally an orally administered agent, Bayer has developed a formulation for topical ophthalmic delivery (BAY-73-4506). A phase 1 study in healthy volunteers established that the topical drop was well tolerated, and animal studies have established efficacy in models of both corneal and CNV.[203–205] A nonhuman primate study found reduction in the development of CNV-type lesions similar to the rates found when using ranibizumab.[204] Based on these encouraging results, a phase II trial was initiated in humans testing regorafenib topical drops in patients with exudative AMD (NCT02222207).

Complement Inhibition.[a]

Complement inhibitors are thought to be a promising class of agents for the treatment of both atrophic and exudative AMD. POT-

4 (AL-78898A, Alcon/Potentia Pharmaceuticals, Fort Worth, TX and Crestwood, KY, USA), a cyclic peptide derivative of Compstatin 13 amino acids in length, is a C3 inhibitor administered by intravitreal injection. Gel-like deposits form in the vitreous when POT-4 is injected at high concentrations (>0.45 mg dose), which may last as long as 6 months, thus providing a sustained-release delivery system. A phase I study of POT-4 in AMD eyes with CNV was completed successfully without any safety concerns at doses up to 1.05 mg (NCT00473928), although the systemic effects of intravitreal administration are unknown. A phase II study was completed in 2013 (NCT01157065), which did not demonstrate any positive results. Further investigation of the compound was terminated. However, in 2014, Apellis Pharmaceuticals acquired the intellectual property rights to POT-4, renamed APL-2. Phase I data are currently being analyzed C3 inhibition should block complement activation arising from many of the currently described complement pathway mutations, as the classical, lectin, fibrinolytic, and alternative pathways all generate the bioactive fragments C3a and C5a and the membrane attack complex (C5b,6,7,8,9) via C3 cleavage (see Fig. 70.3). This targets a relatively large population of AMD patients; however, the broad degree of complement inhibition may theoretically increase risk of intravitreal injection-associated endophthalmitis. In a murine model, it seems that C3 deficiency does not increase the risk of *Staphylococcus aureus* endophthalmitis.[206] In contrast, in a guinea-pig model, complement depletion with cobra venom factor does seem to increase the risk of *S. aureus*, *S. epidermidis*, and *Pseudomonas aeruginosa* endophthalmitis.[207–209] Other treatments related to complement factors are being examined in the context of nonexudative AMD (see below).

Combination Therapies[a]

The principles of combination therapy have been well established in the treatment of infectious diseases such as HIV,[210] or in cancer therapy. The combination of VEGF blockade (e.g., with bevacizumab) with chemotherapy or radiation therapy, for example, results in a greater antitumor effect than with either treatment alone.[211,212] Combining AMD treatments with differing mechanisms of action may have synergistic effects that might result in (1) better visual outcome; (2) reduced frequency of treatment; (3) greater patient convenience (e.g., subconjunctival vs. intravitreal injection); (4) lower risk of adverse events such as endophthalmitis; and/or (5) less likelihood of "escape" (a phenomenon in which cells, e.g., infectious agents or tumor cells, develop alternative pathways that allow them to overcome the inhibition of a pathway essential for their survival or growth). A number of variations have been examined in the past, including retrospective and prospective trials of verteporfin photodynamic therapy with anti-VEGF therapy and/or intraocular or periocular triamcinolone or dexamethasone.[213–227] Newer targeted therapies are discussed below.

Pegpleranib (Fovista) (PDGF Inhibition)

In the early stages of angiogenesis, pericytes contract and reduce their contact with vascular endothelial cells.[228–232] The endothelial cells proliferate and migrate, followed by pericyte migration into the forming vascular bed. During the time that endothelial cells lack pericytes, they are sensitive to VEGF inhibition. Once pericytes reestablish a close relationship with the endothelial cells, they may provide VEGF to the endothelial cells as well as use other signaling systems, such as ang-1/Tie-2,[233] to promote endothelial cell survival, thus rendering the mature capillary network resistant to VEGF-A inhibition with agents such as aflibercept, bevacizumab, and ranibizumab.

Platelet-derived growth factor (PDGF) is produced by platelets, RPE cells, fibroblasts, and macrophages and, among other things, promotes extracellular matrix deposition.[234] PDGF stimulates

pericyte recruitment and promotes maturation of a newly formed vascular bed. There are five members of the PDGF family (all dimers: AA, AB, BB, CC, DD), and endothelial cells primarily express PDGF-B.[235] There are two PDGF receptors, PDGFRα and PDGFRβ, both of which are tyrosine kinases. PDGFβ binds PDGF-B (BB, AB) and PDGF-DD. VEGF impairs vessel maturation by stimulating the formation of VEGFR2-PDGFβ complexes, which suppresses PDGF signaling pathways.[236] PDGF-B mediates pericyte recruitment to the growing endothelial cell tube.

In preclinical models, combination therapy using inhibitors of PDGF and VEGF signaling was superior to monotherapy with VEGF inhibitors in multiple models of angiogenesis.[237] Most importantly, these experiments demonstrated that neovessels become refractory to VEGF-A deprivation as they mature, but combination therapy can induce regression of such vessels. Several agents that target PDGF signaling have been developed, e.g., CR002 (anti-PDGF-D, CuraGen Corp., Branford, CT, USA),[238] mAb 3G3 (anti-PDGFRα, ImClone Systems, Branchburg, NJ, USA/Eli Lilly, Indianapolis, IN, USA),[239] and pegpleranib (Fovista, E10030) (anti-PDGF-B, Ophthotech Corp. New York, NY, USA).

Pegpleranib is a 50 kDa pegylated DNA aptamer that binds PDGF-B with ~300 pM affinity. A phase I trial (NCT01089517) enrolled 57 patients with advanced AMD-associated CNV.[240] Patients were treated with a single dose of 0.03 mg pegpleranib plus three monthly injections of ranibizumab or three monthly doses of pegpleranib (0.3 mg, 1 mg, or 3 mg) combined with three doses of 0.5 mg ranibizumab. Among patients completing follow-up at 4, 8, and 12 weeks, 32% (pegpleranib 0.3-mg cohort), 45% (pegpleranib 1-mg cohort), and 60% (pegpleranib 3-mg cohort) of patients gained at least 15 ETDRS letters. Mean improvement in BCVA was +11.1, +13.4, and +15.7 letters, respectively. Central foveal thickness, as measured by OCT, also decreased significantly, and fluorescein angiography demonstrated regression of the CNV in 85% of eyes. There were no drug-related adverse events. A 24-week phase IIb superiority trial involving 449 patients randomly assigned to receive monthly ranibizumab 0.5 mg or monthly ranibizumab 0.5 mg plus pegpleranib (0.3 mg or 1.5 mg) also was conducted (NCT01089517).[241] The pegpleranib 1.5 mg combination

therapy cohort demonstrated a mean +10.6 ETDRS letter improvement vs. +6.5 letters in the ranibizumab monotherapy cohort (p=.019) (Figs. 70.21–70.22). Improvements in vision, central foveal thickness, and angiographic CNV regression were greater in the combination therapy cohort vs. the monotherapy cohort regardless of CNV subtype. Other than transient intraocular pressure increases in the combination therapy cohort, no safety signals were identified. Twelve month results of two parallel phase III studies (NCT 01944839 and NCT 01940900, 1248 patients enrolled) published in 2015, however, showed that combination therapy with pegpleranib and ranibizumab did not meet the primary endpoint of visual acuity superiority over ranibizumab monotherapy. The 24-month study was terminated early. Another trial (NCT01940887) combining pegpleranib and either bevacizumab or aflibercept is currently underway, and other combination therapies in development may provide synergistic biologic effects that could improve visual outcome, decrease treatment burden, and, ultimately, reduce the overall cost of treatment as well as the incidence of blindness associated with AMD-CNV.

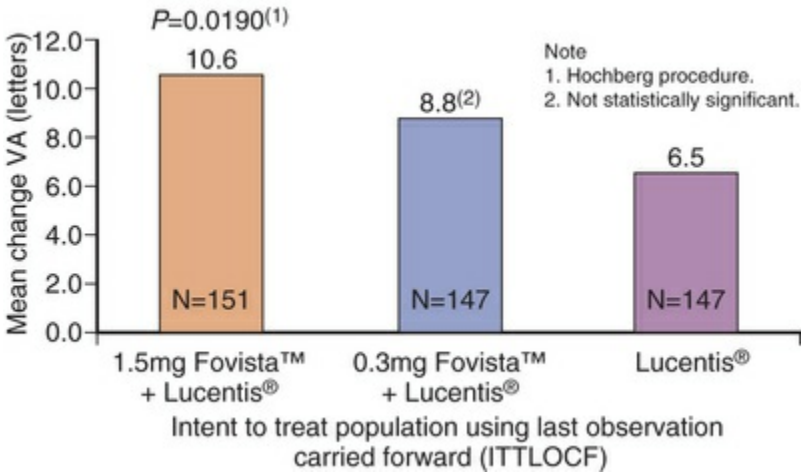

FIG. 70.21 Fovista (anti-PDGF) phase IIb 24-week results. (Reproduced with permission from Ophthotech.)

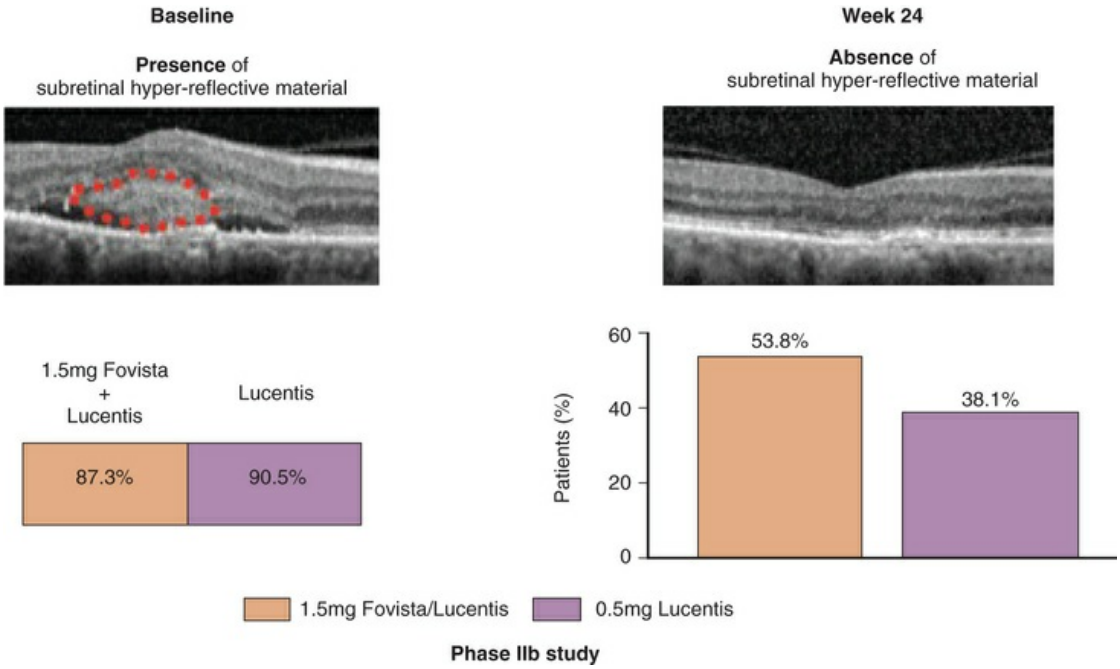

FIG. 70.22 Fovista (anti-PDGF) phase IIb results showing resolution of subretinal hyperreflective material in patients with significant visual gain.

(Reproduced with permission from Ophthotech.)

OHR-102/Squalamine

Squalamine (Ohr Pharmaceuticals, New York, NY, USA) is an antiangiogenic amino sterol derived from the cartilage of the dogfish shark, *Squalus acanthus*, targeting VEGF, PDGF, and basic fibroblast growth factor (bFGF) through calmodulin binding. It has been found to inhibit iris neovascularization when administered by intravenous injection, although it is ineffective when administered by intravitreal injection.[242,243] Squalamine also induces regression of experimental retinopathy of prematurity in a mouse model[244] and was tested in a phase I study of CNV in patients with no safety concerns expressed leading to several phase II trials. Initial visual results were promising, with improvement or stability in those patients receiving higher doses of the drug. Interestingly, the fellow non-study eyes with advanced macular degeneration also showed significant improvement after drug administration. A phase III study was initiated; however, the manufacturer abandoned further development.

Ohr pharmaceuticals later developed a topical formulation of squalamine (0.2%, OHR-102), modified to reduce aqueous

penetration and to maximize transscleral penetration into the choroidal tissue.[245] In the phase II IMPACT study, OHR-102 drops were given twice daily in combination with ranibizumab, compared with ranibizumab with placebo (vehicle drops). Injections were given on a PRN basis according to OCT criteria. The 9-month study enrolled 142 patients. Although results at the midpoint of the study were encouraging for the first 62 enrolled patients completing the study (10 vs. 6 letter improvement in the combination group versus the ranibizumab monotherapy group), by the study's end, there were no significant differences between the combination and monotherapy groups overall (+7.8 compared with +5.3 letters, respectively, with no difference in the number of injections required).[246] However, in subgroup analyses, there was a difference when considering lesions containing classic CNV, with 11 vs. 5 letters gained, 42% vs. 28% gaining 3 lines of vision. Similarly, a higher percentage of patients in this subgroup achieved 4 and 5 lines of vision gain when treated with combination therapy compared with monotherapy. Early post-hoc analyses found that lesion size may have an impact on treatment response as well, as smaller (<10 mm^2) occult lesions had a significantly better response to combination therapy. These data supported a phase III trial in a more targeted patient population.

X-82

The dual-kinase inhibitor X-82 (Tyrogenex, West Palm Beach, FL, USA) is a small molecule that targets the VEGF receptor and PDGF receptor. In the oncology literature, the compound has been advanced as a next generation tyrosine kinase inhibitor that is orally available with an improved safety profile.[247] A phase I dose-escalation study enrolled 35 patients who had previously been treated for exudative AMD, with results presented at ARVO in 2015. Of the 27 patients completing the 24-week treatment, a majority demonstrated either maintenance or improvement from baseline vision, and 89% did not require rescue therapy with ranibizumab.[248] The phase II APEX study has been initiated by Tyrogenex, with visual acuity change and reduction in injections as key endpoints.

Zimura

As discussed previously, complement is believed to play an important role in AMD pathogenesis. Complement factors have been isolated in drusen, and complement factor polymorphisms have been associated with AMD risk. Inhibition of C5 blocks terminal complement activity, but proximal complement functions remain intact, e.g., C3a anaphylatoxin production, C3b opsonization, and immune complex and apoptotic body clearance. Zimura (previously ARC1905; Ophthotech Corp., Princeton, NJ, USA) is an anti-C5 aptamer delivered by intravitreal injection. It binds C5 with high affinity (KD= ~700 pM) and prevents cleavage to C5a and C5b. A phase I trial of Zimura was completed and the results reported in 2010. In this nonrandomized safety study, Zimura was administered with monthly injections with ranibizumab 0.5 mg. There were no safety concerns or dose-limiting toxicities. In 43 patients receiving 6-monthly injections, the mean change in visual acuity at 24 weeks was +13.6, +11.7, and +15.3 letters in the 0.3-mg, 1-mg, and 2-g dosing groups, respectively.[249] Ophthotech has initiated plans for a phase II/III trial. A phase I trial (NCT00950638) for Zimura for GA has also been completed.

Non-Neovascular AMD

Antioxidants, Vitamins, and Cofactors

The rationale for the use of antioxidants, multivitamins, and other cofactors is based upon several lines of evidence, including the essential role of vitamin A in the visual transduction cycle, the known and predicted effects of oxidative stress resulting in reactive oxygen intermediates, and the requirement of certain critical metal ions including zinc in the functioning of critical proteases and other naturally occurring defense mechanisms against oxidative injury. Prior to the release of the data from the AREDS study, there remained some controversy as to whether or not antioxidant multivitamin therapy was efficacious, with some studies suggesting a protective effect, and others not.[42,43,250]

Age-Related Eye Disease Study (AREDS) and AREDS2

The AREDS trial was a large multicenter RCT, which evaluated the effect of high-dose vitamin C and E, beta-carotene, and zinc supplements on AMD progression and visual acuity. A total 4,757 persons were enrolled and stratified into one of four categories of increasing severity of disease. Due to the low rate of progression of Category 1 consisting of drusen area of less than 5 small drusen of 63 μm or less, statistical analysis was only performed on the remaining 3,640 patients with Categories 2, 3, 4. Only the latter two (Categories 3 and 4) were ultimately found to be at more than a trivial risk for progression. Patients in Category 2 with at least one intermediate size druse, but not extensive drusen, had only a 1.3% probability of progression to advanced AMD by year 5 and no meaningful inference could be drawn regarding their risk with or without intervention. Patients in Category 3 had either extensive intermediate drusen, large drusen or non-central GA, and patients in Category 4 had visual acuity of less than 20/32 due to AMD in one eye related either to GA involving the center of the macula or CNV in the fellow eye, but not the study eye, which had visual acuity 20/32 or better. The average follow-up of the 3,640 enrolled study participants aged 55 to 80 was 6.3 years, and by comparison with placebo, patients treated with antioxidants plus zinc demonstrated a statistically significant odds reduction for the development of advanced AMD (odds ratio 0.72, 99% confidence interval, 0.52–0.98). The odds ratios for zinc alone and antioxidants alone were 0.75 and 0.8 respectively, and the odds reduction estimates increased when only patients with Category 3 or Category 4 drusen were included, reducing to 0.66, 0.71, and 0.76 for antioxidants plus zinc, zinc alone, and antioxidants alone, respectively. These data are further reflected in Fig. 70.23.

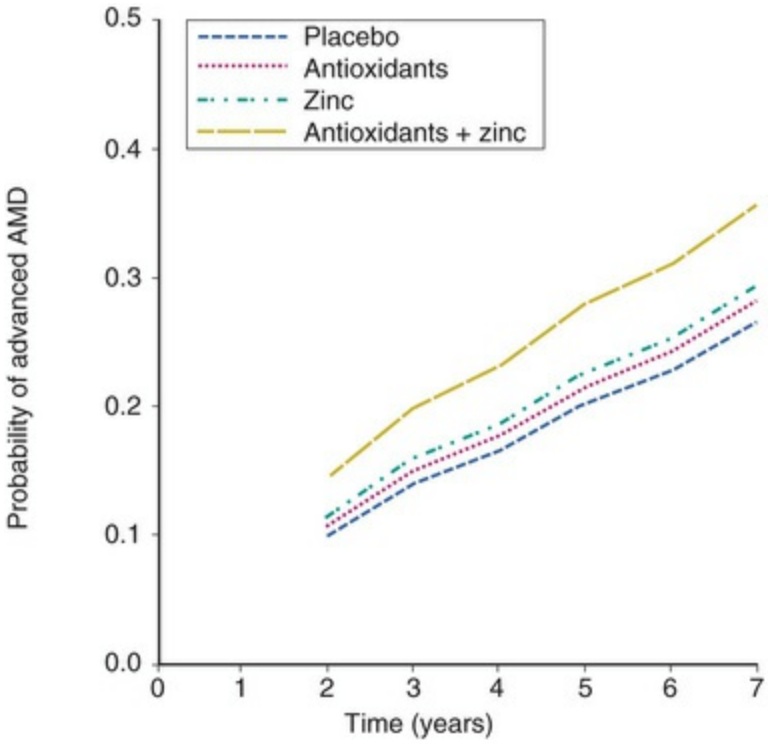

Probability of AMD Event by Year

Treatment	2	3	4	5	2	2
Placebo	0.142	0.197	0.231	0.278	0.311	0.357
Antioxidants	0.112	0.157	0.185	0.226	0.254	0.296
Zinc	0.106	0.149	0.177	0.216	0.243	0.284
Antioxidants + Zinc	0.098	0.139	0.165	0.202	0.229	0.267

FIG. 70.23 Repeated-measures estimates of the probability of loss in the visual acuity score of at least 15 letters in at least one study eye of participants within categories 3 and 4. (Reproduced with permission from AREDS Research Group. Arch Ophthalmol. 2001;119(10):1417-1436.)

Based on these findings, and extrapolation of the US population at risk, it has been estimated that of the 8 million persons in the United States at least age 55 or greater with AMD, if those at highest risk, including Categories 3 and 4, were to receive therapy with the formulation employed in the AREDS trial, as many as 300,000 of the 1.3 million at highest risk for advancement might avoid progression to the severe forms of the disease.[251] Additionally, based upon recent epidemiologic data, exclusion of beta-carotene was recommended for persons with a current history of smoking or a long smoking history based upon a theoretical increased risk of lung cancer.

The macular carotenoids thought to be the principal contributors to macular yellow include lutein and zeaxanthin. One study

suggested that a high dietary intake of these carotenoids protected against AMD, resulting in a 43% reduction in risk for AMD when the upper quartile of use was compared with the lowest quartile.[40] The AREDS reports have supported these findings, showing in cohort studies that those with a high level of dietary intake of lutein and zeaxanthin were less likely to have advanced AMD, as well as large or extensive intermediate drusen.[252] High dietary intake of omega-3 long-chain polyunsaturated fatty acids were also found by the AREDS investigators to be inversely related to progression to both GA as well as neovascular AMD.[37–39] Consequently, the AREDS2 randomized multicenter phase III clinical trial (NCT00345176) was designed to address (1) the role of lutein and zeaxanthin and the omega-3 long-chain polyunsaturated fatty acids docosahexaenoic acid (DHA) and eicosapentaenoic acid (EPA) in prevention of development of GA or CNV; (2) the effect of possible deletion of beta-carotene and lowering the daily zinc oxide dose from 80 mg to 25 mg.

The 4203 AREDS2 study participants (6916 eyes) were randomized to one of four interventions: (1) placebo (the original AREDS supplement, and thus not a true placebo group); (2) lutein (10 mg) and zeaxanthin (2 mg); (3) DHA (350 mg) and EPA (650 mg); (4) both lutein/zeaxanthin and DHA/EPA. A second-tier randomization assigned 3,036 patients (4,987 eyes) to receive (1) the original AREDS supplement; (2) the AREDS supplement without beta-carotene; (3) AREDS supplement with lower dose zinc; or (4) both without beta-carotene and with lower dose zinc. The primary outcome measure was the development of central GA or CNV.

Five-year progression to advanced AMD was similar for all groups in the primary randomization (31% for placebo, 29% for lutein + zeaxanthin, 31% for DHA + EPA, and 30% for lutein + zeaxanthin and DHA + EPA). No intervention resulted in significant reduction in progression to advanced AMD (Fig. 70.24). Similarly, analysis of the secondary randomization showed no difference in progression when lowering zinc or eliminating beta-carotene. There was no effect of any supplement on the risk of moderate visual acuity loss (15 or more letters). All groups in the primary randomization had similar safety outcomes, with no significant differences in serious adverse events; however, in the

secondary randomization, more participants in the beta-carotene group than the no beta-carotene group developed lung cancer (91% of whom were former smokers).

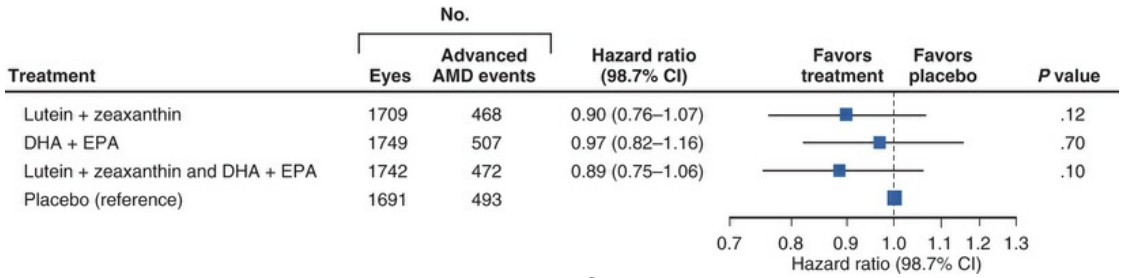

FIG. 70.24 Primary analyses of lutein + zeaxanthin + omega-3 long-chain polyunsaturated fatty acids vs. placebo for treatment of progression to advanced age-related macular degeneration (AMD). (Participants assigned to the placebo group were also given Age-Related Eye Disease Study (AREDS) supplement either within or outside of the secondary randomization for the four variations of the AREDS supplements; thus, there is no true placebo group.) DHA, docosahexaenoic acid; EPA, eicosapentaenoic acid.

(Reproduced with permission from Age-Related Eye Disease Study 2 Research Group. Lutein + zeaxanthin and omega-3 fatty acids for age-related macular degeneration: the Age-Related Eye Disease Study 2 (AREDS2) randomized clinical trial. JAMA. 2013;309(19):2005-15.)

Although the primary analysis of AREDS2 did not show additional benefit when substituting lutein and zeaxanthin for beta-carotene, or when adding DHA and EPA, the potential increased risk of lung cancer in current and former smokers when taking beta-carotene suggested a more favorable safety profile with the naturally occurring macular pigments lutein and zeaxanthin. Additionally, in a prespecified secondary analysis, there was a protective effect associated with lutein and zeaxanthin supplementation for progression to advanced AMD in those patients with the lowest dietary intake of these nutrients. The study also found that the serum levels of lutein and zeaxanthin were lower in those patients who were assigned to the group receiving the supplement including beta-carotene; previous preclinical animal and human studies had suggested that beta-carotene and

lutein + zeaxanthin administered concurrently may result in lower serum and tissue levels of lutein + zeaxanthin due to competitive absorption, leading to the hypothesis that lutein and zeaxanthin may reduce the risk of progression when given without additional beta-carotene.

Additional secondary analysis of the AREDS2 data exploring this hypothesis found that lutein/zeaxanthin alone compared to beta-carotene alone showed a favorable effect of lutein/zeaxanthin in reducing the risk of progression to neovascular AMD, although not central GA (Fig. 70.25). There was no apparent additional synergistic effect when adding beta-carotene to lutein/zeaxanthin, as the hazard ratios for progression remained similar when compared to beta-carotene alone.[253] Lutein/zeaxanthin also compared favorably with beta-carotene for disease progression along the AREDS AMD Scale, as well as for progression to advanced AMD in those patients with bilateral large drusen (although not for those patients with baseline late AMD in one eye). In contrast to AREDS, there was no reduction of vision loss in AREDS2 except in the exploratory analysis of rates of severe vision loss (<20/100). In the secondary analysis of nonsmokers, lung cancer developed more frequently in patients receiving beta-carotene than in those not receiving beta-carotene (91% of whom were former smokers).

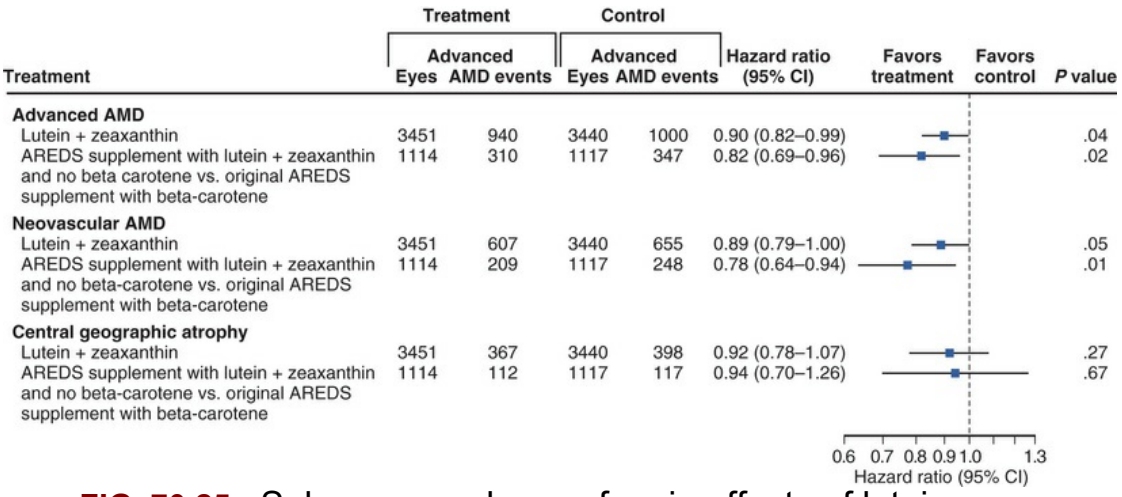

FIG. 70.25 Subgroup analyses of main effects of lutein + zeaxanthin and the comparison of participants randomized to receive lutein + zeaxanthin and Age-

Related Eye Disease Study (AREDS) supplements with lutein + zeaxanthin and without beta carotene vs. those randomized to receive original AREDS supplements with beta-carotene for progression to advanced age-related macular degeneration (AMD) and the two forms of AMD, neovascular AMD and central geographic atrophy. (Reproduced with permission from Age-Related Eye Disease Study 2 Research Group. Lutein + zeaxanthin and omega-3 fatty acids for age-related macular degeneration: the Age-Related Eye Disease Study 2 (AREDS2) randomized clinical trial. JAMA. 2013;309(19):2005-15.)

The AREDS2 data supported the use of supplementation with lutein/zeaxanthin in the reduction of progression to late AMD, and supported the finding in AREDS that beta-carotene increases the risk of lung cancer in current and former smokers. These findings taken together suggested that lutein/zeaxanthin may be a more appropriate carotenoid supplement than beta-carotene, both in safety profile, as well as in protection against the development of neovascular AMD.

Visual Cycle Inhibitors[a]

Visual cycle modulators are intended to reduce the accumulation of toxic fluorophores such as A2E in RPE cells. Fenretinide (ReVision Therapeutics, Inc., San Diego, CA, USA) is a synthetic vitamin A derivative that causes a dose-dependent, reversible reduction in circulating retinal binding protein (RBP) and retinol by competitive displacement of retinol from RBP, as well as interfering with RBP binding to transthyretin (TTR), thus facilitating their elimination via glomerular filtration. In ABCA4$^{-/-}$ mice, fenretinide reduces RPE lipofuscin and A2E accumulation, although it causes modest delays in dark adaptation.[254] Notably, however, despite low blood retinol levels, RPB$^{-/-}$ mice acquire normal vision by 5 months of age when given a vitamin A-sufficient diet.[255,256] Thus, it is not clear that blockade of vitamin A transport to RPE by inhibition of vitamin A binding to RBP will block vitamin A uptake by the RPE during long-term administration unless dietary vitamin A is restricted also. In a phase IIb clinical trial of oral fenretinide, 246 patients were randomized to receive placebo, 100 mg, or a 300 mg daily dose for 24 months (NCT00429936).[257] At the conclusion of the 2-year study,

analysis of GA lesion growth by color fundus photography showed a trend for slowing of lesion growth in the 300-mg fenretinide dose cohort, particularly among patients who had serum RBP levels of ≤2 mg/dL (1.70 ± 0.77 mm^2/year vs. 2.03 ± 1.24 mm^2/year, p=.1848). Moreover, an exploratory and ad hoc analysis of the data revealed that 15 (18.3%) of 82 patients in the placebo arm progressed to CNV, compared with 15 (9.2%) of 163 patients receiving fenretinide at either dose (p=.06), despite the higher baseline risk of developing CNV (based on previous fellow-eye CNV) compared with the placebo group.[257]Although fenretinide can affect dark adaptation[258–265] and ERG readings,[266–269] and is associated with symptoms of dry eye,[263,264] it was generally well tolerated in this study, with four patients (2.5%) withdrawing from the study due to dark adaptation complications, and four other patients in the 300-mg group withdrawing citing visual disturbances.

Emixustat (formerly ACU-442; Acucela, Seattle, WA, USA) is an orally administered compound that inhibits conversion of all-*trans*-retinyl ester to 11-*cis*-retinol via blockade of RPE65 as a means of reducing toxic metabolites of the visual cycle. Emixustat has been shown to reduce lipofuscin and A2E accumulation in the RPE of $ABCA4^{-/-}$ mice. A phase I clinical trial (NCT00942240) in 46 healthy volunteers was completed successfully up to doses of 75 mg.[270] The most common adverse events were vision-related, occurring in 50% of patients receiving the medication, which included dyschromatopsia (32%), unspecified visual disturbance (29%), night blindness (18%), blurred vision (11%), and photophobia (8%). All adverse events were mild or moderate in intensity and were transient in nature, resolving within a few days after onset. There was dose-dependent suppression of the ERG b-wave as expected. Similarly, in a second, multiple-dose, placebo-controlled phase I study, an additional 40 healthy volunteers (30 study medication patients, 10 placebo) were given an oral course of emixustat for 14 days, with doses up to 40 mg. The mean elimination half-life was determined to be 4.6 to 7.9 hours, with peak plasma levels within 3–5 hours after each dose. There was no significant plasma accumulation or systemic adverse events. Visual side-effects were similar to those described above.

A double-masked, dose escalation phase IIa study was completed

with study results reported in 2015 (NCT01002950).[271a] Seventy-two patients with GA were randomized in a 3 : 1 fashion to receive either emixustat (n=54) or placebo (n=18) daily for 90 days, in five dosing cohorts (2, 5, 7, 10 mg given every morning, or 5 mg given every evening). Drug effect on the visual cycle was assessed by measurement of ERG rod sensitivity after photobleaching. After 14 days of study drug administration, there was dose-dependent rod suppression in the emixustat group, with the least suppression in the 2-mg group, and the most suppression in the 10-mg group. One to two weeks after drug cessation, post-bleach amplitudes returned to normal with exception one outlier patient in the 10-mg group that skewed the results in that group. There was no effect on the cone ERG. Fifty-three percent of patients receiving emixustat completed the study, with the higher dosing cohorts (7 and 10 mg) discontinued early because of adverse events, which occurred in 7 of 18 patients in those groups. Eight subjects overall (all receiving study drug) discontinued the study drug due to an adverse event, which were ocular in nature. Ocular adverse events were seen in 93% of emixustat subjects (most commonly visual disturbances such as chromatopsia and delayed dark adaptation), while systemic adverse events were seen in 57%. The majority of these events resolved within 7–14 days after discontinuing the study drug. The phase II study served a proof of concept that emixustat can indeed modulate the visual cycle, with temporary and reversible rod suppression and mild to moderate ocular adverse events. Additional studies are planned; however, it may also be worth noting that histopathologic studies have demonstrated that abnormal fundus autofluorescence in geographic atrophy may result primarily from vertically superimposed or layering of RPE cells rather than intracellular lipofuscin accumulation. As such, there remains some debate regarding the utility of targeting the visual cycle for this disease process.[271b,271c]

Complement Inhibition

Factor D is the rate-limiting enzyme in the activation of the complement alternative pathway. It plays an important role in the positive feedback loop that results in the amplification of

proinflammatory effectors.[272] Lampalizumab (formerly FCFD4514S; Genentech/Roche, South San Francisco, CA, USA) is a monoclonal antibody fragment (Fab) directed against Factor D. An 18-patient, open-label escalating-dose phase Ia clinical trial (NCT00973011) of intravitreal therapy for GA showed that the medication was well tolerated, with no significant adverse events up to the maximum-tested 10 mg dose. The subsequent phase II2 MAHALO study (NCT01229215) enrolled 143 patients (including a 14-patient phase Ib run-in), testing lampalizumab at the 10-mg dose. The placebo-controlled study dosed lampalizumab monthly or bimonthly, compared with sham injections, also given monthly or bimonthly, randomized 1:2:1:2, with twice the number in the treatment groups. The primary study endpoint was the mean change in GA area from baseline to 18 months, as measured by fundus autofluorescence. Other endpoints included GA on color fundus photographs and BCVA. At the study endpoint, there was a 20.4% reduction in the rate of expansion of GA lesions in the monthly lampalizumab injection group relative to the pooled sham groups, which was statistically significant to the predetermined *p*-value of 0.2. There was no difference in rate of GA expansion in the bimonthly lampalizumab group versus sham. In a subgroup analysis of patients with exploratory biomarkers (mutations in CFH, C3, C2/CFB, and CFI, positive in 57% of the patients assayed), there was a 44% reduction relative to sham ($p<.005$, n=28). Final BCVA was worse in all groups relative to baseline, without differences, although the study was not powered to detect differences in visual acuity. There were no significant safety concerns, although there were 7 ocular adverse events in the treatment groups (4 in the monthly group, 3 in the bimonthly group). There was one nonocular adverse event in each of the study groups suspected to be caused by the study drug. The MAHALO study was the first to demonstrate any positive effect on GA progression, with the results prompting a phase III trial.

Inhibition of C5 blocks terminal complement activity, with proximal complement functions remaining intact, e.g., C3a anaphylatoxin production, C3b opsonization, and immune complex and apoptotic body clearance. Previous trials have attempted to slow the rate of GA progression by inhibiting the actions of C5 (or

its cleavage product C5a) without demonstrating efficacy.[95,273] Notably, a double-masked randomized clinical trial of eculizumab, a systemic inhibitor of C5, failed to demonstrate any difference in progression of GA in 30 patients over a 6-month period.[273] However, there is still interest in this area. The monoclonal antibody LFG316 binds C5 with high affinity and prevents its cleavage into C5a and C5b.[274,275] A phase 1 dose-escalation trial in 24 patients with advanced AMD demonstrated safety with a single intravitreal injection of up to 5 mg. There were no significant adverse events, and no change in serum C5 levels or evidence of activation of serum alternative complement pathway. A phase II trial is underway (NCT01527500).

The complement factor C3 is also a target of interest for dry AMD. The cyclic peptide POT-4 was originally developed at the University of Pennsylvania and represented the first complement inhibitor to be tested in patients with AMD. The compound blocks C3 and all downstream effector pathways. A phase I study (NCT00473928) tested a single intravitreal injection of POT-4 in patients with neovascular AMD and was found to be safe and well tolerated.[276] Alcon/Novartis (Fort Worth, Texas, USA) licensed POT-4 and initiated a phase 2 trial, but subsequently terminated its development. Apellis Pharmaceuticals (Crestwood, KY, USA) acquired the rights to POT-4 in 2014 and has continued to develop the technology as APL-2, with the same therapeutic target but with a longer half-life. A phase I trial is in process for neovascular AMD (NCT02461771), with a phase II trial planned for GA (NCT02503332). Fig. 70.26 illustrates the complement pathways and compounds in various stages of investigation.

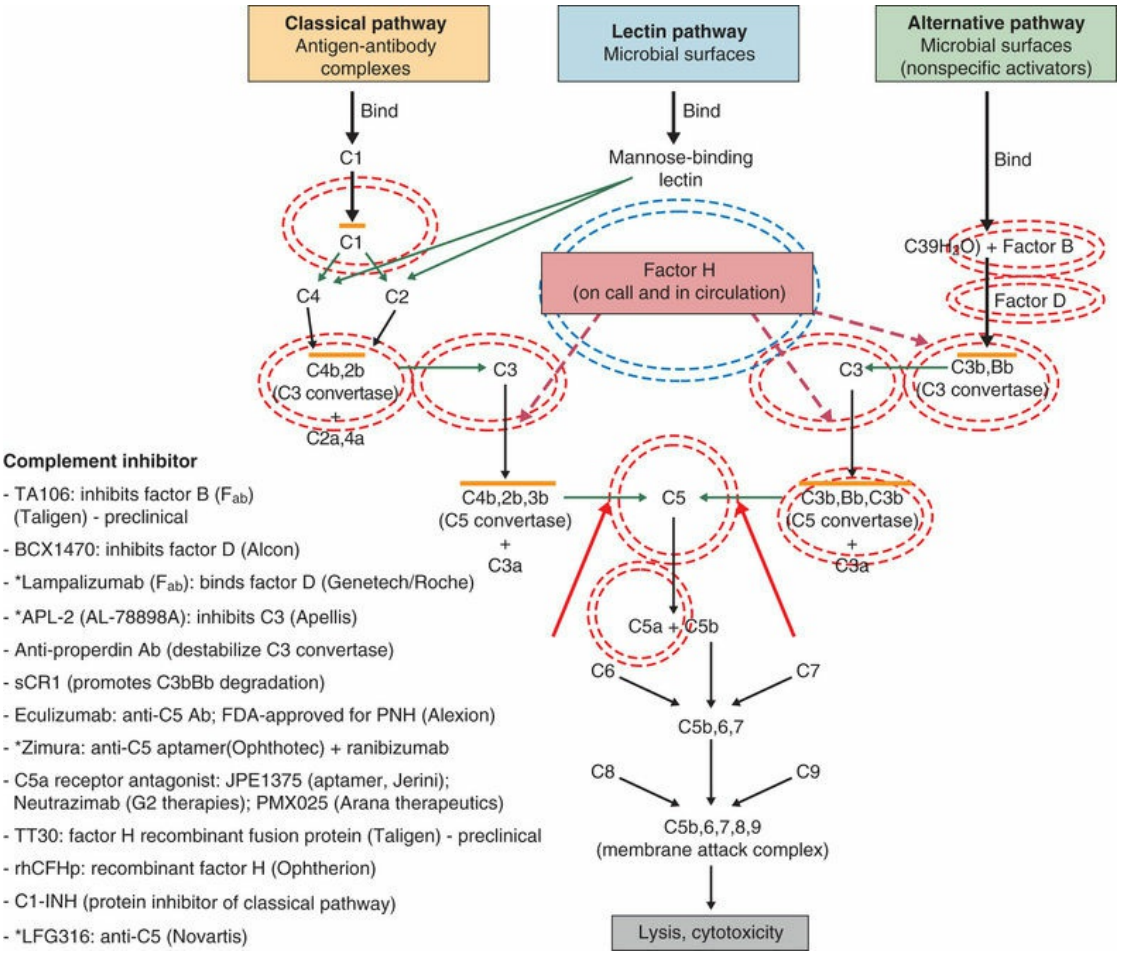

FIG. 70.26 Numerous compounds that modulate the complement pathway are in development for or in clinical trials for AMD treatment. * Currently being investigated for AMD. Red circles indicate the parts of the complement pathway that are being modified. The complement pathway illustrated is adapted from Donoso et al.[277] (Reproduced from Zarbin MA, Rosenfeld PJ. Pathway-based therapies for age-related macular degeneration: an integrated survey of emerging treatment alternatives. Retina 2010; 30: 1350-67, with permission of Springer Science+Business Media.)

Other Agents

Sirolimus

Sirolimus (or rapamycin; MacuSight/Santen, Union City, CA, USA); is a macrocyclic, naturally occurring lactone that was initially isolated from the species *Streptomyces hygroscopicus* and given its name from Rapa Nui (Easter Island) during the course of a search

for novel antifungal agents. Sirolimus interacts with the protein kinase, mechanistic target of rapamycin (mTOR), which regulates various aspects of cell function, including metabolism and apoptotic pathways. Additionally, through its intrinsic immunomodulatory effects, may reduce macrophage chemotaxis and activation, and suppresses T-cell and B-cell proliferation.

It has been shown to inhibit angiogenesis through direct inhibition of vascular endothelial growth factors as well as endothelial cell responses to VEGF.[278] Inhibition has been demonstrated in a murine model of retinopathy of prematurity and laser-induced neovascularization when the drug was administered by an intraperitoneal route.[279] Although sirolimus has been investigated as an agent for neovascular AMD,[280] there is currently more interest as an agent for nonexudative disease.

A single-center, open-label phase I/II study examined subconjunctival administration of sirolimus for the treatment of GA (NCT00766649). The study enrolled 11 patients, 8 of whom completed 24 months of follow-up. Sirolimus was administered quarterly in one eye, with the fellow eye serving as a control. Although sirolimus was well tolerated without significant safety concerns, there was no significant benefit demonstrated.[281] At 24 months, mean GA area increased by 54.5% in the study eye, compared with 39.7% in the fellow eye (p=.41), with significantly more vision loss associated with the study drug (loss of 21 letters compared with 3 letters in the study eye versus the fellow eye). There were no differences in drusen area, retinal thickness, or macular sensitivity. It was postulated that subconjunctival administration may be insufficient to reach the posterior segment of the eye; thus a second study examined the effect of sirolimus delivered via intravitreal injection (NCT01675947). Among the six study participants, two developed accelerated retinal thinning in the treated eye, one of which was associated with paralesional fundus autofluorescence changes. The study was terminated due to safety concerns.[282]

Amyloid

As discussed above, amyloid is thought to be an activator of the complement system in AMD.[106–108] GlaxoSmithKline has developed

a monoclonal antibody to amyloid-β, called GSK933776, which is administered intravenously. Preclinical animal studies demonstrated that the antibody reduced the accumulation amyloid-β and C3a deposition within Bruch's membrane. A phase I trial has been completed and a multicenter, double-masked, placebo-controlled phase II trial is underway.[283]

Increasing Choroidal Blood Flow

Choroidal bloodflow decreases in the normally aging eye, and choroidal hypoperfusion has been implicated in the pathogenesis of AMD.[284–286] Increasing choroidal bloodflow, then, may represent one method of decreasing the risk of progressing to advanced neovascular or atrophic AMD. MacuCLEAR has developed a choroidal vasodilator called MC-1101 that can be given topically. Mechanistically, MC-1101 operates in part through the production nitric oxide, but theoretically without significant systemic side effects due to its route of administration. A phase Ib trial was completed, and demonstrated a significant increase in choroidal bloodflow (over 5-fold) one hour after administration. A phase II/III trial is currently underway (NCT01601483).

Neuroprotection

In many degenerative retinal conditions, such as retinitis pigmentosa, a therapeutic modality of interest is in the area of neuroprotection, exposing the degenerating tissue to an agent that can retard cell population death. Although different diseases processes, apoptotic degeneration appears to play a role in both inherited retinal degenerations as well as macular degeneration, and investigators are exploring some of the same therapeutic principles.[287] Ciliary neurotrophic factor (CNTF) is in the IL-6 cytokine family that has been shown to slow the loss of photoreceptors in multiple animal models of inherited retinal degenerative conditions.[288–290] In a proof-of-concept, randomized phase II clinical trial, CNTF was administered by encapsulated cell technology (ECT-NT-501; see above section for more background on this technology and for its role in neovascular AMD).[186] The study enrolled 51 patients, with 27 patients receiving the high-dose implant, and 12 patients each receiving sham or low-dose implant,

followed for 12 months. Visual acuity remained stable in the high-dose implant group, with 96.3% of patients losing fewer than 15 letters of vision, compared with 75% of the sham group (p=.078). This difference was statistically significant in those with better baseline vision (>20/63): 10/10 patients maintained vision in the high-dose group, compared with 5/9 in the combined low-dose/sham group (p=.033). Macular OCT measurements demonstrated significant increase in volume in patients receiving the study intervention, regardless of dose, and exclusive of any pathologic change (e.g., CNV, macular edema, epiretinal membrane). No change in GA was found in any group. No treatment-related severe adverse events were reported. The study demonstrated a biologic effect of CNTF (increase in OCT macular volume), as well as proof-of-concept for the CNTF ECT implant. However, no further trials for this indication are currently planned.

Brimonidine given for glaucoma has long been believed to offer additional benefit as a neuroprotective agent. Multiple animal models have shown this effect in a number of cell types, including retinal ganglion cells, bipolar cells, and photoreceptors.[291–293] The mechanism of neuroprotection has not been elucidated, but is likely due to induced expression or upregulation of trophic factors such as brain-derived neurotrophic factor (BDNF) and cytokines that inhibit apoptotic pathways and stimuli.[294,295] A brimonidine sustained-release intravitreal implant has been developed by Allergan[296] (Irvine, CA, USA) and has been tested in a 2-year phase II study of GA (NCT00658619). The randomized double-masked sham-controlled trial enrolled 119 patients with bilateral GA, with one eye serving as the study or sham eye, and the fellow eye acting as a sham control. Study eyes were given either a 200 μg or 400 μg implant or a sham treatment at day 1 of the study and again at 6 months, with the primary outcome of change in GA from baseline to 1 year. At the time of writing, a second phase II study has completed enrollment (NCT02087085).

Doxycycline/Matrix Metalloproteinase Inhibitor

As indicated above, the matrix metalloproteinases, such as MMP-2 and -9, are believed to play a role in the process of angiogenesis in AMD, and are known to be expressed in choroidal neovascular

membranes removed from patients with subfoveal CNV.[82]

Doxycycline has long been known to be a potent matrix metalloproteinase (MMP) inhibitor, acting as a noncompetitive inhibitor through its interactions with zinc or calcium within the center of this class of proteins.[297] In an animal model of CNV, doxycycline administration decreased laser-induced CNV size significantly. Based on this activity and the possible association of matrix metalloproteinases with the pathogenesis of macular degeneration, a phase II/III trial has been initiated testing doxycycline for GA.

Home Monitoring for AMD

The goal of current pharmacotherapies for treatment-warranted AMD is to preserve retinal structure and function. Treatment studies have demonstrated better visual outcomes in patients with improved vision at the time of initiating treatment.[298–300] As such, earlier detection of treatment-warranted disease is paramount to improved visual outcomes with treatment.

Because the interval between scheduled clinic visits for patients with AMD may span up to one year, an area of interest has been the development of out-of-office tools to aid in the diagnosis and surveillance of patients for treatment-warranted disease, specifically the development or reactivation of CNV.

Pathology[301] and psychophysical[302] studies have demonstrated that there is an early susceptibility of the parafoveal rod photoreceptors in both dry and wet AMD. Several targeted monitoring tools have been developed. Validation against age-matched controls and with serial measurements versus a given patient's baseline have indicated promise with regard to the detection of de novo and recurrent treatment-warranted disease, respectively.

The utility of at-home self-monitoring remains dependent on patient adherence to the testing procedures and may be improved through better patient education and tools. For example, the Vision and Memory Stimulating Journal (KeepSight; Hebron, CT), which includes an Amsler-type grid for home testing, demonstrated improved adherence to weekly testing (80% vs. 50%, p=.002) and

patient confidence in self-monitoring (p=.002).[317]

Hyperacuity-Based Testing

Hyperacuity, or vernier acuity, relies on the integration of visual input over an area of retina, and as such, hyperacuity tasks may detect subtle defects in the photoreceptor mosaic.

Amsler Grid

The traditional Amsler macular grid is a handheld, paper-based test in which patients fixate centrally on a grid wherein each block subtends about 1 degree of visual angle, noting areas of scotoma or metamorphopsia.[303] Amsler grid testing was found to correlate well with areas of RPE atrophy (r=0.73, p<.001),[304] and in a meta-analysis, to have a sensitivity and specificity to detect neovascular AMD of 64–87% and 91–99%, respectively.[305] As such, it has been a mainstay of out-of-office screening for treatment-warranted AMD since the 1960s.

Preferential Hyperacuity Perimetry/ForeseeHome

ForeseeHome (Notal Vision, Ltd; Tel Aviv, Israel) is a fixed, device-based preferential hyperacuity perimetry (PHP) test that presents patients with dotted-line stimuli within a 14° diameter area of retina, and a subset of the dots are misaligned. Patients are tasked with indicating the location of misalignment.[306] A recent meta-analysis[305] of studies evaluating preferential hyperacuity perimetry testing found that it has a sensitivity and specificity to detect neovascular AMD of 80–89% and 82–91%, respectively. A recent prospective, randomized, unmasked clinical trial comparing the ForeseeHome device plus standard care versus standard care alone demonstrated detection of CNV at an earlier stage of functional loss (20/32 vs. 20/40, loss of 4 vs. 9 ETDRS letters from baseline, p=.021).[307]

Shape Discrimination Hyperacuity/myVisionTrack

myVisionTrack (Vital Art and Science, Inc; Richardson, TX) is a handheld, smartphone-based shape discrimination hyperacuity

(SDH) test in which patients are presented with an alternate forced-choice task to determine which of three circular shapes, subtending a 3° diameter area of retina, is radially distorted.[308] In a cross-sectional study of 32 patients with AMD and 10 age-matched controls, SDH scores in 31 (97%) of the patients with AMD were significantly worse than the mean control score, resulting in a test sensitivity and specificity of 97% and 100%, respectively.[309] In a cross-sectional study of 37 patients with AMD and 27 age-matched controls, worse SDH was correlated with increasing OCT central subfield thickness (r=0.56, p<.0001).[308] In both studies, SDH scores in patients with AMD were significantly worse than controls, to a degree that correlated with severity of disease. Additional studies are ongoing to assess the validity of this test to detect early treatment-warranted AMD.

Rarebit/MultiBitTest

Rarebits are small stimuli presented for short durations that assess the receptive field matrix. MultiBitTest (MBT; Visumetrics AB; Gothenburg, Sweden) is a handheld, smartphone-based rarebit integration test in which patients are tasked with identifying numerical digits that have been segmented into receptive field-sized stimuli, which in aggregate subtend a 7° diameter area of retina. In a cross-sectional study of 28 patients with AMD and 20 aged controls, MBT demonstrated an area under the receiver-operating characteristic curve of 0.95, indicating promise to detect disease.[310]

Perimetry-Based Testing

Perimetry-based tests, such as microperimetry, seek to localize areas of absolute and relative scotoma by applying direct stimuli.[311]

Macular Mapping Test

The Macular Mapping Test (MMT; Aston University; Birmingham, UK) is a computer-based test in which Sloan letters are displayed at eccentricities up to 18° from fixation, which is maintained by a radially symmetric wagon-wheel pattern. The patient is queried on detection and recognition of the letter. In a cross-sectional study of

29 eyes with AMD and 31 eyes of age-matched controls, there was a significant difference in mean MMT scores between eyes with advanced AMD versus controls (p<.001),[312] indicating promise to detect disease.

Luminance-Based Testing

As there is preferential parafoveal rod > cone loss in early AMD,[301] low luminance tasks, such as dark adaptation[313] and photostress recovery,[314] have been found to be affected in patients with AMD.

Low Luminance Visual Acuity/SKILL Card

The Smith–Kettlewell Institute Low Luminance (SKILL) card measures the difference between standard high-contrast versus a low-luminance, low-contrast near visual acuity.[315] In a cross-sectional study of 17 patients with AMD and 20 age-matched controls, there was a significant difference in mean SKILL scores between eyes with advanced AMD versus controls (p=.01).[316]

Summary

A variety of molecules, specifically targeted to different pathologic pathways in AMD, have been identified for their therapeutic potential. Additionally, our understanding of the genetic basis for AMD continues to increase rapidly, which has led to a systematic and rational basis for pharmacotherapy. A number of associated genes and alleles have been identified that confer risk or are protective against the disease, and as the related pathways are elaborated, we are able to not only target these pathways with great specificity, but also identify those individuals who are most likely to benefit from a particular therapy. Research is actively being pursued in preclinical models both in academic laboratories and in the pharmaceutical industry, including a large number of early-stage clinical trials in recent years. The success of VEGF inhibition has shown that targeted therapies are a key component of the treatment of macular degeneration. It is anticipated that agents that can modulate and inhibit various stages of the disease, and especially including those multiple stages relating to RPE function,

the visual transduction cycle, and inflammatory pathways, will find prominent roles either alone or in combination. It is also increasingly likely that not only treatments targeted at specific molecular pathways, but also gene transformation and replacement, should become increasingly important tools in addition to standard VEGF inhibitors and other classes of small molecules and specific monoclonals in the management of this disease.

References

1. Bird AC, Bressler NM, Bressler SB, et al. An international classification and grading system for age-related maculopathy and age-related macular degeneration. The International ARM Epidemiological Study Group. *Surv Ophthalmol*. 1995;39(5):367–374.
2. Ambati J, Ambati BK, Yoo SH, Ianchulev S, Adamis AP. Age-related macular degeneration: etiology, pathogenesis, and therapeutic strategies. *Surv Ophthalmol*. 2003;48(3):257–293.
3. Blumenkranz MS, Russell SR, Robey MG, Kott-Blumenkranz R, Penneys N. Risk factors in age-related maculopathy complicated by choroidal neovascularization. *Ophthalmology*. 1986;93(5):552–558.
4. Ferris FL 3rd. Senile macular degeneration: review of epidemiologic features. *Am J Epidemiol*. 1983;118(2):132–151.
5. Ferris FL 3rd, Fine SL, Hyman L. Age-related macular degeneration and blindness due to neovascular maculopathy. *Arch Ophthalmol*. 1984;102(11):1640–1642.
6. Bressler NM, Hawkins BS, Sternberg P Jr, McDonald HR. Are the submacular surgery trials still relevant in an era of photodynamic therapy? *Ophthalmology*. 2001;108(3):435–436.
7. Macular Photocoagulation Study Group. Argon laser photocoagulation for senile macular degeneration. Results of a randomized clinical trial. *Arch Ophthalmol*. 1982;100(6):912–918.
8. Macular Photocoagulation Study Group. Argon laser photocoagulation for neovascular maculopathy. Three-year

results from randomized clinical trials. *Arch Ophthalmol*. 1986;104(5):694–701.
9. Macular Photocoagulation Study Group. Laser photocoagulation of subfoveal neovascular lesions of age-related macular degeneration. Updated findings from two clinical trials. *Arch Ophthalmol*. 1993;111(9):1200–1209.
10. Slakter JS, Yannuzzi LA, Sorenson JA, Guyer DR, Ho AC, Orlock DA. A pilot study of indocyanine green videoangiography-guided laser photocoagulation of occult choroidal neovascularization in age-related macular degeneration. *Arch Ophthalmol*. 1994;112(4):465–472.
11. Leibowitz HM, Krueger DE, Maunder LR, et al. The Framingham Eye Study monograph: An ophthalmological and epidemiological study of cataract, glaucoma, diabetic retinopathy, macular degeneration, and visual acuity in a general population of 2631 adults, 1973–1975. *Surv Ophthalmol*. 1980;24(Suppl.):335–610.
12. Brantley MA Jr, Fang AM, King JM, Tewari A, Kymes SM, Shiels A. Association of complement factor H and LOC387715 genotypes with response of exudative age-related macular degeneration to intravitreal bevacizumab. *Ophthalmology*. 2007;114(12):2168–2173.
13. Brantley MA Jr, Edelstein SL, King JM, et al. Association of complement factor H and LOC387715 genotypes with response of exudative age-related macular degeneration to photodynamic therapy. *Eye (Lond)*. 2009;23(3):626–631.
14. Tsuchihashi T, Mori K, Horie-Inoue K, et al. Complement factor H and high-temperature requirement A-1 genotypes and treatment response of age-related macular degeneration. *Ophthalmology*. 2011;118(1):93–100.
15. Feng X, Xiao J, Longville B, et al. Complement factor H Y402H and C-reactive protein polymorphism and photodynamic therapy response in age-related macular degeneration. *Ophthalmology*. 2009;116(10):1908–1912.e1.
16. Klein ML, Francis PJ, Rosner B, et al. CFH and LOC387715/ARMS2 genotypes and treatment with antioxidants and zinc for age-related macular degeneration. *Ophthalmology*. 2008;115(6):1019–1025.

17. Klein RJ, Zeiss C, Chew EY, et al. Complement factor H polymorphism in age-related macular degeneration. *Science*. 2005;308(5720):385–389.
18. Edwards AO, Ritter R 3rd, Abel KJ, Manning A, Panhuysen C, Farrer LA. Complement factor H polymorphism and age-related macular degeneration. *Science*. 2005;308(5720):421–424.
19. Francis PJ, Hamon SC, Ott J, Weleber RG, Klein ML. Polymorphisms in C2, CFB and C3 are associated with progression to advanced age related macular degeneration associated with visual loss. *J Med Genet*. 2009;46(5):300–307.
20a. Chen Y, Zeng J, Zhao C, et al. Assessing susceptibility to age-related macular degeneration with genetic markers and environmental factors. *Arch Ophthalmol*. 2011;129(3):344–351.
20b. Johnson LV, Leitner WP, Staples MK, et al. Complement activation and inflammatory processes in Drusen formation and age related macular degeneration. *Exp Eye Res*. 2001;73:887–896.
20c. Andreoli MT, Morrison MA, Kim BJ, et al. Comprehensive analysis of complement factor H and LOC387715/ARMS2/HTRA1 variants with respect to phenotype in advanced age-related macular degeneration. *Am J Ophthalmol*. 2009;148:869–874.
21. Albig AR, Schiemann WP. Fibulin-5 antagonizes vascular endothelial growth factor (VEGF) signaling and angiogenic sprouting by endothelial cells. *DNA Cell Biol*. 2004;23(6):367–379.
22. Klenotic PA, Munier FL, Marmorstein LY, Anand-Apte B. Tissue inhibitor of metalloproteinases-3 (TIMP-3) is a binding partner of epithelial growth factor-containing fibulin-like extracellular matrix protein 1 (EFEMP1). Implications for macular degenerations. *J Biol Chem*. 2004;279(29):30469–30473.
23. Fariss RN, Apte SS, Olsen BR, Iwata K, Milam AH. Tissue inhibitor of metalloproteinases-3 is a component of Bruch's membrane of the eye. *Am J Pathol*. 1997;150(1):323–328.
24. Felbor U, Stohr H, Amann T, Schonherr U, Apfelstedt-Sylla

E, Weber BH. A second independent Tyr168Cys mutation in the tissue inhibitor of metalloproteinases-3 (TIMP3) in Sorsby's fundus dystrophy. *J Med Genet*. 1996;33(3):233–236.
25. Lin RJ, Blumenkranz MS, Binkley J, Wu K, Vollrath D. A novel His158Arg mutation in TIMP3 causes a late-onset form of Sorsby fundus dystrophy. *Am J Ophthalmol*. 2006;142(5):839–848.
26. De La Paz MA, Pericak-Vance MA, Lennon F, Haines JL, Seddon JM. Exclusion of TIMP3 as a candidate locus in age-related macular degeneration. *Invest Ophthalmol Vis Sci*. 1997;38(6):1060–1065.
27. Marmorstein LY, Munier FL, Arsenijevic Y, et al. Aberrant accumulation of EFEMP1 underlies drusen formation in malattia leventinese and age-related macular degeneration. *Proc Natl Acad Sci USA*. 2002;99(20):13067–13072.
28. Chong NH, Alexander RA, Gin T, Bird AC, Luthert PJ. TIMP-3, collagen, and elastin immunohistochemistry and histopathology of Sorsby's fundus dystrophy. *Invest Ophthalmol Vis Sci*. 2000;41(3):898–902.
29. Kamei M, Hollyfield JG. TIMP-3 in Bruch's membrane: changes during aging and in age-related macular degeneration. *Invest Ophthalmol Vis Sci*. 1999;40(10):2367–2375.
30. Stone EM, Lotery AJ, Munier FL, et al. A single EFEMP1 mutation associated with both malattia leventinese and Doyne honeycomb retinal dystrophy. *Nat Genet*. 1999;22(2):199–202.
31. Mata NL, Weng J, Travis GH. Biosynthesis of a major lipofuscin fluorophore in mice and humans with ABCR-mediated retinal and macular degeneration. *Proc Natl Acad Sci USA*. 2000;97(13):7154–7159.
32. Zhang K, Garibaldi DC, Kniazeva M, et al. A novel mutation in the ABCR gene in four patients with autosomal recessive Stargardt disease. *Am J Ophthalmol*. 1999;128(6):720–724.
33. Allikmets R. Further evidence for an association of ABCR alleles with age-related macular degeneration. The International ABCR Screening Consortium. *Am J Hum Genet*. 2000;67(2):487–491.

34. Bernstein PS, Leppert M, Singh N, et al. Genotype-phenotype analysis of ABCR variants in macular degeneration probands and siblings. *Invest Ophthalmol Vis Sci*. 2002;43(2):466–473.
35. Radu RA, Mata NL, Nusinowitz S, Liu X, Sieving PA, Travis GH. Treatment with isotretinoin inhibits lipofuscin accumulation in a mouse model of recessive Stargardt's macular degeneration. *Proc Natl Acad Sci USA*. 2003;100(8):4742–4747.
36. Radu RA, Mata NL, Bagla A, Travis GH. Light exposure stimulates formation of A2E oxiranes in a mouse model of Stargardt's macular degeneration. *Proc Natl Acad Sci USA*. 2004;101(16):5928–5933.
37. SanGiovanni JP, Chew EY, Clemons TE, et al. The relationship of dietary lipid intake and age-related macular degeneration in a case-control study: AREDS Report No. 20. *Arch Ophthalmol*. 2007;125(5):671–679.
38. SanGiovanni JP, Chew EY, Agron E, et al. The relationship of dietary omega-3 long-chain polyunsaturated fatty acid intake with incident age-related macular degeneration: AREDS report no. 23. *Arch Ophthalmol*. 2008;126(9):1274–1279.
39. Sangiovanni JP, Agron E, Meleth AD, et al. ω-3 Long-chain polyunsaturated fatty acid intake and 12-y incidence of neovascular age-related macular degeneration and central geographic atrophy: AREDS report 30, a prospective cohort study from the Age-Related Eye Disease Study. *Am J Clin Nutr*. 2009;90(6):1601–1607.
40. Seddon JM, Ajani UA, Sperduto RD, et al. Dietary carotenoids, vitamins A, C, and E, and advanced age-related macular degeneration. Eye Disease Case-Control Study Group. *JAMA*. 1994;272(18):1413–1420.
41. Beatty S, Koh H, Phil M, Henson D, Boulton M. The role of oxidative stress in the pathogenesis of age-related macular degeneration. *Surv Ophthalmol*. 2000;45(2):115–134.
42. Cho E, Stampfer MJ, Seddon JM, et al. Prospective study of zinc intake and the risk of age-related macular degeneration. *Ann Epidemiol*. 2001;11(5):328–336.

43. Cho E, Seddon JM, Rosner B, Willett WC, Hankinson SE. Prospective study of intake of fruits, vegetables, vitamins, and carotenoids and risk of age-related maculopathy. *Arch Ophthalmol*. 2004;122(6):883–892.
44. Heuberger RA, Mares-Perlman JA, Klein R, Klein BE, Millen AE, Palta M. Relationship of dietary fat to age-related maculopathy in the Third National Health and Nutrition Examination Survey. *Arch Ophthalmol*. 2001;119(12):1833–1838.
45. Zarbin MA, Rosenfeld PJ. Pathway-based therapies for age-related macular degeneration: an integrated survey of emerging treatment alternatives. *Retina*. 2010;30(9):1350–1367.
46. Zarbin MA, Rosenfeld PJ. Review of emerging treatments for age-related macular degeneration. Stratton RD, Hauswirth WW, Gardner TW. *Oxidative stress in applied basic research and clinical practice: Studies on retinal and choroidal disorders*. Humana Press: New York; 2012:1–46.
47. Tomany SC, Wang JJ, Van Leeuwen R, et al. Risk factors for incident age-related macular degeneration: pooled findings from 3 continents. *Ophthalmology*. 2004;111(7):1280–1287.
48. Thornton J, Edwards R, Mitchell P, Harrison RA, Buchan I, Kelly SP. Smoking and age-related macular degeneration: a review of association. *Eye (Lond)*. 2005;19(9):935–944.
49. Darzins P, Mitchell P, Heller RF. Sun exposure and age-related macular degeneration. An Australian case–control study. *Ophthalmology*. 1997;104(5):770–776.
50. Tomany SC, Cruickshanks KJ, Klein R, Klein BE, Knudtson MD. Sunlight and the 10-year incidence of age-related maculopathy: the Beaver Dam Eye Study. *Arch Ophthalmol*. 2004;122(5):750–757.
51. A randomized, placebo-controlled, clinical trial of high-dose supplementation with vitamins C and E, beta carotene, and zinc for age-related macular degeneration and vision loss: AREDS report no. 8. *Arch Ophthalmol*. 2001;119(10):1417–1436.
52a. van Leeuwen R, Tomany SC, Wang JJ, et al. Is medication use associated with the incidence of early age-related

maculopathy? Pooled findings from 3 continents. *Ophthalmology*. 2004;111(6):1169–1175.
52b. Vavvas DG, Daniels AB, Kapsala ZG, et al. Regression of Some High-risk Features of Age-related Macular Degeneration (AMD) in Patients Receiving Intensive Statin Treatment. *EBioMedicine*. 2016;5:198–203.
53. Friedlander M, Theesfeld CL, Sugita M, et al. Involvement of integrins alpha v beta 3 and alpha v beta 5 in ocular neovascular diseases. *Proc Natl Acad Sci USA*. 1996;93(18):9764–9769.
54. Friedlander M, Brooks PC, Shaffer RW, Kincaid CM, Varner JA, Cheresh DA. Definition of two angiogenic pathways by distinct alpha v integrins. *Science*. 1995;270(5241):1500–1502.
55. Miller JW. Vascular endothelial growth factor and ocular neovascularization. *Am J Pathol*. 1997;151(1):13–23.
56. Robinson CJ, Stringer SE. The splice variants of vascular endothelial growth factor (VEGF) and their receptors. *J Cell Sci*. 2001;114(Pt 5):853–865.
57. Ferrara N. Vascular endothelial growth factor: basic science and clinical progress. *Endocr Rev*. 2004;25(4):581–611.
58. Senger DR, Galli SJ, Dvorak AM, Perruzzi CA, Harvey VS, Dvorak HF. Tumor cells secrete a vascular permeability factor that promotes accumulation of ascites fluid. *Science*. 1983;219(4587):983–985.
59. Fukumura D, Gohongi T, Kadambi A, et al. Predominant role of endothelial nitric oxide synthase in vascular endothelial growth factor-induced angiogenesis and vascular permeability. *Proc Natl Acad Sci USA*. 2001;98(5):2604–2609.
60. Sennlaub F, Courtois Y, Goureau O. Inducible nitric oxide synthase mediates retinal apoptosis in ischemic proliferative retinopathy. *J Neurosci*. 2002;22(10):3987–3993.
61. Ishida S, Usui T, Yamashiro K, et al. VEGF164-mediated inflammation is required for pathological, but not physiological, ischemia-induced retinal neovascularization. *J Exp Med*. 2003;198(3):483–489.
62. Usui T, Ishida S, Yamashiro K, et al. VEGF164(165) as the pathological isoform: differential leukocyte and endothelial

responses through VEGFR1 and VEGFR2. *Invest Ophthalmol Vis Sci*. 2004;45(2):368–374.
63. Mayerhofer M, Valent P, Sperr WR, Griffin JD, Sillaber C. BCR/ABL induces expression of vascular endothelial growth factor and its transcriptional activator, hypoxia inducible factor-1alpha, through a pathway involving phosphoinositide 3-kinase and the mammalian target of rapamycin. *Blood*. 2002;100(10):3767–3775.
64. Grossniklaus HE, Ling JX, Wallace TM, et al. Macrophage and retinal pigment epithelium expression of angiogenic cytokines in choroidal neovascularization. *Mol Vis*. 2002;8:119–126.
65. Tolentino MJ, Brucker AJ, Fosnot J, et al. Intravitreal injection of vascular endothelial growth factor small interfering RNA inhibits growth and leakage in a nonhuman primate, laser-induced model of choroidal neovascularization. *Retina*. 2004;24(4):660.
66. Dawson DW, Volpert OV, Gillis P, et al. Pigment epithelium-derived factor: a potent inhibitor of angiogenesis. *Science*. 1999;285(5425):245–248.
67. Folkman J, Ingber DE. Angiostatic steroids. Method of discovery and mechanism of action. *Ann Surg*. 1987;206(3):374–383.
68. Folkman J, Weisz PB, Joullie MM, Li WW, Ewing WR. Control of angiogenesis with synthetic heparin substitutes. *Science*. 1989;243(4897):1490–1493.
69. Fung WE. Interferon alpha 2a for treatment of age-related macular degeneration. *Am J Ophthalmol*. 1991;112(3):349–350.
70. Lai CC, Wu WC, Chen SL, et al. Suppression of choroidal neovascularization by adeno-associated virus vector expressing angiostatin. *Invest Ophthalmol Vis Sci*. 2001;42(10):2401–2407.
71. Mori K, Duh E, Gehlbach P, et al. Pigment epithelium-derived factor inhibits retinal and choroidal neovascularization. *J Cell Physiol*. 2001;188(2):253–263.
72. Mori K, Ando A, Gehlbach P, et al. Inhibition of choroidal neovascularization by intravenous injection of adenoviral

vectors expressing secretable endostatin. *Am J Pathol*. 2001;159(1):313–320.
73. O'Reilly MS, Boehm T, Shing Y, et al. Endostatin: an endogenous inhibitor of angiogenesis and tumor growth. *Cell*. 1997;88(2):277–285.
74. O'Reilly MS, Wiederschain D, Stetler-Stevenson WG, Folkman J, Moses MA. Regulation of angiostatin production by matrix metalloproteinase-2 in a model of concomitant resistance. *J Biol Chem*. 1999;274(41):29568–29571.
75. Hellstrom M, Kalen M, Lindahl P, Abramsson A, Betsholtz C. Role of PDGF-B and PDGFR-beta in recruitment of vascular smooth muscle cells and pericytes during embryonic blood vessel formation in the mouse. *Development*. 1999;126(14):3047–3055.
76. Tolentino MJ. Current molecular understanding and future treatment strategies for pathologic ocular neovascularization. *Curr Mol Med*. 2009;9(8):973–981.
77. Benjamin LE, Golijanin D, Itin A, Pode D, Keshet E. Selective ablation of immature blood vessels in established human tumors follows vascular endothelial growth factor withdrawal. *J Clin Invest*. 1999;103(2):159–165.
78. Benjamin LE, Hemo I, Keshet E. A plasticity window for blood vessel remodelling is defined by pericyte coverage of the preformed endothelial network and is regulated by PDGF-B and VEGF. *Development*. 1998;125(9):1591–1598.
79. Dell S, Peters S, Muther P, Kociok N, Joussen AM. The role of PDGF receptor inhibitors and PI3-kinase signaling in the pathogenesis of corneal neovascularization. *Invest Ophthalmol Vis Sci*. 2006;47(5):1928–1937.
80. Perez-Santonja JJ, Campos-Mollo E, Lledo-Riquelme M, Javaloy J, Alio JL. Inhibition of corneal neovascularization by topical bevacizumab (anti-VEGF) and Sunitinib (anti-VEGF and anti-PDGF) in an animal model. *Am J Ophthalmol*. 2010;150(4):519–528.e1.
81. Crabb JW, Miyagi M, Gu X, et al. Drusen proteome analysis: an approach to the etiology of age-related macular degeneration. *Proc Natl Acad Sci USA*. 2002;99(23):14682–

14687.
82. Anand-Apte B, Pepper MS, Voest E, et al. Inhibition of angiogenesis by tissue inhibitor of metalloproteinase-3. *Invest Ophthalmol Vis Sci*. 1997;38(5):817–823.
83. Takahashi T, Nakamura T, Hayashi A, et al. Inhibition of experimental choroidal neovascularization by overexpression of tissue inhibitor of metalloproteinases-3 in retinal pigment epithelium cells. *Am J Ophthalmol*. 2000;130(6):774–781.
84. Morrissey JH, Tajkhorshid E, Sligar SG, Rienstra CM. Tissue factor/factor VIIa complex: role of the membrane surface. *Thromb Res*. 2012;129(Suppl. 2):S8–10.
85. Garnier D, Milsom C, Magnus N, et al. Role of the tissue factor pathway in the biology of tumor initiating cells. *Thromb Res*. 2010;125(Suppl. 2):S44–50.
86. Regina S, Rollin J, Blechet C, Iochmann S, Reverdiau P, Gruel Y. Tissue factor expression in non-small cell lung cancer: relationship with vascular endothelial growth factor expression, microvascular density, and K-ras mutation. *J Thorac Oncol*. 2008;3(7):689–697.
87. Mullins RF, Russell SR, Anderson DH, Hageman GS. Drusen associated with aging and age-related macular degeneration contain proteins common to extracellular deposits associated with atherosclerosis, elastosis, amyloidosis, and dense deposit disease. *FASEB J*. 2000;14(7):835–846.
88. Cho Y, Cao X, Shen D, et al. Evidence for enhanced tissue factor expression in age-related macular degeneration. *Lab Invest*. 2011;91(4):519–526.
89. Bora PS, Hu Z, Tezel TH, et al. Immunotherapy for choroidal neovascularization in a laser-induced mouse model simulating exudative (wet) macular degeneration. *Proc Natl Acad Sci USA*. 2003;100(5):2679–2684.
90. Tezel TH, Bodek E, Sonmez K, et al. Targeting tissue factor for immunotherapy of choroidal neovascularization by intravitreal delivery of factor VII-Fc chimeric antibody. *Ocul Immunol Inflamm*. 2007;15(1):3–10.
91. Oshima Y, Deering T, Oshima S, et al. Angiopoietin-2

enhances retinal vessel sensitivity to vascular endothelial growth factor. *J Cell Physiol*. 2004;199(3):412–417.
92. Babapoor-Farrokhran S, Jee K, Puchner B, et al. Angiopoietin-like 4 is a potent angiogenic factor and a novel therapeutic target for patients with proliferative diabetic retinopathy. *Proc Natl Acad Sci USA*. 2015;112(23):E3030–9.
93. Bhutto IA, McLeod DS, Hasegawa T, et al. Pigment epithelium-derived factor (PEDF) and vascular endothelial growth factor (VEGF) in aged human choroid and eyes with age-related macular degeneration. *Exp Eye Res*. 2006;82(1):99–110.
94. Amaral J, Becerra SP. Effects of human recombinant PEDF protein and PEDF-derived peptide 34-mer on choroidal neovascularization. *Invest Ophthalmol Vis Sci*. 2010;51(3):1318–1326.
95. Nozaki M, Raisler BJ, Sakurai E, et al. Drusen complement components C3a and C5a promote choroidal neovascularization. *Proc Natl Acad Sci USA*. 2006;103(7):2328–2333.
96. Hageman GS, Luthert PJ, Victor Chong NH, Johnson LV, Anderson DH, Mullins RF. An integrated hypothesis that considers drusen as biomarkers of immune-mediated processes at the RPE–Bruch's membrane interface in aging and age-related macular degeneration. *Prog Retin Eye Res*. 2001;20(6):705–732.
97. Arroyo JG, Michaud N, Jakobiec FA. Choroidal neovascular membranes treated with photodynamic therapy. *Arch Ophthalmol*. 2003;121(6):898–903.
98. Ghazi NG, Jabbour NM, De La Cruz ZC, Green WR. Clinicopathologic studies of age-related macular degeneration with classic subfoveal choroidal neovascularization treated with photodynamic therapy. *Retina*. 2001;21(5):478–486.
99. Schnurrbusch UE, Welt K, Horn LC, Wiedemann P, Wolf S. Histological findings of surgically excised choroidal neovascular membranes after photodynamic therapy. *Br J Ophthalmol*. 2001;85(9):1086–1091.

100. Moshfeghi DM, Kaiser PK, Grossniklaus HE, et al. Clinicopathologic study after submacular removal of choroidal neovascular membranes treated with verteporfin ocular photodynamic therapy. *Am J Ophthalmol*. 2003;135(3):343–350.
101. Celkova L, Doyle SL, Campbell M. NLRP3 inflammasome and pathobiology in AMD. *J Clin Med*. 2015;4(1):172–192.
102. Tseng WA, Thein T, Kinnunen K, et al. NLRP3 inflammasome activation in retinal pigment epithelial cells by lysosomal destabilization: implications for age-related macular degeneration. *Invest Ophthalmol Vis Sci*. 2013;54(1):110–120.
103. Anderson OA, Finkelstein A, Shima DT. A2E induces IL-1ss production in retinal pigment epithelial cells via the NLRP3 inflammasome. *PLoS ONE*. 2013;8(6):e67263.
104. Patel M, Chan CC. Immunopathological aspects of age-related macular degeneration. *Semin Immunopathol*. 2008;30(2):97–110.
105. Penfold PL, Madigan MC, Gillies MC, Provis JM. Immunological and aetiological aspects of macular degeneration. *Prog Retin Eye Res*. 2001;20(3):385–414.
106. Ratnayaka JA, Serpell LC, Lotery AJ. Dementia of the eye: the role of amyloid beta in retinal degeneration. *Eye (Lond)*. 2015;29(8):1013–1026.
107. Bradt BM, Kolb WP, Cooper NR. Complement-dependent proinflammatory properties of the Alzheimer's disease beta-peptide. *J Exp Med*. 1998;188(3):431–438.
108. Johnson LV, Leitner WP, Rivest AJ, Staples MK, Radeke MJ, Anderson DH. The Alzheimer's A beta-peptide is deposited at sites of complement activation in pathologic deposits associated with aging and age-related macular degeneration. *Proc Natl Acad Sci USA*. 2002;99(18):11830–11835.
109. Mori K, Gehlbach PL, Ito YN, Yoneya S. Decreased arterial dye-filling and venous dilation in the macular choroid associated with age-related macular degeneration. *Retina*. 2005;25(4):430–437.
110. Coleman DJ, Silverman RH, Rondeau MJ, Lloyd HO,

Khanifar AA, Chan RV. Age-related macular degeneration: choroidal ischaemia? *Br J Ophthalmol*. 2013;97(8):1020–1023.
111a. Manjunath V, Goren J, Fujimoto JG, Duker JS. Analysis of choroidal thickness in age-related macular degeneration using spectral-domain optical coherence tomography. *Am J Ophthalmol*. 2011;152(4):663–668.
111b. Seddon JM, McLeod DS, Bhutto IA, et al. Histopathological Insights Into Choroidal Vascular Loss in Clinically Documented Cases of Age-Related Macular Degeneration. *JAMA Ophthalmol*. 2016;134(11):1272–1280.
112. Campochiaro PA. Ocular neovascularisation and excessive vascular permeability. *Expert Opin Biol Ther*. 2004;4(9):1395–1402.
113. Hurwitz H, Fehrenbacher L, Novotny W, et al. Bevacizumab plus irinotecan, fluorouracil, and leucovorin for metastatic colorectal cancer. *N Engl J Med*. 2004;350(23):2335–2342.
114. Michels S, Rosenfeld PJ, Puliafito CA, Marcus EN, Venkatraman AS. Systemic bevacizumab (Avastin) therapy for neovascular age-related macular degeneration twelve-week results of an uncontrolled open-label clinical study. *Ophthalmology*. 2005;112(6):1035–1047.
115. Moshfeghi AA, Rosenfeld PJ, Puliafito CA, et al. Systemic bevacizumab (Avastin) therapy for neovascular age-related macular degeneration: twenty-four-week results of an uncontrolled open-label clinical study. *Ophthalmology*. 2006;113(11):2002.e1–2002.e12.
116. Rosenfeld PJ, Moshfeghi AA, Puliafito CA. Optical coherence tomography findings after an intravitreal injection of bevacizumab (avastin) for neovascular age-related macular degeneration. *Ophthalmic Surg Lasers Imaging*. 2005;36(4):331–335.
117. Han DP. Intravitreal human immune globulin in a rabbit model of *Staphylococcus aureus* toxin-mediated endophthalmitis: a potential adjunct in the treatment of endophthalmitis. *Trans Am Ophthalmol Soc*. 2004;102:305–320.
118. Shahar J, Avery RL, Heilweil G, et al. Electrophysiologic

and retinal penetration studies following intravitreal injection of bevacizumab (Avastin). *Retina*. 2006;26(3):262–269.
119. Dib E, Maia M, Longo-Maugeri IM, et al. Subretinal bevacizumab detection after intravitreous injection in rabbits. *Invest Ophthalmol Vis Sci*. 2008;49(3):1097–1100.
120. Mordenti J, Thomsen K, Licko V, et al. Intraocular pharmacokinetics and safety of a humanized monoclonal antibody in rabbits after intravitreal administration of a solution or a PLGA microsphere formulation. *Toxicol Sci*. 1999;52(1):101–106.
121. Mordenti J, Cuthbertson RA, Ferrara N, et al. Comparisons of the intraocular tissue distribution, pharmacokinetics, and safety of 125I-labeled full-length and Fab antibodies in rhesus monkeys following intravitreal administration. *Toxicol Pathol*. 1999;27(5):536–544.
122. Bakri SJ, Kitzmann AS. Retinal pigment epithelial tear after intravitreal ranibizumab. *Am J Ophthalmol*. 2007;143(3):505–507.
123. Miyake T, Sawada O, Kakinoki M, et al. Pharmacokinetics of bevacizumab and its effect on vascular endothelial growth factor after intravitreal injection of bevacizumab in macaque eyes. *Invest Ophthalmol Vis Sci*. 2010;51(3):1606–1608.
124. Nomoto H, Shiraga F, Kuno N, et al. Pharmacokinetics of bevacizumab after topical, subconjunctival, and intravitreal administration in rabbits. *Invest Ophthalmol Vis Sci*. 2009;50(10):4807–4813.
125. Beer PM, Wong SJ, Hammad AM, Falk NS, O'Malley MR, Khan S. Vitreous levels of unbound bevacizumab and unbound vascular endothelial growth factor in two patients. *Retina*. 2006;26(8):871–876.
126. Krohne TU, Eter N, Holz FG, Meyer CH. Intraocular pharmacokinetics of bevacizumab after a single intravitreal injection in humans. *Am J Ophthalmol*. 2008;146(4):508–512.
127. Zhu Q, Ziemssen F, Henke-Fahle S, et al. Vitreous levels of bevacizumab and vascular endothelial growth factor-A in patients with choroidal neovascularization. *Ophthalmology*.

2008;115(10):1750–1755 [1755.e1].
128. Brechner RJ, Rosenfeld PJ, Babish JD, Caplan S. Pharmacotherapy for neovascular age-related macular degeneration: an analysis of the 100% 2008 medicare fee-for-service part B claims file. *Am J Ophthalmol*. 2011;151(5):887–895.e1.
129. Martin DF, Maguire MG, Ying GS, Grunwald JE, Fine SL, Jaffe GJ. Ranibizumab and bevacizumab for neovascular age-related macular degeneration. *N Engl J Med*. 2011;364(20):1897–1908.
130. Arevalo JF, Maia M, Garcia-Amaris RA, et al. Intravitreal bevacizumab for refractory pseudophakic cystoid macular edema: the Pan-American Collaborative Retina Study Group results. *Ophthalmology*. 2009;116(8):1481–1487.
131. Caccavale A, Romanazzi F, Imparato M, Negri A, Morano A, Ferentini F. Central serous chorioretinopathy: a pathogenetic model. *Clin Ophthalmol*. 2011;5:239–243.
132. Cervantes-Castaneda RA, Giuliari GP, Gallagher MJ, et al. Intravitreal bevacizumab in refractory uveitic macular edema: one-year follow-up. *Eur J Ophthalmol*. 2009;19(4):622–629.
133. Ehrlich R, Ciulla TA, Maturi R, et al. Intravitreal bevacizumab for choroidal neovascularization secondary to presumed ocular histoplasmosis syndrome. *Retina*. 2009;29(10):1418–1423.
134. El Matri L, Kort F, Bouraoui R, Karim B, Chebil A, Chaker N. Intravitreal bevacizumab for the treatment of choroidal neovascularization secondary to angioid streaks: one year of follow-up. *Acta Ophthalmol*. 2011;89(7):641–646.
135. Gregori NZ, Rattan GH, Rosenfeld PJ, et al. Safety and efficacy of intravitreal bevacizumab (avastin) for the management of branch and hemiretinal vein occlusion. *Retina*. 2009;29(7):913–925.
136. Mintz-Hittner HA, Kennedy KA, Chuang AZ. Efficacy of intravitreal bevacizumab for stage 3+ retinopathy of prematurity. *N Engl J Med*. 2011;364(7):603–615.
137. Nakanishi H, Tsujikawa A, Yodoi Y, et al. Prognostic factors for visual outcomes 2-years after intravitreal bevacizumab

for myopic choroidal neovascularization. *Eye (Lond)*. 2011;25(3):375–381.
138. Wu L, Arevalo JF, Berrocal MH, et al. Comparison of two doses of intravitreal bevacizumab as primary treatment for macular edema secondary to branch retinal vein occlusions: results of the Pan American Collaborative Retina Study Group at 24 months. *Retina*. 2009;29(10):1396–1403.
139. Rosenfeld PJ, Brown DM, Heier JS, et al. Ranibizumab for neovascular age-related macular degeneration. *N Engl J Med*. 2006;355(14):1419–1431.
140. Brown DM, Kaiser PK, Michels M, et al. Ranibizumab versus verteporfin for neovascular age-related macular degeneration. *N Engl J Med*. 2006;355(14):1432–1444.
141. Brown DM, Michels M, Kaiser PK, Heier JS, Sy JP, Ianchulev T. Ranibizumab versus verteporfin photodynamic therapy for neovascular age-related macular degeneration: two-year results of the ANCHOR study. *Ophthalmology*. 2009;116(1):57–65.e5.
142. Rosenfeld PJ, Schwartz SD, Blumenkranz MS, et al. Maximum tolerated dose of a humanized anti-vascular endothelial growth factor antibody fragment for treating neovascular age-related macular degeneration. *Ophthalmology*. 2005;112(6):1048–1053.
143. Regillo CD, Brown DM, Abraham P, et al. Randomized, double-masked, sham-controlled trial of ranibizumab for neovascular age-related macular degeneration: PIER Study year 1. *Am J Ophthalmol*. 2008;145(2):239–248.
144. Abraham P, Yue H, Wilson L. Randomized, double-masked, sham-controlled trial of ranibizumab for neovascular age-related macular degeneration: PIER study year 2. *Am J Ophthalmol*. 2010;150(3):315–324.e1.
145. Schmidt-Erfurth U, Eldem B, Guymer R, et al. Efficacy and safety of monthly versus quarterly ranibizumab treatment in neovascular age-related macular degeneration: the EXCITE study. *Ophthalmology*. 2011;118(5):831–839.
146. Holz FG, Amoaku W, Donate J, et al. Safety and efficacy of a flexible dosing regimen of ranibizumab in neovascular age-related macular degeneration: the SUSTAIN study.

Ophthalmology. 2011;118(4):663–671.
147. Fung AE, Lalwani GA, Rosenfeld PJ, et al. An optical coherence tomography-guided, variable dosing regimen with intravitreal ranibizumab (Lucentis) for neovascular age-related macular degeneration. *Am J Ophthalmol*. 2007;143(4):566–583.
148. Lalwani GA, Rosenfeld PJ, Fung AE, et al. A variable-dosing regimen with intravitreal ranibizumab for neovascular age-related macular degeneration: year 2 of the PrONTO Study. *Am J Ophthalmol*. 2009;148(1):43–58.e1.
149. Collaborative overview of randomised trials of antiplatelet therapy – I: Prevention of death, myocardial infarction, and stroke by prolonged antiplatelet therapy in various categories of patients. Antiplatelet Trialists' Collaboration. *BMJ (Clin Res)*. 1994;308(6921):81–106.
150. Schmidt-Erfurth U. Clinical safety of ranibizumab in age-related macular degeneration. *Expert Opin Drug Saf*. 2010;9(1):149–165.
151. Busbee BG, Ho AC, Brown DM, et al. Twelve-month efficacy and safety of 0.5 mg or 2.0 mg ranibizumab in patients with subfoveal neovascular age-related macular degeneration. *Ophthalmology*. 2013;120(5):1046–1056.
152. Ho AC, Busbee BG, Regillo CD, et al. Twenty-four-month efficacy and safety of 0.5 mg or 2.0 mg ranibizumab in patients with subfoveal neovascular age-related macular degeneration. *Ophthalmology*. 2014;121(11):2181–2192.
153a. Rosenfeld PJ. Bevacizumab versus ranibizumab for AMD. *N Engl J Med*. 2011;364(20):1966–1967.
153b. Maguire MG, Martin DF, Ying GS, et al. Five-Year Outcomes with Anti-Vascular Endothelial Growth Factor Treatment of Neovascular Age-Related Macular Degeneration: The Comparison of Age-Related Macular Degeneration Treatments Trials. *Ophthalmology*. 2016;123(8):1751–1761.
154. Kodjikian L, Souied EH, Mimoun G, et al. Ranibizumab versus bevacizumab for neovascular age-related macular degeneration: results from the GEFAL noninferiority randomized trial. *Ophthalmology*. 2013;120(11):2300–2309.

155. Krebs I, Schmetterer L, Boltz A, et al. A randomised double-masked trial comparing the visual outcome after treatment with ranibizumab or bevacizumab in patients with neovascular age-related macular degeneration. *Br J Ophthalmol*. 2013;97(3):266–271.
156. Schauwvlieghe A-SME, Dijkman G, Hooymans JMM, et al. Comparing the effectiveness of bevacizumab to ranibizumab in patients with exudative age-related macular degeneration: BRAMD. *Invest Ophthalmol Vis Sci*. 2014;55(13):870.
157. Berg K, Pedersen TR, Sandvik L, Bragadottir R. Comparison of ranibizumab and bevacizumab for neovascular age-related macular degeneration according to LUCAS treat-and-extend protocol. *Ophthalmology*. 2015;122(1):146–152.
158. Holash J, Davis S, Papadopoulos N, et al. VEGF-Trap: a VEGF blocker with potent antitumor effects. *Proc Natl Acad Sci USA*. 2002;99(17):11393–11398.
159. Chappelow AV, Kaiser PK. Neovascular age-related macular degeneration: potential therapies. *Drugs*. 2008;68(8):1029–1036.
160. Cao JSH, Renard RA, et al. Systemic or intravitreal administration of VEGF Trap suppresses vascular leak and leukostasis in the retinas of diabetic rats. *Invest Ophthalmol Vis Sci*. 2006;47.
161. Rudge JS, Thurston G, Davis S, et al. VEGF trap as a novel antiangiogenic treatment currently in clinical trials for cancer and eye diseases, and VelociGene- based discovery of the next generation of angiogenesis targets. *Cold Spring Harb Symp Quant Biol*. 2005;70:411–418.
162. Nguyen QD, Shah SM, Browning DJ, et al. A phase I study of intravitreal vascular endothelial growth factor trap-eye in patients with neovascular age-related macular degeneration. *Ophthalmology*. 2009;116(11):2141–2148.e1.
163. Brown DM, Heier JS, Ciulla T, et al. Primary endpoint results of a phase II study of vascular endothelial growth factor trap-eye in wet age-related macular degeneration. *Ophthalmology*. 2011;118(6):1089–1097.
164. Heier JS, Boyer D, Nguyen QD, et al. The 1-year results of

CLEAR-IT 2, a phase 2 study of vascular endothelial growth factor trap-eye dosed as-needed after 12-week fixed dosing. *Ophthalmology*. 2011;118(6):1098–1106.
165. http://investor.regeneron.com/releasedetail.cfm?ReleaseID=532099 [accessed 12.15.02].
166. http://files.shareholder.com/downloads/REGN/1026966568x1AA6-43DB-8783-EA5C0C4C78DE/REGN_Angiogenesis_Final_021311.pdf [accessed 12.15.02].
167. Heier JS, Brown DM, Chong V, et al. Intravitreal aflibercept (VEGF trap-eye) in wet age-related macular degeneration. *Ophthalmology*. 2012;119(12):2537–2548.
168. Schmidt-Erfurth U, Kaiser PK, Korobelnik JF, et al. Intravitreal aflibercept injection for neovascular age-related macular degeneration: ninety-six-week results of the VIEW studies. *Ophthalmology*. 2014;121(1):193–201.
169. http://investor.regeneron.com/releasedetail.cfm?ReleaseID=585837 [accessed 12.15.02].
170. Zhang M, Zhang J, Yan M, Li H, Yang C, Yu D. Recombinant anti-vascular endothelial growth factor fusion protein efficiently suppresses choridal neovasularization in monkeys. *Mol Vis*. 2008;14:37–49.
171. Suto K, Yamazaki Y, Morita T, Mizuno H. Crystal structures of novel vascular endothelial growth factors (VEGF) from snake venoms: insight into selective VEGF binding to kinase insert domain-containing receptor but not to fms-like tyrosine kinase-1. *J Biol Chem*. 2005;280(3):2126–2131.
172. Zhang M, Yu D, Yang C, et al. The pharmacology study of a new recombinant human VEGF receptor-fc fusion protein on experimental choroidal neovascularization. *Pharm Res*. 2009;26(1):204–210.
173. Huo X, Li Y, Jiang Y, et al. Inhibition of ocular neovascularization by co-inhibition of VEGF-A and PLGF. *Cell Physiol Biochem*. 2015;35(5):1787–1796.
174. Rakic JM, Lambert V, Devy L, et al. Placental growth factor, a member of the VEGF family, contributes to the development of choroidal neovascularization. *Invest*

Ophthalmol Vis Sci. 2003;44(7):3186–3193.
175. Lu X, Sun X. Profile of conbercept in the treatment of neovascular age-related macular degeneration. *Drug Des Devel Ther*. 2015;9:2311–2320.
176. Dugel PU. Results of ESBA 1008, a single-chain antibody fragment, for the treatment of neovascular AMD. ASRS; 8/10/14; San Diego, CA2014.
177. Singerman LW, Weichselberger A, Sallstig P. OSPREY trial: randomized, active-controlled, phase II study to evaluate safety and efficacy of RTH258, a humanized single-chain anti-VEGF antibody fragment, in patients with neovascular AMD. ARVO Annual Meeting Abstract; Denver, CO. *Invest Ophthalmol Vis Sci*. 2015;56(7):4801.
178. Stumpp MT, Binz HK, Amstutz P. DARPins: a new generation of protein therapeutics. *Drug Discov Today*. 2008;13(15–16):695–701.
179. Krohne TU, Liu Z, Holz FG, Meyer CH. Intraocular pharmacokinetics of ranibizumab following a single intravitreal injection in humans. *Am J Ophthalmol*. 2012;154(4):682–686.e2.
180. Souied EH, Devin F, Mauget-Faysse M, et al. Treatment of exudative age-related macular degeneration with a designed ankyrin repeat protein that binds vascular endothelial growth factor: a phase I/II study. *Am J Ophthalmol*. 2014;158(4):724–732.e2.
181. Meyer CH, Krohne TU, Holz FG. Intraocular pharmacokinetics after a single intravitreal injection of 1.5 mg versus 3.0 mg of bevacizumab in humans. *Retina*. 2011;31(9):1877–1884.
182. Winn SR, Hammang JP, Emerich DF, Lee A, Palmiter RD, Baetge EE. Polymer-encapsulated cells genetically modified to secrete human nerve growth factor promote the survival of axotomized septal cholinergic neurons. *Proc Natl Acad Sci USA*. 1994;91(6):2324–2328.
183. Rivera ML, Lelis A, Bouchard B, et al. Pharmacokinetics of a VEGF antagonist delivered by an intraocular encapsulated cell technology implant. ARVO Annual Meeting Abstract; Ft. Lauderdale, FL. *Invest Ophthalmol Vis Sci*. 2012;53:474.

184. Guerrero-Naranjo JL, Quiroz-Mercado H, Sanchez-Bermudez G, et al. Safety of implantation of the NT-503 device in patients with Choroidal neovascularization secondary to age-related macular degeneration. *Invest Ophthalmol Vis Sci*. 2013;54(15):3298.
185. Kauper K, Rivera M, Mills J, et al. Design considerations and performance of a next-generation encapsulated cell technology intraocular implant delivering VEGF-antagonist. ARVO Meeting Abstract; Orlando, FL. *Invest Ophthalmol Vis Sci*. 2014;55:441.
186. Zhang K, Hopkins JJ, Heier JS, et al. Ciliary neurotrophic factor delivered by encapsulated cell intraocular implants for treatment of geographic atrophy in age-related macular degeneration. *Proc Natl Acad Sci USA*. 2011;108(15):6241–6245.
187. Loewenstein AL, Laganovska G. *First-in-human results of a refillable drug delivery implant providing release of ranibizumab in patients with neovascular AMD*. [Paper presented to American Academy of Ophthalmology Retina Subspecialty Day; 11/9/12; Chicago, IL] 2012.
188. Lo R, Li PY, Saati S, Agrawal RN, Humayun MS, Meng E. A passive MEMS drug delivery pump for treatment of ocular diseases. *Biomed Microdevices*. 2009;11(5):959–970.
189. Saati S, Lo R, Li PY, Meng E, Varma R, Humayun MS. Mini drug pump for ophthalmic use. *Trans Am Ophthalmol Soc*. 2009;107:60–70.
190. Gutierrez-Hernandez JC, Caffey S, Abdallah W, et al. One-year feasibility study of replenish micropump for intravitreal drug delivery: a pilot study. *Transl Vis Sci Technol*. 2014;3(4):8.
191. Humayun M, Santos A, Altamirano JC, et al. Implantable micropump for drug delivery in patients with diabetic macular edema. *Transl Vis Sci Technol*. 2014;3(6):5.
192. Lai CM, Shen WY, Brankov M, et al. Long-term evaluation of AAV-mediated sFlt-1 gene therapy for ocular neovascularization in mice and monkeys. *Mol Ther*. 2005;12(4):659–668.
193. Kendall RL, Wang G, Thomas KA. Identification of a

natural soluble form of the vascular endothelial growth factor receptor, FLT-1, and its heterodimerization with KDR. *Biochem Biophys Res Commun*. 1996;226(2):324–328.
194. Mori K, Gehlbach P, Yamamoto S, et al. AAV-mediated gene transfer of pigment epithelium-derived factor inhibits choroidal neovascularization. *Invest Ophthalmol Vis Sci*. 2002;43(6):1994–2000.
195. Maguire AM, Simonelli F, Pierce EA, et al. Safety and efficacy of gene transfer for Leber's congenital amaurosis. *N Engl J Med*. 2008;358(21):2240–2248.
196. Bainbridge JW, Smith AJ, Barker SS, et al. Effect of gene therapy on visual function in Leber's congenital amaurosis. *N Engl J Med*. 2008;358(21):2231–2239.
197. Cideciyan AV, Hauswirth WW, Aleman TS, et al. Human RPE65 gene therapy for Leber congenital amaurosis: persistence of early visual improvements and safety at 1 year. *Hum Gene Ther*. 2009;20(9):999–1004.
198. Bainbridge JW, Mistry A, De Alwis M, et al. Inhibition of retinal neovascularisation by gene transfer of soluble VEGF receptor sFlt-1. *Gene Ther*. 2002;9(5):320–326.
199. Gehlbach P, Demetriades AM, Yamamoto S, et al. Periocular gene transfer of sFlt-1 suppresses ocular neovascularization and vascular endothelial growth factor-induced breakdown of the blood-retinal barrier. *Hum Gene Ther*. 2003;14(2):129–141.
200. Lukason M, DuFresne E, Rubin H, et al. Inhibition of choroidal neovascularization in a nonhuman primate model by intravitreal administration of an AAV2 vector expressing a novel anti-VEGF molecule. *Mol Ther*. 2011;19(2):260–265.
201. Igarashi T, Miyake K, Masuda I, Takahashi H, Shimada T. Adeno-associated vector (type 8)-mediated expression of soluble Flt-1 efficiently inhibits neovascularization in a murine choroidal neovascularization model. *Hum Gene Ther*. 2010;21(5):631–637.
202. Rakoczy EP, Lai CM, Magno AL, et al. Gene therapy with recombinant adeno-associated vectors for neovascular age-related macular degeneration: 1 year follow-up of a phase 1 randomised clinical trial. *Lancet*. 2015;386(10011):2395–2403.

203. Onder HI, Erdurmus M, Bucak YY, Simavli H, Oktay M, Kukner AS. Inhibitory effects of regorafenib, a multiple tyrosine kinase inhibitor, on corneal neovascularization. *Int J Ophthalmol*. 2014;7(2):220–225.
204. Boettger MKK, Richter A, von Degenfeld G, et al. *Topically administered regorafenib eye drops inhibit grade IV lesions in the non-human primate laser CNV model*. [ARVO Meeting Abstract, Denver, CO] 2015.
205. Klar J, Boettger MK, Freundlieb J, Keldenich J, Elenea P, von Degenfeld G. *Effects of the multi-kinase inhibitor regorafenib on ocular neovascularization*. [ARVO Meeting Abstract, Denver, CO] 2015.
206. Engelbert M, Gilmore MS. Fas ligand but not complement is critical for control of experimental Staphylococcus aureus Endophthalmitis. *Invest Ophthalmol Vis Sci*. 2005;46(7):2479–2486.
207. Giese MJ, Mondino BJ, Glasgow BJ, et al. Complement system and host defense against staphylococcal endophthalmitis. *Invest Ophthalmol Vis Sci*. 1994;35(3):1026–1032.
208. Aizuss DH, Mondino BJ, Sumner HL, Dethlefs BA. The complement system and host defense against Pseudomonas endophthalmitis. *Invest Ophthalmol Vis Sci*. 1985;26(9):1262–1266.
209. Ni Z, Hui P. Emerging pharmacologic therapies for wet age-related macular degeneration. *Ophthalmologica*. 2009;223(6):401–410.
210. Mathis S, Khanlari B, Pulido F, et al. Effectiveness of protease inhibitor monotherapy versus combination antiretroviral maintenance therapy: a meta-analysis. *PLoS ONE*. 2011;6(7):e22003.
211. Klement G, Baruchel S, Rak J, et al. Continuous low-dose therapy with vinblastine and VEGF receptor-2 antibody induces sustained tumor regression without overt toxicity. *J Clin Invest*. 2000;105(8):R15–24.
212. Lee CG, Heijn M, di Tomaso E, et al. Anti-Vascular endothelial growth factor treatment augments tumor radiation response under normoxic or hypoxic conditions.

Cancer Res. 2000;60(19):5565–5570.
213. Chan A, Blumenkranz MS, Wu KH, et al. Photodynamic therapy with and without adjunctive intravitreal triamcinolone acetonide: a retrospective comparative study. *Ophthalmic Surg Lasers Imaging*. 2009;40(6):561–569.
214. Chaudhary V, Mao A, Hooper PL, Sheidow TG. Triamcinolone acetonide as adjunctive treatment to verteporfin in neovascular age-related macular degeneration: a prospective randomized trial. *Ophthalmology*. 2007;114(12):2183–2189.
215. Hatta Y, Ishikawa K, Nishihara H, Ozawa S, Ito Y, Terasaki H. Effect of photodynamic therapy alone or combined with posterior subtenon triamcinolone acetonide or intravitreal bevacizumab on choroidal hypofluorescence by indocyanine green angiography. *Retina*. 2010;30(3):495–502.
216. Kovacs KD, Quirk MT, Kinoshita T, et al. A retrospective analysis of triple combination therapy with intravitreal bevacizumab, posterior sub-tenon's triamcinolone acetonide, and low-fluence verteporfin photodynamic therapy in patients with neovascular age-related macular degeneration. *Retina*. 2011;31(3):446–452.
217. Liggett PE, Colina J, Chaudhry NA, Tom D, Haffner G. Triple therapy of intravitreal triamcinolone, photodynamic therapy, and pegaptanib sodium for choroidal neovascularization. *Am J Ophthalmol*. 2006;142(6):1072–1074.
218. Maberley D. Photodynamic therapy and intravitreal triamcinolone for neovascular age-related macular degeneration: a randomized clinical trial. *Ophthalmology*. 2009;116(11):2149–2157.e1.
219. Piermarocchi S, Sartore M, Lo Giudice G, Maritan V, Midena E, Segato T. Combination of photodynamic therapy and intraocular triamcinolone for exudative age-related macular degeneration and long-term chorioretinal macular atrophy. *Arch Ophthalmol*. 2008;126(10):1367–1374.
220. Roth DB, Kulkarni KM, Walsman S, Modi A. Intravitreal triamcinolone acetonide preceding photodynamic therapy for exudative age-related macular degeneration. *Ophthalmic Surg Lasers Imaging*. 2009;40(5):467–471.

221. Sacu S, Michels S, Prager F, et al. Randomised clinical trial of intravitreal Avastin vs photodynamic therapy and intravitreal triamcinolone: long-term results. *Eye (Lond)*. 2009;23(12):2223–2227.
222. Spaide RF, Sorenson J, Maranan L. Combined photodynamic therapy with verteporfin and intravitreal triamcinolone acetonide for choroidal neovascularization. *Ophthalmology*. 2003;110(8):1517–1525.
223. Spaide RF, Sorenson J, Maranan L. Photodynamic therapy with verteporfin combined with intravitreal injection of triamcinolone acetonide for choroidal neovascularization. *Ophthalmology*. 2005;112(2):301–304.
224. Augustin AJ, Puls S, Offermann I. Triple therapy for choroidal neovascularization due to age-related macular degeneration: verteporfin PDT, bevacizumab, and dexamethasone. *Retina*. 2007;27(2):133–140.
225. Bakri SJ, Couch SM, McCannel CA, Edwards AO. Same-day triple therapy with photodynamic therapy, intravitreal dexamethasone, and bevacizumab in wet age-related macular degeneration. *Retina*. 2009;29(5):573–578.
226. Kaiser PK, Boyer DS, Garcia R, et al. Verteporfin photodynamic therapy combined with intravitreal bevacizumab for neovascular age-related macular degeneration. *Ophthalmology*. 2009;116(4):747–755 [755.e1].
227. Forte R, Bonavolonta P, Benayoun Y, Adenis JP, Robert PY. Intravitreal ranibizumab and bevacizumab in combination with full-fluence verteporfin therapy and dexamethasone for exudative age-related macular degeneration. *Ophthalmic Res*. 2011;45(3):129–134.
228. Bergers G, Song S, Meyer-Morse N, Bergsland E, Hanahan D. Benefits of targeting both pericytes and endothelial cells in the tumor vasculature with kinase inhibitors. *J Clin Invest*. 2003;111(9):1287–1295.
229. Bergers G, Song S. The role of pericytes in blood-vessel formation and maintenance. *Neuro Oncol*. 2005;7(4):452–464.
230. von Tell D, Armulik A, Betsholtz C. Pericytes and vascular stability. *Exp Cell Res*. 2006;312(5):623–629.
231. Carmeliet P. Mechanisms of angiogenesis and

arteriogenesis. *Nat Med*. 2000;6(4):389–395.
232. Carmeliet P, Jain RK. Molecular mechanisms and clinical applications of angiogenesis. *Nature*. 2011;473(7347):298–307.
233. Ribatti D, Nico B, Crivellato E. The role of pericytes in angiogenesis. *Int J Dev Biol*. 2011;55(3):261–268.
234. Donovan J, Abraham D, Norman J. Platelet-derived growth factor signaling in mesenchymal cells. *Front Biosci (Landmark Ed)*. 2013;18:106–119.
235. Alvarez RH, Kantarjian HM, Cortes JE. Biology of platelet-derived growth factor and its involvement in disease. *Mayo Clin Proc*. 2006;81(9):1241–1257.
236. Greenberg JI, Shields DJ, Barillas SG, et al. A role for VEGF as a negative regulator of pericyte function and vessel maturation. *Nature*. 2008;456(7223):809–813.
237. Aiello LP, Davis MD, Girach A, et al. Effect of ruboxistaurin on visual loss in patients with diabetic retinopathy. *Ophthalmology*. 2006;113(12):2221–2230.
238. Hawthorne T, Giot L, Blake L, et al. A phase I study of CR002, a fully-human monoclonal antibody against platelet-derived growth factor-D. *Int J Clin Pharmacol Ther*. 2008;46(5):236–244.
239. Stock P, Monga D, Tan X, Micsenyi A, Loizos N, Monga SP. Platelet-derived growth factor receptor-alpha: a novel therapeutic target in human hepatocellular cancer. *Mol Cancer Ther*. 2007;6(7):1932–1941.
240. Boyer DS, Group OA-PiAMDS. Combined inhibition of platelet derived (PDGF) and vascular endothelial (VEGF) growth factors for the treatment of neovascular age-related macular degeneration (NV-AMD) – results of a Phase 1 study. *Invest Ophthalmol Vis Sci*. 2009;50(13):1260.
241. Boyer D. A phase 2b study of Fovista™, a platelet derived growth factor (pdgf) inhibitor in combination with a vascular endothelial growth factor (VEGF) inhibitor for neovascular age-related macular degeneration (AMD). *Invest Ophthalmol Vis Sci*. 2013;54(15):2175.
242. Genaidy M, Kazi AA, Peyman GA, et al. Effect of squalamine on iris neovascularization in monkeys. *Retina*.

2002;22(6):772–778.
243. Jones SR, Kinney WA, Zhang X, Jones LM, Selinsky BS. The synthesis and characterization of analogs of the antimicrobial compound squalamine: 6 beta-hydroxy-3-aminosterols synthesized from hyodeoxycholic acid. *Steroids*. 1996;61(10):565–571.
244. Higgins RD, Yan Y, Geng Y, Zasloff M, Williams JI. Regression of retinopathy by squalamine in a mouse model. *Pediatr Res*. 2004;56(1):144–149.
245. Slakter JS. Interim results from a phase 2 study of squalamine lactate ophthalmic solution 0.2% in the treatment of neovascular age-related macular degeneration (AMD). ASRS; August 12, 2014; San Diego, CA.
246. Slakter JS. Correlation of anatomic and visual outcomes in the phase 2 study of squalamine lactate ophthalmic solution 0.2% (OHR-102) in the Treatment of neovascular age-related macular degeneration (AMD). Macula Society Annual Meeting; 2/27/15; Scottsdale, AZ.
247. Rampurwala MMC, Eickhoff JC, Kolesar J, et al. *Pharmacodynamic study using FLT PET/CT in advanced solid malignancies treated with a sequential combination of X-82 and docetaxel*. [ASCO] 2015 [Chicago, IL].
248. Rosenfeld PJS, Boyer DS, Brown DM, A phase 1 safety study of an orally available tyrosine kinase inhibitor X-82 in previously treated wet AMD patients. ARVO Meeting Abstract; 5/6/15; Denver, CO.
249. Cousins SW. Targeting complement factor 5 in combination with vascular endothelial growth factor (VEGF) inhibition for neovascular age related macular degeneration (AMD): results of a phase 1 study. ARVO Meeting Abstract; 5/3/10; Fort Lauderdale, FL.
250. Newsome DA, Swartz M, Leone NC, Elston RC, Miller E. Oral zinc in macular degeneration. *Arch Ophthalmol*. 1988;106(2):192–198.
251. Bressler NM, Bressler SB, Congdon NG, et al. Potential public health impact of Age-Related Eye Disease Study results: AREDS report no. 11. *Arch Ophthalmol*. 2003;121(11):1621–1624.

252. SanGiovanni JP, Chew EY, Clemons TE, et al. The relationship of dietary carotenoid and vitamin A, E, and C intake with age-related macular degeneration in a case-control study: AREDS report no. 22. *Arch Ophthalmol*. 2007;125(9):1225–1232.
253. Age-Related Eye Disease Study 2 Research G, Chew EY, Clemons TE, et al. Secondary analyses of the effects of lutein/zeaxanthin on age-related macular degeneration progression: AREDS2 report no. 3. *JAMA Ophthalmol*. 2014;132(2):142–149.
254. Radu RA, Han Y, Bui TV, et al. Reductions in serum vitamin A arrest accumulation of toxic retinal fluorophores: a potential therapy for treatment of lipofuscin-based retinal diseases. *Invest Ophthalmol Vis Sci*. 2005;46(12):4393–4401.
255. Quadro L, Blaner WS, Salchow DJ, et al. Impaired retinal function and vitamin A availability in mice lacking retinol-binding protein. *EMBO J*. 1999;18(17):4633–4644.
256. Vogel S, Piantedosi R, O'Byrne SM, et al. Retinol-binding protein-deficient mice: biochemical basis for impaired vision. *Biochemistry*. 2002;41(51):15360–15368.
257. Mata NL, Lichter JB, Vogel R, Han Y, Bui TV, Singerman LJ. Investigation of oral fenretinide for treatment of geographic atrophy in age-related macular degeneration. *Retina*. 2013;33(3):498–507.
258. Decensi A, Torrisi R, Bruno S, et al. Randomized trial of fenretinide in superficial bladder cancer using DNA flow cytometry as an intermediate end point. *Cancer Epidemiol Biomarkers Prev*. 2000;9(10):1071–1078.
259. Follen M, Atkinson EN, Schottenfeld D, et al. A randomized clinical trial of 4-hydroxyphenylretinamide for high-grade squamous intraepithelial lesions of the cervix. *Clin Cancer Res*. 2001;7(11):3356–3365.
260. Camerini T, Mariani L, De Palo G, et al. Safety of the synthetic retinoid fenretinide: long-term results from a controlled clinical trial for the prevention of contralateral breast cancer. *J Clin Oncol*. 2001;19(6):1664–1670.
261. Garaventa A, Luksch R, Lo Piccolo MS, et al. Phase I trial and pharmacokinetics of fenretinide in children with

neuroblastoma. *Clin Cancer Res*. 2003;9(6):2032–2039.
262. Puduvalli VK, Yung WK, Hess KR, et al. Phase II study of fenretinide (NSC 374551) in adults with recurrent malignant gliomas: a North American Brain Tumor Consortium study. *J Clin Oncol*. 2004;22(21):4282–4289.
263. Mariani L, Formelli F, De Palo G, et al. Chemoprevention of breast cancer with fenretinide (4-HPR): study of long-term visual and ophthalmologic tolerability. *Tumori*. 1996;82(5):444–449.
264. Conley B, O'Shaughnessy J, Prindiville S, et al. Pilot trial of the safety, tolerability, and retinoid levels of N-(4-hydroxyphenyl) retinamide in combination with tamoxifen in patients at high risk for developing invasive breast cancer. *J Clin Oncol*. 2000;18(2):275–283.
265. Caruso RC, Zujewski J, Iwata F, et al. Effects of fenretinide (4-HPR) on dark adaptation. *Arch Ophthalmol*. 1998;116(6):759–763.
266. Kaiser-Kupfer MI, Peck GL, Caruso RC, Jaffe MJ, DiGiovanna JJ, Gross EG. Abnormal retinal function associated with fenretinide, a synthetic retinoid. *Arch Ophthalmol*. 1986;104(1):69–70.
267. Decensi A, Torrisi R, Polizzi A, et al. Effect of the synthetic retinoid fenretinide on dark adaptation and the ocular surface. *J Natl Cancer Inst*. 1994;86(2):105–110.
268. Decensi A, Fontana V, Fioretto M, et al. Long-term effects of fenretinide on retinal function. *Eur J Cancer*. 1997;33(1):80–84.
269. Marmor MF, Jain A, Moshfeghi D. Total rod ERG suppression with high dose compassionate Fenretinide usage. *Doc Ophthalmol*. 2008;117(3):257–261.
270. Kubota R, Boman NL, David R, Mallikaarjun S, Patil S, Birch D. Safety and effect on rod function of Acu-4429, a novel small-molecule visual cycle modulator. *Retina*. 2012;32(1):183–188.
271a. Dugel PU, Novack RL, Csaky KG, Richmond PP, Birch DG, Kubota R. Phase ii, randomized, placebo-controlled, 90-day study of emixustat hydrochloride in geographic atrophy associated with dry age-related macular

degeneration. *Retina*. 2015;35(6):1173–1183.
271b. Rudolf M, Vogt SD, Curcio CA, et al. Histologic basis of variations in retinal pigment epithelium autofluorescence in eyes with geographic atrophy. *Ophthalmology*. 2013;120(4):821–828.
271c. Ach T, Tolstik E, Messinger JD, et al. Lipofuscin redistribution and loss accompanied by cytoskeletal stress in retinal pigment epithelium of eyes with age-related macular degeneration. *Invest Ophthalmol Vis Sci*. 2015;56(5):3242–3252.
272. Emlen W, Li W, Kirschfink M. Therapeutic complement inhibition: new developments. *Semin Thromb Hemost*. 2010;36(6):660–668.
273. Yehoshua Z, de Amorim Garcia Filho CA, Nunes RP, et al. Systemic complement inhibition with eculizumab for geographic atrophy in age-related macular degeneration: the COMPLETE study. *Ophthalmology*. 2014;121(3):693–701.
274. Roguska M, Splawski I, Diefenbach-Streiber B, et al. Generation and characterization of LFG316, a fully-human anti-C5 antibody for the treatment of age-related macular degeneration. *Invest Ophthalmol Vis Sci*. 2014;55(13):3433.
275. Carrion A, Etemad-Gilbertson B, Zhou J, Soni A, Roguska M. Characterization of the stoichiometry of human complement C5 binding to LFG316. *Invest Ophthalmol Vis Sci*. 2014;55(13):3432.
276. Kaushal S, Grossi F, Francois C, Slakter J, Group AS. Complement C3 inhibitor POT-4: clinical safety of intravitreal administration. *Invest Ophthalmol Vis Sci*. 2009;50(13):5010.
277. Donoso LA, Kim D, Frost A, Callahan A, Hageman G. The role of inflammation in the pathogenesis of age-related macular degeneration. *Surv Ophthalmol*. 2006;51(2):137–152.
278. Guba M, von Breitenbuch P, Steinbauer M, et al. Rapamycin inhibits primary and metastatic tumor growth by antiangiogenesis: involvement of vascular endothelial growth factor. *Nat Med*. 2002;8(2):128–135.
279. Dejneka NS, Kuroki AM, Fosnot J, Tang W, Tolentino MJ, Bennett J. Systemic rapamycin inhibits retinal and choroidal

neovascularization in mice. *Mol Vis*. 2004;10:964–972.
280. Nussenblatt RB, Byrnes G, Sen HN, et al. A randomized pilot study of systemic immunosuppression in the treatment of age-related macular degeneration with choroidal neovascularization. *Retina*. 2010;30(10):1579–1587.
281. Wong WT, Dresner S, Forooghian F, et al. Treatment of geographic atrophy with subconjunctival sirolimus: results of a phase I/II clinical trial. *Invest Ophthalmol Vis Sci*. 2013;54(4):2941–2950.
282. Petrou PA, Cunningham D, Shimel K, et al. Intravitreal sirolimus for the treatment of geographic atrophy: results of a phase I/II clinical trial. *Invest Ophthalmol Vis Sci*. 2015;56(1):330–338.
283. Wang F, Fries M, Wurzelmann JI, Shearn SP, Schwartz MR, Ozden R. Patient-reported visual function in patients with geographic atrophy secondary to age-related macular degeneration (AMD): baseline characteristics of the BAM114341 cohort. *Invest Ophthalmol Vis Sci*. 2015;56(7):2811.
284. Friedman E. The pathogenesis of age-related macular degeneration. *Am J Ophthalmol*. 2008;146(3):348–349.
285. Xu W, Grunwald JE, Metelitsina TI, et al. Association of risk factors for choroidal neovascularization in age-related macular degeneration with decreased foveolar choroidal circulation. *Am J Ophthalmol*. 2010;150(1):40–47.e2.
286. Grunwald JE, Hariprasad SM, DuPont J, et al. Foveolar choroidal blood flow in age-related macular degeneration. *Invest Ophthalmol Vis Sci*. 1998;39(2):385–390.
287. Dunaief JL, Dentchev T, Ying GS, Milam AH. The role of apoptosis in age-related macular degeneration. *Arch Ophthalmol*. 2002;120(11):1435–1442.
288. Faktorovich EG, Steinberg RH, Yasumura D, Matthes MT, LaVail MM. Photoreceptor degeneration in inherited retinal dystrophy delayed by basic fibroblast growth factor. *Nature*. 1990;347(6288):83–86.
289. LaVail MM, Yasumura D, Matthes MT, et al. Protection of mouse photoreceptors by survival factors in retinal degenerations. *Invest Ophthalmol Vis Sci*. 1998;39(3):592–602.

290. Cayouette M, Behn D, Sendtner M, Lachapelle P, Gravel C. Intraocular gene transfer of ciliary neurotrophic factor prevents death and increases responsiveness of rod photoreceptors in the retinal degeneration slow mouse. *J Neurosci*. 1998;18(22):9282–9293.
291. Ortin-Martinez A, Valiente-Soriano FJ, Garcia-Ayuso D, et al. A novel in vivo model of focal light emitting diode-induced cone-photoreceptor phototoxicity: neuroprotection afforded by brimonidine, BDNF, PEDF or bFGF. *PLoS ONE*. 2014;9(12):e113798.
292. Lee D, Kim KY, Noh YH, et al. Brimonidine blocks glutamate excitotoxicity-induced oxidative stress and preserves mitochondrial transcription factor a in ischemic retinal injury. *PLoS ONE*. 2012;7(10):e47098.
293. Yigit U, Erdenoz S, Uslu U, et al. An immunohistochemical analysis of the neuroprotective effects of memantine, hyperbaric oxygen therapy, and brimonidine after acute ischemia reperfusion injury. *Mol Vis*. 2011;17:1024–1033.
294. Guo X, Namekata K, Kimura A, et al. Brimonidine suppresses loss of retinal neurons and visual function in a murine model of optic neuritis. *Neurosci Lett*. 2015;592:27–31.
295. Pfeiffer N, Lamparter J, Gericke A, Grus FH, Hoffmann EM, Wahl J. Neuroprotection of medical IOP-lowering therapy. *Cell Tissue Res*. 2013;353(2):245–251.
296. Deokule SP, Baffi JZ, Guo H, Nazzaro M, Kaneko H. Evaluation of extended release brimonidine intravitreal device in normotensive rabbit eyes. *Acta Ophthalmol*. 2012;90(5):e344–8.
297. Samtani S, Amaral J, Campos MM, Fariss RN, Becerra SP. Doxycycline-mediated inhibition of choroidal neovascularization. *Invest Ophthalmol Vis Sci*. 2009;50(11):5098–5106.
298. Ying GS, Huang J, Maguire MG, et al. Baseline predictors for one-year visual outcomes with ranibizumab or bevacizumab for neovascular age-related macular degeneration. *Ophthalmology*. 2013;120(1):122–129.
299. Ying GS, Maguire MG, Daniel E, et al. Association of

baseline characteristics and early vision response with 2-year vision outcomes in the Comparison of AMD Treatments Trials (CATT). *Ophthalmology*. 2015;122(12):2523–2531.
300. Lim JH, Wickremasinghe SS, Xie J, et al. Delay to treatment and visual outcomes in patients treated with anti-vascular endothelial growth factor for age-related macular degeneration. *Am J Ophthalmol*. 2012;153(4):678–686 [686.e1-2].
301. Curcio CA, Medeiros NE, Millican CL. Photoreceptor loss in age-related macular degeneration. *Invest Ophthalmol Vis Sci*. 1996;37(7):1236–1249.
302. Owsley C, Jackson GR, Cideciyan AV, et al. Psychophysical evidence for rod vulnerability in age-related macular degeneration. *Invest Ophthalmol Vis Sci*. 2000;41(1):267–273.
303. Crossland M, Rubin G. The Amsler chart: absence of evidence is not evidence of absence. *Br J Ophthalmol*. 2007;91(3):391–393.
304. Tolentino MJ, Miller S, Gaudio AR, Sandberg MA. Visual field deficits in early age-related macular degeneration. *Vision Res*. 1994;34(3):409–413.
305. Faes L, Bodmer NS, Bachmann LM, Thiel MA, Schmid MK. Diagnostic accuracy of the Amsler grid and the preferential hyperacuity perimetry in the screening of patients with age-related macular degeneration: systematic review and meta-analysis. *Eye (Lond)*. 2014;28(7):788–796.
306. Loewenstein A, Malach R, Goldstein M, et al. Replacing the Amsler grid: a new method for monitoring patients with age-related macular degeneration. *Ophthalmology*. 2003;110(5):966–970.
307. Group AHSR, Chew EY, Clemons TE, et al. Randomized trial of a home monitoring system for early detection of choroidal neovascularization home monitoring of the Eye (HOME) study. *Ophthalmology*. 2014;121(2):535–544.
308. Wang YZ, He YG, Mitzel G, Zhang S, Bartlett M. Handheld shape discrimination hyperacuity test on a mobile device for remote monitoring of visual function in maculopathy. *Invest Ophthalmol Vis Sci*. 2013;54(8):5497–5505.

309. Wang YZ, Wilson E, Locke KG, Edwards AO. Shape discrimination in age-related macular degeneration. *Invest Ophthalmol Vis Sci*. 2002;43(6):2055–2062.
310. Winther C, Frisen L. Self-testing of vision in age-related macula degeneration: a longitudinal pilot study using a smartphone-based rarebit test. *J Ophthalmol*. 2015;2015:285463.
311. Dinc UA, Yenerel M, Gorgun E, Oncel M. Assessment of macular function by microperimetry in intermediate age-related macular degeneration. *Eur J Ophthalmol*. 2008;18(4):595–600.
312. Bartlett H, Davies LN, Eperjesi F. The macular mapping test: a reliability study. *BMC Ophthalmol*. 2005;5:18.
313. Flamendorf J, Agron E, Wong WT, et al. Impairments in dark adaptation are associated with age-related macular degeneration severity and reticular pseudodrusen. *Ophthalmology*. 2015;122(10):2053–2062.
314. Dimitrov PN, Robman LD, Varsamidis M, et al. Visual function tests as potential biomarkers in age-related macular degeneration. *Invest Ophthalmol Vis Sci*. 2011;52(13):9457–9469.
315. Schneck ME, Haegerstrom-Portnoy G, Lott LA, Brabyn JA, Gildengorin G. Low contrast vision function predicts subsequent acuity loss in an aged population: the SKI study. *Vision Res*. 2004;44(20):2317–2325.
316. Feigl B, Brown B, Lovie-Kitchin J, Swann P. Cone-mediated multifocal electroretinogram in early age-related maculopathy and its relationships with subjective macular function tests. *Curr Eye Res*. 2004;29(4–5):327–336.
317. Bittner AK, Torr-Brown S, Arnold E, et al. Improved adherence to vision self-monitoring with the Vision and Memory Stimulating (VMS) Journal for non-neovascular age-related macular degeneration during a randomized controlled trial. *J Clin Exp Ophthalmol*. 2014;5(1):320.

[a]Selected text adapted with permission from Zarbin and Rosenfeld, 2010[45] and Zarbin and Rosenfeld, 2012.[46]

[a]Selected text adapted with permission from Zarbin and Rosenfeld, 2010[45] and Zarbin and Rosenfeld, 2012.[46]

[a]Selected text adapted with permission from Zarbin and Rosenfeld, 2010[45] and Zarbin and Rosenfeld, 2012.[46]

[a]Selected text adapted with permission from Zarbin and Rosenfeld, 2010[45] and Zarbin and Rosenfeld, 2012.[46]

71

Pathologic Myopia

Kyoko Ohno-Matsui, Tatsuro Ishibashi

Pathologic myopia is a major cause of legal blindness and low vision worldwide,[1–5] and its prevalence is increasing in modern society, presumably due to an increase of near activities. In patients with pathologic myopia, various kinds of macular lesions develop in the posterior fundus, and these are the cause of visual impairment.[6,7,1–5] There are new ideas concerning the pathogenesis of pathologic myopia and novel treatments for macular complications. Although macular lesions in eyes with pathologic myopia had been an incurable degenerative disorder, the recent application of anti-vascular endothelial growth factor (VEGF) therapy for myopic choroidal neovascularization (CNV)[6–9] and vitreoretinal surgery for myopic traction maculopathy have enabled the treatment of these complications due to pathologic myopia.[10–18] With these advances, pathologic myopia is now a curable disorder in some patients to some extent.

Epidemiology

Myopia is more common among Asian populations, especially in East Asian countries, than among white, black, or Hispanic people. The prevalence of myopia (spherical equivalent [SE], <−0.5 or −1.0 diopters [D]) is reported to range from 17% to 43% among Asian populations.[19–27] Among white populations in Europe, the United States, and Australia, it is reported to be between 13% and 27%.[28–31] In Hispanic and black populations, it is reported to be 17% and 21%, respectively.[29,32] The prevalence of high myopia (SE, <−5.0 or −6.0 D) is also greater in Asian populations, ranging from 1.7% to 9.1%, than that in white, Hispanic, and black populations (2.0%, 2.4%, 1.0%, respectively).[19–32]

Pathologic myopia is one of the major causes of visual impairment and blindness worldwide. For example, myopic macular degeneration is the leading cause of blindness in Japan, the second most common cause in Denmark[33] and in China,[23] and the third cause of blindness in Latinos 40 years and older in the United States.[3] Myopic macular degeneration was the leading cause of impaired vision for persons aged between 55 and 75 years in The Netherlands.[34–36] In Italy and Taiwan, it is the second most common cause of low vision.[37,38] The impact of myopic retinopathy on visual

impairment is of great concern because it is often bilateral, irreversible, and it frequently affects individuals during their most productive ages.[39,40]

To date, three population-based studies have estimated the prevalence of myopic retinopathy. The Blue Mountains Eye Study in Australia, which focused on a white population, reported that the prevalence of myopic retinopathy was 1.2%.[40] In the Beijing Eye Study in China and the Hisayama Study in Japan, the prevalence was 3.1% and 1.7%, respectively.[41] Study participants' characteristics, methodology, and study design (for example, the definition of myopic retinopathy) were different between those studies; therefore the precise racial difference in myopic retinopathy prevalence is unknown. But it may be higher in East Asian populations than in white populations, and the prevalence of high myopia is probably higher as well.

The prevalence of myopic retinopathy is increased with advancing age in those population-based studies. Histologic studies have shown a decreased density of photoreceptors, ganglion cells, retinal pigment epithelium, and optic nerve fibers with age.[42,43] However, several studies using optical coherence tomography (OCT) have examined subjects with healthy eyes with neither high myopia nor hyperopia and reported a negative relationship between retinal thickness and age.[44,45] In addition to the axial elongation of the eyeball in highly myopic eyes, increasing age may contribute to pathogenesis of myopic retinopathy by causing retinal thinning.

Although it is reported that men have longer axial length than women,[46,47] many hospital-based studies showed higher prevalence of myopic retinopathy in women than in men.[48–50] For example, Hayashi et al. showed that of 429 consecutive patients with pathologic myopia, 147 were men and 282 were women, which is about twice as many cases in women than in men.[39] Comparable findings were also observed in population-based studies. In the Blue Mountains Eye Study, the prevalence of myopic retinopathy in men was 0.06% and that in women was 0.4%. In the Hisayama Study, the prevalence of myopic retinopathy in men and in women was 1.2% and 2.2%, respectively. The Beijing Eye Study did not report the prevalence of myopic retinopathy by sex, but the female :

male ratios of the subjects with and without myopic retinopathy were 75 : 57 and 570 : 489, respectively. It suggests that not only greater axial length but other risk factors such as genetic factors and lifestyle risk factors may contribute to the pathogenesis of myopic retinopathy.

Pathogenesis

Hereditary or genetic factors play important roles in the development of pathologic myopia. There is a large international linkage study on familial high myopia, in which linkage analyses were performed on 1201 samples from Asian, African-American, and Caucasian families, finding that the MYP1, MYP3, MYP6, MYP11, MYP12, and MYP14 loci were replicated.[51] Recent genomewide studies identified susceptibility loci at 15q14 and 15q25 for myopia.[52,53] The risk of myopia versus hyperopia showed an odds ratio (OR) 1.88 for homozygous carriers of the risk allele at the top-SNPs in locus 15q14 and OR 1.33 for heterozygous carriers. The 15q14 region contains the *GJD2* gene, encoding Connexin 36, which is associated with neurotransmission in the retina.[54,55] However, the genetic influence on the development of myopic macular degeneration is not clear. The genetic risk factors of age-related macular degeneration related to rs11200638 of HTRA1, and rs1061170 (Y402H) of complement factor H (CFH) did not appear to contribute significantly to the development of CNV in a highly myopic elderly Japanese population.[56] It was reported that the responsiveness of myopic CNV to PDT had a correlation with common coagulation-balance gene polymorphisms.[57]

Various factors such as aging and biomechanical factors in addition to hereditary factors have been considered to contribute to the development of myopic macular degeneration in highly myopic eyes.[58–60] Excessive axial elongation and posterior staphyloma formation are critical features of pathologic myopia, and these are considered important for the development and progression of myopic macular degeneration.[59] Large-scale studies show that a peripapillary crescent, chorioretinal atrophy, and posterior staphyloma are related significantly to increased axial length.[41,59] Above all, the incidence, size, and type of peripapillary crescent

have the strongest correlation with the axial length;[59,61] more than 95% of eyes with an axial length of 26.5 mm or more have a peripapillary crescent, while 0% of eyes with an axial length of 21.4 mm or less have a peripapillary crescent.[59] Chorioretinal atrophy has also been related directly to increased axial length.

In addition to the influence of biomechanical factors, aging is an important factor for the development of posterior staphyloma and subsequent myopic macular degeneration. A posterior staphyloma is rarely found in highly myopic patients younger than 40 years of age.[62] The posterior staphyloma develops as patients age, and this accelerates the further mechanical extension of the posterior fundus, and causes the development of myopic macular degeneration. The incidence of myopic chorioretinal atrophy increases with age, and these changes are rarely seen in persons less than 20 years old.[59,61] Childhood high myopes do not develop myopic macular degeneration or posterior staphyloma.[63]

The development of myopic choroidal neovascularization (myopic CNV) and lacquer cracks are not directly correlated with axial length. The incidence of myopic CNV peaks in the fourth decade. There may be biologic mechanisms of neovascular membrane formation other than axial elongation or aging.[61] Steidl and Pruett[64] reported that eyes with a shallow staphyloma had the high frequency of CNV. They suggested that it is possible that eyes with a shallow staphyloma may be healthier and more metabolically active with well-perfused chorioretinal tissue and good capacity to respond to injury by neovascular ingrowth. It appears that the influence of aging and mechanical factors is rather complicated and different lesions of course may have different pathogenetic influences.

Histopathology

The Sclera

Scleral thinning and localized ectasia of the posterior sclera are characteristic changes of the eyes with pathologic myopia. Vurgese and Jonas reported that in axially elongated eyes, scleral thinning occurred at and posterior to the equator, being more marked closer

to the posterior pole in human eyes.[65] Microscopically, the normal sclera consists of interwoven bands or bundles of collagen fibers.[58] These are usually well integrated and in longitudinal section present a relatively homogeneous appearance throughout their extent. The architectural changes in the longitudinal fibers in pathologic myopia consist of thinning of the collagen bundles, a reduction in refringence of the bundle edges, and the loss of longitudinal fiber striations. The cross-sectional fibers demonstrate dissociation such that the individual fibers separate from one another. There is also a reduction in the size of the individual dissociated fibers. The more advanced examples of architectural disorganization are found in and about the regions of the posterior pole and peripapillary sclera. It has also been reported that the elastic fibers within the sclera showed a definite decrease in the number of fibers.

Electron microscopic analyses showed that a predominance of collagen fibrils of small diameter, usually averaging below 60–70 nm, was found.[58] Fibrils of a very fine diameter were also observed. Also, the cross-sectioned fibrils showed a marked increase in the prevalence of fissured or "star-shaped" forms. Most of the ultramicroscopic alterations seen in the myopic sclera indicate a derangement of the growth and organization of the fibrils. These may be products of defective fibrillogenesis. These aspects of development are thought to be under the control of the acidic glycosaminoglycan composition of the interfibrillar substance. It is also conceivable that this picture corresponds to abnormal fibril growth in the presence of an accentuated breakdown or catabolism of the sclera.

Ohno-Matsui et al. analyzed the scleral thickness and scleral curvature in a large series of highly myopic patients using swept-source OCT.[66] The entire thickness of the sclera was observed in most of the highly myopic eyes, and the mean subfoveal scleral thickness was 227.9 μm in the highly myopic eyes. The curvatures of the inner scleral surface of highly myopic eyes could be divided into curvatures that sloped toward the optic nerve, those that were symmetric and centered on the fovea, those that were asymmetric, and those that were irregular (Fig. 71.1). Irregular scleral curvature was associated with the frequency of myopic macular

complications.

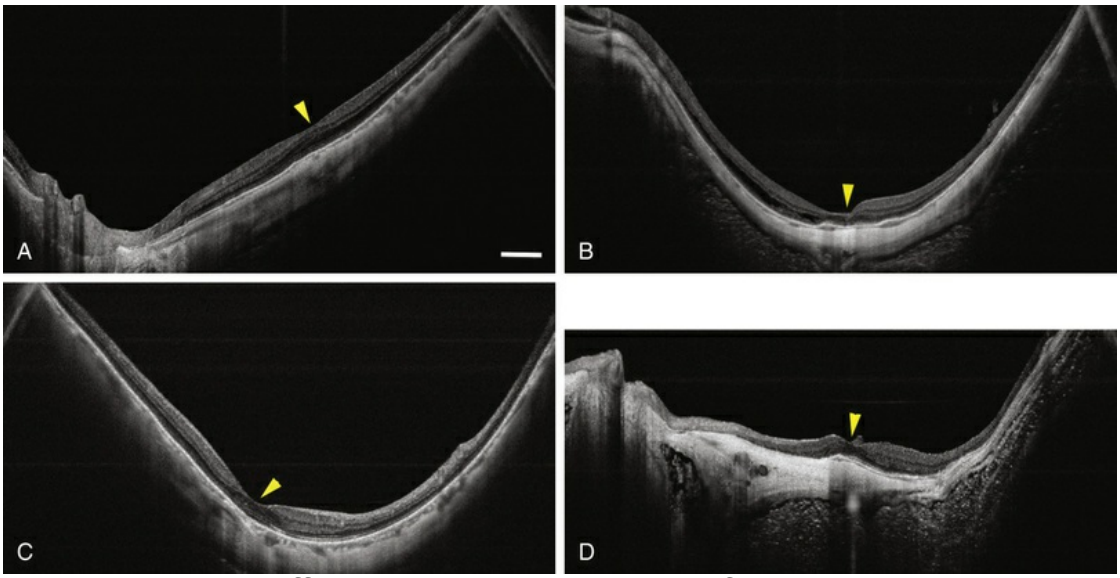

FIG. 71.1 Different curvature patterns of the sclera in highly myopic eyes. (A) The curvature is sloped toward the optic nerve. The curve of inner scleral surface is straight (*arrowhead*), and the optic disc is at the bottom of the posterior segment of the eye. Scale bar: 1 mm. (B) The curvature is symmetric around the fovea. The sclera is strongly bowed posteriorly; however, the curve is symmetric around the fovea (*arrowhead*), and the fovea is situated on the bottom of posterior segment of the eye. (C) Asymmetric curvature around the fovea. The sclera is strongly bowed posteriorly, and the most protruded point is away from the central fovea. The fovea (*arrowhead*) is on the slope. (D) Irregular curvature. The sclera is irregular and does not have a smooth curvature. The *arrowhead* indicates the fovea. (With permission from Ohno-Matsui K, Akiba M, Modegi T, et al. Association between shape of sclera and myopic retinochoroidal lesions in patients with pathologic myopia. Invest Ophthalmol Vis Sci 2012;53(10):6046-61.)

Choroid and Retinal Pigment Epithelium

The degenerative changes found in pathologic myopia initially appear to involve the choriocapillaris–Bruch's membrane–retinal pigment epithelium (RPE) complex. The changes subsequently

affecting the choroid were essentially degenerative and atrophic. Thinning of the choroid and loss of the choriocapillaris were reported (Fig. 71.2). Choroidal vascular occlusions are a prominent feature of the disease, and this process appears to affect the smaller-diameter vessels initially. The choroidal vessels appear to be fewer and to have thinner walls than seen normally. There is a generalized loss of the normal connective tissue framework of the choroid with some degree of compaction of the vessels. Although the large-sized choroidal vessels tend to be most resistant, these, too, may undergo occlusion in the late stages of the disease. Recent studies using enhanced-depth imaging of optical coherence tomography (EDI-OCT) or high penetrance OCT also showed significant thinning of the choroid in highly myopic eyes.[67]

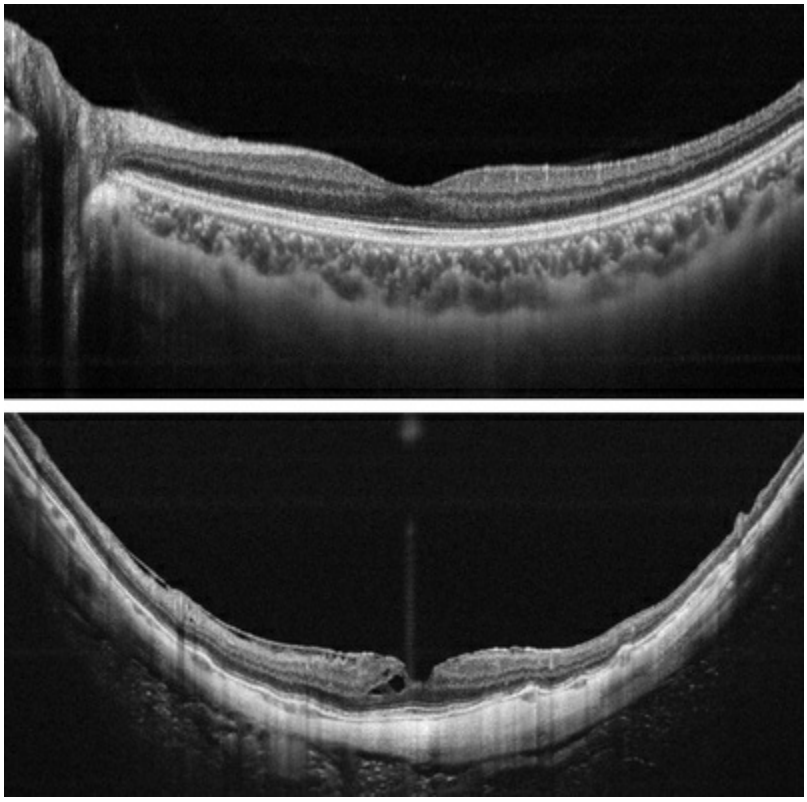

FIG. 71.2 Choroidal thinning in pathologic myopia. In comparison with emmetropic eyes (top), the choroid is extremely thinned in eyes with pathologic myopia (bottom). Large choroidal vessels sporadically remain and indent the overlying retinal pigmented epithelium.

The RPE cells are seen to be flatter and larger than usual, a

possible consequence of passive expansion. Hyperpigmentation, hypopigmentation, and multilayered clumping of the RPE cells may also be seen. Bruch's membrane may show a variety of changes, including thinning, splitting, and rupture.

Animal Models

Rhesus monkeys, chickens, fish, tree shrews, marmosets, and guinea-pigs have long been used as animal models of experimental myopia by inducing form-deprivation myopia by lid suture or by wearing plastic goggles.[68–70] Chicks have long been the main animal model for experimental myopia because myopia accompanying a dramatic increase of the axial length can be induced easily by wearing plastic goggles in about 2 weeks.[71] Therefore, many studies were performed using chick models of experimental myopia. These studies identified responsible factors that cause excessive eye growth. However, the sclera of chickens differs from that of humans. The chicken has the classic vertebrate sclera, consisting of a layer of cartilage surrounded by layers of fibrous connective tissue, whereas in most mammals, including primates and rodents, the cartilage has been lost.

Based on the benefit of having similar scleral components, mice have commonly been used as experimental myopia,[72,73] although there is some drawback that the induced myopia is not as severe as in the chickens because mice are not "visual animals." Mouse model advantages also include the availability of numerous knockout mutants, more advanced gene microarrays for screening the transcriptome, and a completely sequenced genome. Moreover, Olivier et al. reported that mice with conditional inactivation of Lrp2 in eyes demonstrated congenital high myopia. In addition to an excessive elongation of the posterior chamber, the Lpr2-deficient eye had normal intraocular pressure and developed chorioretinal atrophy and staphyloma resembling human pathologic myopia.[74]

In general, animal models of experimental myopia do not develop retinal complications. This might be due to a short lifespan of animals and short duration of myopia. As an exception, Hirata and Negi[75] reported the development of lacquer cracks in chicks with experimental myopia (Fig. 71.3). This result is interesting

because it suggests that lacquer cracks are purely caused by mechanical stretching of the globe and less affected by aging.

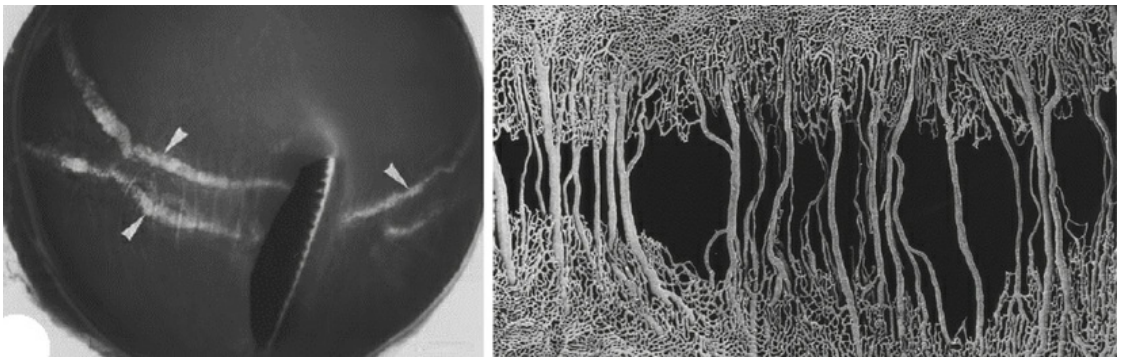

FIG. 71.3 Development of lacquer cracks in chick models of experimental myopia. In the posterior fundus (left), lacquer cracks are observed to course as linear streaks. Electron microscopic photograph at the area of lacquer cracks shows a disruption of choriocapillaris (right). Large choroidal vessels across the lesion are observed. (With permission from Hirata A, Negi A. Lacquer crack lesions in experimental chick myopia. Graefes Arch Clin Exp Ophthalmol 1998;236(2):138-45.)

The transcriptome of neurosensory retina without RPE was analyzed with Affymetrix GeneChip Mouse Genome 430 2.0 arrays after unilateral retinal image degradation by use of frosted goggles in mice,[76] and identified some genes altered including a downregulation of the early growth response 1 (*Egr*-1) gene. The refractions of homozygous *Egr*-1 knockout mice were some 4–5 diopters less hyperopic relative to the wild-type.[77] Zebrafish have also been considered as a model of experimental myopia. Downregulation of zebrafish lumican gene expression manifested ocular enlargement resembling axial myopia due to disruption of the collagen fibril arrangement in the sclera and resulted in scleral thinning.[78] The lumican gene, which encodes one of the major keratan sulfate proteoglycans in the vertebrate cornea and sclera, has been linked to axial myopia in humans. Veth and colleagues[79] have used zebrafish to identify a genetically complex, recessive mutant that shows risk factors for glaucoma including adult-onset severe myopia, elevated intraocular pressure, and progressive retinal ganglion cell pathology. Positional cloning and analysis of a

noncomplementing allele indicated that non-sense mutations in low-density lipoprotein receptor-related protein 2 (lrp2) underlie the mutant phenotype.

Posterior Staphyloma

A posterior staphyloma is an outward protrusion of all layers of the posterior eye globe and is considered a hallmark lesion of pathologic myopia. Until recently there has not been a uniformly accepted definition of a posterior staphyloma; thus, it has been common for authors to refer to abnormalities in the posterior pole of myopic eyes, even those that do not involve an outpouching, as being "staphylomas." Spaide[80] recently proposed a clear definition of a staphyloma as "an outpouching of the wall of the eye that has a radius of curvature that is less than the surrounding curvature of the wall of the eye" (Fig. 71.4) in pathologic myopia.

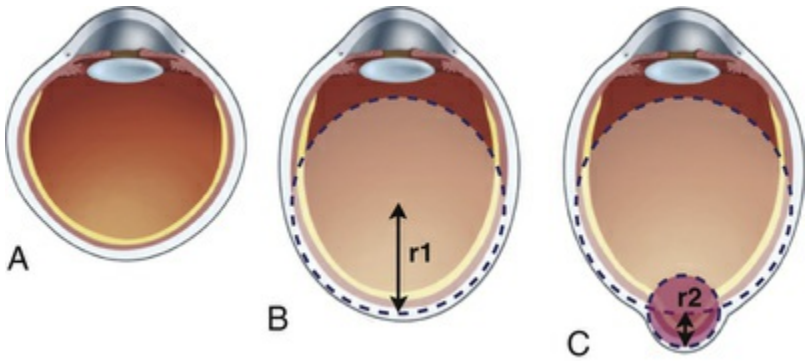

FIG. 71.4 Definition of a posterior staphyloma. (A) Normal eye shape. (B) Axial length elongation occurring in the equatorial region that does not induce any alteration in the curvature of the posterior part of the eye. This eye would have axial myopia but no staphyloma. (C) A second curvature develops in the posterior portion of the eye, and this second curvature has a shorter radius (r_2) of curvature than the surrounding eye wall (r_1). This secondary curve is due to a staphyloma. (With permission from Spaide RF, Ohno-Matsui K, Yannuzzi LA. Pathologic myopia. New York: Springer; 2014.)

There are 10 different types of staphyloma according to Curtin (Fig. 71.5).[62] Types I through V are basic staphylomas, and types VI

through X are compound staphylomas. A posterior staphyloma is not common in children with pathologic myopia, and the incidence of staphyloma is significantly higher in older patients (96.7% in those ≥50 years of age) than in younger patients (80.7% in those <50 years).[46]

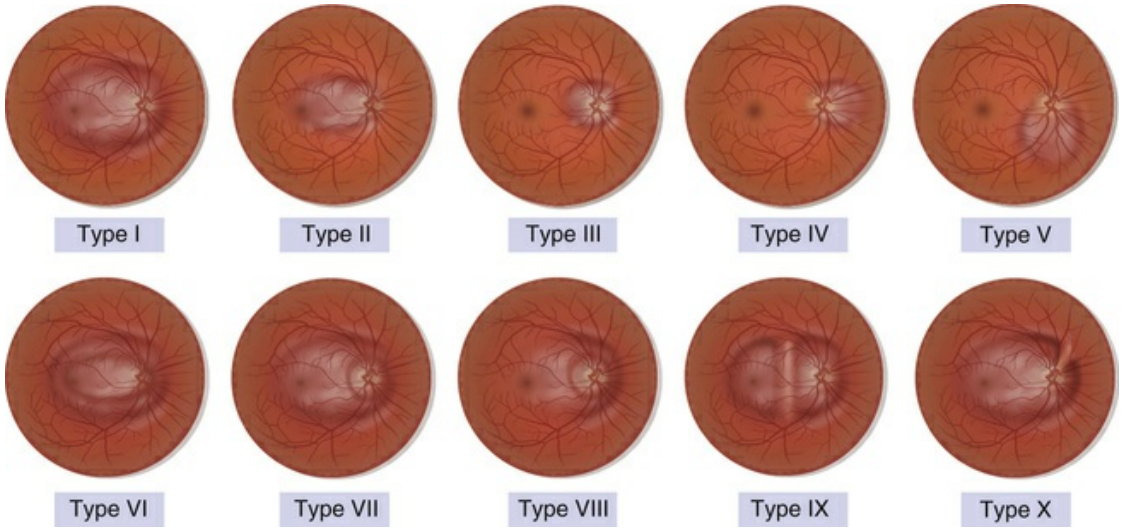

FIG. 71.5 Curtin's classification of posterior staphyloma. (With permission from Curtin BJ. The posterior staphyloma of pathologic myopia. Trans Am Ophthalmol Soc 1977;75:67†86.)

However, this classification was made from the ophthalmoscopic appearances and fundus drawings that made the classification subjective. Also, some of the types are rare, and recent studies using OCT showed that there are more complex irregularities of the scleral curvature[66,81–86] within the area of a staphyloma than Curtin[87] had noted. To overcome these problems, we[88] used three-dimensional magnetic resonance imaging (3D MRI) of the globe and ultrawide-field fundus imaging to analyze the presence and types of the posterior staphyloma based on Spaide's definition. Ohno-Matsui reported that in about a half of highly myopic eyes (mean axial length; 30 mm), the staphyloma was not observed and the eyes were simply elongated (Fig. 71.6). The most frequent type of staphyloma was the wide, macular type (Fig. 71.7), followed by the narrow, macular type. The types of staphyloma have been renamed according to the area: wide-macular, narrow-macular, peripapillary, nasal, inferior, and others to facilitate memorization

(Fig. 71.8).

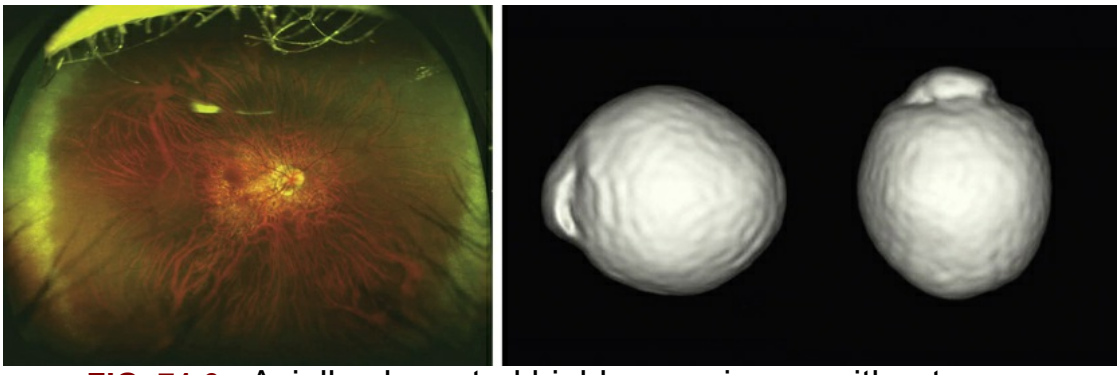

FIG. 71.6 Axially elongated highly myopic eye without having a posterior staphyloma. Wide-field fundus photo (left) shows diffuse chorioretinal atrophy in the posterior fundus. In three-dimensional magnetic resonance imaging (3D MRI) of the globe, the eye is simply elongated and does not have a clear outpouching suggestive of staphyloma in the images viewed from nasally (middle) as well as in the image viewed from inferiorly (right). (With permission from Ohno-Matsui K. Proposed classification of posterior staphylomas based on analyses of eye shape by three-dimensional magnetic resonance imaging. Ophthalmology 2014;121(9):1798-1809.)

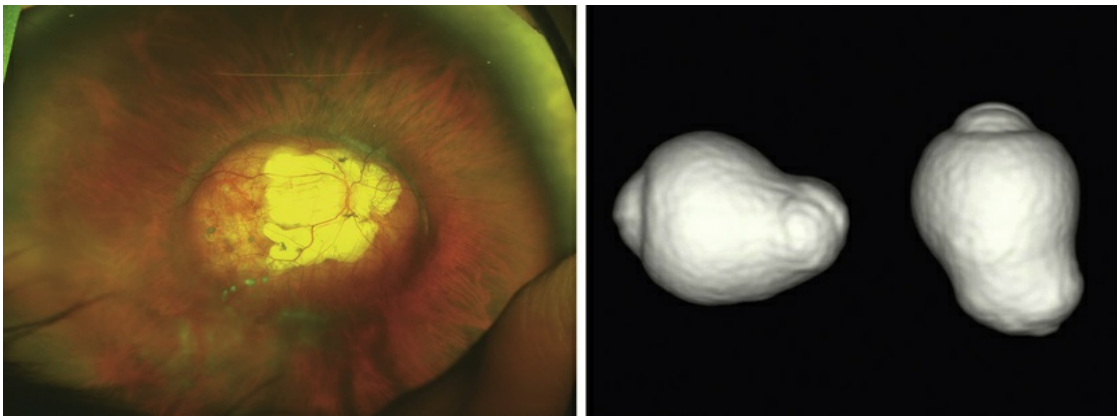

FIG. 71.7 Highly myopic eye with wide, macular staphyloma. Wide-field fundus photo (left) shows macular atrophy and large conus. The upper edge of wide, macular staphyloma is clearly observed. In three-dimensional magnetic resonance imaging (3D MRI) of the globe, an outpouching of wide area of posterior

segment is seen in the image viewed from nasally (middle) as well as that viewed from inferiorly (right).
(With permission from Ohno-Matsui K. Proposed classification of posterior staphylomas based on analyses of eye shape by three-dimensional magnetic resonance imaging. Ophthalmology 2014;121(9):1798-1809.)

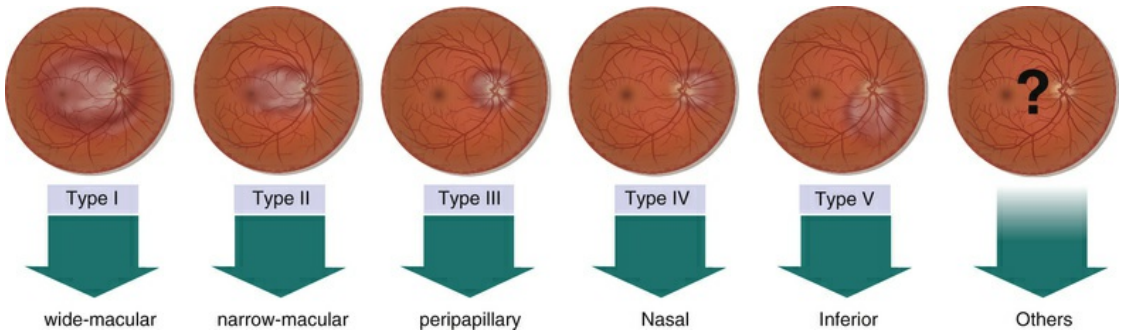

FIG. 71.8 Renaming of types of posterior staphyloma. Curtin's Type I to wide-macular, Type II to narrow-macular, Type III to peripapillary, Type IV to nasal, Type V to inferior, and others.

Classification of Myopic Maculopathy

Various kinds of macular lesions develop in eyes with pathologic myopia, such as diffuse chorioretinal atrophy, patchy chorioretinal atrophy, lacquer cracks, myopic choroidal neovascularization (myopic CNV), CNV-related macular atrophy (Fig. 71.9).[1,2,58,61,64]

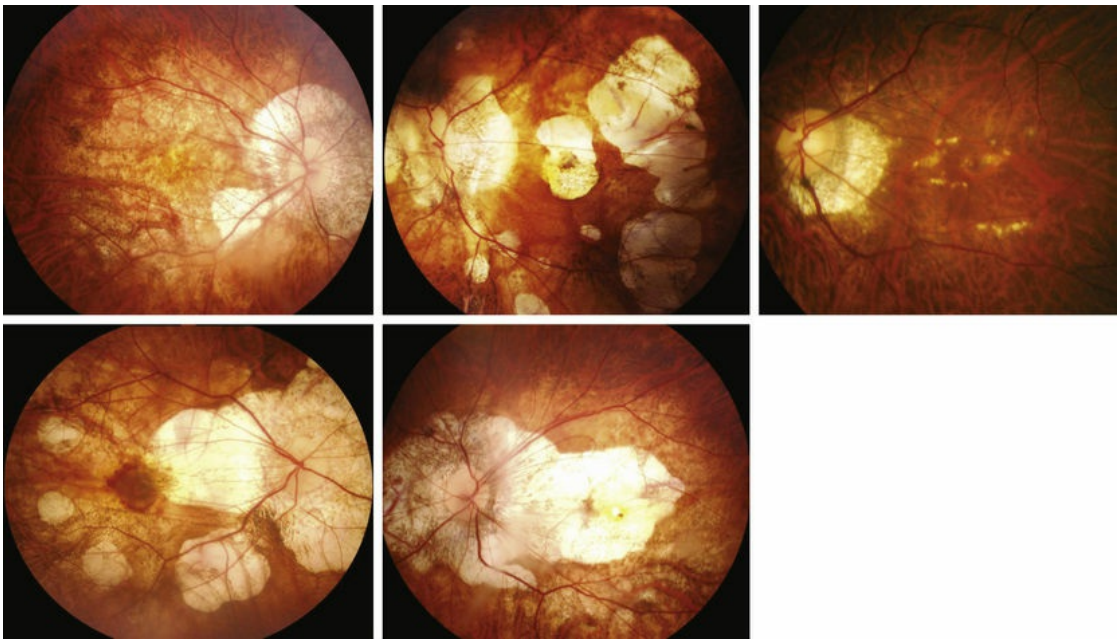

FIG. 71.9 Various lesions of myopic maculopathy. In the top row, diffuse chorioretinal atrophy (left), patchy chorioretinal atrophy (middle), and lacquer cracks (right). In the bottom row, myopic choroidal neovascularization (myopic CNV; left) and macular atrophy (most frequently, CNV-related macular atrophy; right).

Based on the long-term data of natural progression of lesions of myopic maculopathy (Fig. 71.10),[39] Ohno-Matsui and META-PM study group investigators[89] proposed an international classification (Table 71.1). According to the main path of natural progression, five categories were proposed (category 0, no macular lesions; category 1, tessellated fundus; category 2, diffuse chorioretinal atrophy; category 3, patchy chorioretinal atrophy; category 4, macular atrophy). The lesions that develop independently from the main progression pattern were considered "plus lesions," and they included lacquer cracks, myopic CNV, and Fuchs' spot (scar phase of myopic CNV). The eyes with lesions more severe than or equal to category 2 or with "plus lesions" are considered "pathologic myopia."

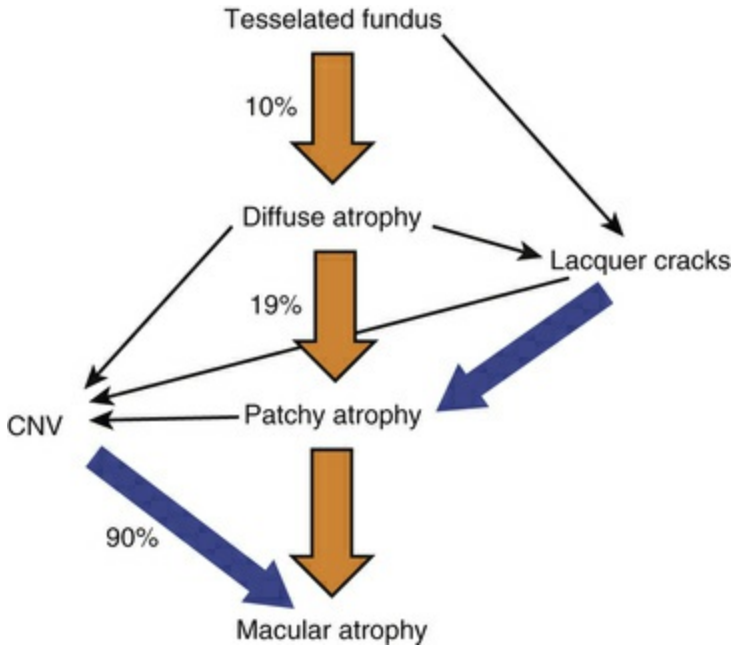

FIG. 71.10 Pattern of natural progression of myopic maculopathy. (With permission from Hayashi K, Ohno-Matsui K, Shimada N, et al. Long-term pattern of progression of myopic maculopathy: a natural history study. Ophthalmology 2010;117(8):1595-1611.)

TABLE 71.1

International Photographic Classification and Grading System for Myopic Maculopathy

	Myopic Maculopathy	"Plus" Lesions
Category 0	No macular lesions	
Category 1	Tessellated fundus	
Category 2	Diffuse chorioretinal atrophy	+ Lacquer cracks (Lc) Myopic choroidal neovascularization Fuchs' spot (Fs)
Category 3	Patchy chorioretinal atrophy	
Category 4	Macular atrophy	

Ohno-Matsui K, Kawasaki R, Jonas JB, et al. International photographic classification and grading system for myopic maculopathy. Am J Ophthalmol 2015;159(5):877-83 e7.

Myopic Chorioretinal Atrophy

Two types of myopic chorioretinal atrophy develop in the posterior fundus. According to Tokoro, there is diffuse chorioretinal atrophy

and patchy chorioretinal atrophy.[6] Diffuse chorioretinal atrophy is observed as yellowish-white and ill-defined chorioretinal atrophy. Diffuse chorioretinal atrophy is characterized by marked thinning of the choroid in OCT images. Due to the disappearance of most of the choroid, only large choroidal vessels sporadically remain. Patchy chorioretinal atrophy is observed as grayish-white and well-defined chorioretinal atrophy. The areas of patchy atrophy develop within an area of diffuse atrophy (Fig. 71.11). The entire choroid does not exist in the area of patchy atrophy accompanying with a loss of retinal pigment epithelium and photoreceptors, the inner retina directly sits on the sclera in OCT images.

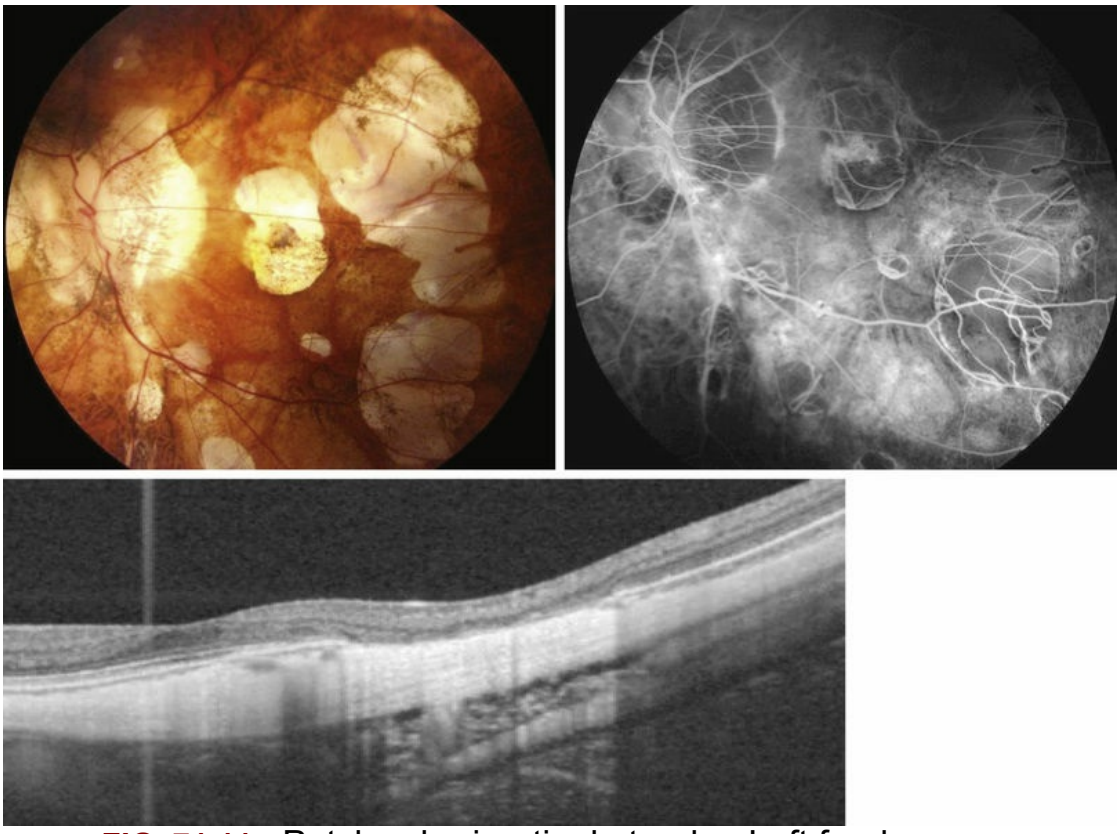

FIG. 71.11 Patchy chorioretinal atrophy. Left fundus (top left) shows multiple areas of whitish, patchy atrophy. Fluorescein angiogram (top right) shows choroidal filling defect in the area of patchy atrophy. Optical coherence tomographic (OCT) image shows a lack of the entire choroid, retinal pigment epithelium, and photoreceptors. The inner retina directly sits on the sclera.

Lacquer Cracks

Lacquer cracks are considered to represent linear ruptures of Bruch's membrane in the macular area of highly myopic eyes and are observed as yellowish linear lesions in the macula. The presence of Bruch's membrane defects has been reported in histopathologic studies.[90] However, due to a lack of clinicopathologic studies, it is not clear whether the yellowish linear lesions observed in highly myopic eyes truly represent rupture of Bruch's membrane. In addition, it is still difficult to detect such a narrow lesion by using OCT.

Lacquer cracks are more easily detected by fluorescein angiography, fundus autofluorescence imaging, and indocyanine green angiography.[64,65] With time, lacquer cracks increase in number and also increase their width (Fig. 71.12).[66] When new lacquer cracks develop, the choriocapillaris is also damaged and subretinal bleeding may occur.[67] Subretinal bleeding without CNV is a visible sign of new lacquer crack formation, and after absorption of bleeding, lacquer cracks appear as yellowish linear lesions. Lacquer cracks are known as precursor lesions of myopic CNV.[65,68] Often, CNV tends to develop along the foveal edge of chorioretinal atrophy that was formed by increased width of lacquer cracks.

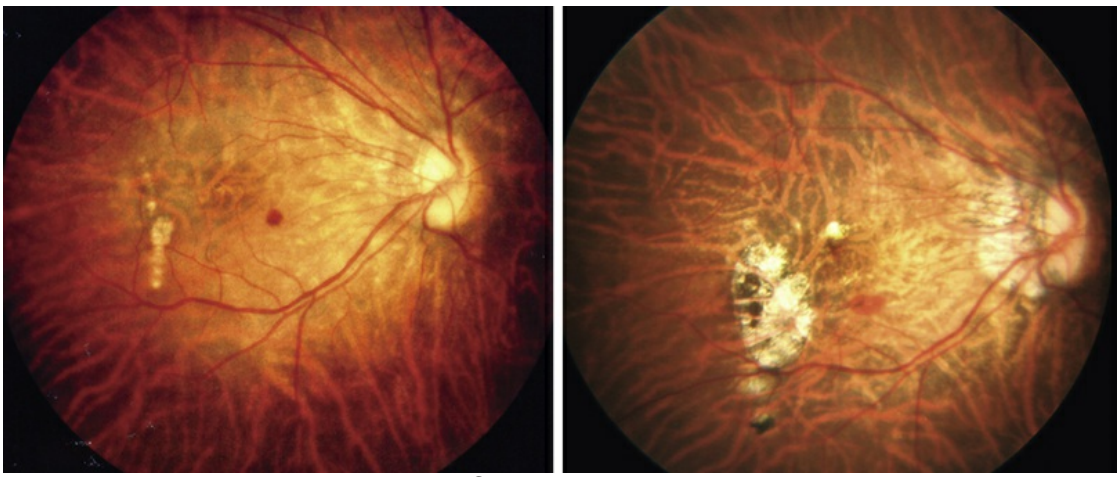

FIG. 71.12 Progression from lacquer cracks to patchy chorioretinal atrophy. Right fundus shows vertically linear lacquer cracks temporal to the fovea (left). Fifteen years later, the width of lacquer cracks has

widened and has progressed to patchy atrophy (right).

As linear lesions that need to be differentiated from lacquer cracks, myopic stretch lines (Fig. 71.13) were reported by Shinohara et al.[91] Myopic stretch lines are considered to represent the proliferation of RPE cells indented by large choroidal vessels in the area with severe diffuse atrophy.

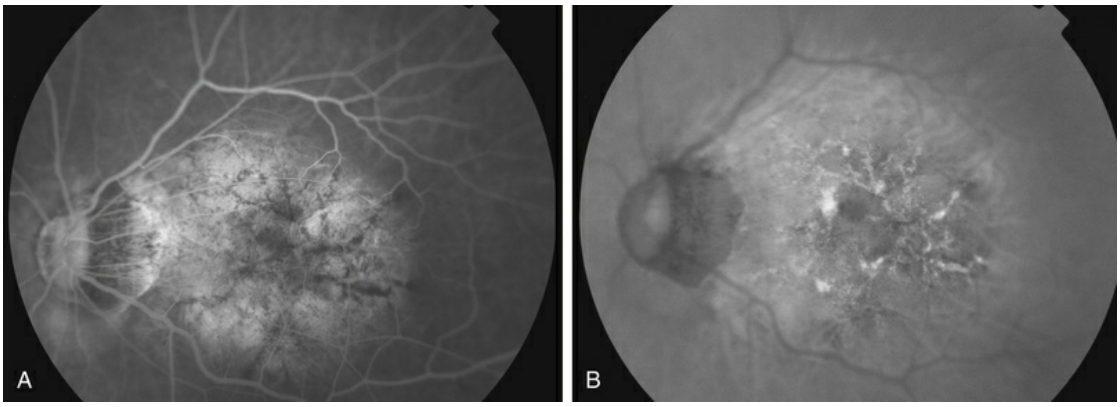

FIG. 71.13 Myopic stretch lines. In fluorescein angiogram (A), the lesions are observed as radial hypofluorescence. In fundus autofluorescence (B), the lesions are seen as a mixture of hyper- and hypoautofluorescence.

Myopic Choroidal Neovascularization

Macular CNV is a one of the most frequent complications that reduce the central vision in patients with pathologic myopia (Fig. 71.14). Myopic CNV develops in 10% of highly myopic patients,[68] and 30% of the patients who have a CNV in one eye eventually develop CNV in the other eye. Due to a thin, stretched fundus, the bleeding does not usually overlie the CNV, and therefore CNV is easily observed ophthalmoscopically. Myopic CNV is almost always so-called classic CNV, and CNV shows distinct hyperfluorescence throughout the entire angiographic phase. Especially for small CNV, fluorescein angiography is a powerful tool to detect CNV.

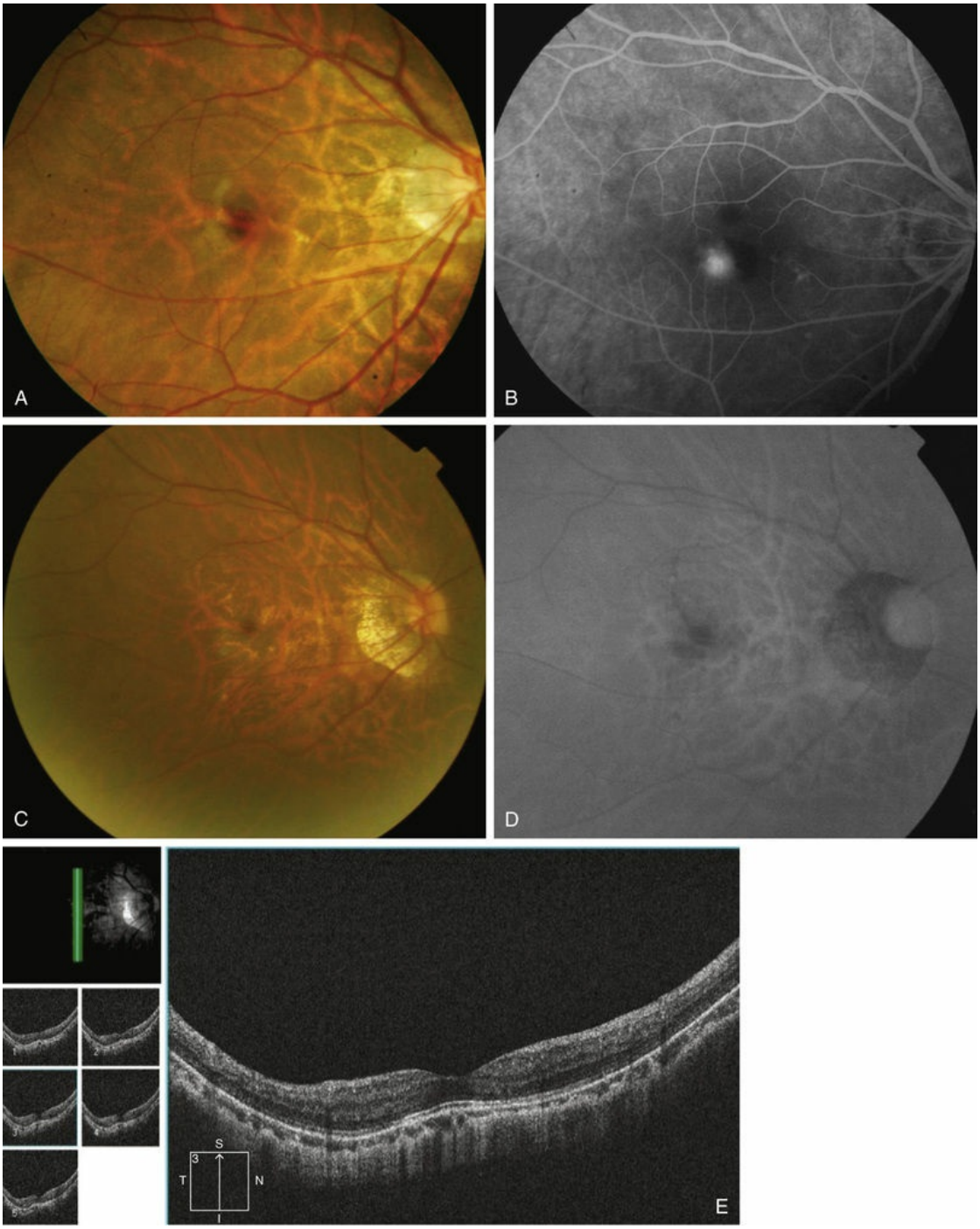

FIG. 71.14 Myopic choroidal neovascularization (CNV) treated with anti-vascular endothelial growth factor. At onset (A,B) small CNV is observed temporal to the fovea in fundus photo (A) and in fluorescein angiogram (B). The best corrected visual acuity (BCVA) is 0.7. Six years after a single injection of intravitreal bevacizumab (C–E), the CNV is barely detectable in fundus image (C) and in optical coherence tomography image (E). Fundus autofluorescence does not show a

development of CNV-related macular atrophy (D). The BCVA is 1.0.

Due to the low activity of the CNV, myopic CNV does not show hyperfluorescence by indocyanine green angiography in most cases. OCT shows CNV as an elevated lesion in the subretinal space; however, most eyes with myopic CNV do not show exudative changes like retinal edema or retinal detachment. Thus, OCT does not differentiate subretinal bleeding with or without CNV in eyes with pathologic myopia.

Natural Course of Myopic CNV

Myopic CNV is not intensely active, and thus has a tendency to regress spontaneously, and progresses from an active phase to a scar phase. In the scar phase, the CNV is covered by proliferated RPE cells and is observed as a dark pigmented spot (Fuchs' spot). After CNV regression, well-defined chorioretinal atrophy gradually develops and enlarges around the Fuchs' spot, and this causes a progressive visual decrease in the long term. This phase is called atrophic CNV.

The prognosis of myopic CNV is poor. A natural history study with 10-year follow-up showed that, at the onset of CNV, 70% had a visual acuity better than 20/200 and 22% had a visual acuity better than 20/40. Three years after the onset of CNV, 56% retained a visual acuity of better than 20/200. At 5 and 10 years after onset, however, visual acuity dropped to 20/200 or less in 89% and 96%, respectively.[37,77] The mechanism by which chorioretinal atrophy develops and enlarges around the regressed CNV in eyes with pathologic myopia is not clear. Because chorioretinal atrophy around the CNV affects the final visual outcome of eyes with myopic CNV, we need to determine the effect of treatment against myopic CNV on chorioretinal atrophy development.

Current Treatment of Myopic CNV

Anti-vascular endothelial growth factor (VEGF) therapy has recently been used as the first-line therapy to treat myopic CNV. Large clinical trials examining the effectiveness and the safety of

ranibizumab and aflibercept have been reported in the REPAIR study,[92] the RADIANCE study,[9] and the MYRROR study.[5] In the REPAIR study,[92] 65 patients with myopic CNV treated with ranibizumab were enrolled across 12 sites. At 12 months, 86% of patients showed improvement in mean score of the best corrected visual acuity (BCVA) and 37% of patients achieved a BCVA gain of ≥15 letters. In the RADIANCE study,[9] 277 patients with visual impairment due to myopic CNV were enrolled and showed that ranibizumab treatment (either guided by vision stabilization or guided by disease stability) was superior to photodynamic therapy on mean average BCVA change from baseline to month 3 through month 12. In the MYRROR study,[5] a total of 122 patients with myopic CNV were assigned either to aflibercept or sham injection. The patients in the intravitreal aflibercept group gained significantly more vision at week 24 and 48 than those in the sham injection group.

Anti-VEGF therapies are especially effective for nonsubfoveal CNV.[93] Some patients with nonsubfoveal myopic CNV show a complete disappearance of CNV over the long term without developing CNV-related macular atrophy (see Fig. 71.13). However, some patients show a development and enlargement of CNV-related macular atrophy with time (Fig. 71.15). The long-term visual outcome of anti-VEGF therapies need to be clarified, since some studies showed a decreased vision in the long term.[6,94] The influence of anti-VEGF therapies on the development of chorioretinal atrophy around myopic CNV also needs to be evaluated. The treatment guideline for myopic CNV has been proposed by Wong et al. (Fig. 71.16).[95]

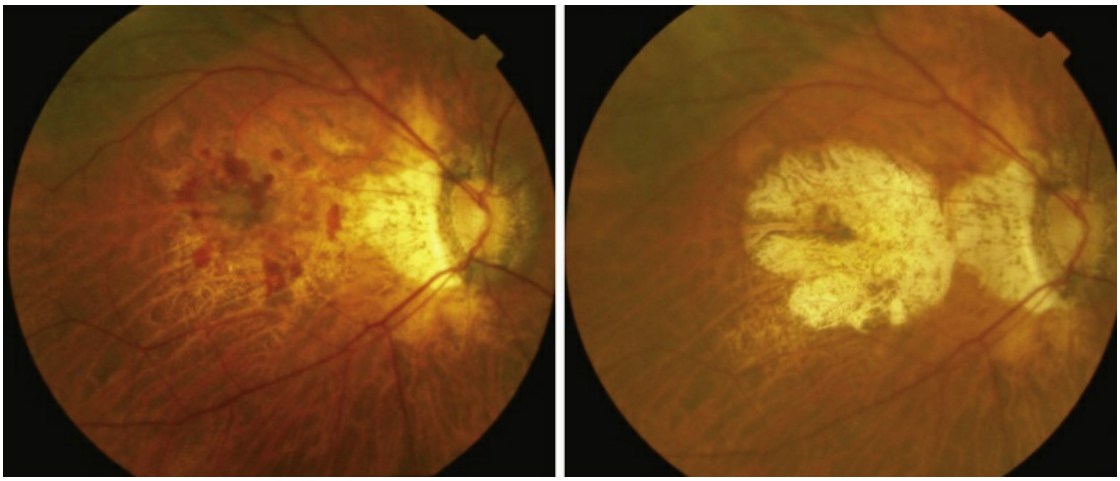

FIG. 71.15 Long-term development of macular atrophy in the eyes treated with anti-vascular endothelial growth factor. At onset (left), the choroidal neovascularization (CNV) accompanying with hemorrhage is observed. The best corrected visual acuity (BCVA) is 0.2. Six years after a single injection of intravitreal bevacizumab (right), the CNV has shrunken and is seen as a tiny Fuchs' spot. However, a large chorioretinal atrophy has developed, and the BCVA has decreased to 0.08.

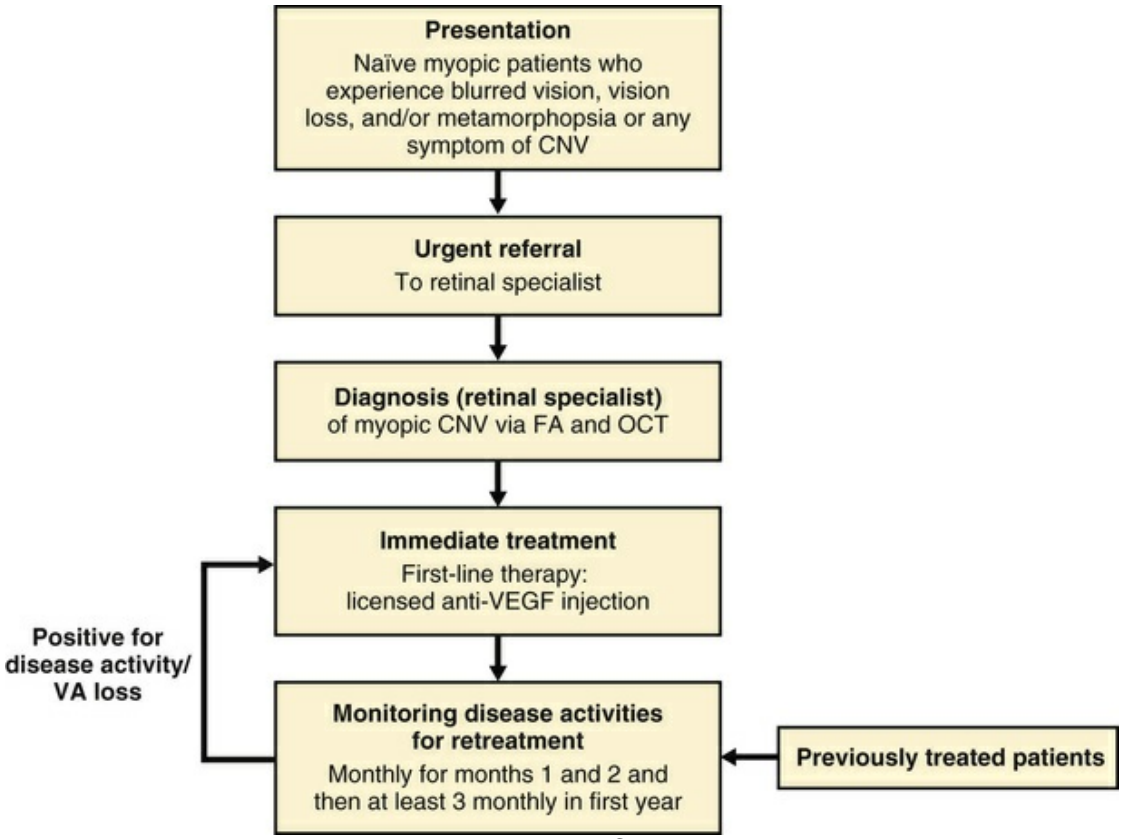

FIG. 71.16 Treatment algorithm for myopic choroidal neovascularization (myopic CNV). *FA,* fluorescein angiography; *OCT,* optical coherence tomography; *VA,* visual acuity; *VEGF,* vascular endothelial growth factor. (With permission from Wong TY, Ohno-Matsui K, Leveziel N, et al. Myopic choroidal neovascularisation: current concepts and update on clinical management. Br J Ophthalmol 2015;99(3):289-96.)

Other Macular Lesions

Dome-Shaped Macula (Fig. 71.17)

The dome-shaped macula (DSM) was first described by Gaucher et al.[92] as a convex protrusion of the macula in highly myopic eyes detected in OCT images. Imamura and Spaide[84] used EDI-OCT and showed that the DSM resulted from a relative localized thickening of the sclera under the macula in highly myopic eyes. Caillaux et al.[82] classified DSM into round dome; horizontal oval-shaped dome; and vertical oval-shaped dome.

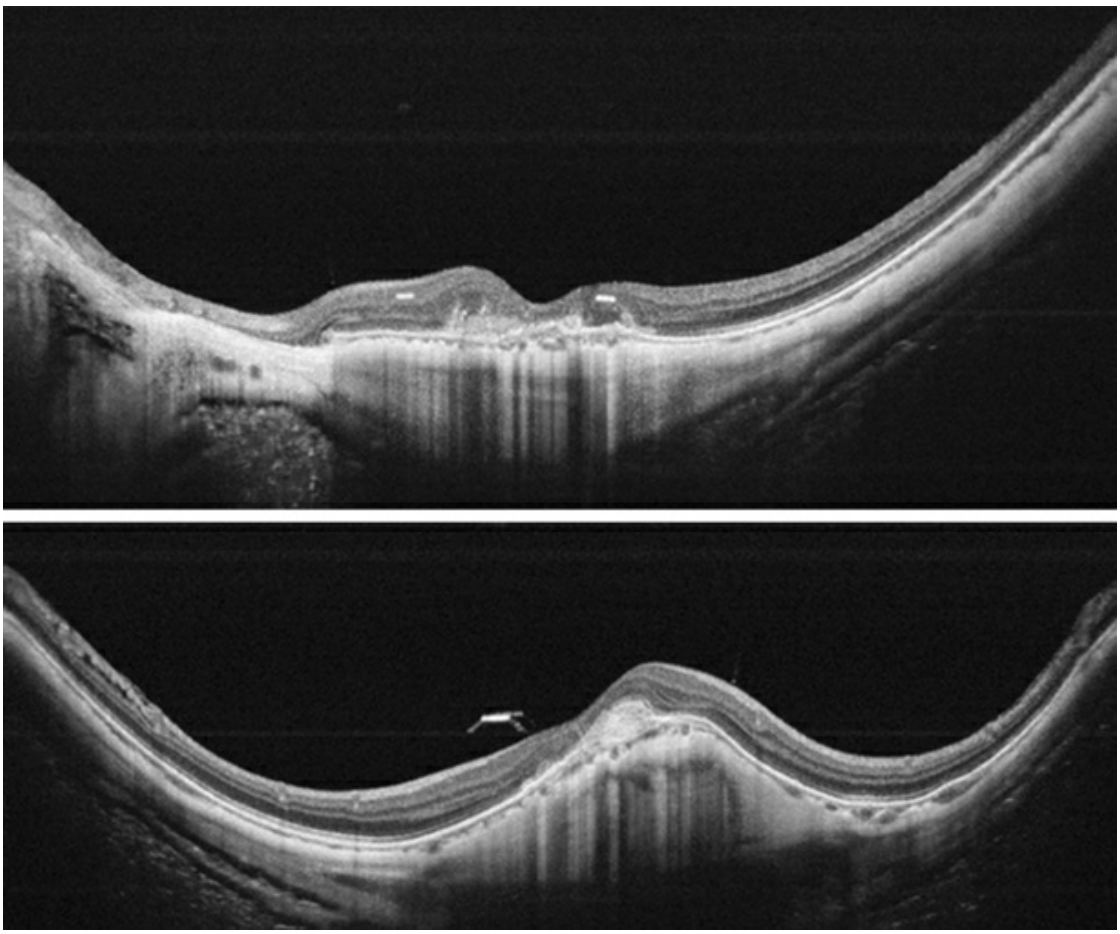

FIG. 71.17 Dome-shaped macula (DSM). In optical coherence tomographic images, the dome-shaped protrusion is obvious in vertical section across the macula (bottom image) due to the subfoveal scleral thickening. DSM is not obvious in horizontal section (top image). The choroidal neovascularization is observed at the top of the dome.

Liang, Ohno-Matsui, and coworkers[96] examined a large series of highly myopic patients and showed that DSM was found in about 20% of highly myopic eyes, suggesting that DSM was a common complication of pathologic myopia. Macular complications such as serous retinal detachment and macular retinoschisis have been reported to occur in eyes with DSM.[96]

Myopic Traction Maculopathy

Myopic macular retinoschisis (also known as myopic foveoschisis[69] or myopic traction maculopathy[70]) was first identified in 1999.[8] Myopic macular retinoschisis is found in 9% of highly myopic eyes

with posterior staphyloma,[71] and 50% of patients progress to more serious complications such as full-thickness macular hole or macular retinal detachment within 2 years.[72] Myopic macular retinoschisis is considered to be caused by various factors. The rigidity of the internal limiting membrane (ILM) can induce significant traction on the retina.[4] OCT examinations of serial sections along the entire posterior vascular arcade showed that the paravascular abnormalities, such as paravascular lamellar holes,[73] vascular microfolds,[73–75] and paravascular retinal cysts,[73] are frequently found in eyes with myopic macular retinoschisis. Although the mechanism of the development of this condition is not fully clear, the glial cells such as astrocytes, which exist abundantly around the retinal vessels, can migrate and proliferate through the paravascular lamellar holes. These cells can produce collagen and facilitate the proliferative and contractile response of ILM. Studies have shown that vitrectomy is useful to treat myopic macular retinoschisis in some patients.[69,76] The development of postoperative or intraoperative full-thickness macular holes is a serious complication. To avoid the mechanical damage to the fovea by ILM peeling, nonfoveolar peeling[15] or foveal-sparing ILM peeling[11] (Fig. 71.18) have been used with a good surgical outcome.

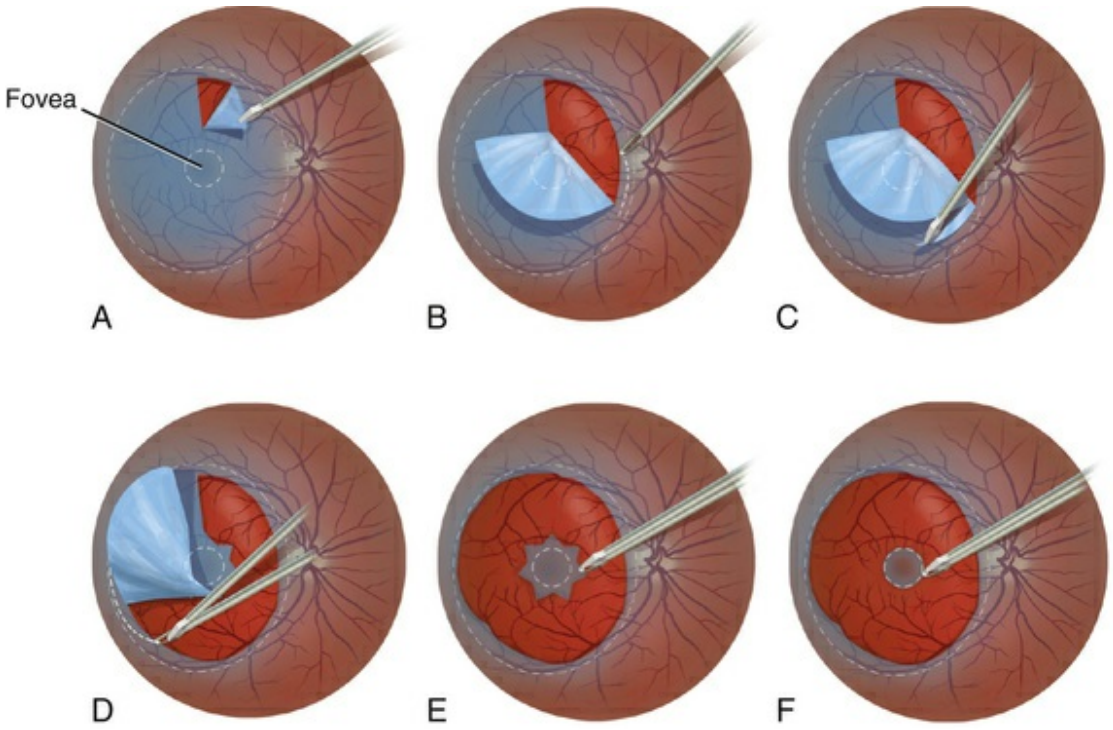

FIG. 71.18 Schematic drawings of fovea-sparing internal limiting membrane (ILM) peeling. Start ILM peeling away from the central fovea. Proceed with the ILM peeling. When the peeled ILM flap comes close to the central fovea, stop and start ILM peeling from a new site. Proceed with ILM peeling from the new site with special attention not to peel the ILM around the central fovea. Start the ILM peeling from several new sites and proceed to peel ILM from the entire macular area away from the central fovea. Trim the ILM that remains on and around the fovea with a vitreous cutter.
(With permission from Shimada N, Sugamoto Y, Ogawa M, et al. Fovea-sparing internal limiting membrane peeling for myopic traction maculopathy. Am J Ophthalmol 2012;24:24.)

Conclusion

Pathologic myopia is a major cause of visual impairment worldwide, and associated visual loss is due to various lesions of myopic macular degeneration that develop secondary to posterior staphyloma formation and progressive thinning of the RPE-choroid with age in addition to an increase of axial length. Among various lesions of myopic macular degeneration, myopic CNV can be treated by application of anti-VEGF therapy or photodynamic therapy. Also, the advance of OCT technology has enabled the evaluation of pathogenic mechanism of myopic macular retinoschisis, and vitrectomy has been proven useful to treat this condition. Further studies evaluating the long-term outcome of anti-VEGF therapy for myopic CNV and vitrectomy to manage myopic macular retinoschisis are expected.

References

1. Ohno-Matsui K. Myopic chorioretinal atrophy. Spaide RF, Ohno-Matsui K, Yannuzzi LA. *Pathologic myopia*. Springer: New York; 2014.
2. Spaide RF. Choroidal neovascularization. Spaide RF, Ohno-Matsui K, Yannuzzi LA. *Pathologic myopia*. Springer: New

York; 2014.
3. Freitas-da-Costa P, Pinheiro-Costa J, Carvalho B, et al. Anti-VEGF therapy in myopic choroidal neovascularization: long-term results. *Ophthalmologica*. 2014;232(1):57–63.
4. Oishi A, Yamashiro K, Tsujikawa A, et al. Long-term effect of intravitreal injection of anti-VEGF agent for visual acuity and chorioretinal atrophy progression in myopic choroidal neovascularization. *Graefes Arch Clin Exp Ophthalmol*. 2013;251(1):1–7.
5. Ikuno Y, Ohno-Matsui K, Wong TY, et al. Intravitreal aflibercept injection in patients with myopic choroidal neovascularization: the MYRROR Study. *Ophthalmology*. 2015;122(6):1220–1227.
6. Ruiz-Moreno JM, Montero JA, Araiz J, et al. Intravitreal anti-vascular endothelial growth factor therapy for choroidal neovascularization secondary to pathologic myopia: six years outcome. *Retina*. 2015;35(12):2450–2456.
7. Adatia FA, Luong M, Munro M, et al. The other CNVM: a review of myopic choroidal neovascularization treatment in the age of anti-vascular endothelial growth factor agents. *Surv Ophthalmol*. 2015;60(3):204–215.
8. Wong TY, Ferreira A, Hughes R, et al. Epidemiology and disease burden of pathologic myopia and myopic choroidal neovascularization: an evidence-based systematic review. *Am J Ophthalmol*. 2014;157(1):9–25.e12.
9. Wolf S, Balciuniene VJ, Laganovska G, et al. RADIANCE: a randomized controlled study of ranibizumab in patients with choroidal neovascularization secondary to pathologic myopia. *Ophthalmology*. 2014;121(3):682–692.e2.
10. Shimada N, Tanaka Y, Tokoro T, et al. Natural course of myopic traction maculopathy and factors associated with progression or resolution. *Am J Ophthalmol*. 2013;156(5):948–957.e1.
11. Shimada N, Sugamoto Y, Ogawa M, et al. Fovea-sparing internal limiting membrane peeling for myopic traction maculopathy. *Am J Ophthalmol*. 2012;24:24.
12. Panozzo G, Mercanti A. Vitrectomy for myopic traction maculopathy. *Arch Ophthalmol*. 2007;125(6):767–772.

13. Johnson MW. Myopic traction maculopathy: pathogenic mechanisms and surgical treatment. *Retina*. 2012;32(Suppl. 2):S205–10.
14. Futagami S, Inoue M, Hirakata A. Removal of internal limiting membrane for recurrent myopic traction maculopathy. *Clin Experiment Ophthalmol*. 2008;36(8):782–785.
15. Ho TC, Chen MS, Huang JS, et al. Foveola nonpeeling technique in internal limiting membrane peeling of myopic foveoschisis surgery. *Retina*. 2012;32(3):631–634.
16. Ho TC, Yang CM, Huang JS, et al. Long-term outcome of foveolar internal limiting membrane nonpeeling for myopic traction maculopathy. *Retina*. 2014;34(9):1833–1840.
17. Kobayashi H, Kishi S. Vitreous surgery for highly myopic eyes with foveal detachment and retinoschisis. *Ophthalmology*. 2003;110(9):1702–1707.
18. Ikuno Y, Sayanagi K, Ohji M, et al. Vitrectomy and internal limiting membrane peeling for myopic foveoschisis. *Am J Ophthalmol*. 2004;137(4):719–724.
19. Dandona R, Dandona L, Naduvilath TJ, et al. Refractive errors in an urban population in Southern India: the Andhra Pradesh Eye Disease Study. *Invest Ophthalmol Vis Sci*. 1999;40(12):2810–2818.
20. Saw SM, Chan YH, Wong WL, et al. Prevalence and risk factors for refractive errors in the Singapore Malay Eye Survey. *Ophthalmology*. 2008;115(10):1713–1719.
21. Wong TY, Foster PJ, Hee J, et al. Prevalence and risk factors for refractive errors in adult Chinese in Singapore. *Invest Ophthalmol Vis Sci*. 2000;41(9):2486–2494.
22. Saw SM, Gazzard G, Koh D, et al. Prevalence rates of refractive errors in Sumatra, Indonesia. *Invest Ophthalmol Vis Sci*. 2002;43(10):3174–3180.
23. Bourne RR, Dineen BP, Ali SM, et al. Prevalence of refractive error in Bangladeshi adults: results of the National Blindness and Low Vision Survey of Bangladesh. *Ophthalmology*. 2004;111(6):1150–1160.
24. Gupta A, Casson RJ, Newland HS, et al. Prevalence of refractive error in rural Myanmar: the Meiktila Eye Study.

Ophthalmology. 2008;115(1):26–32.
25. Wickremasinghe S, Foster PJ, Uranchimeg D, et al. Ocular biometry and refraction in Mongolian adults. *Invest Ophthalmol Vis Sci*. 2004;45(3):776–783.
26. Xu L, Li J, Cui T, et al. Refractive error in urban and rural adult Chinese in Beijing. *Ophthalmology*. 2005;112(10):1676–1683.
27. Sawada A, Tomidokoro A, Araie M, et al. Refractive errors in an elderly Japanese population: the Tajimi study. *Ophthalmology*. 2008;115(2):363–370.e3.
28. Wang Q, Klein BE, Klein R, et al. Refractive status in the Beaver Dam Eye Study. *Invest Ophthalmol Vis Sci*. 1994;35(13):4344–4347.
29. Katz J, Tielsch JM, Sommer A. Prevalence and risk factors for refractive errors in an adult inner city population. *Invest Ophthalmol Vis Sci*. 1997;38(2):334–340.
30. Attebo K, Ivers RQ, Mitchell P. Refractive errors in an older population: the Blue Mountains Eye Study. *Ophthalmology*. 1999;106(6):1066–1072.
31. Wensor M, McCarty CA, Taylor HR. Prevalence and risk factors of myopia in Victoria, Australia. *Arch Ophthalmol*. 1999;117(5):658–663.
32. Tarczy-Hornoch K, Ying-Lai M, Varma R. Myopic refractive error in adult Latinos: the Los Angeles Latino Eye Study. *Invest Ophthalmol Vis Sci*. 2006;47(5):1845–1852.
33. Buch H, Vinding T, La Cour M, et al. Prevalence and causes of visual impairment and blindness among 9980 Scandinavian adults: the Copenhagen City Eye Study. *Ophthalmology*. 2004;111(1):53–61.
34. Cotter SA, Varma R, Ying-Lai M, et al. Causes of low vision and blindness in adult Latinos: the Los Angeles Latino Eye Study. *Ophthalmology*. 2006;113(9):1574–1582.
35. Xu L, Wang Y, Li Y, et al. Causes of blindness and visual impairment in urban and rural areas in Beijing: the Beijing Eye Study. *Ophthalmology*. 2006;113(7):1134.e1–1134.e11.
36. Klaver CC, Wolfs RC, Vingerling JR, et al. Age-specific prevalence and causes of blindness and visual impairment in an older population: the Rotterdam Study. *Arch*

Ophthalmol. 1998;116(5):653–658.
37. Cedrone C, Culasso F, Cesareo M, et al. Incidence of blindness and low vision in a sample population: the Priverno Eye Study, Italy. *Ophthalmology*. 2003;110(3):584–588.
38. Hsu WM, Cheng CY, Liu JH, et al. Prevalence and causes of visual impairment in an elderly Chinese population in Taiwan: the Shihpai Eye Study. *Ophthalmology*. 2004;111(1):62–69.
39. Hayashi K, Ohno-Matsui K, Shimada N, et al. Long-term pattern of progression of myopic maculopathy: a natural history study. *Ophthalmology*. 2010;117(8):1595–1611.
40. Vongphanit J, Mitchell P, Wang JJ. Prevalence and progression of myopic retinopathy in an older population. *Ophthalmology*. 2002;109(4):704–711.
41. Liu HH, Xu L, Wang YX, et al. Prevalence and progression of myopic retinopathy in Chinese adults: the Beijing Eye Study. *Ophthalmology*. 2010;117(9):1763–1768.
42. Panda-Jonas S, Jonas JB, Jakobczyk-Zmija M. Retinal photoreceptor density decreases with age. *Ophthalmology*. 1995;102(12):1853–1859.
43. Gao H, Hollyfield JG. Aging of the human retina. Differential loss of neurons and retinal pigment epithelial cells. *Invest Ophthalmol Vis Sci*. 1992;33(1):1–17.
44. Eriksson U, Alm A. Macular thickness decreases with age in normal eyes: a study on the macular thickness map protocol in the Stratus OCT. *Br J Ophthalmol*. 2009;93(11):1448–1452.
45. Alamouti B, Funk J. Retinal thickness decreases with age: an OCT study. *Br J Ophthalmol*. 2003;87(7):899–901.
46. Lim LS, Saw SM, Jeganathan VS, et al. Distribution and determinants of ocular biometric parameters in an Asian population: the Singapore Malay eye study. *Invest Ophthalmol Vis Sci*. 2010;51(1):103–109.
47. Fotedar R, Wang JJ, Burlutsky G, et al. Distribution of axial length and ocular biometry measured using partial coherence laser interferometry (IOL Master) in an older white population. *Ophthalmology*. 2010;117(3):417–423.
48. Hayashi K, Ohno-Matsui K, Shimada N, et al. Long-term

results of photodynamic therapy for choroidal neovascularization in Japanese patients with pathologic myopia. *Am J Ophthalmol*. 2011;151(1):137–147.e1.
49. Gharbiya M, Giustolisi R, Allievi F, et al. Choroidal neovascularization in pathologic myopia: intravitreal ranibizumab versus bevacizumab – a randomized controlled trial. *Am J Ophthalmol*. 2010;149(3):458–464.e1.
50. Yoshida T, Ohno-Matsui K, Yasuzumi K, et al. Myopic choroidal neovascularization: a 10-year follow-up. *Ophthalmology*. 2003;110(7):1297–1305.
51. Li YJ, Guggenheim JA, Bulusu A, et al. An international collaborative family-based whole-genome linkage scan for high-grade myopia. *Invest Ophthalmol Vis Sci*. 2009;50(7):3116–3127.
52. Solouki AM, Verhoeven VJ, van Duijn CM, et al. A genome-wide association study identifies a susceptibility locus for refractive errors and myopia at 15q14. *Nat Genet*. 2010;42(10):897–901.
53. Hysi PG, Young TL, Mackey DA, et al. A genome-wide association study for myopia and refractive error identifies a susceptibility locus at 15q25. *Nat Genet*. 2010;42(10):902–905.
54. Verhoeven VJ, Hysi PG, Saw SM, et al. Large scale international replication and meta-analysis study confirms association of the 15q14 locus with myopia: the CREAM consortium. *Hum Genet*. 2012;131(9):1467–1480.
55. Verhoeven VJ, Hysi PG, Wojciechowski R, et al. Genome-wide meta-analyses of multiancestry cohorts identify multiple new susceptibility loci for refractive error and myopia. *Nat Genet*. 2013;45(3):314–318.
56. Nakanishi H, Gotoh N, Yamada R, et al. ARMS2/HTRA1 and CFH polymorphisms are not associated with choroidal neovascularization in highly myopic eyes of the elderly Japanese population. *Eye (Lond)*. 2010;24(6):1078–1084.
57. Parmeggiani F, Gemmati D, Costagliola C, et al. Impact of coagulation-balance gene predictors on efficacy of photodynamic therapy for choroidal neovascularization in pathologic myopia. *Ophthalmology*. 2010;117(3):517–523.

58. Curtin BJ. Ocular findings and complications. Curtin BJ. *The myopias*. Harper and Row: New York; 1985.
59. Curtin BJ, Karlin DB. Axial length measurements and fundus changes of the myopic eye. I. The posterior fundus. *Trans Am Ophthalmol Soc*. 1970;68:312–334.
60. Tokoro T. *Atlas of Posterior fundus changes in pathologic myopia*. Springer: Tokyo; 1998:101–123.
61. Tokoro T. *Atlas of posterior fundus changes in pathologic myopia*. Springer-Verlag: Tokyo; 1998:5–22.
62. Hsiang HW, Ohno-Matsui K, Shimada N, et al. Clinical characteristics of posterior staphyloma in eyes with pathologic myopia. *Am J Ophthalmol*. 2008;146(1):102–110.
63. Kobayashi K, Ohno-Matsui K, Kojima A, et al. Fundus characteristics of high myopia in children. *Jpn J Ophthalmol*. 2005;49(4):306–311.
64. Steidl SM, Pruett RC. Macular complications associated with posterior staphyloma. *Am J Ophthalmol*. 1997;123(2):181–187.
65. Vurgese S, Panda-Jonas S, Jonas JB. Scleral thickness in human eyes. *PLoS ONE*. 2012;7(1):6.
66. Ohno-Matsui K, Akiba M, Modegi T, et al. Association between shape of sclera and myopic retinochoroidal lesions in patients with pathologic myopia. *Invest Ophthalmol Vis Sci*. 2012;53(10):6046–6061.
67. Fujiwara T, Imamura Y, Margolis R, et al. Enhanced depth imaging optical coherence tomography of the choroid in highly myopic eyes. *Am J Ophthalmol*. 2009;148(3):445–450.
68. Wiesel TN, Raviola E. Myopia and eye enlargement after neonatal lid fusion in monkeys. *Nature*. 1977;266(5597):66–68.
69. Raviola E, Wiesel TN. An animal model of myopia. *N Engl J Med*. 1985;312(25):1609–1615.
70. Wallman J, Turkel J, Trachtman J. Extreme myopia produced by modest change in early visual experience. *Science*. 1978;201(4362):1249–1251.
71. Troilo D. Experimental studies of emmetropization in the chick. *Ciba Found Symp*. 1990;155:89–102 [discussion 14].
72. Tkatchenko TV, Shen Y, Tkatchenko AV. Mouse experimental myopia has features of primate myopia. *Invest*

Ophthalmol Vis Sci. 2010;51(3):1297–1303.
73. Barathi VA, Boopathi VG, Yap EP, et al. Two models of experimental myopia in the mouse. *Vision Res*. 2008;48(7):904–916.
74. Cases O, Joseph A, Obry A, et al. Foxg1-Cre mediated Lrp2 inactivation in the developing mouse neural retina, ciliary and retinal pigment epithelia models congenital high myopia. *PLoS ONE*. 2015;10(6):e0129518.
75. Hirata A, Negi A. Lacquer crack lesions in experimental chick myopia. *Graefes Arch Clin Exp Ophthalmol*. 1998;236(2):138–145.
76. Brand C, Schaeffel F, Feldkaemper MP. A microarray analysis of retinal transcripts that are controlled by image contrast in mice. *Mol Vis*. 2007;13:920–932.
77. Schippert R, Burkhardt E, Feldkaemper M, et al. Relative axial myopia in Egr-1 (ZENK) knockout mice. *Invest Ophthalmol Vis Sci*. 2007;48(1):11–17.
78. Yeh LK, Liu CY, Kao WW, et al. Knockdown of zebrafish lumican gene (zlum) causes scleral thinning and increased size of scleral coats. *J Biol Chem*. 2010;285(36):28141–28155.
79. Veth KN, Willer JR, Collery RF, et al. Mutations in zebrafish lrp2 result in adult-onset ocular pathogenesis that models myopia and other risk factors for glaucoma. *PLoS Genet*. 2011;7(2):e1001310.
80. Spaide RF. *Staphyloma: Part 1*. Springer: New York; 2013:167–176.
81. Gaucher D, Erginay A, Lecleire-Collet A, et al. Dome-shaped macula in eyes with myopic posterior staphyloma. *Am J Ophthalmol*. 2008;145(5):909–914.
82. Caillaux V, Gaucher D, Gualino V, et al. Morphologic characterization of dome-shaped macula in myopic eyes with serous macular detachment. *Am J Ophthalmol*. 2013;156(5):958–967.
83. Ellabban AA, Tsujikawa A, Muraoka Y, et al. Dome-shaped macular configuration: longitudinal changes in the sclera and choroid by swept-source optical coherence tomography over two years. *Am J Ophthalmol*. 2014;158(5):1062–1070.
84. Imamura Y, Iida T, Maruko I, et al. Enhanced depth imaging

optical coherence tomography of the sclera in dome-shaped macula. *Am J Ophthalmol*. 2011;151(2):297–302.
85. Ohno-Matsui K, Akiba M, Moriyama M. Macular pits and scleral dehiscence in highly myopic eyes with macular chorioretinal atrophy. *Retin Cases Brief Rep*. 2013;7(4):334–337.
86. Pedinielli A, Souied EH, Perrenoud F, et al. In vivo visualization of perforating vessels and focal scleral ectasia in pathological myopia. *Invest Ophthalmol Vis Sci*. 2013;54(12):7637–7643.
87. Curtin BJ. The posterior staphyloma of pathologic myopia. *Trans Am Ophthalmol Soc*. 1977;75:67–86.
88. Ohno-Matsui K. Proposed classification of posterior staphylomas based on analyses of eye shape by three-dimensional magnetic resonance imaging. *Ophthalmology*. 2014;121(9):1798–1809.
89. Ohno-Matsui K, Kawasaki R, Jonas JB, et al. International photographic classification and grading system for myopic maculopathy. *Am J Ophthalmol*. 2015;159(5):877–883.e7.
90. Grossniklaus HE, Green WR. Pathologic findings in pathologic myopia. *Retina*. 1992;12(2):127–133.
91. Shinohara K, Moriyama M, Shimada N, et al. Myopic stretch lines: linear lesions in fundus of eyes with pathologic myopia that differ from lacquer cracks. *Retina*. 2014;34(3):461–469.
92. Tufail A, Narendran N, Patel PJ, et al. Ranibizumab in myopic choroidal neovascularization: the 12-month results from the REPAIR study. *Ophthalmology*. 2013;120(9):1944–1945.e1.
93. Hayashi K, Shimada N, Moriyama M, et al. Two-year outcomes of intravitreal bevacizumab for choroidal neovascularization in Japanese patients with pathologic myopia. *Retina*. 2012;32(4):687–695.
94. Sarao V, Veritti D, Macor S, et al. Intravitreal bevacizumab for choroidal neovascularization due to pathologic myopia: long-term outcomes. *Graefes Arch Clin Exp Ophthalmol*. 2016;254(3):445–454.
95. Wong TY, Ohno-Matsui K, Leveziel N, et al. Myopic

choroidal neovascularisation: current concepts and update on clinical management. *Br J Ophthalmol*. 2015;99(3):289–296.
96. Liang IC, Shimada N, Tanaka Y, et al. Comparison of clinical features in highly myopic eyes with and without a dome-shaped macula. *Ophthalmology*. 2015;122(8):1591–1600.

72

Angioid Streaks

Linda A. Lam

Introduction

The appearance of angioid streaks was initially described by Doyne in 1889 as irregular and radiating lines extending from the optic nerve to the peripheral retina found in an eye with retinal hemorrhages after blunt trauma.[1] The term “angioid streaks” originated as the ophthalmoscopic appearance of the lines was similar to that of blood vessels.[2] Histopathologic studies found that angioid streaks represent irregular dehiscences in the collagenous and elastic portion of Bruch's membrane.[3,4] Associations have been found between angioid streaks and systemic conditions such as pseudoxanthoma elasticum (Grönbald–Strandberg syndrome),[5–7] osteitis deformans (Paget disease),[5,8–10] blood dyscrasias such as sickle-cell anemia,[5,11–13] fibrodysplasia hyperelastica (Ehlers–Danlos syndrome),[5,14] and acromegaly.[5,15] However, angioid streaks may also occur in patients without associated systemic disease.[16] Patients with angioid streaks usually are asymptomatic unless complications such as macular choroidal neovascularization (CNV) develop.[5,16] In cases of macular involvement the prognosis is often poor, with most eyes progressing to legal blindness without treatment.[5,6,16] Multiple therapeutic strategies have been used to treat CNV secondary to angioid streaks, including argon laser photocoagulation,[17–19] transpupillary thermotherapy,[20] photodynamic therapy,[21–23] surgical intervention,[24–26] intravitreal anti-vascular endothelial growth factor (VEGF) treatments with pegaptanib,[27] bevacizumab,[28–34] or ranibizumab,[35-40] aflibercept,[41] and combination therapy.[42–44]

Histopathology

Angioid streaks represent discrete irregular breaks in Bruch's membrane and are often associated with atrophic changes of the overlying retinal pigment epithelium (RPE) and calcific degeneration.[4] Klien proposed a dual mechanism for the development of angioid streaks, including (1) a primary abnormality in the fibers of Bruch's membrane and (2) increased deposits of metal salts or an increasing tendency for their pathologic position.[3] The deposition of calcium may cause Bruch's membrane to be more brittle and to develop choroidal rupture.[4] Immunohistochemical studies show significant calcium deposition and infiltration of vascularized tissue above the RPE from Bruch's membrane in the area of CNV in an eye with angioid streaks.[45]

Tissue metalloproteinase, specifically MMP-9, was found in high concentrations in the excised Bruch's membrane in an area of CNV in an eye with angioid streaks. MMP-9 is known to induce basement membrane destruction and angiogenesis.[45]

In the early stages, angioid streaks are partial breaks of the thickened and calcified Bruch's membrane with thinning of the RPE, events that do not cause anatomic changes in the overlying retinal layers.[46] Subsequently, a full-thickness defect of the Bruch's membrane may occur followed by atrophy of the choriocapillaris, RPE, and photoreceptors. Fibrovascular proliferation from the choroid may occur through the Bruch's membrane break, resulting in CNV and subsequent development of a disciform scar.[4,10,46] This process usually results in slowly progressive macular changes and vision loss. Sudden vision loss can result from a serous or hemorrhagic detachment around the CNV or after mild trauma leading to choroidal rupture and submacular hemorrhage resulting from the brittleness of Bruch's membrane.[4,10]

Systemic Associations

Angioid streaks have been most commonly associated with systemic conditions such as pseudoxanthoma elasticum (Grönbald–Strandberg syndrome),[5–7] osteitis deformans (Paget disease),[5,8–10] fibrodysplasia hyperelastica (Ehlers–Danlos syndrome),[5,14]

acromegaly,[5,15] Marfan syndrome,[6] and blood dyscrasias such as sickle-cell anemia,[11,12] thalassemia,[6] and spherocytosis.[6] Angioid streaks have also been described in patients with the following conditions: alpha-beta-lipoproteinemia, acquired hemolytic anemia, hemochromatosis, hypertension, diabetes, hypercalcinosis, hyperphosphatemia, diffuse lipomatosis, Sturge–Weber syndrome, tuberous sclerosis, neurofibromatosis, microsomia, epilepsy, senile elastosis, cutaneous calcinosis, and trauma[5,6,16] (Box 72.1).

Box 72.1

Systemic Conditions Associated With Angioid Streaks

- Pseudoxanthoma elasticum (Grönbald–Strandberg syndrome)
- Osteitis deformans (Paget disease)
- Fibrodysplasia hyperelastica (Ehlers–Danlos syndrome)
- Acromegaly
- Marfan syndrome
- Sickle-cell anemia
- Thalassemia
- Spherocytosis
- Acquired hemolytic anemia
- Hemochromatosis
- Alpha-beta-lipoproteinemia
- Hypertension
- Diabetes
- Hypercalcinosis
- Hyperphosphatemia

- Diffuse lipomatosis
- Sturge–Weber syndrome
- Neurofibromatosis
- Tuberous sclerosis
- Microsomia
- Epilepsy
- Cutaneous calcinosis
- Trauma

In a large study examining associated systemic diagnosis in 50 patients with angioid streaks, half of the patients were found to have a related systemic condition.[5] Seventeen of the 25 patients were diagnosed also with pseudoxanthoma elasticum (PXE), 5 patients with Paget disease, and 3 patients had sickle-cell disease.[5] The remaining half of the patients with angioid streaks did not demonstrate associated systemic disease.[5]

The most common systemic association of angioid streaks is PXE, an inherited disorder associated with degeneration of the elastic fibers in the dermatologic, gastrointestinal, cardiovascular, and ocular tissues. PXE accounts for 59–87% of cases with angioid streaks.[7] In PXE, the primary finding is elastic fiber degeneration in connective tissue, followed by a secondary calcium deposition.[4,10] In addition to angioid streaks, eyes also demonstrate a so-called "peau d'orange" pigmentary change, reticular pigmentary dystrophy affecting the macula, atrophic lesions of the RPE, crystalline bodies, and optic disc drusen (in 21% of patients with PXE and angioid streaks).[47] By 20 years after first diagnosis, angioid streaks develop in almost all patients with PXE.[16]

In patients with Paget disease, extensive Bruch's membrane calcification and angioid streaks followed by CNV and disciform scarring may develop.[9,10] About 10% of patients with advanced Paget disease develop angioid streaks.[9,10]

Similar significant calcium depositions at Bruch's membrane have been identified using histochemical and electron microscopic studies in patients with sickle-cell hemoglobinopathies.[13] The presence of iron–calcium complexes at the level of Bruch's membrane was previously suggested as an etiology for angioid streaks in patients with hemoglobinopathy; however, histopathologic studies demonstrate no increased iron deposition at the Bruch's membrane.[47] Compared to PXE, a smaller proportion of patients develop CNV and subsequent visual loss.[6]

Ocular Manifestations and Clinical Course

Angioid streaks usually originate from the optic nerve and may either radiate out or surround it concentrically and appear as irregular lines of varying width.[6] The subretinal lines can range in diameter from 50 to 500 μm.[16] The color of angioid streaks varies based on the fundus pigmentation and tends to be reddish in light-colored individuals and brown-colored in darker-pigmented individuals[16] (see Figs. 72.1A–D).

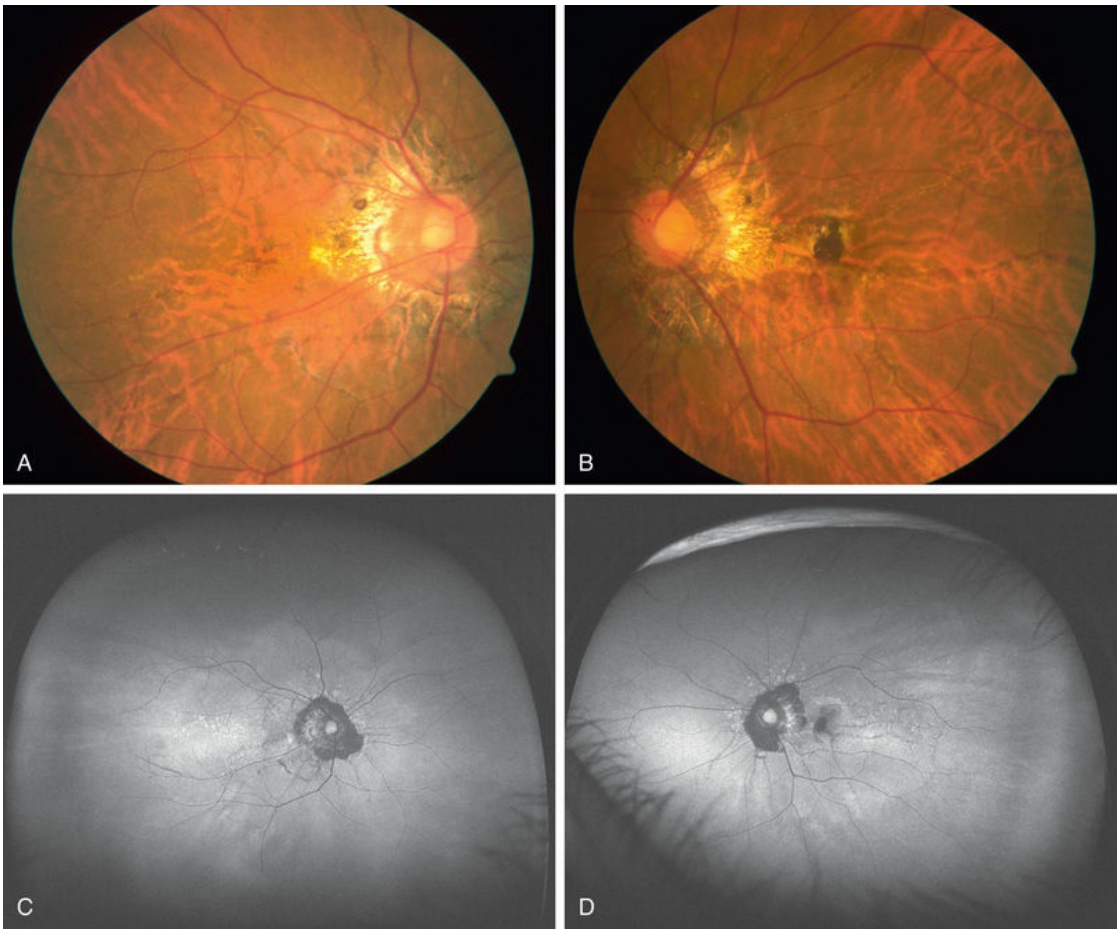

FIG. 72.1 A 63-year-old Asian woman with pseudoxanthoma elasticum and angioid streaks. Wide-field imaging of the right (A) and left (B) eyes shows angioid streaks (darker lines) radiating out from the optic disc. A hyperpigmented scar just nasal to the fovea developed after laser photocoagulation (A). The laser treatment was given prior to the use of intravitreal anti-VEGF therapy. Fundus autofluorescence imaging demonstrates the angioid streaks in the right (C) and left (D) eye. Spectral domain optical coherence tomography in this patient is shown in Fig. 72.3.

Angioid streaks have not been reported in newborns, and few cases have been described in individuals under 10 years of age.[6] Angioid streaks remain over time and do not regress, and the streaks may increase in length and width over time.[48] New streaks may form adjacent to old lesions. Over time, the adjacent RPE and choriocapillaris may develop atrophy.[48]

Most patients with angioid streaks are asymptomatic unless the macula is involved, with the development of traumatic rupture of

the Bruch's membrane or CNV (Figs. 72.1B and 72.2A–B). If the macula is involved, patients may report metamorphopsia or blurred vision.

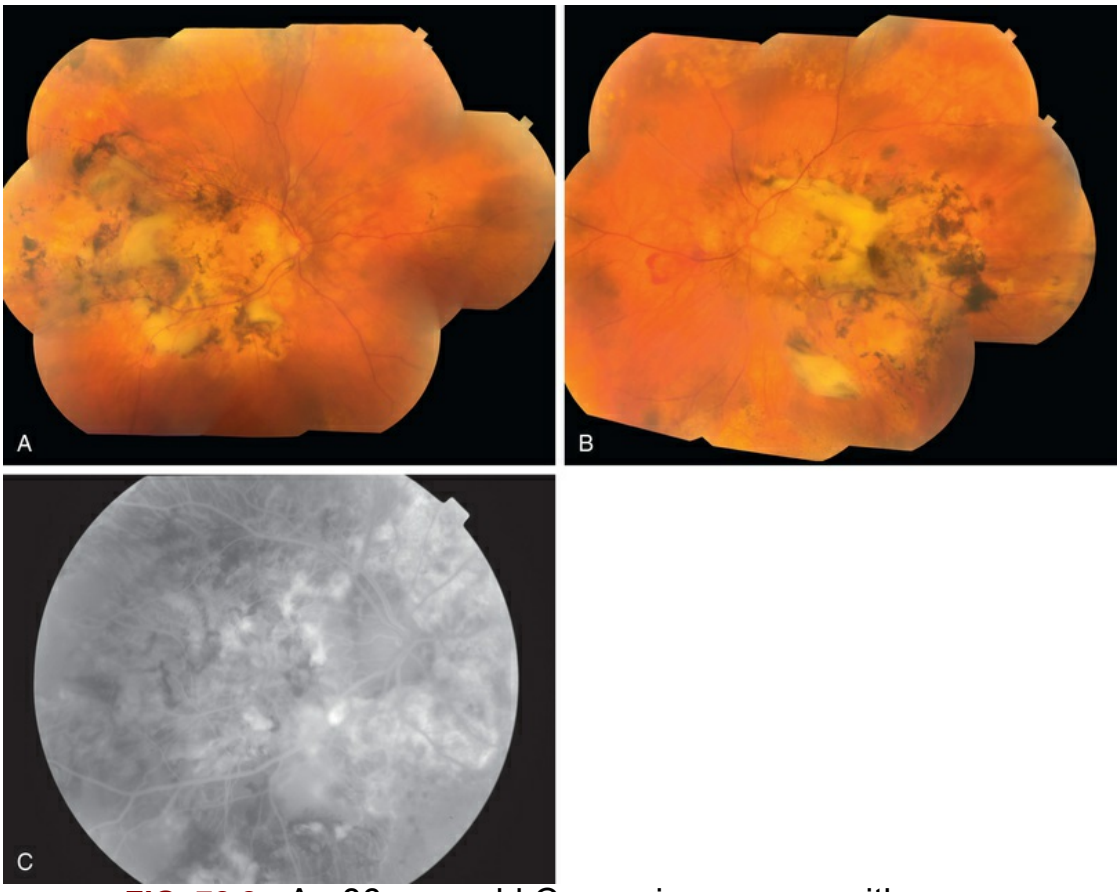

FIG. 72.2 An 86-year-old Caucasian woman with angioid streaks. Extensive disciform scar is found in the macula in both eyes (A,B), with new choroidal neovascularization and subretinal hemorrhage in the peripheral nasal retina in the left eye (B). Fluorescein angiography demonstrates extensive pigmentary changes and disciform scarring in the right eye (C). She underwent multiple intravitreal bevacizumab injections in the right eye, and her visual acuity had improved from $20/100^{-2}$ to 20/60. In the left eye the visual acuity was 20/400.

Patients may demonstrate breaks of Bruch's membrane after mild head or eye injuries, due to the brittleness of the calcified Bruch's membrane. Rupture of Bruch's membrane after trauma may be followed by subretinal hemorrhages. Up to 15% of patients with

angioid streaks develop significant visual loss after mild head injury.

The most common and significant complication of angioid streaks is the development of CNV, which is often bilateral and occurs in 72–86% of eyes with angioid streaks.[16] CNV is usually bilateral but asymmetric, with an interval of approximately 18 months between the development of CNV in initial and fellow eye.[7] Patients with PXE have a higher risk of CNV development compared to patients with other systemic diseases. By age 50, the majority of patients with PXE demonstrate reduced vision less than 20/200. Geographic chorioretinal atrophy (GA) independent of CNV is another cause of visual loss in eyes with PXE.[49] In one series, 8 of 41 (20%) eyes examined with PXE demonstrated GA, with growth of the GA similar to that of atrophic age-related macular degeneration.[49] Pattern dystrophy was found in 46–59% of eyes with PXE.[49]

Ocular Imaging and Diagnosis

Fluorescein Angiography (FA)

Usually the diagnosis of angioid streaks is made on fundoscopic examination, but FA may be helpful to detect the streaks and associated CNV when the findings are subtle. Irregular hyperfluorescence of the angioid streaks occurs during early phase angiography followed by varying degrees of staining during the later phases.[4] In some individuals with deeply pigmented choroidal tissue, the angioid streaks may be difficult to detect angiographically; whereas in lightly pigmented individuals, FA may aid in the identification of the angioid streaks before ophthalmoscopic detection[4] (Fig. 72.2C).

Fundus Autofluorescence (FAF)

Autofluorescence imaging uses light emission from lipofuscin in RPE cells and is considered to reflect RPE metabolic activity. Angioid streaks can show increased or decreased fundus autofluorescence. Autofluorescence often demonstrates RPE

atrophy more extensive than that seen on fundus ophthalmoscopy or FA; therefore, FAF may be a useful noninvasive tool to monitor the progression of the RPE changes related to angioid streaks and CNV (see Figs. 72.1C–D). FAF in eyes with angioid streaks has also been similar to the FAF images from eyes with pattern dystrophy. FAF demonstrated large areas of confluent hypoautofluorescence, demonstrating widespread loss of RPE cells in eyes with PXE.[50]

Indocyanine Green Angiography (ICGA)

A study incorporating the use of multiple modalities (FA, ICGA, FAF, and confocal near-infrared reflectance) in patients with angioid streaks and PXE has suggested a centrifugal spread of progressive calcification of Bruch's membrane that begins at the posterior pole and progresses toward the retinal periphery.[51] A central area of decreased fluorescence centered on the posterior pole on late-phase ICGA, while eccentric areas demonstrated a normal fluorescence on late-phase ICGA.[51]

Spectral Domain Optical Coherence Tomography (SD-OCT)

In eyes with advanced fundus pathology, such as large areas of atrophy and fibrosis, the underlying Bruch's membrane breaks cannot be detected on fundus photography, fluorescein angiography, or fundus autofluorescence imaging.[46] SD-OCT can detect abnormalities in Bruch's membrane as well as subretinal fibrosis and deposits that can be difficult to discern in areas of atrophy on FAF, FA, or ICGA[52] (Fig. 72.3).

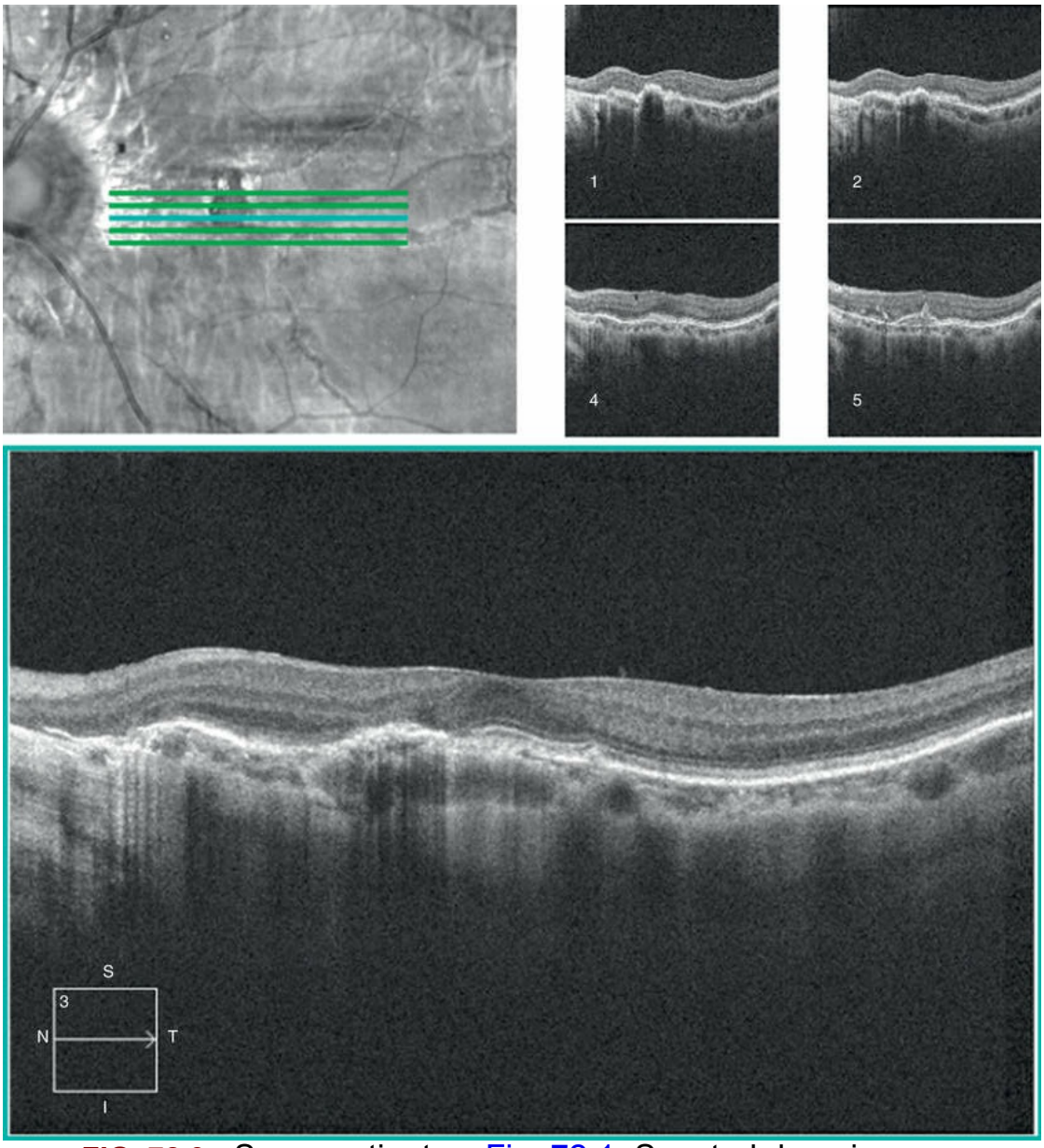

FIG. 72.3 Same patient as Fig. 72.1. Spectral domain optical coherence tomography demonstrates chorioretinal atrophy corresponding to the laser scar nasal to the fovea in the left eye, which has a best corrected visual acuity of 20/25. Visual acuity in the right eye was 20/25.

Swept Source OCT

A prospective case series showed similar mean choroidal thickness in eyes with angioid streaks without CNV compared to normal age-matched controls.[53] However, in those eyes with angioid streaks and CNV, the choroid was much thinner.[53] The degree of choroidal

thinning was found to be independent of CNV treatment history: no difference was found in choroidal thickness in treatment-naïve eyes with CNV versus those previously treated with anti-VEGF or PDT.[53] The small sample size in the study may be insufficient to detect a difference.

Therapy

There is no known prophylaxis except perhaps eye protection to reduce trauma. Current treatment strategies are directed to the eyes with CNV. Untreated CNV results in an average visual acuity of 20/200 by age 50, which was found by pooling data from several studies totaling 147 eyes.[54] One study found a final visual acuity of 20/640 in a group of 26 untreated eyes with either active CNV or disciform scar secondary to angioid streaks.[19] Untreated CNV results in poor visual outcomes in the majority of published reports.

Laser Photocoagulation

Results from laser photocoagulation in the treatment of macular CNV demonstrate a high recurrence rate of up to 77% and poor overall visual outcomes.[17–19] Thermal laser was one of the first therapies used for the treatment of macular CNV (see Fig. 72.1B). In one case series, the eyes treated with laser for macular CNV developed further CNV growth and vision loss.[8] However, other studies suggested that laser treatment for extrafoveal CNV related to angioid streaks resulted in better visual outcomes than untreated eyes.[17] Prophylactic treatment of angioid streaks prior to development of CNV is not recommended.[47] Laser photocoagulation achieves short-term cessation of CNV growth, but given the scotoma created and the early recurrences, other treatment regimens such as anti-VEGF therapy should be considered as first-line therapy.[54] Laser photocoagulation treatment for extrafoveal CNV still remains controversial given the availability of better treatment regimens.

Transpupillary Thermotherapy

Using a diode laser beam with 810 nm wavelength, transpupillary thermotherapy (TTT) may have better penetration to the choriocapillaris and may be less damaging to the RPE. TTT employs a diode with a lower threshold to avoid producing a thermal burn. However, a retrospective study investigating the use of TTT in treatment of subfoveal choroidal neovascularization found no significant long-term benefit in reducing the growth of the CNV or in visual improvement.[20]

Photodynamic Therapy

Data from both retrospective and prospective case series of eyes treated with photodynamic therapy (PDT) demonstrate variability in visual outcomes after treatment.[55] Several early reports investigating PDT use in eyes with angioid streaks suggest a reduction of CNV progression compared to natural history alone.[21,55] A retrospective, placebo-controlled case series found a greater reduction in mean visual acuity over the mean follow-up period of 18 months in untreated (from 20/160 to 20/640) versus PDT-treated eyes (from 20/126 to 20/500).[21] However, another study found mean visual acuity decreased after PDT treatment from 20/400 to 20/600.[56] Extension of an initial study with two additional years of follow-up identified progressive decrease in visual acuity following PDT treatment.[57] In a recent pooled retrospective analysis examining PDT outcomes, the lesion size was found to be increased after PDT treatment and may be indicative of persistent disease activity despite PDT.[54] When compared to natural history, the outcome post-PDT treatment is similar.[23]

Surgical Therapies

Prior to the use of anti-VEGF treatments for CNV, macular translocation and CNV removal were treatment options. Translocation is a surgical technique used to move the macular neuroretina to lie on top of an area of RPE without previous choroidal neovascularization. Varying short-term visual acuity improvement has been reported in a few studies employing macular translocation for CNV-related angioid streaks, but the number of eyes treated (less than 10) was limited.[25,26] Both macular

translocation and CNV removal were associated with frequent complications, such as proliferative vitreoretinopathy, retinal detachment, and hemorrhage. Currently, surgical treatment of CNV is not recommended.[25,26]

Anti-VEGF Treatment

Laser photocoagulation, TTT, and PDT have not been as successful in reducing the degree of visual loss compared with the visual outcomes following anti-VEGF therapy. Treatments with anti-VEGF therapies, such as with bevacizumab,[28–34] ranibizumab,[34–40] and aflibercept,[41] have demonstrated a marked reduction in the rate of visual acuity loss in the treated eyes compared with that in untreated eyes, but again, follow-up is short and randomized trials are lacking. Overall, no obvious difference in efficacy between bevacizumab and ranibizumab was found for CNV therapy in angioid streaks; however, the small number of eyes in each study was insufficient to detect differences in safety or effectiveness.[28–39] Variability in the treatment regimen, with pro re nata (prn) dosing used predominantly in bevacizumab studies, while a monthly regimen was more likely used in ranibizumab-treated eyes, was noted.[54] Currently there is inadequate evidence to show superiority of a prn versus fixed-dosing regimen in CNV treatment in angioid streaks.[54]

Bevacizumab

The majority of eyes with CNV secondary to angioid streaks treated with intravitreal bevacizumab demonstrated an improvement or stabilization in mean visual acuity on long-term follow-up ranging from 12 to 28 months.[28–34] Several retrospective case series reported stabilization or improvement of visual acuity after bevacizumab treatment in 87–100% of eyes with a follow-up ranging from 12 to 28 months.[28–32] Mean visual acuity improved by 3 or more lines in 44–62% of eyes by 12 months after bevacizumab treatment.[29,31]

In a study involving patients with angioid streaks secondary to PXE, the mean visual acuity improved from 20/80 to 20/40 with an average of 6.5 injections over a mean follow-up of 28 months.[28] In the same study, eyes with early disease demonstrated better visual

outcomes, with a mean visual acuity of 20/25 compared to a final mean visual acuity of 20/63 in eyes with advanced disease.[28] Eyes with CNV were initially treated with intravitreal bevacizumab and were followed every 4–6 weeks.[28–32] Retreatment with another bevacizumab injection was given if CNV activity was found.[28,31]

Multiple studies with at least 12-month follow-up reported a mean of approximately four bevacizumab injections (1.25–1.5 mg) given over 12–18 months.[29,30,31] Recurrent CNV is common, occurring in 33% of eyes by 19 months in one case series.[32] Not only can CNV recur at the same location, but new CNV can also develop in a different location requiring retreatment.[32]

Angiographic resolution of the CNV was found in 67% of the eyes by 19 months.[32] At final follow-up between 12 and 19 months, several studies have shown a reduction of central retinal thickness by 67–103 μm after bevacizumab treatment.[29,31]

Despite a majority of eyes demonstrating stable or improved visual acuity at the final follow-up in studies using bevacizumab to treat CNV secondary to angioid streaks, 8–13% of eyes demonstrate further decreased visual acuity.[28,31,32] In the eyes with visual loss after undergoing bevacizumab treatment, the visual decline is postulated to be related to atrophic macular changes and not from active choroidal neovascularization.[28,31]

Ranibizumab

Similar to the visual outcomes in bevacizumab trials, the majority of eyes treated with intravitreal ranibizumab demonstrated improved or stable visual outcomes at final follow-up, ranging from 3 months to 24 months.[35–39] In several prospective and retrospective case series reports, final visual acuity outcomes were stable or improved in 66–93% of eyes treated with ranibizumab (0.3–0.5 mg).[35,36,38,39] While the majority of eyes treated with intravitreal ranibizumab maintained or improved vision, 7–33% of eyes treated with ranibizumab lost vision by the end of the study.[35–39]

In two prospective studies, all eyes were given either three- or four-monthly loading doses of ranibizumab.[38,39] Then an “as needed” treatment protocol was used: another ranibizumab injection was given if CNV activity was detected. An average of 5–7 ranibizumab injections was given in two prospective trials with a

follow-up of 14–16 months, respectively.[38,39] One prospective trial found that 78% of eyes needed retreatment after the first three loading doses of ranibizumab.[39] Angiographic resolution of the CNV after ranibizumab treatment was reported in 66% of eyes.[36] On OCT testing, a mean decrease of 107 μm was shown in one prospective study at one year.[38] Vision loss secondary to retinal degeneration despite CNV resolution has been reported in eyes after treatment with ranibizumab.[40]

Aflibercept

To date, one case report documented aflibercept use in two patients treated with a single injection.[41] Vision improved from 20/25 to 20/20 in one patient at 12 months, whereas the other patient showed a gain of 20/200 to 20/50 after one injection at 9 months.[41]

Combination Therapy

Several studies examined whether combination therapy may be superior to monotherapy.[42–44] One prospective trial investigated the outcomes using reduced fluence PDT (25 J/cm^2) and intravitreal ranibizumab (0.5 mg) for treatment-naïve eyes with CNV related to angioid streaks.[42] At 12 months of follow-up, 9 of the 10 eyes demonstrated stable or improved vision, with 6 eyes showing gains of two or greater lines. One eye had more than 3 lines of decreased vision.[42] A diminished recurrence rate was found, but the visual outcome was similar to that with ranibizumab alone.[42] Another study examining the effect of PDT plus bevacizumab versus bevacizumab alone found similar outcomes with either therapy regimen.[43] One report with 5 eyes noted fewer PDT treatments needed when combined with intraocular triamcinolone injection.[44] Given the small sample size of these studies, further investigations involving combination therapies are needed before determining if added benefit exists over monotherapy with anti-VEGF treatment alone.

Conclusion

Calcification and degeneration in Bruch's membrane account for the

fundus and histopathologic appearance of angioid streaks. Angioid streaks are associated with multiple systemic conditions, including PXE, Paget disease, Ehlers–Danlos syndrome, and various blood dyscrasias such as sickle-cell anemia. Angioid streaks may not significantly affect vision if they remain extramacular or if choroidal neovascularization does not develop. However, choroidal neovascularization has been reported to occur in the majority of eyes with angioid streaks and is often bilateral. Treatments with laser photocoagulation, photodynamic therapy, and surgical interventions have not resulted in sustained visual improvement. However, significant improvement in visual outcomes has been found after using anti-VEGF therapy. Whether the early favorable results are sustained with longer follow-up will require further study. Geographic atrophy also is a contributing factor in visual loss in PXE patients with angioid streaks, and future therapies that inhibit GA progression may be beneficial.

References

1. Doyne RW. Choroidal and retinal changes: the results of blows on the eyes. *Trans Ophthalmol Soc U K*. 1889;9:128.
2. Knapp H. On the formation of dark angioid streaks as unusual metamorphosis of retinal hemorrhage. *Arch Ophthalmol*. 1892;26:289–292.
3. Klien BA. Angioid streaks: a clinical and histopathologic study. *Am J Ophthalmol*. 1947;30:955–968.
4. Gass JDM. Pathogenesis of disciform detachment of the neuroepithelium. VI. Disciform detachment secondary to heredodegenerative, neoplastic and traumatic lesions of the choroid. *Am J Ophthalmol*. 1967;63:689–711.
5. Clarkson JG, Altman RD. Angioid streaks. *Surv Ophthalmol*. 1982;26:235–246.
6. Finger RP, Issa PC, Ladewig MS, et al. Pseudoxanthoma elasticum. *Surv Ophthalmol*. 2009;54:272–285.
7. Connor PJ Jr, Juergens JL, Perry HO, et al. Pseudoxanthoma elasticum and angioid streaks: a review of 106 cases. *Am J Med*. 1961;30:537–543.
8. Clarkson JG. Paget's disease and angioid streaks: One

complication less? *Br J Ophthalmol*. 1991;75:511.
9. Dabbs TR, Skjodt K. Prevalence of angioid streaks and other ocular complications of Paget's disease of bone. *Br J Ophthalmol*. 1990;74:579–582.
10. Gass JDM, Clarkson JG. Angioid streaks and disciform macular detachment in Paget's disease (osteitis deformans). *Am J Ophthalmol*. 1973;75:576–586.
11. Condon PI, Serjeant GR. Ocular findings in elderly cases of homozygous sickle-cell disease in Jamaica. *Br J Ophthalmol*. 1976;60:361–364.
12. Geeraets WJ, Guerry D III. Angioid streaks and sickle-cell disease. *Am J Ophthalmol*. 1960;49:450–470.
13. Jampol LM, Acheson R, Eagle RC Jr, et al. Calcification of Bruch's membrane in angioid streaks with homozygous sickle cell disease. *Arch Ophthalmol*. 1987;105:93–98.
14. Green WR, Friedman-Kien A, Banfield WG. Angioid streaks in Ehlers–Danlos syndrome. *Arch Ophthalmol*. 1966;76:197–204.
15. Paton D. Angioid streaks and acromegaly. *Am J Ophthalmol*. 1963;56:841–842.
16. Georgalas I, Papconstantinou D, Koutsandrea C, et al. Angioid streaks, clinical course, complications, and current therapeutic management. *Ther Clin Risk Manag*. 2009;5:81–89.
17. Gelisken O, Hendriskse F, Deutman AF. A long-term follow-up study of laser coagulation of neovascular membranes in angioid streaks. *Am J Ophthalmol*. 1988;105:299–303.
18. Lim JI, Bressler NM, Marsh MJ, et al. Laser treatment of choroidal neovascularization in patients with angioid streaks. *Am J Ophthalmol*. 1993;116:414–423.
19. Pece A, Avanza P, Galli L, et al. Laser photocoagulation of choroidal neovascularization in angioid streaks. *Retina*. 1997;17:12–16.
20. Ozdek S, Bozan E, Gurelik G, et al. Transpupillary thermotherapy for the treatment of choroidal neovascularization secondary to angioid streaks. *Can J Ophthalmol*. 2007;42:95–100.
21. Karacorlu M, Karacorlu S, Ozdemir H, et al. Photodynamic

therapy with verteporfin for choroidal neovascularization in patients with angioid streaks. *Am J Ophthalmol*. 2002;134:360–366.
22. Menchini U, Virgili G, Introini U, et al. Outcomes of choroidal neovascularization in angioid streaks after photodynamic therapy. *Retina*. 2004;24:763–771.
23. Arias L, Pujol O, Rubio M, Caminal J. Long-term results of photodynamic therapy for the treatment of choroidal neovascularization secondary to angioid streaks. *Graefes Arch Clin Exp Ophthalmol*. 2006;244:753–757.
24. Mennel S, Schmidt JC, Meyer CH. Therapeutic strategies in choroidal neovascularization secondary to angioid streaks. *Am J Ophthalmol*. 2003;136:580–582.
25. Roth DB, Estafanous M, Lewis H. Macular translocation for subfoveal choroidal neovascularization in angioid streaks. *Am J Ophthalmol*. 2001;131:390–392.
26. Thomas MA, Dickinson JD, Melberg NS, et al. Visual results after surgical removal of subfoveal choroidal neovascular membranes. *Ophthalmology*. 1994;101:1384–1396.
27. Cekic O, Gocmez E, Kocabora MS. Management of CNV in angioid streaks by intravitreal use of specific anti-VEGF aptamer (pegaptanib sodium): long-term results. *Curr Eye Res*. 2011;36:492–495.
28. Finger RP, Issa PC, Schmitz-Valckenberg S, et al. Long-term effectiveness of intravitreal bevacizumab for choroidal neovascularization secondary to angioid streaks in pseudoxanthoma elasticum. *Retina*. 2011;10:1–11.
29. El Matri L, Kort F, Bouraoui R, et al. Intravitreal bevacizumab for the treatment of choroidal neovascularization secondary to angioid streaks: one year of follow-up. *Acta Ophthalmol*. 2011;89(7):641–646.
30. Teixeira A, Mattos T, Velletri R, et al. Clinical course of choroidal neovascularization secondary to angioid streaks treated with intravitreal bevacizumab. *Ophthalmic Surg Lasers Imaging*. 2010;41:546–549.
31. Wiegand TW, Rogers AH, McCabe F, et al. Intravitreal bevacizumab treatment of choroidal neovascularization in patients with angioid streaks. *Br J Ophthalmol*. 2009;93:47–

51.
32. Sawa M, Gomi F, Tsujikawa M, et al. Long-term results of intravitreal bevacizumab injection for choroidal neovascularization secondary to angioid streaks. *Am J Ophthalmol*. 2009;148:594.
33. Chang LK, Spaide RF, Brue C, et al. Bevacizumab treatment for subfoveal choroidal neovascularization from causes other than age-related macular degeneration. *Arch Ophthalmol*. 2008;126:941–945.
34. Myung J, Bhatnagar P, Spaide RF, et al. Long-term outcomes of intravitreal antivascular endothelial growth factor therapy for the management of choroidal neovascularization in pseudoxanthoma elasticum. *Retina*. 2010;30:748–755.
35. Carneiro AM, Silva RM, Veludo MJ, et al. Ranibizumab treatment for choroidal neovascularization from causes other than age-related macular degeneration and pathological myopia. *Ophthalmologica*. 2011;225:81–88.
36. Mimoun G, Tilleul J, Leys A, et al. Intravitreal ranibizumab for choroidal neovascularization in angioid streaks. *Am J Ophthalmol*. 2010;150:692–700.
37. Heier JS, Brown D, Ciulla T, et al. Ranibizumab for choroidal neovascularization secondary to causes other than age-related macular degeneration: a phase I clinical trial. *Ophthalmology*. 2011;118:111–118.
38. Ladas ID, Kotsolis AI, Ladas DS, et al. Intravitreal ranibizumab for macular choroidal neovascularization secondary to angioid streaks: one-year results of a prospective study. *Retina*. 2010;30:1185–1189.
39. Vadala M, Pece A, Cipolla S, et al. Angioid streak-related choroidal neovascularization treated by intravitreal ranibizumab. *Retina*. 2010;30:903–990.
40. Hansen MS, Klefter ON, Larsen M. Retinal degeneration and persistent serous detachment in the absence of active choroidal neovascularization in pseudoxanthoma elasticum. *Acta Ophthalmol*. 2014;92:156–157.
41. Vaz-Pereira S, Collaço L, De Salvo G, et al. Intravitreal aflibercept for choroidal neovascularisation in angioid

streaks. *Eye (Lond)*. 2015;10:1038.
42. Artunay O, Yuzbasioglu E, Rasier R, et al. Combination treatment with intravitreal injection of ranibizumab and reduced fluence photodynamic therapy for choroidal neovascularization secondary to angioid streaks: preliminary clinical results of 12-month follow-up. *Retina*. 2011;10:1–8.
43. Donati MC, Virgili G, Bini A, et al. Intravitreal bevacizumab (Avastin) for choroidal neovascularization in angioid streaks: a case series. *Ophthalmologica*. 2009;223:24–27.
44. Pece A, Russo G, Ricci F, et al. Verteporfin photodynamic therapy combined with intravitreal triamcinolone for choroidal neovascularization due to angioid streaks. *Clin Ophthalmol*. 2010;4:525–530.
45. Kazato Y, Shimada H, Nakashizuka H, et al. Immunohistochemical findings of a Bruch's membrane defect and active choroidal neovascularization in angioid streaks. *Jpn J Ophthalmol*. 2011;54:172–174.
46. Dreyer R, Green WR. The pathology of angioid streaks: a study of twenty-one cases. *Trans Pa Acad Ophthalmol Otolaryngol*. 1978;31:158–167.
47. Gass HD. *Stereoscopic atlas of macular diseases: diagnosis and treatment*. 4th ed. Mosby: St. Louis; 1997:118–125.
48. Shilling JS, Black RK. Prognosis and therapy of angioid streaks. *Trans Ophthalmol Soc U K*. 1975;95:301–306.
49. Schoenberger SD, Agarwal A. Geographic chorioretinal atrophy in pseudoxanthoma elasticum. *Am J Ophthalmol*. 2013;165:715–723.
50. Sawa M, Ober MD, Freund KB, et al. Fundus autofluorescence in patients with pseudoxanthoma elasticum. *Ophthalmology*. 2006;113:814–820.
51. Issa PC, Finger RP, Gotting C, et al. Centrifugal fundus abnormalities in pseudoxanthoma elasticum. *Ophthalmology*. 2010;117:1406–1414.
52. Issa PC, Finger RP, Holz FG, et al. Multimodal imaging including spectral domain OCT and confocal near infrared reflectance for characterization of outer retinal pathology in pseudoxanthoma elasticum. *Invest Ophthalmol Vis Sci*.

2009;50:5913–5918.
53. Ellabban AA, Hangai M, Yamashiro K, et al. Tomographic fundus features in pseudoxanthoma elasticum: comparison with neovascular age-related macular degeneration in Japanese patients. *Eye (Lond)*. 2012;26:1086–1094.
54. Gliem M, Finger RP, Fimmers R, et al. Treatment of choroidal neovascularization due to angioid streaks: a comprehensive review. *Retina*. 2013;33:1300–1314.
55. Chan WM, Lim TH, Pece A, et al. Verteporfin PDT for non standard indications: a review of current literature. *Graefes Arch Clin Exp Ophthalmol*. 2010;248:613–626.
56. Shaikh S, Ruby AJ, Williams GA. Photodynamic therapy using verteporfin for choroidal neovascularization in angioid streaks. *Am J Ophthalmol*. 2003;136:1–6.
57. Browning AC, Amoaku WM, Chung AK, et al. Photodynamic therapy for angioid steaks. *Ophthalmology*. 2007;114:1592.

73

Ocular Histoplasmosis

Justis P. Ehlers, Andrew P. Schachat

Treatment

- Laser Photocoagulation
- Photodynamic Therapy
- Anti-VEGF Therapy
- Combination Therapy
- Intravitreal Triamcinolone
- Submacular Surgery and Macular Translocation

Historical Perspective

In 1942 Reid provided the first description of histoplasmosis-associated ophthalmic abnormalities from a patient with acute disseminated histoplasmosis.[1] Following Reid's description, additional reports surfaced of atrophic chorioretinal lesions associated with positive histoplasmin skin testing.[2–4] In 1959 Woods and Wahlen[4] published a series of 62 patients with granulomatous uveitis. Nineteen of these patients "showed a peculiar and consistent pattern of ocular lesions" that included both discrete atrophic, sparsely pigmented or unpigmented, peripheral lesions (frequently referred to as "histo spots") and later cystic lesions in the macula. Skin testing for histoplasmin was positive in all of these 19 patients. Woods and Wahlen concluded that previous benign systemic histoplasmosis was responsible for the ocular findings in these 19 patients.[4] A few years later Schlaegel and Kenney[5] demonstrated that atrophic lesions around the optic nerve were also part of the clinical spectrum of ocular histoplasmosis syndrome (OHS), often called ocular histoplasmosis or presumed ocular histoplasmosis syndrome (POHS).

Clinical Features of Ocular Histoplasmosis

The symptoms associated with ocular histoplasmosis are wide-

ranging and are dependent on the pathology present. Atrophic lesions are typically asymptomatic. The presence of choroidal neovascularization (CNV) often results in variable vision loss and metamorphosia. Recently, an updated review of ocular histoplasmosis outlined many of the clinical features of ocular histoplasmosis, as well as recent shifts in treatment paradigms.[6]

A clinical diagnosis of ocular histoplasmosis is based on the presence of at least two of the following fundus lesions in one or both eyes in the absence of ocular inflammation:[7,8]

- Discrete, focal, atrophic (i.e., punched-out) choroidal scars in the macula or the periphery, smaller in size than the optic disc (histo spots) (Fig. 73.1).

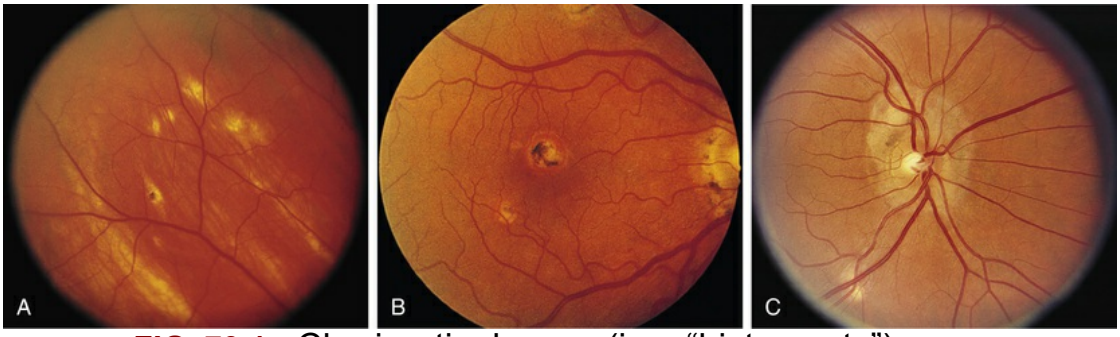

FIG. 73.1 Chorioretinal scars (i.e., "histo spots") characteristic of ocular histoplasmosis. (A) Peripheral histo spots. (B) Macular histo spots. Larger lesion with pigment proliferation may represent spontaneously regressed choroidal neovascularization (CNV). (C) Histo spots and peripapillary scarring. The peripapillary lesion superotemporal and within the peripapillary scarring probably represents spontaneously regressed CNV.

- Peripapillary chorioretinal scarring (i.e., peripapillary atrophy) (Fig. 73.2).

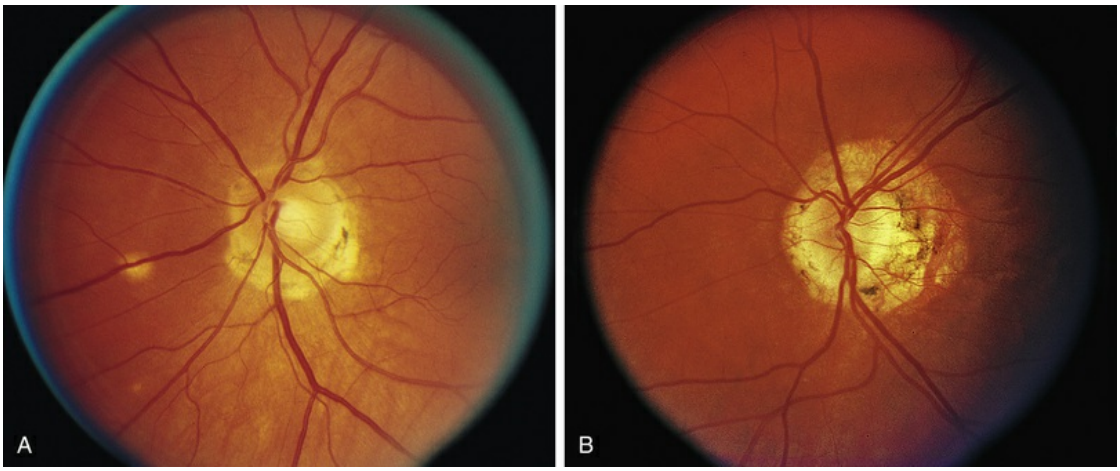

FIG. 73.2 (A,B) Two examples of peripapillary scarring.

- CNV or associated sequelae (hemorrhagic retinal detachment, fibrovascular disciform scar) (Figs. 73.3–73.5).

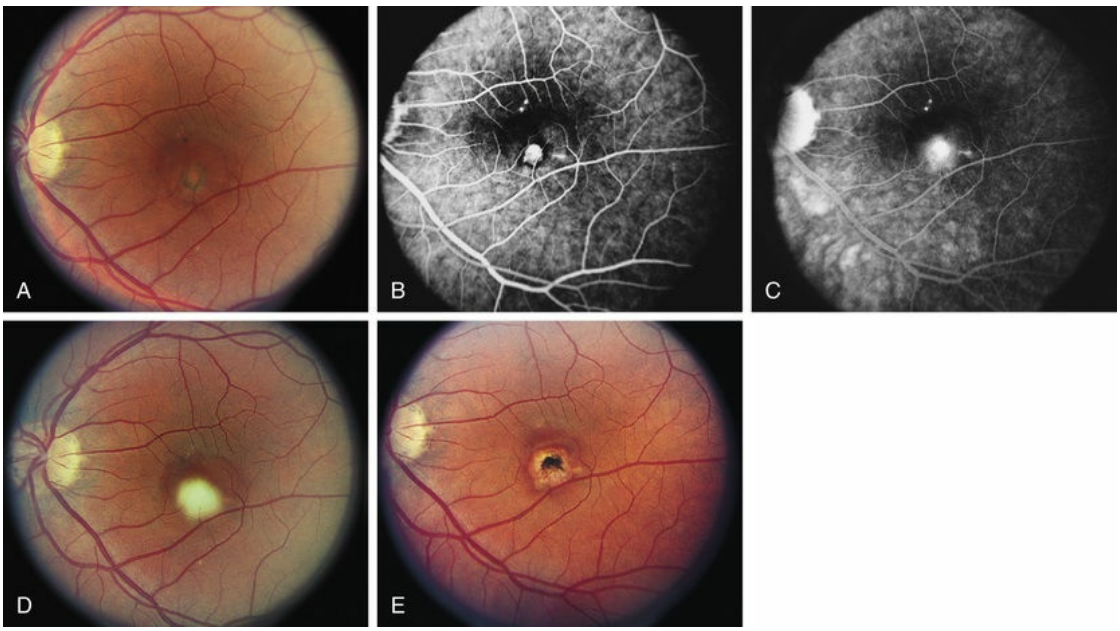

FIG. 73.3 (A) Choroidal neovascularization (CNV) secondary to ocular histoplasmosis with subretinal fluid in the macula. (B) Early frame of fluorescein angiogram shows extrafoveal CNV. (C) Late frame of fluorescein angiogram shows increased leakage of fluorescein dye. (D) Color photograph taken 1 day after laser photocoagulation shows whitening of retina from treatment. (E) Treatment scar 2 years after laser photocoagulation; no evidence of recurrent CNV.

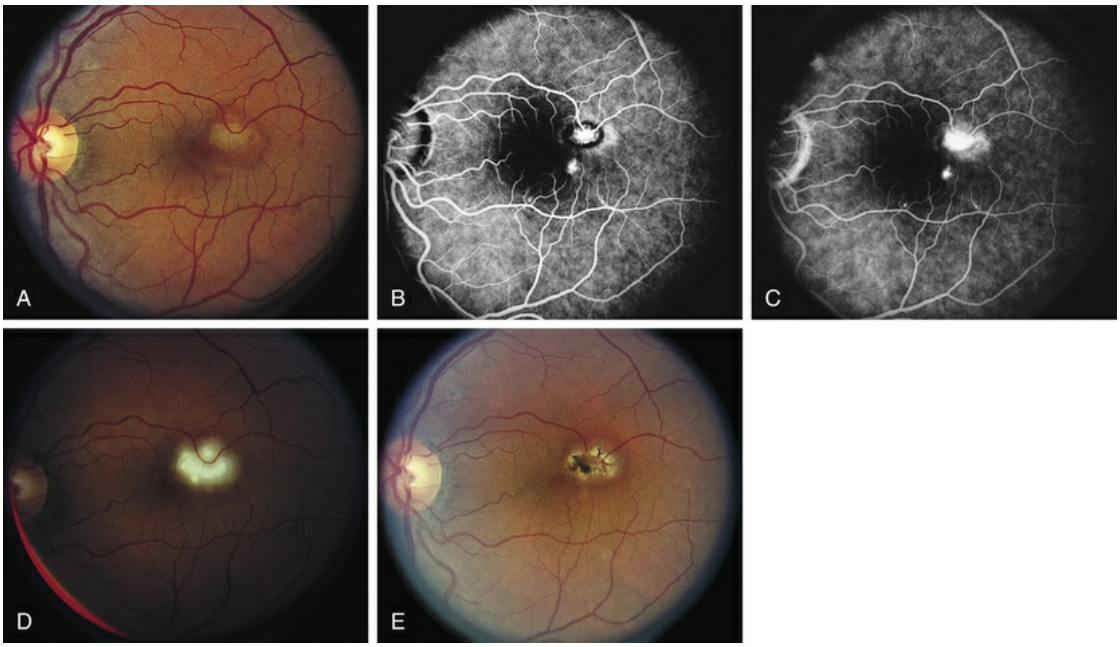

FIG. 73.4 (A) Choroidal neovascularization (CNV) secondary to ocular histoplasmosis with subretinal fluid in the macula. (B) Extrafoveal CNV is visible on this early frame of a fluorescein angiogram. (C) Late frame of fluorescein angiogram shows increased leakage of fluorescein dye from the CNV. (D) Color photograph taken 1 day after laser photocoagulation shows whitening of retina from treatment. (E) Atrophic treatment scar 2.5 years after laser photocoagulation; no evidence of recurrent CNV.

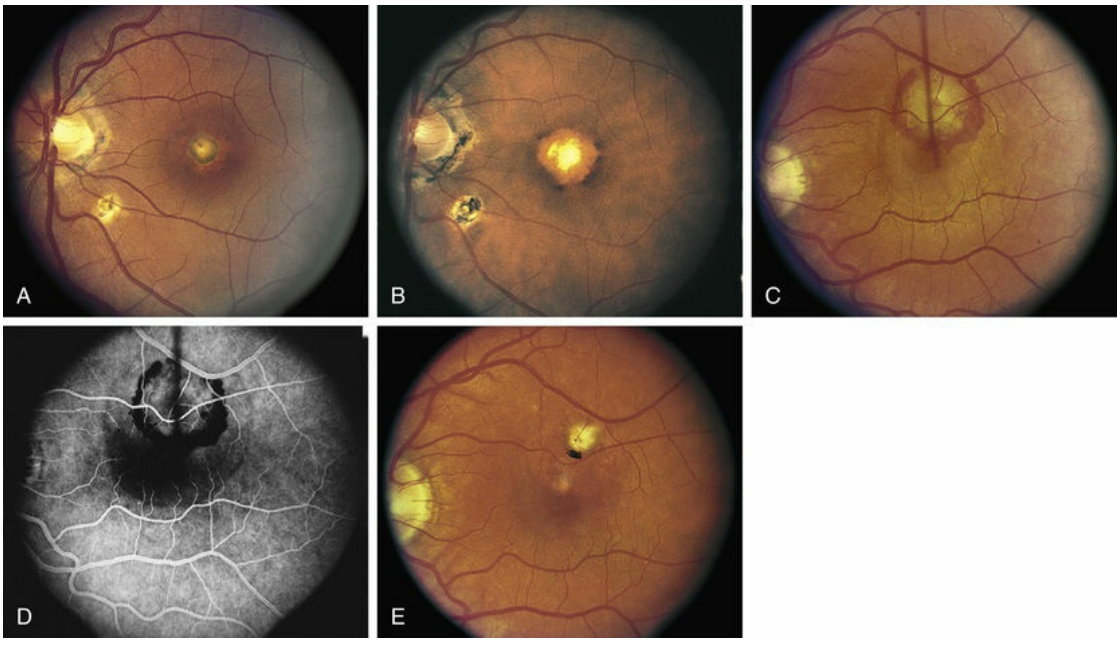

FIG. 73.5 The Macular Photocoagulation Study Group demonstrated that laser treatment of eligible choroidal neovascular lesions was better than no treatment with respect to delaying or preventing loss of visual acuity. However, some CNV regresses spontaneously. These two patients did not have laser treatment of their choroidal neovascularization (CNV), which involuted spontaneously. (A) Juxtafoveal CNV in first patient. (B) Disciform scar 4 years later. (C) This patient had extrafoveal CNV with a rim of hemorrhage visible on the photograph. (D) CNV, hemorrhage, and fluid are all visible on this early frame of a fluorescein angiogram. (E) A small scar with pigment proliferation is visible 4 years later. Visual acuity returned to 20/20 3 months after enrollment and remained at 20/20 throughout the 5-year follow-up period.

Most often both eyes have typical lesions, although the appearance may not be symmetric at initial presentation. The early granulomatous stage of ocular histoplasmosis, as described by Woods and Whalen, is rarely seen clinically.[4,7] The initial focal scars are probably too small to be seen with the ophthalmoscope. Gass[7] has postulated that lymphocytic infiltration of the surrounding tissue produces enlargement of the lesion over a period of years and thus allows it to become clinically detectable.

Differential Diagnosis

The differential diagnosis of ocular histoplasmosis includes a wide spectrum of disorders:

- **Multifocal choroiditis with panuveitis.** Characterized by multiple chorioretinal scars with similar findings to ocular histoplasmosis. Significant anterior and/or posterior inflammation present in the active phase, and there may be associated CNV. One study examined distinguishing features of multifocal choroiditis compared to ocular histoplasmosis.[9] Findings that were more characteristic of multifocal choroiditis included progressive growth of lesions, bridging scars, progressive proliferation of pigment, myopic disc changes, clustering of lesions (e.g., macula, equator), disc swelling, subretinal fibrosis, and narrowed/sheathed

vessels.[9] These features may be particularly important in distinguishing quiescent multifocal choroiditis from ocular histoplasmosis (see Chapter 79, White spot syndromes and related diseases).

- **Myopic degeneration.** Peripapillary atrophy and CNV may be seen in patients with myopic degeneration. Small white focal areas of chorioretinal atrophy along with linear atrophic areas (e.g., lacquer cracks) may also be present in the posterior pole (see Chapter 71, Myopic macular degeneration).
- **Multiple evanescent white dot syndrome (MEWDS).** White lesions of the retinal pigment epithelium (RPE)/outer retina may be present with associated granularity of the fovea. Often the vision is transiently decreased with an associated enlarged blind spot. Mild inflammation may be present. Scarring and permanent chorioretinal lesions are not usually observed (see Chapter 79, White spot syndromes and related diseases).
- **Idiopathic CNV.** A diagnosis of exclusion. Particularly in younger individuals, idiopathic CNV is seen in the absence of other signs of ocular histoplasmosis, age-related macular degeneration (AMD), angioid streaks, and other CNV-related conditions.
- **Choroidal rupture with CNV.** A history of trauma is usually present. A partially circumferential concentric chorioretinal macular scar is typically present and is associated with the CNV. Peripapillary atrophy and associated peripheral chorioretinal atrophy is not present (see Chapter 94, Traumatic chorioretinopathies).
- **Punctate inner choroidopathy.** Minimal to mild inflammation may be present. Atrophic scars may be associated with CNV. Spots are usually smaller than those seen with ocular histoplasmosis. Predominantly seen in women. Peripapillary atrophy is usually not present. Acute symptoms (e.g., photopsias) are usually associated with the initial diagnosis of the white lesions and may correlate with location of lesions (see Chapter 79, White spot syndromes and related diseases).
- **Neovascular AMD.** Typically in older patients (i.e., >50 years). Drusen present. Areas of focal atrophy may be present in the

macula, but the atrophy is not usually seen in the periphery. Peripapillary atrophy is often not present (see Chapter 69, Neovascular (exudative or "wet") age-related macular degeneration).

- **Sarcoidosis.** Scattered active inflammatory choroidal lesions may be present. Usually accompanied by anterior/posterior inflammation. CNV and peripapillary atrophy not typically present. Elevated angiotensin-converting enzyme may be seen. Often associated with hilar adenopathy on chest radiograph or CT scan of the chest (see Chapter 81, Sarcoidosis).

Relationship of Ocular Disease to Systemic Infection

Systemic infection with *Histoplasma capsulatum* via the respiratory tract is thought to be the initial event prior to the development of ocular histoplasmosis. Although a definitive causal relationship between *H. capsulatum* and the ocular disorder has not been demonstrated to satisfy Koch's postulates completely,[10,11] continuing experimental work with primates[12,13] may eventually satisfy this requirement.

Several observations support a causal relationship between *H. capsulatum* and the ocular histoplasmosis syndrome:

- Almost all patients diagnosed as having ocular histoplasmosis in the United States have lived some or all of their lives in an endemic area.[14,15]
- Positive histoplasmin skin testing occurs more frequently in patients with ocular histoplasmosis compared with controls.[15–17]
- Activation of lesions of ocular histoplasmosis has been reported following histoplasmin skin testing.[2–4,17–19]
- DNA from *H. capsulatum* has been isolated from an enucleated eye previously diagnosed with ocular histoplasmosis.[20]
- DNA from *H. capsulatum* has been isolated from the peripheral blood of a patient diagnosed with acute ocular histoplasmosis associated with a systemic illness also consistent with histoplasmosis.[21]

Other observations can be used to question the causal relationship between *H. capsulatum* and the ocular syndrome. In the UK and Europe, a clinical syndrome nearly identical to ocular histoplasmosis may occur.[22–26] These patients have never lived in or visited an endemic area, however, and only a small proportion of Europeans are positive reactors to histoplasmin skin testing.[22–27] Additionally, *H. capsulatum* has not been identified in the UK.[27] Certainly, the possibility exists that an alternate organism may result in a similar ocular syndrome in these areas.[24] Systemic antifungal treatment with amphotericin B has not been shown to be effective for the treatment of the ocular disorder.[28]

Clinical Features of Systemic Infection

Goodwin[29] classified systemic infection based on the immune status of the host and exposure type. The usual histoplasmosis infection is a relatively mild illness with flu-like respiratory symptoms. Most patients do not seek medical care. Studies in Tennessee have demonstrated that almost 90% of children of 13 years of age had positive reactions to histoplasmin skin tests.[30] A great deal of variation has been observed in the distribution of positive reactors by neighborhood of residence.[31,32] Rarely, more severe, even fatal cases of disseminated infection may occur, but these are usually associated with immune system deficiencies, such as acquired immunodeficiency syndrome (AIDS). Occasionally, epidemics of systemic disease outbreak may occur that are often associated with high levels of environmental exposure (e.g., excavations, construction projects in old buildings, work in chicken or other fowl habitats, or exposure in bat-inhabited caves).[33–48]

Epidemiology of Ocular Histoplasmosis

Geographic Distribution of *H. capsulatum* in the United States

The Ohio and Mississippi river valleys make up the largest part of

the "histo belt," where 60% or more of lifelong residents have positive histoplasmin skin testing.[49] Comstock described the major endemic histoplasmosis area as a triangle with its apices in Eastern Nebraska, Central Ohio, and Southwestern Mississippi.[31]

Prevalence and Incidence

The prevalence of asymptomatic ocular histoplasmosis in endemic areas (e.g., Ohio, Maryland) within the United States ranges from 1.6 to 5.3%.[15,16,50] The disciform lesion prevalence rates in the same areas were 0.0–0.1% of the endemic populations.[15,16,50] In those eyes that had atrophic spots, the prevalence of disciform lesions was 4.5%.[50]

The incidence rate of neovascular disciform lesions and atrophic lesions is largely unknown. The development of initial neovascular disciform lesions has been reported at around 2 per 100, 000 population per year.[51] Studies examining the incidence rate of neovascular lesions in fellow eyes have shown a rate of 0.0–12% per year.[52–56]

Age

The median age of patients with vision-threatening disciform lesions has typically been reported to be in the fourth and fifth decade, with an age range of 10–81 years old.[14,18,51,57–60] The median age of persons who have atrophic scars has been reported to be in the fourth, fifth, and sixth decades of life by various investigators.[16,61] These reports are of the age at detection, however, and not necessarily the age of development of the atrophic lesion. It is likely that these lesions develop earlier in life and are only coincidentally discovered during ophthalmic examinations for causes of visual symptoms that may or may not be related to ocular histoplasmosis.

Gender and Race

There is no gender predilection for ocular histoplasmosis. The vast majority of disciform lesions occur in Caucasians with only around a dozen cases reported among African Americans.[62] Interestingly,

histo spots and positive skin tests have been reported in some studies to have similar prevalence among Caucasians and African Americans.[16,63] Other studies have found a much higher prevalence in Caucasians (i.e., nearly 100% of all cases) as compared to Hispanics or African Americans.[15,17,50,57]

Histocompatibility Antigens and Genetic Predisposition

In disciform lesions, both human leukocyte antigen (HLA)-B7 and HLA-DRw2 have been reported to be two to four times more common among cases than controls.[64–66] For histo spots, HLA-DRw2 was twice as common among cases as among controls, but less difference was seen between the groups in regards to HLA-B7.[66,67] These findings suggest an underlying genetic susceptibility or predisposition for development of ocular histoplasmosis. It is unclear whether this genetic predisposition specifically reflects the susceptibility to ocular histoplasmosis or to infection by *H. capsulatum*. Although these associations exist, routine testing for HLA typing in connection with ocular histoplasmosis is not typically performed owing to the lack of significant positive and negative predictive values.

A recent analysis of patients with ocular histoplasmosis identified several genes that confer increased risk of CNV in age-related macular degeneration, including ARMS2, C3, MT-NDH2, and CFH.[68] In this report of 93 patients, 62 eyes had CNV secondary to ocular histoplasmosis and 31 patients had no evidence of CNV. Genetic testing detected no association with CNV risk. Though small, this study suggests alternate genetic risk factors may be at play for CNV secondary to ocular histoplasmosis compared to age-related macular degeneration.

Pathogenesis

Numerous theories regarding the pathogenesis of ocular histoplasmosis have been proposed. The most widely accepted theory involves focal infection of the choroid at the time of systemic infection. The focal inflammatory/infectious process results in an

atrophic scar that disrupts Bruch's membrane. Alternatively, the infection may involve the retinal pigment epithelium and choriocapillaris and may progress rapidly to subretinal hemorrhage, exudation, and a fibrovascular disciform scar (Fig. 73.6).

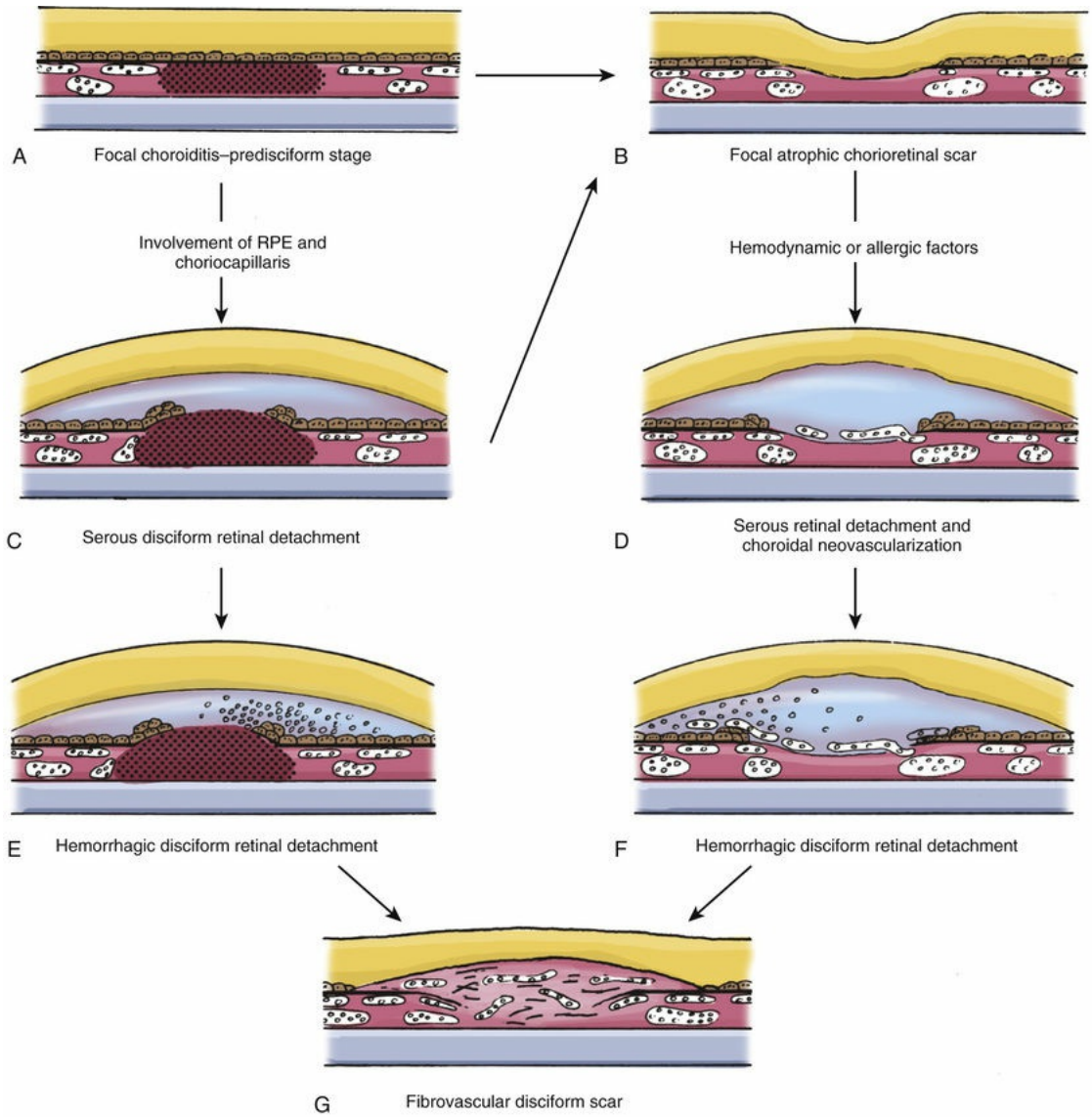

FIG. 73.6 Hypothesized mechanism of the pathogenesis of disciform lesions of ocular histoplasmosis. Focal choroiditis (A) damages the choriocapillaris, retinal pigment epithelium (RPE), and Bruch's membrane and produces an exudative detachment of the retina (B) or hemorrhage into the subretinal space (C). Any of these three stages may resolve, leaving either a focal area of atrophy of the

retinal pigment epithelium, Bruch's membrane, and choroid (D) or, in the case of subretinal hemorrhage, a disciform scar (G). Either in the absence of further inflammation or under the influence of recurrent episodes of inflammation, the choroidal blood vessels surrounding an atrophic chorioretinal scar (D) may decompensate and cause serous exudation, choroidal neovascularization, and transient serous detachment of the retina (E). This process in turn may result in a hemorrhagic detachment of the retina (F) that resolves as a disciform scar (G). (Reproduced with permission from Gass JDM. Stereoscopic atlas of macular diseases, vol. 1: Diagnosis and treatment. St. Louis: Mosby; 1987. p. 6.)

CNV formation may be promoted by multiple factors at the site of the atrophic scar. Disruption of Bruch's membrane provides access to the subretinal space for neovascularization.[69] The fragile vessels are prone to hemorrhage and exudation, often ultimately resulting in disorganization of the RPE and neurosensory retina and, ultimately, a fibrovascular scar.

The initiator for CNV development is unknown. The results from HLA typing suggest a possible genetic predisposition for progression from atrophic scars to disciform lesions in ocular histoplasmosis.[64–67] Other hypotheses have attributed these phenomena to a larger initial inoculum of the fungus,[12,70] reinfection,[4,71] hypersensitivity,[4,15] and the presence of other factors that compromise the vascular system[15,72,73] or the immune system.[74] CNV development has also been associated with proangiogenic factors such as vascular endothelial growth factor.[75]

One recent study examined 568 patients with ocular histoplasmosis, and of those patients, 142 patients were diagnosed with associated CNV.[76] In this study, logistic regression analysis identified age, education level, and smoking as significant risk factors for CNV development. Level of education was inversely associated (weak) with CNV risk (OR 0.95; 95% CI 0.92–0.98). Smoking was the most significant risk factor, with an OR of 2.83 (95% CI 1.8–4.31).[76]

Studying ocular histoplasmosis with animal models has been difficult. Histoplasmosis is known to occur in many species of animals.[77–81] However, efforts to develop an animal model for

ocular histoplasmosis have been hampered by two major factors: (1) nonprimates do not have a macula with its special anatomic, physiologic, and neurologic characteristics; and (2) decades are believed to elapse between initial infection with *H. capsulatum* and the development of characteristic macular lesions. The most promising animal models are primates, in which systemic infection and ocular lesions have been produced.[12,13]

Natural History of Ocular Histoplasmosis and Public Health Implications

Histo spots outside the macular area are typically asymptomatic, although visual symptoms occasionally have been reported that correlate with the location of the atrophic scars.[82] Active CNV may result in sudden decrease in vision secondary to hemorrhage or exudation. The vision loss in this disease often occurs in middle-aged individuals who are in the most active and productive stage of their life.[14,18,51,57–60] Spontaneous recovery of central vision has been reported in the Macular Photocoagulation Study (MPS)[53,58] and by other investigators.[83–85]

Two studies have addressed the public health importance of ocular histoplasmosis as a cause of visual impairment. One study in Tennessee found that ocular histoplasmosis was responsible for 2.8% of visual impairment among applicants for aid for the blind.[51] In Maryland a study comparing the 15-year incidence of visual impairment in those persons with histo spots to those persons without histo spots found that there was no difference in the rates of visual impairment.[52] The Submacular Surgery Trials Research Group found that individuals with unilateral and bilateral CNV cases had significant deficits in visual function, similar to patients with neovascular age-related macular degeneration (AMD).[86] Not surprisingly, the study showed that patients with bilateral CNV had significantly worse functional impairment of all groups, but those with unilateral involvement also had significant functional deficits.[86]

Treatment

Numerous approaches for ocular histoplasmosis management have been suggested, including avoidance of stress, avoidance of aspirin, avoidance of the Valsalva maneuver, hyposensitization to histoplasmin, use of immunosuppressive agents, and photocoagulation.[10] Histoplasmin desensitization,[87] amphotericin B,[18,28] and other prophylactic interventions[88,89] have been tried by many investigators and discarded. No treatment is known to prevent inactive lesions from giving rise to exudative or hemorrhagic neovascular complexes that typically end in disciform macular scars. Systemic corticosteroids also have been suggested, particularly in cases of "active" histo spots and subfoveal CNV.[7] In the era of anti-vascular endothelial growth factor (VEGF) and photodynamic therapy (PDT), however, the use of systemic corticosteroids even in subfoveal cases is now mainly of historic interest. Whether there is a role to manage active histo spots is unclear since many or perhaps most spontaneously involute.

Laser Photocoagulation

Initiated in 1979, the Macular Photocoagulation Study (MPS) Group demonstrated the effectiveness of laser treatment in comparison to no treatment in two randomized clinical trials for patients with well-defined extrafoveal or juxtafoveal CNV.[58,59,90,91] The first trial enrolled 262 patients with well-demarcated extrafoveal CNV.[59,90] The posterior border of these lesions could not be closer than 200 μm from the center of the foveal avascular zone; initial best corrected visual acuity of the affected eye was 20/100 or better. Eligible eyes were randomly assigned to argon laser treatment or to no treatment. The eyes were reexamined twice each year, at which time best corrected VA was measured and color photographs were taken. Fluorescein angiograms were taken at time of study entry, 6 and 12 months after enrollment, and annually thereafter.

In 1983 the MPS Data and Safety Monitoring Committee halted enrollment after concluding that argon laser photocoagulation was beneficial in preventing or delaying large loss of visual acuity compared to observation without treatment. From 18 months

through 5 years, a loss of 6 or more lines of VA was experienced in 10% of treated eyes compared to 40% of untreated controls. Median VA at baseline was 20/25 and after 5 years dropped to 20/40 in the treated group compared to 20/80 in controls.[90] In the laser-treated group, 26% of eyes had persistence of CNV or recurrence of CNV at the scar edge, and 7% developed a new CNV not contiguous with the laser scar.[90]

In 1981 a second trial was initiated by the MPS Group for patients with juxtafoveal CNV.[91] In this trial, best corrected VA at entry was permitted to be as poor as 20/400 in the study eye. A total of 289 eyes were randomized between krypton laser treatment and no treatment. Five years after the trial began, the MPS Data and Safety Monitoring Committee again halted enrollment after concluding that eyes treated with krypton laser were less likely to lose visual acuity than untreated eyes. A loss of 6 or more lines was seen in 11% of the treated eyes compared to about 30% of the controls.[91] Approximately one-third of treated patients had persistent or recurrent CNV contiguous with the zone of laser treatment; and new, noncontiguous areas of CNV developed in 2% of treated eyes.[91] A subgroup analysis by the MPS group of CNV located between the fovea and optic nerve showed that there was no contraindication to treatment of these lesions in the papillomacular bundle with laser.[92] A subset of the MPS Group piloted laser photocoagulation for subfoveal CNV secondary to ocular histoplasmosis but observed no short-term benefit compared to observation.[93]

In view of the very good results with extrafoveal CNV and even juxtafoveal CNV from the MPS studies, laser photocoagulation therapy may be considered for these lesions. Additionally, when compared to anti-VEGF therapy, laser photocoagulation is not as expensive and avoids many of the ocular and possible systemic risks of intravitreal injections with anti-VEGF agents. If subfoveal recurrence or primary subfoveal disease develops, PDT and/or anti-VEGF treatment should be considered (see below).

Photodynamic Therapy

The treatment of subfoveal CNV secondary to ocular

histoplasmosis with PDT was first suggested in 2002.[94] Since that small study, numerous studies have been published examining the use of PDT for ocular histoplasmosis. In fact, PDT is now approved by the United States Food and Drug Administration (FDA) for the treatment of subfoveal CNV secondary to ocular histoplasmosis.

Most of the studies performed for PDT with ocular histoplasmosis have been retrospective case series. In a 2003 retrospective review of 38 eyes with juxtafoveal CNV treated with PDT, treated eyes were more than twice as likely to have visual improvement or stabilization compared to the natural history group in the corresponding MPS clinical trial. Visual acuity improved or stabilized in 69% of eyes, with 44% of eyes improving at least 2 lines. Nearly 40% of eyes had undergone submacular surgery prior to PDT.[95] In 2004 a retrospective review of 11 eyes, of which five had juxtafoveal CNV and six had subfoveal CNV, documented similar findings. Eighty percent of eyes showed vision stabilization or improvement in the juxtafoveal group. Sixty percent of eyes with juxtafoveal lesions achieved a final visual acuity of 20/40 or better. Eyes with subfoveal lesions had similar results, with 83% of eyes having stabilization or improvement in vision. Fifty percent of eyes with subfoveal CNV also had a final visual acuity of 20/40 or better.[96] In 2005 a retrospective review of 23 eyes with juxtafoveal CNV associated with ocular histoplasmosis found that approximately 82% of eyes had visual stabilization (less than 2 line loss) or improvement. Thirty percent of eyes gained more than 2 lines of vision. Approximately 60% of patients required only a single PDT session. Following PDT, submacular surgery was performed in 16% of patients due to CNV progression.[97]

In 2006 a retrospective review of young patients undergoing PDT for CNV secondary to etiologies other than AMD included 6 patients with ocular histoplasmosis with subfoveal CNV. The mean pretreatment acuity in these eyes was 20/50, and the mean final visual acuity was 20/50. Three of these eyes (50%) required at least one retreatment session with PDT. One of 6 patients improved by more than 1 line of VA. Four eyes (67%) maintained their visual acuity (i.e., less than 2 lines lost or gained), one eye gained more than 2 lines of VA, and one eye lost 2 lines.[98]

An uncontrolled prospective trial evaluating PDT for subfoveal

CNV secondary to POHS included 26 eyes. Examination of 22 eyes 2 years following initial treatment revealed that 45% of eyes had gained 1.5 lines or more. Eighteen percent of eyes lost 1.5 lines or more, including 9% of eyes that lost 3 or more lines of VA. The mean number of treatments was 2.9 during the first year and 1 during the second year. After 2 years, only 15% of eyes had persistent angiographic leakage.[99]

Anti-VEGF Therapy

Over the last several years, the use of anti-VEGF agents has transformed the landscape in the treatment of CNV-related disease, particularly neovascular AMD. Case reports and case series suggest that anti-VEGF agents may also be effective in the treatment of CNV secondary to ocular histoplasmosis (Fig. 73.7). In 2007 the first case report was published documenting a 23-year-old female with sudden vision loss to 20/200 with subfoveal CNV. After a single intravitreal injection of bevacizumab, the visual acuity improved to 20/30 by 6 months follow-up.[100] Of course, the control arms of the MPS studies discussed above show that spontaneous involution can occur, but following this case report, retrospective consecutive case series were published examining the use of the intravitreal bevacizumab for the treatment of CNV in ocular histoplasmosis. One study examined intravitreal bevacizumab in 24 treatment-naïve eyes. The mean age was 43 years and the average number of injections was 6.8 per year. After 3 months, visual acuity improved from a mean baseline visual acuity of 20/114 to 20/55 (i.e., approximately 3 lines). Fifty-eight percent of eyes had 20/40 or better vision at final follow-up compared to 21% at baseline. Nine patients had 12 month follow-up and improved from a mean baseline visual acuity of 20/150 to 20/45 (i.e., approximately 6 lines). No significant complications were reported.[101]

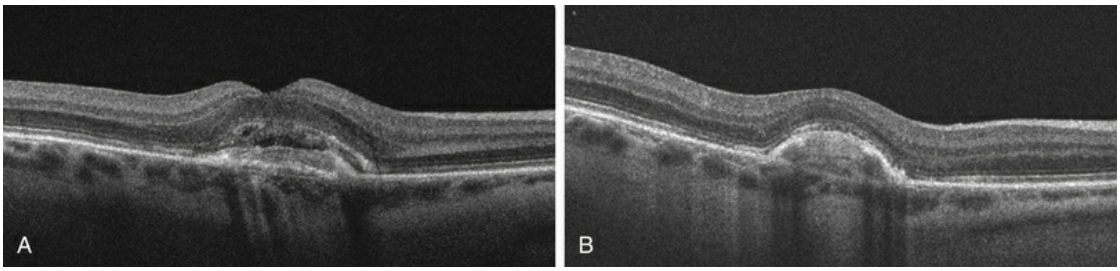

FIG. 73.7 Optical coherence tomography images of subfoveal choroidal neovascularization (CNV). CNV is visible in the subfoveal area with overlying subretinal fluid (A). Following intravitreal bevacizumab therapy, the subretinal fluid is significantly improved although the CNV remains (B).

A second study examined the use of bevacizumab in 28 eyes with CNV secondary to histoplasmosis. All patients included had active CNV with subfoveal fluid and either juxtafoveal or subfoveal CNV. Previous or concurrent PDT was allowed in this study. Seven patients were treatment naïve, 16 were PDT failures, and 5 patients were treated with combination PDT/bevacizumab therapy. The mean age was 46 years and mean follow-up was 5 months. Overall, the mean initial visual acuity was 20/88 and the mean final visual acuity was 20/54. Stability of visual acuity (<1.5 line loss) was seen in 93% of patients. Additionally, 43% of eyes experienced a 3 or more line gain. Both of the studies examining bevacizumab were retrospective, with significant methodologic shortcomings, and the results should be interpreted with caution.[102]

An additional retrospective review reported 54 eyes of 52 patients treated with either bevacizumab or ranibizumab for CNV secondary to histoplasmosis. The mean patient age was 47.6 years. Mean baseline visual acuity was 20/53, and the final mean visual acuity was 20/26 (p<.005). Previous treatment, including PDT, was allowed. Visual acuity improvement was noted in 81% of eyes, stability of visual acuity was recorded in 13% of eyes, and vision loss was reported in 6 % of eyes.[103]

A phase I randomized 12-month clinical trial evaluated ranibizumab for the treatment of CNV secondary to conditions other than AMD has been conducted. This study randomized eyes to monthly ranibizumab or 3-monthly injections followed by an as needed (prn) dosing schedule at monthly visits. Nine eyes (of 30)

with ocular histoplasmosis were included in this trial, four in the monthly arm and five in the prn arm. Prior treatment with other therapeutic modalities was allowed. Subgroup analysis was not performed for each diagnosis included. As a group, mean lines of change from baseline was +7.4 in the monthly injection arm and +5.0 in the prn group. A 3-line or more gain in visual acuity was seen in 66.7% of the monthly arm patients and in 57% in the prn arm. There were no statistically significant differences between the groups at any time point. No serious ocular or systemic adverse events were observed, but larger sample sizes are needed to detect infrequent severe adverse events.[104]

Further research is needed to define better the role of anti-VEGF therapy in the management of CNV secondary to ocular histoplasmosis. Early research suggests that it may have an important role in the management of this condition.

Combination Therapy

Similar to AMD, combination therapy is also being considered for the treatment of CNV secondary to ocular histoplasmosis. Combination therapy may reduce the need for ongoing intravitreal injections. PDT or laser photocoagulation may provide a more enduring effect, compared to anti-VEGF therapy alone. Adding anti-VEGF therapy may reduce the required spot size needed for either laser modality. In 2010, a small retrospective case series examining combination anti-VEGF agents with PDT included three eyes with CNV secondary to ocular histoplasmosis. Treatment consisted of PDT and intravitreal bevacizumab initiated concurrently with retreatment with PDT every 10–12 weeks and with bevacizumab every 4–6 weeks. Retreatment was based on persistent edema or subretinal fluid. Three of 3 (100%) eyes improved 2 lines or more at final follow-up.[105] As outlined in the previous section, a retrospective case series utilizing bevacizumab for CNV secondary to ocular histoplasmosis included five eyes that were treated with concurrent PDT therapy. Subgroup analysis of these five patients revealed that all five eyes experienced stabilization or improvement in visual acuity with a mean gain of 2.4 lines.[102]

In 2012 a retrospective comparative case series was published that examined intravitreal bevacizumab compared to combined intravitreal bevacizumab and PDT. A total of 151 eyes were included in the study, and 104 eyes had at least a 12-month follow-up period. The mean follow-up was 21.1 months. There was no difference in visual acuity at 12 months or 24 months between the bevacizumab monotherapy and combination groups.[106]

Intravitreal Triamcinolone

Given the possible underlying inflammatory pathogenic mechanisms of ocular histoplasmosis, the use of intravitreal steroids may be of use in the treatment of CNV secondary to ocular histoplasmosis. A retrospective case series examined the use of intravitreal triamcinolone in 10 eyes with CNV secondary to ocular histoplasmosis (5 subfoveal and 5 juxtafoveal) was conducted with a median follow-up of 17 months. Visual acuity improved or stabilized in 80% of eyes, including 30% that gained 1 line or more. Twenty percent of eyes lost 1–3 lines of visual acuity, and no eyes lost more than 3 lines of vision. Cataract progression and increased intraocular pressure were concerning ocular side-effects.[107]

Submacular Surgery and Macular Translocation

Prior to PDT and anti-VEGF therapy, submacular surgery for CNV secondary to ocular histoplasmosis was an important treatment alternative for many patients with significant vision loss.[108–110] As with many treatment modalities for CNV, recurrence of CNV is a major issue. In fact, the recurrence rate after submacular surgery is higher than recurrence following laser photocoagulation.[111] In 1997 the National Eye Institute and the National Institutes of Health initiated the Submacular Surgery Trials group H trial in order to compare functional outcomes and quality of life between patients assigned to surgery versus those assigned to observation (Fig. 73.8). The trial included 225 patients non-AMD with subfoveal CNV and visual acuity of 20/50 to 20/800. Of the 225 patients, 192 patients had ocular histoplasmosis. At 2 years, vision had improved or remained

stable in 20% more patients treated with surgery than with observation.[112] This outcome difference was not statistically significant. Subgroup analyses revealed that nearly all of the benefit seen with surgery was in those eyes with 20/100 or worse baseline visual acuity. In this subset of 92 eyes, 76% of surgery eyes remained stable or improved compared to 50% of eyes that were observed. Additionally, quality-of-life scores improved more with surgery.[113]

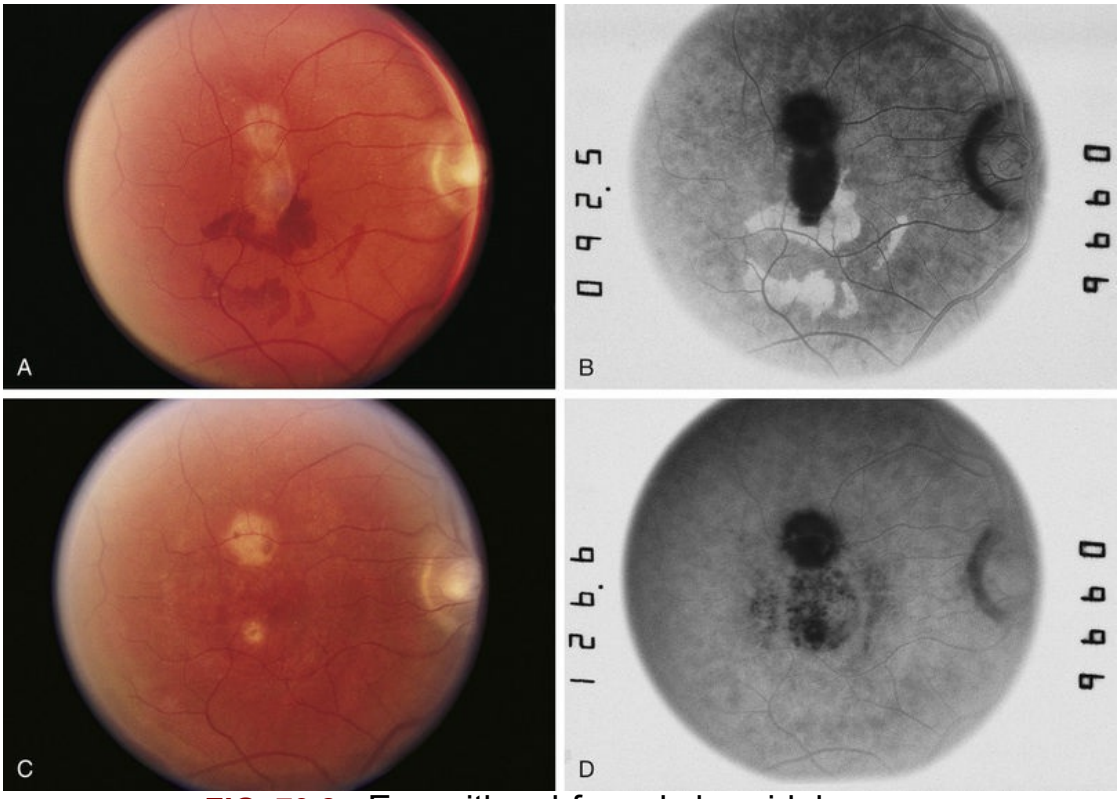

FIG. 73.8 Eye with subfoveal choroidal neovascularization (CNV) treated with submacular surgery in the Submacular Surgery Trials (group H trial). Color photograph (A) and early frame of fluorescein angiogram (B) shows subfoveal CNV in an eye with characteristic lesions of ocular histoplasmosis. Color photograph (C) and early frame of fluorescein angiogram (D) taken 6 months after submacular surgery show a well-demarcated postoperative disturbed area of the retinal pigment epithelium.

Macular translocation has also been utilized for the treatment of

patients with bilateral vision loss associated with ocular histoplasmosis.[114] One report described three cases of ocular histoplasmosis treated with 360° macular translocation. Two of the three eyes showed improvement in visual acuity. Two of the three cases developed recurrent CNV, and two of the three cases developed chronic cystoid macular edema.[114] Limited macular translocation for ocular histoplasmosis has also been reported, but the specific visual acuity results were not separated from the larger study which included predominantly AMD cases so that conclusions cannot be drawn regarding the effectiveness of limited translocation for ocular histoplasmosis.[115] Although surgical intervention remains a viable option in select situations, anti-VEGF therapy and PDT are now the mainstays of treatment for subfoveal and juxtafoveal CNV secondary to ocular histoplasmosis and laser photocoagulation is often advised for extrafoveal CNV.

References

1. Reid JD, Scherer JH, Herbut PA, et al. Systemic histoplasmosis diagnosed before death and produced experimentally in guinea pigs. *J Lab Clin Med*. 1942;27:419–434.
2. Krause AC, Hopkins WG. Ocular manifestation of histoplasmosis. *Am J Ophthalmol*. 1951;39:564–566.
3. Schlaegel TF. Granulomatous uveitis: an etiologic survey of 100 cases. *Trans Am Acad Ophthalmol Otolaryngol*. 1958;62:813–825.
4. Woods AC, Wahlen HE. The probable role of benign histoplasmosis in the etiology of granulomatous uveitis. *Trans Am Ophthalmol Soc*. 1959;57:318–343.
5. Schlaegel TF, Kenney D. Changes around the optic nerve head in presumed ocular histoplasmosis. *Am J Ophthalmol*. 1966;62:454–458.
6. Diaz RI, Sigler EJ, Rafieetary MR, Calzada JI. Ocular histoplasmosis syndrome. *Surv Ophthalmol*. 2015;60(4):279–295.
7. Gass JDM. Stereoscopic atlas of macular diseases. Mosby: St Louis, MO; 1987. *Diagnosis and treatment*. vol. 1.

8. Patz A, Fine SL. Presumed ocular histoplasmosis. Yanuzzi LA, Gitter KA, Schatz H. *The macula: a comprehensive text and atlas*. Williams & Wilkins: Baltimore; 1979.
9. Parnell JR, Jampol LM, Yannuzzi LA, et al. Differentiation between presumed ocular histoplasmosis syndrome and multifocal choroiditis with panuveitis based on morphology of photographed fundus lesions and fluorescein angiography. *Arch Ophthalmol*. 2001;119:208–212.
10. Schlaegel TF. *Ocular histoplasmosis*. Grune & Stratton: New York; 1977.
11. Wong VG, Kwon-Chung KJ, Hill WB. Koch's postulates and experimental ocular histoplasmosis. *Int Ophthalmol Clin*. 1975;15:139–145.
12. Smith RE. Natural history and reactivation studies of experimental ocular histoplasmosis in a primate model. *Trans Am Ophthalmol Soc*. 1982;80:695–757.
13. Jester JV, Smith RE. Subretinal neovascularization after experimental ocular histoplasmosis in a subhuman primate. *Am J Ophthalmol*. 1985;100:252–258.
14. Van Metre TE, Maumenee AE. Specific ocular uveal lesions in patients with evidence of histoplasmosis. *Arch Ophthalmol*. 1964;71:314–324.
15. Ganley JP. Epidemiologic characteristics of presumed ocular histoplasmosis. *Acta Ophthalmol*. 1973;(Suppl. 119):1–63.
16. Asbury T. The status of presumed ocular histoplasmosis: including a report of a survey. *Trans Am Ophthalmol Soc*. 1966;4:371–400.
17. Schlaegel TF, Weber JC, Helveston E, et al. Presumed histoplasmic choroiditis. *Am J Ophthalmol*. 1967;63:919–925.
18. Makley TA, Long JW, Suie T, et al. Presumed histoplasmic chorioretinitis with special emphasis on the present modes of therapy. *Trans Am Acad Ophthalmol Otolaryngol*. 1965;69:443–457.
19. McCulloch C. Histoplasmosis. *Trans Can Opthalmolog Soc*. 1963;26:107–125.
20. Spencer WH, Chan C-C, Shen DF, et al. Detection of *Histoplasma capsulatum* DNA in lesions of chronic ocular

histoplasmosis syndrome. *Arch Ophthalmol*. 2003;121:1551–1555.
21. Hernandez J, Munoz-Cadavid C, Hernandez D, Montoya C, Gonzalez A. Detection of Histoplasma capsulatum DNA in peripheral blood from a patient with ocular histoplasmosis syndrome. *Med Mycol*. 2012;50:202–226.
22. Braunstein RA, Rosen DA, Bird AC. Ocular histoplasmosis syndrome in the United Kingdom. *Br J Ophthalmol*. 1974;58:893–898.
23. Craandijk A. Focal macular choroidopathy. *Doc Ophthalmol*. 1979;48:1–99.
24. Bottoni FG, Deutman AF, Aandekerk AL. Presumed ocular histoplasmosis syndrome and linear streak lesions. *Br J Ophthalmol*. 1989;73:528–535.
25. Suttorp-Schulten MSA, Bollemeijer JG, Bos PJM, et al. Presumed ocular histoplasmosis in the Netherlands – an area without histoplasmosis. *Br J Ophthalmol*. 1997;81:7–11.
26. Ongkosuwito JV, Kortbeek LM, Van der Lelij A, et al. Aetiological study of the presumed ocular histoplasmosis syndrome in the Netherlands. *Br J Ophthalmol*. 1999;83:535–539.
27. Edwards PQ, Billings EL. Worldwide pattern of skin sensitivity to histoplasmin. *Am J Trop Med Hyg*. 1971;20:288–319.
28. Giles CL, Falls HF. Further evaluation of amphotericin-B therapy in presumptive histoplasmosis chorioretinitis. *Am J Ophthalmol*. 1961;51:588–598.
29. Goodwin RA, Shapiro JL, Thurman GH, et al. Disseminated histoplasmosis: clinical and pathologic correlations. *Medicine (Baltimore)*. 1980;95:1–33.
30. Zeidberg LD, Dillon A, Gass RS. Some factors in the epidemiology of histoplasmin sensitivity in Williamson county, Tennessee. *Am J Public Health*. 1951;41:80–89.
31. Comstock GW, Vicens CN, Goodman NL, et al. Differences in the distribution of sensitivity to histoplasmin and isolations of *Histoplasma capsulatum*. *Am J Epidemiol*. 1968;88:195–209.
32. Zeidberg LD. The microdistribution of histoplasmin

sensitivity in an endemic area. *Public Health Monogr*. 1956;39:190–197.
33. Burke DS, Churchill FE, Gaydos JC, et al. Epidemic histoplasmosis in patients with undifferentiated fever. *Mil Med*. 1982;147:466–467.
34. Ryder KW, Jay SJ, Kiblawi SO, et al. Serum angiotensin converting enzyme activity in patients with histoplasmosis. *JAMA*. 1983;249:1888–1889.
35. Weber TR, Grosfeld JL, Kleiman MB, et al. Surgical implications of endemic histoplasmosis in children. *J Pediatr Surg*. 1983;18:486–491.
36. Weinberg GA, Kleiman MB, Grosfeld JL, et al. Unusual manifestations of histoplasmosis in childhood. *Pediatrics*. 1983;72:99–105.
37. Wheat U, Stein L, Corya BC, et al. Pericarditis as a manifestation of histoplasmosis during two large urban outbreaks. *Medicine (Baltimore)*. 1983;62:110–119.
38. Brodsky AL, Gregg MB, Loewenstein MS, et al. Outbreak of histoplasmosis associated with the 1970 Earth Day activities. *Am J Med*. 1973;54:333–342.
39. Schwarz J, Salfelder K, Viloria JE. *Histoplasma capsulatum* in vessels of the choroid. *Ann Ophthalmol*. 1977;9:633–636.
40. Schlech WF, Wheat U, Ho JL, et al. Recurrent urban histoplasmosis, Indianapolis, Indiana, 1980–1981. *Am J Epidemiol*. 1983;118:301–312.
41. Waldman RJ, England AC, Tauxe R, et al. A winter outbreak of acute histoplasmosis in northern Michigan. *Am J Epidemiol*. 1983;117:68–75.
42. Wilcox KR, Waisbren BA, Martin J. The Walworth, Wisconsin, epidemic of histoplasmosis. *Ann Intern Med*. 1958;49:388–418.
43. Younglove RM, Terry RM, Rose NJ, et al. An outbreak of histoplasmosis in Illinois associated with starlings. *IMJ Ill Med J*. 1968;134:259–263.
44. Larrabee WF, Ajello L, Kaufman L. An epidemic of histoplasmosis on the isthmus of Panama. *Am J Trop Med Hyg*. 1978;27:281–285.
45. Loosli CG, Grayston JT, Alexander ER, et al.

Epidemiological studies of pulmonary histoplasmosis in a farm family. *Am J Hyg*. 1952;55:392–401.
46. Bartlett PC, Vonbehren LA, Tewari RP, et al. Bats in the belfry: an outbreak of histoplasmosis. *Am J Public Health*. 1982;72:1369–1372.
47. Morse DL, Gordon MA, Matte T, et al. An outbreak of histoplasmosis in a prison. *Am J Epidemiol*. 1985;122:253–261.
48. Sorley DL, Levin ML, Warren JW, et al. Bat-associated histoplasmosis in Maryland bridge workers. *Am J Med*. 1979;67:623–626.
49. Edwards LB, Acquaviva FA, Livesay VT, et al. An atlas of sensitivity to tuberculin, PPD-B, and histoplasmin in the United States. *Am Rev Respir Dis*. 1969;99:1–132.
50. Smith RE, Ganley JP. An epidemiologic study of presumed ocular histoplasmosis. *Trans Am Acad Ophthalmol Otolaryngol*. 1971;75:994–1005.
51. Feman SS, Podgorski SF, Penn MK. Blindness from presumed ocular histoplasmosis in Tennessee. *Ophthalmology*. 1982;89:1295–1298.
52. Hawkins BS, Ganley JP. Risk of visual impairment attributable to ocular histoplasmosis. *Arch Ophthalmol*. 1994;112:655–666.
53. Macular Photocoagulation Study Group. Five-year follow-up of fellow eyes of individuals with ocular histoplasmosis and unilateral extrafoveal or juxtafoveal choroidal neovascularization. *Arch Ophthalmol*. 1996;114:677–688.
54. Lewis ML, Schiffman JC. Long-term follow-up of the second eye in ocular histoplasmosis. *Int Ophthalmol Clin*. 1983;23:125–135.
55. Watzke RC, Claussen RW. The long-term course of multifocal choroiditis (presumed ocular histoplasmosis). *Am J Ophthalmol*. 1981;91:750–760.
56. Sawelson H, Goldberg RE, Annesley WH, et al. Presumed ocular histoplasmosis syndrome: the fellow eye. *Arch Ophthalmol*. 1976;94:221–224.
57. Gass JDM, Wilkinson CP. Follow-up study of presumed ocular histoplasmosis. *Trans Am Acad Ophthalmol*

Otolaryngol. 1972;76:672–694.
58. Macular Photocoagulation Study Group. Krypton laser photocoagulation for neovascular lesions of ocular histoplasmosis: results of a randomized clinical trial. *Arch Ophthalmol*. 1987;105:1499–1507.
59. Macular Photocoagulation Study Group. Argon laser photocoagulation for ocular histoplasmosis: results of a randomized clinical trial. *Arch Ophthalmol*. 1983;101:1347–1357.
60. Schlaegel TF, Weber JC. Follow-up study of presumed ocular histoplasmic choroiditis. *Am J Ophthalmol*. 1971;71:1192–1195.
61. Smith RE, Ganley JP, Knox DL. Presumed ocular histoplasmosis. II. Patterns of peripheral and peripapillary scarring in persons with nonmacular disease. *Arch Ophthalmol*. 1972;87:251–257.
62. Baskin MA, Jampol LM, Huamonte FU, et al. Macular lesions in blacks with the presumed ocular histoplasmosis syndrome. *Am J Ophthalmol*. 1980;89:77–83.
63. Edwards PQ, Palmer CE. Sensitivity to histoplasmin among negro and white residents of different communities in the USA. *Bull World Health Organ*. 1964;30:575–585.
64. Godfrey WA, Sabates R, Cross DE. Association of presumed ocular histoplasmosis with HLA-B7. *Am J Ophthalmol*. 1978;85:854–858.
65. Braley RE, Meredith TA, Aaberg TM, et al. The prevalence of HLA-B7 in presumed ocular histoplasmosis. *Am J Ophthalmol*. 1978;85:859–861.
66. Meredith TA, Smith RE, Duquesnoy RJ. Association of HLA-DRw2 antigen with presumed ocular histoplasmosis. *Am J Ophthalmol*. 1980;89:70–76.
67. Meredith TA, Smith RE, Braley RE, et al. The prevalence of HLA-B7 in presumed ocular histoplasmosis in patients with peripheral atrophic scars. *Am J Ophthalmol*. 1978;86:325–328.
68. Wilkes M, Miller D, Zanke B, et al. Investigation of Choroidal Neovascularization Risk alleles in ocular histoplasmosis. *Ophthalmology*. 2014;121:1487–1488.
69. Weingeist TA, Watzke RC. Ocular involvement by

Histoplasma capsulatum. *Int Ophthalmol Clin*. 1983;23:33–47.
70. Smith RE, Macy JI, Parrett C, et al. Variations in acute multifocal histoplasmic choroiditis in the primate. *Invest Ophthalmol Vis Sci*. 1978;17:1005–1018.
71. Davidorf FH. The role of T-lymphocytes in the reactivation of presumed ocular histoplasmosis scars. *Int Ophthalmol Clin*. 1975;15:111–124.
72. Gamble CN, Aronson SB, Brescia FB. Experimental uveitis. 1. The production of recurrent immunologic (Auer) uveitis and its relationship to increased uveal vascular permeability. *Arch Ophthalmol*. 1970;84:321–330.
73. Aronson SB, Fish MB, Pollycove M, et al. Altered vascular permeability in ocular inflammatory disease. *Arch Ophthalmol*. 1971;85:455–466.
74. Kaplan HJ, Waldrep JC. Immunological basis of presumed ocular histoplasmosis. *Int Ophthalmol Clin*. 1983;23:19–31.
75. Kwak N, Okamoto N, Wood JM, et al. VEGF is major stimulator in model of choroidal neovascularization. *Invest Ophthalmol Vis Sci*. 2000;41:3158–3164.
76. Chheda L, Ferketich A, Carroll CP, Moyer P, Kurz DE, Kurz PA. Smoking as a risk factor for choroidal neovascularization secondary to presumed ocular histoplasmosis syndrome. *Ophthalmology*. 2012;119:333–338.
77. De Monbreun WA. The dog as a natural host for *Histoplasma capsulatum*: report of a case of histoplasmosis in this animal. *Am J Trop Med*. 1939;19:565–587.
78. Emmons CW, Morlan HB, Hill EL. Histoplasmosis in rats and skunks in Georgia. *Public Health Rep*. 1949;64:1423–1430.
79. Akun RS. Histoplasmosis in a cat. *J Am Vet Med Assoc*. 1950;117:43–44.
80. Menges RW. Histoplasmin sensitivity in animals. *Public Health Monogr*. 1956;39:210–215.
81. Menges RW, Furcolow ML, Hinton A. The role of animals in the epidemiology of histoplasmosis. *Public Health Monogr*. 1956;39:277–281.
82. Rivers MB, Pulido JS, Folk JC. Ill-defined choroidal neovascularization within ocular histoplasmosis scars. *Retina*. 1992;12:90–95.

83. Orlando RG, Davidorf FH. Spontaneous recovery phenomenon in the presumed ocular histoplasmosis syndrome. *Int Ophthalmol Clin*. 1983;23:137–149.
84. Jost BF, Olk RJ, Burgess DR. Factors related to spontaneous visual recovery in the ocular histoplasmosis syndrome. *Retina*. 1987;7:1–8.
85. Campochiaro PA, Morgan KM, Conway BP, et al. Spontaneous involution of subfoveal neovascularization. *Am J Ophthalmol*. 1990;109:668–675.
86. Submacular Surgery Trials Research Group. Health- and vision-related quality of life among patients with ocular histoplasmosis or idiopathic choroidal neovascularization at time of enrollment in a randomized trial of submacular surgery. SST report no. 5. *Arch Ophthalmol*. 2005;123:78–88.
87. Kaiser RJ, Torsch T, O'Connor PR. Prognostic criteria in macular histoplasmic choroiditis. *Int Ophthalmol Clin*. 1975;15:41–49.
88. Makley TA, Long JW, Suie T. Therapy of chorioretinitis presumed to be caused by histoplasmosis. *Int Ophthalmol Clin*. 1975;15:181–195.
89. Schlaegel TF. Corticosteroids in the treatment of ocular histoplasmosis. *Int Ophthalmol Clin*. 1983;23:111–123.
90. Macular Photocoagulation Study Group. Argon laser photocoagulation for neovascular maculopathy: five-year results from randomized clinical trials. *Arch Ophthalmol*. 1991;109:1109–1114.
91. Macular Photocoagulation Study Group. Laser photocoagulation for juxtafoveal choroidal neovascularization: five-year results from randomized clinical trials. *Arch Ophthalmol*. 1994;112:500–509.
92. Macular Photocoagulation Study Group. Laser photocoagulation for neovascular lesions nasal to the fovea: results from clinical trials for lesions secondary to ocular histoplasmosis and idiopathic causes. *Arch Ophthalmol*. 1995;113:56–61.
93. Fine SL, Wood WJ, Isernhagen RD, et al. Laser treatment of subfoveal neovascular membranes of ocular histoplasmosis. *Arch Ophthalmol*. 1993;111:19–20.

94. Saperstein DA, Rosenfeld PJ, Bressler NM, et al. Photodynamic therapy of subfoveal choroidal neovascularization with verteporfin in the ocular histoplasmosis syndrome. One-year results of an uncontrolled, prospective case series. *Ophthalmology*. 2002;109:1499–1505.
95. Busquets MA, Shah GK, Wickens J, et al. Ocular photodynamic therapy with verteporfin for choroidal neovascularization secondary to ocular histoplasmosis syndrome. *Retina*. 2003;23:299–306.
96. Liu JC, Boldt HC, Folk JC, et al. Photodynamic therapy of subfoveal and juxtafoveal choroidal neovascularization in ocular histoplasmosis syndrome: a retrospective case series. *Retina*. 2004;24:863–870.
97. Shah GK, Blinder KJ, Hariprasad SM, et al. Photodynamic therapy for juxtafoveal choroidal neovascularization due to ocular histoplasmosis syndrome. *Retina*. 2005;25:26–32.
98. Lam A, Lee HC, Ho AC, et al. Photodynamic therapy in young patients. *Ophthalmic Surg Lasers Imaging*. 2006;37:182–189.
99. Rosenfeld PJ, Saperstein DA, Bressler NM, Verteporfin in Ocular Histoplasmosis Study Group, et al. Photodynamic therapy with verteporfin in ocular histoplasmosis:uncontrolled, open-label 2-year study. *Ophthalmology*. 2004;111:1725–1733.
100. Adán A, Navarro M, Casaroli-Marano RP, et al. Intravitreal bevacizumab as initial treatment for choroidal neovascularization associated with presumed ocular histoplasmosis syndrome. *Graefes Arch Clin Exp Ophthalmol*. 2007;245:1873–1875.
101. Ehrlich R, Ciulla TA, Maturi R, et al. Intravitreal bevacizumab for choroidal neovascularization secondary to presumed ocular histoplasmosis syndrome. *Retina*. 2009;29:1418–1423.
102. Schadlu R, Blinder KJ, Shah GK, et al. Intravitreal bevacizumab for choroidal neovascularization in ocular histoplasmosis. *Am J Ophthalmol*. 2008;145:875–878.
103. Nielsen J, Fick T, Saggau D, Barnes C. Intravitreal anti-

vascular endothelial growth factor therapy for choroidal neovascularization secondary to ocular histoplasmosis syndrome. *Retina*. 2012;32:468–472.
104. Heier JS, Brown D, Ciulla T, et al. Ranibizumab for choroidal neovascularization secondary to causes other than age-related macular degeneration: a phase I clinical trial. *Ophthalmology*. 2011;118:111–118.
105. Han DP, McAllister JT, Weinberg DV, et al. Combined intravitreal anti-VEGF and verteporfin photodynamic therapy for juxtafoveal and extrafoveal choroidal neovascularization as an alternative to laser photocoagulation. *Eye (Lond)*. 2010;24:713–716.
106. Cionni D, Lewis S, Petersen M, et al. Analysis of Outcomes for Intravitreal bevacizumab in the treatment of choroidal neovascularization secondary to ocular histoplasmosis. *Ophthalmology*. 2012;119:327–332.
107. Rechtman E, Allen VD, Danis RP, et al. Intravitreal triamcinolone for choroidal neovascularization in ocular histoplasmosis syndrome. *Am J Ophthalmol*. 2003;136:739–741.
108. Thomas MA, Kaplan HJ. Surgical removal of subfoveal neovascularization in the presumed ocular histoplasmosis syndrome. *Am J Ophthalmol*. 1991;111:1–7.
109. Thomas MA, Grand MG, Williams DF, et al. Surgical management of subfoveal choroidal neovascularization. *Ophthalmology*. 1992;99:952–968.
110. Thomas MA, Dickinson JD, Melberg NS, et al. Visual results after surgical removal of subfoveal choroidal neovascular membranes. *Ophthalmology*. 1994;101:1384–1396.
111. Melberg NS, Thomas MA, Dickinson JD, et al. Managing recurrent neovascularization after subfoveal surgery in presumed ocular histoplasmosis syndrome. *Ophthalmology*. 1996;108:1064–1068.
112. Submacular Surgery Trials Research Group. Surgical removal vs observation for subfoveal choroidal neovascularization, either associated with the ocular histoplasmosis syndrome or idiopathic. I. Ophthalmic findings from a randomized clinical trial: Submacular

Surgery Trials (SST) group H trial: SST report no. 9. *Arch Ophthalmol*. 2004;122:1597–1611.
113. Submacular Surgery Trials Research Group. Surgical removal vs observation for subfoveal choroidal neovascularization, either associated with the ocular histoplasmosis syndrome or idiopathic. II. Quality-of-life findings from a randomized clinical trial: SST group H trial: SST report no. 10. *Arch Ophthalmol*. 2004;122:1616–1628.
114. Ehlers JP, Maldonado R, Sarin N, et al. Treatment of non-age-related macular degeneration submacular diseases with macular translocation surgery. *Retina*. 2011;31:1337–1346.
115. Ng EW, Fujii GY, Au Eong KG, et al. Macular translocation in patients with recurrent subfoveal choroidal neovascularization after laser photocoagulation for nonsubfoveal choroidal neovascularization. *Ophthalmology*. 2004;111:1889–1893.

74

Polypoidal Choroidal Vasculopathy

Xiaoxin Li

Introduction

Polypoidal choroidal vasculopathy (PCV) is an exudative maculopathy with features similar to neovascular age-related macular degeneration (AMD) with pigment epithelial detachment (PED), and neurosensory detachment, some with hemorrhage. The pathogenesis of PCV is largely unknown, but it is now recognized widely as a subtype of neovascular age-related macular degeneration.

PCV is more common in non-white populations (including blacks, Hispanics, and Asians).[1] The incidence of PCV in Chinese and Japanese patients in exudative AMD has been reported to be much higher than in Caucasians.[2–7] The true prevalence and consequences may be underestimated if indocyanine green angiography (ICGA) is not performed. The widespread availability of ICGA has improved the diagnosis of PCV.

Polypoidal choroidal vasculopathy was first described as polypoidal, subretinal, vascular lesions associated with serous and hemorrhagic detachments of the retinal pigment epithelium (RPE) in a series of patients (10/11 were women) by Yannuzzi et al. at the Annual Meeting of the American Academy of Ophthalmology in 1982.[8] The entity was initially called idiopathic polypoidal choroidal vasculopathy (IPCV). Kleiner et al. in 1984[9] described a peculiar hemorrhagic disorder of the macula, characterized by recurrent subretinal and subretinal pigment epithelium bleeding in middle-aged black women, which they termed posterior uveal bleeding syndrome (PUBS).[10] Later, a study from the same group of authors showed an expanded clinical spectrum for PCV, affecting various ages, both genders, and several racial populations.[11] This chapter will use the PCV nomenclature; the IPCV and PUBS terms are mentioned for historical benefit.

The past decade has witnessed dramatic improvements in the understanding of exudative maculopathy and recognition of the importance of PCV, especially in the Asia–Pacific regions. A PCV Roundtable meeting panel of experts suggest that PCV is defined

angiographically as the presence of single or multiple focal nodular areas of hyperfluorescence arising from the choroidal circulation within the first 6 minutes after injection of indocyanine green, with or without an associated choroidal interconnecting vascular network. The presence of orange–red subretinal nodules with corresponding indocyanine green hyperfluorescence is pathognomonic of PCV.[12] The implication of the definition is obvious but bears repetition. The definition of PCV relies on ICGA. Retina specialists who do not generally utilize ICGA tend not to diagnose PCV. Later in the chapter there is also clinical definition of PCV.

Pathogenesis

PCV is regarded as a primary abnormality of the choroidal vessels, characterized by an inner choroidal vascular network of vessels ending in an aneurysmal bulge or outward projection, often visible as a reddish-orange, spheroid, polyp-like structure. PCV primarily involves the inner choroidal vasculature that is well differentiated from the middle and larger choroid vessels by histology.[13]

Histopathological features have been reported by Kuroiwa from surgically excised specimens from five patients with PCV, who had been diagnosed by ICGA. The results indicated that arteriosclerosis appears to be an important pathologic feature in the choroidal vessels of PCV subjects.[14] In another histopathologic report, by Nakashizuka et al., who examined specimens surgically extracted from five eyes of five PCV patients, the pathologic findings revealed little granulation tissue formation in any of the specimens; on the other hand, all the specimens exhibited a massive exudative change and leaking, all the vessels exhibited hyalinization, and choriocapillaris had disappeared, even in the cases in which RPE had been preserved.[15] This group also demonstrated by immunohistochemistry that PCV is not the same as choroidal neovascularization (CNV). CD-34 is a marker of vascular endothelial expression, and CD-34 staining revealed discontinuity in the vascular endothelium, smooth muscle actin (SMA) was negative in hyalinized vessels, and there was disruption and injury of smooth-muscle cells causing dilation of vessels. VEGF antibody

was negative in vascular endothelial cells. These histopathologic findings indicated that hyalinization of choroidal vessels, like arteriosclerosis, was characteristic of PCV.[15]

The genetic studies with CNV and PCV have been controversial in published papers.[16,17] Recently, we investigated the relationship between CNV of AMD and PCV by performing a series of meta-analyses. We found that many genes have common associations with PCV and CNV. For example, the pooled odds ratio (OR) between SNP rs10490924 (TT : GG, within the *ARMS2* gene, previously identified as LOC387715[18]) and CNV is 4.23 (95% CI 3.535.06), while the pooled OR between this SNP and PCV is 5.13 (95% CI 3.40–7.75) (data unpublished). SNP rs9332739 within complement factor 3 (*C3*) gene also have a common association with CNV (GG : CC, pooled OR 2.12, 95% CI 1.81–2.47) and PCV (pooled OR 3.52, 95%CI 1.43–8.69). Moreover, a similar trend was found in complement factor H (*CFH*, rs1061170, CC : TT) and *SERPING1* (C1 inhibitor, rs2511989 GG : AA). The elastin gene identified by Kondo et al. in 2008 was shown to disrupt the elastic area of the Bruch's membrane. He found that a common elastin gene (ELN) variant was significantly associated with susceptibility to PCV.[19] With the increased knowledge about the genetic determinants for AMD, researchers have tried to find genetic evidence to determine the association between neovascular AMD and PCV. Single-nucleotide polymorphisms (SNP) of *CFH*, replicated in multiple cohorts, have been proved to be associated with both neovascular AMD and PCV, which demonstrates major genetic evidence to support the similarity between neovascular AMD and PCV. One study reported a strong association with PCV ($p<.0005$, with or without adjustment for age and sex). All of the 11 SNPs tested at the *CFH* locus were significantly associated with PCV, and 8 of 11 SNP markers tested showed significant evidence of heterogeneity between AMD and PCV ($p<.05$ for all comparisons) after adjusting for age and sex.[20]

Furthermore, a series of meta-analyses was performed to investigate the pooled OR between the risk factors for CNV and PCV. We found that CNV and PCV have many common risk factors, such as smoking and diabetes. For example, the pooled OR between smoking and CNV is 1.78 (95%CI 1.52–2.09),[21] while the

pooled OR between smoking and PCV is 1.51 (95% CI 1.06–2.16, data unpublished). The pooled OR between diabetes and CNV is 1.66 (95% CI 1.05–2.63),[21] while the pooled OR between diabetes and PCV is 1.94 (95% CI 1.29–2.92, data unpublished). However, the pooled OR between hypertension and CNV is 1.02 (95% CI 0.77–1.35),[21] while the pooled OR between hypertension and PCV is 1.60 (95% CI 1.17–2.18, data unpublished). Therefore, hypertension is only associated with PCV. This is consistent with pathology findings: the PCV lesion has thickened and hyalinized vessel walls, which is similar to that seen in hypertension.[22]

Clinical Features

Demographics

The prevalence of PCV in presumed neovascular AMD was reported as 7.8% in US,[1] 4.0% in Belgian,[23] 9.8% in Italian,[24] 8.2% in Greeek[25], 23.0–54.7% in Japanese,[26] 22.3–49% in Chinese,[7,27] and 24.6%[28] in Korean populations. The prevalence varies with age.[29] In summary, PCV is more prevalent in blacks, Japanese, Chinese, and other Asians than in whites, while the incidence of AMD is very high in whites and low in blacks. The incidence of both diseases is high in Asians.

Although early reports suggested that PCV was a condition predominantly of middle-aged women,[11] and that typically PCV presents one to two decades earlier than classical AMD, it is most commonly diagnosed in patients between the ages of 50 and 65.[30] However, the age of the subjects reported with a mean of 66.1± 9.6 years in Chinese population.[29] Caucasian patients usually present with PCV at an older age.[31] It has subsequently been established that PCV occurs in both genders (and more commonly in Asian men than women).[28] Although women are involved more often than men in some reports, more men still have manifestations of the disorder among Chinese patients.[7,29,31,32] PCV is usually a bilateral disease. The majority of the patients with evidence of PCV in one eye eventually develop similar lesions in the fellow eye.

The natural course of PCV is variable: it may be relatively stable, or there may be repeated bleeding and leakage with vision loss and

chorioretinal atrophy, with or without fibrotic scarring. Reddish-orange nodules alone, or nodules and small subretinal hemorrhage and absence of hard exudates, may still allow a benign clinical course and stable vision.[33,34]

The association of PCV with other conditions is not certain. PCV with severe thrombocytopenia and massive hemorrhage has been reported,[35] and PCV has also been associated with sickle-cell disease and irradiation.[36] Some experts believe it is advisable to screen PCV patients for hypertension and platelet count, but hypertension is common in older patients and is already monitored during medical visits, and the platelet data are not firmly established. The role of hereditary and environmental factors in its etiology is inconclusive and needs further study.

Clinical Findings

Clinically, PCV is characterized by protruding orange-red elevated lesions, often with nodular elevations of the RPE, that can be seen during routine fundus examination using ophthalmoscopy and contact lens slit-lamp biomicroscopy. The nodular elevations of the RPE are easily visible by optical coherence tomography (OCT). PCV is also characterized by nodular lesions only observed when using ICGA. The nodular lesions appear as polyp-like or grape-like clusters (Fig. 74.1).[11,15] The nodular lesions are associated with serous exudation and hemorrhage that may lead to detachment of the RPE and sometimes the neurosensory retina.[34] Associated features are recurrent subretinal hemorrhage and vitreous hemorrhage (Fig. 74.2).

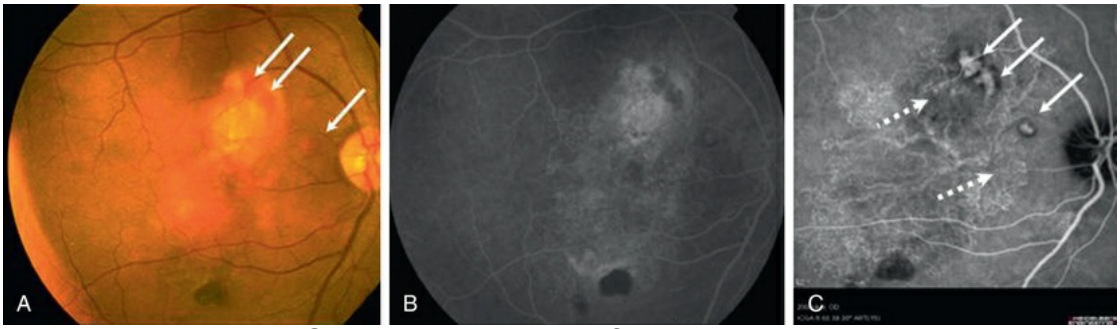

FIG. 74.1 (A) Color photograph of an 53-year-old male with blurred vision in the right eye for 2 years; visual

acuity was 20/200. There are protruded orange–red elevated lesions (*arrows*) in the superior area of the macular. (B) Fluorescein angiogram of the same fundus showing occult choroidal neovascularization. (C) Indocyanine green angiogram at 6 minutes 3 seconds reveals a branching vascular network in the central macular and polypoidal lesions (*arrows*) connecting to a branching vascular network (*dashed arrows*) and corresponding to the orange–red subretinal nodules.

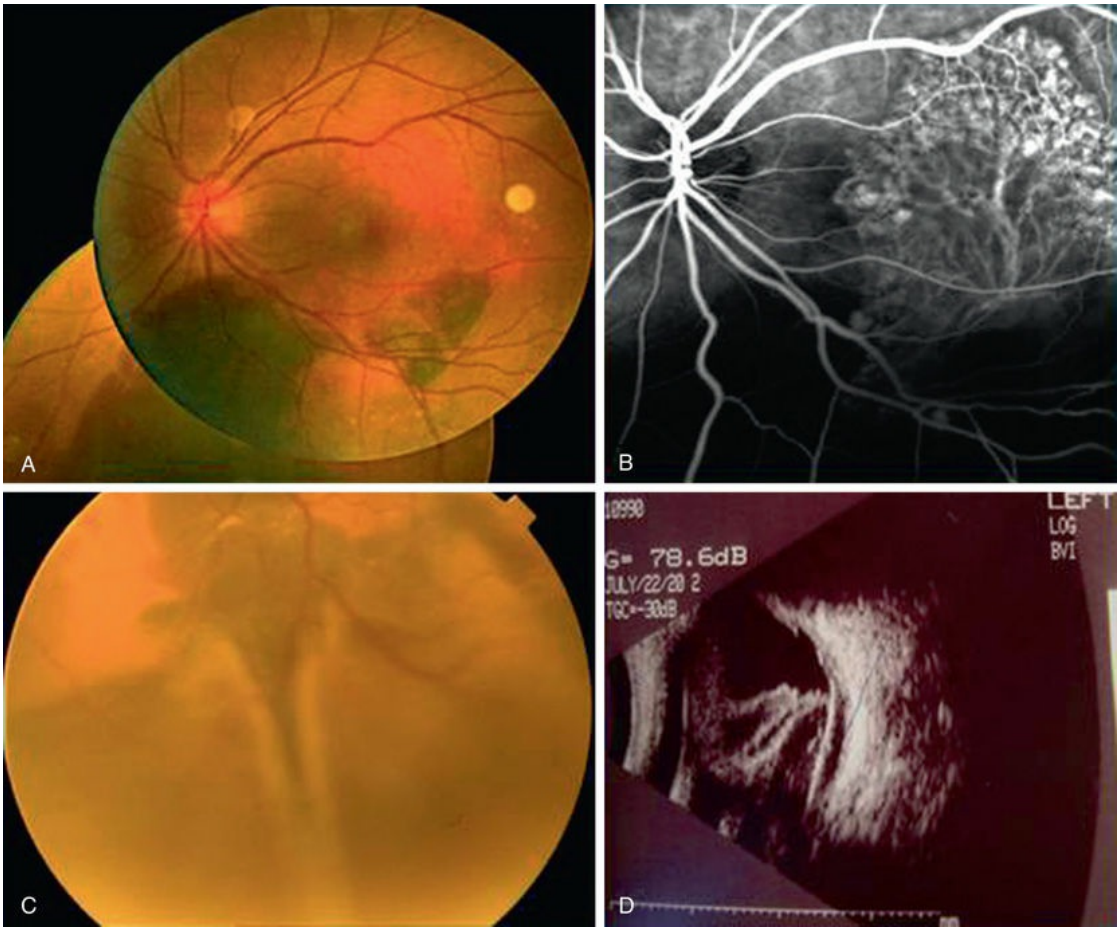

FIG. 74.2 (A) Color photograph of a 65-year-old man with blurred vision for 18 months. There is a large area of protruding orange–red elevated lesion on the temporal side of the fovea. (B) Indocyanine green angiogram from the same fundus. (C) One month later the vision dropped to hand motions and the color photograph showed hemorrhagic retinal detachment inferior to the fovea. (D) One week later subretinal

hemorrhages and bleeding into the vitreous cavity was demonstrated on B-scan ultrasonography.

Nodular lesions are located mainly in the macula area, although this may be ascertainment bias since ICGA tends to look at that area. In one report, 69.5% nodular lesions were located in the macular area, 15% PCV lesions were located under the temporal retinal vascular arcade, and 4.5% PCV lesions were located peripapillary (within one disc diameter of the disc edge). PCV lesions were also located in the midperipheral area.[29]

PCV lesions may be active or inactive (Fig. 74.3). PCV is considered as active if there is clinical, OCT, or fluorescein angiography (FA) evidence of any one of the following: vision loss of 5 or more letters (ETDRS chart); subretinal fluid with or without intraretinal fluid; pigment epithelial detachment; subretinal hemorrhage; or fluorescein leakage (Box 74.1). There are currently no universally recognized criteria for defining disease activity in PCV; treatment should be initiated for active and symptomatic PCV and can be considered for active, asymptomatic PCV.[12]

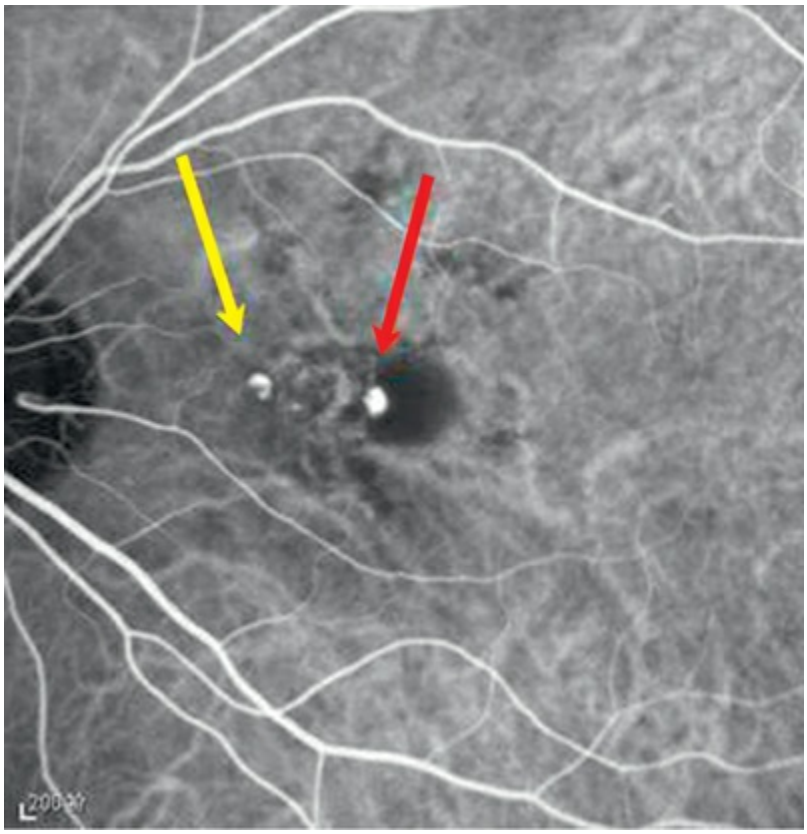

FIG. 74.3 Indocyanine green angiogram of a 73-year-old man with polypoidal choroidal vasculopathy and a 7-month history of decreased visual acuity in his left eye. There are two polyps in the macular region. *Yellow arrowhead* identifies an inactive polyp; *red arrowhead* points to an active polyp with surrounding hypofluorescence.

Box 74.1

Characteristics of Active Polypoidal Choroidal Vasculopathy

- Neurosensory detachment
- Pigment epithelium detachment
- Subretinal lipid exudation
- FA evidence of activity is leaking hyperfluorescence, mostly in an "occult"' pattern
- Subretinal haemorrhage
- Polyp surrounded by fluid (hypofluorescent halo in ICGA)

FA, fluorescein angiography; ICGA, indocyanine green angiography.

Choroidal vascular hyperpermeability, reportedly a characteristic finding in central serous chorioretinopathy (CSC), might play a role in the pathogenesis of PCV. PCV with angioid streaks secondary to pseudoxanthoma elasticum has also been reported in one patient.[37,38]

Some authors reported PCV combined with CNV.[31] PCV theoretically can induce ischemic changes, inflammation, sick RPE, and breaks in Bruch's membrane. These changes could contribute to the development of CNV, and fibrosis and scarring may ensue. The fibrotic scarring can be caused by subretinal bleeding.

Angiographic Features

PCV is better visualized by ICGA than by FA because indocyanine green absorbs and emits near-infrared light, which readily penetrates the RPE, enhancing viewing of choroidal lesions. Also, the higher binding affinity of indocyanine green to plasma proteins means that it does not leak rapidly from the choriocapillaris in the same way as fluorescein.[39] In recent years, ICGA has been accepted as the gold standard for the diagnosis of PCV, and as one of the specific criteria to distinguish PCV from retinal angiomatous proliferation by the angiogram in stereo.[6] The ICGA characteristics of PCV include a branching network of inner choroidal vessels,[2,6,22,40–42] and nodular polypoidal aneurysms or dilations at the edge of these abnormal vessel networks, which correspond to orange subretinal nodules;[2,6,11,21,32,34,40,42] and the presence of single or multiple focal nodular areas of hyperfluorescence (hypofluorescent halo) arising from the choroidal circulation within the first 6 minutes (Box 74.2). Pulsation in polyps and/or associated vasculature has been less extensively reported and can be observed only using video ICGA.[43,44]

Box 74.2

ICGA Characteristics of Polypoidal Choroidal Vasculopathy

- Polypoidal lesions shown on ICGA as typical nodular hyperfluorescence, and one of the following angiographic criteria:
- A branching network of inner choroidal vessels, nodular polypoidal aneurysms or dilations at the edge of these abnormal vessel networks, presence of hypofluorescent halo (in first 6 minutes)
- Pulsation in polyps can be observed only using video ICGA

ICGA, indocyanine green angiography.

ICGA should be considered to assist the diagnosis of PCV when routine ophthalmoscopic examination indicates a serosanguineous maculopathy with one of the following features: clinically visible orange–red subretinal nodules, spontaneous massive subretinal

hemorrhage (if not so severe as to preclude all ICG views), and in some cases with notched or hemorrhagic pigment epithelium detachment (PED), or a lack of response to anti-VEGF therapy. The total lesion area for PCV is the area of all polyps and the branching vascular network (BVN) as viewed by ICGA. This is important for laser and photodynamic treatment modalities.

Classification

PCV was initially classified by the Japanese Study Group on PCV.[2] PCV roundtable meeting panel of experts proposed three categories to subclassify PCV:[12]

1. Quiescent: polyps in the absence of subretinal or intraretinal fluid or hemorrhage

2. Exudative: exudation without hemorrhage, which may include sensory retinal thickening, neurosensory detachment, PED, and subretinal lipid exudation

3. Hemorrhagic: any hemorrhage with or without other exudative characteristics

There are additional classifications for discussion. Akiyuki Kawamura classified PCV into two types: Type 1, both feeder and draining vessels are visible on ICGA and network vessels are numerous; Type 2, neither feeder nor draining vessels are detectable and the number of network vessels is small.[45] Based on the presence of a branching vascular network on ICGA and presence of late leakage from the PCV lesion on FA, Tock Han Lim classified into three types: Type A (interconnecting channels on ICGA) – 22.4%; Type B (branching vascular network with no leakage of FA) – 24.3%; Type C (branching vascular network with late leakage of FA) – 53.3% from 107 patients. The highest rate of moderate visual loss (loss of ≥3 lines) occurred in Type C PCV (57.7% vs. 0% for Types B and A at 5 years, $p<.001$).[46]

Differential Diagnosis

Neovascular Age-Related Macular Degeneration

Some authors categorize PCV as a subtype of neovascular AMD.[6] PCV has been considered to be part of or similar to occult CNV due to similar features (Fig. 74.4A), elevated levels of vascular endothelial growth factor (VEGF), similar histology, and expression of growth factors and receptor antibodies. We view PCV as a distinct condition. It has been documented that the increased levels of VEGF in PCV are lower compared with AMD CNV or myopic CNV. The increase in VEGF levels in PCV is mild to moderate. The clinical features of the PCV are different from those of neovascular AMD. PCV is associated with polyp-like structures projecting from the plane of the inner choroid towards the outer retina or RPE; the RPE is mostly intact, while in neovascular AMD the neovascular tufts arising from the choroid may either invade and perforate Bruch's membrane or grow through defects in Bruch's membrane and proliferate in either sub-RPE space (type I CNV) or in the subsensory retinal space (type II CNV).[47] The ingrowth of new vessels extending from the choroid into the sub-RPE space is the most important histopathologic change of occult CNV (Fig. 74.4B).

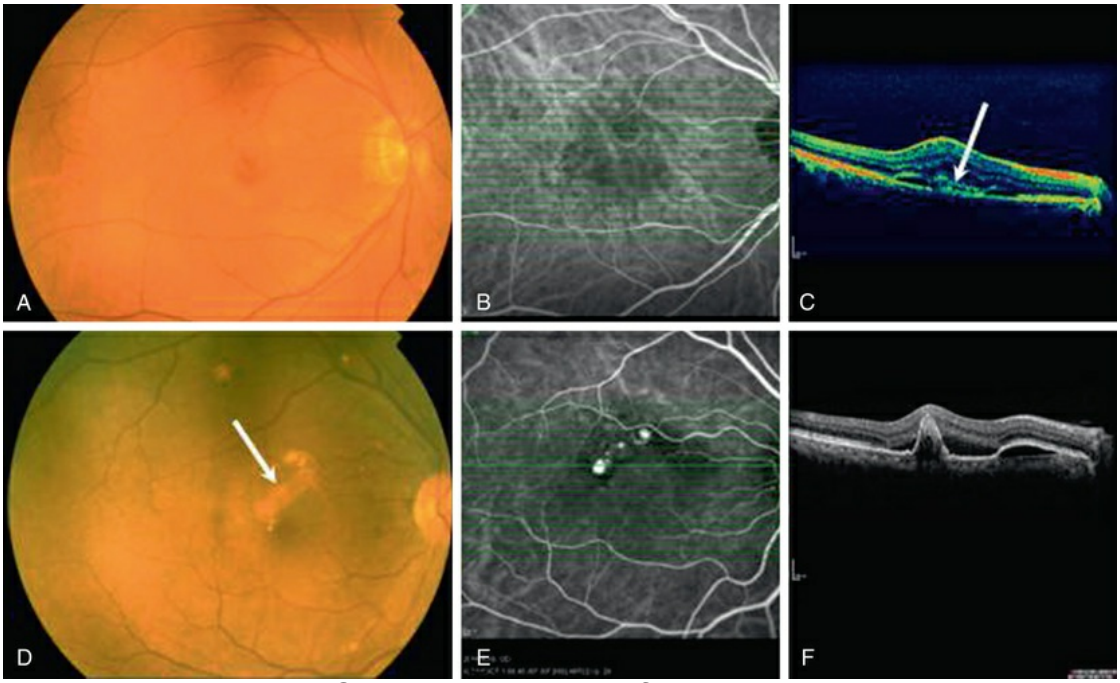

FIG. 74.4 (A) Color photograph of 72-year-old man

with visual acuity 20/20. (B) Indocyanine green angiography (ICGA) demonstrates choroidal neovascularization (CNV) superior to fovea. (C) Optical coherence tomography (OCT) of the same fundus; *arrow* points to the CNV component above the retinal pigment epithelium (RPE) band and the RPE band is broken. (D) Color photograph of 66-year-old woman with visual acuity 20/100, with orange–red subretinal nodules in the macular area (*arrow*). (E) ICGA of the same fundus showed polyps corresponding to the orange–red lesions. (F) OCT of the same fundus showed a detached RPE in a "bent back" form corresponding to the polypoidal lesion with subretinal fluid and a large area RPE detachment.

OCT findings (Figs. 74.4C and F) can assist in understanding the differences in the retinal structures that are affected by these two clinical entities and also may help in the differential diagnosis of PCV and neovascular AMD.[13]

Central Serous Chorioretinopathy

Central serous chorioretinopathy (CSC) is characterized by accumulation of transparent fluid and round, serous detachment of the macular retina. It has been thought to be due to a focal leakage from one or more defects at the level of the RPE, which allow serous fluid from the choriocapillaries to diffuse into the subretinal space. It has been hypothesized that a protracted disturbance in the microcirculation of the choriocapillaries leads to leakage of fluid into the sub-RPE space. A combination of choroidal hyperpermeability and impaired RPE function leads to pooling of fluid in the sub-RPE space with eventual leakage through the RPE into the subretinal space. ICGA has expanded our knowledge of CSC. A consistent finding is the hyperpermeability of the choroid during ICGA in CSC. The multifocal choroid hyperfluorescence patches in the ICG demonstrate multifocal choroid vascular hyperpermeable areas.[42]

PCV masquerading as CSC was reported in CSC with persistent and/or recurrent exudation; a myriad of retinal pigment epithelial changes may evolve that make it difficult to differentiate it from

PCV. In such patients, ICGA is useful in differentiating these two entities. An accurate clinical diagnosis is important since CSC and PCV differ in terms of their risk factors, natural course, visual prognosis, and treatment.[48]

Treatment

Thermal Laser Photocoagulation

Laser photocoagulation has been suggested to be beneficial, albeit with short-term follow-up. The greatest benefit may be for extrafoveal PCV.[49] In some studies that analyzed reported vision outcomes, ICGA-guided laser photocoagulation was successful in stabilizing or improving vision in 55–100% of eyes; however, vision loss occurred in 13–45% of eyes.[32,49–51] Photocoagulation of the whole lesion, compared with polyps only, appears to be more efficacious.[51]

Photodynamic Therapy

Verteporfin photodynamic therapy (PDT) causes regression or resolution of polyps by its angio-occlusive mechanism of action. In the Everest trial, 71.4% achieved complete occlusion of polyps[12] with resolution of exudative changes after less than three treatments, reduces loss of letters on the ETDRS chart to less than 15, with improved vision in 80–100% of patients after 1 year[52,53]. For treatment-naive patients the entire PCV lesion as indicated by ICGA (polyps plus the branching vascular network) should be treated.

Common complications reported with verteporfin-PDT therapy are subretinal hemorrhage, recurrence of PCV with leakage from the branching vascular network (BVN), RPE damage or tear, and fibrous scarring. Subretinal hemorrhage is common and can lead to vitreous hemorrhage and consequently a poor outcome.[52–54] Larger lesion size and a leaking vascular net[53] are risk factors for bleeding after PDT.

Anti-VEGF Therapy

Increased VEGF levels have been observed in PCV patients.[43] Recent studies have demonstrated the usefulness of anti-VEGF therapy for PCV. Reduction in the number of polypoidal complexes was low, achieved in 4/12 (33%) eyes treated with intravitreal ranibizumab[55] and 1/11 (9.09%) eyes with intravitreal bevacizumab.[56]

LAPTOP study is a phase IV prospective multicenter randomized clinical trial with two arms for 12 months: PDT versus ranibizumab, which demonstrated intravitreal ranibizumab is superior to PDT monotherapy in achieving visual gain.[54] The use of intravitreal conbercept has been reported for the management of PCV: 53 patients with PCV were identified at baseline. At month 12, mean changes in best corrected visual acuity (BCVA) from baseline were 14.4±14.1 letter scores for the pooled 0.5 mg group (n=25, p<.001) and 14.2±21.0 letter scores for the 2.0 mg group (n=18, p=.011). A gain of ≥15 letters was observed in 48.0% (12/25) and 44.4% (8/18) of patients receiving 0.5 and 2.0 mg conbercept, respectively.[57] A similar outcome was reported in aflibercept: 48 % and 27% of PCV patients had completely or partially regressed polyps after aflibercept monthly for 3 months.[58]

Combination Therapy

EVEREST is a multicenter, double-masked, ICGA-guided randomized controlled trial studying patients with symptomatic PCV. Eyes were treated with verteporfin PDT monotherapy, 0.5 mg ranibizumab monotherapy, or a combination of these treatments.[1] Both combination therapy and verteporfin PDT monotherapy were superior to ranibizumab monotherapy in achieving complete polyp regression at month 6. Improvements in BCVA and central retinal thickness (CRT) also favored combination therapy.[12]

The authors of a recent relatively large comparative case series reported that with combination verteporfin PDT plus bevacizumab there were better early BCVA outcomes than with verteporfin PDT alone (p=.0016 for the difference between treatments in mean BCVA change from baseline at 3 months and p=.048 at 12 months).[31] Combination therapy also decreased the rate of PDT-related hemorrhages compared with verteporfin PDT monotherapy (3/61

[4.9%] vs. 15/85 [17.6%], respectively), but did not impact the resolution and recurrence of lesions.[31]

These trials support the selection of ICGA-guided verteporfin PDT with or without combination with ranibizumab as standard preferred treatment options.

References

1. Yannuzzi LA, Wong DW, Sforzolini BS, et al. Polypoidal choroidal vasculopathy and neovascularized age-related macular degeneration. *Arch Ophthalmol*. 1999;117:1503–1510.
2. Japanese Study Group of Polypoidal Choroidal V. Criteria for diagnosis of polypoidal choroidal vasculopathy. *Nippon Ganka Gakkai Zasshi*. 2005;109:417–427.
3. Yi C, Ou J, Yian H, Mai G, Yu Q. A case report of idiopathic polypoidal choroidal vasculopathy. *Yan ke xue bao [Eye Science]*. 2001;17:126–129.
4. Liu Y, Wen F, Huang S, et al. Subtype lesions of neovascular age-related macular degeneration in Chinese patients. *Graefes Arch Clin Exp Ophthalmol*. 2007;245:1441–1445.
5. Hwang DK, Yang CS, Lee FL, Hsu WM. Idiopathic polypoidal choroidal vasculopathy. *J Chinese Med Assoc*. 2007;70:84–88.
6. Maruko I, Iida T, Saito M, Nagayama D, Saito K. Clinical characteristics of exudative age-related macular degeneration in Japanese patients. *Am J Ophthalmol*. 2007;144:15–22.
7. Wen F, Chen C, Wu D, Li H. Polypoidal choroidal vasculopathy in elderly Chinese patients. *Graefes Arch Clin Exp Ophthalmol*. 2004;242:625–629.
8. Yannuzzi LA. *Idiopathic polypoidal choroidal vasculopathy*. Macula Society Meeting: Miami, Florida; 1982.
9. Kleiner RC, Johnson RL. Posterior uveal bleeding syndrome. *Ophthalmology*. 1984;91.
10. Kleiner RC, Brucker AJ, Johnston RL. The posterior uveal bleeding syndrome. *Retina*. 1990;10:9–17.
11. Yannuzzi LA, Sorenson J, Spaide RF, Lipson B. Idiopathic

polypoidal choroidal vasculopathy (IPCV). *Retina*. 1990;10:1–8.
12. Koh AH, Expert PCV Panel, Chen LJ, et al. Polypoidal choroidal vasculopathy: evidence-based guidelines for clinical diagnosis and treatment. *Retina*. 2013;33:686–716.
13. Ozawa S, Ishikawa K, Ito Y, et al. Differences in macular morphology between polypoidal choroidal vasculopathy and exudative age-related macular degeneration detected by optical coherence tomography. *Retina*. 2009;29:793–802.
14. Kuroiwa S, Tateiwa H, Hisatomi T, Ishibashi T, Yoshimura N. Pathological features of surgically excised polypoidal choroidal vasculopathy membranes. *Clin Exp Ophthalmol*. 2004;32:297–302.
15. Nakashizuka H, Mitsumata M, Okisaka S, et al. Clinicopathologic findings in polypoidal choroidal vasculopathy. *Invest Ophthalmol Vis Sci*. 2008;49:4729–4737.
16. Dewan A, Liu M, Hartman S, et al. HTRA1 promoter polymorphism in wet age-related macular degeneration. *Science*. 2006;314:989–992.
17. Klein RJ, Zeiss C, Chew EY, et al. Complement factor H polymorphism in age-related macular degeneration. *Science*. 2005;308:385–389.
18. Jiang J, Huang L, Yu X, et al. Overexpression of HTRA1 Leads to Down-regulation of Fibronectin and Functional Changes in RF/6A Cells and HUVECs. *PLoS ONE*. 2012;7(10):e46115.
19. Kondo N, Honda S, Ishibashi K, Tsukahara Y, Negi A. Elastin gene polymorphisms in neovascular age-related macular degeneration and polypoidal choroidal vasculopathy. *Invest Ophthalmol Vis Sci*. 2008;49:1101–1105.
20. Huang L, Li Y, Guo S, et al. Different hereditary contribution of the CFH gene between polypoidal choroidal vasculopathy and age-related macular degeneration in Chinese Han people. *Invest Ophthalmol Vis Sci*. 2014;55:2534–2538.
21. Chakravarthy U, Wong TY, Fletcher A, et al. Clinical risk factors for age-related macular degeneration: a systematic review and meta-analysis. *BMC Ophthalmol*. 2010;10:31.

22. Nakashizuka H, Yuzawa M. Hyalinization of choroidal vessels in polypoidal choroidal vasculopathy. *Surv Ophthalmol*. 2011;56:278–279 [author reply 279].
23. Lafaut BA, Leys AM, Snyers B, Rasquin F, De Laey JJ. Polypoidal choroidal vasculopathy in Caucasians. *Graefes Arch Clin Exp Ophthalmol*. 2000;238:752–759.
24. Scassellati-Sforzolini B, Mariotti C, Bryan R, Yannuzzi LA, Giuliani M, Giovannini A. Polypoidal choroidal vasculopathy in Italy. *Retina*. 2001;21:121–125.
25. Ladas ID, Rouvas AA, Moschos MM, Synodinos EE, Karagiannis DA, Koutsandrea CN. Polypoidal choroidal vasculopathy and exudative age-related macular degeneration in Greek population. *Eye*. 2004;18:455–459.
26. Sho K, Takahashi K, Yamada H, et al. Polypoidal choroidal vasculopathy: incidence, demographic features, and clinical characteristics. *Arch Ophthal*. 2003;121:1392–1396.
27. Tao Y, Hu J, Li XX. Clinical characteristics of 254 cases of polypoidal choroidal vasculopathy. *Chinese J Ocular Fundus Dis*. 2012;28:4.
28. Byeon SH, Lee SC, Oh HS, Kim SS, Koh HJ, Kwon OW. Incidence and clinical patterns of polypoidal choroidal vasculopathy in Korean patients. *Jpn J Ophthalmol*. 2008;52:57–62.
29. Hou J, Tao Y, Li XX, Zhao MW. Clinical characteristics of polypoidal choroidal vasculopathy in Chinese patients. *Graefes Arch Clin Exp Ophthalmol*. 2011;249:975–979.
30. Ciardella AP, Donsoff IM, Yannuzzi LA. Polypoidal choroidal vasculopathy. *Ophthalmol Clin North Am*. 2002;15:537–554.
31. Gomi F, Sawa M, Wakabayashi T, Sasamoto Y, Suzuki M, Tsujikawa M. Efficacy of intravitreal bevacizumab combined with photodynamic therapy for polypoidal choroidal vasculopathy. *Am J Ophthalmol*. 2010;150:48–54.e41.
32. Kwok AK, Lai TY, Chan CW, Neoh EL, Lam DS. Polypoidal choroidal vasculopathy in Chinese patients. *Br J Ophthalmol*. 2002;86:892–897.
33. Okubo A, Arimura N, Abematsu N, Sakamoto T. Predictable

signs of benign course of polypoidal choroidal vasculopathy: based upon the long-term observation of non-treated eyes. *Acta Ophthalmol*. 2010;88:e107–14.
34. Uyama M, Wada M, Nagai Y, et al. Polypoidal choroidal vasculopathy: natural history. *Am J Ophthalmol*. 2002;133:639–648.
35. Lip PL, Hope-Ross MW, Gibson JM. Idiopathic polypoidal choroidal vasculopathy: a disease with diverse clinical spectrum and systemic associations. *Eye*. 2000;14(Pt 5):695–700.
36. Smith RE, Wise K, Kingsley RM. Idiopathic polypoidal choroidal vasculopathy and sickle cell retinopathy. *Am J Ophthalmol*. 2000;129:544–546.
37. Baillif-Gostoli S, Quaranta-El Maftouhi M, Mauget-Faysse M. Polypoidal choroidal vasculopathy in a patient with angioid streaks secondary to pseudoxanthoma elasticum. *Graefes Arch Clin Exp Ophthalmol*. 2010;248:1845–1848.
38. Sasahara M, Tsujikawa A, Musashi K, et al. Polypoidal choroidal vasculopathy with choroidal vascular hyperpermeability. *Am J Ophthalmol*. 2006;142:601–607.
39. Desmettre T, Devoisselle JM, Mordon S. Fluorescence properties and metabolic features of indocyanine green (ICG) as related to angiography. *Surv Ophthalmol*. 2000;45:15–27.
40. Yuzawa M, Mori R, Kawamura A. The origins of polypoidal choroidal vasculopathy. *Br J Ophthalmol*. 2005;89:602–607.
41. Costa RA, Navajas EV, Farah ME, Calucci D, Cardillo JA, Scott IU. Polypoidal choroidal vasculopathy: angiographic characterization of the network vascular elements and a new treatment paradigm. *Progr Retinal Eye Res*. 2005;24:560–586.
42. Spaide RF, Hall L, Haas A, et al. Indocyanine green videoangiography of older patients with central serous chorioretinopathy. *Retina*. 1996;16:203–213.
43. Byeon SH, Lew YJ, Lee SC, Kwon OW. Clinical features and follow-up results of pulsating polypoidal choroidal vasculopathy treated with photodynamic therapy. *Acta Ophthalmol*. 2010;88:660–668.

44. Okubo A, Hirakawa M, Ito M, Sameshima M, Sakamoto T. Clinical features of early and late stage polypoidal choroidal vasculopathy characterized by lesion size and disease duration. *Graefes Arch Clin Exp Ophthalmol*. 2008;246:491–499.
45. Kawamura A, Yuzawa M, Mori R, Haruyama M, Tanaka K. Indocyanine green angiographic and optical coherence tomographic findings support classification of polypoidal choroidal vasculopathy into two types. *Acta Ophthalmol*. 2013;91:e474–81.
46. Tan CS, Ngo WK, Lim LW, Lim TH. A novel classification of the vascular patterns of polypoidal choroidal vasculopathy and its relation to clinical outcomes. *Br J Ophthalmol*. 2014;98:1528–1533.
47. Gass JD. Biomicroscopic and histopathologic considerations regarding the feasibility of surgical excision of subfoveal neovascular membranes. *Am J Ophthalmol*. 1994;118:285–298.
48. Yannuzzi LA, Freund KB, Goldbaum M, et al. Polypoidal choroidal vasculopathy masquerading as central serous chorioretinopathy. *Ophthalmology*. 2000;107:767–777.
49. Lee MW, Yeo I, Wong D, Ang CL. Argon laser photocoagulation for the treatment of polypoidal choroidal vasculopathy. *Eye*. 2009;23:145–148.
50. Nishijima K, Takahashi M, Akita J, et al. Laser photocoagulation of indocyanine green angiographically identified feeder vessels to idiopathic polypoidal choroidal vasculopathy. *Am J Ophthalmol*. 2004;137:770–773.
51. Yuzawa M, Mori R, Haruyama M. A study of laser photocoagulation for polypoidal choroidal vasculopathy. *Jpn J Ophthalmol*. 2003;47:379–384.
52. Chan WM, Lam DS, Lai TY, et al. Photodynamic therapy with verteporfin for symptomatic polypoidal choroidal vasculopathy: one-year results of a prospective case series. *Ophthalmology*. 2004;111:1576–1584.
53. Hirami Y, Tsujikawa A, Otani A, et al. Hemorrhagic complications after photodynamic therapy for polypoidal choroidal vasculopathy. *Retina*. 2007;27:335–341.

54. Oishi A, Kojima H, Mandai M, et al. Comparison of the effect of ranibizumab and verteporfin for polypoidal choroidal vasculopathy: 12-month LAPTOP study results. *Am J Ophthalmol*. 2013;156:644–651.
55. Kokame GT, Yeung L, Lai JC. Continuous anti-VEGF treatment with ranibizumab for polypoidal choroidal vasculopathy: 6-month results. *Br J Ophthalmol*. 2010;94:297–301.
56. Gomi F, Ohji M, Sayanagi K, et al. One-year outcomes of photodynamic therapy in age-related macular degeneration and polypoidal choroidal vasculopathy in Japanese patients. *Ophthalmology*. 2008;115:141–146.
57. Qu J, Cheng Y, Li X, et al. Efficacy of Intravitreal injection of conbercept in polypoidal choroidal vasculopathy subgroup analysis of the AURORA study. *Retina*. 2016;36(5):926–937.
58. Ijiri S, Sugiyama K. Short-term efficacy of intravitreal aflibercept for patients with treatment-naive polypoidal choroidal vasculopathy. *Graefes Arch Clin Exp Ophthalmol*. 2015;253:351–357.

75

Central Serous Chorioretinopathy

Dennis Lam, Sudipta Das, Shirley Liu, Vincent Lee, Lin Lu

Introduction

Albrecht von Graefe first described a disease causing recurrent serous macular detachment and coined the term "central recurrent retinitis" in 1866.[1,2] One hundred years later, Bennet used the term "central serous retinopathy."[3] In 1967, Gass provided the classic description of the pathogenesis and clinical features of this condition and called it idiopathic central serous choroidopathy (CSC).[4–6] Currently, this chorioretinal disorder is known as central

serous chorioretinopathy (CSCR).

CSCR is a disorder with multifactorial etiology and complex pathogenesis. It typically affects middle-aged men and is characterized by serous neurosensory detachment (NSD) of the retina at the posterior pole. Most cases of CSCR are idiopathic and regress spontaneously within 3–4 months with good visual prognosis.[7] However, some patients suffer from a chronic form of the disease with persistent or recurrent serous macular detachment with progressive visual loss. Advances in indocyanine green angiography (ICGA) and optical coherence tomography (OCT) have led to greater understanding of the pathophysiology and treatment for CSCR. Photodynamic therapy (PDT) using lower doses and reduced fluence has revolutionized the treatment of symptomatic CSCR. Recently, evolving treatment options in the form of antivascular endothelial growth factor (anti-VEGF) and mineralocorticoid receptor (MR) antagonists appear to be promising, but more support from randomized controlled trials (RCTs) is needed before incorporating them into regular clinical practice.

Definition, Pathogenesis, Risk Factors, and Epidemiology

Definition

Central serous chorioretinopathy (CSCR or CSC) is a disease characterized by localized and serous detachments of the neurosensory retina with or without focal pigment epithelial detachments (PEDs) and altered retinal pigment epithelium (RPE). The disease causes central visual symptoms due to the presence of serous retinal detachments (SRDs) in the macular area. There are reports of asymptomatic patients presenting with one or multiple episodes of extramacular SRDs, as observed in the contralateral eye of an active CSCR patient or when examining the eyes of relatives of CSCR patients.[8,9]

The disease termed “CSCR” is classically divided into two forms, i.e., acute and chronic. This distinction to some extent depends upon the duration of the SRD and on the presence of extended RPE

changes. The acute form usually resolves within 3–4 months, leaving mostly color discrimination defects in a few patients.[7] The chronic form, which was initially termed as "diffuse retinal epitheliopathy" by Yannuzi et al. in 1992,[10] is characterized by widespread tracks of RPE atrophy showing reduced fundus autofluorescence (FAF) with or without SRD.[11,12] In this chronic form of disease, in addition to chronic SRD and multifocal RPE atrophic areas, there can be irregular RPE detachments and longstanding intraretinal cystoid cavities, usually seen with disease duration longer than 5 years.[13,14]

Pathogenesis

The pathophysiology of CSCR is thought to involve multiple etiologies and mechanisms that ultimately lead to widespread choroidal circulatory abnormalities and subsequent RPE disturbances.[15] The hyperpermeability of the choroid can be due to stasis, ischemia, or inflammation, which is evident with the staining of the inner choroid in mid-phase ICGA.[16–19] This is further supported by the enhanced-depth imaging (EDI-) OCT finding of a thickened choroid in both eyes of patients with CSCR.[20] These hyperpermeable choroidal vessels, hypothesized to cause increased tissue hydrostatic pressure, overcome the barrier function of the RPE and lead to the formation of PEDs. This phenomenon is supported by areas of choroidal staining contiguous with the foci of RPE leakage on fluorescein angiography (FA).[16,21,22] Further increases in hydrostatic pressure in the choroid cause breaches in the RPE that allow fluid to enter into the subretinal space. Choriocapillary nonperfusion, as revealed by areas of hypofluorescence on ICGA in patients with CSCR, leading to choroidal venous dilation and congestion, has also been identified as one of the possible causes.[16–18] Focal loss of polarity of RPE cells has also been attributed to causing CSCR by actively pumping fluid into the subretinal space.[23]

Recently, new research has demonstrated the potential involvement of the aldosterone/mineralocorticoid receptor pathway in the pathogenesis of CSCR. In preclinical animal models, intravitreal injection of aldosterone provoked vasodilation,

thickening, and leakage of the choroidal vessels with elongation of RPE cells and accumulation of subretinal fluid, mimicking CSCR.[24]

Risk Factors

In 1927, Horniker suggested that psychiatric disturbances were linked to CSCR.[25] However, it was Yannuzi in 1987 who observed a definite association between CSCR and the "type-A" personality pattern.[26] Subsequently, antipsychotic medication use, psychologic stress, and depression were described as independent risk factors for CSCR.[27,28] Recently, a possible association between narcissistic personality and CSCR has been suggested by Carlesimo et al.[29] Patients receiving corticosteroid therapy are at higher risk of developing CSCR.[30–32] Though systemic intake of steroids (both oral and intravenous) is an independent risk factor for CSCR,[27,32,33] it has also been described after local administration of steroids via inhaled, intranasal,[34,35] epidural,[36] intraarticular,[37,38] topical dermal,[39] and periocular[40] routes. Furthermore, there are two reports suggesting the aggravation of preexisting CSCR and the induction of CSCR after vitrectomy with intravitreal triamcinolone injection.[41,42] Steroid-induced CSCR is probably an idiosyncratic response in selected individuals, with less male predilection, frequent bilaterality, and commonly atypical presentation.[43,44] Steroid-induced SRD during corticosteroid treatment for posterior uveitis can be deceptive, and prompt discontinuation of steroid therapy should be advocated once the diagnosis is confirmed.[43] CSCR has also been reported following kidney, bone marrow and heart transplantations.[45–48] Conditions that are associated with increased endogenous cortisol production, such as Cushing disease and pregnancy, increase the risk of having CSCR. In pregnancy, the risk is greatest during the third trimester and usually resolves after delivery.[33,49–51] Patients with hypertension and obstructive sleep apnea also have a higher risk of developing CSCR.[52] Abnormalities in coagulation and platelet aggregation have been proposed as risk factors in the pathogenesis of CSCR.[53] Aqueous sample analysis in patients with CSCR showed lower levels of platelet-derived growth factor (PDGF). This suggests PDGF may play a role in the pathogenesis of CSCR.[54] The role of VEGF in CSCR has not been

proven in studies.[55] Gastroesophageal reflux and *Helicobacter pylori* infection have been separately reported to be associated with CSCR and treatment of the above conditions has been shown to accelerate the rate of subretinal fluid resolution.[56–58] Smoking, antihistamines, alcohol consumption, and allergic respiratory diseases are known to increase the risk of CSCR.[59] Recently, oral MEK inhibitors (binimetinib) used for metastatic cancer were shown to produce transient bilateral SRDs in 65% of patients.[60,61] Though use of phosphodiesterase-5 inhibitors (sildenafil, tadalafil, vardenafil) was shown to cause CSCR, there is conflicting evidence in different studies regarding resolution of the disease after their discontinuation.[62,63]

So far, cases of familial CSCR have been reported in the literature, but no clear transmission pattern or genotype has been found to be associated with the disease.[64–66] In a recent analysis of five families, 50% of the eyes from relatives of CSCR patients had a choroid thicker than 395 nm, suggesting that pachychoroid could be one of the phenotypical indicators and that CSCR may be inherited with a possible dominant transmission pattern.[8]

Epidemiology

At present, CSCR ranks after age-related macular degeneration (AMD), diabetic retinopathy (DR), and retinal vein occlusion (RVO) as the most common vision-threatening disease.[67] Men are mostly affected in 72–88% of cases,[68] and the annual incidence in a population-based study was six times higher in men than in women.[69] Recent epidemiologic data confer a higher mean age of affected patients than generally assumed, ranging between 39 and 51 years.[69,70] CSCR has rarely been reported in children.[71] The epidemiology of CSCR in older patients (i.e., older than 50 years of age) shows more bilaterality, features of chronic CSCR, female prevalence, and risk of developing choroidal neovascularization (CNV).[69,72] In this age group one should always consider and exclude other differential diagnoses, such as AMD and polypoidal choroidal vasculopathy (PCV).[73]

Clinical Features

Demographics

The incidence of CSCR varies among different ethnic groups. A suspected higher frequency is noted among Asians and whites as compared to blacks, and in the latter group CSCR behaves more aggressively with poor visual outcome.[73,74] In Asian populations, CSCR is common and both bilateral and multifocal forms are seen more frequently in this population compared to other ethnic groups.[75] Highly elevated SRD and large pigment epithelial detachments (PED) are also noticed in Asian populations, which often get misdiagnosed as Harada's disease.[76]

Symptoms

Acute CSCR patients usually complain of symptoms related to the localization of SRD in the macular area (Fig. 75.1). These are mostly blurred vision, relative central scotoma, metamorphopsia, mild to moderate dyschromatopsia, hypermetropization, micropsia, and reduced contrast sensitivity. The anteriorly displaced neurosensory retina causes the eye to become hyperopic and patients often gain benefit from the addition of hyperopic corrective lenses.

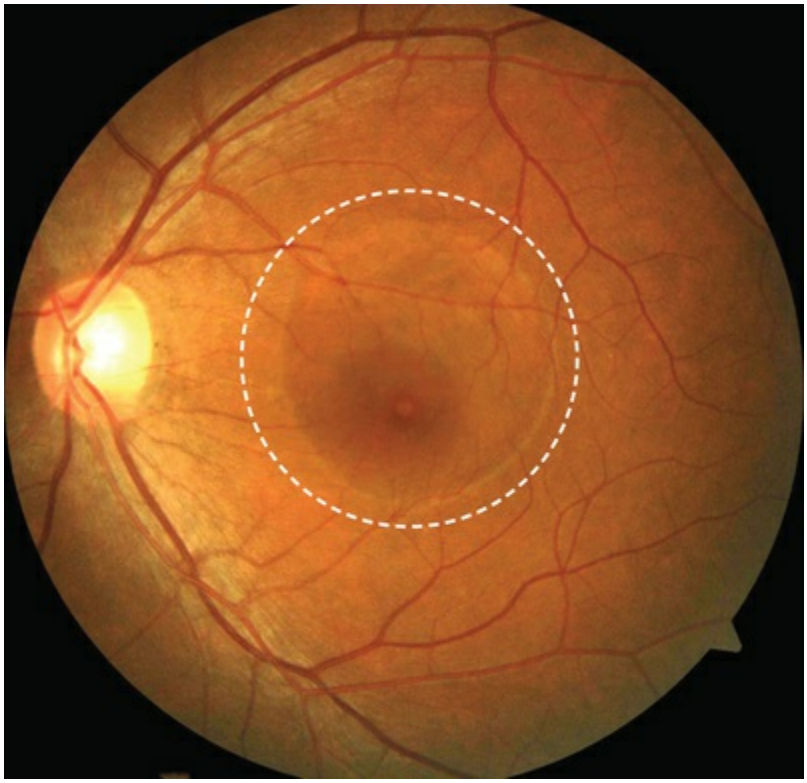

FIG. 75.1 Color fundus of a young male patient with typical central serous chorioretinopathy presenting with circular neurosensory detachment at the posterior pole (*encircled by white ring*).

Signs

The hallmark of acute CSCR is a well-demarcated round or oval-shaped area of NSD over the posterior pole. This can be associated with one or multiple serous PEDs. Though indirect ophthalmoscopy is sufficient to diagnose SRD, sometimes minimal subretinal fluid or small PEDs can be better detected by slit-lamp biomicroscopy using a 78 D lens. In those patients, the loss of foveal reflex provides a clue for diagnosis. Due to increased visibility of xanthophyll pigments, these patients often have a yellow discoloration of the fovea.[4,50,68,77] Phagocytosed photoreceptor outer segments from the outer retina can sometimes appear as tiny yellow dots at the inner surface of the RPE[78] (Fig. 75.2). The subretinal fluid in acute CSCR is usually transparent but occasionally can become turbid due to subretinal or sub-RPE fibrin deposition[4,68] (Fig. 75.3). This fibrin usually dissolves over time but sometimes coalesces to cause subretinal fibrosis leading to a

permanent decrease in vision. Patients with CSCR can also present with inferior bullous exudative retinal detachment.[79,80] In chronic cases there are areas of RPE change and typical RPE atrophic tract in the fundus, which are located inferiorly due to the gravitational effect of longstanding subretinal fluid. They can also present with chronic cystoid macular edema, subretinal lipid deposition, and secondary CNV.

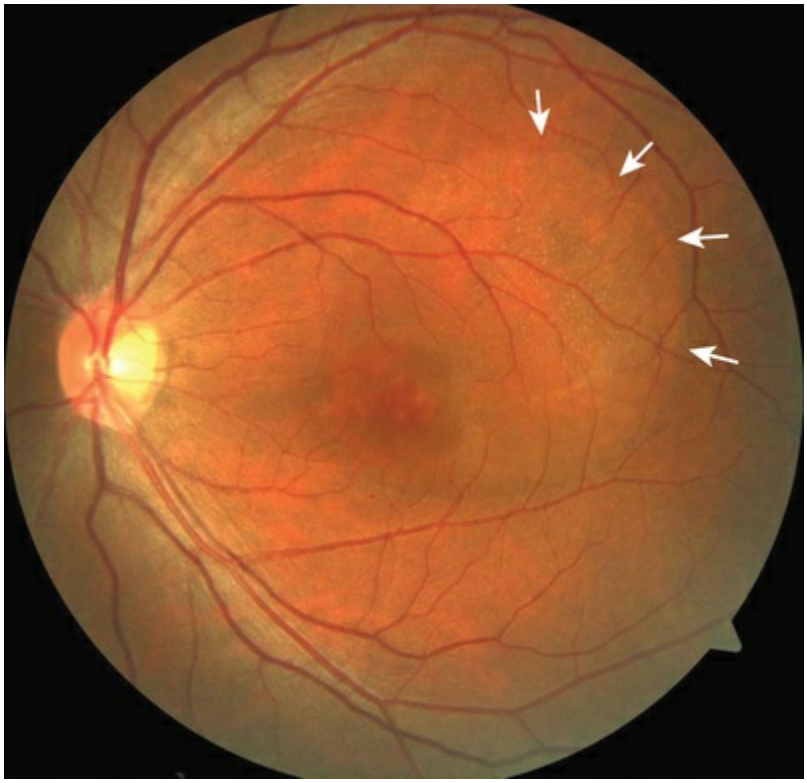

FIG. 75.2 Color fundus photograph of a patient with central serous chorioretinopathy showing neurosensory detachment of the parafoveal region, with yellow dots on the posterior surface of the detached retina (*white arrows*).

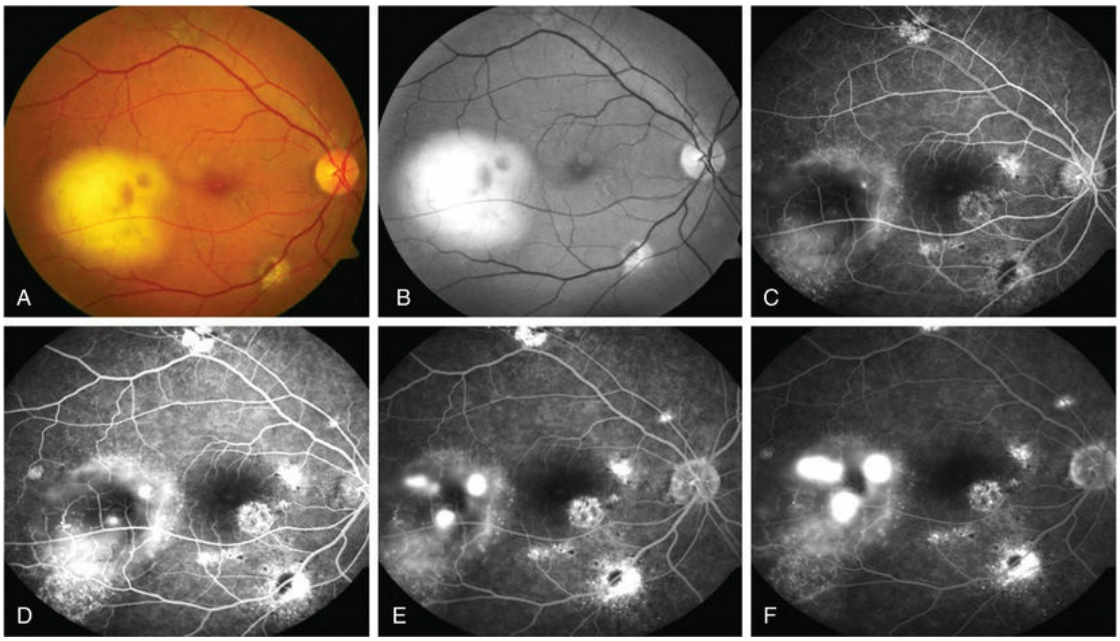

FIG. 75.3 This patient with chronic central serous chorioretinopathy showed organized subretinal fibrin with subretinal fluid temporal to the macula. Fluorescein angiography showed areas of retinal pigment epithelial atrophy with multiple pinpoint leaks adjoining the fibrin.

Differential Diagnosis

Age-Related Macular Degeneration

CSCR, CNV, and PCV can be grouped together on the spectrum of "pachychoroid" conditions.[81] AMD is the most important differential diagnosis in CSCR patients aged 50 years or older.[18] Secondary CNV (mostly type 2) can develop in patients with chronic CSCR during follow-up or after laser photocoagulation. Although each of the diseases has its own characteristic FA and ICGA features, it might be difficult to differentiate between the two because of diffused and ill-defined leakage. OCT may be helpful in those cases by showing the neovascular complex in AMD.

Polypoidal Choroidal Vasculopathy

Because of serous macular detachment, RPE alteration, and choroidal hyperpermeability on ICGA, it can be difficult to

distinguish PCV from chronic CSCR. The important points that favor the diagnosis of polyps are subretinal hemorrhage, branching vascular network, and leaking polyps on ICGA. OCT typically shows serosanguineous, notched or hemorrhagic PED and higher optical density of subretinal fluid.[82]

Optic Disc Pit

Optic disc pits are focal excavations located in the temporal aspect of the optic nerve head creating communication between the vitreous cavity, the subretinal space, and to some extent the subarachnoid space. They have been seen to produce chronic or recurrent serous retinal detachment following schisis of the inner retina in around 45% of cases with variable intraretinal cystoid edema. The diagnosis can be confirmed clinically by careful peripapillary examination and the absence of leakage on FA of optic disc pits.

Inflammatory and Infectious Diseases

Vogt–Koyanagi–Harada (VKH) disease is a multisystemic disorder with bilateral granulomatous panuveitis, which often presents with multiple serous retinal detachments mimicking CSCR. Apart from its systemic, neurologic, and dermatologic signs, the presence of vitritis, increased choroidal thickening on ultrasound, and pinpoint multifocal leaks on FA readily distinguish it from CSCR. Posterior scleritis can also present with serous retinal detachment. In this case, however, patients frequently experience pain on ocular movement and ultrasound B-scans demonstrate thickening of the suprachoroidal space with the characteristic T-sign. Hence, differentiation for these conditions is of utmost importance, as unlike CSCR, systemic steroids are the mainstay of treatment. Other inflammatory conditions causing SRD include sympathetic ophthalmia, uveal effusion syndrome, and benign reactive lymphoid hyperplasia of the choroid. Presumed ocular histoplasmosis syndrome (POHS) is an infectious disease that may cause SRD like CSCR, but it has characteristic punched-out peripheral chorioretinal lesions and peripapillary atrophy.

Autoimmune and Vascular Disorders

Autoimmune diseases such as systemic lupus erythematosus, polyarteritis nodosa, and scleroderma produce fibrinoid necrosis of the choroidal vessels. The disease process itself and sometimes systemic steroid therapy can lead to SRD, complicating the outcome. A few nonautoimmune conditions like malignant hypertension, toxemia during pregnancy, and disseminated intravascular coagulopathy can also present with NSD secondary to choroidal arterial occlusion.

Intraocular Tumors

Various types of choroidal tumors, including choroidal hemangioma, choroidal melanoma, choroidal osteoma and choroidal metastasis, can cause exudative macular detachment mimicking CSCR. It is important to differentiate a malignant and potentially lethal condition from CSCR. Most of the time, large tumors are detected clinically, but sometimes small tumors, especially choroidal hemangiomas, are difficult to discern in the presence of subretinal fluid. Ultrasonography is useful in detecting and differentiating the nature of the tumor. In hemangiomas, ICGA shows a classical "wash-out" phenomenon in late phases of angiography and EDI-OCT shows increased caliber of medium and large choroidal vessels in the tumor with normal choriocapillaries.[83]

Dome-Shaped Macula

Dome-shaped macula is a forward bulge of the macula within a posterior pole staphyloma in myopic eyes; fluctuating serous foveal detachment is observed in around 50% of these eyes.[84] This condition can be associated with pinpoint leakage on FA, small PEDs, and greater subfoveal choroidal thickness on OCT, making it difficult to differentiate from CSCR.[85] SRDs resolve spontaneously in most cases. In chronic and persistent SRDs there are studies reporting good results with half-fluence PDT and oral spironolactone.[86,87]

Ancillary Testing

Optical Coherence Tomography (OCT)

Spectral domain (SD-OCT) and recently, enhanced-depth imaging and swept-source technologies, have made the understanding of CSCR better by allowing better full-depth visualization of the neurosensory retina, RPE, choroid, and choroidal vessels. Hyperreflective dots on SD-OCT seen in the subretinal space and within retinal layers correspond with the hyperautofluorescent area on FAF.[88–90] Throughout the disease process, an increased number of dots tends to correlate with worse final visual acuity.[91] Elongation of photoreceptor outer segments in the area of a macular SRD is a frequent SD-OCT finding in CSCR. Frequently, erosion of photoreceptor outer segments is visible on SD-OCT at the site of leakage, suggesting mechanical abrasion from active flow through the RPE break. Serous PED is seen in 50–100% of CSCR-affected eyes.[92,93] In active CSCR cases, a combination of SD-OCT with FA identified an elevation of the RPE or a PED at the leakage sites in most or all cases[94] (Fig. 75.4). Compared to healthy subjects, increased choroidal thickness has been reported in both affected and fellow eyes of CSCR patients.[94,95] Localization of PEDs in the areas of dilated, large choroidal vessels and thickened choroid on SD-OCT, (Fig. 75.5) and with vascular hyperpermeability on ICGA, suggests the role of choroidal flow deregulation in the pathogenesis of PED.[94] In chronic CSCR, there can be hyperreflective content over the Bruch membrane, creating a "double layer sign" on OCT.[93] Quantitative measurement and thickness maps taken serially can be used to assess disease progression and response to treatment. Treatment response to photodynamic therapy (PDT) when evaluated with EDI-OCT has shown a 20% reduction in subfoveal choroidal thickness one year after half-fluence treatment.[96] Thinning of the outer nuclear layer, chronic cystoid degeneration, and disruption of the ellipsoid zone (junction of the inner and outer segments of the photoreceptors) on OCT are associated with poorer visual outcome.[89]

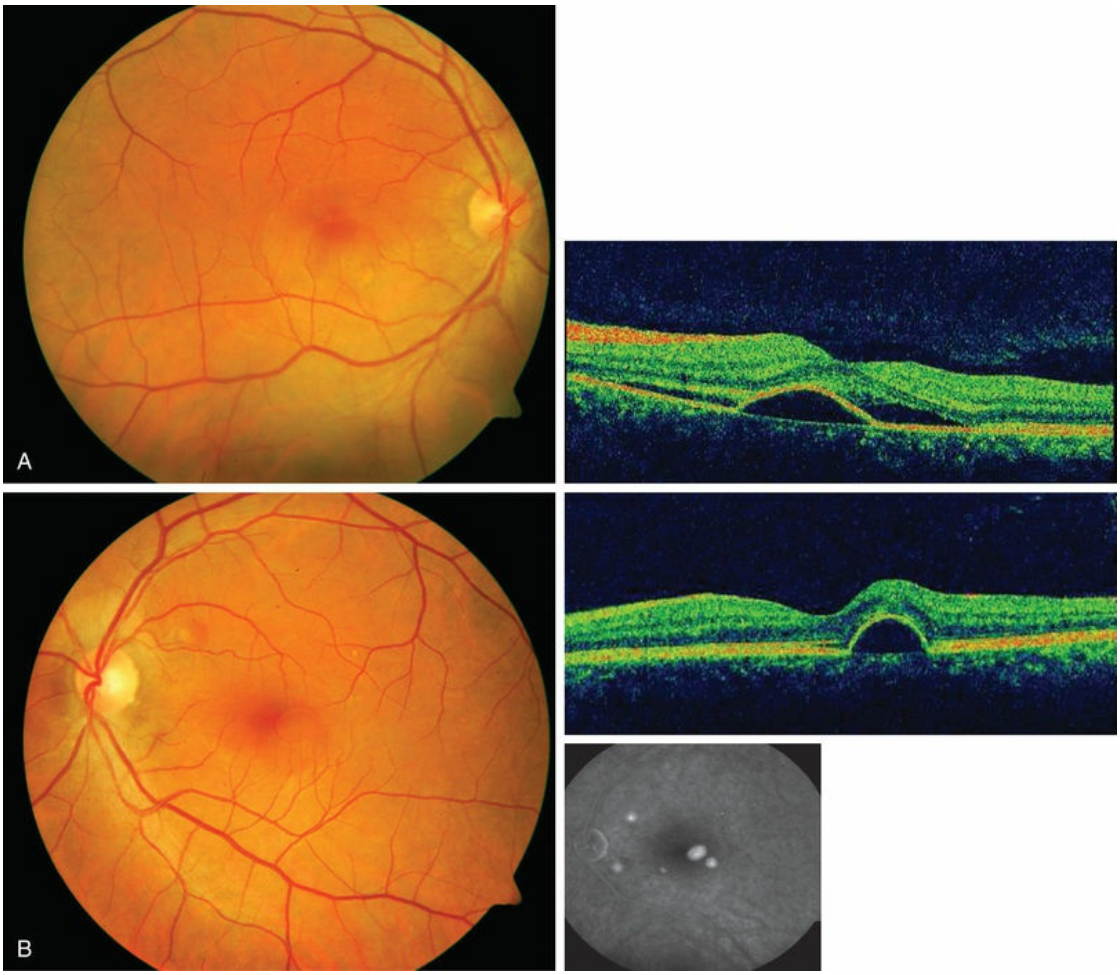

FIG. 75.4 This 45-year-old male presented with a right eye relative scotoma for 3 weeks. (A) Clinical examination showed subretinal fluid together with a pigment epithelium detachment (PED) in the macula. Optical coherence tomography (OCT) shows PED with subretinal fluid. Fluorescein angiogram (FA) showed initial pooling of dye in the PED followed by leakage. (B) Left eye showed PED in fundus photo and OCT with pooling of dye on FA.

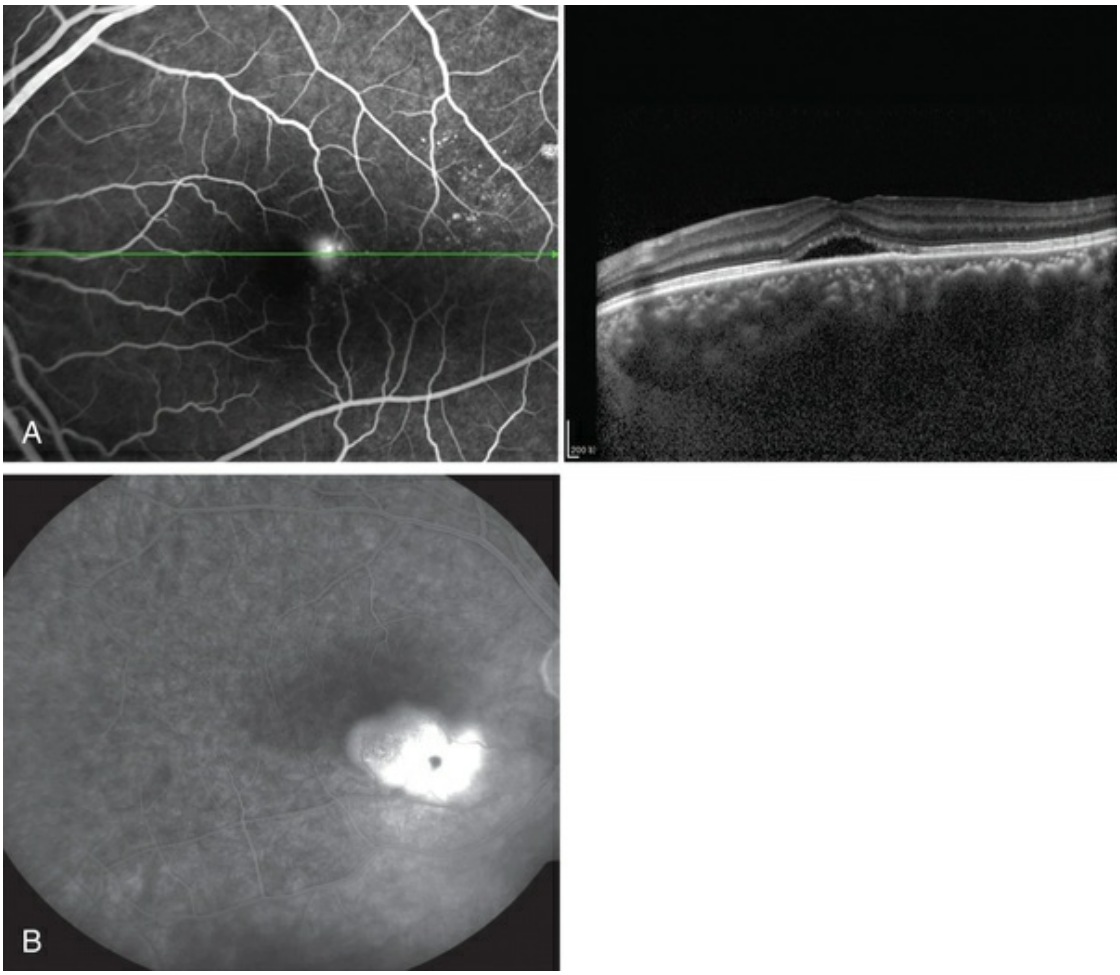

FIG. 75.5 Enhanced-depth imaging spectral domain optical coherence tomography showed an increase of subfoveal choroidal thickness in a patient with acute central serous chorioretinopathy.

Fundus Autofluorescence

FAF mostly originates from the RPE lipofuscin and reflects RPE health. It allows for noninvasive detection of the changes seen at different phases and forms of CSCR. Focal areas of hypoautofluorescence corresponding to the leakage points in acute CSCR are observed in 70–100% of eyes. This supports the hypothesis of a focal RPE defect or detachment[90] (Fig. 75.6). The SRD in acute CSCR also shows hypoautofluorescence due to the masking effect of SRF and elongated photoreceptors. As the disease progresses to become persistent or chronic, with the resolution of subretinal fluid, there is increasing hyperautofluorescence due to the accumulation of non-shed fluorophores. The pattern of this

change in FAF has been shown to correlate with visual acuity.[97] FAF can be pathognomonic in chronic CSCR by multiple hypoautofluorescent "gravitational tracks" with a thin border of surrounding hyperautofluorescence[98,99] (Fig. 75.7).

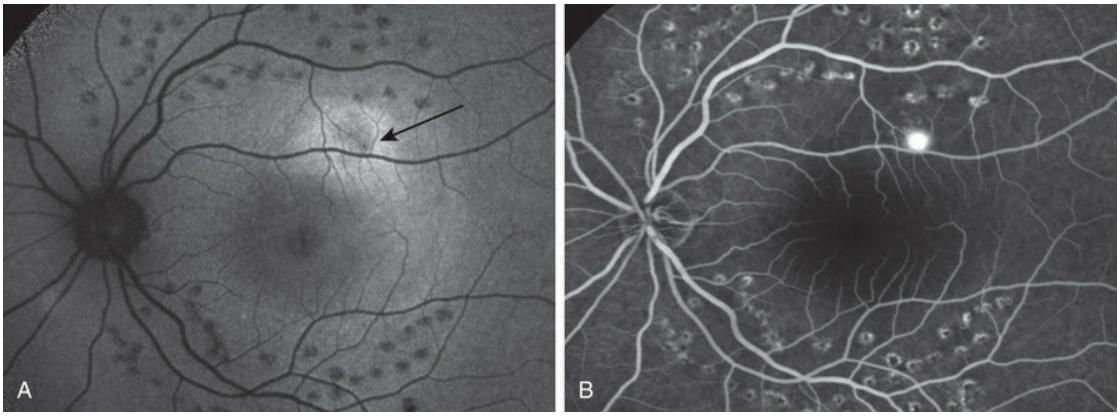

FIG. 75.6 This 38-year-old man with central serous chorioretinopathy was treated with ill-defined laser for submacular fluid before he presented to us with active pinpoint leakage on fluorescein angiography of the left eye. Fundus autofluorescence showed increased autofluorescence suggestive of longstanding subretinal fluid with point hypoautofluorescence (*black arrow*) corresponding with the leak on angiography.

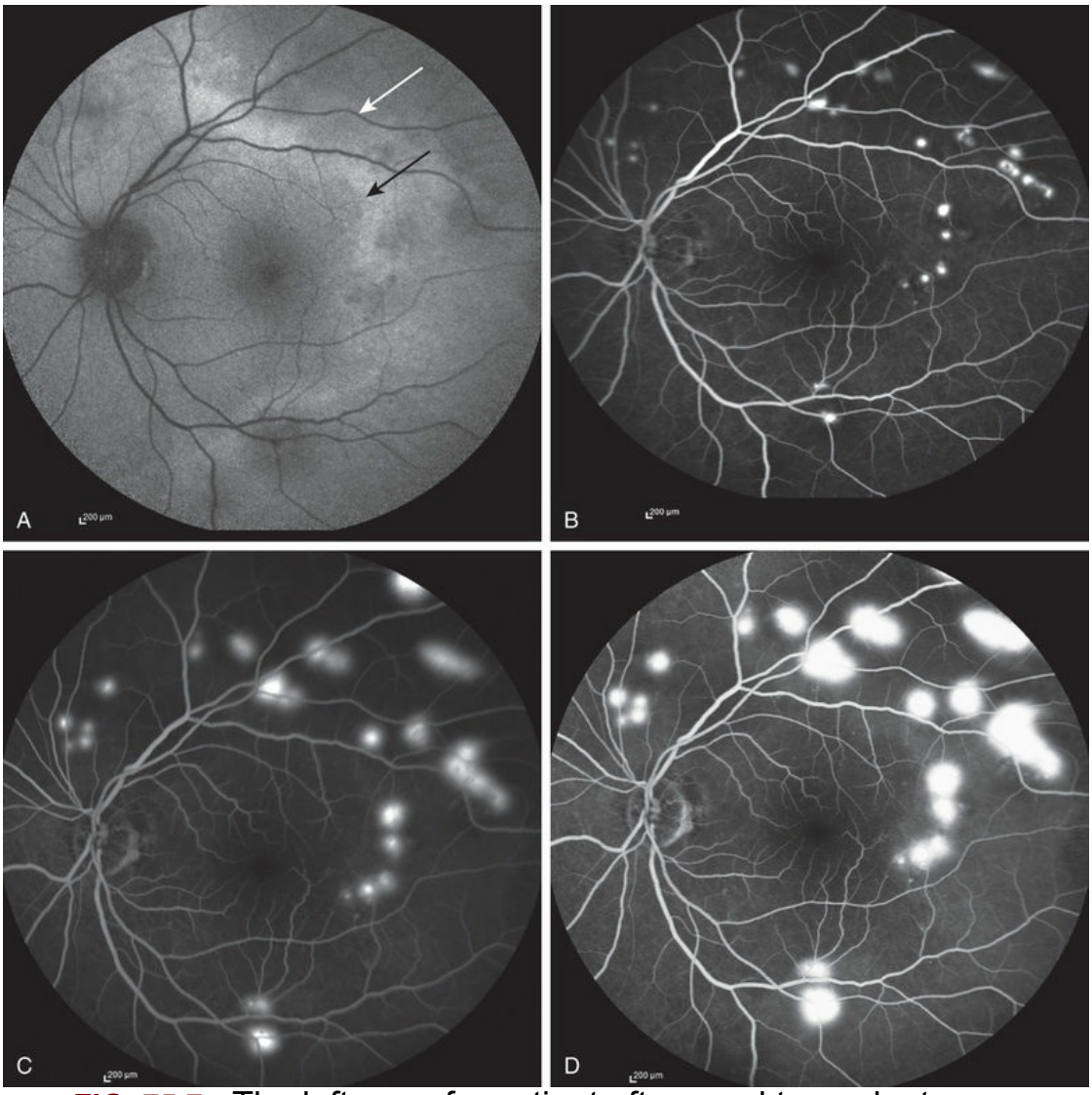

FIG. 75.7 The left eye of a patient after renal transplant on long-term systemic steroids showing multifocal pinpoint leaks in central serous chorioretinopathy. Note the hypoautofluorescent patches (*white arrow*) with surrounding hyperautofluorescence (*black arrow*) suggestive of the chronic nature of the disease.

Fluorescein Angiography (FA)

FA in acute CSCR classically shows leakage in either an inkblot or smokestack pattern. In the former, the leakage starts as a pinpoint in the early phase and then concentrically enlarges in the late phase to appear as an inkblot (Fig. 75.8). In smokestack appearance, the leakage again starts as a pinpoint in the early phase, but gradually the hyperfluorescence ascends and expands to form a mushroom

cloud or umbrella-like appearance. The smokestack pattern (Fig. 75.9) is less frequent and appears in only about 10–15% of patients with acute CSCR, especially in the very early stage.[100] It is caused by an increased protein concentration in the subretinal fluid. Chronic CSCR shows diffuse RPE window defect and patchy hyperfluorescence due to RPE atrophy (Fig. 75.3). Multifocal CSCR would show multiple sites of leakage (Fig. 75.7). FA is also useful in differentiating CSCR from other conditions such as CNV and VKH and helps in diagnosing unnoticed extramacular leaks in the affected or fellow eye.

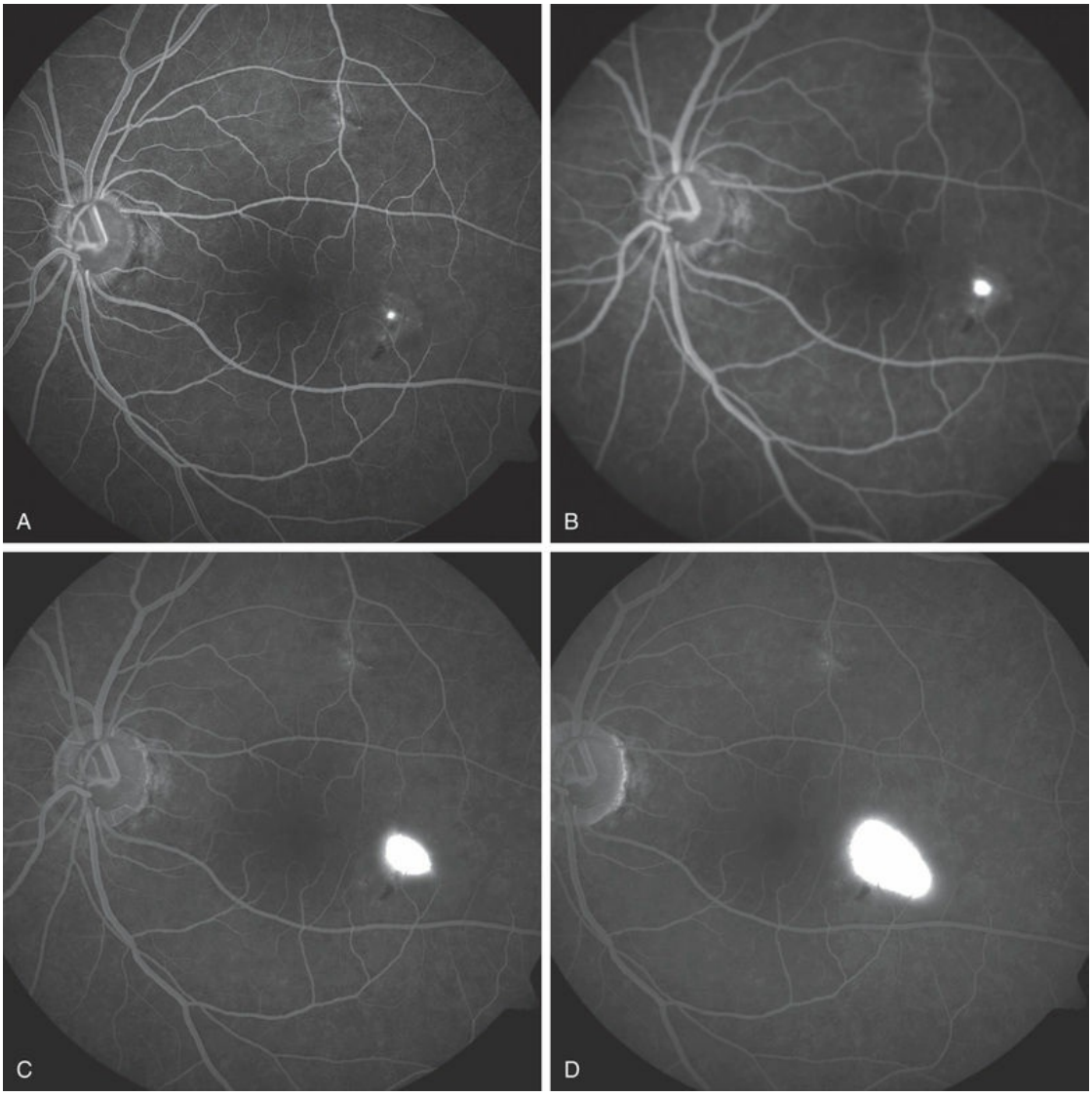

FIG. 75.8 Inkblot leakage (fluorescein angiogram). The hyperfluorescence starts as a pinpoint and then enlarges circumferentially to produce intense

hyperfluorescence in the late phase similar to the appearance of a drop of ink on a piece of paper.

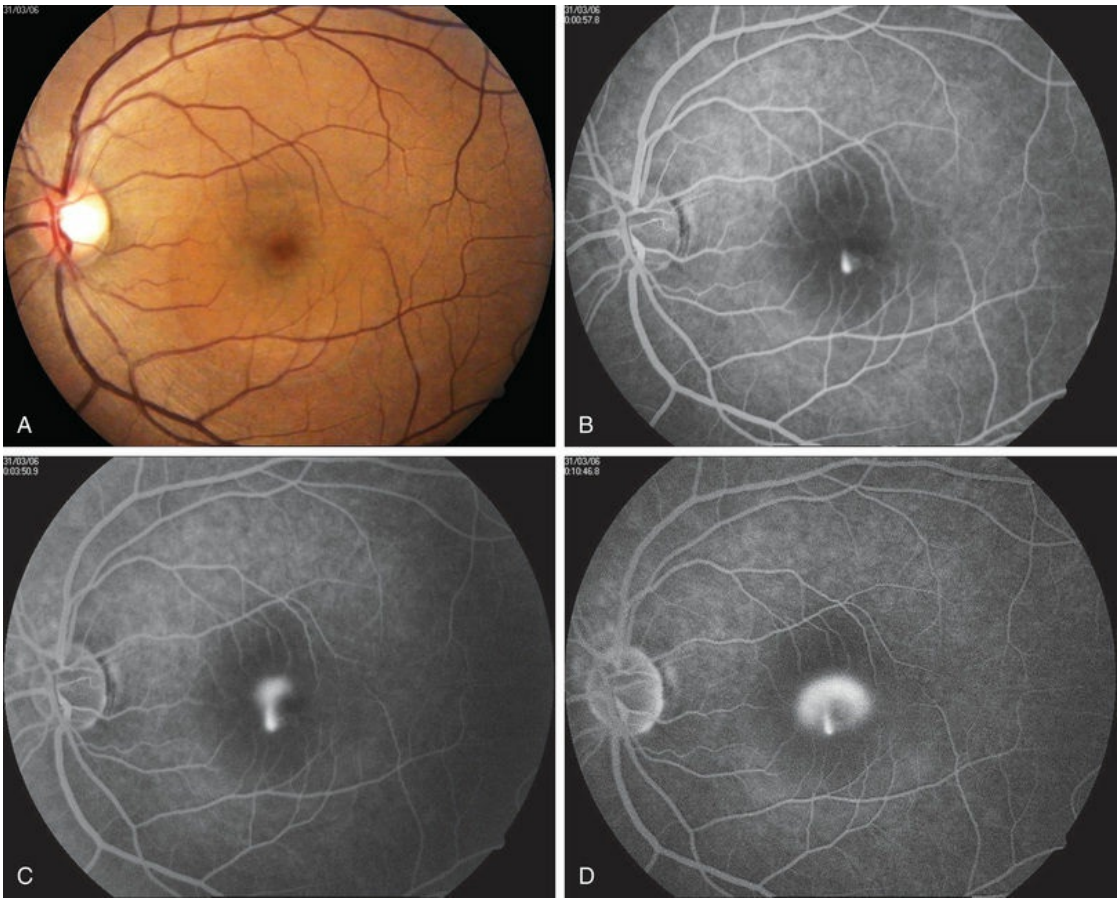

FIG. 75.9 Smokestack appearance(fluorescein angiogram). The hyperfluorescent spot starts as a pinpoint and then diffuses upward and laterally to give a mushroom cloud or umbrella-like appearance.

Indocyanine Green Angiography

ICGA is one of the most important investigations in CSCR because it demonstrates the choroidal vascular changes that contribute to the disease process and can act as a guide to treatments such as photodynamic therapy (PDT). ICGA in CSCR shows delay in choroidal filling in the early phase with hypofluorescent areas resulting from nonperfusion of choriocapillaries. This leads to choroidal venous dilatation that results in geographic areas of

hyperfluorescence, which indicates choroidal hyperpermeability in the mid phase (Fig. 75.10). In the late phase there is either washout or persistent hyperfluorescence. In addition, punctate hyperfluorescent spots are often seen in the mid- and late phases in 80–90% of active CSCR patients.[101] The area of choroidal vascular abnormality seen in ICGA is frequently bilateral and usually much more widespread than the leakage seen on FA.

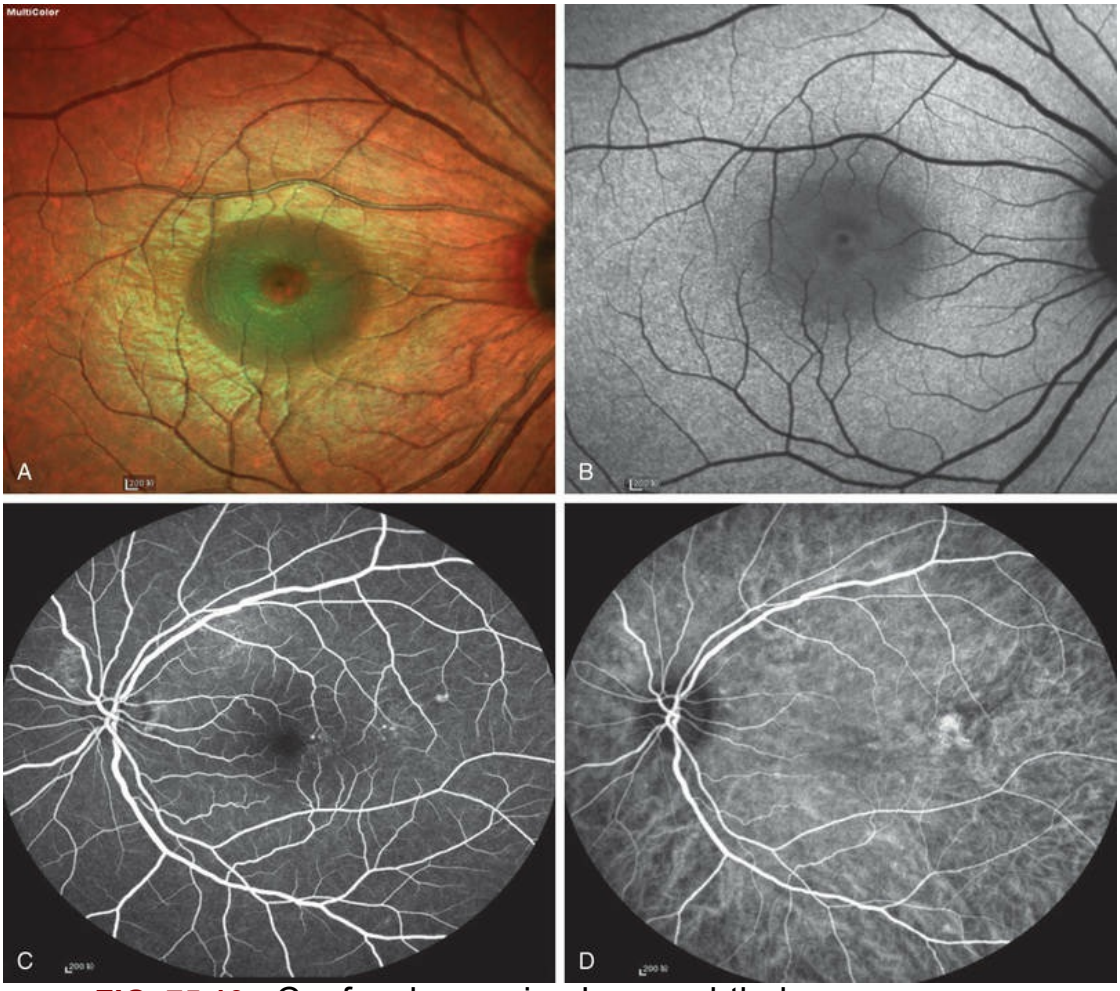

FIG. 75.10 Confocal scanning laser ophthalmoscope allows for simultaneous scanning and provides more information on macular changes in central serous chorioretinopathy patients. (A) Multicolor imaging showing dome-shaped neurosensory detachment (NSD); (B) hypoautofluorescence of NSD; (C) pinpoint leak on fluorescein angiography; and (D) dilated choroidal vessels on indocyanine green angiography.

Multifocal Electroretinography

Multifocal electroretinography (mfERG) can indicate widespread retinal dysfunction in CSCR beyond what is appreciated on clinical examination. First- and second-order kernel mfERG response amplitudes are reduced in patients with CSCR.[102] First-order kernel mfERG amplitudes are reduced in the center and the second-order responses are predominately reduced in the peripheral retina. This suggests that, though outer retinal dysfunction is localized in the center, inner retinal dysfunction might extend beyond the border of visible SRD and can be seen in the fellow eye also. Unlike OCT, mfERG response amplitudes were found to correlate with visual acuity.[102,103] The amplitude of mfERG improves markedly after resolution of subretinal fluid but does not return to baseline.

Microperimetry

Microperimetry allows functional assessment of macular sensitivity in patients with CSCR. In acute CSCR, presence of subretinal fluid causes reduced macular sensitivity in both the central and paracentral areas. It has been shown to improve; however, the condition never reverts to normal after resolution of subretinal fluid with or without treatment.[104,105] More often there are residual focal areas of reduced sensitivity, which correspond to RPE irregularities or defects at the ellipsoid layer on OCT. Moreover, macular sensitivity demonstrated correlation with central macular thickness on OCT and visual acuity, suggesting the existence of structural and functional correlation in CSCR.[106]

Natural History

Most acute CSCR patients show spontaneous visual recovery within 3–4 months. However, some patients may progress to chronic or recurrent diseases, which lead to areas of RPE atrophy and pigmentation in the macular area with subsequent visual loss. Poor visual acuity on presentation and long-standing macular detachment suggest worse prognosis. Up to 50% of patients with CSCR develop recurrence within the first year of presentation.[107] A

history of psychiatric illness, especially depression, is associated with a higher rate of recurrence. A small proportion of patients develop irreversible visual loss due to gross RPE atrophy, subretinal fibrosis, development of CNV (0.3–2% per patient per year)[108] or chronic cystoid macular degeneration (CMD) (Fig. 75.11). According to the study by Ooto et al., eyes with resolved CSCR with 20/20 or better visual acuity had reduced cone density with preserved ellipsoid zone when analyzed with adaptive optics scanning laser ophthalmoscope, compared to controls.[109] This explains the presence of residual symptoms like metamorphopsia, scotoma, reduced contrast and color sensitivity even in patients with well recovered vision after resolution of acute CSCR. Thus, the loss of photoreceptors in eyes with good acuity emphasizes the subclinical functional loss that patients can experience after even a single episode of CSCR.

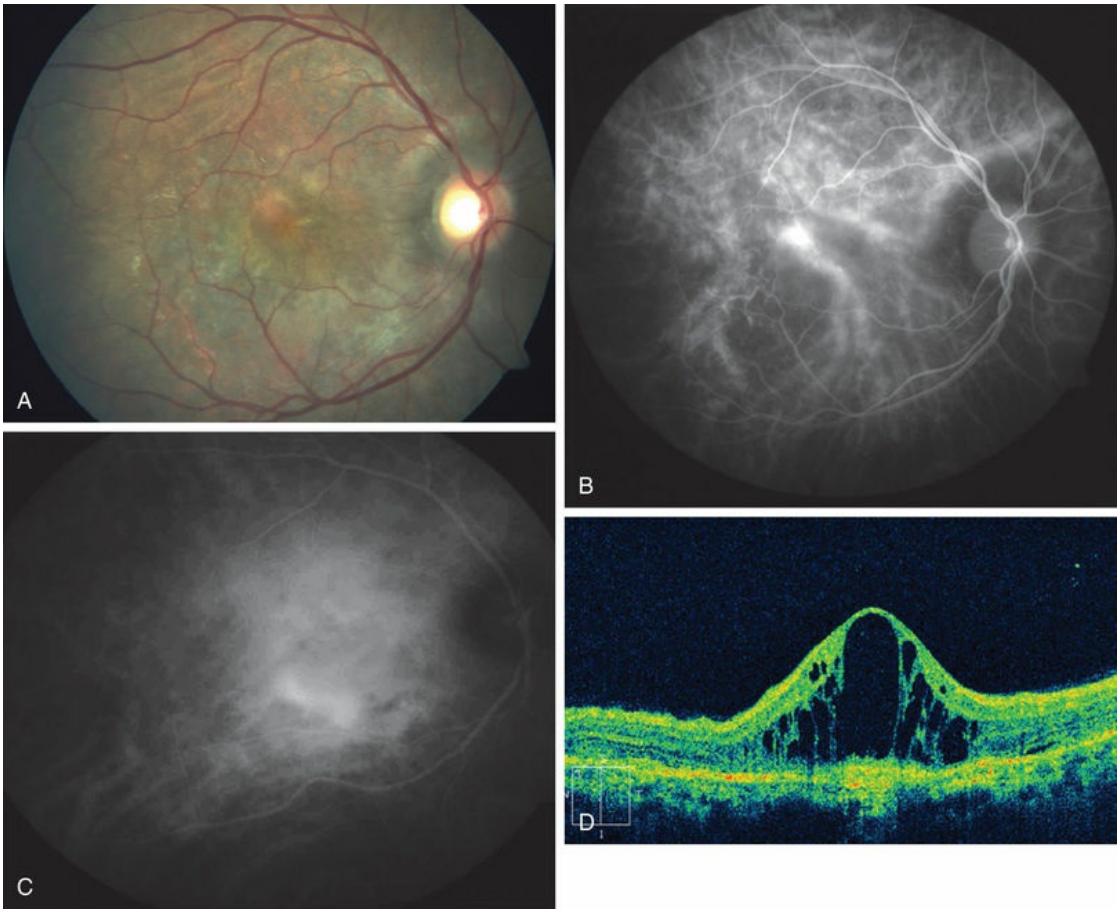

FIG. 75.11 This 52-year-old woman on oral steroids for a long duration presented with longstanding dimness

of vision in both eyes. Her right eye showed gross retinal pigment epithelial defects and chronic cystoid macular degeneration on optical coherence tomography suggestive of chronic central serous chorioretinopathy. Indocyanine green angiography demonstrated dilated choroidal vasculature in the early phase and late diffuse patchy hyperfluorescence.

Treatment

Observation With or Without Removal of Risk Factors

Acute CSCR is a self-limiting disease, with reattachment of the neurosensory retina occurring within 3–4 months in the majority of cases.[19] Because of this favorable natural history, observation has been considered as an appropriate first-line approach. As high levels of endogenous or exogenous corticosteroids have been implicated as an etiology for CSCR, discontinuation of steroids in any form (i.e., systemic, nasal sprays, intraarticular injections, topical ointments) is advocated. Correction of corticosteroid level, when possible, can lead to resolution of detachment in 90% of cases. Lifestyle modification, treatment of sleep apnea, and psychosocial therapies also help in affected CSCR patients prone to psychologic stress.[110,111] In CSCR, recurrences occur in approximately 20–50% of patients within one year. Patients with frequent recurrences or chronic neurosensory retinal detachment for around 4 months may develop foveal attenuation, cystoid macular degeneration, and widespread RPE atrophy, resulting in permanent loss of visual functions.[112] Therefore, though observation is the standard initial management in most cases of acute or classic CSCR, active treatment should be initiated when symptoms persist for more than 3 months.[113] Treatment usually accelerates visual recovery but no treatment can maximize final visual gain.[111] In this situation, any treatment other than observation should be applied judiciously in susceptible patients with persistent serous macular elevation and RPE atrophic areas with subtle leaks on FA.[10,68] Early treatment is recommended in cases where rapid recovery of vision is required

for vocational or other reasons, and also when untreated CSCR has previously resulted in a poor visual outcome in the fellow eye.[114]

Historical Thermal (Argon) Laser Photocoagulation and Micropulsed Diode Laser

Laser photocoagulation, when applied to the RPE leakage points, causes direct thermal sealing effects on focal RPE defects that promote a healing response and favor stimulation of surrounding RPE cells.[115] This often hastens the resolution of NSD but rarely alters final visual outcome or rate of recurrence.[28] This may be due to the fact that zonal hyperperfusion and hyperpermeability of the choriocapillaries, the presumptive pathophysiology in CSCR, are not amenable to laser photocoagulation therapy.[96] This promising treatment method has become less favored in recent years because of significant adverse effects such as permanent scotoma, enlargement of RPE scar, secondary laser-induced CNV formation, and, rarely, inadvertent foveal photocoagulation in cases of subfoveal or juxtafoveal leak.[115–117] Thermal laser photocoagulation is now indicated in the management of CSCR with discrete, solitary extrafoveal leakage points with persistent NSD (Fig. 75.12). Situations with multiple leaks, subfoveal or juxtafoveal leak, and bullous exudative RD are better managed by safety-enhanced PDT rather than argon laser photocoagulation.

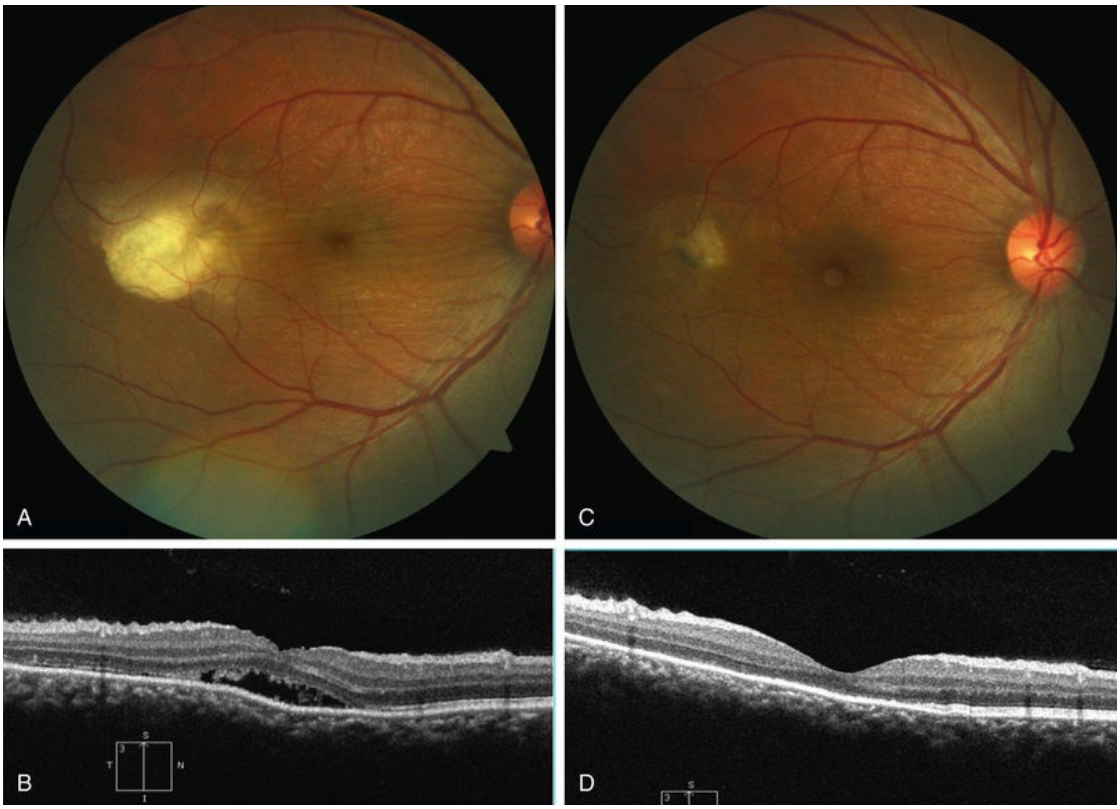

FIG. 75.12 Resolved subretinal fibrin and subretinal fluid in longstanding central serous chorioretinopathy following focal laser to extrafoveal leakage.

There has been a renewed interest in using micropulse diode laser, instead of conventional argon laser photocoagulation, to treat CSCR.[118–122] The diode laser with ultashort 810-nm micropulsed emissions enables subthreshold therapy to the RPE and choroid without a visible burn endpoint, reducing the risk of structural and functional retinal damage. In a series of 30 patients, the diode group had faster visual recovery and better final contrast sensitivity than the argon laser group without any persistent scotoma.[123] A small case series has also demonstrated the beneficial effect of using indocyanine green dye-enhanced micropulse diode laser photocoagulation at the end of 1-year follow-up.[122] Nevertheless, the efficacy and safety of micropulse diode laser in instances involving more than one leakage point, as commonly encountered in chronic CSCR, are not proved and RCTs are necessary to fully substantiate the treatment efficacy and safety of micropulse diode laser in the management of CSCR.

Photodynamic Therapy (PDT)

The results of the TAP and VIP studies in the management of age-related macular degeneration with PDT encouraged some researchers to use PDT in selected CSCR patients.[73,124] There are confirmed reports showing the efficacy and favorable visual outcomes of ICGA-guided PDT to treat CSCR in a majority of cases.[22,125–129] The analyzed mechanism of action of PDT that causes narrowing of choriocapillaries, choroidal hypoperfusion, and choroidal vascular remodeling supports its use as treatment for CSCR, which is thought to be primarily a choroidal vascular disorder; success of PDT has also been shown to depend upon the degree of hyperpermeability on ICGA.[128–132] However, in AMD the use of conventional PDT has revealed RPE atrophy, choriocapillaris ischemia, and secondary CNV as potential vision-threatening complications.[127,128] Therefore, in recent years there has been a constant effort to apply PDT in the safest form to reduce the risk of iatrogenic adverse effects in symptomatic CSCR patients.

Conventional PDT With Normal Dosage and Fluence

The standard PDT for treatment of neovascular AMD is performed using 6 mg/m^2 infusion of verteporfin (Visudyne, Novartis AG, Bülach, Switzerland). A 30-mL infusion of verteporfin is administered for 10 minutes, followed by delivery of laser at 689 nm 15 minutes after the commencement of infusion. A total light energy of 50 J/cm^2, intensity of 600 mW/cm^2, and photosensitization time of 83 seconds is delivered, with a spot size diameter of 1000 μm larger than the greatest linear dimension of the lesion. There has been normalization in calibers of the congested choroidal vasculature with a decrease in extravascular leakage in cases treated with PDT in a few pilot studies.[128] In a recent meta-analysis, all 10 studies that met standard STROBE criteria[133] showed significant improvement in best corrected visual acuity (BCVA) after conventional PDT treatment.[134] However, the possible posttreatment visual loss, potential choroidal ischemia, RPE atrophy, and risk of developing CNV have restricted clinicians from the widespread application of standard dose PDT in CSCR patients.[111,127,135,136]

Safety-Enhanced PDT With Reduced Verteporfin Dosage

As conventional PDT treatment poses certain potential iatrogenic hazards to patient's vision, many studies of CSCR have tried to modify the dosage of verteporfin or reduce the fluence of laser application to enhance the efficacy of PDT while minimizing its side-effects.[111,135] It has been demonstrated that after 10 minutes of infusion, the concentration of verteporfin is greatest in the choroidal circulation and least at the retinal outer segment.[137] In PDT, photochemical response in the choroid is dose–response-dependent and the aims of these studies were to lower the risk of retinochoroidal complications without compromising the vascular remodeling ability of PDT.[96] Safety-enhanced PDT was performed using half the normal dose of verteporfin at 3 mg/m^2 with 10 minutes of infusion, followed by a delivery of 689 nm laser after 5 minutes. A total light energy of 50 J/cm^2 was delivered within 83 seconds.[135] The well-known safety issues, such as impairment of retinal function associated with full-dose PDT, were alleviated in this half-dose regimen.[135,138] In a RCT, Chan and associates showed complete resolution of fluid in 79.5% and 94.9% of the half-dose PDT-treated eyes at 1 and 12 months, respectively, with only 1 recurrence.[135] Recently, one study reporting the long-term results of half-dose PDT in chronic CSCR patients without posterior cystoid retinal degeneration showed a dry macula at 12 months' follow-up for all 27 eyes[139] (Fig. 75.13). Eyes without PED, duration of CSCR for less than 6 months, and age younger than 45 years were more likely to achieve better visual outcome after treatment. Though studies have tried lower doses of verteporfin, it is the 3-mg group that had the best results in terms of BCVA and central foveal thickness (CFT) reduction at 6 months' follow-up[135,140–142] (Fig. 75.14). In spite of the encouraging results on the safety of half-dose PDT in the management of CSCR, it is essential to individualize management plans due to the absence of a large RCT to document treatment complications. The role and limitations of PDT in CSCR should be clearly emphasized to patients, as most of them will have good visual potential, and there have been sporadic observations of transient impairment of multifocal ERG response and development of juxtafoveal CNV with the use of half-dose PDT.[143]

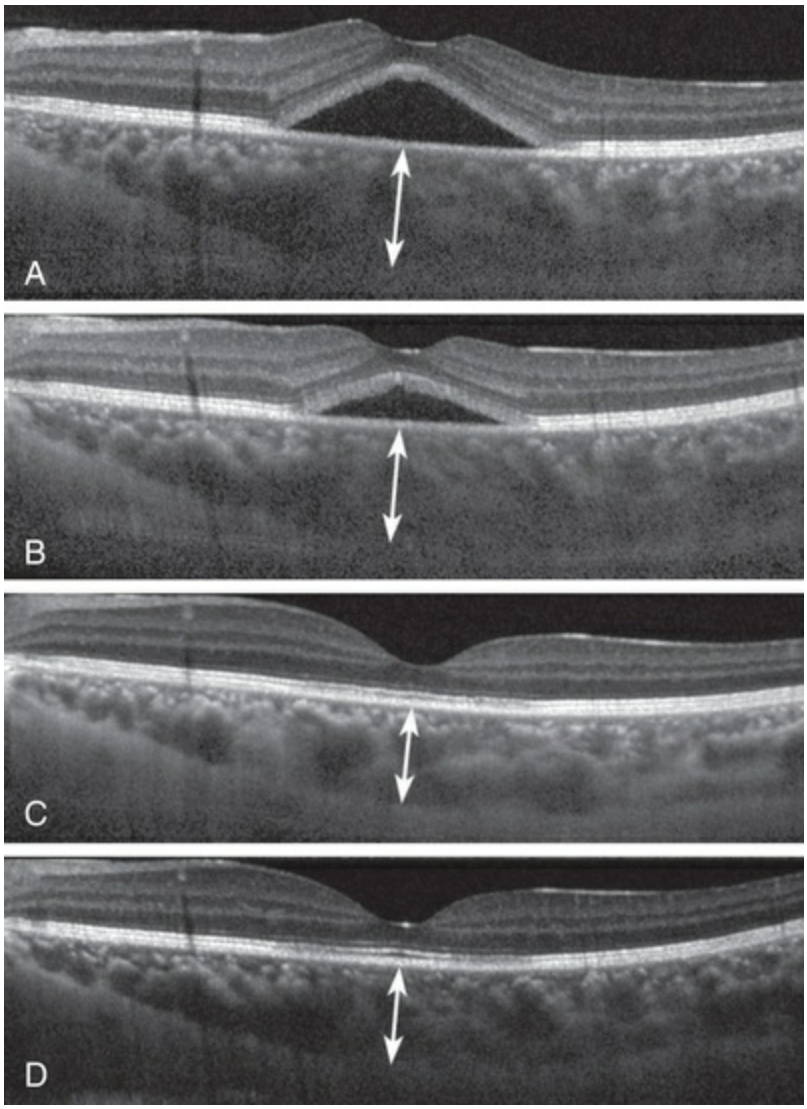

FIG. 75.13 This 33-year-old male presented with a right eye relative scotoma for more than 3 months. (A) Optical coherence tomography (OCT) showed neurosensory detachment of the macula. (B–D) Resolution of subretinal fluid and restoration of normal architecture of the macula after photodynamic treatment (PDT) shown on OCT. On longitudinal follow-up the choroidal thickness has also decreased after PDT.

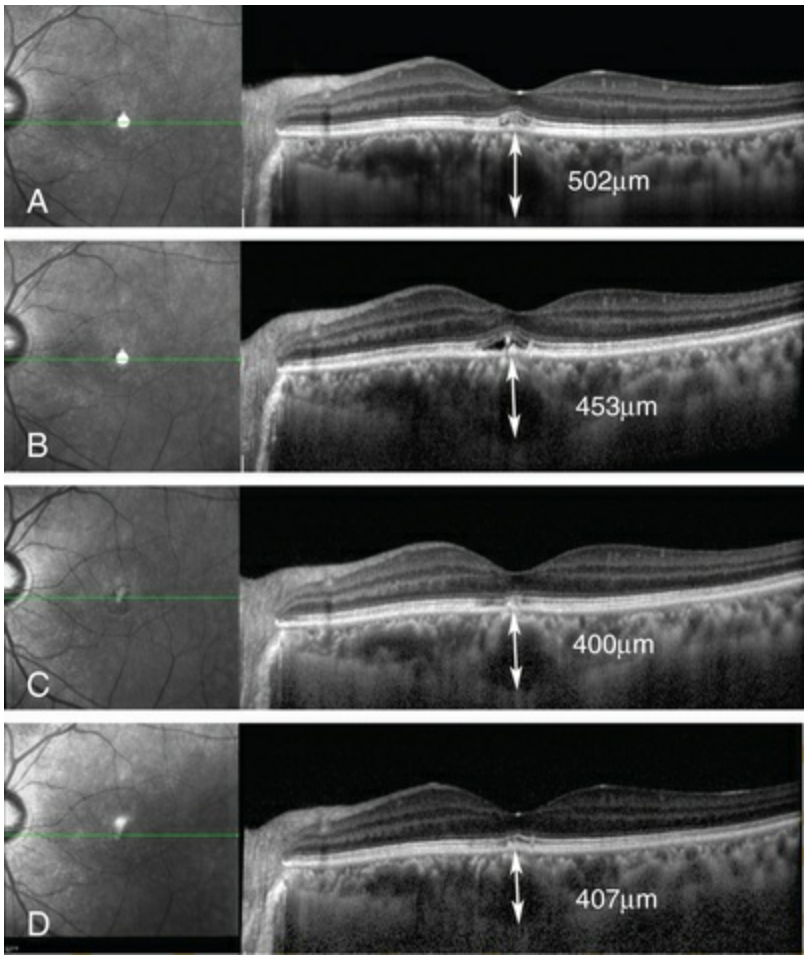

FIG. 75.14 This 42-year-old male presented with a left eye persistent central scotoma for more than 4 months. (A) Optical coherence tomography showed mild neurosensory detachment of the macula (B). (C,D) Resolved subretinal fluid after photodynamic treatment and restoration of relatively normal architecture of the choroid.

Safety-Enhanced PDT With Reduced Laser Fluence

Similar to drug dosage, another parameter that can be modified to enhance the safety of PDT is the intensity of the laser fluence. For instance, improved efficacy and safety profiles of low fluence PDT have been documented in the management of chronic CSCR.[144–146] An RCT by Bae at al.[146] compared half-fluence PDT with intravitreal ranibizumab (0.05 mL) in 16 eyes of chronic CSCR patients and found complete resolution of SRF at 6 months in 75% of the half-fluence group compared to 25% in the ranibizumab group. The low fluence PDT group also showed significant CFT reduction at the

end of 9 months. In two other studies, Shin et al.[145] and Reibaldi et al.[144] compared standard versus half-fluence PDT and both authors reported better BCVA in the half-fluence group at the end of 12-month follow-up compared to the standard group. A recent retrospective study of 56 chronic CSCR patients treated with half-dose and half-fluence PDT divided in equal numbers showed a complete resolution of SRF in 19 (61.3%) and 26 (83.9%) half-fluence-treated eyes at 1 and 12 months, respectively. The corresponding values were 25 (86.2%) and 29 (100%) in the half-dose-treated eyes without any statistical difference in BCVA between the groups. There were 15 and 5 recurrences overall in the half-fluence PDT and half-dose PDT groups, respectively.[147] The meta-analysis by Erikitola et al. also concluded that 100% of the subjects in the reduced fluence group and 42.9% of the subjects in the half-dose group had recurrence within the 1-year follow-up period.[134] Therefore, half-dose PDT can be more cost-effective and superior to half-fluence in keeping the macula dry for a longer period with fewer retreatments. However, the lack of quality RCTs to discern either short-term or long-term safety, coupled with reports of complications, is sufficient to remind clinicians of the importance of caution and individualization when managing CSCR with reduced dose or lowered fluence PDT.

Anti-Vascular Growth Factor (VEGF) Injections

The favorable results of anti-VEGF treatment in macular diseases have led to several studies on anti-VEGF in patients with CSCR. Although CSCR is not associated with increased VEGF aqueous or plasma levels,[148] anti-VEGF therapy was proposed in CSCR to reduce choroidal hyperpermeability.[149] A limited number of interventional case series have reported beneficial effects of bevacizumab in terms of visual acuity improvement and SRF reduction without significant complications.[150–152] Of the two randomized studies, the first by Lim et al. showed no difference in terms of visual acuity gain, CFT reduction, or duration of SRD between the bevacizumab and control groups.[153] The second study by Bae et al. showed a superior effect of half-fluence PDT over

ranibizumab.[146] More recently, aflibercept was used in a pilot study of 12 patients with persistent fluid over 6 months, which showed a moderate effect on SRF and CFT reduction.[154] A recent meta-analysis of 4 studies including acute and chronic CSCR showed no significant improvement with intravitreal bevacizumab compared to observation, PDT, or laser photocoagulation in terms of final visual acuity and central macular thickness.[149] Though the role of bevacizumab,[155] ranibizumab,[156] and aflibercept[157] in CSCR-related CNV is accepted, the long-term benefit and safety issues in different types of CSCR still warrant further study.

Miscellaneous Treatments

Transpupillary Thermotherapy

Transpupillary thermotherapy (TTT) is a long-pulse, low-energy, 810-nm near infrared laser, which causes choroidal vascular thrombosis and is used in the treatment of choroidal tumors. A few people have expressed their preference for performing TTT at the site of focal juxtafoveal leakage instead of using thermal laser.[158] Wei and colleagues were the first to report the use of TTT for CSCR, describing the complete resolution of subretinal fluid 4 weeks after TTT in a case of chronic CSCR with no observed visual improvement.[159] In a large unmasked, nonrandomized, prospective cohort study with unmatched control of 15 eyes, 96% of the 25 treated with TTT experienced complete resolution of neurosensory retinal detachment and focal leakage on FA at 3 months. Visual acuity improved significantly in 92% of cases compared with 33% of the control group.[160] Because of the longer duration of disease in the control group, it is difficult to confidently accept the outcomes in this study. Therefore, well-controlled, properly matched RCTs are warranted to determine the precise role and efficacy of TTT in the management of CSCR.

Systemic Medications

Anticorticosteroid Therapy.

Patients with CSCR commonly have endogenous hypercortisolism, which has resulted in trials of medications targeting cortisol

pathways.[161] These include ketoconazole, mifepristone (RU486), finasteride, rifampin, and antiadrenergic drugs. Ketoconazole interferes with endogenous glucocorticoid production in part by inhibiting the conversion of 11-b-deoxycortisol to cortisol. Two groups have investigated ketoconazole as a treatment for CSCR without any significant benefit.[162] Nielsen and colleagues investigated oral mifepristone, an abortifacient with glucocorticoid receptor antagonist properties, in 16 chronic CSCR subjects with varied response.[163] Finasteride, an inhibitor of 5-alpha-reductase that converts testosterone to the potent androgen dihydrotestosterone, has been investigated in CSCR.[164] Packo et al. found that rifampicin, a semisynthetic antituberculosis antibiotic with an inhibitory effect on endogenous steroid production, caused resolution of macular edema and subretinal fluid in a CSCR patient initially suspected to have tuberculosis. Rifampicin has been investigated in a small series[165] but further research into using corticosteroid antagonists in the treatment of CSCR is warranted. The rationale for adrenergic blockade to treat CSCR is the glucocorticoid-mediated increased expression of adrenergic receptors.[166] Yoshioka's monkey model prevented the development of experimental CSCR by blocking alpha-adrenergic receptors.[167] In a recent retrospective consecutive case series, patients received oral eplerenone, a competitive antagonist to the mineralocorticoid receptor (MR), for chronic CSCR. MR activation in choroidal vessels has been shown to be involved in the pathogenesis of CSCR. A total of 17 eyes of 13 patients treated with 25 and 50 mg of oral eplerenone per day showed an improvement of logMAR visual acuity from 0.42 at baseline to 0.29 and decreased subfoveal thickness from 339.5 μm to 270 μm at 6 months.[168] Though these studies provide hope for the medical management of CSCR, there is a need for extensive research with longer follow-up before these drugs can be accepted as primary oral therapy in CSCR.

Carbonic Anhydrase Inhibitors.

Oral acetazolamide was tried as a treatment for CSCR on the basis that the inhibition of carbonic anhydrase in the RPE seemed to promote resorption of SRF and retinal adhesion.[169] Patients treated with acetazolamide had faster subjective improvement in vision,

but it did not alter final visual outcome or recurrence rates.[170]

Aspirin.

A report showing increased levels of plasminogen activator inhibitor in CSCR patients compared to controls led to the hypothesis that hypercoagulability can play a role in CSCR pathogenesis.[171] In a nonrandomized, open-label case series, 109 patients had more rapid visual recovery, reduced rates of recurrence, and slightly better visual outcome than the control group after an aspirin regimen of one 100-mg tablet daily for 1 month followed by 100-mg on alternating days for 5 months.

Anti-*Helicobacter pylori* Treatment.

A prospective study of 25 *H. pylori*-positive CSCR patients treated with the standard *H. pylori* eradication regimen (metronidazole and amoxicillin 500 mg three times per day for 2 weeks and omeprazole once per day for 6 weeks) demonstrated complete subretinal fluid reabsorption compared to 25 controls, without any effect on final visual outcomes or recurrence rate.[172] The exact pharmacopeia of the above-mentioned systemic treatments for CSCR is not clearly understood and will require well-designed studies to establish their long-term efficacy and safety.

Conclusion

The pathophysiology of CSCR remains uncertain. It is a multifactorial disease and seems to result from a complex interaction of both known and unknown environmental and genetic factors. The role of choroidal vascular hyperpermeability related to the deranged mineralocorticoid pathway in the pathogenesis of CSCR is interesting but needs more scientific support. Though the natural history of CSCR has been thought to be favorable, frequent reports of significant anatomical and functional loss even from a mild course of the disease and the risk of frequent recurrences require early effective treatment. Advances in imaging techniques have not only resulted in more accurate diagnosis and management but have also broadened the horizons for the development of new treatments. To date, we do not have appropriate guidelines for the

management of CSCR and new modes of therapy are being developed regularly. We have tried to emphasize a simple evidence-based diagnostic and treatment algorithm, which can be beneficial for handling CSCR patients in everyday practice (Fig. 75.15). Of the described treatment options, safety-enhanced PDT using lower doses, oral corticosteroid antagonists, intravitreal anti-VEGF therapy, and micropulse diode laser do merit further research. Combination therapies involving the above treatment modalities may have a role in preventing permanent visual loss in this so-called benign disease and thus warrant additional studies in the form of large-scale randomized trials.

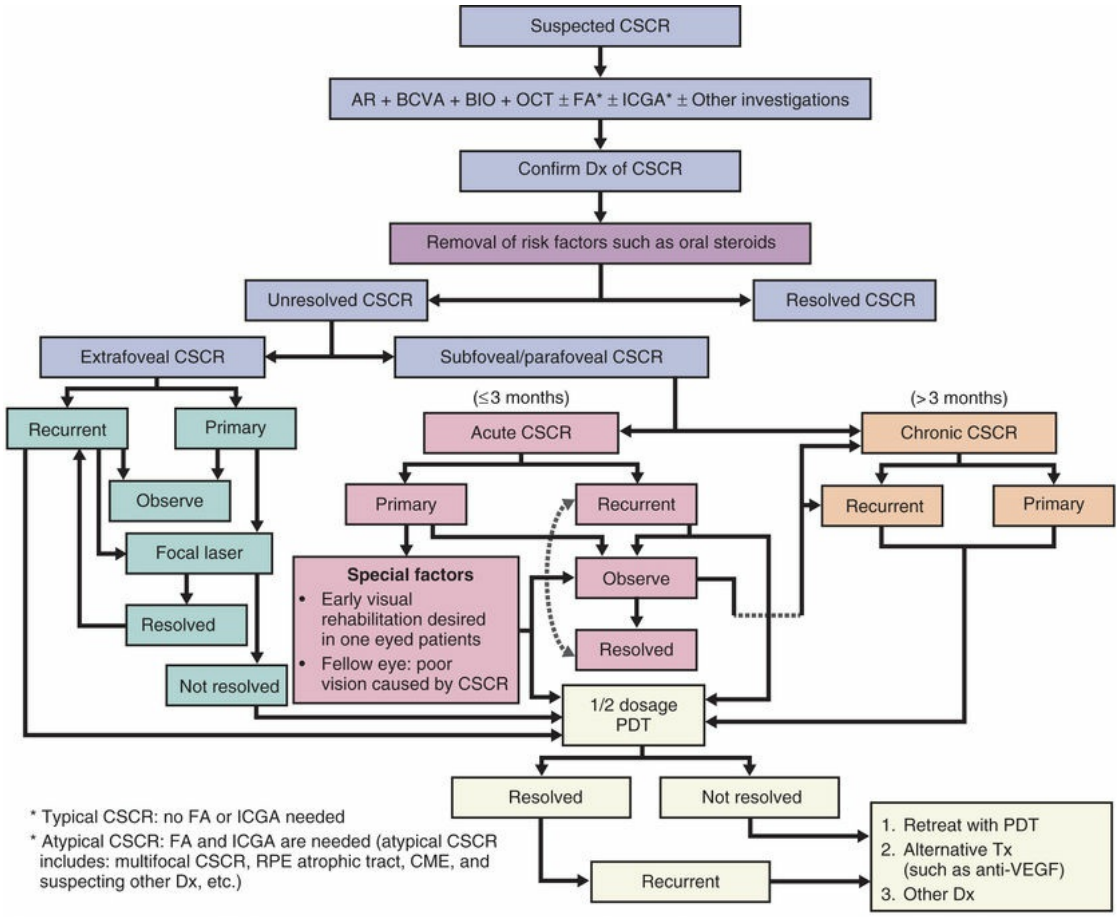

AR = Autorefraction; Anti-VEGF = Anti-vascular endothelial growth factor; BCVA = Best corrected visual acuity; BIO = Binocular indirect ophthalmoscope; CME = Cystoid macular edema; CSCR = Central serous chorioretinopathy; Dx = Diagnosis; FA = Fluorescein angiography; ICGA = Indocyanine green angiography; IV = Intravitreal; OCT= Optical coherence tomography; PDT = Photodynamic therapy; Tx = Treatment

FIG. 75.15 Diagnostic and management algorithm for central serous chorioretinopathy.

References

1. Liu DT, Fok AC, Chan WM, et al. Central serous chorioretinopathy. Ryan SJ. *Retina*. 5th ed. Saunders: St. Louis; 2013 [ch. 72].
2. Von Graefe A. Uebercentralerecidivierende retinitis. *Graefes Arch Clin Exp Ophthalmol*. 1866;12:211–215.
3. Bennet G. Central serous retinopathy. *Br J Ophthalmol*. 1955;39:605–618.
4. Gass JDM. *Stereoscopic atlas of macular diseases*. 4th ed. CV Mosby: St. Louis; 1997:49–70.
5. Gass JDM. Pathogenesis of disciform detachment of the neuro-epithelium. I. General concepts and classification. *Am J Ophthalmol*. 1967;63:573–585.
6. Gass JDM. Pathogenesis of disciform detachment of the neuro-epithelium. II. Idiopathic central serous choroidopathy. *Am J Ophthalmol*. 1967;63:587–615.
7. Baran NV, Gurlu VP, Esgin H. Long-term macular function in eyes with central serous chorioretinopathy. *Clin Experiment Ophthalmol*. 2005;33:369–372.
8. Lehmann M, Bousquet E, Beydoun T, et al. Pachychoroid: an inherited condition? *Retina*. 2015;35(1):10–16.
9. Weenink AC, Borsje RA, Oosterhuis JA. Familial chronic central serous chorioretinopathy. *Ophthalmologica*. 2001;215:183–187.
10. Yannuzzi LA, Slakter JS, Kaufman SR, et al. Laser treatment of diffuse retinal pigment epitheliopathy. *Eur J Ophthalmol*. 1992;2:103–114.
11. Imamura Y, Fujiwara T, Spaide RF. Fundus autofluorescence and visual acuity in central serous chorioretinopathy. *Ophthalmology*. 2011;118:700–705.
12. Teke MY, Elgin U, Nalcacioglu-Yuksekkaya P, et al. Comparison of autofluorescence and optical coherence tomography findings in acute and chronic central serous chorioretinopathy. *Int J Ophthalmol*. 2014;7:350–354.
13. Iida T, Yannuzzi LA, Spaide RF, et al. Cystoid macular degeneration in chronic central serous chorioretinopathy. *Retina*. 2003;23:1–7.

14. Piccolino FC, Longrais DL, Manea RR, et al. Risk factors for posterior cystoid retinal degenerationin central serous chorioretinopathy. *Retina*. 2008;28:1146–1150.
15. Spaide RF, Goldbaum M, Wong DWK, et al. Serous detachment of the retina. *Retina*. 2003;23:820–846.
16. Okushiba U, Takeda M. Study of choroidal vascular lesions in central serous chorioretinopathy using indocyanine green angiography. *Nippon Ganka Gakkai Zasshi*. 1997;101:74–82.
17. Prunte C, Flammer J. Choroidal capillary and venous congestion in central serous chorioretinopathy. *Am J Ophthalmol*. 1996;121:26–34.
18. Spaide RF, Hall L, Haas A, et al. Indocyanine green video angiography of older patients with central serous chorioretinopathy. *Retina*. 1996;16:203–213.
19. Yannuzzi LA. Central serous chorioretinopathy: a personal perspective. *Am J Ophthalmol*. 2010;149:361–363.
20. Imamura Y, Fujiwara T, Margolis R, et al. Enhanced depth imaging optical coherence tomography of the choroid in central serous chorioretinopathy. *Retina*. 2009;29:1469–1473.
21. Uyama M, Matsunaga H, Matsubara T, et al. Indocyanine green angiography and pathophysiology of multifocal posterior pigment epitheliopathy. *Retina*. 1999;19:12–21.
22. Yannuzzi LA, Slakter JS, Gross NE, et al. Indocyanine green angiography – guided photodynamic therapy fortreatment of chronic central serous chorioretinopathy: a pilot study. *Retina*. 2003;23:288–298.
23. Spitznas M. Pathogenesis of central serous retinopathy: a new working hypothesis. *Graefes Arch Clin Exp Ophthalmol*. 1986;224:321–324.
24. Zhao M, Celerier I, Bousquet E, et al. Mineralocorticoid receptor is involved in rat and human ocular chorioretinopathy. *J Clin Invest*. 2012;122:2672–2679.
25. Horniker E. Su di unaforma di retinite central di originevasoneurotica. *Ann Ottalmol*. 1927;55:578–600 [830-840].
26. Yannuzzi LA. Type A behavior and central serous chorioretinopathy. *Trans Am Ophthalmol Soc*. 1986;84:799–

845.
27. Tittl MK, Spaide RF, Wong D, et al. Systemic findings associated with central serous chorioretinopathy. *Am J Ophthalmol*. 1999;128:63–68.
28. Fok AC, Chan PPM, Lam DSC, et al. Risk factors for recurrence of serous macular detachment in untreated patients with central serous chorioretinopathy. *Ophthalmic Res*. 2011;46:160–163.
29. Carlesimo SC, Piazzi G, Leone C, et al. Masuda's central serous chorioretinopathy (CSCR) and its somatic investment in narcissism: our observations on new psychiatric nosography. *Clin Ter*. 2014;165:27–30.
30. Carvalho-Recchia CA, Yannuzzi LA, Negrao S, et al. Corticosteroids and central serous chorioretinopathy. *Ophthalmology*. 2002;109:1834–1837.
31. Karadimas P, Kapetanios A, Bouzas EA. Central serous chorioretinopathy after local application of glucocorticoids for skin disorders. *Arch Ophthalmol*. 2004;122:784–786.
32. Tsai DC, Chen SJ, Huang CC, et al. Risk of central serous chorioretinopathy in adults prescribed oral corticosteroids: a population-based study in Taiwan. *Retina*. 2014;34:1867–1874.
33. Haimovici R, Koh S, Gagnon DR, et al. Risk factors for central serous chorioretinopathy: a case–control study. *Ophthalmology*. 2004;111:244–249.
34. Haimovici R, Gragoudas ES, Duker JS, et al. Central serous chorioretinopathy associated with inhaled or intranasal corticosteroids. *Ophthalmology*. 1997;104:1653–1660.
35. Kleinberger AJ, Patel C, Lieberman RM, et al. Bilateral central serous chorioretinopathy caused by intranasal corticosteroids: a case report and review of the literature. *Laryngoscope*. 2011;121:2034–2037.
36. Kao LY, et al. Bilateral serous retinal detachment resembling central serous chorioretinopathy following epidural steroid injection. *Retina*. 1998;18:479–481.
37. Kassam AA, White W, et al. Loss of visual acuity due to central serous retinopathy after steroid injection into the shoulder bursa. *J Shoulder Elbow Surg*. 2011;20:5–6.

38. Mondal LK, Sarkar K, Datta H, et al. Acute bilateral central serous chorioretinopathy following intra-articular injection of corticosteroid. *Indian J Ophthalmol*. 2005;53:132–134.
39. Ezra N, Taban M, Behroozan D. Central serous chorioretinopathy associated with topical corticosteroids in a patient with psoriasis. *J Drugs Dermatol*. 2011;10:918–921.
40. Baumal CR, Martidis A, Truong SN. Central serous chorioretinopathy associated with periocular corticosteroid injection treatment for HLA-B27-associated iritis. *Arch Ophthalmol*. 2004;122:926–928.
41. Imasawa M, Ohshiro T, Gotoh T, et al. Central serous chorioretinopathy following vitrectomy with intravitreal triamcinolone acetonide for diabetic macular oedema. *Acta Ophthalmol Scand*. 2005;83:132–133.
42. Kocabora MS, Durmaz S, Kandemir N. Exacerbation of central serous chorioretinopathy following intravitreal triamcinolone injection. *Graefes Arch Clin Exp Ophthalmol*. 2008;246:1783–1786.
43. Khairallah M, Kahloun R, et al. Central serous chorioretinopathy, corticosteroids, and uveitis. *Ocul Immunol Inflamm*. 2012;20:76–85.
44. Han JM, Hwang JM, et al. Changes in choroidal thickness after systemic administration of high-dose corticosteroids: a pilot study. *Invest Ophthalmol Vis Sci*. 2014;55:440–445.
45. Cheng LL, Kwok AKH, Wat NMS, et al. Graft-vs-host-disease-associated conjunctival chemosis and central serous chorioretinopathy after bone marrow transplant. *Am J Ophthalmol*. 2002;134:293–295.
46. Chung H, Kim KH, Kim JG, et al. Retinal complications in patients with solid organ or bone marrow transplantations. *Transplantation*. 2007;83:694–699.
47. Farzan K, Rezaei L, et al. Central serous chorioretinopathy following kidney transplantation. *Saudi J Kidney Dis Transpl*. 2014;25:615–620.
48. Kian-Ersi F, Taheri S, Akhlaghi MR. Ocular disorders in renal transplant patients. *Saudi J Kidney Dis Transpl*. 2008;19:751–755.
49. Garg SP, Dada T, Talwar D, et al. Endogenous cortisol

profile in patients with central serous chorioretinopathy. *Br J Ophthalmol*. 1997;81:962–964.
50. Gass JD. Central serous chorioretinopathy and white subretinal exudation during pregnancy. *Arch Ophthalmol*. 1991;109:677–681.
51. Fastenberg DM, Ober RR. Central serous choroidopathy in pregnancy. *Arch Ophthalmol*. 1983;101:1055–1058.
52. Eom Y, Oh J, Kim S, et al. Systemic factors associated with central serous chorioretinopathy in Koreans. *Korean J Ophthalmol*. 2012;26:260–264.
53. Caccavale A, Romanazzi F, Imparato M, et al. Central serous chorioretinopathy: a pathogenetic model. *Clin Ophthalmol*. 2011;5:239–243.
54. Shin MC, Lim JW. Concentration of cytokines in the aqueous humor of patients with central serous chorioretinopathy. *Retina*. 2011;31:1937–1943.
55. Lim JW, Kim MU, Shin MC. Aqueous humor and plasma levels of vascular endothelial growth factor and interleukin-8 in patients with central serous chorioretinopathy. *Retina*. 2010;30:1465–1471.
56. Mansuetta CC, Mason JO, Swanner J, et al. An association between central serous chorioretinopathy and gastroesophageal reflux disease. *Am J Ophthalmol*. 2004;137:1096–1100.
57. Cotticelli L, Borrelli M, D'Alessio AC, et al. Central serous chorioretinopathy and *Helicobacter pylori*. *Eur J Ophthalmol*. 2006;16:274–278.
58. Misiuk-Hojlo M, Michalowska M, Turno-Krecicka A. *Helicobacter pylori* – a risk factor for the development of the central serous chorioretinopathy. *Klin Oczna*. 2009;111:30–32.
59. Tittl MK, Spaide RF, Wong D, et al. Systemic findings associated with central serous chorioretinopathy. *Am J Ophthalmol*. 1999;128:63–68.
60. McCannel TA, Chmielowski B, Finn RS, et al. Bilateral subfoveal neurosensory retinal detachment associated with MEK inhibitor use for metastatic cancer. *JAMA Ophthalmol*. 2014;132:1005–1009.

61. Urner-Bloch U, Urner M, Stieger P, et al. Transient MEK inhibitor-associated retinopathy in metastatic melanoma. *Ann Oncol*. 2014;25:1437–1441.
62. Aliferis K, Petropoulos IK, Farpour B, et al. Should central serous chorioretinopathy be added to the list of ocular side effects of phosphodiesterase 5 inhibitors? *Ophthalmologica*. 2012;227:85–89.
63. Fraunfelder FW, Fraunfelder FT. Central serous chorioretinopathy associated with sildenafil. *Retina*. 2012;28:606–609.
64. Lin E, Arrigg PG, Kim RY. Familial central serous choroidopathy. *Graefes Arch Clin Exp Ophthalmol*. 2000;238:930–931.
65. Oosterhuis JA. Familial central serous retinopathy. *Graefes Arch Clin Exp Ophthalmol*. 1996;234:337–341.
66. Park DW, Schatz H, Gaffney MM, et al. Central serous chorioretinopathy in two families. *Eur J Ophthalmol*. 1998;8:42–47.
67. Wang M, Munch IC, Hasler PW, et al. Central serous chorioretinopathy. *Acta Ophthalmol*. 2008;86:126–145.
68. Spaide RF, Campeas L, Haas A, et al. Central serous chorioretinopathy in younger and older adults. *Ophthalmology*. 1996;103:2070–2079 [discussion 2079e2080].
69. Kitzmann AS, Pulido JS, Diehl NN, et al. The incidence of central serous chorioretinopathy in Olmsted County, Minnesota. *Ophthalmology*. 2008;115:169–173.
70. Tsai DC, Chen SJ, Huang CC, et al. Epidemiology of idiopathic central serous chorioretinopathy in Taiwan, 2013; 2001–2006: a population-based study. *PLoS ONE*. 2013;8:e66858.
71. Kim YC, Kim SD, Kim KS. A case of idiopathic central serous chorioretinopathy in a 12-year-old male treated with bevacizumab. *Korean J Ophthalmol*. 2012;26:391–393.
72. Leibowitz HM, Krueger DE, Maunder LR, et al. The Framingham Eye Study monograph: an ophthalmological and epidemiological study of cataract, glaucoma, diabetic retinopathy, macular degeneration, and visual acuity in a general population of 2631 adults, 1973–1975. *Surv*

Ophthalmol. 1980;24(Suppl.):335–610.
73. Chan WM, Lim TH, Pece A, et al. Verteporfin PDT for non-standard indications a review of current literature. *Graefes Arch Clin Exp Ophthalmol*. 2010;248:613–626.
74. Yannuzzi LA. Type-A behavior and central serous chorioretinopathy. *Retina*. 1987;7:111–131.
75. How AC, Koh AH. Angiographic characteristics of acute central serous chorioretinopathy in an Asian population. *Ann Acad Med Singap*. 2006;35:77–79.
76. Kunavisarut P, Pathanapitoon K, Van S, et al. Chronic central serous chorioretinopathy associated with serous retinal detachment in a series of Asian patients. *Ocul Immunol Inflamm*. 2009;17:269–277.
77. Ie D, Yannuzi LA, Spaide RF, et al. Subretinal exudative deposits in central serous chorioretinopathy. *Br J Ophthalmol*. 1993;77:349–353.
78. Maruko I, Iida T, Ojima A, et al. Subretinal dot like precipitates and yellow material in central serous chorioretinopathy. *Retina*. 2011;31:759–765.
79. Yannuzi LA, Shakin J, Fisher YL, et al. Peripheral retinal detachments and retinal pigment epithelial atrophic tracts secondary to central serous pigment epitheliopathy. *Ophthalmology*. 1984;91:1554–1572.
80. Gass JD. Bullous retinal detachment: an unusual manifestation of idiopathic central serous choroidopathy. *Am J Ophthalmol*. 1973;75:810–821.
81. Pang CE, Freund KB. Pachychoroid neovasculopathy. *Retina*. 2015;35:1–9.
82. Baek J, Park YH. Optical density ratio in the subretinal fluid: differentiating chronic central serous chorioretinopathy and polypoidal choroidal vasculopathy. *Am J Ophthalmol*. 2015;159:386–392.
83. Shields CL, Pellegrini M, Ferenczy SR, et al. Enhanced depth imaging optical coherence tomography of intraocular tumors: from placid to seasick to rock and rolling topography – the 2013 Francesco Orzalesi Lecture. *Retina*. 2014;34:1495–1512.
84. Caillaux V, Gaucher D, Gualino V, et al. Morphologic

characterization of dome-shaped macula in myopic eyes with serous macular detachment. *Am J Ophthalmol*. 2013;156:958–967.
85. Viola F, Dell'Arti L, Benatti E, et al. Choroidal findings in dome-shaped macula in highly myopic eyes: a longitudinal study. *Am J Ophthalmol*. 2015;159:44–52.
86. Chinskey ND, Johnson MW. Treatment of subretinal fluid associated with dome-shaped macula. *Ophthalmic Surg Lasers Imaging Retina*. 2013;44:593–595.
87. Dirani A, Matet A, Beydoun T, et al. Resolution of foveal detachment in dome-shaped macula after treatment by spironolactone: report of two cases and mini-review of the literature. *Clin Ophthalmol*. 2014;8:999–1002.
88. Kon Y, Lida T, Maruko I, et al. The optical tomography ophthalmoscope for examination of central serous chorioretinopathy with precipitates. *Retina*. 2008;28:864–869.
89. Yalcinbayir O, Gelisken O, Akova B, et al. Correlation of spectral domain optical coherence tomography findings and visual acuity in central serous chorioretinopathy. *Retina*. 2014;34:705–712.
90. Iacono P, Battaglia PM, Papayannis A, et al. Acute central serous chorioretinopathy: a correlation study between fundus autofluorescence and spectral-domain OCT. *Graefes Arch Clin Exp Ophthalmol*. 2015;253(11):1889–1897.
91. Landa G, Barnett JA, Garcia PMT, et al. Quantitative and qualitative spectral domain optical coherence tomography analysis of sub-retinal deposits in patients with acute central serous retinopathy. *Ophthalmologica*. 2013;230:62–68.
92. Ahlers C, Geitzenauer W, Stock G, et al. Alterations of intraretinal layers in acute central serous chorioretinopathy. *Acta Ophthalmol*. 2009;87:511–516.
93. Yang L, Jonas JB, Wei W. Optical coherence tomography-assisted enhanced depth imaging of central serous chorioretinopathy. *Invest Ophthalmol Vis Sci*. 2013;54:4659–4665.
94. Yang L, Jonas JB, Wei W. Choroidal vessel diameter in central serous chorioretinopathy. *Acta Ophthalmol*. 2013;91:358–362.

95. Goktas A. Correlation of subretinal fluid volume with choroidal thickness and macular volume in acute central serous chorioretinopathy. *Eye (Lond)*. 2014;28:1431–1436.
96. Maruko I, Iida T, Sugano Y, et al. Subfoveal retinal and choroidal thickness after verteporfin photodynamic therapy for polypoidal choroidal vasculopathy. *Am J Ophthalmol*. 2011;151:594–603.
97. Imamura Y, Fujiwara T, Spaide RF. Fundus autofluorescence and visual acuity in central serous chorioretinopathy. *Ophthalmology*. 2011;118:700–705.
98. Agarwal A. *Gass's Atlas of macular diseases*. 5th ed. WB Saunders: Philadelphia; 2012.
99. Framme C, Walter A, Gabler B, et al. Fundus autofluorescence in acute and chronic-recurrent central serous chorioretinopathy. *Acta Ophthalmol Scand*. 2005;83:161–167.
100. Bujarborua D, Nagpal PN, Deka M. Smokestack leak in central serous chorioretinopathy. *Graefes Arch Clin Exp Ophthalmol*. 2010;248:339–351.
101. Tsujikawa A, Ojima Y, Yamashiro K, et al. Punctate hyperfluorescent spots associated with central serous chorioretinopathy as seen on indocyanine green angiography. *Retina*. 2010;30:801–809.
102. Lai TY, Lai RY, Ngai JW, et al. First- and second-order kernel multifocal electroretinography abnormalities in acute central serous chorioretinopathy. *Doc Ophthalmol*. 2008;116:29–40.
103. Yip YWY, Ngai JWS, Fok ACT, et al. Correlation between functional and anatomical assessments by multifocal electroretinography and optical coherence tomography in central serous chorioretinopathy. *Doc Ophthalmol*. 2010;120:193–200.
104. Reibaldi M, Boscia F, Avitabile T, et al. Functional retinal changes measured by microperimetry in standard-fluence vs. low-fluence photodynamic therapy in chronic central serous chorioretinopathy. *Am J Ophthalmol*. 2011;151:953–960.
105. Senturk F, Karacorlu M, Ozdemir H, et al. Microperimetric

changes after photodynamic therapy for central serous chorioretinopathy. *Am J Ophthalmol*. 2011;151:303–309.
106. Dinc UA, Yenerel M, Tatlipinar S, et al. Correlation of retinal sensitivity and retinal thickness in central serous chorioretinopathy. *Ophthalmologica*. 2010;224:2–9.
107. Yap EY, Robertson DM. The long-term outcome of central serous chorioretinopathy. *Arch Ophthalmol*. 1996;114:689–692.
108. Bandello F, Virgili G, Lanzetta P, Pirracchio A, Menchini U. ICG angiography and retinal pigment epithelial decompensation (CRSC and epitheliopathy). *J Fr Ophthalmol*. 2001;24:448–451.
109. Ooto S, Hangai M, Sakamoto A, et al. High-resolution imaging of resolved central serous chorioretinopathy using adaptive optics scanning laser ophthalmoscopy. *Ophthalmology*. 2010;117:1800–1809 [1809.e1-2].
110. Ross A, Ross AH, Mohamed Q. Review and update of central serous chorio-retinopathy. *Curr Opin Ophthalmol*. 2011;22(3):166–173.
111. Chan WM, Lai TY, Lai RY, et al. Half-dose verteporfin photodynamic therapy for acute central serous chorioretinopathy: one-year results of a randomized controlled trial. *Ophthalmology*. 2008;115:1756–1765.
112. Loo RH, Scott IU, Flynn HW Jr, et al. Factors associated with reduced visual acuity during long-term follow-up of patients with idiopathic central serous chorioretinopathy. *Retina*. 2002;22:19–24.
113. Wang MS, Sander B, Larsen M. Retinal atrophy in idiopathic central serous chorioretinopathy. *Am J Ophthalmol*. 2002;133:787–793.
114. Nicholson B, Noble J, Forooghian F, et al. Central serous chorioretinopathy: update on pathophysiology and treatment. *Surv Ophthalmol*. 2013;58:103–126.
115. Lim JW, Kang SW, Kim YT, et al. Comparative study of patients with central serous chorioretinopathy undergoing focal laser photocoagulation or photodynamic therapy. *Br J Ophthalmol*. 2011;95:514–517.
116. Robertson DM, Ilstrup D. Direct, indirect, and sham laser

photocoagulation in the management of central serous chorioretinopathy. *Am J Ophthalmol*. 1983;95:457–466.
117. Gartner J. Long-term follow-up of an ophthalmologist's central serous retinopathy photocoagulated by sun gazing. *Doc Ophthalmol*. 1987;66:19–33.
118. Sivaprasad S, Elagonz M, McHugh D, et al. Micropulsed diode laser therapy: evolution and clinical applications. *Surv Ophthalmol*. 2010;55:516–530.
119. Gupta B, Elagouz M, McHugh D, et al. Micropulse diode laser photocoagulation for central serous chorioretinopathy. *Clin Experiment Ophthalmol*. 2009;37:801–805.
120. Chen SN, Hwang JF, Tseng LF, et al. Subthreshold diode micropulse photocoagulation for the treatment of chronic central serous chorioretinopathy with juxtafoveal leakage. *Ophthalmology*. 2008;115:2229–2234.
121. Lanzetta P, Furlan F, Morgante L, et al. Nonvisible subthreshold micropulse diode laser (810 nm) treatment of central serous chorioretinopathy: a pilot study. *Eur J Ophthalmol*. 2008;18:934–940.
122. Ricci F, Missiroli F, Regine F, et al. Indocyanine green enhanced sub-threshold diode-laser micropulse photocoagulation treatment of chronic central serous chorioretinopathy. *Graefes Arch Clin Exp Ophthalmol*. 2009;247:597–607.
123. Verma L, Sinha R, Venkatesh P, et al. Comparative evaluation of diode laser versus argon laser photocoagulation in patients with central serous retinopathy: a pilot, randomized controlled trial [ISRCTN84128484]. *BMC Ophthalmol*. 2004;4:15.
124. Chan WM, Lai TY, Tano Y, et al. Photodynamic therapy in macular diseases of Asian populations: when East meets West. *Jpn J Ophthalmol*. 2006;50:161–169.
125. Battaglia Parodi M, Da Pozzo S, Ravalico G. Photodynamic therapy in chronic central serous chorioretinopathy. *Retina*. 2003;23:235–237.
126. Canakis C, Livir-Rallatos C, Panayiotis Z, et al. Ocular photodynamic therapy for serous macular detachment in the diffuse retinal pigment epitheliopathy variant of

idiopathic central serous chorioretinopathy. *Am J Ophthalmol*. 2003;136:750–752.
127. Cardillo Piccolino F, Eandi CM, Ventre L, et al. Photodynamic therapy for chronic central serous chorioretinopathy. *Retina*. 2003;23:752–763.
128. Chan WM, Lam DS, Lai TY, et al. Choroidal vascular remodeling in central serous chorioretinopathy after indocyanine green guided photodynamic therapy with verteporfin: a novel treatment at the primary disease level. *Br J Ophthalmol*. 2003;87:1453–1458.
129. Taban M, Boyer DS, Thomas EL, et al. Chronic central serous chorioretinopathy: photodynamic therapy. *Am J Ophthalmol*. 2004;137:1073–1080.
130. Schlotzer-Schrehardt U, Viestenz A, Naumann GO, et al. Dose-related structural effects of photodynamic therapy on choroidal and retinal structures of human eyes. *Graefes Arch Clin Exp Ophthalmol*. 2002;240:748–757.
131. Schmidt-Erfurth U, Laqua H, Schlotzer-Schrehard U, et al. Histopathological changes following photodynamic therapy in human eyes. *Arch Ophthalmol*. 2002;120:835–844.
132. Ryo I, Miki S, Motokazu T, et al. Association between the efficacy of photodynamic therapy and indocyanine green angiography findings for central serous chorioretinopathy. *Am J Ophthalmol*. 2010;149:441–446.
133. Fung AE, Palanki R, Bakri SJ, et al. Applying the CONSORT and STROBE statements to evaluate the reporting quality of neovascular age-related macular degeneration studies. *Ophthalmology*. 2009;116(2):286–296.
134. Erikitola OC, Crosby Nwaobi R, Lotery AJ, et al. Photodynamic therapy for central serous chorioretinopathy. *Eye (Lond)*. 2014;28:944–957.
135. Lai TYY, Chan WM, Li H, et al. Safety enhanced photodynamic therapy with half dose verteporfin for chronic central serous chorioretinopathy: a short-term pilot study. *Br J Ophthalmol*. 2006;90(7):869.
136. Lee P, Kim K, Lee W. Severe choroidal ischemia following photodynamic therapy for pigment epithelial detachment and chronic central serous chorioretinopathy. *Jpn J*

Ophthalmol. 2009;53(1):52–56.
137. Haimovici R, Kramer M, Miller JW, et al. Localization of lipoprotein-delivered 1–3 benzoporphyrin derivative in the rabbit eye. *Curr Eye Res*. 1997;16:83–90.
138. Fujita K, Yuzawa M, Mori R. Retinal sensitivity after photodynamic therapy with half-dose verteporfin for chronic central serous: short-term results. *Retina*. 2011;31:772–778.
139. Karakus SH, Basarir B, Pinarci EY, et al. Long-term results of half-dose photodynamic therapy for chronic central serous chorioretinopathy with contrast sensitivity changes. *Eye (Lond)*. 2013;27(5):612–620.
140. Koytak A, Erol K, Coskun E, et al. Fluorescein angiography-guided photodynamic therapy with half-dose verteporfin for chronic central serous chorioretinopathy. *Retina*. 2010;30(10):1698.
141. Nicolo M, Zoli D, Musolino M, et al. Association between the efficacy of half-dose photodynamic therapy with indocyanine green angiography and optical coherence tomography findings in the treatment of central serous chorioretinopathy. *Am J Ophthalmol*. 2012;153(3):474–480.
142. Uetani R, Ito Y, Oiwa K, et al. Half-dose vs. one-third-dose photodynamic therapy for chronic central serous chorioretinopathy. *Eye (Lond)*. 2012;26(5):640.
143. Wu ZH, Lai RY, Yip YW, et al. Improvement in multifocal electroretinography after half-dose verteporfin photodynamic therapy for central serous chorioretinopathy: a randomized placebo-controlled trial. *Retina*. 2011;31(7):1378–1386.
144. Reibaldi M, Cardascia N, Longo A, et al. Standard-fluence versus low-fluence photodynamic therapy in chronic central serous chorioretinopathy: a nonrandomized clinical trial. *Am J Ophthalmol*. 2010;149:307–315.
145. Shin JY, Woo SJ, Yu HG, et al. Comparison of efficacy and safety between half-fluence and full-fluence photodynamic therapy for chronic central serous chorioretinopathy. *Retina*. 2011;31:119–126.
146. Bae SH, Heo JW, Kim C, et al. Randomized pilot study of

low-fluence photo-dynamic therapy versus intravitreal ranibizumab for chronic central serous chorioretinopathy. *Am J Ophthalmol*. 2011;152:784–792.
147. Nicoló M, Eandi CM, Alovisi C, et al. Half-fluence versus half-dose photodynamic therapy in chronic central serous chorioretinopathy. *Am J Ophthalmol*. 2014;157:1033–1037.
148. Lim JW, Kim MU, Shin MC. Aqueous humor and plasma levels of vascular endothelial growth factor and interleukin-8 in patients with central serous chorioretinopathy. *Retina*. 2010;30:1465–1471.
149. Chung YR, Seo EJ, Lew HM, et al. Lack of positive effect of intravitreal bevacizumab in central serous chorioretinopathy: meta-analysis and review. *Eye (Lond)*. 2013;27:1339–1346.
150. Arevalo JF, Espinoza JV. Single-session combined photodynamic therapy with verteporfin and intravitreal anti-vascular endothelial growth factor therapy for chronic central serous chorioretinopathy: a pilot study at 12-month follow-up. *Graefes Arch Clin Exp Ophthalmol*. 2011;249:1159–1166.
151. Artunay O, Yuzbasioglu E, Rasier R, et al. Intravitreal bevacizumab in treatment of idiopathic persistent central serous chorioretinopathy: a prospective, controlled clinical study. *Curr Eye Res*. 2010;35:91–98.
152. Lim JW, Kim MU. The efficacy of intravitreal bevacizumab for idiopathic central serous chorioretinopathy. *Graefes Arch Clin Exp Ophthalmol*. 2011;249:969–974.
153. Lim JW, Ryu SJ, Shin MC. The effect of intravitreal bevacizumab in patients with acute central serous chorioretinopathy. *Korean J Ophthalmol*. 2010;24:155–158.
154. Pitcher JD, Witkin AJ, DeCroos FC, et al. A prospective pilot study of intravitreal aflibercept for the treatment of chronic central serous chorioretinopathy: the CONTAIN study. *Br J Ophthalmol*. 2015;99(6):848–852.
155. Chan WM, Lai TYY, Liu DTL, et al. Intravitreal bevacizumab (Avastin) for choroidal neovascularization secondary to central serous chorioretinopathy, secondary to punctate inner choroidopathy, or of idiopathic origin. *Am J*

Ophthalmol. 2007;143:977–983.
156. Konstantinidis L, Mantel I, Zografos L, et al. Intravitreal ranibizumab in the treatment of choroidal neovascularization associated with idiopathic central serous chorioretinopathy. *Eur J Ophthalmol*. 2010;20:955–958.
157. Broadhead GK, Chang A. Intravitreal aflibercept for choroidal neovascularization complicating chronic central serous chorioretinopathy. *Graefes Arch Clin Exp Ophthalmol*. 2015;253(6):979–981.
158. Sharma T, Parikh SD. Transpupillary thermotherapy for juxtafoveal leak in central serous chorioretinopathy. *Ophthalmic Surg Lasers Imaging*. 2010;1–3.
159. Wei SY, Yang CM. Transpupillary thermotherapy in the treatment of central serous chorioretinopathy. *Ophthalmic Surg Lasers Imaging*. 2005;36:412–415.
160. Shukla D, Kolluru C, Vignesh TP, et al. Transpupillary thermotherapy for subfoveal leaks in central serous chorioretinopathy. *Eye (Lond)*. 2008;22:100–106.
161. Jampol LM, Weinreb R, Yannuzzi L. Involvement of corticosteroids and catecholamines in the pathogenesis of central serous chorioretinopathy: a rationale for new treatment strategies. *Ophthalmology*. 2002;109:1765–1766.
162. Golshahi A, Klingmuller D, Holz FG, et al. Ketoconazole in the treatment of central serous chorioretinopathy: a pilot study. *Acta Ophthalmol*. 2010;88(5):576–581.
163. Nielsen JS, Jampol LM. Oral mifepristone for chronic central serous chorioretinopathy. *Retina*. 2011;31:1928–1936.
164. Forooghian F, Meleth AD, Cukras C, et al. Finasteride for chronic central serous chorioretinopathy. *Retina*. 2011;31:766–771.
165. Ravage Z, Packo K. *Rifampin for treatment of central serous chorioretinopathy*. [Abstract, ARVO meeting, 2011. Ft Lauderdale, FL] 2011.
166. Sakaue M, Hoffman BB. Glucocorticoids induce transcription and expression of the alpha 1B adrenergic receptor gene in DTT1 MF-2 smooth muscle cells. *J Clin Invest*. 1991;88:385–389.
167. Yoshioka H. [The etiology of central serous

chorioretinopathy]. *Nippon Ganka Gakkai Zasshi*. 1991;95:1181–1195.
168. Singh RP, Sears JE, Bedi R, et al. Oral eplerenone for the management of chronic central serous chorioretinopathy. *Int J Ophthalmol*. 2015;8(2):310–314.
169. Cox SN, Hay E, Bird AC. Treatment of chronic macular edema with acetazolamide. *Arch Ophthalmol*. 1988;106:1190–1195.
170. Pikkel J, Beiran I, Ophir A, et al. Acetazolamide for central serous retinopathy. *Ophthalmology*. 2002;109:1723–1725.
171. Yamada R, Yamada S, Ishii A, et al. [Evaluation of tissue plasminogen activator and plasminogen activator inhibitor-1 in blood obtained from patients of idiopathic central serous chorioretinopathy.]. *Nippon Ganka Gakkai Zasshi*. 1993;97:955–960.
172. Rahbani-Nobar MB, Javadzadeh A, Ghojazadeh L, et al. The effect of *Helicobacter pylori* treatment on remission of idiopathic central serous chorioretinopathy. *Mol Vis*. 2011;17:99–103.

76

Uveal Effusion Syndrome and Hypotony Maculopathy

Cagri G. Besirli, Mark W. Johnson

Uveal Effusion Syndrome
Hypotony Maculopathy

The clinical observation of abnormal serous fluid accumulation in the outer layer of the ciliary body and choroid is called uveal effusion. This exudative detachment of the choroid and the ciliary body is also known as ciliochoroidal effusion, ciliochoroidal detachment, choroidal effusion, or choroidal detachment. These names are used interchangeably in this chapter. Uveal effusion does not refer to a specific entity, but this name is used as the common term to describe a pathoanatomic condition caused by several ocular and systemic disorders. Uveal effusion is frequently associated with nonrhegmatogenous retinal detachment, secondary to the chronic accumulation of protein-rich fluid in the choroid and

the breakdown of the retinal pigment epithelial fluid barrier. The term "idiopathic uveal effusion syndrome" or "uveal effusion syndrome" in short refers to the presence of ciliochoroidal effusion in an eye with no other known associated ocular or systemic disorder. Uveal effusion syndrome typically occurs spontaneously in an otherwise healthy middle-aged man.

Hypotony maculopathy refers to the structural changes in the macular region and related visual dysfunction that may develop in an eye with low intraocular pressure. In addition to the changes in the macular region, hypotony may be associated with other posterior-segment abnormalities, including optic nerve swelling, vascular tortuosity, and chorioretinal folds. The vision loss may be profound in the setting of persistent ocular hypotony, but visual improvement is typical after intraocular pressure is restored.

Uveal Effusion Syndrome

Introduction

Spontaneous exudative detachment of the choroid and ciliary body was first reported by Schepens and Brockhurst in 1963;[1] these authors used the term "uveal effusion" in their description of this disorder. Almost two decades later, Gass and Jallow in 1982 coined the term "idiopathic uveal effusion syndrome" to describe idiopathic serous detachment of the choroid, ciliary body, and retina.[2] Uveal effusion syndrome is a rare ocular disorder that typically manifests itself in an otherwise healthy middle-aged male. In their original report, Schepens and Brockhurst described 17 patients, only one of whom was female. The diagnosis of uveal effusion syndrome is based on characteristic clinical findings and exclusion of other known causes of uveal effusion. Bilateral involvement is common, and unilateral cases tend to occur in older males. In addition to the accumulation of serous fluid in the ciliary body and choroid, nonrhegmatogenous retinal detachment with marked shifting of the subretinal fluid is commonly observed in patients with uveal effusion syndrome. Retinal detachment often begins inferiorly, as in other causes of exudative retinal detachment. Other ocular findings include dilation of the episcleral

blood vessels, blood in Schlemm's canal, normal intraocular pressure, mild vitreous cells, leopard-spot retinal pigment epithelial alterations, elevation of the subretinal fluid protein levels, and elevation of the cerebrospinal fluid protein. Without treatment, a protracted clinical course with remissions and exacerbations over many months to years may cause significant visual decline and morbidity. Unlike other causes of ciliochoroidal effusion, patients with idiopathic uveal effusion syndrome respond poorly to nonsurgical treatment, including corticosteroids or antimetabolites. Similarly, surgical treatment of nonrhegmatogenous retinal detachment in uveal effusion syndrome using conventional techniques, including scleral buckling or pars plana vitrectomy, fails to reattach the neurosensory retina secondary to persistent serous exudation. In most cases, successful reattachment of the nonrhegmatogenous retinal detachment requires a scleral-thinning procedure, including quadrantic partial-thickness sclerectomies and sclerostomies.

Pathophysiology of Ciliochoroidal Effusions

General Mechanisms

Since idiopathic uveal effusion syndrome represents only a small percentage of ciliochoroidal effusions, it is important to discuss the general mechanisms of serous accumulation in the ciliary body and choroid. Most cases of ciliochoroidal effusion can be classified into one of the following pathophysiologic categories: (1) hydrodynamic; (2) inflammatory; (3) neoplastic; or (4) associated with abnormal sclera.[3] Under physiologic conditions, a normal eye has equilibrium between the transmural hydrostatic pressure gradient, defined as the difference between the intravascular blood pressure and intraocular pressure, and the colloid osmotic pressure gradient of the choriocapillaris (Fig. 76.1). Albumin is the most abundant protein in the choroidal capillaries and is the primary driver of the colloid osmotic pressure. This pressure gradient draws fluid into blood vessels and maintains relative dehydration of the suprachoroidal space due to a low extravascular colloid concentration.[4] Fenestrated capillaries of the choroid allow albumin to escape into the extravascular space. To maintain the colloid

osmotic gradient, albumin leaves the choroid across the sclera, and this transscleral protein flow is facilitated by intraocular pressure.[5–7]

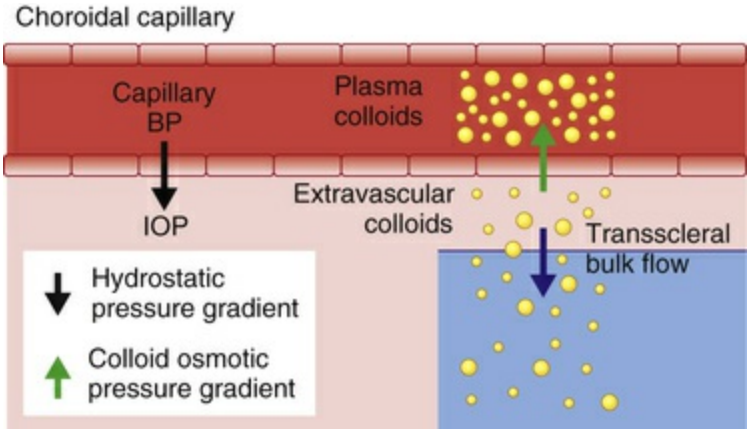

FIG. 76.1 In normal choroidal capillaries, the transmural hydrostatic pressure gradient is in equilibrium with the colloid osmotic pressure gradient. Colloids escaping the fenestrated capillaries move across the sclera by bulk flow, driven by intraocular pressure (*IOP*). *BP*, blood pressure. (From Johnson MW. Uveal Effusion. In: Guyer DR, Yannuzzi, L.A., Chang, S., Shields, J.A., Green, W.R., editor. Retina-Vitreous-Macula. Philadelphia: W.B.Saunders.)

The fluid equilibrium across the layers of the choroid may be disturbed by several factors affecting one or more components of this intricate system.[3] Ocular hypotony decreases the driving force for transscleral protein flow and increases the transmural hydrostatic pressure gradient. These changes then facilitate the accumulation of protein and fluid in the suprachoroidal space. Elevated uveal venous pressure increases the transmural hydrostatic pressure gradient and leads to increased fluid movement into the extravascular space. Vascular competence may be compromised by inflammation, which then increases capillary protein permeability and accumulation of protein in the extravascular space. This reduces the colloid osmotic pressure gradient and the absorption of extravascular fluid into the capillaries. Abnormal scleral composition or thickness may increase resistance to transscleral protein outflow and accumulation of protein-rich fluid in the suprachoroidal space.[8] These alterations are more likely to affect the choroidal fluid dynamics when two or

more are present simultaneously. Indeed, the creation of ciliochoroidal effusion in animal models requires experimental alteration of two or more pathophysiologic factors.[9,10]

Idiopathic and Nanophthalmic Uveal Effusion

In patients with uveal effusion syndrome or the closely related condition of nanophthalmos, abnormal sclera, referred to here as scleropathy, is the most likely primary ocular anomaly affecting choroidal fluid dynamics. In nanophthalmos, scleropathy is congenital in origin and associated with other ocular abnormalities. Acquired scleropathy may be secondary to a systemic disorder, such as the accumulation of amyloid in systemic amyloidosis or mucopolysaccharide in Hunter syndrome.[11,12] In uveal effusion syndrome, scleropathy appears to be secondary to the abnormal accumulation of glycosaminoglycan-like deposits and thickening of the sclera in the absence of any known systemic disorder.[13–15] Ward et al. reported that electron microscopy of excised sclera showed increased glycosaminoglycan-like deposits between the scleral fibers.[15] In a following report, Forrester and colleagues performed histochemical studies on scleras excised from patients with uveal effusion syndrome and showed deposition of the glycosaminoglycan proteodermatan sulfate and a smaller amount of proteochondroitin sulfate, indicating a primary defect in scleral proteodermatan metabolism and representing a form of ocular mucopolysaccharidosis.[13] Histologic similarities between scleras isolated from eyes with uveal effusion syndrome and nanophthalmos were demonstrated by Uyama et al., who found disorganized scleral fibers and proteoglycan deposits in 6 nanophthalmic eyes and 11 non-nanophthalmic eyes with uveal effusion syndrome.[14] As discussed above, abnormal scleral composition increases resistance to transscleral protein outflow, which in turn leads to the accumulation of protein, mostly albumin, in the extravascular space of the choroid and higher colloid osmotic pressure.[8] This results in reduced movement of fluid from the suprachoroidal space into the choroidal capillaries and leads to serous ciliochoroidal effusion. In vitro experimental evidence is consistent with this model, as chondroitinase ABC digestion, which removes glycosaminoglycans, improves scleral transport in human

cadaver eyes.[16]

Ciliochoroidal effusion and nonrhegmatogenous retinal detachment can be successfully treated in patients with uveal effusion syndrome by quadrantic partial-thickness sclerectomies.[17,18] The disappearance of serous fluid after partial-thickness sclerectomies is consistent with the hypothesis that abnormally thickened sclera prevents outflow of protein and suggests that the removal of excess extravascular protein may be improved by reducing scleral thickness and resistance. Under normal conditions, eyes with congenital or acquired scleropathies may have enough redundancy in choroidal protein transport mechanisms to achieve physiologic fluid equilibrium and dehydration of the suprachoroid. However, when choroidal fluid dynamics are further stressed by additional pathologic factors, such as compression of the vortex veins, these compensatory mechanisms may no longer be sufficient to overcome the effect of increased colloids in the suprachoroidal space, which may then lead to increased extravascular fluid retention and ciliochoroidal detachment.

Vortex vein compression was first suggested by Schaffer in 1975 as a possible mechanism of uveal effusion in nanophthalmic eyes following glaucoma filtration surgery.[19] Relative obstruction of venous outflow secondary to compressed vortex veins may cause congestion of the choriocapillaris and alter the transmural hydrostatic pressure gradient, favoring increased retention of fluid in the suprachoroidal space. Brockhurst reported successful reattachment of the retina and resolution of ciliochoroidal effusion in nanophthalmic eyes after surgical decompression of the vortex veins.[20] Additional evidence for the role of increased intravascular pressure secondary to reduced ocular venous drainage in uveal effusion was provided by Casswell and colleagues, who reported resolution of retinal detachment after vortex vein decompression in patients with uveal effusion syndrome.[21] As proposed by Gass, compression of the vortex veins by an abnormally thickened sclera may contribute to increased fluid retention and serous exudation in the choroid and ciliary body in uveal effusion syndrome.[17]

Clinical Features

Ciliochoroidal detachments in uveal effusion syndrome are brown–orange, solid-appearing elevations with smooth, convex surfaces (Fig. 76.2). Transillumination of the globe confirms the serous nature of the exudation. Choroidal detachments do not undulate appreciably with ocular movements, and this helps to distinguish them from rhegmatogenous retinal detachments. In early or mild cases, the diagnosis is suggested when the ora serrata is visible without the use of scleral depression secondary to shallow elevation of the pars plana and peripheral choroid (Fig. 76.3). As the effusion progresses, annular or lobular choroidal detachment may be seen. The characteristic four-lobed configuration results from the attachment of the choroid to the sclera at the vortex vein ampullae. The fluid accumulation is always greater anteriorly, as the anterior connecting fibers attaching choroid to the sclera are long and tangentially oriented, unlike the posterior fibers that are short and run more directly from uvea to sclera.[22]

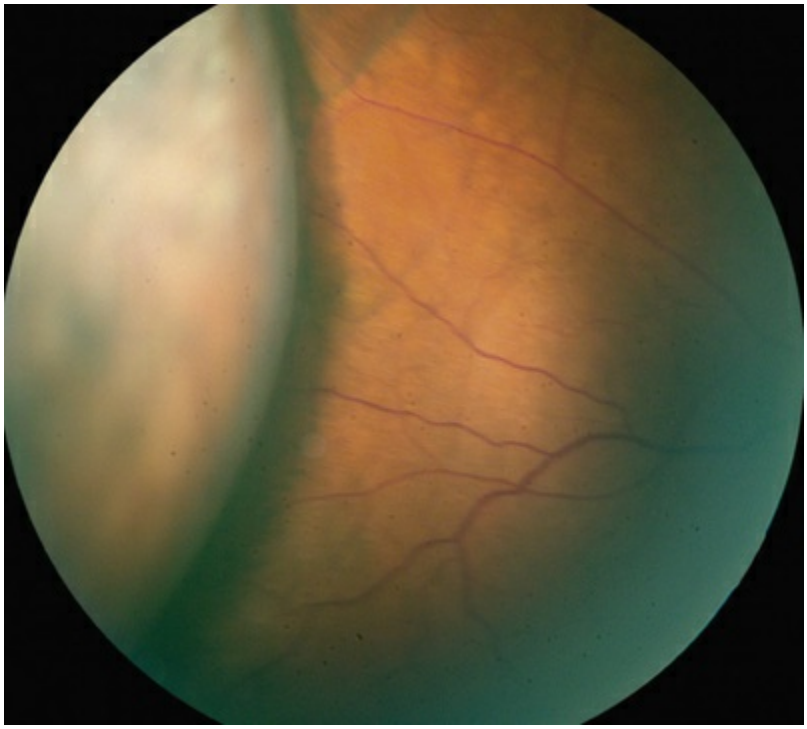

FIG. 76.2 Ciliochoroidal effusion demonstrating the characteristic solid-appearing choroidal elevation with a smooth, convex surface.

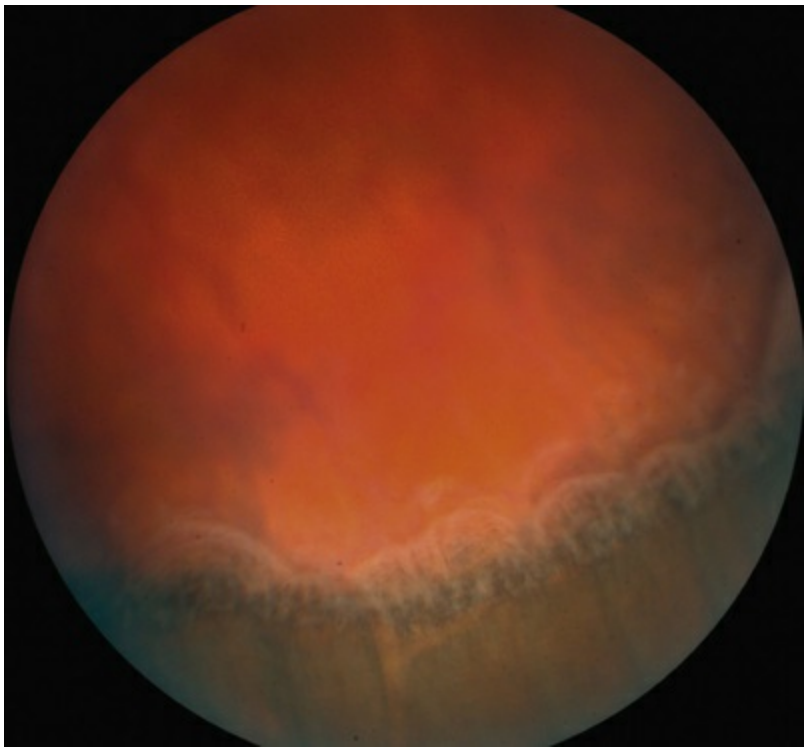

FIG. 76.3 Visible ora serrata without the use of scleral depression secondary to shallow elevation of the pars plana and peripheral choroid in an eye with ciliochoroidal effusion.

Long-standing uveal effusion causes decompensation of the retinal pigment epithelial fluid barrier, resulting in increased protein and fluid accumulation in the subretinal space and development of nonrhegmatogenous retinal detachment (Fig. 76.4). There is greater absorption of fluid from the subretinal space compared with protein outflow, which results in rising protein concentration and marked shifting of subretinal fluid with changes in head position. Progressive subretinal fluid accumulation may lead to total retinal detachment. Chronic serous effusion and subretinal fluid accumulation may result in diffuse depigmentation and multifocal hyperplasia of the retinal pigment epithelium, forming the characteristic clinical finding of leopard spots in the fundus (Figs. 76.4 and 76.5).

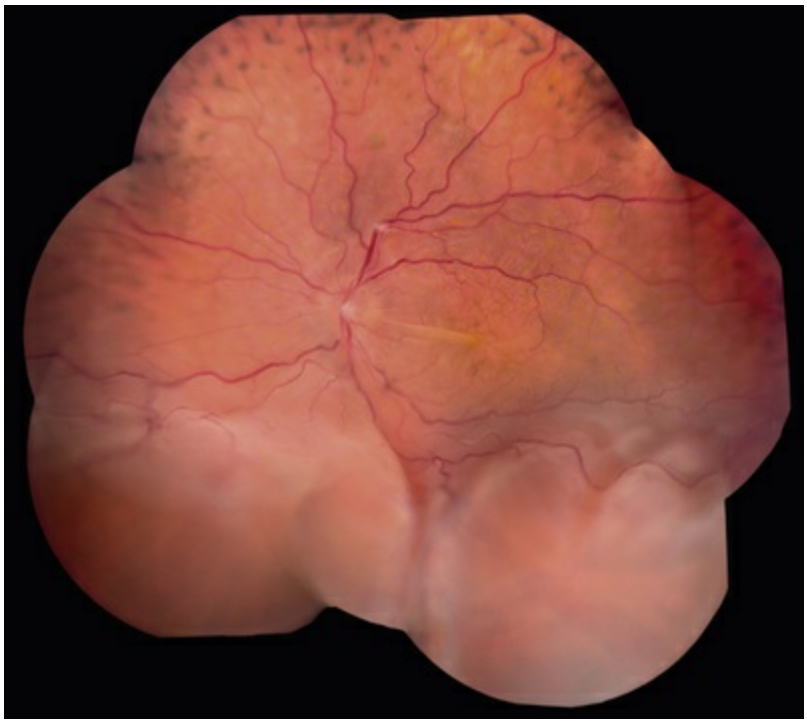

FIG. 76.4 Nonrhegmatogenous retinal detachment in a patient with uveal effusion. Location of the subretinal fluid is dependent on gravity. Leopard-spot retinal pigmentation is apparent superiorly.

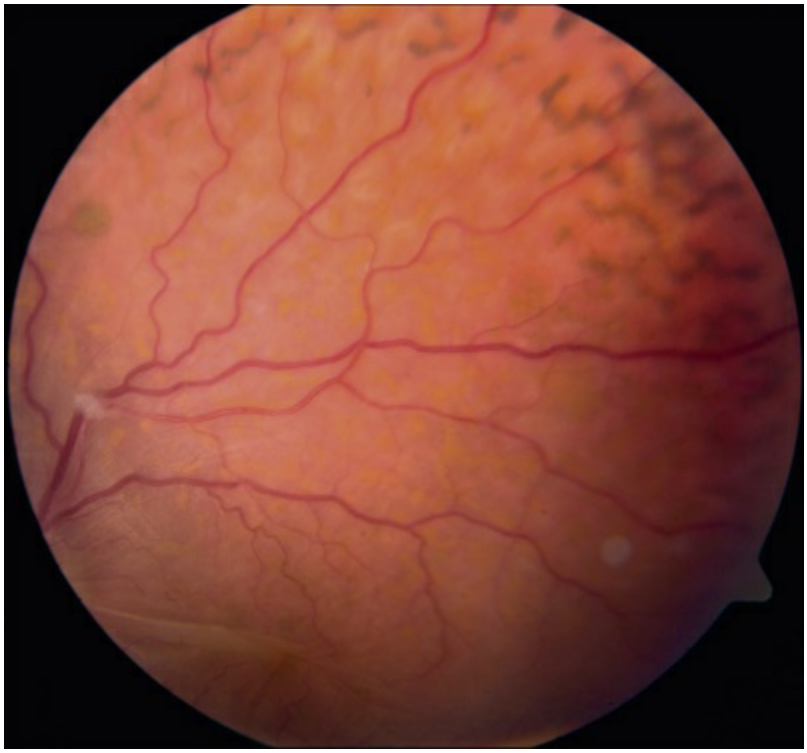

FIG. 76.5 Leopard-spot retinal pigmentation in uveal

effusion syndrome.

Anterior-segment examination in a patient with uveal effusion syndrome may reveal dilation of the episcleral blood vessels. Blood may be present in the Schlemm's canal on gonioscopy. The anterior chamber is free of any signs of inflammation, and the presence of anterior-chamber cell should increase suspicion of another ocular disorder with secondary uveal effusion. Mild vitreous cells may be present. Intraocular pressure is normal in patients with uveal effusion syndrome, and hypotony would indicate the presence of an alternative etiology. Elevation of subretinal fluid protein levels has been documented.[2,23,24] Although not commonly tested today, earlier studies of patients with uveal effusion syndrome demonstrated increased cerebrospinal fluid pressure and protein levels in some cases.[1,2]

Diagnostic Studies

In addition to the clinical examination, ancillary studies are important for the diagnosis of uveal effusion syndrome and, more importantly, for the exclusion of other more common etiologies of ciliochoroidal effusion.

Ophthalmic Ultrasound

B-scan ultrasound examination typically shows a smooth, thick, dome-shaped membrane with little aftermovement.[25] Ciliochoroidal effusion may be distinguished from retinal detachment by extension of the detachment anterior to the ora serrata. Highly bullous ciliochoroidal detachments may extend posteriorly and insert near the edge of the optic nerve. A-scan evaluation demonstrates a thick, 100% spike at tissue sensitivity, which at low sensitivity can often be seen to be double-peaked.[25] In early presentations of uveal effusion syndrome, the only evidence for ciliochoroidal effusion may be subtle degrees of supraciliary effusion on high-frequency ultrasound biomicroscopy. Diffuse, high-reflective thickening of the posterior choroid may be seen (Fig. 76.6). Low-reflective choroidal thickening should raise the suspicion for an infiltrative process secondary to an inflammatory

or neoplastic condition.[25]

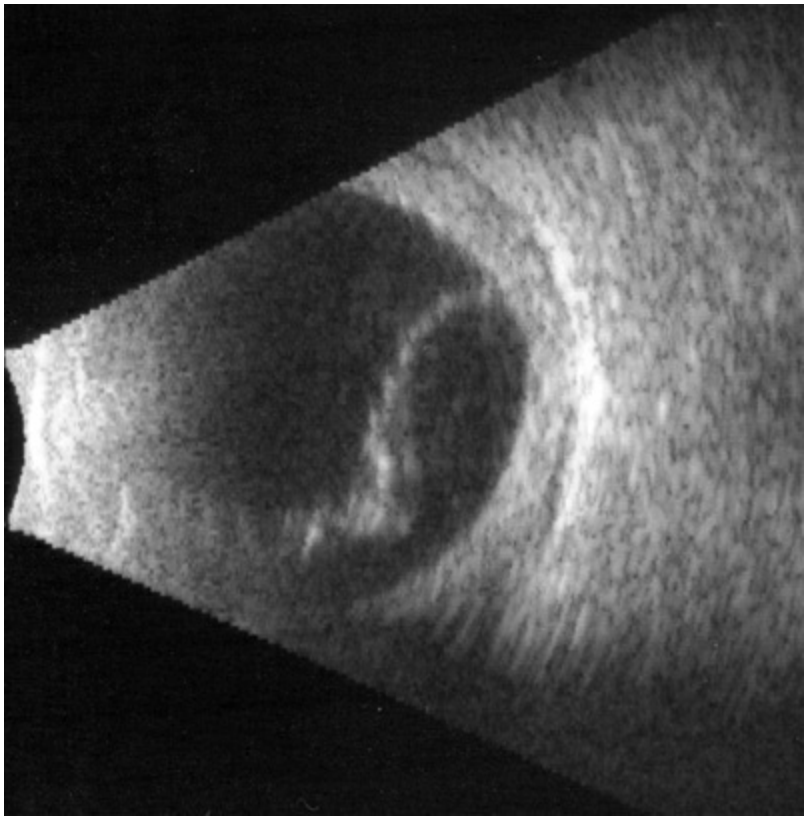

FIG. 76.6 B-scan ultrasound of an eye with uveal effusion syndrome shows choroidal thickening and inferior nonrhegmatogenous retinal detachment.

Angiography and Optical Coherence Tomography

The diagnostic value of fluorescein and indocyanine green angiography and optical coherence tomography is limited in uveal effusion syndrome and serves mostly to exclude other etiologies. Angiography may demonstrate a leopard-spot appearance of hyperfluorescence and hypofluorescence (Fig. 76.7). The presence of focal fluorescein leaks and focal pigment epithelial detachments should increase the suspicion for idiopathic central serous chorioretinopathy as the underlying diagnosis. Multiple pin-point leaks may indicate the presence of an inflammatory or neoplastic choroidal infiltration. Indocyanine green angiography shows diffuse granular choroidal hyperfluorescence in the early phase, indicating marked hyperpermeability of the choroidal vessels.[14]

This choroidal hyperfluorescence persists into the late-phase angiogram and becomes more diffuse, demonstrating increased accumulation of fluid in the choroid. Spectral-domain optical coherence tomography may show focal thickening of the retinal pigment epithelium layer corresponding to the areas of leopard spots.[26]

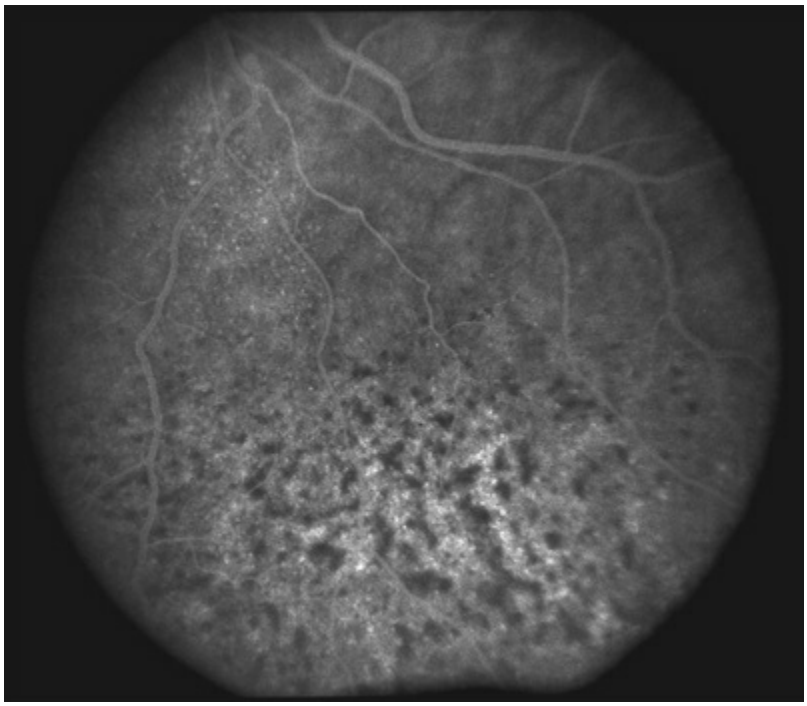

FIG. 76.7 Fluorescein angiogram of a patient with uveal effusion syndrome demonstrating leopard-spot appearance of hyperfluorescence and hypofluorescence.

Differential Diagnosis

Uveal effusion syndrome is a diagnosis of exclusion. The differential diagnosis may be categorized by primary pathogenic factors causing ciliochoroidal effusion (Box 76.1). As discussed above, serous effusions in the ciliary body and choroid generally require the simultaneous presence of multiple pathogenic factors.

Box 76.1

Differential Diagnosis of Ciliochoroidal Effusions

Scleropathies

Congenital

- Uveal effusion syndrome
- Nanophthalmos

Acquired

- Amyloidosis
- Mucopolysaccharidosis

Hydrodynamic factors

Ocular hypotony

- Wound leak
- Overfiltration
- Cyclodialysis
- Penetrating ocular trauma
- Rhegmatogenous retinal detachment
- Ciliary body dysfunction

Elevated uveal venous pressure

- Arteriovenous fistula
- Sturge–Weber syndrome

- Idiopathic prominent episcleral vessels
- Vortex vein compression
- Valsalva maneuver

Malignant hypertension

Inflammatory factors

- After trauma or surgery
- After photocoagulation or cryotherapy
- Drug reaction
- Uveitis
- Scleritis
- Orbital cellulitis
- Idiopathic orbital inflammation

Neoplastic conditions

- Metastatic carcinoma
- Malignant melanoma
- Lymphoproliferative and melanocytic choroidal infiltration

Congenital and Acquired Scleropathies

As discussed above, congenital or acquired scleropathy with abnormal thickening of the sclera significantly alters the choroidal fluid dynamics and may cause uveal effusion, especially in the presence of other pathogenic factors such as vortex vein compression with reduced venous outflow and elevated uveal venous pressure. Uveal effusion syndrome and nanophthalmos can be considered in the same spectrum of diseases with a congenital primary scleral abnormality. Secondary scleral abnormalities are seen in association with systemic disorders, including amyloidosis or mucopolysaccharidosis.[11,12]

Uveal effusion in patients with nanophthalmos is remarkably similar to that seen in the idiopathic uveal effusion syndrome. Nanophthalmos is a pure form of microphthalmia characterized by small eyes and extremely thick sclera with no other identifiable ocular or systemic abnormalities. The axial length is generally less than 20 mm, and high hyperopia (>+7.00 D) is typical. Other findings include small corneal diameter, shallow anterior chamber, high lens-to-eye volume ratio, and strong predisposition to develop angle closure glaucoma.[27] Uveal effusion and nonrhegmatogenous retinal detachment may occur spontaneously and are frequently induced by intraocular surgery in nanophthalmic eyes.[27,28] The detection of nanophthalmos is important prior to any planned intraocular procedure since prophylactic use of sclerectomies may prevent significant postoperative complications secondary to uveal effusion.

Hydrodynamic Effusions

Hydrodynamic factors associated with ciliochoroidal effusion include ocular hypotony, elevated uveal venous pressure, and malignant hypertension. Long-standing low intraocular pressure induces uveal effusion and may in turn be worsened by ciliary body detachment. The most common reason for hypotony is glaucoma filtering or drainage device surgery, especially in the early postoperative period. Resuturing the scleral flap, scleral patch grafting, autologous blood injection, and other methods have been described in the literature to reverse postoperative hypotony.[29–31] Hypotony and uveal effusion complicating anterior-segment surgery are usually secondary to a wound leak or inadvertent

filtering bleb. Other ocular disorders that may lead to hypotony and secondary ciliochoroidal effusion include cyclodialysis, penetrating ocular trauma, rhegmatogenous retinal detachment, and ciliary body dysfunction.

Elevated uveal venous pressure and increased transudation from choroidal vessels may be seen in the setting of carotid–cavernous sinus fistula or dural arteriovenous fistulas. When an intracranial fistula is suspected in a patient with uveal effusion, nonrhegmatogenous retinal detachment, and other associated findings, neuroimaging should be obtained. Patients with idiopathic prominent episcleral vessels or Sturge–Weber syndrome have elevated episcleral venous pressure and likely secondary increase in choriocapillaris pressure, which predisposes them to a higher risk of significant ciliochoroidal effusion during intraocular surgery when the intraocular pressure drops to zero.[32] Compression of the vortex veins and reduction of ocular venous outflow may lead to uveal effusion after scleral buckling surgery.

Malignant hypertension secondary to severe renal disease or pregnancy may lead to ciliochoroidal effusion and nonrhegmatogenous retinal detachment, which usually resolve with blood pressure control.

Inflammatory Factors

In addition to causing hypotony, penetrating trauma may induce marked intraocular inflammation, which leads to increased vascular permeability. Chronic low-grade inflammation with increased permeability of the choriocapillaris may also be seen after intraocular surgery. Transient vascular leakage and serous ciliochoroidal fluid accumulation may be seen after thermal injury from panretinal photocoagulation or transscleral cryotherapy. Inflammation of the uveal tract secondary to autoimmune or infectious etiologies may be complicated by ciliochoroidal effusion and nonrhegmatogenous retinal detachment. A uveitic syndrome is usually suspected in these patients based on other ocular findings. A painful or red eye in a patient with uveal effusion may be secondary to scleritis, idiopathic orbital inflammation, or orbital cellulitis. Careful examination is required to differentiate idiopathic uveal effusion from uveitis, especially if there is no response to

high-dose corticosteroid treatment.[33] A buckle infection should always be in the differential diagnosis of uveal effusion in a patient with scleral inflammation after scleral buckling surgery.

Neoplastic Effusions

Choroidal metastatic tumors or malignant melanoma may infrequently present with ciliochoroidal effusion and nonrhegmatogenous retinal detachment. The diagnosis may only be apparent after an ophthalmic ultrasound in cases with extensive choroidal and subretinal fluid accumulation. In addition to solid tumors of the eye, neoplastic infiltrations and secondary uveal thickening may cause nonrhegmatogenous retinal detachment and occasional serous uveal effusion in lymphoproliferative disorders or melanocytic proliferation.

Treatment of Idiopathic Uveal Effusion Syndrome

Most patients with idiopathic uveal effusion syndrome become symptomatic of their disease when the subretinal fluid from the inferior nonrhegmatogenous retinal detachment progresses superiorly and causes macular detachment. Macular damage can also occur from repeated episodes wherein subretinal fluid shifts into the macula while the patient is lying down. Some patients may initially be misdiagnosed and treated medically for other causes of exudative retinal detachment, which fails to restore vision. Surgical treatment is required to prevent further macular damage by facilitating the resolution of subretinal fluid. In patients with known idiopathic uveal effusion syndrome and an otherwise asymptomatic eye (e.g., fellow eye of a patient with a unilateral presentation), prophylactic treatment with a scleral-thinning procedure should be considered prior to any intraocular surgery in order to prevent postoperative ciliochoroidal effusion and nonrhegmatogenous retinal detachment.

Scleral Thinning Procedures

Gass first described sclerectomy with sclerostomy for the treatment

of uveal effusion syndrome in 1983.[17] The idea of using this procedure in patients with uveal effusion syndrome arose after an unsuccessful attempt at vortex vein decompression in another patient. Gass operated on both eyes of a patient with thick sclera and uveal effusion and amputated or ruptured the vortex veins during attempted decompression. Despite the occurrence of suprachoroidal hemorrhage in both eyes, ciliochoroidal and nonrhegmatogenous detachment resolved in both eyes postoperatively. This observation led him to hypothesize that the excision of large scleral flaps at the sites of vortex veins was responsible for the successful outcome. To test this hypothesis, he performed quadrantic partial-thickness sclerectomies and sclerostomies without vortex vein decompression or drainage of subretinal fluid in both eyes of a patient with long-standing uveal effusion and bullous nonrhegmatogenous retinal detachment. Complete resolution of ciliochoroidal and subretinal fluid occurred 10–12 weeks after surgery.[17] In 1990, Johnson and Gass expanded on this initial result in a retrospective study of 23 eyes of 20 patients with uveal effusion syndrome who underwent a scleral-thinning procedure without vortex vein decompression.[18] The investigators observed complete resolution of subretinal and supraciliochoroidal fluid in 96% of eyes after one or two procedures. The mean time for resolution of uveal effusion and nonrhegmatogenous retinal detachment was 2.4 months. Other investigators reported similar results using scleral-thinning procedures for treatment of uveal effusion and nonrhegmatogenous retinal detachment associated with Hunter syndrome, nanophthalmos, and uveal effusion syndrome.[12,14,21,34,35]

The surgical procedure for scleral thinning involves the creation of 5×7 mm, one-half to two-thirds thickness sclerectomies in each quadrant, centered 1–2 mm anterior to the equator and placed outside the meridian of each vortex vein to avoid its intrascleral course (Fig. 76.8).[17,18,36] The long axis of the sclerectomy is oriented circumferentially. An approximately 2-mm linear sclerostomy may be created in the center of each sclerectomy bed and enlarged with a 1–2-mm scleral punch. Similar scleral-thinning techniques have been reported by others treating nanophthalmic or idiopathic uveal effusion.[14,37] Persistent or recurrent uveal effusion and

nonrhegmatogenous retinal detachment following surgery may be secondary to the fibrosis and scarring of sclerectomies and sclerotomies. An antimetabolite, such as mitomycin-C (MMC), may reduce the risk of recurrent fibrosis following repeat scleral thinning procedure.[38] A novel approach using Ex-PRESS shunt to drain choroidal fluid without sclerotomies has recently been reported.[39]

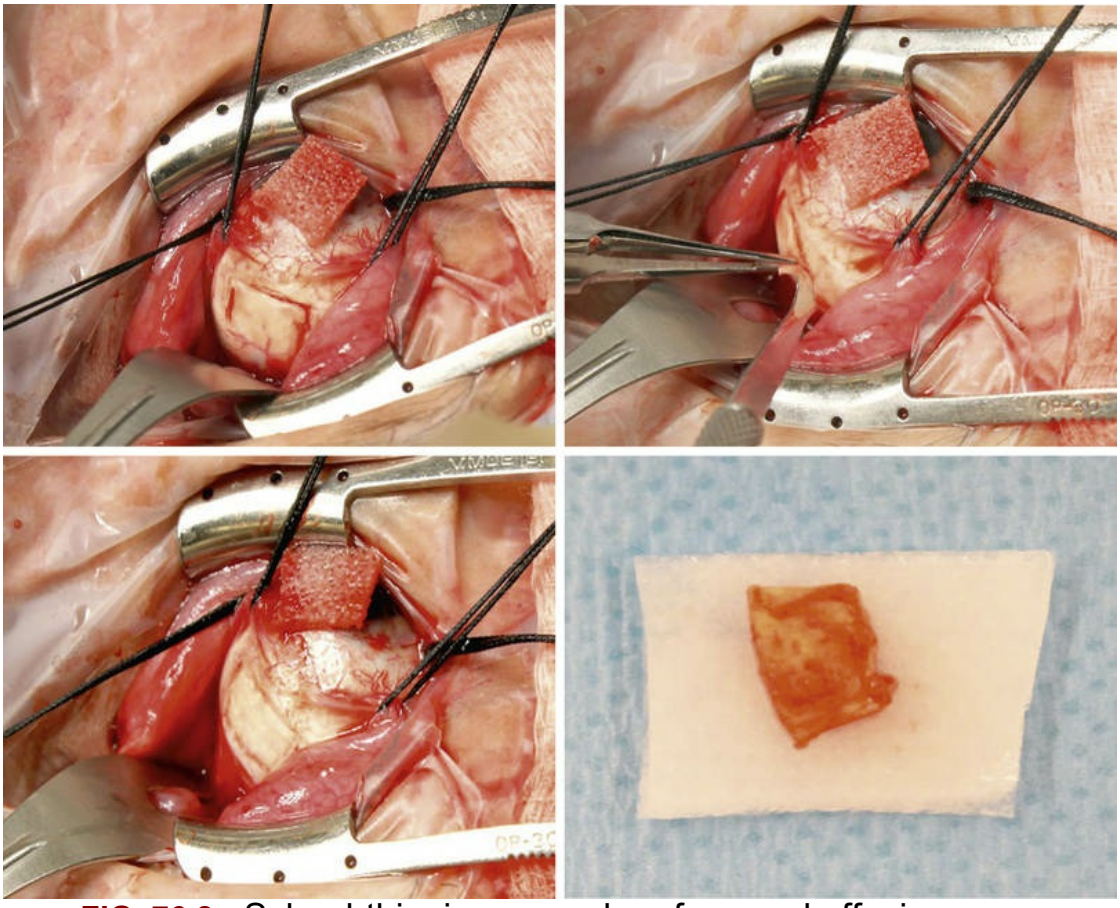

FIG. 76.8 Scleral-thinning procedure for uveal effusion syndrome. Borders of the sclerectomy are outlined with partial-thickness scleral incisions (top left). One-half to two-thirds thickness lamellar scleral dissection is performed (top right), creating a scleral window (bottom left) and an excised section of abnormally thick sclera (bottom right).

Pars Plana Vitrectomy

The extent of visual improvement after scleral-thinning procedures

may be limited by photoreceptor and retinal pigment epithelial damage secondary to chronic retinal detachment. In the series reported by Johnson and Gass, visual acuity improved by 2 or more Snellen lines in 56% of eyes, remained stable in 35% of eyes, and worsened in 9% of eyes.[18] Overall visual acuity was 20/400 or better in 96% of eyes and 20/40 or better in 35% of eyes. Among the 12 of 23 eyes whose final visual acuity was worse than 20/40, the primary vision-limiting factor was atrophic photoreceptor and retinal pigment epithelial damage due to chronic retinal detachment. The mean time for retinal reattachment following scleral-thinning surgery in this series was 2.4 months. To facilitate rapid retinal reattachment and prevent ongoing damage to photoreceptors and the retinal pigment epithelium, Schneiderman and Johnson performed pars plana vitrectomy and internal drainage of subretinal fluid at the time of quadrantic partial-thickness sclerectomies in a 73-year-old man with uveal effusion syndrome and total retinal detachment.[40] This patient's vision improved from hand motions to 20/70 1 year postoperatively. This combined approach of sclerectomies and pars plana vitrectomy for macula-off nonrhegmatogenous retinal detachment in uveal effusion syndrome allows immediate approximation of the photoreceptors and the retinal pigment epithelium and prevents further photoreceptor cell death. An alternative approach is external drainage of the subretinal fluid,[24] which presents significant risk of subretinal hemorrhage, profound ocular hypotony, and difficulty accessing the posteriorly shifting subretinal fluid.

Vortex Vein Decompression

In 1980, Brockhurst reported successful use of scleral-thinning procedure with vortex vein decompression in the treatment of nanophthalmic ciliochoroidal effusion.[20] He described the isolation of the intrascleral portion of the vortex vein and decompressing all four veins. Since scleral-thinning procedures alone are successful in the treatment of uveal effusion syndrome, vortex vein decompression for the treatment of ciliochoroidal effusion in uveal effusion syndrome or nanophthalmos is no longer performed by most vitreoretinal surgeons.

Conclusion

Idiopathic uveal effusion syndrome is a rare condition that typically presents in otherwise healthy middle-aged males with spontaneous detachment of the ciliary body and the peripheral choroid. This condition is frequently associated with nonrhegmatogenous retinal detachment with marked shifting of subretinal fluid due to its exceptionally high protein content. Other ocular findings include dilation of the episcleral blood vessels, blood in Schlemm's canal, normal intraocular pressure, mild vitreous cells, and leopard-spot pigment epithelial alterations. Current evidence indicates that congenital scleropathy manifesting with abnormal accumulation of glycosaminoglycan-like deposits and thickening of the sclera is the primary pathologic anomaly in patients with uveal effusion syndrome. The diagnosis of uveal effusion syndrome is based on characteristic clinical findings and exclusion of the other known causes of ciliochoroidal effusion and nonrhegmatogenous retinal detachment. The natural course is usually prolonged with remissions and exacerbations, and without treatment, patients may experience permanent loss of vision. Treatment is primarily surgical and requires quadrantic partial-thickness sclerectomies and sclerostomies.

Hypotony Maculopathy

Introduction

Loss of central vision may develop in patients with reduced intraocular pressure following trauma or ocular surgery. One of the causes of reduced vision in the setting of hypotony is significant folding of the choroid, neurosensory retina, and retinal pigment epithelium in the posterior pole, termed hypotony maculopathy by Gass in 1972.[41–44] The initial description of fundus changes associated with hypotony dates back to the 1950s, when Dellaporta described patients with reduced vision following glaucoma procedures or perforating eye injuries.[41] He noted that hypotony was associated with several fundus abnormalities, including optic nerve swelling, vascular tortuosity, and chorioretinal folds.[41] The incidence of hypotony maculopathy significantly increased after the

introduction of antimetabolites in glaucoma-filtering surgery.[45–47] Younger age, myopia, and male gender are significant risk factors for the development of hypotony maculopathy after glaucoma procedures.[46–48]

Clinical Features

Posterior-segment examination in patients with hypotony maculopathy shows irregular folding of the neurosensory retina, retinal pigment epithelium, and choroid (Fig. 76.9). These folds are initially broad and indistinct and tend to radiate outward in a branching fashion from the optic disc temporally and appear concentric or irregular nasally. Around the center of the fovea, retinal folds may be arranged in a stellate pattern. The elevated crests of the folds appear yellow with dark narrow troughs in between. Reduction of the ocular anteroposterior diameter causes relative hyperopia. Marked optic disc edema may be present. Retinal vasculature is typically tortuous and may be engorged in some eyes. Anterior-segment examination may show a shallow anterior chamber if there is ciliochoroidal effusion. As the intraocular pressure returns to the normal range, the choroidal folds flatten and may disappear. If the hypotony was chronic, permanent retinal pigment epithelial changes may cause pigmented lines in the fundus.

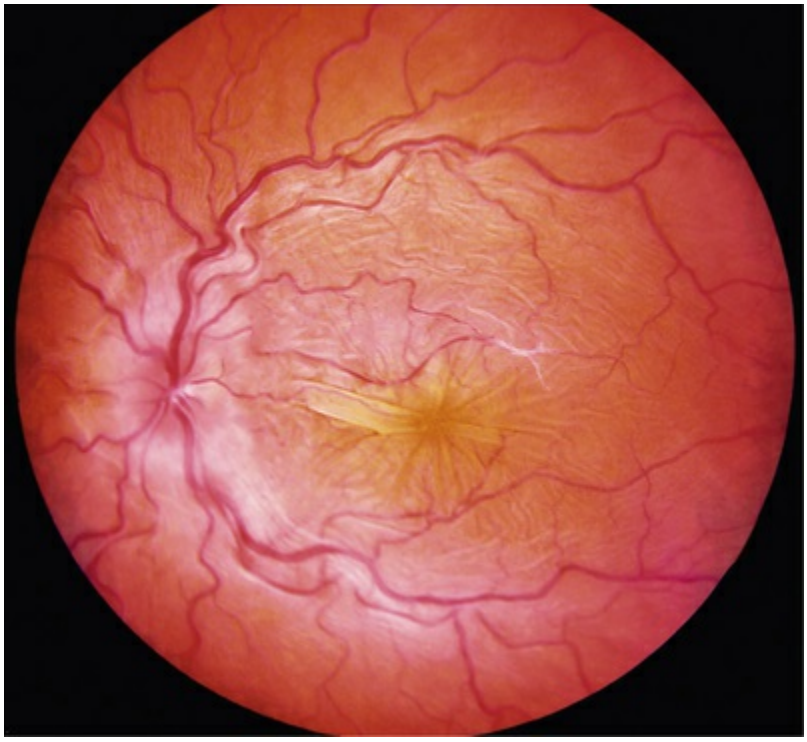

FIG. 76.9 Chorioretinal folds and optic disc edema in a patient with hypotony maculopathy.

Diagnosis

Fluorescein Angiography

Fluorescein angiography is useful in demonstrating chorioretinal folds, especially in mild cases with a normal-appearing fundus examination. In the initial stages of hypotony, fluorescein angiography demonstrates an irregular increase in background choroidal fluorescence corresponding to the crest of the choroidal folds (Fig. 76.10). This produces hyperfluorescent streaks that may be seen in the early arterial phase. The hyperfluorescence of these streaks is multifactorial: (1) thinning of the retinal pigment epithelium on the crest of the folds; (2) pooling of the choroidal fluorescein under the crest; and (3) shorter course of the incident blue and reflected yellow-green light during angiography. The troughs of the folds are occupied by compressed retinal pigment epithelial cells, which reduce the transmission of the background choroidal fluorescence and cause hypofluorescence on angiography. Leakage of fluorescein may be seen in the capillaries of the optic nerve and there is typically no leakage in the retinal

capillaries.[49] In long-standing hypotony, angiography may show permanent alterations in the retinal pigment epithelium. The chorioretinal folds may be differentiated from the folds of the neurosensory retina, which do not alter the background fluorescence.

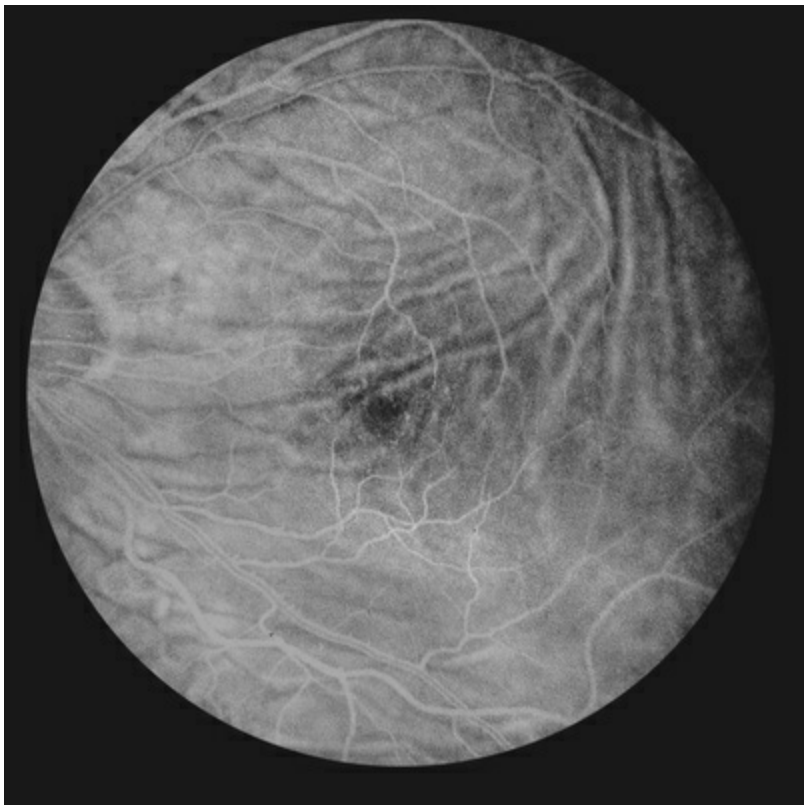

FIG. 76.10 Fluorescein angiogram in hypotony maculopathy demonstrates hyperfluorescent streaks corresponding to the crest of the chorioretinal folds.

Ocular Ultrasound

B-scan ultrasonography typically shows flattening and thickening of the sclera and choroid in the posterior pole[50] (Fig. 76.11). Anterior-segment evaluation with ultrasound biomicroscopy may be useful for the identification of the underlying etiology of hypotony. The presence of a cyclodialysis cleft or anterior ciliary detachment may only be apparent on ultrasound biomicroscopy.[51,52]

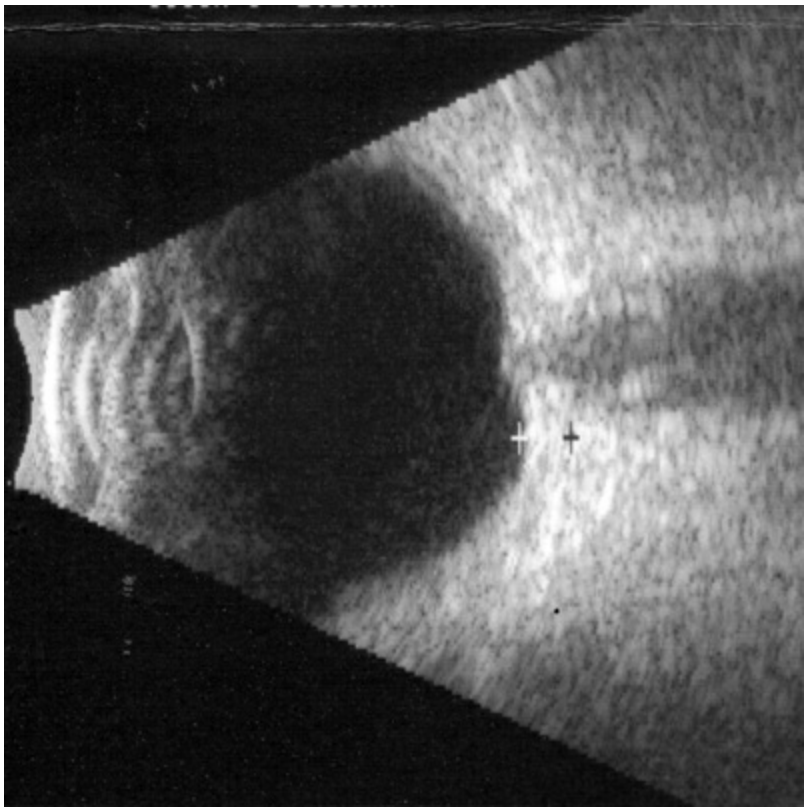

FIG. 76.11 B-scan ultrasonography in a patient with low intraocular pressure showing characteristic flattening and thickening of the sclera and choroid in the posterior pole.

Optical Coherence Tomography

In patients with low intraocular pressure and reduced visual acuity, optical coherence tomography (OCT) imaging of the posterior pole can help to demonstrate subtle chorioretinal folds of the macula that may otherwise be difficult to detect on biomicroscopy[53–55] (Fig. 76.12). High-resolution OCT may detect chorioretinal folding in early hypotony, which may not show any changes in the background choroidal fluorescence during fluorescein angiography.[54] However, the clinical significance of subtle chorioretinal folds detected only by OCT in a patient with unchanged vision is unclear. OCT in a patient with symptomatic hypotony maculopathy and stereotypical biomicroscopic findings typically shows prominent chorioretinal folds (Fig. 76.12).

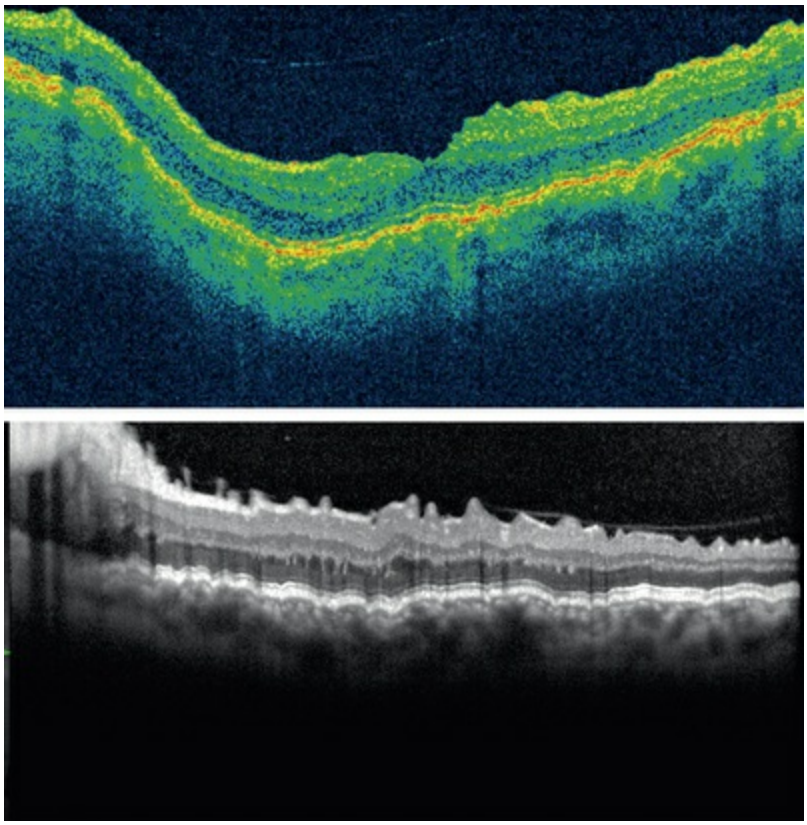

FIG. 76.12 High-resolution optical coherence tomography may demonstrate subtle (top panel) or prominent (bottom panel) chorioretinal folding in hypotony maculopathy.

Pathogenesis

Hypotony

The reduction of intraocular pressure may be secondary to decreased aqueous production or increased aqueous outflow. In most cases, both a reduction in aqueous production and an increase in aqueous outflow are present in a hypotonous eye. Box 76.2 lists various etiologies of decreased intraocular pressure, some of which will be briefly discussed below.

Box 76.2

Causes of Hypotony

Postoperative

- Wound leak

- Overfiltration

Ocular trauma

- Cyclodialysis
- Perforating injury

Inflammatory

- Iridocyclitis

Retinal detachment

Ciliochoroidal detachment

Ciliary body hypoperfusion

- Carotid occlusion
- Giant cell arteritis

Photocoagulation or cryoablation of the ciliary body

Excessive reduction of intraocular pressure by pharmacologic agents

Systemic

- Hyperosmotic agents
- Dehydration
- Uremia
- Diabetic ketoacidosis

- Myotonic dystrophy

Decreased Aqueous Production

Reduced aqueous production is an uncommon etiology of hypotony. The factors that lead to decreased aqueous production may be inflammatory, vascular, or structural. Ciliary body inflammation may compromise the production of aqueous in patients with uveitis. Severe intraocular inflammation in the immediate postoperative period following intraocular surgery may decrease aqueous secretion. Trauma may be associated with significant iridocyclitis and hypotony, which may be worsened by increased aqueous outflow due to a cyclodialysis cleft or globe rupture. Decreased ocular perfusion in patients with vasculitis or arterial occlusion may cause ciliary body ischemia. Other causes of decreased aqueous production include ciliary body detachment secondary to ciliochoroidal effusion, trauma, or proliferative vitreoretinopathy.

Increased Aqueous Outflow

When the aqueous production is no longer sufficient to match the increased outflow, hypotony develops. Most cases of ocular hypotony are secondary to increased aqueous outflow. Under physiologic conditions, the aqueous leaves the eye primarily through the trabecular meshwork and Schlemm's canal in a pressure-dependent manner, with much smaller amounts exiting through uveoscleral outflow. Several factors may increase aqueous outflow, including wound leak after anterior-segment surgery and excessive aqueous filtration after glaucoma filtering or drainage device surgery. After the introduction of antimetabolites in glaucoma-filtering procedures, the incidence of hypotony increased.[45] Antimetabolites inhibit subconjunctival healing and scarring, which would otherwise limit the overfiltration rate. With the introduction of sutureless small-gauge vitrectomy technology, vitreoretinal surgeons encounter ocular hypotony with increasing frequency in their postoperative patients.[56] Ocular trauma may be associated with scleral rupture and wound leak. Postoperative or traumatic cyclodialysis creates a free communication between the

anterior chamber and the suprachoroidal space, increasing the uveoscleral outflow.

Mechanism of Maculopathy

Chorioretinal folds form in the hypotonous eye due to scleral shrinkage and reduction of the inner surface area of the sclera. This loss of surface area then leads to folding of the inner portion of choroid and the outer retina.[57–60] Maculopathy develops when the neurosensory retina is thrown into a series of stellate folds around the center of the fovea. This central stellate retinal wrinkling is caused by the thickened posterior scleral wall and the choroid displacing the normally thick retina surrounding the thin foveola.[49] The folding of the neurosensory retina is the primary cause of vision loss in hypotony maculopathy. The risk of hypotony maculopathy is highest in young myopic patients, and this may indicate that the sclera is more vulnerable to swelling and contraction in young patients.

Mechanism of Optic Disc Edema

Reduced intraocular pressure may lead to broad areas of choroidal swelling and retinal folding around the optic nerve, and this may cause disc edema.[49] Another proposed mechanism is the anterior bowing of the lamina cribrosa and constriction of axonal bundles in the lamina scleralis, causing reduced orthograde and retrograde axoplasmic transport and swelling of the optic nerve.[61] Disc edema may be less impressive in eyes with preexisting optic nerve disease and loss of axons.

Differential Diagnosis

The finding of chorioretinal folds may be seen in any condition that reduces the inner surface area of the sclera secondary to thickening or shrinkage (Box 76.3).

Box 76.3

Differential Diagnosis of Hypotony Maculopathy

- Idiopathic chorioretinal folds

- Retrobulbar mass lesions
- Scleral inflammation
- Scleral buckle
- Choroidal tumors
- Choroidal neovascularization
- Focal chorioretinal scars
- Optic nerve head disorders
- Retinal folds

Idiopathic Chorioretinal Folds

Horizontal macular chorioretinal folds, as well as folds radiating from the optic nerve, may be seen in young hyperopic patients on routine evaluation.[58,62] These idiopathic chorioretinal folds are usually confined to the area around the macula and optic nerve, but may at times involve most of the posterior pole. Patients usually do not report any visual dysfunction. The appearance of the folds is usually symmetric in both eyes, but may occasionally be seen unilaterally. As the name indicates, the etiology of these chorioretinal folds is unknown and may be secondary to the shrinkage of the fibrous tunic of the eye after an inflammatory process during early years of life.[49]

Retrobulbar Mass Lesions

Any space-occupying mass in the orbit may cause scleral edema, choroidal congestion, and chorioretinal folds.[63,64] A mass in the extraconal space may induce astigmatism, whereas intraconal location of a tumor may lead to acquired hyperopia.[63] Both benign and malignant tumors have been reported to present with chorioretinal folds.

Scleral Inflammation

Scleral inflammation with edema, thickening, and choroidal congestion may lead to the development of chorioretinal folds. Thyroid eye disease, idiopathic orbital inflammation, and other autoimmune or infectious uveitic diseases presenting with scleritis may have associated chorioretinal folds.[49,65,66]

Scleral Buckle

Thickening of the sclera in the posterior slope of a scleral buckle may cause occasional chorioretinal folds in patients who underwent rhegmatogenous retinal detachment repair.

Choroidal Tumors

Malignant melanoma or metastatic lesions of the choroid may cause vascular congestion, choroidal edema, and scleral thickening, leading to chorioretinal folds surrounding the tumor.[49]

Choroidal Neovascularization

Spontaneous or laser-induced contraction of subretinal pigment epithelial choroidal neovascular membrane may induce the formation of chorioretinal folds that radiate away from the membrane.[67]

Focal Chorioretinal Scars

Focal scars of the choroid and the retina may sometimes cause contraction and induce chorioretinal folds radiating towards the center of the scar.[68]

Optic Nerve Head Disorders

Idiopathic intracranial hypertension and papilledema may be associated with chorioretinal folds. These folds are usually horizontal in the macula and converge on the nasal side of the swollen optic nerve.[69,70] Chorioretinal folds have also been seen in patients with unexplained optic atrophy.[71] In some patients with increased intracranial pressure, chorioretinal folds may present in the absence of any detectable papilledema and a lumbar puncture with an opening pressure may need to be performed to rule out idiopathic intracranial hypertension.[72]

Retinal Folds

Retinal folds may be mistaken for chorioretinal folds in some eyes. Usually, folds of the neurosensory retina are narrow and seen radiating away from a focal inner retinal contraction caused by macular pucker or outer retinal contraction secondary to a chorioretinal scar (Fig. 76.13).[49] Fluorescein angiography is helpful in differentiating retinal folds from chorioretinal folds, since folds of the neurosensory retina do not change the fluorescence pattern and are not seen on angiography.

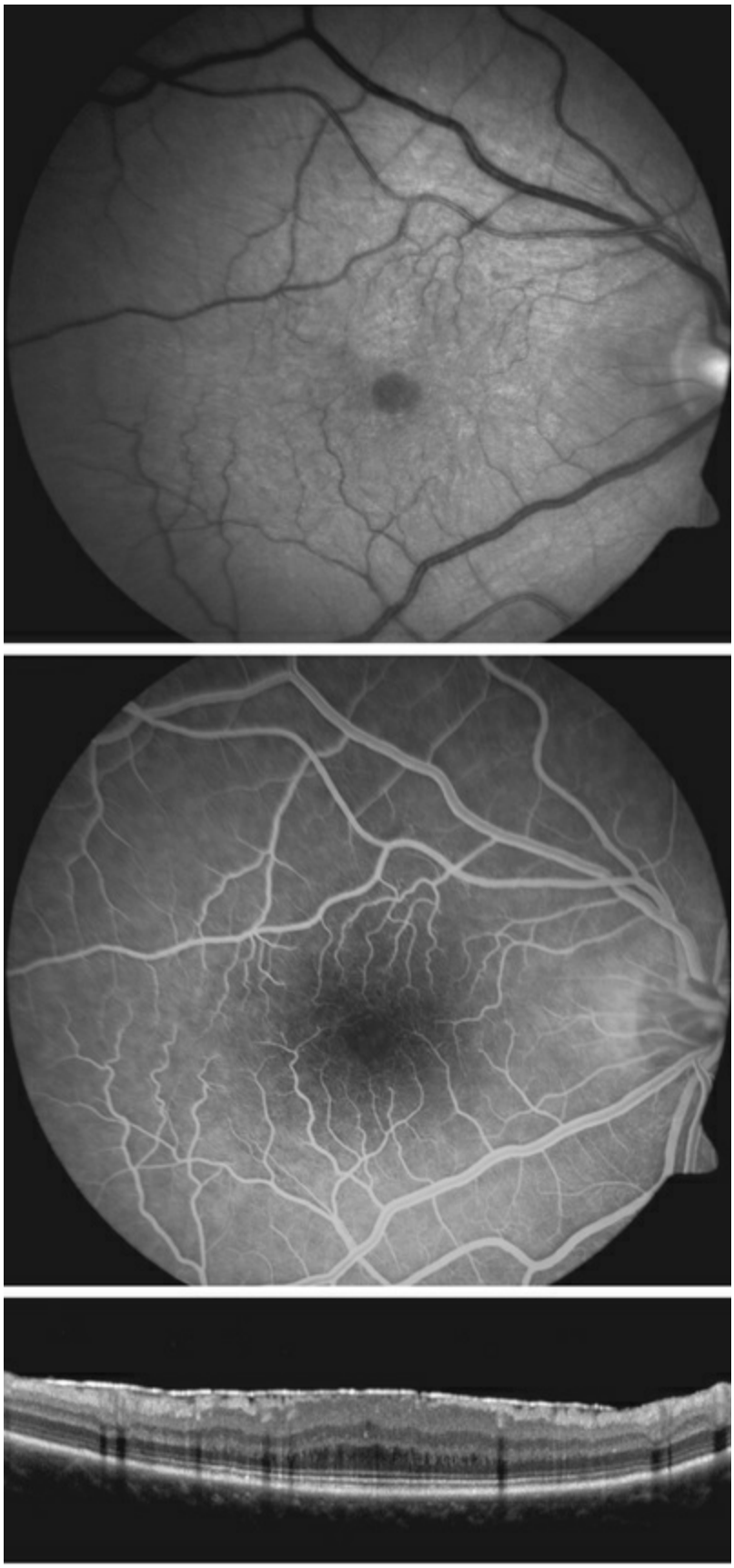

FIG. 76.13 Red-free photo of the posterior pole (top panel) and high-resolution optical coherence tomography (bottom panel) demonstrate fine, subtle

retinal folds associated with an epiretinal membrane. Fluorescein angiogram shows no fluorescence changes associated with these folds (middle panel).

Treatment

The effective treatment of hypotony maculopathy requires correcting the underlying ocular abnormality and restoring normal intraocular pressure. Since postoperative hypotony accounts for a significant portion of hypotony maculopathy patients, treatment is typically managed by an anterior-segment surgeon. Injection of viscoelastic or fluid into the anterior chamber to increase intraocular pressure produces short-lived effects. Wound leaks after anterior-segment surgery need to be addressed immediately with a bandage contact lens or suturing the wound to prevent further aqueous loss. Ocular inflammation requires treatment with a topical or oral corticosteroid. Posttraumatic cyclodialysis cleft may require laser or surgical closure to normalize intraocular pressure. Overfiltration after glaucoma surgery may require resuturing the scleral flap, donor scleral patch graft placement, or autologous blood injection.[29–31,73]

Chorioretinal folds may resolve following the restoration of normal intraocular pressure. In cases of chronic hypotony, the retinal pigment epithelium will show permanent changes, including hyperpigmentation at the troughs of the folds, causing irregularly dark, pigmented lines in the posterior pole detected by fluorescein angiography.[49] The choroid and the sclera return to normal thickness, and the tortuosity and engorgement of the retinal vessels disappear.

Early detection of hypotony maculopathy is important for implementing the necessary measures to restore normal intraocular pressure and recovery of vision. The prognosis for visual recovery depends on the duration of the hypotony and the chronicity of the chorioretinal folds. Prolonged folding of the choroid and the neurosensory retina may cause irreversible structural changes in the macula and poor visual recovery after normalization of the intraocular pressure. However, significant visual improvement may still occur in some patients after treatment of chronic hypotony.[74]

Duker and Schuman reported that pars plana vitrectomy and mechanical flattening of the posterior pole with intraoperative instillation of perfluorocarbon liquid significantly improved visual acuity in a patient who had minimal visual recovery after increasing the intraocular pressure with previous bleb revision.[75] The efficacy of this approach has not been confirmed in larger patient cohorts. Others have advocated internal limiting membrane peeling with gas tamponade in myopic patients with hypotony maculopathy.[76]

Conclusion

Hypotony maculopathy is characterized by folding of the choroid, neurosensory retina, and retinal pigment epithelium in the posterior pole in an eye with low intraocular pressure. The folding of the neurosensory retina is believed to be the primary cause of vision loss. In addition to chorioretinal folds, acquired hyperopia, optic disc edema, and tortuous retinal vasculature may be associated with hypotony maculopathy. Fluorescein angiography demonstrates an irregular increase in background choroidal fluorescence corresponding to the crest of the chorioretinal folds. B-scan ultrasonography shows flattening and thickening of the sclera and choroid in the posterior pole. High-resolution optical coherence tomography allows early detection of chorioretinal folding that may be difficult to diagnose on clinical examination. Early detection and treatment are important for preventing permanent structural changes in the retina and maximizing visual recovery.

References

1. Schepens CL, Brockhurst RJ. Uveal effusion. 1. Clinical picture. *Arch Ophthalmol*. 1963;70:189–201.
2. Gass JD, Jallow S. Idiopathic serous detachment of the choroid, ciliary body, and retina (uveal effusion syndrome). *Ophthalmology*. 1982;89:1018–1032.
3. Johnson MW. Uveal effusion. Guyer DR, Yannuzzi LA, Chang S, et al. *Retina–vitreous–macula*. WB Saunders: Philadelphia; 1999:658–668.

4. Toris CB, Pederson JE, Tsuboi S, et al. Extravascular albumin concentration of the uvea. *Invest Ophthalmol Vis Sci*. 1990;31:43–53.
5. Brubaker RF, Pederson JE. Ciliochoroidal detachment. *Surv Ophthalmol*. 1983;27:281–289.
6. Inomata H, Bill A. Exit sites of uveoscleral flow of aqueous humor in cynomolgus monkey eyes. *Exp Eye Res*. 1977;25:113–118.
7. Alm A, Bill A. Ocular circulation. Moses RA, Hart WM Jr. *Adler's physiology of the eye*. Mosby: St Louis; 1987:199.
8. Jackson TL, Hussain A, Salisbury J, et al. Transscleral albumin diffusion and suprachoroidal albumin concentration in uveal effusion syndrome. *Retina*. 2012;32:177–182.
9. Aaberg TM, Maggiano JM. Choroidal edema associated with retinal detachment repair: experimental and clinical correlation. *Mod Probl Ophthalmol*. 1979;20:6–15.
10. Hawkins WR, Schepens CL. Choroidal detachment and retinal surgery. *Am J Ophthalmol*. 1966;62:813–819.
11. Liew SC, McCluskey PJ, Parker G, et al. Bilateral uveal effusion associated with scleral thickening due to amyloidosis. *Arch Ophthalmol*. 2000;118:1293–1295.
12. Vine AK. Uveal effusion in Hunter's syndrome: eEvidence that abnormal sclera is responsible for the uveal effusion syndrome. *Retina*. 1986;6:57–60.
13. Forrester JV, Lee WR, Kerr PR, et al. The uveal effusion syndrome and trans-scleral flow. *Eye (Lond)*. 1990;4:354–365.
14. Uyama M, Takahashi K, Kozaki J, et al. Uveal effusion syndrome: clinical features, surgical treatment, histologic examination of the sclera, and pathophysiology. *Ophthalmology*. 2000;107:441–449.
15. Ward RC, Gragoudas ES, Pon DM, et al. Abnormal scleral findings in uveal effusion syndrome. *Am J Ophthalmol*. 1988;106:139–146.
16. Boubriak OA, Urban JP, Bron AJ. Differential effects of aging on transport properties of anterior and posterior human sclera. *Exp Eye Res*. 2003;76:701–713.
17. Gass JD. Uveal effusion syndrome: a new hypothesis

concerning pathogenesis and technique of surgical treatment. *Retina*. 1983;3:159–163.
18. Johnson MW, Gass JD. Surgical management of the idiopathic uveal effusion syndrome. *Ophthalmology*. 1990;97:778–785.
19. Calhoun FP Jr. The management of glaucoma in nanophthalmos. *Trans Am Ophthalmol Soc*. 1975;73:97–122.
20. Brockhurst RJ. Vortex vein decompression for nanophthalmic uveal effusion. *Arch Ophthalmol*. 1980;98:1987–1990.
21. Casswell AG, Gregor ZJ, Bird AC. The surgical management of uveal effusion syndrome. *Eye (Lond)*. 1987;1:115–119.
22. Moses RA. Detachment of ciliary body – anatomical and physical considerations. *Invest Ophthalmol*. 1965;4:935–941.
23. Brockhurst RJ, Lam KW. Uveal effusion. II. Report of a case with analysis of subretinal fluid. *Arch Ophthalmol*. 1973;90:399–401.
24. Gass JD. Uveal effusion syndrome: a new hypothesis concerning pathogenesis and technique of surgical treatment. *Trans Am Ophthalmol Soc*. 1983;81:246–260.
25. Green RL, Byrne SF. Diagnostic ophthalmic ultrasound. Ryan SJ. *Retina*. Mosby: St. Louis; 1989.
26. Okuda T, Higashide T, Wakabayashi Y, et al. Fundus autofluorescence and spectral-domain optical coherence tomography findings of leopard spots in nanophthalmic uveal effusion syndrome. *Graefes Arch Clin Exp Ophthalmol*. 2010;248:1199–1202.
27. Singh OS, Simmons RJ, Brockhurst RJ, et al. Nanophthalmos: a perspective on identification and therapy. *Ophthalmology*. 1982;89:1006–1012.
28. Brockhurst RJ. Nanophthalmos with uveal effusion: a new clinical entity. *Arch Ophthalmol*. 1975;93:1989–1999.
29. Cohen SM, Flynn HW Jr, Palmberg PF, et al. Treatment of hypotony maculopathy after trabeculectomy. *Ophthalmic Surg Lasers*. 1995;26:435–441.
30. Haynes WL, Alward WL. Rapid visual recovery and long-term intraocular pressure control after donor scleral patch grafting for trabeculectomy-induced hypotony

maculopathy. *J Glaucoma*. 1995;4:200–201.
31. Haynes WL, Alward WL. Combination of autologous blood injection and bleb compression sutures to treat hypotony maculopathy. *J Glaucoma*. 1999;8:384–387.
32. Bellows AR, Chylack LT Jr, Epstein DL, et al. Choroidal effusion during glaucoma surgery in patients with prominent episcleral vessels. *Arch Ophthalmol*. 1979;97:493–497.
33. Maggio E, Polito A, Prigione G, et al. Uveal effusion syndrome mimicking severe chronic posterior uveitis: a case series of seven eyes of four patients. *Graefes Arch Clin Exp Ophthalmol*. 2016;254(3):545–552.
34. Allen KM, Meyers SM, Zegarra H. Nanophthalmic uveal effusion. *Retina*. 1988;8:145–147.
35. Good WV, Stern WH. Recurrent nanophthalmic uveal effusion syndrome following laser trabeculoplasty. *Am J Ophthalmol*. 1988;106:234–235.
36. Wang BZ, Clark B, McKelvie P, et al. Four quadrant sclerotomies for uveal effusion syndrome. *Eye (Lond)*. 2015;29(4):588–589.
37. Faulborn J, Kolli H. Sclerotomy in uveal effusion syndrome. *Retina*. 1999;19:504–507.
38. Sabrosa NA, Smith HB, MacLaren RE. Scleral punch method with topical mitomycin C for safe revision of failed deep sclerectomy in nanophthalmic uveal effusion syndrome. *Graefes Arch Clin Exp Ophthalmol*. 2009;247:999–1001.
39. Yepez JB, Arevalo JF. Ex-PRESS shunt for choroidal fluid drainage in uveal effusion syndrome type 2: a potentially novel technique. *JAMA Ophthalmol*. 2015;133(4):470–471.
40. Schneiderman TE, Johnson MW. A new approach to the surgical management of idiopathic uveal effusion syndrome. *Am J Ophthalmol*. 1997;123:262–263.
41. Dellaporta A. Fundus changes in postoperative hypotony. *Am J Ophthalmol*. 1955;40:781–785.
42. Gass JDM. Hypotony maculopathy. Bellows JC. *Contemporary ophthalmology, honoring Sir Stewart Duke-Elder*. Williams & Wilkins: Baltimore; 1972:343–366.
43. Hovanesian JA, Higginbotham EJ, Lichter PR, et al. Long-

term visual outcome of ocular hypotension after thermosclerostomy. *Am J Ophthalmol*. 1993;115:603–607.
44. Thomas M, Vajaranant TS, Aref AA. Hypotony Maculopathy: Clinical Presentation and Therapeutic Methods. *Ophthalmol Ther*. 2015;4(2):79–88.
45. Costa VP, Wilson RP, Moster MR, et al. Hypotony maculopathy following the use of topical mitomycin C in glaucoma filtration surgery. *Ophthalmic Surg*. 1993;24:389–394.
46. Jampel HD, Pasquale LR, Dibernardo C. Hypotony maculopathy following trabeculectomy with mitomycin C. *Arch Ophthalmol*. 1992;110:1049–1050.
47. Stamper RL, McMenemy MG, Lieberman MF. Hypotonous maculopathy after trabeculectomy with subconjunctival 5-fluorouracil. *Am J Ophthalmol*. 1992;114:544–553.
48. Fannin LA, Schiffman JC, Budenz DL. Risk factors for hypotony maculopathy. *Ophthalmology*. 2003;110:1185–1191.
49. Gass JDM. *Hypotony maculopathy. Stereoscopic atlas of macular diseases: diagnosis and treatment*. Mosby: St. Louis; 1997:294–295.
50. Cappaert WE, Purnell EW, Frank KE. Use of B-sector scan ultrasound in the diagnosis of benign choroidal folds. *Am J Ophthalmol*. 1977;84:375–379.
51. Chan TK, Talbot JF, Rennie IG, et al. The application of ultrasonic biomicroscopy in the management of traumatic hypotony. *Eye (Lond)*. 2000;14(Pt 5):805–807.
52. Roters S, Engels BF, Szurman P, et al. Typical ultrasound biomicroscopic findings seen in ocular hypotony. *Ophthalmologica*. 2002;216:90–95.
53. Budenz DL, Schwartz K, Gedde SJ. Occult hypotony maculopathy diagnosed with optical coherence tomography. *Arch Ophthalmol*. 2005;123:113–114.
54. Lima VC, Prata TS, Castro DP, et al. Macular changes detected by Fourier-domain optical coherence tomography in patients with hypotony without clinical maculopathy. *Acta Ophthalmol (Copenh)*. 2011;89:e274–7.
55. Martinez de la Casa JM, Garcia Feijoo J, Castillo Gomez A, et al. [Hypotony maculopathy diagnosed by optical coherence

tomography]. *Arch Soc Esp Oftalmol*. 2003;78:567–569.
56. Thompson JT. Advantages and limitations of small gauge vitrectomy. *Surv Ophthalmol*. 2011;56:162–172.
57. Cangemi FE, Trempe CL, Walsh JB. Choroidal folds. *Am J Ophthalmol*. 1978;86:380–387.
58. Leahey AB, Brucker AJ, Wyszynski RE, et al. Chorioretinal folds: a comparison of unilateral and bilateral cases. *Arch Ophthalmol*. 1993;111:357–359.
59. Newell FW. Choroidal folds. The seventh Harry Searls Gradle memorial lecture. *Am J Ophthalmol*. 1973;75:930–942.
60. Newell FW. Fundus changes in persistent and recurrent choroidal folds. *Br J Ophthalmol*. 1984;68:32–35.
61. Minckler DS, Bunt AH. Axoplasmic transport in ocular hypotony and papilledema in the monkey. *Arch Ophthalmol*. 1977;95:1430–1436.
62. Kalina RE, Mills RP. Acquired hyperopia with choroidal folds. *Ophthalmology*. 1980;87:44–50.
63. Friberg TR, Grove AS Jr. Choroidal folds and refractive errors associated with orbital tumors: an analysis. *Arch Ophthalmol*. 1983;101:598–603.
64. Shields JA, Shields CL, Rashid RC. Clinicopathologic correlation of choroidal folds: secondary to massive cranioorbital hemangiopericytoma. *Ophthal Plast Reconstr Surg*. 1992;8:62–68.
65. Krist D, Wenkel H. Posterior scleritis associated with *Borrelia burgdorferi* (Lyme disease) infection. *Ophthalmology*. 2002;109:143–145.
66. Haruyama M, Yuzawa M, Kawamura A, et al. Indocyanine green angiographic findings of chorioretinal folds. *Jpn J Ophthalmol*. 2001;45:293–300.
67. Diskin J, Maguire AM, Margherio RR. Choroidal folds induced with diode endolaser. *Arch Ophthalmol*. 1992;110:754.
68. Johnson RN, Schatz H, McDonald HR. Photic maculopathy: early angiographic and ophthalmoscopic findings and late development of choroidal folds. Case report. *Arch Ophthalmol*. 1987;105:1633–1634.
69. Bird AC, Sanders MD. Choroidal folds in association with

papilloedema. *Br J Ophthalmol*. 1973;57:89–97.
70. Lavinsky J, Lavinsky D, Lavinsky F, et al. Acquired choroidal folds: a sign of idiopathic intracranial hypertension. *Graefes Arch Clin Exp Ophthalmol*. 2007;245:883–888.
71. Sarraf D, Schwartz SD. Bilateral choroidal folds and optic neuropathy: a variant of the crowded disk syndrome? *Ophthalmology*. 2003;110:1047–1052.
72. Griebel SR, Kosmorsky GS. Choroidal folds associated with increased intracranial pressure. *Am J Ophthalmol*. 2000;129:513–516.
73. Schwartz GF, Robin AL, Wilson RP, et al. Resuturing the scleral flap leads to resolution of hypotony maculopathy. *J Glaucoma*. 1996;5:246–251.
74. Delgado MF, Daniels S, Pascal S, et al. Hypotony maculopathy: improvement of visual acuity after 7 years. *Am J Ophthalmol*. 2001;132:931–933.
75. Duker JS, Schuman JS. Successful surgical treatment of hypotony maculopathy following trabeculectomy with topical mitomycin C. *Ophthalmic Surg*. 1994;25:463–465.
76. Nadal J, Carreras E, Canut M, et al. Vitrectomy and internal limiting membrane peeling for macular folds secondary to hypotony in myopes. *Clin Ophthalmol*. 2015;9:859–864.

SECTION 4

Inflammatory Disease/Uveitis

OUTLINE

Inflammation
Infections

Inflammation

OUTLINE

77

Sympathetic Ophthalmia

Daniel Vítor Vasconcelos-Santos, Narsing A. Rao

Introduction

Sympathetic ophthalmia, also known as sympathetic ophthalmitis and sympathetic uveitis, is a rare bilateral diffuse granulomatous uveitis that occurs a few days to several decades after penetrating accidental or surgical trauma to an eye. Both the traumatized eye,

commonly referred to as the "exciting" eye, and the fellow eye, referred to as the "sympathizing" eye, are affected. Injury to and/or incarceration of uveal tissue has been a feature of nearly all cases of sympathetic ophthalmia. The clinical signs and symptoms are usually detected in the sympathizing eye within the first 3 months after trauma to the fellow eye.[1,2]

The notion that injury to one eye may have repercussion in the contralateral eye probably dates back to ancient times, with Hippocrates (460–370 BC), but has also been reported by Agathias, in a compilation from Constantius Cephalis (1000 AD).[1,3] However, it was William Mackenzie, in 1830, who provided the first comprehensive clinical description and pioneered the use of the term "sympathetic ophthalmia" to describe this entity.[1,3] Ernst Fuchs, in 1905, thoroughly detailed the characteristic histopathologic features.[4] The pathogenesis of sympathetic ophthalmia has, however, remained an enigma despite years of study. There is now some experimental evidence implicating an autoimmune delayed hypersensitivity reaction to melanocytes or tyrosinase peptide antigen as a possible pathogenetic mechanism.

Epidemiology

Sympathetic ophthalmia is a relatively rare disease, although exact figures are difficult to determine because the onset or the diagnosis, or both, are often delayed for months to years after the initial injury. In addition, definite histopathologic confirmation is achieved in around only one-third of suspected cases, but may be established histopathologically in others not suspected clinically.[2] In 1972, Liddy and Stuart[5] reported an incidence of sympathetic ophthalmia of 0.19% following penetrating injuries and 0.007% following intraocular surgery. Among the general population, sympathetic ophthalmia has been estimated to affect 0.03 per 100,000 persons per year[6] and possibly corresponds to 1–2% of all uveitis cases.[7] Surgical procedures that may lead to sympathetic ophthalmia include cataract extraction, iridectomy, paracentesis, cyclodialysis, synechialysis, retinal detachment repair, keratectomy, vitrectomy, evisceration, laser cyclophotocoagulation, proton-beam irradiation, and others.[2,3,8]

Although advances in modern surgical techniques may be contributing to a lower incidence of sympathetic ophthalmia, this is probably being partially offset by more aggressive surgical management of severely traumatized eyes, which in the past would have been promptly enucleated. In fact, the epidemiology of sympathetic ophthalmia has been changing, and more cases are now being associated with intraocular surgery,[6,7,9,10] in contrast to accidental penetrating trauma.[3] Pars plana vitrectomy is now one of the leading surgical procedures associated with sympathetic ophthalmia[11] with an estimated risk of around 0.01%;[12] cases have been recently reported even after the advent of small-gauge sutureless vitrectomy surgery.[13,14] For these reasons, sympathetic ophthalmia should not be considered a disappearing disease and thus should not be neglected.

Some studies have shown a male preponderance, but this is believed to be a reflection of the higher incidence of accidental trauma in males. Indeed, when only cases of surgical trauma are considered, the ratio is similar.[15] In Winter's series of 257 cases of sympathetic ophthalmia, there was no difference in age incidence.[16] Other authors have reported relative peaks in childhood and early adult years, thought to reflect a higher incidence of accidental trauma in these ages, and an additional peak in the sixth and seventh decades, thought to represent an increased incidence of surgical procedures among persons in this age group.[17]

Pathogenesis

The exact cause of sympathetic ophthalmia is unknown. Clinical studies have shown that the predominant predisposing factors are accidental penetrating trauma, accounting for approximately 60–70% of cases, and penetrating surgical trauma, accounting for nearly 30%. Recent studies have pointed to an inversion of this proportion, with many cases now being associated with surgical rather than accidental trauma.[6,7,10,11] A small percentage of cases are the result of contusion injuries with occult scleral rupture and perforating corneal ulcers. The common denominator in the overwhelming majority of cases is the presence of a penetrating injury in which wound healing is complicated by incarceration of

the iris, ciliary body, or choroid.[2]

Historically, the pathogenesis of sympathetic ophthalmia had been suspected to be infectious. However, no organisms have ever been isolated from cases of sympathetic ophthalmia, and infective agents have not induced the disease in laboratory animals. Sympathetic ophthalmia may also develop in the setting of posttraumatic or postoperative infectious endophthalmitis, and it is possible that such infection may potentiate the development of sympathetic ophthalmia in these cases[18] and not prevent it, in contrast to what had previously been suggested.[1,19,20] Most cases of sympathetic ophthalmia, however, develop in the absence of intraocular infection.[17]

Several investigators have proposed an immunologic basis for sympathetic ophthalmia, in which a T-cell-mediated autoimmune response against an antigenic protein from the uvea, particularly a uveal tyrosinase peptide, may be involved.[21–25] Marak[26,27] and Wong and colleagues[21] demonstrated enhanced transformation of peripheral lymphocytes from patients with histologically confirmed sympathetic ophthalmia when exposed to homologous uveal-retinal extracts in tissue culture, suggesting that these patients have lymphocytes that are sensitized to some component(s) of uveal-retinal antigen. When antigens extracted from the retina are injected into guinea-pigs, intraocular inflammation similar to sympathetic ophthalmia develops in these animals.[27] Some studies indeed suggest that sympathetic ophthalmia may result from altered T-cell response to one of the soluble proteins associated with the retinal photoreceptor membranes, particularly the retinal S antigen, or to other retinal or choroidal melanocyte antigens.[22–24,27,28] However, recent studies reveal that T-cell immune response to tyrosinase peptide may play a role in the development of sympathetic ophthalmia, as in Vogt–Koyanagi–Harada disease.[23,29–31]

There may be a genetic predisposition to the development of sympathetic ophthalmia. Human leukocyte antigen (HLA) association has been reported in sympathetic ophthalmia, including HLA-A11, HLA-B40, HLA-DR4/DRw53, and HLA-DR4/DQw3 haplotypes.[32,33] Studies from Asia and Europe found a significant correlation between HLA-DRB1*4 and HLA-DQB1*04 and the development of sympathetic ophthalmia.[34–36] A similar association

was also seen in patients with Vogt–Koyanagi–Harada disease. Finally, genetic background may also correlate to disease severity, either through some of those predisposing HLA haplotypes such as HLA-DRB1[34] or through cytokine polymorphisms such as in interleukin (IL)-10, modifying the immune response and the risk of disease recurrence.[37]

Immunopathology

In sympathetic ophthalmia the immunopathologic alterations are similar in both the exciting and sympathizing eyes and typically consist of a diffuse granulomatous inflammation of the uveal tract, made up of lymphocytes, plasma cells, and nests of epithelioid histiocytes; pigment is often present within these epithelioid cells and also within giant cells (Fig. 77.1). In the majority of cases, the inflammatory process does not involve the choriocapillaris or the retina. Absence of necrosis is another characteristic feature. The choroid is diffusely involved and thickened by an infiltration of predominantly lymphocytes, collections of epithelioid cells, and a few giant cells; neutrophils are rarely seen. Plasma cells may be present, particularly in patients treated with corticosteroids. Eosinophils can also be found and are frequently concentrated in the inner choroid, particularly in heavily pigmented individuals. Nodular clusters of epithelioid cells containing pigment are often seen lying between the retinal pigment epithelium (RPE) and Bruch's membrane; these appear clinically as the drusen-like, yellow-white dots known as Dalen–Fuchs nodules (Fig. 77.2).[1,2,4,16,17,38,39] Inflammatory cell infiltration in the iris may result in the clinical appearance of a thickened iris.

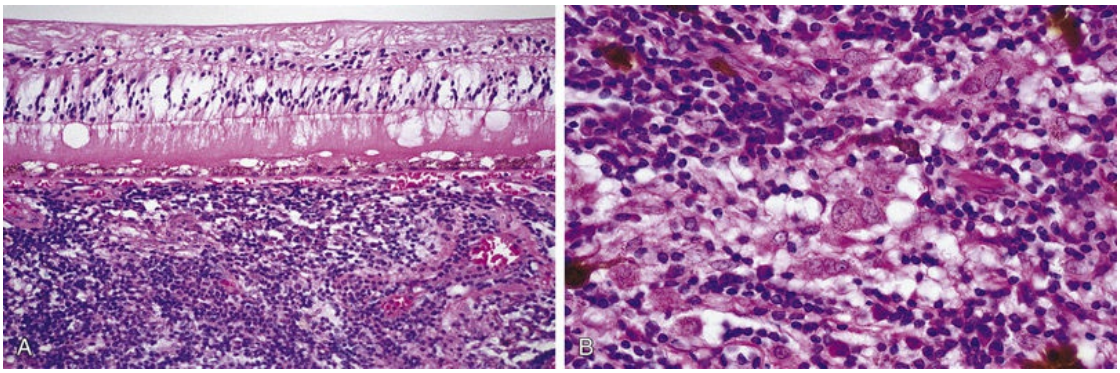

FIG. 77.1 Histopathologic aspects of sympathetic ophthalmia. (A) Note granulomatous inflammation of the choroid with focal serous detachment of the retina (hematoxylin and eosin, ×130). (B) Multinucleated giant cells and epithelioid histiocytes have pigment in their cytoplasm (hematoxylin and eosin, ×565).

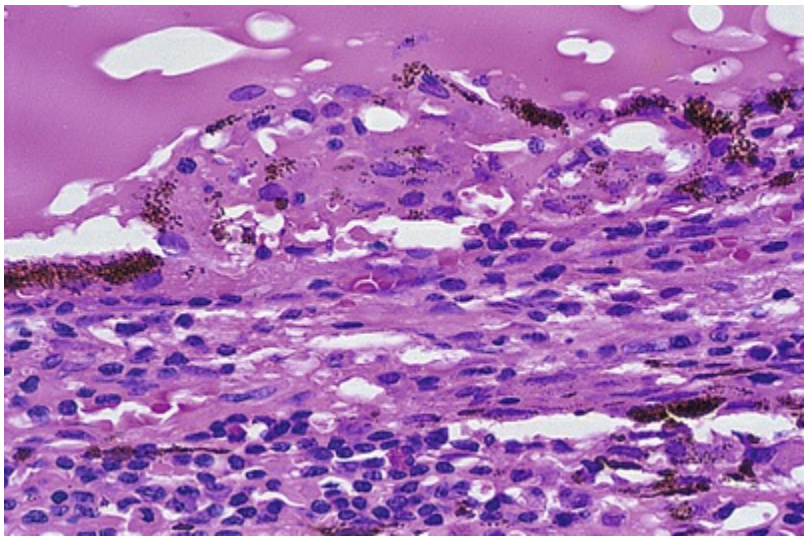

FIG. 77.2 Histopathologically, the Dalen–Fuchs nodule is characterized by focal collections of epithelioid cells at the level of Bruch's membrane (hematoxylin and eosin, ×250).

The retina is usually free of inflammatory infiltrates. However, few enucleated eyes of sympathetic ophthalmia show collections of mononuclear cells around the blood vessels, and occasional involvement in the areas overlying the Dalen–Fuchs nodules, and in the pars plana region. Other pathologic changes include scleral involvement with inflammatory infiltrates around the emissary veins and extension of the granulomatous process into the optic

nerve and surrounding meningeal sheaths, the sites where melanocytes are also present.[1,4,17,40,41] Some of the eyes with characteristic histologic features of sympathetic ophthalmia but also with breaks in the lens capsule may additionally reveal features of phacoanaphylaxis, with zonal granulomatous inflammation around the lens material.[40] Even though typical features of sympathetic ophthalmia include non-necrotizing granulomatous uveitis, there are cases exhibiting atypical features such as nongranulomatous choroiditis, and enucleated eyes with long-standing intraocular inflammation may show chorioretinal adhesions with the inflammatory process involving the choriocapillaris, as seen in chronic Vogt–Koyanagi–Harada disease.[16,40]

Immunohistochemical studies have revealed infiltration of predominantly T lymphocytes in the uveal tract.[38,42] B lymphocytes may also be present, especially in long-standing disease, as well as in individuals receiving corticosteroids.[41,43,44] Among the T lymphocytes, both helper ($CD4^+$) and suppressor/cytotoxic ($CD8^+$) cells have been observed,[38,42] driving a Th1 response with secretion of proinflammatory cytokines such as interferon-γ and IL-2.[45] M1 macrophages have been reported to predominate in the granulomas, with significant expression of IL-23, CCL19, and CXCL11. IL-17 has also been detected in relatively high levels in the inflammatory infiltrate of eyes with SO.[46] Inflammatory cells are probably recruited to the eye by the selective expression of intercellular adhesion proteins in the uveal tract (particularly some integrins),[47] as well as some other molecules in macrophages and RPE cells, including chemokines, such as monocyte chemotactic protein-1 (CCL2/MCP-1) and stromal cell-derived factor-1 (CXCL12/SDF-1), and metalloproteinases, such as gelatinase-B.[44] Relative preservation of the choriocapillaris in the acute phase of the disease process may be associated with secretion of anti-inflammatory cytokines by the RPE.[28] A recent study has shown $CD4^+$ T lymphocytes and melanin-laden macrophages expressing HLA-DR underneath the conjunctiva in the exciting eye, suggesting that antigen processing and presentation may initially take place at that site, further leading to activation of lymphocytes and to the granulomatous response.[48]

Even though the retina seems to be relatively spared in the

pathologic process of sympathetic ophthalmia, tumor necrosis factor-alpha (TNF-α)-mediated mitochondrial oxidative stress has been localized in the outer retina of enucleated human globes with the disease (Fig. 77.3). This was associated with apoptosis of photoreceptors, and such photoreceptor damage could be an early mechanism leading to vision loss in sympathetic ophthalmia.[49,50] Interestingly, overexpression of a heat shock protein, α-A-crystallin, has also been identified in the outer retina of these eyes, being associated with protection against oxidative damage and decreased photoreceptor apoptosis.[51]

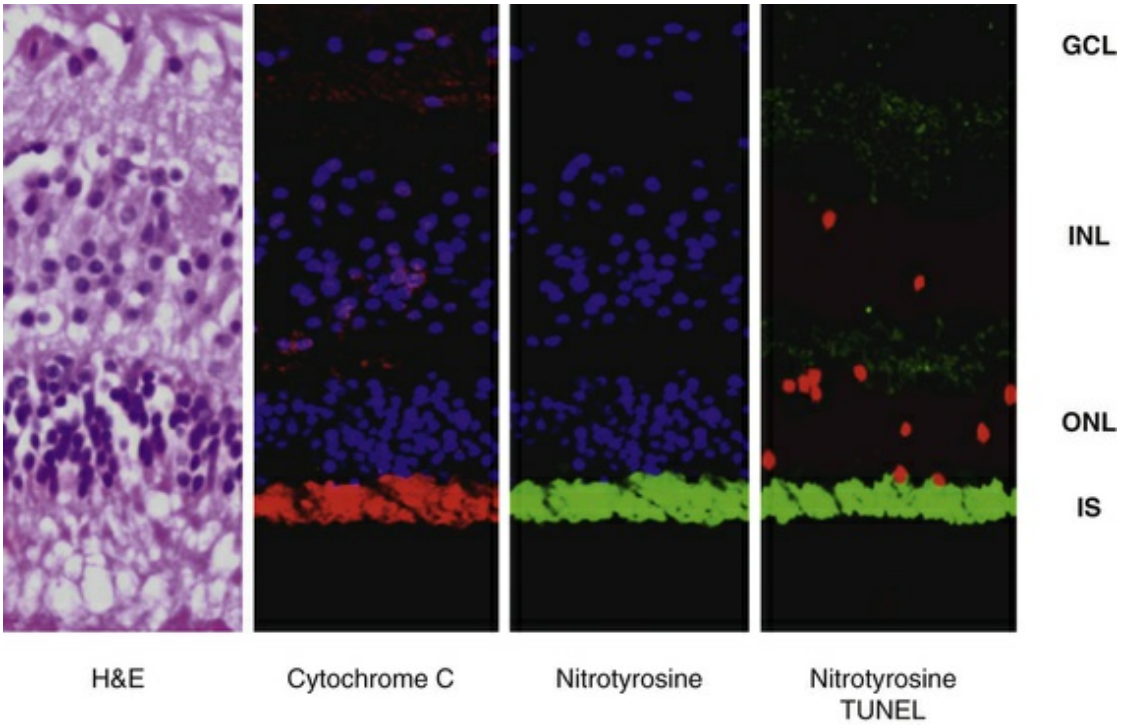

FIG. 77.3 Mitochondrial oxidative stress and apoptosis in the human retina with sympathetic ophthalmia. Cytochrome C and nitrotyrosine are immunolocalized in the inner segments (*IS*) of the photoreceptors. Apoptotic neurons marked by terminal deoxynucleotidyl transferase-mediated dUTP nick end labeling *(TUNEL)* assay are detected primarily in the outer nuclear layer *(ONL)*, and also in the inner nuclear layer (*INL*), but not in the ganglion cell layer (*GCL*). The corresponding hematoxylin and eosin-stained section is seen on the left.

A recent study[52] has also implicated microRNA (small noncoding RNA that negatively regulate gene expression) in the coordination of the immune response in sympathetic ophthalmia. Downregulation of four microRNA (hsa-miR-1, hsa-let-7e, hsa-miR-9, and hsa-miR182) has been associated with the expression of proinflammatory cytokines, particularly TNF-α and nuclear factor-kappa B1 (NF-κB), crucial to the pathogenesis of the disease.[52]

Clinical Findings

The clinical onset of sympathetic ophthalmia is typically heralded by the development of an apparently mild intraocular inflammation in the sympathizing eye and worsening of inflammation in the exciting eye. The interval between the time of injury and the onset of inflammation in the sympathizing eye has been reported to be as short as 5 days and as long as 66 years after trauma.[1,3,53] In general, however, sympathetic ophthalmia rarely develops sooner than 2 weeks after trauma, with 80% of cases occurring within 3 months and 90% within 1 year of the penetrating injury.[2,7,11] The peak incidence occurs between 4 and 8 weeks after accidental trauma, while cases following surgical trauma may have a more delayed onset.[54]

Symptoms in the sympathizing eye include mild pain, photophobia, and increased lacrimation, blurring of vision, visual fatigue, or even paresis of accommodation. The exciting eye may have a decrease in vision and an increase in photophobia. Moreover, both eyes may show ciliary injection and a partially dilated and poorly responsive pupil.[1,2,9,11]

The clinical signs are variable and can be either insidious or fairly rapid in onset. Anterior-segment changes are those of an anterior uveitis, with ciliary injection, keratic precipitates, flare, and inflammatory cells in the anterior chamber. Thickening of the iris and even iris nodules may also be seen, and posterior synechiae are common. Posterior-segment findings in sympathetic ophthalmia include inflammatory cell infiltration of the vitreous, hyperemia and edema of the optic disc, diffuse edema and exudative detachment of the retina, as well as small yellow-white deposits beneath the RPE, so-called Dalen–Fuchs nodules.[1,2,9,11,16,17] Bullous

serous detachments may also be seen in the peripheral retina. Occasionally, multiple deep ill-defined yellowish lesions may be present, corresponding to choroidal granulomas (Fig. 77.4). Inflammatory scleral involvement is rarely seen clinically but is a common finding on microscopic examination of enucleated eyes. With time, patients may develop depigmentation of the choroid leading to the so-called sunset glow fundus, as well as RPE changes, as seen in individuals with chronic Vogt–Koyanagi–Harada disease.[55,56] Although less commonly than in Vogt–Koyanagi–Harada disease, extraocular involvement – including meningismus, dysacusis, vitiligo, poliosis, and alopecia – may also be present in patients with sympathetic ophthalmia.[2,55,57,58]

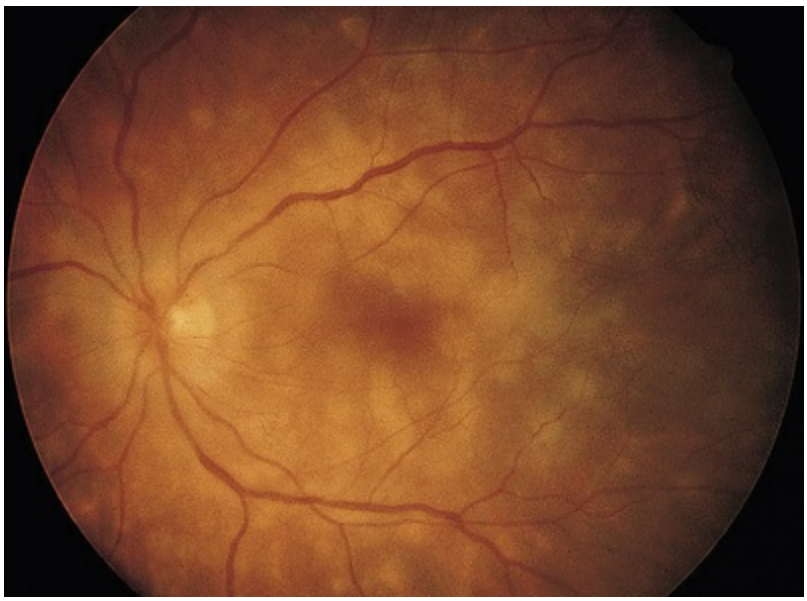

FIG. 77.4 Multiple choroidal granulomas in sympathetic ophthalmia.

Diagnosis

The diagnosis of sympathetic ophthalmia is essentially clinical.[1,2,11] No serologic or immunologic tests are available to aid in the diagnosis. Even though there are no systematized diagnostic criteria, the presence of penetrating ocular trauma (either accidental or surgical) is a fundamental feature. Bilateral intraocular inflammation should also be present and may be accompanied by

exudative retinal detachments and/or optic disc edema early in the disease process, or by choroidal depigmentation (sunset glow fundus) and RPE changes in chronic cases, similarly to Vogt–Koyanagi–Harada disease.[59] However, variations in this clinical presentation can challenge or delay the diagnosis. Some imaging studies, such as fluorescein angiography, indocyanine green angiography (ICGA), B-scan ultrasound, as well as optical coherence tomography (OCT), may be helpful to disclose or delineate better some supportive features of sympathetic ophthalmia.[10]

Fluorescein angiography may typically show multiple progressively fluorescent dots at the level of the RPE (pin-point leakage; Fig. 77.5), as well as disc leakage, as also seen in Vogt–Koyanagi–Harada disease. Coalescence of the dye from these foci occurs in the areas of exudative detachment.[2,60,61] Less frequently there may also be early focal blockage of the background choroidal fluorescence, a finding also noted in acute posterior multifocal placoid pigment epitheliopathy.[62] On ICGA numerous hypofluorescent patches may be visible during the intermediate phase, presumably corresponding to the choroidal granulomas. Some of these may become isofluorescent at the later phases.[63–65]

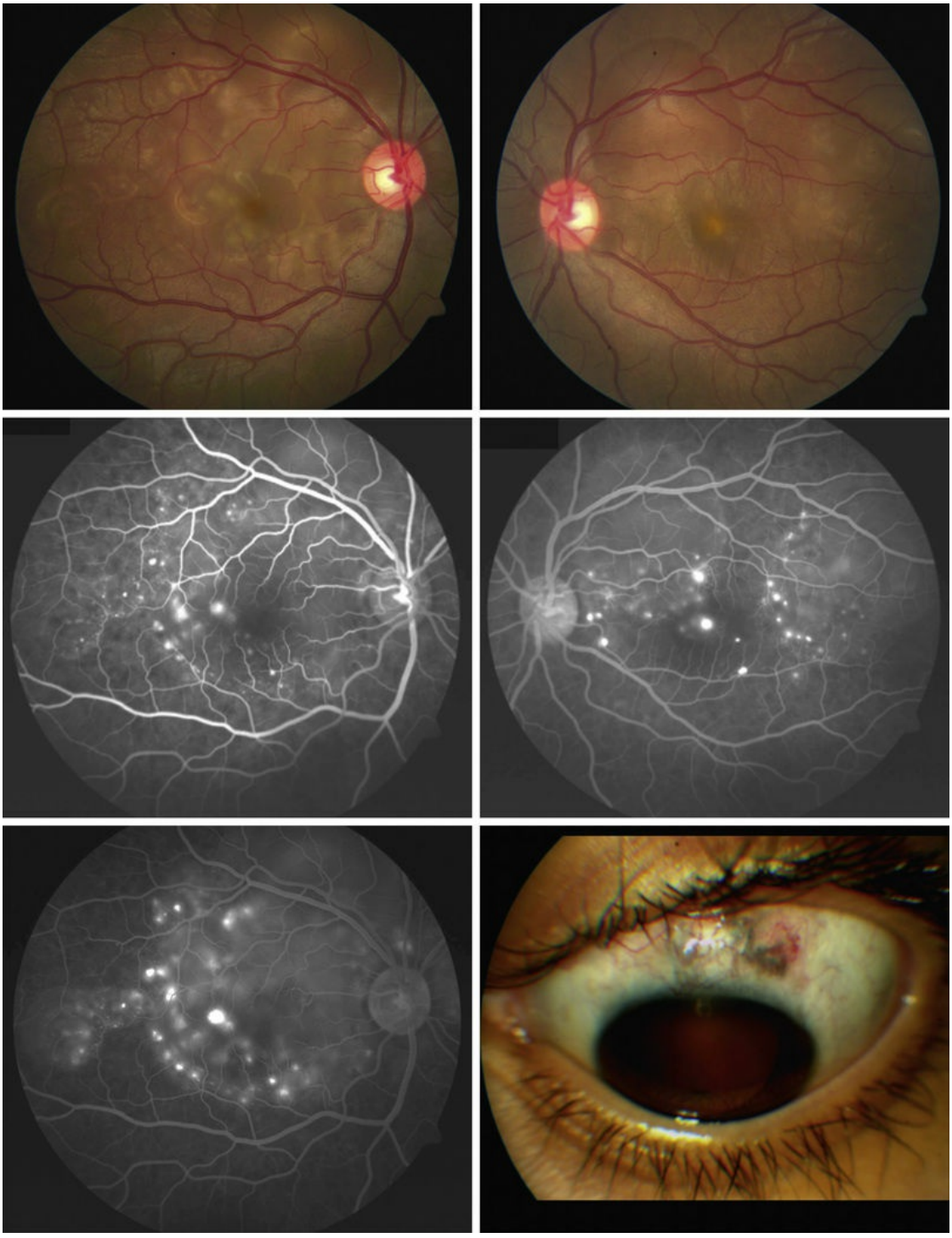

FIG. 77.5 Fundus and angiographic features of sympathetic ophthalmia following a penetrating scleral injury in the left eye. Foci of exudative retinal detachment are seen in the posterior pole of both eyes. Fluorescein angiography reveals multiple pin-point leaks at the level of the retinal pigment epithelium.

Ultrasound examination may reveal choroidal thickening and also areas of exudative retinal detachment, being particularly useful in the exciting eyes with opaque media.[11,18] Usually the choroidal thickening is more prominent around the optic disc and less in the anterior choroid. OCT can nicely delineate the foci of exudative retinal detachment, their resolution following appropriate therapy (Fig. 77.6), as well as progressive decrease in choroidal thickening, changes in the neurosensory retina and in the RPE.[62,66,67]

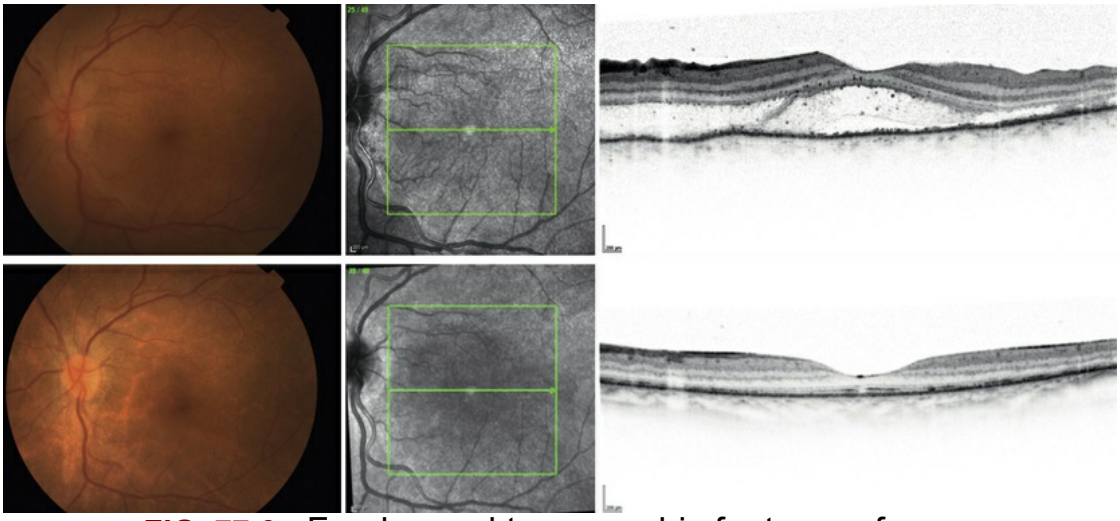

FIG. 77.6 Fundus and tomographic features of sympathetic ophthalmia before (top) and 2 months after (bottom) appropriate treatment with high-dose oral corticosteroid. Complete resolution of the exudative retinal detachment is seen. (Courtesy of Centro Brasileiro de Ciências Visuais, Belo Horizonte, Brazil.)

Especially in those severely traumatized eyes that later require enucleation, histopathologic examination may help to make or confirm the diagnosis.[2,17,18,40,41]

Differential Diagnosis

Sympathetic ophthalmia must be differentiated from several infectious and also other noninfectious uveitides, including syphilis, tuberculosis, sarcoidosis, multifocal choroiditis, and panuveitis. Other bacterial and fungal infections can also produce a granulomatous anterior and/or posterior uveitis, being usually

differentiated by history and associated clinical findings. Infectious endophthalmitis must always be considered following any penetrating trauma to the eye. In particular, less virulent microorganisms such as *Propionibacterium acnes* and some fungi may lead to a picture of chronic endophthalmitis, which should be distinguished from sympathetic ophthalmia. Reactivation of a preexisting uveitis after injury or the development of a posttraumatic iritis or iridocyclitis can also occur.[2,11]

Phacoanaphylatic endophthalmitis can also closely simulate the clinical picture of sympathetic ophthalmia, and these two entities may even coexist in the same eye. Although unilaterality can be a clue, phacoanaphylaxis may also be bilateral, but such bilaterality is rare. The incidence of phacoanaphylaxis in cases of sympathetic ophthalmia has been estimated to range between 4 and 25%. Unlike sympathetic ophthalmia, in bilateral phacoanaphylaxis the eye first involved is usually quiet by the time inflammation begins in the fellow eye. Moreover, ultrasound examination usually reveals predominant thickening of the anterior uveal tract in phacoanaphylactic endophthalmitis, in contrast to sympathetic ophthalmia, in which such thickening is more pronounced in the posterior uveal tract. A careful slit-lamp examination should always be carried out to search for ruptured lens capsule and fragments of lens cortex in the anterior chamber. In phacoanaphylactic endophthalmitis, lens extraction can be curative, thereby avoiding unnecessary enucleation.[18,68]

Vogt–Koyanagi–Harada syndrome is a bilateral granulomatous panuveitis, often associated with a prodrome of meningeal and auditory symptoms. The disease may have clinical and histopathologic features identical to sympathetic ophthalmia in both the acute and in the chronic phase. However, findings such as vitiligo and alopecia are more common in Vogt–Koyanagi–Harada syndrome than in sympathetic ophthalmia. A history of penetrating trauma is helpful in this differential diagnosis.[2,55,56]

Course and Complications

Untreated sympathetic ophthalmia runs a long, variable, and complicated course, marked initially by episodes of active

intraocular inflammation followed by quiescent periods that can last months to several years. With time, the disease may become chronically active, eventually producing irreversible ocular damage and even phthisis bulbi. Long-term complications of sympathetic ophthalmia include cataract, secondary ocular hypertension or hypotony, glaucoma, persistent cystoid macular edema or retinal detachment, chorioretinal scarring (including epiretinal membrane formation), choroidal neovascularization, subretinal fibrosis, and optic atrophy.[2,17,69] In spite of treatment, the overall risk of developing any of these ocular complications reaches 40% per patient per year, with around half of the patients losing vision to <20/40 and roughly one-fourth eventually becoming legally blind.[54]

Therapy

Although corticosteroids have not been shown to be effective in the prevention of sympathetic ophthalmia, they do constitute the mainstay of its therapy.[2,6,9] Large doses of corticosteroids should be given early in the course of the disease and continued for at least 6 months. For the first week, 1.5–2.0 mg/kg of body weight of oral prednisone (or equivalent) is given daily and then gradually tapered over several months, following clinical response of the uveitis. Alternatively, pulse therapy with intravenous methylprednisolone (up to 1 g daily for 3 days), as well as supplementation with sub-Tenon injection of triamcinolone acetonide (20–40 mg), may be considered. Topical corticosteroids and mydriatic/cycloplegic agents are used adjunctively as needed. Special care should be taken to monitor side-effects of the systemic corticosteroids, including periodic measurement of blood pressure, body weight, lipids, blood glucose, as well as gastroduodenal protection and prophylaxis of osteoporosis (with calcium and vitamin D supplementation).[70]

In a number of patients, medical problems or systemic or ophthalmologic complications may prevent the long-term use of high doses of steroids. In these patients, supplemental treatment with immunosuppressive agents (azathioprine, 2–4 mg/kg per day; cyclosporine, 2.5–5 mg/kg per day; mycophenolate mofetil, 1–1.5 g b.i.d.; methotrexate, 15–25 mg/week) has been shown to suppress

inflammation effectively, allow reduction of corticosteroid therapy to nontoxic levels (<10 mg/day), and, in some cases, induce disease remission. Careful monitoring of their side-effects every 4–6 weeks, with the supervision of an internist, is recommended. Bone-marrow suppression, renal and/or hepatic toxicity can occur with prolonged use of these agents.[70] The alkylating agents cyclophosphamide (2–3 mg/kg per day) and chlorambucil (0.1–0.2 mg/kg per day) are reserved for more severe and refractory cases.[70,71] These agents require careful monitoring for side-effects, including hemorrhagic urinary bladder inflammation and development of malignancies. A recent study[72] interestingly confirmed that high-dose short-term chlorambucil (median cumulative dose: 1449 mg; median duration: 14 weeks) may lead to sustained remission in most SO patients refractory to conventional therapy, with minimal adverse effects in a median follow-up of 8 years (range: 4–37 years).

Biologicals, particularly anti-TNF agents such as infliximab and adalimumab, may also be used in cases of sympathetic ophthalmia that are unresponsive to conventional immunomodulatory agents and, in this setting, favorable results have been anecdotally reported in the recent literature.[73–75] However the long-term safety of these agents is still uncertain.[76]

Intraocular corticosteroids, either administered as intravitreal injections (triamcinolone acetonide 4 mg) or as slow-release devices, such as fluocinolone or dexamethasone intravitreal implants, may also be used, especially in individuals who cannot tolerate the systemic medications.[77–80] Special concern should be given to the high risk of cataract and secondary glaucoma associated with these intravitreal devices.

Prevention

The prevention of sympathetic ophthalmia entails careful microsurgical wound toilet and prompt closure of all penetrating injuries. Every attempt should be made to save any eye with a reasonable prognosis for useful vision, but in those eyes with barely discernible or no visual function, and with demonstrable disorganization of the ocular contents, enucleation within 2 weeks after injury is possibly the only way to definitely prevent the

development of sympathetic ophthalmia.[3] At one time it was believed that the use of steroids following penetrating injury would in some instances prevent the development of sympathetic ophthalmia; this has not been proved to be the case.

Enucleation of the exciting eye once sympathetic ophthalmia has commenced has been a topic of considerable controversy. Some studies suggest that early enucleation of the exciting eye may improve the prognosis for the sympathizing eye;[17,81] however, careful review of the data presented in these studies does not support this conclusion.[82] A review by Winter of 257 cases of histologically proven sympathetic ophthalmia indicated no benefit to the sympathizing eye from enucleation of the exciting eye, whether performed briefly before, concomitant with, or subsequent to the development of sympathetic ophthalmia at various elapsed intervals following injury.[16] This was also supported by the results of a prospective study.[6] Indeed, it is possible that the exciting eye may eventually provide the better visual acuity, and its enucleation would therefore deprive the patient of that visual potential.[82]

Another controversy is the possible role of evisceration versus enucleation. Even though evisceration may be technically easier and provides a faster recovery,[83] it may not protect against the development of sympathetic ophthalmia, probably because of retention of uveal remnants in the scleral shell.[84] Cases of sympathetic ophthalmia following evisceration have been described in the older literature.[84,85] Sympathetic ophthalmia after evisceration is rarer nowadays, but recent cases have been anecdotally reported.[86–89] Because this is far less common than in the past,[90,91] and management of sympathetic ophthalmia has significantly improved,[6,9,11] an issue arises whether evisceration should indeed be preferred to enucleation, particularly in blind eyes, after severe trauma and/or infection. Indeed evisceration is increasingly recommended by surgeons in place of enucleation.[10,92] However, this issue is not yet resolved,[65] especially considering the very low incidence of sympathetic ophthalmia and the changing trend from posttraumatic to postsurgical cases.[7,9] An additional complication to this controversy is the risk of inadvertently eviscerating occult tumors,[93] which may even outweigh the risk of sympathetic ophthalmia *per se*. It is advisable that patients with penetrating

ocular injuries, as well as those undergoing intraocular surgeries with an increased risk of sympathetic ophthalmia (such as pars plana vitrectomy), are counseled about the possibility of developing the disease, early or even long after the traumatic or surgical insult.

Prognosis

Before the use of corticosteroids, the visual prognosis of sympathetic ophthalmia was generally poor. However, after the advent of the corticosteroids and more recently of immunosuppressive agents, outcomes dramatically improved.[9,11] Makley and Azar found that, in patients treated solely with systemic corticosteroids, a visual acuity of 20/60 or better was achieved in most of them, but relapses occurred in 60%, sometimes long after initial disease remission.[69] Chan et al. reported visual acuity of 20/40 or better in 50% of patients treated with steroids and immunosuppressive agents.[94] With prompt and aggressive corticosteroid therapy, and immunosuppressive agents, as needed, many eyes with sympathetic ophthalmia should retain reasonable vision.

In conclusion, sympathetic ophthalmia is a serious ocular inflammatory entity, often with many exacerbations and a relentlessly progressive course that may result in very poor vision. Cases associated with penetrating accidental trauma have been decreasing with improved repair of such globes, but, on the other hand, those following intraocular (particularly vitreoretinal) surgery are on the rise. Long-term follow-up of these patients is essential. It is hoped that, with the prompt and aggressive use of corticosteroids early in the course of the disease, and supplementation with immunosuppressive agents when indicated, the prognosis in these patients need not to be as grim as it had been in the past.

References

1. Duke-Elder S. Sympathetic ophthalmitis. Mosby: St. Louis; 1966:558–593. Duke-Elder S. *System of ophthalmology*. vol. 9.
2. Goto H, Rao NA. Sympathetic ophthalmia and Vogt–

Koyanagi–Harada syndrome. *Int Ophthalmol Clin*. 1990;30:279–285.
3. Albert DM, Diaz-Rohena R. A historical review of sympathetic ophthalmia and its epidemiology. *Surv Ophthalmol*. 1989;34:1–14.
4. Brour J, Desjardins L, Lehoang P, et al. Sympathetic ophthalmia after proton beam irradiation for choroidal melanoma. *Ocul Immunol Inflamm*. 2012;20:273–276.
5. Fuchs E. Über sympathisierende Entzündung (nebst Bemerkungen über seröse traumatische Iritis). *Graefes Arch Ophthalmol*. 1905;61:365–456.
6. Liddy L, Stuart J. Sympathetic ophthalmia in Canada. *Can J Ophthalmol*. 1972;7:157–159.
7. Kilmartin DJ, Dick AD, Forrester JV. Prospective surveillance of sympathetic ophthalmia in the UK and Republic of Ireland. *Br J Ophthalmol*. 2000;84:259–263.
8. Sen HN, Nussenblatt RB. Sympathetic ophthalmia: what have we learned? *Am J Ophthalmol*. 2009;148:632–633.
9. Vote BJ, Hall A, Cairns J, et al. Changing trends in sympathetic ophthalmia. *Clin Experiment Ophthalmol*. 2004;32:542–545.
10. Chu XK, Chan CC. Sympathetic ophthalmia: to the twenty-first century and beyond. *J Ophthalmic Inflamm Infect*. 2013;3:49.
11. Castiblanco CP, Adelman RA. Sympathetic ophthalmia. *Graefes Arch Clin Exp Ophthalmol*. 2009;247:289–302.
12. Gass JD. Sympathetic ophthalmia following vitrectomy. *Am J Ophthalmol*. 1982;93:552–558.
13. Cha DM, Woo SJ, Ahn J, et al. A case of sympathetic ophthalmia presenting with extraocular symptoms and conjunctival pigmentation after repeated 23-gauge vitrectomy. *Ocul Immunol Inflamm*. 2010;18:265–267.
14. Haruta M, Mukuno H, Nishijima K, et al. Sympathetic ophthalmia after 23-gauge transconjunctival sutureless vitrectomy. *Clin Ophthalmol*. 2010;4:1347–1349.
15. Wang Y, Chan CC. Gender differences in Vogt–Koyanagi–Harada disease and sympathetic ophthalmia. *J Ophthalmol*. 2014;157803.

16. Winter FC. Sympathetic uveitis; a clinical and pathologic study of the visual result. *Am J Ophthalmol*. 1955;39:340–347.
17. Lubin JR, Albert DM, Weinstein M. Sixty-five years of sympathetic ophthalmia: a clinicopathologic review of 105 cases (1913–1978). *Ophthalmology*. 1980;87:109–121.
18. Rathinam SR, Rao NA. Sympathetic ophthalmia following postoperative bacterial endophthalmitis: a clinicopathologic study. *Am J Ophthalmol*. 2006;141:498–507.
19. Woods AC. Sympathetic ophthalmia: part 2. *Am J Ophthalmol*. 1936;19:100–109.
20. Samuels B. Panophthalmitis and sympathetic ophthalmia. *Arch Ophthalmol*. 1938;20:804–811.
21. Wong VG, Anderson R, O'Brien PJ. Sympathetic ophthalmia and lymphocyte transformation. *Am J Ophthalmol*. 1971;72:960–966.
22. Rao NA, Robin J, Hartmann D, et al. The role of the penetrating wound in the development of sympathetic ophthalmia: experimental observations. *Arch Ophthalmol*. 1983;101:102–104.
23. Sugita S, Sagawa K, Mochizuki M, et al. Melanocyte lysis by cytotoxic T lymphocytes recognizing the MART-1 melanoma antigen in HLA-A2 patients with Vogt–Koyanagi–Harada disease. *Int Immunol*. 1996;8:799–803.
24. Hammer H. Cellular hypersensitivity to uveal pigment confirmed by leucocyte migration tests in sympathetic ophthalmitis and the Vogt–Koyanagi–Harada syndrome. *Br J Ophthalmol*. 1974;58:773–776.
25. Rao NA, Wong VG. Aetiology of sympathetic ophthalmitis. *Trans Ophthalmol Soc U K*. 1981;101:357–360.
26. Marak GE Jr. Recent advances in sympathetic ophthalmia. *Surv Ophthalmol*. 1979;24:141–156.
27. Rao NA, Wacker WB, Marak GE Jr. Experimental allergic uveitis: clinicopathologic features associated with varying doses of S antigen. *Arch Ophthalmol*. 1979;97:1954–1958.
28. Rao NA. Mechanisms of inflammatory response in sympathetic ophthalmia and VKH syndrome. *Eye (Lond)*. 1997;11:213–216.
29. Yamaki K, Ohono S. Animal models of Vogt–Koyanagi–

Harada disease (sympathetic ophthalmia). *Ophthalmic Res*. 2008;40:129–135.
30. Yamaki K, Gocho K, Hayakawa K, et al. Tyrosinase family proteins are antigens specific to Vogt–Koyanagi–Harada disease. *J Immunol*. 2000;165:7323–7329.
31. Kawakami Y, Suzuki Y, Shofuda T, et al. T cell immune responses against melanoma and melanocytes in cancer and autoimmunity. *Pigment Cell Res*. 2000;13(Suppl. 8):163–169.
32. Reynard M, Shulman IA, Azen SP, et al. Histocompatibility antigens in sympathetic ophthalmia. *Am J Ophthalmol*. 1983;95:216–221.
33. Azen SP, Marak GE Jr, Minckler DS, et al. Histocompatibility antigens in sympathetic ophthalmia. *Am J Ophthalmol*. 1984;98:117–119.
34. Kilmartin DJ, Wilson D, Liversidge J, et al. Immunogenetics and clinical phenotype of sympathetic ophthalmia in British and Irish patients. *Br J Ophthalmol*. 2001;85:281–286.
35. Shindo Y, Ohno S, Usui M, et al. Immunogenetic study of sympathetic ophthalmia. *Tissue Antigens*. 1997;49:111–115.
36. Tiercy JM, Rathinam SR, Gex-Fabry M, et al. A shared HLA-DRB1 epitope in the DR beta first domain is associated with Vogt–Koyanagi–Harada syndrome in Indian patients. *Mol Vis*. 2010;16:353–358.
37. Atan D, Turner SJ, Kilmartin DJ, et al. Cytokine gene polymorphism in sympathetic ophthalmia. *Invest Ophthalmol Vis Sci*. 2005;46:4245–4250.
38. Chan CC, Nussenblatt RB, Fujikawa LS, et al. Sympathetic ophthalmia: immunopathological findings. *Ophthalmology*. 1986;93:690–695.
39. Kuo PK, Lubin JR, Ni C, et al. Sympathetic ophthalmia: a comparison of the histopathological features from a Chinese and American series. *Int Ophthalmol Clin*. 1982;22:125–139.
40. Croxatto JO, Rao NA, McLean IW, et al. Atypical histopathologic features in sympathetic ophthalmia: a study of a hundred cases. *Int Ophthalmol*. 1982;4:129–135.
41. Aziz HA, Flynn HW Jr, Young RC, et al. Sympathetic ophthalmia: clinicopathologic correlation in a consecutive case series. *Retina*. 2015;35:1696–1703.

42. Jakobiec FA, Marboe CC, Knowles DM 2nd, et al. Human sympathetic ophthalmia: an analysis of the inflammatory infiltrate by hybridoma-monoclonal antibodies, immunochemistry, and correlative electron microscopy. *Ophthalmology*. 1983;90:76–95.
43. Shah DN, Piacentini MA, Burnier MN, et al. Inflammatory cellular kinetics in sympathetic ophthalmia a study of 29 traumatized (exciting) eyes. *Ocul Immunol Inflamm*. 1993;1:255–262.
44. Abu El-Asrar AM, Struyf S, Van den Broeck C, et al. Expression of chemokines and gelatinase B in sympathetic ophthalmia. *Eye (Lond)*. 2007;21:649–657.
45. Hooks JJ, Chan CC, Detrick B. Identification of the lymphokines, interferon-gamma and interleukin-2, in inflammatory eye diseases. *Invest Ophthalmol Vis Sci*. 1988;29:1444–1451.
46. Furusato E, Shen D, Cao X, et al. Inflammatory cytokine and chemokine expression in sympathetic ophthalmia: a pilot study. *Histol Histopathol*. 2011;26:1145–1151.
47. Kuppner MC, Liversidge J, McKillop-Smith S, et al. Adhesion molecule expression in acute and fibrotic sympathetic ophthalmia. *Curr Eye Res*. 1993;12:923–934.
48. Jayaprakash Patil A, Edward DP, Wong M, et al. The role of perivascular melanophage infiltrates in the conjunctiva in sympathetic ophthalmia. *Ocul Immunol Inflamm*. 2011;19:186–191.
49. Parikh JG, Saraswathy S, Rao NA. Photoreceptor oxidative damage in sympathetic ophthalmia. *Am J Ophthalmol*. 2008;146:866–875.e2.
50. Kaneko Y, Rao NA. Mitochondrial oxidative stress initiates visual loss in sympathetic ophthalmia. *Jpn J Ophthalmol*. 2012;56:191–197.
51. Kase S, Meghpara BB, Ishida S, et al. Expression of α-crystallin in the retina of human sympathetic ophthalmia. *Mol Med Rep*. 2012;5:395–399.
52. Kaneko Y, Wu GS, Saraswathy S, et al. Immunopathologic processes in sympathetic ophthalmia as signified by microRNA profiling. *Invest Ophthalmol Vis Sci*.

2012;53:4197–4204.
53. Zaharia MA, Lamarche J, Laurin M. Sympathetic uveitis 66 years after injury. *Can J Ophthalmol*. 1984;19:240–243.
54. Galor A, Davis JL, Flynn HW Jr, et al. Sympathetic ophthalmia: incidence of ocular complications and vision loss in the sympathizing eye. *Am J Ophthalmol*. 2009;148:704–710.e2.
55. Rao NA, Marak GE. Sympathetic ophthalmia simulating Vogt–Koyanagi–Harada's disease: a clinico-pathologic study of four cases. *Jpn J Ophthalmol*. 1983;27:506–511.
56. Rao NA. Pathology of Vogt–Koyanagi–Harada disease. *Int Ophthalmol*. 2007;27:81–85.
57. Comer M, Taylor C, Chen S, et al. Sympathetic ophthalmia associated with high frequent deafness. *Br J Ophthalmol*. 2001;85:496.
58. Kawashima Y, Noguchi Y, Takase H, et al. Bilateral hearing impairment as the initial symptom of sympathetic ophthalmia. *Am J Otolaryngol*. 2015;36:606–610.
59. Read RW, Holland GN, Rao NA, et al. Revised diagnostic criteria for Vogt–Koyanagi–Harada disease: report of an international committee on nomenclature. *Am J Ophthalmol*. 2001;131:647–652.
60. Dreyer WB Jr, Zegarra H, Zakov ZN, et al. Sympathetic ophthalmia. *Am J Ophthalmol*. 1981;92:816–823.
61. Sharp DC, Bell RA, Patterson E, et al. Sympathetic ophthalmia: histopathologic and fluorescein angiographic correlation. *Arch Ophthalmol*. 1984;102:232–235.
62. Correnti AJ, Read RW, Kimble JA, et al. Imaging of Dalen–Fuchs nodules in a likely case of sympathetic ophthalmia by fluorescein angiography and OCT. *Ophthalmic Surg Lasers Imaging*. 2010;1–3.
63. Bernasconi O, Auer C, Zografos L, et al. Indocyanine green angiographic findings in sympathetic ophthalmia. *Graefes Arch Clin Exp Ophthalmol*. 1998;236:635–638.
64. Saatci AO, Pasa E, Soylev MF, et al. Sympathetic ophthalmia and indocyanine green angiography. *Arch Ophthalmol*. 2004;122:1568–1569.
65. Moshfeghi AA, Harrison SA, Ferrone PJ. Indocyanine green

angiography findings in sympathetic ophthalmia. *Ophthalmic Surg Lasers Imaging*. 2005;36:163–166.
66. Gallagher MJ, Yilmaz T, Cervantes-Castaneda RA, et al. The characteristic features of optical coherence tomography in posterior uveitis. *Br J Ophthalmol*. 2007;91:1680–1685.
67. Gupta V, Gupta A, Dogra MR, et al. Reversible retinal changes in the acute stage of sympathetic ophthalmia seen on spectral domain optical coherence tomography. *Int Ophthalmol*. 2011;31:105–110.
68. Marak GE Jr. Phacoanaphylactic endophthalmitis. *Surv Ophthalmol*. 1992;36:325–339.
69. Makley TA Jr, Azar A. Sympathetic ophthalmia: a long-term follow-up. *Arch Ophthalmol*. 1978;96:257–262.
70. Jabs DA, Rosenbaum JT, Foster CS, et al. Guidelines for the use of immunosuppressive drugs in patients with ocular inflammatory disorders: recommendations of an expert panel. *Am J Ophthalmol*. 2000;130:492–513.
71. Tessler HH, Jennings T. High-dose short-term chlorambucil for intractable sympathetic ophthalmia and Behçet's disease. *Br J Ophthalmol*. 1990;74:353–357.
72. Patel SS, Dodds EM, Echandi LV, et al. Long-term, drug-free remission of sympathetic ophthalmia with high-dose, short-term chlorambucil therapy. *Ophthalmology*. 2014;121:596–602.
73. Gupta SR, Phan IT, Suhler EB. Successful treatment of refractory sympathetic ophthalmia in a child with infliximab. *Arch Ophthalmol*. 2011;129:250–252.
74. Menghini M, Frimmel SA, Windisch R, et al. Efficacy of infliximab therapy in two patients with sympathetic ophthalmia. *Klin Monbl Augenheilkd*. 2011;228:362–363.
75. Kim JB, Jeroudi A, Angeles-Han ST, et al. Adalimumab for pediatric sympathetic ophthalmia. *JAMA Ophthalmol*. 2014;132:1022–1024.
76. Keystone EC. Does anti-tumor necrosis factor-α therapy affect risk of serious infection and cancer in patients with rheumatoid arthritis? A review of longterm data. *J Rheumatol*. 2011;38:1552–1562.
77. Ozdemir H, Karacorlu M, Karacorlu S. Intravitreal

triamcinolone acetonide in sympathetic ophthalmia. *Graefes Arch Clin Exp Ophthalmol*. 2005;243:734–736.
78. Chan RV, Seiff BD, Lincoff HA, et al. Rapid recovery of sympathetic ophthalmia with treatment augmented by intravitreal steroids. *Retina*. 2006;26:243–247.
79. Mahajan VB, Gehrs KM, Goldstein DA, et al. Management of sympathetic ophthalmia with the fluocinolone acetonide implant. *Ophthalmology*. 2009;116:552–557.e1.
80. Bratton ML, He YG, Weakley DR. Dexamethasone intravitreal implant (Ozurdex) for the treatment of pediatric uveitis. *J AAPOS*. 2014;18:110–113.
81. Reynard M, Riffenburgh RS, Maes EF. Effect of corticosteroid treatment and enucleation on the visual prognosis of sympathetic ophthalmia. *Am J Ophthalmol*. 1983;96:290–294.
82. Marak GE Jr. Sympathetic ophthalmia. *Ophthalmology*. 1982;89:1291–1292.
83. O'Donnell BA, Kersten R, McNab A, et al. Enucleation versus evisceration. *Clin Experiment Ophthalmol*. 2005;33:5–9.
84. Ruedemann AD. Sympathetic ophthalmia after evisceration. *Trans Am Ophthalmol Soc*. 1963;61:274–314.
85. Green WR, Maumenee AE, Sanders TE, et al. Sympathetic uveitis following evisceration. *Trans Am Acad Ophthalmol Otolaryngol*. 1972;76:625–644.
86. Griepentrog GJ, Lucarelli MJ, Albert DM, et al. Sympathetic ophthalmia following evisceration: a rare case. *Ophthal Plast Reconstr Surg*. 2005;21:316–318.
87. Androudi S, Theodoridou A, Praidou A, et al. Sympathetic ophthalmia following postoperative endophthalmitis and evisceration. *Hippokratia*. 2010;14:131–132.
88. Zhang Y, Zhang MN, Jiang CH, et al. Development of sympathetic ophthalmia following globe injury. *Chin Med J*. 2009;122:2961–2966.
89. Freidlin J, Pak J, Tessler HH, et al. Sympathetic ophthalmia after injury in the Iraq war. *Ophthal Plast Reconstr Surg*. 2006;22:133–134.
90. du Toit N, Motala MI, Richards J, et al. The risk of sympathetic ophthalmia following evisceration for

penetrating eye injuries at Groote Schuur Hospital. *Br J Ophthalmol*. 2008;92:61–63.
91. Savar A, Andreoli MT, Kloek CE, et al. Enucleation for open globe injury. *Am J Ophthalmol*. 2009;147:595–600.e1.
92. Zheng C, Wu AY. Enucleation versus evisceration in ocular trauma: a retrospective review and study of current literature. *Orbit*. 2013;32:356–361.
93. Eagle RC Jr, Grossniklaus HE, Syed N, et al. Inadvertent evisceration of eyes containing uveal melanoma. *Arch Ophthalmol*. 2009;127:141–145.
94. Chan CC, Roberge RG, Whitcup SM, et al. 32 cases of sympathetic ophthalmia: a retrospective study at the National Eye Institute, Bethesda, MD, from 1982 to 1992. *Arch Ophthalmol*. 1995;113:597–600.

78

Vogt–Koyanagi–Harada Disease

Hiroshi Goto, P. Kumar Rao, Narsing A. Rao

Introduction and Historical Aspects

Vogt–Koyanagi–Harada (VKH) disease is a bilateral granulomatous uveitis often associated with exudative retinal detachment and with extraocular manifestations, such as pleocytosis in the cerebrospinal fluid and, in some cases, vitiligo, poliosis, alopecia, and dysacusis.[1]

Poliosis associated with ocular inflammation was first described by Ali-ibn-Isa, an Arab physician who lived in the 1st century AD (cited by Pattison).[2] This association was reported by Schenkl in 1873,[3] by Hutchinson in 1892,[4] and by Vogt in l906.[5] Harada described a primary posterior uveitis with exudative retinal detachments in association with cerebrospinal fluid pleocytosis.[6]

Three years later, in 1929, Koyanagi described six patients with bilateral chronic iridocyclitis, patchy depigmentation of the skin, patchy hair loss, and whitening of the hair, especially the eyelashes.[7] This constellation of findings was termed "uveitis with poliosis, vitiligo, alopecia, and dysacusis."[7] Babel in 1932[8] and Bruno and McPherson in 1945 combined the findings of Vogt, Koyanagi, and Harada and suggested that these processes represent a continuum of the same disease,[9] thereafter recognized as Vogt–Koyanagi–Harada syndrome.

When a patient presents with the ocular and the extraocular manifestations, the diagnosis of VKH is made with certainty. However, extraocular manifestations such as dysacusis and cutaneous changes are relatively rare, and the dermatologic changes mainly occur late in the course of the disease.[1,10] Because of the variation in clinical presentations of VKH, the American Uveitis Society (AUS) in 1978 recommended the following diagnostic criteria: (1) the absence of any history of ocular trauma or surgery; and (2) the presence of at least three of the following four signs: (a) bilateral chronic iridocyclitis; (b) posterior uveitis, including exudative retinal detachment, forme fruste of exudative retinal detachment, disc hyperemia or edema and "sunset glow" fundus; (c) neurologic signs of tinnitus, neck stiffness, cranial nerve, or central nervous system disorders, or cerebrospinal fluid pleocytosis;

and (d) cutaneous findings of alopecia, poliosis, or vitiligo.[11]

Since VKH manifestations vary depending upon the clinical course, a given patient may not initially present with the features required for the diagnosis of VKH by AUS criteria. Read and Rao evaluated the utility of the existing AUS criteria in 71 consecutive patients with VKH who were diagnosed based on the clinical features and the course of the disease, combined with fluorescein angiography (FA) with or without ultrasonography in selected cases.[12] The authors concluded that AUS criteria for diagnosis of VKH may not be adequate. Taking into account the multisystem nature of VKH and allowing for the different ocular findings present in the early and late stages of the disease, the First International Workshop on VKH proposed revised diagnostic criteria to include clinical manifestations at various stages of disease.[13] The revised diagnostic criteria are summarized in Box 78.1

Box 78.1

Revised Diagnostic Criteria Proposed by the First International Workshop on Vogt–Koyanagi–Harada Disease*

Complete VKH Disease

1. Bilateral ocular involvement (a or b must be met, depending on the stage of disease when the patient is examined)

a. Early manifestations of disease

1) There must be evidence of a diffuse choroiditis (with or without anterior uveitis, vitreous inflammatory reaction, or optic disc hyperemia), which may manifest as one of the following:

a) Focal areas of subretinal fluid, or

b) Bullous serous retinal detachments

2) With equivocal fundus findings, both of the following must be present as well:

a) Focal areas of delay in choroidal perfusion, multifocal areas of pin-point leakage, large placoid areas of hyperfluorescence, pooling within subretinal fluid, and optic nerve staining (listed in order of sequential appearance) by fluorescein angiography, and

b) Diffuse choroidal thickening, without evidence of posterior scleritis by ultrasonography

b. Late manifestations of disease

1) History suggestive of prior presence of findings from la, and either both (2) and (3) below, or multiple signs from (3):

2) Ocular depigmentation (either of the following manifestations is sufficient):

a) Sunset glow fundus, or

b) Sugiura's sign

3) Other ocular signs:

a) Nummular chorioretinal depigmented scars, or

b) Retinal pigment epithelium clumping and/or migration, or

c) Recurrent or chronic anterior uveitis

2. Neurologic/auditory findings (may have resolved by time of examination)

a. Meningismus (malaise, fever, headache, nausea, abdominal pain, stiffness of the neck and back, or a combination of these factors; headache alone is not sufficient to meet the definition of meningismus, however), or

b. Tinnitus, or

c. Cerebrospinal fluid pleocytosis

3. Integumentary finding (not preceding onset of central nervous system or ocular disease)

a. Alopecia, or

b. Poliosis, or

c. Vitiligo

Incomplete VKH Disease (Point 1 and Either 2 or 3 Must Be Present)

1. Bilateral ocular involvement as defined for complete VKH disease

2. Neurologic/auditory findings as defined for complete VKH disease above, or

3. Integumentary findings as defined for complete VKH disease above

Probable VKH Disease

1. Bilateral ocular involvement as defined for complete VKH disease above

*In all cases there should not be a history of penetrating ocular injury or surgery preceding the initial onset of uveitis and no clinical or laboratory evidence suggestive of other ocular disease criteria.

Modified from Read RW, Holland GN, Rao NA, et al. Revised diagnostic criteria for Vogt–Koyanagi–Harada disease: report of an international committee on nomenclature. Am J Ophthalmol 2001;131:647–52.

In the past, constellation of these ocular signs and symptoms warranted the term "syndrome," but in recent years the entity has been well characterized; thereafter the International Workshop on VKH adopted the term Vogt–Koyanagi–Harada disease.[13]

Epidemiology

The incidence of VKH is variable. It appears to be more common in Japan, where it accounts for 6.7% of all uveitis referrals.[14] In the United States it accounts for 1–4% of all uveitis clinic referrals.

VKH tends to affect more pigmented races, such as Asians, Hispanics, American Indians, and Asian Indians.[1,15] In the United States there appears to be variability in the racial distribution of patients with VKH disease.[1,11,16,17] In northern California, VKH was seen mainly in Asians (4l%), followed by whites (29%), Hispanics (16%), and blacks (14%).[17] In contrast, reports from southern California show that 78% of VKH patients were Hispanic while 3% were white, 10% were Asian, and 6% were black.[1] A series reported from the National Institutes of Health (NIH) showed that 50% of VKH patients were white, 35% were black, and 13% were Hispanic.[17] However, most of those patients reported in the NIH series had remote American Indian ancestry. Most studies report that women tend to be affected more frequently than men; however, Japanese investigators have not found such a female predilection.[15] Most patients are in their second to fifth decades of

life, but children may also be affected.[1,18] According to the university hospital-based national survey conducted twice in Japan in the past 10 years, the frequency of VKH disease among all uveitis patients has been stable at about 7%.[19]

Clinical Description

Typical clinical features of VKH include bilateral panuveitis associated with exudative retinal detachment, meningismus associated with headache and pleocytosis of cerebrospinal fluid, tinnitus or hearing loss, and cutaneous changes, such as alopecia, poliosis, and vitiligo. However, all of the cutaneous changes are rarely seen during the initial presentation, and the clinical features vary depending upon the stage of the disease as well as the effect of medical treatment. Presence of ocular and two or more extraocular features is considered as a complete form of VKH disease.[13] Incomplete VKH disease includes bilateral typical ocular involvement plus either neurologic/auditory or cutaneous changes, whereas probable VKH disease is composed of just ocular manifestations.[13] However, some of these probable VKH patients can develop cutaneous manifestations during the chronic or chronic recurrent stage of the disease.

The Prodromal Stage

Initial manifestations of VKH disease may include nonspecific viral-like illness, commonly referred to as a prodromal stage. This stage may last only a few days and may be limited to headaches, nausea, dizziness, fever, orbital pain, and meningism. Light sensitivity and tearing may occur 1–2 days following the above symptoms. These neurologic signs include cranial nerve palsies and optic neuritis. Cerebrospinal fluid analysis usually reveals pleocytosis.

The Acute Uveitic Stage

This stage follows the prodromal phase and presents with blurring of vision in both eyes. One eye may be affected first, followed a few days later by the second eye. Despite a delay in symptoms, careful

examination will reveal bilateral posterior uveitis. This uveitis consists of thickening of the posterior choroid with elevation of the peripapillary retinochoroidal layer, multiple serous retinal detachments (Fig. 78.1), hyperemia, and edema of the optic nerve head.

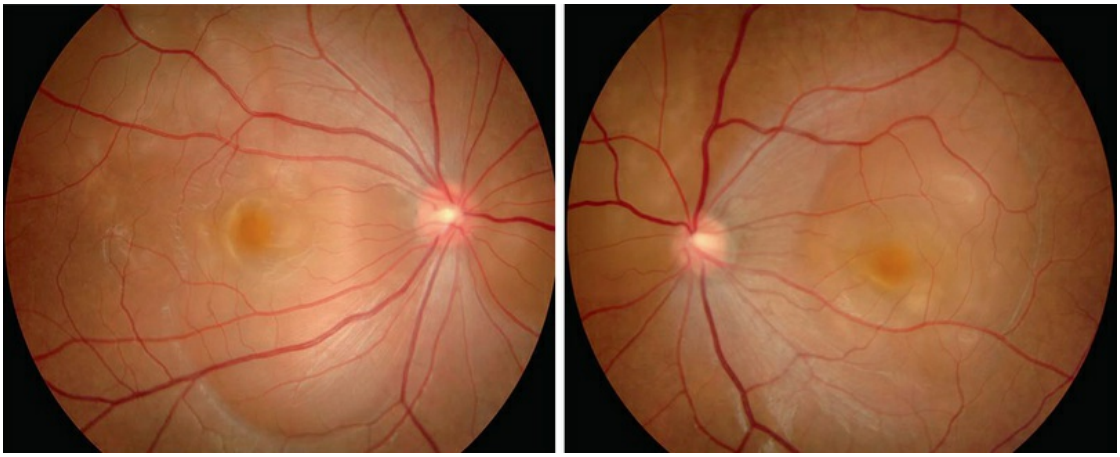

FIG. 78.1 Bilateral multiple serous retinal detachments at the acute uveitis stage of Vogt–Koyanagi–Harada disease.

Rarely VKH disease can present with optic disc hyperemia and edema without serous retinal detachments (Fig. 78.2). VKH patients with optic disc swelling without typical serous retinal detachment are more likely to be female, older individuals, and they develop chronic disease more frequently than patients with the typical VKH presentations.[20]

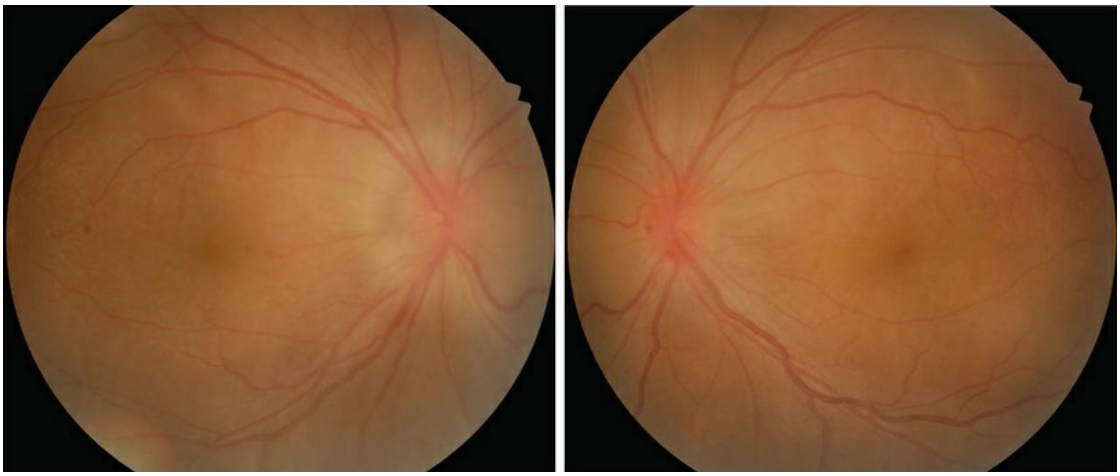

FIG. 78.2 Bilateral hyperemia and edema of the optic disc at the acute uveitis stage of Vogt–Koyanagi–Harada disease without serous retinal detachment.

Thickened choroid can be detected by ultrasonography (Fig. 78.3). Alteration in the retinal pigment epithelium (RPE) associated with multifocal choroidal inflammation is easily observed with FA, which reveals hypofluorescent dots at the early phase followed by multiple focal areas of leakage and subretinal fluid accumulation at the late phase (Fig. 78.4).

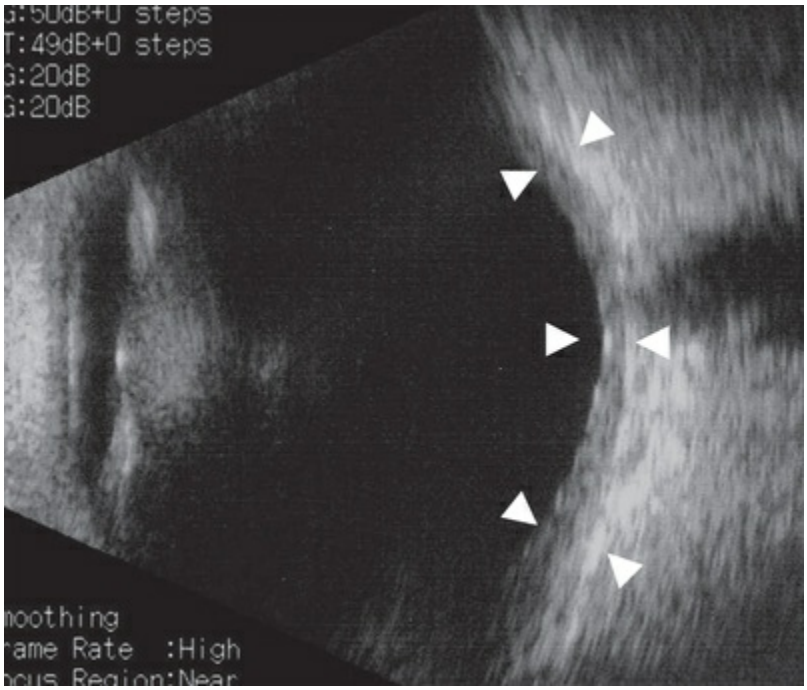

FIG. 78.3 Ultrasonography showing thickened choroid (*arrowheads*).

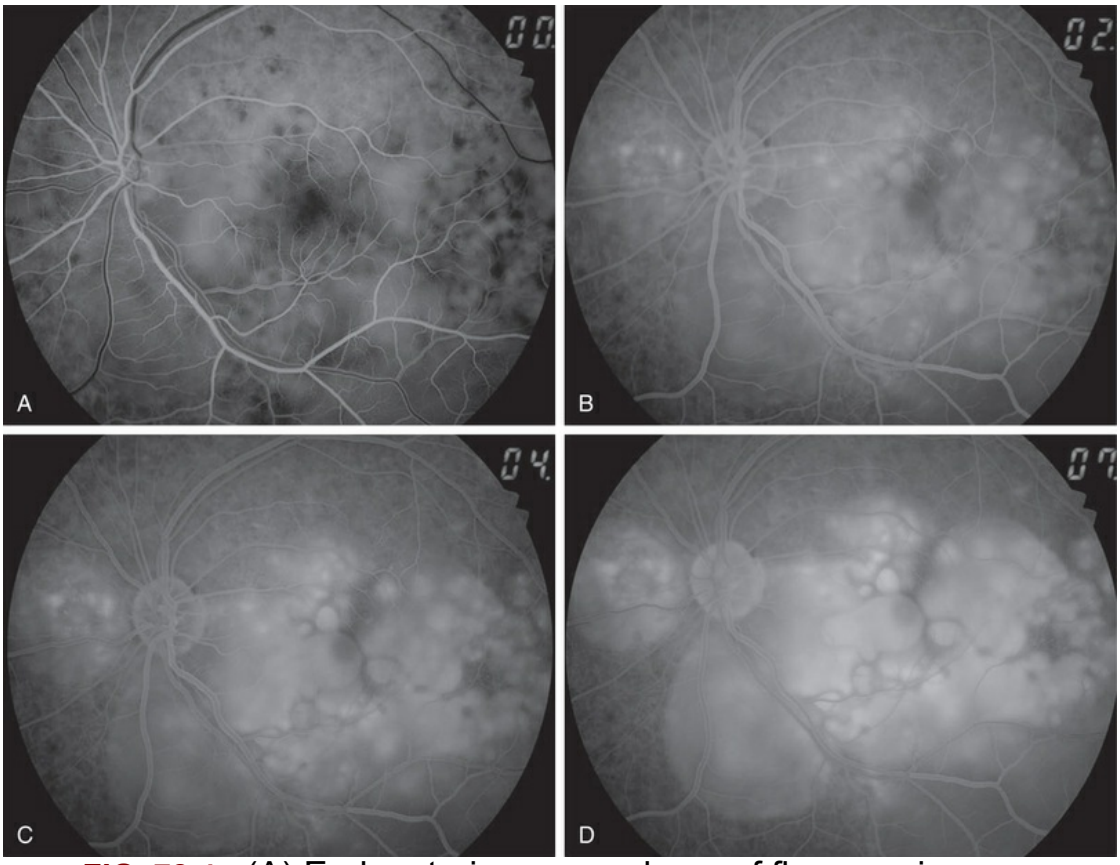

FIG. 78.4 (A) Early arteriovenous phase of fluorescein angiogram exhibiting multiple hypofluorescent dots with irregular hyperfluorescent background. (B) Subsequently, multiple hyperfluorescent dots at the retinal pigment epithelium level are noted. (C) Dye leakage during midphase of the angiogram. (D) Subretinal dye pooling at the area of serous retinal detachment during the late phase.

Indocyanine green angiography (ICGA) (Fig. 78.5) could be useful to evaluate choroidal inflammatory changes, such as early choroidal stromal vessel hyperfluorescence and leakage, and hypofluorescent dark dots at the level of the choroid.[21,22]

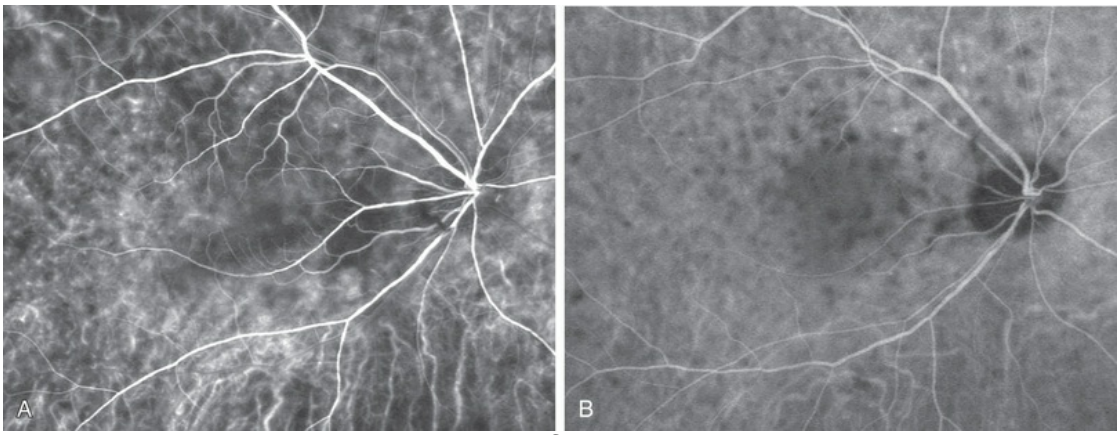

FIG. 78.5 (A) Early phase of the indocyanine green angiogram showing vascular leakage in the choroid. (B) Late phase of angiogram showing multiple hypofluorescent dots.

The inflammation eventually becomes diffuse, extending into the anterior segment and revealing the presence of flare and cells in the anterior chamber. Less commonly, mutton-fat keratic precipitates, small nodules on the iris surface and pupillary margin, may be observed;[1] however, these anterior inflammatory changes are more common in the recurrent phase. The inflammatory infiltrate in the ciliary body and choroid may cause forward displacement of the lens iris diaphragm (Fig. 78.6), leading to acute angle closure glaucoma or annular choroidal detachment.[23,24] These intraocular changes are typically bilateral; rarely, however, the process can be restricted to one eye.[25]

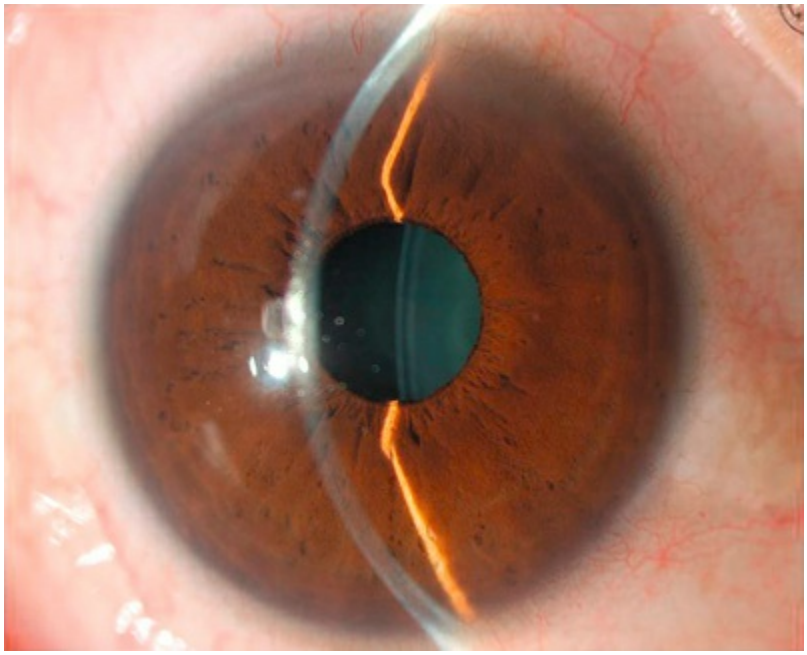

FIG. 78.6 Shallow anterior chamber caused by the anterior displacement of the lens associated with inflammatory infiltrates at the ciliary body.

The Chronic Uveitic Stage

The chronic or convalescent stage occurs several weeks after the acute uveitic stage and is characterized by development of vitiligo (Fig. 78.7), poliosis, and depigmentation of the choroids. Perilimbal vitiligo, also known as Sugiura's sign (Fig. 78.8), may develop at this stage among the patients who have melanosis at the palisade of Vogt, such as Japanese patients.[1,13]

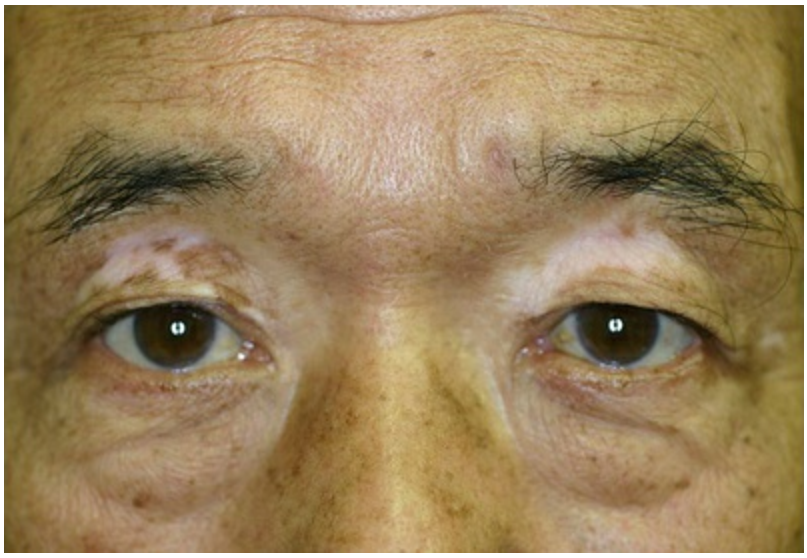

FIG. 78.7 Bilateral upper-eyelid vitiligo.

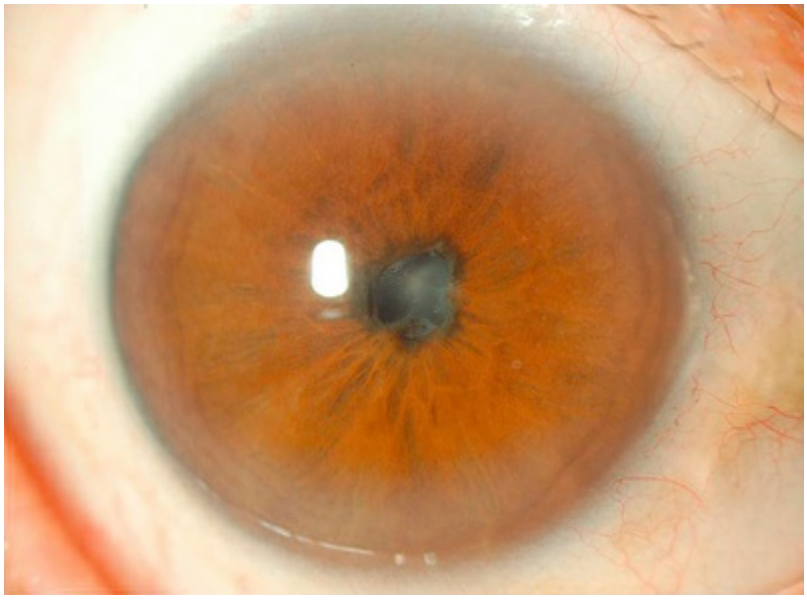

FIG. 78.8 Chronic stage of Vogt–Koyanagi–Harada disease showing extensive posterior synechiae and loss of pigment at the limbus (Sugiura's sign).

Choroidal depigmentation occurs a few months after the uveitic phase. This leads to the characteristic pale disc with a bright red–orange choroid known as sunset glow fundus (Fig. 78.9). In Hispanics, the sunset glow fundus may show foci of RPE changes in the form of hyperpigmentation or hypopigmentation. The juxtapapillary area may show marked depigmentation. At this stage, small, yellow, well-circumscribed areas of chorioretinal

atrophy may appear, mainly in the inferior midperiphery of the fundus. This convalescent phase may last for several months.

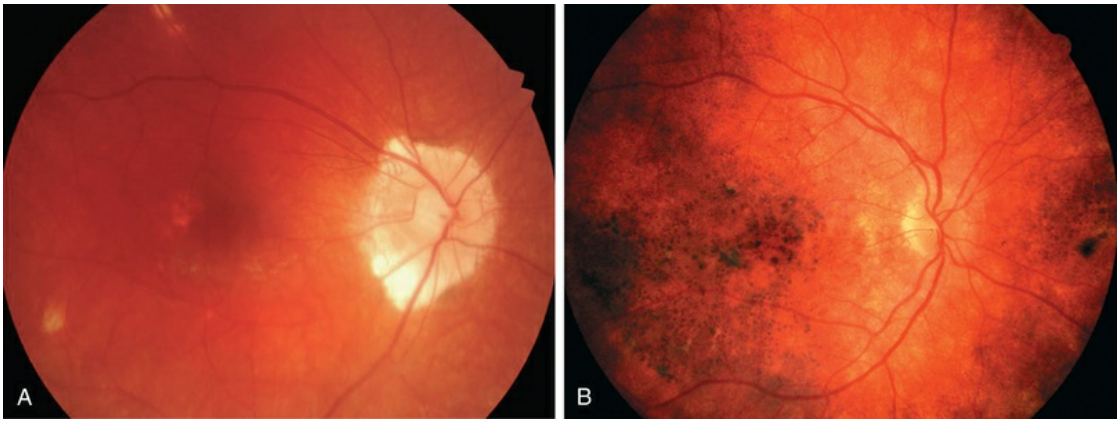

FIG. 78.9 Chronic stage of Vogt–Koyanagi–Harada disease revealing sunset glow fundus with juxtapapillary depigmentation and oval retinal pigment epithelium atrophic lesions in an Asian patient (A) and in a Hispanic patient (B).

The Chronic Recurrent Stage

The chronic recurrent stage consists of a smoldering panuveitis with acute episodic exacerbations of granulomatous anterior uveitis. Recurrent posterior uveitis with exudative retinal detachment is uncommon. The anterior uveitis may be resistant to local and systemic corticosteroid therapy. Iris nodules may be seen during this phase (Fig. 78.10). The most visually debilitating complication of the chronic inflammation during this stage appears to be the development of subretinal neovascular membranes.[26] Posterior subcapsular cataract, as well as glaucoma, either angle closure or open angle, and posterior synechiae, may also be seen.[27,28] Recurrence of the intraocular inflammation may lead to extensive chorioretinal atrophy.

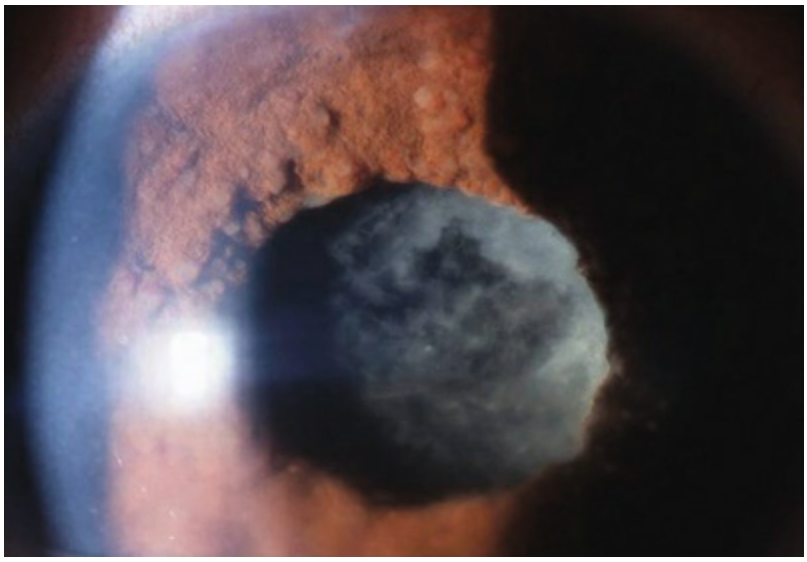

FIG. 78.10 Multiple iris nodules at the iris in chronic recurrent stage.

Frequency of Distinguishing Clinical Features

Clinical features of ocular and extraocular manifestations of 180 patients with VKH disease and 967 patients with non-VKH disease analyzed by stepwise logistic regression models are listed in Table 78.1.[29] In the acute stage, exudative retinal detachment was most likely to be found, whereas in the chronic stage, sunset glow fundus was most common. Prevalence of sunset glow fundus can be low (67.5%) in patients treated with systemic corticosteroid from the initial acute uveitic stage.[27]

TABLE 78.1

Distinguishing Clinical Features of Acute and Chronic Vogt–Koyanagi–Harada Disease[26]

Dependent Variable = VKH	Odds Ratio Estimate (95% CI)	*p* Value
ACUTE DISEASE		
Exudative retinal detachment	>999 (48.02, >999)	<0.0001
Alopecia	81.23 (2.47, >999)	0.01
Disc hyperemia	5.28 (1.02, 27.42)	0.05
Asian	24.48 (2.38, 251.9)	0.007
Hispanic	59.76 (3.77, 948.2)	0.004
CHRONIC DISEASE		
Sunset glow fundus	141.66 (54.65, 367.2)	<0.0001

Vitiligo	11.73 (3.59, 38.33)	<0.0001
Alopecia	3.20 (1.40, 7.31)	0.0005
Nummular chorioretinal scars	2.83 (1.34, 5.98)	0.01
Vitreous cells	0.39 (0.18, 0.83)	0.02
Asian	3.48 (1.60, 7.60)	0.002
Hispanic	13.25 (4.63, 37.88)	0.0003

Reproduced with permission from Rao NA, Gupta A, Dustin L, et al. Frequency of distinguishing clinical features in Vogt–Koyanagi–Harada disease. Ophthalmology 2010;117:591–9 [Table 8].

Pathology and Pathogenesis

VKH is a non-necrotizing diffuse granulomatous inflammation involving the uvea. Although a granulomatous process is the primary feature of the disease, the histopathologic changes vary depending on the stage of the disease.[30] Uvea is thickened by diffuse infiltration of lymphocytes and macrophages, admixed with epithelioid cells and multinucleated giant cells containing melanin granules. The neural retina is detached from the RPE, and the subretinal space contains proteinaceous fluid exudates (Fig. 78.11). Dalen–Fuchs nodules, which represent focal aggregates of epithelioid histiocytes admixed with RPE, are located between Bruch's membrane and the RPE.[31] In the convalescent stage, the choroidal melanocytes decrease in number and disappear (Fig. 78.12), resulting in the sunset glow appearance of the fundus.[31] During the chronic stage, the numerous focal yellowish oval or round lesions seen in the inferior peripheral fundus by ophthalmoscopy histologically display a focal loss of RPE cells and the formation of chorioretinal adhesions.[31] In the longstanding chronic recurrent stage, the RPE and neural retina show degenerative changes (Fig. 78.13). The RPE may reveal hyperplasia and fibrous metaplasia with or without associated subretinal neovascularization.[31]

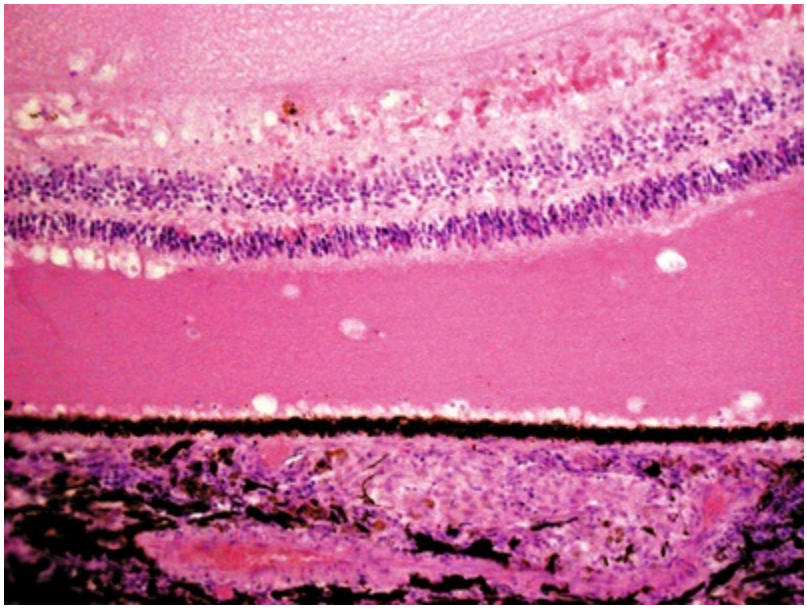

FIG. 78.11 Acute uveitic stage of Vogt–Koyanagi–Harada disease shows serous detachment of the retina, preservation of choriocapillaris from inflammatory cell infiltration, and thickening of choroid from granulomatous inflammatory cell infiltration (hematoxylin and eosin). (Courtesy of Professor H. Inomata.)

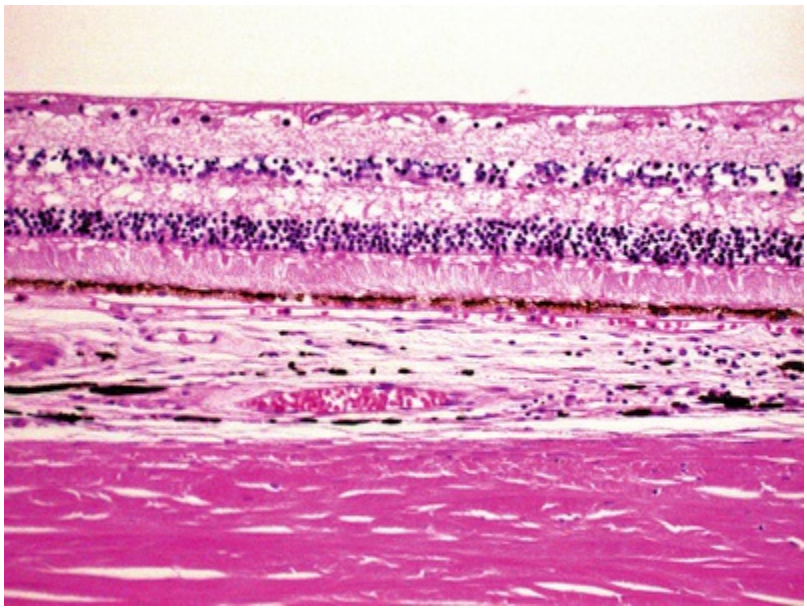

FIG. 78.12 Convalescent stage of Vogt–Koyanagi–Harada disease, exhibiting loss of choroidal melanocytes and infiltration of lymphocytes and plasma cells in the choroid. Note relatively intact retinal pigment epithelium and neurosensory retina

(hematoxylin and eosin). (Courtesy of Professor H. Inomata.)

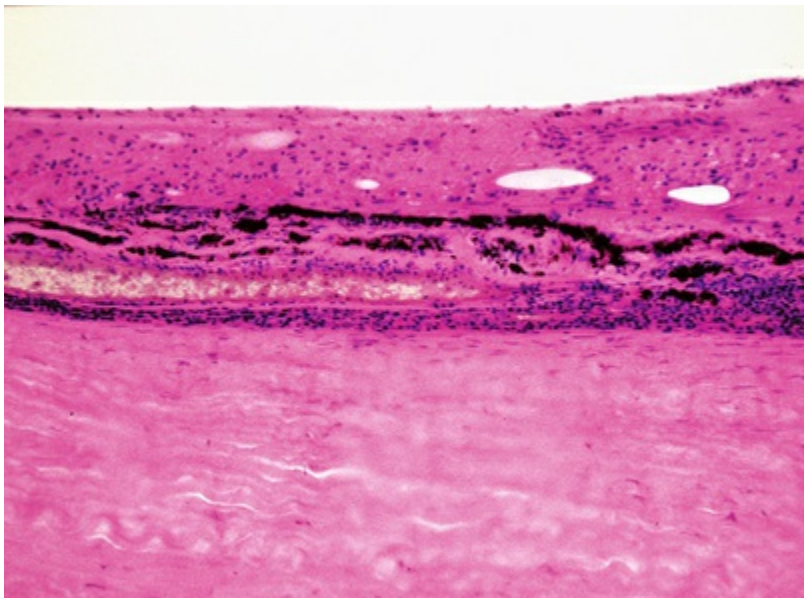

FIG. 78.13 Chronic recurrent stage of Vogt–Koyanagi–Harada disease shows choroidal inflammation, retinal pigment epithelium proliferation, and degeneration of overlying retina (hematoxylin and eosin). (Courtesy of Professor H. Inomata.)

Although the exact cause for the inflammation directed at the melanocytes remains unknown, current evidence suggests that it involves an autoimmune process driven by T lymphocytes against an as-yet unidentified antigen(s) associated with melanocytes.[1,32,33]

The antigenic peptides to induce autoimmune response in the uveal tract may include tyrosinase or tyrosinase-related proteins.[34,35] Experimental animal studies, as well as T-cell clones raised specific to tyrosinase family protein from the peripheral blood of patients with VKH, suggest that autoreactive T cells against tyrosinase and/or tyrosinase-related proteins may play a role in the development of VKH in a genetically susceptible individual.[35]

Cytokines are known to play an important role in the pathogenesis of VKH disease. Interleukin (IL)-21, a member of the IL-2 family exerting pleiotropic effects on the immune system, could be involved in the pathogenesis of VKH disease, possibly by promoting IL-17 secretion.[36]

$CD4^{+}CD25^{high}$ T-regulatory (Treg) cells have been shown to be involved in the pathogenesis of autoimmune diseases. Reduction of number or impaired function of $CD4^{+}CD25^{high}$ Treg cells has been reported in patients with VKH.[37]

There is a strong association with the human leukocyte antigen (HLA) DR4 in Japanese patients with VKH disease, and these patients and individuals from Korea showed predominant alleles of DRB1*0405 and HLA-DRB1 *0410.[38] Significant difference in the prevalence of HLA-DRB1 *0405 between the VKH patients and control subjects was also demonstrated in the Middle East.[39] However, in other racial groups, such as mixed Hispanic individuals from southern California, either HLA-DR1 or HLA-DR4 was found in 84% of patients with VKH disease.[40] Indeed, there was a higher relative risk with HLA-DR1 than HLA-DR4 (4.11 vs. 1.96, respectively). Similar HLA-DR1 and HLA-DR4 subtypes were noted in 89% of mixed Mexican patients.[41] These studies indicate that specific HLA genes may confer risk for development of VKH disease.

Investigations

Imaging Studies

In the vast majority of cases, the diagnosis of VKH disease is a clinical one when the patient presents with ocular and extraocular manifestations. However, when the disease presents without extraocular changes, FA is essential for the diagnosis. ICGA is also useful to evaluate choroidal inflammatory changes.

In patients with inadequate pupillary dilation caused by posterior synechiae or dense vitritis that obscures the view of the fundus, ultrasonography may help to establish the diagnosis.[42] Ultrasound biomicroscopic examination and other recent ophthalmic viewing systems during the uveitic stage may reveal shallow anterior chamber, ciliochoroidal detachment, and thickened ciliary body.

In addition to angiography and ultrasonography, optical coherence tomography (OCT) and scanning laser ophthalmoscopy (SLO) have been found useful for substantiating the diagnosis.

Serous retinal detachment can be clearly observed by OCT (Fig. 78.14). Thickened choroid can be demonstrated by OCT with enhanced depth imaging (Fig. 78.15). OCT has been used not only for supporting diagnosis but for monitoring resolution of the serous retinal detachment[43,44] and choroidal thickness[45,46] with corticosteroids and immunomodulatory therapy. Choroidal undulation and bulging inward in the acute stage are also clearly demonstrated by OCT.[47] In the chronic stage, changes of the RPE can be clearly depicted as decreased fundus autofluorescence[48,49] (Fig. 78.16).

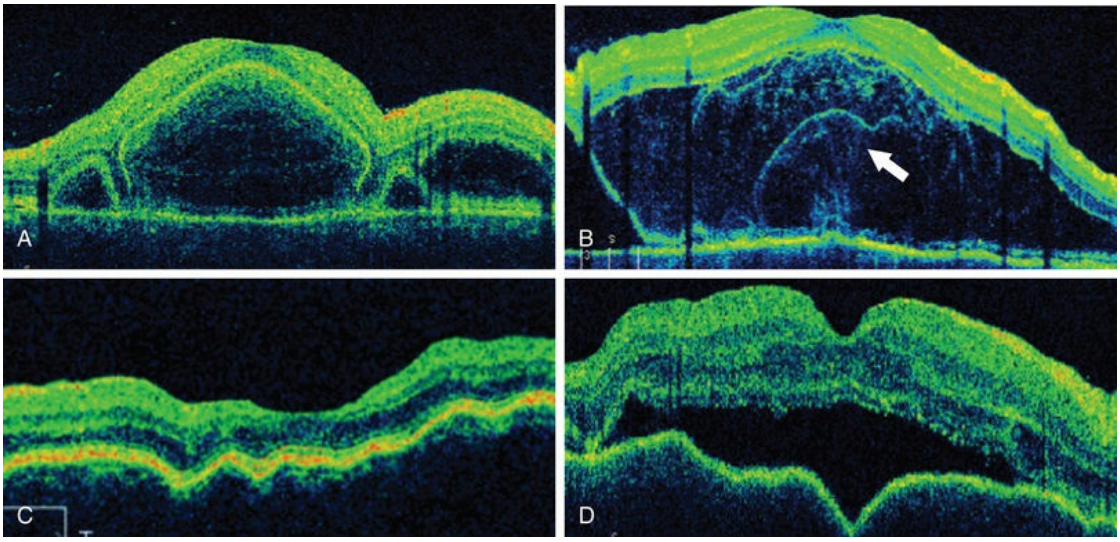

FIG. 78.14 Optical coherence tomography showing serous retinal detachment at the acute uveitic stage. Note the multiple serous retinal detachment with septa (A), presence of fibrin in subretinal space (*arrow*) (B), waving of retinal pigment epithelium (C), and choroidal excavation (D).

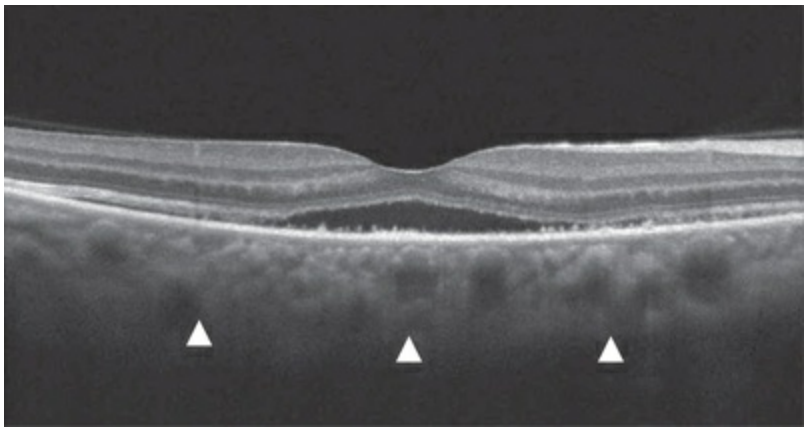

FIG. 78.15 Optical coherence tomography 9 days after systemic corticosteroid therapy showing thickened choroid at the macular area (*arrowheads*).

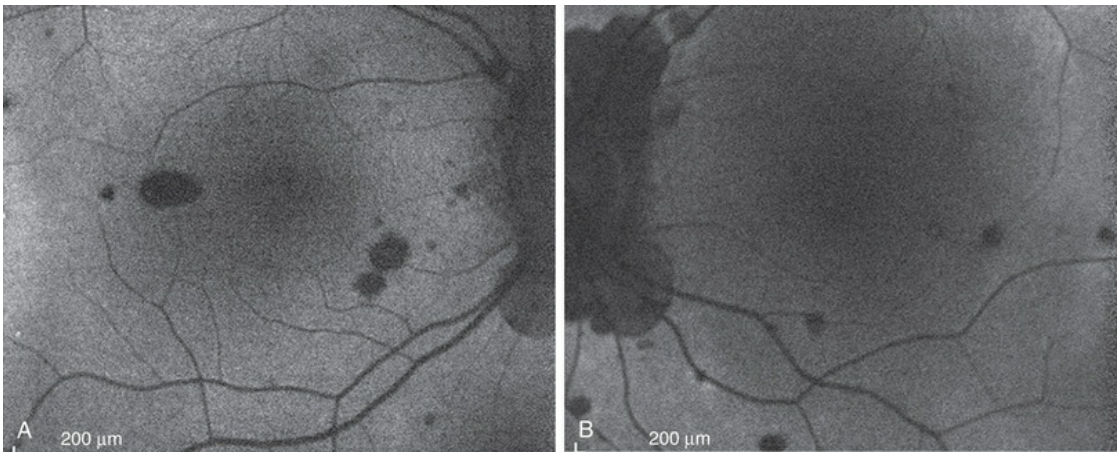

FIG. 78.16 Fundus autofluorescence imaging shows decreased autofluorescence at the atrophic nummular scars.

Lumbar Puncture

Although lumbar puncture is not necessary for the diagnosis of VKH disease with typical ocular and extraocular manifestations, this procedure is a useful adjunctive test in cases with atypical features. Ohno et al. found that more than 80% of patients with VKH disease had cerebrospinal fluid pleocytosis, consisting mostly of lymphocytes.[17] In their study, the pleocytosis was present in 80% of patients within 1 week and in 97% of patients within 3 weeks of the onset of uveitis. The cerebrospinal fluid pleocytosis, however, is

transient and resolves within 8 weeks even in patients who develop recurrences of intraocular inflammation. Cytologic analysis may reveal melanin-containing histiocytes in patients with pleocytosis.[50]

Differential Diagnosis

The differential diagnosis of VKH disease includes sympathetic ophthalmia, uveal effusion syndrome, posterior scleritis, acute posterior multifocal placoid pigment epitheliopathy (APMPPE), and sarcoidosis.[1] Sympathetic ophthalmia can present with bilateral panuveitis associated with retinal detachment and meningismus. However, a history of penetrating ocular injury is the rule in this disorder. Extraocular manifestations, such as dysacusis, vitiligo, poliosis, and alopecia, can occur in sympathetic ophthalmia, but they are rare.[51]

Uveal effusion syndrome may clinically mimic VKH disease. Angiographically, the effusion syndrome may reveal numerous fluorescent blotches in the subretinal space during the serous detachment phase. The syndrome can involve both eyes, although not simultaneously. Unlike VKH disease, the effusion syndrome lacks intraocular inflammation. Posterior scleritis affects predominantly women and is often bilateral. Patients may present with pain, photophobia, and loss of vision, and the vitreous often reveals cells. Exudative retinal detachment and choroidal folds may be noted. Ultrasonography can help to differentiate posterior scleritis from VKH disease. The former reveals flattening of the posterior aspect of the globe, thickening of the posterior coats of the eye, retrobulbar edema, and high internal reactivity of the thickened sclera. Other entities, such as sarcoidosis and APMPPE, can be differentiated based on their clinical features, ultrasonography, and FA.

Treatment

Although data from randomized trials are lacking, early and aggressive use of systemic corticosteroids followed by slow tapering over 3–6 months is the acceptable treatment of choice to suppress the intraocular inflammation and to prevent the

development of complications related to the ocular inflammation.[1] Such treatment may prevent progression of the disease to the chronic recurrent stage and may also reduce the incidence and/or severity of extraocular manifestations. If the ocular inflammation relapses after tapering of systemic corticosteroids, the relapse may reflect too-rapid tapering of the corticosteroids. Such recurrences become increasingly steroid-resistant, and cytotoxic or immunosuppressive agents are usually required to control the inflammation. Patients with inflammatory cell infiltration in the anterior chamber require topical corticosteroids and cycloplegics to reduce ciliary spasm and prevent posterior synechiae formation.

High-dose oral corticosteroids, 1–2 mg/kg per day of prednisone or 200 mg of intravenous methylprednisolone for 3 days, followed by oral administration of high-dose corticosteroids with a slow taper, are the mainstay of therapy for VKH disease.[52,53] The use of intravenous corticosteroids, up to 1 g/day for 3 days, followed by a slow taper has been recommended by some. However, Sasamoto et al. found a similar beneficial effect of decreased intraocular inflammation with either 1 g or 200 mg per day of intravenous corticosteroids.[53] Of course, as is always the case when corticosteroids are prescribed, careful attention to possible risks and side-effects is warranted. The route of systemic administration of corticosteroids includes oral and intravenous injection followed by an oral taper. However, the International VKH Study Group concluded that route of administration had no significantly detectable effect on visual acuity outcome nor on the development of visually significant complications.[54]

Although the initial episode of uveitis can be managed successfully in the majority of cases with intravenous and/or oral corticosteroids, few patients may require additional immunomodulatory agent such as cyclosporine, methotrexate, or mycophenolate mofetil. In contrast, recurrences do not respond as well to systemic corticosteroid treatment.[1] Such patients may show some initial response to sub-Tenon injections of triamcinolone acetonide, but they usually require immunomodulatory agents, such as cyclosporine, methotrexate, azathioprine, mycophenolate mofetil, cyclophosphamide, and chlorambucil.[55–58] Sustained release steroid such as the fluocinolone acetonide intravitreal implant may

provide control of intraocular inflammation and reduce dependency on systemic corticosteroids and/or immunosuppressive agents in patients with the chronic stage of VKH disease.[59]

Cyclosporine 2.5–5 mg/kg per day is generally preferred when the intraocular inflammation is corticosteroid-resistant or when the patient experiences intolerable side-effects from the long-term use of corticosteroids. Recently, biologic agents, rituximab and anti-TNF-α antibody, infliximab have been reported in the management of VKH disease.[60]

Administration of the immunomodulatory agents and biologics requires a careful pretreatment evaluation and careful subsequent evaluations during the follow-up examinations for any side-effects associated with the therapy. Various immunosuppressive and cytotoxic agents used in the treatment of VKH disease are summarized in Box 78.2.

Box 78.2

Immunosuppressive/Cytotoxic Agents Used in the Treatment of Vogt–Koyanagi–Harada Disease

- Corticosteroids[1,53]
- Oral prednisone 1–2 mg/kg per day initially, followed by gradual taper over 3–6 months
- Pulse dose of methylprednisolone 1 g/day for 3 days, followed by gradual tapering of oral prednisone over 3–6 months
- Intravenous methylprednisolone 100–200 mg/day for 3 days, followed by gradual tapering of oral prednisone over 3–6 months
- Immunosuppressive agents[1]
- Cyclosporin 2.5–5 mg/kg per day
- FK506 0.1–0.15 mg/kg per day
- Cytotoxic agents[1]

- Azathioprine 1–2.5 mg/kg per day
- Mycophenolate mofetil 1–3 g/day
- Cyclophosphamide 1–2 mg/kg per day
- Chlorambucil 0.1 mg/kg per day; dose adjusted every 3 weeks to a maximum of 18 mg/day
- Anti-TNF-α monoclonal antibody[59]

Complications and Management

A retrospective analysis of the records of 101 patients with VKH disease followed at the Doheny Eye Institute revealed the development of at least one complication in 51% of eyes.[61] Cataract occurred in 42%, glaucoma in 27%, choroidal neovascularization in 11% (Fig. 78.17), and subretinal fibrosis in 6% (Fig. 78.18). The patients who developed these complications had a significantly longer median duration of disease and significantly more recurrences than did those patients who developed no complications. Moreover, eyes possessing a better visual acuity at presentation had better visual acuity at final follow-up, and patients who developed VKH at a more advanced age had a worse visual acuity.[61]

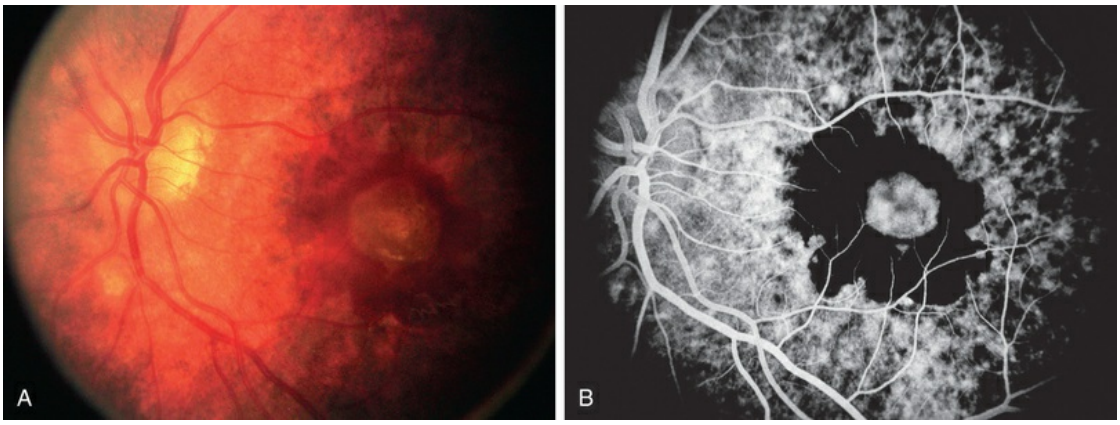

FIG. 78.17 Submacular choroidal neovascular membrane and hemorrhage during the chronic recurrent stage (A); the fluorescein angiogram shows a

typical neovascular membrane (B).

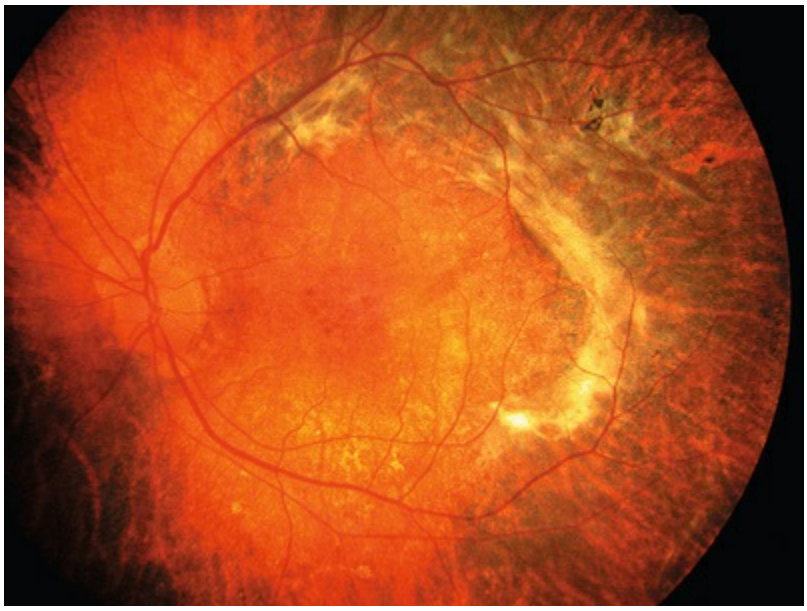

FIG. 78.18 Subretinal fibrosis in a patient with chronic recurrent stage of Vogt–Koyanagi–Harada disease.

There is general agreement that cataract surgery should be delayed until the intraocular inflammation has subsided, at which time safe cataract extraction with posterior-chamber intraocular lens implantation can be successfully accomplished. Occasionally, patients with significant vitreous opacities and debris may require a combined procedure of pars plana vitrectomy and lensectomy.

Angle closure due to peripheral anterior synechiae and posterior synechiae may cause glaucoma.[27] Acute angle closure with elevated intraocular pressure has been reported as a presenting sign of VKH disease. Although sustained elevated intraocular pressure can be controlled by medical therapy alone, most patients require surgical intervention in the form of iridectomy, trabeculectomy with 5-fluorouracil or mitomycin C, and tube-shunt surgery.

Chronic recurrent anterior uveitis and fundus pigmentary disturbances seem to predispose patients to the development of choroidal neovascularization[26] (Fig. 78.18). These subretinal neovascular membranes present with raised masses, which may be associated with subretinal hemorrhage. Fluorescein angiography, ICGA, OCT angiography, and OCT are useful for detecting the

neovascular membranes, and photocoagulation may help with the management. Photodynamic therapy with verteporfin for subfoveal choroidal neovascularization has been attempted with some success.[62] Intravitreal injection of an anti-vascular endothelial growth factor (VEGF) may be an option to treat CNV in eyes with VKH.[63]

Prognosis

In general those VKH patients who are treated with initial high-dose systemic corticosteroids followed by gradual tapering will usually have a fair visual prognosis; nearly two-thirds of these patients retain 20/40 or better visual acuity.[1,53] On average, most patients require treatment for 4–6 months. The complications of chronic recurrent VKH disease include cataract, glaucoma, choroidal neovascularization, subretinal fibrosis, and optic atrophy.[1,52,61,64]

Jap et al. reported that patients treated with low-dose prednisolone (less than 1 mg/kg) had a higher incidence of peripapillary atrophy with increase in recurrences and more frequent episodes.[65]

Conclusion

VKH is a bilateral granulomatous panuveitis typically associated with exudative retinal detachment that can present initially with posterior uveitis associated with focal or multifocal serous retinal detachment, with signs of meningeal irritation and with or without extraocular manifestations such as poliosis, vitiligo, and auditory disturbances. However, in general the cutaneous extraocular manifestations develop during the chronic phase of the disease. In most cases the diagnosis is a clinical one, but the diagnosis of atypical cases may require the use of FA, lumbar puncture, and ultrasonography. VKH is treated initially with high-dose systemic corticosteroids. Successful outcome requires a gradual tapering of the corticosteroids over a 3–6-month period. Complications of this disease include cataract, glaucoma, choroidal neovascularization, and subretinal fibrosis. The overall prognosis for adequately

managed cases is fair, with nearly 60–70% of patients retaining vision of 20/40 or better.

References

1. Moorthy RS, Inomata H, Rao NA. Vogt–Koyanagi–Harada syndrome. *Surv Ophthalmol*. 1995;39:265–292.
2. Pattison EM. Uveo-meningoencephalitic syndrome (Vogt–Koyanagi–Harada). *Arch Neurol*. 1965;12:197–205.
3. Schenkl A. Ein Fall von plötzlich aufgetretener Poliosis circumscripta der Wimpern. *Arch Dermatol Syph*. 1873;5:137–139.
4. Hutchinson J. A case of blanched eyelashes. *Arch Surg*. 1892;4:357.
5. Vogt A. Frühzeitiges Ergrauen der Zilien und Bemerkungen über den sogenannten plötzlichen Eintritt dieser Veränderung. *Klim Monatsbl Augenheilkd*. 1906;44:228–242.
6. Harada E. Beitrag zur klinischen Kenntnis von nichteitriger Choroiditis (choroiditis diffusa acuta). *Acta Soc Ophthalmol Jpn*. 1926;30:356–378.
7. Koyanagi Y. Dysakusis, Alopecia und Poliosis bei schwerter Uveitis nichttraumatischen Ursprungs. *Klin Monatsbl Augenheilkd*. 1929;82:194–211.
8. Babel J. Syndrome de Vogt–Koyanagi (Uveite bilaterale, poliosis, alopecie, vitiligo et dysacousie). *Schweiz Med Wochenschr*. 1932;4:1136–1140.
9. Bruno MG, McPherson SD Jr. Harada's disease. *Am J Ophthalmol*. 1949;32:513–522.
10. Beniz J, Forster DJ, Lean JS, et al. Variations in clinical features of the Vogt–Koyanagi–Harada syndrome. *Retina*. 1991;11:275–280.
11. Snyder DA, Tessler HA. Vogt–Koyanagi–Harada syndrome. *Am J Ophthalmol*. 1980;90:69–75.
12. Read RW, Rao NA. Utility of existing Vogt–Koyanagi–Harada syndrome diagnostic criteria at initial evaluation of the individual patient: a retrospective analysis. *Ocul Immunol Inflamm*. 2000;8:227–234.

13. Read RW, Holland GN, Rao NA, et al. Revised diagnostic criteria for Vogt–Koyanagi–Harada disease: report of an international committee on nomenclature. *Am J Ophthalmol*. 2001;131:647–652.
14. Goto H, Mochizuki M, Yamaki S, et al. Epidemiological survey of intraocular inflammation in Japan. *Jpn J Ophthalmol*. 2007;51:41–44.
15. Shimizu K. Harada's, Behçet's, Vogt–Koyanagi syndromes: are they clinical entities? *Trans Am Acad Ophthalmol Otolaryngol*. 1973;77:281–290.
16. Nussenblatt RB. Clinical studies of Vogt–Koyanagi–Harada's disease at the National Eye Institute, NIH, USA. *Jpn J Ophthalmol*. 1988;32:330–333.
17. Ohno S, Char DH, Kimura SJ, et al. Vogt–Koyanagi–Harada syndrome. *Am J Opthalmlol*. 1977;83:735–740.
18. Forster DJ, Green RL, Rao NA. Unilateral manifestation of the Vogt–Koyanagi–Harada syndrome in a 7-year-old child. *Am J Ophthalmol*. 1991;111:380–382.
19. Ohguro N, Sonoda KH, Takeuchi M, et al. The 2009 prospective multi-center epidemiologic survey of uveitis in Japan. *Jpn J Ophthalmol*. 2012;56:432–435.
20. Okunuki Y, Tsubota K, Kezuka T, et al. Differences in the clinical features of two types of Vogt–Koyanagi–Harada disease: serous retinal detachment and optic disc swelling. *Jpn J Ophthalmol*. 2015;59:103–108.
21. Herbort CP, Mantovani A, Bouchenaki N. Indocyanine green angiography in Vogt–Koyanagi–Harada disease: angiographic signs and utility in patient follow-up. *Int Ophthalmol*. 2007;27:173–182.
22. Miyanaga M, Kawaguchi T, Miyata K, et al. Indocyanine green angiography findings in initial acute pretreatment Vogt–Koyanagi–Harada disease in Japanese patients. *Jpn J Ophthalmol*. 2010;54:377–382.
23. Kawano Y, Tawara A, Nishioka Y, et al. Ultrasound biomicroscopic analysis of transient shallow anterior chamber in Vogt–Koyanagi–Harada syndrome. *Am J Ophthalmol*. 1996;121:720–723.
24. Yamamoto N, Naito K. Annular choroidal detachment in

patients with Vogt–Koyanagi–Harada disease. *Graefes Arch Clin Exp Ophthalmol*. 2004;242:355–358.
25. Usui Y, Goto H, Sakai J, et al. Presumed Vogt–Koyanagi–Harada disease with unilateral ocular involvement: report of three cases. *Graefes Arch Clin Exp Ophthalmol*. 2009;247:1127–1132.
26. Moorthy RS, Chong LP, Smith RE, et al. Subretinal neovascular membranes in Vogt–Koyanagi–Harada syndrome. *Am J Ophthalmol*. 1993;116:164–170.
27. Forster DJ, Rao NA, Hill RA, et al. Incidence and management of glaucoma in Vogt–Koyanagi–Harada syndrome. *Ophthalmology*. 1993;100:613–618.
28. Moorthy RS, Rajeev B, Smith RE, et al. Incidence and management of cataracts in Vogt–Koyanagi–Harada syndrome. *Am J Ophthalmol*. 1999;118:197–204.
29. Rao NA, Gupta A, Dustin L, et al. Frequency of distinguishing clinical features in Vogt–Koyanagi–Harada disease. *Ophthalmology*. 2010;117:591–599.
30. Keino H, Goto H, Usui M. Sunset glow fundus in Vogt–Koyanagi–Harada disease with or without chronic ocular inflammation. *Graefes Arch Clin Exp Ophthalmol*. 2002;240:878–882.
31. Inomata H, Rao NA. Depigmented atrophic lesions in sunset glow fundi of Vogt–Koyanagi–Harada disease. *Am J Ophthalmol*. 2001;131:607–614.
32. Norose K, Yano A. Melanoma specific Th1 cytotoxic T lymphocyte lines in Vogt–Koyanagi–Harada disease. *Br J Ophthalmol*. 1996;80:1002–1008.
33. Sugita S, Sagawa K, Mochizuki M, et al. Melanocyte lysis by cytotoxic T lymphocytes recognizing the MART-1 melanoma antigen in HLA-A2 patients with Vogt–Koyanagi–Harada disease. *Int Immunol*. 1996;8:799–803.
34. Gocho K, Kondo I, Yamaki K. Identification of autoreactive T cells in Vogt–Koyanagi–Harada disease. *Invest Ophthalmol Vis Sic*. 2001;42:2004–2009.
35. Hayakawa K, Ishikawa M, Yamaki K. Ultrastructural changes in rat eyes with experimental Vogt–Koyanagi–Harada disease. *Jpn J Ophthalmol*. 2004;48:222–227.

36. Li F, Yang P, Liu X, et al. Upregulation of interleukin 21 and promotion of interleukin 17 production in chronic or recurrent Vogt–Koyanagi–Harada disease. *Arch Ophthalmol*. 2010;128:1449–1454.
37. Chen L, Yang P, Zhou H, et al. Diminished frequency and function of $CD4^{+}CD25^{high}$ regulatory T cells associated with active uveitis in Vogt–Koyanagi–Harada syndrome. *Invest Ophthalmol Vis Sci*. 2008;49:3475–3482.
38. Shindo Y, Ohno S, Yamamoto T, et al. Complete association of the HLA-DRB1 04 and DQ1 04 alleles with Vogt–Koyanagi–Harada's disease. *Hum Immunol*. 1994;39:169–176.
39. Iqniebi A, Gaafar A, Sheereen A, et al. HLA-DRB1among patients with Vogt–Koyanagi–Harada disease in Saudi Arabia. *Mol Vis*. 2009;15:1876–1880.
40. Weisz JM, Holland GN, Roer LN, et al. Association between Vogt–Koyanagi–Harada syndrome and HLA-DR1 and DR4 in Hispanic patients living in Southern California. *Ophthalmology*. 1995;102:1012–1015.
41. Arellanes-Garcia L, Bautista N, More P, et al. HLA-DR is strongly associated with Vogt–Koyanagi–Harada disease in Mexican Mestizo patients. *Ocul Immunol Inflamm*. 1998;6:93–100.
42. Forster DJ, Cano MR, Green RL, et al. Echographic features of the Vogt–Koyanagi–Harada syndrome. *Arch Ophthalmol*. 1990;108:1421–1426.
43. Yamaguchi Y, Otani T, Kishi S. Tomographic features of serous retinal detachment with multilobular dye pooling in acute Vogt–Koyanagi–Harada disease. *Am J Ophthalmol*. 2007;144:260–265.
44. Ishihara K, Hangai M, Kita M, et al. Acute Vogt–Koyanagi–Harada disease in enhanced spectral-domain optical coherence tomography. *Ophthalmology*. 2009;116:1799–1807.
45. Fong AH, Li KK, Wong D. Choroidal evaluation using enhanced depth imaging spectral domain optical coherence tomography in Vogt–Koyanagi–Harada disease. *Retina*. 2011;31:502–599.
46. Nakai K, Gomi F, Ikuno Y, et al. Choroidal observations in Vogt-Koyanagi-Harada disease using high-penetration

optical coherence tomography. *Graefes Arch Clin Exp Ophthalmol*. 2012;250:1089–1095.
47. Hosoda Y, Uji A, Hangai M, et al. Relationship between retinal lesions and inward choroidal bulging in Vogt–Koyanagi–Harada disease. *Am J Ophthalmol*. 2014;157:1056–1063.
48. Vasconcelos-Santos DV, Sohn EH, Sadda S, et al. Retinal pigment epithelial changes in chronic Vogt–Koyanagi–Harada disease: fundus autofluorescence and spectral domain-optical coherence tomography findings. *Retina*. 2010;30:33–41.
49. Heussen FM, Vasconcelos-Santos DV, Pappuru RR, et al. Ultra-wide-field green-light (532-nm) autofluorescence imaging in chronic Vogt–Koyanagi–Harada disease. *Ophthalmic Surg Lasers Imaging*. 2011;42:272–277.
50. Tsai JH, Sukavatcharin S, Rao NA. Utility of lumbar puncture in diagnosis of Vogt–Koyanagi–Harada disease. *Int Ophthalmol*. 2007;27:189–194.
51. Rao NA, Marak GE. Sympathetic ophthalmia simulating Vogt–Koyanagi–Harada's disease: a clinico-pathologic study of four cases. *Jpn J Ophthalmol*. 1983;27:506–511.
52. Rubsamen PE, Gass JDM. Vogt–Koyanagi–Harada syndrome. Clinical course, therapy, and long-term visual outcome. *Arch Ophthalmol*. 1991;109:682–687.
53. Sasamoto Y, Ohno S, Matsuda H. Studies on corticosteroid therapy in Vogt–Koyanagi–Harada disease. *Ophthalmologica*. 1990;201:162–167.
54. Read RW, Yu F, Accorinti M, et al. Evaluation of the effect on outcomes of the route of administration of corticosteroids in acute Vogt–Koyanagi–Harada disease. *Am J Ophthalmol*. 2006;142:119–124.
55. Bykhovskaya I, Thorne JE, Kempen JH, et al. Vogt–Koyanagi–Harada disease: clinical outcomes. *Am J Ophthalmol*. 2005;140:674–678.
56. Agarwal M, Ganesh SK, Biswas J. Triple agent immunosuppressive therapy in Vogt–Koyanagi–Harada syndrome. *Ocul Immunol Inflamm*. 2006;14:333–339.
57. Abu El-Asrar AM, Al Tamimi M, Hemachandran S, et al.

Prognostic factors for clinical outcomes in patients with Vogt–Koyanagi–Harada disease treated with high-dose corticosteroids. *Acta Ophthalmol*. 2013;91:486–493.
58. Kondo Y, Fukuda K, Suzuki K, et al. Chronic noninfectious uveitis associated with Vogt–Koyanagi–Harada disease treated with low-dose weekly systemic methotrexate. *Jpn J Ophthalmol*. 2012;56:104–106.
59. Khalifa Y, Loh AR, Nisha R, et al. Fluocinolone acetonide intravitreal Implants in Vogt–Koyanagi–Harada disease. *Ocul Immunol Inflamm*. 2009;17:431–433.
60. Wang Y, Gaudio PA. Infliximab therapy for 2 patients with Vogt–Koyanagi–Harada syndrome. *Ocul Immunol Inflamm*. 2008;16:167–171.
61. Read RW, Rechodouni A, Butani N, et al. Complications and prognostic factors in Vogt–Koyanagi–Harada disease. *Am J Ophthalmol*. 2001;131:599–606.
62. Nowilaty SR, Bouhaimed M, Photodynamic Therapy Study Group. Photodynamic therapy for subfoveal choroidal neovascularisation in Vogt–Koyanagi–Harada disease. *Br J Ophthalmol*. 2006;90:982–986.
63. Wu L, Evans T, Saravia M, et al. Intravitreal bevacizumab for choroidal neovascularization secondary to Vogt–Koyanagi–Harada syndrome. *Jpn J Ophthalmol*. 2009;53:57–60.
64. Kuo IC, Rechdouni A, Rao NA, et al. Subretinal fibrosis in a patient with Vogt–Koyanagi–Harada syndrome. *Ophthalmology*. 2000;107:1721–1728.
65. Jap A, Luu CD, Yeo I, et al. Correlation between peripapillary atrophy and corticosteroid therapy in patients with Vogt–Koyanagi–Harada disease. *Eye (Lond)*. 2008;22:240–245.

79

White Spot Syndromes and Related Diseases

Rukhsana G. Mirza, Lee M. Jampol

Introduction

The white spot syndromes (WSS) are a group of diseases characterized by inflammation and dysfunction of the outer retina, retinal pigment epithelium, choroid, or a combination of these. They often present a diagnostic and therapeutic challenge for

clinicians and researchers. The etiologies of WSS remain unknown. This chapter discusses birdshot chorioretinopathy (BCR), acute posterior multifocal placoid pigment epitheliopathy (APMPPE), serpiginous choroiditis, relentless placoid chorioretinitis, persistent placoid maculopathy, multifocal choroiditis (MFC)/punctate inner choroidopathy (PIC), multiple evanescent white dot syndrome (MEWDS), acute zonal occult outer retinopathy (AZOOR), and acute macular neuroretinopathy (AMN). Many entities are included in the differential diagnosis of these diseases. These include granulomatous diseases, such as sarcoid, tuberculosis, and sympathetic ophthalmia; masquerade syndromes like syphilis and intraocular lymphoma; infectious etiologies including toxoplasmosis and pneumocystis choroidopathy; and other entities such as presumed ocular histoplasmosis and Behçet disease.[1] In addition, in some cases, degenerative processes such as drusen may appear similar to the whitish-yellow lesions of WSS.

The WSS each have distinct features, but do share some characteristics. Blurred vision, photopsias, visual field changes, floaters, and changes in contrast sensitivity can occur. Although these entities are thought to be inflammatory in nature, vitritis and iritis are not a necessary finding. The white spots themselves may be subtle or a prominent finding. Inflammatory multifocal chorioretinopathies may actually be a more descriptive term.

The white spot syndromes may present in one or both eyes. When bilateral, they may be asymmetric. The age of onset is generally greater than 50 (other than MEWDS and MFC/PIC) but can range from the second to the sixth decade of life.

An autoimmune etiology has been hypothesized[2] and proposed specifically for birdshot chorioretinopathy, acute zonal occult outer retinopathy (AZOOR), and multiple evanescent white dot syndrome (MEWDS).[3] Infectious causes have been postulated. As yet, no characteristic pattern of antiretinal antibodies has been found. These entities need to be distinguished from entities with known neoplasias such as cancer-associated retinopathy (CAR) or melanoma-associated retinopathy (MAR). There are similar features, including panretinal dysfunction, rapid progression, ERG changes, family history of autoimmune disease, retinal antibody activity on Western blot, and improvement in symptoms with

immunosuppression. It has been shown that there is an increased prevalence of systemic autoimmunity in both patients with WSS and their first- as well as second-degree relatives.[4] This suggests that this group of diseases occurs in families with inherited immune dysregulation that predisposes to autoimmunity.

It has also been suggested that several of these entities may be "related" or even represent a spectrum of the same process. Multifocal choroiditis (MFC), punctate inner choroiditis (PIC), MEWDS, acute macular neuroretinopathy (AMN), and AZOOR share commonalities, and Gass referred to them as the AZOOR complex.[5] These include female preponderance, zones of visual field loss that are usually contiguous to the blind spot, enlarged blind spot, photopsias, and ERG changes such as reduced amplitudes. These diseases are rarely overlapping, and clear distinctions can be made with multimodal imaging techniques. Acute idipathic blind spot enlargment (AIBSE) was previously described by Fletcher and colleagues in 1988[6] and sometimes included with the white spot syndromes. In previous case series characterizing this entity,[7] there were many patients that today could be distinguished as having other distinct WSS. We believe enlarged blind spots may be a feature of the white spots syndromes and other diseases mentioned in this chapter and are not a specific entitiy.

Birdshot Chorioretinopathy

The term birdshot retinochoroidopathy was first used in 1980 by Ryan and Maumenee.[8] It was a descriptive term for patients with multiple small, cream-colored fundus findings. These lesions are scattered around the optic disc and radiate to the equator in a "shotgun" pattern. Other terms such as vitiliginous chorioretinitis have been used.[9] It has come to be known as birdshot chorioretinopathy (BCR) due to the histopathologic evidence that the primary lesions of the disease are in the choroid.[10] It is a bilateral, chronic process with vitritis, retinal vasculitis, and cystoid macular edema (CME). Furthermore, it demonstrates the strongest link between any disease and any HLA class I antigen.[11]

Clinical Course

Clinical Symptoms.

Patients present with complaints of blurred vision, floaters, and photopsias. Most have vision of 20/40 or better.[10] The eye is generally not red or painful. Severe nyctalopia despite normal visual acuity may also be a presenting symptom.[12] Individuals also may describe an alteration in color vision[13] or visual fields.[14] Although Gass described a few patients who concurrently had vitiligo of the skin,[9] BCR is thought to be a purely ocular disease.

Epidemiology.

BCR is a rare chronic posterior uveitis. Shah and colleagues did an extensive review of English literature in 2005 and reported the following epidemiologic characteristics.[10] Birdshot chorioretinopathy accounts for 0.6–1.5% of patients referred to tertiary centers for uveitis, or 6–7.9% of patients with posterior uveitis. There is a slight female predominance in the literature, at 54.1–58%.[10,15] The mean reported age at the onset of disease is 53 years. It is generally not a disease of children. The oldest reported age at onset was 79 years. Patients are predominantly white. Finally, the HLA-A29 allele (which is present in about 7% of Caucasians) is strongly associated with BCR.[16] The presence of this allele has been associated with a risk factor of 50–224 to develop BCR. Ninety percent or more of patients with BCR are HLA-A29-positive. Further sequencing of this allele has uncovered 11 subtypes. The HLA-A29*02 subtype is 20 times more prevalent in Caucasians than the HLA-A29*01 type, and the rest are exceedingly rare.[17] HLA-A29*02 subtype is most commonly associated with BCR.

Fundus Findings.

It is important to recognize that symptoms can precede the onset of the classic fundus findings by several years.[18] There is a range of presentations of the lesions associated with BCR. These birdshot lesions can be oval or round in shape, typically about one-half or one-quarter disc diameter in size. They appear deep to the retina (Fig. 79.1). They can be subtle and be asymmetric between eyes. The

lesions can be distinct or poorly defined and can occasionally coalesce. They tend to cluster near the nerve and most commonly nasal and inferior to the disc.[19,20] There is a pattern of linear radiation away from the nerve to the periphery[7] (Fig. 79.2). They may appear to follow choroidal blood vessels peripherally. There is no hyperpigmentation or clumping noted. The retinal pigment epithelium (RPE) and overlying retina appear intact. There has been a report of these choroidal lesions preceding symptom onset in BCR, but this is not the norm.[21]

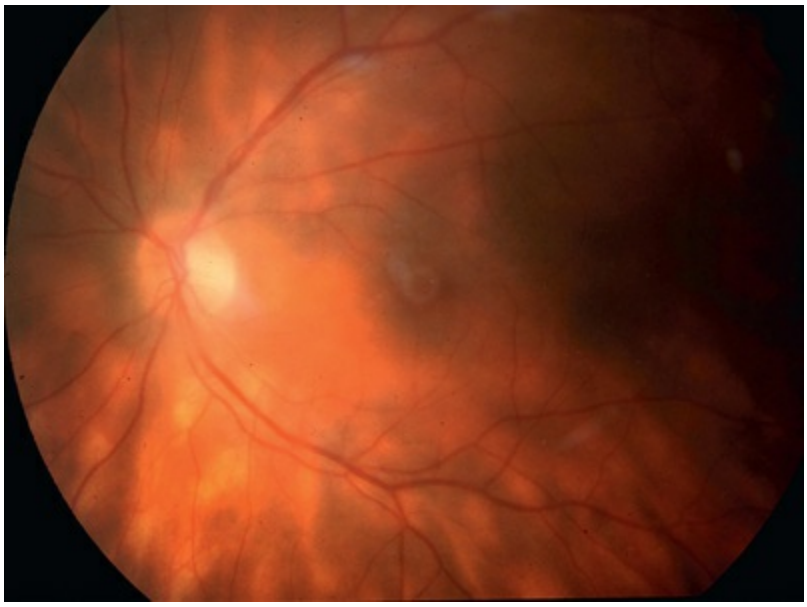

FIG. 79.1 Fundus photo of the left posterior pole showing a hazy view and the distribution of deep, creamy oval lesions.

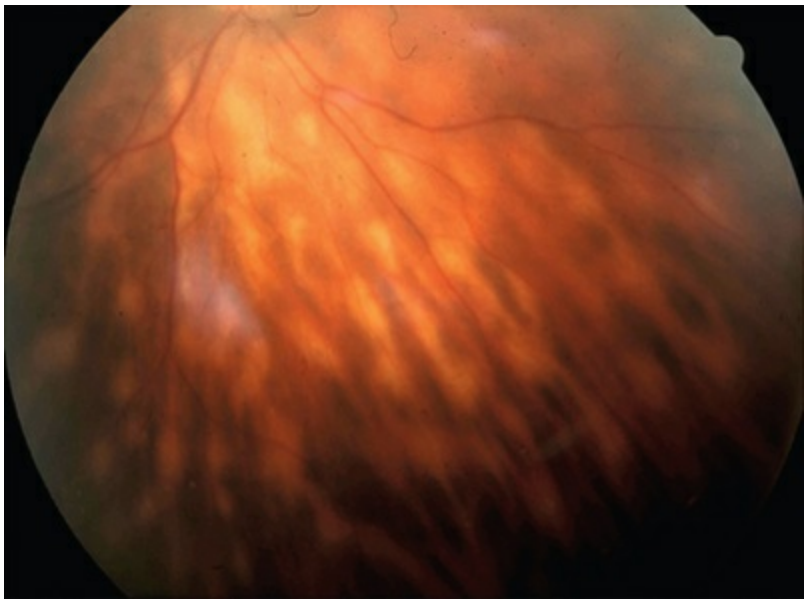

FIG. 79.2 Fundus photo showing the "birdshot" pattern extending linearly from the nerve to the periphery.

Other Ocular Findings.

The anterior segment generally has minimal inflammation without prominent keratic precipitates. Fine keratic precipitates have been described in some series.[20] Due to the mild nature of anterior segment inflammation, posterior synechiae do not occur. Signs of posterior inflammation include retinal vasculitis, optic disc edema, CME (in about 50% of patients),[22] and epiretinal membrane (ERM) formation. Rhegmatogenous retinal detachment has been reported.[8,23,24] Other common findings include diffuse narrowing of the retinal arterioles, perivascular nerve fiber layer hemorrhages, and tortuosity of retinal vessels. Choroidal neovascularization (CNV) can occur.[11,25,26] It has been postulated that this occurs due to the uveitic component causing CNV rather than ischemic factors.[27,28]

A consensus document on the diagnostic criteria for BCR was published in 2006.[29] Required characteristics include bilateral disease, presence of at least three peripapillary lesions inferior or nasal to the optic nerve in at least one eye, low-grade anterior segment inflammation (less than or equal to 1+ cells), and low-grade vitreous inflammation (less than or equal to 2+ vitreous haze). Supportive findings include HLA-A29 positive, retinal vasculitis, and CME. Finally, exclusion criteria include presence of significant keratic precipitates, posterior synechiae, or diagnosis of

infectious, neoplastic, or inflammatory disease that may cause multifocal choroidal lesions.

Clinical Course and Prognosis.

The disease is chronic in nature and does not regress. Again, symptoms of blurred vision, color deficiency, contrast sensitivity issues, and visual field problems may be present for years prior to the onset of fundus lesions. Visual acuity may be normal despite these complaints. It remains a poorly understood disease, and no consensus on management and treatment has been found. Many patients have a slow decline in vision despite treatment.[10]A final visual acuity of 20/40 or better in the best-seeing eye was reported in 75.1% of patients. However, 9.8% of patients were legally blind at follow-up (in the review of literature by Shah and colleagues[10]). Generally, macular edema was the commonest cause of visual decline in 50.5%.[10] Choroidal neovascular membranes developed in 5% of eyes.[25,26] These occur near the optic disc and can be bilateral. Finally, optic disc edema leading to atrophy can also affect visual prognosis. However, in a recent analysis of 46 patients, method of treatment was correlated with visual outcome.[30] Tomkins-Netzer and colleagues categorized patients as either having (1) no treatment, (2) short-term (less than/equal to 1 year) local or systemic treatment, or (3) systemic steroids with second-line immunosuppressants. They found that prognosis for central visual acuity and maintenance of visual fields was improved in patients on long-term immunosuppression compared to short-term therapy.[30]

Imaging

Fluorescein Angiography.

The creamy white spots have variable appearance on fluorescein angiography (FA), and the disease may be more evident clinically than with this mode of imaging (Fig. 79.3). The lesions can hypofluoresce in the early phase, and there can be diffuse hyperfluorescence in the late phases (Fig. 79.4). One theory suggests that the lesions are likely in the outer choroid and associated with large choroidal vessels, thus many of the lesions show neither

hypofluorescence or hyperfluorescence in any phase. The diffuse hyperfluorescence seen may represent a deep inflammatory focus that accumulates fluorescein.[20] Angiographic findings may include increased transit time, leakage from retinal vasculature leading to CME, optic disc hyperfluorescence (Fig. 79.5), and disc or retinal neovascularization.[9,31,32]

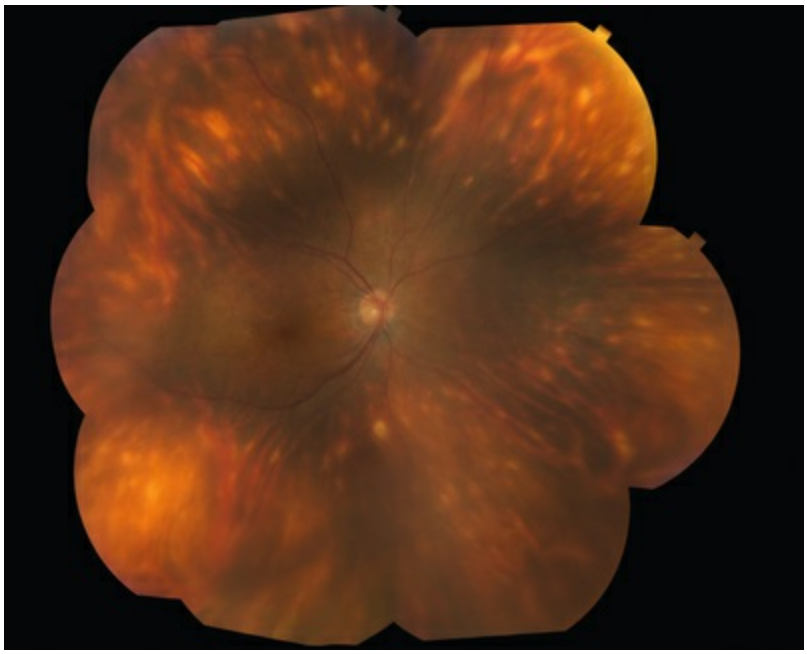

FIG. 79.3 Color montage of right eye showing the distribution of spots.

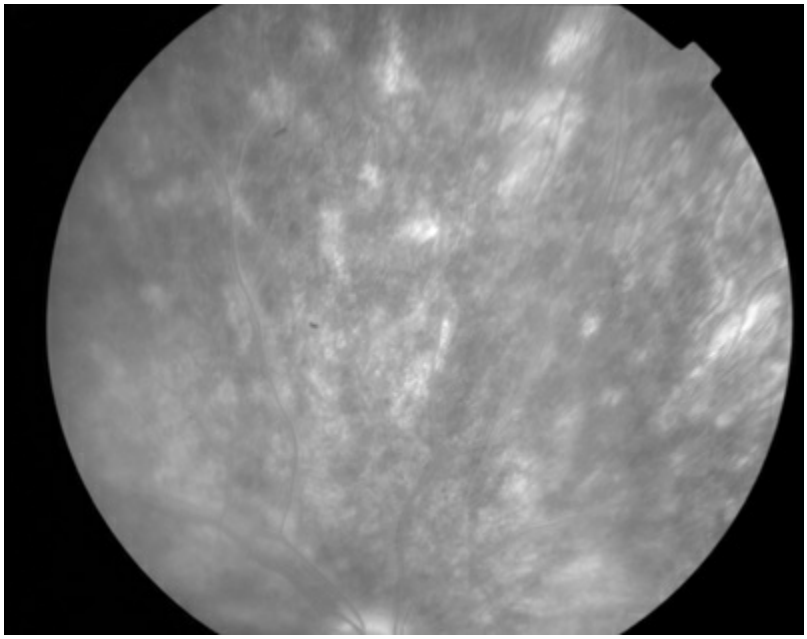

FIG. 79.4 Fluorescein angiography (FA) of periphery showing hyperfluorescence of lesions.

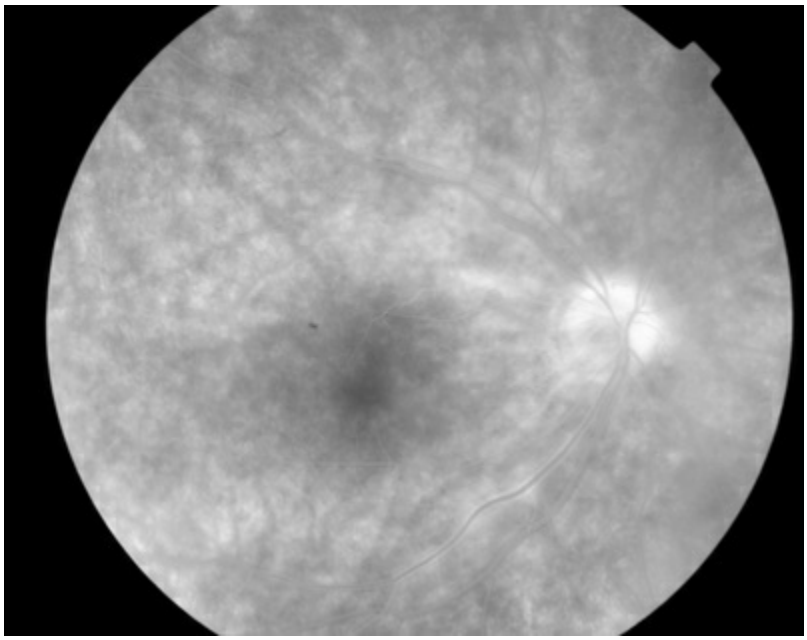

FIG. 79.5 Fluorescein angiography (FA) showing hyperfluorescence of the optic nerve.

Indocyanine Green Angiography.

Indocyanine green angiography (ICGA) is an important diagnostic test. In the active disease,[32] the birdshot lesions appear

hypofluorescent during the intermediate phase of angiography and appear to be bordered by medium-to-large vessels[32–34] (Fig. 79.6). Hypofluorescent lesions can occur prior to clinical lesions.[35] The choroidal vessels appear indistinct. Late in the ICGA, there is diffuse choroidal hyperfluorescence. Theories to explain this early hypofluorescence include choroidal ischemia versus blockage from inflammatory infiltrates. However, in birdshot chorioretinopathy it is agreed upon that the site of the pathology is primarily the choroid. In the acute stages, the inflammatory infiltrates may be denser and block fluorescence. In late stages of the disease, it is thought that the lesions become more atrophic and choroidal vasculature may become more visible. The lesions can become more isofluorescent in this phase of the disease, or they may remain hypofluorescent.[31,32]

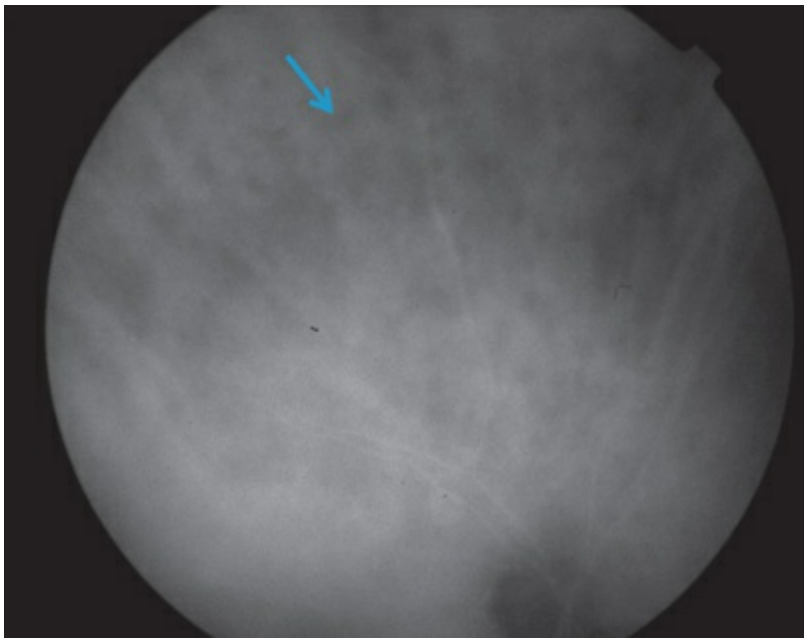

FIG. 79.6 Indocyanine green angiography (ICGA) showing hypofluorescent lesions exceeding the number seen clinically.

Optical Coherence Tomography.

This mode of imaging has primarily been used to follow CME, which is the most common cause of vision loss in BCR[36] (Fig. 79.7). Photoreceptor loss is not a prominent finding early in the course of

this disease. Keane and colleagues created a protocol to scan extramacular retina using enhanced-depth imaging (EDI) optical coherence tomography (OCT).[37] They looked at four locations: superior and inferior to the major vascular arcades, temporal to the the macula, and nasal to the optic nerve in addition to the macula. They found that there is significant thinning of the retina and choroid in the peripheral locations. There was a clear transition zone between the normal and abnormal retina. They suggest using this protocol and looking at the ellipsoid zone to monitor disease progression.[37] They also found discrete outer retinal and choroidal hyperreflective foci, which have been postulated to be inflammatory in nature.[38] Birnbaum and colleagues looked at the findings of 14 patients undergoing treatment and graded clinical symptoms as well as analyzed spectral domain (SD)-OCT with EDI.[39] They described a hyporeflectivity in the suprachoroidal space and found that if this "fluid" was present, it correlated directly to the presence of symptoms.[39] Another series of 11 patients looked at the features of the choroid on SD-OCT. Most patients were clinically inactive.[40] They found that despite clinical inactivity, patients had significantly thinner choroids than age-matched controls.[40]

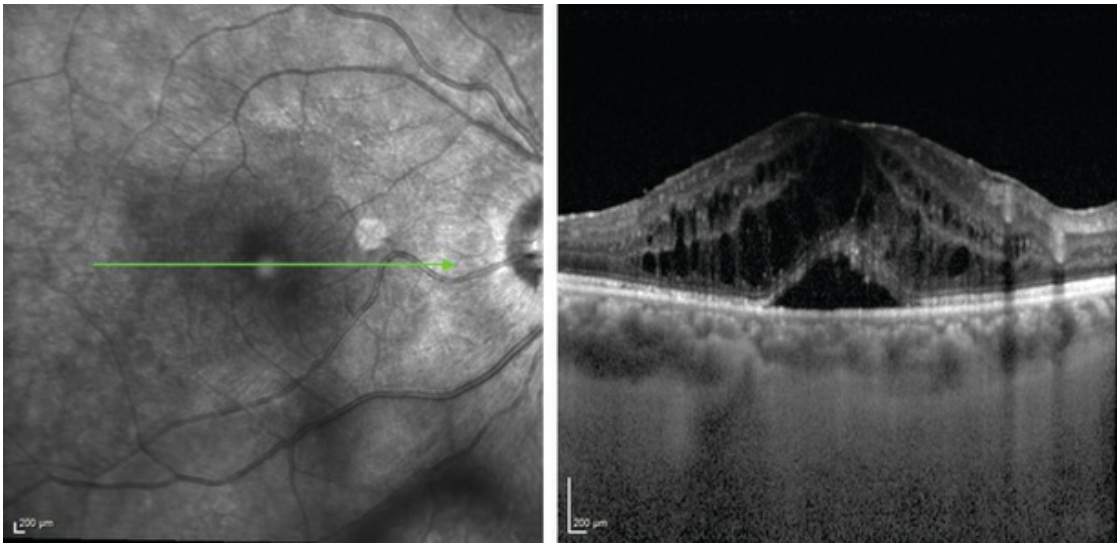

FIG. 79.7 Optical coherence tomography (OCT) showing cystoid macular edema and subfoveal fluid in a patient with birdshot chorioretinitis. (Courtesy of Deborah A. Goldstein, MD.)

Fundus Autofluorescence.

Giuliari and colleagues looked at fundus autofluorescence (FAF) of 18 eyes and found a spectrum of patterns.[36] They found that hypoautofluorescent lesions on FAF did not necessarily correspond to clinical birdshot lesions. Commonly (15/18 eyes) more FAF lesions denoting RPE defects were seen than clinical lesions. Koizumi and colleagues looked at eight patients. They found that some of these hypofluorescent lesions could be placoid in nature and involve the macula.[41] In addition, a perivascular (retinal) linear hypofluorescent FAF pattern was noted by both groups of investigators.[36,41] It was postulated that this finding may suggest that the retinal vessels may play a role in inflammatory-driven damage of the RPE and serve as a conduit for inflammatory factors. The observation that the clinical choroidal lesions did not always correspond to the FAF defects suggests that the choroid and RPE may be affected independently.[41] Furthermore, RPE defects in the macula could also be another cause of vision loss in these individuals. In another multicenter series of 76 patients who underwent wide-field FAF, 80% of patients were observed to have hypoautofluorescent lesions that correlated to decreased vision. They noted a diffuse involvement in the pigment epithelium.[42] FAF may be valuable in evaluating these patients as lesions may be clinically difficult to see.

Electrophysiology

Electroretinogram.

Electroretinography (ERG) is an important test for following BCR. Abnormal electroretinograms (ERGs) were reported in 88.8% of patients.[10] There appear to be two groups of patients: those who develop abnormal ERG early in the disease process and those that develop abnormal results late in the course.[43] Early ERGs may demonstrate supernormal ERG amplitudes, which may be related to retinal inflammation. In this stage, there may be a greater decrease in b-wave amplitude versus a-wave amplitude.[24,43] This is a negative ERG pattern and is not pathognomonic for BCR. It suggests that the Müller and bipolar cells are more affected than the

photoreceptor–retinal pigment epithelium complex. This has been seen in autoimmune retinopathy. Rod dysfunction may occur before cone dysfunction: the rod b-wave may be affected prior to photopic b-wave and flicker response in most patients. In late phases of the disease, there is a progressive decrease in a- and b-wave amplitudes. The 30 Hz flicker implicit time is abnormal in 70% of patients at baseline and is an important marker to follow.[22,44] ERG findings have been noted to improve with treatment.[45] Some authors argue that the reversible nature of the ERG abnormalities suggest a nonischemic etiology.[17] Inflammation of the retinal vasculature could lead to inner retinal dysfunction, while choroidal inflammation could be the cause of altered outer retinal function. Multifocal ERG has also been used and shows impairment as correlated with other functional tests.[46]

Electrooculogram.

Shah and colleagues found that 66.5% of eyes reported in the literature with electrooculography (EOG) findings had abnormal results.[10] Decreased Arden ratios, representing RPE dysfunction, were reported.[43] These ratios further decline with disease progression.

Visual Field Testing

Visual field abnormalities are present in patients with BCR. These include peripheral constriction, enlarged blind spot, central or paracentral scotomas, and generalized diminished sensitivity.[9,19,20,23,47] It is not certain whether these visual field defects occur due to ganglion cell, optic nerve, or outer retinal dysfunction, but it is unlikely that the birdshot lesions themselves cause blind spots.[10] Visual field abnormalities may be reversible with immunosuppression.[48] This is an important component to monitoring this disease.[49]

Systemic Associations

There are no definitive systemic associations. Shah and colleagues'[10] review of the literature revealed hearing loss in some patients.[8,50] As mentioned earlier, cutaneous vitiligo associated with BCR has also

been reported in a few patients.[9,20] In addition, Priem and Oosterhuis reported an increased incidence of vascular disease in their series. Of 102 patients, 16 had hypertension, 5 had coronary artery disease, 2 had a history of cerebrovascular accident, and 2 had a central retinal vein occlusion.[20] These numbers are not impressive considering the age of the patients.

Pathogenesis

The pathogenesis of BCR is unknown. Inflammation appears to be a primary feature. The histopathologic findings in a few eyes with BCR have been reported.[51,52] These suggest that the spots may be related to accumulation of lymphocytes in the choroid at multiple levels, occasionally associated with hemorrhage.[51] BCR appears to be a nongranulomatous nodular choroidal infiltration.[52] Some of the foci were adjacent to the choroidal vessels. The RPE, ciliary body, and iris were not involved. Some lymphocytes were found around the retinal blood vessels and in the optic disc. The lymphocytes were primarily CD^{8+}T-lymphocytes. Inflammation is strongly associated with HLA-A29, which suggests a genetic predisposition to this disease. However, the fact that HLA-A29 is present in 7% of the white population and BCR is so rare tells us other factors are at work. Other genes are highly suspected. Increased interleukin (IL)-17 levels have been found in the aqueous and serum of patients.[22,53] This may represent a T-helper (Th)17-specific autoimmune process. However, initial studies of anti-IL-17 have not been efficacious.[22] Familial history of autoimmunity is likely.[2]

Differential Diagnosis

Birdshot chorioretinopathy can usually be distinguished from other disorders by history and physical findings. However, entities such as pars planitis, intraocular B-cell lymphoma, syphilitic chorioretinitis, sarcoidosis, sympathetic ophthalmia, and other white spot diseases, especially multifocal choroiditis and panuveitis syndrome, should be considered. Indolent nonprogressive multifocal choroidal lesions also give a similar picture and should be considered when unilateral.[54] Sarcoidosis (see Chapter 81, Sarcoidosis) and BCR may be the most difficult to distinguish from each other.[10]

Management/Treatment

In the review of the literature by Shah and colleagues,[10] most cases were treated; however, no definitive guidelines for the initiation of treatment were given. This chronic progressive disease may not be sight-threatening in the early course, but macular edema with retinal damage, photoreceptor dysfunction, RPE atrophy, and optic nerve damage are the end results. Corticosteroids have been the mainstay of treatment. Oral, sub-Tenon, intraocular, and most recently sustained release fluocinolone acetonide[55] have been used. Corticosteroids can reduce CME,[8,24,56,57] inflammation,[24] and optic disc edema.[56] They have also been reported to decrease symptoms such as nyctalopia and issues with contrast sensitivity.[12] Systemic steroids carry their own risks. Local steroid injections increase the risk of cataract and cause glaucoma with repeated dosing. Implantation of a fluocinolone acetonide sustained-release device has been shown to eliminate the need for systemic therapy; however, it also has a high risk of cataract progression and glaucoma.[55,58]

Immunosuppressive Therapy.

Conventional second-line immunosuppression is used when low-dose steroids are not sufficient at controlling disease and for long-term management of refractory cases.[59] The three classes of immunosuppressives have been used. Cyclosporine has been used as it inhibits T lymphocytes and prevents S-Ag-induced experimental uveitis.[11] Low-dose cyclosporine has proven to have positive visual effect in conjunction with steroids or alone.[60] Nephrotoxicity is the primary side-effect, and hypertension can be a problem.[60] Antimetabolites such as azathioprine, mycophenolate mofetil, and methotrexate have been adjunctive or used in monotherapy. Side-effects of these drugs include bone-marrow suppression and hepatotoxicity.[61] Methotrexate showed improved outcomes in one series compared with no treatment or steroid therapy.[62] The use of the alkylating agents cyclophosphamide and chlorambucil has also been reported. Side-effects such as bone-marrow suppression and development of malignancies must be weighed for this class. Daclizumab, a monoclonal antibody against the alpha-subunit of the IL-2 receptor of T cells, has been found to

have value in treating BCR.[61,63] The long-term efficacy of these agents needs to be determined and weighed against potential side-effects. Other biologics, such as infliximab and adalimumab, have also been used with evidence supporting efficacy.[59] A targeted IL-17 human monoclonal antibody, secukinumab, was not found to be effective in early trials.[59] Intravenous immunoglobulin G (IVIG) and interferons (IFNs) have also been studied.[59]

Anti-vascular endothelial growth factor (VEGF) therapy has been documented to be useful in treating CNV associated with inflammatory chorioretinal disorders.[64] Anti-VEGF may have some use in treatment of CME as well.[65] However, it has not been as effective in controlling the inflammatory component.[59] In following our patients, we recommend ERG yearly, Goldmann visual field examination at least yearly, close monitoring of visual acuity, OCT to evaluate epiretinal membranes and CME, and FA to assess disc and retinal vascular leakage.

Summary

Birdshot chorioretinopathy is a bilateral, chronic progressive disease characterized by deep round lesions in a "birdshot" pattern. Symptoms include blurred vision, photopsias, scotomas, nyctalopia, and poor contrast sensitivity. These can develop years before the onset of fundus findings. The process is associated with a low-grade inflammation of the anterior and posterior segments. Visual prognosis is threatened by the ultimate development of CME, RPE, and photoreceptor atrophy, as well as optic nerve atrophy. Chronic immune suppression is the mainstay of therapy.

Placoid Diseases

Acute posterior multifocal placoid pigment epitheliopathy (APMPPE), serpiginous choroiditis (SC), relentless placoid chorioretinitis (RPC), and persistent placoid maculopathy (PPM) are grouped together due to the "placoid" nature of the lesions. The pathophysiology of these lesions is still poorly understood. They share similarities on fluorescein and indocyanine green angiography; there exists a debate regarding the nature of the hypofluorescence that is seen in these studies. Some argue that

primary choroidal ischemia is the cause of the pathology, while others believe that this is blockage from swollen outer retina or RPE. In actuality, it may be a combination of these as newer OCT studies suggest that the outer retinal layer may be a site of primary insult. Attempts have been made, using new multimodal imaging, to separate these conditions. So far, the individual lesions look extremely similar, including OCT imaging. These conditions do, however, differ in their clinical courses and can almost always be separated from each other. APMPPE shows multiple lesions, usually in both eyes, which heal rapidly without the development of marked retinal or choroidal atrophy. Serpiginous choroidits is usually active in one eye; old scars are frequent. The lesions left untreated can develop more atrophy that the lesions of APMPPE. Relentless chorioretinopathy shows continued development of new lesions (unlike the other entities) for many months. It requires immune suppression to stop this process. Persistent placoid maculopathy shows almost symmetric lesions that persist for months and sometimes longer. Although the pathophysiology of the individual lesions may be similar, these clinical findings allow their separation.

The diagnosis may dictate what therapy is necessary. APMPPE shows marked healing, and although there may be permanent damage, it is often not severe. Many retinologists do not treat it, although some use corticosteroids. Serpiginous usually causes more retinal and choroidal atrophy. Immediate therapy is often indicated, usually corticosteriods. Relentless requires long-term immune suppression. Persistent placoid chorioretinopathy may show a response to immune suppression, but definitely requires treatment of the choroidal neovascularization, which often develops. For all of these entities, treatment of choroidal neovascularization is indicated, and where appropriate immune suppression should be used.

Acute Posterior Multifocal Placoid Pigment Epitheliopathy

Acute posterior multifocal placoid pigment epitheliopathy (APMPPE) was first described in 1968 by Gass.[66] He presented three

healthy young female patients who developed the acute onset of bilateral central vision loss associated with multifocal placoid (plate-like) lesions at the level of the outer retina and the RPE, although he had also considered a primary choroiditis. Discussion regarding the site and etiology of the lesions would continue as the disease was further described in later years.[67–76]

Clinical Course

Clinical Symptoms.

Patients present with the onset of central vision loss that may be described as blurred vision, paracentral scotoma, metamorphopsia, "spots" in the vision, and photopsias.[77] Initial vision at presentation is 20/25 or worse in about 77% of eyes and 20/40 or worse in 58%.[77] Lesions can be unilateral or bilateral (more common 75%).[78] If unilateral, the second eye can become involved in a few days or weeks. Headaches, stiff neck, and malaise may accompany these ocular symptoms. A history of an antecedent viral syndrome or recent vaccination may be obtained.

Epidemiology.

Males and females are equally affected, and generally this occurs in young adults, typically between age 20 and 50 with the mean age of onset being 26.[77,78] Recently, Taich and Johnson describe a syndrome resembling APMPPE in older adults (over age 50).[79] These elderly individuals characteristically may have a worse outcome, with moderate or severe vision loss due to the development of geographic atrophy and CNV. These patients resemble the entity persistent placoid maculopathy (see below), and some may not have APMPPE. Generally, APMPPE is not a recurrent disease, but recurrence can rarely occur. A case of 11 recurrences in the span of 15 years has been described.[80]

Fundus Findings.

Gass reported multiple round and confluent cream-colored, flat lesions with indistinct margins scattered in the posterior pole. Classically lesions have not been noted clinically anterior to the equator. However, with newer imaging modalities anterior lesions

can be seen.[81] The lesions are typically bilateral (Figs. 79.8 and 79.9). Fresh lesions can develop over the next few weeks; therefore lesions of differing ages can be visible. The placoid lesions tend to clear centrally initially leaving hypopigmentation. Later there is mild pigment mottling, which develops into condensation of the pigment. Finally an increasing degree of coarse pigment clumping occurs (Fig. 79.10). These lesions can enlarge. In the original article, there was no description of serous macular detachment associated with APMPPE. However, later reports described localized serous retinal detachments,[71,74,82–86] and OCT imaging frequently reveals fluid. A superficial resemblance to Harada disease has been reported based on this feature.[83,87–90] Modern imaging techniques can easily differentiate these two entities. Recently, a staging scheme based on OCT classification has been proposed by Goldenberg and colleagues that correlates to the clinical findings just described.[91] In their four-stage classification system, lesions are described ranging from a subacute phase to resolution phase. Gass commented on how remarkably the choroid and retina remain relatively intact during the course of the disease. Spaide described choroidal infiltrations in the periphery[92] of a patient with acute APMPPE. In addition, multiple authors have described an association with retinal vasculitis,[93–95] and retinal vein occlusion has also been seen.[93,94] Other findings can include subhyaloid hemorrhage[94] and rare CNV.[96] Case reports have also illustrated optic nerve involvement with disc edema.[93,97]

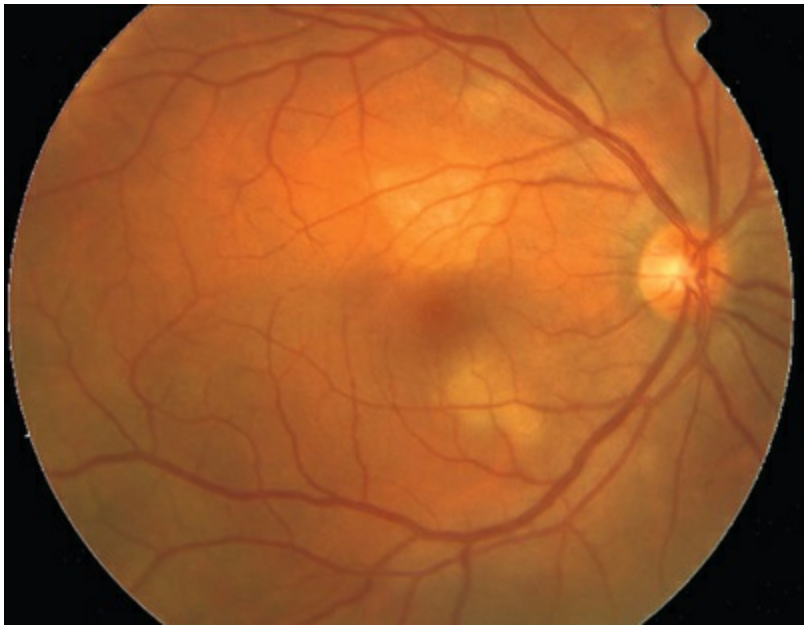

FIG. 79.8 Fundus photo of the right eye showing placoid opacification during the acute phase.

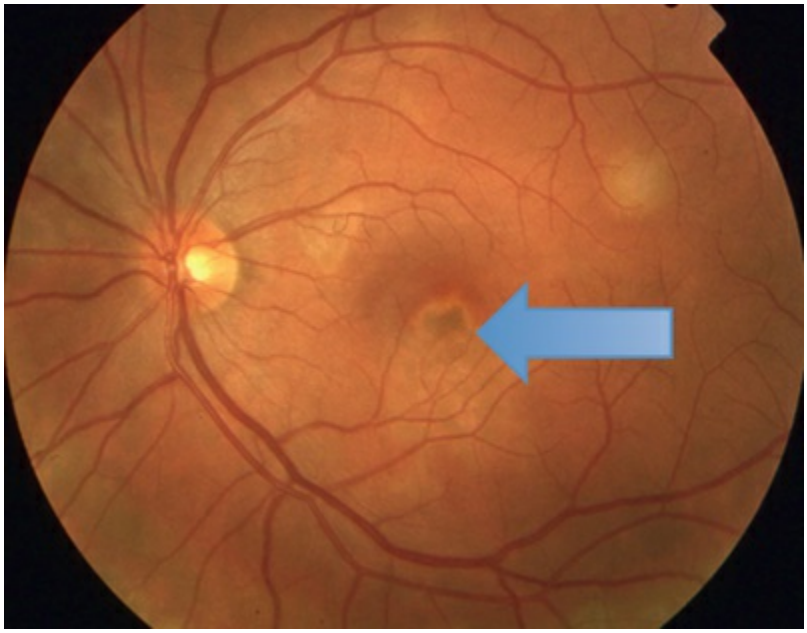

FIG. 79.9 Fundus photo of the left eye. Lesions of differing ages can be seen. Some mild pigment mottling can be seen (*arrow*).

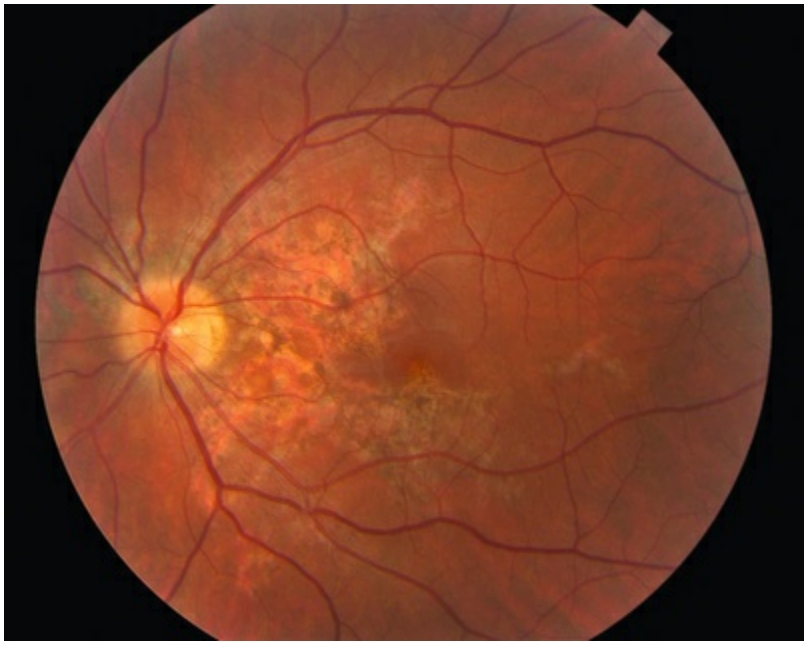

FIG. 79.10 Color fundus photo of healed acute posterior multifocal placoid pigment epitheliopathy.

Other Ocular Findings.

Although vitritis is usually not a prominent component of APMPPE, the degree of ocular inflammation varies widely. An anterior uveitis[98] and granulomatous anterior uveitis[99] have been described. In addition, rare corneal stromal infiltrates[100] have been mentioned.

Clinical Course and Prognosis.

Generally there is improvement of the visual symptoms within 2–4 weeks. APMPPE has a relatively good prognosis when compared with other placoid white spot syndromes. However, Fiore and colleagues[77] reviewed the literature as well as a cohort from their own institution and showed that approximately 50% of patients have an incomplete recovery of central vision and 25% of patients have 20/40 vision or worse. Sixty percent of eyes have residual visual symptoms. Foveal involvement at presentation is an important prognosticator. Eighty-eight percent of eyes without foveal involvement proceed to full central visual recovery in contrast to 53% of eyes that presented with foveal involvement. Unfortunately, approximately 70% of eyes present with foveal involvement. Photoreceptor involvement may ultimately limit

visual prognosis. Progressive improvement of visual acuity usually accompanies the resolution of the lesions. Gass initially reported that visual recovery could continue on for months after the lesions resolved, even up to 6 months.[66] However, most visual recovery occurs within 1 month.[68,70,71,74,77,82]

Imaging

Fluorescein Angiography.

Gass[66] described the lesions in the early phase as nonfluorescent (Fig. 79.11) and that the choroidal fluorescence is obstructed. Later in the angiogram there is a progressive, irregular staining of the lesions (Fig. 79.12). Ryan and Maumenee postulated that this could represent localization to the RPE or choriocapillaris rather than implying an infiltrate of the outer choroid.[67] Gass also stated that the underlying choroidal circulation appeared intact below the healing lesions.[66] However, later ICGA studies suggested that choroidal hypoperfusion did exist.[101,102] This is discussed below. As the process becomes inactive, hyperfluorescence corresponding to window defects in the mottled RPE develops and staining is no longer evident (Fig. 79.13). There may be visibility of the large choroidal vessels in areas of confluent atrophy. However, this does not exist in all areas, implying some RPE remains intact.[72] Either loss of the choriocapillaris or abnormal circulation in the confluent atrophied areas is suggested. In addition to these FA findings, there is also blocked fluorescence from pigment clumping.

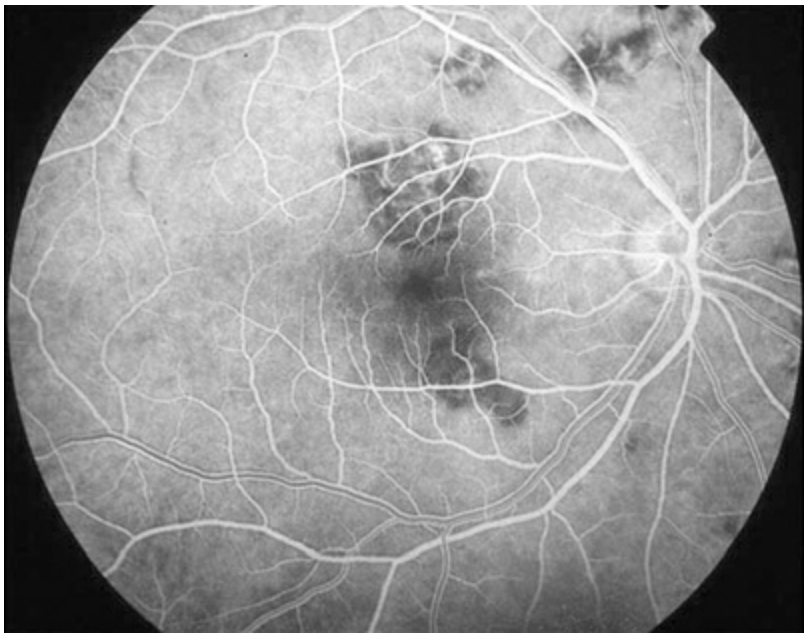

FIG. 79.11 Acute lesion: Fluorescein angiography (FA) shows early hypofluorescence of placoid areas.

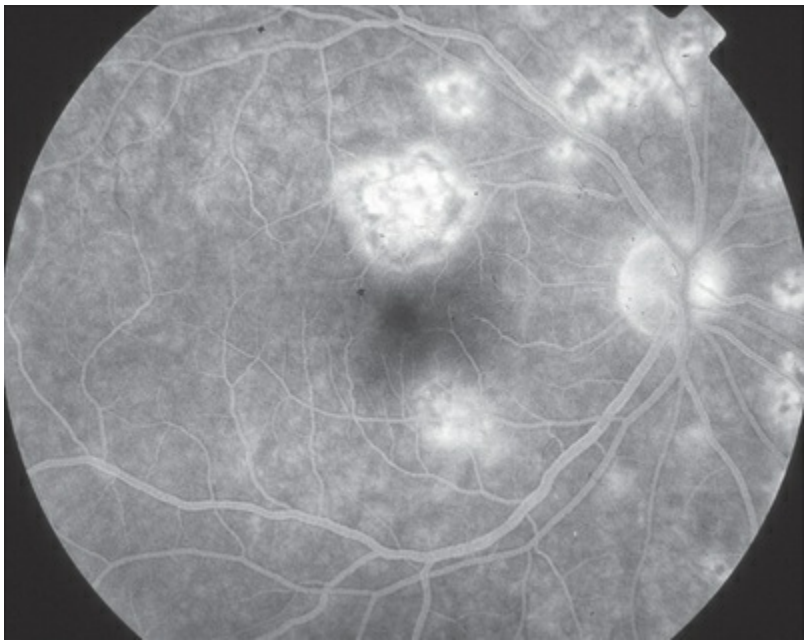

FIG. 79.12 Acute lesion: Fluorescein angiography (FA) in the late phases shows hyperfluorescence.

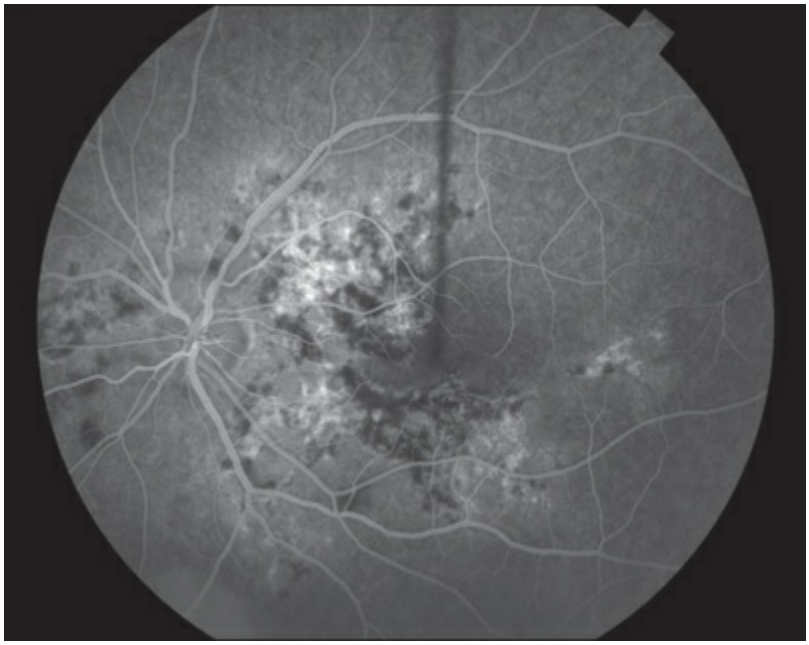

FIG. 79.13 Healed lesion: early fluorescein angiography (FA). As the process becomes inactive, window defects develop. Pigment clumping is seen and blocks fluorescence as well.

The retinal vessels and optic nerve usually are normal;[66,72] however, some reports have described an association with retinal vasculitis, retinal vein occlusions, and disc edema.

Indocyanine Green Angiography.

Since ICGA studies focus on the choroidal circulation, its findings in APMPPE have been important in developing theories of pathogenesis.[102–107] Acute lesions show early hypofluorescence (Fig. 79.14). In the late phases, these lesions become more defined in shape. These areas are more numerous than the placoid lesions seen clinically. As the disease heals, the hypofluorescence in the late phase becomes less defined and smaller. This lends some support to the theory of choroidal ischemia as an underlying factor in the pathogenesis of APMPPE. It is postulated that there is more hypofluorescence in the acute phase due to the additional presence of swollen outer retina or RPE cells in response to choroidal ischemia (clinically presenting as placoid lesions). As these disappear, there is less blockage and thus less hypofluorescence. Photoreceptor damage may also play a role in this as well, as elucidated by OCT studies and discussed below. Studies show that

the hypofluorescence in the late phases can also completely resolve,[101] suggesting that choroidal vasculopathy, if present, may be a transient process.

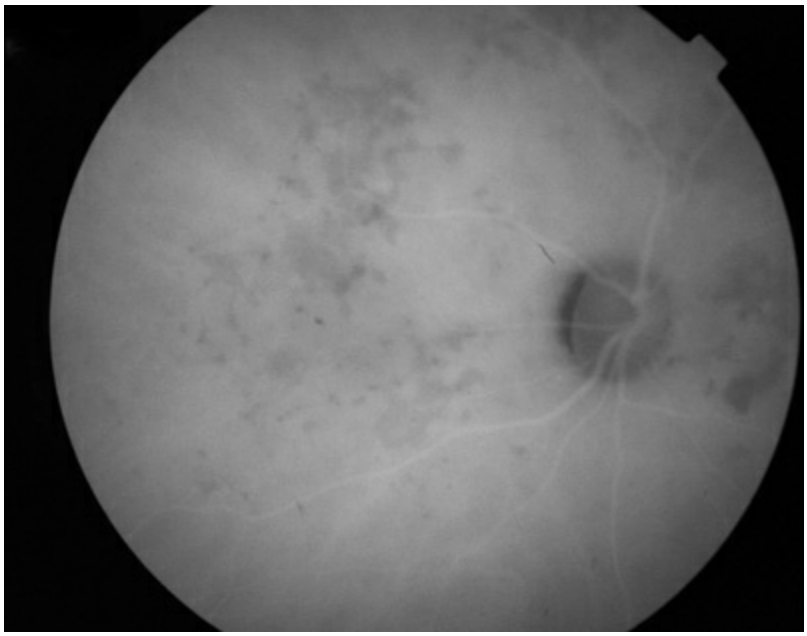

FIG. 79.14 Acute lesion: Indocyanine green angiography (ICGA) shows hypofluorescent areas.

Optical Coherence Tomography.

Many studies have described the OCT findings in APMPPE.[88,108–113] Garg and Jampol reported outer retinal abnormalities in APMPPE using time domain technology. A serous retinal detachment had reflective material within the subretinal fluid (SFR). It was postulated that this was either proteinaceous material or edematous RPE. There was rapid resolution of the serous detachment and the material disappeared.[85]

Lofoco and colleagues showed that in the acute phases the time domain OCT revealed a mild hyperreflective area above the RPE in the photoreceptor layer corresponding to the placoid lesions. Later the OCT scan revealed a nodular hyperreflective lesion in the plane of the RPE with mild underlying backscattering. They theorized that the hyperreflective areas may indicate inflammatory tissue and inflammatory cells or the presence of ischemic edema in the outer retinal layers.[113] As ultra-high resolution (UHR)-OCT developed,

Scheufele and colleagues showed disruption of the outer retina early in the disease (Fig. 79.15). RPE disruption occurs as the lesions heal.[114] Backscatter of lesions was observed in the acute inflammatory phase in UHR as well. They found photoreceptor atrophy as the lesions began to heal and persistence of it post resolution. They suggested that the backscattering of acute lesions in the outer retina represents inflamed or damaged photoreceptor cell bodies. In addition to illustrating photoreceptor and RPE degeneration, spectral domain OCT has also shown that in some patients with fluid associated with the placoid lesions, that there may actually be accumulation of intraretinal fluid (IRF) rather than an exudative retinal detachment.[85,108]

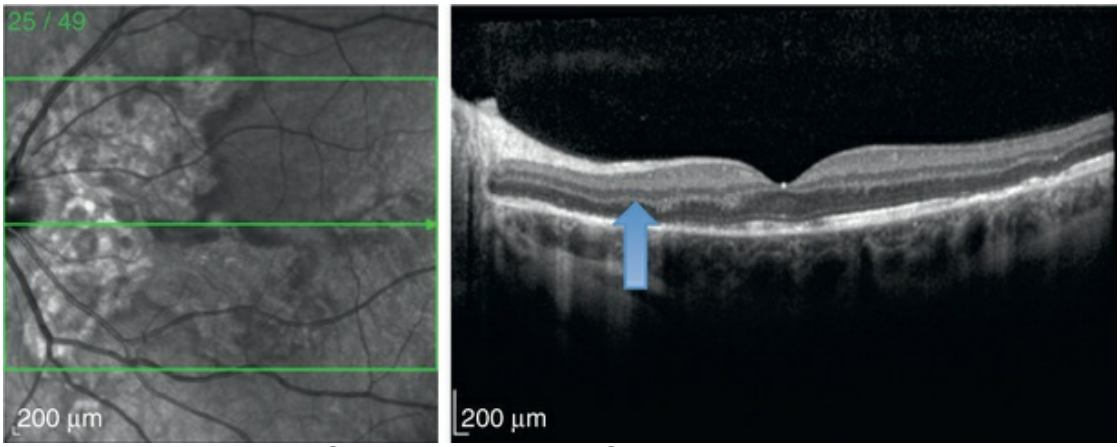

FIG. 79.15 Subacute lesion: Optical coherence tomography (OCT) showing disruption of the outer retina.

Fundus Autofluorescence.

FAF imaging is directed at the retinal pigment epithelial layer and is therefore especially useful in APMPPE. Several studies have described FAF findings[88,110,112,115,116] (Fig. 79.16).

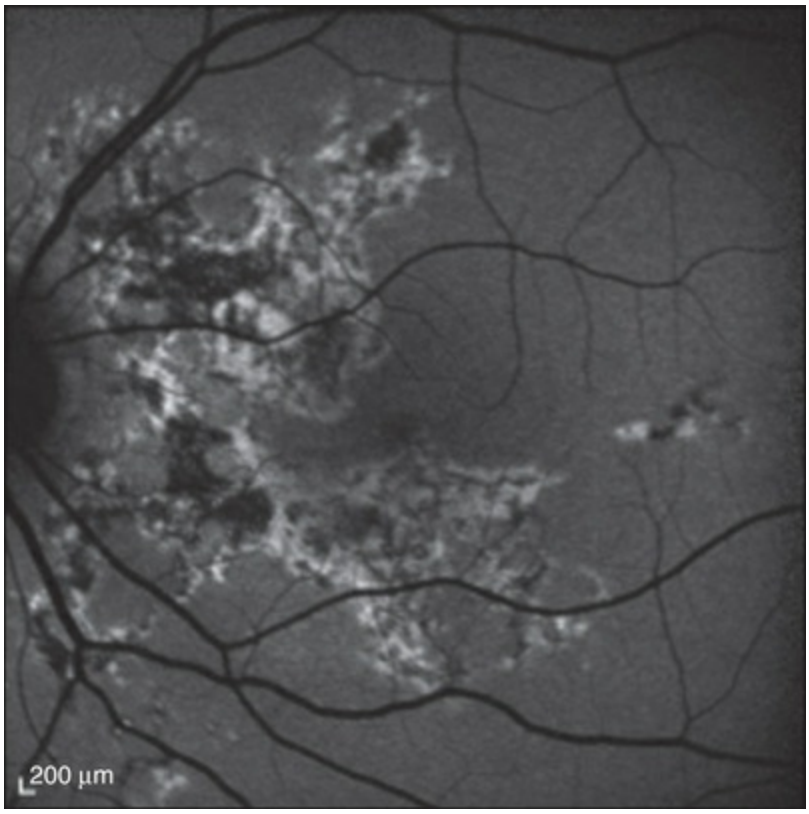

FIG. 79.16 Subacute lesion: Fundus autofluorescence (FAF) shows areas of hyper- and hypoautofluorescence corresponding to clinical changes in pigmentation.

Spaide compared angiographic findings with autofluorescence. He noted that the early hypofluorescence seen on angiogram did not match up precisely with observable changes of the RPE, and he suggested this means there are choriocapillaris perfusion defects. In the late phase of the angiogram, there was staining of some of the lesions. These late-staining lesions matched the size and shape of lesions seen in fundus autofluorescence. As the lesions resolved clinically, they became pigmented centrally with a depigmented halo. On autofluorescence, centrally there was intense hyperautofluorescence, and the depigmented halo was hypoautofluorescent, implying atrophy. He postulated there was a centripetal contraction of the placoid lesions that produced this appearance. He noted the autofluorescence changes lagged behind the clinical appearance. In addition, he found that choroidal abnormalities seemed more numerous on fluorescein and indocyanine green angiography. He concluded the RPE abnormalities were a result of the choroidal abnormalities.[116]

Adaptive Optics.

As an emerging technology, limited description of adaptive optics scanning laser ophthalmoscopy (AO-SLO) is provided in the literature. This imaging modality is currently best at analyzing the cone mosaic. The descriptions of APMPPE show dark annulus corresponding to loss of the imaging of the cone cells in a case of acute APMPPE.[117] They also describe hyperreflective flecks, which correspond to dome-shaped elevations on OCT. Further study is warranted to see the course of these cells as disease progresses.

Electrophysiology

Although these functional studies are not essential in the diagnosis of APMPPE, they do emphasize the role of RPE involvement as described by Fishman and colleagues. The electroretinogram is normal to minimally subnormal. However, abnormal light : dark ratios have been documented on EOG, suggesting a diffuse RPE problem. Furthermore, the ERG and EOG abnormalities can normalize, suggesting that this can be a transient RPE problem.[72] However, despite this good recovery, visual field abnormalities can persist in some cases.[95]

Systemic Associations

APMPPE has been linked to CNS manifestations[118–120] including cerebral vasculitis,[95,121–127] meningo-encephalitis,[128] and stroke.[95,129–133] Cases of APMPPE associated with sixth cranial nerve palsy[134] and transient hearing loss[135] have also been cited. Headaches are a common symptom, and APMPPE has mimicked migraine with aura.[95,136] Although many patients give a history of viral illness, the symptoms of malaise and headaches may thus be more related to a widespread underlying vasculitis. Cerebrospinal fluid analysis has shown pleocytosis,[137] which lends credence to this. The CNS associations are not benign and death, though uncommon, is possible. This has been described in association with a rapid taper of prednisone in one case.[138] There should be a low threshold for neurologic or rheumatologic consultation. MRI and CSF examination are important in these patients.[95] Steroids should be considered for CNS involvement.

Systemic vasculitis[139] has been implicated in APMPPE-like patients and has been described in a P-ANCA-positive patient.[140,141] Other associations with erythema nodosum,[68,76] ulcerative colitis,[142] thyroiditis,[143] nephritis,[144,145] and juvenile rheumatoid arthritis[146] lead to an underlying immune-mediated or inflammatory link. Other associations include granulomatous diseases such as granulomatosis with polyangiitis,[147] pulmonary TB,[148] and sarcoidosis.[121,149]

Pathogenesis

When Gass first described APMPPE, he believed that the abnormalities were primarily at the level of the RPE. He believed that there was blockage of fluorescence due to damaged RPE cells, and these cells stained in the late phases. He stated that the retinal and choroidal circulations looked remarkably intact.[66] Van Buskirk and coworkers first described an alternate theory that choroidal perfusion was the primary problem and that the hypofluorescence seen with angiography was due to lack of perfusion of the choriocapillaris.[76] ICGA studies found that the choroid did appear hypoperfused as described above. However, Fishman and colleagues' study of ERG and EOG revealed that the ERG and thus the retina remained relatively intact compared to the EOG. Therefore, a diffuse RPE process was implicated in the acute phase of the disease. It also confirmed the transitory nature of this process as the EOG could normalize.[72] The fact that the ERG was generally normal did not favor a primary widespread choriocapillaris defect.

Currently, some believe that there is a vascular insult affecting the choroid that may cause partial choroidal ischemia leading to RPE changes and ultimately affect photoreceptors. In addition, the systemic associations of this disease suggest an underlying vasculitis. It is possible that a primary process involving the outer retina and RPE could secondarily cause choroidal abnormalities on angiography. There may be a trigger, either inflammatory or infectious in nature, that incites this process. Furthermore, an association with HLA-B7 and HLA-DR2[150] has been described, and this suggests there are certain individuals who are more susceptible to this process.

Although exact etiology is unknown, there have been

associations with viral illness;[151] specifically, mumps,[152] adenovirus,[153,154] and coxsackievirus B[155] have been mentioned. In half of the cases presented by Ryan and Maumenee, there was an overt viral illness prodrome.[67] In addition to viral infections, an association with bacterial infections has also been described. Two case reports implicate Lyme disease.[156,157] Another case report described APMPPE post acute bacterial infection with group A streptococcus.[158] APMPPE has also been found post various vaccinations such as influenza,[159] varicella,[160] meningococcal C conjugate,[161] and hepatitis B.[162] Molecular mimicry has been implicated in these cases of post-vaccination APMPPE.[159] Sequence similarities between the introduced antigens and the eye could incite an immune reaction.

A delayed-type hypersensitivity (DTH) reaction may bring all these associations together.[105] In this process, there is an activation of sensitized T lymphocytes by various stimuli such as bacteria, viruses, and fungi. Previously primed T cells release lymphokines that then activate macrophages and cytotoxic T cells. Macrophages then give rise to epithelioid cells and giant cells that can lead to granulomas. The systemic associations such as CNS inflammation as mentioned above could be explained in this manner. The fluorescein and ICGA findings could also be explained by a choroidal DTH reaction causing choroidal vascular occlusion.

A thrombotic process of the choroid has also been postulated. Elevated anticardiolipin antibodies were found in a patient with acute APMPPE. These levels were normal a year after resolution of the disease.[163] The association with retinal vein occlusion supports a prothrombotic state. Furthermore, elevated anticardiolipin antibodies have been associated with a number of viral infections and in many cases also associated with thrombosis.[164]

Differential Diagnosis

The diagnosis of APMPPE is made clinically based on examination, time course, and imaging characteristics. Other white spot placoid diseases are in the differential diagnosis and should be considered. These include serpiginous choroidopathy (which should be considered in recurrent, chronic cases), relentless placoid chorioretinitis, which should be thought of in severe, persistent,

and recurrent cases, and persistent placoid maculopathy. Other considerations include diffuse unilateral subacute neuroretinitis, Harada disease,[83,87–89] TB, sarcoid, fungal disease, choroidal metastasis, or lymphomatous infiltrate,[67] and especially syphilis.[165]

Management/Treatment

Laboratory investigations are usually not necessary. Certain investigations may be useful in severe or questionable cases. Spinal fluid analysis for pleocytosis[139] and anticardiolipin antibodies[163] are among them.

No therapy in the management of acute APMPPE has been proven with certainty. A review of the data from the literature on corticosteroids does not provide clear direction.[77] However, some support the use of steroids when there is central nervous system involvement.[166] Recently, the use of tumor necrosis factor (TNF) blockers has been reported in patients with severe APMPPE.[167]

Rarely CNV can develop. Bruch's membrane appears less affected in APMPPE compared to serpiginous choroiditis, and therefore CNV is less prevalent. Anti-VEGF agents have been found to be useful in treating the CNV.[168,169] Photodynamic therapy has been used as well; however, its use is cautioned as it can exacerbate inflammation and possible choroidal ischemia, which are present in the acute stages of APMPPE.[96]

Summary

APMPPE is a bilateral inflammatory process involving the RPE, the choriocapillaris, and outer retina. There is an equal incidence in males and females. A viral prodrome is often associated with this entity. Headaches are a common symptom, and neurologic symptoms need to be addressed. There are characteristic findings on fluorescein angiography, including early hypofluorescence with late staining in the acute phase. This process becomes inactive over the period of weeks without intervention, and in comparison to other WSS it has a relatively good prognosis. The pathogenesis is controversial, and the outer retina may be the primary site of damage, but choroidal hypoperfusion leading to RPE and photoreceptor damage may play a role.

Idiopathic Serpiginous Choroiditis

Serpiginous choroiditis (SC), also previously known as helicoid peripapillary chorioretinal degeneration,[170] geographic helicoid peripapillary choroidopathy,[171] and geographical choroidopathy,[172] is a rare disease of unknown etiology. It is usually eventually bilateral, chronic, and progressive. The lesions involve the outer retina, RPE, choriocapillaris, and large choroidal vessels.[173] Patients present with acute geographic or serpentine lesions that are gray or gray–yellow (due to disruption of the RPE and outer retina).

Clinical Course

Clinical Symptoms.

Patients are often asymptomatic until a lesion affects the fovea. Blurred vision occurs at this point.[174,175] Although this is a bilateral disease, typically the patient becomes symptomatic unilaterally with foveal involvement. Small central or paracentral scotomas may be present. These are absolute in their acute stages and become relative with healing.[175]

Epidemiology.

Idiopathic SC is often a disease of healthy individuals. The onset is usually between the ages of 30 and 70. However, cases of SC have been reported in younger individuals.[175] Most reports of SC involve Caucasians; however, SC has also been reported in Asians,[176] African Americans,[175] and Hispanics.[177] The literature reflects a slight predilection for males.[173] No family history is elicited. One study done in a Finnish population showed a higher prevalence of HLA-B7 in patients with SC.[178]

Fundus Findings.

Two variants of idiopathic SC are seen. The classic appearance[173] starts with one or several geographic patches of gray or creamy yellow placoid lesions in the peripapillary region. It generally progresses with recurrences in a centrifugal manner with finger-like or serpentine projections. In one report, a centripetal direction was described.[174] Acutely, the outer retina appears edematous, and

serous retinal detachments may be seen.[179,180] As these active lesions resolve (with or without) treatment over the next several weeks, extensive RPE and choriocapillaris atrophy occurs (Fig. 79.17). SC has recurrences, and therefore it is common to see old and active lesions at the same time. Recurrences can occur at the edge of old scars (Fig. 79.18), but not always. As the disease becomes chronic, chorioretinal atrophy, subretinal fibrosis, and RPE clumping is seen.[173] Since most patients become symptomatic only when the fovea becomes involved, about two-thirds present with bilateral chorioretinal scarring.[181]

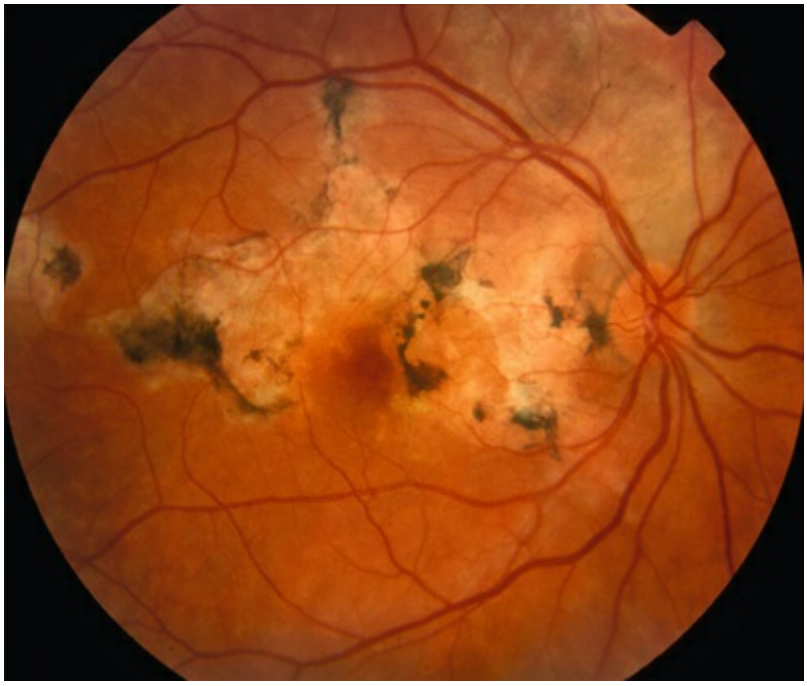

FIG. 79.17 Fundus photo of serpiginous choroiditis showing the geographic projections in the inactive phase. (Courtesy Alice T. Lyon, MD.)

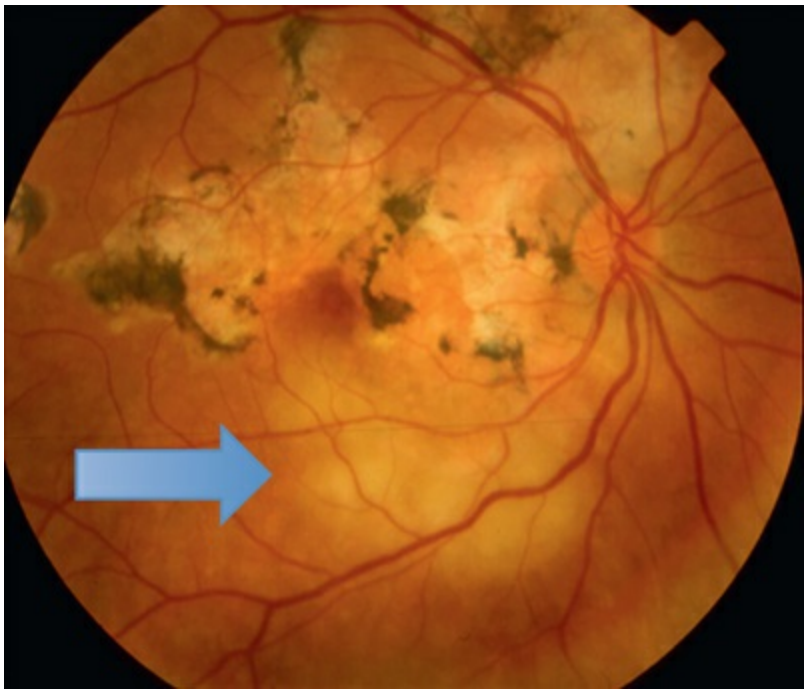

FIG. 79.18 Fundus photo showing acute recurrence of serpiginous choroiditis near the edge of a scar.

Macular serpiginous choroiditis[176,177] is the second variant (Figs. 79.19–79.22). There is no difference in the lesions of macular serpiginous and peripapillary diseases except for location.[178] There is generally a poorer prognosis for the macular variant as the fovea is affected at the start. Vision loss may also be related to subsequent development of CNV.[177] However, Sahu and coworkers, in a more recent report, did not observe CNV in their series.[182] Macular SC may be misdiagnosed as macular degeneration, macular dystrophies, or toxoplasmosis.[173]

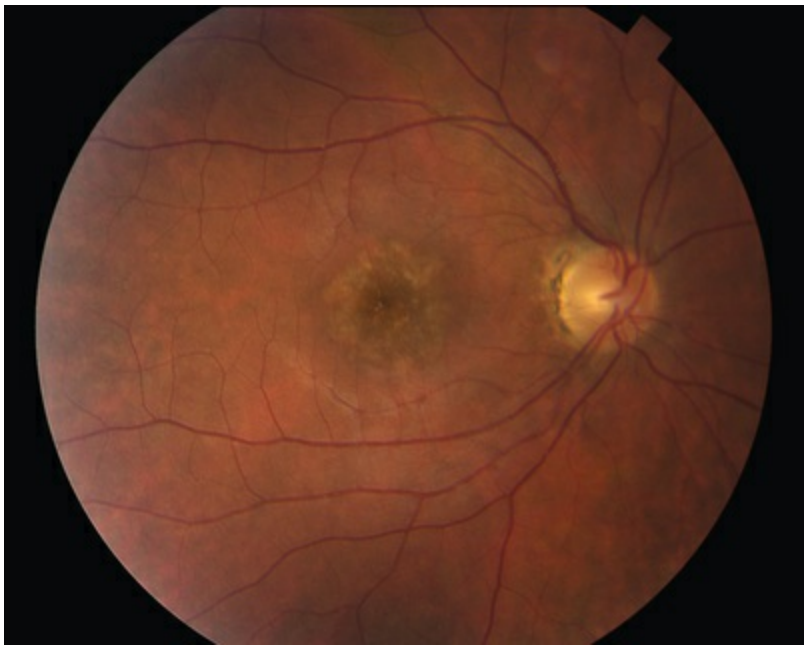

FIG. 79.19 Fundus photo of subacute macular serpiginous choroiditis.

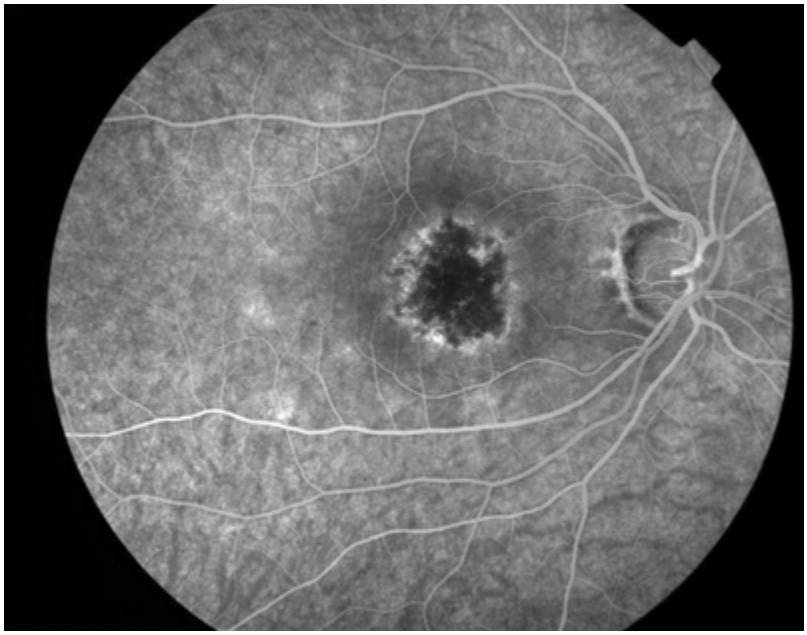

FIG. 79.20 Subacute lesion: early fluorescein angiography (FA) shows hypofluorescence.

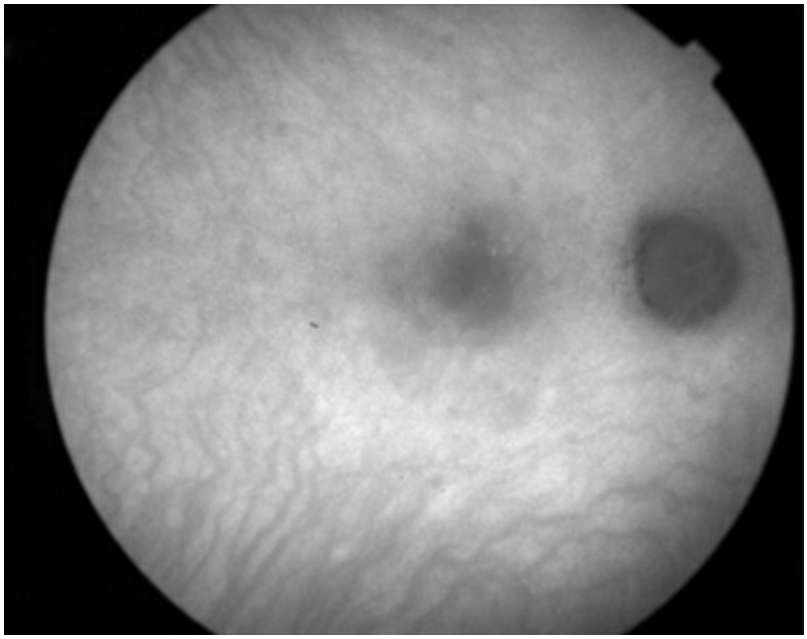

FIG. 79.21 Subacute lesion: Indocyanine green angiography (ICGA) showing hypofluorescence centered in the macula.

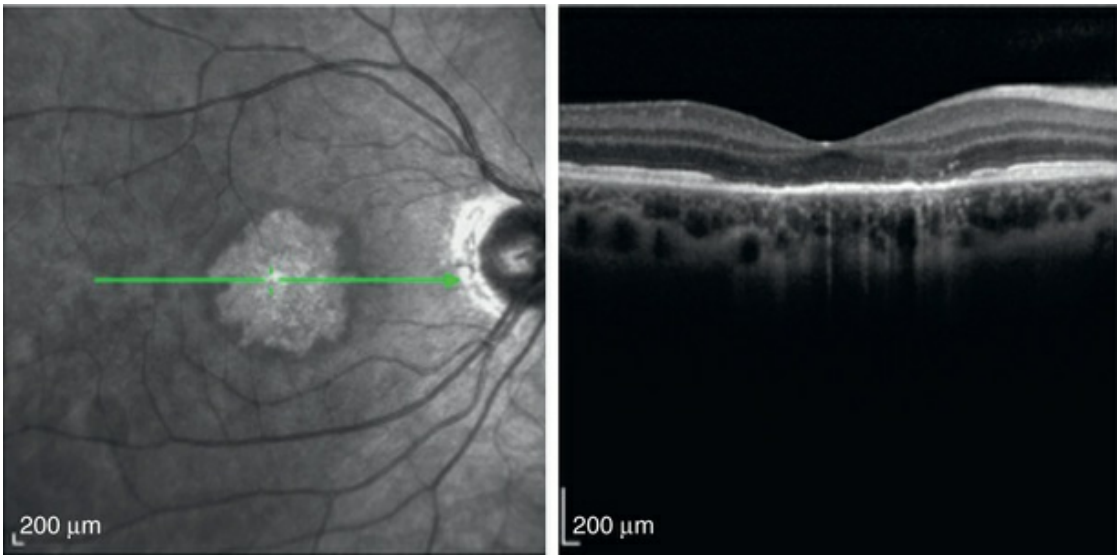

FIG. 79.22 Healed lesion: Optical coherence tomography (OCT) in macular serpiginous choroiditis shows outer retinal disruption.

Other Ocular Findings.

Although idiopathic serpiginous choroiditis is not usually associated with a marked inflammatory response,

nongranulomatous anterior uveitis[183,184] has been seen. More commonly – estimated in about a third of patients – there are fine vitreous cells.[180] The eye is white. Additional retinal findings have been described. These include CNV, which affects 13–20% of eyes,[185–190] vein occlusions,[191,192] retinal vasculitis[192] (usually a periphlebitis), CME,[193] and bilateral full-thickness macular holes.[194] Optic nerve abnormalities such as optic disc edema[174] and disc neovascularization[189] can be seen at the active stage of serpiginous choroiditis.

Clinical Course and Prognosis.

Serpiginous choroiditis is characterized by multiple recurrences at intervals of months to years. Healing of individual lesions takes place in 2[178] to 8 weeks,[173] but new lesions appear later.[174] Generally acute lesions are seen in one eye at a time.

Visual loss is correlated with proximity to the fovea. There can be some incomplete recovery, but due to the recurrences, 75% of untreated patients develop central visual loss in one or both eyes. Final visual acuity is less than 20/200 in up to 25%.[195]

Imaging

Fluorescein Angiography.

In the acute SC, the lesions show hypofluorescence during the early phase of the study[171] (Fig. 79.23). This is may be due to a of blockage by swollen outer retina and RPE and/or nonperfusion of the choriocapillaris. The borders of the lesion may be hyperfluorescent, representing intact choriocapillaris. As the study progresses, the previous hypofluorescent lesions become variably hyperfluorescent, and this intensifies over time, representing staining of the acute lesions (Fig. 79.24). Retinal vascular staining may be seen near active lesions. Pigmentary changes then develop, and there is gradual appearance of atrophy. Angiography at this stage shows mottled hyperfluorescence with increased fluorescence in the late phases representing leakage of dye from the damaged choriocapillaris at the periphery of the lesion. CNV can occur and appears as late leakage, usually at the edge of a scar.

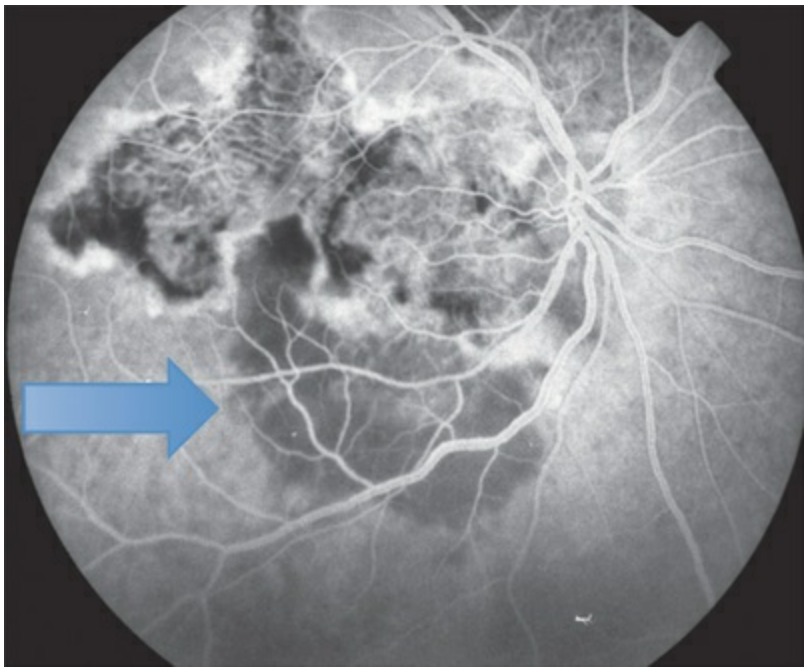

FIG. 79.23 Fluorescein angiography (FA) shows hypofluorescence corresponding to the new lesion (*arrow*). (Courtesy Alice T. Lyon, MD.)

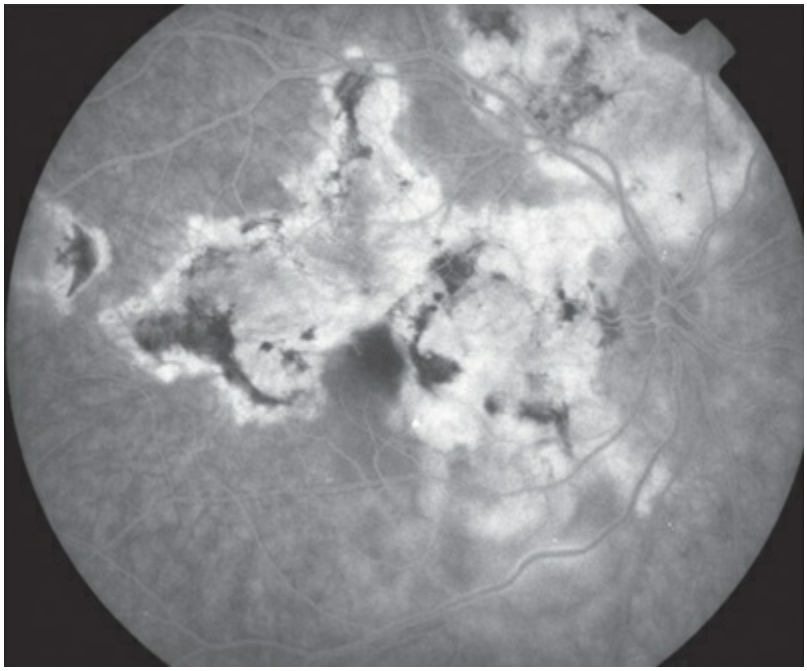

FIG. 79.24 Fluorescein angiography (FA) in the late phases shows that previously hypofluorescent lesions become variably hyperfluorescent.

Indocyanine Green Angiography.

ICGA[196–199] is useful in evaluating SC. Giovannini and colleagues describe how ICGA allows a greater understanding of the disease. In particular, ICGA allowed (1) better staging of SC, revealing choroidal alterations when there was no clinical or FA evidence; (2) better identification of the active lesions, which appear to be larger at the choroidal level in comparison with the corresponding retinal lesions; and (3) persistence of choroidal activity even when the signs of retinal activity had disappeared.[198] The ICGA pattern is characterized by hypofluorescent areas persisting from early to late phases (Fig. 79.25). The hypofluorescence has been reported to be less pronounced in later phases, which may represent delayed perfusion rather than nonperfusion.[200] The hypofluorescent lesions appear more extensive on ICGA in comparison to clinical examination and fluorescein angiography.

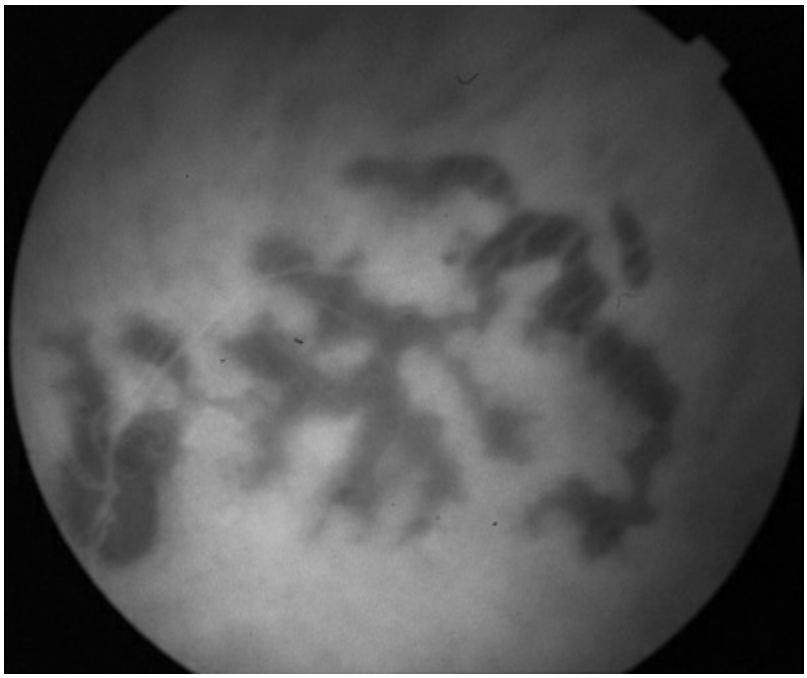

FIG. 79.25 Indocyanine green angiography (ICGA) of this patient with serpiginous choroiditis is characterized by persistent hypofluorescence. (Courtesy Manjot K. Gill, MD.)

Optical Coherence Tomography.

OCT findings have been described.[201–205] Chronic changes seen with

spectral domain OCT illustrates development of retinal atrophy with disruption of the photoreceptor layers in affected areas. There is thinning of the RPE, and IRF including cystic changes can be seen.[201] There is increased reflectance of the choroid and the deeper retinal layers. Opacification of the outer nuclear layer and Henle's layer is seen. Disruption of the photoreceptor inner/outer segments can be seen in active and inactive lesions[202] (Fig. 79.26). It is noted that in acute lesions, the outer retina and choroid are involved with relative sparing of the inner retina. In late cases, due to RPE migration, the inner retina can also show changes.[206] OCT is useful for looking for cystoid macular edema, epiretinal membranes, and choroidal neovascularization, which occur with serpiginous choroiditis.[206]

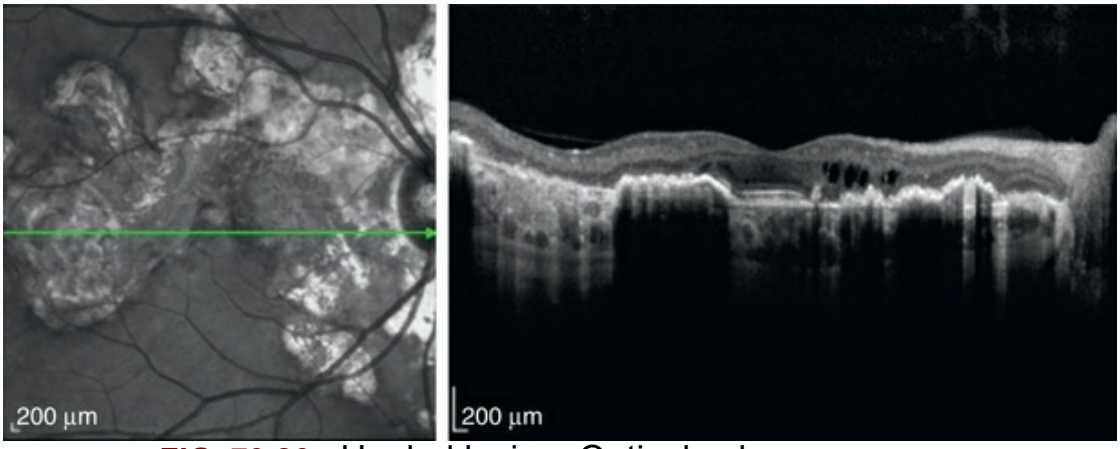

FIG. 79.26 Healed lesion: Optical coherence tomography (OCT) shows retinal atrophy and disruption of the photoreceptor layers. Cystic fluid is seen here as well. The fovea is spared.

Fundus Autofluorescence.

As idiopathic SC affects the RPE, FAF[202,205,207] images are helpful in demarcating this disease. New lesions appear hyperautofluorescent, and old lesions are hypoautofluorescent (Fig. 79.27). Recurrences are characterized by hyperautofluorescent lesions at the borders of old hypoautofluorescent areas.[207] Hyperautofluorescence was detected 2–5 days after the appearance of acute lesions.[205] Piccolino and colleagues compared FAF to ICGA

and OCT and found that the acute hyperautofluorescent areas were less extensive than the apparent perfusion defect delineated by ICGA.[205] When compared to OCT, there was increased reflectance of the photoreceptor layer corresponding to the area of hyperautofluorescence. As the disease progressed, the hyperautofluorescent area became hypoautofluorescent and the photoreceptor changes persisted. This has been confirmed by later studies as well.[208,209] The lesions appear to be homogenous.[207]

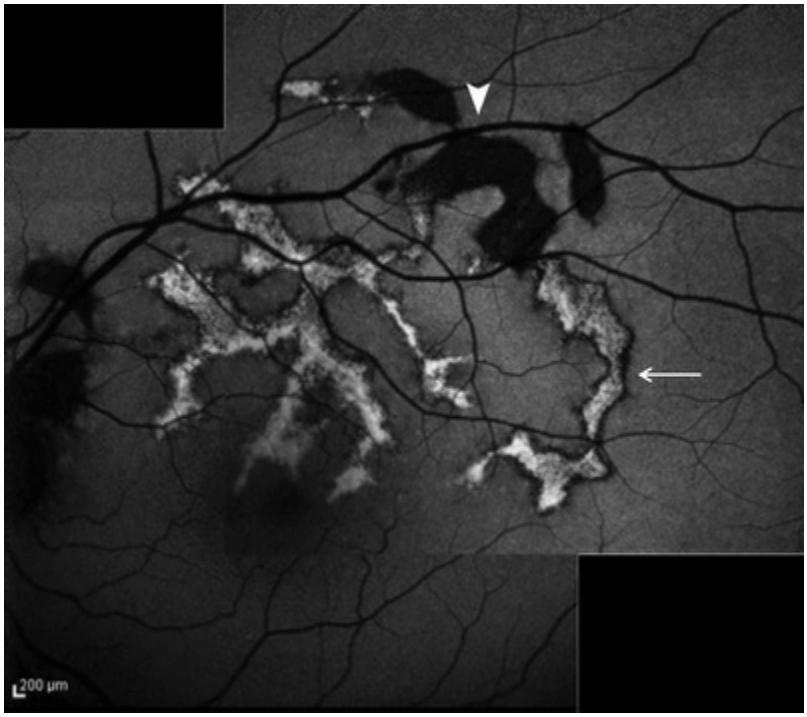

FIG. 79.27 Fundus autofluorescence (FAF) image shows hypoautofluorescent lesions corresponding to old lesions, the subacute lesions are more hyperautofluorescent. (Courtesy Manjot K. Gill, MD.)

Electrophysiology

Results of ERG are normal,[175,180] and EOG is abnormal only when there is extensive disease.[180]

Perimetry.

Goldmann visual field examination shows that scotomas corresponding to an area of activity may not be permanent.[175]

Scotomas corresponding to fundus lesions are present but are not absolute and usually are denser centrally and less peripherally. More recently, microperimetry[210] studies confirm this finding. Microperimetry may be able to detect subclinical lesions.[206]

Systemic Associations

Reports have described SC in patients with various systemic diseases: Crohn's disease,[211] systemic lupus erythematosus (SLE),[212] celiac disease,[213] and extrapyramidal dystonia.[214] These are likely coincidental associations. Systemic vasculitides can cause choroidal ischemic syndromes, which may resemble SC.

Pathogenesis

The pathogenesis of serpiginous choroiditis remains unknown. Postulated etiologies have included autoimmune, infectious, vascular, and degenerative.[173]

The inflammatory nature of the disease is supported by histopathology with inflammatory lymphocytic infiltrate in the choroid (more prominent at the margin of the lesion).[188,215] Clinically, the presence of anterior uveitis, vitritis, and retinal vasculitis also points to an inflammatory etiology. The report of an association with HLA-B7 suggests some individuals are more susceptible to this process.[178] Broekhuyse found a sensitization to S-antigen in SC patients.[216] Acute SC lesions respond to corticosteroids and immune modulating agents consistent with an immune-mediated process.

A microbial origin of SC has been suggested, but the evidence is not convincing. Herpesvirus has been found in aqueous humor,[217] and VZV and HSV DNA were detected in the aqueous of a subset of patients with serpiginous choroiditis, suggesting that these viruses may be involved. Conversely, Akpek and Chan described the lack of herpesvirus DNA in choroidal tissues at autopsy of a patient with SC.[215] No viral DNA was amplified, including HSV, CMV, EBV, VZV, or HHV-8. Furthermore, there are reports of recurrences while on antiviral therapy.[195] Pisa and colleagues studied five patients with SC to assess the presence of fungal infection by the presence of antibodies in human serum samples.[218] Antibodies against *Candida* were apparent in four of the patients.

Vasculopathy, either primary or secondary, has also been proposed.[173,200,219] The clinical presence of phlebitis and branch retinal vein occlusions supports this etiology. King and colleagues noted elevated factor VIII in association with SC.[220] This could lead to an occlusive vascular phenomenon due to vascular endothelial injury as seen in diseases such as scleroderma, Raynaud disease, polymyalgia rheumatica, and temporal arteritis. Fluorescein and ICGA also suggest vascular involvement. Hayreh's early work showed that closure of the cilioretinal vessels could produce lesions that look something like SC.[221] The lack of systemic vascular disease in SC does not support vasculopathy.

Finally, a degenerative etiology has been proposed. The nature of SC's chronic and progressive nature and later onset in life lends some support to this.[173] One case showed an association with unilateral extrapyramidal dystonia,[214] which could be supportive or coincidental. The presence of inflammation and lack of familial inheritance, the sporadic nature of SC, and occasional recovery of vision are not supportive of a degenerative condition.

Differential Diagnosis

APMPPE must be considered. Patients with APMPPE are usually younger. The acute lesions are bilateral and scattered throughout the posterior pole. Recurrences are very rare. CNV is a rare complication in APMPPE compared to serpiginous choroiditis. Visual prognosis is better with APMPPE. Persistent placoid maculopathy and relentless placoid chorioretinitis should also be considered and will be discussed later in this chapter. Other white spot syndromes such as birdshot choroidopathy and multifocal choroiditis and panuveitis syndrome as well as presumed ocular histoplasmosis may also be considerations.

Other diagnostic considerations include tuberculous serpiginous choroiditis (discussed further below and Chapter 85, Mycobacterial infections), sarcoidosis,[222] systemic non-Hodgkin lymphoma,[223] antiphospholipid antibody syndrome,[224] toxoplasmosis,[225] syphilis, and posterior scleritis.[226]

With macular SC, one must think about choroidal ischemia in the differential diagnosis.[177] This can occur with systemic vascular diseases such as systemic lupus erythematosus, toxemia of

pregnancy, disseminated intravascular coagulation, thrombotic thrombocytopenic purpura, and malignant hypertension as an etiology for macular vision loss.

Management/Treatment

Although the diagnosis is suspected by clinical history, examination, and imaging characteristics, a preliminary workup could include TB skin test, chest radiograph, quantiferon gold test if TB is suggested,[227] ACE, VDRL, fluorescent treponemal antibody absorption test, toxoplasma titers, and a viral screen. Abrez and colleagues suggest an aqueous tap if anterior chamber cells are noted with an evaluation by PCR for viral etiology.[184] Indications for doing a more extensive workup include the presence of multifocal lesions, lesions primarily involving the macula and sparing the peripapillary area and cells in the anterior chamber, as well as vitritis.[206]As serpiginous choroiditis is a rare disease, controlled trials comparing treatments are not available. Much of what we know comes from small case series.[228] Due to the relapsing and progressive nature of SC, treatments would ideally address both the acute inflammatory episode and preventing recurrences.

Corticosteroids have been a mainstay of acute treatment and multiple routes of administration have been described: oral prednisone,[179] sub-Tenon triamcinolone, intravenous pulse methylprednisolone therapy,[229] intravitreal triamcinolone acetonide,[230–233] and intravitreous fluocinolone acetonide implant.[234] Systemic prednisone therapy of 60–80 mg/day is a commonly prescribed therapeutic regimen. However, acute lesions in the fovea or threatening the fovea may benefit from immediate intravitreal corticosteroids. Aggressive corticosteroid therapy is useful in treating acute attacks, but since the corticosteroids are tapered, is not useful in preventing recurrences. Relapses are common after tapering the medication. A case report described using an intravitreous fluocinolone acetonide implant that resulted in ongoing control of the disease for 14 months postoperative follow-up.[234] This delivery route avoids the side-effects of systemic corticosteroids. However, cataract and glaucoma from this route of administration are often seen.

Corticosteroids can be used alone or in combination with other

immunosuppressive therapy.[235,236] T-cell inhibitor (cyclosporine),[237,238] antimetabolites (azathioprine),[239] and alkylating agents (cyclophosphamide and chlorambucil)[240,241] have been used. Cyclosporine alone has been used with mixed results. Triple-agent immunosuppression with cyclosporine, azathioprine, and prednisone was described by Hooper and Kaplan.[242] They reported five patients with bilateral SC in whom visual recovery was promoted by this regimen. The therapy was given for 8 weeks prior to tapering. Two patients relapsed. Another study reported four patients maintained on a low dose of triple therapy for 12–69 months. Three patients did achieve remission off the drugs.[235] Alkylating agents have shown some promise, but side-effects, including bone-marrow suppression, nausea, fatigue, as well as one case of development of transitional epithelial carcinoma of the bladder, did occur.[240] For this reason, these agents should probably be reserved for sight-threatening disease that has failed conventional immunosuppressive therapy.[173] Other more recent therapies have included infliximab[243] and interferon-alpha-2a.[206,244] They appear promising, but the risk of systemic side-effects should be weighed. Patients receiving systemic management for SC are often jointly managed with a rheumatologist, internist, or oncologist.

Treatment is also aimed at managing complications of SC. These include CNV and CME. Reports have described the use of anti-VEGF agents for inflammatory chorioretinal disorders.[245–249] CNV in SC appears to be responsive to this treatment. Photodynamic therapy[250,251] has also been used with some success; however, the clinician should be mindful that choroidal ischemia and inflammation is inherent in SC and could be exacerbated by this treatment. For extrafoveal CNV, thermal photocoagulation is possible.

Acetazolamide[252] may be useful in the management of CME related to SC. It is thought that CME develops due to RPE dysfunction. After 2 weeks of treatment, there was complete resolution of CME with improvement of visual acuity in one case report.

Follow-up can include Amsler grid use by the patient to monitor for relapses and foveal involvement.

Tuberculous Serpiginous Choroiditis

Tuberculous serpiginous choroiditis can resemble idiopathic serpiginous choroiditis. Some may call this a serpiginous-like choroidopathy, but the term multifocal serpiginoid choroiditis (MSC) was suggested as a preferred term in a recent major review.[206] TB-related serpiginous choroiditis is associated with more vitritis compared to serpiginous choroiditis. In addition, patients with TB choroiditis have more multifocal lesions involving the periphery. SC has larger lesions compared to TB and is more likely to have lesions extending from the optic nerve head.[253] Fluorescein angiography does not distinguish between these two entities. Fundus autofluorescence may. Hypofluorescence corresponding to RPE loss in SC is more homogeneous compared to the variegated pattern and stippled hyperautofluorescence of tuberculous disease.[205] *Francisella tularensis* and *Bartonella henselae* have also be reported to give a clinical picture like SC.[254] These authors argue that both idiopathic SC and those with an infectious etiology should be grouped together on a spectrum as they give a similar clinical picture.[254] In developing countries, especially India, individuals with evidence of tuberculosis commonly may have serpiginous-like lesions. (See differential diagnosis section below and Chapter 85, Mycobacterial infections). SD-OCT may be useful at differentiating tuberculous SC from idiopathic SC. Choroidal infiltration as has been reported in a case of tuberculous related disease and not in idiopathic SC.[255] FAF may help to distinguish the lesions of SC from TB-related disease. TB-related diseases in general have a stippled hypoautofluorescence corresponding to lesions, which is not as homogenous as SC.[207] (See Chapter 85, Mycobacterial infections for more of a discussion on TB.)

Summary

Idiopathic serpiginous choroiditis is a chronic, progressive, and often bilateral disease. The course of the disease includes destruction of the choriocapillaris, RPE, and atrophy of the overlying retina. Treatment is aimed at immune suppression and carries significant side-effects. Visual prognosis is determined by the proximity of active disease to the fovea. Tuberculous SC must be considered and ruled out.

Relentless Placoid Chorioretinitis

Relentless placoid chorioretinitis (RPC) was described in 2000 by Jones and colleagues.[256] They reported six patients resembling both APMPPE and serpiginous choroiditis, but with an atypical time course and retinal distribution. The term ampiginous has been used to describe similar patients.[257] It is likely that some previous descriptions of multifocal serpiginous[258] and recurrent APMPPE represent this entity.[259]

Clinical Course

Clinical Symptoms.

The commonest complaint is sudden painless blurring.[260] Patients also describe metamorphopsia, floaters, or can initially be asymptomatic.

Epidemiology.

Patients were aged 17–51 in the report by Jones and colleagues.[256] There was no gender predilection. In a series by Jyotirmay and colleagues, a male preponderance was found with a mean age of 34.[260] The patients have no consistent medical disorder or viral prodrome.

Fundus Findings.

In most cases, patients have bilateral posterior creamy-white lesions at the level of the RPE (Fig. 79.28). The lesions (in almost all cases) tend to be smaller than those of APMPPE (approximately one-half disc area)[260] (Fig. 79.29). Lesions can be active in both eyes simultaneously. As they heal, pigmented chorioretinal atrophy develops. Lesions can persist and grow. A hallmark of this disease is the eventual presence of numerous (>50 to hundreds) lesions with involvement anterior and posterior to the equator. This is in contrast to APMPPE, which is mostly limited to the posterior pole. One study found that lesions more commonly appear in the periphery first and in the posterior pole later.[260] The fovea is commonly involved.

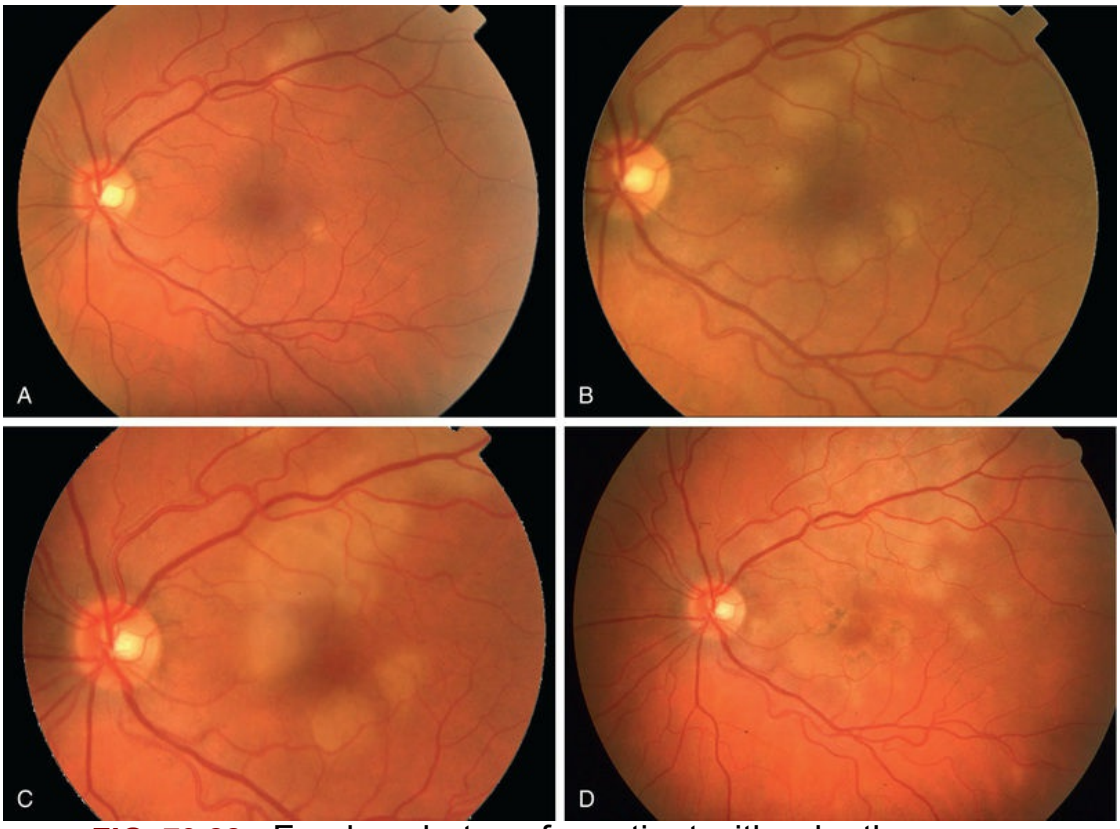

FIG. 79.28 Fundus photos of a patient with relentless placoid chorioretinitis documenting progression (A–D) of posterior creamy white lesions at the level of the retinal pigment epithelium over the course of one month.

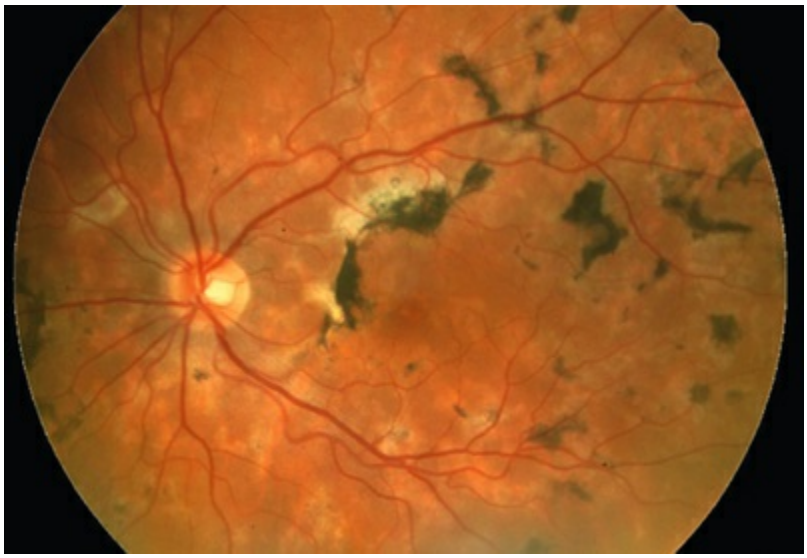

FIG. 79.29 Fundus photo of the same patient 2 years later. Healed lesions show pigmented chorioretinal

atrophy. The fovea is spared.

Other findings have included a mild vitritis, occasional SRF, and disc swelling.[260] In their study of 26 eyes in 16 patients, Jyotirmay and colleagues found subretinal fibrosis, as well as epiretinal membranes as rare findings.[260] Interestingly, CNV is not described.[252,260,261]

Other Ocular Findings.

Jones et al. described a patient with herpetic keratitis and corneal infiltrates in their series. Iritis with keratic precipitates as well as episcleritis can also occur.[256,261]

Clinical Course and Prognosis.

The clinical course is prolonged and relapsing. In four of the original six patients, active lesions were seen bilaterally and concurrently. This is in contrast to serpiginous chorioretinitis in which usually only one eye is active at a time. Pigmented chorioretinal atrophy develops within weeks. Throughout the long clinical course, lesions persisted and grew. There was also the appearance of new lesions for 5–24 months despite therapy, and involved eyes developed 50 or more lesions. Some patients showed recurrences months to years after onset. These can occur after significant periods of inactivity.

Permanent vision loss is usually mild. However, central vision was affected in all untreated cases. Vision dropped as much as 6 lines in the acute stage in Jones et al.'s study.[256] Some patients showed improvement in vision. Patients who received prolonged systemic steroids seemed to have decreased activity and improved visual outcome. Only two out of six patients had a final vision worse than 20/40 in the original series. Jyotirmay and colleagues report a favorable visual outcome in over 96% of their patients.[260]

Imaging

Fluorescein Angiography.

Similar to APMPPE and SC, fluorescein studies reveal early hypofluorescence due to either blockage or choriocapillaris

nonperfusion. Later phases show staining.

Indocyanine Green Angiography.

ICGA shows hypofluorescence in the areas corresponding to the clinical lesions. This persists into the late phases. Again this shows similarity to APMPPE and SC.

Optical Coherence Tomography.

There have been only limited reports. During the active stage of the disease with foveal lesions, the OCT showed subfoveal fluid.[262] In addition, a pigment epithelial detachment with hyperreflectivity of the inner and outer retinal layers was present. Another report described three zones of inflammation via SD-OCT in a patient.[263] Central to the lesion, a dome-shaped elevation involving the IS/OS junction with loss of the IS/OS band and thinning of the RPE associated with SRF was seen. Just peripheral to this, the IS/OS band was thickened and also associated with SRF. The outermost region showed a normal IS/OS band and mildly hyperreflective outer retinal layers. These were three concentric zones (Zone 1–3) that also corresponded to autofluorescence findings.[263] Choroidal thickness has also been reported in a study of three patients. They found that the choroid thickness was no different than the unaffected eye in the quiescent stage.[264] The authors felt that this was a distinguishing feature of RPC and different from other placoid diseases such as SC.[264] Further study is warranted.

Fundus Autofluorescence.

FAF of RPC showed marked hypoautofluorescence in areas of widespread chorioretinal atrophy.[265] In another patient, a "cockade pattern" FAF was described.[263] Central in the lesion (Zone 1) there was dark hypoautofluorescence surrounded by a "white circle" of relative hyperautoflourescence (Zone 2), and the outermost concentric circle was hypoautofluorescent as well (Zone 3), but less so than in Zone 1. The authors correlate this directly to OCT findings as described above.[263]

Electrophysiology

A decrease in the electrooculogram and electroretinogram results (scotopic, photopic, and flicker) has been reported.[256] Other reports do not show this finding.[262]

Systemic Associations

In Jones and colleagues' case series, one patient had Hashimoto thyroiditis and aseptic meningitis. Two other patients presented with nonspecific upper respiratory tract infections.[256] Jyotirmay et al.'s series reported two patients with Hashimoto thyroiditis and one patient with type 1 diabetes mellitus.[260] There has been a recent case report of RPC associated with central nervous system lesions in a 20-year-old male.[266]

Pathogenesis

The similarity to APMPPE and serpiginous choroiditis suggests that there is some common pathophysiology. The reports of concurrent RPC in patients with thyroiditis may indicate inflammatory or immune processes.

Choroidal ischemia, either primary or secondary due to an inflammatory etiology, is a consideration, as it is in APMPPE and SC. The presence of RPC in a patient with CNS lesions may indicate a small-vessel vasculitis.[266]

Differential Diagnosis

APMPPE and serpiginous choroiditis are the main considerations (Table 79.1). Time course as well as the number and location of the lesions distinguish these diseases. There may be some resemblance to other white spot diseases including multifocal choroiditis and birdshot chorioretinopathy. Other processes such as Harada disease, neoplastic infiltration of the choroid, infections such as syphilis, and granulomatous diseases such as tuberculosis and sarcoidosis can also be considered.[256]

TABLE 79.1

Comparison of APMPPE, Serpiginous Choroiditis, and Relentless Placoid Chorioretinitis

	APMPPE	Serpiginous Choroiditis	Relentless Placoid Chorioretinitis
AGE	Young	Young to middle-aged	Young to middle-aged
COURSE	Lesions heal over weeks	Lesions heal over weeks to months	Continued activity, growth of lesions, new lesions
VISUAL OUTCOME	Good	Poor if fovea involved	Poor if fovea involved
OCULAR INVOLVEMENT	Usually posterior pole	Posterior pole, usually peripapillary	Posterior pole and anterior to equator
SYSTEMIC INVOLVEMENT	Headaches, CNS signs	None	None
RECURRENCES	Usually uniphasic	Recurrences contiguous with old lesions	Noncontiguous recurrences
TREATMENT	Often does well without treatment	Immunosuppression	Immunosuppression

CNS, central nervous system.

Management/Treatment

The best regimen is as yet unknown. Jones et al. described decreased activity and improved vision in patients who were treated with prolonged steroids versus patients who were untreated or treated less aggressively.[256] Antiviral therapy was not effective. Immunosuppression with cyclosporine was also described, but recurrence was noted when it was tapered. Mycophenolate mofetil with prednisone was used in one patient who also had CNS lesions.[267] Jyotirmay and colleagues used steroids (including sub-Tenon) in combinations with azathioprine or cyclophosphamide.

Summary

Relentless placoid chorioretinitis is a disease of unknown etiology that resembles APMPPE and serpiginous choroiditis. It has a prolonged and relapsing course. Many creamy lesions appear in the periphery, midperiphery, and macula. They grow in size and eventually heal leaving pigmented chorioretinal atrophy. Commonly active lesions are found bilaterally. A hallmark of this disease is the eventual presence of 50 to hundreds of lesions that are seen throughout the fundus. Despite the vast distribution, including foveal involvement, visual prognosis is fairly good. Aggressive prolonged immunosuppressive therapy appears indicated. The RPE and outer retina appeared involved when looking at the OCT and FAF. The choroid may not be as involved in

this disease based on a small cohort of this rare disease.[264]

Persistent Placoid Maculopathy

Persistent placoid maculopathy (PPM) is a rare disease that superficially resembles macular serpiginous choroiditis but differs in its clinical course and visual prognosis.[268] It was originally described by Golchet and colleagues in 2006. More recently the same group and others have described series of patients using multimodal imaging.[269,270] Atrophy is a common feature of PPM and is a major cause of visual loss.[270] CNV frequently occurs.

Clinical Course

Clinical Symptoms.

Patients present with gradual, painless, decreased vision, more commonly in one eye. Photopsias and decline in color vision can be seen.[268]

Epidemiology.

In the original description there were six patients. Five were men; the range of ages was 50–68. There were no consistent systemic medical problems.[268]

Fundus Findings.

Patients almost always have bilateral almost symmetric whitish plaque-like lesions at the level of the outer retina and RPE (Fig. 79.30). These lesions are centered in the fovea and not contiguous with the optic disc. There is a jigsaw pattern to margins of the lesions. During the course of the disease there is very gradual fading of the whitish lesions in all patients.[268] This can take months to years. This is a distinguishing feature from APMPPE.[270] In addition to the central lesions, satellite lesions have also been show to occur.[270] RPE mottling and pigment clumping without CNV can develop. CNV can be seen leading to an increase in pigmentation, atrophy, or scarring.

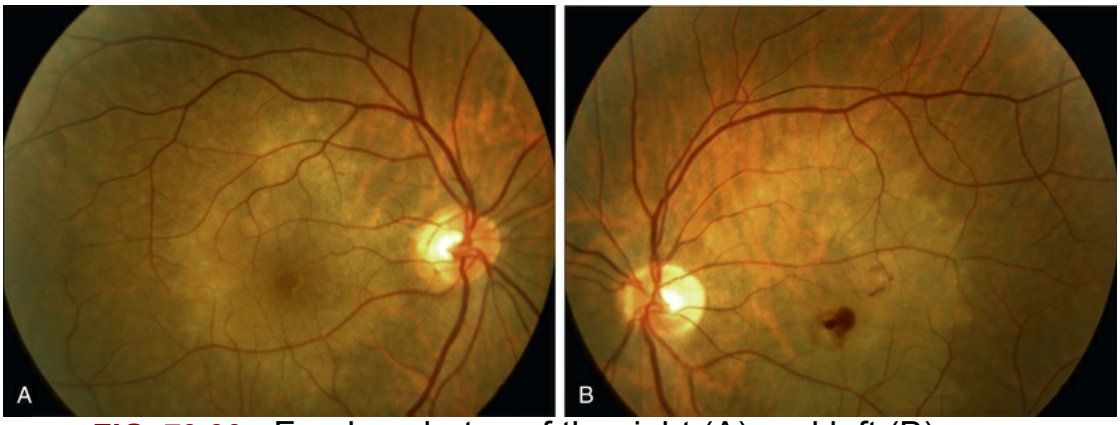

FIG. 79.30 Fundus photos of the right (A) and left (B) eye of a patient with persistent placoid maculopathy. Bilateral whitish plaques are seen. They are centered on the fovea. The left eye also shows a macular hemorrhage consistent with choroidal neovascularization.

Other Ocular Findings.

Patients do not have cells in the anterior chamber, but vitreous cells have been described.[270]

Clinical Course and Prognosis.

This macular disorder superficially resembles macular serpiginous. Vision is often minimally affected until the development of CNV or atrophy.

Imaging

Fluorescein Angiography.

In acute lesions, FA shows early hypofluorescence with hyperfluorescence ranging from filling to mild punctate hyperfluorescence in the late phase. No leakage or staining is seen, unless CNV is present (Figs. 79.31 and 79.32). Optic nerve hyperfluorescence was seen in one patient.[269] In healed lesions, FA is normal unless atrophy or scarring develops. However, some cases do have persistent hypofluorescence.[270]

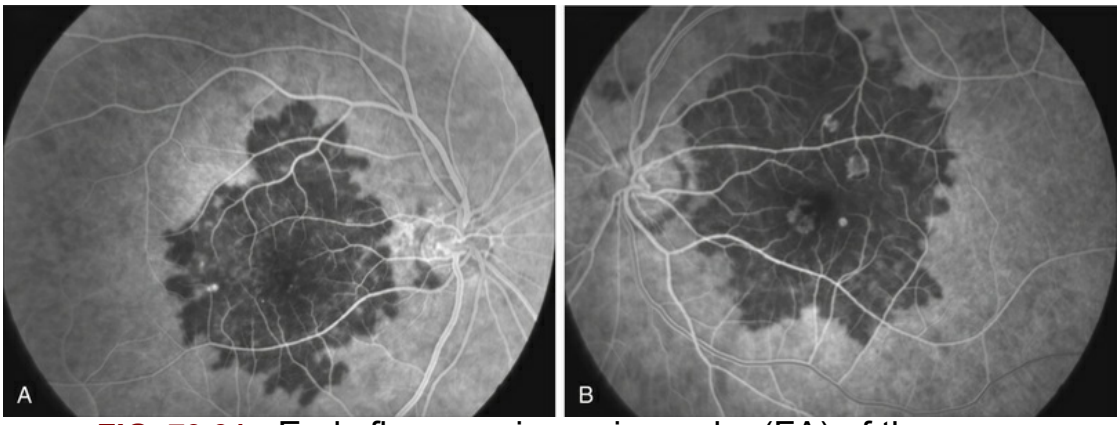

FIG. 79.31 Early fluorescein angiography (FA) of the right (A) and left (B) eye show hypofluorescence corresponding to the clinically seen macular lesions.

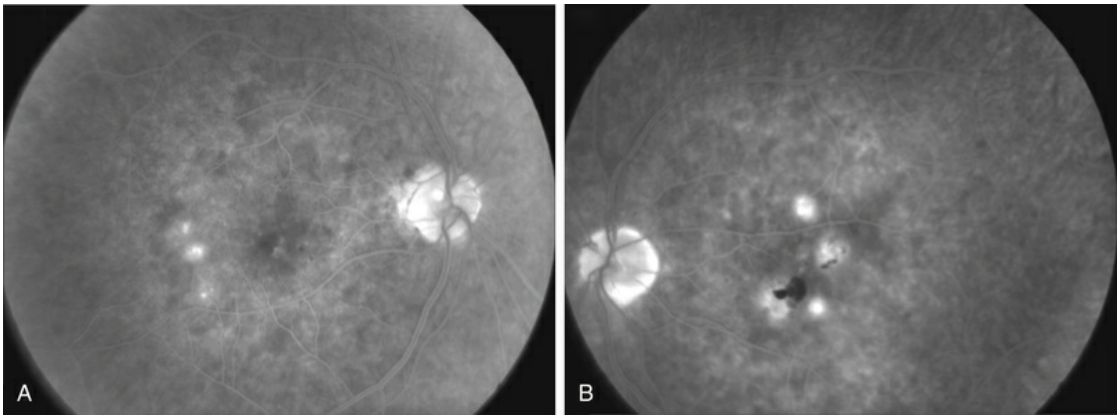

FIG. 79.32 Late fluorescein angiography (FA) of the right (A) and left (B) eye shows that there may be some slight hyperfluorescence corresponding to the lesion. There are some focal areas of hyperfluorescence that corresponds to choroidal neovascularization.

Indocyanine Green Angiography.

ICGA reveals persistent hypofluorescence throughout the angiogram (Fig. 79.33).[270] The large choroidal vessels in the affected areas are seen. In one case, the hypofluorescence showed partial resolution on follow-up.[268]

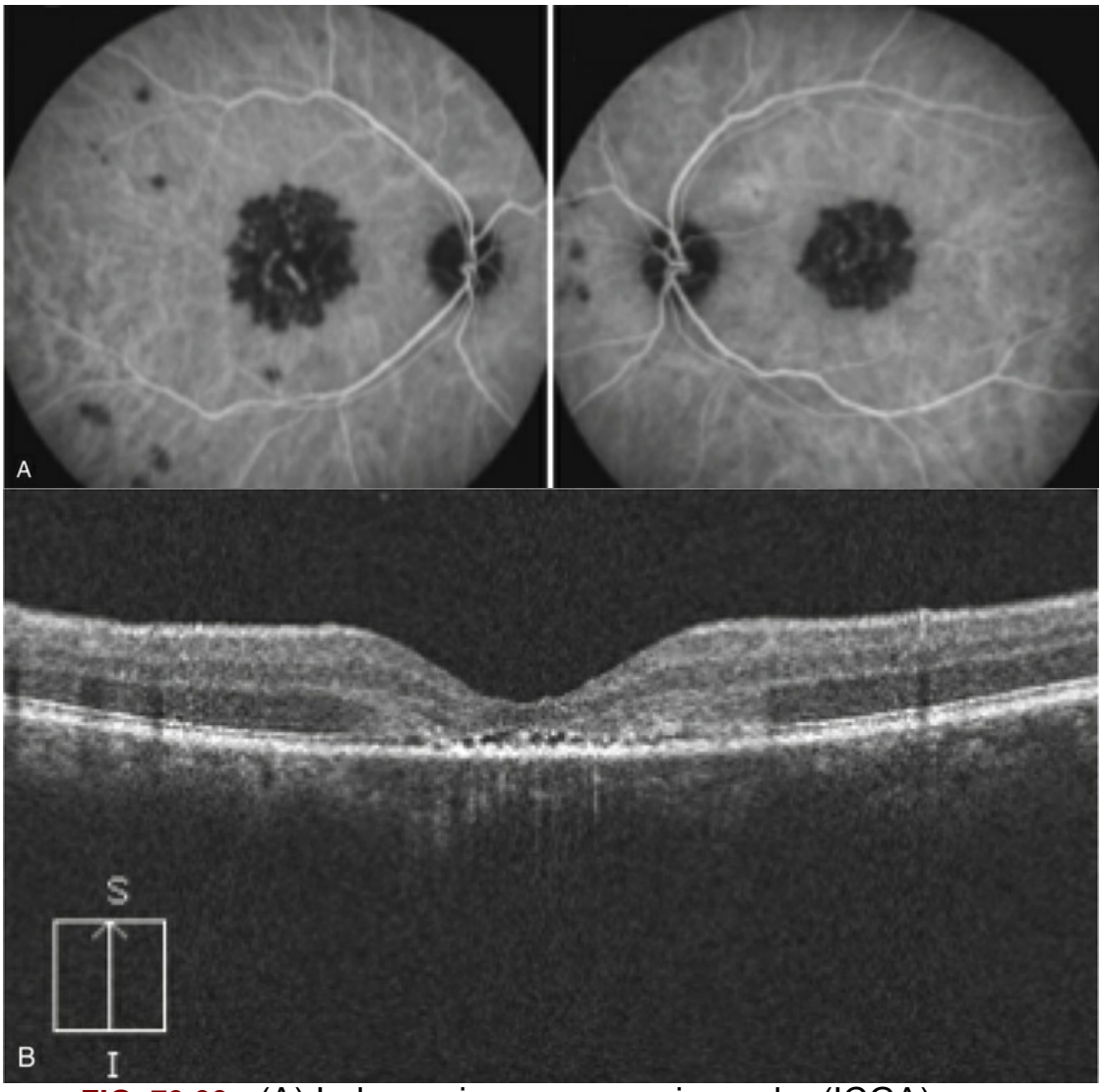

FIG. 79.33 (A) Indocyanine green angiography (ICGA) shows classic central hypofluorescence with other scattered foci in the posterior pole. (B) Optical coherence tomography (OCT) shows opacification of the outer nuclear layer and some foveal thinning with a small amount of subretinal fluid and irregular retinal pigment epithelium.

Optical Coherence Tomography.

Gendy et al. described the multimodal imaging of five patients.[270] The group found hyperreflectivity of the outer nuclear layer (ONL) and disruption of the ELM and the ellipsoid zone in all cases. In some cases there was a hyporeflective sliver at the level of the outer segments. In some cases there was a homogeneous solid isoreflective pattern of the choroidal capillaries underneath areas of

significantly disrupted RPE. In healed lesions a complete restoration of the outer retinal architecture could be seen if progression to atrophy did not occur.

Fundus Autofluorescence.

Hypofluorescence correlating to RPE damage would be expected and has been seen in one case.[271] This was noted in a patient with concurrent CNV. In Gendy et al.'s series, hyperautofluorescence, hypoautofluorescence, and no changes were seen in acute lesions. Healed lesions showed mixed hyper- and hypoautofluorescence in atrophic lesions.[270] FAF can also reveal far peripheral lesions.[269]

Electrophysiology

One patient had a normal electroretinogram.[268]

Systemic Associations

No clear systemic associations are known. Hypertension was common.[268,269]

Pathogenesis

There is similar speculation about pathophysiology as with other placoid white spot entities. Choroidal hypoperfusion,[272] blockage by swollen RPE cells, and inflammatory lesions in the outer retina, or a combination of these, have been suggested to explain the hypofluorescence on ICGA.[272] However, extensive choroidal hypoperfusion would not be expected in patients who maintain good vision. Nika and colleagues suggest that choroidal infiltrates are the primary pathology with secondary RPE and outer retinal changes based on multimodal imaging of a series of three patients treated with immunosuppression.[269]

Differential Diagnosis

In addition to macular serpiginous choroiditis, other considerations include APMPPE, relentless placoid chorioretinitis, and syphilitic posterior placoid chorioretinitis.[268] The time course visual outcome, symmetric white lesions, and common association with CNV distinguishes it from the other white spot entities. The fluorescein

angiogram in syphilis shows late staining unlike PPM, as well as clinical signs of inflammation due to the infectious etiology (see Chapter 87, Spirochetal infections).

Management/Treatment

Oral or periocular corticosteroids have been used with subsequent improvement in vision. More recent case series suggest significant improvement in at least one eye with high-dose steroids.[269] The role of steroids requires further investigation. Anti-VEGF agents have been used to treat CNV, with good results in a few reports.[273–275]

Summary

Persistent placoid maculopathy is a unique placoid white spot entity. Bilateral almost symmetric white lesions centered in the macula and not contiguous with the optic nerve are seen. These fade over months to years. They may be associated with pigmentary changes and atrophy. Visual outcome is related to the development of CNV or atrophy, which are very common.

Multifocal Choroiditis/Punctate Inner Choroidopathy

Idiopathic multifocal choroiditis (MFC) (including punctate inner choroidopathy [PIC]) is a condition characterized by inflammation at the level of the RPE and outer retina. Jampol and colleagues[276,277] have classified MFC and PIC as the same disease as their ophthalmoscopic appearance and clinical courses are similar. Multimodal imaging has further solidified this idea.[277–279] Furthermore, MFC and PIC share haplotypic associations with IL10 and TNF loci.[280] For historic purposes, a brief introduction to each of the conditions is in order. MFC does not appear to be a pure choroiditis. Chorioretinal scars are left by the inflammation. The etiology and pathogenesis of MFC/PIC is unclear

Multifocal Choroiditis

MFC was first described by Nozik and Dorsch in two young

patients in 1973.[281] They reported a chorioretinopathy that resembled presumed ocular histoplasmosis (POHS) but was associated with a bilateral anterior uveitis (see Chapter 73, Ocular histoplasmosis). Later, Dreyer and Gass[282] coined the term multifocal choroiditis and panuveitis, describing 28 patients with uveitis and lesions at the level of the RPE and choriocapillaris. Deutsch and Tessler[283] reported a series of 28 patients in 1984 with what they termed inflammatory pseudohistoplasmosis. Their series included patients with concurrent systemic diseases such as tuberculosis, sarcoidosis, and syphilis. Morgan and Schatz,[284] 2 years later, described 11 patients with a recurrent idiopathic multifocal choroiditis. The term multifocal choroiditis should be further characterized as it is the subject of confusion. MFC can be secondary to other disease: either infectious bacterial (including TB, syphilis, fungal/POHS), viral, or noninfectious (sarcoid).[278] MFC as discussed in this chapter is idiopathic. However, even within the idiopathic category, there is MFC that presents with minimal anterior cell or vitritis and that has a significant cellular reaction – this latter category is sometimes characterized as multifocal choroiditis and panuveitis (MFCPU). MFCPU is commonly seen by our uveitis colleagues. We consider these a spectrum of disease.

Punctate Inner Choroidopathy

PIC was first described in 1984.[285] Watzke reported 10 myopic women with blurred vision, photopsias, or paracentral scotomas with small yellow–white lesions of the inner choroid and RPE. These lesions were associated with overlying SRF. Acute lesions healed to atrophic scars and developed more pigmentation with time. Choroidal neovascular membranes developed in more than half of these individuals.[286] The lesions of PIC are classically limited to only the posterior pole (Figs. 79.34 and 79.35).

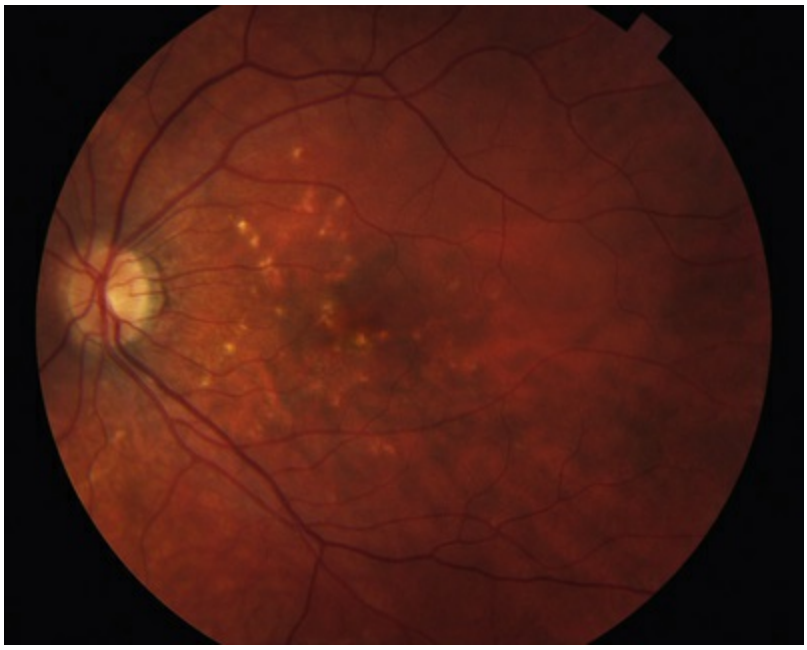

FIG. 79.34 Fundus photo of the posterior pole showing small round lesions that are characteristic.

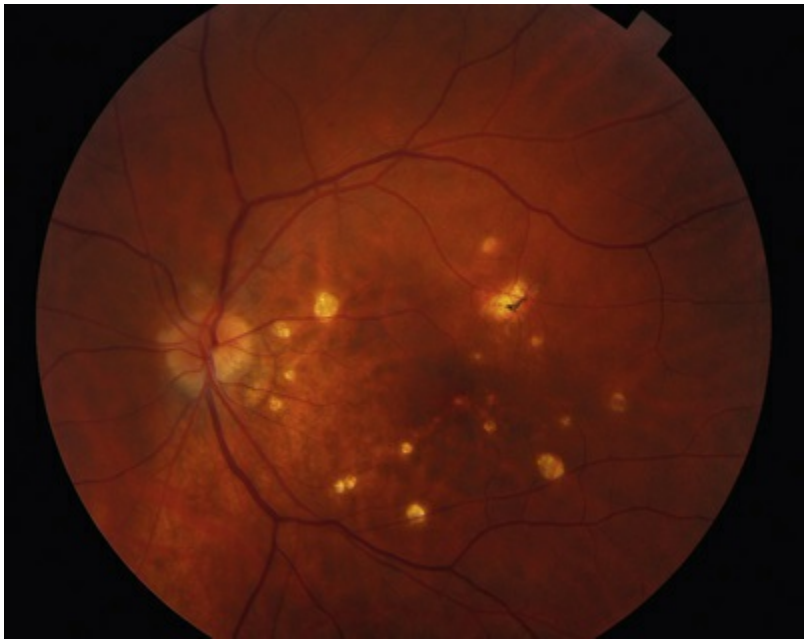

FIG. 79.35 Expansion of scars in the inactive phase is common.

MFC and PIC are considered the same entity by many retina specialists and will be referred to as MFC/PIC or MFC in this chapter.[276,277] In general, PIC is used when the lesions/scars are limited to the posterior pole and MFC when scars are seen in the

periphery as well. However, these distinctions are arbitrary.[277] Some MFC lesions have a significant component of fibrosis that if severe have been called progressive subretinal fibrosis and uveitis syndrome.[287] We consider the fibrosis in the spectrum of the same disease process. MFC can present with photoreceptor loss apart from the focal lesions.[288] We consider this to be MFC with chorioretinal atrophy.[289] If severe, these cases were considered as part of Gass's AZOOR complex, but we now believe these are distinct from AZOOR on multimodal imaging.[288,289]

Clinical Course

Clinical Symptoms.

Patients present with decreased central vision, photopsias, floaters, metamorphopsia, paracentral or temporal scotomas, ocular discomfort, or photophobia. Asymptomatic lesions may be seen. Photopsias often correspond to lesions in the peripapillary area and indicate activity of the disease. Visual acuity can range from 20/20 to light perception. More than half present with vision less than 20/100 in the worse eye.[282,284]

In a survey of 77 people with PIC conducted by Gerstenblith and colleagues,[290] scotomas were the presenting complaint in 91% of patients, followed by blurred vision (86%), photopsias (73%), floaters (69%), metamorphopsia (65%), and decreased peripheral vision (26%). Most (85%) presented with unilateral symptoms.

Epidemiology.

MFC has been reported predominantly in Caucasian,[291] myopic[290] women between the second and sixth decades of life.[282,284] Most affected patients are in their 30s. In addition, most have never lived in areas that are endemic for histoplasmosis. Mean refraction is −4.6 diopters.[292]

Fundus Findings.

In the acute phase, yellow round or oval lesions, ranging in number from one to scores, are seen in the outer retina and RPE. They range in size from 50 to 1000 μm. They occur in the posterior pole, peripapillary region, and midperiphery. The nasal retina often

shows clustering.[293] When limited to the posterior pole[290] (Fig. 79.34), occasionally there is a linear pattern. The initial lesions are sub-RPE, and a neurosensory detachment may be present. These break out into the overlying retina. With time, these spots usually evolve into atrophic chorioretinal scars. After 2–3 years they become more distinct, pigment, and appear similar to the punched-out lesions of POHS (Fig. 79.35). Some lesions disappear without sequelae. CNV commonly develops. The lesions can also be arranged in linear scars (Schlaegel lines) parallel to the ora in the periphery[294] (Fig. 79.36). Previously, this linear appearance was thought to be pathognomonic for POHS.[295,296] Evanescent white lesions resembling MEWDS may be seen. Active lesions can be associated with SRF. As inflammation resolves, the lesions may disappear or become atrophic with a variable amount of pigment ("punched-out" appearance). They can also enlarge in size. There can be bridging subretinal scars between the disciform or atrophic scars.[297] Cantrill and Folk described five patients who developed sharply angulated subretinal scars as the lesions healed.[298] They noted broad scar formation in the macula as the lesions coalesced that could be related to serous and hemorrhagic macular detachment. During active phases, exudative retinal detachment may overlie areas of activity.

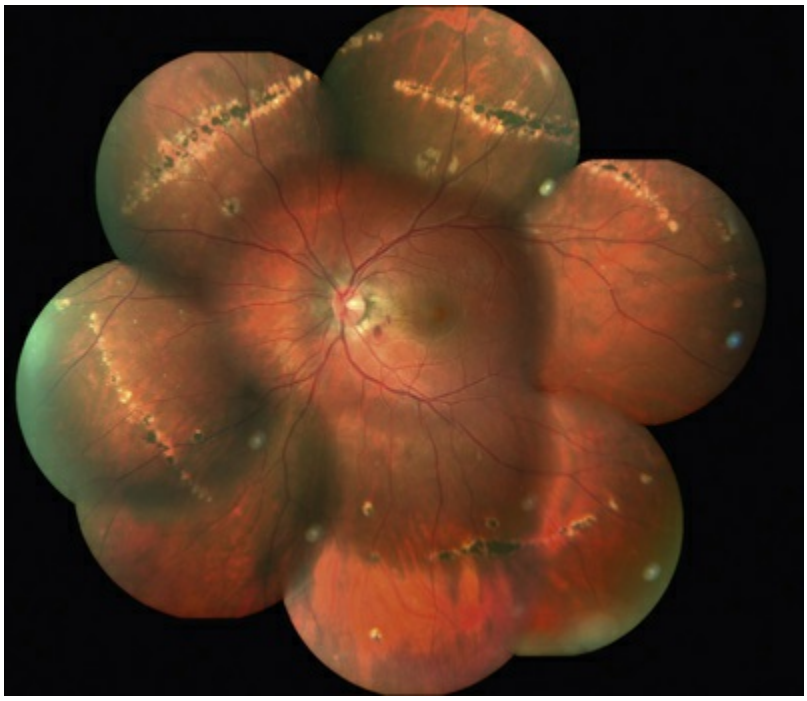

FIG. 79.36 Linear scars parallel to the ora are seen in the periphery. (Courtesy of Medical University of Innsbruck, Austria.)

In recurrent episodes, new chorioretinal lesions may develop. Optic disc edema can be seen, and atrophy may occur. Optic disc neovascularization can very rarely be seen.[283] The peripapillary region may have a characteristic subretinal fibrosis[299] that has been described as a "napkin ring" configuration (Fig. 79.37). The midperiphery may have lobulated lesions resembling flowers. Retinal vessels may be narrowed. Periphlebitis may develop. Cystoid macular edema occurs in 10–20% of individuals. CNV develops in 25–30% of cases and can be the presenting sign.[282,284,291]

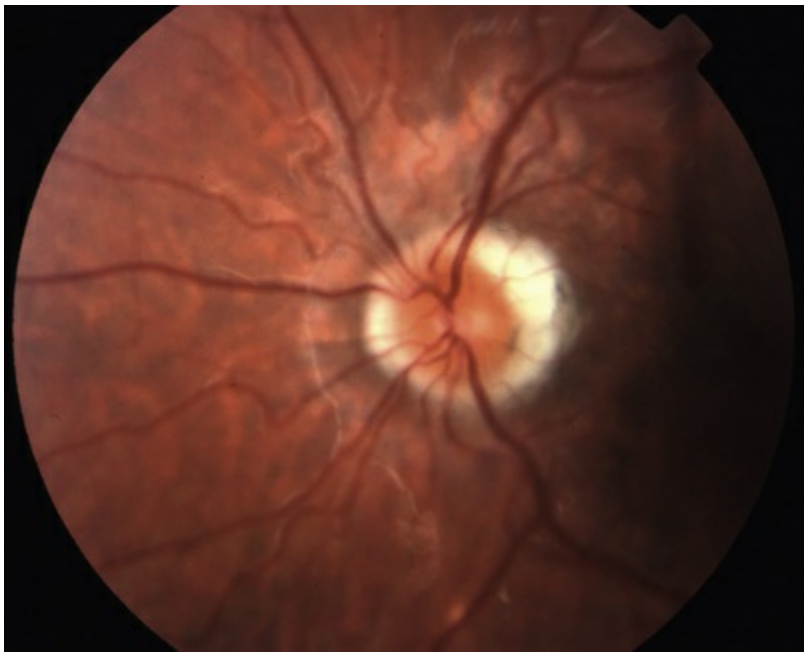

FIG. 79.37 Fundus photo showing a characteristic subretinal fibrosis ("napkin ring").

Multimodal imaging has helped characterize other variants of MFC. Jung and colleagues described 13 cases (21 eyes) of idiopathic MFC with discrete chorioretinal lesions associated with either diffuse (13 eyes), multizonal (6 eyes), or zonal (2 eyes) retinal or chorioretinal atrophy.[288] The outer retinal atrophy occurred around the optic nerve, geographic zones in the mid and far periphery, or diffusely. In diffuse disease, multiple pigmented chorioretinal scars were associated with confluent areas of atrophy and fibrous

proliferation. This occurred along the major vessels and in the peripapillary area. This more commonly occurred bilaterally. The atrophy progressed centripetally, but spared the macula until late in the disease. The atrophy correlated to Goldmann visual fields with either significant constriction or a large scotoma involving the blind spot. ERG showed rod and cone depression. Multifocal ERG showed signal preservation of the central macula but peripheral depression (Fig. 79.38). Multizonal disease was characterized by multiple, atrophic, pigmented chorioretinal scars and geographic atrophy that was hypopigmented. The atrophy was found throughout the fundus, including the peripapillary area and macula. In one patient, multizonal disease progressed to diffuse disease over the course of 14 years. Zonal disease occurred bilaterally in one patient. This patient had the typical lesions of MFC, but a visual field scotoma and a focal peripapillary zone of outer retinal atrophy. ICGA and FAF did not show any defect corresponding to the VF defect, but SD-OCT showed an attenuation of photoreceptors. This indicated a photoreceptor dysfunction rather than an RPE or choroidal dysfunction. Of note, no demarcation line of hyperautofluorescence between normal and abnormal retina occurred in any of these cases. This is an important distinguishing factor from AZOOR.[288] Munk and colleagues described a related variant of MFC with retinal or chorioretinal atrophy. They reported the findings of eight patients in whom MFC/PIC was associated with acute photoreceptor loss or dysfunction out of proportion to the clinically visible lesions.[289] In these patients, OCT showed the typical MFC lesions associated with large zones of attenuation of the external limiting membrane, ellipsoid zone, and interdigitation zones. These areas were hyperautofluorescent on FAF and corresponded to VF loss on formal testing. Full-field ERG often showed depression of both the rods and cones. Some anatomic recovery is possible, but the interdigitation zone remained affected.[289]

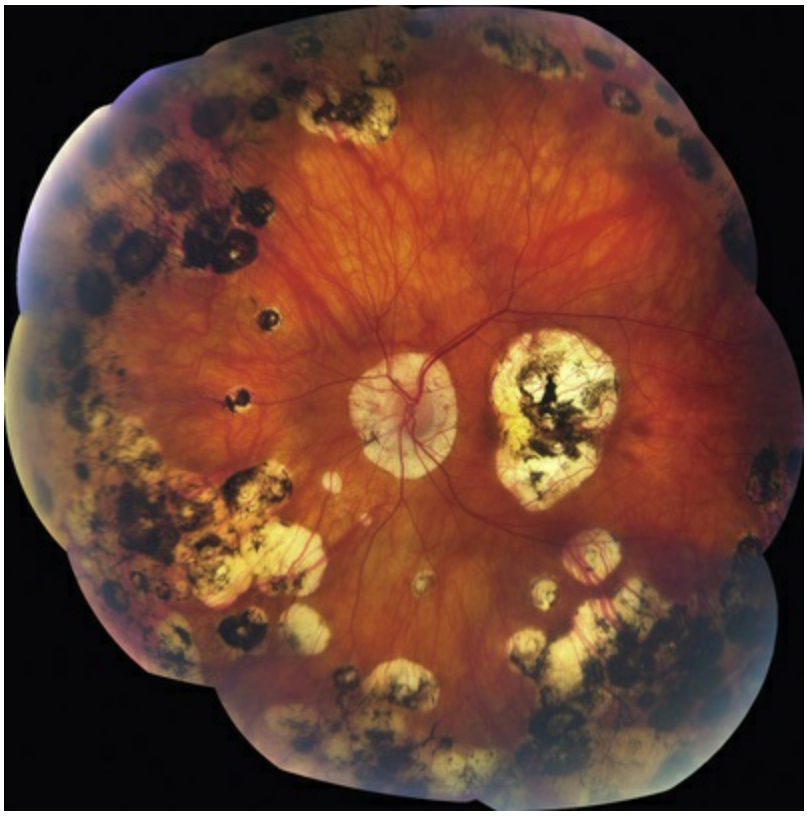

FIG. 79.38 Color fundus photo of multifocal choroiditis with chorioretinal atrophy.

Other Ocular Findings.

MFC/PIC may have no uveitis or a mild to moderate anterior uveitis. Nongranulomatous keratic precipitates and posterior synechiae can be present. Iris abnormalities, such as neovascularization or abnormal avascular areas on fluorescein angiography, have been reported.[300] Vitritis, if present, is usually mild or moderate. Findings may be asymmetric.

Clinical Course and Prognosis.

MFC waxes and wanes, but vision loss can occur. Most patients have recurrent episodes that can involve the central or peripheral vision. These can resolve spontaneously or with the aid of immunosuppressants. Some patients retain excellent vision but have persistent photopsias. About 25% of patients have a more chronic course that involves more inflammation, or CNV. Recurrent inflammation may cause CME, vitreous haze, subretinal scarring, and swelling around old scars (Fig. 79.39). New lesions that are not

contiguous with old scars can develop. CNV is the most common cause of visual loss in MFC and can be seen with either inactive macular scars or recurrent inflammation. The long-term visual prognosis of MFC is variable. Brown and colleagues[293] followed 41 patients (68 eyes) for a mean of 39 months. They found that 66% of eyes ended up with 20/40 vision or better. Only 21% of eyes ended up 20/200 or worse. The majority of the cases with poor vision were due to CNV and less commonly CME. Foveal atrophy and uveitic neovascular glaucoma were other causes in their series. About one-third of patients developed CNV. Thorne and colleagues[301] studied 66 patients (122 eyes) and found that 55% of patients presented with vision worse than 20/50 and 38% presented with vision worse than 20/200. CNV was found in 22% of patients at presentation and was the most common cause of vision loss. Presence of epiretinal membrane and CME were other causes of vision loss. Use of immunosuppressive therapy was associated with an 83% reduction in the risk of posterior pole complications, including new or recurrent CNV. Brown and colleagues followed patients with lesions limited to the posterior pole for a mean length of 51 months.[293] They found that 77% of eyes had a final vision of 20/40 or better. Twenty-three percent had a vision of 20/50 or worse. Twenty percent had a vision of 20/200 or worse. The primary cause of this poor vision was CNV. Essex and colleagues[292] reported the clinical features and outcome of 136 patients (271 eyes) with lesions limited to the posterior pole (PIC) with a mean follow-up of 6.2 years. They found 63 fellow eyes that were normal at presentation. Of these, 56 (88%) remained unchanged. Only 3 (5%) developed lesions, and 4 (6%) developed CNV. In eyes with lesions, 49 of 74 eyes (66%) remained unchanged. New lesions developed in 9 eyes (12%), and CNV developed in 16 (22%). Generally, the prognosis for MFC limited to the posterior pole is very good.[302]

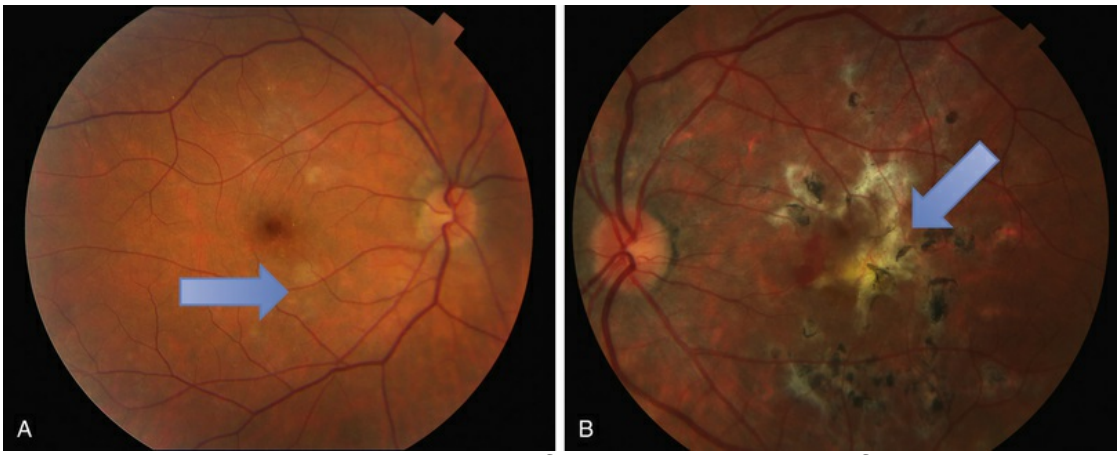

FIG. 79.39 Fundus photos of the right (A) and left (B) eyes. The right eye shows subtle acute lesions (*arrow*). The left eye shows chronic disease. Bridging fibrosis is seen between scars (*thin arrow*).

Imaging

Fluorescein Angiography.

In the acute phase, the clinical lesions appear hypofluorescent on FA. Late in the angiogram, the lesions stain[284] (Figs. 79.40 and 79.41). CNV may be present in the peripapillary or macular areas. In the healed phase, the lesions become atrophic and show a window defect on angiography. A recent study of CNV in MFC revealed that most CNV is classic and clearly demonstrated unless blocked by subretinal blood.[303] The researchers looked at OCT (both stratus and spectralis) and found that CNV could be missed with this mode of imaging. They recommended FA be used in cases with suspected neovascularization. PIC lesions can appear hyperfluorescent in the arterial phase or may appear as blocked fluorescence (Fig. 79.42A). In later phases, the lesions stain[285] (Fig. 79.42B). More lesions are seen on FA than are clinically visible. Tiny punctuate hyperfluorescent lesions may be seen scattered in the posterior pole. In later stages of disease, as the RPE atrophies, window defects are seen. Leakage of fluorescein into the subretinal space is also possible.

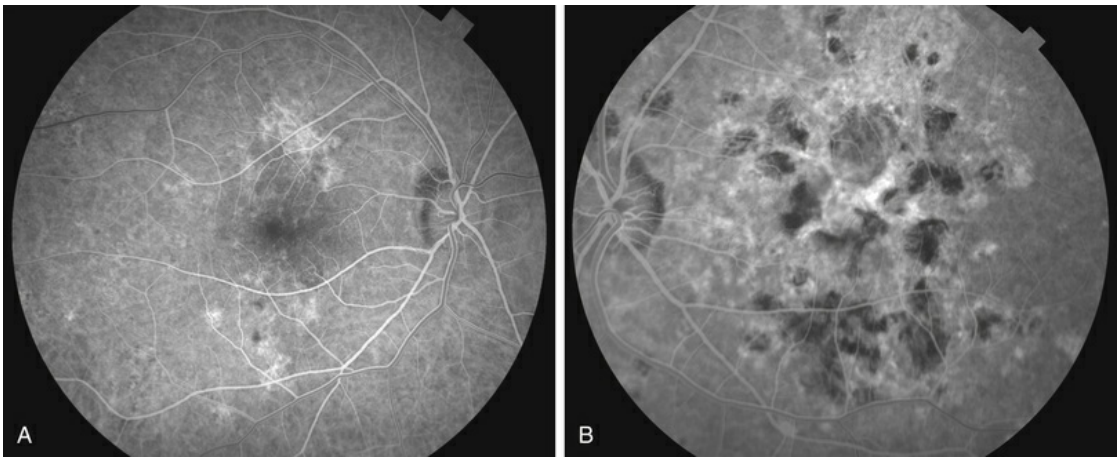

FIG. 79.40 Early fluorescein angiography (FA) of the right (A) and left (B) eye of a patient with new onset of symptoms in the right eye. The left eye has had poor vision for some time.

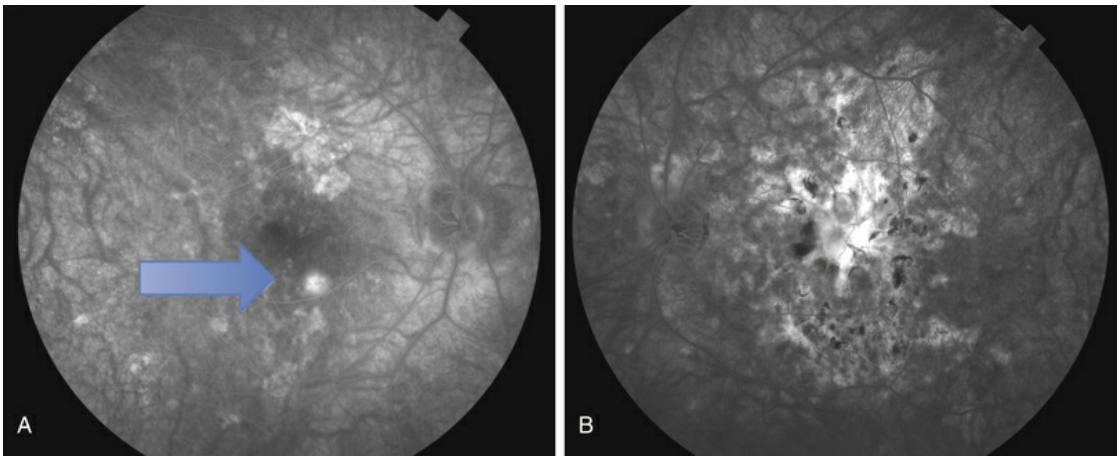

FIG. 79.41 Late fluorescein angiography (FA) of the right (A) and left (B) eye shows an acute hyperfluorescent lesion in the right (*arrow*). The left eye shows staining of the scars.

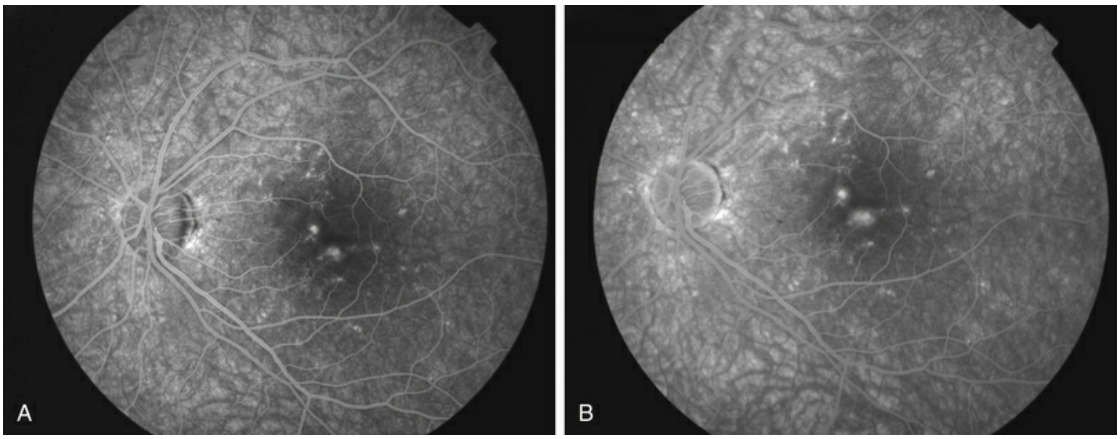

FIG. 79.42 (A,B) Fluorescein angiography shows increasing fluorescence (staining), and some slight leakage of lesions is seen.

Olsen and colleagues described CNV in six patients with PIC.[304] They found that a fibrotic response followed the development of CNV and there was often a dumbbell-shaped pattern of subretinal fibrosis.

Indocyanine Green Angiography.

ICGA shows hypofluorescent round spots that may be far more numerous than seen on clinical examination and fluorescein angiography[305–308] (Fig. 79.43). The MFC/PIC lesions hypofluoresce in the early, middle, and late phases of ICGA[309,310] (Fig. 79.44). Tiffin and colleagues described choroidal vascular abnormalities.[310] In addition to the hypofluorescent lesions that, in some cases, corresponded to clinically seen lesions, larger choroidal vessels were seen crossing these areas. Several choroidal vessels also showed hyperfluorescence of the vessel wall. They postulated focal choroidal ischemia in the areas of hypofluorescence and possibly a vasculitis in the area of hyperfluorescence of the vessel walls.

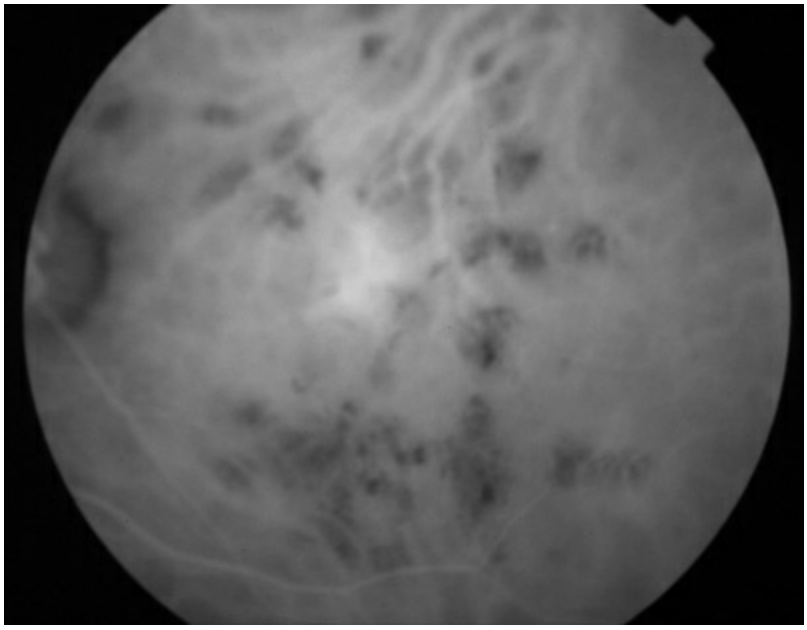

FIG. 79.43 Indocyanine green angiography (ICGA) shows numerous hypofluorescent round spots.

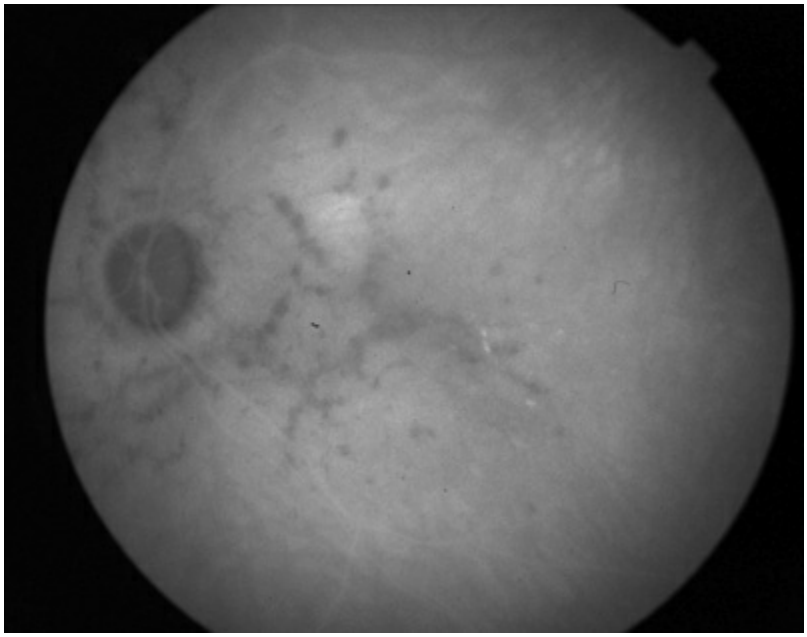

FIG. 79.44 Indocyanine green angiography (ICGA) shows numerous hypofluorescent spots.

Optical Coherence Tomography.

Characterization of the OCT findings of MFC/PIC have been the subject of many major papers.[279,311–313] Spaide and colleagues

describe the acute MFC/PIC lesions as nodular collections below the RPE that begin to rupture allowing the inflammatory material to enter the subretinal space and outer retina[279] (Fig. 79.45). Vance and colleagues describe SD-OCT imaging of acute lesions that showed drusen-like material between the RPE and Bruch's membrane, as well as a localized choroidal hyperreflectivity below the material.[314] These lesions disappear with treatment. Zhang and colleagues described a five-stage evolution of the lesions from choroidal infiltration, development of sub-RPE nodules, chorioretinal nodules, regression, and retinal herniation.[312] Focal choroidal excavation has been noted by us and other authors as well.[315] As discussed earlier, the MFC/PIC lesions can be associated with widespread loss of outer retinal elements beyond the nodular area.[279,288,289]

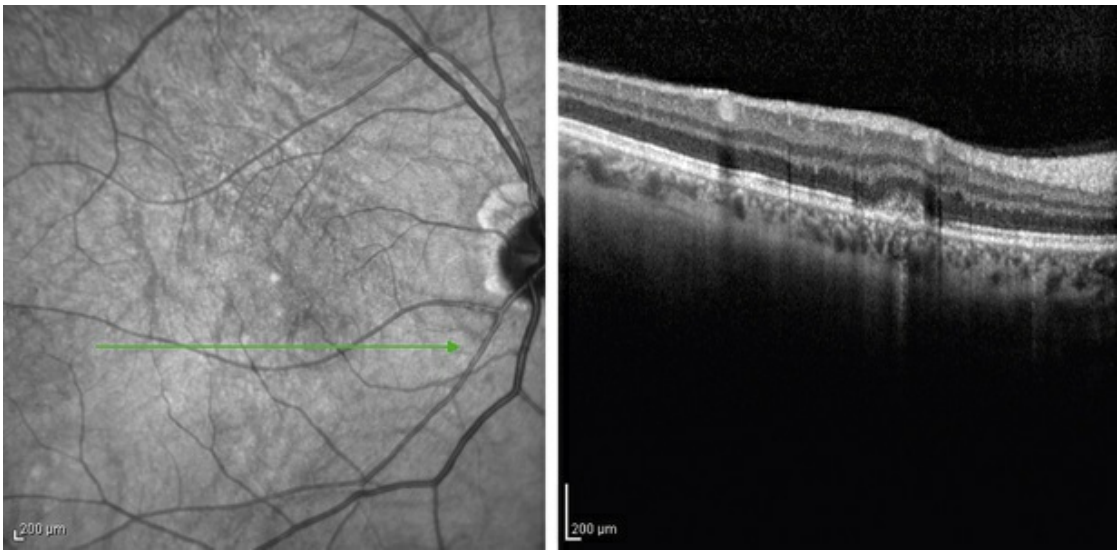

FIG. 79.45 Optical coherence tomography (OCT) of the right eye shows a hyperreflective lesion in the outer retina corresponding to an acute lesion.

CNV is also seen on OCT and can usually be distinguished from the MFC/PIC lesions by the heterogenous nature of the signal, association with IRF/SRF, and larger size of the lesion in comparison to the more homogenous, smaller characteristic of a MFC/PIC lesion.[316] OCT angiography will likely be very useful in identifying CNV when it is uncertain with other testing.

Fundus Autofluorescence.

Hyperautofluorescence was observed in the areas of fresh lesions. This resolved when immunosuppression was instituted. In the majority of patients, punctate hypoautofluorescent spots were seen on FAF corresponding to areas of chorioretinal atrophy (inactive lesions)[317] (Fig. 79.46). Larger plaques of hypoautofluorescence are seen when there is significant atrophy as seen in diffuse and multizonal disease.[288] Hyperautofluorescence is seen early in areas of photoreceptor involvement in patients with acute photoreceptor loss or dysfunction out of proportion to clinically visible lesions.[289]

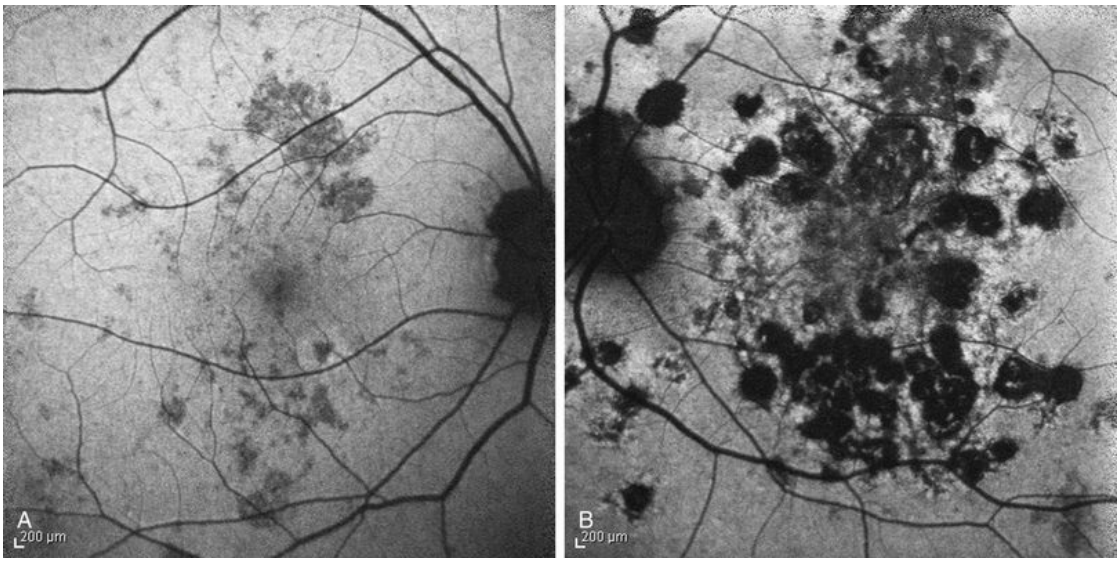

FIG. 79.46 (A,B) Fundus autofluorescence corresponding to inactive lesions that have developed chorioretinal scars.

Electrophysiology

Dreyer and Gass[282] reported ERGs on 29 eyes of 16 patients. They observed normal or borderline results in 41% of patients, moderately reduced results in 17%, and severely reduced results in 21% of eyes. Oh and colleagues used multifocal ERG (mfERG) to study pre- and posttreatment results; however, due to the sensitivity of this test, it becomes almost extinguished with active MFC.[318] Furthermore, full-field ERG shows cone and rod depression in MFC with retinal and choroidal atrophy as well as when it is

associated with photoreceptor loss.[288,289] Electrophysiologic tests are not used commonly in the management of MFC.

Visual Field Testing

Blind spot enlargement as a manifestation of multifocal choroiditis was described in 1991.[319] Enlarged blind spot in the setting of a normal optic nerve has been seen and called acute idiopathic blind spot enlargement (AIBSE). The enlargement is thought to be due to peripapillary retinal dysfunction rather than an optic nerve problem.[320] It can be seen in MFC and MEWDS. This is supported by the fact that color vision and pupillary responses have been reported to be normal in these patients. The enlarged blind spot can resolve with inactivity of disease. Visual field testing may also demonstrate scotomas related to areas of photoreceptor loss, chorioretinal scarring, or serous detachments related to active lesions. Visual fields are an important way to monitor MFC.

Systemic Associations

An association between MFC and Epstein–Barr virus (EBV) has been suggested but never proven.[321] It was postulated that EBV triggers an immune response that starts a persistent intraocular inflammatory response. Immunoglobulin M antibodies directed against the viral capsid antigen or the Epstein–Barr early antigen were present in patients with MFC in one series with none in controls.[321,322] However, this could not be reproduced.[323] Some patients with MFC may also have or develop sarcoidosis. These individuals are often not distinguishable from those who have idiopathic MFC.

Pathogenesis

The cause of MFC/PIC is not understood. It typically affects young, otherwise healthy myopic women. There are yellow lesions are seen at the level of the outer retina as seen by OCT and beginning under the RPE. The lesions of MFC/PIC eventually atrophy and look similar to the punched-out lesions of POHS. CNV can develop, leading to bridging scars and subretinal fibrosis. Patients can also develop blind spots and scotomas that can improve with or without

treatment. Lesions resembling MFC have been reported to occur in patients with other white spot syndromes such as APMPPE and MEWDS.[324,325] Jampol and Becker proposed a common genetic hypothesis for autoimmune involvement in these inflammatory processes.[2] The interplay of genetics, immune dysregulation, and environmental triggers may play a role in the different presentations of these clinical entities. Atan and colleagues[280] studied MFC and PIC and found similarities in the association with a IL-10 haplotype, and negative associations with a TNF haplotype. These genetic loci are known to be associated with noninfectious uveitis and autoimmunity. They state that definitive proof will necessitate genomewide sequence analysis. However, their data support the idea that genetic factors have a strong effect on clinical phenotype.

Differential Diagnosis

The differential diagnosis for MFC/PIC includes presumed ocular histoplasmosis syndrome, sarcoidosis, Vogt–Koyanagi–Harada syndrome, sympathetic ophthalmia, myopic degeneration maculopathy, and other white spot syndromes such as serpiginous choroiditis and birdshot chorioretinopathy.

Infectious etiologies for multifocal choroiditis may be considered given the patient's history and health status. These include viral (herpes simplex, herpes zoster, Epstein–Barr, cytomegalovirus, Coxsackie), bacterial (syphilis, tuberculosis, *Borrelia burgdorfori*, septic choroiditis, metastatic endophthalmitis), fungal (histoplasmosis, *Cryptococcus*, coccidioidomycosis, *Candida*), protozoal (toxoplasmosis, *Pneumocystis carinii*), and worms (diffuse unilateral subacute neuroretinitis). Noninfectious etiologies include sarcoidosis, and neoplasias such as intraocular lymphoma can be considered as well.

Differentiation of MFC and POHS

Both entities may show punched-out chorioretinal scars, peripapillary scarring, and CNV. Classically, the teaching is that the difference between these two entities is the presence of inflammation with MFC and absence with POHS. However, MFC can be present without signs of inflammation. Parnell and

colleagues[297] differentiated MFC from POHS based on clinical features, morphology of photographed fundus lesions, and fluorescein angiography. Clinically, MFC patients may develop photopsias and visual field defects. Clinically, distinctive features of MFC include multiple small white lesions clustered in the macula, nasal retina, or equator, a mixture of acute and inactive lesions, progressive growth of lesions, and subretinal fibrous metaplasia with bridging tissue between scars. Other changes include hyperplastic changes around the nerve ("napkin ring"), myopic-appearing nerve, sheathing of vessels or narrowed vessels, and inflammation seen as CME, vitritis, or disc edema (see Chapter 73, Ocular histoplasmosis.)

Management/Treatment

Treatment is aimed at inflammation and its sequelae (CME and CNV). Multifocal choroiditis may be associated with significant anterior and posterior inflammation. This can be managed with topical, periocular, intraocular, or systemic corticosteroids. Steroid-sparing agents are used when steroids are not tolerated or recurrence is frequent. Even if there is no significant visible inflammation, the MFC/PIC lesions do respond to immunosuppressive drugs. Immunosuppression should certainly be considered if there is progressive development of lesions and photoreceptor involvement.[289] CNV can be managed with anti-VEGF therapy with or without the use of corticosteroids. Anti-VEGF has become the standard management strategy. Amer and Lois[286] in their extensive review of literature on PIC suggest that PDT may best achieve closure of already formed neovascularization, while immunosuppressive agents may be most effective in the early stages of development of CNV. Anti-VEGF therapy has been found to be effective in several studies of CNV caused by MFC[326–329]/PIC.[330–332] An additional complication in these patients due to the demographics (young females) is concomitant pregnancy. Steroid therapy is possible during pregnancy; other agents may affect fertility, and teratogenicity is a risk.

Summary

Multifocal choroiditis/punctate inner choroidopathy is an entity

that presents predominantly in young, healthy, myopic women. It may present unilaterally or bilaterally with lesions that are small and multifocal. With new imaging techniques, the outer retina and RPE seem to be the area of involvement. It has varied outcomes; visual prognosis is generally dependent on the status of the macula and development of CNV or fibrosis. Treatments are aimed at reversing these processes.

Multiple Evanescent White Dot Syndrome

Multiple evanescent white dot syndrome (MEWDS), originally presented at ARVO in 1983 and in print in 1984,[333] is an acute, multifocal, usually unilateral retinopathy affecting young adults. Multiple white dots are seen at the level of the outer retina.

Clinical Course

Clinical Symptoms.

Patients usually have an acute onset of blurred vision in one eye. They also may complain of a blind spot or "spots" in their periphery correlating to a temporal scotoma. Photopsias (especially temporally) are common. Patients also may relate flu-like symptoms.[333]

Epidemiology.

No particular racial or regional predisposition for MEWDS has been reported. There is a strong female predominance (75%). Initial visual acuity ranges from 20/20 to 20/300 and, after an average duration of approximately 6 weeks, almost always returns to normal levels. Patients are young, and cases of MEWDS have been reported in children as young as 10 years old and in patients as old as 67 years old.[334,335] Most patients, however, cluster near the mean age of 27 years. A high prevalence of myopes has been reported.[336,337]

Fundus Findings.

Numerous small (100–200 μm) white dots are seen ophthalmoscopically (Fig. 79.47). The white dots are mostly concentrated in the paramacular area, usually sparing the fovea itself, and are less prominent and numerous beyond the vascular arcades.[333] These small "dots" in the retina are distinguished from larger "spots" seen on multimodal imaging (ICGA, FAF), which appear deeper. The dots appear in late ICGA as small hypofluorescent lesions overlying larger hypofluorescent ones (spots).[338] This is discussed further below. Vitreal cells, retinal venous sheathing, and blurring of the disc margins are often present. The classic macular appearance is a granularity (Fig. 79.48). In atypical cases this may be the primary feature present.[339] The white dots disappear completely after a number of weeks or months. They may be replaced by mild pigment mottling, or rarely chorioretinal scarring resembling multifocal choroiditis. An appearance of transient brown areas has also been described after the white spots resolve. These resemble the lesions of AMN but are more numerous and widespread.[340] In the largest case series recently published, 27 of 32 patients also had optic nerve edema.[337] Rarely, a progressive geographic circumpapillary discoloration, appearing as a large white lesion, can be a presenting sign,[341] and peripapillary scarring may be seen after the acute lesions have healed.[342]

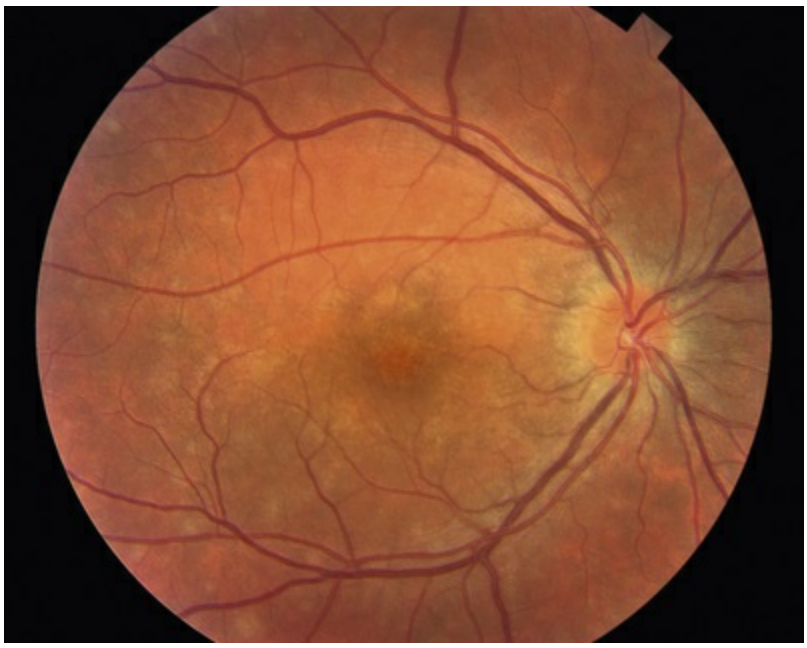

FIG. 79.47 Fundus photo showing subtle numerous white spots. There are also blurred disc margins and foveal granularity.

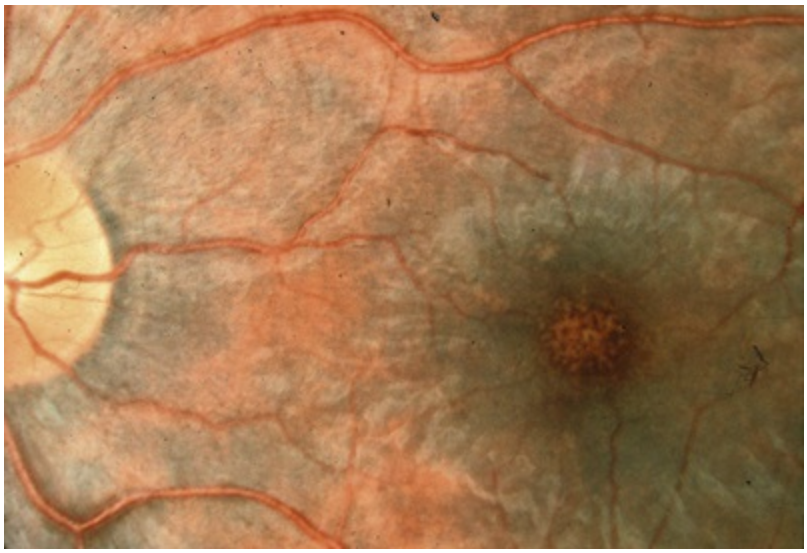

FIG. 79.48 Fundus photo showing granularity of the fovea. This may be the only presenting feature.

Rare instances of late CNV have also been noted with MEWDS.[343,344] Some "idiopathic" cases of CNV could represent MEWDS with resolution of other ocular changes before presentation.[345,346]

Other Ocular Findings.

Mild iritis may be present. Vitritis may be variable.

Clinical Course and Prognosis.

MEWDS is usually a self-limited disease, and recovery of visual function occurs over several weeks (3–10 weeks) with a concurrent dramatic improvement of the electroretinogram (ERG) and early receptor potential (ERP) amplitudes.[333,347] Cases of recurrent MEWDS occur , but determinants predisposing toward recurrence have not been identified.[348] Although usually unilateral, bilateral MEWDS has been reported. Bilateral involvement can be either simultaneous or sequential (seen as recurrence of MEWDS in the opposite eye). Bilateral cases may show asymmetric involvement,

with only one symptomatic eye, or simultaneous symptoms.[337,349]There is a chronic form of MEWDS with evidence of multiple recurrences over many years and involving both eyes.[350] Vision returns to baseline between recurrences in most patients. Some patients complain of visual field disturbances or photopsias even after vision has normalized. Fine and colleagues describe three cases of apparent MEWDS going on to develop a more permanent widespread photoreceptor loss resembling AZOOR.[351] If this occurs, it is extremely rare.

Multimodal imaging of a large series of patients has characterized MEWDS further.[337] OCT has shown that the inflammatory lesions of MEWDS are at the level of the outer retina. (see below). The change in the photoreceptor architecture noted acutely returns to normal.[352,353] The integrity of foveal cones specifically has been studied with OCT and foveal reflection analyzer, and also shows recovery.[354] The foveal granularity is associated with disruption of the IS–OS junction in the fovea with outer retinal swelling. A variety of foveal lesions on OCT have been described.[337] This recovers partially. Although clinical lesions are usually present in one eye, photoreceptor dysfunction has been found to be bilateral in some cases.[353,355] More recent emerging technology, adaptive optics, has been used to show photoreceptor disruption at the cellular level in the acute phase of MEWDS as well.[356] Photoreceptor recovery supports the good prognosis associated with MEWDS. CNV is very rare, but if present can affect visual prognosis.

Imaging

Fluorescein Angiography.

FA findings include early and late hyperfluorescence of the white dots often in a wreath-like pattern; diffuse, but patchy, late staining at the level of the RPE and retina; and disc capillary leakage. The wreath-like hyperfluorescence corresponds to the dots seen clinically, as well as lesions seen on ICGA and FAF.[337] A diffuse noncystoid leakage may be seen in the macula (Figs. 79.49 and 79.50). After resolution of the acute lesions, window defects may be noted in the macula corresponding to the clinical granularity seen

and, less often, elsewhere. Chorioretinal scars with blockage and window defects may occasionally be seen. Of note, in the subacute phase FAF and angiography can still show the lesions after they clinically have resolved.[340] Focal areas of vascular staining are sometimes noted.

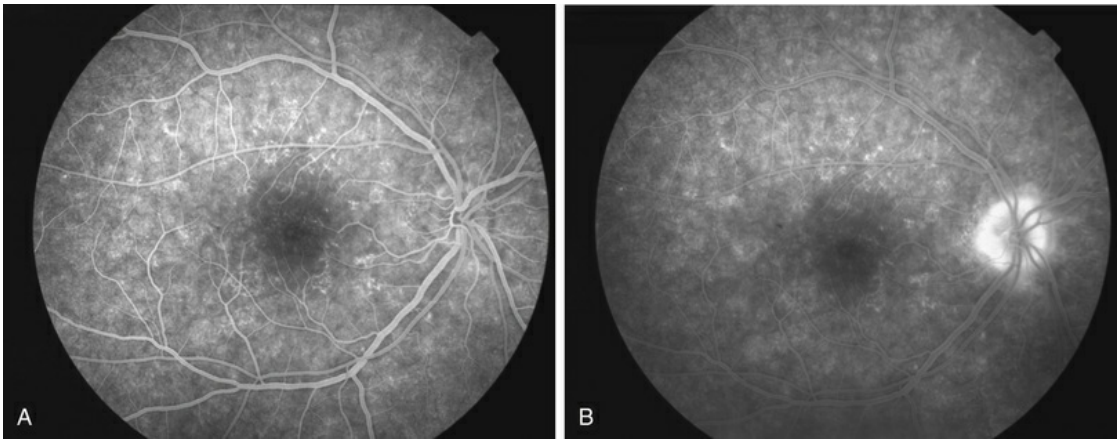

FIG. 79.49 Fluorescein angiography (FA) of the right eye (A) early and (B) late. There is subtle early and late hyperfluorescence of the white dots in a wreath-like pattern. There is late staining of the optic nerve.

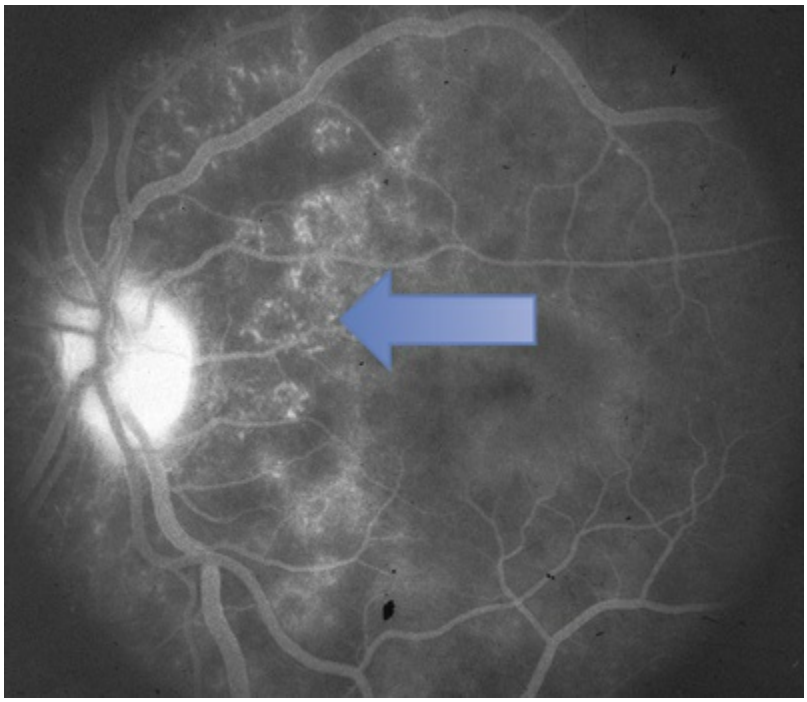

FIG. 79.50 Left eye fluorescein angiography (FA)

close-up of wreath-like pattern (*arrow*); a diffuse, noncystoid leakage is seen in the outer retina in the macula.

Indocyanine Green Angiography.

ICGA in patients with MEWDS shows no abnormalities of large choroidal vessels in the early phase, but hypofluorescent lesions are evident in the late phase, corresponding to the white dots[357] (Fig. 79.51). There can be "spots" that are larger, deeper, and can be confluent appearing as a large plaque of deep retinal hypofluorescence. These hypofluorescent dots and spots are more numerous than those clinically seen. The hypofluorescence in the late phase suggests but does not prove that MEWDS may affect the choriocapillaris, as well as its well-known effect on the photoreceptors.[358,359] These lesions gradually disappear upon recovery,[359,360] but abnormalities on ICGA have been reported to be present up to 9 months after the initial presentation, even after clinical symptoms have resolved.[361,362] Since ICGA reveals lesions not seen clinically or by FA,[363] it has been recommended with some enthusiasm in the patients with MEWDS, mainly to help establish a diagnosis.[364] The blind spot enlargement of MEWDS corresponds to multiple peripapillary lesions, sometimes only detected with ICGA.

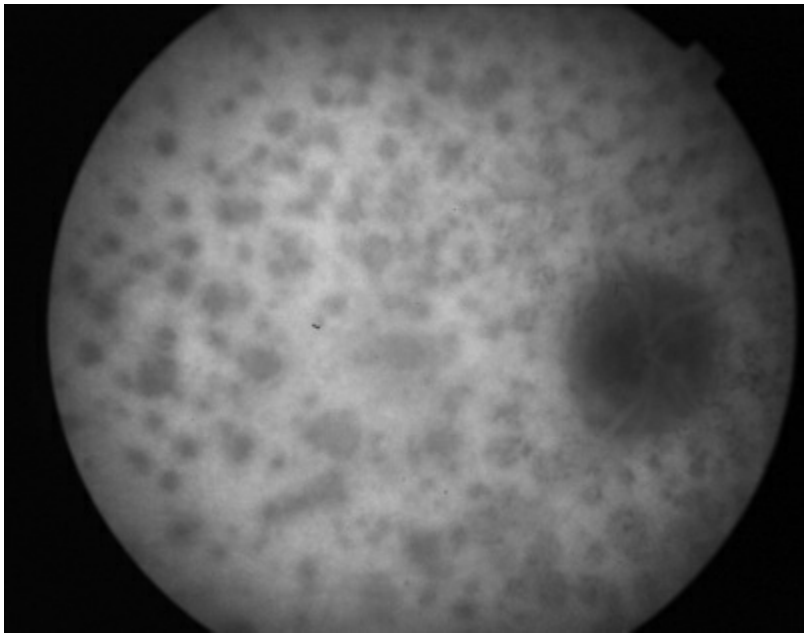

FIG. 79.51 Indocyanine green angiography (ICGA) showing numerous hypofluorescent spots including confluent lesions around the disc.

Laser speckle flowgraphy (LSFG) was recently used to describe the changes to the choroidal circulation in patient with MEWDS.[365] They found that the choroidal blood flow (as defined by mean blur rate (MBR), was decreased in the affected eye as compared to the unaffected eye. Furthermore, it increased in the affected eye by 20.2% at 1 month and 13.3% at 3 months, and this correlated with improving vision. There was no significant change in blood flow in the unaffected eye.[365] It is unclear if these changes are primary or secondary in the pathogenesis of MEWDS. Multimodal imaging analysis, however, strongly suggests that MEWDS is primarily a photoreceptor disease.[337]

Optical Coherence Tomography.

OCT findings were first described using time domain technology. A dome-shaped reflective lesion in the subretinal space was seen corresponding to a clinical white dot. An increased reflectivity in the choroid was seen below this lesion in the acute phase. In the recovery phase, there was a decrease in size of the subretinal material and less reflectivity in the choroid. Ultimately, deep retinal lesions disappeared, but reflectivity was seen in the choroid for several months after active disease.[366] High-resolution OCT revealed disturbance in the ellipsoid zone (EZ also called the IS–OS junction).[367–369] In cases of recurrent MEWDS, a thinning of the outer nuclear layer was seen. RPE disturbance was not a prominent feature.[369] Li and colleagues emphasized that the disruption of the photoreceptor outer segments can be restored anatomically. Functional studies also showed recovery.[353] In addition, although lesions typically occurred unilaterally, the photoreceptor dysfunction is bilateral in most cases.[353] Focal disruption of the EZ[339] is seen even in atypical cases where white dots are not present. In a more recent analysis, these findings have been characterized further. OCT shows multifocal debris in the outer retina and centered on the EZ and also involving the interdigitation zone. In a multimodal analysis, these correspond to the dots seen on fundus photography, FA, and ICGA. Furthermore, confluent spots appear

as a plaque in the outer retina and may be pathognomonic and important in distinguishing MEWDS from other diseases. Protrusions of the hyperreflectant material towards the ONL correspond to the smaller dots seen on fundus photography[337] (Fig. 79.52). Therefore, this study is of particular importance in making the diagnosis of MEWDS (Fig. 79.53). Analysis of the choroid with enhanced-depth imaging suggested a trend towards transient choroidal thickening in the acute phase, and en face imaging showed an unremarkable choroid and choriocapillaris.[337] One published case described a patient with MEWDS who developed acquired focal choroidal excavation suggesting RPE/Bruch's membrane involvement.[370]

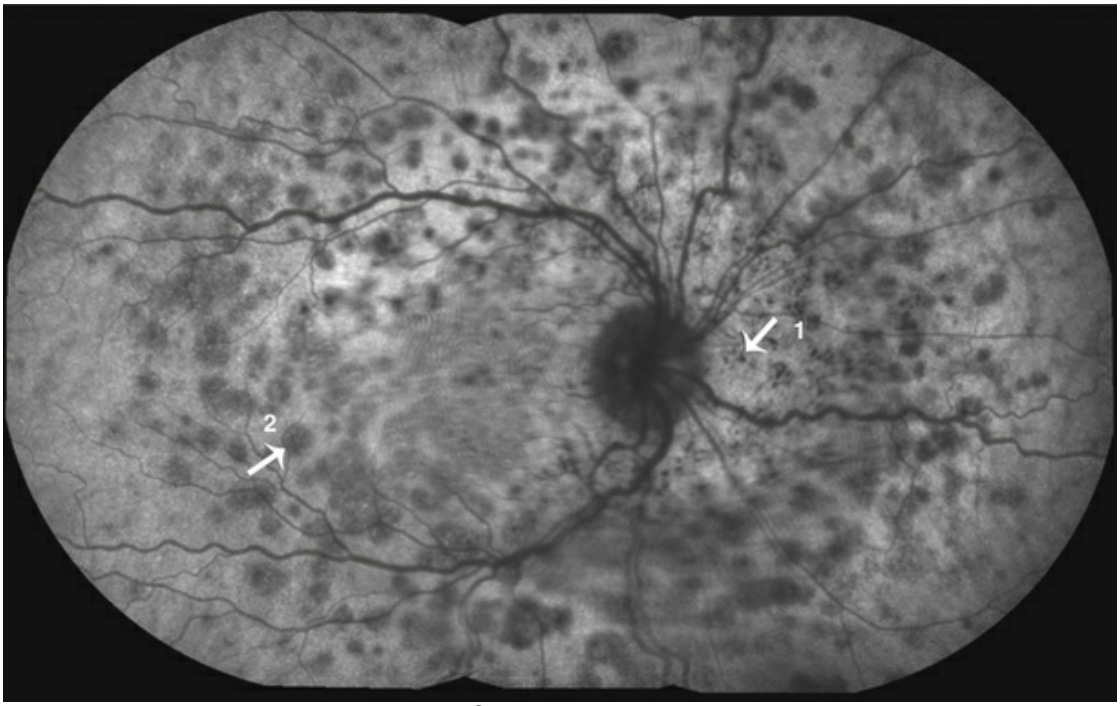

FIG. 79.52 Fundus autofluorescence (FAF) illustrates smaller, more superficial dots (*1*) on larger, deeper spots (*2*) characteristic of multiple evanescent white dot syndrome (MEWDS).

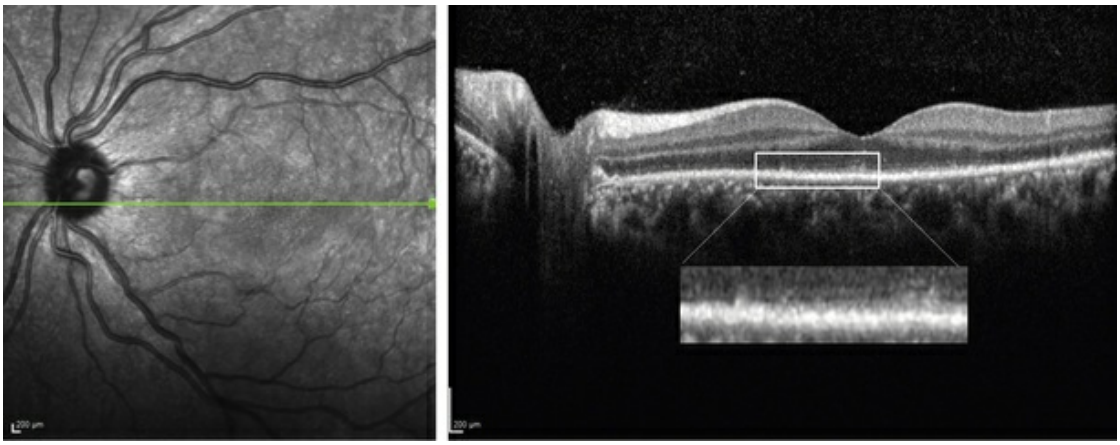

FIG. 79.53 Optical coherence tomography (OCT) shows small projections in the outer retina corresponding to "dots." Near-infrared reflectance imaging highlights the granular fovea.

Fundus Autofluorescence.

Dell'Omo and colleagues studied MEWDS in the acute and subacute phases and characterized specific FAF findings. Hypoautofluorescent areas were seen concentrated around the optic disc and posterior pole. Areas of hyperautofluorescence were seen as well, corresponding to the white dots.[371] Furino and colleagues described this as well.[372] In the recovery phase, many of the hypoautofluorescent lesions faded, while others persisted. The areas of hyperautofluorescence became smaller and more consolidated. They also retracted centripetally, becoming smaller with a ring of hypoautofluorescence around them, or became entirely hypoautofluorescent. In other cases, they disappeared altogether without becoming hypoautofluorescent.[371] These hypoautofluorescent spots generally correlate with the lesions seen with FA and ICGA.

Near-infrared autofluorescence (NIR-FAF) is a modality where a wavelength of 787 nm is used instead of the blue light used in traditional FAF. Some suggest that there may be additional value to seeing the white dots as hypoautoflourescent lesions in this modality[373](Fig. 79.54).

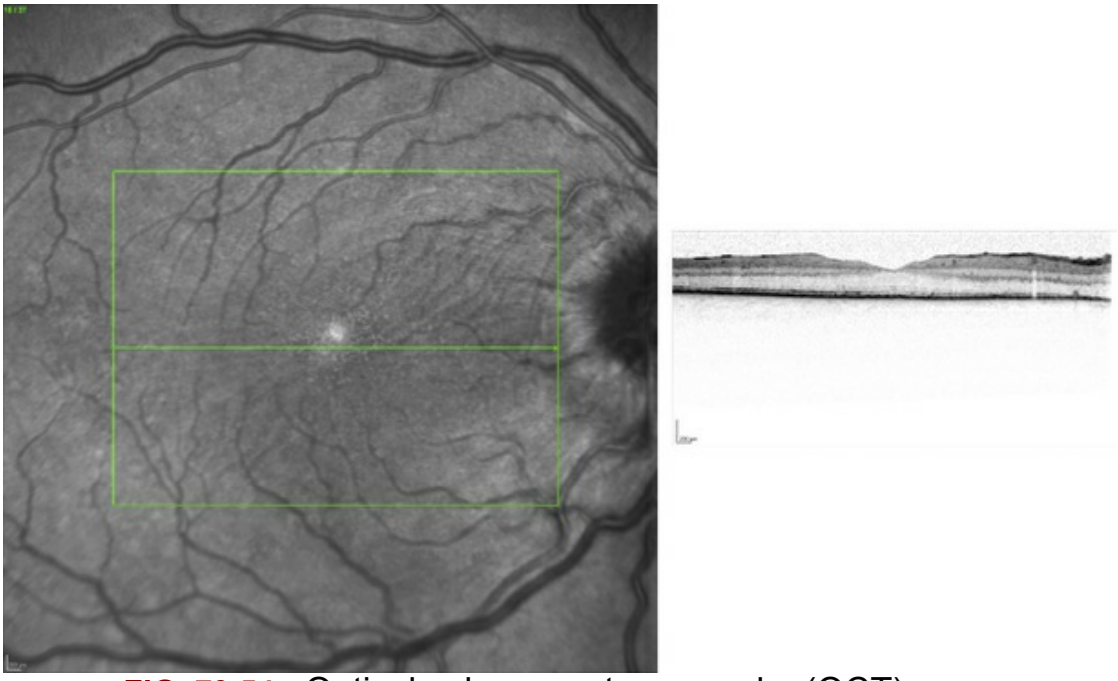

FIG. 79.54 Optical coherence tomography (OCT) through the fovea shows swelling of the outer retinal layers and granules at the level of the retinal pigment epithelium. (Courtesy of Medical University of Vienna.)

Electrophysiology

Electrophysiologic studies in patients with acute MEWDS[347] have found reduced ERG a-wave and reduced ERP amplitudes that would suggest a primary involvement of the outer segments of photoreceptors. Focal ERG studies reveal delayed recovery of oscillatory potential (OP), which implies some inner retinal involvement.[374] Studies[375] have used foveal densitometry and color matching to show that, even with normal ERG findings, abnormalities exist during the active stage of MEWDS at the level of the cone photoreceptor outer segments. A transient metabolic disturbance at the level of the pigment epithelium–photoreceptor complex has been suggested. Multifocal electroretinography (mfERG) shows areas of depression that correspond to scotomas while full-field ERG shows a general depression. These abnormalities resolve after 6 weeks.[376] In addition, mfERG shows supernormal amplitudes of the first-order kernel of N1- and P1-wave amplitudes at the beginning of the disease; these values decrease to normal or subnormal values by 2 weeks and may be

helpful in detecting early stages of MEWDS or for follow-up.[377]

Visual Field Testing

Visual field testing often shows an enlarged blind spot. Testing can range from normal to a generalized depression to cecocentral or arcuate scotomas.[378] Visual field abnormalities may persist for an extended period beyond the resolution of clinical lesions.[379] Newer microperimetry testing also shows enlarged blind spots.[380] In addition, microperimetry has shown decreased retinal sensitivity in areas of EZ abnormalities, when correlated with SD-OCT.[381]

Pathogenesis

We believe that with multimodal imaging we can clearly differentiate MEWDS from other WSS. The cause of MEWDS is unknown.

At the present time we do not have definite evidence for an infectious or immunologic cause for MEWDS. A single patient with chronic relapsing MEWDS was noted to respond to cyclosporine therapy.[382] Laatikainen and Immonen[383] described an increased level of protein in the cerebrospinal fluid in MEWDS patients. The occurrence of MEWDS following varicella infection,[343] vaccination for hepatitis A[384] or hepatitis B,[385] or most recently reported in a young girl after vaccination for human papilloma virus and meningococcus[386] suggests environmental triggers. One case of MEWDS from China with no previous or concurrent illness exhibited increased serum immunoglobulin M (IgM) and IgG values.[387] Recovery of vision in 3 weeks was coincident with the return of the IgM value to normal values. Data from this case suggested that MEWDS might be associated with a viral syndrome, although tests for herpes zoster, herpes simplex, mumps, and measles were inconclusive. Any explanation of the etiology of MEWDS must explain the strong female predominance, the occurrence of occasional chronic relapsing cases, and the excellent visual outcome in almost every case. The HLA locus may be important. A preliminary study found the frequency of HLA-B51 haplotype to be 3.7 times more common in patients with MEWDS than a normal control group.[388,389]

Our present suggestion is that a variety of relatively common

susceptibility genes may be responsible for MEWDS. These predispose to immune dysregulation. Precipitated by environmental triggers, MEWDS may develop. If this theory is true, then patients with MEWDS may demonstrate a family or personal history of autoimmunity. In investigating this, we have found an increased prevalence of autoimmunity in patients with white spot syndromes and their families, but the number of MEWDS cases was very small.[2,4] While the etiology of MEWDS is studied further, we believe that MEWDS is a distinct clinical entity that should not be confused with other WSS.

Differential Diagnosis

The differential diagnosis of MEWDS includes acute posterior multifocal placoid pigment epitheliopathy (APMPPE) and birdshot chorioretinopathy. Other chorioretinopathies such as sarcoidosis and diffuse unilateral subacute neuroretinitis must be considered. In middle-aged or older patients, ocular infiltration by lymphoma must be ruled out.

Patients with MEWDS often present with signs and symptoms suggesting primary optic nerve disease, including disc edema, visual loss, afferent pupillary defect, enlarged blind spot, and other optic nerve field defects. Dodwell et al.[390] reported five cases that were initially misdiagnosed as primary optic nerve disease, as the white spots were subtle findings. Optic nerve involvement in MEWDS could theoretically contribute to the central visual loss, visual field loss, afferent pupillary defect, and even dyschromatopsia. MEWDS should be considered in the differential diagnosis of young, healthy patients who present with unilateral optic nerve dysfunction.[391,392]

The challenge of correctly diagnosing MEWDS lies in its variable, sometimes subtle, presentation and the rapid reversal of the visual loss with disappearance of the white dots. It should be noted that blind spot enlargement may be a feature of MEWDS, MCF/PIC, and perhaps other WSS

Management/Treatment

The natural course of MEWDS is excellent, and no intervention is required. We do not support the use of steroids in MEWDS.

Although CNV is not common in MEWDS, anti-VEGF therapy has been used with success in a few cases.[393,394]

Summary

MEWDS usually presents in young myopic females who may describe a viral prodrome. Generally, clinically the retinopathy is unilateral. Clinically there are three diagnostic findings: (1) grayish-white dots scattered in the posterior pole; (2) foveal granularity; and (3) optic nerve edema. Foveal granularity is the classic hallmark of this condition and defining feature. Multimodal imaging has shown that this is a photoreceptor disease.[337] The course is almost always good, and no intervention is required.

Acute Zonal Occult Outer Retinopathy

Acute zonal occult outer retinopathy (AZOOR) has been linked by Gass to the white spot syndromes (AZOOR complex) although it has no white spots. In the early 1990s, Gass[395] described 13 patients with what he called acute zonal occult outer retinopathy. These were, in general, young, healthy patients, who abruptly developed photopsias and the presence of a scotoma in a local area of the retina. Examination initially showed minimal fundus changes; however, a dense scotoma could be plotted in the involved area. With the passage of time, these zones often developed pigment epithelial mottling, bone spicule pigmentation, and some choroidal atrophy (Fig. 79.55). The changes, when widespread, could resemble retinitis pigmentosa.[396]

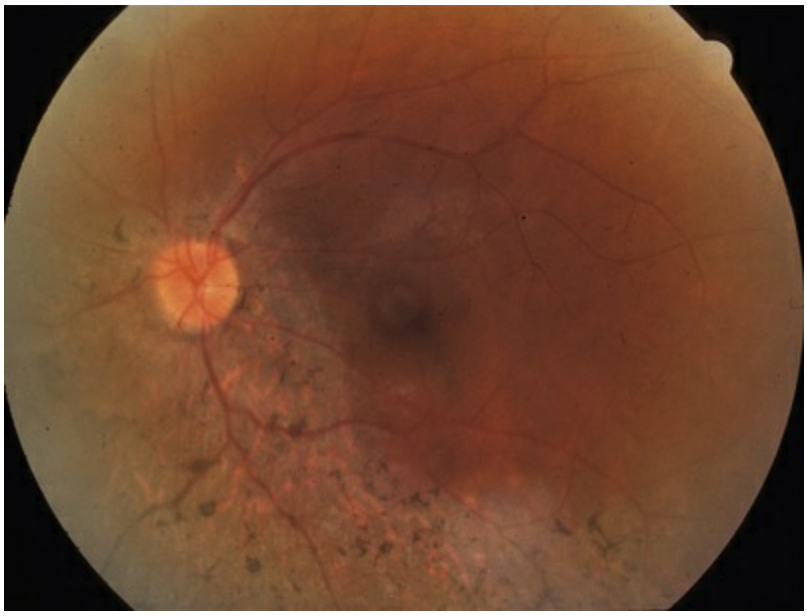

FIG. 79.55 Fundus photo of advanced acute zonal occult outer retinopathy. Pigment epithelial atrophy and bone spicule formation can be seen in continuity with the disc.

Gass[5,397] used the term AZOOR complex. Within this description he included MEWDS, AIBSE, AMN, PIC, and MFC. He felt that these diseases were somehow related; they demonstrated outer retinal dysfunction and usually occurred in young, healthy females. With the advent of multimodal imaging analysis, we believe that AZOOR is a distinct entity and can be distinguished from other white spot diseases.[288,289,398] The term AZOOR complex is thus outdated. The disease has recently been reviewed, and a classification based on multimodal imaging has been described by Mrejen and colleagues and is described in this section.[398]

Clinical Course

Clinical Symptoms.

Patients with AZOOR have the abrupt onset of a scotoma related to outer retinal dysfunction. Most have photopsias. They may complain of central visual disturbance and night vision difficulty.[398] There may be recurrences, new scotomas, or an increase in the size of the scotoma. The scotoma is often contiguous with the optic nerve. The disease may be unilateral initially but some progress to bilaterality.

Epidemiology.

AZOOR is seen in all ethnic groups, although the literature shows a predominance of Caucasians. There is a marked predominance of women. Most patients are young, although occasionally elderly patients are involved. In the United States, a recent review showed a mean age of 47 years (range 17–86). A review of 38 cases in Japan showed a mean age of onset of 33.2 years (range of 15–47 yrs) with a high prevalence (92.3%) of myopia in their population.[399] Some of the patients relate a preceding viral illness. There is no definite association with any systemic diseases. Patients generally present with good vision.[398]

Fundus Findings.

The fundus initially appears normal; subsequently the area of involvement will show retinal atrophy and mottling. The foveal cones appear to be relatively resistant to AZOOR accounting for good vision in many cases. If the onset of symptoms is recent, an abrupt transition can be seen. A gray–white line may be present at onset between normal and involved retina.[398] It is transient and can disappear within weeks. Gass and Stern described this acute annular occult retinopathy (AAOR) as a variant of AZOOR[400] (Figs. 79.56 and 79.57). We now believe these were cases of AZOOR. The gray–white line fades. An orange zone may develop between normal and abnormal retina.[398] The area of involvement is often peripapillary, but usually the central vision is good even if involvement extends to the fovea. Patients can have "skip" lesions with larger areas of involvement (typically peripapillary) and smaller areas elsewhere.[398] The arterioles attenuate with time (Fig. 79.58). The late appearance may resemble sectoral retinitis pigmentosa. The appearance can also resemble diffuse unilateral subacute neuroretinitis (DUSN). CNV is seen rarely.[398,401]

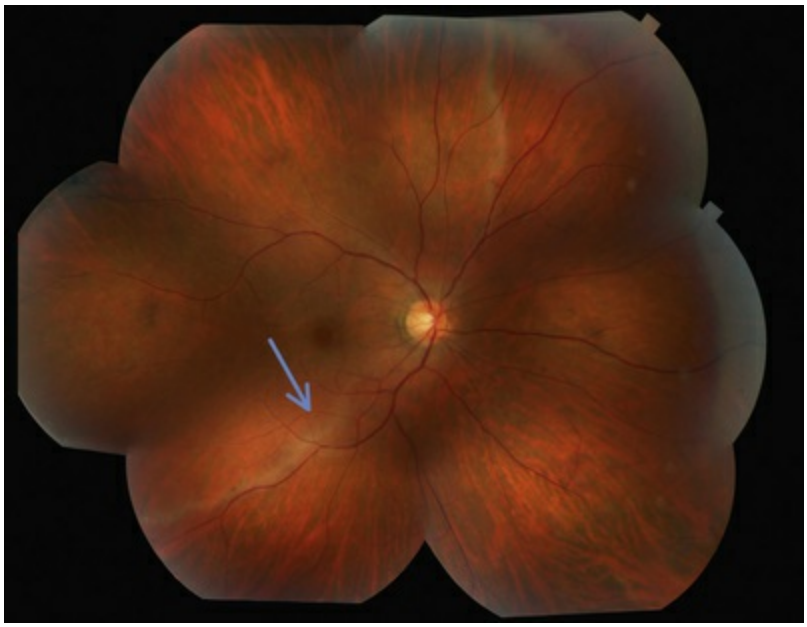

FIG. 79.56 Fundus photo of acute annular occult outer retinopathy. A grey–white line (*arrow*) is present between the normal retina to the right and involved retina to the left. (Courtesy of Manjot K. Gill, MD.)

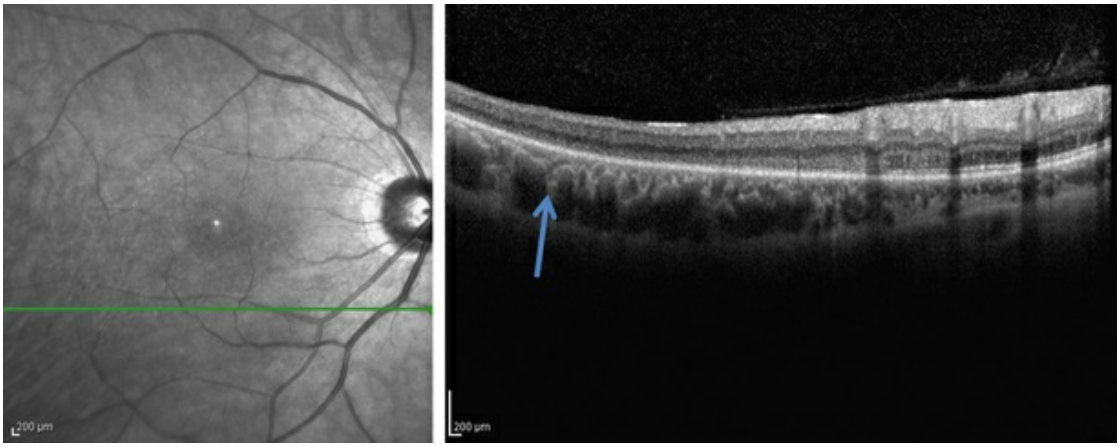

FIG. 79.57 Optical coherence tomography (OCT) shows retinal thinning in the involved area. (Courtesy of Manjot K. Gill, MD.)

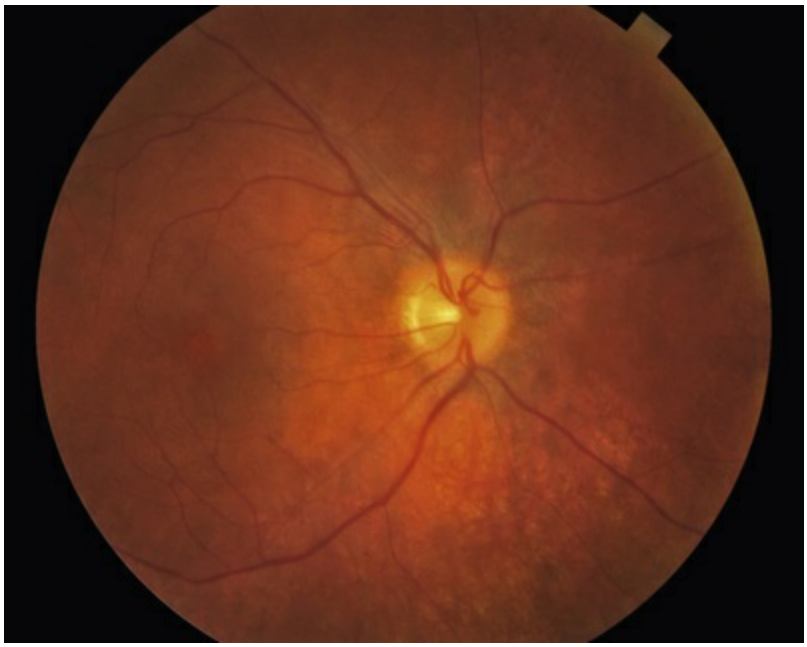

FIG. 79.58 Fundus photo. Subtle fundus changes are seen. Arteriolar attenuation is present.

Other Ocular Findings.

The eyes are quiet without evidence of anterior chamber reaction. There may be a few vitreous cells.[398] Disc leakage, retinal vascular staining (periphlebitis), and some CME may rarely be seen.

Clinical Course and Prognosis.

Patients may show progression, with new areas of retinal involvement. Occasionally there may also be some improvement in visual function in the involved areas. Gass[397] suggested that most cases were active for about 6 months and then stabilized. In a Japanese case series with mean follow-up of 31 months, prognosis was reported to be very good with good visual outcomes and recurrence only in 9 of 38 patients.[399] However, there is little literature on the long-term follow-up of this disease. What we know from the existing literature is that chorioretinal atrophy may lead to severe vision loss, and prognosis is limited based on this.[402] There may exist a spectrum of severity with some showing little fundus change and reversal of abnormalities on imaging[403] to more severe disease that can resemble inherited dystrophies.

Imaging

Fluorescein Angiography.

Initially the fluorescein angiogram may be normal. Then window defects and abnormalities at the level of the pigment epithelium become apparent. Retinal arteriolar narrowing in the areas of involvement may be seen. Retinal vessel staining and leakage may be seen (Fig. 79.59).

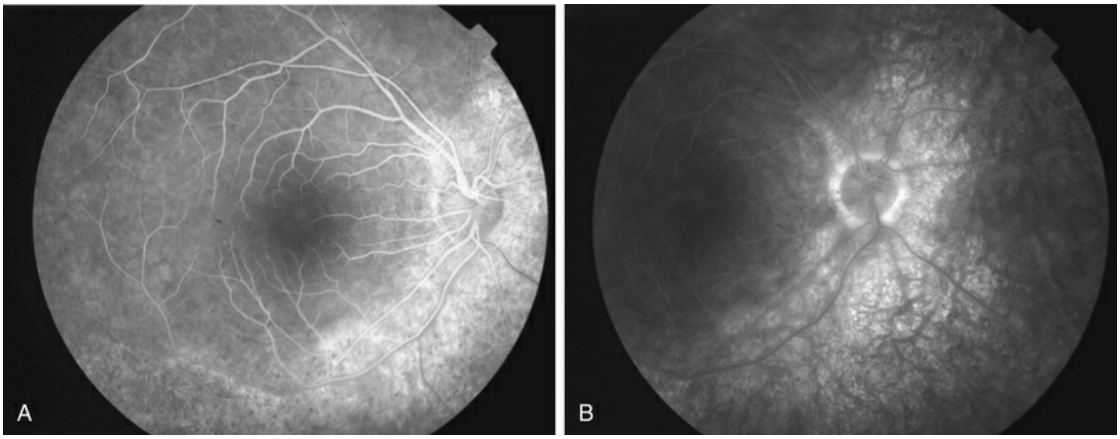

FIG. 79.59 (A,B) Fluorescein angiography (FA) shows peripapillary zonal retinal pigment epithelium abnormalities with window-type defects.

Characteristic "Trizonal" Pattern of Azoor.

Fundus Autofluorescence.

The AZOOR line, the transition from normal to involved retina, is best seen with FAF. It is hyperautofluorescent initially around the zonal area of involvement. With time, it can become discontinuous or beaded in appearance.[398] In some patients there is a diffusely hyperautofluorescent area that is surrounded by speckled hyperautofluorescence. Later these areas become hypoautofluorescent. The peripapillary area is most involved. The three zones of autofluorescence are (1) normal autofluorescence outside the delineating line; (2) speckled hyperautofluorescence bordering the affected area; and (3) hypoautofluorescence in a region of atrophy[398,404,405] (Fig. 79.60).

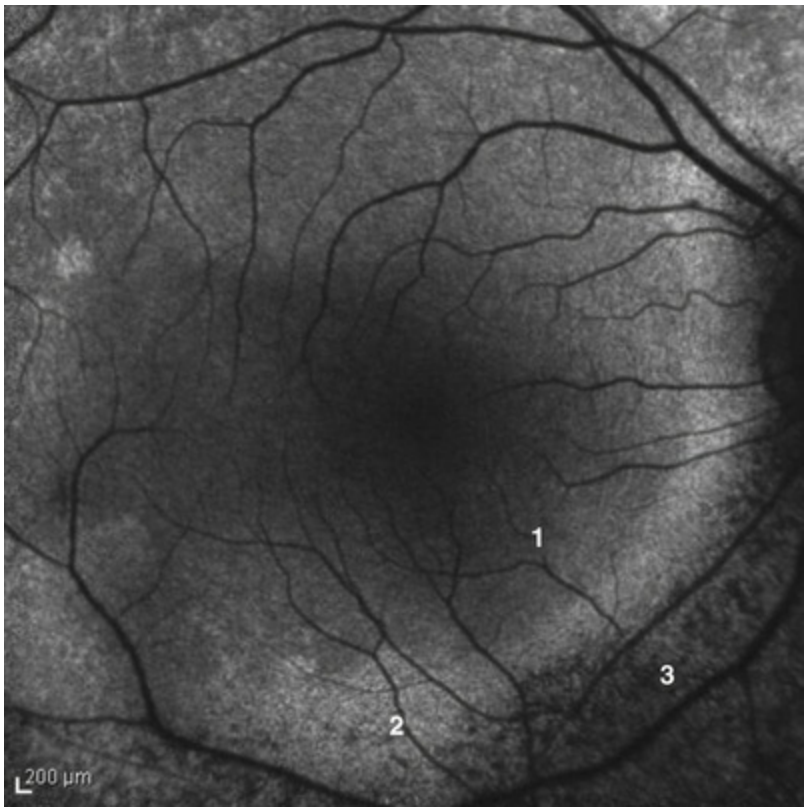

FIG. 79.60 Fundus autofluorescence (FAF) shows the characteristic "trizonal" pattern of autofluorescence. Zone 1 – normal autofluorescence. Zone 2 – speckled hyperautofluorescence. Zone 3 – hypoautofluorescence.

Optical Coherence Tomography.

Spectral domain OCT corresponds to the changes seen on FAF: (1) outside the AZOOR line, the OCT is normal; (2) inside the line, there is presence of subretinal hyperreflective material and there is an absence or irregularity of the ellipsoid zone; (3) with chronicity, atrophy of the RPE and thinning of the retina may be seen with the outer nuclear layer and then the inner nuclear layer thinning. Disruption may extend to the inner retina as well. Choroidal atrophy occurs (Fig. 79.61).[398,405–407]

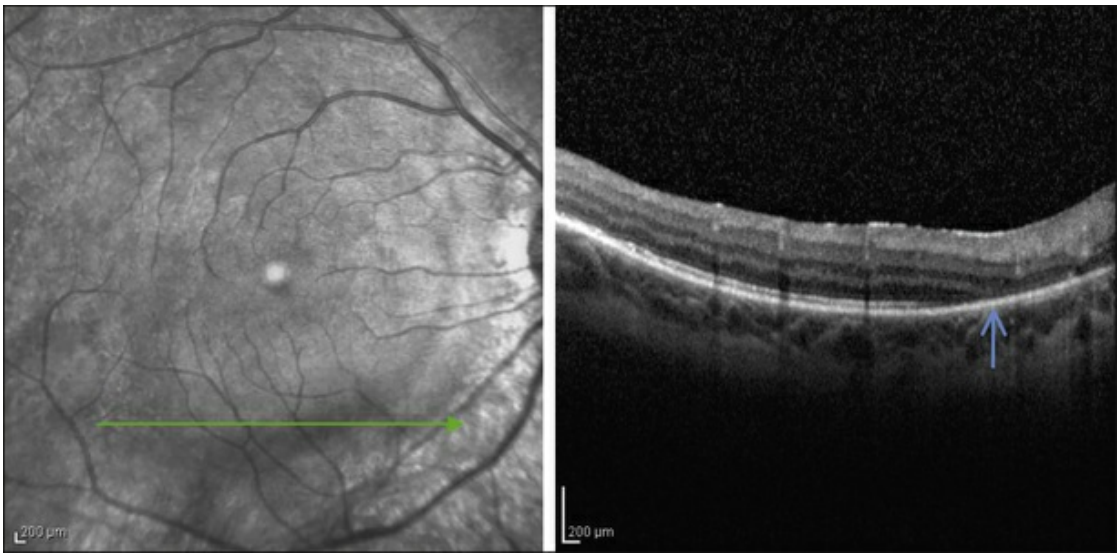

FIG. 79.61 Optical coherence tomography (OCT) shows absence of the ellipsoid zone line in the area of retinal involvement (*arrow*).

Indocyanine Green Angiography.

ICGA may be normal or may show hypofluorescence in the area of involvement. This depends on the stage of disease. In chronic AZOOR, (1) ICGA is normal outside the involved area; (2) there is late extrachoroidal leakage inside the AZOOR line; (3) hypofluorescence is noted due to loss of choriocapillaris within the late lesion.[398]

Visual Field Testing

Scotomas (usually peripheral and temporal) develop often in continuity with the optic disc. These are usually dense. With healing, some improvement may occur, but the functional loss is often permanent (Fig. 79.62).

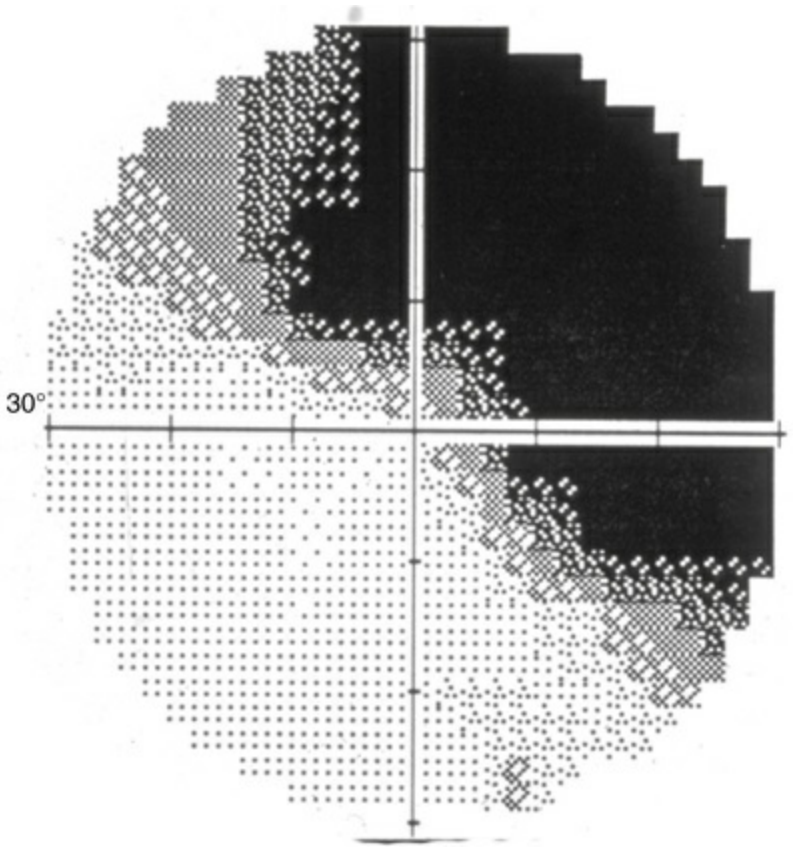

FIG. 79.62 Perimetry shows a dense zonal defect.

Electrophysiology

Focal ERG demonstrates abnormalities in the area of the scotoma. Full-field ERGs are almost always abnormal, if large enough areas of the retina are involved.[397] EOG testing is usually abnormal.

Adaptive Optics Scanning Laser Ophthalmoscopy

This modality is particularly useful in AZOOR as the photoreceptors are primarily involved. A case of a man presenting with AZOOR showed dark areas on AO-SLO corresponding to disruption of the ellipsoid zone on OCT, indicating decreased cone density. As the patient improved, there was reversal of the dark areas to a normal mosaic appearance.[403] In another series, 3 of 4 patients demonstrated focal cone loss and 1 patient demonstrated abnormal cones, but the rods appeared normal.[408] In another series of 12 eyes, 8 eyes had abnormally hyporeflective areas on near-infrared images that corresponded to an abnormal ellipsoid zone on SD-OCT. Cone mosaics were abnormal in the corresponding areas

on AO-SLO.[409]

Systemic Associations

Systemic autoimmune diseases have been noted in some patients with AZOOR.[396] Like other white spot syndromes, it may be occurring in patients with immune dysfunction.[2,4]

Pathogenesis

Mechanisms causing vision loss with the development of AZOOR remain obscure. Could this be an autoimmune attack on the retina? A possible association with systemic autoimmune disease suggests this.[4] In a recent study, three patients with acute AZOOR were evaluated with molecular biological methods and all were found to have antiretinal antibodies.[410] However, no specific antiretinal antibodies have been identified, and the presence of antibodies may be coincidental or a secondary phenomenon (epiphenomenon) not related to the underlying disease process.

Gass suggested that AZOOR is possibly a viral infection, with the virus entering the eye from the optic disc and thus producing peripapillary lesions.[5] There is no evidence supporting an infectious etiology of AZOOR at this point.

Differential Diagnosis

The visual loss of AZOOR must be distinguished from optic neuropathies. OCT should show ellipsoid zone abnormalities in the involved area. It may initially be difficult to distinguish AZOOR from other entities with outer retinal dysfunction, but the characteristic trizonal pattern of multimodal imaging can distinguish these cases. Patients with hereditary retinal diseases (e.g., retinitis pigmentosa) develop changes that can possibly resemble AZOOR. These changes may be sectoral or asymmetric. Some of the patients with hereditary diseases have been shown to have antiretinal antibodies (the role these play in the pathophysiology of the diseases is unproven). Retinal dystrophies are usually bilateral, symmetric, and slowly progressive, distinguishing them from AZOOR. Patients with cancer-associated retinopathy (CAR) or melanoma-associated retinopathy (MAR)

may show outer or inner retinal dysfunction with autoantibodies against the retina. These cases can resemble AZOOR. A poorly defined group of patients have been felt to have "autoimmune retinopathies" without cancer where antiretinal antibodies or cell-mediated immunity may cause retinal dysfunction.[411] The clinical presentation of AZOOR – local and segmental, often peripapillary, or at least contiguous with the disc – helps in the diagnosis.

Management/Treatment

No proven therapy exists. There is only meager evidence of an effect of systemic corticosteroids and other immunosuppressive drugs.[343,412] Antiviral drugs and antibacterial drugs have also been tried. Recently, Mahajan and Stone[413] reported the response of three patients to valaciclovir. Although these patients did show clinical improvement, they were early on in their course and their clinical appearances were not typical for AZOOR. The value of this drug for AZOOR remains uncertain, and we have not found it helpful in our hands.

Summary

AZOOR is a disease of sectoral or zonal outer retinal dysfunction, often adjacent to the optic nerve. Characteristic features include a demarcating AZOOR line at the level of the outer retina, a trizonal pattern of sequential involvement of the outer retina, RPE and choroid (seen on FAF, OCT, and ICGA), and zonal progression. Although the fundus initially appears normal, the development of pigmentary changes occurs. Outer retinal and RPE changes are seen in most cases, and some inflammation may be seen. At the present time there is no definitive evidence of an infectious cause of AZOOR. Autoimmune disease is perhaps suggested by the female predominance. Differentiating this condition from hereditary retinal degenerations, CAR, MAR, and autoimmune retinopathies is necessary, and the trizonal multimodal imaging pattern is often helpful in this process.

Acute Macular Neuroretinopathy

Acute macular neuroretinopathy (AMN) was first described in 1975 by Bos and Deutman.[414] It is an increasingly recognized condition that causes transient or permanent visual changes.[415] The distinct macular lesions of AMN are reddish-brown in appearance and wedge-shaped or flower-like pointing to or encircling the fovea. The level of the retina involved has been controversial. Originally it was thought to be a disease of the inner retina. Newer imaging techniques have shown the middle and outer retina are involved.[416–421] Fawzi and colleagues used multimodal imaging and found that the disease starts at the level of the outer plexiform layer and then rapidly involves the outer retina.[422] Multimodal imaging and clinical associations suggest that vascular compromise is the cause. In understanding this disease, it is important to review that there are three capillary layers of the retina. The superficial capillary plexus (SCP) is the innermost, and when compromised causes cotton-wool spots and hemorrhage. Next, the intermediate capillary plexus (ICP) may be associated with paracentral acute middle maculopathy (PAMM) (discussed further below) when it is ischemic. Finally, an outermost layer, deep capillary plexus (DCP) insult may cause AMN. Reports now appearing suggest that vascular ischemia can damage the three functional layers of the retinal capillaries. One, two, or three of these vascular beds may be involved on a given patient.

Clinical Course

Clinical Symptoms.

Patients complain of decreased vision and paracentral scotomas. A viral prodrome (recently dengue fever has been described),[423] sympathomimetic drug use, anemia, and thrombocytopenia among other associations are now recognized.

Epidemiology.

AMN may occur in young women in the second to fourth decades of life.[414] In a review of the literature, Turbeville reported that 83%

of reported cases to 2002 were women with a mean age of 27 years.[424] Interestingly, 41 cases of AMN were published from 1975 to 2002. From 2002 till 2012, 43 cases were published in the English literature,[425] showing the increased recognition of this disease, largely due to multimodal imaging (especially OCT and near-infrared images).

Fundus Findings.

One or several small lesions are seen surrounding the fovea at the level of the outer retina. These may be round, oval, or petaloid[414,424] (Fig. 79.63). They appear brown or dark red compared to the surrounding retina.[414,418] The lesions are best seen on red-free photography or near-infrared reflectance imaging. Retinal hemorrhages have been reported.[424] No abnormality is obvious in the retinal vessels or optic disc.

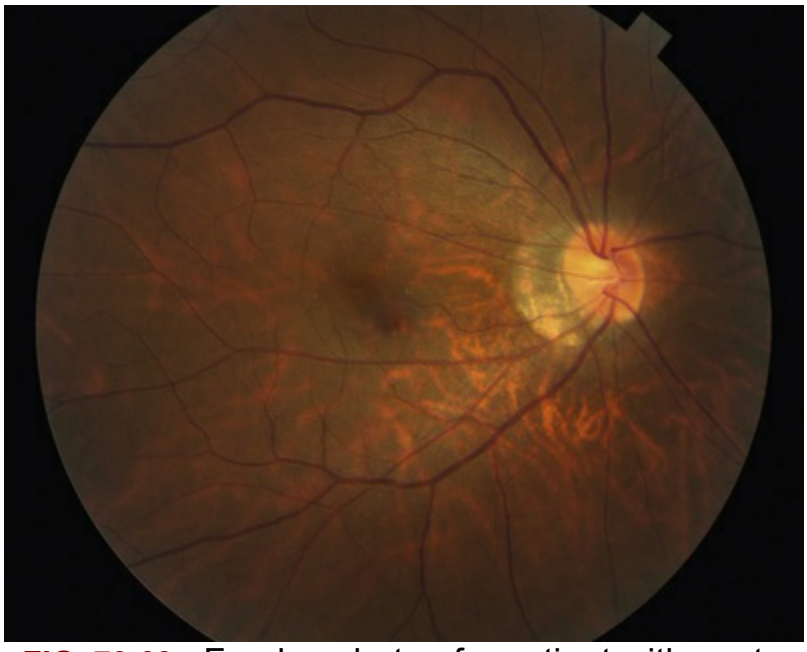

FIG. 79.63 Fundus photo of a patient with acute macular neuroretinopathy. Subtle macular reddish-brown lesions are seen.

Clinical Course and Prognosis.

The disease process may be unilateral or bilateral. Patients are often seen several days after the development of scotomas.[424] The lesions

may develop rapidly or over the course of days to weeks. Turbeville and colleagues noted a different time course in those cases that were related to viral prodrome and those that developed in association with epinephrine. Patients who reported an influenza-like illness had an onset of scotomas generally over days to weeks, though sudden onset was also possible. With time, some of the symptoms and lesions resolved, though patients remain mildly symptomatic. In contrast, all the epinephrine cases were sudden, bilateral, and did not seem to resolve with time. They postulated that this may represent different mechanisms.[424]

Recurrences may occur in one or both eyes. The acute retinal lesions fade but generally do not disappear completely. Complete recovery has been reported in a few cases.[424] Newer imaging techniques as further discussed below suggest that there are persistent anatomical changes in the outer retina despite subjective or clinical improvement.[426]

Imaging

Fluorescein Angiography.

Usually, FA results are normal. Sometimes there may be a slight hypofluorescence corresponding to blockage from the clinically seen lesions.[414,418,427]

Indocyanine Green Angiography.

ICGA is normal.[428]

Optical Coherence Tomography.

Much of the recent literature on AMN is devoted to OCT findings.[415,417,428–435] The infrared images seen with OCT highlight the lesions best. The reddish-brown clinical lesions correspond to focal changes in the photoreceptors[422] (Fig. 79.64). Early SD-OCT findings were described in a 29-year-old woman 3 hours after the onset of symptoms. An isolated hyperreflectivity at the posterior border of the outer plexiform layer was described. Seven days later she developed a wedge-shaped lesion with hyperreflectivity of the ONL and ellipsoid zone, and the outer plexiform layer (OPL) was no longer hyperreflective.[436] The findings on infrared reflectance

and OCT change rapidly over time in the first few weeks. Fawzi and colleagues described eight patients using multimodal imaging in 2012. Hyperreflective bands involving the OPL and ONL occurred acutely. Then disruption of the ellipsoid zone was seen. As the hyperreflectivity subsided, there was thinning of the ONL. The interdigitation line is also affected, and changes may persist even after the ellipsoid zone recovers.[422] En face SD-OCT has been characterized in a case report of bilateral AMN and correlates with Fawzi's description. The patient was imaged 5 months after the onset of symptoms and found to have a thinned ONL and disruption of the ellipsoid and interdigitation zones corresponding to the reddish lesions seen clinically.[437]

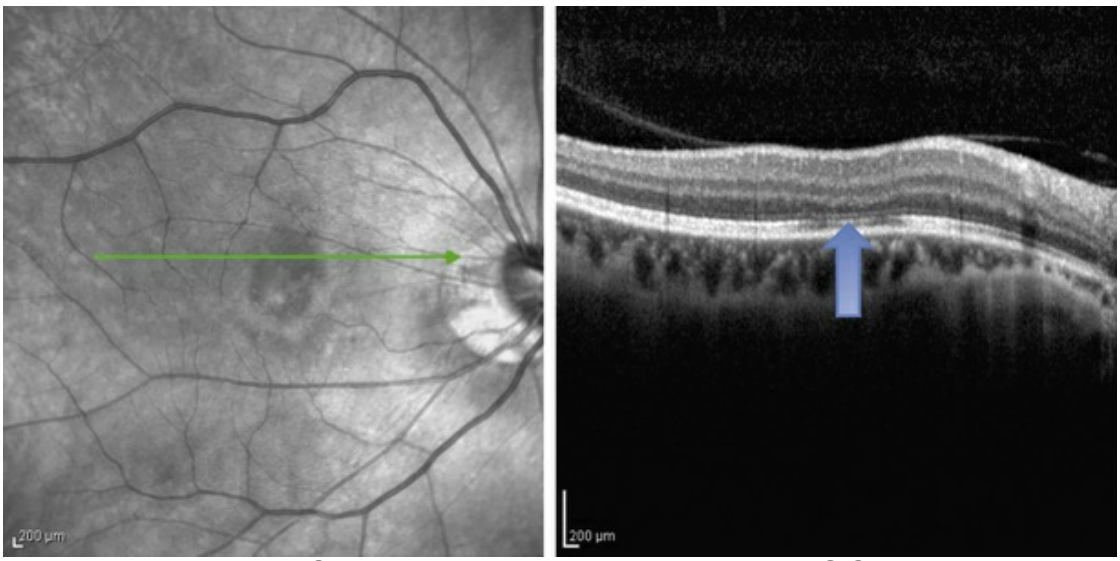

FIG. 79.64 Optical coherence tomography (OCT) shows that the lesions correspond to focal interdigitation zone defects (*arrow*).

Fundus Autofluorescence.

Subtle hypoautofluorescence corresponding to clinical lesions has been reported.[415]

Electrophysiology

Multifocal ERG has shown decreased foveal peaks in affected eyes.[416,434] Researchers using mfERG localize the lesion to the outer

retina affecting the photoreceptor or bipolar cell layer. Changes may persist for longer durations.[438,439] ERG and EOG are generally normal.[440]

Visual Field Testing

Paracentral scotomas are seen corresponding exactly to the shape and location of the clinical lesions. Patients can draw their scotomas on an Amsler grid.[414] When defects are very small, microperimetry may be helpful.[441,442]

Adaptive Optics

AO-SLO has shown that cone photoreceptors are disrupted within areas of defects measured by microperimetry.[443] The area of decreased cone photoreceptor density has also been shown to be larger than the area that was seen on near-infrared imaging or SD-OCT, and it may not completely recover.[444]

Systemic Associations

Oral contraceptive use, flu-like syndrome, dengue fever, anemia, thrombocytopenia, contrast media exposure, caffeine use, epinephrine use, trauma, history of headaches/migraines, postpartum hypotension, diabetes mellitus, and hypotensive shock have all been described in patients who developed AMN.[423–425]

Pathogenesis

Retinal ischemia related to insult to the deep capillary plexus seems to be the etiology. Imaging shows involvement of the photoreceptors and the development of zones of outer retinal thinning. Turbeville and colleagues review theories of pathogenesis, which include hormonal predisposition, infectious processes (44% of reported cases to 2002 had a flu-like syndrome), decreased blood flow to the outer retina causing transient ischemia, and increased thoracic pressure causing a sudden increase in intravascular pressure damaging the blood–retina barrier.[424] The early involvement of the outer plexiform layer, as well as the vascular associations, suggest a vascular insult to the outer capillary network.[422] Given that the OPL is radially oriented, it would make

sense that an ischemic insult in this region could create a wedge-shaped defect.[445] A case report of a 15-year-old girl who presented with concomitant cotton-wool spots and IRF with reddish lesions in both eyes lends support to this theory. OCT imaging revealed typical hyperreflective plaques at the level of the OPL/ONL. The concurrence of cotton-wool spots and AMN lesions in this patient are supportive of a vascular insult as the etiology.[445]

Differential Diagnosis

Entities included in the differential are central serous chorioretinopathy, old inner retinal infarcts, PAMM, and optic neuritis.

Management/Treatment

The disease is self-limited. Visual acuity and visual field defects improve slowly over time, though subtle symptoms may persist. No treatment has been shown effective.

Paracentral Acute Middle Maculopathy

In 2013, Sarraf and colleagues coined the term paracentral acute middle maculopathy (PAMM), a disease whose clinical presentation resembles AMN with reddish lesions and acute scotomas. However, multimodal imaging shows PAMM affects the middle macular layers above the OPL. These layers are bordered by the intermediate (ICP) and deep (DCP) capillary plexus[421] (Fig. 79.65). An association with retinal ischemia was suggested.[421,446] PAMM has been found in other vascular diseases such as diabetes and central retinal vein occlusion.[420] The OCT findings in PAMM show hyperreflectivity at the OPL/INL (inner nuclear layer) junction instead of OPL/ONL as in AMN. Thinning of the INL occurs with time, and no outer retinal abnormalities occur.[421] PAMM resembles AMN clinically; however, there is a different locus of injury. PAMM occurs more commonly than AMN in males, who are older (mean age 47.6 years), and often with vasculopathic risk factors.[419] The clinical similarities with AMN have given insight into a vascular insult of the retinal capillary plexus as a likely common etiology.

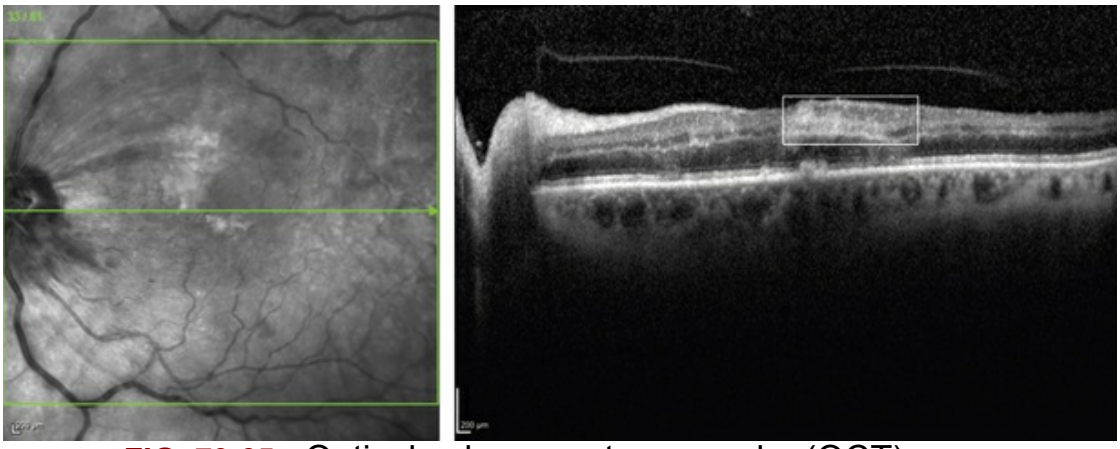

FIG. 79.65 Optical coherence tomography (OCT) shows paracentral acute middle maculopathy lesion. Hyperreflectivity is at the level of the inner nuclear layer.

Summary

AMN is an increasingly recognized condition and should be considered in patients with an acute onset of paracentral scotomas. The typical reddish-brown lesions are found in the macula and are best seen with red-free light or infrared reflectance. AMN involves the outer retina, as evidenced by OCT imaging, and can be distinguished from PAMM in this manner. It is a self-limited process, and no treatment has been proven effective.

Acknowledgment

Evica Simjanoski, CRA, and the retina photographers at Northwestern Medicine for the imaging in this chapter. Lauren Nicosia MD, Northwestern Feinberg School of Medicine, for administrative support of this project.

Supported in part by a grant from Kevin Hitzeman and Mary Dempsey.

References

1. Quillen DA, Davis JB, Gottlieb JL, et al. The white dot syndromes. *Am J Ophthalmol*. 2004;137(3):538–550.
2. Jampol LM, Becker KG. White spot syndromes of the retina:

a hypothesis based on the common genetic hypothesis of autoimmune/inflammatory disease. *Am J Ophthalmol*. 2003;135(3):376–379.
3. Heckenlively JR, Ferreyra HA. Autoimmune retinopathy: a review and summary. *Semin Immunopathol*. 2008;30(2):127–134.
4. Pearlman RB, Golchet PR, Feldmann MG, et al. Increased prevalence of autoimmunity in patients with white spot syndromes and their family members. *Arch Ophthalmol*. 2009;127(7):869–874.
5. Gass JD. Are acute zonal occult outer retinopathy and the white spot syndromes (AZOOR complex) specific autoimmune diseases? *Am J Ophthalmol*. 2003;135(3):380–381.
6. Fletcher WA, Imes RK, Goodman D, et al. Acute idiopathic blind spot enlargement: a big blind spot syndrome without optic disc edema. *Arch Ophthalmol*. 1988;106(1):44–49.
7. Volpe NJ, Rizzo JF, Lessell S. Acute idiopathic blind spot enlargement syndrome: a review of 27 new cases. *Arch Ophthalmol*. 2001;119(1):59–63.
8. Ryan SJ, Maumenee AE. Birdshot retinochoroidopathy. *Am J Ophthalmol*. 1980;89(1):31–45.
9. Gass JD. Vitiliginous chorioretinitis. *Arch Ophthalmol*. 1981;99(10):1778–1787.
10. Shah KH, Levinson RD, Yu F, et al. Birdshot chorioretinopathy. *Surv Ophthalmol*. 2005;50(6):519–541.
11. Nussenblatt RB, Mittal KK, Ryan S, et al. Birdshot retinochoroidopathy associated with HLA-A29 antigen and immune responsiveness to retinal S-antigen. *Am J Ophthalmol*. 1982;94(2):147–158.
12. Ladas JG, Arnold AC, Holland GN. Control of visual symptoms in two men with birdshot retinochoroidopathy using low-dose oral corticosteroid therapy. *Am J Ophthalmol*. 1999;128(1):116–118.
13. Holland GN, Shah KH, Monnet D, et al. Longitudinal cohort study of patients with birdshot chorioretinopathy II: color vision at baseline. *Am J Ophthalmol*. 2006;142(6):1013–1018.
14. Gordon LK, Monnet D, Holland GN, et al. Longitudinal

cohort study of patients with birdshot chorioretinopathy. IV. Visual field results at baseline. *Am J Ophthalmol*. 2007;144(6):829–837.
15. Faia LJ. Gender differences in birdshot chorioretinopathy and the white dot syndromes: do they exist? *J Ophthalmol*. 2014;2014:146768.
16. Priem HA, Kijlstra A, Noens L, et al. HLA typing in birdshot chorioretinopathy. *Am J Ophthalmol*. 1988;105(2):182–185.
17. Monnet D, Brézin AP. Birdshot chorioretinopathy. *Curr Opin Ophthalmol*. 2006;17(6):545–550.
18. Soubrane G, Bokobza R, Coscas G. Late developing lesions in birdshot retinochoroidopathy. *Am J Ophthalmol*. 1990;109(2):204–210.
19. Gasch AT, Smith JA, Whitcup SM. Birdshot retinochoroidopathy. *Br J Ophthalmol*. 1999;83(2):241–249.
20. Priem HA, Oosterhuis JA. Birdshot chorioretinopathy: clinical characteristics and evolution. *Br J Ophthalmol*. 1988;72(9):646–659.
21. Lim L, Harper A, Guymer R. Choroidal lesions preceding symptom onset in birdshot chorioretinopathy. *Arch Ophthalmol*. 2006;124(7):1057–1058.
22. Shao EH, Menezo V, Taylor SR. Birdshot chorioretinopathy. *Curr Opin Ophthalmol*. 2014;25(6):488–494.
23. Fuerst DJ, Tessler HH, Fishman GA, et al. Birdshot retinochoroidopathy. *Arch Ophthalmol*. 1984;102(2):214–219.
24. Kaplan HJ, Aaberg TM. Birdshot retinochoroidopathy. *Am J Ophthalmol*. 1980;90(6):773–782.
25. Soubrane G, Coscas G, Binaghi M, et al. Birdshot retinochoroidopathy and subretinal new vessels. *Br J Ophthalmol*. 1983;67(7):461–467.
26. Brucker AJ, Deglin EA, Bene C, et al. Subretinal choroidal neovascularization in birdshot retinochoroidopathy. *Am J Ophthalmol*. 1985;99(1):40–44.
27. Felder KS, Brockhurst RJ. Neovascular fundus abnormalities in peripheral uveitis. *Arch Ophthalmol*. 1982;100(5):750–754.
28. Henkind P. Ocular neovascularization: the Krill memorial lecture. *Am J Ophthalmol*. 1978;85(3):287–301.
29. Levinson RD, Brezin A, Rothova A, et al. Research criteria

for the diagnosis of birdshot chorioretinopathy: results of an international consensus conference. *Am J Ophthalmol*. 2006;141(1):185–187.
30. Tomkins-Netzer O, Taylor SR, Lightman S. Long-term clinical and anatomic outcome of birdshot chorioretinopathy. *JAMA Ophthalmol*. 2014;132(1):57–62.
31. Howe LJ, Woon H, Graham EM, et al. Choroidal hypoperfusion in acute posterior multifocal placoid pigment epitheliopathy: an indocyanine green angiography study. *Ophthalmology*. 1995;102(5):790–798.
32. Fardeau C, Herbort CP, Kullmann N, et al. Indocyanine green angiography in birdshot chorioretinopathy. *Ophthalmology*. 1999;106(10):1928–1934.
33. Stanga PE, Lim JI, Hamilton P. Indocyanine green angiography in chorioretinal diseases: indications and interpretation: an evidence-based update. *Ophthalmology*. 2003;110(1):15–21 [quiz 22–3].
34. Howe LJ, Stanford MR, Graham EM, et al. Choroidal abnormalities in birdshot chorioretinopathy: an indocyanine green angiography study. *Eye (Lond)*. 1997;11(Pt 4):554–559.
35. Reddy AK, Gonzalez MA, Henry CR, et al. Diagnostic sensitivity of indocyanine green angiography for birdshot chorioretinopathy. *JAMA Ophthalmol*. 2015;133(7):840–843.
36. Giuliari G, Hinkle DM, Foster CS. The spectrum of fundus autofluorescence findings in birdshot chorioretinopathy. *J Ophthalmol*. 2009;2009:567693.
37. Keane PA, Allie M, Turner SJ, et al. Characterization of birdshot chorioretinopathy using extramacular enhanced depth optical coherence tomography. *JAMA Ophthalmol*. 2013;131(3):341–350.
38. Sherif E. When you can have the bird without shooting it!: extramacular enhanced depth optical coherence tomography in birdshot chorioretinopathy. *JAMA Ophthalmol*. 2013;131(10):1369.
39. Birnbaum AD, Fawzi AA, Rademaker A, et al. Correlation between clinical signs and optical coherence tomography with enhanced depth imaging findings in patients with

birdshot chorioretinopathy. *JAMA Ophthalmol*. 2014;132(8):929–935.
40. Young M, Fallah N, Forooghian F. Choroidal degeneration in birdshot chorioretinopathy. *Retina*. 2015;35(4):798–802.
41. Koizumi H, Pozzoni MC, Spaide RF. Fundus autofluorescence in birdshot chorioretinopathy. *Ophthalmology*. 2008;115(5):e15–20.
42. Piffer AL, Boissonnot M, Gobert F, et al. Relevance of wide-field autofluorescence imaging in birdshot retinochoroidopathy: descriptive analysis of 76 eyes. *Acta Ophthalmol*. 2014;92(6):463–469.
43. Hirose T, Katsumi O, Pruett RC, et al. Retinal function in birdshot retinochoroidopathy. *Acta Ophthalmol (Copenh)*. 1991;69(3):327–337.
44. Comander J, Loewenstein J, Sobrin L. Diagnostic testing and disease monitoring in birdshot chorioretinopathy. *Semin Ophthalmol*. 2011;26(4–5):329–336.
45. Holder GE, Robson AG, Pavesio C, et al. Electrophysiological characterisation and monitoring in the management of birdshot chorioretinopathy. *Br J Ophthalmol*. 2005;89(6):709–718.
46. Chiquet C, Berthemy-Pellet S, Altayrac-Bethenod J, et al. Multifocal electroretinogram in birdshot chorioretinopathy. *Retina*. 2015;36(5):1256–1265.
47. Priem HA, De Rouck A, De Laey JJ, et al. Electrophysiologic studies in birdshot chorioretinopathy. *Am J Ophthalmol*. 1988;106(4):430–436.
48. Thorne JE, Jabs DA, Kedhar SR, et al. Loss of visual field among patients with birdshot chorioretinopathy. *Am J Ophthalmol*. 2008;145(1):23–28.
49. Arya B, Westcott M, Robson AG, et al. Pointwise linear regression analysis of serial Humphrey visual fields and a correlation with electroretinography in birdshot chorioretinopathy. *Br J Ophthalmol*. 2015;99(7):973–978.
50. Heaton JM, Mills RP. Sensorineural hearing loss associated with birdshot retinochoroidopathy. *Arch Otolaryngol Head Neck Surg*. 1993;119(6):680–681.
51. Gaudio PA, Kaye DB, Crawford JB. Histopathology of

birdshot retinochoroidopathy. *Br J Ophthalmol*. 2002;86(12):1439–1441.
52. Pulido JS, Canal I, Salomão D, et al. Histological findings of birdshot chorioretinopathy in an eye with ciliochoroidal melanoma. *Eye (Lond)*. 2012;26(6):862–865.
53. Kuiper J, Rothova A, de Boer J, et al. The immunopathogenesis of birdshot chorioretinopathy: a bird of many feathers. *Prog Retin Eye Res*. 2015;44:99–110.
54. Shelsta HN, Jampol LM, Weinberg DV. Indolent nonprogressive multifocal choroidal lesions. *Retina*. 2012;32(2):289–292.
55. Rush RB, Goldstein DA, Callanan DG, et al. Outcomes of birdshot chorioretinopathy treated with an intravitreal sustained-release fluocinolone acetonide-containing device. *Am J Ophthalmol*. 2011;151(4):630–636.
56. Godel V, Baruch E, Lazar M. Late development of chorioretinal lesions in birdshot retinochoroidopathy. *Ann Ophthalmol*. 1989;21(2):49–52.
57. Oh KT, Christmas NJ, Folk JC. Birdshot retinochoroiditis: long term follow-up of a chronically progressive disease. *Am J Ophthalmol*. 2002;133(5):622–629.
58. Bajwa A, Aziz K, Foster CS. Safety and efficacy of fluocinolone acetonide intravitreal implant (0.59 mg) in birdshot retinochoroidopathy. *Retina*. 2014;34(11):2259–2268.
59. Menezo V, Taylor SR. Birdshot uveitis: current and emerging treatment options. *Clin Ophthalmol*. 2014;8:73–81.
60. Vitale AT, Rodriguez A, Foster CS. Low-dose cyclosporine therapy in the treatment of birdshot retinochoroidopathy. *Ophthalmology*. 1994;101(5):822–831.
61. Jap A, Chee SP. Immunosuppressive therapy for ocular diseases. *Curr Opin Ophthalmol*. 2008;19(6):535–540.
62. Rothova A, Ossewaarde-van Norel A, Los LI, et al. Efficacy of low-dose methotrexate treatment in birdshot chorioretinopathy. *Retina*. 2011;31(6):1150–1155.
63. Sobrin L, Huang JJ, Christen W, et al. Daclizumab for treatment of birdshot chorioretinopathy. *Arch Ophthalmol*. 2008;126(2):186–191.

64. Battaglia Parodi M, Iacono P, Verbraak FD, et al. Antivascular endothelial growth factors for inflammatory chorioretinal disorders. *Dev Ophthalmol*. 2010;46:84–95.
65. Hager JL, Lewis RA, Lambert HM. Treatment of cystoid macular edema in a patient with birdshot chorioretinopathy with bevacizumab. *Retin Cases Brief Rep*. 2013;7(1):108–110.
66. Gass JD. Acute posterior multifocal placoid pigment epitheliopathy. *Arch Ophthalmol*. 1968;80(2):177–185.
67. Ryan SJ, Maumenee AE. Acute posterior multifocal placoid pigment epitheliopathy. *Am J Ophthalmol*. 1972;74(6):1066–1074.
68. Deutman AF, Oosterhuis JA, Boen-Tan TN, et al. Acute posterior multifocal placoid pigment epitheliopathy: pigment epitheliopathy of choriocapillaritis? *Br J Ophthalmol*. 1972;56(12):863–874.
69. Deutman AF, Boen-Tan TN, Oosterhuis JA. Proceedings: acute posterior multifocal placoid pigment epitheliopathy. *Ophthalmologica*. 1973;167(5):368–372.
70. Fitzpatrick PJ, Robertson DM. Acute posterior multifocal placoid pigment epitheliopathy. *Arch Ophthalmol*. 1973;89(5):373–376.
71. Savino PJ, Weinberg RJ, Yassin JG, et al. Diverse manifestations of acute posterior multifocal placoid pigment epitheliopathy. *Am J Ophthalmol*. 1974;77(5):659–662.
72. Fishman GA, Rabb MF, Kaplan J. Acute posterior multifocal placoid pigment epitheliopathy. *Arch Ophthalmol*. 1974;92(2):173–177.
73. Lewis RA. Acute posterior multifocal placoid pigment epitheliopathy: a recurrence. *Arch Ophthalmol*. 1975;93(3):235–238.
74. Holt WS, Regan CD, Trempe C. Acute posterior multifocal placoid pigment epitheliopathy. *Am J Ophthalmol*. 1976;81(4):403–412.
75. Scuderi G, Recupero SM, Valvo A. Acute posterior multifocal placoid pigment epitheliopathy. *Ann Ophthalmol*. 1977;9(2):189–194.
76. Van Buskirk EM, Lessell S, Friedman E. Pigmentary

epitheliopathy and erythema nodosum. *Arch Ophthalmol*. 1971;85(3):369–372.
77. Fiore T, Iaccheri B, Androudi S, et al. Acute posterior multifocal placoid pigment epitheliopathy: outcome and visual prognosis. *Retina*. 2009;29(7):994–1001.
78. Jones NP. Acute posterior multifocal placoid pigment epitheliopathy. *Br J Ophthalmol*. 1995;79(4):384–389.
79. Taich A, Johnson MW. A syndrome resembling acute posterior multifocal placoid pigment epitheliopathy in older adults. *Trans Am Ophthalmol Soc*. 2008;106:56–62 [discussion 62–3].
80. Cohen LM, Munk MR, Goldstein DA, Jampol LM. Acute, posterior multifocal placoid pigment epitheliopathy: a case of 11 recurrences over 15 years. *Retin Cases Brief Rep*. 2015;9(3):226–230.
81. Mrejen S, Gallego-Pinazo R, Wald KJ, et al. Acute posterior multifocal placoid pigment epitheliopathy as a choroidopathy: what we learned from adaptive optics imaging. *JAMA Ophthalmol*. 2013;131(10):1363–1364.
82. Bird AC, Hamilton AM. Placoid pigment epitheliopathy: presenting with bilateral serous retinal detachment. *Br J Ophthalmol*. 1972;56(12):881–886.
83. Kayazawa F, Takahashi H. Acute posterior multifocal placoid pigment epitheliopathy and Harada's disease. *Ann Ophthalmol*. 1983;15(1):58–62.
84. Kremer I, Yassur Y. Unilateral atypical retinal pigment epitheliopathy associated with serous retinal detachment. *Ann Ophthalmol*. 1992;24(2):75–77.
85. Garg S, Jampol LM. Macular serous detachment in acute posterior multifocal placoid pigment epitheliopathy. *Retina*. 2004;24(4):650–651.
86. Birnbaum AD, Blair MP, Tessler HH, et al. Subretinal fluid in acute posterior multifocal placoid pigment epitheliopathy. *Retina*. 2010;30(5):810–814.
87. Furusho F, Imaizumi H, Takeda M. One case of Harada disease complicated by acute posterior multifocal placoid pigment epitheliopathy-like recurrence in both eyes. *Jpn J Ophthalmol*. 2001;45(1):117–118.

88. Lee GE, Lee BW, Rao NA, et al. Spectral domain optical coherence tomography and autofluorescence in a case of acute posterior multifocal placoid pigment epitheliopathy mimicking Vogt–Koyanagi–Harada disease: case report and review of literature. *Ocul Immunol Inflamm*. 2011;19(1):42–47.
89. Wright BE, Bird AC, Hamilton AM. Placoid pigment epitheliopathy and Harada's disease. *Br J Ophthalmol*. 1978;62(9):609–621.
90. Williams DF, Mieler WF. Long-term follow-up of acute multifocal posterior placoid pigment epitheliopathy. *Br J Ophthalmol*. 1989;73(12):985–990.
91. Goldenberg D, Habot-Wilner Z, Loewenstein A, et al. Spectral domain optical coherence tomography classification of acute posterior multifocal placoid pigment epitheliopathy. *Retina*. 2012;32(7):1403–1410.
92. Spaide RF, Yannuzzi LA, Slakter J. Choroidal vasculitis in acute posterior multifocal placoid pigment epitheliopathy. *Br J Ophthalmol*. 1991;75(11):685–687.
93. Abu El-Asrar AM, Aljazairy AH. Acute posterior multifocal placoid pigment epitheliopathy with retinal vasculitis and papillitis. *Eye (Lond)*. 2002;16(5):642–644.
94. De Souza S, Aslanides IM, Altomare F. Acute posterior multifocal placoid pigment epitheliopathy associated with retinal vasculitis, neovascularization and subhyaloid hemorrhage. *Can J Ophthalmol*. 1999;34(6):343–345.
95. Thomas BC, Jacobi C, Korporal M, et al. Ocular outcome and frequency of neurological manifestations in patients with acute posterior multifocal placoid pigment epitheliopathy (APMPPE). *J Ophthalmic Inflamm Infect*. 2012;2(3):125–131.
96. Bowie EM, Sletten KR, Kayser DL, et al. Acute posterior multifocal placoid pigment epitheliopathy and choroidal neovascularization. *Retina*. 2005;25(3):362–364.
97. Frohman LP, Klug R, Bielory L, et al. Acute posterior multifocal placoid pigment epitheliopathy with unilateral retinal lesions and bilateral disk edema. *Am J Ophthalmol*. 1987;104(5):548–550.
98. Lowes M. Placoid pigment epitheliopathy presenting as an anterior uveitis: a case report. *Acta Ophthalmol (Copenh)*.

1977;55(5):800–806.
99. Alvi NP, Fishman GA. Granulomatous anterior uveitis presenting with acute posterior multifocal placoid pigment epitheliopathy. *Doc Ophthalmol*. 1995;89(4):347–353.
100. Oh KT, Park DW. Acute posterior multifocal placoid pigment epitheliopathy with corneal stromal infiltrates. *Am J Ophthalmol*. 1998;125(4):556–558.
101. Howe LJ, Woon H, Graham EM, et al. Choroidal hypoperfusion in acute posterior multifocal placoid pigment epitheliopathy: an indocyanine green angiography study. *Ophthalmology*. 1995;102(5):790–798.
102. Dhaliwal RS, Maguire AM, Flower RW, et al. Acute posterior multifocal placoid pigment epitheliopathy: an indocyanine green angiographic study. *Retina*. 1993;13(4):317–325.
103. Schneider U, Inhoffen W, Gelisken F. Indocyanine green angiography in a case of unilateral recurrent posterior acute multifocal placoid pigment epitheliopathy. *Acta Ophthalmol Scand*. 2003;81(1):72–75.
104. Stanga PE, Lim JI, Hamilton P. Indocyanine green angiography in chorioretinal diseases: indications and interpretation: an evidence-based update. *Ophthalmology*. 2003;110(1):15–21 [quiz 22–3].
105. Park D, Schatz H, McDonald HR, et al. Acute multifocal posterior placoid pigment epitheliopathy: a theory of pathogenesis. *Retina*. 1995;15(4):351–352.
106. Van Liefferinge T, Sallet G, De Laey JJ. Indocyanine green angiography in cases of inflammatory chorioretinopathy. *Bull Soc Belge Ophtalmol*. 1995;257:73–81.
107. Yuzawa M, Kawamura A, Matsui M. Indocyanine green video angiographic findings in acute posterior multifocal placoid pigment epitheliopathy. *Acta Ophthalmol (Copenh)*. 1994;72(1):128–133.
108. Montero JA, Ruiz-Moreno JM, Fernandez-Munoz M. Spectral domain optical coherence tomography findings in acute posterior multifocal placoid pigment epitheliopathy. *Ocul Immunol Inflamm*. 2011;19(1):48–50.
109. Cheung CM, Yeo IY, Koh A. Photoreceptor changes in acute

and resolved acute posterior multifocal placoid pigment epitheliopathy documented by spectral-domain optical coherence tomography. *Arch Ophthalmol*. 2010;128(5):644–646.
110. Batioglu F, Ozmert E, Kurt R. Fundus autofluorescence and spectral optical coherence tomography findings in a case with acute posterior multifocal placoid pigment epitheliopathy. *Ann Ophthalmol (Skokie)*. 2008;40(3–4):185–189.
111. Lim LL, Watzke RC, Lauer AK, et al. Ocular coherence tomography in acute posterior multifocal placoid pigment epitheliopathy. *Clin Exp Ophthalmol*. 2006;34(8):810–812.
112. Souka AA, Hillenkamp J, Gora F, et al. Correlation between optical coherence tomography and autofluorescence in acute posterior multifocal placoid pigment epitheliopathy. *Graefes Arch Clin Exp Ophthalmol*. 2006;244(10):1219–1223.
113. Lofoco G, Ciucci F, Bardocci A, et al. Optical coherence tomography findings in a case of acute multifocal posterior placoid pigment epitheliopathy (AMPPPE). *Eur J Ophthalmol*. 2005;15(1):143–147.
114. Scheufele TA, Witkin AJ, Schocket LS, et al. Photoreceptor atrophy in acute posterior multifocal placoid pigment epitheliopathy demonstrated by optical coherence tomography. *Retina*. 2005;25(8):1109–1112.
115. Yeh S, Forooghian F, Wong WT, et al. Fundus autofluorescence imaging of the white dot syndromes. *Arch Ophthalmol*. 2010;128(1):46–56.
116. Spaide RF. Autofluorescence imaging of acute posterior multifocal placoid pigment epitheliopathy. *Retina*. 2006;26(4):479–482.
117. Hong IH, Park SP, Chen CL, et al. Cone photoreceptor abnormalities correlate with vision loss in a case of acute posterior multifocal placoid pigment epitheliopathy. *Ophthalmic Surg Lasers Imaging Retina*. 2014;45(1):74–78.
118. Pagnoux C, Thorne C, Mandelcorn ED, et al. CNS involvement in acute posterior multifocal placoid pigment epitheliopathy. *Can J Neurol Sci*. 2011;38(3):526–528.
119. Althaus C, Unsöld R, Figge C, et al. Cerebral complications

in acute posterior multifocal placoid pigment epitheliopathy. *Ger J Ophthalmol*. 1993;2(3):150–154.
120. Stoll G, Reiners K, Schwartz A, et al. Acute posterior multifocal placoid pigment epitheliopathy with cerebral involvement. *J Neurol Neurosurg Psychiatry*. 1991;54(1):77–79.
121. Prokosch V, Becker H, Thanos S, et al. Acute posterior multifocal placoid pigment epitheliopathy with concurrent cerebral vasculitis and sarcoidosis. *Graefes Arch Clin Exp Ophthalmol*. 2010;248(1):151–152.
122. Massé H, Guyomard JL, Baudet D, et al. Mitoxantrone therapy for acute posterior multifocal placoid pigment epitheliopathy with cerebral vasculitis. *Case Rep Med*. 2009 [2009:481512].
123. de Vries JJ, den Dunnen WF, Timmerman EA, et al. Acute posterior multifocal placoid pigment epitheliopathy with cerebral vasculitis: a multisystem granulomatous disease. *Arch Ophthalmol*. 2006;124(6):910–913.
124. Hsu CT, Harlan JB, Goldberg MF, et al. Acute posterior multifocal placoid pigment epitheliopathy associated with a systemic necrotizing vasculitis. *Retina*. 2003;23(1):64–68.
125. Weinstein JM, Bresnick GH, Bell CL, et al. Acute posterior multifocal placoid pigment epitheliopathy associated with cerebral vasculitis. *J Clin Neuroophthalmol*. 1988;8(3):195–201.
126. Wilson CA, Choromokos EA, Sheppard R. Acute posterior multifocal placoid pigment epitheliopathy and cerebral vasculitis. *Arch Ophthalmol*. 1988;106(6):796–800.
127. Sigelman J, Behrens M, Hilal S. Acute posterior multifocal placoid pigment epitheliopathy associated with cerebral vasculitis and homonymous hemianopia. *Am J Ophthalmol*. 1979;88(5):919–924.
128. Kersten DH, Lessell S, Carlow TJ. Acute posterior multifocal placoid pigment epitheliopathy and late-onset meningo-encephalitis. *Ophthalmology*. 1987;94(4):393–396.
129. Luneau K, Newman NJ, Srivastava S, et al. A case of acute posterior multifocal placoid pigment epitheliopathy with recurrent stroke. *J Neuroophthalmol*. 2009;29(2):111–118.
130. Jaramillo A, Gaete G, Romero P, et al. Acute pontine infarct

in a 16-year-old man with acute posterior multifocal placoid pigment epitheliopathy: a case report. *J Stroke Cerebrovasc Dis*. 2009;18(2):164–166.
131. Bugnone AN, Hartker F, Shapiro M, et al. Acute and chronic brain infarcts on MR imaging in a 20-year-old woman with acute posterior multifocal placoid pigment epitheliopathy. *AJNR Am J Neuroradiol*. 2006;27(1):67–69.
132. Al Kawi A, Wang DZ, Kishore K, et al. A case of ischemic cerebral infarction associated with acute posterior multifocal placoid pigment epitheliopathy, CNS vasculitis, vitamin B(12) deficiency and homocysteinemia. *Cerebrovasc Dis*. 2004;18(4):338–339.
133. Bewermeyer H, Nelles G, Huber M, et al. Pontine infarction in acute posterior multifocal placoid pigment epitheliopathy. *J Neurol*. 1993;241(1):22–26.
134. Gibelalde A, Bidaguren A, Ostolaza JI, et al. Pigmentary epitheliopathy multifocal acute placoid associated with paralysis of VI cranial par. *Arch Soc Esp Oftalmol*. 2009;84(3):159–162.
135. Clearkin LG, Hung SO. Acute posterior multifocal placoid pigment epitheliopathy associated with transient hearing loss. *Trans Ophthalmol Soc U K*. 1983;103(Pt 5):562–564.
136. Spencer BR, Kunimoto DY, Patel DR, et al. Acute multifocal posterior placoid pigment epitheliopathy (AMPPPE) mimicking migraine with aura. *Cephalalgia*. 2009;29(6):694–698.
137. Fishman GA, Baskin M. Jednock N. Spinal fluid pleocytosis in acute posterior multifocal placoid pigment epitheliopathy. *Ann Ophthalmol*. 1977;9(1):36.
138. El Sanhouri A, Sisk RA, Petersen MR. Mortality from cerebral vasculitis associated with rapid steroid taper during treatment of acute posterior multifocal placoid pigment epitheliopathy. *Arch Ophthalmol*. 2012;130(7):935–937.
139. Hedges TR, Sinclair SH, Gragoudas ES. Evidence for vasculitis in acute posterior multifocal placoid pigment epitheliopathy. *Ann Ophthalmol*. 1979;11(4):539–542.
140. Matsuo T, Horikoshi T, Nagai C. Acute posterior multifocal

placoid pigment epitheliopathy and scleritis in a patient with pANCA-positive systemic vasculitis. *Am J Ophthalmol*. 2002;133(4):566–568.
141. Matsuo T. Eye manifestations in patients with perinuclear antineutrophil cytoplasmic antibody-associated vasculitis: case series and literature review. *Jpn J Ophthalmol*. 2007;51(2):131–138.
142. Di Crecchio L, Parodi MB, Saviano S, et al. Acute posterior multifocal placoid pigment epitheliopathy and ulcerative colitis: a possible association. *Acta Ophthalmol Scand*. 2001;79(3):319–321.
143. Jacklin HN. Acute posterior multifocal placoid pigment epitheliopathy and thyroiditis. *Arch Ophthalmol*. 1977;95(6):995–997.
144. Laatikainen LT, Immonen IJ. Acute posterior multifocal placoid pigment epitheliopathy in connection with acute nephritis. *Retina*. 1988;8(2):122–124.
145. Priluck IA, Robertson DM, Buettner H. Acute posterior multifocal placoid pigment epitheliopathy: urinary findings. *Arch Ophthalmol*. 1981;99(9):1560–1562.
146. Bridges WJ, Saadeh C, Gerald R. Acute posterior multifocal placoid pigment epitheliopathy in a patient with systemic-onset juvenile rheumatoid arthritis: treatment with cyclosporin A and prednisone. *Arthritis Rheum*. 1995;38(3):446–447.
147. Chiquet C, Lumbroso L, Denis P, et al. Acute posterior multifocal placoid pigment epitheliopathy associated with Wegener's granulomatosis. *Retina*. 1999;19(4):309–313.
148. Anderson K, Patel KR, Webb L, et al. Acute posterior multifocal placoid pigment epitheliopathy associated with pulmonary tuberculosis. *Br J Ophthalmol*. 1996;80(2):186.
149. Dick DJ, Newman PK, Richardson J, et al. Acute posterior multifocal placoid pigment epitheliopathy and sarcoidosis. *Br J Ophthalmol*. 1988;72(1):74–77.
150. Wolf MD, Folk JC, Panknen CA, et al. HLA-B7 and HLA-DR2 antigens and acute posterior multifocal placoid pigment epitheliopathy. *Arch Ophthalmol*. 1990;108(5):698–700.

151. Nga AD, Ramli N, Mimiwati Z. Post viral acute multifocal posterior placoid pigment epithiopathy in a teenage child. *Med J Malaysia*. 2009;64(2):176–178.
152. Borruat FX, Piguet B, Herbort CP. Acute posterior multifocal placoid pigment epitheliopathy following mumps. *Ocul Immunol Inflamm*. 1998;6(3):189–193.
153. Thomson SP, Roxburgh ST. Acute posterior multifocal placoid pigment epitheliopathy associated with adenovirus infection. *Eye (Lond)*. 2003;17(4):542–544.
154. Azar P, Gohd RS, Waltman D, et al. Acute posterior multifocal placoid pigment epitheliopathy associated with an adenovirus type 5 infection. *Am J Ophthalmol*. 1975;80(6):1003–1005.
155. Hollsten JE, McClintock M, Samy H, Peden M, Kay CN. Fulminant chorioretinitis and papillitis secondary to coxsackievirus B presenting as acute posterior multifocal placoid pigment epitheliopathy with positive response to intravenous immunoglobulin. *Retin Cases Brief Rep*. 2013;7(3):225–231.
156. Augsten R, Pfister W, Königsdörffer E. [Acute posterior multifocal placoid pigment epitheliopathy (APMPPE) and borreliosis]. *Klin Monatsbl Augenheilkd*. 2009;226(6):512–513.
157. Wolf MD, Folk JC, Nelson JA, et al. Acute, posterior, multifocal, placoid, pigment epitheliopathy and Lyme disease. *Arch Ophthalmol*. 1992;110(6):750.
158. Lowder CY, Foster RE, Gordon SM, et al. Acute posterior multifocal placoid pigment epitheliopathy after acute group A streptococcal infection. *Am J Ophthalmol*. 1996;122(1):115–117.
159. Mendrinos E, Baglivo E. Acute posterior multifocal placoid pigment epitheliopathy following influenza vaccination. *Eye (Lond)*. 2010;24(1):180–181.
160. Fine HF, Kim E, Flynn TE, et al. Acute posterior multifocal placoid pigment epitheliopathy following varicella vaccination. *Br J Ophthalmol*. 2010;94(3):282–283 [363].
161. Yang DS, Hilford DJ, Conrad D. Acute posterior multifocal placoid pigment epitheliopathy after meningococcal C conjugate vaccine. *Clin Exp Ophthalmol*. 2005;33(2):219–221.

162. Brézin AP, Massin-Korobelnik P, Boudin M, et al. Acute posterior multifocal placoid pigment epitheliopathy after hepatitis B vaccine. *Arch Ophthalmol*. 1995;113(3):297–300.
163. Uthman I, Najjar DM, Kanj SS, et al. Anticardiolipin antibodies in acute multifocal posterior placoid pigment epitheliopathy. *Ann Rheum Dis*. 2003;62(7):687–688.
164. Uthman IW, Bizri AR, Gharavi AE. Infections and antiphospholipid antibodies. *J Med Liban*. 2000;48(5):324–326.
165. Menon SR, Fleischhauer J, Jost K, et al. Clinical and electrophysiological course of acute syphilitic posterior placoid chorioretinitis. *Klin Monatsbl Augenheilkd*. 2005;222(3):261–263.
166. O'Halloran HS, Berger JR, Lee WB, et al. Acute multifocal placoid pigment epitheliopathy and central nervous system involvement: nine new cases and a review of the literature. *Ophthalmology*. 2001;108(5):861–868.
167. El-Markaby HS, Mohammed TH, El-Raggal TM. Acute posterior multifocal placoid pigment epitheliopathy: role of TNF blocker in severe cases. *Retina*. 2012;32(10):2102–2107.
168. Mavrakanas N, Mendrinos E, Tabatabay C, et al. Intravitreal ranibizumab for choroidal neovascularization secondary to acute multifocal posterior placoid pigment epitheliopathy. *Acta Ophthalmol*. 2010;88(2):e54–5.
169. Battaglia Parodi M, Iacono P, Verbraak FD, et al. Antivascular endothelial growth factors for inflammatory chorioretinal disorders. *Dev Ophthalmol*. 2010;46:84–95.
170. Franceschetti A. A curious affection of the fundus oculi: helicoid peripapillar chorioretinal degeneration. Its relation to pigmentary paravenous chorioretinal degeneration. *Doc Ophthalmol*. 1962;16:81–110.
171. Schatz HS, Maumenee AEM, Patz A. Geographic helicoid peripapillary choroidopathy: clinical presentation and fluorescein angiographic findings. *Trans Am Acad Ophthalmol Otolaryngol*. 1974;78:747–761.
172. Hamilton AM, Bird AC. Geographical choroidopathy. *Br J Ophthalmol*. 1974;58(9):784–797.
173. Lim WK, Buggage RR, Nussenblatt RB. Serpiginous

choroiditis. *Surv Ophthalmol*. 2005;50(3):231–244.
174. Laatikainen L, Erkkilä H. Serpiginous choroiditis. *Br J Ophthalmol*. 1974;58(9):777–783.
175. Weiss H, Annesley WH, Shields JA, et al. The clinical course of serpiginous choroidopathy. *Am J Ophthalmol*. 1979;87(2):133–142.
176. Hardy RA, Schatz H. Macular geographic helicoid choroidopathy. *Arch Ophthalmol*. 1987;105(9):1237–1242.
177. Mansour AM, Jampol LM, Packo KH. Macular serpiginous choroiditis. *Retina*. 1988;8(2):125–131.
178. Erkkilä H, Laatikainen L, Jokinen E. Immunological studies on serpiginous choroiditis. *Graefes Arch Clin Exp Ophthalmol*. 1982;219(3):131–134.
179. Hoyng C, Tilanus M, Deutman A. Atypical central lesions in serpiginous choroiditis treated with oral prednisone. *Graefes Arch Clin Exp Ophthalmol*. 1998;236(2):154–156.
180. Chisholm IH, Gass JD, Hutton WL. The late stage of serpiginous (geographic) choroiditis. *Am J Ophthalmol*. 1976;82(3):343–351.
181. Laatikainen L, Erkkilä H. A follow-up study on serpiginous choroiditis. *Acta Ophthalmol (Copenh)*. 1981;59(5):707–718.
182. Sahu DK, Rawoof A, Sujatha B. Macular serpiginous choroiditis. *Indian J Ophthalmol*. 2002;50(3):189–196.
183. Masi RJ, O'Connor GR, Kimura SJ. Anterior uveitis in geographic or serpiginous choroiditis. *Am J Ophthalmol*. 1978;86(2):228–232.
184. Abrez H, Biswas J, Sudharshan S. Clinical profile, treatment, and visual outcome of serpiginous choroiditis. *Ocul Immunol Inflamm*. 2007;15(4):325–335.
185. Baglivo E, Boudjema S, Pieh C, et al. Vascular occlusion in serpiginous choroidopathy. *Br J Ophthalmol*. 2005;89(3):387–388.
186. Blumenkranz MS, Gass JD, Clarkson JG. Atypical serpiginous choroiditis. *Arch Ophthalmol*. 1982;100(11):1773–1775.
187. Lee DK, Suhler EB, Augustin W, et al. Serpiginous choroidopathy presenting as choroidal neovascularisation. *Br J Ophthalmol*. 2003;87(9):1184–1185.

188. Wu JS, Lewis H, Fine SL, et al. Clinicopathologic findings in a patient with serpiginous choroiditis and treated choroidal neovascularization. *Retina*. 1989;9(4):292–301.
189. Laatikainen L, Erkkilä H. Subretinal and disc neovascularisation in serpiginous choroiditis. *Br J Ophthalmol*. 1982;66(5):326–331.
190. Jampol LM, Orth D, Daily MJ, et al. Subretinal neovascularization with geographic (serpiginous) choroiditis. *Am J Ophthalmol*. 1979;88(4):683–689.
191. Baglivo E, Safran AB, Borruat FX. Multiple evanescent white dot syndrome after hepatitis B vaccine. *Am J Ophthalmol*. 1996;122(3):431–432.
192. Friberg TR. Serpiginous choroiditis with branch vein occlusion and bilateral periphlebitis: case report. *Arch Ophthalmol*. 1988;106(5):585–586.
193. Steinmetz RL, Fitzke FW, Bird AC. Treatment of cystoid macular edema with acetazolamide in a patient with serpiginous choroidopathy. *Retina*. 1991;11(4):412–415.
194. Gregory ME, Bhatt U, Benskin S, et al. Bilateral full thickness macular holes in association with serpiginous choroiditis. *Ocul Immunol Inflamm*. 2009;17(5):328–329.
195. Christmas NJ, Oh KT, Oh DM, et al. Long-term follow-up of patients with serpiginous choroiditis. *Retina*. 2002;22(5):550–556.
196. Squirrell DM, Bhola RM, Talbot JF. Indocyanine green angiographic findings in serpiginous choroidopathy: evidence of a widespread choriocapillaris defect of the peripapillary area and posterior pole. *Eye (Lond)*. 2001;15(Pt 3):336–338.
197. Salati C, Pantelis V, Lafaut BA, et al. A 8 months indocyanine angiographic follow-up of a patient with serpiginous choroidopathy. *Bull Soc Belge Ophtalmol*. 1997;265:29–33.
198. Giovannini A, Mariotti C, Ripa E, et al. Indocyanine green angiographic findings in serpiginous choroidopathy. *Br J Ophthalmol*. 1996;80(6):536–540.
199. Giovannini A, Ripa E, Scassellati-Sforzolini B, et al. Indocyanine green angiography in serpiginous

choroidopathy. *Eur J Ophthalmol*. 1996;6(3):299–306.
200. Van Liefferinge T, Sallet G, De Laey JJ. Indocyanine green angiography in cases of inflammatory chorioretinopathy. *Bull Soc Belge Ophtalmol*. 1995;257:73–81.
201. Punjabi OS, Rich R, Davis JL, et al. Imaging serpiginous choroidopathy with spectral domain optical coherence tomography. *Ophthalmic Surg Lasers Imaging*. 2008;39(Suppl. 4):S95–8.
202. Arantes TE, Matos K, Garcia CR, et al. Fundus autofluorescence and spectral domain optical coherence tomography in recurrent serpiginous choroiditis: case report. *Ocul Immunol Inflamm*. 2011;19(1):39–41.
203. Gallagher MJ, Yilmaz T, Cervantes-Castañeda RA, et al. The characteristic features of optical coherence tomography in posterior uveitis. *Br J Ophthalmol*. 2007;91(12):1680–1685.
204. van Velthoven ME, Ongkosuwito JV, Verbraak FD, et al. Combined en-face optical coherence tomography and confocal ophthalmoscopy findings in active multifocal and serpiginous chorioretinitis. *Am J Ophthalmol*. 2006;141(5):972–975.
205. Cardillo Piccolino F, Grosso A, Savini E. Fundus autofluorescence in serpiginous choroiditis. *Graefes Arch Clin Exp Ophthalmol*. 2009;247(2):179–185.
206. Nazari Khanamiri H, Rao NA. Serpiginous choroiditis and infectious multifocal serpiginoid choroiditis. *Surv Ophthalmol*. 2013;58(3):203–232.
207. Yeh S, Forooghian F, Wong WT, et al. Fundus autofluorescence imaging of the white dot syndromes. *Arch Ophthalmol*. 2010;128(1):46–56.
208. Carreño E, Portero A, Herreras JM, et al. Assesment of fundus autofluorescence in serpiginous and serpiginous-like choroidopathy. *Eye (Lond)*. 2012;26(9):1232–1236.
209. Arantes TE, Matos K, Garcia CR, et al. Fundus autofluorescence and spectral domain optical coherence tomography in recurrent serpiginous choroiditis: case report. *Ocul Immunol Inflamm*. 2011;19(1):39–41.
210. Pilotto E, Vujosevic S, Grgic VA, et al. Retinal function in patients with serpiginous choroiditis: a microperimetry

study. *Graefes Arch Clin Exp Ophthalmol*. 2010;248(9):1331–1337.
211. Ugarte M, Wearne IM. Serpiginous choroidopathy: an unusual association with Crohn's disease. *Clin Exp Ophthalmol*. 2002;30(6):437–439.
212. Fuentes-Paez G, Celis-Sanchez J, Torres J, et al. Serpiginous choroiditis in a patient with systemic lupus erythematosus. *Lupus*. 2005;14(11):928–929.
213. Mulder CJ, Pena AS, Jansen J, et al. Celiac disease and geographic (serpiginous) choroidopathy with occurrence of thrombocytopenic purpura. *Arch Intern Med*. 1983;143(4):842.
214. Richardson RR, Cooper IS, Smith JL. Serpiginous choroiditis and unilateral extrapyramidal dystonia. *Ann Ophthalmol*. 1981;13(1):15–19.
215. Akpek EK, Chan CC, Shen D, et al. Lack of herpes virus DNA in choroidal tissues of a patient with serpiginous choroiditis. *Ophthalmology*. 2004;111(11):2071–2075.
216. Broekhuyse RM, van Herck M, Pinckers AJ, et al. Immune responsiveness to retinal S-antigen and opsin in serpiginous choroiditis and other retinal diseases. *Doc Ophthalmol*. 1988;69(1):83–93.
217. Madhavan HN, Priya K, Biswas J. Current perspectives of herpesviral retinitis and choroiditis. *Indian J Pathol Microbiol*. 2004;47(4):453–468.
218. Pisa D, Ramos M, García P, et al. Fungal infection in patients with serpiginous choroiditis or acute zonal occult outer retinopathy. *J Clin Microbiol*. 2008;46(1):130–135.
219. Babel J. Geographic and helicoid choroidopathies: clinical and angiographic study; attempted classification. *J Fr Ophtalmol*. 1983;6(12):981–993.
220. King DG, Grizzard WS, Sever RJ, et al. Serpiginous choroidopathy associated with elevated factor VIII–von Willebrand factor antigen. *Retina*. 1990;10(2):97–101.
221. Hayreh SS, Baines JA. Occlusion of the posterior ciliary artery. I. Effects on choroidal circulation. *Br J Ophthalmol*. 1972;56(10):719–735.
222. Edelsten C, Stanford MR, Graham EM. Serpiginous

choroiditis: an unusual presentation of ocular sarcoidosis. *Br J Ophthalmol*. 1994;78(1):70–71.
223. Rattray KM, Cole MD, Smith SR. Systemic non-Hodgkin's lymphoma presenting as a serpiginous choroidopathy: report of a case and review of the literature. *Eye (Lond)*. 2000;14(Pt 5):706–710.
224. Tang J, Fillmore G, Nussenblatt RB. Antiphospholipid antibody syndrome mimicking serpiginous choroidopathy. *Ocul Immunol Inflamm*. 2009;17(4):278–281.
225. Mahendradas P, Kamath G, Mahalakshmi B, et al. Serpiginous choroiditis-like picture due to ocular toxoplasmosis. *Ocul Immunol Inflamm*. 2007;15(2):127–130.
226. Sonika, Narang S, Kochhar S, et al. Posterior scleritis mimicking macular serpiginous choroiditis. *Indian J Ophthalmol*. 2003;51(4):351–353.
227. Mackensen F, Becker MD, Wiehler U, et al. QuantiFERON TB-Gold – a new test strengthening long-suspected tuberculous involvement in serpiginous-like choroiditis. *Am J Ophthalmol*. 2008;146(5):761–766.
228. Akpek EK, Ilhan-Sarac O. New treatments for serpiginous choroiditis. *Curr Opin Ophthalmol*. 2003;14(3):128–131.
229. Markomichelakis NN, Halkiadakis I, Papaeythymiou-Orchan S, et al. Intravenous pulse methylprednisolone therapy for acute treatment of serpiginous choroiditis. *Ocul Immunol Inflamm*. 2006;14(1):29–33.
230. Pathengay A. Intravitreal triamcinolone acetonide in serpiginous choroidopathy. *Indian J Ophthalmol*. 2005;53(1):77–79.
231. Wadhwa N, Garg SP, Mehrotra A. Prospective evaluation of intravitreal triamcinolone acetonide in serpiginous choroiditis. *Ophthalmologica*. 2010;224(3):183–187.
232. Adigüzel U, Sari A, Ozmen C, et al. Intravitreal triamcinolone acetonide treatment for serpiginous choroiditis. *Ocul Immunol Inflamm*. 2006;14(6):375–378.
233. Karacorlu S, Ozdemir H, Karacorlu M. Intravitreal triamcinolone acetonide in serpiginous choroiditis. *Jpn J Ophthalmol*. 2006;50(3):290–291.
234. Seth RK, Gaudio PA. Treatment of serpiginous choroiditis

with intravitreous fluocinolone acetonide implant. *Ocul Immunol Inflamm*. 2008;16(3):103–105.
235. Akpek EK, Baltatzis S, Yang J, et al. Long-term immunosuppressive treatment of serpiginous choroiditis. *Ocul Immunol Inflamm*. 2001;9(3):153–167.
236. Vonmoos F, Messerli J, Moser HR, et al. Immunosuppressive therapy in serpiginous choroiditis – case report and brief review of the literature. *Klin Monatsbl Augenheilkd*. 2001;218(5):394–397.
237. Araujo AA, Wells AP, Dick AD, et al. Early treatment with cyclosporin in serpiginous choroidopathy maintains remission and good visual outcome. *Br J Ophthalmol*. 2000;84(9):979–982.
238. Leznoff A, Shea M, Binkley KE, et al. Cyclosporine in the treatment of nonmicrobial inflammatory ophthalmic disease. *Can J Ophthalmol*. 1992;27(6):302–306.
239. Vianna RN, Ozdal PC, Deschênes J, et al. Combination of azathioprine and corticosteroids in the treatment of serpiginous choroiditis. *Can J Ophthalmol*. 2006;41(2):183–189.
240. Akpek EK, Jabs DA, Tessler HH, et al. Successful treatment of serpiginous choroiditis with alkylating agents. *Ophthalmology*. 2002;109(8):1506–1513.
241. Sahin OG. Long-term cyclophosphamide treatment in a case with serpiginous choroiditis. *Case Rep Ophthalmol*. 2010;1(2):71–76.
242. Hooper PL, Kaplan HJ. Triple agent immunosuppression in serpiginous choroiditis. *Ophthalmology*. 1991;98(6):944–951 [discussion 951–2].
243. Seve P, Mennesson E, Grange JD, et al. Infliximab in serpiginous choroiditis. *Acta Ophthalmol*. 2010;88(8):e342–3.
244. Sobaci G, Bayraktar Z, Bayer A. Interferon alpha-2a treatment for serpiginous choroiditis. *Ocul Immunol Inflamm*. 2005;13(1):59–66.
245. Battaglia Parodi M, Iacono P, Verbraak FD, et al. Antivascular endothelial growth factors for inflammatory chorioretinal disorders. *Dev Ophthalmol*. 2010;46:84–95.
246. Rouvas A, Petrou P, Douvali M, et al. Intravitreal

ranibizumab for the treatment of inflammatory choroidal neovascularization. *Retina*. 2011;31(5):871–875.
247. Song MH, Roh YJ. Intravitreal ranibizumab for choroidal neovascularisation in serpiginous choroiditis. *Eye (Lond)*. 2009;23(9):1873–1875.
248. Julián K, Terrada C, Fardeau C, et al. Intravitreal bevacizumab as first local treatment for uveitis-related choroidal neovascularization: long-term results. *Acta Ophthalmol*. 2011;89(2):179–184.
249. Rouvas A, Petrou P, Douvali M, et al. Intravitreal ranibizumab for the treatment of inflammatory choroidal neovascularization. *Retina*. 2011;31(5):871–879.
250. Lim JI, Flaxel CJ, LaBree L. Photodynamic therapy for choroidal neovascularisation secondary to inflammatory chorioretinal disease. *Ann Acad Med Singapore*. 2006;35(3):198–202.
251. Park SP, Ko DA, Chung H, et al. Photodynamic therapy with verteporfin for juxtafoveal choroidal neovascularization in serpiginous choroiditis. *Ophthalmic Surg Lasers Imaging*. 2006;37(5):425–428.
252. Steinmetz RL, Fitzke FW, Bird AC. Treatment of cystoid macular edema with acetazolamide in a patient with serpiginous choroidopathy. *Retina*. 1991;11(4):412–415.
253. Vasconcelos-Santos DV, Rao PK, Davies JB, et al. Clinical features of tuberculous serpiginous-like choroiditis in contrast to classic serpiginous choroiditis. *Arch Ophthalmol*. 2010;128(7):853–858.
254. Khurana RN. Serpiginous choroiditis secondary to Bartonella henselae? *JAMA Ophthalmol*. 2013;131(8):1102.
255. Rifkin LM, Munk MR, Baddar D, et al. A new OCT finding in tuberculous serpiginous-like choroidopathy. *Ocul Immunol Inflamm*. 2015;23(1):53–58.
256. Jones BE, Jampol LM, Yannuzzi LA, et al. Relentless placoid chorioretinitis: a new entity or an unusual variant of serpiginous chorioretinitis? *Arch Ophthalmol*. 2000;118(7):931–938.
257. Nussenblatt RB, Whitcup S, Palestine AG. *Uveitis: fundamentals and clinical practice*. 2nd ed. Mosby: St. Louis;

1996.
258. Arora SK, Gupta V, Gupta A, et al. Diagnostic efficacy of polymerase chain reaction in granulomatous uveitis. *Tuber Lung Dis*. 1999;79(4):229–233.
259. Lyness AL, Bird AC. Recurrences of acute posterior multifocal placoid pigment epitheliopathy. *Am J Ophthalmol*. 1984;98(2):203–207.
260. Jyotirmay B, Jafferji SS, Sudharshan S, et al. Clinical profile, treatment, and visual outcome of ampiginous choroiditis. *Ocul Immunol Inflamm*. 2010;18(1):46–51.
261. Jones NP. Acute posterior multifocal placoid pigment epitheliopathy. *Br J Ophthalmol*. 1995;79(4):384–389.
262. Amer R, Florescu T. Optical coherence tomography in relentless placoid chorioretinitis. *Clin Exp Ophthalmol*. 2008;36(4):388–390.
263. Veronese C, Marcheggiani EB, Tassi F, et al. Early autofluorescence findings of relentless placoid chorioretinitis. *Retina*. 2014;34(3):625–627.
264. Dolz-Marco R, Rodríguez-Ratón A, Hernández-Martínez P, et al. Macular retinal and choroidal thickness in unilateral relentless placoid chorioretinitis analyzed by swept-source optical coherence tomography. *J Ophthalmic Inflamm Infect*. 2014;4:24.
265. Yeh S, Forooghian F, Wong WT, et al. Fundus autofluorescence imaging of the white dot syndromes. *Arch Ophthalmol*. 2010;128(1):46–56.
266. Yeh S, Lew JC, Wong WT, et al. Relentless placoid chorioretinitis associated with central nervous system lesions treated with mycophenolate mofetil. *Arch Ophthalmol*. 2009;127(3):341–343.
267. Chung YM, Yeh TS, Liu JH. Increased serum IgM and IgG in the multiple evanescent white-dot syndrome. *Am J Ophthalmol*. 1987;104(2):187–188.
268. Golchet PR, Jampol LM, Wilson D, et al. Persistent placoid maculopathy: a new clinical entity. *Trans Am Ophthalmol Soc*. 2006;104:108–120.
269. Nika M, Kalyani PS, Jayasundera KT, et al. Pathogenesis of persistent placoid maculopathy: a multimodal imaging

analysis. *Retina*. 2015;35(8):1531–1539.
270. Gendy MG, Fawzi AA, Wendel RT, et al. Multimodal imaging in persistent placoid maculopathy. *JAMA Ophthalmol*. 2014;132(1):38–49.
271. Kovach JL. Persistent placoid maculopathy imaged with spectral domain OCT and autofluorescence. *Ophthalmic Surg Lasers Imaging*. 2010;41(Suppl):S101–3.
272. Khairallah M, Ben Yahia S. Persistent placoid maculopathy. *Ophthalmology*. 2008;115(1):220–221.
273. Parodi MB, Iacono P, Bandello F. Juxtafoveal choroidal neovascularization secondary to persistent placoid maculopathy treated with intravitreal bevacizumab. *Ocul Immunol Inflamm*. 2010;18(5):399–401.
274. Battaglia Parodi M, Iacono P, Verbraak FD, et al. Antivascular endothelial growth factors for inflammatory chorioretinal disorders. *Dev Ophthalmol*. 2010;46:84–95.
275. Eadie JA, Gottlieb JL. Successful treatment of choroidal neovascularization secondary to persistent placoid maculopathy with intravitreal bevacizumab. *Retin Cases Brief Rep*. 2014;8(1):37–40.
276. Jampol LM, Wiredu A. MEWDS, MFC, PIC, AMN, AIBSE, and AZOOR: one disease or many? *Retina*. 1995;15(5):373–378.
277. Essex RW, Wong J, Jampol LM, et al. Idiopathic multifocal choroiditis: a comment on present and past nomenclature. *Retina*. 2013;33(1):1–4.
278. Fung AT, Pal S, Yannuzzi NA, et al. Multifocal choroiditis without panuveitis: clinical characteristics and progression. *Retina*. 2014;34(1):98–107.
279. Spaide RF, Goldberg N, Freund KB. Redefining multifocal choroiditis and panuveitis and punctate inner choroidopathy through multimodal imaging. *Retina*. 2013;33(7):1315–1324.
280. Atan D, Fraser-Bell S, Plskova J, et al. Punctate inner choroidopathy and multifocal choroiditis with panuveitis share haplotypic associations with IL10 and TNF loci. *Invest Ophthalmol Vis Sci*. 2011;52(6):3573–3581.
281. Nozik RA, Dorsch W. A new chorioretinopathy associated

with anterior uveitis. *Am J Ophthalmol*. 1973;76(5):758–762.
282. Dreyer RF, Gass DJ. Multifocal choroiditis and panuveitis: a syndrome that mimics ocular histoplasmosis. *Arch Ophthalmol*. 1984;102(12):1776–1784.
283. Deutsch TA, Tessler HH. Inflammatory pseudohistoplasmosis. *Ann Ophthalmol*. 1985;17(8):461–465.
284. Morgan CM, Schatz H. Recurrent multifocal choroiditis. *Ophthalmology*. 1986;93(9):1138–1147.
285. Watzke RC, Packer AJ, Folk JC, et al. Punctate inner choroidopathy. *Am J Ophthalmol*. 1984;98(5):572–584.
286. Amer R, Lois N. Punctate inner choroidopathy. *Surv Ophthalmol*. 2011;56(1):36–53.
287. Palestine AG, Nussenblatt RB, Parver LM, et al. Progressive subretinal fibrosis and uveitis. *Br J Ophthalmol*. 1984;68(9):667–673.
288. Jung JJ, Khan S, Mrejen S, et al. Idiopathic multifocal choroiditis with outer retinal or chorioretinal atrophy. *Retina*. 2014;34(7):1439–1450.
289. Munk MR, Jung JJ, Biggee K, et al. Idiopathic multifocal choroiditis/punctate inner choroidopathy with acute photoreceptor loss or dysfunction out of proportion to clinically visible lesions. *Retina*. 2015;35(2):334–343.
290. Gerstenblith AT, Thorne JE, Sobrin L, et al. Punctate inner choroidopathy: a survey analysis of 77 persons. *Ophthalmology*. 2007;114(6):1201–1204.
291. Kedhar SR, Thorne JE, Wittenberg S, et al. Multifocal choroiditis with panuveitis and punctate inner choroidopathy: comparison of clinical characteristics at presentation. *Retina*. 2007;27(9):1174–1179.
292. Essex RW, Wong J, Fraser-Bell S, et al. Punctate inner choroidopathy: clinical features and outcomes. *Arch Ophthalmol*. 2010;128(8):982–987.
293. Brown J, Folk JC, Reddy CV, et al. Visual prognosis of multifocal choroiditis, punctate inner choroidopathy, and the diffuse subretinal fibrosis syndrome. *Ophthalmology*. 1996;103(7):1100–1105.
294. Spaide RF, Yannuzzi LA, Freund KB. Linear streaks in multifocal choroiditis and panuveitis. *Retina*.

1991;11(2):229–231.
295. Borodoker N, Cunningham ET, Yannuzzi LA, et al. Peripheral curvilinear pigmentary streak in multifocal choroiditis. *Arch Ophthalmol*. 2002;120(4):520–521.
296. Fonseca RA, Dantas MA, Kaga T, et al. Subretinal fibrosis and linear streaks in multifocal choroiditis. *Arch Ophthalmol*. 2001;119(1):142.
297. Parnell JR, Jampol LM, Yannuzzi LA, et al. Differentiation between presumed ocular histoplasmosis syndrome and multifocal choroiditis with panuveitis based on morphology of photographed fundus lesions and fluorescein angiography. *Arch Ophthalmol*. 2001;119(2):208–212.
298. Cantrill HL, Folk JC. Multifocal choroiditis associated with progressive subretinal fibrosis. *Am J Ophthalmol*. 1986;101(2):170–180.
299. Buerk BM, Rabb MF, Jampol LM. Peripapillary subretinal fibrosis: a characteristic finding of multifocal choroiditis and panuveitis. *Retina*. 2005;25(2):228–229.
300. Wiechens B. Nölle B. Iris angiographic changes in multifocal chorioretinitis with panuveitis. *Graefes Arch Clin Exp Ophthalmol*. 1999;237(11):902–907.
301. Thorne JE, Wittenberg S, Jabs DA, et al. Multifocal choroiditis with panuveitis: incidence of ocular complications and of loss of visual acuity. *Ophthalmology*. 2006;113(12):2310–2316.
302. Leung TG, Moradi A, Liu D, et al. Clinical features and incidence rate of ocular complications in punctate inner choroidopathy. *Retina*. 2014;34(8):1666–1674.
303. Kotsolis AI, Killian FA, Ladas ID, et al. Fluorescein angiography and optical coherence tomography concordance for choroidal neovascularisation in multifocal choroidtis. *Br J Ophthalmol*. 2010;94(11):1506–1508.
304. Olsen TW, Capone A, Sternberg P, et al. Subfoveal choroidal neovascularization in punctate inner choroidopathy: surgical management and pathologic findings. *Ophthalmology*. 1996;103(12):2061–2069.
305. Slakter JS, Giovannini A, Yannuzzi LA, et al. Indocyanine

green angiography of multifocal choroiditis. *Ophthalmology*. 1997;104(11):1813–1819.
306. Vadalà M, Lodato G, Cillino S. Multifocal choroiditis: indocyanine green angiographic features. *Ophthalmologica*. 2001;215(1):16–21.
307. Cimino L, Auer C, Herbort CP. Sensitivity of indocyanine green angiography for the follow-up of active inflammatory choriocapillaropathies. *Ocul Immunol Inflamm*. 2000;8(4):275–283.
308. Levy J, Shneck M, Klemperer I, et al. Punctate inner choroidopathy: resolution after oral steroid treatment and review of the literature. *Can J Ophthalmol*. 2005;40(5):605–608.
309. Akman A, Kadayifçilar S, Aydin P. Indocyanine green angiographic findings in a case of punctate inner choroidopathy. *Eur J Ophthalmol*. 1998;8(3):191–194.
310. Tiffin PA, Maini R, Roxburgh ST, et al. Indocyanine green angiography in a case of punctate inner choroidopathy. *Br J Ophthalmol*. 1996;80(1):90–91.
311. Vance SK, Khan S, Klancnik JM, et al. Characteristic spectral-domain optical coherence tomography findings of multifocal choroiditis. *Retina*. 2011;31(4):717–723.
312. Zhang X, Zuo C, Li M, et al. Spectral-domain optical coherence tomographic findings at each stage of punctate inner choroidopathy. *Ophthalmology*. 2013;120(12):2678–2683.
313. Zarranz-Ventura J, Sim DA, Keane PA, et al. Characterization of punctate inner choroidopathy using enhanced depth imaging optical coherence tomography. *Ophthalmology*. 2014;121(9):1790–1797.
314. Vance SK, Khan S, Klancnik JM, et al. Characteristic spectral-domain optical coherence tomography findings of multifocal choroiditis. *Retina*. 2011;31(4):717–723.
315. Kim H, Woo SJ, Kim YK, et al. Focal choroidal excavation in multifocal choroiditis and punctate inner choroidopathy. *Ophthalmology*. 2015;122(7):1534–1535.
316. Amer R, Priel E, Kramer M. Spectral-domain optical coherence tomographic features of choroidal neovascular

membranes in multifocal choroiditis and punctate inner choroidopathy. *Graefes Arch Clin Exp Ophthalmol*. 2015;253(6):949–957.
317. Haen SP, Spaide RF. Fundus autofluorescence in multifocal choroiditis and panuveitis. *Am J Ophthalmol*. 2008;145(5):847–853.
318. Oh KT, Folk JC, Maturi RK, et al. Multifocal electroretinography in multifocal choroiditis and the multiple evanescent white dot syndrome. *Retina*. 2001;21(6):581–589.
319. Khorram KD, Jampol LM, Rosenberg MA. Blind spot enlargement as a manifestation of multifocal choroiditis. *Arch Ophthalmol*. 1991;109(10):1403–1407.
320. Spaide RF, Koizumi H, Freund KB. Photoreceptor outer segment abnormalities as a cause of blind spot enlargement in acute zonal occult outer retinopathy-complex diseases. *Am J Ophthalmol*. 2008;146(1):111–120.
321. Tiedeman JS. Epstein–Barr viral antibodies in multifocal choroiditis and panuveitis. *Am J Ophthalmol*. 1987;103(5):659–663.
322. Schenck F, Böke W. Retinal vasculitis with multifocal chorioretinitis. *Klin Monatsbl Augenheilkd*. 1990;197(5):378–381.
323. Spaide RF, Sugin S, Yannuzzi LA, et al. Epstein–Barr virus antibodies in multifocal choroiditis and panuveitis. *Am J Ophthalmol*. 1991;112(4):410–413.
324. Mathura JR, Jampol LM, Daily MJ. Multifocal choroiditis and acute posterior multifocal placoid pigment epitheliopathy occurring in the same patient. *Arch Ophthalmol*. 2004;122(12):1881–1882.
325. Bryan RG, Freund KB, Yannuzzi LA, et al. Multiple evanescent white dot syndrome in patients with multifocal choroiditis. *Retina*. 2002;22(3):317–322.
326. Fine HF, Zhitomirsky I, Freund KB, et al. Bevacizumab (Avastin) and ranibizumab (Lucentis) for choroidal neovascularization in multifocal choroiditis. *Retina*. 2009;29(1):8–12.
327. Parodi MB, Iacono P, Kontadakis DS, et al. Bevacizumab vs

photodynamic therapy for choroidal neovascularization in multifocal choroiditis. *Arch Ophthalmol*. 2010;128(9):1100–1103.
328. Chang LK, Spaide RF, Brue C, et al. Bevacizumab treatment for subfoveal choroidal neovascularization from causes other than age-related macular degeneration. *Arch Ophthalmol*. 2008;126(7):941–945.
329. Uparkar M, Borse N, Kaul S, et al. Photodynamic therapy following intravitreal bevacizumab in multifocal choroiditis. *Int Ophthalmol*. 2008;28(5):375–377.
330. Chan WM, Lai TY, Lau TT, et al. Combined photodynamic therapy and intravitreal triamcinolone for choroidal neovascularization secondary to punctate inner choroidopathy or of idiopathic origin: one-year results of a prospective series. *Retina*. 2008;28(1):71–80.
331. Vossmerbaeumer U, Spandau UH, von Baltz S, et al. Intravitreal bevacizumab for choroidal neovascularisation secondary to punctate inner choroidopathy. *Clin Exp Ophthalmol*. 2008;36(3):292–294.
332. Rosen E, Rubowitz A, Ferencz JR. Exposure to verteporfin and bevacizumab therapy for choroidal neovascularization secondary to punctate inner choroidopathy during pregnancy. *Eye (Lond)*. 2009;23(6):1479.
333. Jampol LM, Sieving PA, Pugh D, et al. Multiple evanescent white dot syndrome. I. Clinical findings. *Arch Ophthalmol*. 1984;102(5):671–674.
334. Olitsky SE. Multiple evanescent white-dot syndrome in a 10-year-old child. *J Pediatr Ophthalmol Strabismus*. 1998;35(5):288–289.
335. Lim JI, Kokame GT, Douglas JP. Multiple evanescent white dot syndrome in older patients. *Am J Ophthalmol*. 1999;127(6):725–728.
336. Asano T, Kondo M, Kondo N, et al. High prevalence of myopia in Japanese patients with multiple evanescent white dot syndrome. *Jpn J Ophthalmol*. 2004;48(5):486–489.
337. Marsiglia M, Gallego-Pinazo R, Cunha de Souza E, et al. Expanded clinical spectrum of multiple evanescent white dot syndrome with multimodal imaging. *Retina*.

2016;36(1):64–74.
338. Gross NE, Yannuzzi LA, Freund KB, et al. Multiple evanescent white dot syndrome. *Arch Ophthalmol*. 2006;124(4):493–500.
339. Shelsta HN, Rao RR, Bhatt HK, et al. Atypical presentations of multiple evanescent white dot syndrome without white dots: a case series. *Retina*. 2011;31(5):973–976.
340. Huang J, Spaide R. Appearance of brown areas after resolution of the acute phase of multiple evanescent white dot syndrome. *Retina*. 2004;24(5):814–816.
341. Luttrull JK, Marmor MF, Nanda M. Progressive confluent circumpapillary multiple evanescent white-dot syndrome. *Am J Ophthalmol*. 1999;128(3):378–380.
342. Daniele S, Daniele C, Ferri C. Association of peripapillary scars with lesions characteristic of multiple evanescent white-dot syndrome. *Ophthalmologica*. 1995;209(4):217–219.
343. McCollum CJ, Kimble JA. Peripapillary subretinal neovascularization associated with multiple evanescent white-dot syndrome. *Arch Ophthalmol*. 1992;110(1):13–14.
344. Wyhinny GJ, Jackson JL, Jampol LM, et al. Subretinal neovascularization following multiple evanescent white-dot syndrome. *Arch Ophthalmol*. 1990;108(10):1384–1385.
345. Papadia M, Herbort CP. Idiopathic choroidal neovascularisation as the inaugural sign of multiple evanescent white dot syndrome. *Middle East Afr J Ophthalmol*. 2010;17(3):270–274.
346. Machida S, Fujiwara T, Murai K, et al. Idiopathic choroidal neovascularization as an early manifestation of inflammatory chorioretinal diseases. *Retina*. 2008;28(5):703–710.
347. Sieving PA, Fishman GA, Jampol LM, et al. Multiple evanescent white dot syndrome. II. Electrophysiology of the photoreceptors during retinal pigment epithelial disease. *Arch Ophthalmol*. 1984;102(5):675–679.
348. Aaberg TM, Campo RV, Joffe L. Recurrences and bilaterality in the multiple evanescent white-dot syndrome. *Am J Ophthalmol*. 1985;100(1):29–37.
349. Jost BF, Olk RJ, McGaughey A. Bilateral symptomatic

multiple evanescent white-dot syndrome. *Am J Ophthalmol*. 1986;101(4):489–490.
350. Tsai L, Jampol LM, Pollock SC, et al. Chronic recurrent multiple evanescent white dot syndrome. *Retina*. 1994;14(2):160–163.
351. Fine HF, Spaide RF, Ryan EH, et al. Acute zonal occult outer retinopathy in patients with multiple evanescent white dot syndrome. *Arch Ophthalmol*. 2009;127(1):66–70.
352. Forooghian F, Stetson PF, Gross NE, et al. Quantitative assessment of photoreceptor recovery in atypical multiple evanescent white dot syndrome. *Ophthalmic Surg Lasers Imaging*. 2010;41(Suppl):S77–80.
353. Li D, Kishi S. Restored photoreceptor outer segment damage in multiple evanescent white dot syndrome. *Ophthalmology*. 2009;116(4):762–770.
354. Kanis MJ, van Norren D. Integrity of foveal cones in multiple evanescent white dot syndrome assessed with OCT and foveal reflection analyser. *Br J Ophthalmol*. 2006;90(6):795–796.
355. Li D, Kishi S. Loss of photoreceptor outer segment in acute zonal occult outer retinopathy. *Arch Ophthalmol*. 2007;125(9):1194–1200.
356. Boretsky A, Mirza S, Khan F, et al. High-resolution multimodal imaging of multiple evanescent white dot syndrome. *Ophthalmic Surg Lasers Imaging Retina*. 2013;44(3):296–300.
357. Ie D, Glaser BM, Murphy RP, et al. Indocyanine green angiography in multiple evanescent white-dot syndrome. *Am J Ophthalmol*. 1994;117(1):7–12.
358. Borruat FX, Auer C, Piguet B. Choroidopathy in multiple evanescent white dot syndrome. *Arch Ophthalmol*. 1995;113(12):1569–1571.
359. Obana A, Kusumi M, Miki T. Indocyanine green angiographic aspects of multiple evanescent white dot syndrome. *Retina*. 1996;16(2):97–104.
360. Obana A, Kusumi M, Moriwaki M, et al. Two cases of multiple evanescent white dot syndrome examined with indocyanine green angiography. *Nippon Ganka Gakkai*

Zasshi. 1995;99(2):244–251.
361. Yen MT, Rosenfeld PJ. Persistent indocyanine green angiographic findings in multiple evanescent white dot syndrome. *Ophthalmic Surg Lasers*. 2001;32(2):156–158.
362. Tsukamoto E, Yamada T, Kadoi C, et al. Hypofluorescent spots on indocyanine green angiography at the recovery stage in multiple evanescent white dot syndrome. *Ophthalmologica*. 1999;213(5):336–338.
363. Herbort CP, Borruat FX, de Courten C, et al. Indocyanine green angiography in posterior uveitis. *Klin Monatsbl Augenheilkd*. 1996;208(5):321–326.
364. Stanga PE, Lim JI, Hamilton P. Indocyanine green angiography in chorioretinal diseases: indications and interpretation: an evidence-based update. *Ophthalmology*. 2003;110(1):15–21 [quiz 22–13].
365. Hashimoto Y, Saito W, Saito M, et al. Decreased choroidal blood flow velocity in the pathogenesis of multiple evanescent white dot syndrome. *Graefes Arch Clin Exp Ophthalmol*. 2015;253(9):1457–1464.
366. Amin HI. Optical coherence tomography findings in multiple evanescent white dot syndrome. *Retina*. 2006;26(4):483–484.
367. Gerstenblith AT, Thorne JE, Sobrin L, et al. Punctate inner choroidopathy: a survey analysis of 77 persons. *Ophthalmology*. 2007;114(6):1201–1204.
368. Sikorski BL, Wojtkowski M, Kaluzny JJ, et al. Correlation of spectral optical coherence tomography with fluorescein and indocyanine green angiography in multiple evanescent white dot syndrome. *Br J Ophthalmol*. 2008;92(11):1552–1557.
369. Nguyen MH, Witkin AJ, Reichel E, et al. Microstructural abnormalities in MEWDS demonstrated by ultrahigh resolution optical coherence tomography. *Retina*. 2007;27(4):414–418.
370. Hashimoto Y, Saito W, Noda K, et al. Acquired focal choroidal excavation associated with multiple evanescent white dot syndrome: observations at onset and a pathogenic hypothesis. *BMC Ophthalmol*. 2014;14:135.
371. Dell'Omo R, Mantovani A, Wong R, et al. Natural evolution

of fundus autofluorescence findings in multiple evanescent white dot syndrome: a long-term follow-up. *Retina*. 2010;30(9):1479–1487.
372. Furino C, Boscia F, Cardascia N, et al. Fundus autofluorescence and multiple evanescent white dot syndrome. *Retina*. 2009;29(1):60–63.
373. Battaglia Parodi M, Iacono P, Falcomatà B, et al. Near-infrared fundus autofluorescence in multiple evanescent white-dot syndrome. *Eur J Ophthalmol*. 2015;25(1):43–46.
374. Horiguchi M, Miyake Y, Nakamura M, et al. Focal electroretinogram and visual field defect in multiple evanescent white dot syndrome. *Br J Ophthalmol*. 1993;77(7):452–455.
375. Keunen JE, van Norren D. Foveal densitometry in the multiple evanescent white-dot syndrome. *Am J Ophthalmol*. 1988;105(5):561–562.
376. Chen D, Martidis A, Baumal CR. Transient multifocal electroretinogram dysfunction in multiple evanescent white dot syndrome. *Ophthalmic Surg Lasers*. 2002;33(3):246–249.
377. Feigl B, Haas A, El-Shabrawi Y. Multifocal ERG in multiple evanescent white dot syndrome. *Graefes Arch Clin Exp Ophthalmol*. 2002;240(8):615–621.
378. Nakao K, Isashiki M. Multiple evanescent white dot syndrome. *Jpn J Ophthalmol*. 1986;30(4):376–384.
379. Hamed LM, Glaser JS, Gass JD, et al. Protracted enlargement of the blind spot in multiple evanescent white dot syndrome. *Arch Ophthalmol*. 1989;107(2):194–198.
380. Boscarino MA, Johnson TM. Microperimetry in multiple evanescent white dot syndrome. *Can J Ophthalmol*. 2007;42(5):743–745.
381. Hangai M, Fujimoto M, Yoshimura N. Features and function of multiple evanescent white dot syndrome. *Arch Ophthalmol*. 2009;127(10):1307–1313.
382. Figueroa MS, Ciancas E, Mompean B, et al. Treatment of multiple evanescent white dot syndrome with cyclosporine. *Eur J Ophthalmol*. 2001;11(1):86–88.
383. Laatikainen L, Immonen I. Multiple evanescent white dot syndrome. *Graefes Arch Clin Exp Ophthalmol*. 1988;226(1):37–

40.
384. Fine L, Fine A, Cunningham ET. Multiple evanescent white dot syndrome following hepatitis a vaccination. *Arch Ophthalmol*. 2001;119(12):1856–1858.
385. Baglivo E, Safran AB, Borruat FX. Multiple evanescent white dot syndrome after hepatitis B vaccine. *Am J Ophthalmol*. 1996;122(3):431–432.
386. Cohen SM. Multiple evanescent white dot syndrome after vaccination for human papilloma virus and meningococcus. *J Pediatr Ophthalmol Strabismus*. 2009;25:1–3; 10.3928/01913913-20090616-01 [ePub; Jun].
387. Chung YM, Yeh TS, Liu JH. Increased serum IgM and IgG in the multiple evanescent white-dot syndrome. *Am J Ophthalmol*. 1987;104(2):187–188.
388. Desarnaulds AB, Borruat FX, Herbort CP, et al. Multiple evanescent white dot syndrome: a genetic predisposition? *Klin Monatsbl Augenheilkd*. 1996;208(5):301–302.
389. Borruat FX, Piguet B, Herbort CP. Acute posterior multifocal placoid pigment epitheliopathy following mumps. *Ocul Immunol Inflamm*. 1998;6(3):189–193.
390. Dodwell DG, Jampol LM, Rosenberg M, et al. Optic nerve involvement associated with the multiple evanescent white-dot syndrome. *Ophthalmology*. 1990;97(7):862–868.
391. Fong KS, Fu ER. Multiple evanescent white dot syndrome – an uncommon cause for an enlarged blind spot. *Ann Acad Med Singapore*. 1996;25(6):866–868.
392. Reddy CV, Brown J, Folk JC, et al. Enlarged blind spots in chorioretinal inflammatory disorders. *Ophthalmology*. 1996;103(4):606–617.
393. Battaglia Parodi M, Iacono P, Verbraak FD, et al. Antivascular endothelial growth factors for inflammatory chorioretinal disorders. *Dev Ophthalmol*. 2010;46:84–95.
394. Rouvas AA, Ladas ID, Papakostas TD, et al. Intravitreal ranibizumab in a patient with choroidal neovascularization secondary to multiple evanescent white dot syndrome. *Eur J Ophthalmol*. 2007;17(6):996–999.
395. Gass JD. Acute zonal occult outer retinopathy. Donders Lecture: The Netherlands Ophthalmological Society,

Maastricht, Holland, June 19, 1992. *J Clin Neuroophthalmol*. 1993;13(2):79–97.
396. Monson DM, Smith JR. Acute zonal occult outer retinopathy. *Surv Ophthalmol*. 2011;56(1):23–35.
397. Gass JD, Agarwal A, Scott IU. Acute zonal occult outer retinopathy: a long-term follow-up study. *Am J Ophthalmol*. 2002;134(3):329–339.
398. Mrejen S, Khan S, Gallego-Pinazo R, et al. Acute zonal occult outer retinopathy: a classification based on multimodal imaging. *JAMA Ophthalmol*. 2014;132(9):1089–1098.
399. Saito S, Saito W, Saito M, et al. Acute zonal occult outer retinopathy in Japanese patients: clinical features, visual function, and factors affecting visual function. *PLoS ONE*. 2015;10(4):e0125133.
400. Gass JD, Stern C. Acute annular outer retinopathy as a variant of acute zonal occult outer retinopathy. *Am J Ophthalmol*. 1995;119(3):330–334.
401. Cohen SYM, Jampol LMM. Choroidal neovascularization in peripapillary acute zonal occult outer retinopathy. *Cases Brief Rep*. 2007;1(4):220–222.
402. Hoang QV, Gallego-Pinazo R, Yannuzzi LA. Long-term follow-up of acute zonal occult outer retinopathy. *Retina*. 2013;33(7):1325–1327.
403. Nakao S, Kaizu Y, Yoshida S, et al. Spontaneous remission of acute zonal occult outer retinopathy: follow-up using adaptive optics scanning laser ophthalmoscopy. *Graefes Arch Clin Exp Ophthalmol*. 2015;253(6):839–843.
404. Spaide RF. Collateral damage in acute zonal occult outer retinopathy. *Am J Ophthalmol*. 2004;138(5):887–889.
405. Fujiwara T, Imamura Y, Giovinazzo VJ, et al. Fundus autofluorescence and optical coherence tomographic findings in acute zonal occult outer retinopathy. *Retina*. 2010;30(8):1206–1216.
406. Li D, Kishi S. Loss of photoreceptor outer segment in acute zonal occult outer retinopathy. *Arch Ophthalmol*. 2007;125(9):1194–1200.
407. Spaide RF, Koizumi H, Freund KB. Photoreceptor outer

segment abnormalities as a cause of blind spot enlargement in acute zonal occult outer retinopathy-complex diseases. *Am J Ophthalmol*. 2008;146(1):111–120.
408. Mkrtchyan M, Lujan BJ, Merino D, et al. Outer retinal structure in patients with acute zonal occult outer retinopathy. *Am J Ophthalmol*. 2012;153(4):757–768.
409. Ueno S, Kawano K, Ito Y, et al. Near-infrared reflectance imaging in eyes with acute zonal occult outer retinopathy. *Retina*. 2015;35(8):1521–1530.
410. Tagami M, Matsumiya W, Imai H, et al. Autologous antibodies to outer retina in acute zonal occult outer retinopathy. *Jpn J Ophthalmol*. 2014;58(6):462–472.
411. Heckenlively JR, Ferreyra HA. Autoimmune retinopathy: a review and summary. *Semin Immunopathol*. 2008;30(2):127–134.
412. Chen SN, Yang CH, Yang CM. Systemic corticosteroids therapy in the management of acute zonal occult outer retinopathy. *J Ophthalmol*. 2015;2015:793026.
413. Mahajan VB, Stone EM. Patients with an acute zonal occult outer retinopathy-like illness rapidly improve with valacyclovir treatment. *Am J Ophthalmol*. 2010;150(4):511–518.
414. Bos PJ, Deutman AF. Acute macular neuroretinopathy. *Am J Ophthalmol*. 1975;80(4):573–584.
415. Yeh S, Hwang TS, Weleber RG, et al. Acute macular outer retinopathy (AMOR): a reappraisal of acute macular neuroretinopathy using multimodality diagnostic testing. *Arch Ophthalmol*. 2011;129(3):365–368.
416. El-Dairi M, Bhatti MT, Vaphiades MS. A shot of adrenaline. *Surv Ophthalmol*. 2009;54(5):618–624.
417. Vance SK, Spaide RF, Freund KB, et al. Outer retinal abnormalities in acute macular neuroretinopathy. *Retina*. 2011;31(3):441–445.
418. Miller MH, Spalton DJ, Fitzke FW, et al. Acute macular neuroretinopathy. *Ophthalmology*. 1989;96(2):265–269.
419. Dansingani KK, Freund KB. Paracentral acute middle maculopathy and acute macular neuroretinopathy: related and distinct entities. *Am J Ophthalmol*. 2015;160(1):1–3.

420. Rahimy E, Sarraf D. Paracentral acute middle maculopathy spectral-domain optical coherence tomography feature of deep capillary ischemia. *Curr Opin Ophthalmol*. 2014;25(3):207–212.
421. Sarraf D, Rahimy E, Fawzi AA, et al. Paracentral acute middle maculopathy: a new variant of acute macular neuroretinopathy associated with retinal capillary ischemia. *JAMA Ophthalmol*. 2013;131(10):1275–1287.
422. Fawzi AA, Pappuru RR, Sarraf D, et al. Acute macular neuroretinopathy: long-term insights revealed by multimodal imaging. *Retina*. 2012;32(8):1500–1513.
423. Munk MR, Jampol LM, Cunha Souza E, et al. New associations of classic acute macular neuroretinopathy. *Br J Ophthalmol*. 2016;100(3):389–394.
424. Turbeville SD, Cowan LD, Gass JD. Acute macular neuroretinopathy: a review of the literature. *Surv Ophthalmol*. 2003;48(1):1–11.
425. Aziz HA, Kheir WJ, Young RC, et al. Acute macular neuroretinopathy: a case report and review of the literature, 2002–2012. *Ophthalmic Surg Lasers Imaging Retina*. 2015;46(1):114–124.
426. Chan WM, Liu DT, Tong JP, et al. Longitudinal findings of acute macular neuroretinopathy with multifocal electroretinogram and optical coherence tomography. *Clin Exp Ophthalmol*. 2005;33(4):439–442.
427. O'Brien DM, Farmer SG, Kalina RE, et al. Acute macular neuroretinopathy following intravenous sympathomimetics. *Retina*. 1989;9(4):281–286.
428. Abu el-Asrar AM. Serpiginous (geographical) choroiditis. *Int Ophthalmol Clin*. 1995;35(2):87–91.
429. Rush JA. Acute macular neuroretinopathy. *Am J Ophthalmol*. 1977;83(4):490–494.
430. Feigl B, Haas A. Optical coherence tomography (OCT) in acute macular neuroretinopathy. *Acta Ophthalmol Scand*. 2000;78(6):714–716.
431. Mirshahi A, Scharioth GB, Klais CM, et al. Enhanced visualization of acute macular neuroretinopathy by Heidelberg retina tomography. *Clin Exp Ophthalmol*.

2006;34(6):596–599.
432. Monson BK, Greenberg PB, Greenberg E, et al. High-speed, ultra-high-resolution optical coherence tomography of acute macular neuroretinopathy. *Br J Ophthalmol*. 2007;91(1):119–120.
433. Hughes EH, Siow YC, Hunyor AP. Acute macular neuroretinopathy: anatomic localisation of the lesion with high-resolution OCT. *Eye (Lond)*. 2009;23(11):2132–2134.
434. Maschi C, Schneider-Lise B, Paoli V, et al. Acute macular neuroretinopathy: contribution of spectral-domain optical coherence tomography and multifocal ERG. *Graefes Arch Clin Exp Ophthalmol*. 2011;249(6):827–831.
435. Kuznik-Borkowska A, Cohen SY, Broïdo-Hooreman O, et al. Acute macular neuroretinopathy. *J Fr Ophtalmol*. 2006;29(3):319–322.
436. Baumüller S, Holz FG. Early spectral-domain optical coherence tomography findings in acute macular neuroretinopathy. *Retina*. 2012;32(2):409–410.
437. Affortit AS, Lazrak Z, Leze RH, et al. En face spectral domain optical coherence tomography in a case of bilateral acute macular neuroretinopathy. *Retina*. 2015;35(5):1049–1050.
438. Maturi RK, Yu M, Sprunger DT. Multifocal electroretinographic evaluation of acute macular neuroretinopathy. *Arch Ophthalmol*. 2003;121(7):1068–1069.
439. Browning AC, Gupta R, Barber C, et al. The multifocal electroretinogram in acute macular neuroretinopathy. *Arch Ophthalmol*. 2003;121(10):1506–1507.
440. Sieving PA, Fishman GA, Salzano T, et al. Acute macular neuroretinopathy: early receptor potential change suggests photoreceptor pathology. *Br J Ophthalmol*. 1984;68(4):229–234.
441. Gómez-Torreiro M, Gómez-Ulla F, Bolívar Montesa P, et al. Scanning laser ophthalmoscope findings in acute macular neuroretinopathy. *Retina*. 2002;22(1):108–109.
442. Battaglia Parodi M, Iacono P, Panico D, et al. Microperimetric assessment of the two optical coherence tomography subtypes of acute macular neuroretinopathy.

Clin Experiment Ophthalmol. 2015;43(7):637–642.
443. Hansen SO, Cooper RF, Dubra A, et al. Selective cone photoreceptor injury in acute macular neuroretinopathy. *Retina*. 2013;33(8):1650–1658.
444. Mrejen S, Pang CE, Sarraf D, et al. Adaptive optics imaging of cone mosaic abnormalities in acute macular neuroretinopathy. *Ophthalmic Surg Lasers Imaging Retina*. 2014;45(6):562–569.
445. Groat CL, Ellis BD, Leys MJ. A unique case of acute macular neuroretinopathy associated with cotton wool spots and intraretinal fluid. *Retin Cases Brief Rep*. 2016;10(1):26–31.
446. Tsui I, Sarraf D. Paracentral acute middle maculopathy and acute macular neuroretinopathy. *Ophthalmic Surg Lasers Imaging Retina*. 2013;44(6):S33–5.

80

Autoimmune Retinopathies

Austin R. Fox, H. Nida Sen, Robert B. Nussenblatt, (posthumously)

Introduction

Autoimmune retinopathies (AIR) represent a group of inflammatory mediated retinopathies with otherwise unexplained vision loss associated with visual field deficits, photoreceptor dysfunction as evidenced on electroretinography (ERG), and the presence of circulating autoantibodies targeted against retinal antigens. Clinically, the fundus often appears normal, but some patients may show retinal vascular attenuation, diffuse retinal atrophy with or without pigmentary changes or waxy disc pallor. There are usually few or no intraocular inflammatory cells.[1,2]

AIR presumably results from an immunologic attack on the

retina by antibodies directed against retinal antigens. The first case of vision loss and photoreceptor degeneration associated with cancer was described by Sawyer et al. in 1976.[3] Paraneoplastic retinopathy, as a term, was first used by Klingele and associates in 1984 and has become the more general term used for autoimmune retinopathies associated with systemic malignancy since then.[4] Several forms of autoantibody-mediated retinopathy are described: cancer-associated retinopathy (CAR) syndrome, melanoma-associated retinopathy (MAR) syndrome, or autoimmune retinopathy of other types.[3,5–11] AIR can be categorized in two groups: (i) autoimmune retinopathy associated with cancer or other malignancies (paraneoplastic retinopathy or paraneoplastic autoimmune retinopathy); (ii) autoimmune retinopathy without any evidence of malignancy (nonparaneoplastic autoimmune retinopathy). Cancer-associated retinopathy and other paraneoplastic retinopathies will be covered in Chapter 138 (Remote effects of cancer on the retina). Autoimmune retinopathy is the preferred term for an acquired, presumed immunologically mediated retinopathy caused by antiretinal autoantibodies in the absence of a malignancy. This chapter will emphasize the latter.

Epidemiology and Mechanisms

The prevalence of AIR is unknown, but the condition is believed to be rare. Clinical reports of nonparaneoplastic AIR consist only of case reports and a few small cohorts.[12–15] AIR remains an ill-defined disorder and the lack of standardized diagnostic criteria may be contributing to the underestimation of its prevalence. Though circulating autoantibodies to retinal antigens have been shown to be associated with retinal dysfunction, the mechanisms by which these antibodies cause dysfunction are not entirely understood.[16] Multiple retinal proteins have been found to be antigenic, including recoverin, carbonic anhydrase, α-enolase, arrestin, transducin-β and -α, carbonic anhydrase II, TULP1, neurofilament protein, heat shock proteins, photoreceptor-cell-specific nuclear receptor (PNR), Müller-cell-specific antigen, transient receptor potential cation channel, subfamily M, member 1 (TRPM1), and many other yet-unidentified antigens[17,18] (Table 80.1). Some of these antigens are

retina-specific, such as recoverin and rhodopsin, while others can be found in nonretinal tissues as well, such as enolase. Among these, recoverin and enolase are the most extensively studied antigens in the context of AIR. Recoverin is a 23 kDa calcium-binding protein found in both rods and cones. Enolase is a 48 kDa glycolytic enzyme whose α- and β-isoforms are found in many tissues, and γ-isoform in neuronal tissues.[43] In a large series, more than 30% of patients with antiretinal antibodies tested positive for antienolase antibody.[44] Antibodies against α-enolase appear to be fairly ubiquitous; they are found in multiple autoimmune diseases and even in healthy subjects.[45–48] This has been, in part, attributed to the multifunctional nature of α-enolase.[16,26,49]

TABLE 80.1
Proteins Targeted by Antiretinal Antibodies

Recoverin (23 kD)		CAR, npAIR[6,14,19–25]
Alpha-enolase (46 kD)		CAR, npAIR[14,22,26–29]
Carbonic anhydrase II (CA II) (30 kD)		CAR, npAIR[12,22,30]
Tubby-like protein 1 (TULP-1) (65 kD)		CAR[31]
Heat shock protein 70 (HSC 70) (70 kD)		CAR[21]
Transducin-β (35 kD)		MAR[32]
Transducin-α (40 kD)		CAR, MAR[33]
Arrestin (S-antigen) (48 kD)		MAR, npAIR[22,34]
Interphotoreceptor binding protein (IRBP) (141 kD)		npAIR, MAR[22,35]
Heat shock protein 60 (HSC 60) (61 kD)		CAR, npAIR[36]
Collapsin response mediator protein 2 (CRMP2) (62 kDa)		CAR, MAR, npAIR[36]
Unknown proteins	22 kD, 34 kD, 35 kD, 37 kD, 40 kD, 68 kD	npAIR[15,37,38]
	34 kD, 40 kD, 46 kD, 60 kD, 70 kD	CAR [23,39–42]

Antibodies against the listed proteins were identified in the serum of patients with AIR or AIR-like clinical findings.

CAR, cancer-associated retinopathy; MAR, melanoma-associated retinopathy; npAIR, nonparaneoplastic autoimmune retinopathy.

Of all these antigens, recoverin and CAR has the strongest association. Recoverin has been shown to be expressed by the tumor cells of patients with CAR.[50] While antirecoverin antibody is most specific to CAR, it has also been found in patients with nonparaneoplastic AIR, as well as patients with small-cell lung carcinoma without any retinopathy.[19,20,51] Recoverin and α-enolase have been shown to be highly expressed in cancer cells in patients with paraneoplastic AIR. It is plausible that the disease is triggered

by molecular mimicry between retinal proteins and tumor antigens in cases of paraneoplastic AIR and presumed viral or bacterial proteins in the case of nonparaneoplastic AIR.[27,52,53] Regardless of the presence or absence of malignancy, autoimmune retinopathies appear to share common clinical features.

Experimental studies have attempted to shed light on the pathogenic mechanisms of autoimmune retinopathy. In vitro studies have demonstrated that some of the antiretinal antibodies are, indeed, cytotoxic to retinal cells, and that the cellular internalization of the antibody leads to apoptosis.[21,26,28,54–56] This antibody-mediated apoptosis is independent of complement and involves caspase pathways and intracellular calcium influx. Similarly, in vivo studies showed that intravitreal injection of antirecoverin antibody causes apoptosis of retinal cells and a decrease in ERG responses.[21,57,58] Recoverin also acts as a uveitogenic antigen and can induce autoimmune retinopathy-like disease in animal models leading to reduced scotopic and photopic ERG responses.[59,60] Both in vitro and in vivo studies showed that antirecoverin antibody-triggered apoptosis occurs only in recoverin-positive cells.[61] Antirecoverin antibodies target photoreceptor cells, and anti-α-enolase antibodies appear to target ganglion cells. Antibodies targeting retinal bipolar cells have been associated with MAR. Additionally, injection of immunoglobulins isolated from serum of patients with MAR into the vitreous of monkeys led to ERG changes similar to those observed in MAR, indicating the pathogenicity of the antiretinal antibodies.[62] Evidence from these studies suggests that antiretinal autoantibodies can target virtually any retinal cell type – photoreceptor cells, ganglion cells, bipolar cells – and cause retinal dysfunction.[14,54,63]

It is still unclear, however, why some patients with antiretinal antibodies develop retinopathy while others do not. It has been suggested that antiretinal antibodies may be pathogenic when targeting specific epitopes, resulting in retinal cytotoxicity in CAR patients, while in healthy controls, antiretinal antibodies may target different epitopes without such a consequence.[26] On the other hand, it is a possibility that antiretinal antibodies are an epiphenomenon, resulting secondarily from the pathogenesis of AIR. In addition to studying the role of antiretinal antibodies, future studies are needed

to elucidate the role of cellular immunity in the pathogenesis of AIR, about which little is known.

Studies are also needed to explore other factors (i.e., genetics) potentially contributing to the pathogenesis of nonparaneoplastic AIR. Our group found significantly different frequencies of certain HLA alleles among 18 nonparaneoplastic AIR patients as compared to the general population, however, future studies of larger cohorts are needed to verify potential genetic associations.[64] As more nonparaneoplastic AIR patients are identified, genetic studies may provide insight into the pathogenesis and support the diagnosis of nonparaneoplastic AIR in the future.

Clinical Features

Clinical features of AIR are quite variable. Serum antiretinal autoantibodies have been associated with loss of vision and visual field defects as well as electrophysiologic changes in patients with autoimmune retinopathy, but the exact mechanism has not been fully understood. In particular, the pathogenicity and specificity of these autoantibodies with respect to clinical findings have yet to be determined. Nevertheless, patients with AIR appear to share common clinical features despite the heterogeneity in the detectable circulating antiretinal antibodies.[12,14,65]

The clinical manifestations of nonparaneoplastic AIR is quite variable; there are no clear guidelines or consensus on the diagnosis of autoimmune retinopathy. Commonly recognized clinical manifestations include the following:[12,13]

1. Symptoms: acute or subacute onset of photopsia, dyschromatopsia, nyctalopia, photoaversion, scotomas, sometimes central vision loss.

2. Fundus findings: normal-appearing fundus or waxy disc pallor, attenuated retinal vasculature and retinal pigment epithelial (RPE) atrophy or mottling. There are few or no intraocular inflammatory cells.

3. Psychophysical tests:

a. Visual fields: constricted visual fields, central or paracentral scotomas.

b. Electroretinogram (ERG): ERG can show abnormalities in rods, cones, Müller cells, or bipolar cell responses or a combination of these.

Patients with nonparaneoplastic AIR present with acute or subacute vision loss. Patients typically complain of color vision changes, photosensitivity or photoaversion, and varying degrees of nyctalopia. Other presenting symptoms include floaters; photopsias; scotomas, most commonly paracentral; and constricted visual fields. Of these, photosensitivity, photoaversion, difficulty seeing in bright light, reduced visual acuity, dyschromatopsia and central scotomas are suggestive of cone dysfunction, whereas nyctalopia (night blindness) and midperipheral scotomas are suggestive of rod dysfunction. Depending on the extent and the distinct retinal cell involvement, visual acuity, particularly in the earlier stages, may be deceivingly good. On presentation to a tertiary care center, most patients may have been diagnosed with nonspecific retinal degeneration or isolated cases of retinitis pigmentosa (RP). Fundus examination can be unremarkable or may show signs of retinal degeneration such as waxy disc pallor, attenuated retinal vasculature with or without pigmentary changes, or diffuse atrophy. Though atypical, one case of nonparaneoplastic AIR presenting with severe peripheral retinal vasoocclusion has been reported.[66] There may be mild or no inflammatory cells in the anterior chamber or the vitreous[12,13,67] (Fig. 80.1).

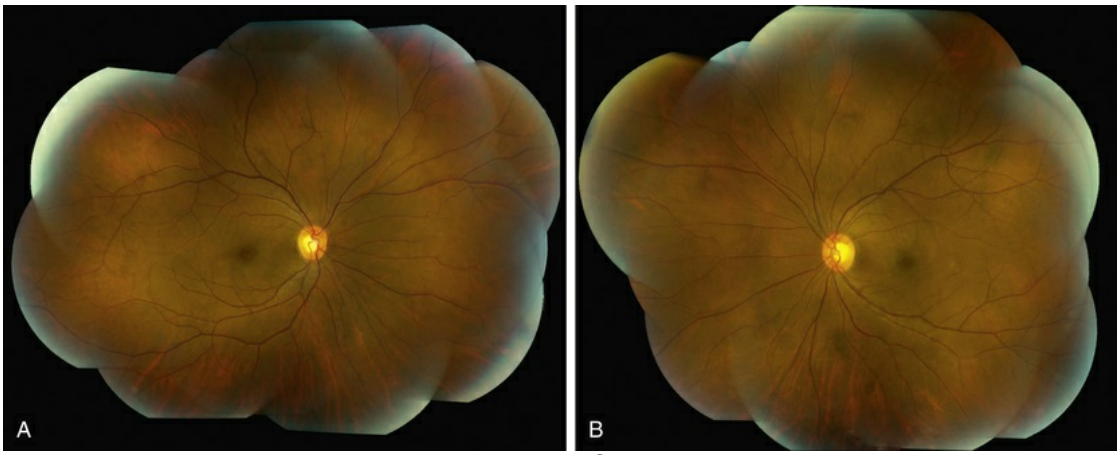

FIG. 80.1 (A,B) Fundus photo of a 57-year-old patient with systemic lupus erythematosus and autoimmune retinopathy. Note the mild attenuation of retinal vasculature and mild optic nerve pallor.

Ancillary testing with fluorescein angiography (FA) or optical coherence tomography (OCT) may show mild retinal vascular staining or leakage, or cystoid macular edema (CME) in some cases.[12,68] Using spectral domain (SD) OCT, a few studies have identified outer retinal abnormalities and decreased central macular thickness in nonparaneoplastic AIR patients.[69–71] These abnormalities may include disruption or loss of the photoreceptor outer and inner segment junction (or ellipsoid zone), loss of the photoreceptor layer, disruption or loss of the external limiting membrane, and outer nuclear layer thinning. On FAF, a parafoveal hyperautofluorescent ring corresponds to these outer retinal abnormalities identified on SD-OCT.[70,71] Similar features on FAF and OCT have been noted in following 24 AIR patients here at the National Eye Institute.[68] However, abnormal FAF findings have not been consistently identified in all nonparaneoplastic AIR patients.

Visual field testing may confirm scotomas and constricted visual fields. While static visual field testing may be better for demonstrating and following central and paracentral scotomas, kinetic visual fields are better for measuring peripheral field constriction. However, kinetic visual fields have the disadvantage of examiner dependence, the need for patient cooperation, intertester variability, and lack of standardization of parameters.[72,73] ERG may demonstrate abnormal rod, cone, Müller cell, and bipolar cell responses and delay in implicit times.[12,13,27,37] However, the

majority of studies involving ERG findings in AIR come from paraneoplastic retinopathies (Fig. 80.2).

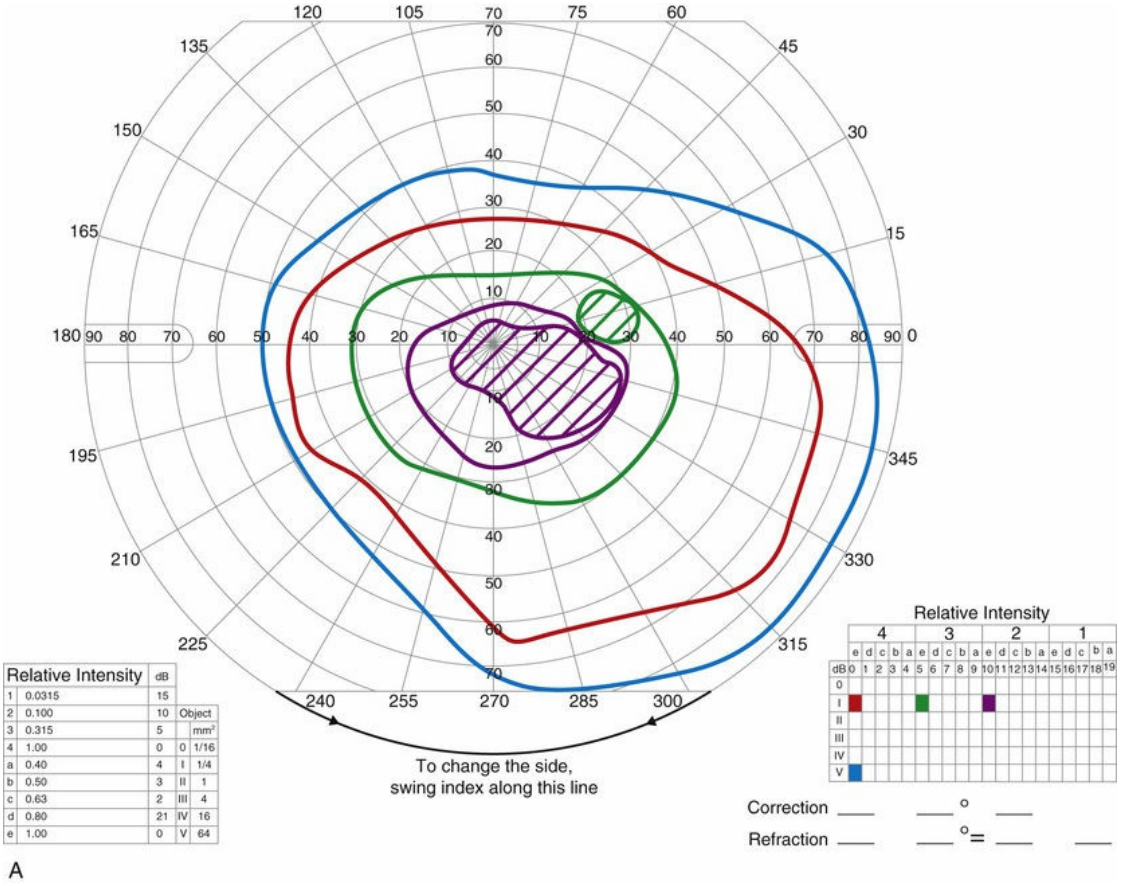

A

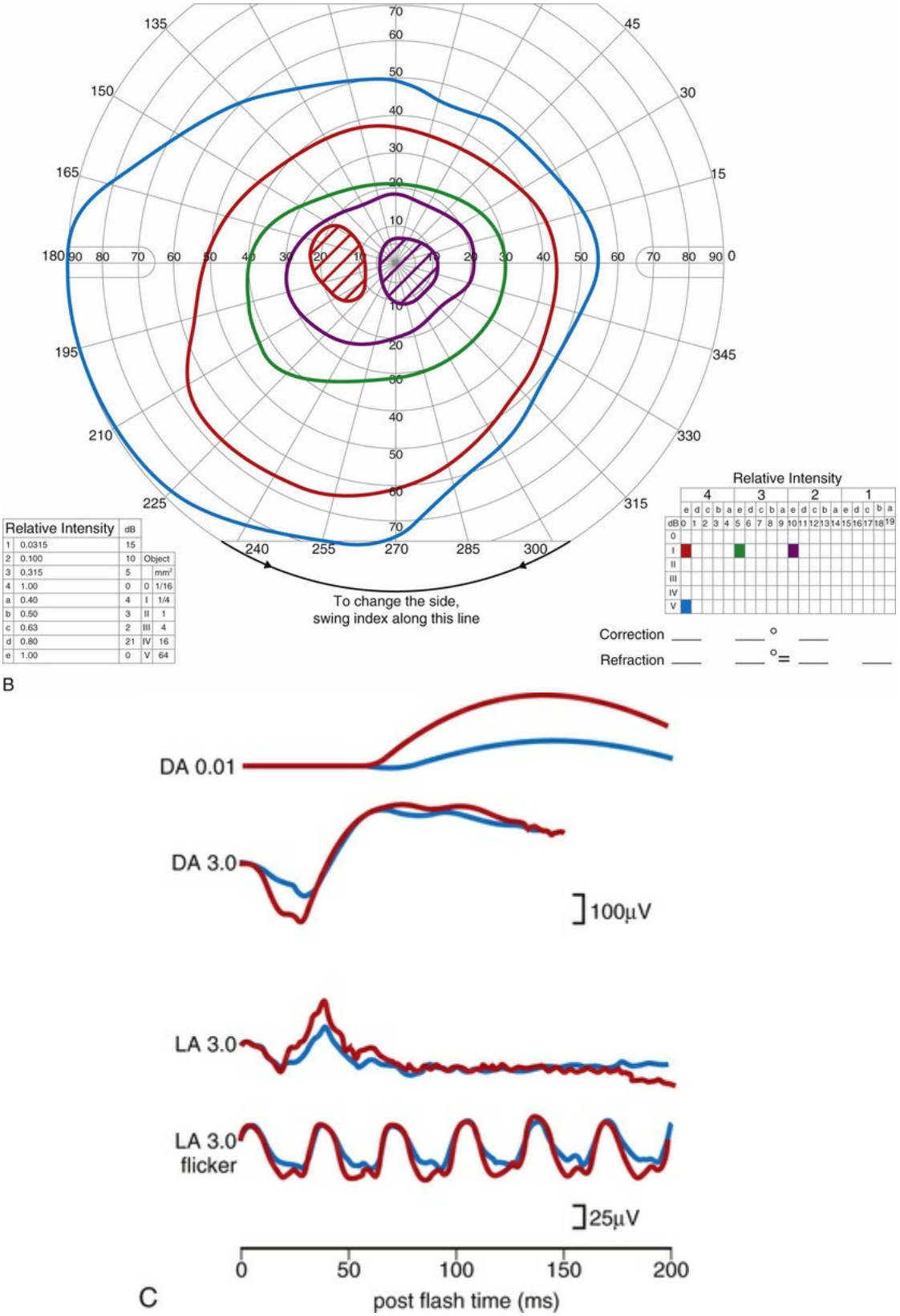

FIG. 80.2 (A–C) Goldman visual field of an autoimmune retinopathy patient shows central and paracentral scotoma in the right (A) and left (B) eye. (C) Electroretinogram (ERG) responses of the same patient show reduced amplitudes for both rod- and

cone-mediated responses. Blue traces indicate baseline ERG recordings; red traces were recorded 1 month after treatment with rituximab (Rituxan®, Genentech, Inc., CA), a chimeric anti-CD20 antibody. Note the improvement in rod-mediated responses. ERGs were recorded according to ISCEV standards. Number indicates flash intensity (cd-s/m^2). Note different scales for dark-adapted (DA) and light-adapted (LA) ERGs. (Courtesy of Brett Jeffrey, PhD.)

AIR is almost always bilateral, although involvement can be asymmetric. There is a female preponderance (63–66%), and average age at diagnosis appears to range from 51 years to 56 years.[12–14] The typical patient would be a middle-aged or older adult in their fifth to sixth decades with no history of visual problems prior to the onset of photopsias, scotomas, and other symptoms consistent with AIR, and no family history of RP. A personal or a family history of systemic autoimmune disease can be common among patients with nonparaneoplastic AIR.[12,15] In fact, cases of nonparaneoplastic AIR have been described in the setting of systemic lupus erythematosus and autoimmune polyglandular syndrome type 1(APS 1).[74–77]

As might be expected for an entity with no consensus in diagnosis, retrospective studies in patients with nonparaneoplastic AIR showed that clinical features vary considerably. In one study, diffuse retinal atrophy was seen in the majority of patients (83%) and pigment deposits in only a small proportion (13%), and macular edema was present in approximately half of the cases, while another study showed pigmentary changes in approximately half of the patients and macular edema in 24%. The most common symptoms at onset were subacute vision loss, photopsias, and nyctalopia. Similarly, in a series of 12 patients with antienolase-associated retinopathy, clinical characteristics included visual loss, normal-appearing fundus except for vascular attenuation in most, optic nerve head pallor in some, and mainly abnormal cone responses. In all of these studies, however, there was a female predominance, and the age at onset was similar.[12–14,27]

Diagnosis

The diagnosis of AIR is difficult as there are no definitive or standardized tests. The presumptive diagnosis relies on the presence of the above clinical manifestations, usually more than one, along with demonstration of serum antiretinal antibodies. Most patients will have more than one antiretinal antibody. If the clinical features of autoimmune retinopathy and the circulating antiretinal antibodies are present, and if there is no apparent cause of visual function abnormalities, including malignancy, at presentation or following a thorough investigation, a diagnosis of nonparaneoplastic AIR is made (Table 80.2).

TABLE 80.2

Diagnostic Criteria for Nonparaneoplastic AIR[a]

Essential Diagnostic Criteria[b]	Supportive Diagnostic Criteria
No apparent cause responsible for visual function abnormality[c]	Symptoms: photopsias, scotomas, dyschromatopsia nyctalopia, photoaversion
ERG abnormality	Systemic autoimmune disease: personal or family history
Presence of serum antiretinal antibodies (ARAs)	Rapidity of onset of vision change (acute or subacute)
Absence of fundus lesions and retinal degeneration or dystrophy that may explain visual function loss[d]	
Absence of overt intraocular inflammation[e]	

[a]Suggested diagnostic criteria following an expert consensus meeting in 2013 (unpublished data).

[b]All essential diagnostic criteria must be present. Supportive diagnostic criteria are not necessary to make the diagnosis of AIR.

[c]Including no evidence of malignancy.

[d]Absence of choroidoretinal lesions (other than incidental/small peripheral benign degenerations, such as pavingstone, lattice, etc., or old toxoplasmosis scar) or absence of retinal dystrophy, retinitis pigmentosa, or other hereditary eye disorders.

[e]Less than +1 intraocular cells/haze present.

In addition to an extensive review of systems and history to rule out any malignancy, a thorough physical exam and basic laboratory investigations accompanied by age- and gender-appropriate investigations are typically undertaken prior to starting treatment. These investigations are best performed or facilitated by an internist

or the primary care physician. Because the diagnosis of AIR is currently presumptive, it is very important that a clear communication between the ophthalmologist and the primary medical team is established regarding the uncertainty of the diagnosis and the possible overlap with paraneoplastic retinopathy, so an appropriate investigation can be undertaken. Imaging with MRI or CT should be guided by the review of systems and the patient's individual risk factors, and, as such, determined by the patient's primary medical team.

Demonstration of serum antiretinal antibodies can be done using various methods, including Western blot (WB), immunohistochemistry (IHC), or enzyme-linked immunosorbent assay (ELISA). Western blot is a protein immunoblot of patients' serum incubated with extracts of a normal donor human retina and shows antiretinal IgG bands. It identifies antibody activity based on size of the protein, and the interpretation relies on intensity of protein bands on a photographic film. The results may be affected by multiple technical factors and lack specificity. For example, a 23-kDa band on WB does not necessarily mean antibody against recoverin; there may be other antigens with the same size. The immunohistochemical detection of antiretinal antibodies, on the other hand, involves fixing patient serum against frozen donor human retina (or monkey or mouse retina) using immunohistochemical staining. Sections are then analyzed using light microscopy to determine which layers of the retina show binding of the antiretinal antibody. The advantage with IHC is the ability to localize the specific site of binding within the retina (Fig. 80.3). ELISA is similar, in principle, to WB and IHC and involves adding various dilutions of patient sera into wells coated with specific retinal proteins, and binding is detected using secondary antibodies.[10,78] All of these techniques, however, lack standardization.[17]

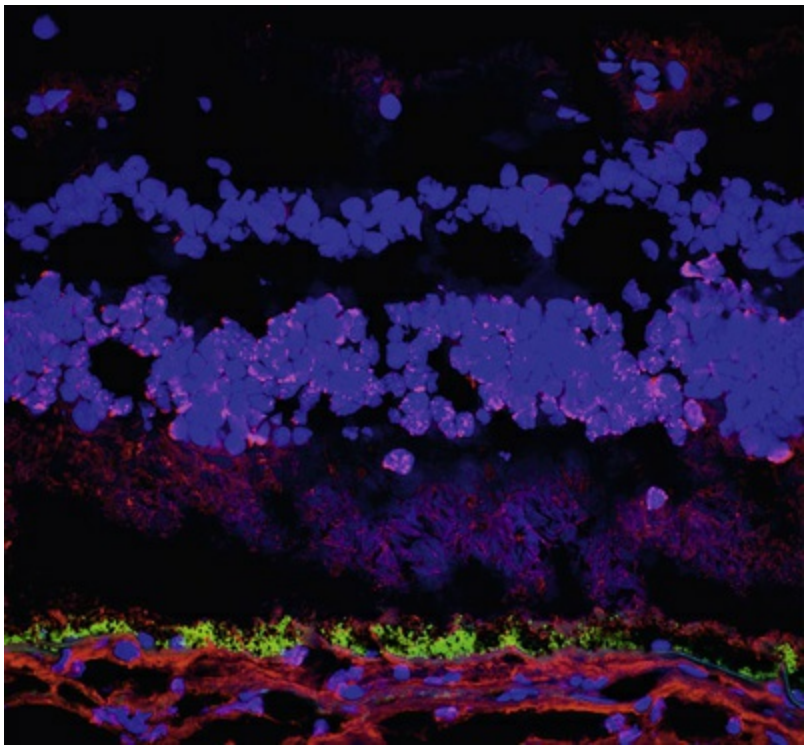

FIG. 80.3 Immunohistochemistry performed using serum of autoimmune retinopathy patient against fresh-frozen human donor retina shows staining at the photoreceptor inner and outer segments as well as outer nuclear layer. (Courtesy of Chi Chao Chan, MD.)

To highlight the lack of standardization and variable methods between laboratories, one study compared the results of antiretinal antibody detection and measurement between two laboratories and found an overall concordance rate of detecting any antiretinal antibodies of 64%, yielding very poor interobserver agreement (kappa = −0.13),[79] and an ARA-specific concordance rate of 36%. Currently, there are few centers in the United States that perform antiretinal antibody testing, and only one center provides these services commercially through a CLIA (clinical laboratory improvement amendments) certified laboratory.[80]

Autoimmune retinopathy, similar to paraneoplastic retinopathy, can be associated with various antiretinal antibodies. Initially, detected autoantibodies in nonparaneoplastic AIR were antirecoverin antibodies.[19] Later, antibodies directed against the inner plexiform layer,[11] Müller cells (35 kDa), or other unidentified retinal proteins have been described.[37,78] One of the most commonly detected antibodies on WB in nonparaneoplastic AIR appears to be

one with a molecular weight of about 35 kDa, which was detected in about 25% of autoimmune retinopathies, whereas antirecoverin antibodies were more commonly associated with the paraneoplastic AIR. Anti-α-enolase antibodies were somewhat equally distributed in both groups.[14] Distinct profiles of multiple antiretinal antibodies, or antiretinal antibody signatures, have been explored and identified in paraneoplastic retinopathies, as well as in age-related macular degeneration (AMD), and it has been suggested that distinct signatures may correlate with a specific subtype or stage of disease.[81–83] As we learn more about antiretinal antibodies and the pathogenesis of nonparaneoplastic AIR, it is likely that unique antiretinal antibody signatures may be identified and aid in the management of nonparaneoplastic AIR.[14]

Moreover, it is important to remember that the mere presence of these autoantibodies does not warrant a diagnosis of AIR, nor does it mean they are pathogenic. Antiretinal antibodies have been detected in patients with other retinal diseases, uveitis, retinal degenerations including AMD, and even in normal controls.[22,84–87] Conversely, they can be negative in patients with clinical features considered typical of AIR.[14] In a large cohort, only 47% of patients who presented with signs and symptoms compatible with AIR had any detectable antiretinal antibodies. Of these, patients with a history of cancer were more likely to have detectable antiretinal antibodies (63.5%) than those who did not (41.1%).[14] The fact that half of patients with symptoms and signs compatible with AIR tested negative for any antiretinal antibody with the techniques currently available highlights the difficulty of diagnosis. The role of antiretinal antibodies in the pathogenesis of AIR has yet to be determined, but understanding such will aid in the diagnosis and management of AIR.

Differential Diagnosis

Since there are no standardized tests for nonparaneoplastic AIR, the differential diagnosis is as challenging as its diagnosis. A variety of retinopathies are associated with the detection of antiretinal antibodies in serum. In addition, the clinical features seen in autoimmune retinopathy are not specific or unique to AIR and can

be seen in other forms of retinopathies.

The spectrum of disorders that may show clinical or laboratory similarities to AIR can be studied in four groups:

1. Paraneoplastic disorders (e.g., CAR, MAR).

2. White-dot syndrome spectrum disorders (e.g., acute zonal occult outer retinopathy).

3. Retinal degenerative disorders (e.g., retinitis pigmentosa, cone–rod dystrophy).

4. Noninfectious and infectious uveitis syndromes.

Paraneoplastic retinopathies, similar to nonparaneoplastic AIR, are characterized by vision loss, photopsias, nyctalopia, and scotomas. Cancer-associated retinopathy is typically associated with antirecoverin antibody, and most commonly associated with small-cell carcinoma of the lung. It is important to remember that a non-neoplastic form of antirecoverin antibody-associated retinopathy has also been described.[6,7,19] MAR occurs in patients with cutaneous melanoma and is characterized by a negative waveform on standardized full-field ERG due to reduction in b-wave amplitudes. In addition to similar symptoms as in nonparaneoplastic AIR, patients tend to have diffuse fundus depigmentation. Paraneoplastic retinopathies typically have a more rapid decline, with rapid progression of vision and visual field loss, as well as ERG changes; spontaneous recovery has not been observed. Vision loss can precede the identification of malignancy.[65,67] It is important to differentiate paraneoplastic retinopathy from nonparaneoplastic AIR because of significant implications for treatment. The features of paraneoplastic retinopathy are covered in detail in Chapter 138 (Remote effects of cancer on the retina).

White dot syndromes such as acute zonal occult outer retinopathy (AZOOR) or multiple evanescent white dot syndrome (MEWDS) have been suggested to be associated with antiretinal antibodies.[78,88] AZOOR and MEWDS have overlapping features and cases of MEWDS evolving into AZOOR have been described.[89]

However, immunohistochemical testing of sera of patients with AZOOR yielded conflicting results in demonstrating antiretinal antibodies.[90] AZOOR can present with symptoms, visual field, and ERG findings similar to nonparaneoplastic AIR; it is typically bilateral but asymmetric, and the majority of patients either stabilize or show partial recovery without treatment. MEWDS, despite having similar symptoms, is a unilateral retinopathy which is characterized by afferent pupillary defect, optic nerve swelling, and spontaneous recovery, and hence is more readily differentiated from AIR. Both AZOOR and MEWDS may show enlarged blind spot on visual fields. In addition, the majority of eyes affected by AZOOR may show fundus autofluorescence abnormalities which have not been observed in AIR.[15,91,92]

Antiretinal antibodies have also been reported to occur in patients with RP, a hereditary retinal degeneration. However, up to 60% of patients with RP may lack a family history of retinal degeneration. Indeed, some patients who are eventually diagnosed as nonparaneoplastic AIR are initially diagnosed as isolated cases of RP. Approximately 10–37% of patients with RP may have circulating antiretinal antibodies.[20,85] Additionally, 90% of patients with RP and macular cysts have circulating antiretinal antibodies on WB, compared with 13% of patients with RP without macular cysts and 6% of controls.[22] Most commonly detected antibodies are targeted against carbonic anhydrase II and α-enolase.[22] In some cases of RP, rapid progression of visual field loss and CME appears to be associated with presence of antiretinal antibodies.[22,85] In retinal degenerations, whether the antibodies precede the onset of retinopathy or whether antiretinal autoantibodies are a consequence of retinal damage is unclear. Additionally, whether the presence of these autoantibodies has a significant impact on clinical course has yet to be determined.

Antiretinal antibodies have also been found in patients with retinal vasculitis, uveitis patients with Vogt–Koyanagi–Harada syndrome (VKH), Behçet disease, and sympathetic ophthalmia. In patients with VKH, antibody reactivity to photoreceptors correlated with disease activity. However, all of these syndromes are characterized by significant intraocular inflammation in addition to their unique fundus findings, making the differentiation rather

unproblematic. Other rare cases of retinopathies associated with antiretinal antibodies include onchocerciasis and ocular toxoplasmosis. Antibodies to retinal pigment epithelium (RPE), neural retina, or photoreceptor layer have been described in these infectious retinopathies.[65,87,93] Typical fundus findings in these entities are helpful in differentiating them from nonparaneoplastic AIR. In all of the aforementioned diseases, it is unclear if the antibodies preceded the retinal disease or if the immune reactivity is simply a consequence of the retinal degenerative process.

Treatment and Prognosis

Various forms of immunomodulatory approaches have been tried in an attempt to treat autoimmune retinopathy. Theoretically, because of the presumed autoimmune nature of the disease, immunosuppression for nonparaneoplastic AIR is the most sensible treatment strategy. However, because of the ambiguity in diagnosis and lack of standardization in therapeutic outcomes, management of AIR poses an enormous challenge. The immunosuppressive therapy can be considered empiric at this time because of our lack of understanding of this condition. If undertaken, a long-term treatment is needed in most cases, and therapy is not helpful once widespread retinal degeneration occurs. Most treatment-related case series and reports are regarding paraneoplastic retinopathy and include surgery to reduce tumor burden, chemotherapy, corticosteroids, intravenous immunoglobulin (IVIG), or plasmapheresis.[23,94–99] Recently, successful treatment of autoimmune retinopathy or associated cancer with more targeted biologic agents have also been reported.[39,100–104]

Immunosuppressive therapy should be administered by a rheumatologist, immunologist, or a uveitis specialist well versed in the management of such therapy. Immunosuppressive agents such as mycophenolate mofetil, cyclosporine, or corticosteroids may help improve visual function in some autoimmune retinopathy patients. In a cohort of 24 nonparaneoplastic AIR patients that received therapy with various combinations of prednisone, cyclosporine, azathioprine, mycophenolate mofetil, or periocular or intravitreal steroid injections, 15 of the 24 showed varying degrees of

improvement in visual acuity or visual field. CME improved in almost half of the patients; unfortunately, ERG was not routinely performed. More recently, remission of nonparaneoplastic AIR after minimal steroid treatment (50 mg daily for 2 weeks) has been observed.[105] Decrease in antiretinal antibodies following treatment may be seen in some cases;[12,23,65,105] however, clinical significance of this finding is unclear.

In addition to systemic and local corticosteroids, most commonly used immunosuppressive agents in the treatment of AIR include intravenous immunoglobulin (IVIG), antimetabolites such as mycophenolate mofetil, azathioprine, and T-cell inhibitors such as cyclosporine.[12] IVIG has multiple mechanisms of action, some of which are not completely understood. When used in the treatment of autoimmune disorders, its effect is believed to be due to its interaction with Fc receptors on effector cells or by acting as antiidiotypic antibodies directed against idiotypes on circulating autoantibodies. This mechanism may be at play in autoantibody-mediated diseases. Other mechanisms may involve clearance of immune complex deposits, presence of neutralizing antibodies in IVIG, or its effect on the number of T-cell subsets, proinflammatory monocytes, or regulatory T cells.[106] IVIG has been used in several uveitic syndromes refractive to conventional therapy. Its use is limited by cost and long infusions. The typical dose ranges between 1 and 2.5 g/kg each infusion, and the infusions can be administered every 4–8 weeks, although different protocols have been used. Major side-effects include hypersensitivity and anaphylactic reactions and thrombotic events.[107] Similarly, plasmapheresis has also been used in paraneoplastic autoimmune retinopathy. Plasmapheresis, also known as therapeutic plasma exchange, involves extracorporeal elimination of large molecular weight plasma proteins from the blood. The regimen for plasmapheresis is determined according to the pathologic substance desired to be removed. To replace volume, albumin, albumin–saline combination, or fresh-frozen plasma can be used; the latter is preferred to avoid depletion of coagulation factors and immunoglobulins. Its effect is believed to be due to removal of immune complexes and immune reactants. The effect may be rapid but is often short-lived; therefore, more sustainable

immunomodulation is often required. Major side-effects include paresthesias, muscle cramps, or urticarial and anaphylactic reactions.[23]

Less frequently, targeted B-cell therapy, such as anti-CD20 monoclonal antibody (Rituximab), has also been used in the treatment of AIR. Rituximab targets CD20 found on B cells, which are the precursors of antibody-secreting plasma cells.[14,101] Although there is anecdotal evidence, the benefit of immunosuppressive therapy in AIR is also not definite. There are no clear guidelines on how to institute and manage immunosuppressives in patients with AIR, owing to the rarity and ambiguity surrounding this entity. Therefore, the treating physician typically extrapolates from guidelines that are established for other ocular inflammatory disorders.[108] These drugs can take several weeks to have an effect, and it may take up to several months to observe a clinical effect in the form of improvement or stabilization on visual fields or ERG. More rapid improvement has been reported in CAR patients treated with IVIG.[23]

Adding to the challenges in the management is the lack of parameters to guide treatment. There have been no clear indicators for prognosis. Whether the autoantibodies would disappear in response to treatment, or whether their disappearance would be accompanied by clinical improvement is still unclear. Regardless, patients treated with immunosuppressives need to be closely monitored for side-effects. The most common side-effects with azathioprine and mycophenolate mofetil are gastrointestinal upset, nausea, and less commonly, vomiting. The most common severe side-effects are reversible bone-marrow suppression and hepatotoxicity. The most serious side-effects of cyclosporine are nephrotoxicitiy which occurs less commonly at lower doses (2–5 mg/kg per day), and hypertension. Regular complete blood count with differential and chemistry panel including hepatic and renal function tests should be performed during therapy. Patients should be encouraged to report any side-effects, as early intervention in the form of discontinuation or dose adjustments can be critical.

The response to treatment is very variable, with more favorable results achieved in paraneoplastic retinopathy, particularly CAR, with a combination of chemotherapy and immunomodulation. It

has also been suggested that those with a family history of autoimmune disorders may be less likely to respond to immunosuppression.[12] Our experience indicates that with treatment only a minority of patients with AIR show improvement in visual function, and some remain stable. This may be due to late presentation to our center with significant loss seen on both ERG and visual fields at presentation. Whether an earlier attempt to treat with immunosuppressives would be more beneficial is not clear. Early treatment attempts would require establishing a clear diagnosis using sensitive and specific assays and more definitive clinical criteria. While most of the immunosuppressives used in the treatment of AIR can be instituted and managed safely, a better understanding of the disease is needed to justify more aggressive and potentially beneficial treatment approaches.

Despite evolving research, the relationship between antiretinal antibodies and retinal dysfunction is not fully understood. Limitations in diagnostic assays also limit therapeutic investigations. Regardless, until more is known the mainstay of treatment remains immunosuppression following a thorough investigation to rule out malignancy. Clearly, additional studies are needed to identify the specificity and pathogenicity of antiretinal antibodies and the appropriate treatment. Efforts to establish diagnostic criteria, including more definitive clinical criteria and a standardized assay for antiretinal antibody detection, have been initiated with the goal to promote collaboration in order to advance understanding and future therapeutic investigations.

References

1. Weinstein JM, Kelman SE, Bresnick GH, et al. Paraneoplastic retinopathy associated with antiretinal bipolar cell antibodies in cutaneous malignant melanoma. *Ophthalmology*. 1994;101:1236–1243.
2. Jacobson DM, Thirkill CE, Tipping SJ. A clinical triad to diagnose paraneoplastic retinopathy. *Ann Neurol*. 1990;28:162–167.
3. Sawyer RA, Selhorst JB, Zimmerman LE, et al. Blindness caused by photoreceptor degeneration as a remote effect of

cancer. *Am J Ophthalmol*. 1976;81:606–613.
4. Klingele TG, Burde RM, Rappazzo JA, et al. Paraneoplastic retinopathy. *J Clin Neuroophthalmol*. 1984;4:239–245.
5. Jacobson DM, Miller NR, Newman NJ. Paraneoplastic diseases of neuro-ophthalmologic interest. *Walsh & Hoyt's clinical neuro-ophthalmology*. 5th ed. Williams & Wilkins: Baltimore, MD; 2008:2497–2551.
6. Thirkill CE, Roth AM, Keltner JL. Cancer-associated retinopathy. *Arch Ophthalmol*. 1987;105:372–375.
7. Keltner JL, Thirkill CE. Cancer-associated retinopathy vs recoverin-associated retinopathy. *Am J Ophthalmol*. 1998;126:296–302.
8. Vaphiades MS, Brown H, Whitcup SM. Node way out: Comments by Keltner JL, Thirkill CE. *Surv Ophthalmol*. 2000;45:77–83.
9. Weinstein JM, Kelman SE, Bresnick GH. Paraneoplastic retinopathy associated with antiretinal bipolar cell antibodies in cutaneous malignant melanoma. *Ophthalmology*. 1994;101:1236–1243.
10. Potter MJ, Thirkill CE, Dam OM. Clinical and immunocytochemical findings in a case of melanoma-associated retinopathy. *Ophthalmology*. 1999;106:2121–2125.
11. Mizener JB, Kimura AE, Adamus G. Autoimmune retinopathy in the absence of cancer. *Am J Ophthalmol*. 1997;123:607–618.
12. Ferreyra HA, Jayasundera T, Khan NW, et al. Management of autoimmune retinopathies with immunosuppression. *Arch Ophthalmol*. 2009;127:390–397.
13. Larson TA, Gottlieb CC, Zein WM, et al. Autoimmune retinopathy: prognosis and treatment. *Invest Ophthalmol Vis Sci*. 2010;51 [E-Abstract 6375].
14. Adamus G, Ren G, Weleber RG. Autoantibodies against retinal proteins in paraneoplastic and autoimmune retinopathy. *BMC Ophthalmol*. 2004;4:5.
15. Mantel I, Ramchand KV, Holder GE, et al. Macular and retinal dysfunction of unknown origin in adults with normal fundi: evidence for an autoimmune pathophysiology. *Exp Mol Pathol*. 2008;84:90–101.

16. Adamus G. Autoantibody-induced apoptosis as a possible mechanism of autoimmune retinopathy. *Autoimmun Rev*. 2003;2:63–69.
17. Forooghian F, Macdonald IM, Heckenlively JR, et al. The need for standardization of antiretinal antibody detection and measurement. *Am J Ophthalmol*. 2008;146(4):489–495.
18. Kondo M, Sanuki R, Ueno S, et al. Identification of autoantibodies against TRPM1 in patients with paraneoplastic retinopathy associated with ON bipolar cell dysfunction. *PLoS ONE*. 2011;6(5):e19911.
19. Whitcup SM, Vistica BP, Milam AH, et al. Recoverin-associated retinopathy: a clinically and immunologically distinctive disease. *Am J Ophthalmol*. 1998;126:230–237.
20. Heckenlively JR, Fawzi AA, Oversier J, et al. Autoimmune retinopathy: patients with antirecoverin immunoreactivity and panretinal degeneration. *Arch Ophthalmol*. 2000;118(11):1525–1533.
21. Ohguro H, Ogawa K, Maeda T, et al. Cancer-associated retinopathy induced by both anti-recoverin and anti-hsc70 antibodies in vivo. *Invest Ophthalmol Vis Sci*. 1999;40(13):3160–3167.
22. Heckenlively JR, Jordan BL, Aptsiauri N. Association of antiretinal antibodies and cystoid macular edema in patients with retinitis pigmentosa. *Am J Ophthalmol*. 1999;127:565–573.
23. Guy J, Aptsiauri N. Treatment of paraneoplastic visual loss with intravenous immunoglobulin: report of 3 cases. *Arch Ophthalmol*. 1999;117:471–477.
24. Polans AS, Burton MD, Haley TL, et al. Recoverin, but not visinin, is an autoantigen in the human retina identified with a cancer-associated retinopathy. *Invest Ophthalmol Vis Sci*. 1993;34:81–90.
25. Keltner JL, Thirkill CE, Tyler NK, et al. Management and monitoring of cancer-associated retinopathy. *Arch Ophthalmol*. 1992;110:48–53.
26. Adamus G, Amundson D, Seigal GM, et al. Anti-enolase α autoantibodies in cancer-associated retinopathy: epitope mapping and cytoxicity on retinal cells. *J Autoimmun*.

1998;11:671–677.
27. Weleber RG, Watzke RC, Shults WT, et al. Clinical and electrophysiologic characterization of paraneoplastic and autoimmune retinopathies associated with antienolase antibodies. *Am J Ophthalmol*. 2005;139:780–794.
28. Ren G, Adamus G. Cellular targets of anti-alpha-enolase autoantibodies of patients with autoimmune retinopathy. *J Autoimmun*. 2004;23:161–167.
29. Adamus G, Aptsiauri N, Guy J, et al. The occurrence of serum autoantibodies against enolase in cancer-associated retinopathy. *Clin Immunol Immunopathol*. 1996;78:120–129.
30. Adamus G, Karren L. Autoimmunity against carbonic anhydrase II affects retinal cell functions in autoimmune retinopathy. *J Autoimmun*. 2009;32:133–139.
31. Kikuchi T, Arai J, Shibuki H, et al. Tubby-like protein 1 as an autoantigen in cancer-associated retinopathy. *J Neuroimmunol*. 2000;103:26–33.
32. Potter MJ, Adamus G, Szabo SM, et al. Autoantibodies to transducin in a patient with melanoma-associated retinopathy. *Am J Ophthalmol*. 2002;134:128–130.
33. Adamus G, Brown L, Weleber RG. Molecular biomarkers for autoimmune retinopathies: significance of anti-transducin-alpha autoantibodies. *Exp Mol Pathol*. 2009;87(3):195–203.
34. Bazhin AV, Dalke C, Willner N, et al. Cancer-retina antigens as potential paraneoplastic antigens in melanoma-associated retinopathy. *Int J Cancer*. 2009;124:140–149.
35. Bianciotto C, Shields CL, Thirkill CE, et al. Paraneoplastic retinopathy with multiple detachments of the neurosensory retina and autoantibodies against interphotoreceptor retinoid binding protein (IRBP) in cutaneous melanoma. *Br J Ophthalmol*. 2010;94:1684–1685 [1696].
36. Adamus G, Bonnah R, Brown L, et al. Detection of autoantibodies against heat shock proteins and collapsin response mediator proteins in autoimmune retinopathy. *BMC Ophthalmol*. 2013;13:48.
37. Peek R, Verbraak F, Coevoet HM, et al. Müller cell-specific autoantibodies in a patient with progressive loss of vision. *Invest Ophthalmol Vis Sci*. 1998;39:1976–1979.

38. Keltner JL, Thirkill CE. The 22-kDa antigen in optic nerve and retinal diseases. *J Neuroophthalmol*. 1999;19:71–83.
39. Espandar L, O'Brien S, Thirkill C, et al. Successful treatment of cancer-associated retinopathy with alemtuzumab. *J Neurooncol*. 2007;83:295–302.
40. Ohkawa T, Kawashima H, Makino S, et al. Cancer-associated retinopathy in a patient with endometrial cancer. *Am J Ophthalmol*. 1996;122:740–742.
41. Murphy MA, Thirkill CE, Hart WM Jr. Paraneoplastic retinopathy: a novel autoantibody reaction associated with small-cell lung carcinoma. *J Neuroophthalmol*. 1997;17:77–83.
42. Masaoka N, Emoto Y, Sasaoka A, et al. Fluorescein angiographic findings in a case of cancer-associated retinopathy. *Retina*. 1999;19:462–464.
43. McAleese SM, Dunbar B, Fothergill JE, et al. Complete amino acid sequence of the neurone-specific gamma isozyme of enolase (NSE) from human brain and comparison with the non-neuronal alpha form (NNE). *Eur J Biochem*. 1988;178:413–417.
44. Adamus G, Wilson DJ. The need for standardization of antiretinal antibody detection and measurement. *Am J Ophthalmol*. 2009;147(3):557 [author reply 557–8].
45. Shin SJ, Kim BC, Kim TI, et al. Anti-alpha-enolase antibody as a serologic marker and its correlation with disease severity in intestinal Behçet's disease. *Dig Dis Sci*. 2011;56(3):812–818.
46. Lee JH, Cho SB, Bang D, et al. Human anti-alpha-enolase antibody in sera from patients with Behçet's disease and rheumatologic disorders. *Clin Exp Rheumatol*. 2009;27(2 Suppl. 53):S63–6.
47. Forooghian F, Adamus G, Sproule M, et al. Enolase autoantibodies and retinal function in multiple sclerosis patients. *Graefes Arch Clin Exp Ophthalmol*. 2007;245(8):1077–1084.
48. Vermeulen N, Arijs I, Joossens S, et al. Anti-alpha-enolase antibodies in patients with inflammatory bowel disease. *Clin Chem*. 2008;54:534–541.
49. Pancholi V. Multifunctional a-enolase: its role in diseases.

Cell Mol Life Sci. 2001;58:902–920.
50. Thirkill CE, Tait RC, Tyler NK, et al. Intraperitoneal cultivation of small-cell carcinoma induces expression of the retinal cancer-associated retinopathy antigen. *Arch Ophthalmol*. 1993;111:974–978.
51. Bazhin AV, Shifrina ON, Savchenko MS, et al. Low titre autoantibodies against recoverin in sera of patients with small cell lung cancer but without a loss of vision. *Lung Cancer*. 2001;34:99–104.
52. Polans A, Witkowska D, Haley T, et al. Recoverin, a photoreceptor-specific calcium-binding protein, is expressed by the tumor of a patient with cancer-associated retinopathy. *Proc Natl Acad Sci USA*. 1995;92:9176–9180.
53. Matsubara S, Yamaji Y, Soto M, et al. Expression of a photoreceptor protein, recoverin, as a cancer-associated retinopathy autoantigen in human lung cancer cell lines. *Br J Cancer*. 1996;74:1419–1422.
54. Adamus G. Autoantibody-induced apoptosis as a possible mechanism of autoimmune retinopathy. *Autoimmun Rev*. 2003;2(2):63–68.
55. Chen W, Elias RV, Cao W, et al. Anti-recoverin antibodies cause the apoptotic death of mammalian photoreceptor cells in vitro. *J Neurosci Res*. 1999;57:706–718.
56. Adamus G, Webb S, Shiraga S, et al. Anti-recoverin antibodies induce an increase in intracellular calcium, leading to apoptosis in retinal cells. *J Autoimmun*. 2006;26:146–153.
57. Adamus G, Machnicki M, Elerding H, et al. Antibodies to recoverin induce apoptosis of photoreceptor and bipolar cells in vivo. *J Autoimmun*. 1998;11:523–533.
58. Adamus G, Machnicki M, Seigel GM. Apoptotic retinal cell death induced by antirecoverin autoantibodies of cancer-associated retinopathy. *Invest Ophthalmol Vis Sci*. 1997;38:283–291.
59. Gery I, Chanaud NP 3rd, Anglade E. Recoverin is highly uveitogenic in Lewis rats. *Invest Ophthalmol Vis Sci*. 1994;35:3342–3345.
60. Lu Y, He S, Jia L, et al. Two mouse models for recoverin-

associated autoimmune retinopathy. *Mol Vis*. 2010;16:1936–1948.
61. Williams RC, Peen E. Apoptosis and cell penetration by autoantibody may represent linked processes. *Clin Exp Rheumatol*. 1999;17:643–647.
62. Lei B, Bush RA, Milam AH, et al. Human melanoma-associated retinopathy (MAR) antibodies alter the retinal ON-response of the monkey ERG in vivo. *Invest Ophthalmol Vis Sci*. 2000;41:262–266.
63. Adamus G, Chan CC. Experimental autoimmune uveitides: multiple antigens, diverse diseases. *Int Rev Immunol*. 2002;21(2–3):209–229.
64. Grange L, Dalal M, Wang Y, et al. HLA polymorphisms and autoimmune markers in non-paraneoplastic autoimmune retinopathy (AIR) [ARVO Abstract]. *Invest Ophthalmol Vis Sci*. 2013;54:2514.
65. Hooks JJ, Tso MO, Detrick B. Retinopathies associated with antiretinal antibodies. *Clin Diagn Lab Immunol*. 2001;8:853–858.
66. Lin CJ, Chen SN, Hwang JF, et al. Nonparaneoplastic autoimmune retinopathy presenting with peripheral retinal vasoocclusion: case report. *Retin Cases Brief Rep*. 2013;7(1):41–45.
67. Chan JW. Paraneoplastic retinopathies and optic neuropathies. *Surv Ophthalmol*. 2003;48:12–38.
68. Dalal M, Grange L, Wang Y, et al. Optical coherence tomography, fundus autofluorescence, and fluorescein angiography in non-paraneoplastic autoimmune retinopathy [ARVO Abstract]. *Invest Ophthalmol Vis Sci*. 2013;54:2516.
69. Abazari A, Allam SS, Adamus G, et al. Optical coherence tomography findings in autoimmune retinopathy. *Am J Ophthalmol*. 2012;153(4):750–756.
70. Lima LH, Greenberg JP, Greenstein VC, et al. Hyperautofluorescent ring in autoimmune retinopathy. *Retina*. 2012;32(7):1385–1394.
71. Pepple KL, Cusick M, Jaffe GJ, et al. SD-OCT and autofluorescence characteristics of autoimmune

retinopathy. *Br J Ophthalmol*. 2013;97(2):139–144 [Erratum in: Br J Ophthalmol 2014;98(5):713].
72. Shapiro LR, Johnson CA. Quantitative evaluation of manual kinetic perimetry using computer simulation. *Appl Opt*. 1990;29:1445–1450.
73. Keltner JL, Johnson CA, Spurr JO, et al. Comparison of central and peripheral visual field properties in the optic neuritis treatment trial. *Am J Ophthalmol*. 1999;128:543–553.
74. Cao X, Bishop RJ, Forooghian F, et al. Autoimmune retinopathy in systemic lupus erythematosus: histopathologic features. *Open Ophthalmol J*. 2009;28(3):20–25.
75. Bourgault S, Baril C, Vincent A, et al. Retinal degeneration in autoimmune polyglandular syndrome type 1: a case series. *Br J Ophthalmol*. 2015;99(11):1536–1542.
76. Breunig A, Lee MS, Miller BS, et al. Autoimmune retinopathy in a patient with autoimmune polyendocrine syndrome type I. *Ocul Immunol Inflamm*. 2013;21(2):153–157.
77. Oray M, Kir N, Tuncer S, et al. Autoimmune retinopathies: a report of 3 cases. *Ocul Immunol Inflamm*. 2013;21(6):424–433.
78. Heckenlively JR, Ferreyra HA. Autoimmune retinopathy: a review and summary. *Semin Immunopathol*. 2008;30:127–134.
79. Faez S, Loewenstein J, Sobrin L. Concordance of antiretinal antibody testing results between laboratories in autoimmune retinopathy. *JAMA Ophthalmol*. 2013;131(1):113–115.
80. *Ocular Immunology Laboratory, Oregon Health & Science University [Online.] Portland, OR: OHS; no date*. http://www.ohsu.edu/xd/health/services/casey-eye/clinical-services/diagnostic-services/upload/Ocular-Immunology-Web-2.pdf.
81. Adamus G, Choi D, Raghunath A, et al. Significance of anti-retinal autoantibodies in cancer-associated retinopathy with gynecological cancers. *J Clin Exp Ophthalmol*. 2013;4(6):307.
82. Adamus G. Latest updates on antiretinal autoantibodies associated with vision loss and breast cancer. *Invest Ophthalmol Vis Sci*. 2015;56(3):1680–1688.
83. Adamus G, Chew EY, Ferris FL, et al. Prevalence of anti-

retinal autoantibodies in different stages of age-related macular degeneration. *BMC Ophthalmol*. 2014;14:154.
84. Heckenlively JR, Aptsiauri N, Nusinowitz S, et al. Investigations of antiretinal antibodies in pigmentary retinopathy and other retinal degenerations. *Trans Am Ophthalmol Soc*. 1996;94:179–200.
85. Cherepanoff S, Mitchell P, Wang JJ, et al. Retinal autoantibody profile in early age-related macular degeneration: preliminary findings from the Blue Mountains Eye Study. *Clin Experiment Ophthalmol*. 2006;34:590–595.
86. Joachim SC, Bruns K, Lackner KJ, et al. Analysis of IgG antibody patterns against retinal antigens and antibodies to alpha-crystallin, GFAP, and alpha-enolase in sera of patients with "wet" age-related macular degeneration. *Graefes Arch Clin Exp Ophthalmol*. 2007;245:619–626.
87. Ko AC, Brinton JP, Mahajan VB, et al. Seroreactivity against aqueous-soluble and detergent-soluble retinal proteins in posterior uveitis. *Arch Ophthalmol*. 2011;129:415–420.
88. Brown J Jr, Folk JC. Current controversies in the white dot syndromes: multifocal choroiditis, punctate inner choroidopathy, and the diffuse subretinal fibrosis syndrome. *Ocul Immunol Inflamm*. 1998;6(2):125–127.
89. Fine HF, Spaide RF, Ryan EH Jr, et al. Acute zonal occult outer retinopathy in patients with multiple evanescent white dot syndrome. *Arch Ophthalmol*. 2009;127(1):66–70.
90. Jacobson SG, Morales DS, Sun XK, et al. Pattern of retinal dysfunction in acute zonal occult outer retinopathy. *Ophthalmology*. 1995;102:1187–1198.
91. Fujiwara T, Imamura Y, Giovinazzo VJ, et al. Fundus autofluorescence and optical coherence tomographic findings in acute zonal occult outer retinopathy. *Retina*. 2010;30:1206–1216.
92. Yeh S, Forooghian F, Wong WT, et al. Fundus autofluorescence imaging of the white dot syndromes. *Arch Ophthalmol*. 2010;128:46–56.
93. Chan CC, Nussenblatt RB, Kim MK, et al. Immunopathology of ocular onchocerciasis. 2. Antiretinal

autoantibodies in serum and ocular fluids. *Ophthalmology*. 1987;94:439–443.
94. Yamamoto S, Hanaya J, Mera K, et al. Recovery of visual function in patient with melanoma-associated retinopathy treated with surgical resection and interferon-beta. *Doc Ophthalmol*. 2012;124(2):143–147.
95. Keltner JL, Thirkill CE, Yip PT. Clinical and immunologic characteristics of melanoma-associated retinopathy syndrome: eleven new cases and a review of 51 previously published cases. *J Neuroophthalmol*. 2001;21:173–187.
96. Palmowski AM, Haus AH, Pfohler C, et al. Bilateral multi-focal chorioretinopathy in a woman with cutaneous malignant melanoma. *Arch Ophthalmol*. 2002;120(12):1756–1761.
97. Jacobzone C, Cochard-Marianowski C, Kupfer I, et al. Corticosteroid treatment for melanoma- associated retinopathy: effect on visual acuity and electrophysiologic findings. *Arch Dermatol*. 2004;140:1258–1261.
98. Subhadra C, Dudek AZ, Rath PP, et al. Improvement in visual fields in a patient with melanoma-associated retinopathy treated with intravenous immunoglobulin. *J Neuroophthalmol*. 2008;28:23–26.
99. Huynh N, Shildkrot Y, Lobo A-M, et al. Intravitreal triamcinolone for cancer-associated retinopathy refractory to systemic therapy. *J Ophthal Inflamm Infect*. 2012;2(3):169–171.
100. Sen HN, Chan CC, Caruso RC, et al. Waldenström's macroglobulinemia-associated retinopathy. *Ophthalmology*. 2004;111:535–539.
101. Mahdi N, Faia LJ, Goodwin J, et al. A case of autoimmune retinopathy associated with thyroid carcinoma. *Ocul Immunol Inflamm*. 2010;18:322–323.
102. Or C, Collins DR, Merkur AB, et al. Intravenous rituximab for the treatment of cancer-associated retinopathy. *Can J Ophthalmol*. 2013;48:35–38.
103. Dy I, Chintapatla R, Preeshagul I, et al. Treatment of cancer-associated retinopathy with rituximab. *J Natl Compr Canc Netw*. 2013;11:1320–1324.

104. Audemard A, de Raucourt S, Miocque S, et al. Melanoma-associated retinopathy treated with ipilimumab therapy. *Dermatology*. 2013;227(2):146–149.
105. Bursztyn LL, Belrose JC, Coupland SG, et al. Remission of nonparaneoplastic autoimmune retinopathy after minimal steroid treatment. *Retin Cases Brief Rep*. 2015;9(2):173–176.
106. Kaveri SV, Lacroix-Desmazes S, Bayry J. The antiinflammatory IgG. *N Engl J Med*. 2008;17(359):307–309.
107. Le Hoang P, Cassoux N, George F, et al. Intravenous immunoglobulin (IVIg) for the treatment of birdshot retinochoroidopathy. *Ocul Immunol Inflamm*. 2000;8:49–57.
108. Jabs DA, Rosenbaum JT, Foster CS, et al. Guidelines for the use of immunosuppressive drugs in patients with ocular inflammatory disorders: recommendations of an expert panel. *Am J Ophthalmol*. 2000;130:492–513.

81

Sarcoidosis

Yasir Jamal Sepah, Aniruddha Agarwal, Douglas A. Jabs, Quan Dong Nguyen

Sarcoidosis is a multisystem granulomatous disorder of unknown etiology characterized by intrathoracic involvement. The disease was first described as early as 1869 by Hutchinson, but its protean manifestations and clinical course still make sarcoidosis a diagnostic and therapeutic challenge for modern-day physicians. Ocular involvement is common and has been reported to occur in approximately 20–50% of patients with sarcoidosis.[1,2] Posterior segment manifestations may account for up to 28% of the lesions seen in patients with ocular sarcoid. Most large case series of patients with uveitis report that approximately 5% of patients with uveitis have biopsy-confirmed systemic sarcoidosis.[3–6]

General Considerations

Epidemiology

Sarcoidosis is worldwide in its distribution, but there is a striking difference in the prevalence between countries. In Japan, the prevalence is as low as 3.7 : 100,000 compared to Finland where the estimated prevalence is 28.2:100,000.[7] Although all races are affected, series in the United States generally show that the disease is more prevalent in blacks than in whites (three to four times more common). It has also been noted that the prevalence of sarcoidosis in black populations of Africa and South America is less than what has been observed in the African American population.[8–10] Both sexes are affected, with the overall frequency showing a slight excess of females (approximately 60%). Sarcoidosis is a disease of young adults, with almost three-fourths of cases occurring in those younger than 40 years of age. Children may be affected, but this is

uncommon.[6,8–11] The clinical course of childhood sarcoidosis is often atypical; that is, there is less frequent pulmonary involvement and more frequent extrathoracic disease.[12,13] A study of 46 Caucasian children from Denmark reported the four most-frequent presenting symptoms to be erythema nodosum (22%), iridocyclitis (22%), peripheral lymphadenopathy (15%), and cutaneous sarcoidosis (7%).[14] Among children, sarcoid-related uveitis must be differentiated from juvenile idiopathic arthritis and familial juvenile systemic granulomatosis.[15–19]

Etiology and Pathogenesis

The etiology of sarcoidosis is unknown. Multiple etiologies have been proposed, including a variety of infectious agents, allergy to pine pollen and peanut dust, chewing pine pitch, and hypersensitivity to chemicals such as beryllium or zirconium. Cigarette smoking and tobacco exposure have also been proposed as independent risk factors for ocular sarcoidosis.[20] To date, there is no conclusive evidence to implicate any of these as an etiologic agent.

Familial studies and human leukocyte antigen (HLA) typing have suggested a possible genetic predisposition, but these studies are far from conclusive.[21] A cooperative multicenter study, A Case Control Etiologic Study of Sarcoidosis (ACCESS), enrolled 736 biopsy-confirmed cases from 10 centers in the United States and suggested a genetic predisposition for sarcoidosis, presenting evidence for the allelic variation at the HLA-DRB1 locus as a contributing factor to the disease. The most significant finding was the relationship between *DRB1*0401* and eye involvement ($p \leq .0008$; odds ratio [OR] 3.49) in the study population. Although only 2% of blacks had a *DRB1*0401* allele, a similar OR was present in both blacks and whites.[22]

Patients with sarcoidosis are characterized by depression of delayed-type hypersensitivity, reflected by T-cell anergy, and skin tests that are often negative. Peripheral blood lymphocytes from patients with sarcoidosis show diminished responses to mitogens.

Bronchoalveolar lavage is useful to determine the immunologic events at the area of active disease in the lungs. These studies have

shown entirely different results from peripheral blood lymphocytes. In the lungs, there is an excess of helper-T lymphocytes ($CD4^+$). These activated helper-T cells spontaneously secrete lymphokines, including interleukin-2 (IL-2), and will activate polyclonal B cells to produce immunoglobulins. These studies have been interpreted to show that an active T-cell-driven immunologic response occurs at the target organ, leading to granuloma formation.[23,24] Studies of bronchoalveolar lavage fluids have suggested that macrophages may also play a role in the pathogenesis of pulmonary sarcoidosis by inducing changes in the pulmonary microvasculature.[25]

Immunohistologic studies of biopsy tissue from patients with sarcoidosis have demonstrated the presence of cells of macrophage lineage and activated T cells in the granuloma. The vast majority of lymphocytes are T cells of the helper subset ($CD4^+$) and express activation markers, including class II antigens and the IL-2 receptor.[26–28]

Clinical Features

The organs most frequently involved in sarcoidosis are the lungs, lymph nodes and spleen, skin, eyes, nervous system, and the musculoskeletal system[1,21,29–31] (Table 81.1).

TABLE 81.1

Organ System Involvement in Sarcoidosis

Organ System	Frequency (%)
Intrathoracic	84–93
Hilar nodes	60–77
Lung parenchyma	40–56
Lymph nodes	23–37
Eyes	11–32
Skin	12–27
Erythema nodosum	4–31
Spleen	1–18
Bones	2–9
Parotid	5–8
Central nervous system	2–7

Intrathoracic Sarcoidosis

Several series have demonstrated that intrathoracic involvement is the most common manifestation of sarcoidosis and occurs in approximately 90% of patients. An abnormality on chest radiograph examination is evident at the onset of sarcoidosis in almost all patients. Chest radiograph abnormalities have been classified according to a simple staging system, which closely correlates with the eventual outcome. Stage 0 is characterized by a normal chest radiograph; stage 1 is characterized by bilateral hilar lymphadenopathy without pulmonary infiltration and is seen in 65% of patients with pulmonary sarcoidosis; stage 2 is characterized by hilar lymphadenopathy associated with pulmonary infiltration and is seen in 22% of patients with sarcoid; stage 3 sarcoid is characterized by pulmonary infiltration with fibrosis but without bilateral hilar adenopathy and occurs in 13% of patients. The overall rates of radiographic resolution are 59%, 39%, and 38% for disease stage 1, 2, and 3, respectively.[1]

Extrapulmonary Lesions

Involvement of the reticuloendothelial system, particularly the extrapulmonary lymph nodes or spleen, or both, is common and occurs in 23–37% of patients with sarcoidosis. Biopsy of a palpable lymph node is often used for histologic confirmation of the diagnosis of sarcoidosis (see below). Skin lesions occur frequently in sarcoidosis and include erythema nodosum, lupus pernio, maculopapular rashes, cutaneous plaques, and subcutaneous nodules. Lupus pernio (dusky-purple infiltration of the skin of the nose) and sarcoid plaques are typically associated with chronic disease, whereas erythema nodosum (especially in the presence of polyarthritis) is typically associated with acute sarcoid or Löfgren syndrome.[32] Neurosarcoidosis occurs in 2–7% of patients with sarcoid. Facial palsy is the most frequent manifestation of neurosarcoidosis. Other presentations include other cranial nerve palsies, papilledema, peripheral neuropathy, meningitis, space-occupying cerebral lesions, cavernous sinus syndrome,[33] and endocrine disorders such as hypopituitarism or diabetes insipidus resulting from space-occupying lesions. Musculoskeletal involvement includes bone cysts in patients with chronic sarcoid, polyarthralgias, and periarthritis in patients with acute sarcoid,

and, less commonly, myopathy from granulomatous lesions within muscles.[1,21,31,33–37]

Investigations

Radiologic Evaluation

Chest X-Ray.

The single best test for the evaluation of patients with suspected sarcoidosis is the chest film, since it may be abnormal in approximately 90% of patients with sarcoid. Although the chest film is the best test for detecting the presence of sarcoidosis, it does not unequivocally establish the diagnosis, though neither does a negative chest radiograph rule out the disease. Among patients with negative chest radiographic, bronchoalveolar lavage may have a high diagnostic value for detecting sarcoid-related uveitis.[38]

High-Resolution Computed Tomography (CT).

The CT findings in sarcoidosis can be divided into three main categories:

1. Parenchymal findings.

2. Large and small airway findings.

3. Mediastinal findings.

The presence of diffuse nodular opacities (1–5 mm) with irregular borders in the perilymphatic distribution typically in the upper and middle lung zones is the most common and almost universal finding in the lung parenchyma.[39] The presence of architectural distortion is also exclusive to sarcoidosis as opposed to other diseases with perilymphatic distribution.[40] "Sarcoid galaxy sign," which is a collection of multiple granulomas and gives the impression of an opacity, is present in 10–20% of patients with pulmonary sarcoidosis.[41] Extensive fibrosis, mostly distributed in the upper and middle zones associated with architectural distortion, is also seen in 20–25% of cases. The presence of air trapping at end expiration has been reported frequently. Terasaki et

al.[42] reported air trapping on expiration in 45 (98%) of their study patients. Davies et al.[43] demonstrated that the extent of air trapping on expiration was correlated with the pulmonary function of the patient.

Large-airway involvement is seen in 1–3% of patients with pulmonary sarcoidosis. This typically presents with tracheal stenosis due to granuloma formation within the tracheal mucosa or submucosa or secondary to lymph node compression from the outside. More than 60% of patients with sarcoidosis are reported to have smooth thickening of the smaller airways.[39]

The classic radiologic finding in the mediastinum of a sarcoid patient is symmetric bilateral hilar adenopathy with some form of paratracheal adenopathy. Symmetry is an important diagnostic feature of the sarcoid hilar adenopathy as it is uncommon in the major diagnostic alternatives, including tuberculosis and lymphoma.[39]

Gallium Scan.

Gallium-67 is a radioactive isotope with a half-life of 78 hours and is administered intravenously to patients as Ga-citrate. The Ga uptake is detected by gamma cameras 48 hours after injection and is assessed in the liver, spleen, thorax, eyes, and lacrimal and salivary glands. Ga scanning has been suggested as a useful diagnostic test for sarcoidosis. The test is again nonspecific, and gallium uptake is seen in other diseases, including Sjögren syndrome, tuberculosis, radiation therapy, and lymphoma. However, signs such as lambda (Ga uptake of parahilar and infrahilar bronchopulmonary lymph nodes) and panda (Ga uptake of lacrimal and salivary glands) on Ga scanning along with bilateral symmetrical hilar lymphadenopathy may be highly specific for sarcoidosis, obviating the need for invasive procedures such as biopsy.[44,45] In addition, it has been proposed that the combination of gallium scanning and an elevated angiotensin-converting enzyme (ACE) level is highly specific for sarcoidosis, but these studies have employed patients specifically chosen for very active sarcoid.[46] As such, these tests may be of less utility in a patient with presumed sarcoid uveitis and no obvious evidence of systemic sarcoidosis. The best use of these tests may be in following patients with active disease.[47,48]

In a study of 22 patients with sarcoid uveitis compared to 70 patients with uveitis secondary to other disorders, Power et al.[49] reported that the sensitivity and specificity of an elevated ACE alone in diagnosing sarcoidosis were 73% and 83%, respectively, and that the sensitivity and specificity of the gallium scan alone were 91% and 84%, respectively. Using the combination of a gallium scan and an elevated serum ACE, the specificity for diagnosing sarcoidosis was 100% and the sensitivity was 73%. The authors concluded that the combination of serum ACE level and whole-body gallium scan might be useful for diagnosing sarcoidosis in patients with uveitis. However, because of the study design inherent in investigating the values of these tests, their actual utility in patients with normal chest radiographs and without clinical evidence of sarcoid remains uncertain. Furthermore, because the reported prevalence of sarcoid uveitis is approximately 5% among patients with biopsy-confirmed systemic sarcoidosis,[3–6] routine screening of all patients with uveitis by both ACE levels and gallium scan may have a low positive predictive value and, therefore, may be misleading. Nevertheless, in selected patients in whom sarcoidosis is highly likely, these tests may be useful.

Magnetic Resonance Imaging (MRI) and Positive Emission Tomography Scan (PET)

Fluorodeoxyglucose PET (^{18}F-FDG PET) scanning has become of great importance in the study and follow-up of patients with cancer. However, in recent years, its role in the diagnosis and management of other conditions such as sarcoidosis has been explored. Although the sensitivity of a whole-body PET scan to detect sarcoid lesions is 80–100%, the findings are nonspecific and histology is required to confirm or rule out sarcoidosis. F-FDG PET/CT may show intense uptake in eyes with active sarcoidosis.[50] In addition, a decrease in FDG uptake correlates well with changes in the magnitude and extent of inflammatory activity among patients with sarcoidosis receiving treatment.[51] Thus, F-FDG PET may be a valuable adjunct in the management of ocular and systemic sarcoidosis.[52]

MRI has been successfully used in the evaluation of organ-specific damage in patients with sarcoidosis, especially cardiac and

musculoskeletal tissue.[46,49,53–56]

Histology

Histologic confirmation (Table 81.2)[57–75] may be required to establish the diagnosis of sarcoid. Sites most often biopsied include the lungs, mediastinal lymph nodes, skin, peripheral lymph nodes, liver, and conjunctiva. Biopsy of clinically evident skin lesions or palpable lymph nodes is frequently performed because of the high yield and low morbidity. Fiberoptic bronchoscopy with transbronchial lung biopsy is positive in 80% of patients with intrapulmonary sarcoidosis. This procedure is routinely performed by pulmonary physicians and has a relatively low morbidity. The next step in such a scenario is cervical mediastinoscopy, which is both highly invasive and an expensive procedure. The requirement of general anesthesia further increases the chances of complications from the procedure. From the patient's perspective it is important that further possibilities of minimally invasive techniques for the diagnosis of sarcoidosis are explored.

TABLE 81.2

Yield of Different Biopsy Sites in the Diagnosis of Sarcoidosis

Technique	Study	Positive/Total	(%)
Liver biopsy	Branson and Park (1954)[57]	48/63	76
	Israel and Sones (1964)[58]	22/24	92
	Klatskin (1976)[59]	17/23	94
Scalene lymph node biopsy	Beahrs et al. (1957)[60]	20/34	59
	Rochlin and Enterline (1958)[61]	27/34	79
	Williams and Webb (1962)[62]	32/39	82
Scalene fat pad biopsy	Romer et al. (1973)[63]	115/142	81
	Rasmussen and Neukirch (1976)[64]	41/99	52
Mediastinoscopy	Carlens (1964)[65]	118/123	96
	Palva (1964)[66]	27/28	96
	Romer et al. (1973)[63]	47/48	98
Lung biopsy, transbronchial	Koerner et al. (1975)[67]	21/23	91
Bronchoscope	Koontz (1978)[68]	74/104	71
Conjunctival biopsy	Crick et al. (1961)[69]	20/79	25
	Bornstein et al. (1962)[70]	16/64	25
	Kahn et al. (1977)[71]	20/60	33
	Solomon et al. (1978)[72]	8/15	57
	Garver (unpublished, 1980)	10/21	48
	Nichols et al. (1980)[73]	30/55	55
	Karcioglu and Brear (1985)[74]	14/28	50
Minor salivary gland biopsy	Nessan and Jacoway (1979)[75]	44/75	58

Modified from Green WR. Inflammatory diseases and conditions of the eye. In: Spencer WH, editor. Ophthalmic Pathology: An Atlas and Textbook, vol. 3. Philadelphia, PA: WB Saunders; 1986.

Development of linear echoendoscopes and subsequent procedures (endoscopic ultrasound-guided fine-needle aspiration [EUS-FNA] and endobronchial ultrasound-guided transbronchial needle aspiration [EBUS-TBNA]) has opened new diagnostic possibilities for sarcoidosis. Both techniques allow real-time monitoring of the needle. Several investigators have reported a high sensitivity of 72–85% for EBUS-TBNA and minimal complications. In a randomized control trial Tremblay et al.[76] have shown that the diagnostic yield of EBUS-guided TBNA (95.8%) versus the conventional TBNA (73.1%) was 22.7% greater. Sensitivity and specificity were 60.9% and 100%, respectively, in the standard TBNA group, and 83.3% and 100%, respectively, in the EBUS-guided TBNA group (absolute increase in sensitivity of 22.5%). EUS-FNA was used for diagnosis of sarcoidosis and had a yield of 82% and sensitivity of 89–94% by assessing noncaseating granulomas in mediastinal nodes.[77] The liver biopsy is often positive in patients with sarcoidosis, but the finding of granulomatous lesions on liver biopsy must be interpreted with caution, as they can be produced by other disorders. Other potential biopsy sites include peripheral lymph nodes and minor salivary glands. Minor salivary gland biopsy is a minimally invasive and easier means for the diagnosis of sarcoidosis.

Conjunctival biopsies are positive in 25–57% of patients with histologically documented sarcoidosis. Variations in these reports are the result of whether clinically evident lesions are biopsied or whether a “blind” conjunctival biopsy is performed. However, the yield can be increased by techniques such as bilateral conjunctival biopsies and serial sectioning of the specimens, and careful inspection of the conjunctiva for any visibly evident nodules which can be biopsied. Transconjunctival lacrimal gland biopsy can also be used for histologic diagnosis, but the procedure is not performed routinely.[47,78]

Immunology

The Kveim skin test was a simple, specific, outpatient skin test

using human sarcoid tissue. It was positive in 78% of patients with sarcoidosis and was helpful in delineating multisystemic sarcoidosis from other granulomatous disorders. The antigen was a saline suspension of human sarcoid tissue prepared from the spleen of a patient suffering from active sarcoidosis. This material was injected intradermally, and the site inspected for nodule formation after 3–6 weeks. A palpable nodule was biopsied, and the finding of noncaseating granulomas on biopsy established the diagnosis of sarcoid.[21,58,79] Concerns about the injection of human tissue, with its potential for disease transmission, have essentially eliminated the use of the Kveim test.

Studies suggest that CD4/CD8 ratios in the vitreous fluid may be high among patients with ocular sarcoidosis. This finding is similar to the observations of higher CD4 cell counts in the bronchoalveolar lavage fluid in patients with pulmonary sarcoidosis.[26–28] In a study of 51 eyes of 38 patients with ocular sarcoidosis (confirmed by International Workshop on Ocular Sarcoidosis [IWOS] criteria), peripheral blood and vitreous T lymphocytes (obtained by pars plana vitrectomy) were analyzed using polymerase chain reaction, and flow cytometry. CD4/CD8 ratios were high among patients with sarcoidosis compared to nonsarcoid controls with a high sensitivity and specificity of 100% and 96.3%, respectively.[80]

Noninvasive Tests

Multiple attempts have been made to find noninvasive tests that could be both sensitive and specific in the diagnosis of sarcoidosis. These have included measurement of serum calcium, urinary calcium, serum lysozyme, and serum immunoglobulins. Although all these may be abnormal in patients with sarcoid, they are nonspecific and nondiagnostic. The serum ACE level has been touted as a useful measurement in the diagnosis of sarcoidosis. The ACE level is frequently abnormal in patients with active sarcoidosis and appears to reflect the total-body granuloma content in such patients. As such, it may be useful in following patients with active sarcoid.[48,58,81] However, it is not diagnostic of sarcoidosis and appears to be of limited utility in the diagnostic dilemma of patients with possible sarcoid uveitis but a normal chest film.

For following patients with active intrapulmonary sarcoid, pulmonary function tests, particularly forced vital capacity, forced expiratory volume, and diffusing capacity, are far more useful. Changes in pulmonary function tests are often used to follow patients with sarcoidosis and to adjust the corticosteroid dosage.[29]

Jabs and Johns[82] reported that over 80% of patients with ocular sarcoid had their ocular lesions at the time of diagnosis of sarcoidosis, and Hunter and Foster[56] reported that 3% of patients with uveitis were diagnosed as having sarcoid after the initial evaluation for a systemic disease revealed no diagnosable systemic disorder. Although patients who present with uveitis should be evaluated for sarcoid, repetitive workups appear to have limited value unless new symptoms arise.

Course and Prognosis

There appear to be two distinct paradigms of sarcoidosis, acute and chronic, with differences in onset, natural history, course, prognosis, and response to treatment. Acute sarcoidosis tends to have an abrupt, explosive onset in young patients and to go into spontaneous remission within 2 years of onset. Acute iritis is often seen in acute sarcoidosis. The response to systemic corticosteroids is generally quite good, and the manifestations may quickly disappear within a week of therapy initiation. The long-term complications of sarcoidosis are minimal. Löfgren syndrome comprises erythema nodosum, bilateral hilar adenopathy, and acute iritis; it generally has a good long-term prognosis.[1,21,31]

Chronic sarcoidosis is defined as disease persistence of greater than 2 years. The disease may have a more insidious onset and generally has intrapulmonary involvement with chronic pulmonary disease as a major source of morbidity. Corticosteroid therapy is generally required and may be prolonged. Chronic ocular disease, particularly chronic uveitis, may be a feature of chronic sarcoidosis.[1,21,29,31,82]

The overall mortality from sarcoidosis is 3–5%, but neurosarcoidosis is associated with a mortality of 10%.[55] Corticosteroids are the mainstay of treatment. Patients with hilar adenopathy without abnormalities of pulmonary function and

without intrapulmonary infiltration may not need systemic corticosteroid treatment.

Ocular Manifestations

Multiple studies have documented the common occurrence of ocular involvement in sarcoidosis and the various ocular manifestations of sarcoid. Frequency estimates vary and have ranged as high as 50%.[55] However, most series report rates that are generally closer to 15–28%.[1,21,31,34,82,83] These differences undoubtedly relate to case ascertainment methods, the patient population studied, definitions of ophthalmic involvement, and the nature of the evaluation conducted. Racial differences influence not only the mode of presentation for ocular sarcoidosis but also the frequency of patients with ocular involvement. When the same diagnostic criteria were applied, Japanese patients with sarcoidosis were found to have ocular disease six times more frequently than Finnish patients, and they were also more likely to present with ocular symptoms of sarcoidosis. In the United States the black population is twice as likely to have ocular disease as opposed to white patients. Furthermore, high frequencies of ocular involvement are reported when keratoconjunctivitis sicca is sought carefully and included as evidence of lacrimal involvement in sarcoidosis.[55]

Sarcoidosis may affect most of the ocular structures, as well as the orbit and adnexa. Ocular lesions described in sarcoidosis include anterior uveitis, iris nodules, conjunctival nodules, scleral nodule,[84,85] and corneal disease with either band keratopathy or interstitial keratitis; posterior segment disease, including chorioretinitis, periphlebitis, chorioretinal nodules, vitreous inflammation, and retinal neovascularization; and orbital disease, including involvement of the lacrimal gland, nasolacrimal duct, optic nerve, and orbital granulomas. The various ocular lesions along with the prevalence estimates are outlined in Table 81.3.

TABLE 81.3

Ocular Manifestations of Sarcoidosis

Ocular Manifestations	Frequency in Patients With Ocular Sarcoid (%)

ANTERIOR SEGMENT DISEASE	
Anterior uveitis	66–70
Acute	15–32
Chronic	39–53
Iris nodules	11–16
Conjunctival lesions	7–47
CORNEA	
Band keratopathy	5–14
Interstitial keratitis	1
POSTERIOR SEGMENT DISEASE	
Vitritis	3–25
Periphlebitis	10–17
Chorioretinitis	11
Choroidal nodules	4–5
Retinal neovascularization	1–5
Orbital and other disease	26
Lacrimal gland	7–60
Keratoconjunctivitis sicca	5–60
Enlargement	7–28
Orbital granuloma	1
Optic nerve granuloma	<1–7

Sarcoidosis accounts for nearly 5% of all the adult uveitis cases and 1% of the pediatric cases. Anterior uveitis is the most common ocular manifestation and occurs in approximately two-thirds of patients with ocular sarcoid. The uveitis may be an acute iridocyclitis or a chronic granulomatous uveitis. Acute iridocyclitis with mutton-fat keratic precipitates is most often seen in patients with acute sarcoid but can be seen in those with chronic sarcoid as well. The prognosis is worse for those with chronic disease, who may develop complications such as secondary glaucoma, cataracts, macular edema, and visual loss. Iris nodules are occasionally seen in association with anterior uveitis in patients with sarcoidosis.

Conjunctival and corneal lesions such as band-shaped keratopathy are less common. These are generally described as conjunctival nodules, which on biopsy reveal the characteristic granuloma formation of sarcoidosis. Occasionally a nonspecific or phlyctenular keratoconjunctivitis is described in association with other mucocutaneous lesions of sarcoidosis. In addition, occasional cases of interstitial keratitis in association with sarcoidosis have been described.

The frequency of orbital, and particularly lacrimal gland, lesions varies widely among series and depends on the patient selection and investigations used. Clinical enlargement is present in less than one-third of patients with ocular sarcoid, but when sought,

keratoconjunctivitis sicca may be present in a greater percentage.[31,34,55,82–84] Orbital granuloma, independent of the lacrimal gland, occurs infrequently.[86–88] Massive lacrimal gland enlargement simulating a lacrimal gland tumor may occur and require orbitotomy and biopsy. Sarcoid granulomas may also manifest as a pseudotumor, affecting the orbital muscles along with the lacrimal gland resulting in swelling, diplopia and restriction of ocular motility.[89–91]

Posterior Segment Disease

Posterior segment lesions are reported to occur in approximately 14–28% of patients with ocular sarcoid.[6,14,31,34,54,55,82,83,92,93] The actual frequency may be higher, since most patients with posterior segment disease also have anterior uveitis. Posterior lesions include vitritis, chorioretinitis, periphlebitis, vascular occlusion, retinal neovascularization, and optic nerve head granulomas.

Vitreous infiltration in patients with sarcoidosis can appear as cellular infiltration, often as a nonspecific vitritis. More classically, however, the lesions demonstrate clumping and an accumulation of vitreous debris, called either “snowballs” or a “string of pearls” (Fig. 81.1). These lesions may be somewhat similar in appearance to those seen in pars planitis, although snowball formation is generally not seen in sarcoid uveitis. Sarcoid granulomas can also present in the optic nerve, peripheral retina, pars plana, and anterior choroid and can be imaged by high-resolution ultrasound biomicroscopy as different forms of uveal thickening.[94]

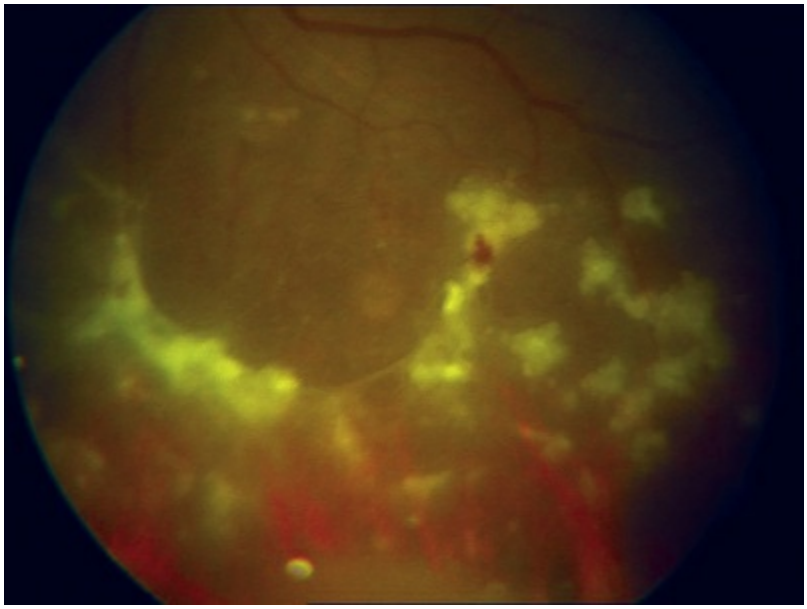

FIG. 81.1 Vitreous inflammation in a patient with sarcoidosis. (Courtesy of Vishali Gupta, MD).

Perivascular sheathing is the second most common finding and occurs in 10–17% of patients with ocular sarcoid. It is generally a midperipheral periphlebitis without significant vascular occlusion (Figs. 81.2 and 81.3). However, a few series have documented the occasional occurrence of occlusive retinal vascular disease, particularly branch retinal vein occlusion (Fig. 81.4). Central retinal vein occlusion is much less common. Histologic studies have demonstrated vascular compromise by the granulomatous inflammatory material.[95,96] More severe forms of periphlebitis have been called "candle-wax drippings" (*taches de bougie*). Arteriolar involvement is very unlikely in patients with sarcoidosis. Sanders and Shilling[97] have described an "acute retinopathy of sarcoidosis" with extensive perivascular sheathing, vascular occlusion, and intraretinal hemorrhages. These cases were complicated by subsequent retinal neovascularization.

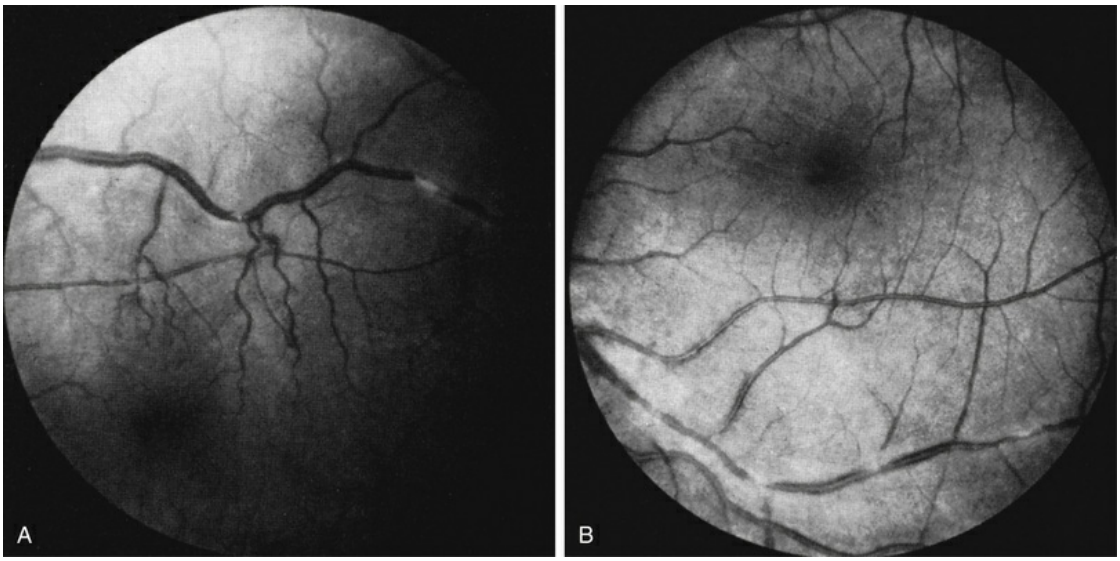

FIG. 81.2 (A, B) Perivascular sheathing in a patient with sarcoidosis. (Reproduced with permission from Green WR. Inflammatory diseases and conditions of the eye. In: Spencer WH, editor. Ophthalmic pathology: an atlas and textbook, vol. 3. Philadelphia, PA: WB Saunders; 1986.)

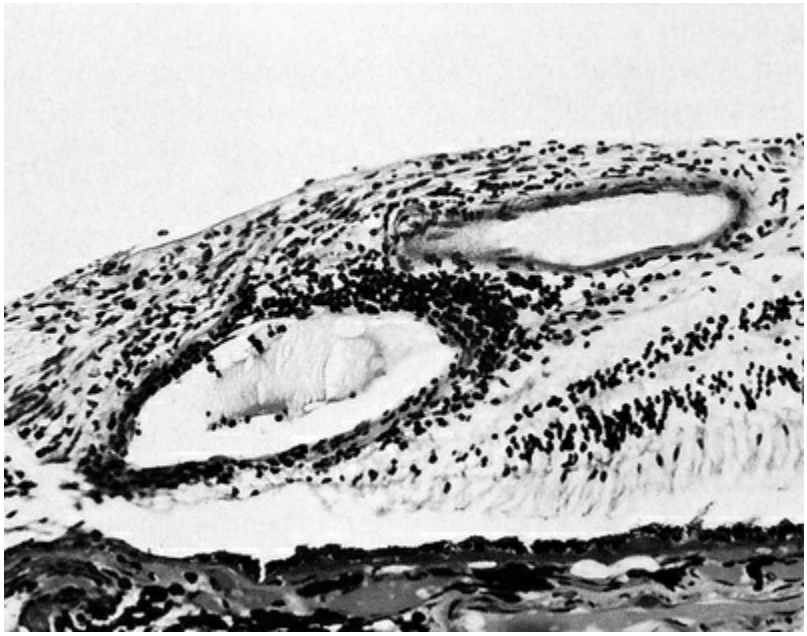

FIG. 81.3 Histopathology of periphlebitis in a patient with sarcoidosis (periodic acid–Schiff reaction; ×225). (Reproduced with permission from Green WR. Inflammatory diseases and conditions of the eye. In: Spencer WH, editor. Ophthalmic pathology: an atlas and textbook, vol. 3. Philadelphia, PA: WB Saunders; 1986.)

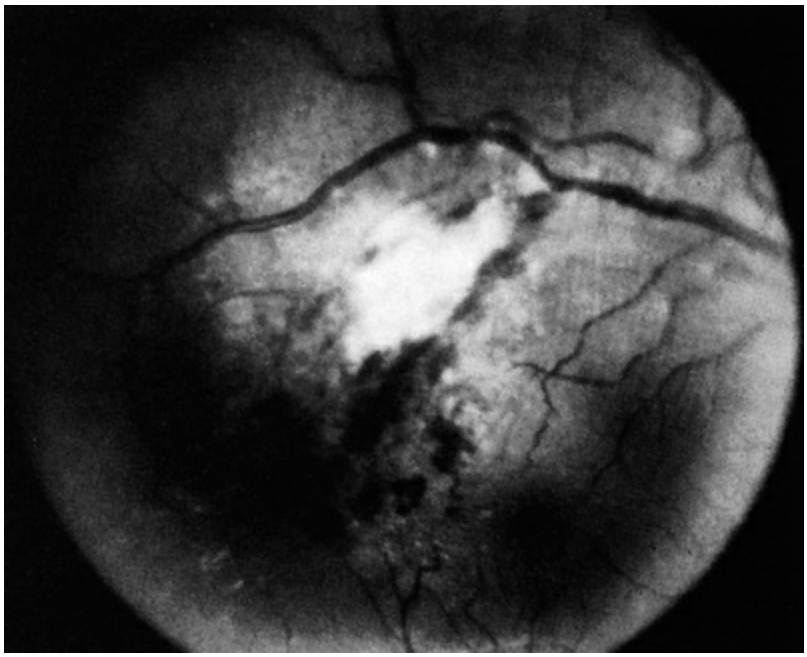

FIG. 81.4 Perifoveal branch vein occlusion in a patient with sarcoidosis.

Deeper chorioretinal lesions have also been reported. These can vary in size from small "Dalen–Fuchs-like" granulomas to large choroidal nodules simulating a metastatic tumor.[98,99] If located in the macular region, these lesions can cause severe visual loss. Exudative retinal detachments are rarely seen in patients with sarcoid uveitis but do occur in those patients with large nodular chorioretinal granulomas. These detachments appear to be an overlying detachment of the neurosensory retina.[5,100]

Visual loss can occur from epiretinal membrane formation and cystoid macular edema in patients with sarcoidosis. Once the inflammation has been controlled, pars plana vitrectomy with membrane peeling may have a beneficial effect on restoring vision, although development of cataract and membrane recurrence may require additional surgeries.[101,102] In one small uncontrolled case series, triamcinolone acetonide was injected into the vitreous cavity to assist the visualization of the vitreous for the vitrectomy,[103] but the role of this approach is uncertain. Complications of ocular sarcoidosis such as epiretinal membranes and macular edema may also be treated effectively using microincision vitrectomy (23- or 25-gauge systems) resulting in remission of ocular inflammation and improvement in visual acuity.[104]

Peripheral retinal neovascularization or neovascularization of the

optic nerve head is present in less than 5% of patients with ocular sarcoid, but can be associated with significant visual loss due to vitreous hemorrhage. Peripheral retinal neovascularization is generally seen in patients with a defined vaso-occlusive disorder such as a branch retinal vein occlusion. The peripheral neovascular lesions may even simulate a sea fan, similar to that seen in sickle-cell disease. Neovascularization of the disc may also develop after a branch or central vein occlusion. The rare occurrence of peripapillary choroidal neovascularization in the absence of uveitis or optic nerve disease has been reported, and described to be responsive to oral corticosteroids.[103] Doxanas and coworkers[105] described a patient with sarcoidosis and a steroid-responsive neovascularization of the optic nerve head without retinal nonperfusion (Fig. 81.5). Hoogstede and Copper[96] described one case of subretinal neovascularization, which they attributed to sarcoid uveitis. Duker et al.[106] reported the clinical features of proliferative sarcoid retinopathy in 11 eyes of seven patients. In these cases the new retinal vessels were associated with concomitant peripheral retinal capillary nonperfusion. The authors suggested that in these patients capillary nonperfusion secondary to microvascular shutdown, rather than a direct effect of inflammation, was the stimulus for the formation of retinal neovascularization.

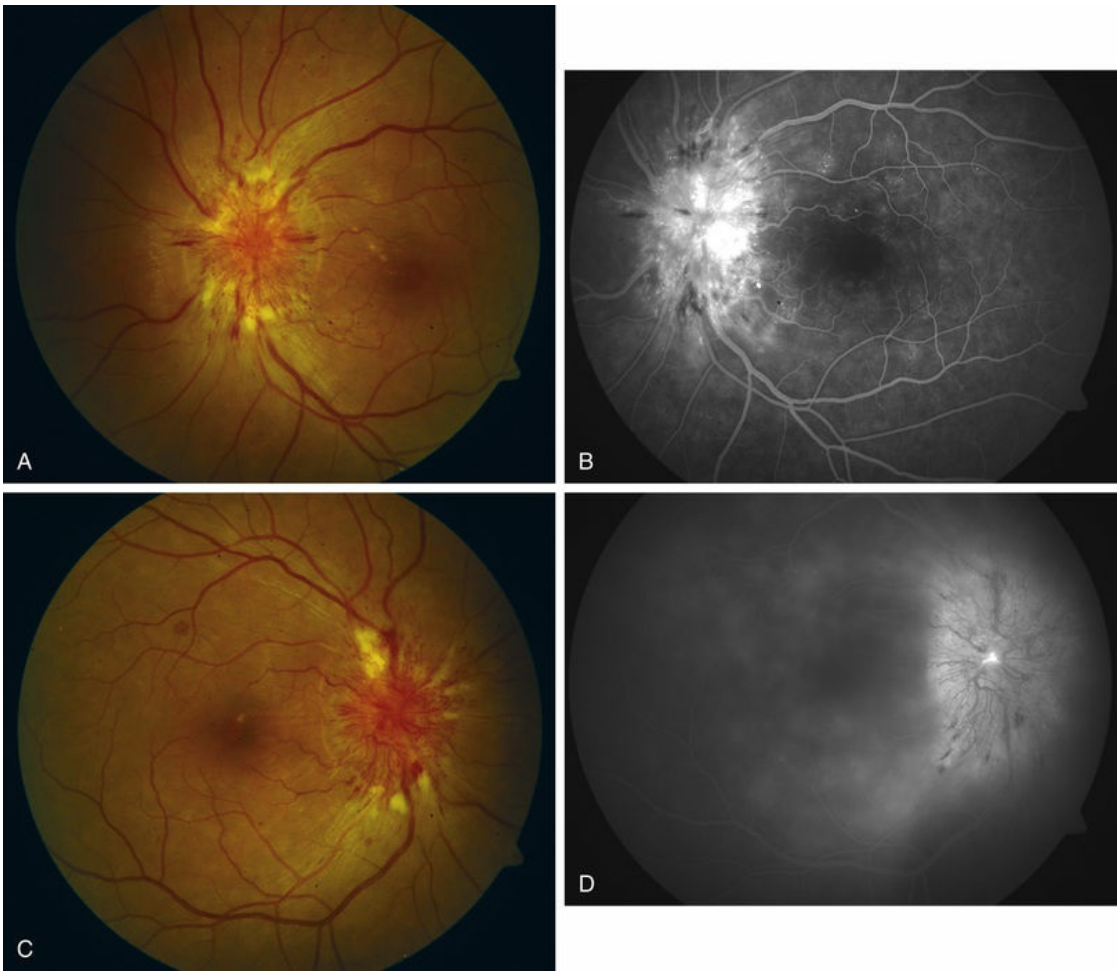

FIG. 81.5 Neovascularization of the optic nerve in a patient with sarcoidosis. Fundus photograph (A) and fluorescein angiogram (B) of the left eye, and fundus photograph (C) and fluorescein angiogram (D) of the right eye of a young female diagnosed with sarcoidosis. (Courtesy of Vishali Gupta, MD).

It has been reported that when posterior-segment involvement is seen in patients with sarcoid uveitis, there is an increased frequency of CNS involvement. In a retrospective review of the literature, Gould and Kaufman[107] suggested that the prevalence of CNS involvement increased from 2% to 30% when fundus lesions were found. However, Spalton and Sanders[108] found no such association, thus leaving the association not well confirmed.

Optic nerve involvement, particularly multiple granulomas of the optic nerve head, occur in 0.5–7.0% of patients with ocular sarcoid[31,34,79,82,108] (Fig. 81.6). Histologic descriptions have shown granuloma formation[79,109] (Fig. 81.7). Optic disc edema without granulomatous invasion of the optic nerve head may be seen in

patients either with chronic uveitis or with papilledema[36] from CNS sarcoid, mimicking conditions such as malignant hypertension.[110] Other manifestations include optociliary shunt vessels and macroaneurysms.[111] Occasionally, isolated sarcoid optic neuropathy (optic atrophy, optic neuritis, optic disc edema) may occur and may be the first manifestation of neurosarcoidosis.[112–114]

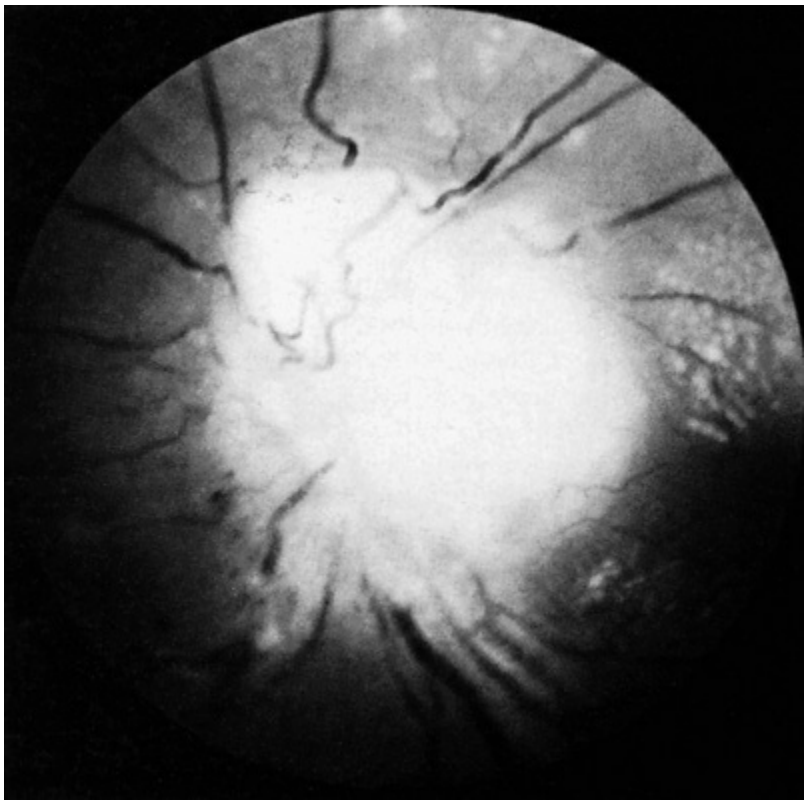

FIG. 81.6 Optic nerve mass in a patient with sarcoidosis. (Courtesy of Robert Nussenblatt, MD.)

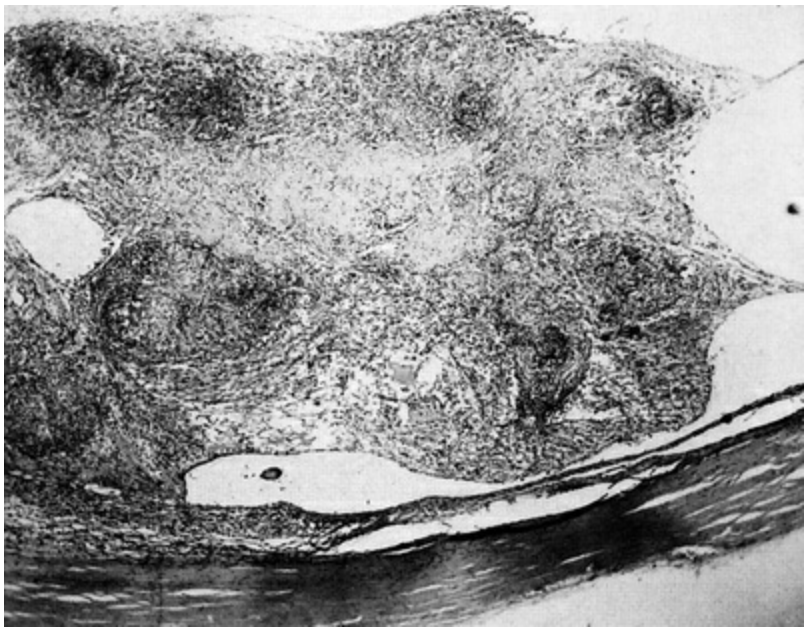

FIG. 81.7 Granulomatous inflammatory mass coming from the optic nerve head in a patient with sarcoidosis (hematoxylin and eosin, ×35). (Reproduced with permission from Green WR. Inflammatory diseases and conditions of the eye. In: Spencer WH, editor. Ophthalmic pathology: an atlas and textbook, vol. 3. Philadelphia, PA: WB Saunders; 1986.)

In addition to these conventionally observable lesions, Mizuno and Takahashi[115] have used cycloscopy to document the common occurrence of lesions in the ciliary processes of patients with intraocular sarcoidosis. In their series, nodules of the ciliary processes were seen in 41% of eyes, waxy exudates in 24%, and cyclitic membrane-like exudates in 3%. Only 20% of eyes with intraocular sarcoid had no observable lesions.

Diagnosis

Ocular sarcoidosis can present as a myriad of signs and symptoms. Such variability in presentation makes the diagnosis challenging and clinicians often need to resort to invasive diagnostic techniques in order to rule out or establish the diagnosis. In 2006 the scientific community came together at the first IWOS in Tokyo, Japan and established criteria for the diagnosis of ocular sarcoidosis when ocular changes are present in the presence or absence of clinical signs of systemic disease. These have been subsequently revised in

2009. The IWOS diagnostic criteria allow ophthalmologists to arrive at one of the following four conclusions with a minimally invasive approach: (1) definite; (2) presumed; (3) probable; and (4) possible ocular sarcoidosis. A summary of the 2006 IWOS diagnostic criteria and laboratory investigation is given in Table 81.4. A proposed outline to the approach in evaluating a patient for possible ocular sarcoid is shown in Fig. 81.8.

TABLE 81.4

Clinical Signs, Laboratory Investigations, and Diagnostic Criteria Proposed by the International Workshop on Ocular Sarcoidosis (2006)

Clinical Signs Suggestive of Ocular Sarcoidosis
1. Mutton-fat KPs (large and small) and/or iris nodules at pupillary margin (Koeppe) or in stroma (Bussacca) 2. Trabecular meshwork (TM) nodules and/or tent-shaped peripheral anterior synechiae (PAS) 3. Snowballs/string-of-pearl vitreous opacities. 4. Multiple chorioretinal peripheral lesions (active and atrophic) 5. Nodular and/or segmental periphlebitis (± candle-wax drippings) and/or macroaneurysm in an inflamed eye 6. Optic disc nodule(s)/granuloma(s) and/or solitary choroidal nodule 7. Bilaterality (assessed by clinical examination or investigational tests showing subclinical inflammation)
Laboratory Investigations in Suspected Ocular Sarcoidosis
1. Negative tuberculin test in a BCG-vaccinated patient or having had a positive PPD (or Mantoux) skin test previously 2. Elevated serum ACE and/or elevated serum lysozyme 3. Chest radiography; look for bilateral hilar lymphadenopathy (BHL) 4. Abnormal liver enzyme tests (any two of alkaline phosphatase, ASAT, ALAT, LDH or GGT) 5. Chest CT scan in patients with negative chest radiograph
Diagnostic Criteria for Ocular Sarcoidosis (Fig. 81.8)
All other possible causes of uveitis, in particular tuberculous uveitis, have to be ruled out.
1. Biopsy supported diagnosis with a compatible uveitis → Definite ocular sarcoidosis 2. Biopsy not done; presence of BHL with a compatible uveitis → Presumed ocular sarcoidosis 3. Biopsy not done and BHL-negative; presence of three of the suggestive intraocular signs and two positive investigational tests → Probable ocular sarcoidosis 4. Biopsy negative, four of the suggestive intraocular signs and two of the investigations are positive → Possible ocular sarcoidosis

ALAT, alanine aminotransferase; ASAT, aspartate aminotransferase; BCG, bacillus Calmette-Guérin; CT, computed tomography; GGT, gamma-glutamyl transferase; KPs, keratic precipitates; LDH, lactate dehydrogenase; PPD, purified protein derivative.

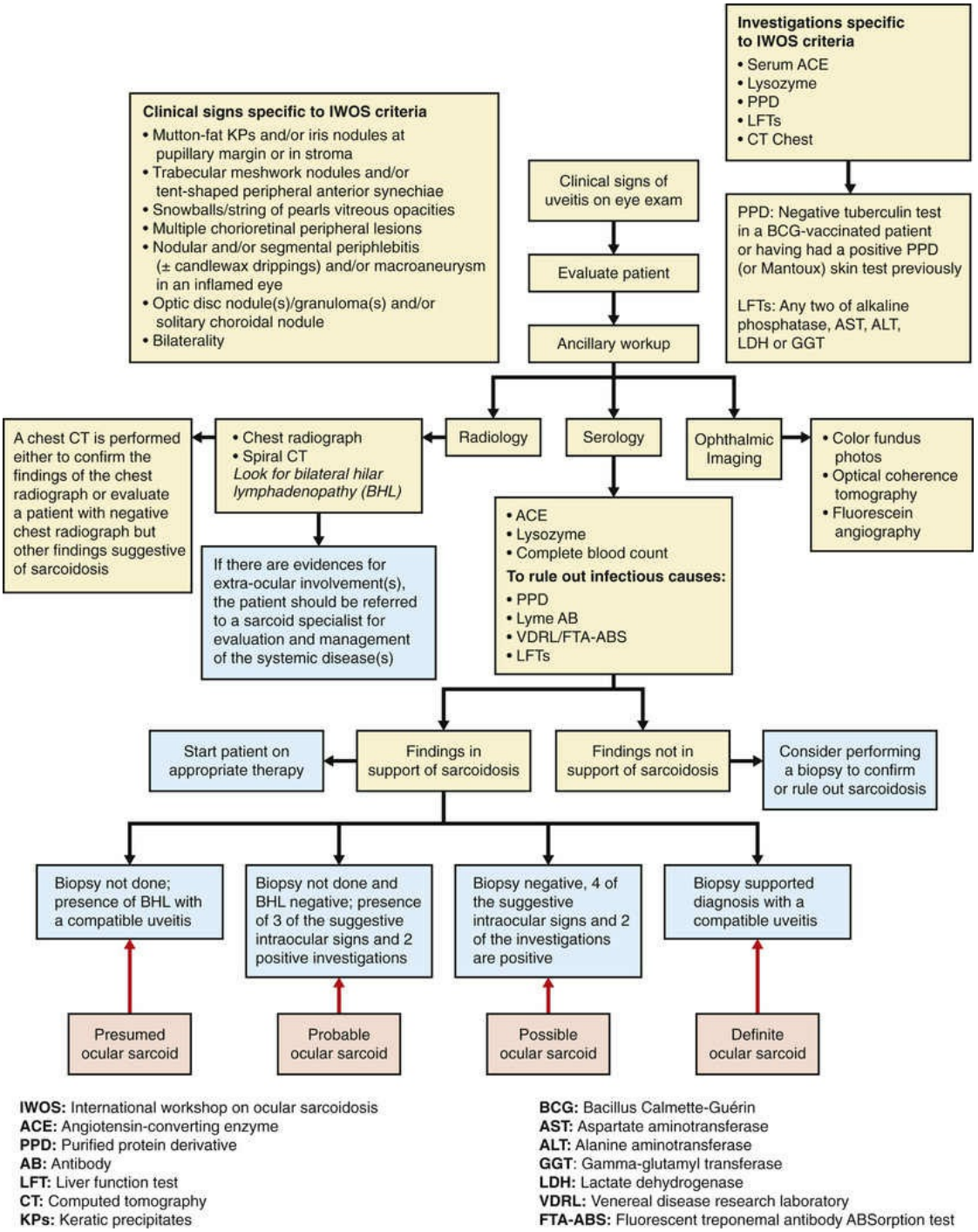

FIG. 81.8 Schematic outline for the evaluation of patients with suspected sarcoidosis.

A survey of 24 uveitis specialists from around the world has suggested that a significant number of ophthalmologists use the IWOS criteria to establish a diagnosis of ocular sarcoidosis.[116] A recent study compared the ocular (such as tent-shaped peripheral anterior synechiae) and systemic findings (such as lung function

tests and bronchoalveolar lavage) findings in both biopsy and nonbiopsy proven cases of ocular sarcoidosis with the criteria proposed by IWOS (n=83). The study results showed that employing the IWOS criteria provides high reliability in diagnosing ocular sarcoidosis.[117] Employing the IWOS diagnostic criteria allows for diagnosis in the absence of a biopsy, provides information for both the clinician and patient with regard to prognosis, and encourages nonspecialists to consider sarcoidosis as a putative diagnosis. Although there are limitations of the IWOS diagnostic criteria, they certainly help to limit the investigations that a patient with suspected sarcoidosis may have to undergo and help the caregiver to formulate a standardized approach towards establishing the diagnosis.

As is the case in any other form of uveitis, there needs to be a systematic approach to establishing a diagnosis of ocular sarcoidosis and ruling out its major differentials. Patients may present with no systemic disease. After carefully ruling out the possibility of an infectious cause of the uveitis, ophthalmologists may follow the IWOS criteria for diagnosis. However, if the clinical and ancillary evidence is not enough to commit to a diagnosis or rule out the possibility in patients with ocular sarcoidosis, a biopsy may be performed. It is important for the ophthalmologist to consider referring patients with suspected sarcoidosis to an internist whenever there is evidence of extrapulmonary involvement or the diagnosis of systemic disease needs to be confirmed.

Course and Prognosis

Karma and coworkers[83] classified the course of ocular sarcoidosis as monophasic, relapsing, or chronic. The three different courses of uveitis correlated with visual outcome. Patients with monophasic uveitis retained 20/30 or better visual acuity in 88% of eyes, with relapsing uveitis in 72% of eyes, and with chronic uveitis in none of the six eyes. Similarly, those with monophasic uveitis had a visual acuity of 20/70 or worse in 12% of eyes, with relapsing uveitis in 28% of eyes, and chronic uveitis in 67% of eyes. Hence the course of uveitis appears to correlate with the long-term visual outcome.

The development of secondary glaucoma in association with sarcoid uveitis appears to be a poor prognostic sign and is associated with severe visual loss. In one series,[82] most of these patients had a panuveitis with both anterior- and posterior-segment involvement associated with the development of secondary glaucoma, suggesting a more severe ocular disease. Treatment should be directed towards promptly suppressing the inflammation and minimizing any potential ocular complications.

In a retrospective study of 60 patients with sarcoid-associated uveitis who were followed at a subspecialty eye care and referral center, Dana et al.[118] identified prognostic factors for visual outcomes in sarcoid uveitis. The factors most strongly associated with both a lack of visual acuity improvement and a final visual acuity worse than 20/40 were (1) delay in presentation to a uveitis subspecialist of greater than 1 year; (2) development of glaucoma; and (3) presence of intermediate or posterior uveitis. There was a substantial increase in the relative odds of both visual improvement and the likelihood of achieving a visual acuity of at least 20/40 among patients in whom systemic corticosteroids were used for treatment. Because patients with more severe disease are more likely to receive systemic corticosteroid therapy, this result strongly supports the use of systemic corticosteroids for selected patients with sarcoid uveitis. Miserocchi et al. evaluated the risk factors for visual outcomes in 44 patients retrospectively, and their multivariate results suggest that only the presence of cystoid macular edema was significantly associated with worse visual outcome.[119]

Therapy

Treatment of any form of uveitis depends upon the initial presentation of the patient, severity of the disease, and accompanying complications. Nonetheless, the goals of therapy remain the same and include preservation of visual acuity, prompt identification of all sources of inflammation, zero tolerance toward any degree of inflammation, and proper management of complications such as macular edema, cataract, and glaucoma. The management of uveitis can be quite complex and may involve

employment of multiple therapeutic options, some of which do have potential significant and serious side-effects. A proposed outline for the management of ocular sarcoidosis is shown in Fig. 81.9. However, it is of the utmost importance to recognize that the approach to the management of each patient should be individualized. The proposed scheme only serves as a generalized recommendation. If there are any concerns regarding the diagnosis and management of a patient with ocular sarcoidosis, it may be beneficial for the patient if he/she can be referred to a uveitis specialist who is experienced in managing the disease.

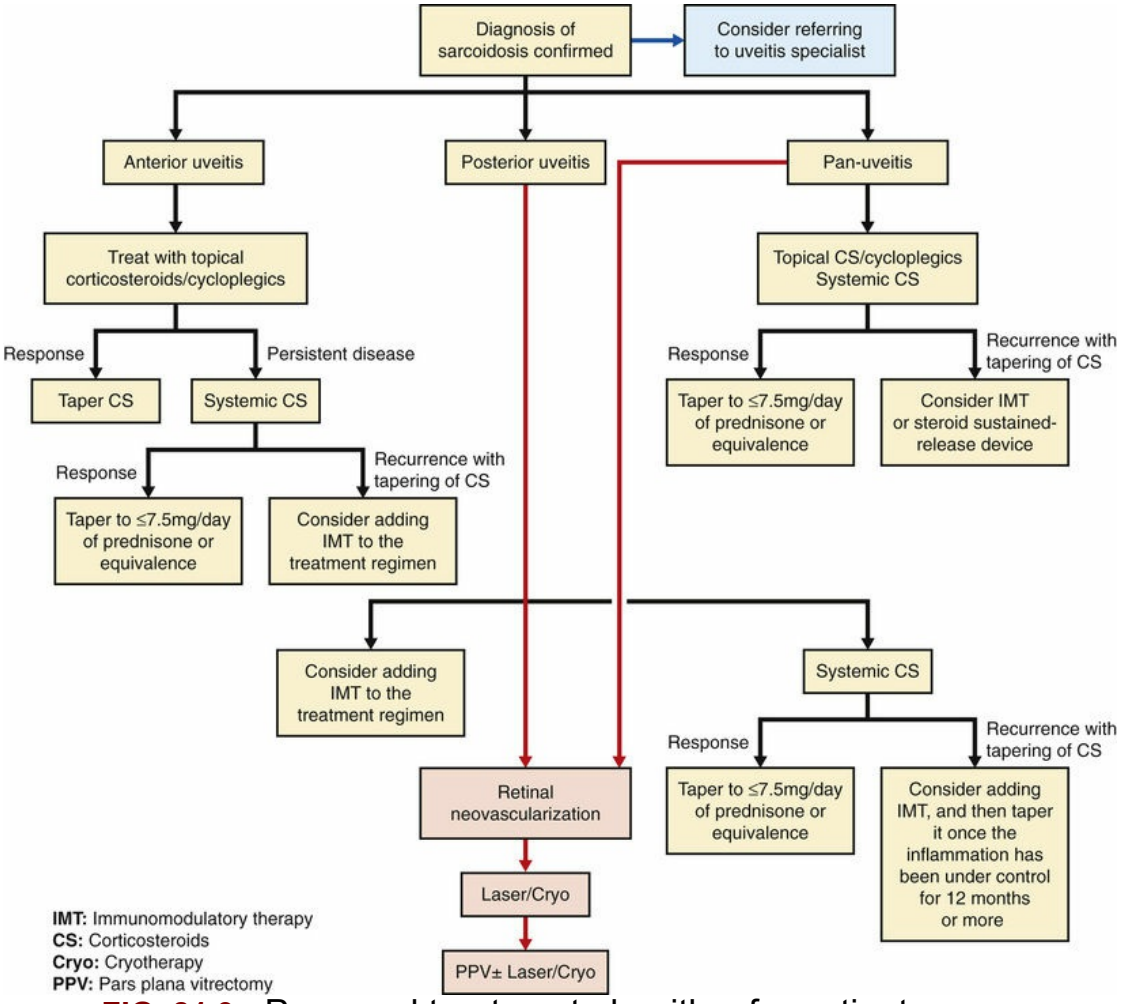

FIG. 81.9 Proposed treatment algorithm for patients with ocular sarcoidosis.

Established Therapy

Treatment of the anterior uveitis associated with sarcoidosis is generally achieved with intensive topical corticosteroids, which may require several months to reach quiescence. In some patients with refractory anterior uveitis, the judicious use of oral corticosteroids may be necessary to suppress the inflammation. Patients with sarcoidosis generally respond to corticosteroid therapy, but chronic therapy may be necessary. Posterior-segment lesions in sarcoidosis generally require the use of systemic corticosteroids. Dosages are often in the range of prednisone 40–80 mg/day initially. Maintenance therapy with systemic corticosteroids should be less than 5 mg/day of prednisone or equivalence. Posterior-segment lesions such as perivascular sheathing and peripheral chorioretinal nodules that are not associated with visual loss may not mandate oral corticosteroid therapy. However, vascular occlusion, neovascularization, macular mass lesions, and optic disc lesions may produce profound visual loss and most likely require corticosteroid therapy.

Although corticosteroids are very effective in controlling inflammation initially, their long-term use is often associated with significant complications and side-effects. The use of steroid-sparing agents is indicated if chronic steroid usage (≥5 mg of prednisone or equivalent daily) is required to control the inflammation. Corticosteroid-sparing agents such as hydroxychloroquine, methotrexate, azathioprine, mycophenolate mofetil, or cyclosporine may be useful in patients with corticosteroid-dependent sarcoidosis in whom corticosteroid side-effects are problematic;[120–123] however, their usages may not be without risk. Patients being treated with these agents, including corticosteroids, require very thorough and experienced clinical oversight by specialists (such as uveitis specialists, rheumatologists, or oncologists) who are familiar with employing such classes of drugs.

Methotrexate,[124] azathioprine,[125,126] and mycophenolate[127] have been widely employed as steroid-sparing agents in the management of chronic uveitis. In a retrospective series of 386 patients, methotrexate was found to control uveitis in 66% of patients.[128] A delay of up to 6 months in response to therapy with methotrexate has also been reported, which has prompted the use

of intraocular injections of the drug.[125] Azathioprine has been reported to be beneficial in patients with ocular sarcoidosis who do not respond to methotrexate. However, in a retrospective study of patients with intermediate uveitis, a 25% rate of discontinuation was noted within the first year of therapy due to toxicity. The use of azathioprine is permitted in pregnant women with several precautions. Mycophenolate mofetil has shown promising results in terms of low toxicity. Deuter et al.[127] reported a success rate of 86% in patients with chronic uveitis treated with mycophenolate with a discontinuation of only 5% due to toxicity. A small series of seven patients diagnosed with sarcoidosis has also reported the drug to be beneficial.[129] Galor et al. reported a response rate of 70%, 42%, and 58% at 6 months for mycophenolate mofetil, methotrexate, and azathioprine, respectively, in 321 patients with nonspecific ocular inflammation.[130] Although the time to response for azathioprine and mycophenolate was similar, the former had more toxicity-related events reported.

Other immunomodulatory therapeutic agents have been employed in the management of sarcoidosis. Baughman and Lower reported a 58% complete and 28% partial improvement in patients with ocular sarcoidosis when treated with leflunomide. Only two of the 28 patients discontinued therapy due to toxicity in this study.[131]

Biologic Agents

Biologics, antagonists of tumor necrosis factor (TNF) such as adalimumab (humanized monoclonal antibody), infliximab (chimeric monoclonal antibody), and etanercept (soluble TNF receptor antagonist) have been reported in small studies to benefit patients with chronic uveitis.[132–136] However, there is a lack of evidence from clinical trials supporting the use of adalimumab and infliximab, while it has been shown in a double-masked randomized clinical trial that etanercept is no better than placebo when treating chronic uveitis.[92,93] Several groups have also reported the development of uveitis in patients receiving anti-TNF therapy[135,137–139] at a significantly higher rate, with etanercept followed by infliximab and adalimumab.[140] Although the mechanism of this phenomenon is not yet fully understood, several

reports of anti-TNF therapy leading to a sarcoidosis-like reaction suggest that a very cautious approach should be taken when using these agents to treat ocular sarcoidosis.

Conclusion

Sarcoidosis is a multiorgan disease with protean manifestations, including ocular involvement. Throughout the years, significant advancements have been made toward the understanding of the pathogenesis of sarcoidosis; however, the etiology of the disease is not completely elucidated. Evidence suggests that the pathophysiology most likely involves T cells. Sarcoid is one of the most common causes of uveitis of all types – anterior, intermediate, and/or posterior. Therefore, it is important for ophthalmologists to recognize that ocular manifestations may be the initial presentation of a patient with sarcoidosis.

The IWOS has established criteria for the diagnosis of ocular sarcoidosis when ocular changes are present in the presence or absence of clinical signs of systemic disease. Such criteria are helpful and should be considered in establishing the diagnosis and asserting its certainty. Managing a patient with ocular sarcoid will depend on whether the disease is unilateral or bilateral, whether there is presence or absence of systemic involvement, and how such involvements are at the time of the ocular disease. It is important for ophthalmologists caring for patients with ocular sarcoid to collaborate with internists, pulmonologists, and sarcoid specialists to provide patients with comprehensive and complete care.

There are existing therapeutic options and approaches that may be used in bringing the disease into quiescence, which should be the goals for both ocular and systemic diseases. In addition, potential new drugs are currently in development that may lead to disease quiescence with fewer side-effects and complications in the future.

References

1. Jamilloux Y, Kodjikian L, Broussolle C, et al. Sarcoidosis and uveitis. *Autoimmun Rev*. 2014;13:840–849.

2. James DG. Sarcoidosis. Wyngaarden JB, Smith LH Jr. *Cecil textbook of medicine*. 17th ed. WB Saunders: Philadelphia; 1985.
3. Henderly DE, Genstler AJ, Smith RE, et al. Changing patterns of uveitis. *Am J Ophthalmol*. 1987;103:131–136.
4. Karma A. Ophthalmic changes in sarcoidosis. *Acta Ophthalmol Suppl*. 1979;1–94.
5. Perkins ES, Folk J. Uveitis in London and Iowa. *Ophthalmologica*. 1984;189:36–40.
6. Rosenbaum JT. Uveitis. An internist's view. *Arch Intern Med*. 1989;149:1173–1176.
7. Jones N, Mochizuki M. Sarcoidosis: epidemiology and clinical features. *Ocul Immunol Inflamm*. 2010;18(2):72–79.
8. Statement on sarcoidosis. Joint statement of the American Thoracic Society (ATS), the European Respiratory Society (ERS) and the World Association of Sarcoidosis and Other Granulomatous Disorders (WASOG) adopted by the ATS Board of Directors and by the ERS Executive Committee, February 1999. *Am J Respir Crit Care Med*. 1999;160:736–755.
9. Rybicki BA, Major M, Popovich J Jr, et al. Racial differences in sarcoidosis incidence: a 5-year study in a health maintenance organization. *Am J Epidemiol*. 1997;145:234–241.
10. Lazarus A. Sarcoidosis: epidemiology, etiology, pathogenesis, and genetics. *Dis Mon*. 2009;55:649–660.
11. James DG, Neville E, Siltzbach LE. A worldwide review of sarcoidosis. *Ann N Y Acad Sci*. 1976;278:321–334.
12. Rosenberg AM, Yee EH, Mackenzie JW. Arthritis in childhood sarcoidosis. *J Rheumatol*. 1983;10:987–990.
13. Seamone CD, Nozik RA. Sarcoidosis and the eye. *Ophthalmol Clin North Am*. 1992;5:567–576.
14. Milman N, Hoffmann AL. Childhood sarcoidosis: long-term follow-up. *Eur Respir J*. 2008;31:592–598.
15. Blain JG, Riley W, Logothetis J. Optic nerve manifestations of sarcoidosis. *Arch Neurol*. 1965;13:307–309.
16. Jabs DA, Houk JL, Bias WB, et al. Familial granulomatous synovitis, uveitis, and cranial neuropathies. *Am J Med*. 1985;78:801–804.

17. Rose CD, Eichenfield AH, Goldsmith DP, et al. Early onset sarcoidosis with aortitis – "juvenile systemic granulomatosis?". *J Rheumatol*. 1990;17:102–106.
18. Scerri L, Cook LJ, Jenkins EA, et al. Familial juvenile systemic granulomatosis (Blau's syndrome). *Clin Exp Dermatol*. 1996;21:445–448.
19. Latkany PA, Jabs DA, Smith Justine R, et al. Multifocal choroiditis in patients with familial juvenile systemic granulomatosis. *Am J Ophthalmol*. 2002;134:897–904.
20. Janot AC, Huscher D, Walker M, et al. Cigarette smoking and male sex are independent and age concomitant risk factors for the development of ocular sarcoidosis in a New Orleans sarcoidosis population. *Sarcoidosis Vasc Diffuse Lung Dis*. 2015;32(2):138–143.
21. James DG. Sarcoidosis. Wyngaarden JB, Smith LH Jr. *Cecil textbook of medicine*. 17th ed. WB Saunders: Philadelphia; 1985.
22. Rossman MD, Thompson B, Frederick M, et al. HLA-DRB1*1101: a significant risk factor for sarcoidosis in blacks and whites. *Am J Hum Genet*. 2003;73:720–735.
23. Crystal RG, Roberts WC, Hunninghake GW, et al. NIH conference. Pulmonary sarcoidosis: a disease characterized and perpetuated by activated lung T-lymphocytes. *Ann Intern Med*. 1981;94:73–94.
24. Hunninghake GW, Crystal RG. Pulmonary sarcoidosis: a disorder mediated by excess helper T-lymphocyte activity at sites of disease activity. *N Engl J Med*. 1981;305:429–434.
25. Meyer KC, Kaminski MJ, Calhoun WJ, et al. Studies of bronchoalveolar lavage cells and fluids in pulmonary sarcoidosis. I. Enhanced capacity of bronchoalveolar lavage cells from patients with pulmonary sarcoidosis to induce angiogenesis in vivo. *Am Rev Respir Dis*. 1989;140:1446–1449.
26. Buechner SA, Winkelmann RK, Banks PM. T-cell subsets in cutaneous sarcoidosis. *Arch Dermatol*. 1983;119:728–732.
27. Chan CC, Wetzig RP, Palestine AG, et al. Immunohistopathology of ocular sarcoidosis: report of a case and discussion of immunopathogenesis. *Arch*

Ophthalmol. 1987;105:1398–1402.
28. Semenzato G, Agostini C, Zambello R, et al. Activated T-cells with immunoregulatory functions at different sites of involvement in sarcoidosis – phenotypic and functional evaluations. *Ann N Y Acad Sci*. 1986;465:56–73.
29. Johns CJ, Schonfeld SA, Scott PP, et al. Longitudinal study of chronic sarcoidosis with low-dose maintenance corticosteroid therapy: outcome and complications. *Ann N Y Acad Sci*. 1986;465:702–712.
30. Mayock RL, Bertrand P, Morrison CE, et al. Manifestations of sarcoidosis: analysis of 145 patients, with a review of nine series selected from the literature. *Am J Med*. 1963;35:67–89.
31. James DG. Ocular sarcoidosis. *Ann N Y Acad Sci*. 1986;465:551–563.
32. Mana J, Marcoval J, Graells J, et al. Cutaneous involvement in sarcoidosis: relationship to systemic disease. *Arch Dermatol*. 1997;133:882–888.
33. Zarei M, Anderson JR, Higgins JN, et al. Cavernous sinus syndrome as the only manifestation of sarcoidosis. *J Postgrad Med*. 2002;48:119–121.
34. Obenauf CD, Shaw HE, Sydnor CF, et al. Sarcoidosis and its ophthalmic manifestations. *Am J Ophthalmol*. 1978;86:648–655.
35. Delaney P. Neurologic manifestations in sarcoidosis: review of the literature, with a report of 23 cases. *Ann Intern Med*. 1977;87:336–345.
36. James DG, Zatouroff MA, Trowell J, et al. Papilloedema in sarcoidosis. *Br J Ophthalmol*. 1967;51:526–529.
37. Sugo A, Seyama K, Yaguchi T, et al. Cardiac sarcoidosis with myopathy and advanced A-V nodal block in a woman with a previous diagnosis of sarcoidosis. *Nihon Kyobu Shikkan Gakkai Zasshi*. 1995;33:1111–1118.
38. Caspers LE, Ebraert H, Makhoul D, Willermain F, Michel O. Broncho-alveolar lavage (BAL) for the diagnosis of sarcoidosis uveitis. *Ocul Immunol Inflamm*. 2014;22(2):102–109.
39. Wilson AG, Hansell DM. Immunologic diseases of the lung.

Armstrong P, Wilson AG, Hansell DM. *Imaging of the diseases of the chest*. Mosby: London; 2000:637–688.
40. Nishino M, Lee KS, Itoh H, et al. The spectrum of pulmonary sarcoidosis: variations of high-resolution CT findings and clues for specific diagnosis. *Eur J Radiol*. 2010;73:66–73.
41. Nakatsu M, Hatabu H, Morikawa K, et al. Large coalescent parenchymal nodules in pulmonary sarcoidosis: "sarcoid galaxy" sign. *AJR Am J Roentgenol*. 2002;178(6):1389–1393.
42. Terasaki H, Fujimoto K, Muller NL, et al. Pulmonary sarcoidosis: comparison of findings of inspiratory and expiratory high-resolution CT and pulmonary function tests between smokers and nonsmokers. *AJR Am J Roentgenol*. 2005;185:333–338.
43. Davies CW, Tasker AD, Padley SP, et al. Air trapping in sarcoidosis on computed tomography: correlation with lung function. *Clin Radiol*. 2000;55:217–221.
44. Sulavik SB, Spencer RP, Weed DA, et al. Recognition of distinctive patterns of gallium-67 distribution in sarcoidosis. *J Nucl Med*. 1990;31(12):1909–1914.
45. Rodrigues T, Rocha E, Barcelos A. Ocular and parotid sarcoidosis – panda sign. *Acta Reumatol Port*. 2014;39(4):345–346.
46. Nosal A, Schleissner LA, Mishkin FS, et al. Angiotensin-I-converting enzyme and gallium scan in noninvasive evaluation of sarcoidosis. *Ann Intern Med*. 1979;90:328–331.
47. Weinreb RN. Diagnosing sarcoidosis by transconjunctival biopsy of the lacrimal gland. *Am J Ophthalmol*. 1984;97:573–576.
48. Rohatgi PK, Ryan JW, Lindeman P. Value of serial measurement of serum angiotensin converting enzyme in the management of sarcoidosis. *Am J Med*. 1981;70:44–50.
49. Power WJ, Neves RA, Rodriguez A, et al. The value of combined serum angiotensin-converting enzyme and gallium scan in diagnosing ocular sarcoidosis. *Ophthalmology*. 1995;102:2007–2011.
50. Jung RS, Mittal BR, Maturu NV, et al. Ocular sarcoidosis: does (18)F-FDG PET/CT have any role? *Clin Nucl Med*.

2014;39(5):464–466.
51. Sobic-Saranovic DP, Grozdic IT, Videnovic-Ivanov J, et al. Responsiveness of FDG PET/CT to treatment of patients with active chronic sarcoidosis. *Clin Nucl Med*. 2013;38(7):516–521.
52. Soussan M, Augier A, Brillet PY, et al. Functional imaging in extrapulmonary sarcoidosis: FDG-PET/CT and MR features. *Clin Nucl Med*. 2014;39(2):e146–59.
53. Akbar JJ, Meyer CA, Shipley RT, et al. Cardiopulmonary imaging in sarcoidosis. *Clin Chest Med*. 2008;29:429–443 [viii].
54. Mana J. Magnetic resonance imaging and nuclear imaging in sarcoidosis. *Curr Opin Pulm Med*. 2002;8:457–463.
55. Crick RP, Hoyle C, Smellie H. The eyes in sarcoidosis. *Br J Ophthalmol*. 1961;45:461–481.
56. Hunter DG, Foster CS. Isolated ocular sarcoidosis – late development of systemic manifestations in uveitis patients. *Invest Ophthalmol Vis Sci*. 1991;32:681.
57. Branson JH, Park JH. Sarcoidosis hepatic involvement: presentation of a case with fatal liver involvement; including autopsy findings and review of the evidence for sarcoid involvement of the liver as found in the literature. *Ann Intern Med*. 1954;40:111–145.
58. Israel HL, Sones M. Selection of biopsy procedures for sarcoidosis diagnosis. *Arch Intern Med*. 1964;113:255–260.
59. Klatskin G. Hepatic granulomata: problems in interpretation. *Ann N Y Acad Sci*. 1976;278:427–432.
60. Beahrs OH, Woolner LB, Kirklin JW, et al. Carcinomatous transformation of mixed tumors of the parotid gland. *AMA Arch Surg*. 1957;75:605–613 [discussion 604–13].
61. Rochlin DB, Enterline HT. Prescalene lymph node biopsies; a report of 142 cases. *Am J Surg*. 1958;96:372–378.
62. Williams TK, Webb WR. Prescalene node biopsy. An evaluation. *Arch Surg*. 1962;84:261–264.
63. Romer F, Paulsen S, Antonius V, et al. Sarcoidosis in a Danish "amt". A retrospective epidemiologic study of sarcoidosis in Ringkobing Amt from 1960 to 1969. *Dan Med Bull*. 1973;20:112–120.

64. Rasmussen SM, Neukirch F. Sarcoidosis: a clinical study with special reference to the choice of biopsy procedure. *Acta Med Scand*. 1976;199:209–216.
65. Carlens E. Biopsies in connection with bronchoscopy and mediastinoscopy in sarcoidosis: a comparison. *Acta Med Scand Suppl*. 1964;425:237–238.
66. Palva T. Mediastinal sarcoidosis. *Acta Otolaryngol Suppl*. 1964;188:258.
67. Koerner SK, Sakowitz AJ, Appelman RI, et al. Transbronchial lung biopsy for the diagnosis of sarcoidosis. *N Engl J Med*. 1975;293:268–270.
68. Koontz CH. Lung biopsy in sarcoidosis. *Chest*. 1978;74:120–121.
69. Crick RP, Hoyle C, Smellie H. The eyes in sarcoidosis. *Br J Ophthalmol*. 1961;45:461–481.
70. Bornstein JS, Frank MI, Radner DB. Conjunctival biopsy in the diagnosis of sarcoidosis. *N Engl J Med*. 1962;267:60–64.
71. Khan F, Wessely Z, Chazin SR, et al. Conjunctival biopsy in sarcoidosis: a simple, safe, and specific diagnostic procedure. *Ann Ophthalmol*. 1977;9:671–676.
72. Solomon DA, Horn BR, Byrd RB, et al. The diagnosis of sarcoidosis by conjunctival biopsy. *Chest*. 1978;74:271–273.
73. Nichols CW, Eagle RC Jr, Yanoff M, et al. Conjunctival biopsy as an aid in the evaluation of the patient with suspected sarcoidosis. *Ophthalmology*. 1980;87:287–291.
74. Karcioglu ZA, Brear R. Conjunctival biopsy in sarcoidosis. *Am J Ophthalmol*. 1985;99:68–73.
75. Nessan VJ, Jacoway JR. Biopsy of minor salivary glands in the diagnosis of sarcoidosis. *N Engl J Med*. 1979;301:922–924.
76. Tremblay A, Stather DR, Maceachern P, et al. A randomized controlled trial of standard vs endobronchial ultrasonography-guided transbronchial needle aspiration in patients with suspected sarcoidosis. *Chest*. 2009;136:340–346.
77. Annema JT, Veselic M, Rabe KF. Endoscopic ultrasound-guided fine-needle aspiration for the diagnosis of sarcoidosis. *Eur Respir J*. 2005;25:405–409.
78. Weinreb RN, Tessler H. Laboratory diagnosis of ophthalmic

sarcoidosis. *Surv Ophthalmol*. 1984;28:653–664.
79. Green WR. Inflammatory disease and conditions of the eye. Spencer WH. *Ophthalmic pathology: an atlas and textbook*. WB Saunders: Philadelphia, PA; 1986.
80. Kojima K, Maruyama K, Inaba T, et al. The CD4/CD8 ratio in vitreous fluid is of high diagnostic value in sarcoidosis. *Ophthalmology*. 2012;119(11):2386–2392.
81. Baarsma GS, La Hey E, Glasius E, et al. The predictive value of serum angiotensin converting enzyme and lysozyme levels in the diagnosis of ocular sarcoidosis. *Am J Ophthalmol*. 1987;104:211–217.
82. Jabs DA, Johns CJ. Ocular involvement in chronic sarcoidosis. *Am J Ophthalmol*. 1986;102:297–301.
83. Karma A, Huhti E, Poukkula A. Course and outcome of ocular sarcoidosis. *Am J Ophthalmol*. 1988;106:467–472.
84. Qazi FA, Thorne JE, Jabs DA. Scleral nodule associated with sarcoidosis. *Am J Ophthalmol*. 2003;136:752–754.
85. Hessen M, Eberhart C, Butler N, et al. Sarcoidosis presenting as scleral nodule. *Ocul Immunol Inflamm*. 2014;22(4):311–313.
86. Khan JA, Hoover DL, Giangiacomo J, et al. Orbital and childhood sarcoidosis. *J Pediatr Ophthalmol Strabismus*. 1986;23:190–194.
87. Collison JM, Miller NR, Green WR. Involvement of orbital tissues by sarcoid. *Am J Ophthalmol*. 1986;102:302–307.
88. Faller M, Purohit A, Kennel N, et al. Systemic sarcoidosis initially presenting as an orbital tumour. *Eur Respir J*. 1996;474–476.
89. Kobak S, Topaloglu A, Öncel G, et al. Sarcoidosis presenting as orbital pseudotumor. *Reumatismo*. 2015;67(2):78–81.
90. Hannanachi Sassi S, Dhouib R, Kanchal F, et al. Orbital tumor revealing a systemic sarcoidosis. *Acta Med Iran*. 2015;53(3):195–197.
91. Kang JJ, Aakalu VK, Lin A, et al. Orbital granuloma annulare as presentation of systemic sarcoidosis. *Orbit*. 2013;32(6):372–374.
92. Foster CS, Tufail F, Waheed NK, et al. Efficacy of etanercept in preventing relapse of uveitis controlled by methotrexate. *Arch Ophthalmol*. 2003;121:437–440.

93. Smith JA, Thompson DJ, Whitcup SM, et al. A randomized, placebo-controlled, double-masked clinical trial of etanercept for the treatment of uveitis associated with juvenile idiopathic arthritis. *Arthritis Rheum*. 2005;53:18–23.
94. Gentile RC, Berinstein DM, Liebmann J, et al. High-resolution ultrasound biomicroscopy of the pars plana and peripheral retina. *Ophthalmology*. 1998;105:478–484.
95. Gass JD, Olson CL. Sarcoidosis with optic nerve and retinal involvement. *Arch Ophthalmol*. 1976;94:945–950.
96. Hoogstede HA, Copper AC. A case of macular subretinal neovascularisation in chronic uveitis probably caused by sarcoidosis. *Br J Ophthalmol*. 1982;66:530–535.
97. Sanders MD, Shilling JS. Retinal, choroidal, and optic disc involvement in sarcoidosis. *Trans Ophthalmol Soc U K*. 1976;96:140–144.
98. Suryaprakash V, Kanungo S, Biswas J. Peripheral choroidal nodules in a case of proven systemic sarcoidosis. *Indian J Ophthalmol*. 2013;61(6):291–292.
99. Chen L, Xu G. Extensive choroidal infiltrates in choroidal biopsy proven ocular sarcoidosis. *Retin Cases Brief Rep*. 2013;7(1):69–70.
100. Letocha CE, Shields JA, Goldberg RE. Retinal changes in sarcoidosis. *Can J Ophthalmol*. 1975;10:184–192.
101. Kiryu J, Kita M, Tanabe T, et al. Pars plana vitrectomy for cystoid macular edema secondary to sarcoid uveitis. *Ophthalmology*. 2001;108:1140–1144.
102. Kiryu J, Kita M, Tanabe T, et al. Pars plana vitrectomy for epiretinal membrane associated with sarcoidosis. *Jpn J Ophthalmol*. 2003;47:479–483.
103. Sonoda KH, Enaida H, Ueno A, et al. Pars plana vitrectomy assisted by triamcinolone acetonide for refractory uveitis: a case series study. *Br J Ophthalmol*. 2003;87:1010–1014.
104. Takayama K, Tanaka A, Shibata M, et al. Evaluation of microincision vitrectomy surgery using wide-viewing system for complications with ocular sarcoidosis. *Medicine (Baltimore)*. 2015;94(7):e559.
105. Doxanas MT, Kelley JS, Prout TE. Sarcoidosis with neovascularization of the optic nerve head. *Am J*

Ophthalmol. 1980;90:347–351.
106. Duker JS, Brown GC, McNamara JA. Proliferative sarcoid retinopathy. *Ophthalmology*. 1988;95:1680–1686.
107. Gould H, Kaufman HE. Sarcoid of the fundus. *Arch Ophthalmol*. 1961;65:453–456.
108. Spalton DJ, Sanders MD. Fundus changes in histologically confirmed sarcoidosis. *Br J Ophthalmol*. 1981;65:348–358.
109. Kelley JS, Green WR. Sarcoidosis involving the optic nerve head. *Arch Ophthalmol*. 1973;89:486–488.
110. Sharma A, Sagar V, Singla V, et al. Inflammatory optic disc edema due to sarcoidosis mimicking malignant hypertension. *Int J Rheum Dis*. 2014; 10.1111/1756-185X [e-pub ahead of print].
111. Yokoi K, Oshita M, Goto H. Retinal macroaneurysm associated with ocular sarcoidosis. *Jpn J Ophthalmol*. 2010;54(5):392–395.
112. Ing EB, Garrity JA, Cross SA, et al. Sarcoid masquerading as optic nerve sheath meningioma. *Mayo Clin Proc*. 1997;72:38–43.
113. Katz B. Disc edema, transient obscurations of vision, and a temporal fossa mass. *Surv Ophthalmol*. 1991;36:133–139.
114. Mansour AM. Sarcoid optic disc edema and optociliary shunts. *J Clin Neuroophthalmol*. 1986;6:47–52.
115. Mizuno K, Takahashi J. Sarcoid cyclitis. *Ophthalmology*. 1986;93:511–517.
116. Wakefield D, Zierhut M. Controversy: ocular sarcoidosis. *Ocul Immunol Inflamm*. 2010;18:5–9.
117. Agrawal R, Gonzalez-Lopez JJ, Meier F, et al. Ocular and systemic features of sarcoidosis and correlation with the International Workshop for Ocular Sarcoidosis diagnostic criteria. *Sarcoidosis Vasc Diffuse Lung Dis*. 2015;32(3):237–245.
118. Dana MR, Merayo-Lloves J, Schaumberg DA, et al. Prognosticators for visual outcome in sarcoid uveitis. *Ophthalmology*. 1996;103:1846–1853.
119. Miserocchi E, Modorati G, Di Matteo F, et al. Visual outcome in ocular sarcoidosis: retrospective evaluation of risk factors. *Eur J Ophthalmol*. 2011;21(6):802–810.
120. Gedalia A, Molina JF, Ellis GS, et al. Low-dose methotrexate

therapy for childhood sarcoidosis. *J Pediatr*. 1997;130:25–29.
121. Kaye O, Palazzo E, Grossin M, et al. Low-dose methotrexate: an effective corticosteroid-sparing agent in the musculoskeletal manifestations of sarcoidosis. *Br J Rheumatol*. 1995;34:642–644.
122. Lower EE, Baughman RP. Prolonged use of methotrexate for sarcoidosis. *Arch Intern Med*. 1995;155:846–851.
123. Mathur A, Kremer JM. Immunopathology, rheumatic features, and therapy of sarcoidosis. *Curr Opin Rheumatol*. 1992;4:76–80.
124. Samson CM, Waheed N, Baltatzis S, et al. Methotrexate therapy for chronic noninfectious uveitis: analysis of a case series of 160 patients. *Ophthalmology*. 2001;108:1134–1139.
125. Taylor SR, Habot-Wilner Z, Pacheco P, et al. Intraocular methotrexate in the treatment of uveitis and uveitic cystoid macular edema. *Ophthalmology*. 2009;116:797–801.
126. Muller-Quernheim J, Kienast K, Held M, et al. Treatment of chronic sarcoidosis with an azathioprine/prednisolone regimen. *Eur Respir J*. 1999;14:1117–1122.
127. Deuter CME, Doycheva D, Stuebiger N, et al. Mycophenolate sodium for immunosuppressive treatment in uveitis. *Ocul Immunol Inflamm*. 2009;17:415–419.
128. Kempen JH, Altaweel MM, Holbrook JT, et al. The multicenter uveitis steroid treatment trial: rationale, design, and baseline characteristics. *Am J Ophthalmol*. 2010;149:550–561.e10.
129. Bhat P, Cervantes-Castaneda RA, Doctor PP, et al. Mycophenolate mofetil therapy for sarcoidosis-associated uveitis. *Ocul Immunol Inflamm*. 2009;17:185–190.
130. Galor A, Perez VL, Hammel JP, et al. Comparison of antimetabolite drugs as corticosteroid-sparing therapy for noninfectious ocular inflammation. *Ophthalmology*. 2008;115:1826–1832.
131. Baughman RP, Lower EE. Leflunomide for chronic sarcoidosis. *Sarcoidosis Vasc Diffuse Lung Dis*. 2004;21:43–48.
132. Reiff A, Takei S, Sadeghi S, et al. Etanercept therapy in children with treatment-resistant uveitis. *Arthritis Rheum*. 2001;44:1411–1415.

133. Baughman RP, Bradley DA, Lower EE. Infliximab in chronic ocular inflammation. *Int J Clin Pharmacol Ther*. 2005;43:7–11.
134. Galor A, Perez VL, Hammel JP, et al. Differential effectiveness of etanercept and infliximab in the treatment of ocular inflammation. *Ophthalmology*. 2006;113:2317–2323.
135. Tynjala P, Lindahl P, Honkanen V, et al. Infliximab and etanercept in the treatment of chronic uveitis associated with refractory juvenile idiopathic arthritis. *Ann Rheum Dis*. 2007;66:548–550.
136. Diaz-Llopis M, Garcia-Delpech S, Salom D, et al. Adalimumab therapy for refractory uveitis: a pilot study. *J Ocul Pharmacol Ther*. 2008;24:351–361.
137. Schmeling H, Horneff G. Etanercept and uveitis in patients with juvenile idiopathic arthritis. *Rheumatology (Oxford)*. 2005;44:1008–1011.
138. Hashkes PJ, Shajrawi I. Sarcoid-related uveitis occurring during etanercept therapy. *Clin Exp Rheumatol*. 2003;21:645–646.
139. Riancho-Zarrabeitia L, Calvo-Río V, Blanco R, et al. Anti-TNF-α therapy in refractory uveitis associated with sarcoidosis: multicenter study of 17 patients. *Semin Arthritis Rheum*. 2015;45(3):361–368.
140. Lim LL, Fraunfelder FW, Rosenbaum JT. Do tumor necrosis factor inhibitors cause uveitis? A registry-based study. *Arthritis Rheum*. 2007;56:3248–3252.

82

Intermediate Uveitis

Phoebe Lin, Glenn J. Jaffe

Introduction

Intermediate uveitis is defined anatomically, according to the Standardized Uveitis Nomenclature working group, as intraocular inflammation in which the primary site is the vitreous, but it commonly involves the peripheral retina as well.[1] The origin of the inflammatory cells includes the ciliary body pars plana, the peripheral retinal vessels, and the peripheral choroid. Previously used terminology for this entity includes pars planitis, peripheral uveitis, peripheral cyclitis, hyalitis, and vitritis. The term “pars planitis” now specifically refers to a subcategory of idiopathic intermediate uveitis characterized by the presence of snowbanks

and snowballs, which will be described in more detail below.

Epidemiology and Demographics

Because the currently used nomenclature for uveitis was agreed upon in 2005, prevalence and incidence figures for this anatomic category of uveitis are sparse. Although various groups have reported the frequency of intermediate uveitis in their uveitis practices, ranging from 4 to 15.4%, these figures are subject to referral bias since the reports originate from tertiary care referral clinics.[2–6] In pediatric uveitis, it accounts for up to 25% of cases.[7,8] The overall population prevalence of different types of uveitis based on anatomic location, including intermediate uveitis, has been investigated in several population studies since 2005. Gritz and Wong found a prevalence ratio for intermediate uveitis of 4.0 per 100, 000 persons in a cross-sectional retrospective study using a database of individuals in northern California receiving care through a single large health-maintenance organization.[9] The incidence was 1.5 per 100, 000 person-years. These figures were reported with the stipulation that the prevalence may have been underestimated because a significant proportion of included patients did not have dilated fundus examinations, and the anatomic uveitis location was, therefore, unknown. Another study utilizing the Veterans Affairs database in the Pacific Northwest region found that the prevalence of intermediate uveitis was approximately 3.3 per 100 ,000 persons.[10] The annual incidence of pars planitis in Olmstead County, Minnesota, was 2.08 per 100, 000 persons.[11]

Although intermediate uveitis can occur at any age, it tends to occur in a younger age range. Average age of onset was 31 years (range 8–64 years) in one study,[12] and 30 years (range 6–76 years) in another.[13] There appears to be no gender predilection for this anatomic subtype of uveitis, although certain entities that can cause intermediate uveitis, such as sarcoidosis, have a strong female bias.[14] In certain uveitis practices, such as that reported by Thorne and colleagues, intermediate uveitis appears to be slightly more common in women (66.4%).[13] Racial predilection likely depends on the etiology, but there appears to be no race preference in pars

planitis.

Presentation and Clinical Findings

The most common symptoms of intermediate uveitis include blurry vision and floaters, whereas pain, redness, and photophobia are less common than in other types of uveitis. Although typically bilateral over time (74.5–80% bilateral),[3,12,13,15] it is frequently asymmetric and may begin unilaterally. Findings on clinical examination at onset include anterior vitreous cells or diffuse vitreous haze, and, to a lesser extent, anterior chamber involvement. Vitreous haze is graded on a scale of 0–4+ based on the level of optic nerve and retinal vessel obscuration.[16] Snowballs (see below for discussion on histopathology) are whitish inflammatory vitreous opacities in clusters frequently found in the inferior vitreous cavity (Fig. 82.1). Snowbanks are identified as whitish-gray confluent preretinal membranes most commonly seen along the inferior pars plana, and peripheral retina (Fig. 82.2A). Over time, these may develop into organized fibrovascular membranes that are prone to vitreous hemorrhage and retinal detachment. The vascular component of this snowbank is continuous with the retinal vessels (Fig. 82.2B). Commonly, a peripheral vasculitis manifested by perivascular sheathing is seen in intermediate uveitis and may indicate an increased probability of associated systemic disease.[12] According to one study, periphlebitis in the setting of intermediate uveitis was associated with an increased rate of multiple sclerosis (MS) or optic neuritis (Fig. 82.3).[17] It is important to note that sarcoidosis can also present as an isolated periphlebitis or as granulomatous inflammation in the form of snowballs. Periphlebitis in sarcoidosis can present with a wide spectrum of appearances, from scant focal periphlebitis to exudative candle-wax drippings (taches de bougie) (Fig. 82.4). Yellowish peripheral punched-out chorioretinal lesions that might represent active or old choroidal granulomas are highly suspicious for sarcoidosis, although once these are present, the anatomical designation is panuveitis rather than intermediate uveitis. Obliterative peripheral vasculitis may result in peripheral neovascularization and resultant vitreous hemorrhage (Fig. 82.5). Cystoid macular edema (CME) is a common finding, occurring in

over 40% of individuals at diagnosis of intermediate uveitis (Fig. 82.6).[13] Campbell et al. demonstrated that peripheral vascular leakage (PVL) seen on ultra-wide-field fluorescein angiography in eyes with uveitis, including those with intermediate uveitis, may be associated with higher rates of ocular complications such as CME, at least at the time of discovery of the PVL.[18] Clinically apparent optic nerve edema also occurs in a small percentage of patients with intermediate uveitis. Other noteworthy complications include retinoschisis (Fig. 82.7), which occurs in pars planitis frequently, and exudative retinal detachment.[19]

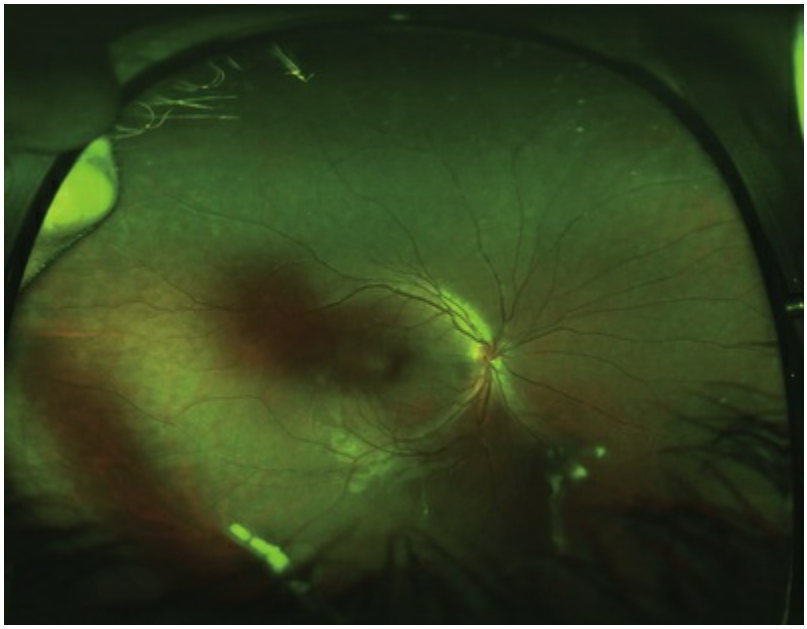

FIG. 82.1 Snowballs seen in the inferior and mid-vitreous cavity in a 14-year-old boy with pars planitis.

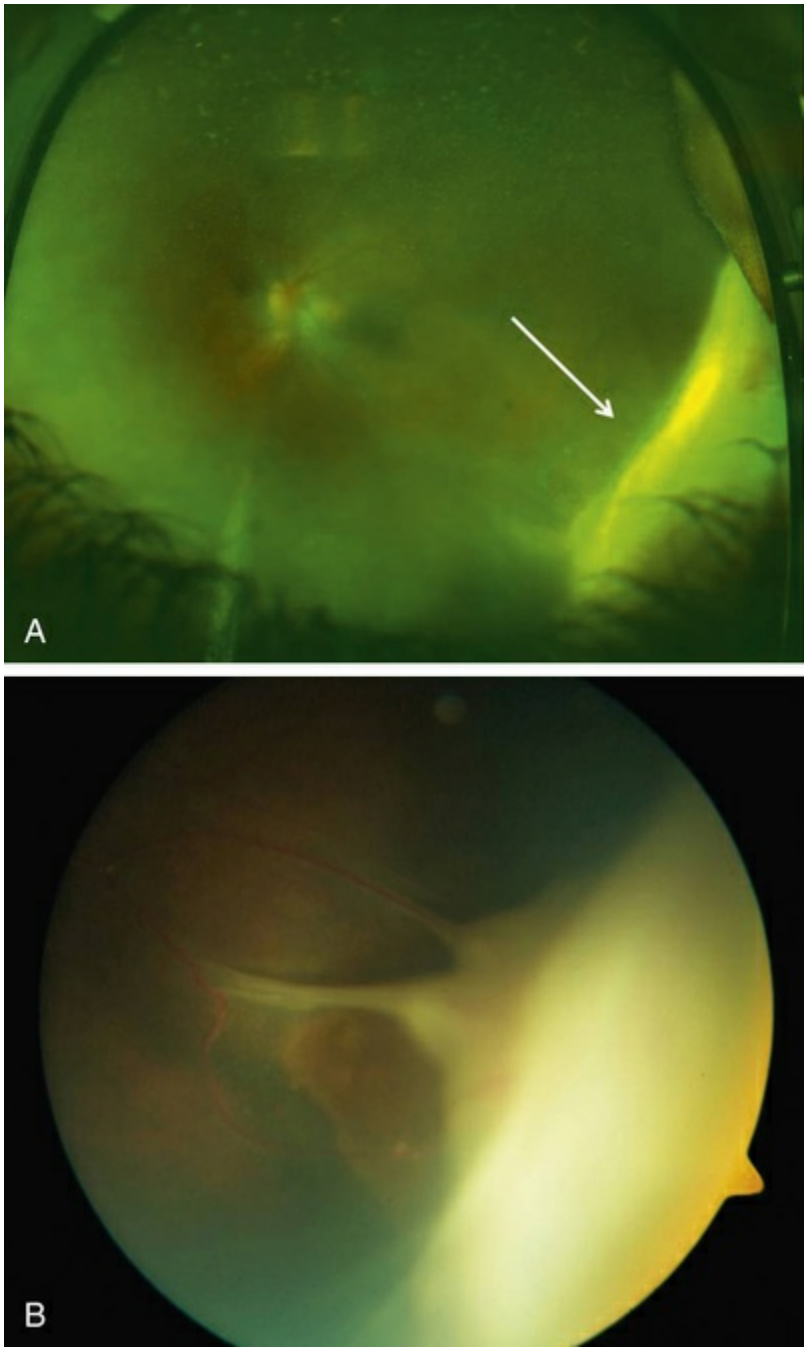

FIG. 82.2 Inferotemporal pars plana snowbank in a patient with idiopathic unilateral pars planitis. (A) Ultrawide-field fundus image. Snowbank noted by *white arrow*. (B) Retinal vessel (*red arrow*) incorporated into snowbank in magnified view of snowbank from same patient as in panel A.

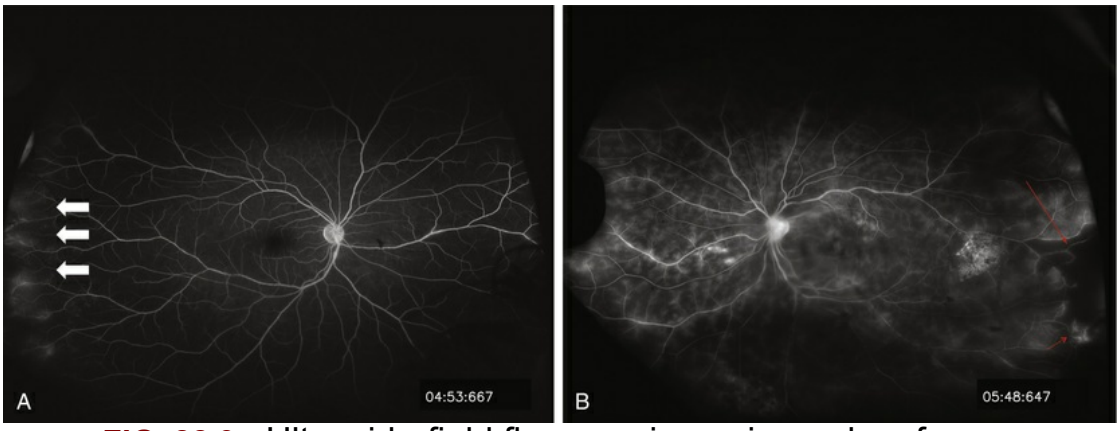

FIG. 82.3 Ultrawide-field fluorescein angiography of (A) right and (B) left eyes of a 31-year-old woman presenting with bilateral asymmetric intermediate uveitis, who was later diagnosed with multiple sclerosis. In panel A *white arrows* show peripheral vascular leakage. In panel B *red arrows* show peripheral nonperfusion (*long solid arrow*) and early retinal neovascularization (*short dotted arrow*). Panel B also demonstrates diffuse retinal venular leakage.

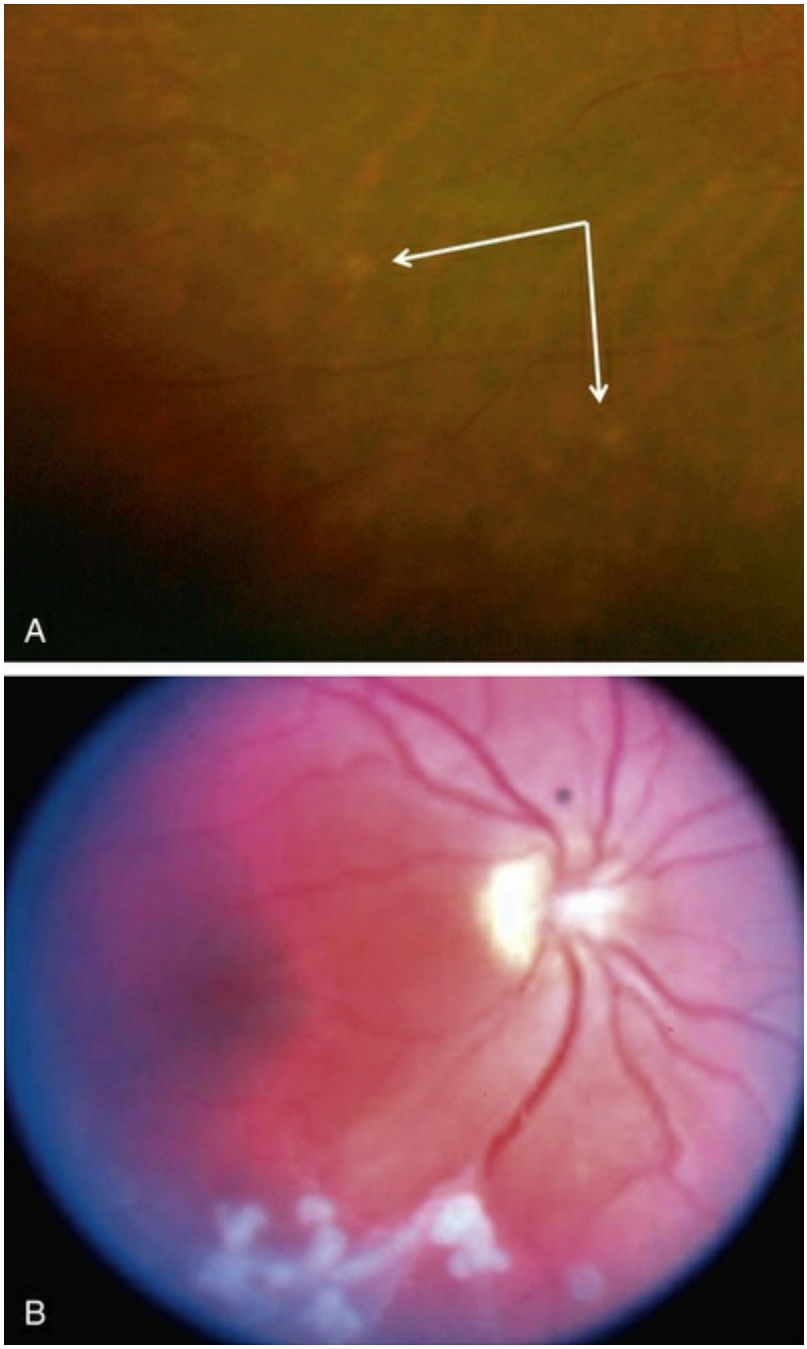

FIG. 82.4 (A) Focal periphlebitis (*arrows*) in a patient with sarcoid intermediate uveitis. (B) Granulomatous exudative periphlebitis (candle-wax drippings or taches de bougie in intermediate uveitis due to sarcoidosis).

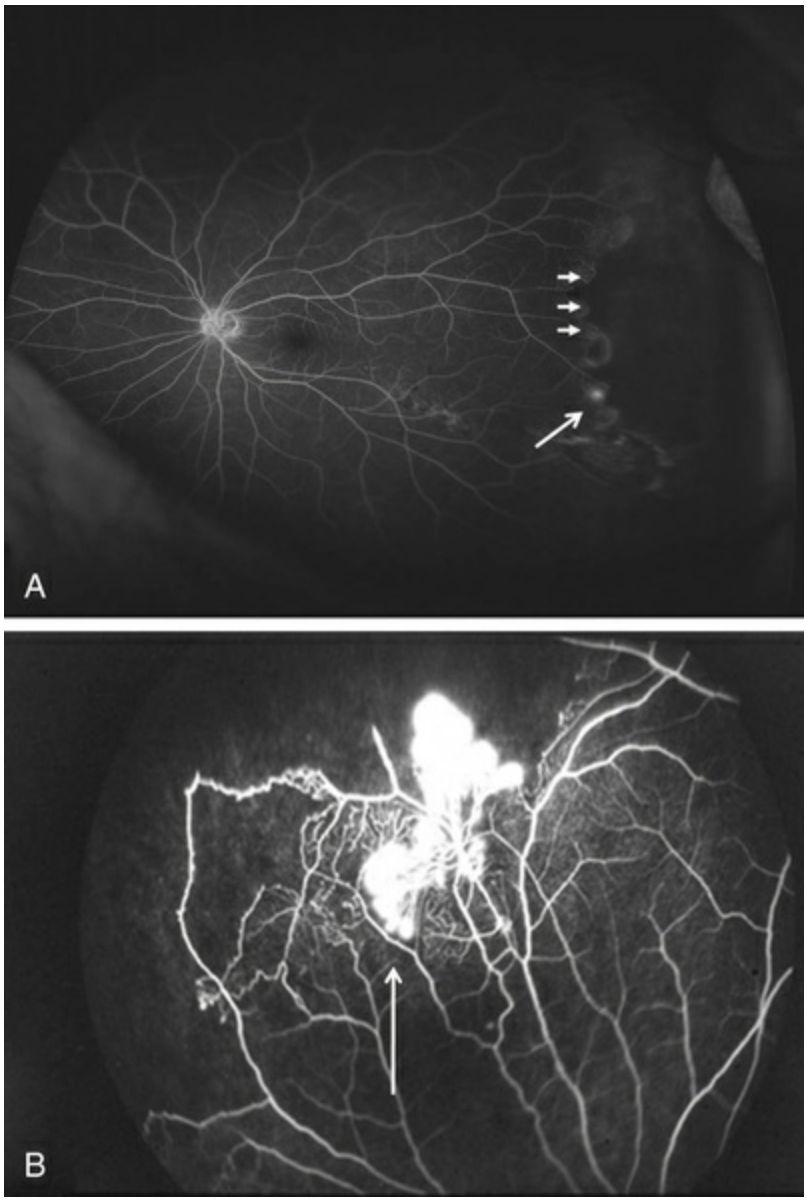

FIG. 82.5 Peripheral nonperfusion and neovascularization (NV) in 2 patients with sarcoidosis-associated intermediate uveitis. (A) Wide-field fluorescein angiography showing severe peripheral nonperfusion (*short arrows*) and an early neovascular tuft (*long arrow*). (B) Advanced peripheral NV (*arrow*).

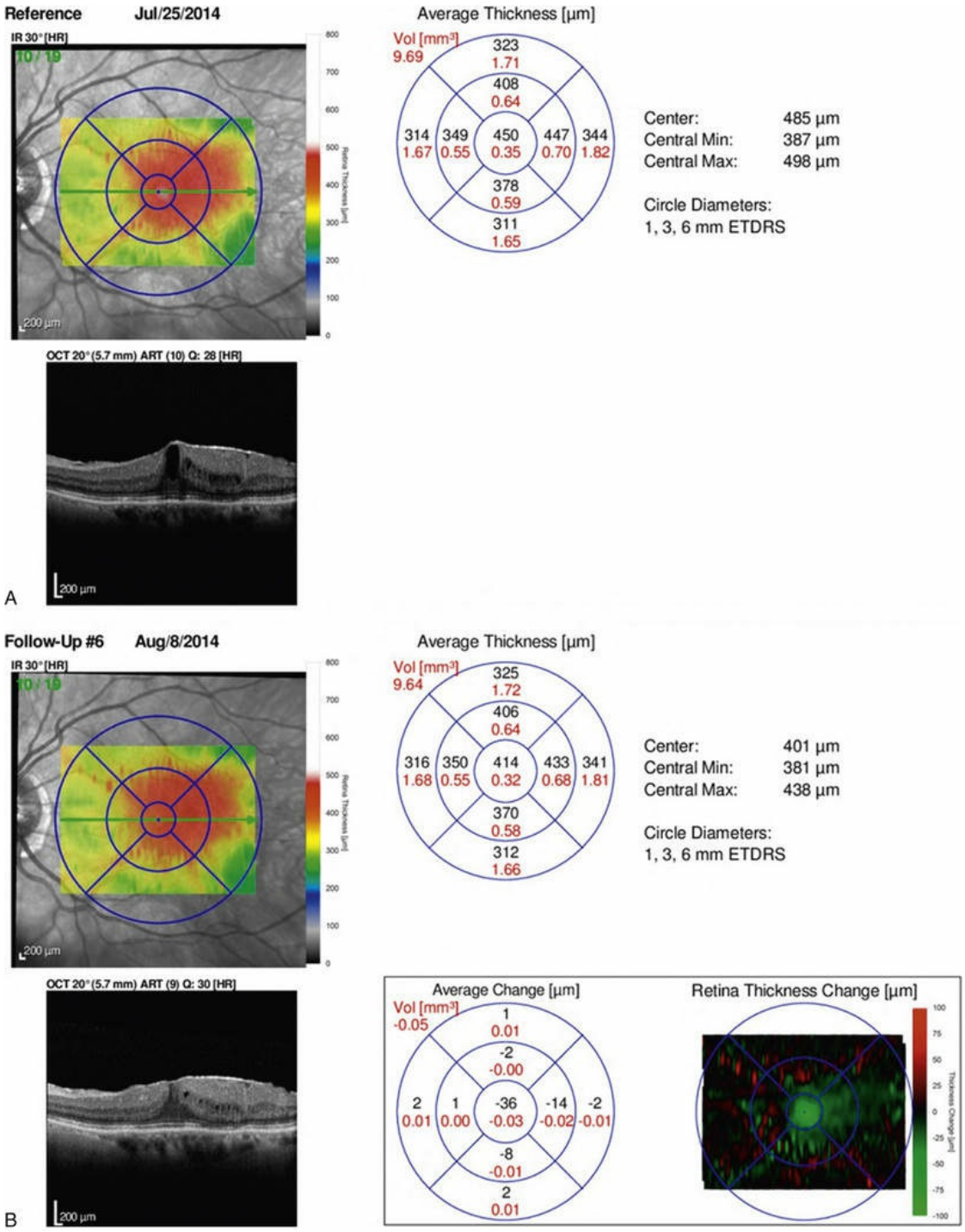

FIG. 82.6 Spectral domain optical coherence tomography demonstrating unilateral cystoid macular edema in a patient with intermediate uveitis before (A) and after (B) treatment with a posterior sub-Tenon Kenalog injection. This patient also has an epiretinal membrane causing a stellate configuration of thickening of the retina.

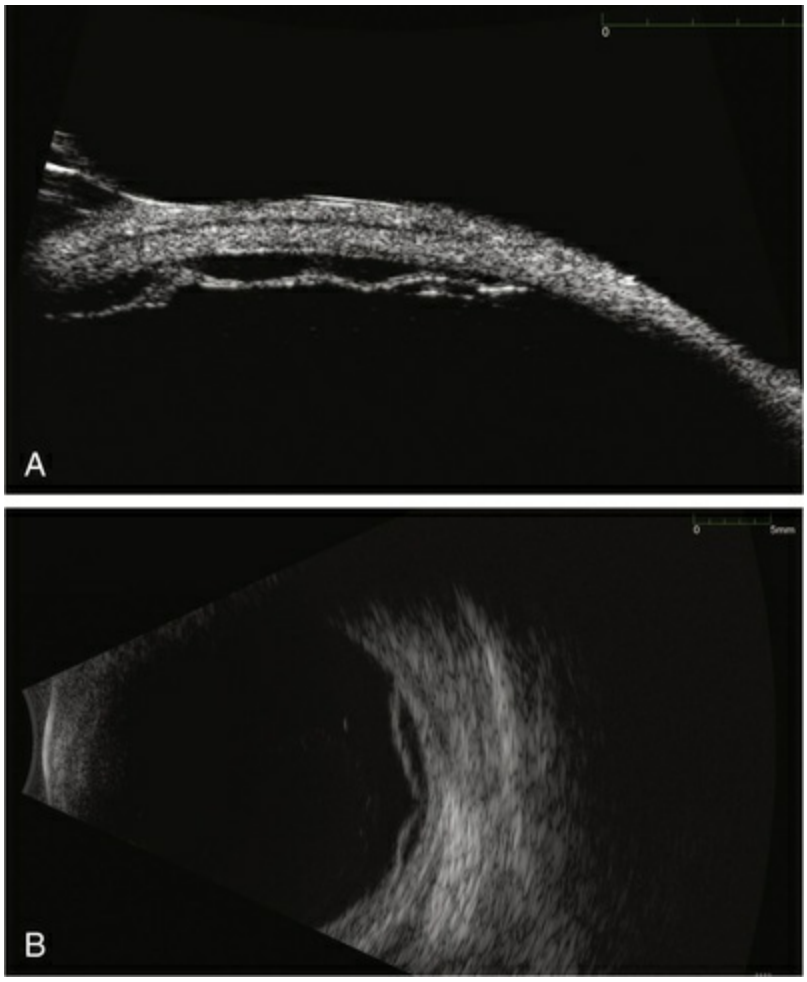

FIG. 82.7 (A) Pars plana snowbank and schisis demonstrated by ultrasound biomicroscopy, and retinoschisis on B-scan ultrasound (B), both from the same 7-year-old boy with pars planitis.

Imaging

Although the majority of cases of intermediate uveitis are diagnosed by clinical examination, various imaging modalities give useful adjunctive information to guide diagnosis and management. For instance, in the setting of media opacity from cataract, ultrasound biomicroscopy (UBM) can be used to detect pars plana exudates (Fig. 82.7). Identification of cyclitic membranes by UBM can be of great value in preoperative planning. B-scan ultrasonography can be used to diagnose and measure macular thickening with a great degree of accuracy, sensitivity, and specificity in the setting of media opacity or intolerance to

fluorescein angiography and optical coherence tomography (OCT).[20] B-scan can also be used to document the extent of retinoschisis (Fig. 82.7). Fluorescein angiography is useful to detect CME, vasculitis, peripheral nonperfusion, and peripheral neovascularization (see Fig. 82.3). OCT is important to identify and follow CME as a gauge of disease activity in intermediate uveitis.[21] In some cases, concentric macular retinal thickening without frank CME, as determined by OCT, can be used to monitor response to treatment.[22]

Differential Diagnosis and Workup

The cause of intermediate uveitis can be determined by investigating the presence of systemic findings or historical clues. Although the vast majority of cases are idiopathic (nearly 70%),[23] the most common known inflammatory etiologies include sarcoidosis and MS, whereas infectious causes can include syphilis, Lyme disease, and tuberculosis (Box 82.1). Pars planitis is, by definition, idiopathic intermediate uveitis characterized by the presence of snowbanks and snowballs. Thorne et al. found that 36% of their intermediate uveitis patients had pars planitis.[13] In one study by Rodriguez et al., 22.2% of cases of intermediate uveitis at a referral center were due to sarcoidosis, whereas 8.0% were due to MS.[23] One out of 112 cases at this center was due to Lyme disease. Two other studies, 14.8 and 16.2%, respectively, had MS.[17,24]

Box 82.1

Differential Diagnosis of Intermediate Uveitis

Infectious

- Lyme disease (*Borrelia burgdorferi*)
- Syphilis (*Treponema pallidum*)
- Toxocariasis (*Toxocara canis*)
- Toxoplasmosis (*Toxoplasma gondii*)

- Tuberculosis (*Mycobacterium tuberculosis*)
- Cat-scratch disease (*Bartonella, Rochalimaea*)
- Whipple's disease (*Tropheryma whippelli*)
- HTLV-1
- Hepatitis C
- Epstein–Barr virus
- Endophthalmitis (*Propionibacterium acnes*, indolent fungal infection)

Immune

- Sarcoidosis
- Multiple sclerosis
- Inflammatory bowel disease
- Behçet disease
- Idiopathic
- Pars planitis

Masquerade

- Lymphoma (usually B-cell, NHL)
- Leukemia
- Amyloidosis
- Other neoplasms: retinoblastoma, uveal melanoma
- Irvine–Gass syndrome (CME with subtle inflammation)

HTLV-1, human T-lymphotropic virus-1; NHL, non-Hodgkin's lymphoma; CME, cystoid macular edema.

Tests that warrant investigation in all patients with intermediate uveitis include rapid plasma reagin and fluorescent treponemal antibody absorption test to test for syphilis, chest radiography, angiotensin-converting enzyme (ACE), and tuberculin skin test with anergy panel to evaluate sarcoidosis and tuberculosis. If clinical suspicion is high for sarcoidosis in the setting of a negative ACE and chest radiograph, one should consider a gallium scan, pulmonary function tests, or a chest computed tomography scan. A careful review of systems should be performed to determine if there are risks associated with MS, including urinary retention, neurologic weakness or symptoms, or evidence of previous optic neuritis (Table 82.1).[25] In a significant number of patients, as is the case in our experience, pars planitis can be the first manifestation of a central nervous system demyelinating process, so it is important to elicit the appropriate history and keep a low threshold for the diagnosis of MS. Because there is growing evidence that early treatment of MS with systemic interferon therapy may reduce long-term disability, it is important to consider this systemic association seriously upon initial presentation.[26–28] Evaluation by a neurologist, magnetic resonance imaging (MRI) of the brain, and cerebrospinal fluid studies should be considered in new-onset intermediate uveitis, even without the above symptoms, given that early disease can by asymptomatic.

TABLE 82.1
Systemic Symptoms and Signs of Multiple Sclerosis by Site

Anatomic Location	Symptoms	Signs
Cerebrum	Cognitive impairment	Deficits in attention, reasoning, and executive function; dementia (late)
	Depression	Flat affect
	Hemisensory and motor	Upper motor neuron signs
Optic nerve	Unilateral vision loss	rAPD, Uhthoff phenomenon (exacerbation in hot temperatures), Pulfrich effect (difficulty judging path of oncoming cars)
Cerebellum	Tremor	Action tremor
	Clumsiness and poor balance	Gait ataxia

Brainstem	Diplopia, oscillopsia	INO, nystagmus
	Vertigo	
	Impaired swallowing	
	Impaired speech	
Spinal cord	Weakness	
	Stiffness and painful spasms	Spasticity, Lhermitte's sign (painful electric-shock sensation down spine upon neck flexion)
	Bladder dysfunction	
	Retention	
	Frequency, urgency	
Other	Pain	
	Fatigue	
	Temperature sensitivity and exercise intolerance	

INO, internuclear ophthalmoplegia; rAPD, relative afferent papillary defect.

Modified from Compston A, Coles A. Multiple sclerosis. Lancet 2008;372:1502–17.

If there is a history of exposure to deer or ticks, especially if the patient lives or travels in an endemic area, and there is an associated history of a target lesion or systemic flu-like symptoms, then *Borrelia burgdorferi* antibody should be tested. Exposure to cats might prompt serum antibody testing for *Bartonella*.[29] In the elderly population, intraocular lymphoma should be suspected and there should be a lower threshold to perform diagnostic vitrectomy, especially if there is limited response to corticosteroids.[30,31] If intraocular lymphoma is highly suspected, a lumbar puncture for cytologic evaluation of the cerebrospinal fluid and neuroimaging are adjunctive diagnostic tests to consider. Bilateral pars planitis has been found in patients who have human T-cell lymphotropic virus type 1 (HTLV-1) infection, which is endemic in Japan, the Caribbean islands, parts of Central Africa, and South America.[32] The latter can be diagnosed with serologic testing for antibodies against HTLV-1. Gastrointestinal disturbances associated with a pars planitis-like clinical presentation should prompt referral to a gastroenterologist since it has been reported in association with inflammatory bowel disease and Whipple's disease.[33,34] Other masquerade syndromes, such as intermediate uveitis secondary to tumor necrosis from retinoblastoma or uveal melanoma or even metastasis from other types of systemic cancer, must be evaluated in the appropriate clinical settings.[35] Finally, mild vitritis and CME in the setting of recent cataract surgery should prompt consideration of pseudophakic CME. One should consider indolent

endogenous or exogenous endophthalmitis as a possibility if there is a poor response or worsening with corticosteroids in the setting of the appropriate risk factors, such as immunocompromised state or recent intraocular surgery.

Histopathology and Pathophysiology

On histopathologic examination, snowballs are isolated vitreous granulomas consisting of lymphocytes, macrophages, epithelioid cells, and multinucleated giant cells.[36] Snowbanks consist of collapsed vitreous collagen, membranous fibroglial cells, blood vessels, and lymphocytes, as well as hyperplastic pars plana nonpigmented epithelium.[37] Periphlebitis is denoted by lymphocytic infiltration and cuffing of the peripheral retinal venules.[36] Because the term "intermediate uveitis" is an anatomic designation, one should avoid assigning a single etiologic or pathophysiologic process to it given that various systemic diseases and infectious processes can result in inflammation in this anatomical location. The pathogenesis of the autoimmune causes of intermediate uveitis involves overlapping principles, as well as some distinguishing characteristics, and will be discussed here for pars planitis and sarcoidosis.

Pars Planitis

Although it is thought that noninfectious intermediate uveitis arises from an autoimmune response, the antigenic stimulus has not yet been clearly identified. Bora et al. described a novel 36 kDa nucleopore complex protein that was found to be six to eight times higher in the sera of 81% of active pars planitis patients compared with controls ($p<.05$).[38] The exact function of this protein and its role in the pathogenesis of pars planitis are unknown, although there are indications that other nucleopore complex proteins may be involved in myeloid leukemogenesis and autoantibody formation.[39,40] Wetzig et al. found that endstage idiopathic intermediate uveitis in a familial case of bilateral intermediate uveitis was characterized immunopathologically by a predominance of $CD4^+$ T lymphocytes and overwhelming

predominance of glial cells in the pars plana snowbank; the latter is a characteristic unique to this type of uveitis.[41] It has been proposed that pars planitis represents a similar pathoetiologic entity as MS, although with expression either isolated to the eye or starting in the eye.[42] Indeed, patients with MS have increased circulating $CD54^+$ lymphocytes and antibodies that recognize glial proteins.[43] Raja et al.[24] discovered that a human leukocyte antigen (HLA)-DR15 allele, which is known to be associated with MS, was significantly associated with pars planitis compared with controls (odds ratio, 2.86; p=0.004). Although no specific autoantigen has been clearly determined, components of vitreous, in addition to the glial elements mentioned above, have been implicated. Circulating lymphocytes isolated from pars planitis patients appear to proliferate in response to type II collagen.[37] Furthermore, Hultsch produced a clinical entity similar to pars planitis by giving owl monkeys multiple intravitreal injections of hyaluronic acid.[44]

Interleukin (IL-)8, a cytokine that is involved in neutrophil and T-lymphocyte recruitment, and soluble intercellular adhesion molecule 1 (sICAM-1), which is expressed at sites of inflammation to aid in leukocyte adhesion and migration, were elevated in the blood of patients with intermediate uveitis compared to controls. Furthermore, elevated sICAM-1 and IL-8 were associated with development of systemic disease. Elevated IL-8 was associated with signs of inflammatory activity such as periphlebitis and the presence of vitreous exudates. Rather than explaining the pathogenesis of this ocular condition, these markers may be indicators of systemic disease or activity, even in the absence of systemic symptoms.[45,46]

Sarcoidosis

Sarcoidosis is also thought to be a $CD4^+$ T-lymphocyte-mediated process in the eye and in other actively affected tissues. Efforts to elucidate an infectious cause for sarcoidosis have met with little success. Patients with active sarcoidosis have a predominantly Th1 cytokine profile with elevated levels of IL-2 and interferon-gamma, and diminished levels of IL-4. Despite the predominance of $CD4^+$ T cells in ocular tissues affected by the disease, elevated peripheral

levels of immunoglobulin, B-cell hyperactivity in the peripheral blood, and a loss of delayed-type hypersensitivity to the tuberculin skin test (anergy) argues for an unusual partitioning of the immune response.[43,47] We have found that approximately 50% of patients with sarcoid-associated uveitis are anergic to delayed-type hypersensitivity testing.[48] The latter observations underline the importance of an anergy panel to accompany a tuberculin skin test in the initial workup of intermediate uveitis. HLA associations in sarcoidosis also differ from pars planitis and have not been clearly elucidated. In one study by Rossman et al., ocular sarcoidosis was associated with the HLA-DRB1*0401 allele in both blacks and whites.[49]

Treatment

Unilateral Disease

Once an infectious cause has been ruled out, the primary treatment of choice is corticosteroids. If an underlying systemic condition is suspected, then systemic treatment with appropriate referral to a rheumatologist or infectious disease specialist is warranted. For unilateral noninfectious intermediate uveitis in the absence of systemic disease, periocular corticosteroids are initiated (Fig. 82.8), although some clinicians utilize systemic steroids. In our practice, posterior sub-Tenon Kenalog is given at 40 mg/mL, 1 mL total. If there is little to no response in 3–4 weeks, a second injection can be given, or alternatively, if the patient is pseudophakic and does not have glaucoma, an intravitreal injection of preservative-free triamcinolone acetonide can be offered. If smoldering uveitic CME is present without other evidence of active inflammatory disease, a trial of topical corticosteroids in combination with nonsteroidal antiinflammatory drops can be applied prior to considering either periocular or intravitreal corticosteroids.[50] Topical difluprednate is also very effective in treating uveitic CME associated with intermediate uveitis, but causes a higher rate of elevated intraocular pressure than prednisolone acetate and was as high as 50% in pediatric uveitis patients in one study.[51] Alternatively, bevacizumab has been investigated for its efficacy in treating uveitic CME. In a

study comparing intravitreal bevacizumab with intravitreal triamcinolone acetonide for uveitic CME, after removing the effect on cataract formation the triamcinolone group appeared to have significantly better visual acuity outcomes. Triamcinolone was also more effective in reducing macular thickness than bevacizumab.[52]

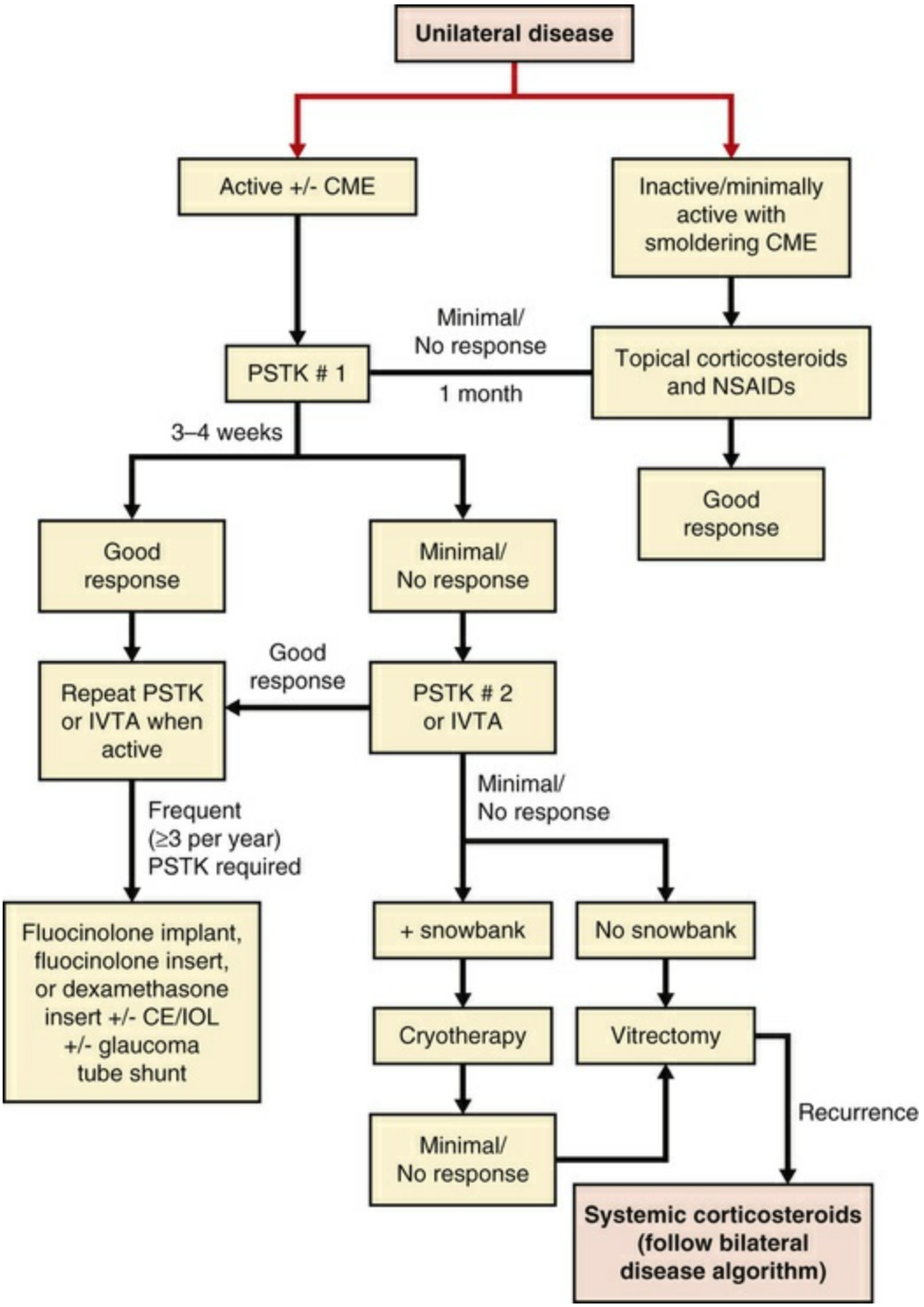

FIG. 82.8 Treatment algorithm for unilateral disease. CME, cystoid macular edema; PSTK, posterior sub-Tenon Kenalog; IVTA, intravitreal triamcinolone acetonide; CE/IOL, cataract extraction with intraocular lens implant; NSAIDs, nonsteroidal antiinflammatory drugs.

If the patient has benefited from periocular or intraocular corticosteroid, but has documented recurrence when the corticosteroids have waned, then a corticosteroid intravitreal implant can be considered, especially if the patient is already pseudophakic (Fig. 82.9). If the patient is phakic, combined lens extraction, intraocular lens implantation, and insertion of a fluocinolone acetonide sustained drug delivery system (Retisert) can be performed.[53] If the patient has known glaucoma, then combined glaucoma tube shunt and fluocinolone implant surgery should be considered and has been found to be effective.[54] In young patients, combined surgery should proceed only after achieving relative quiescence given the robust inflammatory response after incisional surgery and careful consideration of the loss of accommodation that will occur after removing the crystalline lens. Alternatively, a dexamethasone intravitreal insert (Ozurdex)[55] or the fluocinolone acetonide nonbiodegradable insert (Iluvien) can be injected through the pars plana into the vitreous cavity to circumvent the need for incisional surgery, although the latter is not yet FDA approved for the treatment of uveitis. If there is little to no response after two corticosteroid injections (either posterior sub-Tenon or intravitreal), then therapeutic/diagnostic vitrectomy can be considered. If a snowbank is present, cryotherapy can be applied but tends to be more effective if applied to 3 clock-hours or less of snowbanking.[56] Peripheral laser photocoagulation has also been used to treat pars planitis, resulting in a decrease in the amount of corticosteroid needed and in decreased vitritis, although the rate of epiretinal membrane increased.[57] If peripheral neovascularization occurs, then targeted peripheral laser to areas of nonperfusion is indicated. Finally, oral prednisone can be used, applying the algorithm for bilateral disease below.

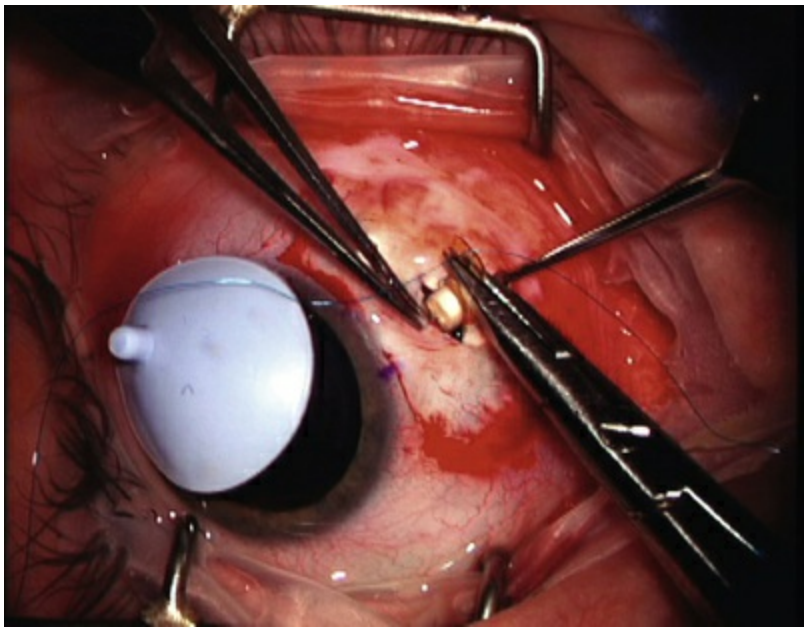

FIG. 82.9 Fluocinolone acetonide implant placement.

Bilateral Disease

Bilateral disease usually warrants treatment with systemic corticosteroids, starting at 1 mg/kg per day tapered to the lowest levels required to achieve quiescence over a 2-month period. If greater than 10 mg of oral prednisone is required for longer than 4 months, or when treating children, in whom long-term corticosteroids can cause growth retardation, steroid-sparing immunosuppressives should be initiated (Fig. 82.10). If one is not aware of the systemic risks or does not choose to monitor appropriately for systemic risks, referral to or co-management with an internist or rheumatologist is highly recommended.

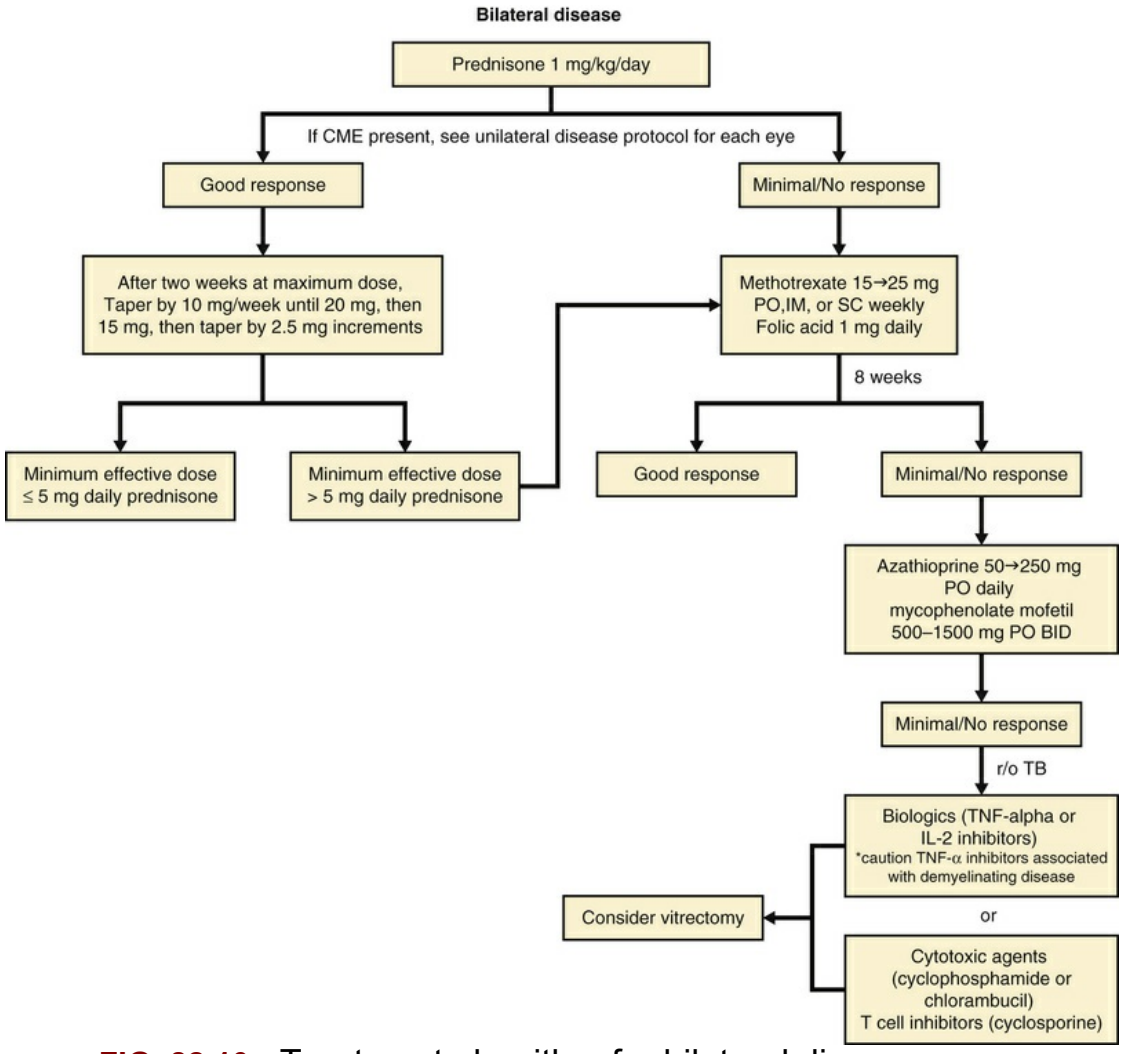

FIG. 82.10 Treatment algorithm for bilateral disease.

We have had good success treating sarcoidosis-associated intermediate and panuveitis with methotrexate starting at 12.5–15 mg PO weekly and escalating to 25 mg PO weekly, along with folic acid, 1 mg/day. Dosage is based on treatment response and tolerability. Because of its relative safety in children, methotrexate is often used as a first-line agent with a short course of bridging corticosteroids. It should be noted that methotrexate should not be used in pregnancy given its teratogenicity and fetal abortive effects. Common side-effects of methotrexate include nausea, vomiting, and oral stomatitis. If gastrointestinal side-effects prevent oral dosing, intramuscular or subcutaneous injections can be administered instead. Hepatotoxicity, cytopenia, and interstitial pneumonitis can also occur with methotrexate use. Liver function tests and complete blood counts are evaluated before initiation of therapy and should be monitored every 8–12 weeks thereafter. The

dose of methotrexate should be reduced if the aspartate aminotransferase or alanine aminotransferase level is more than twice normal on two separate occasions, but any elevation may warrant at least dose reduction. In the first study on the use of methotrexate in ocular sarcoidosis, 100% of 11 patients decreased their dosage of corticosteroids, 86% successfully discontinued prednisone, and 90% had preserved or improved visual acuity, although all patients in this study had panuveitis rather than isolated intermediate uveitis.[58] In a multicentered retrospective study in which methotrexate was used to treat noninfectious uveitis patients of all anatomical subtypes, methotrexate was found to be moderately effective in controlling inflammation, although the side-effect profile was beneficial.[59] Information regarding the effectiveness of methotrexate on the intermediate uveitis subgroup in the latter study was difficult to interpret given that 76.2% were inactive at the time of starting methotrexate.

In patients unable to tolerate methotrexate or who fail to achieve treatment success on this agent, other antimetabolites, including azathioprine or mycophenolate mofetil, can be initiated. Galor et al. compared the three antimetabolites in the treatment of noninfectious ocular inflammation in a retrospective cohort study. They suggested that mycophenolate mofetil controlled inflammation more rapidly than methotrexate, when "control of inflammation" was defined by quiescent inflammation on ≤10 mg oral prednisone.[60] There were several caveats in the latter study, however, including significantly younger age in the methotrexate group and the use of prior immunosuppressive drug therapy in the azathioprine and mycophenolate groups. If antimetabolites are minimally effective, a course of cytotoxic agents (cyclophosphamide or chlorambucil) or T-cell inhibitors (cyclosporine) can be given with close attention to toxic side-effects. Alternatively, the tumor necrosis factor-alpha (TNF-α) inhibitors adalimumab or infliximab can be initiated in combination with methotrexate,[61] although it is important to note that there are a number of reports of these biologics causing demyelinating disease such as MS and progressive multifocal leukoencephalopathy.[62] Because they have also been implicated in the reactivation of latent tuberculosis,[63] an updated tuberculin skin test should be performed

prior to initiating these drugs. If the patient is anergic to the tuberculin skin test due to sarcoidosis, a quantiFERON tuberculosis test can be performed.[64]

The anti-IL-2 receptor biologic daclizumab and infliximab have both been used to treat ocular sarcoidosis with success.[65,66] Etanercept is a TNF-alpha inhibitor that is no longer used as often in the treatment of uveitis since it has been associated with increased inflammation or lack of ocular inflammation control. In one study of 22 uveitis patients who received anti-TNF-α therapy, infliximab was more effective than etanercept in controlling ocular inflammation.[67] It is possible that other biologics targeting additional inflammatory cytokines such as IL-6 (e.g., tocilizumab), may prove to be successful in the treatment of noninfectious intermediate uveitis as well.[68]

The results of the Multicenter Uveitis Steroid Treatment trial, comparing systemic antiinflammatory therapy with the fluocinolone acetonide surgical implant for intermediate, posterior, and panuveitis[69] demonstrated no significant difference in visual acuity outcome at 24 months, but improved control of uveitis activity, vitreous haze, and a trend towards better control of CME in the implant group. The rate of ocular complications, such as elevated intraocular pressure requiring glaucoma surgery or cataracts, was significantly higher in the implant group, as expected, whereas adverse systemic events, while infrequent in both groups, were slightly lower in the implant group, although the risk of hospitalization did not differ between the two groups.[69] The MUST follow-up study showed similar results out to 54 months, although a 21% crossover rate from systemic immunosuppression to the implant after the initial study ended suggests possible underestimation of the advantages of the implant group.[70] Also, while the implant group had a more rapid reduction in macular edema at 6 months, by 48 months the two groups were similar. The irreversible damage that can occur to the retina with macular edema would argue for faster control with the implant. Given the relative costs of the two treatment paradigms, it would be reasonable to consider implant therapy for unilateral noninfectious intermediate, posterior, or panuveitis cases in which there are no systemic manifestations of disease, or any cases in which systemic

treatment fails or is intolerable, as long as ocular side-effects such as glaucoma are treated aggressively.

Diagnostic and Therapeutic Vitrectomy

Diagnostic and therapeutic vitrectomy is considered in patients who are not responsive to the above treatment regimens or if intraocular lymphoma is highly suspected. In a prospective randomized study, Tranos et al. demonstrated better visual acuity and improved fluorescein angiographic CME characteristics after vitrectomy, compared with standard medical therapy consisting of systemic corticosteroids and immunosuppressives. However, this study was underpowered to achieve statistical significance.[71] A number of other studies also appear to show a moderate level of success in treating CME with pars plana vitrectomy, which is thought to be effective by debulking soluble and cellular vitreous inflammatory mediators and by allowing easier access to the vitreous cavity of aqueous inhibitory molecules such as transforming growth factor-ß and alpha-melanocyte-stimulating hormone.[72–74] We perform a diagnostic vitrectomy if an infectious source such as herpetic viral infection or toxoplasmosis is suspected but cannot be confirmed using other methods, or if intraocular lymphoma is suspected, in which case the specimen is sent for cytopathologic evaluation and/or flow cytometry. If intraocular lymphoma is diagnosed, a neurologic workup and MRI may be necessary to determine if there is central nervous system disease. If isolated to the eye or in the setting of central nervous system lymphoma with a recurrence restricted to the eye, orbital irradiation or intravitreal rituximab alone or in combination with methotrexate can be administered with success.[75–77]

Clinical Course and Complications

Clinical Course

Patients with inflammatory intermediate uveitis often have a favorable visual acuity outcome. In one study of patients with pars planitis, mean visual acuity after 10 years of follow-up was 20/30,

75% maintained a visual acuity of 20/40 or better, and one-third maintained normal visual acuity without treatment.[11] In a study by Kalinina Ayuso and colleagues, younger age at onset decreased the visual prognosis and increased the rates of complications;[78] however, another study showed higher rates of remission in patients who presented at a younger age. Mean time to remission in the latter study, which occurred at a rate of 34%, was 8.6 years.[12]

Complications

Causes of vision loss in intermediate uveitis include CME, uveitic glaucoma, retinal detachment, vitreous hemorrhage, cataracts, and epiretinal membranes. Band keratopathy, especially prominent in children with chronic intermediate uveitis, can also cause vision loss. Chronic CME accounts for most cases of permanent visual loss, and occurred at a rate of 41.2% over 15 years according to one large retrospective cohort study, and at a rate of 45.7% in a separate study.[11,13] Concentric retinal macular thickening can also be seen in patients with intermediate uveitis, although it does not necessarily need to be treated.[22] The 15-year rates of cataract and epiretinal membranes were 34.2% and 44.4%, respectively, in the report by Donaldson et al.[11] An increased rate of CME appears to be associated with cigarette smoking. In one large case–control study, the odds ratio of a smoker (versus a nonsmoker) having intermediate uveitis with CME was 8.4 compared with an odds ratio of 1.5 in intermediate uveitis without CME.[4] In the report from Thorne et al., the odds ratio of having CME at presentation was 3.9 compared with a reference group of patients who had never smoked.[13]

In the late stages of intermediate uveitis peripheral neovascular and fibrous membranes can extend on to the ciliary body to form cyclitic and/or retrolenticular membranes, resulting in ciliary body detachment and hypotony. Prevention of progression to this stage is the mainstay of management. Once this develops, surgical intervention can be attempted to remove the cyclitic membrane and reverse hypotony to prevent phthisis, but success in improving visual outcome is poor.[79] Retinal detachment in the setting of active inflammatory disease should be repaired after relative quiescence is

achieved, if possible. Combined surgery with fluocinolone implant and placement of silicone oil can be considered given the lipophilic nature of fluocinolone and its ability to be dispersed throughout the silicone oil.[80]

References

1. Jabs DA, Nussenblatt RB, Rosenbaum JT. Standardization of uveitis nomenclature for reporting clinical data. Results of the First International Workshop. *Am J Ophthalmol*. 2005;140:509–516.
2. Bonfioli AA, Damico FM, Curi AL, et al. Intermediate uveitis. *Semin Ophthalmol*. 2005;20:147–154.
3. Lai WW, Pulido JS. Intermediate uveitis. *Ophthalmol Clin North Am*. 2002;15:309–317.
4. Lin P, Loh AR, Margolis TP, et al. Cigarette smoking as a risk factor for uveitis. *Ophthalmology*. 2010;117:585–590.
5. Lin P, Tessler HH, Goldstein DA. Family history of inflammatory bowel disease in patients with idiopathic ocular inflammation. *Am J Ophthalmol*. 2006;141:1097–1104.
6. Henderly DE, Genstler AJ, Smith RE, et al. Changing patterns of uveitis. *Am J Ophthalmol*. 1987;103:131–136.
7. Kump LI, Cervantes-Castaneda RA, Androudi SN, et al. Analysis of pediatric uveitis cases at a tertiary referral center. *Ophthalmology*. 2005;112:1287–1292.
8. Tugal-Tutkun I, Havrlikova K, Power WJ, et al. Changing patterns in uveitis of childhood. *Ophthalmology*. 1996;103:375–383.
9. Gritz DC, Wong IG. Incidence and prevalence of uveitis in Northern California; the Northern California Epidemiology of Uveitis Study. *Ophthalmology*. 2004;111:491–500 [discussion].
10. Suhler EB, Lloyd MJ, Choi D, et al. Incidence and prevalence of uveitis in Veterans Affairs Medical Centers of the Pacific Northwest. *Am J Ophthalmol*. 2008;146:890–896.e8.
11. Donaldson MJ, Pulido JS, Herman DC, et al. Pars planitis: a 20-year study of incidence, clinical features, and outcomes. *Am J Ophthalmol*. 2007;144:812–817.

12. Vidovic-Valentincic N, Kraut A, Hawlina M, et al. Intermediate uveitis: long-term course and visual outcome. *Br J Ophthalmol*. 2009;93:477–480.
13. Thorne JE, Daniel E, Jabs DA, et al. Smoking as a risk factor for cystoid macular edema complicating intermediate uveitis. *Am J Ophthalmol*. 2008;145:841–846.
14. Tugal-Tutkun I, Aydin-Akova Y, Guney-Tefekli E, et al. Referral patterns, demographic and clinical features, and visual prognosis of Turkish patients with sarcoid uveitis. *Ocul Immunol Inflamm*. 2007;15:337–343.
15. Althaus C, Sundmacher R. Intermediate uveitis: epidemiology, age and sex distribution. *Dev Ophthalmol*. 1992;23:9–14.
16. Madow B, Galor A, Feuer WJ, et al. Validation of a photographic vitreous haze grading technique for clinical trials in uveitis. *Am J Ophthalmol*. 2011;152:170–176.
17. Malinowski SM, Pulido JS, Folk JC. Long-term visual outcome and complications associated with pars planitis. *Ophthalmology*. 1993;100:818–824 [discussion 25].
18. Campbell JP, Beardsley RM, Palejwala NV, et al. Peripheral vascular leakage in uveitis: clinical and angiographic findings. *Ophthalmology*. 2015;122(6):1269–1270.
19. Pollack AL, Mcdonald HR, Johnson RN, et al. Peripheral retinoschisis and exudative retinal detachment in pars planitis. *Retina*. 2002;22:719–724.
20. Lai JC, Stinnett SS, Jaffe GJ. B-scan ultrasonography for the detection of macular thickening. *Am J Ophthalmol*. 2003;136:55–61.
21. de Smet MD, Okada AA. Cystoid macular edema in uveitis. *Dev Ophthalmol*. 2010;47:136–147.
22. Castellano CG, Stinnett SS, Mettu PS, et al. Retinal thickening in iridocyclitis. *Am J Ophthalmol*. 2009;148:341–349.
23. Rodriguez A, Calonge M, Pedroza-Seres M, et al. Referral patterns of uveitis in a tertiary eye care center. *Arch Ophthalmol*. 1996;114:593–599.
24. Raja SC, Jabs DA, Dunn JP, et al. Pars planitis: clinical features and class II HLA associations. *Ophthalmology*.

1999;106:594–599.
25. Compston A, Coles A. Multiple sclerosis. *Lancet*. 2008;372:1502–1517.
26. Curkendall SM, Wang C, Johnson BH, et al. Potential health care cost savings associated with early treatment of multiple sclerosis using disease-modifying therapy. *Clin Ther*. 2011;33:914–925.
27. Jacobs LD, Beck RW, Simon JH, et al. Intramuscular interferon beta-1a therapy initiated during a first demyelinating event in multiple sclerosis. CHAMPS Study Group. *N Engl J Med*. 2000;343:898–904.
28. Comi G, Filippi M, Barkhof F, et al. Effect of early interferon treatment on conversion to definite multiple sclerosis: a randomised study. *Lancet*. 2001;357:1576–1582.
29. Ormerod LD, Dailey JP. Ocular manifestations of cat-scratch disease. *Curr Opin Ophthalmol*. 1999;10:209–216.
30. Sabet-Peyman EJ, Eberhart CG, Janjua K, et al. Persistent intermediate uveitis associated with latent manifestation of facial large B-cell non-Hodgkin lymphoma. *Ocul Immunol Inflamm*. 2009;17:322–324.
31. Mruthyunjaya P, Jumper JM, McCallum R, et al. Diagnostic yield of vitrectomy in eyes with suspected posterior segment infection or malignancy. *Ophthalmology*. 2002;109:1123–1129.
32. Buggage RR. Ocular manifestations of human T-cell lymphotropic virus type 1 infection. *Curr Opin Ophthalmol*. 2003;14:420–425.
33. Boskovich SA, Lowder CY, Meisler DM, et al. Systemic diseases associated with intermediate uveitis. *Cleve Clin J Med*. 1993;60:460–465.
34. Thaler S, Grisanti S, Klingel K, et al. Intermediate uveitis and arthralgia as early symptoms in Whipple's disease. *Int J Infect Dis*. 2010;14(Suppl. 3):e388–9.
35. Soheilian M, Mirbabai F, Shahsavari M, et al. Metastatic cutaneous melanoma to the vitreous cavity masquerading as intermediate uveitis. *Eur J Ophthalmol*. 2002;12:324–327.
36. Eichenbaum JW, Friedman AH, Mamelok AE. A clinical and histopathological review of intermediate uveitis (“pars

planitis"). *Bull N Y Acad Med*. 1988;64:164–174.
37. Pederson JE, Kenyon KR, Green WR, et al. Pathology of pars planitis. *Am J Ophthalmol*. 1978;86:762–774.
38. Bora NS, Bora PS, Tandhasetti MT, et al. Molecular cloning, sequencing, and expression of the 36 kDa protein present in pars planitis. Sequence homology with yeast nucleopore complex protein. *Invest Ophthalmol Vis Sci*. 1996;37:1877–1883.
39. Courvalin JC, Lassoued K, Bartnik E, et al. The 210-kD nuclear envelope polypeptide recognized by human autoantibodies in primary biliary cirrhosis is the major glycoprotein of the nuclear pore. *J Clin Invest*. 1990;86:279–285.
40. Kraemer D, Wozniak RW, Blobel G, et al. The human CAN protein, a putative oncogene product associated with myeloid leukemogenesis, is a nuclear pore complex protein that faces the cytoplasm. *Proc Natl Acad Sci USA*. 1994;91:1519–1523.
41. Wetzig RP, Chan CC, Nussenblatt RB, et al. Clinical and immunopathological studies of pars planitis in a family. *Br J Ophthalmol*. 1988;72:5–10.
42. Nissenblatt MJ, Masciulli L, Yarian DL, et al. Pars planitis – a demyelinating disease? *Arch Ophthalmol*. 1981;99:697.
43. Boyd SR, Young S, Lightman S. Immunopathology of the noninfectious posterior and intermediate uveitides. *Surv Ophthalmol*. 2001;46:209–233.
44. Hultsch E. Peripheral uveitis in the owl monkey: experimental model. *Mod Probl Ophthalmol*. 1977;18:247–251.
45. Klok AM, Luyendijk L, Zaal MJ, et al. Elevated serum IL-8 levels are associated with disease activity in idiopathic intermediate uveitis. *Br J Ophthalmol*. 1998;82:871–874.
46. Klok AM, Luyendijk L, Zaal MJ, et al. Soluble ICAM-1 serum levels in patients with intermediate uveitis. *Br J Ophthalmol*. 1999;83:847–851.
47. Bianco A, Spiteri MA. Peripheral anergy and local immune hyperactivation in sarcoidosis: a paradox or birds of a feather. *Clin Exp Immunol*. 1997;110:1–3.
48. Chow JH, Mettu PS, Srivastava SK, Jaffe GJ. PPD and

positive skin test controls in the evaluation of anergy in uveitis patients. *Invest Ophthalmol Vis Sci*. 2008;49(13):799.
49. Rossman MD, Thompson B, Frederick M, et al. HLA-DRB1*1101: a significant risk factor for sarcoidosis in blacks and whites. *Am J Hum Genet*. 2003;73:720–735.
50. Hogewind BF, Zijlstra C, Klevering BJ, et al. Intravitreal triamcinolone for the treatment of refractory macular edema in idiopathic intermediate or posterior uveitis. *Eur J Ophthalmol*. 2008;18:429–434.
51. Slabaugh MA, Herlihy E, Ongchin S, et al. Efficacy and potential complications of difluprednate use for pediatric uveitis. *Am J Ophthalmol*. 2012;153(5):932–938.
52. Soheilian M, Rabbanikhah Z, Ramezani A, et al. Intravitreal bevacizumab versus triamcinolone acetonide for refractory uveitic cystoid macular edema: a randomized pilot study. *J Ocul Pharmacol Ther*. 2010;26:199–206.
53. Chieh JJ, Carlson AN, Jaffe GJ. Combined fluocinolone acetonide intraocular delivery system insertion, phacoemulsification, and intraocular lens implantation for severe uveitis. *Am J Ophthalmol*. 2008;146:589–594.
54. Malone PE, Herndon LW, Muir KW, et al. Combined fluocinolone acetonide intravitreal insertion and glaucoma drainage device placement for chronic uveitis and glaucoma. *Am J Ophthalmol*. 2010;149:800–806.e1.
55. Ghosn CR, Li Y, Orilla WC, et al. Treatment of experimental anterior and intermediate uveitis by a dexamethasone intravitreal implant. *Invest Ophthalmol Vis Sci*. 2011;52:2917–2923.
56. Okinami S, Sunakawa M, Arai I, et al. Treatment of pars planitis with cryotherapy. *Ophthalmologica*. 1991;202:180–186.
57. Pulido JS, Mieler WF, Walton D, et al. Results of peripheral laser photocoagulation in pars planitis. *Trans Am Ophthalmol Soc*. 1998;96:127–137 [discussion 37–41].
58. Dev S, McCallum RM, Jaffe GJ. Methotrexate treatment for sarcoid-associated panuveitis. *Ophthalmology*. 1999;106:111–118.
59. Gangaputra S, Newcomb CW, Liesegang TL, et al.

Methotrexate for ocular inflammatory diseases. *Ophthalmology*. 2009;116:2188–2198.e1.
60. Galor A, Jabs DA, Leder HA, et al. Comparison of antimetabolite drugs as corticosteroid-sparing therapy for noninfectious ocular inflammation. *Ophthalmology*. 2008;115:1826–1832.
61. Neri P, Zucchi M, Allegri P, et al. Adalimumab (Humira): a promising monoclonal anti-tumor necrosis factor alpha in ophthalmology. *Int Ophthalmol*. 2011;31:165–173.
62. Li SY, Birnbaum AD, Goldstein DA. Optic neuritis associated with adalimumab in the treatment of uveitis. *Ocul Immunol Inflamm*. 2010;18:475–481.
63. Salgado E, Gomez-Reino JJ. The risk of tuberculosis in patients treated with TNF antagonists. *Expert Rev Clin Immunol*. 2011;7:329–340.
64. Milman N, Soborg B, Bo Svendsen C, et al. Quantiferon test for tuberculosis screening in sarcoidosis patients. *Scand J Infect Dis*. 2011;43(9):728–735.
65. Gallagher M, Quinones K, Cervantes-Castaneda RA, et al. Biological response modifier therapy for refractory childhood uveitis. *Br J Ophthalmol*. 2007;91:1341–1344.
66. Lindstedt EW, Baarsma GS, Kuijpers RW, et al. Anti-TNF-alpha therapy for sight threatening uveitis. *Br J Ophthalmol*. 2005;89:533–536.
67. Galor A, Perez VL, Hammel JP, et al. Differential effectiveness of etanercept and infliximab in the treatment of ocular inflammation. *Ophthalmology*. 2006;113:2317–2323.
68. Adan A, Mesquida M, Llorenc V, et al. Tocilizumab treatment for refractory uveitis-related macular edema. *Graefes Arch Clin Exp Ophthalmol*. 2013;251(11):2627–2632.
69. Kempen JH, Altaweel MM, Holbrook JT, et al. Randomized comparison of systemic anti-inflammatory therapy versus fluocinolone acetonide implant for intermediate, posterior, and panuveitis: the Multicenter Uveitis Steroid Treatment Trial. *Ophthalmology*. 2011;118:1916–1926.
70. Multicenter Uveitis Steroid Treatment (MUST) Trial Research Group. Benefits of systemic anti-inflammatory therapy versus fluocinolone acetonide intraocular implant

for intermediate uveitis, posterior uveitis, and panuveitis: fifty-four month results of the multicenter uveitis steroid treatment (MUST) trial and follow-up study. *Ophthalmology*. 2015;122(10):1967–1975.
71. Tranos P, Scott R, Zambarakji H, et al. The effect of pars plana vitrectomy on cystoid macular oedema associated with chronic uveitis: a randomised, controlled pilot study. *Br J Ophthalmol*. 2006;90:1107–1110.
72. Becker M, Davis J. Vitrectomy in the treatment of uveitis. *Am J Ophthalmol*. 2005;140:1096–1105.
73. Dugel PU, Rao NA, Ozler S, et al. Pars plana vitrectomy for intraocular inflammation-related cystoid macular edema unresponsive to corticosteroids: a preliminary study. *Ophthalmology*. 1992;99:1535–1541.
74. Verbraeken H. Therapeutic pars plana vitrectomy for chronic uveitis: a retrospective study of the long-term results. *Graefes Arch Clin Exp Ophthalmol*. 1996;234:288–293.
75. Levy-Clarke GA, Chan CC, Nussenblatt RB. Diagnosis and management of primary intraocular lymphoma. *Hematol Oncol Clin North Am*. 2005;19:739–749 [viii].
76. Pe'er J, Hochberg FH, Foster CS. Clinical review: treatment of vitreoretinal lymphoma. *Ocul Immunol Inflamm*. 2009;17:299–306.
77. Smith JR, Rosenbaum JT, Wilson DJ, et al. Role of intravitreal methotrexate in the management of primary central nervous system lymphoma with ocular involvement. *Ophthalmology*. 2002;109:1709–1716.
78. Kalinina Ayuso V, ten Cate HA, van den Does P, et al. Young age as a risk factor for complicated course and visual outcome in intermediate uveitis in children. *Br J Ophthalmol*. 2011;95:646–651.
79. Yu EN, Paredes I, Foster CS. Surgery for hypotony in patients with juvenile idiopathic arthritis-associated uveitis. *Ocul Immunol Inflamm*. 2007;15:11–17.
80. Dayani PN, Chow J, Stinnett SS, et al. Pars plana vitrectomy, fluocinolone acetonide implantation, and silicone oil infusion for the treatment of chronic, refractory uveitic hypotony. *Am J Ophthalmol*. 2011;152:849–856.e1.

83

Rheumatic Disease

Alastair K. Denniston, Benjamin Rhodes, Mary Gayed, David Carruthers, Caroline Gordon, Philip I. Murray

Introduction

An Approach to the Assessment of the Patient With Possible Rheumatic Disease

Patients may present to the ophthalmologist with a known rheumatic disease, and it may be assumed that the ophthalmic problem is a manifestation of their rheumatic disease. Alternatively, patients may present who do not have a known diagnosis of rheumatic disease. In this group it is important to know which ophthalmic conditions are associated with rheumatic disease and to be aware that some are common to many rheumatic diseases, such as keratoconjunctivitis sicca, and scleritis. Therefore, one must have knowledge of those diseases and how to differentiate between them. This will involve taking a full ophthalmic and medical history, performing a detailed examination, and ordering appropriate investigations.

Common Ocular Presentations of Rheumatic Disease

Keratoconjunctivitis Sicca and Other Corneal Presentations

Keratoconjunctivitis sicca (KCS, or "dry-eye syndrome") is a common ocular manifestation of a number of rheumatic diseases including rheumatoid arthritis (RA), systemic lupus erythematosus (SLE), scleroderma, and relapsing polychondritis. Symptoms vary from slight irritation and burning in mild disease to severe pain and blurred vision arising from increasing corneal involvement. Clinical examination using slit-lamp biomicroscopy reveals a small or absent tear meniscus with a tear film break-up time of less than 10 seconds. Corneal abnormalities, which may be highlighted with fluorescein drops and a cobalt blue light, include punctate epitheliopathy, mucus filaments, strands, and plaques. Additional staining with Rose Bengal or Lissamine Green drops reveals a characteristic interpalpebral pattern, with greatest staining nasal and temporal to the corneal limbus. Tear production, as measured by Schirmer's test, is reduced. Wetting of the test strip by less than 5 mm after 5 minutes in the unanesthetized eye indicates severe tear deficiency. It should be noted that the correlation of dry eye symptoms with observed disease is poor. Many more patients report "dry eyes" than have visible disease, and many asymptomatic patients do have some degree of keratoconjunctivitis sicca.[1]

Other less common corneal presentations of rheumatic disease include the sight-threatening peripheral ulcerative keratitis (PUK). The etiology is uncertain, but it has been suggested that immune complex deposition at the corneal limbus results in an obliterative vasculitis and stromal melt. It is most commonly associated with RA or systemic vasculitis, in particular granulomatosis with polyangiitis (previously known as Wegener's granulomatosis).[2,3] Clinical features include variable pain and redness and reduced vision, uni/bilateral peripheral corneal ulceration with epithelial defect and stromal thinning, associated limbal inflammation, and scleritis.

Scleritis/Episcleritis

Scleritis.

Inflammation of the sclera is an extremely painful, potentially blinding condition. It may be classified according to location (anterior – 90%, or posterior – 10%), distribution (diffuse or nodular), and destruction (necrotizing or non-necrotizing). The majority of anterior scleritis is non-necrotizing (diffuse or nodular), and necrotizing disease may occur with and without inflammation.

Scleritis is associated with systemic disease in around 40–50% of patients, of which most are cases of a rheumatic disease, such as RA, granulomatosis with polyangiitis, relapsing polychondritis, SLE, sarcoidosis, polyarteritis nodosa, inflammatory bowel disease, psoriatic arthritis, ankylosing spondylitis, and gout.[4] It is commonest in middle-aged women. Scleritis is bilateral in 50% of cases, but both eyes may not be affected at the same time.[5] The pain (constant/deep/boring) can be so severe that it may wake the patient at night. The eye has an intense red/dark red appearance. The globe may be very tender to touch. A bluish hue implies scleral thinning from previous active scleritis due to the underlying blue/black uveal tissue showing through the translucent sclera. Scleral thinning can eventually result in high degrees of astigmatism. The degree of redness and scleral thinning is more easily seen under room light or in daylight than by the slit lamp. Topical phenylephrine 2.5% causes blanching of the more superficial episcleral vessels but does not change the engorgement of deeper scleral vessels and can often help differentiate between scleritis and episcleritis. The most severe type is necrotizing anterior scleritis with inflammation. Apart from the severe pain and redness, there may be tearing and photophobia. White avascular areas surrounded by injected edematous sclera are present that may lead to scleral necrosis. An associated anterior uveitis suggests advanced disease. Complications of scleritis include peripheral ulcerative keratitis, acute stromal keratitis, sclerosing keratitis, uveitis, cataract, astigmatism, glaucoma, and globe perforation.

Posterior scleritis is uncommon but is probably underdiagnosed. It is a potentially sight-threatening condition. It may be overlooked on account of more obvious anterior scleral inflammation or

because there is isolated posterior disease and thus the eye appears white and quiet (often despite severe symptoms). It is associated with systemic disease (usually RA or systemic vasculitis) in up to one-third of cases. There is mild–severe deep pain (may be referred to brow or jaw), reduced vision, diplopia, and hypermetropic shift. The eye is white (unless anterior involvement) but may be associated with lid edema, proptosis, lid retraction, restricted motility, shallow anterior chamber, choroidal folds, annular choroidal detachment, exudative retinal detachments, macular edema, and optic disc edema. Diagnosis (and response to therapy) may be assisted by B-scan ultrasonography with measurement of scleral thickening and fluid in the Tenon space (T-sign).

Episcleritis.

This common condition is a benign, recurrent inflammation of the episclera. Being superficial it is easily distinguished from deeper scleral inflammation, in that it is less painful and the involved vessels blanch on instillation of topical phenylephrine 2.5%. It is more common in young women, often self-limiting, and may require little or no treatment. It is not usually associated with any systemic disease, although around 10% may have an underlying rheumatic disease.[6]

Uveitis

Acute Anterior Uveitis.

In acute anterior uveitis (AAU) patients typically present with pain, photophobia, redness, and blurred vision. Examination findings are of anterior segment inflammation, including circumlimbal injection, keratic precipitates (especially inferior), anterior chamber (AC) flare, cells, and fibrin (fibrin is a key feature in HLA-B27-associated uveitis). A hypopyon is suggestive of HLA-B27-associated disease, Behçet disease, or severe intraocular infection.[7] Posterior synechiae are common in both idiopathic and HLA-B27-associated AAU, and every effort should be made to break them at time of presentation. Vitreous cells may be seen as "spill-over" inflammation, but vitritis is not a dominant feature. Occasionally cystoid macular edema (CME) may be seen (especially in HLA-B27 disease), but this is

more commonly a feature of intermediate, posterior, or pan-uveitis. It is estimated that up to one-third of patients with AAU have ankylosing spondylitis (AS).[8] Treatment is with intensive topical corticosteroid and mydriatic. If severe, subconjunctival corticosteroid and mydriatic, oral corticosteroid or even intravenous corticosteroid may be given. Recurrent disease (especially if frequent or severe) may be an indication for maintenance systemic treatment.

Chronic Anterior Uveitis.

In chronic anterior uveitis (CAU) patients are typically asymptomatic, so the condition may be picked up on routine optometric review or in screening in the context of juvenile idiopathic arthritis (JIA). Anterior chamber cells and flare are noted, and with time posterior synechiae, cataract, band keratopathy, and secondary glaucoma are common.

Intermediate Uveitis.

This is defined anatomically as the predominant amount of inflammation being in the vitreous. Patients typically present with floaters but may have reduced vision in the context of associated CME. Examination findings include vitritis, retinal periphlebitis, snowball vitreous opacities, and snowbanks at the vitreous base. It is commonly idiopathic but may be associated with systemic disease; the main rheumatic disease association is with sarcoidosis, but multiple sclerosis is also a recognized cause.

Posterior Uveitis.

Patients typically present with visual symptoms, arising from retinal and/or choroidal inflammation; an associated retinal vasculitis may be seen. A number of rheumatic diseases may be associated with posterior uveitis, including Behçet disease and sarcoidosis.

Panuveitis.

In panuveitis (inflammation involving anterior chamber, vitreous, and retina/choroid) the presentation is usually with visual problems (reduced acuity, floaters) with redness, photophobia, and pain

being a more minor feature.

Other Retinal Presentations

Retinal vasculitis may be associated with Behçet disease, sarcoidosis, systemic vasculitis, and SLE, but may also be associated with infections (herpesviruses, toxoplasma) and nonrheumatic systemic diseases (such as multiple sclerosis).

Orbital Presentations

Rheumatic diseases – notably ANCA-associated vasculitis (ANCA = antineutrophil cytoplasmic antibodies) and SLE – may be associated with orbital inflammation or periorbital edema. Orbital inflammation may present with reduced vision, acute proptosis, lid edema, conjunctival injection and chemosis, reduced ocular motility, and raised intraocular pressure. It may be misdiagnosed as orbital cellulitis, thyroid-associated ophthalmopathy, or another form of orbital inflammation. Inflammation sometimes includes a myositis that may be demonstrated by imaging using CT and B-scan ultrasound (enlargement of extraocular muscles).

Neuro-Ophthalmic Presentations

Neuro-ophthalmic complications of rheumatic disease are most commonly seen in the systemic vasculitides and include optic neuropathy, ocular motility abnormalities, and retrochiasmal lesions. They are discussed in more detail under the specific rheumatic diseases (see below).

Investigations

The investigations ordered will depend on the history and examination findings. A baseline set of tests might include full blood count, erythrocyte sedimentation rate, C-reactive protein, urea and electrolytes, liver function tests, rheumatoid factor, antinuclear antibody, antineutrophil cytoplasmic antibody, angiotensin-converting enzyme, uric acid, syphilis serology, chest radiograph, and urinalysis.

Therapeutic Considerations

Many patients will require systemic treatment, such as corticosteroids, immunosuppressants (methotrexate, azathioprine, mycophenolate mofetil, cyclosporine), and biologics (anti-TNF, rituximab – anti-CD20) for their rheumatic and ophthalmic disease. Where possible this should be undertaken in conjunction with a rheumatologist who has an expertise in this type of therapy. Ophthalmologists should prescribe these drugs only if they have a detailed knowledge of their action, route of administration, side-effects, and how to monitor for them, as the treatments themselves have potentially serious complications. Most patients with sight-threatening disease are likely to be prescribed oral corticosteroid, and these have numerous, well-recognized side-effects, including glucocorticoid-induced bone disease.[9] Fortunately, in patients with ocular inflammation the commonly used immunosuppressants do not appear to increase overall or cancer mortality.[10]

Disease-Specific Section

Rheumatoid Arthritis

General Considerations

Rheumatoid arthritis (RA) is a chronic disease which is characterized by synovial inflammation that typically affects the small joints of the hands and feet in a symmetrical distribution. It can lead to joint destruction and may be associated with systemic features including sight-threatening ocular disease. Early treatment of disease is felt to be important to limit long-term damage.

Epidemiology

RA is the commonest of the inflammatory arthritides, with an incidence of around 3 in 10, 000 per annum and a prevalence of 1% among adults in industrialized nations.[11–13] Epidemiologic risk factors include age (increases with age), female gender (3–5 times greater risk than male),[13] and smoking.[14]

Articular and Systemic Disease

The diagnosis of rheumatoid arthritis requires the presence of chronic polyarticular joint inflammation, which is characterized by pain and stiffness, tenderness, and joint swelling. In contrast to noninflammatory degenerative arthritis such as osteoarthritis, patients commonly complain of morning stiffness that improves with exercise.[15] All synovial joints may be affected including the metacarpophalangeal joints (MCPJs), proximal interphalangeal joints (PIPs), the interphalangeal joint of the thumb, metatarsophalangeal joints (MTPJs), wrist, elbows, hip joints, knees, and the atlantoaxial joint.[15] Typically, however, there is symmetric involvement of the wrists, MCPJs, PIPJs, and MTPJs with sparing of the distal interphalangeal joints.

Damage to joints and periarticular structures due to uncontrolled inflammation can, with time, give rise to the classical deforming appearances of advanced rheumatoid arthritis including ulnar deviation, "Swan-neck," and Boutonniere deformities ("rheumatoid hands").

Numerous extraarticular features have been reported in rheumatoid arthritis.[16] The commonest, affecting up to 30%, are solid lesions within the subcutaneous tissues of extensor surfaces known as rheumatoid nodules. Pleural disease, often asymptomatic and presenting as pleural thickening or small pleural effusion, is also reasonably common.[17] More serious extraarticular manifestations include pulmonary fibrosis, vasculitis, vasculitic neuropathy, and pericarditis. Other systemic complications include systemic amyloidosis and a chronic anemia and/or leucopenia. The combination of RA, splenomegaly, and leucopenia is known as Felty syndrome.[18] It is now recognized that rheumatoid arthritis is an important risk factor for atherosclerosis and premature cardiovascular mortality.[19] The incidence of severe, nonpulmonary extraarticular features of rheumatoid arthritis, particularly vasculitis, appears to be declining.[16] Whether this is related to changing treatment regimens is uncertain.

In addition to clinical assessment, the diagnosis of rheumatoid arthritis may be supported by systemic investigations such as the measurement of inflammatory markers, rheumatoid factor, and anticitrullinated protein antibodies (ACPA). ACPA in particular has high sensitivity and specificity for rheumatoid arthritis and may

predict the development of destructive disease.[20] New American/European classification criteria for rheumatoid arthritis were published in 2010, which reflect the clinical emphasis on early disease identification prior to the development of joint damage, combined with the clinical utility of anti-CCP antibodies (Box 83.1).

Box 83.1

The 2010 American College of Rheumatology (ACR)/European League Against Rheumatism (EULAR) Classification Criteria for Rheumatoid Arthritis

The criteria are aimed at classification of newly presenting patients. In addition, patients with erosive disease typical of rheumatoid arthritis (RA) with a history compatible with prior fulfillment of the 2010 criteria should be classified as having RA.

Target Population (Who should be tested?)

1. Patients that have at least 1 joint with definite clinical synovitis (swelling)

2. Patients with the synovitis not better explained by another disease

Classification Criteria for RA

(Score-based algorithm: add score of categories A–D; a score of >6/10 is needed for classification of a patient as having definite RA.)

	Score
A. Joint Involvement	
1 large joint	0
2–10 large joints	1
1–3 small joints (with or without involvement of large joints)	2
4–10 small joints (with or without involvement of large joints)	3
>10 joints (at least 1 small joint)	5
B. Serology (at least 1 test result is needed for classification)	
Negative RF *and* negative ACPA	0
Low-positive RF *or* low-positive ACPA	2
High-positive RF *or* high-positive ACPA	3
C. Acute-Phase Reactants (at least 1 test result is needed for classification)	
Normal CRP *and* normal ESR	0
Abnormal CRP *or* abnormal ESR	1
D. Duration of Symptoms	

<6 weeks	0
≥6 weeks	1

Adapted from Aletaha D, Neogi T, Silman AJ, et al. 2010 Rheumatoid Arthritis Classification Criteria: an American College of Rheumatology/European League Against Rheumatism collaborative initiative. Arthritis Rheum 2010;62:2569–81.

Ocular Disease

In RA, anterior segment disease is more common than posterior segment disease. Common anterior segment disease includes keratoconjunctivitis sicca, Sjögren syndrome, episcleritis, scleritis, and various forms of keratitis.

Scleritis occurs in 1–6% of patients with RA and in up to 14% of patients with rheumatoid vasculitis.[2,4,5] Scleritis in the context of RA may present with severe pain and may be diffuse or nodular, anterior or posterior, and necrotizing or non-necrotizing in pattern.[6] Of greatest concern is scleromalacia performans, in which scleral destruction is not typically painful and not associated with visible signs of inflammation.[2,6] Episcleritis may also be seen in the context of RA.[6,22]

Corneal complications of RA are wide-ranging with varying risk of perforation. Marginal keratitis without apparent inflammation may result in peripheral thinning giving rise to the appearance of "contact lens cornea." More significant are peripheral ulcerative keratitis and keratolysis ("corneal melt"), both of which have a high risk of perforation.[2] Necrotizing keratitis or scleritis in the context of RA are associated with increased mortality.[23]

Posterior segment lesions in RA include posterior scleritis and rarely a retinal vasculitis. Retinal vasculitis is probably underdiagnosed. In one study of 60 patients with RA the rate of retinal vasculitis was 18% even in the absence of clinical features of retinal vasculitis.[24] This study is supported by a number of case reports describing typical retinal vasculitis associated with fluorescein angiographic evidence of leakage and a single case of retinal exudation in the context of scleritis that the authors attribute to vasculitis.[25,26]

Treatment-related ocular complications of RA include cataract (corticosteroid), elevated intraocular pressure (corticosteroid), and retinopathy (chloroquine and to a lesser extent

hydroxychloroquine).

Treatment

Treatment of Systemic Disease.

The goals of treatment in RA are to alleviate symptoms, including pain and loss of function, and to prevent joint damage. Comprehensive management guidelines were published by the American College of Rheumatology (ACR) in 2012 and the European League Against Rheumatism in 2013, and these largely agree in their management recommendations.[27,28] Current best practice is to treat early and aggressively, with frequent therapy escalation until disease activity is low or absent. First-line treatment is typically with methotrexate used as monotherapy or in combination (concurrently or sequentially) with other traditional synthetic disease-modifying agents. Patients who fail to respond to this approach will escalate to a targeted biologic DMARD (typically an anti-TNF biologic as first line with tocilizumab (anti-interleukin-6), rituximab (anti-CD20), and abatacept (fusion protein of CTLA-4 and IgG) as alternatives). Tofacitinib, a synthetic janus kinase inhibitor, is available in the United States.

Treatment of Ocular Disease.

Mild superficial ocular disease (such as mild keratoconjunctivitis sicca or episcleritis) may be adequately controlled with topical therapies such as artificial tear substitutes.[29] Non-necrotizing anterior scleritis may be managed with oral NSAIDs, but necrotizing disease frequently requires systemic corticosteroid. Uncontrolled ocular inflammation warrants escalation of systemic treatment that should be coordinated with a rheumatologist. In addition, sight-threatening inflammation such as necrotizing scleritis or corneal melt requires urgent rescue therapy such as pulsed intravenous methylprednisolone.[2] In our practice we administer up to three pulses of 500–1000 mg methylprednisolone on consecutive days that is usually followed by commencing or increasing a course of oral corticosteroid (in addition to DMARD/biologic therapy).

Seronegative Spondyloarthropathies

General Considerations

Spondyloarthropathy (SpA) is a term used to describe a group of interrelated inflammatory arthropathies affecting the axial skeleton, synovium, and extraarticular sites (Box 83.2).[30,31] This group of conditions includes ankylosing spondylitis, reactive arthritis, inflammatory bowel disease-related arthritis, juvenile spondyloarthropathies, and psoriatic arthritis. Clinical manifestations include inflammatory back pain, sacroiliitis, enthesitis (inflammation of the entheses, where tendons or ligaments insert into the bone), dactylitis (inflammation of an entire digit), uveitis, and usually an asymmetric arthritis that affects lower limbs. These diseases are often subclassified as either axial SpA (where disease predominantly affects the back and sacroiliac joints) or peripheral SpA (where enthesitis, arthritis, and dactylitis predominates).[30,31] Overlapping or undifferentiated disease patterns are well recognized. There is a strong association with the class I MHC molecule HLA-B27. Based on a systematic review, which included nearly 30 ,000 patients, the mean prevalence of uveitis in spondyloarthropathies has been estimated at 33% overall, with acute anterior uveitis being the most common type seen.[32]

Box 83.2

The Assessment of Spondyloarthritis International Society (ASAS) Criteria for Axial and Peripheral Spondyloarthritis[30,31]

Axial Spondyloarthropathy

Consider in patients aged <45 years with ≥3 months back pain *and*

- *Either* – Sacroliitis on imaging* + ≥1 spondyloarthritis clinical features†
- *Or* – HLA-B27 positive + ≥2 spondyloarthritis clinical features

Peripheral Spondyloarthropathy

Consider in patients with arthritis or enthesitis or dactylitis *and*

- *Either* ≥1 of psoriasis, inflammatory bowel disease, preceding

infection, HLA-B27, uveitis, or sacroiliitis on imaging

- *Or* ≥2 of arthritis, enthesitis, dactylitis, history of inflammatory back pain, or a positive family history

*Sacroiliitis on Imaging

- Definite radiographic sacroiliitis according to modified New York criteria (radiographic axial spondyloarthropathy)
- Active inflammation on MRI highly suggestive of sacroiliitis associated with spondyloarthropathy (if radiographic features absent then termed nonradiographic spondyloarthropathy)

†Spondyloarthritis Clinical Features

- Inflammatory back pain
- Arthritis
- Enthesitis (heel)
- Uveitis
- Dactylitis
- Psoriasis
- Inflammatory bowel disease
- Good response to NSAIDS
- Positive family history for spondyloarthritis
- HLA-B27
- Elevated CRP

Epidemiology

Spondyloarthropathies occur particularly in individuals who are

positive for HLA-B27, but additional environmental factors are also thought to play a role. Spondyloarthropathies as a whole have a prevalence of 0.5–1.9% of the population.

Ankylosing Spondylitis

General Considerations.

Ankylosing spondylitis (AS) is an HLA-B27-associated chronic inflammatory axial arthritis typically presenting in young men with a strong association with anterior uveitis. The traditional classification scheme (the Modified New York criteria) required the presence of radiographic sacroiliitis along with the symptoms and signs of inflammatory back pain. The increasing use of sensitive modalities such as MRI has identified a group of patients with inflammatory disease but no radiographic changes, and this has led to a concept of nonradiographic axial SpA and a new set of classification criteria for axial SpA that incorporates this concept (Box 83.2).[30] Whether patients with nonradiographic axial SpA will all inevitably develop ankylosing spondylitis is currently unknown.

Epidemiology.

AS is the commonest of the spondyloarthropathies. Its prevalence varies between 0.1 and 0.4% of the population, depending on the frequency of HLA-B27 in that population. This results in significant geographic variation with low rates of in South Africa and Japan, higher rates in Germany compared to other European countries, and very high rates in the natives of Eurasia and the North American circumpolar/sub-Arctic areas.[33] AS is commoner in males, with a male : female ratio of 2–3 : 1, although it has been suggested that it may be underdiagnosed in females due to them having milder disease.[34]

Articular and Systemic Disease.

The hallmark of AS is inflammatory back pain that presents with buttock pain and early morning stiffness (minimum 30 minutes), that is relieved by exercise and NSAIDs, and worse with rest.[35] The shoulders and hips are regarded as axial joints and are affected in up to 50% of patients.[36] In AS an asymmetric oligoarthritis is

uncommon but may be a predictor of more severe disease if it presents early in the disease course.[36]

Enthesitis can occur at any enthesis but is most commonly seen in the foot at the insertion of the Achilles tendon and of the plantar fascia onto the calcaneus. The classic cardiac abnormalities in AS are aortitis, aortic regurgitation, and conduction abnormalities, but symptomatic disease is rare.[37]

Disease is monitored using a combination of instruments, including BASDAI (Bath Ankylosing Spondylitis Assessment Index), BASFI (Bath Ankylosing Spondylitis Function Index), inflammatory markers (CRP/ESR), Visual Analogue Scale, swollen joint count, and radiographs of spine and pelvis.

Ocular Disease.

The commonest ocular complication of AS is recurrent AAU. It is almost always unilateral but may affect both eyes sequentially (described as "flip-flop" pattern). Rarely the anterior uveitis may become persistent. The presentation is of typical AAU, but inflammation is classically more severe (often with fibrin in the anterior chamber) and recurrences more frequent than in idiopathic AAU.[38–40] Hypopyon may also be present in severe cases. AAU may lead to sight loss via recurrent or persistent CME, secondary glaucoma, and cataract.[38–40] Treatment-related ocular complications of AS include cataract and elevated intraocular pressure (secondary to corticosteroid usage).

Treatment

Treatment of Systemic Disease.

The goal of treatment in AS is to relieve pain and to restore and maintain posture and movement to as near normal as possible. This is achieved through lifelong physical therapy and medical treatment. NSAIDs (nonsteroidal antiinflammatory drugs) are an effective treatment and are recommended as first-line therapy in many national guidelines.[41,42] There is little evidence to support the use of steroids or DMARDs (disease-modifying antirheumatic drugs such as sulfasalazine and methotrexate) in axial SpA, although they may be some use in treating peripheral

manifestations.[43] Five TNF-inhibitors (etanercept, infliximab, adalimumab, certolizumab, and golimumab) are authorized for the treatment of ankylosing spondylitis, and are typically used when active disease is not adequately controlled after a trial of a number of NSAID agents. Meta-analyses strongly support the efficacy of these agents in axial SpA.[43,44]

Treatment of Ocular Disease.

The mainstay of treatment for AS-associated AAU is intensive topical corticosteroids and a mydriatic (as for idiopathic AAU), but it should be noted that subconjunctival treatment and oral corticosteroids are more commonly required to adequately control inflammation in HLA-B27-associated versus idiopathic AAU. Anti-TNF agents, such as infliximab, etanercept, and adalimumab, as part of studies for the treatment of the underlying AS can also reduce the frequency of AAU recurrences.[45,46]

Reactive Arthritis (Previously Known as Reiter Syndrome)

General Considerations.

Reactive arthritis (ReA) is a sterile inflammation of the joints triggered by an infection, associated with frequently occurring extraarticular symptoms.

Epidemiology.

There are a few population-based studies which have estimated the incidence to be between 1 and 30 per 100, 000 per annum.[47] HLA-B27 is positive in 60–80% of patients with reactive arthritis. The most commonly associated infections are urogenital (*Chlamydia trachomatis*) or gastrointestinal (*Yersinia*, *Salmonella*, *Shigella*, and *Campylobacter*).[47–50]

Articular and Systemic Disease.

Characteristically patients will have an asymmetric oligoarthritis of the large lower limb joints, with involvement often occurring in an additive or migratory pattern. The upper limbs and small joints

(usually PIP joints) can also be affected. Other features include inflammatory lower back pain similar to AS, dactylitis, enthesitis, erythema nodosum, keratoderma blennorrhagica (skin lesions on the soles of feet that mimic pustular psoriasis), and a distinctive genital rash called circinate balanitis.[47,48]

Ocular Disease.

The commonest ocular complication of ReA is anterior segment disease. Conjunctivitis forms part of the classical triad of ReA but is usually only seen at first presentation and early in the disease. Of more consequence is recurrent AAU that may occur in up to 50% of patients, although in only up to 20% patients at the initial attack.[40,48] As described for other forms of AAU, these attacks may be associated with spillover vitreous cells and CME, and very rarely optic disc edema.

Rarely ReA may be associated with panuveitis or multifocal choroiditis;[51,52] the rarity of such cases is underlined by many series of ReA patients in which no cases of panuveitis or posterior uveitis were identified.[48,53]

Treatment

Treatment of Systemic Disease.

The underlying infection should be treated as appropriate.[47,54] Acute arthritis can be treated with NSAIDs and intraarticular corticosteroids. DMARDs such as sulphasalazine or methotrexate should be considered in patients with a prolonged disease course, while case reports suggest anti-TNF biologic drugs may be helpful in severe resistant cases.[47,54]

Treatment of Ocular Disease.

ReA-associated AAU is treated as for idiopathic AAU with intensive topical corticosteroids and a mydriatic. As noted previously for other HLA-B27-associated AAU, subconjunctival treatment and oral corticosteroids may be required to adequately control inflammation. Rare cases of posterior segment inflammation are likely to require systemic immunosuppression.

Inflammatory Bowel Disease

General Considerations.

Peripheral and axial arthritis are associated with inflammatory bowel disease (IBD), especially Crohn's disease and ulcerative colitis.

Epidemiology.

The incidence of peripheral arthritis is reported to be between 5% and 10% in ulcerative colitis and 10% and 20% in Crohn's disease, respectively.[55] Men and women are affected equally. Spondylitis occurs in 1–26% of patients with IBD, and males are more often affected than females. In addition, the prevalence of AS in IBD (1–6%) is higher than in the general population.[55]

Articular and Systemic Disease.

IBD-related arthritis is often a clinical diagnosis as radiology is often normal with no joint erosion or deformity. Some authors have classified two distinct types of arthritis: type 1 (pauciarticular) and type 2 (polyarticular).[55,56]

Ocular Disease.

Ophthalmic complications are estimated to occur in 3.5–12% of patients with IBD, occurring more commonly earlier in the disease.[57] The commonest ocular complications of IBD are uveitis, episcleritis, and scleritis.

Uveitis is usually of recurrent AAU type, occurring in around 5% of IBD patients, but in up to 50% of IBD patients who are also positive for HLA-B27.[58] Less commonly, a chronic bilateral anterior uveitis may be seen, which has a female gender preponderance.[59] Scleritis is a well-recognized feature of IBD and has been reported to parallel the activity of the bowel disease. Scleritis is usually anterior but may be posterior; it may be non-necrotizing or necrotizing, leading to a risk of scleromalacia perforans.[60] Retinal artery occlusions and ischemic optic neuropathy are reported and may reflect the prothrombotic tendency seen in some patients with IBD. Other reported associations with IBD include keratitis, retinal vasculitis, posterior uveitis, cystoid macular edema, optic neuritis,

neuroretinitis, Brown's syndrome, and orbital myositis.[60] A recent community survey also suggested that there is a high prevalence of "dry eye" (up to 42%), which was associated with 5-aminosalicylate use, although it was not clear if this was causative or a surrogate marker of disease activity.[61] Interestingly, a family history of IBD has been proposed as an independent risk factor for the development of idiopathic ocular inflammation, including uveitis.[62]

Treatment

Treatment of Systemic Disease.

Treatment depends on the severity of symptoms. Patients with mild oligoarthritis usually respond to relative rest, physiotherapy, and intraarticular corticosteroid injections.[55,56] Most of the patients respond to NSAIDs because they control the symptoms and joint and enthesis inflammation, but they do not stop joint destruction, and they may have significant side-effects including exacerbation of IBD and produce small intestine and colon ulcers. Hence, they are recommended for patients with mild exacerbations, to control symptoms in arthritis flares, but their use must be limited to the minimal effective dose and time.[55,56]

Type 1 arthritis is related to disease activity and therefore therapy of the underlying IBD is the treatment of choice. Treatment of type 2 IBD arthritis and axial arthropathies generally requires long-term treatment with a DMARD, such as sulfasalazine or methotrexate. In addition, treatment with systemic or intraarticular corticosteroids can be used.[55] A number of IBD patients will also be using anti-TNF agents to control their bowel symptoms.

Treatment of Ocular Disease.

IBD-associated AAU is treated as for idiopathic AAU with intensive topical corticosteroids and a mydriatic; it should be noted that the more chronic form of anterior uveitis may require more prolonged treatment.[63] The treatment of scleritis will depend on the pattern and severity of disease seen but will often require immunosuppression.[63]

Psoriatic Arthritis

General Considerations.

Psoriatic arthritis (PsA) is traditionally diagnosed by the combination of an inflammatory arthritis (peripheral arthritis and/or sacroiliitis or spondylitis), psoriasis, and the absence of serologic tests for rheumatoid factor.[30] In 2006, however, the CASPAR (ClASsification Criteria for Psoriatic ARthritis) was developed (Box 83.3). This has been demonstrated to have high sensitivity and specificity for the diagnosis of PsA (see below).[30,64]

Box 83.3

The CASPAR Criteria for Psoriatic Arthritis

Presence of

Inflammatory articular disease (joint, spine or enthesis)

and
At least 3 points scored from the following

Current psoriasis (2 points), a personal history of psoriasis (1 point), or a family history of psoriasis (1 point)

Typical psoriatic nail dystrophy (1 point); this includes onycholysis, pitting, hyperkeratosis

Dactylitis (1 point): current or previous episode noticed by rheumatologist

Juxtaarticular new bone formation (1 point): hand or foot X-rays

Rheumatoid factor-negative (1 point): preferably by enzyme-linked immunosorbent assay

Modified with permission from Taylor W, Gladman D, Helliwell P, et al. Classification criteria for psoriatic arthritis: development of new criteria from a large international study. Arthritis Rheum 2006;54:2665–73.

Epidemiology.

Psoriatic arthritis (PsA) can occur at any age but is commonest between 30 and 50 years of age. It affects males and females equally.[30,65] The exact prevalence of PsA is unknown, but it is estimated to affect 0.3–1% of the US population and 7–42% of

patients with psoriasis.[30,65,66]

Articular and Systemic Disease.

PsA can cause a variety of articular symptoms, varying from an isolated monoarthritis to an extensive destructive arthritis. Articular involvement can be divided into five subtypes: DIP (distal interphalangeal) joint involvement, mono/oligoarticular, symmetric polyarthritis, arthritis mutilans, and spondyloarthropathy. It is important that patients with long-standing PsA have cervical spine radiographs before a general anesthetic, as there can be a clinically silent erosive/inflammatory arthritis causing atlantoaxial or subaxial instability, as in RA.[67] Dactylitis or "sausage digit" occurs in 30–40% of patients with PsA. In addition 20–40% of patients have symptomatic enthesitis generally affecting the foot at the insertion of the Achilles tendon and of the plantar fascia onto the calcaneus.[64,68] There appears no correlation between the severity of skin psoriasis and joint involvement, but skin symptoms do tend to precede joint symptoms. Psoriasis can be assessed using a variety of tools including PASI (Psoriasis Area and Severity Index), health assessment questionnaires, and Psoriatic Arthritis Response Criteria (PsARC).

Ocular Disease.

Ophthalmic complications are estimated to occur in 10% of patients with psoriasis[69] and 31% of patients with PsA.[70] The most common presentations are conjunctivitis (up to 20%) or uveitis (7%).[70] Paiva and coworkers compared the nature of uveitis in PsA to that seen with a previous cohort of spondyloarthropathy patients. Interestingly this suggested that PsA-associated uveitis was more likely to be insidious in onset (19% vs. 3%), bilateral (38% vs. 7%), chronic in duration (31% vs. 6%), or posterior (44% vs. 17%).[71] Episcleritis, scleritis, keratoconjunctivitis sicca, and keratitis are also reported.[69,70]

Treatment

Treatment of Systemic Disease.

NSAIDs are normally used for musculoskeletal symptoms, based

on the evidence from other rheumatic diseases.[72] Intraarticular corticosteroid can be used, but oral corticosteroids should be used cautiously as they can be associated with a "poststeroid flare" of cutaneous disease. Typically, nonbiologic disease-modifying drugs (for example methotrexate, sulfasalazine, and leflunomide) are used as first-line treatment, with methotrexate also being an effective treatment for cutaneous psoriasis.[43] Clinician experience suggests these can be effective for many people, and they continue to feature in the majority of treatment guidelines; however, reviews, meta-analyses, and a randomized controlled trial of methotrexate really fail to demonstrate a clear statistical benefit from these agents, so there remains some uncertainty over their role.[73]

All licensed anti-TNF agents (etanercept/infliximab/adalimumab/certolizumab/golimumab) are effective at treating peripheral arthritis, as well as enthesitis, and dactylitis and cutaneous psoriasis.[43] They are recommended for use in patients with an active peripheral arthritis despite traditional treatment. Where access is available, two other treatment options have been approved in psoriatic arthritis: ustekinumab, a monoclonal antibody targeting the common p40 subunit of IL-12/IL-23 inhibitor, and apremilast, an oral inhibitor of phosphodiesterase 4, which has immunomodulatory effects.[43]

Treatment of Ocular Disease.

PsA-associated AAU is treated as for idiopathic AAU with intensive topical corticosteroids and a mydriatic, but more persistent anterior uveitis may require prolonged treatment. Cataract, which may be associated with chronic intraocular inflammation, corticosteroid usage, and possibly P-UVA treatment,[74] requires surgical treatment with appropriate immunosuppressive perioperative care.

Juvenile Idiopathic Arthritis

General Considerations

Juvenile idiopathic arthritis (JIA) is the most common rheumatic disease occurring in childhood. It is characterized by persistent inflammation of the joints, with onset prior to age 16 years.

Epidemiology

The reported incidence of JIA varies between 0.8 to 23 per 100, 000 per annum, with a prevalence rate between 7 and 400 per 100, 000 children. There are reported differences between different ethnic groups: JIA is more frequent in children of European descent than in children of African, Asian, or East Indian origin.[75]

Articular and Systemic Disease

JIA is classified using the ILAR (International League of Associations of Rheumatologists) classification (Box 83.4). The main clinical feature of JIA is defined as "swelling within a joint or limitation in range of movement with joint pain or tenderness, which persists for a minimum of 6 weeks, observed by a physician and which is not due to primary mechanical disorders or to other identifiable causes."[76]

Box 83.4

The International League of Associations of Rheumatologists (ILAR) Classification of Juvenile Idiopathic Arthritis

Systemic Arthritis

Definition: Arthritis in one or more joints with or preceded by fever of at least 2 weeks' duration that is documented to be daily ("quotidian") for at least 3 days, and accompanied by one or more of the following:

1. Evanescent (nonfixed) erythematous rash

2. Generalized lymph node enlargement

3. Hepatomegaly and/or splenomegaly

4. Serositis

Exclusions (below): a, b, c, d

Oligoarthritis

Definition: Arthritis affecting 1–4 joints during the first 6 months of disease. Two subcategories are recognized:

1. Persistent oligoarthritis: Affecting not more than 4 joints throughout the disease course

2. Extended oligoarthritis: Affecting a total of more than 4 joints after the first 6 months of disease

Exclusions (below): a, b, c, d, e

Polyarthritis (Rheumatoid Factor Negative)

Definition: Arthritis affecting 5 or more joints during the first 6 months of disease; a test for RF is negative.
Exclusions (below): a, b, c, d, e

Polyarthritis (Rheumatoid Factor Positive)

Definition: Arthritis affecting 5 or more joints during the first 6 months of disease; two or more tests for RF at least 3 months apart during the first 6 months of disease are positive.
Exclusions (below): a, b, c, e

Psoriatic Arthritis

Definition: Arthritis and psoriasis, or arthritis and at least two of the following:

1. Dactylitis

2. Nail pitting or onycholysis

3. Psoriasis in a first-degree relative

Exclusions (below): b, c, d, e

Enthesitis-Related Arthritis

Definition: Arthritis and enthesitis, or arthritis or enthesitis, with at least two of the following:

1. The presence of or a history of sacroiliac joint tenderness and/or inflammatory lumbosacral pain

2. The presence of HLA-B27 antigen

3. Onset of arthritis in a male over 6 years of age

4. Acute (symptomatic) anterior uveitis

5. History of ankylosing spondylitis, enthesitis-related arthritis, sacroiliitis with inflammatory bowel disease, Reiter syndrome, or acute anterior uveitis in a first-degree relative

Exclusions (below): a, d, e

Undifferentiated Arthritis

Definition: Arthritis that fulfills criteria in no category or in two or more of the above categories.

Exclusions

The principle of this classification is that all categories of JIA are mutually exclusive. This principle is reflected in the list of possible exclusions for each category:

a) Psoriasis or a history of psoriasis in the patient or first-degree relative

b) Arthritis in an HLA-B27-positive male beginning after the 6th birthday

c) Ankylosing spondylitis, enthesitis-related arthritis, sacroiliitis with inflammatory bowel disease, Reiter syndrome, or acute anterior uveitis, or a history of one of these disorders in a first-degree relative

d) The presence of IgM rheumatoid factor on at least two occasions at least 3 months apart

e) The presence of systemic JIA in the patient

The application of exclusions is indicated under each category and may change as new data become available.

Reproduced with permission from Petty RE, Southwood TR, Manners P, et al. International League of Associations for Rheumatology classification of juvenile idiopathic arthritis: second revision, Edmonton, 2001. J Rheumatol 2004;31:390–2.

Ocular Disease

The major ocular manifestation of JIA is uveitis. Uveitis is present in around 10% of JIA patients at presentation but may occur in up to one-third of patients at some point during their disease although the exact estimate depends on the type of population sampled.[77–81] Inflammation is typically a chronic anterior uveitis with a white eye, which is usually bilateral (70%) but may initially present with unilateral disease. Recurrent acute anterior uveitis is less commonly seen and when it does occur is usually in the context of HLA-B27.

The risk of developing uveitis in association with JIA has been stratified according to age of onset, type of arthritis, and the presence of ANA, with uveitis occurring in up to half of the highest-risk group (oligoarticular – persistent and extended, ANA-positive disease). Interestingly, a recent study has suggested that age and ANA status may be less useful in predicting risk in boys (versus girls).[82] It should be noted that the gold standard for determining ANA is via immunofluorescence on HEp-2 cells; ELISA-determined ANA was not found to be predictive.[83] Antihistone antibodies are also associated with risk of uveitis but are less widely used in clinical practice.[83] Since the chronic anterior uveitis has minimal if any of the symptoms commonly associated with inflammation, screening is recommended. The recommendations of the American Academy of Pediatrics are summarized in Table 83.1.[84]

TABLE 83.1

American Academy of Pediatrics Guidelines on Frequency of Ophthalmologic Examination in Patients With Juvenile Idiopathic Arthritis

Type	ANA	Age at Onset (yr)	Duration of Disease (yr)	Risk Category	Eye Examination Frequency (mth)
Oligoarthritis or polyarthritis	+	≤6	≤4	High	3
	+	≤6	>4	Moderate	6
	+	≤6	>7	Low	12
	+	>6	≤4	Moderate	6
	+	>6	>4	Low	12
	−	≤6	≤4	Moderate	6
	−	≤6	>4	Low	12
	−	>6	NA	Low	12
Systemic disease	NA	NA	NA	Low	12

(fever, rash)					

Recommendations for follow-up continue through childhood and adolescence.

ANA, antinuclear antibodies; NA, not applicable; mth, month; yr, year.

Reproduced with permission from Cassidy J, Kivlin J, Lindsley C, Nocton J. Ophthalmologic examinations in children with juvenile rheumatoid arthritis. Pediatrics 2006;117:1843–5.

JIA-associated uveitis is more commonly seen in girls,[81] but male gender is a risk factor for worse disease, with significantly higher rates of CME by 5 years of follow-up (50% vs. 4%) and need for cataract surgery (59% vs. 32%). Other reported predictors of worse outcome are uveitis present at time of diagnosis[85,86] and elevated laser flare values.[87]

The key sight-threatening complications of JIA-associated uveitis are band keratopathy (60%), cataract (40%), glaucoma (10–25%), and CME (10%). Posterior synechiae are present in most cases.[77,88,89] Less commonly, vitritis and a peripheral retinal vasculitis are reported.[77,80,88,89]

Treatment

Treatment of Systemic Disease.

The management of JIA is based on a combination of medical treatment, physical and occupational therapy, and surgical management. NSAIDs can be used for all types of mild JIA, to treat pain and stiffness. Oral corticosteroids must be used minimally in children because of the effects on bone and growth; the main indications are severe fever, serositis, and macrophage activation syndrome. Intraarticular corticosteroids can be used, and encouraging results have been reported in children with monoarthritis.[90] Methotrexate is used for patients with polyarthritis; other DMARDs that have been shown to be effective include sulfasalazine and leflunomide. Etanercept can be used in patients who fail to respond to methotrexate therapy and has been demonstrated to be effective in both the short- and long-term management of JIA.[91–93] Infliximab was not shown to be superior to placebo in polyarticular JIA.[94] Adalimumab is licensed for use in JIA and was found to be effective in children with polyarticular JIA.[95] Abatacept is an alternative biologic agent which is a selective

T-cell co-stimulator inhibitor. In randomized controlled trials (RCTs) abatacept was superior to placebo in children with polyarticular arthritis, including those who were anti-TNF treatment failures.[96,97] There is some concern regarding the potential increased risk of cancers in children using anti-TNF agents.[98] Further studies are being undertaken to investigate the potential future role of other biologics, including rituximab, IL(interleukin)-1, and IL-6 antagonists.

Treatment of Ocular Disease.

Systemic immunosuppression is usually required to control both the systemic disease and its ocular manifestations, although some children may require only topical corticosteroid and a mydriatic. What constitutes a "safe" level of topical corticosteroid usage in children is controversial. In a recent retrospective study by Thorne and coworkers, topical corticosteroid use was associated with development of cataract, and this was independent of active uveitis or presence of posterior synechiae.[99] Importantly, there appeared to be no significant increase of cataract when chronic administration was no more than twice daily.[99] The need for frequent topical corticosteroid to control the uveitis usually requires the introduction of methotrexate often given by the subcutaneous route weekly rather than orally. If methotrexate cannot adequately control the inflammation, then it requires the addition of an anti-TNF agent; adalimumab appears to be the drug of choice, with effective control of the uveitis in 16/18 children in one study.[100] There are some reports of uveitis occurring in association with etanercept.[101]

Cataract surgery is challenging and requires very careful preparation, perioperative care, and intensive postoperative management. It is vital that the patient's carers are fully aware of the importance of adherence to prescribed therapy and follow-up visits. Traditionally cataract removal for these patients was by pars plana vitrectomy/lensectomy followed by aphakia, but it is now more common to use intraocular lenses at the time of surgery.[102–104] Postoperative posterior synechiae and intraocular lens deposits are common, but overall visual improvement is encouraging, with a recent series of 17 eyes reporting an improvement in visual acuity

of 2 lines or more in all patients with no increase of CME, glaucoma, or hypotony,[103] but it should be noted that other studies do report significant rates of secondary glaucoma and CME.[104]

Systemic Lupus Erythematosus

General Considerations

Systemic lupus erythematosus (SLE) is a multisystem autoimmune disease predominantly affecting women of childbearing age. The 1997 American College of Rheumatology classification criteria remain widely used (Box 83.5), although an alternative set of classification criteria were proposed by the Systemic Lupus International Collaborating Clinics (SLICC) group in 2012.[105,106] Although similar in outline, the SLICC criteria have greater sensitivity, at the expense of some specificity, by considering a broader range of clinical manifestations (especially in dermatologic and neurologic categories) and immunologic manifestations (for example low complement). By requiring the presence of at least one immunologic feature, the SLICC criteria do not support the concept of "seronegative lupus."

Box 83.5

The 1997 Updated American College of Rheumatology Criteria for Systemic Lupus Erythematosus

For the purposes of clinical trials, a diagnosis of SLE is made on the presence of at least four out of 11 criteria being present simultaneously or sequentially.

1. **Malar rash**
   Fixed erythema, flat or raised, over the malar eminences, tending to spare the nasolabial folds

2. **Discoid rash**
   Erythematous raised patches with adherent keratotic scaling and follicular plugging; atrophic scarring may occur in older lesions

3. **Photosensitivity**
   Skin rash as a result of unusual reaction to sunlight, by patient

history or physician observation

4. **Oral ulcers**
   Oral or nasopharyngeal ulceration, usually painless, observed by physician

5. **Nonerosive arthritis**
   Involving 2 or more peripheral joints, characterized by tenderness, swelling, or effusion

6. **Pleuritis or pericarditis**

(a) Pleuritis: convincing history of pleuritic pain or rubbing heard by a physician or evidence of pleural effusion
or

(b) Pericarditis: documented by electrocardiogram or rub or evidence of pericardial effusion

7. **Renal disorder**

(a) Persistent proteinuria > 0.5 g per day or > than 3+ if quantitation not performed
or

(b) Cellular casts: may be red cell, hemoglobin, granular, tubular, or mixed

8. **Neurologic disorder**

(a) Seizures: in the absence of offending drugs or known metabolic derangements, e.g., uremia, ketoacidosis, or electrolyte imbalance
or

(b) Psychosis: in the absence of offending drugs or known metabolic derangements, e.g., uremia, ketoacidosis, or electrolyte imbalance

9. **Hematologic disorder**
At least one of the following:

(a) Hemolytic anemia – with reticulocytosis

(b) Leucopenia <4000/mm^3 on ≥2 occasions

(c) Lymphopenia <1500/mm^3 on ≥ 2occasions

(d) Thrombocytopenia <100 ,000/mm^3 in the absence of offending drugs

. **Immunologic disorder**
At least one of the following:

(a) Anti-DNA: antibody to native DNA in abnormal titer

(b) Anti-Sm: presence of antibody to Sm nuclear antigen

(c) Positive finding of antiphospholipid antibodies on:

1. An abnormal serum level of IgG or IgM anticardiolipin antibodies

2. A positive test result for lupus anticoagulant using a standard method, *or*

3. A false-positive test result for at least 6 months confirmed by *Treponema pallidum* immobilization or fluorescent treponemal antibody absorption test

. **Positive antinuclear antibody**
An abnormal titer of antinuclear antibody by immunofluorescence or an equivalent assay at any point in time and in the absence of potential drug causes

Modified from Hochberg MC. Updating the American College of Rheumatology revised criteria for the classification of systemic lupus erythematosus. Arthritis Rheum 1997;40:1725.

Epidemiology

SLE has a prevalence of around 28 cases per 100, 000,[107] predominantly affecting women of child-bearing age (15–45 years); the female : male ratio peak is 12 : 1. SLE is more common in non-Caucasians, in whom it is both more severe and earlier in onset.

Articular and Systemic Disease

SLE is a systemic disease that can cause constitutional or organ-specific symptoms. The skin, mucous membranes, joints, kidney, brain, serous membranes, lung, heart, and occasionally the gastrointestinal tract may all be involved.[105,107] Arthritis in SLE can be divided into a deforming and nondeforming arthropathy. Constitutional symptoms consist of fever, malaise, fatigue, weight loss, lymphadenopathy, and anorexia.[107] There are multiple cutaneous manifestations of lupus: commonly these include photosensitivity (>50% of patients), butterfly/malar rash, painful/painless oral ulcers, diffuse alopecia, and livedo reticularis.[107]

Renal disease is one of the most serious SLE manifestations and a prognostic indicator of disease severity. Renal biopsy is used to determine the class of nephropathy as classified by the International Society of Nephrology (ISN)/Renal Pathology Society

(RPS) guidelines.[108]

Neuropsychiatric SLE (NPSLE) is a major diagnostic and treatment problem. The ACR has provided classification criteria, describing central and peripheral types of neurologic involvement that may be found in lupus patients.[107]

Pulmonary features of SLE include pleurisy, pneumonitis, pulmonary hemorrhage, pulmonary embolism, pulmonary hypertension, and diaphragmatic weakness causing shrinking lungs. Pericarditis is the most common cardiac manifestation; others include myocarditis, endocarditis, accelerated atherosclerosis, and, rarely, pericardial tamponade.[107]

Abdominal pain, nausea, vomiting, and diarrhea occur in up to 50% of SLE patients. Gastrointestinal involvement includes mesenteric vasculitis (high risk of death), aseptic peritonitis (with or without ascites), subacute bowel obstruction, hepatitis, sclerosing cholangitis, protein-losing enteropathy, pancreatitis, and ascites.[109]

Cytopenias, including anemia, leucopenia, or thrombocytopenia, are commonly associated with SLE; they may be immune-mediated or due to other factors, e.g., menstrual losses. Antiphospholipid antibodies and lupus anticoagulant are found in about 30–40% of patients, associated with venous and arterial thrombosis, recurrent fetal loss, preeclampsia, headache, and epilepsy.[107]

A firm diagnosis of lupus is made based on appropriate clinical findings and the measurement of at least one antibody. There are a number of antibodies associated with SLE, the most common being ANA (antinuclear antibody). Other associated autoantibodies include anti-dsDNA (double stranded DNA) in approximately 60% of patients, the highly specific anti-Sm antibody (Smith proteins) in 10–30% of patients, and anti-RNP (ribonucleoprotein) also in 10–30% of patients.[105–107]

Ocular Disease

Ophthalmic complications are common in SLE, affecting up to one-third of patients. The commonest complication is keratoconjunctivitis sicca, but sight-threatening posterior segment and neuro-ophthalmic disease is also seen (reviewed by Sivaraj and coworkers).[110]

Common ocular surface diseases related to SLE include KCS

(25% of SLE patients).[111,112] Peripheral ulcerative keratitis is a rare but serious complication requiring urgent immunosuppression.[2]

Episcleritis is observed in 1–2% and scleritis in 1% of patients with SLE.[6,113] Scleritis may be anterior or posterior, necrotizing or non-necrotizing, and may indicate activity of the underlying disease.

Occasionally SLE may cause orbital inflammation and present with acute proptosis, lid edema, conjunctival injection and chemosis, reduced ocular motility, and elevated intraocular pressure, with myositis and panniculitis also reported.[114,115] Orbital inflammation may also be associated with posterior scleritis.

Lupus retinopathy was first described by Bergmeister in 1929. Its prevalence is estimated at around 10%, although this is variable depending on the population studied.[116] The classic clinical picture is of cotton-wool spots, retinal hemorrhages, and vascular abnormalities (arterial narrowing with capillary dilation, and venous dilation and tortuosity) (Figs. 83.1–83.3). Additional features may include retinal edema, hard exudates, and microaneurysms. Retinopathy is usually bilateral but may be asymmetric.[117]

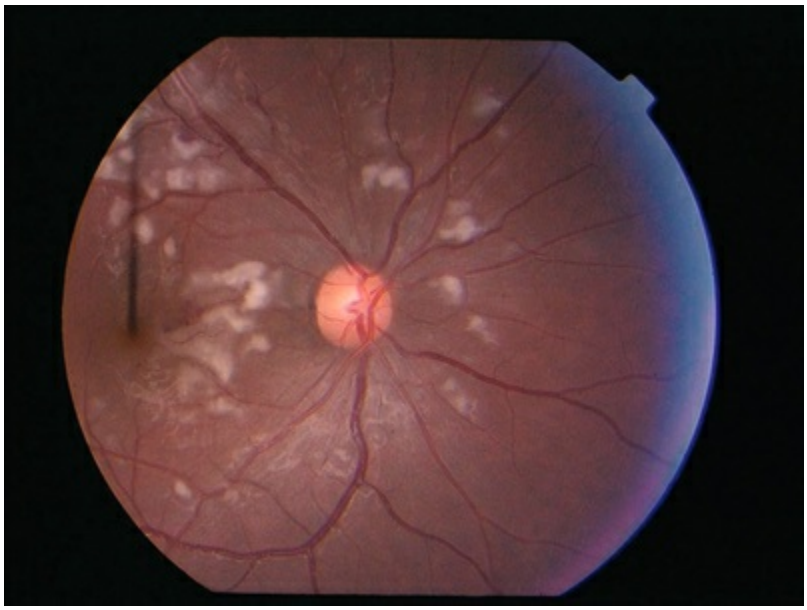

FIG. 83.1 Acute lupus retinopathy with cotton-wool spots, arterial narrowing, venous dilation, and tortuosity.

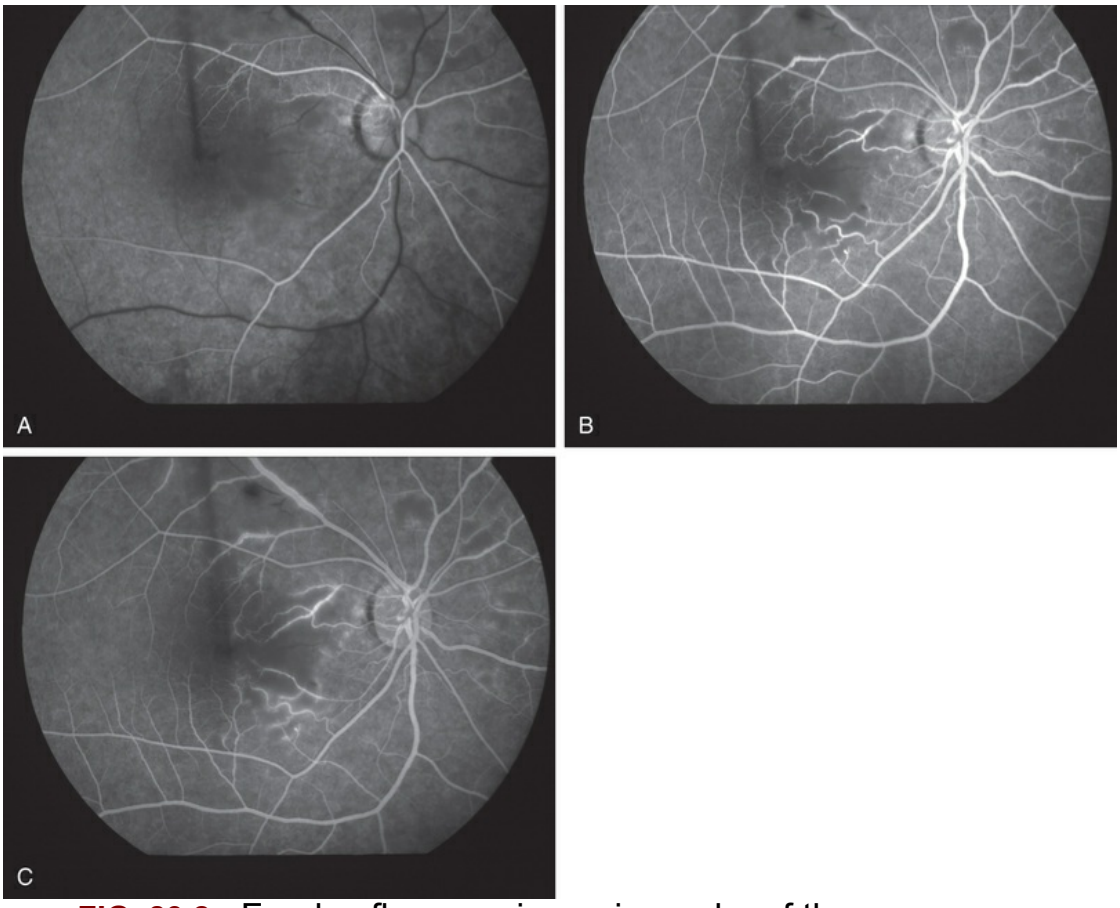

FIG. 83.2 Fundus fluorescein angiography of the same patient: (A) early, (B) arteriovenous, and (C) late phases demonstrating capillary “dropout,” vessel wall staining, and leakage.

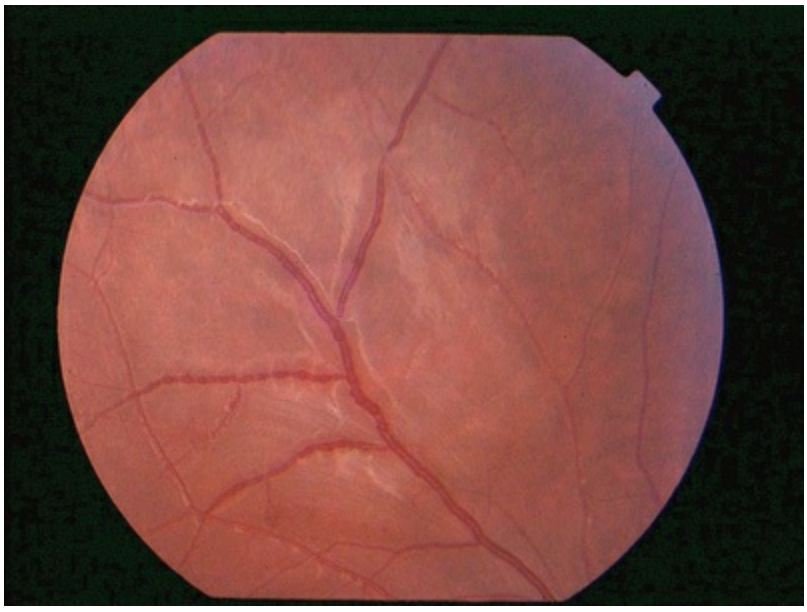

FIG. 83.3 Detail of the same patient showing venous beading.

Severe vaso-occlusive retinopathy is much less common but potentially devastating. Whereas mild retinopathy may be picked up as an incidental finding, vaso-occlusive retinopathy usually presents with visual symptoms such as reduced acuity, visual field loss, and distortion. In addition it is strongly associated with the life-threatening complication of CNS lupus.[118] The clinical appearance is of widespread arteriolar occlusion and capillary nonperfusion. Subsequently neovascularization is common (up to 72% cases) (Figs. 83.4 and 83.5)[118] and may be complicated by vitreous hemorrhage (up to 63%), retinal traction, and detachment (up to 27%).[118] The occurrence of vaso-occlusive disease is strongly associated with the presence of antiphospholipid antibodies (up to fourfold increased risk).[119] Primary antiphospholipid syndrome (i.e., antiphospholipid antibodies in the absence of SLE or any other systemic disease) may be associated with a similar severe vaso-occlusive retinopathy but with cotton-wool spots being less common. The severe vaso-occlusive retinopathy is sometimes described as a retinal vasculitis, but this is not generally supported by histologic examination.[120]

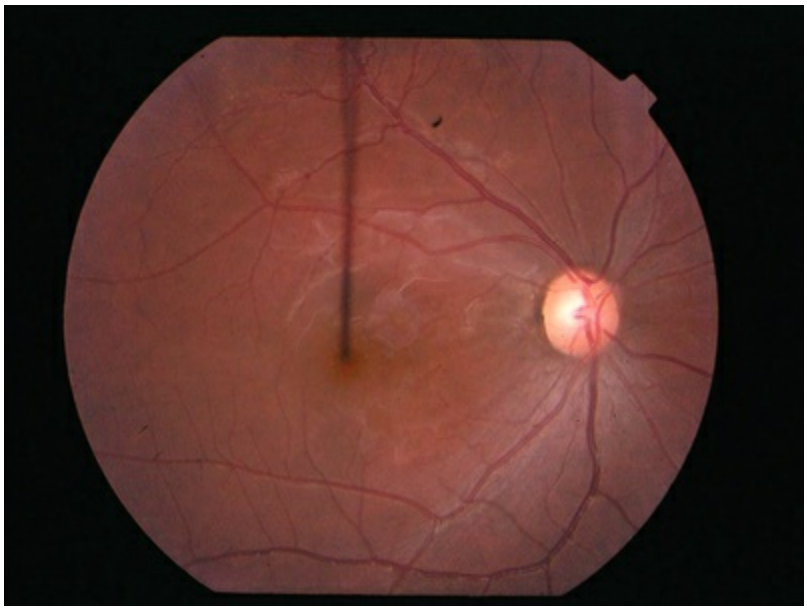

FIG. 83.4 The same patient one year later, showing resolution of cotton-wool spots. Careful examination,

however, reveals two areas of abnormal neovascularization.

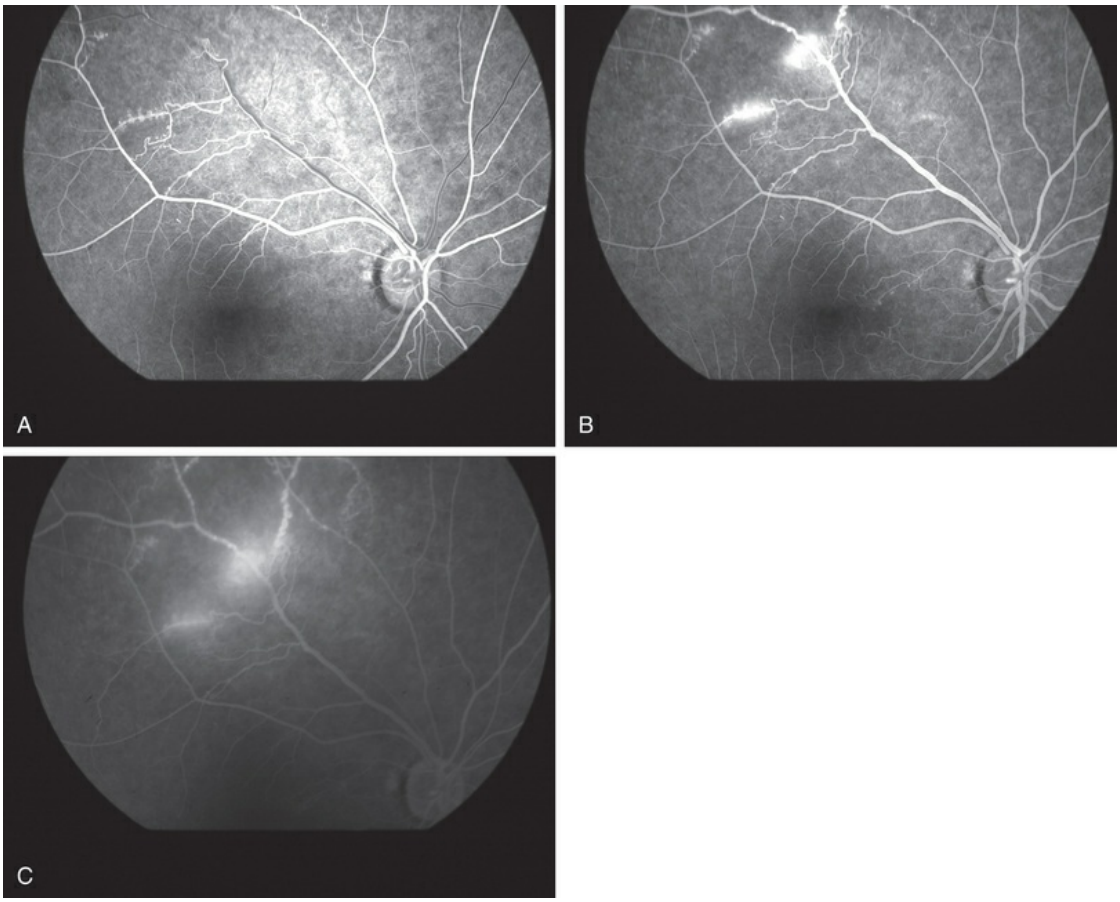

FIG. 83.5 Fundus fluorescein angiography of the same patient: (A) early, (B) arteriovenous, and (C) late phases demonstrating the presence of active new vessels. These did not resolve with immunosuppression and required sectoral laser photocoagulation.

Occlusion of the larger retinal vessels may occur and again is associated with the presence of antiphospholipid antibodies. Manifestations include branch retinal arteriolar or central retinal artery occlusion (B/CRAO) (Fig. 83.6), branch or central retinal vein occlusion (B/CRVO), and combined retinal arterial and venous occlusions.[118,120]

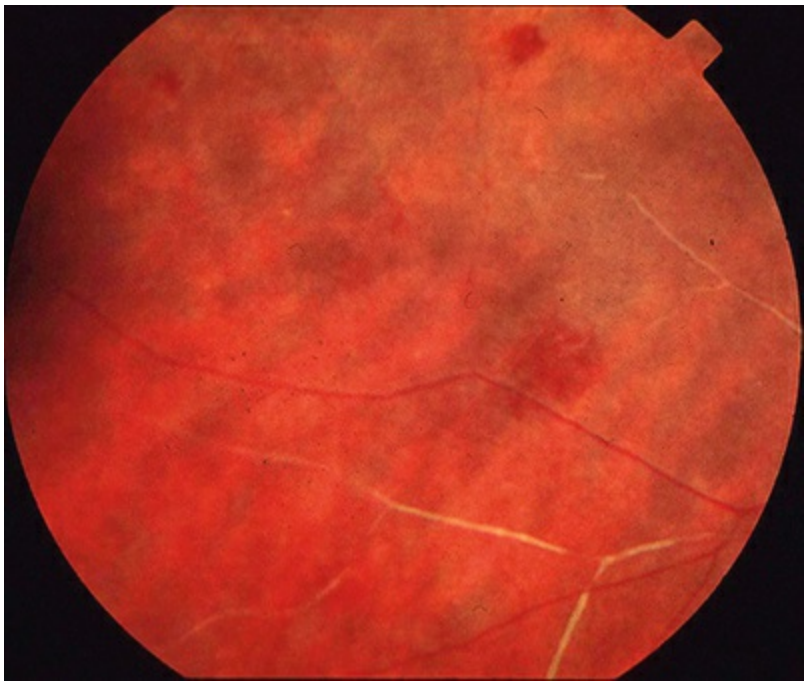

FIG. 83.6 Branch retinal arteriole occlusion in a patient with systemic lupus erythematosus and antiphospholipid syndrome.

Other retinal manifestations of SLE include an unusual bilateral pigmentary retinopathy that may resemble retinitis pigmentosa but is proposed to be ischemic in origin.[121] Coexisting systemic hypertension may result in features of hypertensive retinopathy. Choroidal involvement in SLE (lupus choroidopathy) may also cause significant visual morbidity. Choroidopathy results in single or multifocal serous detachments of the retina and retinal pigment epithelium (RPE), which may mimic idiopathic central serous chorioretinopathy (CSC).[122] The degree of visual symptoms depends on the anatomic location of the detachment(s). These serous detachments may become extensive over time but conversely may reverse with control of the underlying systemic disease.[122] Fluorescein angiography (and indocyanine green angiography) is helpful as it not only demonstrates typical CSC-like leakage from the choroid into the subretinal and sub-RPE spaces but also demonstrates the degree of choroidal ischemia.

Optic nerve disease is uncommon (about 1% patients with SLE). The spectrum of disease described includes anterior and posterior ischemic optic neuropathy, and acute optic neuritis (which is also thought to be ischemic in origin).[123] Bilateral optic disc swelling in

SLE may arise due to either idiopathic intracranial hypertension or accelerated systemic hypertension, both of which are more common in SLE.

Other neuro-ophthalmic complications of SLE include ocular motility abnormalities (causes include brain stem infarcts, cranial neuropathies, tenosynovitis, myositis, and Miller–Fisher syndrome), nystagmus, ptosis, and migraine.[110]

Finally, it should be noted that patients with SLE are immunosuppressed (both due to disease and treatment) and may present with severe intraocular infections. Retinal necrosis due to herpes simplex virus, varicella-zoster virus, and cytomegalovirus have been reported. Other ocular infections include tuberculous choroidal abscess and nocardia endophthalmitis.[124,125]

Treatment

Treatment of Systemic Disease.

The treatment of SLE is tailored to the severity of disease. General lifestyle advice includes avoidance of sunlight and use of sun block. Patients should have regular disease assessments and be screened for SLE complications, such as infection, diabetes, hyperlipidemia, and hypertension. Women of childbearing age should be advised regarding the importance of good disease control before conception, the need for close monitoring during pregnancy, and the risk of postpartum disease flare.

Mild cases with intermittent rashes, arthritis, and other mucocutaneous features can usually be treated with corticosteroid creams, short courses of NSAIDs, and hydroxychloroquine (<6.5 mg/kg per day). Patients with more severe disease manifestations (such as nephritis, gastrointestinal vasculitis, or central nervous system disease) are likely to need azathioprine, methotrexate, mycophenolate mofetil, or cyclophosphamide as immunosuppressive agents, combined with a variable dose of oral steroid. If conservative treatment and traditional DMARDs fail, then biologics should be considered.

Rituximab is a monoclonal antibody against the B-lymphocyte marker CD20 expressed on B cells, it has been used in SLE patients since 2002, but not without controversy. Although two randomized

controlled trials failed to demonstrate statistical efficacy, most clinicians regard it as an effective treatment strategy for antibody-mediated disease manifestations such as arthritis and nephritis, and this is supported by a large meta-analysis of open-label registries.[126] It may also have significant "steroid-sparing" effects, allowing a lower dose of concomitant steroid to achieve disease control.[127] It therefore remains widely used, particularly in refractory nephritis. An alternative biologic agent, belimumab, neutralizes soluble B-lymphocyte stimulator (BLyS – also known as BAFF), a B-cell activating factor that induces B-cell proliferation and maintains survival. Efficacy in patients with moderately active nonrenal lupus was assessed in two masked, randomized, placebo-controlled trials.[128] It has been approved for use in the United States but has not yet obtained worldwide authorization in all publically funded healthcare systems.

Treatment of Ocular Disease.

In SLE, control of the systemic disease often improves the ophthalmic disease. The presence of severe ophthalmic disease should prompt the rheumatologist to look for evidence of systemic activity, and warrants escalation of systemic therapy. Additional local and regional treatments may also be indicated depending on the type of ocular complication. For example, KCS may benefit from a range of treatments, including tear replacement therapy (preservative-free preparations preferred), punctal occlusion, lid hygiene, topical corticosteroids or cyclosporine, and environmental measures.[110]

Mild anterior segment inflammation may respond to topical corticosteroids (keratitis or anterior uveitis) or topical NSAIDs (episcleritis). In more severe anterior segment inflammation, such as scleritis or disease affecting the posterior segment or orbit, systemic treatment is required. Non-necrotizing scleritis may respond to oral NSAIDs, but most severe inflammatory disease will require high-dose systemic corticosteroid often in combination with the immunosuppressive agents listed above. Significant retinal vascular occlusions associated with antiphospholipid antibodies may be treated with warfarin or low-dose acetylsalicylic acid (in addition to immunosuppression). Retinal neovascularization

usually requires panretinal photocoagulation. Persistent vitreous hemorrhage or traction retinal detachment may require vitreoretinal surgery.[110,118]

Sjögren Syndrome

General Considerations

Sjögren syndrome is a slowly progressive, inflammatory autoimmune disease primarily affecting the exocrine glands.

Epidemiology

Sjögren syndrome predominantly affects females in the fourth to fifth decade of life. The female : male ratio is 9 : 1. In a population-based study in Minnesota, incidence of Sjögren syndrome was estimated to be 3.9 per 100, 000 per year.[129]

Articular and Systemic Disease

Sjögren syndrome is clinically characterized by sicca symptoms: dry eyes and mouth due to failure of the salivary and mucosal glands. Sjögren syndrome may be primary or secondary to a preexisting disorder such as SLE, rheumatoid arthritis, systemic sclerosis, vasculitis, autoimmune thyroid disease, or primary biliary cirrhosis.[130,131]

The primary syndrome is associated with hypergammaglobulinemia with very high total IgG levels and strongly positive antinuclear antibody, rheumatoid factor, and anti-Ro and anti-La antibody levels. The extraglandular manifestations include arthralgia, Raynaud phenomenon, peripheral neuropathy, myositis, liver and interstitial nephritis, or renal tubular acidosis. Immune complex deposition resulting from ongoing B-cell hyperactivity is associated with increased morbidity and lymphoma risk.[130]

Ocular Disease

The cardinal ocular sign of Sjögren syndrome is keratoconjunctivitis sicca (KCS), which may range from mild irritation in its early stage to severe tear deficiency with ocular surface inflammation and

damage resulting in severe visual loss.[1] Assessment of tear production, tear stability, and careful examination of the ocular surface are key.[1] Posterior segment disease is rare. Rosenbaum and Bennett described a series of eight patients with Sjögren syndrome and uveitis, reporting that in all cases the disease was bilateral and chronic; in their report they describe anterior and posterior disease (but no chorioretinitis) with posterior synechiae, cataract, and pars plana exudation being common.[132]

Treatment

Treatment of Systemic Disease.

Sjögren syndrome is a chronic disease with a wide clinical spectrum, making it necessary for regular follow-up. Treatment of sicca symptoms is essential and includes general measures such as avoidance of dry atmospheres, humidification of rooms, and chewing sugarless chewing gum.[131] Hydroxychloroquine can be effective for treating the subgroup of Sjögren sufferers who have inflammatory myalgias and arthralgias. Anti-TNF-α agents have not shown clinical efficacy. Rituximab also did not show a statistically significant effect in a recent randomized controlled trial, although further trials are due to report shortly[131,133]

Treatment of Ocular Disease.

The treatment of KCS is predominantly with frequent use of preservative-free tear substitutes, with a range of viscosities to suit the patient, their visual needs, and even the time of day. RCTs have shown topical 0.05% cyclosporine to be beneficial for patients with moderate to severe dry eye disease.[134,135] In the presence of associated inflammation of the ocular surface, topical glucocorticoids may be required.[29]

Sarcoidosis

This is dealt with separately in Chapter 81 (Sarcoidosis).

Familial Juvenile Systemic Granulomatosis

(Blau Syndrome)

General Considerations

Familial juvenile systemic granulomatosis (Blau syndrome or Jabs syndrome) is a rare autosomal dominant disorder, associated with mutations in the *NOD2/CARD 15* gene.[136–139] It was described by Blau in 1985, as a triad of polyarthritis, iritis, and granulomatous papulosquamous rash.

Epidemiology

Little is known about the epidemiology of familial juvenile systemic granulomatosis. It is thought to occur worldwide, with equal gender and race distribution.[138] All affected members carry one of a number of *NOD2/CARD 15* mutations.[138, 140] Not all affected individuals have the complete triad of symptoms.

Articular and Systemic Disease

Familial juvenile systemic granulomatosis presents with a polyarticular arthritis, associated with synovial and tenosynovial cysts, resulting in swelling of the affected joints and tendons.[138] Campylodactyly (multidigit contracture of the interphalangeal joints) can occur secondary to inflammation.[138]

Familial juvenile systemic granulomatosis can be distinguished from childhood sarcoidosis by the absence of pulmonary involvement.[138,141] The rash is described as papuloerythematous and usually affects the trunk and extremities.[138] In addition, familial juvenile systemic granulomatosis can be associated with a large vessel vasculitis and cranial nerve palsies;[138] Crohn's disease is reported to occur in 30% of patients.[142]

Ocular Disease

The cardinal ocular sign of familial juvenile systemic granulomatosis is a chronic anterior uveitis or panuveitis with multifocal choroiditis.[143] Complications of uveitis are common, including cataract, glaucoma, band keratopathy, and CME. Also reported are subepithelial corneal infiltrates, optic disc edema, ischemic optic neuropathy, and retinal vasculopathy.[143,144]

Treatment

Treatment of Systemic Disease.

Treatment for familial juvenile systemic granulomatosis is largely empirical. Prednisone can be used (dose will be dependent on the severity of disease).[138,139] Immunosuppressive agents, such as methotrexate and azathioprine, have been used with little effect.[138,139] There are also isolated reports of benefit from infliximab and anakinra (IL-1 receptor antagonist) in refractory cases.[138,139]

Treatment of Ocular Disease.

Due to the chronicity of disease, long-term immunosuppression is generally required[144] that may be supplemented with topical and local treatment (as described previously) when needed for flares of ocular disease.

Systemic Sclerosis

General Considerations

Systemic sclerosis (also called scleroderma) is a multisystem disease of unknown etiology, with immunologic, vascular, and fibrotic abnormalities. There is characteristic tissue thickening and fibrosis, often with involvement of internal organs. The most recent classification criteria were published in 2013.[145]

Epidemiology

The precise estimate for the incidence and prevalence of systemic sclerosis are unknown. This is likely due to a combination of true variation over different populations and differences in case ascertainment and disease classification.[146] Reported prevalence estimates in North America have varied from 13.8 cases per 100, 000 from 1950 to 1979 to 28.6 cases per 100, 000 in 1985, while a Canadian study estimated the prevalence in Quebec in 2003 to be 44.3 cases per 100 ,000.[146,147] Systemic sclerosis is more common in women, with a female : male ratio of 4–6 : 1. Multiple studies have demonstrated increased incidence and severity of scleroderma in people of African descent.

Articular and Systemic Disease

Cutaneous manifestations may initially present with inflammation, edema, and reduced sweat and oil production. The characteristic cutaneous features include sclerodactyly, scleroderma, Raynaud phenomenon, digital ulceration, telangiectasia, calcinosis, and perioral radial furrowing. Gastrointestinal effects include esophageal dysmotility, gastroesophageal reflux disease (GORD), and intestinal dysmotility.[145]

Pulmonary disease (including pulmonary fibrosis and pulmonary arterial hypertension) is the leading cause of mortality in systemic sclerosis.

Systemic sclerosis patients will for the most part have a positive ANA (85–90%). The mutually exclusive presence of scleroderma-associated antibodies (including anticentromere, antitopoisomerase-1 (Scl-70) and anti-RNA polymerase III) are increasingly recognized as having important prognostic implications.[148]

Ocular Disease

Ocular involvement is common, particularly of the eyelids and anterior segment. Lid involvement occurs in up to two-thirds of patients, resulting in progressive skin tightness, blepharophimosis, and occasionally lagophthalmos. Small lid telangiectasia occurs in up to 21% of patients.[149,150] Ocular surface disease is also very common, with KCS affecting up to 79% patients. KCS may occur as part of secondary Sjögren syndrome. It should be noted when interpreting IOP measurements in scleroderma that central corneal thickness increases during the first eight years of disease and may affect IOP readings.[151,152]

Although retinopathy may be seen in patients with scleroderma. it is usually in the context of secondary hypertension, and is of a clinical appearance typical of hypertensive retinopathy (cotton-wool spots, exudation, neuroretinal edema, hemorrhages). Milder retinal changes may also occur in normotensive patients with scleroderma, as shown by Ushiyama et al. where 34% of normotensive scleroderma patients (vs. 8% controls) had retinal findings such as hard exudates and vascular tortuosity.[116] Other reported retinal features include combined CRVO and CRAO,

bilateral CRVO, BRVO, and parafoveal telangiectasia. Interestingly, fundus fluorescein angiography (FFA) studies suggest that abnormality of the choroidal vasculature occurs in around one-third of patients, with hyperfluorescence in the late phase corresponding with areas of hypopigmentation.[153] Other reported ocular complications include cranial nerve palsies, Brown syndrome, and ophthalmoplegia.[154]

Treatment

Treatment of Systemic Disease.

Systemic sclerosis is a heterogeneous condition, with varying degrees of severity. Treatment strategies are aimed at the vascular, immunologic, or fibrotic manifestations of disease and need to be individualized depending on the patient and their disease manifestations.[155] Digital ulceration is typically managed with conventional vasodilators, escalating to sildenafil (phosphodiesterase type V inhibitor) and bosentan (endothelin receptor antagonist) in severe cases. Sildenafil, bosentan, and intravenous prostacyclin are used for pulmonary hypertension. Corticosteroids are commonly used at low doses for inflammatory arthritis, but there is no convincing trial evidence. Methotrexate has been demonstrated to be effective for skin manifestations in early disease and may help joint disease, while mycophenolate mofetil is an effective alternative for skin, lung, and joint disease. The efficacy of cyclophosphamide for scleroderma-associated lung fibrosis has been demonstrated and subsequently replicated in a clinical trial setting.[156] In patients with severe diffuse cutaneous systemic sclerosis, autologous hematopoietic stem cell transplantation has proven more effective than cyclophosphamide for skin and lung disease, albeit with considerable procedure-related mortality and morbidity.[157,158]

Tocilizumab (anti-interleukin-6) is another agent showing early promise in systemic sclerosis, and its role needs to be clarified in larger clinical trials.

Treatment of Ocular Disease.

Keratoconjunctivitis sicca may usually be controlled with topical

therapy as previously described.[29] In addition to systemic immunosuppression, treatment of blood pressure is an important factor in preventing or treating retinopathy.

Polymyositis and Dermatomyositis

General Considerations

Polymyositis and dermatomyositis are inflammatory myopathies, characterized by proximal muscle weakness and often a variety of cutaneous and systemic features.

Epidemiology

Several classification criteria have been proposed; the most frequent are the Bohan and Peter criteria (Box 83.6).[159] The precise incidence of myositis is unknown but is estimated to be between 2 and 10 new cases per million persons at risk per year.[160] The reported female : male incidence ratio is 2.5 : 1.[160] Similar to SLE and systemic sclerosis, there is a higher incidence in people of African descent, with a younger age of onset.

Box 83.6

The Bohan and Peter Criteria for the Diagnosis of Polymyositis and Dermatomyositis

Individual Criteria

1. Symmetric proximal muscle weakness

2. Muscle biopsy evidence of myositis

3. Increase in serum skeletal muscle enzymes

4. Characteristic electromyography pattern

5. Typical rash of dermatomyositis

Diagnostic criteria

Polymyositis:

Definite: all of 1–4

Probable: any three of 1–4

Possible: any two of 1–4

Dermatomyositis:

Definite: 5 plus any three of 1–4

Probable: 5 plus any two of 1–4

Possible: 5 plus any one of 1–4

Modified from Bohan A, Peter JB. Polymyositis and dermatomyositis (first of two parts). N Engl J Med 1975;292:344–7.

Myositis can be associated with other autoimmune conditions, particularly scleroderma and mixed connective tissue disease, and occasionally in SLE, RA, and Sjögren syndrome. Recent interest has focused on a range of myositis-associated autoantibodies that may have utility for classification and prognostication in the inflammatory myositides.[161]There is an increased risk of malignancy in both polymyositis and dermatomyositis. The greatest risk is in dermatomyositis (standardized incidence ratio (SIR): 3.0) which is associated with ovarian, lung, pancreatic, stomach, colorectal, and non-Hodgkin lymphoma. Antitranscriptional intermediary factor 1 γ (anti-TIF-1γ) antibodies may be seen in cancer-associated dermatomyositis. Polymyositis is associated with a significant but lower increased risk (SIR: 1.2–1.5), of malignancy, particularly non-Hodgkin lymphoma, and lung and bladder cancer.[162]

Articular and Systemic Disease

Myositis often presents as a subtle, progressive, painless symmetrical weakness over 3–6 months, affecting proximal more than distal muscles.[163] Dermatomyositis is associated with

characteristic skin manifestations including a heliotrope rash (purplish rash over the periorbital area), Gottron papules (scaly or erythematous papules and plaques over bony prominences, particularly elbows and knees), and an erythematous rash over anterior chest and upper back and shoulders. Subcutaneous calcinosis (nodules or plaques of calcification over the elbows, forearms, knuckles, axillae, or buttocks), occurs particularly in juvenile dermatomyositis, but occasionally also in adult cases.[163]

Arthralgias and synovitis of small or large joints may occur in patients with myositis, even without an associated connective tissue disease. A deforming arthropathy of the proximal and distal interphalangeal joints occurs typically in patients with inflammatory myopathy and antisynthetase antibodies.[163] Interstitial lung disease is also more likely to develop in patients with anti-Jo-1 or other antisynthetase antibodies. Subclinical cardiac involvement including myocarditis, pericarditis, arrhythmias, and congestive cardiac failure have been reported. Gastrointestinal tract musculature involvement may occur, causing dysphonia, dysphagia, pseudo-obstruction, or malabsorption.[163]

Ocular Disease

The classic heliotrope eyelid eruption of dermatomyositis is a familiar periocular sign of disease. Actual ocular involvement with myositis of the extraocular muscles is rare.[164] A retinopathy with cotton-wool spots is described in both these conditions, most commonly seen in children and usually (but not exclusively) in the context of systemic vasculitis. Retinopathy is usually mild, but in its severe retinal vasculitis form may lead to permanent visual loss.[165,166] Conjunctivitis, anterior uveitis, and episcleritis are also reported.[166,167]

Treatment

Treatment of Systemic Disease.

There are no large RCTs exploring the treatment of myositis, so treatment is based on case series, open-label trials, and small RCTs. General measures for treating are rehabilitation, avoidance of aspiration, and sun protection. Primary initial therapy is oral

corticosteroid.[163,168] Initially patients should be treated with prednisone 1 mg/kg, daily for 4–6 weeks before tapering the dose, but in more severe disease intravenous methylprednisolone up to 1 g/day for three consecutive days is recommended. Immunosuppressant therapy at an early stage may be required to facilitate corticosteroid reduction and side-effects from corticosteroids, and the first choice agents are methotrexate and azathioprine. In severe cases, in particular those associated with vasculitis or interstitial lung disease, cyclophosphamide has been recommended.[163,168] Intravenous immunoglobulin has been proposed in patients with rapidly progressing disease, and alternative agents include cyclosporine and mycophenolate mofetil. In a randomized controlled trial of Rituximab for inflammatory myopathy, no statistical difference was seen in comparison with placebo when looking at the primary endpoint, but 83% in the treatment group did improve.[169] Anti-TNF biologics are ineffective or may even worsen outcome.

Treatment of Ocular Disease.

Systemic immunosuppression is required to control both the systemic disease and its ocular manifestations. Vasculitis regimens such as intravenous cyclophosphamide and methylprednisolone are commonly used.[167]

Relapsing Polychondritis

General Considerations.

Relapsing polychondritis is a rare autoimmune disease of unknown etiology, primarily affecting cartilaginous structures throughout the body.

Epidemiology.

Relapsing polychondritis has an estimated incidence rate of 3.5 per million per annum; the peak onset is between 40 and 60 years. Equal frequency has been reported in both genders and all racial groups. Over 30% of cases are associated with existing autoimmune and hematologic conditions, including RA, SLE, Sjögren syndrome,

AS, lymphoma, and IBD.[170]

Articular and Systemic Disease

Relapsing polychondritis is a multisystem disease that can affect the cartilaginous structures in the eyes, ears, nose, laryngotracheobronchial, and costal cartilages (Table 83.2). It causes inflammation of hyaline cartilage with a predilection for ear cartilage.[171] Involvement of the parasternal joints, including the sternoclavicular, costochondral, and manubriosternal articulations, is typical for this condition. Peripheral joint disease is reported in 70% of patients and is usually nonerosive and asymmetric.[171]

TABLE 83.2
Systemic Features of Relapsing Polychondritis

Organ Involvement	Clinical Manifestation
Ear	External inflammation, loss of hearing, tinnitus, vertigo
Eye	Episcleritis, scleritis, ulcerative keratitis, uveitis, proptosis
Nose	Crusting, rhinorrhea, epistaxis, saddle nose
Large airways	Hoarseness, aphonia, wheezing, inspiratory stridor, nonproductive cough, dyspnea
Joints	Parasternal joints, peripheral joints (mono- or oligoarticular)
Heart	Aortic and mitral valvular disease
Skin	Aphthous ulcers, purpura, papules, nodules or ulcerations

Reproduced with permission from Lahmer T, Treiber M, von Werder A, et l. Relapsing polychondritis: an autoimmune disease with many faces. Autoimmun Rev 2010;9:540–6.

Ocular Disease

Ophthalmic disease occurs in around half of patients with relapsing polychondritis. In a series of 112 patients, Isaak and coworkers reported that 19% patients had ocular symptoms at the onset of disease, with 51% developing ocular symptoms during the course of disease. Episcleritis (39%) and scleritis (14%) are common.[172] Anterior uveitis was reported as just 9% in the Isaak series but has been reported to be as prevalent as 30% in other series.[173] Other anterior segment findings include KCS and peripheral ulcerative keratitis.[174] The commonest posterior segment presentation is posterior scleritis, which may be severe and be associated with

serous retinal detachments and frank proptosis.[175–177] Retinopathy consisting of cotton-wool spots and intraretinal hemorrhages is reported to occur in up to 9% of patients. Other posterior segment features are branch or central retinal vein occlusions and ischemic optic neuropathy.[172] Cranial neuropathies may also be seen.

Treatment

Treatment of Systemic Disease.

First-line therapy for relapsing polychondritis is corticosteroid, initially started at 1 mg/kg prednisone daily; if necessary, three pulses IV methylprednisolone can be administered. Immunosuppressives should be used for severe disease causing organ compromise or where corticosteroids have not provided a satisfactory response within a few weeks. The choice of immunosuppressant is empirical; the most commonly used agents are cyclophosphamide, azathioprine, cyclosporine, and methotrexate.[170] There are case reports reporting success with anti-TNF agents (etanercept/infliximab/adalimumab), anakinra, and rituximab.[178]

Treatment of Ocular Disease.

Systemic immunosuppression is required to control both the systemic disease and its severe ocular manifestations. Vasculitis regimens may be required. Anterior uveitis, episcleritis, and KCS may be additionally controlled with topical therapy as previously described.

Primary Systemic Vasculitis

The vasculitides are a heterogeneous group of diseases involving inflammation of blood vessels with subsequent tissue destruction and/or organ damage. The vasculitides can be considered to be primary or secondary (commonly associated with another connective tissue disease or infection). They are predominantly arterial in nature, though capillaries and less commonly veins are involved. Local tissue disruption is caused by inflammatory cell infiltrate in the vessel wall and subsequent tissue ischemia from

vessel occlusion. The primary systemic vasculitides are an uncommon group of diseases (combined annual incidence >100 new cases per million).[179] Classification is usually based on the predominantly affected vessel (Box 83.7). Recently the term ANCA-associated vasculitis (AAV) has been used to describe those small vessel conditions where there are similar immunopathologic tissue mechanisms: granulomatosis with polyangiitis (GPA, Wegener's granulomatosis), microscopic polyangiitis (MPA), and eosinophilic granulomatosis with polyangiitis (EGPA, Churg–Strauss syndrome).[180,181]

Box 83.7

Classification of Vasculitides According to the Chapel Hill Consensus

Primary Vasculitides

Large artery

Giant cell arteritis

Takayasu arteritis

Medium artery

Polyarteritis nodosa

Kawasaki disease

Small artery and vein

Granulomatosis with polyangiitis (Wegener's granulomatosis)[a]

Microscopic polyangiitis*

Eosinophilic granulomatosis with polyangiitis (EGPA,

Churg–Strauss syndrome)

Henoch–Schonlein purpura

Leukocytoclastic vasculitis

Essential cryoglobulinemic vasculitis

Other

Behçet disease

Cogan syndrome

Secondary Vasculitides

Connective tissue disease

Hepatitis B/C

Human immunodeficiency virus (HIV)

Recently, Watts et al. have suggested a possible fourth category, no predominant vessel size, to describe Behçet disease, primary central nervous system (CNS) vasculitis and Cogan syndrome.[180]

[a]These vasculitides are associated with ANCA.

Modified from Jennette JC, Falk RJ, Andrassy K, et al. Nomenclature of systemic vasculitides. Proposal of an international consensus conference. Arthritis Rheum 1994;37:187–92.

In parallel with advances in our understanding of the immunobiology of the vasculitides, it is becoming increasingly recognized that therapy for vasculitis needs to be tailored to the specific diagnosis and the phase of disease in that individual. An understanding of the natural history of the specific conditions and

assessment to identify the extent and activity of disease is required to achieve this.

Progression and Prognosis of Primary Systemic Necrotizing Vasculitis

Classification of the vasculitides is most often based on the size of vessel involved (Box 83.7).[182] The initial and predominant inflammatory process is granulomatous in some cases, with the vasculitic phase of the illness only presenting later. This is typical of GPA, where constitutional and upper respiratory symptoms may be present for several years prior to diagnosis, thus delaying the commencement of appropriate therapy and adding to the morbidity and mortality of the condition.

Though the vasculitides are characteristically relapsing diseases, the frequency of relapse depends on the specific underlying diagnosis. In polyarteritis nodosa (PAN) the risk is low, which contrasts with ANCA-associated vasculitides where relapse is as high as 50%.[183] Prior to the introduction of effective therapy, the 5-year survival of systemic necrotizing vasculitis (SNV) was only 15%; corticosteroids improved this figure to 48%, while the combination corticosteroids and cyclophosphamide (CP) gave a significant improvement, with 5-year survival reaching 80%. However, this improved survival came at a cost, with recurrent flares of disease activity leading to the accumulation of organ damage, with appreciable morbidity also related to drug toxicity.

Aims of Therapy

The aim of therapy in SNV must be to suppress disease activity so that organ damage is limited.

Clinical tools to assess disease activity and damage are used to aid in assessment and management of these complex diseases. These scoring systems have predictive value for severe disease where patients are at higher risk of mortality, thus supporting a more aggressive approach to therapy. The Birmingham Vasculitis Activity Score (BVAS) provides a weighted numeric score based on the specific organ involved and the severity of that involvement. A high score reflects either critical organ involvement or multisystem

disease and predicts a higher mortality.[184] The Vasculitis Damage Index (VDI) is a cumulative score where items of organ damage must be present for a period of at least 3 months and be attributable to effects of the disease, its therapy, or other undefined causes. A high VDI score identifies a subgroup of patients with more severe or fatal disease.[185]

Thorough clinical assessment to differentiate vasculitis localized to a single organ (such as ocular vasculitis) from more systemic disease is important, as the former group may not require systemic immunosuppression. Use of a systematic approach in clinical assessment, such as that provided on the BVAS form, can help clinicians identify previously unsuspected disease symptoms or signs, such as purpura or vascular bruits. Urinalysis is a simple critical investigation to identify renal involvement. Laboratory tests may provide supportive evidence of active systemic disease. A rise in C-reactive protein indicates active inflammation in the absence of infection. The presence of ANCA supports a diagnosis of one of the AAV but should not on its own prompt introduction of immunosuppressive therapy without appropriate clinical features. MPO-ANCA is seen in MPA and EGPA, while PR3-ANCA is most commonly seen in GPA. Tissue samples for histopathologic examination may be needed to confirm a diagnosis and exclude alternatives such as infection or malignancy. Therefore, a combination of clinical tools and laboratory investigations can help support a diagnosis of SNV and help differentiate disease activity, where immunosuppressive therapy may be required, from irreversible organ damage, where more therapy may be potentially harmful.

A diagnosis of vasculitis is not an indication to commence aggressive therapy in every patient. Some small vessel disease, such as Henoch–Schonlein purpura (HSP) or isolated leukocytoclastic vasculitis (LCV), where an initiating event is identified, may be self-limiting and need no therapy. Corticosteroids alone may be enough for the large vessel vasculitides. It is the AAV and PAN where a more aggressive approach is indicated to minimize organ damage. The approach outlined below can also be applied to other vasculitides where there is critical organ-threatening disease (such as sight-threatening scleritis in rheumatoid vasculitis).

Induction Stage.

Cyclophosphamide in combination with corticosteroids are the drugs of choice for remission induction. Continuous oral cyclophosphamide (2 mg/kg daily) in conjunction with oral prednisone (1 mg/kg reducing to 10 mg daily by 3 months) induces remission in most by 3 months.[186] Remission induction takes longer in some patients, increasing the risk of drug-related toxicity. A safer and equally effective approach is to use intermittent pulses of intravenous cyclophosphamide.[187] The pulse interval is an important factor and a suggested induction regimen has been provided (Table 83.3).

TABLE 83.3

Pulse Cyclophosphamide Induction Regimen

Drug Doses	**Methylprednisolone 10 mg/kg plus Cyclophosphamide 15 mg/kg**
Dose interval	0, 2, 4, 7, 10, 13 weeks Switch after six pulses to consolidation phase with monthly infusions ×3. If in remission, maintenance treatment with methotrexate or azathioprine can be commenced
Dose reductions	Age (>70 years), renal impairment, infection, neutropenia
Toxicity	Nausea, alopecia, neutropenia, infertility, hemorrhagic cystitis

Maintenance Stage.

At 6 months, cyclophosphamide should be switched to milder maintenance therapy, such as azathioprine (2 mg/kg daily) or methotrexate. Cotrimoxazole has also been shown to reduce the relapse rate in GPA, possibly by eliminating nasal carriage of *Staphylococcus aureus*. Other maintenance agents that have been used in small series include cyclosporine, leflunomide, and mycophenolate mofetil. The duration that maintenance therapy should be continued is not clear, but in diseases where the relapse rate is high (e.g., AAV) therapy should probably be continued for 3–5 years.

Adjuvant Therapy.

Where disease control is proving difficult and in the presence of severe organ involvement, pulses of methylprednisolone (1 g on

three consecutive days) may be used but should not delay the commencement of cyclophosphamide. Plasma exchange and intravenous immunoglobulin are other potential treatment modalities.

Treatment of Relapse.

Fewer items of damage accumulate after relapse than at first presentation,[185] but for major relapses a short course of cyclophosphamide (six pulses), with an early transfer to maintenance methotrexate, azathioprine, or cyclosporine, is one approach. Patients with recurrent relapses may be exposed to several courses of cyclophosphamide, increasing the risk of drug-related toxicity (bladder cancer, infertility, myelodysplasia). Methotrexate may be used as an alternative to cyclophosphamide for less severe relapse.

Alternative Approaches to Therapy.

A number of alternative therapies have been trialed. A short course of higher-dose pulsed cyclophosphamide may induce an early remission, but has an increased risk of neutropenia and infection. Autologous stem cell transplantation after intensive immunosuppression has been successfully carried out in a few patients with severe unremitting disease. Anti-T-cell monoclonal antibodies (Campath-1H and anti-CD4) have produced dramatic responses in some patients. Anti-TNF agents have not shown any benefit over standard therapy,[188] although several case reports suggest a benefit in some cases of treatment-resistant vasculitis. More promising results have been shown using the B-cell depleting anti-CD20 antibody rituximab, which is now used in some cases for remission induction or maintenance therapy.[189]

Large Vessel Vasculitides

Giant Cell Arteritis

General Considerations.

Giant cell arteritis (GCA) or temporal arteritis is a vasculitis that typically affects elderly patients, and is highly corticosteroid-

responsive. Symptoms tend to begin insidiously, most commonly headaches, scalp tenderness, myalgias, fever, anorexia, and weight loss.[190] In some cases, however, disease can present abruptly with a major complication such as loss of vision.[191]

Epidemiology.

GCA is predominantly a disease of the elderly. It rarely affects those under 50 years, with a mean age of presentation of 70–75 years. There is a 2 : 1 female : male ratio. It is estimated to affect approximately 220 patients per million per year.[180,192,193]

Articular and Systemic Disease.

GCA targets branches of the external carotid artery; patient symptoms include headaches, scalp tenderness, and jaw and tongue claudication. There is an increased risk of transient ischemic attack (TIA) or stroke, as a result of arteritis of the vertebral and basilar arteries. Systemic features of GCA, such as fever, malaise, fatigue, weakness, anorexia, weight loss, and depression are present in 40–50% of patients. The arteritic process can involve other large vessels and subclavian or brachial arteries presenting with upper limb claudication or an aortitis (thoracic > abdominal) is well recognized in 10–20% of patients. There is thought to be an association with polymyalgia rheumatica.[194]

Ocular Disease.

Many patients present with temporal headache but no visual loss, but anterior ischemic optic neuropathy (AION) due to arteritis of the short posterior ciliary arteries is the major complication of GCA, and typically presents as acute painless loss of vision. The diagnosis is straightforward when seen with devastating loss of vision (often perception of light), a relative afferent pupillary defect, and typical optic disc edema in the context of systemic features typical of the disease. With time, optic atrophy ensues with complete loss of vision. Nevertheless in some patients it is difficult to distinguish between an arteritic and nonarteritic cause of AION. Failure to differentiate these two can be catastrophic as involvement of the second eye in arteritic AION ranges from 10% if treated to 95% if untreated. A detailed ocular and general history is essential and

examination reveals a tender, thickened, nonpulsatile superficial temporal artery. Characteristically there is an elevated erythrocyte sedimentation rate (ESR) and C-reactive protein (CRP). A definitive diagnosis is made on temporal artery biopsy (TAB), but a positive biopsy is not always required to make a diagnosis (American College of Rheumatology classification criteria for GCA – Box 83.8).[195] Nevertheless, all patients with a clinical and/or laboratory diagnosis, or where the diagnosis is in doubt, should have therapy instigated and a TAB performed. A TAB is normally performed within 48–72 hours of commencing corticosteroid therapy. A recent study has shown that on 459 cases of biopsy-proven GCA the odds of a positive biopsy were 1.5 times greater with an ESR of 47–107 mm/h, 5.3 times greater with a CRP >2.45 mg/dL, and 4.2 times greater with platelets >400 /μL.[196]

Box 83.8

The American College of Rheumatology 1990 Criteria for the Classification of Giant Cell Arteritis

The presence of *three or more* of the following five criteria is associated with 93.5% sensitivity and 91.2% sensitivity for giant cell arteritis (GCA).

1. Age ≥50 years at disease onset
2. New onset of localized headache
3. Temporal artery tenderness or decreased pulse
4. ESR ≥50 mm/h
5. Arterial biopsy with necrotizing arteritis with a predominance of mononuclear cell infiltrates or granulomatous process with multinucleate giant cells

Reproduced with permission from Hunder GG, Bloch DA, Michel BA, et al. The American College of Rheumatology 1990 criteria for the classification of giant cell arteritis. Arthritis Rheum 1990;33:1122–8.

More problematic are those presenting with posterior ischemic optic neuropathy (with an apparently normal optic disc in the acute

phase) and who may not report typical features; in the series by Hayreh, around 10% of the IONs seen were posterior ischemic optic neuropathy (PION).[191] The estimates of visual loss from GCA vary widely from 13% to 70%, with lower estimates being seen in a recent series that may reflect improved diagnosis and earlier treatment. The visual loss is usually severe (<20/200), and visual recovery is uncommon despite appropriate therapy.[197] Visual field loss may be complete, altitudinal, or occasionally an arcuate (Bjerrum-type) scotoma. Amaurosis fugax may be a warning of impending ION or other serious ischemic pathology. An ischemic retinopathy with cotton-wool spots (and sometimes retinal hemorrhages) may be seen and can precede optic nerve involvement.[198,199] Other ophthalmic complications of biopsy-proven GCA include cilioretinal artery occlusion (CRAO), and ocular ischemic syndrome occurring in about 14%, 20%, and 1%, respectively, of patients. Occasionally there is extraocular muscle dysfunction with symptoms of transient or permanent diplopia.[191]

Treatment.

Corticosteroids are the mainstay of treatment, with almost all patients who present to a rheumatologist responding to 40–60 mg oral prednisone. Those patients presenting to an ophthalmologist with or without vision loss should have three intravenous pulses of methylprednisolone 1 g for 3 days, then oral prednisone 1 mg/kg daily. Corticosteroid taper can occur after 4 weeks with resolution of symptoms and a fall in inflammatory markers.[200] It is reasonable to aim for a dose of 15 mg by 3 months of therapy. In addition, low-dose aspirin (to reduce the risk of arterial thrombus and visual loss) and bone protection (bisphosphonates and calcium and vitamin D supplementation) with or without a proton pump inhibitor could be considered.[200] On average, 18 months of corticosteroid treatment is required, but up to 40% may need long-term therapy due to relapsing disease. A corticosteroid sparing agent may need to be introduced, such as methotrexate, azathioprine, and leflunomide. There is no evidence that they are beneficial when used at disease onset but may be helpful in relapsing disease to minimize corticosteroid dose and thus side-effects. Recently, encouraging results have been demonstrated with the biologics infliximab,

etanercept, rituximab, and tociluzimab.[201–203]

Takayasu's Arteritis

General Considerations.

Takayasu's arteritis is a rare inflammatory disease of unknown etiology, characterized by granulomatous vasculitis affecting large arteries, in particular the aorta and its main branches.

Epidemiology.

Takayasu's arteritis is very rare, with an annual incidence of 2.6 per million in North America and 1.2 per million in Japan. It is classically described in women of childbearing age of Southeast Asian, South African, and Latin American background[204–206] (see Box 83.9[207]).

Box 83.9

The American College of Rheumatology Criteria for the Classification of Takayasu Arteritis

For purposes of classification, a patient is said to have Takayasu arteritis if *at least three* of these six criteria are present. The presence of any three or more criteria yields a sensitivity of 90.5% and a specificity of 97.8%.

1. Age at disease onset <40 years
   Development of symptoms or findings related to Takayasu arteritis at age under 40 years

2. Claudication of extremities
   Development and worsening of fatigue and discomfort in muscles of one or more extremities while in use, especially the upper extremities

3. Decreased brachial artery pulse
   Decreased pulsation of one or both brachial arteries

4. BP difference >10 mmHg
   Difference of >10 mmHg in systolic blood pressure between arms

5. Bruit over subclavian arteries or aorta
   Bruit audible on auscultation over one or both subclavian arteries or abdominal aorta

6. Arteriogram abnormality
   Arteriographic narrowing or occlusion of the entire aorta, its primary branches, or large arteries in the proximal upper or lower extremities, not due to arteriosclerosis, fibromuscular dysplasia, or similar causes; changes usually focal or segmental

Reproduced with permission from Arend WP, Michel BA, Bloch DA, et al. The American College of Rheumatology 1990 criteria for the classification of Takayasu arteritis. Arthritis Rheum 1990;33:1129–34.

Articular and Systemic Disease.

At the time of diagnosis, 10–20% of patients are clinically asymptomatic and the disease is diagnosed incidentally on vascular examination. The most common findings on examination are hypertension, bruits, diminished or absent pulses, and asymmetric blood pressure readings in the extremities. Of symptomatic patients, 80–90% can present with either systemic or vascular symptoms, or a combination of both. Systemic features include fever, malaise, weight loss, arthralgia, and night sweats.[204–206]

Vascular symptoms are more common and are as a result of active vasculitis or vascular damage from previous inflammation resulting in stenosis or aneurysm formation. Involvement of the carotid and vertebral arteries can lead to central nervous system involvement. Clinically patients may be asymptomatic or have symptoms including transient ischemic attacks, stroke, dizziness, syncope, headache, or visual changes. Mesenteric involvement is common. The most common cardiac manifestation is aortic regurgitation. Cutaneous manifestations such as erythema nodosum and pyoderma granulosum have been observed in 3–28% of patients.[204–206]

Ocular Disease.

Ophthalmic disease occurs in around one-third of patients with Takayasu arteritis. The most common ocular complication is hypertensive retinopathy (16–30%), followed by Takayasu

retinopathy (13–15%) and ocular ischemic syndrome (around 4%).[208,209] Takayasu retinopathy may progress from small vessel dilation (stage 1), to microaneurysms (stage 2), arteriovenous anastomoses (stage 3), and finally additional complications, such as retinal neovascularization and vitreous hemorrhage (stage 4).[208] Other recognized complications include AION, PION, and neovascular glaucoma. The presence of ischemic ocular complications is associated with nonrecordable right upper limb blood pressure.[209]

Treatment.

Corticosteroids are the mainstay of treatment. Initially it is recommended that prednisone is started at 1 mg/kg daily (maximum 60 mg/day), for a month then tapered gradually.[210,211] If patients have severe disease or refractory disease, steroid-sparing agents need to be considered.

Corticosteroid-sparing agents that can be considered are azathioprine (2 mg/kg daily) and methotrexate (20–25 mg/week).[210,212] Other agents with limited data available include cyclophosphamide, mycophenolate mofetil, leflunomide and minocycline, and the biologic agents infliximab, tocilizumab, and abatacept.[210,212]

Nonmedical interventions such as angioplasty, stent insertion, arterial reconstruction, and bypass grafting may also be required.[210,211]

Medium Vessel Vasculitides

Polyarteritis Nodosa

General Considerations.

Polyarteritis nodosa (PAN) is a necrotizing inflammation of medium vessels with or without glomerulonephritis, which can be secondary to hepatitis B, and is ANCA-negative.

Epidemiology.

PAN is a very uncommon disease, being estimated to occur at less than 1 per million per year (United Kingdom data). The major

environmental risk factor is hepatitis B; other associated viruses are HIV and parvovirus B19.[193]

Articular and Systemic Disease.

PAN has a wide spectrum of disease, ranging from very mild limited disease to life-threatening organ involvement. Arthralgia or arthritis may be present in up to 50% of patients. An intermittent, asymmetric, predominantly lower limb, nondeforming arthritis may occur in up to 20% of cases. Myalgias may occur in up to 50% of patients.[213,214]

Cutaneous features are seen in 25–60%: these include infarctions, ulcerations, livedo reticularis, subcutaneous nodules, and ischemic changes of distal digits.[215] Peripheral neuropathy or mononeuritis multiplex may be seen. CNS involvement with headaches, seizures, cranial nerve dysfunction, stroke, and cerebral hemorrhage are less common. Renal involvement can result in hypertension as a result of renal artery stenosis or renal impairment/failure due to multiple microaneurysms and infarcts as a consequence of vascular occlusion. Abdominal pain, which can occur in up to 70% of patients as a result of gastrointestinal involvement, can be severe, with bowel ischemia occurring.[213,214]

Ocular Disease.

Ophthalmic disease occurs in around 10–20% of patients with PAN and may reflect direct ocular involvement or be secondary to its systemic effects (notably hypertension from renal disease). Retinal disease includes retinal vasculitis and hypertensive retinopathy. Other ophthalmic complications include peripheral ulcerative keratitis, episcleritis, scleritis (both anterior and posterior), serous retinal detachments, ischemic optic neuropathy, cranial neuropathies, and cerebral disease resulting in visual field defects.[216–218]

Treatment.

Pulsed intravenous cyclophosphamide and corticosteroids has been found to achieve better disease control and sustained remission compared to corticosteroids alone, but the long-term survival remains unchanged.[219,220] Patients with hepatitis-associated PAN are

recommended to have high-dose corticosteroid therapy tapered over 2 weeks, followed by antiviral agents and plasma exchange.[219,220]

Kawasaki Disease

General Considerations.

Kawasaki disease predominantly affects young children and is the most common cause of acquired heart disease in the United States and Japan. It is the second commonest vasculitis of childhood after Henoch–Schonlein purpura.

Epidemiology.

The highest incidence rate is in Japan – 216 cases per 100 ,000 per year in children under 5 years of age – with a peak incidence at between 9 and 11 months of age.[221] There are possible familial and infectious links.[193]

Articular and Systemic Disease.

Kawasaki disease is usually defined as a persistent fever for a minimum of 5 days with a minimum of four out of the following: (1) polymorphous rash; (2) bilateral conjunctival injection without exudates; (3) oropharyngeal involvement, including red fissured lips, strawberry tongue, and red pharynx without exudates; (4) peripheral changes including edema of extremities, sole erythema, and periungual desquamation; and (5) cervical lymphadenopathy. Arthritis of the small joints is common and is associated with a bluish discoloration over the PIPs. Axial arthropathy and effusions can also occur, but the articular symptoms will usually resolve after the acute phase.[222,223]

The most serious manifestation is that of the cardiovascular system, which can result in aneurysms (especially the coronary arteries), myocarditis, and congestive cardiac failure. Other clinical manifestations include gastrointestinal manifestations, urethritis, facial nerve palsy (rare), and sensorineural hearing loss.[222,223]

Ocular Disease.

Bilateral conjunctival injection without purulent discharge is one of

the hallmarks of Kawasaki disease. Additionally, bilateral anterior uveitis is common in the first week of illness.[224] Rare ocular manifestations include optic neuritis and ophthalmic artery obstruction.[225]

Treatment.

Kawasaki disease is treated with a single intravenous (IV) dose of immunoglobulin and high-dose aspirin. The aspirin dose can be reduced once the fever finishes. If patients fail to respond to the first dose of IV immunoglobulin, treatment options include a repeat infusion, infliximab, IV methylprednisolone, and plasmapheresis.[226–229]

Small Vessel Vasculitides

Granulomatosis With Polyangiitis (Wegener's Granulomatosis)

General Considerations.

Granulomatosis with polyangiitis (GPA) is a multisystem disease of unknown etiology, characterized by granulomatous inflammation, tissue necrosis, and varying degrees of vasculitis. It can affect any organ, but has a predilection for the upper respiratory tract, lungs, and kidneys.

Epidemiology.

GPA has a slight male predominance, and is more common in Caucasians. GPA is a rare disease, with a prevalence ranging from 3 per 100, 000 in the United States to up to 16 per 100 ,000 in Northern Europe.[230,231] GPA predominantly affects older individuals, but 15% of cases have been reported in childhood.[232] GPA is highly associated with PR3 (proteinase 3) ANCA.[233]

Articular and Systemic Disease.

Musculoskeletal symptoms can occur in up to 60% of patients. Commonly a migratory polyarthritis affecting the large joints or a polyarthritis can occur.

Presenting symptoms in up to 75% of patients will be of upper

respiratory tract disease (nasal, sinus, tracheal, and/or ear abnormalities). The "saddle nose deformity" results from nasal bridge collapse, and other nasal manifestations include nasal pain, stuffiness, crusts, epistaxis, mucosal erosion, and septal perforation. A characteristic feature of mouth involvement is "strawberry gums," an intense gingivitis that responds to systemic treatment. A serious complication is subglottic stenosis secondary to tracheal inflammation and scarring, as this may require a tracheostomy.[3] Nonspecific systemic features may occur, particularly during active disease, which include fever, malaise, arthralgias, anorexia, and weight loss.[3]

Pulmonary involvement may present as cough, hemoptysis, dyspnea, or pleuritic or other forms of chest pain; however one-third of patients with pulmonary lesions have asymptomatic disease. Renal involvement occurs in about 80% of GPA patients.

Ocular Disease.

Ophthalmic disease occurs in around 50% of patients in this condition and is an important cause of morbidity and blindness, with vision loss occurring in around 8%.[3] Although orbital disease is the most common ocular complication of the disease, almost any part of the ophthalmic system may be affected.

Orbital disease occurs in up to 20% of patients with GPA. It may present with acute or subacute proptosis, and may be associated with ocular motility disturbance (resulting in diplopia), and optic nerve compression or infiltration potentially leading to blindness. Severe proptosis may also lead to sight-threatening exposure keratopathy. It should be noted that although proptosis is common in these patients, chronic orbital inflammation may lead to orbital socket contraction with enophthalmos, restrictive ophthalmopathy, and chronic pain.[234]

Important nonorbital presentations of GPA include scleritis (7–10% of patients), peripheral ulcerative keratitis, and an ulcerative conjunctivitis with a chronic cicatrizing course.[235] The scleritis may be anterior or posterior; necrotizing scleritis is often associated with corneal disease (marginal corneal ulcer/PUK). Uveitis is uncommon (around 3%). Anterior, posterior and panuveitis have all been described in this context and may be isolated or associated with

scleritis.[236,237] Retinal vasculitis may occur and ranges in severity from cotton-wool spots to severe vaso-occlusive disease, with neovascularization and related consequences. Neuro-ophthalmic consequences most commonly occur secondary to orbital involvement, but may also arise due to vasculitis causing ischemic optic neuropathy. In a study of 59 patients with ANCA-associated vasculitis and ocular inflammation, 75% had scleritis, and with time these patients had a 2.75-fold higher mortality than other patients with inflammatory eye disease.[238]

Treatment.

Like other vasculitides, the suggested treatment to induce remission is pulsed intravenous cyclophosphamide with oral steroids.[219,239] Corticosteroid-sparing agents that can be substituted for cyclophosphamide once remission has been achieved are methotrexate or azathioprine. If disease is limited, then methotrexate in combination with oral corticosteroid can be used rather than cyclophosphamide.[219] Biologics are now increasingly used in the management, initially infliximab and more recently rituximab.[240] Rituximab is used for remission induction when cyclophosphamide is contraindicated and as remission maintenance in those where risk of relapse is high. It has been used in sight threatening ocular and orbital disease.[189,241] Treatment is primarily directed against the systemic disease, although it should be noted that the severity of ophthalmic involvement may be an important factor in escalating therapy.

Microscopic Polyangiitis

General Considerations.

Microscopic polyangiitis (MPA) is a necrotizing vasculitis, predominantly affecting small vessels, associated with MPO (myeloperoxidase) ANCA.

Epidemiology.

MPA has an incidence of 5 per million per year, with a peak age of onset of between 65 and 75 years; it is more common in men.[231]

Articular and Systemic Disease.

Renal involvement is very common, affecting up to 90% of patients. Rapidly progressive glomerulonephritis may occur, resulting in acute renal failure necessitating renal dialysis. Varying degrees of pulmonary involvement can occur; these can range from mild dyspnea to life-threatening pulmonary hemorrhage. Involvement of both the central and peripheral nervous system is described and includes peripheral neuropathy, mononeuritis multiplex, cerebral hemorrhage/infarction, seizures, or headache. Other systemic manifestations include cardiac, gastrointestinal, otorhinolaryngeal, and venous thromboembolism.[215,242,243]

Ocular Disease.

Ophthalmic disease is rare in MPA, with one series noting ocular involvement in only 1 of 85 patients with MPA.[242] In small case series and isolated reports the following ophthalmic complications have been noted: scleritis, anterior uveitis with hypopyon, retinal vasculitis (ranging from cotton-wool spots to neovascularization and vitreous hemorrhage), and peripheral nonulcerative keratitis.[244,245]

Treatment.

Recommended treatment for severe MPA is oral corticosteroid with pulsed intravenous cyclophosphamide to induce remission.[219,239] In milder active disease (no threatened vital organ disease or damage), methotrexate or azathioprine and oral corticosteroid can be used, but there is a higher risk of relapse.[239] If patients have failed to achieve remission and have persistent low activity, IV immunoglobulin can be used to achieve remission.[219] There is increasing data on the use of biologics, mainly rituximab for the same indications as for GPA.[246]

Eosinophilic Granulomatosis with Polyangiitis

General Considerations.

Eosinophilic granulomatosis with polyangiitis (EGPA, Churg–Strauss syndrome) is a primary, multisystem, eosinophilic vasculitis

associated with upper and lower respiratory tract disease and ANCA.

Epidemiology.

EGPA is estimated to have a prevalence of 10 to 15 per million. The mean age of diagnosis is 55 years. It has equal gender incidence.[247]

Articular and Systemic Disease.

EGPA can affect virtually any organ system in the body. Systemic symptoms include fever, weight loss, arthralgias, and, rarely, arthritis.[247]

Pulmonary involvement is nearly universal in EGPA with 96–100% having asthma. Other pulmonary manifestations include pulmonary infiltrates, pulmonary hemorrhage, and pleural effusions.

Peripheral neuropathy occurs commonly (65–75%), usually with mononeuritis multiplex. CNS involvement may include cranial nerve palsies, ischemic optic neuropathy, cerebral hemorrhage or infarction, convulsions, coma, and psychosis.

Abdominal pain is the most common gastrointestinal symptom. Cardiac involvement includes eosinophilic endomyocarditis, coronary vasculitis, valvular heart disease, congestive heart failure, hypertension, and pericarditis. Skin lesions are common and typically include nonthrombocytopenic palpable purpura, with erythematous, maculopapular, or pustular lesions being reported. Renal involvement is fairly typical, but unlike other necrotizing vasculitides such as GPA or microscopic polyangiitis, renal failure is rare.[247–249]

Ocular Disease.

Ophthalmic disease may arise from two processes: vasculitis and granuloma formation. Clinical presentations include conjunctival nodules,[250] peripheral ulcerative keratitis, episcleritis, scleritis, uveitis (rare), retinal vasculitis,[251] retinal artery occlusion, ischemic optic neuropathy, cranial neuropathies,[252] and orbital disease (presenting with an orbital inflammatory syndrome).[251]

Treatment.

As with other ANCA-positive vasculitides, remission induction is normally achieved with oral corticosteroids and cyclophosphamide or with a DMARD such as methotrexate or azathioprine in less severe disease.[219,239] Rituximab is currently undergoing clinical trials, but there have been promising results published.[253]

Ocular Complications of Rheumatologic Therapies

General

Ocular complications of rheumatologic therapies may relate to (1) direct drug-specific toxic effects, such as chloroquine retinopathy, (2) indirect drug-specific side-effects, such as corticosteroid-induced ocular hypertension resulting in secondary glaucoma, and (3) drug nonspecific complications relating to immunosuppression, such as opportunistic infections.

Corticosteroids

Most treatment-related visual morbidity is associated with corticosteroid treatment. The association between posterior subcapsular cataract and exogenous corticosteroids is well established.[254] Cataract surgery in patients with rheumatic diseases is generally successful, although there must be strict control of any intraocular inflammation prior to surgery and in the postoperative phase. Prognosis will be worse if there is visually significant posterior segment disease. Increased intraocular pressure due to exogenous corticosteroids may occur in up to 30% of the normal population, with 5% experiencing an increase of more than 15 mmHg (reviewed by Clark[255]). Corticosteroid-induced ocular hypertension must be monitored and treated where there is a risk of progression to secondary glaucoma.

Antimalarials

The aminoquinolines chloroquine and hydroxychloroquine have been widely used in the treatment of SLE. These drugs can cause a

reversible, visually insignificant keratopathy (cornea verticillata) and, more importantly, an irreversible sight-threatening maculopathy. Clinical progression is of loss of the foveal reflex followed by a fine granular appearance of the macula and finally a "bull's-eye" maculopathy presenting as a central scotoma. Endstage disease includes generalized atrophy, peripheral pigmentation, arteriolar attenuation, and optic atrophy.[256]

Retinopathy is rare with hydroxychloroquine when used at currently recommended doses (<6.5 mg/kg daily), but increases markedly towards 1% after 5–7 years of usage or a cumulative dose of 1000 g of hydroxychloroquine.[257,258] The risk with chloroquine is thought to be significantly greater, with an increased risk at over 460 g chloroquine. In both cases, risk increases with increasing dose, increasing duration, and reduced renal function. The American Academy of Ophthalmology (AAO) 2011 guidelines recommend screening for all patients at baseline or within first year of use, and to start annual screening after 5 years of use (or earlier if additional risk factors).[258] Assessments should include dilated retinal examinations and white 10–2 automated visual field testing which should be interpreted with a low threshold for abnormality and with retesting if abnormalities are seen. Additionally, they recommend that one or more of the following should be performed where available: spectral domain optical coherence tomography, multifocal electroretinography, or fundus autofluorescence.[258] High-risk patients include those on a dose of >6.5 mg/kg, with a duration of >5 years, obese patients, those with renal or hepatic disease, those with preexisting retinal disease, or those over the age of 60 years.[258] Amsler grid testing is no longer recommended. Although fundus examinations are advised for documentation, the aim is to detect changes before visible maculopathy. The AAO authors stress the importance of counseling patients regarding the risk of toxicity and the rationale for screening.

References

1. The definition and classification of dry eye disease: report of the Definition and Classification Subcommittee of the International Dry Eye WorkShop (2007). *Ocul Surf*.

2007;5:75–92.
2. Galor A, Thorne JE. Scleritis and peripheral ulcerative keratitis. *Rheum Dis Clin North Am*. 2007;33:835–854 [vii].
3. Tarabishy AB, Schulte M, Papaliodis GN, et al. Wegener's granulomatosis: clinical manifestations, differential diagnosis, and management of ocular and systemic disease. *Surv Ophthalmol*. 2010;55:429–444.
4. Akpek EK, Thorne JE, Qazi FA, et al. Evaluation of patients with scleritis for systemic disease. *Ophthalmology*. 2004;111:501–516.
5. Galor A, Thorne JE, Jabs DA. Rheumatic disease and scleritis. *Ophthalmology*. 2007;114:1232.
6. Watson PG, Hayreh SS. Scleritis and episcleritis. *Br J Ophthalmol*. 1976;60:163–191.
7. Zaidi AA, Ying GS, Daniel E, et al. Hypopyon in patients with uveitis. *Ophthalmology*. 2010;117:366–372.
8. Rothova A, van Veenedaal WG, Linssen A, et al. Clinical features of acute anterior uveitis. *Am J Ophthalmol*. 1987;103:137–145.
9. Weinstein RS. Clinical practice. Glucocorticoid-induced bone disease. *N Engl J Med*. 2011;365:62–70.
10. Kempen JH, Daniel E, Dunn JP, et al. Overall and cancer related mortality among patients with ocular inflammation treated with immunosuppressive drugs: retrospective cohort study. *BMJ*. 2009;339:b2480.
11. Symmons D, Turner G, Webb R, et al. The prevalence of rheumatoid arthritis in the United Kingdom: new estimates for a new century. *Rheumatology (Oxford)*. 2002;41:793–800.
12. Gabriel SE, Crowson CS, O'Fallon WM. The epidemiology of rheumatoid arthritis in Rochester, Minnesota, 1955–1985. *Arthritis Rheum*. 1999;42:415–420.
13. Gabriel SE. The epidemiology of rheumatoid arthritis. *Rheum Dis Clin North Am*. 2001;27:269–281.
14. Sugiyama D, Nishimura K, Tamaki K, et al. Impact of smoking as a risk factor for developing rheumatoid arthritis: a meta-analysis of observational studies. *Ann Rheum Dis*. 2010;69:70–81.
15. Majithia V, Geraci SA. Rheumatoid arthritis: diagnosis and

management. *Am J Med*. 2007;120:936–939.
16. Turesson C. Extra-articular rheumatoid arthritis. *Curr Opin Rheumatol*. 2013;25:360–366.
17. Lake F, Proudman S. Rheumatoid arthritis and lung disease: from mechanisms to a practical approach. *Semin Respir Crit Care Med*. 2014;35:222–238.
18. Balint GP, Balint PV. Felty's syndrome. *Best Pract Res Clin Rheumatol*. 2004;18:631–645.
19. Nurmohamed MT, Heslinga M, Kitas GD. Cardiovascular comorbidity in rheumatic diseases. *Nat Rev Rheumatol*. 2015;11(12):693–704.
20. Schellekens GA, Visser H, de Jong BA, et al. The diagnostic properties of rheumatoid arthritis antibodies recognizing a cyclic citrullinated peptide. *Arthritis Rheum*. 2000;43:155–163.
21. Aletaha D, Neogi T, Silman AJ, et al. 2010 Rheumatoid arthritis classification criteria: an American College of Rheumatology/European League Against Rheumatism collaborative initiative. *Arthritis Rheum*. 2010;62:2569–2581.
22. Akpek EK, Uy HS, Christen W, et al. Severity of episcleritis and systemic disease association. *Ophthalmology*. 1999;106:729–731.
23. Foster CS, Forstot SL, Wilson LA. Mortality rate in rheumatoid arthritis patients developing necrotizing scleritis or peripheral ulcerative keratitis: effects of systemic immunosuppression. *Ophthalmology*. 1984;91:1253–1263.
24. Giordano N, D'Ettorre M, Biasi G, et al. Retinal vasculitis in rheumatoid arthritis: an angiographic study. *Clin Exp Rheumatol*. 1990;8:121–125.
25. Martin MF, Scott DG, Gilbert C, et al. Retinal vasculitis in rheumatoid arthritis. *Br Med J (Clin Res Ed)*. 1981;282:1745–1746.
26. Matsuo T, Koyama T, Morimoto N, et al. Retinal vasculitis as a complication of rheumatoid arthritis. *Ophthalmologica*. 1990;201:196–200.
27. Singh JA, Furst DE, Bharat A, et al. 2012 Update of the 2008 American College of Rheumatology (ACR) recommendations for the use of disease-modifying anti-

rheumatic drugs and biologics in the treatment of rheumatoid arthritis (RA). *Arthritis Care Res*. 2012;64:625–639.
28. Smolen JS, Landewé R, Breedveld FC, et al. EULAR recommendations for the management of rheumatoid arthritis with synthetic and biological disease-modifying antirheumatic drugs: 2013 update. *Ann Rheum Dis*. 2013;0:1–18.
29. Management and therapy of dry eye disease: report of the Management and Therapy Subcommittee of the International Dry Eye WorkShop (2007). *Ocul Surf*. 2007;5:163–178.
30. Rudwaleit M, van der Heijde D, Landewé R, et al. The development of assessment of Spondyloarthritis International Society classification criteria for axial spondyloarthritis (part II): validation and final selection. *Ann Rheum Dis*. 2009;68:777–783.
31. Rudwaleit M, van der Heijde D, Landewé R, et al. The Assessment of Spondyloarthritis International Society classification criteria for peripheral spondyloarthritis and for spondyloarthritis in general. *Ann Rheum Dis*. 2011;70:25–31.
32. Zeboulon N, Dougados M, Gossec L. Prevalence and characteristics of uveitis in the spondyloarthropathies: a systematic literature review. *Ann Rheum Dis*. 2008;67:955–959.
33. Gabriel SE, Michaud K. Epidemiological studies in incidence, prevalence, mortality, and comorbidity of the rheumatic diseases. *Arthritis Res Ther*. 2009;11:229.
34. Lee W, Reveille JD, Davis JC Jr, et al. Are there gender differences in severity of ankylosing spondylitis? Results from the PSOAS cohort. *Ann Rheum Dis*. 2007;66:633–638.
35. van der Heijde D, Lie E, Kvien TK, et al. ASDAS, a highly discriminatory ASAS-endorsed disease activity score in patients with ankylosing spondylitis. *Ann Rheum Dis*. 2009;68:1811–1818.
36. Zochling J, van der Heijde D, Burgos-Vargas R, et al. ASAS/EULAR recommendations for the management of

ankylosing spondylitis. *Ann Rheum Dis*. 2006;65:442–452.
37. Palazzi C, Salvarani C, D'Angelo S, et al. Aortitis and periaortitis in ankylosing spondylitis. *Joint Bone Spine*. 2011;78:451–455.
38. Rosenbaum JT. Acute anterior uveitis and spondyloarthropathies. *Rheum Dis Clin North Am*. 1992;18:143–151.
39. Linssen A, Dekker-Saeys AJ, Dijkstra PF, et al. The use of HLA-B27 as a diagnostic and prognostic aid in acute anterior uveitis (AAU) in The Netherlands. *Doc Ophthalmol*. 1986;64:217–223.
40. Tay-Kearney ML, Schwam BL, Lowder C, et al. Clinical features and associated systemic diseases of HLA-B27 uveitis. *Am J Ophthalmol*. 1996;121:47–56.
41. Escalas C, Trijau S, Dougados M. Evaluation of the treatment effect of NSAIDs/TNF blockers according to different domains in ankylosing spondylitis: results of a meta-analysis. *Rheumatology (Oxford)*. 2010;49:1317–1325.
42. Braun J, van den Berg R, Baraliakos X, et al. 2010 update of the ASAS/EULAR recommendations for the management of ankylosing spondylitis. *Ann Rheum Dis*. 2011;70:896–904.
43. Soriano ER, Acosta-Felquer MR, Luong P, et al. Pharmacological treatment of psoriatic arthritis and axial spondyloarthritis with traditional biologic and non-biologic DMARDs. *Best Pract Clin Res Rheumatol*. 2014;28:793–806.
44. Callhoff J, Sieper J, Weiss A, et al. Efficacy of TNFalpha blockers in patients with ankylosing spondylitis and non-radiographic axial spondyloarthritis: a meta-analysis. *Ann Rheum Dis*. 2014;10:205–322.
45. Rudwaleit M, Rodevand E, Holck P, et al. Adalimumab effectively reduces the rate of anterior uveitis flares in patients with active ankylosing spondylitis: results of a prospective open-label study. *Ann Rheum Dis*. 2009;68:696–701.
46. Braun J, Baraliakos X, Listing J, et al. Decreased incidence of anterior uveitis in patients with ankylosing spondylitis treated with the anti-tumor necrosis factor agents infliximab and etanercept. *Arthritis Rheum*. 2005;52:2447–2451.

47. Selmi C, Gershwin EG. Diagnosis and classification of reactive arthritis. *Autoimmun Rev*. 2014;13:546–549.
48. Lee DA, Barker SM, Su WP, et al. The clinical diagnosis of Reiter's syndrome: ophthalmic and nonophthalmic aspects. *Ophthalmology*. 1986;93:350–356.
49. Saari KM, Kauranen O. Ocular inflammation in Reiter's syndrome associated with *Campylobacter jejuni* enteritis. *Am J Ophthalmol*. 1980;90:572–573.
50. Saari KM, Vilppula A, Lassus A, et al. Ocular inflammation in Reiter's disease after *Salmonella* enteritis. *Am J Ophthalmol*. 1980;90:63–68.
51. Needham AD, Harding SP, Carey P. Bilateral multifocal choroiditis in Reiter syndrome. *Arch Ophthalmol*. 1997;115:684–685.
52. Conway RM, Graham SL, Lassere M. Incomplete Reiter's syndrome with focal involvement of the posterior segment. *Aust N Z J Ophthalmol*. 1995;23:63–66.
53. Rosenbaum JT. Characterization of uveitis associated with spondyloarthritis. *J Rheumatol*. 1989;16:792–796.
54. Leirisalo-Repo M. Reactive arthritis. *Scand J Rheumatol*. 2005;34:251–259.
55. Rothfuss KS, Stange EF, Herrlinger KR. Extraintestinal manifestations and complications in inflammatory bowel diseases. *World J Gastroenterol*. 2006;12:4819–4831.
56. Rodriguez-Reyna TS, Martinez-Reyes C, Yamamoto-Furusho JK. Rheumatic manifestations of inflammatory bowel disease. *World J Gastroenterol*. 2009;15:5517–5524.
57. Hopkins DJ, Horan E, Burton IL, et al. Ocular disorders in a series of 332 patients with Crohn's disease. *Br J Ophthalmol*. 1974;58:732–737.
58. Greenstein AJ, Janowitz HD, Sachar DB. The extra-intestinal complications of Crohn's disease and ulcerative colitis: a study of 700 patients. *Medicine (Baltimore)*. 1976;55:401–412.
59. Lyons JL, Rosenbaum JT. Uveitis associated with inflammatory bowel disease compared with uveitis associated with spondyloarthropathy. *Arch Ophthalmol*. 1997;115:61–64.
60. Ghanchi FD, Rembacken BJ. Inflammatory bowel disease

and the eye. *Surv Ophthalmol*. 2003;48:663–676.
61. Cury DB, Moss AC. Ocular manifestations in a community-based cohort of patients with inflammatory bowel disease. *Inflamm Bowel Dis*. 2010;16:1393–1396.
62. Lin P, Tessler HH, Goldstein DA. Family history of inflammatory bowel disease in patients with idiopathic ocular inflammation. *Am J Ophthalmol*. 2006;141:1097–1104.
63. Soukiasian SH, Foster CS, Raizman MB. Treatment strategies for scleritis and uveitis associated with inflammatory bowel disease. *Am J Ophthalmol*. 1994;118:601–611.
64. Taylor W, Gladman D, Helliwell P, et al. Classification criteria for psoriatic arthritis: development of new criteria from a large international study. *Arthritis Rheum*. 2006;54:2665–2673.
65. Shbeeb M, Uramoto KM, Gibson LE, et al. The epidemiology of psoriatic arthritis in Olmsted County, Minnesota, USA, 1982–1991. *J Rheumatol*. 2000;27:1247–1250.
66. Ibrahim G, Waxman R, Helliwell PS. The prevalence of psoriatic arthritis in people with psoriasis. *Arthritis Rheum*. 2009;61:1373–1378.
67. Jenkinson T, Armas J, Evison G, et al. The cervical spine in psoriatic arthritis: a clinical and radiological study. *Br J Rheumatol*. 1994;33:255–259.
68. van Romunde LK, Cats A, Hermans J, et al. Psoriasis and arthritis. II. A cross-sectional comparative study of patients with "psoriatic arthritis" and seronegative and seropositive polyarthritis: clinical aspects. *Rheumatol Int*. 1984;4:61–65.
69. Rehal B, Modjtahedi BS, Morse LS, et al. Ocular psoriasis. *J Am Acad Dermatol*. 2011;65:1202–1212.
70. Lambert JR, Wright V. Eye inflammation in psoriatic arthritis. *Ann Rheum Dis*. 1976;35:354–356.
71. Paiva ES, Macaluso DC, Edwards A, et al. Characterisation of uveitis in patients with psoriatic arthritis. *Ann Rheum Dis*. 2000;59:67–70.
72. Nash P, Clegg DO. Psoriatic arthritis therapy: NSAIDs and traditional DMARDs. *Ann Rheum Dis*. 2005;64(Suppl. 2):ii74–7.
73. Kingsley GH, Kowalczyk A, Taylor H, et al. A randomized

placebo-controlled trial of methotrexate in psoriatic arthritis. *Rheumatology (Oxford)*. 2012;51:1368–1377.
74. Current status of oral PUVA therapy for psoriasis. Eye protection revisions. *J Am Acad Dermatol*. 1982;6:851–855.
75. Saurenmann RK, Rose JB, Tyrrell P, et al. Epidemiology of juvenile idiopathic arthritis in a multiethnic cohort: ethnicity as a risk factor. *Arthritis Rheum*. 2007;56:1974–1984.
76. Petty RE, Southwood TR, Manners P, et al. International League of Associations for Rheumatology classification of juvenile idiopathic arthritis: second revision, Edmonton, 2001. *J Rheumatol*. 2004;31:390–392.
77. BenEzra D, Cohen E, Behar-Cohen F. Uveitis and juvenile idiopathic arthritis: a cohort study. *Clin Ophthalmol*. 2007;1:513–518.
78. Berk AT, Kocak N, Unsal E. Uveitis in juvenile arthritis. *Ocul Immunol Inflamm*. 2001;9:243–251.
79. Boone MI, Moore TL, Cruz OA. Screening for uveitis in juvenile rheumatoid arthritis. *J Pediatr Ophthalmol Strabismus*. 1998;35:41–43.
80. Chylack LT Jr. The ocular manifestations of juvenile rheumatoid arthritis. *Arthritis Rheum*. 1977;20:217–223.
81. Saurenmann RK, Levin AV, Feldman BM, et al. Prevalence, risk factors, and outcome of uveitis in juvenile idiopathic arthritis: a long-term followup study. *Arthritis Rheum*. 2007;56:647–657.
82. Saurenmann RK, Levin AV, Feldman BM, et al. Risk factors for development of uveitis differ between girls and boys with juvenile idiopathic arthritis. *Arthritis Rheum*. 2010;62:1824–1828.
83. Nordal EB, Songstad NT, Berntson L, et al. Biomarkers of chronic uveitis in juvenile idiopathic arthritis: predictive value of antihistone antibodies and antinuclear antibodies. *J Rheumatol*. 2009;36:1737–1743.
84. Cassidy J, Kivlin J, Lindsley C, et al. Ophthalmologic examinations in children with juvenile rheumatoid arthritis. *Pediatrics*. 2006;117:1843–1845.
85. Ayuso VK, Ten Cate HA, van der Does P, et al. Male gender and poor visual outcome in uveitis associated with juvenile

idiopathic arthritis. *Am J Ophthalmol*. 2010;149:987–993.
86. Kalinina AV, Ten Cate HA, van der Does P, et al. Male gender as a risk factor for complications in uveitis associated with juvenile idiopathic arthritis. *Am J Ophthalmol*. 2010;149:994–999.
87. Christoph T, Carsten H, Martin R, et al. Elevated laser flare values correlate with complicated course of anterior uveitis in patients with juvenile idiopathic arthritis. *Acta Ophthalmol*. 2011;896:e521–7.
88. Key IIISN, Kimura SJ. Iridocyclitis associated with juvenile rheumatoid arthritis. *Am J Ophthalmol*. 1975;80:425–429.
89. Rosenberg AM, Oen KG. The relationship between ocular and articular disease activity in children with juvenile rheumatoid arthritis and associated uveitis. *Arthritis Rheum*. 1986;29:797–800.
90. Beukelman T, Guevara JP, Albert DA. Optimal treatment of knee monarthritis in juvenile idiopathic arthritis: a decision analysis. *Arthritis Rheum*. 2008;59:1580–1588.
91. Prakken B, Albani S, Martini A. Juvenile idiopathic arthritis. *Lancet*. 2011;377:2138–2149.
92. Giannini EH, Ilowite NT, Lovell DJ, et al. Long-term safety and effectiveness of etanercept in children with selected categories of juvenile idiopathic arthritis. *Arthritis Rheum*. 2009;60:2794–2804.
93. Lovell DJ, Giannini EH, Reiff A, et al. Etanercept in children with polyarticular juvenile rheumatoid arthritis. Pediatric Rheumatology Collaborative Study Group. *N Engl J Med*. 2000;342:763–769.
94. Ruperto N, Lovell DJ, Cuttica R, et al. A randomized, placebo-controlled trial of infliximab plus methotrexate for the treatment of polyarticular-course juvenile rheumatoid arthritis. *Arthritis Rheum*. 2007;56:3096–3106.
95. Lovell DJ, Ruperto N, Goodman S, et al. Adalimumab with or without methotrexate in juvenile rheumatoid arthritis. *N Engl J Med*. 2008;359:810–820.
96. Ruperto N, Lovell DJ, Quartier P, et al. Long-term safety and efficacy of abatacept in children with juvenile idiopathic arthritis. *Arthritis Rheum*. 2010;62:1792–1802.

97. Ruperto N, Lovell DJ, Quartier P, et al. Abatacept in children with juvenile idiopathic arthritis: a randomised, double-blind, placebo-controlled withdrawal trial. *Lancet*. 2008;372:383–391.
98. Diak P, Siegel J, La GL, et al. Tumor necrosis factor alpha blockers and malignancy in children: forty-eight cases reported to the Food and Drug Administration. *Arthritis Rheum*. 2010;62:2517–2524.
99. Thorne JE, Woreta FA, Dunn JP, et al. Risk of cataract development among children with juvenile idiopathic arthritis-related uveitis treated with topical corticosteroids. *Ophthalmology*. 2010;117:1436–1441.
100. Biester S, Deuter C, Michels H, et al. Adalimumab in the therapy of uveitis in childhood. *Br J Ophthalmol*. 2007;91:319–324.
101. Lim LL, Fraunfelder FW, Rosenbaum JT. Do tumor necrosis factor inhibitors cause uveitis? A registry-based study. *Arthritis Rheum*. 2007;56:3248–3252.
102. Quinones K, Cervantes-Castaneda RA, Hynes AY, et al. Outcomes of cataract surgery in children with chronic uveitis. *J Cataract Refract Surg*. 2009;35:725–731.
103. Grajewski RS, Zurek-Imhoff B, Roesel M, et al. Favourable outcome after cataract surgery with IOL implantation in uveitis associated with juvenile idiopathic arthritis. *Acta Ophthalmol*. 2012;90(7):657–662.
104. Kotaniemi K, Penttila H. Intraocular lens implantation in patients with juvenile idiopathic arthritis-associated uveitis. *Ophthalmic Res*. 2006;38:318–323.
105. Hochberg MC. Updating the American College of Rheumatology revised criteria for the classification of systemic lupus erythematosus. *Arthritis Rheum*. 1997;40:1725.
106. Petri M, Orbai A, Alarcón GS, et al. Derivation and validation of systemic lupus international collaborating clinics classification criteria for systemic lupus erythematosus. *Arthritis Rheum*. 2012;64:2677–2686.
107. Smith PP, Gordon C. Systemic lupus erythematosus: clinical presentations. *Autoimmun Rev*. 2010;10:43–45.

108. Weening JJ, D'Agati VD, Schwartz MM, et al. The classification of glomerulonephritis in systemic lupus erythematosus revisited. *Kidney Int*. 2004;65:521–530.
109. Sultan SM, Ioannou Y, Isenberg DA. A review of gastrointestinal manifestations of systemic lupus erythematosus. *Rheumatology (Oxford)*. 1999;38:917–932.
110. Sivaraj RR, Durrani OM, Denniston AK, et al. Ocular manifestations of systemic lupus erythematosus. *Rheumatology (Oxford)*. 2007;46:1757–1762.
111. Jensen JL, Bergem HO, Gilboe IM, et al. Oral and ocular sicca symptoms and findings are prevalent in systemic lupus erythematosus. *J Oral Pathol Med*. 1999;28:317–322.
112. Read RW. Clinical mini-review: systemic lupus erythematosus and the eye. *Ocul Immunol Inflamm*. 2004;12:87–99.
113. Lachmann SM, Hazleman BL, Watson PG. Scleritis and associated disease. *Br Med J*. 1978;1:88–90.
114. Stavrou P, Murray PI, Batta K, et al. Acute ocular ischaemia and orbital inflammation associated with systemic lupus erythematosus. *Br J Ophthalmol*. 2002;86:474–475.
115. Grimson BS, Simons KB. Orbital inflammation, myositis, and systemic lupus erythematosus. *Arch Ophthalmol*. 1983;101:736–738.
116. Ushiyama O, Ushiyama K, Koarada S, et al. Retinal disease in patients with systemic lupus erythematosus. *Ann Rheum Dis*. 2000;59:705–708.
117. Coppeto JR. Retinopathy and systemic lupus erythematosus. *Arch Ophthalmol*. 1984;102:1748–1749.
118. Jabs DA, Fine SL, Hochberg MC, et al. Severe retinal vaso-occlusive disease in systemic lupus erythematous. *Arch Ophthalmol*. 1986;104:558–563.
119. Asherson RA, Merry P, Acheson JF, et al. Antiphospholipid antibodies: a risk factor for occlusive ocular vascular disease in systemic lupus erythematosus and the "primary" antiphospholipid syndrome. *Ann Rheum Dis*. 1989;48:358–361.
120. Graham EM, Spalton DJ, Barnard RO, et al. Cerebral and retinal vascular changes in systemic lupus erythematosus.

Ophthalmology. 1985;92:444–448.
121. Sekimoto M, Hayasaka S, Noda S, et al. Pseudoretinitis pigmentosa in patients with systemic lupus erythematosus. *Ann Ophthalmol*. 1993;25:264–266.
122. Jabs DA, Hanneken AM, Schachat AP, et al. Choroidopathy in systemic lupus erythematosus. *Arch Ophthalmol*. 1988;106:230–234.
123. Jabs DA, Miller NR, Newman SA, et al. Optic neuropathy in systemic lupus erythematosus. *Arch Ophthalmol*. 1986;104:564–568.
124. Wang JC, Chuah GC, Yap EY. Tuberculous choroidal granulomas in a patient with systemic lupus erythematosus: a case report. *Int Ophthalmol*. 2001;24:107–109.
125. Ishibashi Y, Watanabe R, Hommura S, et al. Endogenous Nocardia asteroides endophthalmitis in a patient with systemic lupus erythematosus. *Br J Ophthalmol*. 1990;74:433–436.
126. Beckwith H, Lightstone L. Rituximab in systemic lupus erythematosus and lupus nephritis. *Nephron Clin Pract*. 2014;128:250–254.
127. Condon MB, Ashby D, Pepper RJ, et al. Prospective observational single-centre cohort study to assess the effectiveness of treating lupus nephritis with rituximab and mycophenolate mofetil but no oral steroids. *Ann Rheum Dis*. 2013;72:1280–1286.
128. Lutalo PM, D'Cruz DP. Update on belimumab for the management of systemic lupus erythematosus. *Expert Opin Biol Ther*. 2014;14:1701–1708.
129. Pillemer SR, Matteson EL, Jacobsson LT, et al. Incidence of physician-diagnosed primary Sjögren syndrome in residents of Olmsted County, Minnesota. *Mayo Clin Proc*. 2001;76:593–599.
130. Fox RI. Sjögren's syndrome. *Lancet*. 2005;366:321–331.
131. Mavragani CP, Moutsopoulos NM, Moutsopoulos HM. The management of Sjögren's syndrome. *Nat Clin Pract Rheumatol*. 2006;2:252–261.
132. Rosenbaum JT, Bennett RM. Chronic anterior and posterior

uveitis and primary Sjogren's syndrome. *Am J Ophthalmol*. 1987;104:346–352.
133. Devauchelle-Pensec V, Mariette X, Jousse-Joulin S, et al. Treatment of primary Sjögren's syndrome with rituximab: a randomized trial. *Ann Intern Med*. 2014;160:233–242.
134. Sall K, Stevenson OD, Mundorf TK, et al. Two multicenter, randomized studies of the efficacy and safety of cyclosporine ophthalmic emulsion in moderate to severe dry eye disease. CsA Phase 3 Study Group. *Ophthalmology*. 2000;107:631–639.
135. Barber LD, Pflugfelder SC, Tauber J, et al. Phase III safety evaluation of cyclosporine 0.1% ophthalmic emulsion administered twice daily to dry eye disease patients for up to 3 years. *Ophthalmology*. 2005;112:1790–1794.
136. Rothova A. Ocular involvement in sarcoidosis. *Br J Ophthalmol*. 2000;84:110–116.
137. Fretzayas A, Moustaki M, Vougiouka O. The puzzling clinical spectrum and course of juvenile sarcoidosis. *World J Pediatr*. 2011;7:103–110.
138. Wouters CH, Maes A, Foley KP, et al. Blau syndrome, the prototypic auto-inflammatory granulomatous disease. *Pediatr Rheumatol Online J*. 2014;12:33.
139. Punzi L, Furlan A, Podswiadek M, et al. Clinical and genetic aspects of Blau syndrome: a 25-year follow-up of one family and a literature review. *Autoimmun Rev*. 2009;8:228–232.
140. Rose CD, Wouters CH, Meiorin S, et al. Pediatric granulomatous arthritis: an international registry. *Arthritis Rheum*. 2006;54:3337–3344.
141. James DG. A comparison of Blau's syndrome and sarcoidosis. *Sarcoidosis*. 1994;11:100–101.
142. Geha RS, Notarangelo LD, Casanova JL, et al. Primary immunodeficiency diseases: an update from the International Union of Immunological Societies Primary Immunodeficiency Diseases Classification Committee. *J Allergy Clin Immunol*. 2007;120:776–794.
143. Latkany PA, Jabs DA, Smith JR, et al. Multifocal choroiditis in patients with familial juvenile systemic granulomatosis. *Am J Ophthalmol*. 2002;134:897–904.

144. Latkany P. Blau syndrome. *Ophthalmology*. 2004;111:853–854.
145. Van den Hoogen F, Khanna D, Fransen J, et al. 2013 classification criteria for systemic sclerosis: an American college of rheumatology/European league against rheumatism collaborative initiative. *Ann Rheum Dis*. 2013;72:1747–1755.
146. Bernatsky S, Joseph L, Pineau CA, et al. Scleroderma prevalence: demographic variations in a population-based sample. *Arthritis Rheum*. 2009;61:400–404.
147. Chifflot H, Fautrel B, Sordet C, et al. Incidence and prevalence of systemic sclerosis: a systematic literature review. *Semin Arthritis Rheum*. 2008;37:223–235.
148. Nihtyanova SI, Denton CP. Autoantibodies as predictive tools in systemic sclerosis. *Nat Rev Rheumatol*. 2010;6:112–116.
149. West RH, Barnett AJ. Ocular involvement in scleroderma. *Br J Ophthalmol*. 1979;63:845–847.
150. Horan EC. Ophthalmic manifestations of progressive systemic sclerosis. *Br J Ophthalmol*. 1969;53:388–392.
151. Emre S, Kayikcioglu O, Ates H, et al. Corneal hysteresis, corneal resistance factor, and intraocular pressure measurement in patients with scleroderma using the Reichert ocular response analyzer. *Cornea*. 2010;29:628–631.
152. Serup J, Serup L. Increased central cornea thickness in localized scleroderma morphoea. *Metab Pediatr Syst Ophthalmol*. 1985;8:11–14.
153. Serup L, Serup J, Hagdrup H. Fundus fluorescein angiography in generalized scleroderma. *Ophthalmic Res*. 1987;19:303–308.
154. Tailor R, Gupta A, Herrick A, et al. Ocular manifestations of scleroderma. *Surv Ophthalmol*. 2009;54:292–304.
155. Kowal-Bielecka O, Landewe R, Avouac J, et al. EULAR recommendations for the treatment of systemic sclerosis: a report from the EULAR Scleroderma Trials and Research group EUSTAR. *Ann Rheum Dis*. 2009;68:620–628.
156. Tashkin DP, Elashoff E, Clements PJ, et al. Scleroderma Lung Study Research Group. Cyclophosphamide versus

placebo in scleroderma lung disease. *N Engl J Med*. 2006;354:655–666.
157. Burt RK, Shah SJ, Dill K, et al. Autologous non-myeloablative haemopoietic stem-cell transplantation compared with pulse cyclophosphamide once per month for systemic sclerosis (ASSIST): an open-label, randomized phase 2 trial. *Lancet*. 2011;378:498–506.
158. Van Laar JM, Farge D, Sont JK, et al. Autologous hematopoietic stem cell transplantation vs intravenous pulse cyclophosphamide in diffuse cutaneous systemic sclerosis: a randomized clinical trial. *JAMA*. 2014;311:2490–2498.
159. Bohan A, Peter JB. Polymyositis and dermatomyositis first of two parts. *N Engl J Med*. 1975;292:344–347.
160. Mastaglia FL, Phillips BA. Idiopathic inflammatory myopathies: epidemiology, classification, and diagnostic criteria. *Rheum Dis Clin North Am*. 2002;28:723–741.
161. Tansley SL, McHugh NJ. Myositis specific and associated autoantibodies in the diagnosis and management of juvenile and adult idiopathic inflammatory myopathies. *Curr Rheumatol Rep*. 2014;16:464.
162. Hill CL, Zhang Y, Sigurgeirsson B, et al. Frequency of specific cancer types in dermatomyositis and polymyositis: a population-based study. *Lancet*. 2001;357:96–100.
163. Dalakas M. Inflammatory muscle disease. *N Engl J Med*. 2015;372:1734–1747.
164. Susac JO, Garcia-Mullin R, Glaser JS. Ophthalmoplegia in dermatomyositis. *Neurology*. 1973;23:305–310.
165. Yeo LM, Swaby DS, Situnayake RD, et al. Irreversible visual loss in dermatomyositis. *Br J Rheumatol*. 1995;34:1179–1181.
166. Cohen BH, Sedwick LA, Burde RM. Retinopathy of dermatomyositis. *J Clin Neuroophthalmol*. 1985;5:177–179.
167. Backhouse O, Griffiths B, Henderson T, et al. Ophthalmic manifestations of dermatomyositis. *Ann Rheum Dis*. 1998;57:447–449.
168. McHugh N. Disease management dermatomyositis/polymyositis. *Rheumatology (Oxford)*. 2011;50:12–14.

169. Oddis CV, Reed AM, Aggarwal R, et al. Rituximab in the treatment of refractory adult and juvenile dermatomyositis and adult polymyositis: a randomized, placebo-phase trial. *Arthritis Rheum*. 2013;65:314–324.
170. Lahmer T, Treiber M, von Werder A, et al. Relapsing polychondritis: an autoimmune disease with many faces. *Autoimmun Rev*. 2010;9:540–546.
171. Balsa A, Expinosa A, Cuesta M, et al. Joint symptoms in relapsing polychondritis. *Clin Exp Rheumatol*. 1995;13:425–430.
172. Isaak BL, Liesegang TJ, Michet CJ Jr. Ocular and systemic findings in relapsing polychondritis. *Ophthalmology*. 1986;93:681–689.
173. Matas BR. Iridocyclitis associated with relapsing polychondritis. *Arch Ophthalmol*. 1970;84:474–476.
174. Messmer EM, Foster CS. Vasculitic peripheral ulcerative keratitis. *Surv Ophthalmol*. 1999;43:379–396.
175. Magargal LE, Donoso LA, Goldberg RE, et al. Ocular manifestations of relapsing polychondritis. *Retina*. 1981;1:96–99.
176. Anderson B Sr. Ocular lesions in relapsing polychondritis and other rheumatoid syndromes. The Edward Jackson memorial lecture. *Am J Ophthalmol*. 1967;64:35–50.
177. McKay DA, Watson PG, Lyne AJ. Relapsing polychondritis and eye disease. *Br J Ophthalmol*. 1974;58:600–605.
178. McCarthy EM, Cunnane G. Treatment of relapsing polychondritis in the era of biological agents. *Rheumatol Int*. 2010;30:827–828.
179. Basu N, Watts R, Bajema I, et al. EULAR points to consider in the development of classification and diagnostic criteria in systemic vasculitis. *Ann Rheum Dis*. 2010;69:1744–1750.
180. Watts RA, Suppiah R, Merkel PA, et al. Systemic vasculitis – is it time to reclassify? *Rheumatology (Oxford)*. 2011;50:643–645.
181. Falk RJ, Gross WL, Guillevin L, et al. Granulomatosis with polyangiitis Wegener's: an alternative name for Wegener's granulomatosis. *Arthritis Rheum*. 2011;63:863–864.
182. Jennette JC, Falk RJ, Andrassy K, et al. Nomenclature of

systemic vasculitides: proposal of an international consensus conference. *Arthritis Rheum*. 1994;37:187–192.
183. Gordon M, Luqmani RA, Adu D, et al. Relapses in patients with a systemic vasculitis. *QJM*. 1993;86:779–789.
184. Luqmani RA, Bacon PA, Moots RJ, et al. Birmingham Vasculitis Activity Score (BVAS) in systemic necrotizing vasculitis. *QJM*. 1994;87:671–678.
185. Exley AR, Carruthers DM, Luqmani RA, et al. Damage occurs early in systemic vasculitis and is an index of outcome. *QJM*. 1997;90:391–399.
186. Langford CA, Talar-Williams C, Barron KS, et al. Use of a cyclophosphamide-induction methotrexate-maintenance regimen for the treatment of Wegener's granulomatosis: extended follow-up and rate of relapse. *Am J Med*. 2003;114:463–469.
187. Adu D, Pall A, Luqmani RA, et al. Controlled trial of pulse versus continuous prednisolone and cyclophosphamide in the treatment of systemic vasculitis. *QJM*. 1997;90:401–409.
188. Morgan MD, Drayson MT, Savage CO, et al. Addition of infliximab to standard therapy for ANCA-associated vasculitis. *Nephron Clin Pract*. 2011;117:c89–97.
189. Stone JH, Merkel PA, Spiera R, et al. Rituximab versus cyclophosphamide for ANCA-associated vasculitis. *N Engl J Med*. 2010;363:221–232.
190. Hunder GG. Clinical features of GCA/PMR. *Clin Exp Rheumatol*. 2000;18:S6–8.
191. Hayreh SS, Podhajsky PA, Zimmerman B. Ocular manifestations of giant cell arteritis. *Am J Ophthalmol*. 1998;125:509–520.
192. Direskeneli H, Aydin SZ, Kermani TA, et al. Development of outcome measures for large-vessel vasculitis for use in clinical trials: opportunities, challenges, and research agenda. *J Rheumatol*. 2011;38:1471–1479.
193. Watts RA, Scott DG. Epidemiology of the vasculitides. *Semin Respir Crit Care Med*. 2004;25:455–464.
194. Cantini F, Niccoli L, Storri L, et al. Are polymyalgia rheumatica and giant cell arteritis the same disease? *Semin Arthritis Rheum*. 2004;33:294–301.

195. Hunder GG, Bloch DA, Michel BA, et al. The American College of Rheumatology 1990 criteria for the classification of giant cell arteritis. *Arthritis Rheum*. 1990;33:1122–1128.
196. Walvick MD, Walvick MP. Giant cell arteritis: laboratory predictors of a positive temporal artery biopsy. *Ophthalmology*. 2011;118:1201–1204.
197. Danesh-Meyer H, Savino PJ, Gamble GG. Poor prognosis of visual outcome after visual loss from giant cell arteritis. *Ophthalmology*. 2005;112:1098–1103.
198. Melberg NS, Grand MG, Dieckert JP, et al. Cotton-wool spots and the early diagnosis of giant cell arteritis. *Ophthalmology*. 1995;102:1611–1614.
199. Johnson MC, Lee AG. Giant cell arteritis presenting with cotton wool spots. *Semin Ophthalmol*. 2008;23:141–142.
200. Ghosh P, Borg FA, Dasgupta B. Current understanding and management of giant cell arteritis and polymyalgia rheumatica. *Expert Rev Clin Immunol*. 2010;6:913–928.
201. Hoffman GS, Cid MC, Rendt-Zagar KE, et al. Infliximab for maintenance of glucocorticosteroid-induced remission of giant cell arteritis: a randomized trial. *Ann Intern Med*. 2007;146:621–630.
202. Martinez-Taboada VM, Rodriguez-Valverde V, Carreno L, et al. A double-blind placebo controlled trial of etanercept in patients with giant cell arteritis and corticosteroid side effects. *Ann Rheum Dis*. 2008;67:625–630.
203. Bhatia A, Ell PJ, Edwards JC. Anti-CD20 monoclonal antibody (rituximab) as an adjunct in the treatment of giant cell arteritis. *Ann Rheum Dis*. 2005;64:1099–1100.
204. Cong XL, Dai SM, Feng X, et al. Takayasu's arteritis: clinical features and outcomes of 125 patients in China. *Clin Rheumatol*. 2010;29:973–981.
205. Hall S, Barr W, Lie JT, et al. Takayasu arteritis: a study of 32 North American patients. *Medicine (Baltimore)*. 1985;64:89–99.
206. Nasu T. Takayasu's truncoarteritis in Japan: a statistical observation of 76 autopsy cases. *Pathol Microbiol (Basel)*. 1975;43:140–146.
207. Arend WP, Michel BA, Bloch DA, et al. The American

College of Rheumatology 1990 criteria for the classification of Takayasu arteritis. *Arthritis Rheum*. 1990;33:1129–1134.
208. Chun YS, Park SJ, Park IK, et al. The clinical and ocular manifestations of Takayasu arteritis. *Retina*. 2001;21:132–140.
209. Peter J, David S, Danda D, et al. Ocular manifestations of Takayasu arteritis: a cross-sectional study. *Retina*. 2011;31:1170–1178.
210. Mukhtyar C, Guillevin L, Cid MC, et al. EULAR recommendations for the management of large vessel vasculitis. *Ann Rheum Dis*. 2009;68:318–323.
211. Park MC, Lee SW, Park YB, et al. Clinical characteristics and outcomes of Takayasu's arteritis: analysis of 108 patients using standardized criteria for diagnosis, activity assessment, and angiographic classification. *Scand J Rheumatol*. 2005;34:284–292.
212. Valsakumar AK, Valappil UC, Jorapur V, et al. Role of immunosuppressive therapy on clinical, immunological, and angiographic outcome in active Takayasu's arteritis. *J Rheumatol*. 2003;30:1793–1798.
213. Pettigrew HD, Teuber SS, Gershwin ME. Polyarteritis nodosa. *Compr Ther*. 2007;33:144–149.
214. Dillon MJ, Eleftheriou D, Brogan PA. Medium-size-vessel vasculitis. *Pediatr Nephrol*. 2010;25:1641–1652.
215. Kluger N, Pagnoux C, Guillevin L, et al. Comparison of cutaneous manifestations in systemic polyarteritis nodosa and microscopic polyangiitis. *Br J Dermatol*. 2008;159:615–620.
216. Blodi FC, Sullivan PB. Involvement of the eyes in periarteritis nodosa. *Trans Am Acad Ophthalmol Otolaryngol*. 1959;63:161–165.
217. Moore JG, Sevel D. Corneo-scleral ulceration in periarteritis nodosa. *Br J Ophthalmol*. 1966;50:651–655.
218. Yamamoto S, Takeuchi S. Episcleritis as the primary clinical manifestation in a patient with polyarteritis nodosa. *Jpn J Ophthalmol*. 2000;44:151–153.
219. Mukhtyar C, Guillevin L, Cid MC, et al. EULAR recommendations for the management of primary small

and medium vessel vasculitis. *Ann Rheum Dis*. 2009;68:310–317.
220. Gayraud M, Guillevin L, le TP, et al. Long-term followup of polyarteritis nodosa, microscopic polyangiitis, and Churg–Strauss syndrome: analysis of four prospective trials including 278 patients. *Arthritis Rheum*. 2001;44:666–675.
221. Nakamura Y, Yashiro M, Uehara R, et al. Epidemiologic features of Kawasaki disease in Japan: results of the 2007–2008 nationwide survey. *J Epidemiol*. 2010;20:302–307.
222. Gedalia A, Cuchacovich R. Systemic vasculitis in childhood. *Curr Rheumatol Rep*. 2009;11:402–409.
223. Gedalia A. Kawasaki disease: an update. *Curr Rheumatol Rep*. 2002;4:25–29.
224. Ohno S, Miyajima T, Higuchi M, et al. Ocular manifestations of Kawasaki's disease (mucocutaneous lymph node syndrome). *Am J Ophthalmol*. 1982;93:713–717.
225. Farvardin M, Kashef S, Aleyasin S, et al. Sudden unilateral blindness in a girl with Kawasaki disease. *J Pediatr Ophthalmol Strabismus*. 2007;44:303–304.
226. Ogata S, Bando Y, Kimura S, et al. The strategy of immune globulin resistant Kawasaki disease: a comparative study of additional immune globulin and steroid pulse therapy. *J Cardiol*. 2009;53:15–19.
227. Imagawa T, Mori M, Miyamae T, et al. Plasma exchange for refractory Kawasaki disease. *Eur J Pediatr*. 2004;163:263–264.
228. Sundel RP, Burns JC, Baker A, et al. Gamma globulin re-treatment in Kawasaki disease. *J Pediatr*. 1993;123:657–659.
229. Sundel RP, Baker AL, Fulton DR, et al. Corticosteroids in the initial treatment of Kawasaki disease: report of a randomized trial. *J Pediatr*. 2003;142:611–616.
230. Schilder AM. Wegener's granulomatosis vasculitis and granuloma. *Autoimmun Rev*. 2010;9:483–487.
231. Ntatsaki E, Watts RA, Scott DG. Epidemiology of ANCA-associated vasculitis. *Rheum Dis Clin North Am*. 2010;36:447–461.
232. Mahr AD, Neogi T, Merkel PA. Epidemiology of Wegener's granulomatosis: lessons from descriptive studies and analyses of genetic and environmental risk determinants.

Clin Exp Rheumatol. 2006;24:S82–91.
233. Rao NV, Wehner NG, Marshall BC, et al. Characterization of proteinase-3 PR-3, a neutrophil serine proteinase: structural and functional properties. *J Biol Chem*. 1991;266:9540–9548.
234. Talar-Williams C, Sneller MC, Langford CA, et al. Orbital socket contracture: a complication of inflammatory orbital disease in patients with Wegener's granulomatosis. *Br J Ophthalmol*. 2005;89:493–497.
235. Robinson MR, Lee SS, Sneller MC, et al. Tarsal-conjunctival disease associated with Wegener's granulomatosis. *Ophthalmology*. 2003;110:1770–1780.
236. Tanihara H, Nakayama Y, Honda Y. Wegener's granulomatosis with rapidly progressive retinitis and anterior uveitis. *Acta Ophthalmol (Copenh)*. 1993;71:853–855.
237. Huong du LT, Tran TH, Piette JC. Granulomatous uveitis revealing Wegener's granulomatosis. *J Rheumatol*. 2006;33:1209–1210.
238. Watkins AS, Kempen JH, Choi D, et al. Ocular disease in patients with ANCA-positive vasculitis. *J Ocul Biol Dis Infor*. 2009;3:12–19.
239. Lapraik C, Watts R, Bacon P, et al. BSR and BHPR guidelines for the management of adults with ANCA associated vasculitis. *Rheumatology (Oxford)*. 2007;46:1615–1616.
240. Booth A, Harper L, Hammad T, et al. Prospective study of TNFalpha blockade with infliximab in anti-neutrophil cytoplasmic antibody-associated systemic vasculitis. *J Am Soc Nephrol*. 2004;15:717–721.
241. Taylor SR, Salama AD, Joshi L, et al. Rituximab is effective in the treatment of refractory ophthalmic Wegener's granulomatosis. *Arthritis Rheum*. 2009;60:1540–1547.
242. Guillevin L, Durand-Gasselin B, Cevallos R, et al. Microscopic polyangiitis: clinical and laboratory findings in eighty-five patients. *Arthritis Rheum*. 1999;42:421–430.
243. Lhote F, Cohen P, Genereau T, et al. Microscopic polyangiitis: clinical aspects and treatment. *Ann Med Interne (Paris)*. 1996;147:165–177.

244. Hara A, Ohta S, Takata M, et al. Microscopic polyangiitis with ocular manifestations as the initial presenting sign. *Am J Med Sci*. 2007;334:308–310.
245. Gallagher MJ, Ooi KG, Thomas M, et al. ANCA associated pauci-immune retinal vasculitis. *Br J Ophthalmol*. 2005;89:608–611.
246. Walsh M, Jayne D. Rituximab in the treatment of anti-neutrophil cytoplasm antibody associated vasculitis and systemic lupus erythematosus: past, present and future. *Kidney Int*. 2007;72:676–682.
247. Noth I, Strek ME, Leff AR. Churg–Strauss syndrome. *Lancet*. 2003;361:587–594.
248. Guillevin L, Cohen P, Gayraud M, et al. Churg–Strauss syndrome. Clinical study and long-term follow-up of 96 patients. *Medicine (Baltimore)*. 1999;78:26–37.
249. Masi AT, Hunder GG, Lie JT, et al. The American College of Rheumatology 1990 criteria for the classification of Churg–Strauss syndrome (allergic granulomatosis and angiitis). *Arthritis Rheum*. 1990;33:1094–1100.
250. Margolis R, Kosmorsky GS, Lowder CY, et al. Conjunctival involvement in Churg–Strauss syndrome. *Ocul Immunol Inflamm*. 2007;15:113–115.
251. Takanashi T, Uchida S, Arita M, et al. Orbital inflammatory pseudotumor and ischemic vasculitis in Churg–Strauss syndrome: report of two cases and review of the literature. *Ophthalmology*. 2001;108:1129–1133.
252. Weinstein JM, Chui H, Lane S, et al. Churg–Strauss syndrome (allergic granulomatous angiitis). Neuro-ophthalmologic manifestations. *Arch Ophthalmol*. 1983;101:1217–1220.
253. Pepper RJ, Fabre MA, Pavesio C, et al. Rituximab is effective in the treatment of refractory Churg–Strauss syndrome and is associated with diminished T-cell interleukin-5 production. *Rheumatology (Oxford)*. 2008;47:1104–1105.
254. West SK, Valmadrid CT. Epidemiology of risk factors for age-related cataract. *Surv Ophthalmol*. 1995;39:323–334.
255. Clark AF, Wordinger RJ. The role of steroids in outflow resistance. *Exp Eye Res*. 2009;88:752–759.

256. Hobbs HE, Sorsby A, Freedman A. Retinopathy following chloroquine therapy. *Lancet*. 1959;2:478–480.
257. Lee AG. Hydroxychloroquine screening. *Br J Ophthalmol*. 2005;89:521–522.
258. Marmor MF, Kellner U, Lai TY, et al. Revised recommendations on screening for chloroquine and hydroxychloroquine retinopathy. *Ophthalmology*. 2011;118:415–422.

Infections

OUTLINE

84

HIV-Associated Infections

Igor Kozak, J. Allen McCutchan, William R. Freeman

Introduction

Acquired immunodeficiency syndrome (AIDS) is a potentially fatal multisystem syndrome characterized by profound disruption of the immune system and a propensity for various opportunistic infections and neoplasms. AIDS is caused by either of two human immunodeficiency viruses (HIV-1 [formerly HTLV-3] or HIV-2).[1–3] HIV-1 entered humans from chimpanzees nearly a century ago and, after passing unrecognized among West Africans,[4,5] came to the United States via Haiti in the 1970s. AIDS was recognized first in 1981 as outbreaks of usual opportunistic infections (OIs) in homosexual men in three American cities.

Ocular involvement occurs in up to 73% of AIDS patients,[6,7] with the most common lesions being a retinal vasculopathy consisting of cotton-wool spots, retinal hemorrhages, and infectious retinopathy such as cytomegalovirus (CMV), herpetic, toxoplasmic, or luetic retinitis.

Epidemiology of HIV Infection and AIDS

By 2012, an estimated 1.2 million people were living with HIV in the United States.[8] Since 1996 AIDS has been converted from an inevitably progressive and fatal disease into a manageable chronic condition by three-drug regimens referred to as highly active or combination antiretroviral therapy (HAART or CART). HIV is spread by homosexual and heterosexual intercourse, blood exposures through shared needles among intravenous drug users, or peripartum or by breast-feeding of infants.[9–11]

Occupational Exposure to HIV

The average risk of HIV transmission in healthcare workers after percutaneous exposure to HIV-infected blood is approximately 0.3% without treatment.[12,13] This risk is further lowered by double-gloving and is probably much lower in the ophthalmic setting.[14] Postexposure prophylaxis (PEP) with two or three antiretroviral

drugs appears likely to dramatically reduce the transmission of HIV even after high-risk injuries.[15] Because PEP should be started as soon as possible after injury, healthcare institutions should have well-developed procedures that provide for expert consultation and ready access to a combination of drugs for persons at high risk of injuries, such as surgeons, invasive proceduralists, and phlebotomists.

Currently, for percutaneous injuries, the US Public Health Service recommends 4 weeks of treatment with a two-drug regimen if the exposure is less severe (solid needle and superficial injury) and the source patient has asymptomatic HIV infection or known low viral load (<1500 RNA copies/mL [class I patient]). An expanded three-drug regimen is recommended if the exposure is severe (large-bore hollow needle, deep puncture, visible blood on device, or needle used in patient's artery or vein) or if the source patient has symptomatic HIV infection, AIDS, acute seroconversion, or known high viral load (class II patient). The recommended two-drug regimens for HIV/PEP are (1) tenofovir plus emtricitabine or (2) zidovudine plus lamivudine. Tenofovir is generally better tolerated, but should not be used in persons with renal insufficiency. Three-drug regimens involve adding ritonavir-boosted (/r) lopinavir/r or darunavir/r. Alternatives for constructing an expanded regimen in cases of resistance, drug interactions, or intolerance include darunavir/r, atazanavir/r, or raltegravir. For mucous membrane or nonintact skin exposures, the two-drug regimen is recommended for all small volume exposures (a few drops) and large volume (major blood splash) exposure in a class I patient, with three-drug expanded regimens recommended for large volume exposure in a class II patient.[13]

HIV Virology and Pathogenesis

HIV infection usually gradually depletes CD4 lymphocytes, resulting in decreased blood levels of this crucial subset of “helper” T cells.[16] AIDS patients typically become ill only after $CD4^+$ helper T cells reach less than 200/μL, a level that no longer supports cell-mediated immunity at levels needed to contain infections by select opportunistic viral, bacterial, or fungal pathogens.

Understanding of HIV infection was revolutionized by the development in the mid-1990s of assays that measured the levels of HIV in the blood. All stages of HIV infection were seen to be characterized by a high rate of viral replication in most patients. Levels of plasma HIV-1 RNA predict the rate of clinical progression in HIV patients.[17–23] Both high replication and an error-prone reverse transcription process promote frequent mutations in the HIV genome that result in the emergence of variants that can better resist either control by the host's antibody and cell-mediated immune responses or by antiretroviral drugs, if drugs are present in insufficient numbers or at low blood levels that fail to fully suppress HIV replication. Under selective pressure from antiretroviral agents, mutations that confer a decreased sensitivity to individual drugs are selected and stored in latent cells where they last for decades.[24–27]

Therapy of HIV Infections

Treatment of HIV has evolved rapidly, with the development of more than 30 drugs (as of 2011) that fall into at least four classes based on which of the steps in HIV replication they inhibit (Table 84.1). These steps include (1) binding to receptors and entry into the host cell; (2) reverse transcription of HIV RNA to proviral DNA; (3) integration of proviral DNA into the host cell genome; and (4) maturation of HIV after budding by the action of HIV protease.[28] Coadministration of drugs from several of the classes delays or prevents the emergence of drug-resistant HIV by minimizing viral replication. However, HIV may develop resistance to all available therapy because (1) patients have difficulty maintaining high levels of adherence over long periods and (2) cross-resistance is common to drugs within a class.[29–32] After failure of a regimen, the next combination of drugs is less likely to be successful in fully suppressing HIV replication, which is the necessary condition for prolonged success. For details of recent expert guidelines on HIV therapy consult Guidelines for the Use of Antiretroviral Agents in HIV-1-Infected Adults and Adolescents, which is constantly updated and available at this NIH website: http://www.aidsinfo.nih.gov/ContentFiles/AdultandAdolescentGL.p

TABLE 84.1

Currently Licensed Antiretroviral Drugs in the United States in 2011 by Class

Brand Name	Generic Name	Manufacturer Name
MULTICLASS COMBINATION PRODUCTS		
Atripla	efavirenz, emtricitabine, and tenofovir disoproxil fumarate	Bristol–Myers Squibb and Gilead Sciences
NUCLEOSIDE REVERSE TRANSCRIPTASE INHIBITORS (NRTIS)		
Combivir	lamivudine and zidovudine	GlaxoSmithKline
Emtriva	emtricitabine, FTC	Gilead Sciences
Epivir	lamivudine, 3TC	GlaxoSmithKline
Epzicom	abacavir and lamivudine	GlaxoSmithKline
Retrovir	zidovudine, azidothymidine, AZT, ZDV	GlaxoSmithKline
Trizivir	abacavir, zidovudine, and lamivudine	GlaxoSmithKline
Truvada	tenofovir disoproxil fumarate and emtricitabine	Gilead Sciences, Inc.
Videx EC	enteric-coated didanosine, ddI EC	Bristol–Myers Squibb
Videx	didanosine, dideoxyinosine, ddI	Bristol–Myers Squibb
Viread	tenofovir disoproxil fumarate, TDF	Gilead
Zerit	stavudine, d4T	Bristol–Myers Squibb
Ziagen	abacavir sulfate, ABC	GlaxoSmithKline
NONNUCLEOSIDE REVERSE TRANSCRIPTASE INHIBITORS (NNRTIS)		
Edurant	rilpivirine	Tibotec Therapeutics
Intelence	etravirine	Tibotec Therapeutics
Rescriptor	delavirdine, DLV	Pfizer
Sustiva	efavirenz, EFV	Bristol–Myers Squibb
Viramune (immediate release)	nevirapine, NVP	Boehringer Ingelheim
Viramune XR (extended release)	nevirapine, NVP	Boehringer Ingelheim
PROTEASE INHIBITORS (PIS)		
Agenerase	amprenavir, APV	GlaxoSmithKline
Aptivus	tipranavir, TPV	Boehringer Ingelheim
Crixivan	indinavir, IDV,	Merck
Fortovase	saquinavir (no longer marketed)	Hoffmann–La Roche
Invirase	saquinavir mesylate, SQV	Hoffmann–La Roche
Kaletra	lopinavir and ritonavir, LPV/RTV	Abbott Laboratories
Lexiva	fosamprenavir calcium, FOS-APV	GlaxoSmithKline
Norvir	ritonavir, RTV	Abbott Laboratories
Prezista	darunavir	Tibotec, Inc.
Reyataz	atazanavir sulfate, ATV	Bristol–Myers Squibb
Viracept	nelfinavir mesylate, NFV	Agouron Pharmaceuticals
FUSION INHIBITORS		
Fuzeon	enfuvirtide, T-20	Hoffmann–La Roche & Trimeris
ENTRY INHIBITORS – CCR5 CO-RECEPTOR ANTAGONIST		
Selzentry	maraviroc	Pfizer
HIV INTEGRASE STRAND TRANSFER INHIBITORS		
Isentress	raltegravir	Merck & Co., Inc.

Clinical Spectrum of HIV

HIV infection and disease is highly variable in presentation and includes asymptomatic, various chronic or recurring constitutional signs and symptoms, and a plethora of opportunistic conditions. The "acute retroviral syndrome," that is, early or primary infection with HIV, is characterized by fever, pharyngitis, skin rash, arthralgias, malaise, mucosal ulcerations, and neurologic manifestations such as aseptic meningitis.[33]

Patients chronically infected with HIV may present with a prodrome of generalized, nontender lymph node enlargement, fevers and night sweats, weight loss, and diarrhea for weeks or months, formerly termed AIDS-related complex (ARC). Nearly all HIV-seropositive patients will progress to AIDS, but a small minority, called "long-term nonprogressors" or "elite controllers," suppress their infections naturally (without treatment) to the point of very low or undetectable levels of plasma HIV. Although highly active antiretroviral therapy (HAART) often reduces plasma viremia of HIV-1 to undetectable levels, latent viral reservoirs of resting CD4 lymphocytes persist for years and reappear in the blood if therapy is stopped.[34]

Opportunistic infections are responsible for the deaths of most AIDS patients, but consequences of coinfections with hepatitis C and B, such as hepatic insufficiency or hepatocellular carcinoma, have become increasingly important, in part because HIV promotes progression of these infections.[35] The most common pathogens encountered in AIDS patients are cytomegalovirus (CMV), *Candida albicans*, *Pneumocystis jiroveci* (formerly *carinii*), *Mycobacterium tuberculosis* and *M. avium-intracellulare*, *Cryptococcus neoformans*, herpes simplex virus (HSV), *Cryptosporidium* spp., *Toxoplasma gondii*, and varicella-zoster virus (VZV).[3,36] CMV retinitis can be the initial sign of tissue-invasive systemic CMV infection in these patients, although it is restricted to patients with advanced immunosuppression ($CD4^+$ count less than 50/μL). CMV may present also in the gastrointestinal tract, brain and spinal cord, or other organs.[37]

Infection Control Related to HIV

The US Centers for Disease Control and Prevention (CDC) recommendations for universal precautions to prevent the occupational transmission of HIV and other bloodborne viruses in the healthcare setting were provided in 1988 and have not been amended.[38]

The CDC provided specific guidelines for ophthalmologic examinations in addition to the general recommendations. The use of gloves (especially if the skin of the examiner is compromised in any way) and good handwashing technique after procedures or examinations involving the eye are recommended because HIV may be present in tears.

Sterilization of all instruments and equipment that come into contact with the eye in all patients is necessary using gas or steam autoclaving or a 5- to 10-minute soak in one of the following solutions: 3% hydrogen peroxide solution, 10% solution of sodium hypochlorite (common household bleach), or 70% ethanol or isopropanol. Instruments disinfected in this manner should be rinsed in water and dried before reuse.[39,40] Damage to tonometer tips has been reported with the use of 70% isopropanol; thus a 5- to 10-minute soak in 3% H_2O_2 or 1 : 10 dilution of household bleach may be preferable.[41] It should be noted that there is no evidence of HIV transmission through contact with tears or instruments used to examine these patients.[39]

Contact lenses used in trial fittings on all patients should be disinfected by use of any commercially available cleaning method or solution.[42] Inactivation of HIV by various disinfectants on surfaces has been reviewed.[43] Guidelines for preventing transmission of HIV through transplantation of human tissue and organs (including corneal transplants) have been set forth.[44] Specific recommendations for postexposure management of needlestick injuries or mucosal membrane exposures to secretions from patients with HIV infection have been published.[45]

Ocular Findings in AIDS: An Overview

HIV has been detected in the cornea,[46] conjunctival epithelium,[47]

and in tears,[46] but at very low titers. Ocular manifestations of AIDS may be seen in up to 100% of patients. They are less common, but may be seen in patients with earlier, symptomatic HIV infection.[48] Most common are cotton-wool spots and other noninfectious retinopathies,[49] CMV retinitis, and conjunctival Kaposi sarcoma, followed less frequently by herpes zoster ophthalmicus,[50,51] retinal toxoplasmosis, choroidal *P. carinii* infection, herpes simplex and herpes zoster retinitis (acute retinal necrosis [ARN]), and cryptococcal choroiditis.[6,52–59]

Iritis may occur in association with viral retinitis but especially with CMV; it is mild. Acute iritis may be associated with the use of oral rifabutin (used for the treatment and prophylaxis of mycobacterial infections) or intravenous cidofovir used for CMV retinitis.[60]

Choroidal infection with *Cryptococcus*, *Pneumocystis*, *M. tuberculosis*, *Aspergillus*, *Toxoplasma*, *Histoplasma*, and *M. avium-intracellulare* usually is associated with systemic infection.[61,62] *Histoplasma capsulatum* chorioretinitis and endophthalmitis,[63] *Paracoccidioidomycosis brasiliensis* chorioretinitis,[64] keratitis sicca, cranial nerve paralysis, Roth's spots, papilledema, perivasculitis, and fungal corneal ulcers are rare but have been reported.[65]

Noninfectious Retinopathy

Noninfectious retinopathy refers to cotton-wool spots, retinal hemorrhages, and microvascular abnormalities that do not progress, enlarge, or cause visual symptoms. No infectious cause of these lesions has been demonstrated, and they appear to represent nonspecific retinal microvascular disease. A correlation between the number of cotton-wool spots and decreased cerebral blood flow (as shown by technetium 99^{m} hexamethylpropyleneamine oxime single photon emission computed tomography) was shown in 25 patients with AIDS or symptomatic HIV infection.[66]

Cotton-wool spots are the most common ocular lesion seen in AIDS, occurring in 25–50% of patients[6,67] and in up to 75% of cases by autopsy examination.[57] In one study, up to 92% of AIDS patients were found to have evidence of retinovascular disease when examined using fluorescein angiography.[67] Cotton-wool spots seen

by ophthalmoscopy are a result of microinfarction of the nerve fiber layer of the retina. In AIDS these lesions usually are confined to the posterior pole near the optic disc[67] (Fig. 84.1). Histopathologic study of retinal cotton-wool spots in AIDS patients has demonstrated that these lesions have pathologic features identical to those seen in cotton-wool spots of other cause. Similar to the cotton-wool spots seen in other systemic diseases, this lesion in AIDS demonstrates no associated inflammation, no cells in the vitreous, and no vascular leakage on fluorescein angiography (Fig. 84.2). Attempts to isolate organisms from cotton-wool spots in the hope of explaining their cause in AIDS as infectious have been unsuccessful, and the cause of this lesion in AIDS remains elusive.[6,57,68,69]

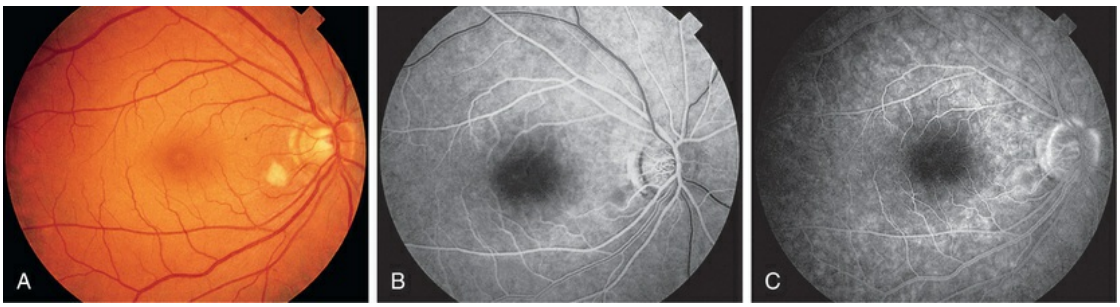

FIG. 84.1 (A) Retinal cotton-wool spot seen inferotemporal to the disc. (B) Early fluorescein angiogram shows blockage and possible nonperfusion. (C) Late angiogram shows staining, presumably from damaged retinal microvasculature.

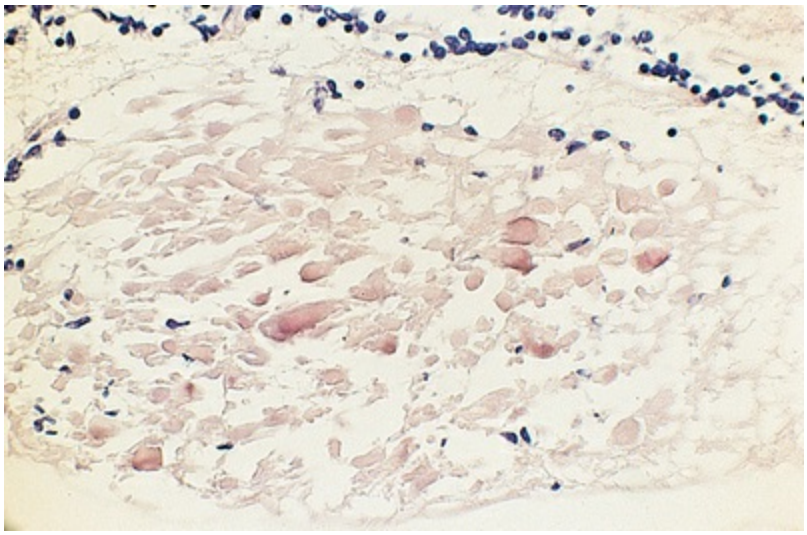

FIG. 84.2 Photomicrograph of retinal cotton-wool spot shows cytoid bodies and swelling of the nerve fiber layer of the retina. Retinal cellular elements are seen at the top of the photograph.

Cotton-wool spots have been speculated to be harbingers of CMV retinitis or perhaps sites of susceptibility to CMV infection, but substantiation of these ideas is lacking. Histopathologic studies of eyes at autopsy have failed to show clear evidence of a viral cause of cotton-wool spots.[70–72]

We have reported that noninfectious retinopathy is not seen in HIV-seronegative men and is rare in ARC, but it is very common in patients with AIDS even in the absence of active opportunistic ophthalmic infection.[48] It is striking that this lesion may be seen in 50–75% of AIDS patients, and studies using multiple examinations indicate that the more frequently these patients are examined, the higher the incidence may be.[6,49] Cotton-wool spots probably are ophthalmoscopically visible for 6–12 weeks, and owing to the transient nature of the lesion and its apparent noninfectious cause, treatment is not indicated at this time.[73] On in vivo imaging they cause the "hyper-reflective sign"[74] followed by inner retina thinning years after their disappearance.[75]

In a cross-sectional study, the median CD4 count (per microliter [μL]) in patients with cotton-wool spots was 14 cells (range 0–160) and was 8 cells (range 0–42) in patients with CMV retinitis.[76] In the absence of other systemic vascular disease, such as hypertension or diabetes mellitus, AIDS must be considered in the differential diagnosis of cotton-wool spots owing to their very high prevalence

in these patients. Whether these lesions are an early manifestation of AIDS remains to be elucidated, but they may be apparent in HIV-infected persons before the onset of opportunistic infections.[48]

Morphologic studies have shown that the number of retrobulbar optic nerve fibers in patients with AIDS is decreased compared with the number of optic nerve fibers in normal control eyes as a result of axonal degeneration and an associated decrease in the number of optic nerve axons.[77–80] Infarctions of the nerve fiber layer develop in most patients with AIDS, and the number of such infarctions increases over time.[6,49] Visual dysfunction associated with multiple nerve fiber layer infarctions may be manifested by defects in color-vision and contrast-sensitivity testing in patients with AIDS.[81–83,]

Interestingly, in vivo studies of the retinal nerve fiber layer have shown both broad and slit-like defects, suggesting that retinal nerve fiber loss and optic nerve fiber loss are related to subclinical vision loss in HIV patients without infectious retinitis.[74,84] Electroretinographic studies of HIV patients without retinitis also have shown retinal dysfunction.[85,86] The complex of above-mentioned vision abnormalities has been termed HIV neuroretinal disorder with an incidence in HIV patients between 16% to 50% after 20 years of AIDS diagnosis.[87,88] The molecular biology of HIV retinopathy and possible pathophysiology of HIV neuroretinal disorder has been published recently.[89]

Retinal hemorrhages are seen in AIDS in association with CMV retinitis, cotton-wool spots, and as an isolated finding. These lesions have been reported in up to 30%[52,67,90] of AIDS patients, and autopsy evidence of retinal hemorrhages has been reported to be as high as 40%. Retinal hemorrhages usually take the form of flame-shaped lesions in the posterior pole, dot-blot hemorrhages, or as punctate intraretinal hemorrhages peripherally (Fig. 84.3). Occasionally the hemorrhage is manifested as Roth's spots (hemorrhage with a white central area).[52,67] The pattern of retinal hemorrhages changes over time. The hemorrhages do not appear to be related to a bleeding diathesis or coagulopathy, but rather seem to be a manifestation of AIDS itself.[6] Vision loss from retinal hemorrhage has not been described, and treatment is conservative if the lesions are not associated with CMV retinitis or septicemia.

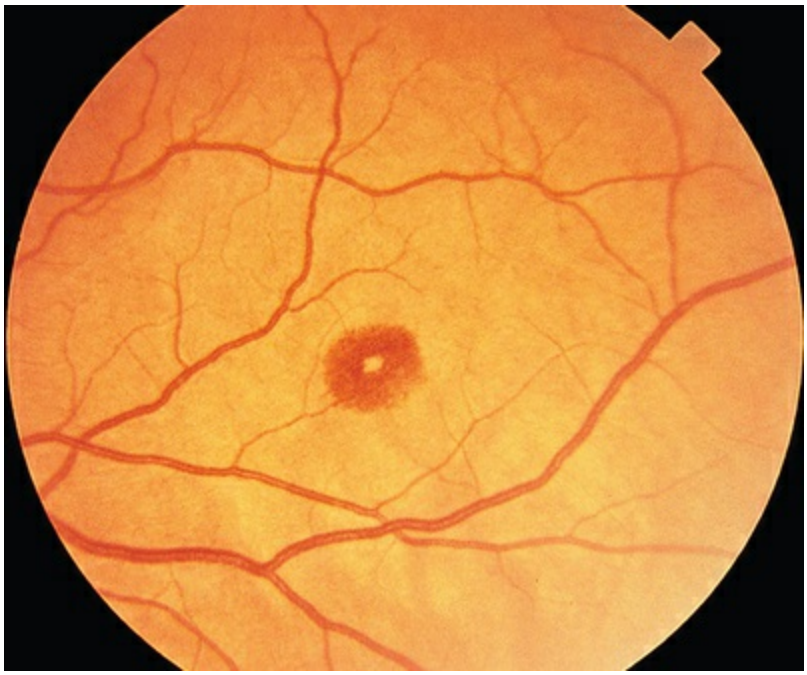

FIG. 84.3 White, centered retinal hemorrhage (Roth spot) seen in an HIV-infected patient. These lesions do not progress.

Microvascular pathologic findings in AIDS, as demonstrated by fluorescein angiography, include microaneurysms, telangiectasias, focal areas of nonperfusion, and capillary loss.[67] These changes are similar to the changes seen in diabetes mellitus. The histologic findings of periodic acid–Schiff (PAS)-positive thickening of blood vessels and precapillary arteriolar closure also correlate with the findings in diabetes mellitus.

Branch or central retinal vein occlusion, branch retinal artery occlusion, and ischemic maculopathy have been reported in HIV patients without infectious retinitis. The incidence is unknown. It is possible that the cause may be related to lupus anticoagulant and other clotting abnormalities seen in HIV-infected patients.[91,92] Abnormalities of retinal blood flow have also been reported in HIV patients and may contribute to the pathogenesis of microvascular abnormalities.[93–96]

Infectious Retinopathy

Cytomegalovirus Retinitis

Pathogenesis, Diagnosis, and Clinical Manifestations

CMV infection is a major cause of morbidity and mortality in AIDS. CMV retinitis has been reported to occur in 15–40% of AIDS patients with the rate declining since the arrival of HAART.[37,52,97,98] In contrast to the noninfectious lesions of AIDS, CMV retinitis demands aggressive treatment to prevent severe visual loss.[6,99,100] Patients with active CMV disease may have systemic symptoms of fever, arthralgia, and pneumonitis, or leukopenia, retinitis, or hepatitis; blood cultures and urine specimens may be positive for CMV. CMV retinitis often is the presenting sign of systemic CMV infection, and all patients should be thoroughly evaluated for systemic disease.

The clinical presentation of CMV retinitis in AIDS is similar in many respects to CMV retinitis found in iatrogenically immunosuppressed patients and infants with cytomegalic inclusion disease.[101,102] Correlation of the clinical and typical pathologic findings at autopsy has been demonstrated.[103] Specifically, it is known that CMV is a neurotropic virus with a tendency to infect neural tissues and the retina. Necrosis of the retina in AIDS-associated CMV retinitis is typical, with pathognomonic cytomegaly and minimal inflammatory cells present in the lesions. Choroidal involvement is rare, and whether vascular endothelium is involved is unclear. These lesions also may appear as noncontiguous patches rather than the more commonly seen contiguous spreading lesion. Antigens to CMV have been found by immunofluorescence, immunoperoxidase staining, and DNA hybridization techniques.[104,105] The most distinctive anterior segment finding is the presence of fine stellate keratic precipitates on the corneal endothelium.[106] Retinal vascular nonperfusion and retinal neovascularization resulting from CMV retinitis and choroiditis also have been reported.[107]

CMV is a slowly progressive necrotizing retinitis that may affect the posterior pole, the periphery, or both, and may be unilateral or bilateral. Involved retinal areas appear as white intraretinal lesions, areas of infiltrate, and often necrosis along the vascular arcades in the posterior pole. In addition, prominent retinal hemorrhages often are present within the necrotic area or along its leading edge (Fig. 84.4). Peripherally, CMV retinitis occurs commonly; it tends to have a less intense white appearance, with areas of granular, white

retinitis that may or may not demonstrate associated retinal hemorrhage (Fig. 84.5). As the retinitis progresses, an area of atrophic, avascular retina may remain with underlying retinal pigment epithelial atrophy or hyperplasia.[6,37,108] Peripheral CMV retinitis is common in AIDS patients who initially may report only floaters with or without a visual field deficit. Wide-angle fundus photography and fluorescein angiography may be of benefit if the diagnosis is uncertain. These techniques may be used to document progression of retinitis, and fluorescein leakage in areas of retinitis may be helpful in confirming the diagnosis (Fig. 84.6).

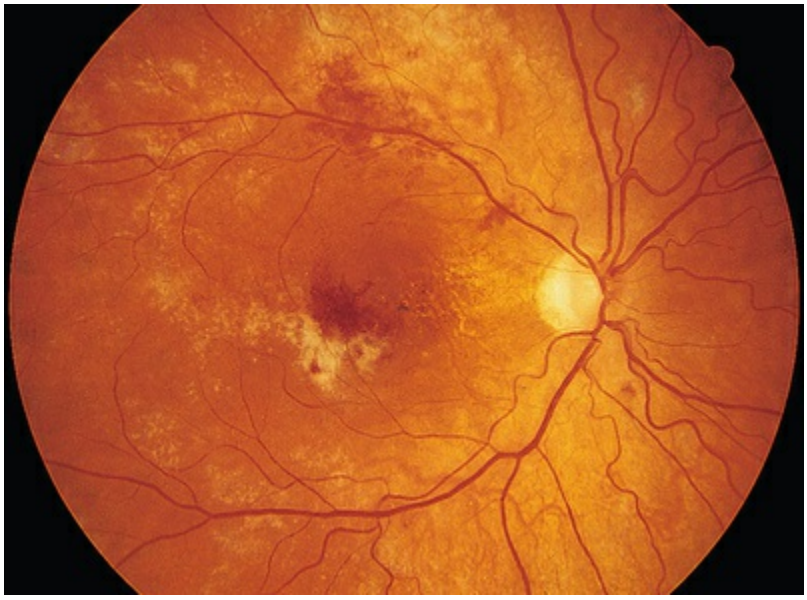

FIG. 84.4 CMV retinitis with hemorrhagic areas are seen superior to the fovea and a more dense area just below the fovea. Borders are opaque and associated with variable amounts of hemorrhage.

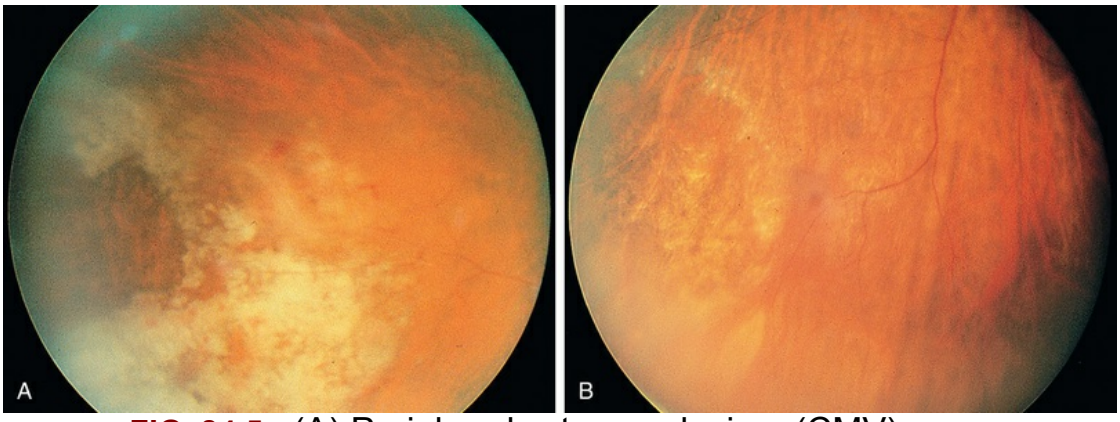

FIG. 84.5 (A) Peripheral cytomegalovirus (CMV) retinitis without retinal hemorrhage is characterized by white areas of retinal necrosis. (B) After healing, CMV retinitis leaves behind a glial scar without opacification (not same eye as in panel A). Often only minimal pigmentary changes are seen.

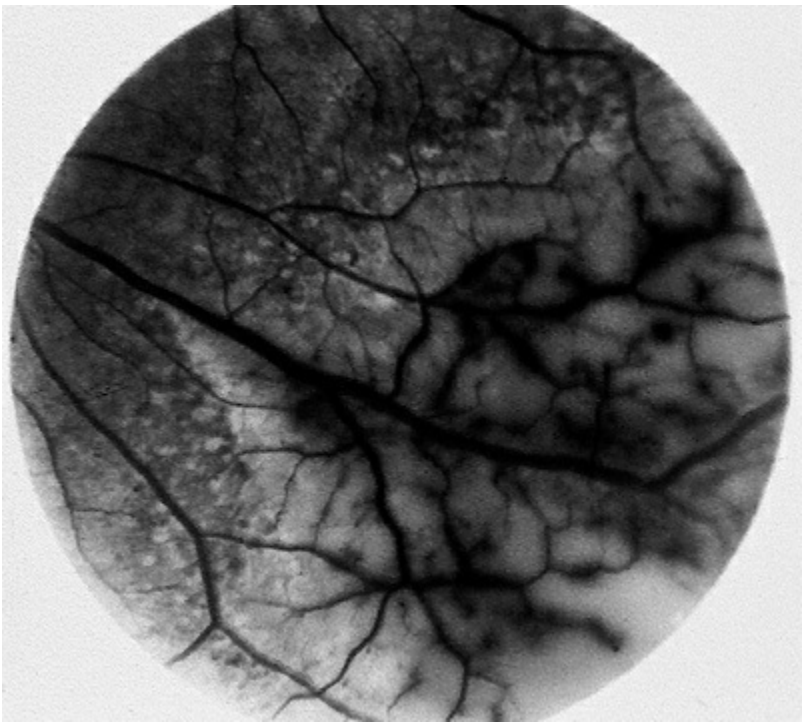

FIG. 84.6 Fluorescein angiogram of cytomegalovirus (CMV) retinitis lesion shows lack of perfusion and blockage, as well as staining and leakage of fluorescein from damaged retinal vessels.

Reactivation of CMV retinitis is characterized by reopacification of the border of the lesion followed by advancement. Smoldering

retinitis (Fig. 84.7) and subtle reactivation may be difficult to recognize without prior fundus photographs. Several studies have shown that wide-angle fundus photographs are a more sensitive indicator of retinitis progression than is clinical examination by indirect ophthalmoscopy.[109,110]

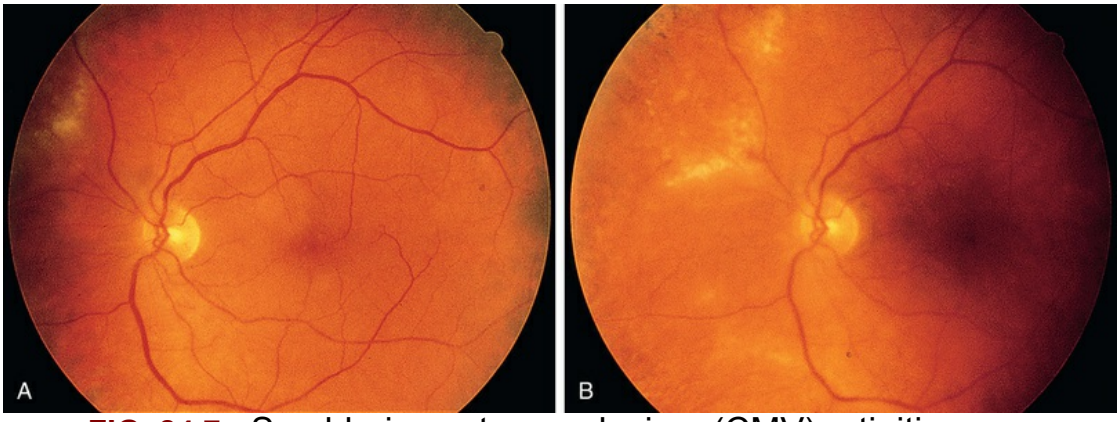

FIG. 84.7 Smoldering cytomegalovirus (CMV) retinitis is a low grade of retinitis border activity that is associated with slow progression of retinitis. It may be difficult to diagnose without fundus photographs. (A) Low grade CMV lesion. (B) Lesion has progressed slowly over 2 months.

Several investigators have shown that untreated CMV retinitis is inexorably progressive in AIDS patients.[6,52,102,104,110,111] As in our experience, untreated CMV becomes bilateral in the vast majority of patients. In an observational study of 26 patients treated for CMV retinitis, vision scores decreased with greater abnormalities found on ophthalmologic examination. Visual symptoms were most strongly related to findings in the worse eye. Patients reported considerable impairment, including blurred vision (42%), difficulty reading (40%), difficulty driving (44%), treatment interference with social activities (40%), and substantial trouble with vision (50%).[112] Treatment of AIDS-related CMV retinitis minimizes loss of vision and may protect previously uninfected eyes, prolonging visual independence.[113]

Recurrent CMV retinitis exhibiting a foveal-sparing pattern within 1500 mm of the foveola has been described and occurs primarily in patients with recurrent CMV retinitis resistant to

treatment ("clinically resistant"), particularly that which has arisen temporally. Despite its foveolar proximity and ultimate significant loss of function, the pattern of progression allows for preservation of useful foveal vision for longer periods than would have been expected.[114]

Other manifestations of CMV retinitis include retinal edema, attenuated vessels, perivascular sheathing, and exudative retinal detachment[115] (Fig. 84.8). In addition, vitritis and anterior uveitis are often seen, and optic atrophy may occur as a late manifestation resulting from widespread retinal destruction. CMV occasionally may be demonstrated in vitreous biopsy specimens in these patients.[103] The yield may be higher in the presence of marked vitritis because CMV is a cell-associated virus. Other causes of retinitis, including herpes simplex retinitis,[101,116] toxoplasmosis,[62] candidal infection, Behçet disease, syphilis, acute retinal necrosis,[117,118] and subacute sclerosing panencephalitis, usually can be distinguished from CMV on clinical grounds, although this may not be the case in retinitis caused by other members of the herpesvirus family.[117] CMV has a very characteristic clinical appearance, but the lesions in CMV retinitis vary from patient to patient, and it is important to maintain a high index of suspicion for the above infections, especially in light of frequent superinfection of AIDS patients with multiple organisms.[6,90,91]

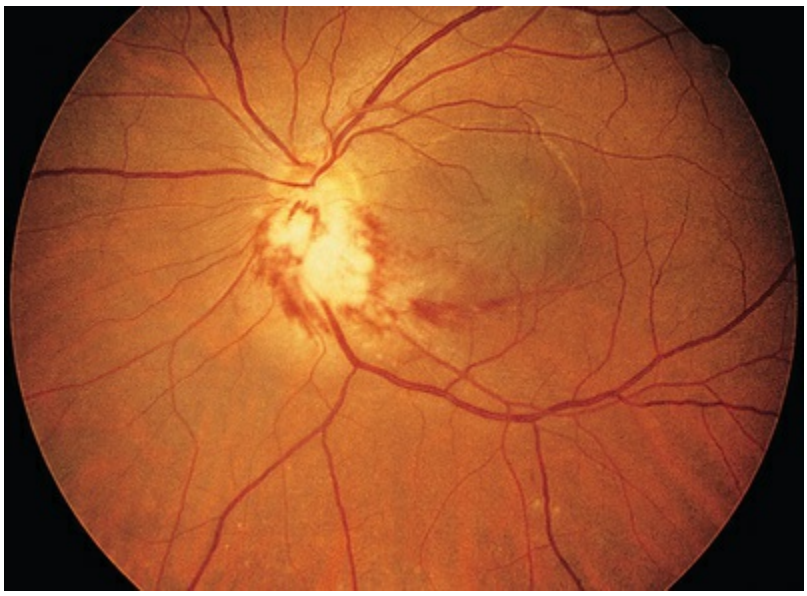

FIG. 84.8 Cytomegalovirus (CMV) affecting the

perifoveal area or the optic nerve can result in an exudative retinal detachment often involving the macula. If there has not been actual involvement of a vital structure, treatment may result in improvement of central vision.

CMV retinitis is a reflection of underlying active systemic CMV infection. In almost all cases it is a blinding disease if not controlled. Thus, in the face of changing mental status, development of focal signs on neurologic examination, or other symptoms consistent with subacute encephalitis in AIDS patients, a comprehensive ophthalmologic examination is indicated, and an increased index of suspicion of CMV infection of the CNS and possible CMV retinitis is warranted. There is also evidence that patients with CMV retinitis, especially peripapillary disease, have a much higher incidence of CMV encephalitis. CMV infection of the brain, optic nerves, and retinas from 47 consecutive autopsies of patients with AIDS was examined.[119] Immunocytochemistry demonstrated CMV infection in 11 (23%) brains, 2 (2%) of 94 optic nerves, and 38 (40%) of 94 retinas. Ten (91%) of 11 patients with CMV encephalitis had concurrent retinitis. While 10 (42%) of 24 patients with CMV retinitis had CMV encephalitis, when the retinitis included the peripapillary region, 75% had encephalitis. The optic nerve parenchyma usually was not infected histologically despite extensive peripapillary retinitis. The strength of these associations suggests that CMV retinitis defines a group of patients with AIDS at risk for development of CMV encephalitis (relative risk, 9.5%), especially when the retinitis involves the peripapillary region (relative risk, 13%). Furthermore, in patients with AIDS without CMV retinitis, central nervous system symptoms are unlikely to be attributable to CMV encephalitis.[119] The pathologic correlation between ocular and cerebral lesions in patients with AIDS has been reviewed.[120]

CMV retinitis is less frequent in children with AIDS, with reported rates of approximately 5–6%, though rates of extraocular CMV are higher than in adults. CMV retinitis has been reported in young children with high absolute CD4 counts, though these counts are low relative to the child's age. Older children tend to have low absolute CD4 counts, similar to adults. There is a higher incidence

of bilateral and posterior pole disease in children, however this is likely due in part to delays in diagnosis in children from lack of subjective vision complaints.[120–123]

Screening Techniques for Retinal and Systemic CMV Infection

Screening for CMV retinitis is a difficult problem. Many patients who are CMV-viremic or -viruric may not have end-organ disease, and studies employing quantitative CMV polymerase chain reaction (PCR) in plasma or CMV antigenemia have not been able to definitively predict the development of CMV retinitis.[124] Currently no laboratory marker exists that reliably predicts the occurrence of clinical CMV retinitis.

Urine is culture-positive for CMV in more than 50% of homosexual men and the majority of AIDS patients; thus urine culture may not be of diagnostic value. Serology in AIDS patients is nonspecific, and documentation of rising CMV titers is unusual.[6,104] Studies of newly diagnosed CMV retinitis patients indicate that many are CMV culture-negative in the blood. Positive blood cultures for CMV, fever, and weight loss are associated with more extensive CMV retinitis at the time of diagnosis.[125] The results of virologic blood assays for CMV also have been associated with clinical outcome in patients with CMV retinitis.[126] Therefore assays for the detection of CMV antigenemia may be a simple and rapid means of identifying those patients with unilateral retinitis at highest risk of developing CMV retinitis of the fellow eye or of visceral CMV disease if intravitreal injections or implants are used as the sole treatment for CMV retinitis.[127]

A positive PCR result supports the clinical diagnosis and may be useful for monitoring response to antiviral treatment. By prospective monitoring for increases in plasma CMV DNA copy number, it may be possible to identify HIV-seropositive patients who are at imminent risk for development of symptomatic CMV retinitis.[128]

It is also reasonable and practical to use the CD4 cell count as a threshold below which to screen patients, since the risk of CMV retinitis increases at CD4 cell counts below 50/μL.[74] The incidence and prevalence of CMV retinitis in a cohort study of patients with

CD4 cell counts below 0.10×10^9/L (100/μL) revealed a 25% chance for the development of CMV retinitis by 4 years of follow-up. Among those subjects in whom CMV retinitis developed, about 19% had retinitis before a CD4 cell count of less than 0.05×10^9/L (<50/μL) was observed, and 81% had CMV retinitis after the CD4 cell count reached this threshold.[129] In the HAART era, some patients may develop CMV retinitis with CD4 counts above 100/μL, probably because of incomplete restoration of the immune repertoire against CMV.[130]

A technique for screening for central CMV retinitis, entoptic perimetry, which employs patient visualization of moving particles on a computer monitor, appears to have a very high sensitivity and specificity (over 90%) in detecting CMV retinitis within the central 30-degrees radius of fixation[84] (Fig. 84.9).

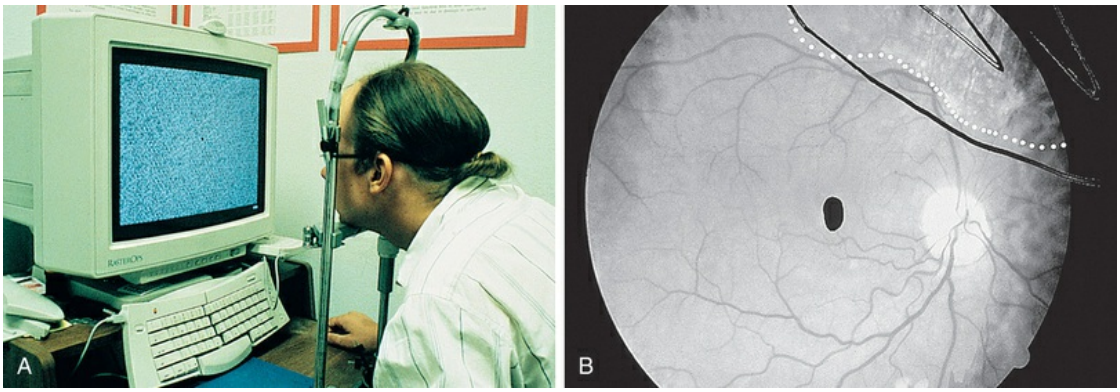

FIG. 84.9 Entoptic perimetry can allow detection of cytomegalovirus (CMV) retinitis lesions. (A) The patient is asked to view particle motion programmed on a monitor. (B) An overlay of the CMV lesion (dotted white border) and the patient's own sketch of the scotoma seen (black line).

Techniques for detection of CMV DNA based on PCR are increasingly being applied to ocular fluids; however, the clinical significance of such findings can sometimes be unclear. The application of PCR-based methods to ocular fluids made a useful contribution to the treatment of the patients.[131]

This appears to be a sensitive and specific diagnostic assay that could assist in the diagnosis of CMV retinitis.[132] PCR detection of CMV DNA has been reported to be a more sensitive method than

analysis of locally produced antibodies by calculating a Goldman–Witmer coefficient to determine local ocular antibody production. There is also an immune predisposition to the development of CMV retinitis in patients with AIDS.[133,134]

Treatment of CMV Retinitis

The treatment of CMV retinitis has been reviewed.[135,136] Treatment may be systemic, local, or a combination of the two. There are currently four medications approved by the US Food and Drug Administration (FDA) for the treatment of CMV retinitis: ganciclovir, valganciclovir, cidofovir, foscarnet. Fomivirsen, the first antisense drug with a relatively long duration of action, is no longer available in the United States.

Systemic Therapy of CMV Retinitis.

CMV retinitis may be treated systemically or intravitreally. However, systemic treatment is associated with less spread of CMV retinitis from one eye to the other.[136] In addition, local treatment including the sustained release ganciclovir implant has been shown to be associated with higher risk of the development of systemic CMV.[137,138]

Systemic CMV may cause gastrointestinal disease, with colitis being the most common manifestation as well as esophagitis. Systemic CMV diagnosis may be difficult and usually requires histopathologic evidence of CMV infection. The cumulative incidence of systemic CMV disease that becomes clinically apparent is approximately 25%.[139] Therefore, although systemic CMV disease may not be clinically apparent at the time of diagnosis of CMV retinitis, some experts believe that initial systemic therapy may be warranted despite the inconvenience, expense, and potential toxicities.

Intravenous Ganciclovir.

Ganciclovir is a nucleoside analog of 2-deoxyguanosine, similar to acyclovir.[140] Despite its structural similarities with acyclovir, ganciclovir is much more active in vitro against CMV than acyclovir.[141] Ganciclovir inhibits all herpesviruses, including CMV,

by preventing DNA elongation. CMV lacks the virally specified thymidine kinase (TK) that converts ganciclovir (or acyclovir) to its monophosphate form.[142] TK-altered strains resistant to acyclovir are as sensitive to ganciclovir as the unaltered parent strains. Thus ganciclovir is phosphorylated to its triphosphate form much more efficiently than acyclovir which accounts for the greater activity of ganciclovir against CMV.[143]

The majority of AIDS patients treated with ganciclovir respond within 2–4 weeks with decreased retinal opacification and stabilization of the retinitis[97] (Fig. 84.10). Ganciclovir is commercially available as an intravenous and oral formulation (and also is included in an intraocular device), and indefinite maintenance therapy is necessary as long as the patient remains in immune failure with a CD4 count below 50/μL. An intravenous loading dose of 5 mg/kg every 12 hours for 14–21 days should be followed by maintenance doses of 5 mg/kg per day. If the drug is discontinued, retinitis often recurs within 10–21 days, continuing its progression at the borders of healed areas.[97] Recurrences have been common, even during maintenance therapy, being reported 3 weeks to 5 months after institution of therapy and occurring in 30–40% of patients.[97] Many investigators have found that discontinuation or delay of ganciclovir therapy results in nearly 100% recurrence of retinitis, at which time reinstitution of the loading dose regimen often is necessary.[142,144,145] Multiple series in patients with AIDS and CMV retinitis have shown response rates of 80–100%, with 60–80% of patients achieving a remission with ganciclovir therapy.[37,145–149]

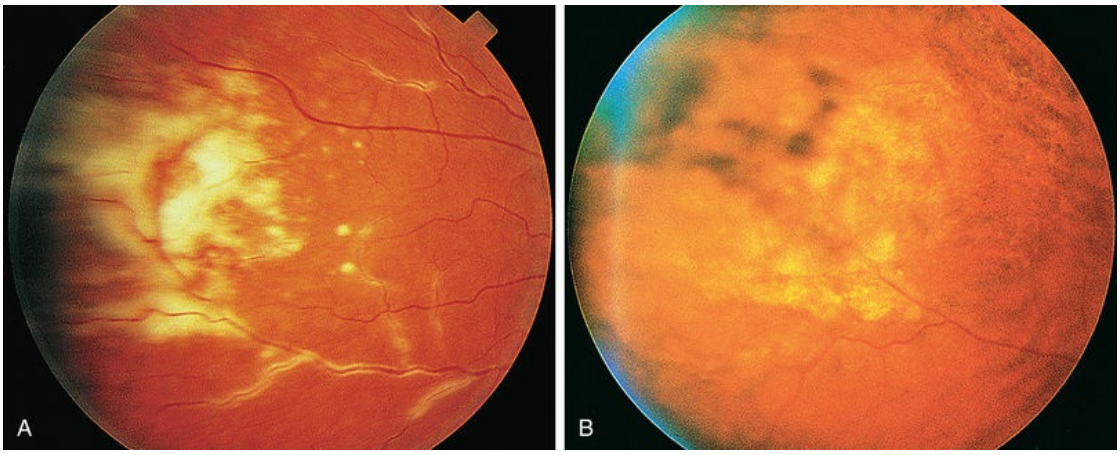

FIG. 84.10 (A) Active peripheral cytomegalovirus (CMV) retinitis with secondary retinal vasculitis. (B) The area is healed after intravenous ganciclovir therapy. Note absence of border opacification. Also seen are pigmentary changes characteristic of healed CMV.

The treatment of CMV retinitis usually includes an induction phase followed by a maintenance phase to prevent relapse. Before the advent of HAART, relapse occurred almost universally, given a sufficiently long period after induction courses of ganciclovir. Therapy therefore continued for a lifetime. The median time to relapse in patients treated with just an induction dose is 3–4 weeks.[145]

Most clinicians use a 14-day induction course of intravenous ganciclovir consisting of 5 mg/kg per day every 12 hours and indefinite maintenance of 5 mg/kg per day. Lower doses and every-other-day dosing schedules have been associated with high rates of early relapse. Since treatment may be lifelong if the patient's CD4 count cannot be elevated with anti-HIV therapy, usually a permanent or semipermanent indwelling venous catheter is placed at the onset of therapy if intravenous therapy is chosen as maintenance therapy. Ganciclovir requires modification of dosing in the presence of renal insufficiency.

Side-effects of ganciclovir include granulocytopenia, neurologic dysfunction, abnormal liver function tests, and rarely, thrombocytopenia. The most serious toxicity is granulocytopenia, which may occur in up to one-third of patients when defined as less than 500 neutrophils per microliter.[145] Granulocytopenia is generally reversible, and this adverse effect is exacerbated when used with AZT.[150] The use of colony-stimulating factors rGM-CSF (recombinant granulocyte–macrophage colony-stimulating factor) and rG-CSF (recombinant granulocyte colony-stimulating factor) for reversing or preventing neutropenia may be useful.

The prevalence of CMV resistance to ganciclovir is unknown, but ever-increasing induction regimens may be necessary to control CMV retinitis. Strains of CMV that develop resistance to ganciclovir may remain susceptible to foscarnet. Because of the question of ganciclovir resistance, a trial of combined vs. alternating foscarnet–

ganciclovir maintenance therapy has been reported to be effective.[151]

Visual acuity depends on the location of the involved retina, and involvement of the fovea or optic nerve may result in decreased visual acuity even if there has been a response to therapy. Ganciclovir has been shown to be effective in preserving visual acuity. For example, 73% of eyes maintained a visual acuity of 20/40 or better when treated with ganciclovir.[152]

Oral Ganciclovir.

Oral ganciclovir (FDA approved, 1994) can be used for maintenance therapy of CMV retinitis after it has been healed with intravenous ganciclovir therapy. Studies using this drug regimen have shown efficacy, but it is clear that oral ganciclovir is less effective than intravenous ganciclovir for many patients.

Perhaps the most common use of oral ganciclovir is in patients being treated with intravitreal therapy (injections of cidofovir or ganciclovir implant) to prevent systemic CMV disease. Such use of oral ganciclovir also may reduce the incidence of CMV in the fellow eye if it is not involved.[153,154] Oral ganciclovir for prophylaxis or treatment of CMV retinitis has been replaced by oral valganciclovir, which provides much higher blood levels.

Valganciclovir.

Valganciclovir, the valine ester of ganciclovir, is an orally administered formulation of ganciclovir. The valine ester confers enhanced permeability and absorption of the molecule through the cell membranes of the gut. Once in the bloodstream, the valine ester is cleaved from the molecule by esterases, rendering plasma levels of ganciclovir comparable to those achieved with intravenous ganciclovir administration. A single-dose randomized crossover pharmacokinetic study reported the absolute ganciclovir bioavailability after oral valganciclovir administration is 60.9% compared to 5.6% bioavailability of oral ganciclovir.[155] A randomized crossover dose-ranging study determined that plasma levels of ganciclovir after an 875 mg dose of valganciclovir are similar to the plasma levels achieved with a dose of 5 mg/kg of intravenous ganciclovir (AUC 24.8 mg/ml per hour vs. 26 mg/ml

per hour). The authors suggested the 900 mg dose of valganciclovir would approximate the AUC value of the 5 mg/kg dose of IV ganciclovir.[156]

Valganciclovir has been studied for induction therapy for CMV retinitis. Martin et al. (Valganciclovir Study Group) reported a multicenter randomized, controlled clinical trial comparing oral valganciclovir 900 mg twice a day for 3 weeks' induction therapy followed by 900 mg daily for 1 week maintenance therapy with intravenous ganciclovir 5 mg/kg twice a day for 3 weeks' induction therapy followed by 5 mg/kg once daily for one week of maintenance therapy. After 4 weeks both groups received continued maintenance therapy with 900 mg valganciclovir daily. Eighty patients with newly diagnosed CMV retinitis were randomized to each group in a 1 : 1 ratio. Primary endpoint was photographically determined progression of CMV retinitis within 4 weeks after the initiation of treatment. In the valganciclovir group, 9.9% of patients had progression of CMV retinitis within the first 4 weeks compared to 10.0% of patients assigned to IV ganciclovir. This 0.1 percentage point difference was not significant (95% CI −9.7 to 10.0). Secondary endpoints included the achievement of a prospectively defined successful response to induction therapy and the time to progression of CMV retinitis. Seventy-seven percent of patients receiving IV ganciclovir and 71.9% of patients receiving oral valganciclovir achieved a satisfactory response to induction therapy. This 5.2 percentage point difference was not significant (95% CI −20.4 to 10.1). The median times to progression of retinitis were 125 days in the IV ganciclovir group and 160 days in the oral valganciclovir group. The relative risk of progression of retinitis in the valganciclovir group compared to the ganciclovir group was 0.90 (95 CI 0.58–1.38). Diarrhea was the most common adverse effect during the study and occurred more frequently in the valganciclovir group compared to the ganciclovir group (19% vs. 10%, p=.11). Neutropenia occurred with similar frequency in each group. Catheter-related side-effects were seen more frequently in the IV ganciclovir group than in the valganciclovir group.[157] No clinical trials have been published specifically comparing efficacy of valganciclovir for maintenance therapy of CMV retinitis.

Lalezari et al. (Roche Valganciclovir Study Group) reported a

large safety study of valganciclovir. The adverse event profile was similar to that reported from previous studies of intravenous and oral ganciclovir. Adverse events of note were diarrhea (38%), nausea (23%), fever (18%), neutropenia (absolute neutrophil count <500 cells/μL) (10%), anemia (hemoglobin <8.0 g/dL) (12%), and thrombocytopenia (platelet count <25, 000 cells/μL) (2%).[158]

In summary, oral valganciclovir offers the obvious advantage of extreme effectiveness against CMV retinitis without the difficulties and inconveniences of intravenous administration. Furthermore, because valganciclovir is converted to ganciclovir in the bloodstream, its pharmacologic safety profile, including side-effects, is no different than that of intravenously administered ganciclovir. Thus oral valganciclovir is an effective and safe alternative to intravenous ganciclovir for the treatment of CMV retinitis. Oral ganciclovir has become unavailable but is now supplanted by valganciclovir.

Foscarnet.

The second drug for the treatment of CMV retinitis in patients with AIDS was licensed by the FDA in 1993. Foscarnet is a pyrophosphate analog with broad antiviral activity via inhibition of viral polymerases, such inhibition not being dependent on activation or phosphorylation by viral or cellular enzymes. Foscarnet inhibits DNA chain elongation by preventing pyrophosphate exchange.[159]

Foscarnet inhibits the DNA polymerase of CMV and other herpesviruses (HSV-1, HSV-2, VZV, and Epstein–Barr virus [EBV]) and the replication of HIV in vitro and in vivo.[160] Both herpesvirus and HIV replication may be inhibited by therapeutically achievable concentrations of foscarnet. Since the drug is not metabolized and is excreted by the kidney, the dosage must be adjusted for renal insufficiency. Foscarnet also has been used successfully to treat HIV-infected patients with acyclovir-resistant HSV and VZV infections, in addition to CMV retinitis. Foscarnet acts directly on the viral polymerase of all herpesviruses and on the reverse transcriptase of HIV-1. Resistance of CMV to foscarnet is associated with mutations in the genes of these polymerases. Cross-resistance to antiviral drugs is likely to be an increasing problem, since

patients with AIDS are living longer as a result of HAART and of the drugs used in the prophylaxis of various opportunistic infections, as well as because of the experience gained in the management of HIV-related problems.

Foscarnet has been shown to be useful against ganciclovir-resistant herpesviruses, such as CMV, because a mutation in a DNA polymerase gene conferring resistance to ganciclovir and acyclovir differs from the region conferring resistance to foscarnet.[161] Foscarnet also is an effective inhibitor of the HIV reverse transcriptase enzyme and acts in a dose-dependent manner. AZT and foscarnet have synergistic activity in vitro against HIV, and in vivo foscarnet has activity against HIV as measured by surrogate markers.[162]

The use of foscarnet salvage therapy in patients with CMV retinitis who are intolerant of or resistant to ganciclovir was studied in AIDS patients with CMV retinitis who had documented hematologic intolerance or resistance to ganciclovir therapy. This study showed that in patients intolerant of ganciclovir, salvage foscarnet therapy resulted in a longer time to retinitis progression than reported previously in historic controls who terminated ganciclovir therapy. In patients who exhibited clinical resistance to ganciclovir, foscarnet appeared to have efficacy in controlling retinitis. No significant differences in either efficacy or toxicity were observed in the range of foscarnet maintenance doses studied.[163]

A large, randomized, multicenter, blinded clinical trial (the Foscarnet–Ganciclovir Cytomegalovirus Retinitis Trial) compared ganciclovir with foscarnet in the treatment of CMV retinitis in patients with AIDS. No difference was reported between the treatment groups in the rate of progression of retinitis; however, the median survival was 8.5 months in the ganciclovir group and 12.6 months in the foscarnet group. Excess mortality was reported in a subset of patients in the foscarnet group whose renal function was compromised at entry. Differences in mortality could not be explained entirely on the basis of less antiretroviral therapy in the ganciclovir group, which suggests beneficial interactions between foscarnet and antiretroviral nucleosides. These results indicate that, for patients with AIDS and CMV retinitis, treatment with foscarnet initially offers a survival advantage over treatment with

ganciclovir, although foscarnet was not as well tolerated as ganciclovir.[164]

A marginally prolonged survival seen in patients treated with foscarnet compared with those treated with ganciclovir may have been due to a direct effect on HIV replication. Both drugs had a suppressive effect on circulating p24 antigen, which was predictive of improved survival. The inhibitory effect on CMV replication also may have a beneficial effect on limiting HIV replication.[165]

A randomized, controlled, comparative trial of foscarnet and ganciclovir demonstrated that they equally controlled CMV retinitis but that foscarnet was associated with a longer survival. However, foscarnet was less well tolerated than ganciclovir, primarily because of the nature of its side-effects. Since foscarnet and ganciclovir have different side-effects, initial treatment of CMV retinitis should be individualized.[166]

The most frequently reported major adverse effect associated with foscarnet administration is nephrotoxicity, with dose-limiting toxicity occurring frequently and cases of acute renal failure having been observed. Symptomatic hypocalcemia has been reported and may be responsible for arrhythmias and seizures, and the risk is increased by concurrent administration of intravenous pentamidine. Bone-marrow suppression with neutropenia, anemia, and thrombocytopenia can be seen with foscarnet administration. Neutropenia was reported to be less common with foscarnet than with ganciclovir (14% vs. 34%).[164]

Practical guidelines for the use of foscarnet include administration through an infusion pump to avoid the potential consequences of overdose or too rapid infusion, adequate hydration of patients with saline loading[167] to reduce the risk of nephrotoxicity, avoidance of administration of other potentially nephrotoxic agents, and monitoring of renal function two or three times per week during induction therapy and once per week during maintenance therapy, with the dosage being recalculated on the basis of patient weight and serum creatinine. Studies of foscarnet doses have suggested that patients receiving high maintenance doses (120 mg/kg per day) have slower rates of retinitis progression.[168,169]

Foscarnet is active against HIV, and studies have shown that it

raises the CD4 count transiently and decreases viral antigenemia (p24 antigen). Because of its efficacy against CMV and HIV, it would appear to be a potentially effective agent for treating HIV-infected patients; however, it is currently only available for intravenous administration, and its use is associated with substantial toxicity (see above).[162,170]

Cidofovir.

Cidofovir, (S)-1-[3-hydroxy-2-(phosphonylmethoxy)propyl]cytosine, formerly known as HPMPC, was the first antiviral nucleotide analog available for the treatment of CMV retinitis. Cidofovir is active in uninfected cells, may act preemptively, and may retain activity against ganciclovir-resistant strains. Preclinical studies showed the major toxicity of cidofovir to be dose-, schedule-, and species-dependent nephrotoxicity. The concomitant administration of probenecid protects animal models against cidofovir-induced nephrotoxicity. Four treatment modifications are indicated clinically to reduce the incidence of cidofovir-related nephrotoxicity: dose reduction or interruption for changes in renal function; concomitant administration of probenecid; administration of 1 liter of normal saline 1 hour before infusion; and extension of the dosing interval.[171]

The treatment of CMV retinitis with intravenous cidofovir was demonstrated to be effective in slowing the progression of peripheral CMV retinitis in patients with previously untreated CMV retinitis and AIDS. Intravenous cidofovir also has been used for long-term suppression of CMV retinitis. Biweekly therapy (after induction therapy) was reported to have a time to progression of CMV retinitis of 120 days in one randomized, controlled trial[172] and 2.5 months in another randomized, controlled trial.[173,174] Treatment and subsequent maintenance of CMV retinitis with 20 μg of intravitreously injected cidofovir, given at 5- to 6-week intervals, also is safe and highly effective.[175]

Treatment with parenteral cidofovir is complicated by nephrotoxicity, which can be reduced with saline hydration and concomitant administration of probenecid. Despite these additional treatments, the long-term reports from the HPMPC Peripheral Cytomegalovirus Retinitis Trial showed a rate of proteinuria of 1.22

per patient-year and a rate of elevated serum creatinine of 0.41 per patient-year. Thus many patients may have difficulty tolerating cidofovir for a prolonged time. Neutropenia has also been reported with cidofovir.

Unfortunately parenteral cidofovir has also been found to have ocular toxicity, including a high incidence of iritis (up to 50%), including recurrent iritis, and a risk of profound ocular hypotony with vision loss, similar to the iritis and hypotony seen with intravitreal injections of cidofovir.[176–178] It has been estimated in one study that cidofovir-related iritis developed in half of patients within approximately 4 months. The long-term reports from the HPMPC Peripheral Cytomegalovirus Retinitis Trial showed a rate of cidofovir-associated uveitis of 0.20 per person-year and a rate of significant ocular hypotony of 0.16 per patient-year.[174] Thus in the setting of iritis in HIV-infected patients, use of systemic cidofovir or rifabutin should be considered potential causes of iritis, and these drugs may need to be discontinued.

Nephrotoxicity may be cumulative in some patients and appears to be related to toxicity in the proximal tubule. This "secretory toxicity" also may be responsible for the hypotony and iritis that the drug causes when given intravenously or intravitreously. The ciliary body and the proximal tubule of the kidney have many similarities in terms of the mechanism involved in the secretion of fluids across epithelia. Oral administration of probenecid before and after the intravenous infusion appears to help ameliorate the nephrotoxicity of the drug, but the ocular side-effects of iritis and hypotony occur despite concomitant probenecid administration.

CMV Resistance.

Many patients taking chronic maintenance therapy for CMV retinitis develop resistant virus. Development of in vitro resistance of CMV to ganciclovir and foscarnet and disease progression has been shown in several small studies,[179,180] and mechanisms of resistance to ganciclovir have been described.[180] In one prospective, randomized study of 207 patients with newly diagnosed CMV retinitis, drug-resistant CMV occurred in four of nine ganciclovir-treated patients and in none of five foscarnet-treated patients.[126] In patients with CMV retinitis and AIDS treated with either oral or

intravenous ganciclovir, isolates of CMV after a median exposure of 75 and 165 days, respectively, showed increasing resistance in vitro.[181] Jabs et al. reported that the cumulative incidence of ganciclovir resistance at 9 months was 27.5%.[180] Similar incidence rates of resistance occur for foscarnet and cidofovir.[182] In addition, the incidence of resistance to valganciclovir appears to be similar to that for ganciclovir.[183]

Resistance to an anti-CMV drug can be described as phenotypic, expressed as an inhibitory concentration 50% greater than a certain threshold (IC50). This is determined typically via plaque reduction assays, DNA hybridization assays, or antigen-reduction assays that require large amounts of viable virus, often requiring culturing.[180,184–186] Genotypic resistance is defined by the presence of a mutation in the CMV genome conferring resistance to a particular drug. PCR amplification techniques allow fast detection of resistance-conferring mutations in the viral genome, requiring only small amounts of viral nucleic acids and can use nonviable virus.[187–189] Low-level ganciclovir resistance is typically associated with mutations in the CMV *UL97* gene. *UL97* codes for a phosphotransferase that catalyzes the first step of ganciclovir activation to the triphosphate form. High-level ganciclovir resistance is typically caused by mutations in both the CMV *UL97* and *UL54* genes. *UL54* codes for the cytomegalovirus DNA polymerase.[190] Mutations in the *UL54* gene are also responsible for foscarnet and cidofovir resistance.[190–194] *UL54* mutations responsible for foscarnet resistance are usually distinct from those causing ganciclovir–cidofovir resistance. However, low-grade ganciclovir–foscarnet cross-resistance has been reported, plus Chou et al. reported a DNA polymerase mutation causing resistance to ganciclovir, cidofovir, and foscarnet.[180,188–192]

Treatment Strategies in Resistant CMV.

When clinically resistant retinitis appears, many clinicians employ an alternative antiviral agent systemically; intravenous cidofovir or foscarnet are alternatives. Unfortunately, as mentioned above, there can be cross-resistance between CMV isolates resistant to ganciclovir and resistant to cidofovir and/or foscarnet; this must be borne in mind in such patients. The probability of developing

foscarnet or cidofovir resistance while taking these drugs appears similar to the rates of development of resistance to ganciclovir.[182] For this reason, clinicians often employ intravitreal therapies including the ganciclovir intraocular device when systemic therapy begins to fail. Intravitreal therapies appear to be more effective in such circumstances, largely because they deliver higher doses of anti-CMV medication to the retina.[195] In such circumstances, it is recommended to continue to treat the patient with some form of systemic therapy, often oral valganciclovir, to help prevent systemic CMV infection or infection of the fellow eye. Studies have shown that treatment with the ganciclovir implant alone is associated with a higher risk of contralateral CMV retinitis and extraocular CMV.[196,197]

Combination Therapies: Ganciclovir–Foscarnet.

Several studies have shown that combinations of foscarnet and ganciclovir are more effective in the treatment of recurrent or resistant retinitis than is continued monotherapy.[99,197] Such combination intravenous therapy also has been shown to be safe and effective in children with CMV retinitis.[198] Unfortunately, combination intravenous therapy with these two drugs necessitates multiple intravenous infusions daily and has a marked negative effect on patients' lifestyle. Combination of IV foscarnet and oral valganciclovir has supplanted this combination intravenous therapy.

The combination of foscarnet and ganciclovir in patients with AIDS and CMV retinitis who have relapsed has been shown to be more effective than either agent given alone;[151] however, combination therapy was associated with the greatest negative impact of treatment on quality-of-life measures.

To determine the best therapeutic systemic regimen for treatment of relapsed CMV retinitis, a multicenter randomized controlled clinical trial of 279 patients with AIDS and either persistently active or relapsed CMV retinitis was reported. Patients were randomized to one of three therapeutic regimens: induction with foscarnet sodium at 90 mg/kg intravenously every 12 hours for 2 weeks, followed by maintenance at a dosage of 120 mg/kg per day (foscarnet group); induction with ganciclovir sodium at 5 mg/kg

intravenously every 12 hours for 2 weeks followed by maintenance at 10 mg/kg per day (ganciclovir group); or continuation of previous maintenance therapy plus induction with the other drug (either ganciclovir or foscarnet) for 2 weeks followed by maintenance therapy with both drugs, ganciclovir sodium at 5 mg/kg per day and foscarnet sodium at 90 mg/kg per day (combination therapy group). The mortality rate was similar among the three groups. Median survival times were as follows: foscarnet group, 8.4 months; ganciclovir group, 9.0 months; and combination therapy group, 8.6 months (p=.89). Comparison of retinitis progression revealed that combination therapy was the most effective regimen for controlling the retinitis. The median times to retinitis progression were as follows: foscarnet group, 1.3 months; ganciclovir group, 2.0 months; and combination therapy group, 4.3 months (p=.001). Although no difference could be detected in visual acuity outcomes, visual field loss and retinal area involvement on fundus photographs both paralleled the progression results, with the most favorable results in the combination therapy group. The rates of visual field loss were as follows: foscarnet group, 28 degrees per month; ganciclovir group, 18 degrees per month; combination therapy group, 16 degrees per month (p=.009). The rates of increase of retinal area involved by CMV were as follows: foscarnet group, 2.47% per month; ganciclovir group, 1.40% per month; and combination therapy group, 1.19% per month (p=.04). Although side-effects were similar among the three treatment groups, combination therapy was associated with the greatest negative impact of treatment on quality-of-life measures. This study suggests that for patients with AIDS and CMV retinitis whose retinitis has relapsed and who can tolerate both drugs, combination therapy appears to be the most effective therapy for controlling CMV retinitis.[151] Small series suggest that combined intravitreal injections of ganciclovir and foscarnet may be effective in treating CMV retinitis when the infection is clinically resistant to either intravitreal drug alone.[199]

Summary of Initial Systemic CMV Retinitis Treatment

The initial treatment of CMV retinitis is usually oral valganciclovir 900 mg twice a day for induction therapy of approximately 3 weeks

followed by 900 mg daily for maintenance therapy. Intravenous ganciclovir can be used if a patient has a contraindication to oral treatment such as malabsorption. The dose for intravenous ganciclovir is 5 mg/kg twice a day for induction therapy for 2–3 weeks followed by maintenance therapy at 5 mg/kg daily or 6 mg/kg 5 days/week. Induction therapy with intravenous foscarnet is dosed at 90 mg/kg twice a day for approximately 2 weeks followed by maintenance therapy at 120 mg/kg daily. Intravenous cidofovir for induction therapy is dosed at 5 mg/kg weekly for approximately 3 weeks followed by maintenance therapy dosed at 3–5 mg/kg every 2 weeks.

Intraocular Therapy of Viral Retinitis

Ganciclovir.

Because of the difficulties associated with systemic ganciclovir, foscarnet, and cidofovir, interest in local administration has increased. Obviously, intraocular (or periocular) treatment will not affect the systemic CMV infection, but in some patients, especially those with systemic toxicity resulting from the drug, local administration may have certain advantages.

In 40 patients with primary CMV retinitis involving 57 eyes, all had received one 14-day course of intravenous ganciclovir and all were free of other end-organ CMV disease. All affected eyes received weekly intravitreal injections of 400 mg of ganciclovir for maintenance therapy. Median survival of patients was at least 13 months. Fifteen patients had 19 new opportunistic infections during the observation period, but none developed new nonocular CMV disease. Active retinitis recurred in 68.4% of the eyes while receiving maintenance therapy, with a median time to progression of 14.7 weeks. CMV retinitis occurred in 30.4% of the previously uninvolved eyes (follow-up 3.1 years). Bacterial endophthalmitis complicated treatment in one eye, and retinal detachment developed in five eyes. Thus the long-term treatment of CMV retinitis with weekly intraocular injections of ganciclovir was associated with survival and ocular outcomes similar to those reported with systemic ganciclovir.[200]

Intravitreal ganciclovir also was shown to be an effective

alternative to systemic ganciclovir in patients with severe neutropenia and in patients who chose to continue receiving systemic zidovudine or didanosine.[201] Injections of high-dose intravitreal ganciclovir using a 2 mg dose revealed that weekly 2 mg injections appear to offer superior control of retinitis for periods of months or longer.[202] Highly concentrated ganciclovir solution for intravitreal injection also reduced repeated amaurosis and ocular pain and was reported by patients to have improved their comfort and quality of life, thus increasing their compliance to treatment and reducing side-effects, as compared with usual protocols.[203]

Foscarnet.

Intravitreal foscarnet at a dose of 2.4 mg per injection given one or two times weekly also appears to be a safe and effective treatment method for CMV retinitis. Resistance to this treatment regimen may develop, however.[204] High-dose intravitreal foscarnet for CMV retinitis was shown to be a safe, effective, and useful alternative in patients with intolerance to intravenous therapy.[205]

Ganciclovir Intraocular Device.

An intraocular sustained-release ganciclovir delivery implant that releases drug into the vitreous is commercially available.[206] These surgically implanted, time-release implants have been shown to be more effective than intravenous ganciclovir alone in delaying the progression of CMV retinitis.[137,207,208]

Insertion of the device requires a pars plana incision and a partial vitrectomy. The implant is sewn into the pars plana behind the lens.[206] Insertion of the ganciclovir intraocular device (GIOD) requires trimming the strut of the device so that it is nearly flush with the drug pellet. A 5.5-mm incision can be made 4 mm posterior to the limbus with a microvitreoretinal blade or similar instrument (Fig. 84.11). A unimanual bipolar intraocular cautery can be used to coagulate bleeding choroid. It is important to ensure that the incision is full-thickness, since the device can be inserted inadvertently under the pars plana. A suture is placed through the preplaced hole (the surgeon must make the hole) in the strut of the device; 8–0 Prolene can be used. The device is anchored in the middle of the wound, and running or interrupted sutures can be

used to close the wound. Astigmatism can result from overzealous wound closure; this is usually transient. This procedure can be performed in an outpatient setting under local anesthesia.

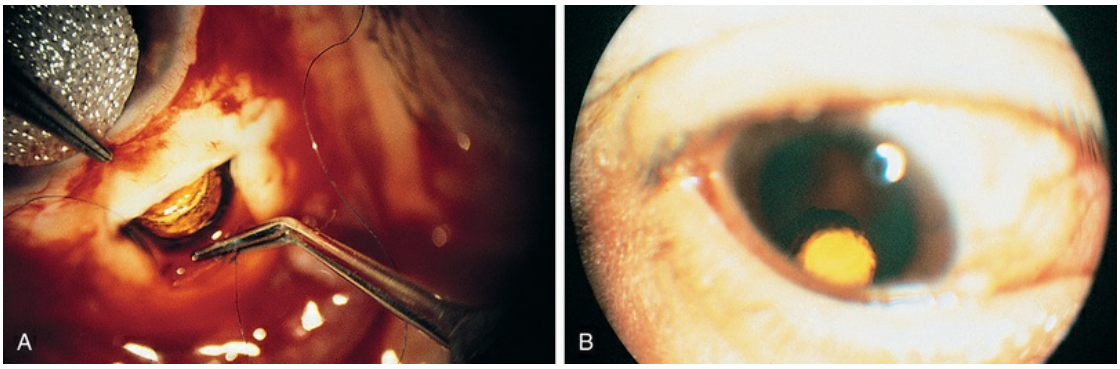

FIG. 84.11 (A) Insertion of ganciclovir intraocular device. (B) The device can be seen inferotemporally through a dilated pupil.

Despite the relative ease of insertion, it has become clear that the risk of retinal detachment in the first 2 months after insertion is substantially higher than if other methods are used to control retinitis, though in the long term there is no statistical difference in retinal detachment rate.[206,209–211] In addition, the risk of postoperative endophthalmitis appears to be a real one, with incidences on the order of 1% or sometimes higher.[212] The intravitreal levels attained by this drug are over twice those after intravenous administration, and this appears to be associated with a lower incidence of resistance and progression of retinitis. This is particularly true in newly diagnosed cases, but failure can occur in up to 25% of such cases within the first 2 months. In a study of 91 implants in 70 eyes, GIOD was effective as an adjunct to continued systemic therapy in those patients with recurrent CMV retinitis.[208] Intraocular sustained-release implants have been used to treat acute CMV disease and to prevent recurrence. Pathology studies of eyes having undergone implantation with the GIOD have shown no evidence of intraocular toxicity.[204] It is not certain whether implants should be exchanged at the 7-month time period or whether retinitis should be allowed to reactivate before replacing the implant.

Intravitreal Cidofovir.

Another form of intraocular therapy is intravitreal cidofovir (HPMPC), which is injected every 6 weeks. This work was initiated after discovery of long-acting properties of the drug in the eye. The safety and efficacy of intravitreal cidofovir for CMV retinitis in humans were reported in a phase I/II unmasked, consecutive case series in a single-center institutional referral practice. Eligible patients with AIDS had active CMV retinitis in at least one eye, despite adequate intravenous therapy with ganciclovir or foscarnet, were intolerant to intravenous therapy, were noncompliant with intravenous therapy, or refused intravenous therapy. In a preliminary safety study (group 1), 10 eyes of nine patients received 14 injections of cidofovir while being treated concurrently with intravenous ganciclovir. In a dose-escalating efficacy study (group 2), eight eyes of seven patients received 11 injections of cidofovir as sole treatment for CMV retinitis. The primary outcome was time to retinitis progression. In group 1 eyes receiving 20 μg of cidofovir, the median time to retinitis progression was between 49 and 92 days (mean, 78 days). In group 2 eyes treated with 20 μg of cidofovir with probenecid, the median time to retinitis progression was 64 days (mean 63 days). Hypotony occurred in the two eyes treated with a 100 μg dose of cidofovir and in one of three eyes receiving a 40 μg dose. No adverse effects resulted from the remaining 20 μg cidofovir injections. Cidofovir was found to be safe and effective for the local treatment of CMV retinitis, providing a long duration of antiviral effect (Fig. 84.12).[213]

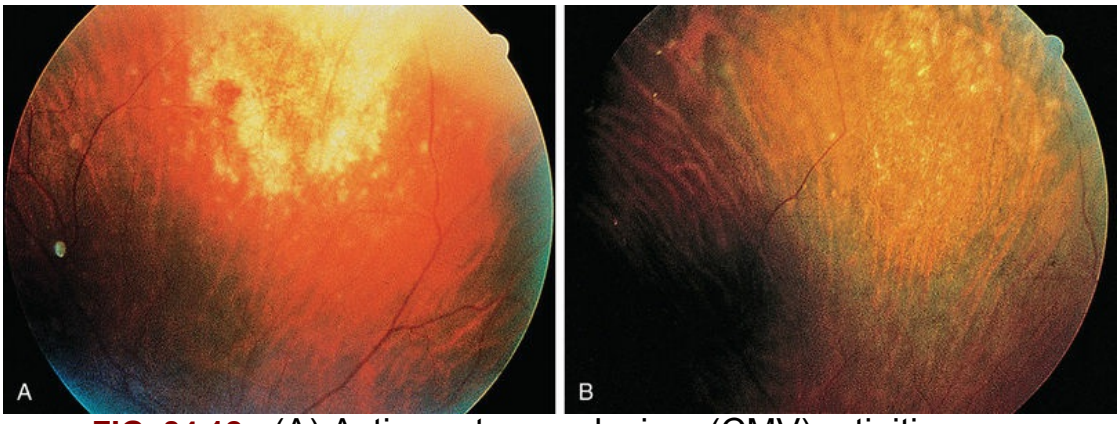

FIG. 84.12 (A) Active cytomegalovirus (CMV) retinitis with no systemic treatment. The eye was injected with a single injection of cidofovir 20 μg via the pars plana.

(B) The retinitis remains healed 53 days later, with no other therapy.

It was then shown that injections of 20 μg of intravitreal HPMPC resulted in complete suppression of CMV replication with no advancement of retinitis borders when given every 6 weeks.[178,213–217] This medication must be given with oral probenecid. Probenecid 2 g is given orally 2 hours before, and 1 g 2 hours and 8 hours after injection.

Two types of adverse events may occur after intravitreal cidofovir injection: iritis and hypotony. The incidence of these is not dissimilar to what is seen after intravenous administration. The incidence of iritis can be reduced from 70% to 18% if oral probenecid is used, and it is now recommended universally. Iritis can be managed with topical steroids and cycloplegia; however, it may lead to cataract and synechiae in the long term. A mild, asymptomatic 20% reduction in intraocular pressure (IOP) is seen almost universally after cidofovir injection, and this appears to be of no concern. The mechanism of this has been defined by ultrasound biomicroscopy, which has disclosed that severe hypotony after cidofovir injections is associated with ciliary body atrophy.[214] Reduction in aqueous flow has been demonstrated by aqueous fluorophotometry. This effect on secretory epithelia also is probably responsible for the nephrotoxicity of the drug when given intravenously. Indeed, probenecid also is given before and after each intravenous infusion to prevent uptake by the proximal tubule of the kidney and associated nephrotoxicity. Profound hypotony with vision loss occurs in approximately 1% of injections.

A retrospective, cohort study described iritis and hypotony after treatment with intravenous cidofovir for CMV retinitis in association with intraocular inflammation.[176] Eleven cases of iritis (26%) occurred among 43 patients. In six cases the iritis was bilateral. Patients who experienced iritis were more likely to have been previously treated for CMV retinitis (p=.03), to be diabetic (p=.05), or to be receiving protease inhibitors (p=.001). The onset of iritis occurred at a mean (±SD) of 4.9 ± 1.8 days after a cidofovir dose and after a mean (±SD) of 4.2 ± 1.6 doses of cidofovir. Six eyes of four patients had hypotony. Five eyes of five patients had a persistent decrease in visual acuity of at least 2 Snellen lines. Acute

intraocular inflammation may occur with or without hypotony after intravenous cidofovir therapy, similar to the reactions seen after intravitreous administration. Cidofovir therapy can be continued in some patients if medical necessity warrants, but inflammation may recur or permanent hypotony develop.

A lower cidofovir dose (10 μg) has been used to investigate methods of reducing the toxicity of intravitreal cidofovir. This dose is effective in healing retinitis in 75% of patients, but the response in 25% is inadequate. The 10 μg dose, however, is not associated with a significant incidence of iritis or IOP lowering. Cidofovir should be diluted in a sterile manner by a pharmacist. It can be diluted in normal saline and frozen for extended periods in single-dose vials.

The efficacy and safety of HPMPC injections given every 5–6 weeks for the maintenance treatment of CMV retinitis with 20 μg intravitreally injected was shown to be highly effective, with only rare episodes of reactivation and progression.[178]

A correlation between IOP and CD4 T-lymphocyte counts in patients with HIV with and without CMV retinitis has been described.[218] IOP was measured with calibrated Goldmann applanation tonometers in two groups of patients. Group A included 84 HIV patients (120 eyes) with CMV retinitis, and group B included 110 HIV patients (183 eyes) without CMV retinitis; 33 patients without HIV (66 eyes) were included as a control group. Step-wise regression analysis of IOP included correlation with CMV retinitis (presence, extent, and activity), CD4 T-lymphocyte count, age, and gender. The mean IOP was 9.8 mmHg in group A, 12.6 mmHg in group B, and 16.1 mmHg in the control group. All three groups were statistically different from each other when IOP was compared ($p<.0001$). Step-wise regression showed that low CD4 T-lymphocyte count and extent of CMV retinitis both correlated to low IOP. These results demonstrate that IOP is lower than normal in patients with HIV and that decreased CD4 T-lymphocyte count is the major factor associated with low IOP, accounting for 20% of the effect. The extent of CMV retinitis accounts for 8% of the effect.

Fomivirsen.

Fomivirsen, formerly called ISIS 2922, was approved by the FDA in August 1998 for the treatment of CMV retinitis in AIDS patients

intolerant of or who have a contraindication to other CMV regimens or who were insufficiently responsive to previous treatments for CMV retinitis. Fomivirsen is the first of a class of antisense oligonucleotides. This compound possesses potent anti-CMV activity, but does not target the CMV viral DNA polymerase. Fomivirsen is a 21-base synthetic phosphorothioate oligonucleotide designed to be complementary to CMV mRNA that encodes for the major immediate early region (IE2) proteins of CMV. Binding to this location results in specific inhibition of gene expression that is critical to production of essential viral proteins.[219–221]

Following intravitreal administration, the rate of vitreous clearance of fomivirsen is first-order with a half-life of approximately 55 hours in humans. Measurable concentrations of drug are not detected in the systemic circulation after intravitreal injection, making the interaction of fomivirsen with systemic drugs unlikely. Preclinical studies of fomivirsen by Freeman and associates suggested that this type of antiviral antisense compound does inhibit viral replication; however, it did cause changes in the RPE and intraocular inflammation at doses only moderately higher than the dose needed to treat retinitis by the intravitreal route.[222]

The Vitravene Study Group published the data from the clinical trials involving fomivirsen. Two prospective randomized open-label controlled clinical trials (US/Brazilian and EuroCanadian Studies) compared two fomivirsen regimens for the treatment of reactivated CMV retinitis or CMV retinitis that was persistently active despite other anti-CMV treatments. The more intense schedule (regimen A) included 61 patients (67 eyes) and consisted of three weekly 330 μg (0.05 ml) intravitreal injections for induction, then 330 μg every 2 weeks for maintenance therapy. The less intense schedule (regimen B) included 32 patients (39 eyes) and utilized a 330 μg injection for induction on day 1 and day 15, then 330 μg injections every 4 weeks for maintenance therapy. The study endpoint was time to progression based on masked evaluation of serial fundus photos. Eligibility criteria included AIDS patients with active CMV retinitis who had failed prior treatment with ganciclovir, foscarnet, or cidofovir.[223]

In the US/Brazilian study, median time to progression was 106 days (interpolated median 88.6 days) for regimen A and 267 days

(interpolated median 111.3 days) for regimen B (p=.2179 Wilcoxon rank sum test; 0.2950 log rank). In the EuroCanadian study the median time to progression was not determinable for regimen A; only four patients progressed (25th percentile 91 days). The median time to progression for regimen B was 403 days (interpolated median 182 days).[224]

The safety and toxicity of fomivirsen was also reported by the Vitravene study group. The most often reported adverse events were anterior chamber inflammation and increased IOP. Retinal pigment epitheliopathy occurred in 5 : 10 patients in the trial for newly diagnosed CMV retinitis with the 330 μg dose; this prompted a change to the reported 165 μg dose used for the remainder of the study. No episodes of retinal pigment epitheliopathy were reported with the 165 μg dose. No patients developed retinal pigment epitheliopathy in the 330 μg less intense regimen.

Independent of the randomized clinical trials, there have been reports of Vitravene-induced peripheral retinal toxicity and serious inflammation with vision loss. In clinical practice fomivirsen has been used as a fourth-line drug for CMV retinitis resistant to other therapy. The approved dose of fomivirsen is 330 μg intravitreally every 2 weeks for induction therapy for two doses followed by 330 μg intravitreally every month for maintenance therapy. Fomivirsen is no longer available in the United States.[225]

Rhegmatogenous Retinal Detachment in CMV Retinitis

Retinal detachment is a common cause of vision loss in patients with CMV retinitis. In the pre-HAART era, the incidence rate of retinal detachment in patients with CMV retinitis was approximately 33% per eye per year.[145,152,211,226–230] The incidence of retinal detachment in immunosuppressed patients with CMV retinitis was believed to be higher in patients treated with anti-CMV therapies, specifically ganciclovir.[231–232] These retinal detachments were characterized by multiple peripheral breaks in areas of healed atrophic retinitis, and in some patients severe proliferative vitreoretinopathy (PVR) resulted (Fig. 84.13).[233] Detachment occurred from weeks to months after institution of intravenous ganciclovir therapy and was frequently bilateral.

Retinal detachment may also complicate the course of CMV retinitis.

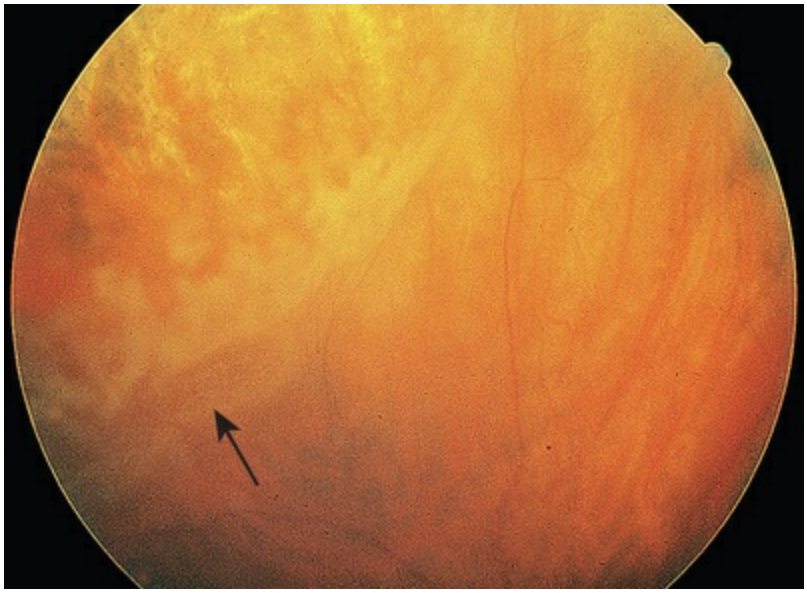

FIG. 84.13 Retinal breaks (*arrow*) are seen just peripheral to the area of border opacification; the retina is detached.

However, it now appears that rhegmatogenous retinal detachment is associated with healed or active CMV retinitis due to breaks in the necrotic retina.[233] Results of a multicenter, prospective, randomized, controlled clinical trial analyzing incidence and risk factors for rhegmatogenous retinal detachment in a population of patients with newly diagnosed CMV retinitis treated with foscarnet vs. ganciclovir revealed that retinal detachment in patients with CMV retinitis is unrelated to the type of intravenous therapy used or to refractive error. The median time to retinal detachment in an involved eye with CMV retinitis and free of retinal detachment at baseline was 18.2 months.[227]

Studies have confirmed that the risk factors for retinal detachment in eyes with CMV retinitis include the extent of peripheral CMV disease, as well as retinitis activity and involvement of the anterior retina near the vitreous base.[211,231–233] This is logical, considering that in most cases the causative retinal breaks are within or at the border of healed CMV retinitis lesions. A recent report from SOCA investigators has confirmed increased

prevalence and incidence of epiretinal membranes in eyes with inactive extramacular CMV retinitis.[234] In addition, any intervention that violates the vitreous (e.g., vitreous biopsy or insertion of the ganciclovir implant) would be expected to accelerate the development of vitreous detachment or liquefaction, which would increase the risk of retinal detachment.[207,209,211]

With the advent of HAART therapy the incidence of CMV retinitis-related retinal detachment has decreased by 60%. The success of HAART in the reduction of retinal detachment risk may be related to the improved immune control over CMV replication, thus protecting against progression of disease to larger lesion sizes. The altered pattern of inflammation with HAART-mediated immune improvement may also change the course of vitreous detachment, a key step in the development of CMV-related detachments, thus altering the retinal detachment risk.[207,211,235]

Patients with AIDS and CMV retinitis are surviving longer as a result of the use of HAART and improved treatment of opportunistic infections. As a result, though the incidence rate of retinal detachment is lower, the overall prevalence of retinal detachment may become an increasingly common cause of visual morbidity in these patients. In the pre-HAART era, the incidence and outcome of retinal detachment complicating CMV retinitis were studied at two London AIDS centers. Patients with CMV retinitis were identified prospectively and underwent standard treatment. Retinal detachments were diagnosed during regular follow-up. If retinal reattachment surgery was performed, a standard procedure of vitrectomy and internal tamponade with silicone oil was employed. Of 147 patients with CMV retinitis, 41 (28%) developed retinal detachments (47 eyes); 43 detachments were rhegmatogenous and four were exudative. At the last clinic visit, eight eyes (53%) maintained a visual acuity of 6/60 or better. The visual results of surgery are good in selected patients, bearing in mind the progressive nature of the underlying disease and poor life expectancy.[236]

Vitrectomy with silicone oil tamponade also was studied in eyes with retinal detachments related to CMV retinitis or acute retinal necrosis.[237] Anatomic reattachment was achieved in all eyes, and preservation of ambulatory vision was achieved in most eyes.

Visual acuity was limited by concomitant optic nerve disease in some eyes. The authors noted that surgical repair employing silicone oil produces excellent results and that prognosis for vision is strongly related to preoperative visual acuity.

Treatment of retinal detachment consists of vitrectomy, posterior hyaloid removal, and intraocular tamponade with silicone oil or long-acting gas.[237] Retinal reattachment surgery in 29 eyes of 24 patients with AIDS and retinal detachment associated with CMV retinitis was described by Freeman et al.[238] In this study the total retinal reattachment rate was 76%, and the macular attachment rate was 90% after one operation. The mean postoperative visual acuity (best corrected) was 20/60, but in some patients visual acuity decreased because of progressive CMV retinitis. Prophylactic laser photocoagulation of fellow eyes did not appear to prevent retinal detachment (Fig. 84.14).

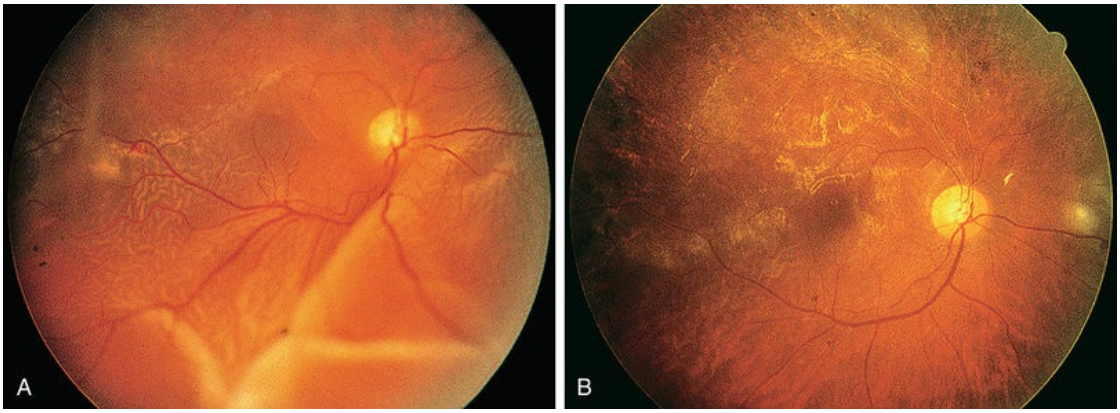

FIG. 84.14 (A) Preoperatively the macula has been shallowly detached, associated with a rhegmatogenous cytomegalovirus (CMV)-related retinal detachment. (B) Postoperatively the retina is reattached; silicone oil is in place, and the visual acuity is 20/40. Good visual recovery may be possible even with macula-off detachments because the detachment may be shallow as the vitreous is well formed; the retina may not be completely detached from the macula, and the macular detachments may be shallow.

The repair of retinal detachment in eyes with viral retinitis is complex and is performed using a combination of pars plana vitrectomy, internal tamponade (usually with silicone oil or a long-

acting gas such as perfluoropropane), and endolaser often combined with scleral buckling.[239] Pneumatic retinopexy can cause retinal traction and seldom is useful in these eyes. The most common causes of rhegmatogenous retinal detachment in AIDS patients with viral retinitis are acute retinal necrosis syndrome and previously treated CMV retinitis. In these eyes PVR occasionally is established at the time of detachment or has the potential to occur as a result of multiple retinal breaks and necrosis combined with intraocular inflammation. Scleral buckling alone often is unsuccessful in these cases because of the numerous areas of retinal necrosis and break formation. Retinal breaks are often not apparent until the time of vitrectomy, and the configurations of the retinal detachments are atypical because of peripheral retinal scarring and adhesion to the pigment epithelium and choroid. Thus in these eyes rhegmatogenous retinal detachments may not extend to the ora serrata. In eyes with CMV retinitis, we have favored an approach using complete delamination of the posterior hyaloid combined with endodrainage and permanent tamponade with silicone oil, although we have had good success with intraocular long-acting gases in cases of more limited retinitis and retinal detachment. Patients with AIDS and CMV retinitis appear to be surviving longer, and survival after retinal reattachment surgery has been increased to between 6 months and 2 years.[233]

To determine if scleral buckling is of any benefit in surgical repair of CMV-associated retinal detachment if combined with vitrectomy, silicone oil, and inferior midperipheral endolaser, 22 consecutive eyes with CMV-associated retinal detachments were repaired with vitrectomy and endolaser to all breaks and to the inferior midperipheral retina using silicone oil without scleral buckling. Results were compared with another series of 56 consecutive eyes undergoing vitrectomy, silicone oil injection, endolaser to all breaks, and 360 degrees encircling scleral buckling. Total retinal reattachment rates were 84% for group 1 and 86% for group 2. Rates of macular reattachment were 91% for group 1 and 91% for group 2. Mean best postoperative refracted visual acuity was 20/66 for group 1 and 20/67 for group 2. Median best postoperative refracted visual acuity was 20/74 for group 1 and 20/80 for group 2. These differences between the two groups were not statistically

significant. Patients who underwent surgery with the macula attached had a better postoperative visual outcome. Thus, scleral buckling may not be necessary in CMV-related retinal detachment if repaired with vitrectomy, silicone oil, and inferior midperipheral endolaser.[240] Elimination of scleral buckling may reduce intraoperative time, patient morbidity, and the risk of an accidental needle-stick. Patients with macula-on retinal detachments also should be considered for surgery before macular detachment occurs.[241]

The long-term visual results of CMV retinal detachment surgery are still in question, however, and visual acuity may be limited by factors such as refractive problems resulting from silicone oil and cataract[232,242,243] (Fig. 84.15). In addition, posterior capsule fibrosis is very common if subsequent cataract surgery is performed in the presence of silicone oil. Methods to reduce visual acuity loss from cataract include judicious use of gas tamponade with scleral buckling instead of silicone oil and removal of silicone oil prior to or at the time of cataract surgery. Posterior capsule fibrosis can be treated with Nd : YAG capsulotomy, though success is higher if the silicone oil has been previously removed.[244]

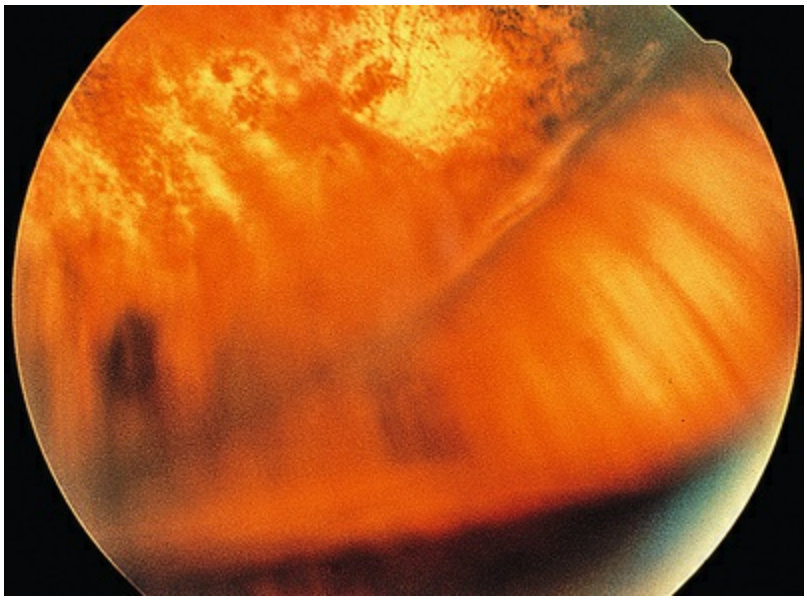

FIG. 84.15 Postoperatively, inferior retinal redetachment posterior to scleral buckle with use of silicone oil. The detachment has been walled off by laser that was applied intraoperatively. Inferior laser

photocoagulation may obviate the need for encircling scleral buckling in cytomegalovirus (CMV)-related retinal detachments.

The general operative approach to these eyes is by pars plana vitrectomy, and the surgeon should leave the lens intact whenever possible. After the vitreous gel is removed, all epiretinal membranes are segmented and traction is removed, allowing the retina to become mobile. In some cases the peripheral vitreous gel is adherent to the necrotic peripheral retina and cannot be removed without causing further retinal damage. The use of a soft-tipped extrusion needle may allow the surgeon to remove the posterior hyaloid over broad areas of the retina. A posterior retinotomy is made, and, if an endoretinal biopsy is to be performed, it is done at the location of the posterior retinotomy that will be used for internal drainage.[233,239] A pneumohydraulic exchange is made through the retinotomy site, attaching the retina and filling the eye with air using a constant-pressure, sterile, air-delivery pump. Retinopexy is placed around all breaks in eyes to be treated with a long-acting gas. The peripheral retina may be encircled with either a small buckle or a band to relieve vitreous base traction, which may become a problem later in these inflamed eyes. In eyes with widespread retinal necrosis, most surgeons use silicone oil because it permanently tamponades all retinal breaks, including future sites of retinal necrosis and break formation.

In the HAART era, PVR may be seen in CMV detachment. This may be due to immune recovery uveitis causing a propensity to intraocular inflammation.[245–247] The management of CMV-related rhegmatogenous retinal detachments has been reviewed.[248] Certainly, it may be useful in acute retinal necrosis (ARN) because rhegmatogenous retinal detachment develops in a large number of patients with ARN. Similar considerations apply in bilateral healed CMV retinitis. The difficulty in both diseases is that all areas of retinal involvement must be surrounded with three rows of argon laser treatment. It is often impossible to carry out treatment to the ora serrata, however, and fluid may leak anteriorly and cause retinal detachment despite treatment. In addition, subretinal fluid may break through a wall of laser treatment if the mass of detached retina and subretinal fluid is relatively large. For this reason most

surgeons advocate placement of a panretinal type of pattern within the area of healing retinitis as well.[249–251]

HIV Disease/CMV Retinitis in the HAART Era

Since the advent of HAART many patient have had dramatic restoration of immune system function. This also may be associated with a sustained drop in the plasma HIV viral load to low or undetectable levels. This suppression of plasma viremia may be prolonged; however, the HIV genome may still be found.[37,252] As mentioned earlier, with the prevalent use of HAART, the incidence of CMV retinitis has decreased approximately 75%.[253–256] For patients with CMV retinitis on HAART the risk of vision loss is lower,[253] the risk of retinal detachment is approximately 60% less, and long-term survival is much higher.[211,253]

In fact, for patients who have healed CMV retinitis and respond to HAART, discontinuation of maintenance therapy for CMV disease has been shown to be safe in a subset of patients.[253,257–262] We have found that some of these patients may discontinue anti-CMV therapy without reactivation of retinitis (Fig. 84.16). These data suggest that HAART therapy also is permitting at least partial immune reconstitution in some patients. Thus a trial of withdrawal of CMV therapy may be indicated in some patients with good response to HAART therapy and well-healed CMV retinitis. Patients should have a sustained CD4 count elevation of over 100 cells/μL for at least 3–6 months before discontinuing anti-CMV treatment and should be carefully monitored for reactivation. Reactivation of CMV retinitis may occur after successful HAART therapy when the CD4 count diminishes.[263] In addition, some patients may develop CMV retinitis on HAART with CD4 counts above 100/μL, probably because of incomplete restoration of the immune repertoire against CMV.[130]

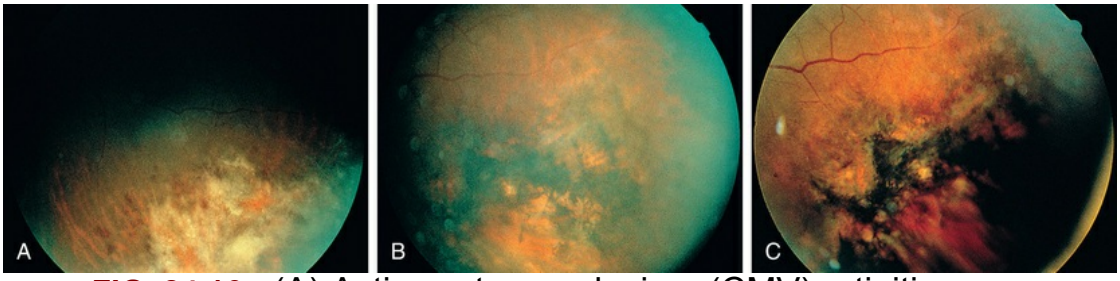

FIG. 84.16 (A) Active cytomegalovirus (CMV) retinitis required treatment with systemic ganciclovir. (B) The patient was subsequently treated with highly active antiretroviral therapy, with increase in $CD4^+$ cell count to over 100 cells/μL. The retinitis had remained healed. (C) The patient's systemic anti-CMV therapy was withdrawn, and the retinitis has remained healed for over 6 months. The $CD4^+$ cell count remains over 100.

The effects of HAART on the natural history of other AIDS-related opportunistic disorders have been summarized[264,265] and reflect the improvement or resolution of changes in the natural history of these disorders with inflammatory syndromes. The development of CMV retinitis relatively soon after initiation of HAART has been described.[265]

Immune Recovery Uveitis.

In conjunction with the dramatic improvements in the immune system reported in some patients on HAART therapy, inflammation at sites of opportunistic infections is common, and related to recovery of immunity with effective antiretroviral therapy.[266] The syndrome has been described in the eye as "immune recovery vitritis" or "immune recovery uveitis" (IRU).[267–274]

Immune recovery uveitis appears to occur in eyes with healed CMV lesions in patients with immune reconstitution on HAART. The incidence rate of this phenomenon has varied, with reports from 0.11 to 0.83 per person-year in HAART responders with CMV retinitis.[271,273] Jabs et al. reported the frequency of IRU at 15.5% of 200 prevalent cases of CMV retinitis.[274] Arevalo et al. reported IRU in 37.5% of 32 patients.[275] Eyes in which CMV retinitis lesions involve large surface areas of retina seem to be at higher risk for the development of IRU.[276] Previous treatment with cidofovir may also be a risk factor.[277] Patients with IRU exhibit signs of inflammation

such as iritis, vitritis, macular edema, and epiretinal membrane formation (Fig. 84.17).[278–282] Cataract, vitreomacular traction, PVR, optic disc and retinal neovascularization, panuveitis with hypopyon, and uveitic angle closure glaucoma with posterior synechia have also been reported in IRU.[283–289] Vision loss from these inflammatory sequelae may range from mild to moderate and is usually associated with macular edema and associated macular surface changes or cataract in most cases.

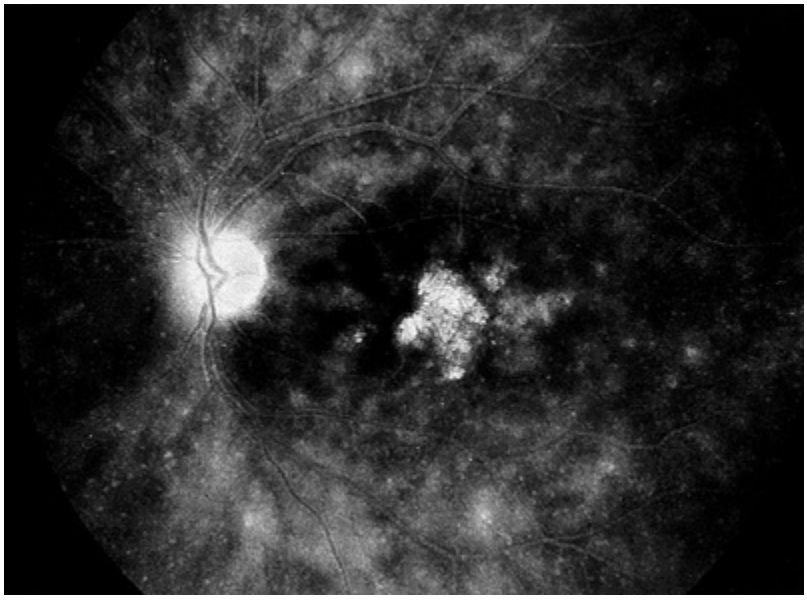

FIG. 84.17 Macular edema in a patient with immune recovery uveitis.

The pathophysiology of IRU is not well understood. One hypothesis is that once the CMV retinitis is healed and the immune system is reconstituted, the patient can mount an inflammatory response to residual CMV antigens in retinal glial cells in or adjacent to the necrotic CMV lesion. Another hypothesis is that control of CMV retinitis is incomplete in certain individuals with continued subclinical virus or viral protein production that stimulates the immune system. It has been reported that CMV antigens persist in cells of all retinal layers at the borders of clinically healed CMV lesions and in CMV-infected retinal glial cells after treatment with ganciclovir.[288–290]

Periocular steroids may be used successfully to treat this disorder, but ophthalmologists should be aware of CD4 cell counts.

It appears that if the CD4 cell count is elevated above 60/μL, treatment of immune recovery vitritis can be carried out without reactivation of retinitis (Fig. 84.13).[268,283] One case of reactivated CMV retinitis has been reported after treatment of IRU with periocular steroids.[291] Intravitreal triamcinolone is also effective in reducing macular edema; however, caution is needed not to reactivate retinitis.[292]

Other Complications of CMV Retinitis

Central visual loss in AIDS patients with CMV retinitis occurs in two forms: direct macular tissue destruction and secondary involvement as part of rhegmatogenous retinal detachment. We treated 32 patients (35 eyes) with macular exudation that caused reversible visual loss and initially manifested as neurosensory retinal detachment and lipid exudates. Of 35 eyes, 25 showed papillary or peripapillary active retinitis and 10 showed retinitis 1500–3000 μm from the fovea. Of 23 eyes with reduced vision that were followed up until healing of the retinitis and resolution of subretinal fluid and lipid exudates, 22 (96%) showed visual improvement with anti-CMV treatment. Our findings suggest that macular exudation is a reversible cause of visual loss in patients with CMV retinitis.[115]

Cystoid macular edema can occur in the setting of resolving CMV retinitis in patients with immunodeficiency other than AIDS. This entity is distinct from serous macular exudation, which can occur in patients with AIDS with active CMV retinitis involving the posterior pole.[293]

Herpetic Retinitis

Acute Retinal Necrosis in HIV Patients

ARN has been reported in AIDS patients.[294] It is a devastating disease characterized by the acute onset of a fulminant panuveitis with confluent, well-demarcated areas of retinitis, plus prominent anterior uveitis, occlusive retinal and choroidal vasculitis, vitritis, and papillitis.[54,117,295,296] In most cases the cause of the clinical syndrome of ARN is VZV but HSV can also cause ARN. The retinitis is characterized by deep retinal whitening, minimal

hemorrhage, and a rapid progression. In some cases, ARN in AIDS patients may be preceded by VZV optic neuropathy.[297] A history of preceding cutaneous zoster infection may be helpful in making the diagnosis in such cases.[298,299] In addition, the CD4 count is usually above 60/μL.[297] The new diagnostic criteria for ARN that do not include immune status of the patient have been published recently.[300]

No evidence of retinal vascular abnormalities may be present either clinically or angiographically early in the course of ARN. Retinal detachment is a common sequela, with multiple retinal breaks evident within areas of retinal necrosis. Retinal atrophy, often accompanied by PVR, is a common end-stage finding, and there may be associated anterior uveitis, scleritis, and ocular hypotension.[117]

Large numbers of herpesvirus particles in retinal tissue affected with ARN have been demonstrated by electron microscopy using endoretinal biopsy techniques. Virus may be detectable only during the acute phase of the disease.[117,301] Necrotic retinal tissue or retina reduced to thin glial remnants may not demonstrate virus. The difficulty in growing virus from these specimens is consistent with the hypothesis of VZV as the causative agent, since VZV is difficult to isolate and grow in vitro. CMV initially was believed to be the presumed infectious agent of ARN, but subsequent studies have not confirmed this.[302]

Studies employing endoretinal biopsy and PCR techniques have enabled definitive identification and culture of the causative virus, which has important diagnostic and therapeutic implications. Recent studies have suggested that combination antiviral therapy given intravenously (usually acyclovir or ganciclovir in combination with foscarnet), if given promptly, can arrest the disease and salvage vision.[197] Retinal detachment in VZV retinitis is common (up to two-thirds of patients) and may be associated with PVR or retinal shortening. Repair with vitrectomy and silicone oil after relief of traction with membrane segmentation and sometimes retinotomy may result in useful vision.[197,303] Prophylactic barrier laser around lesions should be considered to lower the risk of retinal detachment in ARN.

Ganciclovir has good efficacy against all herpesviruses but has a

lower therapeutic index and must be given indefinitely because it acts as a virostatic agent. Determination of a specific viral cause early in the course of the disease when large numbers of viral particles are present is therefore imperative. Both HSV and VZV may be sensitive to acyclovir. However, VZV requires higher serum concentrations than HSV. Treatment for ARN in AIDS patients is usually based on established treatment for non-HIV-infected patients. Acyclovir intravenously 500 mg/m^2 or 10 mg/kg every 8 hours is effective, followed by oral famciclovir 500 mg t.i.d., acyclovir 800 mg five times a day or valacyclovir 1000 mg t.i.d. for maintenance therapy.[93] Duration of maintenance therapy is controversial, with reports of contralateral ARN infection decades later. This may support lifetime maintenance therapy, especially in immunosuppressed AIDS patients. Valacyclovir 1000 mg t.i.d. has been reported effective for initial treatment of ARN in a small series of immunocompetent individuals.[304] Intravenous foscarnet may be used in acyclovir resistant cases.[305] Corticosteroids have been used to decrease vitritis in immunocompetent patients with ARN, but steroids are usually contraindicated in HIV patients with advanced immunosuppression.[93]

Progressive Outer Retinal Necrosis

Progressive outer retinal necrosis (PORN) is another variant of herpetic retinitis in AIDS patients and is nearly always caused by VZV. The incidence of PORN has decreased during the HAART era.[306] It has been described in association with VZV as the onset of retinitis either succeeded by or coincident with an eruption of dermatomal zoster.[307] Most patients with this syndrome have had low CD4 cell counts (i.e., below 50/μL). PORN syndrome is an extremely rapid progressive necrotizing retinitis characterized by early patchy multifocal deep outer retinal lesions (Fig. 84.18) with late diffuse thickening of the retina, absence of vascular inflammation, and minimal to no vitreous inflammation.[308] Severe vision loss develops as a result of a widespread retinal necrosis and from retinal detachment, the latter reported in up to 70% of patients in early studies.[308–313] Perivascular clearing of the retinal opacification is characteristic of PORN syndrome (Fig. 84.19).

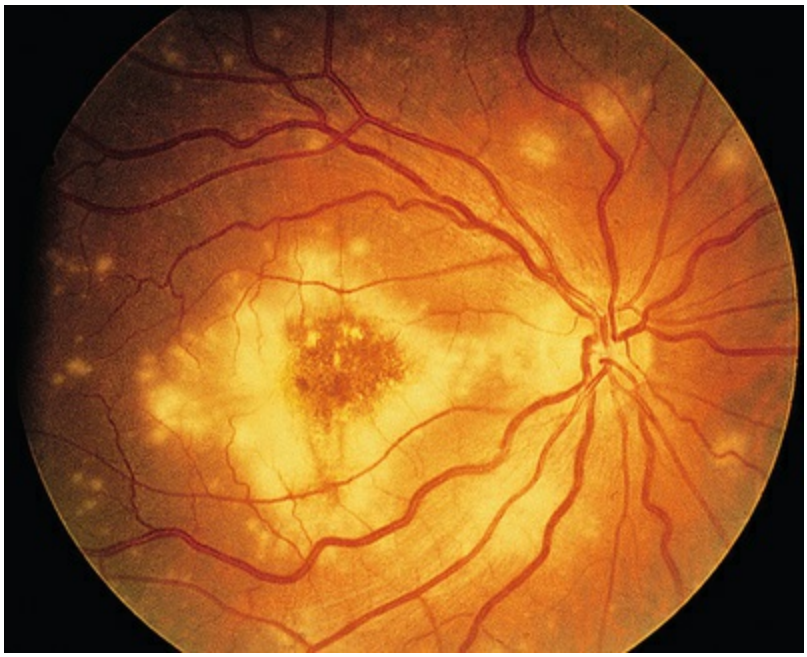

FIG. 84.18 Deep, round retinal lesions seen superior to the optic disc are characteristic of varicella-zoster retinitis in AIDS patients, also termed progressive outer retinal necrosis (PORN) syndrome.

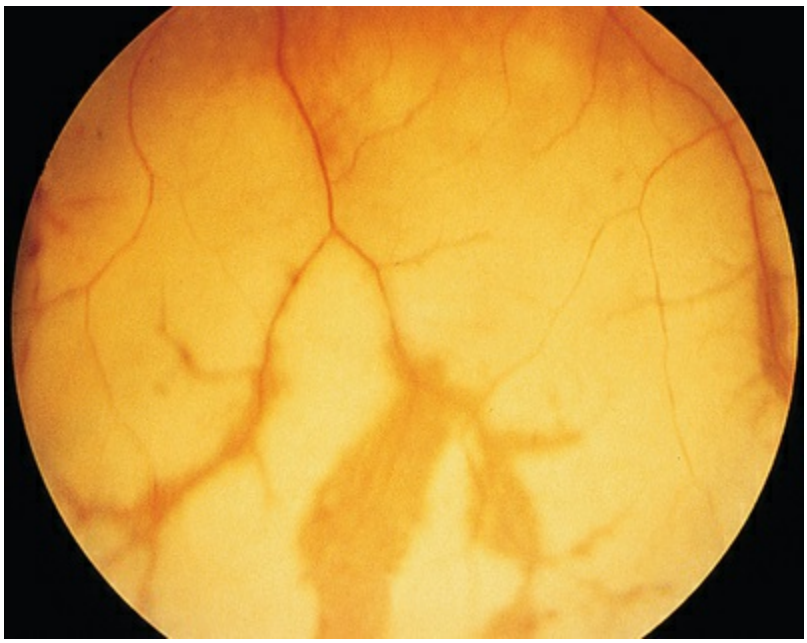

FIG. 84.19 Varicella-zoster retinitis in an HIV patient shows retinal opacification and perivascular "clearing." The perivascular edema and necrosis is cleared first; the tissue is not spared.

Therapy of PORN often requires immediate high-dose anti-zoster or -HSV therapy. The earliest reports of treatment of PORN with single intravenous antivirals, primarily acyclovir showed poor visual results. Engstrom et al. reported final vision of no light perception (NLP) in 67% of 63 eyes within 4 weeks.[307] Poor outcomes with intravenous acyclovir were possibly due to development of HSV or VZV resistance to acyclovir in patients who developed PORN while on prophylactic anti-HSV therapy with acyclovir. Recent studies have shown improved visual outcomes employing combination intravenous and intravitreal antiviral treatment. Scott et al.[308] reported final vision of 20/80 or better in 5 of 11 eyes (45%) with only two of 11 eyes (18%) progressing to NLP vision utilizing a regimen of intravitreal ganciclovir and foscarnet plus intravenous foscarnet and intravenous ganciclovir or oral valganciclovir. In addition, the authors' data suggested that laser demarcation may be beneficial to decrease the rate of retinal detachment. Combination of antiviral drugs and HAART preserved vision in a report by Kim et al.[314]

Nonviral Intraocular Infections in AIDS Patients

Nonviral intraocular infections have been reported in AIDS patients. Autopsy studies have documented numerous infections. Many of the opportunistic infections seen in patients with AIDS can be prevented with appropriate prophylactic agents.[315]

Pneumocystis carinii Choroidopathy

In 1987 Macher and associates[316] described a patient with AIDS with disseminated pneumocystosis, and choroidal *P. carinii* (now *P. jiroveci*) was found at autopsy; no clinical correlation was reported. In 1989 Rao and colleagues[58] reported the histopathologic findings in an autopsy series of three patients with AIDS who clinically demonstrated yellow choroidal infiltrates while receiving aerosolized pentamidine for *P. carinii* pneumonia (PCP) prophylaxis. In two cases a presumptive diagnosis of disseminated pneumocystosis was made by ophthalmologic examination. Histopathologically, the choroidal infiltrates were eosinophilic,

acellular, vacuolated, and frothy, with the infiltrates within the choroidal vessels and choriocapillaris. Both Gomori's methenamine-silver stain and electron microscopy demonstrated organisms.

In 1989 Freeman et al. described a woman with AIDS with multifocal, slowly enlarging, round-to-oval lesions in the choroid.[317] Fluorescein angiography revealed early hypofluorescence with late staining of the lesions, which appeared deep to the retinal circulation, without evidence of retinal involvement or inflammation (Fig. 84.20). A transscleral choroidal biopsy revealed, by electron microscopy, cystic structures characteristic of *P. carinii* within necrotic choroid.

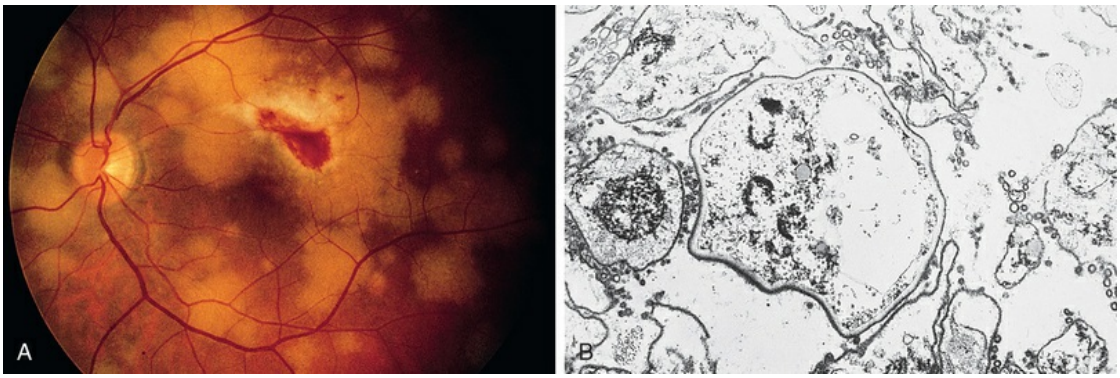

FIG. 84.20 (A) Pneumocystis choroiditis. The round lesions are associated with minimal inflammation. Overlying the lesions in the superior portion of the macula is a typical cytomegalovirus (CMV) retinitis lesion. (B) Electron micrograph of *Pneumocystis carinii* organisms seen after choroidal biopsy.

A multicenter study of pneumocystis choroidopathy in 1991 reported 21 patients with AIDS and presumed *P. carinii* choroidopathy.[318] The lesions were characteristically yellow to pale yellow, appeared in the choroid, and were found in the posterior pole. They enlarged slowly before systemic antipneumocystis therapy and eventually resolved. Of 21 patients, 18 were receiving topical therapy with aerosolized pentamidine. There was little evidence of retinal destruction by visual acuity and visual field testing. The choroidal infiltrates were not associated with vitreous inflammation unless another infectious retinitis was present. Resolution of choroiditis took from 6 weeks to 4 months after

systemic therapy. Survival after the diagnosis ranged from 2 to 36 weeks.

The CDC recommends double-strength trimethoprim–sulfamethoxazole (TMP–SMX) daily or three times weekly for primary prophylaxis of PCP when CD4 counts are below 200/ml, with alternatives including dapsone, dapsone plus pyrimethamine and leucovorin, aerosolized pentamidine administered by the Respirgard II nebulizer, and atovaquone.[319] PCP is the most common AIDS-defining opportunistic infection. Choroidal *P. carinii* infection appears to have been more common when the prophylactic use of nonsystemically absorbed aerosolized pentamidine for PCP was widespread. The choroidal lesions of *P. carinii* appear as pale, cream- or orange-colored, space-occupying lesions from several hundred to several thousand micrometers in size and they rarely are symptomatic or lead to a decrease in visual acuity. The lesions may be unilateral or bilateral.[58,317–322] *P. carinii* choroidopathy appears to be a marker for disseminated pneumocystosis and should be treated systemically. The need for maintenance systemic therapy for choroidopathy has not been established.

Although the diagnosis of disseminated pneumocystosis may be suggested by the characteristic appearance of *P. carinii* choroidopathy, isolated retinal disease may rarely be the earliest clinical manifestation of disseminated pneumocystosis. The incidence of *P.carinii* choroiditis has decreased, probably because of more widespread use of systemic PCP prophylaxis such as trimethoprim–sulfamethoxazole, immune restoration from HAART, and decreased use of aerosolized pentamidine for prophylaxis and therapy.[319]

Ocular Toxoplasmosis

Toxoplasmosis is a common CNS opportunistic infection in patients with AIDS. Ocular toxoplasmosis is much less common,[62,323–325] with reported incidence of 3% in HIV-infected patients in France.[326] US incidence is decreased in the HAART era by immune restoration and primary toxoplasmosis prophylaxis with TMP–SMX for those with CD4 counts less than 200/ml.[93] Eight patients with presumed ocular toxoplasmic retinochoroiditis were described in 1988 by

Holland et al.[62] In two cases the diagnosis was confirmed histologically. Lesions were usually bilateral (5/8) and multifocal, with vitreous inflammation noted clinically. Therapy resulted in remission, but reactivation and disease progression followed in two of three patients when therapy was stopped. Three patients had retinal tears or detachment as a result of severe retinal necrosis. The ocular lesions were the first manifestation of toxoplasmosis in four of five patients with disseminated disease, although all patients had preexisting HIV infection, and in four the diagnosis of AIDS had not been made. In four of five patients with no evidence of nonocular infection, evidence of *Toxoplasma* was demonstrated in the CNS (encephalitis or brain abscess). No patient had evidence of preexisting chorioretinal scars, and all had IgG antibodies to *T. gondii* at the time of diagnosis. Ocular disease was believed to be secondary to reactivation of *Toxoplasma* or to newly acquired or newly disseminated disease to the eye from nonocular sites of disease (Fig. 84.21).

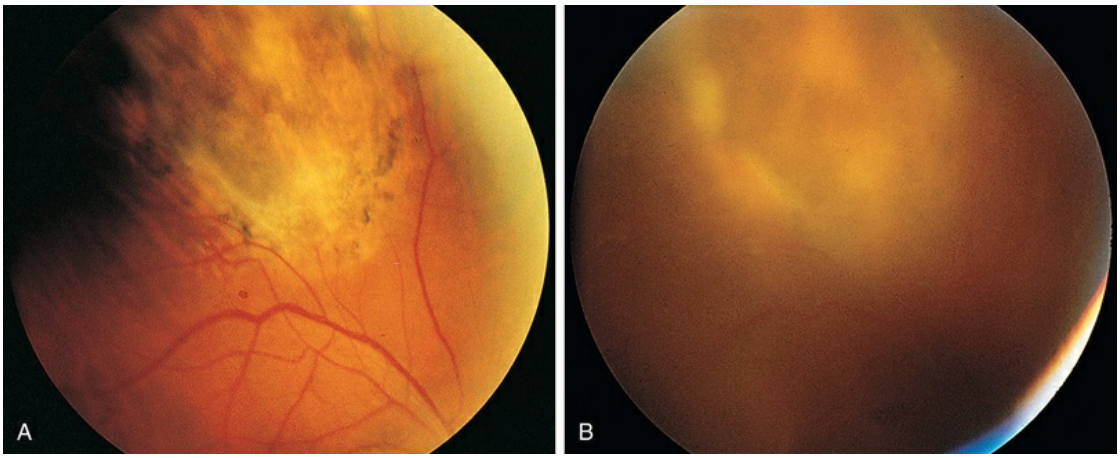

FIG. 84.21 (A) Toxoplasmosis retinitis in an HIV patient who was healed after antitoxoplasmosis therapy with clindamycin. (B) Systemic treatment for toxoplasmosis was withdrawn 6 months later, and the retinitis reactivated.

Retinal toxoplasmosis in HIV infection may present as a focal necrotizing nonhemorrhagic retinitis that does not heal spontaneously and may simulate ARN, CMV, or luetic retinitis.[93,327] Prominent vitreous and anterior chamber reaction, relative absence

of retinal hemorrhage, and thick, densely opaque yellow-white lesions with smooth nongranular borders suggest toxoplasmosis. Endoretinal biopsy or PCR techniques may be useful if diagnosis is difficult.[93,328,329]

Ocular toxoplasmosis often presents differently in AIDS compared to immunocompetent individuals, spreading as a contiguous or multifocal retinitis. AIDS patients more often have extensive areas of retinal necrosis plus multiple areas of active infection.[330,331] Histopathologic studies show absent to scant inflammatory cells in the infected retina of immunocompromised patients. AIDS patients can develop ocular toxoplasmosis in the absence of preexisting chorioretinal scars. This pattern combined with frequent systemic toxoplasmosis at diagnosis suggests that acquired disease is more common than reactivation of congenital disease.[93,332] For immunocompetent individuals, current evidence also suggests that most patients with ocular toxoplasmosis were infected postnatally, even though the risk of ocular toxoplasmosis is higher from congenital infection[333] (Fig. 84.21). Ocular toxoplasmosis in AIDS patients has also been reported to cause miliary disease, optic neuritis, panophthalmitis, and acute unilateral iridocyclitis without retinal lesions.[334,335] Ocular toxoplasmosis is diagnosed clinically and using PCR from a vitreous fluid sample.

Ocular, as well as disseminated, toxoplasmosis in patients with AIDS is treated with standard antitoxoplasma regimens used in immunocompetent patients such as sulfadiazine (4–6 g/day) or clindamycin in sulfa-allergic patients plus pyrimethamine/leucovorin, with apparent response rates of 80%. TMP–SMX was reported in a small (77 patients) randomized trial to be effective and better tolerated than pyrimethamine–sulfadiazine.[336–338] Other treatments for patients unable to tolerate sulfa drugs such as azithromycin or atovaquone have been primarily studied for CNS toxoplasmosis in AIDS patients and ocular toxoplasmosis in immunocompetent patients.[339] Atovaquone was originally synthesized as an antimalarial and has been shown to have activity against both *P. carinii* and *T. gondii*. Ocular toxoplasmosis in patients with AIDS frequently recurs when medical therapy is terminated so maintenance therapy generally is

given. Corticosteroids may be given as adjunctive therapy for intracranial toxoplasmosis to reduce cerebral edema, although this is unproved; systemic corticosteroids are sometimes given to reduce inflammation in ocular disease, although these should be administered cautiously in HIV-infected patients. In addition, resolution of ocular toxoplasmosis in AIDS patients has been seen without corticosteroid therapy.[62]

Toxoplasma retinitis is decreasing because of more widespread use of HAART and of prophylaxis, such as TMP–SMX. Currently the CDC recommends consideration of discontinuing maintenance therapy (sulfadiazine plus pyrimethamine/leucovorin with clindamycin used in sulfa-allergic patients) for toxoplasma encephalitis if a patient maintains a CD4 count above 200/μL for greater than 6 months.

Fungal Diseases

Candida albicans

Since HIV can be a consequence of intravenous drug use, which is also associated with candidemia, it is surprising that candida endophthalmitis is not seen more frequently in HIV patients. Focal retinal and chorioretinal lesions and endophthalmitis from *Candida* spp. have been described in patients with AIDS.[55,340] Traditional therapy for candida endophthalmitis has been systemic amphotericin B. However, limited vitreous penetration has resulted in treatment failures, plus adverse effects including nephrotoxicity discourage its use.[341] Trials comparing oral fluconazole to intravenous amphotericin B for systemic candidemia in immunocompetent patients suggested equivalent efficacy with fluconazole being the less toxic.[342] Vitrectomy and intravitreal amphotericin B can be helpful in cases failing systemic therapy.

Cryptococcus neoformans

Cryptococcal infections may occur in 5–10% of patients with AIDS[343] and are associated with both direct and indirect ocular complications. Cryptococcal infection is a common occurrence in

AIDS, resulting in meningitis and secondary ocular involvement. Chorioretinitis, endophthalmitis, or both, caused by direct intraocular invasion of the organism, have been described in immunosuppressed patients.[344,345] Visual loss caused by cryptococcal infection has been demonstrated to result from invasion of the visual pathways, including the optic nerve, tract, and chiasm.

The treatment of cryptococcal disease in patients with AIDS usually consists of an "induction" phase of about 2 weeks followed by a "consolidation" phase of about 8 weeks. Amphotericin B (>7 mg/kg per day) is most commonly used for induction, if possible combined with 5-flucytosine 100 mg/kg daily in four divided doses. If necessary because of toxicity, amphotericin can be replaced by fluconazole (800–1200 mg/day); a third phase of prolonged maintenance therapy with oral fluconazole (200 mg/day) is continued unless CD4 counts are above 200/μL. Ophthalmologic complications of cryptococcal meningitis were seen infrequently before the description of AIDS.

Histoplasmosis

Histoplasmosis was initially reported in patients with AIDS in 1982, and in the next eight years more than 100 systemic cases were reported,[346] mostly disseminated disease that presents as fevers without localized symptoms. The treatment of histoplasmosis in patients with AIDS usually consists of an induction phase with amphotericin B followed by a lifelong maintenance phase with either amphotericin B or itraconazole.[347]

Gonzales et al. reported bilateral endogenous endophthalmitis in an HIV-positive patient presenting with severe subretinal exudation, choroidal granulomas, and intraretinal hemorrhage leading to bilateral exudative retinal detachments. Vitreous cultures grew *Histoplasma capsulatum* var. *capsulatum*. Treatment involved systemic and bilateral intravitreal amphotericin B plus vitrectomy/scleral buckle in one eye.[348] Ala-Kauhaluoma et al. reported a case of panuveitis in disseminated histoplasmosis in an HIV patient treated with liposomal amphotericin B, HAART, and topical steroids that ended up with anterior segment scarring.[349]

Aspergillosis

Endogenous endophthalmitis caused by *Aspergillus fumigatus* rarely has been described in AIDS and can arrive in the eye hematogenously or through extension to the orbit from adjacent sinuses. One case of disseminated, invasive aspergillosis with ocular involvement noted at autopsy was described in 13 patients with pulmonary aspergillosis; no clinical correlation of ocular findings was reported.[350] Whereas four cases of orbital aspergillosis in HIV were reported, ocular aspergillosis is very rare in the HIV population.[351,352]

Coccidioidomycosis

To our knowledge, no cases of ocular coccidioidomycosis have been described in patients with AIDS. In a retrospective review of 77 patients with HIV infection and coccidioidomycosis, no case of endogenous endophthalmitis secondary to coccidioidomycosis was described, although disseminated disease (including meningitis) was described in a majority of patients.[353] Other unusual mycotic infections causing endophthalmitis, some in association with chorioretinitis, but not necessarily HIV-seropositive patients, are reviewed by McDonnell and Green.[354]

Paracoccidioidomycosis

Severe CNS plus ocular infection with *Paracoccidioides brasiliensis* that simulated CNS and ocular toxoplasmosis has been reported in a pregnant HIV-positive patient. The infection caused severe iridocyclitis, vitritis, plus a granulomatous chorioretinal lesion also involving the optic nerve that ultimately progressed to retinal detachment, NLP vision, and enucleation despite treatment.[355]

Advances in Antifungal Therapy

Fungal endophthalmitis traditionally has been treated with intravenous amphotericin B. Limitation of vitreous penetration plus systemic toxicity limit its effectiveness. Flucytosine and fluconazole

have higher vitreous penetration but are limited by lack of broad coverage against many of the organisms typically seen in fungal endophthalmitis. As a result, vitrectomy and intravitreal amphotericin B is usually recommended in serious fungal endophthalmitis or cases unresponsive to systemic therapy.[356]

The triazole antifungal medications fluconazole, itraconazole, voriconazole, posaconazole, and ravuconazole are orally available and are less toxic drugs that can treat a variety of fungal organisms.[357–361]

Older drugs such fluconazole, which treats candidal infection, and cryptococci and itraconazole, which treat histoplasmosis and aspergillosis, remain valuable. Voriconazole has been shown to have mean aqueous and vitreous minimum inhibitory concentrations for 90% of isolates (MIC90) for a wide spectrum of yeast and molds, including *Candida* and *Aspergillus* spp. after oral administration. Voriconazole and posaconazole have also been reported to successfully treat fungal endophthalmitis that was unresponsive to traditional antifungal agents.[362] Voriconazole and posaconazole have been shown to have efficacy against *Candida albicans* isolates from HIV patients.[361]

Bacterial Retinitis

Syphilis

Concurrent ocular syphilis appears to be more common in HIV-infected than in uninfected persons. Ophthalmic manifestations of syphilis usually occur during or shortly after the secondary stage. Syphilitic uveitis and chorioretinitis in HIV-infected patients have been described. Nine patients with ocular syphilis and concurrent HIV infection were described by McLeish and colleagues in 1990.[363] They found iridocyclitis in three of 15 eyes, vitritis in one eye, retinitis or neuroretinitis in five eyes, papillitis in two eyes, optic perineuritis in two eyes, and retrobulbar neuritis in two eyes. The three of nine patients with AIDS had the worst initial visual acuities. Six of nine had concomitant neurosyphilis. Benzathine benzylpenicillin, the only treatment in three of the patients, led to relapses in all three. Seven of nine patients treated with high-dose

intravenous penicillin responded dramatically to therapy with no evidence of relapse.

Concurrent ocular syphilis and neurosyphilis reported in two patients with HIV infection, in addition to a review of 13 other HIV-infected patients with ocular syphilis, revealed that 11 of the 13 HIV-infected patients with ocular syphilis had neurosyphilis.[364] The authors stress that neuro-ophthalmic syphilis may be the presenting feature of HIV infection and that ocular syphilis is strongly associated with concurrent neurosyphilis in patients that are HIV-seropositive (Fig. 84.22).

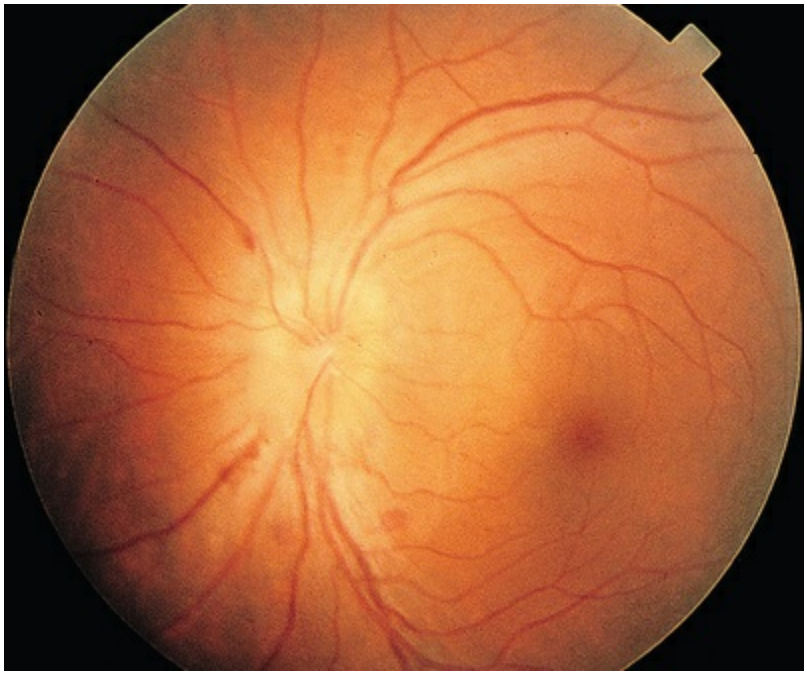

FIG. 84.22 Papillitis and vitritis from syphilis in an HIV-positive patient. Intravenous penicillin resolved the findings.

Necrotizing retinitis has been reported in a patient with HIV and syphilis. In some cases the appearance of luetic retinitis as a focal expanding white lesion may simulate CMV retinitis, ARN, or toxoplasmic retinitis. Marked inflammation of the vitreous and anterior chamber usually accompanies syphilitic retinal disease with posterior synechiae and keratic precipitates.[365]

Standard treatment of primary and secondary syphilis with 2.4 million units of intramuscular benzathine penicillin in patients with

and without HIV infection produce similar excellent clinical responses. Serologic responses to therapy (reducing nontreponemal antibody to unreactive levels), the primary method for ascertaining adequate treatment, are less certain in HIV patients.[366]

For retinitis, treatment for neurosyphilis with intravenous penicillin should be used and ceftriaxone may be used when penicillin is contraindicated. With regard to diagnosis, false-negative serum rapid plasma reagin (RPR) and Venereal Disease Research Laboratories (VDRL) may occur uncommonly with HIV infection. Thus additional, more specific tests are recommended in this population (i.e., fluorescent treponemal antibody, absorbed [FTA-ABS]).[367]

Invasive Diagnostic Techniques for Retinal Disease

In difficult cases, biopsy of the vitreous, choroid, or retina may allow for diagnosis of retinal disease. Vitreous biopsy may yield a diagnosis if a moderate to heavy cellular infiltrate is present. Most modern vitrectomy machines use sterile, disposable tubing and cassettes so that vitreous washings obtained are sterile. These washings may be filtered or centrifuged for appropriate stains, cultures, and cytologic study.

An alternative method may be used to obtain undiluted vitreous at the time of pars plana vitrectomy. After the infusion cannula can be visualized within the eye, the cannula is connected to a sterile, constant-air infusion pump, and a vitrectomy is carried out under air. In phakic eyes, a minus-power contact lens is used to visualize the retina under air. In this way the entire volume of the vitreous cavity may be removed in an undiluted form for study.

Appropriate processing of vitreous obtained as part of a diagnosis is mandatory, and the testing performed should reflect the differential diagnosis. Where infection is suspect, plating of undiluted vitreous on appropriate culture media for aerobic bacteria (chocolate and blood agar, brain–heart media), anaerobic bacteria (thioglycolate media and cooked meat broth), media for acid-fast bacilli, and fungal culture media is imperative and should

be done in the operating room. Smears of the undiluted gel should be stained for these etiologic agents, and cytologic smears also should be obtained. In addition, histopathologic stains are useful in ruling out intraocular neoplasms, particularly intraocular lymphoma. Other important diagnostic aids include the use of cytospin preparations that concentrate the cells in vitreous washings, and the use of cell blocks, should enough cellular material be present in a vitreous specimen. The choice of fixatives should be considered carefully. In general, the use of electron microscopic fixatives such as glutaraldehyde may destroy the antigenicity of proteins, rendering immunostaining impossible. Buffered paraformaldehyde will preserve many antigens, although in some cases, frozen, nonfixed tissue is required. In situ hybridization may work on fixed or fresh tissue and can be valuable in determining the presence of pathogenic DNA.[368]

PCR techniques also may be useful in analyzing aqueous or vitreous specimens in difficult cases. Nonfixed fluids are best; they can be frozen for later evaluation or processed fresh. In cases of active retinitis, the test is very sensitive, although it may be somewhat nonspecific because it may detect CMV in the blood in the absence of retinal infection. Choroidal biopsies may be indicated when infiltrative processes of the choroid are seen clinically. Fungal, bacterial, protozoal, or parasitic disease may cause metastatic focal or diffuse infiltrative lesions in the choroid. Tuberculous disease and neoplastic disorders, including lymphoma, also may produce such lesions. All such diseases respond temporarily, if at all, to steroid therapy, and in many cases the diagnosis cannot be made by study of vitreous cells. Before undertaking this diagnostic procedure, prior arrangements for appropriate histologic examination of all materials obtained must be made, since the amount of material that can be obtained is usually small. Any cultures to be taken should be performed by direct plating of the tissue onto the appropriate media in the operating room, as outlined above.

Thorough preoperative examination of the posterior segment is necessary. The choroidal lesion to be biopsied must be well localized. Echography can be used to gain further information regarding the consistency of the lesion and the presence of

subretinal or suprachoroidal fluid. It can also be useful in determining if an intraocular lesion has extraocular extension. It is best to select a site distant from the macular area; a nasal area of involvement is best.

In the operating room, the conjunctiva is removed from the limbus 360 degrees, and all four rectus muscles are isolated. Tenon's capsule is cleaned from the quadrant to be biopsied, and the margins of the lesion are marked. It is advantageous to choose a site where a serous or exudative retinal detachment is present overlying the lesion in question because this provides an added margin of safety. A half-thickness scleral dissection is performed 5–10 mm^2 and fashioned into a "trap door." Preplaced 5–0 polyester sutures can be used to allow the trap door to be closed quickly. A smaller area of underlying sclera is closed by diathermy to prevent bleeding, and then an area 3–4 mm on each side is resected. Care is taken to remove choroid and not retina. The trap door is then closed with 5-0 polyester sutures, and the area of resection is examined with the indirect ophthalmoscope. Some sclera should be visible if a full-thickness choroidal biopsy was performed. Retinal incarceration in the biopsy site is a potential source of problems and may have to be addressed using internal pars plana surgical techniques. Vitreous in the biopsy implies retinal incarceration or a retinal break that must be repaired using pars plana vitrectomy techniques. Using this technique, embolic bacterial endophthalmitis, pneumocystis choroidopathy, and other pathologic entities may be diagnosed. Because of the potential to damage the retina or perforate the eye, in some cases it may be preferable to perform a pars plana vitrectomy before choroidal biopsy. This will allow maintenance of intraocular pressure, as well as rapid internal access to the retina should complications arise.

Endoretinal biopsy has been reported to be of value in the diagnosis of viral retinitis. Freeman et al.[117] first reported this technique in 1986. We pursued this technique in patients with CMV retinitis (Fig. 84.23). After healing of retinitis with ganciclovir, rhegmatogenous retinal detachment developed in a large number of these patients as a result of numerous breaks in areas of necrotic and healed retina. We showed in several eyes that persistent infection was present, as viral particles were seen. At this time we

do not recommend endoretinal biopsy for all cases of viral retinitis. Rather, we treat such cases with the appropriate antiviral drug and await a response. Response may not indicate a specific viral cause, however, because some drugs treat multiple viruses. In certain cases it is helpful to obtain an etiologic diagnosis. As new antiviral and immunostimulating drugs become available, viral retinitis may not take on the so-called classic clinical appearance, and aggressive diagnostic techniques may become more important. Currently we obtain endoretinal biopsies at the time of pars plana vitrectomy to repair rhegmatogenous retinal detachments in these patients. During these procedures, undiluted vitreous specimens are taken for viral cultures, and in some cases in situ nucleic acid hybridization studies are done. The retinal biopsy (described below) is divided into three small pieces, and each is placed on a small wedge of sterile paper or on an agar sandwich in the operating room using the operating microscope. Tissue is fixed in glutaraldehyde for electron microscopy, as well as in buffered formalin for light microscopy and some immunologic studies. The third piece of tissue may be frozen for further immunologic studies or cultured for virus. It is important to remember that the choice of fixative and tissue preparation technique is critically important; if an incorrect choice is made, it may not be possible to arrive at a diagnosis. Even when obtaining an endoretinal biopsy, the vitreous should also be examined because vitreous biopsy in cases of infectious retinitis may be positive for the causative organism. One can also perform endoretinal biopsy in nondetached retinas. The preliminary results in animals have been encouraging, and refinement of these techniques in the future may shed light on a variety of retinal disorders.

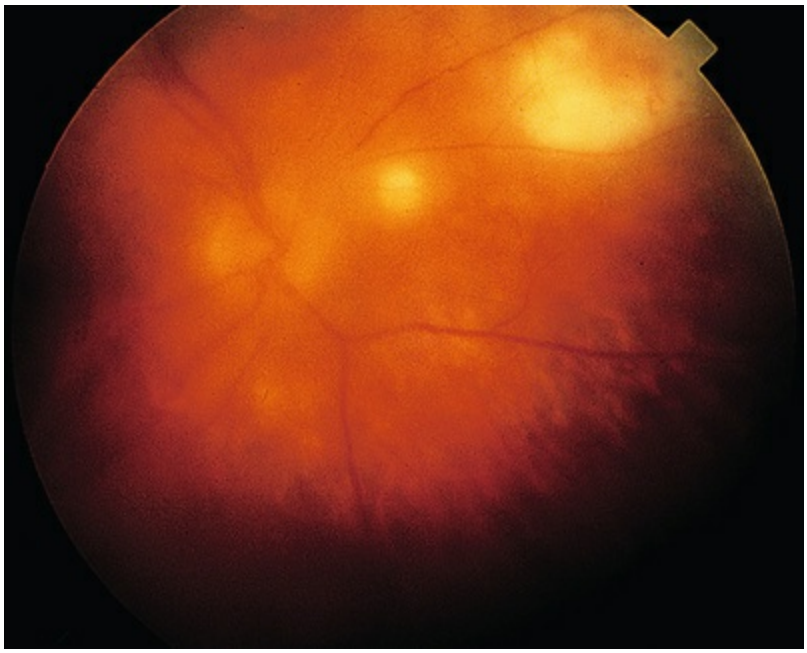

FIG. 84.23 Retinal lymphoma in an HIV-positive patient can present as an atypical retinitis. Diagnosis was made by endoretinal biopsy.

In eyes undergoing endoretinal biopsy a pars plana vitrectomy with complete removal of the hyaloid is performed. The biopsy site also is used for internal drainage. To determine the etiologic diagnosis, it is important to make this location at the junction of healed and normal or active retinitis. Vessels are cauterized only posterior to the biopsy site. We prefer to use the pointed 20-gauge intraocular unimanual bipolar cautery. Low power must be used, and major vessels posterior to the biopsy site are cauterized. Using motorized vertical cutting scissors, a rectangular strip of retina is excised, which crosses the site of active retinitis or the leading border. The strip may be 2 mm wide and 3–5 mm long. It is chosen from an area of necrotic or gliotic nonfunctional retina so that no visual loss occurs. Removal of the tissue from the eye through the 20-gauge sclerotomy with a forceps may crush and mutilate the tissue, so, instead, we prefer to guide the tissue toward the sclerotomy with a pick or pick forceps. The tissue is released, and the instrument is then removed from the eye while the infusion bottle is elevated to the high position. In this way the tissue is hydraulically directed into the sclerotomy site and plugs it. The tissue is gently teased out of the sclerotomy with a 0.12 mm forceps and spread over the cornea, removing all folds.

Any ocular tissue, but particularly small endoretinal biopsy specimens, must be processed with care. The surgeon must decide in advance on the location of the area to be biopsied and the fixatives and numbers of specimens to be processed. We have developed a mount that allows more facile mounting of retinal biopsy specimens.[368] The agar–albumin sandwich technique allows the small piece of retinal tissue to be floated onto a slab of clear agar and then "glued" to it with liquid agar that has been warmed in a microwave oven. When the tissue is draped on the agar, it can be readily identified and not lost during processing. Multiple sections of the tissue can then be cut for processing and immunostaining. The technique also works well for electron microscopy and other morphologic studies.

Antiretroviral Therapy

Expert guidelines for use of these drugs are continuously updated.[369,370] Many other antiretroviral agents are undergoing preclinical and clinical studies. Currently available drugs do not eradicate latent HIV infection, which returns when drugs are stopped (Table 84.1). When used in combination, they usually decrease viral replication, improve immunologic status, reduce risk of infectious complications, and prolong life. Drugs active against the patient's HIV strain should always be used in combination for full potency and prevention of resistance.

References

1. Review of draft for revision of HIV infection classification system and expansion of AIDS surveillance case definition. *MMWR Morb Mortal Wkly Rep*. 1991;40:787.
2. Revision of the CDC surveillance case definition for acquired immunodeficiency syndrome. Council of State and Territorial Epidemiologists; AIDS Program, Center for Infectious Diseases. *MMWR Morb Mortal Wkly Rep*. 1987;36(Suppl. 1):1S–15S.
3. CDC. HIV prevalence estimates. *MMWR Morb Mortal Wkly Rep*. 2008;57(39):1073–1076.

4. Deeks SG, Smith M, Holodniy M, et al. HIV-1 protease inhibitors: a review for clinicians. *JAMA*. 1997;277:145–153.
5. Zhu T, Korber BT, Nahmias AJ, et al. An African HIV-1 sequence from 1959 and implications for the origin of the epidemic. *Nature*. 1998;391:594–597.
6. Freeman WR, Lerner CW, Mines JA, et al. A prospective study of the ophthalmologic findings in the acquired immune deficiency syndrome. *Am J Ophthalmol*. 1984;97:133–142.
7. Jabs DA, Green R, Fox R, et al. Ocular manifestations of acquired immune deficiency syndrome. *Ophthalmology*. 1989;96:1092–1099.
8. Hall HI, An Q, Tang T, et al. Prevalence of diagnosed and undiagnosed HIV infection – United States, 2008–2012. *MMWR Morb Mortal Wkly Rep*. 2015;64(2):657–662.
9. Hogg RS, Health KV, Yi B, et al. Improved survival among HIV-infected individuals following initiation of antiretroviral therapy. *JAMA*. 1998;279:450–454.
10. Palella FJ, Delaney KM, Moorman AC, et al. Declining morbidity and mortality among patients with advanced human immunodeficiency virus infection. *N Engl J Med*. 1998;338:853–860.
11. Padian NS, Shiboski SC, Jewell NP. Female-to-male transmission of human immunodeficiency virus. *JAMA*. 1991;266:1664–1667.
12. *Centers for Disease Control and Prevention [Online]*. [Atlanta, GA: CDC; 2002. Surveillance of healthcare personnel with HIV/AIDS, as of December 2002] http://www.cdc.gov/ncidod/hip/BLOOD/hivpersonnel.htm.
13. US Public Health Service. Updated US public health service guidelines for the management of occupational exposures to HBV, HCV, and HIV and recommendations for postexposure prophylaxis. *MMWR Recomm Rep*. 2005;541–547.
14. Marcus R. Surveillance of health care workers exposed to blood from patients infected with the human immunodeficiency virus. *N Engl J Med*. 1988;319:1118–1123.
15. Cardo DM, Culver DH, Ciesielski CA, et al. A case–control

study of HIV seroconversion in health care workers after percutaneous exposure. *N Engl J Med*. 1997;137:1485–1490.
16. Fauci AS. Immunopathogenic mechanisms of HIV infection. *Ann Intern Med*. 1996;124:654–663.
17. Coombs RW, Welles SL, Hooper C, et al. Association of plasma human immunodeficiency virus type 1 RNA level with risk of clinical progression in patients with advanced infection. *J Infect Dis*. 1996;174:704–712.
18. Hughes MD, Johnson VA, Hirsch MS. Monitoring plasma HIV-1RNA levels in addition to CD4 lymphocyte count improves assessment of antiretroviral therapeutic response. *Ann Intern Med*. 1997;127:929–938.
19. Mellors JW, Kingsley LA, Rinaldo CR Jr, et al. Quantitation of HIV-1 RNA in plasma predicts outcome after seroconversion. *Ann Intern Med*. 1995;122:573–579.
20. Mellors JW, Rinaldo CR Jr, Gupta P, et al. Prognosis in HIV-1 infection predicted by the quantity of virus in plasma. *Science*. 1996;272:1167–1170.
21. Mellors JW, Munoz A, Giorgi JV, et al. Plasma viral load and CD4 lymphocytes as prognostic markers of HIV-1 infection. *Ann Intern Med*. 1997;126:946–954.
22. O'Brien WA, Hartigan PM, Martin D, et al. Changes in plasma HIV-1 RNA and CD4 lymphocyte counts and the risk of progression to AIDS. *N Engl J Med*. 1996;334:426–431.
23. Welles SL, Jackson JB, Yen-Lieberman B, et al. Prognostic value of plasma human immunodeficiency virus type 1 (HIV-1) RNA levels in patients with advanced HIV-1 disease and with little or no zidovudine therapy. *J Infect Dis*. 1996;174:696–703.
24. Feinberg MB. Changing the natural history of HIV disease. *Lancet*. 1996;348:239–246.
25. Havlir DV, Richman DD. Viral dynamics of HIV: implications for drug development and therapeutic strategies. *Ann Intern Med*. 1996;124:984–994.
26. Ho DD, Neumann AU, Perelson AS, et al. Rapid turnover of plasma virions and CD4 lymphocytes in HIV-1 infection. *Nature*. 1995;373:123–126.
27. Perelson AS, Newmann AU, Markowitz M, et al. HIV-1

dynamics in vivo: virion clearance rate, infected cell life-span, and viral generation time. *Science*. 1996;271:1582–1586.
28. McDonald CK, Kuritzkes DR. Human immunodeficiency virus type 1 protease inhibitors. *Arch Intern Med*. 1997;157:951–959.
29. Gulick RM, Mellor JW, Havlir D, et al. Treatment with indinavir, zidovudine, and lamivudine in adults with human immunodeficiency virus infection and prior antiretroviral therapy. *N Engl J Med*. 1997;337:734–739.
30. Hammer SM, Squires KE, Hughes MD, et al. A controlled trial of two nucleoside analogues plus indinavir in persons with human immunodeficiency virus infection and CD4 cell counts of 200 per cubic millimeter or less. *N Engl J Med*. 1997;337:725–733.
31. Ledergerber B, Egger M, Opravil M, et al. Clinical progression and virological failure on highly active antiretroviral therapy in HIV-1 patients: a prospective cohort study. Swiss HIV Cohort Study. *Lancet*. 1999;353:863–881.
32. Cervia JS, Smith MA. Enfuvirtide (T-20): a novel human immunodeficiency virus type 1 fusion inhibitor. *Clin Infect Dis*. 2003;37:1102–1106.
33. Pedersen C, Lindhardt BO, Jensen BL, et al. Clinical course of primary HIV infection: consequences for subsequent course of infection. *Br Med J*. 1989;299:154–157.
34. Chun T, Stuyver L, Mezell S, et al. Presence of an inducible HIV-1 latent reservoir during highly active antiretroviral therapy. *Proc Natl Acad Sci USA*. 1997;94:13193–13197.
35. Joshi D, O'Grady J, Dietrich D, et al. Increasing burden of liver disease in patients with HIV infection. *Lancet*. 2011;377(9772):1198–1209.
36. Update: Acquired Immunodeficiency Syndrome – United States. *MMWR Morb Mortal Wkly Rep*. 1986;35:757–766.
37. Henderly DE, Freeman WR, Smith RE, et al. Cytomegalovirus retinitis as the initial manifestation of the acquired immune deficiency syndrome. *Am J Ophthalmol*. 1987;103:316–320.
38. Update: Universal precautions for prevention of

transmission of human immunodeficiency virus, hepatitis B virus, and other bloodborne pathogens in health-care settings. *MMWR Morb Mortal Wkly Rep*. 1988;37:377–388.
39. Leads from the MMWR. Recommendations for preventing possible HTLV-III/LAV virus from tears. *JAMA*. 1985;254:1429.
40. Update: Acquired Immunodeficiency Syndrome – United States. *MMWR Morb Mortal Wkly Rep*. 1985;35:17–21.
41. Key CB, Whitman J. Alcohol soaking damages applanation tonometer heads. *Arch Ophthalmol*. 1986;104:800.
42. Vogt M, Ho DD, Bakar S, et al. Safe disinfection of contact lenses after contamination with HTLV-III. *Ophthalmology*. 1986;93:771–774.
43. Sattar SA. Springthorpe vs Survival and disinfectant inactivation of the human immunodeficiency virus: a critical review. *Rev Infect Dis*. 1991;13:430–447.
44. Centers for Disease Control and Prevention, Department of Health and Human Services. Guidelines for preventing transmission of human immunodeficiency virus through transplantation of human tissue and organs. *MMWR Morb Mortal Wkly Rep*. 1994;43:1–17.
45. Centers for Disease Control and Prevention. Update: provisional Public Health Service recommendations for chemoprophylaxis after occupational exposure to HIV. *MMWR Morb Mortal Wkly Rep*. 1996;45:468–472.
46. Ablashi DV, Sturzenegger S, Hunter EA, et al. Presence of HTLV-III in tears and cells from the eyes of AIDS patients. *J Exp Pathol*. 1987;3:693–703.
47. Fujikawa LS, Salahuddin SZ, Ablashi D, et al. Human T-cell leukemia/lymphotropic virus type III in the conjunctival epithelium of a patient with AIDS. *Am J Ophthalmol*. 1985;100:507–509.
48. Freeman WR, Chen A, Henderly D, et al. Prognostic and systemic significance of non-infectious AIDS associated retinopathy. *Invest Ophthalmol Vis Sci*. 1987;28(Suppl.):9.
49. Freeman WR, Chen A, Henderly DE, et al. Prevalence and significance of acquired immunodeficiency syndrome-related retinal microvasculopathy. *Am J Ophthalmol*.

1989;107:229–235.
50. Cole EL, Meisler DM, Calabrese LH, et al. Herpes zoster ophthalmicus and acquired immune deficiency syndrome. *Arch Ophthalmol*. 1984;102:1027–1029.
51. Sandor EV, Millman A, Croxson TS, et al. Herpes zoster ophthalmicus in patients at risk for the acquired immune deficiency syndrome (AIDS). *Am J Ophthalmol*. 1986;101:153–155.
52. Holland GN, Pepose JS, Pettit TH, et al. Acquired immune deficiency syndrome, ocular manifestations. *Ophthalmology*. 1983;90:859–873.
53. Kestelyn P, Van de Perre P, Rouvroy D, et al. A prospective study of the ophthalmologic findings in the acquired immune deficiency syndrome in Africa. *Am J Ophthalmol*. 1985;100:230–238.
54. Lipson BK, Freeman WR, Beniz J, et al. Optic neuropathy associated with cryptococcal arachnoiditis in AIDS patients. *Am J Ophthalmol*. 1989;107:523–527.
55. Morinelli EN, Dugel PU, Riffenburgh R, et al. Infectious multifocal choroiditis in patients with acquired immune deficiency syndrome. *Ophthalmology*. 1993;100:1014–1021.
56. Pepose JS, Hilborne LH, Cancilla PA, et al. Concurrent herpes simplex and cytomegalovirus retinitis and encephalitis in the acquired immune deficiency syndrome (AIDS). *Ophthalmology*. 1984;91:1669–1677.
57. Pepose JS, Nestor MS, Holland GN, et al. An analysis of retinal cotton-wool spots and cytomegalovirus retinitis in the acquired immunodeficiency syndrome. *Am J Ophthalmol*. 1983;95:118–119.
58. Rao NA, Zimmerman PL, Boyer D, et al. A clinical, histopathologic, and electron microscopic study of *Pneumocystis carinii* choroiditis. *Am J Ophthalmol*. 1989;107:218–228.
59. Weiss A, Margo CE, Ledord DK, et al. Toxoplasmic retinochoroiditis as an initial manifestation of the acquired immune deficiency syndrome. *Am J Ophthalmol*. 1986;101:248–249.
60. Arevalo JF, Russack V, Freeman WR. New ophthalmic

manifestations of presumed rifabutin-related uveitis. *Ophthalmic Surg Lasers*. 1997;28:321–324.
61. Glasgow BJ, Engstrom RE Jr, Holland GN, et al. Bilateral endogenous fusarium endophthalmitis associated with acquired immunodeficiency syndrome. *Arch Ophthalmol*. 1996;114:873–877.
62. Holland GN, Engstrom RE, Glasgow BJ, et al. Ocular toxoplasmosis in patients with the acquired immunodeficiency syndrome. *Am J Ophthalmol*. 1988;106:653–667.
63. Gonzales CA, Scott IU, Chaudhry NA, et al. Endogenous endophthalmitis caused by *Histoplasma capsulatum* var. *capsulatum*: a case report and literature review. *Ophthalmology*. 2000;107:725–729.
64. Finamor LP, Muccioli C, Martins MC, et al. Ocular and central nervous system paracoccidioidomycosis in a pregnant woman with acquired immunodeficiency syndrome. *Am J Ophthalmol*. 2002;134:456–459.
65. Santos C, Parker J, Dawson C, et al. Bilateral fungal corneal ulcers in a patient with AIDS-related complex. *Am J Ophthalmol*. 1985;102:118–119.
66. Geier SA, Schielke E, Klauss V, et al. Retinal microvasculopathy and reduced cerebral blood flow in patients with acquired immunodeficiency syndrome. *Am J Ophthalmol*. 1992;113:100–101.
67. Newsome DA, Green W, Miller ED, et al. Microvascular aspects of acquired immune deficiency syndrome retinopathy. *Am J Ophthalmol*. 1984;98:590–601.
68. Freeman WR, O'Connor GR. Acquired immune deficiency syndrome retinopathy, pneumocystis, and cotton-wool spots. *Am J Ophthalmol*. 1984;98:235–237.
69. Kwok S, O'Donnell JJ, Wood IS. Retinal cotton-wool spots in a patient with *Pneumocystis carinii* infection. *N Engl J Med*. 1982;307:184–185.
70. Faber DW, Wiley CA, Bergeron-Lynn G, et al. Role of human immunodeficiency virus and cytomegalovirus in the pathogenesis of retinitis and retinal vasculopathy in AIDS patients. *Invest Ophthalmol Vis Sci*. 1992;33:2345–2353.

71. Gonzalez CR, Wiley CA, Arevalo JF, et al. Polymerase chain reaction detection of cytomegalovirus and human immunodeficiency virus-1 in the retina of patients with acquired immune deficiency syndrome with and without cotton-wool spots. *Retina*. 1996;16:305–311.
72. Honrubia FM, Ferrer E, Torron C, et al. Study of the retinal fiber layer in patients with acquired immunodeficiency syndrome. *Ger J Ophthalmol*. 1994;3:1–4.
73. Mansour AM, Rodenko G, Dutt R. Half-life of cotton wool spots in the acquired immunodeficiency syndrome. *Int J STD AIDS*. 1990;1:132–133.
74. Kozak I, Bartsch DU, Cheng L, et al. In vivo histology of cotton-wool spots using high resolution optical coherence tomography. *Am J Ophthalmol*. 2006;141(4):748–750.
75. Gomez ML, Mojana F, Bartsch DU, et al. Imaging of long-term retinal damage after resolved cotton wool spots. *Ophthalmology*. 2009;116(12):2407–2414.
76. Kuppermann BD, Petty JG, Richman DD, et al. Cross-sectional prevalence of CMV retinitis in AIDS patients: correlation with CD4 counts. *Invest Ophthalmol Vis Sci*. 1992;33:750.
77. Sadun AA, Pepose JS, Madigan MC, et al. AIDS-related optic neuropathy: a histological, virological and ultrastructural study. *Graefes Arch Clin Exp Ophthalmol*. 1995;233:387–398.
78. Sadun AA, Tenhula WN, Heller KB. Optic nerve pathology associated with AIDS: ultrastructural changes. [ARVO Abstract]. *Invest Ophthalmol Vis Sci*. 1990;31(Suppl.):1792.
79. Tenhula WN, Sadun AA, Heller KB, et al. Optic nerve axon losses in AIDS. Morphometric comparisons. [ARVO Abstract]. *Invest Ophthalmol Vis Sci*. 1990;31(Suppl.):1793.
80. Kozak I, Bartsch DU, Cheng L, et al. Objective analysis of retinal damage in HIV-positive patients in the HAART era using OCT. *Am J Ophthalmol*. 2005;139(2):295–301.
81. Quiceno JI, Capparelli E, Sadun AA, et al. Visual dysfunction without retinitis in patients with acquired immunodeficiency syndrome. *Am J Ophthalmol*. 1992;113:8–13.
82. Barteselli G, Chhablani J, Gomez ML, et al. Visual function

assessment in simulated real-life situations in HIV-infected subjects. *PLoS ONE*. 2014;9(5):e97023.
83. Shah KH, Holland GN, Yu F, et al. Contrast sensitivity and color vision in HIV-infected individuals without infectious retinopathy. *Am J Ophthalmol*. 2006;142(2):284–292.
84. Plummer DJ, Arevalo JF, Fram N, et al. Effectiveness of entoptic perimetry for locating peripheral scotomas caused by cytomegalovirus retinitis. *Arch Ophthalmol*. 1996;114:828–831.
85. Latkany PA, Holopigian K, Lorenzo-Latkany M, et al. Electroretinographic and psychophysical findings during early and late stages of human immunodeficiency virus infection and cytomegalovirus retinitis. *Ophthalmology*. 1997;104:445–453.
86. Falkenstein IA, Bartsch DU, Azen SP, et al. Multifocal electroretinography in HIV-positive patients without infectious retinitis. *Am J Ophthalmol*. 2008;146(4):579–588.
87. Freeman WR, Van Natta ML, Jabs DA, et al. Vision function in HIV-infected individuals without retinitis: report of the Studies of Ocular Complications of AIDS Research Group. *Am J Ophthalmol*. 2008;145:453–462.
88. Jabs DA, Drye L, Van Natta ML, et al. Incidence and long-term outcomes of the human immunodeficiency virus neuroretinal disorder in patients with AIDS. *Ophthalmology*. 2015;122(4):760–768.
89. Kozak I, Sasik R, Freeman WR, et al. A degenerative retinal process in HIV-associated non-infectious retinopathy. *PLoS ONE*. 2013;8(9):e74712.
90. Holland GN, Gottlieb MS, Foos RY. Retinal cotton-wool patches in acquired immunodeficiency syndrome. *N Engl J Med*. 1982;307:1702.
91. Conway MD, Tong P, Olk RJ. Branch retinal artery occlusion (BRAO) combined with branch retinal vein occlusion (BRVO) and optic disc neovascularization associated with HIV and CMV retinitis. *Int Ophthalmol*. 1995–1996;19:249–252.
92. Cunningham ET Jr, Levinson RD, Jampol LM, et al. Ischemic maculopathy in patients with acquired immunodeficiency

syndrome. *Am J Ophthalmol*. 2001;132:727–733.
93. Levinson RD, Dunn JP, Holland GN. Ophthalmic disorders associated with selected primary and acquired immunodeficiency diseases. *Duane's clinical ophthalmology*. Harper and Row: Hagerstown; 2004 [CD-ROM; ch. 40].
94. Dejaco-Ruhswurm I, Kiss B, Rainer G, et al. Ocular blood flow in patients infected with human immunodeficiency virus. *Am J Ophthalmol*. 2001;132:719–725.
95. Lim MC, Cumberland WG, Minassian SL, et al. Decreased macular leukocyte velocity in HIV-infected individuals. *Am J Ophthalmol*. 2001;132:710–718.
96. Dadgostar H, Holland GN, Huang X, et al. Hemorheologic abnormalities associated with HIV infection: in vivo assessment of retinal microvascular blood flow. *Invest Ophthalmol Vis Sci*. 2006;47(9):3933–3938.
97. Henderly DE, Freeman WR, Causey DM, et al. Cytomegalovirus retinitis and response to therapy with ganciclovir. *Ophthalmology*. 1987;94:425–434.
98. Jabs DA, Bartlett JG. AIDS and ophthalmology: a period of transition. *Am J Ophthalmol*. 1997;124:227–233.
99. Studies of Ocular Complications of AIDS Research Group in collaboration with the AIDS Clinical Trials Group. Foscarnet–ganciclovir cytomegalovirus retinitis trial 4 – visual outcomes. *Ophthalmology*. 1994;101:1250–1261.
100. Collaborative DHPG Treatment Study Group. Treatment of serious cytomegalovirus infections with 9-(1,3-dihydroxy-2-propoxymethyl) guanine in patients with AIDS and other immunodeficiencies. *N Engl J Med*. 1986;314:801–805.
101. Cogan DG. Immunosuppression and eye disease. *Am J Ophthalmol*. 1977;83:777–788.
102. Egbert PR, Pollard RB, Gallagher JG, et al. Cytomegalovirus retinitis in immunosuppressed hosts. II. Ocular manifestations. *Ann Intern Med*. 1980;93:664.
103. DeVenecia G, Zu Rhein GM, Pratt MV, et al. Cytomegalic inclusion retinitis in an adult, a clinical, histopathologic, and ultrastructural study. *Arch Ophthalmol*. 1971;86:44.
104. Friedman AH, Orellana J, Freeman WR, et al. Cytomegalovirus retinitis: a manifestation of the acquired

immune deficiency syndrome (AIDS). *Br J Ophthalmol*. 1983;67:372–380.
105. Kennedy PGE, Newsome DA, Hess J, et al. Cytomegalovirus but not human T lymphotropic virus type III/lymphadenopathy associated virus detected by in-situ hybridization in retinal lesions in patients with the acquired immune deficiency syndrome. *Br Med J*. 1986;293:162–164.
106. Brody JM, Butrus SI, Laby DM, et al. Anterior segment findings in AIDS patients with cytomegalovirus retinitis. *Graefes Arch Clin Exp Ophthalmol*. 1995;233:374–376.
107. Saran BR, Pomilla PV. Retinal vascular nonperfusion and retinal neovascularization as a consequence of cytomegalovirus retinitis and cryptococcal choroiditis. *Retina*. 1996;16:510–512.
108. Palestine AG, Stevens G, Lane HC, et al. Treatment of cytomegalovirus retinitis with dihydroxy propoxymethyl guanine. *Am J Ophthalmol*. 1986;101:95–101.
109. Studies of Ocular Complications of AIDS Research Group in collaboration with the AIDS Clinical Trials Group. Assessment of cytomegalovirus retinitis – clinical evaluation vs centralized grading of fundus photographs. *Arch Ophthalmol*. 1996;114:791–805.
110. Studies of Ocular Complications of AIDS Research Group in collaboration with the AIDS Clinical Trials Group. Clinical vs photographic assessment of treatment of cytomegalovirus retinitis. Foscarnet–ganciclovir cytomegalovirus retinitis trial report 8. *Arch Ophthalmol*. 1996;114:848–855.
111. Roarty JD, Fisher EJ, Nussbaum JJ. Long-term visual morbidity of cytomegalovirus retinitis in patients with acquired immune deficiency syndrome. *Ophthalmology*. 1993;100:1685–1688.
112. Wu AW, Coleson LC, Holbrook J, et al. Measuring visual function and quality of life in patients with cytomegalovirus retinitis: development of a questionnaire. [for; Studies of Ocular Complications of AIDS Research Group] *Arch Ophthalmol*. 1996;114:841–847.
113. Bloom PA, Sandy CJ, Migdal CS, et al. Visual prognosis of

AIDS patients with cytomegalovirus retinitis. *Eye (Lond)*. 1995;9:697–702.
114. Luckie AP, Ai E. A foveal-sparing pattern of cytomegalovirus retinitis in the acquired immunodeficiency syndrome. *Aust N Z J Ophthalmol*. 1996;24:53–59.
115. Gangan PA, Besen G, Munguia D, et al. Macular serous exudation in patients with acquired immunodeficiency syndrome and cytomegalovirus retinitis. *Am J Ophthalmol*. 1994;118:212–219.
116. Minkler DS, Mcleon EB, Shaw CM, et al. Herpes virus hominis encephalitis and retinitis. *Arch Ophthalmol*. 1976;94:89–95.
117. Freeman WR, Thomas EL, Rao NA, et al. Demonstration of herpes group virus in the acute retinal necrosis syndrome. *Am J Ophthalmol*. 1986;102:701–709.
118. Young SJ, Bird AC. Bilateral acute retinal necrosis. *Br J Ophthalmol*. 1978;62:581–590.
119. Bylsma SS, Achim CL, Wiley CA, et al. The predictive value of cytomegalovirus retinitis for cytomegalovirus encephalitis in acquired immunodeficiency syndrome. *Arch Ophthalmol*. 1995;113:89–95.
120. Leger F, Vital C, Vital A, et al. Pathologic correlations between ocular and cerebral lesions in 36 AIDS patients. *Clin Neuropathol*. 1997;16:45–48.
121. Livingston PG, Kerr NC, Sullivan JL. Ocular disease in children with vertically acquired human immunodeficiency virus infection. *J AAPOS*. 1998;2:177–181.
122. Du LT, Coats DK, Kline MW, et al. Incidence of presumed cytomegalovirus in HIV-infected pediatric patients. *J AAPOS*. 1999;3:245–249.
123. Baumal CR, Levin AV, Read SE. Cytomegalovirus retinitis in immunosuppressed children. *Am J Ophthalmol*. 1999;127:550–558.
124. Rasmussen L, Zipeto D, Wolitz RA, et al. Risk for retinitis in patients with AIDS can be assessed by quantitation of threshold levels of cytomegalovirus DNA burden in blood. *J Infect Dis*. 1997;176:1146–1155.
125. Studies of Ocular Complications of AIDS Research Group in

collaboration with the AIDS Clinical Trials Group. Foscarnet–ganciclovir cytomegalovirus retinitis trial 5 – clinical features of cytomegalovirus retinitis at diagnosis. *Am J Ophthalmol*. 1997;124:141–157.
126. Studies of Ocular Complications of AIDS Research Group in collaboration with the AIDS Clinical Trials Group. Cytomegalovirus (CMV) culture results, drug resistance, and clinical outcome in patients with AIDS and CMV retinitis treated with foscarnet or ganciclovir. *J Infect Dis*. 1997;176:50–58.
127. Pannuti CS, Kallas EG, Muccioli C, et al. Cytomegalovirus antigenemia in acquired immunodeficiency syndrome patients with untreated cytomegalovirus retinitis. *Am J Ophthalmol*. 1996;122:847–852.
128. Rasmussen L, Morris S, Zipeto D, et al. Quantitation of human cytomegalovirus DNA from peripheral blood cells of human immunodeficiency virus-infected patients could predict cytomegalovirus retinitis. *J Infect Dis*. 1995;171:177–182.
129. Hoover DR, Peng Y, Saah A, et al. Occurrence of cytomegalovirus retinitis after human immunodeficiency virus immunosuppression. *Arch Ophthalmol*. 1996;114:821–827.
130. Song MK, Schrier RD, Smith IL. Paradoxical activity of CMV retinitis in patients receiving highly active antiretroviral therapy. *Retina*. 2002;22:262–267.
131. Mitchell SM, Fox JD. Aqueous and vitreous humor samples for the diagnosis of cytomegalovirus retinitis. *Am J Ophthalmol*. 1995;120:252–253.
132. McCann JD, Margolis TP, Wong MG, et al. A sensitive and specific polymerase chain reaction-based assay for the diagnosis of cytomegalovirus retinitis. *Am J Ophthalmol*. 1995;120:219–226.
133. Schrier RD, Freeman WR, Wiley CA, et al. Immune predispositions for cytomegalovirus retinitis in AIDS. The HNRC Group. *J Clin Invest*. 1995;95:1741–1746.
134. Dunn JP, Martin DF. *Medscape from WebMD Ophthalmology*. [Sep 30; Treatment of cytomegalovirus (CMV) retinitis in

the era of highly active antiretroviral therapy; [Online with account] http://medscape.com/viewprogram/663; 2003.
135. Jabs DA. Cytomegalovirus retinitis and the acquired immunodeficiency syndrome – bench to bedside: LXVII Edward Jackson Memorial lecture. *Am J Ophthalmol*. 2011;151(2):198–216.
136. Stalder N, Sudre P, Olmari M, et al. Cytomegalovirus retinitis: decreased risk of bilaterality with increased use of systemic treatment. Swiss HIV Cohort Study Group. *Clin Infect Dis*. 1997;24:620–624.
137. Martin DF, Kuppermann BD, Wolitz RA, et al. Oral ganciclovir for patients with cytomegalovirus retinitis treated with a ganciclovir implant. Roche Ganciclovir Study Group. *N Engl J Med*. 1999;340:1063–1070.
138. Jabs DA, Martin BK, Forman MS. Cytomegalovirus resistance to ganciclovir and clinical outcomes of patients with cytomegalovirus retinitis. *Ophthalmology*. 2003;135:26–34.
139. Chiron Ganciclovir Implant Study Group. *A randomized, controlled, multicenter clinical trial of sustained-release intraocular ganciclovir implant in AIDS patients with CMV retinitis (abstract 1215). Program and abstracts of the Thirty-fifth Interscience Conference on Antimicrobial Agents and Chemotherapy (San Francisco)*. American Society for Microbiology: Washington, DC; 1995.
140. Bach MC, Bagwell SP, Knapp NP, et al. 9-(1,3-dihydroxy-2-propoxymethyl) guanine for cytomegalovirus infections in patients with the acquired immunodeficiency syndrome. *Ann Intern Med*. 1985;103:381.
141. Sha BE, Benson CA, Deutsch TA, et al. Suppression of cytomegalovirus retinitis in persons with AIDS with high-dose intravenous acyclovir. *J Infect Dis*. 1991;164:777–780.
142. Biron KK, Stanat SC, Sorrell JB, et al. Metabolic activation of the nucleoside analog 9-[[2-hydroxy-1-(hydroxymethyl) ethoxy]methyl] guanine in human diploid fibroblasts infected with human cytomegalovirus. *Proc Natl Acad Sci USA*. 1985;82:2473–2477.
143. Field AK, Daview ME, Dewitt C, et al. 9-[[2-hydroxy-1-

(hydroxymethyl)ethoxy]methyl] guanine: a selective inhibitor of herpes group virus replication. *Proc Natl Acad Sci USA*. 1983;80:4139–4143.
144. Anand R, Font RL, Fish RH, et al. Pathology of cytomegalovirus retinitis treated with sustained release intravitreal ganciclovir. *Ophthalmology*. 1993;100:1032–1039.
145. Jabs DA, Enger C, Bartlett JG. Cytomegalovirus retinitis and acquired immunodeficiency syndrome. *Arch Ophthalmol*. 1989;107:75–80.
146. Holland GN, Sidikaro Y, Kreiger AE, et al. Treatment of cytomegalovirus retinopathy with ganciclovir. *Ophthalmology*. 1987;94:815–823.
147. Jacobson MA, O'Donnell JJ, Porteous D, et al. Retinal and gastrointestinal disease due to cytomegalovirus in patients with the acquired immune deficiency syndrome: prevalence, natural history, and response to ganciclovir therapy. *Q J Med*. 1988;67:473–486.
148. Orellana J, Teich SA, Friedman AH, et al. Combined short- and long-term therapy for the treatment of cytomegalovirus retinitis using ganciclovir (BW B759U). *Ophthalmology*. 1987;94:831–838.
149. Studies of Ocular Complications of AIDS Research Group in collaboration with the AIDS Clinical Trials Group. Mortality in patients with the acquired immunodeficiency syndrome treated with either foscarnet or ganciclovir for cytomegalovirus retinitis. *N Engl J Med*. 1992;326:213–220.
150. Hoechst H, Dieterich D, Bozzette S, et al. Toxicity of combined ganciclovir and zidovudine for cytomegalovirus disease associated with AIDS. *Ann Intern Med*. 1990;113:111–117.
151. Studies of Ocular Complications of AIDS Research Group in collaboration with the AIDS Clinical Trials Group. Combination foscarnet and ganciclovir therapy vs monotherapy for the treatment of relapsed cytomegalovirus retinitis in patients with AIDS: the cytomegalovirus retreatment trial. *Arch Ophthalmol*. 1996;114:23–33.
152. Gross JG, Bozzette SA, Mathews WC, et al. Longitudinal study of cytomegalovirus retinitis in acquired immune

deficiency syndrome. *Ophthalmology*. 1990;97:681–686.
153. Spector SA, McKinley GF, Lalezari JP, et al. Oral ganciclovir for the prevention of cytomegalovirus disease in persons with AIDS. *N Engl J Med*. 1996;334:1491–1497.
154. Oral Ganciclovir European and Australian Cooperative Study Group. Intravenous vs oral ganciclovir: European/Australian comparative study of efficacy and safety in the prevention of cytomegalovirus retinitis recurrence in patients with AIDS. The Oral Ganciclovir European and Australian Cooperative Study Group. *AIDS*. 1995;9:471–477.
155. Jung D, Dorr A. Single-dose pharmacokinetics of valganciclovir in HIV- and CMV-seropositive subjects. *J Clin Pharmacol*. 1999;39:800–804.
156. Brown F, Banken L, Saywell K, et al. Pharmacokinetics of valganciclovir and ganciclovir following multiple oral dosages of valganciclovir in HIV- and CMV-seropositive volunteers. *Clin Pharmacokinet*. 1999;37:167–176.
157. Martin DF, Sierra-Madero J, Walmsley S, et al. A controlled trial of valganciclovir as induction therapy for cytomegalovirus retinitis. *N Engl J Med*. 2002;346:1119–1126.
158. Lalezari J, Lindley J, Walmsley S, et al. A safety study of oral valganciclovir maintenance treatment of cytomegalovirus retinitis. *J Acquir Immune Defic Syndr*. 2002;30:392–400.
159. Crumpacker CS. Mechanism of action of foscarnet against viral polymerases. *Am J Med*. 1992;92(Suppl. 2A):3–7.
160. Bergdahl S, Sonnerbor A, Larsson A, et al. Declining levels of HIV p24 antigen in serum during treatment with foscarnet. *Lancet*. 1988;1:1052.
161. Crumpacker CS, Kowalsky PN, Oliver SA, et al. Resistance of herpes simplex virus to 9-[[2-(hydroxymethyl) ethoxy]methyl] guanine (2-NDG); physical mapping of drug synergism within the viral DNA polymerase locus. *Proc Natl Acad Sci USA*. 1984;81:1556–1560.
162. Jacobson MA, Crowe S, Levy J, et al. Effect of foscarnet therapy on infection with human immunodeficiency virus in patients with AIDS. *J Infect Dis*. 1988;158:862–865.

163. Jacobson MA, Wulfsohn M, Feinberg JE, et al. Phase II dose-ranging trial of foscarnet salvage therapy for cytomegalovirus retinitis in AIDS patients intolerant of or resistant to ganciclovir (ACTG protocol 093). AIDS Clinical Trials Group of the National Institute of Allergy and Infectious Diseases. *AIDS*. 1994;8:451–459.
164. Studies of Ocular Complications of AIDS Research Group in collaboration with the AIDS Clinical Trials Group. Morbidity and toxic effects associated with ganciclovir or foscarnet therapy in a randomized cytomegalovirus retinitis trial. *Arch Intern Med*. 1995;155:65–74.
165. Studies of Ocular Complications of AIDS Research Group in collaboration with AIDS Clinical Trials Group. Antiviral effects of foscarnet and ganciclovir therapy on human immunodeficiency virus p24 antigen in patients with AIDS and cytomegalovirus retinitis. *J Infect Dis*. 1995;172:613–621.
166. Jabs DA. Controversies in the treatment of cytomegalovirus retinitis: foscarnet vs ganciclovir. *Infect Agents Dis*. 1995;4:131–142.
167. Deray G, Martinez F, Katlama C, et al. Foscarnet nephrotoxicity: mechanism, incidence, and prevention. *Am J Nephrol*. 1989;9:316–321.
168. Holland GN, Levinson RD, Jacobson MA. Dose-related difference in progression rates of cytomegalovirus retinopathy during foscarnet maintenance therapy. AIDS Clinical Trials Group Protocol 915 Team. *Am J Ophthalmol*. 1995;119:576–586.
169. Berthe P, Baudouin C, Garraffo R, et al. Toxicologic and pharmacokinetic analysis of intravitreal injections of foscarnet, either alone or in combination with ganciclovir. *Invest Ophthalmol Vis Sci*. 1994;35:1038–1045.
170. Palestine AG, Polis MA, De Smet MD, et al. A randomized controlled trial of foscarnet in the treatment of cytomegalovirus retinitis in patients with AIDS. *Ann Intern Med*. 1991;115:665–673.
171. Lalezari JP. Cidofovir: a new therapy for cytomegalovirus retinitis. *J Acquir Immune Defic Syndr*. 1997;14(Suppl. 1):22–26.

172. Lalezari JP, Stagg RJ, Kuppermann BD, et al. Intravenous cidofovir for peripheral cytomegalovirus retinitis in patients with AIDS: a randomized, controlled trial. *Ann Intern Med*. 1997;126:257–263.
173. Studies of Ocular Complications of AIDS Research Group in collaboration with the AIDS Clinical Trials Group. Long-term follow-up of patients with AIDS treated with parenteral cidofovir for cytomegalovirus: the HPMPC Peripheral Cytomegalovirus Retinitis Trial. *AIDS*. 2000;14:1571–1581.
174. Studies of Ocular Complications of AIDS Research Group in collaboration with the AIDS Clinical Trials Group. Parenteral cidofovir for cytomegalovirus retinitis in patients with AIDS: the HPMPC peripheral cytomegalovirus retinitis trial – a randomized, controlled trial. *Ann Intern Med*. 1997;126:264–274.
175. Rahhal FM, Arevalo JF, Chavez de la Paz E, et al. Treatment of cytomegalovirus retinitis with intravitreous cidofovir in patients with AIDS: a preliminary report. *Ann Intern Med*. 1996;125:98–103.
176. Davis JL, Taskintuna I, Freeman WR, et al. Iritis and hypotony after treatment with intravenous cidofovir for cytomegalovirus retinitis. *Arch Ophthalmol*. 1997;115:733–737.
177. Kirsch LS, Arevalo JF, Chavez de la Paz E, et al. Intravitreal cidofovir (HPMPC) treatment of cytomegalovirus retinitis in patients with acquired immune deficiency syndrome. *Ophthalmology*. 1995;102:533–543.
178. Rahhal FM, Arevalo JF, Munguia D, et al. Intravitreal cidofovir for the maintenance treatment of cytomegalovirus retinitis. *Ophthalmology*. 1996;103:1078–1083.
179. Jabs DA, Dunn JP, Enger C, et al. Cytomegalovirus retinitis and viral resistance: prevalence of resistance at diagnosis, 1994. Cytomegalovirus Retinitis and Viral Resistance Study Group. *Arch Ophthalmol*. 1996;114:809–814.
180. Jabs DA, Enger C, Dunn JP, et al. Cytomegalovirus retinitis and viral resistance: 4. Ganciclovir resistance. *J Infect Dis*. 1998;177:770–773.

181. Drew WL, Stempton MJ, Andrews J, et al. Cytomegalovirus (CMV) resistance in patients with CMV retinitis and AIDS treated with oral or intravenous ganciclovir. *J Infect Dis*. 1999;179:1352–1355.
182. Jabs DA, Enger C, Forman M, et al. Incidence of foscarnet resistance and cidofovir resistance in patients treated for cytomegalovirus retinitis. The Cytomegalovirus Retinitis and Viral Resistance Study Group. *Antimicrob Agents Chemother*. 1998;42:2240–2241.
183. Boivin G, Gilbert C, Gaudreau A, et al. Rate of emergence of cytomegalovirus (CMV) mutations in leukocytes of patients with acquired immunodeficiency syndrome who are receiving valganciclovir as induction and maintenance therapy for CMV retinitis. *J Infect Dis*. 2001;184:1598–1602.
184. Drew WL, Miner RC, Saleh E, et al. Antiviral susceptibility of cytomegalovirus: criteria for detecting resistance to antivirals. *Clin Diagn Virol*. 1993;1:179–185.
185. Landry ML, Stanat S, Biron K, et al. A standardized plaque reduction assay for determination of drug susceptibilities of cytomegalovirus clinical isolates. *Antimicrob Agents Chemother*. 2000;44:688–692.
186. Cihlar T, Fuller MD, Cherrington JM. Characterization of drug resistance-associated mutations in the human cytomegalovirus DNA polymerase gene by using recombinant mutant viruses generated from overlapping DNA fragments. *J Virol*. 1998;72:5927–5936.
187. Weinberg A, Jabs DA, Chou S, et al. Mutations conferring foscarnet resistance in a cohort of patients with acquired immunodeficiency syndrome and cytomegalovirus retinitis. *J Infect Dis*. 2003;187:777–784.
188. Spector SA, Hsia K, Wolf D, et al. Molecular detection of human cytomegalovirus and determination of genotypic ganciclovir resistance in clinical specimens. *Clin Infect Dis*. 1995;21(Suppl. 2):S170–3.
189. Erice A. Resistance of human cytomegalovirus to antiviral drugs. *Clin Microbiol Rev*. 1999;12:286–297.
190. Smith KL, Cherrington JM, Jiles RE, et al. High-level resistance of cytomegalovirus to ganciclovir is associated

with alterations in both the UL97 and DNA polymerase genes. *J Infect Dis*. 1997;176:69–77.
191. Chou S, Lurain NS, Weinberg A, et al. Interstrain variation in the human cytomegalovirus DNA polymerase sequence and its effect on the genotypic diagnosis of antiviral drug resistance. *Antimicrob Agents Chemother*. 1999;43:1500–1502.
192. Chou S, Marousek G, Parenti DM, et al. Mutation in region III of the DNA polymerase gene conferring foscarnet resistance in cytomegalovirus isolates from 3 subjects receiving prolonged antiviral therapy. *J Infect Dis*. 1998;178:526–530.
193. Gilbert C, Bestman-Smith J, Boivin G. Resistance of herpesvirus to antiviral drugs: clinical impacts and molecular mechanisms. *Drug Resist Update*. 2002;5:88–114.
194. Hu H, Jabs DA, Forman MS, et al. Comparison of cytomegalovirus (CMV) UL97 gene sequences in the blood and vitreous of patients with acquired immunodeficiency syndrome and CMV retinitis. *J Infect Dis*. 2002;185:861–867.
195. Arevalo JF, Gonzalez C, Capparelli EV, et al. Intravitreous and plasma concentrations of ganciclovir and foscarnet after intravenous therapy in patients with AIDS and cytomegalovirus. *J Infect Dis*. 1995;172:951–956.
196. Jabs DA, Martin BK, Forman MS, et al. Cytomegalovirus resistance to ganciclovir and clinical outcomes of patients with cytomegalovirus retinitis. *Am J Ophthalmol*. 2003;135:26–34.
197. Kuppermann BD, Flores-Aguilar M, Quiceno J, et al. Combination ganciclovir and foscarnet therapy in the treatment of clinically resistant cytomegalovirus retinitis in patients with the acquired immune deficiency syndrome. *Am J Ophthalmol*. 1993;111:1359–1366.
198. Walton RC, Whitcup SM, Mueller BU, et al. Combined intravenous ganciclovir and foscarnet for children with recurrent cytomegalovirus retinitis. *Ophthalmology*. 1995;102:1865–1870.
199. Desatnik HR, Foster RE, Lowder CY. Treatment of clinically resistant cytomegalovirus retinitis with combined intravitreal injections of ganciclovir and foscarnet. *Am J*

Ophthalmol. 1996;122:121–123.
200. Hodge WG, Lalonde RG, Sampalis J, et al. Once-weekly intraocular injections of ganciclovir for maintenance therapy of cytomegalovirus retinitis: clinical and ocular outcome. *J Infect Dis*. 1996;174:393–396.
201. Montero MC, Pastor M, Buenestado C, et al. Intravitreal ganciclovir for cytomegalovirus retinitis in patients with AIDS. *Ann Pharmacother*. 1996;30:717–723.
202. Young S, Morlet N, Besen G, et al. High-dose (2000-microgram) intravitreous ganciclovir in the treatment of cytomegalovirus retinitis. *Ophthalmology*. 1998;105:1404–1410.
203. Baudouin C, Chassain C, Caujolle C, et al. Treatment of cytomegalovirus retinitis in AIDS patients using intravitreal injections of highly concentrated ganciclovir. *Ophthalmologica*. 1996;210:329–335.
204. Tognon MS, Turrini B, Masiero G, et al. Intravitreal and systemic foscarnet in the treatment of AIDS-related CMV retinitis. *Eur J Ophthalmol*. 1996;6:179–182.
205. Diaz-Llopis M, Espana E, Munoz G, et al. High dose intravitreal foscarnet in the treatment of cytomegalovirus retinitis in AIDS. *Br J Ophthalmol*. 1994;78:120–124.
206. Sandorn GE, Anand R, Torti RE, et al. Sustained-release ganciclovir therapy for treatment of cytomegalovirus retinitis: use of an intravitreal device. *Arch Ophthalmol*. 1992;110:188–195.
207. Martin DF, Parks DJ, Mellow SD, et al. Treatment of cytomegalovirus retinitis with an intraocular sustained-release ganciclovir implant: a randomized controlled clinical trial [see comments]. *Arch Ophthalmol*. 1994;112:1531–1539.
208. Marx JL, Kapusta MA, Patel SS, et al. Use of the ganciclovir implant in the treatment of recurrent cytomegalovirus retinitis. *Arch Ophthalmol*. 1996;114:815–820.
209. Martin DF, Ferris FL, Brothers RJ, et al. Retinal detachment in eyes treated with a ganciclovir implant [Letter]. *Arch Ophthalmol*. 1995;113:1355.
210. Martin DF, Dunn JP, Davis JL, et al. Use of the ganciclovir

implant for the treatment of cytomegalovirus retinitis in the era of potent antiretroviral therapy: recommendations of the International AIDS Society – USA panel. *Am J Ophthalmol*. 1999;127:329–339.
211. Kempen JH, Jabs DA, Dunn JP, et al. Retinal detachment risk in cytomegalovirus retinitis related to the acquired immunodeficiency syndrome. *Arch Ophthalmol*. 2001;119:33–40.
212. Shane TS, Martin DF. Endophthalmitis after ganciclovir implant in patients with AIDS and cytomegalovirus retinitis. *Am J Ophthalmol*. 2003;136:649–654.
213. Kirsch LS, Arevalo JF, De Clercq E, et al. Phase I/II study of intravitreal cidofovir for the treatment of cytomegalovirus retinitis in patients with the acquired immunodeficiency syndrome. *Am J Ophthalmol*. 1995;119:466–476.
214. Banker AS, Arevalo JF, Munguia D, et al. Intraocular pressure and aqueous humor dynamics in patients with AIDS treated with intravitreal cidofovir (HPMPC) for cytomegalovirus retinitis. *Am J Ophthalmol*. 1997;124:168–180.
215. Besen B, Flores-Aguilar M, Assil KK, et al. Long-term therapy for herpes retinitis in an animal model with high-concentrated liposome-encapsulated HPMPC. *Arch Ophthalmol*. 1995;113:661–668.
216. Kirsch LS, Arevalo JF, Chavez de la Paz E, et al. Intravitreal cidofovir (HPMPC) treatment of cytomegalovirus retinitis in patients with acquired immune deficiency syndrome [published erratum appears in Ophthalmology 102:702, 1995]. *Ophthalmology*. 1995;102:533–542 [discussion 542–3].
217. Taskintuna I, Rahhal FM, Arevalo JF, et al. Low-dose intravitreal cidofovir (HPMPC) therapy of cytomegalovirus retinitis in patients with acquired immune deficiency syndrome. *Ophthalmology*. 1997;104:1049–1057.
218. Arevalo JF, Munguia D, Faber D, et al. Correlation between intraocular pressure and CD4 T-lymphocyte counts in patients with human immunodeficiency virus with and without cytomegalovirus retinitis. *Am J Ophthalmol*. 1996;122:91–96.

219. Azad RF, Driver VB, Tanaka K, et al. Antiviral activity of a phosphorothioate oligonucleotide complementary to RNA of the human cytomegalovirus major immediate-early region. *Antimicrob Agents Chemother*. 1993;37:1945–1954.
220. Anderson KP, Fox MC, Brown-Driver V, et al. Inhibition of human cytomegalovirus immediate-early gene expression by an antisense oligonucleotide complementary to immediate-early RNA. *Antimicrob Agents Chemother*. 1996;40:2004–2011.
221. The Vitravene Study Group. A randomized controlled clinical trial of intravitreous fomivirsen for treatment of newly diagnosed peripheral cytomegalovirus retinitis in patients with AIDS. *Am J Ophthalmol*. 2002;133:467–474.
222. Freeman WR. Retinal toxic effects associated with intravitreal fomivirsen. *Arch Ophthalmol*. 2001;119:458.
223. The Vitravene Study Group. Randomized dose-comparison studies of intravitreous fomivirsen for treatment of cytomegalovirus retinitis that has reactivated or is persistently active despite other therapies in patients with AIDS. *Am J Ophthalmol*. 2002;133:475–483.
224. The Vitravene Study Group. Safety of intravitreous fomivirsen for treatment of cytomegalovirus retinitis patients with AIDS. *Am J Ophthalmol*. 2002;133:484–498.
225. Jabs DA, Griffiths PD. Fomivirsen for the treatment of cytomegalovirus retinitis. *Am J Ophthalmol*. 2002;133:552–556.
226. Kempen JH, Jabs DA, Wilson LA, et al. Risk of vision loss in patients with cytomegalovirus retinitis and the acquired immunodeficiency syndrome. *Arch Ophthalmol*. 2003;121:466–476.
227. Freeman WR, Friedberg DN, Berry C, et al. Risk factors for development of rhegmatogenous retinal detachment in patients with cytomegalovirus retinitis. *Am J Ophthalmol*. 1993;116:713–720.
228. Studies of Ocular Complications of AIDS (SOCA) Research Group in Collaboration with the AIDS Clinical Trials Group (ACTG). Rhegmatogenous retinal detachment in patients with cytomegalovirus retinitis. Foscarnet–Ganciclovir

Cytomegalovirus Retinitis Trial. *Am J Ophthalmol*. 1997;124:61–70.
229. Broughton WL, Cupples HP, Parver LM. Bilateral retinal detachment following cytomegalovirus retinitis. *Arch Ophthalmol*. 1978;96:618–624.
230. Freeman WR, Henderly DE, Wan WL. Rhegmatogenous retinal detachment in treated cytomegalovirus retinitis: prevalence, pathophysiology, and treatment. *Am J Ophthalmol*. 1987;103:527–536.
231. Sidikaro Y, Silver L, Holland GN, et al. Rhegmatogenous retinal detachments in patients with AIDS and necrotizing retinal infections. *Ophthalmology*. 1991;98:129–135.
232. Irvine AR. Treatment of retinal detachment due to cytomegalovirus retinitis in patients with AIDS. *Trans Am Ophthalmol Soc*. 1991;89:349–363.
233. Freeman WR, Quiceno JI, Crapotta JA, et al. Surgical repair of rhegmatogenous retinal detachment in immunosuppressed patients with cytomegalovirus retinitis. *Ophthalmology*. 1992;99:466–474.
234. Kozak I, Vaidya V, van Natta ML, et al. The prevalence and incidence of epiretinal membranes in eyes with inactive extramacular CMV retinitis. *Invest Ophthalmol Vis Sci*. 2014;55(7):4304–4312.
235. Freeman WR. Retinal detachment in cytomegalovirus retinitis: should our approach be changed? *Retina*. 1999;19:27–33.
236. Sandy CJ, Bloom PA, Graham EM, et al. Retinal detachment in AIDS-related cytomegalovirus retinitis. *Eye (Lond)*. 1995;9:277–281.
237. Regillo CD, Vander JF, Duker JS, et al. Repair of retinitis-related retinal detachments with silicone oil in patients with acquired immunodeficiency syndrome. *Am J Ophthalmol*. 1992;113:21–27.
238. Freeman WR. Application of vitreoretinal surgery to inflammatory and infectious diseases of the posterior segment. *Int Ophthalmol Clin*. 1992;32:15–33.
239. Nasemann JE, Mutsch A, Wiltfang R, et al. Early pars plana vitrectomy without buckling procedure in cytomegalovirus

retinitis-induced retinal detachment. *Retina*. 1995;15:111–116.
240. Garcia RF, Flores-Aguilar M, Quiceno JI, et al. Results of rhegmatogenous retinal detachment repair in cytomegalovirus retinitis with and without scleral buckling. *Ophthalmology*. 1995;102:236–245.
241. Davis JL, Chuang EL. Management of retinal detachment associated with CMV retinitis in AIDS patients. *Eye (Lond)*. 1992;6:28–34.
242. Tanna AP, Kempen JH, Dunn JP. Incidence and management of cataract after retinal detachment repair with silicone oil in immune compromised patients with cytomegalovirus retinitis. *Am J Ophthalmol*. 2003;136:1009–1015.
243. Irvine AR, Lonn L, Schwartz D, et al. Retinal detachment in AIDS: long-term results after repair with silicone oil. *Br J Ophthalmol*. 1997;81:180–183.
244. Meldrum ML, Aaberg TM, Patel A, et al. Cataract extraction after silicone oil repair of retinal detachments due to necrotizing retinitis. *Arch Ophthalmol*. 1996;114:885–892.
245. Azen SP, Scott IU, Flynn HW Jr, et al. Silicone oil in the repair of complex retinal detachments. A prospective observational multicenter study. *Ophthalmology*. 1998;105:1587–1597.
246. Karavellas MP, Song M, MacDonald JC, et al. Long-term posterior and anterior segment complications of immune recovery uveitis associated with cytomegalovirus retinitis. *Am J Ophthalmol*. 2000;130:57–64.
247. Baumal CR, Reichel E. Management of cytomegalovirus-related rhegmatogenous retinal detachments. *Ophthalmic Surg Lasers*. 1998;29:916–925.
248. Althaus C, Loeffler KU, Schimkat M, et al. Prophylactic argon laser coagulation for rhegmatogenous retinal detachment in AIDS patients with cytomegalovirus retinitis. *Graefes Arch Clin Exp Ophthalmol*. 1998;236:359–364.
249. Davis JL, Hummer J, Feuer WJ. Laser photocoagulation for retinal detachment and retinal tears in cytomegalovirus retinitis. *Ophthalmology*. 1997;104:2053–2060 [discussion

2060–1].
250. McCluskey P, Grigg J, Playfair TJ. Retinal detachments in patients with AIDS and CMV retinopathy: a role for laser photocoagulation. *Br J Ophthalmol*. 1995;79:153–156.
251. Meffert SA, Ai E. Laser photocoagulation prophylaxis for CMV retinal detachments. *Ophthalmology*. 1998;105:1353–1355.
252. Finzi D, Hermankova M, Pierson T, et al. Identification of a reservoir for HIV-1 in patients on highly active antiretroviral therapy. *Science*. 1997;278:1295–1300.
253. Kempen JH, Martin BK, Wu AW, et al. The effect of cytomegalovirus retinitis on the quality of life of patients with AIDS in the era of highly active antiretroviral therapy. *Ophthalmology*. 2003;110:987–995.
254. Palella FJ Jr, Delaney KM, Moorman AC, et al. Declining morbidity and mortality among patients with advanced human immunodeficiency virus infection. HIV Outpatient Study Investigators. *N Engl J Med*. 1998;338:853–860.
255. Varani S, Spezzacatena P, Manfredi R, et al. The incidence of cytomegalovirus (CMV) antigenemia and CMV disease is reduced by highly active antiretroviral therapy. *Eur J Epidemiol*. 2000;16:433–437.
256. Deayton JR, Wilson P, Sabin CA, et al. Changes in the natural history of cytomegalovirus retinitis following the introduction of highly active antiretroviral therapy. *AIDS*. 2000;14:1163–1170.
257. MacDonald JC, Torriani FJ, Morse LS, et al. Lack of reactivation of cytomegalovirus (CMV) retinitis after stopping CMV maintenance therapy in AIDS patients with sustained elevations in CD4 T cells in response to highly active antiretroviral therapy. *J Infect Dis*. 1998;177:1182–1187.
258. Jabs DA, Bolton SG, Dunn JP, et al. Discontinuing anticytomegalovirus therapy in patients with immune reconstitution after combination antiretroviral therapy. *Am J Ophthalmol*. 1998;126:817–822.
259. MacDonald JC, Karavellas MP, Torriani FJ, et al. Highly active antiretroviral therapy-related immune recovery in

AIDS patients with cytomegalovirus retinitis. *Ophthalmology*. 2000;107:877–881.
260. Curi AL, Muralha A, Muralha L, et al. Suspension of anticytomegalovirus maintenance therapy following immune recovery due to highly active antiretroviral therapy. *Br J Ophthalmol*. 2001;85:471–473.
261. Whitcup SM, Fortin E, Lindblad AS, et al. Discontinuation of anticytomegalovirus therapy in patients with HIV infection cytomegalovirus. *JAMA*. 1999;282:1633–1671.
262. Vrabec TR, Baldassano VF, Whitcup SM. Discontinuation of maintenance therapy in patients with quiescent cytomegalovirus retinitis and elevated CD4 counts. *Ophthalmology*. 1998;105:1259–1264.
263. Miller CJ, Baker JV, Bomann AM, et al. Adjudicated morbidity and mortality outcomes by age among individuals with HIV infection on suppressive antiretroviral therapy. *PLoS ONE*. 2014;9(4):e95061.
264. Michelet C, Arvieux C, Francois C, et al. Opportunistic infections occurring during highly active antiretroviral treatment. *AIDS*. 1998;12:1815–1822.
265. Jacobson MA, Zegans M, Pavan PR, et al. Cytomegalovirus retinitis after initiation of highly active antiretroviral therapy. *Lancet*. 1997;349:1443–1445.
266. Walker NF, Scriven J, Meintjes G, et al. Immune reconstitution inflammatory syndrome in HIV-infected patients. *HIV AIDS (Auckl)*. 2015;7:49–64.
267. Karavellas MP, Lower CY, Macdonald JC, et al. Immune recovery vitreitis associated with inactive cytomegalovirus retinitis: a new syndrome. *Arch Ophthalmol*. 1998;116:169–175.
268. Otiti-Sengeri J, Meenken C, van den Horn GJ, et al. Ocular immune reconstitution inflammatory syndromes. *Curr Opin HIV AIDS*. 2008;3:432–437.
269. Holland GN. Pieces of a puzzle: toward better understanding of intraocular inflammation associated with human immunodeficiency virus infection. *Am J Ophthalmol*. 1998;125:383–385.
270. Zegans ME, Walton RC, Holland GN, et al. Transient

vitreous inflammatory reactions associated with combination antiretroviral therapy in patients with AIDS and cytomegalovirus retinitis. *Am J Ophthalmol*. 1998;125:292–300.
271. Holland GN. Immune recovery uveitis. *Ocul Immunol Inflamm*. 1999;7:215–221.
272. Karavellas MP, Plummer DJ, Macdonald JC, et al. Incidence of immune recovery vitreitis in cytomegalovirus retinitis patients following institution of successful highly active antiretroviral therapy. *J Infect Dis*. 1999;179:697–700.
273. Nguyen QD, Kempen JH, Bolton SG, et al. Immune recovery uveitis in patients with AIDS and cytomegalovirus retinitis after highly active antiretroviral therapy. *Am J Ophthalmol*. 2000;129:634–639.
274. Jabs DA, Van Natta ML, Kempen JH, et al. Characteristics of patients with cytomegalovirus retinitis in the era of highly active antiretroviral therapy. *Am J Ophthalmol*. 2002;133:48–61.
275. Arevalo JF, Mendoza AJ, Ferretti Y. Immune recovery uveitis in AIDS patients with cytomegalovirus retinitis treated with highly active antiretroviral therapy in Venezuela. *Retina*. 2003;23:495–502.
276. Karavellas MP, Azen SP, Macdonald JC, et al. Immune recovery vitreitis in AIDS: clinical predictors, sequella, and treatment outcomes. *Retina*. 2001;21:1–9.
277. Song M, Azen SP, Buley A, et al. Effect of anti-cytomegalovirus therapy on the incidence of immune recovery uveitis in AIDS patients with healed cytomegalovirus retinitis. *Am J Ophthalmol*. 2003;136:696–702.
278. Newsome R, Casswell T, O'Moore E, et al. Cystoid macular oedema in patients with AIDS and cytomegalovirus retinitis on highly active antiretroviral therapy. *Br J Ophthalmol*. 1998;82:456–457.
279. Silverstein BE, Smith JH, Sykes SO, et al. Cystoid macular edema associated with cytomegalovirus retinitis in patients with acquired immunodeficiency syndrome. *Am J Ophthalmol*. 1998;125:412–415.

280. Whitcup SM. Cytomegalovirus retinitis in the era of highly active antiretroviral therapy. *JAMA*. 2000;283:653–657.
281. Karavellas MP, Song MK, Macdonald JC, et al. Long-term posterior and anterior segment complications of immune recovery uveitis associated with cytomegalovirus retinitis. *Am J Ophthalmol*. 2000;130:57–64.
282. Sanislo SR, Lowder CY, Kaiser PK. Optic nerve head neovascularization in a patient with inactive cytomegalovirus retinitis and immune recovery. *Am J Ophthalmol*. 1998;126:318–320.
283. Canzano JC, Reed JB, Morse LS. Vitreomacular traction syndrome following highly active antiretroviral therapy in AIDS patients with cytomegalovirus retinitis. *Retina*. 1998;18:443–447.
284. Robinson MR, Csasky KG, Lee SS, et al. Fibrovascular changes misdiagnosed as cytomegalovirus retinitis reactivation in a patient with immune recovery. *Clin Infect Dis*. 2004;38:139–141.
285. Biswas J, Choudhry S, Kumarasamy, et al. Immune recovery vitreitis presenting as panuveitis following therapy with protease inhibitors. *Indian J Ophthalmol*. 2000;48:313–315.
286. Goldberg DE, Freeman WR. Uveitic angle closure glaucoma in a patient with inactive cytomegalovirus and immune recovery uveitis. *Ophthalmic Surg Lasers*. 2002;33:421–425.
287. Goldberg DE, Wang H, Azen SP, et al. Long term visual outcome of patients with cytomegalovirus retinitis treated with highly active antiretroviral therapy. *Br J Ophthalmol*. 2003;87:853–855.
288. Kuppermann BD, Holland GN. Immune recovery uveitis. *Am J Ophthalmol*. 2000;130:103–106.
289. Urban B, Bakunowicz-Lazarcyk A, Michalczuk M. Immune recovery uveitis: pathogenesis, clinical symptoms, and treatment. *Mediators Inflamm*. 2014;2014:971417.
290. D'Alessandro L, Bottaro E. Reactivation of CMV retinitis after treatment with subtenon corticosteroids for immune recovery uveitis in patients with AIDS. *Scand J Infect Dis*. 2002;34:780–782.

291. Morrison VL, Kozak I, LaBree LD, et al. Intravitreal triamcinolone acetate for the treatment of immune recovery uveitis macular edema. *Ophthalmology*. 2007;114(2):334–339.
292. Shah AM, Oster SF, Freeman WR. Viral retinitis after intravitreal triamcinolone injection in patients with predisposing medical comorbidities. *Am J Ophthalmol*. 2010;149(3):433–440.
293. Maguire AM, Nichols CW, Crooks GW. Visual loss in cytomegalovirus retinitis caused by cystoid macular edema in patients without the acquired immune deficiency. *Ophthalmology*. 1996;103:601–605.
294. Omerod LD, Larkin JA, Margo CA, et al. Rapidly progressive herpetic retinal necrosis: a blinding disease characteristic of advanced AIDS. [see commentary by C.L. Lowder, pp. 46–47]. *Clin Infect Dis*. 1998;26:34–35.
295. Stewart MW. Herpetic (non-cytomegalovirus) retinal infections in patients with the acquired immunodeficiency syndrome. *Curr HIV Res*. 2013;11(3):210–219.
296. Duker JS, Blumenkranz MS. Diagnosis and management of the acute retinal necrosis (ARN) syndrome. *Surv Ophthalmol*. 1991;35:327–343.
297. Friedlander S, Rahhal FM, Ericson L, et al. Optic neuropathy preceding acute retinal necrosis in acquired immunodeficiency syndrome. *Arch Ophthalmol*. 1996;114:1481–1485.
298. Culbertson WW, Atherton SS. Acute retinal necrosis and similar retinitis syndromes. *Int Ophthalmol Clin*. 1993;33:129–143.
299. Sellitti TP, Huang AJ, Schiffman J, et al. Association of herpes zoster ophthalmicus with acquired immunodeficiency syndrome and acute retinal necrosis. *Am J Ophthalmol*. 1993;116:297–301.
300. Takase H, Okada AA, Goto H, et al. Development and validation of new diagnostic criteria for acute retinal necrosis. *Jpn J Ophthalmol*. 2015;59(1):14–20.
301. Abe T, Tsuchida K, Tamai M. A comparative study of the polymerase chain reaction and local antibody production in acute retinal necrosis syndrome and cytomegalovirus

retinitis. *Graefes Arch Clin Exp Ophthalmol*. 1996;234:419–424.
302. Weinberg DV, Lyon AT. Repair of retinal detachments due to herpes varicella-zoster virus retinitis in patients with acquired immune deficiency syndrome. *Ophthalmology*. 1997;104:279–282.
303. Schlingemann RO, Bruinenberg M, Wertheim-Van Dillen P, et al. Twenty years' delay of fellow eye involvement in herpes simplex virus type 2-associated bilateral acute retinal necrosis syndrome. *Am J Ophthalmol*. 1996;122:891–892.
304. Aslanides IM, De Souza S, Wong DTW, et al. Oral valacyclovir in the treatment of acute retinal necrosis syndrome. *Retina*. 2002;22:352–354.
305. Chatis PA, Miller CH, Schrager LE, et al. Successful treatment with foscarnet of an acyclovir-resistant mucocutaneous infection with herpes simplex virus in a patient with the acquired immunodeficiency syndrome. *N Engl J Med*. 1989;320:297–300.
306. Pavesio CE, Mitchell SM, Barton K, et al. Progressive outer retinal necrosis (PORN) in AIDS patients: a different appearance of varicella-zoster retinitis. *Eye (Lond)*. 1995;9:271–276.
307. Engstrom RJ, Holland GN, Margolis TP, et al. The progressive outer retinal necrosis syndrome. A variant of necrotizing herpetic retinopathy in patients with AIDS. *Ophthalmology*. 1994;101:1488–1502.
308. Scott IU, Luu KM, Davis JL. Intravitreal antivirals in the management of patients with acquired immunodeficiency syndrome with progressive outer retinal necrosis. *Arch Ophthalmol*. 2002;120:1219–1222.
309. Ciulla TA, Rutledge BK, Morley MG, et al. The progressive outer retinal necrosis syndrome: successful treatment with combination antiviral therapy. *Ophthalmic Surg Lasers*. 1998;29:198–206.
310. Margolis TP, Lowder CY, Holland GN, et al. Varicella-zoster virus retinitis in patients with the acquired immunodeficiency syndrome. *Am J Ophthalmol*. 1991;112:119–131.

311. Spaide RF, Martin DF, Teich SA, et al. Successful treatment of progressive outer retinal necrosis syndrome. *Retina*. 1996;16:479–487.
312. Meffert SA, Kertes PJ, Lim P, et al. Successful treatment of progressive outer retinal necrosis using high-dose intravitreal ganciclovir. *Retina*. 1997;17:560–562.
313. Perez-Blasquez E, Traspas R, Marin IM, et al. Intravitreal ganciclovir treatment in progressive outer retinal necrosis. *Am J Ophthalmol*. 1997;124:418–421.
314. Kim SJ, Equi R, Belair ML, et al. Long-term preservation of vision in progressive outer retinal necrosis treated with combination antiviral drugs and highly active antiretroviral therapy. *Ocul Immunol Inflamm*. 2007;15:425–427.
315. Kaplan JE, Benson C, Holmes KK, et al. Guidelines for Prevention and Treatment of Opportunistic Infections in HIV-Infected Adults and Recommendations of the U.S. Public Health Service and the Infectious Disease Society of America. *MMWR Recomm Rep*. 2009;58(RR04):1–198.
316. Macher AM, Bardenstein DS, Zimmerman LE. *Pneumocystis carinii* choroiditis in a male homosexual with AIDS and disseminated pulmonary and extrapulmonary *P. carinii* infection. *N Engl J Med*. 1987;236:1092.
317. Freeman WR, Gross JG, Labelle J, et al. *Pneumocystis carinii* choroidopathy: a new clinical entity. *Arch Ophthalmol*. 1989;107:863–867.
318. Shami MJ, Freeman WR, Friedberg D, et al. A multicenter study of pneumocystis choroidopathy. *Am J Ophthalmol*. 1991;112:15–22.
319. Centers for Disease Control and Prevention. *HIV/AIDS surveillance report*. 1999:2–38 [11].
320. Dugel PU, Rao NA, Forster DJ, et al. *Pneumocystis carinii* choroiditis after long-term aerosolized pentamidine therapy. *Am J Ophthalmol*. 1990;110:113–117.
321. Foster RE, Lowder CY, Meisler DM, et al. Presumed *Pneumocystis carinii* choroiditis: unifocal presentation, regression with intravenous pentamidine, and choroiditis recurrence. *Ophthalmology*. 1991;98:1360–1365.
322. Sneed SR, Blodi CF, Berger BB, et al. *Pneumocystis carinii*

choroiditis in patients receiving inhaled pentamidine. *N Engl J Med*. 1989;322:936–937.
323. Gagliuso DJ, Teich SA, Friedman AH, et al. Ocular toxoplasmosis in AIDS patients. *Trans Am Ophthalmol Soc*. 1990;88:63–66 [discussion 86-88].
324. Parke DW II, Font RL. Diffuse toxoplasmic retinochoroiditis in a patient with AIDS. *Arch Ophthalmol*. 1986;104:571–575.
325. Heinemann MH, Gold JMW, Maisel J. Bilateral toxoplasma retinochoroiditis in a patient with acquired immune deficiency syndrome. *Retina*. 1986;6:224.
326. Cochereau-Massin I, LeHoang P, Lautier-Frau M, et al. Ocular toxoplasmosis in human immunodeficiency virus-infected patients. *Am J Ophthalmol*. 1992;114:130–135.
327. Elkins BS, Holland GN, Opremcak EM, et al. Ocular toxoplasmosis misdiagnosed as cytomegalovirus retinopathy in immunocompromised patients. *Ophthalmology*. 1994;101:499–507.
328. Berger BB, Egwuagu CE, Freeman WR, et al. Miliary toxoplasmic retinitis in acquired immunodeficiency syndrome. *Arch Ophthalmol*. 1993;111:373–376.
329. Cano-Parra JL, Diaz-Llopis ML, Cordoba JL, et al. Acute iridocyclitis in a patient with AIDS diagnosed as toxoplasmosis by PCR. *Ocul Immunol Inflamm*. 2000;8:127–130.
330. Moshfeghi DM, Dodds EM, Couto CA, et al. Diagnostic approaches to severe, atypical toxoplasmosis mimicking acute retinal necrosis. *Ophthalmology*. 2004;111:716–725.
331. Moorthy RS, Smith RE, Rao NA. Progressive ocular toxoplasmosis in patients with acquired immunodeficiency syndrome. *Am J Ophthalmol*. 1993;115:742–747.
332. Holland GN. Ocular toxoplasmosis: a global reassessment. Part II: Disease manifestations and management. *Am J Ophthalmol*. 2004;137:1–17.
333. Holland GN. Ocular toxoplasmosis: a global reassessment. Part I: Epidemiology and course of disease. *Am J Ophthalmol*. 2003;136:973–988.
334. Grossniklaus HE, Specht CS, Allaire G, et al. *Toxoplasma gondii* retinochoroiditis and optic neuritis in acquired

immune deficiency syndrome. Report of a case. *Ophthalmology*. 1990;97:1342–1346.
335. Rehder JR, Burnier MBJ, Pavesio CE, et al. Acute unilateral toxoplasmic iridocyclitis in an AIDS patient. *Am J Ophthalmol*. 1988;106:740–741.
336. Torre D, Casari S, Speranza F, et al. Randomized trial of trimethoprim–sulfamethoxazole versus pyrimethamine–sulfadiazine for therapy of toxoplasmic encephalitis in patients with AIDS. *Antimicrob Agents Chemother*. 1998;2:1346–1349.
337. Jacobson JM, Hafner R, Remington J, et al. Dose-escalation, phase I/II study of azithromycin and pyrimethamine for the treatment of toxoplasmic encephalitis in AIDS. *AIDS*. 2001;15:583–589.
338. Bosch-Driessen LH, Verbraak FD, Suttorp-Schulten MSA, et al. A prospective, randomized trial of pyrimethamine and azithromycin vs pyrimethamine and sulfadiazine for the treatment of ocular toxoplasmosis. *Am J Ophthalmol*. 2002;134:34–40.
339. Pearson PA, Piracha AR, Sen H, et al. Atovaquone for the treatment of toxoplasma retinochoroiditis in immunocompetent patients. *Ophthalmology*. 1999;106:148–153.
340. Friedman AH. The retinal lesions of the acquired immune deficiency syndrome. *Trans Am Ophthalmol Soc*. 1984;82:447–491.
341. Edwards JE, Foos RY, Montomerie JZ, et al. Ocular manifestations of candida septicemia: review of seventy-six cases of hematogenous candida endophthalmitis. *Medicine (Baltimore)*. 1974;53:47–75.
342. Rex JH, Bennet JE, Sugar AM, et al. A randomized trial comparing fluconazole with amphoteracin B for the treatment of candidemia in patients without neutropenia. *N Engl J Med*. 1994;331:1325–1330.
343. Panther LA, Sande MA. Cryptococcal meningitis in AIDS. Sande MA, Volberding PA. *The medical management of AIDS*. 2nd ed. WB Saunders: Philadelphia; 1997.
344. Shields JA, Wright DM, Augsburger JJ, et al. Cryptococcal

chorioretinitis. *Am J Ophthalmol*. 1980;89:210.
345. Wykoff CA, Albini TA, Couvillion SS, et al. Intraocular cryptococcoma. *Arch Ophthalmol*. 2009;127(5):700–702.
346. Wheat LJ, Connolly-Stringfield PA, Baker RL, et al. Disseminated histoplasmosis in the acquired immune deficiency syndrome: clinical findings, diagnosis and treatment, and review of the literature. *Medicine (Baltimore)*. 1990;69:361–374.
347. Wheat J, Hafner R, Wulfsohn M, et al. Prevention of relapse of histoplasmosis with itraconazole in patients with the acquired immunodeficiency syndrome. *Ann Intern Med*. 1993;118:610–616.
348. Gonzales CA, Scott IU, Chaudhry NA, et al. Endogenous endophthalmitis caused by *Histoplasma capsulatum* var. *capsulatum*: a case report and literature review. *Ophthalmology*. 2000;107:725–729.
349. Ala-Kauhaluoma M, Aho I, Ristola M, et al. Involvement of intraocular structures in disseminated histoplasmosis. *Acta Ophthalmol*. 2010;88(4):493–496.
350. Denning DW, Follansbee SE, Scolaro M, et al. Pulmonary aspergillosis in the acquired immunodeficiency syndrome. *N Engl J Med*. 1991;324:654–662.
351. Kronish JW, Johnson TE, Gilberg SM, et al. Orbital infections in patients with human immunodeficiency virus infection. *Ophthalmology*. 1996;103(9):1483–1492.
352. Perri P, Campa C, Incorvaia C, et al. Endogenous *Aspergillus versicolor* endophthalmitis in an immuno-competent HIV-positive patient. *Mycopathologia*. 2005;160(3):259–261.
353. Fish DG, Ampel NM, Galgiani JN, et al. Coccidioidomycosis during human immunodeficiency virus infection: a review of 77 patients. *Medicine (Baltimore)*. 1990;69:384–391.
354. McDonnell PJ, Green WR. Endophthalmitis. Mandell GL, Gordon RG, Bennett JE. *Principles and practice of infectious diseases*. 4th ed. Churchill Livingstone: New York; 1995.
355. Finamor LP, Muccioli C, Martins MC, et al. Ocular and central nervous system paracoccidioidomycosis in a pregnant woman with acquired immunodeficiency syndrome. *Am J Ophthalmol*. 2002;134:456–459.

356. Brod RD, Flynn HW, Miller D. Endogenous fungal endophthalmitis. *Duane's clinical ophthalmology*. Harper and Row: Hagerstown; 2007 [CD-ROM. ch 11].
357. Hariprasad SM, Mieler WF, Holz ER, et al. Determination of vitreous, aqueous, and plasma concentration of orally administered voriconazole in humans. *Arch Ophthalmol*. 2004;122:42–47.
358. Schiller DS, Fung HB. Posaconazole: an extended-spectrum triazole antifungal agent. *Clin Ther*. 2007;29(9):1862–1886.
359. Riddell J 4th, Comer GM, Kauffman CA. Treatment of endogenous fungal endophthalmitis: focus on new antifungal agents. *Clin Infect Dis*. 2011;52:648–653.
360. Garbino J, Ondrusova A, Baligvo E, et al. Successful treatment of *Paecilomyces lilacinus* endophthalmitis with voriconazole [published correction appears in Scand J Infect Dis 2003; 35:79]. *Scand J Infect Dis*. 2002;34:701–703.
361. Kim JE, Perkins SL, Harris GJ. Voriconazole treatment of fungal scleritis and epibulbar abscess resulting from scleral buckle infection. *Arch Ophthalmol*. 2003;121:735–737.
362. Ruhnke M, Schmidt-Westhausen A, Trautmann M. In vitro activities of voriconazole (UK-109,496) against fluconazole-susceptible and -resistant *Candida albicans* isolates from oral cavities of patients with human immunodeficiency virus infection. *Antimicrob Agents Chemother*. 1997;41:575–577.
363. Tucker JD, Li JZ, Robbins GK, et al. Ocular syphilis among HIV-infected patients: a systematic analysis of the literature. *Sex Transm Infect*. 2011;87:4–8.
364. McLeish WM, Pulido JS, Holland S, et al. The ocular manifestations of syphilis in the human immunodeficiency virus type 1-infected host. *Ophthalmology*. 1990;97:196–203.
365. Levy JH, Liss RA, Maguire AM. Neurosyphilis and ocular syphilis in patients with concurrent human immunodeficiency virus infection. *Retina*. 1989;9:175–180.
366. Gass JDM, Braunstein RA, Chenoweth RG. Acute syphilitic posterior placoid chorioretinitis. *Ophthalmology*. 1990;97:1288–1297.
367. Farhi D, Benhaddou N, Grange P, et al. Clinical and serologic baseline and follow-up features of syphilis

according to HIV status in the post-HAART era. *Medicine (Baltimore)*. 2009;88:331–340.
368. Freeman WR, Wiley CA. In situ nucleic acid hybridization. *Surv Ophthalmol*. 1988;34:187–192.
369. Schneiderman TE, Faber DW, Gross JG, et al. The agar–albumin sandwich technique for processing retinal biopsy specimens. *Am J Ophthalmol*. 1989;108:567–571.
370. *HHS Panel on Antiretroviral Guidelines for Adults and Adolescents [Internet]*. [Department of Health and Human Services; Oct 14; Guidelines for the use of antiretroviral agents in HIV-1-infected adults and adolescents] http://www.aidsinfo.nih.gov/ContentFiles/AdultandAdoles 2011.

85

Mycobacterial Infections

Sivakumar R. Rathinam, Perumalsamy Namperumalsamy

Introduction

Ocular mycobacterial infection represents an important form of extrapulmonary infection which encompasses tubercular as well as nontubercular mycobacterial (NTM) diseases in and around the eye. It presents with diverse clinical manifestations because of the

number of factors that are related to the microbe and the host. In spite of recent revolutionary advances in diagnostic technologies, establishing the diagnosis as well as treating the disease are clinical challenges. Mycobacterial diseases have been known to affect humans for more than a century and it still continues to be a global health concern. There are several challenges as far as tuberculosis (TB) is concerned. To list a few, TB stands as the most common opportunistic infection in human immunodeficiency virus (HIV)-positive patients in many developing countries. In 2013, an estimated 1.1 million of the 9 million people (13%) who developed TB were HIV-positive; 1.5 million people died from TB, including 360,000 people with concomitant HIV infection, which equates to about 4100 deaths a day.[1] Yet another global threat is the emergence of multidrug resistant (MDR-TB) and extensively drug-resistant strains of tuberculosis (XDR-TB). In 2013, the World Health Organization has estimated that globally 20.5% of previously treated and 3.5% of new TB patients have had MDR-TB which translates into an estimated 480,000 patients. Of them an estimated 9.0% had extensively drug resistant TB (XDR-TB).[2] Another important concern is the emergence of NTM infections, both in immune competent and immune compromised individuals in previously unrecognized settings and with new clinical manifestations.[3] Clinical manifestations of NTM simulate typical tuberculosis. Lack of better laboratory tools for differentiation, lack of treatment guidelines, and resistance to routine antitubercular treatment challenge the early management of mycobacterial infections. There is also a need to develop a consensus in investigations and treatment guidelines for ocular tuberculosis.[1]

Pulmonary and Extrapulmonary Tuberculosis

Tuberculosis is an infection caused by a rod-shaped, nonspore-forming, aerobic bacterium, *Mycobacteria tuberculosis*. Bacilli spread by small airborne droplets from infected patients. Once the droplet nuclei are inhaled, the bacilli settle in the airways. If the infection is not contained by the immune system, in around 3–8 weeks, local

spread and spread to regional lymph nodes in the lungs occurs. Subsequent spread to other organs results in extrapulmonary tuberculosis (EPTB). EPTB is reported to be increasing over the last several years.[4] Organs affected in EPTB include lymph nodes, pleura, central nervous system, eyes, musculoskeletal system, genitourinary tract, and gastrointestinal tract. Symptoms and clinical presentations of EPTB are variable and depend on the organ involved. Unlike pulmonary TB patients, EPTB patients are less likely to present with cough, dyspnea, hemoptysis, abnormal chest radiograph, night sweats, weight loss, anorexia, or fatigue. They may present with higher rates of abdominal pain, diarrhea, infertility, monoarticular joint pain, headache, meningismus, or lymphadenopathy depending upon the organ involved. Ocular tuberculosis represents an extrapulmonary dissemination of the bacilli primarily from lungs. However, patients with ocular TB may have a normal chest radiograph and negative chest complaints; alternatively they may have evidence of other forms of EPTB such as tubercular lymphadenitis. Ophthalmologists have to include appropriate questions in the history and consider extraocular systems whenever a tubercular etiology is suspected. It is essential to rule out EPTB and involvement of other systems in patients who may appear only to harbor pulmonary tuberculosis.

Ocular Tuberculosis

Three classic forms of ocular tuberculosis have been described. Direct ocular infection from an exogenous source may involve ocular adnexa, conjunctiva, sclera, or cornea. The second form results from a hypersensitivity reaction to distant foci of infection causing episcleritis, phlyctenulosis, and occlusive retinal vasculitis of the type observed in Eales disease. The third form relates to the hematogenous spread of *M. tuberculosis* from pulmonary or extrapulmonary sites.

Tuberculosis is one of the most common causes of infectious uveitis in tropical countries.[5–7] It is either unilateral or asymmetrically bilateral, characterized by a chronic and insidious course. Anatomically, tubercular uveitis may present as anterior, intermediate, posterior, or pan uveitis; more often a granulomatous

than nongranulomatous uveitis. The manifestations of ocular tuberculosis are numerous (Figs. 85.1–85.5).Clinical signs of ocular tuberculosis based on anatomical location are given in Table 85.1.

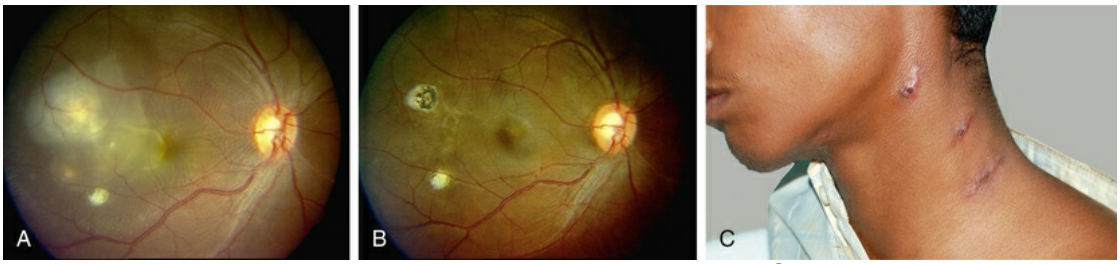

FIG. 85.1 Patient #1. (A) Pretreatment fundus photograph of right eye showing a choroidal tubercle with adjoining exudative detachment. A healed scar is below the active lesion. (B) Post antitubercular treatment fundus photograph of the right eye showing healed scars with resolution of exudative detachment. (C) Multiple tubercular cervical sinuses in the neck of the same patient

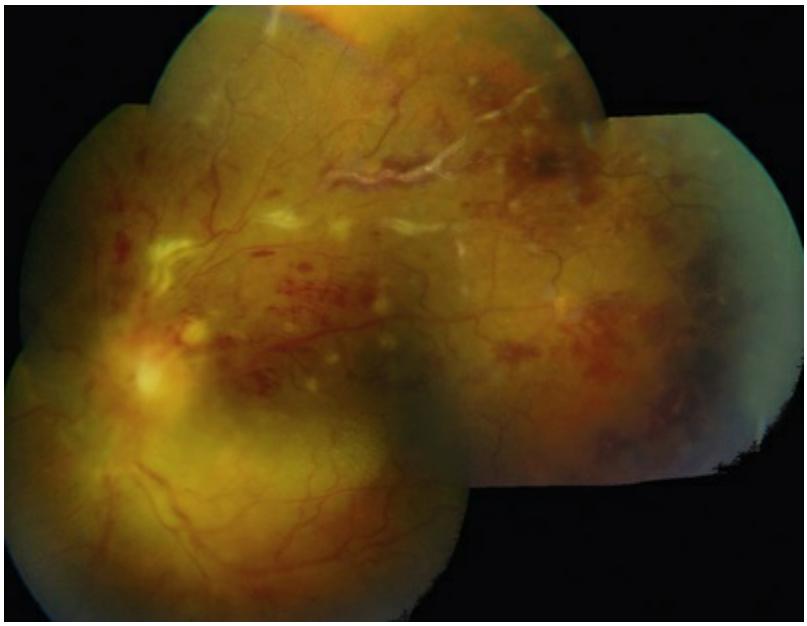

FIG. 85.2 Patient #2. Fundus photograph showing tubercular disc granuloma, vasculitis, and multifocal retinitis in a smear-positive pulmonary tuberculosis patient.

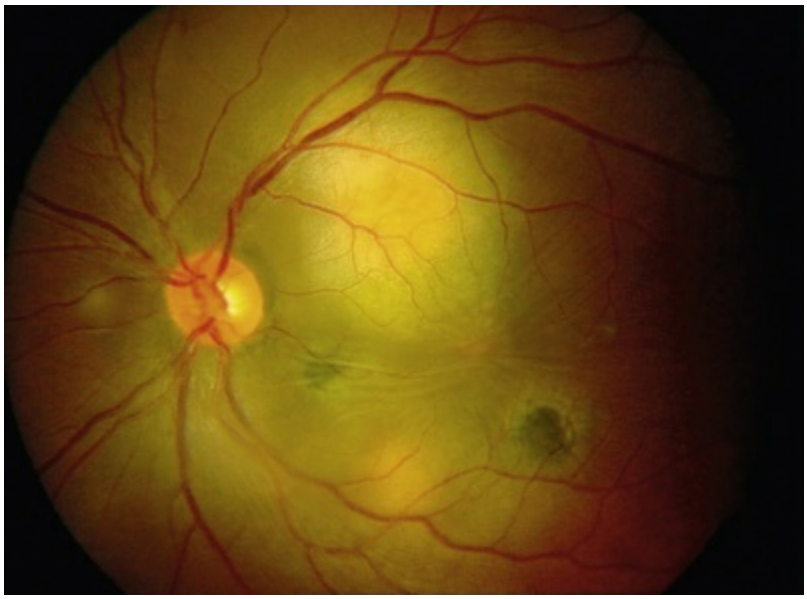

FIG. 85.3 Patient #3. Fundus photograph showing old healed choroiditis as well as active recurrent lesions with varying chronology of choroidal lesions in the right eye. Mantoux skin test was necrotic and chest radiograph showed calcified lymph nodes.

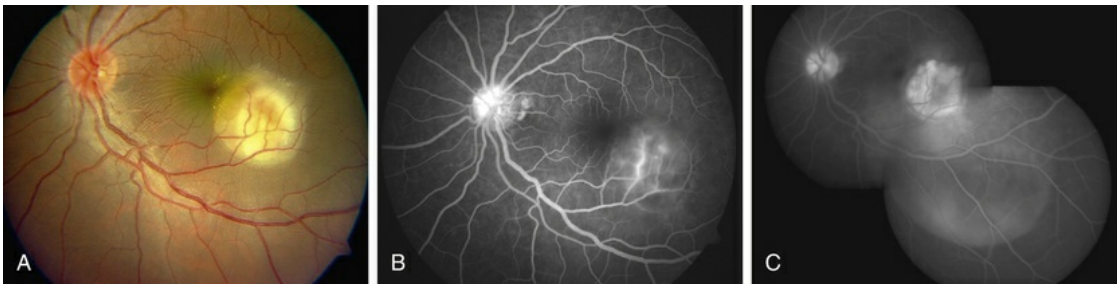

FIG. 85.4 Patient #4. (A) Choroidal tubercle with choroidal folds, with shallow serous retinal detachment. (B) Fundus fluorescein angiogram shows vascular staining and perivascular leakage overlying the lesion suggestive of active retinal vasculitis. (C) Fundus fluorescein angiogram shows a well-demarcated choroidal tubercle showing increasing hyperfluorescence with pooling of dye in the area of neurosensory detachment in the late phase extending beyond the tubercle with late disc staining.

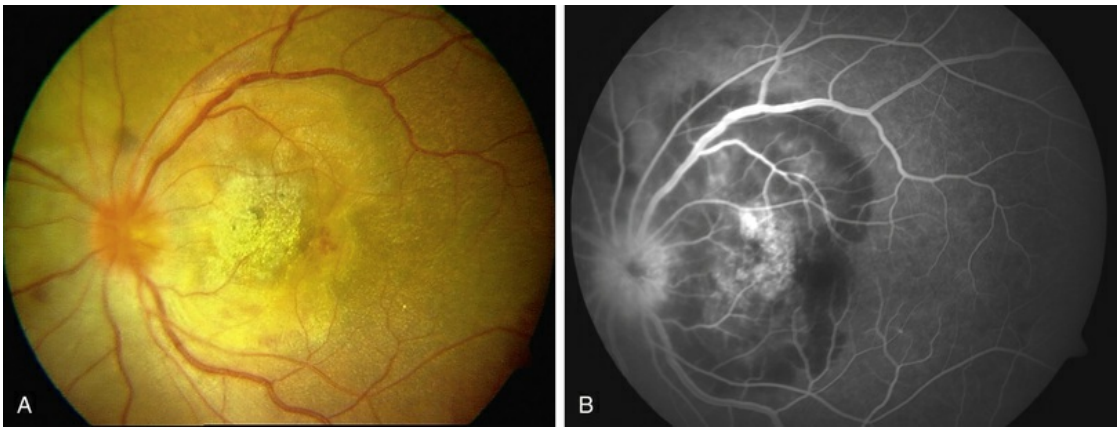

FIG. 85.5 Patient #5. (A) Pretreatment fundus photograph of the left eye showing serpiginous-like choroiditis partly healed in the center with an active peripheral lesion, disc hyperemia with vitreous reaction. Vitreous was positive for real-time polymerase chain reaction for *Mycobacterium tuberculosis*. (B) Fundus fluorescein angiogram of the same patient showing hyperfluorescence in the older central lesion and hypofluorescence in the active peripheral lesion, vessel wall staining, and disc staining.

TABLE 85.1
Clinical Signs: Ocular Mycobacterial Infections

Primary Site of Inflammation	Clinical Signs
Lids, adnexa, sclera, and cornea	Lupus vulgaris Recurrent episcleritis/scleritis, necrotizing scleritis, posterior scleritis, interstitial keratitis Sclerokerato uveitis
Lacrimal apparatus	Lacrimal gland adenitis, dacryocystitis
Orbit	Tuberculoma, tubercular abscess
Anterior uveitis	Nongranulomatous/granulomatous uveitis Hypopyon Anterior chamber granulomas
Intermediate uveitis	Recurrent, granulomatous
Posterior uveitis	Choroidal tubercles Choroidal tuberculoma Multifocal chorioretinitis Subretinal abscess Serpiginouschoroiditis Perivascular healed chorioretinal scars
Pan uveitis	Endophthalmitis Panophthalmitis Primary vasculitis

	Exudative retinal vasculitis Haemorrhagicvasculitis
Optic nerve	Optic disc granuloma Optic neuritis Neuroretinitis Optic atrophy

Anterior segment inflammation may show granulomatous keratic precipitates, iris granulomas that result in posterior synechiae, and complicated cataract. Posterior segment signs such as multifocal chorioretinitis with pigmented scars and exudative retinal hemorrhagic periphlebitis (Fig. 85.2) with uveitis are highly suggestive of tubercular etiology.[5] Presence of perivascular healed chorioretinal scars in such patients would also suggest a tubercular cause. Serpiginous-like choroiditis (SLC) of presumed tubercular etiology closely mimics classic serpiginous choroidopathy (SC) (Figs. 85.5A–B). However, patients with SLC are more likely to have multifocal scattered highly pigmented lesions with vitreous cells in contrast to classic SC, which is characteristically seen in peripapillary area.[5,6] Intermediate uveitis of tuberculosis and sarcoidosis closely mimic each other. It is granulomatous and recurrent; unlike sarcoidosis, tubercular intermediate uveitis does not respond to steroid and immunosuppressive treatment. In patients with choroidal tubercles, fundus fluorescein angiography may show initial "hypofluorescence" and then a late hyperfluorescence of the tubercles. Vessel wall staining, vascular leakage, disc staining and pooling of dye in the area of exudative detachment are other signs commonly seen in fluorescein angiography (Figs. 85.4B–C).

Thus tubercular uveitis has variable presentation making the clinical diagnosis challenging. To help the clinician, diagnostic criterion has been recommended. Diagnosis is considered as definitive TB only when the bacilli are isolated from the ocular tissues. The criterion for presumed tuberculous uveitis is reported to be presence of any one of the following clinical signs, such as choroidal granuloma, broad-based posterior synechiae, retinal vasculitis with or without choroiditis, or serpiginous-like choroiditis with a positive tuberculin skin test (TST) or QuantiFERONTB Gold test, or any other relevant tests, such as chest radiograph and computed tomography.[5] Good response to antitubercular treatment and absence of recurrence further supports

the diagnosis of presumed ocular tuberculosis.

Differential Diagnosis

Granulomatous uveitis may also be seen in patients with herpes simplex or varicella zoster infection, phacoantigenic uveitis, sarcoidosis, syphilis, leprosy, Vogt–Koyanagi–Harada disease and sympathetic ophthalmia. Other causes of choroidal granulomas include syphilis, sarcoidosis, and fungal lesions.[5,6]

Pathogenesis

Tissue damage in ocular tuberculosis is not only a direct consequence of infection but it is also due to nonresolving inflammation that results from a sensitive balance between protective immunity and destructive pathology.[8] Molecular studies and sequencing of the *M. tuberculosis* genome have identified specific and highly immunogenic antigens. These are the so-called 6-kDa early secretory antigenic target (ESAT-6) and the 10-kDa culture filtrate protein (CFP-10). They are capable of eliciting vigorous helper T-cell responses with resultant cytotoxicity in cellular models. They cause cell lysis and may enable the bacteria to invade and spread within the alveolar epithelium. Recent studies indicate ESAT-6 may also stimulate the trafficking of infected macrophages into the granulomas, to utilize the granulomas as foci of macrophage recruitment, infection, and subsequent bacterial dissemination.[8]

Host genetic factors appear to play a role in disease severity. Abnormalities in the genes encoding the IFN-gamma (IFN-γ) receptor chain and genes encoding IL-12 are important in determining the susceptibility to disseminated mycobacterial disease.[9] Pulmonary alveolar macrophages express complement and toll-like receptors and destroy the bacteria when they fuse with lysosomes. However, the mycobacteria can inhibit fusion with lysosomes and may then thrive in the phagosome. Retinal pigment epithelium (RPE) shares several functions with the macrophages, including expression of toll-like receptors and complement and phagocytosis of bacteria. Clinicopathologic study combined with molecular analysis revealed distribution of the mycobacteria in the

RPE in spite of the inflammatory process seen in retina and uvea. The authors suggest a possibility of reactivation of sequestered organisms in cases of recurrent inflammation.[10]

Nontuberculous Mycobacterial Infections

More recently, nontuberculous mycobacterial (NTM) disease appears to be increasing.[11] The genus *Mycobacterium* contains more than 125 species; these saprophytic mycobacteria are ubiquitous in the environment and may be present in soil, water, and dust particles. Both rapid and slow-growing NTM have been implicated in ocular infection, *M. chelonae* and *M. abscessus* are often reported to result in severe and progressive endophthalmitis. NTM endophthalmitis has been reported after uncomplicated phacoemulsification and intraocular lens implantation, laser in situ keratomileusis, endothelial keratoplasty, scleral buckling, and intravitreal injections.[12] Difficulty in management is mainly due to delay in the diagnosis and varying sensitivity to antibiotics. In many studies, initial cultures took variable periods to demonstrate growth or failed entirely to show the causative organism. Etiologies were often misdiagnosed as *Propionibacterium acnes*, nocardial or fungal endophthalmitis.[12] NTM are resistant to most conventional antimycobacterial drugs but are sensitive to a variety of other antibiotics. Amikacin, moxifloxacin, and to a lesser extent levofloxacin and ciprofloxacin demonstrate significant effectiveness against NTM.[13] Biofilm forming nonpigmented rapidly growing mycobacteria have also been shown to result in endophthalmitis. These organisms show resistance to eradication strategies, resistance to innate host immune responses and to antibiotics.[14] Large gaps still exist in our knowledge on ocular NTM infection. Accurate biomarkers to predict exposure, latency, relapse, and resistant diseases are being investigated and not yet available for clinical use.

Latent Tuberculosis

Latent tuberculosis infection (LTBI) is diagnosed when there is a positive TST in an asymptomatic person with no clinical or radiographic signs of active tuberculosis. The clinical relevance of

this condition is that 5–15% of persons with latent infection may progress to active tuberculosis during their lifetimes.[15] After entry into the human system, organisms can either begin to proliferate immediately, causing primary TB, or be cleared by the immune system. Alternatively, by slowing their metabolism or becoming dormant, they adapt to stressful conditions generated by the infected host and remain silent to the immune system. When the environmental conditions are favorable, activation may result in clinically apparent disease. Simplified, evidence-based management algorithms are available, and we believe clinicians should consult and follow international and national guidelines to manage the patients with latent tuberculosis.[16]

Laboratory Evaluation

A complete systemic history and examination are fundamental steps in the evaluation of all patients with ocular tuberculosis and may reveal evidence of pulmonary and other extrapulmonary tuberculosis. Recent advances in diagnostic tools for tuberculous infection, including molecular biology techniques, IFN-γ release assays, and radiodiagnostics have improved the specificity of the diagnosis. However, all these investigations have their own strengths and limitations.[17] The suboptimal specificity and sensitivity of existing diagnostic tools delay the diagnosis and treatment of active ocular infection. Clear understanding of their principles and proper test selection are needed to obtain relevant clinical support.

Positive reaction after Mantoux or TST intradermal injection of tuberculin purified protein derivative (PPD) indicate a successful cellular immune response by the patient. The antigen used in TST is a mixture of more than 200 proteins derived from *M. tuberculosis*. They can cross-react with BCG and NTM antigens undermining the specificity of the test. Hence TST has limited specificity; a positive result may not confirm disease. The American Thoracic Society and the United States Centers for Disease Control (CDC) consider reactions of 5 mm or more to be positive in very high-risk individuals (e.g., abnormal chest radiograph, HIV patients), 10 mm or more in high-risk patients (e.g., patients from endemic areas),

and 15 mm or more in patients with no identified risk factors. In addition, a negative test does not rule out TB. In a study on patients with histopathologically proven ocular tuberculosis, 40% had negative TST results.[18]

To study the immune response of patient, novel in vitro tests have been developed using ESAT-6 and CFP-10 proteins (see Pathogenesis). Commercially available QuantiFERON (QFT) and TSPOT.TB are commonly known as interferon-gamma release assays (IGRA). T cells, collected from the patient, are exposed to these specific tubercular antigens. The assay measures the IFN-γ released by sensitized T cells of the patient. The CDC guidelines state that IGRAs can be used in all situations in which the TST is currently used. Canada and United Kingdom national guidelines suggest using IGRAs only to confirm a positive TST.[19] Although these tests were originally designed to screen for latent tuberculosis, they have been tested in active systemic and ocular tuberculosis cohorts as well. A meta-analysis on IGRA concludes that the diagnostic sensitivities of both IGRAs are higher than that of TSTs and the specificities are lower.[20] TST and QFT were found equally predictive of progression to TB disease; QFT was not found superior to TST in a cohort of adolescents in a high systemic TB burden population from South Africa,[21] as well as in uveitis.[22] It is claimed that the QFT result together with the TST may increase the sensitivity.[23] However, positive and negative predictive values of IGRA depend on prevalence of TB in that population. As far as systemic TB is concerned, there is increasing evidence that IGRAs perform differently in high-burden compared to low-burden countries. Because of the low prevalence of TB in the United States, the low pretest probability, and low positive predictive value, IGRAs may not be useful as a standard part of the uveitis work-up.[24] The lack of a gold standard for diagnosis of TB infection prevents an effective and interpretable comparison of the IGRAs and the TST in ocular tuberculosis.[24]

Radiologic examination of the chest may reveal infiltrations, cavitation, hilar lymphadenopathy, pleural effusion, fibrotic, or calcific lesion in some patients. The predominant route of infection to ocular tissues is by hematogenous spread from the lungs, however the pulmonary focus may not be evident clinically or

radiographically in all patients. In a cohort of histopathologically proven ocular TB patients, 57% of patients had negative chest radiograph results.[18] Hence an initial negative workup does not rule out the infection, and repeat workup may be needed. More recently, high resolution computed tomography of the chest was found to be a useful tool in the diagnosis of granulomatous uveitis. Some centers further recommend use of positron emission tomography/CT guided lymph node identification for biopsy to aid the diagnosis of tuberculosis-associated uveitis.[25]

Isolation of *M. tuberculosis* by culture remains the cornerstone for diagnosis; however, isolation from inflamed ocular tissue is not always possible. Whenever it is possible, the specimen is often too small for all the procedures, such as Ziehl–Neelsen staining, inoculation in liquid and solid media, species identification, and drug susceptibility testing. Biopsy specimens may be obtained for histopathologic analysis from either the iris or by retinochoroidal biopsy. The absence of acid-fast bacilli or of caseating necrosis in the biopsy specimen does not rule out tuberculosis. In such circumstances either anterior chamber fluid or vitreous can be subjected to molecular diagnostic testing. Diagnosis based on detection of mycobacterial DNA through PCR and real time PCR are becoming the method of choice because of rapid test results and the ability to test in a very small sample.[18] The sensitivity of the multiplex, multitargeted PCR assay has been reported to be better than single targeted assays.[26,27] The WHO recommends the use of Xpert MTB/RIF, a fully automated real-time nucleic acid amplification technology, for rapid and simultaneous detection of TB and rifampicin resistance. The test provides accurate results in less than 2 hours and has minimal bio-safety requirements, training, and can be housed in nonconventional laboratories.[28] Xpert MTB/RIF is currently used only for sputum samples. Studies are needed to understand its potential role in ocular fluids.

Resistance to anti-TB drugs may be caused by chromosomal mutations in genes encoding drug targets resulting in MDR-TB. Proper management of MDR-TB relies on early recognition of drug resistance. Clinical diagnosis of drug resistance is checked by drug susceptibility testing. It is performed on all positive mycobacterial cultures on Middlebrook 7H10 agar with 1% proportional method

for isoniazid, rifampicin, ethambutol, streptomycin, ciprofloxacin, and kanamycin. Drug susceptibility testing by conventional mycobacterial culture is slow and elaborate, requiring sequential procedures for the diagnosis. Several molecular diagnostic tests such as the Sanger-based DNA sequencing methods are expected to lead to faster identification of MDR and XDR strains.[29]

Treatment

Antitubercular therapy is highly effective in reducing the recurrences of uveitis in patients with manifest TB. The systemic management of TB is complex and requires the input of infectious disease experts. The WHO recommends new patients with both pulmonary TB and extrapulmonary TB to be treated with a four-drug regimen (isoniazid 5 mg/kg daily, rifampicin 10 mg/kg daily, ethambutol 15 mg/kg daily, and pyrazinamide 20–25 mg/kg daily). Ethambutol and pyrazinamide are stopped after 2 months and isoniazid and rifampicin are continued for 4–6 months. Corticosteroids seem to have a potential benefit in patients with tubercular pericarditis and meningitis.[30] Similarly, steroids are used in ocular TB as well. More evidence is required on the dose and duration of corticosteroid treatment in ocular infections.

Tuberculosis with HIV coinfection represents a significant challenge, affecting millions of people worldwide. The treating physician has to consider drug interactions, overlapping side-effects, high pill burden, and risk of immune reconstitution inflammatory syndrome. Specific guidelines should be followed with special attention to the CD4 count and drug interactions.[31] In such patients, initiation of concomitant antitubercular and antiretroviral therapy may result in exacerbation of inflammation and clinical deterioration.[32] Either addition of corticosteroids or delaying the administration of HAART treatment is advised.

Hepatotoxic effects are seen with all first-line antituberculosis therapies and usually present as nausea, vomiting, and abdominal pain in the right upper quadrant. In most patients, even if hepatotoxic effects develop, severe liver injury can be avoided and antituberculosis therapy can be completed by following a comprehensive management algorithm.[33] Drug dosage and adverse

reactions are summarized in Table 85.2.

TABLE 85.2
Five Groups of Antituberculosis Drugs

Drug	Dose	Adverse Reaction	Additional Information
GROUP 1: FIRST-LINE ORAL ANTITUBERCULOSIS DRUGS			
(Use all possible drugs)			
Isoniazid	4–6 mg/kg (up to 300 mg)	Transient increase in hepatic enzyme Peripheral neuropathy	Use during pregnancy is considered safe Crosses the blood–brain barrier,
Rifampicin	8–12 mg/kg	Hepatotoxicity: Thrombocytopenia	Used during pregnancy
Ethambutol	15–20 mg/kg	Reversible dose-related; retrobulbar neuritis, typically begin 3–6 months after the start of therapy Hepatotoxicity	Does not cross meninges Better ocular penetration Crosses placental barrier, but considered safe in pregnancy
Pyrazinamide	20–25 mg/kg	Pruritus Hepatotoxicity	Safe during pregnancy Crosses the blood–brain barrier
GROUP 2: FLUOROQUINOLONES	**GROUP 3: INJECTABLE DRUGS**	**GROUP 4**	**GROUP 5**
(A fluoroquinolone should always be included in the treatment of MDR or XDR tuberculosis)	(There should always be an injectable drug in the treatment of MDR and XDR tuberculosis)	(Use all the necessary drugs to make up at least four active basic drugs; start with ethionamide, cycloserine; finally aminosalicylic acid)	(Less-effective drugs or drugs on which clinical data are sparse)
Ofloxacin (15 mg/kg)	Streptomycin (15 mg/kg)	Ethionamide/prothionamide (15 mg/kg)	Clofazimine (100 mg)
Levofloxacin (15 mg/kg)	Kanamycin (15 mg/kg)	Cycloserine/terizidone (15 mg/kg)	Amoxicillin with clavulanate (875/125 mg every 12 h)
Moxifl oxacin (7 · .5–10 mg /kg)	Amikacin (15 mg/kg)	P-aminosalicylic acid (acid salt) 150 mg/kg	Linezolid (600 mg)
	Capreomycin (15 mg/kg)		Imipenem (500–1000 mg every 6 h)
			Clarithromycin (500 mg/12 h)

			Thioacetazone (150 mg)

MDR, multidrug-resistant tuberculosis; XDR, extensively drug-resistant tuberculosis.

Drug-Resistant Tuberculosis

MDR tuberculosis is defined as the disease caused by organisms that are resistant to isoniazid and rifampicin, which are two first-line anti-TB drugs. XDR-TB is defined as tuberculosis that is caused by organisms resistant to isoniazid and rifampicin and to any one of the fluoroquinolones and at least one of the injectable second-line drugs. MDR and XDR tuberculosis are generally thought to have high morbidity and mortality rates, and drug-resistant strains have evolved mainly due to incomplete or improper treatment of TB patients. MDR and XDR-TB are now global threats.[2] In the vast majority of clinical settings in the developing world, culture and drug-susceptibility testing are not available. Most cases likely go undetected due to insufficient laboratory infrastructure for diagnosis.[34,35] At present, MDR-TB is treated by a combination of eight to ten drugs with therapies lasting up to 18–24 months; only four of these drugs were actually developed to treat TB. Such suboptimal therapy leads to almost 30% of MDR-TB patients experiencing treatment failure. The current situation necessitates the immediate identification of new and more potent drugs.[36,37] However, when the drugs are chosen in a stepwise selection process through five groups on the basis of efficacy, safety, and cost, with the right combination and rational use, a better prognosis can be obtained.[38] Drug dosages for MDR and XDR-TB (Group 2–5) are given in Table 85.2. Linezolid is an off-label use for MDR-TB. There are scattered case reports of optic neuropathy secondary to this drug. A baseline ophthalmologic evaluation is recommended before its use.[39]

Detection of drug resistance is possible only in culture isolates, because of challenges in isolating the organisms from the eye; drug susceptibility testing is difficult in ocular TB. This has serious implications specifically in uveitis. When a trial of antitubercular treatment fails in presumed ocular TB, there is a very high possibility for the uveitis specialist to assume a nontubercular

etiology and to start corticosteroids or immunosuppressive treatment to control inflammation.[35] In such situations molecular diagnostic studies may be of help.

According to the WHO 2015 Millennium Development Goal (MDG) of halting and reversing TB, worldwide TB incidence fell at an average rate of about 1.5% per year between 2000 and 2013. Globally, the TB mortality rate fell by an estimated 45% between 1990 and 2013, and TB prevalence rate fell by 41% during the same period.[2] If success is continued and quality care is provided as per the International Standard of TB Care, it is anticipated the incidence of extrapulmonary tuberculosis, including ocular TB, will decline.

References

1. Cunningham ET, Rathinam SR, Albini TA, et al. Tuberculous uveitis. *Ocul Immunol Inflamm*. 2015;23(1):2–6.
2. World Health Organization. *Global tuberculosis control 2014*. [Geneva: World Health Organization] http://www.who.int/tb/publications/global_report/en/.
3. Griffith DE, Aksamit T, Brown-Elliott BA, et al. An official ATS/IDSA statement: diagnosis, treatment, and prevention of nontuberculous mycobacterial diseases. *Am J Respir Crit Care Med*. 2007;15:367–416.
4. Gonzalez OY, Adams G, Teeter LD, et al. Extra-pulmonary manifestations in a large metropolitan area with a low incidence of tuberculosis. *Int J Tuberc Lung Dis*. 2003;7:1178–1185.
5. Gupta A, Bansal R, Gupta V, et al. Ocular signs predictive of tubercular uveitis. *Am J Ophthalmol*. 2010;149:562–570.
6. Vasconcelos-Santos DV, Rao PK, Davies JB, et al. Clinical features of tuberculous serpiginouslike choroiditis in contrast to classic serpiginous choroiditis. *Arch Ophthalmol*. 2010;128:853–858.
7. Rathinam SR, Namperumalsamy P. Global variation and pattern changes in epidemiology of uveitis. *Indian J Ophthalmol*. 2007;55:173–183.
8. Dorhoi A, Reece ST, Kaufmann SHE. For better or for worse: the immune response against Mycobacterium

tuberculosis balances pathology and protection. *Immunol Rev*. 2011;240:235–251.
9. Krishnan N, Robertson BD, Thwaites G. The mechanisms and consequences of the extra-pulmonary dissemination of Mycobacterium tuberculosis. *Tuberculosis (Edinb)*. 2010;90:361–366.
10. Rao NA, Saraswathy S, Smith RE. Tuberculous uveitis: distribution of Mycobacterium tuberculosis in the retinal pigment epithelium. *Arch Ophthalmol*. 2006;124:1777–1779.
11. Shenai S, Rodrigues C, Mehta A. Time to identify and define non-tuberculous mycobacteria in a tuberculosis-endemic region. *Int J Tuberc Lung Dis*. 2010;14:1001–1008.
12. Matieli LCV, De Freitas D, Sampaio J, et al. Mycobacterium abscessus endophthalmitis: treatment dilemma and review of the literature. *Retina*. 2006;26:826–829.
13. Caballero AR, Marquart ME, O'Callaghan RJ, et al. Effectiveness of fluoroquinolones against Mycobacterium abscessus in vivo. *Curr Eye Res*. 2006;31:23–29.
14. Holland SP, Pulido JS, Miller D, et al. Biofilm and scleral buckle-associated infections: a mechanism for persistence. *Ophthalmology*. 1991;98:933–938.
15. Getahun H, Matteelli A, Chaisson RE, et al. Latent Mycobacterium tuberculosis infection. *N Engl J Med*. 2015;372:2127–2135.
16. World Health Organization. *Guidelines on the management of latent tuberculosis infection*. [Geneva: World Health Organization] http://www.who.int/tb/publications/latent-tuberculosis-infection/en/.
17. Vasconcelos-Santos DV, Zierhut M, Rao NA. Strengths and weaknesses of diagnostic tools for tuberculous uveitis. *Ocul Immunol Inflamm*. 2009;17:351–355.
18. Wroblewski KJ, Hidayat AA, Neafie RC, et al. Ocular tuberculosis: a clinicopathologic and molecular study. *Ophthalmology*. 2011;118:772–777.
19. Schluger NW, Burzynski J. Recent advances in testing for latent TB. *Chest*. 2010;138:1456–1463.
20. Sester M, Sotgiu G, Lange C, et al. Interferon-γ release assays for the diagnosis of active tuberculosis: a systematic

review and meta-analysis. *Eur Respir J*. 2011;37:100–111.
21. Mahomed H, Hawkridge T, Verver S, et al. The tuberculin skin test versus QuantiFERON TB GoldH in predicting tuberculosis disease in an adolescent cohort study in South Africa. *PLoS ONE*. 2011;6(3):e17984.
22. Babu K, Satish V, Satish S, et al. Utility of QuantiFERON TB gold test in a south Indian patient population of ocular inflammation. *Indian J Ophthalmol*. 2009;57:427–430.
23. Marcus A, Hla MH, Soon-Phaik C. Diagnosis of tuberculous uveitis: clinical application of an interferon-gamma release assay. *Ophthalmology*. 2009;116:1391–1396.
24. Albini TA, Karakousis PC, Rao NA. Interferon-gamma release assays in the diagnosis of tuberculous uveitis. *Am J Ophthalmol*. 2008;146:486–488.
25. Doycheva D, Deuter C, Hetzel J, et al. The use of positron emission tomography/CT in the diagnosis of tuberculosis-associated uveitis. *Br J Ophthalmol*. 2011;95(9):1290–1294.
26. Sharma K, Gupta V, Bansal R, et al. Novel multi-targeted polymerase chain reaction for diagnosis of presumed tubercular uveitis. *J Ophthalmic Inflamm Infect*. 2013;3:25.
27. Kataria P, Kumar A, Bansal R, et al. devR PCR for the diagnosis of intraocular tuberculosis. *Ocul Immunol Inflamm*. 2015;23:47–52.
28. World Health Organization. *Tuberculosis diagnostics Xpert MTB/RIF test*. http://who.int/tb/features_archive/factsheet_xpert.pdf.
29. Campbell PJ, Morlock GP, Sikes RD, et al. Molecular detection of mutations associated with first- and second-line drug resistance compared with conventional drug susceptibility testing of Mycobacterium tuberculosis. *Antimicrob Agents Chemother*. 2011;55:2032–2041.
30. Kadhiravan T, Deepanjali S. Role of corticosteroids in the treatment of tuberculosis: an evidence-based update. *Indian J Chest Dis Allied Sci*. 2010;52:153–158.
31. Curran A, Falcó V, Pahissa A, et al. Management of tuberculosis in HIV-infected patients. *AIDS Rev*. 2012;14(4):231–246.
32. Rathinam SR, Lalitha P. Paradoxical worsening of ocular

tuberculosis in HIV patients after antiretroviral therapy. *Eye (Lond)*. 2007;21:667–668.
33. Senousy BE, Belal SI, Draganov PV. Hepatotoxic effects of therapies for tuberculosis. *Nat Rev Gastroenterol Hepatol*. 2010;7:543–556.
34. Koul A, Arnoult E, Lounis N, et al. The challenge of new drug discovery for tuberculosis. *Nature*. 2011;469:483–490.
35. Rathinam SR. Treating uveitis in the developing world setting. *Int Ophthalmol Clin*. 2010;50:219–228.
36. Rao NA, Irfan M, Soomro MM, et al. Drug resistance pattern in multidrug resistance pulmonary tuberculosis patients. *J Coll Physicians Surg Pak*. 2010;20(4):262–265.
37. Shahid SK. Newer patents in antimycobacterial therapy. *Pharm Pat Anal*. 2015;4(3):219–238.
38. Caminero JA, Sotgiu G, Zumla A, et al. Best drug treatment for multidrug-resistant and extensively drug-resistant tuberculosis. *Lancet Infect Dis*. 2010;10:621–629.
39. Agrawal R, Addison P, Saihan Z, et al. Optic neuropathy secondary to Linezolid for multidrug-resistant mycobacterial spinal tuberculosis. *Ocul Immunol Inflamm*. 2015;23:90–92.

86

Eales Disease

Dhananjay Shukla, Perumalsamy Namperumalsamy

Introduction

Eales disease is an idiopathic, occlusive perivasculitis affecting the peripheral retina, leading to retinal nonperfusion, new vessel formation, and recurrent vitreous hemorrhages. Eales disease was reported from the United Kingdom, United States, and Canada in the latter half of the 19th century and early 20th century.[1,2] The eponym originated from the first description by Henry Eales of a syndrome of recurrent vitreous hemorrhage in young men with epistaxis and constipation.[3] Most cases in the last decade have been reported from the Indian subcontinent, with a few reports from the

Middle East.[4–13] However, the incidence of Eales disease appears to have declined globally, due probably to improved general health and living standards and reduced incidence of tuberculosis (TB),[1,2,10] as well as to improved etiologic diagnosis in a heterogeneous group of allegedly primary vasculitides, previously amalgamated as presumed Eales disease.[14] Most patients are healthy young men, aged 20–40 years; the mean age of onset is generally earlier in Asians than in Caucasians.[2,15–17]

Clinical Features and Natural History

Three sequential vascular responses that determine the natural course of Eales disease are inflammation, occlusion, and neovascularization.[1,2,10,15] Most patients are asymptomatic at the stages of inflammation and occlusion. The disease starts quietly as multiple, peripheral inflammatory branch retinal vein occlusions: fine, solid white lines representing venous sheathing are the commonest clinical presentation (Fig. 86.1).[1,2] As active vasculitis slowly resolves, the fuzzy vascular sheathing, with indistinct margins, becomes well defined and distinct. Retinal arteries may be involved later, but their involvement is not central to the disease presentation,[1] and is generally suggestive of other conditions like systemic vasculitides.[11,18] Other clinical features that suggest alternative inflammatory etiologies are exudative or focal vasculitis; cotton-wool spots;[11,18] and central retinal involvement including macular and optic disc edema, choroiditis, anterior uveitis, and vitritis.[2,14]

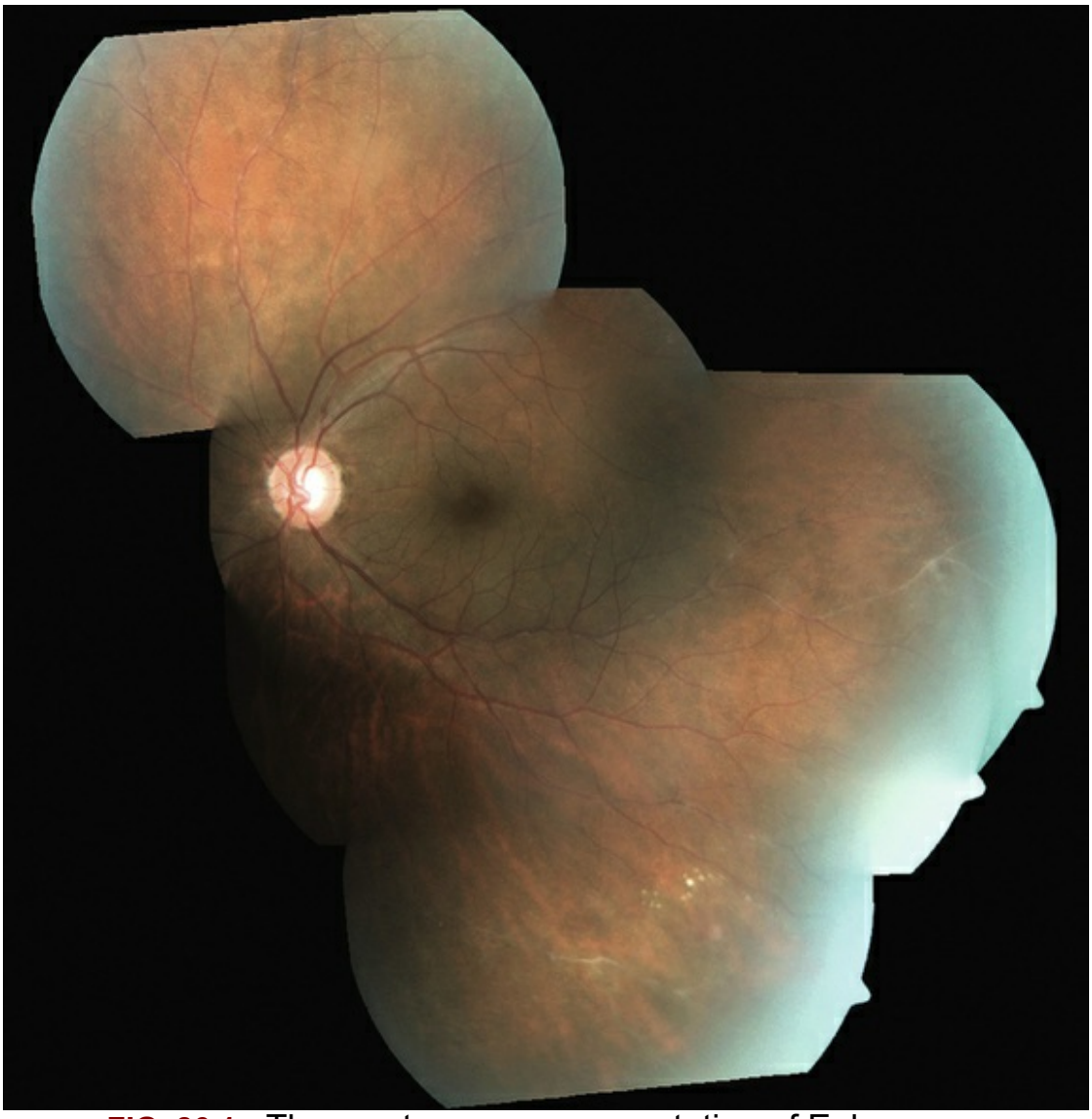

FIG. 86.1 The most common presentation of Eales disease is solid columns of occlusive sheathing in peripheral veins, as seen here in superior, inferior, and inferotemporal periphery. A few hard exudates inferiorly suggest resolved retinal edema. The posterior pole and visual acuity are unaffected.

As the occlusions are primarily venous, they occur gradually, allowing development of compensatory phenomena like collaterals, microaneurysms, capillary telangiectasia, corkscrew vessels, and venous beading; some of these changes may be observed by careful examination of the apparently uninvolved fellow eye of a patient with unilateral involvement. Prolonged and extensive retinal nonperfusion eventually leads to peripheral neovascularization in up to 80% of eyes; disc neovascularization is rare.[2,4,15] New vessels

bleed into the vitreous, resulting in the classic presentation of Eales disease: a sudden, unilateral blurring of vision or floaters[15,17] (Fig. 86.2). Vision often improves, but recurrences are common. The second eye is ultimately affected in 50–90% of cases, after a gap of 3–10 years.[2,4,14,15] Isolated episodes of vitreous hemorrhage usually settle down without visual deficit; recurrent bleeds lead to progressive contraction of vitreous cortex, resulting in traction retinal detachments, secondary retinal tears, and epimacular membranes.[1] Though anterior segment neovascularization occurs in a small fraction of eyes, the prognosis is better than what is typically associated with iris neovascularization.[4]

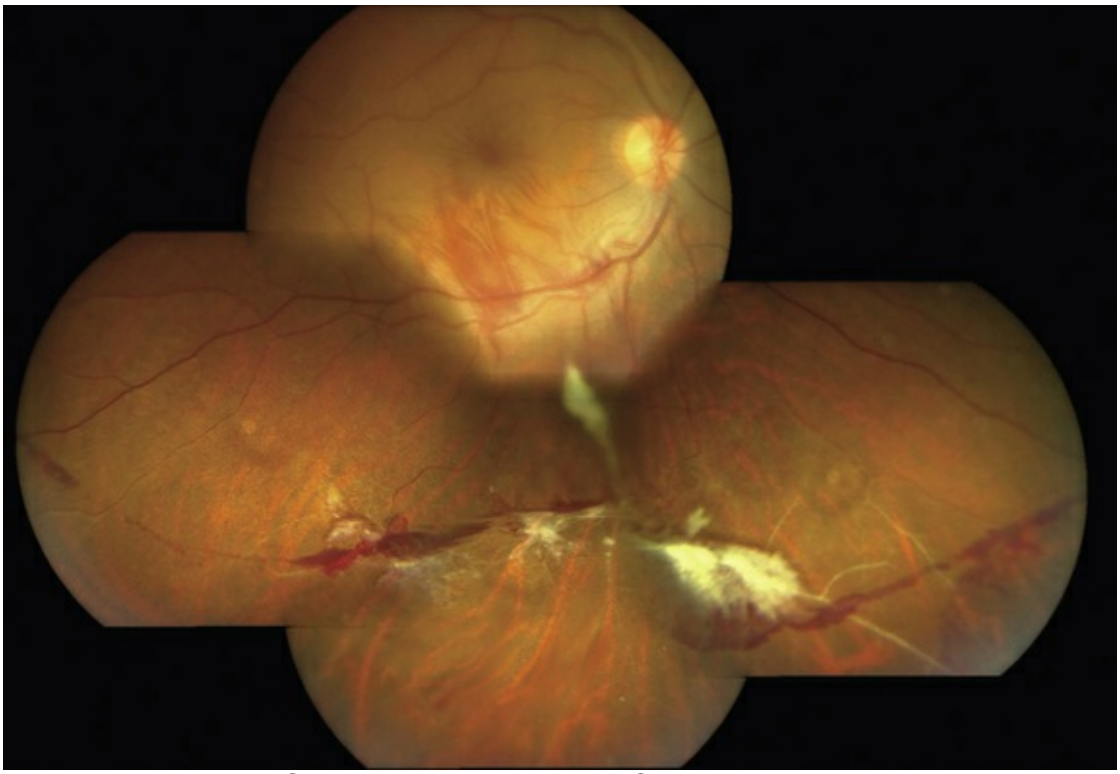

FIG. 86.2 Classic presentation of Eales disease is floaters or blurring of vision due to vitreous hemorrhage from peripheral new vessels. Recurrent bleeds, along with preceding inflammation, lead to epiretinal membrane formation, which is beginning at the posterior pole. Note the linear, extensive sheathing of the peripheral retinal vessels.

Charamis graded the evolution of Eales disease into four stages. Stage I was characterized by mild peripheral perivasculitis; stage II

by extensive inflammation involving larger vessels; neovascularization and vitreous hemorrhage heralded stage III; and tractional complications marked stage IV.[19] A system for grading Eales disease on the basis of the degree and extent of retinal vasculopathy, neovascular proliferations, and vitreous hemorrhage has also been proposed.[20] However, the course of the disease is variable, and a fixed sequence of stages may not be followed consistently.[1,2]

Pathology and Pathogenesis

The classic histopathologic connotation of the term "vasculitis" is a type III hypersensitivity reaction with deposition of immune complexes in the vessel wall, leading to vessel wall destruction.[21,22] This rheumatologic definition is not applicable to retinal vasculitis in general, and Eales disease in particular, which represents perivascular cuffing with inflammatory cells, graded by clinical appearance rather than vascular caliber or type of immune response.[11,21,22] Most authors have therefore used the terms "vasculitis" and "perivasculitis" interchangeably in the context of Eales disease.

Central to the visually debilitating complications of Eales disease is retinal hypoxia. Inflammation causes hypoxia by an increase in the metabolic demands of cells and a reduction in metabolic substrates caused by inflammatory vascular occlusion. Hypoxia in turn triggers further inflammation, setting up a vicious cycle.[23] This sequence suggest a pathogenetic role for both angiogenic factors and inflammatory cytokines in Eales disease, in a manner similar to noninflammatory vascular diseases like diabetic retinopathy. A simultaneous upregulation of vascular endothelial growth factor (VEGF), and interleukins (IL)-6 and IL-9 has indeed been observed during the proliferative phases of both diabetic retinopathy and Eales disease.[7] Other biochemical analyses have also implicated retinal autoimmunity, angiogenic growth factors, and oxidative stress in causing inflammation and neovascularization in Eales disease.[2] Recent serologic and genetic studies have reinforced the role of cell-mediated immunity in Eales disease, particularly interleukins and tumor necrosis factor-alpha.[9,12] Raised serum

homocysteine has also been proposed to cause both vascular damage and oxidative stress in Eales disease.[24]

The pathogenesis of inflammatory vascular occlusions in Eales disease remains unclear. Systemic association with neurologic, vestibuloauditory, hematologic, and parasitic diseases and infections have been proposed but never proven.[2,15] The most frequently reported association is with systemic TB. While viable organisms have not been demonstrated from the eyes with Eales disease, polymerase chain reaction-based studies have identified mycobacterial DNA in vitreous and epiretinal tissue.[25,26] These findings make the case for hypersensitivity to tuberculoprotein; the case is reinforced by the presence of tuberculin skin test positivity in the majority of patients.[2] This concept continues to be popular among current researchers.[11] Several other studies have, however, disputed this notion by demonstrating Mantoux positivity in healthy controls, as well as Mantoux negativity among Eales patients.[2,15,27]

Differential Diagnosis

Eales disease is a diagnosis of exclusion (Fig. 86.3). Several ocular and systemic inflammatory and noninflammatory diseases cause retinal vascular sheathing or occlusion, which may closely resemble Eales disease. However, a battery of investigations is not necessary for every patient. A detailed history and a thorough systemic examination rule out most of the mimicking diseases; only a few tailored investigations are required to clinch the diagnosis.

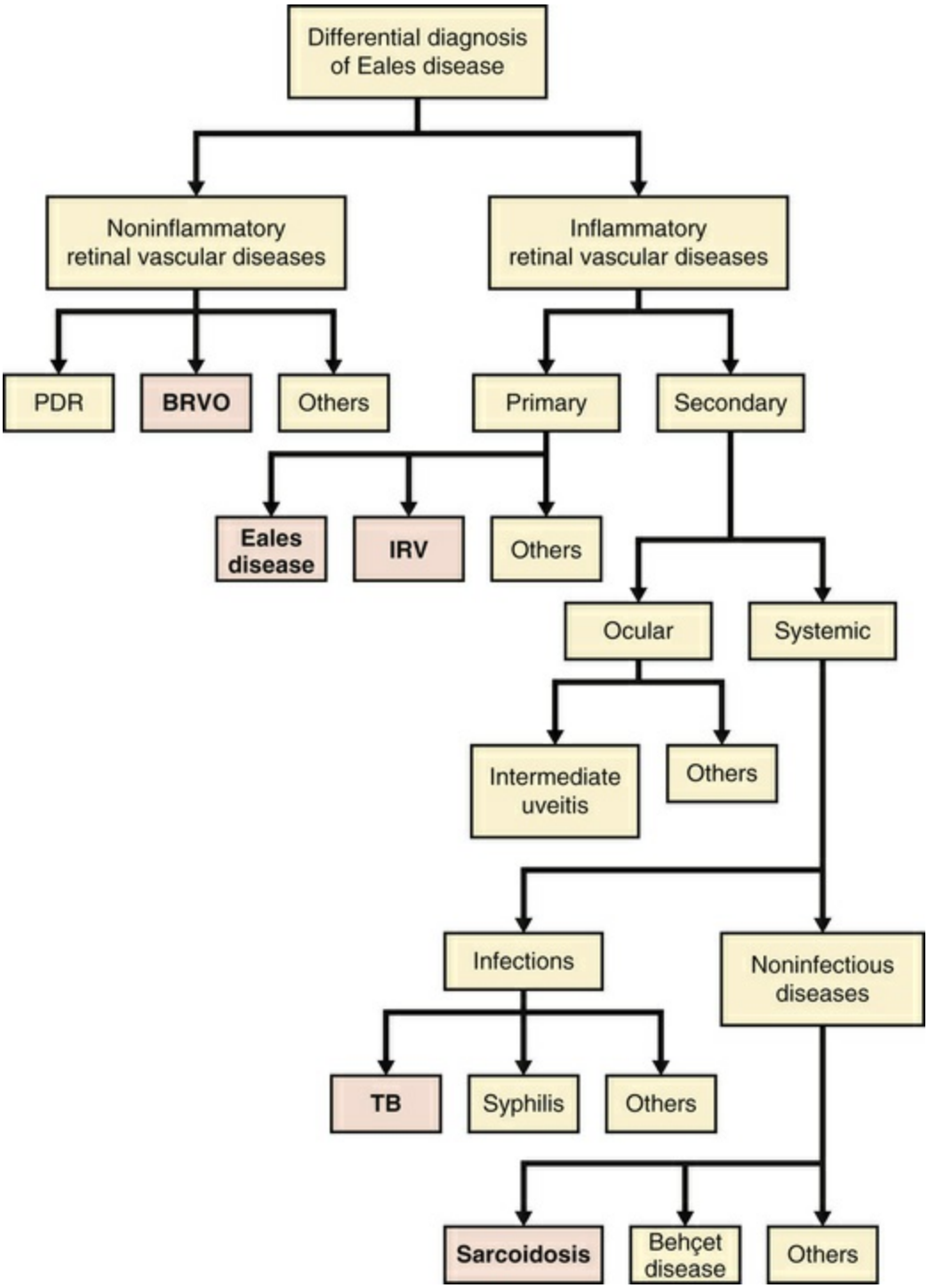

FIG. 86.3 Differential diagnosis of Eales disease. PDR, proliferative diabetic retinopathy; BRVO, branch retinal vein occlusion; IRV, idiopathic retinal vasculitis; TB, tuberculosis.

Among noninflammatory vascular occlusions, primary branch retinal vein occlusion mimics Eales most closely. The former occurs at an arteriovenous crossing; the crossing artery is frequently sclerosed. The occlusions are not multiple and peripheral like Eales,

and affect older age groups. Proliferative diabetic retinopathy may also exhibit sheathing of vessels during active stage (as part of the appearance labeled "featureless retina") or at involutional stage. Central retinal vein occlusion in a young adult should be investigated for inflammatory etiology (see diagnostic workup, below) because it represents a rare presentation of Eales.[1] Coats disease, familial exudative vitreoretinopathy (FEVR), and sickle-cell disease also show similar peripheral nonperfusion and should be ruled out. Though Coats disease also occurs in male patients, they are typically younger and have unilateral disease with prominent telangiectasia, more exudation, and less neovascularization or vitreous hemorrhage. FEVR and sickle-cell retinopathy have distinctive clinical and angiographic features, as well as familial and systemic associations respectively, to distinguish them from Eales disease.

Ocular inflammatory conditions like intermediate uveitis, endophthalmitis, multifocal choroiditis, and birdshot retinopathy may have associated retinal vasculitis, but primary lesions are generally prominent and unmistakable. Systemic TB should be ruled out in every case of retinal vasculitis because of its endemic presence, especially in the Southeast Asian region.[28] TB typically causes severe perivasculitis along with granulomatous anterior uveitis, retinal hemorrhages, moderate vitritis and focal choroiditis.[28] Syphilis, like TB, needs to be screened by default because of its recent reemergence with HIV, as well as its varied presentations.[29] Retinal periphlebitis occurs in about half the cases of leptospirosis, the most widespread zoonosis globally. Nongranulomatous uveitis, vitritis, and papillitis help in differentiation.[30] Retinal vasculitis can also occur along with necrotizing retinitis, though arteries are involved more commonly.[11]

Like TB and syphilis, sarcoidosis has no pathognomonic signs and needs to be ruled out in most ocular inflammations. Sarcoid vasculitis is typically segmental and nodular, with snowball vitreous exudates and granulomatous uveitis. Diagnosis is based on key ophthalmic signs and laboratory investigations.[31] Although uncommon, Behçet disease is the classic presentation of occlusive retinal vasculitis along the Silk Route (see below). It involves both arteries and veins, and is accompanied by severe uveitis, vitritis,

and retinal infiltrates; orogenital aphthoses are diagnostic.[32] Systemic vasculitides like systemic lupus erythematosus (SLE) have been erroneously linked with retinal vasculitis in the literature.[22] Their retinal effects are typically mediated through secondary hypertension (e.g., cotton-wool spots, superficial hemorrhages) and manifest as arterial rather than venous occlusions.[33]

Primary Retinal Vasculitis

Once the diseases causing secondary vasculitis are ruled out, the two main conditions which remain in the picture are Eales disease and idiopathic retinal vasculitis. When (1) the vasculitis is more posterior, sectoral, and exudative; (2) neovascularization, vitreous hemorrhage, and recurrences are uncommon; and (3) presentation is gender-neutral, the term "idiopathic retinal vasculitis" is preferred over "Eales disease."[2] The differentiation is indeed semantic, and the disease workup remains the same (see below), leading some authorities to suggest that the term "Eales disease" should be discontinued.[34] However, classic Eales disease has the unusual combination of minimal peripheral vascular inflammation but extensive vascular occlusions and neovascularization leading to recurrent vitreous hemorrhages, justifying the eponym.[2,14]

Diagnostic Workup for Eales Disease

The purpose of the workup is to search for a cause for vasculitis and to rule out infections. This is best done by meticulous history-taking and systemic examination; laboratory investigations should be tailored to the positive findings from history and examination.[35]

After considering the age and sex of the patient, one should elicit information about residence and travel (see below), occupation, and eating habits, all of which may help with the diagnosis of leptospirosis, syphilis, and toxoplasmosis. Similarly, cough, fever, and night sweats (TB or sarcoidosis); joint pain and swelling (SLE, Behçet disease); orogenital ulcerations (Behçet disease, syphilis); recurrent abortions and sexually transmitted disease (syphilis, HIV); skin rashes, nodules, or vesicles (SLE, Behçet disease, sarcoidosis); and neurologic symptoms (sarcoidosis, multiple

sclerosis) reveal underlying diseases that should be investigated further.

A detailed examination for systemic disease, especially for skin and mucosa, joints, and respiratory and central nervous systems, by an internist rules out important systemic associations, some of which may be life-threatening. Only a few basic screening investigations are universally required in retinal vasculitis, which the ophthalmologist should order before referral to the internist: a complete hemogram, peripheral smear, erythrocyte sedimentation rate, tuberculin skin test, chest radiography, rapid plasma reagin (RPR for syphilis), enzyme-linked immunosorbent assay for HIV, and urinalysis are sufficient to screen for most common diseases causing retinal vasculitis; further investigations are required only when history, examination, and/or aforementioned investigations point towards a specific disease.[11,35]

Fluorescein angiography helps mainly to identify peripheral new vessels and the extent of retinal nonperfusion, bordered by compensatory phenomena like collaterals and microaneurysms (Fig. 86.4). Active vasculitis appears as leakage from the stained vessel walls, though it can be detected clinically. B-scan ultrasound is a key presurgical investigation to assess the retinal status, posterior vitreous detachment (PVD), and tractional membranes obscured by vitreous hemorrhage. While assessing PVD, one must beware of vitreoschisis and an anomalous PVD, both common in Eales disease.[36] Recently, ultra-wide-field imaging has expanded the photographic, autofluoroscent, and angiographic views of retinal vasculitis, revealing undetected sheathed/blocked vessels, capillary dropouts, and neovascularization.[37,38] The additional information improved disease monitoring in half of the patients and changed the line of management in four-fifths of them.[37] On the other hand, microstructural imaging with adaptive optics technology has also been reported to enhance the early detection of subtle or subclinical retinal vasculitis.[39]

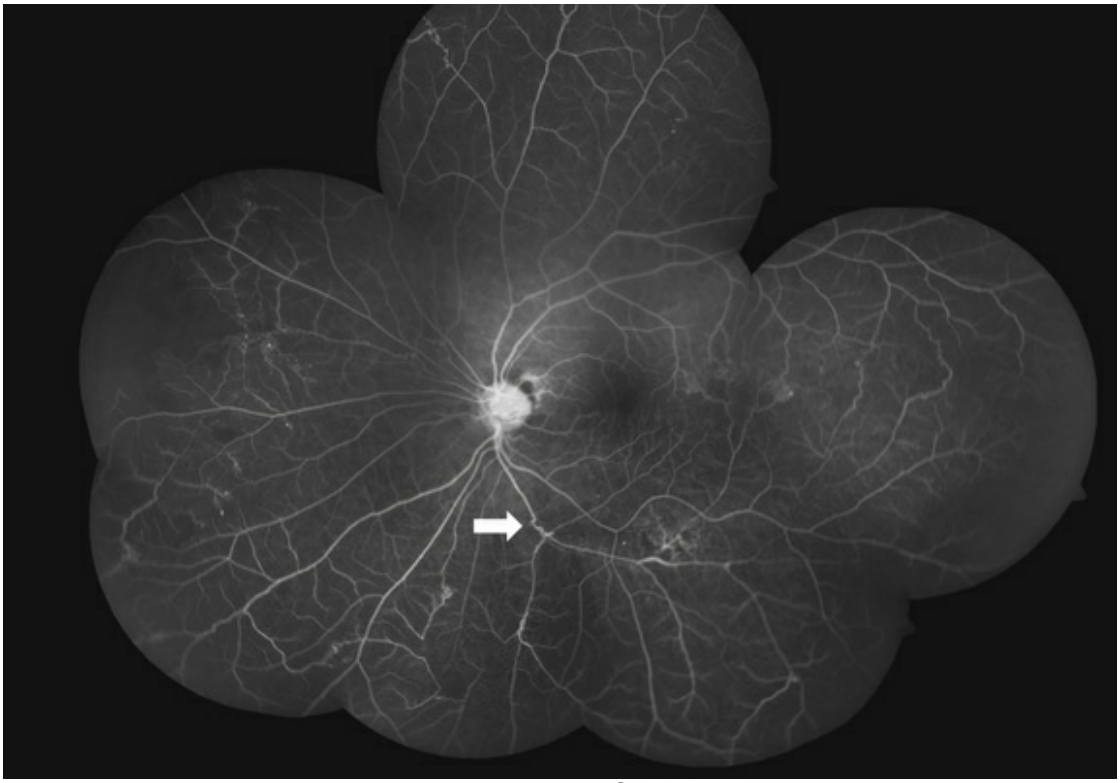

FIG. 86.4 Midphase angiogram of a patient with Eales disease showing scattered peripheral areas of capillary microaneurysms, telangiectasia, collateral formation, and retinal nonperfusion, most prominent at 3:00 and 9:00 meridians. The posterior pole is largely unaffected. The inflammatory sheathing of inferotemporal retinal vein from the first branching downwards (*arrow*) is not apparent due to resolution of active vasculitis.

Epidemiologic Spectrum of Retinal Vasculitis

There is considerable geographic variation in the ophthalmologists' perspective on what retinal vasculitis represents, alone or with concurrent uveitis. The default association in the Indian subcontinent is with TB or Eales disease;[1,2,34,40] in the Middle or Far East (including China and Japan) and the Mediterranean region, retinal vasculitis means Behçet disease;[40,41] sarcoidosis is the most common association in the United States, Japan, and The Netherlands;[40,42] and in South America, Europe, Australia, and

Africa, toxoplasmosis is the first intraocular inflammation to rule out.[40,43] The infective etiologies are typically more common in the developing countries, whereas noninfectious vasculitis is the norm in the developed world.[40] The ethnic/cultural subtext in etiologic diagnosis must also be kept in mind (TB or Eales in Indians; sarcoidosis in Scandinavians and African-Americans; Behçet disease in East Asians; and toxoplasmosis in Europeans, native Australians, and South Americans).[40–45]The migration of ethnic groups across the globe has complicated the epidemiologic profile of retinal vasculitis to some extent,[45] but broad causative associations remain relevant. Finally, irrespective of the geographic and ethnic riders, retinal vasculitis as the *predominant* feature of posterior uveitis has only a few key systemic associations: TB, sarcoidosis, and Behçet disease.[28,41,42]

Management

Patients with resolved vasculitis and clear media should be followed up at 6–12-month intervals. When the vision is good and the macula is healthy, minimal peripheral vasculitis may also be observed, though with close follow-up.[2,34,35]

Once systemic and ocular infections have been ruled out by history, examination, and investigations, corticosteroids are the mainstay of treatment for active vasculitis. Periocular depot corticosteroids like triamcinolone acetonide, 40 mg/mL, are effective in most cases with unilateral disease.[46] When the vasculitis is bilateral or severe, or when there is inadequate response to periocular injections, systemic corticosteroids (typically, oral prednisolone, 1 mg/kg body weight per day) should be considered.[46] In the authors' experience, corticosteroids by these two routes are almost always enough to control the inflammation in Eales disease; immunosuppressive agents are rarely required. A small short-term case series reported successful resolution of active vasculitis in Eales disease with intravitreal injection of triamcinolone acetonide, 4 mg/0.1 mL.[5] The rationale of choosing the intravitreal over the sub-Tenon route and the potential predicament of bilateral treatment were not explained. In the presence of a positive tuberculin test, some investigators

recommend antitubercular therapy.[1,15,28,34] However, its role in the treatment of Eales disease is unproven and controversial, and should be decided by an internist.[2]

Once the proliferative stage is reached, peripheral scatter photocoagulation in the ischemic areas bordering the neovascularization is the treatment of choice.[1,2,4,10,14,15,34] Treatment should be extended posteriorly according to the posterior spread of the retinal nonperfusion and the presence of posterior or disc neovascularization.[2] Scatter photocoagulation is not recommended in the absence of neovascularization for peripheral retinal nonperfusion, which is nearly universal in Eales disease.[20] Photocoagulation is also contraindicated in the presence of active vasculitis, which is likely to flare up and release more angiogenic factors, aggravating neovascularization (Fig. 86.5).[2] Pretreatment with corticosteroids sometimes mitigates the need for subsequent photocoagulation as well.

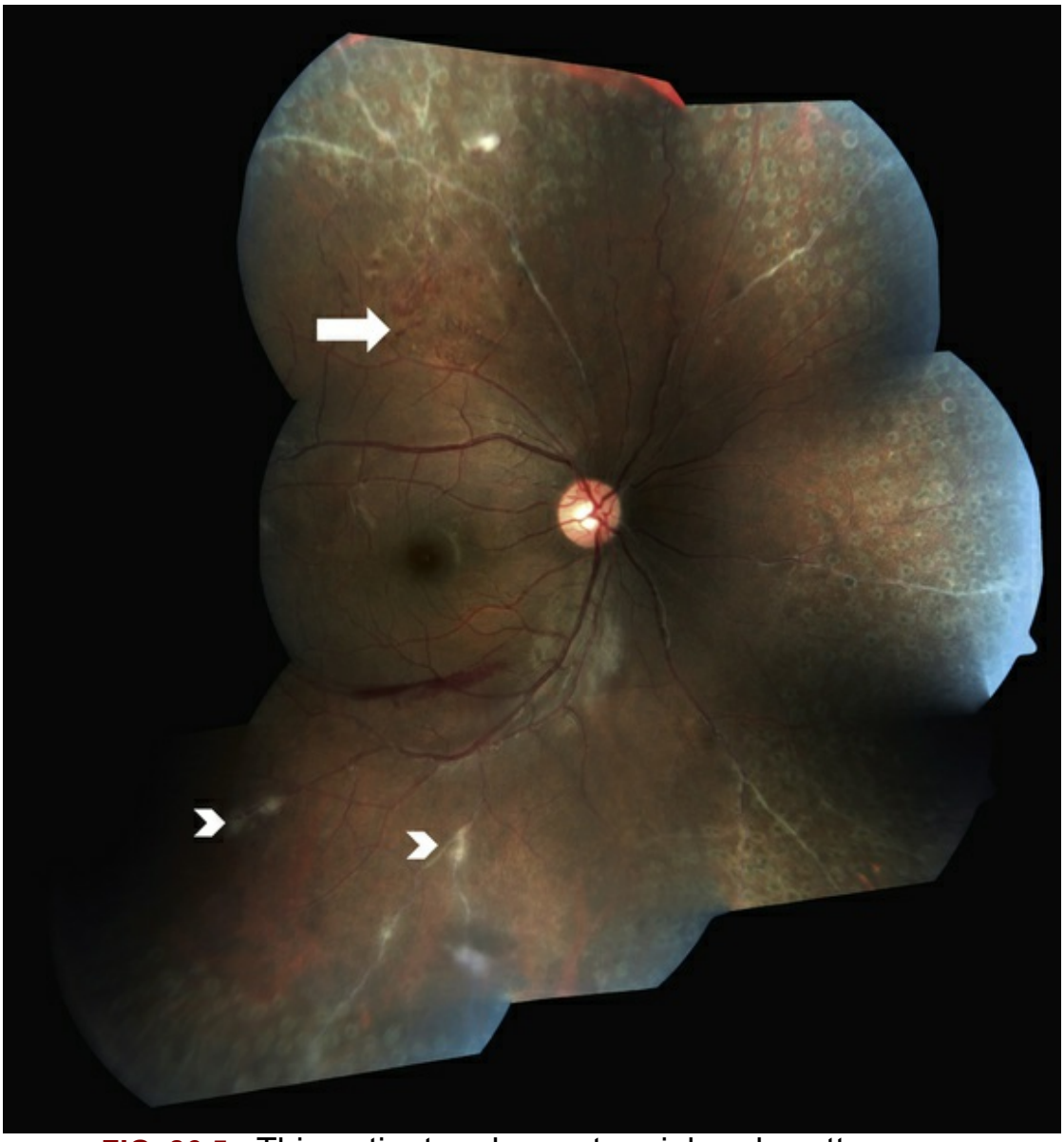

FIG. 86.5 This patient underwent peripheral scatter photocoagulation for postinflammatory neovascularization in Eales disease. The picture shows a simultaneous recurrence of neovascularization (*arrow*) and vascular inflammation (*arrowheads*): the inflammation was treated before neovascularization. Note the lack of involvement of the posterior pole.

Persistent vitreous hemorrhage is the most frequent indication for vitrectomy. Early intervention (within 3–6 months) begets better visual outcomes;[47] epimacular membranes or extramacular retinal detachment warrant consideration of early vitrectomy; and macular detachment mandates immediate vitrectomy. Results of vitrectomy

in Eales disease have been reported for about three decades; however, there is marked discrepancy in the reported outcomes due to variability in case selection, mainly PVD status and retinal detachment.[4,8,36,47] With modern surgical instrumentation, good surgical outcomes are possible in spite of incomplete or anomalous PVD and tractional sequelae (Fig. 86.6).[8] Over the past decade, the surgical instrumentation and inclination have irrevocably shifted towards small gauge (23–27G) sutureless vitrectomy for the entire vitreoretinal surgical spectrum, including Eales disease, excellent outcomes and faster recuperation are now common.[48] However, encircling belt-buckle may improve the surgical outcomes in the presence of peripheral tractional membranes.[8] Recently, anti-VEGF drugs like bevacizumab and ranibizumab have been used as adjuvants to scatter photocoagulation and vitrectomy. While bevacizumab probably has merit in treating neovascularization refractory to scatter photocoagulation[6] and as an adjuvant to vitrectomy, it cannot substitute vitrectomy for vitreous hemorrhage in Eales disease, and can precipitate tractional complications.[13,49] The patient should always be cautioned about the need for vitrectomy prior to anti-VEGF injection.

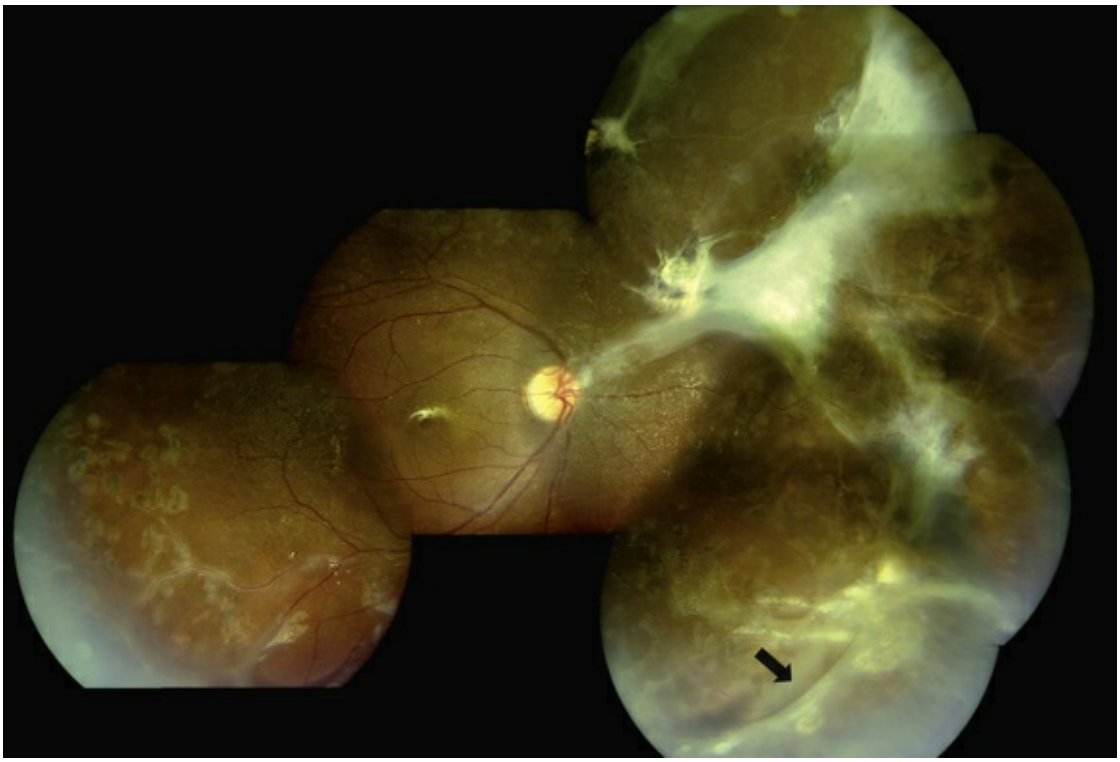

FIG. 86.6 Postvitrectomy view of an eye with persistent vitreous hemorrhage and membranes due to Eales disease: Note the relatively spared macula in spite of a large nasal residual tractional band with multiple attachments. Peripheral scatter photocoagulation marks are visible all around; indentation of the encircling belt buckle is seen inferonasally (*arrow*).
(Reproduced with permission from Shukla D, Kanungo S, Prasad NM, et al. Surgical outcomes for vitrectomy in Eales' disease. Eye 2008;22:900–4.)

Summary

Though numerous ocular and systemic diseases cause retinal vasculitis, isolated retinal vasculitis, as seen in Eales disease, has few systemic associations.[50] A detailed history and clinical examination, and specific investigations as indicated by the positive findings, are cost-effective and sufficient. Once the diagnosis of Eales disease is established, most cases are usually observed;[14] corticosteroids are required when vasculitis is significant. Peripheral scatter photocoagulation is effective in the proliferative disease, but should be delayed in favor of corticosteroids in the presence of active inflammation. Recurrent vitreous hemorrhage and tractional complications require consideration of early vitrectomy. With judicious use of medical and surgical treatment options, visual prognosis is good in most cases. While corticosteroids and scatter photocoagulation remain the standard of care, pharmacotherapy using antiangiogenic molecules, antioxidants, and antibodies against specific inflammatory cytokines may play a larger role in the future treatment of this enigmatic disease.[2,7,9,12,34]

References

1. Patnaik B, Nagpal PN, Namperumalsamy P, et al. Eales disease: clinical features, pathophysiology, etiopathogenesis. *Ophthalmol Clin North Am*. 1998;11:601–618.
2. Biswas J, Sharma T, Gopal L, et al. Eales disease – an

update. *Surv Ophthalmol*. 2002;47:197–214.
3. Eales H. Retinal haemorrhages associated with epistaxis and constipation. *Brim Med Rev*. 1880;9:262.
4. Atmaca LS, Batioglu F, Atmaca Sonmez P. A long-term follow-up of Eales' disease. *Ocul Immunol Inflamm*. 2002;10:213–221.
5. Ishaq M, Feroze AH, Shahid M, et al. Intravitreal steroids may facilitate treatment of Eales' disease (idiopathic retinal vasculitis): an interventional case series. *Eye (Lond)*. 2007;21:1403–1405.
6. Kumar A, Sinha S. Rapid regression of disc and retinal neovascularization in a case of Eales disease after intravitreal bevacizumab. *Can J Ophthalmol*. 2007;42:335–336.
7. Murugeswari P, Shukla D, Rajendran A, et al. Proinflammatory cytokines and angiogenic and anti-angiogenic factors in vitreous of patients with proliferative diabetic retinopathy and Eales' disease. *Retina*. 2008;28:817–824.
8. Shukla D, Kanungo S, Prasad NM, et al. Surgical outcomes for vitrectomy in Eales' disease. *Eye (Lond)*. 2008;22:900–904.
9. Saxena S, Pant AB, Khanna VK, et al. Interleukin-1 and tumor necrosis factor-alpha: novel targets for immunotherapy in Eales disease. *Ocul Immunol Inflamm*. 2009;17:201–206.
10. Das T, Pathengay A, Hussain N, et al. Eales' disease: diagnosis and management. *Eye (Lond)*. 2010;24:472–482.
11. El-Asrar AMA, Herbort CP, Tabbara KF. A clinical approach to the diagnosis of retinal vasculitis. *Int Ophthalmol*. 2010;30:149–173.
12. Sen A, Paine SK, Chowdhury IH, et al. Association of interferon-gamma, interleukin-10, and tumor necrosis factor-alpha gene polymorphisms with occurrence and severity of Eales' disease. *Invest Ophthalmol Vis Sci*. 2011;52:171–178.
13. Patwardhan SD, Azad R, Shah BM, et al. Role of intravitreal bevacizumab. In: Eales disease with dense vitreous hemorrhage: a prospective randomized control study.

Retina. 2011;31:866–870.
14. Schubert HD. Eales' disease. Guyer DR, Yannuzzi LA, Chang S, et al. *Retina – vitreous – macula*. W.B. Saunders: Philadelphia; 1999:415–420.
15. Das T, Biswas J, Kumar A, et al. Eales' disease study. *Indian J Ophthalmol*. 1994;42:3–18.
16. Elliot AJ. Recurrent intraocular hemorrhage in young adults (Eales's disease); a report of 31 cases. *Trans Am Ophthalmol Soc*. 1954;52:811–875.
17. Spitznas M, Meyer-Schwicherath G, Stephan B. The clinical picture of Eales' disease. *Albrecht Von Graefes Arch Klin Exp Ophthalmol*. 1975;73–85.
18. Stanford MR, Verity DH. Diagnostic and therapeutic approach to patients with retinal vasculitis. *Int Ophthalmol Clin*. 2000;40:69–83.
19. Charamis J. On the classification and management of the evolutionary course of Eales' disease. *Trans Ophthalmol Soc U K*. 1965;85:157–160.
20. Das TP, Namperumalsamy P. *Photocoagulation in Eales' disease: results of prospective randomised clinical study*. [Presented at XXVI International Congress of Ophthalmology, Singapore] 1990.
21. Graham EM, Stanford MR, Whitcup SM. Retinal vasculitis. Pepose JS, Holland GN, Wilhelmus KR. *Ocular infection and immunity*. Mosby: St. Louis; 1996:538–551.
22. Rosenbaum JT, Ku J, Ali A, et al. Patients with retinal vasculitis rarely suffer from systemic vasculitis. *Semin Arthritis Rheum*. 2012;41:859–865.
23. Eltzschig HK, Carmeliet P. Hypoxia and inflammation. *N Engl J Med*. 2011;17:656–665.
24. Bharathselvi M, Biswas J, Selvi R, et al. Increased homocysteine, homocysteine-thiolactone, proteinhomocysteinylation and oxidative stress in the circulation of patients with Eales' disease. *Ann Clin Biochem*. 2013;50:330–338.
25. Biswas J, Therese L, Madhavan HN. Use of polymerase chain reaction in detection of *Mycobacterium tuberculosis* complex DNA from vitreous sample of Eales' disease. *Br J*

Ophthalmol. 1999;83:994.
26. Madhavan HN, Therese KL, Gunisha P, et al. Polymerase chain reaction for detection of *Mycobacterium tuberculosis* in epiretinal membrane in Eales' disease. *Invest Ophthalmol Vis Sci*. 2000;41:822–825.
27. Muthukkaruppan V, Rengarajan K, Chakkalath HR, et al. Immunological status of patients of Eales' disease. *Indian J Med Res*. 1989;90:351–359.
28. Bansal R, Sharma A, Gupta A. Ocular tuberculosis. *Expert Rev Ophthalmol*. 2015;7:341–349.
29. Chao JR, Khurana RN, Fawzi AA, et al. Syphilis: reemergence of an old adversary. *Ophthalmology*. 2006;113:2074–2079.
30. Shukla D, Rathinam SR, Cunningham ET Jr. Leptospiral uveitis in the developing world. *Int Ophthalmol Clin*. 2010;50:113–124.
31. Herbort CP, Rao NA, Mochizuki M. International criteria for the diagnosis of ocular sarcoidosis: results of the First International Workshop on Ocular Sarcoidosis (IWOS). *Ocul Immunol Inflamm*. 2009;17:160–169.
32. Davatchi F, Shahram F, Chams-Davatchi C, et al. Behçet's disease in Iran: analysis of 6500 cases. *Int J Rheum Dis*. 2010;13:367–373.
33. Aristodemou P, Stanford M. Therapy insight: the recognition and treatment of retinal manifestations of systemic vasculitis. *Nat Clin Pract Rheumatol*. 2006;2:443–451.
34. Biswas J, Ravi RK, Naryanasamy A, et al. Eales' disease – current concepts in diagnosis and management. *J Ophthalmic Inflamm Infect*. 2013;3:11.
35. George RK, Walton RC, Whitcup SM, et al. Primary retinal vasculitis: systemic associations and diagnostic evaluation. *Ophthalmology*. 1996;103:384–389.
36. Badrinath SS, Gopal L, Sharma T, et al. Vitreoschisis in Eales' disease: pathogenic role and significance in surgery. *Retina*. 1999;19:51–54.
37. Mesquida M, Llorenç V, Fontenla JR, et al. Use of ultra-wide-field retinal imaging in the management of active

Behçet retinal vasculitis. *Retina*. 2014;34:2121–2127.
38. Reznicek L, Seidensticker F, Stumpf C, et al. Systematic analysis of wide-field fundus autofluorescence (FAF) imaging in posterior uveitis. *Curr Eye Res*. 2014;39:164–171.
39. Errera MH, Coisy S, Fardeau C, et al. Retinal vasculitis imaging by adaptive optics. *Ophthalmology*. 2014;121:1311–1312.e2.
40. London NJ, Rathi nam SR, Cunningham ET Jr. The epidemiology of uveitis in developing countries. *Int Ophthalmol Clin*. 2010;50:1–17.
41. Khairallah M, Accorinti M, Muccioli C, et al. Epidemiology of Behçet disease. *Ocul Immunol Inflamm*. 2012;20:324–335.
42. Jones N, Mochizuki M. Sarcoidosis: epidemiology and clinical features. *Ocul Immunol Inflamm*. 2010;18:72–79.
43. Wakefield D, Chang JH. Epidemiology of uveitis. *Int Ophthalmol Clin*. 2005;45:1–13.
44. Chang JH, Landers J, Henderson TR, et al. Prevalence of uveitis in indigenous populations presenting to remote clinics of central Australia: the Central Australian Ocular Health Study. *Clin Experiment Ophthalmol*. 2012;40:448–453.
45. Llorenç V, Mesquida M, Sainz de la Maza M, et al. Epidemiology of uveitis in a Western urban multiethnic population. The challenge of globalization. *Acta Ophthalmol*. 2015;93(6):561–567.
46. George RK, Nussenblatt RB. Treatment of retinal vasculitis. *Ophthalmol Clin North Am*. 1998;11:673–680.
47. Kumar A, Kumar A, Tiwari HK, et al. Comparative evaluation of early vs. deferred vitrectomy in Eales' disease. *Acta Ophthalmol Scand*. 2000;78:77–78.
48. Khanduja S, Gupta S, Sinha S, et al. Surgical outcomes of minimally invasive vitrectomy surgery in Eales' disease. *Nepal J Ophthalmol*. 2013;5:182–189.
49. Kumar A, Sehra SV, Thirumalesh MB, et al. Secondary rhegmatogenous retinal detachment following intravitreal bevacizumab in patients with vitreous hemorrhage or tractional retinal detachment secondary to Eales' disease. *Graefes Arch Clin Exp Ophthalmol*. 2012;250:685–690.
50. Saurabh K, Das R, Biswas J, et al. Profile of retinal vasculitis

in a tertiary eye care center in Eastern India. *Indian J Ophthalmol*. 2011;59:297–301.

87

Spirochetal Infections

Julie H. Tsai, Narsing A. Rao

Introduction

The history of spirochetal infections in the eye extends back to the first reported observations of spirochetes isolated from the nervous system.[1] Today, the most common spirochetal organisms encountered in the tissues of the eye and ocular adnexae are *Treponema pallidum*, the infectious entity causing syphilis; *Borrelia burgdorferi sensu lato* complex, a diverse group of spirochetes that cause Lyme disease (LD); and *Leptospira* species, which upon infection produces a host of local and systemic findings typical of leptospirosis. Diagnosis of spirochetal infections of the eye requires a high degree of clinical suspicion as well as early recognition for more effective treatment.

Syphilitic Uveitis

Infection with the spirochete *T. pallidum* results in the ocular and systemic findings associated with syphilis. Sexual transmission is the most common means of inoculation, though direct contact with an active lesion or spread via transfusion are also potential routes of infection. Prior to the advent of penicillin, the disease was associated with high morbidity and mortality; however, as the antibiotic became widely available, the incidence of syphilitic disease dropped steeply. In recent years, changing socioeconomic factors and increases in high-risk sexual behavior, infection with human immunodeficiency virus (HIV), and antibiotic resistance have all contributed to resurgence of the disease. Worldwide, there

are an estimated 10 million new cases of syphilis annually, and increases in reported cases are seen most commonly in cases of men who have sex with men (MSM) and those who are coinfected with HIV.[2,3]

While uncommon, ocular manifestations are typically associated with neurosyphilis, which can occur early or late in the course of infection.[4] Symptoms can be seen roughly 2–6 months after initial infection.[5] The most common ocular finding is uveitis, which can present as anterior, intermediate, posterior or panuveitis.[6]

Epidemiology and Pathogenesis

The only known reservoir for syphilis is in the human, and historically infection had been limited to populations with poor hygiene, limited access to healthcare, and low socioeconomic status. The most current surveillance data in the United States indicates that the rate of primary and secondary syphilis has more than doubled between the years of 2005 and 2013: from 2.1 cases to 5.3 cases per 100,000 population. Specifically, the greatest percentage increases are seen in young men (149.4% in those ages 20–24 from 2005 to 2009, and 48.4% in ages 25–29 from 2009 to 2013), particularly among MSM.[2,6] Due to such high rates of infection within the younger population and particularly in urban areas in the western United States, recent expansion of syphilis testing in nonclinical settings have been made available to the public via online testing labs as well as social media apps on smartphone platforms.[7,8] This provides an additional avenue for detecting new cases and offers innovative online syphilis prevention information with easily available testing and partner notification tools; however, the impact on public health surveillance has yet to be determined.

The local and systemic response to *T. pallidum* is complex, and is initiated as the bacteria enter the body through intact mucosa. Local invasion of the tissues ensues, and dissemination occurs via blood and the lymphatic system. On the microscopic level, lymphocytic infiltration is seen, either diffuse or focal, surrounding the blood vessels of affected organs. In the eye, this can be found in the iris, ciliary body, and choroid, along with chronic granulomatous inflammation, including epithelioid histiocytes and multinucleated

giant cells. Mononuclear cells, sensitized T lymphocytes, macrophages, and plasma cells can also be seen. This inflammation and the resulting adaptive immune response cause the tissue destruction characteristic of syphilis.

Local antibodies are also produced against the lipid, protein, and lipoprotein components of *T. pallidum*. The majority of bacteria are eradicated by opsonization and engulfed by macrophages. Those organisms that are resistant to phagocytosis may persist locally at the site of inoculation. Dissemination can occur despite the development of the humoral and cellular response, and without treatment, the bacteria can persist in the human host for decades, resulting in continued transmission and end-organ damage.[9]

Ocular Manifestations

Uveitis is the most common ocular finding, ranging from 0.7% to 16.4% in recent epidemiologic studies, with higher rates of occurrence in patients coinfected with HIV.[6,10] Findings can include keratic precipitates and iritis in the anterior segment of the eye, manifesting as either granulomatous or nongranulomatous inflammation. Dilated iris capillaries may also be noted (roseola), and these dilated and tortuous vessels may be a result of obliterative endarteritis. Posterior manifestations include vitritis, vasculitis, papillitis, periphlebitis, exudative retinal detachment, uveal effusion, central retinal vein occlusion, subretinal neovascular membrane formation, retinal necrosis, and neuroretinitis.[6,10–12] Acute syphilitic posterior placoid chorioretinitis can often be seen in the macula or juxtapapillary locations.[13,14] The yellow or gray placoid lesions often have atrophic centers and are flat, with no evidence of fluid or hemorrhage. Fluorescein angiography reveals early hypofluorescence and late stain of the lesion with distinctive "leopard spot" hypofluorescence (Fig. 87.1). In patients with HIV, posterior uveitis is more common, presenting as a dense vitritis or diffuse, creamy retinitis with overlying punctuate retinal precipitates.[6,11,15,16]

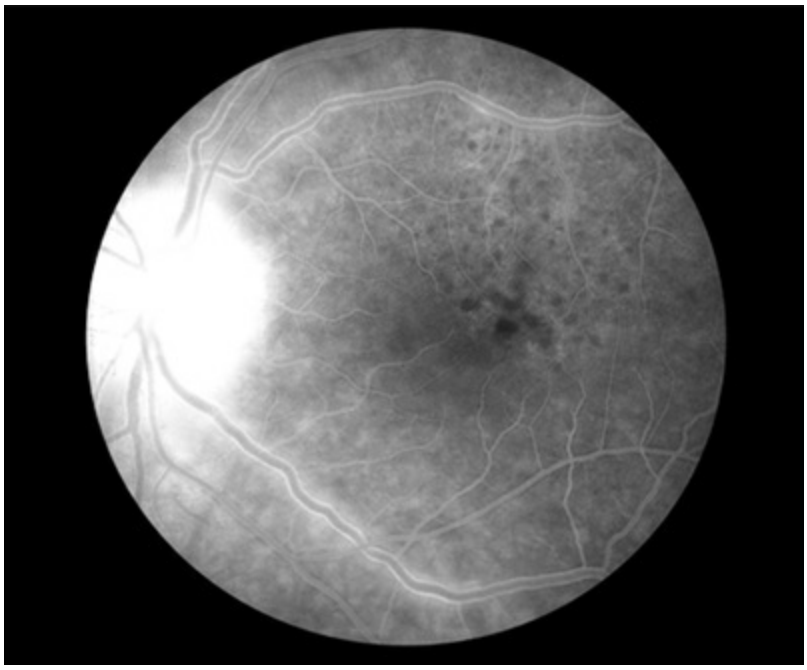

FIG. 87.1 Late fluorescein angiographic image of the left eye in a patient with ocular syphilis with focal hypofluorescence, leakage of the optic disc, and staining of the retinal veins. (Reproduced with permission from Chao JR, Khurana RN, Fawzi AA, et al. Syphilis: reemergence of an old enemy. Ophthalmology 2006;113:2074–9.)

Other ocular findings include interstitial keratitis of the cornea; chancre and nonspecific papillary reaction of the conjunctiva; episcleral and scleral inflammation; and inflammation of the optic nerve presenting as optic neuritis. Cataract can also be seen, both in congenital as well as acquired disease. Glaucoma in syphilis is often due to uveitis, though it may occur in either congenital or acquired infection. Lastly, the classic pupillary finding in syphilis (Argyll Robertson pupil) is seen in late syphilis or early neurosyphilis, manifesting with anisocoria and light–near dissociation upon clinical testing.

Findings in neurosyphilis are variable and dependent on the stage of disease. Stroke-like symptoms due to vasculitis and vascular compromise in early neurosyphilis may affect the cranial nerve nuclei as well as the centers for saccadic and smooth pursuit. Focal intracranial gummas may cause visual field deficits and superior orbital fissure syndrome, depending on the location of origination. Horner's syndrome and internuclear ophthalmoplegia may also be observed. Late neurosyphilis may result in general

paresis and tabes dorsalis.

Diagnosis

A high level of clinical suspicion is required for the appropriate diagnosis of syphilitic uveitis, due to its variable clinical presentation and atypical presentation in HIV-infected individuals. Appropriate laboratory studies can aid in confirming the diagnosis and rule out other disease entities. Visualization of the organism in lesion exudates or tissue via dark-field microscopy with immunofluorescent staining is considered the gold standard and the quickest and most direct approach for establishing the diagnosis; however, the availability of such facilities limits its utility in clinical practice.[17] In addition, these tests are highly specific, but not very sensitive for widespread detection of infection.

Serologic testing with nontreponemal and treponemal tests is most commonly used in ophthalmic clinical practice. Nontreponemal tests detect the antibody to cardiolipin cholesterol antigen, and most clinicians are familiar with the Venereal Disease Research Laboratory (VDRL) and rapid plasma reagin (RPR) tests. These tests are best suited for general screening in a population with a low prevalence of syphilis, as well as for monitoring treatment efficacy as the titers decrease with appropriate therapy.

Treponemal tests, such as the fluorescent treponemal antibody absorption tests (FTA-ABS) and the microhemagglutinin assay for *T. pallidum* (MHA-TP), are more specific than the nontreponemal tests and may be just as sensitive. However, they are more expensive and a proportionate increase in false positives can occur if they are applied to a low-risk population. Thus, they may be used initially in patients who have a high probability of infection. Generally, once these tests are positive, the patient remains positive for life.

Newer treponemal tests, such as enzyme immunoassays (EIA) and chemiluminescence assays (CIA) utilizing specific treponemal antigens, have recently been approved by the Food and Drug Administration (FDA) and are recommended by the Centers for Disease Control and Prevention (CDC) as initial screening tests for syphilis (http://www.cdc.gov/std/syphilis/Syphilis-Webinar.htm).

These EIA/CIA tests are qualitative, have specific IgM and IgG antitreponemal antibodies (for detection of early and late syphilis, respectively) and also remain positive for life. The new "reverse sequence" algorithm allows for the capture of those individuals with either very early disease or late findings (e.g., neurosyphilis with ocular complications) who would be positive by treponemal-specific testing but negative by RPR. These discordant results are expected due to the high sensitivity and low specificity of the EIA/CIA tests; thus, a confirmatory treponema particle agglutination test would be submitted (Fig. 87.2). The use of a singular type of serologic test is insufficient for diagnosis, as each has its limitations, specifically the false-positive test results in patients without syphilis. False-positive test results may be associated with certain infections (e.g., Lyme disease, leptospirosis, malaria) and medical conditions (e.g., autoimmune disorders, intravenous drug use, pregnancy).

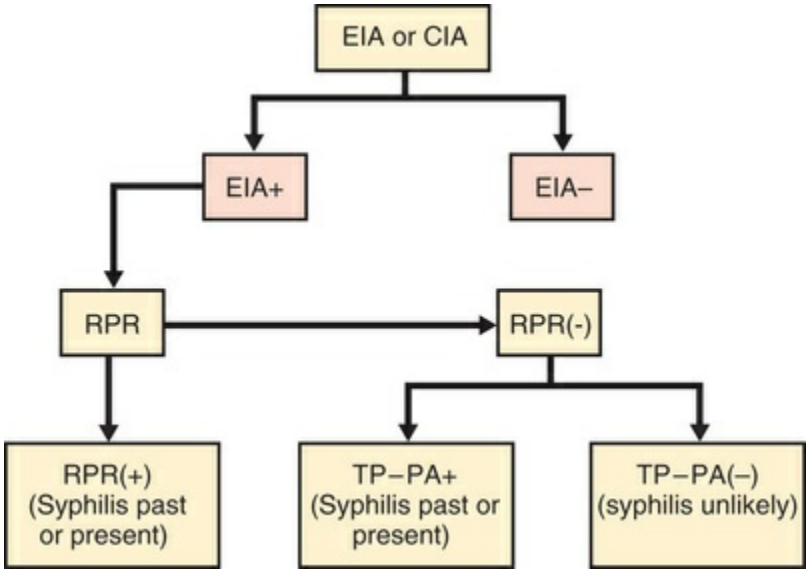

FIG. 87.2 Reverse sequencing algorithm for detection of syphilis. The testing protocol begins with an immunoassay for treponemal antibodies. Negative results rule out syphilis, but a positive result is followed by a nontreponemal quantitative test. A positive nontreponemal test is considered diagnostic of syphilis infection, either past or present. Further confirmation can be performed with a sensitive and specific treponemal agglutination test, such as the TP-PA.

Abbreviations: CIA, chemiluminescence immunoassay; EIA, enzyme immunoassay; RPR, rapid plasma regain; TP-PA, treponemal pallidum particle agglutination.

(Adapted from the Centers for Disease Control and Prevention webinar on reverse sequencing syphilis screening, http://www.cdc.gov/std/syphilis/Syphilis-Webinar.htm).

Other testing modalities include polymerase chain reaction (PCR) assays and rapid specific treponemal tests. PCR assays, if available, should be conducted on frozen specimens (shipped according to the laboratory specifications), but cannot discern between live or dead organisms. The rapid tests, which may use as little as 10–50 μL of sample, are considered to be equivalent to the older specific treponemal antibody tests and have similar limitations in terms of distinguishing active versus inactive infection.[18,19]

For HIV-infected individuals, these serologic tests are often accurate and reliable for diagnosis and following therapeutic response. Atypical results (i.e., unusually high/low/fluctuating titers) without corresponding clinical findings suggestive of early syphilis should prompt further investigation to confirm the diagnosis.[20] False-negative tests may occur due to insufficient production of antibody to the bacterial proteins, or an overall lack of immunoreactivity.

In neurosyphilis, cerebrospinal fluid (CSF) analysis, along with VDRL and FTA-ABS tests, may need to be considered in confirming the diagnosis of neurosyphilis.[4] CSF FTA-ABS is often too sensitive and thus the role of this test is still controversial. CSF VDRL does have the advantage over CSF FTA-ABS in cases requiring differentiation of current active infection from past infection. Leukocytosis and elevated protein concentrations can be seen in the CSF and these findings are often present for more than 1 year in those individuals with neurologic symptoms. This is consistent with neurosyphilis and warrants treatment even if test results are negative.

Differential Diagnosis

The clinical findings and possible differential diagnoses for syphilitic uveitis are listed in Table 87.1. The most critical diagnosis

to make may be acute syphilitic posterior chorioretinitis, and one must rule out acute posterior multifocal placoid pigment epitheliopathy and atypical serpiginous choroidopathy. In these instances, the use of intravitreal steroid or systemic immunosuppressive therapy for treatment of these conditions may unmask an underlying infection.[14] It is important to emphasize that a high degree of clinical suspicion is vital in order to make the diagnosis, and that serologic confirmation is required.

TABLE 87.1

Differential Diagnosis of Ocular Syphilis With Laboratory Workup

Disease/Disorder	Possible Serologic/Laboratory Testing
Toxoplasmosis	IgM-ELISA, IgG-ELISA for antibodies to *Treponema gondii*
Rubella	IgM-ELISA, IgG-ELISA for rubella; rubella titer
Cytomegalovirus (CMV)	CMV DNA PCR
Human immunodeficiency virus (HIV)	ELISA
Herpes simplex virus (HSV)	Diagnostic viral culture, HSV-1/HSV-2 serologic assays
Varicella-zoster virus (VZV)	Diagnostic viral culture, antibody assays
HLA-B27-related uveitis	HLA-B27 genetic testing
Primary intraocular lymphoma	Cytology on vitreous or aqueous humor; neuroradiologic and CSF studies
Sarcoidosis	Angiotensin-converting enzyme (ACE) level
Tuberculosis	PPD, QuantiFERON gold testing
Idiopathic uveitis	Diagnosis of exclusion after testing for other uveitic entities

CSF, cerebrospinal fluid; ELISA, enzyme-linked immunosorbent assay; HLA, human leukocyte antigen; IgM/IgG, immunoglobulin M/G; PCR, polymerase chain reaction; PPD, purified protein derivative.

Treatment

The clinician who diagnoses syphilitic infection in a patient has two responsibilities: to report the case to the state Department of Health;[21] and to determine if he or she is comfortable in managing and following the therapeutic regimen for the patient. A survey of infectious disease practitioners conducted in 2008 found variation in the management of syphilis among the experts, particularly in cases where patients were coinfected with HIV.[17] It is the recommendation of the authors that the ophthalmologist treat the patient in consultation with an infectious disease specialist.

Penicillin G is the preferred treatment for all stages of syphilis

(Table 87.2). The dose, route of administration, and duration of therapy are determined by the stage and clinical findings. Sexual partners of the infected individual also need to be evaluated and treated.[21] For patients with a penicillin allergy, alternative antibiotics may be used; however, as the other medications are not as effective as penicillin, skin testing and desensitization are recommended, especially in those patients who are coinfected with HIV. As for patients diagnosed with congenital syphilis, treatment with aqueous penicillin G or procaine penicillin G via intravenous administration is recommended. Other antibiotics such as ceftriaxone and ampicillin have been used, but there is no optimal therapy for congenital syphilis noted at this time.

TABLE 87.2

Recommended Treatment of Syphilis

Stage of Disease	Preferred Treatment	Alternative Treatment
Primary, secondary, or early latent	Benzathine penicillin G 2.4 million units im, single dose	Doxycycline 100 mg po b.i.d. ×2 weeks or tetracycline 500 mg po q.i.d. ×2 weeks
Late latent, latent syphilis of unknown duration, tertiary stage, or those who fail primary therapy	Benzathine penicillin G 2.4 million units im, administered weekly ×3 weeks	Doxycycline 100 mg po b.i.d. ×4 weeks or tetracycline 500 mg po q.i.d. ×4 weeks
Neurosyphilis	Aqueous penicillin G 3–4 million units iv every 4 hours ×10–14 days	Procaine penicillin 2.4 million units im daily ×10–14 days and probenecid 500 mg po q.i.d. ×10–14 days

Notes: (1) Human immunodeficiency virus-positive patients should be treated with penicillin at all stages of infection, and those allergic to penicillin should be desensitized and then treated with the full regimen. (2) All patients with tertiary syphilis should have a cerebrospinal fluid analysis and be evaluated for neurosyphilis.

(Adapted from Centers for Disease Control and Prevention. Sexually transmitted diseases treatment guidelines, 2010. MMWR 2010;59:26–40.)

Syphilitic uveitis or other ocular manifestations associated with neurosyphilis should be treated according to the recommendations for neurosyphilis.[4] A CSF examination is recommended for all patients with syphilitic eye disease to guide therapy. The recommended regimen is aqueous crystalline penicillin G delivered intravenously, as no alternative has been proven scientifically effective. In those patients who have failed primary therapy and

show evidence of tertiary syphilis, asymptomatic neurosyphilis may be present and may warrant evaluation of the CSF.[22] With regard to neurosyphilis in the HIV-positive patient, treatment with intravenous penicillin utilizing the neurosyphilis recommendations results in rapid resolution of findings. It is important to note that therapy must be of a duration and dose sufficient to cure neurosyphilis, regardless of CSF findings.[20]

Success with therapy may be evaluated by improvement in clinical findings and seroconversion or low titers upon nontreponemal testing. The published criteria for treatment of early syphilis describe four- to eightfold decrease in nontreponemal titers that should occur by 3–6 months, respectively. It is important to realize that these criteria cannot be used in monitoring treatment efficacy in HIV-positive patients, and aggressive treatment regimens are recommended in this population.

Once the infection has been appropriately treated, adjunctive therapy with corticosteroids may be applied for any residual ocular inflammation. Topical corticosteroids are beneficial for anterior uveitis and interstitial keratitis, whereas systemic corticosteroid therapy may be required in order to resolve symptoms of residual scleritis, posterior uveitis, or optic neuritis. Corticosteroid regimens should always be administered concurrently with antibiotic therapy.

Course and Outcome

Outcomes of syphilitic uveitis and systemic disease are dependent on early diagnosis and appropriate antibiotic therapy. These cases often result in full visual recovery and improvement in other systemic findings. Untreated cases of syphilitic uveitis often lead to worsening of intraocular inflammation, development of glaucoma secondary to chronic uveitis, and retinal necrosis. Chronic vitritis and optic atrophy may also occur. Treatment in HIV-positive individuals should be initiated early and aggressively, utilizing the regimen recommended for neurosyphilis.

Uveitis Associated With Lyme

Disease

LD is a multisystem disorder found in North America, Europe, and Asia caused by the tick-borne spirochete *Borrelia burgdorferi sensu lato*, a complex of 13 closely related species in the genus *Borrelia*. In the United States the majority of manifestations are caused by infection with *B. burgdorferi sensu stricto* (hereafter known as *B. burgdorferi*), transmitted by the *Ixodes* tick species, whereas in Europe and Asia, the disease is mainly caused by *B. garinii* and *B. afzelii*, respectively.

The disease can be broken down into stages: stage 1, which often begins days to weeks after the tick bite and is denoted by the pathognomonic finding of erythema migrans in conjunction with fever, malaise, and arthralgias; stage 2, which is the phase of dissemination of the spirochete to multiple organs in the days, weeks, or months after infection; and stage 3, which often occurs after a disease-free period lasting months to years.

In all cases, a history of tick bite may be absent in 50% of individuals.[23] The dissemination to multiple organ systems, particularly the skin, heart, joints, and nervous system, along with neurologic manifestations (e.g., cranial and peripheral neuropathies and meningoencephalitis), is the hallmark of stage 2 disease.[24] Chronic arthritis and conduction defects may also develop.[25] The lymphocytoma, another skin lesion, may develop, especially on the earlobe or breast, and the initial erythema migrans fades and reappears.[24] These findings may take days, weeks, or even months to manifest clinically.

The third or late stage of disease often occurs after a disease-free period lasting months to years, and may occur despite adequate antibiotic therapy.[26] Chronic symptoms mark this phase of infection, and common conditions include chronic relapsing arthritis of the knee; acrodermatitis chronica atrophicans, a rash that results in atrophy of the skin and underlying structures; and late neurologic manifestations (e.g., encephalopathy, demyelination, and dementia).[24,26,27]

Ocular disease can manifest at any stage of infection. Though well documented, the majority of cases persist in case reports and case series, with few definitive, large-scale studies in the scientific

literature.

Epidemiology and Pathogenesis

In the United States, the endemic areas are clustered around three regions: (1) the northeast, down as far south to Virginia, with hyperendemic regions in Connecticut and New York; (2) the Midwest, in the states of Michigan, Wisconsin, and Minnesota; and (3) the west, primarily in northern California. Certain areas of Europe and Asia are also affected, particularly in regions with a temperate climate. It is unclear why there is a preponderance of cases localized to the northeastern United States.[25]

The pathogenesis of the disease is similar to that induced by the spirochete *T. pallidum*, and follows in three distinct stages. The first stage, or early infection, is believed to be due to spirochetemia. After an incubation period of 3–32 days, the spirochete multiplies and induces proinflammatory responses in both the innate and adaptive immune systems. This is clinically observed as the characteristic skin rash, erythema migrans, at the site of the tick bite.[25] Within days to weeks, *B. burgdorferi* can be recovered from many areas of the body. All affected tissues show some infiltration of lymphocytes and plasma cells, along with vascular damage (e.g., mild vasculitis or hypervascular occlusion).

The immunologic response of the host to parasitic invasion is the likely etiology for the manifestations of stage 2 and 3 disease.[28] The specific immunoglobulin M (IgM) response provides for polyclonal B-cell activation and increased levels of circulating immune complexes, while the specific IgG response develops over weeks in response to spirochetal polypeptides and nonprotein antigens. Spirochetal killing is primarily due to bactericidal B-cell responses and utilizes the complement pathway. For the majority of cases, the innate and adaptive response is capable of controlling widespread dissemination of the disease without antibiotic therapy; however, without appropriate therapy, *B. burgdorferi* can survive for several years in particular loci, such as joints, skin, and nervous system.[25] Recent reports seem to support this observation, as *in vitro* studies indicate that these infectious strains are capable of forming cystic bodies and biofilm aggregates, and current antibiotics have varying

effects on these different morphologic forms.[29,30]

Ocular Manifestations

Ocular findings are less prominent compared to the significant systemic manifestations and can appear at any stage of disease. Conjunctivitis is the most common finding, present in 11% of patients with early-stage Lyme disease.[31] Ophthalmologists are generally not consulted as the nonspecific findings of conjunctival and periorbital inflammation are mild in nature and self-limiting. Neuro-ophthalmic complications are associated with stage 2 disease and commonly manifest as ocular motility problems due to cranial nerve palsies, optic neuritis, papilledema, and pseudotumor cerebri in the setting of meningoencephalitis.[26,32–34] Stromal keratitis, episcleritis, and symblepharon formation have been reported in stage 3 disease.[35]

Intraocular inflammation often presents as chorioretinitis and vitreous inflammation, though there have been a variety of clinical presentations associated with LD.[32,36,37] Vitreous involvement may be nonspecific, with or without associated retinal pathology, such as retinal vasculitis.[37] Clinically, the presence of disc edema in the setting of posterior-segment inflammation may be related to chronic posterior-segment inflammation rather than the neurologic involvement from borreliosis (Fig. 87.3). Appropriate neuro-ophthalmic testing should be undertaken to evaluate the potential of other central nervous system complications.

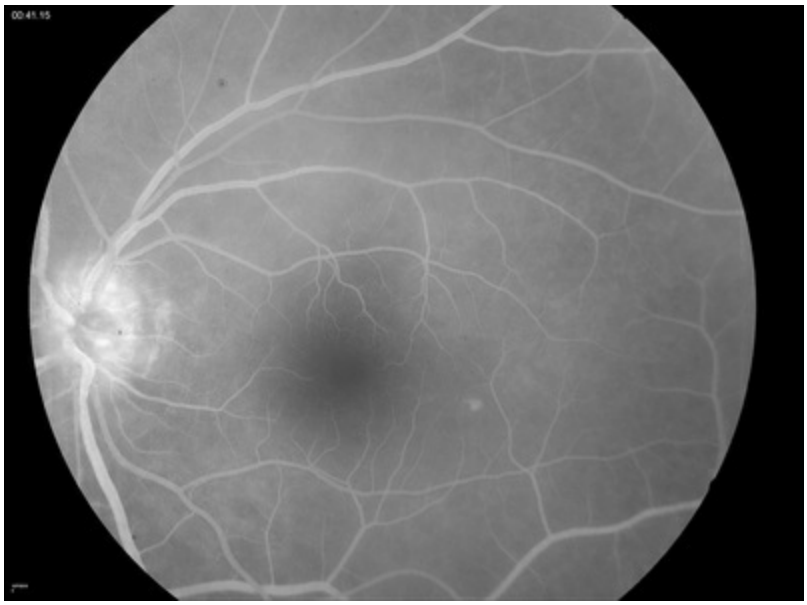

FIG. 87.3 Fluorescein angiogram depicting disc edema and mild vitritis in a 44-year-old Caucasian male with positive serology for Lyme borreliosis. There is a nonspecific window defect temporal to the fovea.
(Courtesy of Thomas J. Federici, MD.)

Diagnosis

The clinical diagnosis of LD is dependent on the following: appearance of the pathognomonic skin rash (erythema migrans) in a patient with a history of tick bite and/or residence in an endemic region; or the appearance of the skin lesion in addition to involvement of two organ systems in those patients without a history of a tick bite or residence in a nonendemic region. The diagnostic criteria for Lyme disease as recommended by the CDC are listed in Table 87.3.[38]

TABLE 87.3
Diagnostic Criteria and Case Classification of Lyme Disease

DEFINITION
Erythema migrans (EM), or at least one advanced manifestation, as defined below, and laboratory confirmation of infection
ADVANCED MANIFESTATIONS
Musculoskeletal System
Recurrent, brief attacks (lasting weeks or months) of objective joint swelling in one or a few joints, sometimes followed by chronic arthritis in one or a few joints; manifestations not considered criteria for diagnosis include chronic progressive arthritis, not preceded by brief

attacks, and chronic symmetrical polyarthritis; arthralgia, myalgia, or fibromyalgia syndromes alone are not criteria for musculoskeletal involvement
Nervous System
Any of the following, alone or in combination: lymphocytic meningitis; cranial neuritis, particularly facial palsy (may be bilateral); radiculoneuropathy; or, rarely, encephalomyelitis (must be confirmed by showing antibody production against *Borrelia burgdorferi* in the cerebrospinal fluid, demonstrated by a higher titer of antibody in cerebrospinal fluid than in serum); headache, fatigue, paresthesia, or mild stiff neck alone are not criteria for neurologic involvement
Cardiovascular System
Acute-onset, high-grade (2 or 3) atrioventricular conduction defects that resolve in days to weeks and are sometimes associated with myocarditis; palpitations, bradycardia, bundle branch block, or myocarditis are not criteria for cardiovascular involvement
CLASSIFICATION
Suspected
• A case of EM where there is no known exposure and no laboratory evidence of infection, *or* • A case with laboratory evidence of infection but no clinical information available (e.g., a laboratory report)
Probable
Any other case of physician-diagnosed Lyme disease that has laboratory evidence of infection
Confirmed
• A case of EM with a known exposure, *or* • A case of EM with laboratory evidence of infection and without a known exposure, *or* • A case with at least one late manifestation (e.g., musculoskeletal, nervous system, or cardiac) that has laboratory evidence of infection.

Adapted from "Lyme Disease (*Borrelia burgdorferi*) 2011 Case Definition", available from http://www.cdc.gov/nndss/conditions/lyme-disease/case-definition/2011/.

Culture of *B. burgdorferi* from peripheral blood, areas of skin rash, and CSF provides for definitive diagnosis.[39,40] However, positive cultures are often difficult to obtain as they mainly occur early on in the disease process. In these cases, sensitivity is highest in tissue culture, with the positive rates of culture dropping significantly for plasma and CSF.[25] For ocular disease, serologic testing is often more helpful in diagnosis as these manifestations can occur several years after initial inoculation. These results, along with a clinical history suggestive of infection, provide the basis for diagnosis of LD.

The CDC recommends a two-step approach in which serologic samples are tested: first, an enzyme-linked immunosorbent assay (ELISA) is performed to detect the presence of IgG and IgM specific for *B. burgdorferi*. For those individuals suspected of acquiring LD overseas, a specific C6 peptide ELISA is recommended as the other serologic tests may not detect the European and Asian strains.[41] Equivocal results are then tested by Western blotting. According to CDC criteria, the IgM Western blot is considered positive if two of the following three bands are present: 23, 39, and 41 kDa, though the combination of the 23- and 41-kDa bands may still be

considered a false-positive result. The IgG Western blot may be considered to be positive if five of the following 10 bands are present: 18, 23, 28, 30, 39, 41, 45, 58, 66, and 93 kDa.[41] The results still need to be interpreted with care, as a portion of the normal population has IgG reactivity to the 41-kDa flagellar antigen of the spirochete and thus the presence of the band alone cannot be utilized in serologic diagnosis.[25]

As a final note of caution: these tests, though commonly used, can be insensitive during the first few weeks of infection, prior to the development of host antibody response. Actively infected individuals will have a positive IgG response. For those patients with active disease lasting more than 4–8 weeks, an elevated IgM response is likely to be a false positive, and thus an IgM response should not be used to support the diagnosis of an infection after that time period.[25] In instances where the disease course is much more aggressive and severe than initially anticipated, coinfection with *Babesia microti* or *Ehrlichia phagocytophila* (causing human babesiosis and granulocytic anaplasmosis, respectively) should be considered.[42,43]

Differential Diagnoses

Given the various ocular manifestations of LD, the clinician needs to rule out both infectious and noninfectious etiologies with similar clinical presentations. In terms of other infectious etiologies, findings on the clinical examination as well as appropriate serologic/diagnostic tests should be undertaken to rule out syphilis, tuberculosis, viral meningitis/encephalitis, viral keratitis, infectious arthritis and mononucleosis, and mumps. Examination should also incorporate the following noninfectious etiologies in the differential diagnosis: sarcoidosis, collagen vascular diseases, vasculitis, Vogt–Koyanagi–Harada syndrome, and multiple sclerosis.

Treatment

Therapy for LD consists of antibiotic treatment for the systemic infection, though preventive measures (i.e., protective clothing, repellents, and acaricides), landscape modifications, and tick checks are often the best defense against infection as they reduce exposure.

Vaccination was once offered to individuals between the ages of 15 and 70 years who may travel to or live in endemic regions;[44] however, the vaccine is no longer available. In addition, a single dose of doxycycline (200 mg) is no longer recommended for prophylaxis after a documented tick bite; rather, appropriate antibiotic therapy for a minimum of 10–20 days is preferred.[45,46]

With regard to management of ocular findings, the most effective treatment strategy remains unclear.[32] Systemic therapy should be initiated in consultation with an infectious disease specialist (Table 87.4). Diplopia secondary to cranial nerve palsies should be addressed according to the severity of patient symptoms. Adjunct corticosteroids have been beneficial in treating the specific ocular manifestations: topical applications for anterior-segment manifestations (e.g., keratitis and episcleritis), and intravitreous injections for macular edema.[35,47–49] Systemic corticosteroids have been utilized in more severe cases of ocular inflammation, such as vision-threatening uveitis, scleritis, or optic neuritis; however, the use may be controversial, as a higher incidence of relapses has been observed. Inadequate treatment in the early stages may lead to relapses and development of late-stage manifestations.[26] Treatment of concomitant infections should also be addressed if the clinical findings persist despite prolonged antibiotic therapy.

TABLE 87.4
Treatment of Lyme Disease

EARLY INFECTION – LOCAL OR DISSEMINATED
Adults
Doxycycline 100 mg orally twice daily for 14–21 days
Amoxicillin 500 mg orally three times a day for 14–21 days
In case of doxycycline/amoxicillin allergy:
Cefuroxime 500 mg orally twice daily for 14–21 days
Erythromycin 250 mg orally four times daily for 14–21 days
Children
Amoxicillin 50 mg/kg body weight per day in three divided doses for 14–21 days
In case of penicillin allergy:
Cefuroxime 30 mg/kg per day in two divided doses for 14–21 days
NEUROLOGIC AND/OR OCULAR ABNORMALITIES (EARLY OR LATE)
Adults
Ceftriaxone 2 g iv once a day for 14–28 days
Cefotaxime 2 g iv every 8 hours for 14–28 days
In case of ceftriaxone or penicillin allergy:
Doxycycline 100 mg orally 3 times a day for 30 days

Children	
	Ceftriaxone 75–100 mg/kg per day (maximum 2 g) iv once a day for 14–28 days
	Cefotaxime 150 mg/kg per day in three to four divided doses (maximum 6 g) for 14–28 days

Notes: (1) Avoid doxycycline in pregnant women. (2) Chronic Lyme disease symptoms seen in late disease may require long-term antibiotic therapy (2 or more months of oral antibiotics, or 1 or more months of iv antibiotics).

Adapted from Steere AC. Lyme disease. N Engl J Med 2001;345:115–25.

Disease Course and Outcome

The majority of patients respond well to systemic antibiotic therapy; however, posterior uveitis, stromal keratitis, and neurotrophic keratitis can be slow to respond to treatment. Untreated disease can have a relapsing course for several years, though the number of patients with chronic symptoms, most notably arthritis, decreases 10–20% each year, with few individuals having symptoms beyond 5 years.[25] In "chronic Lyme disease" or posttreatment Lyme disease syndrome (PTLDS), no consensus has been reached with respect to prolonged antibiotic therapy.[50]

Ocular Leptospirosis

Leptospirosis is a zoonotic infection with a worldwide distribution, with higher incidence in tropical and subtropical climates. Initially described in 1886, infection causes a severe condition characterized by acute fever, malaise, and uveitis. Most human infection may be asymptomatic, and there is a wide spectrum of disease presentation which ranges from nonspecific febrile illness to multiorgan involvement associated with high mortality rates.

Systemic disease begins with nonspecific symptoms of headache, fevers, myalgias, malaise, and conjunctival chemosis with or without subconjunctival hemorrhage. The fevers may be mild, moderate, or severe. Anicteric disease affects 80–90% of patients, but 10–15% go on to develop severe systemic septicemia or multiorgan failure (icteric leptospirosis, or Weil disease) and mortality ranges from less than 5% to 30%.[51,52] Poor prognostic factors include involvement of the liver, renal failure, rhabdomyolysis, and altered sensorium.[53]

Epidemiology and Pathogenesis

The genus *Leptospira* consists of two strains: *L. interrogans*, which causes the infectious disease in humans, and *L. biflexa*, which is a saprophytic strain. The natural reservoir for *Leptospira* is wild animals, particularly rodents, but dogs and other domestic livestock may also be affected. The spirochete colonizes the renal tubules of the animal host, and survives excretion in the urine. It also survives as a free-living organism in contaminated soil or water. Individuals at high risk for infection include abattoir workers, farmers, veterinarians, miners, and sewerage workers who contract the disease via direct contact with diseased animals. Indirect contact is more common after exposure to wet soil or water through occupational exposure or recreational exposures (e.g., water sports in either fresh or sea water, ecotourism in endemic regions) as the spirochete has the ability to enter the human body through intact mucosa or abraded epidermis. The appearance of this rural tropical disease in urban centers of developing regions is often secondary to a lack of sanitation in areas of rapid expansion and growth. Sporadic outbreaks have also been reported in developed countries.[54,55]

Hematogenous dissemination allows the organisms to invade the central nervous system and aqueous humor of the eye; transendothelial migration occurs via systemic vasculitis, resulting in a broad spectrum of presentations, including pulmonary hemorrhage, damage to the renal tubule structures, and hepatic cell destruction.[56] It is unclear which mechanism allows for *Leptospira* to cause infection in ocular and systemic infection: innate bacterial virulence factors, direct tissue damage secondary to hemolytic toxins, or innate host immune responses.

Ocular Manifestations

In the acute phase of infection, the incidence of ocular signs ranges from 2% to 90% of cases, suggesting that the majority of findings may be nonspecific and diagnosed only when there is a high index of suspicion. Conjunctival hyperemia, chemosis, and subconjunctival hemorrhage are most commonly seen in these cases. Changes in the retinal vasculature and the presence of retinal

hemorrhages have been reported, along with disc hyperemia and retinal vasculitis.[54]

After the initial septicemic phase, a period of relative quiescence ranging from 2 days to 4 years precedes the development of ocular symptoms, which can vary from a localized anterior uveitis to diffuse panuveitis. Findings are generally nongranulomatous, though granulomatous reactions may be seen in rare cases. Anterior-segment findings can include hypopyon (in 12% of cases), a fibrinous reaction, and cataract. In rare cases, spontaneous absorption of the lens opacity has been reported. The symptoms of photophobia, blurred vision, and pain are generally self-limited.[57]

In the posterior segment, vitritis is common, with vitreous strands or veil opacities that attach to the optic disc. There may be other vitreous precipitates in the posterior vitreous, along with snowbanking. Nonocclusive vasculitis, periphlebitis, choroiditis, and papillitis have also been described.[54]

Diagnosis

Clinical diagnosis of systemic and ocular leptospirosis is difficult given the nonspecific symptoms and variable presentations reported in the literature (Table 87.5). The clinician cannot rely on the examination alone; rather, a high index of suspicion in an endemic region, or in individuals who may have exposure due to socioeconomic or recreational factors, needs to be taken into account, along with laboratory testing for confirmation of clinical suspicion.

TABLE 87.5

Differential Diagnosis of Leptospirosis

HLA-B27-related uveitis	Sarcoidosis
Behçet disease	Syphilis
Eales disease	Toxoplasmosis
Endophthalmitis	Leprosy
Tuberculosis	

HLA, human leukocyte antigen.

The gold standard for laboratory testing is the microscopic agglutination test (MAT), which is comprised of the agglutination

of live leptospiras by titrated amounts of patient serum. A fourfold change in the titer or seroconversion is considered positive, with a compatible clinical presentation. Of note, false negatives can occur if the infection is due to a serovar not present in the testing panel, and false positives can also occur if there are any residual antibodies to a prior exposure in an endemic area. In chronic cases, a titer of 1 : 100 is considered a positive test. The main difficulty in obtaining MAT testing lies in that large numbers of leptospiral cultures need to be maintained; thus, only large reference laboratories are able to conduct this laboratory test. Other diagnostic procedures, including a *Leptospira* dipstick test, ELISA, and microscopic slide agglutination tests, have replaced the MAT for more routine use. PCR for the detection of leptospiral DNA may be more sensitive in early identification of Leptospira outbreaks.[58]

Treatment

Antibiotic therapy for systemic disease is extremely effective. Supportive care should be initiated for those individuals suffering from multiorgan involvement. Intravenous penicillin G has been effective for severe systemic infection, but for less severe presentations, doxycycline given 100 mg twice daily for 1 week was shown to be effective in eradicating leptospiras from all target organs within 3 days. There does not seem to be any difference between the appropriate use of intravenous penicillin, intravenous cephalosporin, doxycyline, or azithromycin, but they have not been tested to the same extent as intravenous penicillin.[59]

Treatment for leptospiral uveitis includes local administration of corticosteroids, with dose and route of delivery dependent on the location, laterality, and severity of the symptoms. It is unclear if systemic antibiotic therapy during the early phase of infection provides any protective role in the prevention of immunologic sequelae such as uveitis, though a recent study suggests that those treated in the septicemic phase developed only mild disease.[60]

Disease Course and Outcome

Visual recovery and potential are generally good, with one large series reporting that more than 50% of patients regained 20/20

vision.[57] Most patients have mild disease (anicteric) and recover within 1–2 weeks. For systemic disease, mortality varies from less than 1% to more than 20%, and is dependent on the severity of disease and involvement of multiple organ systems.[52]

References

1. Nichols HJ. Observations on a strain of *Spirochaeta pallida* isolated from the nervous system. *J Exp Med*. 1914;19(4):362–371.
2. Patton ME, Su JR, Nelson R, et al. Primary and secondary syphilis – United States, 2005–2013. *MMWR Morb Mortal Wkly Rep*. 2014;63(18):402–406.
3. World Health Organization. *Global incidence and prevalence of selected curable sexually transmitted infections 2008*. World Health Organization: Geneva; 2012.
4. Marra M. Update on neurosyphilis. *Curr Infect Dis Rep*. 2009;11(2):127–134.
5. Durnian JM, Naylor G, Saeed AM. Ocular syphilis: the return of an old acquaintance. *Eye (Lond)*. 2004;18(4):440–442.
6. Davis JL. Ocular syphilis. *Curr Opin Ophthalmol*. 2014;25(6):513–518.
7. Levine DK, Scott KC, Klausner JD. Online syphilis testing – confidential and convenient. *Sex Transm Dis*. 2005;32(2):139–141.
8. Dockterman E. STD tests: There's an app for that. *Time*. January 7, 2014 http://healthland.time.com/2014/01/07/std-tests-theres-an-app-for-that/.
9. Peeling RW, Hook EW 3rd. The pathogenesis of syphilis: the great mimicker, revisited. *J Pathol*. 2006;208(2):224–232.
10. Jones NP. The Manchester Uveitis Clinic: the first 3000 patients – epidemiology and casemix. *Ocul Immunol Inflamm*. 2015;23(2):118–126.
11. Kuo IC, Kapusta MA, Rao NA. Vitritis as the primary manifestation of ocular syphilis in patients with HIV infection. *Am J Ophthalmol*. 1998;125(3):306–311.
12. Passo MS, Rosenbaum JT. Ocular syphilis in patients with

human immunodeficiency virus infection. *Am J Ophthalmol*. 1988;106(1):1–6.
13. Gass JD, Braunstein RA, Chenoweth RG. Acute syphilitic posterior placoid chorioretinitis. *Ophthalmology*. 1990;97(10):1288–1297.
14. Song JH, Hong YT, Kwon OW. Acute syphilitic posterior placoid chorioretinitis following intravitreal triamcinolone acetonide injection. *Graefes Arch Clin Exp Ophthalmol*. 2008;246(12):1775–1778.
15. Browning DJ. Posterior segment manifestations of active ocular syphilis, their response to a neurosyphilis regimen of penicillin therapy, and the influence of human immunodeficiency virus status on response. *Ophthalmology*. 2000;107(11):2015–2023.
16. Villanueva AV, Sahouri MJ, Ormerod LD, et al. Posterior uveitis in patients with positive serology for syphilis. *Clin Infect Dis*. 2000;30(3):479–485.
17. Dowell D, Polgreen PM, Beekmann SE, et al. Dilemmas in the management of syphilis: a survey of infectious diseases experts. *Clin Infect Dis*. 2009;49(10):1526–1529.
18. Behrhof W, Springer E, Brauninger W, et al. PCR testing for *Treponema pallidum* in paraffin-embedded skin biopsy specimens: test design and impact on the diagnosis of syphilis. *J Clin Pathol*. 2008;61(3):390–395.
19. Borelli S, Monn A, Meyer J, et al. Evaluation of a particle gel immunoassay as a screening test for syphilis. *Infection*. 2009;37(1):26–28.
20. Gordon SM, Eaton ME, George R, et al. The response of symptomatic neurosyphilis to high-dose intravenous penicillin G in patients with human immunodeficiency virus infection. *N Engl J Med*. 1994;331(22):1469–1473.
21. Chorba TL, Berkelman RL, Safford SK, et al. Mandatory reporting of infectious diseases by clinicians. *JAMA*. 1989;262(21):3018–3026.
22. Workowski KA, Bolan GA. Centers for Disease Control and Prevention Sexually Transmitted Disease Treatment Guidelines 2015. *MMWR Recomm Rep*. 2015;64(RR–03):1–137.

23. Reik L Jr, Burgdorfer W, Donaldson JO. Neurologic abnormalities in Lyme disease without erythema chronicum migrans. *Am J Med*. 1986;81(1):73–78.
24. Duray PH, Steere AC. Clinical pathologic correlations of Lyme disease by stage. *Ann N Y Acad Sci*. 1988;539:65–79.
25. Steere AC. Lyme disease (Lyme borreliosis) due to *Borrelia burgdorferi*. Bennett JE, Dolin R, Blaser MJ. *Mandell, Douglas and Bennett's principles and practice of infectious disease*. 8th ed. Churchill-Livingstone: Philadelphia; 2015:2725–2735.
26. Winterkorn JM. Lyme disease: neurologic and ophthalmic manifestations. *Surv Ophthalmol*. 1990;35(3):191–204.
27. Rahn DW. Lyme disease: clinical manifestations, diagnosis, and treatment. *Semin Arthritis Rheum*. 1991;20(4):201–218.
28. Glickstein L, Moore B, Bledsoe T, et al. Inflammatory cytokine production predominates in early Lyme disease in patients with erythema migrans. *Infect Immun*. 2003;71(10):6051–6053.
29. Sapi E, Bastian SL, Mpoy CM, et al. Characterization of biofilm formation by *Borrelia burgdorferi* in vitro. *PLoS ONE*. 2012;7(10):e48277.
30. Sapi E, Kaur N, Anyanwu S, et al. Evaluation of in-vitro antibiotic susceptibility of different morphological forms of *Borrelia burgdorferi*. *Infect Drug Resist*. 2011;4:97–113.
31. Zaidman GW. The ocular manifestations of Lyme disease. *Int Ophthalmol Clin*. 1997;37(2):13–28.
32. Lesser RL, Kornmehl EW, Pachner AR, et al. Neuro-ophthalmologic manifestations of Lyme disease. *Ophthalmology*. 1990;97(6):699–706.
33. Karma A, Seppala I, Mikkila H, et al. Diagnosis and clinical characteristics of ocular Lyme borreliosis. *Am J Ophthalmol*. 1995;119(2):127–135.
34. Jacobson DM, Frens DB. Pseudotumor cerebri syndrome associated with Lyme disease. *Am J Ophthalmol*. 1989;107(1):81–82.
35. Zaidman GW. Episcleritis and symblepharon associated with Lyme keratitis. *Am J Ophthalmol*. 1990;109(4):487–488.
36. Rothova A, Kuiper H, Spanjaard L, et al. Spiderweb vitritis in Lyme borreliosis. *Lancet*. 1991;337(8739):490–491.

37. Mikkila HO, Seppala IJ, Viljanen MK, et al. The expanding clinical spectrum of ocular Lyme borreliosis. *Ophthalmology*. 2000;107(3):581–587.
38. Centers for Disease Control and Prevention. *Lyme Disease (*Borrelia burgdorferi*)*. [Case Definition] http://www.cdc.gov/nndss/conditions/lyme-disease/case-definition/2011/; 2011.
39. Wormser GP, Bittker S, Cooper D, et al. Comparison of the yields of blood cultures using serum or plasma from patients with early Lyme disease. *J Clin Microbiol*. 2000;38(4):1648–1650.
40. Berger BW, Johnson RC, Kodner C, et al. Cultivation of *Borrelia burgdorferi* from erythema migrans lesions and perilesional skin. *J Clin Microbiol*. 1992;30(2):359–361.
41. Wormser GP, Schriefer M, Aguero-Rosenfeld ME, et al. Single-tier testing with the C6 peptide ELISA kit compared with two-tier testing for Lyme disease. *Diagn Microbiol Infect Dis*. 2013;75(1):9–15.
42. Krause PJ, Telford SR 3rd, Spielman A, et al. Concurrent Lyme disease and babesiosis. Evidence for increased severity and duration of illness. *JAMA*. 1996;275(21):1657–1660.
43. Krause PJ, McKay K, Thompson CA, et al. Disease-specific diagnosis of coinfecting tickborne zoonoses: babesiosis, human granulocytic ehrlichiosis, and Lyme disease. *Clin Infect Dis*. 2002;34(9):1184–1191.
44. Recommendations for the use of Lyme disease vaccine. Recommendations of the Advisory Committee on Immunization Practices (ACIP). *MMWR Recomm Rep*. 1999;48(RR–7):1–17 [21–5].
45. Wormser GP, Dattwyler RJ, Shapiro ED, et al. The clinical assessment, treatment, and prevention of Lyme disease, human granulocytic anaplasmosis, and babesiosis: clinical practice guidelines by the Infectious Diseases Society of America. *Clin Infect Dis*. 2006;43(9):1089–1134.
46. Cameron DJ, Johnson LB, Maloney DL. Evidence assessments and guideline recommendations in Lyme disease: the clinical management of known tick bites,

erythema migrans rashes, and persistent disease. *Expert Rev Anti Infect Ther*. 2014;12(9):1103–1135.
47. Orlin SE, Lauffer JL. Lyme disease keratitis. *Am J Ophthalmol*. 1989;107(6):678–680.
48. Flach AJ, Lavoie PE. Episcleritis, conjunctivitis, and keratitis as ocular manifestations of Lyme disease. *Ophthalmology*. 1990;97(8):973–975.
49. Reibaldi M, Faro S, Motta L, et al. Intravitreal triamcinolone for macular edema in Lyme disease. *Graefes Arch Clin Exp Ophthalmol*. 2008;246(3):457–458.
50. Krupp LB, Hyman LG, Grimson R, et al. Study and treatment of post Lyme disease (STOP-LD): a randomized double masked clinical trial. *Neurology*. 2003;60(12):1923–1930.
51. Leptospirosis: an emerging public health problem. *Wkly Epidemiol Rec*. 2011;86(6):45–50.
52. Martins MG, Matos KT, da Silva MV, et al. Ocular manifestations in the acute phase of leptospirosis. *Ocul Immunol Inflamm*. 1998;6(2):75–79.
53. Dupont H, Dupont-Perdrizet D, Perie JL, et al. Leptospirosis: prognostic factors associated with mortality. *Clin Infect Dis*. 1997;25(3):720–724.
54. Rathinam SR. Ocular manifestations of leptospirosis. *J Postgrad Med*. 2005;51(3):189–194.
55. Morgan J, Bornstein SL, Karpati AM, et al. Outbreak of leptospirosis among triathalon participants and community residents in Springfield, Illinois, 1998. *Clin Infect Dis*. 2002;34(12):1593–1599.
56. Haake DA, Levett PN. *Leptospira* species (Leptospirosis). Bennett JE, Dolin R, Blaser MJ. *Mandell, Douglas and Bennett's principles and practice of infectious disease*. 8th ed. Churchill-Livingstone: Philadelphia; 2015:2714–2720.
57. Rathinam SR, Rathnam S, Selvaraj S, et al. Uveitis associated with an epidemic outbreak of leptospirosis. *Am J Ophthalmol*. 1997;124(1):71–79.
58. Picardeau M, Bertherat E, Jancloes M, et al. Rapid tests for diagnosis of leptospirosis: current tools and emerging technologies. *Diagn Microbiol Infect Dis*. 2014;78(1):1–8.

59. Brett-Major DM, Coldren R. Antibiotics for leptospirosis. *Cochrane Database Syst Rev*. 2012;(2) [CD008264].
60. Pappachan JM, Mathew S, Thomas B, et al. The incidence and clinical characteristics of the immune phase eye disease in treated cases of human leptospirosis. *Indian J Med Sci*. 2007;61(8):441–447.

88

Ocular Toxoplasmosis

Rubens Belfort Jr., Claudio Silveira, Cristina Muccioli

Introduction

Toxoplasmosis is a common zoonosis caused by the infection with *Toxoplasma gondii*, and one of the most important cause of infectious retinal disease and posterior uveitis. Toxoplasmosis can cause severe, life-threatening disease, especially in newborns and

immunosuppressed patients, but the majority of *T. gondii* infections in immunocompetent patients remain asymptomatic.[1,2]

In the eye toxoplasmosis can cause blindness secondary to the retinitis present in the posterior pole of the eye or vitreoretinal complications in the acute or recurrent form of the disease.[3] Ocular toxoplasmosis (OT) represents 50–85% of the posterior uveitis cases in Brazil and 25% in the United States.[4] The prevalence of OT in the United States is not well determined but ranges from 0.6% to 2% according to published reports, and in Brazil the prevalence ranges from 10% to 17.7%.[5]

OT may occur either in a congenital or a postnatal acquired form and in both the eye may be affected during the acute phase of the infection or more commonly many months to years later[6] (Box 88.1).

Box 88.1

Myths in Ocular Toxoplasmosis

All cases congenital

Must present retinochoroiditis

Vertical transmission (pregnancy) only once

Cats and meat are the only source

Nothing to prevent ocular form

No treatment to avoid recurrences

All patients need antitoxoplasmic drugs for 4–6 weeks

Recurrences are related only to local factors

Beef is probably not important in the transmission of toxoplasmosis, and undercooked lamb, pork, and chicken are the major culprits, as well as food and environment contaminated by the feces of infected cats, organ transplantation, and blood transfusion.[7] Recently, water has been associated with the transmission of OT in different continents.[8]

Fetal toxoplasmosis tends to occur only when the woman acquires the first infection during or months before the pregnancy

and is more severe, and a more frequent cause of abortion, in the first months of pregnancy. In a fetus infected later on, milder infections develop and children are born often with subclinical infections. OT will develop up to decades later, being bilateral in up to 85% of patients.[9] It is known though that rarely even women with IgG serum antibodies against *Toxoplasma* may not be protected against transmitting congenital toxoplasmosis to a fetus.[10]

Biology, Life Cycle, and Transmission of the Organism

T. gondii is an obligate, intracellular protozoan parasite that undergoes a life cycle that includes both sexual and asexual reproduction. The sexual cycle occurs exclusively in felines (definitive hosts), which shed a large number of infectious oocysts in their feces once in their lifetime and usually for a few weeks. Members of the cat family are therefore its definitive hosts, but hundreds of other species, including mammals, birds, and reptiles, may serve as intermediate hosts,[11] The parasite can be found in the host's tissues and body fluids, such as saliva, milk, semen, urine, and peritoneal fluid.[12]

T. gondii exists in three infectious forms: the oocyst, the tachyzoite, and the bradyzoite (also called the tissue cyst). Once ingested by the intermediate hosts, the disease causes the production of tachyzoites and under the pressure of the immune response forms tissue cysts, the bradyzoites, that are very resistant and may remain in the retina as well as the central nervous system and many muscles of the organism, such as the tongue, heart etc., for many years.[13] They can remain dormant in the host without tissue damage and, for reasons that are unknown, after many years may rupture, causing reactivation of the ocular acute and recurrent disease.[14]

Strains/Clonal Populations – Haplogroups Genetics

The ability to identify parasite types may now provide new insights into the pathogenesis of this disease, and, ultimately, become an

important diagnostic and prognostic tool.[15]

The majority of strains identified in Europe and North America are classified into three distinct genotypes (type I, II, and III). Type I strains are very virulent and types II and III are less so. All of them can cause disease in humans. Type I strains are considered to be more often associated with postnatally acquired ocular infections, and type II strains are more associated with congenital infections and toxoplasmic encephalitis.[16] Atypical strains as well as mixed infections have being identified in many parts of the world and seem to be common in Brazil.[17] The make-up of *T. gondii* is more complex than previously recognized and suggests that unique or divergent genotypes may contribute to different clinical outcomes of toxoplasmosis in different localities.[18]

Atypical toxoplasmic retinochoroiditis as well as variations in the clinical presentation and severity of disease has been attributed to several factors, including the genetic heterogeneity of the host and the genotype of the parasite responsible for infection.[19]

Pathogenesis

Serologic evidence of previous toxoplasm infection is present in 20–70% of individuals in different countries, depending on a variety of factors, including climate, hygiene, and dietary habits, and there is not always a correlation between the prevalence of serum antibodies and the frequency of ocular disease.[20] Different factors such as the pathogenicity of the toxoplasmosis strains may play an important role.[21]

Ocular toxoplasmosis in immunocompetent patients is characterized histologically by foci of granulomatous chorioretinal inflammation and coagulative necrosis of the retina with sharply demarcated borders. Inflammatory changes can be widespread in the eye and involve choroid, iris, and trabecular meshwork. Immunosuppressed patients with ocular toxoplasmosis present both tachyzoites and tissue cysts in areas of retinal necrosis and within retinal pigment epithelial cells.[22] Parasites can occasionally be found in the iris, choroid, vitreous, and optic nerve. The lesions tend to be diffuse and often active in both eyes.[23,24]

Ocular Disease

The retina is the primary site of *T. gondii* infection in the eye and the hallmark is a necrotizing retinochoroiditis satellite to old hyperpigmented scars and accompanied by vitreous inflammation and anterior uveitis. Retinal vasculitis is also present. OT is characterized by recurrent episodes of necrotizing retinochoroiditis thought to be caused by the proliferation of live organisms that emerge from tissue cysts and or inflammatory reaction triggered by autoimmune mechanisms.[25]

The most common clinical signs of active ocular toxoplasmosis are blurring or loss of vision and floaters. Depending on the location of the lesions and the anterior chamber and vitreous inflammation, patients can be more or less symptomatic.[26]

The diagnosis is clinical and based on the ocular examination, the exclusion of the differential diagnosis and the presence of circulating antibodies for toxoplasmosis. The ocular exam comprises biomicroscopy and indirect ophthalmoscopy. In special cases other procedures such as OCT or fluorescein angiography may be necessary.[27]

Toxoplasmic retinochoroiditis can be associated with severe morbidity if disease extends to structures critical for vision, including the macula and optic nerve, if there is damage to the eye from inflammation, or if there are complications such as retinal detachment or neovascularization.[28] The timing of recurrences varies between individuals and is unpredictable also regarding the site of the recurrence and its clinical presentation.[29]

Toxoplasmic retinochoroiditis lesions have the same characteristics, whether they result from congenital or acquired infections. The acute and new lesions are usually intensely white, focal lesions with overlying vitreous inflammatory haze. Active lesions that are accompanied by a severe vitreous inflammatory reaction will have the classic “headlight in the fog” appearance. Anterior uveitis characterized by inflammatory cells in the aqueous, medium-sized keratic precipitates, and posterior synechiae are present.[30]

Eyes with active toxoplasmic retinochoroiditis will occasionally develop retinal vasculitis with vascular sheathing and hemorrhages

in response to reactions between circulating antibodies and local *T. gondii* antigens.[31] Typically hyperpigmented scars of old and inactive lesions are present and recurrent lesions occur at the border of healed scar as a satellite lesion.[32]

In most cases toxoplasmic retinochoroiditis is a self-limited disease. Untreated lesions generally begin to heal after 1 or 2 months, although the time course is variable, and in some cases active disease may persist for months.[33]

As a lesion heals, its borders become more defined, and after several months may become hyperpigmented. Large scars will have an atrophic center that is devoid of all retinal and choroidal elements; the underlying sclera gives the lesion its white center.[34]

Recent evidence has also suggested that patients with recent acquired infection may present with vitritis or even anterior uveitis in the absence of retinochoroiditis.[35]

The association between Fuchs heterochromic cyclitis and ocular toxoplasmosis has been reported in different countries and the pathologic mechanisms remain unknown.[36]

Laboratory

Toxoplasmic retinochoroiditis is diagnosed clinically. Parasites are found rarely in intraocular fluids, and invasive diagnostic tests such as retinal biopsy are associated with serious risks that prevent their routine use. Different serologic tests exist and should be used only to confirm past exposure to *T. gondii*; it is inappropriate to base a diagnosis of ocular toxoplasmosis on the presence of antibodies alone. The IgG serum antibodies can persist at high titers for years after an acute infection, and there is a high prevalence of such antibodies in the general population. Because active retinal lesions are usually foci of recurrent disease, serum IgG titers may be low and IgM may be absent. The serologic determination of IgA antiboidies may help to determine the time of the primary infection since they last for less time in the serum.[37]

The development of molecular biology techniques has allowed the identification of *T. gondii* DNA in the aqueous humor and the vitreous, as well as ocular tissue sections, of patients with presumed toxoplasmic retinochoroiditis by PCR techniques even

when organisms are not identified on histopathologic examination.[38,39]

The differential diagnoses comprise infectious diseases such as rubeola, cytomegalovirus, syphilis, herpes simplex, tuberculosis, and toxocariasis. Noninfectious conditions like retinal and choroidal coloboma, retinoblastoma, retinopathy of prematurity, gyrate atrophy, retinal vascular membrane, serpiginous choroidopathy among others have to be excluded in some presentations.[40]

Outcomes and Complications

Toxoplasmic retinochoroiditis can result in permanent loss of vision because of retinal necrosis, uveitis and its complications. Central vision will be lost if lesions affect the fovea, maculopapillary bundle, or optic disc. Other reported complications include macular edema, retinal neovascularization, vascular occlusion, and vitreoretinal lesions such as vitreous hemorrhage and epiretinal membranes. Subretinal neovascular membranes may be a cause of sudden loss of vision. Rhegmatogenous and traction retinal detachments may occur as well as secondary glaucoma and cataracts.[41]

Treatment and Prevention

There are many questions surrounding the treatment of ocular toxoplasmosis. Available drugs do not eliminate tissue cysts and cannot prevent chronic infection. No treatment has proven to be superior or even more efficient than nothing. It is accepted that steroids decrease the inflammation and therefore can lead to better vision function; they should not be used without antitoxoplasmic drugs in order to avoid the worsening of the infection.[42] But the role of the antitoxoplasmic drugs has never been scientifically proven and it is possible its effect would be limited to the first days of the retinitis. There is no cure for toxoplasmosis since the tissue cysts are resistant to the available drugs and remain viable for many years.[43]

The combination of pyrimethamine, sulfadiazine, and corticosteroids, which is considered “classic” therapy for ocular

toxoplasmosis (Box 88.2), is the most common drug combination used and considered the best option.[44] Therapy with trimethoprim and sulfamethoxazole probably is equally effective and has fewer side-effects and better patient compliance. It may be considered though as having a higher risk to cause severe allergic reactions because of the long life of sulfamethoxazole.[45] Other drugs, such as systemic or intraocular clindamycin, have also been used.[46,47]

Box 88.2

Typical Therapy for Ocular Toxoplasmosis

Pyrimethamine

75 mg to 100 mg loading dose given over 24 hours, followed by 25–50 mg daily for 4–6 weeks depending on clinical response.

Sulfadiazine

2.0–4.0 g loading dose initially, followed by 1.0 g given 4 times daily for 4–6 weeks, depending or clinical response.

Prednisone

40–60 mg daily for 2–6 weeks depending on clinical response; taper off before discontinuing trimethoprim–sulfamethoxazole.

Folinic acid

5.0 mg tablet or 3.0 mg intravenous preparation given orally, 2 to 3 times weekly during pyrimethamine therapy.

The length of treatment depends on the individual clinical picture.

Steroid treatment is often administered systemically and always associated with antitoxoplasmic drugs. Local drops are used when anterior uveitis is present.[48]

Traditional short-term treatments of active toxoplasmic retinochoroiditis lesions do not prevent subsequent recurrences. There is no cure for OT since none of the available drugs penetrates the cyst.[49]

The association of trimethoprim–sulfamethoxazole (TMP–SMX)

given for many months may decrease the number of recurrences and should be considered in higher-risk patients.[50]

A study performed after 10 years, with the objective to evaluate the benefits of the use of the combination of TMP–SMX, showed no difference in the recurrence rate in both groups, suggesting that the prophylactic treatment effect disappears when the treatment is stopped. Thus, long-term intermittent treatment with TMP–SMX can reduce the rate of recurrent toxoplasmic retinochoroiditis only when the patient is being treated.[51]

Long-term therapy may play a role in the management of ocular toxoplasmosis in specific situations. It might be most appropriate for individuals or populations with demonstrated histories of frequent and severe recurrences. It might also be considered for people at greatest risk of vision loss, such as those with retinochoroidal scars adjacent to the fovea, where any reactivation can result in profound vision loss.[51]

Prevention of toxoplasmosis is debatable, and it is unknown if patients with the acquired benign systemic form of the disease should be treated in every case, and specifically in children, to decrease the population of tissue cysts and therefore avoid or decrease the later ocular involvement.[52]

Surgery to cataract secondary to severe inflammation should be performed to restore vision and to allow fundus examination in order to identify new lesions as well as retinal complications secondary to the uveitis. As a rule, patients with cataract secondary to ocular toxoplasmosis should be operated with good results after 3 months of the uveitis being inactive.[53]

Local treatment with intravitreal injections of clindamycin and dexamethasone without concomitant systemic therapy is a treatment option in patients with allergies or inadequate responses to oral medications.[54,55,56]

References

1. Weiss LM, Dubey JP. Toxoplasmosis: a history of clinical observations. *Int J Parasitol*. 2009;39(8):895–901.
2. Commodaro AG, Belfort RN, Rizzo LV, et al. Ocular toxoplasmosis: an update and review of the literature. *Mem*

Inst Oswaldo Cruz. 2009;104(2):345–350.
3. Nussenblatt RB. Ocular toxoplasmosis. Nussenblatt RB, Whitcup SM, Palestine AG. *Uveitis: fundamentals and clinical practice*. 2nd ed. Mosby–Year Book, Inc: St. Louis, MO; 1996:211–228.
4. Jones JL, Kruszon-Moran D, Wilson M, et al. *Toxoplasma gondii* infection in the United States: seroprevalence and risk factors. *Am J Epidemiol*. 2001;154:357–365.
5. Holland GN. Ocular toxoplasmosis: a global reassessment. Part I: epidemiology and course of disease. *Am J Ophthalmol*. 2003;136(6):973–988.
6. Holland GN, O'Connor GR, Belfort R, et al. Toxoplasmosis. Pepose JS, Holland GN, Wilhelmus KR. *Ocular Infection and Immunity*. Mosby–Year Book, Inc: St. Louis, MO; 1996:1183–1223.
7. Montoya JG, Liesenfeld O. Toxoplasmosis. *Lancet*. 2004;363(9425):1965–1976.
8. Bowie WR, King AS. Outbreak of toxoplasmosis associated with municipal drinking water. *Lancet*. 1997;350:173–178.
9. Garza-Leon M, Muccioli C, Arellanes-Garcia L. Toxoplasmosis in pediatric patients. *Int Ophthalmol Clin*. 2008;48:75–85.
10. Silveira C, Ferreira R, Muccioli C, et al. Toxoplasmosis transmitted to a newborn from the mother infected 20 years earlier. *Am J Ophthalmol*. 2003;136(2):370–371.
11. Remington JS, McLeod R, Thulliez P, et al. Toxoplasmosis. Remington JS, Klein J. *Infectious diseases of the fetus and newborn infant*. 5th ed. WB Saunders: Philadelphia; 2001:205–346.
12. Belfort R Jr, Muccioli C. Toxoplasmosis ocular. AMOLCA: Venezuela; 2008:81–88. Fernando Arévalo J, Graue-Wiechers F, Quiroz-Mercado H, et al. *Uveítis y tumores intraoculares temas selectos*. vol. 1.
13. Tenter AM, Heckeroth AR, Weiss LM. Toxoplasma gondii: from animals to humans. *Int J Parasitol*. 2000;30(12–13):1217–1258.
14. Silveira C, Vallochi AL, Rodrigues da Silva U, et al. Toxoplasma gondii in the peripheral blood of patients with

acute and chronic toxoplasmosis. *Br J Ophthalmol*. 2011;95(3):396–400.
15. Howe DK, Honoré S, Derouin F, et al. Determination of genotypes of Toxoplasma gondii strains isolated from patients with toxoplasmosis. *J Clin Microbiol*. 1997;35(6):1411–1414.
16. Vallochi AL, Muccioli C, Martins MC, et al. The genotype of Toxoplasma gondii strains causing ocular toxoplasmosis in humans in Brazil. *Am J Ophthalmol*. 2005;139(2):350–351.
17. Vaudaux JD, Muccioli C, James ER, et al. Identification of an atypical strain of Toxoplasma gondii as the cause of a waterborne outbreak of toxoplasmosis in Santa Isabel do Ivai, Brazil. *J Infect Dis*. 2010;202(8):1226–1233.
18. Grigg ME, Ganatra J, Boothroyd JC, et al. Unusual abundance of atypical strains associated with human ocular toxoplasmosis. *J Infect Dis*. 2001;184(5):633–639.
19. Bottós J, Miller RH, Belfort RN, UNIFESP Toxoplasmosis Group, et al. Bilateral retinochoroiditis caused by an atypical strain of Toxoplasma gondii. *Br J Ophthalmol*. 2009;93(11):1546–1550.
20. Talabani H, Asseraf M, Yera H, et al. Contributions of immunoblotting, real-time PCR, and the Goldmann–Witmer coefficient to diagnosis of atypical toxoplasmic retinochoroiditis. *J Clin Microbiol*. 2009;47(7):2131–2135.
21. Saeij JP, Boyle JP, Boothroyd JC. Differences among the three major strains of Toxoplasma gondiiand their specific interactions with the infected host. *Trends Parasitol*. 2005;21:476–481.
22. Holland GN. Ocular toxoplasmosis: a global reassessment. Part II: Disease manifestations and management. *Am J Ophthalmol*. 2004;137:1–17.
23. Holland GN, Engstrom RE Jr, Glasgow BJ, et al. Ocular toxoplasmosis in patients with the acquired immunodeficiency syndrome. *Am J Ophthalmol*. 1988;106(6):653–667.
24. Rehder JR, Burnier MB Jr, Pavesio CE, et al. Acute unilateral toxoplasmic iridocyclitis in an AIDS patient. *Am J Ophthalmol*. 1988;106(6):740–741.

25. Arevalo JF, Belfort R Jr, Muccioli C, et al. Ocular toxoplasmosis in the developing world. *Int Ophthalmol Clin*. 2010;50(2):57–69.
26. Bonfioli AA, Orefice F. Toxoplasmosis. *Semin Ophthalmol*. 2005;20(3):129–141.
27. Pereira A, Orefice F. Toxoplasmosis. Foster CS, Vitale AT. *Diagnosis and treatment of uveitis*. W.B. Saunders: Philadelphia, PA; 2001:385–410.
28. Bosch-Driessen LH, Karimi S, Stilma JS, et al. Retinal detachment in ocular toxoplasmosis. *Ophthalmology*. 2000;107(1):36–40.
29. Holland GN, Crespi CM, ten Dam-van Loon N, et al. Analysis of recurrence patterns associated with toxoplasmic retinochoroiditis. *Am J Ophthalmol*. 2008;145(6):1007–1013.
30. Rothova A. Ocular manifestations of toxoplasmosis. *Curr Opin Ophthalmol*. 2003;14(6):384–388.
31. Smith JR, Cunningham ET Jr. Atypical presentations of ocular toxoplasmosis. *Curr Opin Ophthalmol*. 2002;13(6):387–392.
32. Hovakimyan A, Cunningham ET Jr. Ocular toxoplasmosis. *Ophthalmol Clin North Am*. 2002;15(3):327–332.
33. Tabbara KF. Ocular toxoplasmosis. *Int Ophthalmol*. 1990;14(5–6):349–351.
34. Pleyer U, Torun N, Liesenfeld O. Ocular toxoplasmosis. *Ophthalmologe*. 2007;104(7):603–615 [quiz 616].
35. Holland GN, Muccioli C, Silveira C, et al. Intraocular inflammatory reactions without focal necrotizing retinochoroiditis in patients with acquired systemic toxoplasmosis. *Am J Ophthalmol*. 1999;128(4):413–420.
36. Toledo de Abreu M, Belfort R Jr, Hirata PS. Fuchs' heterochromic cyclitis and ocular toxoplasmosis. *Am J Ophthalmol*. 1982;93(6):739–744.
37. Vallochi AL, Nakamura MV, Schlesinger D, et al. Ocular toxoplasmosis: more than just what meets the eye. *Scand J Immunol*. 2002;55:324–328.
38. Matos K, Muccioli C, Belfort Junior R, et al. Correlation between clinical diagnosis and PCR analysis of serum, aqueous, and vitreous samples in patients with

inflammatory eye disease. *Arq Bras Oftalmol*. 2007;70:109–114.
39. Fekkar A, Bodaghi B, Touafek F, et al. Comparison of immunoblotting, calculation of the Goldmann–Witmer coefficient, and real-time PCR using aqueous humor samples for diagnosis of ocular toxoplasmosis. *J Clin Microbiol*. 2008;46(6):1965–1967.
40. Vasconcelos-Santos DV, Dodds EM, Oréfice F. Review for disease of the year: differential diagnosis of ocular toxoplasmosis. *Ocul Immunol Inflamm*. 2011;19(3):171–179.
41. London NJ, Hovakimyan A, Cubillan LD, et al. Prevalence, clinical characteristics, and causes of vision loss in patients with ocular toxoplasmosis. *Eur J Ophthalmol*. 2011;21(6):811–819.
42. Stanford MR, Gilbert RE. Treating ocular toxoplasmosis: current evidence. *Mem Inst Oswaldo Cruz*. 2009;104(2):312–315.
43. Stanford MR, See SE, Jones LV, et al. Antibiotics for toxoplasmic retinochoroiditis: an evidence-based systematic review. *Ophthalmology*. 2003;110:926–931 [quiz 931-2].
44. Rothova A, Meenken C, Buitenhuis HJ, et al. Therapy for ocular toxoplasmosis. *Am J Ophthalmol*. 1993;115:517–523.
45. Soheilian M, Sadoughi MM, Ghajarnia M, et al. Prospective randomized trial of trimethoprim/sulfamethoxazole versus pyrimethamine and sulfadiazine in the treatment of ocular toxoplasmosis. *Ophthalmology*. 2005;112(11):1876–1882.
46. Soheilian M, Ramezani A, Azimzadeh A, et al. Randomized trial of intravitreal clindamycin and dexamethasone versus pyrimethamine, sulfadiazine, and prednisolone in treatment of ocular toxoplasmosis. *Ophthalmology*. 2011;118(1):134–141.
47. Lasave AF, Díaz-Llopis M, Muccioli C, et al. Intravitreal clindamycin and dexamethasone for zone 1 toxoplasmic retinochoroiditis at twenty-four months. *Ophthalmology*. 2010;117(9):1831–1838.
48. Bosch-Driessen EH, Rothova A. Sense and nonsense of corticosteroid administration in the treatment of ocular toxoplasmosis. *Br J Ophthalmol*. 1998;82:858–860.

49. Holland GN, Crespi CM, ten Dam-van Loon N, et al. Analysis of recurrence patterns associated with toxoplasmic retinochoroiditis. *Am J Ophthalmol*. 2008;145(6):1007–1013.
50. Silveira C, Belfort R Jr, Muccioli C, et al. The effect of long-term intermittent trimethoprim/sulfamethoxazole treatment on recurrences of toxoplasmic retinochoroiditis. *Am J Ophthalmol*. 2002;134:41–46.
51. Silveira C, Muccioli C, Nussenblatt R, et al. The effect of long-term intermittent trimethoprim/sulfamethoxazole treatment on recurrences of toxoplasmic retinochoroiditis: 10 years of follow-up. *Ocul Immunol Inflamm*. 2015;23(3):246–247.
52. McLeod R, Kieffer F, Sautter M, et al. Why prevent, diagnose and treat congenital toxoplasmosis? *Mem Inst Oswaldo Cruz*. 2009;104(2):320–344.
53. Van Gelder RN, Leveque TK. Cataract surgery in the setting of uveitis. *Curr Opin Ophthalmol*. 2009;20(1):42–45.
54. Zamora YF, Arantes T, Reis FA, et al. Local treatment of toxoplasmic retinochoroiditis with intravitreal clindamycin and dexamethasone. *Arq Bras Oftalmol*. 2015;78(4):216–219.
55. Kishore K, Conway MD, Peyman GA. Intravitreal clindamycin and dexamethasone for toxoplasmic retinochoroiditis. *Ophthalmic Surg Lasers*. 2001;32(3):183–192.
56. Baharivand N, Mahdavifard A, Fouladi RF. Intravitreal clindamycin plus dexamethasone versus classic oral therapy in toxoplasmic retinochoroiditis: a prospective randomized clinical trial. *Int Ophthalmol*. 2013;33(1):39–46.

89

Helminthic Disease

Marcos Ávila, David Isaac

Introduction

Helminths have plagued mankind since before the era of our earliest recorded history.[1] It is possible to recognize features of helminthic infections from the ancient writings of Hippocrates, Egyptian medical papyri, and the Bible.[2] Nematode worms or roundworms are a class of one of the most important phylum of the Helminths (Nemathelminthes) and include the major intestinal human worms (e.g., *Ascaris lumbricoides*, *Trichuris trichiura*, *Necator americanus*, *Ancylostoma duodenale*, *Strongyloides stercoralis*), animal worms (e.g., *Toxocara canis*, *Toxocara cati*, *Ancylostoma caninum*, *Baylisascaris procyonis*), and the filarial worms that can cause lymphatic filariasis (e.g., *Wuchereria bancrofti*, *Brugia malayi*) or onchocerciasis (*Onchocerca volvulus*).[1] The other phylum of the Helminths is called Platyhelminths, which is divided into trematodes (e.g., *Schistosoma mansoni*) and cestodes (e.g., *Taenia*

solium, *Taenia saginata*). Many kinds of adult worms cannot develop on their own and parasitize human intestine; some in their larval stage can infect humans directly, causing tissue damage that includes the eye.[3] It is estimated that almost 1 billion people worldwide, especially in tropical areas and developing countries, are infected with one or more helminths.[4] This chapter discusses the most common helminthic diseases that affect the posterior segment of the eye: ocular toxocariasis, diffuse unilateral subacute neuroretinitis (DUSN), ocular onchocerciasis, and cysticercosis.

Ocular Toxocariasis

Toxocariasis is an infection caused by the nematode *T. canis* and less frequently by other roundworms such as *T. cati*.[3,5,6] Systemic effects of *Toxocara* infestation in the human are termed visceral larval migrans (VLM). VLM is usually a self-limited disease and typically affects young children from 6 months to 4 years of age.[5] Findings associated with the disorder range from a mild to moderate eosinophilia in an asymptomatic patient, fever, pallor, anorexia, malaise, hepatomegaly, and transient infiltrates of the lungs in symptomatic VLM to, more infrequently, a fulminating and fatal disease associated with pneumonia, congestive heart failure, or convulsions.[3,5,7] Ocular toxocariasis is unusual in adults but is an important cause of visual impairment during childhood, accounting for approximately 1% of all cases of uveitis among all ages in referral centers in the United States and Japan[8,9] and 3% of panuveitis in Switzerland.[10] Exact correlation between VLM and ocular toxocariasis is not well determined but patients with systemic disease rarely present with ocular involvement. In one study of 245 cases of VLM, only 5% had any indication of ocular disease.[11]

History

In 1907 Leiper first described the infestation of humans with canine nematodes.[12] Later, Wilder, in 1950, described nematode ocular infection.[13] In her study Wilder reviewed the histopathology of 46 eyes primarily enucleated for suspicion of intraocular malignancy,

and nematode larvae were found in 24 eyes. Two years later Beaver and coworkers identified a *Toxocara* species larva in a liver biopsy from a child with visceral lesions and eosinophilia, identifying the etiological agent with this previously reported syndrome in children.[14] Nichols, in 1956, reported identifying *T. canis* (Toxocaridae family) in specimens originally studied by Wilder who first thought the worm to be part of family Ancylostomidae.[15] These studies demonstrated a common etiology for systemic and ocular diseases. In 1959 Irvine and Irvine[16] described histologic findings in a 4-year-old child presenting with strabismus, decreased vision, and retinal detachment. The eye was enucleated for suspicion of a tumor but an eosinophilic abscess with *Toxocara canis* larva on the pars plana region was demonstrated. This patient differed from cases reported by Wilder[13] since the patient presented with clear media and the retina could be examined. In 1960 Ashton[17] described four histopathologically proven cases of *Toxocara* endophthalmitis that presented with a posterior pole granuloma in a distinct fashion that represented a third classic form of this disorder. Duguid, in 1961,[18] described a case series of ocular toxocariasis and emphasized the difference between the posterior pole granuloma and diffuse chronic endophthalmitis, suggesting that clinical diagnosis could be performed in certain cases. In 1971 Wilkinson and Welch[19] reported 41 cases of proven or presumed ocular toxocariasis. Eyes with chronic endophthalmitis and leukocoria were much more likely to have been enucleated, whereas eyes with the posterior or peripheral isolated and visible granulomas were usually diagnosed clinically, and enucleation was not performed to confirm the diagnosis. Since then, several other relatively unusual forms of ocular *Toxocara* have been described and these are briefly discussed later. Association of *T. canis* and diffuse unilateral subacute neuroretinitis will be discussed separately in this chapter.

Parasitology

The *Toxocara* genus comprises 21 species, including *T. canis* which is the most common cause of toxocariasis.[3,5,6,20] *T. canis* is a natural parasite of dogs and occasionally can infest human and other

paratenic hosts such as rodents and rabbits.[21] Adult worms are cylindrical and long, measuring from 75 to 120 mm. Male worms are longer than females and in their development undergo five different stages from larvae to adult parasite.[20] Adult forms are found only on the small intestine of puppies until 6 months of age (definitive host) and pregnant and lactating bitches. In older dogs and humans the cycle is not complete, and because of this only the definitive host where worms reach sexual maturation can shed eggs in feces. To understand the pathogenesis of *T. canis* and the development of VLM and ocular toxocariasis it is necessary to understand the parasite life cycle.

Eggs lacking an embryo are shed in the feces of the definitive host (puppies). The eggs then develop an embryo and become infective in the environment in 2–6 weeks. Following ingestion by dogs or other parasite hosts, the infective eggs hatch and larvae penetrate the intestine wall and are carried by the circulation to a wide variety of tissues (liver, heart, lungs, brain, muscle, eyes). In the human and in adult dogs, this completes the life cycle, and the parasites are usually enclosed by an inflammatory granulomatous response that is primarily eosinophilic, although the larvae may remain viable for years under such conditions.[3,5,22,23] During pregnancy, the host response in the infected bitch is altered, and previously encysted larvae may resume migration,[23] crossing the placenta and affecting the canine fetus. In puppies, larvae reaching the lungs are coughed up and swallowed and, reaching the small intestine, they quickly mature into adult worms that produce infectious ova that are passed in fecal material. Prenatal infection is the primary route of transmission to puppies; however, they can become infected after birth by ingestion of milk or feces from an infected nursing bitch.[6,22] The infection rate in puppies may approach 100%,[24,25] and they start to shed over 200, 000 eggs per day in feces from 3 to 6 weeks after initial infestation and may shed eggs until they are about 6 months old when the mature worms die[20] (Fig. 89.1).

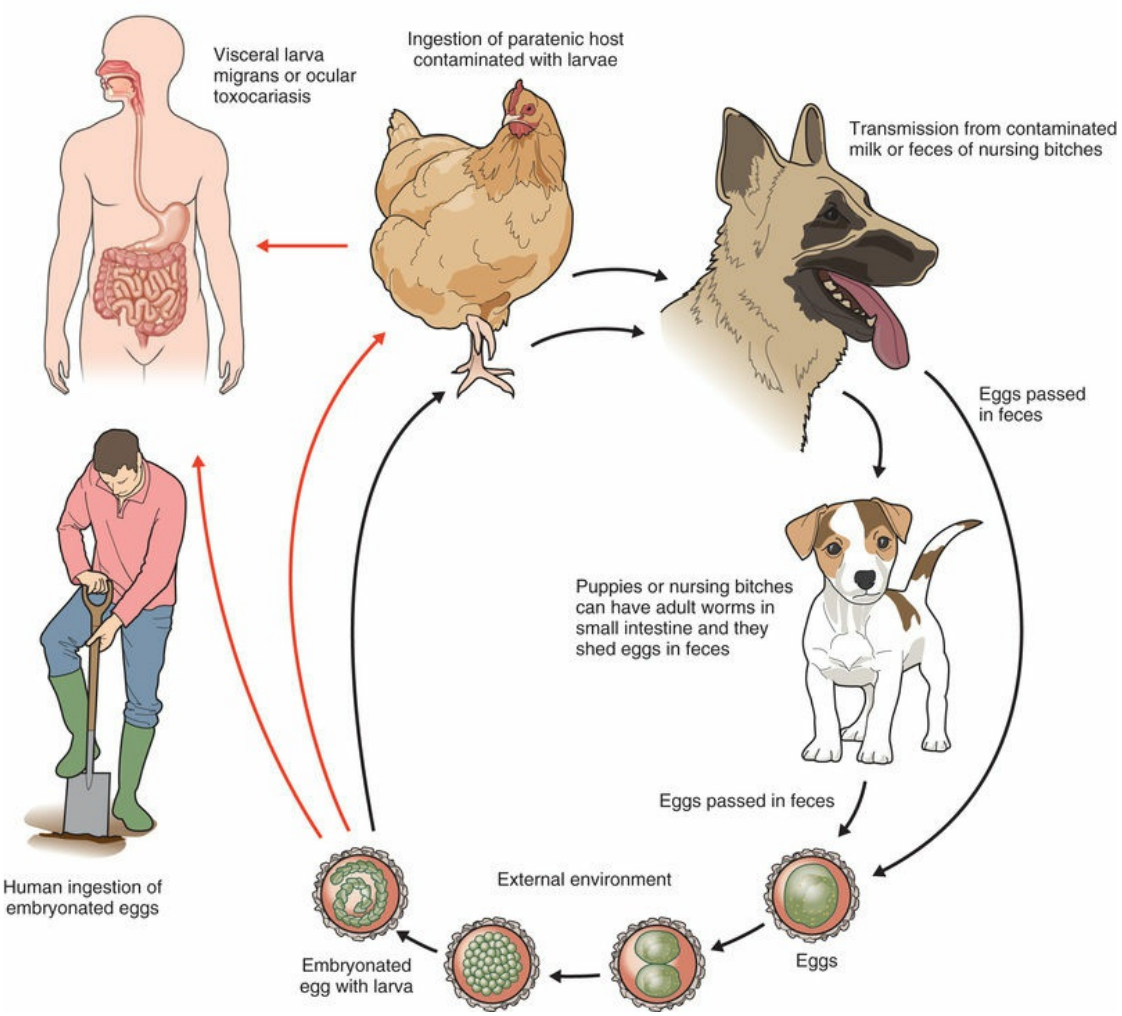

FIG. 89.1 Life cycle of *Toxocara canis*. Parasites mature and complete their cycle of life in puppies and pregnant bitches. Embryonated eggs are shed in feces and they mature in the external environment. Humans become infested by ingestion of embryonated eggs from contaminated soil or larvae from paratenic hosts. Larvae are disseminate to organs originating visceral larva migrans or ocular toxocariasis.

Pathophysiology

Humans can be infested by ingestion of embryonated eggs or larvae. Eggs can be ingested accidentally after contact with puppies or by geophagia of soil containing embryonated eggs.[26–28] Outdoor parks and playgrounds (sandboxes) can be highly contaminated with embryonated eggs of *Toxocara,* since in this environment people routinely walk their pets.[29–33] Under optimal conditions

embryonated eggs may remain viable for years.[34] Direct contact with untreated puppies is also an important form of transmission. Amaral et al. have shown that perianal hair from stray as well as owned dogs had embryonated eggs in 24% of cases, and 99% of the total number of eggs were found in puppies.[25] A less frequent method of transmission is the ingestion of larvae from contaminated meat. Several studies described infection by eating raw meat or liver from animals such as cows, chicken, and ducks.[35–37]

After ingesting embryonated ova, the parasites mature in the small intestine and transform to second stage larvae which penetrate the intestine wall, enter the lymphatic and portal circulation, and are disseminated to liver and lungs. Then the larvae reach the heart and are disseminated to other organs such as brain, kidney, heart, muscle, and eyes.[20] In human beings the parasites are enclosed by an inflammatory granulomatous reaction and the parasites do not evolve further.[22] The eosinophilic granuloma comprise the larva enveloped by a central core of eosinophils surrounded by mononuclear cells, histiocytes, epithelioid cells, and giant cells. Because of the inability of the parasite to mature into an adult form in humans, a search for *T. canis* ova in human feces is inevitably unrewarding.[38]

T. canis can cause either VLM or ocular toxocariasis, and the clinical manifestation depends on factors such as host immunologic condition, inflammatory response, number of eggs/larvae ingested, frequency of ingestion, and localization of the second stage larvae in human tissues.[20] A large amount of ingested embryonated eggs may lead to a rapid increase in eosinophilia and rising antibody levels.[20] One study has shown that the degree of systemic eosinophilia in VLM has been correlated with level of exposure to *Toxocara* larvae.[39] A lower exposure to embryonated eggs may produce lower levels of antibodies and eosinophilia and may permit wider larval migration, reaching the eye.[20] Intraocular involvement by *T. canis* tends to occur in young patients, but in individuals who have developed ocular toxocariasis the age of onset is usually older than patients with VLM.[7,13,22,40] Mean age of presentation for systemic VLM is 2 years[5] versus 7.5 years for ocular toxocariasis.[11]

Clinical Presentations

Although the average age of presentation is around 8 years for ocular toxocariasis,[5,11] the age at presentation may range from 2 to 30 years,[11,41] and individual cases have been reported in adults with age up to 62 years.[41,42] *Toxocara canis* infection in adults and very young children is rare, probably because of better hygiene habits of adults and less contact with puppies, sandboxes, and geophagia.

The ocular involvement is typically unilateral, and bilateral disease is quite rare.[20,43] Patients usually present with unilateral visual impairment, leukokoria, and/or strabismus in a relatively quiet eye. Careful slit-lamp examination can show cells in the anterior chamber (73%) and vitreous (100%),[44] and vitritis causing decrease in visual acuity was reported in 53% in one series.[9]

Based on ophthalmoscopic findings, ocular toxocariasis can be classified into these categories: peripheral granuloma, posterior pole granuloma, chronic endophthalmitis, or atypical presentations.

The presence of a retinal granuloma is the most common finding in ocular toxocariasis. Wilkinson and Welch,[19] in a study with 41 eyes diagnosed with the disease, reported that a peripheral granulomatous mass with relatively clear media was the most common form of presentation, being seen in 18 of 41 (44%) cases. Stewart et al.,[9] in 2005, described 22 cases of ocular toxocariasis, and in 50% of them peripheral granuloma was diagnosed. However, an isolated posterior pole inflammatory mass was the most common form of presentation in a series of 100 cases reported by Hagler et al.[45] and in 53% of 30 cases published by Oréfice and coworkers.[44]

Shields,[7] in a review in 1984, divided ocular toxocariasis into nine different categories, including DUSN.[7] Despite *T. canis* being described as one of the possible nematodes to cause DUSN, other roundworms are also causes of DUSN and therefore the disorder will be discussed separately in this chapter.

Peripheral Granuloma

The peripheral granuloma, also described as the peripheral inflammatory mass form of *Toxocara* endophthalmitis, is usually seen in a quiet eye with varying levels of decreased vision and strabismus.[19] The vitreous and anterior chamber show mild to

moderate reaction. Intense vitritis can occur; however, at diagnosis the vitreous is generally clear. Peripheral granuloma presents as a dense, white inflammatory mass in the periphery of the retina. Localized traction on the retina may result in the production of a typical retinal fold from the periphery to the optic nerve (Fig. 89.2). This mass may be quite localized, spherical, and similar to those observed in the posterior pole. Fibrocellular bands may be observed running from a peripheral inflammatory mass to the more posterior retina or the optic nerve (Fig. 89.3). The prognosis in eyes with peripheral granulomatous inflammation is usually relatively good and visual acuity can be preserved. By the time this diagnosis is made, active inflammation is usually not progressive.[19] Ultrasound biomicroscopy study of 15 eyes with peripheral toxocariasis has shown alterations such as vitreous membranes in 86.6%, granuloma in 73.3%, pseudocysts in 53.3%, and thickening of ciliary body in 40% of studied eyes.[46] Intraretinal and epiretinal traction bands can lead to production of both traction and rhegmatogenous retinal detachments, macular displacement and distortion, and optic nerve dysfunction.

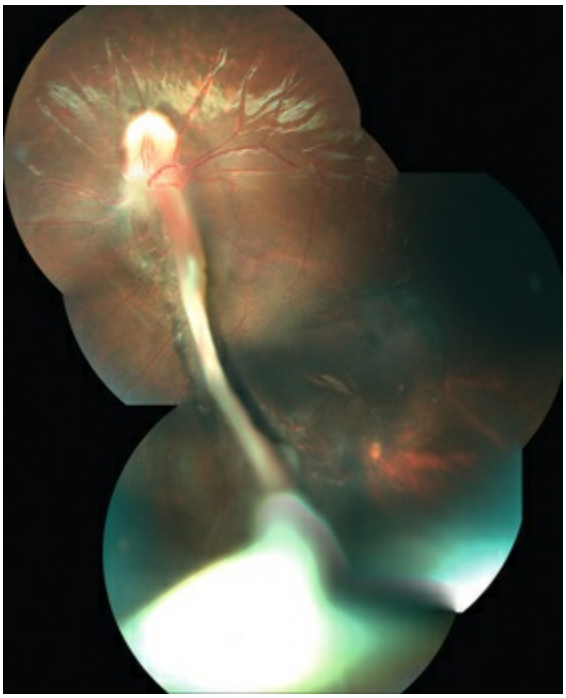

FIG. 89.2 Peripheral granuloma. Composite fundus photography showing peripheral granuloma (white mass) and retinal fold towards optic nerve head. There

is hyperpigmentation of surrounding retinal pigmented epithelium and macular displacement inferiorly.

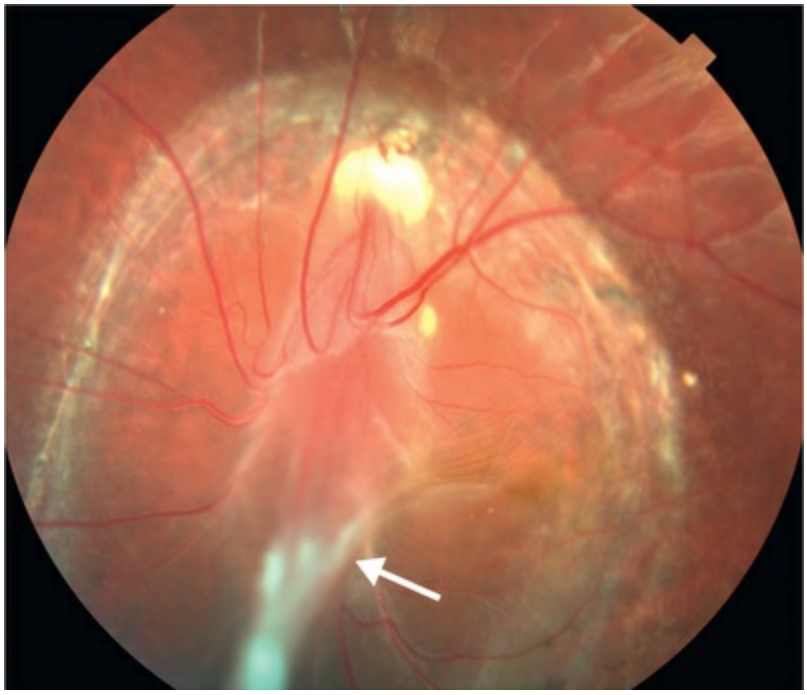

FIG. 89.3 Fibrocellular bands running from a peripheral granuloma to the optic nerve head (*arrow*).

Posterior Pole Granuloma

Posterior pole granuloma presents as white or gray spherical intraretinal or subretinal granuloma affecting the posterior pole. Most of the time it is diagnosed in a cicatricial stage when the lesion appears as a well-defined subretinal mass, measuring from 500 to 3000 μm, with no hemorrhage or exudates. Traction bands running from the mass to the surrounding retina may be observed. With cicatricial granulomas, there is very mild or no anterior chamber reaction and a low amount of cells in the vitreous cavity. Perilesional retina can show hyperpigmentation of retinal pigmented epithelium (RPE) and wrinkling of internal limiting membrane (Fig. 89.4). An optical coherence tomography case report has shown that the granuloma presents as a well-defined subretinal mass above the RPE (Fig. 89.5).[47] Active disease can show different stages of severity from mild anterior chamber and vitreous reaction

to a very intense vitritis, as seen in the chronic endophthalmitis form of the disease. During the active phase the posterior pole granuloma is observed as an ill-defined hazy mass surrounded by retinal exudates or hemorrhages.[19,20] A granuloma is usually seen in the posterior pole temporal to the optic nerve head; however, the occurrence of optic nerve granuloma has been described.[48] Due to posterior pole involvement, patients present with central visual impairment and can have strabismus and leukokoria. Macular lesions may be observed in association with peripheral inflammatory masses, and choroidal neovascularization may occur as a late complication.[45,49,50]

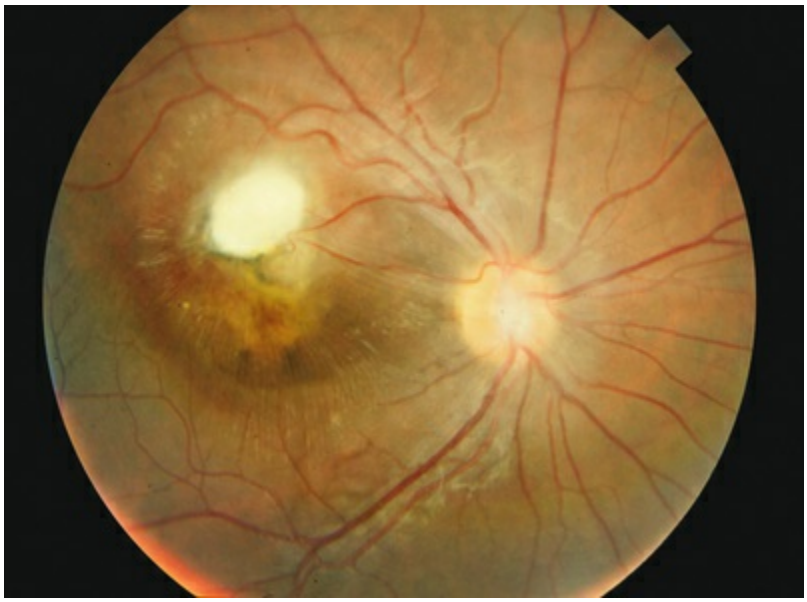

FIG. 89.4 Posterior pole granuloma. A posterior pole granuloma with surrounding retinal pigmented epithelium changes and internal retina wrinkling.
(Courtesy of Fernando Oréfice, MD, and Editora Cultura Médica.)

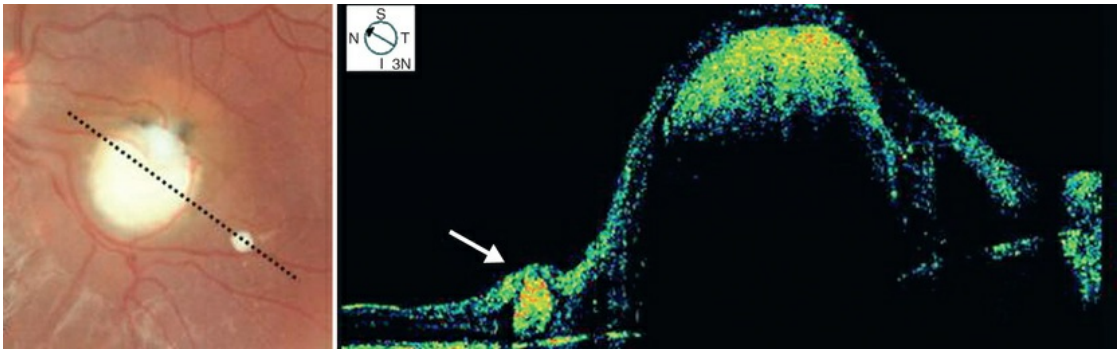

FIG. 89.5 Optical coherence tomography of a posterior pole granuloma showing its subretinal location. (Courtesy of Aline do Lago Coutinho, MD.)

Chronic Endophthalmitis

Patients with chronic endophthalmitis are typically younger than those with more localized granulomatous forms of the disease. There is usually relatively clear media.[19] Localized granulomatous forms may be a late presentation of an acute form of the disease that had healed without development of retinal detachment or phthisis bulbi. As the vitreous clears it is possible to visualize the retinal lesions.[19] The history is usually negative for trauma, intraocular surgery, or bacterial and fungal endophthalmitis. However, a history of playing in sandboxes in public places and geophagia may be obtained.[19,27,28] External inspection usually reveals a quiet eye, but severe intraocular inflammation can be present. In such cases leukokoria may be seen. Patients present with anterior chamber reaction that can vary from moderate to intense granulomatous reaction and can lead to hypopyon and posterior synechiae. The vitreous shows dense cellular infiltration with hazy media that can clear or develop cyclitic membranes, retinal traction, and detachment that can be diagnosed ultrasonographically.[51] If vitreous clears, a localized granuloma can be seen. The prognosis in this form of endophthalmitis depends primarily on the degree of intravitreal organization and the development of complications such as retrolental membranes, cataract, glaucoma, retinal detachment, and phthisis bulbi.

Atypical Presentations

Atypical forms of ocular toxocariasis have been reported. Most of

them had a presumed diagnosis. These include optic nerve granuloma and optic neuritis;[48] motile subretinal nematode,[52] which more recently many consider to be an early phase of DUSN; diffuse chorioretinitis;[7] conjunctivitis; keratitis; and lens involvement, including motile intralenticular larva and cataract.[7,22]

Diagnosis

Definitive diagnosis of ocular toxocariasis is obtained by means of histologic demonstration of the larva or fragments of it in affected tissues. This evaluation is rarely performed, and clinical signs, epidemiology (age, geophagia, contact with puppies, playing in sandboxes), imaging, and serologic tests are sufficient to permit the diagnosis despite the fact they do not confirm the presence of the parasite. Clinical presentation of localized granuloma in the periphery and posterior pole are very typical in many cases and a presumed diagnosis is made. In cases of chronic endophthalmitis when fundus examination is not possible due to media opacification, specific ancillary tests such as ultrasonography or CT scan can help in establishing the differential diagnosis.

The enzyme-linked immunosorbent assay (ELISA) is the current serum test of choice to detect exposure to *T. canis*.[7] Intraocular fluids (aqueous humor, vitreous) can also be used to detect antibodies in a suspected case of ocular toxocariasis with a negative serum ELISA test.[7,41,53] The ELISA test employs antigens secreted by the second-stage larva and recombinant antigens have been produced from them that add even greater specificity to an already-reliable test (approximately 92%). The ELISA has a reasonably high degree of sensitivity as well (approximately 78%), at a titer greater than 1 : 32.[54] The immunodiagnostic tests used for VLM are not as reliable for ocular toxocariasis, and eosinophil count is not usually increased in these patients. Centers for Disease Control and Prevention consider serum ELISA titers less than 1 : 32 to be insignificant in the diagnosis of systemic toxocariasis[55] but others have stated that a serum titer of 1 : 8 is sufficient to support a diagnosis of ocular toxocariasis if the patient has signs and symptoms compatible with that disorder.[45] A positive test may represent a previous contact with the parasite and it does not

necessarily mean that the patient suffers from either VLM or ocular toxocariasis. Ellis and coworkers have shown that 23% of 333 kindergarten children in rural North Carolina without signs of ocular toxocariasis exhibited a serum titer ≥1 : 32, and 32% had a titer ≥1 : 16.[55] Prestes-Carneiro and coworkers have shown that 14% of 182 randomly studied patients in rural São Paulo, Brazil, presented positive ELISA tests for *T. canis*.[56] Thus a positive serum titer cannot be used to confirm absolutely a diagnosis of ocular toxocariasis, although the absence of any serologic evidence of *Toxocara* infestation does not exclude the diagnosis but may assist in reducing the odds of this organism being the cause of ocular disease. Oréfice and coworkers studying 30 cases of presumed ocular toxocariasis found a positive ELISA test in 88% of them.[44] Another study has shown that only 45% of patients with clinically diagnosed ocular toxocariasis had titers higher than 1 : 32.[54]

Cytologic study of aqueous humor or vitrectomy samples may also be helpful in confirming the diagnosis of ocular toxocariasis. The presence of eosinophils in intraocular fluids is consistent with intraocular *Toxocara*. Remnants of *Toxocara* organisms have occasionally been recovered from vitrectomy specimens obtained at surgery.[57]

Differential Diagnosis

Differential diagnosis of ocular toxocariasis includes retinoblastoma, toxoplasmosis, other causes of endophthalmitis and uveitis, retinopathy of prematurity, Coats disease, persistent hyperplastic primary vitreous, and familial exudative vitreoretinopathy. In localized granulomas with clear media, diagnosis can be determined by clinical evaluation (indirect binocular ophthalmoscope). In eyes with severe vitreous opacification, it may be impossible to make the appropriate diagnosis on the basis of morphologic features alone and considering the differential diagnosis is important.

Retinoblastoma

Retinoblastoma is the most common intraocular malignancy of childhood and also the most important entity frequently confused

with ocular toxocariasis.[7] The first report of nematode intraocular endophthalmitis by Wilder[13] included enucleated eyes for suspicion of intraocular retinoblastoma. Shields and coworkers[58] reported that among 500 consecutive patients referred to them with leukokoria, 42% had pseudoretinoblastoma and among them 15.6% had a final diagnosis of ocular toxocariasis. Patients with retinoblastoma are usually diagnosed before 2 years of age, being younger than a typical child with ocular toxocariasis. Sporadic retinoblastomas are more frequently confused with ocular toxocariasis since most of them are unilateral, and lack a family history of the malignancy. On ophthalmic evaluation, retinoblastoma usually does not present signs of intraocular inflammation, with clear vitreous and lack of posterior synechiae, cataract or cyclitic membranes, and the tumor presents a growing pattern that does not occur in toxocariasis granulomas.[7] In cases with opaque media the differential diagnosis is harder. Ultrasonography and CT scan may be very valuable in demonstrating an intraocular mass and calcifications of a retinoblastoma or vitreous organization and tractional membranes, which is more frequently observed in ocular toxocariasis. In cases where the differential diagnosis is difficult, evaluation of intraocular fluids by ELISA or cytology may be of particular importance. If retinoblastoma is suspected, however, biopsy should be avoided and consultation with other experts may be a better path to reliable diagnosis. Risks and concerns relating to sampling retinoblastoma tissue are discussed in the oncology section of this book.

Toxoplasmosis

The typical lesion seen with protozoal *Toxoplasma gondii* infection is focal granulomatous and necrotizing retinochoroiditis. It appears as a whitish or yellowish lesion, slightly elevated and with poorly defined limits.[20] During active disease, severe vitritis frequently occurs and in this case a differential diagnosis with chronic endophthalmitis caused by *Toxocara* can be very difficult. Ultrasonographic study can show vitreous membranes and an elevated mass that are more common in toxocariasis. Serologic studies of antibodies to both parasites can be helpful in establishing differential diagnosis.

Other Forms of Endophthalmitis and Uveitis

Bacterial endophthalmitis is frequently related to a recent history of trauma or intraocular surgery. These acute infections produce much more intraocular inflammation than a typical toxocariasis case. Endogenous endophthalmitis is rare, but an indolent infection may be nearly impossible to distinguish from nematode endophthalmitis. In such cases, laboratory diagnostic methods may be of value in determining the etiology. Pars planitis or chronic cyclitis is a condition that typically occurs in an older age group than that in which ocular toxocariasis occurs. Hogan and coworkers[59] described a case of pars planitis in which subsequent histologic examination demonstrated that the etiology was *T. canis*.

Retinopathy of Prematurity

Patients with retinopathy of prematurity (ROP) have a positive history of prematurity and low birth weight, which is not common in ocular toxocariasis. ROP is usually diagnosed soon after birth, and nontreated patients can develop cicatricial signs such as high myopia, temporal macular dragging, peripheral retinal folds, and, in more severe disease, ROP stage V (retrolental fibroplasia). ROP affects both eyes while ocular toxocariasis is almost always unilateral. Morphologic features of ROP may be very similar to those of peripheral cicatricial ocular toxocariasis. In both conditions a peripheral white retinal mass may be associated with a fold of retina extending from the posterior pole to the granuloma.

Coats Disease

Coats disease is a unilateral condition that affects predominantly young males in the same age group as does toxocariasis. Ophthalmoscopic and fluorescein angiographic evaluation show classic intraretinal telangiectatic vessels with association with yellow intraretinal and subretinal exudates. In later stages retinal detachment may be present and the differential diagnosis with ocular toxocariasis may be more difficult. In Coats disease vitreous shows no signs of marked inflammation and epiretinal membrane formation is not seen.

Persistent Hyperplastic Primary Vitreous

Persistent hyperplastic primary vitreous (PHPV) is a congenital condition usually diagnosed within the first few weeks of life and presents itself almost always unilaterally. PHPV presents frequently with a retrolental fibrovascular mass that may be confused with toxocariasis. The involved eye is typically microphthalmic, and this feature is not common in ocular toxocariasis.

Familial Exudative Vitreoretinopathy

Familial exudative vitreoretinopathy is an inherited disorder with typically bilateral occurrence. This disorder is associated with peripheral vascular abnormalities, pronounced exudation, vitreoretinal traction, and folds of retina extending from the posterior pole to a peripheral type of mass.

Treatment

Most ocular toxocariasis cases are diagnosed when there is a focal granuloma but no longer vitreous or surrounding active inflammation. In such cases treatment with anthelmintics or corticosteroids is not helpful and surgical treatment is considered when there is clinical cataract, vitreous membranes or opacification, or in cases of retinal detachment.

Medical therapy should be considered in cases of active inflammation. Topical and systemic corticosteroids are useful in managing acute inflammatory reaction and may reduce vitreous opacification and reduce or prevent membrane formation.[7,19,48,60,61] Topical mydriatics may prevent posterior synechia and secondary angle closure secondary to seclusio pupillae.[20] The exact role of anthelmintic therapy in ocular toxocariasis remains unclear and it is not proven that the use of this therapy can kill intraocular larva.[7] Despite this, the use of anthelmintic drugs or combination of them with corticosteroids has been reported with favorable results.[52,62] Anthelmintic drugs such as thiabendazole and diethylcarbamazine have been recommended in selected cases of VLM,[60] and nowadays albendazole is the current drug of choice in the treatment of VLM,[30] showing its superiority over thiabendazole.[63] For the treatment of VLM currently recommended therapy is albendazole 400 mg twice

a day for 5 days.[64] Treatment of ocular disease was described as a dose of 200 mg albendazole twice a day for one month.[20] If a subretinal larva is observed it can be destroyed with photocoagulation.[7] Intravitreal ranibizumab has been described to treat choroidal neovascularization secondary to ocular toxocariasis.[65]

Ocular surgery is indicated mainly in cases of ocular toxocariasis with retinal detachment[43,66,67] and pars plana vitrectomy is the preferred technique, allowing release of membrane traction and retinal reattachment in more than 70% of cases in some series.[45,67,68] Other indications for surgery include management of vitreous opacification, cataract, and glaucoma. Hagler and coworkers[45] reported 17 consecutive cases of retinal detachment secondary to ocular toxocariasis. In this report the retina was successfully reattached in 12 (71%) cases, and vision remained stable or improved in 15 (88%) of the 17 eyes. Small et al.[67] reported 12 cases of retinal detachment with a postoperative reattachment after vitreous surgery in 10 (83%), and visual acuity improved in 7 (70%) of the anatomic successes. Recently Giuliari and coworkers[68] presented 45 cases treated surgically for complicated ocular toxocariasis. Pars plana vitrectomy was the technique of choice in 58% of the cases, 38% had peripheral granuloma, and postoperative visual acuity was equal or better than 20/300 in 60% of the eyes studied.

The most important approach to the management of ocular toxocariasis and VLM is prevention, decreasing the risk of ingestion of *T. canis* embryonated eggs or larvae. Effective measures include anthelmintic treatment of newborn puppies, as well as nursing and lactating bitches after each pregnancy; hygienic disposal of dog feces; avoiding contact of children at risk with potentially contaminated animals; avoiding eating raw meat of possible hosts; stopping children from playing in sandboxes in places where people walk their dogs; and improving hygiene habits in children, among others.

Diffuse Unilateral Subacute Neuroretinitis

DUSN is an ocular disease caused by the presence of a nematode worm in the subretinal space. The disease affects predominantly children and young adults and often causes unilateral severe visual loss. In the acute stage it presents with an appearance of subacute retinitis, optic disc swelling, and mild to moderate vitritis, while in late stages there is retinal and optic disc atrophy, retinal vessel narrowing, and severe visual impairment.

History and Etiology

In 1978 Gass and Scelfo first described a clinical syndrome in which only one eye of a healthy child or young adult was affected.[69] Features of the syndrome include insidious, usually severe loss of peripheral and central vision; vitritis; diffuse and focal pigment epithelial derangement with relative sparing of the macula; narrowing of the retinal vessels; optic atrophy; increased retinal circulation time; and subnormal electroretinographic findings.[69] Initially the syndrome was termed "unilateral retinal wipeout syndrome." Later, after recognition of signs of acute stages of the disease, the syndrome was named diffuse unilateral subacute neuroretinitis. The nematodal etiology of the syndrome was not yet clear, but from 36 patients reported, two revealed the presence of a subretinal worm at fundus examination, and both larvae were suspected to be from the *Toxocara* genus.[69,70] Later, in 1983, Gass and Braunstein described two different-sized nematodes causing the disease and postulated that the cause was probably not *T. canis*. The geographic distribution of both was different, and the smaller worm (from 400–1000 μm in length) was proposed to be a larva of *Ancylostoma caninum*, while the larger one (from 1500 to 2000 μm in length) remained uncertain.[71] One year later, Kazacos and coworkers suggested that the larger larva previously described[71] was *Baylisascaris procyonis*, an intestinal nematode of raccoons and squirrels associated with central nervous system infections.[72,73] Association of DUSN and neural larva migrans has been reported, and indirect immunofluorescence assays on serum and cerebrospinal fluid of one patient were positive for *B. procyonis*.[74] Other case reports of DUSN with confirmed serologic evidence of *B. procyonis* infestation were reported and support its etiology as the

larger nematode to cause DUSN.[75,76]

The exact etiology of the smaller larva remains unclear. Despite the first impression of the larvae being *Toxocara*,[70] later Gass and Braunstein[71] opined that *T. canis* might not be the cause of DUSN due to lack of consistent serologic evidence, the length of second-stage larva of *T. canis* being smaller than the small worm described, the clinical features being different than other forms of ocular toxocariasis, and the worldwide prevalence of *T. canis* not fitting with the limited distribution of DUSN. Gass theorized that *A. caninum*, a common parasite of dogs, could be the causative agent because it is a frequent cause of cutaneous larval migrans in the southeastern United States, its infective third-stage larva measures approximately 650 μm, it can survive in host tissues for months to years without changing size or shape, and cutaneous larval migrans had immediately preceded the onset of DUSN in some patients.[77] Casella and coworkers[78] also described cases of DUSN and cutaneous larva migrans, reinforcing that *A. caninum* could be a probable cause of the disease in Brazil. Cunha de Souza and Nakashima[79] successfully extracted a subretinal worm in a 9-year-old Brazilian boy through a retinotomy after pars plana vitrectomy. This larva was morphologically similar to third-stage *T. canis* based on length of body and esophagus, tapered tail, and mouth shape. *Toxocara canis* causes visceral larva migrans and *A. caninum* causes cutaneous larva migrans, and there is evidence that both can be related to DUSN; thus confirmation of one as causative agent does not necessarily exclude the other as a possible cause. Cases of DUSN caused by non-nematode worm were reported by McDonald and coworkers. In such cases the larva related to DUSN was *Alaria mesocercaria*, a trematode worm.[80] Despite this report, nematodes are described as the main etiologic factors in DUSN. Among them, some filariae, such as *Dirofilaria*,[81–83] have been proposed to cause the disease, but *B. procyonis* as the large worm and *A. caninum* and/or *T. canis* as the small worms are the most probable etiologic factors.

Epidemiology

DUSN is an endemic disease in the southeastern United States

where the smaller worm (400–1000 μm) is most often seen and in the northern-midwestern part of the country where the larger worm (1500–2000 μm) is mostly related to the disease.[71,77] Its occurrence has been described also in the Caribbean,[9] Canada,[84] Germany,[85] Spain,[86] China,[87] and India.[82,83,88] It is endemic in South America, with most cases described in Brazil[78,89–92] and Venezuela.[93] In South America, DUSN is caused by a smaller worm, although in one case report a larger worm was found as the etiologic factor (Fig. 89.6).[94]

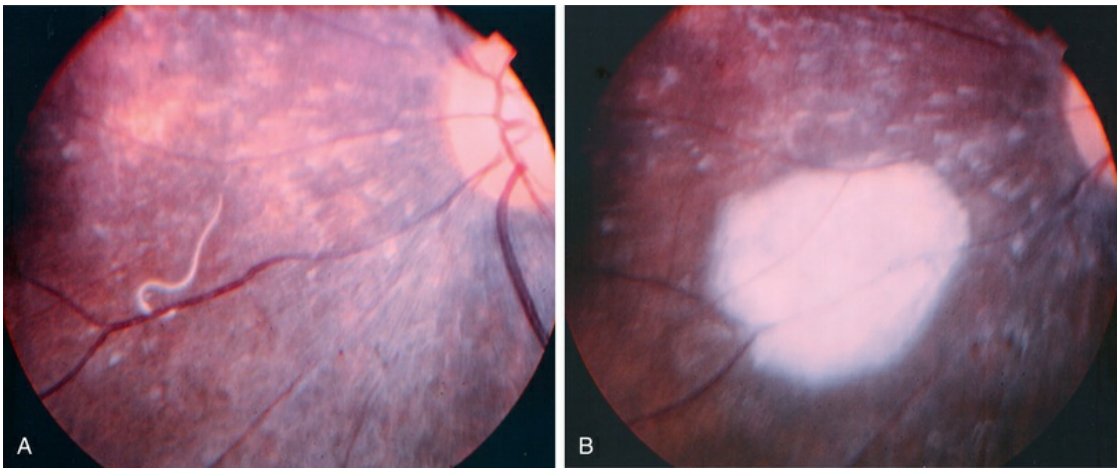

FIG. 89.6 Subretinal large nematode (A). Retinal aspect after photocoagulation of the nematode (B).

(Reproduced with permission from Cialdini AP, Souza EC, Avila MP. The first South American case of diffuse unilateral subacute neuroretinitis caused by a large nematode. Arch Ophthalmol. 1999;117:1431–2. Copyright © 1996 American Medical Association. All rights reserved.)

DUSN typically affects healthy patients in the second and third decades of life,[69,71] with a higher incidence in the male gender. In the typical disease only one eye is affected and a single motile subretinal nematode can be identified. Cases of nematodes infesting both eyes[91] or two nematodes infesting the same eye[85] are less frequently reported.

Pathophysiology

The complete pathophysiology of DUSN is not clearly determined, but it is presumed that DUSN develops as a local reaction of outer

retina to toxic products released by subretinal worm.[69] These products would also produce a toxic reaction to inner retina. Through the years there is a progressive loss of ganglion cells, secondary arterial narrowing, and optic atrophy.[78] Gass and Scelfo[70] reported histopathologic findings from one eye of a patient with clinical evidence of DUSN. Histopathologic analysis has shown a nongranulomatous vitritis, retinitis, and retinal and optic nerve perivasculitis. An extensive degeneration of the peripheral retina, mild degeneration of the posterior retina, retinal pigmented epithelium (RPE), choroiditis, and mild optic nerve atrophy were also observed. There was no eosinophilic reaction as usually seen in the typical granuloma of ocular toxocariasis. Histopathologic data were not sufficient to explain severe visual loss in this case (light perception), which contributed to speculation about the role of functional mechanisms in causing visual damage such as an inflammatory and/or toxic aggression towards retinal bipolar cells.[95] Recently Gomes and coworkers[96] and Casella and coworkers[97] described two case series of patients with DUSN studied by means of time domain optical coherence tomography (OCT). In both series the OCT main finding was diffuse atrophy of the retinal nerve fiber layer. Berbel et al. described normal choroidal thickness despite retinal atrophy measured by spectral domain OCT with enhanced depth imaging.[98] The variability of the inflammatory signs and tissue damage seen in patients with the disease may reflect differences in host immune response to the organism or the characteristics of the nematode itself.[99]

Clinical Presentation

Clinical features of DUSN can be divided into early and late stages.

Early Stage

Most patients with DUSN are asymptomatic or have mild symptoms in this stage of the disease.[91] Main symptoms include central or paracentral scotoma, floaters, mild to moderate visual loss, and ocular discomfort.[70] Signs include afferent pupillary defect; mild to moderate vitritis; optic disc swelling; vasculitis; and/or narrowing of retinal vessels. Less frequently, posterior

segment signs include retinal and subretinal hemorrhages, serous exudation, and choroidal neovascularization.[70] The anterior segment is typically calm, although occasionally anterior uveitis may be present. The most characteristic retinal finding is the presence of recurrent crops of evanescent, multifocal, gray-white or yellow lesions at the level of the outer retina (Fig. 89.7). These active lesions are typically clustered in posterior pole, and the larva may be found in the surrounding area.[77] These lesions disappear in 1–2 weeks as the worm moves to other retinal area. Less than 1% of the lesions can lead to a focal chorioretinal scar that simulates that seen in the presumed ocular histoplasmosis syndrome.

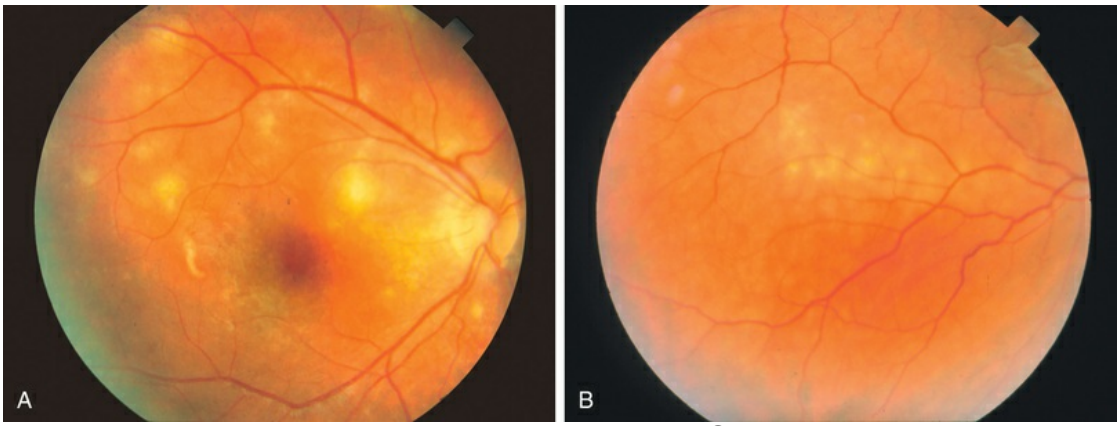

FIG. 89.7 Early stage presumed DUSN. Fundus photographs showing typical retinal finding: crops of multifocal, gray-white, or yellow lesions at the level of the outer retina. (Courtesy of Fernando Oréfice, MD and Editora Cultura Médica.)

Late Stage

Frequently in children, visual loss is insidious, and the patient comes to medical attention during the late stages of the disease.[99] If the nematode is not recognized and the condition is not treated, the disease evolves to its late stage. Main symptoms include a dense central or paracentral scotoma and severe permanent visual loss, while signs include an afferent pupillary defect in the affected eye, progressive optic atrophy, narrowing of the retinal arteries, and marked focal and/or diffuse degenerative changes in the RPE. The nematode may survive for 4 years or longer and may be found in

the subretinal space even after the development of retinal and optic disc changes[99] (Fig. 89.8).

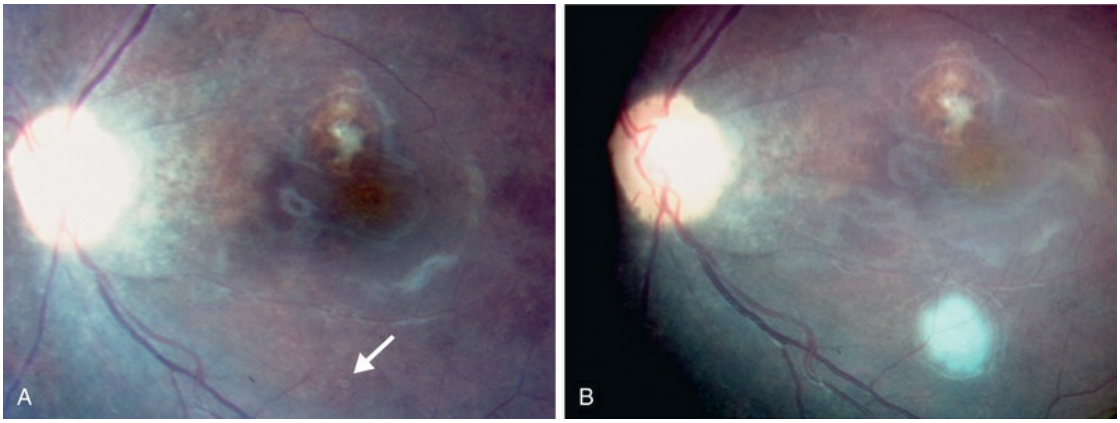

FIG. 89.8 (A) *Arrow* indicates the location of a subretinal nematode in the macular region. This case represents a late stage of DUSN with optic disc pallor, retinal pigmented epithelium changes, and vascular narrowing. (B) Same eye after photocoagulation of the nematode. (Courtesy of Arnaldo Cialdini, MD.)

Diagnosis

Definitive diagnosis of DUSN is based on identification of subretinal nematode after observation of clinical aspects that raise suspicion of the disease. Indirect ophthalmoscopy is important in making the correct diagnosis and in locating the cluster of active gray-white outer retinal lesions. These lesions are typically found in acute stages of the disease and, if they are present, the nematode will usually be found biomicroscopically in their vicinity.[99] If these lesions are absent, a detailed search of the entire fundus using a contact lens may locate the worm (Fig. 89.9). The rates of nematode identification in previous studies has varied from 33% to 52%.[93,96,100] A case report has shown that scanning laser ophthalmoscopy enhances contrast between the nematode and the ocular fundus and improves visualization and location of a moving worm.[101] In cases in which nematode is not located on fundus examination, a presumed diagnosis is established based on clinical findings, epidemiology, and ancillary exams.

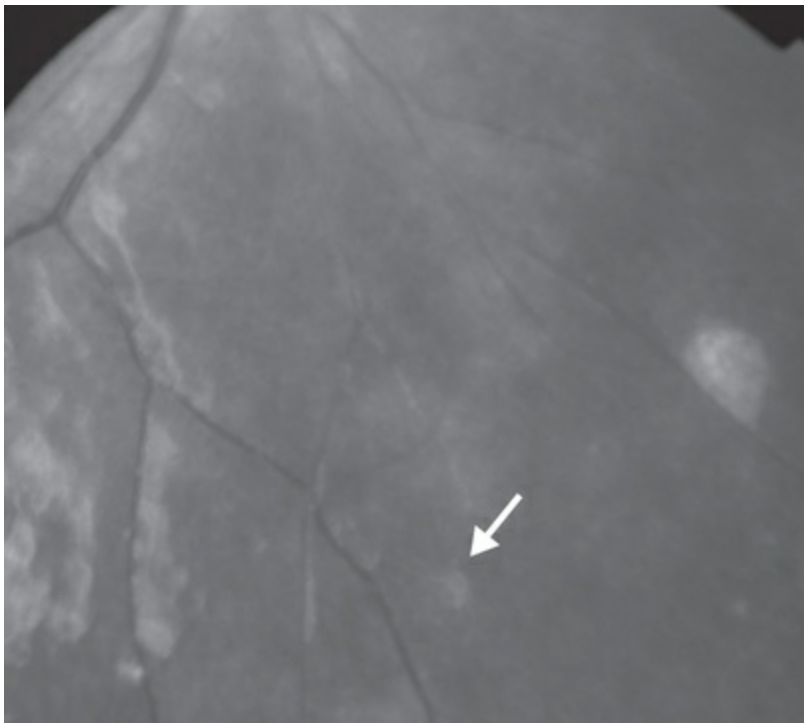

FIG. 89.9 Red-free retinography showing subretinal nematode (*arrow*) located on nasal-inferior retina.

Fluorescein angiography (FA) findings are different in acute and late stages of DUSN. During the early stages of the disease FA shows leakage of dye from the optic nerve head and perivenous phlebitis.[70] The active gray-white lesions exhibit early hypofluorescence and hyperfluorescence with staining in late phases of the angiogram. The aspect of the lesions on FA is very similar to the fluorescein pattern found in other white dot syndromes; however, in multiple evanescent white dot syndrome (MEWDS) the lesions are hyperfluorescent on early angiogram. In early stages of the disease there are also minimal changes in RPE and cystoid macular edema may occur. In late stages of DUSN, FA shows diffuse hyperfluorescence from RPE window defects and delay in retinal perfusion (Fig. 89.10). Indocyanine green angiography (ICGA) shows multiple small round hypofluorescent lesions that persist during all angiograms. Their aspect is similar to lesions found in birdshot chorioretinopathy.[102]

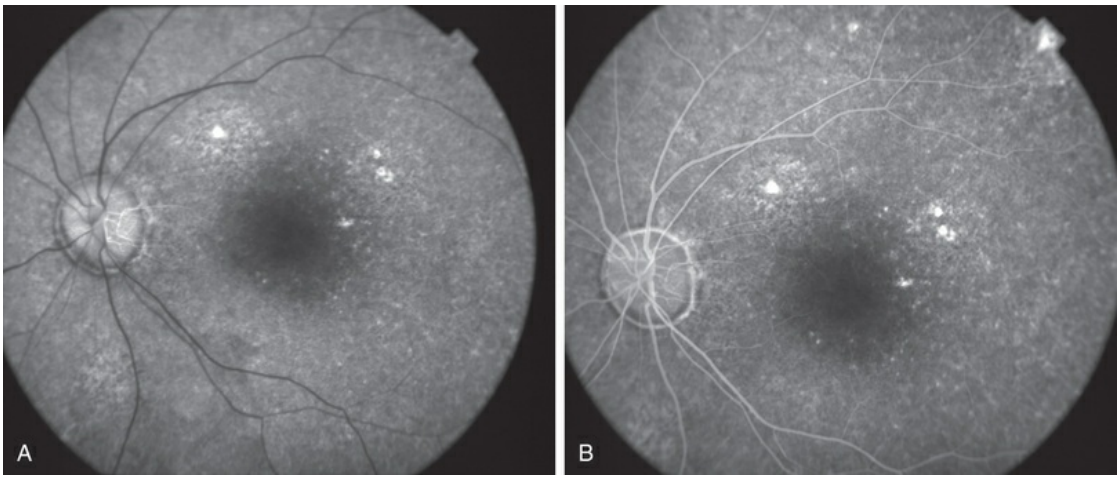

FIG. 89.10 Fluorescein angiography performed in a late stage of DUSN, showing diffuse hyperfluorescence from retinal pigmented epithelium window defects and delay in retinal perfusion.

The electroretinogram (ERG) may be normal in the very early stage of the disease, however it typically varies from subnormal to severely decreased as the retinopathy progress. During all stages of the disease the b-wave is more affected than the a-wave, possibly due to a toxic effect of the nematode and its products to retinal bipolar cells.[95] Rarely the ERG is extinguished[70,71] and the unaffected eye presents normal ERG. Eradication of the nematode in one case resulted in improvement in multifocal ERG amplitudes.[103]

OCT shows diffuse retinal thinning and diffuse retinal nerve layer atrophy.[96,97] Casella and coworkers also described focal retinal edema in areas affected by the worm and have shown the topography of subretinal worm by means of OCT[97] (Fig. 89.11). Gomes et al., studying 38 patients with DUSN, described statistical significance between retinal nerve fiber thickness and worse visual acuity.[96]

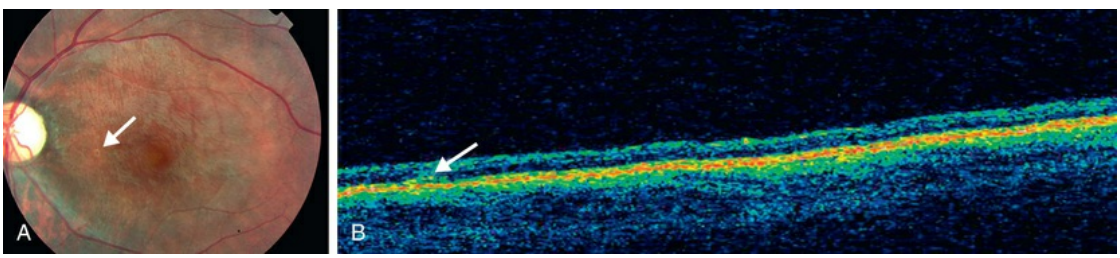

FIG. 89.11 (A) Color fundus photograph showing subretinal nematode (*arrow*). (B) Optical coherence

tomography showing retinal atrophy and nematode in subretinal space (*arrow*). (Images courtesy of Antônio Marcelo Casella, MD.)

Serologic studies, stool examinations, and peripheral blood smears are of little value in making the diagnosis of DUSN.[70] Toxocaral and *B. procyonis* antibody titers have been suggested as diagnostic tools to try to characterize which nematode is producing the disease.[72] Recent study showed that ELISA cross-reactivity between them may be present and suggests a Western blot analysis to complete serologic differentiation between *Toxocara* and *Baylisascaris* as cause of larva migrans.[104] ELISA test has been also used for serologic characterization of cutaneous larva migrans caused by *A. caninum*.[105]

Differential Diagnosis

DUSN can mimic several other chorioretinal diseases.[77] The disease presents differently in early and late stages and the differential diagnosis will be described separately for better comprehension.

In the early stages of DUSN, the typically seen gray-white lesions can mimic many other infectious and inflammatory conditions (Fig. 89.7). In DUSN, typical lesions occur in outer retina and after healing they normally present few or no RPE scars. In other infections such as toxoplasmosis, cytomegalovirus, and bacterial or fungal retinitis generally the inner retina is affected and there is prominent chorioretinal scarring left in the area of the retinitis. DUSN may also mimic white dot syndromes such as acute posterior multifocal placoid pigment epitheliopathy (APMPPE), serpiginous choroiditis, MEWDS, multifocal choroiditis with panuveitis (MFC), and birdshot chorioretinopathy.[102] These entities are discussed in other chapters in more detail. Briefly, unlike DUSN, the active lesions in APMPPE and serpiginous choroiditis are accompanied by loss of visual acuity only when the lesions involve the center of the fovea, and they always cause permanent visible alterations in the pigment epithelium. APMPPE and serpiginous choroiditis occur in adults and are generally bilateral. In APMPPE, the electro-oculogram may be abnormal but the ERG is normal, and visual prognosis is good. Serpiginous choroiditis has a

worse prognosis than APMPPE and electrophysiologic tests are normal. MEWDS occurs in young adults; it is more frequent in women and may be distinguished from DUSN by a frequent history of an antecedent flu-like illness and photopsia, widely scattered gray-white outer retinal lesions, an enlarged blind spot, hyperfluorescent dots seen from the early phases of fluorescein angiography (in DUSN lesions are initially hypofluorescent), a decrease in the ERG a-wave that normalizes as symptoms fade, and return of the fundus and visual function to normal in most patients within several months.[99] Birdshot chorioretinopathy often occurs in middle-aged women, is bilateral, and is frequently associated with positive HLA-A29. Fundus changes include moderate vitritis and multiple scattered yellowish rounded lesions that may resemble DUSN lesions. Fluorescein angiography shows hypofluorescent lesions and may demonstrate active retinovascular leakage along the large retinal vessels, small vessel leakage, and cystoid or diffuse macular edema. Circulation times are often delayed and the vessels empty much more rapidly than in a normal eye.[101] Other uveitis can mimic DUSN. In Behçet disease, the white lesions involve the inner retina and the patient usually has other systemic manifestations of the disorder, including oral and/or genital ulcers, arthritis, and erythema nodosum. Patients with DUSN occasionally may demonstrate perivenous candle-wax-dripping exudate or subretinal exudate similar to that seen in patients with sarcoidosis.[77]

In late stage of the disease after fading of gray-white lesions and development of scattered focal chorioretinal scars, the fundus of patients with DUSN may be mistaken for the presumed ocular histoplasmosis syndrome (POHS). POHS is frequently bilateral, shows normal RPE between the focal scars, presents clear vitreous without inflammatory cells, and there is a lack of optic atrophy and retinal vessel narrowing. Retinitis pigmentosa (RP) is another important differential diagnostic entity. The presence of bone-spicule RPE hyperpigmentation, bilaterality, and posterior subcapsular cataract are common in RP but rare in DUSN.[99] Other causes of optic atrophy may mimic DUSN, such as trauma, retrobulbar or intracranial tumors, and sustained occlusion of ophthalmic artery.

Treatment

Prompt identification of the early signs of the disease allows treatment that can prevent late manifestations and encourage visual recovery/preservation. Treatment of DUSN can be performed with either photocoagulation of the nematode when it is identified during fundus examination (careful searching often with a contact lens is needed) or systemic anthelmintic drugs when the diagnosis is presumed. Photocoagulation of the subretinal worm is the current treatment of choice (see Figs. 89.6 and 89.8). It causes minimal or no posttreatment exacerbation of inflammation and is successful in causing prompt and permanent inactivation of the disease. Visual acuity improvement depends on the stage of the diagnosis.

Initially the use of oral anthelmintic was considered ineffective,[71] but further studies have shown that thiabendazole is effective in the treatment of patients with a moderate degree of vitritis associated with a breakdown in the blood–retinal barrier.[106–108] Subsequently, ivermectin has been tried as a less toxic alternative to thiabendazole.[109] However, Casella and coworkers reported that ivermectin failed to kill a nematode that was subsequently identified and destroyed with laser photocoagulation.[110] Two studies report case series of successful treatment of DUSN with albendazole[100,111] (Fig. 89.12). Cunha de Souza and coworkers[100] and Malaguido and coworkers[111] report the use of albendazole 400 mg/daily for 30 days with fading of active lesions and visual recovery. In patients with late-stage DUSN some degree of improvement of vision was observed. No adverse side-effects were observed in both studies, and this therapy has been advocated in cases of presumed DUSN where the nematode is not located.[91,112]

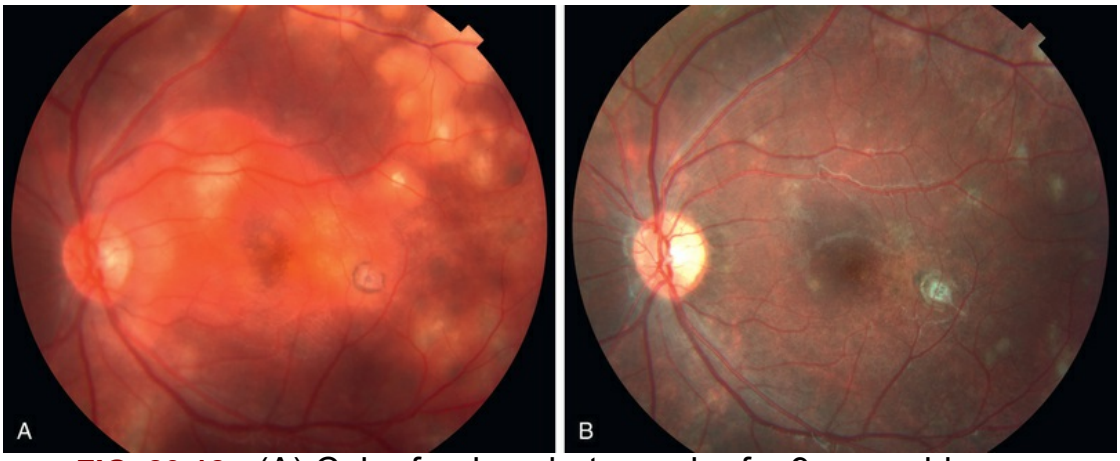

FIG. 89.12 (A) Color fundus photograph of a 9-year-old boy with unilateral multifocal retinitis diagnosed as presumed early stage of DUSN. (B) Appearance after 45 days. The patient was treated with albendazole 400 mg/day twice a day for 30 days. Visual acuity improved from 20/200 (A) to 20/70 (B).

Onchocerciasis

Onchocerciasis (river blindness) is caused by the microfilarial stage of the nematode *Oncocerca volvulus*. More than 99% of infected people live in 31 sub-Saharan African countries, but the disease also exists in some regions in Latin America (Brazil, Guatemala, Mexico, and Venezuela) and Yemen.[92,113,114] According to the World Health Organization, onchocerciasis is the world's second leading cause of preventable blindness and its prevalence is estimated at 37 million individuals worldwide.[114,115] The filariae cause dermatitis, subcutaneous nodules due to encapsulation of parasites in fibrous tissue, and eye disease. The disease is transmitted by an insect of the genus *Simulium* (Blackflies) which breed in fast-flowing rivers and streams, lending the name "river blindness." The vector ingests microfilariae during a blood-meal from a sick human. Then the parasites develop into infectious stages and are transmitted to other persons on subsequent bites. Humans are the only definitive known host.[113]

Clinical Presentation

Ocular onchocerciasis can involve any part of the eye and disease manifestations are characterized either as posterior or anterior eye disease.[116]

Anterior eye disease prevalence has been described ranging from 43 to 48% of affected individuals in studied populations. The most frequently diagnosed anterior eye disease is the presence of microfilariae in the anterior chamber associated or not with iridocyclitis, followed by punctate epithelial keratitis, corneal microfilariae, sclerosing keratitis, and neovascularization leading to visual impairment and blindness in one or both eyes in 2–4% of patients.[117,118]

Posterior eye disease prevalence ranges from 34% to 75% of affected patients.[117,118] Posterior segment lesions include atrophy of RPE and choroid mainly in the posterior pole, hyperpigmentation clumping of RPE, white and shiny intraretinal deposits, retinitis, subretinal fibrosis, neuritis, and optic nerve atrophy.[117–120] Patients may present with visual field loss and poor night vision, and in patients with hyperpigmentation of RPE a differential diagnosis with retinitis pigmentosa is important. Another important differential diagnostic consideration is hypovitaminosis A, which can cause also night blindness and intraretinal white spots.

Treatment and Prevention

Through the years the prevalence of ocular onchocerciasis is falling in endemic areas. This fact is due to several task forces of the World Health Organization in Africa and the Americas to reduce vector breeding and also to the treatment of patients with the disease, preventing blindness in affected and contamination of healthy individuals.

Ivermectin is a safe and effective microfilaricidal drug which has been donated by Merck and Company since 1987 to be delivered through mass drug administration programs to control onchocerciasis. Ivermectin rapidly kills the microfilariae and reduces the lifespan of adult worms. This therapeutic scheme is administered twice each year, and the goal of these programs was to treat at least 85% of the population at risk and completely eliminate transmission of the parasite in Africa and America by the

year 2012.[113] By the end of 2011, transmission was interrupted in 10 of 13 active locations throughout Latin America. In 2013 and 2014, respectively Colombia and Ecuador were declared free of river blindness by the World Health Organization[114]. In 2012, approximately 99 million treatments for onchocerciasis were administered in Africa, and the World Health Organization leads a consortium the main purpose of which is complete elimination of onchocerciasis by 2025.[121]

Cysticercosis

Cysticercosis is the infestation of human tissues by *Cysticercus cellulosae*, the larval form of *Taenia solium*, a common pork parasite that can cause taeniasis in man. The ingestion of contaminated and uncooked meat containing cysticerci leads to development of taeniasis, the infestation of human small intestine by the adult tapeworm of *T. solium* (definitive host). Cysticercosis occurs when the intermediate host (e.g., pork, man) ingests eggs of *T. solium* from contaminated food or water, or by autoinfection of the definitive host when there is accidental ingestion of eggs shed in the host feces.[122,123] The ingested eggs develop into larvae, which penetrate the small intestine wall, reaching lymphatics and vascular system. The larvae then spread to highly vascularized organs such as brain, heart, muscles, and eyes, where they become a cystic structure containing the scolex named cysticercus (metacestode).[124] Cysticerci may remain viable in the ocular and central nervous system for years, and ocular manifestations can be devastating as the cysticercus increases in size or dies releasing toxic products leading to a profound inflammatory reaction, causing blindness in 3–5 years.[125]

Clinical Presentation

The central nervous system is the most affected system and neurocysticercosis is the most commonly diagnosed form of cysticercosis.[126] Neurocysticercosis is the main cause of acquired seizures worldwide. The disease can also lead to encephalopathy, meningeal signs, obstructive hydrocephalus, and other neurologic

abnormalities.[127] Cysticerci appear as cystic lesions on computed tomography (CT) or magnetic resonance imaging (MRI), and when calcified appear as hyperdense spots on radiographs.

Eyes and adnexal tissues are affected in 13–46% of infected individuals.[122] Cysticerci may be present in virtually all ocular and adnexal structures such as in the eyelids, orbit, extraocular muscles, subconjunctival space, anterior chamber, vitreous and subretinal space.[123,126,128–130] Vitreous and subretinal locations are the most often diagnosed locations of ocular cysticercosis, ranging from 68 to 74% of studied cases, and 41% occurred either subretinally or intraretinally in one series.[122,126] The parasite reaches the eye through posterior ciliary arteries to the subretinal space. A subretinal cysticercus is seen ophthalmoscopically as a cyst in subretinal space containing one scolex that usually presents as a white spot inside the cyst (Fig. 89.13). Associated findings may be observed, such as retinal pigmented epithelium hyperpigmentation, serous retinal detachment, retinal edema and/or hemorrhages, and severe uveitis in later stages (Fig. 89.14). Intravitreous cysticercus presents as a well-defined translucent floating cyst that can produce undulating movement, especially when stimulated by light. Epiretinal membranes or RPE changes in the spot where the parasites traverse the retina may be observed (Fig. 89.15).[124,128,131,132] Ultrasonography may be used to confirm the cystic nature of the parasite, and MRI has been suggested to confirm ultrasonographic findings as well as determine the presence of possible other cysts in orbit or brain.[130]

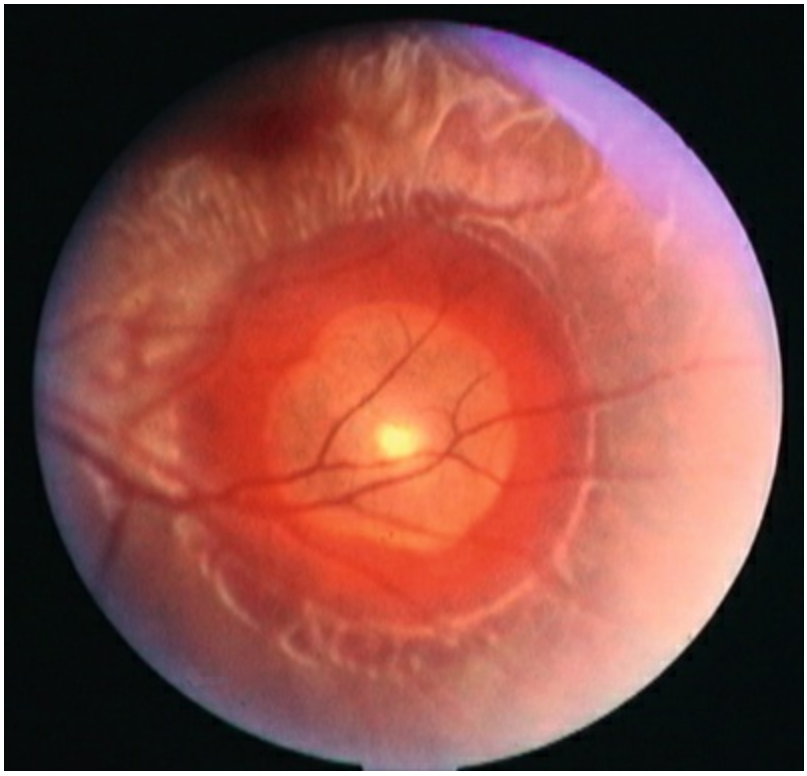

FIG. 89.13 Subretinal cysticercus in the posterior pole surrounded by hemorrhage.

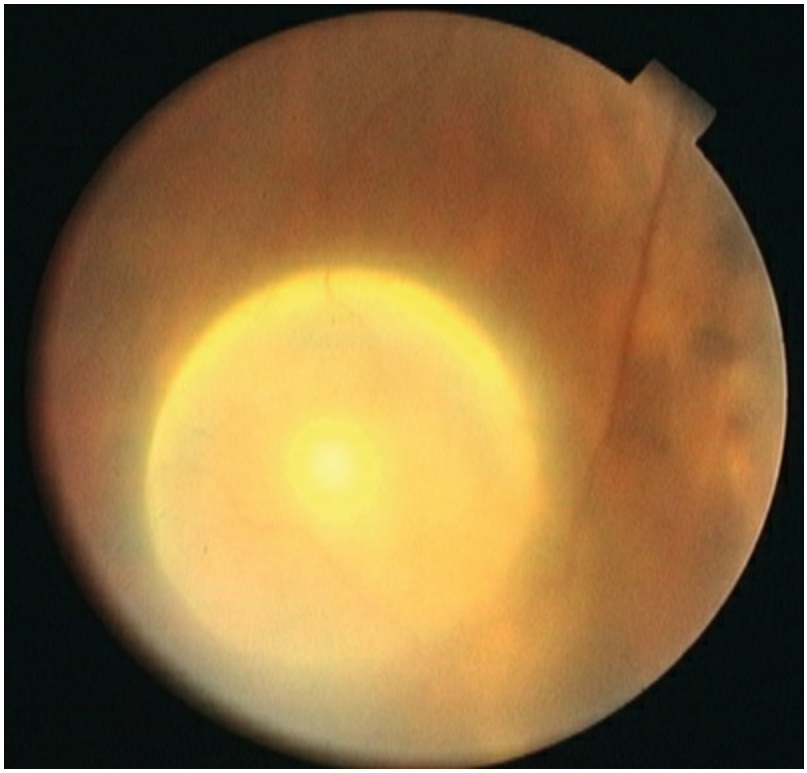

FIG. 89.14 Subretinal cysticercus located in the inferior

retina.

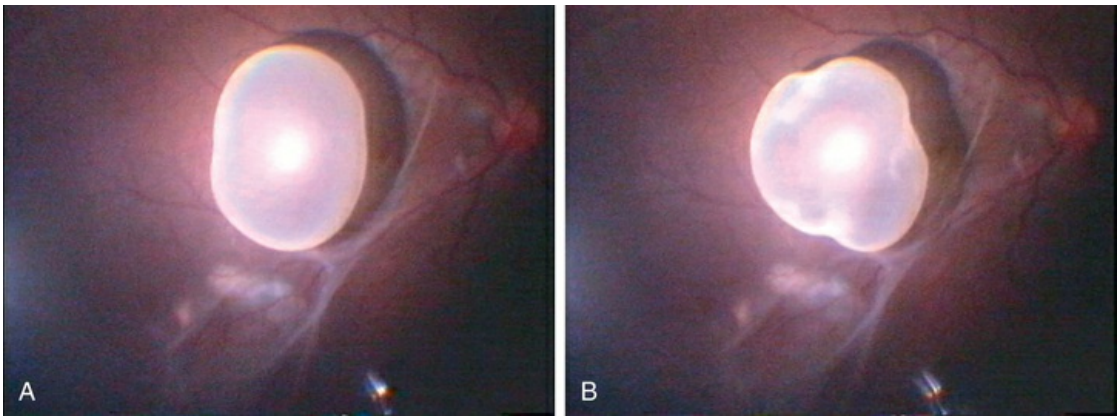

FIG. 89.15 Intravitreal cysticercus. It is possible to see an epiretinal membrane and pigmented epithelium changes inferiorly. This is the possible site from where the parasite passed from the subretinal space to the vitreous cavity. During vitrectomy it was possible to detect cyst movements as the light pipe was directed to it.

Treatment

Intraocular cysticercosis is treated with surgical removal.[131–133] Treatment with systemic drugs has not been succesful[134] and killing the cyst without removing it might produce severe uveitis. An intravitreal cysticercus can be removed by pars plana vitrectomy, and the subretinal cyst removal can be performed by either vitrectomy or transcleral removal.[131] The cysticercus should be removed unharmed, avoiding its rupture and release of intracystic material in the vitreous cavity; however, there are reports of successful suction of the cyst during vitrectomy with the vitreous cutter,[131,132] and rupture of intravitreal or partial removal of the subretinal cyst during vitrectomy followed by administration of intravitreous and systemic corticosteroids without postoperative significant inflammation.[124,133]

References

1. Hotez PJ, Brindley PJ, Bethony JM, et al. Helminth infections: the great neglected tropical diseases. *J Clin Invest*. 2008;118:1311–1321.
2. Cox FEG. History of human parasitology. *Clin Microbiol Rev*. 2002;15:595–612.
3. Glickman LT, Magnaval J. Zoonotic roundworm infections. *Infect Dis Clin North Am*. 1993;7:717–732.
4. Hotez PJ, Molyneux DH, Fenwick A, et al. Control of neglected tropical diseases. *N Engl J Med*. 2007;357:1018–1027.
5. Zinkham WH. Systemic visceral larval migrans. Ryan SJ, Smith RE. *Selected topics on the eye in systemic disease*. Grune & Stratton: New York; 1979:167–175.
6. Schantz PM. Of worms, dogs, and human hosts: continuing challenges for veterinarians in prevention of human diseases. *J Am Vet Med Assoc*. 1994;204:1023–1028.
7. Shields JA. Ocular toxocariasis: a review. *Surv Ophthalmol*. 1984;28:361–381.
8. Goto H, Mochizuki M, Yamaki K, et al. Epidemiological survey of intraocular inflammation in Japan. *Jpn J Ophthalmol*. 2007;51:41–44.
9. Stewart JM, Cubillan LD, Cunningham ET Jr. Prevalence, clinical features, and causes of vision loss among patients with ocular toxocariasis. *Retina*. 2005;25:1005–1013.
10. Tran VT, Auer C, Guex-Crosier Y, et al. Epidemiological characteristics of uveitis in Switzerland. *Int Ophthalmol*. 1994–1995;18:293–298.
11. Brown DH. Ocular *Toxocara canis* II. Clinical review. *J Pediatr Ophthalmol*. 1970;7:182–191.
12. Leiper RT. Two new genera of nematodes occasionally parasitic in man. *Br Med J*. 1907;1:1296–1298.
13. Wilder HC. Nematode endophthalmitis. *Trans Am Acad Ophthalmol Otolaryngol*. 1950;55:99–109.
14. Beaver PC, Snyder CH, Carrera GM, et al. Chronic eosinophilia due to visceral larva migrans. *Pediatrics*. 1952;9:7–19.
15. Nichols RL. The etiology of visceral larva migrans. I. Diagnostic morphology of infective second-stage *Toxocara*

larvae. *J Parasitol*. 1956;42:349–362.
16. Irvine WC, Irvine AR Jr. Nematode endophthalmitis: *Toxocara canis* – report of one case. *Am J Ophthalmol*. 1959;47:185–191.
17. Ashton N. Larval granulomatosis of the retina due to Toxocara. *Br J Ophthalmol*. 1960;44:129–148.
18. Duguid IM. Features of ocular infestation by *Toxocara*. *Br J Ophthalmol*. 1961;45:789–796.
19. Wilkinson CP, Welch RB. Intraocular *Toxocara*. *Am J Ophthalmol*. 1971;71:921–930.
20. Rocha IML, Oréfice F, Soares IP, et al. Toxocaríase. Oréfice F. *Uveíte clínica e cirúrgica*. 2nd ed. Cultura Médica: Rio de Janeiro; 2005.
21. Chieffi PP, Santos SV, Queiroz ML, et al. Human toxocariasis: contribution by Brazilian researchers. *Rev Inst Med Trop S Paulo*. 2009;51:301–308.
22. Molk R. Ocular toxocariasis: a review of the literature. *Ann Ophthalmol*. 1983;15:216–231.
23. Ottesen EA. Visceral larval migrans and other unusual helminth infections. Mandell GL, Douglas RG, Bennett JE. *Principles and practice of infectious diseases*. 2nd ed. John Wiley: New York; 1979.
24. Mok CH. Visceral larva migrans: a discussion based in review of literature. *Clin Pediatr*. 1968;7:565–573.
25. Amaral HL, Rassier GL, Pepe MS, et al. Presence of *Toxocara canis* eggs on the hair of dogs: a risk factor for visceral larva migrans. *Vet Parasitol*. 2010;174:115–118.
26. Marmor M, Glickman L, Shofer F, et al. *Toxocara canis* infection of children: epidemiological and neuropsychological findings. *Am J Public Health*. 1987;77:554–559.
27. Schantz PM, Meyer D, Glickman LT. Clinical, serologic, and epidemiologic characteristics of ocular toxocariasis. *Am J Trop Med Hyg*. 1979;28:24–28.
28. Schantz PM, Weis PE, Pollard ZF, et al. Risk factors for toxocaral ocular larva migrans: a case–control study. *Am J Public Health*. 1980;70:1269–1272.
29. Queiroz ML, Simonsen M, Paschoalotti MA, et al. Frequency

of soil contamination by *Toxocara canis* eggs in the south region of São Paulo municipality (SP, Brazil) in a 18 month period. *Rev Inst Med Trop Sao Paulo*. 2006;48:317–319.
30. Despommier D. Toxocariasis: clinical aspects, epidemiology, medical ecology, and molecular aspects. *Clin Microbiol Rev*. 2003;16:265–272.
31. Castillo D, Paredes C, Zanartu C. Environmental contamination with *Toxocara* spp. eggs in public squares and parks from Santiago, Chile, 1999. *Bol Chil Parasitol*. 2000;55:86–91.
32. Giacometti A, Cirioni O, Fortuna M. Environmental and serological evidence for the presence of toxocariasis in the urban area of Ancona, Italy. *Eur J Epidemiol*. 2000;16:1023–1026.
33. Akdemir C. Visceral larva migrans among children in Kütahya (Turkey) and an evaluation of playgrounds for *T. canis* eggs. *Turk J Pediatr*. 2010;52:158–162.
34. Borg OA, Woodruff AW. Prevalence of ova of *Toxocara* species in public places. *Br Med J*. 1973;4:470–472.
35. Yoshikawa M, Nishiofuku M, Moriya K, et al. A familial case of visceral toxocariasis due to consumption of raw bovine liver. *Parasitol Int*. 2008;57:525–529.
36. Hoffmeister B, Glaeser S, Flick H, et al. Cerebral toxocariasis after consumption of raw duck liver. *Am J Trop Med Hyg*. 2007;76:600–602.
37. Morimatsu Y, Akao N, Akiyoshi H, et al. A familial case of visceral larva migrans after ingestion of raw chicken livers: appearance of specific antibody in bronchoalveolar lavage fluid of the patients. *Am J Trop Med Hyg*. 2006;75:303–306.
38. Wilkinson CP. Ocular toxocariasis. Ryan SJ. *Retina*. 4th ed. Elsevier: London; 2005.
39. Glickman LT, Schantz PM. Epidemiology and pathogenesis of zoonotic toxocariasis. *Epidemiol Rev*. 1981;3:230–250.
40. Bass JL, Mehta KA, Glickman LT, et al. Clinically inapparent *Toxocara* infection in children. *N Engl J Med*. 1983;308:723–724.
41. Alabiad CR, Albini TA, Santos CI, et al. Ocular toxocariasis in a seronegative adult. *Ophthalmic Surg Lasers Imaging*.

2010;2:1–3.
42. Raistrick ER, Hart JC. Ocular toxocariasis in adults. *Br J Ophthalmol*. 1976;60:365–370.
43. Benitez-del Castillo JM, Herreros G, Guillen JL, et al. Bilateral ocular toxocariasis demonstrated by aqueous humor enzyme-linked immunosorbent assay. *Am J Ophthalmol*. 1995;119:514–516.
44. Oréfice F, Boratto LM, Silva HF. Presumível toxocaríase ocular – revisão de 30 casos (1978–1989) – Relato de dois casos atípicos. *Rev Bras Oftalmol*. 1991;50:92–101.
45. Hagler WS, Pollard ZF, Jarrett WH, et al. Results of surgery for ocular *Toxocara canis*. *Ophthalmology*. 1981;88:1081–1086.
46. Cella W, Ferreira E, Torigoe AM, et al. Ultrasound biomicroscopy findings in peripheral vitreoretinal toxocariasis. *Eur J Ophthalmol*. 2004;14(2):132–136.
47. do Lago A, Andrade R, Muccioli C, et al. Optical coherence tomography in presumed subretinal toxocara granuloma: case report. *Arq Bras Oftalmol*. 2006;69:403–405.
48. Bird AC, Smith JL, Curtin VT. Nematode optic neuritis. *Am J Ophthalmol*. 1970;69:72–77.
49. Gass JDM. *Stereoscopic atlas of macular diseases*. 4th ed. Mosby: St. Louis; 1997.
50. Monshizadeh R, Ashrafzadeh MT, Rumelt S. Choroidal neovascular membrane: a late complication of inactive *Toxocara* chorioretinitis. *Retina*. 2000;20:219–220.
51. Wan WL, Cano MR, Pince KJ, et al. Echographic characteristics of ocular toxocariasis. *Ophthalmology*. 1991;98:28–32.
52. Rubin ML, Kaufman HE, Tierney JP, et al. An intraretinal nematode (a case report). *Trans Am Acad Ophthalmol Otolaryngol*. 1968;72:855–866.
53. Sharkey JA, McKay PS. Ocular toxocariasis in a patient with repeatedly negative ELISA titers to *Toxocara canis*. *Br J Ophthalmol*. 1993;77:253–254.
54. Schantz PM. *Toxocara* larva migrans now. *Am J Trop Med Hyg*. 1989;41:21–34.
55. Ellis GS Jr, Pakalnis VA, Worley G, et al. *Toxocara canis* infestation: clinical and epidemiological associations with

seropositivity in kindergarten children. *Ophthalmology*. 1986;93:1032–1037.
56. Prestes-Carneiro LE, Souza DH, Moreno GC, et al. Toxocariasis/cysticercosis seroprevalence in a long-term rural settlement, São Paulo, Brazil. *Parasitology*. 2009;136:681–689.
57. Maguire AM, Green WR, Michels RG, et al. Recovery of intraocular *Toxocara canis* by pars plana vitrectomy. *Ophthalmology*. 1990;97:675–680.
58. Shields JA. Differential diagnosis of retinoblastoma. Guyer DR, Yannuzzi LA, Chang S, et al. *Retina–vitreous–macula*. W.B. Saunders: Philadelphia; 1999.
59. Hogan MJ, Kimura SJ, Spencer WH. Visceral larval migrans and peripheral retinitis. *JAMA*. 1965;194:1345–1347.
60. O'Connor GR. Chemotherapy of toxoplasmosis and toxocariasis. Srinivasan BD. *Ocular therapeutics*. Masson: New York; 1980.
61. Barisan-Asenbauer T, Maca SM, Hauff W, et al. Treatment of ocular toxocariasis with albendazole. *J Ocul Pharm Therapeut*. 2001;17:287–294.
62. Seong S, Moon D, Lee DK, et al. A case of ocular toxocariasis successfully treated with albendazole and triamcinolone. *Korean J Parasitol*. 2014;52(5):537–540.
63. Sturchler D, Schubarth P, Gualzata M, et al. Thiabendazole vs albendazole in treatment of toxocariasis: a clinical trial. *Ann Trop Med Parasitol*. 1989;83:473–478.
64. Hotez PJ. *Toxocara canis*. Burg FD, Wald ER, Ingelfinger JR, et al. *Gellis and Kaganís current pediatric therapy*. 15th ed. W.B. Saunders: Philadelphia; 1995:683–684.
65. Lyall DA, Hutchison BM, Gaskell A, et al. Intravitreal ranibizumab in the treatment of choroidal neovascularisation secondary to ocular toxocariasis in a 13-year-old boy. *Eye*. 2010;24:1730–1731.
66. Amin HI, McDonald HR, Han DP, et al. Vitrectomy update for macular traction in ocular toxocariasis. *Retina*. 2000;20:80–85.
67. Small KW, McCuen BW, de Juan E, et al. Surgical management of retinal traction caused by ocular

toxocariasis. *Am J Ophthalmol*. 1989;108:10–14.
68. Giuliari GP, Ramirez G, Cortez RT. Surgical treatment of ocular toxocariasis: anatomic and functional results in 45 patients. *Eur J Ophthalmol*. 2011;21(4):490–494.
69. Gass JDM, Scelfo R. Diffuse unilateral subacute neuroretinitis. *J R Soc Med*. 1978;71:95–111.
70. Gass JD, Gilbert WR Jr, Guerry RK, et al. Diffuse unilateral subacute neuroretinitis. *Ophthalmology*. 1978;85:521–545.
71. Gass JD, Braunstein RA. Further observations concerning the diffuse unilateral subacute neuroretinitis syndrome. *Arch Ophthalmol*. 1983;101:1689–1697.
72. Kazacos KR, Raymond LA, Kazacos EA, et al. The raccoon ascarid: a probable cause of human ocular larva migrans. *Ophthalmology*. 1985;92:1735–1744.
73. Kazacos KR, Vestre WA, Kazacos EA, et al. Diffuse unilateral subacute neuroretinitis syndrome: probable cause. *Arch Ophthalmol*. 1984;102:967–968.
74. Mets MB, Noble AG, Basti S, et al. Eye findings of diffuse unilateral subacute neuroretinitis and multiple choroidal infiltrates associated with neural larva migrans due to *Baylisascaris procyonis*. *Am J Ophthalmol*. 2003;135:888–890.
75. Goldberg MA, Kazacos KR, Boyce WM, et al. Diffuse unilateral subacute neuroretinitis. Morphometric, serologic and epidemiologic support for *Baylisascaris* as a causative agent. *Ophthalmology*. 1993;100:1695–1701.
76. Brasil OF, Lewis H, Lowder CY. Migration of *Baylisascaris procyonis* into the vitreous. *Br J Ophthalmol*. 2006;90:1203–1204.
77. Gass JDM. Mosby: St. Louis; 1997:622–628. *Stereoscopic atlas of macular diseases: diagnosis and treatment*. vol. 4.
78. Casella AMB, Machado RA, Tsuro A, et al. Would *Ancylostoma caninum* be one of the agents of diffuse unilateral subacute neuroretinitis (D.U.S.N) in Brazil? *Arq Bras Oftalmol*. 2001;64:473–476.
79. Cunha de Souza E, Nakashima Y. Diffuse unilateral subacute neuroretinitis. Report of transvitreal surgical removal of a subretinal nematode. *Ophthalmology*. 1995;102:1183–1186.

80. McDonald HR, Kazacos KR, Schatz H, et al. Two cases of intraocular infection with *Alaria mesocercaria* (Trematoda). *Am J Ophthalmol*. 1994;117:447–455.
81. Parsons HE. Nematode chorioretinitis: report of a case, with photographs of a viable worm. *Arch Ophthalmol*. 1952;47:799–800.
82. Nath R, Gogoi R, Bordoloi N, et al. Ocular dirofilariasis. *Indian J Pathol Microbiol*. 2010;53:157–159.
83. Myint K, Sahay R, Mon S, et al. "Worm in the eye": the rationale for treatment of DUSN in south India. *Br J Ophthalmol*. 2006;90(9):1125–1127.
84. Yuen VH, Chang TS, Hooper PL. Diffuse unilateral subacute neuroretinitis syndrome in Canada. *Arch Ophthalmol*. 1996;114:1279–1282.
85. Kuchle M, Knorr HL, Medenblik-Frysch S, et al. Diffuse unilateral subacute neuroretinitis syndrome in a German most likely caused by the raccoon roundworm, *Baylisascaris procyonis*. *Graefes Arch Clin Exp Ophthalmol*. 1993;231:48–51.
86. Harto MA, Rodriguez-Salvador V, Avino JA, et al. Diffuse unilateral subacute neuroretinitis in Europe. *Eur J Ophthalmol*. 1999;9:58–62.
87. Cai J, Wei R, Zhu L, et al. Diffuse unilateral subacute neuroretinitis in China. *Arch Ophthalmol*. 2000;118:721–722.
88. Natesh S, Harsha K, Nair U, et al. Subretinal worm and repeat laser photocoagulation. *Middle East Afr J Ophthalmol*. 2010;17:183–185.
89. Souza EC, Cunha SL, Gass JD. Diffuse unilateral subacute neuroretinitis in South America. *Arch Ophthalmol*. 1992;110:1261–1263.
90. Souza EC, Abujamra S, Nakashima Y, et al. Diffuse bilateral subacute neuroretinitis: first patient with documented nematodes in both eyes. *Arch Ophthalmol*. 1999;117:1349–1351.
91. Oréfice F, Garcia CAA, Paranhos FRL, et al. Neuroretinite subaguda unilateral difusa (DUSN). Oréfice F. *Uveíte clínica e cirúrgica*. 2nd ed. Cultura Médica: Rio de Janeiro; 2005.
92. Sabrosa NA, Zajdenweber M. Nematode infections of the eye: toxocariasis, onchocerciasis, diffuse unilateral subacute

neuroretinitis, and cysticercosis. *Ophthalmol Clin North Am*. 2002;15:351–356.
93. Cortez R, Denny JP, Muci-Mendoza R, et al. Diffuse unilateral subacute neuroretinitis in Venezuela. *Ophthalmology*. 2005;112(12):2110–2114.
94. Cialdini AP, Souza EC, Avila MP. The first South American case of diffuse unilateral subacute neuroretinitis caused by a large nematode. *Arch Ophthalmol*. 1999;117:1431–1432.
95. Oréfice F, Gonçalves ER, Siqueira RC, et al. Estudo de 21 casos de neuroretinite subaguda unilateral difusa (DUSN): dois casos com larva móvel sub-retiniana. *Rev Bras Oftalmol*. 1994;53:23–45.
96. Gomes AH, Garcia CA, Segundo P de S, et al. Optic coherence tomography in a patient with diffuse unilateral subacute neuroretinitis. *Arq Bras Oftalmol*. 2009;72:185–188.
97. Casella AM, Farah ME, Souza EC, et al. Retinal nerve fiber layer atrophy as relevant feature for diffuse unilateral subacute neuroretinitis (DUSN): case series. *Arq Bras Oftalmol*. 2010;73:182–185.
98. Berbel RF, Casella AM, de Souza EC, et al. Evaluation of patients with diffuse unilateral subacute neuroretinitis by spectral domain optical coherence tomography with enhanced depth imaging. *Clin Ophthalmol*.2014;8:1081–1087.
99. Davis JL, Gass JDM, Olsen KR. Diffuse unilateral subacute neuroretinitis. Ryan SJ. *Retina*. 4th ed. Elsevier: London; 2005.
100. de Souza EC, Casella AM, Nakashima Y, et al. Clinical features and outcomes of patients with diffuse unilateral subacute neuroretinitis treated with oral albendazole. *Am J Ophthalmol*. 2005;140:437–445.
101. Moraes LR, Cialdini AP, Avila MP, et al. Identifying live nematodes in diffuse unilateral subacute neuroretinitis by using the scanning laser ophthalmoscope. *Arch Ophthalmol*. 2002;120:135–138.
102. Quillen DA, Davis JB, Gottlieb JL, et al. The white dot syndromes. *Am J Ophthalmol*. 2004;137:538–550.
103. Martidis A, Greenberg PB, Rogers AH, et al. Multifocal electroretinography response after laser photocoagulation

of a subretinal nematode. *Am J Ophthalmol*. 2002;133:417–419.
104. Dangoudoubiyam S, Kazacos KR. Differentiation of larva migrans caused by *Baylisascaris procyonis* and *Toxocara* species by Western blotting. *Clin Vaccine Immunol*. 2009;16:1563–1568.
105. Kwon IH, Kim HS, Lee JH, et al. A serologically diagnosed human case of cutaneous larva migrans caused by *Ancylostoma caninum*. *Korean J Parasitol*. 2003;41:233–237.
106. Gass JD, Callanan DG, Bowman CB. Successful oral therapy for diffuse unilateral subacute neuroretinitis. *Trans Am Ophthalmol Soc*. 1991;89:97–112.
107. Maguire AM, Zarbin MA, Conner TB, et al. Ocular penetration of thiabendazole. *Arch Ophthalmol*. 1952;108:1675.
108. Gass JDM, Callanan DG, Bowman CB. Oral therapy in diffuse unilateral subacute neuroretinitis. *Arch Ophthalmol*. 1992;110:675–680.
109. Callanan DG, Davis JL, Cohen SM, et al. The use of ivermectin in diffuse unilateral subacute neuroretinitis. *Ophthalmology*. 1993;100(9 Suppl.):114–115.
110. Casella AM, Farah ME, Belfort R Jr. Anthelmintic drugs in diffuse unilateral subacute neuroretinitis. *Am J Ophthalmol*. 1998;125:109–111.
111. Malaguido MR, Casella AM, Malaguido DR. Clinical treatment of diffuse unilateral subacute neuroretinitis with albendazole. *Arq Bras Oftalmol*. 2007;70:814–822.
112. Rosa AA, Rodrigues Neto TS. Diffuse unilateral subacute neuroretinitis (DUSN): current update. *Arq Bras Oftalmol*. 2013;76(4):256–260.
113. Report from the 2009 Inter-American Conference on Onchocerciasis: Progress towards eliminating river blindness in the Region of the Americas. *Wkly Epidemiol Rec*. 2010;85(33):321–326.
114. *World Health Organization Fact Sheet no. 374. Onchocerciasis*. http://www.who.int/mediacentre/factsheets/fs374/en; 2015.
115. Reddy M, Gill SS, Kalkar SR, et al. Oral drug therapy for multiple neglected tropical diseases: a systematic review.

JAMA. 2007;298:1911–1924.
116. Hall LR, Pearlman E. Pathogenesis of onchocercal keratitis (river blindness). *Clin Microbiol Rev*. 1999;12:445–453.
117. Newland HS, White AT, Greene BM, et al. Ocular manifestations of onchocerciasis in a rain forest area of west Africa. *Br J Ophthalmol*. 1991;75:163–169.
118. Kayembe DL, Kasonga DL, Kayembe PK, et al. Profile of eye lesions and vision loss: a cross-sectional study in Lusambo, a forest-savanna area hyperendemic for onchocerciasis in the Democratic Republic of Congo. *Trop Med Int Health*. 2003;8:83–89.
119. Semba RD, Murphy RP, Newland HS, et al. Longitudinal study of lesions of the posterior segment in onchocerciasis. *Ophthalmology*. 1990;97:1334–1341.
120. Bird AC, Anderson J, Fuglsang H. Morphology of posterior segment lesions of the eye in patients with onchocerciasis. *Br J Ophthalmol*. 1976;60:2–20.
121. Anon. Meeting of the International Task Force for Disease Eradication, January 2014. *Wkly Epidemiol Rec*. 2014;89(15):153–160.
122. Duke-Elders S, Perkins ES. *System of ophthalmology: inflammations of the uveal tract: uveitis*. Mosby: St. Louis; 1966:478–487.
123. Orefice F. *Uveíte clínica e cirúrgica: texto e atlas*. Cultura Médica: Rio de Janeiro; 2000:705–713.
124. Pantaleão GR, Borges de Souza AD, Rodrigues EB, et al. The use of systemic and intravitreous steroid in inflammation secondary to intraocular cysticercosis: case report. *Arq Bras Oftalmol*. 2007;70:1006–1009.
125. Junior L. Ocular cysticercosis. *Am J Ophthalmol*. 1949;32:523–548.
126. Wittig EO. Ocular cysticercosis: an epidemiological study. *Arq Neuropsiquiatr*. 2001;59:693–701.
127. Shandera WX, Kass JS. Neurocysticercosis: current knowledge and advances. *Curr Neurol Neurosci Rep*. 2006;6:453–459.
128. Kruger-Leite E, Jalkh AE, Quiroz H, et al. Intraocular cysticercosis. *Am J Ophthalmol*. 1985;99:252–257.

129. Rath S, Honavar SG, Naik M, et al. Orbital cysticercosis: clinical manifestations, diagnosis, management, and outcome. *Ophthalmology*. 2010;117:600–605.
130. Chung GW, Lai WW, Thulborn KR, et al. Magnetic resonance imaging in the diagnosis of subretinal cysticercosis. *Am J Ophthalmol*. 2002;134:931–932.
131. Sharma T, Sinha S, Shah N, et al. Intraocular cysticercosis: clinical characteristics and visual outcome after vitreoretinal surgery. *Ophthalmology*. 2003;110:996–1004.
132. Avila MP, Cialdini AP, Pereira AE, et al. *Live cysticercus/Giant intraocular foreign bodies. Best of Show Video Awards*. [Annual Meeting, American Academy of Ophthalmology – Final Program] 2003:301.
133. Passos E, Frasson MC, Nehemy MB. Vitrectomia para o tratamento de cisticerco intrarretiniano. *Rev Bras Oftalmol*. 1996;55:841–845.
134. Santos R, Chavarria M, Aguirre AE. Failure of medical treatment in two cases of intraocular cysticercosis. *Am J Ophthalmol*. 1984;97:249–250.

90

Endogenous Endophthalmitis

Bacterial and Fungal

Ajay E. Kuriyan, Stephen G. Schwartz, Janet L. Davis, Harry W. Flynn Jr.

Epidemiology and Risk Factors

Endogenous endophthalmitis remains an uncommon but serious

cause of intraocular inflammation.[1] The incidence may be increasing, due to several factors. An increasing number of immunocompromised patients are receiving antineoplastic agents, immunomodulating agents, and newer broad-spectrum antimicrobial agents, all of which may reduce normal flora.[1,2] Low-birthweight premature infants and patients with a history of intravenous substance abuse are at increased risk for endogenous endophthalmitis.[3–5] Other reported risk factors include long-term intravenous line placement, peripheral hyperalimentation, systemic corticosteroids, abdominal surgery, hemodialysis, human immunodeficiency virus (HIV) infection, systemic malignancy, diabetes mellitus, pregnancy or postpartum state, massive systemic trauma, alcoholism, hepatic insufficiency, and genitourinary manipulation.[1,6–9]

A series of 64 cases over 10 years reported a culture positivity rate of 64%. Of culture-positive cases, fungi (predominantly *Candida* spp.) were isolated in 66%, Gram-negative bacteria in 19%, and Gram-positive bacteria in 15%.[10] Fungal cases were generally associated with better visual outcomes.[10] Another study found that among endogenous fungal endophthalmitis cases, better visual outcomes were associated with yeast species (e.g., *Candida* spp.) compared to mold species (e.g., *Aspergillus* spp.).[11]

Clinical Assessment of the Patient

Infectious endophthalmitis may be categorized by the cause of the infection and by the characteristic timing of clinical signs/symptoms.[12] One proposed categorization scheme is presented in Box 90.1.[13] In general, endogenous endophthalmitis is suspected in a patient without risk factors for exogenous endophthalmitis, such as prior surgery, intravitreal injection, trauma, or keratitis. Patients with endogenous endophthalmitis may present with varying degrees of pain, inflammation, and visual loss. In the anterior chamber, cell and flare, fibrin, posterior synechiae, and hypopyon may occur. In the posterior segment, findings may include vitreous opacification and chorioretinitis, including hemorrhage, cotton-wool spots, retinal opacification, and vasculitis. An insidious onset, focal vitreous opacities, and

chorioretinal infiltrates suggest fungal etiology. Relatively more rapid progression and more severe intraocular inflammation suggest bacterial etiology.

Box 90.1

Classification of Endophthalmitis and Common Causative Organisms

Acute-onset postoperative endophthalmitis

Coagulase-negative staphylococci

Staphylococcus aureus

Streptococcus spp.

Chronic (delayed-onset) postoperative endophthalmitis

Propionibacterium acnes

Candida parapsilosis

Coagulase-negative staphylococci

Filtering bleb-associated endophthalmitis

Streptococcus spp.

Staphylococcus spp.

Haemophilus influenza

Posttraumatic endophthalmitis

Staphylococcus spp.

Bacillus cereus

Endogenous endophthalmitis

Candida albicans

Aspergillus spp.

Staphylococcus aureus

Gram-negative organisms

Endophthalmitis associated with microbial keratitis

Gram-negative organisms

Staphylococcus aureus

Fusarium spp.

Endophthalmitis associated with intravitreal injection

Coagulase-negative staphylococci

Streptococcus spp.

Adapted from Schwartz SG, Flynn HW Jr, Scott IU. Endophthalmitis: classification and current management. Expert Rev Ophthalmol 2007;2:385–96.

Endogenous endophthalmitis may present as a relatively mild and nonspecific anterior uveitis.[14] Early in the clinical course, the clinical features may be subtle, making the diagnosis difficult. The rate of initial misdiagnosis has been reported as high as 63% in one large series.[15] A differential diagnosis of endogenous endophthalmitis is presented in Box 90.2.

Box 90.2

Differential Diagnosis of Endogenous Endophthalmitis

Uveitis

Anterior/intermediate

Pars planitis

Posterior

Vogt–Koyanagi–Harada disease

Posterior scleritis

Sarcoidosis

Syphilis

Tuberculosis

Sympathetic ophthalmia

Intraocular lymphoma

Lyme disease

Tumor necrosis with inflammation

Retinoblastoma

Disseminated toxoplasmosis

Disseminated viral retinitis

Vitreous metastases

Occlusive diseases of the choriocapillaris

Disseminated intravascular coagulation

Thrombotic thrombocytopenic purpura

Asteroid hyalosis

Cases may be classified according to several criteria. One published classification scheme for endogenous bacterial endophthalmitis used zones of anatomic involvement (Box 90.3).[16] Another scheme, designed for endogenous fungal endophthalmitis, also used anatomic criteria (Box 90.4); in this series, the stage at initial diagnosis was statistically correlated to the final visual acuity.[17]

Box 90.3

Anatomic Classification of Endogenous Bacterial Endophthalmitis

Focal: One or a few discrete foci in the iris, ciliary body, retina, or choroid

Anterior diffuse: Severe generalized signs of inflammation in the anterior segment

Posterior diffuse: Intense inflammatory reaction in vitreous, obscuring the fundus

Panophthalmitis: Severe involvement of anterior segment, posterior segment, and orbital structures

Adapted from Greenwald MJ, Wohl LG, Sell CH. Metastatic bacterial endophthalmitis: a contemporary reappraisal. Surv Ophthalmol 1986;31:81–101.

Box 90.4

Classification of Endogenous Fungal

Stage I: Chorioretinal changes without extension into the vitreous cavity

Stage II: Fungal mass penetrating through the internal limiting membrane and budding into the vitreous cavity

Stage III: Vitreous opacity resulting in a blurred fundus

Stage IV: Vitreous opacity plus retinal detachment

Adapted from Takebayashi H, Mizota A, Tanaka M. Relation between stage of endogenous fungal endophthalmitis and prognosis. Graefes Arch Clin Exp Ophthalmol 2006;244:816–20.

Medical Evaluation of the Patient

In contrast to patients with other categories of endophthalmitis, nearly all patients with endogenous endophthalmitis have an identifiable systemic infection and require at least some degree of systemic evaluation. Generally, the medical evaluation is performed in consultation with an infectious disease specialist or other medical specialist. A high index of suspicion should be maintained because both the ophthalmic and systemic symptoms are quite variable. In one series, 43% of patients with endogenous endophthalmitis had no nonocular symptoms.[18] Endogenous endophthalmitis may present prior to the onset of systemic symptoms[19] or may occur in patients later found to have no other systemic infection.[20] In one series, the rate of negative systemic workup was over 40%.[21] In a patient not known to have systemic infection, intraocular cultures (aqueous and/or vitreous) may be necessary to confirm the diagnosis. Intraocular cultures are also important in patients who progress despite treatment with empiric antimicrobial therapy.

Obtaining cultures from multiple sites may be necessary to make a specific diagnosis. In one series of patients with endogenous bacterial endophthalmitis, the rate of diagnostic cultures was 74% for vitreous, 72% for blood, and 96% overall.[22] The rates of positive cultures are lower in patients with endogenous fungal

endophthalmitis. Rates of positive cultures have been reported in the range of 44–70%,[23] and as low as 18% in one series.[24] One study reported the highest rate of diluted vitrectomy cassette vitreous specimens culture positivity using a combination of both a membrane filter system and blood culture bottle.[25] Although polymerase chain reaction-based identification of organisms is not routinely performed, it may provide higher rates of organism identification than routine culture techniques.[26,27]

Endogenous Bacterial Endophthalmitis

Endogenous bacterial endophthalmitis is reported to comprise between 2% and 8% of all cases of infectious endophthalmitis (Fig. 90.1).[22] Many bacteria have been reported to cause endogenous endophthalmitis.[28] Gram-positive agents associated with bacterial endogenous endophthalmitis include *Staphylococcus aureus*,[29] group B *Streptococcus*,[30] *Streptococcus pneumoniae*,[31,32] *Streptococcus bovis*,[33] *Enterococcus faecalis*,[34,35] *Propionibacterium acnes*,[36] *Listeria monocytogenes*,[37] *Bacillus* spp.,[38] *Nocardia* spp.,[39,40] and others. Gram-negative agents associated with bacterial endogenous endophthalmitis include *Klebsiella pneumoniae*,[41–44] *Pseudomonas aeruginosa*,[45,46] *Escherichia coli*,[47] *Neisseria meningitidis*,[48] *Proteus* spp.,[49] *Salmonella* serotype B,[50] *Serratia marcescens*,[51] and others.

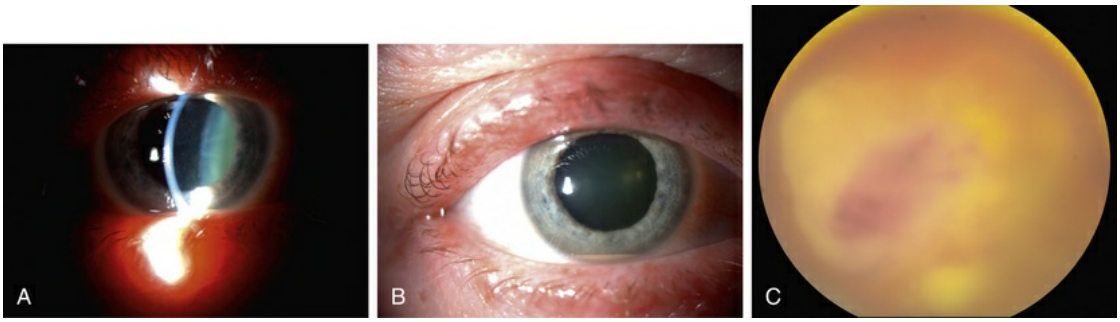

FIG. 90.1 Endogenous Klebsiella pneumonia endophthalmitis. (A) Note anterior chamber cell and flare. (B) Note hypopyon. (C) Note vitreous opacification overlying macular chorioretinitis and associated hemorrhage. (Case courtesy of Lisa C. Olmos, MD, MBA.)

Endogenous Fungal Endophthalmitis

Over 50,000 species of fungi have been reported, yet fewer than 200 of these are associated with clinical disease in humans and even fewer have been reported to cause endogenous endophthalmitis (Box 90.5). Fungi may be differentiated using several criteria, but are commonly divided between unicellular yeasts and multicellular molds. Molds contain tubular structures (hyphae). Some fungi may grow with both yeast-like and mold-like morphology in tissues or culture. Fungi may also be classified by pigmentation (moniliaceous versus dematiaceous), virulence (pathogenic versus opportunistic), and clinical presentation (cutaneous, subcutaneous, or systemic).

Box 90.5

Fungal Isolates

Yeasts and yeast-like isolates

Candida species

C. albicans

C. parapsilosis

C. tropicalis

C. glabrata

Cryptococcus neoformans

Trichosporon beigelii

Sporobolomyces salmonicolor

Hyaline molds – septate (colorless hyphae)

Aspergillus spp.

A. fumigatus

A. niger

A. glaucus

A. flavus

Pseudoallescheria boydii

Fusarium spp.

F. solani

F. oxysporum

Bipolaris hawaiiensis

Paecilomyces spp.

Penicillium spp.

Hyaline molds – aseptate (colorless hyphae)

Mucor spp.

Absidia spp.

Rhizopus spp.

Dematiaceous molds (colored hyphae)

Scedosporium spp.

S. apiopsermum

S. prolificans

Cladophialophora bantiana

Phialemoniunm curvatum

Dimorphic molds

Blastomyces dermatitidis

Histoplasma capsulatum

Sporothrix schenckii

Coccidioides immitis

Candida albicans is the most common yeast isolate and the most common overall fungal isolate in patients with endogenous fungal endophthalmitis.[52,53] *C. albicans* may be found as a commensal organism in the gastrointestinal tract and mucous membranes of healthy individuals.[54] Although the organism is of low virulence to healthy individuals, candidemia is associated with relatively high rates of morbidity and mortality.[55] In one series, the mortality rate among patients with candidemia and endogenous *Candida* endophthalmitis was 77%.[56] *Candida* endophthalmitis is strongly associated with intravenous drug abuse.[57] Other *Candida* species reported to cause endophthalmitis include *C. tropicalis*, *C. parapsilosis*, *C. glabrata*, *C. guilliermondii*, *C. krusei*, and *C. dubliniensis*. Among patients with diagnosed candidemia, reported rates of endogenous endophthalmitis range from less than 3%[58] to 44%.[59] The prevalence of *Candida* endophthalmitis may be decreasing, as systemic antifungals are now more commonly prescribed for

patients with positive blood cultures.[60] The most characteristic clinical sign of *Candida* endophthalmitis is one or more creamy white, well-circumscribed chorioretinal lesions, less than 1 mm in diameter, most commonly in the posterior pole, with an overlying haze of vitreous inflammatory cells (Figs. 90.2 and 90.3). Yellow or fluffy-white vitreous opacities, sometimes connected by strands of inflammatory material ("string of pearls" configuration), may be noted.[61] A subretinal abscess has been reported in a patient with endogenous *C. albicans* endophthalmitis.[62] The initial misdiagnosis rate may be high; one series reported this rate to approach 50%.[3]

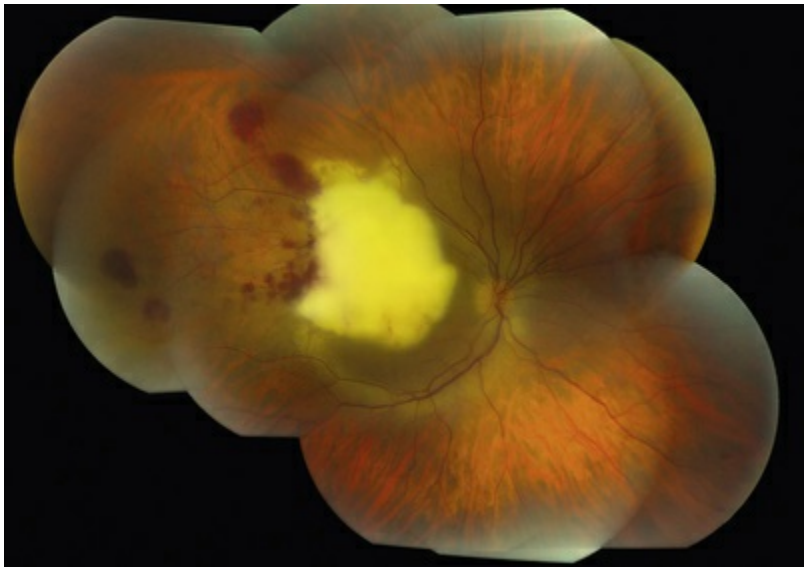

FIG. 90.2 Endogenous *Candida* endophthalmitis. Note creamy white chorioretinal lesion, with associated retinal hemorrhage and evidence of vasculitis.

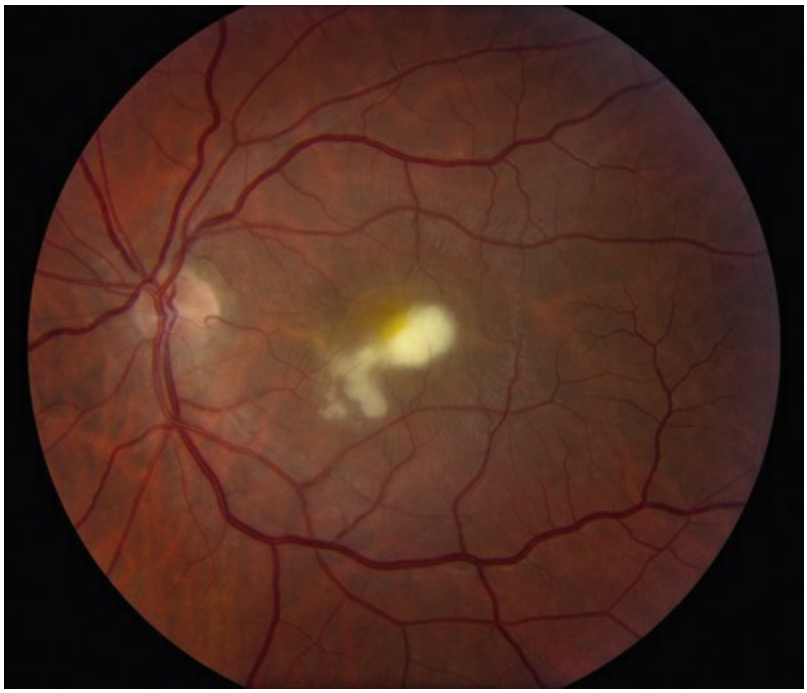

FIG. 90.3 Macular chorioretinitis, clinically suspected endogenous *Candida* endophthalmitis. This patient was an intravenous drug abuser and improved with empiric oral fluconazole. (Case courtesy of Jeffrey K. Moore, MD.)

Aspergillus is the most common mold isolate and the second most common overall fungal isolate in patients with endogenous fungal endophthalmitis.[52] Reported risk factors include chronic pulmonary disease, liver transplantation,[63] and treatment with systemic corticosteroids, but rare cases are reported in apparently immunocompetent individuals.[64] Endogenous *Aspergillus* endophthalmitis is associated with a characteristic central macular chorioretinal inflammatory lesion.[65] A gravitational layering (pseudohypopyon) of inflammatory exudates in either the preretinal (subhyaloid) or subretinal space may be noted with the macular lesion. Additionally, *Aspergillus* endophthalmitis may be associated with retinal vascular occlusion, choroidal vascular occlusion, exudative retinal detachment, and/or diffuse hemorrhagic retinal necrosis.[66,67]

Cryptococcus neoformans is associated with meningitis and visual loss through a variety of mechanisms, including cryptococcomas in the visual pathway, optic neuritis, and elevated intracranial pressure.[68] *C. neoformans* may cause endophthalmitis, which is typically characterized by nonspecific intraocular inflammation,

making initial misdiagnosis relatively common. The most common presentation is a multifocal chorioretinitis.[69] Successful outcomes have been reported with a combination of systemic amphotericin B and fluconazole with intravitreal amphotericin B.[70] *Coccidioides immitis* endophthalmitis is associated with chronic pulmonary or disseminated coccidioidomycosis.[71] Endogenous endophthalmitis is infrequently reported.[72] Asymptomatic patients with systemic coccidioidomycosis may have inactive chorioretinal scars, suggesting prior intraocular involvement.[73] Alternatively, a case of ocular coccidiomycosis has been reported 22 years following treatment of systemic disease.[74] Rare causes of endogenous fungal endophthalmitis include *Histoplasma capsulatum*,[75] *Sporothrix schenckii*,[76] *Fusarium solani*,[77,78] and others.

The Infectious Disease Society of America recommends ophthalmic evaluation for all patients with fungemia. These recommendations are mainly based on older studies, which found rates of ocular involvement in fungemic patients as high as 37%.[79–81] More recent studies have found rates of ocular involvement in fungemic patients ranging from 1 to 16%.[82–85] The lower rates of ocular involvement are attributed to increased use of intravenous triazoles which have higher intraocular bioavailability than intravenous amphotericin B.[86] Routine ocular screening of verbal asymptomatic fungemic patients is controversial. Although a very small number of verbal patients with fungal endophthalmitis were asymptomatic, the screening results may not change the patient management and may not be cost-effective.[82–85]

Treatment Strategies

Although successful treatment of chorioretinitis in a patient with systemic candidiasis has been reported after simply removing an infected catheter,[87] most patients with endogenous endophthalmitis require treatment with systemic antimicrobial agents. The choroid and retina are highly vascular structures, which suggests that systemic pharmacotherapy may be sufficient to treat infections confined to these structures, while severe intravitreal involvement may require intravitreal agents.[86] In patients not responding to systemic therapy, intravitreal therapy should be considered. There

is no current consensus regarding the precise role of surgical techniques, such as pars plana vitrectomy (PPV). The Endophthalmitis Vitrectomy Study (EVS) did not enroll patients with endogenous endophthalmitis, and therefore its results are not directly applicable to these patients.[88] However, PPV and intravitreal injection of antifungals are an important treatment option in patients who fail to respond to initial intravitreal and systemic antifungal treatments.

Systemic Pharmacotherapies

Although the EVS reported no additional benefit using systemic amikacin and ceftazidime, patients with endogenous bacterial endophthalmitis are generally treated with systemic antimicrobials in order to manage systemic infections. The selection of systemic pharmacotherapies is frequently made in consultation with an infectious disease or other medical specialist. The management is typically individualized based on the severity of the ocular and systemic infections.

Systemic antimicrobials are associated with variable intravitreal penetration. For example, in a prospective study, intravenous teicoplanin was reported to have poor intravitreal penetration.[89] A more recent series of patients with postoperative endophthalmitis reported that systemic meropenem and linezolid offered no additional benefits.[90]

Alternatively, both systemic gatifloxacin[91] and moxifloxacin[92] have been reported to reach potentially therapeutic intraocular drug levels in the noninflamed eye, but their specific benefit in the treatment of endogenous bacterial endophthalmitis remains unproven. Systemic gatifloxacin is no longer commercially available, due to an associated dysglycemia in some patients.[93] Additionally, systemic fluoroquinolones are associated with other serious adverse events, including tendinopathy, especially in the elderly and in patients taking systemic corticosteroids.[94]

A case report demonstrated that after a single dose of intravenous daptomycin, intravitreal concentrations of daptomycin were approximately 28% of the serum concentration, suggesting a potential role for this drug in the treatment of endogenous bacterial

endophthalmitis.[95]

Systemic antibiotics may not prevent the onset of endogenous bacterial endophthalmitis. One case report documented that *P. aeruginosa* endophthalmitis involved the second eye despite initiation of intravenous ceftazidime.[96]

Commonly used systemic antifungals are reviewed in Box 90.6.

Box 90.6

Systemic Antifungal Agents

Amphotericin B 0.6–1 mg/kg per day IV

Azole compounds

Fluconazole 400–1600 mg/day oral or IV

Itraconazole 400–800 mg/day oral or IV

Voriconazole 6 mg/kg/day oral or IV

Posaconazole 400–800 mg/day oral or IV

Echinocandins

Caspofungin 70 mg loading dose, then 50 mg/day IV

Micafungin 50–150 mg/day IV

Anidulafungin 50–100 mg/day

IV, intravenous.

Amphotericin B has been widely used in the treatment of various fungal infections. An alternative liposomal formulation is also available,[97] but experience with this formulation in the treatment of endogenous fungal endophthalmitis is limited at this time.[98,99] Amphotericin B is administered intravenously and is generally effective in the treatment of infections due to *Candida*,[100]

Aspergillus,[101] *Blastomyces*,[102] *Coccidioides*,[72] and other fungi. The use of amphotericin B is limited by multiple toxic effects, including renal failure, chills, fever, vomiting, nausea, diarrhea, dyspnea, malaise, anemia, arrhythmia, hypokalemia, and hearing loss.[103] The intravitreal penetration of systemic amphotericin B is relatively poor, and although successful treatment of *Candida* endophthalmitis has been reported using systemic amphotericin B alone,[104] this approach has a high rate of treatment failure.[105] Either a systemic agent with better intraocular penetration, or combined systemic and intravitreal treatment, is generally selected.

Azoles collectively represent an alternative antifungal drug class. The imidazoles (miconazole and ketoconazole) were used historically, but largely have been replaced by the newer triazoles (fluconazole, itraconazole, voriconazole, and posaconazole), although a case report documented a good outcome in endogenous *Aspergillus terreus* endophthalmitis using intravitreal amphotericin B, oral ketoconazole, and topical natamycin.[106]

Fluconazole has excellent gastrointestinal absorption and may be used orally or intravenously.[107] Intraocular penetration from the systemic circulation is generally excellent.[108] A case report documented good outcomes in a patient with bilateral endogenous *C. albicans* endophthalmitis using intravenous fluconazole and PPV in one eye only.[109] Fluconazole (with or without PPV) has also been reported to successfully treat endophthalmitis caused by *C. tropicalis*,[110] *Coccidioides immitis*,[111] and *Cryptococcus neoformans*.[112] Fluconazole is generally well tolerated, with gastrointestinal disturbance as the major reported toxicity.[113] Oral fluconazole may be an appropriate antifungal choice in patients with chorioretinitis outside the posterior pole,[114] in patients who have been initially treated with intravenous amphotericin B,[115] and in patients at risk for toxicity.

Itraconazole may also be prescribed orally but is used infrequently in the treatment of endogenous endophthalmitis.[116] It has relatively more effectiveness against *Aspergillus* than the other azoles,[113] but intraocular penetration is relatively poor.

Voriconazole is a synthetic second-generation azole derived from fluconazole. It may be used orally or intravenously. Voriconazole is generally effective against most *Candida* species (including those

resistant to fluconazole, such as *C. krusei* and *C. glabrata*),[117] as well as *Aspergillus* and *Cryptococcus*.[118] Voriconazole has excellent intravitreal penetration from the systemic circulation.[119] Oral voriconazole alone has been reported to successfully manage a patient with presumed endogenous *Candida* endophthalmitis.[120]

Posaconazole is a newer azole with efficacy against *Candida*, *Aspergillus*, and *Zygomycetes*.[121] Relatively little is known about its intraocular penetration. Successful treatment of refractory *Fusarium* deep keratitis or endophthalmitis has been reported with oral (or oral plus topical) posaconazole.[122,123]

Commonly used echinocandins include caspofungin, micafungin, and anidulafungin. These are newer agents and, compared with amphotericin B and the azoles, relatively little has been reported about their use in endogenous endophthalmitis. Caspofungin may be effective against *C. albicans* resistant to azoles.[124] One case report documented successful treatment of *C. glabrata* endophthalmitis using only systemic caspofungin.[125] A second report documented treatment of *A. fumigatus* endophthalmitis resistant to intravitreal amphotericin and systemic voriconazole with systemic caspofungin.[126] Another study found that eight eyes with endogenous fungal endophthalmitis in patients treated with intravenous micafungin had intravitreal levels of micafungin (measured from vitrectomy sample) above the minimal inhibitory concentration.[127]

Intravitreal Pharmacotherapies

In endogenous endophthalmitis, intravitreal pharmacotherapies may be used as adjunctive therapies to systemic medications.

The EVS did not enroll patients with endogenous endophthalmitis, and its results are not directly applicable,[88] although many principles are relevant. The EVS used intravitreal vancomycin and amikacin, which achieved broad-spectrum coverage of both gram-positive and gram-negative organisms. In a patient with bacteremia due to a known organism, targeted pharmacotherapy may be considered in patients with suspected ocular involvement. To reduce the risk of aminoglycoside toxicity, ceftazidime or ceftriaxone may be considered as an alternative to

amikacin. Ceftazidime may precipitate when mixed with vancomycin, but this does not appear to affect its clinical efficacy.[128] Injecting antibiotics through separate syringes is generally recommended. Intravitreal daptomycin has been reported to be safe and effective in treating one case of bilateral endogenous endophthalmitis secondary to vancomycin resistant *S. aureus*.[129]

Intravitreal antifungals are listed in Box 90.7. Animal studies have suggested that intravitreal amphotericin B, 5–10 μg, is generally nontoxic.[130] A case series of patients inadvertently treated with very high doses reported severe noninfectious panophthalmitis, but ultimately good visual outcomes, following treatment with doses as high as 500 μg.[131] Intravitreal amphotericin B alone, without systemic therapy, has been reported to successfully treat endogenous *Candida* endophthalmitis.[132] A case report documented good outcomes using PPV, intravitreal liposomal amphotericin B, and systemic fluconazole in a patient with bilateral endogenous *C. albicans* endophthalmitis.[133]

Box 90.7

Intravitreal Antifungal Agents

Amphotericin B 0.005–0.01 mg/0.1 ml

Voriconazole 0.1 mg/0.2 ml

Caspofungin 0.1 mg/0.1 ml

Fluconazole (experimental)

Flucytosine (experimental)

Intravitreal fluconazole has been tested in animal models,[134,135] but does not appear to be any more effective than intravitreal amphotericin B and is thus rarely used clinically.[112] Intravitreal ketoconazole has been reported safe in a rabbit model,[136] but its use has not been reported in humans.

Based on animal models, intravitreal voriconazole appears to be nontoxic up to doses of 100 μg and may be less toxic to the retina than intravitreal amphotericin B.[137] Intravitreal voriconazole, with or without PPV, has been reported to successfully treat patients

with endogenous fungal endophthalmitis,[138] including in a patient resistant to PPV with repeated injections of intravitreal amphotericin B and systemic voriconazole.[139] The combination of intravitreal amphotericin B and voriconazole has been shown to be effective in a series of patients with exogenous filamentous fungal endophthalmitis.[140] One study found of exogenous fungal endophthalmitis isolates found 100% sensitivity to intravitreal voriconazole, compared to 69% sensitivity to intravitreal amphotericin B.[141]

Intravitreal corticosteroids (e.g., dexamethasone 400 μg) may be a helpful adjunct in some patients with bacterial or fungal endophthalmitis, by reducing inflammation.[142] Generally, corticosteroids should be withheld until proper antimicrobials have been initiated, especially in patients with suspected fungal disease.

Surgical Treatments

Although there is no general agreement on exactly which patients will benefit from PPV,[104] surgical treatments are typically reserved for patients with established vitreous involvement.[143] PPV offers the advantages of removing infectious organisms from the vitreous cavity and providing ample material for cultures. Disadvantages of PPV include surgical risks, such as retinal detachment, choroidal detachment, or sclerotomy site leakage. One large series reported improved outcomes in patients treated with PPV.[15] In patients with endogenous fungal endophthalmitis treated with PPV and systemic antifungals, adjunctive intravitreal antifungals were not used in one series of *Candida* cases.[110] In phakic patients with an uninvolved crystalline lens, lensectomy is not required at the time of vitreous surgery.[144,145]

Vitreous needle tap may be useful in hospitalized patients who are poor surgical candidates or in facilities where access to PPV instrumentation and support staff is limited (Fig. 90.4). Patients who fail to respond to tap and inject should be considered for PPV during subsequent follow-up.

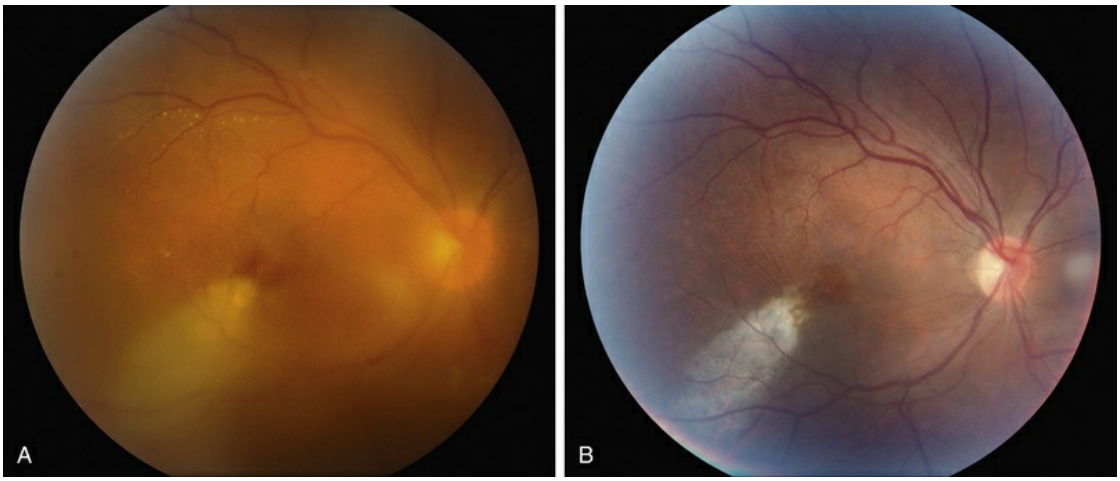

FIG. 90.4 (A) Endogenous methicillin-resistant *Staphylococcus aureus* endophthalmitis. Note white subretinal lesion with overlying vitritis. (B) Four months after treatment with intravitreal vancomycin and ceftazidime, as well as systemic vancomycin, the patient improved. Note clear vitreous and subretinal scar.

Suggested Management

In patients with clinically suspected endogenous endophthalmitis, the history, physical findings, and blood cultures may be useful to determine an etiology. Because of the relative infrequency of these cases (especially bacterial cases), there are no generally established treatment guidelines.[15]

An insidious onset, diffuse vitreous opacities, and chorioretinal infiltrates suggest fungal etiology. Rapid progression and more severe intraocular inflammation suggest bacterial etiology. Other causes of vitreous cellular inflammation should be considered, including toxoplasmosis, sarcoidosis, syphilis, neoplastic etiologies, pars planitis, and dehemoglobinized vitreous hemorrhage.

In patients with clinically suspected endogenous endophthalmitis, consultation with an infectious disease or other medical specialist should be considered to search for evidence of bacteremia/fungemia or other organ involvement. Patients with chorioretinal infiltrates with no or mild vitreous cells may be initially managed with systemic antimicrobials and close observation. Patients with moderate or severe vitreous

inflammation, or patients with milder disease who progress despite systemic therapy, may be treated with systemic antimicrobials, as well as PPV with intravitreal antimicrobials.

Using a high index of suspicion and these treatment suggestions, many patients will achieve good anatomic and visual outcomes. Unfortunately, some patients with endogenous endophthalmitis will lose vision despite prompt and appropriate therapy.

References

1. Smith SR, Kroll AJ, Lou PL, Ryan EA. Endogenous bacterial and fungal endophthalmitis. *Int Ophthalmol Clin*. 2007;47(2):173–183.
2. Chakrabarti A, Shivaprakash MR, Singh R, et al. Fungal endophthalmitis: fourteen years' experience from a center in India. *Retina*. 2008;28(10):1400–1407.
3. Schiedler V, Scott IU, Flynn HW, Davis JL, Benz MS, Miller D. Culture-proven endogenous endophthalmitis: clinical features and visual acuity outcomes. *Am J Ophthalmol*. 2004;137(4):725–731.
4. Aziz HA, Berrocal AM, Sisk RA, et al. Intraocular infections in the neonatal intensive care unit. *Clin Ophthalmol*. 2012;6:733–737.
5. Basu S, Kumar A, Kapoor K, Bagri NK, Chandra A. Neonatal endogenous endophthalmitis: a report of six cases. *Pediatrics*. 2013;131(4):e1292–7.
6. Rahman W, Hanson R, Westcott M. A rare case of peripartum endogenous bacterial endophthalmitis. *Int Ophthalmol*. 2011;31(2):113–115.
7. Vaziri K, Pershing S, Albini TA, Moshfeghi DM, Moshfeghi AA. Risk factors predictive of endogenous endophthalmitis among hospitalized patients with hematogenous infections in the United States. *Am J Ophthalmol*. 2015;159(3):498–504.
8. Lee S, Um T, Joe SG, et al. Changes in the clinical features and prognostic factors of endogenous endophthalmitis: fifteen years of clinical experience in Korea. *Retina*. 2012;32(5):977–984.
9. Lim HW, Shin JW, Cho HY, et al. Endogenous

endophthalmitis in the Korean population: a six-year retrospective study. *Retina*. 2014;34(3):592–602.
10. Connell P, O'Neill E, Fabinyi D, et al. Endogenous endophthalmitis: 10-year experience at a tertiary referral centre. *Eye*. 2011;25(1):66–72.
11. Sridhar J, Flynn HW Jr, Kuriyan AE, Miller D, Albini T. Endogenous fungal endophthalmitis: risk factors, clinical features, and treatment outcomes in mold and yeast infections. *J Ophthalmic Inflamm Infect*. 2013;3(1):60.
12. Schwartz SG, Flynn HW Jr. Update on the prevention and treatment of endophthalmitis. *Expert Rev Ophthalmol*. 2014;9(5):425–430.
13. Schwartz SG, Flynn HW Jr, Scott IU. Endophthalmitis: classification and current management. *Expert Rev Ophthalmol*. 2007;2(3):385–396.
14. Chhabra MS, Noble AG, Kumar AV, Mets MB. Neisseria meningitidis endogenous endophthalmitis presenting as anterior uveitis. *J Pediatr Ophthalmol Strabismus*. 2007;44(5):309–310.
15. Jackson TL, Eykyn SJ, Graham EM, Stanford MR. Endogenous bacterial endophthalmitis: a 17-year prospective series and review of 267 reported cases. *Surv Ophthalmol*. 2003;48(4):403–423.
16. Greenwald MJ, Wohl LG, Sell CH. Metastatic bacterial endophthalmitis: a contemporary reappraisal. *Surv Ophthalmol*. 1986;31(2):81–101.
17. Takebayashi H, Mizota A, Tanaka M. Relation between stage of endogenous fungal endophthalmitis and prognosis. *Graefes Arch Clin Exp Ophthalmol*. 2006;244(7):816–820.
18. Khan A, Okhravi N, Lightman S. The eye in systemic sepsis. *Clin Med*. 2002;2(5):444–448.
19. Kim S, Seo SW, Park J, Chung I. Bilateral endophthalmitis as the initial presentation of bacterial meningitis. *Korean J Ophthalmol*. 2009;23(4):321–324.
20. Shankar K, Gyanendra L, Hari S, Dev Narayan S. Culture proven endogenous bacterial endophthalmitis in apparently healthy individuals. *Ocul Immunol Inflamm*. 2009;17(6):396–399.

21. Binder MI, Chua J, Kaiser PK, Procop GW, Isada CM. Endogenous endophthalmitis: an 18-year review of culture-positive cases at a tertiary care center. *Medicine (Baltimore)*. 2003;82(2):97–105.
22. Okada AA, Johnson RP, Liles WC, D'Amico DJ, Baker AS. Endogenous bacterial endophthalmitis: report of a ten-year retrospective study. *Ophthalmology*. 1994;101(5):832–838.
23. Anand AR, Madhavan HN, Neelam V, Lily TK. Use of polymerase chain reaction in the diagnosis of fungal endophthalmitis. *Ophthalmology*. 2001;108(2):326–330.
24. McDonnell PJ, McDonnell JM, Brown RH, Green WR. Ocular involvement in patients with fungal infections. *Ophthalmology*. 1985;92(5):706–709.
25. Rachitskaya AV, Flynn HW Jr, Wong J, Kuriyan AE, Miller D. A 10-year study of membrane filter system versus blood culture bottles in culturing vitrectomy cassette vitreous in infectious endophthalmitis. *Am J Ophthalmol*. 2013;156(2):349–354.
26. Jayasudha R, Narendran V, Manikandan P, Prabagaran SR. Identification of polybacterial communities in patients with postoperative, posttraumatic, and endogenous endophthalmitis through 16S rRNA gene libraries. *J Clin Microbiol*. 2014;52(5):1459–1466.
27. Hong BK, Lee CS, Van Gelder RN, Garg SJ. Emerging techniques for pathogen discovery in endophthalmitis. *Curr Opin Ophthalmol*. 2015;26(3):221–225.
28. Jackson TL, Paraskevopoulos T, Georgalas I. Systematic review of 342 cases of endogenous bacterial endophthalmitis. *Surv Ophthalmol*. 2014;59(6):627–635.
29. Major JC, Engelbert M, Flynn HW Jr, Miller D, Smiddy WE, Davis JL. Staphylococcus aureus endophthalmitis: antibiotic susceptibilities, methicillin resistance, and clinical outcomes. *Am J Ophthalmol*. 2010;149(2):278–283.
30. Sparks J, Recchia F, Weitkamp J. Endogenous group B streptococcal endophthalmitis in a preterm infant. *J Perinatol*. 2007;27(6):392–394.
31. Torii H, Miyata H, Sugisaka E, Ichikawa Y, Shinoda K, Inoue M. Bilateral endophthalmitis in a patient with bacterial

meningitis caused by Streptococcus pneumoniae. *Ophthalmologica*. 2008;222(5):357–359.
32. Kuriyan AE, Weiss KD, Flynn HW Jr, et al. Endophthalmitis caused by streptococcal species: clinical settings, microbiology, management, and outcomes. *Am J Ophthalmol*. 2014;157(4):774–780.
33. Gupta M, Durand ML, Sobrin L. Vancomycin resistance in ocular infections. *Int Ophthalmol Clin*. 2011;51(4):167–181.
34. Rishi E, Rishi P, Nandi K, Shroff D, Therese KL. Endophthalmitis caused by Enterococcus faecalis: a case series. *Retina*. 2009;29(2):214–217.
35. Kim H, Kim S, Chung I, et al. Emergence of Enterococcus species in the infectious microorganisms cultured from patients with endophthalmitis in South Korea. *Infection*. 2014;42(1):113–118.
36. Montero J, Ruiz-Moreno J, Rodriguez A, Ferrer C, Sanchis E, Alio J. Endogenous endophthalmitis by Propionibacterium acnes associated with leflunomide and adalimumab therapy. *Eur J Ophthalmol*. 2006;16(2):343.
37. Augsten R, Königsdörffer E, Dawczynski J, Schröder K, Pfister W. Endogene Endophthalmitis, verursacht durch Listeria monocytogenes. *Klin Monatsbl Augenheilkd*. 2004;221(12):1054–1056.
38. Miller JJ, Scott IU, Flynn HW Jr, et al. Endophthalmitis caused by Bacillus species. *Am J Ophthalmol*. 2008;145(5):883–888.
39. Kawakami H, Sawada A, Mochizuki K, Takahashi K, Muto T, Ohkusu K. Endogenous Nocardia farcinica endophthalmitis. *Jpn J Ophthalmol*. 2010;54(2):164–166.
40. Silva RA, Young R, Sridhar J. Nocardia choroidal abscess: risk factors, treatment strategies, and visual outcomes. *Retina*. 2015;35(10):2137–2146.
41. Ang M, Jap A, Chee S. Prognostic factors and outcomes in endogenous Klebsiella pneumoniae endophthalmitis. *Am J Ophthalmol*. 2011;151(2):338–344.
42. Sridhar J, Flynn HW Jr, Kuriyan AE, Dubovy S, Miller D. Endophthalmitis caused by Klebsiella species. *Retina*. 2014;34(9):1875–1881.

43. Kashani AH, Eliott D. The emergence of Klebsiella pneumoniae endogenous endophthalmitis in the USA: basic and clinical advances. *J Ophthalmic Inflamm Infect*. 2013;3(1):28.
44. Park G, Kim S, Kim H, et al. Klebsiella pneumoniae as the most frequent pathogen of endogenous endophthalmitis. *Korean J Med*. 2012;82(2):200–207.
45. Motley WW III, Augsburger JJ, Hutchins RK, Schneider S, Boat TF. Pseudomonas aeruginosa endogenous endophthalmitis with choroidal abscess in a patient with cystic fibrosis. *Retina*. 2005;25(2):202–207.
46. Sridhar J, Kuriyan AE, Flynn HW Jr, Miller D. Endophthalmitis caused by Pseudomonas aeruginosa: clinical features, antibiotic susceptibilities, and treatment outcomes. *Retina*. 2015;35(6):1101–1106.
47. Tseng C, Liu PY, Shi Z, et al. Endogenous endophthalmitis due to Escherichia coli: case report and review. *Clin Infect Dis*. 1996;22(6):1107.
48. Balaskas K, Potamitou D. Endogenous endophthalmitis secondary to bacterial meningitis from Neisseria meningitidis: a case report and review of the literature. *Cases J*. 2009;2:149.
49. Leng T, Flynn HW Jr, Miller D, Murray TG, Smiddy WE. Endophthalmitis caused by proteus species: antibiotic sensitivities and visual acuity outcomes. *Retina*. 2009;29(7):1019–1024.
50. Rachitskaya AV, Flynn HW Jr, Davis JL. Endogenous endophthalmitis caused by salmonella serotype B in an immunocompetent 12-year-old child. *Arch Ophthalmol*. 2012;130(6):802–804.
51. Tan N, Galvante PR, Chee SP. Endogenous Serratia marcescens endophthalmitis: an atypical presentation. *Eye*. 2014;28(1):108–109.
52. Ness T, Pelz K, Hansen LL. Endogenous endophthalmitis: microorganisms, disposition and prognosis. *Acta Ophthalmol Scand*. 2007;85(8):852–856.
53. Lingappan A, Wykoff CC, Albini TA, et al. Endogenous fungal endophthalmitis: causative organisms, management

strategies, and visual acuity outcomes. *Am J Ophthalmol*. 2012;153(1):162–166.
54. Underhill DM, Iliev ID. The mycobiota: interactions between commensal fungi and the host immune system. *Nature Rev Immunol*. 2014;14(6):405–416.
55. Pappas PG, Rex JH, Lee J, et al. A prospective observational study of candidemia: epidemiology, therapy, and influences on mortality in hospitalized adult and pediatric patients. *Clin Infect Dis*. 2003;37(5):634–643.
56. Menezes AV, Sigesmund DA, Demajo WA, Devenyi RG. Mortality of hospitalized patients with Candida endophthalmitis. *Arch Intern Med*. 1994;154(18):2093–2097.
57. Connell PP, O'Neill EC, Amirul Islam FM, et al. Endogenous endophthalmitis associated with intravenous drug abuse: seven-year experience at a tertiary referral center. *Retina*. 2010;30(10):1721–1725.
58. Scherer WJ, Lee K. Implications of early systemic therapy on the incidence of endogenous fungal endophthalmitis. *Ophthalmology*. 1997;104(10):1593–1598.
59. Bross J, Talbot GH, Maislin G, Hurwitz S, Strom BL. Risk factors for nosocomial candidemia: a case-control study in adults without leukemia. *Am J Med*. 1989;87(6):614–620.
60. Donahue SP, Hein E, Sinatra RB. Ocular involvement in children with candidemia. *Am J Ophthalmol*. 2003;135(6):886–887.
61. Nagao M, Saito T, Doi S, et al. Clinical characteristics and risk factors of ocular candidiasis. *Diagn Microbiol Infect Dis*. 2012;73(2):149–152.
62. Kaburaki T, Takamoto M, Araki F, et al. Endogenous Candida albicans infection causing subretinal abscess. *Int Ophthalmol*. 2010;30(2):203–206.
63. Hashemi SB, Shishegar S, Nikeghbalian S, et al. Endogenous Aspergillus endophthalmitis occurring after liver transplantation: a case report. *Transplant Proc*. 2009;41(7):2933–2935.
64. Logan S, Rajan M, Graham E, Johnson E, Klein J. A case of aspergillus endophthalmitis in an immuncompetent woman: intra-ocular penetration of oral voriconazole: a case

report. *Cases J*. 2010;3:31.
65. Weishaar PD, Flynn HW Jr, Murray TG, et al. Endogenous Aspergillus endophthalmitis: clinical features and treatment outcomes. *Ophthalmology*. 1998;105(1):57–65.
66. Jampol LM, Dyckman S, Maniates V, Tso M, Daily M, O'Grady R. Retinal and choroidal infarction from Aspergillus: clinical diagnosis and clinicopathologic correlations. *Trans Am Ophthalmol Soc*. 1988;86:422–440.
67. Georgala A, Layeux B, Kwan J, et al. Inaugural bilateral Aspergillus endophthalmitis in a seriously immunocompromised patient. *Mycoses*. 2011;54(5):e631–3.
68. Rex JH, Larsen RA, Dismukes WE, Cloud GA, Bennett JE. Catastrophic visual loss due to Cryptococcus neoformans meningitis. *Medicine (Baltimore)*. 1993;72(4):207–224.
69. Henderly DE, Liggett PE, Rao NA. Cryptococcal chorioretinitis and endophthalmitis. *Retina*. 1987;7(2):75–79.
70. Shwu-Jiuan S, Yi-Chung C, Ni-Wen K, Jao-Hsien W, Chia-Jung C. Endogenous cryptococcal endophthalmitis. *Ophthalmology*. 1998;105(2):377–381.
71. Zakka KA, Foos RY, Brown WJ. Intraocular coccidioidomycosis. *Surv Ophthalmol*. 1978;22(5):313–321.
72. Blumenkranz MS, Stevens DA. Endogenous coccidioidal endophthalmitis. *Ophthalmology*. 1980;87(10):974–984.
73. Rodenbiker HT, Ganley JP, Galgiani JN, Axline SG. Prevalence of chorioretinal scars associated with coccidioidomycosis. *Arch Ophthalmol*. 1981;99(1):71–75.
74. Stone JL, Kalina RE. Ocular coccidioidomycosis. *Am J Ophthalmol*. 1993;116(2):249–250.
75. Gonzales CA, Scott IU, Chaudhry NA, et al. Endogenous endophthalmitis caused by Histoplasma capsulatum var. capsulatum: a case report and literature review. *Ophthalmology*. 2000;107(4):725–729.
76. Cartwright MJ, Promersberger M, Stevens GA. Sporothrix schenckii endophthalmitis presenting as granulomatous uveitis. *Br J Ophthalmol*. 1993;77(1):61–62.
77. Jorgensen JS, Prause JU, Kiilgaard JF. Bilateral endogenous Fusarium solani endophthalmitis in a liver-transplanted patient: a case report. *J Med Case Rep*. 2014;8:101.

78. Malavade SS, Mai M, Pavan P, Nasr G, Sandin R, Greene J. Endogenous Fusarium endophthalmitis in hematologic malignancy: short case series and review of literature. *Infect Dis Clin Pract*. 2013;21(1):6–11.
79. Parke DW, Jones DB, Gentry LO. Endogenous endophthalmitis among patients with candidemia. *Ophthalmology*. 1982;89(7):789–796.
80. Klein JJ, Watanakunakorn C. Hospital-acquired fungemia: its natural course and clinical significance. *Am J Med*. 1979;67(1):51–58.
81. Brooks RG. Prospective study of Candida endophthalmitis in hospitalized patients with candidemia. *Arch Intern Med*. 1989;149(10):2226–2228.
82. Ghodasra DH, Eftekhari K, Shah AR, VanderBeek BL. Outcomes, impact on management, and costs of fungal eye disease consults in a tertiary care setting. *Ophthalmology*. 2014;121(12):2334–2339.
83. Adam MK, Vahedi S, Nichols MM, et al. Inpatient ophthalmology consultation for fungemia: prevalence of ocular involvement and necessity of funduscopic screening. *Am J Ophthalmol*. 2015;160(5):1078–1083.
84. Oude Lashof AM, Rothova A, Sobel JD, et al. Ocular manifestations of candidemia. *Clin Infect Dis*. 2011;53(3):262–268.
85. Dozier CC, Tarantola RM, Jiramongkolchai K, Donahue SP. Fungal eye disease at a tertiary care center: the utility of routine inpatient consultation. *Ophthalmology*. 2011;118(8):1671–1676.
86. Riddell J 4th, Comer GM, Kauffman CA. Treatment of endogenous fungal endophthalmitis: focus on new antifungal agents. *Clin Infect Dis*. 2011;52(5):648–653.
87. Dellon AL, Stark WJ, Chretien PB. Spontaneous resolution of endogenous Candida endophthalmitis complicating intravenous hyperalimentation. *Am J Ophthalmol*. 1975;79(4):648–654.
88. Results of the Endophthalmitis Vitrectomy Study. A randomized trial of immediate vitrectomy and of intravenous antibiotics for the treatment of postoperative

bacterial endophthalmitis. Endophthalmitis Vitrectomy Study Group. *Arch Ophthalmol*. 1995 Dec;113(12):1479–1496.
89. Briggs M, McDonald P, Bourke R, Smith G, McGalliard J, Wong D. Intravitreal penetration of teicoplanin. *Eye*. 1998;12(2):252–255.
90. Tappeiner C, Schuerch K, Goldblum D, Zimmerli S, Fleischhauer JC, Frueh BE. Combined meropenem and linezolid as a systemic treatment for postoperative endophthalmitis. *Klin Monatsbl Augenheilkd*. 2010;227(4):257–261.
91. Hariprasad SM, Mieler WF, Holz ER. Vitreous and aqueous penetration of orally administered gatifloxacin in humans. *Arch Ophthalmol*. 2003;121(3):345–350.
92. Hariprasad SM, Shah GK, Mieler WF, et al. Vitreous and aqueous penetration of orally administered moxifloxacin in humans. *Arch Ophthalmol*. 2006;124(2):178–182.
93. Park-Wyllie LY, Juurlink DN, Kopp A, et al. Outpatient gatifloxacin therapy and dysglycemia in older adults. *N Engl J Med*. 2006;354(13):1352–1361.
94. Mehlhorn AJ, Brown DA. Safety concerns with fluoroquinolones. *Ann Pharmacother*. 2007;41(11):1859–1866.
95. Sheridan KR, Potoski BA, Shields RK, Nau GJ. Presence of adequate intravitreal concentrations of daptomycin after systemic intravenous administration in a patient with endogenous endophthalmitis. *J Hum Pharmacol Drug Ther*. 2010;30(12):1247–1251.
96. Chan W, Liu DT, Fan DS, Lau TT, Lam DS. Failure of systemic antibiotic in preventing sequential endogenous endophthalmitis of a bronchiectasis patient. *Am J Ophthalmol*. 2005;139(3):54950.
97. Rex JH, Walsh TJ, Sobel JD, et al. Practice guidelines for the treatment of candidiasis. Infectious Diseases Society of America. *Clin Infect Dis*. 2000;30(4):662–678.
98. Darling K, Singh J, Wilks D. Case report: Successful treatment of Candida glabrata endophthalmitis with amphotericin B lipid complex (ABLC). *J Infect*. 2000;40(1):92–94.
99. Virata SR, Kylstra JA, Brown JC, Wohl DA, Cohen MS.

Worsening of endogenous Candida albicans endophthalmitis during therapy with intravenous lipid complex amphotericin B. *Clin Infect Dis*. 1999;28(5):1177–1178.
100. Griffin JR, Pettit TH, Fishman LS, Foos RY. Blood-borne Candida endophthalmitis: a clinical and pathologic study of 21 cases. *Arch Ophthalmol*. 1973;89(6):450–456.
101. Roney P, Barr CC, Chun CO, Raff MJ. Endogenous aspergillus endophthalmitis. *Rev Infect Dis*. 1986;8(6):955–958.
102. Lewis H, Aaberg TM, Fary DR, Stevens TS. Latent disseminated blastomycosis with choroidal involvement. *Arch Ophthalmol*. 1988;106(4):527–530.
103. Lemke A, Kiderlen A, Kayser O. Amphotericin B. *Appl Microbiol Biotechnol*. 2005;68(2):151–162.
104. Kinyoun JL. Treatment of Candida endophthalmitis. *Retina*. 1982;2(4):215–222.
105. Green WR, Bennett JE, Good RD. Ocular penetration of amphotericin B: a report of laboratory studies and a case report of postsurgical cephalosporium endophthalmitis. *Arch Ophthalmol*. 1965;73(6):769–775.
106. Dave VP, Majji AB, Suma N, Pappuru RR. A rare case of Aspergillus terreus endogenous endophthalmitis in a patient of acute lymphoid leukemia with good clinical outcome. *Eye (Lond)*. 2011;25(8):1094–1096.
107. Humphrey MJ, Jevons S, Tarbit MH. Pharmacokinetic evaluation of UK-49,858, a metabolically stable triazole antifungal drug, in animals and humans. *Antimicrob Agents Chemother*. 1985;28(5):648–653.
108. Savani DV, Perfect JR, Cobo LM, Durack DT. Penetration of new azole compounds into the eye and efficacy in experimental Candida endophthalmitis. *Antimicrob Agents Chemother*. 1987;31(1):6–10.
109. Annamalai T, Fong KCS, Choo MM. Intravenous fluconazole for bilateral endogenous Candida endophthalmitis. *J Ocular Pharmacol Therapeut*. 2011;27(1):105–107.
110. Christmas NJ, Smiddy WE. Vitrectomy and systemic

fluconazole for treatment of endogenous fungal endophthalmitis. *Ophthalmic Surg Lasers*. 1996;27(12):1012–1018.
111. Wan WL, Kuhak BM, Smith MD, Oster HA, Luttrull KJ. Treatment of ocular fungal infections with oral fluconazole. *Am J Ophthalmol*. 1995;119(4):477–481.
112. Urbak S, Degn T. Fluconazole in the management of fungal ocular infections. *Ophthalmologica*. 1994;208(3):147–156.
113. Como JA, Dismukes WE. Oral azole drugs as systemic antifungal therapy. *N Engl J Med*. 1994;330(4):263–272.
114. Edwards JE Jr, Bodey GP, Bowden RA, et al. International Conference for the Development of a Consensus on the Management and Prevention of Severe Candidal Infections. *Clin Infect Dis*. 1997;25(1):43–59.
115. Akler ME, Vellend H, McNeely DM, Walmsley SL, Gold WL. Use of fluconazole in the treatment of candidal endophthalmitis. *Clin Infect Dis*. 1995;20(3):657–664.
116. Van't Wout J, Novakova I, Verhagen C, Fibbe W, De Pauw B, Van der Meer J. The efficacy of itraconazole against systemic fungal infections in neutropenic patients: a randomised comparative study with amphotericin B. *J Infect*. 1991;22(1):45–52.
117. Pappas PG, Rex JH, Sobel JD, et al. Guidelines for treatment of candidiasis. *Clin Infect Dis*. 2004;38(2):161–189.
118. Scott LJ, Simpson D. Voriconazole: a review of its use in the management of invasive fungal infections. *Drugs*. 2007;67(2):269–298.
119. Hariprasad SM, Mieler WF, Holz ER, et al. Determination of vitreous, aqueous, and plasma concentration of orally administered voriconazole in humans. *Arch Ophthalmol*. 2004;122(1):42–47.
120. Biju R, Sushil D, Georgy NK. Successful management of presumed Candida endogenous endophthalmitis with oral voriconazole. *Indian J Ophthalmol*. 2009;57(4):306–308.
121. Morris MI. Posaconazole: a new oral antifungal agent with an expanded spectrum of activity. *Am J Health Syst Pharm*. 2009;66(3):225–236.
122. Sponsel WE, Graybill JR, Nevarez HL, Dang D. Ocular and

systemic posaconazole (SCH-56592) treatment of invasive Fusarium solani keratitis and endophthalmitis. *Br J Ophthalmol*. 2002;86(7):829–830.
123. Tu EY, McCartney DL, Beatty RF, Springer KL, Levy J, Edward D. Successful treatment of resistant ocular fusariosis with posaconazole (SCH-56592). *Am J Ophthalmol*. 2007;143(2):222–227.
124. Bennett J. Antimicrobial agents: antifungal agents. Hardman JGLL. *Goodman and Gilman's The pharmacological basis of therapeutics*. McGraw–Hill: New York; 2001:1295–1312.
125. Sarria JC, Bradley JC, Habash R, Mitchell KT, Kimbrough RC, Vidal AM. Candida glabrata endophthalmitis treated successfully with caspofungin. *Clin Infect Dis*. 2005;40(5):e46–8.
126. Durand ML, Kim IK, D'Amico DJ, et al. Successful treatment of Fusarium endophthalmitis with voriconazole and Aspergillus endophthalmitis with voriconazole plus caspofungin. *Am J Ophthalmol*. 2005;140(3):552–554.
127. Mochizuki K, Sawada A, Suemori S, et al. Intraocular penetration of intravenous micafungin in inflamed human eyes. *Antimicrob Agents Chemother*. 2013;57(8):4027–4030.
128. Kwok AK, Hui M, Pang CP, et al. An in vitro study of ceftazidime and vancomycin concentrations in various fluid media: implications for use in treating endophthalmitis. *Invest Ophthalmol Vis Sci*. 2002;43(4):1182–1188.
129. Buzzacco DM, Carroll CP. Intravitreal daptomycin in a case of bilateral endogenous endophthalmitis. *Arch Ophthalmol*. 2012;130(7):940–941.
130. Axelrod AJ, Peyman GA, Apple DJ. Toxicity of intravitreal injection of amphotericin B. *Am J Ophthalmol*. 1973;76(4):578–583.
131. Payne JF, Keenum DG, Sternberg P, Thliveris A, Kala A, Olsen TW. Concentrated intravitreal amphotericin B in fungal endophthalmitis. *Arch Ophthalmol*. 2010;128(12):1546–1550.
132. Brod RD, Flynn HW Jr, Clarkson JG, Pflugfelder SC, Culbertson WW, Miller D. Endogenous Candida

endophthalmitis: management without intravenous amphotericin B. *Ophthalmology*. 1990;97(5):666–674.
133. Koç A, Onal S, Yenice O, Kazokoglu H. Pars plana vitrectomy and intravitreal liposomal amphotericin B in the treatment of Candida endophthalmitis. *Ophthalmic Surg Lasers Imaging*. 2010;1-3.
134. Schulman JA, Peyman G, Fiscella R, et al. Toxicity of intravitreal injection of fluconazole in the rabbit. *Can J Ophthalmol*. 1987;22(6):304–306.
135. Velpandian T, Narayanan K, Nag TC, Ravi AK, Gupta SK. Retinal toxicity of intravitreally injected plain and liposome formulation of fluconazole in rabbit eye. *Indian J Ophthalmol*. 2006 Dec;54(4):237–240.
136. Yoshizumi MO, Banihashemi AR. Experimental intravitreal ketoconazole in DMSO. *Retina*. 1988;8(3):210–215.
137. Gao H, Pennesi ME, Shah K, et al. Intravitreal voriconazole: an electroretinographic and histopathologic study. *Arch Ophthalmol*. 2004;122(11):1687–1692.
138. Chang YF, Yang CS, Lee FL, Lee SM. Voriconazole for Candida endophthalmitis. *Ophthalmology*. 2012;119(11):2414–2415.
139. Kramer M, Kramer MR, Blau H, Bishara J, Axer-Siegel R, Weinberger D. Intravitreal voriconazole for the treatment of endogenous Aspergillus endophthalmitis. *Ophthalmology*. 2006;113(7):1184–1186.
140. Mithal K, Pathengay A, Bawdekar A, et al. Filamentous fungal endophthalmitis: results of combination therapy with intravitreal amphotericin B and voriconazole. *Clin Ophthalmol*. 2015;9:649.
141. Silva RA, Sridhar J, Miller D, Wykoff CC, Flynn HW Jr. Exogenous fungal endophthalmitis: an analysis of isolates and susceptibilities to antifungal agents over a 20-year period (1990–2010). *Am J Ophthalmol*. 2015;159(2):257–264.
142. Schulman JA, Peyman GA. Intravitreal corticosteroids as an adjunct in the treatment of bacterial and fungal endophthalmitis: a review. *Retina*. 1992;12(4):336–340.
143. Snip RC, Michels RG. Pars plana vitrectomy in the management of endogenous Candida endophthalmitis. *Am*

J Ophthalmol. 1976;82(5):699–704.
144. Huang SS, Brod RD, Flynn HW Jr. Management of endophthalmitis while preserving the uninvolved crystalline lens. *Am J Ophthalmol*. 1991;112(6):695–701.
145. Townsend J, Pathengay A, Flynn HW Jr, Miller D. Management of endophthalmitis while preserving the uninvolved crystalline lens. *Clin Ophthalmol*. 2012;6:453–457.

91

Acute Retinal Necrosis Syndrome

G. Atma Vemulakonda, Jay S. Pepose, Russell N. Van Gelder

Definition

In 1971 Urayama and coworkers[1] reported six cases of an apparently new syndrome characterized by acute necrotizing retinitis, vitritis, retinal arteritis, choroiditis, and late-onset rhegmatogenous retinal detachment. Young and Bird[2] described two similar cases in 1978 and gave the syndrome the acronym BARN (bilateral acute necrosis syndrome). With the subsequent recognition of unilateral and asynchronous bilateral cases, the disease has been termed simply *acute retinal necrosis syndrome*, or ARN syndrome. ARN syndrome is characterized by the initial onset of episcleritis or scleritis, periorbital pain, and anterior uveitis,

which may be granulomatous or stellate in appearance. This is followed by decreased vision resulting from vitreous opacification, necrotizing retinitis, and, in some cases, optic neuritis or neuropathy. The retinitis appears as deep, multifocal, yellow–white patches, typically beginning in the peripheral fundus (Figs. 91.1 and 91.2) and then becoming concentrically confluent and spreading toward the posterior pole (Figs. 91.3–91.5); the macula frequently is spared. An active vasculitis is present, with perivascular hemorrhages, sheathing, and terminal obliteration of arterioles by thrombi. The phase of active retinitis usually lasts 4–6 weeks, during which time an exudative retinal detachment may occur.[3–8]

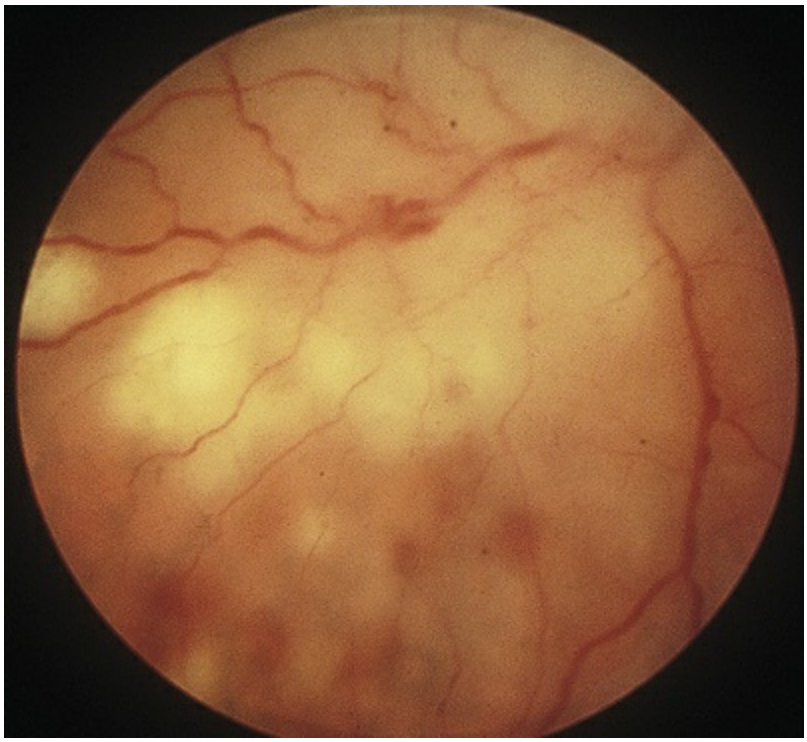

FIG. 91.1 Typical fundus appearance of early acute retinal necrosis syndrome demonstrating necrotizing peripheral retinitis, intraretinal hemorrhage, and vitritis.

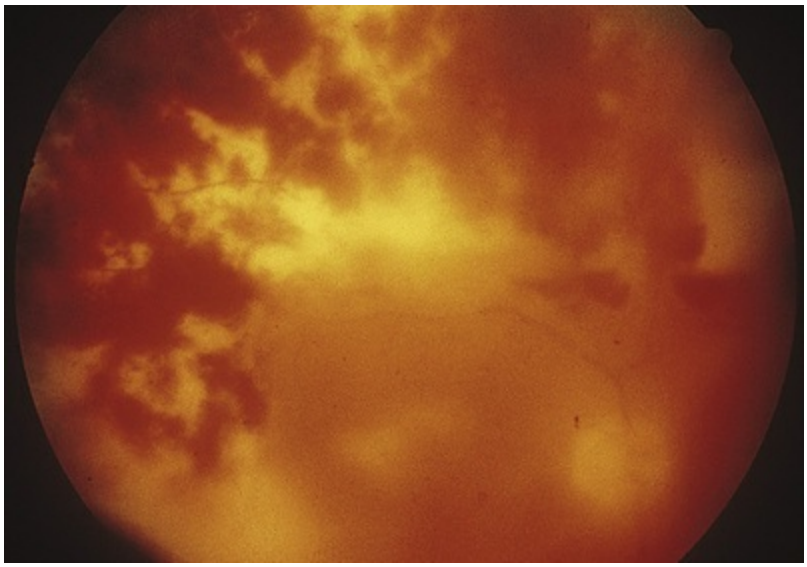

FIG. 91.2 White patches of retinal necrosis are seen in the periphery with isolated areas of necrosis more posterior early in the course of acute retinal necrosis.

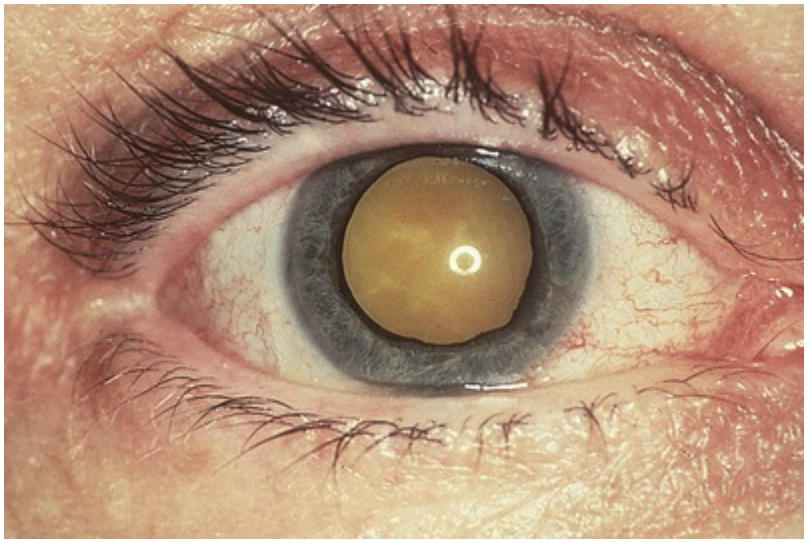

FIG. 91.3 Marked vitritis associated with acute retinal necrosis syndrome. Episcleritis and keratic precipitates are also often seen early in the syndrome.

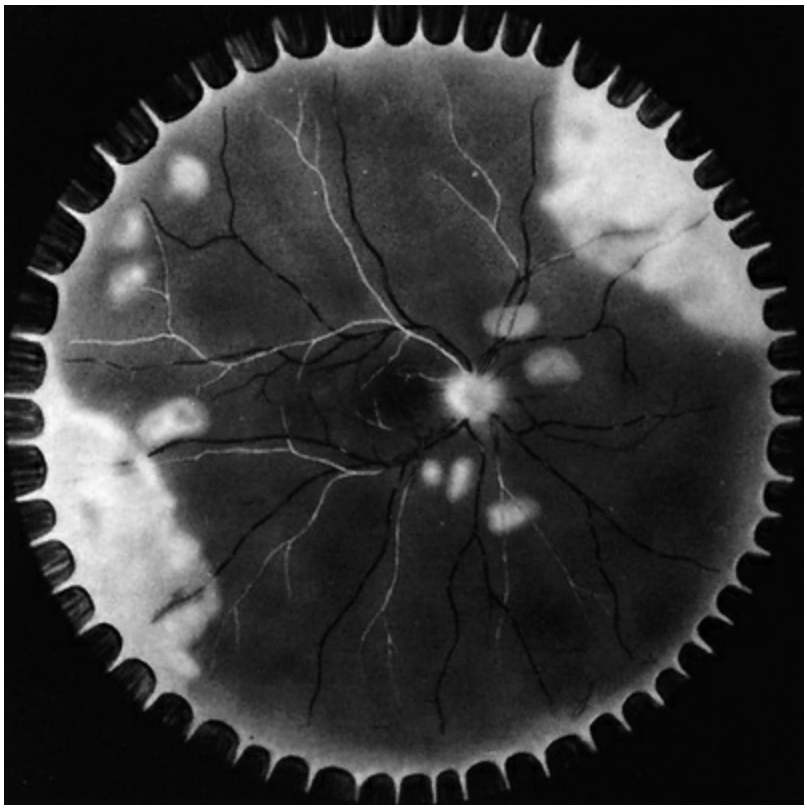

FIG. 91.4 Fundus appearance in early acute retinal necrosis syndrome, with areas of peripheral retinal whitening and arterial vasculitis. Disease at this stage is often accompanied by marked vitritis and intraretinal hemorrhage.

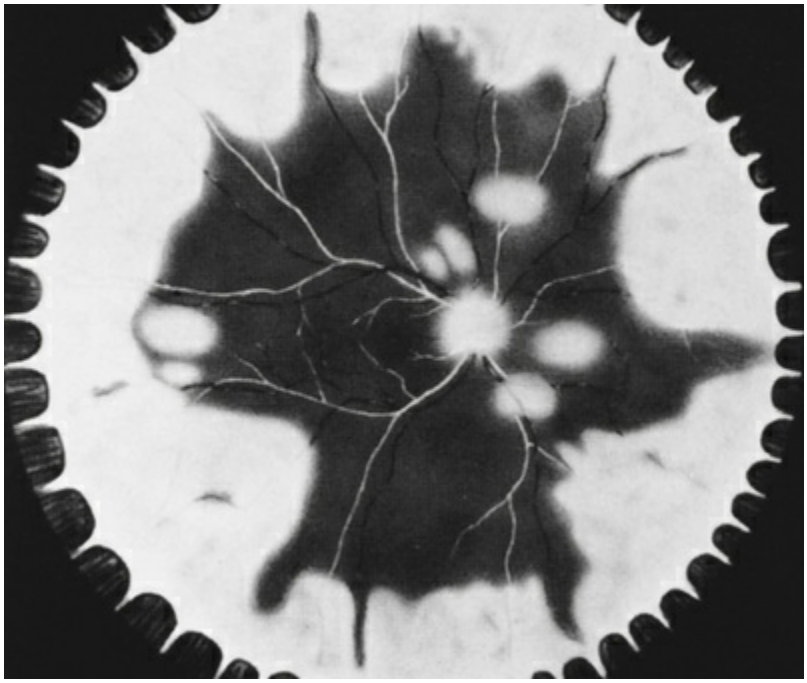

FIG. 91.5 The peripheral retinitis becomes confluent for 360 degrees and is accompanied by an obliterative vasculitis and papillitis.

With resolution, pigmentation of the peripheral lesions begins at their posterior margins, leaving a scalloped appearance (Fig. 91.6), frequently accompanied by retinal breaks at the junction of normal and necrotic retina. Giant retinal pigment epithelial tears may develop.[9] A rhegmatogenous retinal detachment has been observed in approximately 75% of untreated eyes, generally within 1–2 months after the onset of the disease, although earlier detachments have been noted, particularly in cases associated with herpes simplex virus (HSV).[3,6,8,10] Vitreous inflammation may lead to organization and proliferative vitreoretinopathy,[11] adding a traction component to the retinal detachment (Fig. 91.7). Vision may also decrease as a result of anterior ischemic optic neuropathy.

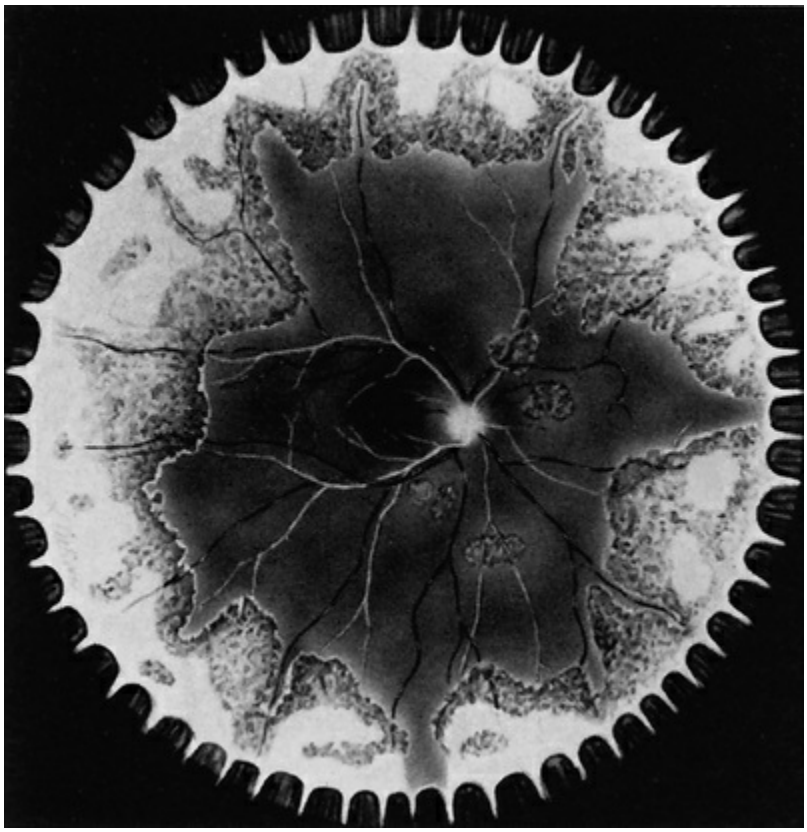

FIG. 91.6 During the resolution of active retinitis, the lesions become pigmented starting at their posterior margins, leaving a scalloped border between necrotic and normal-appearing retina.

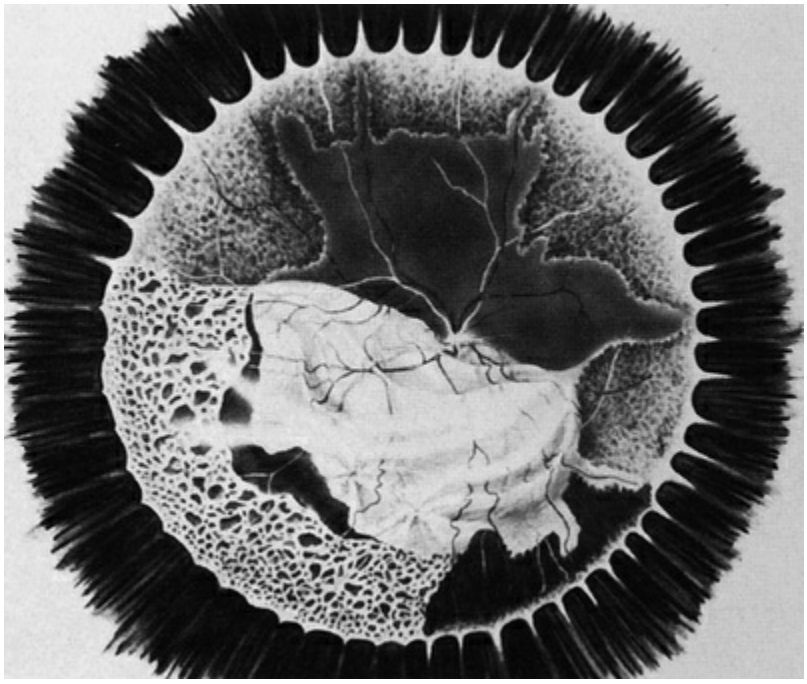

FIG. 91.7 Retinal breaks and the onset of proliferative vitreoretinopathy can lead to a combined traction–rhegmatogenous retinal detachment 1–2 months after the onset of the acute retinal necrosis syndrome. (From Clarkson JG, Blumenkranz MS, Culbertson WW, et al. Ophthalmology 91:1665-1668, 1984.)

Computed tomography[12–14] and ultrasonography[14] have revealed enlargement of the optic nerve sheath in ARN cases associated with prominent optic disc edema. ARN patients can develop meningoencephalitis and must be closely evaluated for this.[15] Even in ARN patients who are not immunocompromised and who have no clinical evidence of encephalitis, magnetic resonance imaging of selected cases has shown lesions of the lateral geniculate, optic tracts, and chiasm,[16] suggesting viral spread through the central nervous system by axoplasmic transport from retinal ganglion cells. An explanation for this has been shown in mouse models, where there is evidence to show that HSV1 infection may progress through the optic chiasm from one eye to the other and along the visual pathways leading to meningoencephalitis.[17]

The contralateral eye is involved in approximately 36% of untreated ARN cases, usually within 6 weeks of the onset of disease

in the first eye.[9,18] However, the second eye can be affected as late as 46 years after involvement of the first eye, and the fellow eye has become involved even after acyclovir treatment for ARN in the first eye.[19] Mild forms of ARN syndrome, characterized by patchy, peripheral retinal opacification, have been reported. These mild cases did not become rapidly confluent or lead to detachment.[20] It is unclear whether this atypical presentation is a result of intense acyclovir and corticosteroid therapy or a reflection of a wide range of disease severity. In addition, less involved forms of ARN have been reported after primary varicella.[21]

Patient Population

The British Ophthalmological Surveillance Unit reported an incidence for ARN syndrome of 0.63 cases per million population per year, with age range from 10 to 94 and nearly equal incidence in men and women.[22] ARN syndrome occurs most commonly in otherwise healthy patients. However, ARN patients may demonstrate subclinical immune dysfunction. In one review of 216 patients with ARN, impaired cellular immunity was noted in 16%.[23] Skin testing of patients with ARN revealed anergy in five of seven tested cases and abnormal lymphocyte proliferative indices in one-third.[24] The significance of cutaneous anergy is unclear, however, since patients with zoster infections frequently demonstrate anergy.[25] Specific HLA haplotypes may increase the relative risk of developing ARN syndrome, such as the HLA-DQw7 antigen and phenotype Bw62 and DR4 in white patients in the United States[26] and HLA-Aw33, B44, and DRw6 in Japanese patients.[27] Pleocytosis of the cerebrospinal fluid frequently accompanies the syndrome,[9,13,28] and intrathecal production of antibodies against herpesviruses has been demonstrated in selected cases.[4] Some patients present with ARN before, after, or at the same time as they show skin manifestations of varicella-zoster infection[29,30] (e.g., primary varicella, herpes zoster ophthalmicus, or Ramsay Hunt syndrome). Unilateral ARN also has been noted after herpes simplex keratitis.[31] Diffuse cerebral atrophy and labyrinthine deafness have been reported following ARN,[32] and some investigators have suggested that ARN be considered as one of the

uveomeningeal syndromes.[14]

Acute necrotizing retinitis that is clinically identical to ARN or shares many features with ARN has been reported in immunocompromised patients. ARN was first described in immunocompromised patients in 1985;[33] the largest case series described 26 cases of ARN in AIDS patients, noting a generally fulminant course.[34] The cause of the retinitis in these immunocompromised patients may be particularly diverse or multifactorial. For example, an AIDS patient died after an ARN-like syndrome with concurrent encephalitis, and herpes simplex viral antigens were localized in the central nervous system at postmortem examination.[35] In contrast, several immunocompromised patients have presented with ARN in association with skin manifestations of zoster.[36] Although ARN syndrome initially was defined as manifesting in otherwise healthy patients, many authorities have broadened the diagnostic criteria to include immunocompromised hosts.[36–39] It is the evolution of clinical signs and symptoms, and not the specific pathogen or immune status of the patient, that serves as the sole basis by which ARN syndrome has been defined (see Differential Diagnosis, below).

Several systemic medications and conditions appear to increase risk of ARN syndrome. There are several reports of ARN following natalizumab therapy for multiple sclerosis.[40,41] There have also been several reports of ARN syndrome following immunizations for varicella zoster [42,43] and influenza,[44] although these cases appear very rarely. HSV viral encephalitis has also been recognized as a risk factor for subsequent ARN syndrome.[45–48]

Numerous reports have documented ARN syndrome following intraocular or periocular steroid injections.[49–51] ARN syndrome has also been reported following intravitreal dexamethasone implant (Ozurdex®)[52] and intravitreal fluocinolone acetonide implant (Retisert®).[53] However, in a review of cases of postinjection viral retinitis, 23 of 30 reported cases were cytomegalovirus (CMV) retinitis, with only six reported cases of HSV or varicella-zoster virus (VZV) ARN.[54] The incidence of ARN syndrome following intravitreal or periocular steroid injection is presently unknown but appears rare.

Etiology

Considerable evidence points to multiple members of the herpesvirus family in the etiology of ARN syndrome. In numerous studies, VZV has been the most frequent virus isolated,[55] up to 66.7%.[56] VZV was isolated in tissue culture from the vitreous of a blind eye enucleated early in the course of the disease, and specific varicella-zoster antigens were identified in retinal tissue by immunocytologic staining[57] (Fig. 91.8). VZV was identified by electron microscopy in necrotic retinal tissue (Fig. 91.9) in two other cases of ARN.[58] Varicella-zoster DNA in intraocular fluids of ARN cases has been confirmed by polymerase chain reaction (PCR),[59] and Witmer quotients of paired serum to intraocular fluid antibody levels have been diagnostic of varicella-zoster in numerous cases.[60,61] Varicella-zoster antigens have been demonstrated in vitreous aspirates of patients with ARN syndrome.[62]

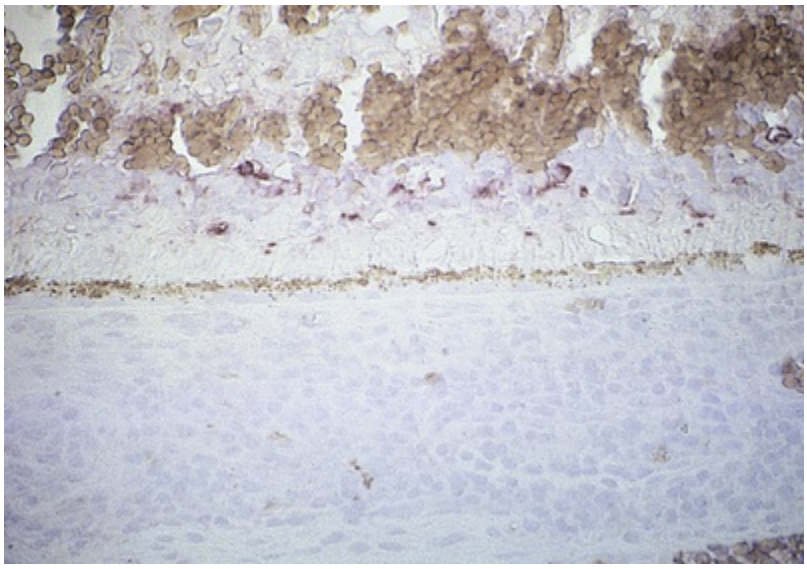

FIG. 91.8 Varicella-zoster antigens (brown) are seen in cells scattered in all layers of a necrotic retina.

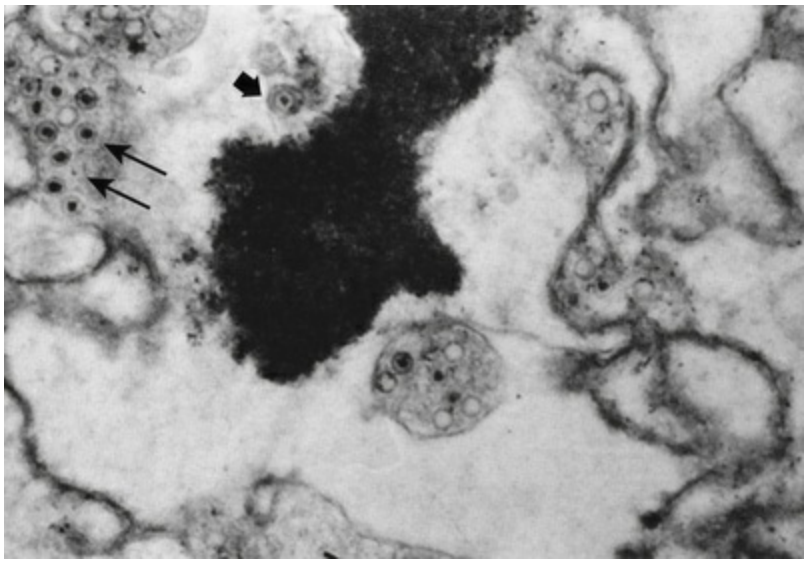

FIG. 91.9 Ultrastructural studies of necrotic retina reveal multiple 100-nm nucleocapsids (*double arrows*) and enveloped virions typical of a herpes-type virus.
(Courtesy MS Blumenkranz.)

Restriction endonuclease patterns of the ARN virus isolate were similar to those of typical varicella-zoster strains and showed similar sensitivities to a panel of antiviral drugs.[63] Although strain heterogeneity has been observed in the varicella-zoster viruses associated with ARN syndrome,[64] the data thus do not support the notion that the ARN virus represents a mutant strain of VZV with significant alterations in either the viral thymidine kinase or DNA polymerase genes. It therefore remains enigmatic why an "old virus" should give rise to a "new" syndrome.

Numerous reports have suggested that other members of the herpesvirus family may cause ARN.[56] A number of studies have implicated HSV because of concurrent herpes simplex skin lesions,[65] the detection of herpes simplex antigens on vitreous cells,[7] the presence of immune complexes containing herpes simplex antigens in aqueous or serum,[66] the documentation of intraocular antibody synthesis directed against HSV,[61] diagnostic changes in serum antibody levels to herpes simplex, PCR detection of herpes simplex,[67] or the culture of herpes simplex from vitreous humor.[3,8,57] Several cases have been described of ARN caused by reactivation of HSV type 2.[59,67,68] Interestingly, patients with herpes simplex type 2 appear to be much younger (mean 21 years) than those with either herpes simplex type 1 or varicella zoster (mean age 40 years).[61,69,70]

The proportion of ARN syndrome patients with disease caused by HSV-2 may be higher in Japan than in the United States, perhaps coincident with changing epidemiologic distributions of HSV-1 vs HSV-2 in this population.[71,72] Patients with ARN syndrome caused by herpes simplex type 1 appear to have a higher risk of encephalitis or meningitis than those with disease caused by varicella-zoster.[45–48,69,73]

In one study,[74] CMV was cultured and CMV antigens were demonstrated in retinal tissue from a case of ARN, but megalic cells or electron-dense cytoplasmic inclusions were not identified. In another case the PCR yielded positive results for CMV in one immunocompetent individual whose vitreous was negative for varicella-zoster and HSV types 1 and 2.[75] Epstein–Barr virus has also been postulated in some cases of ARN syndrome,[76,77] with one reported case showing histopathologic confirmation.[78] However, caution should be applied in making this diagnosis as EBV has been found in 20% of normal cadaveric eyes.[79] While one study found EBV by PCR in 16.7% of ARN cases, each case was also positive for VZV by PCR.[56] Human herpes virus 6 (HHV-6) is a more recently discovered HHV and has also been rarely associated with an ARN-like presentation.[80,81]

Pathologic Features

Studies of blind eyes enucleated early in the course of ARN have demonstrated retinal necrosis, hemorrhage, and considerable vitreous debris. The retinal necrosis is full thickness, and an underlying choroiditis is present that may be granulomatous (Fig. 91.10). Varicella-zoster virus DNA and antigens have been identified in lymphoid cells within choroidal infiltrates in an eye enucleated in the late stage of disease.[82] Eosinophilic intranuclear inclusions within cells of all layers of retina and retinal pigment epithelium were the first clues suggesting a possible viral etiology by a member of the herpes group.[58] There is histologic evidence of retinal arteritis (Fig. 91.11), although no virus particles have been detected in vascular endothelium. Deposits of immune complexes containing varicella-zoster viral antigens have been demonstrated in retinal vessel walls by immunocytologic methods and may play a

role in the vasculitis seen during active stages. The perivasculitis is not restricted to retinal vessels alone and can involve the extraocular muscles (Fig. 91.12). Immune complexes with herpes simplex also have been identified in intraocular fluids in ARN cases.

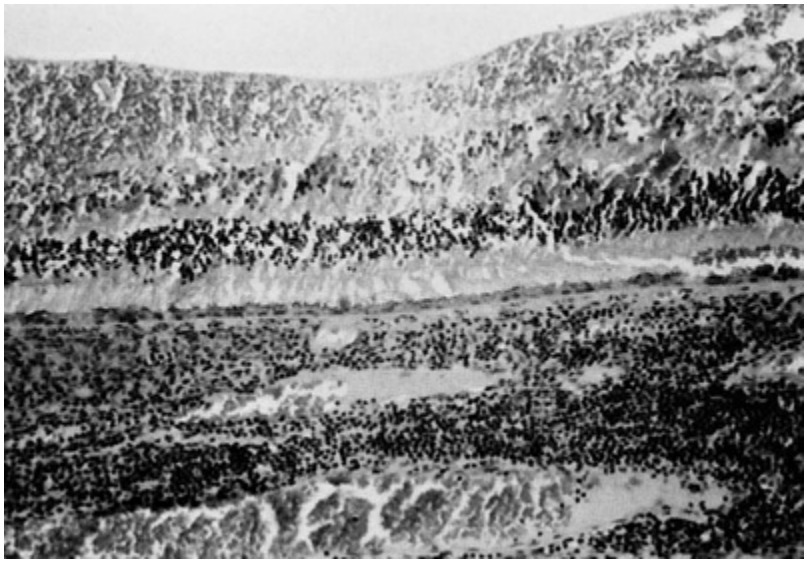

FIG. 91.10 Photomicrograph of a case of acute retinal necrosis shows full-thickness retinal necrosis with an underlying granulomatous choroiditis. (Courtesy Robert Y Foos.)

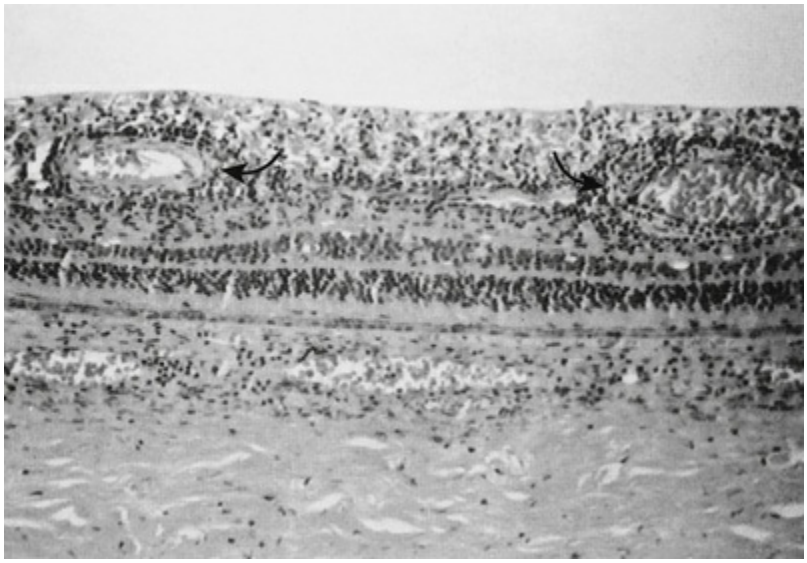

FIG. 91.11 Histologic evidence of retinal vasculitis

(*arrows*) in acute retinal necrosis. (Courtesy Robert Y Foos.)

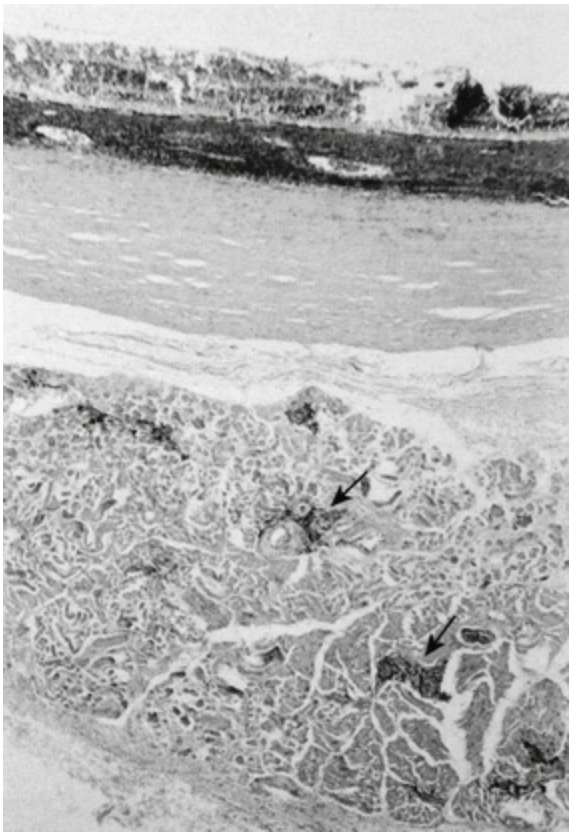

FIG. 91.12 Foci of perivascular inflammation (*arrows*) are seen in the inferior oblique muscle in a case of acute retinal necrosis. (Courtesy Robert Y Foos.)

Ultrastructural studies of retinal tissue have revealed 180 mm virions containing icosahedral capsids, consistent with particles of the herpes group[58] (see Fig. 91.8). The optic nerve may be largely necrotic and heavily infiltrated with plasma cells, but no virus particles or antigens have been seen in the optic nerve. It is possible that the absence of viral antigens or particles reflects more the time point in the course of the disease when enucleation was performed in these rare cases than conclusive evidence regarding acute optic nerve infection. The multifocal, deep retinitis observed early in the course of ARN is compatible with either bloodborne spread of virus or transmission to the eye through a bilateral nerve pathway. An animal model of ARN using herpes simplex virus suggests that spread to the contralateral eye occurs by retrograde axonal

transport between the suprachiasmatic nucleus of the hypothalamus and the contralateral retina.[83]

Retinal necrosis in ARN probably is the result of multiple factors, including a direct lytic viral infection of retina, immune complex disease mediating an obliterative arteritis, choroidal inflammation and occlusion, T-cell mediated inflammation, and vitreous inflammation. All these elements contribute and lead to a combined traction-rhegmatogenous retinal detachment.

Differential Diagnosis

The American Uveitis Society released its criteria for diagnosis of acute retinal necrosis syndrome in 1994.[39] Under this definition, diagnosis of ARN syndrome is dependent solely on the observed clinical findings and their progression. Neither the identification of an etiologic agent nor knowledge of the patient's immune status is required to render a diagnosis of ARN syndrome. The diagnostic criteria are divided into mandatory and supporting categories and are summarized in Table 91.1. By this definition, retinal lesions presumptively caused by herpesviruses (but not part of other well-recognized syndromes such as CMV retinitis or progressive outer retinal necrosis [see below]) are covered under the umbrella term *necrotizing herpetic retinopathy*. A similar set of disease criteria has been suggested by the Japanese ARN study group.[84]

TABLE 91.1

American Uveitis Society Criteria for Diagnosis of Acute Retinal Necrosis Syndrome

Required Clinical Criteria	Supporting Clinical Criteria
One or more foci of retinal necrosis with discrete borders, located in peripheral retina	Optic neuropathy/atrophy
Rapid progression of disease in the absence of therapy	Scleritis
Circumferential spread of disease	Pain
Evidence of occlusive vasculopathy and arteriolar involvement	
A prominent inflammatory reaction in the vitreous and anterior chamber	

The differential diagnosis of ARN includes CMV retinopathy, syphilitic retinitis, toxoplasmosis (particularly in

immunocompromised hosts), large cell lymphoma, and acute multifocal hemorrhagic retinal vasculitis. A more extensive differential diagnosis includes toxocariasis, fungal or bacterial retinitis, pars planitis, Behçet disease, sarcoidosis, commotio retinae, central retinal artery or ophthalmic artery occlusion, ischemic ocular syndrome, collagen-vascular disease, intraocular leukemia/lymphoma (including T-cell-mediated[85]) and retinoblastoma.

ARN syndrome is distinguished from a separate form of varicella-zoster retinitis reported in human immunodeficiency virus (HIV)-infected patients, sometimes referred to as "progressive outer retinal necrosis syndrome" or PORN.[66,86] This latter entity shares an etiologic agent with some cases of ARN but is otherwise distinct. It is characterized by multifocal, patchy choroidal, and deep posterior retinal opacification that initially may be parafoveal. Additional features differentiating this syndrome from ARN include the absence of vitreous or anterior chamber inflammation or signs of active vasculitis. PORN progresses rapidly from the posterior pole to involve the entire retina, resulting in widespread retinal necrosis and atrophy. Despite a common etiologic agent, varicella-zoster retinitis should not be referred to as ARN syndrome. Indeed, the two diseases may even affect different eyes of the same patient.[87]

Although ARN syndrome is a clinical diagnosis established on the basis of a constellation of evolving signs and symptoms, which may be pathognomonic in many cases, in atypical or difficult diagnostic cases ancillary clinical history or laboratory tests can support the diagnosis. It is important to assess the patient's level of immunocompetence, since knowledge of seropositivity to HIV and syphilis may help to establish the appropriate specific diagnosis. Diagnostic vitrectomy is appropriate in cases of uncertain diagnosis. The most sensitive and specific method for the detection of herpes viruses in vitreous specimens is the polymerase chain reaction (PCR). PCR assays are capable of detecting a single varicella zoster virion from vitreous biopsy.[88] Simultaneous PCR for multiple herpes viruses has been used to screen for an etiologic agent in atypical cases of ARN and has implicated both CMV[88] and HSV[59] as potentially causative. PCR can be performed in multiplex for VZV, HSV, CMV, and toxoplasmosis.[89] Sensitivity for each, even

in multiplex testing, is at least 10 genomes per microliter. With application of quantitative PCR (qPCR), accurate estimates of pathogen load can be achieved.[90,91] Quantitative PCR may be used to follow disease response to antiviral agents.[92] The great sensitivity of PCR can be problematic, however; assays that yield false positive results, likely through amplification of latent virus in host tissue, have been reported.[88] False-negative results can also occur. Consensus has not yet been reached regarding the negative predictive value of a negative PCR test for viral DNA. PCR requires meticulous technical performance to avoid specificity problems and is best performed by a laboratory with considerable experience with this method. In most cases, aqueous and/or vitreous sampling for PCR has become the diagnostic test of choice when faced with viral retinitis.[56,93,94]

In cases in which PCR is negative but clinical suspicion is high, endoretinal biopsy may be appropriate. Taking the biopsy from the transition zone between normal and necrotic retina during the acute phase of the disease greatly increases its diagnostic yield. Obtaining paired serum and intraocular fluid specimens and calculation of a modified Goldmann–Witmer coefficient (GWC) may be calculated to confirm diagnosis. With the increased use of PCR, GWC testing is used less frequently, and is not widely available clinically.[56,93,94] However, GWC testing may be more valuable in late stages of disease, as viral DNA disappears but immunologic responses increase.[60,95]

Treatment and Prognosis

Treatment of ARN syndrome is complex and must be individualized in response to the many pathogenic and temporal facets of the disorder, as well as to the specific vitreoretinal pathologic findings at hand. Cases of ARN associated with mild or minimal inflammation have been reported in which ARN did not progress to extensive retinal necrosis, traction, or detachment.[20,21] Controlled, randomized, prospective treatment studies on ARN have not been conducted given the relative rarity of this disease, so current recommendations are based solely on anecdotal data and case series. Early studies indicated that the natural history of classic

ARN syndrome carries a generally poor prognosis in untreated eyes,[9] with only 28% of affected eyes obtaining a final vision better than 20/200 because of rhegmatogenous retinal detachment (75% of affected eyes), optic nerve dysfunction, or macular abnormality. The advent of antiviral therapy and vitrectomy techniques[96] has decreased this level of vision loss to less than one-third of cases in recent years.[12] In one series of cases that were detected early and treated aggressively with acyclovir and laser photocoagulation, outcome for 13 eyes of 12 patients showed 20/40 or better vision in 46% of eyes and 20/400 or better in 92%,[97] (although it should be noted that the use of prophylactic laser photocoagulation has become more controversial that it was in the past,[98,99] see below). Another recent outcome study of 62 eyes of 53 patients showed less favorable results, with surgical intervention required in 51% of patients and good functional outcome seen in 45%.[100] Outcome seems to be dependent on virus type. In one retrospective study of 81 eyes of 74 patients, VZV was associated with significantly worse visual acuity outcomes and a 2.5-fold higher risk of retinal detachment than in HSV-affected eyes.[101] Meghpara et al.[99] reviewed 25 eyes of 25 patients with at least 1 year of follow-up, of whom half had received intravitreal antivirals and all patients had received systemic treatment. They noted 5 of 25 eyes developed retinal detachment, with greater extent of retinitis at presentation being the major risk factor for poor outcome.

Acyclovir has been used in an effort to limit the direct cytopathic effect of virus on retinal tissue. Based on the dose required for a 50% reduction of virus plaques in tissue culture (ED_{50}), oral administration of acyclovir results in subtherapeutic serum levels; in contrast, intravenous acyclovir (13 mg/kg every 8 hours) results in an intravitreal acyclovir level[4] over three times the ARN ED_{50}. After intravenous administration of acyclovir to ARN patients (1500 mg/m^2 per day in three divided doses), retinal lesions were first noted to regress 3.9 days after the beginning of therapy, new lesions did not develop, and existing lesions did not progress.[19] Historically, intravenous therapy for 5–10 days was followed by oral acyclovir at the zoster dosage (800 mg orally five times daily, assuming normal renal function) for up to 6 weeks after the onset of infection, and longer in immunocompromised patients.

Valacyclovir (1 g orally three times daily) or famciclovir[102,103] (500 mg orally three times daily) may also be used following intravenous acyclovir administration. Side-effects of acyclovir include decreased renal function, gastrointestinal irritation, phlebitis, central nervous system dysfunction, and hypersensitivity reactions. Acyclovir has potent antiviral action against varicella-zoster virus, HSV types 1 and 2 (both of which have been implicated in ARN), and Epstein–Barr virus, but it has low activity against CMV. Valganciclovir is active against VZV, HSV, and CMV, but is FDA-approved at present only for CMV retinitis.

In recent years, many clinicians have moved to outpatient use of oral antivirals for treatment induction of ARN.[104–106] Prodrugs such as valacyclovir and famciclovir have high systemic absorption, are active against VZV and HSV, and may be used for prophylaxis against involvement of the second eye.[3,107] Valganciclovir, another prodrug, has been used in other cases.[108] Treatment algorithms have used oral valacyclovir 1 g 3 times daily, oral famciclovir 500 mg 3 times daily, or valganciclovir 450–900 mg 2 times daily until complete resolution of retinitis was observed. Some clinicians have used higher doses of valacyclovir, 2 g 3–4 times daily, to achieve resolution,[109] although there is some risk of renal impairment or mental status changes at this higher dose.[110] These medications are then generally slowly tapered over 1.5 to 75.7 months.[98,111] Recent studies have not found a significant superiority of intravenous over oral treatment induction, but these studies have been retrospective and limited by the relative rarity of this disease. Given the risk of encephalitis particularly in patients with HSV-1-associated disease, close monitoring of patient mental status is warranted.

Recent studies have suggested an adjunctive role for intravitreal antiviral medication in the treatment of ARN syndrome. Ganciclovir (typically 2–4 mg/0.1 mL) and foscarnet (2.4 mg/0.1 mL) have been utilized, with injections typically repeated at 48-72 hours depending in clinical response. Early administration of intravitreal antivirals also provides an opportunity for vitreous sampling (akin to the "tap and inject" for endophthalmitis), allowing for PCR-based identification of causative virus. In one small series, three patients treated with intravitreal ganciclovir as well as intravenous foscarnet, ganciclovir, or acyclovir led to excellent outcomes,[112]

while in another series three patients responded to intravitreal antiviral treatment despite progression on intravenous acyclovir.[113] A similar approach has been employed for progressive outer retinal necrosis.[114,115] In one series of 81 eyes with ARN syndrome, intravitreal foscarnet was associated with a 40% lower rate of retinal detachment than eyes treated solely with systemic therapy.[101] Yeh et al.[116,117] compared 12 patients receiving intravitreal and systemic antivirals to 12 patients receiving only systemic therapy. This group found that patients receiving combination therapy were more likely to gain visual acuity and less likely to develop detachment, with progression to severe vision loss at 0.13 per patient year in the combination group compared with 0.54 per patient year in the systemic-only group. However, Tibbetts et al.[118] studied a cohort of 58 ARN patients of whom 36 were treated with acyclovir only and 22 were treated with either newer agents and/or intravitreal antivirals, and found equivalent outcomes for the groups, with 24% of each group achieving 20/200 or worse vision.

Acute decreases in vision in ARN patients can result from ischemic optic neuropathy and have led to trials of anticoagulants such as aspirin, along with high-dose oral steroids early after initiation of antiviral therapy. Systemic corticosteroids also may limit intraocular inflammation and the vitreous reaction, but are generally begun only after 24–48 hours of intravenous acyclovir. Virus particles or antigens have not been observed in the optic nerve in ARN, and it appears that the optic nerve dysfunction is caused by ischemia from swollen vascular endothelial cells, thrombotic arteriolar occlusion, and infiltration of the optic nerve by inflammatory cells. Hyperaggregation of platelets has been reported in six of seven patients with bilateral ARN studied, as determined by adenosine 5-diphosphate aggregation testing and partial prothrombin times.[119] Optic nerve dysfunction has been reported in ARN patients despite anticoagulation therapy or antiplatelet therapy. Studies have employed optic nerve sheath fenestration in conjunction with acyclovir therapy in a small group of ARN patients with optic neuropathy and disc edema, with reported improvement in final vision in six of eight eyes.[14] Better results were obtained in the subgroup that underwent

decompression within 12 days of the onset of the optic neuropathy.

In early studies prior to current antiviral management techniques, the second eye became involved in 36% of ARN patients, usually within 6 weeks of the first eye's involvement.[19] More recent studies have suggested a fellow-eye involvement rate of ~3% with appropriate antiviral treatment.[118] The duration of systemic treatment to prevent fellow-eye involvement is not well established but generally risk is felt to be decreased in 6–12 weeks, although one report suggested significantly reduced fellow-eye involvement when systemic treatment was carried out greater than 14 weeks.[120] However, bilateral ARN has been reported up to 46 years after the first eye was affected,[121,122] raising a question as to utility of very long-term or life-long prophylaxis in patients who have lost vision in one eye from ARN syndrome. Risk of second-eye involvement may also be dependent on the etiologic agent causing disease. Additionally, rare cases of reactivation in the originally affected eye have been reported.[123]

Retinal tears at the junction of normal and necrotic retina, as well as subsequent proliferative retinopathy creating a complicated combined traction–rhegmatogenous retinal detachment, pose a difficult problem in the management of ARN. Whereas Peyman et al.[7,18] obtained good results in selected patients with intravenous and intravitreal acyclovir in conjunction with prophylactic vitrectomy and scleral buckles in an uncontrolled study of active ARN cases that had not yet developed detachment, others have not been able to prevent retinal detachment by similar management,[124] while still others have found decreased incidence of secondary detachment, but no improvement in final mean visual acuity.[125] In a study of 13 eyes of 12 ARN patients, the incidence of retinal detachment despite intravenous acyclovir therapy was 84%, suggesting that antiviral therapy alone does not effectively preclude retinal detachment.

The use of prophylactic laser has been an issue of great debate in recent years. Several studies have demonstrated the benefit of prophylactic laser photocoagulation posterior to areas of active retinitis,[28,58,97,126] while others have found no decrease in the risk of retinal detachment.[98,127] One reason for this variability may be the small sample sizes used in these studies. Investigators have also

postulated that generally the eyes receiving prophylactic photocoagulation have less vitritis, which allows for treatment. It is thought that vitritis over necrotic retina increases the risk of retinal detachment. They further reason that the eyes unable to receive prophylactic photocoagulation because of media opacity are at higher risk for retinal detachment than those with less vitritis and subsequently clearer media.[98] Without prospective randomized controlled studies, this question may not be definitively answered.

One study found that retinal detachments appear to occur anywhere from 9 to 148 days from the onset of symptoms, so these eyes should be carefully examined at each office visit.[56] With the use of modern microsurgical techniques, including intravitreal silicone oil, air–fluid exchange, demarcating laser photocoagulation, and a long-acting gas tamponade, a high percentage of retinas can be anatomically reattached. In one recent study of 12 eyes of 10 patients with follow-up of mean 4.4 years undergoing retinal detachment surgery, there were no cases of redetachment or of hypotony. [128] However, patients must be carefully selected, and it must be kept in mind that patients with known optic atrophy or minimal vision because of macular pucker or dysfunction before detachment are unlikely to obtain improved visual function despite anatomically successful retinal reattachment. Several studies have looked at whether prophylactic vitrectomy might improve outcomes.[129–131] However, the largest study of 48 eyes treated with prophylactic vitrectomy versus 56 eyes treated conventionally[132] found no improvement in outcome in the group treated prophylactically.

ARN syndrome remains a relatively recently described, potentially visually devastating disorder with multifactorial pathogenesis. Its successful management appears to depend on further advances in antiviral chemotherapy, control of the ischemic vasculopathy, and prevention of proliferative vitreoretinopathy.

References

1. Urayama A, Yamada N, Sasaki T, et al. Unilateral acute uveitis with retinal periarteritis and detachment. *Jpn J Clin Ophthalmol*. 1971;25:607–619.

2. Young NJ, Bird AC. Bilateral acute retinal necrosis. *Br J Ophthalmol*. 1978;62(9):581–590.
3. Duker JS, Nielsen JC, Eagle RC Jr, et al. Rapidly progressive acute retinal necrosis secondary to herpes simplex virus, type 1. *Ophthalmology*. 1990;97(12):1638–1643.
4. el Azazi M, Samuelsson A, Linde A, et al. Intrathecal antibody production against viruses of the herpesvirus family in acute retinal necrosis syndrome. *Am J Ophthalmol*. 1991;112(1):76–82.
5. Lewis ML, Culbertson WW, Post JD, et al. Herpes simplex virus type 1: a cause of the acute retinal necrosis syndrome. *Ophthalmology*. 1989;96(6):875–878.
6. Margolis T, Irvine AR, Hoyt WF, et al. Acute retinal necrosis syndrome presenting with papillitis and arcuate neuroretinitis. *Ophthalmology*. 1988;95(7):937–940.
7. Peyman GA, Goldberg MF, Uninsky E, et al. Vitrectomy and intravitreal antiviral drug therapy in acute retinal necrosis syndrome: report of two cases. *Arch Ophthalmol*. 1984;102(11):1618–1621.
8. Watanabe J, Ashida M, Funaki A, et al. [A case of acute retinal necrosis syndrome caused by herpes simplex virus type 1]. *Nippon Ganka Gakkai Zasshi*. 1989;93(1):65–71.
9. Fox GM, Blumenkranz M. Giant retinal pigment epithelial tears in acute retinal necrosis. *Am J Ophthalmol*. 1993;116(3):302–306.
10. Matsuo T, Date S, Tsuji T, et al. Immune complex containing herpesvirus antigen in a patient with acute retinal necrosis. *Am J Ophthalmol*. 1986;101(3):368–371.
11. Ahmadieh H, Soheilian M, Azarmina M, et al. Surgical management of retinal detachment secondary to acute retinal necrosis: clinical features, surgical techniques, and long-term results. *Jpn J Ophthalmol*. 2003;47(5):484–491.
12. Litoff D, Catalano RA. Herpes zoster optic neuritis in human immunodeficiency virus infection. *Arch Ophthalmol*. 1990;108(6):782–783.
13. Sergott RC, Anand R, Belmont JB, et al. Acute retinal necrosis neuropathy: clinical profile and surgical therapy. *Arch Ophthalmol*. 1989;107(5):692–696.

14. Sergott RC, Belmont JB, Savino PJ, et al. Optic nerve involvement in the acute retinal necrosis syndrome. *Arch Ophthalmol*. 1985;103(8):1160–1162.
15. Cardine S, Chaze PA, Bourcier F, et al. [Bilateral acute retinal necrosis syndrome associated with meningoencephalitis caused by herpes simplex virus 2. A case report]. *J Fr Ophtalmol*. 2004;27(7):795–800.
16. Farrell TA, Wolf MD, Folk JC, et al. Magnetic resonance imaging in a patient with herpes zoster keratouveitis and contralateral acute retinal necrosis. *Am J Ophthalmol*. 1991;112(6):735–736.
17. Labetoulle M, Kucera P, Ugolini G, et al. Neuronal pathways for the propagation of herpes simplex virus type 1 from one retina to the other in a murine model. *J Gen Virol*. 2000;81(Pt 5):1201–1210.
18. Carney MD, Peyman GA, Goldberg MF, et al. Acute retinal necrosis. *Retina*. 1986;6(2):85–94.
19. Blumenkranz MS, Culbertson WW, Clarkson JG, et al. Treatment of the acute retinal necrosis syndrome with intravenous acyclovir. *Ophthalmology*. 1986;93(3):296–300.
20. Matsuo T, Nakayama T, Koyama T, et al. A proposed mild type of acute retinal necrosis syndrome. *Am J Ophthalmol*. 1988;105(6):579–583.
21. Kelly SP, Rosenthal AR. Chickenpox chorioretinitis. *Br J Ophthalmol*. 1990;74(11):698–699.
22. Cochrane TF, Silvestri G, McDowell C, et al. Acute retinal necrosis in the United Kingdom: results of a prospective surveillance study. *Eye (Lond)*. 2012;26(3):370–377 [quiz 378].
23. Rochat C, Herbort CP. [Acute retinal necrosis syndrome. Lausanne cases, review of the literature and new physiopathogenetic hypothesis]. *Klin Monatsbl Augenheilkd*. 1994;204(5):440–449.
24. Rochat C, Polla BS, Herbort CP. Immunological profiles in patients with acute retinal necrosis. *Graefes Arch Clin Exp Ophthalmol*. 1996;234(9):547–552.
25. Pepose JS. Skin test with varicella-zoster virus antigen for ophthalmic herpes zoster. *Am J Ophthalmol*. 1984;98(6):825–

827.
26. Holland GN, Cornell PJ, Park MS, et al. An association between acute retinal necrosis syndrome and HLA-DQw7 and phenotype Bw62, DR4. *Am J Ophthalmol*. 1989;108(4):370–374.
27. Ichikaw T, Sakai J, Usui M. HLA antigens of patients with Kirisawa's uveitis and herpetic keratitis. *Atarashii Ganka*. 1989;6:107–114.
28. Sternberg P Jr, Han DP, Yeo JH, et al. Photocoagulation to prevent retinal detachment in acute retinal necrosis. *Ophthalmology*. 1988;95(10):1389–1393.
29. Browning DJ, Blumenkranz MS, Culbertson WW, et al. Association of varicella zoster dermatitis with acute retinal necrosis syndrome. *Ophthalmology*. 1987;94(6):602–606.
30. Yeo JH, Pepose JS, Stewart JA, et al. Acute retinal necrosis syndrome following herpes zoster dermatitis. *Ophthalmology*. 1986;93(11):1418–1422.
31. Sado K, Kimura T, Hotta Y, et al. Acute retinal necrosis syndrome associated with herpes simplex keratitis. *Retina*. 1994;14(3):260–263.
32. Severin M, Neubauer H. Bilateral acute vascular retinal necrosis. *Ophthalmologica*. 1981;182(4):199–203.
33. Neetens A, Stevens W, Taelman R, et al. Immune deficiency and necrotising retinopathy. *Bull Soc Belge Ophtalmol*. 1985;215:73–86.
34. Batisse D, Eliaszewicz M, Zazoun L, et al. Acute retinal necrosis in the course of AIDS: study of 26 cases. *AIDS*. 1996;10(1):55–60.
35. Freeman WR, Thomas EL, Rao NA, et al. Demonstration of herpes group virus in acute retinal necrosis syndrome. *Am J Ophthalmol*. 1986;102(6):701–709.
36. Jabs DA, Schachat AP, Liss R, et al. Presumed varicella zoster retinitis in immunocompromised patients. *Retina*. 1987;7(1):9–13.
37. Chambers RB, Derick RJ, Davidorf FH, et al. Varicella-zoster retinitis in human immunodeficiency virus infection: case report. *Arch Ophthalmol*. 1989;107(7):960–961.
38. Freeman WR, Wiley CA, Gross JG, et al. Endoretinal biopsy

in immunosuppressed and healthy patients with retinitis: indications, utility, and techniques. *Ophthalmology*. 1989;96(10):1559–1565.
39. Holland GN. Standard diagnostic criteria for the acute retinal necrosis syndrome. Executive Committee of the American Uveitis Society. *Am J Ophthalmol*. 1994;117(5):663–667.
40. Van Tassel SH, Gupta MP, Orlin A, et al. Progressive outer retinal necrosis in a multiple sclerosis patient on natalizumab. *Neurology*. 2015;84(21):2198–2199.
41. Saraiva VS. Acute retinal necrosis and immune reconstitution inflammatory syndrome in a natalizumab-treated patient with multiple sclerosis. *Retin Cases Brief Rep*. 2015;9(3):195–197.
42. Gonzales JA, Levison AL, Stewart JM, et al. Retinal necrosis following varicella-zoster vaccination. *Arch Ophthalmol*. 2012;130(10):1355–1356.
43. Charkoudian LD, Kaiser GM, Steinmetz RL, et al. Acute retinal necrosis after herpes zoster vaccination. *Arch Ophthalmol*. 2011;129(11):1495–1497.
44. Rothova A, de Groot JD, Mudrikova T. Reactivation of acute retinal necrosis after flu H1N1 vaccination. *Br J Ophthalmol*. 2011;95(2):291.
45. Maertzdorf J, Van der Lelij A, Baarsma GS, et al. Herpes simplex virus type 1 (HSV-1)-induced retinitis following herpes simplex encephalitis: indications for brain-to-eye transmission of HSV-1. *Ann Neurol*. 2000;48(6):936–939.
46. Gaynor BD, Wade NK, Cunningham ET Jr. Herpes simplex virus type 1 associated acute retinal necrosis following encephalitis. *Retina*. 2001;21(6):688–690.
47. Gain P, Chiquet C, Thuret G, et al. Herpes simplex virus type 1 encephalitis associated with acute retinal necrosis syndrome in an immunocompetent patient. *Acta Ophthalmol Scand*. 2002;80(5):546–549.
48. Kim C, Yoon YH. Unilateral acute retinal necrosis occurring 2 years after herpes simplex type 1 encephalitis. *Ophthalmic Surg Lasers*. 2002;33(3):250–252.
49. Shah AM, Oster SF, Freeman WR. Viral retinitis after

intravitreal triamcinolone injection in patients with predisposing medical comorbidities. *Am J Ophthalmol*. 2010;149(3):433–440.e1.
50. Aggermann T, Stolba U, Brunner S, et al. Endophthalmitis with retinal necrosis following intravitreal triamcinolone acetonide injection. *Ophthalmologica*. 2006;220(2):131–133.
51. Toh T, Borthwick JH. Acute retinal necrosis post intravitreal injection of triamcinolone acetonide. *Clin Experiment Ophthalmol*. 2006;34(4):380–382.
52. Kucukevcilioglu M, Eren M, Yolcu U, et al. Acute retinal necrosis following intravitreal dexamethasone (Ozurdex(R)) implant. *Arq Bras Oftalmol*. 2015;78(2):118–119.
53. Ramaiya KJ, Rao PK. Herpetic necrotizing retinitis following flucinolone acetonide intravitreal implant. *Ocul Immunol Inflamm*. 2011;19(1):72–74.
54. Takakura A, Tessler HH, Goldstein DA, et al. Viral retinitis following intraocular or periocular corticosteroid administration: a case series and comprehensive review of the literature. *Ocul Immunol Inflamm*. 2014;22(3):175–182.
55. Muthiah MN, Michaelides M, Child CS, et al. Acute retinal necrosis: a national population-based study to assess the incidence, methods of diagnosis, treatment strategies and outcomes in the UK. *Br J Ophthalmol*. 2007;91(11):1452–1455.
56. Lau CH, Missotten T, Salzmann J, et al. Acute retinal necrosis features, management, and outcomes. *Ophthalmology*. 2007;114(4):756–762.
57. Culbertson WW, Blumenkranz MS, Pepose JS, et al. Varicella zoster virus is a cause of the acute retinal necrosis syndrome. *Ophthalmology*. 1986;93(5):559–569.
58. Culbertson WW, Blumenkranz MS, Haines H, et al. The acute retinal necrosis syndrome. Part 2: Histopathology and etiology. *Ophthalmology*. 1982;89(12):1317–1325.
59. Cunningham ET Jr, Short GA, Irvine AR, et al. Acquired immunodeficiency syndrome-associated herpes simplex virus retinitis: clinical description and use of a polymerase chain reaction-based assay as a diagnostic tool. *Arch Ophthalmol*. 1996;114(7):834–840.
60. Pepose JS, Flowers B, Stewart JA, et al. Herpesvirus

antibody levels in the etiologic diagnosis of the acute retinal necrosis syndrome. *Am J Ophthalmol*. 1992;113(3):248–256.
61. Van Gelder RN, Willig JL, Holland GN, et al. Herpes simplex virus type 2 as a cause of acute retinal necrosis syndrome in young patients. *Ophthalmology*. 2001;108(5):869–876.
62. Soushi S, Ozawa H, Matsuhashi M, et al. Demonstration of varicella-zoster virus antigens in the vitreous aspirates of patients with acute retinal necrosis syndrome. *Ophthalmology*. 1988;95(10):1394–1398.
63. Pepose JS, Biron K. Antiviral sensitivities of the acute retinal necrosis syndrome virus. *Curr Eye Res*. 1987;6(1):201–205.
64. Abe T, Sato M, Tamai M. Variable R1 region in varicella zoster virus in fulminant type of acute retinal necrosis syndrome. *Br J Ophthalmol*. 2000;84(2):193–198.
65. Ludwig IH, Zegarra H, Zakov ZN. The acute retinal necrosis syndrome: possible herpes simplex retinitis. *Ophthalmology*. 1984;91(12):1659–1664.
66. Margolis TP, Lowder CY, Holland GN, et al. Varicella-zoster virus retinitis in patients with the acquired immunodeficiency syndrome. *Am J Ophthalmol*. 1991;112(2):119–131.
67. Rahhal FM, Siegel LM, Russak V, et al. Clinicopathologic correlations in acute retinal necrosis caused by herpes simplex virus type 2. *Arch Ophthalmol*. 1996;114(11):1416–1419.
68. Thompson WS, Culbertson WW, Smiddy WE, et al. Acute retinal necrosis caused by reactivation of herpes simplex virus type 2. *Am J Ophthalmol*. 1994;118(2):205–211.
69. Ganatra JB, Chandler D, Santos C, et al. Viral causes of the acute retinal necrosis syndrome. *Am J Ophthalmol*. 2000;129(2):166–172.
70. Tan JCH, Byles D, Stanford MR, et al. Acute retinal necrosis in children caused by herpes simplex virus. *Retina*. 2001;21(4):344–347.
71. Hashido M, Lee FK, Nahmias AJ, et al. An epidemiologic study of herpes simplex virus type 1 and 2 infection in Japan based on type-specific serological assays. *Epidemiol*

Infect. 1998;120(2):179–186.
72. Itoh N, Matsumura N, Ogi A, et al. High prevalence of herpes simplex virus type 2 in acute retinal necrosis syndrome associated with herpes simplex virus in Japan. *Am J Ophthalmol*. 2000;129(3):404–405.
73. Tada Y, Negoro K, Morimatsu M, et al. Findings in a patient with herpes simplex viral meningitis associated with acute retinal necrosis syndrome. *AJNR Am J Neuroradiol*. 2001;22(7):1300–1302.
74. Rungger-Brandle E, Roux L, Leuenberger PM. Bilateral acute retinal necrosis (BARN): identification of the presumed infectious agent. *Ophthalmology*. 1984;91(12):1648–1658.
75. Silverstein BE, Conrad D, Margolis TP, et al. Cytomegalovirus-associated acute retinal necrosis syndrome. *Am J Ophthalmol*. 1997;123(2):257–258.
76. Kramer S, Brummer C, Zierhut M. Epstein–Barr virus associated acute retinal necrosis. *Br J Ophthalmol*. 2001;85(1):114.
77. Gallego-Pinazo R, Harto M, Garcia-Medina JJ, et al. Epstein–Barr virus and acute retinal necrosis in a 5-year-old immunocompetent child. *Clin Ophthalmol*. 2008;2(2):451–455.
78. Schaal S, Kagan A, Wang Y, et al. Acute retinal necrosis associated with Epstein–Barr virus: immunohistopathologic confirmation. *JAMA Ophthalmol*. 2014;132(7):881–882.
79. Chodosh J, Gan YJ, Sixbey JW. Detection of Epstein–Barr virus genome in ocular tissues. *Ophthalmology*. 1996;103(4):687–690.
80. Papageorgiou E, Ch'ng S, Kulkarni A, et al. Fourth cranial nerve palsy and bilateral acute retinal necrosis following human herpesvirus 6 infection of the central nervous system. *Ocul Immunol Inflamm*. 2014;22(3):228–232.
81. Sugita S, Shimizu N, Watanabe K, et al. Use of multiplex PCR and real-time PCR to detect human herpes virus genome in ocular fluids of patients with uveitis. *Br J Ophthalmol*. 2008;92(7):928–932.
82. Rummelt V, Wenkel H, Rummelt C, et al. Detection of varicella zoster virus DNA and viral antigen in the late

stage of bilateral acute retinal necrosis syndrome. *Arch Ophthalmol*. 1992;110(8):1132–1136.
83. Vann VR, Atherton SS. Neural spread of herpes simplex virus after anterior chamber inoculation. *Invest Ophthalmol Vis Sci*. 1991;32(9):2462–2472.
84. Takase H, Okada AA, Goto H, et al. Development and validation of new diagnostic criteria for acute retinal necrosis. *Jpn J Ophthalmol*. 2015;59(1):14–20.
85. Levy-Clarke GA, Buggage RR, Shen D, et al. Human T-cell lymphotropic virus type-1 associated T-cell leukemia/lymphoma masquerading as necrotizing retinal vasculitis. *Ophthalmology*. 2002;109(9):1717–1722.
86. Forster DJ, Dugel PU, Frangieh GT, et al. Rapidly progressive outer retinal necrosis in the acquired immunodeficiency syndrome. *Am J Ophthalmol*. 1990;110(4):341–348.
87. Gariano RF, Berreen JP, Cooney EL. Progressive outer retinal necrosis and acute retinal necrosis in fellow eyes of a patient with acquired immunodeficiency syndrome. *Am J Ophthalmol*. 2001;132(3):421–423.
88. Short GA, Margolis TP, Kuppermann BD, et al. A polymerase chain reaction-based assay for diagnosing varicella-zoster virus retinitis in patients with acquired immunodeficiency syndrome. *Am J Ophthalmol*. 1997;123(2):157–164.
89. Dabil H, Boley ML, Schmitz TM, et al. Validation of a diagnostic multiplex polymerase chain reaction assay for infectious posterior uveitis. *Arch Ophthalmol*. 2001;119(9):1315–1322.
90. Dworkin LL, Gibler TM, Van Gelder RN. Real-time quantitative polymerase chain reaction diagnosis of infectious posterior uveitis. *Arch Ophthalmol*. 2002;120(11):1534–1539.
91. Asano S, Yoshikawa T, Kimura H, et al. Monitoring herpesvirus DNA in three cases of acute retinal necrosis by real-time PCR. *J Clin Virol*. 2004;29(3):206–209.
92. Bernheim D, Germi R, Labetoulle M, et al. Time profile of viral DNA in aqueous humor samples of patients treated

for varicella-zoster virus acute retinal necrosis by use of quantitative real-time PCR. *J Clin Microbiol*. 2013;51(7):2160–2166.
93. Cottet L, Kaiser L, Hirsch HH, et al. HSV2 acute retinal necrosis: diagnosis and monitoring with quantitative polymerase chain reaction. *Int Ophthalmol*. 2009;29(3):199–201.
94. Asano S, Yoshikawa T, Kimura H, et al. Monitoring herpesvirus DNA in three cases of acute retinal necrosis by real-time PCR. *J Clin Virol*. 2004;29(3):206–209.
95. Luyendijk L, vd Horn GJ, Visser OH, et al. Detection of locally produced antibodies to herpes viruses in the aqueous of patients with acquired immune deficiency syndrome (AIDS) or acute retinal necrosis syndrome (ARN). *Curr Eye Res*. 1990;9(Suppl.):7–11.
96. Blumenkranz M, Clarkson J, Culbertson WW, et al. Vitrectomy for retinal detachment associated with acute retinal necrosis. *Am J Ophthalmol*. 1988;106(4):426–429.
97. Crapotta JA, Freeman WR, Feldman RM, et al. Visual outcome in acute retinal necrosis. *Retina*. 1993;13(3):208–213.
98. Tibbetts MD, Shah CP, Young LH, et al. Treatment of acute retinal necrosis. *Ophthalmology*. 2010;117(4):818–824.
99. Meghpara B, Sulkowski G, Kesen MR, et al. Long-term follow-up of acute retinal necrosis. *Retina*. 2010;30(5):795–800.
100. Roy R, Pal BP, Mathur G, et al. Acute retinal necrosis: clinical features, management and outcomes – a 10-year consecutive case series. *Ocul Immunol Inflamm*. 2014;22(3):170–174.
101. Wong R, Pavesio CE, Laidlaw DA, et al. Acute retinal necrosis: the effects of intravitreal foscarnet and virus type on outcome. *Ophthalmology*. 2010;117(3):556–560.
102. Figueroa MS, Garabito I, Gutierrez C, et al. Famciclovir for the treatment of acute retinal necrosis (ARN) syndrome. *Am J Ophthalmol*. 1997;123(2):255–257.
103. Klein JL, Sandy C, Migdal CS, et al. Famciclovir in AIDS-related acute retinal necrosis. *AIDS*. 1996;10(11):1300–1301.
104. Figueroa MS, Garabito I, Gutierrez C, et al. Famciclovir for

the treatment of acute retinal necrosis (ARN) syndrome. *Am J Ophthalmol*. 1997;123(2):255–257.
105. Aslanides IM, De Souza S, Wong DT, et al. Oral valacyclovir in the treatment of acute retinal necrosis syndrome. *Retina*. 2002;22(3):352–354.
106. Emerson GG, Smith JR, Wilson DJ, et al. Primary treatment of acute retinal necrosis with oral antiviral therapy. *Ophthalmology*. 2006;113(12):2259–2261.
107. Pepose JS. The potential impact of the varicella vaccine and new antivirals on ocular disease related to varicella-zoster virus. *Am J Ophthalmol*. 1997;123(2):243–251.
108. Savant V, Saeed T, Denniston A, et al. Oral valganciclovir treatment of varicella zoster virus acute retinal necrosis. *Eye (Lond)*. 2004;18(5):544–545.
109. Guex-Crosier Y, Meylan PR. High dosage of oral valaciclovir as an alternative treatment of varicella zoster acute retinal necrosis syndrome. *Eye (Lond)*. 2006;20(2):247.
110. Guney E, Akcay BI, Erdogan G, et al. Systemic side effects of antiviral therapy in a patient with acute retinal necrosis. *Ocul Immunol Inflamm*. 2014;22(3):233–235.
111. Aizman A, Johnson MW, Elner SG. Treatment of acute retinal necrosis syndrome with oral antiviral medications. *Ophthalmology*. 2007;114(2):307–312.
112. Chau Tran TH, Cassoux N, Bodaghi B, et al. Successful treatment with combination of systemic antiviral drugs and intravitreal ganciclovir injections in the management of severe necrotizing herpetic retinitis. *Ocul Immunol Inflamm*. 2003;11(2):141–144.
113. Luu KK, Scott IU, Chaudhry NA, et al. Intravitreal antiviral injections as adjunctive therapy in the management of immunocompetent patients with necrotizing herpetic retinopathy. *Am J Ophthalmol*. 2000;129(6):811–813.
114. Scott IU, Luu KM, Davis JL. Intravitreal antivirals in the management of patients with acquired immunodeficiency syndrome with progressive outer retinal necrosis. *Arch Ophthalmol*. 2002;120(9):1219–1222.
115. Roig-Melo EA, Macky TA, Heredia-Elizondo ML, et al. Progressive outer retinal necrosis syndrome: successful

treatment with a new combination of antiviral drugs. *Eur J Ophthalmol*. 2001;11(2):200–202.
116. Yeh S, Suhler EB, Smith JR, et al. Combination systemic and intravitreal antiviral therapy in the management of acute retinal necrosis syndrome. *Ophthalmic Surg Lasers Imaging Retina*. 2014;45(5):399–407.
117. Flaxel CJ, Yeh S, Lauer AK. Combination systemic and intravitreal antiviral therapy in the management of acute retinal necrosis syndrome (an American Ophthalmological Society thesis). *Trans Am Ophthalmol Soc*. 2013;111:133–144.
118. Tibbetts MD, Shah CP, Young LH, et al. Treatment of acute retinal necrosis. *Ophthalmology*. 2010;117(4):818–824.
119. Ando F, Kato M, Goto S, et al. Platelet function in bilateral acute retinal necrosis. *Am J Ophthalmol*. 1983;96(1):27–32.
120. Jeon S, Kakizaki H, Lee WK, et al. Effect of prolonged oral acyclovir treatment in acute retinal necrosis. *Ocul Immunol Inflamm*. 2012;20(4):288–292.
121. La Cava M, Abbouda A, Restivo L, et al. Delayed onset of bilateral acute retinal necrosis syndrome: a 46-year interval. *Semin Ophthalmol*. 2015;30(2):146–149.
122. Falcone PM, Brockhurst RJ. Delayed onset of bilateral acute retinal necrosis syndrome: a 34-year interval. *Ann Ophthalmol*. 1993;25(10):373–374.
123. Matsuo T, Nakayama T, Baba T. Same eye recurrence of acute retinal necrosis syndrome. *Am J Ophthalmol*. 2001;131(5):659–661.
124. Blumenkranz M, Clarkson J, Culbertson WW, et al. Visual results and complications after retinal reattachment in the acute retinal necrosis syndrome: the influence of operative technique. *Retina*. 1989;9(3):170–174.
125. Hillenkamp J, Nölle B, Bruns C, et al. Acute retinal necrosis: clinical features, early vitrectomy, and outcomes. *Ophthalmology*. 2009;116(10):1971–1975.e2.
126. Han DP, Lewis H, Williams GA, et al. Laser photocoagulation in the acute retinal necrosis syndrome. *Arch Ophthalmol*. 1987;105(8):1051–1054.
127. McDonald HR, Lewis H, Kreiger AE, et al. Surgical management of retinal detachment associated with the

acute retinal necrosis syndrome. *Br J Ophthalmol*. 1991;75(8):455–458.
128. Almeida DR, Chin EK, Tarantola RM, et al. Long-term outcomes in patients undergoing vitrectomy for retinal detachment due to viral retinitis. *Clin Ophthalmol*. 2015;9:1307–1314.
129. Matsuo T. Timing of prophylactic and early vitrectomy for first-presenting or recurrent acute retinal necrosis syndrome. *Acta Med Okayama*. 2012;66(6):493–497.
130. Luo YH, Duan XC, Chen BH, et al. Efficacy and necessity of prophylactic vitrectomy for acute retinal necrosis syndrome. *Int J Ophthalmol*. 2012;5(4):482–487.
131. Ishida T, Sugamoto Y, Sugita S, et al. Prophylactic vitrectomy for acute retinal necrosis. *Jpn J Ophthalmol*. 2009;53(5):486–489.
132. Iwahashi-Shima C, Azumi A, Ohguro N, et al. Acute retinal necrosis: factors associated with anatomic and visual outcomes. *Jpn J Ophthalmol*. 2013;57(1):98–103.

SECTION 5

Miscellaneous

OUTLINE

92

Drug Toxicity of the Posterior Segment

Michael T. Andreoli, Robert A. Mittra, William F. Mieler

Introduction

A variety of systemic (and select topical and intravitreal) medications are associated with retinal abnormalities and/or toxicity. Fortunately, in the majority of cases the loss of visual function is minimal or even at times reversible, following discontinuation of the inciting drug. Nevertheless, permanent or progressive visual loss may occur in some instances. We present

those medications known to produce a well-described anomaly and have omitted others that have not been definitively proven to cause retinal abnormalities. The medications are grouped according to the type of retinal toxicity they produce, and they are summarized in Box 92.1.

Box 92.1

Patterns of Retinal Toxicity

Disruption of the retina and retinal pigment epithelium

Chloroquine derivatives

Chloroquine

Hydroxychloroquine

Phenothiazines

Thioridazine

Chlorpromazine

Quinine sulfate

Clofazimine

Deferoxamine

Corticosteroid preparations

Cisplatin and BCNU (carmustine)

Vascular damage

Quinine sulfate

Cisplatin and BCN

Talc

Oral contraceptives

Aminoglycoside antibiotics

Vancomycin

Interferon (carmustine)

Ergot alkaloids

Phenylpropanolamine

Cystoid macular edema

Epinephrine

Latanoprost

Nicotinic acid

Paclitaxel/docetaxel

Fingolimod

Retinal folds

Acetazolamide

Chlorthalidone

Ethoxzolamide

Hydrochlorothiazide

Metronidazole

Sulfa antibiotics

Triamterene

Topiramate

Crystalline retinopathy

Tamoxifen

Canthaxanthin

Methoxyflurane

Talc

Nitrofurantoin

Uveitis

Rifabutin

Cidofovir

Miscellaneous

Digoxin

Methanol

MEK inhibitors

Disruption of the Retina and Retinal Pigment Epithelium

Chloroquine Derivatives

Chloroquine

Chloroquine was first used as an antimalarial drug in World War II. Currently it is prescribed for treatment of amebiasis, rheumatoid arthritis, systemic lupus erythematosus, and in countries primarily outside the United States, for prophylaxis against malaria. Retinal toxicity with degeneration of the RPE and neurosensory retina as a result of long-term daily use of chloroquine has been well described.[1–7] However, most cases of retinopathy have developed when a higher than currently recommended dose (3 mg/kg/day using lean body weight) was used.[8] A daily dose exceeding 250 mg

with a total cumulative dose between 100 and 300 g is customarily needed to develop features of toxicity.[9] One study showed a 19% incidence of chloroquine retinopathy in patients taking a mean daily dose of 329 mg.[10] Conversely, with strict adherence to a low dose per diem, the incidence of retinal abnormalities is minimal even when cumulative doses reach over 1000 g.[11]

A paracentral scotoma may be the earliest manifestation of retinal toxicity and can precede the development of any ophthalmoscopic or ERG abnormality.[12] Subtle macular pigment stippling with a loss of the foveal light reflex (Fig. 92.1) usually appears on fundus examination before the development of a classic bull's-eye maculopathy, in which a ring of depigmentation surrounded by an area of hyperpigmentation is seen centered on the fovea (Fig. 92.2). Visual acuity decreases when the RPE abnormalities involve the center of the fovea. The peripheral retina can display pigment mottling, which may, in severe cases, develop into the appearance of primary tapetoretinal degeneration with narrowed retinal vessels, optic disc pallor, and eventual blindness (Fig. 92.3).

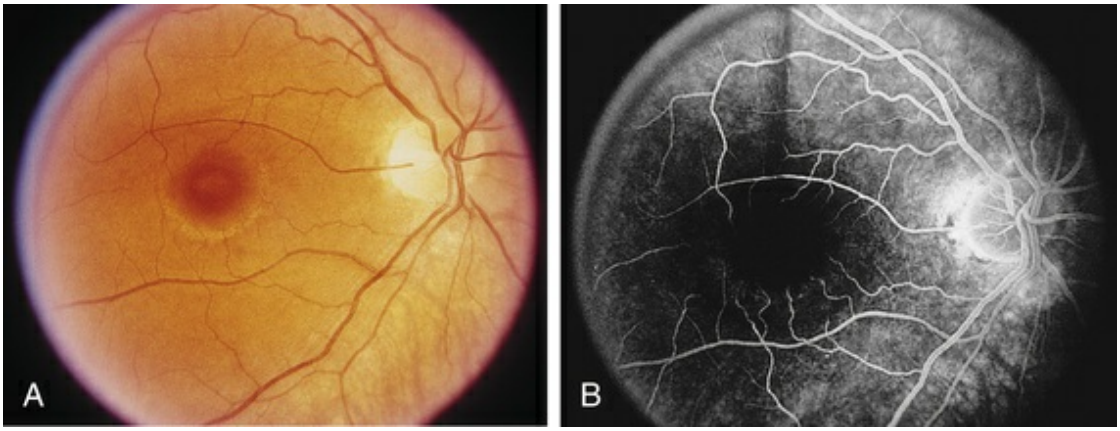

FIG. 92.1 Early chloroquine toxicity. Photograph (A) and fluorescein angiogram (B) show early perifoveal pigmentary changes. (Reproduced with permission from Mieler WF. Focal points. American Academy of Ophthalmology, December 1997.)

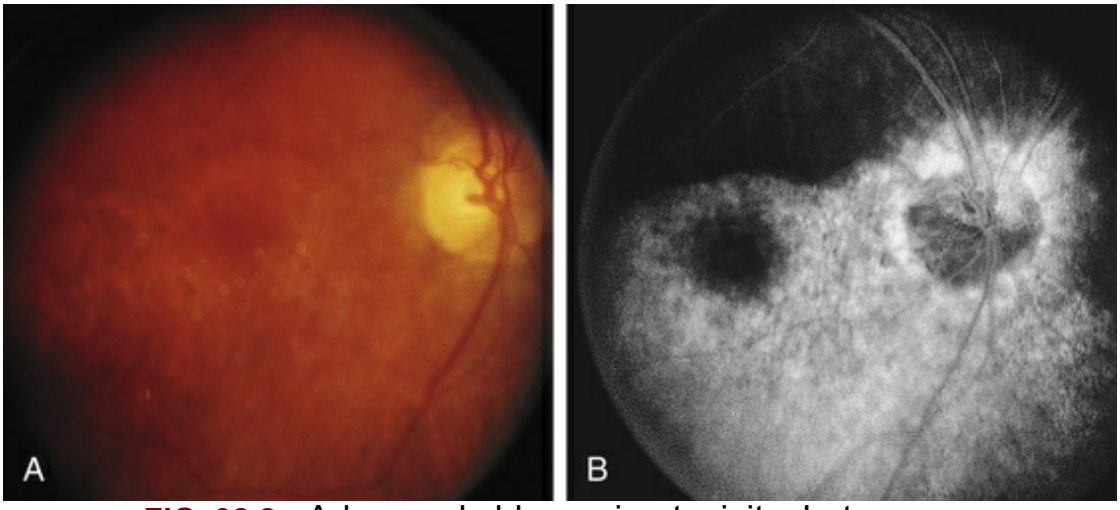

FIG. 92.2 Advanced chloroquine toxicity. Later photograph (A) and fluorescein angiogram (B) from the patient in Fig. 92.1 show marked progression with advanced widespread pigmentary changes. (Reproduced with permission from Mieler WF. Focal points. American Academy of Ophthalmology, December 1997.)

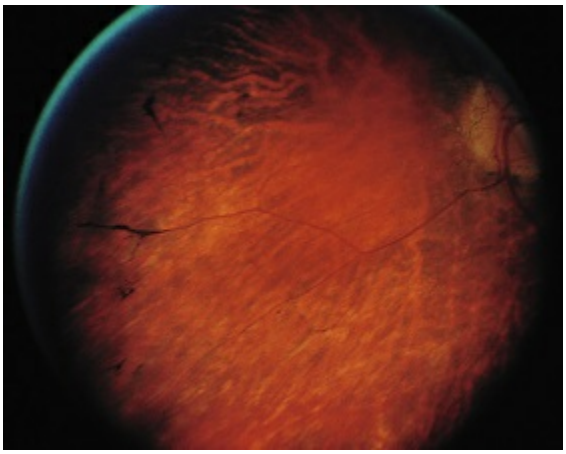

FIG. 92.3 Chloroquine retinopathy. Photograph shows bone-spicule pigmentary changes that can develop in advanced cases. The appearance is similar to endstage retinitis pigmentosa.

After the cessation of chloroquine treatment, early subtle macular changes may possibly revert back to normal. Although far advanced cases may progress despite discontinuation of the drug, most patients remain stable with long-term follow-up.[13,14] Chloroquine, however, is very slowly excreted from the body. It has been detected in the plasma, red blood cells, and urine of patients 5

years after their last known ingestion.[15] This prolonged presence may account for the rare cases of delayed onset of chloroquine retinopathy seen up to 7 years or longer after discontinuation.[16,17]

Fluorescein angiography (FA) may be helpful in the early demonstration of pigment abnormalities in the macula (see Figs. 92.1 and 92.2). There is minimal evidence of damage to the choriocapillaris on FA in the areas of pigment disturbance. The electroretinogram (ERG) and electro-oculogram (EOG) may be abnormal early, although the EOG is sometimes supernormal initially and is not as helpful diagnostically.[18] Histopathologic sections demonstrate loss of retinal pigment epithelium (RPE) pigmentation with an accumulation of pigment-laden cells in the outer retinal layers with damage and reduction of photoreceptors.[19] Electron microscopic studies reveal more widespread damage to the retina, especially the ganglion cell layer.[20] The retinal nerve fiber layer thickness has been shown to be significantly decreased compared to normal in patients on chloroquine therapy and is correlated to the daily dose taken.[21] Fundus autofluorescence (FAF) and optical coherence tomography (OCT) findings suggest that the ganglion cell layer is affected by toxicity initially, especially surrounding the retinal vasculature.[22]

Like the phenothiazines (to be discussed later in this section), chloroquine is bound by melanin and concentrated in the RPE and uveal tissues.[23] It appears that chloroquine toxicity may be mediated by disruption of lysosomal function in the RPE and neural retina and by inhibition of critical enzymes and interference with their metabolic function.[16,24,25]

With the availability of hydroxychloroquine, a less toxic though quite similar medication, use of chloroquine has steadily waned. Screening for toxicity has been more fully evaluated recently for hydroxychloroquine (see below), and similar testing is likely appropriate for chloroquine as well. Color vision can be abnormal in early toxicity and use of the Standard Pseudoisochromatic Plates Part 2 (SPP-2) or the American Optical Hardy Rand Rittler (AO-HRR) color vision plates provides adequate sensitivity and specificity for detection of abnormalities.[26,27] Multifocal ERG testing may be abnormal in early toxicity even when other tests such as visual field and full-field ERG are normal.[28,29]

Hydroxychloroquine

Given the incidence of toxicity with chloroquine, most rheumatologists prefer hydroxychloroquine for the treatment of rheumatoid arthritis (RA) and systemic lupus erythematosus (SLE). Although it can produce a retinopathy identical to chloroquine, its occurrence is much less common.[30–33] Toxicity involving decreased visual acuity, paracentral scotoma, and a bull's-eye maculopathy has been documented (Figs. 92.4 and 92.5).[34–39] Many of these patients received above the recommended daily dosage of 6.5 mg/kg per day, but the classic fundus findings have been reported at lower doses as well.[34,36,39–41] Screening for toxicity becomes more important the longer the patient has been taking the drug as toxicity approaches 1% after 5–7 years of therapy and/or a cumulative dose of 1000 g.[42–44]

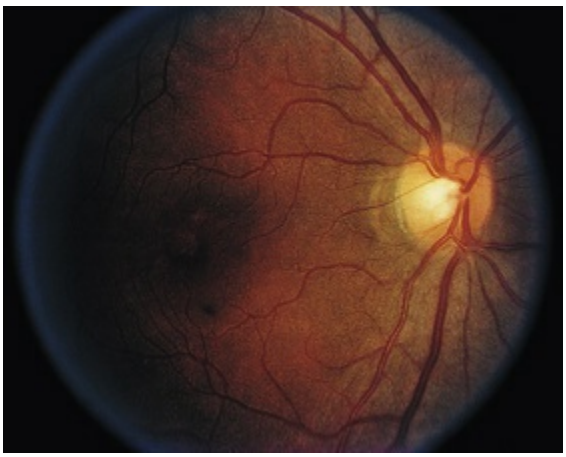

FIG. 92.4 Hydroxychloroquine toxicity. Photograph displays nonspecific pigmentary changes in the central macula.

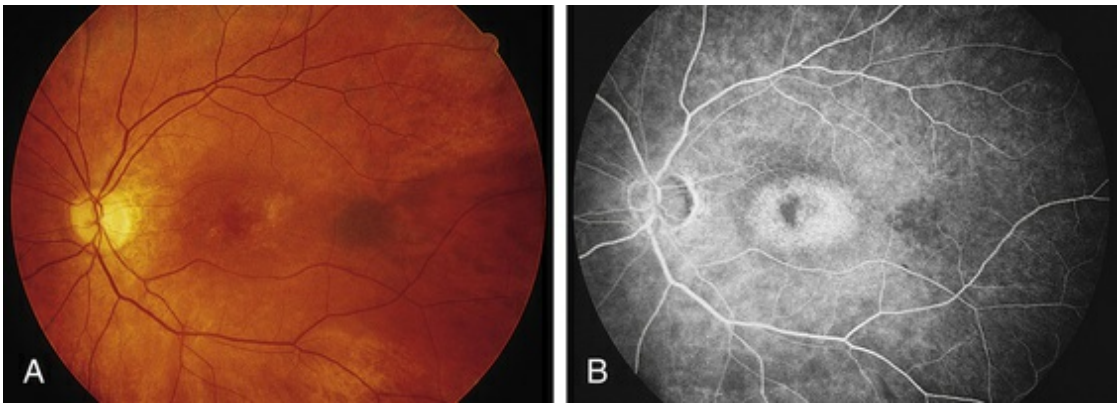

FIG. 92.5 Hydroxychloroquine toxicity. Photograph (A) and fluorescein angiogram (B) show a marked bull's-eye maculopathy, virtually identical to what has been described in association with chloroquine maculopathy. The patient was of short stature.

Several authors have questioned the utility of screening given the low yield, high cost, and the difficulty in diagnosing the condition early enough to prevent damage.[45–48] Nevertheless, if retinal and functional changes are detected early, severe visual impairment can be averted.[41,49]

The revised American Academy of Ophthalmology guidelines for screening include a baseline examination performed at the commencement of therapy.[50] Screening examinations during the first 5 years of therapy can be performed during routine ophthalmic examination (interval to be determined by the age of the patient and the presence or absence of retinal or macular disease). Earlier recommendations emphasized dosing by weight. As most patients are given 400 mg/day of hydroxychloroquine, this dose is acceptable for all except for those with short stature (generally 5 feet 2 inches or less in height). These patients should be given a dose based on their ideal body weight, otherwise overdosage may occur.[51] Furthermore, the dosage may need to be altered if the patient has renal or liver dysfunction.

After 5 years of therapy, screening should be performed at least annually.[43] Current guidelines are centered around tests found to detect early toxicity often prior to any appreciable fundus findings. Patients should have a Humphrey 10–2 automated visual field test (HVF 10–2) with a white test object and in addition should have one of three objective tests at each screening: multifocal

electroretinogram (mf-ERG),[42,52–56] spectral domain OCT (SD-OCT),[57–59] and/or FAF[60] (Fig. 92.6). Any abnormalities of the pattern deviation on the HVF 10–2 need to be taken seriously and the test repeated to confirm its reproducibility. In most situations, SD-OCT should also be obtained, particularly since SD-OCT testing is so readily available. While abnormalities on FAF are generally associated with concerns for active disease, the test has not yet been shown to be reliably predictable as a screening tool for future toxicity.

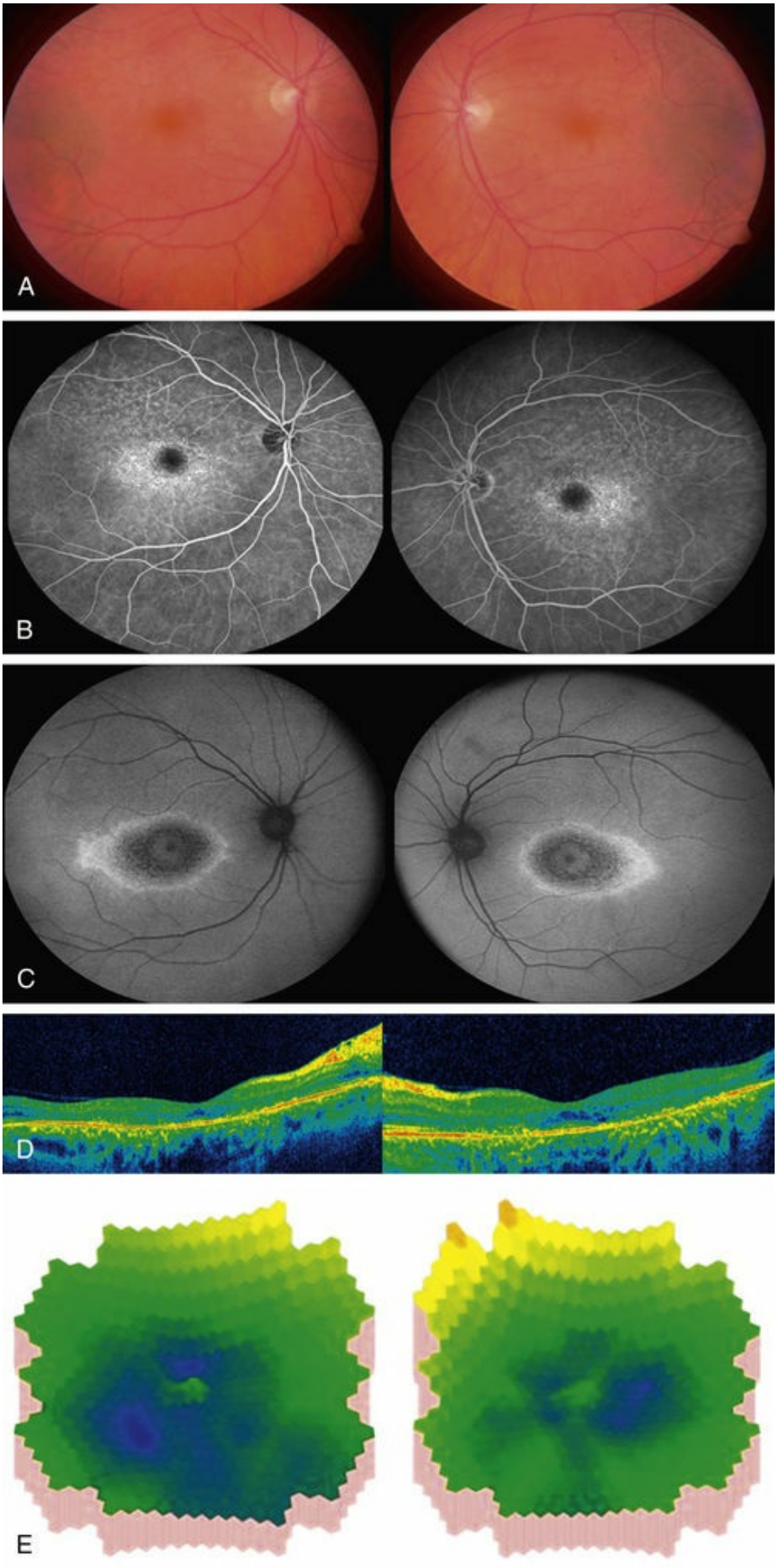
A
B
C
D
E

FIG. 92.6 Screening tests for hydroxychloroquine toxicity. Color photograph (A) showing mild macular pigment mottling in a patient on hydroxychloroquine. Fluorescein angiogram (B) demonstrates hyperfluorescence in the area of the perifoveal pigmentary changes. Fundus autofluorescence (C) shows a perifoveal hypoautofluorescence with a border of hyperautofluorescence. Spectral domain optical coherence tomography (D) shows atrophy of the outer nuclear layer and disruption of the ellipsoid segment. Multifocal electroretinogram (E) shows diminished paracentral waveforms. (Courtesy of David Sarraf, MD, Los Angeles, CA.)

Adjunctive testing now allows for earlier detection of hydroxychloroquine toxicity. FAF has become a widely employed imaging tool with a fairly high sensitivity for recognition of early toxicity. Mild retinopathy may show a paracentral ring of increased FAF, while more advanced stages may present as pericentral mottled loss of FAF with increased FAF in the adjacent retina. Late stages may demonstrate a complete loss of pericentral FAF.[60] Many regard mf-ERG as the most definitive test of toxicity. An analysis of mf-ERG findings in long-term hydroxychloroquine users revealed multiple patterns of abnormalities – paracentral loss, foveal loss, peripheral loss, and generalized loss.[52] The SD-OCT abnormalities associated with hydroxychloroquine toxicity include discontinuity of the ellipsoid zone, thinning of the outer nuclear layer and hyperscattering of the outer segment level (Fig. 92.7).[57] However, perifoveal thinning of the inner plexiform and ganglion cell layers on OCT may precede structural changes to the photoreceptors.[59]

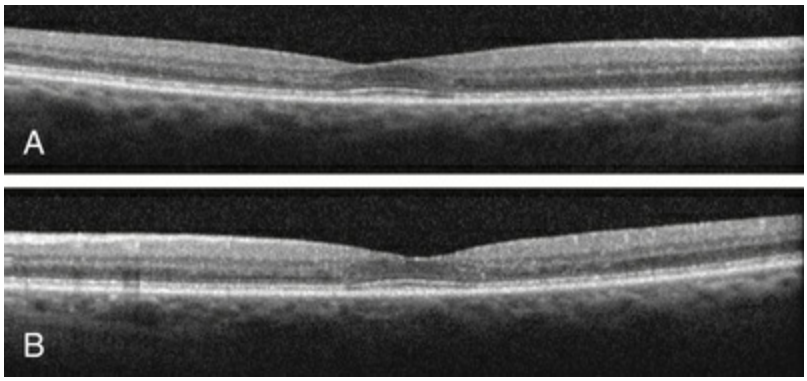

FIG. 92.7 Hydroxychloroquine toxicity: optical coherence tomography image of (A) the right and (B) the left eye, demonstrating perifoveal atrophy of the outer retinal layers and attenuation of the ellipsoid segment in a patient taking hydroxychloroquine for nine years.

As noted in the preceding paragraph, it is imperative to discuss the risk of toxicity with patients and the rationale for screening (to detect, but not necessarily prevent visual loss). If ocular toxicity occurs,[35,37,38,61] and is recognized at an early stage, efforts should be made to communicate this directly to the prescribing physician so that alternative treatment options can be discussed with the patient. In almost all cases, cessation of the drug should be suggested.

In early 2016, the American Academy of Ophthalmology task force on screening recommendations for hydroxychloroquine retinopathy published new updated guidelines in the journal *Ophthalmology*.[62] The 2016 guidelines have lowered the recommended safe dosage to <5.0 mg/kg per day of real body weight. Additionally, it is important to recognize that patients of Asian descent tend to have perifoveal retinopathy, rather than central macular involvement. Annual screening, especially after 5 years of hydroxychloroquine usage, should be performed with Humphrey VF 10–2 and SD-OCT. Finally, one needs to be aware that coexisting renal disease and/or concurrent usage of tamoxifen may increase or hasten development of hydroxychloroquine retinopathy.

Phenothiazines

Thioridazine

Blurred vision, dyschromatopsia (reddish or brownish discoloration of vision), and nyctalopia characterize acute toxicity with thioridazine.[63] In the earliest stages the fundus appearance may be normal or display only mild granular pigment stippling (Fig. 92.8). An intermediate stage is characterized by circumscribed nummular areas of RPE loss from the posterior pole to the midperiphery[64] (Fig. 92.9A). FA reveals disruption of the choriocapillaris in these zones of pigment rarefaction (Fig. 92.9B). In late stages of thioridazine toxicity, widespread areas of depigmentation alternating with hyperpigmented plaques, vascular attenuation, and optic atrophy are seen[65] (Fig. 92.10).

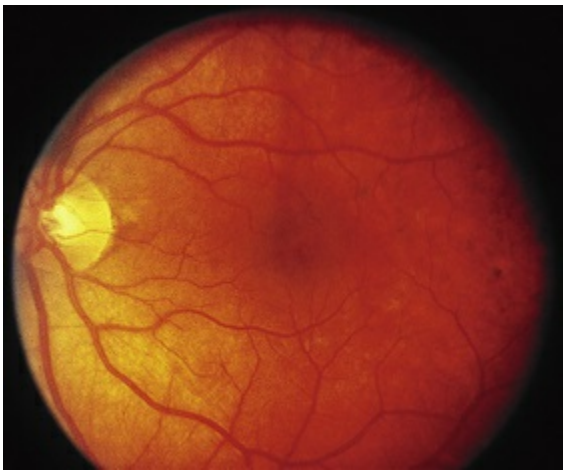

FIG. 92.8 Early thioridazine toxicity. Photograph shows mild granular pigment stippling temporal to the macular region.

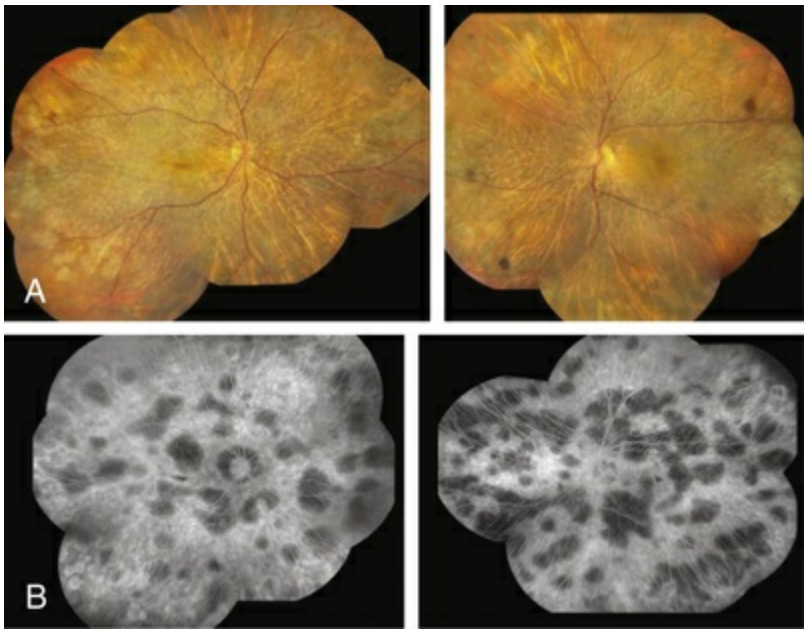

FIG. 92.9 Intermediate thioridazine toxicity. Fundus photograph (A) and fluorescein angiogram (B) show central and peripheral nummular pigmentary changes with corresponding atrophy of the choriocapillaris.

(Courtesy of David Sarraf, MD, Los Angeles, CA.)

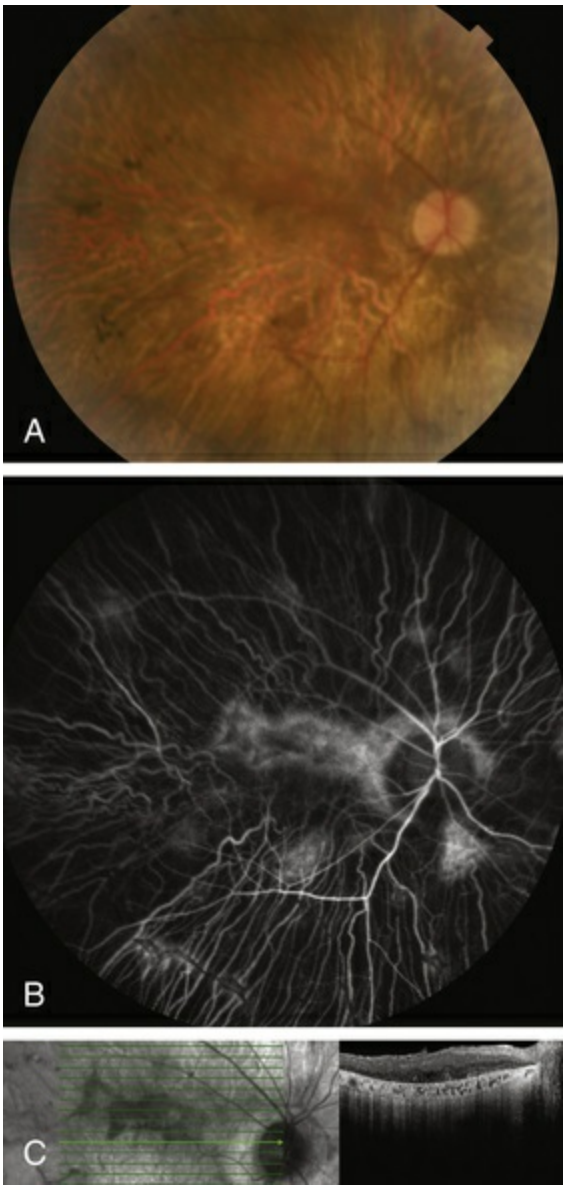

FIG. 92.10 Endstage thioridazine toxicity. Photograph (A) and fluorescein angiogram (B) show diffuse pigmentary and choriocapillaris atrophy, optic atrophy, and vascular attenuation. This severe endstage disease resembles choroideremia. (C) Optical coherence tomography demonstrates outer retinal atrophy with mild cystic changes. (Courtesy of Daniel Kiernan, MD, New York, NY.)

Retinal toxicity from thioridazine is dependent more on the total daily dose than on the cumulative amount of drug received.[66] With higher daily doses, toxicity can occur rapidly, even within the first two weeks of therapy.[67] Toxicity is rare at dosages less than 800 mg/day. Nonetheless, a few cases have been reported with lower

doses given over several years.[68–72] As a result, many now suggest that any patient taking thioridazine, regardless of the daily dose, should be monitored for the development of visual symptoms or fundus changes.

In the initial stages of toxicity, visual field testing can reveal mild constriction, paracentral scotomas, or ring scotomas. ERG is either normal or shows decreased oscillatory potentials. In the later stages, both the rod and cone functions of the ERG, as well as EOG, are markedly abnormal.[73] If the drug is stopped early, ERG testing often improves over the first year.[74] Histologic studies demonstrate that atrophy and disorganization of photoreceptor outer segments occurs primarily, with a secondary loss of the RPE and choriocapillaris.[65]

The early fundus changes associated with thioridazine often progress despite discontinuation of therapy.[64] It is unclear whether this degeneration represents continued toxicity of the drug or a delayed expansion of chorioretinal scarring to areas of subclinical, preexisting damage.[74] Visual function, in contrast to fundus appearance, usually improves over the first year after a toxic reaction, but there has been one report of severe progressive decline in vision after cessation of the drug.[75]

The mechanism of thioridazine-mediated toxicity remains unknown. Many phenothiazines bind melanin granules of the RPE and uveal tissue, but not all commonly instigate retinal toxicity.[76–78] The compound NP-207 (piperidyl-chlorophenothiazine hydrochloride) has a remarkably similar chemical structure to thioridazine, including the same piperidyl side chain. NP-207 was never marketed because of the pronounced pigmentary retinopathy that developed during early clinical trials.[79] This piperidyl side chain is not present in other phenothiazines such as chlorpromazine, which exhibit much less retinal toxicity. Experimental studies demonstrate that phenothiazines both alter enzyme kinetics and inhibit oxidative phosphorylation with subsequent abnormalities in rhodopsin synthesis.[80–82] Other studies postulate that phenothiazine toxicity is due to the drug's effect on the dopamine receptors in the retina.[83] Further study is necessary to determine whether these observed effects are involved in the pathogenesis of thioridazine toxicity.

A review of the daily and cumulative drug dosage is essential in patients taking thioridazine. Baseline fundus photography and possibly ERG testing may be helpful if future toxicity develops. Given the many antipsychotic medications available today, consideration of alternative agents may be discussed with the patient's psychiatrist. At the earliest sign of toxicity, thioridazine should be discontinued.

Chlorpromazine

Chlorpromazine is a piperazine similar to thioridazine but lacks the piperidyl side chain as mentioned above. The compound binds strongly to melanin and can cause hyperpigmentation in the skin, conjunctiva, cornea, lens, and retina[84–90] (Fig. 92.11). Other ocular effects include oculogyric crisis, miosis, and blurred vision caused by paralysis of accommodation. Usual doses range from 40 to 75 mg/day, but dosages up to 800 mg/day are not uncommon.

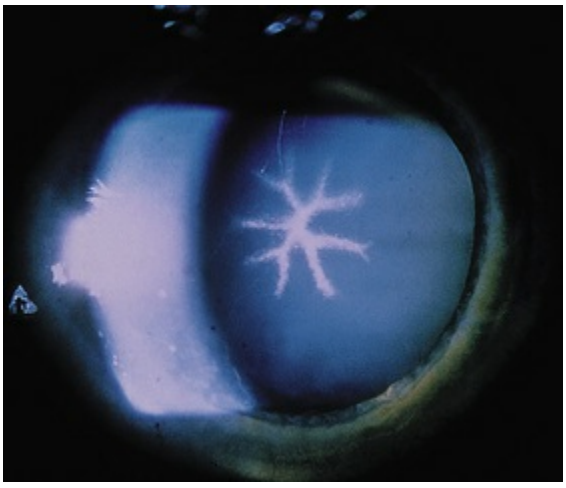

FIG. 92.11 Typical chlorpromazine-induced anterior stellate lens opacities. These findings are generally not felt to be of visual significance.

Retinal toxicity from chlorpromazine is rare. When massive doses are given (e.g., 2400 mg/day for 12 months), pigmentary changes may occur in the retina with attenuation of retinal vessels and optic nerve pallor[87] (Fig. 92.12). Similar to thioridazine, the development and extent of toxicity are more closely related to daily dosage than total amount of drug taken.

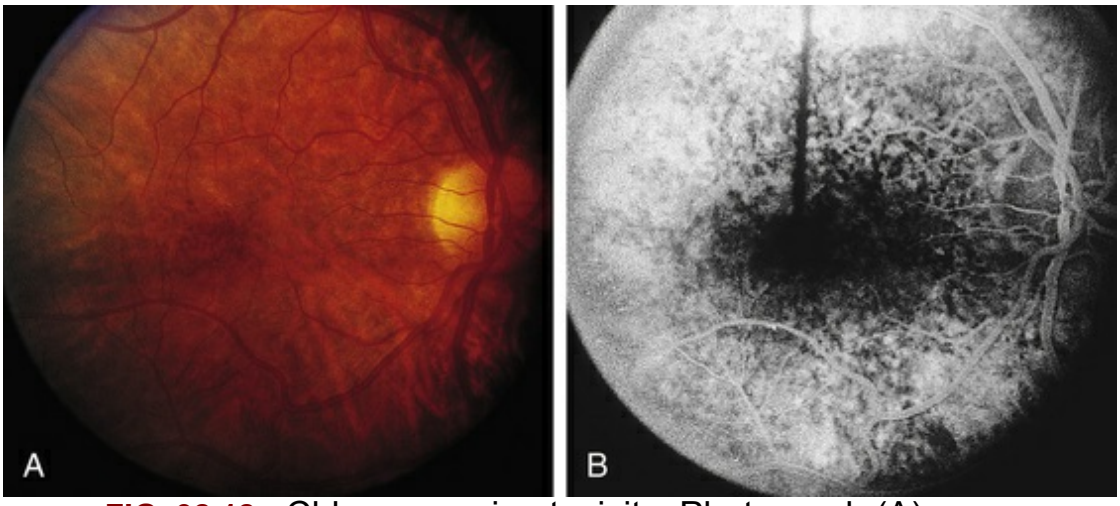

FIG. 92.12 Chlorpromazine toxicity. Photograph (A) and fluorescein angiogram (B) show granular pigmentary changes, though less severe than those generally seen with thioridazine.

MEK Inhibitors

A new class of chemotherapy agents selectively inhibiting the mitogen-activated protein kinase/extracellular signal-regulated kinase (MAPK/ERK) kinase, also referred to as the MEK enzyme, has shown promising results for systemic malignancies. To date, trametinib is the only FDA-approved medication in this class, although binimetinib, selumetinib, and cobimetinib are actively being researched. These drugs have demonstrated particular efficacy for select metastatic cutaneous and uveal melanoma. However, frequent retinal toxicity has recently been recognized. The typical ocular side-effect described is multifocal serous retinal detachment. Pigment epithelial detachment, optic neuropathy, retinal vein occlusion, retinal hemorrhage, cystoid macular edema, and anterior chamber inflammation have also been reported.[91–97] Retinopathy has been described in patients undergoing treatment for metastatic melanoma, metastatic cholangiocarcinoma, and metastatic rectal cancer.

A large proportion of patients with objective signs of retinal toxicity remain asymptomatic. A detailed study of 35 patients on binimetinib therapy for melanoma demonstrated subretinal fluid visible on OCT in approximately three-quarters of patients, affecting the subfoveal region in 85% of these patients. The

subretinal fluid can be quite shallow and extend laterally for large distances. FA and SD-OCT imaging did not exhibit areas of choroidal abnormality or focal RPE defect. Additionally, EOG was abnormal in over 90% of tested patients. Thus, the authors concluded that the retinal toxicity was secondary to a panretinal dysfunction of the RPE. While visual acuity returned to the pretreatment baseline in nearly all patients, EOG findings remained subnormal beyond resolution of the subretinal fluid. In some patients, full-field ERG showed a decreased B-wave, while multifocal ERG showed a diminished response. Furthermore, an array of antiretinal and anti-RPE antibodies were positive in a subset of patients.[91] There have been reports of retinal vein occlusion while on MEK inhibitor therapy. However, given the potentially hypercoagulable state of patients with metastatic malignancy, a causative relationship has not yet been established.[97] A small number of uveitis cases possibly related to MEK inhibitor treatment have been described. Both iritis[93] and panuveitis[98] have been published. However, the panuveitis patient was receiving both trametinib and the B-raf inhibitor dabrafenib, so the underlying etiology of the condition is uncertain.[98]

Subretinal fluid typically reverses with 2–6 weeks of ongoing therapy or discontinuation of treatment (Fig. 92.13).[92] Some pigment epithelial detachments have resolved spontaneously. Macular edema may be responsive to topical steroid or nonsteroidal antiinflammatory agents.[94] Inflammatory episodes have resolved with steroid treatment and stopping therapy. Discontinuation or decreased dosing may be considered for sight-threatening toxicity.[94] Given the relatively minor visual changes and reversibility of ocular toxicity, full ophthalmologic work-up of all patients on these agents has not been advocated at this time.[92]

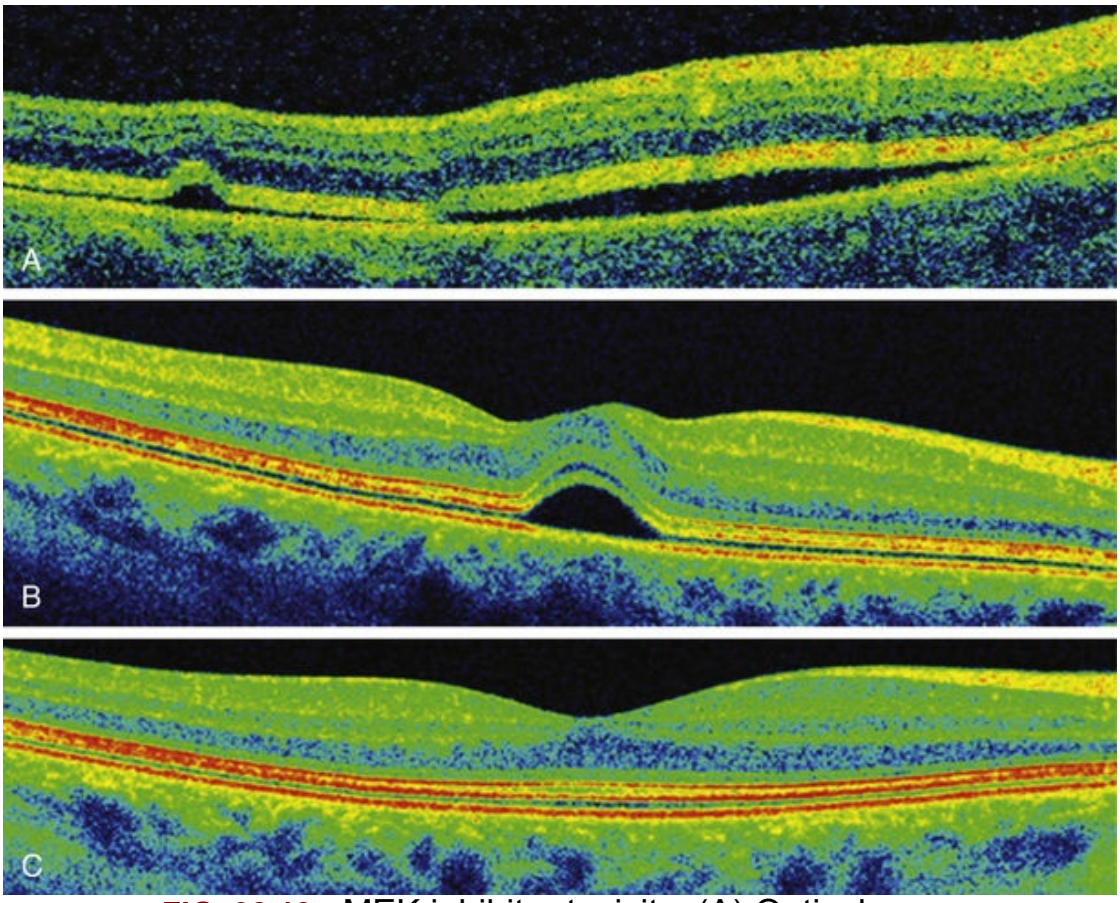

FIG. 92.13 MEK inhibitor toxicity. (A) Optical coherence tomography demonstrating multifocal neurosensory retinal detachments, which were seen bilaterally, 2 weeks after starting pimasertib. Resolution of subretinal fluid was seen 1 week after discontinuation. (B) Fluid accumulation was again seen 2 weeks after rechallenge at half dose, which resolved after being at the lower dose for 1 month (C). (Courtesy of Michael Chilov, MD, Sydney, Australia.)

Quinine Sulfate

Quinine sulfate was first used for the treatment of malaria in World War II, but it currently is prescribed for the management of nocturnal muscle cramps or "restless leg syndrome." The recommended daily dose is less than 2 g. Signs of systemic toxicity occur with doses greater than 4 g, and the fatal oral dose is 8 g. Ocular toxicity with quinine develops after an overdose, either by accidental ingestion or by attempted abortion or suicide. Rarely, chronic ingestion at low levels can result in ocular toxicity as well.[91]

With an overdose, a syndrome known as *cinchonism* is rapidly produced, consisting of nausea, vomiting, headache, tremor, and sometimes hypotension and loss of consciousness. When patients awake they often are completely blind and have dilated, unreactive pupils.[92] In the acute stages of toxicity, fundus examination reveals mild venous dilation with minimal retinal edema and normal arterial caliber. The FA displays minimal abnormalities. ERG testing shows an acute slowing of the a-wave with increased depth, loss of oscillatory potentials, and a decreased b-wave.[93] EOG and visual-evoked potential (VEP) testing are also abnormal.

Over the next few days visual acuity returns, but the patient is left with a small central island of vision. There is a progressive attenuation of the retinal arterioles with the development of optic disc pallor over the next few weeks to months and iris depigmentation can occur[94] (Fig. 92.14). Early investigators believed the mechanism of quinine toxicity to be vascular in origin. This was based primarily on the fundus appearance several weeks after ingestion, which showed marked arteriolar attenuation and optic disc pallor.[92,95] More recent experimental and clinical studies have demonstrated minimal involvement of the retinal vasculature in the early stages of quinine toxicity.[92,95,96] Furthermore, ERG and histologic studies show that the site of toxicity is likely the retinal ganglion, bipolar, and photoreceptor cells.[92,96] Findings on SD-OCT demonstrate inner retinal atrophy.[97] The exact mechanism of quinine toxicity is unidentified, but some have suggested that it may act as an acetylcholine antagonist and disrupt cholinergic transmission in the retina.[98]

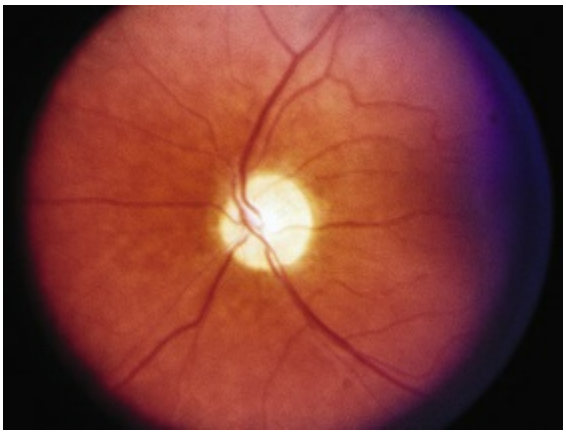

FIG. 92.14 Quinine toxicity. Photograph illustrates the characteristic optic nerve head pallor with diffuse arteriolar attenuation approximately 2 months after an intentional overdose of the medication.

Clofazimine

Clofazimine is a red phenazine dye that has been used to treat dapsone-resistant leprosy, psoriasis, pyoderma gangrenosum, discoid lupus, and more recently, *Mycobacterium avium*-complex infections in AIDS patients. With treatment over several months, clofazimine crystals may accumulate in the cornea. Two cases of bull's-eye maculopathy with pigmentary retinopathy (Fig. 92.15) have been reported in AIDS patients with doses of 200–300 mg/day (total dose, 40–48 g).[99,100] Visual acuity was mildly affected, with reduced scotopic, photopic, and flicker ERG amplitudes. Cessation of treatment may result in the clearance of the corneal deposits but does not appear to affect the retinopathy.

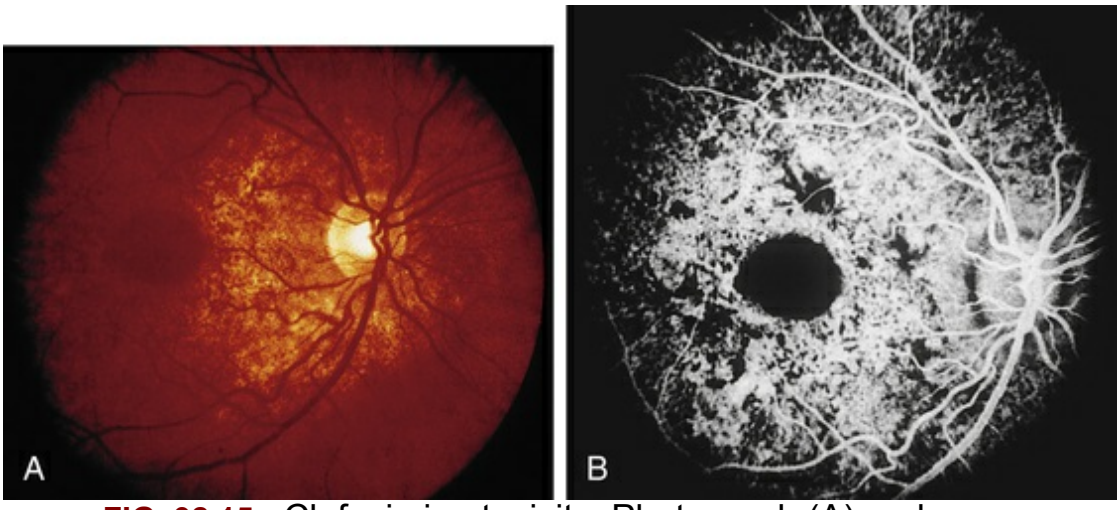

FIG. 92.15 Clofazimine toxicity. Photograph (A) and fluorescein angiogram (B) show moderate macular pigmentary changes in a bull's-eye pattern.

Dideoxyinosine (DDI)

A midperipheral pigmentary retinopathy was initially reported in

three children with AIDS receiving high-dose therapy with the antiviral 2′, 3′-dideoxyinosine.[101] The cases were associated with ERG and EOG changes. More recently, similar phenotypes have been observed in adults, with chorioretinal atrophy anterior to the vascular arcades with corresponding hypoautofluorescence or mottled hyperautofluorescence and hypoautofluorescence (Fig. 92.16). SD-OCT confirms severe chorioretinal atrophy in these regions.[102] The retinal toxicity typically stabilizes after discontinuation of the medication, yet some degree of continued pigment degradation may occur years later

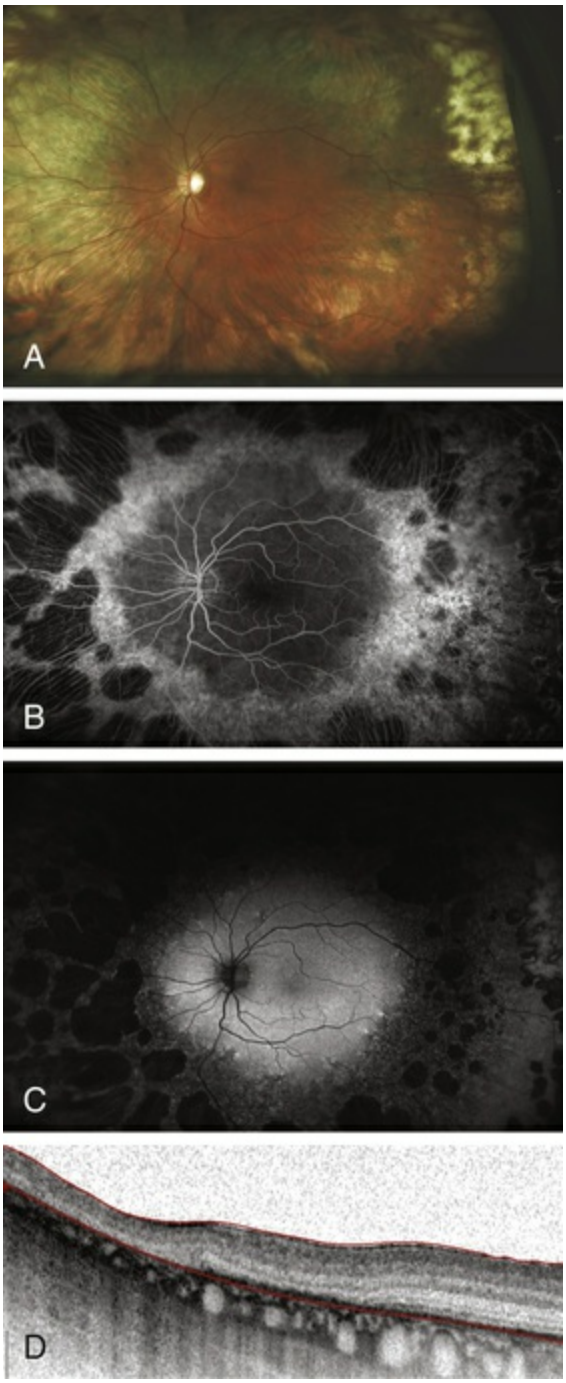

FIG. 92.16 Dideoxyinosine (DDI) toxicity. Fundus photograph (A) showing severe midperipheral retinal pigmentary mottling in an adult having been exposed to DDI in the past. Fluorescein angiogram (B) highlights the retinal pigment epithelium (RPE) changes. Fundus autofluorescence (C) demonstrates patches of peripheral hypoautofluorescence. Optical coherence tomography (D) shows outer retinal and RPE atrophy. (Courtesy of David Sarraf, MD, Los Angeles, CA.)

Deferoxamine

Intravenous and subcutaneous administration of deferoxamine has been used to treat patients who require repeated blood transfusions and subsequently develop complications of iron overload. High-dose intravenous and subcutaneous therapy has produced visual loss, nyctalopia, peripheral and central field loss, and reduced ERG amplitudes and EOG ratios.[103,104] The fundus examination can be normal initially, or there may be a faint graying of the macula.[105] Pigmentary changes in the macula and periphery develop within a few weeks and are particularly highlighted by FA (Fig. 92.17).[106] In some instances, toxicity may present as vitelliform macular lesions.[107] Accumulated material has been shown to deposit within the outer retina or in Bruch's membrane-RPE complex on OCT.[108] Return of visual function occurs with cessation of therapy. Deferoxamine chelates many metals other than iron, and it is possible that the mechanism of toxicity may involve the removal of copper from the RPE.[103] Histopathologic changes occur primarily in the RPE and include loss of microvilli from the apical surface, patchy depigmentation, vacuolation of the cytoplasm, swelling and calcification of mitochondria, and disorganization of the plasma membrane.[109]

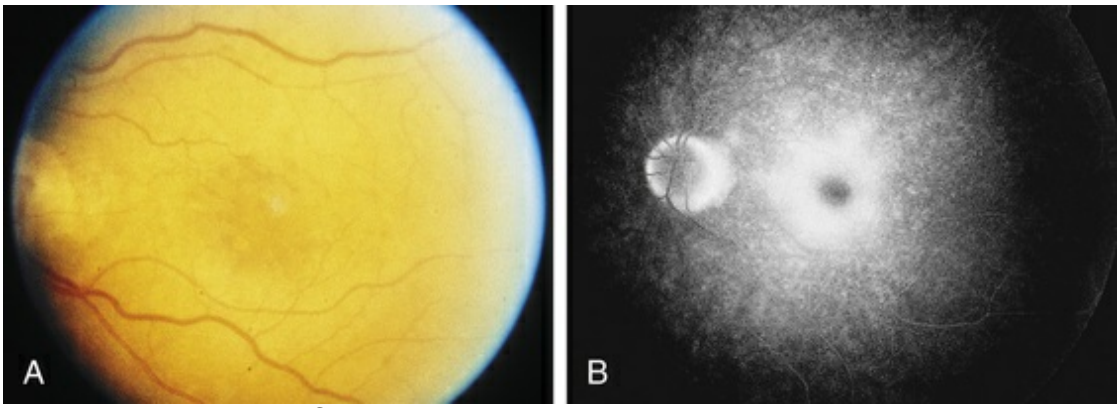

FIG. 92.17 Deferoxamine toxicity. Photograph (A) and fluorescein angiogram (B) show a diffuse pigmentary retinopathy with macular and retinal edema.

Corticosteroid Preparations

The vehicles of several common corticosteroid preparations have been shown to cause retinal necrosis when inadvertently injected into the eye[110,111] (Fig. 92.18). The corticosteroids themselves probably have a minimal toxic effect on the retina.[112] Celestone Soluspan, with its vehicle benzalkonium chloride, and Depo-Medrol, with myristyl gamma-picolinium chloride, caused the most extensive retinal damage in an experimental study comparing several depot steroids.[102] If one of these agents is inadvertently injected, immediate surgical removal should be instituted.

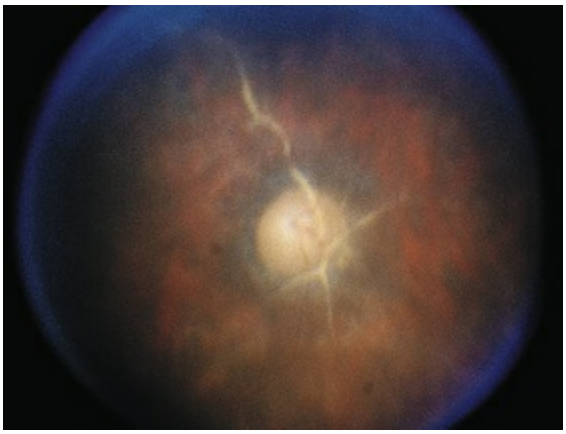

FIG. 92.18 Inadvertent intraocular corticosteroid injection. Photograph shows endstage retinopathy, with sclerotic vessels and diffuse pigmentary changes, after an inadvertent intraocular injection of corticosteroid.

Cisplatin and BCNU (Carmustine)

Cisplatin and BCNU are used for the treatment of malignant gliomas and metastatic breast cancer. Three different types of retinal toxicity have been reported with these agents. One type of change consists of a pigmentary retinopathy of the macula with markedly decreased visual acuity and frequently abnormal electrophysiologic testing. This pigmentary change has been reported after administration of combined intraarterial cisplatin and BCNU and with cisplatin alone for malignant glioma.[113,114] These findings probably are the result of platinum toxicity of the retina. Severe bilateral visual loss was reported after intravenous

cisplatin in a patient that received four times the intended dose for treatment of lymphoma.[115] Later histology showed a splitting of the outer plexiform layer.

A second type of retinopathy has been described and consists of cotton-wool spots, intraretinal hemorrhages, macular exudate, and optic neuropathy with disc swelling. This was reported in the setting of high-dose chemotherapy with cisplatin, cyclophosphamide, carmustine, and autologous bone-marrow transplantation for metastatic breast cancer.[116] The third type of change involves a vascular retinopathy or optic neuropathy, which can include arterial occlusion, vasculitis, and papillitis. This has been seen in approximately 65% of patients receiving intraarterial BCNU alone or combined with cisplatin for malignant glioma.[114] These fundus changes are associated with a profound visual loss that begins about 6 weeks after the start of therapy. Other ocular effects may include orbital pain, chemosis, secondary glaucoma, internal ophthalmoplegia, and cavernous sinus syndrome. Injection of medication above the ophthalmic artery can still result in toxicity.[107] The visual loss usually is progressive, and no treatment is known.

Miscellaneous Agents

Overdose of potassium iodate, an iodized salt used for iodine supplementation in areas endemic for goiter, has been shown to cause profound visual loss and extensive fundus pigmentary abnormalities.[108] FA reveals RPE window defects and ERG and VEP testing show marked impairment of retinal function. Visual acuity may improve slowly over several months. There have been two cases of pigmentary retinopathy with diminished ERG amplitudes reported after administration of denileukin diftitox.[117]

Vascular Damage and/or Occlusion

Quinine Sulfate

See above, in the section Disruption of the retina and retinal pigment epithelium.

Cisplatin and BCNU (Carmustine)

See above, in the section Disruption of the retina and retinal pigment epithelium.

Talc

A characteristic retinopathy consisting of small, white, glistening crystals concentrated in the end arterioles of the posterior pole has been described in intravenous drug abusers[118–120] (Fig. 92.19). These addicts crush oral medications such as methylphenidate hydrochloride (Ritalin) or methadone HCl and then create an aqueous suspension by adding water and heating the mixture. The solution is subsequently drawn up into a syringe, with occasional attempts at filtering the mixture with cotton fibers, gauze, or cigarette filters. These oral medications contain talc (hydrous magnesium silicate) as inert filler material; after intravenous administration, talc particles embolize to the pulmonary vasculature, where the larger particles are trapped. After repeated injections over months to years, collateral vasculature develops, allowing the particles to enter the systemic circulation and embolize to other organs, including the eye. Even before shunt development, particles smaller than 7 μm can traverse the pulmonary capillary bed and enter the retinal circulation.[121]

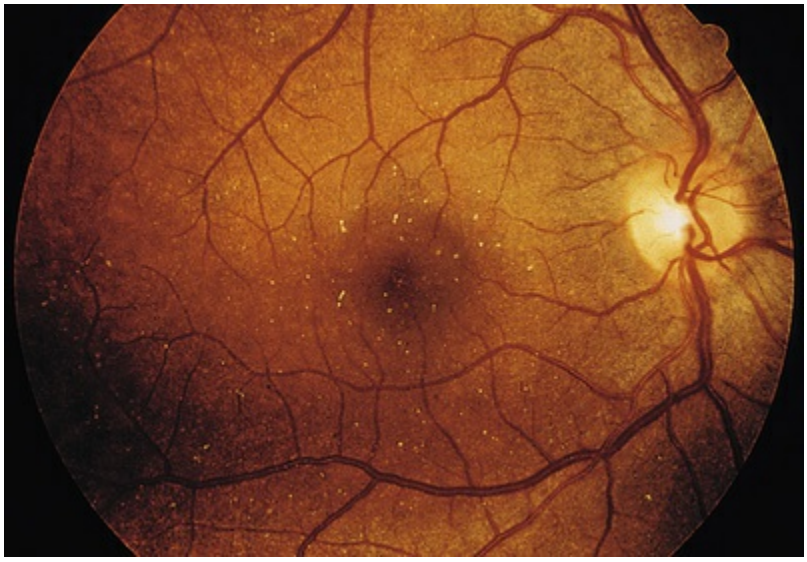

FIG. 92.19 Talc retinopathy. Characteristic perifoveal

yellow-white glistening crystals.

Once a large number of talc particles lodge in the small arterioles of the retinal vasculature, a characteristic picture of an ischemic retinopathy begins to develop. Capillary nonperfusion, microaneurysm formation, cotton-wool spots, and venous loops can all be seen. In severe cases optic disc and peripheral neovascularization and vitreous hemorrhage can develop[122–124] (Fig. 92.20). An experimental model of talc retinopathy in monkeys has demonstrated with light and electron microscopic techniques that the vascular abnormalities induced are very similar to other ischemic retinopathies seen in humans, such as sickle cell and hypertensive retinopathy.[125–127]

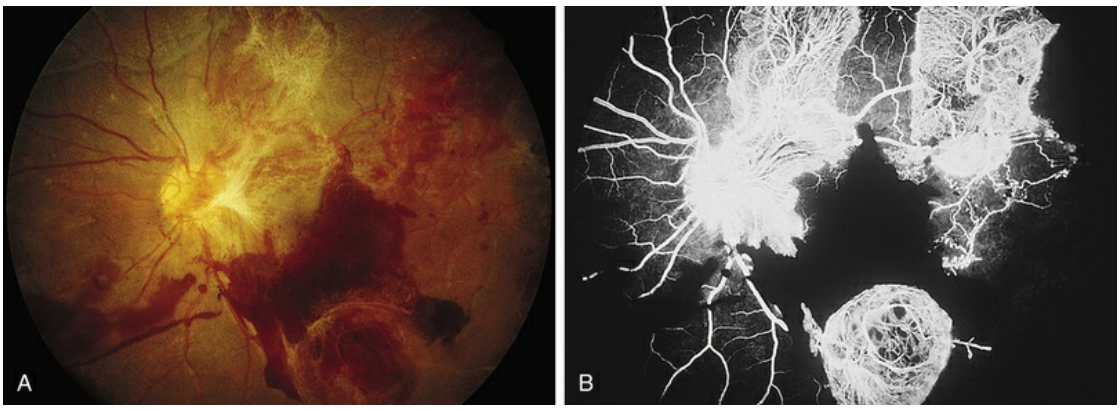

FIG. 92.20 Ischemic talc retinopathy. Photograph (A) and fluorescein angiogram (B) show widespread capillary dropout, neovascularization, and preretinal hemorrhage.

Once talc retinopathy is diagnosed, an attempt at educating the patient as to the cause of the disorder is indicated. Treatment of neovascularization and vitreous hemorrhage should be undertaken using laser photocoagulation and pars plana vitrectomy if necessary in a manner similar to that used for sickle cell or proliferative diabetic retinopathy.

Oral Contraceptives

Oral contraceptives have been implicated in some cases of central retinal vein occlusion (CRVO), retinal and cilioretinal artery

obstruction, and retinal edema occurring in young women.[128–134] The synthetic estrogen and progesterone contained in contraceptive pills are thought to adversely affect coagulation factors and induce a hypercoagulable state leading to thromboembolic complications. Most of the studies reporting ocular complications are from the 1960s and 1970s, when the estrogen concentrations used in "the pill" were much higher (Fig. 92.21). Some recent prospective studies have failed to show an increased incidence of ocular complications with the drug, though one large study showed an increase in "retinal vascular findings".[135–137]

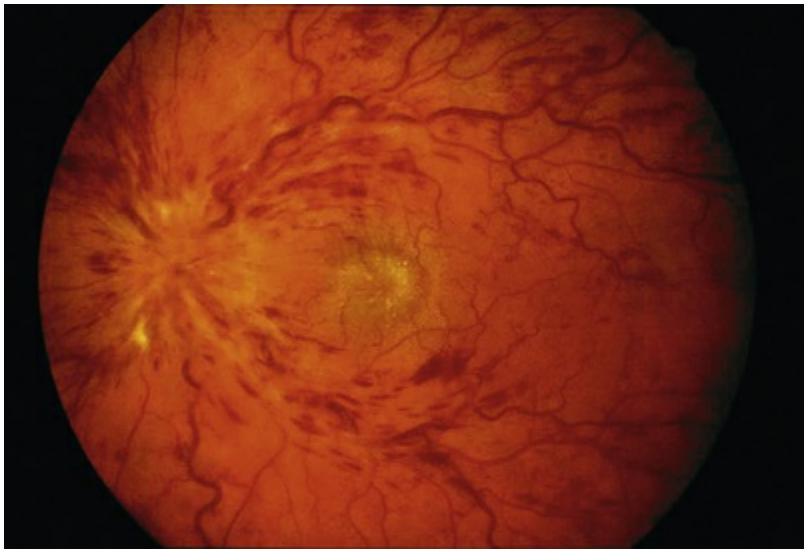

FIG. 92.21 Nonischemic central retinal vein occlusion (CRVO) in a 40-year-old hypertensive female on oral contraceptives. Upon stopping the oral contraceptives, the CRVO resolved without treatment.

Aminoglycoside Antibiotics (Intraocular)

Retinal toxicity from aminoglycoside antibiotics has been reported after inadvertent intraocular injection of massive doses, intravitreal injection for bacterial endophthalmitis, prophylactic intravitreal injection after pars plana vitrectomy, prophylactic subconjunctival injections after routine ocular surgery, and with the use of small amounts in the infusion fluid during cataract extraction.[138–141] Gentamicin is the most toxic antibiotic in the aminoglycoside

family, followed by tobramycin and amikacin.[142] Massive doses result in early superficial and intraretinal hemorrhages, retinal edema, cotton-wool patches, arteriolar narrowing, and venous beading[141] (Fig. 92.22). Fluorescein angiography reveals severe vascular nonperfusion in the acute stages. Visual loss is profound, and late rubeosis iridis, neovascular glaucoma, pigmentary retinopathy, and optic atrophy are common. Intravitreal injection of smaller doses thought to be safe for the eye (100–400 μg) can still cause toxicity with less severe fundus changes.[139–141] The major preservatives found in injectable gentamicin (methylparaben, propylparaben, sodium bisulfite, and edetate disodium) likely play an additive role in its ocular toxicity, along with a quite acidic formulation.

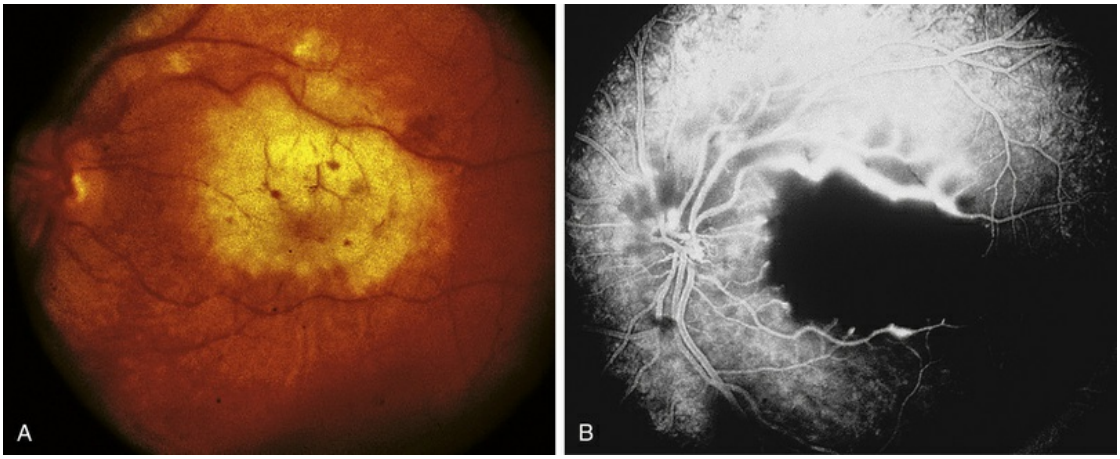

FIG. 92.22 Intraocular gentamicin injection. Photograph (A) and fluorescein angiogram (B) show acute macular necrosis, with virtually complete cessation of blood flow where presumably the medication came in contact with the retina while the patient was in a supine position during the early postoperative timeframe.

A number of factors appear to affect the extent of toxicity observed with similar doses of these medications. Peyman found that retinal toxicity could be enhanced with an intravitreal injection directed at the posterior pole with the bevel of the needle pointed toward the retina, and Zachary and Forster demonstrated that an increased rate of injection during intraocular administration could

also increase the retinal toxicity observed.[143,144] One investigator stated that eyes that have undergone a previous pars plana vitrectomy are at greater risk for gentamicin toxicity, but an experimental model has shown no difference between eyes that had cataract extraction alone compared with those that underwent lensectomy and vitrectomy.[145,146] Finally, increased ocular pigmentation protects the rabbit retina from aminoglycoside toxicity and may explain some of the wide variability seen with intraocular exposure in humans.[147,148]

Although clinical aminoglycoside toxicity appears to affect the retinal vasculature primarily, pathologic studies have revealed that gentamicin in small doses causes the formation of abnormal lamellar lysosomal inclusions in the RPE, and larger doses cause increasing amounts of retinal necrosis, first of the outer then inner segments.[107,142,149,150] Histologically, vessel closure appears to result from granulocytic plugging.

Prevention of aminoglycoside toxicity can be accomplished by abandoning the use of these medications as routine prophylaxis following intraocular surgery, eliminating them from intraocular infusion fluids used in vitrectomy and cataract surgery, and using alternative medications for the treatment of bacterial endophthalmitis. Animal studies have demonstrated that thinned sclera alone without perforation can result in markedly elevated intraocular gentamicin levels after subconjunctival injection.[151] If inadvertent intraocular injection does occur, immediate pars plana vitrectomy with posterior segment lavage should be performed.[152,153] Since there is some evidence that gravity plays a role in the predilection of gentamicin-induced toxicity for the macula, the patient should be placed upright as soon as possible after surgery.[154]

Vancomycin (Intracameral)

Intracameral vancomycin injection has increased in popularity for endophthalmitis prophylaxis following cataract extraction.[155,156] To date, several case series of severe hemorrhagic occlusive vasculitis have been published (Fig. 92.23).[157–159] The toxicity appears to be immune-mediated and manifests a week or so following the

cataract surgery. With the delay in development of the occlusive vasculitis, several bilateral cases have been described, especially when the two eyes are operated on in close time proximity. Despite aggressive treatment including high dose corticosteroids, antiviral medication, and pars plana vitrectomy, visual outcomes are often very poor.[158] Clinicians must also monitor closely for neovascular glaucoma and treat as necessary. Additionally, some authors have suggested a potentially increased incidence of cystoid macular edema has been found in the setting of intracameral vancomycin administration.[160]

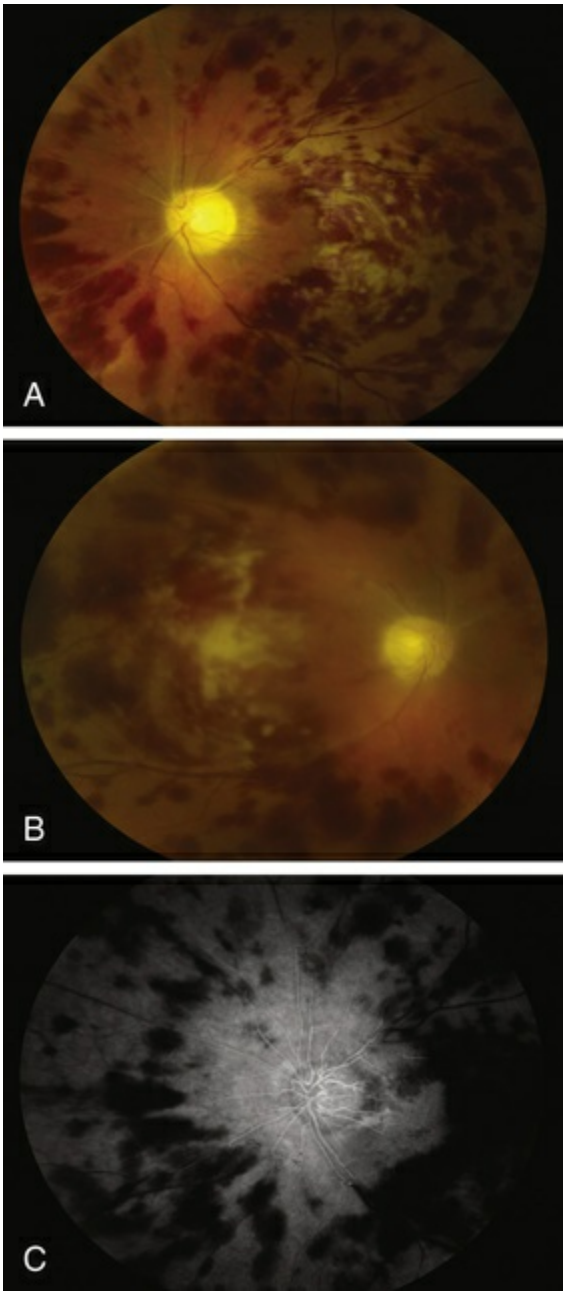

FIG. 92.23 Vancomycin toxicity. Fundus photograph of the left (A) and right (B) eye demonstrating a severe bilateral hemorrhagic occlusive retinal vasculitis following cataract extraction with intracameral injection of vancomycin. Fluorescein angiogram (C) exhibits extensive nonperfusion. (Courtesy of Stephen Russell, MD, Iowa City, IA.)

Interferon

Interferon-α is used to treat Kaposi sarcoma, hemangiomas of

infancy, chronic hepatitis C, melanoma, renal cell carcinoma and in chemotherapy protocols for leukemia, lymphoma, and hemangiomatosis. Interferon therapy has been associated with the development of multiple cotton-wool spots associated with retinal hemorrhages[161–163] (Fig. 92.24). Optic disc edema, branch arterial and venous occlusion, central retinal venous obstruction, anterior ischemic optic neuropathy, and cystoid macular edema have been reported with the more severe findings observed in patients receiving high-dose therapy.[164–168] Visual acuity usually is not affected if the fundus findings are limited to cotton-wool spots and intraretinal hemorrhage. Changes are noted within the first 4–8 weeks of therapy and are seen more frequently in diabetic and hypertensive patients[169] (Fig. 92.25).

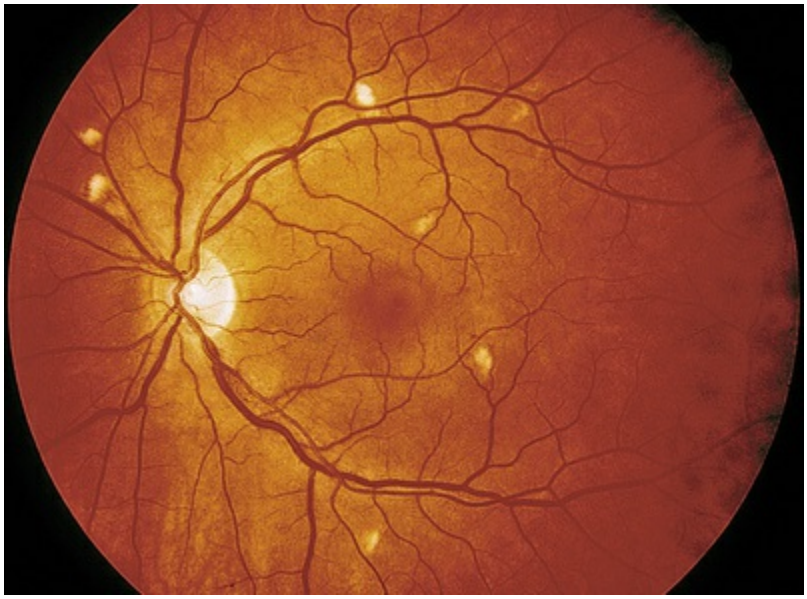

FIG. 92.24 Interferon retinopathy, consisting primarily of multiple cotton-wool spots dispersed throughout the posterior pole. The findings resolved following cessation of therapy.

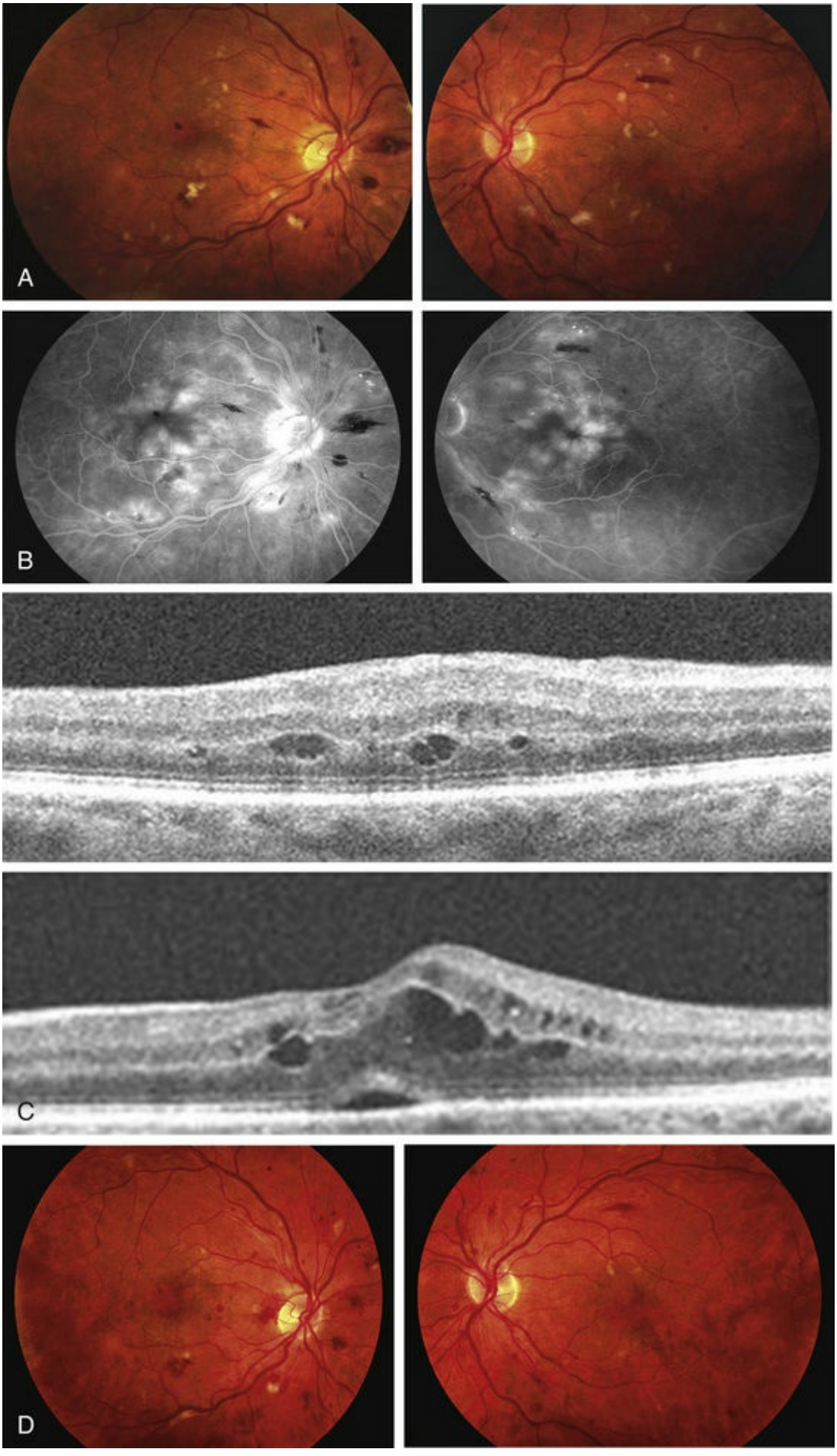
A
B
C
D

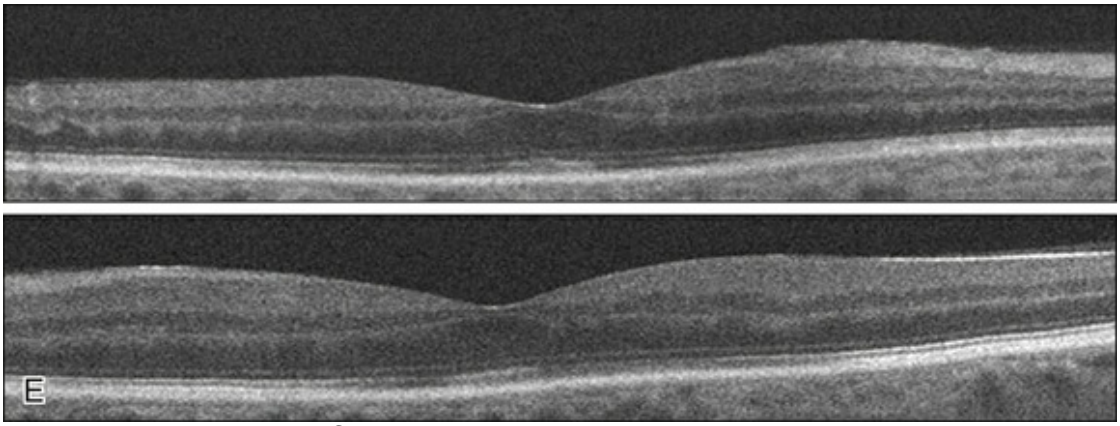

FIG. 92.25 Interferon microangiopathy. Photograph (A) and fluorescein angiogram (B) showing multiple cotton-wool spots and microangiopathy in a patient being treated for hepatitis C. Spectral domain optical coherence tomography (SD-OCT) (C) documents mild cystoid macular edema. Once the interferon was discontinued, photograph (D), taken one month later, documents significant resolution of the cotton-wool spots.SD-OCT (E) shows resolution of the cystoid macular edema. (Courtesy of Joseph Maguire, MD, Philadelphia, PA.)

Intravitreal injection of interferon-α-2b is well tolerated in the rabbit eye up to dosages of 1 million units; 2 million units causes a vitreous haze, and intraretinal hemorrhages.[170] Interferon toxicity may be caused by an increase in immune complex deposition and activated complement C5a with leukocyte infiltration. EOG testing may become abnormal in early toxicity.[171]

Miscellaneous Agents

Ergot alkaloids in higher than recommended doses have been reported to cause retinal vasoconstriction,[172,173] and over-the-counter phenylpropanolamine used in appetite suppressants and decongestants has been implicated in one case of central retinal vein occlusion.[174]

Gemcitabine is a chemotherapeutic agent used for non-small-cell lung carcinoma, breast, ovarian, and pancreatic cancers. It has been associated with one case of Purtscher-like retinopathy with vascular nonperfusion[175] (Fig. 92.26).

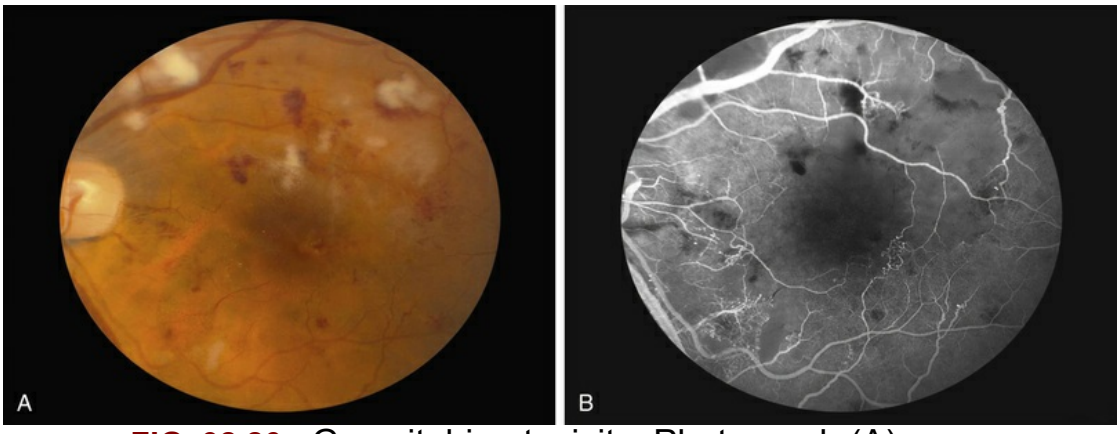

FIG. 92.26 Gemcitabine toxicity. Photograph (A) documents multiple cotton-wool spots, while the fluorescein angiogram (B) shows extensive capillary nonperfusion in a patient being treated for lung carcinoma.

Cystoid Macular Edema

Epinephrine (Topical)

The use of epinephrine compounds in glaucoma has decreased with the advent of newer, more efficacious agents. Topical epinephrine can cause macular edema in aphakic eyes, indistinguishable clinically and angiographically from postoperative aphakic cystoid macular edema (CME). In the largest controlled study, 28% of aphakic eyes treated with epinephrine and 13% of untreated aphakic eyes had macular edema, a difference that was statistically significant.[176] Most cases of CME resolve with cessation of epinephrine usage. This medication should be avoided in the treatment of the glaucomatous aphakic and pseudophakic eyes.

Nicotinic Acid

High doses of niacin have been used to reduce serum lipid and cholesterol levels. Better-tolerated HMG-CoA reductase inhibitor agents have curtailed their utilization, though there has been a recent resurgence in their use in both monotherapy and combination therapy with statins. At doses greater than 1.5 g/day, a minority of patients will report blurred central vision, sometimes

associated with a paracentral scotoma or metamorphopsia.[177] FA fails to demonstrate vascular leakage despite the typical clinical appearance of CME[178,179] (Fig. 92.27). This has led to speculation of a direct toxic effect on Müller cells, resulting in intracellular edema.[180] OCT reveals cystoid spaces in the inner nuclear and outer plexiform layers.[181,182] With cessation of treatment, the CME resolves, and vision generally returns to normal. Given the rarity of this condition, only patients who are taking high-dose niacin and who have visual symptoms should be evaluated.

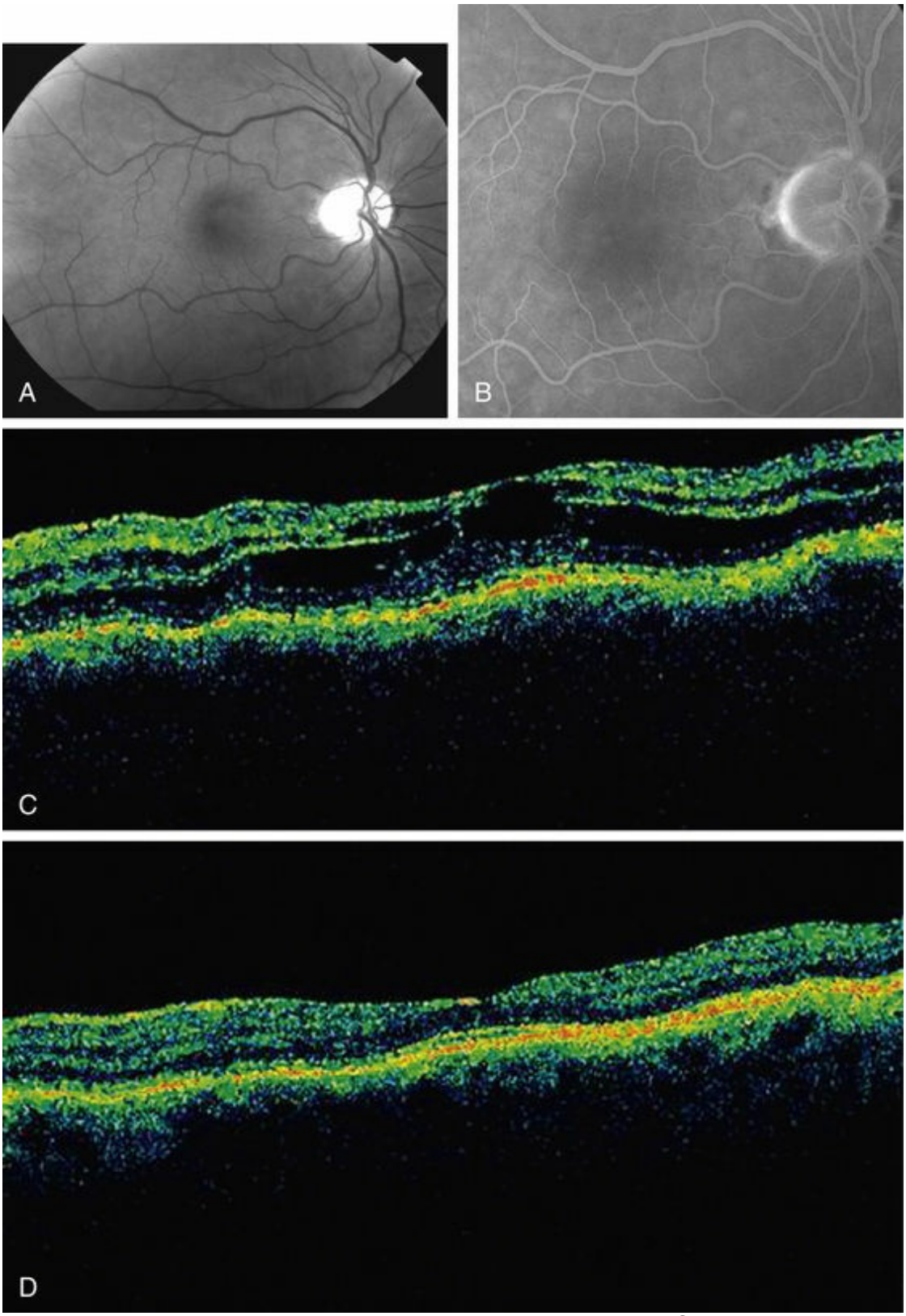

FIG. 92.27 Nicotinic acid maculopathy. Red-free photograph (A) shows blunted foveal reflex, while the fluorescein angiogram (B) shows minimal late leakage. A time domain optical coherence tomography (OCT) (C) shows mild macular edema. The nicotinic acid was

discontinued, and two weeks later, the OCT (D) returned to normal. The findings were bilateral. (Courtesy of Lawrence A Yannuzzi, MD, New York City, NY.)

Latanoprost (Topical)

Latanoprost is a prostaglandin analogue that is used for the control of a variety of forms of glaucoma. Although initial human and animal studies did not show an association between latanoprost and CME, recent case reports and studies have documented that approximately 2–5% of susceptible patients with glaucoma may develop CME and anterior uveitis, which resolves after discontinuation of the drug[183–190] (Fig. 92.28). This may be caused by the preservative used in the drug formulation.[191] Patients with CME who are taking latanoprost should undergo a trial off the medication before initiating further therapy for the edema. High-risk CME patients, such as those with a history of recent surgery or uveitis, should be managed with other agents.

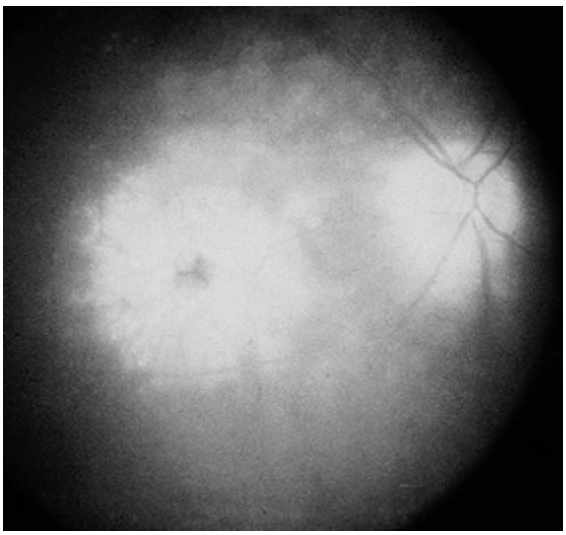

FIG. 92.28 Latanoprost-associated cystoid macular edema. Angiogram shows characteristic fluorescein filling of the cystic spaces.

Paclitaxel/Docetaxel

Paclitaxel and docetaxel are similar antimicrotubule agents that are used for treatment of breast, lung, and prostate cancer. They have both been associated with angiographically negative CME (Fig. 92.29). The edema appears to respond on occasion to cessation of the taxel agent, or to treatment with topical or systemic acetazolamide, and/or intravitreal anti-VEGF therapy.[192,193]

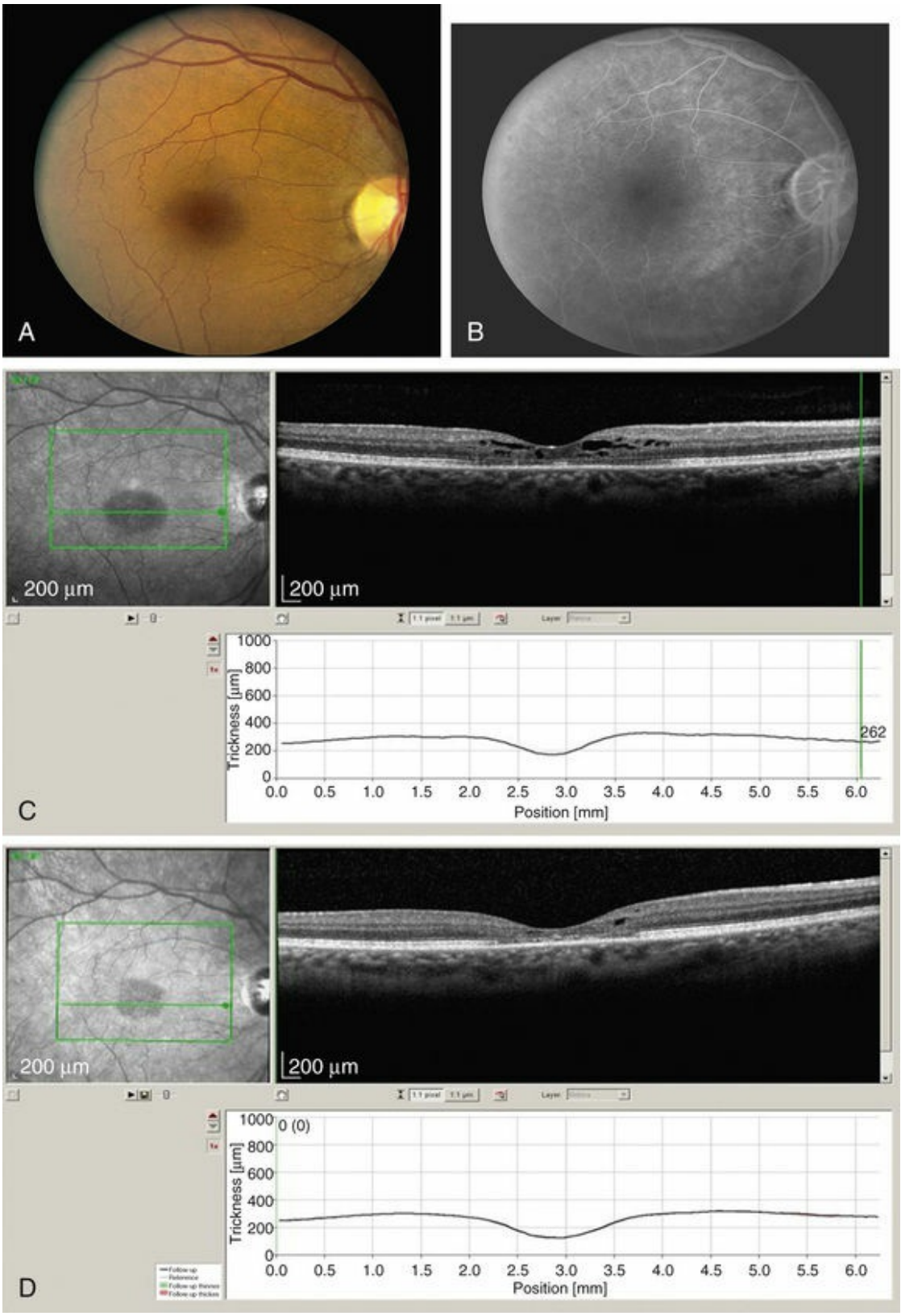

FIG. 92.29 Paclitaxel maculopathy. Photograph (A) showing a blunted foveal reflex in a patient on paclitaxel for treatment of metastatic breast carcinoma. The fluorescein angiogram (B) shows minimal late leakage of dye, though spectral domain optical

coherence tomography (SD-OCT) (C) shows intraretinal cystic spaces. Upon treatment with topical carbonic anhydrase inhibitors, the cystic spaces on SD-OCT (D) gradually resolved. The findings were bilateral.

Fingolimod

Fingolimod (Gilenya) is an immunomodulatory agent targeting the sphingosine-1-phosphate receptor for the treatment of multiple sclerosis. This medication has been implicated in the development of cystoid macular edema, usually within 4 months of treatment initiation. The incidence of macular edema ranged from 0.3% to 1.2%, depending on the dosage. OCT localizes the cysts to the inner nuclear layer, and to a lesser extent, the outer nuclear layer. There may be associated perifoveal leakage on FA. Most cases resolve with discontinuation of the drug and administration of topical antiinflammatory agents.[194]

Retinal Folds

Sulfa Antibiotics, Acetazolamide, Chlorthalidone, Disothiazide, Ethoxzolamide, Hydrochlorothiazide, Metronidazole, Sulfonamide, Topiramate, Triamterene

Several medications, most with a structure similar to sulfanilamide, as those listed above, can cause a syndrome of transient acute myopia, retinal folds, and anterior chamber shallowing. This is thought to occur as a result of ciliary body swelling, choroidal effusion, or both, or with swelling of the lens itself with subsequent forward rotation of the lens–iris diaphragm.[195–204] Retinal folds in the macula are typically seen in young patients with this syndrome, but an FA does not reveal retinal leakage (Figs. 92.30 and 92.31). The folds presumably develop as a result of vitreous traction on the macula that is caused by the forward shift of the lens and iris

diaphragm. The folds typically resolve following discontinuation of the offending medication. It should be noted, however, that on occasion, topiramate may lead to development of angle closure glaucoma.

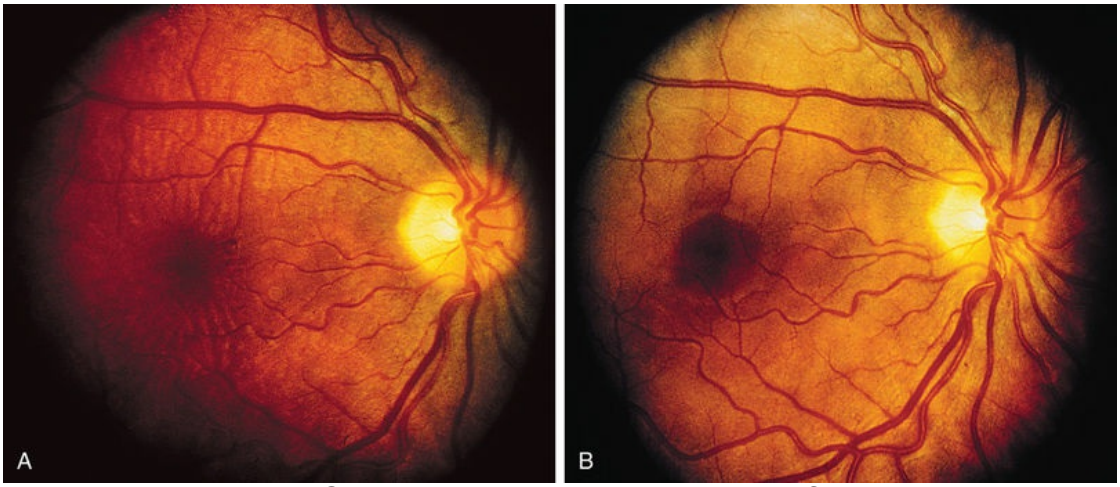

FIG. 92.30 Chlorthalidone-induced retinal folds. Photograph (A) shows perifoveal retinal folds associated with chlorthalidone therapy, which resolve within 2 weeks following discontinuation of the drug (B).

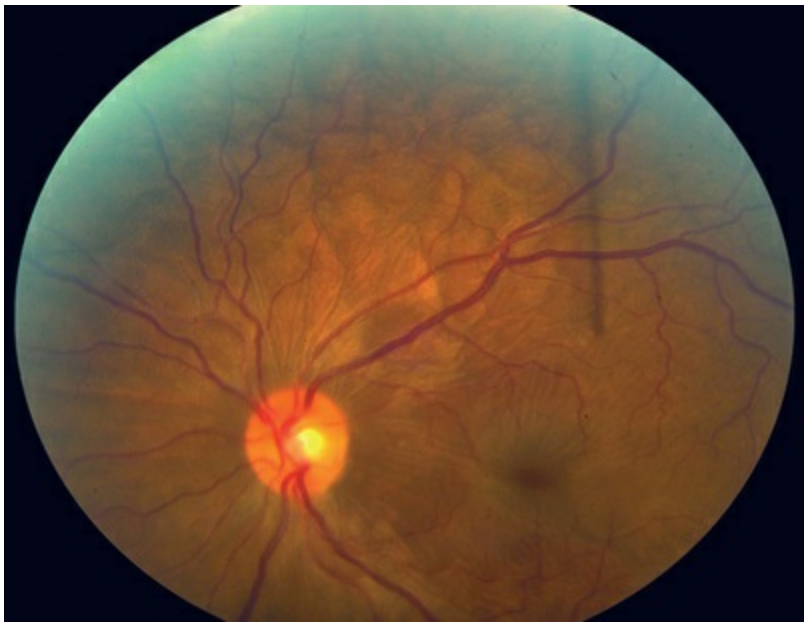

FIG. 92.31 Topiramate-induced retinal folds. Fundus photograph demonstrating macular and extramacular

striae in a patient on topiramate.

Crystalline Retinopathy

Tamoxifen

Tamoxifen is an antiestrogen agent used in the treatment of estrogen-receptor-positive tumors such as advanced breast carcinoma (and in some estrogen-receptor-negative tumors such as hepatocellular carcinoma) and as adjuvant therapy after surgical resection of early disease. Retinal toxicity consisting of decreased visual acuity and color vision with white intraretinal crystalline deposits, macular edema, and punctate retinal pigmentary changes can occur.[205] The intraretinal deposits appear to reside in the inner retina and are most numerous in paramacular areas (Fig. 92.32). Early reports involved patients who had received high doses (60–100 mg/day, total dosage >100 g) of the drug over 1 year.[206] More recent studies have demonstrated that chronic low-dose administration (10–20 mg/day) with as little as 7.7 g total, also can cause ocular toxicity.[207–210] Even asymptomatic patients may exhibit intraretinal crystalline formation.[211] Visual function and edema improve after discontinuation of the drug, but the refractile deposits remain.

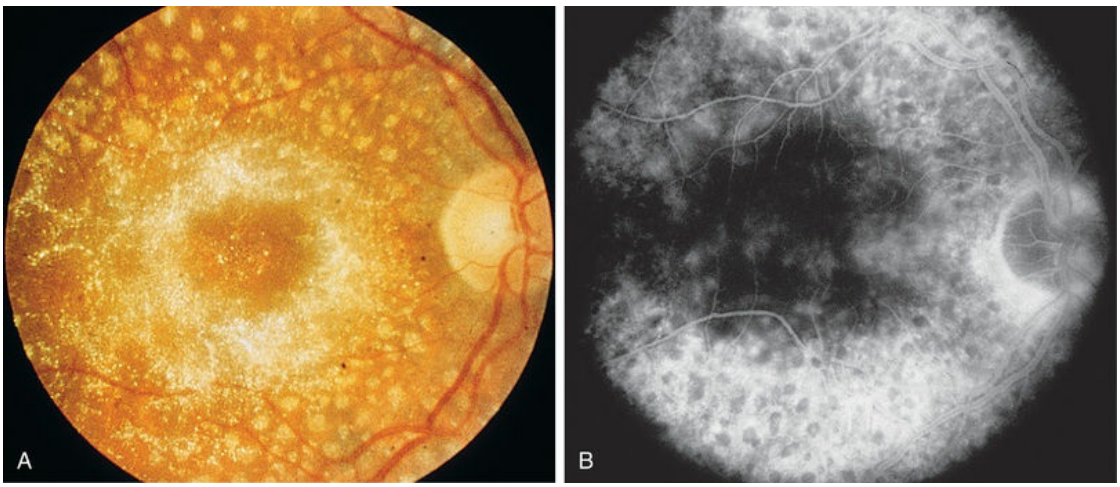

FIG. 92.32 Tamoxifen crystalline retinopathy. Characteristic yellow–white macular crystals are seen in a perifoveal distribution. The crystals were not felt to

be of visual significance.

There has been a recent upturn in cases of tamoxifen-induced retinal crystals, as patients with aggressive glioblastoma are now being treated with 100–200 mg of tamoxifen on a daily basis (Fig. 92.33). Concurrent CME may be treated with intravitreal anti-VEGF therapy.

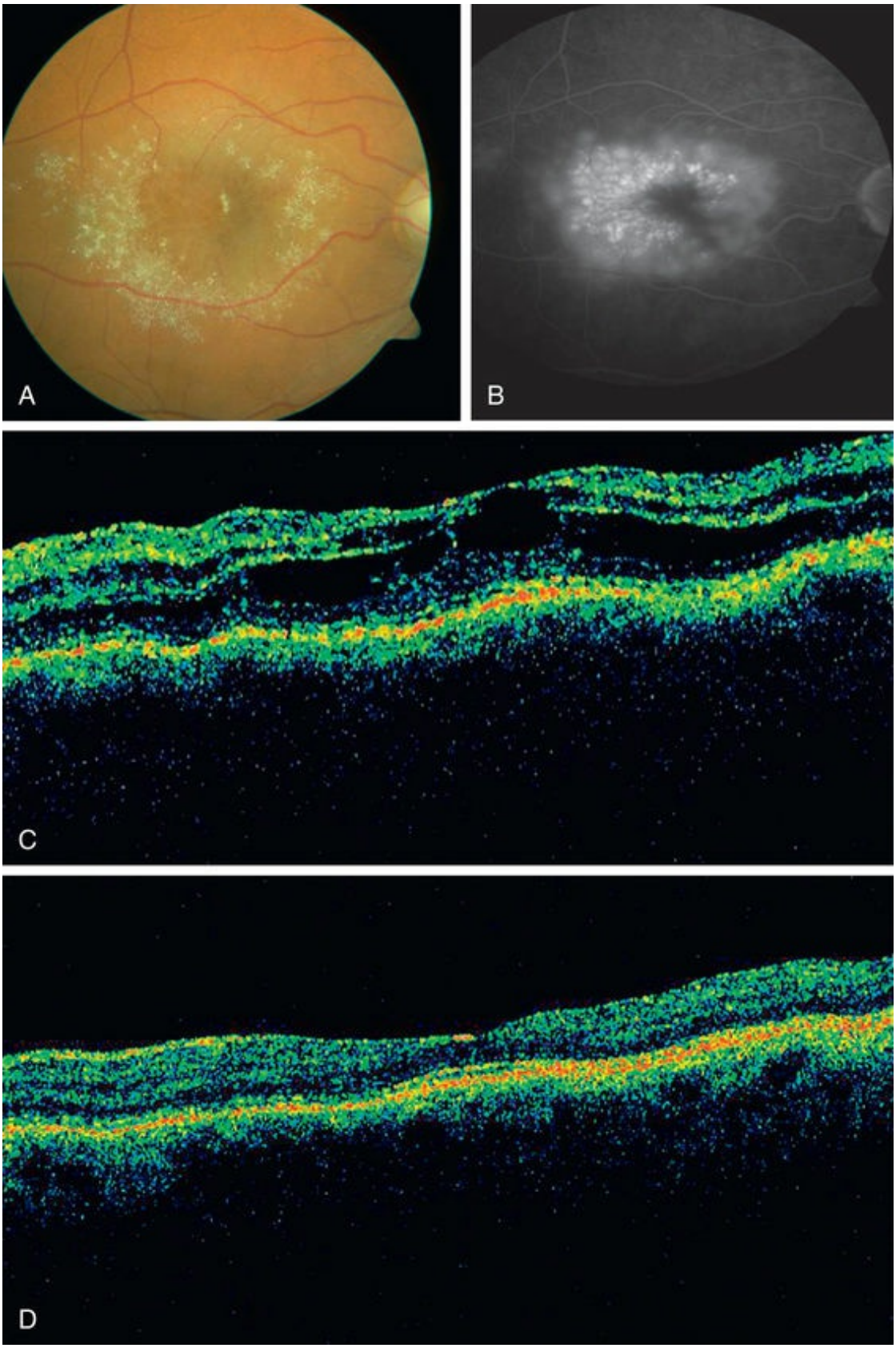

FIG. 92.33 Tamoxifen crystalline retinopathy in a patient with advanced glioblastoma being treated with high-dose tamoxifen. Photograph (A) shows perifoveal crystals, while the fluorescein angiogram (B) shows

diffuse cystoid macular edema (CME). Time domain optical coherence tomography (OCT) (C) confirms the findings of diffuse CME. A follow-up OCT (D) several months later, following administration of intravitreal bevacizumab, shows resolution of the CME. The findings were bilateral. (Courtesy of David Sarraf, MD, Los Angeles, CA.)

FA demonstrates late focal staining in the macula consistent with CME. Decreased photopic and scotopic a- and b-wave amplitude is noted on ERG testing.[212] Light microscopy reveals lesions confined to the nerve fiber and inner plexiform layers, which stain positive for glycosaminoglycans. Small (3–10 μm) intracellular and large (30–35 μm) extracellular lesions within axons are noted on electron microscopy.[206] The lesions appear to represent products of axonal degeneration similar to corpora amylacea. Experimentally, tamoxifen inhibits glutamate uptake by RPE cells.[213] OCT findings in lower-dose therapy interestingly do not show an increase in macular edema, but rather a foveal cyst with disruption of the photoreceptor line, while high-dose therapy can show CME.[214–216]

Decreased vision with bilateral optic disc swelling and retinal hemorrhages has been reported in a patient just 3 weeks after commencement of therapy with tamoxifen. These findings resolved completely after the drug was stopped.[217] It is unclear whether the findings in this patient were related to the more commonly seen toxic effects. Optic neuropathy with tamoxifen has been reported as well.[218] With current low-dose therapy (10–20 mg/day), retinal lesions are rare, and routine examination of asymptomatic patients is not indicated.[211,219] If a patient taking tamoxifen is noted to have intraretinal crystals, FA should be performed, primarily to rule out juxtafoveal telangiectasis, which can have similar-appearing lesions.[220] With confirmed evidence of toxicity causing a visual disturbance, the medication should be stopped. In asymptomatic patients who truly need the medication for treatment of their systemic cancer, continuation of the medication is reasonable with close monitoring of the ocular findings. For persistent macular edema, which has been noted after prolonged high-dose therapy seen following cessation of the drug, antivascular endothelial growth factor (anti-VEGF) injection may be beneficial.[221]

Canthaxanthin

Canthaxanthin is a naturally occurring carotenoid. It is used as a food-coloring agent, for skin pigmentation in the treatment of vitiligo, and for the treatment of photosensitivity disorders such as erythropoietic protoporphyria, psoriasis, and photosensitive eczema. It also has been used over-the-counter in high doses as an oral tanning agent. Many reports have described a characteristic ring-shaped deposition of yellow-orange crystals in the superficial retina with high doses (usually a total dose greater than 19 g over 2 years)[222–224] (Fig. 92.34). The crystals appear more prominently in eyes with preexisting retinal disease and with concurrent use of beta-carotene.[222,225]

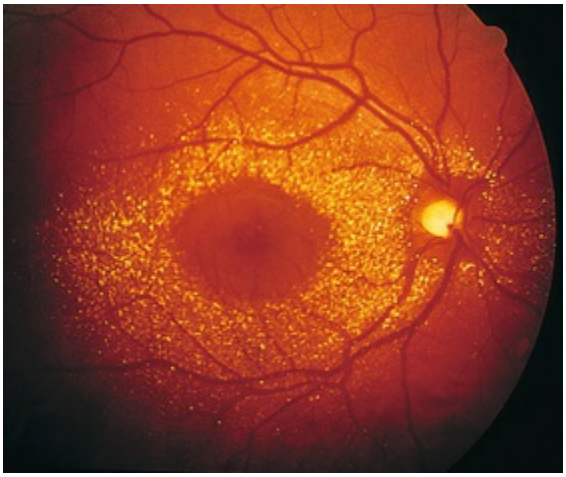

FIG. 92.34 Canthaxanthin retinopathy. Prominent perifoveal punctate yellow deposits in a doughnut-shaped ring surrounding the macula.

Patients usually are asymptomatic, and FA usually is normal. There have been published reports of both normal and abnormal ERG, EOG, dark adaptation, and static threshold perimetry.[226–229] Although only clinically evident in the macula, the lipid-soluble crystals are found pathologically in the entire inner retina and ciliary body.[230] The crystals are, as would be expected, larger and more numerous surrounding the fovea. Canthaxanthin crystals are localized to the spongy degeneration of the inner neuropil and are associated with atrophy of the Müller cells. Interestingly, a single case report showed OCT localization of crystals to the outer

plexiform layer.[231] An experimental model of canthaxanthin-induced retinopathy also has demonstrated RPE cell vacuolization and disruption of phagolysosomes.[232]

With discontinuation of treatment, deposits may slowly clear over many years.[233,234] This slow reversal correlates with the detection of high plasma levels of canthaxanthin many months after discontinuation of the drug. Rarely, a fundus picture identical to canthaxanthin maculopathy can be seen in patients who have no known history of extradietary canthaxanthin.[235] A high dietary intake concurrent with preexisting retinal disease is thought to partially explain this phenomenon.

Methoxyflurane

Methoxyflurane is an inhalational anesthetic, which, if used for extended periods, especially in patients with renal insufficiency, causes irreversible renal failure as a result of deposition of calcium oxalate crystals in the kidney. These crystals are also deposited elsewhere throughout the body. Fundus examination of these patients reveals numerous yellow-white punctate lesions in the posterior pole and periarterially[236,237] (Fig. 92.35). The deposits are located histologically in both the RPE and inner retina.[238,239]

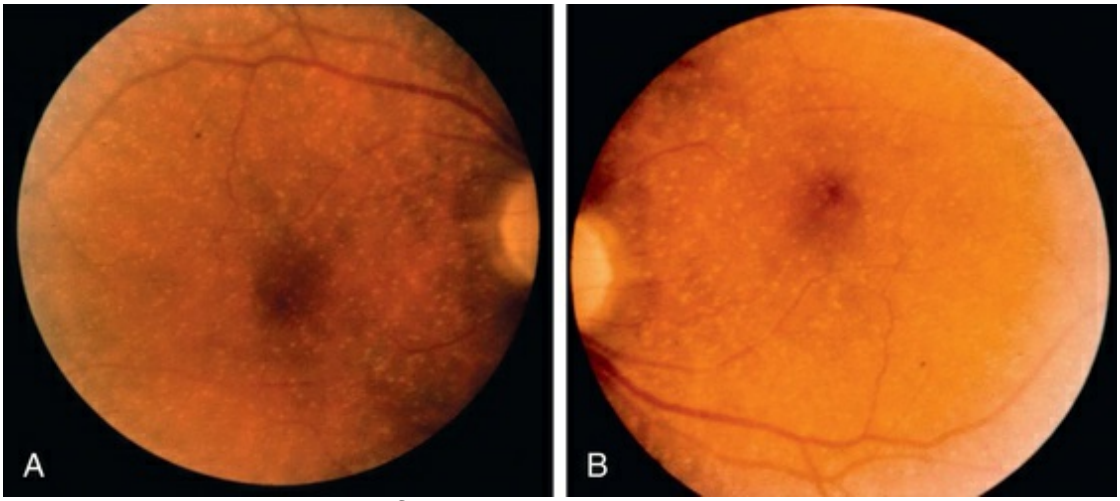

FIG. 92.35 Methoxyflurane crystals. (A,B) Photographs document intraretinal crystals dispersed throughout the posterior pole in a patient subjected to methoxyflurane anesthesia who developed postoperative renal failure.

Talc

See above section Vascular damage and/or occlusion.

Miscellaneous Agents

A single case of crystalline retinopathy following 19 years of nitrofurantoin (Macrodantin) use has been reported.[240] Three cases of rapid visual loss with fludarabine phosphate, a nucleoside analog, during treatment for SLE or metastatic melanoma were reported, with two of the cases exhibiting deep yellow retinal flecks.[241] Three patients receiving long-term ritonavir therapy as part of a highly active antiretroviral therapy regimen were reported to have a retinal pigment epitheliopathy, parafoveal telangiectasis, and intraretinal crystal deposits.[242]

Uveitis

Rifabutin

Rifabutin is a semisynthetic rifamycin antibiotic that is used for the treatment and prevention of disseminated *Mycobacterium avium*-complex (MAC) infection in patients with and without AIDS.[243–251] A small percentage of patients treated with higher doses of rifabutin (>450 mg/day) for systemic MAC infection, or lower doses (300 mg/day) for prophylaxis against MAC, can develop uveitis.[252] The uveitis usually is bilateral and can be severe enough to cause a hypopyon that simulates infectious endophthalmitis.[253] It can occur from 2 weeks to 14 months after initiation of the drug.[251] Concomitant use of clarithromycin and/or fluconazole (or itraconazole), especially when lower doses of rifabutin are used, greatly increases the chance of a uveitic episode.[254] Both systemic fluconazole and clarithromycin elevate rifabutin levels by inhibiting metabolism of the drug via the hepatic microsomal cytochrome P-450.[249] Although most cases have reported mainly an anterior uveitis and corneal endothelial deposits, posterior vitritis and retinal vasculitis have been described as well.[243,255]

Rifabutin-associated uveitis can be treated successfully with

topical corticosteroids or by decreasing or discontinuing the medication. Long-term use may result in ERG abnormalities.[256] Patients without systemic MAC infection who are taking rifabutin for prophylaxis and also are taking fluconazole or clarithromycin should be warned about the potential for uveitis and counseled as to its signs and symptoms.

Cidofovir

Cidofovir, also known as HPMPC, is a nucleotide analogue that inhibits viral DNA polymerase and is used for the treatment of cytomegalovirus (CMV) retinitis.[257–266] Cidofovir therapy, with both intravenous and intravitreous (20 μg) routes of administration, has been associated with an anterior uveitis, hypotony, and visual loss.[267] These complications can be treated and sometimes prevented with the use of topical corticosteroids, cycloplegics, and oral probenecid. Cidofovir has been shown experimentally and clinically to cause a direct toxic effect to the ciliary body, with a resulting iritis and intraocular pressure decrease.[257,265] Although a 10-μg intravitreous dose had fewer side effects, it is also much less effective against CMV retinitis.[266] Investigations continue to try to determine the optimal dose and route of administration of cidofovir.

Latanoprost

See the drugs listed under the section Cystoid macular edema.

Miscellaneous

Cardiac Glycosides

Cardiac glycosides such as digoxin are used in the treatment of chronic heart failure and as antiarrhythmic agents. Although these drugs do not cause a characteristic fundus abnormality, ocular symptoms including blurred vision, scintillating scotomas, and xanthopsia (yellowing of vision) are common.[268,269] These changes probably are caused by direct toxicity to the photoreceptors. The visual symptoms are reversible with discontinuation of the drug.

Methanol

Methanol occasionally is ingested by alcoholics. Visual blurring and field deficits are seen within 18 hours. Early fundus findings include optic nerve hyperemia and retinal edema, and late findings include optic atrophy[270–277] (Fig. 92.36). OCT findings have shown the optic nerve head swelling with adjacent edema of the retinal nerve fiber layer.[278] Optic nerve toxicity is mediated by formic acid, a breakdown product of methanol, which directly affects the inner retina and optic nerve. The degree of systemic acidosis correlates well with the extent of visual dysfunction. Early hemodialysis is effective in removing methanol from the body, but if visual recovery is not evident by 6 days, it often remains permanently decreased.

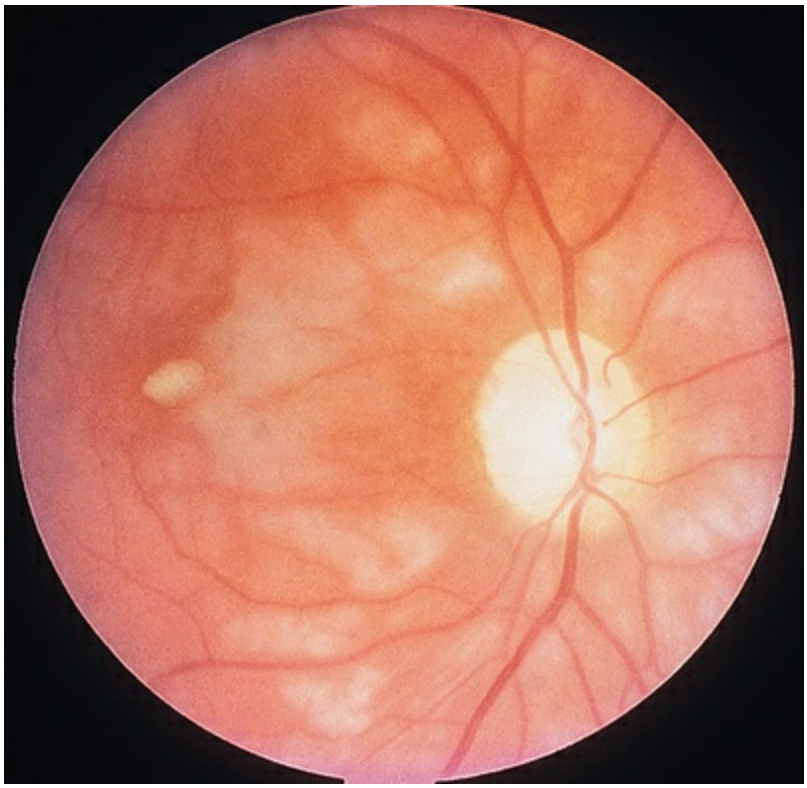

FIG. 92.36 Methanol poisoning. Acute changes revealing peripapillary retinal whitening and edema.

Vigabatrin

Vigabatrin is used for treatment of epilepsy and has been associated

with optic atrophy and visual field defects.[279,280]

Sildenafil, Tadalafil, Vardenafil

Sildenafil, tadalafil, and vardenafil are a class of drugs that are potent inhibitors of phosophodiesterase-5 (PDE-5) and are used for the treatment of erectile dysfunction. Sildenafil also blocks PDE-6, though with only about one-tenth of its effect on PDE-5. PDE-6 is a key enzyme in the phototransduction cascade, and sildenafil modifies this cascade in photoreceptor outer segments causing a rise in cyclic guanosine monophosphate (cGMP). Commonly, patients notice a bluish dyschromatopsia (dose dependent) 1–2 hours after ingestion and this has been associated with a significant transient depression in the ERG in at least one study, though others have shown minimal to no effect on the ERG.[281–290] There appears to be no appreciable effect to slight increase in choroidal circulation with use of sildenafil on the ocular circulation and no adverse effects on those with early age-related macular degeneration.[291–296] There have been reported cases of nonarteritic ischemic optic neuropathy, central serous retinopathy, and cilioretinal artery obstruction with use of sildenafil and tadalafil.[297–309] The true incidence of nonarteritic ischemic optic neuropathy in comparison to age-matched controls is not known.

Summary

Although there are thousands of systemic medications, only a small number of these agents produce retinal abnormalities and/or toxicity. Retinal toxicity can occur when agents are used at standard therapeutic levels, and also when they are used in excess or for nonapproved indications. The mechanism by which toxicity develops is unknown in many cases. With numerous new medications reaching the market annually, ophthalmologists need to maintain a high index of suspicion that patients' symptoms and/or clinical findings may be related to one or more of their medications.

Acknowledgment

The National Registry of Drug-Induced Ocular Side Effects is a valuable resource when checking for possible drug-induced ocular problems (www.eyedrugregistry.com).

References

1. Cambiaggi A. Unusual ocular lesions in a case of systemic lupus erythematosus. *Arch Ophthalmol*. 1957;57(3):451–453.
2. Henkind P, Rothfield NF. Ocular abnormalities in patients treated with synthetic antimalarial drugs. *N Engl J Med*. 1963;269.
3. Hobbs HE, Eadie SP, Somerville F. Ocular lesions after treatment with chloroquine. *Br J Ophthalmol*. 1961;45(4):284–297.
4. Hobbs HE, Sorsby A, Freedman A. Retinopathy following chloroquine therapy. *Lancet*. 1959;2:478–480.
5. Marks JS. Chloroquine retinopathy: is there a safe daily dose? *Ann Rheum Dis*. 1982;41(1):52–58.
6. Nylander U. Ocular damage in chloroquine therapy. *Acta Ophthalmol*. 1967;Suppl 92:1–71.
7. Okun E, Gouras P, Bernstein H. Chloroquine retinopathy. *Arch Ophthalmol*. 1963;69:59–71.
8. Ochsendorf FR, Runne U. Chloroquine: consideration of maximum daily dose (3.5 mg/kg ideal body weight) prevents retinopathy. *Dermatology*. 1996;192(4):382–383.
9. Tobin DR, Krohel G, Rynes RI. Hydroxychloroquine. Seven-year experience. *Arch Ophthalmol*. 1982;100(1):81–83.
10. Finbloom DS, Silver K, Newsome DA, et al. Comparison of hydroxychloroquine and chloroquine use and the development of retinal toxicity. *J Rheumatol*. 1985;12(4):692–694.
11. Mackenzie AH, Scherbel AL. A decade of chloroquine maintenance therapy: rate of administration governs incidence of retinotoxicity. *Arthritis Rheum*. 1968;11:496.
12. Hart WM, Burde RM, Johnston GP, et al. Static perimetry in chloroquine retinopathy. Perifoveal patterns of visual field

depression. *Arch Ophthalmol*. 1984;102(3):377–380.
13. Brinkley JR, Dubois EL, Ryan SJ. Long-term course of chloroquine retinopathy after cessation of medication. *Am J Ophthalmol*. 1979;88(1):1–11.
14. Carr RE, Henkind P, Rothfield N, et al. Ocular toxicity of antimalarial drugs: long-term follow-up. *Am J Ophthalmol*. 1968;66(4):738–744.
15. Rubin M, Bernstein HN, Zvaifler NJ. Studies on the pharmacology of chloroquine. *Arch Ophthalmol*. 1963;70:80–87.
16. Ehrenfeld M, Nesher R, Merin S. Delayed-onset chloroquine retinopathy. *Br J Ophthalmol*. 1986;70(4):281–283.
17. Sassani JW, Brucker AJ, Cobbs W, et al. Progressive chloroquine retinopathy. *Ann Ophthalmol*. 1983;15(1):19–22.
18. Heckenlively JR, Martin D, Levy J. Chloroquine retinopathy. *Am J Ophthalmol*. 1980;89(1):150–151.
19. Wetterholm DH, Winter FC. Histopathology of chloroquine retinal toxicity. *Arch Ophthalmol*. 1964;71:82–87.
20. Ramsey MS, Fine BS. Chloroquine toxicity in the human eye: histopathologic observations by electron microscopy. *Am J Ophthalmol*. 1972;73(2):229–235.
21. Bonanomi MT, Dantas NC, Medeiros FA. Retinal nerve fibre layer thickness measurements in patients using chloroquine. *Clin Experiment Ophthalmol*. 2006;34(2):130–136.
22. Kellner U, Kellner S, Weinitz S. Chloroquine retinopathy: lipofuscin- and melanin-related fundus autofluorescence, optical coherence tomography and multifocal electroretinography. *Adv Ophthalmol*. 2008;116(2):119–127.
23. Bernstein H, Zvaifler N, Rubin M. The ocular deposition of chloroquine. *Invest Ophthalmol*. 1963;2:384–392.
24. Mahon GJ, Anderson HR, Gardiner TA. Chloroquine causes lysosomal dysfunction in neural retina and implications for retinopathy. *Curr Eye Res*. 2003;28:277–284.
25. Ivanina TA, Zueva MV, Lebedeva MN, et al. Ultrastructural alterations in rat and cat retina and pigment epithelium induced by chloroquine. *Graefes Arch Clin Exp Ophthalmol*. 1983;220(1):32–38.
26. Vu BL, Easterbrook M, Hovis JK. Detection of color vision

defects in chloroquine retinopathy. *Ophthalmology*. 1999;106(9):1799–1803 [discussion 1804].
27. Neubauer AS, Samari-Kermani K, Schaller U, et al. Detecting chloroquine retinopathy: electro-oculogram versus colour vision. *Br J Ophthalmol*. 2003;87(7):902–908.
28. Kellner U, Kraus H, Foerster MH. Multifocal ERG in chloroquine retinopathy: regional variance of retinal dysfunction. *Graefes Arch Clin Exp Ophthalmol*. 2000;238(1):94–97.
29. Tzekov R. Full-field ERG in diabetic retinopathy: a screening tool. *Graefes Arch Clin Exp Ophthalmol*. 2015;253(7):987–988.
30. Grierson DJ. Hydroxychloroquine and visual screening in a rheumatology outpatient clinic. *Ann Rheum Dis*. 1997;56(3):188–190.
31. Levy GD, Munz SJ, Paschal J, et al. Incidence of hydroxychloroquine retinopathy in 1,207 patients in a large multicenter outpatient practice. *Arthritis Rheum*. 1997;40(8):1482–1486.
32. Rynes RI. Ophthalmologic considerations in using antimalarials in the United States. *Lupus*. 1996;5(Suppl. 1):S73–4.
33. Coyle JT. Hydroxychloroquine retinopathy. *Ophthalmology*. 2001;108(2):243–244.
34. Falcone PM, Paolini L, Lou PL. Hydroxychloroquine toxicity despite normal dose therapy. *Ann Ophthalmol*. 1993;25(10):385–388.
35. Johnson MW, Vine AK. Hydroxychloroquine therapy in massive total doses without retinal toxicity. *Am J Ophthalmol*. 1987;104(2):139–144.
36. Mavrikakis M, Papazoglou S, Sfikakis PP, et al. Retinal toxicity in long term hydroxychloroquine treatment. *Ann Rheum Dis*. 1996;55(3):187–189.
37. Shearer RV, Dubois EL. Ocular changes induced by long-term hydroxychloroquine (plaquenil) therapy. *Am J Ophthalmol*. 1967;64(2):245–252.
38. Weiner A, Sandberg MA, Gaudio AR, et al. Hydroxychloroquine retinopathy. *Am J Ophthalmol*. 1991;112(5):528–534.

39. Weiser A, Sandberg MA, Gaadio AR, et al. Hydroxychloroquine retinopathy. *Am J Ophthalmol*. 1991;121:582–584.
40. Bienfang D, Coblyn JS, Liang MH, et al. Hydroxychloroquine retinopathy despite regular ophthalmologic evaluation: a consecutive series. *J Rheumatol*. 2000;27(11):2703–2706.
41. Browning DJ. Hydroxychloroquine and chloroquine retinopathy: screening for drug toxicity. *Am J Ophthalmol*. 2002;133(5):649–656.
42. Lyons JS, Severns ML. Detection of early hydroxychloroquine retinal toxicity enhanced by ring ratio analysis of multifocal electroretinography. *Am J Ophthalmol*. 2007;143(5):801–809.
43. Mavrikakis I, Sfikakis PP, Mavrikakis E, et al. The incidence of irreversible retinal toxicity in patients treated with hydroxychloroquine: a reappraisal. *Ophthalmology*. 2003;110(7):1321–1326.
44. Wolfe F, Marmor MF. Rates and predictors of hydroxychloroquine retinal toxicity in patients with rheumatoid arthritis and systemic lupus erythematosus. *Arthritis Care Res*. 2010;62(6):775–784.
45. Easterbrook M, Bernstein H. Ophthalmological monitoring of patients taking antimalarials: preferred practice patterns. *J Rheumatol*. 1997;24(7):1390–1392.
46. Morsman CD, Livesey SJ, Richards IM, et al. Screening for hydroxychloroquine retinal toxicity: is it necessary? *Eye*. 1990;4(Pt 4):572–576.
47. Shipley M, Silman A. Should patients on hydroxychloroquine have their eyes examined regularly? *Br J Rheumatol*. 1997;36(5):514–515.
48. Silman A, Shipley M. Ophthalmological monitoring for hydroxychloroquine toxicity: a scientific review of available data. *Br J Rheumatol*. 1997;36(5):599–601.
49. Easterbrook M. Hydroxychloroquine retinopathy. *Ophthalmology*. 2001;108(12):2158–2159.
50. Marmor MF, Kellner U, Lai TY, et al. American Academy of Ophthalmology. Revised recommendations on screening

for chloroquine and hydroxychloroquine retinopathy. *Ophthalmology*. 2011;118(2):415–422.
51. Michaelides M, Stover NB, Francis PJ, et al. Retinal toxicity associated with hydroxychloroquine and chloroquine: risk factors, screening, and progression despite cessation of therapy. *Arch Ophthalmol*. 2011;129(1):30–39.
52. Maturi RK, Yu M, Weleber RG. Multifocal electroretinographic evaluation of long-term hydroxychloroquine users. *Arch Ophthalmol*. 2004;122(7):973–981.
53. Penrose PJ, Tzekov RT, Sutter EE, et al. Multifocal electroretinography evaluation for early detection of retinal dysfunction in patients taking hydroxychloroquine. *Retina*. 2003;23(4):503–512.
54. Moschos MN, Moschos MM, Apostolopoulos M, et al. Assessing hydroxychloroquine toxicity by the multifocal ERG. *Doc Ophthalmol*. 2004;108(1):47–53.
55. Lai TY, Chan WM, Li H, et al. Multifocal electroretinographic changes in patients receiving hydroxychloroquine therapy. *Am J Ophthalmol*. 2005;140(5):794–807.
56. Lai TY, Ngai JW, Chan WM, et al. Visual field and multifocal electroretinography and their correlations in patients on hydroxychloroquine therapy. *Doc Ophthalmol*. 2006;112(3):177–187.
57. Rodriguez-Padilla JA, Hedges TR 3rd, Monson B, et al. High-speed ultra-high-resolution optical coherence tomography findings in hydroxychloroquine retinopathy. *Arch Ophthalmol*. 2007;125(6):775–780.
58. Stepien KE, Han DP, Schell J, et al. Spectral-domain optical coherence tomography and adaptive optics may detect hydroxychloroquine retinal toxicity before symptomatic vision loss. *Trans Am Ophthalmol Soc*. 2009;107:28–33.
59. Pasadhika S, Fishman GA, Choi D, et al. Selective thinning of the perifoveal inner retina as an early sign of hydroxychloroquine retinal toxicity. *Eye*. 2010;24(5):756–762 [quiz 63].
60. Kellner U, Renner AB, Tillack H. Fundus autofluorescence

and mfERG for early detection of retinal alterations in patients using chloroquine/hydroxychloroquine. *Invest Ophthalmol Vis Sci*. 2006;47(8):3531–3538.
61. Maturi RK, Folk JC, Nichols B, et al. Hydroxychloroquine retinopathy. *Arch Ophthalmol*. 1999;117(9):1262–1263.
62. Marmor MF, Kellner U, Lai TY, et al. American Academy of Ophthalmology. Recommendations on Screening for Chloroquine and Hydroxychloroquine Retinopathy (2016 Revision). *Ophthalmology*. 2016;123(6):1386–1394.
63. Weekley RD, Potts AM, Reboton J, et al. Pigmentary retinopathy in patients receiving high doses of a new phenothiazine. *Arch Ophthalmol*. 1960;64:65–76.
64. Meredith TA, Aaberg TM, Willerson WD. Progressive chorioretinopathy after receiving thioridazine. *Arch Ophthalmol*. 1978;96(7):1172–1176.
65. Miller FS, Bunt-Milam AH, Kalina RE. Clinical-ultrastructural study of thioridazine retinopathy. *Ophthalmology*. 1982;89(12):1478–1488.
66. Connell MM, Poley BJ, McFarlane JR. Chorioretinopathy associated with thioridazine therapy. *Arch Ophthalmol*. 1964;71:816–821.
67. Hagopian V, Stratton DB, Busiek RD. Five cases of pigmentary retinopathy associated with thioridazine administration. *Am J Psychiatry*. 1966;123(1):97–100.
68. Hamilton JD. Thioridazine retinopathy within the upper dosage limit. *Psychosomatics*. 1985;26(10):823–824.
69. Heshe J, Engelstoft FH, Kirk L, et al. Retinal injury developing under thioridazine treatment. *Nord Psykiatr Tidsskr*. 1961;15:442–447.
70. Lam RW, Remick RA. Pigmentary retinopathy associated with low-dose thioridazine treatment. *Can Med Assoc J*. 1985;132(7):737.
71. Neves MS, Jordon K, Dragt H. Extensive chorioretinopathy associated with very low dose thioridazine. *Eye*. 1990;4(Pt 5):767–770.
72. Tekell JL, Silva JA, Maas JA, et al. Thioridazine-induced retinopathy. *Am J Psychiatry*. 1996;153(9):1234–1235.
73. Miyata M, Imai H, Ishikawa S, et al. Change in human

electroretinography associated with thioridazine administration. *Ophthalmologica*. 1980;181(3–4):175–180.
74. Marmor MF. Is thioridazine retinopathy progressive? Relationship of pigmentary changes to visual function. *Br J Ophthalmol*. 1990;74(12):739–742.
75. Chaudhry IA, Shamsi FA, Weitzman ML. Progressive severe visual loss after long-term withdrawal from thioridazine treatment. *Eur J Ophthalmol*. 2006;16(4):651–653.
76. Potts AM. The concentration of phenothiazines in the eye of experimental animals. *Invest Ophthalmol Vis Sci*. 1962;1:522–530.
77. Potts AM. The reaction of uveal pigment in vitro with polycyclic compounds. *Invest Ophthalmol Vis Sci*. 1964;3:405–416.
78. Potts AM. Further studies concerning accumulation of polycyclic compounds on uveal melanin. *Invest Ophthalmol Vis Sci*. 1964;3:399–404.
79. Kinross-Wright JT. Clinical trial of a new phenothiazine compound NP-207. *Psychiatr Res Rep Am Psychiatr Assoc*. 1956;4:89–94.
80. Bonting SL, Caravaggio LL, Canady MR. Studies on sodium potassium-activated adenosine triphosphatase. X Occurrence in retinal rods and relation to rhodopsin. *Exp Eye Res*. 1964;3:47–56.
81. Cerletti A, Taeschler M, Weidmann H. Pharmacologic studies on the structure-activity relationship of hydroxyindole alkylamines. *Adv Pharmacol*. 1968;6(Pt B):233–246.
82. Muirhead JF. Drug effects on retinol oxidation: retinal alcohol:NAD^+ oxidoreductase. *Invest Ophthalmol*. 1967;6(6):635–641.
83. Fornaro P, Calabria G, Corallo G, et al. Pathogenesis of degenerative retinopathies induced by thioridazine and other antipsychotics: a dopamine hypothesis. *Adv Ophthalmol*. 2002;105(1):41–49.
84. DeLong SL, Poley BJ, McFarlane JR. Ocular changes associated with long-term chlorpromazine therapy. *Arch Ophthalmol*. 1965;73:611–617.

85. Mathalone MB. Eye and skin changes in psychiatric patients treated with chlorpromazine. *Br J Ophthalmol*. 1967;51(2):86–93.
86. Oshika T. Ocular adverse effects of neuropsychiatric agents. Incidence and management. *Drug Saf*. 1995;12(4):256–263.
87. Siddal JR. The ocular toxic findings with prolonged and high dosage chlorpromazine intake. *Arch Ophthalmol*. 1965;74:460–464.
88. Wolf ME, Richer S, Berk MA, et al. Cutaneous and ocular changes associated with the use of chlorpromazine. *Int J Clin Pharmacol Ther Toxicol*. 1993;31(8):365–367.
89. Webber SK, Domniz Y, Sutton GL, et al. Corneal deposition after high-dose chlorpromazine hydrochloride therapy. *Cornea*. 2001;20(2):217–219.
90. Razeghinejad MR, Nowroozzadeh MH, Zamani M, et al. In vivo observations of chlorpromazine ocular deposits in a patient on long-term chlorpromazine therapy. *Clin Experiment Ophthalmol*. 2008;36(6):560–563.
91. Horgan SE, Williams RW. Chronic retinal toxicity due to quinine in Indian tonic water. *Eye*. 1995;9(Pt 5):637–638.
92. Brinton GS, Norton EW, Zahn JR, et al. Ocular quinine toxicity. *Am J Ophthalmol*. 1980;90(3):403–410.
93. Lochhead J, Movaffaghy A, Falsini B, et al. The effect of quinine on the electroretinograms of children with pediatric cerebral malaria. *J Infect Dis*. 2003;187(8):1342–1345.
94. Traill A, Patmaraj R, Zamir E. Quinine iris toxicity. *Arch Ophthalmol*. 2007;125(3):430.
95. Bacon P, Spalton DJ, Smith SE. Blindness from quinine toxicity. *Br J Ophthalmol*. 1988;72(3):219–224.
96. Buchanan TA, Lyness RW, Collins AD, et al. An experimental study of quinine blindness. *Eye*. 1987;1(Pt 4):522–524.
97. Christoforidis J, Ricketts R, Loizos T, et al. Optical coherence tomography findings of quinine poisoning. *Clin Ophthalmol*. 2011;5:75–80.
98. Canning CR, Hague S. Ocular quinine toxicity. *Br J Ophthalmol*. 1988;72(1):23–26.
99. Craythorn JM, Swartz M, Creel DJ. Clofazimine-induced

bull's-eye retinopathy. *Retina*. 1986;6(1):50–52.
100. Cunningham CA, Friedberg DN, Carr RE. Clofazamine-induced generalized retinal degeneration. *Retina*. 1990;10(2):131–134.
101. Whitcup SM, Butler KM, Caruso R, et al. Retinal toxicity in human immunodeficiency virus-infected children treated with 2',3'-dideoxyinosine. *Am J Ophthalmol*. 1992;113(1):1–7.
102. Piccolino FC, Pandolfo A, Polizzi A, et al. Retinal toxicity from accidental intraocular injection of depo-medrol. *Retina*. 2002;22(1):117–119.
103. Davies SC, Marcus RE, Hungerford JL, et al. Ocular toxicity of high-dose intravenous desferrioxamine. *Lancet*. 1983;2(8343):181–184.
104. Mehta AM, Engstrom RE Jr, Kreiger AE. Deferoxamine-associated retinopathy after subcutaneous injection. *Am J Ophthalmol*. 1994;118(2):260–262.
105. Gass JDM. *Stereoscopic atlas of macular diseases: diagnosis and treatment*. Mosby: St. Louis; 1997.
106. Haimovici R, D'Amico DJ, Gragoudas ES, Deferoxamine Retinopathy Study G, et al. The expanded clinical spectrum of deferoxamine retinopathy. *Ophthalmology*. 2002;109(1):164–171.
107. Margo CE, Murtagh FR. Ocular and orbital toxicity after intracarotid cisplatin therapy. *Am J Ophthalmol*. 1993;116(4):508–509.
108. Singalavaniga A, Ruangvaravate N, Dulayajinda D. Potassium iodate toxic retinopathy: a report of five cases. *Retina*. 2000;20:378–383.
109. Rahi AH, Hungerford JL, Ahmed AI. Ocular toxicity of desferrioxamine: light microscopic histochemical and ultrastructural findings. *Br J Ophthalmol*. 1986;70(5):373–381.
110. Hines J, Vinores SA, Campochiaro PA. Evolution of morphologic changes after intravitreous injection of gentamicin. *Curr Eye Res*. 1993;12(6):521–529.
111. Pendergast SD, Eliott D, Machemer R. Retinal toxic effects following inadvertent intraocular injection of Celestone Soluspan. *Arch Ophthalmol*. 1995;113(10):1230–1231.
112. McCuen BW, Bessler M, Tano Y, et al. The lack of toxicity of

intravitreally administered triamcinolone acetonide. *Am J Ophthalmol*. 1981;91(6):785–788.
113. Kupersmith MJ, Seiple WH, Holopigian K, et al. Maculopathy caused by intra-arterially administered cisplatin and intravenously administered carmustine. *Am J Ophthalmol*. 1992;113(4):435–438.
114. Miller DF, Bay JW, Lederman RJ, et al. Ocular and orbital toxicity following intracarotid injection of BCNU (carmustine) and cisplatinum for malignant gliomas. *Ophthalmology*. 1985;92(3):402–406.
115. Katz BJ, Ward JH, Digre KB, et al. Persistent severe visual and electroretinographic abnormalities after intravenous Cisplatin therapy. *J Neuroophthalmol*. 2003;23(2):132–135.
116. Khawly JA, Rubin P, Petros W, et al. Retinopathy and optic neuropathy in bone marrow transplantation for breast cancer. *Ophthalmology*. 1996;103(1):87–95.
117. Ruddle JB, Harper CA, Hönemann D, et al. A denileukin diftitox (Ontak) associated retinopathy? *Br J Ophthalmol*. 2006;90(8):1070–1071.
118. Atlee WE. Talc and cornstarch emboli in eyes of drug abusers. *JAMA*. 1972;219(1):49–51.
119. Murphy SB, Jackson WB, Pare JA. Talc retinopathy. *Can J Ophthalmol*. 1978;13(3):152–156.
120. Tse DT, Ober RR. Talc retinopathy. *Am J Ophthalmol*. 1980;90(5):624–640.
121. Schatz H, Drake M. Self-injected retinal emboli. *Ophthalmology*. 1979;86(3):468–483.
122. Friberg TR, Gragoudas ES, Regan CD. Talc emboli and macular ischemia in intravenous drug abuse. *Arch Ophthalmol*. 1979;97(6):1089–1091.
123. Brucker AJ. Disk and peripheral retinal neovascularization secondary to talc and cornstarch emboli. *Am J Ophthalmol*. 1979;88(5):864–867.
124. Kresca LJ, Goldberg MF, Jampol LM. Talc emboli and retinal neovascularization in a drug abuser. *Am J Ophthalmol*. 1979;87(3):334–339.
125. Jampol LM, Setogawa T, Rednam KR, et al. Talc retinopathy in primates: a model of ischemic retinopathy: I. Clinical

studies. *Arch Ophthalmol*. 1981;99(7):1273–1280.
126. Kaga N, Tso MO, Jampol LM, et al. Talc retinopathy in primates: a model of ischemic retinopathy. II. A histopathologic study. *Arch Ophthalmol*. 1982;100(10):1644–1648.
127. Kaga N, Tso MO, Jampol LM. Talc retinopathy in primates: a model of ischemic retinopathy. III. An electron microscopic study. *Arch Ophthalmol*. 1982;100(10):1649–1657.
128. Gombos GM, Moreno DH, Bedrossian PB. Retinal vascular occlusion induced by oral contraceptives. *Ann Ophthalmol*. 1975;7(2):215–217.
129. Goren SB. Retinal edema secondary to oral contraceptives. *Am J Ophthalmol*. 1967;64(3):447–449.
130. Lyle TK, Wybar K. Retinal vasculitis. *Br J Ophthalmol*. 1961;45(12):778–788.
131. Perry HD, Mallen FJ. Cilioretinal artery occlusion associated with oral contraceptives. *Am J Ophthalmol*. 1977;84(1):56–58.
132. Stowe GC, Zakov ZN, Albert DM. Central retinal vascular occlusion associated with oral contraceptives. *Am J Ophthalmol*. 1978;86(6):798–801.
133. Varga M. Recent experiences on the ophthalmologic complications of oral contraceptives. *Ann Ophthalmol*. 1976;8(8):925–934.
134. Walsh FB, Clark DB, Thompson RS, et al. Oral contraceptives and neuro-ophthalmologic interest. *Arch Ophthalmol*. 1965;74(5):628–640.
135. Garg SK, Chase HP, Marshall G, et al. Oral contraceptives and renal and retinal complications in young women with insulin-dependent diabetes mellitus. *JAMA*. 1994;271(14):1099–1102.
136. Petersson GJ, Fraunfelder FT, Meyer SM. Oral contraceptives. *Ophthalmology*. 1981;88:368–371.
137. Vessey MP, Hannaford P, Mant J, et al. Oral contraception and eye disease: findings in two large cohort studies. *Br J Ophthalmol*. 1998;82(5):538–542.
138. Balian JV. Accidental intraocular tobramycin injection: a case report. *Ophthalmic Surg*. 1983;14(4):353–354.
139. Campochiaro PA, Conway BP. Aminoglycoside toxicity – a

survey of retinal specialists. Implications for ocular use. *Arch Ophthalmol*. 1991;109(7):946–950.
140. Campochiaro PA, Lim JI. Aminoglycoside toxicity in the treatment of endophthalmitis. The Aminoglycoside Toxicity Study Group. *Arch Ophthalmol*. 1994;112(1):48–53.
141. McDonald HR, Schatz H, Allen AW, et al. Retinal toxicity secondary to intraocular gentamicin injection. *Ophthalmology*. 1986;93(7):871–877.
142. D'Amico DJ, Caspers-Velu L, Libert J, et al. Comparative toxicity of intravitreal aminoglycoside antibiotics. *Am J Ophthalmol*. 1985;100(2):264–275.
143. Peyman GA, Vastine DW, Crouch ER. Clinical use of intravitreal antibiotics to treat bacterial endophthalmitis. *Trans Am Acad Ophthalmol Otolaryngol*. 1974;78:862–875.
144. Zachary IG, Forster RK. Experimental intravitreal gentamicin. *Am J Ophthalmol*. 1976;82(4):604–611.
145. Rosenbaum JD, Krumholz DM, Metz DM. Gentamicin retinal toxicity after cataract surgery in an eye that underwent vitrectomy. *Ophthalmic Surg Lasers*. 1997;28(3):236–238.
146. Talamo JH, D'Amico DJ, Hanninen LA, et al. The influence of aphakia and vitrectomy on experimental retinal toxicity of aminoglycoside antibiotics. *Am J Ophthalmol*. 1985;100(6):840–847.
147. Kane A, Barza M, Baum J. Intravitreal injection of gentamicin in rabbits. Effect of inflammation and pigmentation on half-life and ocular distribution. *Invest Ophthalmol Vis Sci*. 1981;20(5):593–597.
148. Zemel E, Loewenstein A, Lei B, et al. Ocular pigmentation protects the rabbit retina from gentamicin-induced toxicity. *Invest Ophthalmol Vis Sci*. 1995;36(9):1875–1884.
149. Brown GC, Eagle RC, Shakin EP, et al. Retinal toxicity of intravitreal gentamicin. *Arch Ophthalmol*. 1990;108(12):1740–1744.
150. Conway BP, Tabatabay CA, Campochiaro PA, et al. Gentamicin toxicity in the primate retina. *Arch Ophthalmol*. 1989;107(1):107–112.
151. Loewenstein A, Zemel E, Vered Y, et al. Retinal toxicity of

gentamicin after subconjunctival injection performed adjacent to thinned sclera. *Ophthalmology*. 2001;108(4):759–764.
152. Chu TG, Ferreira M, Ober RR. Immediate pars plana vitrectomy in the management of inadvertent intracameral injection of gentamicin. A rabbit experimental model. *Retina*. 1994;14(1):59–64.
153. Burgansky Z, Rock T, Bartov E. Inadvertent intravitreal gentamicin injection. *Eur J Ophthalmol*. 2002;12(2):138–140.
154. Lim JI, Anderson CT, Hutchinson A, et al. The role of gravity in gentamicin-induced toxic effects in a rabbit model. *Arch Ophthalmol*. 1994;112(10):1363–1367.
155. Anijeet DR, Palimar P, Peckar CO. Intracameral vancomycin following cataract surgery: An eleven-year study. *Clin Ophthalmol*. 2010;4:321–326.
156. Shorstein NH, Winthrop KL, Herrinton LJ. Decreased postoperative endophthalmitis rate after institution of intracameral antibiotics in a Northern California eye department. *J Cataract Refract Surg*. 2013;39(1):8–14.
157. Nicholson LB, Kim BT, Jardon J, et al. Severe bilateral ischemic retinal vasculitis following cataract surgery. *Ophthalmic Surg Lasers Imaging Retina*. 2014;45(4):338–342.
158. Witkin AJ, Shah AR, Engstrom RE, et al. Postoperative hemorrhagic occlusive retinal vasculitis: expanding the clinical spectrum and possible association with vancomycin. *Ophthalmology*. 2015;122(7):1438–1451.
159. Lenci LT, Chin EK, Carter C, et al. Ischemic retinal vasculitis associated with cataract surgery and intracameral vancomycin. *Case Rep Ophthalmol Med*. 2015;2015:683194.
160. Axer-Siegel R, Stiebel-Kalish H, Rosenblatt I, et al. Cystoid macular edema after cataract surgery with intraocular vancomycin. *Ophthalmology*. 1993;111(3):350–356.
161. Guyer DR, Tiedeman J, Yannuzzi LA, et al. Interferon-associated retinopathy. *Arch Ophthalmol*. 1993;111(3):350–356.
162. Kawano T, Shigehira M, Uto H, et al. Retinal complications during interferon therapy for chronic hepatitis C. *Am J Gastroenterol*. 1996;91(2):309–313.

163. Schulman JA, Liang C, Kooragayala LM, et al. Posterior segment complications in patients with hepatitis C treated with interferon and ribavirin. *Ophthalmology*. 2003;110(2):437–442.
164. Kiratli H, Irkeç M. Presumed interferon-associated bilateral macular arterial branch obstruction. *Eye (Lond)*. 2000;14(Pt 6):920–922.
165. Tokai R, Ikeda T, Miyaura T, et al. Interferon-associated retinopathy and cystoid macular edema. *Arch Ophthalmol*. 2001;119(7):1077–1079.
166. Hejny C, Sternberg P, Lawson DH, et al. Retinopathy associated with high-dose interferon alfa-2b therapy. *Am J Ophthalmol*. 2001;131(6):782–787.
167. Fraunfelder FW, Fraunfelder FT. Interferon alfa-associated anterior ischemic optic neuropathy. *Ophthalmology*. 2011;118(2):408–411 [e1-2].
168. Rubio JE Jr, Charles S. Interferon-associated combined branch retinal artery and central retinal vein obstruction. *Retina*. 2003;23(4):546–548.
169. Wilson RL, Ross RD, Wilson LM. Interferon-associated retinopathy in a young, insulin-dependent diabetic patient. *Retina*. 2000;20:413–415.
170. Kertes PJ, Britton WA Jr, Addison DJ, et al. Toxicity of intravitreal interferon alpha-2b in the rabbit. *Can J Ophthalmol*. 1995;30(7):355–359.
171. Crochet M, Ingster-Moati I, Even G, et al. [Retinopathy caused by interferon alpha associated with ribavirin therapy and the importance of the electro-oculogram: a case report]. *J Fr Ophtalmol*. 2004;27(3):257–262.
172. Gupta DR, Strobos RJ. Bilateral papillitis associated with Cafergot therapy. *Neurology*. 1972;22(8):793–797.
173. Mindel JS, Rubenstein AE, Franklin B. Ocular ergotamine tartrate toxicity during treatment of Vacor-induced orthostatic hypotension. *Am J Ophthalmol*. 1981;92(4):492–496.
174. Gilmer G, Swartz M, Teske M, et al. Over-the-counter phenylpropanolamine: a possible cause of central retinal vein occlusion. *Arch Ophthalmol*. 1986;104(5):642.

175. Banach MJ, Williams GA. Purtscher retinopathy and necrotizing vasculitis with gemcitabine therapy. *Arch Ophthalmol*. 2000;118(5):726–727.
176. Thomas JV, Gragoudas ES, Blair NP, et al. Correlation of epinephrine use and macular edema in aphakic glaucomatous eyes. *Arch Ophthalmol*. 1978;96(4):625–628.
177. Fraunfelder FW, Fraunfelder FT, Illingworth DR. Adverse ocular effects associated with niacin therapy. *Br J Ophthalmol*. 1995;79(1):54–56.
178. Gass JD. Nicotinic acid maculopathy. *Am J Ophthalmol*. 1973;76(4):500–510.
179. Millay RH, Klein ML, Illingworth DR. Niacin maculopathy. *Ophthalmology*. 1988;95(7):930–936.
180. Jampol LM. Niacin maculopathy. *Ophthalmology*. 1988;95(12):1704–1705.
181. Spirn MJ, Warren FA, Guyer DR, et al. Optical coherence tomography findings in nicotinic acid maculopathy. *Am J Ophthalmol*. 2003;135(6):913–914.
182. Dajani HM, Lauer AK. Optical coherence tomography findings in niacin maculopathy. *Can J Ophthalmol*. 2006;41(2):197–200.
183. Hoyng PF, Rulo AH, Greve EL, et al. Fluorescein angiographic evaluation of the effect of latanoprost treatment on blood–retinal barrier integrity: a review of studies conducted on pseudophakic glaucoma patients and on phakic and aphakic monkeys. *Surv Ophthalmol*. 1997;41(Suppl. 2):S83–8.
184. Rowe JA, Hattenhauer MG, Herman DC. Adverse side effects associated with latanoprost. *Am J Ophthalmol*. 1997;124(5):683–685.
185. Warwar RE, Bullock JD, Ballal D. Cystoid macular edema and anterior uveitis associated with latanoprost use. Experience and incidence in a retrospective review of 94 patients. *Ophthalmology*. 1998;105(2):263–268.
186. Halpern DL, Pasquale LR. Cystoid macular edema in aphakia and pseudophakia after use of prostaglandin analogs. *Semin Ophthalmol*. 2002;17(3–4):181–186.
187. Wand M, Gaudio AR, Shields MB. Latanoprost and cystoid

macular edema in high-risk aphakic or pseudophakic eyes. *J Cataract Refract Surg*. 2001;27(9):1397–1401.
188. Furuichi M, Chiba T, Abe K, et al. Cystoid macular edema associated with topical latanoprost in glaucomatous eyes with a normally functioning blood-ocular barrier. *J Glaucoma*. 2001;10(3):233–236.
189. Lima MC, Paranhos A Jr, Salim S, et al. Visually significant cystoid macular edema in pseudophakic and aphakic patients with glaucoma receiving latanoprost. *J Glaucoma*. 2000;9(4):317–321.
190. Schumer RA, Camras CB, Mandahl AK. Latanoprost and cystoid macular edema: is there a causal relation? *Curr Opin Ophthalmol*. 2000;11(2):94–100.
191. Miyake K, Ibaraki N. Prostaglandins and cystoid macular edema. *Surv Ophthalmol*. 2002;47(Suppl. 1):S203–18.
192. Joshi MM, Garretson BR. Paclitaxel maculopathy. *Arch Ophthalmol*. 2007;125(5):709–710.
193. Telender DG, Sarraf D. Cystoid macular edema with Docetaxel chemotherapy and the fluid retention syndrome. *Semin Ophthalmol*. 2007;22:151–153.
194. Zarbin MA, Jampol LM, Jager RD, et al. Ophthalmic evaluations in clinical studies of fingolimod (FTY720) in multiple sclerosis. *Ophthalmology*. 2013;120(7):1432–1439.
195. Grinbaum A, Ashkenazi I, Avni I, et al. Transient myopia following metronidazole treatment for Trichomonas vaginalis. *JAMA*. 1992;267(4):511–512.
196. Ryan EH Jr, Jampol LM. Drug-induced acute transient myopia with retinal folds. *Retina*. 1986;6(4):220–223.
197. Soylev MF, Green RL, Feldon SE. Choroidal effusion as a mechanism for transient myopia induced by hydrochlorothiazide and triamterene. *Am J Ophthalmol*. 1995;120(3):395–397.
198. Sen HA, O'Halloran HS, Lee WB. Case reports and small case series: topiramate-induced acute myopia and retinal striae. *Arch Ophthalmol*. 2001;119(5):775–777.
199. Rhee DJ, Goldberg MJ, Parrish RK. Bilateral angle-closure glaucoma and ciliary body swelling from topiramate. *Arch Ophthalmol*. 2001;119(11):1721–1723.

200. Medeiros FA, Zhang XY, Bernd AS, et al. Angle-closure glaucoma associated with ciliary body detachment in patients using topiramate. *Arch Ophthalmol*. 2003;121(2):282–285.
201. Fraunfelder FW, Fraunfelder FT, Keates EU. Topiramate-associated acute, bilateral, secondary angle-closure glaucoma. *Ophthalmology*. 2004;111(1):109–111.
202. Craig JE, Ong TJ, Louis DL, et al. Mechanism of topiramate-induced acute-onset myopia and angle closure glaucoma. *Am J Ophthalmol*. 2004;137(1):193–195.
203. Mahesh G, Giridhar A, Saikumar SJ, et al. Drug-induced acute myopia following chlorthalidone treatment. *Indian J Ophthalmol*. 2007;55(5):386–388.
204. Sankar PS, Pasquale LR, Grosskreutz CL. Uveal effusion and secondary angle-closure glaucoma associated with topiramate use. *Arch Ophthalmol*. 2001;119(8):1210–1211.
205. Alwitry A, Gardner I. Tamoxifen maculopathy. *Arch Ophthalmol*. 2002;120(10):1402.
206. Kaiser-Kupfer MI, Kupfer C, Rodrigues MM. Tamoxifen retinopathy. A clinicopathologic report. *Ophthalmology*. 1981;88(1):89–93.
207. Chang T, Gonder JR, Ventresca MR. Low-dose tamoxifen retinopathy. *Can J Ophthalmol*. 1992;27(3):148–149.
208. Griffiths MF. Tamoxifen retinopathy at low dosage. *Am J Ophthalmol*. 1987;104(2):185–186.
209. Pavlidis NA, Petris C, Briassoulis E, et al. Clear evidence that long-term, low-dose tamoxifen treatment can induce ocular toxicity. A prospective study of 63 patients. *Cancer*. 1992;69(12):2961–2964.
210. Noureddin BN, Seoud M, Bashshur Z, et al. Ocular toxicity in low-dose tamoxifen: a prospective study. *Eye*. 1999;13(Pt 6):729–733.
211. Heier JS, Dragoo RA, Enzenauer RW, et al. Screening for ocular toxicity in asymptomatic patients treated with tamoxifen. *Am J Ophthalmol*. 1994;117(6):772–775.
212. McKeown CA, Swartz M, Blom J, et al. Tamoxifen retinopathy. *Br J Ophthalmol*. 1981;65(3):177–179.
213. Maenpaa H, Mannerstrom M, Toimela T. Glutamate uptake

is inhibited by tamoxifen and toremifene in cultured retinal pigment epithelial cells. *Pharmacol Toxicol*. 2002;91:116–122.
214. Gualino V, Cohen SY, Delyfer M-N, et al. Optical coherence tomography findings in tamoxifen retinopathy. *Am J Ophthalmol*. 2005;140(4):757–758.
215. Park SS, Zawadzki RJ, Truong SN, et al. Microcystoid maculopathy associated with tamoxifen use diagnosed by high-resolution fourier-domain optical coherence tomography. *Retin Cases Brief Rep*. 2009;3(1):33–35.
216. Bourla DH, Sarraf D, Schwartz SD. Peripheral retinopathy and maculopathy in high-dose tamoxifen therapy. *Am J Ophthalmol*. 2007;144(1):126–128.
217. Ashford AR, Donev I, Tiwari RP, et al. Reversible ocular toxicity related to tamoxifen therapy. *Cancer*. 1988;61(1):33–35.
218. Colley SM, Elston JS. Tamoxifen optic neuropathy. *Clin Experiment Ophthalmol*. 2004;32(1):105–106.
219. Nayfield SG, Gorin MB. Tamoxifen-associated eye disease: a review. *J Clin Oncol*. 1996;14(3):1018–1026.
220. Kalina RE, Wells CG. Screening for ocular toxicity in asymptomatic patients treated with tamoxifen. *Am J Ophthalmol*. 1995;119(1):112–113.
221. Bourla DH, Gonzales CR, Mango CW, et al. Intravitreous vascular endothelial growth factor (VEGF) inhibitor therapy for tamoxifen induced macular edema. *Semin Ophthalmol*. 2007;22(2):87–88.
222. Chang TS, Aylward W, Clarkson JG, et al. Asymmetric canthaxanthin retinopathy. *Am J Ophthalmol*. 1995;119(6):801–802.
223. Lonn LI. Canthaxanthin retinopathy. *Arch Ophthalmol*. 1987;105(11):1590–1591.
224. Espaillat A, Aiello LP, Arrigg PG, et al. Canthaxanthine retinopathy. *Arch Ophthalmol*. 1999;117(3):412–413.
225. Cortin P, Boudreault G, Rousseau AP, et al. Retinopathy due to canthazanthine: 2. Predisposing factors. *Can J Ophthalmol*. 1984;19(5):215–219.
226. Boudreault G, Cortin P, Corriveau LA, et al. Canthaxanthine retinopathy: 1. Clinical study in 51 consumers. *Can J*

Ophthalmol. 1983;18(7):325–328.
227. Harnois C, Cortin P, Samson J, et al. Static perimetry in canthaxanthin maculopathy. *Arch Ophthalmol*. 1988;106(1):58–60.
228. Metge P, Mandirac-Bonnefoy C, Bellaube P. Thesaurismose retinienne à la canthaxanthine. *Bull Mem Soc Fr Ophtalmol*. 1984;95:547–549.
229. Weber U, Goerz G, Hennekes R. Carotenoid retinopathy. I. Morphologic and functional findings. *Klin Monatsbl Augenheilkd*. 1985;186(5):351–354.
230. Daicker B, Schiedt K, Adnet JJ, et al. Canthaxanthin retinopathy: an investigation by light and electron microscopy and physicochemical analysis. *Graefes Arch Clin Exp Ophthalmol*. 1987;225(3):189–197.
231. Chan A, Ko TH, Duker JS. Ultrahigh-resolution optical coherence tomography of canthaxanthine retinal crystals. *Ophthalmic Surg Lasers Imaging*. 2006;37(2):138–139.
232. Scallon LJ, Burke JM, Mieler WF, et al. Canthaxanthine-induced retinal pigment epithelial changes in the cat. *Curr Eye Res*. 1988;7(7):687–693.
233. Harnois C, Samson J, Malenfant M, et al. Canthaxanthin retinopathy: anatomic and functional reversibility. *Arch Ophthalmol*. 1989;107(4):538–540.
234. Leyon H, Ros AM, Nyberg S, et al. Reversibility of canthaxanthin deposits within the retina. *Acta Ophthalmol*. 1990;68(5):607–611.
235. Oosterhuis JA, Remky H, Nijman NM, et al. Canthaxanthin retinopathy without intake of canthaxanthin. *Klin Monatsbl Augenheilkd*. 1989;194(2):110–116.
236. Bullock JD, Albert DM. Flecked retina: appearance secondary to oxalate crystals from methoxyflurane anesthesia. *Arch Ophthalmol*. 1975;93(1):26–31.
237. Novak MA, Roth AS, Levine MR. Calcium oxalate retinopathy associated with methoxyflurane abuse. *Retina*. 1988;8(4):230–236.
238. Albert DM, Bullock JD, Lahav M, et al. Flecked retina secondary to oxalate crystals from methoxyflurane anesthesia: clinical and experimental studies. *Trans Sect*

Ophthalmol Am Acad Ophthalmol Otolaryngol. 1975;79(6):OP817–26.
239. Wells CG, Johnson RJ, Qingli L, et al. Retinal oxalosis: a clinicopathologic report. *Arch Ophthalmol*. 1989;107(11):1638–1643.
240. Ibanez HE, Williams DF, Boniuk I. Crystalline retinopathy associated with long-term nitrofurantoin therapy. *Arch Ophthalmol*. 1994;112(3):304–305.
241. Bishop RJ, Ding X, Heller CK, et al. Rapid vision loss associated with fludarabine administration. *Retina*. 2010;30(8):1272–1277.
242. Roe RH, Jumper JM, Gualino V, et al. Retinal pigment epitheliopathy, macular telangiectasis, and intraretinal crystal deposits in HIV-positive patients receiving ritonavir. *Retina*. 2011;31(3):559–565.
243. Arevalo JF, Russack V, Freeman WR. New ophthalmic manifestations of presumed rifabutin-related uveitis. *Ophthalmic Surg Lasers*. 1997;28(4):321–324.
244. Becker K, Schimkat M, Jablonowski H. Anterior uveitis associated with rifabutin medication in AIDS patients. *Infection*. 1996;24:36–38.
245. Jacobs DS, Piliero PJ, Kuperwaser MG, et al. Acute uveitis associated with rifabutin use in patients with human immunodeficiency virus infection. *Am J Ophthalmol*. 1994;118(6):716–722.
246. Karbassi M, Nikou S. Acute uveitis in patients with acquired immunodeficiency syndrome receiving prophylactic rifabutin. *Arch Ophthalmol*. 1995;113(6):699–701.
247. Kelleher P, Helbert M, Sweeney J, et al. Uveitis associated with rifabutin and macrolide therapy for Mycobacterium avium intracellulare infection in AIDS patients. *Genitourin Med*. 1996;72(6):419–421.
248. Nichols CW. Mycobacterium avium complex infection, rifabutin, and uveitis – is there a connection? *Clin Infect Dis*. 1996;22(Suppl. 1):S43–7 [discussion S7].
249. Rifai A, Peyman GA, Daun M, et al. Rifabutin-associated uveitis during prophylaxis for Mycobacterium avium

complex infection. *Arch Ophthalmol*. 1995;113(6):707.
250. Saran BR, Maguire AM, Nichols C, et al. Hypopyon uveitis in patients with acquired immunodeficiency syndrome treated for systemic Mycobacterium avium complex infection with rifabutin. *Arch Ophthalmol*. 1994;112(9):1159–1165.
251. Tseng AL, Walmsley SL. Rifabutin-associated uveitis. *Ann Pharmacother*. 1995;29(11):1149–1155.
252. Bhagat N, Read RW, Rao NA, et al. Rifabutin-associated hypopyon uveitis in human immunodeficiency virus-negative immunocompetent individuals. *Ophthalmology*. 2001;108(4):750–752.
253. Khan MA, Singh J, Dhillon B. Rifabutin-induced uveitis with inflammatory vitreous infiltrate. *Eye*. 2000;14(Pt 3A):344–346.
254. Saha N, Bansal S, Bishop F, et al. Bilateral hypopyon and vitritis associated with rifabutin therapy in an immunocompetent patient taking itraconazole. *Eye*. 2009;23(6):1481.
255. Chaknis MJ, Brooks SE, Mitchell KT, et al. Inflammatory opacities of the vitreous in rifabutin-associated uveitis. *Am J Ophthalmol*. 1996;122(4):580–582.
256. Ponjavic V, Gränse L, Bengtsson Stigmar E, et al. Retinal dysfunction and anterior segment deposits in a patient treated with rifabutin. *Acta Ophthalmol Scand*. 2002;80(5):553–556.
257. Banker AS, Arevalo JF, Munguia D, et al. Intraocular pressure and aqueous humor dynamics in patients with AIDS treated with intravitreal cidofovir (HPMPC) for cytomegalovirus retinitis. *Am J Ophthalmol*. 1997;124(2):168–180.
258. Davis JL, Taskintuna I, Freeman WR, et al. Iritis and hypotony after treatment with intravenous cidofovir for cytomegalovirus retinitis. *Arch Ophthalmol*. 1997;115(6):733–737.
259. Friedberg DN. Hypotony and visual loss with intravenous cidofovir treatment of cytomegalovirus retinitis. *Arch Ophthalmol*. 1997;115(6):801–802.

260. Jabs DA. Cidofovir. *Arch Ophthalmol*. 1997;115(6):785–786.
261. Kirsch LS, Arevalo JF, De Clercq E, et al. Phase I/II study of intravitreal cidofovir for the treatment of cytomegalovirus retinitis in patients with the acquired immunodeficiency syndrome. *Am J Ophthalmol*. 1995;119(4):466–476.
262. Kirsch LS, Arevalo JF, Paz EC. de la Intravitreal cidofovir (HPMPC) treatment of cytomegalovirus retinitis in patients with acquired immune deficiency syndrome. *Ophthalmology*. 1995;102:533–543.
263. Lea AP, Bryson HM. Cidofovir. *Drugs*. 1996;52(2):225–230 [discussion 31].
264. Rahhal FM, Arevalo JF, Munguia D, et al. Intravitreal cidofovir for the maintenance treatment of cytomegalovirus retinitis. *Ophthalmology*. 1996;103(7):1078–1083.
265. Taskintuna I, Banker AS, Rao NA, et al. An animal model for cidofovir (HPMPC) toxicity: intraocular pressure and histopathologic effects. *Exp Eye Res*. 1997;64(5):795–806.
266. Taskintuna I, Rahhal FM, Arevalo JF, et al. Low-dose intravitreal cidofovir (HPMPC) therapy of cytomegalovirus retinitis in patients with acquired immune deficiency syndrome. *Ophthalmology*. 1997;104(6):1049–1057.
267. Wang L, Damji KF, Chialant D, et al. Hypotony after intravenous cidofovir therapy for the treatment of cytomegalovirus retinitis. *Can J Ophthalmol*. 2002;37(7):419–422.
268. Blair JR, Mieler WF. Retinal toxicity associated with commonly encountered systemic agents. *Int Ophthalmol Clin*. 1995;35(4):137–156.
269. Weleber RG, Shults WT. Digoxin retinal toxicity. Clinical and electrophysiological evaluation of a cone dysfunction syndrome. *Arch Ophthalmol*. 1981;99(9):1568–1572.
270. Baumbach GL, Cancilla PA, Martin-Amat G, et al. Methyl alcohol poisoning. IV. Alterations of the morphological findings of the retina and optic nerve. *Arch Ophthalmol*. 1977;95(10):1859–1865.
271. Eells JT, Makar AB, Noker PE, et al. Methanol poisoning and formate oxidation in nitrous oxide-treated rats. *J Pharmacol Exp Ther*. 1981;217(1):57–61.

272. Gilger AP, Potts AM. Studies on the visual toxicity of methanol: the role of acidosis in experimental methanol poisoning. *Am J Ophthalmol*. 1955;39(2 Pt 2):63–86.
273. Hayreh MS, Hayreh SS, Baumbach GL, et al. Methyl alcohol poisoning III. Ocular toxicity. *Arch Ophthalmol*. 1977;95(10):1851–1858.
274. Ingemansson SO. Clinical observations on ten cases of methanol poisoning with particular reference to ocular manifestations. *Acta Ophthalmol*. 1984;62(1):15–24.
275. Martin-Amat G, McMartin KE, Hayreh SS, et al. Methanol poisoning: ocular toxicity produced by formate. *Toxicol Appl Pharmacol*. 1978;45(1):201–208.
276. Martin-Amat G, Tephly TR, McMartin KE, et al. Methyl alcohol poisoning. II. Development of a model for ocular toxicity in methyl alcohol poisoning using the rhesus monkey. *Arch Ophthalmol*. 1977;95(10):1847–1850.
277. Treichel JL, Murray TG, Lewandowski MF, et al. Retinal toxicity in methanol poisoning. *Retina*. 2004;24(2):309–312.
278. Fujihara M, Kikuchi M, Kurimoto Y. Methanol-induced retinal toxicity patient examined by optical coherence tomography. *Jpn J Ophthalmol*. 2006;50(3):239–241.
279. Frisen L, Malmgren K. Characterization of vigabatrin-associated optic atrophy. *Acta Ophthalmol Scand*. 2003;81:466–473.
280. Malmgren K, Ben-Menachem E, Frisén L. Vigabatrin visual toxicity: evolution and dose dependence. *Epilepsia*. 2001;42(5):609–615.
281. Vobig MA. Retinal side-effects of sildenafil. *Lancet*. 1999;353(9162):1442.
282. Vobig MA, Klotz T, Staak M, et al. Retinal side-effects of sildenafil. *Lancet*. 1999;353(9150):375.
283. Zrenner E. No cause for alarm over retinal side-effects of sildenafil. *Lancet*. 1999;353(9150):340–341.
284. Marmor MF. Sildenafil (Viagra) and ophthalmology [Editorial]. *Arch Ophthalmol*. 1999;117(4):518–519.
285. Marmor MF, Kessler R. Sildenafil (Viagra) and ophthalmology. *Surv Ophthalmol*. 1999;44(2):153–162.
286. Luu JK, Chappelow AV, McCulley TJ, et al. Acute effects of

sildenafil on the electroretinogram and multifocal electroretinogram. *Am J Ophthalmol*. 2001;132(3):388–394.
287. Jagle H, Jagle C, Serey L. Dose-dependency and time-course of electrophysiologic short-term effects of Viagra: a case study. *Doc Ophthalmol*. 2005;110:247–254.
288. Jagle H, Jagle C, Serey L, et al. Visual short-term effects of Viagra: double-blind study in healthy young subjects. *Am J Ophthalmol*. 2004;137(5):842–849.
289. Zoumalan CI, Zamanian RT, Doyle RL. ERG evaluation of daily, high-dose sildenafil usage. *Doc Ophthalmol*. 2008;118:225–231.
290. Cordell WH, Maturi RK, Costigan TM, et al. Retinal effects of 6 months of daily use of tadalafil or sildenafil. *Arch Ophthalmol*. 2009;127(4):367–373.
291. Birch DG, Toler SM, Swanson WH, et al. A double-blind placebo-controlled evaluation of the acute effects of sildenafil citrate (Viagra) on visual function in subjects with early-stage age-related macular degeneration. *Am J Ophthalmol*. 2002;133(5):665–672.
292. Grunwald JE, Metelitsina T, Grunwald L. Effect of sildenafil citrate (Viagra) on retinal blood vessel diameter. *Am J Ophthalmol*. 2002;133(6):809–812.
293. Grunwald JE, Siu KK, Jacob SS, et al. Effect of sildenafil citrate (Viagra) on the ocular circulation. *Am J Ophthalmol*. 2001;131(6):751–755.
294. Harris A, Kagemann L, Ehrlich R, et al. The effect of sildenafil on ocular blood flow. *Br J Ophthalmol*. 2008;92(4):469–473.
295. McCulley TJ, Luu JK, Marmor MF, et al. Effects of sildenafil citrate (Viagra) on choroidal congestion. *Ophthalmologica*. 2002;216(6):455–458.
296. Metelitsina TI, Grunwald JE, DuPont JC, et al. Effect of Viagra on the foveolar choroidal circulation of AMD patients. *Exp Eye Res*. 2005;81(2):159–164.
297. Akash R, Hrishikesh D, Amith P, et al. Case report: association of combined nonarteritic anterior ischemic optic neuropathy (NAION) and obstruction of cilioretinal artery with overdose of Viagra. *J Ocul Pharmacol Ther*.

2005;21(4):315–317.
298. Allibhai ZA, Gale JS, Sheidow TS. Central serous chorioretinopathy in a patient taking sildenafil citrate. *Ophthalmic Surg Lasers Imaging*. 2004;35(2):165–167.
299. Pomeranz HD, Bhavsar AR. Nonarteritic ischemic optic neuropathy developing soon after use of sildenafil (Viagra): a report of seven new cases. *J Neuroophthalmol*. 2005;25(1):9–13.
300. Pomeranz HD, Smith KH, Hart WM, et al. Sildenafil-associated nonarteritic anterior ischemic optic neuropathy. *Ophthalmology*. 2002;109(3):584–587.
301. Tripathi A, O'Donnell NP. Branch retinal artery occlusion; another complication of sildenafil. *Br J Ophthalmol*. 2000;84(8):934–935.
302. Bollinger K, Lee MS. Recurrent visual field defect and ischemic optic neuropathy associated with tadalafil rechallenge. *Arch Ophthalmol*. 2005;123(3):400–401.
303. Carter JE. Anterior ischemic optic neuropathy and stroke with use of PDE-5 inhibitors for erectile dysfunction: cause or coincidence? *J Neurol Sci*. 2007;262(1–2):89–97.
304. Escaravage GK, Wright JD, Givre SJ. Tadalafil associated with anterior ischemic optic neuropathy. *Arch Ophthalmol*. 2005;123(3):399–400.
305. Fraunfelder FW, Fraunfelder FT. Central serous chorioretinopathy associated with sildenafil. *Retina*. 2008;28(4):606–609.
306. Gedik S, Yilmaz G, Akova YA. Sildenafil-associated consecutive nonarteritic anterior ischaemic optic neuropathy, cilioretinal artery occlusion, and central retinal vein occlusion in a haemodialysis patient. *Eye*. 2007;21(1):129–130.
307. Hayreh SS. Erectile dysfunction drugs and non-arteritic anterior ischemic optic neuropathy: is there a cause and effect relationship? *J Neuroophthalmol*. 2005;25(4):295–298.
308. Peter NM, Singh MV, Fox PD. Tadalafil-associated anterior ischaemic optic neuropathy. *Eye*. 2005;19(6):715–717.
309. Quiram P, Dumars S, Parwar B, et al. Viagra-associated serous macular detachment. *Graefes Arch Clin Exp*

Ophthalmol. 2005;243(4):339–344.

93

Photic Retinal Injuries

Mechanisms, Hazards, and Prevention

Andrew Symons, Helen Chan, Martin A. Mainster

Photic retinal injuries are uncommon. Managing them effectively requires knowledge of how intense light interacts with the retina and choroid. Recent advances in retinal imaging have improved our understanding of these interactions.

Photic injuries occur when light is absorbed by tissue chromophores. Melanin and hemoglobin are the most effective retinal light absorbers.[1–3] Light is also absorbed by lipofuscin, macular pigment and photopigments for visual and nonvisual photoreception.[4,5] Absorption spectra describe how light absorption varies by wavelength. Melanin and lipofuscin absorption increase steadily with decreasing wavelength. Other absorption spectra peak at specific wavelengths.[1,2,4,5]

Optical radiation includes 400–700 nm visible light and shorter wavelength ultraviolet (UV) radiation (UV-C, 100–280 nm; UV-B, 280–320 nm; UV-A, 320–400 nm). The cornea shields the retina from UV radiation below 300 nm.[6] The crystalline lens protects the retina from most UV-B and UV-A radiation, but crystalline lenses under 30 years of age may transmit a small amount of potentially harmful UV-B radiation.[6–8] Other ocular defense mechanisms against UV radiation and intense visible light include eyebrow shadowing, corneal reflection of light not incident perpendicular to its surface

(Fresnel law), and the pupillary, aversion, squint and blink responses.[9–11]

Retinal light exposure is specified using parameters including optical energy (joule), exposure (joule/cm^2), power (watt) and irradiance (watt/cm^2).[3] Optical power is high when energy is delivered quickly in brief exposures. Exposure and irradiance are high when optical energy and power are confined to small areas, respectively.

Light can produce beneficial or harmful photomechanical, photothermal, and/or photochemical retinal effects.[12–16]

Photomechanical Effects

The most common signs of acute photomechanical retinal trauma are retinal hemorrhages and/or holes.

Photomechanical Mechanisms

Surgical photomechanical effects include photodisruption, photofragmentation, and photovaporization.[16] Photodisruption occurs in Nd : YAG laser capsulotomy and lamellar keratectomy when infrared laser energy ionizes target tissue molecules, producing plasma and a rapidly expanding shock wave that dissects target tissue.[17] Photofragmentation occurs in excimer laser photorefractive keratectomy when UV laser energy breaks bonds in corneal surface molecules and residual energy volatilizes molecular fragments. Photovaporization occurs in holmium laser sclerostomy and erbium laser phacolysis when rapid water vapor expansion excavates target tissues.

Most accidental photomechanical retinal injuries are caused by very brief laser exposures ranging in duration from a hundred femtoseconds (10^{-15} sec) to microseconds (10^{-6} sec).[18–22] Their very high retinal irradiances (power densities) produce tissue heating and expansion that cause immediate thermomechanical chorioretinal distortion and bleeding. Photovaporization may occur, but retinal irradiances are generally far too low for other photomechanical effects. Most victims experience a brilliant light flash followed by immediate monocular vision loss. An audible

sound (pop) and/or momentary pain occur infrequently at the time of the laser accident.

Photomechanical Retinal Injuries

A few photomechanical laser accidents occur each year.[19–22] Most are caused by laboratory research lasers and military rangefinders or target designators.[20–27] Iatrogenic injuries have also been reported.[28–30] Injuries can be prevented by effective laser safety training and proper protective eyewear. Surgical Q-switched and femtosecond laser systems have numerous safeguards that limit high optical irradiances to small, restricted spatial volumes.

Initial vision loss depends on a laser injury's retinal location and associated chorioretinal disruption and bleeding.[21,23,24,31] Blood can spread laterally in subhyaloid, subretinal or sub-retinal pigment epithelium (RPE) spaces. Chorioretinal scars form and evolve. Vision may improve over days to months. Prognosis is excellent for less severe injuries that do not involve the fovea. Patients should be followed for macular holes and choroidal neovascularization (CNV) that can develop in the months following an injury (Fig. 93.1).[25,30,32–37]

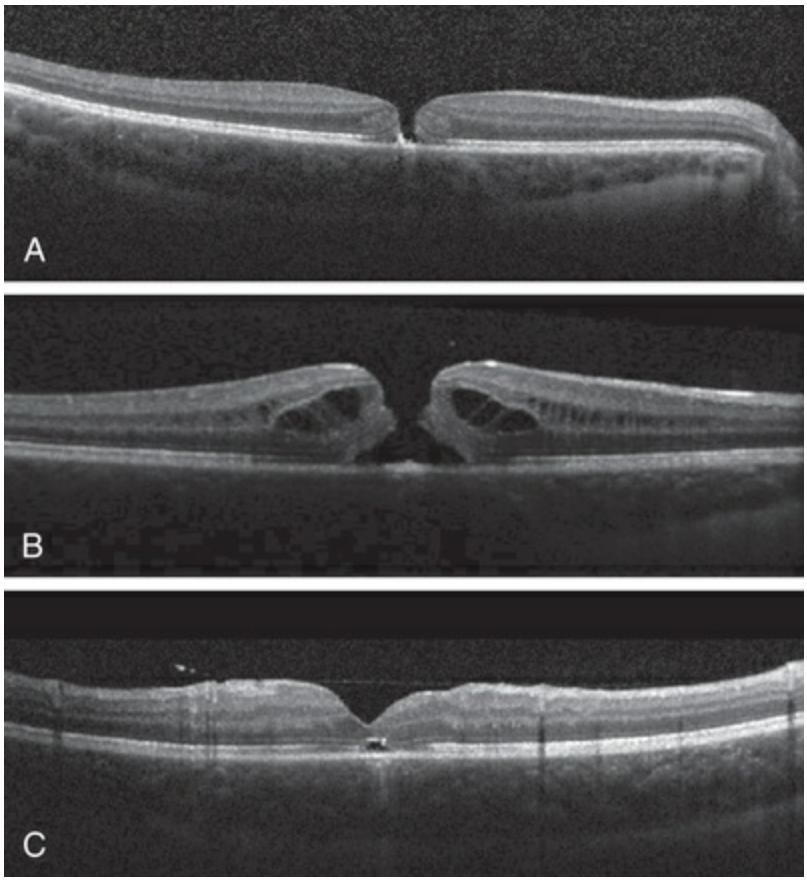

FIG. 93.1 The most common signs of acute photomechanical retinal trauma are retinal hemorrhages and/or holes. Exposure to very high retinal irradiance laser radiation produces tissue heating and expansion that causes immediate chorioretinal distortion and bleeding. Symptoms depend on the extent and retinal location of injuries. In this case, an 11-year-old boy was injured by blue-light from a powerful handheld consumer laser. One week later, his visual acuity was 20/300 and a small full-thickness macular hole was present in his right eye (A). The hole enlarged markedly over the next 2 months (B) and vitrectomy with internal limiting membrane peeling was performed. The hole was closed (C) and visual acuity improved to 20/160 post-operatively.

Treatment

Optical coherence tomography (OCT) and fluorescein angiography

are valuable for evaluating, managing, and documenting real and alleged injuries. Anti-inflammatory and neuroprotective drugs for reducing laser damage have been studied experimentally,[38,39] but clinical trials of their efficacy have been impractical because injuries are uncommon. Macular holes may close and CNV may resolve spontaneously but conventional macular hole surgery and anti-VEGF therapy are potentially useful when needed.[23,26,30,32–36]

Diagnosis of Real Laser Injuries

In actual laser accidents, (1) the light source is usually known, (2) typical chorioretinal damage occurs, (3) there is an unambiguous temporal relationship between the laser incident and serious visual symptoms, (4) the severity of visual symptoms is commensurate with the extent of retinal damage demonstrable with retinal imaging and examination, and (5) typical chorioretinal remodeling occurs after the injury.[40]

Most laser injuries and noninjurious laser exposures are painless.[40] Eye rubbing after a laser incident can cause painful self-inflicted corneal abrasions sometimes falsely attributed to the laser exposure.[40–42] Real retinal laser injuries do not cause chronic headache or other somatic complaints, including head, neck or jaw pain.[40]

The ease of laser injury diagnosis is directly proportional to the severity of the laser injury.[40] In ambiguous cases, subtle retinal findings have an excellent visual prognosis. When a retinal laser injury is alleged and objective findings are absent or within normal limits, diagnosis of laser injury should be deferred pending a rigorous review of the patient's retinal findings, ophthalmic and systemic tests, clinical course, and past medical history. A guideline has been published for this type of analysis.[40]

Pressure from patients or attorneys to reach quick conclusions in alleged but inapparent laser injuries should be resisted.[40,43] Organic retinal laser injuries do not cause chronic pain, and if a significant visual abnormality is present, it should be reproducible and consistent with a significant chorioretinal abnormality.[40]

Photothermal Effects

The most common signs of acute photothermal retinal trauma are ophthalmoscopically visible photocoagulation burns without hemorrhage or holes.

Photothermal Mechanisms

Photocoagulation occurs when intense light is absorbed mostly by melanin in the RPE and choroid. Light energy is converted into heat, increasing the temperature of directly exposed pigmented tissues.[2,3,44] Heat conduction spreads temperature elevation to adjacent sites. Overlying neural retina damaged by heat conduction loses its transparency and becomes visible as a focal white lesion ("burn") because it scatters white fundus illumination light back at an observer. Retinal burns increase in size over time due to post-exposure scarring and collateral chorioretinal damage that is not apparent immediately after the exposure.[2]

Standard clinical photocoagulation produces immediately visible burns with increases in retinal temperature exceeding 20 °C.[1] Photomechanical effects occur at roughly three times the laser exposure needed for a visible lesion. Invisible lesions that are apparent only with fluorescein angiography or autofluorescence imaging occur at half to a fourth of the exposure needed to produce ophthalmoscopically visible lesions. In clinical parlance, "subthreshold" means ophthalmoscopically invisible or "subvisible".[3] Subthreshold photocoagulation can produce beneficial therapeutic effects with low temperature rises that produce minimal or no apparent retinal damage.[45]

Most accidental photothermal retinal injuries are caused by pulsed laser exposures ranging in duration from a microsecond to a few seconds. Retinal irradiance is high enough for photocoagulation but too low for photomechanical effects. The magnitude and duration of chorioretinal temperature elevation determine the severity of a retinal burn, along with lesion size, fundus pigmentation and chorioretinal sequelae.[3,21] Photothermal and photomechanical retinal injuries are managed similarly. Injuries should be followed for retinal holes and CNV that can

develop within a few months of the injury.[34,46–51]

Photothermal Retinal Injuries

Industrial and military photothermal laser accidents are less common than photomechanical ones because they require a narrow range of lower retinal irradiances.

Operating Room or Medical Office Injuries

Most medical laser accidents go unreported for legal reasons.[40] Indirect ophthalmoscope photocoagulator beams and their reflections are potentially hazardous for many meters. Bystanders should put on protective eyewear before these systems are switched from standby to treatment mode. Protective operating microscope filters should be in place and the laser delivery probe inside a patient's eye before an endoscopic photocoagulator is switched to treatment mode.[52]

Slit-Lamp Photocoagulators

Slit-lamp photocoagulator operators are protected from backscattered laser light by optical filters.[53] Laser beam reflections are theoretically hazardous for bystanders up to 2 meters from a flat-surfaced contact lens,[54] so they should wear laser safety glasses or goggles effective for the laser treatment wavelength. No injury of this type has ever been reported.

Laser Pointers and Other Consumer Laser Devices

Laser pointers marketed in the United States are regulated by the Food and Drug Administration (FDA).[41,42,55] They are supposed to produce less than 5 mW (milliWatt) of power (Class 3A) and have warning labels cautioning users not to stare into the laser beam. Brief accidental or inadvertent laser pointer exposures do not cause retinal damage because they are terminated typically in less than 0.25 seconds by normal aversion responses to uncomfortable, dazzling light.[41,55]

Staring deliberately into a laser pointer beam for more than 10 seconds is hazardous and has caused retinal injuries.[41,42,56–58] A laser

pointer injury occurred in an 11-year-old girl who stared into a red laser pointer beam for more than 10 seconds because her classmates wanted to see if her pupil would constrict.[56] Prominent foveolar pigment mottling occurred in her affected eye, along with an initial decrease in visual acuity to 20/60. Pigment mottling faded and visual acuity normalized over several months.

Powerful "handheld laser systems" with dangerous output powers ranging from 20 to 1000 mW (Class 3B or 4) can appear identical to laser pointers and be purchased over the Internet. Low cost has made them available to children, adults who may not observe warning labels, and rioters. These devices are photocoagulators, not laser pointers. They have already caused serious photothermal and photomechanical retinal injuries and represent an increasing public health concern.[47,49,57,59–61] A powerful 100 mW consumer handheld laser resembling a laser pointer caused an injury in a 12-year-old boy who stared for several seconds into its beam reflected by a mirror (Fig. 93.2).[62] Visual acuity reduced to 20/60 and foveolar pigment mottling occurred. Spectral domain OCT of this case and many similar cases demonstrated focal loss of the ellipsoid zone and an area of hyperreflectivity adjacent to the RPE.[48,50,51,62–69] Fundus autofluorescence may show heterogeneous hyperautofluorescence in injured retinal areas.[51,65,70]

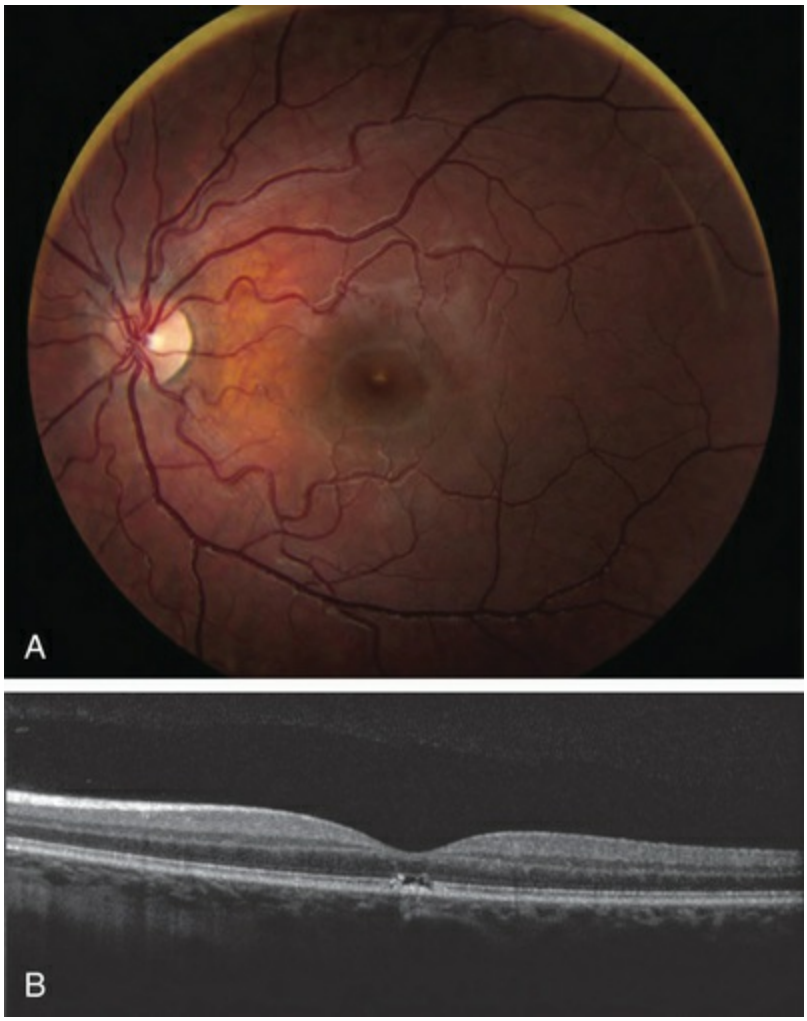

FIG. 93.2 Acute photothermal injury causes photocoagulation burns or pigment changes without hemorrhage or holes. Retinal injury occurred in a 12-year-old boy who deliberately stared for several seconds into a green handheld laser beam reflected by a mirror. Visual acuity reduced to 20/60 and foveolar pigment mottling occurred. Spectral domain optical coherence tomography demonstrated focal loss of the ellipsoid zone and an area of hyperreflectivity adjacent to the retinal pigment epithelium. Visual acuity normalized over several months. (Reproduced with permission from Weng CY, Baumal CR, Albini TA, et al. Self-induced laser maculopathy in an adolescent boy utilizing a mirror. Ophthalmic Surg Lasers Imaging Retina 2015;46(4): 485-488.)

Lasers have been inappropriately marketed as toys for young children.[48,61,66,68,71] Lasers in recreational lightshows have also caused serious photothermal retinal injuries in bystanders.[72,73]

Photochemical Effects

The most common signs of acute photochemical retinal trauma are yellow–white small foveolar lesions in solar and welding arc maculopathy, and larger often extrafoveal lesions in operating microscope and endoilluminator injuries.

Photochemical Mechanisms

Accidental photochemical retinal injuries (known as photic retinopathy or retinal phototoxicity) are caused by prolonged intense light exposures that probably would be well tolerated if experienced only momentarily.[5] They occur at chorioretinal temperature elevations too low for photothermal damage, at illuminances far exceeding normal environmental levels, in exposures lasting from seconds to minutes. Optical radiation produces highly reactive oxygen radicals that can damage retinal cell membranes, proteins, carbohydrates, and nucleic acids. The extent of a photochemical retinal injury depends on individual defense mechanisms, the location and area of exposed retina, and the duration, intensity, and spectrum of the light exposure.[5,10,12,74–76]

Photic retinopathy does not occur unless acute cellular damage is so excessive that it acutely overwhelms retinal repair mechanisms.[5,52] Patients safely undergo bright but much lower irradiances in ophthalmic imaging studies and light therapy for seasonal affective disorder.[12,52,77]

Action spectra characterize how effectively different wavelengths cause a photochemical effect.[78] Photic retinopathy can be divided into photosensitizer- and photopigment-mediated phototoxicities which have different action spectra.[4,5,79]

The hazardousness of photosensitizer-mediated retinal phototoxicity increases rapidly with decreasing wavelength.[5,74] This is similar to the absorption spectrum of lipofuscin in the RPE, which is its primary mediator.[80,81] Thus, UV radiation is much more hazardous than visible light. In an aphakic eye, UV radiation, violet light (400–440 nm) and blue light (440–500 nm) account for 67%, 18%, and 14% of potential retinal phototoxicity, respectively.[82,83] Photosensitizer-mediated phototoxicity is the basis for the

international consensus aphakic standard Aλ phototoxicity function used to estimate industrial acute retinal phototoxicity risks.[84]

In an adult phakic eye, the retina has the additional shielding of crystalline lens attenuation of UV radiation and shorter wavelength visible light. That is why the international consensus phakic standard Bλ phototoxicity function peaks at 440 nm in the blue part of the spectrum. The Bλ function is often termed a "blue light hazard" function, even though blue light has far less retinal phototoxicity than violet light or UV radiation.[4,5,84]

The hazardousness of photopigment-mediated retinal phototoxicity peaks around 500 nm (blue–green), similar to the luminous sensitivity of scotopic vision because the photopigment rhodopsin mediates both processes.[5,85,86] This type of photic retinopathy requires only 1% of the retinal irradiance needed for photosensitizer-mediated phototoxicity,[10,79,87,88] but experimental studies were performed with highly light-sensitive nocturnal rodents whose primary photopigment is rhodopsin.[5,85,88]

Clinical findings are similar in solar or welding arc maculopathies, and operating microscope and endoilluminator injuries.[5,52]

Photochemical Retinal Injuries

Solar and Welder's Maculopathy

Fig. 93.3 shows a typical yellow–white solar maculopathy lesion.[89,90] In the acute setting, OCT imaging demonstrates a full-thickness hyperreflective lesion.[91–94] Central retinal dysfunction has also been shown on multifocal electroretinography.[95] Lesions fade over several weeks, resolving completely or leaving foveolar distortion, pigment mottling, or even a macular hole.[89] Welding arc injuries produce similar clinical abnormalities.[5,96,97] Welder's maculopathy is extremely rare but it may be underreported because its transient clinical symptoms may be masked by those of associated photokeratitis.[5,8,98]

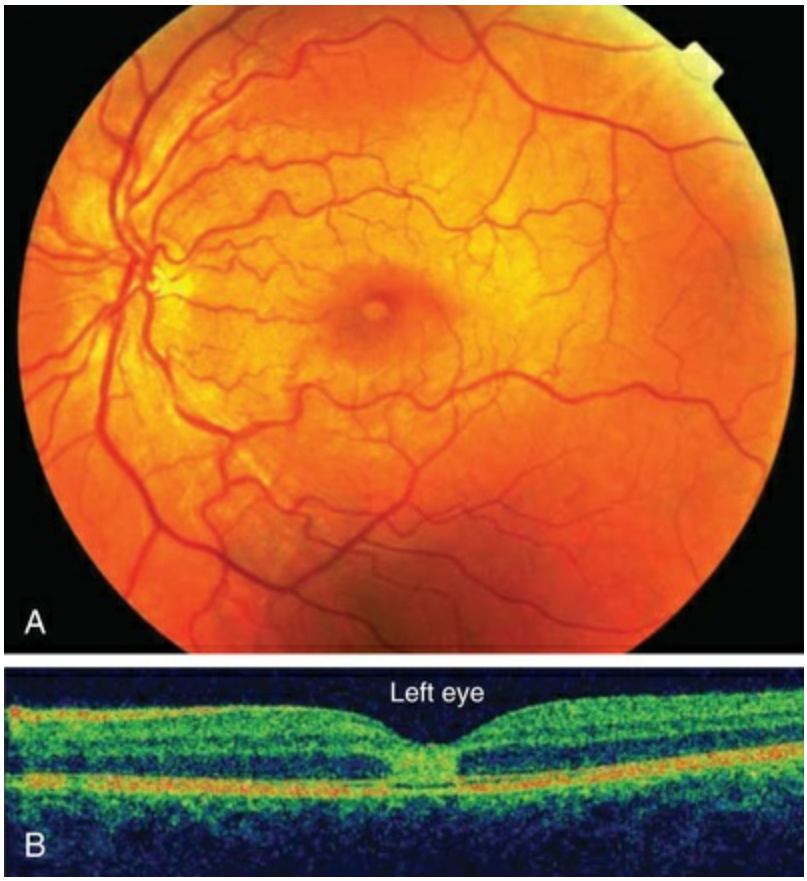

FIG. 93.3 Acute solar maculopathy typically produces a small yellow–white foveolar lesion, as seen in this patient who presented with visual acuity of 20/40 after gazing directly at the sun. Optical coherence tomography in the acute setting demonstrated full-thickness foveal hyperreflection. The lesions faded and visual acuity returned to 20/30 in the 3 months following the injury. (Reproduced with permission from Levy S, Sheck L, Guest S. OCT appearances in acute solar retinopathy. Arch Ophthalmol 2012;130:1540.)

Common visual complaints after acute solar or welding arc injury are blurred vision, central scotoma, and erythropsia. Post-injury visual acuity may be normal or decreased to the 20/40 to 20/200 range. Visual acuity usually returns to 20/20 to 20/40 over 6 months.[5,89] Fluorescein angiography may be normal or may show foveal RPE defects in more severe injuries.[89,93,99–103] Fundus autofluorescence may be normal or demonstrate focal hypoautofluorescence.[93,94,100] The characteristic OCT finding months to years after injury is a well-defined outer retinal hyporeflective gap in the ellipsoid and interdigitation zones, as shown in Fig. 93.4

for a welding arc injury.[5,92,93,97,100,102–112]

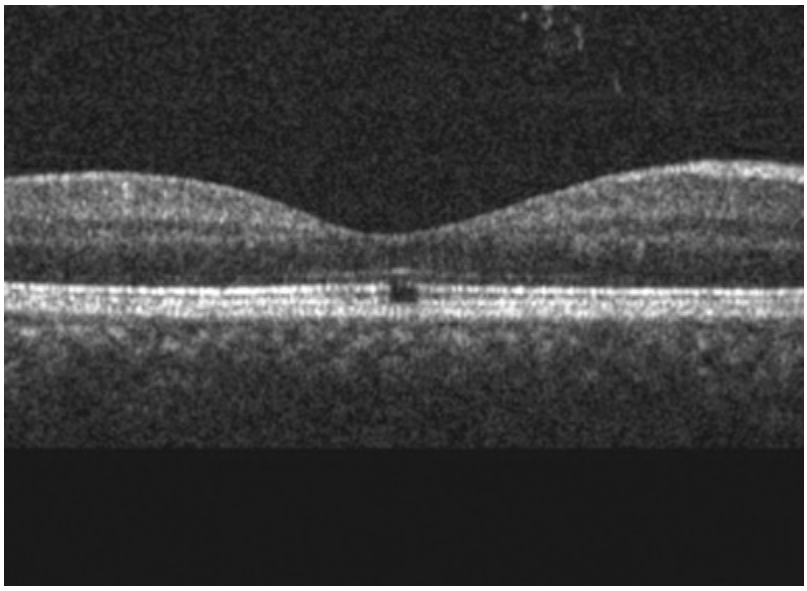

FIG. 93.4 Optical coherence tomography (OCT) images taken months to years after solar or welding arc injuries usually reveal a well-defined foveolar outer retinal hyporeflective space.[5,97,104,108] This 34-year-old male had been welding since 11 years of age and complained of vision loss for 5 months prior to the OCT study. A horizontal scan through his fovea shows largely normal retinal pigment epithelium and external limiting membrane hyperreflective bands but interruption of ellipsoid and interdigitation zone hyperreflective bands. These OCT findings are consistent with chronic damage to photoreceptor inner and outer segment segments.[89] (Courtesy of Suman Pilli, MD, Muralidhar Ogoti, MD, and Vishwanath Kalluri, MD.)

The histopathology of solar retinopathy has been studied in volunteers who stared at the sun monocularly for 10 to 60 minutes before enucleation for choroidal melanoma.[90,113] Photoreceptor damage included vesiculation and fragmentation of photoreceptor outer segment lamellae, mitochondrial swelling, and nuclear pyknosis.[90,113] Cones appeared to be more damage-resistant than rods, possibly accounting for good visual outcomes after some injuries.[113] RPE damage was variable.[90,113] Imaging and histopathologic data to date do not permit determination of

whether solar and welding arc injuries are primarily of RPE and/or photoreceptor origin.

Foveomacular retinitis is a term used to describe foveal abnormalities resembling photic retinopathy. It occurs after blunt ocular trauma and whiplash injury[114–116] and in people with no history of mechanical or photic trauma.[117,118] Outbreaks were reported in military personnel during World War II and again from 1966 to 1973,[119–122] which were ascribed to solar exposure.[121,123] This is consistent with reports of solar maculopathy in young people who have been sunbathing but not sungazing,[124,125] possibly due to Henle layer fiberoptic channeling of short-wavelength photons from perifoveal regions to the center of the fovea (Fig. 93.5).[126]

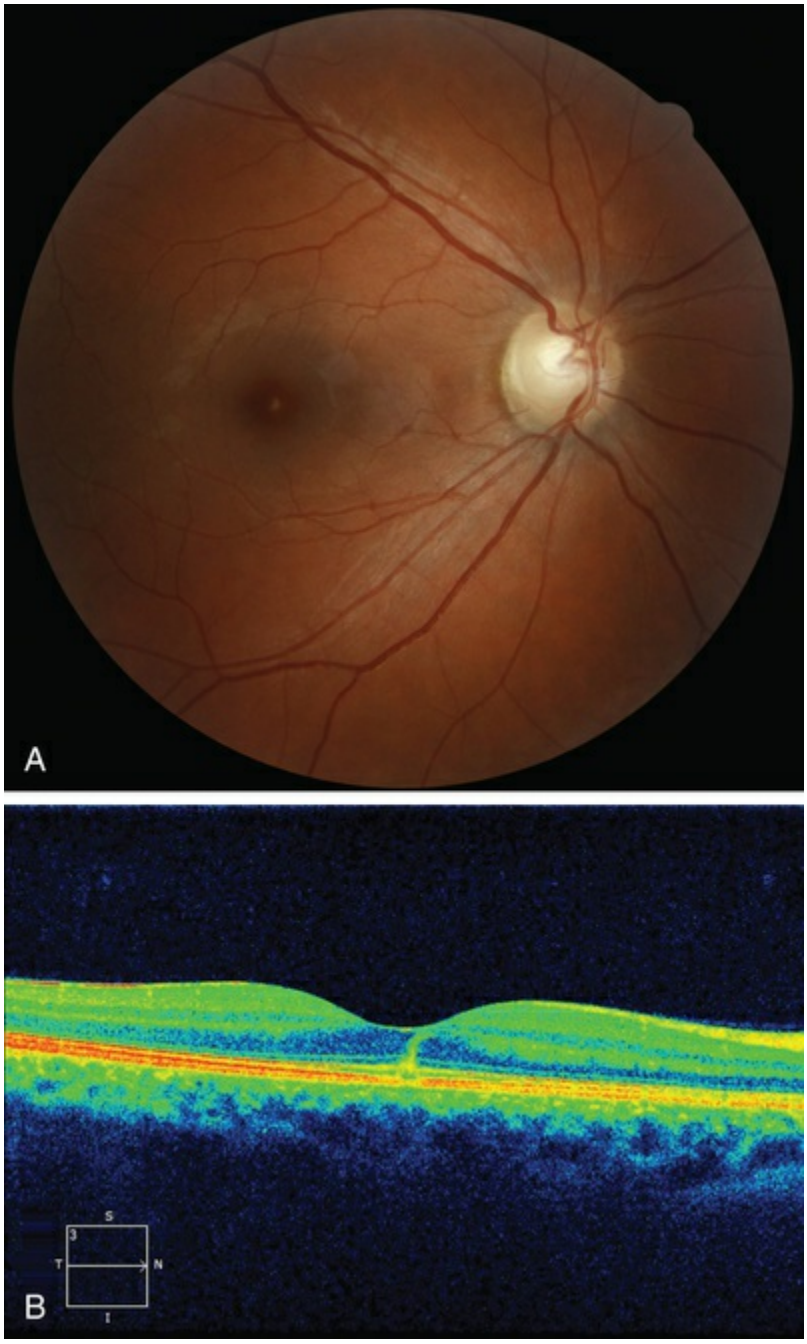

FIG. 93.5 Acute solar maculopathy typically causes a small yellow–white foveolar lesion with full-thickness optical coherence tomography hyperreflectivity. This patient had a localized, less severe injury when he gazed at an eclipse at low solar inclination. These findings may be consistent with Henle layer fiberoptic channeling of photons to the central fovea. (Image courtesy of Daniel Chiu, FRANZCO.)

Momentary solar observation is safe or it would be dangerous to look upwards on a bright sunny day. Even at noontime on a clear

day, direct solar observation with a 3-mm pupil diameter causes only a 4 °C retinal temperature rise, far too low for photocoagulation.[127] Thus, typical solar maculopathy is photochemical not photothermal damage. Conversely, solar observation with a dilated 7-mm pupil produces a 22 °C retinal temperature increase, well above the 10 °C threshold for retinal photocoagulation.[44,127] Telescope-assisted solar observation produces even higher retinal temperature increases.[127,128]

Solar eclipse observation is particularly hazardous because pupillary dilation can occur and increase retinal irradiance.[128] There are many indirect methods for safely viewing solar eclipses.[128,129] Sungazing injuries have been reported to occur during hypoglycemia, drug abuse, psychosis, and religious rituals.[5,103] Sunglasses are not safe for sungazing and pupillary dilation potentially associated with their use may increase the risk of solar injury.[9,12,129] Prolonged solar observation causes the most damage, especially with pharmacologically dilated pupils.

Photokeratitis is a common welding arc accident, but welder's maculopathy is an unusual event. When welders fail to use appropriate eye protection filters, younger workers are at greater risk for retinal injury because of their clear ocular media. The UV-B window in the crystalline lens discussed previously closes by roughly 30 years of age.[6–8] At younger ages, some highly phototoxic UV-B welding arc radiation may be transmitted to the retina, possibly accounting for welding arc maculopathy and welders' reportedly increased risk of uveal melanoma.[6,8] Photic injuries have also been caused by UV-B radiation and/or short wavelength visible light from a femtosecond laser plasma[130] and a short-circuiting high-tension electric circuit.[131]

Experimental photic retinopathy is enhanced by elevated body temperature,[85,132,133] so increased body temperature from a hot day, exercise, or fever could increase the risk of retinal phototoxicity, perhaps accounting for the age-old admonishment to protect children with fevers from bright sunlight.[5] Darker chorioretinal pigmentation could increase local chorioretinal temperature rise associated with solar observation, perhaps further increasing the risk of damage. The fovea is at greatest risk for solar damage in direct sungazing, but foveal injuries in young adults who have been

sunbathing but not sungazing may occur because of crystalline lens UV-B transmission and/or Henle fiberoptic transmission of short wavelength photons toward the fovea.[126]

Operating Microscope and Endoilluminator Injuries

Typical operating microscope injuries are oval lesions measuring 0.5–2 disc diameters in size.[134,135] Damage sites are often inferior to the fovea due to microscope tilt and illumination positioning.[136,137] Fiberoptic endoilluminators can cause comparable lesions elsewhere,[138] as shown in Fig. 93.6. Injuries have occurred in corneal, cataract, glaucoma, and retinal surgery.[134,135,139–141] Photochemical retinal damage is localized primarily to photoreceptors and the RPE as in solar and welder's maculopathies.[142–144]

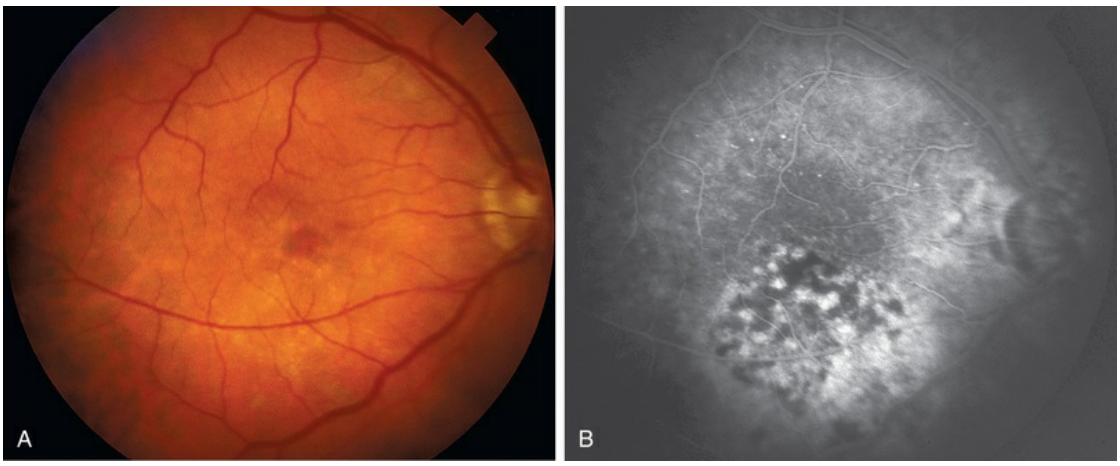

FIG. 93.6 An operating microscope injury in a 67-year-old male with diabetes who had undergone an intraocular lens exchange operation 1 year earlier. The oval-shaped area of retinal pigment epithelial degeneration inferior to the fovea was not prominent ophthalmoscopically, as shown in the fundus photograph (A), but the lesion was quite apparent in the fluorescein angiogram taken on the same day (B).

Lesion size, location, and severity determine vision loss from an operating microscope injury. Lesions initially have a yellow–white appearance sometimes accompanied by a shallow serous neural retinal detachment. This finding resolves rapidly, followed by local

RPE atrophy and pigment mottling. Chronic lesions are usually much less apparent ophthalmoscopically than angiographically, as shown in Figs. 93.6A–B, respectively. Lesions may also appear as localized areas of hyperautofluorescence.[145] Fig. 93.7A is the OCT image of a 70-year-old female with an operating microscope injury temporal to her fovea and also central cystoid macular edema (CME) shortly after complicated cataract surgery. The OCT image in Fig. 93.7B taken years after the resolution of the CME shows persistent chorioretinal scarring at the site of operating microscope injury,[145] consistent with histopathologic findings in human and animal studies.[142–144] Imaging and histopathologic data to date do not permit determination of whether operating microscope and endoilluminator injuries are arise primarily in the RPE or photoreceptors or a combination of both.

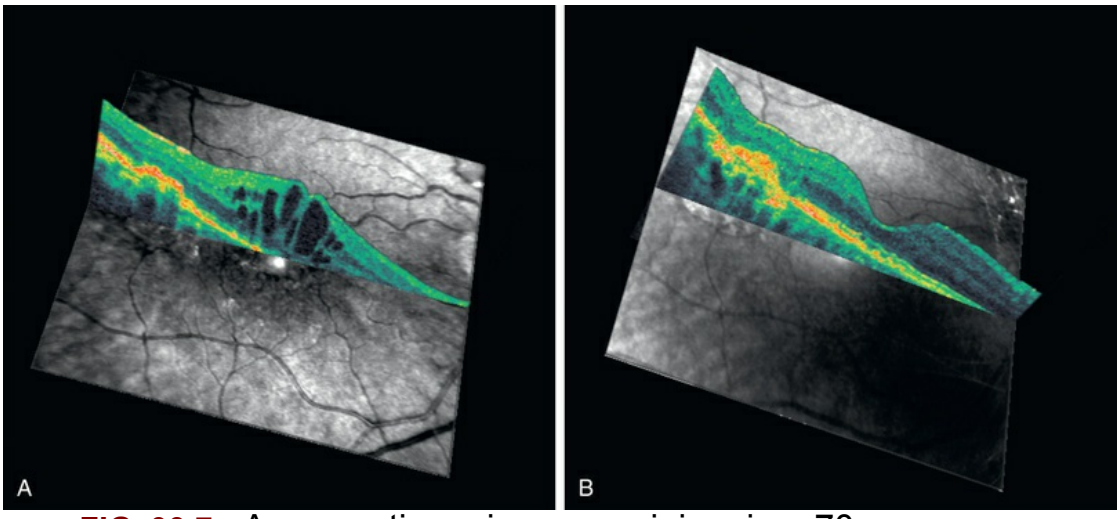

FIG. 93.7 An operating microscope injury in a 70-year-old female who had recently undergone complicated cataract surgery for a partially subluxated crystalline lens due to a tennis ball injury. Initial foveal cystoid macular edema and a serous neural retinal detachment associated with the operating microscope lesion (A) gradually resolved. Prominent chorioretinal scarring (B) is present in the region of the operating microscope lesion 3 years later, long after resolution of the cystoid macular edema. (Image courtesy of Richard B. Rosen, MD)

The risk of operating microscope injury is potentially increased

by higher body temperature,[132] increased chorioretinal pigmentation (theoretically increasing local light absorption and thermal enhancement of retinal phototoxicity),[5] oxygen administration during surgery (hypothetically increasing retinal free radical production),[146] and photosensitizing medications such as hydroxychloroquine, hydrochlorothiazide, furosemide, allopurinol, and the benzodiazepines.[147–149] Diabetes mellitus and hypertension may also increase retinal phototoxicity risks.[150]

Faster cataract surgery reduces the risk of operating microscope injury,[151] as does minimizing operating microscope intensity and discontinuing photosensitizing medications preoperatively when possible.[5,149] Other potentially useful techniques include maintaining patients' eyes in downgaze, using corneal occluders, and avoiding supplemental oxygen use and/or elevated patient core body temperatures.[5,152,153] Operating microscopes produce minimal UV radiation,[154–156] so UV-blocking filters are of little value. One study reported that UV-blocking intraocular lenses reduce postoperative CME,[157] but three subsequent studies refuted that conclusion.[158–160] Reducing operating microscope violet and blue light illumination hypothetically decreases acute retinal phototoxicity risks, but blue light is important for tissue visualization.[5]

Indocyanine green (ICG) is useful for retinal angiography and staining the inner limiting membrane (ILM) during macular hole surgery. ICG fluorescence can persist for months after ICG-assisted vitreoretinal surgery.[161] Visual field defects have occurred after these procedures and may be multifactorial in origin.[162] RPE damage possibly of phototoxic origin has been reported,[163] however alternate mechanisms such as physical trauma to the retinal nerve fiber layer should also be considered. The potential risks and benefits of ILM staining with ICG and alternative vital dyes continue to be evaluated.[164]

Ophthalmoscope and Fundus Camera Exposure

Indirect ophthalmoscopes and fundus cameras produce dazzling exposures and transient afterimages, but there is no evidence that they cause photochemical or thermal retinal injury in routine clinical use.[12,165–168] A 15-minute indirect ophthalmoscope exposure

focused on a single retinal area can cause a localized phototoxic injury in an anesthetized rhesus monkey,[132] but that certainly is not a clinical light exposure. No immediate or long-term retinal abnormalities could be detected after similar exposures were attempted in human volunteers with blind eyes or those requiring enucleation.[169] These results are consistent with instrumentation data showing that fundus camera, indirect ophthalmoscope, and scanning laser ophthalmoscope retinal irradiances are lower than experimentally determined damage thresholds.[12,165,166,168,170] Anterior segment slit-lamp photography has been reported to cause photic retinopathy under unusual circumstances.[171]

Sixty-second stabilized retinal exposures accelerated local retinal degeneration in dogs with rhodopsin gene mutations, prompting recommendation that retinal photography and clinical light exposure be minimized in patients with retinitis pigmentosa.[172] Human and canine retinas differ significantly,[172] and the experimental exposures were 10,000 times longer than 2-msec clinical fundus camera flashes.[168] Light exposure has never been proven to adversely affect the clinical course of retinitis pigmentosa and even light deprivation does not prevent its progression.[173] No current scientific evidence suggests the need for retinal disease-specific light exposure safety standards.[168] Nonetheless, regardless of a patient's condition, clinical retinal imaging should be performed only when necessary and patient comfort dictates that clinical procedures always be carried out at the lowest clinically effective retinal illumination levels.[12,168]

Safety Standards

Safety standards that affect laser users include the voluntary American National Standard Institute (ANSI) Standards "Safe Use of Lasers" (ANSI Z136.1-2007)[174,175] and "Safe Use of Lasers in Health Care Facilities" (ANSI Z136.3-2005).[176] The ANSI Z136.1 Standard is similar to the International Standard IEC 60825-1. ANSI standards are technically "voluntary," but regulatory groups use them to assess medical laser facility safety and litigants use them to scrutinize purported injuries.[177,178]

Safety standards that affect laser manufacturers include the FDA

regulatory "Laser Performance Standard" (21 CFR1040). This standard requires manufacturers to equip laser devices with features such as emission indicators and keyed switches. There are also specific standards for ophthalmic devices such as slit lamps and endoilluminators.

ANSI standards define four laser classes.[174,178] Class 1 lasers are considered incapable of causing damaging ocular exposures and do not require control measures. Their maximum power output in the visible spectrum ranges from 0.0004 mW or less for blue or green light to 0.024 mW or less for red light. Class 2, 3a, and 3b lasers produce laser power that is less than 1 mW, between 1 and 5 mW, and between 5 and 500 mW, respectively. Laser pointers are Class 3a devices. Some dangerous Class 3b handheld laser devices are identical in appearance to laser pointers. Class 4 lasers include potentially hazardous industrial, military or medical lasers that generate more than 500 mW of laser power. Safety standards assign control measures to each laser class.[174,176]

Practical Considerations

Control measures are designed to decrease the risk of laser accidents.[128,177,178] "Engineering" controls are protective measures built into laser systems such as housings, labels, and interlocks. "Administrative" and "procedural" controls are designed to assure the proper use of potentially hazardous laser systems. They include written protocols for (1) operating, maintaining, and servicing laser systems; (2) assuring proper personnel education and training; and (3) using appropriate protective eyewear.

For an ophthalmic laser facility, the ANSI Z136.3-2005 standard recommends that (1) a "Laser Safety Officer" be given local safety oversight responsibility, (2) a warning sign with the signal word "danger" be displayed on the outside of the closed treatment room door during any laser procedure, (3) personnel wear laser eye protection in the nominal hazard zone where diffuse reflections and stray beams could be hazardous, and (4) operators be trained in the safe use of their laser equipment.[176,177] From a practical perspective, the nominal hazard zone is the treatment or operating room in which a surgical laser is located. The laser safety office is

responsible for assuring that (1) protective eyewear is available and used appropriately, (2) personnel using lasers are trained properly, and (3) laser safety measures are audited regularly.

Conclusion

Light can cause photomechanical (thermomechanical), photothermal (photocoagulation), or photochemical (photic retinopathy) retinal damage. Accidental laser injuries are preventable with protective eyewear. Clinical retinal photocoagulation does not cause chronic pain and neither do accidental retinal laser injuries. Visual abnormalities from an alleged laser injury should be correlated with chorioretinal abnormalities. Powerful handheld laser devices that appear identical to laser pointers can be retinal photocoagulators. The only common clinical photochemical injuries are solar and welding arc maculopathies and operating microscope and endoilluminator injuries. Solar maculopathy can occur with or without sungazing. People under 30 years of age are at greatest risk to photic retinopathy because of the UV-B window in their crystalline lenses.

References

1. Mainster MA, White TJ, Allen RG. Spectral dependence of retinal damage produced by intense light sources. *J Opt Soc Am*. 1970;60:848–855.
2. Mainster MA. Wavelength selection in macular photocoagulation. Tissue optics, thermal effects, and laser systems. *Ophthalmology*. 1986;93:952–958.
3. Mainster MA. Decreasing retinal photocoagulation damage: principles and techniques. *Semin Ophthalmol*. 1999;14:200–209.
4. Mainster MA. Violet and blue light blocking intraocular lenses: photoprotection versus photoreception. *Br J Ophthalmol*. 2006;90:784–792.
5. Mainster MA, Boulton M. Retinal phototoxicity, Chapter 174. Albert DM, Miller JW, Blodi BA, et al. *Principles and practice of ophthalmology*. 3rd ed. Elsevier: London;

2008:2195–2205.
6. Boettner EA, Wolter JR. Transmission of the ocular media. *Invest Ophthalmol*. 1962;1:776–783.
7. Barker FM, Brainard GC. *The direct spectral transmittance of the excised human lens as a function of age, (FDA 785345 0090 RA)*. US Food and Drug Administration: Washington, DC; 1991.
8. Mainster MA, Turner PL. Ultraviolet-B phototoxicity and hypothetical photomelanomagenesis: intraocular and crystalline lens photoprotection. *Am J Ophthalmol*. 2010;149:543–549.
9. Sliney DH. Eye protective techniques for bright light. *Ophthalmology*. 1983;90:937–944.
10. Mainster MA. Light and macular degeneration: a biophysical and clinical perspective. *Eye*. 1987;1:304–310.
11. Stamper DA, Lund DJ, Molchany JW, et al. Human pupil and eyelid response to intense laser light: implications for protection. *Percept Mot Skills*. 2002;95:775–782.
12. Mainster MA, Ham WT Jr, Delori FC. Potential retinal hazards: instrument and environmental light sources. *Ophthalmology*. 1983;90:927–932.
13. Mainster MA. Finding your way in the photoforest: laser effects for clinicians. *Ophthalmology*. 1984;91:886–888.
14. Marshall J. Structural aspects of laser-induced damage and their functional implications. *Health Phys*. 1989;56:617–624.
15. Mainster MA. Photic retinal injury. Ryan SJ. *Retina*. Mosby-Year Book, Inc.: St. Louis; 1989:749–757.
16. Mainster MA. Classification of ophthalmic photosurgery. *Lasers Light Ophthalmol*. 1994;6:65–67.
17. Mainster MA, Ho PC, Mainster KJ. Nd:YAG laser photodisruptors. *Ophthalmology*. 1983;Suppl:45–47.
18. Gabel VP, Birngruber R, Lorenz B, et al. Clinical observations of six cases of laser injury to the eye. *Health Phys*. 1989;56:705–710.
19. Thach AB, Lopez PF, Snady-McCoy LC, et al. Accidental Nd:YAG laser injuries to the macula. *Am J Ophthalmol*. 1995;119:767–773.
20. Barkana Y, Belkin M. Laser eye injuries. *Surv Ophthalmol*.

2000;44:459–478.
21. Mainster MA. Retinal laser accidents: mechanisms, management and rehabilitation. *J Laser Appl*. 2000;12:3–9.
22. Harris MD, Lincoln AE, Amoroso PJ, et al. Laser eye injuries in military occupations. *Aviat Space Environ Med*. 2003;74:947–952.
23. Chen YJ. Vitrectomy and microperimetry of an accidental macular hole caused by Nd:YAG laser. *Case Rep Ophthalmol*. 2010;1:80–84.
24. Milani P, Pierro L, Pece A, et al. Retinal photoreceptor focal disruption secondary to accidental Nd:YAG laser exposure. *Int Ophthalmol*. 2011;31:409–412.
25. Cho A, Sakai T, Akiyama G, et al. Femtosecond laser-induced macular hole followed by spectral domain optical coherence tomography. *Clin Exp Ophthalmol*. 2013;41:812–815.
26. Fernandez MP, Modi YS, John VJ, et al. Accidental Nd:YAG laser-induced macular hole in a pediatric patient. *Ophthalmic Surg Lasers Imaging Retina*. 2013;44 Online:e7–10.
27. Scollo P, Herath G, Lobo A. Retinal injury by industrial laser burn. *Occup Med (Lond)*. 2014;64:220–222.
28. Liyanage SE, Kumaran N, De Alwis D. Macular burns resulting from the accidental use of selective laser trabeculoplasty mode during a laser capsulotomy. *Br J Ophthalmol*. 2014;98:141–142.
29. Chen SN, Lu CW, Hu X, et al. A case of accidental retinal injury by cosmetic laser. *Eye (Lond)*. 2014;28:906–907.
30. Kontadakis GA, Karagiannis D, Kandarakis AS. Macular injury with rapid onset of choroidal neovascularization from laser epilation. *JAMA Ophthalmol*. 2015;133:488–490.
31. Baillif S, Paoli V, Francheschetti C, et al. Retinal injury following ND-Yag laser treatment of symptomatic vitreous floaters. *J Franc Ophtalmol*. 2011;34:589–591.
32. Ciulla TA, Topping TM. Surgical treatment of a macular hole secondary to accidental laser burn. *Arch Ophthalmol*. 1997;115:929–930.
33. Newman DK, Flanagan DW. Spontaneous closure of a macular hole secondary to an accidental laser injury. *Br J*

Ophthalmol. 2000;84:1075.
34. Sasahara M, Noami S, Takahashi M, et al. Optical coherence tomographic observations before and after macular hole formation secondary to laser injury. *Am J Ophthalmol*. 2003;136:1167–1170.
35. Nehemy M, Torqueti-Costa L, Magalhaes EP, et al. Choroidal neovascularization after accidental macular damage by laser. *Clin Exp Ophthalmol*. 2005;33:298–300.
36. Ying HS, Symons RC, Lin KL, et al. Accidental Nd:YAG laser-induced choroidal neovascularization. *Lasers Surg Med*. 2008;40:240–242.
37. Sou R, Kusaka S, Ohji M, et al. Optical coherence tomographic evaluation of a surgically treated traumatic macular hole secondary to Nd:YAG laser injury. *Am J Ophthalmol*. 2003;135:537–539.
38. Brown J Jr, Hacker H, Schuschereba ST, et al. Steroidal and nonsteroidal antiinflammatory medications can improve photoreceptor survival after laser retinal photocoagulation. *Ophthalmology*. 2007;114:1876–1883.
39. Shulman S, Belokopytov M, Dubinsky G, et al. Ameliorative effect of PN-277 on laser-induced retinal damage. *Graefes Arch Clin Exp Ophthalmol*. 2009;247:343–348.
40. Mainster MA, Stuck BE, Brown J Jr. Assessment of alleged retinal laser injuries. *Arch Ophthalmol*. 2004;122:1210–1217.
41. Mainster MA, Timberlake GT, Warren KA, et al. Pointers on laser pointers. *Ophthalmology*. 1997;104:1213–1214.
42. Mainster MA. Blinded by the light–not!. *Arch Ophthalmol*. 1999;117:1547–1548.
43. Mainster MA, Sliney DH, Marshall J, et al. But is it really light damage? *Ophthalmology*. 1997;104:179–180.
44. Mainster MA, White TJ, Tips JH, et al. Retinal-temperature increases produced by intense light sources. *J Opt Soc Am*. 1970;60:264–270.
45. Luttrull JK, Musch DC, Mainster MA. Subthreshold diode micropulse photocoagulation for the treatment of clinically significant diabetic macular oedema. *Br J Ophthalmol*. 2005;89:74–80.
46. Bernstein PS, Steffensmeier A. Optical coherence

tomography before and after repair of a macular hole induced by an unintentional argon laser burn. *Arch Ophthalmol*. 2005;123:404–405.
47. Dhoot DS, Xu D, Srivastava S. High-powered laser pointer injury resulting in macular hole formation. *J Pediatr*. 2014;164:668 e1.
48. Raoof N, Chan TK, Rogers NK, et al. "Toy" laser macular burns in children. *Eye (Lond)*. 2014;28:231–234.
49. Petrou P, Patwary S, Banerjee PJ, et al. Bilateral macular hole from a handheld laser pointer. *Lancet*. 2014;383:1780.
50. Alsulaiman SM, Alrushood AA, Almasaud J, et al. High-power handheld blue laser-induced maculopathy: the results of the King Khaled Eye Specialist Hospital Collaborative Retina Study Group. *Ophthalmology*. 2014;121:566–572.e1.
51. Bhavsar KV, Wilson D, Margolis R, et al. Multimodal imaging in handheld laser-induced maculopathy. *Am J Ophthalmol*. 2015;159:227–231.e2.
52. Mainster MA, Turner PL. Retinal injuries from light: mechanisms, hazards and prevention, Chapter 109. Ryan SJ, Hinton DR, Schachat AP, et al. *Retina*. 4th ed. Elsevier: London; 2006:1857–1870.
53. Mainster MA. Ophthalmic laser surgery: principles, technology, and technique. *Trans New Orleans Acad Ophthalmol*. 1985;33:81–101.
54. Jenkins DL. *Hazard evaluation of the coherent model 900 photocoagulator laser system, non-ionizing radiation protection specialty study no. 25-42-0310-79 (NTIS no. ADA 068713)*. U.S. Army Environment Hygiene Agency: Aberdeen Proving Ground, MD; 1979.
55. Sliney DH, Dennis JE. Safety concerns about laser pointers. *J Laser Applications*. 1994;6:159–164.
56. Sell CH, Bryan JS. Maculopathy from handheld diode laser pointer. *Arch Ophthalmol*. 1999;117:1557–1558.
57. Ziahosseini K, Doris JP, Turner GS. Laser eye injuries: maculopathy from handheld green diode laser pointer. *BMJ*. 2010;340:c2982.
58. Fujinami K, Yokoi T, Hiraoka M, et al. Choroidal

neovascularization in a child following laser pointer-induced macular injury. *Jpn J Ophthalmol*. 2010;54:631–633.
59. Wyrsch S, Baenninger PB, Schmid MK. Retinal injuries from a handheld laser pointer. *N Engl J Med*. 2010;363:1089–1091.
60. Ueda T, Kurihara I, Koide R. A case of retinal light damage by green laser pointer (Class 3b). *Jpn J Ophthalmol*. 2011;55:428–430.
61. Yiu G, Itty S, Toth CA. Ocular safety of recreational lasers. *JAMA Ophthalmol*. 2014;132:245–246.
62. Weng CY, Baumal CR, Albini TA, et al. Self-induced laser maculopathy in an adolescent boy utilizing a mirror. *Ophthalmic Surg, Lasers Imaging Retina*. 2015;46:485–488.
63. Hossein M, Bonyadi J, Soheilian R, et al. SD-OCT features of laser pointer maculopathy before and after systemic corticosteroid therapy. *Ophthalmic Surg Lasers Imaging*. 2011;42:e135–8.
64. Turaka K, Bryan JS, Gordon AJ, et al. Laser pointer induced macular damage: case report and mini review. *Int Ophthalmol*. 2012;32:293–297.
65. Rusu I, Sherman J, Gallego-Pinazo R, et al. Spectral-domain optical coherence tomography and fundus autofluorescence findings in a case of laser pointer-induced maculopathy. *Retin Cases Brief Rep*. 2013;7:371–375.
66. Xu M, Lin T. Bilateral central scotomas following laser pointer misuse. CMAJ. *Canad Med Assoc J*. 2014;186:E341.
67. Lally DR, Duker JS. Foveal injury from a red laser pointer. *JAMA Ophthalmol*. 2014;132:297.
68. Lee GD, Baumal CR, Lally D, et al. Retinal injury after inadvertent handheld laser exposure. *Retina*. 2014;34:2388–2396.
69. Noble C, Blice J. Permanent retinal injury from recreational laser pointer. *Military Med*. 2015;180:e378–80.
70. Dirani A, Chelala E, Fadlallah A, et al. Bilateral macular injury from a green laser pointer. *Clin Ophthalmol*. 2013;7:2127–2130.
71. Obana A, Brinkmann R, Gohto Y, et al. A case of retinal injury by a violet light-emitting diode. *Retin Cases Brief Rep*. 2011;5:223–226.

72. Boosten K, Van Ginderdeuren R, Spileers W, et al. Laser-induced retinal injury following a recreational laser show: two case reports and a clinicopathological study. *Bull Soc Belge Ophtalmol*. 2011;11-6.
73. Jeon S, Lee WK. Inner retinal damage after exposure to green diode laser during a laser show. *Clin Ophthalmol*. 2014;8:2467–2470.
74. Ham WT Jr, Mueller HA, Sliney DH. Retinal sensitivity to damage from short wavelength light. *Nature*. 1976;260:153–155.
75. Lawwill T. Three major pathologic processes caused by light in the primate retina: a search for mechanisms. *Trans Am Ophthalmol Soc*. 1982;80:517–579.
76. Sliney DH, Mellerio J, Gabel VP, et al. What is the meaning of threshold in laser injury experiments? Implications for human exposure limits. *Health Phys*. 2002;82:335–347.
77. Gallin PF, Terman M, Reme CE, et al. Ophthalmologic examination of patients with seasonal affective disorder, before and after bright light therapy. *Am J Ophthalmol*. 1995;119:202–210.
78. Sliney DH. How light reaches the eye and its components. *Int J Toxicol*. 2002;21:501–509.
79. van Norren D, Gorgels TG. The Action Spectrum of Photochemical Damage to the Retina: A Review of Monochromatic Threshold Data. *Photochem Photobiol*. 2011;87(4):747–753.
80. Rozanowska M, Jarvis-Evans J, Korytowski W, et al. Blue light-induced reactivity of retinal age pigment. In vitro generation of oxygen-reactive species. *J Biol Chem*. 1995;270:18825–18830.
81. Boulton M, Rozanowska M, Rozanowski B. Retinal photodamage. *J Photochem Photobiol B*. 2001;64:144–161.
82. Mainster MA, Turner PL. Blue-blocking IOLs decrease photoreception without providing significant photoprotection. *Surv Ophthalmol*. 2010;55:272–289.
83. Mainster MA. Blue-blocking intraocular lenses and pseudophakic scotopic sensitivity. *J Cataract Refract Surg*. 2006;32:1403–1404.

84. Threshold limit values for chemical substances physical agents: biological exposure indices. American Conference of Governmental Industrial Hygienists: Cincinnati; 1997.
85. Noell WK, Walker VS, Kang BS, et al. Retinal damage by light in rats. *Invest Ophthalmol*. 1966;5:450–473.
86. Griswold MS, Stark WS. Scotopic spectral sensitivity of phakic and aphakic observers extending into the near ultraviolet. *Vision Res*. 1992;32:1739–1743.
87. Kremers JJ, van Norren D. Two classes of photochemical damage of the retina. *Lasers Light Ophthalmol*. 1988;2:41–52.
88. Mellerio J. Light effects on the retina. Albert DM, Jakobiec FA. *Principles and practice of ophthalmology*. W.B. Saunders: Philadelphia; 1994:1326–1345.
89. Gass JDM. *Stereoscopic atlas of macular diseases*. 3rd ed. Mosby-Year Book, Inc.: St. Louis; 1987.
90. Tso MO, La Piana FG. The human fovea after sungazing. *Trans Am Acad Ophthalmol Otolaryngol*. 1975;79:OP788–95.
91. Levy S, Sheck L, Guest S. OCT appearances in acute solar retinopathy. *Arch Ophthalmol*. 2012;130:1540.
92. Hossein M, Bonyadi J, Soheilian R, et al. Spectral-domain optical coherence tomography features of mild and severe acute solar retinopathy. *Ophthalmic Surg Lasers Imaging*. 2011;42 Online:e84–6.
93. Chen KC, Jung JJ, Aizman A. High definition spectral domain optical coherence tomography findings in three patients with solar retinopathy and review of the literature. *Open Ophthalmol J*. 2012;6:29–35.
94. Brue C, Mariotti C, De Franco E, et al. Solar retinopathy: a multimodal analysis. *Case Reports Ophthalmol Med*. 2013;2013:906920.
95. Schatz P, Eriksson U, Ponjavic V, et al. Multifocal electroretinography and optical coherence tomography in two patients with solar retinopathy. *Acta Ophthalmol Scand*. 2004;82:476–480.
96. Naidoff MA, Slinkey DH. Retinal injury from a welding arc. *Am J Ophthalmol*. 1974;77:663–668.
97. Lucas RS, Harper CA, McCombe MF, et al. Optical coherence tomography findings in welder's maculopathy.

Retin Cases Brief Rep. 2007;1:169–171.
98. Magnavita N. Photoretinitis: an underestimated occupational injury? *Occup Med (Lond)*. 2002;52:223–225.
99. Kaushik S, Gupta V, Gupta A. Optical coherence tomography findings in solar retinopathy. *Ophthalmic Surg Lasers Imaging*. 2004;35:52–55.
100. Comander J, Gardiner M, Loewenstein J. High-resolution optical coherence tomography findings in solar maculopathy and the differential diagnosis of outer retinal holes. *Am J Ophthalmol*. 2011;152:413–419 e6.
101. Cho HJ, Yoo ES, Kim CG, et al. Comparison of spectral-domain and time-domain optical coherence tomography in solar retinopathy. *Korean J Ophthalmol*. 2011;25:278–281.
102. Kung YH, Wu TT, Sheu SJ. Subtle solar retinopathy detected by fourier-domain optical coherence tomography. *J Chinese Med Assoc*. 2010;73:396–398.
103. Jain A, Desai RU, Charalel RA, et al. Solar retinopathy: comparison of optical coherence tomography (OCT) and fluorescein angiography (FA). *Retina*. 2009;29:1340–1345.
104. Steinkamp PN, Watzke RC, Solomon JD. An unusual case of solar retinopathy. *Arch Ophthalmol*. 2003;121:1798–1799.
105. Charbel Issa P, Fleckenstein M, Scholl HP, et al. Confocal scanning laser ophthalmoscopy findings in chronic solar retinopathy. *Ophthalmic Surg Lasers Imaging*. 2008;39:497–499.
106. Chen RW, Gorczynska I, Srinivasan VJ, et al. High-speed ultrahigh-resolution optical coherence tomography findings in chronic solar retinopathy. *Retin Cases Brief Rep*. 2008;2:103–105.
107. Symons RC, Mainster MA, Goldberg MF. Solar maculopathy in a young child. *Br J Ophthalmol*. 2010;94(9):1258–1259.
108. Pilli S, Ogoti M, Kalluri V. Fourier-domain optical coherence tomography findings in welder's maculopathy. *Ophthalmic Surg Lasers Imaging*. 2010;9:1–5.
109. Garg SJ, Martidis A, Nelson ML, et al. Optical coherence tomography of chronic solar retinopathy. *Am J Ophthalmol*. 2004;137:351–354.

110. Jorge R, Costa RA, Quirino LS, et al. Optical coherence tomography findings in patients with late solar retinopathy. *Am J Ophthalmol*. 2004;137:1139–1143.
111. Saxena S, Mishra N, Meyer CH. Three-dimensional spectral domain optical coherence tomography in chronic exposure to welding arc. *BMJ Case Rep*. 2014;2014.
112. Jabbarpoor Bonyadi MH. Early and late spectral domain optical coherence tomography features of acute welding maculopathy. *J Ophthal Vis Res*. 2013;8:391–392.
113. Hope-Ross MW, Mahon GJ, Gardiner TA, et al. Ultrastructural findings in solar retinopathy. *Eye*. 1993;7(Pt 1):29–33.
114. Grey RH. Foveo-macular retinitis, solar retinopathy, and trauma. *Br J Ophthalmol*. 1978;62:543–546.
115. Kelley JS, Hoover RE, George T. Whiplash maculopathy. *Arch Ophthalmol*. 1978;96:834–835.
116. Abebe MT, De Laey JJ. Foveomacular retinitis as a result of ocular contusion. *Bull Soc Belge Ophtalmol*. 1992;243:171–175.
117. Kuming BS. Foveomacular retinitis. *Br J Ophthalmol*. 1986;70:816–818.
118. Jacobs NA. Foveomacular retinitis. *Br J Ophthalmol*. 1987;71:563.
119. Cordes FC. A type of foveomacular retinitis observed in the U.S. Navy. *Am J Ophthalmol*. 1944;27:803–816.
120. Kerr LM, Little HL. Foveomacular retinitis. *Arch Ophthalmol*. 1966;76:498–504.
121. Ritchey CL, Ewald RA. Sun gazing as the cause of foveomacular retinitis. *Am J Ophthalmol*. 1970;70:491–497.
122. Marlor RL, Blais BR, Preston FR, et al. Foveomacular retinitis, an important problem in military medicine: epidemiology. *Invest Ophthalmol*. 1973;12:5–16.
123. Wergel FLJ, Brenner EH. Solar retinopathy foveomacular retinitis. *Ann Ophthalmol*. 1975;7:495–503.
124. Gladstone GJ, Tasman W. Solar retinitis after minimal exposure. *Arch Ophthalmol*. 1978;96:1368–1369.
125. Yannuzzi LA, Fisher YL, Krueger A, et al. Solar retinopathy: a photobiological and geophysical analysis. *Trans Am Ophthalmol Soc*. 1987;85:120–158.

126. Mainster MA. Henle fibers may direct light toward the center of the fovea. *Lasers Light Ophthalmol*. 1988;2:79–86.
127. White TJ, Mainster MA, Wilson PW, et al. Chorioretinal temperature increases from solar observation. *Bull Mathematical Biophys*. 1971;33:1–17.
128. Sliney DH, Wolbarsht ML. *Safety with lasers and other optical sources: a comprehensive handbook*. Plenum Press: New York; 1980.
129. Mainster MA. Solar eclipse safety. *Ophthalmology*. 1998;105:9–10.
130. Yang X, Jiang F, Song Y, et al. Accidental macular injury from prolonged viewing of a plasma flash produced by a femtosecond laser. *Ophthalmology*. 2010;117:972–975.
131. Gardner TW, Ai E, Chrobak M, et al. Photic maculopathy secondary to short-circuiting of a high-tension electric current. *Ophthalmology*. 1982;89:865–868.
132. Friedman E, Kuwabara T. The retinal pigment epithelium. IV. The damaging effects of radiant energy. *Arch Ophthalmol*. 1968;80:265–279.
133. Rinkoff J, Machemer R, Hida T, et al. Temperature-dependent light damage to the retina. *Am J Ophthalmol*. 1986;102:452–462.
134. Fishman GA. Light-induced maculopathy from surgical microscopes during cataract surgery. Ernest JT. *The 1985 year book of ophthalmology*. Mosby–Year Book, Inc.: St. Louis; 1985:177–180.
135. Michels M, Sternberg P Jr. Operating microscope-induced retinal phototoxicity: pathophysiology, clinical manifestations and prevention. *Surv Ophthalmol*. 1990;34:237–252.
136. Brod RD, Olsen KR, Ball SF, et al. The site of operating microscope light-induced injury on the human retina. *Am J Ophthalmol*. 1989;107:390–397.
137. Pavilack MA, Brod RD. Site of potential operating microscope light-induced phototoxicity on the human retina during temporal approach eye surgery. *Ophthalmology*. 2001;108:381–385.
138. Michels M, Lewis H, Abrams GW, et al. Macular

phototoxicity caused by fiberoptic endoillumination during pars plana vitrectomy. *Am J Ophthalmol*. 1992;114:287–296.
139. Khwarg SG, Geoghegan M, Hanscom TA. Light-induced maculopathy from the operating microscope. *Am J Ophthalmol*. 1984;98:628–630.
140. Robertson DM, Feldman RB. Photic retinopathy from the operating room microscope. *Am J Ophthalmol*. 1986;101:561–569.
141. Mares-Perlman JA, Brady WE, Klein BE, et al. Diet and nuclear lens opacities. *Am J Epidemiol*. 1995;141:322–334.
142. Parver LM, Auker CR, Fine BS. Observations on monkey eyes exposed to light from an operating microscope. *Ophthalmology*. 1983;90:964–972.
143. Irvine AR, Wood I, Morris BW. Retinal damage from the illumination of the operating microscope: an experimental study in pseudophakic monkeys. *Arch Ophthalmol*. 1984;102:1358–1365.
144. Green WR, Robertson DM. Pathologic findings of photic retinopathy in the human eye. *Am J Ophthalmol*. 1991;112:520–527.
145. Mansour AM, Yunis MH, Medawar WA. Ocular coherence tomography of symptomatic phototoxic retinopathy after cataract surgery: a case report. *J Med Case Reports*. 2011;5:133.
146. Jaffe GJ, Irvine AR, Wood IS, et al. Retinal phototoxicity from the operating microscope: the role of inspired oxygen. *Ophthalmology*. 1988;95:1130–1141.
147. Ferguson J. Photosensitivity due to drugs. *Photodermatol Photoimmunol Photomed*. 2002;18:262–269.
148. Long VW, Woodruff GH. Bilateral retinal phototoxic injury during cataract surgery in a child. *J AAPOS*. 2004;8:278–279.
149. Manzouri B, Egan CA, Hykin PG. Phototoxic maculopathy following uneventful cataract surgery in a predisposed patient. *Br J Ophthalmol*. 2002;86:705–706.
150. Khwarg SG, Linstone FA, Daniels SA, et al. Incidence, risk factors, and morphology in operating microscope light retinopathy. *Am J Ophthalmol*. 1987;103:255–263.
151. Kleinmann G, Hoffman P, Schechtman E, et al. Microscope-

induced retinal phototoxicity in cataract surgery of short duration. *Ophthalmology*. 2002;109:334–338.
152. O'Brien DP, Francis IC. The corneal quilt: a protective device designed to reduce intraoperative retinal phototoxicity. *Ophthalmic Surg*. 1994;25:191–194.
153. Kraff MC, Lieberman HL, Jampol LM, et al. Effect of a pupillary light occluder on cystoid macular edema. *J Cataract Refract Surg*. 1989;15:658–660.
154. Jampol LM, Kraff MC, Sanders DR, et al. Near-UV radiation from the operating microscope and pseudophakic cystoid macular edema. *Arch Ophthalmol*. 1985;103:28–30.
155. Keates RH, Genstler DE. UV radiation. *Ophthalmic Surg*. 1982;13:327.
156. Sliney DH, Armstrong BC. Radiometric analysis of surgical microscope lights for hazards analyses. *Appl Opt*. 1986;25:1882–1889.
157. Kraff MC, Sanders DR, Jampol LM, et al. Effect of an ultraviolet-filtering intraocular lens on cystoid macular edema. *Ophthalmology*. 1985;92:366–369.
158. Colin J, Ropars YM, Bonissent JF, et al. Cystoid macular oedema and intraocular lenses with ultraviolet filters. *J Eur Implant Soc*. 1987;4:5–10.
159. Clarke MP, Yap M, Weatherill JR. Do intraocular lenses with ultraviolet absorbing chromophores protect against macular oedema? *Acta Ophthalmol (Copenh)*. 1989;67:593–596.
160. Komatsu M, Kanagami S, Shimizu K. Ultraviolet-absorbing intraocular lens versus non-UV-absorbing intraocular lens: comparison of angiographic cystoid macular edema. *J Cataract Refract Surg*. 1989;15:654–657.
161. Ciardella AP, Schiff W, Barile G, et al. Persistent indocyanine green fluorescence after vitrectomy for macular hole. *Am J Ophthalmol*. 2003;136:174–177.
162. Uemura A, Kanda S, Sakamoto Y, et al. Visual field defects after uneventful vitrectomy for epiretinal membrane with indocyanine green-assisted internal limiting membrane peeling. *Am J Ophthalmol*. 2003;136:252–257.
163. Engelbrecht NE, Freeman J, Sternberg P Jr, et al. Retinal

pigment epithelial changes after macular hole surgery with indocyanine green-assisted internal limiting membrane peeling. *Am J Ophthalmol*. 2002;133:89–94.
164. Thompson JT, Haritoglu C, Kampik A, et al. Should indocyanine green be used to facilitate removal of the internal limiting membrane in macular hole surgery. *Surv Ophthalmol*. 2009;54:135–138.
165. Delori FC, Parker JS, Mainster MA. Light levels in fundus photography and fluorescein angiography. *Vision Res*. 1980;20:1099–1104.
166. Delori FC, Pomerantzeff O, Mainster MA. Light levels in ophthalmic diagnostic instruments. *Proc Soc Photo Optical Instrum Enginering*. 1980;229:154–160.
167. Klingbeil U. Safety aspects of laser scanning ophthalmoscopes. *Health Phys*. 1986;51:81–93.
168. Mainster MA, Turner PL. Retinal examination and photography are safe … is anyone surprised? *Ophthalmology*. 2010;117:197–198.
169. Robertson DM, Erickson GJ. The effect of prolonged indirect ophthalmoscopy on the human eye. *Am J Ophthalmol*. 1979;87:652–661.
170. Delori FC, Webb RH, Sliney DH. Maximum permissible exposures for ocular safety (ANSI 2000), with emphasis on ophthalmic devices. *J Opt Soc Am A Opt Image Sci Vis*. 2007;24:1250–1265.
171. Kohnen S. Light-induced damage of the retina through slit-lamp photography. *Graefes Arch Clin Exp Ophthalmol*. 2000;238:956–959.
172. Cideciyan AV, Jacobson SG, Aleman TS, et al. In vivo dynamics of retinal injury and repair in the rhodopsin mutant dog model of human retinitis pigmentosa. *Proc Natl Acad Sci USA*. 2005;102:5233–5238.
173. Berson EL. Light deprivation and retinitis pigmentosa. *Vision Res*. 1980;20:1179–1184.
174. American National Standard for the Safe Use of Lasers, ANSI Z136.1-2007. American National Standards Institute: Washington, DC; 2007.
175. Sliney DH, Wolborsht ML. Safety standards and

measurement techniques for high intensity light sources. *Vision Res*. 1980;20:1133–1141.
176. American National Standard for the Safe Use of Lasers in Health Care Facilities, ANSI Z136.3-2005. American National Standards Institute: Washington, DC; 2005.
177. Sliney DH, Trokel SL. *Medical lasers and their safe use*. Springer-Verlag: New York; 1993.
178. Sliney DH, Mainster MA. Ophthalmic laser safety: tissue interactions, hazards and protection. *Ophthalmol Clinics North Am*. 1998;11:157–164.

94

Traumatic Chorioretinopathies

Dean Eliott, Thanos D. Papakostas

Introduction

Ocular trauma consists of closed globe injuries and open globe injuries. A closed globe is defined as the absence of a full-thickness defect of the cornea and/or sclera. Nonpenetrating posterior segment ocular trauma includes blunt trauma applied directly to the eye in the setting of a closed globe and trauma to other parts of the body that indirectly affects the eye. The ophthalmologist must be familiar with the wide variety of posterior segment manifestations of nonpenetrating trauma to perform appropriate evaluation and treatment. The prevention of ocular trauma is of equal importance. The ophthalmologist should encourage the use of protective eyewear in the industrial workplace and during athletic events, and the use of polycarbonate spectacle lenses in the trauma patient with an intact fellow eye cannot be overemphasized.

Blunt trauma accounts for 51–66% of ocular injuries,[1–3] and posterior segment involvement includes commotio retinae, choroidal rupture, sclopetaria, macular holes, and conditions associated with traumatic retinal detachment such as vitreous base avulsion, retinal dialysis, retinal tears, and giant retinal tears; remote systemic trauma with indirect ocular involvement consists of Purtscher retinopathy, Terson syndrome, Valsalva retinopathy, and shaken baby syndrome.

The pathogenesis of posterior segment involvement from blunt ocular trauma includes coup injury, contrecoup injury, and direct ocular compression.[4] A coup injury is damage at the site of impact, as seen with sclopetaria. In a contrecoup injury, damage occurs at tissue interfaces opposite the site of impact. This occurs with commotio retinae, posterior choroidal rupture, and traumatic

macular hole. Anteroposterior ocular compression results in equatorial stretching because the eye has a fixed volume, and vitreous base avulsion and retinal dialysis occur via that mechanism.[5] The pathogenesis of ocular manifestations from remote trauma is varied and is discussed with each clinical entity.

Direct Ocular Injury

Commotio Retinae

In 1873, Berlin[6] described retinal whitening following blunt trauma to the globe. The condition, now known as commotio retinae, is characterized by transient opacification of the deep retina opposite the site of impact (a contrecoup injury) (Fig. 94.1). The findings may vary from a small area of subtle retinal whitening to widespread marked retinal opacification. If the posterior pole is involved, the fovea is often spared, resulting in a pseudo cherry-red spot. Vision may be affected if the macula is involved, but it usually returns to normal in several days when the opacification resolves.[7,8] With more severe injury, visual loss may persist, and the opacification may be replaced by mottling of the retinal pigment epithelium[7,9] or intraretinal pigment deposition.[10,11]

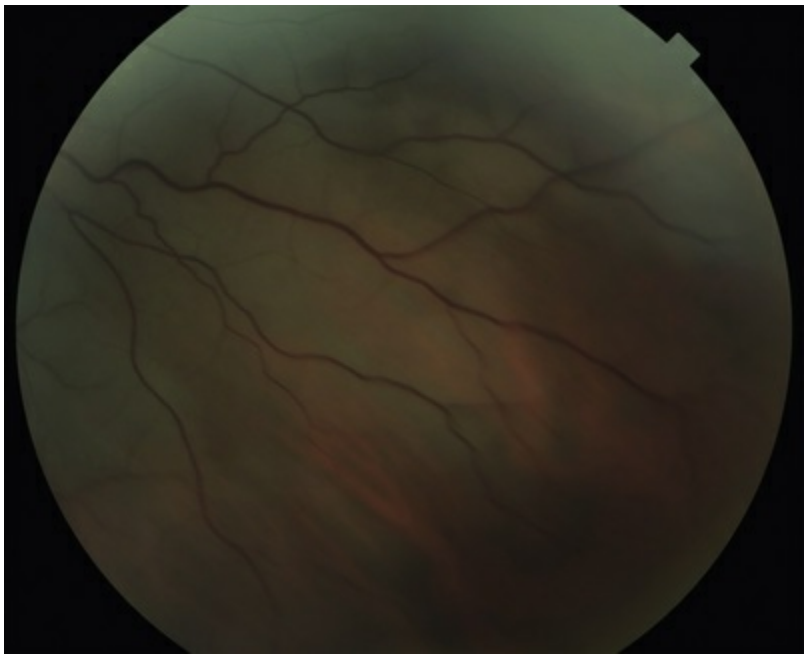

FIG. 94.1 Commotio retinae in a 23-year-old man who

was struck in the eye with a finger while playing football. (Courtesy of Lucia Sobrin, Massachusetts Eye and Ear.)

The blood–retinal barrier has been studied extensively in both animals and humans with commotio retinae. Francois and De Laey[12] and Hart et al.[7] found no leakage on fluorescein angiography (FA) performed on patients immediately after trauma. Gregor and Ryan[13] performed fluorescein angioscopy on pigs immediately after trauma and found no leakage from retinal blood vessels but detected staining of the retinal pigment epithelium that resolved within 24 hours. Blood–retinal barrier disruption at the level of the retinal pigment epithelium was demonstrated in morphologic studies using the horseradish peroxidase tracer technique. Kohno et al.[14] noted no leakage on fluorescein angiography in Rhesus monkeys with commotio retinae, and no disruption of the blood–retinal barrier was found using horseradish peroxidase. Pulido and Blair[15] performed fluorescein angiography and vitreous fluorophotometry on 10 patients with unilateral macular commotio retinae an average of 16 hours after trauma. Fluorescein angiography showed no leakage and vitreous fluorophotometry yielded no difference in the vitreous penetration in the traumatized versus untraumatized eyes of the same patient. The authors concluded that, because vitreous fluorophotometry is highly sensitive in detecting low levels of leakage, breakdown of the blood–retinal barrier is not a major pathophysiologic factor in producing commotio retinae. Mansour et al.[16] reported the histopathologic findings obtained within 24 hours after injury in a human eye with commotio retinae. They noted that only a minimal amount of albumin was detected immunohistochemically around retinal vessels and presented this as additional evidence that the blood–retinal barrier is relatively intact and therefore does not play a major role in the pathogenesis of commotio retinae.

The pathogenesis of commotio retinae, based on histopathologic studies, has included extracellular edema, intracellular edema (of glial cells), and photoreceptor outer segment disruption. Berlin[6] postulated that extracellular edema resulted in the loss of retinal transparency, and the condition became known as “Berlin's edema.” Subsequent histopathologic studies in animals revealed a

different pathogenesis. In an experimental model in pigs, Hart et al.[7,9] and Blight and Hart[17] demonstrated intracellular edema of retinal glial elements. Blight and Hart,[18] in the same model, also found photoreceptor outer segment fragmentation and intracellular edema of the retinal pigment epithelium. Sipperley et al.[19] detected disruption of only the photoreceptor outer segment in an owl monkey model. Using Rhesus monkeys, Kohno et al.[14] demonstrated disruption of photoreceptor outer segments in addition to intracellular edema in Müller cells, retinal pigment epithelial cells, nerve fibers, and the outer plexiform layer axons of photoreceptor cells. Mansour et al.[16] found disruption of the photoreceptor outer segment and damage to the adjacent retinal pigment epithelium in a histopathologic report of a human eye. The authors attributed the susceptibility of the outer segments to the architecture of the retina, particularly the Müller cell skeletal system, because Müller cells occupy the retina from the internal limiting membrane to the photoreceptor inner segments and support all cellular layers except the photoreceptor outer segments.

Souza-Santos et al.[20] described the morphologic characteristics in 11 eyes with commotio retinae using spectral domain optical coherence tomography (OCT) and also evaluated its utility in prognosis and follow-up. Cases with severe trauma had acute disruption of the ellipsoid zone and hyperreflectivity of the overlying retina and were regularly associated with retinal atrophy, pigment disturbance, and poor visual prognosis. Ahn et al.[21] described the OCT features of macular commotio and its association with anatomic and visual outcomes. They also proposed a grading system based on the morphology of the OCT: increased ellipsoid zone reflectivity with disappearance of the thin hyporeflective optical space (grade 1), cone outer segment tips (COST) defect only (grade 2), COST and ellipsoid zone defects (grade 3), and COST, ellipsoid zone, and external limiting membrane defects (grade 4). Eyes with higher grades at baseline had worse visual and anatomic outcomes.

In summary, trauma may induce a mechanical distortion of the retinal elements via deformation of the vitreous, resulting in transient deep retinal opacification, termed “commotio retinae.” The blood–retinal barrier appears to be intact, and the fundus

changes are probably caused by disruption of the photoreceptor outer segments. The condition typically resolves, but persistent visual loss and retinal pigment changes may occur in severe cases.

Choroidal Rupture

In 1854,Von Graefe[22] described crescent-shaped lesions of the posterior pole resulting from trauma to the globe. These usually are single lesions located temporal to the disc in a concentric fashion. Known as choroidal ruptures, these lesions, in fact, are tears of the choroid, Bruch's membrane, and retinal pigment epithelium.

There are both direct and indirect choroidal ruptures. Direct ruptures are located anteriorly at the site of impact (coup injury) and are oriented parallel to the ora. Direct choroidal ruptures are relatively rare and are thought to be caused by compression necrosis.[23] Indirect choroidal ruptures occur opposite the site of impact (contrecoup injury) and appear as the typical curvilinear shaped lesion of the posterior pole (Fig. 94.2), oriented concentric with the disc margin. Trauma induces compressive forces that rupture the relatively inelastic Bruch's membrane and its adherent choriocapillaris (resulting in acute subretinal hemorrhage), as well as the retinal pigment epithelium (resulting in late pigment changes). The retina and sclera do not rupture because the retina is relatively elastic, whereas the sclera has strength sufficient to resist these forces.[24] Patients with pseudoxanthoma elasticum have been shown to have a relatively brittle Bruch's membrane, and these patients are particularly susceptible to choroidal rupture following relatively minor ocular trauma.

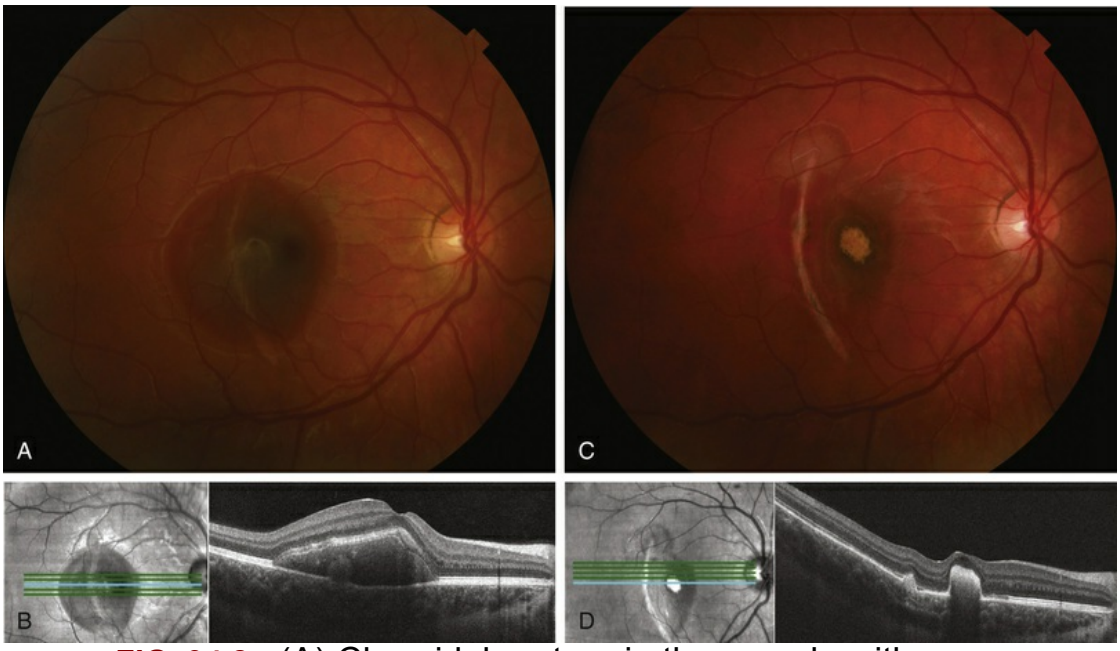

FIG. 94.2 (A) Choroidal rupture in the macula with associated subretinal hemorrhage in an 11-year-old boy who sustained blunt trauma to his right eye with a baseball cap. Visual acuity is 20/100. (B) Optical coherence tomography (OCT) scan showing the area of the choroidal rupture as a discontinuity in Bruch's membrane. There is subretinal hyperreflective material consistent with the subretinal hemorrhage. (C) Five weeks later most of the blood has resolved except there is a small amount of dehemoglobinized subretinal blood at the fovea. There is also subretinal fluid at the superior edge of the choroidal rupture consistent with the development of a choroidal neovascular membrane. Visual acuity is 20/100. (D) OCT scan showing subretinal hyperreflective material in the area of the choroidal rupture and subfoveal hyperreflective material in the area of the dehemoglobinized hemorrhage. (Courtesy of Shizuo Mukai, Massachusetts Eye and Ear.)

Since the initial injury often involves subretinal hemorrhage, the crescent-shaped lesion may not become visible ophthalmoscopically until the overlying hemorrhage resolves. If the macula is involved by the rupture or the accompanying subretinal hemorrhage (or if there is other evidence of macular injury, such as commotio retinae or macular hole), visual acuity usually is reduced. In a report by Hart et al.,[25] initial visual acuity was 20/200 or worse

in all 10 patients with posterior pole choroidal ruptures; six of these patients ultimately improved to 20/30 or better. The choroidal rupture typically develops a gliotic scar within a few weeks, and hyperpigmentation develops at the margins of the healed lesions (Fig. 94.2). The lesions should be followed closely because choroidal neovascularization from the margins may develop at any time. Patients should be instructed to report any changes in central vision (e.g., reduced visual acuity, metamorphopsia), and the examination should focus on the presence of subretinal fluid, hemorrhage, and lipid. Several authors[26,27] have described late hemorrhagic detachment of the pigment epithelium secondary to subretinal pigment epithelial neovascularization, and others have reported serous detachment of the macula from subretinal neovascularization.[8,24,28,29] Many of these patients suffered visual loss months to years following the initial injury and, in some cases, laser photocoagulation resulted in resolution of the choroidal neovascular membrane.[24,28,29] An additional potential complication of choroidal rupture is chorioretinal vascular anastomosis.[30]

FA is useful in evaluating acute choroidal ruptures and cases of suspected choroidal neovascularization. In the acute setting, FA may aid in the detection and localization of small choroidal ruptures and suspected ruptures beneath subretinal hemorrhage. Fluorescein initially may leak from the ruptured choroidal vessels into the outer retina, but this resolves within a few days.[25] Healed choroidal ruptures typically demonstrate early hypofluorescence within the rupture because of the damaged choriocapillaris (the large choroidal vessels usually are intact) and late hyperfluorescence from diffusion from the surrounding intact choriocapillaris. In cases with choroidal neovascularization, FA demonstrates early lacy subretinal vessels with late leakage into the subretinal space.[31]

In choroidal ruptures, fundus autofluorescence typically reveals hypoautofluorescence within the rupture due to loss of pigment epithelium. There is an associated hyperautofluorescence of the rupture rim, likely due to pigment epithelial hyperplasia at the margins of the rupture,[32] which has been well documented clinically and histologically.[33,34] In cases with associated subretinal hemorrhage, there is blocked autofluorescence from the blood.

In a histopathologic report of cases by Aguilar and Green,[35] most ruptures initially were associated with hemorrhage, usually in the subretinal space and occasionally involving the choroid and vitreous. Fibroblastic activity usually was present by 1–2 weeks and a well-developed scar was present by 1 month after injury. In some cases, the retina overlying the choroidal rupture exhibited atrophy and thinning due to the loss of outer layers. Retinal pigment epithelial hyperplasia at the margins of the lesion was common. In three eyes with healed choroidal ruptures, foci of chronic inflammation (lymphocytes) were present in the inner choroid and subretinal space. Choroidal neovascularization from the margin of the choroidal rupture, extending under the retinal pigment epithelium, was present in one eye, and choroidal neovascularization extending into the subretinal space was found in two eyes. The authors concluded that new choroidal blood vessels are common in the healing process and that these vessels usually regress as the scarring process evolves.

Nair et al.[36] described the morphological patterns of indirect choroidal rupture based on spectral domain OCT. Two types of choroidal rupture were seen. The first type seen (type 1) was a forward protrusion of the retinal pigment epithelium (RPE)–choriocapillaris layer with an acutely angled pyramid or dome shape. This was associated with either a small loss of continuity of the retinal pigment epithelial layer or elevated RPE–choriocapillaris projection accompanied by a significant quantity of subretinal hemorrhage. The second type (type 2) was a larger area of disruption of the RPE–choriocapillaris layer, photoreceptor ellipsoid zone, and external limiting membrane, with a posteriorly directed concave contour depression and downward sliding of tissues into the defect. The study included 18 eyes of 18 patients. At presentation, 10 eyes were observed to have type 1 and eight to have type 2. Of the 18 eyes, one with type 1 and two with type 2 developed choroidal neovascularization (16.6%).

In a study of all cases of choroidal rupture diagnosed at Massachusetts Eye and Ear Infirmary between 1993 and 2001,[37] 111 cases were identified. Sixty-eight percent of ruptures occurred in the macula, with 37% being foveal and 31% extrafoveal. Thirty-two percent were peripheral. A majority (61%) of patients had one

rupture, while 21% had two ruptures, 11% had three ruptures, and 7% had four or more ruptures. Two patients (10%) developed choroidal neovascularization between 1 and 18 months after the initial trauma. Longer ruptures also exhibited an increased risk of choroidal neovascularization (0% in ruptures <1.10 mm in length, 11% in ruptures 1.10–2.35 mm, and 50% in ruptures >2.35 mm; p=.03). Ruptures within the arcades and older age also increased the risk of choroidal neovascularization.

Multiple treatment modalities have been reported for choroidal neovascularization secondary to choroidal rupture. These include thermal laser photocoagulation,[38] photodynamic therapy,[39,40] surgical excision,[38,41,42] and more recently intravitreal injection of anti-vascular endothelial growth factor (VEGF) agents. There are several case reports of intravitreal injection of the monoclonal antibody to VEGF, bevacizumab, producing an improvement in visual acuity and resolution of leakage in subfoveal,[43,44] juxtafoveal,[45] and extrafoveal choroidal neovascularization.[46] These studies report stability 9 months,[44] 3 months,[45] and 1 month[46] after treatment of subfoveal, juxtafoveal, and extrafoveal CNV, respectively. Although there are no reports of longer follow-up, the limited data suggest that anti-VEGF agents may produce a more durable response than laser or photodynamic therapy.

In summary, trauma-induced indirect choroidal ruptures occur as crescent-shaped lesions of the posterior pole. These lesions initially can be associated with subretinal hemorrhage and later may develop hyperpigmentation at the margins. Vision initially is affected if the lesion involves the fovea, but late visual loss also may occur if choroidal neovascularization develops. A variety of treatment options are available for patients who develop choroidal neovascularization.

Sclopetaria (Traumatic Chorioretinal Rupture)

Rupture of the choroid and retina (known as sclopetaria or chorioretinal rupture) may occur after nonpenetrating ocular trauma in which a high-velocity projectile strikes or passes tangential to the globe. The condition is rare and has been described

by numerous terms, including chorioretinitis proliferans,[47] traumatic proliferating choroidoretinitis,[48] retinitis proliferans,[49] and acute retinal necrosis.[50] Goldzieher[51] described the first case in 1901, caused by a gunshot wound, and used the term "chorioretinitis sclopetaria." Because the pathogenesis is not inflammatory, the terms sclopetaria and chorioretinal rupture currently are accepted.

The appearance of the fundus is characterized by an area of absent retina, retinal pigment epithelium, Bruch's membrane, and choroid in the same quadrant as the projectile injury (Fig. 94.3). The lesion often extends posteriorly to involve the macula. Bare sclera is visible ophthalmoscopically, but may not be apparent acutely because there may be overlying vitreous hemorrhage and adjacent intraretinal and subretinal hemorrhage. With resolution of the hemorrhage, the lesion ultimately develops irregular, scarred, pigmented borders, and the posterior hyaloid usually remains attached.

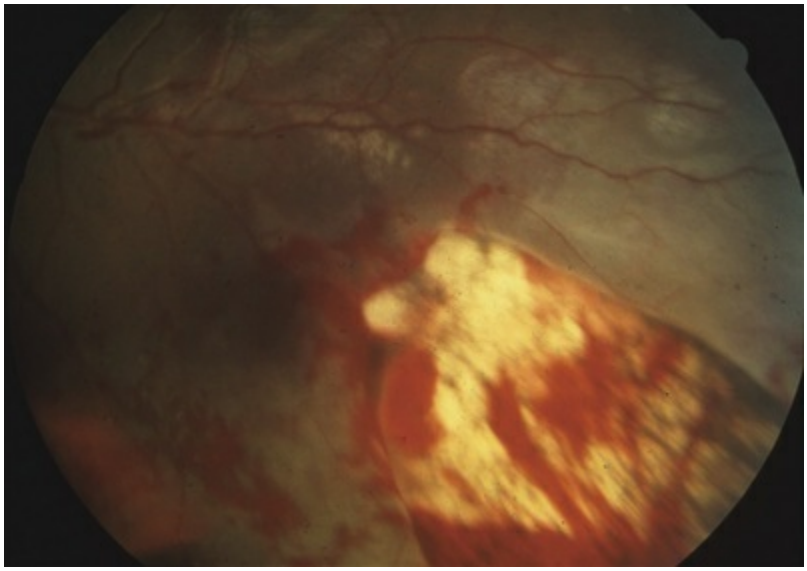

FIG. 94.3 Sclopetaria. Inferotemporal area of bare sclera, pigment, and hemorrhage in a 19-year-old man after a shotgun injury. Pellets passed tangential to the globe and lodged in the orbit. Ocular findings also included commotion retinae, choroidal rupture, and macular hole. (Courtesy of Daniel F. Martin, Cole Eye Institute, reproduced with permission from Eliott D, Avery R. Nonpenetrating posterior segment trauma. Ophthalmology Clinics of North America, Volume 8, Number 4, December 1995.)

Sclopetaria typically is seen following a high-velocity projectile injury to the orbit, usually caused by a shotgun or BB pellet. The missile directly strikes or passes tangential to the globe and often remains in the orbit. Sclopetaria is an example of a coup injury because damage occurs at the site of impact. High velocity projectiles cause rapid deformation of the globe and a sudden increase in the tensile stresses in the ocular tissues. These stresses may exceed the tensile strength of the retina and choroid, but not the relatively elastic posterior hyaloid or the relatively strong sclera. Rupture of the retina and choroid is followed by retraction of these tissues to expose the sclera.[52]

Martin et al.[52] reported eight eyes of seven patients with sclopetaria. A shotgun or BB pellet was the projectile in five of these patients. Seven of eight eyes were managed initially by observation only. One eye was treated with a prophylactic scleral buckle. The retina remained attached in all cases for at least 6 months. Late complications included vitreous hemorrhage in two eyes and retinal detachment in two eyes. The vitreous hemorrhages occurred in the setting of posterior vitreous detachment and one of these eyes required vitrectomy. The retinal detachments were due to breaks at a site distant from the original chorioretinal rupture. The authors concluded that the risk of retinal detachment is low, and they attributed this to an intact posterior hyaloid, which prevents access of liquid vitreous into the subretinal space, and to the adhesion of the retina to the choroid, because these tissues retract as a single unit and prevent access of fluid to the subretinal space.

Ahmadabadi et al.[53] reported the largest series with 13 eyes of 13 patients. The mean follow-up was 37 months. Vitrectomy was performed in two patients with dense vitreous hemorrhage, and one of these patients had retinal detachment, which was treated with silicone oil tamponade. Final visual acuity ranged from 20/1200 to no light perception. The retina remained attached in all eyes during follow-up.

A more recent report[54] described three consecutive patients with traumatic chorioretinal rupture who developed retinal detachment at 1, 2, and 3 weeks after the trauma. In the first case, the underlying retinal breaks were likely created by severe traction from the chorioretinal rupture site. In the second case, the retinal

defect was a small hole at the edge of the superior sclopetaria lesion, associated with early PVR. In the third case, there were multiple breaks in severely atrophic retina at the posterior edge of the lesion. In both cases 1 and 3, proliferative vitreoretinopathy resulted in redetachments that required further intervention.

In summary, sclopetaria or chorioretinal rupture is a rare manifestation of high-velocity projectile injuries to the globe that can lead to rupture of the retina, retinal pigment epithelium, Bruch's membrane, and choroid and leads to retraction of these tissues to expose bare sclera. Regular follow-up is necessary because complications include retinal detachment and vitreous hemorrhage.

Traumatic Macular Hole

While the vast majority of macular holes are idiopathic, they may also develop after blunt ocular trauma. Knapp, in 1869, and Noyes, in 1875 were the first to describe full-thickness macular holes occurring in that setting.[4] Fuchs, in 1901,[55] reported a posttraumatic inner lamellar macular hole. Macular holes have been seen in association with commotio retinae, subretinal hemorrhage, choroidal rupture, and whiplash injury.[4,5] Cox et al.[56] reported that macular holes occur in 6.3% of eyes after blunt trauma, and a subsequent study by Giovinazzo et al.[57] reported the presence of macular cysts or holes in 4% of boxers. Macular holes also have been associated with nontraumatic retinal conditions such as epiretinal membrane, central retinal vein occlusion, and myopia. In addition, they may be occur after surgery for rhegmatogenous retinal detachment,[58,59] and they may be idiopathic.[60]

The clinical features and FA appearance are similar for all full-thickness macular holes, regardless of the cause. Visual acuity typically is 20/40 to 20/400, and symptoms include metamorphopsia and central scotoma. The lesion appears as a full-thickness, round, sharply defined hole in the center of the macula with a surrounding cuff of subretinal fluid and intraretinal cystic changes. The size is variable, but most idiopathic holes measure 200–500 μm in diameter (one-third disc diameter or smaller). Frangieh et al.[61] studied 44 eyes and found that the largest macular holes (up to 1.5

mm in diameter) were associated with blunt trauma (0.86 mm average diameter versus 0.66 mm for nontraumatic macular holes; Fig. 94.4). FA in eyes with macular holes characteristically demonstrates a retinal pigment epithelial window defect in the center of the macula in the early transit phase. In the mid-phase, a surrounding halo of lighter fluorescence may be present. In the late phase, the fluorescence gradually fades.[31]

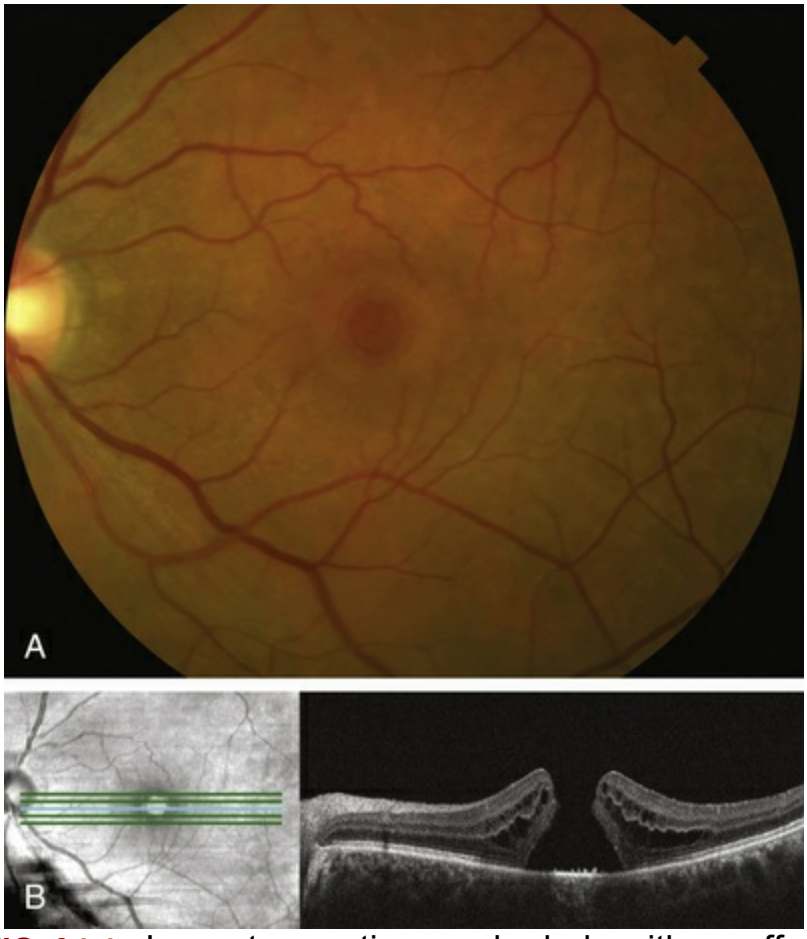

FIG. 94.4 Large traumatic macular hole with a cuff of subretinal fluid.

Huang et al.[62] described the morphologic features of traumatic macular holes based on OCT. Seventy-three consecutive patients with traumatic macular holes were included in the study. Traumatic macular holes were classified into five morphologic types with varying average retinal thicknesses, apical areas, and basal areas. Patients who presented >90 days after injury had greater average retinal thickness (p=.03) and apex areas (p=.002)

compared with those who presented within 90 days. Older patients developed more circular holes, i.e., less eccentricity of the apex (p=.04) and base (p=.01). None of the morphologic parameters investigated in the current study correlated with visual acuity. Patients who presented later in the clinical course or who had greater average retinal thicknesses tended to have better vision (p=.11 and p=.07, respectively).

Mechanisms of macular hole formation following blunt ocular trauma include postcontusion necrosis with cystoid degeneration and anteroposterior vitreofoveal traction.[27] Severe ocular contusion may result in cystoid macular edema. Rupture of the inner retinal layer occasionally occurs, resulting in a lamellar hole; rupture of both the inner and outer retinal layers results in a full-thickness macular hole. The sequence of cystoid degeneration, cyst coalescence, and full-thickness macular hole formation may take months to years.[61] Vitreofoveal traction may produce a macular hole because the vitreous adheres tightly to the retina at the fovea.[30,60] A sudden separation of the posterior hyaloid from the retina at the macula may produce a dehiscence of retinal tissue at the fovea. However, most traumatic macular holes have an attached hyaloid.

Macular holes usually are stable lesions, but progression to retinal detachment occurs rarely.[63] Margherio and Schepens[64] reported that macular holes were present in 10 of 758 eyes (1.3%) with traumatic retinal detachment. Because macular holes rarely are an isolated cause of rhegmatogenous retinal detachment, a thorough examination of the peripheral retina is essential. Prophylactic photocoagulation to the edge of traumatic macular holes is not necessary but, in cases with resultant retinal detachment, vitrectomy with fluid–gas exchange and endophotocoagulation has been performed.

Several studies have reported the use of vitrectomy for traumatic macular hole with an overall single operation success rate of 83%.[65–72] Intraocular gas tamponade is a key component of any surgical attempt to repair macular holes. It is thought that the surface tension of gas at the site of the hole provides a seal that prevents reaccumulation of the intraretinal fluid as the hole closes with time.

Other vitreous substitutes such as silicone oil have been tried for macular hole closure. Ghoraba and Ellakwa[69] published a study involving 22 patients who underwent vitrectomy with silicone oil or intraocular gas for traumatic macular hole. Silicone oil was used in children, in patients with large holes, and in those unable to comply with strict positioning. Despite a selection bias for the use of silicone oil in children, the difference in average age of the two groups was <1 year. With a single surgery, traumatic macular hole closure was achieved in 67% with silicone oil and 92% with perfluoropropane gas.

Miller et al.[68] reported the long-term outcome of traumatic macular holes. Twenty-eight patients were identified with a mean initial visual acuity of logMAR 1.3 (20/400) and a mean follow-up of 2.2 years. Eleven holes (39.3%) closed spontaneously in median 5.7 weeks. Eleven underwent vitrectomy with a median time to intervention of 35.1 weeks. Vision improved in closed holes (p<.01), whether spontaneously (p<.01) or via vitrectomy (p=.04), but it did not improve in holes that did not close (p=.22). There was no relation between initial OCT dimensions and final hole closure status, although there was a trend toward small dimensions for those that closed spontaneously.

Traumatic Retinal Detachment and Associated Conditions

Retinal Detachment

Approximately 10–20% of patients with rhegmatogenous retinal detachment (Fig. 94.5) report a history of blunt ocular trauma,[73–76] and in children, the majority of retinal detachments occur in the setting of trauma. When the vitreous suddenly is deformed and shifted, retinal tearing may occur in areas with firm vitreoretinal adhesion, such as the vitreous base, the fovea, areas of lattice degeneration, and chorioretinal scars. The vitreous base is the most significant of these locations, and retinal damage at the vitreous base may result in retinal dialysis, peripheral retinal tears, and giant retinal tears. Indeed, Goffstein and Burton[74] reported that retinal dialyses account for 53% of traumatic retinal detachments; giant retinal tears, 16%; retinal flap tears with adherent vitreous

(horseshoe tears), 11%; and tears at the edge of lattice degeneration, 8%. (In nontraumatic retinal detachment, retinal dialyses account for 5%; giant retinal tears, 2%; retinal flap tears, 45%; and lattice degeneration, 38%.) In this same report,[74] the mean age of patients with traumatic retinal detachment was 28 years (vs. 53 years for nontraumatic retinal detachment) and 78% of patients were male (vs. 50% for nontraumatic retinal detachment). An earlier study by Cox et al.[56] described similar age and sex distributions.

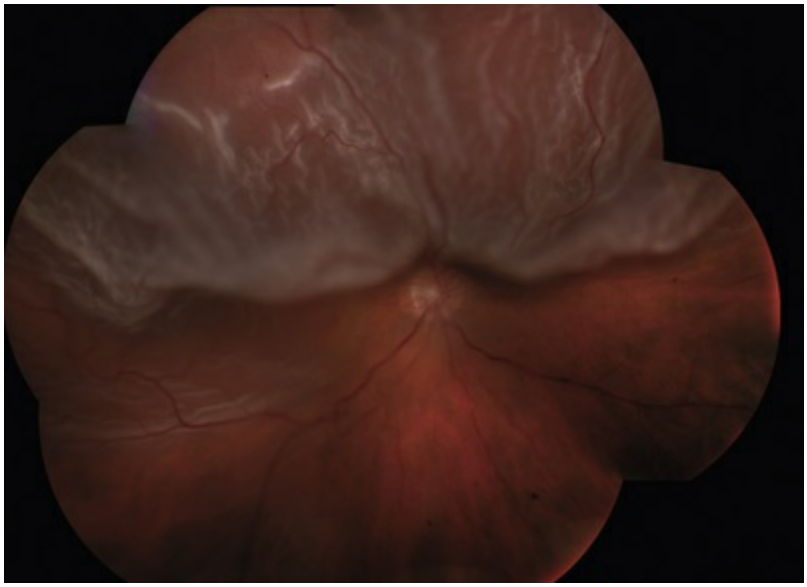

FIG. 94.5 Traumatic retinal detachment involving the macula.

Many patients with retinal detachment report a history of trauma but it often is difficult to establish a direct causal relationship. According to Goffstein and Burton,[74] factors suggesting trauma-induced retinal detachment include unilateral vitreoretinal pathology, retinal dialysis or giant retinal tear, age younger than 40 years, interval from trauma to diagnosis of retinal detachment less than 2 years, and objective evidence of trauma.

Vitreous Base Avulsion

The vitreous base normally is strongly adherent to the pars plana and peripheral retina. With blunt ocular trauma, the vitreous base may be avulsed from these structures, and this may be an isolated finding or associated with retinal dialysis or a giant retinal tear. Cox

et al.[56] reported this finding in 26% of patients with traumatic retinal detachment.

In the absence of retinal detachment, patients may be asymptomatic or may complain of floaters. Examination of the fundus reveals an arcuate band elevated from the peripheral retina. When the superior vitreous base is avulsed, it may appear draped over the superior peripheral retina (Fig. 94.6). Occasionally, fragments of pars plana epithelium remain adherent to the disinserted vitreous base. Avulsion of the vitreous base is pathognomonic of ocular trauma, and its presence should prompt a careful examination for associated ocular injury. Cryopexy to the edges of the avulsed vitreous base may prevent retinal breaks and retinal detachment.

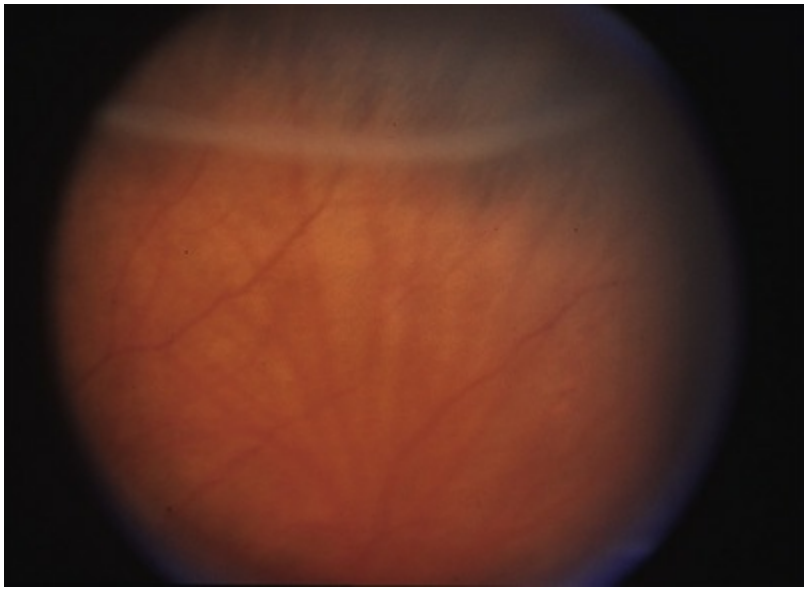

FIG. 94.6 Superior mid-peripheral fundus demonstrating draped ribbon-like opacity (avulsed vitreous base). Cryopexy was performed to the peripheral retina in the region of the vitreous base avulsion. This 40-year-old woman was a victim of domestic violence; the fellow eye had a giant retinal tear with retinal detachment and underwent scleral buckling surgery. Visual acuity remained 20/20 in both eyes. (Reproduced with permission from Eliott D, Avery R. Nonpenetrating posterior segment trauma. Ophthalmology Clinics of North America, Volume 8, Number 4, December 1995.)

Retinal Dialysis

The retina normally is adherent to the pars plana epithelium at the ora serrata. Retinal dialysis is a discontinuity or separation of the retina from the pars plana at the ora, and it may result in retinal detachment. Retinal dialysis occurs in the inferotemporal quadrant in 66% of cases, followed by the superonasal quadrant in 14%, the superotemporal quadrant in 10%, the inferonasal quadrant in 4%, and more than one quadrant in 6%.[77] Most dialyses are traumatic,[78] but developmental[77] and genetic[31] causes also have been proposed. All patients with a history of blunt ocular trauma should undergo scleral depression to assess for retinal dialysis (after an open globe is ruled out).

Patients with retinal dialysis may be asymptomatic or may complain of floaters. If retinal detachment also is present, patients may note loss of peripheral visual field if the detachment extends posterior to the equator or loss of visual acuity if the macula is involved. The vitreous is typically attached in eyes with retinal dialysis, and there may be pigment clumps in the inferior vitreous in cases with associated chronic retinal detachment. Indirect ophthalmoscopy reveals a slit at the ora that opens with scleral depression, and serrations within the dialysis are less prominent than normal (Fig. 94.7). If retinal detachment is present, it often is localized and elevated minimally, especially if the dialysis is small or located inferiorly. Trauma occurs most commonly in young patients with a formed vitreous, which often limits the extent of the detachment. In these patients, the retinal detachment may remain stable or progress slowly. Indeed, Ross[78] noted that one or more demarcation lines were present in 46% of patients with retinal dialysis. With posterior vitreous detachment or avulsion of the vitreous base, the retinal detachment is more likely to extend posteriorly or become highly elevated. Retinal dialysis is treated with photocoagulation or cryopexy as prophylaxis for retinal detachment. The treatment of retinal dialysis with retinal detachment is scleral buckling surgery. The success rate of scleral buckling surgery is approximately 90%[78,79] and visual acuity of 20/100 or better ultimately is achieved in two-thirds of patients.[78]

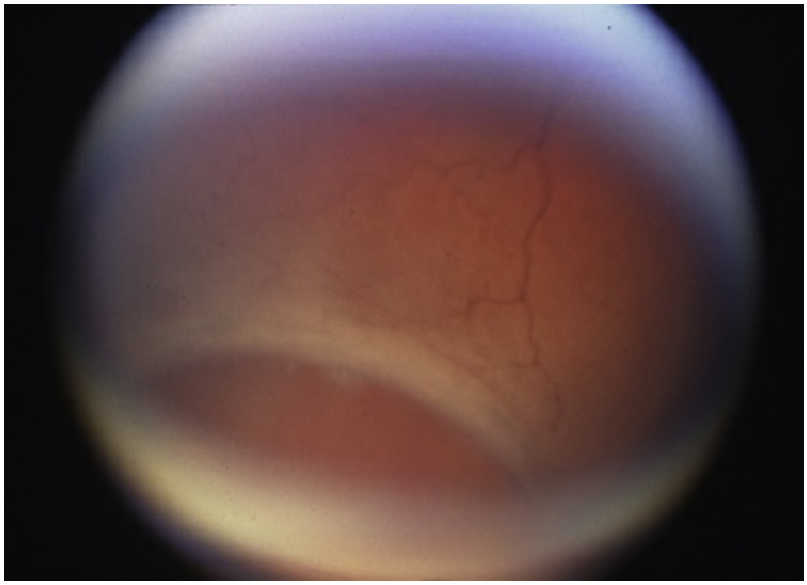

FIG. 94.7 Inferotemporal retinal dialysis in a 65-year-old woman who suffered blunt ocular trauma 2 years prior in a motor vehicle accident. Visual acuity is 20/30. The patient underwent scleral buckling surgery.

(Reproduced with permission from Eliott D, Avery R. Nonpenetrating posterior segment trauma. Ophthalmology Clinics of North America, Volume 8, Number 4, December 1995.)

Retinal Tears

Areas of strong vitreoretinal adhesion are particularly susceptible to traumatic damage. Horseshoe-shaped retinal tears and operculated retinal holes may result from trauma-induced vitreoretinal traction. These lesions may be found anywhere in the peripheral retina, but often are located at areas of lattice degeneration or at the edges of chorioretinal scars. Formed vitreous is attached to the elevated flap of a horseshoe tear and to the operculum in an operculated hole. In either case, liquid vitreous may pass through the retinal break, and traumatic retinal tears therefore are more likely than retinal dialyses to result in retinal detachment. This is especially true for horseshoe tears because vitreous traction on the retinal flap holds the tear open.

Patients may be asymptomatic or may complain of floaters or photopsia. Floaters may be particularly severe if vitreous hemorrhage results from a torn retinal vessel within the retinal tear. If retinal detachment also is present, patients may complain of loss of peripheral visual field or reduction in visual acuity, depending

on the extent of the detachment. Traumatic retinal tears are treated with photocoagulation or cryopexy as prophylaxis for retinal detachment. Scleral buckling surgery may be performed for retinal detachment associated with traumatic retinal tears, and the success rate exceeds 80%.[56] Vitrectomy is also a common procedure for traumatic retinal detachment.

Giant Retinal Tears

Giant retinal tears (GRTs) are retinal breaks extending circumferentially more than 3 clock-hours (equal to or greater than 90°), and they occur in the presence of a posterior vitreous detachment. They are oriented circumferentially, and there may be a radial extension posteriorly at one or both ends. GRTs occur at the posterior edge of the vitreous base. They differ from dialyses in that the anterior edge of a GRT is a strip of attached retina under the vitreous base. In addition, the state of the vitreous is critical in making this distinction. In eyes with GRTs the posterior hyaloid is detached while in eyes with retinal dialysis the vitreous remains attached. It is important to differentiate GRTs from retinal dialysis, as the latter carries a different natural history and is managed in a different manner. In GRTs, retinal detachment often develops because liquid vitreous easily enters the subretinal space. In some cases, the posterior edge of the tear is folded over the posterior pole (inverted posterior retinal flap), making it difficult to determine the status of the macula (Fig. 94.8).

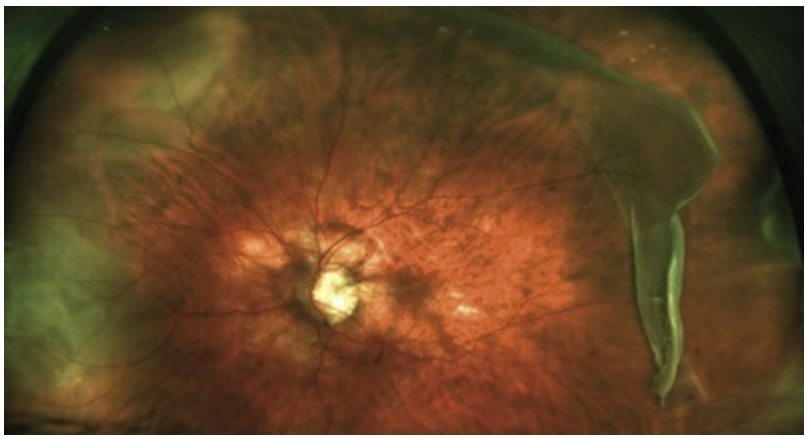

FIG. 94.8 Temporal giant retinal tear and associated retinal detachment. There is also a nasal retinal

detachment. (Courtesy of Yoshi Yonekawa and George Williams, Associated Retina Consultants, William Beaumont Hospital.)

The treatment of GRTs without retinal detachment is usually scleral buckling surgery. Some giant tears can be treated with cryopexy or photocoagulation, but there is a risk of developing a retinal detachment prior to the formation of an adequate chorioretinal adhesion.

Retinal detachments associated with GRTs are challenging cases and success rates were historically poor. Prior to the introduction of vitrectomy, GRTs were managed with scleral bucking combined with intraocular tamponade with either air or silicone oil, and the success rates were 51–65%.[80,81] These cases were technically and physically challenging for the retinal surgeon, as they required the use of specially designed operating tables with the surgeon operating in a supine "car-mechanic" fashion.

For GRTs associated with retinal detachment, the treatment depends on several factors, including the size of the tear, the location of the edges of the tear, the presence of an inverted posterior retinal flap, and the presence of proliferative vitreoretinopathy. Some GRTs fewer than 4 clock-hours in size without an inverted flap and without evidence of proliferative vitreoretinopathy may be treated successfully with scleral buckling surgery. The remainder of GRTs with retinal detachment usually are managed by vitrectomy with fluid–gas exchange with or without a scleral buckle. Some surgeons prefer the additional presence of a buckle if the edges of the GRT are located in the inferior clock-hours. Lensectomy may be performed in some cases, especially in cases with proliferative vitreoretinopathy, to facilitate removal of anterior vitreous.

The introduction of vitrectomy revolutionized the treatment of GRTs and the introduction of heavy liquids was associated with increased retinal reattachment rates. Perfluorocarbon liquid is an essential adjunct in GRTs with an inverted posterior retinal flap. Kreiger[82] proposed meticulous vitreous base shaving and showed that retinal reattachment can sometimes be achieved without the use of adjunctive scleral buckling. Primary retinal reattachment rates with vitrectomy alone range between 77% and 94%[82–87] and

between 68% and 96% when vitrectomy is combined with a scleral buckle.[83,88–95] Based on the current literature, it is difficult to determine the impact of adjunctive scleral buckling to vitrectomy in GRTs. Visual acuity improved postoperatively in at least half of the patients in most studies, and vision deteriorated in up to 40% when compared with the presenting visual acuity. Factors associated with higher redetachment rates were age below 30 years, female gender, prior vitrectomy, GRT extent greater than 180°, and the presence of preoperative proliferative vitreoretinopathy.[92] The rate of proliferative vitreoretinopathy is higher for GRTs than for detachments due to smaller tears, in part because retinal pigment epithelial cells are dispersed easily within the vitreous cavity as a result of the large size of the tear.

Optic Nerve Avulsion

Optic nerve avulsion is a catastrophic event that occurs after nonpenetrating or penetrating ocular trauma, when an object enters between the globe and the orbital wall and displaces the eye.[96,97] Patients experience an acute loss of vision, and often the vision is very poor to the level of no light perception. Optic nerve avulsions can be complete or partial. Complete avulsion is characterized by complete separation of the retina from the optic nerve, and the lamina cribrosa is retracted from the scleral rim. Funduscopic findings in complete optic nerve avulsion include extensive hemorrhages around the optic nerve, vitreous hemorrhage, excavation of the optic nerve and hemorrhage within the optic nerve and central retinal artery occlusion (Fig. 94.9). Possible pathophysiologic mechanisms include sudden extreme rotation of the globe or sudden rise in the intraocular pressure that forces the nerve out of the scleral wall. Unfortunately, there is no treatment for this devastating condition and final visual acuity is usually very poor.[98]

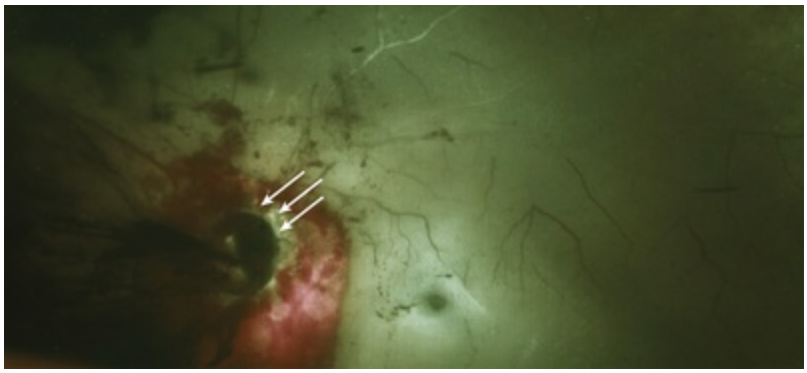

FIG. 94.9 Avulsed optic nerve in a 15-year-old boy who presented with immediate vision loss after he fell onto a rock, striking his left eye. There were no signs of globe rupture or laceration. The area of the optic nerve head was excavated and filled with hemorrhage (*arrows*) with blood emanating into the vitreous. There was also a ring of peripapillary hemorrhage and central retinal artery occlusion. (Reproduced with permission from Modjtahedi et al. Optic nerve head avulsion: Clinical, radiographic and sonographic correlations. Ophthalmology, 2015, volume 122, issue 12, page 2442.)

Indirect Ocular Injury

Purtscher Retinopathy

In 1910, Purtscher[99] described multiple patches of superficial retinal whitening, intraretinal hemorrhages, and papillitis in five patients following severe head trauma. He postulated that the whitening was caused by lymphatic extravasations caused by a sudden increase in intracranial pressure.[99,100] The pathognomonic *Purtscher flecken* appear in about 50% of the patients. These are polygonal areas of retinal whitening in the inner retina, between retinal arterioles and venules and have a characteristic zone of normal appearing retina extending for an average of 50 μm on either side of the vessels. The findings typically are bilateral, but unilateral cases have been described.[101,102] In apparent unilateral cases, the fellow eye may demonstrate very subtle findings.[103]

Although Purtscher's patients experienced visual loss, presenting visual acuity may range from 20/20 to counting fingers. An afferent pupillary defect and central or paracentral scotomas may be present. The fundus changes may be seen immediately and may

progress for 1–2 days following trauma (Fig. 94.10). The fluorescein angiographic findings are variable and include normal choroidal filling, focal areas of retinal arteriolar obstruction, patches of capillary nonperfusion, venous staining, and disc leakage.[101–104]

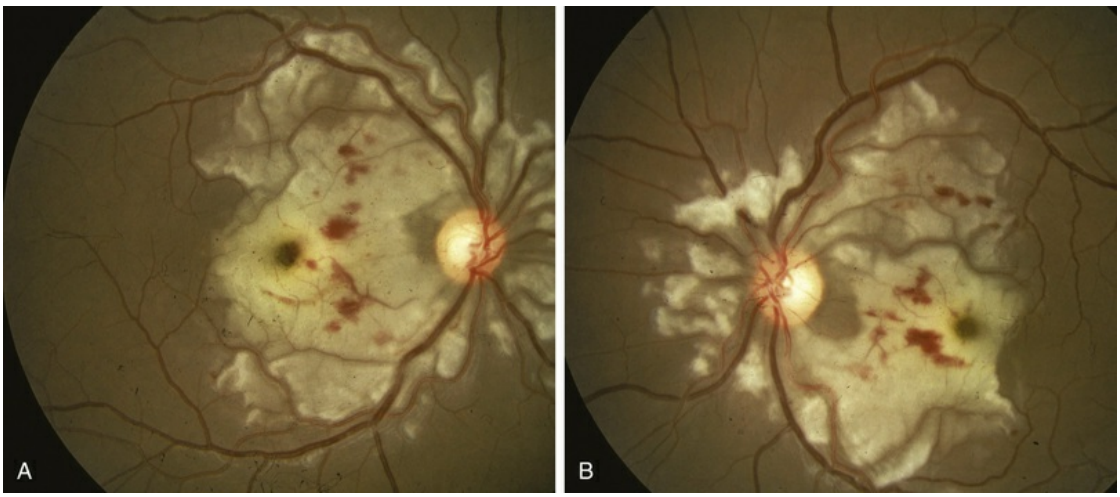

FIG. 94.10 Purtscher retinopathy. (A) Right eye demonstrating patches of superficial retinal whitening throughout the posterior pole in a 30-year-old man 2 days after he was assaulted and suffered head trauma. Visual acuity is 20/100 in both eyes. (B) Left eye shows symmetric involvement. (Reproduced with permission from Eliott D, Avery R. Nonpenetrating posterior segment trauma. Ophthalmology Clinics of North America, Volume 8, Number 4, December 1995.)

Agrawal et al.[100] reviewed clinical data from 24 eyes of 15 patients with Purtscher retinopathy. Without treatment, 50% of eyes improved at least 2 lines and 23% improved at least 4 lines at last follow-up. Only 1 of the 24 eyes had worse vision than at presentation. The course is unpredictable because some patients experience resolution of visual loss and fundus changes (over a several-month period), whereas others develop permanent visual loss associated with macular pigmentary disturbance, nerve fiber layer dropout, and optic atrophy.[101,104] Isolated case reports may suggest that treatment of Purtscher retinopathy with high-dose, intravenous steroids may be beneficial.

The typical setting for Purtscher retinopathy is severe head trauma in the absence of direct trauma to the globe, but a similar appearance of the fundus may develop in a variety of traumatic

injuries and diseases. These include acute pancreatitis,[101,105–107] as well as chronic panceatitis,[108] long bone fracture,[109] chest compression injuries,[103,110] air embolization,[101] amniotic fluid embolization,[111] childbirth,[112] hydrostatic pressure syndrome,[113] and connective tissue diseases such as lupus, scleroderma, dermatomyositis,[27] and thrombotic thrombocytopenic purpura.

The pathogenesis of retinal findings for all of the aforementioned conditions is uncertain, but acute pancreatitis and long bone fracture can lead to fat embolization.[105,107,114] Fat embolization syndrome occurs in up to 5% of patients with long bone fractures and may be fatal. Signs appear within 24 hours after injury and include tachycardia, tachypnea, pyrexia, mental status changes, seizures, focal neurologic signs, petechial hemorrhages, and lipuria.[114–116] Retinal findings are present in 50–60% of patients with fat embolization syndrome and include cotton-wool spots, blot hemorrhages, intravenous fat, and central retinal artery occlusion.[109,115,117–119]

Additional pathogenic mechanisms have been proposed, including arteriolar occlusion from air or amniotic fluid embolization,[101] arteriolar or venous damage resulting from elevated intravascular pressure,[120] and complement-induced granulocyte aggregation.[106,121] Severe trauma can activate the clotting and complement systems, and acute pancreatitis has been shown to activate complement. Complement C5A levels are elevated in patients with Purtscher retinopathy from acute pancreatitis.[121,122] Complement C5A causes intravascular leucoaggregates measuring 60–80 μm in diameter. In an animal model, similar retinal lesions have been observed after infusion of glass beads measuring 15–75 μm into the carotid artery.[123] Blodi et al.[112] suggested the retinal arteriolar embolization theory, most likely secondary to granulocyte aggregates or "leukoemboli," formed in response to complement activation. Features of Purtscher retinopathy that support this concept include sudden onset, multifocal lesions, otherwise healthy retinal vessels, and the characteristic distribution of ischemic patches.[112]

Terson Syndrome

In 1881, Litten[124] reported intraocular hemorrhage in association with subarachnoid hemorrhage, and, in 1900, Terson[125] described vitreous hemorrhage in association with any form of intracranial hemorrhage. Subsequently known as Terson syndrome, the retinal and vitreous hemorrhage most commonly occurs after subarachnoid hemorrhage, the majority resulting from spontaneous rupture of an intracranial aneurysm.[126] Approximately 20% of patients with subarachnoid hemorrhage may develop the condition.[113] Terson syndrome also may occur after subdural hemorrhage, the majority resulting from trauma.[126] Stienen et al.[127] studied the incidence of Terson syndrome in patients with aneurysmal subarachnoid hemorrhage in 60 patients admitted to the hospital. Eleven (18.3%) were noted to have Terson syndrome within 24 hours after aneurysm rupture. Compared with the non-Terson syndrome group, patients with Terson syndrome had worse outcomes, including a significantly higher mortality (36.4 vs. 10.2%; p=.028).

Kuhn et al.[128] studied prospectively the incidence of Terson syndrome with vitreous hemorrhage in patients with subarachnoid hemorrhage. Any type of intraocular hemorrhage was found in 17% of eyes in patients with subarachnoid hemorrhage; vitreous hemorrhage was present in 8%. All patients with vitreous hemorrhage and 89% of the patients with other types of intraocular hemorrhage had a history of coma compared with 46% of those without intraocular hemorrhage (p=.0003).

The vitreous hemorrhage often results in limited visualization of the posterior pole, and multiple preretinal, intraretinal, and subretinal hemorrhages are often present in the peripapillary region (Fig. 94.11). In some cases, a dome-shaped accumulation of blood spans the temporal arcades. Schultz et al.[126] reported the long-term visual outcome in 30 eyes with Terson syndrome. The mean age was 36 years and 11 of 19 patients had bilateral involvement. Presenting visual acuity ranged from 20/20 to light perception. Sixty-three percent of eyes developed a clinically apparent epiretinal membrane; this resulted in significant visual loss in two eyes. With a mean follow-up of 48 months, 83% of eyes achieved visual acuity of 20/50 or better. Half of these eyes had undergone vitrectomy while half were managed conservatively.[126]

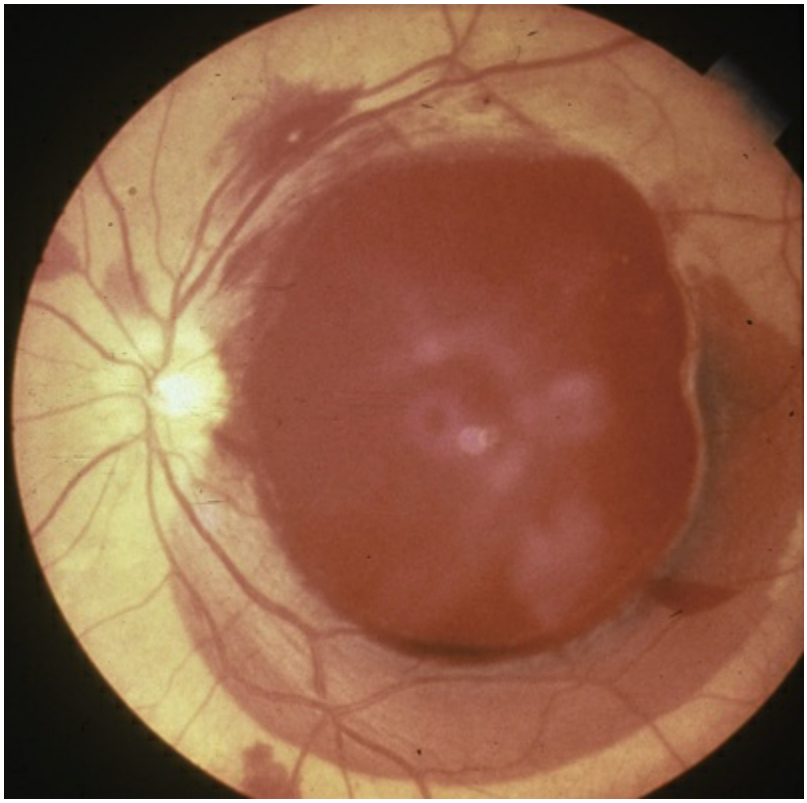

FIG. 94.11 Terson syndrome with hemorrhages in multiple layers. There is a large sub-internal limiting membrane hemorrhage, multiple intraretinal white-centered hemorrhages, and a large area of subretinal hemorrhage.

The pathogenesis of Terson syndrome remains controversial. An early report postulates that hemorrhage in the subarachnoid space can dissect within the optic nerve sheath to enter the eye.[129] This hypothesis cannot explain the presence of preretinal hemorrhage, as there is no direct communication between the subarachnoid space and the vitreous cavity.[119] The mechanism cited most frequently proposes that intracranial hemorrhage produces an acute elevation of intracranial pressure that is transmitted within the optic nerve sheath to obstruct the venous drainage from the eye. This acute rise in venous pressure causes distension and rupture of the fine papillary and retinal capillaries, often resulting in significant hemorrhage.[130–133] The hemorrhage may spread to the subretinal space, within the retina, the subinternal limiting membrane space, the subhyaloid space, or the vitreous cavity.

Vanderlinden and Chisholm[134] first described blood between the retina and the internal limiting membrane in Terson syndrome.

Keithahn et al.[135] reported two adults with perimacular folds spanned by a glistening membrane. In one of these patients, this membrane was shown by electron microscopy to be internal limiting membrane.[135]

The typical clinical course consists of gradual resolution of the vitreous hemorrhage, but vitrectomy may produce good results as well.[126,133,136–138] Indications for vitrectomy include visually immature eyes, in which early rehabilitation may prevent amblyopia, and bilateral Terson syndrome.[126] Indications for conservative management include rapidly clearing vitreous hemorrhage, unilateral involvement with a normal fellow eye, associated ocular damage that precludes good vision, and poor health.[126] In the report by Schultz et al.,[126] ultimate visual outcome was independent of presenting visual acuity, the location of peripapillary hemorrhage, the presence of a dome-shaped lesion, the location of intracranial hemorrhage, and the method of treatment (vitrectomy versus observation). Although there was no difference in the final vision in eyes that underwent vitrectomy compared with eyes managed conservatively, visual recovery was significantly faster in eyes managed with vitrectomy. Sharma et al.[139] reported 15 eyes of 11 patients with Terson syndrome that underwent vitrectomy. Visual acuity of 20/40 or better was achieved in 14 eyes (93.3%). The mean follow-up time was 18 months. Ritland et al.[140] reported 22 eyes with Terson syndrome managed with vitrectomy. Twelve cases underwent unilateral vitrectomy and five had bilateral surgery. The interval between intracranial hemorrhage and vitrectomy was 1–10 months (mean 5.9 months). During a mean follow-up of 23 months (range 1–69 months) visual acuity improved in 21 of 22 eyes. Preoperative visual acuity was ≤0.1 in 20 of 22 eyes, while postoperative visual acuity was ≥0.5 in 16 of 21 eyes. One eye experienced vision loss due to subtotal retinal detachment with massive epiretinal membrane formation and proliferative vitreoretinopathy. Poor visual outcomes were mainly caused by retinal detachment (seven eyes, in which three were associated with proliferative vitreoretinopathy), epiretinal membrane (seven eyes), and optic atrophy (one eye).

Skevas et al.[141] analyzed the need for surgical intervention in Terson syndrome and the rate of Terson syndrome, as well as the

effect of vitrectomy with or without internal limiting membrane peeling. The rate of Terson syndrome was 19.6% (20/102). Eight (9 eyes) of the 20 patients with Terson syndrome (40% of the patients with Terson syndrome) underwent a vitrectomy for nonclearing vitreous hemorrhage. In four patients (4 eyes; 20% of patients with Terson syndrome), internal limiting membrane peeling was considered necessary because of subinternal limiting membrane blood. The mean interval between subarachnoid hemorrhage and vitrectomy was 4.4 months (range, 3–5 months). Postoperative follow-up was 6.4 months. Visual acuity improved in all patients.

Valsalva Retinopathy

The Valsalva maneuver is defined as a sudden elevation in intrathoracic or intraabdominal pressure against a closed glottis. In 1972, Duane[142] described "Valsalva hemorrhagic retinopathy" resulting from rupture of superficial retinal capillaries associated with sudden elevation of ocular venous pressure. Incompetent or absent valves in the venous system of the head and neck allow transmission of thoracic or abdominal pressure into the eye.[142,143] Typical activities producing Valsalva retinopathy include heavy lifting, coughing, vomiting, and straining during bowel movement. Gass[27] described the classic dumbbell-shaped red elevation beneath the internal limiting membrane in or near the central macula; larger round or oval hemorrhages also may be seen (Fig. 94.12). Occasionally, the subinternal limiting membrane hemorrhage breaks through to the subhyaloid space or vitreous cavity.[142] In almost all cases the hemorrhages eventually resolve and vision returns to normal.

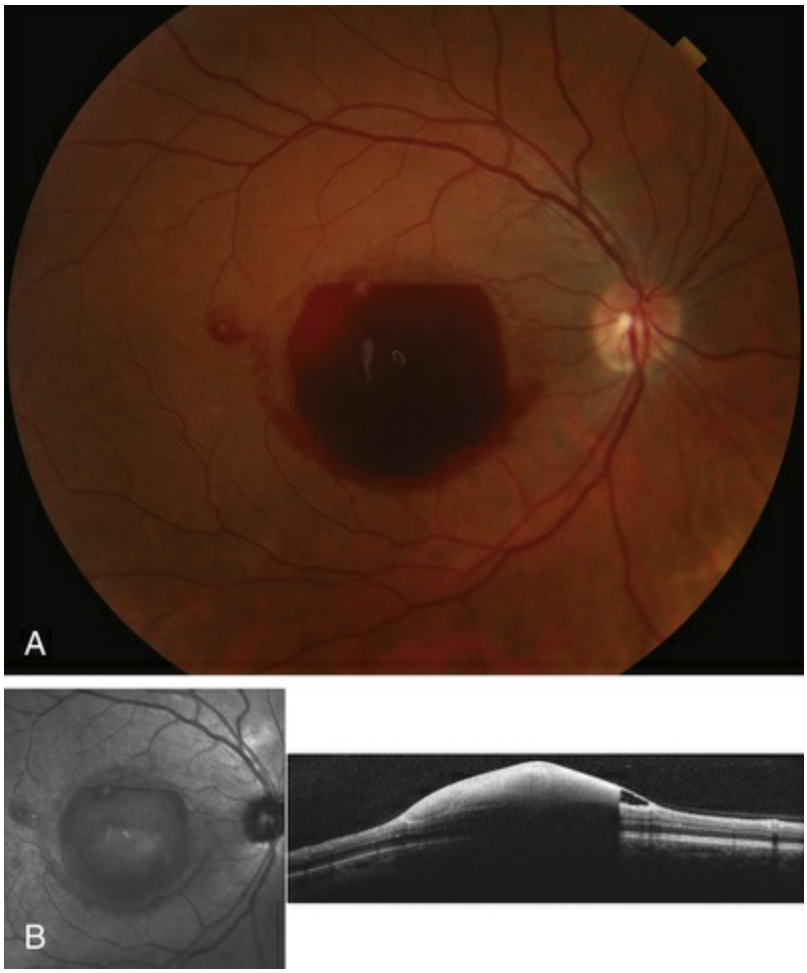

FIG. 94.12 (A) Valsalva retinopathy associated with coughing after waking from general anesthesia in a 41-year-old woman. There is a sub-internal limiting membrane (ILM) hemorrhage in the macula. (B) Vertical optical coherence tomography scan showing the sub-ILM hemorrhage.

Shaken Baby Syndrome

Approximately 30–40% of physically abused children develop ophthalmic manifestations.[144,145] The most common findings include retinal hemorrhages (Fig. 94.13), cotton-wool spots, perimacular retinal folds and vitreous hemorrhage,[27,144] but retinal detachment, retinal folds,[146] retinoschisis,[147] and peripheral chorioretinal atrophy[148] also have been described. Caffey[149] was the first to demonstrate the association between manual shaking of an infant with whiplash-induced intraocular and intracranial hemorrhage. The head accounts for approximately 10% of the weight of an

infant. Because newborns have poorly developed neck muscles, the shaking maneuver causes rapid acceleration–deceleration of the infant's head and may result in whiplash-induced retinal hemorrhages. Hypoxic ischemic brain injury has been shown to account for the cerebral pathology in shaken baby syndrome.[150] Caputo et al.[151] reported three babies with nonaccidental head trauma that presented with traction retinal detachment and retinal ischemia. Bielory et al.[152] also reported three cases of shaken baby syndrome with bilateral peripheral nonperfusion.

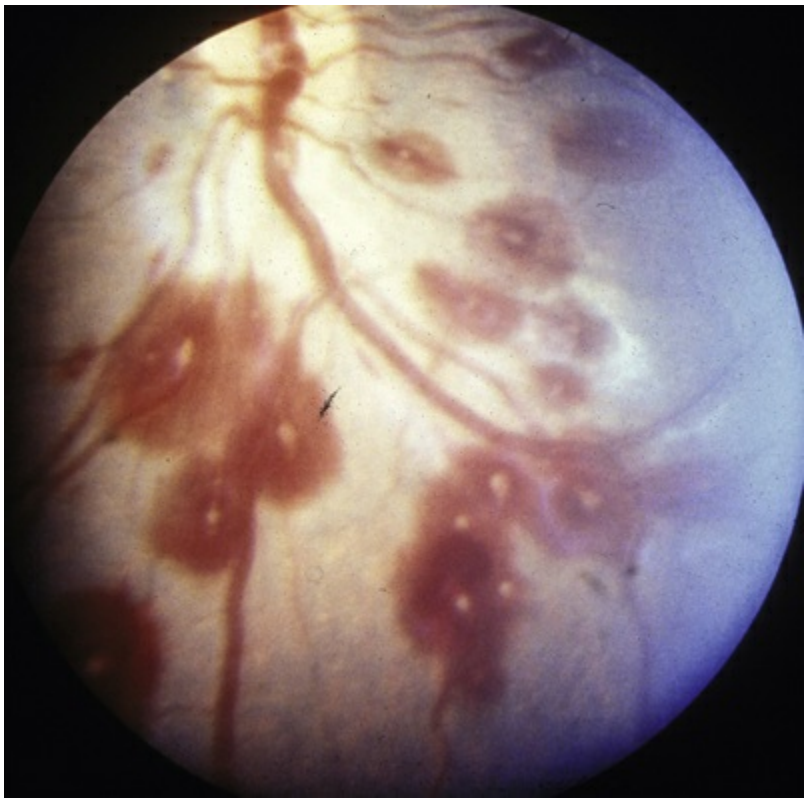

FIG. 94.13 Presumed shaken baby syndrome. Multiple white-centered intraretinal hemorrhages in an 8-month old boy who was found unresponsive with multiple fractures. He was admitted to the intensive care unit for suspected child abuse. (Reproduced with permission from Eliott D, Avery R. Nonpenetrating posterior segment trauma. Ophthalmology Clinics of North America, Volume 8, Number 4, December 1995.)

Muni et al.[153] reported the optical coherence tomography (OCT) findings in three babies with nonaccidental head trauma. Handheld spectral domain OCT documented focal posterior vitreous

separation in four of the six eyes, multilayered retinoschisis in one eye, disruption of the foveal architecture and foveolar detachment in one eye, and disinsertion of the internal limiting membrane or inner retinoschisis in one eye. Handheld spectral domain OCT documented preretinal hemorrhages in all six eyes.

The presence of retinal hemorrhages should arouse suspicion of possible child abuse, especially in infants with additional injuries. Because ocular findings are the presenting signs of child abuse in approximately 5% of cases, the ophthalmologist may play a critical role in the recognition of this serious situation.

Conclusion

It is essential that the ophthalmologist is familiar with the wide variety of posterior segment manifestations of nonpenetrating trauma. A timely and thorough evaluation is critical for accurate diagnosis and appropriate treatment, and awareness of potential late complications is important in the long-term management of the trauma patient. The ophthalmologist also must play a role in the prevention of eye trauma by stressing the use of protective eyewear, especially for the trauma patient with an intact fellow eye.[154]

References

1. LaRoche GR, McIntyre L, Schertzer RM. Epidemiology of severe eye injuries in childhood. *Ophthalmology*. 1988;95:1603–1607.
2. Liggett PE, Pince KJ, Barlow W, et al. Ocular trauma in an urban population. Review of 1132 cases. *Ophthalmology*. 1990;97:581–584.
3. Rapoport I, Romem M, Kinek M, et al. Eye injuries in children in Israel. A nationwide collaborative study. *Arch Ophthalmol*. 1990;108:376–379.
4. Wolter JR. Coup-contrecoup mechanism of ocular injuries. *Am J Ophthalmol*. 1963;56:785–796.
5. Kelley JS, Hoover RE, George T. Whiplash maculopathy. *Arch Ophthalmol*. 1978;96:834–835.

6. Berlin R. Sogenannten commotio retinae. So-called commotio retinae. *Klin Monatsbl Augenheilkd*. 1873;1:42–78.
7. Hart JC, Frank HJ. Retinal opacification after blunt non-perforating concussional injuries to the globe. A clinical and retinal fluorescein angiographic study. *Trans Ophthalmol Soc U K*. 1975;95:94–100.
8. Hart CD, Raistrick R. Indirect choroidal tears and late onset serosanguinous maculopathies. *Graefes Arch Clin Exp Ophthalmol*. 1982;218:206–210.
9. Hart JC, Blight R, Cooper R, et al. Electrophysiological and pathological investigation of concussional injury. An experimental study. *Trans Ophthalmol Soc U K*. 1975;95:326–334.
10. Cogan DG. Pseudoretinitis pigmentosa. Report of two traumatic cases of recent origin. *Arch Ophthalmol*. 1969;81:45–53.
11. Crouch ER, Apple DJ. Posttraumatic migration of retinal pigment epithelial melanin. *Am J Ophthalmol*. 1974;78:251–254.
12. François J, De Laey JJ. Fluoroangiographic study of traumatic chorioretinal angiopathy. *Bull Soc Belge Ophtalmol*. 1970;156:577–589.
13. Gregor Z, Ryan SJ. Blood–retinal barrier after blunt trauma to the eye. *Graefes Arch Clin Exp Ophthalmol*. 1982;219:205–208.
14. Kohno T, Ishibashi T, Inomata H, et al. Experimental macular edema of commotio retinae: preliminary report. *Jpn J Ophthalmol*. 1983;27:149–156.
15. Pulido JS, Blair NP. The blood–retinal barrier in Berlin's edema. *Retina*. 1987;7:233–236.
16. Mansour AM, Green WR, Hogge C. Histopathology of commotio retinae. *Retina*. 1992;12:24–28.
17. Blight R, Hart JC. Histological changes in the internal retinal layers produced by concussive injuries to the globe. An experimental study. *Trans Ophthalmol Soc U K*. 1978;98:270–277.
18. Blight R, Hart JC. Structural changes in the outer retinal layers following blunt mechanical non-perforating trauma

to the globe: an experimental study. *Br J Ophthalmol*. 1977;61:573–587.
19. Sipperley JO, Quigley HA, Gass DM. Traumatic retinopathy in primates. The explanation of commotio retinae. *Arch Ophthalmol*. 1978;96:2267–2273.
20. Souza-Santos F, Lavinsky D, Moraes NS, et al. Spectral-domain optical coherence tomography in patients with commotio retinae. *Retina*. 2012;32:711–718.
21. Ahn SJ, Woo SJ, Kim KE, et al. Optical coherence tomography morphologic grading of macular commotio retinae and its association with anatomic and visual outcomes. *Am J Ophthalmol*. 2013;156:994–1001.e1.
22. Von Graefe A. Ze Falle von Rupture der Choroida. *Graefes Arch Clin Exp Ophthalmol*. 1854;1:402.
23. Kaufer G, Zimmeman LE. Direct rupture of the choroid. *Arch Ophthalmol*. 1966;75:384–385.
24. Hilton GF. Late serosanguineous detachment of the macula after traumatic choroidal rupture. *Am J Ophthalmol*. 1975;79:997–1000.
25. Hart JC, Natsikos VE, Raistrick ER, et al. Indirect choroidal tears at the posterior pole: a fluorescein angiographic and perimetric study. *Br J Ophthalmol*. 1980;64:59–67.
26. Gitter KA, Slusher M, Justice J. Traumatic hemorrhagic detachment of retinal pigment epithelium. *Arch Ophthalmol*. 1968;79:729–732.
27. Gass J. *Stereoscopic atlas of macular diseases*. Mosby Year Book: St. Louis; 1987.
28. Fuller B, Gitter KA. Traumatic choroidal rupture with late serous detachment of macula. Report of successful argon laser treatment. *Arch Ophthalmol*. 1973;89:354–355.
29. Smith RE, Kelley JS, Harbin TS. Late macular complications of choroidal ruptures. *Am J Ophthalmol*. 1974;77:650–658.
30. Goldberg MF. Chorioretinal vascular anastomoses after perforating trauma to the eye. *Am J Ophthalmol*. 1978;85:171–173.
31. Bressler SB, Bressler NM. *Traumatic maculopathies. Eye trauma*. Mosby Year Book: St. Louis; 1991.
32. Lavinsky D, Martins EN, Cardillo JA, et al. Fundus

autofluorescence in patients with blunt ocular trauma. *Acta Ophthalmol*. 2011;89:e89–94.
33. Aguilar JP, Green WR. Choroidal rupture. A histopathologic study of 47 cases. *Retina*. 1984;4:269–275.
34. Kempster RC, Green WR, Finkelstein D. Choroidal rupture. Clinicopathologic correlation of an unusual case. *Retina*. 1996;16:57–63.
35. Aguilar JP, Green WR. Choroidal rupture. A histopathologic study of 47 cases. *Retina*. 1984;4:269–275.
36. Nair U, Soman M, Ganekal S, et al. Morphological patterns of indirect choroidal rupture on spectral domain optical coherence tomography. *Clin Ophthalmol*. 2013;7:1503–1509.
37. Ament CS, Zacks DN, Lane AM, et al. Predictors of visual outcome and choroidal neovascular membrane formation after traumatic choroidal rupture. *Arch Ophthalmol*. 2006;124:957–966.
38. Gross JG, King LP, de Juan E, et al. Subfoveal neovascular membrane removal in patients with traumatic choroidal rupture. *Ophthalmology*. 1996;103:579–585.
39. Harissi-Dagher M, Sebag M, Gauthier D, et al. Photodynamic therapy in young patients with choroidal neovascularization following traumatic choroidal rupture. *Am J Ophthalmol*. 2005;139:726–728.
40. Conrath J, Forzano O, Ridings B. Photodynamic therapy for subfoveal CNV complicating traumatic choroidal rupture. *Eye (Lond)*. 2004;18:946–947.
41. Abri A, Binder S, Pavelka M, et al. Choroidal neovascularization in a child with traumatic choroidal rupture: clinical and ultrastructural findings. *Clin Experiment Ophthalmol*. 2006;34:460–463.
42. Gotzaridis EV, Vakalis AN, Sethi CS, et al. Surgical removal of sequential epiretinal and subretinal neovascular membranes in a patient with traumatic choroidal rupture. *Eye (Lond)*. 2003;17:790–791.
43. Yadav NK, Bharghav M, Vasudha K, et al. Choroidal neovascular membrane complicating traumatic choroidal rupture managed by intravitreal bevacizumab. *Eye*. 2009;23:1872–1873.

44. Chanana B, Azad RV, Kumar N. Intravitreal bevacizumab for subfoveal choroidal neovascularization secondary to traumatic choroidal rupture. *Eye*. 2009;23:2125–2126.
45. Artunay O, Rasier R, Yuzbasioglu E, et al. Intravitreal bevacizumab injection in patients with choroidal neovascularization due to choroid rupture after blunt-head trauma. *Int Ophthalmol*. 2009;29:289–291.
46. De Benedetto U, Battaglia Parodi M, Knutsson KA, et al. Intravitreal bevacizumab for extrafoveal choroidal neovascularization after ocular trauma. *J Ocul Pharmacol Ther*. 2012;28:550–552.
47. Duke-Elder S, MacFaul PA. *Pt. 1: Mechanical Injuries. System of Ophthalmology*. 1972.
48. Doherty WB. Some of the most important ocular and orbital wounds in war. *Am. J. Ophth.*1942;25:135–149.
49. Nover A, Blodi FC. *The ocular fundus: methods of examination and typical findings*. Lea & Febiger: Philadelphia; 1987.
50. Bloome MA, Ruiz RS, Russo CE, et al. Acute retinal necrosis. *Ann Ophthalmol*. 1979;11:723–728.
51. Goldzieher W. Beitrag zur Pathologie der orbitalen Schussverletzungen. *Z Augenheilkd*. 1901;6:277–285.
52. Martin DF, Awh CC, McCuen BW, et al. Treatment and pathogenesis of traumatic chorioretinal rupture (sclopetaria). *Am J Ophthalmol*. 1994;117:190–200.
53. Ahmadabadi MN, Karkhaneh R, Roohipoor R, et al. Clinical presentation and outcome of chorioretinitis sclopetaria: a case series study. *Injury*. 2010;41:82–85.
54. Papakostas TD, Yonekawa Y, Wu D, et al. Retinal detachment associated with traumatic chorioretinal rupture. *Ophthalmic Surg Lasers Imaging Retina*. 2014;45:451–455.
55. Fuchs E. Zur Veranderung der macula lutea nach contusion. *Z. Augenheilkd*. 1901;6.
56. Cox MS, Schepens CL, Freeman HM. Retinal detachment due to ocular contusion. *Arch Ophthalmol*. 1966;76:678–685.
57. Giovinazzo VJ, Yannuzzi LA, Sorenson JA, et al. The ocular complications of boxing. *Ophthalmology*. 1987;94:587–596.
58. Avins LR, Krummenacher TR. Macular holes after

pneumatic retinopexy. Case reports. *Arch Ophthalmol*. 1988;106:724–725.
59. Runge PE, Wyhinny GJ. Macular hole secondary to pneumatic retinopexy. Case report. *Arch Ophthalmol*. 1988;106:586–587.
60. Gass JD. Idiopathic senile macular hole. Its early stages and pathogenesis. *Arch Ophthalmol*. 1988;106:629–639.
61. Frangieh GT, Green WR, Engel HM. A histopathologic study of macular cysts and holes. *Retina*. 1981;1:311–336.
62. Huang J, Liu X, Wu Z, et al. Classification of full-thickness traumatic macular holes by optical coherence tomography. *Retina*. 2009;29:340–348.
63. Aaberg TM, Blair CJ, Gass JD. Macular holes. *Am J Ophthalmol*. 1970;69:555–562.
64. Margherio RR, Schepens CL. Macular breaks. 2. Management. *Am J Ophthalmol*. 1972;74:233–240.
65. Azevedo S, Ferreira N, Meireles A. Management of pediatric traumatic macular holes – case report. *Case Rep Ophthalmol*. 2013;4:20–27.
66. Barreau E, Massin P, Paques M, et al. Surgical treatment of post-traumatic macular holes. *J Fr Ophtalmol*. 1997;20:423–429.
67. Kuhn F, Morris R, Mester V, et al. Internal limiting membrane removal for traumatic macular holes. *Ophthalmic Surg Lasers*. 2001;32:308–315.
68. Miller JB, Yonekawa Y, Eliott D, et al. Long-term follow-up and outcomes in traumatic macular holes. *Am J Ophthalmol*. 2015;160:1255–1258.e1.
69. Ghoraba HH, Ellakwa AF, Ghali AA. Long term result of silicone oil versus gas tamponade in the treatment of traumatic macular holes. *Ophthalmology*. 2012;6:49–53.
70. Amari F, Ogino N, Matsumura M, et al. Vitreous surgery for traumatic macular holes. *Retina*. 1999;19:410–413.
71. Brasil OFM, Brasil OM. Management of traumatic macular holes: case report. *Arq Bras Oftalmol*. 2008;71:581–584.
72. Chow DR, Williams GA, Trese MT, et al. Successful closure of traumatic macular holes. *Retina*. 1999;19:405–409.
73. Dumas JJ. Retinal detachment following contusion of the

eye. *Int Ophthalmol Clin*. 1967;7:19–38.
74. Goffstein R, Burton TC. Differentiating traumatic from nontraumatic retinal detachment. *Ophthalmol*. 1982;89:361–368.
75. Haimann MH, Burton TC, Brown CK. Epidemiology of retinal detachment. *Arch Ophthalmol*. 1982;100:289–292.
76. Schepens CL, Marden D. Data on the natural history of retinal detachment. Further characterization of certain unilateral nontraumatic cases. *Am J Ophthalmol*. 1966;61:213–226.
77. Zion VM, Burton TC. Retinal dialysis. *Arch Ophthalmol*. 1980;98:1971–1974.
78. Ross WH. Traumatic retinal dialyses. *Arch Ophthalmol*. 1981;99:1371–1374.
79. Hagler WS. Retinal dialysis: a statistical and genetic study to determine pathogenic factors. *Trans Am Ophthalmol Soc*. 1980;78:686–733.
80. Norton EW, Aaberg T, Fung W, et al. Giant retinal tears. I. Clinical management with intravitreal air. *Trans Am Ophthalmol Soc*. 1969;67:374–393.
81. Freeman HM, Schepens CL, Couvillion GC. Current management of giant retinal breaks. II. *Trans Am Acad Ophthalmol Otolaryngol*. 1970;74:59–74.
82. Kreiger AE, Lewis H. Management of giant retinal tears without scleral buckling. Use of radical dissection of the vitreous base and perfluoro-octane and intraocular tamponade. *Ophthalmology*. 1992;99:491–497.
83. Ang GS, Townend J, Lois N. Epidemiology of giant retinal tears in the United Kingdom: the British Giant Retinal Tear Epidemiology Eye Study (BGEES). *Invest Ophthalmol Vis Sci*. 2010;51:4781–4787.
84. Ambresin A, Wolfensberger TJ, Bovey EH. Management of giant retinal tears with vitrectomy, internal tamponade, and peripheral 360 degrees retinal photocoagulation. *Retina*. 2003;23:622–628.
85. Batman C, Cekiç O. Vitrectomy with silicone oil or long-acting gas in eyes with giant retinal tears: long-term follow-up of a randomized clinical trial. *Retina*. 1999;19:188–192.

86. Chang S, Lincoff H, Zimmerman NJ, et al. Giant retinal tears. Surgical techniques and results using perfluorocarbon liquids. *Arch Ophthalmol*. 1989;107:761–766.
87. Rofail M, Lee LR. Perfluoro-n-octane as a postoperative vitreoretinal tamponade in the management of giant retinal tears. *Retina*. 2005;25:897–901.
88. Ghosh YK, Banerjee S, Savant V, et al. Surgical treatment and outcome of patients with giant retinal tears. *Eye (Lond)*. 2004;18:996–1000.
89. Goezinne F, Heij EC, Berendschot TTJM, et al. Low redetachment rate due to encircling scleral buckle in giant retinal tears treated with vitrectomy and silicone oil. *Retina*. 2008;28:485–492.
90. Ie D, Glaser BM, Sjaarda RN, et al. The use of perfluoro-octane in the management of giant retinal tears without proliferative vitreoretinopathy. *Retina*. 1994;14:323–328.
91. Mathis A, Pagot V, Gazagne C, Malecaze F. Giant retinal tears. Surgical techniques and results using perfluorodecalin and silicone oil tamponade. *Retina*. 1992;12:S7–10.
92. Scott IU, Murray TG, Flynn HW, et al. Outcomes and complications associated with giant retinal tear management using perfluoro-n-octane. *Ophthalmology*. 2002;109:1828–1833.
93. Sirimaharaj M, Balachandran C, Chan WC, et al. Vitrectomy with short term postoperative tamponade using perfluorocarbon liquid for giant retinal tears. *Br J Ophthalmol*. 2005;89:1176–1179.
94. Unlü N, Kocaoğlan H, Acar MA, et al. The management of giant retinal tears with silicone oil. *Eur J Ophthalmol*. 2003;13:192–195.
95. Verstraeten T, Williams GA, Chang S, et al. Lens-sparing vitrectomy with perfluorocarbon liquid for the primary treatment of giant retinal tears. *Ophthalmology*. 1995;102:17–20.
96. Foster BS, March GA, Lucarelli MJ, et al. Optic nerve avulsion. *Arch Ophthalmol*. 1997;115:623–630.
97. Chaudhry IA, Shamsi FA, Al-Sharif A, et al. Optic nerve

avulsion from door-handle trauma in children. *Br J Ophthalmol*. 2006;90:844–846.
98. Sturm V, Menke MN, Bergamin O, et al. Longterm follow-up of children with traumatic optic nerve avulsion. *Acta Ophthalmol*. 2010;88:486–489.
99. Purtscher O. Noch unbekannte befunde nach schadeltrauma. [Unknown findings after head trauma.]. *Ber Dtsch Ophthalmol Ges*. 1910;36:294–301.
100. Agrawal A, McKibbin M. Purtscher's retinopathy: epidemiology, clinical features and outcome. *Br J Ophthalmol*. 2007;91:1456–1459.
101. Burton TC. Unilateral Purtscher's retinopathy. *Ophthalmology*. 1980;87:1096–1105.
102. Fischbein F, Safir A. Monocular Purtscher's retinopathy. A fluorescein angiographic study. *Arch Ophthalmol*. 1971;85:480–484.
103. Kelley JS. Purtscher's retinopathy related to chest compression by safety belts. Fluorescein angiographic findings. *Am J Ophthalmol*. 1972;74:278–283.
104. Beckingsale AB, Rosenthal AR. Early fundus fluorescein angiographic findings and sequelae in traumatic retinopathy: case report. *Br J Ophthalmol*. 1983;67:119–123.
105. Inkeles DM, Walsh JB. Retinal fat emboli as sequela to acute pancreatitis. *Am J Ophthalmol*. 1975;80:935–938.
106. Jacob HS, Goldstein IM, Shapiro I, et al. Sudden blindness in acute pancreatitis. Possible role of complement-induced retinal leukoembolization. *Arch Intern Med*. 1981;141:134–136.
107. Kincaid MC, Green WR, Knox DL, et al. A clinicopathological case report of retinopathy of pancreatitis. *Br J Ophthalmol*. 1982;66:219–226.
108. Sharma AG, Kazim NA, Eliott D, et al. Purtscher's retinopathy that occurred 6 months before acute pancreatitis. *Am J Ophthalmol*. 2006;141:205–207.
109. Chuang EL, Miller FS, Kalina RE. Retinal lesions following long bone fractures. *Ophthalmology*. 1985;92:370–374.
110. Madsen PH. Traumatic retinal angiopathy (Purtscher). *Ophthalmologica*. 1972;165:453–458.

111. Chang M, Herbert WN. Retinal arteriolar occlusions following amniotic fluid embolism. *Ophthalmology*. 1984;91:1634–1637.
112. Blodi BA, Johnson MW, Gass JD, et al. Purtscher's-like retinopathy after childbirth. *Ophthalmology*. 1990;97:1654–1659.
113. Lyle DJ, Stapp JP, Button RR. Ophthalmologic hydrostatic pressure syndrome. *Am J Ophthalmol*. 1957;44:652–657.
114. Thomas JE, Ayyar DR. Systemic fat embolism. A diagnostic profile in 24 patients. *Arch Neurol*. 1972;26:517–523.
115. Adams CB. The retinal manifestations of fat embolism. *Injury*. 1971;2:221–224.
116. Gurd AR, Wilson RI. The fat embolism syndrome. *J Bone Joint Surg B*. 1974;56B:408–416.
117. Blake J. Ocular embolism. *Trans Ophthalmol Soc U K*. 1975;95:88–93.
118. Dieckert JP. Posterior segment trauma. *Albert and Jakobiec's Principles and practice of ophthalmology*. 3rd ed. Saunders/Elsevier: Philadelphia; 2000:5113–5119.
119. Williams DF, Mieler WF, Williams GA. Posterior segment manifestations of ocular trauma. *Retina*. 1990;10(Suppl. 1):S35–44.
120. Beck JP, Collins JA. Theoretical and clinical aspects of posttraumatic fat embolism syndrome. *Instr Course Lect*. 1973.
121. Jacob HS, Craddock PR, Hammerschmidt DE, et al. Complement-induced granulocyte aggregation: an unsuspected mechanism of disease. *N Engl J Med*. 1980;302:789–794.
122. Shapiro I, Jacob HS. Leukoembolization in ocular vascular occlusion. *Ann Ophthalmol*. 1982;14:60–62.
123. Ashton N, Henkind P. Experimental occlusion of retinal arterioles: using graded glass Ballotini. *Br J Ophthalmol*. 1965;49:225–234.
124. Litten M. Ueber einige vom allegmein-klinischen Standpunkt aus interessante Augenveranderungen. *Berl Klin Wochnschr*. 1881;18:23–27.
125. Terson A. De l'hémorrhagie dans le corps vitre au cours de

l'hémorrhagie cerebrale. *Clin Ophthalmol.*1900;6:309–312.
126. Schultz PN, Sobol WM, Weingeist TA. Long-term visual outcome in Terson syndrome. *Ophthalmology*. 1991;98:1814–1819.
127. Stienen MN, Lücke S, Gautschi OP, et al. Terson haemorrhage in patients suffering aneurysmal subarachnoid haemorrhage: a prospective analysis of 60 consecutive patients. *Clin Neurol Neurosurg*. 2012;114:535–538.
128. Kuhn F, Morris R, Witherspoon CD, et al. Terson syndrome. *Ophthalmology*. 1998;105:472–477.
129. Daubler FH, Marlow SB. A case of hemorrhage into the optic nerve sheaths as a direct extension from a diffuse intrameningeal hemorrhage caused by rupture of aneurysms of a cerebral artery. *Arch Ophthalmol*. 1917;46:553–556.
130. Khan SG, Frenkel M. Intravitreal hemorrhage associated with rapid increase in intracranial pressure (Terson's syndrome). *Am J Ophthalmol*. 1975;80:37–43.
131. Muller PJ, Deck JH. Intraocular and optic nerve sheath hemorrhage in cases of sudden intracranial hypertension. *J Neurosurg*. 1974;41:160–166.
132. Toosi SH, Malton M. Terson's syndrome – significance of ocular findings. *Ann Ophthalmol*. 1987;19:7–12.
133. Weingeist TA, Goldman EJ, Folk JC, et al. Terson's syndrome. Clinicopathologic correlations. *Ophthalmology*. 1986;93:1435–1442.
134. Vanderlinden RG, Chisholm LD. Vitreous hemorrhages and sudden increased intracranial pressure. *J Neurosurg*. 1974;41:167–176.
135. Keithahn MA, Bennett SR, Cameron D, et al. Retinal folds in Terson syndrome. *Ophthalmology*. 1993;100:1187–1190.
136. Clarkson JG, Flynn HW, Daily MJ. Vitrectomy in Terson's syndrome. *Am J Ophthalmol*. 1980;90:549–552.
137. Isernhagen RD, Smiddy WE, Michels RG, et al. Vitrectomy for nondiabetic vitreous hemorrhage. Not associated with vascular disease. *Retina*. 1988;8:81–87.
138. van Rens GH, Bos PJ, van Dalen JT. Vitrectomy in two cases

of bilateral Terson syndrome. *Doc Ophthalmol*. 1983;56:155–159.
139. Sharma T, Gopal L, Biswas J, et al. Results of vitrectomy in Terson syndrome. *Ophthalmic Surg Lasers*. 2002;33:195–199.
140. Ritland JS, Syrdalen P, Eide N, et al. Outcome of vitrectomy in patients with Terson syndrome. *Acta Ophthalmol Scand*. 2002;80:172–175.
141. Skevas C, Czorlich P, Knospe V, et al. Terson's syndrome – rate and surgical approach in patients with subarachnoid hemorrhage: a prospective interdisciplinary study. *Ophthalmology*. 2014;121:1628–1633.
142. Duane TD. Valsalva hemorrhagic retinopathy. *Am J Ophthalmol*. 1973;75:637–642.
143. Ravin JG, Meyer RF. Fluorescein angiographic findings in a case of traumatic asphyxia. *Am J Ophthalmol*. 1973;75:643–647.
144. Harley RD. Ocular manifestations of child abuse. *J Pediatr Ophthalmol Strabismus*. 1980;17:5–13.
145. Jensen AD, Smith RE, Olson MI. Ocular clues to child abuse. *J Pediatr Ophthalmol Strabismus*. 1971;8:270–272.
146. Riffenburgh RS, Sathyavagiswaran L. Ocular findings at autopsy of child abuse victims. *Ophthalmology*. 1991;98:1519–1524.
147. Greenwald MJ, Weiss A, Oesterle CS, Friendly DS. Traumatic retinoschisis in battered babies. *Ophthalmology*. 1986;93:618–625.
148. Harcourt B, Hopkins D. Permanent chorio-retinal lesions in childhood of suspected traumatic origin. *Trans Ophthalmol Soc U K*. 1973;93:199–205.
149. Caffey J. The whiplash shaken infant syndrome: manual shaking by the extremities with whiplash-induced intracranial and intraocular bleedings, linked with residual permanent brain damage and mental retardation. *Pediatrics*. 1974;54:396–403.
150. Parizel PM, Ceulemans B, Laridon A, et al. Cortical hypoxic-ischemic brain damage in shaken-baby (shaken impact) syndrome: value of diffusion-weighted MRI. *Pediatr Radiol*. 2003;33:868–871.

151. Caputo G, De Haller R, Metge F, et al. Ischemic retinopathy and neovascular proliferation secondary to shaken baby syndrome. *Retina*. 2008;28:S42–6.
152. Bielory BP, Dubovy SR, Olmos LC, et al. Fluorescein angiographic and histopathologic findings of bilateral peripheral retinal nonperfusion in nonaccidental injury: a case series. *Arch Ophthalmol*. 2012;130:383–387.
153. Muni RH, Kohly RP, Sohn EH, et al. Handheld spectral domain optical coherence tomography finding in shaken-baby syndrome. *Retina*. 2010;30(4 Suppl.):S45–50.
154. Eliott D, Avery RL. Nonpenetrating posterior segment trauma. *Ophthalmol Clin North Am*. 1995;8(4):647–666.

95

Pregnancy-Related Diseases

Sid Schechet, Janet S. Sunness

Retinal and Choroidal Disorders in Pregnancy

Preeclampsia, Eclampsia, and "HELLP" ("Hemolysis, Elevated Liver Enzymes, and Low Platelets") Syndrome

Preeclampsia typically develops in the second half of pregnancy and is characterized by hypertension, edema, and proteinuria. In healthy women, preeclampsia is generally seen in first pregnancies, with an incidence estimated at 5%.[1] Risk factors for preeclampsia include very young or advanced maternal age, multifetal pregnancy, hemolytic disease of the newborn, diabetes mellitus, chronic systemic hypertension, and renal disease. Eclampsia is preeclampsia with seizures that usually occur late in pregnancy. The HELLP Syndrome consists of hemolysis, elevated liver enzymes, and low platelets. Its incidence ranges from 0.5 to 0.9% of all pregnancies, and 10–20% of those with severe preeclampsia or eclampsia.[2]

Preeclampsia and eclampsia place the fetus at risk due to placental vascular insufficiency. In the early 1900s, severe retinal arteriolar narrowing was believed to reflect placental vascular insufficiency and to be an indication for pregnancy termination and much attention was paid to retinal findings. With improved medical and obstetrical management of hypertension and other aspects of preeclampsia, retinal findings are no longer used to assess this disease.

Early reports gave impressive rates of visual disturbances. Scotomas, diplopia, dimness of vision, and photopsias were noted in 25% of patients with severe preeclampsia and up to 50% of patients with eclampsia.[3] Recent studies, discussed below, suggest

that the rate of visual disturbances has markedly decreased with improved medical management of preeclampsia. Nevertheless, comprehensive ophthalmic examination should be performed, at least for symptomatic patients. Although photic stimuli may predispose to seizures in susceptible patients, the benefits of an ophthalmic examination outweigh the small risk of seizure when an examination is indicated.[4]

Preeclampsia and eclampsia have been associated with hypertensive-like retinopathy; serous retinal detachments; yellow, opaque retinal pigment epithelium (RPE) lesions; arterial and venous occlusive disease; and cortical blindness. HELLP syndrome has been associated specifically with serous retinal detachments. Early studies of retinal disorders in preeclampsia have been discussed in previous works,[5] and an updated review is presented below.

Retinopathy in Preeclampsia and Eclampsia

Retinal arteriolar constriction is the most common funduscopic change seen in preeclampsia; edema, exudates, hemorrhages, and cotton-wool spots are uncommon. The cause of retinal arteriolar narrowing seems to be central retinal artery vasospasm as suggested by increased central retinal artery blood flow velocity.[6] The retinal arteriolar attenuation generally resolves after delivery, presumably due to normalization of central retinal artery blood flow. Pathologically attenuated retinal microvasculature can be seen early in pregnancy, before the onset of preeclampsia, and can be predictive of later development of the disease. Lupton followed normotensive pregnant women with retinal vessel analysis and blood pressure measurements throughout gestation, and he found that those who later developed preeclampsia had significant attenuation early in gestation.[7]

Early twentieth-century studies reported rates of arteriolar attenuation in preeclamptic patients as high as 40–100%.[8] By the end of the twentieth century, studies were showing much lower rates of these arterial changes. A retrospective study of fluorescein angiograms in preeclamptic patients by Schreyer identified normal retinal vessel caliber in 16 of 16 patients, while 4 of 14 patients with

preexisting chronic systemic hypertension had mild retinopathy.[9] Jaffe prospectively demonstrated a statistically significant difference in reduced arteriolar caliber and arteriovenous ratio between those with severe preeclampsia when compared to healthy controls, but there was no difference between those with mild preeclampsia and controls.[10] Neudorfer found that only 14.8% of preeclamptic women had pathologic findings, specifically those with severe preeclampsia and higher systolic blood pressure. Also, all of the visually symptomatic women had findings, while only 1 asymptomatic woman had findings.[11] The difference in the reported prevalence of retinopathy between the early and recent literature is probably related to better medical management of preeclampsia and its complications. Further, these studies suggest that arteriolar narrowing may be more common in those with severe preeclampsia, those with visual symptoms, and those with chronic preexisting hypertension than those with mild preeclampsia.

Li found that in pregnant women every 10-mmHg increase in mean arterial blood pressure was associated with a 1.9-μm reduction in retinal arteriolar caliber. Of note, retinal venous caliber and vascular tortuosity were *not* associated with blood pressure measures.[12] Li found that narrower maternal retinal arteriolar caliber was significantly associated with decreased infant head circumference and birthweight at delivery, reflecting the relative uteroplacental insufficiency.[13] Similarly, Gupta correlated the severity of retinopathy in preeclampsia to the level of placental insufficiency and intrauterine fetal growth retardation. In this study though, the severity of retinopathy did not correlate with the degree of systolic or diastolic hypertension. Interestingly, serum uric acid levels also had a statistically significant positive correlation with retinopathy in this group, but the meaning of this finding is unknown.[14]

It should be briefly mentioned that in the past few years, with improved imaging modalities, retinochoroidal thickening has been shown to occur not only in those with preeclampsia but additionally in those with a normal pregnancy.[15]

Choroidopathy in Preeclampsia, Eclampsia,

and HELLP Syndrome

Choroidal dysfunction is a common ocular complication of preeclampsia and eclampsia, seen clinically as serous retinal detachments or yellow RPE lesions. Fig. 95.1 shows bilateral serous retinal detachments in a 28-year-old female with severe preeclampsia one day after delivery.[16] The serous retinal detachments usually are bilateral and bullous but occasionally are cystic.[4,15] Vigil-De Gracia reviewed 28 cases of serous retinal detachments in patients with severe preeclampsia, eclampsia, or HELLP syndrome. Of these, 89% had bilateral retinal detachments, 69% were diagnosed postpartum, and all patients had complete recovery of vision with clinical management within 2–12 weeks.[17]

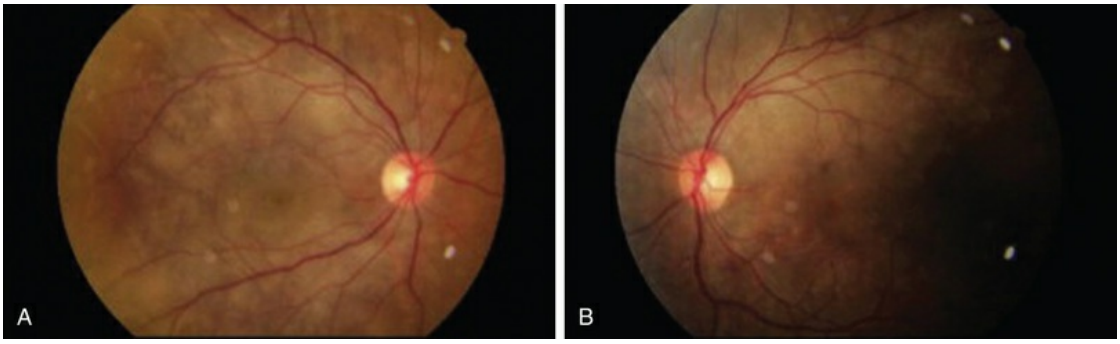

FIG. 95.1 Color fundus photograph depicting bilateral serous retinal detachments in a 28-year-old female with severe preeclampsia one day after delivery.
(Reproduced with permission from Chen KH, Chen LR. Bilateral retinal detachment with subsequent blindness in a pregnant woman with severe preeclampsia. Taiwan J Obstet Gynecol. 2013;52(1):142-4).

In the early twentieth century, serous retinal detachments were seen in 1% of severely preeclamptic patients and about 10% of eclamptic patients.[18,19] More recently, Saito retrospectively evaluated women with severe preeclampsia or eclampsia and found that 65% had serous retinal detachments and 58% had RPE lesions. RPE lesions were usually located in the macular or peripapillary regions: 92% were solitary or grouped, and 8% were large and diffuse. After delivery, all serous retinal detachments and RPE lesions resolved, but three eyes with geographic RPE lesions developed significant chorioretinal atrophy.[20] The apparent

historical increase in the incidence of serous detachments and RPE lesions is almost certainly due to improved examination instrumentation and diagnostic testing.

The etiology of choroidal dysfunction is thought to be ischemic based on fluorescein angiography, limited histopathologic study, and the presence of Elschnig spots on resolution[21] and indocyanine green angiography.[22] Posterior ciliary artery vasospasm, hypoalbuminemia, and microangiopathic anemia during HELLP syndrome also contribute to the incidence of serous retinal detachments.

Although serous retinal detachment and RPE dysfunction can cause marked loss of visual acuity, these changes fully resolve postpartum and most patients return to normal vision within a few weeks (unless atrophy develops). Some patients have residual RPE changes in the macula. Years later, these changes can mimic a macular dystrophy or tapetoretinal degeneration.[23] Rare patients may develop optic atrophy if chorioretinal atrophy is extensive.[18]

Saito has suggested that serous detachments are more specific to preeclampsia and eclampsia, whereas retinopathy is seen more often in preeclampsia superimposed on preexisting hypertension.[24] Retinopathy is associated with higher levels of blood pressure than is serous detachment.[25] Although retinopathy was believed to be a reflection of possible placental insufficiency and possible adverse neonatal outcome, serous retinal detachment is not an additional risk factor.[21]

Postpartum serous detachments have been reported in preeclamptic patients,[26–28] and there are rare reports of exudative detachments in patients *without* preeclampsia.[29,30] While these serous retinal detachments may be mechanistically distinct, they also resolve over several weeks.

Other Ocular Changes Seen in Preeclampsia, Eclampsia, and HELLP Syndrome

Cortical blindness that appears late in pregnancy or postpartum is an uncommon complication of severe preeclampsia and eclampsia. The etiology of vision loss may be occipital ischemia in watershed areas from vasospasm,[31–34] possibly related to extracellular

hypercalcemia,[35] ischemia from antiphospholipid antibody-related vascular occlusion,[36] vasogenic edema,[37-44] petechial[43] or larger hemorrhages,[44,45] hypertensive encephalopathy,[46,47] ischemia from hypotension during delivery,[48] or as part of a postictal state.[49] Most patients recover normal vision over several weeks. A prospective study by Cunningham showed that 15/15 women with cortical blindness experienced complete recovery over 4 hours to 8 days. CT scanning was obtained in 13/15 and MRI scanning in 5/15, revealing edema and petechial hemorrhages in the occipital cortex.[43]

The presence of large intracranial hemorrhages may portend a worse prognosis in terms of both mortality and visual recovery. Akan evaluated CT scans from 22 patients with neurologic complications from eclampsia and found that 2 of the 3 patients who died had massive intracranial hemorrhages.[44] Drislane found that among 4 patients with severe preeclampsia and multifocal cerebral hemorrhages, 1 died and the 3 others developed prolonged cognitive deficits.[45]

Cortical vision loss has been reported in eight patients with HELLP syndrome.[49–54] Other ocular disorders reported associated with HELLP syndrome include vitreous hemorrhage[55] and bilateral anterior ischemic optic neuropathy that resolved within months.[56]

Other ocular disorders reported associated with preeclampsia and eclampsia include ischemic optic neuropathy[57] and optic neuritis,[58,59] ischemic papillophlebitis,[60] peripheral retinal neovascularization,[61] choroidal neovascularization,[62] macular edema,[63] macular ischemia,[64] a tear of the retinal pigment epithelium,[65] and bilateral Purtscher's retinopathy.[66] Retinal arterial and venous occlusions, potential causes of irreversible visual loss, have been reported in patients with preeclampsia and will be discussed below.

Central Serous Chorioretinopathy

Central serous chorioretinopathy (CSC) is caused by localized RPE dysfunction resulting in the accumulation of subretinal fluid. People between the ages of 20 and 50 years are typically affected, and there is an 8 : 1 male predominance.[67] Pregnancy may predispose some women to CSC. The limited amount of

information available concerning CSC in pregnancy makes it difficult to determine whether CSC during pregnancy is typical CSC coincident with pregnancy, or if it is a separate disorder possibly related to the hormonal hypercoagulability or hemodynamic changes of pregnancy.

Only a few dozen cases of CSC associated with pregnancy are reported in the medical literature.[68–79] Unlike the serous retinal detachments observed in preeclampsia and eclampsia, CSC is generally unilateral. The women were all previously healthy, and no cases were associated with preeclampsia or eclampsia. No patients had antecedent eye disease other than refractive error. Primiparas and multiparas were both represented. Most of the cases developed in the third trimester, and all resolved spontaneously within a few months after delivery. There were no cases of significant visual sequelae.

Pregnancy-associated CSC may recur in the context of, or outside of, subsequent pregnancies. CSC recurred in at least two women, always in the same eye, in subsequent pregnancies. One patient had four successive pregnancies with CSC,[69] and one had two successive pregnancies complicated by CSC.[75] One woman developed CSC one month postpartum in two successive pregnancies,[76] and one patient experienced a recurrence of CSC outside the context of pregnancy.[71]

There is an increased incidence of subretinal white exudates (presumably fibrin) in pregnancy-associated CSC (~90%) compared to CSC in males and nonpregnant women (~10%). Sunness reported that 3 of 4 patients with pregnancy-related CSC had subretinal exudates.[71] Gass found that 6/6 cases of pregnancy related CSC had subretinal exudates compared to only 6/50 of nonpregnancy related cases.[72] However, a report of 3 pregnant women with CSC had no exudates,[80] and a large analysis of 17,000 pregnant women found a prevalence of CSC to be 0.008%, with 50% having exudates.[78] The cause of this higher prevalence of subretinal exudates in pregnant women is unknown.

Occlusive Vascular Disorders

An increase in the level of clotting factors and clotting activity

occurs during pregnancy.[81] Several pathologic sources of thrombosis and embolic events can also occur. One review of ischemic cerebrovascular disease suggested that pregnancy is associated with a 13-fold increase in the risk of cerebral infarctions compared to nonpregnant women.[82] This increased risk of vaso-occlusive disease may also manifest as retinal or choroidal vascular occlusions.

Retinal Artery Occlusion

Two cases of unilateral central retinal artery occlusion (CRAO),[83,84] one case of bilateral CRAO,[85] five cases of unilateral branch retinal artery occlusion (BRAO),[86,87] and 3 cases of bilateral multiple BRAO[82] have been reported in association with pregnancy and in the absence of additional risk factors. Two cases of cilioretinal artery occlusion have been reported.[88,89] Several cases of arteriolar occlusion were associated with preeclampsia,[85,90] and one was associated with disc edema.[87] Five of the thirteen cases (38.5%) occurred within 24 hours of delivery, suggesting that this is a particularly susceptible period. Two of the patients with unilateral BRAO also were found to have mild transient protein S deficiency upon further systemic workup.[91]

In addition to the aforementioned cases, Blodi reported that multiple retinal arteriolar occlusions were seen within 24 hours after childbirth in four women. Two patients were preeclamptic and required cesarean section. One of the two also had evidence of cerebral infarctions. The third patient had hypertension, pancreatitis, and premature labor. The fourth was a previously healthy 16-year-old who had an oxytocin-induced labor and had a generalized seizure 2 hours after delivery. The patients reported decreased vision, and all had fundus findings characterized by retinal patches characteristic of ischemia and intraretinal hemorrhages that were similar to Purtscher's retinopathy. After resolution, patients were left with focal arteriolar narrowing and optic disc pallor. The visual acuities ranged from 20/20 to 4/200 with visual field defects corresponding to the areas of occlusion. The authors suggest that complement-induced leukoemboli could have caused the retinal arteriolar occlusions.[90]

At least eight additional cases of pregnancy-associated BRAO have been reported in the literature.[92–98] However, all of these cases had significant additional risk factors for vascular occlusion. Since pregnancy is a common condition, it is difficult to know whether these cases represent true pregnancy associations. One case was associated with intramuscular progesterone therapy for a threatened abortion.[92] Three cases that occurred postpartum were associated with hypercoagulability from protein C[93] or protein S[90,94] deficiency. Two cases were associated with thromboembolic occlusions attributed to mitral valve prolapse[95] and amniotic fluid embolism.[96] The final two cases developed BRAO in the first trimester in association with migraine headaches.[97] Ten more cases of BRAO were reported specifically in the context of Susac syndrome, which will be discussed below.

Susac Syndrome

Susac syndrome (SS) is a clinical triad of encephalopathy, branch retinal artery occlusion (BRAO), and sensory neural hearing loss (SNHL), first described by Susac in 1979.[99] It is a rare syndrome with 304 cases reported in the literature as of 2013.[100] SS is more common in females between the ages of 20 and 40 years of age. SS is thought to be due to an autoimmune-mediated vascular endothelial injury, and therefore reported treatments include immunosuppressive/immunomodulatory, anticoagulation, and early induction of labor. There have been 10 cases of SS presenting or recurring during pregnancy with findings of one or multiple BRAOs, more often bilaterally.[101–108] One series reported three patients with recurrence of disease that occurred months to years after the onset of SS.[106] It appears that pregnancy may affect the course of SS, with BRAO occurring as an initial presentation or recurrence of disease during pregnancy or in the postpartum period. It should be noted that SS has a variable course and is not self-limited as previously thought. A pregnant female with a BRAO should be evaluated for possible SS, and those with SS should be followed closely during pregnancy and in the postpartum period.

Retinal Vein Occlusion

Retinal vein occlusion associated with pregnancy is rare. Few pregnancy-related central retinal vein occlusions (CRVO) have been reported to date, and we are not aware of any branch retinal vein occlusions.[109–115] Most cases were unilateral; some cases improved but not completely; and some cases were associated with preeclampsia, eclampsia, HELLP syndrome, or an undiagnosed arteriovenous malformation. A recent Korean study found a prevalence of 33 pregnancy-related retinal vein occlusions (RVO) in 1.8 million women during their study period, of which 36.4% had preeclampsia or eclampsia. They hypothesized that pregnancy was not a risk factor for RVO, but preeclampsia/eclampsia was.[115]

Disseminated Intravascular Coagulopathy

Disseminated intravascular coagulopathy (DIC) is an acute, life-threatening process of widespread microvascular thrombosis due to uncontrolled activation of the hemostatic system leading to multiorgan failure. It is reported to occur in 0.03–0.35% of pregnancies and is associated with obstetrical complications such as abruptio placentae, uterine atony, HELLP syndrome, and more.[116] This process has a tendency to occlude the posterior choroidal vessels leading to RPE ischemia, dysfunction of the RPE pump mechanism, and subsequent serous retinal detachments in the macular and peripapillary regions.[117–120] The development of serous retinal detachments in pregnancy, especially late pregnancy, may be an early ocular sign of DIC.[120] These detachments tend to be bilateral and symptomatic. With recovery from the systemic disorder, vision generally returns to normal with only residual pigmentary changes.[117,120] Patel reported a case of bilateral retinochoroidal infarction associated with preeclampsia and DIC with permanent vision loss.[121]

Thrombotic Thrombocytopenic Purpura

Thrombotic thrombocytopenic purpura (TTP) is a rare, idiopathic, acute, systemic coagulopathy characterized by platelet consumption and thrombus formation in small vessels. TTP occurs at any age with a peak incidence in the third decade of life and a female to male preponderance of 3:2. Visual changes occur in

approximately 8–20% of cases due to thrombus formation in the choriocapillaris with secondary RPE ischemia.[122–128] Clinical findings are usually bilateral and include serous retinal detachments, yellow spots at the level of the RPE, and localized arteriolar narrowing. Sequelae include RPE pigmentary changes and Elschnig spots with a return to baseline vision over several weeks to months in most cases. There are several reported cases of peripartum and early postpartum associated TTP with the aforementioned ocular findings. All cases were managed via systemic treatment of the TTP with generally good visual outcomes.[122,123] HELLP, DIC, and TTP are discussed in more detail in Chapter 63, Coagulopathies.

Amniotic Fluid Embolism

Amniotic fluid embolism is a serious complication of pregnancy with high mortality. Those who survive the initial event usually develop DIC[129] with the potential ocular complications described above. Two patients developed multiple BRAOs, presumably related to particulate material from the amniotic fluid.[96,130] One of these patients was a 28 year-old who developed the BRAOs during labor. Fig. 95.2 is a color fundus photograph of the right eye (left side of image), demonstrating parafoveal edema and glial optic disc remnants, and of the left eye (right side of image), demonstrating macular BRAO by multiple glistening particles with diffuse superficial retinal edema. Figs. 95.3A–B are intravenous fluorescein angiography images delineating the parafoveal capillary nonperfusion and occluded vessels (indicated by arrows), respectively.[96] Another patient had massive blood loss from an amniotic fluid embolism leading to severe unilateral ischemic optic neuropathy.[131]

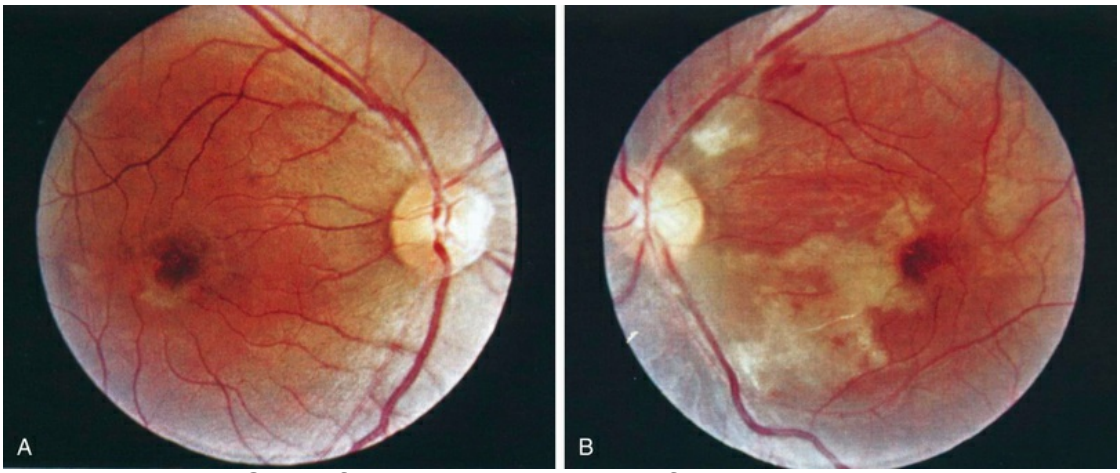

FIG. 95.2 Color fundus photograph of the right eye (A), demonstrating parafoveal edema and glial optic disc remnants, and of the left eye (B), demonstrating macular branch retinal artery occlusion (BRAO) by multiple glistening particles with diffuse superficial retinal edema. (Reproduced with permission from Chang M, Herbert WN. Retinal arteriolar occlusions following amniotic fluid embolism. Ophthalmology 1984;91:1634–7.)

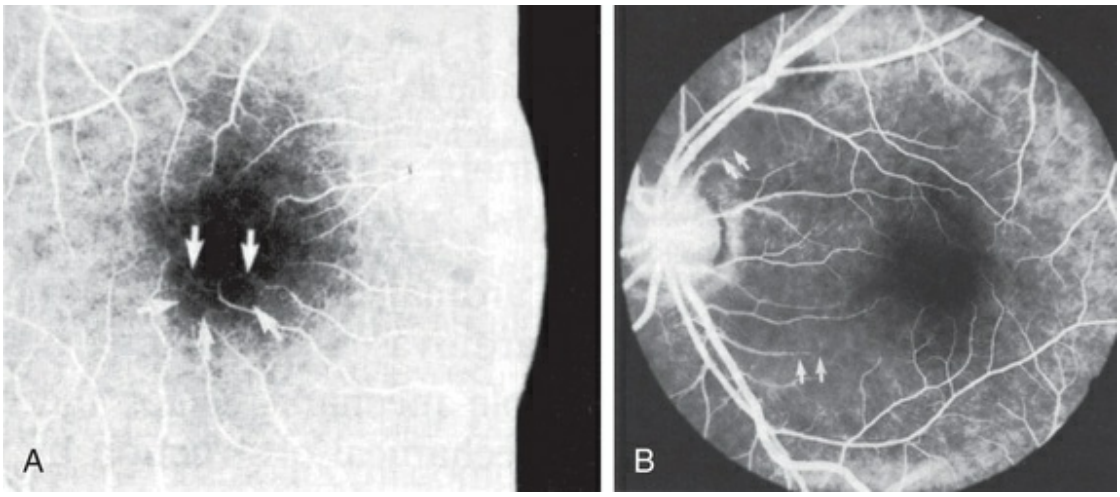

FIG. 95.3 (A,B) Intravenous fluorescein angiography images of the eye from Fig. 95.2 with *arrows* delineating the parafoveal capillary nonperfusion in (A) and occluded vessels in (B). (Reproduced with permission from Chang M, Herbert WN. Retinal arteriolar occlusions following amniotic fluid embolism. Ophthalmology 1984;91:1634–7).

Uveal Melanoma

Pregnancy is heralded by a hormone-dependent hyperpigmentation and well-known cutaneous changes like chloasma and darkening of preexisting nevi owing to increased levels of melanocyte-stimulating hormone in pregnancy.[132] Although estrogen and progesterone may stimulate melanogenesis, there is no evidence that this can cause malignant transformation of melanocytic cells.

A case–control study by Holly et al. found a decreased risk of uveal melanoma for women who had ever been pregnant with an increase in protective effect with more live births. The largest effect was observed between nulliparous and parous women.[133] Others, however, have reported a trend toward a larger-than-expected number of ocular melanomas presenting during pregnancy.[134,135] There are also a number of anecdotal reports of uveal melanomas presenting or growing rapidly during pregnancy.[136–141] These reports led to speculation that uveal melanoma may be hormone-responsive, but two studies have failed to show any estrogen or progesterone receptor expression in ocular melanomas.[139,142] A large retrospective study showed no association of uveal melanoma with the use of oral contraceptives or hormone replacement therapy.[143] It is possible that other hormones may be involved[139] or that tumor growth may be related to pregnancy-associated immune modulation.

Pregnancy-related uveal melanoma does not seem to differ histologically from uveal melanoma not associated with pregnancy. Shields reported that among 10 pregnancy-related choroidal melanomas evaluated after enucleation, the tumors did not differ in cell type, mitotic activity, and other features when compared to a matched group of tumors in nonpregnant women.[144]

The treatment of pregnancy-associated uveal melanoma has been described in two studies. Among 16 cases reported by Shields, 10 eyes were enucleated, four received plaque radiotherapy during or after pregnancy, and two cases were observed. Among 14 of 16 patients who elected to carry the pregnancy to term, all delivered healthy babies with no infant or placental metastases.[144] Romanowska-Dixon reported eight cases in which there were no treatment-related pregnancy complications. The authors do suggest

that brachytherapy is safer towards the end of pregnancy or after delivery.[145]

Childbearing may be associated with improved survival in uveal melanoma. Egan et al. performed a large prospective cohort study in which death rates from metastasis were 25% higher in nulliparous women and men than in women who had given birth. The protective influence of parity was greatest in the first 3 years of follow-up and increased with the number of live births.[146] These results contradict a small earlier study by the same group that concluded rates of metastasis were not higher among women who reported pregnancies or oral contraceptive use.[147] A much smaller study by Shields also showed similar 5-year survival between pregnant and nonpregnant women with posterior uveal melanoma.[144]

Other Changes Arising in Pregnancy

Two choroidal osteomas presenting during pregnancy have been reported,[148,149] one with visual loss due to choroidal neovascularization.[148] Macular neuroretinopathy,[150,151] Valsalva maculopathy,[152] and cystoid macular edema[153] have been observed in the immediate postpartum period. Placental metastases from orbital rhabdomyosarcoma[154] and primary ocular melanoma[155] have been reported.

Preexisting Conditions

Diabetic Retinopathy

The prevalence of diabetic retinopathy (DR) in pregnant women with type 1 diabetes mellitus (DM) has been reported in the range of 57–62%, while pregnant women with type 2 DM have DR in the range of 17–28%.[156] Well-controlled blood glucose and adequate glycosylated hemoglobin (HbA_{1c}) before conception and throughout the pregnancy may reduce the risk of spontaneous abortion, congenital anomalies, and fetal morbidity.[157–159] Two studies suggest that the severity of diabetic retinopathy may be a significant factor in predicting adverse fetal outcomes, and

glycemic control may or may not counteract these adverse fetal effects.[160,161]

Diabetic women who may become pregnant should establish excellent glucose control before conception, since the major period of fetal organogenesis may take place before the mother is even aware that she is pregnant. In addition, a diabetic woman's retinopathy status should be evaluated and stabilized prior to conception. This is particularly important for patients with severe nonproliferative (NPDR) or proliferative diabetic retinopathy (PDR) because scatter laser photocoagulation may reduce progression during pregnancy.[162] Laser treatment or intravitreal injections for diabetic macular edema (DME) before pregnancy may also be important, although the effects of pregnancy on macula edema have not been adequately studied.

Data from the Diabetes in Early Pregnancy Study (DIEP), a study of 155 insulin-dependent diabetic pregnancies,[163] the Diabetic Control and Complications Trial[164] (DCCT), and the previous data summarized by Sunness[162] all provide evidence that better metabolic control before pregnancy diminishes the progression of DR. The institution of tight glycemic control is associated with short-term DR progression.[163,165–167] Nerve fiber layer infarctions commonly are associated with the institution of tight metabolic control of chronic hyperglycemic patients. One study described the retinopathy status of 13 patients managed by insulin pump during pregnancy. Two patients who had a rapid decrease in the HbA_{1c} level developed acute ischemic changes and ultimately PDR.[168] However, a study of 102 type 1 diabetic pregnant women found no correlation between progression of DR and decline in HbA_{1c} levels or prevalence of severe hypoglycemia.[169] It is prudent to stabilize the patient's diabetic status before becoming pregnant if at all possible so that there are no abrupt changes in glycemic control. The long-term benefits of adequate blood glucose control outweigh concerns about the transient worsening of retinopathy that has been associated with the sudden imposition of tight glycemic control.

The frequency of ophthalmic follow-up of a diabetic patient during pregnancy is determined by her baseline retinopathy status. North American ophthalmologic guidelines recommend that a diabetic woman planning pregnancy within 12 months should be

examined by an ophthalmologist, undergo repeat evaluation in the first trimester, and examinations after that should occur at intervals based on the initial findings.[160,170,171] Attendance at a prepregnancy ophthalmologic evaluation was associated with receiving adequate future eye screening and treatment.[165]

Short- and Long-Term Effects of Pregnancy on Diabetic Retinopathy

Since there is a high rate of regression of DR during the postpartum period, one must consider short-term and long-term changes separately. The DCCT research group reported that pregnant women in the conventional treatment group were 2.9 times more likely to progress three or more levels from baseline retinopathy status than nonpregnant women. The odds ratio peaked during the second trimester and persisted as long as twelve months after delivery.[164] One study of short-term effects included 16 women with mild NPDR. Progression during pregnancy was compared to progression between six and fifteen months postpartum in the same women. The number of microaneurysms (MAs) showed a rapid increase between the 28th and 35th weeks of pregnancy. Six months postpartum the number of MAs decreased but in most cases remained higher than the baseline level and remained stable over the subsequent 9-month postpartum period.[172]

Three other studies compared short-term progression of retinopathy between separate control groups of nonpregnant women and pregnant women over the same time period. The first compared the course of DR in 93 pregnant women and 98 nonpregnant women. Progression was observed in 16% of the pregnant group compared to only 6% in the nonpregnant patients. Furthermore, more (32%) of the nonpregnant group had retinopathy at baseline compared to the pregnant cohort (22%), so one might have expected more progression in the nonpregnant group, making these findings more significant.[173] A second study compared 39 nonpregnant women, 46% with DR at baseline, to 53 pregnant diabetic women, 57% with DR at baseline over a 15-month period. In the nonpregnant group the MAs remained stable, dot–blot hemorrhages appeared in three patients (8%), and no nerve fiber layer infarctions developed. In the pregnant group, MAs

increased moderately, and dot–blot hemorrhages and nerve fiber layer infarctions increased markedly. One patient with NDPR from the pregnant group developed PDR.[174] In the third study, there were 133 pregnant and 241 nonpregnant women, and all were statistically equivalent in terms of baseline retinopathy levels. Within each quartile of HbA_{1c}, pregnant women had a greater tendency to have worsening of retinopathy, and the nonpregnant women had a greater tendency to have improvement in their level of DR during the follow-up interval.[175]

A few studies recorded the long-term effects of pregnancy on DR. The first included 40 women followed for 12 months postpartum. Among 19 study participants with no retinopathy at baseline, 30% developed mild NPDR during the second and third trimester. By one year postpartum none had clinically detectable retinopathy. Among the 21 women with retinopathy at baseline, 11 worsened during pregnancy and 2 developed PDR. None of these 11 women had regressed to their initial retinopathy status by one year postpartum.[176] The second study compared 28 diabetic pregnant women to 17 nulliparous matched controls over a 7-year period. Only 5 of 26 (19.2%) women who had been pregnant experienced progression of retinopathy compared to 8 of 16 (50%) nulliparous women, suggesting that pregnancy does not affect long-term progression and may even afford a protective effect.[177] A third study of 30 women who had completed at least one successful pregnancy found no increase in the rate of development of PDR after 2 years of follow-up compared to matched controls.[178] These studies suggest that over time having a history of pregnancy does not appear to confer a higher risk of development/progression of DR.

Two studies suggest that the number of prior pregnancies does not appear to be a long-term factor in the severity of retinopathy present when duration of diabetes is taken into account.[179,180] In fact, a cross-sectional European study reported lower levels of retinopathy in diabetics with multiple pregnancies compared with women matched for age and duration of diabetes.[181] It is not clear if this improved status was caused by a prolonged period of tight metabolic control and better patient education or if pregnancy confers a long-term protective effect. Another possibility involves

the bias that only women with better metabolic control may have undergone the stress of multiple pregnancies.

There has been anecdotal concern that the act of labor can cause significant progression of DR, including vitreous hemorrhage. The second stage of labor includes a series of strong Valsalva maneuvers that may increase intraocular pressure (IOP) and cause retinal hemorrhages. A study by Feghali sought to determine the association between expulsive efforts during the second stage of labor and progression of DR in 192 pregnant women with adequately controlled type 1 DM. There was no difference in DR progression between those who had elective cesarean delivery, those who had cesarean delivery prior to the second stage of labor, and those who had cesarean or vaginal delivery during the second stage. They concluded that vaginal delivery should not be denied to pregnant women with controlled type I diabetes.[182]

The Role of Baseline Retinopathy Status, Duration of Diabetes, and Metabolic Control

The major determinants of the progression of DR in a pregnant woman are the degree of retinopathy and duration of diabetes at the onset of pregnancy.[162,163,174,183–189] Therefore, women with diabetes are encouraged to complete childbearing early in their adult life.[190] The baseline level of retinopathy at conception is the major risk factor for progression of retinopathy, according to the DIEP. When a logistic regression model was used to separate the influence of diabetes duration (shorter duration being less than 15 years, longer duration being more than 15 years) from the effect of a worse baseline level of NPDR, the baseline retinopathy was quite significant but the duration of retinopathy was not. Analysis of pregnant patients with moderate to severe DR in the DIEP showed deterioration (defined as a two-step or more worsening determined on the final scale of the modified Airlie House Diabetic Retinopathy Classification) in 55% of patients with shorter duration and 50% of patients with longer duration of diabetes. However, the rates of development of PDR during pregnancy were 39% of patients with longer duration of diabetes and only 18% of patients with shorter duration of diabetes. The HbA_{1c} level at the beginning of pregnancy was used in the DIEP as a measure of metabolic control. Women

with HbA_{1c} levels of 6 standard deviations (SD) or more from the control mean had a statistically significant higher risk of progression of retinopathy during pregnancy when compared with patients with baseline HbA_{1c} levels within 2 SD of the control mean.[163]

A prospective study of 179 pregnancies in 139 women with type-1 diabetes found that women with moderate to severe DR at baseline had progression in 30%, while only 3.7% progressed with less severe baseline retinopathy.[187] Similarly, in a smaller prospective study of 54 women with type-1 diabetes, there was DR progression in 9.1% with no baseline DR, 20% with NPDR at baseline, and 58.3% with PDR at baseline.[189]

Studies show that duration of diabetes correlates with DR progression, and they delineate that in various ways. One study found that there was a 10% progression rate of DR in women who had type 1 diabetes for 10–19 years compared to a 0% progression rate of those with diabetes less than 10 years.[187] Another study found that women with type 1 diabetes who had DR progression during or soon after pregnancy had an average diabetes onset at age 14 compared to 19 years in those who had no DR progression.[188] Lastly, pregnant women with type 2 diabetes who had progression of DR had diabetes on average for 6.7 years, as opposed to 3.3 years in those who had no progression.[186]

The DCCT group also evaluated the effect of pregnancy on microvascular complications. Pregnant women in the intensive treatment group had a 1.63-fold greater risk of retinopathy progression during pregnancy than nonpregnant women, compared to a 2.48-fold greater risk in the conventional treatment group.[164]

Risk Factors for Progression of Diabetic Retinopathy During Pregnancy

Nephropathy and systemic hypertension are additional risk factors for the progression of DR during pregnancy. A well-known association exists between nephropathy and retinopathy in nonpregnant diabetic patients. One study in pregnant diabetics showed that 8 of 9 patients in whom DME developed during

pregnancy had proteinuria of more than 1 gram per day.[167] Several studies report elevated systolic blood pressure as a risk factor for the progression of DR.[165,169,185,191–193] The DIEP found a 1.3 odds ratio for two-step progression of retinopathy for every 10-mmHg increase in systolic blood pressure.[163]

Progression of Diabetic Retinopathy According to Baseline Status

The following discussion of the progression of retinopathy during pregnancy is subdivided according to the baseline level of retinopathy present. Many of the studies did not use the more recent classification recommended by the Early Treatment Diabetic Retinopathy Study (ETDRS). Whenever possible, the results have been organized according to this classification.[194] All diabetic women, regardless of retinopathy status, should at least have a complete ophthalmic exam before conception, during the first and third trimesters, and within one year after delivery.

Gestational Diabetes

In four studies,[195–198] comprising 397 pregnant women with gestational diabetes, only two women had retinopathy, and both had just one MA each.[195] One of the studies was a 12-year prospective study and did not demonstrate an increased risk of diabetic retinopathy.[195] However, retinal vascular tortuosity in gestational diabetics has been reported, and some degree of tortuosity persisted at 5 months postpartum.[199] There is one case report of a previously healthy nulliparous woman with gestational diabetes diagnosed at 8 weeks' gestation. Glycemic control was instituted, and the patient developed bilateral PDR by 31 weeks' gestation. The patient had a markedly elevated HbA_{1c} level at initial diagnosis suggesting that she may have been diabetic before becoming pregnant.[200] It appears that routine examinations have little utility in gestational diabetics.

No Initial Retinopathy

Summarizing several studies, of 674 pregnant diabetic women with no initial DR, 86 (13%) developed NPDR and only one developed

PDR.[162,163,169,186,189,201,202] Sunness summarized nine studies that included 484 diabetic pregnancies (included in the 674 patients above) with no initial retinopathy. In 23 cases with progression for which postpartum follow-up was available, there was some regression of the nonproliferative changes in 57% of patients.[162]

Mild Nonproliferative Diabetic Retinopathy

Hellstedt monitored MA formation and disappearance rates in diabetic pregnant women. They found that there is continuous turnover of MAs during pregnancy with MA count increasing during pregnancy, peaking at 3 months postpartum, and then declining back to baseline.[203] Six studies with 79 pregnant diabetic women with mild NPDR showed that 24.1% developed increased nonproliferative changes, while 2.5% had proliferative changes.[162,163,186,201,202]

Moderate to Severe Nonproliferative Diabetic Retinopathy

Four studies[163,186,201,202] and one large review by Sunness[162] included 297 diabetic pregnant women with moderate to severe NPDR at baseline. Forty-four percent had nonproliferative retinopathy progression, while 9.1% had proliferative changes. Pregnant diabetic women with moderate to severe NPDR should have a complete examination before conception, during the first and second trimesters, every 4–6 weeks thereafter, and within one year after delivery.

Proliferative Diabetic Retinopathy

Compiling the results of two large reviews[162,204] and three additional smaller studies,[175,185,189] 36.7% of 278 pregnant diabetic women with PDR at baseline had progression of retinopathy (ranging from 22% to 63%).

Optimal treatment of proliferative disease before pregnancy reduces the risk of progression during pregnancy. In the 1988 Sunness review,[162] those patients who had scatter laser photocoagulation before pregnancy showed a 26% rate of progression of their proliferative disease and visual loss compared

to 58% of patients without prior treatment. Those patients with complete regression of proliferative disease before pregnancy did not demonstrate progression of proliferative disease during pregnancy. In Rahman's study, out of 12 women with PDR, 4 had laser prior to pregnancy with only one woman having progression during pregnancy. Out of the 8 women who had no laser prior to pregnancy, 6 had retinopathy progression. Three patients had laser treatment during the second trimester with complete immediate regression, and the other 3 had laser treatment during the third trimester with regression taking 3–4 months.[189] Reece found somewhat different results in an earlier study. In this analysis, half of the patients with proliferative disease who underwent laser treatment prior to pregnancy required additional scatter treatment during pregnancy. In addition, 65% of patients who had proliferative disease during pregnancy required photocoagulation postpartum. No patient had proliferative disease that did not respond to laser photocoagulation.[205]

It appears that it is not predictable whether proliferative retinopathy will regress or not at the end of pregnancy or in the postpartum period. One study found that 4/5 women who developed PDR during pregnancy had spontaneous regression to nonproliferative status within 2 months postpartum.[176] However, one study of 8 women with PDR reported no regression by 3 months postpartum[185] and another study of 16 women with PDR showed no regression in 12 years postpartum.[206]

The possibility of spontaneous regression of PDR is a factor to consider when determining if laser photocoagulation is indicated during pregnancy. Most retina specialists would aggressively treat patients who have high-risk PDR; some retinal specialists would treat one eye or both in cases that are not high risk, given the problem of rapid progression during pregnancy. After consideration of high-risk factors such as high initial HbA_{1c} and duration of diabetes, these decisions must be made on a case-by-case basis. Pregnant diabetic women with PDR should have a complete examination before conception and bimonthly during pregnancy, with close follow-up in the postpartum period.

Vitreous hemorrhage during labor and delivery has been reported in a few cases.[207] Currently, no evidence justifies

performing a cesarean section on the basis of proliferative retinopathy alone, given the availability of vitrectomy for the treatment of nonclearing vitreous hemorrhage.[162]

Diabetic Macular Edema in Pregnancy

Diabetic macular edema (DME) that involves or threatens the fovea is currently treated with anti-VEGF injections, with or without focal laser photocoagulation, outside the context of pregnancy in order to reduce the risk of moderate vision loss. Patients who develop DME during pregnancy or have DME at conception frequently have different prognoses than nonpregnant patients as spontaneous resolution during or after pregnancy has been reported.[186,208]

Two out of 80 type 2 diabetic women who became pregnant while having DME had regression of the edema as their HbA_{1c} levels improved.[186] Sinclair and Nessler reported that 16 of 56 eyes in diabetic women with initial proliferative or nonproliferative retinopathy developed DME during pregnancy. Of these 16 eyes, 14 had improvement in visual acuity and resolution of DME postpartum without laser treatment.[208]

In general, pregnant women with DME should not be treated during pregnancy because of the high rate of postpartum spontaneous improvement. Possible exceptions include cases in which lipid is threatening the fovea or severe, progressive DME develops early in pregnancy. Due to the lack of adequate safety data regarding the use of anti-VEGF treatments (discussed below), the authors recommend focal laser photocoagulation in the rare case where treatment during pregnancy is indicated. However, further study of pregnant women with DME is needed.

Diabetic Retinopathy and Maternal and Fetal Wellbeing

Advanced diabetic retinopathy has been considered a risk factor for adverse fetal outcomes because it may reflect more widespread systemic disease. Pregnancies associated with NPDR may not be at higher risk for adverse fetal outcomes.[204] However, Klein reported an adverse fetal outcome in 43% of women with PDR compared to only 13% of women with NPDR.[160] Another study of 20 pregnancies of 17 women with PDR reported spontaneous abortion in 2 cases,

stillbirth in 1 case, and 3 had major congenital anomalies.[205] Sameshima reported that among 60 pregnant diabetic women, the 7 with PDR had a significantly higher incidence of fetal distress.[209] A final study of 26 women with PDR reported serious neonatal morbidity and mortality (19% and 12%, respectively).[210] A prospective study of 205 women with type 1 diabetes found that low newborn birthweight was associated with retinopathy progression. However, retinopathy progression was not associated with earlier delivery, macrosomia, respiratory distress syndrome, neonatal hypoglycemia, or neonatal death.[211]

Improved medical and obstetrical management has improved the outcome of diabetic pregnancies. In a study of 22 pregnancies complicated by retinopathy and nephropathy in which good glycemic control was present antepartum and throughout pregnancy, there were no infant deaths and only 1 case of mild respiratory distress syndrome.[161] A retrospective study of 482 diabetic pregnancies reported only 3 perinatal deaths, which was statistically equivalent to nonpregnant deliveries over the same period.[212]

Three studies suggest an association between DR and the development of preeclampsia. Hiilesmaa followed 683 consecutive pregnancies with type 1 diabetes and found that retinopathy was a statistically significant independent predictor of preeclampsia.[213] A second study looked retrospectively at 65 pregnant type 1 diabetic patients and reported that deterioration of retinopathy occurred more frequently in those with preeclampsia than those without preeclampsia.[214] Lastly, Gordin followed 158 pregnant type 1 diabetics for 16 years and found that those with pregnancy-induced hypertension and/or preeclampsia had an increased risk of developing severe DR later in life.[187] Perhaps central retinal artery vasospasm associated with preeclampsia exacerbates retinal ischemia that occurs in DR.

Toxoplasmic Retinochoroiditis

The likelihood of congenital toxoplasmosis occurring in the offspring of a mother with active retinochoroiditis or chorioretinal scars is often a concern. This usually is unfounded, however, since

congenital toxoplasmosis in the fetus results only from infection of the mother that occurs during the pregnancy itself. The presence of focal toxoplasmic retinochoroiditis or scars in a patient reflects congenital infection of that patient in essentially all cases and not new infection of the mother.[215] Therefore, the fetus of a woman with active retinochoroiditis or scars should not be at risk for contracting congenital toxoplasmosis. A study of 18 pregnant patients with active toxoplasmosis or scars, some with elevated toxoplasmosis titers, found that no infants developed congenital toxoplasmosis.[216]

One study of 50 pregnant women[217] and another of 17[218] found that recurrence rates of ocular toxoplasmosis are not higher during pregnancy and may in fact be lower. The ocular characteristics of active ocular toxoplasmosis during pregnancy when compared to attacks during the nonpregnant periods are no different in terms of the severity, duration, or outcome of the attacks.[219]

Noninfectious Uveitis

Noninfectious uveitis (anterior, intermediate, posterior, or pan) tends to improve during pregnancy but may worsen in the postpartum period. For example, six patients with preexisting Vogt–Koyanagi–Harada (VKH) syndrome have been reported to improve during pregnancy, but all had flare-ups of disease postpartum.[220–222] However, there have been reports of VKH syndrome[223,224] developing de novo during pregnancy, punctate inner choroidopathy (PIC)[225] developing de novo after miscarriage, and sarcoid uveitis[226] developing de novo during the postpartum period.

More specifically, uveitis activity tends to decrease from the second trimester onwards, with the third trimester being associated with the lowest disease activity.[227–230] Rabiah retrospectively evaluated 76 pregnancies of 50 women with noninfectious uveitis including VKH syndrome, Behçet disease, and idiopathic uveitis. A worsening of uveitis occurred within the first 4 months of pregnancy in 64% of pregnancies and later in pregnancy in 22%. No flare-up occurred in 28%. An early pregnancy worsening was typical of VKH and idiopathic uveitis. Postpartum worsening occurred in 64% and was characteristic of Behçet disease.[227] Chiam

retrospectively evaluated 47 women with noninfectious uveitis reporting flare-up rates of 1.188, 0.540, and 0.972 per person year in prepregnancy, gestation, and postpartum, respectively. Additionally, it was shown that flare-up rates decreased from the first to third trimesters, and that flare-up rates rebounded by 6 months postpartum but did not differ from pre-pregnancy rates.[229]

The severity of uveitis flare-ups was not significantly different between pregnancy and nonpregnant periods, whether assessed by analyzing anterior chamber cell count,[229] or by noting flare-up duration and type of therapy prescribed.[227]

The amelioration of uveitis during pregnancy, and the relapse that often occurs postpartum, is thought to be due to the complex hormonal and immunologic changes that occur to a woman during and after pregnancy.

Other Retinal Disorders

The stress of labor and delivery does not appear to pose a risk for rhegmatogenous retinal detachment (RD) in high myopes. This conclusion is based on three studies examining pregnant women with ocular history of myopia, RD, retinal holes, lattice degeneration, with no RD found after delivery.[231–233]

Rapid growth of choroidal hemangiomas,[134] and the development of exudative retinal detachments associated with hemangiomas[234] have been reported during pregnancy. The hemangioma may regress in the postpartum period.[235] These changes have been attributed to pregnancy-related hormonal perturbations.

There are eight reported cases of endogenous endophthalmitis that occurred after miscarriage with dilatation and curettage,[236] spontaneously during normal pregnancy,[237] after spontaneous abortion[237,238,] after cesarean section,[237] and after a vaginal delivery albeit with a 1-week history of premature rupture of membranes.[239] Most of the reported cases had poor visual outcomes, with three cases having RD. The infectious etiologies included *Klebsiella pneumoniae*, *Bacillus mycoides*, *Sphingomonas paucimobilis*, and *Candida albicans*. Treatment is beyond the scope of this chapter, but it should be mentioned that fluoroquinolones and voriconazole should be avoided during pregnancy and in nursing mothers, while

cephalosporins and amphotericin B are considered safe to use.[237]

Retinitis pigmentosa (RP) is sometimes characterized by a sudden pregnancy-associated deterioration in visual fields after a period of relative stability. It is difficult to determine whether changes are related to pregnancy or are just coincidental. Five to ten percent of women with RP who have been pregnant reported worsening during pregnancy[162,240] and did not return to baseline after delivery.[162] There is one report in the literature of visual field deterioration during pregnancy, which resolved in the postpartum period.[59] One case reported pericentral retinal degeneration that worsened during pregnancy.[241]

Diagnostic Testing and Therapy

Fluorescein crosses the placenta and enters the fetal circulation in humans.[242] No reports of teratogenic effects in humans have been reported to the National Registry of Drug-Induced Ocular Side Effects.[162] European investigators have performed research studies involving the administration of fluorescein to 22 pregnant diabetic women and noticed no adverse effects on the fetus.[243] Another study of neonatal outcome of 105 patients who underwent fluorescein angiography (FA) during pregnancy showed no increased rate of adverse neonatal outcomes.[244] This study, however, included only 41 cases of FA during the first trimester, the time when teratogenic effects are more likely to take place and are more severe. Nevertheless, one survey reported that 77% of retinal specialists never perform FA on a patient they know is pregnant.[245] In another survey, 89% of retina specialists who had seen a pregnant woman who required FA withheld testing out of fear of teratogenicity or lawsuit.[246] We recommend that FA in pregnant women can be considered if the results would change the management of a vision-threatening problem and appropriate informed consent is obtained.

Indocyanine green does not cross the placenta, is highly bonded to plasma proteins, and is metabolized by the liver. Reports of only 6 cases of the use of indocyanine green angiography (ICGA) during pregnancy have been published.[22,247] In a survey of 520 retina specialists, 105 had withheld ICGA out of fear of teratogenicity or

lawsuit during pregnancy and only 24% thought it was safe to use ICGA in a pregnant patient. The authors suggest that current practice patterns concerning the use of ICGA in pregnancy may be unnecessarily restrictive.[246] Like FA, we recommend that ICGA in pregnant women can be considered if the results would change the management of a vision-threatening problem and appropriate informed consent is obtained.

Photodynamic Therapy

Pregnant rats exposed to verteporfin at 40 times the human dose have a high incidence of microphthalmia.[248] Accidental exposure to verteporfin for photodynamic therapy during pregnancy has been reported in three cases. Rosen treated a woman with punctate inner choroidopathy with verteporfin and bevacizumab while she was 1–2 weeks pregnant, before the patient knew of her conception. The pregnancy and childbirth were uncomplicated and yielded a healthy term infant who had no abnormality for at least the first 3 months of life.[249] De Santis reported a similar accidental exposure in the third week of pregnancy without any deleterious effects in the patient or child up to 26 months of life.[250] Rodrigues reported a case of accidental exposure to verteporfin in a 45-year-old woman with a 25-week fetus. The pregnancy appeared to be unaffected, and the child was healthy through 16 months of follow-up.[251] With regard to PDT during pregnancy, caution is recommended.

Anti-VEGF Therapy

Anti-vascular endothelial growth factor (anti-VEGF) medications have not been well evaluated during pregnancy. Bevacizumab may have an inhibitory effect on pregnancy development based on rat studies. Rats were repeatedly injected either with intraperitoneal bevacizumab or saline during early gestation. The size and number of gestational sacs and serum β-CG levels were significantly lower in those with bevacizumab.[252] Systemic bevacizumab and ranibizumab are contraindicated in pregnancy by the manufacturer and classed as “category C” by the United States Food and Drugs Administration (FDA).[253] Additionally, the FDA recently classed intravitreal aflibercept as category C.[254]

There are 14 cases in the literature of pregnant women being treated with intravitreal bevacizumab or ranibizumab: 13 patients with bevacizumab, 1 patient with ranibizumab.[249,255–260] Eleven patients were treated during the first trimester, and 3 patients were treated in the second or third trimester. Eleven patients had normal deliveries with healthy newborns. One patient with a complicated pregnancy history, who was treated with bevacizumab in the first trimester, had an urgent cesarean section at 29 weeks for preeclampsia. The infant initially suffered from bradycardia, respiratory issues, and intraventricular hemorrhages, but stabilized weeks later.[251] Two other patients suffered miscarriages 7 and 10 days after being treated with intravitreal bevacizumab during the first trimester.[255] It is unknown whether the miscarriages were incidental or perhaps related to the bevacizumab injections.

There is insufficient information to conclude that intravitreal administration of anti-VEGF use is safe during pregnancy, nor is there definitive evidence to suggest that it causes harm to the fetus. Further well-designed studies are required, and until such data become available, caution should be exercised.

Conclusion

Information about the effects of pregnancy on the course of retinal disease is limited. In most cases the direct cause of pregnancy effects is only speculative and based on what is known about systemic changes in the mother. As our understanding of the natural course of retinal and choroidal diseases and of the effects of pregnancy on the eye improves, the ophthalmic management of both pregnant and nonpregnant patients will improve.

References

1. Powe CE, Levine RJ, Karumanchi SA. Preeclampsia, a disease of the maternal endothelium: the role of antiangiogenic factors and implications for later cardiovascular disease. *Circulation*. 2011;123:2856–2869.
2. Haram K, Svendsen E, Abildgaard U. The HELLP syndrome: clinical issues and management. A review. *BMC*

Pregnancy Childbirth. 2009;9:8.
3. Dieckmann WJ. *The toxemias of pregnancy*. 2nd ed. Mosby: St. Louis; 1952.
4. Folk JC, Weingeist TA. Fundus changes in toxemia. *Ophthalmology*. 1981;88:1173–1174.
5. Sunness JS, Gass JDM, Singerman U, et al. Retinal and choroidal changes in pregnancy. Singerman U, Jampol LM. *Retinal and choroidal manifestations of systemic disease*. Williams & Wilkins: Baltimore; 1991.
6. Belfort MA. The effect of magnesium sulphate on blood flow velocity in the maternal retina in mild preeclampsia: a preliminary color flow Doppler study. *Br J Obstet Gynaecol*. 1992;99:641–645.
7. Lupton SJ, Chiu CL, Hodgson LA, et al. Changes in retinal microvascular caliber precede the clinical onset of preeclampsia. *Hypertension*. 2013;62(5):899–904.
8. Wagener HP. Arterioles of the retina in toxemia of pregnancy. *JAMA*. 1933;101:1380–1384.
9. Schreyer P, Tzadok J, Sherman DJ, et al. Fluorescein angiography in hypertensive pregnancies. *Int J Gynaecol Obstet*. 1991;34:127–132.
10. Jaffe G, Schatz H. Ocular manifestations of preeclampsia. *Am J Ophthalmol*. 1987;103:309–315.
11. Neudorfer M, Spierer O, Goder M, et al. The prevalence of retinal and optical coherence tomography findings in preeclamptic women. *Retina*. 2014;34(7):1376–1383.
12. Li LJ, Cheung CY, Ikram MK, et al. Blood pressure and retinal microvascular characteristics during pregnancy: Growing Up in Singapore Towards Healthy Outcomes (GUSTO) Study. *Hypertension*. 2012;60(1):223–230.
13. Li LJ, Aris I, Su LL, et al. Associations of maternal retinal vasculature with subsequent fetal growth and birth size. *PLoS ONE*. 2015;10(4):e0118250.
14. Gupta A, Kaliaperumal S, Setia S, et al. Retinopathy in preeclampsia: association with birth weight and uric acid level. *Retina*. 2008;28:1104–1110.
15. Gitter HA, Heuser BP, Sarin LK, et al. Toxemia of pregnancy: an angiographic interpretation of fundus

changes. *Arch Ophthalmol*. 1968;80:449–454 [16].
16. Chen KH, Chen LR. Bilateral retinal detachment with subsequent blindness in a pregnant woman with severe pre-eclampsia. *Taiwan J Obstet Gynecol*. 2013;52(1):142–144.
17. Vigil-De Gracia P, Ortega-Paz L. Retinal detachment in association with pre-eclampsia, eclampsia, and HELLP syndrome. *Int J Gynaecol Obstet*. 2011;114(3):223–225.
18. Fry WE. Extensive bilateral retinal detachment in eclampsia with complete reattachment. *Arch Ophthalmol*. 1929;1:609–614.
19. Hallum AV. Eye changes in hypertensive toxemia of pregnancy. *JAMA*. 1936;106:1649–1651.
20. Saito Y, Tano Y. Retinal pigment epithelial lesions associated with choroidal ischemia in preeclampsia. *Retina*. 1998;18:103–108.
21. Oliver M, Uchenik D. Bilateral exudative retinal detachment in eclampsia without hypertensive retinopathy. *Am J Ophthalmol*. 1980;90:792–796.
22. Valluri S, Adelberg DA, Curtis RS, et al. Diagnostic indocyanine green in preeclampsia. *Am J Ophthalmol*. 1996;122:672–677.
23. Gass JDM, Pautler SE. Toxemia of pregnancy: pigment epitheliopathy masquerading as a heredomacular dystrophy. *Trans Am Ophthalmol Soc*. 1985;83:114–130.
24. Saito Y, Omoto T, Kidoguchi K, et al. The relationship between ophthalmoscopic changes and classification of toxemia in toxemia of pregnancy. *Nippon Ganka Gakkai Zasshi*. 1990;94:870–874.
25. Sadowsky A, Serr DM, Landau J. Retinal changes and fetal prognosis in the toxemias of pregnancy. *Obstet Gynecol*. 1956;8:426–431.
26. Bos AM, van Loon AJ, Ameln JG. Serous retinal detachment in preeclampsia. *Ned Tijdschr Geneeskd*. 1999;143:2430–2432.
27. Chatwani A, Oyer R, Wong S. Postpartum retinal detachment. *J Reprod Med*. 1989;34:842–844.
28. Song YS, Kinouchi R, Ishiko S, et al. Hypertensive choroidopathy with eclampsia viewed on spectral-domain optical coherence tomography. *Graefes Arch Clin Exp*

Ophthalmol. 2013;251(11):2647–2650.
29. Bosco JAS. Spontaneous nontraumatic retinal detachments in pregnancy. *Am J Obstet Gynecol*. 1961;82:208–212.
30. Brismar C, Schimmelpfennig W. Bilateral exudative retinal detachment in pregnancy. *Acta Ophthalmol*. 1989;67:699–702.
31. Yamaguchi K, Fukuuchi Y, Nogawa S, et al. Recovery of decreased local cerebral blood flow detected by the xenon/CT CBF method in a patient with eclampsia. *Keio J Med*. 2000;49:71–74.
32. Neihaus L, Meyer BU, Hoffmann KT. Transient cortical blindness in EHP caused by cerebral vasospasm. *Nervenarzt*. 1999;70:931–934.
33. Kesler A, Kaneti H, Kidron D. Transient cortical blindness in preeclampsia with indication of generalized vascular endothelial damage. *J Neuroophthalmol*. 1998;18:163–165.
34. Duncan R, Hadley D, Bone I, et al. Blindness in eclampsia: CT and MRI imaging. *J Neurol Neurosurg Psychiatry*. 1989;52:899–902.
35. Kaplan PW. Reversible hypercalcemic vasoconstriction with seizure and blindness: a paradigm for eclampsia. *Clin Electroencephalogr*. 1998;29:120–123.
36. Branch DW, Andres R, Digre KB, et al. The association of antiphospholipid antibodies with severe preeclampsia. *Obstet Gynecol*. 1989;73:541–545.
37. Do DV, Rismondo V, Nguyen QD. Reversible cortical blindness in preeclampsia. *Am J Ophthalmol*. 2002;134:916–918.
38. Hiruta M, Fukuda H, Hiruta A, et al. Emergency cesarean section in a patient with acute cortical blindness and eclampsia. *Masui*. 2002;51:670–672.
39. Apollon KM, Robinson JN, Schwartz RB, et al. Cortical blindness in severe preeclampsia: CT, MRI, and SPECT findings. *Obstet Gynecol*. 2000;95:1017–1019.
40. Davila M, Pensado A, Rama P, et al. Cortical blindness as symptom of preeclampsia. *Rev Esp Anestesiol Reanim*. 1998;45:189–200.
41. Shieh T, Kosasa TS, Tomai E, et al. Transient blindness in a preeclamptic patient secondary to cerebral edema. *Hawaii*

Med J. 1996;55:116–117.
42. Beeson JH, Duda EE. CT scan demonstration of cerebral edema in eclampsia preceded by blindness. *Obstet Gynecol*. 1982;60:529–532.
43. Cunningham FG, Fernandez CO, Hernandez C. Blindness associated with preeclampsia and eclampsia. *Am J Obstet Gynecol*. 1995;172:1291–1298.
44. Akan H, Kucac M, Bolat O, et al. The diagnostic value of cranial CT in complicated eclampsia. *J Belge Radiol*. 1993;76:304–306.
45. Drislane FW, Wang AM. Multifocal cerebral hemorrhage in eclampsia and severe preeclampsia. *J Neurol*. 1997;244:194–198.
46. Wijman CA, Beijer IS, van Dijk GW, et al. Hypertensive encephalopathy: does not only occur at high blood pressure. *Ned Tijdschr Geneeskd*. 2002;146:969–973.
47. Leibowitz HA, Hall PE. Cortical blindness as a complication of eclampsia. *Ann Emerg Med*. 1984;13:365–367.
48. Borromeo CJ, Blike GT, Wiley CW, et al. Cortical blindness in a preeclamptic patient after a cesarean delivery complicated by hypotension. *Anesth Analg*. 2000;91:609–611.
49. Levavi H, Neri A, Zoldan J, et al. Preeclampsia, "HELLP" syndrome and postictal cortical blindness. *Acta Obstet Gynecol Scand*. 1987;66:91–92.
50. Ertan AK, Kujat CH, Jost WH, et al. HELLP syndrome-amausosis in sinus thrombosis with complete recovery. *Geburtshilfe Frauenheilkd*. 1994;54:646–648.
51. Ebert AD, Hopp HS, Entezami M, et al. Acute onset of blindness during labor: report of a case of transient cortical blindness in association with HELLP syndrome. *Eur J Obstet Gynecol Reprod Biol*. 1999;84:111–113.
52. Crosby ET, Preston R. Obstetrical anesthesia for a parturient with preeclampsia, HELLP syndrome and acute cortical blindness. *Can J Anaesth*. 1998;45:452–459.
53. Tung CF, Peng YC, Chen Gh, et al. HELLP syndrome with acute cortical blindness. *Zhonghua Yi Xue Za Zhi*. 2001;64:482–485.
54. Erbagci I, Karaca M, Ugur MG, et al. Ophthalmic

manifestations of 107 cases with hemolysis, elevated liver enzymes and low platelet count syndrome. *Saudi Med J*. 2008;29:1160–1163.
55. Leff SR, Yarian DR, Masciulli L, et al. Vitreous hemorrhage as a complication of HELLP syndrome. *Br J Ophthalmol*. 1990;74:498.
56. Maramattom BV. Anterior ischemic optic neuropathy as a manifestation of HELLP syndrome. *Case Rep Crit Care*. 2014;2014:671976.
57. Beck RW, Gamel JW, Willcourt RJ, et al. Acute ischemic optic neuropathy in severe preeclampsia. *Am J Ophthalmol*. 1980;90:342–346.
58. Sommerville-Lange LB. A case of permanent blindness due to toxemia of pregnancy. *Br J Ophthalmol*. 1950;34:431–434.
59. Wagener H. Lesions of the optic nerve and retina in pregnancy. *JAMA*. 1934;103:1910–1913.
60. Price J, Marouf L, Heine MW. New angiographic findings in toxemia of pregnancy. *Ophthalmology*. 1986;93(Suppl.):125.
61. Brancato P, Menchini U, Bandello F. Proliferative retinopathy and toxemia of pregnancy. *Ann Ophthalmol*. 1987;19:182–183.
62. Curi AL, Jacks A, Pevisio C. Choroidal neovascular membrane presenting as a complication of preeclampsia in a patient with antiphospholipid syndrome. *Br J Ophthalmol*. 2000;84:1080.
63. Theodossiadis PG, Kollia AK, Gogas P, et al. Retinal disorders in preeclampsia studied with optical coherence tomography. *Am J Ophthalmol*. 2002;133:707–709.
64. Shaikh S, Ruby AJ, Piotrowski M. Preeclampsia related chorioretinopathy with Purtscher's-like findings and macular ischemia. *Retina*. 2003;23:247–250.
65. Menchini U, Lanzetta P, Virgili G, et al. Retinal pigment epithelium tear following toxemia of pregnancy. *Eur J Ophthalmol*. 1995;5:139–141.
66. Singh K, Jain D, Wallang B. Purtscher's retinopathy in pre-eclampsia: a blinding combination. *Int Ophthalmol*. 2014;34(1):103–106.
67. Todd KC, Hainsworth DP, Lee LR, et al. Longitudinal

analysis of central serous chorioretinopathy and sex. *Can J Ophthalmol*. 2002;37:405–408.
68. Normalina M, Zainal M, Alias D. Central serous choroidopathy in pregnancy. *Med J Malaysia*. 1998;53:439–441.
69. Khairallah M, Nouira F, Gharsallah R, et al. Central serous chorioretinopathy in a pregnant woman. *J Fr Ophtalmol*. 1996;19:216–221.
70. Quillen DA, Gass DM, Brod RD, et al. Central serous chorioretinopathy in women. *Ophthalmology*. 1996;103:72–79.
71. Sunness JS, Haller JA, Fine SL. Central serous chorioretinopathy and pregnancy. *Arch Ophthalmol*. 1993;111:360–364.
72. Gass JD. Central serous chorioretinopathy and white subretinal exudation in pregnancy. *Arch Ophthalmol*. 1991;109:677–681.
73. Fastenberg DM, Ober RR. Central serous choroidopathy in pregnancy. *Arch Ophthalmol*. 1983;101:1055–1058.
74. Chumbley LC, Frank RN. Central serous retinopathy and pregnancy. *Am J Ophthalmol*. 1974;77:158–160.
75. Cruysberg JR, Deutman AF. Visual disturbances during pregnancy caused by central serous choroidopathy. *Br J Ophthalmol*. 1982;66:240–241.
76. Bedrossian RH. Central serous retinopathy and pregnancy. *Am J Ophthalmol*. 1974;78:152.
77. Chakraborti C, Samanta SK, Faiduddin K, et al. Bilateral central serous chorioretinopathy in pregnancy presenting with severe visual loss. *Nepal J Ophthalmol*. 2014;6(12):220–223.
78. Said-Ahmed K, Moustafa G, Fawzy M. Incidence and natural course of symptomatic central serous chorioretinopathy in pregnant women in a maternity hospital in Kuwait. *Middle East Afr J Ophthalmol*. 2012;19(3):273–276.
79. Hirji N, Watt L, Richardson E. Central serous chorioretinopathy secondary to childbirth. *BMJ Case Rep*. 2010;2010 [pii: bcr1020103387].

80. Al-Mujaini A, Wali U, Ganesh A, et al. Natural course of central serous chorioretinopathy without subretinal exudates in normal pregnancy. *Can J Ophthalmol*. 2008;43:588–590.
81. Brenner B. Haemostatic changes in pregnancy. *Thromb Res*. 2004;114(5–6):409–414.
82. Wiebers DO. Ischemic cerebrovascular complications of pregnancy. *Arch Neurol*. 1985;42:1106–1113.
83. Ayaki M, Yokoyama N, Furukawa Y. Postpartum CRAO simulating Purtscher's retinopathy. *Ophthalmologica*. 1995;209:37–39.
84. LaMonica CB, Foye GJ, Silberman L. A case of sudden CRAO and blindness in pregnancy. *Obstet Gynecol*. 1987;69:433–435.
85. Lara-Torre E, Lee MS, Wolf MA, et al. Bilateral retinal occlusion progressing to longlasting blindness in severe preeclampsia. *Obstet Gynecol*. 2002;100:940–942.
86. Gull S, Prentice A. BRAO in pregnancy. *Br J Obstet Gynaecol*. 1994;101:77–78.
87. Humayun M, Kattah J, Cupps TR, et al. Papillophlebitis and arteriolar occlusion in a pregnant woman. *J Clin Neuroophthalmol*. 1992;12:226–229.
88. Basu A, Eyong E. Cilioretinal arterial occlusion phenomenon: a rare cause of loss of vision in pregnancy. *Eur J Obstet Gynecol Reprod Biol*. 2008;137:251–252.
89. Ozdamar Y, Gurlevik U, Acaroglu G, et al. Combined cilioretinal artery and partial central retinal vein occlusion in the postpartum period. *Retin Cases Brief Rep*. 2010;4(2):99–101.
90. Blodi BA, Johnson MW, Gass JD, et al. Purtscher's-like retinopathy after childbirth. *Ophthalmology*. 1990;97:1654–1659.
91. Vela JI, Diaz-Cascajosa J, Crespi J, et al. Protein S deficiency and retinal arteriolar occlusion in pregnancy. *Eur J Ophthalmol*. 2007;17:1004–1006.
92. Lanzetta P, Crovato S, Pirrachio A, et al. Retinal arteriolar obstruction with progestin treatment of threatened abortion. *Acta Ophthalmol Scand*. 2002;80:667–669.

93. Nelson ME, Talbot JF, Preston FE. Recurrent multiple branch retinal arteriolar occlusions in a patient with protein C deficiency. *Graefes Arch Clin Exp Ophthalmol*. 1989;227:443–447.
94. Greven CM, Weaver RG, Owen J, et al. Protein S deficiency and bilateral branch retinal artery occlusion. *Ophthalmology*. 1991;98:33–34.
95. Bergh PA, Hollander D, Gregori CA, et al. Mitral valve prolapse and thromboembolic disease in pregnancy: a case report. *Int J Gynaecol Obstet*. 1988;27:133–137.
96. Kim IT, Choi JB. Occlusions of branch retinal arterioles following amniotic fluid embolism. *Ophthalmologica*. 2002;21:305–308.
97. Brown GC, Magargal LE, Shields JA. Retinal arterial obstruction in children and young adults. *Ophthalmology*. 1981;88:18–25.
98. Chung YR, Kim JB, Lee K, et al. Retinal artery occlusion in a healthy pregnant patient (unilateral BRAO). *Korean J Ophthalmol*. 2008;22:70–71.
99. Susac JO, Hardman JM, Selhorst JB. Microangiopathy of the brain and retina. *Neurology*. 1979;29(3):313–316.
100. Dörr J, Krautwald S, Wildemann B, et al. Characteristics of Susac syndrome: a review of all reported cases. *Nat Rev Neurol*. 2013;9(6):307–316.
101. Deane KD, Tyler KN, Johnson DW, et al. Susac syndrome and pregnancy: disease management. *J Clin Rheumatol*. 2011;17(2):83–88.
102. Hua le H, Donlon SL, Okuda DT. A case of Susac syndrome with cervical spinal cord involvement on MRI. *J Neurol Sci*. 2014;337(1–2):228–231.
103. Feresiadou A, Eriksson U, Larsen HC, et al. Recurrence of Susac syndrome following 23 years of remission. *Case Rep Neurol*. 2014;6(2):171–175.
104. Gordon DL, Hayreh SS, Adams HP Jr. Microangiopathy of the brain, retina, and ear: improvement without immunosuppressive therapy. *Stroke*. 1991;22(7):933–937.
105. Engeholm M, Leo-Kottler B, Rempp H, et al. Encephalopathic Susac's syndrome associated with livedo

racemosa in a young woman before the completion of family planning. *BMC Neurol*. 2013;13:185.
106. Aubart-Cohen F, Klein I, Alexandra JF, et al. Long-term outcome in Susac syndrome. *Medicine (Baltimore)*. 2007;86(2):93–102.
107. Coppeto JR, Currie JN, Monteiro ML, et al. A syndrome of arterial-occlusive retinopathy and encephalopathy. *Am J Ophthalmol*. 1984;98(2):189–202.
108. MacFadyen DJ, Schneider RJ, Chisholm IA. A syndrome of brain, inner ear and retinal microangiopathy. *Can J Neurol Sci*. 1987;14(3):315–318.
109. Chew EY, Trope GE, Mitchell BJ. Diurnal intraocular pressure in young adults with central retinal vein occlusion. *Ophthalmology*. 1987;94:1545–1549.
110. Gabsi S, Rekik R, Gritli N, et al. Occlusion of the central retinal vein in a 6-month pregnant woman. *J Fr Ophtalmol*. 1994;17:350–354.
111. Gonzalvo FJ, Abecia E, Pinilla I, et al. Central retinal vein occlusion and HELLP syndrome. *Acta Ophthalmol Scand*. 2000;78:596–598.
112. Ozdamar Y, Gurlevik U, Acaroglu G, et al. Combined cilioretinal artery and partial central retinal vein occlusion in the postpartum period. *Retin Cases Brief Rep*. 2010;4(2):99–101.
113. Wester ST, Murray TG. Retinal arteriovenous malformation presenting with retinal vein occlusion during pregnancy. *Retin Cases Brief Rep*. 2010;4(2):112–115.
114. Rahman I, Saleemi G, Semple D, et al. Pre-eclampsia resulting in central retinal vein occlusion. *Eye (Lond)*. 2006;20:955–957.
115. Park SJ, Choi NK, Seo KH, et al. Retinal vein occlusion and pregnancy, pre-eclampsia, and eclampsia: the results from a nationwide, population-based study using the national claim database. *PLoS ONE*. 2015;10(3):e0120067.
116. Erez O, Mastrolia SA, Thachil J. Disseminated intravascular coagulation in pregnancy: insights in pathophysiology, diagnosis and management. *Am J Obstet Gynecol*. 2015;213(4):452–463.

117. Bjerknes T, Askvik J, Albrechtsen S, et al. Retinal detachment in association with preeclampsia and abruptio placentae. *Eur J Obstet Gynecol Reprod Biol*. 1995;60:91–93.
118. Cogan DG. Fibrin clots in the choriocapillaris and serous detachment of the retina. *Ophthalmologica*. 1976;172:298–307.
119. Martin VA. Disseminated intravascular coagulopathy. *Trans Ophthalmol Soc U K*. 1978;98:506–507.
120. Hoines J, Buettner H. Ocular complications of disseminated intravascular coagulation (DIC) in abruptio placentae. *Retina*. 1989;9:105–109.
121. Patel N, Riordan-Eva P, Chong V. Persistent visual loss after retinochoroidal infarction in pregnancy-induced hypertension and disseminated intravascular coagulation. *J Neuroophthalmol*. 2005;25:128–130.
122. Benson DO, Fitzgibbons JF, Goodnight SH. The visual system in thrombotic thrombocytopenic purpura. *Ann Ophthalmol*. 1980;12:413–417.
123. Kovács EM, Molvarec A, Rigó J Jr, et al. Bilateral serous retinal detachment as a complication of acquired peripartum thrombotic thrombocytopenic purpura bout. *J Obstet Gynaecol Res*. 2011;37(10):1506–1509.
124. Larcan A, Lambert H, Laprevote-Heully MC, et al. Acute choriocapillaris occlusions in pregnancy and puerperium. *J Mal Vasc*. 1985;10:213–219.
125. Coscas G, Gaudric A, Dhermy P, et al. Choriocapillaris occlusion in Moschowitz's disease. *J Fr Ophtalmol*. 1981;4:101–111.
126. Kovács EM, Molvarec A, Rigó J Jr, et al. Bilateral serous retinal detachment as a complication of acquired peripartum thrombotic thrombocytopenic purpura bout. *J Obstet Gynaecol Res*. 2011;37(10):1506–1509.
127. Titah C, Abisror N, Affortit A, et al. Bilateral serous detachment of retina: an unusual mode of revelation of thrombotic thrombocytopenic purpura of favorable outcome with plasma exchange. *Graefes Arch Clin Exp Ophthalmol*. 2014;252(1):181–183.
128. Zhao C, Qu Y, Sui R, et al. Delayed visual recovery in pregnancy-associated thrombotic thrombocytopenic

purpura with bilateral serous retinal detachment. *Doc Ophthalmol*. 2013;126(2):163–169.
129. Sperry K. Amniotic fluid embolism. *JAMA*. 1986;255:2183–2203.
130. Chang M, Herbert WN. Retinal arteriolar occlusions following amniotic fluid embolism. *Ophthalmology*. 1984;91:1634–1637.
131. Fischbein FI. Ischemic retinopathy following amniotic fluid embolization. *Am J Ophthalmol*. 1969;67:351–357.
132. Cunningham GF, MacDonald PC, Grant NF. *Williams obstetrics*. 19th ed. Appleton & Lange: Norwalk, CT; 1993:215.
133. Holly EA, Aston DA, Ahn DK, et al. Uveal melanoma, hormonal and reproductive factors in women. *Cancer Res*. 1991;51:1370–1372.
134. Reese AB. *Tumors of the eye*. 2nd ed. Hoeber Medical Division, Harper & Row: New York; 1963:366–370.
135. Zinkhan M, Stang A, Jöckel KH, et al. Having children, social characteristics, smoking and the risk of uveal melanoma: a case-control study. *Ophthalmic Epidemiol*. 2013;20(6):360–368.
136. Borner R, Goder G. Melanoblastoma der uvea and schwangerschaft. *Klin Monatsbl Augenheilkd*. 1966;149:684.
137. Frenkel M, Klein HZ. Malignant melanoma of the choroids in pregnancy. *Am J Ophthalmol*. 1966;62:910.
138. Pack GT, Scharnagel IM. The prognosis for malignant melanoma in the pregnant woman. *Cancer*. 1951;4:324.
139. Seddon JM, MacLaughlin DT, Albert DM, et al. Uveal melanomas presenting during pregnancy and the investigation of oestrogen receptors in melanomas. *Br J Ophthalmol*. 1982;66:695.
140. Siegel R, Amslie WH. Malignant ocular melanoma during pregnancy. *JAMA*. 1963;185:542.
141. Lee CS, Yang WI, Shin KJ, et al. Rapid growth of choroidal melanoma during pregnancy. *Acta Ophthalmol*. 2011;89(3):e290–1.
142. Foss AJ, Alexander RA, Guille MJ, et al. Estrogen and progesterone receptor analysis in ocular melanomas.

Ophthalmology. 1995;102:431–435.
143. Behrens T, Kaerlev L, Cree I, et al. Hormonal exposures and the risk of uveal melanoma. *Cancer Causes Control*. 2010;21:1625–1634.
144. Shields CL, Shields JA, Eagle RC, et al. Uveal melamona and pregnancy. A report of 16 cases. *Ophthalmology*. 1991;98:1667–1673.
145. Romanowska-Dixon B. Melanoma of choroids during pregnancy:case report. *Klin Oczna*. 2002;104:395–397.
146. Egan KM, Quinn JL, Gragoudas ES. Childbearing history associated with improved survival in choroidal melanoma. *Arch Ophthalmol*. 1999;117:939–942.
147. Egan KM, Walsh SM, Seddon JM, et al. An evaluation of reproductive factors on the risk of metastases from uveal melanoma. *Ophthalmology*. 1993;100:1160–1166.
148. Gass JD. *Stereoscopic atlas of macular diseases: a funduscopic and angiographic presentation*. 4th ed. Mosby: St. Louis; 1997:218–219.
149. McLeod BK. Choroidal osteoma presenting in pregnancy. *Br J Ophthalmol*. 1988;72(8):612–614.
150. Gass JD. *Stereoscopic atlas of macular diseases: a funduscopic and angiographic presentation*. 4th ed. Mosby: St. Louis; 1997:693–695.
151. Gass JDM. *Stereoscopic atlas of macular diseases: a funduscopic and angiographic presentation*. 3rd ed. Mosby: St. Louis; 1987:512–513.
152. Gass JD. *Stereoscopic atlas of macular diseases: a funduscopic and angiographic presentation*. 4th ed. Mosby: St. Louis; 1997:752–754.
153. Gass JDM. *Stereoscopic atlas of macular diseases: a funduscopic and angiographic presentation*. 3rd ed. Mosby: St. Louis; 1987:380–383.
154. Oday MP, Nielsen P, Al Bozom I. Orbital rhabdomyosarcoma metastatic to the placenta. *Am J Obstet Gynecol*. 1994;171:1382–1383.
155. Marsh RW, Chu NM. Placental metastasis from primary ocular melanoma: a case report. *Am J Obstet Gynecol*. 1996;174:1654–1655.

156. Errera MH, Kohly RP, da Cruz L. Pregnancy-associated retinal diseases and their management. *Surv Ophthalmol*. 2013;58(2):127–142.
157. Bendon RW, Mimouni F, Khouri J, et al. Histopathology of spontaneous abortion in diabetic pregnancies. *Am J Perinatol*. 1990;7:207–210.
158. Mills J, Simpson JL, Driscoll SG, et al. Incidence of spontaneous abortion among normal women and insulin-dependent diabetic women whose pregnancies were identified within 21 days of conception. *N Engl J Med*. 1988;319:1617–1623.
159. Miller E, Hare JW, Cloherty JP, et al. Elevated maternal hemoglobin A_{1c} in early pregnancy and major congenital anomalies in infants of diabetic mothers. *N Engl J Med*. 1981;304:1331–1334.
160. Klein BK, Klein RK, Meuer SM, et al. Does the severity of diabetic retinopathy predict pregnancy outcome? *J Diabet Complications*. 1988;2:179.
161. Jovanovic R, Jovanovic L. Obstetric management when normoglycemia is maintained in diabetic pregnant women with vascular compromise. *Am J Obstet Gynecol*. 1984;149:617–623.
162. Sunness JS. The pregnant woman's eye. *Surv Ophthalmol*. 1988;32:219–238.
163. Diabetes in Early Pregnancy Study Group, Chew EY, James LM, Metzger BE. Metabolic control and progression of retinopathy. *Diabetes Care*. 1995;18:631–637.
164. Diabetes Control and Complications Trial Research Group. Effect of pregnancy on microvascular complications in the diabetes control and complications trial. *Diabetes Care*. 2000;24:1084–1091.
165. Egan AM, McVicker L, Heerey A, et al. Diabetic retinopathy in pregnancy: a population-based study of women with pregestational diabetes. *J Diabetes Res*. 2015;2015:310239.
166. Kroc Collaborative Study Group. Diabetic retinopathy after two years of intensified insulin treatment. Follow-up of the Kroc Collaborative Study. *JAMA*. 1988;260(1):37–41.
167. Chang S, Fuhrmann M, the Diabetes in Early Pregnancy

Study Group. Pregnancy, retinopathy, normoglycemia: a preliminary analysis. *Diabetes*. 1985;34(Suppl.):39.
168. Laatikainen L, Teramo K, Hieta-Heikurainen H, et al. A controlled study of the influence of continuous subcutaneous insulin infusion treatment on diabetic retinopathy during pregnancy. *Acta Med Scand*. 1987;221:367–376.
169. Vestgaard M, Ringholm L, Laugesen CS, et al. Pregnancy-induced sight-threatening diabetic retinopathy in women with Type 1 diabetes. *Diabet Med*. 2010;27(4):431–435.
170. Kentucky Diabetic Retinopathy Group. Guidelines for eye care in patients with diabetes mellitus. *Arch Intern Med*. 1989;149:769–770.
171. Hooper P, Boucher MC, Colleaux K, et al. Contemporary management of diabetic retinopathy in Canada: from guidelines to algorithm guidance. *Ophthalmologica*. 2014;231(1):2–15.
172. Soubrane G, Canivet J, Coscas G. Influence of pregnancy on the evolution of background retinopathy: preliminary results of a prospective fluorescein angiography study. Ryan JJ, Dawson AK, Little HL. *Retinal diseases*. Grune & Stratton: New York; 1985:15–20.
173. Ayed S, Jeddi A, Dagfous F, et al. Aspects evolutifs de la retinopathie diabetique pendant la grosse. *J Fr Ophtalmol*. 1992;15:474.
174. Moloney JM, Drury MI. The effect of pregnancy on the natural course of diabetic retinopathy. *Am J Ophthalmol*. 1982;93:745.
175. Klein BK, Mosse SE, Klein R. Effect of pregnancy on progression of diabetic retinopathy. *Diabetes Care*. 1990;13:34.
176. Serup L. Influence of pregnancy on diabetic retinopathy. *Acta Endocrinol Suppl (Copenh)*. 1986;277:122.
177. Kaaja R, Sjoberg L, Hellsted T, et al. Long-term effects of pregnancy on diabetic complications. *Diabet Med*. 1996;13:165–169.
178. Hemachandra A, Ellis D, Lloyd CE, et al. The influence of pregnancy on IDDM complications. *Diabetes Care*.

1995;18:950–954.
179. Klein BK, Klein R. Gravity and diabetic retinopathy. *Am J Epidemiol*. 1984;119:564.
180. Lipman MJ, Kranias G, Bene CH, et al. The effect of multiple pregnancies on diabetic retinopathy. *Ophthalmology*. 1993;100:141.
181. Chaturvedi N, Stephenson JM, Fuller JH. The relationship between pregnancy and long-term maternal complications in the EURODIAB IDDM complications study. *Diabet Med*. 1995;18:950–954.
182. Feghali M, Khoury JC, Shveiky D, et al. Association of vaginal delivery efforts with retinal disease in women with type I diabetes. *J Matern Fetal Neonatal Med*. 2012;25(1):27–31.
183. Aiello LM, Rand LI, Briones JC, et al. Nonocular clinical risk factors in the progression of diabetic retinopathy. Little HL, Jack RL, Patz A, et al. *Diabetic retinopathy*. Thieme-Stratton: New York; 1983:21–32.
184. Dibble CM, Kochenour NK, Wocley RJ, et al. Effect of pregnancy on diabetic retinopathy. *Obstet Gynecol*. 1982;59:699.
185. Rosenn B, Miodovnik M, Kranias G, et al. Progression of diabetic retinopathy in pregnancy: association with hypertension. *Am J Obstet Gynecol*. 1992;166:1214.
186. Rasmussen KL, Laugesen CS, Ringholm L, et al. Progression of diabetic retinopathy during pregnancy in women with type 2 diabetes. *Diabetologia*. 2010;53(6):1076–1083.
187. Temple RC, Aldridge VA, Sampson MJ, et al. Impact of pregnancy on the progression of diabetic retinopathy in type 1 diabetes. *Diabet Med*. 2001;18:573–577.
188. Lauszus F, Klebe JG, Bek T. Diabetic retinopathy in pregnancy during tight metabolic control. *Acta Obstet Gynecol Scand*. 2000;79:367–370.
189. Rahman W, Rahman FZ, Yassin S, et al. Progression of retinopathy during pregnancy in type 1 diabetes mellitus. *Clin Experiment Ophthalmol*. 2007;35(3):231–236.
190. Beetham WP. Diabetic retinopathy in pregnancy. *Trans Am Ophthalmol Soc*. 1950;48:205.

191. Teuscher A, Schnell H, Wilson PWF. Incidence of diabetic retinopathy and relationship to baseline plasma glucose and blood pressure. *Diabetes Care*. 1988;11:246–251.
192. Berk MA, Miodovnik M, Mimouni F. Impact of pregnancy on complications of insulin-dependent diabetes mellitus. *Am J Perinatol*. 1988;5:359.
193. Gordin D, Kaaja R, Forsblom C, et al. Pre-eclampsia and pregnancy-induced hypertension are associated with severe diabetic retinopathy in type 1 diabetes later in life. *Acta Diabetol*. 2013;50(5):781–787.
194. Early Treatment Diabetic Retinopathy Study Research Group. Fundus photographic risk factors for the progression of diabetic retinopathy. *Ophthalmology*. 1991;98:823.
195. Horvat M, MacLean H, Goldberg L, et al. Diabetic retinopathy in pregnancy: a 12-year prospective study. *Br J Ophthalmol*. 1980;64:398.
196. Acmaz G, Atas M, Gulhan A, et al. Assessment of macular peripapillary nerve fiber layer and choroidal thickness changes in pregnant women with gestational diabetes mellitus, healthy pregnant women, and healthy non-pregnant women. *Med Sci Monit*. 2015;21:1759–1764.
197. Macfarlane DP, O'Sullivan EP, Dorman S, et al. The utility of retinal screening in gestational diabetes. *Diabet Med*. 2013;30(8):1009–1010.
198. Puza SW, Malee MP. Utilization of routine ophthalmologic examinations in pregnant diabetic patients. *J Matern Fetal Med*. 1996;5:7–10.
199. Boone MI, Farber ME, Jovanovic-Peterson L, et al. Increased retinal vascular tortuosity in gestational diabetes mellitus. *Ophthalmology*. 1989;96:251.
200. Hagay Z, Schachter M, Pollack A, et al. Development of proliferative retinopathy in a gestational diabetes patient following rapid metabolic control. *Eur J Obstet Gynecol Reprod Biol*. 1994;57:211.
201. Axer-Sieger R, Hod M, Fink-Cohen S, et al. Diabetic retinopathy during pregnancy. *Ophthalmology*. 1996;103:1815.

202. Lapolla A, Cardone C, Negrin P, et al. Pregnancy does not induce or worsen retinal and peripheral nerve dysfunction in insulin-dependent diabetic women. *J Diabetes Complications*. 1998;12:74–80.
203. Hellstedt T, Kaaja R, Teramo L, et al. The effect of pregnancy on mild diabetic retinopathy. *Graefes Arch Clin Exp Ophthalmol*. 1997;235:437–441.
204. Rodman HM, Singerman LJ, Aiello LM, et al. Diabetic retinopathy and its relationship to pregnancy. Merkatz IR, Adam PAJ. *The diabetic pregnancy, a perinatal perspective*. Grune & Stratton: New York; 1979:73–91.
205. Reece E, Lockwood C, Tuck S, et al. Retinal and pregnancy outcomes in the presence of diabetic proliferative retinopathy. *J Reprod Med*. 1994;39:799.
206. Chan WC, Lim LT, Quinn MJ, et al. Management and outcome of sight-threatening diabetic retinopathy in pregnancy. *Eye (Lond)*. 2004;18(8):826–832.
207. Kitzmiller JL, Aiello LM, Kaldany LM, et al. Diabetic vascular disease complicating pregnancy. *Clin Obstet Gynecol*. 1981;24:107.
208. Sinclair SH, Nessler C, Foxman B, et al. Macular edema and pregnancy in insulin-dependent diabetes. *Am J Ophthalmol*. 1984;97:154.
209. Sameshima H, Kai M, Kajiya S, et al. Retinopathy and perinatal outcome in diabetic pregnancy. *Nippon Sanka Fujinka Gakkai Zasshi*. 1995;47:1048–1054.
210. Lauszus FF, Gron PL, Klebe JG. Pregnancies complicated by diabetic proliferative retinopathy. *Acta Obstet Gynecol Scand*. 1998;77:814–818.
211. McElvy SS, Demarini S, Miodovnik M, et al. Fetal weight and progression of diabetic retinopathy. *Obstet Gynecol*. 2001;97:587–592.
212. Zhu L, Nakabayashi M, Takeda Y. Statistical analysis of perinatal outcomes in pregnancy complicated with diabetes mellitus. *J Obstet Gynaecol Res*. 1997;23:555–563.
213. Hiilesmaa V, Suhonen L, Teramo K. Glycaemic control is associated with preeclampsia but not with pregnancy-induced hypertension in women with type 1 diabetes

mellitus. *Diabetologia*. 2000;43:1534–1539.
214. Lovestam-Adrian M, Agardh CD, Aberg A, et al. Preeclampsia is a potent risk factor for deterioration of retinopathy during pregnancy in type 1 diabetic patients. *Diabet Med*. 1997;14:1059–1065.
215. Perkins ES. Ocular toxoplasmosis. *Br J Ophthalmol*. 1973;57:1–17.
216. Oniki S. Prognosis of pregnancy in patients with toxoplasmic retinochoroiditis. *Jpn J Ophthalmol*. 1983;27:166–174.
217. Braakenburg AM, Crespi CM, Holland GN, et al. Recurrence rates of ocular toxoplasmosis during pregnancy. *Am J Ophthalmol*. 2014;157(4):767–773.e2.
218. Reich M, Ruppenstein M, Becker MD, et al. Risk of recurrence of preexisting ocular toxoplasmosis during pregnancy. *Ocul Immunol Inflamm*. 2015;23(3):240–245.
219. Braakenburg AM, Rothova A. Clinical features of ocular toxoplasmosis during pregnancy. *Retina*. 2009;29:627–630.
220. Snyder DA, Tessler HH. Vogt–Koyanagi–Harada syndrome. *Am J Ophthalmol*. 1980;90:69–75.
221. Steahly LP. Vogt–Koyanagi–Harada syndrome and pregnancy. *Am J Ophthalmol*. 1990;22:59–62.
222. Taguchi C, Ikeda E, Hikita N, et al. A report of two cases suggesting positive influence of pregnancy on uveitis activity. *Nippon Ganka Gakkai Zasshi*. 1999;103:66–71.
223. Friedman Z, Granat M, Neumann E. The syndrome of Vogt–Koyanagi–Harada and pregnancy. *Metab Pediatr Ophthalmol*. 1980;4:147–149.
224. Matsubara S, Kuwata T, Ohkawara Y, et al. Headache in late pregnancy: a symptom for Vogt–Koyanagi–Harada disease. *Arch Gynecol Obstet*. 2011;283(6):1423–1425.
225. Rao VG, Rao GS, Narkhede NS. Flare up of choroiditis and choroidal neovasculazation associated with punctate inner choroidopathy during early pregnancy. *Indian J Ophthalmol*. 2011;59:145–148.
226. Hyman BN. Postpartum uveitis. *Ann Ophthalmol*. 1976;8:677–680.
227. Rabiah PK, Vitale AT. Noninfectious uveitis and pregnancy.

Am J Ophthalmol. 2003;136:91–98.
228. Chiam NP, Lim LL. Uveitis and gender: the course of uveitis in pregnancy. *J Ophthalmol*. 2014;2014:401915.
229. Chiam NP, Hall AJ, Stawell RJ, et al. The course of uveitis in pregnancy and postpartum. *Br J Ophthalmol*. 2013;97(10):1284–1288.
230. Kump LI, Cervantes-Castañeda RA, Androudi SN, et al. Patterns of exacerbations of chronic non-infectious uveitis in pregnancy and puerperium. *Ocul Immunol Inflamm*. 2006;14(2):99–104.
231. Neri A, Grausbord R, Kremer I, et al. The management of labor in high myopic patients. *Eur J Obstet Gynecol Reprod Biol*. 1985;19:277–279.
232. Landau D, Seelenfreund MH, Tadmor O, et al. The effect of normal childbirth on eyes with abnormalities predisposing to rhegmatogenous retinal detachment. *Graefes Arch Clin Exp Ophthalmol*. 1995;233:598–600.
233. Prost M. Severe myopia and delivery. *Klin Oczna*. 1996;98:129–130.
234. Cohen VM, Rundle PA, Rennie IG. Choroidal hemangiomas with exudative retinal detachments during pregnancy. *Arch Ophthalmol*. 2002;120:862–864.
235. Pitta C, Bergen R, Littwin S. Spontaneous regression of a choroidal hemangioma following pregnancy. *Ann Ophthalmol*. 1979;11:772–774.
236. Chen SJ, Chung YM, Liu JH. Endogenous Candida endophthalmitis after induced abortion. *Am J Ophthalmol*. 1998;125:873–875.
237. Sahu C, Kumar K, Sinha MK, et al. Review of endogenous endophthalmitis during pregnancy including case series. *Int Ophthalmol*. 2013;33(5):611–618.
238. Doshi RR, Wender JD, Jumper JM, et al. Endogenous Candida albicans endophthalmitis following spontaneous abortion and IUD removal. *Ophthalmic Surg Lasers Imaging*. 2011;42 Online:e132–4.
239. Rahman W, Hanson R, Westcott M. A rare case of peripartum endogenous bacterial endophthalmitis. *Int Ophthalmol*. 2011;31(2):113–115.

240. Yoser SL, Heckenlively JR, Friedman L, et al. Evaluation of clinical findings and common symptoms in retinitis pigmentosa. *Invest Ophthalmol Vis Sci*. 1987;28(Suppl.):112.
241. Hayaska S, Ugomori S, Kanamori M, et al. Pericentral retinal degeneration deteriorates during pregnancies. *Ophthalmologica*. 1990;200:72–76.
242. Samples JR, Meyer SM. Use of ophthalmic medications in pregnant and nursing women. *Am J Ophthalmol*. 1988;106:616–623.
243. Soubrane G, Canivet J, Coscas G. Influence of pregnancy on the evolution of background retinopathy: preliminary results of a prospective fluorescein angiography study. Ryan SJ, Dawson AK, Little HL. *Retinal diseases*. Grune & Stratton: New York; 1985.
244. Greenberg F, Lewis RA. Safety of fluorescein angiography during pregnancy. *Am J Ophthalmol*. 1990;110:323–324 [(Letter)].
245. Halperin LS, Olk RJ, Soubrane G, et al. Safety of fluorescein angiography during pregnancy. *Am J Ophthalmol*. 1990;109:563–566.
246. Fineman MS, Maguire JI, Fineman SW, et al. Safety of indocyanine green angiography during pregnancy: a survey of the retina, vitreous, and macula societies. *Arch Ophthalmol*. 2001;119:353–355.
247. Iida T, Hagimura N, Otani T, et al. Choroidal vascular lesions in serous retinal detachment viewed with indocyanine green angiography. *Nippon Ganka Gakkai Zasshi*. 1996;100:817–824.
248. US Food and Drug Administration. *Visudyne(TM) (verteporfin for injection)*. www.accessdata.fda.gov/drugsatfda_docs/label/2008/02111 2008.
249. Rosen E, Rubowitz A, Ferencz JR. Exposure to verteporfin and bevacizumab therapy for choroidal neovascularization secondary to punctate inner choroidopathy during pregnancy. *Eye (Lond)*. 2009;23:1479.
250. De Santis M, Carducci B, De Santis L, et al. First case of post-conception Verteporfin exposure: pregnancy and

neonatal outcome. *Acta Ophthalmol Scand*. 2004;82:623–624.
251. Rodrigues M, Meira D, Batista S, et al. Accidental pregnancy exposure to verteporfin: obstetrical and neonatal outcomes: a case report. *Aust N Z J Obstet Gynaecol*. 2009;49:236–237.
252. Kaygusuz I, Eser A, Inegol Gumus I, et al. Effect of anti-vascular endothelial growth factor antibody during early fetal development in rats. *J Matern Fetal Neonatal Med*. 2014;27(17):1744–1748.
253. http://www.accessdata.fda.gov/drugsatfda_docs/label/2013/
254. http://www.fda.gov/Safety/MedWatch/SafetyInformation/u
255. Petrou P, Georgalas I, Giavaras G, et al. Early loss of pregnancy after intravitreal bevacizumab injection. *Acta Ophthalmol*. 2010;88(4):e136.
256. Tarantola RM, Folk JC, Boldt HC, et al. Intravitreal bevacizumab during pregnancy. *Retina*. 2010;30:1405–1411.
257. Sullivan L, Kelly SP, Glenn A, et al. Intravitreal bevacizumab injection in unrecognised early pregnancy. *Eye (Lond)*. 2014;28(4):492–494.
258. Introini U, Casalino G, Cardani A, et al. Intravitreal bevacizumab for a subfoveal myopic choroidal neovascularization in the first trimester of pregnancy. *J Ocul Pharmacol Ther*. 2012;28(5):553–555.
259. Sarhianaki A, Katsimpris A, Petropoulos IK, et al. Intravitreal administration of ranibizumab for idiopathic choroidal neovascularization in a pregnant woman. *Klin Monatsbl Augenheilkd*. 2012;229(4):451–453.
260. Wu Z, Huang J, Sadda S. Inadvertent use of bevacizumab to treat choroidal neovascularisation during pregnancy: a case report. *Ann Acad Med Singapore*. 2010;39(2):143–145.

96

Optic Disc Anomalies, Drusen, Pits, and Associated Retinal Pathology

Rustum Karanjia, S. Khizer R. Khaderi, Alfredo A. Sadun

Optic Disc Anomalies

A variety of congenital optic disc anomalies challenge the clinical acumen of ophthalmologists, internists, and pediatricians. Since some of these abnormalities are known by various names, it is worthwhile reviewing the general categories.

Megalopapilla

Megalopapilla is a rare anomaly of the optic disc, involving thinning of the nerve fiber across a large optic nerve head, and is often associated with large refractive errors and with midline congenital deformities.[1]

Aplasia

Aplasia of the optic nerve head is very rare, probably represents an

extreme form of optic nerve head hypoplasia, and may be associated with the absence or gross maldevelopment of the globe.[1]

Hypoplasia

Optic disc hypoplasia is a congenital underdevelopment of the optic nerve head with a reduced number of axons. Hypoplastic optic discs are often underdiagnosed and may vary in level of development, leading to variable levels of visual acuity and visual field defects.[2] Small crowded hyperopic discs can have the appearance of a hypoplastic optic disc but this is an anatomical variant in a small hyperopic eye.

Papilledema

Papilledema is elevation of the optic nerve due to elevated intracranial pressure. Thus for a diagnosis of papilledema the intracranial pressure must be measured, typically by lumbar puncture opening pressure in the lateral decubitus position. An elevated disc or nerve fiber layer swelling without elevated intracranial pressure is optic disc edema not papilledema.

Pseudopapilledema

Pseudopapilledema is disc elevation in the absence of nerve fiber layer edema. This can occur for a variety of reasons, including optic nerve head drusen, diabetic papillitis, vascular disorders including central retinal vein occlusion, intraocular and peripapillary inflammation, Leber's hereditary optic neuropathy, hamartomas, and infiltrative processes including infection and neoplasms.[3]

Congestion of the Optic Nerve Head

Most causes of pseudopapilledema are acquired and relate to an underlying ocular or systemic disease. The most common congenital cause of congestion at the optic nerve head is optic disc drusen.[4,5]

While not typically present at birth, optic disc drusen first develop between the disc surface and the lamina cribrosa.[6] They

can cause elevation of the optic nerve head and anomalous branch patterns of the retinal vasculature.[7] Typically optic disc drusen become more noticeable over time and can appear on the surface of the optic nerve head by the end of the first decade of life.[7] Disc drusen are discussed in greater detail below.

Cavities in the Optic Nerve Head

Excavated and colobomatous defects of the optic nerve head encompass a spectrum of abnormalities, including tilted discs, peripapillary staphylomas, morning glory disc anomalies, colobomas, and congenital optic disc pits. Optic disc pits were regarded as atypical colobomas by Greear.[8]

Optic disc pits should probably be considered one manifestation along a spectrum of cavitary optic disc anomalies. Slusher and coworkers[9] described a family of 35 members spanning five generations with an autosomal dominant pattern of congenital optic disc abnormalities. Remarkably, a myriad of morphologic variations of phenotype were expressed, including optic disc pits, morning glory syndrome, and coloboma of the optic nerve. One gene defect can result in a variety of optic disc abnormalities; the traditional classification schemes that describe varieties of cavitary optic disc anomalies should therefore be reconsidered.

Anatomy

A brief review of the anatomy and embryology of the optic nerve head permits a better understanding of these abnormalities.

The retinal ganglion cells of each retina contribute approximately 1.2 million unmyelinated axons that converge at a point approximately 4 mm nasal to the foveola, through which they exit the globe, acquire a myelin sheath, and form the optic nerve. These axons project to various primary visual nuclei in the brain,[10] constitute a fiber tract rather than a nerve, and, as such, have histologic and functional similarities to brain tissue. The optic nerve is enclosed by three meningeal sheaths that are contiguous with the meningeal coverings of the brain. Before exiting the eye, however, the axons of the retinal ganglion cells must converge centripetally,

make a sharp turn, traverse the lamina cribrosa, form nerve bundles enclosed by connective tissue septa, and then, once posterior to the lamina cribrosa, become ensheathed by myelin (Fig. 96.1).[11]

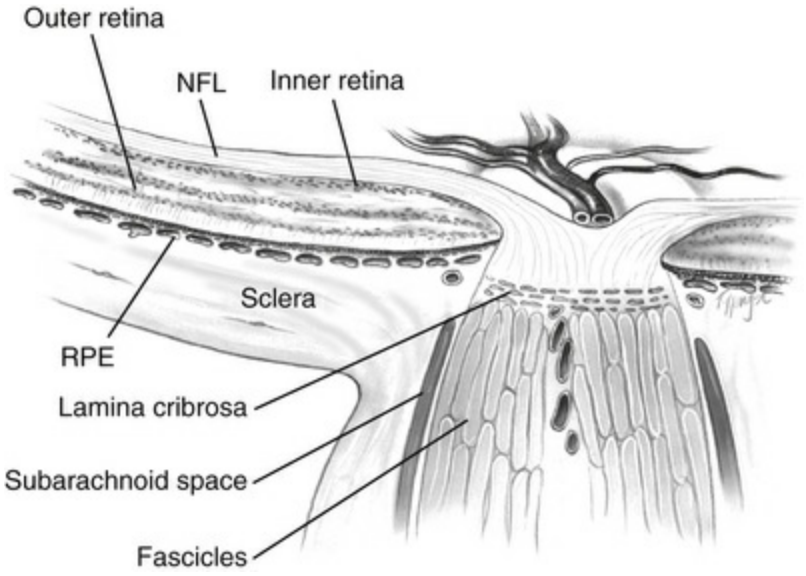

FIG. 96.1 Axial view of optic nerve head and surrounding tissues. Fibers from the retina collect at the optic disc, pass down through the lamina cribrosa, become myelinated, and form fascicles. Note the three parts of the optic nerve: I, anterior portion (retinal); II, midportion (prelaminar or choroidal); III, posterior portion (lamina cribrosa or scleral) at optic nerve head. *NFL*, nerve fiber layer; *RPE*, retinal pigment epithelium.

Thus, the optic nerve head is remarkable in several respects. Axons deriving from the retina become part of the nerve, go from an unmyelinated to a myelinated state, traverse the sieve-like lamina cribrosa, are partitioned into groups by glial columns, and go from an area of high intraocular pressure to relatively low interstitial pressure. Not surprisingly, anomalies of structure at this critical juncture often lead to marked physiologic consequences.[12]

Optic Disc Drusen

In 1856 Müller[13] described concretions of the optic nerve head from a series of histopathologic studies of eyes. This was followed in

1868 by Liebrich,[14] who described the fundus appearance of optic disc drusen and made the link to the histopathology findings of Müller.[13] Nieden introduced the word *Drusenbildung* (German) to describe the concretions.[15,16] Optic disc drusen are composed of acellular concretions predominantly made up of calcium but can also contain amino and nucleic acids, mucopolysaccharides, and iron.[16]

There is no known genetic predisposition for the formation of optic disc drusen. Retrospective studies of relatives of individuals with optic disc drusen found that only one of 27 relatives of seven probands with optic disc drusen also had optic disc drusen.[17] The primary pathogenesis of optic disc drusen also remains unknown, with some hypothesizing an inherited dysplasia of the optic disc and its blood supply. Vascular maldevelopment has been theorized to cause increased transudate release into the intercellular space which in turn acts as a nidus for the formation of optic disc drusen.[17,18]

Optic disc drusen are usually found incidentally on routine examination, with a clinical prevalence reported of 1 in 500 eyes.[19,20] Histopathologic studies, however, have reported a prevalence of approximately 1 in 40[21] with 60% of the drusen buried deep in the optic nerve tissue.[16] The lack of diagnostic techniques to examine the deep portions of the optic nerve head might account for the difference in prevalence as the initial studies were published prior to the advent of B-scan ultrasonography in 1977.[16] Some studies have also reported a higher incidence in women, and there is some discordance in the literature about the percentage of cases which are bilateral, ranging from 69% to 91.2%.[16] This may reflect the asymmetric nature of optic disc drusen and how no single modality can detect all optic disc drusen.[22] There is no clear pattern of inheritance in optic disc drusen, and this may be compounded by the inheritance pattern of optic disc size, which by itself may be a risk factor for optic disc drusen.[15]

Optic disc drusen are the most common cause of pseudopapilledema and distinguishing them from true optic disc edema is of clinical importance. True disc edema is potentially a life threatening process, unlike the more benign nature of optic disc drusen.[5,22]

Visual Defects

Optic disc drusen are associated with two major types of visual field defects. The first is the result of direct compression or displacement of the fibers by the drusen and is typically arcuate in nature, usually in the inferior nasal quadrant.[23] The second is an enlarged blind spot, which is likely related to pseudopapilledema or leaking blood vessels.[24,25]

The visual field defects may be present from childhood[6] and may progress over time. The progression, however, is slow and patients may not be aware of the field defect without formal visual field testing. The reported frequency of visual field defects varies widely, from 24% to 87%, with the highest occurrence in eyes with superficial optic disc drusen.[26–28]

It is unusual for optic disc drusen to impair central acuity by direct compression of the axons in the papillomacular bundle.[16] This is in part due to the decreased number of fibers in the temporal region of the optic disc which would require the optic disc drusen to be much larger before they are able to affect the papillomacular bundle. In cases where the vision has been affected there is typically an accompanying severe visual field defect,[29–31]

Optic disc drusen alter the conformation of the vasculature and are able to displace blood vessels. This can cause transient visual loss, or in some cases anterior ischemic optic neuropathy can occur.[12,32] In a study of 20 patients with optic disc drusen-associated anterior ischemic optic neuropathy (AION), Purvin reported that patients with optic disc drusen and AION were typically younger and more likely to have transient visual obscurations prior to the episode of AION. Interestingly the optic disc drusen patients with AION also had the same vascular risk factors associated with AION in the general population, suggesting that risk factor modification is important in decreasing the likelihood of AION in optic disc drusen patients.[32]

Importantly, patients with optic disc drusen can have other pathologies responsible for their vision loss and there have been case reports of field defects caused by intracranial tumors being misdiagnosed as optic disc drusen.[30,33] It is therefore essential to ensure that there is no other reason for vision loss in patients with optic disc drusen, especially when there is decreased acuity without

visual field changes.

Detection

The appearance of the optic nerve head with optic disc drusen can be quite variable, with some discs showing superficial drusen that are readily visible.[16] There are several techniques that can be used to help identify optic disc drusen which take advantage of various properties of the drusen.

The simplest technique is by direct visualization with fundoscopy. This technique can be further enhanced by looking for autofluorescence, a characteristic of optic disc drusen first described in the 1960s (Fig. 96.2).[34–36] However, autofluorescence is only seen in superficial drusen and in some series is present in as few as 12% of cases.[22]

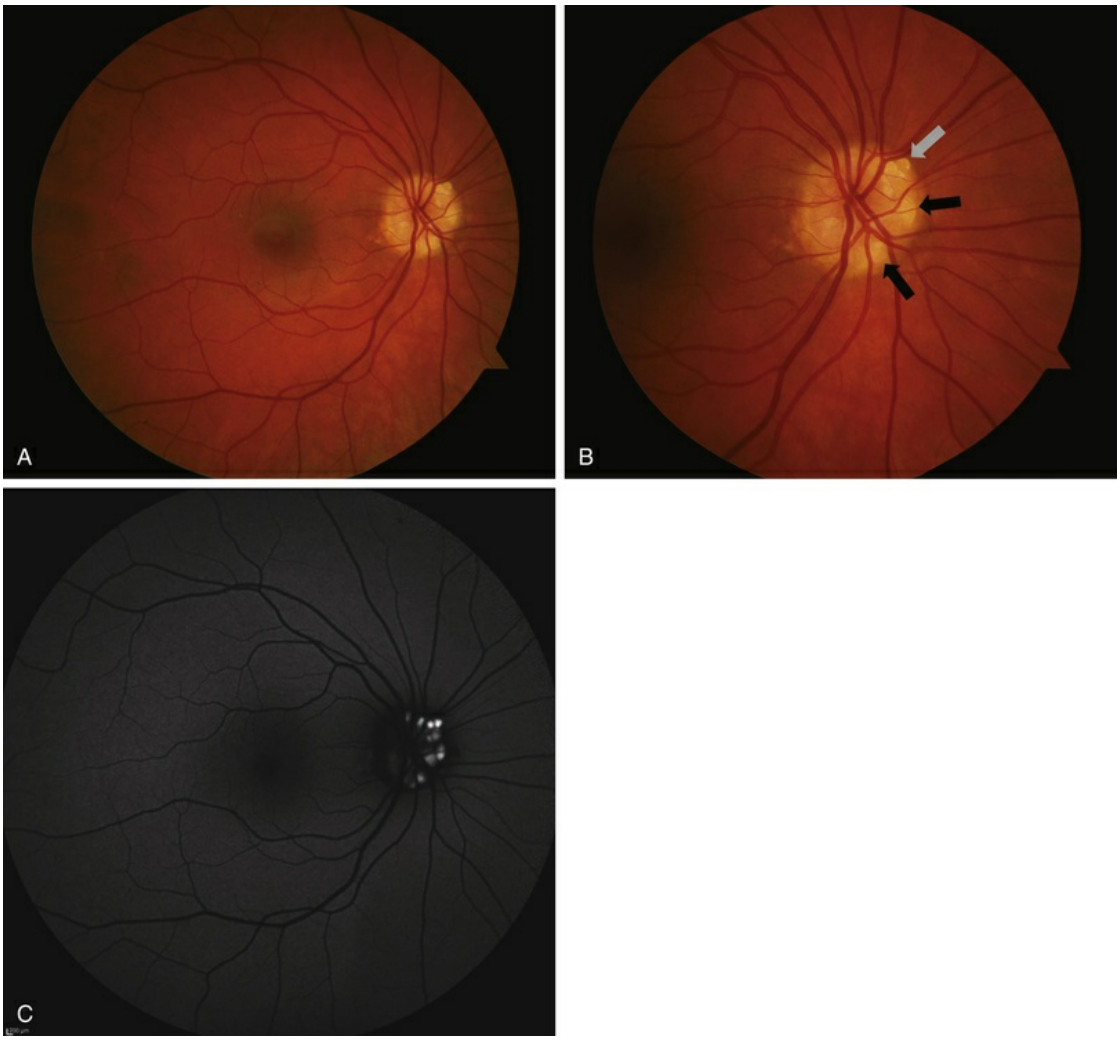

FIG. 96.2 Fundus photograph of patient with optic nerve drusen: (A) low magnification and (B) high magnification color funds photos of the left eye showing obscuration of the disc margin, absence of a central cup and elevation of the disc due to drusen (*arrows*). (C) Fundus autofluorescence image of the same eye showing characteristic autofluorescence of optic disc drusen.

Combining autofluorescence with fluorescin angiography can help distinguish drusen from papilledema. Pineles was able to demonstrate that optic disc drusen showed a characteristic pattern of early (25%) or late (29%) nodular staining and circumferential parapapillary staining (80%) which was distinct from the leakage seen with papilledema.[22]

The depth of disc drusen can, however, pose a problem for superficial imaging techniques, and the main method for looking for buried drusen until recently has been ultrasonography. The use of B-scan ultrasound to detect optic disc drusen was described as far back as the 1970s.[37] Taking advantage of the inherent high reflectivity of calcium, which is present in drusen, it is possible to detect drusen with low gain (Fig. 96.3). The technique is also useful for detecting buried drusen, but the echogenicity of drusen is dependent on the calcium content. While there are no reports of the percentage of drusen that are calcified, some studies have found less than 50% of buried drusen are detected by ultrasound.[38] The variable degree of calcification also hampers the ability of CT scans to detect optic disc drusen. CT scans are further limited by sectioning, as slices greater than 1.5 mm can easily miss drusen in the optic nerve head.

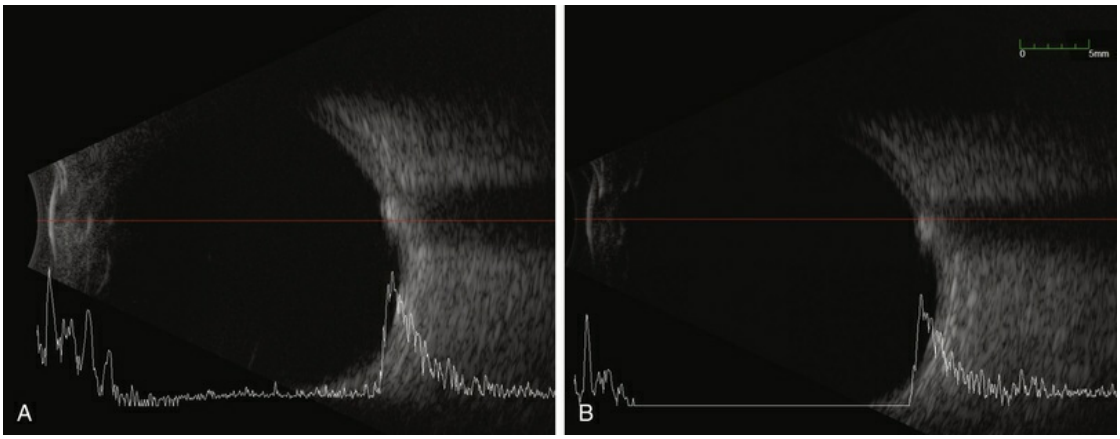

FIG. 96.3 B-scan ultrasound images of the optic nerve from the same patient with optic disc drusen demonstrating the inherent high reflectivity of calcium present in the drusen and the ability to detect the drusen at both high (A) and low (B) gain.

Buried drusen can also be detected by spectral domain optical coherence tomography (OCT)[39] and more recently, enhanced depth OCT[40] (Fig. 96.4). These devices provide an unprecedented ability to evaluate optic disc drusen to the depth of the lamina cribrosa and to evaluate the interplay with structures of the optic nerve. A direct comparison of enhanced depth OCT and B-scan ultrasound has yet to be published, but it is clear that no single modality is perfect for detecting drusen and a combination of modalities in the right clinical context is required to make the appropriate diagnosis.[22]

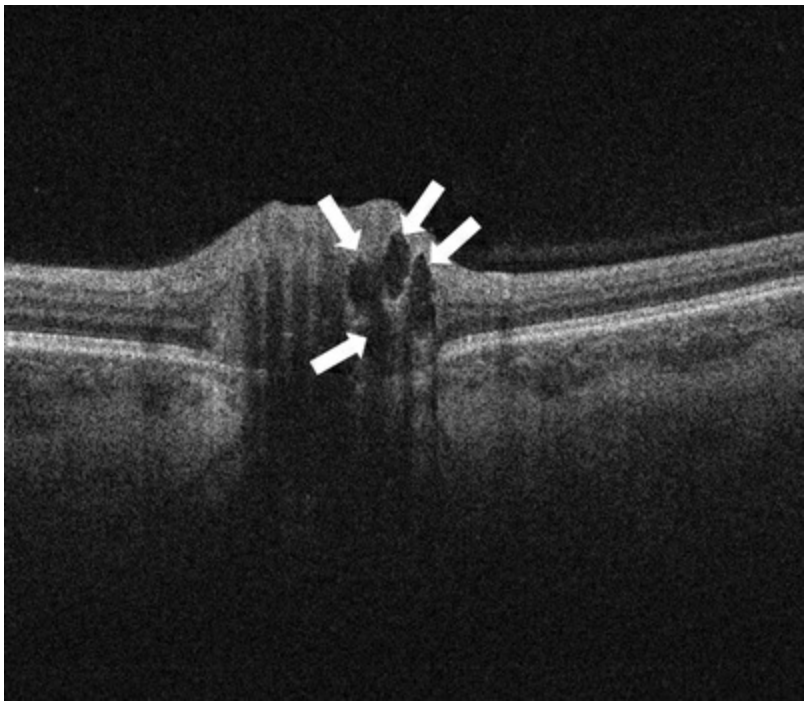

FIG. 96.4 Enhanced depth optical coherence tomography of optic nerve drusen from the same patient showing clearly demarcated superficial and deep drusen (*arrows*) corresponding to area of *gray arrow* of Fig. 96.2B.

Associated Retinal Changes

The retinal vasculature in eyes with optic disc drusen is often anomalous with increased tortuosity, vascular loops, and abnormal branching patterns including optociliary shunt vessels[7,41] There is also an increased incidence of cilioretinal arteries in patients with optic disc drusen with up to 40% of patients having the vascular aberration versus 15% in the normal population.[42,43]

These vascular anomalies appear to predispose patients with optic disc drusen to vascular occlusions including central retinal artery (CRAO) and central retinal vein occlusions (CRVO). The first description of a vascular disturbance associated with optic disc drusen was in 1895 when Gifford described an 11-year-old girl with a central retinal artery occlusion.[44] As with Gifford's case report, patients with optic disc drusen who suffer from a CRAO tend to be younger than individuals who do not have optic disc drusen, but the presence of optic disc drusen alone is usually insufficient to

cause a CRAO. Most cases are associated with other known risk factors for CRAO, including hypertension, contraceptive use, and migraines.[16]

Unlike CRAOs, the anatomical changes caused by optic disc drusen may alone increase the risk of CRVO. The presence of drusen alters the flow dynamics of the central retinal vein by altering the path and potentially constricting the vascular diameter.[45] As a result drusen may represent an independent risk factor for CRVO.

Optic disc drusen are also associated with subretinal neovascularization. Typically in a juxtapapillary location, the neovascularization extends towards the macula but rarely involves it.[46] The neovascular membranes, however, may be associated with hemorrhages that can disrupt vision. Some case reports describe relatively good vision in optic disc drusen-associated neovascular membranes without treatment, but there are also cases of neovascular membrane extending subfoveally causing permanent visual impairment.[28]

Hemorrhages can also occur with optic disc drusen in the absence of a subretinal neovascularization. These spontaneous hemorrhages occur with an incidence of up to 10%.[16] There are four anatomical variations of hemorrhages associated with optic disc drusen: (1) hemorrhages that extend into the vitreous; (2) splinter hemorrhages of the retinal nerve fiber layer; (3) deep hemorrhages of the optic disc; and (4) peripapillary hemorrhages, which may extend into the macula.[16] These hemorrhages do not typically cause visual impairments except when they extend into the macula, which is not common.[29] The pathophysiology of retinal hemorrhages in optic disc drusen is unclear, with some proposing that they are the result of enlarging drusen which can erode into the blood vessels or cause venous stasis leading to hemorrhage.[16]

Treatment

There is no proven treatment for optic disc drusen, and as patients with optic disc drusen often do not suffer from vision loss, treatment may not be warranted. Once the diagnosis is established, however, regular examinations are important to ensure that

treatable complications of optic disc drusen are appropriately managed.

The presence of optic disc drusen can predispose the patient to glaucomatous optic nerve damage at lower intraocular pressures. Assessment for glaucoma can also be complicated by the presence of the optic disc drusen as a small crowded nerve can mask the appearance of cupping. Furthermore, OCT retinal nerve fiber layer (RNFL) measurements may be distorted by the presence of optic disc drusen necessitating serial monitory of both RNFL and visual fields.

Glaucoma may coexist with optic disc drusen[47] and determining which portion of the field loss is due to glaucoma and which is due to optic disc drusen is difficult. In the presence of visual field damage, lowering the IOP should be considered, particularly in patients with field loss at a young age, as the natural attrition of the optic nerve that occurs with aging may be worse in patients with optic disc drusen. The use of pressure-lowering medications should consider the risks and benefits, tailored to each individual patient. Regardless of treatment, serial monitoring with visual fields and OCT RNFL is warranted to assess for progression.

Unlike typical glaucoma, which is a degenerative process in older patients, individuals with optic disc drusen may develop glaucomatous changes at a younger age as optic nerve fibers in the presence of optic disc drusen appear to be compromised and more sensitive to IOP.[16]

Management of vascular complications associated with optic disc drusen such as CRAO and CRVO is similar to the management of these disorders in the absence of drusen (see Chapter 54, Retinal artery occlusions; Chapter 56, Branch retinal vein occlusion; Chapter 57, Central retinal vein occlusion). The presence of a neovascular membrane was historically treated with photocoagulation depending on the location.[48] More recently, anti-VEGF agents such as ranibizumab have been used with some success.[49] Unlike age-related macular degeneration, treatment of neovascularization in optic disc drusen is not always required as the prognosis is usually good.[47]

Optic Disc Pits

In 1882, Wiethe described abnormalities in both optic discs of a 62-year-old woman.[50] His description of dark-gray depressions in the optic nerve heads was probably the first report of optic disc pits. Since Wiethe's initial description, excavations of the optic disc have variously been described as craters, holes, cavities, and, most recently, congenital pits of the optic nerve head.

Studies suggest that optic pits occur in approximately 1 in 10, 000 eyes, although there is considerable variance among studies.[8,51] Men and women are equally affected. Approximately 10–15% of optic disc pits are bilateral. Most optic disc pits are nonfamilial; however, there are a few reports with an autosomal dominant pattern of inheritance.[52] One such report describes a family for which several members had small iris colobomas, some in combination with the pit, providing insight as to the etiology.[53] About 70% of the pits are on the temporal side of the disc, and about 20% are situated centrally; the remainder are found inferiorly, superiorly, and nasally.[54]

Serous retinal detachments may be associated with optic disc pits. These may occur at any age but are most frequent in early adulthood. However, there have been reports of associated retinal detachment occurring as early as 6 years of age and in patients as old as in the ninth decade of life.[55] Some have suggested that the clinical course differs and leads to better visual acuity in children as spontaneous resolution is the rule.[55,56] Through the analysis of stereoscopic transparencies, it has been proposed that the fluid that enters through the optic disc pit actually travels between the inner and outer layers of the retina to produce a retinoschisis.[57,58] OCT has shown such inner retinal schises preceding outer-layer detachment.[59] Following this, detachment of the outer retinal layer may occur as a secondary process.[59] Although no histopathologic studies have confirmed this, the application of OCT has provided compelling evidence for at least two levels of retinal separation (Fig. 96.5).[60] OCT has also been used to demonstrate a marked reduction in thickness of the retinal nerve fiber layer in the quadrant corresponding to the optic nerve pit.[61]

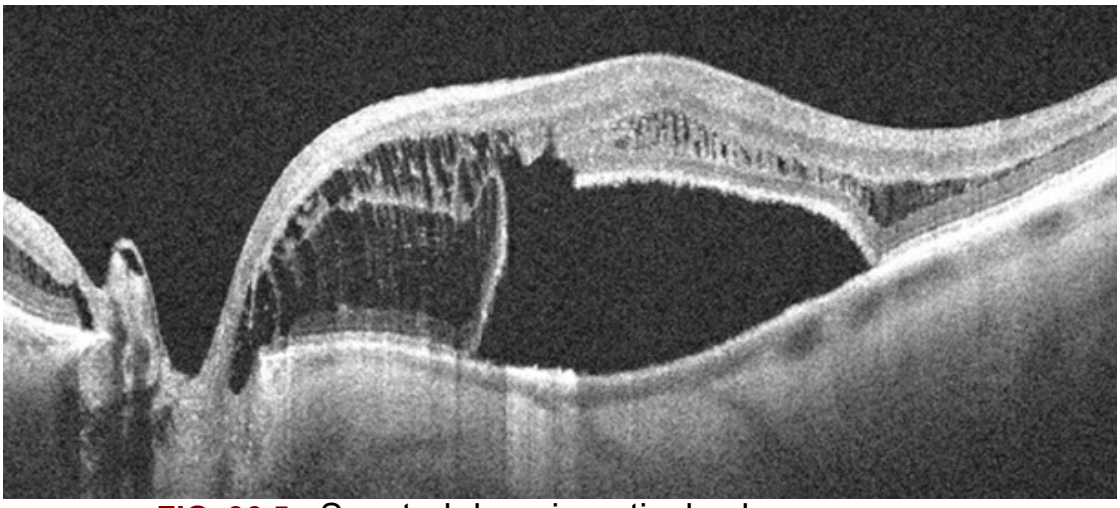

FIG. 96.5 Spectral domain optical coherence tomography image of optic disc pit maculopathy, with cystoid spaces and schisis in multiple layers as well as subretinal fluid.

In the series from Brown et al.,[54] most optic disc pits were gray in color, although they varied from yellow to black. Their size can range from minute to large, occupying most of the surface of the optic disc.

Visual Defects

The optic disc pit is most often associated with two types of visual field defects.[62] The first type is exemplified by arcuate scotomas that probably reflect the absence of the wedge of nerve fibers displaced by the optic disc pit. Larger pits may be associated with large Bjerrum-type scotomas or even altitudinal visual field defects. Nasal or temporal steps are often detectable; less frequently, paracentral scotomas and generalized constriction may be seen.[54] However, Walsh and Hoyt[63] reviewed several studies that demonstrated only an enlarged blind spot as a forme fruste of the visual field defect in association with optic pits.

The second type of visual field defect is that associated with serous detachment of the macula. In 1960 Kranenburg[64] described the association of optic nerve pits and central serous retinopathy. He found that 16 of his 24 patients with optic disc pits had serous detachments of the macula, with corresponding central scotomas or other central visual field changes.

Associated Retinal Changes

Optic nerve head pits that are centrally located are least likely to be associated with retinal changes. Optic disc pits along the rim of the optic disc are usually seen in association with peripapillary chorioretinal atrophy and retinal pigment epithelium changes (Fig. 96.6). These peripapillary changes may develop over time with or without central serous retinal detachments. In following the development of a serous macular detachment, Walsh and Hoyt[63] described the appearance of what they termed an "occult hole" in the optic nerve head.

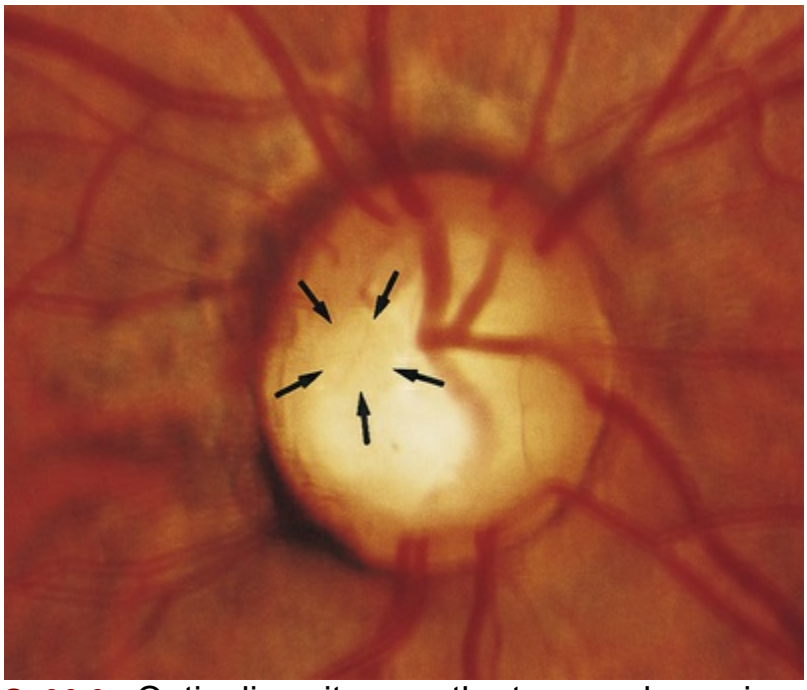

FIG. 96.6 Optic disc pits near the temporal margin are common and are most likely to lead to serous macular detachments (*arrows*).

Serous detachment of the macula is now known as a common complication of the optic disc pit. The natural history of this complication has been well described by Sobol et al.[65] They followed 15 patients with optic disc pits and macular detachments for an average of 9 years and found that 80% lost vision to 20/200 or worse. The visual loss was generally complete within 6 months of presentation. Long-term macular changes included full-thickness or laminar (through the outer retina), retinal holes, retinal pigment

epithelium mottling, and general cystic changes of the macula.[65] Vascular telangiectasis has been reported in connection with intraschistic hemorrhage from a temporal optic disc pit.[66]

A gray fibroglial membrane appears to overlie the pit in many cases (Fig. 96.7). This membrane may be intact or may incompletely cover the pit. The fact that patients with serous macular detachments almost invariably have defects in their diaphanous membrane has prompted theories on how optic nerve pits lead to serous macular detachments.

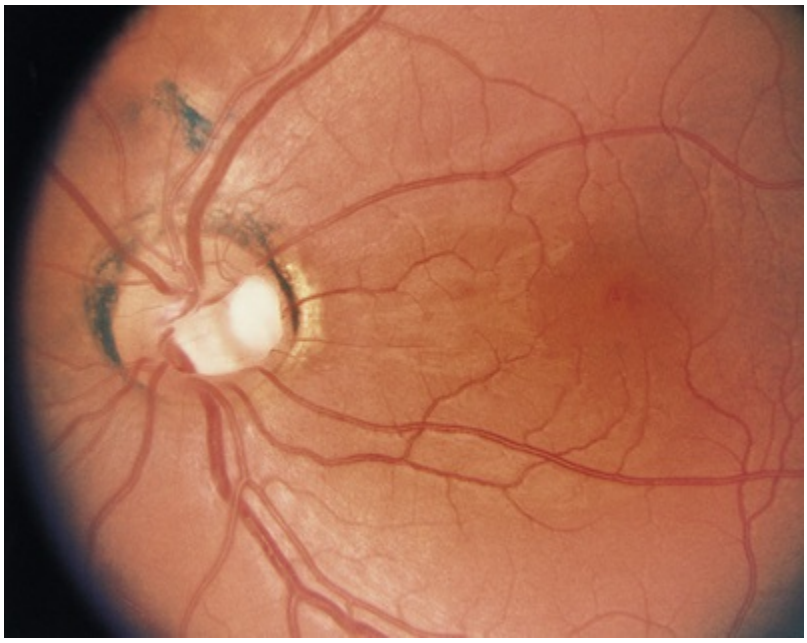

FIG. 96.7 Optic nerve pit. Note overlying gray fibroglial membrane.

Macular Detachment

Several investigators have estimated that between 40% and 50% of patients with optic nerve pits have either an associated nonrhegmatogenous, serous retinal detachment, or retinal changes suggestive of previous detachment.[54,67] The macular serous detachment (or retinoschisis) seen in association with optic disc pits appears most commonly when the pit is located in the temporal region of the optic disc and in larger pits. Conversely, small pits and those located more centrally are less likely to lead to serous

retinal detachments.[54,64]

Appearance of Maculopathy

In 1908, Reis[68] described a case of an optic nerve pit with associated maculopathy. However, this association was not taken seriously until Petersen,[69] in 1958, described several patients with what he called crater-like holes in the optic disc; these patients also had a central serous chorioretinopathy. This relationship was firmly emphasized by Kranenburg[64] in 1960, who described 24 cases of optic disc pits. One-third of these patients had serous retinal detachments, and another third had macular changes that he interpreted as reflecting a previous episode of nonrhegmatogenous serous retinal detachment.

Most of the retinal detachments are temporal to the disc and confined between the superior and inferior vascular arcades. Infrequently, a serous retinal detachment is located outside the arcades if the pit is situated on the nasal side of the optic disc. Often, the serous retinal detachment is contiguous with the optic disc, sometimes through a visible isthmus of subretinal fluid.

The serous macular detachments are generally low (less than 1.0 mm in height). The elevated retina often contains cystic regions that have been demonstrated on histologic examination to exist within the inner nuclear layer.[51] Occasionally the cystic areas rupture outward, producing a lamellar macular hole that, unlike idiopathic lamellar macular holes, retains an intact internal limiting membrane.

The variability of the retinal separation is also consistent with an alternative description of the maculopathy proposed by Lincoff and colleagues.[70] In a case report they provide clear OCT evidence of a schisis cavity between the inner and outer retina and a larger outer-layer retinal detachment. The two are connected by a hole in the outer layer near the fovea.[70]

Course of Associated Serous Macular Detachment

It is difficult to determine the time interval between the beginning

of a serous macular detachment and the earliest visual changes, because the patient usually seeks evaluation after symptoms of blurred vision and metamorphopsia occur secondary to foveal involvement. However, Brown and Tasman[71] described one case in which the retinal detachment started at the temporal margin of the optic disc. This serous retinal detachment expanded slowly in a temporal direction until, after several months, it covered the entire macular area. They also described small yellow precipitates seen under the elevated retina late in the course of serous macular detachment.

In analyzing their 15 patients followed over an average of 9 years, Sobol et al.[65] found that most eyes with optic disc pits presented with visual acuities of about 20/40–20/60. However, each patient lost three or more lines of vision within the next 6 months. After 6 months, a few of those patients got worse and a few got better. Ultimately, only 20% of the patients maintained visual acuities of better than 20/200.[65] Generally, however, patients with optic disc pits present later in the course of their macular detachments when their visual acuities are already worse than 20/70.[71]

Theories of Pathophysiology

By 1960 it was clear that serous macular detachments often occurred as complications of optic disc pits. Ferry[51] had the opportunity to histologically examine two eyes with optic disc pits associated with macular detachments. He suggested that progressive gliosis and "contraction of the retinal elements" contained in the pit produced a traction detachment of the macula. In 1964 Sugar[72] suggested that fluid from the vitreous cavity could enter the subretinal space through a macular hole. However, this is most unlikely because macular holes seen with optic pits are usually lamellar and are only infrequently seen in association with the serous detachment.

Fluorescein angiography may reveal late hyperfluorescence of the optic disc pit.[67] It was therefore postulated that blood vessels in this area leaked fluid, which then entered the subretinal space.[67] However, Brown et al.[54] reported that many patients with serous macular detachments had no leakage on their fluorescein

angiogram.

Others have speculated that there may be a direct source of fluid from the choroid that penetrates through Bruch's membrane under the macular detachment; it was hypothesized that peripapillary chorioretinal atrophic changes permitted this leakage.[73] However, fluorescein angiographic findings do not support this theory. Moreover, many other diseases produce extensive chorioretinal atrophy that does not lead to serous macular detachment.[54]

A few investigators,[74] including Gass,[75] have suggested that cerebrospinal fluid may leak from the optic nerve subarachnoid space into the optic pit and from there into the subretinal space. However, intrathecal fluorescein injections in humans and in animals and histologic studies have failed to demonstrate any such connection.[51,52,76,77]

Currently, the most widely accepted explanation is that originally proposed by Sugar[78] in 1962 and later endorsed by Brockhurst[79] in 1975. It was postulated that fluid from the vitreous leaked through the optic disc pit to fill the subretinal space (Fig. 96.8). In corroboration of this theory, Brown et al.[54] demonstrated that more than 75% of patients with optic disc pits and associated serous macular detachments have posterior vitreous detachments. This would allow liquefied vitreous to be contiguous with the optic disc cavity. Moreover, most of the patients in their series who had pits without macular serous elevations did not have posterior vitreous detachments.[54] Additionally, Brown and his colleagues[77] demonstrated experimentally in dogs a direct connection between the posterior vitreous space and the subretinal space via a congenital optic disc pit. Irvine et al.[74] demonstrated in vivo that there is a continuity between the posterior vitreous cavity and the optic nerve subarachnoid space by observing bubbles percolating out of an optic nerve sheath window after pars plana vitrectomy and gas injection.

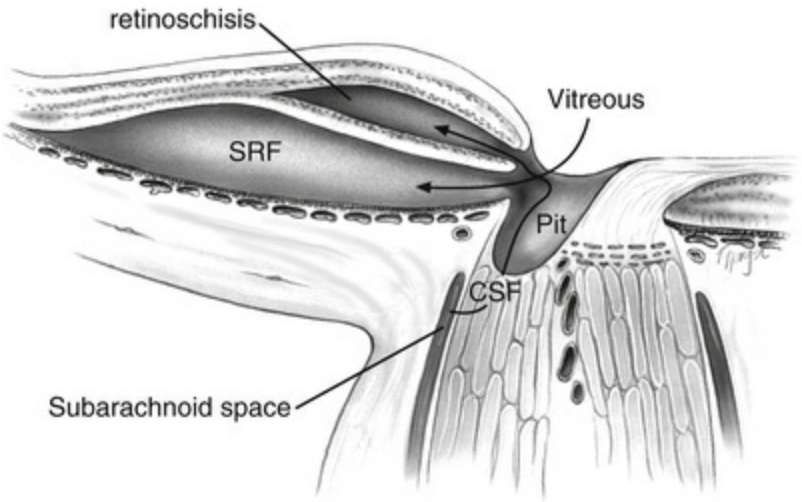

FIG. 96.8 Schematic drawing of axial view of optic nerve head. Various theories describe mechanisms by which fluid enters the subretinal space. Cerebrospinal fluid (*CSF*) could derive from the subarachnoid space. However, the more widely accepted explanation is that fluid in the vitreous space passes into the optic pit and from there directly into the subretinal space. An optic disc pit located near the margin of the optic nerve head is far more likely to permit fluid to leak subretinally. *CSF*, cerebrospinal fluid; *SRF*, subretinal fluid.

The most recent variation on these theories of pathophysiology is that proposed by Lincoff et al.[70] who suggested that the primary communication from the optic disc pit is to the retina temporal to the optic disc.[57] Fluid slips under the inner retina, lifting it and the nerve fiber layer up and away from the outer retina. This has been corroborated by OCT[60] and extended to show both this retinoschisis and an outer retinal detachment connected by a hole in the outer retinal layer (see Fig. 96.6).

Although the theory of direct vitreous fluid entry via the optic pit into the subretinal space is appealing, it does not explain why serous macular detachments tend to occur first in young adulthood. Brown and Tasman[71] suggest that posterior vitreous detachments may be a precipitating factor. Another possibility is the role of macular traction, which occurs with age.

Prognosis

Although the optic nerve head pits, being congenital, are stationary,

their associated retinal abnormalities may be progressive. The prognosis for return of vision after serous macular detachment is variable. Walsh and Hoyt[63] described a patient followed between the ages of 14 and 23 years who developed multiple serous macular detachments that remitted to near-normal vision after each episode. A more rigorous study was conducted by Brown et al.[54] in a group of 20 eyes with optic disc pits and serous macular detachments. These eyes were followed for 5 years, untreated. The mean visual acuity at the end of this time was about 20/80. The authors found very little correlation between the visual acuity at the time of detachment and the long-term visual outcome. They also noted that some detachments resolved spontaneously, whereas others persisted for years. Most patients still had some subretinal macular fluid present after 5 years. Other macular changes, as described above, also persisted. Long-term studies confirm the earlier impressions that untreated macular detachments caused by optic disc pits have an overall poor prognosis.[65]

Treatment

Given the rarity of optic disc pits, most studies examining purported treatments are small and nonrandomized, leading to difficulty in coming to a consensus on the best management for the associated serous macular detachments. Observation, systemic steroids, optic nerve sheath decompression, and scleral buckling procedures have not been demonstrated to be very effective.[79] However, several series have favorably compared the outcome of photocoagulated eyes with untreated eyes in the resolution of the serous macular detachment and in final visual outcome.[74,79,80] The argon laser procedure was used in most of these series to produce photocoagulation burns in one or several rows between the area of serous retinal detachment and the optic disc. The burns were usually applied to areas of elevated retina. Brockhurst,[79] Gass,[80] and Theodossiadis[81] used similar photocoagulation protocols, and all reported that their patients were likely to have good resolution of the serous detachment to a flat macula.

Combining their results, 15 of the 18 patients in these three series had reattachments of their maculas, as opposed to only 5 of 20

untreated patients in the series of Brown et al.[54] However, the difference in final visual outcome between the treated and untreated groups was less pronounced. The photocoagulated eyes in the three studies had ultimate visual acuities that averaged a little worse than 20/80. This does not compare favorably with the 20/80 final visual outcome in the series of Brown et al. In making a similar comparison, Brown and Tasman[71] concluded that photocoagulation therapy is effective for flattening the retinal detachment, but not for improving final visual outcome.

A macular buckling procedure successfully treated cases of serous detachment in optic disc pit. In such cases, OCT showed a resultant closure of the connection between the pit and the retinoschisis with resolution of the schisis.[82] Multifocal electroretinography was performed in 10 patients with optic disc pit with serous macular detachment before and after treatment with macular buckling procedures.[83] Improvement was measured in all eyes at 12 months, though often this was not accompanied by an increase in visual acuity.[83] Follow-up evaluation 11 years after surgery found that the patients maintained the improvement they had achieved 2 years postoperatively, suggesting a good long-term result.[84] Silicon oil has also been used successfully in cases of macular hole in association with the optic disc pit.[85]

More recent attempts to combine photocoagulation therapy with posterior vitrectomy and gas–fluid exchange have led to more encouraging long-term visual outcomes.[86] Bonnet[87] looked at 25 eyes with optic disc pits in 24 patients who presented with visual loss due to serous macular detachments. High-magnification biomicroscopy and fluorescein angiography of these eyes revealed evidence of vitreous traction on the retina and on the optic nerve head. Most particularly, Bonnet noted that none of the patients had posterior vitreous detachments at presentation and that in the 2 patients that subsequently developed a posterior vitreous detachment, reattachment of the macula occurred spontaneously. Fluorescein dye was seen to stain the optic nerve head, especially at the pit and temporal margin of the disc. This dye leakage was not seen in cases that underwent surgical peeling of the posterior vitreous face. Moreover, Bonnet observed a small hole in the roof of the optic pit in several cases, and small bubbles of gas passing from

the vitreous cavity into the subretinal space via the optic disc pit in a case that underwent vitrectomy and gas injection but not photocoagulation. Hence, Bonnet concluded that macular detachments in optic disc pits have a rhegmatogenous component (at the optic disc), that they are associated with vitreous traction, and that the subretinal fluid comes from the vitreous space via the optic disc pit.[87]

Cox and colleagues[88] looked at three treatment approaches. They concluded that the combination of vitrectomy plus gas tamponade plus photocoagulation of the retina temporal to the disc was more effective than vitrectomy and gas or photocoagulation alone. They obtained short-term surgical success in all of their 8 eyes and long-term attachment in 4 out of 8 eyes using the three-part combination therapy.[88] Others have also obtained good anatomic results in optic disc pit with macular detachment using the combination of vitrectomy, air–fluid exchange, and photocoagulation in patients whose final visual acuities averaged 20/60.[89] Various precipitating events may combine with the mechanism described above, leading to macular detachment by vitreous fluid entry into the subretinal space via the optic disc pit.

Novel techniques for treatment of optic disc pit-associated serous macular detachments have also been described. Spaide et al.[90] published a case report describing the use of a bent 25-gauge needle to create half-thickness cuts to the inner retina. This maneuver was combined with a vitrectomy in an attempt to allow intraretinal and subretinal fluid to escape. This procedure did not use intraocular gas to avoid premature closure of the surgical fenestrations and the posterior hyaloid was left intact. One month after surgery, the patient's visual acuity improved from 8/400 preoperatively to 20/20. Schaal et al.[91] described a similar procedure with the use of a 27-gauge cannula to make three-quarter-depth cuts, in combination with a limited preretinal vitrectomy.

Jalil et al.[92] actively drained subretinal fluid with a 42-gauge cannula. This procedure included vitrectomy, induction of posterior vitreous detachment, and internal limiting membrane peel, but without the use of laser photocoagulation around the retinotomy site. Fluid–air exchange followed by internal gas tamponade with 14% C_3F_8 concluded the procedure. The patient's preoperative

visual acuity of 1.00 logMAR improved at 8-months follow-up to 0.4 logMAR. Ziahosseini et al.[93] utilized a similar approach with the addition of argon laser to the cannula insertion site.

References

1. Sadun AA, Yanoff M. Biomedical foundations of ophthalmology. Duane TD, Jaeger EA. *Clicial ophthalmology*. Harper & Row: Philadelphia, PA; 1986.
2. Nelson M, Lessell S, Sadun AA. Optic nerve hypoplasia and maternal diabetes mellitus. *Arch Neurol*. 1986;43(1):20–25.
3. Liu GT, Volpe NJ, Galetta SL. *Neuro-ophthalmology diagnosis and management*. 2nd ed. WB Saunders: Philadelphia, PA; 2010.
4. Kheterpal S, Good PA, Beale DJ, et al. Imaging of optic disc drusen: a comparative study. *Eye (Lond)*. 1995;9(Pt 1):67–69.
5. Carta A, Favilla S, Prato M, et al. Accuracy of funduscopy to identify true edema versus pseudoedema of the optic disc. *Invest Ophthalmol Vis Sci*. 2012;53(1):1–6.
6. Hoover DL, Robb RM, Petersen RA. Optic disc drusen in children. *J Pediatr Ophthalmol Strabismus*. 1988;25(4):191–195.
7. Rosenberg MA, Savino PJ, Glaser JS. A clinical analysis of pseudopapilledema. I: Population, laterality, acuity, refractive error, ophthalmoscopic characteristics, and coincident disease. *Arch Ophthalmol*. 1979;97(1):65–70.
8. Greear JN. Pits, or crater-like holes in the optic disk. *Arch Ophthalmol*. 1942;28:467–483.
9. Slusher MM, Weaver RG Jr, Greven CM, et al. The spectrum of cavitary optic disc anomalies in a family. *Ophthalmology*. 1989;96(3):342–347.
10. Sadun AA, Schaecter JD. Tracing axons in the human brain: a method utilizing light and TEM techniques. *J Electron Microsc Techn*. 1985;2:175–186.
11. Hogan MJ, Alvarado JA, Weddell JE. *Histology of the human eye: an atlas and textbook*. WB Saunders: Philadephia, PA; 1971.
12. Sadun AA, Currie JN, Lessell S. Transient visual obscurations with elevated optic discs. *Ann Neurol*.

1984;16(4):489–494.
13. Müller H. Anatomische Beiträge zur Ophthalmologie. *Archiv für Opthalmologie*. 1856;2:1.
14. Liebrich R. Contribution to discussion on Iwanoff A. Ueber Neuritis Optics. *Kiln Monatsbl Augenheilkd*. 1868;6:426–427.
15. Parsons JH. *Pathology of the eye*. GP Putnam: New York; 1904.
16. Auw-Haedrich C, Staubach F, Witschel H. Optic disk drusen. *Surv Ophthalmol*. 2002;47(6):515–532.
17. Antcliff RJ, Spalton DJ. Are optic disc drusen inherited? *Ophthalmology*. 1999;106(7):1278–1281.
18. Sacks JG, O'Grady RB, Choromokos E, et al. The pathogenesis of optic nerve drusen: a hypothesis. *Arch Ophthalmol*. 1977;95(3):425–428.
19. Lorentzen SE. Drusen of the optic disk: a clinical and genetic study. *Acta Ophthalmol (Copenh)*. 1966;(Suppl. 90):1–180.
20. You QS, Xu L, Wang YX, et al. Prevalence of optic disc drusen in an adult Chinese population: the Beijing Eye Study. *Acta Ophthalmol*. 2009;87(2):227–228.
21. Friedman AH, Gartner S, Modi SS. Drusen of the optic disc: a retrospective study in cadaver eyes. *Br J Ophthalmol*. 1975;59(8):413–421.
22. Pineles SL, Arnold AC. Fluorescein angiographic identification of optic disc drusen with and without optic disc edema. *J Neuroophthalmol*. 2012;32(1):17–22.
23. François P. Les verrucosités hyalines de la papille. *Annales d'Oculistique*. 1949;182:249–278.
24. Lorentzen SE. Optic disc drusen. *Acta Ophthalmol (Copenh)*. 1983;61(2):335–336.
25. Pietruschka G, Priess G. Clinical importance and prognosis of drusen of the disc. *Klin Monbl Augenheilkd*. 1973;162(3):331–341.
26. Mustonen E. Pseudopapilloedema with and without verified optic disc drusen. A clinical analysis II: visual fields. *Acta Ophthalmol (Copenh)*. 1983;61(6):1057–1066.
27. Mustonen E. Pseudopapilloedema with and without verified optic disc drusen: a clinical analysis I. *Acta Ophthalmol (Copenh)*. 1983;61(6):1037–1056.
28. Savino PJ, Glaser JS, Rosenberg MA. A clinical analysis of

pseudopapilledema. II: Visual field defects. *Arch Ophthalmol*. 1979;97(1):71–75.
29. Sanders TE, Gay AJ, Newman M. Drusen of the optic disk-hemorrhagic complications. *Trans Am Ophthalmol Soc*. 1970;68:186–218.
30. Beck RW, Corbett JJ, Thompson HS, et al. Decreased visual acuity from optic disc drusen. *Arch Ophthalmol*. 1985;103(8):1155–1159.
31. Knight CL, Hoyt WF. Monocular blindness from drusen of the optic disk. *Am J Ophthalmol*. 1972;73(6):890–892.
32. Purvin V, King R, Kawasaki A, et al. Anterior ischemic optic neuropathy in eyes with optic disc drusen. *Arch Ophthalmol*. 2004;122(1):48–53.
33. Reifler DM, Kaufman DI. Optic disk drusen and pseudotumor cerebri. *Am J Ophthalmol*. 1988;106(1):95–96.
34. Sanders MD, Ffytche TJ. Fluorescein angiography in the diagnosis of drusen of the disc. *Trans Ophthalmol Soc U K*. 1967;87:457–468.
35. Wise GN, Henkind P, Alterman M. Optic disc drusen and subretinal hemorrhage. *Trans Am Acad Ophthalmol Otolaryngol*. 1974;78(2):OP212–19.
36. Walker ER, Frederickson RG, Mayes MD. The mineralization of elastic fibers and alterations of extracellular matrix in pseudoxanthoma elasticum: ultrastructure, immunocytochemistry, and X-ray analysis. *Arch Dermatol*. 1989;125(1):70–76.
37. Friedman AH, Beckerman B, Gold DH, et al. Drusen of the optic disc. *Surv Ophthalmol*. 1977;21(5):373–390.
38. Kurz-Levin MM, Landau K. A comparison of imaging techniques for diagnosing drusen of the optic nerve head. *Arch Ophthalmol*. 1999;117(8):1045–1049.
39. Yi K, Mujat M, Sun W, et al. Imaging of optic nerve head drusen: improvements with spectral domain optical coherence tomography. *J Glaucoma*. 2009;18(5):373–378.
40. Silverman AL, Tatham AJ, Medeiros FA, et al. Assessment of optic nerve head drusen using enhanced depth imaging and swept source optical coherence tomography. *J Neuroophthalmol*. 2014;34(2):198–205.

41. Erkkila H. The central vascular pattern of the eyeground in children with drusen of the optic disk. *Albrecht Von Graefes Arch Klin Exp Ophthalmol*. 1976;199(1):1–10.
42. Erkkila H. Clinical appearance of optic disc drusen in childhood. *Albrecht Von Graefes Arch Klin Exp Ophthalmol*. 1975;193(1):1–18.
43. Lorentzen SE. Incidence of cilioretinal arteries. *Acta Ophthalmol (Copenh)*. 1970;48(3):518–524.
44. Gifford H. An unusual case of hyaline bodies in the optic nerve. *Arch Ophthalmol*. 1895;24:395.
45. Ring CP, Pearson TC, Sanders MD, et al. Viscosity and retinal vein thrombosis. *Br J Ophthalmol*. 1976;60(6):397–410.
46. Wessing A. *Fluoreszenzangiographie der Retina*. Georg Thieme Verlag: Stuttgart; 1968.
47. Samples JR, van Buskirk M, Shults WT, et al. Optic nerve head drusen and glaucoma. *Arch Ophthalmol*. 1985;103(11):1678–1680.
48. Harris MJ, Fine SL, Owens SL. Hemorrhagic complications of optic nerve drusen. *Am J Ophthalmol*. 1981;92(1):70–76.
49. Gregory-Evans K, Rai P, Patterson J. Successful treatment of subretinal neovascularization with intravitreal ranibizumab in a child with optic nerve head drusen. *J Pediatr Ophthalmol Strabismus*. 2009; 10.3928/01913913-20090818-03 [Aug 21 [E-pub].
50. Wiethe T. Ein Fall von angeborener Deformitat der Sehnervenpapille. *Arch Augenheilkd*. 1881;11:4–19.
51. Ferry AP. Macular detachment associated with congenital pit of the optic nerve head. pathologic findings in two cases simulating malignant melanoma of the choroid. *Arch Ophthalmol*. 1963;70:346–357.
52. Kalina RE, Conrad WC. Letter: Intrathecal fluorescein for serous macular detachment. *Arch Ophthalmol*. 1976;94(8):1421.
53. Singerman LJ, Mittra RA. Hereditary optic pit and iris coloboma in three generations of a single family. *Retina*. 2001;21(3):273–275.
54. Brown GC, Shields JA, Goldberg RE. Congenital pits of the optic nerve head. II. Clinical studies in humans.

Ophthalmology. 1980;87(1):51–65.
55. Brodsky MC. Congenital optic pit with serous maculopathy in childhood. *J AAPOS*. 2003;7(2):150 [author reply].
56. Yuen CH, Kaye SB. Spontaneous resolution of serous maculopathy associated with optic disc pit in a child: a case report. *J AAPOS*. 2002;6(5):330–331.
57. Lincoff H, Lopez R, Kreissig I, et al. Retinoschisis associated with optic nerve pits. *Arch Ophthalmol*. 1988;106(1):61–67.
58. Lincoff H, Yannuzzi L, Singerman L, et al. Improvement in visual function after displacement of the retinal elevations emanating from optic pits. *Arch Ophthalmol*. 1993;111(8):1071–1079.
59. Lincoff H, Kreissig I. Optical coherence tomography of pneumatic displacement of optic disc pit maculopathy. *Br J Ophthalmol*. 1998;82(4):367–372.
60. Krivoy D, Gentile R, Liebmann JM, et al. Imaging congenital optic disc pits and associated maculopathy using optical coherence tomography. *Arch Ophthalmol*. 1996;114(2):165–170.
61. Meyer CH, Rodrigues EB, Schmidt JC. Congenital optic nerve head pit associated with reduced retinal nerve fibre thickness at the papillomacular bundle. *Br J Ophthalmol*. 2003;87(10):1300–1301.
62. Simpson DE. Optic nerve pit. *J Am Optom Assoc*. 1987;58(2):118–120.
63. Walsh FB, Hoyt WF. *Clinical neuro-ophthalmology*. 3rd ed. Williams & Wilkins: Baltimore, MD; 1969.
64. Kranenburg EW. Crater-like holes in the optic disc and central serous retinopathy. *Arch Ophthalmol*. 1960;64:912–924.
65. Sobol WM, Blodi CF, Folk JC, et al. Long-term visual outcome in patients with optic nerve pit and serous retinal detachment of the macula. *Ophthalmology*. 1990;97(11):1539–1542.
66. Quinn SM, Charles SJ. Telangiectasis as a cause of intra-schitic haemorrhage in optic disc pit maculopathy. *Acta Ophthalmol Scand*. 2004;82(1):93–95.
67. Gordon R, Chatfield RK. Pits in the optic disc associated

with macular degeneration. *Br J Ophthalmol*. 1969;53(7):481–489.
68. Reis W. Eine wenig bekannte typische Missbildung am Sehnerveneintritt: umschriebene Grubenbildung auf der Papilla n. optici. *Z Augenheilkd*. 1908;19:505–528.
69. Petersen HP. Pits or crater-like holes in the optic disc. *Acta Ophthalmol (Copenh)*. 1958;36(3):435–443.
70. Lincoff H, Schiff W, Krivoy D, et al. Optic coherence tomography of optic disk pit maculopathy. *Am J Ophthalmol*. 1996;122(2):264–266.
71. Brown GC, Tasman WS. *Congenital anomalies of the optic disk*. Grune & Stratton: New York; 1983.
72. Sugar HS. An explanation for the acquired macular pathology associated with congenital pits of the optic disc. *Am J Ophthalmol*. 1964;57:833–835.
73. Wise G, Dollery C, Henkind P. *The retinal circulation*. Harper & Row: New York; 1971.
74. Irvine AR, Crawford JB, Sullivan JH. The pathogenesis of retinal detachment with morning glory disc and optic pit. *Retina*. 1986;6(3):146–150.
75. Gass JD. Serous detachment of the macula: secondary to congenital pit of the optic nervehead. *Am J Ophthalmol*. 1969;67(6):821–841.
76. Brown GC, Shields JA, Patty BE, et al. Congenital pits of the optic nerve head. I: Experimental studies in collie dogs. *Arch Ophthalmol*. 1979;97(7):1341–1344.
77. Brown GC, Shields JA, Patty BE, et al. Congenital optic pits and serous retinal detachment. *Trans Pa Acad Ophthalmol Otolaryngol*. 1979;32(2):151–154.
78. Sugar HS. Congenital pits in the optic disc with acquired macular pathology. *Am J Ophthalmol*. 1962;53:307–311.
79. Brockhurst RJ. Optic pits and posterior retinal detachment. *Trans Am Ophthalmol Soc*. 1975;73:264–291.
80. Gass JDM. *Stereoscopic atlas of macular diseases*. Mosby: St. Louis; 1977.
81. Theodossiadis G. Evolution of congenital pit of the optic disk with macular detachment in photocoagulated and nonphotocoagulated eyes. *Am J Ophthalmol*. 1977;84(5):620–

631.
82. Theodossiadis GP, Theodossiadis PG. Optical coherence tomography in optic disk pit maculopathy treated by the macular buckling procedure. *Am J Ophthalmol*. 2001;132(2):184–190.
83. Theodossiadis G, Theodossiadis P, Malias J, et al. Preoperative and postoperative assessment by multifocal electroretinography in the management of optic disc pits with serous macular detachment. *Ophthalmology*. 2002;109(12):2295–2302.
84. Theodossiadis GP, Chatziralli IP, Theodossiadis PG. Macular buckling in optic disc pit maculopathy in association with the origin of macular elevation: 13-year mean postoperative results. *Eur J Ophthalmol*. 2015;25(3):241–248.
85. Bechmann M, Mueller AJ, Gandorfer A, et al. Macular hole surgery in an eye with an optic pit. *Am J Ophthalmol*. 2001;132(2):263–264.
86. Pahwa V. Optic pit and central serous detachment. *Indian J Ophthalmol*. 1985;33(3):175–176.
87. Bonnet M. Serous macular detachment associated with optic nerve pits. *Graefes Arch Clin Exp Ophthalmol*. 1991;229(6):526–532.
88. Cox MS, Witherspoon CD, Morris RE, et al. Evolving techniques in the treatment of macular detachment caused by optic nerve pits. *Ophthalmology*. 1988;95(7):889–896.
89. Schatz H, McDonald HR. Treatment of sensory retinal detachment associated with optic nerve pit or coloboma. *Ophthalmology*. 1988;95(2):178–186.
90. Spaide RF, Fisher Y, Ober M, et al. Surgical hypothesis: inner retinal fenestration as a treatment for optic disc pit maculopathy. *Retina*. 2006;26(1):89–91.
91. Schaal KB, Wrede J, Dithmar S. Internal drainage in optic pit maculopathy. *Br J Ophthalmol*. 2007;91(8):1093.
92. Jalil A, Stavrakas P, Dhawahir-Scala FE, et al. Drainage of subretinal fluid in optic disc pit maculopathy using subretinal 42-gauge cannula: a new surgical approach. *Graefes Arch Clin Exp Ophthalmol*. 2010;248(5):751–753.

93. Ziahosseini K, Sanghvi C, Muzaffar W, et al. Successful surgical treatment of optic disc pit maculopathy. *Eye (Lond)*. 2009;23(6):1477–1479.

97

Retina-Related Clinical Trials

A Resource Bibliography

Barbara S. Hawkins, Usha Chakravarthy

Introduction

The subspecialty of Retina has seen some of the most innovative changes in the field of ophthalmology, largely owing to ground-breaking randomized clinical trials, with several or many centers

typically participating, conducted to test new treatment strategies or to compare two or more effective strategies for the management of ocular complications of diabetes, age-related macular degeneration, and retinal vaso-occlusive disease, among others. During the past four decades, large clinical trials of interventions for retinal disorders have laid the foundations for evidence-based clinical practice; foremost among these was the Diabetic Retinopathy Study, which was one of the first initiatives of the National Eye Institute upon its creation as one of the United States National Institutes of Health. The Diabetic Retinopathy Study was one of the largest and best-conducted clinical trials of the safety and effectiveness of panretinal photocoagulation in diabetic retinopathy. This trial provided ophthalmologists with the evidence that was needed to show that proliferative diabetic retinopathy could be managed effectively with laser and also demonstrated the potential of the retinal community to generate the evidence base for treatment of retinal disorders through a networked approach. Since the Diabetic Retinopathy Study, the number of clinical trials in retinal disorders has burgeoned, with increasing sponsorship from industry and agencies in other countries.

The purpose of this chapter is to provide the retinal specialist with a bibliography of selected publications in peer-reviewed journals that report information from important clinical trials of interventions for common retinal disorders. The organization of the citations is by retinal condition and then by specific randomized trials or sets of trials, with trials that focus on the same condition grouped together. The order of the conditions is chronologic by publication of findings from the first major clinical trial. Whenever a randomized trial was conducted as part of a larger study, was preceded by a pilot study, or was continued as an observational study, selected publications from the pilot study or from the follow-up study have been included in the bibliography for the clinical trial. The focus is on large, typically multicenter, randomized trials.

Some publications from early trials have been omitted but may be found in previous editions of this textbook. Cochrane systematic reviews published in the *Cochrane Database of Systematic Reviews* have been cited for many interventions for retinal disorders. Publications from many small trials have been cited within the

Cochrane systematic reviews.

Diabetic Retinopathy and Diabetic Macular Edema

Diabetic Retinopathy Study (DRS)

The historical importance of the DRS is described above.

Diabetic Retinopathy Study Research Group. Preliminary report on effects of photocoagulation therapy. Am J Ophthalmol 1976;81:383–96.

Diabetic Retinopathy Study Research Group. Photocoagulation treatment of proliferative diabetic retinopathy: the second report of Diabetic Retinopathy Study findings. Ophthalmology 1978;85:82–106.

Diabetic Retinopathy Study Research Group. Four risk factors for severe visual loss in diabetic retinopathy: the third report from the Diabetic Retinopathy Study. Arch Ophthalmol 1979;97:654–5.

Diabetic Retinopathy Study Research Group. Photocoagulation treatment of proliferative diabetic retinopathy: a short report of long range results. Diabetic Retinopathy Study (DRS) report number 4. International Congress series no. 500, Diabetes 1979. In: Waldhausl WK, editor. Proceedings of the 10th Congress of the International Diabetes Federation. Amsterdam: Excerpta Medica; 1979. p. 789–94.

Diabetic Retinopathy Study Research Group. Diabetic Retinopathy Study report number 6: Design, methods, and baseline results. Invest Ophthalmol Vis Sci 1981;21:149–208.

Diabetic Retinopathy Study Research Group. Diabetic Retinopathy Study report number 7: A modification of the Airlie House classification of diabetic retinopathy. Invest Ophthalmol Vis Sci 1981;21:210–26.

Diabetic Retinopathy Study Research Group. Photocoagulation treatment of proliferative diabetic retinopathy. Clinical application of Diabetic Retinopathy Study (DRS) findings. DRS report number 8. Ophthalmology 1981;88:583–600.

Ferris FL, Podgor MJ, Davis MD, et al. Macular edema in Diabetic Retinopathy Study patients. Diabetic Retinopathy Study report number 12. Ophthalmology 1987;94:754–60.

UK Multicentre Controlled Study

This randomized trial of photocoagulation for diabetic maculopathy was sponsored by the British Diabetic Association and the Wellcome Trust and was conducted concurrently with the DRS.

Multicentre Controlled Study Coordinating Committee. Photocoagulation treatment of diabetic maculopathy. Interim report of a multicentre controlled study. Lancet 1975;2:1110–3.

Multicentre Controlled Study Coordinating Committee. Proliferative diabetic retinopathy: treatment with xenon-arc photocoagulation. Interim report of multicentre controlled randomised controlled trial. Br Med J 1977;1:739–41.

Diabetic Retinopathy Vitrectomy Study (DRVS)

The primary goal of the DRVS was to compare early vitrectomy with conventional management of severe vitreous hemorrhage secondary to diabetic retinopathy.

Diabetic Retinopathy Vitrectomy Study Research Group. Two-year course of visual acuity in severe proliferative diabetic retinopathy with conventional management. Diabetic Retinopathy Vitrectomy Study (DRVS) report no. 1. Ophthalmology 1985;92:492–502.

Diabetic Retinopathy Vitrectomy Study Research Group. Early vitrectomy for severe vitreous hemorrhage in diabetic

retinopathy. Two-year results of a randomized trial. Diabetic Retinopathy Vitrectomy Study report 2. Arch Ophthalmol 1985;103:1644–52.

Diabetic Retinopathy Vitrectomy Study Research Group. Early vitrectomy for severe proliferative diabetic retinopathy in eyes with useful vision. Results of a randomized trial – Diabetic Retinopathy Vitrectomy Study report 3. Ophthalmology 1988;95:1307–20.

Diabetic Retinopathy Vitrectomy Study Research Group. Early vitrectomy for severe proliferative diabetic retinopathy in eyes with useful vision. Clinical application of results of a randomized trial – Diabetic Retinopathy Vitrectomy Study report 4. Ophthalmology 1988;95:1321–34.

Diabetic Retinopathy Vitrectomy Study Research Group. Early vitrectomy for severe vitreous hemorrhage in diabetic retinopathy. Four-year results of a randomized trial: Diabetic Retinopathy Vitrectomy Study report 5. Arch Ophthalmol 1990;108:958–64.

Early Treatment Diabetic Retinopathy Study (ETDRS)

The ETDRS was designed to evaluate the effectiveness of laser photocoagulation and aspirin, together and singly, in delaying or preventing progression of early diabetic retinopathy to more severe stages and blindness and to determine the optimum time to initiate photocoagulation in diabetic retinopathy. Initiation of the ETDRS was a motivating factor in the development of a new visual acuity chart for use in prospective clinical research studies; articles that report on the design and evaluation of the chart are listed at the end of the ETDRS bibliography.

Early Treatment Diabetic Retinopathy Study Research Group. Photocoagulation for diabetic macular edema. Early Treatment Diabetic Retinopathy Study report number 1. Arch Ophthalmol 1985;103:1796–806.

Early Treatment Diabetic Retinopathy Study Research Group. Treatment techniques and clinical guidelines for photocoagulation of diabetic macular edema. Early Treatment Diabetic Retinopathy Study report number 2. Ophthalmology 1987;94:761–74.

Early Treatment Diabetic Retinopathy Study Research Group. Techniques for scatter and local photocoagulation treatment of diabetic retinopathy: Early Treatment Diabetic Retinopathy Study report no. 3. Int Ophthalmol Clin 1987;27:254–64.

Kinyoun J, Barton F, Fisher M et al. Detection of diabetic macular edema: ophthalmoscopy versus photography – Early Treatment Diabetic Retinopathy Study report number 5. Ophthalmology 1989;96:746–51.

Early Treatment Diabetic Retinopathy Study Research Group. Early Treatment Diabetic Retinopathy Study design and baseline patient characteristics. ETDRS report number 7. Ophthalmology 1991;98:741–56.

Early Treatment Diabetic Retinopathy Study Research Group. Effects of aspirin treatment on diabetic retinopathy: ETDRS report number 8. Ophthalmology 1991;98:757–65.

Early Treatment Diabetic Retinopathy Study Research Group. Early photocoagulation for diabetic retinopathy: ETDRS report number 9. Ophthalmology 1991;98:766–85.

Early Treatment Diabetic Retinopathy Study Research Group. Grading diabetic retinopathy from stereoscopic color fundus photographs – an extension of the modified Airlie House classification. ETDRS report number 10. Ophthalmology 1991;98:786–806.

Early Treatment Diabetic Retinopathy Study Research Group. Classification of diabetic retinopathy from fluorescein angiograms. ETDRS report number 11. Ophthalmology 1991;98:807–22.

Early Treatment Diabetic Retinopathy Study Research Group. Fundus photographic risk factors for progression of diabetic retinopathy: ETDRS report number 12. Ophthalmology 1991;98:823–33.

Early Treatment Diabetic Retinopathy Study Research Group. Fluorescein angiographic risk factors for progression of diabetic retinopathy: ETDRS report number 13. Ophthalmology 1991;98:834–40.

Early Treatment Diabetic Retinopathy Study Investigators. Aspirin effects on mortality and morbidity in patients with diabetes mellitus: Early Treatment Diabetic Retinopathy Study report 14. JAMA 1992;268:1292–300.

Ferris FL. Early photocoagulation in patients with either type I or type II diabetes. Trans Am Ophthalmol Soc 1996;94:505–36.

Davis MD, Fisher MR, Gangnon RE, et al. Risk factors for high-risk proliferative diabetic retinopathy and severe visual loss: Early Treatment Diabetic Retinopathy Study report no. 18. Invest Ophthalmol Vis Sci 1998;39:233–52.

Early Treatment Diabetic Retinopathy Study Research Group. Focal photocoagulation treatment of diabetic macular edema. Relationship of treatment effect to fluorescein angiographic and other retinal characteristics at baseline: ETDRS report no. 19. Arch Ophthalmol 1995;113:1144–55.

Chew EY, Klein ML, Murphy RP, et al. Effects of aspirin on vitreous/preretinal hemorrhage in patients with diabetes mellitus: Early Treatment Diabetic Retinopathy Study report no. 20. Arch Ophthalmol 1995;113:52–5.

Fong DS, Ferris FL, Davis MD, et al. Causes of severe visual loss in the Early Treatment Diabetic Retinopathy Study: ETDRS report no. 24. Am J Ophthalmol 1999;127:137–41.

Chew EY, Benson WE, Remaley NA, et al. Results after lens extraction in patients with diabetic retinopathy: Early Treatment

Diabetic Retinopathy Study report number 25. Arch Ophthalmol 1999;117:1600–6.

Chew EY, Ferris FL, Csaky KG, et al. The long-term effects of laser photocoagulation treatment in patients with diabetic retinopathy: The Early Treatment Diabetic Retinopathy Study Follow-up Study. Ophthalmology 2003;110:1683-9.

Cusick M, Davis MD, Meleth AD, et al for the Early Treatment Diabetic Retinopathy Study (ETDRS) Research Group. Associations of mortality and diabetes complications in patients with type 1 and type 2 diabetes. Early Treatment Diabetic Retinopathy Study report no. 27. Diabetes Care 2005;28:617–25.

Barton FB, Fong DS, Knatterud GL, et al. Classification of Farnsworth–Munsell 100-hue test results in the Early Treatment Diabetic Retinopathy Study. Am J Ophthalmol 2004;138:119–24.

Gangnon RE, Davis MD, Hubbard LD, et al. A severity scale for diabetic macular edema developed from ETDRS data. Invest Ophthalmol Vis Sci 2008;49:5041–7.

Drummond MF, Davies LM, Ferris FL. Assessing the costs and benefits of medical research: the Diabetic Retinopathy Study. Soc Sci Med1992;94(9):973-81.

Ferris FL, Kassoff A, Bresnick GH, et al. New visual acuity charts for clinical research. Am J Ophthalmol 1982;94:91–6.

Ferris FL, Sperduto RD. Standardized illumination for visual acuity testing in clinical research. Am J Ophthalmol 1982;94:97–8.

Ferris FL, Freidlin V, Kassoff A, et al. Relative letter and position difficulty on visual acuity charts from the Early Treatment Diabetic Retinopathy Study. Am J Ophthalmol 1993;116:735–40.

Diabetes Control and Complications Trial (DCCT)

The DCCT was designed to compare intensive with conventional glucose control with respect to development and progression of early vascular and neurologic complications of insulin-dependent diabetes mellitus. The DCCT was sponsored by several institutes of the US National Institutes of Health, including the National Eye Institute, and various corporate sponsors. A follow-up study of members of the DCCT cohort, the Epidemiology of Diabetes Interventions and Complications (EDIC), was undertaken to assess the long-term effects of intensive and conventional diabetes therapy during the DCCT.

Diabetes Control and Complications Trial Research Group. The Diabetes Control and Complications Trial (DCCT): Design and methodologic considerations for the feasibility phase. Diabetes 1986;35:530–45.

Diabetes Control and Complications Trial Research Group. The Diabetes Control and Complications Trial (DCCT): Results of feasibility study. Diabetes Care 1987;10:1–10.

Diabetes Control and Complications Trial Research Group. The effect of intensive treatment of diabetes on the development and progression of long-term complications in insulin-dependent diabetes mellitus. N Engl J Med 1993;329:977–86.

Diabetes Control and Complications Trial Research Group. Effect of intensive diabetes treatment on the development and progression of long-term complications in adolescents with insulin-dependent diabetes mellitus: Diabetes Control and Complications Trial. J Pediatr 1994;125:177–88.

Diabetes Control and Complications Trial Research Group. The effect of intensive diabetes treatment on the progression of diabetic retinopathy in insulin-dependent diabetes mellitus. The Diabetes Control and Complications Trial. Arch Ophthalmol 1995;113:36–51.

Diabetes Control and Complications Trial Research Group. Progression of retinopathy with intensive versus conventional

treatment in the Diabetes Control and Complications Trial. Ophthalmology 1995;102:647–61.

Diabetes Control and Complications Trial (DCCT) Research Group. Effect of intensive diabetes management on macrovascular events and risk factors in the Diabetes Control and Complications Trial. Am J Cardiol 1995;75:894–903.

Diabetes Control and Complications Trial Research Group. The relationship of glycemic exposure (HbA1c) to the risk of development and progression of retinopathy in the Diabetes Control and Complications Trial. Diabetes 1995;44:968–83.

Diabetes Control and Complications Trial Research Group. Influence of intensive diabetes treatment on quality-of-life outcomes in the Diabetes Control and Complications Trial. Diabetes Care 1996;19:195–203.

Diabetes Control and Complications Trial Research Group. The absence of a glycemic threshold for the development of long-term complications: the perspective of the Diabetes Control and Complications Trial. Diabetes 1996;45:1289–98.

Diabetes Control and Complications Trial Research Group. Lifetime benefits and costs of intensive therapy as practiced in the Diabetes Control and Complications Trial. JAMA 1996;276:1400–15.

Diabetes Control and Complications Trial Research Group. Effect of intensive therapy on residual β-cell function in patients with type I diabetes in the Diabetes Control and Complications Trial. Ann Intern Med 1998;128:517–23.

Diabetes Control and Complications Trial Research Group. Early worsening of diabetic retinopathy in the Diabetes Control and Complications Trial. Arch Ophthalmol 1998;116:874–86.

Epidemiology of Diabetes Interventions and Complications (EDIC) Research Group. Design, implementation, and preliminary results of a long-term follow-up of the Diabetes Control and

Complications Trial cohort. Diabetes Care 1999;22:99–111.

Diabetes Control and Complications Trial/Epidemiology of Diabetes Interventions and Complications Research Group. Retinopathy and nephropathy in patients with type I diabetes four years after a trial of intensive therapy. N Engl J Med 2000;342:381–9.

Diabetes Control and Complications Trial Research Group. Effect of pregnancy on microvascular complications in the Diabetes Control and Complications Trial. Diabetes Care 2000;23:1084–91.

Diabetes Control and Complications Trial (DCCT)/ Epidemiology of Diabetes Interventions and Complications (EDIC) Research Group. Beneficial effects of intensive therapy of diabetes during adolescence: outcomes after the conclusion of the Diabetes Control and Complications Trial (DCCT). J Pediatr 2001;139:804–12.

Writing Team for the Diabetes Control and Complications Trial/Epidemiology of Diabetes Interventions and Complications Research Group. Effect of intensive therapy on the microvascular complications of type 1 diabetes mellitus. JAMA 2002;287:2563–9.

Lyons TJ, Jenkins AJ, Zheng D, et al. Diabetic retinopathy and serum lipoprotein subclasses in the DCCT/EDIC cohort. Invest Ophthalmol Vis Sci 2004;45:910–8.

Nathan DM, Cleary PA, Backlund JY, et al. for the Diabetes Control and Complications Trial/Epidemiology of Diabetes Interventions and Complications (DCCT/EDIC) Study Research Group. Intensive diabetes treatment and cardiovascular disease in patients with type 1 diabetes. N Engl J Med 2005;353(25):2643–53.

Diabetes Control and Complications Trial/Epidemiology of Diabetes Interventions and Complications Research Group. Prolonged effect of intensive therapy on the risk of retinopathy complications in patients with type 1 diabetes mellitus. Arch Ophthalmol 2008;126(12):1707–15.

Hubbard LD, Sun W, Cleary PA, et al. for the Diabetes Control and Complications Trial/Epidemiology of Diabetes Interventions and Complications Study Research Group. Comparison of digital and film grading of diabetic retinopathy severity in the Diabetes Control and Complications Trial/Epidemiology of Diabetes Interventions and Complications Study. Arch Ophthalmol 2011;129(6):718–26.

Lachin JM, Genuth S, Nathan DM, et al. for the DCCT/EDIC Research Group. Effect of glycemic exposure on the risk of microvascular complications in the Diabetes Control and Compllications Trial — revisited. Diabetes 2008;57:995-1001.

Jacobson AM, Braffett BH, Cleary PA, et al. for the DCCT/EDIC Research Group. The long-term effects of type 1 diabetes treatment and complications on health-related quality of life. Diabetes Care 2013;36:3131-36.

UK Prospective Diabetes Study (UKPDS)

Since 1983, the UKPDS investigators have published more than 75 articles to report findings from this prospective study.

Kohner EM, Aldington SJ, Stratton IM, et al. United Kingdom Prospective Diabetes Study, 30: Diabetic retinopathy at diagnosis of non-insulin-dependent diabetes mellitus and associated risk factors. Arch Ophthalmol 1998;116:297–303.

United Kingdom Prospective Diabetes Study Group. Intensive blood-glucose control with sulphonylureas or insulin compared with conventional treatment and risk of complications in patients with type 2 diabetes (UKPDS 33). Lancet 1998;352:837–53.

United Kingdom Prospective Diabetes Study (UKPDS) Group. Tight blood pressure control and risk of macrovascular and microvascular complications in type 2 diabetes: UKPDS 38. Br Med J 1998;317:705–13.

Stratton IM, Kohner EM, Aldington SJ, et al. UKPDS 50: Risk factors

for incidence and progression of retinopathy in type II diabetes over 6 years from diagnosis. Diabetologia 2001;44:156–63.

Gray A, Clarke P, Farmer A, et al. Implementing intensive control of blood glucose concentration and blood pressure in type 2 diabetes in England: cost analysis (UKPDS 63). Br Med J 2002;325:860–5.

UK Prospective Diabetes Study (UKPDS) Group. Risks of progression of retinopathy and vision loss related to tight blood pressure control in type 2 diabetes mellitus (UKPDS 69). Arch Ophthalmol 2004;122:1631–40.

Stratton IM, Cull CA, Adler AI, et al. Additive effects of glycaemia and blood pressure exposure on risk of complications in type 2 diabetes: a prospective observational study (UKPDS 75). Diabetologia 2006;49:1761–9.

Diabetic Retinopathy Clinical Research Network (DRCRnet)

The DRCRnet investigators have conducted a number of randomized clinical trials and observational studies of diabetic retinopathy. A complete list of publications from the DRCRnet is maintained on the DRCRnet Public Web Site (http://drcrnet.jaeb.org/Publications.aspx [cited 2015 28 Sep]).

Diabetic Retinopathy Clinical Research Network. A phase 2 randomized clinical trial of intravitreal bevacizumab for diabetic macular edema. Ophthalmology 2007;114(10):1860–7.

Bhavsar AR, Ip MS, Glassman AR for the DRCRnet and the SCORE Study Group. The risk of endophthalmitis following intravitreal triamcinolone injection in the DRCRnet and SCORE clinical trials. Am J Ophthalmol 2007;144:454–6.

Writing Committee for the Diabetic Retinopathy Clinical Research Network. Comparison of the modified Early Treatment Diabetic Retinopathy Study and mild macular grid laser photocoagulation

strategies for diabetic macular edema. Arch Ophthalmol 2007;124:469–80.

Diabetic Retinopathy Clinical Research Network. A randomized trial comparing intravitreal triamcinolone acetonide and focal/grid photocoagulation for diabetic macular edema. Ophthalmology 2008;115:1447–59.

Scott IU, Bressler NM, Bressler SB, et al. and the Diabetic Retinopathy Clinical Research Network. Agreement between clinician and reading center gradings of diabetic retinopathy severity level at baseline in a phase 2 study of intravitreal bevacizumab for diabetic macular edema. Retina 2008;28:38–40.

Diabetic Retinopathy Clinical Research Network. Three-year follow up of a randomized trial comparing focal/grid photocoagulation and intravitreal triamcinolone for diabetic macular edema. Arch Ophthalmol 2009;127(3):245–51.

Bressler NM, Edwards AR, Beck RW, et al. for the Diabetic Retinopathy Clinical Research Network. Exploratory analysis of diabetic retinopathy progression through 3 years in a randomized clinical trial that compares intravitreal triamcinolone acetonide with focal/grid photocoagulation. Arch Ophthalmol 2009;127(12):1566–71.

Bhavsar AR, Googe JM, Stockdale CR, et al. for the Diabetic Retinopathy Clinical Research Network. Risk of endophthalmitis after intravitreal drug injections when topical antibiotics are not required. The Diabetic Retinopathy Clinical Research Network Laser-Ranibizumab-Triamcinolone Clinical Trials. Arch Ophthalmol 2009;127(12):1581-3.

Scott IU, Danis RP, Bressler SB, et al. for the Diabetic Retinopathy Clinical Research Network. Effect of focal/grid photocoagulation on visual acuity and retinal thickening in eyes with non-center-involved diabetic macular edema. Retina 2009;29:613-7.

Diabetic Retinopathy Clinical Research Network. Randomized trial

evaluating ranibizumab plus prompt or deferred laser or triamcinolone plus prompt laser for diabetic macular edema. Ophthalmology 2010;117:1064–77.

Aiello LP, Edwards AR, Beck RW, et al. for the Diabetic Retinopathy Clinical Research Network. Factors associated with improvement and worsening of visual acuity 2 years after focal/grid photocoagulation for diabetic macular edema. Ophthalmology 2010;117:946-53.

Lauer AK, Bressler NM, Edwards AR for the Diabetic Retinopathy Clinical Research Network. Frequency of intraocular pressure increase within days after intravitreal triamcinolone injections in the Diabetic Retinopathy Clinical Research Network. Arch Ophthalmol 2011;129(8):1097-9.

Diabetic Retinopathy Clinical Research Network Writing Committee: Googe J, Brucker AJ, Bressler NM, et al. Randomized trial evaluating short-term effects of intravitreal ranibizumab or triamcinolone acetonide on macular edema after focal/grid laser for diabetic macular edema in eyes also receiving panretinal photocoagulation. Retina 2011;31:1009–27.

Diabetic Retinopathy Clinical Research Network. Expanded 2-year follow-up of ranibizumab plus prompt or deferred laser or triamcinolone plus prompt laser for diabetic macular edema. Ophthalmology 2011;118:609-14.

Dewan V, Lambert D, Edler J, et al. Cost-effectiveness analysis of ranibizumab plus prompt or deferred laser or triamcinolone plus prompt laser for diabetic macular edema. Ophthalmology 2012;119(8):1879-84.

Glassman AR, Stockdale CE, Beck R, et al. for the Diabetic Retinopathy Clinical Research Network. Evaluation of masking study participants to intravitreal injections in a randomized clinical trial. Arch Ophthalmol 2012;130(2):190-4.

Diabetic Retinopathy Clinical Research Network. Randomized

clinical trial evaluating intravitreal ranibizumab or saline for vitreous hemorrhage from proliferative diabetic retinopathy. JAMA Ophthalmol 2013;131(3):283-93.

Bressler SB, Qin H, Melia M, et al. for the Diabetic Retinopathy Clinical Research Network. Exploratory analysis of the effect of intravitreal ranibizumab or triamcinolone on worsening of diabetic retinopathy in a randomized clinical trial. JAMA Ophthalmol 2013;131(8):1033-40.

Bressler SB, Almukhtar T, Aiello LP, et al. for the Diabetic Retinopathy Clinical Research Network. Green or yellow laser treatment for diabetic macular edema. Exploratory assessment within the Diabetic Retinopathy Clinical Research Network. Retina 2013;33:2080-8.

Bhavsar AR, Torres K, Bressler NM, et al. for the Diabetic Retinopathy Clinical Research Network. Evaluation of results 1 year following use of short-term ranibizumab for vitreous hemorrhage due to proliferative diabetic retinopathy. JAMA Ophthalmology 2014;132(7):889-90.

Bressler SB, Almukhtar T, Bhorade A, et al. for the Diabetic Retinopathy Clinical Research Network. Repeated intravitreous ranibizumab injections for diabetic macular edema and the risk of sustained elevation of intraocular pressure or the need for ocular hypotensive treatment. JAMA Ophthalmol 2015;133(5):589-97.

Elman MJ, Ayala A, Bressler NM, et al. for the Diabetic Retinopathy Clinical Research Network. Intravitreal ranibizumab for diabetic macular edema with prompt versus deferred laser treatment: 5-year randomized trial results. Ophthalmology 2015;122:375-81.

Diabetic Retinopathy Clinical Research Network. Aflibercept, bevacizumab, or ranibizumab for diabetic macular edema. N Engl J Med 2015;372:1193-203.

Bressler SB, Melia M, Glassman AR, et al. for the Diabetic Retinopathy Clinical Research Network. Ranibizumab plus

prompt or deferred laser for diabetic macular edema in eyes with vitrectomy before anti-vascular endothelial growth factor therapy. Retina 2015;35(12):2516-28.

Other Intervention Trials

Sorbinil Retinopathy Trial Research Group. A randomized trial of sorbinil, an aldose reductase inhibitor, in diabetic retinopathy. Arch Ophthalmol 1990;108:1234–44.

Krypton Argon Regression of Neovascularization Study Research Group. Randomized comparison of krypton versus argon scatter photocoagulation for diabetic disc neovascularization. Ophthalmology 1993;100:1655–64.

Chaturvedi N, Sjolie A-K, Stephenson JM, et al. and the EUCLID Study Group. Effect of lisinopril on progression of retinopathy in normotensive people with type 1 diabetes. Lancet 1998;351:28–31.

ACCORD Eye Study

Chew EY, Ambrosius WT, Howard LT, et al. for the ACCORD Study Group. Rationale, design, and methods of the Action to Control Cardiovascular Risk in Diabetes Eye Study (ACCORD-EYE). Am J Cardiol 2007;99(Suppl):103i-111i.

ACCORD Study Group and ACCORD Eye Study Group. Effects of medical therapies on retinopathy progression in type 2 diabetes. N Engl J Med 2010;363:233–44.

Ambrosius WT, Danis RP, Goff DC, et al. for the ACCORD Study Group. Lack of association between thiazolidinediones and macular edema in type 2 diabetes. Arch Ophthalmol 2010;128(3):312–8.

Gangaputra S, Lovato JP, Hubbard L, et al. for the ACCORD Eye Research Group. Comparison of standardized clinical classification with fundus photograph grading for the assessment of diabetic retinopathy and diabetic macular edema severity.

Retina 2013;33:1393-9.

Chew EY, Davis MD, Danis RP, et al for the Action to Control Cardiovascular Risk in Diabetes Eye Study Research Group. The effects of medical management on the progression of diabetic retinopathy in persons with type 2 diabetes. The Action to Control Cardiovascular Risk in Diabetes (ACCORD) Eye Study. Ophthalmology 2014;121:2443-51.

ADVANCE/AdRem

Stolk RP, Vingerling JR, Cruickshank JK, et al. on behalf of the AdRem project team and ADVANCE management committee. Rationale and design of the AdRem study: Evaluating the effects of blood pressure lowering and intensive glucose control on vascular retinal disorders in patients with type 2 diabetes mellitus. Contemp Clin Trials 2007;28:6–17.

Stolk RP, Thom SAMcG, van Schooneveld MJ, et al. on behalf of the AdRem Project Team and ADVANCE Management Committee. Retinal vascular lesions in patients with Caucasian and Asian origin with type 2 diabetes. Baseline results from the ADVANCE Retinal Measurements (AdRem) study. Diabetes Care 2008;31:708–13.

Beulens JWJ, Patel A, Vingerling JR, et al. on behalf of the AdRem project team and ADVANCE management committee. Effects of blood pressure lowering and intensive glucose control on the incidence and progression of retinopathy in patients with type 2 diabetes mellitus: a randomised controlled trial. Diabetologia 2009;52:2027–36.

Lee CC, Stolk RP, Adler AI, et al. on behalf of the AdRem project team and ADVANCE management committee. Association between alcohol consumption and diabetic retinopathy and visual acuity – the AdRem Study. Diabet Med 2010;27:1130–7.

DA VINCI Study

Do DV, Schmidt-Erfurth U, Gonzalez VH, et al. The DA VINCI Study: Phase 2 primary results of VEGF Trap-Eye in patients with diabetic macular edema. Ophthalmology 2011;118:1819-1826.

Do DV, Nguyen QD, Boyer D, et al. for the DA VINCI Study Group. One-year outcomes of the DA VINCI study of VEGF Trap-Eye in eyes with diabetic macular edema. Ophthalmology 2012;119:1658-65.

Dexamethasone DDS Study

Haller JA, Kuppermann BD, Blumenkranz MS, et al. for the Dexamethasone DDS Phase II Study Group. Randomized controlled study of an intervitreous dexamethasone drug delivery system in patients with diabetic macular edema. Arch Ophthalmol 2010;128(3):289-96.

Kuppermann BD, Chou C, Weinberg DV, et al. for the Dexamethasone DDS Phase II Study Group. Intravitreous dexamethasone effects on different patterns of diabetic macular edema. Arch Ophthalmol 2010;128(5):642-3.

DIRECT

Sjolie AK, Klein R, Porta M, et al. for the DIRECT Programme Study Group. Effect of candesartan on progression and regression of retinopathy in type 2 diabetes (DIRECT-Protect 2): a randomised placebo-controlled trial. Lancet 2008;372:1385–93.

Chaturvedi N, Porta M, Klein R, et al. for the DIRECT Programme Study Group. Effect of candesartan on prevention (DIRECT-Prevent 1) and progression (DIRECT-Protect 1) of retinopathy in type 1 diabetes: randomised, placebo-controlled trials. Lancet 2008;372:1394–402.

Sjolie AK, Klein R, Torta M, et al. Retinal microaneurysm count predicts progression and regression of diabetic retinopathy. Post-hoc results from the DIRECT Programme. Diabet Med 2011;28:345-51.

FAME

Campochiaro PA, Brown DM, Pearson A, et al. for the FAME Study Group. Long-term benefit of sustained-delivery fluocinolone acetonide vitreous inserts for diabetic macular edema. Ophthalmology 2011;118:626-35.

Campochiaro PA, Brown DM, Pearson A, et al. for the FAME Study Group. Sustained delivery fluocinolone acetamide vitreous inserts provide benefit for at least 3 years in patients with diabetic macular edema. Ophthalmology 2012;119:2125-32.

Macugen 1013 Study

Macugen Diabetic Retinopathy Study Group. A phase II randomized double-masked trial of pegaptanib, an anti-vascular endothelial growth factor aptamer, for diabetic macular edema. Ophthalmology 2005;112:1747-57.

Sultan MB, Zhou D, Loftus J, et al. for the Macugen 1013 Study Group. A phase 2/3, multicenter, randomized, double-masked, 2-year trial of pegaptanib sodium for the treatment of diabetic macular edema. Ophthalmology 2011;118:1107-18.

Loftus JV, Sultan MB, Pleil AM for the Macugen 1013 Study Group. Changes in vision- and health-related quality of life in patients with diabetic macular edema treated with pegaptanib sodium or sham. Invest Ophthalmol Vis Sci 2013;52(10):7498-7505.

PKC-DRS Studies

PKC–DRS Study Group. The effect of ruboxistaurin on visual loss in patients with moderately severe to very severe nonproliferative diabetic retinopathy. Initial results of the Protein Kinase C β inhibitor Diabetic Retinopathy Study (PKC-DRS) multicenter randomized clinical trial. Diabetes 2005;54:2188-97.

PKC–DRS Group. Effect of ruboxistaurin on visual loss in patients with diabetic macular retinopathy. Ophthalmology

2006;113:2221-30.

Davis MD, Sheetz MJ, Aiello LP, et al. for the PKC–DRS Study Group. Effect of ruboxistaurin on the visual acuity decline associated with long-standing diabetic macular edema. Invest Ophthalmol Vis Sci 2009;50:1-4.

Sheetz MJ, Aiello LP, Shahri N, et al. for the MBDV Study Group. Effect of ruboxistaurin (RBX) on visual acuity decline over a 6-year period with cessation and reinstitution of therapy. Results of an open-label extension of the Protein Kinase C Diabetic Retinopathy Study 2 (PKC-DRS2). Retina 2011;31:1053-9.

Aiello LP, Vignati L, Sheetz MJ, et al. for the PKC–DRS and PKC–DRS2 Study Groups. Oral protein kinase C β inhibition using ruboxistaurin. Efficacy, safety, and causes of vision loss among 813 patients (1,392 eyes) with diabetic retinopathy in the Protein Kinase C β inhibitor-Diabetic Retinopathy Study and the Protein Kinase C β inhibitor-Diabetic Retinopathy Study 2. Retina 2011;31:2084-94.

READ-2

Nguyen QD, Shah SM, Heier JS, et al. for the READ-2 Study Group. Primary end point (six months) results of the Ranibizumab for Edema of the mAcula in Diabetes (READ-2) Study. Ophthalmology 2009;116:2175–81.

Nguyen QD, Shah SM, Khwaja AA, et al. for the READ-2 Study Group. Two-year outcomes of the Ranibizumab for Edema of the mAcula in Diabetes (READ-2) Study. Ophthalmology 2010;117:2146–51.

Do DV, Nguyen QD, Khwaja AA, et al. for the READ-2 Study Group. Ranibizumab for Edema of the Macula in Diabetes Study. 3-year outcomes and the need for prolonged frequent treatment. JAMA Ophthalmol 2013;131(2):130-45.

RESTORE

Mitchell P, Bandello F, Schmidt-Erfurth U et al. on behalf of the RESTORE Study Group. The RESTORE Study. Ranibizumab monotherapy or combined with laser versus laser monotherapy for diabetic macular edema. Ophthalmology 2011;118:615-25.

Mitchell P, Annemans L, Gallagher M, et al. Cost-effectiveness of ranibizumab in treatment of diabetic macular edema (DME) causing visual impairment: evidence from the RESTORE trial. Br J Ophthalmol 2012;96:688-93.

Mitchell P, Bressler N, Tolley K, et al. for the RESTORE Study Group. Patient-reported visual function outcomes improve after ranibizumab treatment in patients with vision impairment due to diabetic macular edema. Randomized clinical trial. JAMA Ophthalmol 2013;131(10):1339-47.

Lang GE, Berta A, Eldem BM, et al for the RESTORE Extension Study Group. Two-year safety and efficacy of ranibizumab 0.5 mg in diabetic macular edema. Ophthalmology 2013;120:2004-12.

Schmidt-Erfurth U, Lang GL, Holz FG, et al. on behalf of the RESTORE Extension Study Group. Three-year outcomes of individualized ranibizumab treatment of patients with diabetic macular edema. The RESTORE Extension Study. Ophthalmology 2014;121:1045-53.

RISE/RIDE

Nguyen QD, Brown DM, Marcus MD, et al. on behalf of the RISE and RIDE Research Group. Ranibizumab for diabetic macular edema. Results from 2 phase III randomized trials: RISE and RIDE. Ophthalmology 2012;119:789-801.

Brown DM, Nguyen QD, Marcus DM, et al. on behalf of the RIDE and RISE Research Group. Long-term outcomes of ranibizumab therapy for diabetic macular edema: The 36-month results from two phase III trials, RISE and RIDE. Ophthalmology 2013;120:2013-22.

Bressler NM, Varma R, Suner IJ, et al. for the RIDE and RISE Research Groups. Vision-related function after ranibizumab treatment for diabetic macular edema. Results from RIDE and RISE. Ophthalmology 2014;121:2461-2472.

Domalpally A, Ip MS, Ehrlich JS. Effects of intravitreal ranibizumab on retinal hard exudates in diabetic macular edema. Findings from the RIDE and RISE phase III clinical trials. Ophthalmology 2015;122:779-86.

Brown GC, Brown MM, Turpcu A, et al. The cost-effectiveness of ranibizumab for the treatment of diabetic macular edema. Ophthalmology 2015;122:1416-25.

VISTA and VIVID

Korobelnik J-F, Do DV, Schmidt-Urfurth U, et al. Intravitreal aflibercept for diabetic macular edema. Ophthalmology 2014;121:2247-54.

Brown DM, Schmidt-Urfurth U, Do DV, et al. Intravitreal aflibercept for diabetic macular edema. 100-week results from the VISTA and VIVID studies. Ophthalmology 2015;122:2044-52.

Other Trials

DAMAD Study Group Effect of aspirin alone and aspirin plus dipyridamole in early diabetic retinopathy: a multicenter randomized controlled clinical trial. Diabetes 1989;39:491-8.

Halbert RJ, Leung K-M, Nichol JM, et al. Effect of multiple patient reminders in improving diabetic retinopathy screening. Diabetes Care 1999;22:752-5.

Gillies MC, Simpson JM, Gaston C, et al. Five-year results of a randomized trial with open-label extension of triamcinolone acetonide for refractory diabetic macular edema. Ophthalmology 2009;116:2182–7.

Soheilian M, Ramezani A, Obudi A, et al. Randomized trial of intravitreal bevacizumab alone or combined with triamcinolone versus macular photocoagulation in diabetic macular edema. Ophthalmology 2009;116:1142-50.

Gillies MC, McAllister IL, Zhu M, et al. Pretreatment with intravitreal triamcinolone before laser for diabetic macular edema: 6-month results of a randomized, placebo-controlled trial. Invest Ophthalmol Vis Sci 2010;51(5):2322-8.

Massin P, Bandello F, Garweg JG, et al. Safety and efficacy of ranibizumab in diabetic macular edema (RESOLVE study). Diabetes Care 2010;33:2399-405.

Avitabile T, Bonfiglio V, Castiglione F, et al. Severe proliferative diabetic retinopathy treated with vitrectomy or panretinal photocoagulation: A monocenter randomized controlled clinical trial. Can J Ophthalmol 2011;46(4):345-51.

Gillies MC, McAllister IL, Zhu M, et al. Intravitreal triamcinolone prior to laser treatment of diabetic macular edema: 24-month results of a randomized controlled trial. Ophthalmology 2011;118:866-872.

Pearson PA, Comstock TI, Ip M, et al. Fluocinolone acetonide intravitreal implant for diabetic macular edema: A 3-year multicenter, randomized, controlled clinical trial. Ophthalmology 2011;118:1580-7.

Soheilian M, Garfami KH, Ramezani A, et al. Two-year results of a randomized trial of intravitreal bevacizumab alone or combined with triamcinolone versus laser in diabetic macular edema. Retina 2012;32:314-321.

Lum JX, McGhee SM, Gangwani RA, et al. Screening for diabetic retinopathy with or without a copayment in a randomized controlled trial: Influence of the inverse care law. Ophthalmology 2013;120:1247-53.

Cochrane Systematic Reviews of Interventions for Diabetic Retinopathy/Macular Edema

Martine-Zapata MJ, Marti-Carvajal AJ, Sola I, et al. Anti-vascular endothelial growth factor for proliferative diabetic retinopathy. Cochrane Database of Systematic Reviews 2014, Issue 11, Art. No.: CD008721. doi: 10.1002/14651858.CD008721.pub2.

Virgili G, Parravano M, Menchini F, et al. Anti-vascular endothelial growth factor for diabetic macular edema. Cochrane Database of Systematic Reviews 2014, Issue 10, Art. No.: CD007419. doi: 10.1002/14651858.CD007419.pub4.

Evans JR, Michelessi M, Virgili G. Laser photocoagulation for proliferative diabetic retinopathy. Cochrane Database of Systematic Reviews 2014, Issue 11, Art. No.: CD011234. doi: 10.1002/14651858/CD011234.pub2.

Do DV, Wang X, Vedula SS, et al. Blood pressure control for diabetic retinopathy. Cochrane Database of Systematic Reviews 2015, Issue 1, Art. No.: CD006127. doi: 10.1002/14651858/CD006127.pub2.

Vein Occlusions

Branch Vein Occlusion Study (BVOS)

The BVOS was sponsored by the National Eye Institute and designed to assess in eyes with retinal branch vein occlusion whether scatter photocoagulation could prevent development of neovascularization, peripheral scatter photocoagulation could prevent vitreous hemorrhage, and macular photocoagulation would improve visual acuity in eyes with macular edema and visual acuity of 20/40 or worse. Argon laser photocoagulation improved visual acuity in eyes with macular edema secondary to retinal branch vein occlusion, macular edema, and visual acuity of 20/40 or worse, with a gain of 2 or more lines of visual acuity in

more laser-treated eyes than untreated eyes.

Finkelstein D, Clarkson J, Diddie K, et al. Branch vein occlusion: retinal neovascularization outside the involved segment. Ophthalmology 1982;89:1357–61.

Branch Vein Occlusion Study Group. Argon laser photocoagulation for macular edema in branch vein occlusion. Am J Ophthalmol 1984;98:271–82.

Branch Vein Occlusion Study Group. Argon laser scatter photocoagulation for prevention of neovascularization and vitreous hemorrhage in branch vein occlusion: a randomized clinical trial. Arch Ophthalmol 1986;104:34–41.

Central Vein Occlusion Study (CVOS)

The CVOS included two randomized trials and two observational studies in its design. The goals of the CVOS were: (1) to determine whether photocoagulation therapy could prevent iris neovascularization in eyes with central vein occlusion and evidence of ischemic retina; (2) to assess whether grid photocoagulation could reduce loss of central visual acuity due to macular edema secondary to central vein occlusion; and (3) to describe the course and prognosis for eyes with central vein occlusion.

Central Vein Occlusion Study Group. Central Vein Occlusion Study of photocoagulation. Manual of operations. Online J Curr Clin Trials 1993,Oct 2; Doc. No. 92.

Central Vein Occlusion Study Group. Baseline and early natural history report. The Central Vein Occlusion Study. Arch Ophthalmol 1993;111:1087–95.

Clarkson JG, Central Vein Occlusion Study Group. Central Vein Occlusion Study: Photographic protocol and early natural history. Trans Am Ophthalmol Soc 1994;92:203–13.

Central Vein Occlusion Study Group. Evaluation of grid pattern photocoagulation for macular edema in central vein occlusion.

The Central Vein Occlusion Study Group M report. Ophthalmology 1995;102:1425–33.

Central Vein Occlusion Study Group. A randomized clinical trial of early panretinal photocoagulation for ischemic central vein occlusion. The Central Vein Occlusion Study Group N report. Ophthalmology 1995;102:1434–4.

Central Vein Occlusion Study Group. Natural history and clinical management of central retinal vein occlusion. Arch Ophthalmol 1997;115:486–91.

Standard Care vs COrticosteroid for REtinal Vein Occlusion Study (SCORE)

Scott IU, VanVeldhuisen PC, Oden N, et al., SCORE Study Investigator Group. SCORE Study report 1: Baseline associations between central retinal thickness and visual acuity in patients with retinal vein occlusion. Ophthalmology 2009;116(3):504–12.

Scott IU, Blodi BA, Ip MS, et al., SCORE Study Investigator Group. SCORE Study report 2: Interobserver agreement between investigator and reading center classification of retinal vein occlusion type. Ophthalmology 2009;116(4):756–61.

Ip MS, Oden NL, Scott IU, et al., SCORE Study Investigator Group. SCORE Study report 3: Study design and baseline characteristics. Ophthalmology 2009;116(9):1770–7.

Domalpally A, Blodi BA, Scott IU, et al., SCORE Study Investigator Group. The Standard Care vs. Corticosteroid for Retinal Vein Occlusion (SCORE) Study system for evaluation of optical coherence tomograms: SCORE Study report no. 4. Arch Ophthalmol 2009;127(11):1461–7.

Ip MS, Scott IU, VanVeldhuisen PC, et al., SCORE Study Research Group. A randomized trial comparing the efficacy and safety of intravitreal triamcinolone with observation to treat vision loss

associated with macular edema secondary to central vein occlusion: Standard Care vs Corticosteroid for Retinal Vein Occlusion (SCORE) Study report no. 5. Arch Ophthalmol 2009;127(6):1101–4.

Scott IU, Ip MS, VanVeldhuisen PC, et al., SCORE Study Research Group. A randomized trial comparing the efficacy and safety of intravitreal triamcinolone with standard care to treat vision loss associated with macular edema secondary to branch retinal vein occlusion: Standard Care vs Corticosteroid for Retinal Vein Occlusion (SCORE) Study report no. 6. Arch Ophthalmol 2009;127(9):1115–28.

Scott IU, Oden NL, VanVeldhuissen PC, et al., SCORE Study Investigator Group. SCORE Study report 7: Incidence of intravitreal silicone oil droplets associated with staked-on vs Luer cone syringe design. Am J Ophthalmol 2009;148(5):725–32.

Oden N, VanVeldhuisen PC, Scott IU, et al., SCORE Study Investigator Group. SCORE Study report 8: Closed tests for all pairwise comparisons of means. Drug Inform J 2010;44:405–20.

Blodi BA, Domalpally AM, Scott IU, et al. for the SCORE Study Research Group. Standard Care vs. Corticosteroid for Retinal Vein Occlusion (SCORE) Study system for evaluation of stereoscopic color fundus photographs and fluorescein angiograms. SCORE Study Report 9. Arch Ophthalmol 2010;128(9):1140–5.

Scott IU, VanVeldhuisen PC, Oden NL, for the Standard Care versus COrticosteroid for REtinal Vein Occlusion Study Investigator Group. Baseline predictors of visual acuity and retinal thickness outcomes in patients with retinal vein occlusion: Standard Care versus Corticosteroid for Retinal Vein Occlusion Study report 10. Ophthalmology 2011;118:345–52.

Chan CK, Ip MS, VanVeldhuisen PC, et al. for the SCORE Study Investigator Group. SCORE Study report no. 11. Incidences of neovascular events in eyes with retinal vein occlusion.

Ophthalmology 2011;118:1364–72.

Weinberg DV, Wahle AE, Ip MS, et al. for the SCORE Study Investigator Group. SCORE Study report 12. Development of venous collaterals in the Score [sic] Study. Retina 2013;33:287-95.

Domalpally A, Peng Q, Danis R, et al. and the SCORE Study Research Group. Association of outer retinal layer morphology with visual acuity in patients with retinal vein occlusion: SCORE Study report 13. Eye 2012;26:919-24.

Scott IU, VanVeldhuisen PC, Oden NL, et al. for the SCORE Study Investigator Group. Baseline characteristics and response to treatment in participants with hemiretinal compared with branch retinal or central retinal vein occlusion in the Standard Care vs COrticosteroid for REtinal Vein Occlusion (SCORE) Study. SCORE Study report 14. Arch Ophthalmol 2012;130(12):1517-24.

Aref AA, Scott IU, Oden NL, et al. for the SCORE Study Investigative Group. Incidence, risk factors, and timing of elevated intraocular pressure after intravitreal triamcinolone acetonide injection for macular edema secondary to retinal vein occlusion. SCORE Study report 15. JAMA Ophthalmol 2015;133(9):1022-9.

BRAVO

Campochiaro PA, Heier JS, Feiner L, et al. for the BRAVO Investigators. Ranibizumab for macular edema following branch retinal vein occlusion: six-month primary end point results of a phase III study. Ophthalmology 2010;117:1102–12.

Brown DM, Campochiaro PA, Bhisitkul RB, et al. Sustained benefit from ranibizumab for macular edema following branch retinal vein occlusions: 12-month outcomes of a phase III study. Ophthalmology 2011;118:1594–602.

Bhisukul RB, Campochiaro PA, Shapiro H, et al. Predictive value in retinal vein occlusions of early versus late or incomplete

ranibizumab response defined by optical coherence tomography. Ophthalmology 2013;120:1057-63.

COPERNICUS

Boyer D, Heier J, Brown DM, et al. Vascular endothelial growth factor Trap-Eye for macular edema secondary to central retinal vein occlusion. Six-month results of the phase 3 COPERNICUS Study. Ophthalmology 2012;119:1024-32.

Brown DM, Heier JS, Clark L, et al. Intravitreal aflibercept injection for macular edema secondary to central retinal vein occlusion: 1-year results from the phase 3 COPERNICUS Study. Am J Ophthalmol 2013;155(3):429-37.

GALILEO

Holz FG, Roider J, Ogura Y, et al. VEGF Trap-Eye for macular oedema secondary to central retinal vein occlusion: 6-month results of the phase III GALILEO study. Br J Ophthalmol 2013:97:278-84.

Korobelnik J-F, Holz FG, Roider J, et al. for the GALILEO Study Group. Intravitreal aflibercept injection for macular edema resulting from central retinal vein occlusion. One-year results of the phase 3 GALILEO Study. Ophthalmology 2014;121:202-208.

GENEVA

Haller JA, Bandello F, Belfort R, et al. for the OZURDEX GENEVA Study Group. Randomized, sham-controlled trial of dexamethasone intravitreal implant in patients with macular edema due to retinal vein occlusion. Ophthalmology 2010;117:1134-48.

Haller JA, Bandello F, Belfort R, for the Ozurdex GENEVA Study Group. Dexamethasone intravitreal implant in patients with macular edema related to branch or central retinal vein occlusion.

Twelve-month study results. Ophthalmology 2011;118:2453-60.

Yeh W-S, Haller JA, Lanzetta P, et al. Effect of the duration of macular edema on clinical outcomes in retinal vein occlusion treated with dexamethasone intravitreal implant. Ophthalmology 2012;119:1180-8.

Kuppermann BD, Haller JA, Bandello F, et al. Onset and duration of visual acuity improvement after dexamethasone intravitreal implant in eyes with macular edema due to retinal vein occlusion. Retina 2014;34:1743-9.

CRUISE, HORIZON, SHORE

Brown DM, Campochiaro PA, Singh RP, et al. for the CRUISE Investigators. Ranibizumab for macular edema following central retinal vein occlusion. Six-month primary end point results of a phase III study. Ophthalmology 2010;117:1124–39.

Heier JS, Campochiaro PA, Yau L, et al. Ranibizumab for macular edema due to retinal vein occlusions: long-term follow-up in the HORIZON trial. Ophthalmology 2012;119:802-9.

Campochiaro PA, Wykoff CC, Singer M, et al. Monthly versus as-needed ranibizumab injections in patients with retinal vein occlusion. The SHORE Study. Ophthalmology 2014;121:2432-42.

Cochrane Systematic Reviews

Mitry D, Bunce C, Charteris D. Anti-vascular endothelial growth factor for macular oedema secondary to branch retinal vein occlusion. Cochrane Database of Systematic Reviews. 2013, Issue 1, Art. No.: CD009510. doi: 10.1002/14651858.CD009510.pub2.

Braithwaite T, Nanji AA, Lindsley K, et al. Anti-vascular endothelial growth factor for macular oedema secondary to central retinal vein occlusion. Cochrane Database of Systematic Reviews 2014, Issue 5, Art. No.: CD007325. doi:

10.1002/14651858.CD007325.pub3.

Lam FC, Chia SN, Lee RMH. Macular grid laser photocoagulation for branch retinal vein occlusion. Cochrane Database of Systematic Reviews 2015, Issue 5, Art. No.: CD008732. doi: 10.1002/14651858.CD008732.pub2.

Gewaily D, Muthuswamy K, Greenberg PB. Intravitreal steroids versus observation for macular edema secondary to central retinal vein occlusion. Cochrane Database of Systematic Reviews 2015, Issue 9, Art. No. 007324. doi: 10.1002/14651858.CD007324.pub3.

Age-Related Macular Degeneration and Other Conditions Associated With Choroidal Neovascularization

Because of the numerous trials that have been conducted for these conditions during the past three decades, the clinical trials cited have been subdivided by type of intervention. A Cochrane systematic review has summarized the findings from all Cochrane reviews of interventions for neovascular age-related macular degeneration:

Evans JR, Virgili G, Gordon I, et al. Interventions for neovascular age-related macular degeneration. Cochrane Database of Systematic Reviews 2009, Issue 1, Art. No.: CD007650. doi: 10.1002/14651858.CD007650.

Laser Treatment

Macular Photocoagulation Study (MPS)

The MPS was initiated in 1979 under the sponsorship of the National Eye Institute to evaluate laser photocoagulation for choroidal neovascularization secondary to age-related macular degeneration and ocular histoplasmosis. In addition, small trials of laser photocoagulation for idiopathic choroidal neovascularization

were conducted. In total, the MPS Group conducted eight multicenter randomized trials of laser photocoagulation of choroidal neovascularization. The 1982 publication from the MPS Study Group reports the early results of the first randomized trial to demonstrate a benefit of a treatment for this retinal disorder. Findings from the MPS trials informed both scientific and methodologic aspects of the designs of many subsequent trials of treatments for neovascular age-related macular degeneration.

Macular Photocoagulation Study Group. Argon laser photocoagulation for senile macular degeneration: results of a randomized clinical trial. Arch Ophthalmol 1982;100:912–8.

Macular Photocoagulation Study Group. Argon laser photocoagulation for ocular histoplasmosis: results of a randomized clinical trial. Arch Ophthalmol 1983;101:1347–57.

Macular Photocoagulation Study Group. Argon laser photocoagulation for idiopathic neovascularization: results of a randomized clinical trial. Arch Ophthalmol 1983;101:1358–61.

Macular Photocoagulation Study Group. Recurrent choroidal neovascularization after argon laser photocoagulation for neovascular maculopathy. Arch Ophthalmol 1986;104:503–12.

Macular Photocoagulation Study Group. Argon laser photocoagulation for neovascular maculopathy: three-year results from randomized clinical trials. Arch Ophthalmol 1986;104:694–701.

Macular Photocoagulation Study Group. Krypton laser photocoagulation for neovascular lesions of ocular histoplasmosis: results of a randomized clinical trial. Arch Ophthalmol 1987;105:1499–1507.

Macular Photocoagulation Study Group. Persistent and recurrent neovascularization after krypton laser photocoagulation for neovascular lesions of ocular histoplasmosis. Arch Ophthalmol 1989;107:344–52.

Chamberlin JA, Bressler NM, Bressler SB, et al. The use of fundus photographs and fluorescein angiograms in the identification and treatment of choroidal neovascularization in the Macular Photocoagulation Study. Ophthalmology 1989;96:1526–34.

Macular Photocoagulation Study Group. Krypton laser photocoagulation for neovascular lesions of age-related macular degeneration: results of a clinical trial. Arch Ophthalmol 1990;108:816–24.

Macular Photocoagulation Study Group. Persistent and recurrent neovascularization after krypton laser photocoagulation for neovascular lesions of age-related macular degeneration. Arch Ophthalmol 1990;108:825–31.

Macular Photocoagulation Study Group. Krypton laser photocoagulation for idiopathic neovascular lesions: results of a randomized clinical trial. Arch Ophthalmol 1990;108:832–7.

Bressler SB, Maguire MG, Bressler NM, et al. Relationship of drusen and abnormalities of the retinal pigment epithelium to the prognosis of neovascular macular degeneration. Arch Ophthalmol 1990;108:1442–7.

Folk JC, Blackhurst DW, Alexander J, et al. Pretreatment fundus characteristics as predictors of recurrent choroidal neovascularization. Arch Ophthalmol 1991;109:1193–4.

Macular Photocoagulation Study Group. Argon laser photocoagulation for neovascular maculopathy: five-year results from randomized clinical trials. Arch Ophthalmol 1991;109:1109–14.

Macular Photocoagulation Study Group. Laser photocoagulation of subfoveal neovascular lesions in age-related macular degeneration: results of a randomized clinical trial. Arch Ophthalmol 1991;109:1220–31.

Macular Photocoagulation Study Group. Laser photocoagulation of subfoveal recurrent neovascular lesions in age-related macular

degeneration: results of a randomized clinical trial. Arch Ophthalmol 1991;109:1232–41.

Macular Photocoagulation Study Group. Subfoveal neovascular lesions in age-related macular degeneration: guidelines for evaluation and treatment in the Macular Photocoagulation Study. Arch Ophthalmol 1991;109:1242–57.

Fine SL, Wood WJ, Singerman LJ, et al. Laser treatment for subfoveal neovascular membranes in ocular histoplasmosis syndrome: results of a pilot randomized clinical trial. Arch Ophthalmol 1993;111:19–20.

Macular Photocoagulation Study Group. Five-year follow-up of fellow eyes of patients with age-related macular degeneration and unilateral extrafoveal choroidal neovascularization. Arch Ophthalmol 1993;111:1189–99.

Macular Photocoagulation Study Group. Laser photocoagulation of subfoveal neovascular lesions of age-related macular degeneration. Updated findings from two clinical trials. Arch Ophthalmol 1993;111:1200–9.

Macular Photocoagulation Study Group. Visual outcome after laser photocoagulation for subfoveal choroidal neovascularization secondary to age-related macular degeneration: the influence of initial lesion size and initial visual acuity. Arch Ophthalmol 1994;112:480–8.

Macular Photocoagulation Study Group. Persistent and recurrent neovascularization after laser photocoagulation for subfoveal choroidal neovascularization of age-related macular degeneration. Arch Ophthalmol 1994;112:489–99.

Macular Photocoagulation Study Group. Laser photocoagulation for juxtafoveal choroidal neovascularization. Five-year results from randomized clinical trials. Arch Ophthalmol 1994;112:500–9.

Macular Photocoagulation Study (MPS) Group. Evaluation of argon green vs krypton red laser for photocoagulation of subfoveal

choroidal neovascularization in the Macular Photocoagulation Study. Arch Ophthalmol 1994;112:1176–84.

Macular Photocoagulation Study Group. Laser photocoagulation for neovascular lesions nasal to the fovea. Results from clinical trials for lesions secondary to ocular histoplasmosis or idiopathic causes. Arch Ophthalmol 1995;113:56–61.

Macular Photocoagulation Study Group. The influence of treatment extent on the visual acuity of eyes treated with krypton laser for juxtafoveal choroidal neovascularization. Arch Ophthalmol 1995;113:190–4.

Macular Photocoagulation Study Group. Occult choroidal neovascularization. Influence on visual outcome in patients with age-related macular degeneration. Arch Ophthalmol 1995;114:400–12.

Macular Photocoagulation Study Group. Five-year follow-up of fellow eyes of individuals with ocular histoplasmosis and unilateral extrafoveal or juxtafoveal choroidal neovascularization. Arch Ophthalmol 1996;114:677–88.

Macular Photocoagulation Study Group. Risk factors for choroidal neovascularization in the second eye of patients with juxtafoveal or subfoveal choroidal neovascularization secondary to age-related macular degeneration. Arch Ophthalmol 1997;115:741–7.

Jefferys JL, Alexander J, Hiner CJ, et al. for the Macular Photocoagulation Study Group. Reproducibility of gradings of retinal photographs of eyes with subfoveal choroidal neovascularization and age-related macular degeneration in the Macular Photocoagulation Study. Ophthalmic Epidemiol 2008;15:191–201.

Complications of AMD Prevention Trial (CAPT)

CAPT was a multicenter randomized trial designed to evaluate low-intensity laser treatment of large drusen as a method of preventing vision loss among patients at risk of choroidal

neovascularization and other manifestations of advanced age-related macular degeneration. CAPT was preceded by a pilot study, the Choroidal Neovascularization Prevention Trial (CNVPT).

Choroidal Neovascularization Prevention Trial Research Group. Laser treatment in eyes with large drusen: short-term effects seen in a pilot randomized clinical trial. Ophthalmology 1998;105:11–23.

Choroidal Neovascularization Prevention Trial Research Group. Choroidal neovascularization in the Choroidal Neovascularization Prevention Trial. Ophthalmology 1998;105:1364–72.

Ho AC, Maguire MG, Yoken et al., Choroidal Neovascularization Prevention Trial Research Group. Laser-induced drusen reduction improves visual function at 1 year. Ophthalmology 1999;106:1367-74.

Kaiser RS, Berger JW, Maguire MG, et al., Choroidal Neovascularization Prevention Trial Research Group. Laser burn intensity and the risk for choroidal neovascularization in the CNVPT fellow eye study. Arch Ophthalmol 2001;119:826–32.

Choroidal Neovascularization Prevention Trial Research Group. Laser treatment in fellow eyes with large drusen: updated findings from a pilot randomized clinical trial. Ophthalmology 2003;110:971–8.

Complications of Age-related Macular Degeneration Prevention Trial Study Group. Complications of Age-related Macular Degeneration Prevention Trial (CAPT): rationale, design and methodology. Clin Trials 2004;1:91–107.

Complications of Age-related Macular Degeneration Prevention Trial Research Group. Baseline characteristics, the 25-item National Eye Institute Visual Functioning Questionnaire, and their associations in the Complications of Age-related Macular Degeneration Prevention Trial (CAPT). Ophthalmology

2004;111:1307–16.

Complications of Age-related Macular Degeneration Prevention Trial Research Group. Laser treatment in patients with bilateral large drusen. Ophthalmology 2006;113:1974–86.

Maguire MG, Alexander J, Fine SL and the Complications of Age-related Macular Degeneration Prevention Trial (CAPT) Research Group. Characteristics of choroidal neovascularization in the Complications of Age-related Macular Degeneration Prevention Trial. Ophthalmology 2008;115:1468–73.

Complications of Age-related Macular Degeneration Prevention Trial (CAPT) Research Group. Risk factors for choroidal neovascularization and geographic atrophy in the Complications of Age-related Macular Degeneration Prevention Trial. Ophthalmology 2008;115:1474–9.

Ying G, Maguire MG, Liu C, et al. for the Complications of Age-related Macular Degeneration Prevention Trial Research Group. Night vision symptoms and progression of age-related macular degeneration in the Complications of Age-related Macular Degeneration Prevention Trial. Ophthalmology 2008;115:1876–82.

Ying G, Maguire MG, Alexander J, et al. for the Complications of Age-Related Macular Degeneration Prevention Trial (CAPT) Research Group. Description of the Age-related Eye Disease Study 9-step severity scale applied to participants in the Complications of Age-related Macular Degeneration Prevention Trial. Arch Ophthalmol 2009;127:1147–51.

Maguire MG, Ying G, McCannel CA, et al. for the Complications of Age-related Macular Degeneration Prevention Trial (CAPT) Research Group. Statin use and the incidence of advanced age-related macular degeneration in the Complications of Age-related Macular Degeneration Prevention Trial. Ophthalmology 2009;116:2381–5.

Ying G, Maguire MG for the Complications of Age-related Macular

Degeneration Prevention Trial Research Group. Development of a risk score for geographic atrophy in [the] Complications of Age-related Macular Degeneration Prevention Trial. Ophthalmology 2011;118:332–8.

Brader HS, Ying G-S, Martin ER, et al., for the Complications of Age-Related Macular Degeneration Trial (CAPT) Research Group. Characteristics of incident geographic atrophy in the Complications of Age-Related Macular Degeneration Prevention Trial. Ophthalmology 2013;120:1871-1879.

Prophylactic Treatment of Nonexudative Age-Related Macular Degeneration (PTAMD)

Olk RJ, Friberg TR, Stickney KL, et al. Therapeutic benefits of infrared (810-nm) diode laser macular grid photocoagulation in prophylactic treatment of neoexudative age-related macular degeneration. Two-year results of a randomized pilot study. Ophthalmology 1999;106:2082–90.

Friberg TR, Musch DC, Lim JI, et al. PTAMD Study Group. Prophylactic Treatment of Age-related Macular Degeneration report number 1: 810-nanometer laser to eyes with drusen. Unilaterally eligible patients. Ophthalmology 2006;113:612–22.

Drusen Laser Study

Owens SL, Bunce C, Brannon AJ, et al., Drusen Laser Study Group. Prophylactic laser treatment appears to promote choroidal neovascularization in high-risk ARM: results of an interim analysis. Eye 2003;17:623-7.

Owens SL, Bunce C, Brannon AJ, et al., Drusen Laser Study Group. Prophylactic laser treatment hastens choroidal neovascularization in unilateral age-related maculopathy: Final results of the Drusen Laser Study. Am J Ophthalmol 2006;141:276-81.

Other Trials of Laser to Treat or Prevent Choroidal Neovascularization

Moorfields Macular Study Group. Treatment of senile disciform macular degeneration: a single-blind randomized trial by argon laser photocoagulation. Br J Ophthalmol 1982;66:745-53.

Yassur Y, Axer-Siegel R, Gohen S, et al. Treatment of neovascular senile maculopathy at the foveal capillary free zone with red krypton laser. Retina 1982;2:127-33.

Coscas G, Soubrane G, Ramahefasolo C, et al. Perifoveal laser treatment for subfoveal choroidal new vessels in age-related macular degeneration: results of a randomized clinical trial. Arch Ophthalmol 1991;109:1258–65.

Canadian Ophthalmology Study Group. Argon green vs krypton red laser photocoagulation of extrafoveal choroidal neovascular lesions: one-year results in age-related macular degeneration. Arch Ophthalmol 1993;111:181–5.

Canadian Ophthalmology Study Group. Argon green vs krypton red laser photocoagulation for extrafoveal choroidal neovascularization. One-year results in ocular histoplasmosis. Arch Ophthalmol 1994;112:1166–73.

Cochrane Systematic Reviews

Virgili G, Bini A. Laser photocoagulation for neovascular age-related macular degeneration. Cochrane Database of Systematic Reviews 2007, Issue 3, Art. No.: CD004763. doi: 10.1002/14651858.CD004763.pub2.

Parodi MB, VIrgili G, Evans JR. Laser treatment of drusen to prevent progression to advanced age-related macular degeneration. Cochrane Database of Systematic Reviews 2009, Issue 3, Art. No.: CD006537. doi: 10.1002/14651858.CD006537.pub2.

Photodynamic Therapy

Multicenter randomized clinical trials of verteporfin were initiated

in 1996 under industry sponsorship.

Treatment of Age-Related Macular Degeneration With Photodynamic Therapy (TAP) and Verteporfin in Photodynamic Therapy (VIP)

Treatment of Age-Related Macular Degeneration with Photodynamic Therapy (TAP) Study Group. Photodynamic therapy of subfoveal choroidal neovascularization in age-related macular degeneration with verteporfin: one-year results of 2 randomized clinical trials – TAP report 1. Arch Ophthalmol 1999;117:1329–45.

Treatment of Age-Related Macular Degeneration with Photodynamic Therapy (TAP) Study Group. Photodynamic therapy of subfoveal choroidal neovascularization in age-related macular degeneration with verteporfin: two-year results of 2 randomized clinical trials – TAP report 2. Arch Ophthalmol 2001;119:198–207.

Treatment of Age-Related Macular Degeneration with Photodynamic Therapy (TAP) Study Group. Verteporfin therapy of subfoveal choroidal neovascularization in patients with age-related macular degeneration: additional information regarding baseline lesion composition's impact on vision outcomes – TAP report no. 3. Arch Ophthalmol 2002;120:1443–54.

Rubin GS, Bressler NM, Treatment of Age-Related Macular Degeneration with Photodynamic Therapy (TAP) Study Group. Effects of verteporfin therapy on contrast sensitivity: results from the Treatment of Age-Related Macular Degeneration with Photodynamic Therapy (TAP) investigation – TAP report no. 4. Retina 2002;22:536–44.

Treatment of Age-Related Macular Degeneration with Photodynamic Therapy (TAP) Study Group. Verteporfin therapy for subfoveal choroidal neovascularization in age-related macular degeneration: three-year results of an open-label extension of 2 randomized clinical trials – TAP report no. 5. Arch Ophthalmol

2002;120:1307–14.

Bressler SB, Pieramici DJ, Koester JM, et al. Natural history of minimally classic subfoveal choroidal neovascular lesions in the Treatment of Age-Related Macular Degeneration with Photodynamic Therapy (TAP) investigation. Outcomes potentially relevant to management – TAP report no. 6. Arch Ophthalmol 2004;122:325–9.

Verteporfin in Photodynamic Therapy (VIP) Study Group. Photodynamic therapy of subfoveal choroidal neovascularization in pathologic myopia with verteporfin. 1-year results of a randomized clinical trial – VIP report no. 1. Ophthalmology 2001;108:841–52.

Verteporfin in Photodynamic Therapy Study Group. Verteporfin therapy of subfoveal choroidal neovascularization in age-related macular degeneration: two-year results of a randomized clinical trial including lesions with occult with no classic choroidal neovascularization – Verteporfin in Photodynamic Therapy report no. 2. Am J Ophthalmol 2001;131:541–60.

Verteporfin in Photodynamic Therapy (VIP) Study Group. Verteporfin therapy of subfoveal choroidal neovascularization in pathologic myopia: 2-year results of a randomized clinical trial – VIP report no. 3. Ophthalmology 2003;110:667–73.

Treatment of Age-Related Macular Degeneration with Photodynamic Therapy (TAP) and Verteporfin in Photodynamic Therapy (VIP) Study Groups. Effect of baseline lesion size, visual acuity, and lesion composition on visual acuity changes from baseline with and without verteporfin therapy in choroidal neovascularization secondary to age-related macular degeneration – TAP and VIP report no. 1. Am J Ophthalmol 2003;136:407–18.

Treatment of Age-Related Macular Degeneration with Photodynamic Therapy (TAP) and Verteporfin in Photodynamic Therapy (VIP) Study Groups. Photodynamic therapy of subfoveal

choroidal neovascularization with verteporfin. Fluorescein angiographic guidelines for evaluation and treatment – TAP and VIP report no. 2. Arch Ophthalmol 2003;121:1253–68.

Treatment of Age-Related Macular Degeneration with Photodynamic Therapy (TAP) and Verteporfin in Photodynamic Therapy (VIP) Study Groups. Acute severe visual acuity decrease after photodynamic therapy with verteporfin: case reports from randomized clinical trials – TAP and VIP report no. 3. Am J Ophthalmol 2004;137:683–96.

Treatment of Age-Related Macular Degeneration with Photodynamic Therapy (TAP) and Verteporfin in Photodynamic Therapy (VIP) Study Groups. Verteporfin therapy of subfoveal choroidal neovascularization in age-related macular degeneration: meta-analysis of 2-year safety results in three randomized clinical trials: TAP and VIP report no. 4. Retina 2004;24:1–12.

Other Trials

Japanese Age-Related Macular Degeneration Trial (JAT) Study Group. Japanese Age-Related Macular Degeneration Trial (JAT): 1-year results of photodynamic therapy with verteporfin in Japanese patients with subfoveal choroidal neovascularization secondary to age-related macular degeneration. Am J Ophthalmol 2003;136:1049–61.

Schmidt-Erfurth U, Sacu S for the Early Retreatment Study Group. Randomized multicenter trial of more intense and standard early verteporfin treatment of neovascular age-related macular degeneration. Ophthalmology 2008;115:134-40.

Cochrane Systematic Review

Wormald R, Evans JR, Smeeth LL, et al. Photodynamic therapy for neovascular age-related macular degeneration. Cochrane Database of Systematic Reviews 2007, Issue 3, Art. No.: CD002030. doi: 10.1002/14651858.CD002030.pub3.

Surgical Removal of Choroidal Neovascularization

Submacular Surgery Trials (SST)

Grossniklaus HE, Green WR, for the Submacular Surgery Trials Research Group. Histopathologic and ultrastructural findings of surgically excised choroidal neovascularization. Arch Ophthalmol 1998;116:745–9.

Submacular Surgery Trials Pilot Study Investigators. Submacular Surgery Trials randomized pilot trial of laser photocoagulation versus surgery for recurrent choroidal neovascularization secondary to age-related macular degeneration. I. Ophthalmic outcomes. Submacular Surgery Trials Pilot Study report number 1. Am J Ophthalmol 2000;130:387–407.

Submacular Surgery Trials Pilot Study Investigators. Submacular Surgery Trials randomized pilot trial of laser photocoagulation versus surgery for recurrent choroidal neovascularization secondary to age-related macular degeneration. II. Quality of life outcomes. Submacular Surgery Trials Pilot Study report number 2. Am J Ophthalmol 2000;130:408–18.

Submacular Surgery Trials Research Group. Responsiveness of the National Eye Institute Visual Function Questionnaire to changes in visual acuity: findings in patients with subfoveal choroidal neovascularization. SST report no. 1. Arch Ophthalmol 2003;121:531–9, [Correction: Arch Ophthalmol 2003;121:1513.]

Submacular Surgery Trials Research Group. Clinical trial performance of community-based compared with university-based practices: lessons from the Submacular Surgery Trials. SST report no. 2. Arch Ophthalmol 2004;122:857–63.

Childs AL, the Submacular Surgery Trials Patient-Centered Outcomes Subcommittee for the Submacular Surgery Trials Pilot Study Investigators. Responsiveness of the SF-36 Health Survey to changes in visual acuity among patients with subfoveal

choroidal neovascularization. Am J Ophthalmol 2004;137:373–5.

Sadda SR, Pieramici DJ, Marsh MJ, et al. Changes in lesion size after submacular surgery for subfoveal choroidal neovascularization in the Submacular Surgery Trials Pilot Study. Retina 2004;24:888–99.

Orr PR, Marsh MJ, Hawkins BS, et al. Evaluation of the Traveling Vision Examiner Program of the Submacular Surgery Trials Pilot Study. Ophthalmic Epidemiol 2005;12:47–57.

Submacular Surgery Trials Research Group. Effect of order of administration of health-related quality of life instruments on responses. SST report no. 3. Qual Life Res 2005;14:493–500.

Submacular Surgery Trials Research Group. Health- and vision-related quality of life among patients with choroidal neovascularization secondary to age-related macular degeneration at time of enrollment in randomized trials of submacular surgery. SST report no. 4. Am J Ophthalmol 2004;138:91–108.

Submacular Surgery Trials Research Group. Health- and vision-related quality of life among patients with ocular histoplasmosis or idiopathic choroidal neovascularization at time of enrollment in a randomized trial of submacular surgery. Submacular Surgery Trials report no. 5. Arch Ophthalmol 2005;123:78–88.

Submacular Surgery Trials Research Group. Patients' perceptions of the value of current vision: assessment of preference values among patients with subfoveal choroidal neovascularization – the Submacular Surgery Trials (SST) Vision Preference Value Scale: SST report no. 6. Arch Ophthalmol 2004;122:1856–67.

Submacular Surgery Trials Research Group. Histopathological and ultrastructural features of surgically-excised subfoveal choroidal neovascular lesions: SST report no. 7. Arch Ophthalmol 2005;123:914–21.

Submacular Surgery Trials Research Group. Guidelines for interpreting retinal photographs and coding findings in the

Submacular Surgery Trials (SST): SST report no. 8. Retina 2005;25:253–68.

Submacular Surgery Trials Research Group. Surgical removal versus observation for subfoveal choroidal neovascularization, either associated with the ocular histoplasmosis syndrome or idiopathic. I. Ophthalmic findings from a randomized clinical trial: Submacular Surgery Trials Group H Trial. SST report no. 9. Arch Ophthalmol 2004;122:1597–611.

Submacular Surgery Trials Research Group. Surgical removal versus observation for subfoveal choroidal neovascularization, either associated with the ocular histoplasmosis syndrome or idiopathic. II. Quality-of-life findings from a randomized clinical trial: SST Group H Trial. SST report no. 10. Arch Ophthalmol 2004;122:1616–28.

Submacular Surgery Trials Research Group. Surgery for subfoveal choroidal neovascularization in age-related macular degeneration: ophthalmic findings. SST report no. 11. Ophthalmology 2004;111:1967–80.

Submacular Surgery Trials Research Group. Surgery for subfoveal choroidal neovascularization in age-related macular degeneration: quality-of-life findings. SST report number 12. Ophthalmology 2004;111:1981–92.

Submacular Surgery Trials Research Group. Surgery for hemorrhagic choroidal neovascular lesions of age-related macular degeneration: ophthalmic findings. SST report no. 13. Ophthalmology 2004;111:1993–2006.

Submacular Surgery Trials Research Group. Surgery for hemorrhagic choroidal neovascular lesions of age-related macular degeneration: quality-of-life findings. SST report no. 14. Ophthalmology 2004;111:2007–14.

Miskala PH, Bresser NB, Meinert CL. Relative contributions of reduced vision and general health to NEI-VFQ scores in patients

with neovascular age-related macular degeneration. Arch Ophthalmol 2004;122:758-66.

Miskala PH, Bressler NM, Meinert CL. Is adjustment of National Eye Institute Visual Function Questionnaire scores for general health necessary in randomized trials? Am J Ophthalmol 2004;137:961-3.

Submacular Surgery Trials Research Group. Comparison of 2D reconstructions of surgically excised subfoveal choroidal neovascularization with fluorescein angiographic features: SST report no. 15. Ophthalmology 2006;113:267–79.

Grossniklaus HE, Wilson DJ, Bressler SB, et al., for the Submacular Surgery Trials Research Group. Clinicopathologic studies of eyes that were obtained postmortem from four patients who were enrolled in the Submacular Surgery Trial: SST report no. 16. Am J Ophthalmol 2006;141:93–104.

Submacular Surgery Trials Research Group. Surgical removal vs observation for idiopathic or ocular histoplasmosis syndrome-associated subfoveal choroidal neovascularization. III. Vision Preference Value Scale findings from the randomized Group H Trial: SST report no. 17. Arch Ophthalmol 2008;126:1626–32.

Submacular Surgery Trials Research Group. Comparison of methods to identify incident cataract in eyes of patients with neovascular maculopathy. Submacular Surgery Trials report no. 18. Ophthalmology 2008;115:127–33.

Submacular Surgery Trials Research Group. Evaluation of minimum clinically meaningful changes in scores on the National Eye Institute Visual Function Questionnaire (NEI-VFQ). SST report no. 19. Ophthalmic Epidemiol 2007;14(4):205–15.

Submacular Surgery Trials Research Group. Incident choroidal neovascularization in fellow eyes of patients with unilateral subfoveal choroidal neovascularization secondary to age-related macular degeneration. SST report no. 20 from the Submacular

Surgery Trials Research Group. Arch Ophthalmol 2007;125:1323–30.

Submacular Surgery Trials Research Group. Risk factors for second eye progression to advanced age-related macular degeneration. SST report no. 21. Retina 2009;29:1080–90.

Solomon SD, Dong LM, Haller JA, et al. on behalf of the SST Research Group and the SST Adverse Event Review Committee. Risk factors for rhegmatogenous retinal detachment in the Submacular Surgery Trials. SST report no. 22. Retina 2009;29:819–24.

Radiotherapy

Radiation Therapy for Age-related Macular Degeneration (RAD) Study Group. A prospective, randomized, double-masked trial on radiation therapy for neovascular age-related macular degeneration (RAD Study). Ophthalmology 1999;106:2239-47.

Kobayashi H, Kobayahsi K. Age-related macular degeneration: Long-term results of radiotherapy for subfoveal neovascular membranes. Am J Ophthalmol 2000;130:617–35.

Hart PM, Chakravarthy U, Mackenzie G, et al. Visual outcomes in the Subfoveal Radiotherapy Study: A randomized controlled trial of teletherapy for age-related macular degeneration. Arch Ophthalmol 2002;120:1029–38.

Stevenson MR, Hart PM, Chakravarthy U, et al. Visual functioning and quality of life in the Subfoveal Radiotherapy Study (SFRADS): SFRADS report 2. Br J Ophthalmol 2005;89:1045-51.

Zambarakji HJ, Lane AM, Ezra E, et al. Proton beam irradiation for neovascular age-related macular degeneration. Ophthalmology 2006;113:2012–9.

Dugel PU, Bebchuk JD, Nau J, et al., CABERNET Study Group. Epimacular brachytherapy for neovascular age-related macular

degeneration: a randomized, controlled trial (CABERNET). Ophthalmology 2013;120:317-27.

Jackson TE, Dugel PU, Bebchuk JD, et al. for the CABERNET Study Group. Epimacular brachytherapy for neovascular age-related macular degeneration (CABERNET). Fluorescein angiography and optical coherence tomography. Ophthalmology 2013;120:1597-603

.Jackson TI, Chakravarthy U, Kaiser PK, et al. on behalf of the INTREPID Study Group. Stereotactic radiotherapy for neovascular age-related macular degeneration. 52-week safety and efficacy results of the INTREPID Study. Ophthalmology 2013;120:1893-900.

Cochrane Systematic Review

Evans JR, Sivagnanavel V, Chong V. Radiotherapy for neovascular age-related macular degeneration. Cochrane Database of Systematic Reviews 2010, Issue 5, Art. No.: CD004004. doi: 10.1002/14651858.CD004004.pub3.

Anti-VEGF Therapy for Choroidal Neovascularization

Anti-vascular endothelial growth factor agents for treatment of neovascular age-related macular degeneration and neovascularization secondary to other conditions have changed the treatment paradigm and the prognosis for patients with these conditions. Trials of anti-VEGF agents for neovascular age-related macular degeneration have been sponsored primarily by industry.

VISION

Gragoudas ES, Adamis AP, Cunningham ET, et al. for the VEGF Inhibition Study in Ocular Neovascularization Clinical Trial Group. Pegaptanib for neovascular age-related macular degeneration. N Engl J Med 2004;351:2805–16.

VEGF Inhibition Study in Ocular Neovascularization (V.I.S.I.O.N.) Clinical Trial Group. Pegaptanib sodium for neovascular age-related macular degeneration. Two-year safety results of the two prospective, multicenter, controlled clinical trials. Ophthalmology 2006;113:992–1001.

VEGF Inhibition Study in Ocular Neovascularization (V.I.S.I.O.N.) Clinical Trial Group. Two-year efficacy results of the 2 randomized controlled clinical trials of pegaptanib for neovascular age-related macular degeneration. Ophthalmology 2006;113:1508-21.

Leys A, Zlateva G, Shah SNet al. Quality of life in patients with age-related macular degeneration: results from the VISION Study. Eye 2008;22:792-798.

MARINA

Rosenfeld PJ, Brown DM, Heier JS, et al. for the MARINA Study Group. Ranibizumab for neovascular age-related macular degeneration. N Engl J Med 2006;355:1419–31.

Kaiser PK, Blodi BA, Shapiro H, et al., for the MARINA Study Group. Angiographic and optical coherence tomographic results of the MARINA study of ranibizumab in neovascular age-related macular degeneration. Ophthalmology 2007;114:1868–75.

Boyer DS, Antoszyk AN, Awh CC, et al. for the MARINA Study Group. Subgroup analysis of the MARINA study of ranibizumab in neovascular age-related macular degeneration. Ophthalmology 2007;114:246–52.

Chang TS, Bressler NM, Fine JT, et al. for the MARINA Study Group. Improved vision-related function after ranibizumab treatment of neovascular age-related macular degeneration. Results of a randomized clinical trial. Arch Ophthalmol 2007;125(11):1460–9.

ANCHOR

Brown DM, Kaiser PK, Michels M, et al. for the ANCHOR Study Group. Ranibizumab versus verteporfin for neovascular age-related macular degeneration. N Engl J Med 2006;355:1432–44.

Kaiser PK, Brown DM, Zhang K, et al. Ranibizumab for predominantly classic neovascular age-related macular degeneration: subgroup analysis of first-year ANCHOR results. Am J Ophthalmol 2007;144:850-7.

Brown DM, Michels M, Kaiser PK, et al. for the ANCHOR Study Group. Ranibizumab versus verteporfin photodynamic therapy for neovascular age-related macular degeneration: two-year results of the ANCHOR study. Ophthalmology 2009;116:57–65.

Bressler NM, Chang TS, Fine JT, et al. for the Anti-VEGF Antibody for the Treatment of Predominantly Classic Choroidal Neovascularization in Age-Related Macular Degeneration (ANCHOR) Research Group. Improved vision-related function after ranibizumab vs photodynamic therapy: a randomized clinical trial. Arch Ophthalmol 2009;127(1):13–21.

PIER

Regillo CD, Brown DM, Abraham P, et al. on behalf of the PIER Study Group. Randomized, double-masked, sham-controlled trial of ranibizumab for neovascular age-related macular degeneration: PIER Study year 1. Am J Ophthalmol 2008;145:239–48.

Abraham P, Vue H, Wilson L. Randomized, double-masked, sham-controlled trial of ranibizumab for neovascular age-related macular degeneration: PIER Study year 2. Am J Ophthalmol 2010;150:315-24.

Brown DM, Tuomi L, Shapiro H, for the PIER Study Group. Anatomical measures as predictors of visual outcomes in ranibizumab-treated eyes with neovascular age-related macular degeneration. Retina 2013;33:23-34.

Pooled Findings From Ranibizumab Trials

Bressler NM, Chang TS, Suner IJ, et al. for the MARINA and ANCHOR Research Groups. Vision-related function after ranibizumab treatment by better- or worse-seeing eye. Clinical trial results from MARINA and ANCHOR. Ophthalmology 2010;117:747-758.

Barbazetto I, Sarol N, Shapiro H, et al. Dosing regimens and the frequency of macular hemorrhages in neovascular age-related macular degeneration treated with ranibizumab. Retina 2010;30:1376-85.

Barbazetto IA, Saroj N, Shapiro H, et al. Incidence of new choroidal neovascularization in fellow eyes of patients treated in the MARINA and ANCHOR trials. Am J Ophthalmol 2010;149:939-946.

Rosenfeld PJ, Shapiro H, Tuomi L, et al. for the MARINA and ANCHOR Study Groups. Characteristics of patients losing vision after 2 years of monthly dosing in the phase III ranibizumab clinical trials. Ophthalmology 2011;118:523–30.

Wolf S, Holz FG, Korobelnik J-F, et al. Outcomes following three-line vision loss during treatment of neovascular age-related macular degeneration: subgroup analyses from MARINA and ANCHOR. Br J Ophthalmol 2011;95:1713-8.

Cunningham ET, Feiner L, Chang C, et al. Incidence of retinal pigment epithelial tears after intravitreal ranibizumab injection for neovascular age-related macular degeneration. Ophthalmology 2011;118:2447-52.

Bressler NM, Boyer DS, Williams DF, et al. Cerebrovascular accidents in patients treated for choroidal neovascularization with ranibizumab in randomized controlled trials. Retina 2012;32:1821-8.

Zweifel SA, Saroj N, Shapiro H, Freund KB. The effect of fellow eye

visual acuity on visual acuity of study eyes receiving ranibizumab for age-related macular degeneration. Retina 2012;32:1243-9.

Bressler NM, Chang TS, Varma R, et al. Driving ability reported by neovascular age-related macular degeneration patients after treatment with ranibizumab. Ophthalmology 2013;120:160-8.

Weinberg DV, Shapiro H, Ehrlich JS. Ranibizumab treatment outcomes in phakic versus pseudophakic eyes. An individual patient data analysis of 2 phase 3 trials. Ophthalmology 2013;120:1278-82.

Singer MA, Awh CC, Sadda S, et al. HORIZON: An open-label extension trial of ranibizumab for choroidal neovascularization secondary to age-related macular degeneration. Ophthalmology 2012;119:1175-83.

Rofagha S, Bhisitkul RB, Boyer DS, et al. for the SEVEN-UP Study Group. Seven-year outcomes in ranibizumab-treated patients in ANCHOR, MARINA, and HORIZON. A multicenter cohort study (SEVEN-UP). Ophthalmology 2013;120:2292-9.

Other Single Anti-VEGF Agents

ABC Trial

Patel PJ, Bunce C, Tufail A for the ABC Trial Investigators. A randomized, double-masked phase III/IV study of the efficacy and safety of Avastin®(bevacizumab) intravitreal injections compared to standard therapy in subjects with choroidal neovascularization secondary to age-related macular degeneration: clinical trial design. Trials 2008;9:56.

Patel PJ, Chen FK, Rubin GS, et al. Intersession repeatability of visual acuity scores in age-related macular degeneration. Invest Ophthalmol Vis Sci 2008;49:4347–52.

Patel PJ, Chen FK, Rubin GS, et al. Intersession repeatability of

contrast sensitivity scores in age-related macular degeneration. Invest Ophthalmol Vis Sci 2009;50:2621–5.

Tufail A, Patel PJ, Egan C, et al. Bevacizumab for neovascular age related macular degeneration (ABC Trial): multicentre randomised double masked study. Br Med J 2010;340:c2459.

Keane PA, Patel PJ, Ouyang Y, et al. Effects of retinal morphology on contrast sensitivity and reading ability in neovascular age-related macular degeneration. Invest Ophthalmol Vis Sci 2010;51:5431–7.

Patel PJ, Chen FK, Da Cruz L, et al. for the ABC Trial Study Group. Contrast sensitivity outcomes in the ABC Trial: A randomized trial of bevacizumab for neovascular age-related macular degeneration. Invest Ophthalmol Vis Sci 2011;52:3089–93.

Patel PJ, Chen FK, Da Cruz L, et al. Test–retest variability of reading performance metrics using MNREAD in patients with age-related macular degeneration. Invest Ophthalmol Vis Sci 2011;52:3854–9

Schmidt-Erfurth U, Eldom B, Guymer R, et al. for the EXCITE Study Group. Efficacy and safety of monthly versus quarterly ranibizumab treatment in neovascular age-related macular degeneration: The EXCITE Study. Ophthalmology 2011;115:831-9.

Li Z, Hu Y, Sun X, et al. on behalf of the Neovascular Age-Related Macular Degeneration Treatment Trial Using Bevacizumab (NATTB). Bevacizumab for neovascular age-related macular degeneration in China. Ophthalmology 2012;119:2087-2093.

Heier JS, Brown DM, Chong V, et al. for the VIEW 1 and VIEW 2 Study Groups. Intravitreal aflibercept (VEGF Trap-Eye) in wet age-related macular degeneration. Ophthalmology 2012;119:2537-48.

Wolf S, Balciunienne VJ, Laganovska G, et al. on behalf of the RADIANCE Study Group. RADIANCE: A randomized controlled study of ranibizumab in patients with choroidal neovascularization secondary to pathologic myopia.

Ophthalmology 2014;121L682-92.

Ranibizumab and Photodynamic Therapy

Heier JA, Boyer DS, Ciulla TA, et al. for the FOCUS Study Group. Ranibizumab combined with verteporfin photodynamic therapy in neovascular age-related macular degeneration. Year 1 results of the FOCUS Study. Arch Ophthalmol 2006;124:1532-42.

Antoszyk A, Chung CY, Singh A, on behalf of the FOCUS Study Group. Ranibizumab combined with verteporfin photodynamic therapy in neovascular age-related macular degeneration (FOCUS): Year 2 results. Am J Ophthalmol 2008;145:862-74.

Kaiser PK, Boyer DS, Cruess AF, et on behalf of the DENALI Study Group. Verteporfin plus ranibizumab for choroidal neovascularization in age-related macular degeneration. Twelve-month results of the DENALI Study. Ophthalmology 2012;119:1001-1010.

Larsen M, Schmidt-Erfurth U, Lanzetta P, et al. for the MONT BLANC Study Group. Verteporfin plus ranibizumab for choroidal neovascularization in age-related macular degeneration. Twelve-month MONT BLANC Study results. Ophthalmology 2012;119:992-1000.

Comparative Effectiveness of Anti-VEFG Agents

Comparison of Age-related Macular Degeneration Treatments Trials (CATT)

Martin DF, Maguire MG, Fine SL. Identifying and eliminating the roadblocks to comparative effectiveness research. N Engl J Med 2010;363:105–7.

CATT Research Group. Ranibizumab and bevacizumab for neovascular age-related macular degeneration. N Engl J Med 2011;364:1897–908.

Comparison of Age-Related Macular Degeneration Treatments Trials (CATT) Research Group. Ranibizumab and bevacizumab for treatment of neovascular age-related macular degeneration. Two-year results. Ophthalmology 2012;119:1388–98.

DeCroos FC, Toth CA, Sunnett SS, et al. for the CATT Research Group. Optical coherence tomography grading reproducibility during the Comparison of Age-related Macular Degeneration Treatments Trials. Ophthalmology 2012;119:2549-57.

Ying G-S, Huang J, Maguire MG, et al. on behalf of the Comparison of Age-related Macular Degeneration Treatments Trials Research Group. Baseline predictors for one-year visual outcomes with ranibizumab or bevacizumab for neovascular age-related macular degeneration. Ophthalmology 2013;120:122-9.

Hagstrom SA, Ying G-S, Pauer GJT, et al. for the Comparison of AMD Treatments Trials Research Group. Pharmacogenetics for genes associated with age-related macular degeneration in the Comparison of AMD Treatments Trials (CATT). Ophthalmology 2013;120:593-9.

Jaffe GJ, Martin DF, Toth CA, et al. for the Comparison of Age-related Macular Degeneration Treatments Trials Research Group. Macular morphology and visual acuity in the Comparison of Age-related Macular Degeneration Treatments Trials. Ophthalmology 2013;120:1860-70.

Maguire MG, Daniel E, Shah AR, et al. for the Comparison of Age-related Macular Degeneration Treatments Trials Research Group. Incidence of choroidal neovascularization in the fellow eye in the Comparison of Age-related Macular Degeneration Treatments Trials. Ophthalmology 2013;120:2035-41.

Hagstrom SA, Ying G-S, Pauer GJT, et al. for the Comparison of Age-Related Macular Degeneration Treatments Trials (CATT) Research Group. *VEGFA* and *VEGFR2* gene polymorphisms and response to anti-vascular endothelial growth factor therapy. Comparison of Age-related Macular Degeneration Treatments

Trials (CATT). JAMA Ophthalmol 2014;132(5):521-7.

Grunwald JE, Daniel E, Huang J, et al. for the CATT Research Group. Risk of geographic atrophy in the Comparison of Age-related Macular Degeneration Treatments Trials. Ophthalmology 2014;121:150-61.

Daniel E, Toth CA, Grunwald JE, et al. for the Comparison of Age-related Macular Degeneration Treatments Trials Research Group. Risk of scar in the Comparison of Age-related Macular Degeneration Treatments Trials. Ophthalmology 2014;121:656-66.

Kim BJ, Ying G-S, Huang J, et al. on behalf of the CATT Research Group. Sporadic visual acuity loss in the Comparison of Age-related Macular Degeneration Treatments Trials (CATT). Am J Ophthalmol 2014;158:128-35.

Ying G-S, Kim BJ, Maguire MG, et al. for the CATT Research Group. Sustained visual acuity loss in the Comparison of Age-related Macular Degeneration Treatments Trials. JAMA Ophthalmol 2014;132(8):915-21.

Altaweel AA, Daniel E, Martin DF, et al. for the Comparison of Age-related Macular Degeneration Treatments Trials (CATT) Research Group. Outcomes of eyes with lesions composed of >50% blood in the Comparison of Age-related Macular Degeneration Treatments Trials (CATT). Ophthalmology 2015;122:391-8.

Grunwald JE, Pistilli M, Ying G-S, et al. for the Comparison of Age-related Macular Degeneration Treatments Trials Research Group. Growth of geographic atrophy in the Comparison of Age-related Macular Degeneration Treatments Trials. Ophthalmology 2015;122:809-16.

Meredith TA, McCannel CA, Barr C, et al. for the Comparison of Age-related Macular Degeneration Treatments Trials Research Group. Postinjection endophthalmitis in the Comparison of Age-related Macular Degeneration Treatments Trials Research Group.

Comparison of Age-related Macular Degeneration Treatments Trials (CATT). Ophthalmology 2015;122:817-21.

Ciulla TA, Ying G-S, Maguire MG, et al. for the Comparison of Age-related Macular Degeneration Treatments Trials Research Group. Influence of the vitreomacular interface on treatment outcomes in the Comparison of Age-related Macular Degeneration Treatments Trials. Ophthalmology 2015;122:1203-11.

Toth CA, DeCroos FC, Ying G-S, et al. Identification of fluid on optical coherence tomography by treating ophthalmologists versus a reading center in the Comparison of Age-related Macular Degeneration Treatments Trials. Retina 2015;35:1303-14.

Willoughby AS, Ying G-S, Toth CA, et al. for the Comparison of Age-related Macular Degeneration Treatments Trials Research Group. Subretinal hyperreflective material in the Comparison of Age-related Macular Degeneration Treatments Trials. Ophthalmology 2015;122:1846-53.

Inhibit VEGF in Age-Related Choroidal Neovascularization (Ivan)

IVAN Study Investigators. Ranibizumab versus bevacizumab to treat neovascular age-related macular degeneration. One-year findings from the IVAN randomized trial. Ophthalmology 2012;119:1399–411.

Chakravarthy U, Harding SP, Rogers, et al. for the IVAN study investigators. Alternative treatments to inhibit VEGF in age-related choroidal neovascularization: 2-year findings of the IVAN randomized controlled trial. Lancet 2013;382:1258-67.

Lotery AJ, Gibson J, Cree AJ, et al. for the Alternative Treatments to Inhibit VEGF in Patients with Age-Related Choroidal Neovascularization (IVAN) Study Group. Pharmacogenetic associations with vascular endothelial growth factor inhibition in participants with neovascular age-related macular degeneration in the IVAN Study. Ophthalmology 2013;120:2637-43.

Dakin HA, Wordsworth S, Rogers CA, et al. on behalf of the IVAN Study Investigators. Cost-effectiveness of ranibizumab and bevacizumab for age-related macular degeneration: 2-year findings from the IVAN randomised trial. BMJ Open 2014;4(7):e005094.

Hagstrom SA, Ying G-S, Maguire MG, et al. for the IVAN Study Investigators. *VEGFR2* gene polymorphisms and response to anti-vascular endothelial growth factor therapy in age-related macular degeneration. Ophthalmology 2015;122:1563-8.

Other Comparative Effectiveness Trials of Anti-VEGF Agents

Krebs I, Schmetterer L, Boltz A, et al. for the MANTA Research Group. A randomised double-masked trial comparing the visual outcome after treatment with ranibizumab or bevacizumab in patients with neovascular age-related macular degeneration. Br J Ophthalmol 2012:97(3):266-71.

Kodjikian L, Souied EH, Mimoun G, et al. for the GEFAL Study Group. Ranibizumab versus bevacizumab for neovascular age-related macular degeneration: Results from the GEFAL noninferiority randomized trial. Ophthalmology 2013;120:2300-09.

Berg K, Pedersen TR, Sandvik L, Bragadottir R. Comparison of ranibizumab and bevacizumab for neovascular age-related macular degeneration according to LUCAS treat-and-extend protocol. Ophthalmology 2015;122:146-52.

Cochrane Systematic Review

Solomon SD, Lindsley K, Vedula SS, et al. Anti-vascular endothelial growth factor for neovascular age-related macular degeneration. Cochrane Database of Systematic Reviews 2014, Issue 8, Art. No.:CD005139. doi: 10.1002/14651858.CD005139.pub3/

Other Pharmacologic Treatments for Choroidal Neovascularization

Pharmacological Therapy for Macular Degeneration Study Group. Interferon alfa-2 is ineffective for patients with choroidal neovascularization secondary to age-related macular degeneration. Results of a randomized placebo-controlled clinical trial. Arch Ophthalmol 1997;115:865–72.

Christen WG, Glynn RJ, Ajani UA, et al. Age-related maculopathy in a randomized trial of low-dose aspirin among US physicians. Arch Ophthalmol 2001;119:1143-9.

Christen WG, Glynn RJ, Chew EY, et al. Low-dose aspirin and medical record-confirmed age-related macular degeneration in a randomized trial of women. Ophthalmology 2009;116:2386-92.

Anecortave Acetate Clinical Study Group. Anecortave acetate as monotherapy for treatment of subfoveal neovascularization in age-related macular degeneration. Twelve-month clinical outcomes. Ophthalmology 2003;110:2372–85.

Slakter JS, Bochow T, D'Amico DJ, et al., Anecortave Acetate Clinical Study Group. Anecortave acetate (15 milligrams) versus photodynamic therapy for treatment of subfoveal neovascularization in age-related macular degeneration. Ophthalmology 2006;113:3–13.

Gillies MC, Simpson JM, Penfold P, et al. A randomized clinical trial of a single dose of intravitreal triamcinolone acetonide for neovascular age-related macular degeneration. One-year results. Arch Ophthalmol 2003;121:667–73.

Gillies MC, Simpson JM, Billson FA, et al. Safety of an intra vitreal injection of triamcinolone. Results from a randomized clinical trial. Arch Ophthalmol 2004;122:336–40.

Cohen SY, Bourgeois H, Corbe C, et al. Randomized clinical trial: France DMLA2. Effect of trimetazidine on exudative and

nonexudative age-related macular degeneration. Retina 2012;32:834-843.

Guymer RH, Baird PN, Varsamidis M, et al. Proof of concept, randomized, placebo-controlled study of the effect of simvastatin on the course of age-related macular degeneration. PLOS One 2013;8(12):e83759.

Kuppermann BD, Thomas EL, deSmet MD, Grillone LR, for the Vitrase for Vitreous Hemorrhage Study Groups. Pooled efficacy results from two multinational randomized controlled clinical trials of a single intravitreous injection of highly purified ovine hyaluronidase (Vitrase®) for the management of vitreous hemorrhage. Am J Ophthalmol 2005;140:573-84.

Kuppermann BD, Thomas EL, deSmet MD, et al., for the Vitrase for Vitreous Hemorrhage Study Groups. Safety results of two phase III trials of an intravitreous injection of highly purified ovine hyaluronidase (Vitrase®) for the management of vitreous hemorrhage. Am J Ophthalmol 2005;140:585-97.

Cochrane Systematic Reviews

Geltzer A, Turalba A, Vedula SS. Surgical implantation of steroids with antiangiogenic characteristics for treating neovascular age-related macular degeneration. Cochrane Database of Systematic Reviews 2013, Issue 1, Art. No.: CD005022. doi: 10.1002/14651858.cd005022.pub3.

Gehlbach P, Li T, Hatef E. Statins for age-related macular degeneration. Cochrane Database of Systematic Reviews 2015, Issue 2, Art. No.:CD006927. doi: 10.1002/14651858.CD006927.pub4.

Dietary and Other Oral Supplements

Newsome DA, Swartz M, Leone NC, et al. Oral zinc in macular degeneration. Arch Ophthalmol 1988;106:192-8.

Stur M, Tittl M, Beitner A, et al. Oral zinc and the second eye in age-related macular degeneration. Invest Ophthalmol Vis Sci 1996;17:1225-35.

Newsome DA. A randomized, prospective, placebo-controlled clinical trial of a novel zinc-moncysteine compound in age-related macular degeneration. Curr Eye Res 2008;33(7):591-8.

Age-Related Eye Disease Study (AREDS)

The goal of the AREDS investigators was to assess the clinical course of age-related macular degeneration and age-related cataract. The AREDS design included two prevention trials of high-dose vitamin and mineral supplements for patients at risk of age-related macular degeneration and age-related cataract.

Age-Related Eye Disease Study Research Group. The Age-Related Eye Disease Study (AREDS): design implications. AREDS report no. 1. Control Clin Trials 1999;20:573–600.

Age-Related Eye Disease Study Research Group. The Age-Related Eye Disease Study (AREDS): a clinical trial of zinc and antioxidants. AREDS report no. 2. J Nutr 2000;130(Suppl):1516–9.

Age-Related Eye Disease Study Research Group. Risk factors associated with age-related macular degeneration. A case-control study in the Age-Related Eye Disease Study: Age-Related Eye Disease Study report number 3. Ophthalmology 2000;107:2224–32.

Age-Related Eye Disease Study Research Group. The Age-Related Eye Diseases Study system for classifying age-related macular degeneration from stereoscopic color fundus photographs: the Age-Related Eye Disease Study report number 6. Am J Ophthalmol 2001;132:668–81.

Age-Related Eye Disease Study Research Group. The effect of five-year zinc supplementation on serum zinc, serum cholesterol, and hematocrit in persons assigned to treatment group in the Age-Related Eye Disease Study: AREDS report no. 7. J Nutr

2002;132:697–702.

Age-Related Eye Disease Study Research Group. A randomized, placebo-controlled clinical trial of high-dose supplementation with vitamins C and E, beta carotene, and zinc for age-related macular degeneration and vision loss. AREDS report no. 8. Arch Ophthalmol 2001;119:1417-36.

Clemons TE, Chew EY, Bressler SB, et al. National Eye Institute Visual Function Questionnaire in the Age-Related Eye Disease Study (AREDS). AREDS report no. 10. Arch Ophthalmol 2003;121:211–7.

Age-Related Eye Disease Study Research Group. Potential public health impact of Age-Related Eye Disease Study results. AREDS report no. 11. Arch Ophthalmol 2003;121:1621–4.

Age-Related Eye Disease Study Research Group. Associations of mortality with ocular disorders and an intervention of high-dose antioxidants and zinc in the Age-Related Eye Disease Study. AREDS report no. 13. Arch Ophthalmol 2004;122:716–26.

Age-Related Eye Disease Study Research Group. Responsiveness of the National Eye Institute Visual Function Questionnaire to progression to advanced age-related macular degeneration, vision loss, and lens opacity. AREDS report no. 14. Arch Ophthalmol 2005;123:1207–14.

Rankin MW, Clemons TE, McBee WL, Age-Related Eye Disease Study (AREDS) Research Group. Correlation analysis of the in-clinic and telephone batteries from the AREDS cognitive function ancillary study. AREDS report no. 15. Ophthalmol Epidemiol 2005;12:271–7.

Age-Related Eye Disease Study Research Group. Cognitive impairment in the Age-Related Eye Disease Study. AREDS report no. 16. Arch Ophthalmol 2006;124:537–43.

Age-Related Eye Disease Study Research Group. The Age-Related Eye Disease Study severity scale for age-related macular

degeneration. AREDS report no. 17. Arch Ophthalmol 2005;123:1484–98.

Age-Related Eye Disease Study Research Group. A simplified severity scale for age-related macular degeneration. AREDS report no. 18. Arch Ophthalmol 2005;123:1570–4.

Age-Related Eye Disease Study Research Group. Risk factors for the incidence of advanced age-related macular degeneration in the Age-Related Eye Disease Study (AREDS). AREDS report no. 19. Ophthalmology 2005;112:533–9.

Age-Related Eye Disease Study Research Group. The relationship of dietary lipid intake and age-related macular degeneration in a case–control study. AREDS report no. 20. Arch Ophthalmol 2007;126:671–9.

Age-Related Eye Disease Study Research Group. Centrum use and progression of age-related cataract in the Age-Related Eye Disease Study (AREDS). AREDS report no. 21. Ophthalmology 2006;113:1264–70.

Age-Related Eye Disease Study Research Group. The relationship of dietary carotenoid and vitamin A, E, and C intake with age-related macular degeneration in a case–control study. AREDS report no. 22. Arch Ophthalmol 2007;123:1225–32.

SanGiovanni JP, Chew EY, Agron E, et al. for the Age-Related Eye Disease Study Research Group. The relationship of dietary ω-3 long-chain polyunsaturated fatty acid intake with incident age-related macular degeneration. AREDS report no. 23. Arch Ophthalmol 2008;126(9):1274–9.

Chew EY, Sperduto RD, Milton RC, et al. Risk of advanced age-related macular degeneration after cataract surgery in the Age-Related Eye Disease Study. AREDS report 25. Ophthalmology 2009;116:297–303.

AREDS Research Group. Change in area of geographic atrophy in the Age-Related Eye Disease Study. AREDS report number 26.

Arch Ophthalmol 2009;127:1168–74.

Forooghian F, Agron E, Clemons TE, et al. for the AREDS Research Group. Visual acuity outcomes after cataract surgery in patients with age-related macular degeneration: Age-Related Eye Disease Study report no. 27. Ophthalmology 2009;116:2093–100.

Cukras C, Agron E, Klein ML, et al. for the Age-Related Eye Disease Study Research Group. Natural history of drusenoid pigment epithelial detachment in age-related macular degeneration: Age-Related Eye Disease Study report no. 28. Ophthalmology 2010;117:489–99.

Chew EY, Clemons TE, Agron E, et al. for the Age-Related Eye Disease Study Research Group. Long-term effects of vitamins C and E, β-carotene, and zinc on age-related macular degeneration. AREDS report no. 35. Ophthalmology 2013;120:1604-11.

Chew EY, Clemons TE, Agron E, et al. for the Age-Related Eye Disease Study Research Group. Ten-year follow-up of age-related macular degeneration in the Age-Related Eye Disease Study. AREDS report no. 36. JAMA Ophthlamol 2014;132(3):272-277.

Chew EY, Klein ML, Clemons TE, et al. for the Age-Related Eye Disease Study Research Group. No clinically significant association between *CFH* and *ARMS2* genotypes and response to nutritional supplements. AREDS report no. 38. Ophthalmology 2014;121:2173-80.

Feeny AK, Tadarati M, Freund DE, et al. Automated segmentation of geographic atrophy of the retinal epithelium via random forests in AREDS color fundus images. Comput Biol Med 2015;65:124-36.

Kankanabalit S, Burlina PM, Wolfson, et al. Automated classification of severity of age-related macular degeneration from fundus photographs. Invest Opthalmol Vis Sci 2013;54:1789-96.

Age-Related Eye Disease Study 2 (AREDS2)

Hubbard LD, Danis RP, Neider MW, et al., Age-Related Eye Disease 2 Research Group. Brightness, contrast, and color balance of digital versus film retinal images in the Age-Related Eye Disease Study 2. Invest Ophthalmol Vis Sci 2008;49:3269–82.

AREDS2 Research Group. The Age-Related Eye Disease Study 2 (AREDS2). Study design and baseline characteristics (AREDS2 report number 1). Ophthalmology 2012;119:2282-9.

Age-Related Eye Disease Study 2 (AREDS2) Research Group. Lutein + zeaxanthin and omega-3 fatty acids for age-related macular degeneration. The Age-Related Eye Disease Study 2 (AREDS2) randomized clinical trial. JAMA 2013;309(19):2005-15.

Domalpally A, Danis RP, Chew EY, et al. for the Age-Related Eye Disease 2 Research Group. Evaluation of optimized digital fundus reflex photographs for lens opacities in the Age-Related Eye Disease Study 2: AREDS2 report 7. Invest Ophthalmol Vis Sci 2013;54:5989-5994.

Carotenoids in Age-Related Eye Disease Study (CAREDS)

Moeller SM, Parekh N, Tinker L, et al. for the CAREDS Research Study Group. Associations between intermediate age-related macular degeneration and lutein and zeaxanthin in the Carotenoids in Age-Related Eye Disease Study (CAREDS). Ancillary study of the Women's Health Initiative. Arch Ophthalmol 2006;124:1151-62.

LaRowe TL, Mares JA, Snodderly DM, et al. for the CAREDS Macular Pigment Study Group. Macular pigment density and age-related maculopathy in the Carotenoids in Age-Related Eye Disease Study: An ancillary study of the Women's Health Initiative. Ophthalmology 2008;115:876-83.

Parekh N, Voland RP, Moeller SM, et al. for the CAREDS Research

Study Group. Association between dietary fat intake and age-related macular degeneration in the Carotenoids in Age-Related Eye Disease Study (CAREDS). An ancillary study of the Women's Health Initiative. Arch Ophthalmol 2009;127(11):1483-93.

Carotenoids in Age-Related Maculopathy (CARMA) Study

Neelam K, Hogg RE, Stevenson MR, et al. Carotenoids and co-antioxidants in age-related maculopathy: design and methods. Ophthalmic Epidemiol 2008;15:389-401.

Beatty S, Chakravarthy U, Nolan JM, et al. Secondary outcomes in a clinical trial of carotenoids with coantioxidants versus placebo in early age-related macular degeneration. Ophthalmology 2013;120:600-6.

Other Trials of Dietary Supplements

Christen WG, Manson JE, Glynn RJ, et al. Beta carotene supplementation and age-related maculopathy in a randomized trial of US physicians. Arch Ophthalmol 2007;125:333–9.

Christen WG, Glynn RJ, Chew EY, et al. Folic acid, pyridoxine, and cyanocobalamin combination treatment and age-related macular degeneration in women. The Women's Antioxidant and Folic Acid Cardiovascular Study. Arch Intern Med 2009;169:335–41.

Christen WG, Glynn RJ, Chew EY, et al. Vitamin E and age-related macular degeneration in a randomized trial of women. Ophthalmology 2010;117:1163–8.

Christen WC, Glynn RJ, Sesso HD, et al. Vitamins E and C and medical record-confirmed age-related macular degeneration in a randomized trial of male physicians. Ophthalmology 2012;119:1642-9.

Piermarocchi S, Saviano S, Parisi V, et al. for the CARMIS Study Group. Carotenoids in Age-Related Maculopathy Italian Study

(CARMIS): two-year results of a randomized study. Br J Ophthalmol 2012;22(2):216-25.

Souied EH, Delcourt C, Querques G, et al. for the Nutritional AMD Treatment 2 Study Group. Oral docosahexaenoic acid in the prevention of exudative age-related macular degeneration. The Nutritional AMD Treatment 2 Study. Ophthalmology 2013;120:1619-31.

Cochrane Systematic Reviews

Evans JR, Lawrenson JG. Antioxidant vitamin and mineral supplements for preventing age-related macular degeneration. Cochrane Database of Systematic Reviews 2012, Issue 6, Art. No.: CD000253. doi: 10.1002/14651858/CD000253.pub3.

Lawrence JG, Evans JR. Omega 3 fatty acids for preventing or slowing the progression of age-related macular degeneration. Cochrane Database of Systematic Reviews 2015, Issue 4, Art. No.: CD010015. doi: 10.1002/14651858.CD010015.pub3.

Other Interventions

Multicenter Investigation of Rheopheresis for AMD (MIRA-1) Study Group, Pulido JS. Multicenter prospective randomized, double-masked, placebo-controlled study of rheopheresis to treat nonexudative age-related macular degeneration: Interim analysis. Trans Am Ophthalmol Soc 2002;100:85-107.

Brody BL, Roch-Levecq A-C, Gamst AC, et al. Self-management of age-related macular degeneration and quality of life. A randomized controlled trial. Arch Ophthalmol 2002;120:1477-83.

Soderberg A-C, Algvere PV, Hengstler JC, et al. Combination therapy with low-dose transpupillary thermotherapy and intravitreal ranibizumab for neovascular age-related macular degeneration: a 24-month prospective randomised clinical study. Br J Ophthalmol 2012;96:214-218.

Rovner BW, Casten RJ, Hegel MT, et al. Improving function in age-related macular degeneration. A randomized clinical trial. Ophthalmology 2013;120:1649-55.

Retinopathy of Prematurity

Initiation of the Multicenter Trial of Cryotherapy for Retinopathy of Prematurity (CRYO-ROP) was stimulated by an increase in the incidence of retinopathy of prematurity following a decline after early clinical trials demonstrated that exposure to 100% oxygen in incubators had been responsible for the epidemic of retinopathy of prematurity in the United States in the 1950s. Increased incidence in the 1970s and 1980s was attributable to advances in neonatal medicine that had increased survival among very-low-birthweight premature infants. CRYO-ROP was designed to determine the safety and efficacy of transscleral cryotherapy of the peripheral retina in selected low-birthweight infants with retinopathy of prematurity and to study the natural history of retinal vessel development and outcome in such children. Following completion of CRYO-ROP, additional trials were undertaken to evaluate proposed approaches to reduce the complications of retinopathy of prematurity, all with sponsorship by the National Eye Institute, either alone or in collaboration with other institutes of the National Institutes of Health.

Multicenter Trial of Cryotherapy for Retinopathy of Prematurity (CRYO-ROP)

Cryotherapy for Retinopathy of Prematurity Cooperative Group. Multicenter Trial of Cryotherapy for Retinopathy of Prematurity: preliminary results. Arch Ophthalmol 1988;106:471–9.

Cryotherapy for Retinopathy of Prematurity Cooperative Group. Multicenter Trial of Cryotherapy for Retinopathy of Prematurity: preliminary results. Pediatrics 1988;81:697–706.

Phelps DL, Phelps CE. Cryotherapy in infants with retinopathy of

prematurity. A decision model for treating one or both eyes. JAMA 1989;261:1751–6.

Palmer EA. Results of US randomized clinical trial of cryotherapy for ROP (CRYO-ROP). Doc Ophthal 1990;74:245–51.

Cryotherapy for Retinopathy of Prematurity Cooperative Group. Multicenter Trial of Cryotherapy for Retinopathy of Prematurity: three-month outcome. Arch Ophthalmol 1990;108:195–204.

Watzke RC, Robertson JE, Palmer EA, et al. Photographic grading in the Retinopathy of Prematurity Cryotherapy trial. Arch Ophthalmol 1990;108:950–5.

Dobson V, Quinn GE, Biglan AW, et al. Acuity card assessment of visual function in the Cryotherapy for Retinopathy of Prematurity trial. Invest Ophthalmol Vis Sci 1990;31:1702–8.

Cryotherapy for Retinopathy of Prematurity Cooperative Group. Multicenter Trial of Cryotherapy for Retinopathy of Prematurity: one-year outcome – structure and function. Arch Ophthalmol 1990;108:1408–16.

Palmer EA, Hardy RJ, Davis BR, et al. Operational aspects of terminating randomization in the Multicenter Trial of Cryotherapy for Retinopathy of Prematurity. Control Clin Trials 1991;12:277–92.

Hardy RJ, Davis BR, Palmer EA, et al. Statistical considerations in terminating randomization in the Multicenter Trial of Cryotherapy for Retinopathy of Prematurity. Control Clin Trials 1991;12:293–303.

Palmer EA, Flynn JT, Hardy RJ, et al. Incidence and early course of retinopathy of prematurity. Ophthalmology 1991;98:1628–40.

Phelps DL, Brown DR, Tung B, et al. 28-day survival rates of 6676 neonates with birth weights of 1250 grams or less. Pediatrics 1991;87:7–17.

Quinn GE, Dobson V, Barr CC, et al. Visual acuity in infants after vitrectomy for severe retinopathy of prematurity. Ophthalmology 1991;98:5–13.

Gilbert WS, Dobson V, Quinn GE, et al. The correlation of visual function with posterior retinal structure in severe retinopathy of prematurity. Arch Ophthalmol 1992;110:625–31.

Summers G, Phelps DL, Tung B, et al. Ocular cosmesis in retinopathy of prematurity. Arch Ophthalmol 1992;110:1092–7.

Evans MS, Wallace PR, Palmer EA. Fundus photography in infants. J Ophthalm Photo 1993;15:38–9.

Cryotherapy for Retinopathy of Prematurity Cooperative Group. Multicenter trial of Cryotherapy for Retinopathy of Prematurity: 3-year outcome – structure and function. Arch Ophthalmol 1993;111:339–44.

Reynolds J, Dobson V, Quinn GE, et al. Prediction of visual function in eyes with mild to moderate posterior pole residua of retinopathy of prematurity. Arch Ophthalmol 1993;111:1050–6.

Schaffer DB, Palmer EA, Plotsky DF, et al. Prognostic factors in the natural course of retinopathy of prematurity. Ophthalmology 1993;100:230–7.

Cryotherapy for Retinopathy of Prematurity Cooperative Group. The natural ocular outcome of premature birth and retinopathy. Status at 1 year. Arch Ophthalmol 1994;112:903–12.

Dobson V, Quinn GE, Summers CG, et al. Effect of acute-phase retinopathy of prematurity on grating acuity development in the very low birth weight infant. Invest Ophthalmol Vis Sci 1994;35:4236–44.

Quinn GE, Dobson V, Biglan A, et al. Correlation of retinopathy of prematurity in fellow eyes in the Cryotherapy for Retinopathy of Prematurity study. Arch Ophthalmol 1995;113:469–73.

Dobson V, Quinn GE, Saunders RA, et al. Grating visual acuity in eyes with retinal residua of retinopathy of prematurity. Arch Ophthalmol 1995;113:1172–7.

Dobson V, Quinn GE, Tung B, et al. Comparison of recognition and grating acuities in very-low-birth-weight children with and without retinal residua of retinopathy of prematurity. Invest Ophthalmol Vis Sci 1995;36:692–702.

Cryotherapy for Retinopathy of Prematurity Cooperative Group. Multicenter Trial of Cryotherapy for Retinopathy of Prematurity: Snellen visual acuity and structural outcome at 5½ years after randomization. Arch Ophthalmol 1996;114:417–24.

Kivlin JD, Biglan AW, Gordon RA, et al. Early retinal vessel development and iris vessel dilation as factors in retinopathy of prematurity. Arch Ophthalmol 1996;114:150–4.

Quinn GE, Dobson V, Barr CC, et al. Visual acuity of eyes after vitrectomy for retinopathy of prematurity: follow-up at 5½ years. Ophthalmology 1996;103:595–600.

Gilbert WS, Quinn GE, Dobson V, et al. Partial retinal detachment at 3 months after threshold retinopathy of prematurity. Long-term structural and functional outcome. Arch Ophthalmol 1996;114:1085–91.

Quinn GE, Dobson V, Hardy RJ, et al. Visual fields measured with double-arc perimetry in eyes with threshold retinopathy of prematurity from the Cryotherapy for Retinopathy of Prematurity trial. Ophthalmology 1996;103:1432–7.

Dobson V, Quinn GE, Abramov I, et al. Color vision measured with pseudoisochromatic plates at five-and-a-half years in eyes of children from the CRYO-ROP study. Invest Ophthalmol Vis Sci 1996;37:2467–74.

Bartholomew PA, Chao J, Evans JL, et al. Acceptance/use of the Teller acuity card procedure in the clinic. Am Orthop J

1996;46:99–105.

Saunders RA, Donahue ML, Christmann LM, et al. Racial variation in retinopathy of prematurity. Arch Ophthalmol 1997;115:604–8.

Bremer DL, Palmer EA, Fellows RR, et al. Strabismus in premature infants in the first year of life. Arch Ophthalmol 1998;116:329–33.

Quinn GE, Dobson V, Kivlin J, et al. Prevalence of myopia between 3 months and 5½ years in preterm infants with and without retinopathy of prematurity. Ophthalmology 1998;105:1292–300.

Repka MX, Summers CG, Palmer EA, et al. The incidence of ophthalmologic interventions in children with birth weights less than 1251 grams. Results through 5½ years. Ophthalmology 1998;105:1621–7.

Dobson V, Quinn GE, Siatkowski RM, et al. Agreement between grating acuity at age 1 year and Snellen acuity at age 5½ years in the preterm child. Invest Ophthalmol Vis Sci 1999;40:496–503.

Harvey EM, Dobson V, Tung B, et al. Interobserver agreement for grating acuity and letter acuity assessment in 1- to 5½ -year-olds with severe retinopathy of prematurity. Invest Ophthalmol Vis Sci 1997;40:1565–76.

Repka MX, Palmer EA, Tung B, et al. Involution of retinopathy of prematurity. Arch Ophthalmol 2000;118:645–9.

Quinn GE, Dobson V, Siatkowski RM, et al. Does cryotherapy affect refractive error? Results from treated versus control eyes in the Cryotherapy for Retinopathy of Prematurity trial. Ophthalmology 2001;108:343–7.

Cryotherapy for Retinopathy of Prematurity Cooperative Group. Multicenter trial of Cryotherapy for Retinopathy of Prematurity: ophthalmological outcomes at 10 years. Arch Ophthalmol 2001;119:1110–8.

Cryotherapy for Retinopathy of Prematurity Cooperative Group. Effect of retinal ablative therapy for threshold retinopathy of prematurity: results of Goldmann perimetry at the age of 10 years. Arch Ophthalmol 2001;119:1120–5.

Cryotherapy for Retinopathy of Prematurity Cooperative Group. Contrast sensitivity at age 10 years in children who had threshold retinopathy of prematurity. Arch Ophthalmol 2001;119:1129–33.

Editorial Committee for the Cryotherapy for Retinopathy of Prematurity Cooperative Group. Multicenter Trial of Cryotherapy for Retinopathy of Prematurity. Natural history of ROP: ocular outcome at 5½ years in premature infants with birth weights less than 1251 g. Arch Ophthalmol 2002;120:595–9.

Hardy RJ, Palmer EA, Dobson V, et al. Risk analysis of prethreshold retinopathy of prematurity. Arch Ophthalmol 2003;121:1697–701.

Cryotherapy for Retinopathy of Prematurity Cooperative Group. 15-year outcomes following threshold retinopathy of prematurity. Final results from the Multicenter Trial of Cryotherapy for Retinopathy of Prematurity. Arch Ophthalmol 2005;123:311–8.

Cryotherapy for Retinopathy of Prematurity Cooperative Group. Visual acuity at 10 years in Cryotherapy for Retinopathy of Prematurity (CRYO-ROP) Study eyes. Arch Ophthalmol 2006;124:199–202.

Multicenter Study of Light Reduction in Retinopathy of Prematurity (LIGHT-ROP)

Reynolds JD, Hardy RJ, Kennedy KA, et al. Lack of efficacy of light reduction in preventing retinopathy of prematurity. N Engl J Med 1998;338:1572–6.

LIGHT-ROP Cooperative Group. The design of the multicenter study of Light Reduction in Retinopathy of Prematurity (LIGHT-ROP). J Pediatr Ophthalmol Strabismus 1999;36:257–63.

Kennedy KA, Fielder AR, Hardy RJ, et al. Reduced lighting does not improve medical outcomes in very-low-birth-weight infants. J Pediatr 2001;139:527–31.

Reynolds JD, Dobson V, Quinn GE, et al. for the CRYO-ROP and LIGHT-ROP Cooperative Groups. Evidence-based screening criteria for retinopathy of prematurity. Natural history data from the CRYO-ROP and LIGHT-ROP studies. Arch Ophthalmol 2002;120:1470-6.

Supplemental Therapeutic Oxygen for Prethreshold Retinopathy of Prematurity (STOP-ROP)

STOP-ROP Multicenter Study Group. Supplemental Therapeutic Oxygen for Prethreshold Retinopathy of Prematurity (STOP-ROP), a randomized, controlled trial. I: Primary outcomes. Pediatrics 2000;105:295–310.

Oden NL, Phelps DL, the STOP-ROP Multicenter Study Group. Statistical issues related to early closure of STOP-ROP, a group-sequential trial. Control Clin Trials 2003;24:28–38.

Engel RR, Oden NL, Cohen GR, et al., STOP-ROP Multicenter Study Group. Influence of prior assignment on refusal rates in a trial of supplemental oxygen for retinopathy of prematurity. Paediatr Preinat Epidemiol 2006;20(4):348-59.

Early Treatment for Retinopathy of Prematurity (ETROP or EARLY-ROP)

Early Treatment for Retinopathy of Prematurity Cooperative Group. Revised indications for the treatment of retinopathy of prematurity. Results of the Early Treatment for Retinopathy of Prematurity randomized trial. Arch Ophthalmol 2003;121:1684–96.

Hardy RJ, Good WV, Dobson V, et al. for the Early Treatment for Retinopathy of Prematurity Cooperative Group. Multicenter trial of early treatment for retinopathy of prematurity: Study design.

Control Clin Trials 2004;24:311–26.

Good WV on behalf of the Early Treatment for Retinopathy of Prematurity Copperative Group. Final results of the Early Treatment for Retinopathy of Prematurity (ETROP) randomized trial. Trans Am Ophthalmol Soc 2004;102:233-250.

Davitt BV, Dobson V, Good WV, et al. for the Early Treatment for Retinopathy of Prematurity Cooperative Group. Prevalence of myopia at 9 months in infants with high-risk prethreshold retinopathy of prematurity. Ophthalmology 2005;112:1564–8.

Repka MX, Tung B, Good WV, et al. Outcome of eyes developing retinal detachment during the Early Treatment for Retinopathy of Prematurity Study (ETROP). Arch Opthalmol 2006;124:24–30.

VanderVeen DK, Coats DK, Dobson V, et al. for the Early Treatment for Retinopathy of Prematurity Cooperative Group. Prevalence and course of strabismus in the first year of life for infants with prethreshold retinopathy of prematurity. Arch Ophthalmol 2006;124:766–73.

Early Treatment for Retinopathy of Prematurity Cooperative Group. The Early Treatment for Retinopathy of Prematurity Study: structural findings at age 2 years. Br J Ophthalmol 2006;90:1378–82.

Quinn GE, Dobson V, Davitt BV, et al. on behalf of the Early Treatment for Retinopathy of Prematurity Cooperative Group. Progression of myopia and high myopia in the Early Treatment for Retinopathy of Prematurity Study. Findings to 3 years of age. Ophthalmology 2008;115:1058–64.

Davitt BV, Dobson V, Quinn GE, et al. on behalf of the Early Treatment for Retinopathy of Prematurity Cooperative Group. Astigmatism in the Early Treatment for Retinopathy of Prematurity Study. Findings to 3 years of age. Ophthalmology 2009;116:332-9.

Early Treatment for Retinopathy of Prematurity Cooperative

Group. Final visual acuity results in the Early Treatment for Retinopathy of Prematurity Study. Arch Ophthalmol 2010;128:663–71.

Early Treatment for Retinopathy of Prematurity Cooperative Group. Visual field extent at 6 years of age in children who had high-risk prethreshold retinopathy of prematurity. Arch Ophthalmol 2011;129:127–32.

Early Treatment for Retinopathy of Prematurity Cooperative Group. Grating visual acuity results in the Early Treatment for Retinopathy of Prematurity Study. Arch Ophthalmol 2011;129:840–6.

Repka MX, Tung B, Good WV, et al. Outcome of eyes developing retinal detachment during the Early Treatment for Retinopathy of Prematurity Study. Arch Ophthalmol 2011;129(9):1175-9.

Wheeler DT, Dobson V, Chuang MF, et al. Retinopathy of prematurity in infants weighing less than 500 grams at birth enrolled in the Early Treatment for Retinopathy of Prematurity Study. Ophthalmology 2011;118:1146-51.

VanderVeen DK, Bremer DL, Fellows RR, et al., Early Treatment for Retinopathy of Prematurity Cooperative Group. Prevalence and course of strabismus through age 6 years in participants of the Early Treatment for Retinopathy of Prematurity randomized trial. J AAPOS 2011;14(6):536-40.

Wallace DK, Bremer DL, Good WV, et al. Correlation of recognition visual acuity with posterior retinal structure in advanced retinopathy of prematurity. Arch Ophthalmol 2012;130(12):1512-6.

Bremer DL, Rogers DL, Good WV, et al. Glaucoma in the Early Treatment for Retinopathy of Prematurity (ETROP) Study. J AAPOS 2012;16(5):449-52.

Siatkowski RM, Good WV, Summers CG, et al. Clinical characteristics of children with severe visual impairment but

favorable retinal structural outcomes from the Early Treatment for Retinopathy of Prematurity (ETROP) Study. J AAPOS 2013;17(2):129-34.

Bevacizumab Eliminates the Angiogenic Threat for Retinopathy of Prematurity (BEAT-ROP)

Mintz-Hittner HA, Kennedy KA, Chuang AZ, for the BEAT-ROP Cooperative Group. Efficacy of intravitreal bevacizumab for Stage 3+ retinopathy of prematurity. N Engl J Med 2011;364:603-15.

Geloneck MM, Chuang AX, Clark WL, et al. for the BEAT-ROP Cooperative Group. Refractive outcomes following bevacizumab monotherapy compared with conventional laser treatment: A randomized clinical trial. JAMA Ophthalmol 2014;132(11):1327-33.

Posterior Uveitis

Multicenter Uveitis Steroid Treatment (MUST) Trial

Multicenter Uveitis Steroid Treatment Trial Research Group. The Multicenter Uveitis Steroid Treatment Trial: Rationale, design, and baseline characteristics. Am J Ophthalmol 2010;149:550-61.

Madow B, Galor A, Feuer WJ, et al. Validation of a photographic vitreous haze grading technique for clinical trials in uveitis. Am J Ophthalmol 2011;152:170-6.

Sugar EA, Jabs DA, Altaweel MM, et al. on behalf of the Multicenter Uveitis Steroid Treatment (MUST) Trial Research Group. Identifying a clinically meaningful threshold for change in uveitic macular edema evaluated by optical coherence tomography. Am J Ophthamol 2011;152:1044-52.

Multicenter Uveitis Steroid Treatment (MUST) Trial Research

Group. Randomized comparison of systemic anti-inflammatory therapy versus fluocinolone acetonide implant for intermediate, posterior, and panuveitis: The Multicenter Uveitis Steroid Treatment Trial. Ophthalmology 2011;118:1916-1926.

Gangaputra SS, Altaweel MM, Peng Q, et al. for the MUST Trial Research Group. Morphologic assessment for glaucoma in the Multicenter Uveitis Steroid Treatment (MUST) Trial. Ocular Immunol Inflamm 2011;19:267-74.

Sen HN, Drye LT, Goldstein DA, et al. for the Multicenter Uveitis Steroid Treatment (MUST) Trial Research Group. Hypotony in patients with uveitis: The Multicenter Uveitis Steroid Treatment (MUST) Trial. Ocular Immunol Inflamm 2012;20(2):104-12.

Taylor SRJ, Lightman SL, Sugar EA, et al. The impact of macular edema on visual function in intermediate, posterior, and panuveitis. Ocular Immunol Inflamm 2012;20(3):171-81.

Domapally A, Altaweel MM, Kempen, et al. for the MUST Trial Research Group. Optical coherence tomography evaluation in the Multicenter Uveitis Steroid Treatment (MUST) Trial. Ocular Immunol Inflamm 2012;20(6):443-7.

Frick KD, Drye LT, Kempen JH, et al., Multicenter Uveitis Steroid Treatment (MUST) Trial Research Group. Associations among visual acuity and vision- and health-related quality of life among patients in the Multicenter Uveitis Steroid Treatment Trial. Invest Ophthalmol Vis Sci 2012;53(3):1169-76.

Kempen JH, Sugar EA, Jaffe GJ, et al., for the Multicenter Uveitis Steroid Treatment (MUST) Trial Research Group. Fluorescein angiography versus optical coherence tomography for diagnosis of uveitic macular edema. Ophthalmology 2013;120(9):1852-9.

Multicenter Uveitis Steroid Treatment (MUST) Trial Research Group. Cost-effectiveness of fluocinolone acetonide implant versus systemic therapy for noninfectious intermediate, posterior, and panuveitis. Ophthalmology 2014;121(10):1855-62.

Multicenter Uveitis Steroid Treatment (MUST) Trial Research Group. Benefits of systemic anti-inflammatory therapy versus fluocinolone acetonide intraocular implant for intermediate uveitis, posterior uveitis, and panuveitis. Fifty-four-month results of the Multicenter Uveitis Steroid Treatment (MUST) Trial and Follow-up Study. Ophthalmology 2015;122(10):1967-75.

Multicenter Uveitis Steroid Treatment (MUST) Trial Follow-up Study Research Group. Quality of life and risks associated with systemic anti-inflammatory therapy versus fluocinolone acetonide intraocular implant for intermediate uveitis, posterior uveitis, or panuveitis: Fifty-four-month results of the Multicenter Uveitis Steroid TreatmentTrial and Follow-up Study. Ophthalmology 2015;122(10):1976-86.

Other Trials for Posterior Uveitis

Jaffe GJ, Martin D, Callanan D, et al for the Flucinolone Acetonide Uveitis Study Group. Fluocinolone acetonide implant (Retisert) for noninfectious posterior uveitis. Thirty-four-week results of a multicenter randomized clinical study. Ophthalmology 2006;113:1020-27.

Callanan DG, Jaffe GJ, Marin DF, et al. Treatment of posterior uveitis with a fluocinolone acetonide implant. Three-year clinical trial results. Arch Ophthalmol 2008;126:1191–201.

Pavesio C, Zierhut M, Bairi K, et al. for the Fluocinolone Acetonide Study Group. Evaluation of an intravitreal fluocinolone acetonide implant versus standard systemic therapy in noninfectious posterior uveitis. Ophthalmology 2010;117:567-75.

Lowder C, Belfort B, Lightman S, et al. Dexamethasone intravitreal implant for noninfectious intermediate or posterior uveitis. Arch Ophthalmol 2011;129:545–53.

Soheilian M, Ramezani A, Azimzadeh A, et al. Randomized trial of intravitreal clindamycin and dexamethasone versus pyrimethamine, sulfadiazine, and prednisolone in treatment of

ocular toxoplasmosis. Ophthalmology 2011;118:134–41.

Lowder C, Belfort R, Lightman S, et al. for the Ozurdex HURON Study Group. Dexamethasone intravitreal implant for noninfectious intermediate or posterior uveitis. Arch Ophthalmol 2011;129(5):545-53.

Sangwan VS, Pearson PA, Paul H, et al. Use of the fluocinolone acetonide intravitreal implant for the treatment of noninfectious posterior uveitis. 3-year results of a randomized clinical trial in a predominantly Asian population. Ophthalmol Ther 2015;4(1):1-19.

Other Retinal and Retina-Related Conditions

Collaborative Ocular Melanoma Study (COMS)

The COMS was conducted to compare length of survival after radiotherapy or standard enucleation for primary treatment of choroidal melanoma. Two randomized trials were completed: the COMS randomized trial of iodine-125 brachytherapy and the COMS randomized trial of pre-enucleation external beam radiation. A small nonrandomized observational study of small choroidal melanoma was conducted at a subset of COMS centers. A parallel prospective study of quality of life among patients in the brachytherapy trial (COMS-QOLS) also was conducted. The COMS design and findings are discussed in detail in Chapter 154 (Collaborative Ocular Melanoma Study), which cites most publications from the COMS; only primary outcome publications are provided here.

Collaborative Ocular Melanoma Study Group. The Collaborative Ocular Melanoma Study (COMS) randomized trial of pre-enucleation radiation of large choroidal melanoma. II: Initial mortality findings. COMS report no. 10. Am J Ophthalmol 1998;125:779–96.

Collaborative Ocular Melanoma Study Group. The COMS randomized trial of iodine 125 brachytherapy for choroidal melanoma, III: Initial mortality findings. COMS report no. 18. Arch Ophthalmol 2001;119:969–82.

Collaborative Ocular Melanoma Study Group. The Collaborative Ocular Melanoma Study (COMS) randomized trial of pre-enucleation radiation of large choroidal melanoma. IV. Ten-year mortality findings and prognostic factors. COMS report no. 24. Am J Ophthalmol 2004;138:936–51.

Collaborative Ocular Melanoma Study – Quality of Life Study Group. Quality of life after I-125 brachytherapy versus enucleation for choroidal melanoma: 5-year results from the Collaborative Ocular Melanoma Study. COMS-QOLS report no. 3. Arch Ophthalmol 2006;124:226–36.

Collaborative Ocular Melanoma Study Group. The COMS randomized trial of iodine 125 brachytherapy for choroidal melanoma. V. Twelve-year mortality rates and prognostic factors. COMS report no. 28. Arch Ophthalmol 2006;124:1684–93.

Studies of the Ocular Complications of AIDS (SOCA)

In order to address issues regarding treatment of eye involvement, primarily cytomegalovirus retinitis, in patients with the acquired immune deficiency syndrome (AIDS), the National Eye Institute has sponsored SOCA, a clinical trials network. Most of the SOCA clinical trials have been conducted in collaboration with the AIDS Clinical Trials Group. Several of the trials also had industry sponsorship. A longitudinal observational study (LSOCA) was undertaken by the SOCA investigators to provide information on ocular complications during the HAART era.

Studies of Ocular Complications of AIDS (SOCA) Research Group, in collaboration with the AIDS Clinical Trials Group (ACTG). Studies of Ocular Complications of AIDS foscarnet–ganciclovir cytomegalovirus retinitis trial: 1. Rationale, design, and methods. Control Clin Trials 1992;13:22–39.

Studies of Ocular Complications of AIDS Research Group, in collaboration with the AIDS Clinical Trials Group. Mortality in patients with the acquired immunodeficiency syndrome treated with either foscarnet or ganciclovir for cytomegalovirus retinitis. N Engl J Med 1992;326:213–20.

Clinical Trials Group. Foscarnet–ganciclovir cytomegalovirus retinitis trial: 4. Visual outcomes. Ophthalmology 1994;101:1250–61.

Studies of Ocular Complications of AIDS Research Group in collaboration with the AIDS Clinical Trials Group. Morbidity and toxic effects associated with ganciclovir or foscarnet therapy in a randomized cytomegalovirus retinitis trial. Arch Intern Med 1995;155:65–74.

Studies of Ocular Complications of AIDS Research Group, in collaboration with the AIDS Clinical Trials Group. Antiviral effects of foscarnet and ganciclovir therapy on human immunodeficiency virus p24 antigen in patients with AIDS and cytomegalovirus retinitis. J Infect Dis 1995;172:613–21.

Studies of Ocular Complications of AIDS Research Group, in collaboration with the AIDS Clinical Trials Group. Combination foscarnet and ganciclovir therapy vs monotherapy for the treatment of relapsed cytomegalovirus retinitis in patients with AIDS: the Cytomegalovirus Retreatment trial. Arch Ophthalmol 1996;114:23–33.

Studies of Ocular Complications of AIDS Research Group, in collaboration with the AIDS Clinical Trials Group. Clinical vs photographic assessment of treatment of cytomegalovirus retinitis: Foscarnet–Ganciclovir Cytomegalovirus Retinitis Trial report 8. Arch Ophthalmol 1996;114:848–55.

Wu AW, Coleson LC, Holbrook J, et al. Measuring visual function and quality of life in patients with cytomegalovirus retinitis: development of a questionnaire. Arch Ophthalmol 1996;114:841–7.

Studies of Ocular Complications of AIDS Research Group, in collaboration with the AIDS Clinical Trials Group. Assessment of cytomegalovirus retinitis: clinical evaluation vs centralized grading of fundus photographs. Arch Ophthalmol 1996;114:791–805.

Studies of Ocular Complications of AIDS Research Group, in collaboration with the AIDS Clinical Trials Group. MSL-109 adjuvant therapy for cytomegalovirus retinitis in patients with acquired immunodeficiency syndrome: the Monoclonal Antibody Cytomegalovirus Retinitis Trial. Arch Ophthalmol 1997;115:1528–36. [Correction: Arch Ophthalmol 1998;116:296.]

Studies of Ocular Complications of AIDS Research Group, in collaboration with the AIDS Clinical Trials Group. Parenteral cidofovir for cytomegalovirus retinitis in patients with AIDS: the HPMPC Peripheral Cytomegalovirus Retinitis trial. A randomized, controlled trial. Ann Intern Med 1997;126:264–74.

Studies of Ocular Complications of AIDS (SOCA) Research Group, in collaboration with the AIDS Clinical Trials Group (ACTG). Rhegmatogenous retinal detachment in patients with cytomegalovirus retinitis: the Foscarnet–Ganciclovir Cytomegalovirus Retinitis trial. Am J Ophthalmol 1997;124:61–70.

Studies of Ocular Complications of AIDS Research Group in collaboration with the AIDS Clinical Trials Group. Foscarnet–Ganciclovir Cytomegalovirus Retinitis Trial: 5. Clinical features of cytomegalovirus retinitis at diagnosis. Am J Ophthalmol 1997;124:141–57.

Studies of Ocular Complications of AIDS Research Group, in collaboration with the AIDS Clinical Trials Group. Cytomegalovirus (CMV) culture results, drug resistance, and clinical outcome in AIDS patients with CMV treated with either foscarnet or ganciclovir. J Infect Dis 1997;176:50–8.

Holbrook JT, Davis MD, Hubbard LD, et al. Risk factors for advancement of cytomegalovirus retinitis in patients with

acquired immunodeficiency syndrome. Arch Ophthalmol 2000;118:1196–204.

Holbrook JT, Meinert CL, Van Natta ML, et al. Photographic measures of cytomegalovirus retinitis as surrogates for visual outcomes in treated patients. Arch Ophthalmol 2001;119:554–63.

Martin BK, Gilpin AMK, Jabs DA, et al. for the Studies of Ocular Complications of AIDS Research Group. Reliability, validity, and responsiveness of general and disease-specific quality of life measures in a clinical trial for cytomegalovirus retinitis. J Clin Epidemiol 2001;54:376–86.

Studies of Ocular Complications of AIDS Research Group in collaboration with the AIDS Clinical Trials Group. The ganciclovir implant plus oral ganciclovir versus parenteral cidofovir for the treatment of cytomegalovirus retinitis in patients with acquired immunodeficiency syndrome: The Ganciclovir Cidofovir Cytomegalovirus Retinitis Trial. Am J Ophthalmol 2001;131:457–67.

Jabs DA, Gilpin AMK, Min Y-I, et al. for the Studies of Ocular Complications of AIDS Research Group. HIV and cytomegalovirus viral load and clinical outcomes in AIDS and cytomegalovirus retinitis patients: Monoclonal Antibody Cytomegalovirus Retinitis Trial. AIDS 2002;16:877–87.

Holbrook JT, Jabs DA, Weinberg DV, et al. for the Studies of Ocular Complications of AIDS (SOCA) Research Group. Visual loss in patients with cytomegalovirus retinitis and acquired immunodeficiency syndrome before widespread availability of highly active antiretroviral therapy. Arch Ophthalmol 2003;121:99–107.

Dunn JP, Van Natta M, Foster G, et al. for the Studies of Ocular Complications of AIDS Research Group. Complications of ganciclovir implant surgery in patients with cytomegalovirus retinitis. The Ganciclovir Cidofovir Cytomegalovirus Retinitis Trial. Retina 2004;24:41–50.

Jabs DA, Van Natta M, Thorne JE, et al. for the Studies of the Ocular Complications of AIDS Research Group. Course of cytomegalovirus retinitis in the era of highly active antiretroviral therapy. I. Retinitis progression. Ophthalmology 2004;111:2224–31.

Jabs DA, Van Natta M, Thorne JE, et al. for the Studies of the Ocular Complications of AIDS Research Group. Course of cytomegalovirus retinitis in the era of highly active antiretroviral therapy. 2. Second eye involvement and retinal detachment. Ophthalmology 2004;111:2232–9.

Kempen JH, Min Y-I, Freeman WR, et al. for the Studies of the Ocular Complications of AIDS Research Group. Risk of immune recovery uveitis in patients with AIDS and cytomegalovirus retinitis. Ophthalmology 2006;113:684–94.

Thorne JE, Jabs DA, Kempen JH, et al. for the Studies of Ocular Complications of AIDS Research Group. Incidence of and risk factors for visual acuity loss among patients with AIDS and cytomegalovirus retinitis in the era of highly active antiretroviral therapy. Ophthalmology 2006;113:1432–40.

Thorne JE, Jabs DA, Kempen JH, et al. for the Studies of Ocular Complications of AIDS Research Group. Causes of visual acuity loss among patients with AIDS and cytomegalovirus retinitis in the era of highly active antiretroviral therapy. Ophthalmology 2006;113:1441–5.

Thorne JE, Jabs DA, Kempen JH, et al. for the Studies of Ocular Complications of AIDS Research Group. Incidence of and risk factors for visual acuity loss among patients with AIDS and cytomegalovirus retinitis in the era of highly active antiretroviral therapy. Ophthalmology 2007;114:787–93.

Jabs DA, Van Natta ML, Holbrook JT, et al. for the Studies of the Ocular Complications of AIDS Research Group. Longitudinal Study of the Ocular Complications of AIDS. 1. Ocular diagnoses at enrollment. Ophthalmology 2007;114:780-6.

Jabs DA, Van Natta ML, Holbrook JT, et al for the Studies of the Ocular Complications of AIDS Research Group. Longitudinal Study of the Ocular Complications of AIDS. 2. Ocular examination results at enrollment. Ophthalmology 2007;114:787-93.

Gangaputra S, Pak JW, Peng W, et al. for the Studies of the Ocular Complications of AIDS Research Group. Transition from film to digital fundus photography in the Longitudinal Studies of the Ocular Complications of AIDS. Retina 2012;32:600-605.

Trials of Interventions for Retinitis Pigmentosa

Berson EL, Rosner B, Sandberg MA, et al. A randomized trial of vitamin A and vitamin E supplementation for retinitis pigmentosa. Arch Ophthalmol 1993;111:761–72.

Sandberg MA, Weigel-DeFranco C, Rosner B, et al. The relationship between visual field size and electroretinogram amplitude in retinitis pigmentosa. Invest Ophthalmol Vis Sci 1996;37:1693–8.

Berson EL, Rosner B, Sandberg MA, et al. Clinical trial of docosahexaenoic acid in patients with retinitis pigmentosa receiving vitamin A treatment. Arch Ophthalmol 2004;122:1297–305.

Berson EL, Rosner B, Sandberg MA, et al. Further evaluation of docosahexaenoic acid in patients with retinitis pigmentosa receiving vitamin A treatment: subgroup analyses. Arch Ophthalmol 2004;122:1306–14.

Berson EL, Rosner B, Sandberg MA, et al. Clinical trial of lutein in patients with retinitis pigmentosa receiving vitamin A. Arch Ophthalmol 2010;128:403–11.

Adackapara CA, Sunness JS, DiBernardo CW, et al. Prevalence of cystoid macular edema and stability of OCT retinal thickness in eyes with retinitis pigmentosa during a 48-week lutein trial. Retina 2008;28:103–10.

Retinal Surgery

Silicone Study

The Silicone Study was conducted to compare postoperative tamponade effectiveness of intraocular silicone oil with that of long-acting gas for managing retinal detachment complicated by proliferative vitreoretinopathy.

Azen SP, Irvine AR, Davis MD, et al. The validity and reliability of photographic documentation of proliferative vitreoretinopathy. Ophthalmology 1989;96:352–7.

Lean JS, Stern WH, Irvine AR, et al. Classification of proliferative vitreoretinopathy used in the Silicone Study. Ophthalmology 1989;96:765–71.

Azen SP, Boone DC, Barlow W, et al. Methods, statistical features, and baseline results of a standardized, multicentered ophthalmological surgical trial: the Silicone Study. Control Clin Trials 1991;12:438–55.

Silicone Study Group. Vitrectomy with silicone oil or sulfur hexafluoride gas in eyes with severe proliferative vitreoretinopathy: results of a randomized clinical trial. Silicone Study report 1. Arch Ophthalmol 1992;110:770–9.

Silicone Study Group. Vitrectomy with silicone oil or perfluoropropane gas in eyes with severe proliferative vitreoretinopathy: results of a randomized clinical trial. Silicone Study report 2. Arch Ophthalmol 1992;110:780–92.

McCuen BW, Azen SP, Stern W, et al. Vitrectomy with silicone oil or with perfluoropropane gas in eyes with severe proliferative vitreoretinopathy. Silicone Study report 3. Retina 1993;13:279–84.

Barr CC, Lai MY, Lean JS, et al. Postoperative intraocular pressure abnormalities in the Silicone Study. Silicone Study report 4. Ophthalmology 1993;100:1629–35.

Blumenkranz MS, Azen SP, Aaberg T, et al. Relaxing retinotomy with silicone oil or long-acting gas in eyes with severe proliferative vitreoretinopathy. Silicone Study report 5. Am J Ophthalmol 1993;116:557–64.

Hutton WL, Azen SP, Blumenkranz MS, et al. The effects of silicone oil removal. Silicone Study report 6. Arch Ophthalmol 1994;112:778–85.

Abrams GW, Azen SP, Barr CC, et al. The incidence of corneal abnormalities in the Silicone Study. Silicone Study report 7. Arch Ophthalmol 1995;113:764–9.

Cox MS, Azen SP, Barr CC, et al. Macular pucker after successful surgery for proliferative vitreoretinopathy. Silicone Study report 8. Ophthalmology 1995;102:1884–91.

Lean J, Azen SP, Lopez PF, et al. The prognostic utility of the Silicone Study classification system. Silicone Study report 9. Arch Ophthalmol 1996;114:286–92.

Diddie KR, Azen SP, Freeman HM, et al. Anterior proliferative vitreoretinopathy in the Silicone Study. Silicone Study report 10. Ophthalmology 1996;103:1092–9.

Abrams GW, Azen SP, McCuen BW, et al. Vitrectomy with silicone oil or long-acting gas in eyes with severe proliferative vitreoretinopathy: results of additional and long-term follow-up. Silicone Study report 11. Arch Ophthalmol 1997;115:335–44.

Macular Hole Trials

Kim JW, Freeman WR, El-Haig W, et al. for the Vitrectomy for Macular Hole Study Group. Baseline characteristics, natural history, and risk factors to progression in eyes with stage 2 macular holes. Results from a prospective randomized clinical trial. Ophthalmology 1996;102:1818-29.

Kim JW, Freeman WR, Azen SP, et al., Vitrectomy for Macular Hole

Study Group. Prospective randomized trial of vitrectomy or observation for stage 2 macular holes. Am J Ophthalmol 1996;121:605-14.

Freeman WR, Azen SP, Kim JW, et al. Vitrectomy for the treatment of full-thickness stage 3 or 4 macular holes: results of a multicenter randomized clinical trial. Arch Ophthalmol 1997;115:11–21.

Tadayoni R, Vicaut E, Devin F, et al. A randomized controlled trial of alleviated positioning after small macular hole surgery. Ophthalmology 2011;118:150–5.

Ezra E, Gregor ZJ, for the Moorfields Macular Hole Study Group. Surgery for idiopathic full-thickness macular hole. Two-year results of a randomized clinical trial comparing natural history, vitrectomy, and vitrectomy plus autologous serum: Moorfields Macular Hole Study Group report no. 1. Arch Ophthalmol 2004;122:224-36.

Guillaubey A, Malvitte L, LaFontaine PO, et al. Comparison of face-down and seated position after idiopathic macular hole surgery: A randomized clinical trial. Am J Ophthalmol 2008;146:128-34.

Lois N, Burr J, Norrie J, et al. for the Full-thickness macular hole and Internal Limiting Membrane peeling Study (FILMS) Group. Clinical and cost-effectiveness of internal limiting membrane peeling for patients with idiopathic full thickness macular hole. Protocol for a randomised controlled trial: FILMS (Full-thickness macular hole and Internal Limiting Membrane peeling Study). Trials 2008;9:61.

Lois N, Burr J, Norrie J, et al. for the Full-thickness Macular Hole and Internal Limiting Membrane Peeling Study (FILMS) Group. Internal limiting membrane peeling versus no peeling for idiopathic full-thickness macular hole: A pragmatic randomized controlled trial. Invest Ophthalmol Vis Sci 2011;52(3):1586-92.

SPR Study

Heimann H, Hellmich M, Bornfeld N, et al. Scleral buckling versus primary vitrectomy in rhegmatogenous retinal detachment (SPR Study): design issues and implications. SPR Study report no. 1. Graefes Arch Clin Exp Ophthalmol 2001;239(8):567-74.

SPR Study Group. Scleral buckling versus primary vitrectomy in rhegmatogenous retinal detachment study (SPR Study): recruitment list evaluation. Study report no. 2. Graefes Arch Clin Esp Ophthalmol 2007;245(2):803-9.

Heussen N, Hilgers RD, Heimann H, et al., SPR Study Group. Scleral buckling versus primary vitrectomy in rhegmatogenous retinal detachment study (SPR study): multiple-event analysis of risk factors for reoperations. SPR Study report no. 4. Acta Ophthalmol 2011;89(7):622-8.

SPR Study Group. Scleral buckling versus primary vitrectomy in rhegmatogenous retinal detachment study (SPR Study): predictive factors for functional outcome. Study report no. 6. Graefes Arch Clin Exp Ophthalmol 2011;249(8):1129-36.

Feltgen N, Heimann H, Hoerauf H, et al. for the SPR Study Investigators. Scleral buckling versus primary vitrectomy in rhegmatogenous retinal detachment study (SPR Study): Risk assessment of anatomical outcome. SPR Study report no. 7. Acta Ophthalmologica 2013;91(3):282-7.

Microplasmin for Intravitreous Injection-Traction Release Without Surgical Treatment (MIVI-TRUST) Trials

Stalmans P, Benz MS, Gandorfer A, for the MIVI-TRUST Study Group. Enzymatic vitreolysis with ocriplasmin for vitreomacular traction and macular holes. N Engl J Med 2012;367:606-15.

Haller JA, Stalmans P, Benz MS, et al. for the MIVI-TRUST Study Group. Efficacy of intravitreal ocriplasmin for treatment of vitreomacular adhesion. Subgroup analyses from two randomized trials. Ophthalmology 2015;122:117-122.

Varma R, Haller JA, Kaiser PK. Improvement in patient-reported visual function after ocriplasmin for vitreomacular adhesion. Results of the Micoplasmin for Intravitreous Injection-Traction Release without Surgical Treatment (MIVI-TRUST) Trials. JAMA Ophthalmol 2015;133(9):997-1004.

Folger PA, Toth CA, DeCroos FC, et al. Assessment of retinal morphology with spectral and time domain OCT in the phase III trials of enzymatic vitreolysis. Invest Ophthalmol Vis Sci 2012;53(11):7395-401.

Other Retinal Surgery Trials

Tornambe PE, Hilton GF, the Retinal Detachment Study Group. Pneumatic retinopexy. A multicenter randomized controlled clinical trial comparing pneumatic retinopexy with scleral buckling. Ophthalmology 1989; 96:772-84.

Tornambe PE, Hilton GF, Brinton DA, et al. Pneumatic retinopexy: Two-year follow-up study of the multicenter clinical trial comparing pneumatic retinopexy with scleral buckling. Ophthalmology 1991;98(7):1115-23.

Asaria RHY, Kon CH, Bunce C, et al. Adjuvant 5-fluorouracil and heparin prevents proliferative vitreoretinopathy. Results from a randomized, double-blind, controlled clinical trial. Ophthalmology 2001;108:1179-83.

Wickham L, Bunce C, Wong D, et al. Randomized controlled trial of combined 5-fluorouracil and low-molecular-weight heparin in the management of unselected rhegmatogenous retinal detachments undergoing primary vitrectomy. Ophthalmology 2007;114:698-794.

Williams GA, Haller JA, Kuppermann BD, et al. for the Dexamethasone DDS Phase II Study Group. Dexamethasone posterior segment drug delivery system in the treatment of macular edema resulting from uveitis or Irvine–Gass syndrome. Am J Ophthamol 2009;147:1049-54.

Ahmadieh H, Shoeibi N, Entezari M, et al. Intravitreal bevacizumab for prevention of early postvitrectomy hemorrhage in diabetic patients. A randomized clinical trial. Ophthalmology 2009;116:1943–8.

Entezari M, Ramezani A, Ahmadieh H, et al. Cryotherapy of sclerotomy sites for prevention of late post-vitrectomy diabetic hemorrhage: a randomized clinical trial. Grafes Arch Clin Exp Ophthalmol 2010;248:13-9.

Ahn J, Woo SJ, Chung H, Park KH. The effect of adjunctive intravitreal bevacizumab for preventing postvitrectomy hemorrhage in proliferative diabetic retinopathy. Ophthalmology 2011;118:2218-26.

Cochrane Systematic Reviews

Cornish KS, Lois N, Scott N, et al. Vitrectomy with internal limiting membrane (ILM) peeling versus vitrectomy with no peeling for idiopathic full-thickness macular holes (FTMH). Cochrane Database of Systematic Reviews 2013, Issue 6, Art. No.: CD009306. doi: 10.1002/14651858.CD009306.pub2.

Solebo AL, Lange CAK, Bunce C, et al. Face-down positioning or posturing after macular hole surgery. Cochrane Database of Systematic Reviews 2011, Issue 12, Art. No.:CD008228. doi: 10.1002/14651858.CD008228.pub2.

Sundaram V, Barsam A, Virgili G. Intravitreal low molecular weight heparin and 5-fluorouracil for the prevention of proliferative vitreoretinopathy following retinal reattachment surgery. Cochrane Database of Systematic Reviews 2013, Issue 1, Art. No.:CD006421. doi: 10.1002/14651858.CD006421.pub3.

Hatef E, Sena DF, Fallano KA, et al. Pneumatic retinopexy versus scleral buckle for repairing simple rhegmatogenous retinal detachments. Cochrane Database of Systematic Reviews 2015, Issue 5, Art. No.:CD008350. doi: 10.1002/14651858.CD008350.pub2.

Volume Three

OUTLINE

PART 1

Surgical Retina

OUTLINE

SECTION 1

The Pathophysiology of Retinal Detachment and Associated Problems

OUTLINE

98

Pathogenetic Mechanisms of Retinal Detachment

Sebastian Wolf, Martin Zinkernagel

Introduction

The term retinal detachment is used to describe a separation of the neurosensory retina from the retinal pigment epithelium (RPE). This chapter discusses the mechanisms that keep the retina attached and the pathogenetic mechanisms that cause the most commonly encountered types of retinal detachments. Details of specific types

of retinal detachment and their treatment are addressed in other chapters.

Major Types

Retinal detachments can be classified into categories based on the presence of a tractional component.[1] Those with a tractional component include rhegmatogenous, tractional, combined tractional–rhegmatogenous, and central retinal detachments in myopic eyes. Retinal detachments without tractional components include exudative and hemorrhagic retinal detachments.

The most common form is rhegmatogenous (derived from the Greek word *rhegma*, meaning break) retinal detachment, which occurs as the result of a full-thickness retinal break secondary to or in combination with vitreous traction. The second category, traction retinal detachment, occurs when vitreoretinal adhesions mechanically detach the retina from the underlying RPE. In combined tractional–rhegmatogenous retinal detachments the tractional component precedes the retinal break and therefore is the causative component. Retinal detachment without a tractional component can be caused by subretinal fluid production due to a process, such as a tumor or inflammation, or by blood and/or serum accumulation in the subretinal space.

Accumulation of subretinal fluid is a feature of all retinal detachments. When the normal physiologic forces that maintain contact between the retina and the RPE (e.g., the metabolic pump of the RPE,[2] the osmotic pressure of the choroid,[3] and the more minor mechanical forces of the interphotoreceptor matrix) are compromised or overwhelmed, a retinal detachment occurs. Various pathologic conditions can upset the balance of the normal transretinal pressure gradient and result in subretinal fluid accumulation.[4]

Rhegmatogenous Retinal Detachment

As noted above, rhegmatogenous retinal detachments are those arising from one or more full-thickness retinal breaks in combination with vitreous traction.[1]

Most of these are "horseshoe tears" occurring at sites of strong vitreoretinal adhesions, most commonly at the irregular posterior margin of the vitreous base during posterior vitreous detachment (PVD). They are more common in the superior temporal quadrant followed by the superior nasal quadrant. "U-tears," another term for horseshoe tears, consist of a flap in which its apex is pulled anteriorly by the vitreous while the base remains attached to the retina (Fig. 98.1). The actual tear consists of two anterior extensions (horns) running forward from the apex.

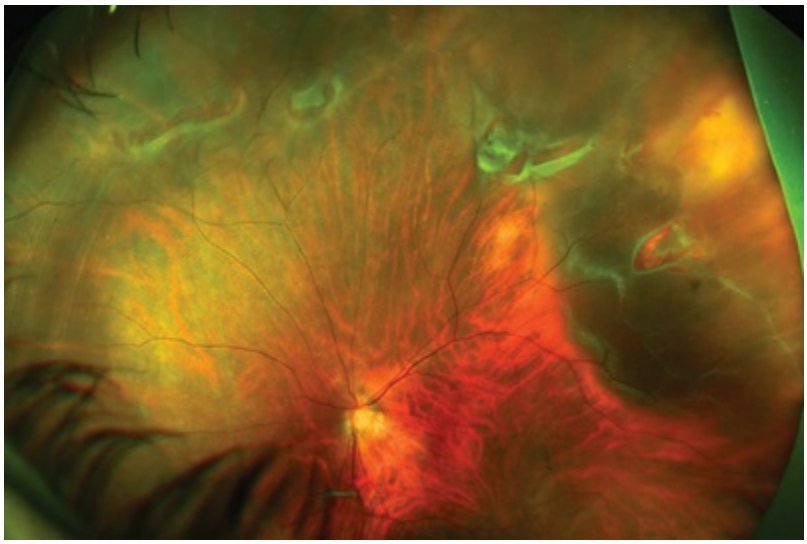

FIG. 98.1 Rhegmatogenous retinal detachments with multiple full-thickness retinal breaks.

The term "retinal break" refers either to a retinal tear or to a retinal hole. Retinal tears are commonly associated with well-defined vitreoretinal traction at the posterior margin of the vitreous base during PVD. In contrast, retinal holes occur more commonly as a result of localized retinal atrophy or deterioration. The overlying operculum generally indicates relief of vitreoretinal traction in this area.[5–7]

In some cases, however, operculated retinal holes may be associated with vitreous traction in the near vicinity of the hole. This is especially true for retinal holes within lattice lesions. These round holes may behave like tears with persistent traction and have a higher likelihood to lead to rhegmatogenous detachment.

The characteristics of a rhegmatogenous retinal detachment are

(1) the existence of abnormal mobility of partially liquefied vitreous gel; (2) tractional forces that can precipitate a retinal break; and (3) the presence of a retinal break that will allow the passage of liquefied vitreous into the subretinal space (Fig. 98.2). All three factors need to be present to cause a rhegmatogenous retinal detachment. For example, if a tear or hole is present in the absence of tractional forces and liquid vitreous, it is unlikely that the retina will detach. Examination of postmortem eyes indicates that approximately 5–10% of eyes have full-thickness retinal defects without any apparent detachment.[8] A spontaneous rhegmatogenous retinal detachment is usually preceded by a PVD. With age, fragmentation of collagen fibers and an aggregation of proteoglycans around these fragments are believed to be responsible for destabilizing the vitreous gel and leading to liquefaction (syneresis).[9,10] The subsequent reduced volume of the vitreous gel is associated with the collapse and aggregation of the collagen fibrillar network. The liquefied vitreous gel may coalesce into a large lacuna, which mimics a true PVD.[11]

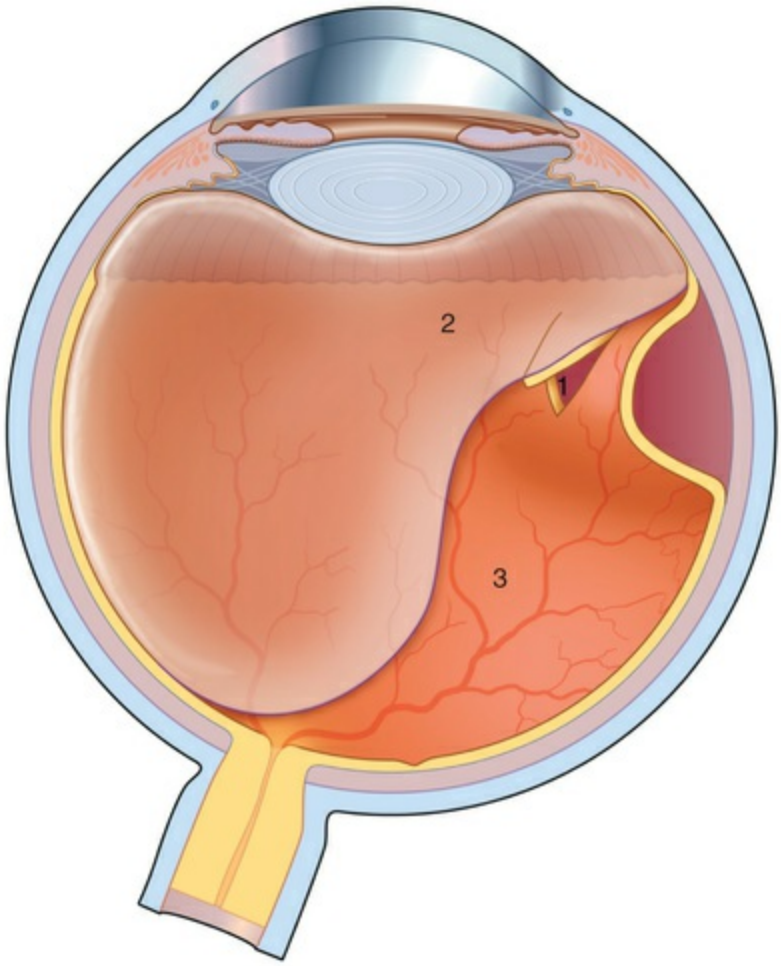

FIG. 98.2 Characteristics of rhegmatogenous retinal detachment. *1* The presence of a retinal break. *2* Tractional forces from the vitreous on the retinal break. *3* Existence of liquefied vitreous able to pass through the retinal break into the subneurosensory space.

When the denser posterior vitreous cortex ruptures, the liquefied vitreous can pass into the subhyaloid space and separate the posterior vitreous surface from the internal limiting membrane of the retina producing a true PVD. Vitreous syneresis can be seen with the slit lamp in more than 90% of patients after the age of 40 years.[12] Both the degree of vitreous liquefaction and the prevalence of PVD are age-related.[10] In one study PVD was found in 27% of patients aged 60–69 years and in 63% of patients after age 70.[13] Other factors that accelerate liquefaction of vitreous gel include enzymatic vitreolysis with ocriplasmin, cataract extraction, high myopia, inflammation, and trauma.[14,15]

In the presence of a PVD, the condensed vitreous moves about

within the vitreous cavity, and rotational movements of the eye exert traction where the vitreous remains attached to the retina, most often at the vitreous base. These tractional forces may lead to a retinal break.

Ocular trauma can lead to traumatic complete or partial PVD which may result in retinal breaks and subsequent rhegmatogenous retinal detachment. In young patients trauma may lead to retinal dialysis which represents a disinsertion of the retina at the ora serrata and is generally not associated with PVD. Dialyses, in general and following trauma, are more common in the inferotemporal quadrant although most of the dialyses in the superonasal quadrant are associated with a definite history of preceding trauma.[16] Giant retinal tears (circumferential retinal breaks of ≥90°) commonly arise from circumferential vitreous traction in the region of the posterior vitreous base, in the presence of a PVD. Giant retinal tears most commonly develop just posterior to the ora but also may be found at the equator (15%) and sometimes posterior to the equator.[17,18] Most giant retinal tears are idiopathic. However trauma, previous surgery, myopia, and inherited vitreoretinopathies have been reported to be risk factors.[19] Inherited vitreoretinopathies include a group of genetic disorders that result in abnormalities of the vitreous and retina with susceptibility to rhegmatogenous retinal detachment (RRD). The most common hereditary vitreoretinopathy is associated with the Stickler syndromes.[20,21] This inherited condition is associated primarily with the *COL2A* gene and also with the *COL11A1* gene.[22] Rhegmatogenous retinal detachment is a very common complication in these patients.[23,24]

Rhegmatogenous retinal detachments originating posterior to the equator are characteristic for high myopia.[25] Posterior pole retinal detachments are very rare, accounting for approximately 1% of retinal detachments in the United States, but the prevalence may be much higher in Asia.[26,27] Most of the nontraumatic retinal breaks located in the posterior pole are secondary to macular holes and associated with a posterior staphyloma.[20] We found that posterior breaks may also be associated with the use of ocriplasmin (Fig. 98.3). Vitreoretinal traction based on epiretinal membranes after incomplete posterior vitreous separation ("vitreoschisis")[28,29] and

reduced retinal adherence to the choroid due to RPE atrophy[30] are speculated to be pathophysiologic factors in retinal detachments associated with myopic macular holes. Some authors believe that operative failure in these instances is related to axial elongation and posterior staphyloma formation.[31]

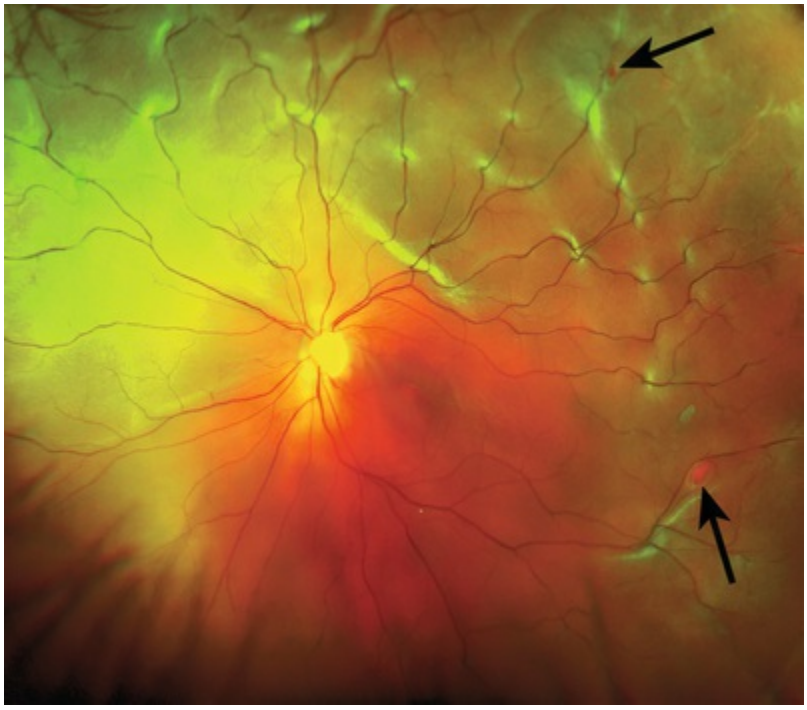

FIG. 98.3 Rhegmatogenous retinal detachments 1 week after ocriplasmin injection. The posterior breaks are marked with *arrows*.

Aphakia and pseudophakia are commonly associated with peripheral retinal breaks at the posterior edge of the vitreous base near the ora serrata. In this region the retina is relatively thin and less developed. The incidence of retinal detachment associated with cataract extraction has decreased with the changes in surgical technique over the years, from intracapsular cataract extraction and aphakic correction to phacoemulsification, combined with the placement of a posterior chamber intraocular lens in the presence of an intact posterior lens capsule.[32] The incidence of retinal detachment depends on the technique of cataract extraction surgery, ranging from 1% to 8.1% with intracapsular cataract extraction, from 0% to 7.5% with extracapsular cataract extraction and up to 1.8% for phacoemulsification surgery.[33–36]

This is attributed by some to a forward shift of the vitreous after cataract surgery: Modern phacoemulsification surgery has been associated with PVD induction of up to 60% one year after surgery.[37] Rowe et al.[38] predicted that 10 years after either phacoemulsification or extracapsular cataract extraction, the cumulative probability of retinal detachment was 5.5 times higher than expected. The incidence of subsequent detachments in fellow eyes of patients experiencing a pseudophakic rhegmatogenous retinal detachment in their first eye has been reported to be 7.8% over a mean follow-up period of 57.4 months.[39] Nd:YAG laser posterior capsulotomy is associated with an increased incidence of subsequent retinal detachment.[40]

Various intraocular inflammatory and infectious conditions can cause vitreous gel liquefaction, PVD, and retinal breaks. Ocular toxoplasmosis,[41] ocular toxocariasis,[42] and pars planitis[43] are associated with morphologic vitreoretinal changes leading to vitreoretinal traction and retinal breaks. Some forms of infectious retinitis, such as acute retinal necrosis syndrome and cytomegalovirus retinitis, can result in multiple small breaks along the border between atrophic and normal retina and within necrotic retina.[44,45] Uveitis itself is an overall risk factor for a rhegmatogenous retinal detachment.[46] In addition, patients presenting with a rhegmatogenous retinal detachment from uveitis will also have a higher rate of proliferative vitreoretinopathy (PVR) at presentation and an overall worse prognosis.[46] However, uveitis may also be masqueraded by a longstanding rhegmatogenous detachment.

Retinal detachment resulting from retinoschisis is a subcategory of rhegmatogenous retinal detachment. This occurs when there are holes in both the inner and outer layers of the retina, allowing fluid to enter the retinoschisis cavity and the subretinal space and hence produce a retinal detachment. The incidence of retinal detachment with retinoschisis was up to 1.6% in a large series of patients with retinal detachment.[47]

Tractional Retinal Detachment

The second most common cause of tractional retinal detachment is

that from vitreoretinal forces that mechanically pull the retina away from the underlying RPE. Tractional retinal detachments are commonly seen in diabetic retinopathy, PVR, penetrating trauma, branch retinal vein occlusion, and retinopathy of prematurity (ROP). Tractional forces can occur within the vitreous body, on the inner surface of the retina, or even beneath the retina as in subretinal fibrosis. In the majority of cases, the traction is associated with a clinically apparent membrane. Such membranes typically have fibroblasts and glial and RPE cells as cellular constituents. Experimental evidence has demonstrated the contractile nature of these groups of cells.[48]

In contrast to the rhegmatogenous retinal detachment, which often has a convex, even bullous, surface, the typical traction retinal detachment has a more concave surface and is likely to be more localized, often not extending to the ora serrata (Fig. 98.4).

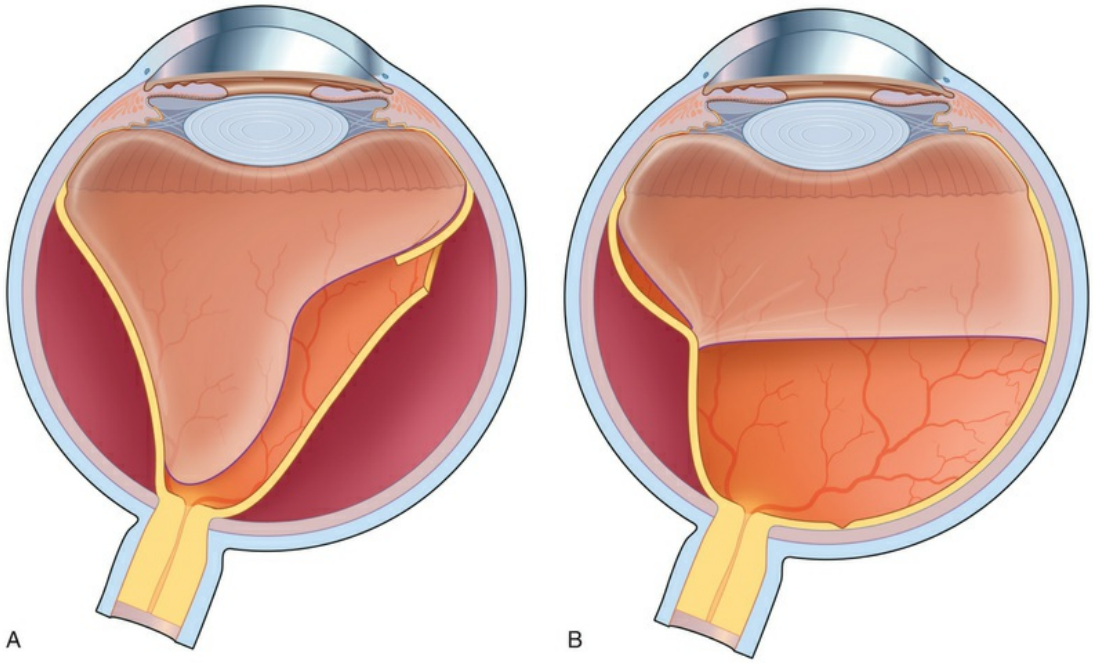

FIG. 98.4 (A) Rhegmatogenous retinal detachment with a bullous configuration. (B) Traction retinal detachment with a concave surface.

Tractional retinal detachments are a common feature of diabetic retinopathy.[49] Contracture of the vitreous gel often occurs in eyes with proliferative retinopathy. As the vitreous gel contracts with

the fibrovascular tissue, these vessels and the underlying retina are drawn anteriorly toward the vitreous base. Because of relatively strong vitreoretinal adhesions along the temporal arcades these areas are most prone to detach, and the detachment can spread both peripherally and centrally toward the macula. Diabetics who develop posterior neovascularization in childhood are prone to this form of traction retinal detachment. However, traction detachments related to diabetes do not inevitably go on to involve the macula. In one series, only 14% progressed to macular detachment within 1 year.[50]

ROP is the leading cause of childhood blindness in the United States, with more than 500 new cases diagnosed each year (see Chapter 118, Surgical management of retinopathy of prematurity). Approximately 90% and in some series up to 100% of ROP, stages 1 and 2, regress. However, it has been reported that up to 17% of infants with aggressive posterior ROP develop a tractional retinal detachment.[51] A gestational age of less than 29.5 weeks, posterior zone 1 disease, and preretinal hemorrhages before laser treatment were identified as the most significant risk factors despite photocoagulation. The pathophysiology is believed to be from endothelial cell proliferation at the junction of the vascularized and avascular retina and migration onto the vitreous scaffold. Contraction of these membranes and the marked adherence of the posterior hyaloid to the retina can produce a complete retinal detachment if untreated.[52]

Retinal vascular diseases such as Eales disease and Coats disease can occasionally cause a fibrous proliferation and membrane formation in the vitreous and a secondary tractional retinal detachment in addition to primarily causing exudative retinal detachments.[53,54]

With the introduction of anti-vascular endothelial growth factor (VEGF) agents for the treatment of exudative and neovascular retinal diseases, there have been concerns that anti-VEGF treatment may lead to contraction of fibrovascular tissue thereby increasing tractional forces leading to tractional detachment.[55,56]

Combined Tractional and

Rhegmatogenous Retinal Detachment

Some retinal detachments combine tractional and rhegmatogenous components. Such detachments are characterized by a full-thickness retinal break and a significant tractional component. Despite the presence of a retinal hole, these detachments are often not bullous and have a concave appearance. They tend to remain localized but may progress to become complete retinal detachments.

Combined tractional–rhegmatogenous retinal detachments are most often seen in proliferative diabetic retinopathy (Fig. 98.5A), PVR, proliferative sickle-cell retinopathy, and penetrating intraocular injuries. PVR (see Chapter 101, Pathogenesis of proliferative vitreoretinopathy, and Chapter 111, Proliferative vitreoretinopathy) is a complication of a rhegmatogenous retinal detachment and is the most common cause of failure of surgical repair of these cases, occurring in 7–10% of primary operations and in a higher percentage of reoperations (Figs. 98.5B–C).[57] In general, PVR develops when cells are dispersed into the vitreous cavity through a retinal break. These cells form membranes on the inner retina surface and on the posterior vitreous surface capable of redetaching the retina and may lead to the reopening of retinal breaks or the creation of new ones.[58]

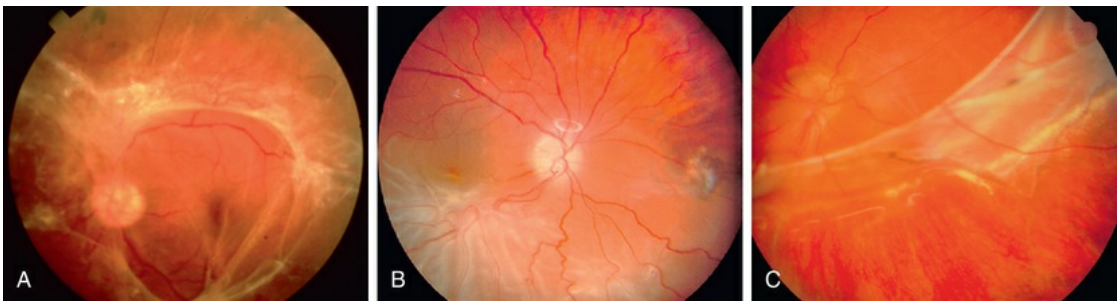

FIG. 98.5 (A) Epiretinal membranes originating together with neovascularizations from the optic disc and the temporal vascular arcade. (B) Two posterior starfolds and inferior retinal detachment under silicone complicating rhegmatogenous retinal detachment. (C) Subretinal strand detaching formerly attached retina from the periphery to the posterior pole of the eye.

Macular pucker has some cellular features in common with PVR

but is usually not classified as this entity. It is not classically associated with retinal breaks and usually not complicated by retinal detachment. Macular pucker has a much better overall prognosis compared with PVR, even though it often compromises central vision. The formation of abnormal membranes on the outer retinal surface is clinically known as subretinal fibrosis. Subretinal fibrosis can disrupt the normal intercellular relationship between the photoreceptors and RPE, thus preventing the regeneration of photoreceptor outer segments after reattachment. (For more details see Chapter 101, Pathogenesis of proliferative vitreoretinopathy.)

In advanced proliferative diabetic retinopathy, combined tractional–rhegmatogenous retinal detachments generally start as tractional retinal detachments that are secondarily complicated by posterior retinal breaks. At this stage, they often have the appearance of a mobile retina with a convex surface and may extend to the ora serrata. The retinal break is commonly located near an area of fibrovascular proliferation.

Exudative and Hemorrhagic Retinal Detachment

Retinal detachments can occur in the absence of a retinal break or vitreoretinal traction. These detachments are the result of a collection of subretinal fluid secondary to diseases of the choroid and RPE or of the retina itself. The RPE is largely responsible for the absorption of the subretinal fluid. Normally, the RPE maintains retinal adherence and absorbs subretinal fluid by means of active transport, creation of an osmotic gradient, and, to a lesser degree, hydrostatic forces. Exudative retinal detachments occur when the balance between fluid production and fluid absorption is disrupted, either by damage to the RPE or by excessive fluid production. Inflammatory diseases and neoplastic lesions are the leading causes of exudative (serous) retinal detachments. Exudative conditions include Vogt–Koyanagi–Harada disease, posterior scleritis, collagen vascular disease, malignant hypertension, sympathetic ophthalmia, preeclampsia, and neoplasms such as malignant melanoma, choroidal hemangioma, and metastatic lesions of the choroid. In

conditions such as central serous chorioretinopathy (idiopathic central serous choroidopathy), the metabolic activity of the RPE can be diffusely compromised,[59] and subretinal fluid is presumably less effectively absorbed. Hyperpermeability of choroidal vessels as demonstrated by indocyanine green angiography are also seen as part of the disease process.[60] Steroids as well as hypercortisolism are risk factors for the development and exacerbation of central serous chorioretinopathy.[61] Retinal vascular diseases, including Coats disease (Fig. 98.6) and familial exudative vitreoretinopathy, may cause excessive production of subretinal fluid and exudates and, consequently, an exudative retinal detachment.[62] Paraproteinemia has been reported to cause serous macular detachment, responding poorly to therapy.[63] "Idiopathic uveal effusion" can produce a serous retinal detachment along with a similar detachment of the choroid, possibly resulting from impaired choroidal venous outflow. This condition when associated with nanophthalmos (mean axial length 16 mm) or high hyperopia (mean +16 diopters) is associated with disorganization of collagen fiber bundles and deposits of proteoglycans in the scleral matrix and can be successfully managed by sclerectomies.[64]

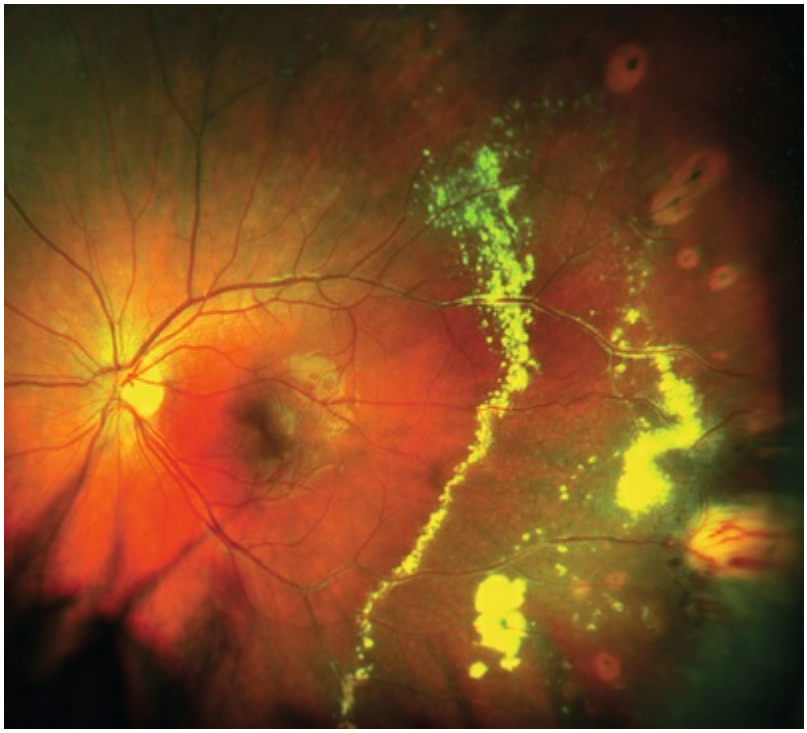

FIG. 98.6 Exudative retinal detachment: Patient is a

12-year-old boy with an extensive exudative retinal detachment due to Coats disease.

Subretinal blood may occur with trauma especially after contusion. Drainage of subretinal blood facilitates retinal RPE apposition, and adequate retinopexy of retinal tears may help to accomplish long-term anatomic attachment in eyes with massive subretinal hemorrhage or bullous retinal detachment.[65] Presumed ocular histoplasmosis syndrome, polypoidal choroidal neovascularization, trauma, and subretinal neovascular membranes, as seen in age-related macular degeneration, may also produce massive hemorrhagic retinal detachment.[55] For the latter the use of anticoagulant medication is a major risk factor, besides high blood pressure and cardiovascular disease.[56] Blood has been proven toxic to the retina and to the retinal pigment epithelium.[66] Displacement of subretinal blood using a gas bubble for subretinal hemorrhage in neovascular age-related macular degeneration decreases the blood's toxicity to the foveal photoreceptors.[67]

A peripheral localization of subretinal hemorrhage is often misinterpreted as choroidal melanoma (pseudomelanoma).[68] Suprachoroidal hemorrhage has been observed after filtering surgery, cataract surgery, trauma, and pars plana vitrectomy.[69,70]

Risk factors for suprachoroidal hemorrhage include high preoperative intraocular pressure, previous retinal detachment, age, gender, and the use antiplatelet or anticoagulant drugs.[69,71]

Conclusion

Retinal detachment is the result of various conditions that compromise or overwhelm the normal physiologic forces that maintain contact between the retina and the RPE. The retinal detachments can be classified as detachments with and without a tractional component. The major types of detachment with tractional components are rhegmatogenous, tractional, and combined tractional–rhegmatogenous, whereas exudative and hemorrhagic detachments have no tractional component. The mechanisms that lead to the first types of retinal detachment include liquefaction of the vitreous gel and the interaction between

retinal traction and retinal breaks. The mechanism of traction retinal detachment is the vitreoretinal traction that mechanically pulls the retina away from the RPE. The mechanisms for exudative and hemorrhagic retinal detachment involve excessive production of fluid, such as from a neoplasm, reduced RPE function, such as from inflammation, poor outflow, such as with idiopathic uveal effusion syndrome, and blood, such as from choroidal neovascularization. Each type of retinal detachment requires treatment addressing the underlying pathogenic process.

References

1. Kuhn F, Aylward B. Rhegmatogenous retinal detachment: a reappraisal of its pathophysiology and treatment. *Ophthalmic Res*. 2014;51(1):15–31.
2. Hughes BA, Miller SS, Machen TE. Effects of cyclic AMP on fluid absorption and ion transport across frog retinal pigment epithelium. Measurements in the open-circuit state. *J Gen Physiol*. 1984;83(6):875–899.
3. Negi A, Marmor MF. The resorption of subretinal fluid after diffuse damage to the retinal pigment epithelium. *Invest Ophthalmol Vis Sci*. 1983;24(11):1475–1479.
4. Machemer R. The importance of fluid absorption, traction, intraocular currents, and chorioretinal scars in the therapy of rhegmatogenous retinal detachments. XLI Edward Jackson memorial lecture. *Am J Ophthalmol*. 1984;98(6):681–693.
5. Byer NE. What happens to untreated asymptomatic retinal breaks, and are they affected by posterior vitreous detachment? *Ophthalmology*. 1998;105(6):1045–1049 [discussion 1049–50].
6. Byer NE. Clinical study of retinal breaks. *Trans Am Acad Ophthalmol Otolaryngol*. 1967;71(3):461–473.
7. Byer NE. The natural history of asymptomatic retinal breaks. *Ophthalmology*. 1982;89(9):1033–1039.
8. Okun E. Gross and microscopic pathology in autopsy eyes. III. Retinal breaks without detachment. *Am J Ophthalmol*. 1961;51:369–391.

9. Neal RE, Bettelheim FA, Lin C, et al. Alterations in human vitreous humour following cataract extraction. *Exp Eye Res*. 2005;80(3):337–347.
10. Sebag J. Ageing of the vitreous. *Eye (Lond)*. 1987;1(Pt 2):254–262.
11. Heller MD, Straatsma BR, Foos RY. Detachment of the posterior vitreous in phakic and aphakic eyes. *Mod Probl Ophthalmol*. 1972;10:23–36.
12. Foos RY, Wheeler NC. Vitreoretinal juncture. Synchysis senilis and posterior vitreous detachment. *Ophthalmology*. 1982;89(12):1502–1512.
13. Steinberg RH. Research update: report from a workshop on cell biology of retinal detachment. *Exp Eye Res*. 1986;43(5):695–706.
14. Sebag J, Balazs EA. Human vitreous fibres and vitreoretinal disease. *Trans Ophthalmol Soc U K*. 1985;104(Pt 2):123–128.
15. Stalmans P, Benz MS, Gandorfer A, et al. Enzymatic vitreolysis with ocriplasmin for vitreomacular traction and macular holes. *N Engl J Med*. 2012;367(7):606–615.
16. Tasman W. Peripheral retinal changes following blunt trauma. *Trans Am Ophthalmol Soc*. 1972;70:190–198.
17. Freeman HM, Schepens CL, Couvillion GC. Current management of giant retinal breaks. II. *Trans Am Acad Ophthalmol Otolaryngol*. 1970;74(1):59–74.
18. Schepens CL, Freeman HM. Current management of giant retinal breaks. *Trans Am Acad Ophthalmol Otolaryngol*. 1967;71(3):474–487.
19. Ang GS, Townend J, Lois N. Epidemiology of giant retinal tears in the United Kingdom: the British Giant Retinal Tear Epidemiology Eye Study (BGEES). *Invest Ophthalmol Vis Sci*. 2010;51(9):4781–4787.
20. Snead MP, McNinch AM, Poulson AV, et al. Stickler syndrome, ocular-only variants and a key diagnostic role for the ophthalmologist. *Eye (Lond)*. 2011;25(11):1389–1400.
21. Snead MP, Yates JR. Clinical and molecular genetics of Stickler syndrome. *J Med Genet*. 1999;36(5):353–359.
22. Ahmad NN, Ala-Kokko L, Knowlton RG, et al. Stop codon in the procollagen II gene (COL2A1) in a family with the

Stickler syndrome (arthro-ophthalmopathy). *Proc Natl Acad Sci USA*. 1991;88(15):6624–6627.
23. Stickler GB, Hughes W, Houchin P. Clinical features of hereditary progressive arthro-ophthalmopathy (Stickler syndrome): a survey. *Genet Med*. 2001;3(3):192–196.
24. Fincham GS, Pasea L, Carroll C, et al. Prevention of retinal detachment in Stickler syndrome: the Cambridge prophylactic cryotherapy protocol. *Ophthalmology*. 2014;121(8):1588–1597.
25. Ripandelli G, Parisi V, Friberg TR, et al. Retinal detachment associated with macular hole in high myopia: using the vitreous anatomy to optimize the surgical approach. *Ophthalmology*. 2004;111(4):726–731.
26. Riordan-Eva P, Chignell AH. Full thickness macular breaks in rhegmatogenous retinal detachment with peripheral retinal breaks. *Br J Ophthalmol*. 1992;76(6):346–348.
27. Zhang CF, Hu C. High incidence of retinal detachment secondary to macular hole in a Chinese population. *Am J Ophthalmol*. 1982;94(6):817–819.
28. Stirpe M, Michels RG. Retinal detachment in highly myopic eyes due to macular holes and epiretinal traction. *Retina*. 1990;10(2):113–114.
29. Oshima Y, Ikuno Y, Motokura M, et al. Complete epiretinal membrane separation in highly myopic eyes with retinal detachment resulting from a macular hole. *Am J Ophthalmol*. 1998;126(5):669–676.
30. Morita H, Ideta H, Ito K, et al. Causative factors of retinal detachment in macular holes. *Retina*. 1991;11(3):281–284.
31. Ichibe M, Yoshizawa T, Murakami K, et al. Surgical management of retinal detachment associated with myopic macular hole: anatomic and functional status of the macula. *Am J Ophthalmol*. 2003;136(2):277–284.
32. Wilkinson CP. Retinal detachment following intraocular lens implantation. *Graefes Arch Clin Exp Ophthalmol*. 1986;224(1):64–66.
33. Francois J, Verbraeken H. Complications in 1,000 consecutive intracapsular cataract extractions. *Ophthalmologica*. 1980;180(3):121–128.

34. Javitt JC, Street DA, Tielsch JM, et al. National outcomes of cataract extraction. Retinal detachment and endophthalmitis after outpatient cataract surgery. Cataract Patient Outcomes Research Team. *Ophthalmology*. 1994;101(1):100–105 [discussion 106].
35. Binkhorst CD. Five hundred planned extracapsular extractions with irido-capsular and iris clip lens implantation in senile cataract. *Ophthalmic Surg*. 1977;8(3):37–44.
36. Erie JC, Raecker MA, Baratz KH, et al. Risk of retinal detachment after cataract extraction, 1980-2004: a population-based study. *Ophthalmology*. 2006;113(11):2026–2032.
37. Mirshahi A, Hoehn F, Lorenz K, et al. Incidence of posterior vitreous detachment after cataract surgery. *J Cataract Refract Surg*. 2009;35(6):987–991.
38. Rowe JA, Erie JC, Baratz KH, et al. Retinal detachment in Olmsted County, Minnesota, 1976 through 1995. *Ophthalmology*. 1999;106:154–159.
39. Sharma MC, Chan P, Kim RU, et al. Rhegmatogenous retinal detachment in the fellow phakic eyes of patients with pseudophakic rhegmatogenous retinal detachment. *Retina*. 2003;23(1):37–40.
40. Ambler JS, Constable IJ. Retinal detachment following Nd:YAG capsulotomy. *Aust N Z J Ophthalmol*. 1988;16(4):337–341.
41. Shields JA. Ocular toxocariasis: a review. *Surv Ophthalmol*. 1984;28(5):361–381.
42. Stewart JM, Cubillan LD, Cunningham ET Jr. Prevalence, clinical features, and causes of vision loss among patients with ocular toxocariasis. *Retina*. 2005;25(8):1005–1013.
43. Heinz C, Schoonbrood S, Heiligenhaus A. Intermediate uveitis in children and young adults: differences in clinical course, associations and visual outcome. *Br J Ophthalmol*. 2014;98(8):1107–1111.
44. Rhegmatogenous retinal detachment in patients with cytomegalovirus retinitis: the Foscarnet–Ganciclovir Cytomegalovirus Retinitis Trial. The Studies of Ocular

Complications of AIDS (SOCA) Research Group in collaboration with the AIDS Clinical Trials Group (ACTG). *Am J Ophthalmol*. 1997;124(1):61–70.
45. Davis JL, Hummer J, Feuer WJ. Laser photocoagulation for retinal detachments and retinal tears in cytomegalovirus retinitis. *Ophthalmology*. 1997;104(12):2053–2060 [discussion 2060–1].
46. Kerkhoff FT, Lamberts QJ, van den Biesen PR, et al. Rhegmatogenous retinal detachment and uveitis. *Ophthalmology*. 2003;110(2):427–431.
47. Mitry D, Singh J, Yorston D, et al. The predisposing pathology and clinical characteristics in the Scottish Retinal Detachment Study. *Ophthalmology*. 2011;118(7):1429–1434.
48. Kim LA, Wong LL, Amarnani DS, et al. Characterization of cells from patient-derived fibrovascular membranes in proliferative diabetic retinopathy. *Mol Vis*. 2015;21:673–687.
49. Massin P, Haouchine B, Gaudric A. Macular traction detachment and diabetic edema associated with posterior hyaloidal traction. *Am J Ophthalmol*. 2001;132(4):599–600.
50. Charles S, Flinn CE. The natural history of diabetic extramacular traction retinal detachment. *Arch Ophthalmol*. 1981;99(1):66–68.
51. Sanghi G, Dogra MR, Katoch D, et al. Aggressive posterior retinopathy of prematurity: risk factors for retinal detachment despite confluent laser photocoagulation. *Am J Ophthalmol*. 2013;155(1):159–164.e2.
52. Weinberg DV, Lyon AT, Greenwald MJ, et al. Rhegmatogenous retinal detachments in children: risk factors and surgical outcomes. *Ophthalmology*. 2003;110(9):1708–1713.
53. Patwardhan SD, Azad R, Shah BM, et al. Role of intravitreal bevacizumab in Eales disease with dense vitreous hemorrhage: a prospective randomized control study. *Retina*. 2011;31(5):866–870.
54. Shields JA, Shields CL, Honavar SG, et al. Clinical variations and complications of Coats disease in 150 cases: the 2000 Sanford Gifford Memorial Lecture. *Am J Ophthalmol*. 2001;131(5):561–571.

55. Kumar A, Sehra SV, Thirumalesh MB, et al. Secondary rhegmatogenous retinal detachment following intravitreal bevacizumab in patients with vitreous hemorrhage or tractional retinal detachment secondary to Eales' disease. *Graefes Arch Clin Exp Ophthalmol*. 2012;250(5):685–690.
56. Ramasubramanian A, Shields CL. Bevacizumab for Coats' disease with exudative retinal detachment and risk of vitreoretinal traction. *Br J Ophthalmol*. 2012;96(3):356–359.
57. Rachal WF, Burton TC. Changing concepts of failures after retinal detachment surgery. *Arch Ophthalmol*. 1979;97(3):480–483.
58. Pennock S, Haddock LJ, Mukai S, et al. Vascular endothelial growth factor acts primarily via platelet-derived growth factor receptor alpha to promote proliferative vitreoretinopathy. *Am J Pathol*. 2014;184(11):3052–3068.
59. von Ruckmann A, Fitzke FW, Fan J, et al. Abnormalities of fundus autofluorescence in central serous retinopathy. *Am J Ophthalmol*. 2002;133(6):780–786.
60. Spaide RF, Hall L, Haas A, et al. Indocyanine green videoangiography of older patients with central serous chorioretinopathy. *Retina*. 1996;16(3):203–213.
61. Carvalho-Recchia CA, Yannuzzi LA, Negrao S, et al. Corticosteroids and central serous chorioretinopathy. *Ophthalmology*. 2002;109(10):1834–1837.
62. Yamane T, Yokoi T, Nakayama Y, et al. Surgical outcomes of progressive tractional retinal detachment associated with familial exudative vitreoretinopathy. *Am J Ophthalmol*. 2014;158(5):1049–1055.
63. Mansour AM, Arevalo JF, Badal J, et al. Paraproteinemic maculopathy. *Ophthalmology*. 2014;121(10):1925–1932.
64. Uyama M, Takahashi K, Kozaki J, et al. Uveal effusion syndrome: clinical features, surgical treatment, histologic examination of the sclera, and pathophysiology. *Ophthalmology*. 2000;107(3):441–449.
65. Han DP, Mieler WF, Schwartz DM, et al. Management of traumatic hemorrhagic retinal detachment with pars plana vitrectomy. *Arch Ophthalmol*. 1990;108(9):1281–1286.
66. Bhisitkul RB, Winn BJ, Lee OT, et al. Neuroprotective effect

of intravitreal triamcinolone acetonide against photoreceptor apoptosis in a rabbit model of subretinal hemorrhage. *Invest Ophthalmol Vis Sci*. 2008;49(9):4071–4077.
67. Chang W, Garg SJ, Maturi R, et al. Management of thick submacular hemorrhage with subretinal tissue plasminogen activator and pneumatic displacement for age-related macular degeneration. *Am J Ophthalmol*. 2014;157(6):1250–1257.
68. Shields CL, Salazar PF, Mashayekhi A, et al. Peripheral exudative hemorrhagic chorioretinopathy simulating choroidal melanoma in 173 eyes. *Ophthalmology*. 2009;116(3):529–535.
69. Chandra A, Xing W, Kadhim MR, et al. Suprachoroidal hemorrhage in pars plana vitrectomy: risk factors and outcomes over 10 years. *Ophthalmology*. 2014;121(1):311–317.
70. Mei H, Xing Y, Yang A, et al. Suprachoroidal hemorrhage during pars plana vitrectomy in traumatized eyes. *Retina*. 2009;29(4):473–476.
71. Speaker MG, Guerriero PN, Met JA, et al. A case–control study of risk factors for intraoperative suprachoroidal expulsive hemorrhage. *Ophthalmology*. 1991;98(2):202–209 [discussion 210].

99

Nonrhegmatogenous Retinal Detachment

Po-Ting Yeh, Chung-May Yang, Chang-Hao Yang, Chang-Ping Lin

Introduction

A wide variety of diseases may present with sensory retinal detachment without retinal breaks. Nonrhegmatogenous retinal detachment may be exudative in nature or caused by vitreoretinal traction. Some diseases with elevated retina may have both exudative and traction components. Occasionally, communication between the subretinal space and other structures of the eye, such

as the vitreous cavity, may lead to retinal detachment. In exudative retinal detachment, the subretinal fluid may be confined to a localized area, usually the posterior pole, or may extend to the periphery, even forming bullous retinal detachment. The characteristic feature of a significant exudative retinal detachment is the presence of shifting subretinal fluid.[1] The fluid shifts to the most dependent location when patients change body position. The surface of the detached retina is usually smooth; however, retinal folding may occur in some diseases associated with subretinal fibrosis. To reach an accurate diagnosis among many diseases presenting with exudative retinal detachment, careful fundus examination, fluorescein angiography (FA), indocyanine green angiography (ICGA), optical coherence tomography (OCT), ultrasonography, computed tomography (CT), and magnetic resonance imaging (MRI) may be necessary.

Pathophysiology

There are three potential sources for fluid accumulation within or under the retina: vitreous fluid, retinal vessels, and choroidal vessels. The main route for vitreous water turnover is by way of the retina, choroid, and the vortex veins. Choriocapillaries of the choroidal circulation, a single-layered capillary structure with numerous fenestrations on the vessel walls, are freely permeable to the intravascular fluid. The main mechanisms for keeping the retina in a dehydrated state are the presence of inner and outer blood–retinal barriers, and the fluid movement across the retinal pigment epithelium (RPE). The inner barrier is made of an endothelial tight junction of the retinal vessels; the outer barrier is produced by the tight junction of retinal pigment epithelial cells. Three mechanisms guarantee the one-way movement of fluid across the RPE: (1) active transport of the RPE; (2) plasma oncotic force, which is higher in the choroidal side; and (3) hydrostatic pressure. Thus, RPE and retinal vascular endothelium are of utmost importance to keep the retina dry in the normal condition. When the RPE is injured, the tight junction may be damaged, causing breakdown of the outer retinal barrier; further, the active transport of fluid may be affected, compromising the unilateral mode of fluid movement. Any disease

capable of significantly increasing the permeability of the choroidal capillaries along with afflicting an injury on the RPE causing breakdown of the outer barrier may result in the accumulation of subretinal fluid. Alternatively, diseases affecting the retinal vascular endothelium causing significant breakdown of the inner barrier may lead to fluid first gathering in the intraretinal space and then gaining access into the subretinal space, if the amount surpasses the intraretinal water retention capacity.

Besides the anatomical structures and physiologic properties restricting fluid entering the subretinal space, adequate fluid outflow is required for the retina to maintain a state of dehydration. There are several outflow pathways that function to drain fluid: vitreoretinal–choroidal outflow carries the vitreous fluid to the RPE and to the choroid through the pumping action of RPE as previously mentioned; the uveoscleral outflow pathway in turn carries the fluid from the choroid to leave the eye through choroidal vortex outflow; transscleral outflow allows protein and fluid draining out through the emissary channels. When diseases cause outflow obstruction, fluid may accumulate in the subretinal space or/and suprachoroidal space, leading to exudative or hemorrhagic retinal detachment or choroidal detachment. In this chapter, commonly encountered disease categories associated with exudative retinal detachment and other nonrhegmatogenous retinal detachment unrelated to traction will be summarized.

Idiopathic

Central Serous Chorioretinopathy

Central serous chorioretinopathy (CSC) is a relatively benign retinal disease characterized by a circular area of serous detachment of the posterior retina usually in young and middle-aged healthy persons. While CSC is mostly self-limiting, there are clinical variants of this disease that have atypical presentations and may reduce the vision tremendously. Most of these atypical CSCs or variant CSCs are associated with excessive accumulation of fluid beneath the sensory retina or RPE. These atypical manifestations can be separated into two major categories: acute bullous retinal detachment and chronic

CSC.

Bullous Retinal Detachment

Some patients with acute bullous retinal detachment (bullous RD) may have the following medical history: long-term corticosteroid taken for systemic diseases, such as systemic lupus erythematosus (SLE), rheumatoid arthritis (RA), or renal or cardiac transplantation; regular taking of herb drugs (some may contain steroid-like ingredients or have steroid added to the drug); or under steroid treatment for presumed Harada disease. Other affected patients do not have a specific history of steroid intake.

Bullous RD usually has an acute onset with simultaneous or sequential involvement of the two eyes. Fundus examinations reveal multiple areas of serous RD in the posterior retina with lower bullous RD. There may be multiple retinal pigment epithelial detachment (RPED) and one or more grayish or yellow patches of subretinal exudates mimicking focal chorioretinitis (Fig. 99.1). In some cases, retinal folds may form by the contraction of fibrinous patches or fibrotic membrane or bands on the outer surface of the detached retina. Small scattered yellowish granular subretinal deposits may have a tendency to settle along the retinal vessels (Fig. 99.2). The vitreous is usually clear, but may have 1–2 plus cells. The disc is not hyperemic.

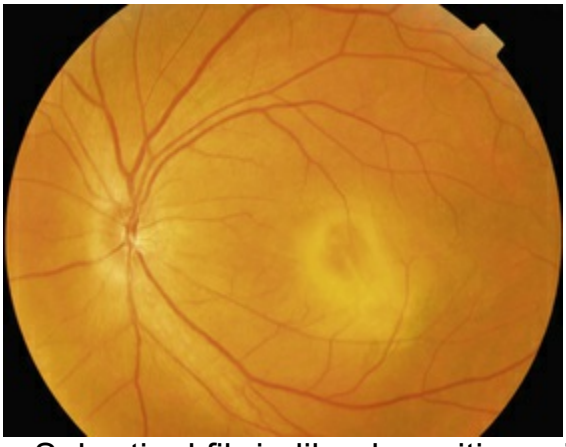

FIG. 99.1 Subretinal fibrin-like deposition mimicking chorioretinitis in a case of acute bullous detachment.

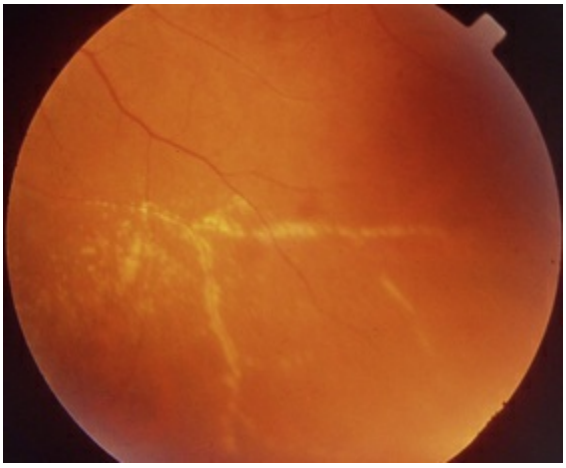

FIG. 99.2 Exudates along retinal vessels in a case of bullous retinal detachment.

FA shows multiple hyperfluorescent spots or patches with late enlargement; intense fluorescein leakage from the edge of the RPE detachment may be seen and correlates with the focal grayish-white or yellow patches seen in the color fundus. Retinal vessels show no leakage.

ICGA shows an ill-defined hyperfluorescent area, which may become more intense in the late phase, suggesting choroidal permeability alteration.

OCT may show retinal pigment epithelial detachment with or without sensory detachment adjacent to or overlying it; the subretinal fluid may be clear or slightly turbid with multiple granular deposits above the RPE and on the outer surface of the detached retina, sometimes forming incomplete septa within the subretinal space (Fig. 99.3); subretinal fibrinous mount with surrounding sensory detachment may be seen.[2] Recent studies show thickened choroid in the involved eyes as well as the fellow eyes.[3,4]

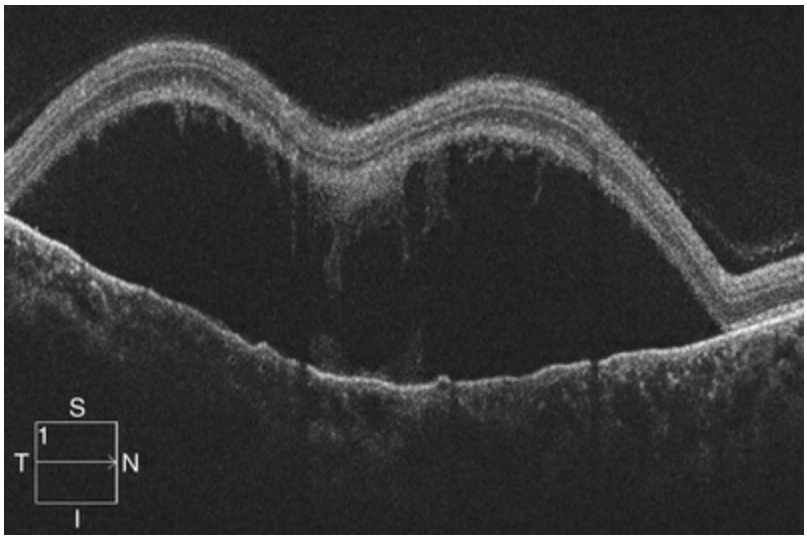

FIG. 99.3 Optical coherence tomography image in a case of acute bullous detachment showing subretinal incomplete vertical septa.

Complications of bullous RD include large RPE tear; broad retinal folding; submacular plaques or fibrotic bands; peripheral paravascular exudates; and peripheral retinal telangiectasia, occlusion, or even fibrovascular proliferation.[2,5] Peripheral vascular changes may be secondary to longstanding sensory detachment.

In treating bullous RD, systemic steroids should be discontinued; patients should keep the head elevated during sleep to prevent fluid shifting to the macular area; FA-guided laser to the leaking points may decrease the subretinal fluid. Once the fluid level recedes, FA should be repeated to identify persistent leaking points and other leaking sites previously hidden by the detached retina. Multiple sessions of laser treatment are usually needed for complete fluid reabsorption. If subretinal fluid (SRF) persists after the measures described above, external drainage of SRF may be undertaken.[6] Care should be taken to make sure that the surgical drainage site is posterior enough to access the subretinal space, which is in the dependent area. Alternatively, pars plana vitrectomy with perfluorocarbon liquid injection and simultaneous external drainage through anterior sclerotomy may be performed, followed by focal laser to the exposed leaking sites and air–fluid exchange. The effect of vitrectomy with internal drainage and silicone oil tamponade is controversial. Recently, bevacizumab injection has been shown to rapidly reduce active fluid leakage into

the subretinal space as well as to decrease the deposition of fibrinous or proteinaceous substances.[7] Photodynamic therapy (PDT) with reduced fluence may also reduce choroidal hyperpermeability and facilitate subretinal fluid reabsorption with RPE tear being the major complication.[8] Prognosis of bullous RD is variable and is affected by the duration of macular detachment, the presence of submacular fibrosis, the development of submacular RPE tears, and occurrence of fibrovascular proliferation under the macula or in the periphery.

Differential diagnoses of bullous RD include diseases associated with large areas of retinal detachment. Harada disease is the most common disease confused with bullous detachment. Both have bilateral exudative detachment with multiple leaking sites and normal retinal vasculatures. Hyperemic discs, vitreous cells, pin-point leaking spots, subretinal RPE folding radiating from the disc, choroidal thickening, and the unique OCT pictures showing outer retinal septated spaces containing optically heterogeneous substances favor the diagnosis of Harada disease. Misdiagnosis may lead to the use of steroid and aggravation of bullous RD. The condition may sometimes be mistaken for rhegmatogenous RD and wrongly operated upon. Other causes of unilateral or bilateral exudative RD should be ruled out, such as hypertensive retinopathy, collagen vascular diseases, leukemia, toxemia, choroidal metastasis, uveal effusion, posterior scleritis, multifocal choroiditis (tuberculosis, syphilis, Lyme), chorioretinitis, sarcoidosis, and lymphoma. Polypoidal choroidal vasculopathy (PCV) may mimic CSC, and severe PCV without subretinal hemorrhage may have similar manifestations to bullous detachment.

Chronic Central Serous Chorioretinopathy

Because of the characteristic angiographic picture of multiple areas of RPE disturbance with late staining or mild leakage, the condition is also named RPE decompensation, diffuse retinal pigment epitheliopathy. This entity should not be confused with typical CSC with persistent subretinal fluid. It is more commonly seen in middle-aged patients of Hispanic or Asian extraction. Personal and medical history may elicit chronic steroid usage.

Typical clinical manifestation is multiple poorly defined areas of chronic persistent or recurrent retinal detachment in the posterior pole. Subtle or obvious areas of RPE changes are noted in the posterior pole and in the juxtapapillary regions; a gravity tract-forming vertical band or reverse funnel-shaped depigmentation, along with pigment migration or bone-spicule pattern of pigmentary changes within the tract and in the inferior part of the retina, are usually found (Fig. 99.4); shallow or bullous detachment in the inferior retina is a frequent finding.

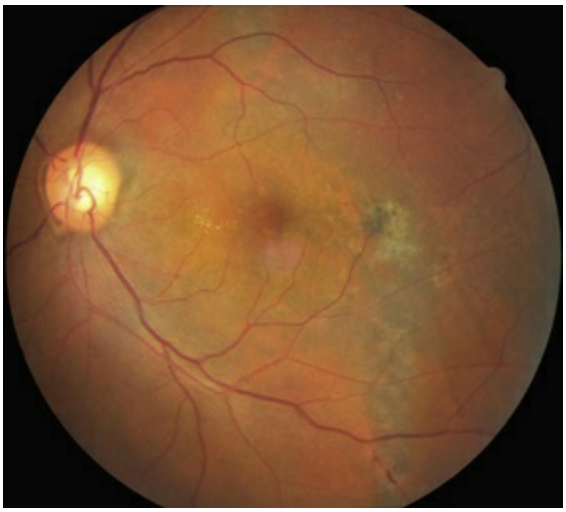

FIG. 99.4 Retinal pigment epithelium changes and gravity tract in a case of chronic central serous chorioretinopathy.

FA may show patchy hyperfluorescent areas or mottled hyperfluorescent areas corresponding to, and more obvious than, those areas of pigmentary changes found ophthalmoscopically. These areas may show late dye leakage or staining of different degrees. Round enlarging spots or jet spots commonly seen in typical CSC may be noticed within or in between the hyperfluorescent areas. Band- or reverse funnel-shaped gravity tracts of window defect changes are usually present. Peripheral vessels within the area of retinal detachment may show leakage, vascular occlusion, or neovascularization.

OCT examination may reveal subretinal fluid under the macula or several areas of retinal detachment separated by attached retina; some may have localized submacular fluid similar to acute CSC.

There may be cystic changes in the overlying retina, suggesting a chronic condition.

Photocoagulation remains the main treatment method. Conventional laser or the more recently developed micropulse laser to leaking points and areas of RPE changes with late fluorescein staining and leakage may stop the leakage.[9] PDT with reduced fluence has been advocated to treat leaking points and areas with late oozing shown on FA with good effect. Intravitreal bevacizumab has also been shown to have some therapeutic effect.[10] However, the prognosis is guarded because of multiple recurrence and permanent macular RPE disturbance.

Uveal Effusion Syndrome

Patients with idiopathic uveal effusion syndrome (IUES) are usually middle-aged men with normal ocular size, presenting with unilateral or bilateral serous choroidal, ciliary, and retinal detachment. There may be central vision decrease or distortion secondary to macular serous detachment or upper visual field defect from lower serous retinal detachment. External eye examination may reveal episcleral vessel dilation; the anterior chamber is usually free of cells; intraocular pressure (IOP) is normal; there may be blood in the Schlemm's canal; and vitreous cells are common findings. Initial disease severity ranges from macular serous detachment with insignificant ciliary and choroidal detachment to obvious ciliochoroidal detachment and bullous retinal detachment. The protein concentration of the subretinal fluid is 2.5–3 times that of the normal plasma. The fellow eye may be affected within a few weeks or a few months after lesions developed in the first eye. The disease may have a protracted course, with wax and wane of the subretinal fluid, eventually leaving areas of mixed RPE atrophy and pigment clumps in a leopard-spot pattern. Some patients may develop a yellowish plaque of exudation in the macular area or severe chorioretinal degeneration causing visual field loss.

FA may not show specific leaking points in the early stage of the disease. As disease progresses FA may highlight the leopard-spot pattern, which was not obvious in fundus examination; choroidal

perfusion may be slow, and focal leaking areas in multiple places may be seen.

Ultrasonography or ultrasound biomicroscopy (UBM) can clearly demonstrate ciliochoroidal detachment, and usually form an annular pattern in the periphery, even before detectable fundus changes. There is no thickened sclera and sub-Tenon fluid adjacent to the optic nerve to form the classic T-sign of the posterior ocular coat typical of posterior scleritis.

Histopathologic examination shows accumulation of protein-rich extracellular materials in the suprachoroidal and subretinal spaces. Choroidal vessels are dilated without inflammatory cell infiltration. Subarachnoid space around the optic disc is enlarged. The sclera shows deranged fibers with deposition of glycosaminoglycans within.[11] Cell culture of the scleral cells reveals intracellular deposition of a glycogen-like substance.[12] Histopathologic studies have shown disorganization of collagen fiber bundles and variation in size of collagen fibrils in nanophthalmic eyes and eyes with short axial length.[11,13] A loss of chondroitin sulfate proteoglycan was observed in nanophthalmic sclerae. This alteration may be related to the abnormal organization of collagen fibrils.[13]

The pathogenesis is unclear, possibly related to congenital anomaly of the sclera and vortex veins hypoplasia. Excessive glycosaminoglycans accumulate within the sclera, combined with defective vortex veins, resulting in decreased drainage of extravasated protein through scleral emissary channels of the transscleral outflow pathway; fluid drainage is also compromised from the decreased function of uveoscleral outflow pathways, leading to excessive protein and fluid accumulation in the suprachoroidal space. Later on, the protein and fluid enter the subretinal space when the extracellular protein concentration becomes equal to that within the vessels. Protein in the suprachoroidal space around the disc may gain access to the subarachnoid space and subdural space resulting in an increase in the CSF protein content even without pleocytosis in 50% of the patients.[14] Forrester and associates believe that IUES is a kind of ocular mucopolysaccharidosis, with the initial defect resting in the proteodermatan synthesis and/or degradation by the scleral fibroblasts.[15] Other evidence also shows that abnormal

mucopolysaccharides of the sclera play an important role in the pathogenesis of IUES. IOP is usually within normal limits because the IOP rising tendency from uveoscleral outflow obstruction is neutralized by decreased aqueous production from the ciliochoroidal detachment.

Best treatment methods have been debated. Vortex vein decompression with scleral resection was initially advocated to treat uveal effusion associated with nanophthalmos. Gass believed that the treatment effect had less to do with vortex vein decompression than with scleral resection to facilitate protein and fluid drainage through the sclera.[16] He suggested partial-thickness sclerectomies or full-thickness sclerectomies. After treatment, exudation may gradually disappear within a few months (Fig. 99.5). However, chorioretinal degeneration may continue to develop from chronic mild recurrence of exudation or abnormal metabolism of mucopolysaccharide.

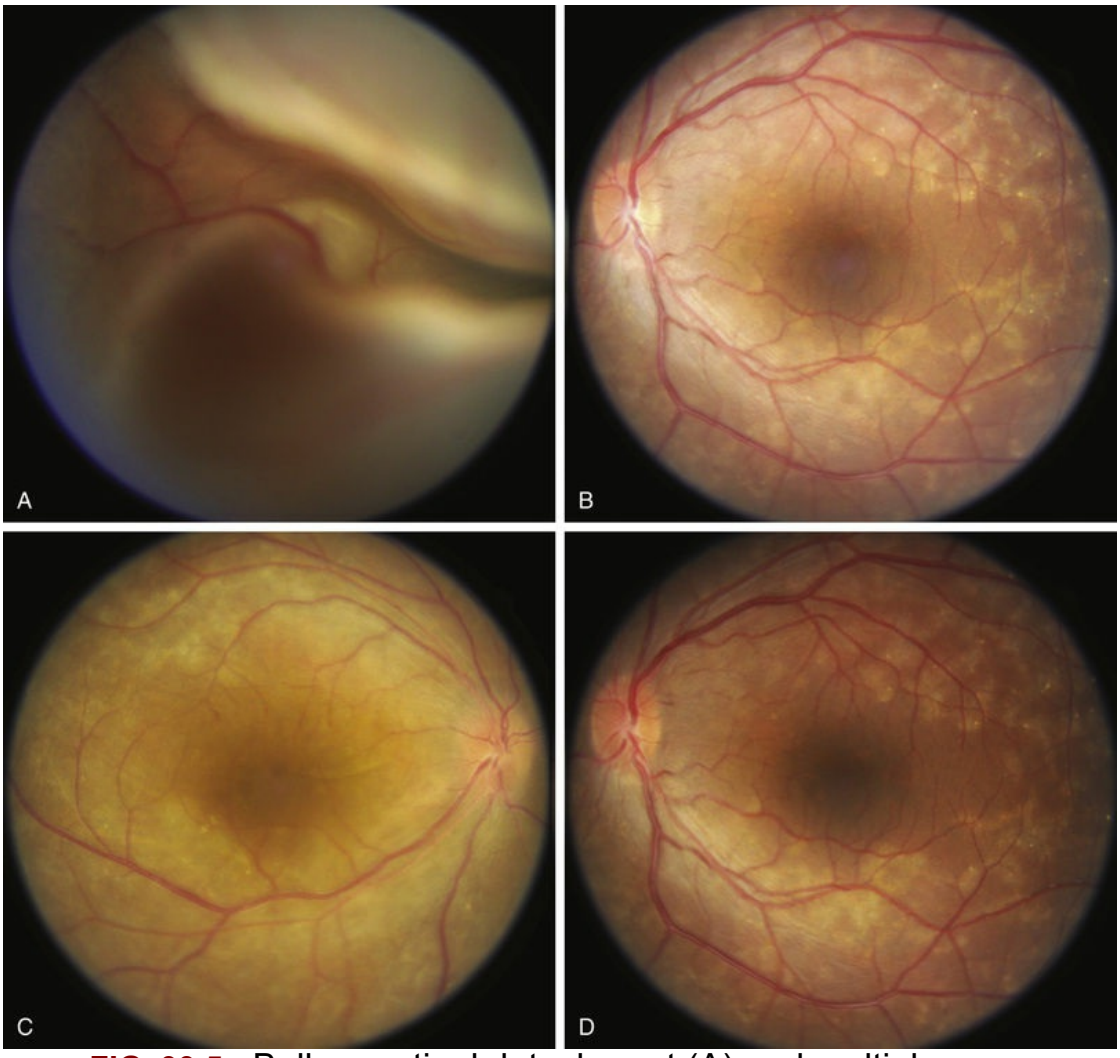

FIG. 99.5 Bullous retinal detachment (A) and multiple subretinal yellow patches (B) in a 36-year-old nanophthalmos patient. One year after sclerectomy in two quadrants, the retina became flat and showed similar yellow patches as the fellow eye (C). The fellow eye had the same changes as the other did one year ago (D).

Other diseases capable of causing uveal effusion include nanophthalmos, dural arteriovenous fistula, scleritis, Harada disease, diffuse tumors of the uveal tract, prolonged hypotony, etc.

Leopard-spot pigmentation may appear in systemic large cell lymphoma, leukemia, bilateral uveal melanocytic proliferation, and organ transplant chorioretinopathy.

Vascular

Coats Disease

This is a nonfamilial developmental retinal vasculopathy. The disease is more common in males, is usually unilaterally affected, and may occur in infants. Symptoms often develop in children or young adults; one-third had symptoms onset over 30 years of age. All vessels – arteries and veins alike – would be affected, showing telangiectasis combined with a large amount of hard exudates; hemorrhagic retinopathy is occasionally seen. On the other hand, a minor form of the disease mainly involving juxtafoveolar areas may occur; decreased vision will not occur until adulthood when hard exudates and edema develop in the macula. The prognosis is directly influenced by the size of the involved area. Occasionally, other vascular anomalies may appear in the lesion eye or the fellow eye, such as macular macrovessels or arterial tortuosity (Fig. 99.6). The condition may be occasionally associated with other abnormalities such as progressive facial hemiatrophy, facial scapulohumeral muscular dystrophy and deafness, or Alport syndrome.[17] It may rarely accompany systemic vascular anomalies.

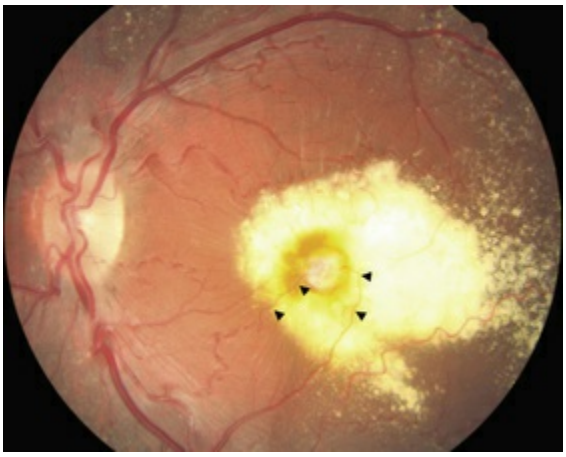

FIG. 99.6 Retinal arterial tortuosity in a case of Coats disease. The fundus picture shows dense macular exudates with submacular fibrosis, retinochoroidal anastomosis, indicated by arrowheads.

Fundus examinations reveal changes of various severities. The mild form presents with focal telangiectasia and microaneurysms, usually at the temporal side of the macula, with or without mild hard exudates. The moderate form ranges from cystoid macular

edema with significant hard exudates surrounding the area containing telangiectatic vessels or microaneurysms, to the more extensive vascular abnormalities with massive exudates which may gain access to the subretinal space. The severe form shows wide and scattered vascular lesions, with hard exudates accumulating around the disc and in the posterior pole, causing exudative detachment. The macula may be detached with massive intraretinal and subretinal exudates, which later may transform to organized subretinal disciform mass or atrophic scar. These changes are likely to be found in infants and children, who visit the ophthalmic clinic because of manifest strabismus secondary to unilateral poor vision or abnormal red reflex from massive exudates in the posterior pole. The accumulation of exudates in the macula may be due to gravity-induced migration of subretinal exudates toward the central area during sleep. The deposition of lipid-rich substance along with macrophage evolves into fibrous tissue. Retinal or choroidal vessels may grow into the lesion to form a disciform scar. The most advanced form presents with bullous detachment with the retina coming in direct contact with the crystalline lens; cholesterol crystals accumulate in the subretinal space.[18] There may be dilated abnormal vessels, hard exudates, or hemorrhage on the surface or in the retina. However, the abnormal tortuous vessels do not dip into the subretinal space, a sign typical of exophytic retinoblastoma.

FA clearly demonstrates aneurysmal dilatation of retinal vessels, including arteries, veins, and capillaries; capillary nonperfusion is also obvious. Normal-appearing vessels do not show dye leakage. Cystoid macular edema may be noted.

The clinical course varies. The macula may not be involved initially until later in life if the lesions are peripherally located, especially in the lower part of the retina. Retinal neovascularization is uncommon despite a wide area of capillary nonperfusion. However, some severe cases develop increasing capillary nonperfusion leading to neovascularization with subsequent vitreous hemorrhage, vitreous membrane formation, exudative and tractional retinal detachment, and neovascular glaucoma, resulting in no light perception; others may develop intraocular inflammation or even acute orbital cellulitis secondary to stimulation from toxic products. Some patients develop mid-

peripheral or peripheral elevated, organized exudative nodule or mass, yellowish in color and mixed with hemorrhagic patches, similar to granuloma, exophytic retinal capillary hemangioma or melanoma (Fig. 99.7). Occasionally, spontaneous resolution may occur.

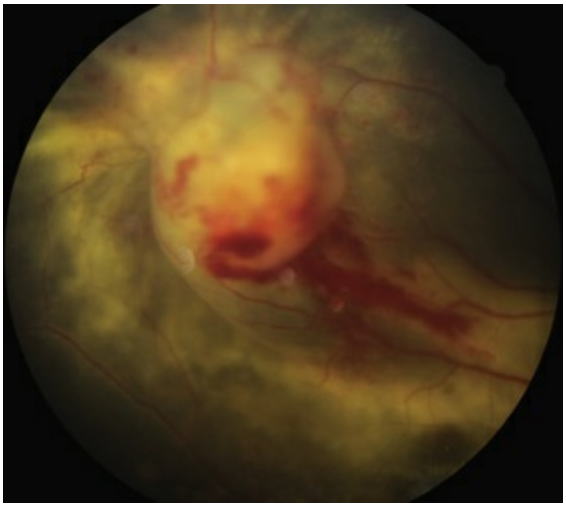

FIG. 99.7 Mid-peripheral elevated exudative nodule surrounded by massive exudates in a 17-year-old boy with Coats disease.

Histopathologic studies show irregular dilation of affected retinal arteries, veins, and capillaries; PAS-positive exudates may be seen in the outer retinal layer; lipid-laden macrophages are seen in the outer retina and the subretinal space. In the severe form of the disease in infants, severe vascular endothelial proliferation and hemorrhagic infarction may be observed. Genetic testing has revealed a somatic mutation on the *NDP* gene on chromosome Xp11.2.

Treatment usually involves laser or cryotherapy aiming at the lesions to decrease exudates and preserve vision (Fig. 99.8). For severe exudative detachment, external drainage should be performed first, followed by cryotherapy to the abnormal vessels. Scleral buckling may facilitate retinal reattachment, enhance the effect of cryotherapy, and promote regression of abnormal vessels. However, new lesions may develop in nearby or remote areas. Follow-up is crucial to detect and treat new lesions. Sector panretinal photocoagulation (PRP) may be used for a nonperfusion

area. For severe cases, vitrectomy to release vitreous traction with external subretinal fluid drainage, laser, or cryo may be considered. Recently, repeated intravitreal injection of bevacizumab has been reported to reduce subretinal fluid, facilitating subsequent laser or cryotherapy.[19]

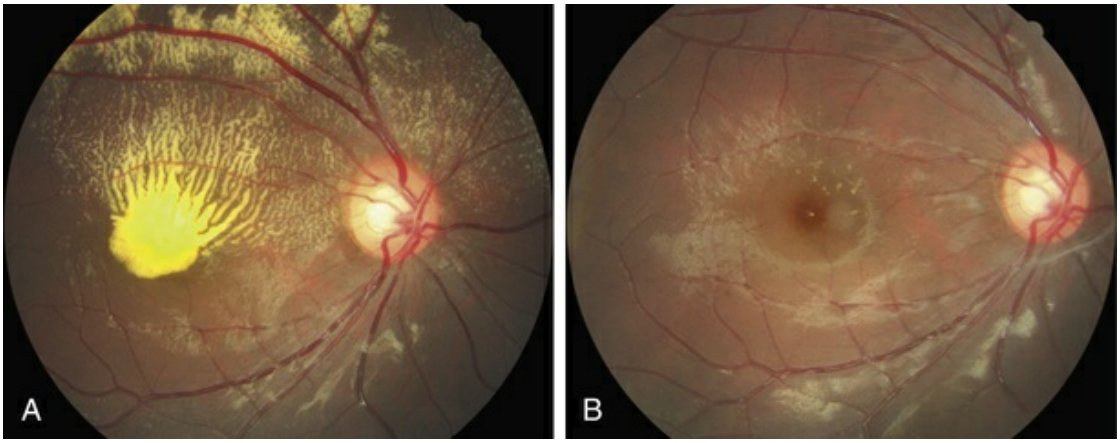

FIG. 99.8 (A) Coats disease. (B) Resolution of hard exudates 1 year after peripheral cryotherapy to the abnormal vascular structures.

Differential diagnoses include all possible causes of white pupil in infants. Localized telangiectasis associated with arterial and venous aneurysms and exudates may be similar to cavernous hemangioma of the retina, acquired retinal macroaneurysm, old branch retinal vein occlusion, bilateral idiopathic retinitis, vasculitis, aneurysms, and neuroretinitis (IRVAN).

Accelerated Hypertension and Pregnancy-Induced Hypertension

Prolonged or severe hypertension may damage the retinal vascular system, choroidal circulation, and disc circulation. The difference in vascular structures, autoregulation, and tissue resistance determines the different susceptibility of these three systems to increased blood pressure. Although leakage from retinal vessels and the optic disc may be a source of subretinal fluid, hypertension-induced choroidopathy is the main category that causes exudative retinal detachment.

While chronic moderate hypertension is rarely associated with choroidopathy, choroidal ischemia is more frequently associated with accelerated hypertension. Unlike retinal circulation, choroidal vessels do not possess autoregulation; the blood flow during fluctuation of systemic blood pressure is mainly regulated by sympathetic tone. When blood pressure is high, raised sympathetic tone can prevent direct pressure damage to the choriocapillaries; however, if there is a rapid rise in blood pressure, excessively increased sympathetic tone may prompt severe constriction of choroidal arteries and arterioles, leading to ischemic changes of the choriocapillaries. Choroidopathy may be separated into three stages: (1) acute ischemic phase; (2) chronic occlusive phase; and (3) chronic reparative phase.[20] In the first two phases, fundus examination may observe white or reddish patches in the outer retina, possibly caused by RPE necrosis; exudative detachment is often present. FA may show a large confluent area or scattered areas of choroidal filling delay; in the mid and late phases, multiple dots or a mosaic pattern of hyperfluorescence from RPE leakage may be seen. In the reparative phase, large areas of irregular REP atrophy, Elschnig spots (a central hyperpigmented lesion surrounded by a hypopigmented ring of RPE changes), or Siegrist spots (spots of pigmentary changes similar to Elschnig spots arranged linearly along choroidal vessels in the equatorial region) may be seen; exudative detachment disappears, but choroidal delayed filling remains.

Pregnancy-Induced Hypertension

About 1–2% of pregnant women who develop severe hypertension, proteinuria, and edema during the third trimester suffer from vision impairment secondary to exudative retinal detachment. Exudative detachment may be limited to the macular area or appear as bullous detachment. The retina may or may not show cotton-wool patches or other changes secondary to hypertension retinopathy (Fig. 99.9). Yellowish-white patches of RPE necrosis may be seen. FA shows delayed choroidal filling and multiple leaking points where RPE has been damaged. After delivery, with control of hypertension, exudative detachment rapidly subsides.

Most patients have good visual recovery. The posterior pole may show RPE changes forming hyperpigmented lines or patches mixed with yellow spots of RPE atrophy. The bilateral changes may be mistaken for macular dystrophy. Severe cases may have extensive exudative detachment. Widespread RPE changes similar to tapetoretinal dystrophy and severely compromised vision may result. The cause of chorioretinal changes in pregnancy-induced hypertension is not clear. Blood pressure may not be very high before the onset of exudative detachment. Affected patients may have other symptoms and signs related to disseminated intravascular coagulation, such as hemolysis, low platelet count, and elevation of liver enzymes. It is possible that mechanisms capable of inducing disseminated intravascular coagulation (see below) are also functional in the choroid, causing choroidal ischemia, RPE damage, and exudative detachment.

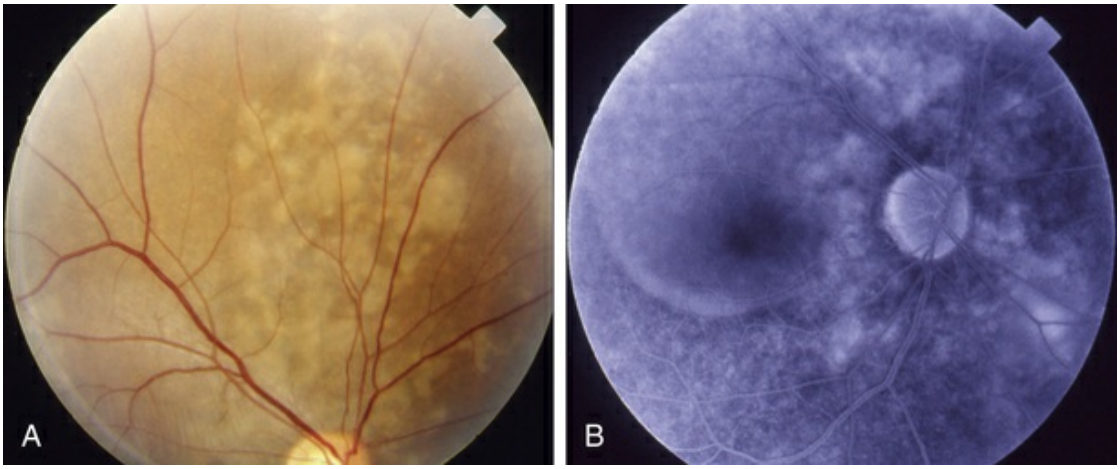

FIG. 99.9 Color photograph (A) and fluorescein angiography image (B) showing exudative retinal detachment and multiple subretinal yellow patches in a case of pregnancy-induced hypertension.

Diabetic Retinopathy

Severe diabetic macular edema (DME) may sometimes accompany localized macular detachment. Fluid leaking out from the vessels first accumulates within the retina; beyond a certain critical point, fluid may gain access into the subretinal space causing sensory

detachment. Severe macular edema not only leads to detachment but may be associated with massive hard exudates (Fig. 99.10). Hard exudates are one of the independent risk factors for vision decrease.[21] In addition to vascular hyperpermeability related to diabetic vasculopathy, taut posterior hyaloid membrane may also contribute to macular edema and localized detachment either from the mechanical traction force or from traction-induced increased vascular permeability.

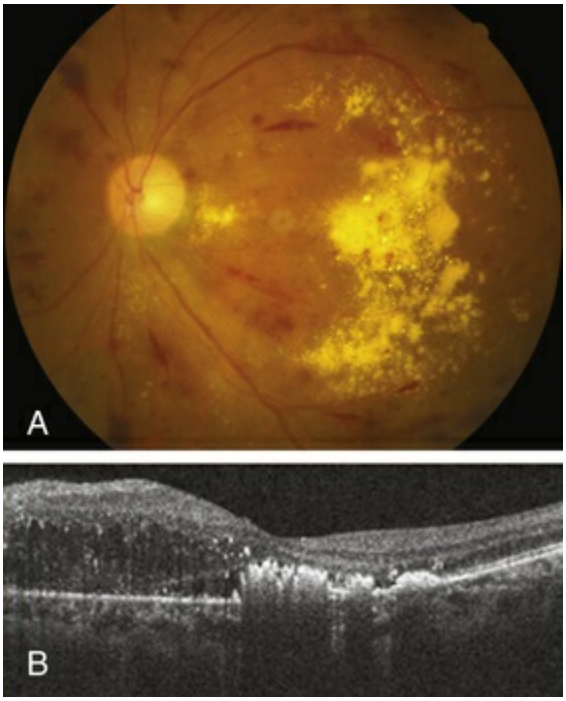

FIG. 99.10 Color photograph (A) and optical coherence tomography image (B) showing massive hard exudates with macular cystic changes and sensory retinal detachment in diabetic retinopathy.

Clinically, early fundus changes leading to severe macular edema may present as a central retinal vein occlusion-like picture with flame-shaped hemorrhage around the disc and scattered perivascular exudates but without FA evidence of disc leakage and venous delayed filling. In other cases, multiple clusters of microaneurysms may distribute in the posterior pole, accompanied by significant capillary nonperfusion. Sensory detachment and massive exudates may later develop. Exudative detachment combined with macular edema represents severe breakdown of the

inner retinal barrier. Laser alone has little effect in such cases. Multiple sessions of intravitreal anti-VEGF (vascular endothelial growth factors) alone or in combination with sub-Tenon or intravitreal steroid administration may effectively flatten down the retina in most cases. It has not been confirmed if subsequent focal laser to the leaking vascular segments or microaneurysms may obtain a more lasting effect. However, the Diabetic Retinopathy Clinical Research Network, as well as other multicenter clinical studies, showed no additional effect of focal laser compared with multiple sessions of intravitreal anti-VEGF using the studies' protocol in treating DME.[22–26] In some cases, exudative detachment is present without significant cystoid macular edema. It may be because the edema is in a resolving phase; thus the response to treatment may be quicker. In severe cases, exudates may consolidate and deposit within or below the macula. If the condition does not improve after several sessions of medical treatment, pars plana vitrectomy combined with hyaloid membrane and internal limiting membrane removal may be performed to reduce edema and hard exudates (Fig. 99.11).[27] Because the development of massive hard exudates indicates that the retina is in a relatively hypoxic state or has already gone into the early proliferative stage, panretinal photocoagulation during the operation is required to inhibit production of angiogenic factors, which may induce further macular edema or neovascularization, leading to postoperative vitreous hemorrhage or even neovascular glaucoma.[27] In the case of preexisting posterior vitreous detachment, epiretinal membrane peeling and internal limiting membrane peeling may be considered.[28] Massive exudates usually form submacular plaques, affecting vision severely. After surgery, the plaque may reduce in size but does not disappear completely, leaving residual fibrosis or crystal-like deposition, causing permanent decrease of vision. Surgical removal of subretinal exudates through iatrogenic retinotomy has been reported;[29] the effect has not been firmly established. Patients with severe edema should have a systemic check-up, including blood pressure, blood lipid, and renal function; any abnormalities should be treated, as these may interfere with local response to the treatment.

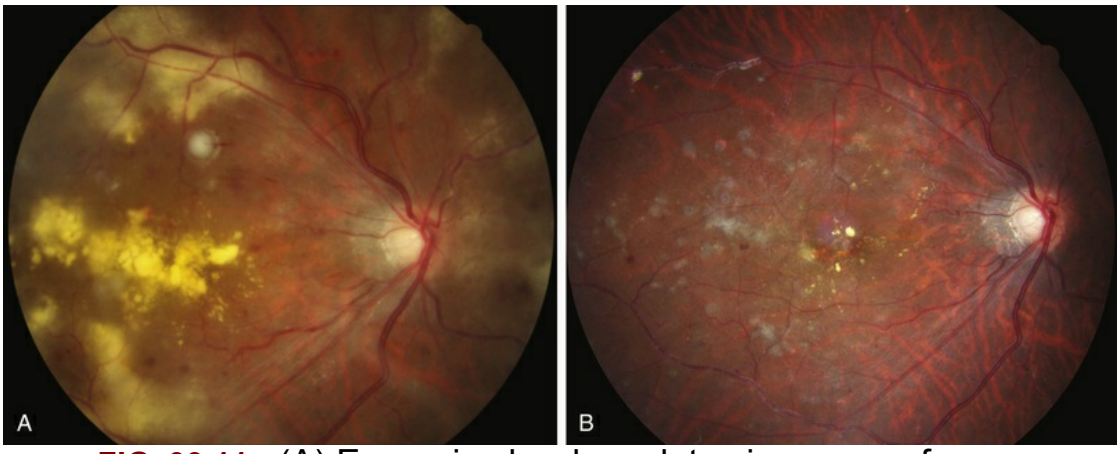

FIG. 99.11 (A) Excessive hard exudates in a case of diabetic retinopathy. (B) Reabsorption of hard exudates 8 months after vitrectomy, posterior hyaloid removal, and scattered laser. Best-corrected visual acuity improved from 20/800 to 20/200.

Vascular Occlusive Diseases

Severe retinal vein occlusion occasionally is accompanied by serous retinal detachment. Exudative detachment has been described in branch, hemispherical, and central retinal vein occlusion (CRVO). Vascular leakage from congested retinal veins outside the macular area is the major source of subretinal fluid at the fovea. In addition, ischemic retina produces angiogenic factors, such as VEGF, which in turn increase vascular permeability. Both increased intravascular pressure and vascular permeability cause leakage of fluid and blood components into the subretinal space. In eyes with retinal vein occlusion, serous RD is typically located beneath the fovea, and the height of the RD was greatest in the fovea (Fig. 99.12).

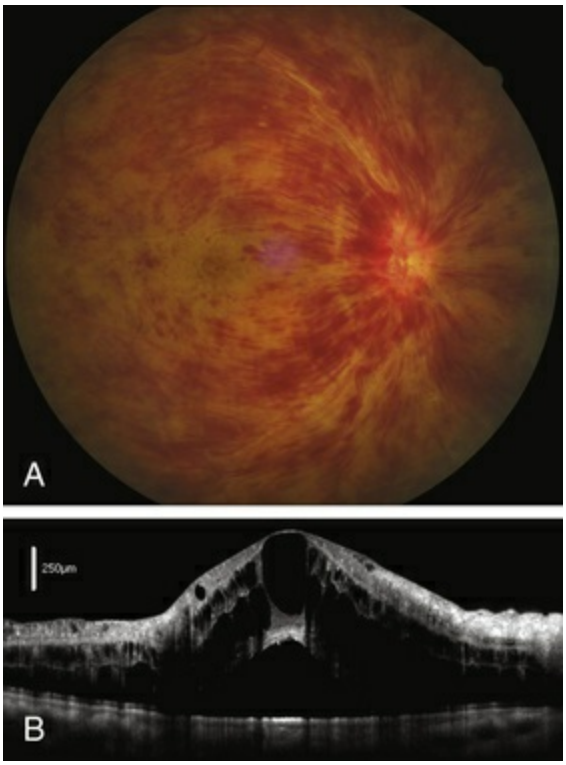

FIG. 99.12 Color photograph (A) and optical coherence tomography image (B) showing central retinal vein occlusion with marked macular edema and localized sensory macular detachment.

Recent studies with OCT revealed that macular serous retinal detachment is a common complication of retinal vein occlusion. Serous RD secondary to branch retinal vein occlusion was first described by Spaide et al.[30] Of the 14 eyes included in that study, 10 (71.4%) had serous RD. Yamaguchi et al. studied 109 eyes with branch retinal vein occlusion (BRVO) by OCT examination, and found that the incidence of serous RD was higher in the group with major BRVO (63%) than in the group with macular BRVO (21%).[31] Ozdemir et al. found a high incidence (81.8%) of serous macular detachment in CRVO.[32] In a series of 91 patients with retinal vein occlusion examined by OCT, Tsujikawa et al. reported that 76 eyes (83.5%) had serous RD involving the fovea.[33] They suggested from their observations that in eyes with retinal vein occlusion a small pointed RD developed initially just beneath the fovea, but subsequently changed into a dome-shaped RD; the foveal architecture, especially that of the Müller cell cone, might be involved in the formation of serous RD.

Application of laser photocoagulation to the affected area of

branch retinal vein occlusion has been reported to treat serous RD and can lead to resolution of subretinal fluid. The beneficial effect of laser treatment may be due to the ablation of ischemic retina, decrease of the production of VEGF, closure of incompetent vessels, and stimulation of RPE to enhance the reabsorption of fluid. Intravitreal injection of bevacizumab, ranibizumab, triamcinolone, and Ozurdex has been reported to treat serous RD due to retinal vein occlusion;[34–38] repeated injection may be necessary for frequent recurrence of macular edema. Laser or surgical instrument-induced chorioretinal anastomosis has been reported to achieve resolution of macular edema;[39–41] vitrectomy with ILM peeling has also been used with variable results.[42,43]

The visual prognosis of serous RD in retinal vein occlusion is variable. In an eye with serous RD associated with retinal vein occlusion, the outer retinal discontinuity does not necessarily lead to poor vision. If the surrounding outer segment of the foveal photoreceptors is preserved, good visual acuity will retain after macular edema and serous RD resolve. However, even after complete resolution of the macular edema and serous RD, diffuse disorganization of the outer photoreceptor layer beneath the fovea often results in poor visual acuity (see Fig. 99.13 online). In addition, a dome-shaped RD sometimes accompanies a focal defect of the outer segment of the photoreceptors above the serous RD. When the defect involves the fovea, visual prognosis is usually poor.

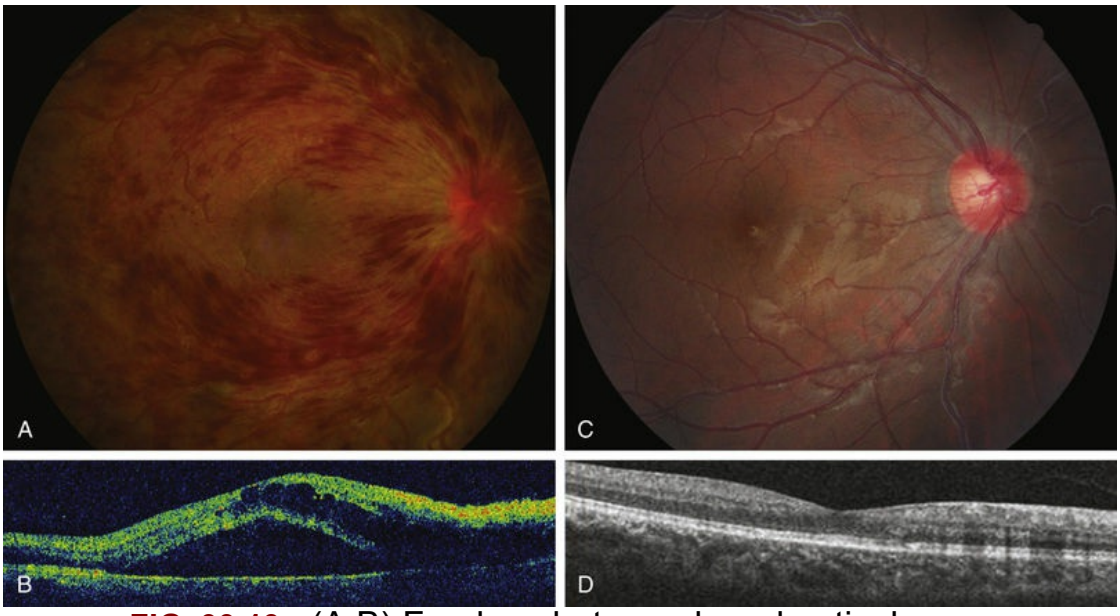

FIG. 99.13 (A,B) Fundus photograph and optical coherence tomography image showing severe macular edema in a case of nonischemic central retinal vein occlusion. (C,D) Resolution of macular edema after intravitreal bevacizumab 1.25 mg twice and posterior sub-Tenon triamcinolone acetonide 40 mg.

Collagen Vascular Diseases

Collagen vascular diseases such as systemic lupus chorioretinopathy during exacerbation of the disease activity may show similar choroidopathy and retinopathy as hypertension-induced changes. Blood pressure may or may not be high. Exudative detachment may develop secondary to breakdown of outer retinal barriers from RPE damage. It should be noticed that exudative detachment can also appear during the quiescent phase of the disease when large doses of steroid treatment have been given, similar to CSC with bullous RD. While steroid should be used in the first condition, it should be withheld or reduced when a CSC-like condition develops.

Inflammatory and Infectious

Vogt–Koyanagi–Harada Syndrome

Vogt–Koyanagi–Harada (VKH) syndrome is a multisystem

inflammatory disease capable of causing neurologic, ocular, and cutaneous symptoms. The ocular involvement includes anterior and posterior uveitis. Multiple serous retinal detachments (SRD) with congested disc is the typical finding. Bullous retinal detachment may appear in severe cases. VKH has been found to be linked with human leukocyte antigen DR4 (HLA-DR4) and HLA-DRw53, with strongest associated risk for HLA-DRB1*0405 haplotype.

These associations are high in many populations, including Japanese, Hispanic, Korean, Indian, Italian, Mexican, and Chinese.[44]

The course of VKH includes three phases: acute, convalescent, and chronic phases. The presentation of VKH usually starts with headache, associated with or followed by red eye, blurred vision, tinnitus, and vertigo. Ophthalmic signs include anterior chamber and vitreous cellular reaction and multiple patchy SRD or bullous detachment. In mild form, the vitreous cells are scanty; only mild choroidal folding with slightly hyperemic disc may be seen. The symptoms of headache along with disc edema and mild pleocytosis in cerebral spinal fluid may be mistakenly diagnosed as aseptic meningitis.

FA shows an early patchy choroidal hypofluorescent area with later multiple pinpoint leakage and dye pooling, usually forming multiple lobulated pattern. The early hypofluorescence and late hyperfluorescence of the scattered mildly elevated yellowish-white lesions may resemble acute posterior multifocal placoid pigment epitheliopathy. ICGA may show early hyperfluorescent choroidal stromal vessels, hypofluorescent dark dots in the intermittent phase, and diffuse late choroidal hyperfluorescence.[45] The hypofluorescent dark dots most probably represent the inflammatory foci. In longstanding VKH disease, 75% of patients have such persistent disease-related choroidal inflammation shown in ICGA.[45,46]

OCT has unique features. In addition to the usual pattern of subretinal fluid accumulation, the subretinal space may develop cystic spaces external to the external limiting membrane (Fig. 99.14); the floors of the cystoid spaces consist mainly of a membranous structure, continuous with the line representing the junction of the photoreceptor inner and outer segments in attached areas. It has

been suggested the membranous structures are composed not only of inflammatory products, but also of retinal tissue, probably the outer segment. The inner choroid may have a wavy appearance.

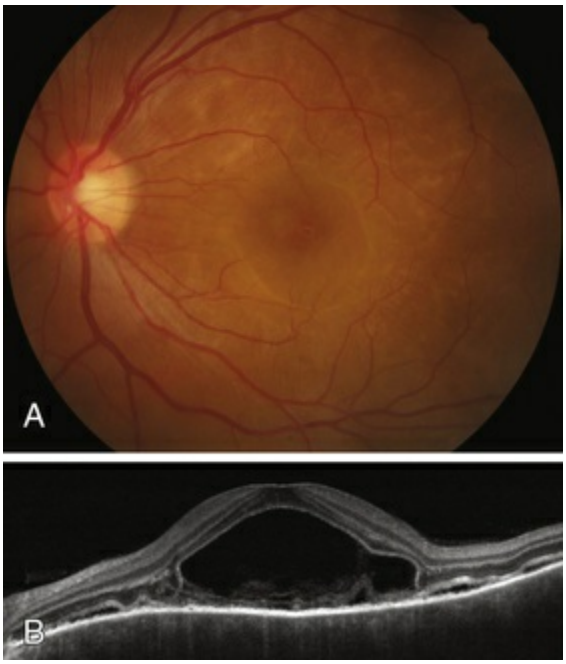

FIG. 99.14 Color photograph (A) in a case of Vogt–Koyanagi–Harada syndrome showing exudative retinal detachment in the posterior pole. Optical coherence tomography image (B) showing multilobulated sensory detachment and cysts formation in the outer retinal area.

The treatment of choice in acute stage is high-dose corticosteroid. Some advocate the use of pulse therapy with methylprednisolone 1 g daily in divided doses followed by gradual tapering over 2–3 months. Insufficient dosage may result in more frequent relapse of the disease. When steroid is tapered too early or too fast, recurrence of serous detachment may occur. Restarting high-dose steroid or supplementary periocular injection of triamcinolone may be required. In severe cases of VKH, immunosuppressive treatment may be needed. The prognosis is usually good unless there is chronic inflammation or choroidal neovascularization (CNV).

In the convalescent stage there may be skin and hair changes, including hair loss, alopecia, and vitiligo 2–3 months after the disease onset. Sunset glow appearance of the fundus, which

indicates diffuse loss of melanin pigment in the RPE and the choroid, may develop. Pigmented lines radiating from the disc after the subsidence of choroidal thickening indicate previous acute inflammation (Fig. 99.15). Scattered punched-out whitish lesions in the peripheral retina (corresponding to the histologic diagnosis of Dalen–Fuchs nodules) are often visible. Recurrence after the convalescent stage usually takes the form of chronic iritis instead of exudative detachment. Subfoveal CNV may occur in around 2% of patients with VKH and may require intravitreal injection of an anti-VEGF agent.

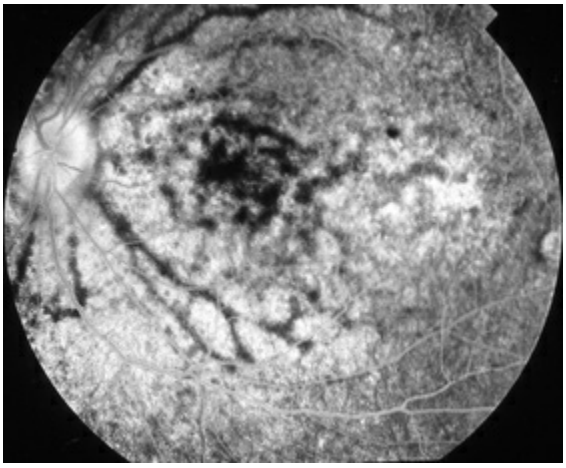

FIG. 99.15 Fluorescein angiography highlighting the radiating pigmented line in a case of convalescent Vogt–Koyanagi–Harada syndrome.

Around 10–20% of VKH may evolve into chronic inflammation. Chronic inflammation manifests as chronic anterior uveitis in most cases. The management of chronic VKH frequently involves the use of cyclosporine. It is the chronic anterior uveitis that results in most of the complications from this disease, such as cataract and glaucoma.

Sympathetic Ophthalmia

Sympathetic ophthalmia (SO) is a bilateral granulomatous uveitis that occurs after ocular trauma or intraocular surgery to an eye. The disease incidence is about 0.3% of eyes with nonsurgical ocular wounds; it is 0.01% for surgical wounds. The inflammation may

develop in the contralateral sympathizing eye as early as 2 weeks after trauma to the initial exciting eye. About half of the cases develop this disorder within 1 year after injury. In surgically induced SO, although this disorder is more likely to occur in eyes suffering from multiple intraocular surgeries for complicated vitreoretinal lesions, simple transscleral subretinal fluid drainage procedure has been reported to be associated with SO.[47]

SO has various types of fundus changes, from one similar to multifocal choroiditis with minimal subretinal fluid to one resembling VKH with evident exudative detachment. The clinical course and treatment response resemble those of VKH in many aspects.

The presenting symptoms include blurred vision, especially accommodation deficit-associated near vision reduction, redness, and ocular pain. The classic clinical signs include cells in the anterior and posterior chambers, multiple patchy or confluent serous detachments, and peripheral scattered cream-colored patches corresponding to Dalen–Fuchs nodules. FA also shows early multiple pinpoint leakage and late subretinal pooling. At the convalescent stage, skin and hair changes can also appear. The mainstay of treatment is corticosteroid. In corticosteroid-resistant cases, immunosuppressive agents may be required. Choroidal neovascular membrane can occur at the late stage. The treatment of choice for CNV is anti-VEGF agents.

Posterior Scleritis

The presenting symptoms of posterior scleritis are blurred vision and ocular pain associated with eye movement. Clinical signs include serous retinal detachment, choroidal folding on fundus examination, multiple pinpoint leakage in FA, and the pathognomonic T-sign by ultrasonography. When there is additional disc swelling and proptosis, CT scan or MRI should be performed to rule out pseudotumor. In rare conditions, posterior scleritis may present with solitary mass instead of diffuse scleritis.[48]

Posterior scleritis is a subgroup of scleritis, which also includes anterior scleritis. The etiology and treatment of posterior scleritis are similar to those of anterior scleritis, except that the anterior

necrotizing type is very rare in posterior scleritis. Reports from most university or tertiary referral centers found that about half of the scleritis cases were associated with systemic diseases. Rheumatoid arthritis is the most commonly associated systemic disease, followed by Wegener granulomatosis and relapsing polychondritis. In community-based referral practice, one-third of the scleritis cases are associated with systemic diseases; most develop after the diagnosis of the systemic disease. Rheumatoid arthritis is the leading cause, with spondyloarthropathy and infectious origin being the second and the third most common etiologies.[49] Other systemic diseases associated with scleritis include: Cogan syndrome, herpes simplex and zoster, aspergillosis, inflammatory bowel disease, and sarcoidosis.

Topical corticosteroid only is successful in controlling scleritis in less than 10% of cases. Noninfectious, non-necrotizing scleritis should be initially treated with topical corticosteroids and oral nonsteroidal antiinflammatory drugs (NSAIDs). Patients with necrotizing scleritis or those with non-necrotizing scleritis recalcitrant to NSAIDs are often started on oral prednisone. If the patient does not respond to the treatment within a month, immunomodulatory therapy (IMT) may be introduced. Steroid-sparing IMT may include antimetabolites (i.e., methotrexate azathioprine and mycophenolate mofetil); alkylating agents (i.e., chlorambucil and cyclophosphamide); T-cell inhibitors (i.e., cyclosporine and tacrolimus); tumor necrosis factor-alpha inhibitors (i.e., infliximab or adalimumab), and rituximab – a chimeric monoclonal antibody against CD-20 found on B cells. Subconjunctival and sub-Tenon triamcinolone injections are another therapeutic alternative.[50]

Infections Associated With Exudative Detachment

Many pathogens, including bacteria, rickettsia, fungus, and viruses have been reported to be able to infect either the choroid or the retina and result in exudative retinal detachment. Increased choroidal vascular permeability from infection-induced inflammation is the major reason for the fluid accumulation. The

visual recovery after appropriate treatment varies.

Bacterial Infection

Syphilis, *Mycobacterium tuberculosis*, cat scratch disease from *Bartonella henselae*, and brucellosis have been reported to cause exudative retinal detachment.

Ocular syphilis may sometimes be concurrent with human immunodeficiency virus (HIV) infection, leading to a more violent and destructive course.[51] Ocular syphilis with or without concurrent HIV infection may be associated with exudative retinal detachment.

Exudative retinal detachment may be seen in severe cases of intraocular tuberculosis. Subretinal neovascularization may later develop and result in choroidal hemorrhage in some cases.

Peripapillary serous retinal detachment and central serous chorioretinopathy-like manifestations have been reported in patients with cat scratch syndrome.[52] The exudates may be absorbed spontaneously, with or without antibiotic treatment, but some severe neuroretinitis cases may be left with optic disc pallor, abnormal color sensation, and a relative afferent papillary defect.[53]

Brucellosis invading the eye is rare, but every structure of the eye could be involved by the disease. The clinical presentations are visual loss, optic disc edema, and serous retinal detachment.[54]

Fungal Infection

Ocular fungal infection usually comes from systemic fungemia, which causes multifocal choroiditis. In ocular fungal infection, serous and hemorrhagic retinal detachments have been found. In some diabetic or immunocompromised patients, mucormycosis may be a fatal fungal infection. Severe rhino-orbital mucormycosis complicated by serous retinal detachment and retinal necrosis has been reported.[55]

Viral Infection

The most common viruses capable of causing serous retinal detachment belong to the herpesvirus family. The *Herpesviridae*

induce acute retinal necrosis, vitritis, retinal arteritis, retinal hemorrhage, exudative retinal detachment, and optic neuropathy. Cytomegalovirus (CMV) retinitis usually occurs in HIV-infected patients. CMV retinitis may also have simultaneous rhegmatogenous and exudative retinal detachment.[56]

Other Infections

Ocular toxoplasmosis is caused by *Toxoplasma gondii*, which is a cosmopolitan protozoan parasite. Clinically, ocular toxoplasmosis may cause retinal vasculitis and focal necrotizing retinochoroiditis, which presents as an oval or circular yellow-white elevated lesion with overlying vitritis. In nearly half of ocular toxoplasmosis cases, serous retinal detachment occurs during active toxoplasmic retinochoroiditis and responds well to conventional therapy, regardless of the total fluid volume.[57] Q fever is a zoonosis caused by infection with *Coxiella burnetii* (*Rickettsia burnetti*), a strictly intracellular organism. Q fever might alter immune system and induce autoimmunoreactive disease. Therefore, it could unleash VKH syndrome or simulate a VKH syndrome via a similar immunologic process and result in exudative retinal detachment.[58]

Degenerative

Age-Related Macular Degeneration and Polypoidal Choroidal Vasculopathy

In age-related macular degeneration (AMD) with CNV, serous and hemorrhagic detachment of the retina occurs frequently. The neovascular membrane causes leakage of serous exudates and red blood cells into the sub-RPE space and subsequently into the subsensory retinal space. Fundus examination typically reveals a light-grayish elevated mass corresponding to a serous and hemorrhagic detachment of the RPE and sensory retina. This mass-like lesion should be differentiated from choroidal melanoma. FA is helpful in the differential diagnosis. In AMD with CNV, the new vessels leak and present as a hyperfluorescent area, and the hemorrhagic lesion shows hypofluorescence because it is blocked

by the subretinal blood. A melanoma shows mottled hyperfluorescence in the early phase and increased staining in the late phase. In addition, a mass-like lesion induced by CNV tends to change configurations within a short period of time. A disciform scar eventually evolves from CNV with massive exudates. Extensive hemorrhagic macular detachment may lead to a breakthrough vitreous hemorrhage; the color of the vitreous opacity tends to be yellow instead of red, indicating the presence of old blood or blood degeneration products in the vitreous. In rare cases, massive hemorrhage from active lesion or disciform scar may cause severe hemorrhagic choroidal and retinal detachment (Fig. 99.16).

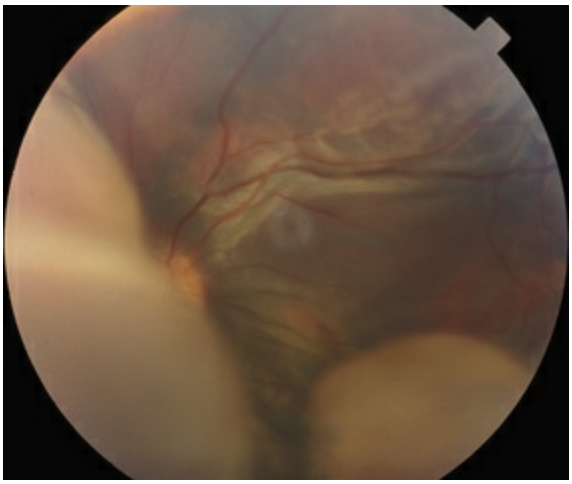

FIG. 99.16 Massive subretinal, sub-RPE (retinal pigment epithelium), and suprachoroidal hemorrhage in a case of age-related macular degeneration.

Polypoidal choroidal vasculopathy has been recognized recently as a distinct exudative macular disorder.[59] It is generally thought to be a primary choroidal vascular abnormality characterized by two distinct components: a complex of branching vascular networks and multiple, terminal, reddish-orange, aneurysms, or polypoidal lesions. Clinically, PCV shows multiple, recurrent serosanguineous detachments of the RPE and neurosensory retina secondary to leakage and bleeding from choroidal vascular lesions (Fig. 99.17).[60] It may be a cause of severe hemorrhagic choroidal and retinal detachment. Whether PCV is a variant of exudative AMD has not been definitively determined. However, there are significant

differences between PCV and exudative AMD in the demographic profile, fundus pictures, natural history, visual outcomes, and response to different treatment modalities. ICGA to identify the characteristic polypoidal vascular dilations is the main method for definite diagnosis of PCV. Recently, OCT has been used extensively to study exudative macular lesions. OCT images can also distinguish the exudative changes associated with PCV from that with exudative AMD. In the study reported by Ozawa et al., serous RD were observed in 78% of the eyes with PCV and in 53% of the eyes with exudative AMD.[61] In addition, eyes with a PCV had a greater height of serous RD, and a higher incidence of large sensory detachment than eyes with exudative AMD. The active polypoidal lesions tend to leak more severely, and the fluid from polypoidal lesions may leak into the subretinal space through the RPE and cause large serous RD, although polypoidal lesions are situated beneath the RPE.

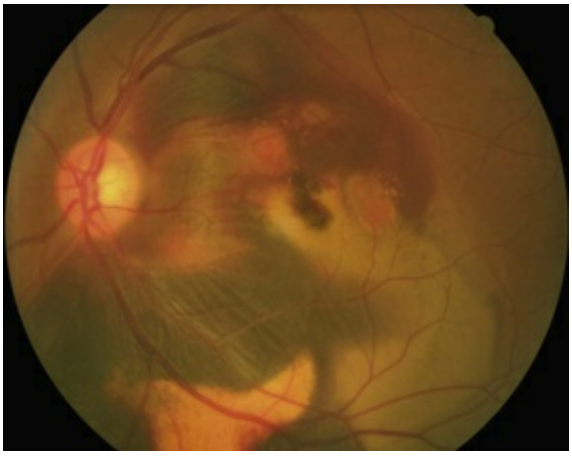

FIG. 99.17 Color fundus photograph in a case of polypoidal choroidal vasculopathy showing multiple orange-colored subretinal nodules, hemorrhagic retinal pigment epithelial detachment, subretinal hemorrhage, and sensory detachment.

In some cases of PCV, a serous neurosensory detachment at the macula without hemorrhage is the major clinical feature associated with RPE atrophy. FA shows only multifocal areas of granular hyperfluorescence. This type of PCV can masquerade as CSC. ICGA might help to establish a more definitive diagnosis. Yannuzzi et al.

reported a series of 13 patients who were previously diagnosed with CSC, but with further evaluation and follow-up, were diagnosed with PCV.[62] These eyes showed the characteristics of exudative macular detachments with a small-caliber, polypoidal vascular abnormality revealed by ICGA. Therefore, the authors recommended that ICGA should be done in the following situations: (1) patients not at risk of CSC, based on age, sex, or race; (2) eyes with persistent serous detachment at the macula associated with lipid accumulation; and (3) recurrent serous detachments with subretinal blood.

Peripheral exudative hemorrhagic chorioretinopathy is an uncommon chorioretinal mass-like lesion. It is characterized by an increased patient age, female preponderance, frequent pigment epithelium detachment, temporal equatorial location, and a highly hemorrhagic and exudative presentation, sometimes extending to the macula. It shares many features with PCV, including polyp-like choroidal telangiectases, abnormal choroidal vascular networks, and exudative and hemorrhagic presentation.[63] In the study done by Mantel et al., ICGA showed hyperfluorescent polyp-like structures in the choroid of the lesion area in 69% of eyes and an abnormal choroidal vascular network in 50% of eyes. OCT showed the typical dome-shaped elevation of the pigment epithelium over the vascular polyps.[64] The relationship between peripheral exudative hemorrhagic chorioretinopathy and PCV needs further investigation.

The serosanguineous retinal detachments in AMD or PCV can be managed by surgical intervention. Pneumatic displacement of submacular hemorrhage from the macula by intravitreal injection of expansile gas with or without tPA is now the first treatment of choice in most cases (see Fig. 99.18 online).[65] Major complications include vitreous hemorrhage and rhegmatogenous retinal detachment. Vitrectomy with subretinal injection of tissue plasminogen activator (tPA) and use of perfluorocarbon liquid to evacuate the liquefied clot from the submacular space has been reported.[66] Oshima et al. described the surgical results of patients with massive subretinal hemorrhage extending to the periphery and involving two or more quadrants with hemorrhagic and bullous retinal detachment.[67] tPA was injected intravitreally 12–24

hours preoperatively; vitrectomy was performed with peripheral retinotomy, drainage of the subretinal hemorrhage through the retinotomy using perfluorocarbon liquid, and finally gas tamponade with postoperative prone positioning. However, the final visual outcome is limited by the underlying macular pathology.

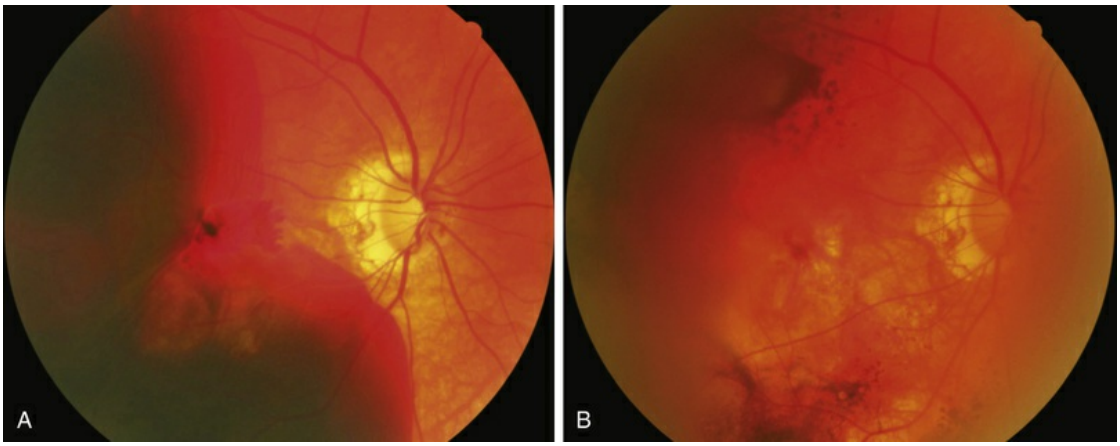

FIG. 99.18 (A) Massive subretinal hemorrhage in a case of polypoidal choroidal vasculopathy. (B) Reabsorption of the blood after pneumatic displacement with 0.2 mL C_3F_8 and intravitreal injection of bevacizumab 1.25 mg.

Tumor and Malignancy

Choroidal Hemangioma

Choroidal hemangioma (CH) can be separated into the focal, solitary type and the diffuse choroidal thickening type. Both may be associated with extensive exudative retinal detachment.

Patients with focal choroidal hemangioma are mostly middle-aged men or women, complaining of unilateral vision decrease or distortion. Fundus examinations may find localized elevated orange-colored lesions ranging in size from 2 disc diameters (DD) to 10 DD in the juxtapapillary, macular, or extramacular area in the posterior pole. The surface is usually smooth, but retinal thickening with cystic space may be seen above the lesion. Yellow specks or

yellowish-white plaque of fibrous metaplasia sometimes exist between the tumor and the overlying retina. The lesion usually does not have pigmentary proliferation within but may have a mild hyperpigmented ring around it. Exudative detachment above and surrounding the tumor or in the inferior peripheral retina, may develop. Cystoid macular edema (CME) may be present when the macula is involved. Gravity tract of pigmentary disturbance may be seen between the tumor and the lower detached retina. Although the detachment is usually limited, severe bullous detachment may occur (see Fig. 99.19 online). Vision is affected by the presence of submacular tumor, submacular fluid or CME.

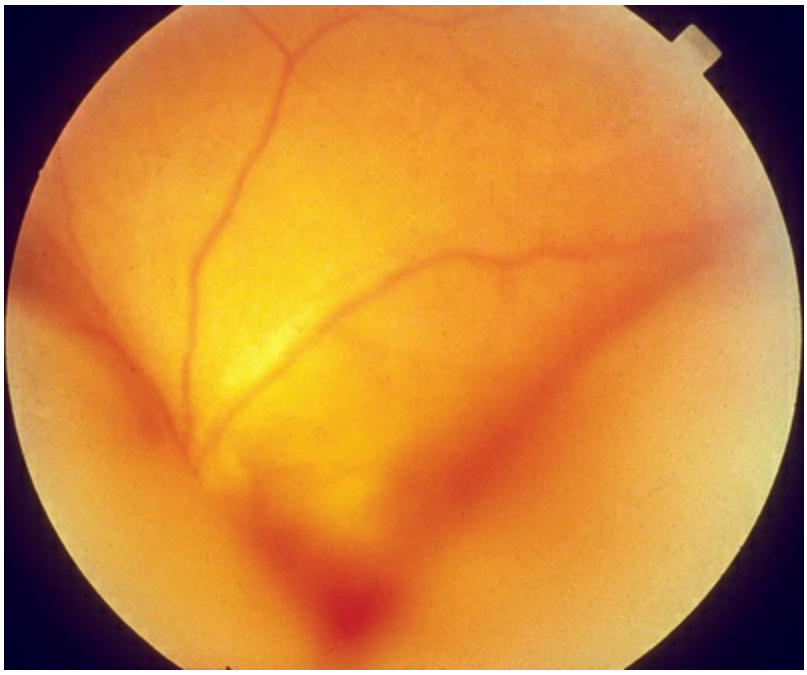

FIG. 99.19 Bullous retinal detachment in a case of solitary choroidal hemangioma.

FA shows the characteristic features of perfusion of large vessels within the tumor in the prearterial phase followed by irregular hyperfluorescence on the tumor surface; a multiloculated pattern of cystoid macular edema may appear in the late phase.[68] A ring of hypofluorescence may be seen surrounding the tumor. In small tumors without significant retinal or pigmentary changes, the lesion shows only mild hyperfluorescence, sometimes difficult to distinguish from the surrounding normal choroid. ICGA

examination can demonstrate tumor vessels in the early phase more clearly.

OCT demonstrates choroidal elevation, RPE disturbance, cystic change in the overlying retina, and subretinal fluid (Fig. 99.20). Schisis-like change may be seen in the outer retina over or adjacent to the tumor, sometimes during treatment sessions of PDT or transpupillary thermotherapy (TTT). Ultrasonography shows high internal reflectivity.[69]

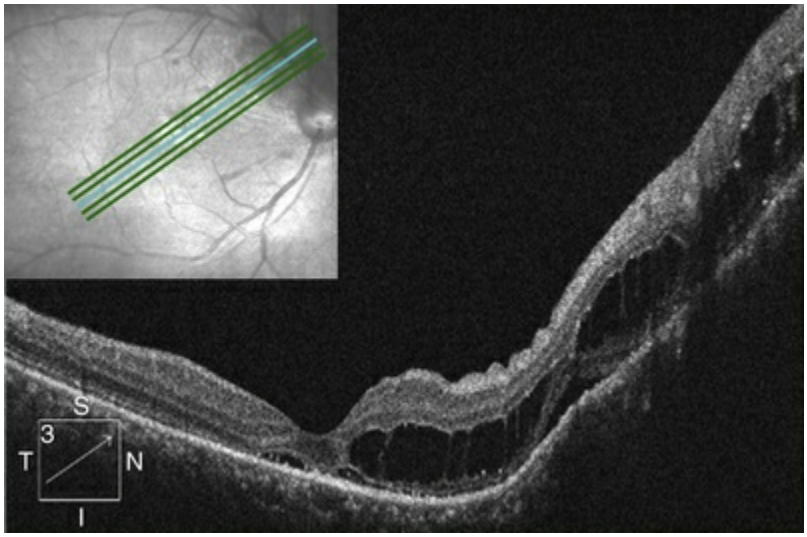

FIG. 99.20 Optical coherence tomography images in a case of choroidal hemangioma showing macular fluid pocket and cystic changes overlying the tumor.

Histologically, cavernous choroidal hemangioma consists of large, dilated, thin-walled vessels with few stromal tissues and blends into surrounding normal choroidal vessels.

Tumors not causing macular changes do not need treatment. Conventionally, an extramacular tumor with submacular fluid accumulation is treated with a laser, aiming at the leaking tumor surface. Multiple sessions of treatment may be necessary to obtain submacular fluid reabsorption. The tumor size may or may not be reduced with this treatment modality. ICGA-enhanced diode laser is another treatment option to facilitate fluid reabsorption. Recently, TTT and PDT have been advocated to treat the tumor.[70,71] With one or a few sessions of treatment at an interval of 2–3 months, fluid reabsorption and tumor reduction, and in some instances, complete

flattening down of the tumor, may occur (see Fig. 99.21 online). Large tumors may be treated with transscleral cryotherapy, thermotherapy, external beam irradiation, or episcleral plaque. In severe cases, the tumor may be hidden under the detached retina, thus inaccessible to laser or other treatment. In such cases, surgical drainage of the subretinal fluid may be performed to reexpose the tumor for a better treatment effect. Alternatively, repeated injection of bevacizumab may be used to facilitate fluid reabsorption.[72] The effect of this treatment has not been well established.

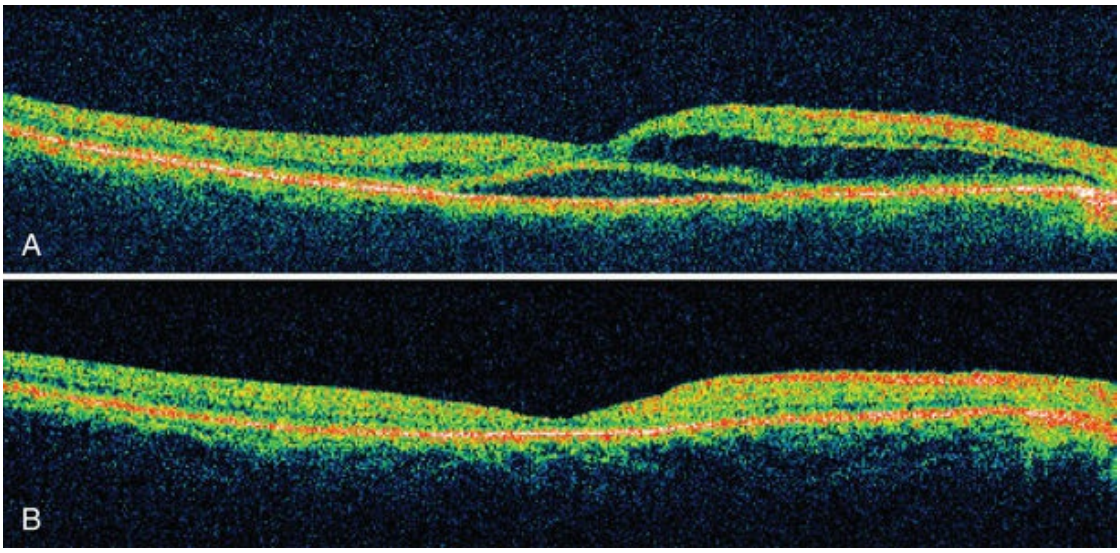

FIG. 99.21 (A) Optical coherence tomography image of the macular area in a case with upper part choroidal hemangioma showing submacular fluid and intraretinal cysts. (B) Resolution of the macular changes after photodynamic therapy to the choroidal hemangioma.

The second type is Sturge–Weber syndrome with diffuse choroidal hemangioma. Compared with the fellow eye, the lesion eye has a more reddish fundus background color; normal choroidal markings are not visible (Fig. 99.22). This may be the only significant fundus finding in some cases. Most cases had mild tortuosity of retinal vessels or scattered pigmentary changes of various degrees. Ultrasonography may detect a thickened choroid. Other more severely affected cases may present with bullous RD, associated with glaucoma secondary to increased resistance of aqueous outflow or abnormalities of the trabecular meshwork.

There may be focal choroidal thickening in addition to diffuse thickening. FA may show minimal abnormality or only patchy hypofluorescent and hyperfluorescent areas from pigmentary disturbance. Late phase leakage and cystoid space may be seen in cases with exudative retinal detachment.

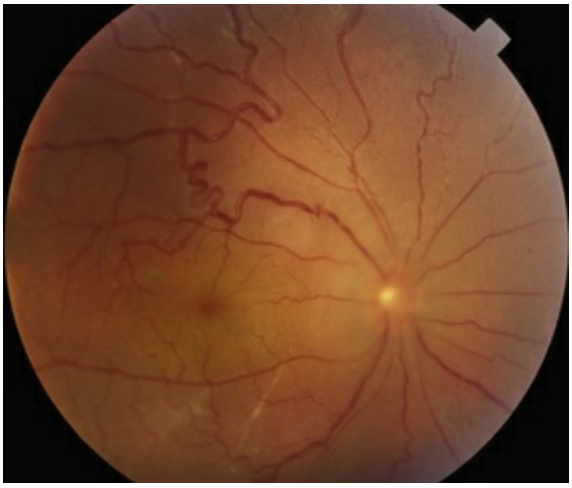

FIG. 99.22 Diffuse choroidal hemangioma with dark red background color, indistinct choroidal markings, and tortuous retinal vessels.

Glaucoma in Sturge–Weber syndrome is difficult to control with medication and usually requires operation. A filtering operation is frequently complicated by severe choroidal detachment, with spontaneous recovery in most cases. For exudative detachment with potentially useful vision, argon laser photocoagulation may be performed to the leaking area to facilitate subretinal fluid reabsorption. Other treatment modalities include low-dose external beam irradiation (1200–2000 cGy) divided into several sessions.[73] Recently, PDT applied with multiple spots and sessions has been used to treat diffuse choroidal hemangioma aiming to reduce exudative detachment as well as choroidal thickness.[74] Further studies may be needed to confirm its usage.

Choroidal Melanoma

Choroidal melanoma is commonly associated with exudative retinal detachment. The tumor lesion is often found during a routine eye examination or during specific fundus check-up for

blurred vision or visual field defect secondary to a macula involved sensory detachment or enlarged tumor itself. Flashing lights may be a complaint during tumor growth or tumor invading into the retina.

Melanoma often presents as a wide-based or dome-shaped pigmented mass under the retina (see Fig. 99.23 online). A small tumor may contain orange pigment on the surface and part or the entire lesion may be amelanotic. Exudative detachment may develop above and surrounding the tumor or in the lower dependent part away from the tumor location. During tumor growth, choroidal melanoma may invade choroidal capillaries, leading to subretinal hemorrhage. It may later break through the Bruch's membrane to form a pigmented or amelanotic mushroom-like lesion. Tumor vessels may be visible, especially if the part above the Bruch's membrane is amelanotic. When the tumor breaks through the Bruch's membrane, it may cause choroidal, subretinal, or vitreous hemorrhage. Melanoma may invade the optic disc causing disc edema. When invading the vitreous, it may cause pigment dispersion within the vitreous and pigment deposition on the surface of the retina. When invading the retina, the drainage vein may become tortuous and engorged. Rarely, the tumor may assume a diffuse growing pattern causing diffuse choroidal thickening.[75] Clinically the diffuse lesion is a more aggressive type than the dome-shaped lesion, and more likely to invade the optic disc and spread outside the sclera, thus having a much worse prognosis.

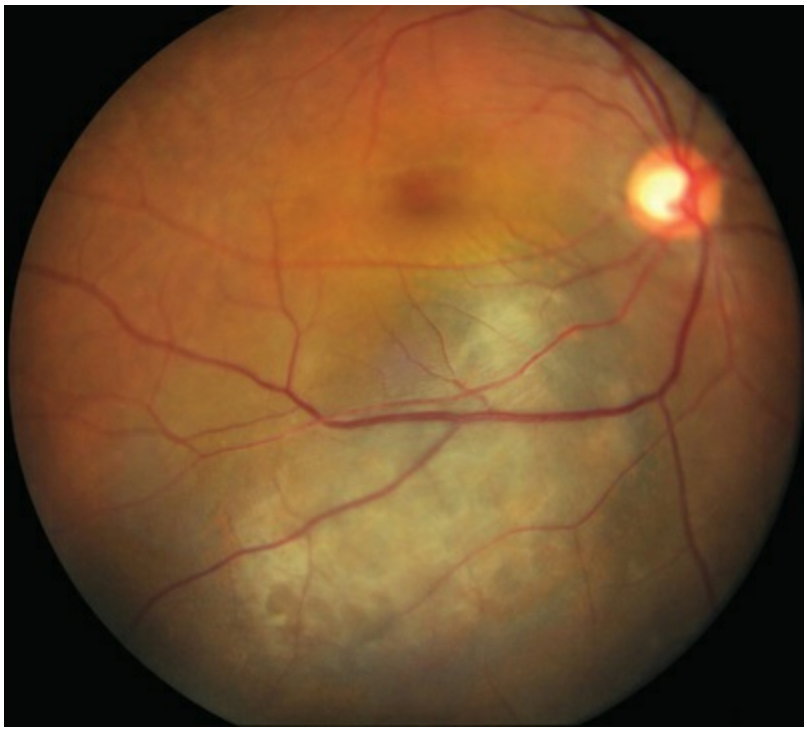

FIG. 99.23 Malignant choroidal melanoma inferior to the macula.

Histopathologic studies have shown that different tumors may contain different types of cells: spindle A, B, epithelioid cells, or mixed cell types. Epithelioid cell type has the worse visual prognosis. On FA, a typical lesion shows early pinpoint hyperfluorescence with late leakage. If there is a Bruch's membrane breakthrough, both tumor vessels and retinal vessels can be seen, presenting the so-called double-circulation sign.[76] ICGA may show tumor vessels in the late stage. Ultrasonography is valuable in showing the size, height and nodular extraocular extension. Typical lesions present as dome- or mushroom-shaped choroidal elevation with acoustic hollowness and choroidal excavation. A scan usually shows an initial spike with rapid attenuation in tumors with compact spindle A or B cell types.[77] The epithelioid cell type is more prone to have a moderate high and low spike within the tumor. MRI inevitably shows the paramagnetic effect of melanin with T1, T2 reverse sign: the lesion shows a hyperdense image in T1 and hypodense in T2, in reverse to the vitreous density (see Fig. 99.24 online).[78] In uncertain cases, fine-needle biopsy with 25-gauge needle through the pars plana into the tumor to obtain cells may be used for cytologic examinations.

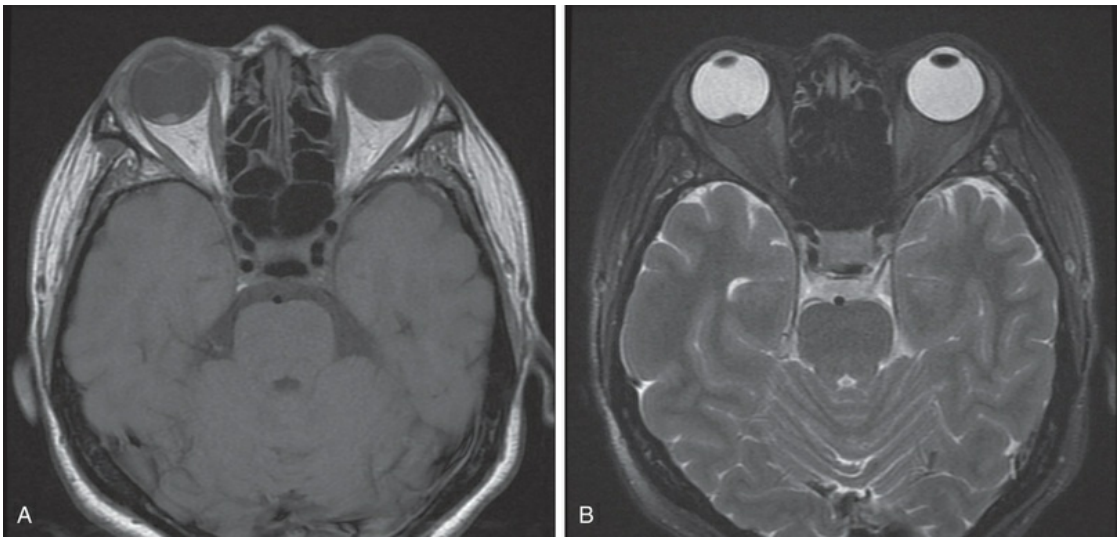

FIG. 99.24 Magnetic resonance imaging study of the above-mentioned case showing typical hyperintense T1 (A) and hypointense T2 (B) images with respect to the vitreous.

Malignant melanoma should be differentiated with choroidal nevi. Important points favoring the diagnosis of melanoma include (1) dome-shaped elevation over 3 mm; (2) orange pigmentation on the surface; (3) sensory detachment over and surrounding the tumor in the absence of CNV; (4) evidence of Bruch's membrane breakthrough; (5) multiple pinpoint leakage on FA.

Some investigators suggest that any melanocytic lesion having a basal diameter greater than 16 mm and a height more than 3 mm should be considered as malignant; lesions with typical fundus picture and showing signs of growth and a basal diameter greater than 2.5 mm should also be considered as malignant and should be treated as such. Others suggest that size itself is not the only element to consider, and emphasis should be put on signs of acute or chronic changes. The following signs indicate chronic changes and favor a benign condition: (1) the tumor shows areas of fibrous metaplasia, presenting either as a fibrotic plaque or CNV; (2) there is evidence of subretinal pigment clumps or intraretinal pigment migration or gravity tract indicating longstanding exudative detachment; (3) drusen is present.

Treatment choice should consider growth potential, size, location, and age. For a small tumor, laser may be used to treat only the leaking points to promote reabsorption of subretinal fluid if exudative detachment involves the macula.[79] For definite small-

sized malignant melanoma, consider laser or transpupillary thermotherapy.[80,81] PDT has been used with mixed results. For medium-sized or large posterior tumors, radiation with plaque or charged particles may be considered. Co-60 plaques or I-125 episcleral plaques are commonly used.[82] Ruthenium-106 plaques have also been widely used in Europe.[83] Other treatment options include photoirradiation similar to PDT for AMD, local resection, ultrasonic hyperthermia and irradiation, and radiation plaque with photocoagulation. Teletherapy with gamma knife or cyberknife may be used. Severe inflammatory reaction is the most common complication.

The Collaborative Ocular Melanoma Study (COMS) found that preoperative radiation for large choroidal melanomas (height >8 mm, basal diameter >16 mm) does not improve 5-year survival; enucleation and brachytherapy have a similar rate of survival for medium-sized tumors (height 3–8 mm, basal diameter ≤16 mm).[84] However, there is evidence from a clinical series that failure to achieve local control after radiation therapy, even when treated by subsequent enucleation, is associated with an increased risk of metastasis.[85]

Metastatic Tumors

Metastatic tumors are the most common malignant neoplasms of the eye,[86,87] with the choroid being the most common site for tumor growth. The breast was the first and the lung the second most common primary site for both choroidal and orbital metastases.[87] Approximately one-third of patients have no history of primary cancer at the time of ocular diagnosis.[87] About 50% of these patients fail to have a primary site detected, despite systemic evaluation by medical oncologists. The most common presenting symptom of intraocular metastasis was blurred vision. When visual acuity was affected, it usually decreased to the range of 20/200 to counting fingers. Other presenting symptoms included flashes, floaters, and pain. The symptom of pain is rarely found in patients with other primary uveal malignancies, such as malignant melanoma.

On fundus examination, typical choroidal metastases show one or more solitary yellow, creamy, flat, or slightly elevated lesions

with overlying pigment disturbance forming a spotted pattern usually located in the posterior retina; bilateral involvement is found in 20–40%, and multifocal in 20%; three-quarters are associated with exudative detachment. It is not possible to determine the origin of the lesions from examining the fundus alone.

FA of most metastatic carcinomas shows hypofluorescence in the arterial and early venous phases and progressive hyperfluorescence in the subsequent frames. Pinpoint foci of hyperfluorescence appear over the tumor in the venous phase and persist in the late angiograms. There may be moderate late hyperfluorescence of the serous subretinal fluid adjacent to the metastatic tumor. FA has limited value in determining the origin of the choroidal tumors, but is useful in differentiating metastatic tumors from non-neoplastic conditions, such as inflammatory processes, subretinal neovascular membranes, and organized hemorrhage.

Ultrasonography shows that metastatic tumors tend to be flat and extend in surface area rather than thickness. Most choroidal metastases have a plateau- or dome-shaped contour and measure approximately 3–4 mm in thickness. Thicker tumors generally were observed with metastases from the gastrointestinal tract, kidney, lung, and prostate. Shield and associates reported that the mean thickness was 4 mm for metastatic gastrointestinal cancers.[87]

A CT scan demonstrates the presence and configuration of intraocular metastases. On MRI, metastatic carcinomas are characteristically isointense or slightly hyperintense to the vitreous on T1-weighted images and hypointense to the vitreous on T2-weighted images. They show mild to moderate enhancement with gadolinium-enhanced examination.

Other ancillary ophthalmic procedures may aid in the diagnosis of metastatic tumors, including radioactive phosphorus test, fine-needle aspiration biopsy, and wedge biopsy.

Differential diagnoses of choroidal metastasis include amelanotic melanoma, amelanotic choroidal nevus, choroidal osteoma, choroidal hemangioma, posterior scleritis, and rhegmatogenous retinal detachment.

Workup for a choroidal metastasis includes an MRI of the head to rule out brain metastases and to determine the extent of the tumor.

The incidence of central nervous system (CNS) metastases increases from 6% to 28% after development of ocular metastasis.[88] Patients with an unknown primary site of origin should obtain a thorough physical examination and have a chest radiograph and a mammogram. In women without breast cancer and in men, the evaluation should be directed initially towards the detection of a primary tumor in the lung, alimentary tract, kidney, thyroid, pancreas, and other organs. Kole et al. suggested that positron emission positron emission tomography (PET)-CT might be helpful for detecting a malignancy of unknown origin.[89]

Common treatment options include chemotherapy, external beam radiation, plaque radiation, hormone therapy, resection, observation, and combination therapy (Fig. 99.25). TTT has been proposed to enhance reabsorption of subretinal fluid.[90]

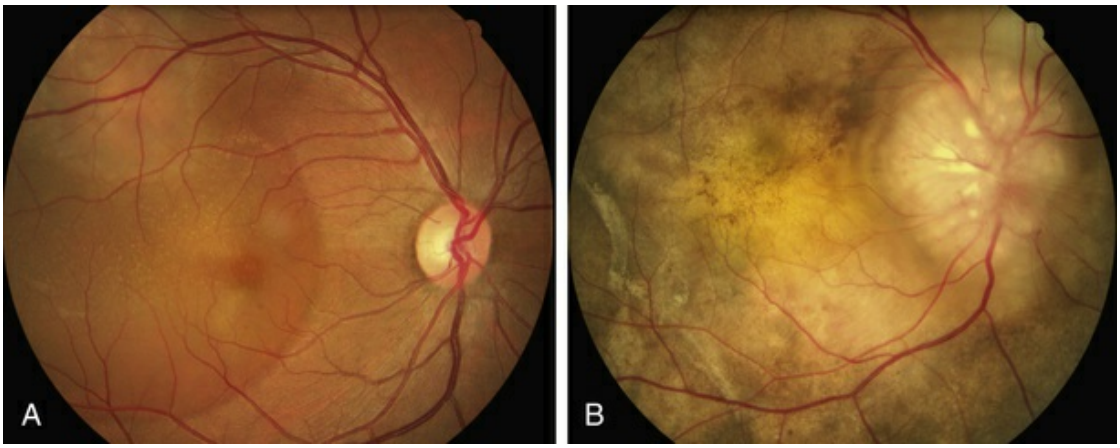

FIG. 99.25 Choroidal metastasis in a case of breast adenocarcinoma. Choroidal tumor with localized sensory detachment and subretinal deposit was noted initially (A). Rapid tumor enlargement was noted in subsequent examinations. Resolution of the tumor with widespread retinal pigment epithelium changes was noted after systemic chemotherapy. Note the presence of tumor infiltration of the optic disc (B).

Prognosis is poor for patients diagnosed with choroidal metastasis. The average survival time is 8–9 months after diagnosis.[91] Cutaneous tumors have the worst prognosis (of 1–2 months survival time), and breast tumors have the best prognosis (7–31 months). Data of 36 patients with choroidal metastases were

collected in 11 years in a teaching hospital in Taiwan. The mean age was 53.9 ± 12.8 years. The primary sites of tumors were lung in 18 (50%); breast in 8 (22.2%); gastrointestinal tract in 3 (8.3%); pancreas in 2 (5.6%); ovary in 2 (5.6%); kidney in 1 (2.8%); liver in 1 (2.8%), and unknown in 1 (2.8%).[92]

Lymphoma

Primary intraocular lymphoma (PIOL) is a rare disease and can rarely induce serous retinal detachment. It belongs to a subset of primary central nervous system lymphoma (PCNSL). Up to 80% of PIOL patients have CNS involvement at the time of, or following, PIOL diagnosis. Around one-quarter of PCNSL patients develop intraocular involvement.[93] It is known as the most important cause of the uveitis masquerade syndrome (see Chapter 82, Intermediate uveitis and Chapter 126, Diagnostic and therapeutic vitrectomy for uveitis). The clinical signs include cellular infiltration of the vitreous, which mimics vitritis, and multiple creamy subretinal infiltrative mounds with surface pigmented clumps (Fig. 99.26). Some cases may show localized subretinal yellowish infiltration with exudative detachment or intraretinal infiltration resembling acute retinal necrosis. The diagnosis of PIOL requires a high index of suspicion. When elderly patients develop vitreous opacity with vitreous cells, PIOL should be kept in the list of differential diagnoses, especially when the so-called vitritis is refractory to corticosteroid treatment. When there is a suspicion of PIOL, pars plana vitrectomy and lumbar puncture are the two important diagnostic procedures. Cytologic examination of the vitreous sample leads to a definite diagnosis. A negative result is likely to occur when patients are receiving treatment with corticosteroid. Some found a higher interleukin (IL)-10 level, or higher IL-10 to IL-6 ratio, in the vitreous of patients with PIOL. Although the cytokine levels are not diagnostic of PIOL, they are useful adjuncts to the cytologic examination. When the clinical suspicion of PIOL is high, and IL-10 level or IL-10 to IL-6 ratio is high, even if the initial vitrectomy and lumbar puncture are negative, more aggressive diagnostic procedures are warranted. In some cases with only scanty vitreous infiltration, cytologic examination of samples from a

subretinal biopsy may be required.[94]

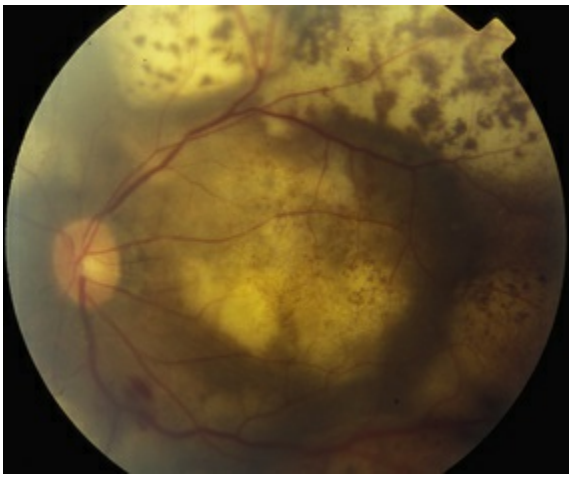

FIG. 99.26 Intraocular lymphoma showing multiple yellowish subretinal mounts with overlying pigmented clumps.

The treatment of choice for PCNSL, with or without PIOL, is high-dose methotrexate intravenously, which can pass the blood–brain barrier and blood–ocular barrier and reach the therapeutic level in the vitreous. Some advocate additional intravitreal methotrexate (0.4 mg/0.1 mL) injections in patients with PCNSL and PIOL (Fig. 99.27). The side-effects of intravitreal methotrexate injection include corneal epithelial toxicity and cataract. In relapsing cases with intraocular involvement only, treatment success has been reported with intravitreal injection of methotrexate only. In refractory cases, radiotherapy on the brain and the involved eye may be an option. However, recurrence is the rule with radiotherapy only. Intravitreal rituximab is a promising alternative for treatment of PIOL, with no significant side-effect.[95]

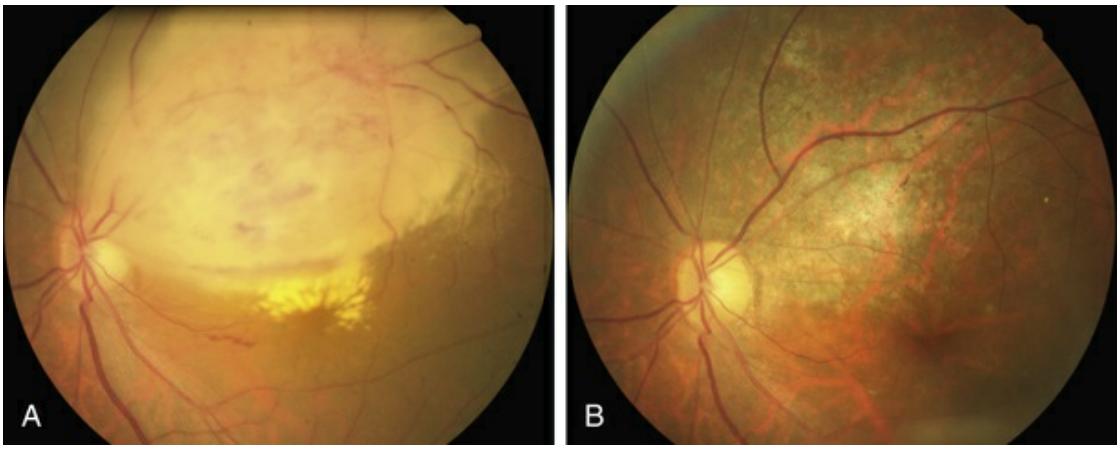

FIG. 99.27 (A) Color fundus photograph in a case of cytology-proven intraocular lymphoma showing massive subretinal infiltration of lymphomatous cells and exudative retinal detachment. (B) Resolution of the exudates after systemic chemotherapy and intravitreal injection of methotrexate.

Leukemia

About 40–70% of the patients with leukemia have eye involvement.[96] Pathologic changes from anterior segment to posterior segment may occur, including corneal ring ulcer, iris infiltration, glaucoma, retinopathy, choroidopathy, and optic neuropathy.[96] Structural alteration may be caused by direct leukemic cell infiltration or by accompanied hematologic abnormalities, such as anemia, hyperviscosity, or both.[96] Posterior segment manifestations are usually associated with retinal vascular changes, retinal hemorrhage or even retinal infiltrations. Exudative retinal detachment may occasionally be seen secondary to leukemic choroidopathy.[96]

Previous study has shown about half of leukemia cases have uveal infiltration.[97] Most do not have clinical symptoms or fundus changes. Ultrasonography may show mild choroidal thickening. Some patients may present with localized or diffuse leopard-spot changes secondary to retinal pigment epithelium damage by either extensive leukemic infiltration of the choroid capillaries or chemotherapy. Focal or diffuse choroidal elevation may occasionally be seen from choroidal infiltration of leukemia, especially acute lymphocytic lymphoma. Exudative detachment

may occur as well as RPE detachment (Fig. 99.28). When localized, it may be similar to CSCR; in more extensive detachment, FA may show pinpoint leakage secondary to RPE damage, similar to Harada disease, posterior scleritis, or other infiltrative diseases of the choroid. Systemic chemotherapy may prompt reabsorption of subretinal fluid.[98] During this process, numerous yellow exudate-like patches may be seen beneath the retina (Fig. 99.29).

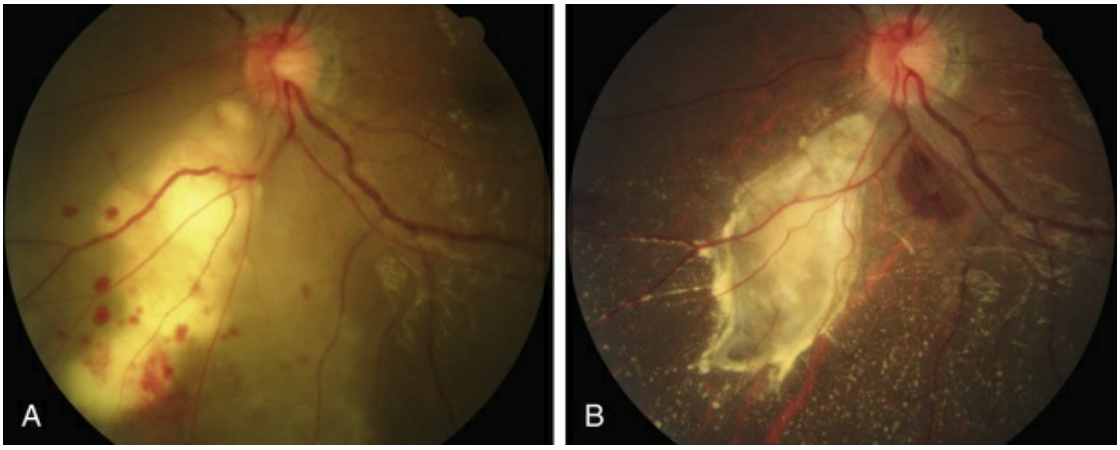

FIG. 99.28 (A) Confluent nodular subretinal infiltration with surrounding exudative detachment in the left eye in a case of acute myelocytic leukemia. (B) Resolution of the lesions with residual subretinal exudates after systemic chemotherapy.

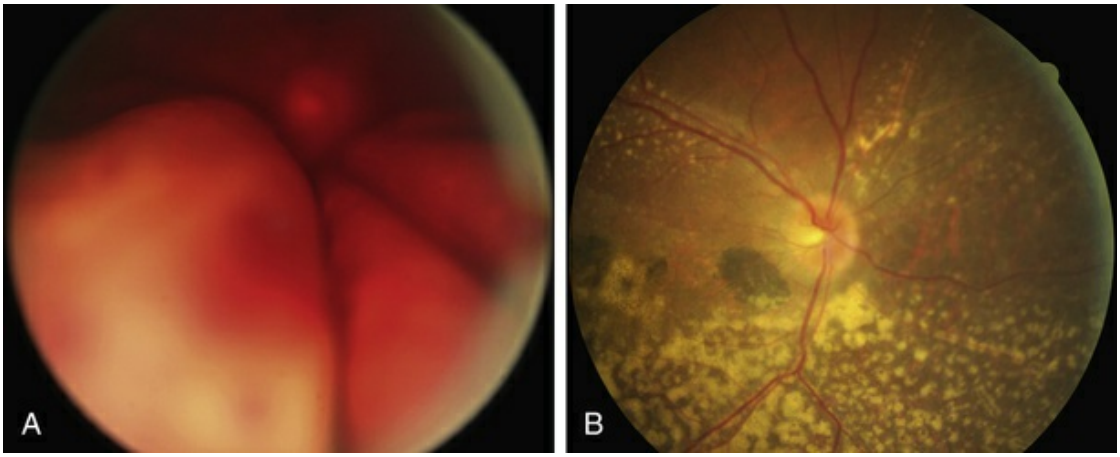

FIG. 99.29 (A) Hemorrhagic choroidal detachment and retinal detachment in a case of acute leukemia. (B) Resolution of the lesions with residual subretinal

exudates after systemic chemotherapy.

Others

Other benign tumors, such as osteoma or astrocytoma, may be associated with exudative retinal detachment adjacent to the lesion site. (Fig. 99.30).

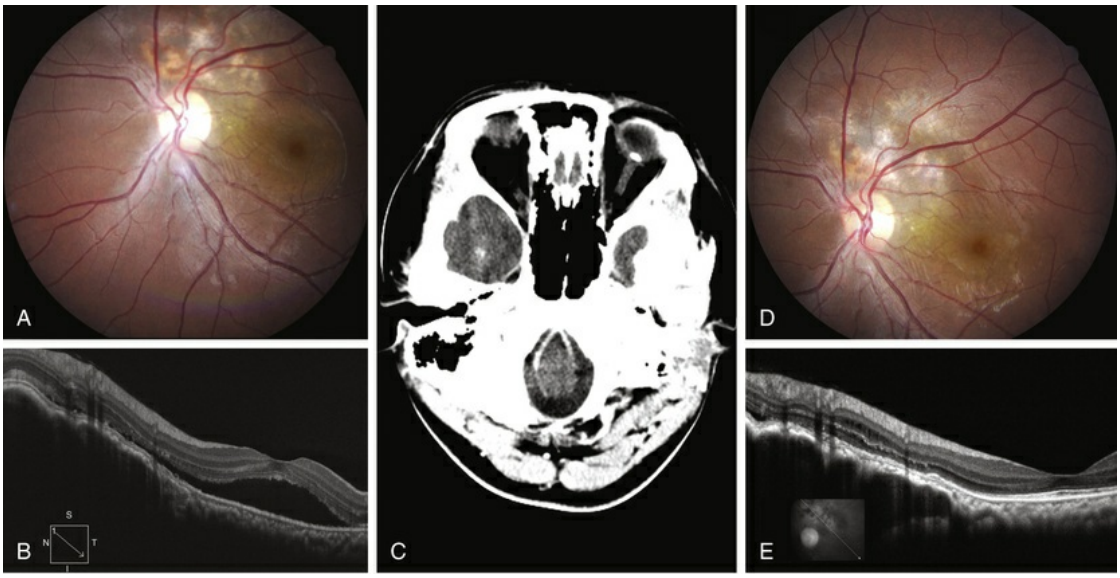

FIG. 99.30 Choroidal osteoma in a 25-year-old woman. The lesion was in the upper juxtapapillary area with localized retinal detachment involving the macula in the left eye (A,B). CT scan (C) shows the lesion to be calcified. Subretinal fluid subsided after one session of transpupillary thermotherapy (D,E).

Disc Anomalies

Optic Nerve Pit

Optic pit is a congenital defect within the optic nerve head and appears as a gray dimple. It varies in size but on average is less than one-third of the DD in width. Clinical examination shows a localized excavation of the disc that typically measures less than one-half of the DD; 50% of the pits locate on the temporal side, and

one-third locate centrally without association with retinal detachment. The incidence of the disease is 1/11 000;[99] 25–75% (40%) are associated with retinal detachment.[100] The condition is unilateral in 90% of cases. In 85% of cases, the abnormal optic disc is larger than the contralateral one. The color of the pit may be gray, yellow, or, less frequently, black. Various juxtapapillary changes including peripapillary retinal pigment epithelial change or choroidal atrophy or both are present in 95%. Visual field defect is caused by retinal elevation in 40% and enlarged optic pit in 60%. The patterns of visual field defect are nasal and temporal steps, altitudinal defects, paracentral scotomas, arcuate scotomas, or generalized or localized constriction.[99] The macula may show the following changes: serous macular elevation, macular cystic degeneration and schisis formation, or macular mottling without evidence of RD. Schisis and RD may be present simultaneously (see Fig. 99.31 online). There is communication between the schisis cavity or subretinal space and the optic disc pit. Retinal detachment including schisis occurs in 40% of cases, usually extending into the macular region or slightly beyond.[101] Larger pit, temporal location pit, and macular hole may be predisposing factors for RD. Longstanding serous retinal detachment can eventually lead to cystic degeneration of the macula and loss of pigment in the underlying retinal pigment epithelium. Lamellar and, rarely, a full-thickness macular hole may develop. Spontaneous resolution of the macular detachment is reported in 25% of cases.

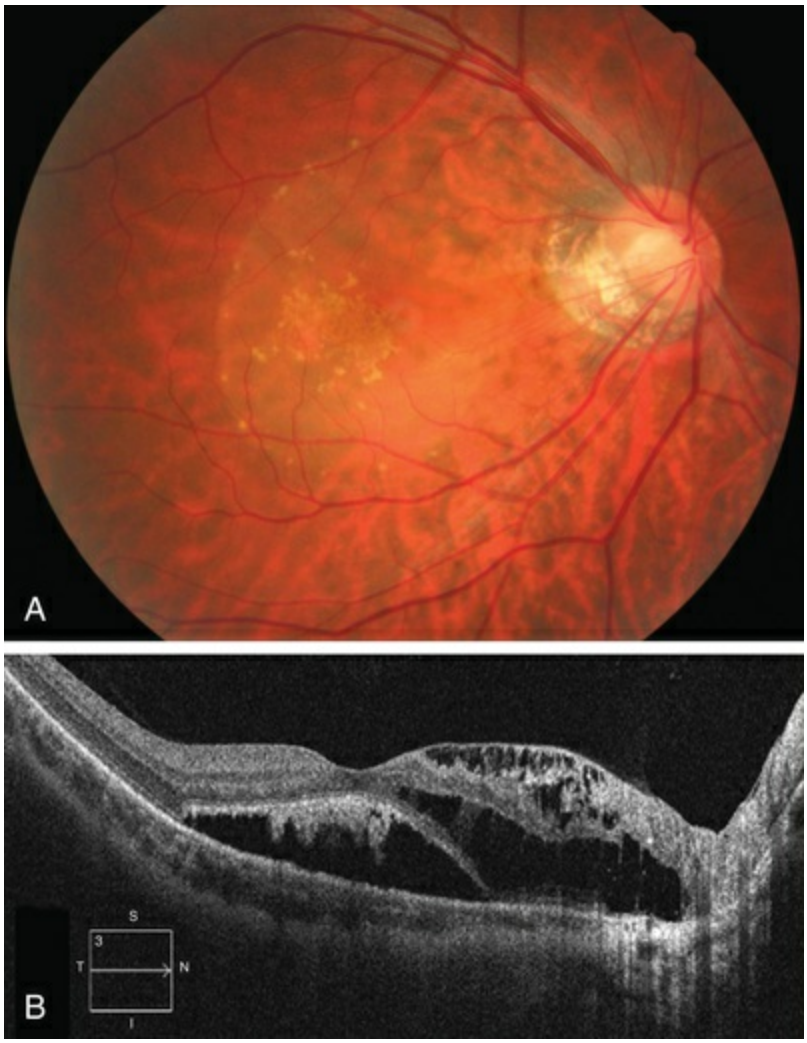

FIG. 99.31 Color fundus picture (A) and optical coherence tomography image (B) showing optic pit with macular sensory detachment with subretinal yellow deposit and retinoschisis nasal to the fovea.

The origin of the schisis fluid or subretinal fluid remains controversial. A Collie dog model suggested a connection between the vitreous cavity and the subretinal space (India ink).[102] OCT may show a thin fenestrated sheet of tissue covering the pit. In addition, some patients treated with vitrectomy and tamponade have gas extending into or under the retina postoperatively. Regenbogen et al. proposed the idea that subretinal fluid could be derived from cerebrospinal fluid.[99,103] Lincoff and Kreissig suggested fluid emanating from an optic disc pit was creating a schisis-like separation of the inner layers of the retina. A detachment of the outer layers from pigment epithelium was a secondary process that began in the center of the macula and did not connect with the optic

disc pit.[104]

The natural course of untreated RD was poor. VA eventually may drop to less than 20/100 in 50–80%, especially when macular detachment develops.

Persistent macular elevation may require surgery (Fig. 99.32). The greater the separation between the peripapillary RPE and the retina, the less the chance of a successful treatment. Laser photocoagulation (along the disc margin adjacent to RD), pneumatic displacement, pars plana vitrectomy, pars plana vitrectomy with autologous platelets, and macular buckling (vertically at posterior pole) have been reported.[104–106] Cox and associates compared various surgical modalities. They concluded that combined surgery of vitrectomy, gas injection, and laser photocoagulation to the temporal margin of the disc is the most effective therapy.[106]

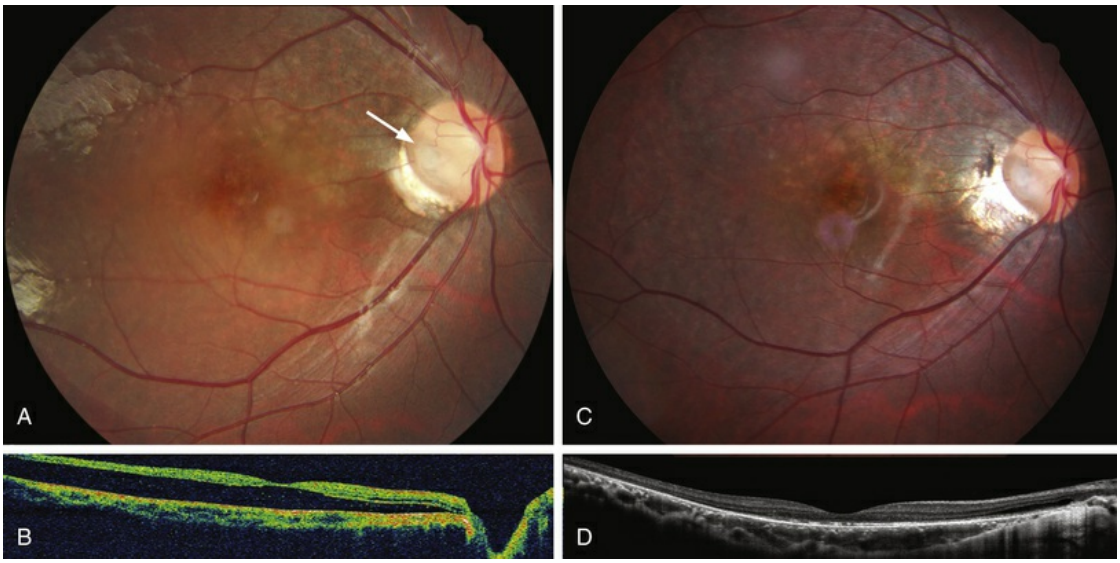

FIG. 99.32 Color fundus photograph (A) and optical coherence tomography (OCT) image (B) showing optic pit (*arrow*) with macular sensory detachment. Color fundus photograph (C) and OCT image (D) showing resolution of the subretinal fluid after one procedure of gas tamponade and three sessions of laser photocoagulation on the temporal margin of the disc.

In some cases, macular RD and schisis were noted without a pit. It may be due to a small pit or chronic CSCR. In some of these cases,

a sheet of tissue with small fenestration may be detected over the disc margin with OCT.

Differential diagnosis includes: macular schisis with/without optic pit; macular detachment with/without optic pit; CSC; myopic and age-related macular degeneration; peripapillary detachment in pathologic myopia (PDPM); malignancy; and PCV.

Morning Glory Syndrome

Morning glory syndrome (MGS) is a congenital optic disc anomaly caused by abnormal closure of the embryonic fissure with outward herniation of the disc and peripapillary tissues. It is characterized by a large-sized excavated disc overlaid with a tuft of glial tissue on the center and surrounded by an elevated pigmented ring. Narrow and straight retinal vessels cross the disc margin in a radial pattern. The disease may be diagnosed in infants or young children because of strabismus or other associated anomalies such as cataract, microphthalmos, or anterior segment anomaly or in school-age children, after vision screening. The visual acuity is usually below 20/200. Some rare cases with minor changes may be found during routine eye examinations.

RD is noted in about one-third of the cases.[107] It may be confined to the peripapillary area or involve a large part of the entire retina (Fig. 99.33). The detachment may be rhegmatogenous or nonrhegmatogenous; the cause is difficult to determine from clinical presentation alone, although bullous detachment is more likely to occur in rhegmatogenous detachment. Definite diagnosis relies on the identification of retinal breaks, which are usually small and slit-like on the surface or margin of the abnormal disc. Because of poor contrast, retinal breaks are difficult to find preoperatively. During operation, SRF may be seen coming out from the hidden break by active or passive suction.

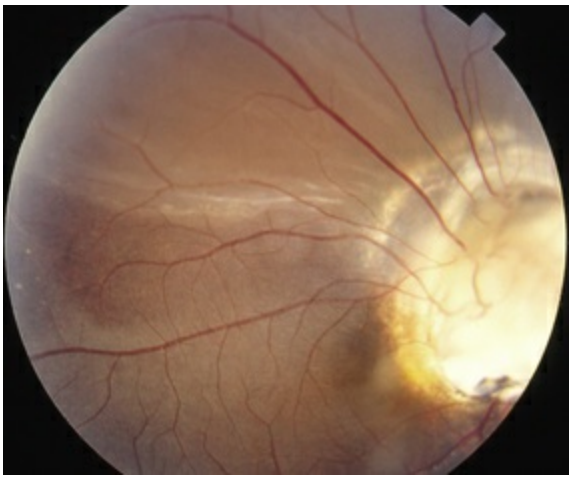

FIG. 99.33 Color fundus photograph showing a case of morning glory syndrome with sensory retinal detachment of the upper retina.

For nonrhegmatogenous detachment, the condition may undergo spontaneous improvement and recurrence. The source of fluid is debated. There may be communication between the subretinal space and subarachnoid space or the vitreous cavity, as in the optic pit. The fact that certain cases had a successful reattachment after an optic nerve fenestration operation suggests that CSF may be an important source of the subretinal fluid.[108,109]

Localized detachment may be observed and more widespread detachment may be treated with vitrectomy, posterior hyaloid and glial tissue removal, internal drainage, and laser around the break, if found. Intractable cases may be treated with silicone oil tamponade, although there is a small danger of silicone oil migrating to the optic nerve sheath. An optic nerve fenestration procedure may be done for cases that did not respond to vitrectomy.

Peripapillary Intrachoroidal Cavitation

Peripapillary intrachoroidal cavitation (ICC) is a yellow-orange lesion usually located in the inferior aspect of the optic disc in a high-myopic eye. ICC has been thought to be a stable lesion without causing vision disturbance. However, in rare patients, macular detachment may develop; vision may thus be compromised. Clinical and imaging studies suggest the accumulation of subretinal fluid may have originated from the

communicating tracts with ICC, which in turn may have communication with the vitreous cavity (Fig. 99.34). The best treatment method is unknown, although intravitreal gas tamponade has been shown to prompt macular reattachment.[110,111] This condition has recently been reported in non-high-myopic eyes.[110]

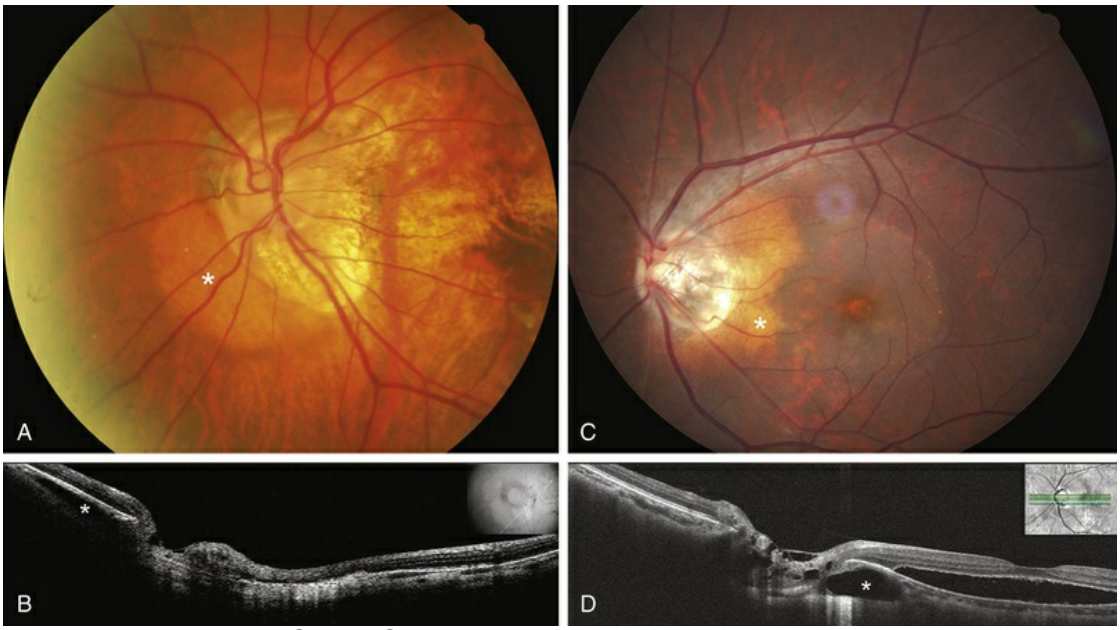

FIG. 99.34 Color fundus photograph (A) and optical coherence tomography (OCT) image (B) showing intrachoroidal cavitation (ICC) situated at the nasal lower juxtapapillary area in a high-myopic patient. Color fundus photograph (C) and OCT image (D) showing peripapillary ICC with macular detachment in a high-myopic patient.

Other Conditions

Postsurgical Exudative Retinal Detachment

Transient exudative detachment in the early postoperative period may sometimes be seen after diabetic vitrectomy, especially if excessive photocoagulation (Fig. 99.35) or peripheral cryotherapy has been done. The detachment is usually located in the inferior

part; significant fluid is noticed 1 or 2 days after surgery. Choroidal detachment may also develop. Sometimes the fluid accumulates in the posterior pole causing severe decrease of vision a few days after surgery. In such cases, ultrasonography demonstrates dome-shaped macular elevation; the condition usually improves within 1–2 weeks. Management of the exudative detachment requires careful examination and proper monitoring of intraocular pressure. If the detachment is associated with abnormally low IOP, rhegmatogenous retinal detachment should be highly suspected.

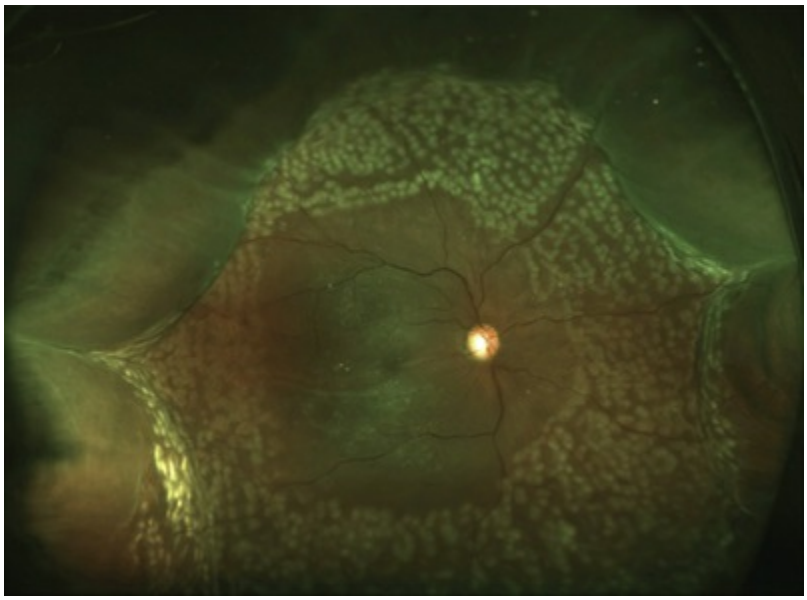

FIG. 99.35 Serous choroidal detachments and submacular fluid after panretinal photocoagulation (360°). Visual acuity improved to 20/20 after the fluid resorbed. (Courtesy of Dr. Yong Ren and Dr. Chirag Jhaveri.)

Exudative detachment may occur after scleral buckling and cryopexy to treat rhegmatogenous retinal detachment.[112] Excessive high circumferential buckle placement or multiple vortex veins compression may induce choroidal detachment with or without exudative retinal detachment. Old age and a medical history of cardiovascular disease are risk factors.[112] Excessive cryopexy may induce exudative retinal detachment causing delayed reabsorption or transient increase of subretinal fluid. As long as retinal breaks sit on the buckle, no specific treatment needs to be done. Choroidal detachment may be treated with systemic steroid especially if the

anterior chamber depth becomes shallow or intraocular pressure is high.

Kim et al. have reported that around 20% patients were found to have multiple subretinal fluid blebs after successful retinal detachment surgeries, especially in young patients. Serial measurements of subretinal fluid blebs using spectral domain (SD)-OCT showed these blebs might result from the active reattachment of retinal pigment epithelium and photoreceptors during the resolution of retinal detachment.[113]

Retinopathy with prematurity treated with laser may develop acute exudative retinal detachment.[114] The condition may respond well to systemic steroid or intravitreal steroid injection.

External drainage may induce choroidal hemorrhage entering into the subretinal space in the detached area. If subretinal blood deposits under the macula, visual acuity may be greatly compromised. The complication rate is high if drainage is done after cryotherapy because of the engorgement of choroidal vessels. To avoid this complication, one should perform external drainage as infrequently as possible or shift to vitrectomy when drainage is judged necessary with a scleral buckling procedure. Once subretinal hemorrhage and choroidal hemorrhage occur, gas injection with head-down positioning may help to push the blood away from the macula.[115,116] Simultaneous use of intravitreal tPA to better mobilize the blood clot has been advocated.[117]

Prolonged hypotony during or after intraocular surgery may induce serous or hemorrhagic choroidal detachment with or without exudative or hemorrhagic retinal detachment. This complication may occur in cataract operations, either phacoemulsification or extracapsular cataract extraction; filtering operation for glaucoma; penetrating keratoplasty; secondary intraocular lens implantation, especially sutured lens; or vitrectomy. The popularization of small gauze vitrectomy may result in more cases experiencing postoperative hypotony secondary to sclerotomy wound leakage, leading to choroidal detachment, particularly in high myopic eyes.[118] Indications and timing for surgical intervention depend on the extent of the detachment, the degree of blood clot lysis within the suprachoroidal space, the level of intraocular pressure, severity of

the symptoms, and whether or not rhegmatogenous retinal detachment exists. Additional information is available online.

Serous choroidal detachment with normal intraocular pressure and without rhegmatogenous retinal detachment can be safely followed. High intraocular pressure not controllable by medication, loss of intraocular contents, and a high suspicion of rhegmatogenous retinal detachment are indications for surgery. A 1–2-week waiting period, during which time systemic steroid may be administered, is required for the partial lysis of the suprachoroidal blood clot. During surgery, the surgeon should make certain that the tip of the infusion cannula is placed within the intraocular cavity. Drainage sclerotomy should be placed where choroid is most elevated. Suprachoroidal drainage and intraocular infusion should proceed at the same time to keep intraocular pressure and to obtain a maximal drainage. Pars plana vitrectomy is then performed to release vitreous traction, followed by perfluorocarbon liquid infusion to settle the retina and push the residual blood out through the drainage sclerotomy.

Disseminated Intravascular Coagulopathy

Disseminated intravascular coagulopathy (DIC) may result in an abnormal clotting state. A variety of systemic conditions are associated with DIC, including malignancy, malignant or pregnancy-induced hypertension, abruptio placentae, collagen vascular diseases, burns, sepsis, and organ transplantation. DIC tends to cause excessive fibrin clot formation, leading to occlusion of small blood vessels in the choroidal, rather than the retinal, circulation. This is thought to be caused by rapid deceleration, followed by stasis of blood in the choriocapillaries. The thrombus formation results in fibrinoid necrosis and disruption of the overlying RPE, which may result in serous RD.

Post-Organ Transplantation or Hemodialysis Exudative Detachment

There are two types of fundus changes: type 1 has orange-colored RPE proliferation mixed with RPE atrophic changes, forming a

leopard-spot pattern, associated with exudative retinal detachment. FA shows multiple RPE leaking points, but no RPE detachment. Subretinal fluid usually disappears within weeks or months; recurrence is common. The onset of the lesions may not be related to graft rejection. Most patients are under treatment with steroid or other antimetabolites such as cyclosporine or azathioprine. The lesions are compatible with acute RPE damage. The RPE flecks may resemble fundus flavimaculatus. The underlying cause may be due to choroidal ischemia secondary to localized intravascular coagulopathy. The other type shows multifocal RPE detachment associated with subretinal serofibrinous substance and bullous detachment, similar to atypical CSC.[119,120] The condition tends to develop in patients under hemodialysis or after kidney transplantation. Most reported hemodialysis cases were taking systemic steroids. The pathogenesis may be similar to those inducing atypical CSC, and laser photocoagulation or PDT with reduced fluence to the leaking areas may be effective in flattening down the retina.

Miscellaneous

Other conditions associated with localized or extensive exudative retinal detachment include familial exudative vitreoretinopathy, acute exudative polymorphous vitelliform maculopathy, retinoblastoma, reactive lymphoid hyperplasia, bilateral diffuse uveal melanocytic proliferation, carotid–cavernous fistula, and systemic diseases such as chronic renal failure, hypoalbuminemia.

Conclusion

Many diseases are capable of developing exudative retinal detachment secondary to imbalance between inflow and outflow of the fluid across the retina. The majority are caused by the increased permeability of choroidal vessels along with RPE dysfunction. Some are caused by excessive leakage from retinal vessels, and less often, caused by outflow obstruction. Treatment should be directed to the underlying mechanisms and aimed to correct the etiology.

References

1. Schepens CL. *Retinal detachment and allied diseases*. Saunders: Philadelphia; 1983:224–226.
2. Wang M, Sander B, la Cour M, et al. Clinical characteristics of subretinal deposits in central serous chorioretinopathy. *Acta Ophthalmol Scand*. 2005;83(6):691–696.
3. Lehmann M, Wolff B, Vasseur V, et al. Retinal and choroidal changes observed with 'en face' enhanced-depth imaging OCT in central serous chorioretinopathy. *Br J Ophthalmol*. 2013;97(9):1181–1186.
4. Ferrara D, Mohler KJ, Waheed N, et al. En face enhanced-depth swept-source optical coherence tomography features of chronic central serous chorioretinopathy. *Ophthalmology*. 2014;121(3):719–726.
5. Schatz H, McDonald HR, Johnson RN, et al. Subretinal fibrosis in central serous chorioretinopathy. *Ophthalmology*. 1995;102(7):1077–1088.
6. Yang CM, Lin CP. Bullous retinal detachment in a patient with central serous chorioretinopathy. *J Formos Med Assoc*. 1998;97(10):711–714.
7. Seong HK, Bae JH, Kim ES, et al. Intravitreal bevacizumab to treat acute central serous chorioretinopathy: short-term effect. *Ophthalmologica*. 2009;223(5):343–347.
8. Canakis C, Conway MD, Livir-Rallatos C, et al. Ocular photodynamic therapy in choroidal neovascularization complicating idiopathic central serous chorioretinopathy. *Ophthalmic Surg Lasers Imaging*. 2004;35(2):168–171.
9. Chen SN, Hwang JF, Tseng LF, et al. Subthreshold diode micropulse photocoagulation for the treatment of chronic central serous chorioretinopathy with juxtafoveal leakage. *Ophthalmology*. 2008;115(12):2229–2234.
10. Schaal KB, Hoeh AE, Scheuerle A, et al. Intravitreal bevacizumab for treatment of chronic central serous chorioretinopathy. *Eur J Ophthalmol*. 2009;19(4):613–617.
11. Uyama M, Takahashi K, Kozaki J, et al. Uveal effusion syndrome: clinical features, surgical treatment, histologic examination of the sclera, and pathophysiology.

Ophthalmology. 2000;107(3):441–449.
12. Shiono T, Shoji A, Mutoh T, et al. Abnormal sclerocytes in nanophthalmos. *Graefes Arch Clin Exp Ophthalmol*. 1992;230(4):348–351.
13. Fukuchi T, Sawada H, Seki M, et al. Changes of scleral sulfated proteoglycans in three cases of nanophthalmos. *Jpn J Ophthalmol*. 2009;53(2):171–175.
14. Schepens CL, Brockhurst RJ. Uveal effusion. 1: Clinical picture. *Arch Ophthalmol*. 1963;70:189–201.
15. Forrester JV, Lee WR, Kerr PR, et al. The uveal effusion syndrome and trans-scleral flow. *Eye (Lond)*. 1990;4(Pt 2):354–365.
16. Gass JD. Uveal effusion syndrome: a new hypothesis concerning pathogenesis and technique of surgical treatment. *Retina*. 1983;3(3):159–163.
17. Desai UR, Sabates FN. Long-term follow-up of facioscapulohumeral muscular dystrophy and Coats' disease. *Am J Ophthalmol*. 1990;110(5):568–569.
18. Eagle RCJ. Coats' disease. Eagle RCJ. *Eye pathology*. WB Saunders: Philadelphia; 1999:214–215.
19. Stergiou PK, Symeonidis C, Dimitrakos SA. Coats' disease: treatment with intravitreal bevacizumab and laser photocoagulation. *Acta Ophthalmol*. 2009;87(6):687–688.
20. Kishi S, Tso MO, Hayreh SS. Fundus lesions in malignant hypertension. I: A pathologic study of experimental hypertensive choroidopathy. *Arch Ophthalmol*. 1985;103(8):1189–1197.
21. Chew EY, Klein ML, Ferris FL 3rd, et al. Association of elevated serum lipid levels with retinal hard exudate in diabetic retinopathy. Early Treatment Diabetic Retinopathy Study (ETDRS) Report 22. *Arch Ophthalmol*. 1996;114(9):1079–1084.
22. Diabetic Retinopathy Clinical Research Network, Elman MJ, Qin H, et al. Intravitreal ranibizumab for diabetic macular edema with prompt versus deferred laser treatment: three-year randomized trial results. *Ophthalmology*. 2012;119(11):2312–2318.
23. Jampol LM, Bressler NM, Glassman AR. Revolution to a

new standard treatment of diabetic macular edema. *JAMA*. 2014;311(22):2269–2270.
24. Ishibashi T, Li X, Koh A, et al. The REVEAL Study: ranibizumab monotherapy or combined with laser versus laser monotherapy in Asian patients with diabetic macular edema. *Ophthalmology*. 2015;122(7):1402–1415.
25. Comyn O, Sivaprasad S, Peto T, et al. A randomized trial to assess functional and structural effects of ranibizumab versus laser in diabetic macular edema (the LUCIDATE study). *Am J Ophthalmol*. 2014;157(5):960–970.
26. Elman MJ, Ayala A, Bressler NM, et al. Intravitreal ranibizumab for diabetic macular edema with prompt versus deferred laser treatment: 5-year randomized trial results. *Ophthalmology*. 2015;122(2):375–381.
27. Yang CM. Surgical treatment for severe diabetic macular edema with massive hard exudates. *Retina*. 2000;20(2):121–125.
28. Gandorfer A, Messmer EM, Ulbig MW, et al. Resolution of diabetic macular edema after surgical removal of the posterior hyaloid and the inner limiting membrane. *Retina*. 2000;20(2):126–133.
29. Takaya K, Suzuki Y, Mizutani H, et al. Long-term results of vitrectomy for removal of submacular hard exudates in patients with diabetic maculopathy. *Retina*. 2004;24(1):23–29.
30. Spaide RF, Lee JK, Klancnik JK Jr, et al. Optical coherence tomography of branch retinal vein occlusion. *Retina*. 2003;23(3):343–347.
31. Yamaguchi Y, Otani T, Kishi S. Serous macular detachment in branch retinal vein occlusion. *Retina*. 2006;26(9):1029–1033.
32. Ozdemir H, Karacorlu M, Karacorlu S. Serous macular detachment in central retinal vein occlusion. *Retina*. 2005;25(5):561–563.
33. Tsujikawa A, Sakamoto A, Ota M, et al. Serous retinal detachment associated with retinal vein occlusion. *Am J Ophthalmol*. 2010;149(2):291–301.e5.
34. Karacorlu M, Karacorlu SA, Ozdemir H, et al. Intravitreal

triamcinolone acetonide for treatment of serous macular detachment in central retinal vein occlusion. *Retina*. 2007;27(8):1026–1030.
35. Ferencz JR, Rosen E, Tam G, et al. Treatment of total exudative retinal detachment due to central retinal vein occlusion by intravitreal bevacizumab in a patient with p-ANCA vasculitis. *Clin Ophthalmol*. 2007;1(3):347–351.
36. Cinal A, Ziemssen F, Bartz-Schmidt KU, et al. Intravitreal bevacizumab for treatment of serous macular detachment in central retinal vein occlusion. *Graefes Arch Clin Exp Ophthalmol*. 2011;249(4):513–520.
37. Coscas G, Coscas F, Zucchiatti I, et al. SD-OCT pattern of retinal venous occlusion with cystoid macular edema treated with Ozurdex(R). *Eur J Ophthalmol*. 2011;21(5):631–636.
38. Gallego-Pinazo R, Dolz-Marco R, Pardo-Lopez D, et al. Ranibizumab for serous macular detachment in branch retinal vein occlusions. *Graefes Arch Clin Exp Ophthalmol*. 2013;251(1):9–14.
39. McAllister IL, Gillies ME, Smithies LA, et al. Factors promoting success and influencing complications in laser-induced central vein bypass. *Ophthalmology*. 2012;119(12):2579–2586.
40. McAllister IL, Gillies ME, Smithies LA, et al. The Central Retinal Vein Bypass Study: a trial of laser-induced chorioretinal venous anastomosis for central retinal vein occlusion. *Ophthalmology*. 2010;117(5):954–965.
41. Chen SN, Huang YC. Full-thickness retinochoroidal incision in the management of central retinal vein occlusion. *J Ophthalmol*. 2015;2015:853539.
42. Raszewska-Steglinska M, Gozdek P, Cisiecki S, et al. Pars plana vitrectomy with ILM peeling for macular edema secondary to retinal vein occlusion. *Eur J Ophthalmol*. 2009;19(6):1055–1062.
43. Sato S, Inoue M, Yamane S, et al. Outcomes of microincision vitrectomy surgery with internal limiting membrane peeling for macular edema secondary to branch retinal vein occlusion. *Clin Ophthalmol*. 2015;9:439–444.

44. Damico FM, Kiss S, Young LH. Vogt–Koyanagi–Harada disease. *Semin Ophthalmol*. 2005;20(3):183–190.
45. Herbort CP, Mantovani A, Bouchenaki N. Indocyanine green angiography in Vogt–Koyanagi–Harada disease: angiographic signs and utility in patient follow-up. *Int Ophthalmol*. 2007;27(2-3):173–182.
46. da Silva FT, Hirata CE, Sakata VM, et al. Indocyanine green angiography findings in patients with long-standing Vogt–Koyanagi–Harada disease: a cross-sectional study. *BMC Ophthalmol*. 2012;12:40.
47. Gupta V, Gupta A, Dogra MR. Posterior sympathetic ophthalmia: a single centre long-term study of 40 patients from North India. *Eye (Lond)*. 2008;22(12):1459–1464.
48. Sainz de la Maza M, Foster CS, Jabbur NS. Scleritis associated with systemic vasculitic diseases. *Ophthalmology*. 1995;102(4):687–692.
49. Raiji VR, Palestine AG, Parver DL. Scleritis and systemic disease association in a community-based referral practice. *Am J Ophthalmol*. 2009;148(6):946–950.
50. Rachitskaya A, Mandelcorn ED, Albini TA. An update on the cause and treatment of scleritis. *Curr Opin Ophthalmol*. 2010;21(6):463–467.
51. Passo MS, Rosenbaum JT. Ocular syphilis in patients with human immunodeficiency virus infection. *Am J Ophthalmol*. 1988;106(1):1–6.
52. Matsuo T, Kato M. Submacular exudates with serous retinal detachment caused by cat scratch disease. *Ocul Immunol Inflamm*. 2002;10(2):147–150.
53. Wade NK, Levi L, Jones MR, et al. Optic disk edema associated with peripapillary serous retinal detachment: an early sign of systemic *Bartonella henselae* infection. *Am J Ophthalmol*. 2000;130(3):327–334.
54. Tunc M, Durukan H. Bilateral severe visual loss in brucellosis. *Ocul Immunol Inflamm*. 2004;12(3):233–236.
55. Kim IT, Shim JY, Jung BY. Serous retinal detachment in a patient with rhino-orbital mucormycosis. *Jpn J Ophthalmol*. 2001;45(3):301–304.
56. Sandy CJ, Bloom PA, Graham EM, et al. Retinal detachment

in AIDS-related cytomegalovirus retinitis. *Eye (Lond)*. 1995;9(Pt 3):277–281.
57. Ouyang Y, Li F, Shao Q, et al. Subretinal fluid in eyes with active ocular toxoplasmosis observed using spectral domain optical coherence tomography. *PLoS ONE*. 2015;10(5):e0127683.
58. Udaondo P, Garcia-Delpech S, Salom D, et al. Q fever: a new ocular manifestation. *Clin Ophthalmol*. 2011;5:1273–1275.
59. Yannuzzi LA, Sorenson J, Spaide RF, et al. Idiopathic polypoidal choroidal vasculopathy (IPCV). *Retina*. 1990;10(1):1–8.
60. Yannuzzi LA, Wong DW, Sforzolini BS, et al. Polypoidal choroidal vasculopathy and neovascularized age-related macular degeneration. *Arch Ophthalmol*. 1999;117(11):1503–1510.
61. Ozawa S, Ishikawa K, Ito Y, et al. Differences in macular morphology between polypoidal choroidal vasculopathy and exudative age-related macular degeneration detected by optical coherence tomography. *Retina*. 2009;29(6):793–802.
62. Yannuzzi LA, Freund KB, Goldbaum M, et al. Polypoidal choroidal vasculopathy masquerading as central serous chorioretinopathy. *Ophthalmology*. 2000;107(4):767–777.
63. Goldman DR, Freund KB, McCannel CA, et al. Peripheral polypoidal choroidal vasculopathy as a cause of peripheral exudative hemorrhagic chorioretinopathy: a report of 10 eyes. *Retina*. 2013;33(1):48–55.
64. Mantel I, Schalenbourg A, Zografos L. Peripheral exudative hemorrhagic chorioretinopathy: polypoidal choroidal vasculopathy and hemodynamic modifications. *Am J Ophthalmol*. 2012;153(5):910–922.e2.
65. Fang IM, Lin YC, Yang CH, et al. Effects of intravitreal gas with or without tissue plasminogen activator on submacular haemorrhage in age-related macular degeneration. *Eye (Lond)*. 2009;23(2):397–406.
66. Lewis H. Intraoperative fibrinolysis of submacular hemorrhage with tissue plasminogen activator and surgical drainage. *Am J Ophthalmol*. 1994;118(5):559–568.

67. Oshima Y, Ohji M, Tano Y. Pars plana vitrectomy with peripheral retinotomy after injection of preoperative intravitreal tissue plasminogen activator: a modified procedure to drain massive subretinal haemorrhage. *Br J Ophthalmol*. 2007;91(2):193–198.
68. Shields CL, Honavar SG, Shields JA, et al. Circumscribed choroidal hemangioma: clinical manifestations and factors predictive of visual outcome in 200 consecutive cases. *Ophthalmology*. 2001;108(12):2237–2248.
69. Liu W, Zhang Y, Xu G, et al. Optical coherence tomography for evaluation of photodynamic therapy in symptomatic circumscribed choroidal hemangioma. *Retina*. 2011;31(2):336–343.
70. Othmane IS, Shields CL, Shields JA, et al. Circumscribed choroidal hemangioma managed by transpupillary thermotherapy. *Arch Ophthalmol*. 1999;117(1):136–137.
71. Boixadera A, Garcia-Arumi J, Martinez-Castillo V, et al. Prospective clinical trial evaluating the efficacy of photodynamic therapy for symptomatic circumscribed choroidal hemangioma. *Ophthalmology*. 2009;116(1):100–105.e1.
72. Sagong M, Lee J, Chang W. Application of intravitreal bevacizumab for circumscribed choroidal hemangioma. *Korean J Ophthalmol*. 2009;23(2):127–131.
73. Gottlieb JL, Murray TG, Gass JD. Low-dose external beam irradiation for bilateral diffuse choroidal hemangioma. *Arch Ophthalmol*. 1998;116(6):815–817.
74. Anand R. Photodynamic therapy for diffuse choroidal hemangioma associated with Sturge–Weber syndrome. *Am J Ophthalmol*. 2003;136(4):758–760.
75. Shields CL, Shields JA, De Potter P, et al. Diffuse choroidal melanoma. Clinical features predictive of metastasis. *Arch Ophthalmol*. 1996;114(8):956–963.
76. Augsburger JJ, Golden MI, Shields JA. Fluorescein angiography of choroidal malignant melanomas with retinal invasion. *Retina*. 1984;4(4):232–241.
77. Farah ME, Byrne SF, Hughes JR. Standardized echography in uveal melanomas with scleral or extraocular extension.

Arch Ophthalmol. 1984;102(10):1482–1485.
78. Bond JB, Haik BG, Mihara F, et al. Magnetic resonance imaging of choroidal melanoma with and without gadolinium contrast enhancement. *Ophthalmology*. 1991;98(4):459–466.
79. Char DH, Bove R, Phillips TL. Laser and proton radiation to reduce uveal melanoma-associated exudative retinal detachments. *Am J Ophthalmol*. 2003;136(1):180–182.
80. Shields JA, Glazer LC, Mieler WF, et al. Comparison of xenon arc and argon laser photocoagulation in the treatment of choroidal melanomas. *Am J Ophthalmol*. 1990;109(6):647–655.
81. Shields CL, Shields JA, Perez N, et al. Primary transpupillary thermotherapy for small choroidal melanoma in 256 consecutive cases: outcomes and limitations. *Ophthalmology*. 2002;109(2):225–234.
82. Diener-West M, Earle JD, Fine SL, et al. The COMS randomized trial of iodine 125 brachytherapy for choroidal melanoma, III: initial mortality findings. COMS Report No. 18. *Arch Ophthalmol*. 2001;119(7):969–982.
83. Kleineidam M, Guthoff R, Bentzen SM. Rates of local control, metastasis, and overall survival in patients with posterior uveal melanomas treated with ruthenium-106 plaques. *Radiother Oncol*. 1993;28(2):148–156.
84. The COMS randomized trial of iodine 125 brachytherapy for choroidal melanoma: V. Twelve-year mortality rates and prognostic factors: COMS Report No. 28. *Arch Ophthalmol*. 2006;124(12):1684–1693.
85. Egan KM, Ryan LM, Gragoudas ES. Survival implications of enucleation after definitive radiotherapy for choroidal melanoma: an example of regression on time-dependent covariates. *Arch Ophthalmol*. 1998;116(3):366–370.
86. Shields JA. Metastatic tumors to the uvea. *Int Ophthalmol Clin*. 1993;33(3):155–161.
87. Shields CL, Shields JA, Gross NE, et al. Survey of 520 eyes with uveal metastases. *Ophthalmology*. 1997;104(8):1265–1276.
88. Demirci H, Shields CL, Chao AN, et al. Uveal metastasis

from breast cancer in 264 patients. *Am J Ophthalmol*. 2003;136(2):264–271.
89. Kole AC, Nieweg OE, Pruim J, et al. Detection of unknown occult primary tumors using positron emission tomography. *Cancer*. 1998;82(6):1160–1166.
90. Wang TJ, Chen MS, Yang CM, et al. Subthreshold transpupillary thermotherapy for early resolution of foveal subretinal fluid in choroidal metastasis. *Retina*. 2006;26(4):391–395.
91. Shields CL. Plaque radiotherapy for the management of uveal metastasis. *Curr Opin Ophthalmol*. 1998;9(3):31–37.
92. Wang TJ, Yang CM, Ho TC, et al. Metastatic choroidal tumors in Taiwan: an 11-year experience. *Am J Ophthalmol*. 2005;140(4):735–737.
93. Mochizuki M, Singh AD. Epidemiology and clinical features of intraocular lymphoma. *Ocul Immunol Inflamm*. 2009;17(2):69–72.
94. Coupland SE, Chan CC, Smith J. Pathophysiology of retinal lymphoma. *Ocul Immunol Inflamm*. 2009;17(4):227–237.
95. Pe'er J, Hochberg FH, Foster CS. Clinical review: treatment of vitreoretinal lymphoma. *Ocul Immunol Inflamm*. 2009;17(5):299–306.
96. Kincaid MC, Green WR. Ocular and orbital involvement in leukemia. *Surv Ophthalmol*. 1983;27(4):211–232.
97. Robb RM, Ervin LD, Sallan SE. An autopsy study of eye involvement in acute leukemia of childhood. *Med Pediatr Oncol*. 1979;6(2):171–177.
98. Miyamoto K, Kashii S, Honda Y. Serous retinal detachment caused by leukemic choroidal infiltration during complete remission. *Br J Ophthalmol*. 2000;84(11):1318–1319.
99. Brown GC, Shields JA, Goldberg RE. Congenital pits of the optic nerve head. II. Clinical studies in humans. *Ophthalmology*. 1980;87(1):51–65.
100. Krivoy D, Gentile R, Liebmann JM, et al. Imaging congenital optic disc pits and associated maculopathy using optical coherence tomography. *Arch Ophthalmol*. 1996;114(2):165–170.
101. Imamura Y, Zweifel SA, Fujiwara T, et al. High-resolution

optical coherence tomography findings in optic pit maculopathy. *Retina*. 2010;30(7):1104–1112.
102. Brown GC, Shields JA, Patty BE, et al. Congenital pits of the optic nerve head. I: Experimental studies in collie dogs. *Arch Ophthalmol*. 1979;97(7):1341–1344.
103. Regenbogen L, Stein R, Lazar M. Macular and juxtapapillary serous retinal detachment associated with pit of optic disc. *Ophthalmologica*. 1964;148:247–251.
104. Lincoff H, Kreissig I. Optical coherence tomography of pneumatic displacement of optic disc pit maculopathy. *Br J Ophthalmol*. 1998;82(4):367–372.
105. Garcia-Arumi J, Guraya BC, Espax AB, et al. Optical coherence tomography in optic pit maculopathy managed with vitrectomy-laser-gas. *Graefes Arch Clin Exp Ophthalmol*. 2004;242(10):819–826.
106. Cox MS, Witherspoon CD, Morris RE, et al. Evolving techniques in the treatment of macular detachment caused by optic nerve pits. *Ophthalmology*. 1988;95(7):889–896.
107. Haik BG, Greenstein SH, Smith ME, et al. Retinal detachment in the morning glory anomaly. *Ophthalmology*. 1984;91(12):1638–1647.
108. Coll GE, Chang S, Flynn TE, et al. Communication between the subretinal space and the vitreous cavity in the morning glory syndrome. *Graefes Arch Clin Exp Ophthalmol*. 1995;233(7):441–443.
109. Irvine AR, Crawford JB, Sullivan JH. The pathogenesis of retinal detachment with morning glory disc and optic pit. *Retina*. 1986;6(3):146–150.
110. Ando Y, Inoue M, Ohno-Matsui K, et al. Macular detachment associated with intrachoroidal cavitation in nonpathological myopic eyes. *Retina*. 2015;35(10):1943–1950.
111. Chen TC, Yang CH, Sun JP, et al. Macular retinal detachment associated with intrachoroidal cavitation in myopic patients. *Graefes Arch Clin Exp Ophthalmol*. 2015;253(9):1437–1446.
112. Maruyama Y, Yuuki T, Kimura Y, et al. Ciliary detachment after retinal detachment surgery. *Retina*. 1997;17(1):7–11.
113. Kim YK, Ahn J, Woo SJ, et al. Multiple subretinal fluid blebs

after successful retinal detachment surgery: incidence, risk factors, and presumed pathophysiology. *Am J Ophthalmol*. 2014;157(4):834–841.
114. Kim MJ, Kim SJ, Yu YS. The risk for retinal detachment associated with hemorrhages pre- and postlaser treatment in retinopathy of prematurity. *Retina*. 2008;28(10):1451–1457.
115. Chen SN, Ho CL, Kuo YH, et al. Intravitreous tissue plasminogen activator injection and pneumatic displacement in the management of submacular hemorrhage complicating scleral buckling procedures. *Retina*. 2001;21(5):460–463.
116. Gopalakrishan M, Giridhar A, Bhat S, et al. Pneumatic displacement of submacular hemorrhage: safety, efficacy, and patient selection. *Retina*. 2007;27(3):329–334.
117. Hassan AS, Johnson MW, Schneiderman TE, et al. Management of submacular hemorrhage with intravitreous tissue plasminogen activator injection and pneumatic displacement. *Ophthalmology*. 1999;106(10):1900–1906 [discussion 6-7].
118. Bourla DH, Bor E, Axer-Siegel R, et al. Outcomes and complications of rhegmatogenous retinal detachment repair with selective sutureless 25-gauge pars plana vitrectomy. *Am J Ophthalmol*. 2010;149(4):630–634.e1.
119. Gass JD. Bullous retinal detachment and multiple retinal pigment epithelial detachments in patients receiving hemodialysis. *Graefes Arch Clin Exp Ophthalmol*. 1992;230(5):454–458.
120. Fawzi AA, Holland GN, Kreiger AE, et al. Central serous chorioretinopathy after solid organ transplantation. *Ophthalmology*. 2006;113(5):805–813.e5.

100

Degenerative Retinoschisis

David Reed, Sunir J. Garg

Definitions and Pathology

First reported in 1933 by Bartels,[1] degenerative retinoschisis results from an acquired splitting of the retinal layers. It is closely related

to cystoid degeneration – cyst-like spaces within the retinal layers that extend approximately 3 mm posteriorly from the ora serrata and occur in nearly all adults. Histologically, cystoid degeneration is subdivided into typical and reticular types. Typical cystoid degeneration develops in the outer plexiform layer immediately adjacent to the ora serrata. In contrast, reticular cystoid degeneration arises within the nerve fiber layer immediately posterior to typical cystoid degeneration. Scleral depression helps to visualize cystoid degeneration but clinical differentiation between the two types is difficult.

Retinoschisis results from coalescence of cystoid degeneration into frank splitting of the retinal layers (Fig. 100.1). Retinoschisis likewise has typical and reticular forms that localize histologically to the outer plexiform layer and to the nerve fiber layer, respectively.[2] A viscous fluid, rich in mucopolysaccharide, gradually accumulates between the layers. The etiology of retinoschisis is unknown.

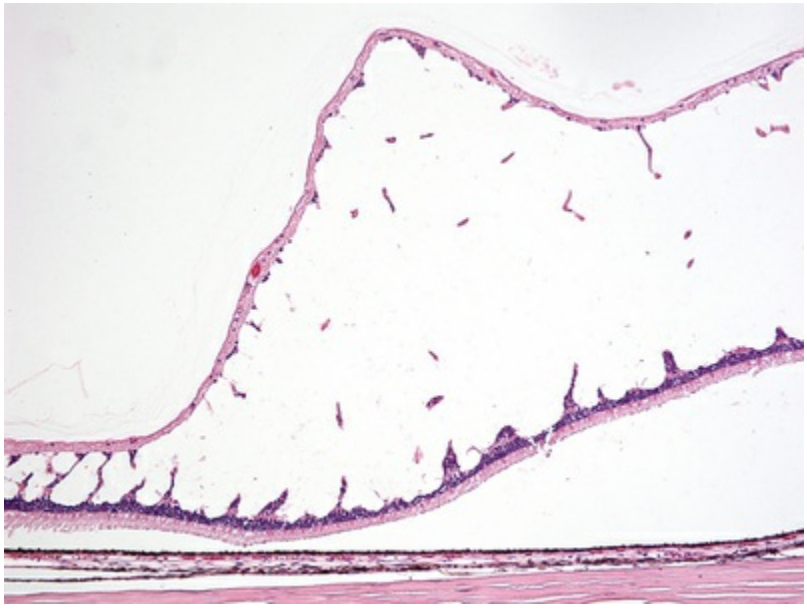

FIG. 100.1 Typical cystoid degeneration leading into typical retinoschisis. (Courtesy of Ralph Eagle, MD.)

Retinal breaks can occur within the inner retinal layer, the outer retinal layer, or both, and do not necessarily cause a retinal detachment.[3] In fact, as there is no path for the intraschisis fluid to enter the subretinal space, inner layer breaks by themselves cannot

lead to a retinal detachment.

Two types of retinal detachments are associated with retinoschisis:

1. **Schisis-detachment** describes a situation in which outer layer holes without inner layer holes enable intraschisis fluid to migrate into the subretinal space.[3]

2. **Progressive rhegmatogenous retinal detachment (RRD) associated with retinoschisis** occurs when breaks in both the inner and outer layers allow liquefied vitreous to gain access to the subretinal space.

Retinoschisis

Although degenerative retinoschisis may occasionally be present in young adults, most patients are over age 50.[3] It occurs in 1–4% of the population over age 50,[4,5] is bilateral in 85%, and is found equally between the sexes.[3] In contrast to retinal detachment and myopic foveal schisis, degenerative retinoschisis is associated with hyperopia, although it may develop in any eye.

In contrast to a retinal detachment, which causes a sloped relative or absolute scotoma, areas of retinoschisis cause a sharply demarcated absolute scotoma on visual field testing. However, even patients with very posterior retinoschisis are almost always asymptomatic.[3]

Ophthalmoscopically, retinoschisis usually appears as a thin and smooth elevation of the peripheral retina (Fig. 100.2), best appreciated with scleral depression. Although the corrugated appearance of an acute, symptomatic rhegmatogenous retinal detachment would rarely be confused for retinoschisis, it is important to differentiate retinoschisis from a chronic, subclinical retinal detachment typically associated with small atrophic holes. Table 100.1 compares features of retinoschisis and rhegmatogenous retinal detachment**.** Retinoschisis occurs in the inferotemporal quadrant in 70% and in the superotemporal quadrant in 30% of affected eyes.[3] Seventy-five percent of cases are postequatorial in furthest extent.[3] During scleral depression, the entire schisis area is

displaced inward as a unitary enclosed structure. This feature helps to differentiate it from a retinal detachment, in which scleral indentation tends to decrease the area of elevation as subretinal fluid escapes through retinal breaks into the vitreous cavity. Small white dots colloquially called "snowflakes" may be present. These are thought to be Müller cell footplates and/or neurons that bridge or formerly bridged the schisis cavity. The retinal vessels in the affected area may be sclerotic. Also, in contrast to retinal detachment, because the photoreceptors and retinal pigment epithelium remain in contact with each other, application of laser will cause whitening of the outer layer of retinoschisis.[6]

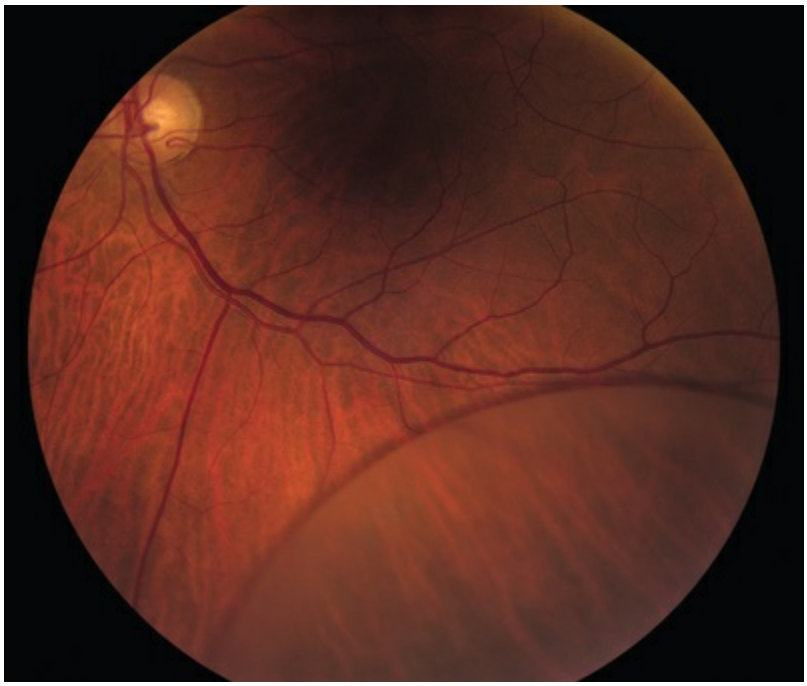

FIG. 100.2 Bullous retinoschisis is seen inferotemporally.

TABLE 100.1

A Comparison of Retinoschisis and Retinal Detachment

	Retinoschisis	Retinal Detachment
Typical patient age	Middle age to elderly	Middle age
Refractive association	Hyperopia	Myopia
Symptoms	Almost always absent	Acute: present Chronic: absent
Scotoma	Absolute	Relative

Avitreous hemorrhage or pigment	Absent	Common
Location	Inferotemporal, Superotemporal	Acute: Usually superior Chronic: Usually inferior
Texture	Smooth	Acute: Corrugated Chronic: Smooth
Müller footplates	Common	Absent
Mobility	Relatively immobile	Acute: Often very mobile Chronic: May be relatively immobile
Movement with scleral depression	Moves as single unit	Height decreases
Color with scleral depression	"White with pressure" may be seen in outer layer	No "white with pressure"
Breaks	May be present	Present
Lattice in elevated retina	Unlikely	Suggestive
Retinal pigment epithelium	Normal (unless associated with retinal detachment, current or regressed)	Acute: Normal Chronic: Atrophy and demarcation lines may be present
Optical coherence tomography	Splitting of retinal layers	Subretinal fluid
Effect of laser application through retinal break[6]	Through inner layer break: Uptake	Through full-thickness break: no uptake
Natural history	Progression rare and if present, slow	Acute: Progressive Chronic: May be nonprogressive or slowly progressive

Typical and reticular retinoschisis cannot be distinguished by assessing retinal layer thickness ophthalmoscopically, but the following clues point toward one or the other: (1) typical retinoschisis is low-lying, while reticular is bullous; (2) typical retinoschisis is located anterior to the equator while reticular retinoschisis may be located posterior to the equator; (3) outer layer holes are only seen in the reticular form.[2]

Ultrasonography is of limited utility in cases of suspected retinoschisis, and it is not precise enough to differentiate retinoschisis from retinal detachment based on thickness of the elevated retinal layer. There are, however, some signals on ultrasonography that can be useful. A-scan ultrasonography of retinoschisis produces a single-peaked spike.[7] B-scan ultrasonography of retinoschisis shows a low-lying or dome-shaped, relatively immobile retinal elevation. A serous choroidal detachment also appears as a dome-shaped, immobile elevation on B-scan. However, the elevated layer of a choroidal detachment is notably thicker than retinoschisis and causes a double-peaked spike

on A-scan.[7]

Optical coherence tomography (OCT) of retinoschisis shows exquisite, in vivo detail of the anatomy of the retinoschisis (Fig. 100.3). OCT is a reliable and useful means of distinguishing between retinoschisis and retinal detachment. In retinoschisis the outer retina is in contact with retinal pigment epithelium (RPE), whereas in retinal detachment the outer retina is separated from the RPE. The peripheral location of retinoschisis can be difficult to image with OCT, but wide-field OCT may make it easier to image peripheral pathology.

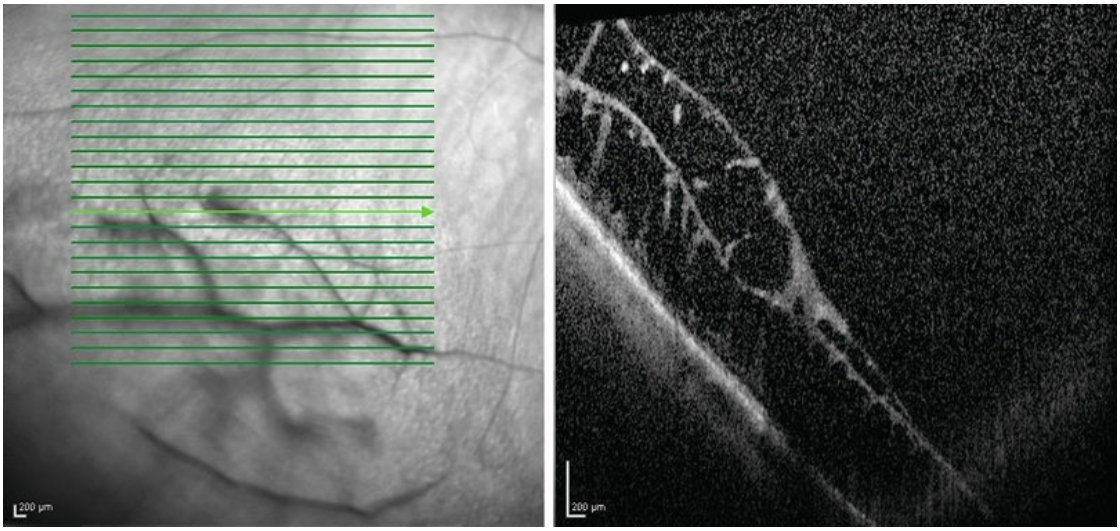

FIG. 100.3 Optical coherence tomography shows both schisis of the middle retina and bullous schisis of the nerve fiber layer.

A large series of 218 eyes, none of which received treatment during an average follow-up of 9 years, gives us the best natural history data available for retinoschisis.[3] Enlargement of the schisis cavity occurred infrequently: lateral expansion occurred in 6%, height increased in 5%, and posterior extension even up to 3 disc diameters from the macula occurred in 3% of eyes. No cases of macular involvement occurred. Among those who had posterior extension of the schisis cavity, the rate of progression was slow (on the order of 2.5 disc diameters/10 years). None of the patients in the study reported symptoms and none was treated. Reports of retinoschisis enlargement involving the macula are exceedingly

rare.[8–11] Neither posterior vitreous detachment nor cataract surgery appeared to destabilize the retinoschisis. This observation may be explained by the fact that retinoschisis is an intraretinal abnormality and is not caused by traction at the vitreoretinal interface.

A large variety of variably invasive techniques have been reported for the treatment of retinoschisis, including diathermy, cryopexy, photocoagulation, several types of scleral surgery (e.g., resection or plication), scleral buckling, external drainage of schisis fluid, and pars plana vitrectomy with internal drainage.[3,12] No treatment has been shown to definitively halt posterior progression of retinoschisis, while complications from even a relatively noninvasive treatment with laser retinopexy have been reported.[13] It is reasonable to follow patients with retinoschisis every one to two years.

Summary

Differentiating degenerative retinoschisis from retinal detachment is very important. Degenerative retinoschisis is usually asymptomatic and nonprogressive, even when very posterior. Proposed treatments for it have not proven to be effective and may cause complications. Therefore, degenerative retinoschisis should be observed without treatment.

Retinoschisis With Retinal Breaks

Reticular retinoschisis may feature inner and/or outer layer breaks. Inner layer breaks are usually small, round, and difficult to detect (Fig. 100.4). As they cannot result in retinal detachment without concomitant outer layer breaks, they are less clinically significant than outer layer breaks.

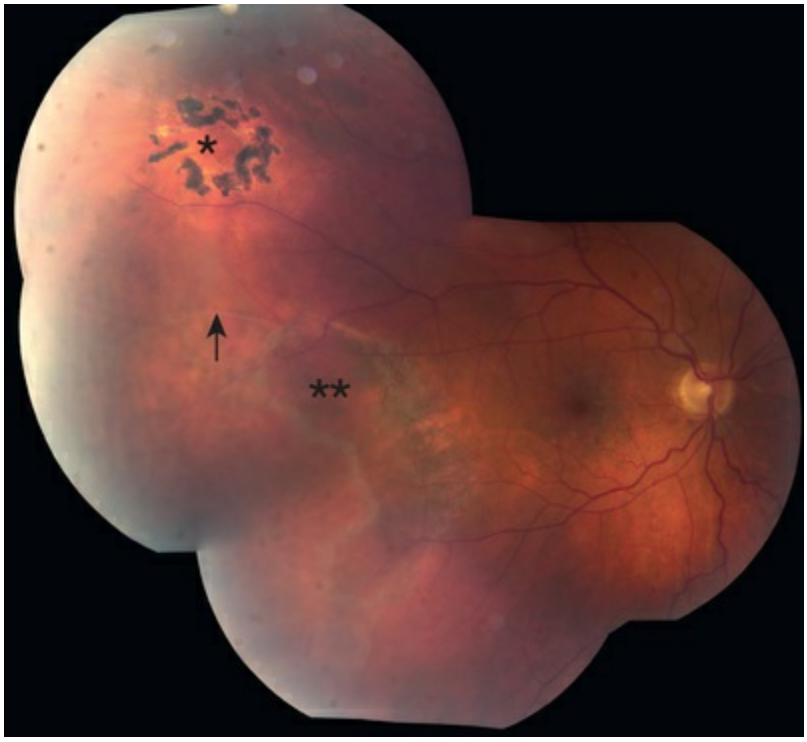

FIG. 100.4 Laser retinopexy had been attempted to surround the round inner layer break superotemporally (*), but the telltale laser uptake within the break proves that this is an inner layer break of retinoschisis, not a full-thickness hole. Temporal to the macula is an irregularly-shaped outer layer break (**). The smudged pigment along the posterior border of the outer layer break suggests chronic subretinal fluid at the edge of the break. The extent of this posterior fluid was followed for 3 years without treatment and remained stable. Nearly the entire temporal periphery is a region of retinoschisis, and a sclerotic vessel is seen within it (*arrow*).

The prevalence of outer layer breaks in eyes with retinoschisis is between 11% and 24%.[3,14,15] Measuring 1–3 disc areas or more, outer layer breaks are usually larger than inner layer breaks. Outer layer breaks are also often posterior to the equator and may have rolled edges (Figs. 100.4 and 100.5A–B).

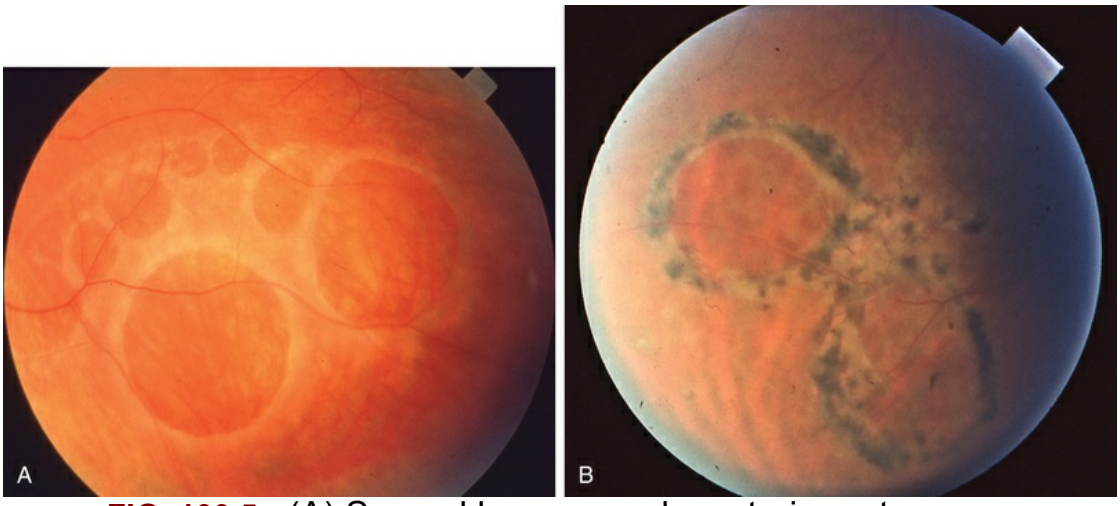

FIG. 100.5 (A) Several large, round, posterior outer layer breaks. (B) Demarcation lines around outer layer breaks denote chronicity. Note the retinal vessels traversing the outer layer breaks. (Courtsey of William Tasman, MD.)

It has been suggested that large outer layer breaks may be more susceptible to progression to retinal detachment.[16–18] In Byer's natural history study, 14/24 (58%) of eyes with outer layer breaks developed a schisis-detachment. Twenty-five out of 218 (11%) eyes had or developed retinal breaks. Five eyes had breaks in both layers. However, none of the patients in this study developed symptoms or underwent treatment.[3]

Because outer layer breaks are asymptomatic, generally have a favorable natural history, and treatments may result in complications, observation alone is reasonable. However, until more conclusive data is available, the surgeon's judgment and patient's wishes should be taken into account on a case-by-case basis. Follow-up every 6 months is reasonable.

Summary

Retinoschisis with inner and/or outer retinal breaks is unlikely to result in progressive retinal detachment. Observation alone is reasonable.

Schisis-Detachment

Schisis-detachment occurs when, in the absence of an inner layer break, intraschisis fluid migrates through an outer layer break into the subretinal space. Schisis-detachment was seen in 14/24 (58%) eyes with outer layer breaks and 14/218 (6.4%) of eyes with retinoschisis.[3] Since schisis-detachments usually do not progress posterior to the posterior border of the schisis cavity, they are almost always asymptomatic.

Four clues pointing to a schisis-detachment include:[19]

- An outer layer break is present.
- The appearance of the schisis is not uniform in height, texture, or transparency.
- There may be a curved yellowish line deep to the inner layer corresponding to the outer layer.
- There may be a pigmented demarcation line in chronic cases.

Symptomatic posterior extension of the subretinal fluid posterior to the area of schisis is rare (Fig. 100.6).[16,20,21] When the fluid does progress posteriorly, it does so very slowly.[21] The relative stability of a schisis-detachment likely is due in part to the viscous nature of the intraschisis fluid, resulting in only some of the fluid traversing the outer layer break into the subretinal space.[19]

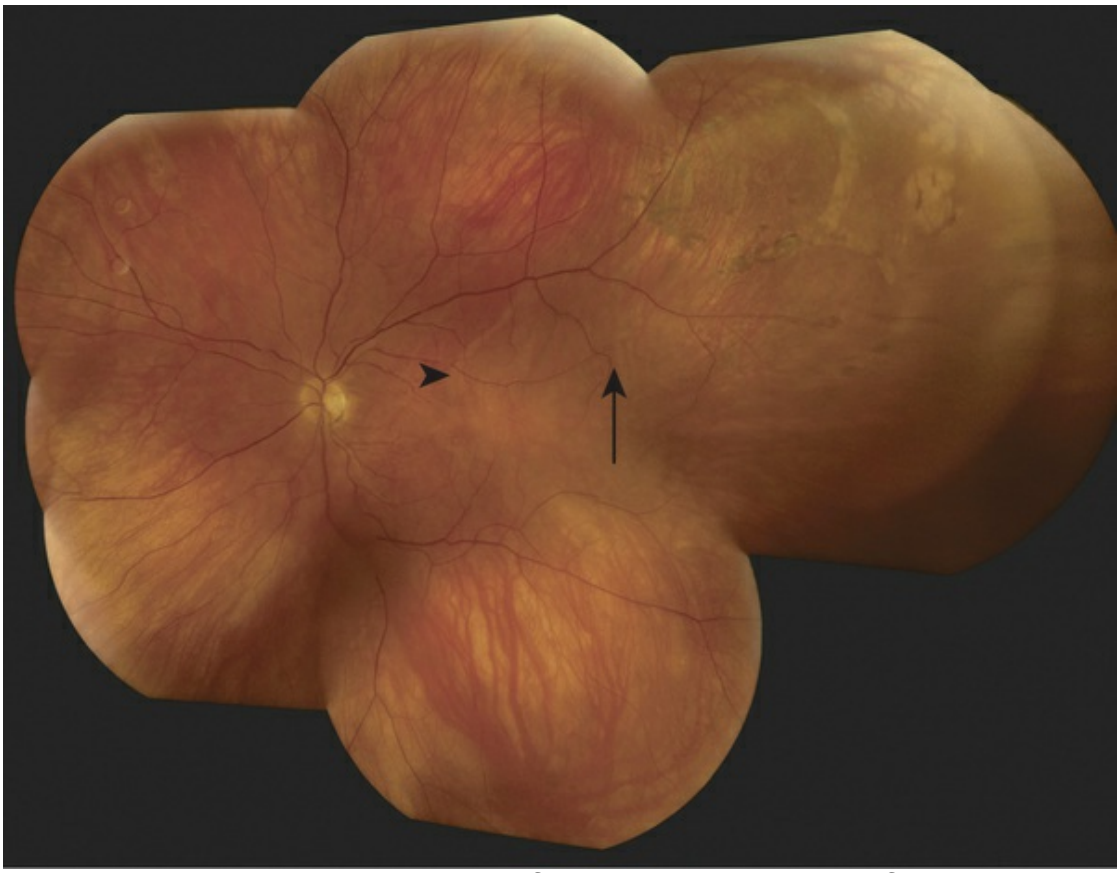

FIG. 100.6 A rare case of posterior extension of subretinal fluid from schisis detachment. Note the two large superotemporal outer wall breaks. The posterior extent of the schisis cavity is seen at the temporal macula (*arrow*). The posterior extent of the subretinal fluid (*arrowhead*) involves the fovea.

Natural history data reported by Byer shows that patients with schisis-detachment are usually asymptomatic and stable with long-term follow up.[3] Even patients with very posterior schisis-detachments can remain stable for many years.[19] Therefore, observation is reasonable in asymptomatic patients, although again, the surgeon's judgment and patient's wishes should be taken into account until more definitive data are available. Patients with schisis-detachment can be followed every 6 months or so.

Cases with posterior, symptomatic extension of subretinal fluid are exceedingly rare. When they do occur, the posterior fluid is shallow; a large progressive retinal detachment does not develop.[22] A 1972 report of 25 cases of schisis-detachment showed 100% success in reattaching the outer layer using several modalities: scleral buckle, diathermy, cryopexy, and laser retinopexy.[23]

However, posterior buckling of outer layer breaks can cause significant macular distortion, requiring removal of the implants.[16] A combination of cryotherapy to the outer retinal breaks, external drainage of subretinal fluid, and intraocular air has also been successful in a small number of patients.[24] More recently, 18 patients with symptomatic schisis-detachment with large posterior outer layer breaks were variously treated with laser retinopexy, cryopexy, scleral buckling, and/or vitrectomy. Although they achieved anatomic success in 13/18, visual acuity improved in only 3 and worsened in 6.[25] Given the rarity of cases of symptomatic schisis-detachment in the literature, there can be no definitive opinion on the best management; surgeon judgment based on solid surgical principles must guide clinical decisions. With current technology, however, it is likely that the often posterior outer layer breaks are best treated using vitrectomy techniques. The special considerations in addressing retinal detachment associated with retinoschisis are discussed in the next section.

Summary

Schisis-detachment is a common finding in eyes with outer layer breaks. It is rarely symptomatic and observation alone is reasonable. The optimal treatment in the rare cases with symptomatic posterior extension of fluid is not known.

Progressive Rhegmatogenous Retinal Detachment Associated With Retinoschisis

Concomitant inner and outer layer breaks (which are likely not in the same area of the schisis) can result in liquefied vitreous accessing the subretinal space and creating a progressive RRD. Progressive RRD associated with retinoschisis is uncommon and has been calculated to occur in only 0.05% of patients with retinoschisis. Progressive RRD is much less common than schisis-detachment. Byer calculated that the ratio of progressive RRD to schisis-detachment is 1 to 178.[3]

Like most RRDs, these progressive RRDs associated with retinoschisis are usually symptomatic. Examination reveals an opacified, corrugated retina typical of acute retinal detachment, but with evident outer layer breaks. Inner layer breaks may be difficult to detect (Fig. 100.7).[22]

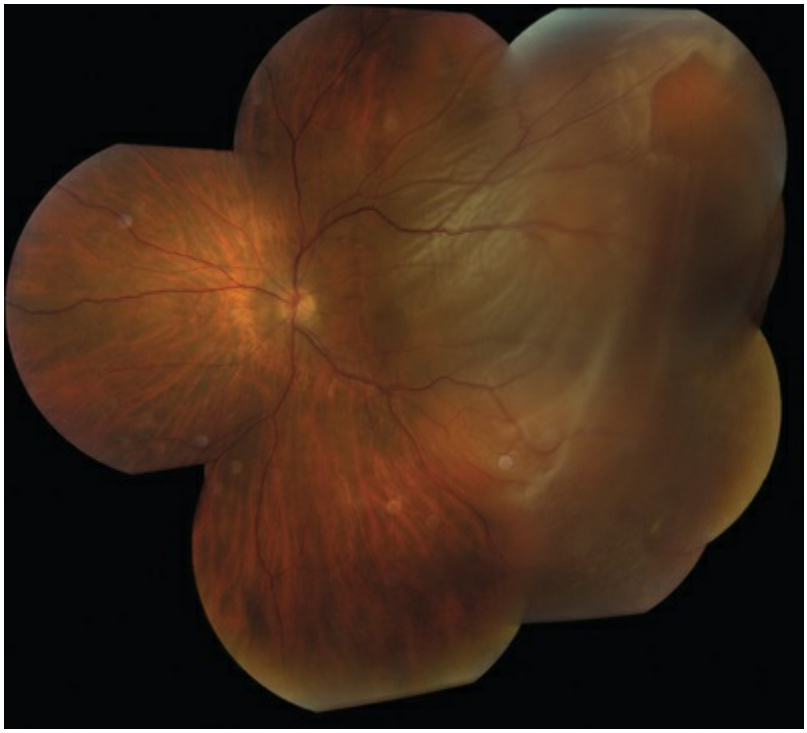

FIG. 100.7 A progressive rhegmatogenous retinal detachment associated with retinoschisis. Elevated, opacified, corrugated retina is seen, with subretinal fluid extending through the macula. A large superotemporal outer layer break is present, but no inner layer breaks are easily identified. Note the retinal vessels traversing the outer layer break.

Progressive RRD associated with retinoschisis clearly requires treatment. A 1973 report using cryopexy with scleral buckling and SF6 gas boasted a 96% anatomic success.[26] Another small study reported scleral buckling techniques being successful in 5/6 patients.[17] In the 1990s, several authors reported the use of pars plana vitrectomy for progressive RRD associated with retinoschisis.[27–29] One study with an average follow-up 11 years reported anatomic success in 43/45 (96%) with scleral buckle and 6/6 with pars plana vitrectomy.[30] In a retrospective comparison of

scleral buckle and pars plana vitrectomy, other authors found that the scleral buckle group had a somewhat better final best-corrected visual acuity and single surgery success rate than the pars plana vitrectomy group (76% vs 62%). The authors concluded that scleral buckle was superior to pars plana vitrectomy in eyes with peripheral outer layer breaks and that pars plana vitrectomy should be reserved for eyes with posterior outer layer breaks.[31]

It appears that treatment of progressive RRD associated with retinoschisis follows the same principles as treatment of any RRD, but with a few special considerations. First, the primary surgical goal is to close the outer wall breaks; treating inner wall breaks and collapsing the schisis cavity is optional.[22] If the schisis cavity is collapsed intraoperatively, it will likely recur postoperatively. Even if the schisis cavity remains collapsed, the scotoma from this area is not reversed.[32,33]

Pars plana vitrectomy and/or scleral buckle may be used to fix the RRD. Factors favoring pars plana vitrectomy include posterior location of outer wall breaks and presence of PVD. Anterior location of outer wall breaks and absence of PVD favor scleral buckle.[31] When performing pars plana vitrectomy, a drainage retinotomy in the inner wall overlying the outer wall break may be created to drain subretinal fluid.[22] Alternatively, the inner wall of the schisis cavity may be resected entirely. Although this technique could theoretically help to elucidate the anatomy and help identify outer layer breaks, outer layer breaks can usually be readily identified, particularly once the retina is flattened. Furthermore, resecting the inner wall of the schisis cavity could lead a surgeon into the accidental resection of full-thickness retina. Endolaser can then be used to treat all breaks, followed by gas or oil tamponade, as usual.[22]

Summary

Progressive RRD associated with retinoschisis is unlikely to develop in most patients with retinoschisis – even those with breaks. It is symptomatic and progressive. Fortunately, surgical treatment is often effective and should be instituted promptly.

Conclusions

Clinical differentiation of retinoschisis and retinal detachment is important because these entities have different natural histories and require different management. Retinoschisis, retinoschisis with retinal breaks, and schisis-detachment all have favorable natural histories and so observation is generally warranted. The only clear indications for treatment are cases of symptomatic posterior extension of schisis-detachments (which are rare) and progressive RRD. Treatment of these disorders utilizes the same surgical principles as treatment of RRD without retinoschisis and is generally effective.

Acknowledgments

We acknowledge Dr Norman Byer, for his foundational work on the natural history of retinoschisis; Dr. William Benson, for generously providing numerous images and critically reviewing the figures for accuracy of description; and Elaine Gonzalez, RN, ophthalmic photographer, for her unflagging efforts to obtain publication-quality images for use in this chapter.

References

1. Bartels M. Uber die Entstehung von Netzhautablösungen. *Klin Monatsbl Augenheilkd*. 1933;91:437–450.
2. Straatsma BR, Foss RY. Typical and reticular degenerative retinoschisis. *Am J Ophthalmol*. 1973;75(4):551–575.
3. Byer NE. Long-term natural history study of senile retinoschisis with implications for management. *Ophthalmology*. 1986;93:1127–1136.
4. Byer NE. Clinical study of senile retinoschisis. *Arch Ophthalmol*. 1968;79(1):36–44.
5. Buch H, Vinding T, Nielsen N. Prevalence and long-term natural course of retinoschisis among elderly individuals. *Ophthalmol*. 2007;114:751–755.
6. Lincoff H, Kreissig I, Stopa M. A modified laser test for the identification of retinoschisis. *Am J Ophthalmol*.

2003;136(5):925–926.
7. Guthoff RF, Stachs O, Labriola LT. Diagnostic ophthalmic ultrasound. Ryan S. *Retina*. 5th ed. Saunders: St Louis; 2013:227–284.
8. Okun E, Cibis PA. The role of photocoagulation in the management of retinoschisis. *Arch Ophthalmol*. 1964;72:309–314.
9. Brockhurst RJ. Cryotherapy in the management of senile retinoschisis. [Discussion of: Dobbie JG] *Trans Am Acad Ophthalmol Otolaryngol*. 1969;73:1060.
10. DeSclafani M, Wagner A, Humphrey W, et al. Pigmentary changes in acquired retinoschisis. *Am J Ophthalmol*. 1988;105:291–293.
11. Gass JDM. *Stereoscopic atlas of macular diseases*. 3rd ed. Mosby: St Louis; 1987:720–721.
12. Yu S, Gao Y, Liang X, et al. Acquired retinoschisis resolved after 23Gauge pars plana vitrectomy in posterior microphthalmos. *BMC Ophthalmol*. 2014;14(1):65.
13. Johnson DL, Nieto JC, Ip MS. Retinal detachment due to an outer retinal tear following laser prophylaxis for retinoschisis. *Arch Ophthalmol*. 2008;126(12):1775–1776.
14. Shea M, Schepens CL, von Pirquet SR. Retinoschisis. I: Senile type. *Arch Ophthalmol*. 1960;63:1–9.
15. Hirose T, Marcil G, Schepens CL, et al. Acquired retinoschisis: observations and treatment. Pruett RC, Regan DJ. *Retina Congress*. Appleton–Century–Croft: New York; 1972:489–503.
16. Sulonen JM, Wells CG, Barricks ME, et al. Degenerative retinoschisis with giant outer layer breaks and retinal detachment. *Am J Ophthalmol*. 1985;99:114–121.
17. Ambler JS, Meyers SM, Zegarra H, et al. The management of retinal detachment complicating degenerative retinoschisis. *Am J Ophthalmol*. 1989;107:171–176.
18. Schwarze H, Laqua H. Retinoschisis mit zentral gelegenem Auszenschictriesenrisz und Begleitamotio. *Klin Monatsbl Augenheilkd*. 1990;197:50–52.
19. Byer NE. Perspectives on the management of the complications of senile retinoschisis. *Eye (Lond)*.

2002;16(4):359–364.
20. Ambler JS, Gutman FA. Retinal detachment and retinoschisis. *Ophthalmology*. 1991;98(1):1.
21. Watzke RC, Folk JC, Lauer AK. Foveal involvement by acquired retinoschisis: long-term visual outcomes. *Retina*. 2013;33(3):606–612.
22. Regillo CD, Custis PH. Surgical management of retinoschisis. *Curr Opin Ophthalmol*. 1997;8(3):80–86.
23. Cox MS Jr, Gutow RF. The treatment of breaks and detachment of the outer layer in degenerative retinoschisis. Pruett RC, Regan DJ. *Retina Congress*. Appleton–Century–Croft: New York; 1972:505–510.
24. Ambler JS, Gass JD, Gutman FA. Symptomatic retinoschisis-detachment involving the macula. *Am J Ophthalmol*. 1991;112(1):8–14.
25. Hoerauf H, Joachimmeyer E, Laqua H. Senile schisis detachment with posterior outer layer breaks. *Retina*. 2001;21(6):602–612.
26. Hagler WS, Woldoff HS. Retinal detachment in relation to senile retinoschisis. *Trans Am Acad Ophthalmol Otolaryngol*. 1973;77(2):OP99–113.
27. Sneed SR, Blodi CF, Folk JC, et al. Pars plana vitrectomy in the management of retinal detachments associated with degenerative retinoschisis. *Ophthalmology*. 1990;97:470–474.
28. Lomeo MD, Diaz-Rohena R, Lambert HM. Use of perfluorocarbon liquid in the repair of retinoschisis retinal detachments. *Ophthalmic Surg Lasers*. 1996;27:778–781.
29. Aslan O, Batman C, Cekic O, et al. The use of perfluorodecalin in retinal detachments with retinoschisis. *Ophthalmic Surg Lasers*. 1998;29:818–821.
30. Dotrelová D. Surgical treatment of progressive and symptomatic retinal detachment in senile retinoschisis. *Sb Lek*. 2002;103(2):109–131.
31. Gotzaridis EV, Georgalas I, Petrou P, et al. Surgical treatment of retinal detachment associated with degenerative retinoschisis. *Semin Ophthalmol*. 2014;29(3):136–141.
32. Lincoff H, Sarup V, Uram D, et al. *Progression and regression*

of retinoschisis in a single patient. [Online] Retinal Physician] http://www.retinalphysician.com/articleviewer.aspx?articleID=104284; 2010.
33. Byer NE. Spontaneous regression of senile retinoschisis. *Arch Ophthalmol*. 1972;88(2):207–209.

101

Pathogenesis of Proliferative Vitreoretinopathy

Peter Wiedemann, Yanors Yandiev, Yan-Nian Hui

Introduction

Proliferative vitreoretinopathy (PVR) is a nonangiogenic fibrotic disease caused by a complex cellular reaction representing a vitreoretinal wound-healing response that results in a characteristic clinical appearance. PVR can be induced by diverse events including rhegmatogenous retinal detachment (RRD), surgical intervention, or trauma. PVR is the leading cause for failure in surgical repair of RRD.

PVR is reported to have an incidence of 5–10% of all RRD,[1] and it is believed to be the most common cause of ultimate failure of a surgery for RRD. A high rate of PVR has also been reported following posterior segment procedures or disorders such as giant retinal tears, macular relocation surgery, endoresection of tumors, and chip implantation. Nearly one-third of human immunodeficiency virus (HIV)-positive patients with cytomegalovirus retinitis-related retinal detachment (RD) had PVR at first surgery.[2] In children, postoperative PVR occurs in higher incidence and is characterized by a rapid and aggressive

development.[3] PVR is also a common complication of ocular injuries, with the highest frequency after perforating and penetrating wounds.[4] PVR is a specific indication for vitrectomy.

The changing understanding of PVR pathogenesis is reflected in the different classification systems. Initially, it was assumed to be primarily due to changes in the vitreous gel ("massive vitreous retraction," "massive preretinal retraction"). Then the involvement of cells was recognized, and the condition was retermed "massive periretinal proliferation."[5] The Retina Society classification was an attempt to categorize the severity of the disease by biomicroscopic parameters.[6] A major problem of this system was that it did not reflect prognosis and surgical difficulty. The Cologne classification[7] and the Silicone Oil Study classification[8] took these aspects into account by separating anterior and posterior PVR. The updated Retina Society classification is a compromise, which describes severity (A, B, C), localization, and updated grade and contraction type.[9] A future classification should provide additional relevant clinical information, such as the biologic activity and the degree of surgical difficulty.[10]

Clinically, early stages of PVR are characterized by an increased reflectance and a cellophane appearance of the inner retinal surface. Additionally, tortuosity of both small and larger vessels is regularly observed. The pathologic hallmarks of advanced PVR include periretinal membrane formation, causing surface wrinkling and single or multifocal star-folds (Fig. 101.1). In the final stages, multidirectional tractional forces produced by posterior and/or anterior PVR form a narrow or closed funnel of the detached retina.[11]

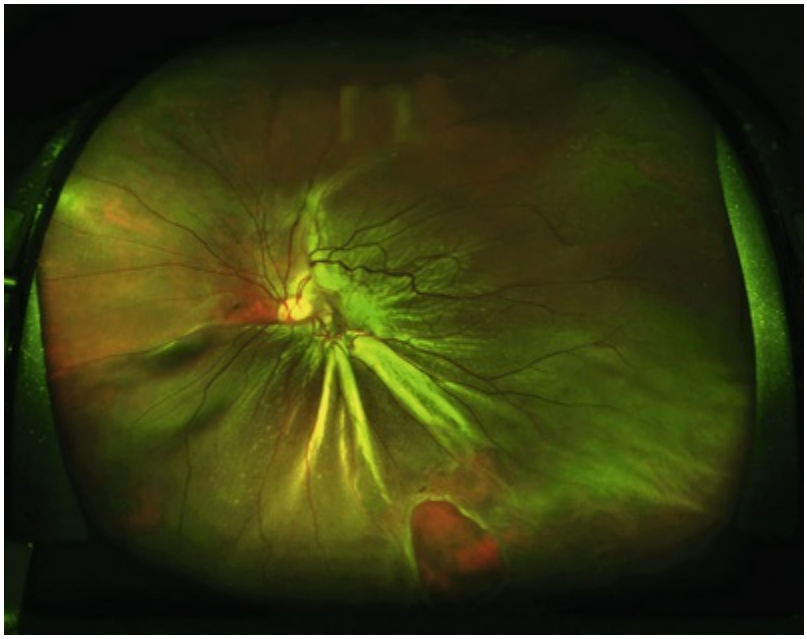

FIG. 101.1 Human proliferative vitreoretinopathy showing typical surface wrinkling and multifocal star-folds after rhegmatogenous retinal detachment.

A retinal break is a prerequisite for the development of PVR. Almost all risk factors for PVR are associated with intravitreal dispersion of retinal pigment epithelial (RPE) cells or the breakdown of the blood–retinal barrier (BRB).[12,13] The size of breaks, the extent of detachment, the presence of preoperative inflammation or low-grade PVR, and iatrogenic complications are important factors in the pathogenesis of severe PVR after the surgery for RRD.[14,15]

Several investigators have underlined the parallels between PVR and the general wound-healing process.[16,17] PVR develops in a sequence of three overlapping phases: inflammation, cellular proliferation, and extracellular matrix (ECM) remodeling. The time course of PVR development is poorly investigated. Clinical data show that on average it takes 4–8 weeks for PVR development after surgery.[10,18] Detailed chronobiology was evaluated in the experimental animal model of PVR induced by macrophages. The inflammation phase is initiated immediately in response to macrophage injection. Cellular proliferation can be detected as early as days 4 ± 7 and peaks on days 10 ± 14. The scarring-induced RD occurs during the second and third weeks after macrophage injection.[19]

Cellular Basis of PVR

After the recognition of the cellular basis of PVR, the identification of cells involved in the PVR process and their roles has been the subject of a large number of experimental and clinical-morphologic studies. The interplay between various cytokines/growth factors (GF), matrix proteins, and the different cell types drives the undesirable formation of periretinal membranes.[20]

Composition of Membranes

The hallmark of the PVR process is the formation of periretinal fibrocellular membranes and intraretinal fibrosis. Membrane formation results from an interaction of retinal and extraretinal cells with components of the ECM. The membranes consist of cells of different origins: retinal glial cells (including Müller cells, microglia cells, and fibrous astrocytes), epithelial cells from the RPE and ciliary body, hyalocytes, blood-borne immune cells (macrophages, lymphocytes, and neutrophils), fibrocytes, and finally myofibrocytes.

The composition of the membranes changes with time, from early cellular to late paucicellular and rather fibrotic membranes.[21] In fibroproliferative membranes, glial cells, RPE cells, and fibrocytes transdifferentiate into contractile myofibrocytes,[22] which generate tractional forces through the expression of the contractile protein α-smooth-muscle actin. Fibroblastic transdifferentiation of cells causes a reduction in cell-specific proteins such as glial fibrillary acidic protein (GFAP; glial cells) and cytokeratins (RPE cells), while proteins involved in motility and proliferation such as α-smooth-muscle actin (which is normally not expressed by the cells) are upregulated.[22–24] This cellular transdifferentiation may be the reason for the paradox that relatively few glial and pigment epithelial cells can be detected in periretinal membranes with the commonly used immunocytochemical markers.

RPE Cells and Epithelial–Mesenchymal Transition

RPE cells are the major cell type involved in the development of PVR. The major pathologic process is the epithelial mesenchymal transition (EMT), in which epithelial cells morphologically and phenotypically transdifferentiate into mesenchymal cells.[25] Pathogenetic steps in the proliferative tractional cascade include EMT, proliferation[26] and directional migration of transformed RPE cells, resulting in the formation of traction-generating fibrocellular membranes in the vitreous and on both surfaces of the retina.

During disease progression, RPE cells lose cell–cell adhesion, undergo EMT, and deposit ECM leading to tissue fibrosis. When RRD occurs cytokines leak into the subretinal space and induce resident RPE cells to migrate, which is the initial step of PVR.[27] RPE cell migration is a complex process that includes changes in cell attachment, spreading, and cytoskeletal reorganization, and it is regulated by cell matrix, matrix-dependent enzymes, cytokines, and GF. Migration is also mediated by cell membrane-associated signaling.[28] The disruption and loss of cell–cell contacts initiate EMT and proliferation of RPE cells.[29,30]

EMT is an important process during normal development in which epithelial cells transform to mesenchymal cells, show alterations in polarized organization and intercellular adhesion, and become migratory and invasive. Its critical role has also been recognized in numerous pathologic conditions, including tumor progression and fibrosis. EMT plays a critical role in PVR. When RPE cells gain access through retinal breaks into the vitreous cavity, they adhere to the detached retina and undergo EMT. During EMT, RPE cells lose their epithelial phenotypes and acquire mesenchymal, fibroblast-like properties and phenotype. Various factors such as cytokines,[31] modified GF signaling,[32] loss of normal matrix adhesion, and changes in cell–cell adhesion profile may initiate the EMT process. Characteristic features of EMT are the upregulation of α-smooth-muscle actin and vimentin, the loss of the zona occludens protein ZO-1, the reduced intercellular adhesion, and the increased motility and enhanced migration,[33] which is supported by the enhanced matrix metalloproteinases (MMPs) activity.

Glial Cells

Whereas the role of RPE cells has been widely discussed in the literature over the last 40 years, the impact of glial cells on the pathogenesis of PVR was frequently overlooked. Glial cells and, in particular, Müller cells, play a central role in retinal physiology. They support the neuronal activity, the integrity of the BRB, and maintain the ionic and osmotic homeostasis. Virtually all retinal diseases are associated with reactive gliosis, which is characterized by cellular hypertrophy and upregulation of the intermediate filaments vimentin and GFAP. Müller cells are active players in all forms of retinal injury and disease.[34] Moreover, Müller cell gliosis is associated with proliferation, and PVR is a key example of massive and long-lasting cellular proliferation.[35] Reactive gliosis is observed within minutes after experimental RD and proceeds so long as the retina remains detached.[36] In the course of PVR, Müller cells proliferate and migrate out of the retina where they are a constant part of fibrocellular membranes. Fibroproliferative membranes are focally connected to the retina via hypertrophied processes of Müller cells, rising from the retinal tissue into the membranes.[1,37,38]

The proliferation of Müller cells is accompanied by alterations in their membrane conductance. Müller cells of patients with PVR, and those from animal models of PVR, display a severe downregulation of the potassium conductance mediated by inwardly rectifying potassium (Kir) channels.[39–42] The downregulation of functional Kir channels causes a depolarization of the cells which is a prerequisite for the reentry of the cells into the proliferation cycle.[43] Moreover, the impaired retinal potassium homeostasis may favor neuronal hyperexcitation and glutamate toxicity. Therefore, the depolarization of Müller cells may contribute to an impairment of the regular glial–neuronal interactions in the retina and, thus, to the neuronal degeneration observed in PVR.[44] Furthermore, activated Müller cells may act as modulators of immune and inflammatory processes, for example by producing proinflammatory cytokines.[45] Reactive gliosis is a limiting factor in the recovery of vision after retinal reattachment.[38] In the healthy retina, Müller cells serve as soft, compliant embedding for neurons and also as a soft substrate required for neurite growth and facilitating neuronal plasticity.[46] The hypertrophied and proliferating glial cells fill the spaces left by

dying neurons and degenerated axons and generate so-called glial scars. Reactive gliosis is associated with an increased stiffness of Müller cells.[47] Such rigid glial scars may constitute a mechanical obstacle for regenerative axon growth. Therefore, attempts to reduce Müller cell gliosis may be a promising tool to inhibit retinal degeneration and to support neuroregeneration after retinal reattachment.[38,44] Internal limiting membrane peeling seems to reduce the occurrence of a postoperative ERM, considered an early sign of PVR, in patients with primary RRD.[48,49]

Blood-Borne Cells

Inflammation is an important step in the pathogenesis of PVR and is associated with influx of blood-derived cells into the retinal tissue and vitreous. Blood-borne cells such as macrophages and fibrocytes are frequently found in PVR membranes. Macrophage-like cells might be also derived from RPE cells which have undergone EMT. Circulating fibrocytes and macrophages may function as precursors of myofibroblasts in PVR membranes and may contribute to the fibrocellular membranes directly.[50,51] Hyalocytes (cells in the cortical vitreous) belong to the monocyte/macrophage lineage and play a significant role in the synthesis of ECM, modulation of immune reaction, and modulation of inflammation. The strong contractile properties of hyalocytes suggest also a critical role in the genesis of PVR.[52]

Stimulation of Cellular Proliferation and Migration

There is a great deal of evidence supporting the idea that soluble factors including GF and cytokines play a central role in the pathogenesis of PVR, inducing key cellular responses such as chemotaxis, proliferation, migration, and extracellular matrix remodeling.[53] **Growth factors** are proteins that bind to receptors on the cell surface, with the primary result of activating cellular proliferation and/or differentiation. **Cytokines** specifically denote signaling proteins that are used extensively in cellular communication. They often exhibit growth factor activity and can

exert autocrine, paracrine, and endocrine effects as do the hormones. **Interleukins** are cytokines specifically directed to leucocytes. Many soluble factors contribute to PVR, but the evidence accumulated so far is greatest for the factors below.

Blood Components (Thrombin, Fibronectin, Plasmin)

A breakdown of the BRB is a characteristic and essential event in the pathogenesis of PVR. Serum that enters the retina and vitreous seems to play an important role in the transmission of mitogenic signals to both Müller cells and RPE cells. **Thrombin**, a serum component, stimulates the proliferation of retinal glial cells and otherwise quiescent RPE cells.[54–58] Thrombin levels are significantly higher in the vitreous of patients with established PVR, and it is involved in the activation of proinflammatory and profibrotic pathways.[59] Thrombin is known to promote actin stress fiber formation, an important determinant of EMT and migration of RPE cells via autocrine activation of PDGF-receptor signaling. Coagulation cascade-induced EMT of RPE may thus contribute to the formation of fibrotic retinal membranes in PVR.[60] **Fibronectin** stimulates the migration of glial cells[54] and plays an important role in ECM remodeling (see below). The vitreous of experimental PVR animals and retinal surgery patients contains the serum-derived protease **plasmin**. It is responsible for the generation of active platelet-derived growth factor-C (PDGF-C), which is the major PDGF isoform involved in the development of PVR.[61]

Platelet-Derived Growth Factor (PDGF)

PDGF seems to play a critical role in the development of PVR. Vitreal PDGF could be detected in eight out of nine PVR patients, but rarely in patients with other vitreoretinal diseases.[61] Both PDGF and PDGF receptor (PDGFR) are present in PVR membranes.[62] RPE and retinal glial cells produce PDGFs and possess their receptors.[62] PDGF is a potent chemoattractant and mitogen for many cell types, including RPE and glial cells.[63]

Among the four PDGF family members, PDGF-C was the predominant isoform in PVR specimens.[61] Plasmin is the major PDGF-C processing protease.[64] Both RPE and glial cells express activated PDGFRα receptors.[65] Abundant binding of PDGF-C to

PDGFRα explains why PDGFRα activation is more important in the pathogenesis of PVR than PDGFRβ activation.[61] In a rabbit model of PVR, delivery of retrovirus containing a dominant negative PDGFRα suppresses the development of RD.[66] Furthermore, oral administration of tyrosine kinase inhibitors, which block signaling through PDGF receptors, reduce PDGF-induced epiretinal membrane formation and RD in transgenic mice.[67] It has been shown recently that PDGFRα can also be activated by other GF.[68] This indirect activation of PDGFRα involves the formation of intracellular reactive oxygen species (ROS). Vitreous is able to tirelessly activate PDGFRα by engaging a ROS-mediated, self-perpetuating loop.[69] Initial studies have shown that vitreal injection of the antioxidant N-acetyl cysteine prevents the development of experimental PVR.[70]

Transforming Growth Factor-Beta (TGFβ)

The cytokine TGF-β is implicated in the tissue contraction in different fibrous diseases including proliferative diabetic retinopathy and PVR.[71,72] The vitreous of PVR patients contains high levels of TGF-β.[73] TGF-β was also localized to subretinal strands of PVR patients.[74] Müller cells are one source of TGF-β in the retina.[75] Experimental RD increases the expression of TGF-β and TGF receptor II in Müller cells and in hypertrophied Müller cell processes that contribute to the formation of periretinal membranes.[76] Secretion of TGF-β2 in nonpolarized RPE cells is significantly higher supporting the contention that loss of polarity of RPE in PVR leads to rise of intravitreal TGF-β2.[77] TGF-β-treated RPE cells differentiate along a myofibroblast pathway.[33] Differentially expressed microRNAs play potential roles in TGF-β-induced EMT in RPE cells.[78,79] Snail transcription factor was activated in TGF-β1-induced EMT.[80] TGF-β-activated kinase 1 (TAK1), is a key player in the EMT process.[81] Furthermore, gene transfer of a soluble TGF-β type II receptor (which traps TGF-β) suppresses the progression of experimental PVR.[82] These experimental and clinical studies indicate that inhibition of TGF-β signaling could be a therapeutic approach to prevent the progression of PVR. The contraction inhibitor simvastatin could prevent PVR progression in a dose-dependent manner.[83] TGF-β

likely mediates cicatricial contraction via activation of the Rho-kinase (ROCK) pathway; this pathway is also activated by various other GF. It makes it an interesting therapeutic target for treating PVR.[84,85]

Insulin-Like Growth Factors (IGF)

The IGF system is known to be present in the vitreous. Studies on RPE and Müller glial cells responsiveness to IGF system indicated that both IGF-1 and IGF-2 are extremely potent tractional force promoters, an activity relevant to PVR pathobiology.[22,86] GFs and their binding proteins have been shown to exhibit both protective and deleterious effects in ocular disease. IGFBP-5 has recently been linked to mediating fibrosis in PVR but also reduces neovascularization.[87] IGFBP-6 participates in the development of PVR and might play a protective role.[88] The regulatory balance between IGF and IGF binding proteins can have profound impact on target tissues.

Monocyte Chemotactic Protein-1 (MCP1)

The chemokine MCP-1 has a role during the initial stage of PVR. In experimental RD, the expression of MCP-1 increases within one hour, and the MCP-1 protein level increases within six hours of detachment.[89] MCP-1 stimulates the migration of RPE cells; this effect is inhibited by dexamethasone.[90] MCP-1 was detected in a substantial percent of vitreous samples of patients with PVR.[91]

Basic Fibroblast Growth Factor (bFGF)

Many observations show that bFGF may be a putative target for PVR therapy. bFGF levels are raised in PVR vitreous.[92] Fibroproliferative membranes contain bFGF.[93] The vitreous bFGF expression levels in PVR-D patients were notably higher than those in PVR-C, vitreous hemorrhage, and control group.[94] A blockade of integrin receptors inhibits bFGF-stimulated RPE cell attachment, migration, and invasion.[95]

Hepatocyte Growth Factor (HGF)

HGF (also known as scatter factor) is a multipotential cytokine that

plays a role in scattering of retinal cells, chemotaxis, and EMT.[96,97] Increased expression level of HGF has been shown in vitreous and in epiretinal PVR membranes.[98,99] In epiretinal membranes of patients with PVR the expression of HGF and its receptor, the c-Met tyrosine kinase, can be localized in various cell types, including glial and RPE cells.[62,100]

Connective Tissue Growth Factor (CTGF)

Both in vivo and in vitro studies demonstrate that CTGF is a crucial factor in the pathogenesis of PVR.[101] CTGF is upregulated in a model of RPE monolayer scrape wounding in vitro. Recombinant human CTGF protein could stimulate RPE migration in a dose-dependent manner; this effect is suppressed by dexamethasone.[102] CTGF is expressed in fibroproliferative membranes and vitreous samples from patients with PVR.[99,103] During the development of PVR the expression of CTGF in epiretinal membranes increases from early to late stage, and localizes to RPE cells in early stage and to glial cells in the late stage of PVR.[62]

Epidermal Growth Factor (EGF)

EGF may activate RPE cells in PVR[104] by inducing migration and proliferation through the EGF–EGFR–MAPK signal pathway in a concentration-dependent manner.[105] EGF could also promote integrin-α5 expression, which subsequently activates RPE cells.[106] In addition, EMT of RPE cells could be induced by EGF.[33]

Vascular Endothelial Growth Factor (VEGF)

VEGF is a regulatory mediator of cellular proliferation and vascular permeability. Anti-VEGF therapy is widely used to treat retinal or choroidal neovascular disorders. The VEGF concentration in the vitreous of PVR patients is significantly higher when compared with RD and macular hole.[107] VEGF is also expressed in PVR membranes.[108] Chronic PVR is often associated with neovascularization in the far periphery of the retina, the ciliary body, and the anterior segment, and VEGF is likely implicated in the induction of neovascularization. As an autocrine and paracrine stimulator, VEGF secreted by RPE, glial, and other cells may

contribute to the progression of fibrovascular membrane formation. Remarkably, VEGF activates not only VEGF receptors but promotes PVR by a noncanonical ability to engage PDGFRα.[109]

Cytokine-Mediated Inflammation (Interleukins and TNF-α)

It has been suggested that cytokine-mediated pathways of inflammation play an important role in the development of PVR. Inflammatory cells, RPE cells, and retinal glial cells are possible sources of interleukin (IL)-6, IL-1β, TNF-α and interferon-gamma (INF-γ) in the PVR vitreous.[42] Cytokines in the vitreous[110] may stimulate important cellular processes, including migration, proliferation, and production of ECM. In the early stage and proliferative phase of experimental PVR, cytokines are present in large amounts in the vitreous ("storm of cytokines"); the cytokine levels decrease to normal in the remodeling (scarring) phase.[111] Under inflammatory conditions and initiated by tumour necrosis factor-alpha (TNF-α), a key mediator of ocular inflammation, the ability of RPE cells to maintain the BRB and immune privilege may be lost and proliferation of RPE cells is facilitated.[112] This emphasizes the role of proinflammatory cytokines in the pathogenesis of PVR.

ECM Remodeling and Myofibroblasts

The ECM is composed of a dynamic and complex array of collagens, glycoproteins, glycosaminoglycans, and proteoglycans. All these molecules form the substrate surrounding the cells and tissues to provide a mechanical and structural support and modulate autocrine signaling loops and the recruitment of cells.[113] Moreover, the ECM interacts with the cytoskeleton and with cytokines to transmit biological signals that affect the cell behavior, development, migration, proliferation, transdifferentiation, contraction, and remodeling. Integrins and proteoglycans on the cell surface are the main adhesion receptors that promote signal transduction.[114] Bruch's membrane and the interphotoreceptor matrix are specialized types of ECM that surround the RPE and

photoreceptors. At early stages of RRD and PVR, the neural retina layer detaches from the RPE layer, resulting in a disintegration of the interphotoreceptor matrix.[115] RRD causes a dissociation of RPE cells from Bruch's membrane and a dispersion of the cells into the vitreal cavity (grade A PVR). The time-dependent increase in the extracellular matrix content of PVR membranes suggests that components of the ECM stimulate its production in an autocrine/paracrine manner.[10]

The wound-healing process is a complex and dynamic process of restoring tissue structures and proper organ function. It is detrimental for tissue function when it becomes excessive such as in PVR. ECM components play a central role in all phases of PVR. ECM remodeling with fibrocellular membrane contraction is a culmination of this process. During the remodeling phase, transdifferentiated RPE, glial, and blood-borne cells can generate tractional forces through contraction of vitreal and newly synthesized ECM resulting in retinal surface wrinkling, star-fold formation, and tractional RD. The synthesis and deposition of ECM components on both sides of the retina is a key event of the remodelling phase. Structural proteins, adhesive proteins and antiadhesive proteins are three components of the ECM in PVR membranes.[113] Collagen (which includes various types), one of the major structural proteins and components of PVR membranes,[10] may be produced by RPE, glial, and fibroblast-like cells.[116–118] The expression of fibronectin, an adhesion protein, in the normal retina is low; under pathologic conditions, its concentration in the vitreous humor increases quickly.[119] Fibronectin promotes adhesion between cells and ECM and might stimulate RPE cells to migrate toward membranes.[120] In addition, fibronectin amplifies the EMT of RPE cells induced by TGF-β.[121] TGF-β also induces the synthesis of ECM components such as collagens and fibronectin.[85,116,122] The function of antiadhesive proteins is contrary to adhesive proteins. Antiadhesive thrombospondin in PVR membranes could facilitate the activated cells to detach from the ECM and to migrate into the wounded area.[123] The balance between MMPs and tissue inhibitors of MMPs (TIMPs) regulates the turnover of the ECM and the tissue remodeling associated with PVR. Cellular components of PVR membranes, including RPE cells, glial cells, and fibroblasts,

synthesize MMPs.[124] The expression of MMP-2 and MMP-9 is upregulated dramatically in PVR membranes.[94] In addition, MMP activity may be required for ECM contraction.[125]

Myofibroblasts play a key role in tissue remodeling. They are the predominant cellular component of PVR epiretinal membranes.[126] They participate in a variety of phenomena and originate from different precursor cells suggesting that the term myofibroblast describes a functional status rather than fixed cell type.[127] The transformation of RPE, glial, and blood-borne cells to myofibroblasts is characterized by expression of α-smooth-muscle actin, a contractive protein that is thought to be essential for tractional force generation.[127] Transmembrane integrins at the myofibroblast surface link bundles of actin microfilaments with ECM. Through this mechanotransduction system, the contractile force generated by stress fibers can be transmitted to the surrounding ECM.[128] Cytokines and the components of ECM modulate the contractile activities of myofibroblasts. Serum components and the members of PDGF, IGF, and (TGF)-β families are considered to be the major mediators of ECM contraction.[22,129]

In an experimental animal model, intravitreal injections of RPE cells or mixtures of RPE and glial cells show a progressively contractive response.[130] Transdifferentiated RPE cells can attach to individual strands of collagen and pull collagen by alternating extension and retraction of the lamellipodia.[131] Vitreous cortex, which consists of densely packed collagen fibrils, may form a scaffold for fibrocellular proliferation and is an active player in the remodeling process. The studies of cell-mediated gel contraction demonstrate that vitreous samples from PVR patients contain sufficient amounts of biologically active factors to induce ECM contraction.[129,132] Clinical data also support the role of vitreous as PVR-stimulating milieu. A tamponade with heavy silicone oil can displace the PVR milieu from the inferior fundus to the upper retina resulting in upper PVR.[133] Removal of the vitreous (scaffold and PVR-stimulated milieu) is a rational treatment goal for PVR.

Biomarkers and Genetic Profiling

Intensive development of molecular biology techniques has

permitted identification of a wide variety of cellular and biological characteristics of PVR, and the search for predictive molecular risk factors (biomarkers) of PVR susceptibility was intensified in recent years. To find proteins that are specifically involved in distinct pathophysiologic events of PVR, vitreous proteomes were investigated. Significant differences were detected in the composition of vitreous proteins between control and PVR samples.[134,135] More than 100 PVR-specific proteins have been identified, including proteins involved in metabolic dysfunction, immune responses, and cytoskeleton remodeling. While the cytoskeletal and metabolic proteins, such as enolases, are downregulated in severe PVR, complement components, the serine proteinase inhibitor (serpin), and proteins involved in cell proliferation are upregulated.[136–139] In addition, the vitreous of PVR patients contains increased levels of MMPs. The vitreal content of MMPs (MMP-1, -2, -3, -8, -9, and TIMP-1)[140] and chemokine CXCL-1[141] correlates with the grade of PVR. The elevation of the vitreal content of inflammation-associated proteins such as α1-antitrypsin, apolipoprotein A-IV, serum albumin, and transferrin is consistent with the significance of inflammation in the pathogenesis of PVR.[142] This suggests that steroids might be helpful as adjuvant therapy of PVR.[143] Kininogen 1 (essential for assembly of the kallikrein–kinin system) is one of the relatively high-abundant proteins in the vitreous *and* serum of PVR patients and may thus represent a serum biomarker of PVR.[137] Laser flare photometry allows simple risk estimation for later PVR development. Elevated laser flare values correspond to an altered profibrotic intraocular cytokine milieu.[144]

Attempts to assess the genetic contribution to PVR have also been made.[145] Interestingly, a strong genetic association between the tumor necrosis factor locus and PVR was observed which underlines the importance of inflammation in the pathogenesis of PVR.[146] Genetic profiling of patients with RRD might improve the predictability of PVR in addition to or in combination with the well-known clinical biomarkers.[147,148]

Conclusion

The pathogenesis of PVR is incompletely understood. We certainly

are not able to prevent this terrible complication.[149] At present PVR can be considered as an excessive vitreoretinal wound healing process characterized by the phases of inflammation, proliferation, and remodeling (Fig. 101.2). Once the vicious cycle of detachment and "storm of cytokines" has started, a permanent functional failure due to structural retinal changes is initiated. PVR is a complex syndrome, which involves impairment of metabolic function, remodeling of the cytoskeleton and ECM, immune responses, and inflammation. Multiple different cellular and soluble factors are involved in the pathogenesis. Therefore, therapeutic options based on the inhibition of one factor or phenomenon may be regarded with skepticism.

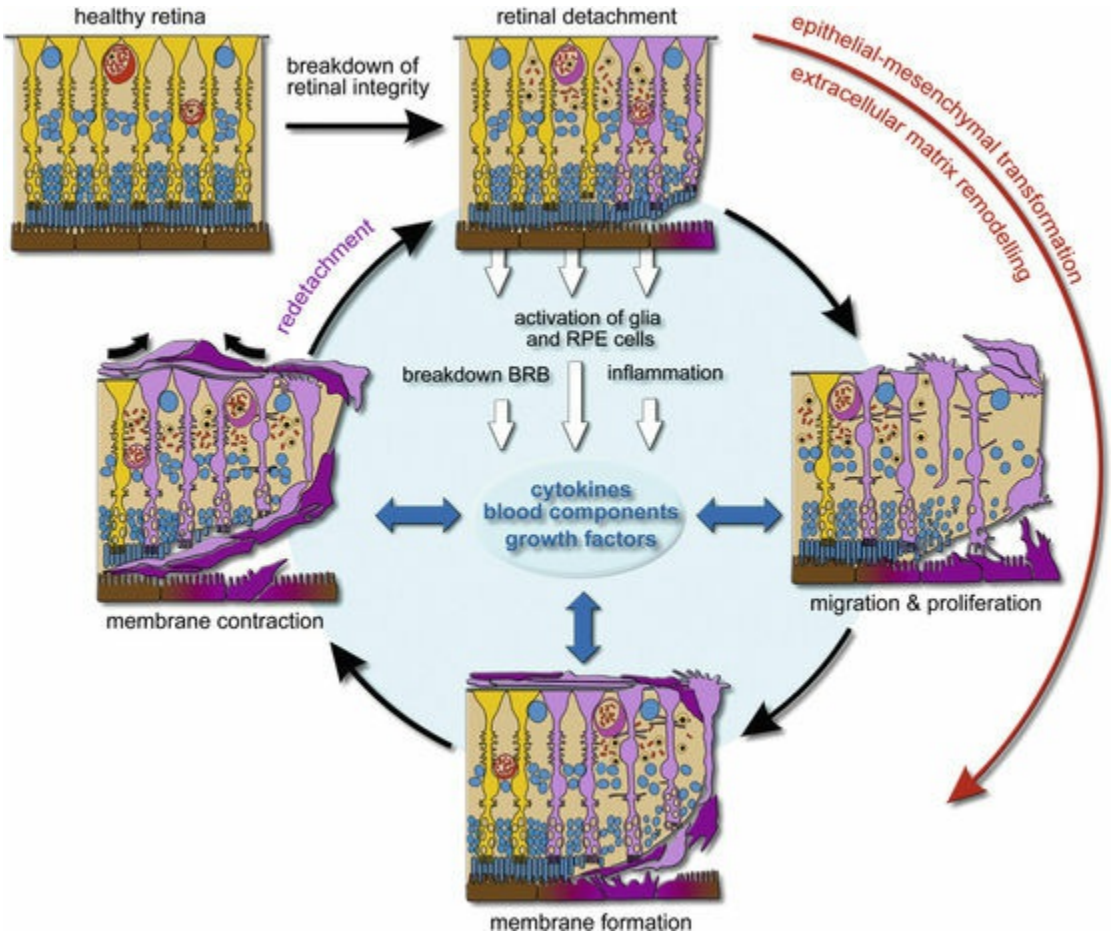

FIG. 101.2 The vicious cycle of proliferative retinopathy. The breakdown of the retinal integrity is accompanied by breakdown of the blood–retinal barrier (BRB) and inflammatory tissue reaction. These processes result in an influx of blood-derived cells and

soluble factors including growth and inflammatory factors, serum, fibrin, and metalloproteinases into the vitreous and retina. The factors stimulate the scattering, migration, and proliferation of the cells of retinal and extraretinal origins followed by periretinal membrane formation. Myofibroblastic transdifferentiation of cells within the fibroproliferative membranes during epithelial–mesenchymal transition and extracellular matrix remodelling cause membrane contraction resulting in fixed (re)detachment of the retina. (Drawing by J. Grosche, Leipzig.)

Further research to understand the relative importance of distinct factors in the formation and progression of PVR may lead to more effective therapeutic approaches for the treatment of PVR. Until then surgery is the treatment of choice. Removal of activated cells and membranes and "complete" vitreous removal is a rational treatment goal achieved by surgery. However, consensus regarding a preferred surgical strategy remains controversial.[150] In the future, combined analysis of clinical risk factors and biomarkers should improve the identification of patients at high risk of PVR formation and may allow targeted application of appropriate adjunctive therapy to preserve vision.

References

1. Charteris DG, Sethi CS, Lewis GP, et al. Proliferative vitreoretinopathy – developments in adjunctive treatment and retinal pathology. *Eye*. 2002;16(4):369–374.
2. Kunavisarut P, Bijlsma WR, Pathanapitoon K, Patikulsila D, Choovuthayakorn J, Rothova A. Proliferative vitreoretinopathy in human immunodeficiency virus-infected patients in the era of highly active antiretroviral therapy. *Am J Ophthalmol*. 2010;150(2):218–222.
3. Scott IU, Flynn HW Jr, Azen SP, Lai MY, Schwartz S, Trese MT. Silicone oil in the repair of pediatric complex retinal detachments: a prospective, observational, multicenter study. *Ophthalmology*. 1999;106(7):1399–1407 [discussion 407-8].

4. Feng K, Wang CG, Hu YT, et al. Clinical features and prognosis of eyeball rupture: eye injury vitrectomy study. *Clin Exp Ophthalmol*. 2015;43(7):629–636.
5. Laqua H, Machemer R. Glial cell proliferation in retinal detachment (massive periretinal proliferation). *Am J Ophthalmol*. 1975;80(4):602–618.
6. The Retina Society Terminology Committee. The classification of retinal detachment with proliferative vitreoretinopathy. *Ophthalmology*. 1983;90(2):121–125.
7. Heimann K, Wiedemann P. *Proliferative vitreoretinopathy*. Kaden Verlag: Heidelberg; 1989.
8. Lean JS, Stern WH, Irvine AR, Azen SP. Classification of proliferative vitreoretinopathy used in the silicone study. The Silicone Study Group. *Ophthalmology*. 1989;96(6):765–771.
9. Machemer R, Aaberg TM, Freeman HM, Irvine AR, Lean JS, Michels RM. An updated classification of retinal detachment with proliferative vitreoretinopathy. *Am J Ophthalmol*. 1991;112(2):159–165.
10. Pastor JC, de la Rua ER, Martin F. Proliferative vitreoretinopathy: risk factors and pathobiology. *Progr Retinal Eye Res*. 2002;21(1):127–144.
11. Iandiev I, Bringmann A, Wiedemann P. Proliferative vitreoretinopathy – pathogenesis and therapy. *Klin Monatsbl Augenheilkd*. 2010;227(3):168–174.
12. Nagasaki H, Shinagawa K. Risk factors for proliferative vitreoretinopathy. *Curr Opin Ophthalmol*. 1995;6(3):70–75.
13. Nagasaki H, Shinagawa K, Mochizuki M. Risk factors for proliferative vitreoretinopathy. *Progr Retinal Eye Res*. 1998;17(1):77–98.
14. Girard P, Mimoun G, Karpouzas I, Montefiore G. Clinical risk factors for proliferative vitreoretinopathy after retinal detachment surgery. *Retina*. 1994;14(5):417–424.
15. Wickham L, Ho-Yen GO, Bunce C, Wong D, Charteris DG. Surgical failure following primary retinal detachment surgery by vitrectomy: risk factors and functional outcomes. *Br J Ophthalmol*. 2011;95(9):1234–1238.
16. Weller M, Wiedemann P, Heimann K. Proliferative

vitreoretinopathy – is it anything more than wound healing at the wrong place? *Int Ophthalmol*. 1990;14(2):105–117.
17. Kirchhof B, Sorgente N. Pathogenesis of proliferative vitreoretinopathy. Modulation of retinal pigment epithelial cell functions by vitreous and macrophages. *Develop Ophthalmol*. 1989;16:1–53.
18. Mietz H, Heimann K. Onset and recurrence of proliferative vitreoretinopathy in various vitreoretinal disease. *Br J Ophthalmol*. 1995;79(10):874–877.
19. Hui YN, Hu D. Prevention of experimental proliferative vitreoretinopathy with daunomycin and triamcinolone based on the time course of the disease. *Graefes Arch Klin Exp Ophthalmol*. 1999;237(7):601–605.
20. Sadaka A. Giuliari GP. Proliferative vitreoretinopathy: current and emerging treatments. *Clin Ophthalmol*. 2012;6:1325–1333.
21. Hiscott PS, Grierson I, McLeod D. Natural history of fibrocellular epiretinal membranes: a quantitative, autoradiographic, and immunohistochemical study. *Br J Ophthalmol*. 1985;69(11):810–823.
22. Guidry C. The role of Muller cells in fibrocontractive retinal disorders. *Progr Retinal Eye Res*. 2005;24(1):75–86.
23. Sramek SJ, Wallow IH, Stevens TS, Nork TM. Immunostaining of preretinal membranes for actin, fibronectin, and glial fibrillary acidic protein. *Ophthalmology*. 1989;96(6):835–841.
24. McGillem GS, Dacheux RF. Rabbit retinal Muller cells undergo antigenic changes in response to experimentally induced proliferative vitreoretinopathy. *Exp Eye Res*. 1999;68(5):617–627.
25. Chen Z, Shao Y, Li X. The roles of signaling pathways in epithelial-to-mesenchymal transition of PVR. *Mol Vis*. 2015;21:706–710.
26. Stern J, Temple S. Retinal pigment epithelial cell proliferation. *Exp Biol Med (Maywood)*. 2015;240(8):1079–1086.
27. Liu Y, Cao GF, Xue J, et al. Tumor necrosis factor-alpha (TNF-alpha)-mediated in vitro human retinal pigment

epithelial (RPE) cell migration mainly requires Akt/mTOR complex 1 (mTORC1), but not mTOR complex 2 (mTORC2) signaling. *Eur J Cell Biol*. 2012;91(9):728–737.
28. He S, Kumar SR, Zhou P, et al. Soluble EphB4 inhibition of PDGF-induced RPE migration in vitro. *Invest Ophthalmol Vis Sci*. 2010;51(1):543–552.
29. Tamiya S, Liu L, Kaplan HJ. Epithelial-mesenchymal transition and proliferation of retinal pigment epithelial cells initiated upon loss of cell-cell contact. *Invest Ophthalmol Vi Sci*. 2010;51(5):2755–2763.
30. Pratt CH, Vadigepalli R, Chakravarthula P, Gonye GE, Philp NJ, Grunwald GB. Transcriptional regulatory network analysis during epithelial-mesenchymal transformation of retinal pigment epithelium. *Mol Vis*. 2008;14:1414–1428.
31. Takahashi E, Haga A, Tanihara H. Merlin regulates the epithelial-to-mesenchymal transition of ARPE-19 cells via TAK1-p38MAPK-mediated activation. *Invest Ophthalmol Vis Sci*. 2015;56(4):2449–2458.
32. Mony S, Lee SJ, Harper JF, Barwe SP, Langhans SA. Regulation of Na,K-ATPase beta1-subunit in TGF-beta2-mediated epithelial-to-mesenchymal transition in human retinal pigmented epithelial cells. *Exp Eye Res*. 2013;115:113–122.
33. Lee H, O'Meara SJ, O'Brien C, Kane R. The role of gremlin, a BMP antagonist, and epithelial-to-mesenchymal transition in proliferative vitreoretinopathy. *Invest Ophthalmol Vis Sci*. 2007;48(9):4291–4299.
34. Wang X, Fan J, Zhang M, Sun Z, Xu G. Gene expression changes under cyclic mechanical stretching in rat retinal glial (Muller) cells. *PLoS ONE*. 2013;8(5):e63467.
35. Bringmann A, Pannicke T, Grosche J, et al. Muller cells in the healthy and diseased retina. *Progr Retinal Eye Res*. 2006;25(4):397–424.
36. Geller SF, Lewis GP, Fisher SK. FGFR1, signaling, and AP-1 expression after retinal detachment: reactive Muller and RPE cells. *Invest Ophthalmol Vis Sci*. 2001;42(6):1363–1369.
37. Charteris DG, Downie J, Aylward GW, Sethi C, Luthert P. Intraretinal and periretinal pathology in anterior

proliferative vitreoretinopathy. *Graefes Arch Klin Exp Ophthalmol*. 2007;245(1):93–100.
38. Fisher SK, Lewis GP. Muller cell and neuronal remodeling in retinal detachment and reattachment and their potential consequences for visual recovery: a review and reconsideration of recent data. *Vision Res*. 2003;43(8):887–897.
39. Bringmann A, Francke M, Pannicke T, et al. Human Müller glial cells: altered potassium channel activity in proliferative vitreoretinopathy. *Invest Ophthalmol Vis Sci*. 1999;40(13):3316–3323.
40. Francke M, Pannicke T, Biedermann B, et al. Loss of inwardly rectifying potassium currents by human retinal glial cells in diseases of the eye. *Glia*. 1997;20(3):210–218.
41. Francke M, Faude F, Pannicke T, et al. Electrophysiology of rabbit Muller (glial) cells in experimental retinal detachment and PVR. *Invest Ophthalmol Vis Sci*. 2001;42(5):1072–1079.
42. Bringmann A, Wiedemann P. Involvement of Müller glial cells in epiretinal membrane formation. *Graefes Arch Klin Exp Ophthalmol*. 2009;247(7):865–883.
43. Bringmann A, Francke M, Pannicke T, et al. Role of glial K(+) channels in ontogeny and gliosis: a hypothesis based upon studies on Müller cells. *Glia*. 2000;29(1):35–44.
44. Francke M, Faude F, Pannicke T, et al. Glial cell-mediated spread of retinal degeneration during detachment: a hypothesis based upon studies in rabbits. *Vis Res*. 2005;45(17):2256–2267.
45. Drescher KM, Whittum-Hudson JA. Evidence for induction of interferon-alpha and interferon-beta in retinal glial cells of Müller. *Virology*. 1997;234(2):309–316.
46. Lu YB, Franze K, Seifert G, et al. Viscoelastic properties of individual glial cells and neurons in the CNS. *Proc Natl Acad Sci USA*. 2006;103(47):17759–17764.
47. Lu YB, Iandiev I, Hollborn M, et al. Reactive glial cells: increased stiffness correlates with increased intermediate filament expression. *FASEB J*. 2011;25(2):624–631.
48. Nam KY, Kim JY. Effect of internal limiting membrane

peeling on the development of epiretinal membrane after pars plana vitrectomy for primary rhegmatogenous retinal detachment. *Retina*. 2015;35(5):880–885.
49. Hejsek L, Dusova J, Stepanov A, Rozsival P. Internal limiting membrane peeling as prophylaxis of epimacular membrane formation in eyes undergoing vitrectomy for rhegmatogenous retinal detachement. *Ceska Slovenska Oftalmol*. 2014;70(3):98–101.
50. Abu El-Asrar AM, Struyf S, Van Damme J, Geboes K. Circulating fibrocytes contribute to the myofibroblast population in proliferative vitreoretinopathy epiretinal membranes. *Br J Ophthalmol*. 2008;92(5):699–704.
51. Lin ML, Li YP, Li ZR, Lin JX, Zhou XL, Liang D. Macrophages acquire fibroblast characteristics in a rat model of proliferative vitreoretinopathy. *Ophthalm Res*. 2011;45(4):180–190.
52. Sakamoto T, Ishibashi T. Hyalocytes: essential cells of the vitreous cavity in vitreoretinal pathophysiology? *Retina*. 2011;31(2):222–228.
53. Wiedemann P. Growth factors in retinal diseases: proliferative vitreoretinopathy, proliferative diabetic retinopathy, and retinal degeneration. *Surv Ophthalmol*. 1992;36(5):373–384.
54. Puro DG, Mano T, Chan CC, Fukuda M, Shimada H. Thrombin stimulates the proliferation of human retinal glial cells. *Graefes Arch Klin Exp Ophthalmol*. 1990;228(2):169–173.
55. Parrales A, Palma-Nicolas JP, Lopez E, Lopez-Colome AM. Thrombin stimulates RPE cell proliferation by promoting c-Fos-mediated cyclin D1 expression. *J Cell Physiol*. 2010;222(2):302–312.
56. Parrales A, Lopez E, Lopez-Colome AM. Thrombin activation of PI3K/PDK1/Akt signaling promotes cyclin D1 upregulation and RPE cell proliferation. *Biochim Biophys Acta*. 2011;1813(10):1758–1766.
57. Parrales A, Lopez E, Lee-Rivera I, Lopez-Colome AM. ERK1/2-dependent activation of mTOR/mTORC1/p70S6K regulates thrombin-induced RPE cell proliferation. *Cell Signal*. 2013;25(4):829–838.

58. Ruiz-Loredo AY, Lopez E, Lopez-Colome AM. Thrombin promotes actin stress fiber formation in RPE through Rho/ROCK-mediated MLC phosphorylation. *J Cell Physiol*. 2011;226(2):414–423.
59. Bastiaans J, van Meurs JC, Mulder VC, et al. The role of thrombin in proliferative vitreoretinopathy. *Invest Ophthalmol Vis Sci*. 2014;55(7):4659–4666.
60. Bastiaans J, van Meurs JC, van Holten-Neelen C, et al. Thrombin induces epithelial-mesenchymal transition and collagen production by retinal pigment epithelial cells via autocrine PDGF-receptor signaling. *Invest Ophthalmol Vis Sci*. 2013;54(13):8306–8314.
61. Lei H, Hovland P, Velez G, et al. A potential role for PDGF-C in experimental and clinical proliferative vitreoretinopathy. *Invest Ophthalmol Vis Sci*. 2007;48(5):2335–2342.
62. Cui JZ, Chiu A, Maberley D, Ma P, Samad A, Matsubara JA. Stage specificity of novel growth factor expression during development of proliferative vitreoretinopathy. *Eye*. 2007;21(2):200–208.
63. Chan CM, Chang HH, Wang VC, Huang CL, Hung CF. Inhibitory effects of resveratrol on PDGF-BB-induced retinal pigment epithelial cell migration via PDGFRbeta, PI3K/Akt and MAPK pathways. *PLoS ONE*. 2013;8(2):e56819.
64. Lei H, Velez G, Hovland P, Hirose T, Kazlauskas A. Plasmin is the major protease responsible for processing PDGF-C in the vitreous of patients with proliferative vitreoretinopathy. *Invest Ophthalmol Vis Sci*. 2008;49(1):42–48.
65. Cui J, Lei H, Samad A, et al. PDGF receptors are activated in human epiretinal membranes. *Exp Eye Res*. 2009;88(3):438–444.
66. Ikuno Y, Kazlauskas A. An in vivo gene therapy approach for experimental proliferative vitreoretinopathy using the truncated platelet-derived growth factor alpha receptor. *Invest Ophthalmol Vis Sci*. 2002;43(7):2406–2411.
67. Saishin Y, Saishin Y, Takahashi K, Seo MS, Melia M, Campochiaro PA. The kinase inhibitor PKC412 suppresses

epiretinal membrane formation and retinal detachment in mice with proliferative retinopathies. *Invest Ophthalmol Vis Sci*. 2003;44(8):3656–3662.
68. Lei H, Velez G, Hovland P, Hirose T, Gilbertson D, Kazlauskas A. Growth factors outside the PDGF family drive experimental PVR. *Invest Ophthalmol Vis Sci*. 2009;50(7):3394–3403.
69. Lei H, Kazlauskas A. A reactive oxygen species-mediated, self-perpetuating loop persistently activates platelet-derived growth factor receptor alpha. *Mol Cell Biol*. 2014;34(1):110–122.
70. Lei H, Velez G, Cui J, et al. N-acetylcysteine suppresses retinal detachment in an experimental model of proliferative vitreoretinopathy. *Am J Pathol*. 2010;177(1):132–140.
71. Saika S, Yamanaka O, Okada Y, et al. TGF beta in fibroproliferative diseases in the eye. *Front Biosci*. 2009;1:376–390.
72. Hoerster R, Muether PS, Vierkotten S, Hermann MM, Kirchhof B, Fauser S. Upregulation of TGF-ss1 in experimental proliferative vitreoretinopathy is accompanied by epithelial to mesenchymal transition. *Graefes Arch Klin Exp Ophthalmol*. 2014;252(1):11–16.
73. Kita T, Hata Y, Kano K, et al. Transforming growth factor-beta2 and connective tissue growth factor in proliferative vitreoretinal diseases: possible involvement of hyalocytes and therapeutic potential of Rho kinase inhibitor. *Diabetes*. 2007;56(1):231–238.
74. Winkler J, Hoerauf H. TGF-ss and RPE-derived cells in taut subretinal strands from patients with proliferative vitreoretinopathy. *Eur J Ophthalmol*. 2011;21(4):422–426.
75. Anderson DH, Guerin CJ, Hageman GS, Pfeffer BA, Flanders KC. Distribution of transforming growth factor-beta isoforms in the mammalian retina. *J Neurosci Res*. 1995;42(1):63–79.
76. Guerin CJ, Hu L, Scicli G, Scicli AG. Transforming growth factor beta in experimentally detached retina and periretinal membranes. *Exp Eye Res*. 2001;73(6):753–764.

77. Hirsch L, Nazari H, Sreekumar PG, et al. TGF-beta2 secretion from RPE decreases with polarization and becomes apically oriented. *Cytokine*. 2015;71(2):394–396.
78. Chen X, Ye S, Xiao W, Luo L, Liu Y. Differentially expressed microRNAs in TGFbeta2-induced epithelial-mesenchymal transition in retinal pigment epithelium cells. *Int J Mol Med*. 2014;33(5):1195–1200.
79. Li M, Li H, Liu X, Xu D, Wang F. MicroRNA-29b regulates TGF-beta1-mediated epithelial-mesenchymal transition of retinal pigment epithelial cells by targeting AKT2. *Exp Cell Res*. 2016;345(2):115–124.
80. Li H, Li M, Xu D, Zhao C, Liu G, Wang F. Overexpression of Snail in retinal pigment epithelial triggered epithelial-mesenchymal transition. *Biochem Biophys Res Comm.*2014;446(1):347–351.
81. Dvashi Z, Goldberg M, Adir O, Shapira M, Pollack A. TGF-beta1 induced transdifferentiation of RPE cells is mediated by TAK1. *PLoS ONE*. 2015;10(4):e0122229.
82. Oshima Y, Sakamoto T, Hisatomi T, Tsutsumi C, Ueno H, Ishibashi T. Gene transfer of soluble TGF-beta type II receptor inhibits experimental proliferative vitreoretinopathy. *Gene Ther*. 2002;9(18):1214–1220.
83. Kawahara S, Hata Y, Kita T, et al. Potent inhibition of cicatricial contraction in proliferative vitreoretinal diseases by statins. *Diabetes*. 2008;57(10):2784–2793.
84. Kita T, Hata Y, Arita R, et al. Role of TGF-beta in proliferative vitreoretinal diseases and ROCK as a therapeutic target. *Proc Natl Acad Sci USA*. 2008;105(45):17504–17509.
85. Itoh Y, Kimoto K, Imaizumi M, Nakatsuka K. Inhibition of RhoA/Rho-kinase pathway suppresses the expression of type I collagen induced by TGF-beta2 in human retinal pigment epithelial cells. *Exp Eye Res*. 2007;84(3):464–472.
86. Mukherjee S, Guidry C. The insulin-like growth factor system modulates retinal pigment epithelial cell tractional force generation. *Invest Ophthalmol Vis Sci*. 2007;48(4):1892–1899.
87. Nguyen DV, Li Calzi S, Shaw LC, Kielczewski JL, Korah HE,

Grant MB. An ocular view of the IGF-IGFBP system. *Growth Hormone IGF Res*. 2013;23(3):45–52.
88. Zhao HM, Sheng MJ, Yu J. Expression of IGFBP-6 in a proliferative vitreoretinopathy rat model and its effects on retinal pigment epithelial cell proliferation and migration. *Int J Ophthalmol*. 2014;7(1):27–33.
89. Nakazawa T, Matsubara A, Noda K, et al. Characterization of cytokine responses to retinal detachment in rats. *Mol Vis*. 2006;12:867–878.
90. Han QH, Hui YN, Du HJ, Zhang WJ, Ma JX, Wang SY. Migration of retinal pigment epithelial cells in vitro modulated by monocyte chemotactic protein-1: enhancement and inhibition. *Graefes Arch Klin Exp Ophthalmol*. 2001;239(7):531–538.
91. Abu el-Asrar AM, Van Damme J, Put W, et al. Monocyte chemotactic protein-1 in proliferative vitreoretinal disorders. *Am J Ophthalmol*. 1997;123(5):599–606.
92. Asaria RH, Kon CH, Bunce C, et al. Silicone oil concentrates fibrogenic growth factors in the retro-oil fluid. *Br J Ophthalmol*. 2004;88(11):1439–1442.
93. Hueber A, Wiedemann P, Esser P, Heimann K. Basic fibroblast growth factor mRNA, bFGF peptide and FGF receptor in epiretinal membranes of intraocular proliferative disorders (PVR and PDR). *Int Ophthalmol*. 1996;20(6):345–350.
94. Liang X, Li C, Gao R, et al. Quantitative study of basic fibroblast growth factor in vitreous with proliferative vitreoretinopathy. *Eye Science*. 2000;16(1):7–10.
95. Hoffmann S, He S, Jin M, et al. A selective cyclic integrin antagonist blocks the integrin receptors alphavbeta3 and alphavbeta5 and inhibits retinal pigment epithelium cell attachment, migration and invasion. *BMC Ophthalmol*. 2005;5:16.
96. Briggs MC, Grierson I, Hiscott P, Hunt JA. Active scatter factor (HGF/SF) in proliferative vitreoretinal disease. *Invest Ophthalmol Vis Sci*. 2000;41(10):3085–3094.
97. Lashkari K, Rahimi N, Kazlauskas A. Hepatocyte growth factor receptor in human RPE cells: implications in

proliferative vitreoretinopathy. *Invest Ophthalmol Vis Sci*. 1999;40(1):149–156.
98. Grierson I, Heathcote L, Hiscott P, Hogg P, Briggs M, Hagan S. Hepatocyte growth factor/scatter factor in the eye. *Progr Retinal Eye Res*. 2000;19(6):779–802.
99. Hinton DR, He S, Jin ML, Barron E, Ryan SJ. Novel growth factors involved in the pathogenesis of proliferative vitreoretinopathy. *Eye*. 2002;16(4):422–428.
100. Hollborn M, Krausse C, Iandiev I, et al. Glial cell expression of hepatocyte growth factor in vitreoretinal proliferative disease. *Lab Invest*. 2004;84(8):963–972.
101. Abu El-Asrar AM, Imtiaz Nawaz M, Kangave D, Siddiquei MM, Geboes K. Osteopontin and other regulators of angiogenesis and fibrogenesis in the vitreous from patients with proliferative vitreoretinal disorders. *Mediators Inflamm*. 2012;2012:493043.
102. Guo CM, Wang YS, Hu D, et al. Modulation of migration and $Ca2^{+}$ signaling in retinal pigment epithelium cells by recombinant human CTGF. *Curr Eye Res*. 2009;34(10):852–862.
103. Kita T, Hata Y, Miura M, Kawahara S, Nakao S, Ishibashi T. Functional characteristics of connective tissue growth factor on vitreoretinal cells. *Diabetes*. 2007;56(5):1421–1428.
104. Liang CM, Tai MC, Chang YH, et al. Glucosamine inhibits epidermal growth factor-induced proliferation and cell-cycle progression in retinal pigment epithelial cells. *Mol Vis*. 2010;16:2559–2571.
105. Yan F, Hui YN, Li YJ, Guo CM, Meng H. Epidermal growth factor receptor in cultured human retinal pigment epithelial cells. *Int J Ophthalmol*. 2007;221(4):244–250.
106. Chen Z, Chen CZ, Gong WR, Li JP, Xing YQ. Integrin-alpha5 mediates epidermal growth factor-induced retinal pigment epithelial cell proliferation and migration. *Pathobiology*. 2010;77(2):88–95.
107. Ogata N, Nishikawa M, Nishimura T, Mitsuma Y, Matsumura M. Inverse levels of pigment epithelium-derived factor and vascular endothelial growth factor in the vitreous of eyes with rhegmatogenous retinal detachment

and proliferative vitreoretinopathy. *Am J Ophthalmol*. 2002;133(6):851–852.
108. Armstrong D, Augustin AJ, Spengler R, et al. Detection of vascular endothelial growth factor and tumor necrosis factor alpha in epiretinal membranes of proliferative diabetic retinopathy, proliferative vitreoretinopathy and macular pucker. *Int J Ophthalmol*. 1998;212(6):410–414.
109. Pennock S, Haddock LJ, Mukai S, Kazlauskas A. Vascular endothelial growth factor acts primarily via platelet-derived growth factor receptor alpha to promote proliferative vitreoretinopathy. *Am J Pathol*. 2014;184(11):3052–3068.
110. Kon CH, Occleston NL, Aylward GW, Khaw PT. Expression of vitreous cytokines in proliferative vitreoretinopathy: a prospective study. *Invest Ophthalmol Vis Sci*. 1999;40(3):705–712.
111. Hui Y, Shi Y, Zhang X, Yang K, Yu C. TNF-alpha, IL-8 and IL-6 in the early inflammatory stage of experimental PVR model induced by macrophages. *[Zhonghua yan ke za zhi] Chin J Ophthalmol*. 1999;35(2):140–143.
112. Korthagen NM, van Bilsen K, Swagemakers SM, et al. Retinal pigment epithelial cells display specific transcriptional responses upon TNF-alpha stimulation. *Br J Ophthalmol*. 2015;99(5):700–704.
113. Kim SH, Turnbull J, Guimond S. Extracellular matrix and cell signalling: the dynamic cooperation of integrin, proteoglycan and growth factor receptor. *J Endocrinol*. 2011;209(2):139–151.
114. Byron A, Morgan MR, Humphries MJ. Adhesion signalling complexes. *Curr Biol*. 2010;20(24):R1063–7.
115. Hou X, Han QH, Hu D, et al. Mechanical force enhances MMP-2 activation via p38 signaling pathway in human retinal pigment epithelial cells. *Graefes Archiv Klin Exp Ophthalmol*. 2009;247(11):1477–1486.
116. Hollborn M, Reichenbach A, Wiedemann P, Kohen L. Contrary effects of cytokines on mRNAs of cell cycle- and ECM-related proteins in hRPE cells in vitro. *Curr Eye Res*. 2004;28(3):215–223.
117. Jerdan JA, Pepose JS, Michels RG, et al. Proliferative

vitreoretinopathy membranes: an immunohistochemical study. *Ophthalmology*. 1989;96(6):801–810.
118. Hollborn M, Faude F, Wiedemann P, Kohen L. Elevated proto-oncogene and collagen mRNA expression in PVR retinas. *Graefes Arch Klin Exp Ophthalmol*. 2003;241(5):439–446.
119. George B, Chen S, Chaudhary V, Gonder J, Chakrabarti S. Extracellular matrix proteins in epiretinal membranes and in diabetic retinopathy. *Curr Eye Res*. 2009;34(2):134–144.
120. Ioachim E, Stefaniotou M, Gorezis S, Tsanou E, Psilas K, Agnantis NJ. Immunohistochemical study of extracellular matrix components in epiretinal membranes of vitreoproliferative retinopathy and proliferative diabetic retinopathy. *Eur J Ophthalmol*. 2005;15(3):384–391.
121. Gamulescu MA, Chen Y, He S, et al. Transforming growth factor beta2-induced myofibroblastic differentiation of human retinal pigment epithelial cells: regulation by extracellular matrix proteins and hepatocyte growth factor. *Exp Eye Res*. 2006;83(1):212–222.
122. Khankan R, Oliver N, He S, Ryan SJ, Hinton DR. Regulation of fibronectin-EDA through CTGF domain-specific interactions with TGFbeta2 and its receptor TGFbetaRII. *Invest Ophthalmol Vis Sci*. 2011;52(8):5068–5078.
123. Hiscott P, Paraoan L, Choudhary A, Ordonez JL, Al-Khaier A, Armstrong DJ. Thrombospondin 1, thrombospondin 2 and the eye. *Progr Retinal Eye Res*. 2006;25(1):1–18.
124. Visse R, Nagase H. Matrix metalloproteinases and tissue inhibitors of metalloproteinases: structure, function, and biochemistry. *Circ Res*. 2003;92(8):827–839.
125. Sheridan CM, Occleston NL, Hiscott P, Kon CH, Khaw PT, Grierson I. Matrix metalloproteinases: a role in the contraction of vitreo-retinal scar tissue. *Am J Pathol*. 2001;159(4):1555–1566.
126. Abu El-Asrar AM, Missotten L, Geboes K. Expression of myofibroblast activation molecules in proliferative vitreoretinopathy epiretinal membranes. *Acta Ophthalmol*. 2011;89(2):e115–21.
127. Hinz B, Gabbiani G. Fibrosis: recent advances in

myofibroblast biology and new therapeutic perspectives. *F1000 Biol Rep.*2010;2:78.
128. Tomasek JJ, Gabbiani G, Hinz B, Chaponnier C, Brown RA. Myofibroblasts and mechano-regulation of connective tissue remodelling. *Nat Rev Mol Cell Biol*. 2002;3(5):349–363.
129. Kita T. Molecular mechanisms of preretinal membrane contraction in proliferative vitreoretinal diseases and ROCK as a therapeutic target. *Nippon Ganka Gakkai Zasshi*. 2010;114(11):927–934.
130. Peters MA, Burke JM, Clowry M, Abrams GW, Williams GA. Development of traction retinal detachments following intravitreal injections of retinal Müller and pigment epithelial cells. *Graefes Arch Klin Exp Ophthalmol*. 1986;224(6):554–563.
131. Glaser BM, Cardin A, Biscoe B. Proliferative vitreoretinopathy: the mechanism of development of vitreoretinal traction. *Ophthalmology*. 1987;94(4):327–332.
132. Beutel J, Luke M, Bartz-Schmidt KU, Grisanti S. Vitreal-induced RPE cell traction. Investigation of pathological vitreous samples in an in vitro contraction model. *Ophthalmologe*. 2009;106(10):893–898.
133. Joussen AM, Lux A, Kirchhof B. Shifting of the proliferative vitreoretinopathy milieu after tamponade with heavy silicone oil in eyes prone to proliferative vitreoretinopathy and bleeding. *Br J Ophthalmol*. 2009;93(1):128–129.
134. Ricker LJ, Altara R, Goezinne F, Hendrikse F, Kijlstra A, La Heij EC. Soluble apoptotic factors and adhesion molecules in rhegmatogenous retinal detachment. *Invest Ophthalmol Vis Sci*. 2011;52(7):4256–4262.
135. Ricker LJ, Kijlstra A, Kessels AG, et al. Interleukin and growth factor levels in subretinal fluid in rhegmatogenous retinal detachment: a case-control study. *PLoS ONE*. 2011;6(4):e19141.
136. Grisanti S, Wiedemann P, Weller M, Heimann K, Zilles K. The significance of complement in proliferative vitreoretinopathy. *Invest Ophthalmol Vis Sci*. 1991;32(10):2711–2717.
137. Yu J, Liu F, Cui SJ, et al. Vitreous proteomic analysis of

proliferative vitreoretinopathy. *Proteomics*. 2008;8(17):3667–3678.
138. Kuo HK, Chen YH, Huang F, Wu YC, Shiea J, Wu PC. The upregulation of zinc finger protein 670 and prostaglandin D2 synthase in proliferative vitreoretinopathy. *Graefes Arch Klin Exp Ophthalmol*. 2016;254(2):205–213.
139. Coral K, Angayarkanni N, Madhavan J, et al. Lysyl oxidase activity in the ocular tissues and the role of LOX in proliferative diabetic retinopathy and rhegmatogenous retinal detachment. *Invest Ophthalmol Vis Sci*. 2008;49(11):4746–4752.
140. Symeonidis C, Papakonstantinou E, Souliou E, Karakiulakis G, Dimitrakos SA, Diza E. Correlation of matrix metalloproteinase levels with the grade of proliferative vitreoretinopathy in the subretinal fluid and vitreous during rhegmatogenous retinal detachment. *Acta Ophthalmol*. 2011;89(4):339–345.
141. Symeonidis C, Androudi S, Georgalas I, et al. Chemokine CXCL-1: activity in the vitreous during proliferative vitreoretinopathy. *Clin Exp Immunol*. 2015;181(2):338–342.
142. Shitama T, Hayashi H, Noge S, et al. Proteome profiling of vitreoretinal diseases by cluster analysis. *Proteomics Clin Appl*. 2008;2(9):1265–1280.
143. Shi H, Guo T, Liu PC, et al. Steroids as an adjunct for reducing the incidence of proliferative vitreoretinopathy after rhegmatogenous retinal detachment surgery: a systematic review and meta-analysis. *Drug Des Devel Ther*. 2015;9:1393–1400.
144. Hoerster R, Hermann MM, Rosentreter A, Muether PS, Kirchhof B, Fauser S. Profibrotic cytokines in aqueous humour correlate with aqueous flare in patients with rhegmatogenous retinal detachment. *Br J Ophthalmol*. 2013;97(4):450–453.
145. Sanabria Ruiz-Colmenares MR, Pastor Jimeno JC, Garrote Adrados JA, Telleria Orriols JJ, Yugueros Fernandez MI. Cytokine gene polymorphisms in retinal detachment patients with and without proliferative vitreoretinopathy: a preliminary study. *Acta Ophthalmol Scand*. 2006;84(3):309–

313.
146. Rojas J, Fernandez I, Pastor JC, et al. A strong genetic association between the tumor necrosis factor locus and proliferative vitreoretinopathy: the retina 4 project. *Ophthalmology*. 2010;117(12):2417 [23.e1–2].
147. Pastor-Idoate S, Rodriguez-Hernandez I, Rojas J, et al. BAX and BCL-2 polymorphisms, as predictors of proliferative vitreoretinopathy development in patients suffering retinal detachment: the Retina 4 project. *Acta Ophthalmol*. 2015;93(7):e541–9.
148. Rojas J, Fernandez I, Pastor JC, et al. Predicting proliferative vitreoretinopathy: temporal and external validation of models based on genetic and clinical variables. *Br J Ophthalmol*. 2015;99(1):41–48.
149. Claes C, Lafeta AP. Proliferative vitreoretinopathy. *Dev Ophthalmology*. 2014;54:188–195.
150. Khan MA, Brady CJ, Kaiser RS. Clinical Management of proliferative vitreoretinopathy: an update. *Retina*. 2015;35(2):165–175.

102

Pathophysiology of Ocular Trauma

Sun Young Lee

Introduction

Ocular trauma is a major cause of ocular morbidity and a leading cause of monocular visual loss. It is estimated that over 2 million eye injuries occur in the United States each year.[1] Children and young adults are particularly at risk, and consequently, society suffers significant socioeconomic loss, as well as human loss, from these common injuries. In 1990, national projections estimated that more than 227, 000 hospital days and US$175–200 million in hospital charges alone result from ocular injuries every year.[2]

A classification of ocular trauma with standardized terminology was developed by Kuhn and associates.[3] The International Society of Ocular Trauma subsequently used this terminology to develop a classification system for mechanical injuries of the eye (Box 102.1). This system has proved useful for describing ocular trauma without miscommunication and for facilitating the delivery of optimal patient care.

Box 102.1

Standardized Classification of Ocular Trauma

Closed globe

- Contusion (no full-thickness wound)
- Lamellar laceration (partial-thickness wound of the eye wall)

Open globe (full-thickness wound of the eye wall)

- Rupture
- Laceration
- Penetrating (single entry wound; no exit wound)
- Perforating (separate entry and exit wounds by same agent)
- Intraocular foreign body (retained foreign object that caused entry wound)

Different types of ocular injuries have different pathophysiologic and therapeutic ramifications; therefore, knowledge of the initial mechanism of injury to the macula or optic nerve is critical for determining visual prognosis.[4–6] Subsequent wound healing responses leading to intraocular proliferation, tractional retinal detachment, and posttraumatic proliferative vitreoretinopathy (PVR) can play major roles in determining the final visual outcome.[4,6–9]

Before the use of vitrectomy, wound closure often left vitreous incarcerated in the lips of the scleral or corneal edges of the wound, providing a scaffold for future proliferation. In the first large prospective study, conducted between 1952 and 1970, only 6% of patients with open-globe injury gained visual acuity of 5/200 or better.[10] Our improved understanding of wound healing and the advent of vitrectomy techniques in the 1970s permitted more successful repair of posterior segment wounds and resulted in a marked decrease in enucleations.[8,9,11,12]

This chapter reviews the pathophysiology and the therapeutic aspects related to open-globe injury involving the posterior segment. (See also Chapter 94, Traumatic chorioretinopathies; Chapter 101, Pathogenesis of proliferative vitreoretinopathy; and Chapter 114, Surgery for ocular trauma.)

Anatomic Change

While the direct damage to the ocular tissue depends upon the nature of trauma, the integrity of the vitreoretinal barrier is commonly disrupted by ocular trauma. The vitreous is normally attached to all contiguous structures, including the posterior lens capsule, the pars plana of the ciliary body, the retina, and the optic disc, but the strength of this attachment varies. The vitreous is most firmly attached at its base and is relatively firmly attached to the lens, fovea–parafoveal area, margin of the optic nerve head, and along major retinal blood vessels.[13] Weakening of the vitreoretinal interface induced by mechanical force can lead to acute posterior vitreous detachment (PVD) from the retina. When the detachment reaches a point of firmer attachment to the retina, typically the vitreous base, it exerts traction on the retina. The abrupt PVD

and/or prolapse and incarceration of the vitreous through the penetrating wound predispose the eye to vitreous traction on the retina and tractional retinal detachment (Fig. 102.1).[14–18]

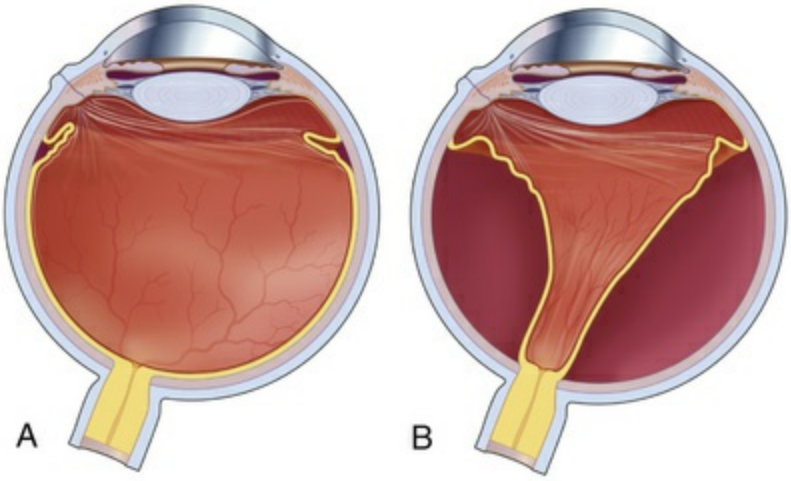

FIG. 102.1 The development of tractional retinal detachment can be related to two mechanisms. (A) Vitreous is incarcerated in the wound, and fibrous ingrowth from the wound along the vitreous scaffold may result in traction on the peripheral retina, rolling forward at the vitreous base and junctions of the ora serrata. (B) The contraction of epiretinal fibrous tissue on the surface of the peripheral and equatorial retina may result in shortening of the retina. Either of these mechanisms, but usually a combination of both, results in tractional retinal detachment. (Reproduced with permission from Cleary PE, Ryan SJ. Method of production and natural history of experimental posterior penetrating eye injury in the rhesus monkey. Am J Ophthalmol 1979;88:212–20.)

Breakdown of the blood–retina barrier after trauma is a key triggering mechanism in the wound healing sequence. The blood–retinal barrier (BRB) consists of tight junctions between the retinal capillary endothelial cells (inner BRB) and the retinal pigment epithelial (RPE) cells (outer BRB). Disruption of this highly specialized barrier system leads to migration of inflammatory cells and leakage of serum components, allowing a profound change in the biochemical milieu of the retina and vitreous.

Histopathologic Findings

In reviewing the histopathology of enucleated human eyes, one must be cognizant of the bias of ascertainment of the specimen. Before the introduction of vitreous surgery in 1970, many more injured eyes were enucleated, whether because the eye had become blind and painful in the late stage or as prophylaxis against the possibility of sympathetic ophthalmia in an earlier stage. Regardless of the indication for enucleation, the pathologist and reader must always consider that the circumstances are dictated by clinical indications and not for reasons of optimal timing to determine pathogenesis. We, therefore, review literature from enucleated eyes and then consider experimental models to better understand the pathophysiology.

Histopathologic evaluation of human eyes enucleated after penetrating trauma has shown that healing of limbal and scleral wounds was more rapid than healing of corneal wounds.[17] As early as 4 days after injury, fibroblastic proliferation had occurred from the episclera, and by 1 week, from the stroma of the ciliary body and choroid. At 2 weeks, a mass of vascularized fibrous tissue joined the wound edges; and by 4–6 weeks, a dense fibrous scar had formed. This fibrous ingrowth in limbal or scleral wounds occurred in relation to vitreous incarceration and damage to the lens and/or vitreous hemorrhage. Condensation of vitreous fibrils over the vitreous base was followed by PVD. Typically, the vitreous remained attached anteriorly, and the condensed vitreous fibrils remained attached to the peripheral retina, frequently radiating from a limbal or scleral wound associated with fibroblasts (Fig. 102.2). Retinal detachment was present in most eyes. Although retinal tears were found in a few eyes, it was impossible to exclude a rhegmatogenous component since not all eyes were serially sectioned. Retinal hemorrhage and choroidal hemorrhage were common within the first 2 months and 2 weeks of injury, respectively. Epiretinal membranes were present over both the peripheral and posterior retina by 6 weeks after injury. Subretinal membranes were delicate, branching, and dendritic in appearance 1 and 2 weeks after injury and were thickened and attached to folds in the retina in later phases. Intraocular inflammatory infiltrate,

mainly monocytes, was prominent in the anterior chamber or vitreous. Almost all eyes contained some macrophages, either lining the PVD or accumulated in areas of subretinal hemorrhage. Fibroblastic proliferation within the vitreous was present in the area of the wound, resulting in a cyclitic membrane in the early weeks after injury and containing fibroblast-like cells 2 months after injury.

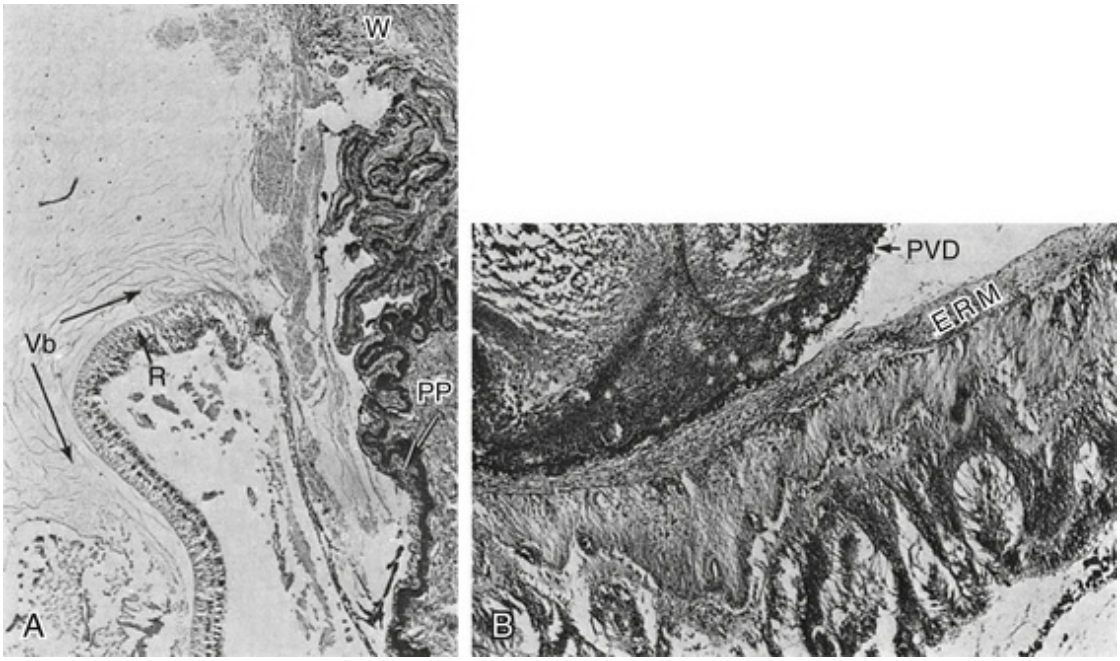

FIG. 102.2 (A) Photomicrograph showing the appearance of the peripheral retina in the vitreous base 2 months after a penetrating injury. The peripheral retina (*R*) is detached and appears to be pulled forward over the pars plana (*PP*). The vitreous is condensed and vitreous fibrils are incarcerated in a peripheral corneal wound (*W*). The vitreous was detached from the posterior retina, but remains attached to the peripheral retina over the vitreous base (*Vb*). (B) Photomicrograph showing a multilayered epiretinal membrane (*ERM)* on the surface of the posterior retina in an eye enucleated 2 months after a penetrating injury. A posterior vitreous detachment (*PVD*) is present and a blood clot is loculated within the vitreous gel. The posterior hyaloid is lined with red cell debris. The epiretinal membrane lies between the posterior hyaloid and the inner limiting membrane of the retina. In adjacent sections, full-thickness retinal

folds were present (hematoxylin and eosin, ×37).
(Reproduced with permission from Winthrop SR, Cleary PE, Minckler DS, et al. Penetrating eye injuries: a histopathological review. Br J Ophthalmol 1980;64:809–17.)

Experimental Models

Human specimens obtained from surgery, such as periretinal membranes, vitreous aspirates, and enucleated eyes, provide information about the pathophysiology of open-globe injury.[17,18] However, since these specimens often represent only the advanced stages of disease and since they encompass the secondary effects of retinal detachment and PVR, their contributions to our understanding of the complex mechanism of trauma-induced injury are somewhat limited. Therefore, animal models that reproduce various types of ocular trauma have played an important role in our understanding of their pathogenesis.

Cleary and Ryan developed penetrating injury models in rabbits and rhesus monkeys using a standard technique.[19–24] A knife wound was made using a stab incision through the pars plana and then lengthened to 8 mm with scissors. Vitreous gel prolapsed through the wound and the vitreous face was ruptured in a manner similar to that encountered in the perforated human eye. The wound was then carefully closed and 0.5 mL of autologous blood was injected into the midvitreous. With this standardized method, tractional retinal detachment was achieved with remarkable reproducibility. During the second week after injury, the blood changed to a contracted clot and the posterior vitreous detached. As early as 4 weeks after the injury, fibrous tissue grew from the wound into the vitreous, the blood clot formed fibrous tissue, and the posterior vitreous detached. Epiretinal membranes became visible around this time and progressed for up to 15 weeks. The retinal detachment typically occurred between 6 and 11 weeks after the injury. The configuration of the retinal detachment was indicative of the key processes involved. When the vitreous detached posteriorly, the anteroperipheral portion of the vitreous remained firmly attached to the peripheral retina in the area of the vitreous base.

Subsequently, the peripheral retina was dragged forward toward the pars plana through its entire circumference, forming a funnel-shaped configuration with full-thickness folds.[19,20,25] The presence of intravitreal blood was a potent stimulant to the development of this cascade of the wound healing process. Some 73% of 25 monkey eyes with intravitreal blood injections developed tractional retinal detachments as opposed to only 24% of eyes that received only balanced salt solution injections.[19]

Penetrating injuries in human eyes are often accompanied by contusions. An animal model used to study this combination employed pigs because pig sclera is sturdy enough to withstand a blunt pellet injury.[26–28] An airgun delivered a pellet to the limbus of a pig eye with standardized force at impact. An 8-mm incision was then made in the pars plana as previously described. The main features were the development of intravitreal proliferation and tractional retinal detachment. Additionally, subretinal hemorrhage was frequently associated, leading to subretinal fibrous membrane formation.

Animal models are useful in reproducing the findings observed in ocular trauma in humans; and furthermore, these models are valuable for evaluating surgical techniques and therapeutic drugs.[29,30] For instance, the morphology of the wound and the efficacy of vitrectomy have been studied in this animal model of a contusion injury. Because of initial uveal engorgement and inflammatory swelling, early surgical intervention was hazardous. The findings support the clinical impression that vitrectomy in traumatized eyes with a substantial contusive component is best delayed for 1 or 2 weeks.[26,27] (This is discussed in more detail in Chapter 114, Surgery for ocular trauma.)

A human RPE culture system is another useful means of investigating the RPE cell's behavioral patterns, such as the migration, proliferation, and alteration of its phenotype, and the growth factors and cytokine-secreting patterns in order to understand the process of PVR.[31–36]

Wound Healing and Traumatic Proliferative Vitreoretinopathy

Wound healing in the eye is similar to that in other bodily tissues, consisting of three phases: exudation/inflammation, proliferation, and regeneration.[37] The typical wound healing response in the anatomic setting of the eye and the vitreoretinal relationship explain the development of tractional retinal detachment after penetrating ocular injury.

Open-globe injury results in a breakdown of the blood–retinal barrier and allows the entry of a variety of cells into the intraocular milieu, causing the expression of a variety of chemokines, inflammatory cytokines, and growth factors that affect the adjacent RPE, fibroblasts, and glial cells. In response, these previously resting cells undergo proliferation and migration as they change their pattern of gene expression, resulting in alterations of their own cytokine, extracellular matrix, and receptor profiles. Some cells – myofibroblasts, for example – proliferate and produce strong contractile forces that oppose the physiologic forces that normally keep the retina attached and a tractional retinal detachment occurs. Following the natural course, proliferation is accompanied by a progressive accumulation of extracellular collagen and by a decrease in inflammation and inflammatory mediators.[18,20] This wound healing process is central to the final common pathway that leads to tractional retinal detachment and posttraumatic PVR in open-globe injury (Fig. 102.3).

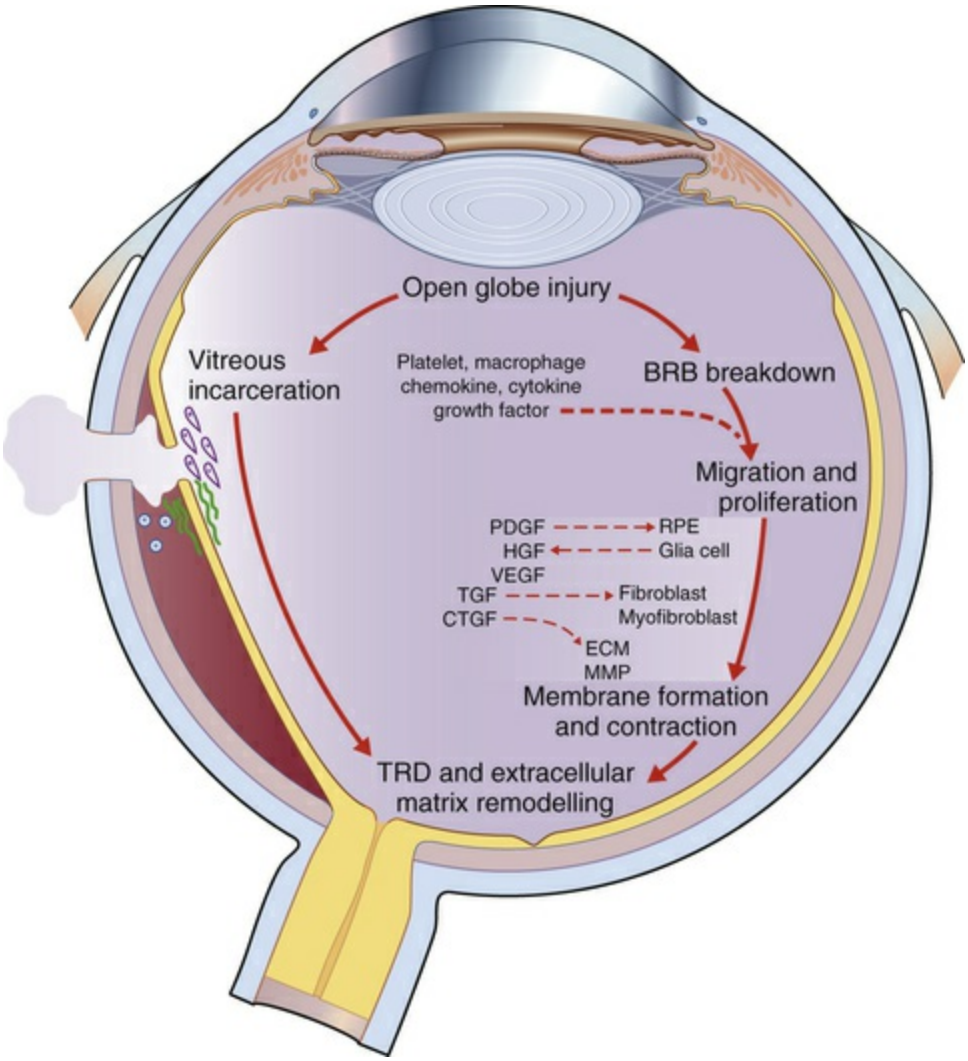

FIG. 102.3 Traumatic proliferative vitreoretinopathy pathway. Abbreviations: *BRB,* blood–retinal barrier; *RPE,* retinal pigment epithelium; *PDGF,* platelet-derived growth factor; *HGF,* hepatocyte growth factor; *VEGF,* vascular endothelial growth factor; *TGF,* tissue growth factor; *CTGF,* connective tissue growth factor; *ECM,* extracellular matrix; *MMP,* matrix metalloproteinase; *TRD,* tractional retinal detachment.

Accordingly, when interpreting human tissues, it is important to emphasize the stage of the wound healing response: the early stage is characterized by many cells, including a range of inflammatory cells, myofibroblasts, RPE, etc. The late stage is characterized by fewer cells of a chronic variety and more extracellular matrix, e.g., collagen.

Cellular Constituents

Epiretinal membranes removed during vitreous surgery for PVR after injury have been analyzed to gain an understanding of the origin and characteristics of their cellular constituents.[38–40] Depending on the nature of the injury and the stage of the response, these membranes contain variable numbers of cells that are phenotypically identified as inflammatory cells, RPE cells, glial cells, fibroblasts, and myofibroblasts.

Inflammatory cells are among the earliest cell types to appear in the wound healing response. They may be attracted to the wound by chemokines upregulated in traumatized retinal tissue, by breakdown of the blood–retinal barrier, or as a response to intraocular blood.[31,41–45] The cytokine products of these cells may be critical for the activation of other retinal cell types, further recruitment of inflammatory cells, and formation of collagen. Macrophages are a constant feature of experimental tractional retinal detachment.[42,43] In the primate model of posterior penetrating injury, macrophages are present before the invasion and proliferation of fibroblast or RPE cells.[19,20] The finding of cellular and humoral immune responses to retinal antigens following retinal detachment and experimental PVR has suggested the possibility of an autoimmune component in PVR, although the evidence for a pathogenic role of such a response is incomplete.[45–48]

The RPE cell is central to the pathophysiologic response seen in posttraumatic PVR. The RPE cells have critical characteristics, including migration and proliferation.[32,33,38] The posttraumatic stimuli that are specifically responsible for RPE changes are not completely understood. RPE cell growth appears to be regulated by both paracrine and autocrine stimulation. RPE cells were shown to proliferate and form multilayered colonies of dedifferentiated RPE cells within 24 hours of retinal detachment in cats.[49] They were also consistently found in the membranes of animal models of penetrating injury.[20,22,26] Additionally, cultured RPE cells, just like RPE cells under the detached retina, produce mitogenic and chemotactic growth factors, such as platelet-derived growth factor (PDGF) and hepatocyte growth factor (HGF), and possess receptors for each of these growth factors. RPE cells respond not only to growth factors from RPE cells (autocrine) but also to those from surrounding tissue or from serum (paracrine), resulting in

recruitment of additional RPE cells, and thus augmenting the process.[34–36,50–56] In response to these stimulations, RPE cells may undergo epithelial-to-mesenchymal transition (EMT) altering their phenotype to cells with a macrophage, fibroblast, or myofibroblast morphology.[32,33,38] This fibroblastic RPE may synthesize and remodel the matrix on the retinal surface, contributing to the formation of the membrane. It was demonstrated that the proportion of RPE in human membranes varies according to the age of the membrane. The number of RPE cells is greater in early (<4 months) specimens and declines progressively as the membranes mature with more advanced extracellular matrices.[57]

Glial cells, identified by their typical morphologic characteristics and immunoreactivity to glial fibrillary acidic protein (GFAP), were found in neurosensory retina and membrane from full-thickness retinectomy specimens obtained at surgery for PVR, with increased expression correlated to the severity of degeneration after trauma.[57–60] Glial cells appear to be involved in PVR formation through migration onto the surface of the retina and may be involved in remodeling of intraretinal synapses, possibly contributing to visual recovery after retinal injury.

Fibroblastic proliferation is critical to the progression of the posttraumatic proliferative response. Although fibroblasts are typically derived from RPE and glial cells, the immunohistochemical markers for these cells are missing in some fibroblasts, making their derivation uncertain.[38,61,62] In studies using an animal model of globe perforation with long posterior wounds and injection of intravitreal blood, where membranes extended from the wounds and β-galactosidase-labeled Tenon fibroblasts were identified in the vitreous and membrane, it was determined that at least some of the fibroblasts may have originated from Tenon layer at the wound edge (Fig. 102.4).[20,24,25,63,64]

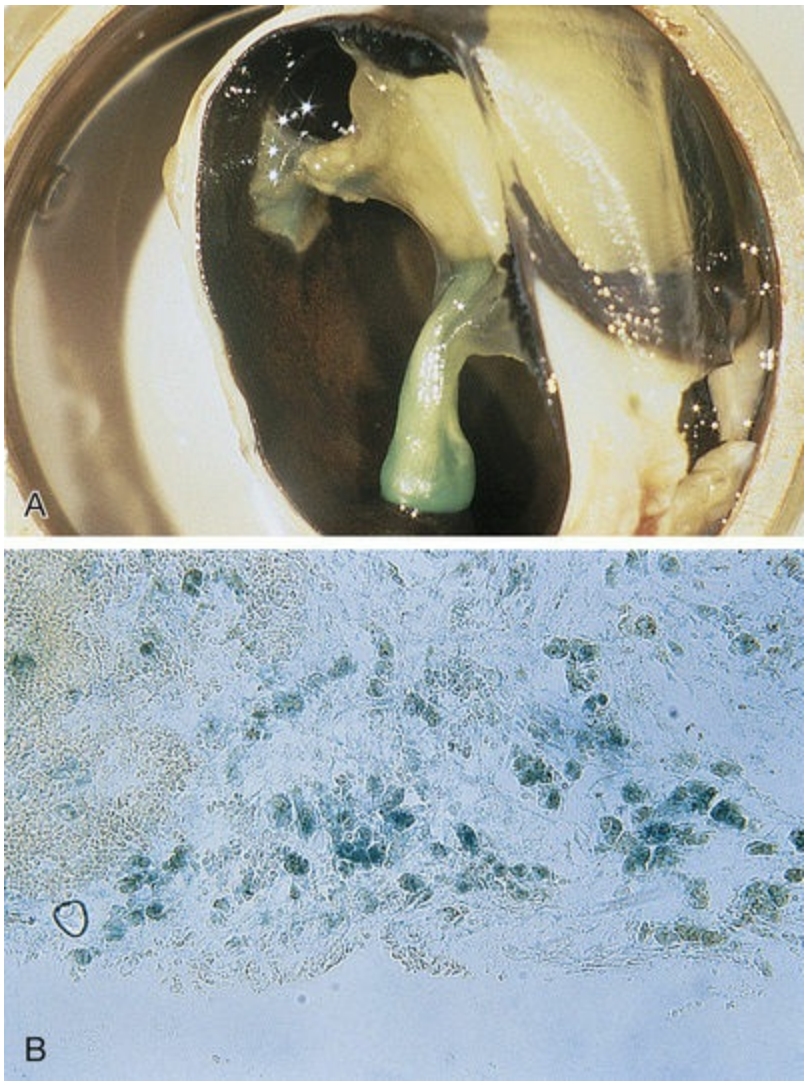

FIG. 102.4 Tenon fibroblasts in proliferative vitreoretinopathy membranes in an experimental ocular trauma model. Fibroblasts were transduced using a retroviral vector to express beta-galactosidase. These labeled cells were injected into Tenon's capsule of rabbits, and 2 days later a double perforation was performed. Animals developed funnel retinal detachment with vitreous membranes extending between the wounds at 30 days. Staining of the specimen with X-gal resulted in a blue color in labeled cells. (A) The vitreous strand from the posterior Tenon wound is blue, indicating that it contains labeled cells from the Tenon's capsule. (B) A microscopic section shows many labeled (blue) cells within the membrane. (Reproduced with permission from Santos RO, Murata T, Cui JZ et al. The role of Tenon fibroblasts in the pathogenesis of proliferative vitreo-retinopathy due to perforating eye injury. ARVO abstract 1998;517.)

Myofibroblasts are an important component of wound contraction in granulation tissue. Similarly, although the origin of these cells is unknown, RPE cells, fibroblasts, and other cell types have been implicated.[38,61,62] Ultrastructural analysis showing that myofibroblasts contain myofibrils and smooth muscle actin suggests that these myofibroblasts may produce contractile forces that cause contraction of the vitreous, retina, and membrane in PVR.[65–67] This force of cellular traction may be transmitted directly by cellular attachment to the adjacent tissue or indirectly through traction on collagen fibrils that are attached to the tissue. Experimental work suggested an alternative mechanism of membrane contraction involving the interaction of RPE cells and collagen.[14] Collagen fibers are pulled by the RPE cells by alternating extension and retraction of their lamellipodia. Collagen is piled up adjacent to the RPE cell with subsequent tissue shortening.

Growth Factors

Several growth factors appear to play critical roles, including platelet-derived growth factor (PDGF), vascular endothelial growth factor (VEGF), hepatocyte growth factor (HGF), transforming growth factor-β (TGF-β) and connective tissue growth factor (CTGF). The abundance of these growth factors in both vitreous and PVR membranes suggests that they play an important role in the wound healing response.[31,34–36,55,56,68]

The PDGF signaling network is comprised of five ligands (PDGF-AA, PDGF-BB, PDGF-AB, PDGF-CC, and PDGF-DD) and two receptors (PDGFR-α and PDGFR-β). Platelet-derived growth factor may be released from platelet α-granules after tissue damage or from endogenous retinal cells such as RPE cells. As a potent mitogenic and chemotactic stimulant for RPE and glial cells, PDGF receptor (PDGFR) signaling seems to play a central role in the development of PVR.[36,69] Analysis of epiretinal membranes from patients with PVR shows that PDGFRs are activated in these membranes.[70] Experimental studies using an organ culture model showed that RPE cell-mediated retinal contraction can be inhibited by neutralizing antibodies against PDGF, and studies using a mouse fibroblast-induced model of PVR showed that PVR was

diminished when fibroblasts isolated from PDGF-receptor knockout mice were used.[71,72] However, recent evidence suggests that experimental PVR depends on PDGFR-α, which can be activated by a much larger spectrum of growth factors rather than the concentration of PDGF only. Neutralizing PDGF does not effectively attenuate experimental PVR, however inhibition of PDGFRα activation prevents the development of PVR.[73] Non-PDGF growth factors such as epidermal growth factor (EGF), fibroblast growth factor (FGF), insulin, HGF, and VEGF-A can indirectly activate PDGFRα without engaging its ligand-binding domain.[74–76] Indirect activation of PDGFRα by non-PDGF family growth factors appears to promote PVR by chronic activation of Akt and suppression of p53.[77]

Vascular endothelial growth factor also has been localized to PVR membranes. Recent study showed that VEGF-A competitively blocks PDGF-dependent PDGFR-α activation.[76] Further study showed that neutralization of VEGF-A inhibits non-PDGF-mediated activation, which protects against PVR.[78]

Hepatocyte growth factor is also mitogenic and chemotactic for RPE cells and was found in the vitreous of patients with PVR.[34,50,51,53] Experimentally, cultured human RPE cells responded to HGF by epithelial-to-mesenchymal shape change and by cell migration response that increased with increasing concentrations of HGF.[34,50,51,53] Activation of mitogen-activated protein kinases (MAPK) is a component of the HGF-induced RPE change.[54] This response was reduced in the presence of neutralizing antibody.[51] In vivo studies in rabbits have shown that overexpression of HGF in RPE leads to subretinal proliferation of RPE.[55]

Transforming growth factor-β is known to play a crucial role as a potent fibrotic factor in EMT and is overexpressed in the vitreous of patients with PVR.[79–80] The contractile effect of hyalocyte-containing collagen gels correlates with vitreal concentration of activated TGF-β2.[81] Similarly, there is strong immunoreactivity for CTGF in human PVR membranes, and CTGF N-terminal fragment accumulates in the vitreous of patients with PVR.[82] CTGF functions as a downstream mediator of TGF-β action on fibroblasts and RPE where it stimulates cell migration and cell matrix deposition.[34,82] In vivo studies have shown that CTGF promotes the development of

highly fibrotic PVR membranes in rabbits.[82] Recently, CTGF has been shown to promote the profibrotic activities of TGF-β by regulating fibronectin-extra domain A (EDA) through protein–protein interactions between CTGF and both TGF-β and TGF-β receptor II.[83]

In addition to various growth factors, proinflammatory cytokines such as tumor necrosis factor-α and interleukin appear to have dramatic effects on many cell types, including RPE, and may alter cellular function by stimulating proliferation, migration, and expression of cell surface integrin and cell adhesion molecule, as well as extracellular matrix production and invasiveness.[35,84–85] It was also shown that infiltrating macrophages or resident RPE or glial cells may be the source of these cytokines.[35,68] A strong association has been found between a polymorphism in the tumor necrosis factor locus and PVR in a case–control study.[86]

The stage specificity of growth factor expression during PVR development has been described, where PDGF-AA is expressed uniformly throughout all stages of PVR, while HGF expression peaks during mid-stage, and CTGF expression is highest during late-stage PVR. These results may be applicable to a stage-specific therapeutic approach for PVR.[87]

Extracellular Matrix

In addition to cellular response, extracellular matrices (ECM) are important components of human PVR membranes, similar to the wound healing process in other organs. Initially, the formation of a fibrin-rich membrane can be observed.[88–89] Intraocular fibrin may provide a structure for the formation of complex membranes by stimulating the migration of RPE cells along the fibrin sheets.[90] Subsequently, membrane is characterized by the presence of interstitial collagens I and III and fibronectin within the membranes.[57,84,91–92] The collagens and fibronectin may be derived from RPE, glial cells, or macrophages, although the most consistent association is with RPE. Similar patterns of ECM expression are found in experimental PVR produced by injection of fibroblasts in the rabbit.[93] Provisional ECM components (collagen I, fibronectin) in PVR membranes may play important roles in the progression of

the wound healing response by stimulating the RPE and glial cells through activation of integrin receptors, resulting in altered cell behavior, including chemotaxis and migration.[85,94]

The wound healing process of PVR involves the unbalanced action of matrix metalloproteinases (MMPs) and tissue inhibitors of MMPs in the degradation and contraction of extracellular matrix.[95–98] MMP-9 and MMP-2 are the major MMPs that have been detected in vitreous samples and proliferative membranes of PVR patients.[96–97,99] In in vitro models of collagen contraction mediated by the RPE, synthetic MMP inhibitors have shown an anticontraction effect in a dose-dependent manner.[100]

Special Conditions

Traumatic Endophthalmitis

Endophthalmitis is a particularly devastating complication of open-globe injury, with a higher reported rate of infection after open-globe injuries (from 3.1% to 31%) in the absence of intraocular foreign body (IOFB) when compared with intraocular surgery (up to 0.1%).[101] Approximately 75% of all posttraumatic culture-positive endophthalmitis cases are infected by gram-positive organisms, with *Bacillus* species causing about 20% of the infections.[102] Risk factors associated with the development of endophthalmitis include the presence of an IOFB, lens rupture, delayed timing of primary repair, age >50 years, female gender, large wound size, location of wound, ocular tissue prolapse, placement of a primary intraocular lens, and rural location.[103-105]

The incidence of infectious endophthalmitis after penetrating injury with IOFB was reported higher, varying from 1.3% to 60%.[101,105-106] A delay in IOFB removal or primary repair of the wound more than 24 hours after the injury have been associated with the increased risk of endophthalmitis[107] (see also Chapter 90, Endogenous endophthalmitis).

Intraocular Foreign Body

The presence of an IOFB affects visual prognosis in three ways: (1)

in the structural damage induced by the IOFB (e.g., retinal tear); (2) as a vehicle for delivery of infectious agents; and (3) in the chemistry of the IOFB (e.g., pure copper is very inflammatory).

Preoperative retinal detachment, the location and the size of IOFB, and scleral or corneoscleral entry wound are predictive of a postoperative retinal detachment.[102,106,108] IOFBs also have a related higher risk of endophthalmitis, which increases dramatically when the IOFB is of a non-metallic material.[106] A chronically retained iron IOFB results in an extinguished electroretinogram and blindness, referred to as ocular siderosis, when there is progressive deposition of iron in the ocular tissues. Collections of dense ferritin particles are seen in the cytoplasm and organelles of ocular cells, and it has been hypothesized that these large accumulations cause physical damage that kills retinal cells.[109] Copper IOFBs are of particular concern because they can rapidly elicit a sterile endophthalmitis-like reaction with hypopyon and retinal detachment. Ionization of copper causes changes in the neurosensory retina that, if left untreated, can lead to loss of vision within a few hours.[110]

Posttraumatic infection and the presence of an IOFB are likely to increase the risk of PVR. Definitive treatment involves vitrectomy, removal of the IOFB, and intravitreal as well as systemic antibiotic therapy.[111]

Combat Ocular Injury

The main mechanism of open-globe injury in the military population is secondary to blast explosions, e.g., from improvised explosive devices (IEDs). Blast-associated injuries have been demonstrated to result in poor functional outcomes despite surgical intervention because of the surgical complexities and extensive blunt ocular concussive damage.[112–113]

Intraocular foreign bodies in combat-related ocular injury may have a reduced risk of endophthalmitis since they are usually propelled with high velocity from the explosion and may attain high temperatures, leading to self-sterilization. Predictably, visual outcomes were substantially associated with the depth of penetration of the IOFBs rather than with the timing of removal.[113]

Therapeutic Aspects

Surgical Approach

Throughout the literature on the pathophysiology of ocular trauma and related wound healing processes, vitrectomy is shown to be beneficial in that it removes the blood, vitreous scaffolds, and other stimuli for PVR (see Chapter 114, Surgery for ocular trauma, for a description of trauma principles and treatment techniques). Although progress in instrumentation and surgical techniques has provided dramatic improvements in anatomic repair, including repairing the laceration, reattaching the retina, and removing IOFBs after open-globe injury, a variety of late complications may develop, including new or recurrent retinal detachment and progressive proliferative membranes.[114–115] Therefore, pharmacologic approaches have been studied to modify the wound healing process by inhibiting the development of PVR.

Pharmacologic Approach

Corticosteroids reduce intraocular inflammation and adversely affect wound healing.[116] Machemer and Tano et al. suggested intravitreal application of steroids to suppress inflammation locally and to reduce proliferation of cells in patients with aggressive PVR.[117,118] Since soluble cortisone is washed out of the eye within approximately 24 hours after a single intravitreal injection, the use of crystalline triamcinolone has been described for the treatment of PVR. As part of its wide utilization for a number of other retinal diseases, intravitreal triamcinolone is now commonly used in PVR.[119] However, posttraumatic PVR is a long-term complication that may require drug release over months, and long-term injections of triamcinolone are associated with complications, such as elevated intraocular pressure, cataract formation, and endophthalmitis.[120]

Antiproliferative drugs have been considered for the treatment of PVR, and a wide spectrum of drugs such as 5-fluorouracil, daunomycin, cyclosporine, mitomycin C, hypericin, and Taxol have been tested in experimental models or human clinical trials to decrease uncontrolled mitogenic activity of the cells at the

vitreoretinal interface.[30,121–128] However, none of these drugs was entirely satisfactory because their inhibitory effects were transient, and most have a narrow therapeutic window.[127–128]

Agents that block growth factors and their signaling also have been considered to modify the wound healing process. Targeting PDGFR-α, HGF, and protein kinase C through approaches such as direct-binding blockers, receptor blockers, and gene therapy seem to have potential in experimental models but further tests in humans are required prior to clinical use.[129–132] The recent study demonstrated non-PDGF-mediated activation of PDGFR-α involves the development of PVR and the inhibition of this pathway via neutralization of VEGF-A using ranibizumab resulted in a protection for the development of PVR in rabbit models.[78] These findings suggest that inhibitors of PDGFR-α and the related pathway would be a potential target to prevent development of PVR, but it needs to be further studied for the treatment of PVR.

Various MMP inhibitors have been suggested to reduce the severity of PVR because cell-mediated collagen contraction and cell migration and invasion in PVR are mediated by MMPs, and these inhibitors may be adjunctive to other pharmacologic approaches.[95–97,100]

Although these therapies would likely be of no use in the treatment of an established membrane, their possible use in the prevention of intraocular proliferation in specific high-risk populations with ocular trauma is being explored. Recent advances in drug delivery to the vitreous and retina including injectable particles and implantable devices may be even more helpful for these pharmacologic approaches for the treatment of PVR.[133]

Conclusion

Severe open-globe injuries continue to be a major cause of ocular morbidity. The advent of vitrectomy with adjunct procedures in the 1970s has led to more successful anatomic results and a decreased rate of enucleation. Functional success, however, remains limited. In addition to the nature of the injury and the location and extent of the initial damage, the subsequent wound healing process contributes further anatomical and functional damage. Wound

healing in the eye occurs in a manner and with processes and cell cycles similar to that of other bodily tissues. Injury to the vitreous and breakdown of the blood–retinal barrier are major risk factors for the development of PVR with the expression of a variety of cytokines and growth factors that exert effects on the RPE, fibroblasts, and glial cells. These cells proliferate, migrate, change their pattern of gene expression, and develop preretinal membranes. The contractile properties of these cells may overcome the normal adhesion between the neurosensory retina and the RPE, causing a traction retinal detachment to occur.

Vitreous surgery and adjunct procedures remain the primary mode of therapy as these treatments eliminate stimulating factors and remove the scaffold for proliferation. Future progress may include pharmacologic approaches. There are theoretical reasons to favor strategies that emphasize the inhibition of cellular proliferation, inhibition of growth factors and cytokines, or inhibition of intracellular signaling pathways, or possibly the alteration of cellular function through gene therapy. For the future, these approaches need to be further studied, not only to moderate wound healing but to restore functional vision loss.

References

1. Haring RS, Canner JK, Haider AH, et al. Ocular injury in the United States: emergency department visits from 2006–2011. *Injury*. 2016;47(1):104–108.
2. Tielsch JM, Parver LM. Determinants of hospital charges and length of stay for ocular trauma. *Ophthalmology*. 1990;97:231–237.
3. Kuhn F, Morris R, Witherspoon D, et al. A standard classification of ocular trauma. *Ophthalmology*. 1996;103:240–243.
4. de Bustros S, Michels RG, Glaser BM. Evolving concepts in the management of posterior segment penetrating ocular injuries. *Retina*. 1990;10:S72–5.
5. Fuller DG, Hutton WL. Prediction of postoperative vision in eyes with severe trauma. *Retina*. 1990;10:S20–34.
6. Shock JP, Adams D. Long-term visual acuity results after

penetrating and perforating ocular injuries. *Am J Ophthalmol*. 1985;100:714–718.
7. Esmaeli B, Elner SG, Schork MA, et al. Visual outcome and ocular survival after penetrating trauma: a clinicopathologic study. *Ophthalmology*. 1995;102:393–400.
8. Pieramici DJ, MacCumber MW, Humayun MU, et al. Open-globe injury: update on types of injuries and visual results. *Ophthalmology*. 1996;103:1798–1803.
9. Soheilian M, Peyman GA, Wafapoor H, et al. Surgical management of traumatic retinal detachment with perfluorocarbon liquid. The Vitreon Study Group. *Int Ophthalmol*. 1996–1997;20:241–249.
10. Cherry PMH. Rupture of the globe. *Arch Ophthalmol*. 1972;88:498–507.
11. Moon C, Lee J, Sohn J, et al. The result of consecutive vitrectomy in penetrating ocular injury. *J Korean Ophthalmol Soc*. 1996;37:1937–1945.
12. Spiegel D, Nasemann J, Nawrocki J, et al. Severe ocular trauma managed with primary pars plana vitrectomy and silicone oil. *Retina*. 1997;17:275–285.
13. Fine BS, Tousimis AJ. The structure of the vitreous body and the suspensory ligaments of the lens. *Arch Ophthalmol*. 1961;65:95–110.
14. Glaser BM, Cardin A, Biscoe B. Proliferative vitreoretinopathy: the mechanism of development of vitreoretinal traction. *Ophthalmology*. 1987;94:327–332.
15. Hsu HT, Patterson R, Ryan SJ. Traumatic posterior vitreous detachment: scanning electron microscopy of an experimental model in the monkey eye. *Scan Electron Microsc*. 1984;(Pt 3):1361–1368.
16. Matsumoto B, Blanks JC, Ryan SJ. Topographic variations in the rabbit and primate internal limiting membrane. *Invest Ophthalmol Vis Sci*. 1984;25:71–82.
17. Winthrop SR, Cleary PE, Minckler DS, et al. Penetrating eye injuries: a histopathological review. *Br J Ophthalmol*. 1980;64:809–817.
18. Punnonen E. Pathological findings in eyes enucleated because of perforating injury. *Acta Ophthalmol (Copenh)*.

1990;68:265–269.
19. Cleary PE, Ryan SJ. Method of production and natural history of experimental posterior penetrating eye injury in the rhesus monkey. *Am J Ophthalmol*. 1979;88:212–220.
20. Cleary PE, Ryan SJ. Histology of wound, vitreous, and retina in experimental posterior penetrating eye injury in the rhesus monkey. *Am J Ophthalmol*. 1979;88:221–231.
21. Cleary PE, Ryan SJ. Experimental posterior penetrating eye injury in the rabbit. I. Method of production and natural history. *Br J Ophthalmol*. 1979;63:306–311.
22. Cleary PE, Ryan SJ. Experimental posterior penetrating eye injury in the rabbit. II. Histology of wound, vitreous, and retina. *Br J Ophthalmol*. 1979;63:312–321.
23. Cleary PE, Jarus G, Ryan SJ. Experimental posterior penetrating eye injury in the rhesus monkey: vitreous–lens admixture. *Br J Ophthalmol*. 1980;64:801–808.
24. Cleary PE, Minckler DS, Ryan SJ. Ultrastructure of traction retinal detachment in rhesus monkey eyes after a posterior penetrating ocular injury. *Am J Ophthalmol*. 1980;90:829–845.
25. Hsu HT, Ryan SJ. Natural history of penetrating ocular injury with retinal laceration in the monkey. *Graefes Arch Clin Exp Ophthalmol*. 1986;224:1–6.
26. Gregor Z, Ryan SJ. Combined posterior contusion and penetrating injury in the pig eye. II. Histological features. *Br J Ophthalmol*. 1982;66:799–804.
27. Gregor Z, Ryan SJ. Combined posterior contusion and penetrating injury in the pig eye: III. A controlled treatment trial of vitrectomy. *Br J Ophthalmol*. 1983;67:282–285.
28. Gregor Z, Ryan SJ. Combined posterior contusion and penetrating injury in the pig eye. I. A natural history study. *Br J Ophthalmol*. 1982;66:793–798.
29. Chen YS, Vinores SA, Campochiaro PA. *Simultaneous expression of vascular endothelial growth factor (VEGF) and its receptors in epiretinal membrane. ARVO abstract*. 1996:577.
30. Wiedemann P, Sorgente N, Ryan SJ. Proliferative vitreoretinopathy: the rabbit cell injection model for screening of antiproliferative drugs. *J Pharmacol Methods*. 1984;12:69–78.

31. Kruger EF, Nguyen QD, Ramos-Lopez M, et al. Proliferative vitreoretinopathy after trauma. *Int Ophthalmol Clin*. 2002;42:129–143.
32. Abe T, Durlu YK, Tamai M. The properties of retinal pigment epithelial cells in proliferative vitreoretinopathy compared with cultured retinal pigment epithelial cells. *Exp Eye Res*. 1996;63:201–210.
33. Campochiaro PA, Jerdan JA, Glaser BM, et al. Vitreous aspirates from patients with proliferative vitreoretinopathy stimulate retinal pigment epithelial cell migration. *Arch Ophthalmol*. 1985;103:1403–1405.
34. Hinton DR, He S, Jin ML, et al. Novel growth factors involved in the pathogenesis of proliferative vitreoretinopathy. *Eye*. 2002;16:422–428.
35. Limb GA, Earley O, Jones SE, et al. Expression of mRNA coding for TNF alpha, IL-1 beta and IL-6 by cells infiltrating retinal membranes. *Graefes Arch Clin Exp Ophthalmol*. 1994;232:646–651.
36. Campochiaro PA, Glaser BM. Platelet-derived growth factor is chemotactic for human retinal pigment epithelial cells. *Arch Ophthalmol*. 1985;103:576–579.
37. Irvin TT. The healing wound. Bucknall TE, Ellis H. *Wound healing for surgeons*. Bailliere Tindall: London; 1984:3–28.
38. Kampik A, Kenyon KR, Michels RG, et al. Epiretinal and vitreous membranes. Comparative study of 56 cases. *Arch Ophthalmol*. 1981;99:1445–1454.
39. Schwartz D, de Ia Cruz ZC, Green WR, et al. Proliferative vitreoretinopathy. Ultrastructural study of 20 retroretinal membranes removed by vitreous surgery. *Retina*. 1988;8:275–281.
40. Rentsch FJ. The ultrastructure of preretinal macular fibrosis. *Graefes Arch Clin Exp Ophthalmol*. 1977;203:321–337.
41. Topping TM, Abrams GW, Machemer R. Experimental double-perforating injury of the posterior segment in rabbit eyes: the natural history of intraocular proliferation. *Arch Ophthalmol*. 1979;97:735–742.
42. Leibovich SJ, Ross R. The role of macrophage in wound repair: a study with hydrocortisone and antimacrophage

serum. *Am J Pathol*. 1975;78:71–100.
43. Charteris DG, Hiscott P, Robey HL, et al. Inflammatory cells in proliferative vitreoretinopathy subretinal membranes. *Ophthalmology*. 1993;100:43–46.
44. Baudouin C, Fredi-Reygrobellet D, Brignole F, et al. Growth factors in vitreous and subretinal fluid cells from patients with proliferative vitreoretinopathy. *Ophthalmic Res*. 1993;25:52–59.
45. Charteris DG, Hiscott P, Grierson I, et al. Proliferative vitreoretinopathy: lymphocytes in epiretinal membranes. *Ophthalmology*. 1992;99:1364–1367.
46. Grisanti S, Heimann K, Wiedemann P. Immune response to specific molecules of the retina in proliferative vitreoretinal disorders. *Graefes Arch Clin Exp Ophthalmol*. 1994;232:302–307.
47. Baudouin C, Fredi-Reygrobeilet D, Gordon WC, et al. Immunohistologic study of epiretinal membranes in proliferative vitreoretinopathy. *Am J Ophthalmol*. 1990;110:593–598.
48. Grisanti S, Wiedemann P, Weller M, et al. The significance of complement in proliferative vitreoretinopathy. *Invest Ophthalmol Vis Sci*. 1991;32:2711–2717.
49. Anderson DH, Stern WH, Fisher SK, et al. The onset of pigment epithelial proliferation after retinal detachment. *Invest Ophthalmol Vis Sci*. 1981;21:10–16.
50. Grieson I, Heathcote L, Hiscott P, et al. Hepatocyte growth factor/scatter factor in the eye. *Prog Retin Eye Res*. 2000;19:779–802.
51. Briggs MC, Grierson I, Hiscott P, et al. Active scatter factor (HGF/SF) in proliferative vitreoretinal disease. *Invest Ophthalmol Vis Sci*. 2000;41:3085–3094.
52. Lashikari K, Rahimi N, Kazlauskas A. Hepatocyte growth factor receptor in human RPE cells: implications in proliferative vitreoretinopathy. *Invest Ophthalmol Vis Sci*. 1999;40:149–156.
53. Jin M, Chen Y, He S, et al. Hepatocyte growth factor and its role in the pathogenesis of retinal detachment. *Invest Ophthalmol Vis Sci*. 2004;45:323–329.

54. Liou GI, Matragoon S, Samuel S, et al. MAP kinase and beta-catenin signaling in HGF induced RPE migration. *Mol Vis*. 2002;8:483–493.
55. Robbins SG, Mixon RN, Wilson DJ, et al. Platelet-derived growth factor ligands and receptors immunolocalized in proliferative retinal diseases. *Invest Ophthalmol Vis Sci*. 1994;35:3649–3663.
56. Westra I, Robbins SG, Wilson DJ, et al. Time course of growth factor staining in a rabbit model of traumatic retinal detachment. *Graefes Arch Clin Exp Ophthalmol*. 1995;233:573–581.
57. Morino I, Hiscott P, McKechnie N, et al. Variation in epiretinal membrane components with clinical duration of the proliferative tissue. *Br J Ophthalmol*. 1990;74:393–399.
58. Jerdan JA, Pepose JS, Michels RG, et al. Proliferative vitreoretinopathy membranes: an immunohistochemical study. *Ophthalmology*. 1989;96:801–810.
59. Sethi CS, Lewis GP, Fisher SK, et al. Glial remodeling and neural plasticity in human retinal detachment with proliferative vitreoretinopathy. *Invest Ophthalmol Vis Sci*. 2005;46:329–342.
60. Charteris DG, Downie J, Aylward GW, et al. Intraretinal and periretinal pathology in anterior proliferative vitreoretinopathy. *Graefes Arch Clin Exp Ophthalmol*. 2007;245:93–100.
61. Gabbiani G. The cellular derivation and the life span of the myofibroblast. *Pathol Res Pract*. 1996;192:708–711.
62. Hui YN, Sorgente N, Ryan SJ. Ultrastructures of the glial epiretinal membrane induced by activated macrophages. *Clin Med J (Engl)*. 1992;105:577–581.
63. Hsu HT, Ryan SJ. Experimental retinal detachment in the rabbit: penetrating ocular injury with retinal laceration. *Retina*. 1986;6:66–69.
64. Santos RO, Murata T, Cui JZ, et al. *The role of tenon fibroblasts in the pathogenesis of proliferative vitreo-retinopathy due to perforating eye injury. ARVO abstract*. 1998:517.
65. Desmoulière A. Factors influencing myofibroblast differentiation during wound healing and fibrosis. *Cell Biol*

Int. 1995;19:471–476.
66. Jester JV, Petroll WM, Barry PA, et al. Expression of alpha-smooth muscle (alpha-SM) actin during corneal stromal wound healing. *Invest Ophthalmol Vis Sci*. 1995;36:809–819.
67. Sakamoto T, Hinton DR, Sakamoto H, et al. Collagen gel contraction induced by retinal pigment epithelial cells and choroidal fibroblasts involves the protein kinase C pathway. *Curr Eye Res*. 1994;13:451–459.
68. Limb GA, Alam A, Earley O, et al. Distribution of cytokine proteins within epiretinal membranes in proliferative vitreoretinopathy. *Curr Eye Res*. 1994;13:791–798.
69. Harvey AK, Roberge F, Hjelmeland LM. Chemotaxis of rat retinal glia to growth factors found in repairing wounds. *Invest Ophthalmol Vis Sci*. 1987;28:1092–1099.
70. Cui J, Lei H, Samad A, et al. PDGF receptors are activated in human epiretinal membranes. *Exp Eye Res*. 2009;88:438–444.
71. Carrington L, McLeod D, Boulton M. IL-10 and antibodies to TGF-β2 and PDGF inhibit RPE-mediated retinal contraction. *Invest Ophthalmol Vis Sci*. 2000;41:1210–1216.
72. Andrews A, Balciunaite E, Leong FL, et al. Platelet-derived growth factor plays a key role in proliferative vitreoretinopathy. *Invest Ophthalmol Vis Sci*. 1999;40:2683–2689.
73. Lei H, Rheaume MA, Cui J, et al. A novel function of p53: a gatekeeper of retinal detachment. *Am J Pathol*. 2012;181:866–874.
74. Lei H, Velez G, Hovland P, et al. Growth factors outside the PDGF family drive experimental PVR. *Invest Ophthalmol Vis Sci*. 2009;50:3394–3403.
75. Campochiaro PA, Hackett SF, Vinores SA, et al. Platelet-derived growth factor is an autocrine growth stimulator in retinal pigment epithelial cells. *J Cell Sci*. 1994;107:2459–2469.
76. Pennock S, Kazlauskas A. Vascular endothelial growth factor A competitively inhibits platelet-derived growth factor (PDGF)-dependent activation of PDGF receptor and subsequent signaling events and cellular responses. *Mol Cell Biol*. 2012;32:1955–1966.

77. Lei H, Velez G, Kazlauskas A. Pathological signaling via platelet-derived growth factor receptor α involves chronic activation of Akt and suppression of p53. *Mol Cell Biol*. 2011;31:1788–1799.
78. Pennock S, Kim D, Mukai S, et al. Ranibizumab is a potential prophylaxis for proliferative vitreoretinopathy, a nonangiogenic blinding disease. *Am J Pathol*. 2013;182:1659–1670.
79. Yokoyama K, Kimoto K, Itoh Y, et al. The PI3K/Akt pathway mediates the expression of type I collagen induced by TGF-β2 in human retinal pigment epithelial cells. *Graefes Arch Clin Exp Ophthalmol*. 2012;250:15–23.
80. Kimoto K, Nakatsuka K, Matsuo N, et al. p38 MAPK medicates the expression of type I collagen induced by TGF-beta 2 in human retinal pigment epithelial cells ARPE-19. *Invest Ophthalmol Vis Sci*. 2004;45:24317.
81. Kita T, Hata Y, Arita R, et al. Role of TGF-beta in proliferative vitreoretinal diseases and ROCK as a therapeutic target. *Proc Natl Acad Sci USA*. 2008;105:17504–17509.
82. He S, Chen Y, Khankan R, et al. Connective tissue growth factor as a mediator of intraocular fibrosis. *Invest Ophthalmol Vis Sci*. 2008;49:4078–4088.
83. Khankan R, Oliver N, He S, et al. Regulation of fibronectin-EDA through CTGF domain-specific interactions with TGF-beta2 and its receptor TGF-betaRII. *Invest Ophthalmol Vis Sci*. 2011;52:5068–5078.
84. Casaroli Marano RP, Vilaró S. The role of fibronectin, laminin, vitronectin and their receptors on cellular adhesion in proliferative vitreoretinopathy. *Invest Ophthalmol Vis Sci*. 1994;35:2791–2803.
85. Hunt RC, Pakalnis VA, Choudhury P, et al. Cytokines and serum cause alpha-2 beta-1 integrin-mediated contraction of collagen gels by cultured retinal pigment epithelial cells. *Invest Ophthalmol Vis Sci*. 1994;35:955–963.
86. Rojas J, Fernandez I, Pastor JC, et al. A strong genetic association between the tumor necrosis factor locus and proliferative vitreoretinopathy: the retina 4 project.

Ophthalmology. 2010;117:2417–2423.
87. Cui JZ, Chiu A, Maberley D, et al. Stage specificity of novel growth factor expression during development of proliferative vitreoretinopathy. *Eye*. 2007;21:200–208.
88. Jaffe GJ, Schwartz D, Han DP, et al. Risk factors for postvitrectomy fibrin formation. *Am J Ophthalmol*. 1990;109:661–667.
89. Johnson RN, Blankenship G. A prospective, randomized, clinical trial of heparin therapy for postoperative intraocular fibrin. *Ophthalmology*. 1988;95:312–317.
90. Vidaurri-Leal JS, Glaser BM. Effect of fibrin on morphologic characteristics of retinal pigment epithelial cells. *Arch Ophthalmol*. 1984;102:1376–1379.
91. Scheiffarth OF, Kampik A, Günther H, et al. Proteins of the extracellular matrix in vitreoretinal membranes. *Graefes Arch Clin Exp Ophthalmol*. 1988;226:357–361.
92. Tervo K, Latvala T, Suomalainen VP, et al. Cellular fibronectin and tenascin in experimental perforating scleral wounds with incarceration of the vitreous. *Graefes Arch Clin Exp Ophthalmol*. 1995;233:168–172.
93. Spee C, Soriano D, Kohen L, et al. *ECM production during the time course of PVR in a rabbit model. ARVO abstract*. 1994:3651.
94. Robbins SG, Brem RB, Wilson DJ, et al. Immunolocalization of integrins in proliferative retinal membranes. *Invest Ophthalmol Vis Sci*. 1994;35:3475–3485.
95. Hiscott P, Sheridan C, Magee RM, et al. Matrix and the retinal pigment epithelium in proliferative retinal disease. *Prog Retin Eye Res*. 1999;18:167–190.
96. Webster L, Chignell AH, Limb GA. Predominance of MMP-1 and MMP-2 in epiretinal and subretinal membranes of proliferative vitreoretinopathy. *Exp Eye Res*. 1999;68:91–98.
97. Kon CH, Occleston NL, Charteris D, et al. A prospective study of matrix metalloproteinases in proliferative vitreoretinopathy. *Invest Ophthalmol Vis Sci*. 1998;39:1524–1529.
98. Sheridan CM, Occleston NL, Hiscott P, et al. Matrix metalloproteinases: a role in the contraction of vitreo-retinal scar tissue. *Am J Pathol*. 2001;159:1555–1566.

99. Symeonidis C, Papakonstantinou E, Androudi S, et al. Interleukin-6 and the matrix metalloproteinase response in the vitreous during proliferative vitreoretinopathy. *Cytokine*. 2011;54:212–217.
100. Ozerdem U, Mach-Hofacre B, Keefe K, et al. The effect of prinomastat (AG3340), a synthetic inhibitor of matrix metalloproteinases, on posttraumatic proliferative vitreoretinopathy. *Ophthalmic Res*. 2001;33:20–23.
101. Ahmed Y, Schimel AM, Pathengay A, et al. Endophthalmitis following open-globe injuries: endophthalmitis following open-globe injuries. *Eye*. 2012;26:212–217.
102. Alfaro DV, Roth D, Liggett PE. Posttraumatic endophthalmitis: causative organisms, treatment, and prevention. *Retina*. 1994;14:206–211.
103. Andreoli CM, Andreoli MT, Kloek CE, et al. Low rate of endophthalmitis in a large series of open globe injuries. *Am J Ophthalmol*. 2009;147 [601–8.e2].
104. Boldt HC, Pulido JS, Blodi CF, et al. Rural endophthalmitis. *Ophthalmology*. 1989;96:1722–1726.
105. Thompson JT, Parver LM, Enger CL, et al. Infectious endophthalmitis after penetrating injuries with retained intraocular foreign bodies. National Eye Trauma System. *Ophthalmology*. 1993;100:1468–1474.
106. Jonas JB, Knorr HLJ, Budde WM. Prognostic factors in ocular injuries caused by intraocular or retrobulbar foreign bodies. *Ophthalmology*. 2000;107:823–828.
107. Wani VB, Al-Ajmi M, Thalib L, et al. Vitrectomy for posterior segment intraocular foreign bodies: visual results and prognostic factors. *Retina*. 2003;23:654–660.
108. Parrish CM, O'Day DM. Traumatic endophthalmitis. *Int Ophthalmol Clin*. 1987;27:112–119.
109. Tawara A. Transformation and cytotoxicity of iron in siderosis bulbi. *Invest Ophthalmol Vis Sci*. 1986;27:226–236.
110. Mester V, Kuhn F. Intraocular foreign bodies. *Ophthalmol Clin North Am*. 2002;15:235–242.
111. Jonas J, Budde WM. Early versus late removal of retained intraocular foreign bodies. *Retina*. 1999;19:193–197.

112. Bajaire B, Oudovitchenko E, Morales E. Vitreoretinal surgery of the posterior segment for explosive trauma in terrorist warfare. *Graefes Arch Clin Exp Ophthalmol*. 2006;244:991–995.
113. Colyer MH, Chun DW, Bowker KS, et al. Perforating globe injuries during operation Iraqi Freedom. *Ophthalmology*. 2008;115:2087–2093.
114. Cox MS, Freeman HM. Retinal detachment due to ocular penetration. I. Clinical characteristics and surgical results. *Arch Ophthalmol*. 1978;96:1354–1361.
115. Chiquet C, Gain P, Zech JC, et al. Risk factors for secondary retinal detachment after extraction of intraocular foreign bodies. *Can J Ophthalmol*. 2002;37:168–176.
116. Pessa ME, Bland KI, Copelend EM III. Growth factors and determinants of wound repair. *J Surg Res*. 1987;42:207–217.
117. Machemer R. Proliferative vitreoretinopathy (PVR): a personal account of its pathogenesis and treatment. Proctor lecture. *Invest Ophthalmol Vis Sci*. 1988;29:1771–1783.
118. Tano Y, Sugita G, Abrams G, et al. Inhibition of intraocular proliferation with intravitreal corticosteroids. *Am J Ophthalmol*. 1980;89:131–136.
119. Jonas JB, Hayler JK, Panda-Jonas S. Intravitreal injection of crystalline cortisone as adjunctive treatment of proliferative vitreoretinopathy. *Br J Ophthalmol*. 2000;84:1064–1067.
120. Ozkiriş A, Erkiliç K. Complications of intravitreal injection of triamcinolone acetonide. *Can J Ophthalmol*. 2005;40:63–68.
121. van Bockxmeer FM, Martin CE, Thompson DE, et al. Taxol for the treatment of proliferative vitreoretinopathy. *Invest Ophthalmol Vis Sci*. 1985;26:1140–1147.
122. Harris MS, Sakamoto T, Kimura H, et al. Hypericin inhibits cell growth and induces apoptosis in retinal pigment epithelial cells: possible involvement of protein kinase C. *Curr Eye Res*. 1996;15:255–262.
123. Murphy TL, Sakamoto T, Hinton DR, et al. Migration of retinal pigment epithelium cells in vitro is regulated by protein kinase C. *Exp Eye Res*. 1995;60:683–695.
124. Tahara YR, Sakamoto TR, Oshima YR, et al. The antidepressant hypericin inhibits progression of

experimental proliferative vitreoretinopathy. *Curr Eye Res*. 1999;19:323–329.
125. Wiedemann P, Hilgers RD, Bauer P, et al. Adjunctive daunorubicin in the treatment of proliferative vitreoretinopathy: results of a multicenter clinical trial. Daunomycin Study Group. *Am J Ophthalmol*. 1998;126:550–559.
126. Asaria RH, Kon CH, Bunce C, et al. Adjuvant 5-fluorouracil and heparin prevents proliferative vitreoretinopathy: results from a randomized, double-blind, controlled clinical trial. *Ophthalmology*. 2001;108:1179–1183.
127. Steinhorst UH, Hatchell DL, Chen EP, et al. Ocular toxicity of daunomycin: effects of subdivided doses on the rabbit retina after vitreous gas compression. *Graefes Arch Clin Exp Ophthalmol*. 1993;231:591–594.
128. Penha FM, Rodrigues EB, Maia M, et al. Retinal and ocular toxicity in ocular application of drugs and chemicals – part II: retinal toxicity of current and new drugs. *Ophthalmic Res*. 2010;44:205–224.
129. Ikuno Y, Leong FL, Kazlauskas A. Attenuation of experimental proliferative vitreoretinopathy by inhibiting the platelet-derived growth factor receptor. *Invest Ophthalmol Vis Sci*. 2000;41:3107–3116.
130. Ikuno Y, Kazlauskas A. An in vivo gene therapy approach for experimental proliferative vitreoretinopathy using the truncated platelet-derived growth factor alpha receptor. *Invest Ophthalmol Vis Sci*. 2002;43:2406–2411.
131. Date K, Matsumoto K, Shimura H, et al. HGF/NK4 is a specific antagonist for pleiotrophic actions of hepatocyte growth factor. *FEBS Lett*. 1997;420:1–6.
132. Hinton DR, He S, Graf K, et al. Mitogen-activated protein kinase activation mediates PDGF-directed migration of RPE cells. *Exp Cell Res*. 1998;239:11–15.
133. Guidetti B, Azéma J, Malet-Martino M, et al. Delivery systems for the treatment of proliferative vitreoretinopathy: materials, devices and colloidal carriers. *Curr Drug Deliv*. 2008;5:7–19.

SECTION 2

Retinal Reattachment: General Surgical Principles and Techniques

OUTLINE

103

The Biomechanics of Scleral Buckles in the Treatment of Retinal Detachment

John T. Thompson

Introduction

The use of scleral buckles in conjunction with chorioretinal adhesions around retinal breaks forms the basis of therapy for some uncomplicated rhegmatogenous retinal detachments. Other techniques for retinal reattachment, such as the use of vitrectomy and a gas bubble or pneumatic retinopexy, are described in other chapters. Understanding the biomechanics of scleral buckles helps the surgeon to choose when their use is most appropriate for retinal

detachment repair. This chapter examines the physical effects of scleral buckles on the eye and the mechanism of action of scleral buckles in promoting retinal reattachment.

Effects of Scleral Buckles on the Geometry of the Eye

The scleral buckle alters the shape of the eye, depending primarily on the type of buckling material used, the location and tension of the scleral sutures, and the circumferential tightening of an encircling buckle. The changes in the geometry of the eye may have a number of secondary effects that may be clinically important to the patient. These include changes in the axial length of the eye, induced spherical equivalent and astigmatic refractive errors, changes in the volume of the eye, and altered compliance (ocular rigidity) after scleral buckle placement. Some of these effects are also beneficial in helping to reattach the retina.

Axial Length Changes After Scleral Buckles

The axial length of the eye may change after placement of a scleral buckle. Radial soft silicone sponges appear to induce little change in the axial length of the eye. Segmental scleral buckles may cause a hyperopic shift while encircling scleral buckles may produce increases or decreases in axial length, depending on the scleral buckle material, the location of the buckle, and the height of the buckle.[1,2] Hard silicone encircling buckles most commonly increase the axial length of the eye,[3–5] although some eyes show no apparent change in axial length after placement of an encircling buckle.[6,7] Occasionally, high encircling silicone buckles may decrease the axial length of the eye.[4,8]

The changes in axial length induced by circumferential scleral buckles can be understood by analyzing the geometry of the eye with an encircling buckle in place. If a circumferential buckle is tightened around the equator of the eye, the first effect is to decrease the circumference of the eye in coronal cross-section, causing the eye to assume an elliptical shape in horizontal cross-

section. The normally spherical human eye acquires the shape of a prolate spheroid after placement of a broad circumferential buckle (Fig. 103.1). The eye is still circular in coronal cross-section, because the encircling buckle constricts the equator of the eye into a circle of smaller circumference. The eye becomes more elliptical in sagittal and horizontal cross-section. A decrease in the circumference of the eye caused by indentation from a scleral buckle in the coronal plane is accompanied by an increase in the anteroposterior dimension of the eye (Fig. 103.1) in the sagittal and horizontal planes as the eye becomes elongated by the equatorial constriction from the encircling scleral buckle. This change from a sphere to a prolate spheroid occurs primarily because of the relative inelasticity of the sclera at physiologic intraocular pressures in the fluid-filled eye. If the circumferential buckle is tightened high enough, the eye will assume the shape of a dumbbell. The anteroposterior axial length of the eye decreases at very high circumferential buckle heights because part of the circumference of the sclera in the horizontal and sagittal cross-sections is used to create the dumbbell-shaped indentation in the sclera (Fig. 103.1).

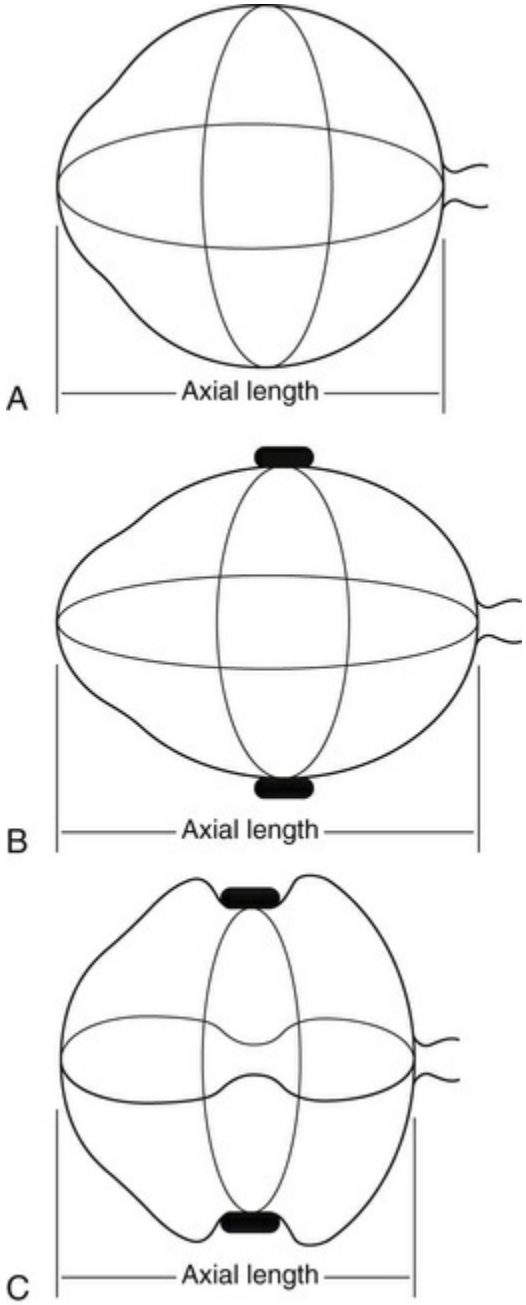

FIG. 103.1 (A) The normal spherical shape of the eye. (B) The spherical eye acquires the shape of a prolate spheroid after placement of a moderately high circumferential buckle. Horizontal and sagittal cross-sections of an eye with a broad circumferential buckle at moderate buckle heights show an ellipse. Coronal cross-section of an eye with a circumferential buckle shows a circle. The anteroposterior axial length of the eye increases at moderate buckle heights. (C) The eye acquires a dumbbell shape at very high circumferential buckle heights. Coronal cross-section of an eye with a very high circumferential buckle still shows a circle, but the sagittal and horizontal cross-sections show a

dumbbell shape. The axial length of the eye decreases at very high buckle heights.

Placement of two mattress sutures per quadrant to invaginate the sclera beneath a circumferential buckle has additional effects on the geometry and axial length of the eye. Indentation of the sclera by tightening mattress sutures around a circumferential hard silicone exoplant causes a decrease in the axial length of the eye if there is no concomitant circumferential shortening of the encircling buckle.[4] The mattress sutures pull together the anterior and posterior sclera where the suture bites are anchored, decreasing the axial length of the eye. As the mattress sutures are tightened, the sclera is indented by the circumferential buckle beneath the mattress sutures, causing the eye to acquire a dumbbell shape in horizontal and sagittal cross-sections.

These two effects, circumferential shortening and scleral invagination by mattress sutures, must be considered in understanding the geometry of the eye after placement of an encircling scleral buckle. The first effect, circumferential shortening, increases the axial length by changing the shape of the eye from a sphere to a prolate spheroid with mild to moderate circumferential tightening of an encircling buckle. The second effect, invagination of the sclera around a broad encircling element with mattress sutures, contributes to a decrease in the axial length of the eye.

The increases in axial length from circumferential shortening of the eye predominate over decreases in axial length from scleral invagination at low to moderate buckle heights, producing a shift toward myopia. The decreases in axial length from scleral invagination tend to predominate over increases in axial length at very high buckle heights. Some eyes with moderate to high circumferential buckles have no net change in axial length when the circumferential shortening and scleral invagination precisely balance. It would be desirable to try to adjust circumferential buckle to minimize axial length changes, but this is difficult to achieve, since other factors, such as support of the retinal breaks and relief of vitreoretinal traction, are more important surgical goals.

A geometric model to explain the effects of circumferential scleral buckles on the axial length and to predict these axial length changes was developed to improve the predictability of these axial length

changes. The geometric model of the effects of scleral buckles on axial length is based on the following assumptions: First, the overall contour of the eye with a scleral buckle is assumed to be an ellipse. Second, the circumference of the eye is constant, because the buckle does not stretch or shrink the sclera substantially. Fig. 103.2 gives a gross estimate of the circumference of the indented eye wall (which equals π times axial length) after a scleral buckle, based on the preoperative perimeter of the eye and the amount of indentation of the eye wall by the scleral buckle at the equator. The axial length of the eye can then be calculated following placement of the scleral buckle, using the formula to solve for the axial length to predict the effect of the scleral buckle on refraction.

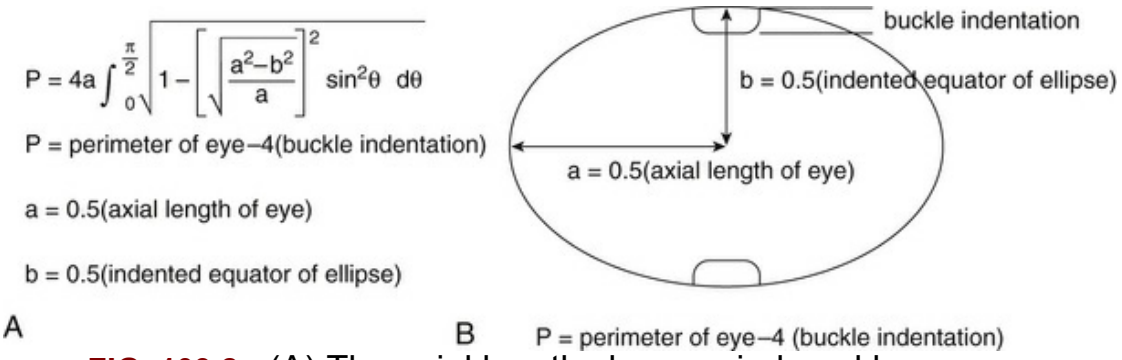

FIG. 103.2 (A) The axial length changes induced by a circumferential scleral buckle may be estimated grossly by this formula by solving the equation for 'a' if the original circumference of the eye, the amount of buckle indentation, and equatorial shortening of the eye are known. (B) Geometric model relating circumferential buckle shortening, scleral indentation, and axial length.

Refractive Errors Caused by Scleral Buckles

Three primary types of refractive error can be induced by scleral buckles used for retinal reattachment. The first type is an astigmatic error caused by changes in the corneal curvature; the second type is a change in the spherical equivalent induced by changes in axial length, anterior chamber depth, or position of the crystalline lens. The third are higher-order aberrations that were found to be greater

when segmental scleral buckles are used rather than circumferential buckles.[9] The higher-order aberrations persist at least 3 months but may improve over time.

Astigmatic Errors

Regular and irregular corneal astigmatism are most likely to result from placement of segmental or radial exoplants.[8,10–13] Some astigmatic errors may be persistent, requiring correction,[1] although many astigmatic errors improve within several months following surgery.[14] Corneal astigmatism usually results when a high, anterior radial buckle is placed. The indentation of a radial buckle in the anterior sclera can be transmitted to the cornea because of the inelasticity of both the sclera and the cornea. If the eye were highly elastic like a balloon, indentation of the eye from a radial buckle would be present only directly under the buckle. The radial buckle would have no effect on the surrounding sclera. Because the sclera is less elastic than the rubber skin of a balloon, the radial buckle causes some indentation in the surrounding sclera beyond the extent of the buckle itself. The greatest astigmatic errors occur in eyes in which a segmental buckle spans one to two quadrants.[15] Encircling circumferential buckles of uniform width rarely produce substantial astigmatism.

Spherical Equivalent Errors

Changes in refraction from scleral buckles caused by changes in axial length and lens position are more common than astigmatic errors. Most eyes with encircling buckles have a small shift toward myopia; this is associated with an increase in axial length.[5,8,16] Shallowing of the anterior chamber associated with displacement of the lens anteriorly in phakic eyes with an encircling buckle may also contribute to a shift toward myopia.[8] Anterior displacement of the lens becomes less pronounced several months after retinal reattachment in most eyes.[16] The buckle height decreases substantially in eyes with radial buckles over a period of months, while buckle height does not decrease as much in eyes with circumferential buckles.[17] Some eyes with high circumferential scleral exoplants have a shift in refraction toward hyperopia.[7] The changes in axial length and refractive error with different scleral

buckles are reported in the literature and are summarized in Table 103.1. When scleral buckles are placed in children, the scleral buckle may retard growth-related increases in the axial length of the eye, causing the eye to develop less myopia than the fellow eye.[21]

TABLE 103.1

Changes in Axial Length and Refractive Error with Different Scleral Buckles

Authors	Buckle Type	Axial Length (mm)	Refraction (diopter)
Jacklin[18]	Narrow band	−1.3	
Rubin[8]	2-mm band, low buckle	+0.44	−1.25
	2-mm band, moderate buckle	+1.09	−1.89
	2-mm band, high buckle	−0.35	+0.47
Burton et al.[19]	Implant + explant	No net change	
Larsen and Syrdalen[5]	2-mm band	+0.98	
Kiernan et al.[7]	Half of a 7.5-mm sponge	No net change	No net change
Smiddy et al.[20]	Band ± tire	+0.99	−2.75

Change in Refractive Error Over Time

The change in refractive error induced by the scleral buckle also tends to normalize after several months due to two main factors. (1) In eyes with silicone bands such as #40 and #240-style, there is a stress relaxation of the band over time.[22] This can be understood by taking a rubber band and stretching it to near breaking. The amount of force needed to stretch the rubber band to the same length decreases with successive stretching cycles. This explains why the buckling effect from an encircling band tends to decrease over time. (2) In eyes with silicone sponges or tires held in place by sutures, the scleral invagination caused by the suture also decreases over time as the suture erodes the sclera where the suture enters and exits the scleral tunnel. This also decreases the buckling effect and refractive changes months to years following surgery.

Scleral Chord Versus Scleral Arc Length

The curvature of the spherical globe must be considered when distances on the surface of the globe are measured. Calipers are commonly used to measure distances for placement of scleral sutures and to measure the shortest line between two points on the

spherical globe, which is called the scleral chord length (Fig. 103.3). The distance measured along the curved surface of the globe between two points is the scleral arc length. The scleral chord length measured by the calipers is always shorter than the scleral arc length.[23] The scleral arc length can be calculated from the scleral chord length, and vice versa, using the formula in Fig. 103.4. Scleral arc length and scleral chord length are similar when the chord length is a small percentage of the radius of the globe. A caliper setting (chord length) of 8 mm corresponds to a scleral arc length of 8.16 mm, a 2% error; a caliper setting of 13 mm corresponds to a scleral arc length of 13.74 mm, a 5.7% error. The discrepancy between scleral chord length and scleral arc length increases nonlinearly whenever calipers are used to measure large distances on the globe.

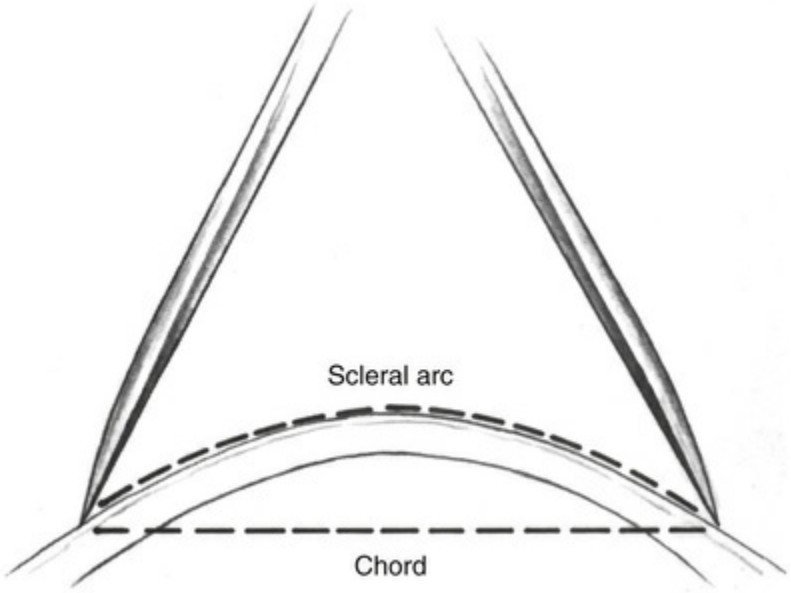

FIG. 103.3 Calipers are used to measure distances for placement of sutures around scleral buckles and to measure the shortest distance between two points on the sclera (scleral chord length). The distance between two points on the surface of the sclera (scleral arc length) is always longer than the scleral chord length.

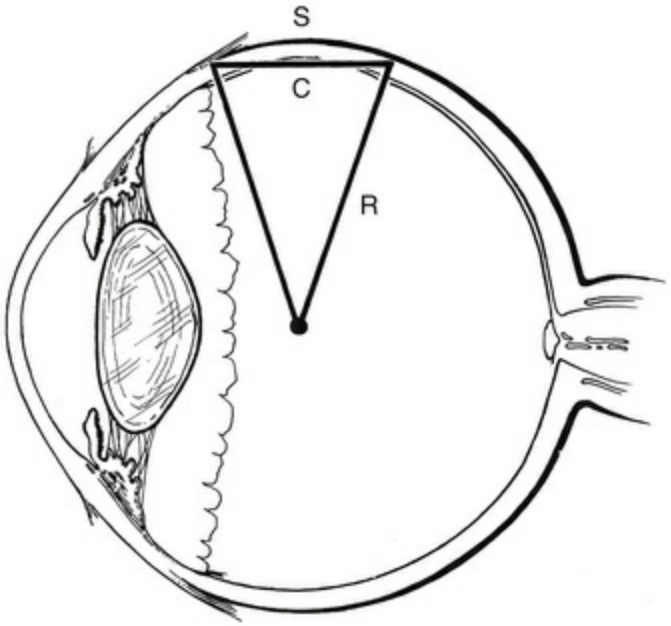

FIG. 103.4 The scleral arc length (*S*) can be calculated from the scleral chord length (*C*) and vice versa. The inverse sin in the formula must be calculated in degrees to obtain the scleral arc length. The difference between the scleral arc length and the scleral chord length increases nonlinearly with larger distances measured by the calipers. *R*, radius of eye.

Effects on the Internal Geometry of the Eye

It is the buckling effect created by an episcleral buckle that is desirable in closing retinal breaks and relieving vitreoretinal traction. Intrascleral buckles were used in the early days of retinal detachment repair but are not currently used due to the difficulty in creating large, partial-thickness scleral flaps. The geometry of the episcleral scleral buckle and the technique of scleral buckle and suture placement determine the shape and height of the indentation. It may be desirable to create a high buckling effect in the treatment of certain retinal detachments, and suture placement is important in these eyes. Deep suture bites of at least 4–5 mm long are needed to allow maximum tension to be placed on the suture and transmitted to the scleral buckle. Superficial or short scleral suture bites tend to tear through the sclera and decrease the

effective buckle height. The tearing strength of 4–0 silk sutures through the sclera measured by a tensile strength tester is significantly greater for deep suture bites (50–90% depth) than for superficial suture bites (20–30% depth) (Thompson, unpublished data).

The major variables that determine the internal geometry of indentation induced by the scleral buckle exoplant include (1) shape of the buckle; (2) composition of the buckle (silicone sponge versus hard silicone); (3) suture placement with respect to the dimensions of the buckle; (4) suture tension; (5) distribution of tension from the suture to the buckle; and (6) intraocular pressure. An analysis of scleral indentation from a 5-mm radial silicone sponge showed that the following factors decreased indentation: (1) placement of the suture bites too close or too far apart; (2) high intraocular pressure; (3) short suture bites in the sclera; (4) loose sutures; and (5) use of a half-thickness sponge compared with a full-thickness sponge. Factors that increased scleral indentation included (1) low intraocular pressure and (2) tight sutures.[24,25]

The orientation of the scleral buckle also helps to determine the topography of the indentation in the sclera. Radial buckles appear to offer advantages in the support of a solitary horseshoe-shaped retinal tear.[26–28] Moderate to high circumferential encircling scleral buckles cause radial folding of the retina. This radial folding occurs because the encircling buckle forces a reduction in the normal circumference of the eye in the equatorial meridian. The sclera and retina are unable to shrink to the new, smaller circumference, so the "excess" retina, choroid, and sclera are thrown into radial folds to conform to the smaller circumference of the eye induced by the encircling buckle (Fig. 103.5). The circumferential shortening of the eye beneath an encircling buckle is the basis of the fishmouth phenomenon (Fig. 103.6).[29,30] Wedge-shaped buckles and radial scleral buckles minimize the risk of the fishmouth phenomenon because they cause less circumferential shortening over the retinal tear than do encircling scleral buckles.

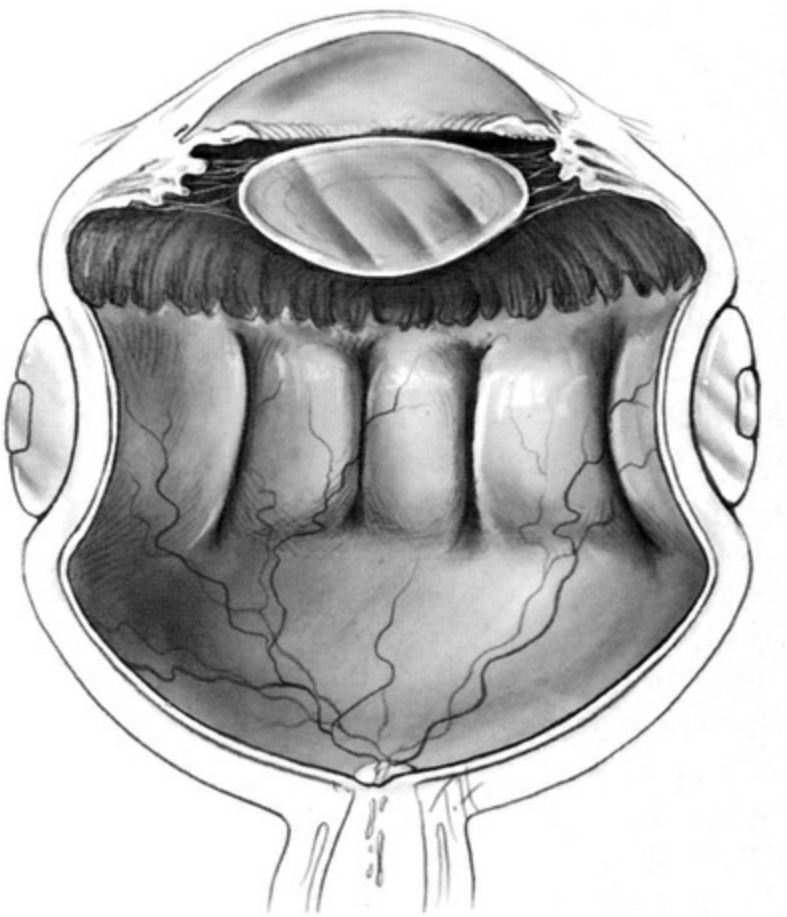

FIG. 103.5 Radial retinal folds on a broad encircling buckle induced by shortening the circumference of the eye. The sclera, choroid, and retina are unable to shrink to the smaller globe circumference beneath the scleral buckle indentation, so the “excess” retina on the buckle is thrown into folds.

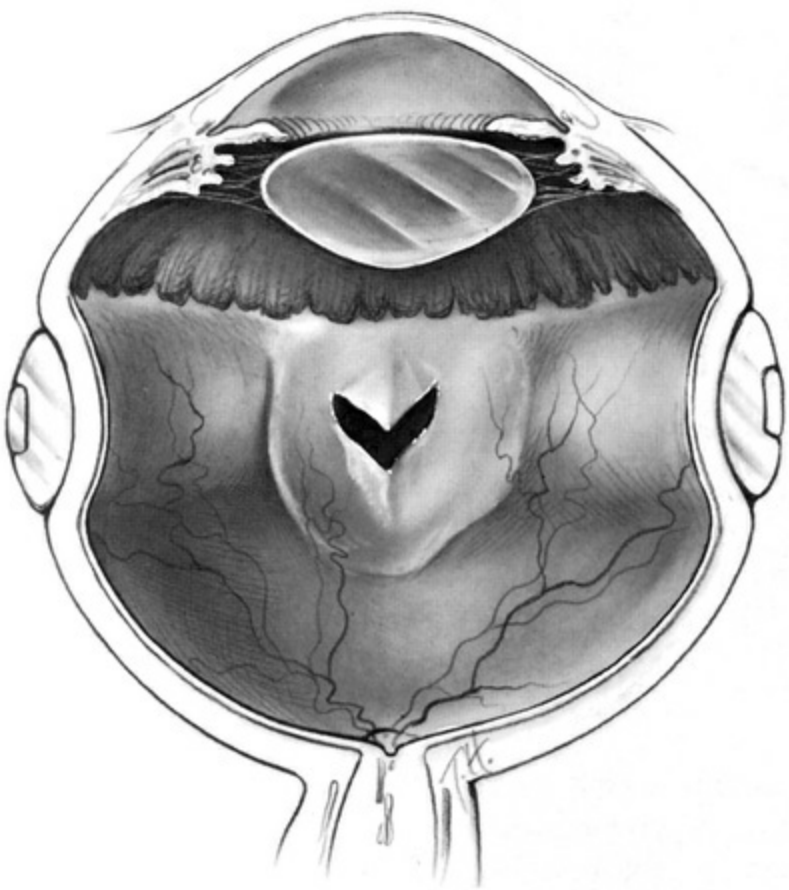

FIG. 103.6 The fishmouth phenomenon results when a radial fold bisects a retinal tear. The radial fold tends to keep the tear from settling on the buckle and may lead to persisting retinal detachment. The fishmouth phenomenon is most commonly produced by circumferential shortening of the globe from an encircling buckle, causing a radial fold to pass through a horseshoe-shaped retinal tear. Minimizing the circumferential shortening of the eye with a radial or wedge-shaped buckle decreases the likelihood of the fishmouth phenomenon.

Circumferential encircling buckles are necessary in some eyes because of multiple retinal breaks, circumferential vitreoretinal traction, or circumferential shortening of the retina caused by epiretinal membranes. Anterior circumferential vitreoretinal traction caused by cell-mediated contraction of the vitreous base or peripheral epiretinal membranes associated with funnel-shaped retinal detachments in eyes with proliferative vitreoretinopathy decrease the effective circumference of the peripheral retina. A broad circumferential encircling buckle is preferable in this

situation because it reduces the circumference of the eye wall, allowing reapposition of the retina against the retinal pigment epithelium (RPE). This can allow the surgeon to avoid having to perform circumferential retinectomy to remove the foreshortened retina. The risks and benefits of radial or encircling circumferential buckles must be evaluated in each circumstance so as to choose the optimal geometry of the scleral buckle for the particular retinal tear and retinal detachment configuration.

Volume Changes in the Eye After Scleral Buckles

Indentation of the eye wall by a scleral buckle displaces fluid from the vitreous cavity, causing a reduction in the volume of the vitreous cavity. This occurs because a sphere contains the largest volume of fluid with the least surface area. The amount of fluid displaced depends on the buckle type and configuration. The amount of volume displacement is small for most buckles but can be substantial for broader encircling buckles. Estimation of the intraocular volume of an eye with a scleral buckle is important in several circumstances: (1) estimation of how much fluid must be withdrawn from the vitreous cavity or drained from the subretinal space to permit placement of a specific scleral buckle; (2) injection of pharmacologic agents such as antibiotics or antimetabolites into the vitreous, when therapeutic and toxic concentrations must be considered; and (3) injection of expansile gases into the vitreous. The volume displacement of a scleral buckle can be predicted as a function of the following variables: (1) the axial length of the eye = 2× internal radius; (2) the buckle width measured anterior and/or posterior to the equator; (3) the buckle circumference; and (4) the buckle height. The formula for determining volume displacement by a scleral buckle is given in Fig. 103.7. A 5-mm radial silicone sponge displaces only about 0.2 mL, or 5%, of the vitreous cavity volume.[31] This is why placement of a radial sponge in a nondrainage procedure only occasionally elevates the intraocular pressure substantially. A 2.5-mm-wide silicone encircling band (#240 style) displaces about 0.5 mL, or 12%, of the vitreous cavity volume.[31] A 7-mm-wide hard silicone encircling buckle (#287 style)

displaces from 1.3 mL (33%) to 1.7 mL (43%) of the vitreous cavity volume of a phakic eye, depending on the buckle geometry and height.[31] The decrease in vitreous cavity volume increases with increasing buckle width and height for circumferential buckles, as shown in Table 103.2. Magnetic resonance imaging has been used to confirm the decreased volume of the eye induced by scleral buckles. An encircling band in this study reduced the vitreous cavity volume by an average of 1.7 mL.[32]

$$V = c \frac{\pi}{360} (2\,rh\text{-}h^2)\,(w1 + w2)$$

V - Volume displaced (mm^3)
c - Circumference of buckle (degrees)
r - Internal radius of eye (mm)
h - Height of buckle (mm)
w1 - Width of buckle anterior to equator (mm)
w2 - Width of buckle posterior to equator (mm)

FIG. 103.7 Indentation of the sclera by a scleral buckle displaces fluid from the vitreous cavity. The ocular volume displacement from a scleral buckle is a function of the circumference of the buckle, the radius of the eye, the height of the buckle, and the width of the buckle (1 mL = 1000 mm^3).

TABLE 103.2

Estimated Vitreous Cavity Volume Displacement of Scleral Buckles

Scleral Buckle	Vitreous Cavity Volume Displacement (mL)
Half of 5-mm sponge	0.09–0.15
3×5 mm sponge	0.11–0.20
5-mm round sponge	0.14–0.22
#240 style (circumferential)	0.47–0.48
#276 style (circumferential)	1.08–1.13
#287 style (circumferential)	1.32–1.57
#280 style (circumferential)	1.82–1.88

Data from Thompson JT, Michels RG. Volume displacement of scleral buckle. Arch Ophthalmol 1985;103:1822–4.

Scleral Buckles, Ocular Rigidity, and Corneal

Hysteresis

Placement of a scleral buckle changes the normal ocular rigidity. Ocular rigidity is the change in intraocular pressure for a given change in intraocular volume and is a measure of the elasticity of the eye. Intraocular pressure normally increases rapidly as microliter volumes are injected into the eye. The increase in intraocular pressure (ocular rigidity) is decreased in eyes with an encircling scleral buckle because the volume of the vitreous cavity was decreased with placement of a scleral buckle.[33,34] This decrease in volume is related to changes in the shape of the eye caused by the scleral buckle.[31] As the intraocular pressure is increased by injection of saline solution or gas into the eye, the eye becomes less elliptical and more spherical as the sutures holding the buckle are stressed or the encircling band is stretched. The net effect is to decrease the buckling effect and to increase the intraocular volume such that the intraocular pressure does not rise as rapidly as in the normal eye. This effect can be better understood by considering an eye with an encircling buckle and no invagination by scleral sutures. If water is injected into the eye, the encircling buckle will stretch as the eye assumes a more spherical shape. Once the buckle has stretched so that the eye returns to its original spherical shape (before placement of the buckle), the intraocular pressure will increase rapidly. The changes in ocular rigidity have several important clinical ramifications. First, methods of measuring intraocular pressure that depend on a standard ocular rigidity, such as the indentation tonometry (Schiøtz), electronic indentation tonometry (Tonopen®), pneumotonometer, and ocular response analyzer (ORA), are less accurate in eyes with scleral buckles. The ORA tends to underestimate true IOP.[35] Second, an injection of fluid or gas into an eye with a scleral buckle will cause less elevation of intraocular pressure than injection of the same volume into a normal eye, if all other factors are equal. Placement of an intraocular gas bubble into the vitreous also itself reduces ocular rigidity because the gas in the vitreous cavity is more compressible than the vitreous fluid it replaces. This has been confirmed in a study showing that eyes with scleral buckles and small intraocular gas bubbles have less increase in intraocular pressure with air travel than eyes without scleral buckles.[36] Eyes with reduced ocular

rigidity from an intraocular gas bubble and an encircling scleral buckle require even larger volumes of fluid aspiration to reduce the intraocular pressure than normal eyes with elevated intraocular pressure.[37]

Corneal hysteresis is a property that measures the elasticity of the cornea by comparing the difference in pressure at which the cornea is depressed by an air jet compared to the pressure at which it bends back to its normal shape. The presence of a scleral buckle in eyes with vitrectomy increases corneal hysteresis compared to eyes without a scleral buckle, and this had secondary effects on intraocular pressure measurements.[35]

Scleral Buckles and Ocular Blood Flow

Encircling scleral buckles also change ocular blood flow.[38] This does not create clinically recognizable problems in most patients undergoing scleral buckle for retinal reattachment but can create ocular ischemia or peripheral visual field defects.[39] As a result, a few surgeons advocate cutting the circumferential band routinely after the retina has reattached to improve ocular blood flow.[40]

Effects of Scleral Buckles on the Rpe and Retina

A number of forces are associated with the production of retinal tears and detachments, and there are also forces that promote attachment of the retina. Scleral buckles act to alter the former and enhance the latter.

An Overview of Forces Acting on the Retina

Vitreoretinal traction forces play an important role in the pathogenesis of retinal tears, rhegmatogenous retinal detachments, and traction retinal detachments. Forces that act on the retina have both magnitude and direction and are best represented by vectors. A force vector is represented graphically by an arrow with a length and a direction. The length of the vector is proportional to the magnitude of the force, and the direction indicates the direction

along which the force acts (Fig. 103.8). Simple arithmetical operations can be performed on vectors to determine the net force produced by two forces acting on the same point. The simplest way to add vectors is to draw the vectors so that the arrowhead of the first vector connects to the tail of the second vector. A new vector, which is the sum of the two vectors, is drawn from the tail of the first vector to the head of the second vector (Fig. 103.8).

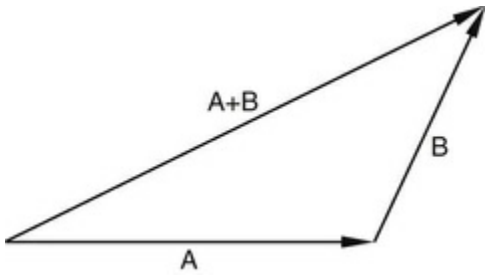

FIG. 103.8 Vitreoretinal traction forces have both magnitude and direction. These forces can be represented by vectors. Simple arithmetical operations, such as addition of vectors *A* and *B*, can be performed by drawing the resultant vector *A* + *B* from the tail of *A* to the arrowhead of *B*.

A second important concept is the equilibrium of vector forces. If two vector forces of equal magnitude simultaneously act in opposite directions on the same point, there is no displacement of the object at that point. A simple example of equilibrium involving opposing vector forces is found in localized vitreous traction on the retina at the edge of a posterior vitreous detachment (PVD). If the force of vitreous traction on the retina at the edge of a PVD is counterbalanced by retinal adherence to the eye wall, no tear will develop. If vitreous traction on the retina exceeds photoreceptor adherence to the RPE and retinal tensile strength, a retinal tear will develop to reestablish equilibrium (Fig. 103.9). Vector algebra can be used to understand how various forces acting on the retina lead to retinal tears, traction retinal detachments, and rhegmatogenous retinal detachments. Scleral buckles help to alter the magnitude and direction of these vectors, thus promoting closure of retinal breaks and retinal reattachment.

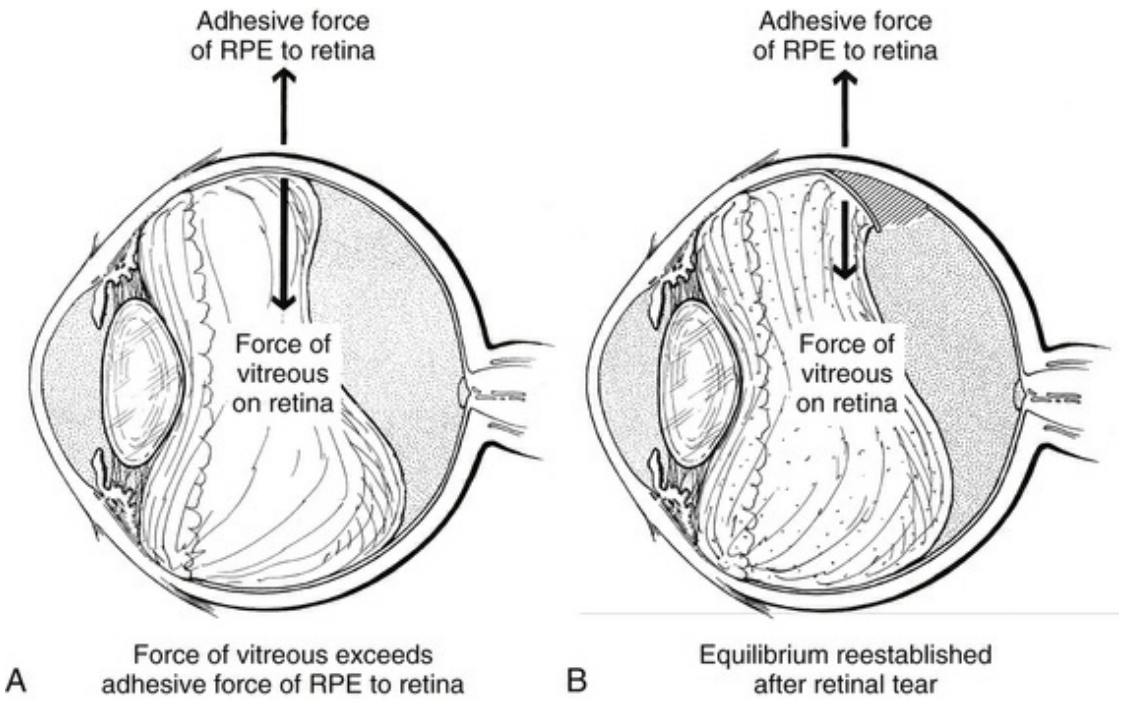

FIG. 103.9 (A) A retinal tear will result if the force of a posterior vitreous detachment exceeds the adhesive force of the retinal pigment epithelium (RPE) to the retina and the tensile strength of the retina. (B) The retinal tear reestablishes equilibrium between the traction of the posterior hyaloid on the retina and the adhesive force of the RPE.

Forces That Lead to Retinal Tears and Detachments

Most retinal breaks are caused by a combination of forces, including vitreous traction and fluid movement during rotary ocular movements, and sometimes traction associated with epiretinal membranes.

Vitreous Traction

Vitreous traction may be exerted in many different directions (i.e., perpendicular, tangential, or oblique) with respect to the curved surface of the retina. An example of relatively pure perpendicular (or radial) vitreous traction occurs with a superior horseshoe-shaped tear resulting from posterior vitreous detachment (Fig. 103.10). As the posterior hyaloid detaches, gravity causes the

vitreous gel to pull away from the superior retina. A focal adhesion of the vitreous to the retina may cause a tear to develop if the force exerted by the vitreous on the retina exceeds the adherence of the photoreceptors to the RPE and the tensile strength of the retina. The force exerted by the vitreous is primarily perpendicular or oblique to the surface of the retina. The importance of gravitational forces on the vitreous in the genesis of retinal tears is emphasized by the observation that most horseshoe-shaped tears occur in the superior retina. An example of relatively pure tangential traction on the surface of the retina occurs with a localized epiretinal membrane causing distortion of the macula (Fig. 103.11). Most of the traction from an epiretinal membrane occurs tangentially on the surface of the retina, although there is a small inward radial component to this traction because of the concave shape of the eye wall.[41]

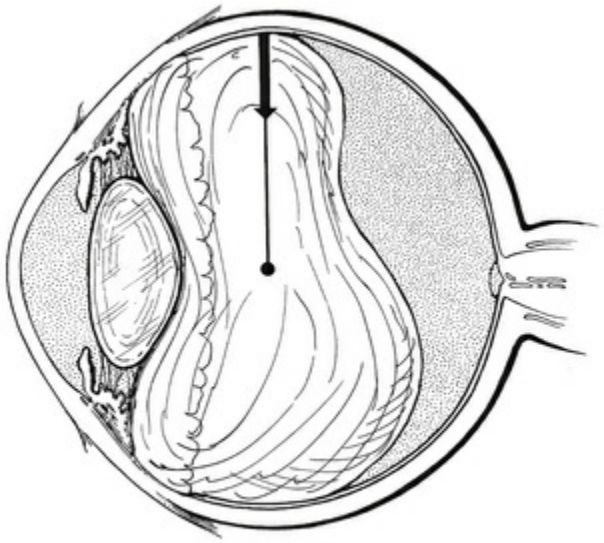

FIG. 103.10 Radial retinal traction. The force of gravity on the vitreous in vitreoretinal attachment to the superior retina causes traction on the retina directed radially toward the center of the eye. Radial retinal traction is more likely to lead to a retinal tear than is tangential retinal traction. Gravitational forces of the vitreous on the retina can explain the greater incidence of superior horseshoe-shaped retinal tears.

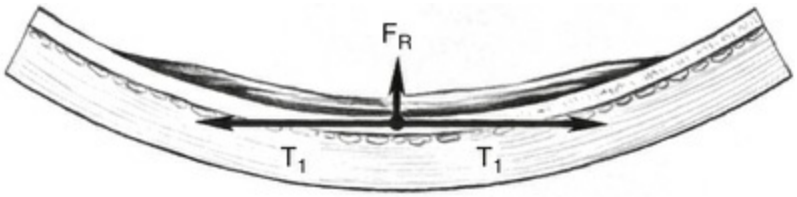

FIG. 103.11 Tangential retinal traction. The elastic force of an epiretinal membrane adherent to the surface of the retina causes relatively pure tangential retinal traction (T_1). The traction is parallel to the curved surface of the retina at each point on the retina. There is also a small inward radial component to the traction (F_R), caused by the epiretinal membrane because of the curved surface of the eye.

It appears that radial traction on the retina is more likely to produce retinal breaks than is tangential traction. Most vitreoretinal traction causing a retinal tear, traction retinal detachment, or rhegmatogenous retinal detachment is oblique to the surface of the retina. Oblique vitreoretinal traction can be separated into orthogonal vectors (oriented at 90°) composed of varying mixtures of radial and tangential traction (Fig. 103.12). Some of the forces that can cause traction on the retina include (1) gravitational forces on the vitreous gel attached to the retina, particularly when the vitreous is adherent to a localized area in the superior retina and surrounded by an area of vitreous detachment; (2) inertial forces transmitted from the vitreous to the retina during ocular movements or blunt trauma; (3) contraction of the vitreous gel at sites of vitreoretinal attachment caused by cellular proliferation; and (4) contractile fibrocellular membranes on the surface of the retina posterior to a PVD. Myopic eyes with long axial lengths have higher shearing forces on the retina with saccadic eye movements than emmetropic eyes, which may predispose them to develop retinal tears.[42]

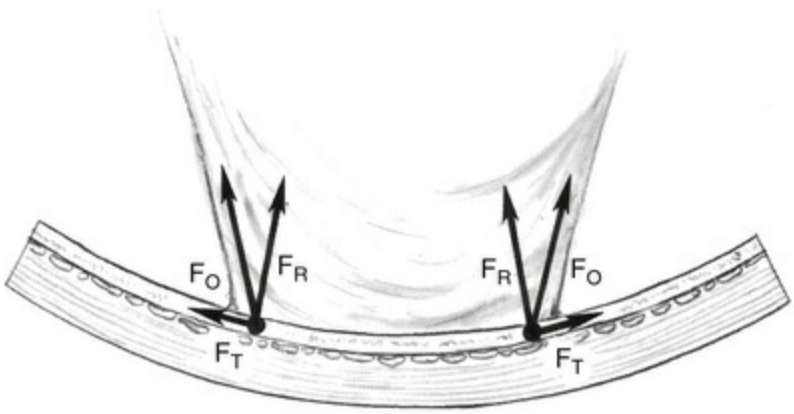

FIG. 103.12 Vitreoretinal traction oblique to the surface of the retina is composed of different mixtures of radial and tangential traction. An oblique vector (F_O) resulting from vitreoretinal traction can be divided into orthogonal vectors consisting of a radial vector (F_R) directed toward the center of the eye and a vector tangent to the surface of the retina (F_T).

Fluid Movement and Retinal Breaks

Retinal traction can be created by saccadic eye movements in eyes with posterior vitreous detachment, and this traction may lead to retinal tears.[43] Fluid currents in eyes with retinal tears may allow fluid to move from the vitreous cavity into the subretinal space, creating a rhegmatogenous retinal detachment. Rotational eye movements appear to be especially important in forcing fluid through a retinal tear, leading to retinal detachment.[44,45] Fluid movement associated with rotational eye movements appears more likely to cause a retinal detachment when vitreous traction elevates the flap of a retinal tear than when a retinal hole is present without vitreous traction. The elevated retinal flap with vitreous traction may trap vitreous fluid and funnel it into the tear. The vitreous fluid can then act as a wedge, interposing itself between the retina and the RPE as the eye rotates (Fig. 103.13).[46] Once the normal adhesion of the retina to the RPE is disrupted, rotational eye movements can force additional fluid into the subretinal space, thereby extending the retinal detachment. A retinal hole in the absence of vitreous traction does not catch the vitreous fluid from rotational eye movements as easily and thus is less likely to lead to retinal detachment. If retinal detachment occurs, continued fluid

flux through the retinal tear is important in maintaining and enlarging the retinal detachment.[47–49]

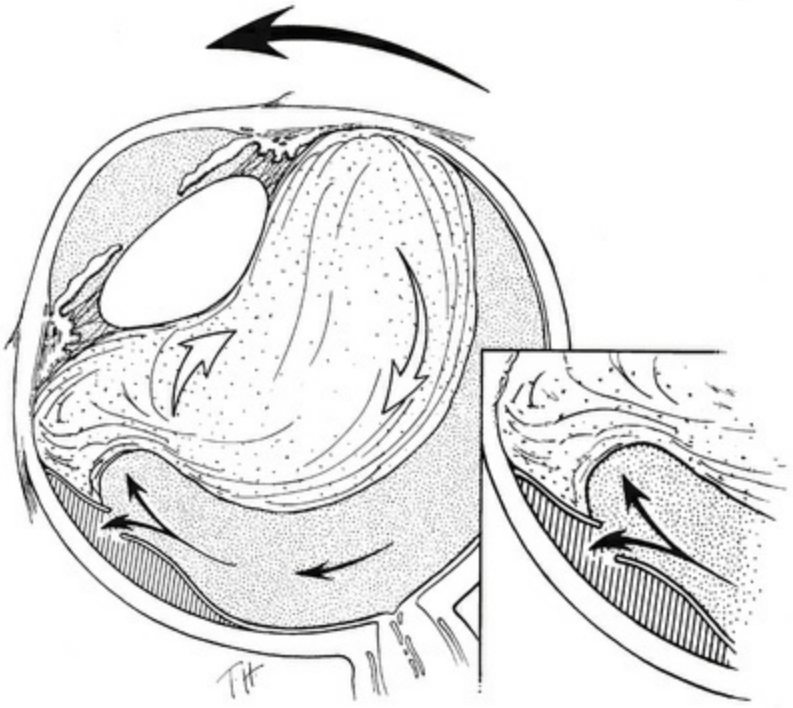

FIG. 103.13 Rotation of the eye causes traction on the retina at the insertion of the vitreous gel to the retina at the vitreous base. The inertia of the vitreous fluid may dissect under the flap of a horseshoe-shaped tear, resulting in retinal detachment. Additional fluid may be forced under the retina with rotational eye movements.

(Reproduced with permission from Wilkinson CP, Rice TA. Michels' retinal detachment. 2nd ed. St. Louis: Mosby; 1997.)

Epiretinal Membranes, Cellular Proliferation, and Retinal Breaks

Epiretinal membranes with cellular proliferation on the surface of the retina may also cause retinal breaks and retinal detachment. As the epiretinal membranes contract, they seek the shortest distance between areas of attachment to the concave inner surface of the retina. The shortest distance between two points on the curved retinal surface is a straight line, or chord; the shortest distance between three points on the curved retinal surface is a series of lines

within a single plane. The epiretinal membrane that initially conforms to the concave inner surface of the retina can cause a traction detachment of the retina in the configuration of a plane. The planar configuration occurs because this will minimize the tangential tension within the epiretinal membrane (Fig. 103.14). In most instances the vitreous gel also contributes to the traction retinal detachment. Attachment of the vitreous gel to fibrocellular epiretinal membranes may produce additional radial or oblique traction on the retina, leading to more complicated configurations of retinal detachments such as the table-top traction retinal detachment sometimes seen in eyes with severe proliferative diabetic retinopathy (Fig. 103.15). These radial, tangential, and oblique forces on the retina may also cause retinal breaks, creating a traction–rhegmatogenous retinal detachment. The biomechanics of these detachments are much more complicated because their configuration is determined by an equilibrium of vitreoretinal traction, retinal elasticity, and fluid flux through retinal breaks and absorption of subretinal fluid. The detached retina will assume the configuration that balances all of these synergistic and opposing forces.

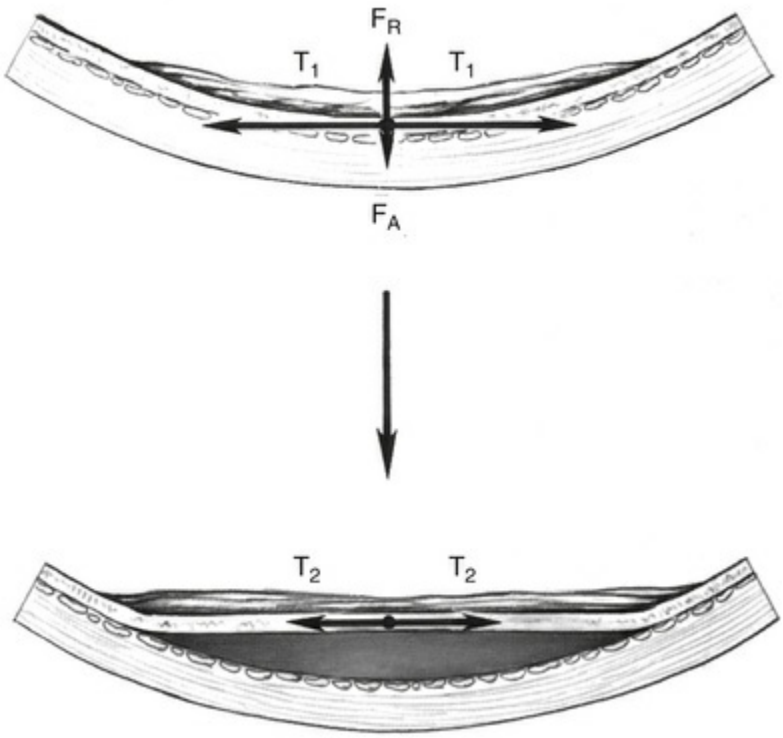

FIG. 103.14 Tangential tension in an epiretinal membrane (T_1) with its associated radial retinal traction (F_R) may exceed the adhesive force of the retina to the retinal pigment epithelium (RPE). A localized traction retinal detachment will occur if the radial retinal traction (F_R) exceeds the adhesive force of the RPE to the retina ($F_R > F_A$). The traction detachment eliminates the radial force pulling the retina away from the eye wall (F_R) and also minimizes the tension in the epiretinal membrane ($T_2 < T_1$).

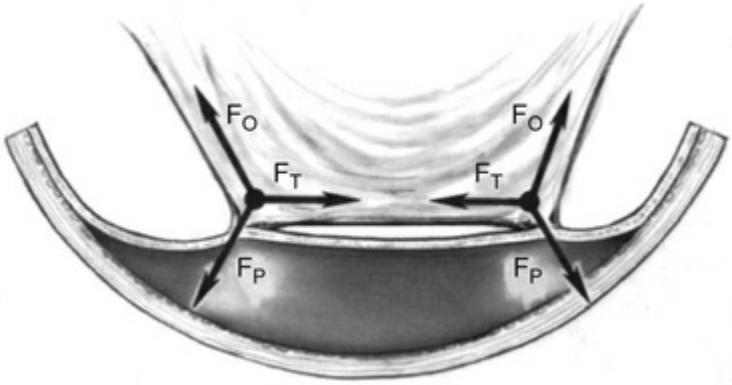

FIG. 103.15 The configuration of a table-top traction retinal detachment in equilibrium is determined by a combination of tangential (*FT*) and oblique (*FO*) vitreoretinal traction forces. This is opposed by forces that promote retinal reattachment, such as the absorption of subretinal fluid (*FP*).

Forces That Promote Attachment of the Retina

A number of physiologic forces maintain or attempt to restore attachment of the neurosensory retina to the RPE (see Chapter 31, Cellular effects of detachment and reattachment on the neural retina and retinal pigment epithelium). Adhesions between the neurosensory retina and RPE/choroid also assist in maintaining reattachment. Scleral buckles alter the effects of vitreous traction, epiretinal membranes, and fluid movement.

Physiologic Adhesion Between Retina and RPE

Several factors promote adhesion between the retina and the RPE. First, adhesion of the RPE and photoreceptors is assisted by a viscous mucopolysaccharide substance between the villous processes of the RPE interdigitating with the photoreceptors.[50] This appears to account for only a small component of the adhesion between the retina and the RPE. Second, an oncotic pressure difference between the choroid and subretinal space makes another small contribution to promoting adhesion of the retina to the RPE.[51,52] The oncotic pressure difference arises because proteins in the choroid cannot easily pass through the RPE and Bruch's membrane into the subretinal space.[53] Third, hydraulic forces on the retina promote adhesion of the retina to the RPE. The hydraulic forces are a result of intravitreal fluid pushing against the retina at a physiologic intraocular pressure. The hydraulic forces are produced by more rapid passage of fluid from the subretinal space through the sclera than from the vitreous through the retina.[54] The hydraulic forces have been compared to an inner tube (the retina) forced against the inner wall of a tire (the sclera). Hydraulic forces are independent of the RPE pump and explain why the retina can remain attached after removal of the choroid and RPE in an eye wall resection, such as is sometimes used for removal of a choroidal melanoma.[55] Hydraulic forces would be expected to produce a lower pressure in the subretinal space than in the intravitreal space. However, attempts to measure this small pressure difference directly have not been successful.[56] Finally, the most important factor maintaining retinal attachment is the RPE pump, which actively removes fluid from the subretinal space, promoting adhesion of the RPE to the photoreceptors.[27] These four types of force maintain apposition of the retina and the RPE.

Several properties of the RPE–photoreceptor adhesion are important in determining the types of retinal tears and retinal detachments that can occur with vitreoretinal traction. The adhesive force between the RPE and photoreceptors paradoxically appears to be weaker with small tractional forces than larger tractional forces in vitro.[57] The variability of the strength of adhesion between the retina and the RPE as a function of the tractional force on the retina is a result of the viscoelastic properties of the mucopolysaccharide

holding the retina and the RPE together. These viscoelastic properties can be understood by considering the force required to pull adhesive tape off a surface. The adhesion of the adhesive tape to a surface is lower at lower rates of traction than at higher rates of traction. Hence, the adhesion of the retina to the RPE would be expected to be lower at lower rates of traction than at a higher rate of traction.[57]

The retina itself also behaves like a viscoelastic substance when tractional forces cause elongation of the retina. The retina has greater elongation at lower peeling rates than at higher peeling rates.[57,58] Smaller tractional forces on the retina exerted over a longer period of time tend to produce larger traction retinal detachments than do larger tractional forces over a short period.[59] This can explain why relatively minimal chronic vitreous traction can produce an extensive traction retinal detachment, whereas larger forces from short-lived vitreous traction associated with ocular trauma may produce no retinal tears or detachment. The forces required to produce retinal tears and detachments are greater in vivo than in vitro because of active metabolic processes, such as the RPE pump, that favor retinal adhesion.[60] The presence of vitreous traction, retinal breaks, and fluid currents in the eye may overcome these adhesive forces, leading to retinal detachment. The scleral buckle and chorioretinal adhesion counteract the forces that detach the retina and help reestablish an adhesion between the retina and the RPE.

Thermal Chorioretinal Adhesions

Three different thermal modalities can be used to create a chorioretinal adhesion around retinal breaks associated with a retinal detachment. The first is diathermy, whereby an electric current is applied to the external sclera. The current passes through the sclera, creating a burn that includes sclera, RPE, and retina. A chorioretinal adhesion or scar is created when the RPE undergoes proliferation at the site of the burn. The second type of thermal adhesion is cryopexy, whereby a freeze is applied to the external sclera or occasionally internally on the retinal surface. The freeze passes through sclera, RPE, and retina to create a thermal-induced scar. Cryopexy causes minimal change to the sclera compared with

diathermy, which causes some scleral necrosis. The third type of thermal adhesion is created by the laser. This type of adhesion is placed internally by focusing the laser on the retina. The laser energy is absorbed primarily by the pigmented RPE and choroid, leading to a chorioretinal scar. Laser photocoagulation causes no change to the underlying sclera.

The final chorioretinal adhesions formed by diathermy, cryopexy, and laser have similar strengths and are certainly adequate to maintain apposition of the retina and the RPE if there is no substantial traction on the retina. The rapidity of onset of the chorioretinal adhesion is not the same for these three methods, however. Laser photocoagulation appears to induce a more rapid chorioretinal adhesion than cryopexy or diathermy.[61,62] The chorioretinal adhesion induced by laser photocoagulation starts within 24 hours of treatment and increases rapidly within 3 days, whereas the adhesion formed by cryopexy or diathermy takes at least several days to start to form and does not reach maximum strength until about 2 weeks.[61,62] Cryopexy given at the time of scleral buckle for retinal reattachment and laser photocoagulation 1 month later have similar efficacy in maintaining retinal reattachment in one randomized trial.[63]

Scleral Buckles and Vitreous Traction

Scleral buckles help in several ways to counteract the forces that tend to detach the retina. Indentation of the eye wall produced by the scleral buckle can decrease vitreous traction on the retinal tear in rhegmatogenous retinal detachment. Scleral buckles may also decrease vitreous traction in traction retinal detachments, causing the detachment to decrease in size or to resolve completely. Vitreous traction causing elevation of the retinal break in a traction–rhegmatogenous retinal detachment may perpetuate the retinal detachment by allowing fluid from the vitreous cavity to pass through the retinal break into the subretinal space. The scleral buckle relieves this vitreoretinal traction by decreasing the magnitude and possibly changing the direction of the vitreous traction on the retinal tear. Circumferential scleral buckles help to decrease transretinal traction by decreasing the diameter and circumference of the vitreous base. This effect can be understood by

comparing the vitreous to a spring and applying Hook's law. The force exerted by a stretched spring is greater than a spring with minimal stretch (Fig. 103.16). The force of stretch is directly proportional to the distance the spring is stretched. Reducing the diameter of the vitreous cavity in the vitreous base with a circumferential buckle decreases the transvitreal traction, shifting the equilibrium back toward retinal reattachment. Optical coherence tomography has been used to image the retina overlying scleral buckles and has confirmed that residual vitreous traction and unsupported retinal breaks are important causes of persisting retinal detachment.[64] The capability of the scleral buckle to relieve traction and promote retinal adhesion has been confirmed when scleral buckles are used to treat retinal detachments without the use of any chorioretinal adhesions. Two randomized trials found no difference in retinal reattachment rates with the use of scleral buckles, whether or not any retinopexy was used.[65,66]

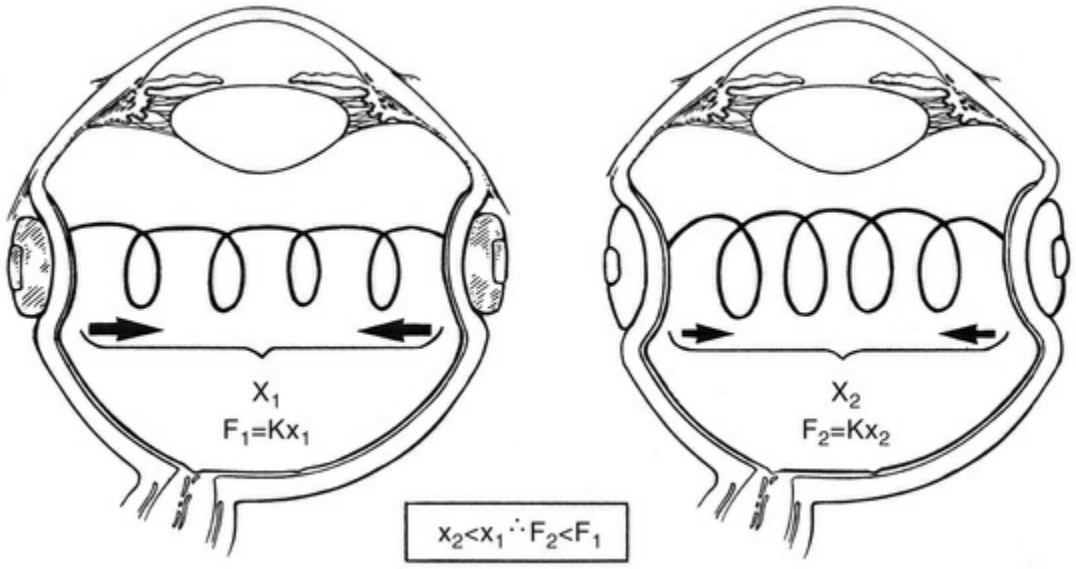

FIG. 103.16 The transvitreal contractile force is the product of a constant (K) and the transvitreal distance (x_1 or x_2). The transvitreal force with a low circumferential buckle (F_1) is greater than the transvitreal force with a high circumferential buckle (F_2) since the transvitreal distance with the low circumferential buckle (x_1) is greater than the transvitreal distance with the high circumferential buckle (x_2). (Reproduced with permission from Wilkinson CP, Rice TA.

Michels' retinal detachment. 2nd ed. St. Louis: Mosby; 1997.)

Scleral Buckles and Traction on the Retinal Surface

Cellular epiretinal proliferation adherent to the surface of the retina may also promote traction retinal detachment by exerting traction on the retina or may precipitate a rhegmatogenous detachment if the force is strong enough to tear the retina. An epiretinal membrane on the surface of the retina produces retinal traction along the concave eye wall. This traction is composed of two vectors. The first is tangential to the retina and is caused by tension in the contractile epiretinal membrane. The second is directed radially inward, toward the center of the eye, and is a result of tangential traction on a curved surface (Fig. 103.17). At each point along the epiretinal membrane is a small force tangential to the retina and a small force directed inward toward the center of the eye. The force directed radially inward tends to pull the epiretinal membrane and retina away from the RPE. This radial force is normally counterbalanced by adhesion of the retina to the RPE. If the tension on the epiretinal membrane becomes great enough, the radial inward force may exceed the RPE adhesive capacity, causing a traction retinal detachment or retinal tear (see Fig. 103.14).

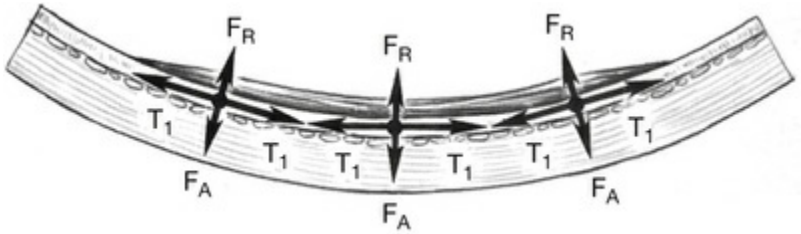

FIG. 103.17 Tension from an epiretinal membrane adherent to the concave surface of the retina produces a tangential force (T_1) and a radial force (F_R) at each point on the epiretinal membrane. The radial force tends to pull the retina off the retinal pigment epithelium (RPE). This inward radial force is normally counterbalanced by the adhesive force of the RPE to retina (F_A), such that $F_R < F_A$.

The radial force from tangential traction on the retina can be

approximated by the formula in Fig. 103.18.[41] The radial inward force on the retina per unit length is proportional to the tension of the epiretinal membrane. The greater the tension within the epiretinal membrane, the greater the radial inward force tending to detach the retina. The radial inward force from the epiretinal membrane is inversely proportional to the radius of curvature of the eye wall. Hence, an epiretinal membrane on an eye with a small radius of curvature exerts more radial inward force on the retina than does the same epiretinal membrane on an eye with a large radius of curvature, if all other variables are equal.

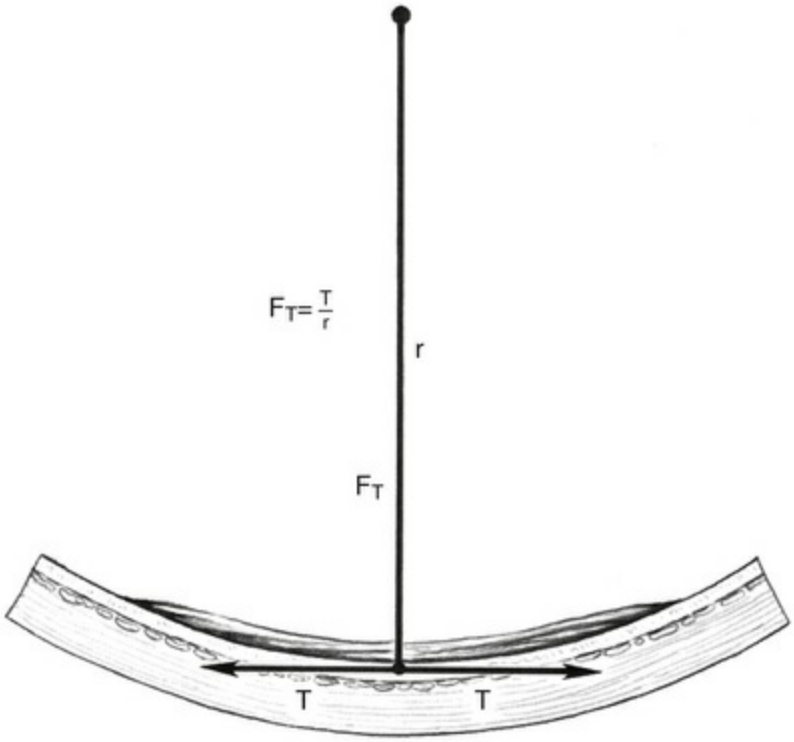

FIG. 103.18 The magnitude of the inward radial force from an epiretinal membrane on the concave surface of the retina (F_T) can be calculated from the tension on the retina (T) and the radius of curvature of the eye (r). The radial force per unit length of the epiretinal membrane is proportional to the tension in the epiretinal membrane and inversely proportional to the radius of curvature of the eye wall.

The formula in Fig. 103.18 also explains how scleral buckles help to promote retinal reattachment in eyes with breaks adjacent to

epiretinal membranes and in eyes with traction retinal detachments secondary to epiretinal proliferation. The scleral buckle alters the shape of the eye wall from the normal concave contour to a convex contour over the scleral buckle. Without the scleral buckle, the radial force induced by the epiretinal membrane on the retina is directed inward toward the center of the eye. With the scleral buckle, the radial force is directed toward the convex center of curvature of the radial buckle (Fig. 103.19). The scleral buckle reverses the direction of the radial force induced by the epiretinal membrane from an inward force, tending to detach the retina, to an outward force, promoting retinal reattachment. Furthermore, because the convex radius of curvature of the retina on the scleral buckle is much smaller than the concave radius of curvature of the eye, the magnitude of the radial outward force promoting retinal reattachment with a scleral buckle is larger than the original radial inward force tending to detach the retina.

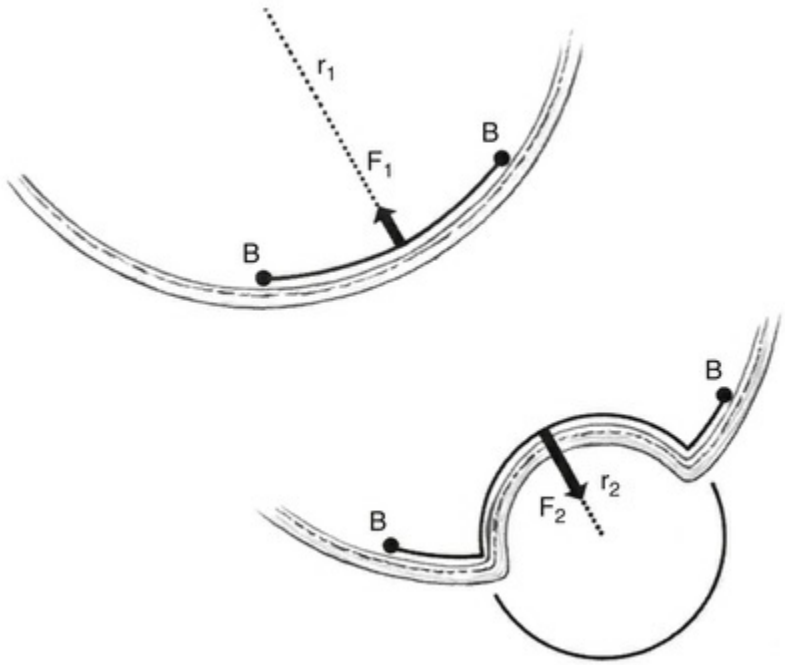

FIG. 103.19 A scleral buckle reverses the direction of the radial inward force on the retina (F_1) to an outward force (F_2), thereby promoting retinal reattachment of an epiretinal membrane. *B* is the site of attachment of the epiretinal membrane. The magnitude of the force promoting retinal reattachment is greater than the original inward force that tended to detach the retina.

This occurs because the radius of curvature of the sclera over the scleral buckle (r_2) is smaller than the radius of curvature of the normal concave eye wall (r_1).

This analysis of vector forces induced by an epiretinal membrane can be understood by considering a tight surgical glove on a hand. When the hand is cupped, the glove will lift off the palm of the hand because the glove is like a tight trampoline bridging the edges of the concave surface of the palm of the hand. The glove on a cupped hand is analogous to an epiretinal membrane lifting the retina off the RPE. Traction retinal detachments would always occur with epiretinal proliferation on the surface of the retina if no adhesive forces were present to counterbalance the radial inward force on the retina from the epiretinal membrane. When the palm of the hand is flattened and hyperextended, the elastic surgical glove is pulled tightly against the palm of the hand. The force vector that pulled the surgical glove off the cupped hand reverses when the hand is hyperextended, pulling the glove against the convex surface of the palm of the hand. This is analogous to the effect of a scleral buckle changing the concave eye wall to a convex configuration, promoting retinal reattachment. Radial scleral buckles may also assist in closure of retinal breaks by stretching the retina slightly on the scleral buckle, since the retina must conform to the increased arc length of the scleral buckle (Fig. 103.20).[26]

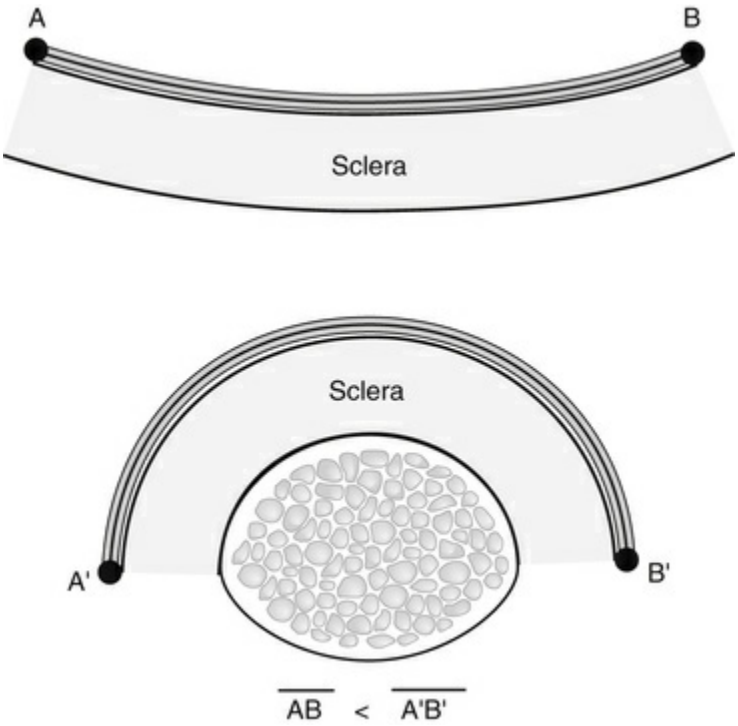

FIG. 103.20 The retina is stretched when a scleral buckle is used to indent the eye wall. The distance from *A* to *B* on the upper diagram is less than the distance from *A'* to *B'* on the lower diagram since the retina must now conform to the longer outer circumference of the buckle and sclera rather than the shorter inner circumference of the nonbuckled sclera.

Scleral Buckles and Fluid Movement

Fluid currents associated with rotational movements of the eye are important in creating and maintaining retinal detachments, as discussed previously.[45] Scleral buckles may alter the direction and magnitude of fluid currents in eyes with retinal detachment, decreasing the movement of vitreous fluid through tears into the subretinal space. Scleral buckles may change the fluid flux through retinal tears. The distance between the RPE and a retinal tear is reduced when the eye wall is indented by a scleral buckle. This displaces the preexisting subretinal fluid away from the tear and helps to bring the RPE and the retinal tear closer together. The distance from the retinal tear to the RPE is important in determining whether the retina will reattach or remain detached. The closer the retinal tear is to the RPE, the greater the force promoting retinal reattachment. A quantitative model of retinal

reattachment force was developed to try to predict the magnitude of retinal reattachment forces in eyes with rhegmatogenous retinal detachment treated with a radial buckle (Fig. 103.21).[47] The retinal reattachment force in this model results from the absorption of subretinal fluid by the RPE pump, which brings the retina and the RPE into closer apposition. This model predicts that the retinal reattachment force is inversely proportional to the cube of the distance from the retinal hole to the RPE on the buckle. Halving the distance from the retinal tear to the buckle causes an eightfold increase in the retinal reattachment force. This analysis would predict that most retinal tears within 3 mm of the RPE will spontaneously reattach without drainage of subretinal fluid, and this appears to be confirmed by clinical observations.[47] A subsequent finite element analysis using this model made the somewhat surprising prediction that rapid eye movements may actually help to reattach the retina better than relative ocular immobility, which has been advocated for years to help absorb persisting subretinal fluid.[67]

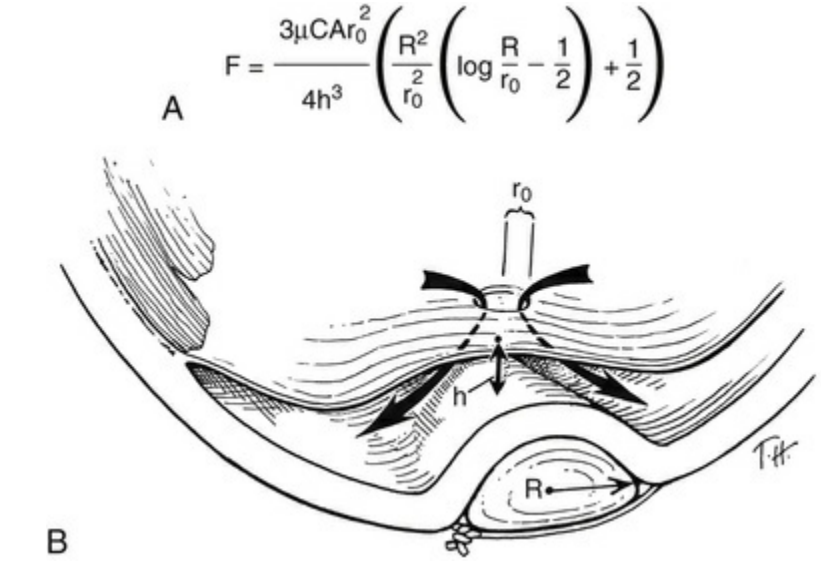

FIG. 103.21 (A) Absorption of subretinal fluid by the retinal pigment epithelium (RPE) in an eye with a cylindrical radial buckle induces a flow of fluid from the subretinal space into the RPE and a secondary flow of fluid from the vitreous to the subretinal space. This creates a force that pushes the detached retina toward the RPE. The force of retinal reattachment (F) is

proportional to the viscosity of vitreous cavity fluid (μ), the choroidal absorption rate (C), the radius of the cylindrical buckle (R), and the area of RPE exposed by the retinal detachment (A). The force of retinal reattachment is inversely proportional to the height of detachment (h) and the radius of the retinal break (r_0) as long as the buckle is larger than the retinal hole. (B) Reduced flow of liquid vitreous through a retinal break (*arrows*) into the subretinal space compared with the rate of fluid absorption by the pigment epithelium induces a force that tends to flatten the retina against the pigment epithelium. This force depends on the radius of the retinal break (r), the distance the break is separated from the scleral buckle (h), and the radius of the scleral buckle (R). (Panel B reproduced with permission from Wilkinson CP, Rice TA. Michels' retinal detachment. 2nd ed. St. Louis: Mosby; 1997.)

Scleral buckles can also displace vitreous fluid away from the tear, plugging the tear with solid vitreous gel. The movement of fluid from the vitreous cavity through the tear is impeded when the tear is occluded by solid vitreous gel.[68] Larger scleral buckles may displace more of the liquid vitreous, leaving solid vitreous gel in the vitreous cavity to plug retinal breaks. If additional tamponade of retinal breaks is needed, intraocular gas bubbles can eliminate or decrease the movement of vitreous fluid through the retinal break because of the high surface tension at the gas–water interface at the site of the retinal tear. It takes only approximately 0.625 mL of air injected into the vitreous cavity to cover 4 clock-hours of the peripheral retina, as shown in Fig. 103.22.[46] The use of supplemental intravitreal air and appropriate positioning of the bubble to cover the retinal tear(s) is very helpful when there is substantial persisting subretinal fluid around the retinal break(s).

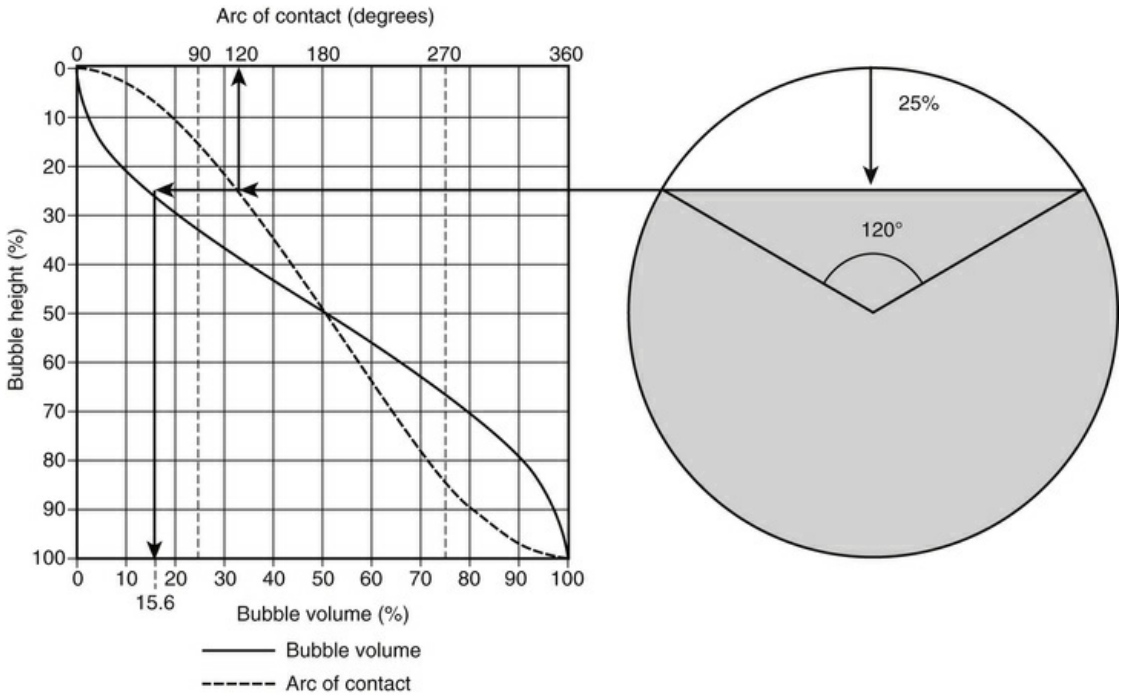

FIG. 103.22 Relationship of meniscus height of the intraocular gas bubble, bubble volume, and arc of contact within the eye. A gas bubble with a meniscus height of 25% displaces 15.6% of the volume of the vitreous cavity with an arc of contact of 120° degrees or 4 clock-hours. A relatively small intraocular gas bubble volume can provide tamponade to retinal breaks between the 8:00 and 4:00 meridian with appropriate head positioning when there is persisting subretinal fluid around a retinal break. (Reproduced with permission from Wilkinson CP, Rice TA. Michels' retinal detachment. 2nd ed. St. Louis: Mosby; 1997.)

Scleral buckles help to reduce vitreous traction and diminish the flux of vitreous fluid through retinal tears, thus promoting reapposition of the retina to the RPE. The combination of relief of vitreoretinal traction by the scleral buckle and formation of a chorioretinal adhesion helps to maintain attachment of the retina postoperatively. It is the equilibrium between the forces promoting retinal attachment and the forces promoting retinal detachment that determines whether the retina remains attached or detached.

Conclusion

Scleral buckles play an important role in the treatment of

rhegmatogenous retinal detachments by changing the geometry and physiology of the eye. Scleral buckles may cause secondary changes in axial length, corneal topography, and intraocular volume as a result of changes in the geometry of the eye. Forces that normally maintain retinal attachment include the mucopolysaccharide "glue" between the photoreceptors and the RPE, an oncotic pressure difference between the choroid and the subretinal space, hydraulic forces on the retina from vitreous fluid, and the RPE pump. Retinal detachment occurs when the forces promoting retinal attachment are overwhelmed by forces promoting retinal detachment. Forces that can lead to retinal detachment include vitreous traction, retinal tears, and cellular epiretinal proliferation. The normal ocular homeostasis may be disrupted by a retinal tear, and a new equilibrium is then established that can create a retinal detachment. The scleral buckle helps to alter this equilibrium favorably through changes in the vitreous fluid dynamics and geometry of the vitreoretinal interface. The use of a scleral buckle helps to overcome the forces tending to detach the retina in most eyes, allowing successful treatment of rhegmatogenous retinal detachments.

References

1. Hayashi H, Hayashi K, Nakao F, et al. Corneal shape changes after scleral buckling surgery. *Ophthalmology*. 1997;104:831–837.
2. Okada Y, Nakamura S, Kubo E, et al. Analysis of changes in corneal shape and refraction following scleral buckling surgery. *Jpn J Ophthalmol*. 2000;44:132–138.
3. Flament J. Etude optico-echographique des modifications biometriques de l'axe antero-posterieur de l'oeil provoquées par quelques techniques de la chirurgie chorioretinienne. *Arch Ophtalmol (Paris)*. 1973;33:397–412.
4. Harris MJ, Blumenkranz MS, Wittpenn J, et al. Geometric alterations produced by encircling scleral buckles: biometric and clinical considerations. *Retina*. 1987;7:14–19.
5. Larsen JS, Syrdalen P. Ultrasonographic study on changes in axial eye dimensions after encircling procedure in retinal

detachment surgery. *Acta Ophthalmol*. 1979;57:337–343.
6. Burton TC. Irregular astigmatism following episcleral buckling procedure with the use of silicone rubber sponges. *Arch Ophthalmol*. 1973;90:447–448.
7. Kiernan JP, Leveille AS, Morse PH. Axial length following scleral buckling. *Retina*. 1982;2:176–178.
8. Rubin ML. The induction of refractive errors by retinal detachment surgery. *Trans Am Ophthalmol Soc*. 1975;73:452–490.
9. Okamoto F, Yamane N, Okamoto C, et al. Changes in higher-order aberrations after scleral buckling surgery for rhegmatogenous retinal detachment. *Ophthalmology*. 2008;115:1216–1221.
10. Goel R, Crewdson J, Chignell AH. Astigmatism following retinal detachment surgery. *Br J Ophthalmol*. 1983;67:327–329.
11. Mensher JH, Burton TC. Corneal curvature changes after scleral buckling. Mosby: St. Louis; 1974. Blodi FC. *Current concepts in ophthalmology*. vol. 4.
12. Wang HZ, Chen MT, Chang CH, et al. The changes in ocular axial length and corneal curvatures after scleral buckling for retinal detachment. *Kaohsiung J Med Sci*. 1994;10:77–83.
13. Wolter JR. Regular astigmatism resulting from retinal detachment surgery in a young man with a disinsertion. *J Pediatr Ophthalmol*. 1967;4:27–29.
14. Weinberger D, Lichter H, Loya N, et al. Corneal topographic changes after retinal and vitreous surgery. *Ophthalmology*. 1999;106:1521–1524.
15. Kinoshita M, Tanihara H, Negi A, et al. Vector analysis of corneal astigmatism after scleral buckling surgery. *Ophthalmologica*. 1994;208:250–253.
16. Fiore JV Jr, Newton JC. Anterior segment changes following the scleral buckling procedure. *Arch Ophthalmol*. 1970;84:284–287.
17. Theodossiadis GP, Maniakis SG, Ladas ID, et al. The persistence of buckle height in relation to orientation of buckle fixation: an ultrasonographic study. *Acta Ophthalmol*. 1994;72:315–318.

18. Jacklin HN. Postoperative refractive changes following various scleral buckling techniques. Pruett RC, Regan CJ. *Retina congress*. Appleton–Century–Crofts: New York; 1972.
19. Burton TC, Herron BE, Ossoinig KC. Axial length changes after retinal detachment surgery. *Am J Ophthalmol*. 1977;83:59–62.
20. Smiddy WE, Loupe DN, Michels RG, et al. Refractive error changes after scleral buckling surgery. *Arch Ophthalmol*. 1989;107:1469–1471.
21. Sato T, Kawasaki T, Okuyama M, et al. Refractive changes following scleral buckling surgery in juvenile retinal detachment. *Retina*. 2003;23:629–635.
22. Hinrichsen G, Eherhardt A, Sringer H. Mechanical behavior of cerclage material consisting of silicone rubber. *Albrecht Von Graefes Arch Klin Exp Ophthalmol*. 1979;211:251–258.
23. Thompson JT, Michels RG. Comparison of chord length and scleral arc length when placing sutures for episcleral exoplants. *Retina*. 1985;5:225–226.
24. Boldrey EE. Variation of technique of episcleral sponge placement: effect on scleral indentation for retinal detachment repair. *Ann Ophthalmol*. 1981;13:743–746.
25. Draeger J, Guthoff R, Moeller J. Correlations between intraocular pressure and resulting scleral indentation after detachment surgery. *Ophthalmic Res*. 1982;14:466–472.
26. Goldbaum MH, Smithline M, Poole TA, et al. Geometric analysis of radial buckling. *Am J Ophthalmol*. 1975;79:958–965.
27. Lincoff H. The rationale for radial buckling. *Mod Probl Ophthalmol*. 1974;12:484–491.
28. Lincoff H, Kreissig I. Advantages of radial buckling. *Am J Ophthalmol*. 1975;79:955–957.
29. Pruett RC. The fishmouth phenomenon. I. Clinical characteristics and surgical options. *Arch Ophthalmol*. 1977;95:1777–1781.
30. Pruett RC. The fishmouth phenomenon. II. Wedge scleral buckling. *Arch Ophthalmol*. 1977;95:1782–1787.
31. Thompson JT, Michels RG. Volume displacement of scleral buckle. *Arch Ophthalmol*. 1985;103:1822–1824.

32. Shi MG, Qiao BD, Zhou YX. The volume and dimensions of eyeball analyzed by MRI following encircling scleral buckles. *Zhonghua Yan Ke Za Zhi*. 2006;24:150–154.
33. Friberg TR, Fourman SB. Scleral buckling and ocular rigidity. *Arch Ophthalmol*. 1990;108:1622–1627.
34. Johnson MW, Han DP, Hoffman KE. The effect of scleral buckling on ocular rigidity. *Ophthalmology*. 1990;97:190–195.
35. Ruiz-de-Gopegui E, Ascaso FJ, DelBuey MA, et al. Effects of encircling scleral buckling on the morphology and biomechanical properties of the cornea. *Arch Soc Esp Oftalmol*. 2011;86:363–367.
36. Noble J, Kanchanaranya N, Devenyi RG, et al. Evaluating the safety of air travel for patients with scleral buckles and small volumes of intraocular gas. *Br J Ophthalmol*. 2014;98:1226–1229.
37. Simone JN, Whitacre MM. The effect of intraocular gas and fluid volumes on intraocular pressure. *Ophthalmology*. 1990;97:238–243.
38. Movaffaghy A, Pharmakakis NM, Chamot SR. Effect of squatting on sub-foveal blood flow defect in pseudophakic eyes operated by cerclage. *Klin Monatsbl Augenheilkd*. 2001;21:323–326.
39. Kimura I, Shinoda K, Eshita T, et al. Relaxation of encircling buckle improved choroidal blood flow in a patient with visual field defect following encircling procedure. *Jpn J Ophthalmol*. 2006;50:554–556.
40. Lincoff H, Stopa M, Kreissig I, et al. Cutting the encircling band. *Retina*. 2006;26:650–654.
41. Michels RG, Thompson JT, Rice TA, et al. Effect of scleral buckling on vector forces caused by epiretinal membranes. *Am J Ophthalmol*. 1987;104:667–669.
42. David T, Smye S, James T, et al. Time-dependent stress and displacement of the eye wall tissue of the human eye. *Med Eng Phys*. 1997;19:131–139.
43. Repetto R, Tatone A, Testa A, et al. Traction on the retina induced by saccadic eye movements in the presence of posterior vitreous detachment. *Biomech Model Mechanobiol*. 2011;10:191–202.

44. Lindner K. Über die Herstellung von Modellen zu Modellversuchen der Netzhautabhebung. *Klin Monatsbl Augenheilkd*. 1933;90:289–300.
45. Rosengren B, Osterlin S. Hydrodynamic events in the vitreous space accompanying eye movements. *Ophthalmologica*. 1976;173:513–524.
46. Wilkinson CP, Rice TA. *Michels' retinal detachment*. 2nd ed. Mosby: St. Louis; 1997.
47. Hammer ME. Retinal reattachment forces created by absorption of subretinal fluid. *Doc Ophthalmol Proc Ser*. 1981;25:61–75.
48. Pederson JE, Cantrill HL. Experimental retinal detachment. V. Fluid movement through the retinal hole. *Arch Ophthalmol*. 1984;102:136–139.
49. Tsuboi S, Taki-Noie J, Emi K, et al. Fluid dynamics in eyes with rhegmatogenous retinal detachments. *Am J Ophthalmol*. 1985;99:673–676.
50. Berman ER, Bach G. The acid mucopolysaccharides of cattle retina. *Biochem J*. 1968;108:75–88.
51. Marmor MF, Abdul-Rahim AS, Cohen DS. The effect of metabolic inhibitors on retinal adhesion and subretinal fluid resorption. *Invest Ophthalmol Vis Sci*. 1980;19:893–903.
52. Negi A, Marmor MF. The resorption of subretinal fluid after diffuse damage to the retinal pigment epithelium. *Invest Ophthalmol Vis Sci*. 1983;24:1475–1479.
53. Toris CB, Pederson JE. Experimental retinal detachment. VII. Intravenous horseradish peroxidase diffusion across the blood–retinal barrier. *Arch Ophthalmol*. 1984;102:752–756.
54. Fatt I, Shantinath K. Flow conductivity of retina and its role in retinal adhesion. *Exp Eye Res*. 1971;12:218–226.
55. Foulds WS. Do we need a retinal pigment epithelium (or choroid) for the maintenance of retinal apposition? *Br J Ophthalmol*. 1985;69:237–239.
56. Maurice DM, Salmon J, Zauberman H. Subretinal pressure and retinal adhesion. *Exp Eye Res*. 1971;12:212–217.
57. deGuillebon H, Zauberman H. Experimental retinal detachment: biophysical aspects of retinal peeling and stretching. *Arch Ophthalmol*. 1972;87:545–548.

58. Hammer ME, Peters H, Wu W. Basic mechanical properties of retina in simple elongation. *Invest Ophthalmol Vis Sci*. 1987;28(Suppl.):116.
59. Zauberman H, deGuillebon H, Holly FJ. Retinal traction in vitro: biophysical aspects. *Invest Ophthalmol*. 1972;11:46–55.
60. Zauberman H. deGuillebon H. Retinal traction in vivo and postmortem. *Arch Ophthalmol*. 1972;87:549–554.
61. Bloch D, O'Connor P, Lincoff H. The mechanism of the cryosurgical adhesion. III. Statistical analysis. *Am J Ophthalmol*. 1971;71:666–673.
62. Yoon YH, Marmor MF. Rapid enhancement of retinal adhesion by laser photocoagulation. *Ophthalmology*. 1988;95:1385–1388.
63. Lira RP, Takasaka I, Arieta CE, et al. Cryotherapy vs laser photocoagulation in scleral buckle surgery: a randomized clinical trial. *Arch Ophthalmol*. 2010;128:1519–1522.
64. Oster SF, Mojana F, Freeman WR. Spectral-domain optical coherence tomography imaging of postoperative scleral buckles. *Retina*. 2011;31:1493–1499.
65. Figueroa MS, Corte MD, Sbordone S, et al. Scleral buckling technique without retinopexy for treatment of rhegmatogenous: a pilot study. *Retina*. 2002;22:288–293.
66. Mahdizadeh M, Masoumpour M, Ashraf H. Anatomical retinal reattachment after scleral buckle with and without retinopexy: a pilot study. *Acta Ophthalmol*. 2008;86:297–301.
67. Foster WJ, Dowla N, Joshi SY, et al. The fluid mechanics of scleral buckling surgery for the repair of retinal detachment. *Graefes Arch Clin Exp Ophthalmol*. 2010;248:31–36.
68. Foulds WS. The vitreous in retinal detachment. *Trans Ophthalmol Soc U K*. 1975;95:412–416.

104

Techniques of Scleral Buckling

Paul Sullivan

Introduction

While almost any rhegmatogenous detachment can be managed with scleral buckling, there has been a trend towards increased use of pneumatic retinopexy and primary vitrectomy.[1] This chapter describes the techniques used in scleral buckling. The choice between buckling and other techniques is covered in Chapter 109

(Optimal procedures for retinal detachment repair).

The term "buckle" refers to deformation of a structure under stress. Sometimes the term "buckle" is used synonymously with some form of encircling explant, while others use the term to describe local explants.[2] In this chapter, the term is used in the more generic sense to imply any type of explant.

Different schools of buckling technique have arisen with divergent views in particular on the role of encirclement and subretinal fluid drainage.[3] This chapter has been written to reflect this diversity of practice.

Buckling of the sclera to close retinal breaks was initially achieved using combinations of lamellar scleral dissection with compression sutures until it was shown that it could be achieved more efficiently using scleral implants[4] and subsequently explants.[5,6] Scleral implants are now of purely historical interest. Likewise diathermy, which was used extensively in the past to achieve retinopexy,[4] has been supplanted by photocoagulation and cryotherapy. There have also been subsequent refinements of the basic technique of scleral buckling, including intraocular gas injection and subretinal fluid drainage. However, in contrast with other areas of vitreoretinal surgery, there have been no major innovations in the basic technique of scleral buckling in the past 20 years. (See Video 104.1 online for a demonstration of scleral buckling technique.)

Surgical Anatomy

Coats of the Eye

The conjunctiva is adherent to the sclera at the limbus, so the radial incisions to enter the subconjunctival plane have to be made just behind the limbus. The conjunctiva becomes friable with age and care must be taken to avoid tearing and buttonholing. Nontoothed forceps (such as notched forceps) are used to grasp the conjunctiva.

The Tenon capsule is a layer of fascia that envelops the globe from the limbus to the optic nerve (Fig. 104.1). It is pierced by the extraocular muscles. A glove-like sleeve of fascia extends anteriorly (to the rectus insertions) and posteriorly (for several millimeters)

along the muscles from the points at which they pierce the Tenon capsule. Between the rectus muscles anteriorly these sleeves are joined by a layer of fascia: the intermuscular septum. The intermuscular septum and fascial sleeves of the recti are sometimes collectively referred to as the posterior Tenon capsule. The result of this complex arrangement is that several layers of tissue have to be incised to get access to the surface of the sclera (or sub-Tenon space). The anterior Tenon capsule may be dissected away from the sclera along with the conjunctiva (to which it is adherent by small fascial filaments). The intermuscular septum is then divided separately. Care must be taken when stripping fascia off the rectus muscles because ligaments from the recti to the wall of the orbit are functionally important in the actions of the muscle.[7]

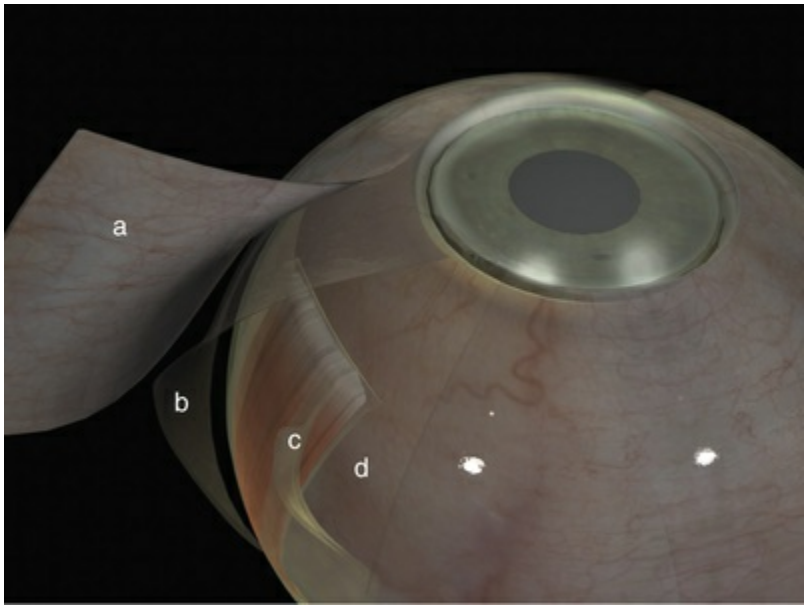

FIG. 104.1 Tenon's capsule. *(a)* Conjunctiva and *(b)* the anterior Tenon capsule have been dissected to reveal *(c)* the "posterior Tenon" glove-like extensions of the Tenon capsule along the recti and the associated intermuscular septum. Bare sclera *(d)* lies under this.

The thickness of the sclera varies. It is thickest around the optic nerve (1.2 mm) and thinnest under the recti behind their insertions, so attempts to pass scleral sutures under the muscles are particularly hazardous. Where scleral mattress sutures are more

typically passed, at the equator, it is approximately 1 mm thick. Passage of sutures is facilitated by the lamellar arrangement of collagen fibers, which allows spatulated (or "side cutting") needles to follow a plane between lamellae.

Extraocular Muscles

The recti are adherent to the sclera at the spiral of Tillaux. The location of this ring corresponds approximately to that of the ora serrata (Fig. 104.2).[8] Circumferential scleral tires are therefore often placed as anteriorly as the rectus muscle insertions will allow. In this position they support the retina as far anteriorly as the ora serrata ("break ora occlusive buckling").

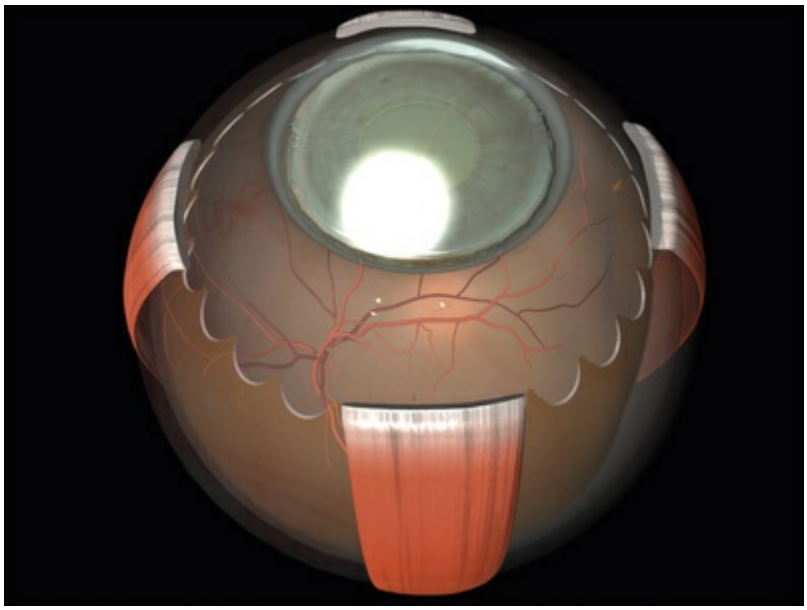

FIG. 104.2 The ora serrata and the spiral of Tillaux (rectus insertions). The sclera has been rendered transparent to reveal the relationship between the ora serrata and the muscle insertions. Buckling anteriorly as far as the rectus insertions prevents anterior leakage.

The superior oblique muscle runs laterally from the trochlea to its insertion under the superior rectus. Passage of a superior rectus muscle hook from the temporal side of the muscle reduces the risk of inadvertently "hooking" the superior oblique, as well as does

keeping the sweep of the hook preequatorial. The superior oblique insertion is frequently encountered on the temporal side of the muscle where it can be an obstacle to scleral suturing. Division of a small (<⅓) portion of the insertion to facilitate suturing seems to have little effect on ocular motility. Note that a vortex vein is usually present under the temporal edge of the superior oblique insertion.

The inferior oblique muscle passes under the lateral rectus muscle. The chance of inadvertently hooking it while passing a muscle hook under the lateral rectus is reduced by passing the hook from the superior side.

Choroidal Vasculature

The long posterior arteries (as well as their corresponding nerves) run anteriorly from the equator at 3 and 9 o'clock and may be damaged by heavy photocoagulation or subretinal fluid drainage in these meridia (Fig. 104.3 online).

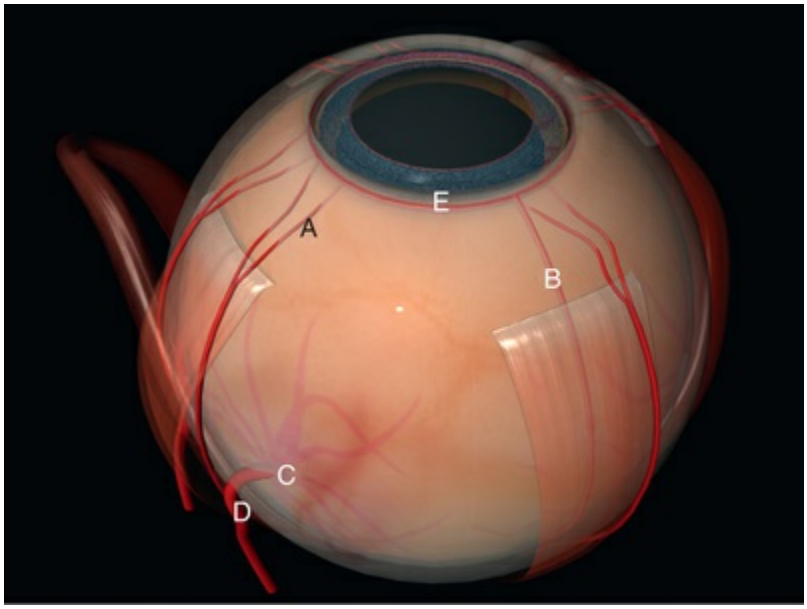

FIG. 104.3 The choroidal vasculature. Surgical trauma should be minimized to all of these structures. *A*, anterior ciliary artery; *B*, long posterior ciliary artery; *C*, vortex ampulla; *D*, vortex vein; *E*, greater arterial circle of the iris.

The anatomy of the vortex veins is somewhat variable but one tends to leave the globe either side of the vertical recti just behind the equator. They may be inadvertently hooked along with a vertical rectus muscle if the muscle hook is passed behind the equator. Injury to the vortex veins may result in interruption to the venous drainage from the choroid and choroidal detachment. When operating near the vertical recti, the vortex veins should be identified to prevent injury.

The choriocapillaris itself is very vascular and prone to bleed when penetrated. Because the vortex veins tend to be located near the vertical recti, subretinal fluid drainage is carried out closer to the horizontal than to the vertical recti whenever possible.

The anterior ciliary arteries are useful indicators of the meridia of the rectus muscle insertions (Fig. 104.4). As they supply the arterial circles of the iris, surgical trauma (including diathermy) should be minimized.

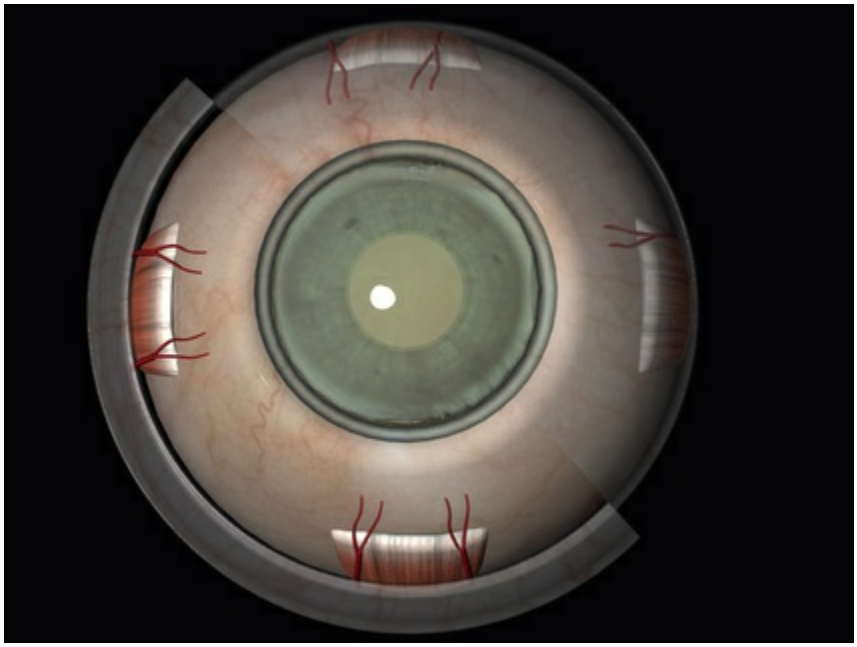

FIG. 104.4 The anterior ciliary arteries. A useful indicator of the location of the rectus positions especially in reoperations. Note that the lateral rectus only has one.

Innervation

Sensory nerves from the globe and bulbar conjunctiva pass through the ciliary ganglion. Local anesthesia in this region, for example, sub-Tenon anesthesia, will therefore anesthetize the globe effectively. The innervation of the lids and palpebral conjunctiva is by the lacrimal, frontal, and infraorbital nerves, which do not pass through the muscle cone. Blockage of the ciliary ganglion alone does not therefore reliably provide adequate analgesia for buckling surgery.

Preoperative Assessment

A careful preoperative assessment is required in every case. Having taken a careful history (and noted relevant systemic health problems and past ophthalmic history), the anterior and posterior segments of the eye are carefully examined using slit-lamp biomicroscopy and indirect ophthalmoscopy. A particular note is made of the following:

- Macular involvement
- Features suggesting that the retinal detachment is nonrhegmatogenous (see also Chapter 99, Nonrhegmatatogenous retinal detachment)
- The presence of vitreous detachment
- Significant ocular co-pathology, which may affect management (e.g., glaucomatous optic neuropathy, aphakia with vitreous in the anterior chamber, a history of strabismus surgery)
- The number and position of the retinal breaks.

Finding the Retinal Break

Missed retinal breaks are an important cause of surgical failure, so the preoperative examination should be very thorough.[9] Even when a break has been found, it is essential to complete examination of the retina, as most retinal detachments have more than one break.[10] Their location is carefully documented on a chart that can be referred to subsequently during surgery (Fig. 104.5). These drawings should show the location of retinal breaks in relation to easily visible retinal landmarks such as small hemorrhages,

vascular bifurcations, and areas of pigmentation.

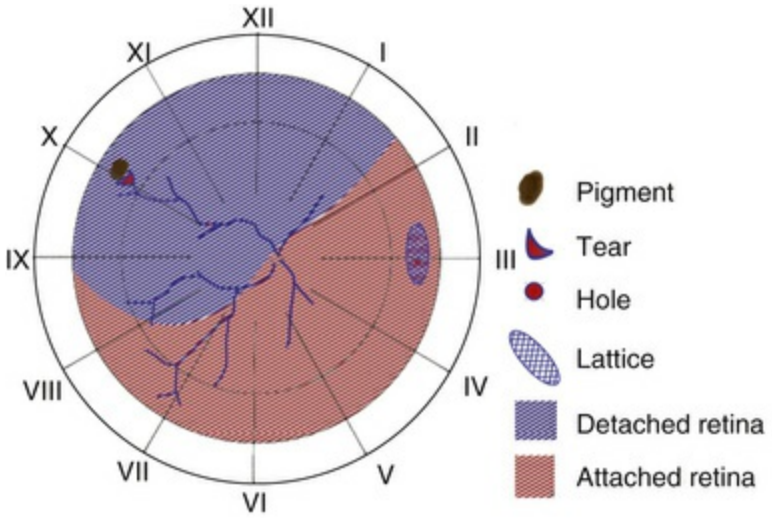

FIG. 104.5 A retinal drawing – note the emphasis on easily visible features that can act as guides to the location of breaks intraoperatively. The outer circle corresponds to the location of the junction between the pars plana and the pars plicata. The middle circle represents the location of the ora serrata.The inner circle represents the location of the equator of the globe.

This carefully documented preoperative assessment has many advantages. If in doubt, an area of retina can be reexamined alternately with indirect ophthalmoscopy and slit-lamp biomicroscopy to establish whether a break is truly present. The drawings made can be referred to if the retinal view becomes obscured during surgery. If the breaks are not easily seen, the other retinal features on the drawings provide useful reference points to their location.

In children and uncooperative patients, it may be impossible to establish the position of the retinal breaks preoperatively. One is then forced to rely on the intraoperative examination under anesthesia.

Lincoff's Rules

Lincoff has shown how the location of retinal breaks determines the distribution of subretinal fluid (Fig. 104.6).[11] Review of the retinal

drawings will therefore determine whether the break location is consistent with the subretinal fluid distribution. When the distribution of fluid does not seem to obey Lincoff's rules, reexamine the retina to ensure that no breaks have been missed.

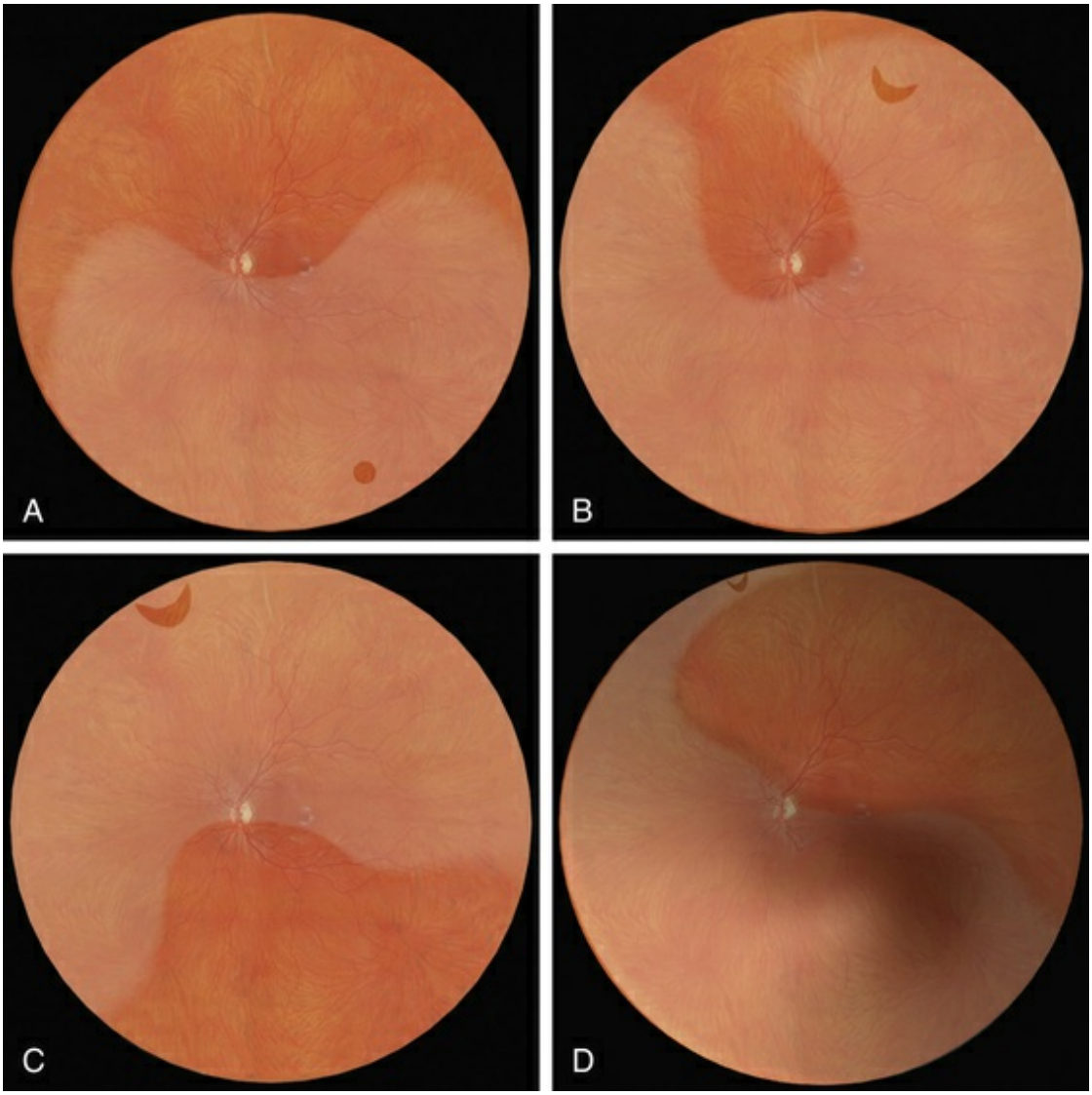

FIG. 104.6 The location of retinal breaks can be deduced from careful analysis of the topography of the detachment as described by Harvey Lincoff. (A) An inferior detachment slightly higher on the temporal side pointing to a break on that side. (B) A subtotal retinal detachment – the break is usually close to the upper border of the fluid on the side it is highest. (C) The fluid crosses the midline superiorly implying a superior break near 12 o'clock. The fluid has tracked down further nasal implying the break is slightly to the nasal

side. (D) The presence of bullae implies a superior break. A shallow sinus of fluid leads to a small superonasal break.

Scheduling Surgery

In "macular on" retinal detachment, urgent surgery should generally be scheduled to prevent detachment of the macula. Cases with tractional tears tend to progress very rapidly and should be treated urgently. Asymptomatic retinal detachments and detachments without tractional breaks (e.g., those due to retinal dialyses, atrophic retinal breaks in young myopes, and cases with "tide marks") progress more slowly. Some delay, if it allows optimal conditions for surgery, may then be acceptable.

Reducing eye and head movements seems to reduce the rate at which subretinal fluid accumulates. Bed rest, eye patching, and rectus sutures have all been used to reduce the amount of subretinal fluid. This may prevent extension of subretinal fluid to the macula and make it easier to identify retinal breaks. It may also avoid the need for subretinal fluid drainage.[12] Such measures are rarely practical now, as most retinal detachment care takes place in an ambulatory or semiambulatory setting.[13]

Preparation for Surgery

Anesthesia

General anesthesia provides ideal operating conditions for younger patients, uncooperative patients, and for reoperations (when local anesthesia may be less effective).

Peribulbar administration of a 50 : 50 mix of lidocaine and bupivacaine, particularly when used with adjunctive Hyalase, provides excellent anesthesia and akinesia. Its action is not limited to the nerves that travel in the muscle cone or the sub-Tenon space.

In theory, sub-Tenon anesthesia alone should be insufficient (see above). In practice, sub-Tenon anesthesia gives anesthesia equivalent to other techniques,[14] presumably due to overspill of anesthetic agents to the peribulbar space. A particular advantage of

sub-Tenon anesthesia is the ease with which it can be "topped up" intraoperatively.[15] Sub-Tenon anesthesia may also be a useful adjunct to general anesthesia[16] both to block the vagus (preventing bradycardia or asystole from rectus muscle traction) and for analgesia in the immediate postoperative period. The presence of buckles and scarring may make this technique more difficult and less effective in reoperations.

Positioning the Head for Surgery

Surgical access is best when the orbital rim is horizontal. This is achieved by extending the neck slightly and tilting the nose away from the operated eye (Fig. 104.7 online). Once in the correct position the head may be fixed with a loop of clinical adhesive tape.

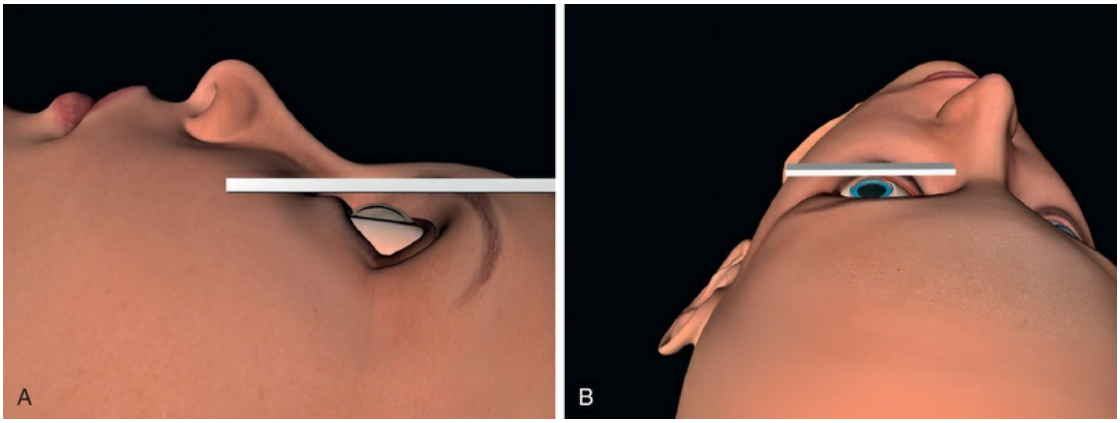

FIG. 104.7 Improving surgical access by flattening the orbital rim: (A) extension of the neck; (B) slightly tilting the head.

Preparation and Draping

The skin and lashes are cleaned with a disinfecting solution such as povidone iodine. A diluted aqueous iodine solution can be instilled in the conjunctival sac (avoiding the use of undiluted or alcohol-based preparations for this). The skin should be thoroughly dried before application of a sterile self-adhesive drape. Providing these steps are taken, it should be possible to tuck the eyelashes under the lid when the lid speculum is introduced, and it is therefore

unnecessary to trim the lashes preoperatively.

If the palpebral aperture is deemed too narrow, a lateral canthotomy may be performed.

Surgical Steps

Conjunctival Peritomy

Neat incisions with later anatomic reposition of the conjunctival edge prevents a number of unpleasant sequelae. Conjunctival misalignment with heaped scars may cause tear film dysfunction. Buttonholing the conjunctiva may lead to Tenon prolapse and delay healing. Recession of the peritomy edge leaves bare sclera and makes subsequent reoperation difficult.

A circumferential limbal peritomy with radial relieving incisions is made.[17] The conjunctiva 3–4 mm behind the limbus is grasped with forceps and gently lifted creating a radial pleat of conjunctiva (Fig. 104.8). A blunt-tipped spring scissors is used to make a vertical radial cut. A second cut is often needed to extend the incision through the Tenon capsule down to the sclera. Great care is taken not to tear the conjunctiva. The spring scissors can easily be used in either hand and the orientation varied as the incision progresses. A gentle spreading action of the scissors under the conjunctiva breaks the weak trabecular adhesions to the episcleral tissue.

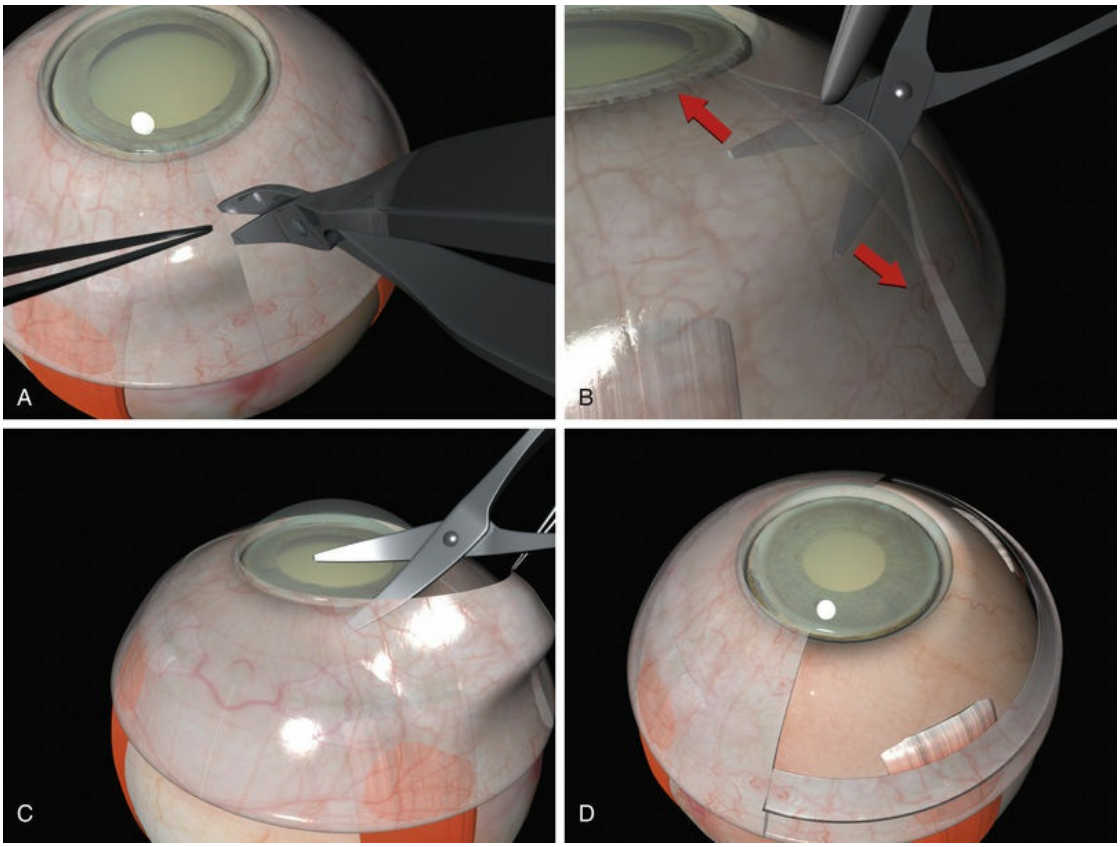

FIG. 104.8 Limbal peritomy. (A) The conjunctiva is grasped with a nontoothed forceps and elevated to create a pleat. Radial division of this with spring scissors initiates the peritomy. (B) Spreading action with blunt scissors to break the trabecular adhesions to the sclera. (C) Extension of incision around the limbus. (D) 180° peritomy for segmental buckle.

A slight modification of this technique with the circumferential incision 2 mm behind the limbus leaves a frill that may be useful during closure (Fig. 104.9).

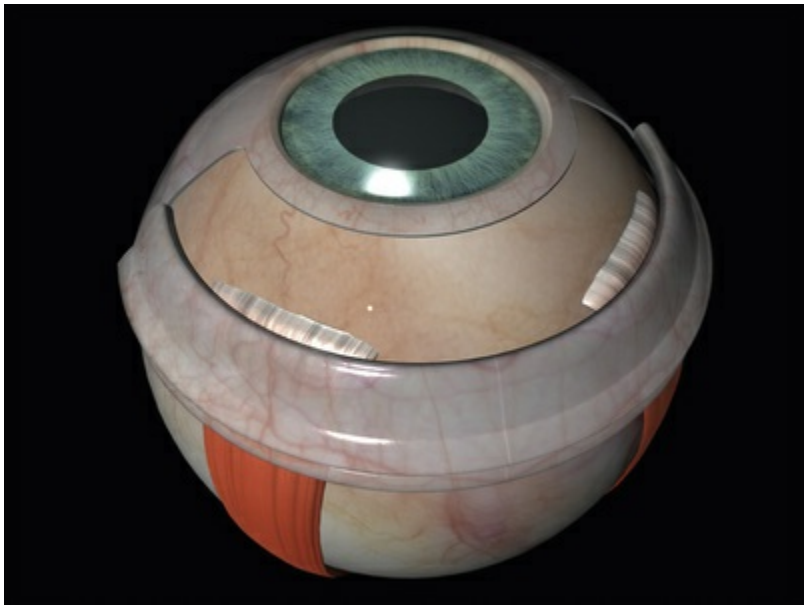

FIG. 104.9 A 180° peritomy with a 2-mm limbal frill of conjunctiva to facilitate closure.

The extent of the peritomy depends on the size of the buckle planned. A 360° peritomy is not required if a local explant is planned. Note that it is not necessary to perform a 360° peritomy purely to sling all four muscles as rectus bridle sutures can be passed transconjunctivally.

Slinging Rectus Muscles

Between two and four rectus muscles are slung depending on the planned size of the buckle.

A closed pair of blunt scissors is pushed through the intermuscular septum between two recti. The opening created is enlarged by spreading the blades (Fig. 104.10). In this way, the sub-Tenon space is opened and bare posterior sclera is exposed.

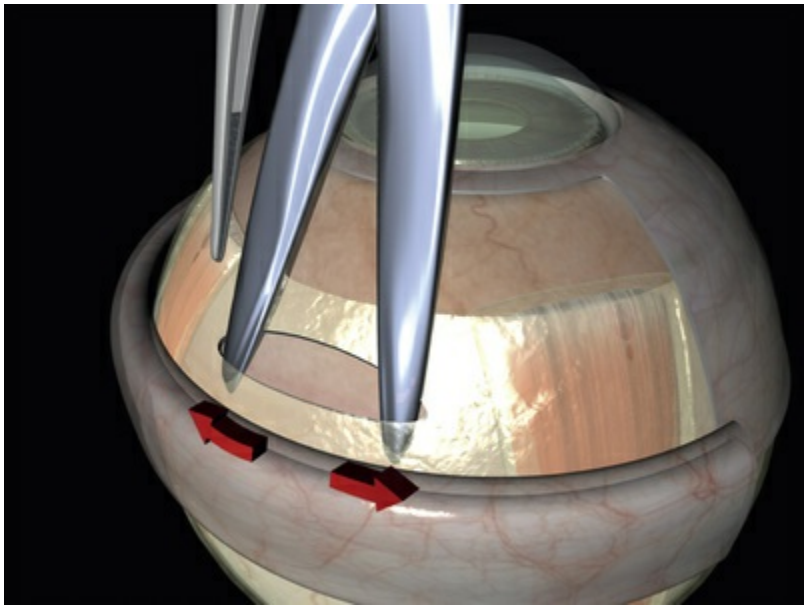

FIG. 104.10 Opening the intermuscular septum by spreading with blunt scissors. This opens the sub-Tenon space, exposing the posterior sclera.

The muscle is engaged with a sweeping posterior and circumferential movement around the globe employing a specialized muscle hook (Fig. 104.11 online). Very posterior "sweeps" risk damage to the vortex veins. Once a rectus has been successfully hooked, the globe moves with the hook. If the muscle is inadvertently split, a second hook can be passed from the opposite side of the muscle. The remaining anterior fibers of the intermuscular septum are now cut off or swept off. This dissection should be limited to the fascia required to visualize the sclera.

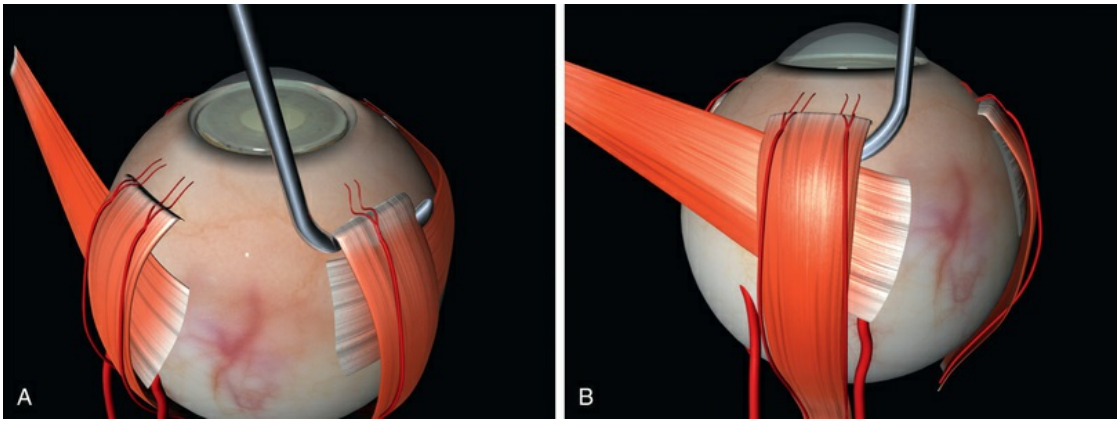

FIG. 104.11 Passage of muscle hooks to avoid the obliques – the lateral rectus from above (A) and the

superior rectus from the temporal side (B).

A large braided (e.g., 2-0 silk) bridle suture is passed under the muscle. There are various ways of achieving this involving reverse passage of the suture under the muscle (to avoid engaging the tip in the sclera). Alternatively, a modified muscle hook with a threading eyelet at its tip can be used.[18] These bridle sutures can be clipped to the surgical drape to position and stabilize the globe thereafter (e.g., while suturing). When free movement of the globe is desirable (e.g., when searching for breaks), the clips are released.

The sclera is now inspected for dark ectatic areas (Fig. 104.12). Suturing and even cryotherapy or indentation at these sites can be perilous, so their early identification is essential.

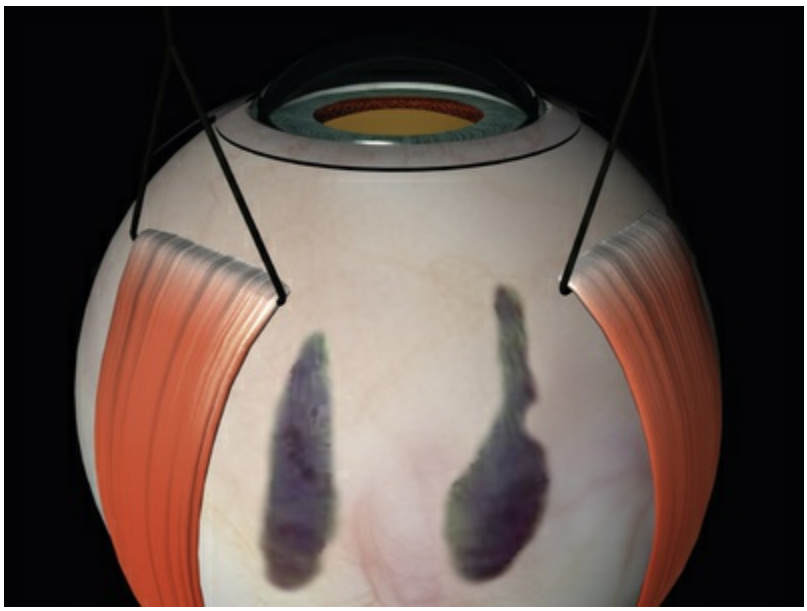

FIG. 104.12 Scleromalacia. The sclera is examined for any areas of thin sclera at the start of surgery. Surgical manipulation is avoided in these areas because of the risk of scleral perforation.

Reoperations

Special precautions must be taken during revision surgery.

Adhesions are invariably present between the conjunctiva and sclera. A cutting action with the scissors is more effective than a

spreading action in breaking these. Care must be taken to avoid delaminating into the sclera or buttonholing conjunctiva.

A fibrous capsule forms around old explants. Incising this capsule exposes the surface of the explant. The plane thereby opened up is useful for slinging rectus muscles. The muscle hooks are placed around the muscles over the explants before these are removed. The rest of the periexplant capsule is then trimmed flush with the sclera. The sclera is often very thin in the bed of longstanding buckles, especially encircling elements. No attempt is made therefore to dissect capsule off the bed of the buckle. Particular care must be taken when dissecting the capsule from the very thin sclera under the rectus muscles. The scissors are gently lifted away from the globe while closing the blades.

Examination Under Anesthesia and Break Localization

A careful indented examination under anesthesia of the whole peripheral retina is now carried out to confirm the location of the retinal breaks. The preoperative drawings provide a useful reference if they are difficult to locate.

Most surgeons employ indirect ophthalmoscopy using a sterile condensing lens. Some surgeons advocate microscopic visualization using endoillumination (such as a chandelier inserted through the pars plana) in combination with an indirect viewing system such as the Biom.[19]

The location of each break is marked on the sclera. This essential step is carried out while the cornea is clear and allows planning of the rest of the operation. The sclera is indented under indirect ophthalmoscopic indentation using a fine (but not sharp) tipped instrument such as a Gass scleral indenter.[20] Once the indent is seen to correspond to the position of a retinal break, sustained (for several seconds) indentation is applied. The resulting transient scleral thinning produces a focal area of scleral translucency, and the underlying choroid shows through. This point is then marked with very gentle diathermy or a surgical marker pen. If a marker pen is used, the sclera is dried both before and after the application to prevent the dye spreading. Several marks are made for larger

breaks.

Errors in break localization may lead to buckle malposition. Localization errors tend to be radial (i.e., determining how far back a break is) rather than circumferential (determining its clock hour). For example, if a retinal break is highly elevated (as in a bullous detachment), parallax errors may make the break seem more posterior than it truly is (Fig. 104.13).

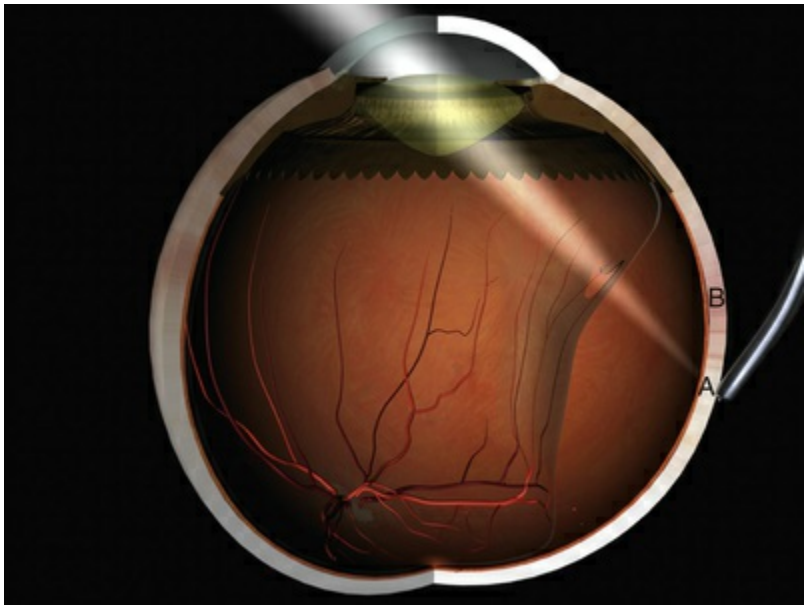

FIG. 104.13 Break localization error. When breaks are highly elevated, they appear more posterior than they really are due to parallax. *A*, apparent location; *B*, actual location.

Parallax errors may be avoided by draining subretinal fluid and then reforming the globe with air (the DACE – drain, air, cryotherapy, explant – operation) (Fig. 104.14).[21,22] The view of the retina through the gas bubble can be challenging for those not experienced with this technique.

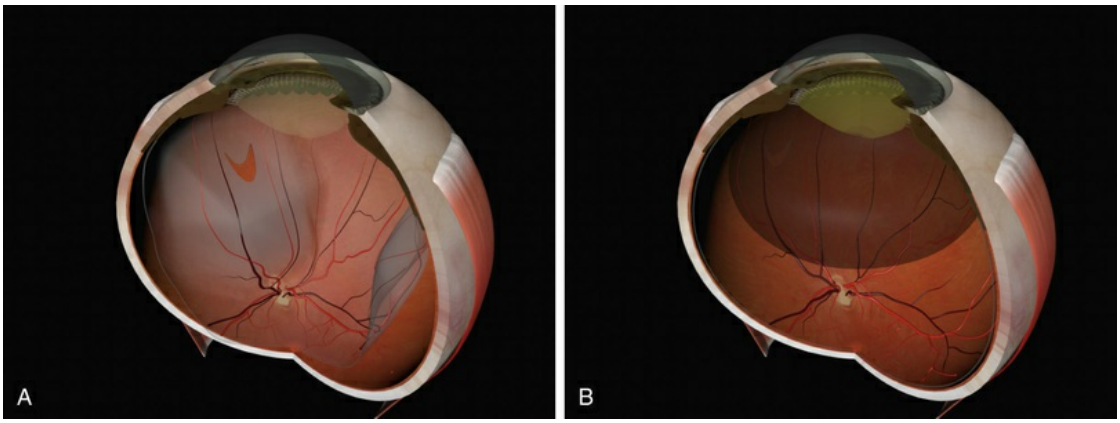

FIG. 104.14 Bullous retinal detachment: (A) managed with the DACE (drain, air, cryotherapy, explant) procedure. (B) The operation starts with subretinal fluid drainage and air injection. This aids subsequent break localization.

The development of corneal opacity greatly complicates surgery, particularly if it develops in the early stages of the procedure. This should be avoided by using preservative-free drops for preoperative pupil dilatation and avoiding the corneal epithelium desiccation by periodic irrigation with saline or use of a coating of dispersive viscoelastic. If corneal epithelial edema develops, the view may be transiently improved by rolling a damp cotton bud over the cornea accompanied by slight downward pressure on the globe. If this fails, corneal epithelial debridement may become necessary.

Retinopexy

The indent from the explant closes retinal breaks, but retinopexy is required to produce an enduring bond between the retina and the retinal pigment epithelium that will persist even if the indent disappears.[23]

Retinopexy was initially achieved using diathermy in association with lamellar scleral dissection and scleral implants.[4] Cryotherapy has supplanted diathermy because it can be performed without scleral dissection and the treatment can be monitored ophthalmoscopically. More recently photocoagulation has also been used.

Cryotherapy

The technique of cryotherapy is described in detail in Chapter 110 (Prevention of retinal detachment). The aim is to produce freezing of healthy retina surrounding all the retinal breaks. The treatment is monitored using the indirect ophthalmoscope. When the indent from the tip of the cryoprobe is seen under a retinal break, the cryoprobe is activated. After a few seconds one observes whitening of the retina. Smaller breaks can be treated with a single application. The break is seen as a darker area within the freeze, and this is useful in confirming that the whole break has been treated. Larger breaks may need several applications. These are applied by working methodically around the edges of the break to ensure contiguous burns with minimal overlap (Fig. 104.15). Refreezing and freezing of the bare central RPE in large breaks are avoided to reduce the risk of RPE dispersion.[24]

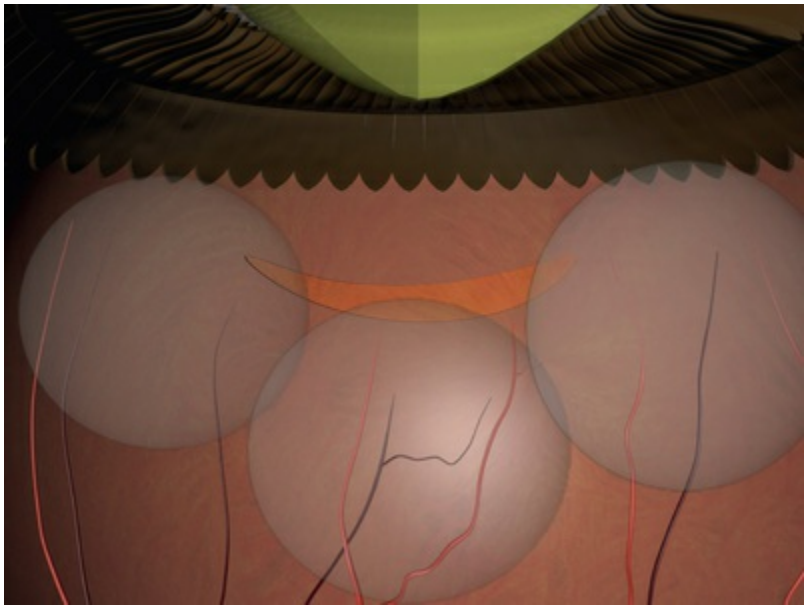

FIG. 104.15 Confluent cryotherapy burns with minimal overlap.

One can envisage the immediate tissue reaction as an ice ball expanding outwards progressively in every direction from the tip of the probe for as long as the cryoprobe is active. Some factors (the insulating effect of an intervening rectus muscle, the heat sink effect of the choroidal circulation) impede the development of a visible

reaction on the retina. Others (reduced choroidal blood flow in high myopia, the insulating effect of intraocular gas) hasten the development of retinal freezing. The effect of subretinal fluid is particularly important.

In the presence of shallow subretinal fluid, the indentation of the tip of the cryoprobe approximates the pigment epithelium to the retina and both freeze almost simultaneously. If the breaks are more elevated, the pigment epithelium cannot be opposed to the retina. Freezing of the pigment epithelium can then be clearly seen to precede freezing of the retina, sometimes by several seconds (Fig. 104.16). In this situation, what is the optimal end point of treatment: freezing of the pigment epithelium or the retina? This is a particularly important question given the concern about potential adverse effects of excessive cryotherapy on other tissues.[25–27] In an experimental model the adhesions produced by freezing of the retinal pigment epithelium alone lacked the microvillous interdigitations normally present between pigment epithelium and retina. The resulting chorioretinal adhesion was weaker than when the freeze was allowed to extend to the retina.[28] In practice, the chorioretinal adhesions that develop from freezing of the pigment epithelium alone seem to be sufficient. A further advantage of freezing the retina, however, is that the "lighting up" of the retinal breaks is a useful confirmation that all the edges of the break have been treated.

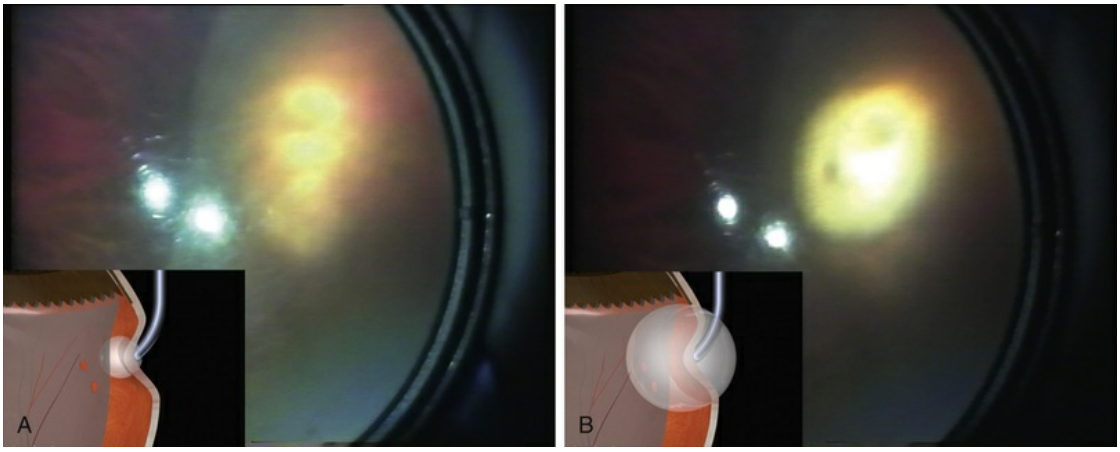

FIG. 104.16 Cryotherapy in the presence of subretinal fluid. Freezing of the retinal pigment epithelium is seen to occur first (A). As the ice ball gets bigger, freezing of

the retina with lighting up of the breaks (B).

In the presence of bullous subretinal fluid, it may be impossible to approximate the retina to the retinal pigment epithelium. In this situation, subretinal fluid drainage is probably safer than very heavy cryotherapy, which may cause severe postoperative vitritis.

The tip of the cryoprobe must be allowed to thaw completely before attempted withdrawal, otherwise choroidal hemorrhage and even scleral avulsion may occur.

Cryotherapy to the disc or macula (Fig. 104.17) occurs when the indentation from the shaft of the probe is mistaken for its tip ("shaft indentation") (Fig. 104.18). This cognitive problem can be avoided by encouraging trainees to intentionally indent posteriorly (without actually activating the cryoprobe!) (Fig. 104.19). They then become familiar with the distinctive appearance of shaft indentation.

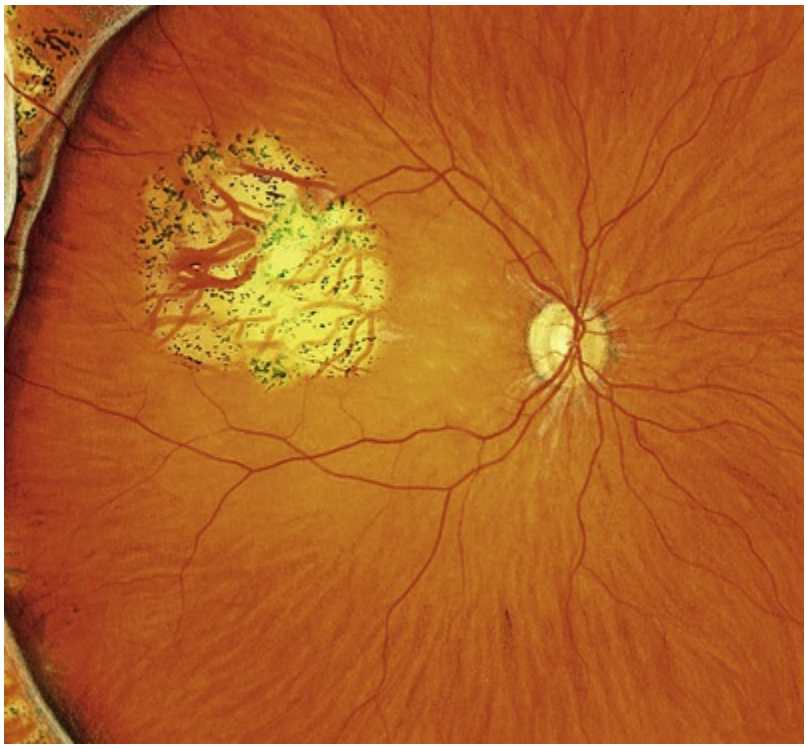

FIG. 104.17 Inadvertent cryotherapy to the posterior pole.

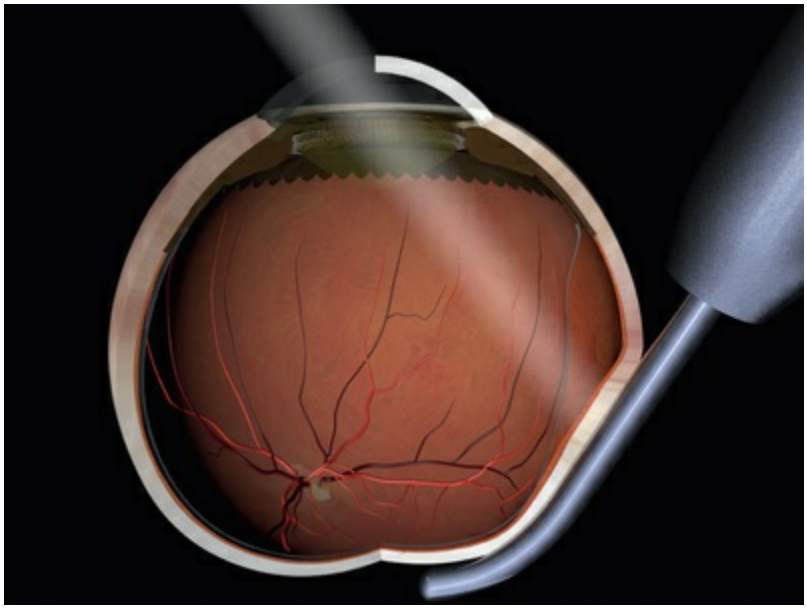

FIG. 104.18 Shaft indentation – a cause of posterior cryotherapy.

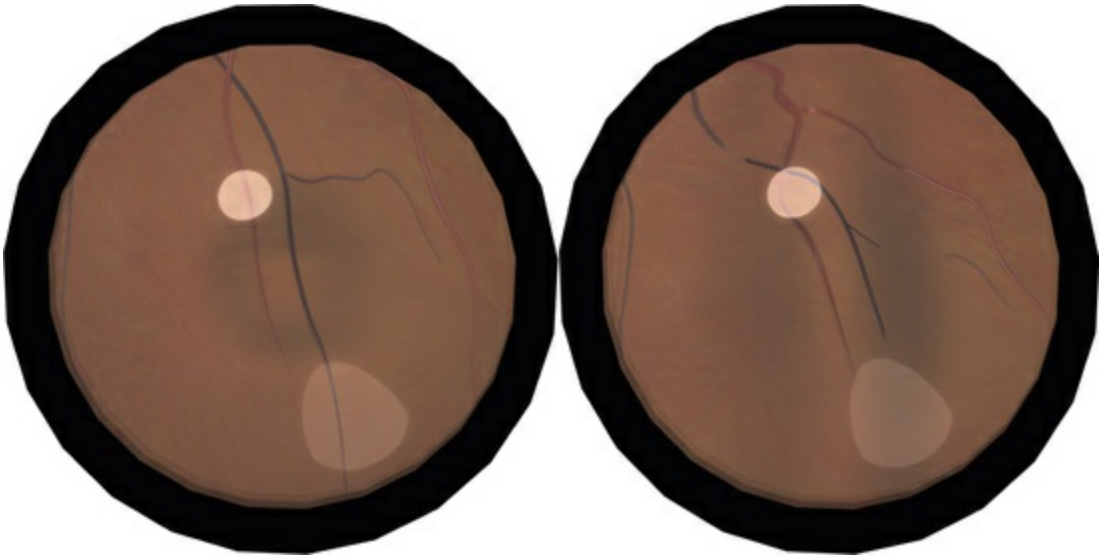

FIG. 104.19 The appearance of shaft indentation (right) compared with tip indentation (left).

Beginners find cryotherapy on anterior breaks challenging because the cryoprobe has a tendency to slip over the surface of the eye. This can be overcome with counter-traction from the bridle sutures on the opposite recti (Fig. 104.20). Alternatively, the cryoprobe is intentionally placed anterior to the break and the globe rotated using the tip of the probe. The pressure of the probe is then

slightly released while the indent from the probe is viewed using indirect ophthalmoscopy. As the globe returns slowly to the primary position, the tip indentation is seen to move. When the indentation of the tip is under the break, a very small increase in the pressure applied stabilizes the globe and the cryoprobe is activated.

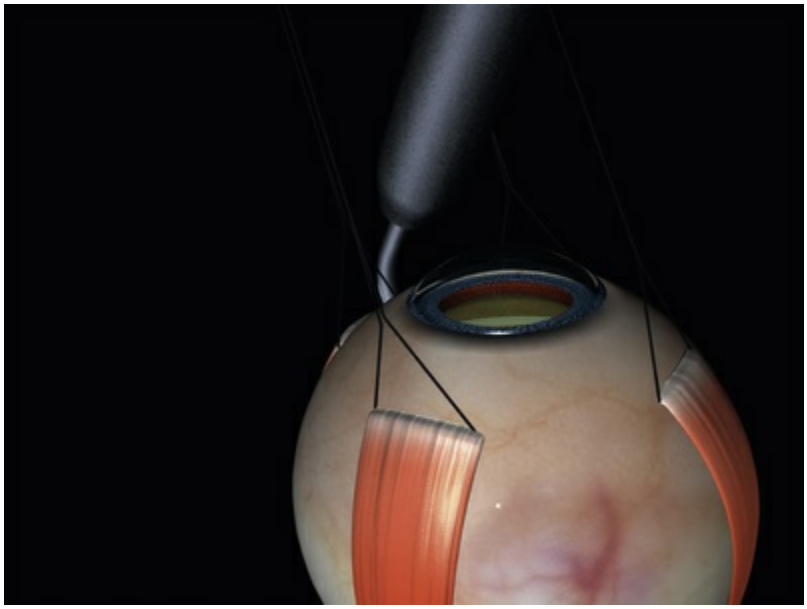

FIG. 104.20 Additional bridle sutures to stabilize the globe during treatment of large anterior breaks, e.g., a dialysis.

Diode Laser

The delivery technique of transscleral diode laser uses a probe that indents the sclera under indirect ophthalmoscopic visualization. A diode laser aiming beam facilitates accurate placement of the tip. The endpoint of treatment can be difficult to titrate, particularly in blonde fundi, and overtreatment with choroidal hemorrhage and scleral thinning may occur during the learning curve.[29] The theoretical advantages of diode laser (less inflammation, blood–ocular barrier breakdown, and pigment dispersion) do not seem to translate into clinical practice as a large randomized trial failed to find any advantage over cryotherapy.[30]

Photocoagulation

Photocoagulation may be applied several days to weeks postoperatively once the retina has reattached.[31,32] While visual recovery was faster in the postoperative laser retinopexy groups, the final anatomic and visual results are comparable to cryopexy. Photocoagulation on the buckle is uncomfortable and requires the use of regional anesthesia. The main disadvantage of this technique is the need for an additional procedure.

Choice of Retinopexy Technique

Intraoperative cryopexy remains a quick and simple technique. The search for an alternative means of producing retinopexy is driven by the belief that cryotherapy is inherently dangerous. This view has been challenged.[33]

Manipulation of the globe after cryotherapy causes release of pigment into the vitreous cavity,[24] and some surgeons prefer to carry out cryotherapy at a later operative stage.

Choice of Scleral Explant

Knowledge of the location of all the retinal breaks and their elevation allows planning of the rest of the operation, including the choice of scleral explant.

The aim of placing an explant is the creation of an indentation in the wall of the eye which provides adequate support to all the elevated retinal breaks. Areas of detachment where there are no breaks do not require support. Breaks in areas of attached retina can be treated with retinopexy alone.

Historically, a number of materials have been used in the manufacture of explants.[34] None of these seem to be as well tolerated as silicone rubber which is biologically inert and can be left in situ indefinitely.[6,35]

Two types of cylindrical silicone explant are currently in regular use: solid silicone tires and silicone sponges consisting of air-filled cells (Fig. 104.21). Early silicone sponges had communicating air cells and an increased risk of infection,[36] but this problem has been much reduced by the use of sponges with closed air cells.

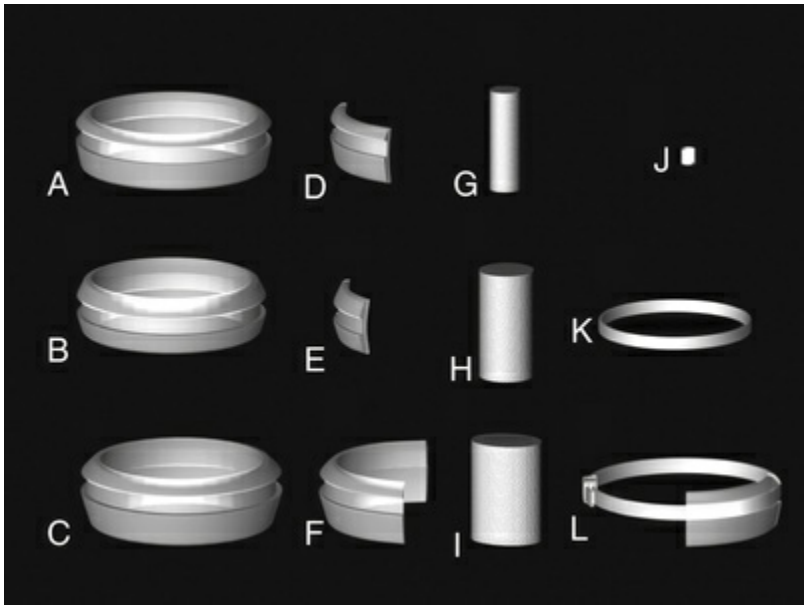

FIG. 104.21 Various types of explant may be used. Solid silicone tires of various sizes and profiles *(A–C)* are trimmed to the desired size *(D–F)*. Silicone sponges also come in various sizes *(G,H)* and may have a circular or oval cross-section *(I)*. Watzke sleeves *(J)* are used with bands *(K)* and silicone tires to create encirclements *(L)*.

Solid silicone is, for practical purposes, noncompressible. Silicone sponges, because of their cellular composition, are easily deformable and compressible. When a sponge is initially sutured, the sponge is compressed and the intraocular pressure rises. As the intraocular pressure subsequently falls to physiologic levels, the sponge expands facilitating closure of elevated retinal breaks. (Details of the mechanism of action of scleral buckles are described in Chapter 103, The effects and action of scleral buckles in the treatment of retinal detachment.)

The height of the indentation produced by an explant is a factor of the bite separation and the diameter of the explant. Silicone tires are generally thinner than sponges and therefore produce lower indents. When used to treat elevated breaks, an adjunctive measure such as subretinal fluid drainage or gas injection is more likely to be necessary if a circumferential tire is used.

The profile of the resulting indent also differs. Tires tend to produce broad indentation of uniform, albeit relatively low height. Sponges, particularly those with a circular cross-sectional profile,

are much higher centrally. Accurate localization in the transverse meridian is therefore critical when using a sponge with a circular cross-sectional profile.

The design of solid silicone tires reflects their original use as circumferential scleral implants. There is a groove on the upper surface with a rectangular profile to accommodate an overlying band. It was subsequently found that they can be used as explants.[37] Some surgeons dispense with the band and use them as purely local explants.

Silicone tires are usually oriented circumferentially. Sponges may be oriented either circumferentially or radially. The geometry of the indent favors radial orientation of sponges when treating retinal tears.[2] While the choice between tires and sponges is to some extent a matter of surgeon preference, their different physical properties favor their use in different situations depending on the number, size, and location of retinal breaks. This can be illustrated by some examples:

Example 1: A detachment with a single elevated equatorial tractional tear (Fig. 104.22). This may be closed successfully using a single radial sponge without drainage of subretinal fluid. If a silicone tire is used in the same situation, the indent may not be high enough to close retinal breaks without subretinal fluid drainage and/or gas injection.

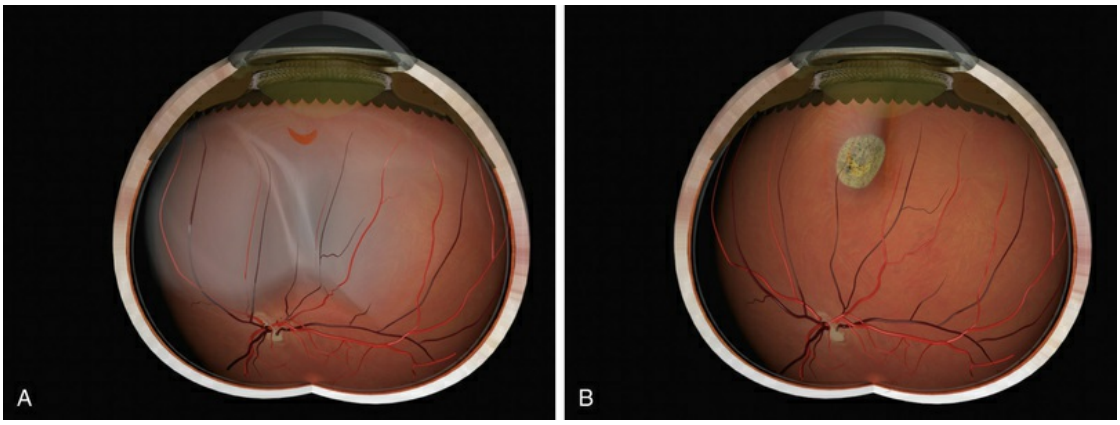

FIG. 104.22 (A) Elevated tear closed by (B) radial sponge (nondrainage).

Example 2: A detachment due to a series of round retinal holes (Fig. 104.23). The holes are anterior to the equator at various distances from the ora. They may be treated with a circumferential explant. A very high indent is not required because there is no traction on the breaks and the fluid is very shallow. As the distance from the ora varies the broader indentation from a tire can close all the breaks.

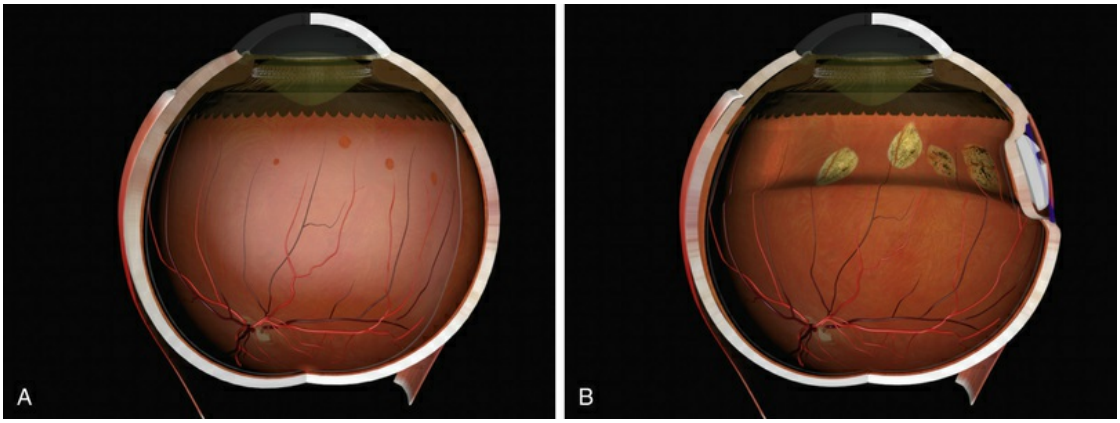

FIG. 104.23 (A) Atrophic round holes (varying distances from the ora) closed with (B) a broad tire.

Example 3: A pseudophakic eye with a total retinal detachment. Good visualization of the peripheral retina is impeded by peripheral capsule opacification and limited pupil dilatation (Fig. 104.24). No tears are seen. An internal approach using pars plana vitrectomy has many advantages here.[38] If this is not possible, an encircling tire may be used. The buckle may be secured just behind the rectus muscle insertions to support the anterior retina where the breaks are likely to be located. The tire supports the whole area of subretinal fluid ("dry-to-dry" buckling). The placement of an encircling silicone band in the groove of the tire maintains the height of the indent so that undetected retinal breaks remain closed.

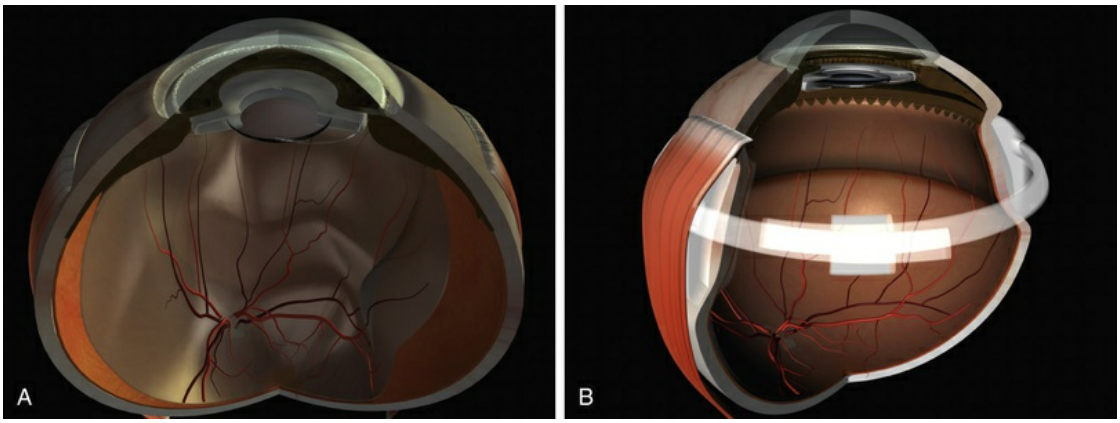

FIG. 104.24 (A) Extensive detachment in a pseudophakic eye with poor peripheral fundal view. The breaks are likely to be quite anterior. (B) An encircling tire has been used to close them.

Example 4: Three tractional tears are present (Fig. 104.25). They can be treated with separate radial sponges or with a single circumferential buckle.

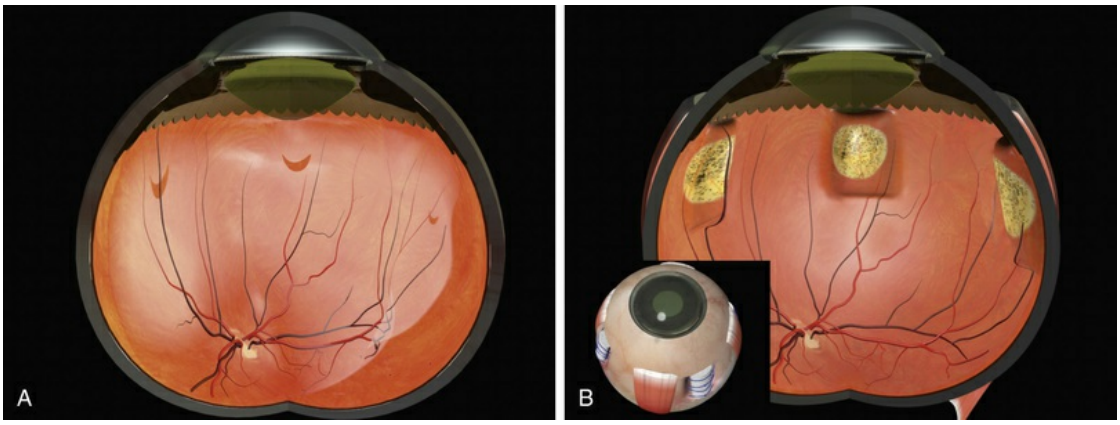

FIG. 104.25 (A,B) Multiple tears closed with sponges.

Example 5: Three tractional tears are again present, but they are too close together to be easily closed with individual radial sponges (Fig. 104.26). A "raft" of radial sponges sewn side-to-side is possible, but a circumferential buckle is an easier option. A high circumferential sponge may be used, but it can be difficult to close all the breaks because of the variable distances from the limbus. Furthermore, high circumferential sponges are particularly likely to result in fishmouthing (Fig. 104.27). A

circumferential tire combined with subretinal fluid drainage and/or gas injection may be used.

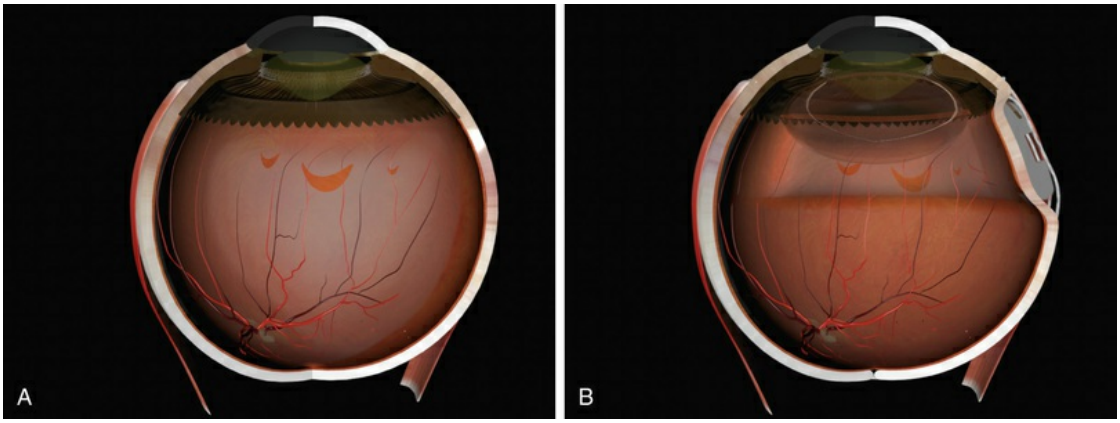

FIG. 104.26 (A) Multiple tears closed with (B) a tire and gas bubble.

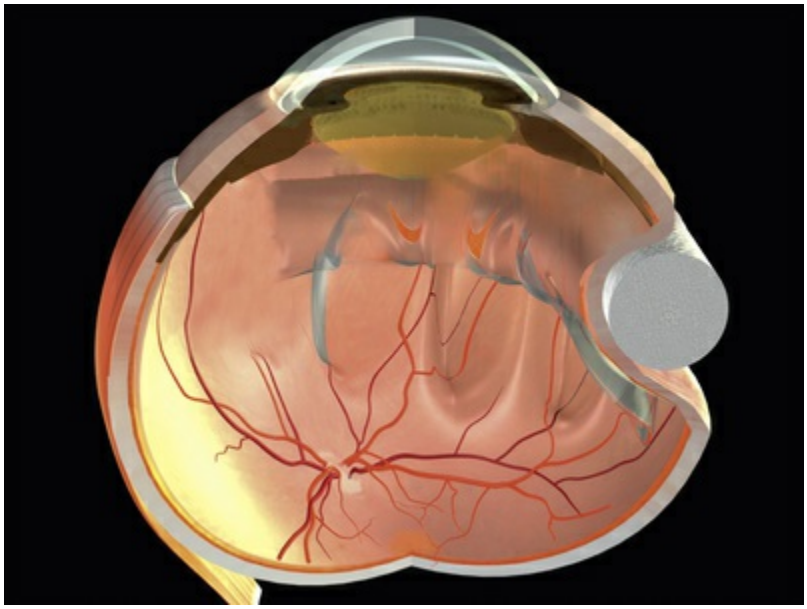

FIG. 104.27 Fishmouthing. The high indentation causes radial redundancy folds which keep breaks open.

Example 6: A retinal dialysis. Provided the indent is high enough (a 3-mm circumferential sponge usually works well), it does not need to be very wide and subretinal fluid drainage is usually

unnecessary (Fig. 104.28).[39]

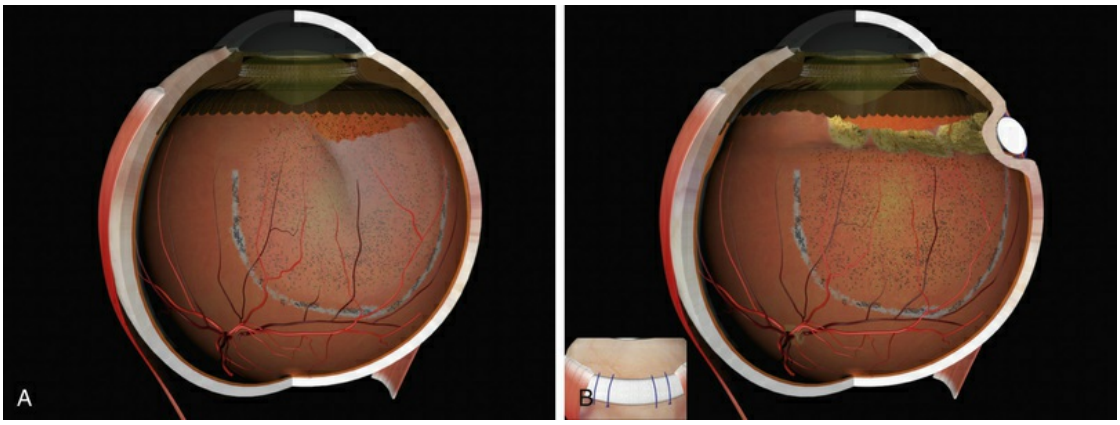

FIG. 104.28 (A) Chronic dialysis closed by (B) an anterior circumferential 3-mm sponge.

Scleral Sutures

Once the breaks have been marked, the size and position of the required buckle should be apparent so that partial-thickness scleral mattress sutures can be preplaced. Some surgeons prefer to carry out this step later in the operation following cryotherapy.

The desirable physical properties of scleral sutures are durability, biocompatibility, and ease of handling. Monofilament nylon and polyester both possess all these properties. A braided surface modified polyester is slightly easier to handle than a monofilament suture: the friction between throws of the knot makes it easier to tie the knot under tension. Nylon, however, has better "memory," and several throws will keep the tension in the knot without resorting to slip knots or holding the knot between throws.

The suture bites are oriented parallel to the long axis of the explant (i.e., radial suture bites for a radial explant, circumferential bites for a circumferential explant).

The distance between the bites is significantly greater than the width of the explant. This allows the sclera to partially envelop the explant, creating the indent. For example, when suturing a 5-mm sponge, the bites are placed 8 mm apart. Silicone tires generally need a bite separation 2 mm greater than their width. Failure to space the bites sufficiently reduces the height of the indent. Calipers

are used to ensure accurate bite separation (Fig. 104.29). The bites pass in opposite directions so that the mattress suture has a box configuration and the sutures do not cross over on the buckle. Crossing over of the sutures reduces the length of the indent (Fig. 104.30). A box suture may be difficult to achieve with posterior radial bites, as it is easier and safer to pass a bite anteroposteriorly than it is to pass it posteroanteriorly. Use of a double-armed suture allows two anteroposterior passes of the needle. Alternatively, a figure-of-eight suture may be converted to a box suture by dividing the suture between the bites (Fig. 104.31).

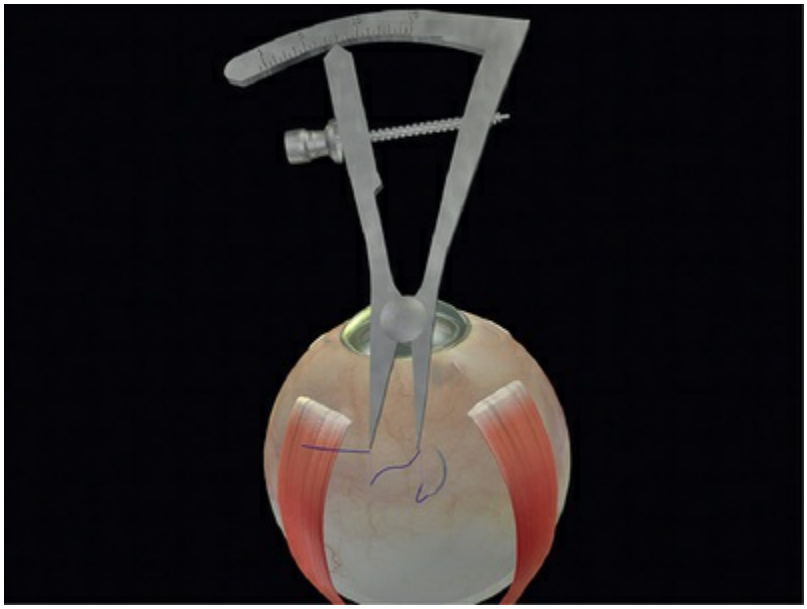

FIG. 104.29 Calipers used to ensure the correct suture bite separation – in this case 8 mm for a 5-mm sponge.

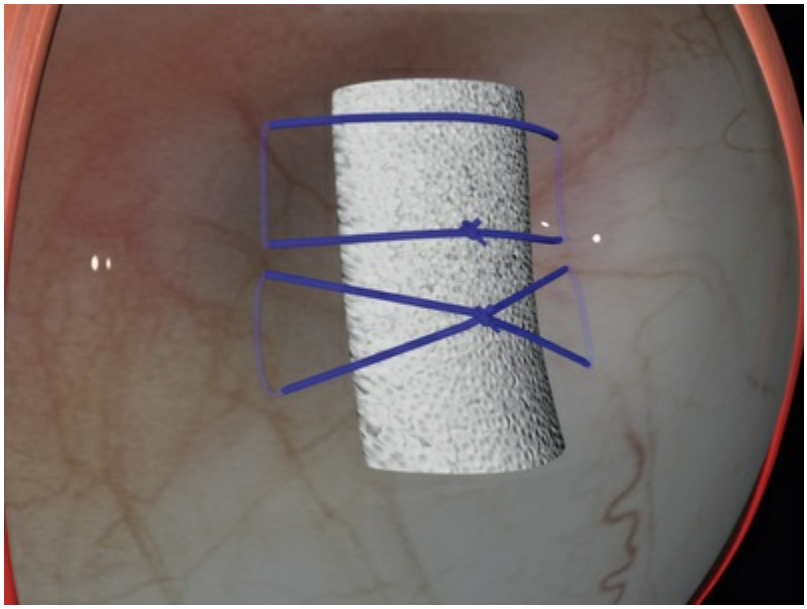

FIG. 104.30 A crossed mattress suture (bottom) does not support the ends of the sponge as well as a box suture (top).

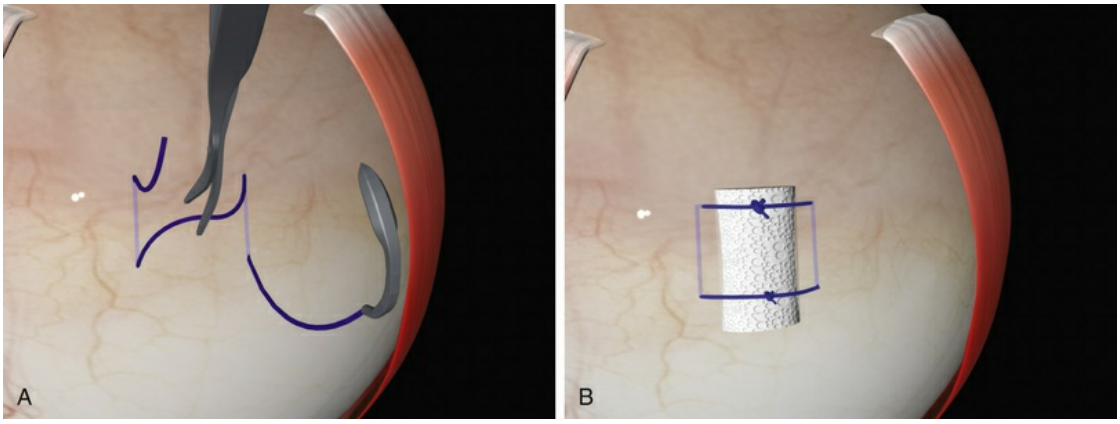

FIG. 104.31 Conversion of (A) a crossed mattress suture to (B) a box mattress suture.

Mattress sutures should have a square configuration, with the bites parallel to each other and the long axis of the buckle. Irregular nonparallel sutures cause less-effective indentation (Fig. 104.32).

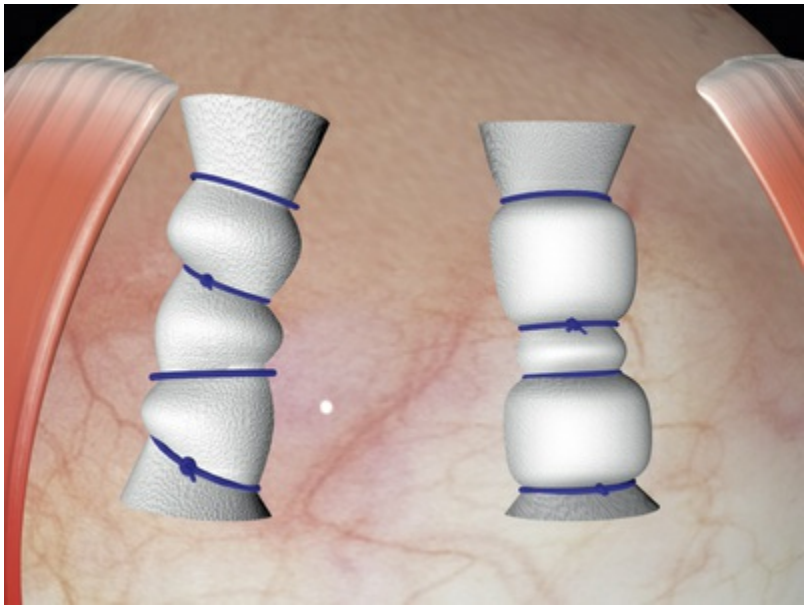

FIG. 104.32 Irregular untidy sutures give uneven indents.

The sutures need to be placed partial thickness (½–⅓) through the sclera. As the sclera is only 1 mm thick, care needs to be taken to avoid scleral perforation. A spatulated needle rather than a cutting needle is used. The spatulated needle profile has a flat top and bottom and cutting lateral edges (Fig. 104.33). The sclera has a pseudolamellar structure.[40] When appropriately used, a spatulated needle tends to glide between the scleral lamellae.

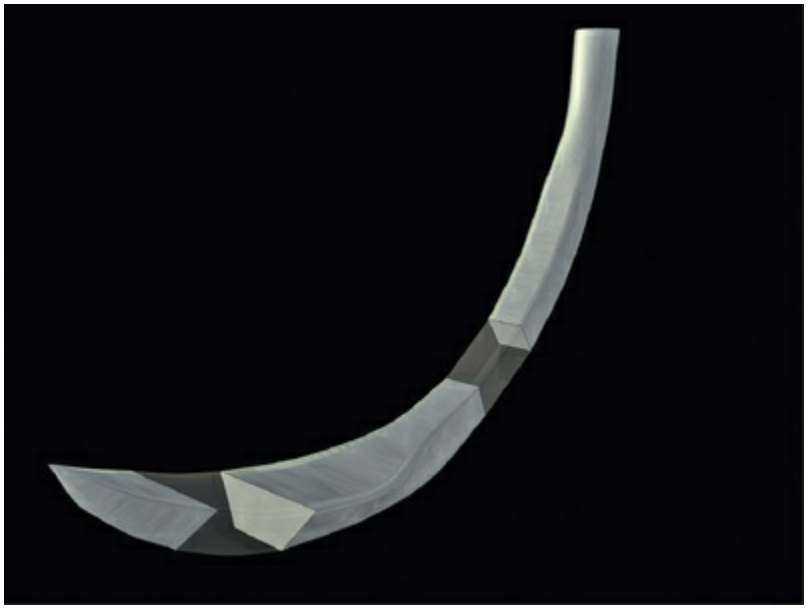

FIG. 104.33 The structure of a spatulated needle. The

side cutting tip favors its passage at a constant depth between scleral lamellae. This is a 3/8 circle needle – a 1/2 circle may be needed when access is difficult (e.g., posterior scleral sutures).

When suturing (and whenever putting needles in the globe, e.g., during drainage) a forceps held in the nondominant hand is used to grasp a rectus insertion. This positions and fixates the globe for the suture and also allows the intraocular pressure to be adjusted if the eye is very soft. The spatulated needle is mounted 2/3 of the distance from its tip in a curved (e.g., Barraquer) needleholder.

The tip of the needle is placed on the sclera so that the tangent of the tip is parallel with the surface of the eye. It is important to ensure the needle does not bank, as this may cause the needle to cut out laterally (Fig. 104.34). When placing posterior sutures, this is easiest to achieve while sitting on the opposite side of the eye from the surgical area (Fig. 104.35). In fact it is a good principle to always operate "over the cornea," as this gives better access to the recesses of the sub-Tenon space.

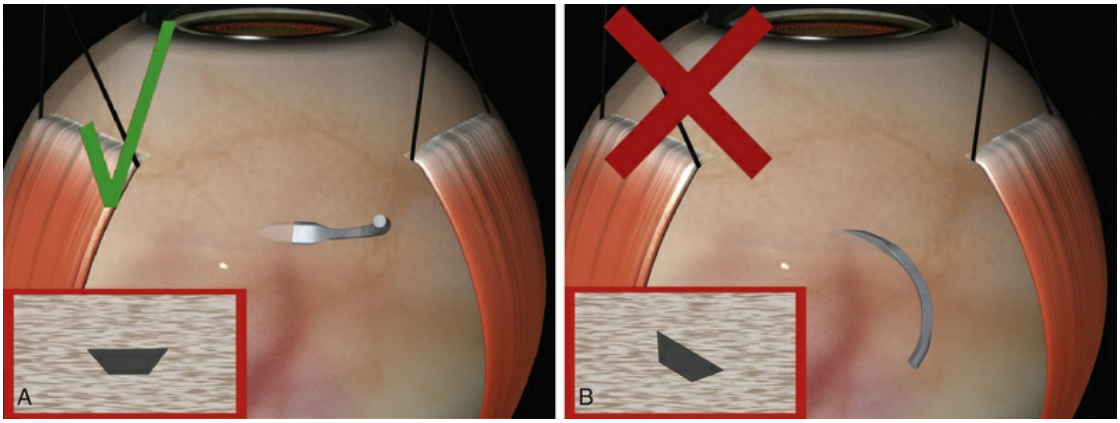

FIG. 104.34 A spatulated flat should be laid flat on the sclera (A) – if it banks (B), it may cut out.

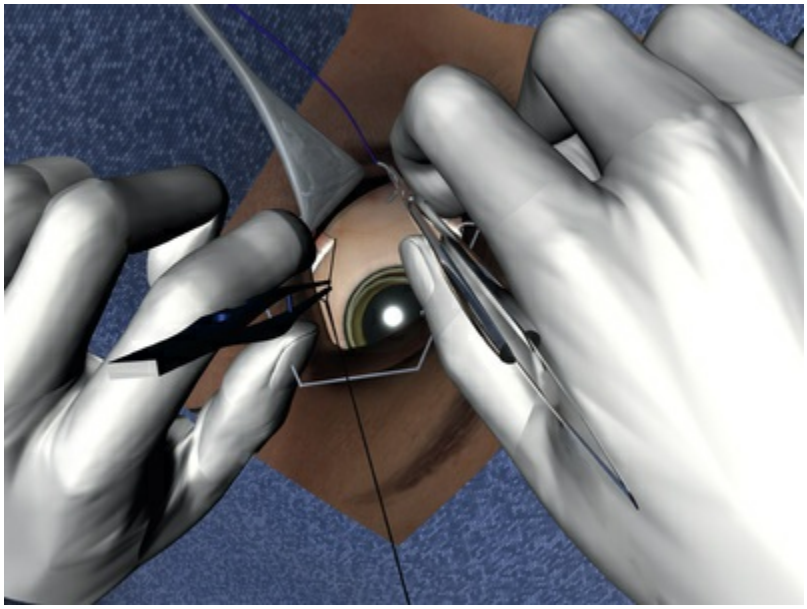

FIG. 104.35 Operate from the other side (“over the cornea”) for access to the posterior sub-Tenon space.

Gentle downward pressure creates a small indent (Fig. 104.36). The needle is now advanced, keeping the tangent of its tip parallel to the surface of the eye. This causes it to advance progressively deeper into the sclera. Once it has reached the desired depth, no more downward pressure is applied. The spatulated design of the needle allows it to glide (or delaminate) between the scleral lamellae at a constant depth.

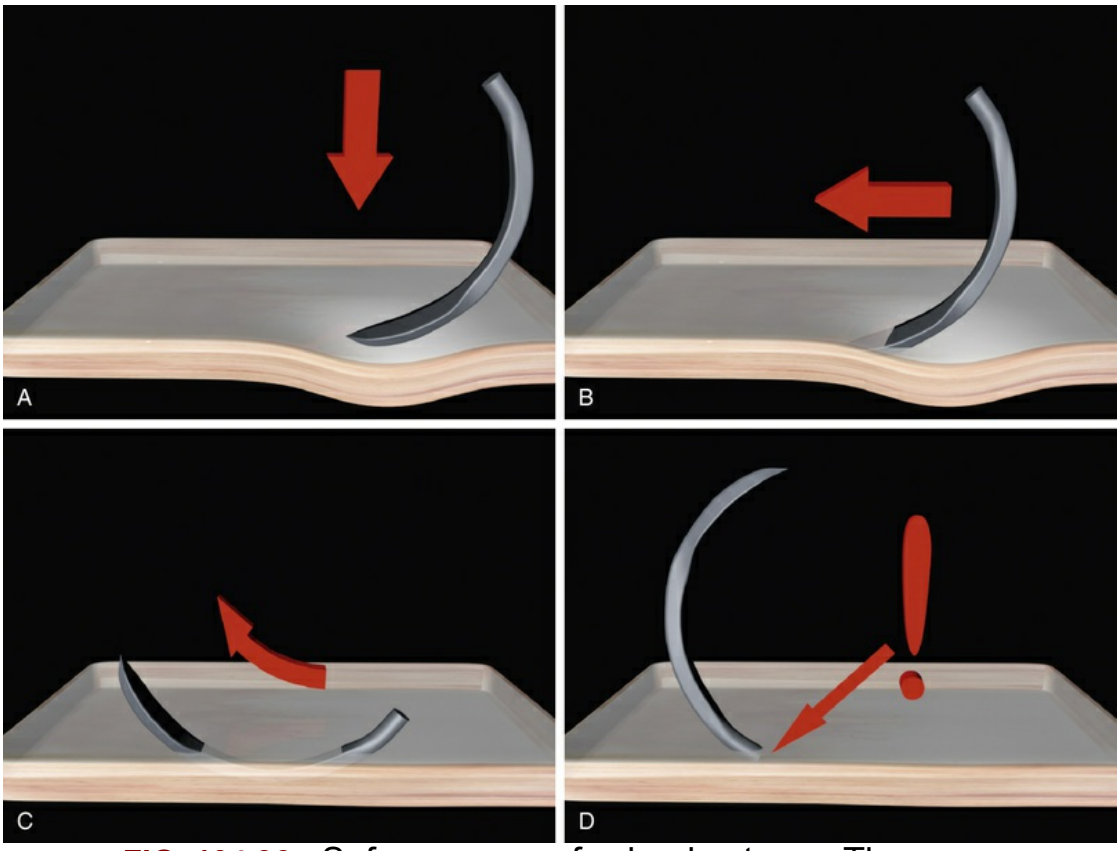

FIG. 104.36 Safe passage of scleral sutures. The depth of the needle is gauged by its visibility throughout. At the correct depth the body of the needle is just visible as it passes through the sclera. If it is very clearly visible, the needle track may be too superficial and the suture may tear out when tied. If the body of the needle is not visible at all, it may have penetrated the sclera.

The depth of the needle passage is monitored continuously during its passage through the sclera. At a depth of 500 μm, the needle is only just visible. The depth of the needle can be varied during the pass. Downward pressure while advancing the needle will take it deeper into the sclera and slight rotation (or lifting) of the needle can be used to reduce its depth. While care must be taken not to perforate the sclera, the entrance and exit from the sclera should not be too shallow (Fig. 104.37). If the start or end of the bite is very superficial, the sutures may partially tear out under tension. Once the bite is deemed of adequate length (usually 4–5 mm), the needle is rotated to bring the tip out of the sclera.

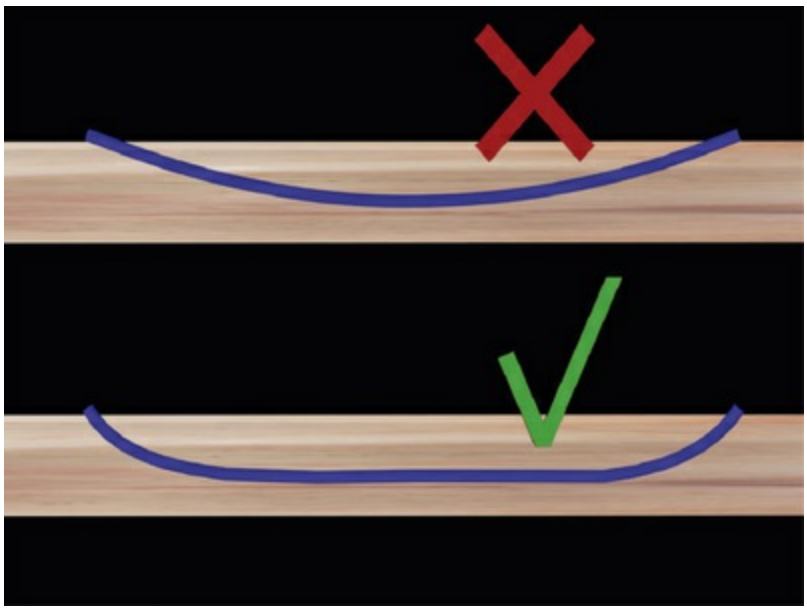

FIG. 104.37 Suture track. If the entry or exit is too shallow, the suture may cut out.

Great care must be taken with the heel of the needle at this stage to prevent it penetrating the sclera. A good rule is to focus one's attention on the heel rather than the tip once the tip is clear of the sclera.

With experience, it is possible to modify this technique by initially engaging the scleral fibers more vertically with the tip before flattening the tip, indenting, and advancing the needle.

The consequences of deep sutures depend on the state of the underlying retina. If the perforation occurs at a site with deep subretinal fluid, the retina is generally unaffected, and unless there is significant hemorrhage, there are no adverse consequences. If a deep suture is passed in an area of attached retina, a retinotomy may be created which will require retinopexy. In any event, the suture can act as a conduit for microorganisms to enter the eye and should be replaced. Deep sutures anterior to the spiral of Tillaux (as used for circumferential explants) do not injure the retina.

Tying the Sutures

The aspiring vitreoretinal surgeon should have a good understanding of basic surgical principles. The properties of surgeon's knots (Fig. 104.38A) and slip knots (Fig. 104.38B) are particularly important.[41] Scleral mattress sutures have to be tied under tension to create an indent. There are a number of ways of

doing this.

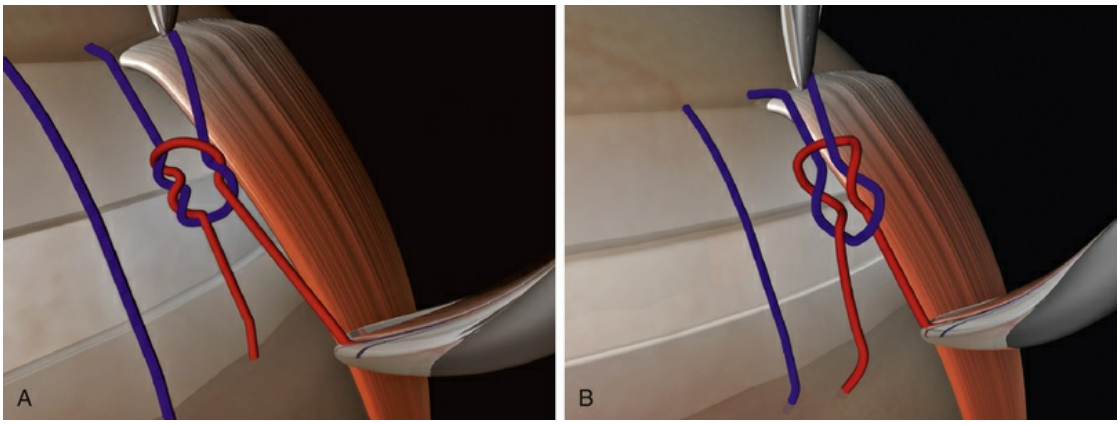

FIG. 104.38 Surgical knots. The ends have been colored differently to highlight the knot architecture. A surgeon's knot (A) is a square (or reef) knot with an extra forward throw. It is secure and compact but will slacken between the forward and backward throws unless the tension in the forward throws is maintained by grasping them with a second instrument. Alternately, multiple forward throws will maintain their tension. The tension in the knot cannot be easily adjusted unlike a slip knot (B), which can be easily tightened if using a low friction material. Note that the knot is inherently less stable unless extra turns of the suture are then added.

A slip knot (1–1–1) can be tightened on the second throw. In this case, two single throws are made without the special care needed to produce a surgeon's knot. A slip knot generally occurs by default. One easy way of ensuring this is to do a single “forward throw” first and then a single “reverse” or “backward” throw but to pull the suture ends in the same direction on both throws (i.e., not to alternate the direction of pull as one would with a surgeon's knot). Knot slippage requires low suture friction and is easier to achieve with synthetic monofilament sutures such as nylon and virtually impossible with Ethibond. Slip knots require extra throws after the tension has been adjusted to prevent later slippage and loosening of the knot.

A “locking” knot, where the two ends of the sutures are pulled firmly to one end between throws, maintains its tension after the

first throw (although a double or even treble first throw is required). This can be achieved using any suture material.

A surgeon's knot (similar to a reef knot but with a 2–1 structure) can be used if the assistant holds the knot with a pair of forceps between the first and second throws to maintain the tension of the first throw. The resulting knot is very compact.

Alternatively, one can rely on the friction and "memory" of a large number of throws to maintain the tension between the second and third throws. The resulting knot is bulkier than a surgeon's knot.

The use of releasable bow knots allows subsequent retying to adjust the height of the buckle. The bow can finally be converted to a surgeon's knot by cutting the loop and pulling on the shorter end of the cut suture through the knot.

Prominent suture ends may erode through the conjunctiva and ultimately lead to extrusion of the buckle. Once the knots have been tied securely, the sutures should therefore be rotated bimanually to leave the knot lying posteriorly (Fig. 104.39). If nylon is used, the ends should be trimmed close to the knot.

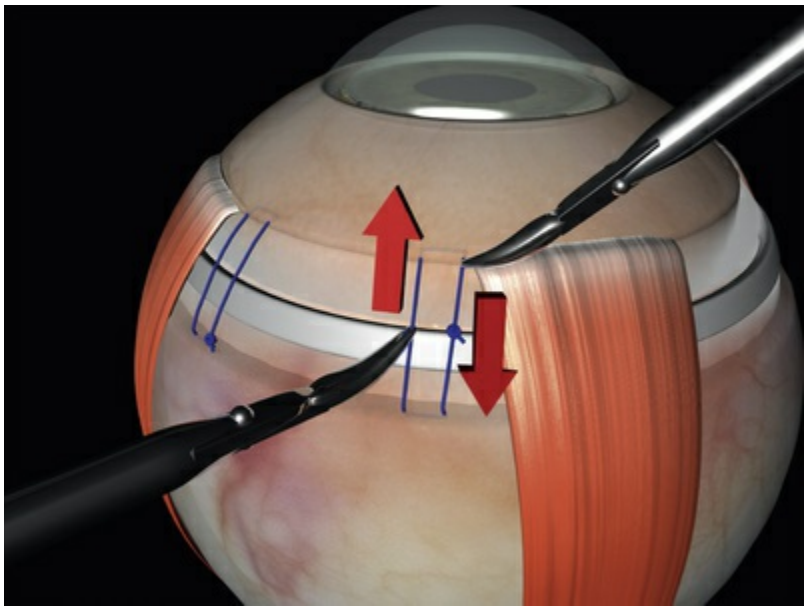

FIG. 104.39 Bimanual suture rotation to leave knots lying posteriorly.

Subretinal Fluid Drainage

Indications for Drainage

There is no consensus on the role of subretinal fluid drainage. Approximation of retinal breaks alone is sufficient to cause retinal reattachment (see also Chapter 103, The effects and action of scleral buckles in the treatment of retinal detachment).[42] Subretinal fluid drainage has been used to lower intraocular pressure, but this can be achieved in other ways, for example by paracentesis.[43] The anterior chamber depth is quickly restored particularly in myopic and pseudophakic eyes, allowing repeated paracentesis. A randomized controlled trial of medium complexity cases showed no advantage of subretinal fluid drainage.[44]

It is easier to state which eyes do not require subretinal fluid drainage. Scleral buckling is particularly effective in closing breaks without vitreous detachment. Detachments due to atrophic round holes and retinal dialysis can therefore usually be managed without subretinal fluid drainage. Conversely, most retinal surgeons will drain subretinal fluid in eyes with highly elevated tractional tears, very long-standing detachments or proliferative vitreoretinopathy (PVR). The decision whether to drain subretinal fluid is not made in isolation but is part of the overall planning of the surgery. For example, the choice of buckle or the need for intraocular air injection may influence the decision to drain. A case that could be managed with a nondrainage technique using a radial sponge may require subretinal fluid drainage if a circumferential solid silicone tire is used. While subretinal fluid drainage was previously in as many as 75% of cases, the trend towards increasing use of vitrectomy and pneumatic retinopexy in more bullous detachments has reduced the number of cases in which external subretinal fluid drainage is necessary in many surgeons' practices.[45]

Technique of Drainage

Timing.

Subretinal fluid drainage may be carried out at various stages in the operation. The DACE (drain, air, cryotherapy, explant) sequence was developed for bullous retinal detachments. Subretinal fluid

drainage followed by air injection to reform the globe prevents parallax errors during break localization. It has also been argued that cryotherapy may cause vascular congestion of the choriocapillaris and that subretinal fluid drainage should not therefore follow cryotherapy.[46] In practice, subretinal fluid drainage does not appear any more hazardous when performed after cryotherapy.[47] It can even be performed at the end of the operation.[48]

Location of Drain Sites.

The long ciliary neurovascular complexes run at 3 and 9 o'clock, and these sites should be avoided, as should the area around the vortex veins. Sites adjacent to (but not under) the horizontal recti are optimal from the perspective of avoiding choroidal vasculature.[46]

Draining anteriorly may carry a lower rate of hemorrhage, but drainage may be less complete than if the drainage is carried out more posteriorly. Drainage near the equator is usually a reasonable compromise. One advantage of draining "in the bed of the buckle" is that any retinal incarceration or break will be supported once the buckle is tightened. The planned drain site should be examined by indirect ophthalmoscopy immediately before drainage is carried out to ensure that the subretinal fluid is deep enough. Drainage where the subretinal fluid is very shallow risks not just incomplete drainage but retinal injury.

Drainage Techniques.

There are a number of different ways of draining subretinal fluid. Each relies on different strategies to avoid complications, such as choroidal hemorrhage and retinal incarceration. The techniques can be classified as either two-stage techniques in which a large (cut down) sclerostomy with separate choroidotomy is made or those in which a very small sclerostomy and choroidotomy are made together.

Cut Down Techniques.

A scleral incision 3 mm in length is made in the sclera, repeatedly spreading the edges, then incising the base of the resulting groove

(Fig. 104.40 online). The choroid becomes increasingly visible in the base of the incision. Finally, a small knuckle of bare choroid protrudes slightly.

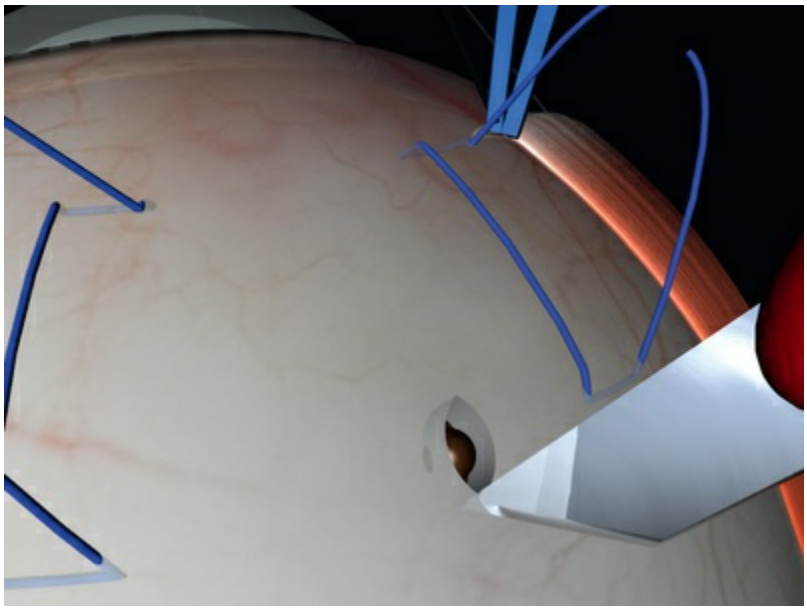

FIG. 104.40 Sclerostomy for a cut down drain. Note location in the posterior bed of the buckle.

The choroidotomy can be made with a needle. Transillumination may be used to visualize and avoid larger choroidal vessels, but there is still a risk of hemorrhage from the choriocapillaris.

Thermal choroidotomy may be used to reduce the risk of bleeding with this technique. A diathermy needle may be used to coagulate the choroidal vessels[49] and a diathermy needle used to perforate the choroid.[50] Alternatively, photocoagulation may be used. The tip of a laser endoprobe is positioned very close to the knuckle of choroid (Fig. 104.41). The laser is activated for 1–2 seconds at very high power (600 mW) until subretinal fluid is seen welling forward. The high beam divergence makes unintentional retinotomy unlikely, and this technique has been used successfully in the presence of quite shallow subretinal fluid.[51] Use of an indirect laser for this step avoids the expense of an endolaser probe.[52]

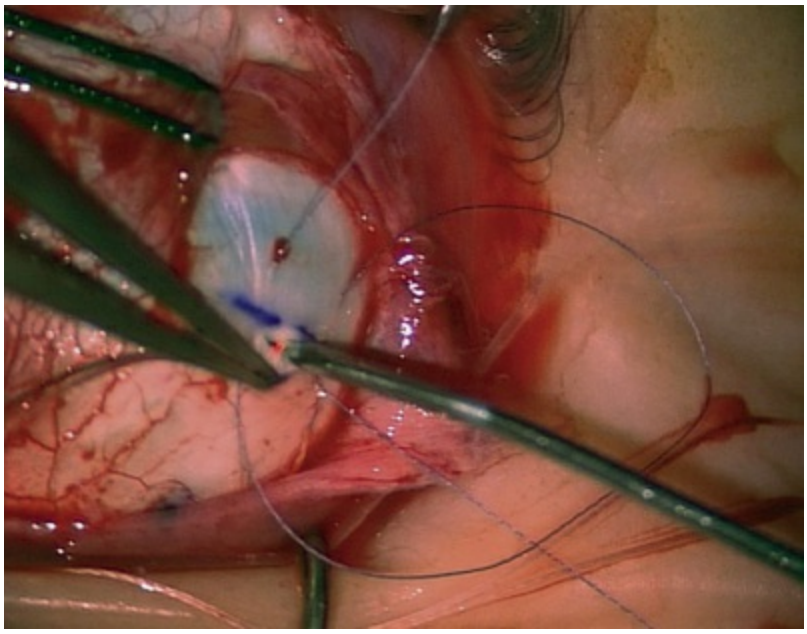

FIG. 104.41 Thermal choroidotomy using a laser endoprobe.

Single-Stage Techniques.

Charles has described a technique using a 25-gauge hypodermic needle attached to an open syringe under ophthalmoscopic visualization (Fig. 104.42). The needle enters the globe anteriorly and is passed under the buckle and obliquely posteriorly in the subretinal space.[53] Retinal incarceration is extremely unlikely, and any retinal breaks created will be in the bed of the buckle and therefore supported. An increased risk of intraocular bleeding has been reported however.[54] This may be averted by increasing the intraocular pressure to close the choroidal vascular bed, for example, by tightening an encircling band prior to drainage.[48]

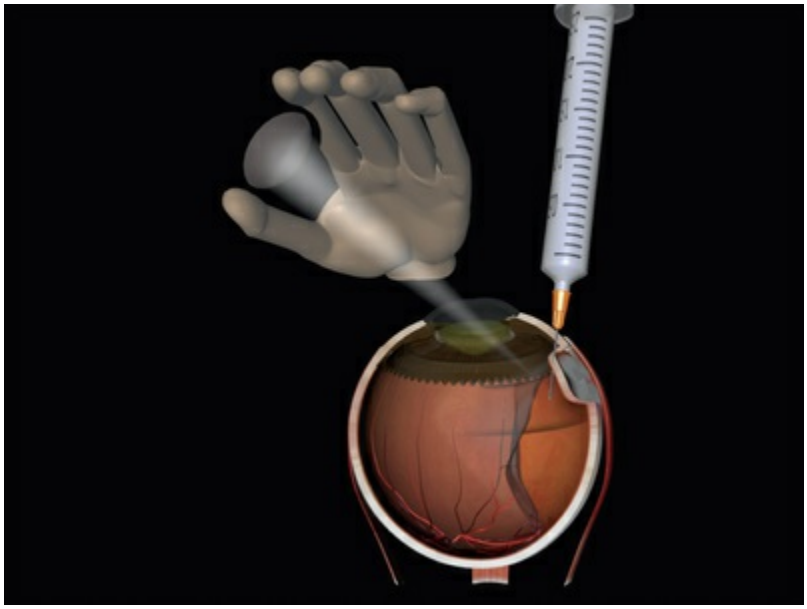

FIG. 104.42 Hypodermic needle drain. Note the bevel faces away from the retina.

Suture needle drains use a spatulated needle held in a locking needleholder with 2.5 mm of the tip protruding (limiting the depth of penetration) (Fig. 104.43 online).[55] Very firm pressure on the globe with a forceps at a rectus insertion elevates the intraocular pressure, closing the choriocapillaris before and for 5 minutes after the drain. A single rapid and decisive stab is made into the sclera and the needle immediately withdrawn.

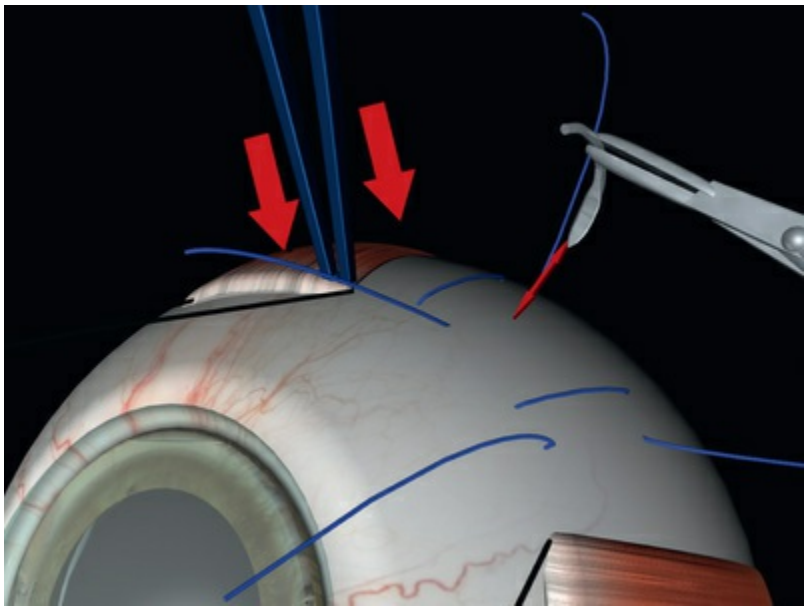

FIG. 104.43 Suture needle drain. Note firm pressure on

the globe to close the choroidal vasculature.

It is also possible to penetrate the sclera and choroid together using a specially designed diathermy needle that cauterizes to reduce the risk of hemorrhage.[56]

Comparison of Techniques.

While performing cut down drainage, intraocular pressure elevation is avoided to prevent retinal incarceration. In needle drainage on the other hand there is no risk of incarceration (because the choroidotomy is so small) and a high intraocular pressure is desirable to reduce the risk of bleeding. When operating on bullous detachments, very rapid release of fluid can make it difficult to maintain a sufficient intraocular pressure, and this may account for the increased risk of subretinal hemorrhage with this technique.[57]

After Drainage

Whichever drainage technique is used, it is prudent to be prepared for postoperative hypotony. Prolonged hypotony is dangerous during buckling surgery. It may lead to suprachoroidal effusions and hemorrhage,[58] hyphema, and pupil constriction. The scleral sutures should therefore have been preplaced ready for tying and a syringe of air or saline with a small-bore needle at hand to reform the globe.

If subretinal fluid does not flow, or stops earlier than anticipated, the drain site is inspected to exclude a retinal incarceration and reassess the depth of subretinal fluid at the drain site. Star-shaped folds radiating from the drain site indicate a retinal incarceration (Fig. 104.44). It is not generally possible to re-posit the incarcerated retina in the eye and dangerous to try. The site of the incarceration is supported by an explant to relieve traction at this site, combined with retinopexy if there is also a retinal break.

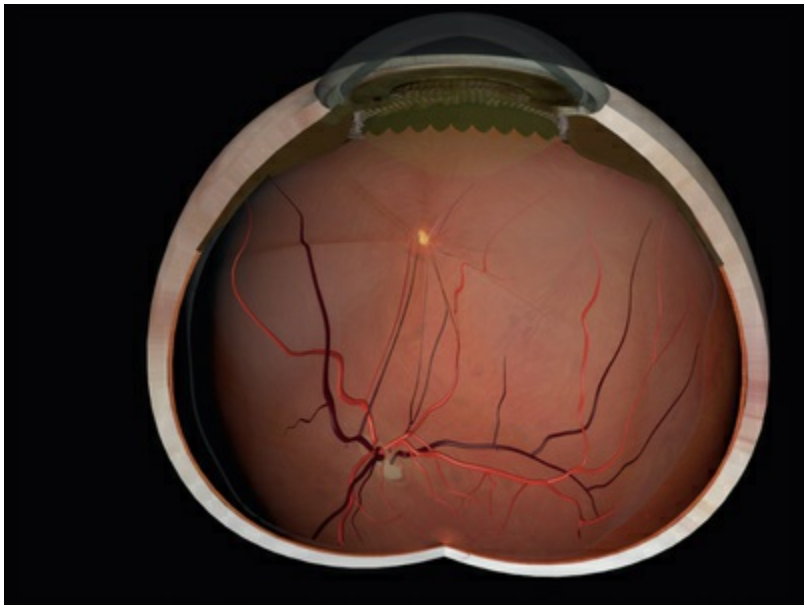

FIG. 104.44 Retinal incarceration.

If there is deep subretinal fluid at the drain site, gentle massage of the globe or distracting the sclerostomy edges may reestablish flow, otherwise a fresh choroidotomy may be needed.

The major complication of subretinal fluid drainage is choroidal hemorrhage. Subretinal blood tends to gravitate to the most dependent area of subretinal fluid – the macula if this is detached. The rate at which this occurs is probably contingent on the viscosity of the subretinal fluid (and therefore the chronicity of the detachment). It can have serious consequences for visual recovery, so steps should be taken first to limit bleeding and second, to displace the hemorrhage. First the intraocular pressure is elevated, either by tightening sutures or intravitreal injection (cut down drains should be closed with the prepared sutures if this is done). The patient's head may also be tilted towards the drain site. Subfoveal hemorrhage may be displaced pneumatically[59] or removed subsequently by vitrectomy.[60]

Air Injection

When only small holes are present, a soft globe may be reformed with saline, but in the presence of large tears, the fluid quickly leaves the eye and the eye will re-soften. The surface tension of a gas bubble prevents its passage through breaks. An additional advantage of air and gas injections is their ability to supplement the

external buckling effect with internal tamponade of breaks. The major disadvantage of using air or gas is that they may make fundal view difficult particularly if the injection technique is poor. The gas injection technique is described in detail in Chapter 107 (Pneumatic retinopexy), but there are some special considerations relating to the use of gases in buckling surgery.

Use of air or gas to reform a collapsed globe entails injecting into a soft eye. A number of modifications to the basic pneumatic retinopexy technique can make this easier. Use of an air pump can be particularly helpful for the less-experienced surgeon (Fig. 104.45). A 23-gauge needle is attached to the air line and the pump pressure set at a physiologic level (i.e., 20 mmHg) before being clamped. The needle is introduced into the eye taking the precautions described in Chapter 107 (Pneumatic retinopexy). The clamp on the air line is released, and air rapidly enters the vitreous cavity until the preset pressure on the pump is reached. The rate of air flow is optimal and the final pressure physiologic. This technique is relatively forgiving of errors in placement of the needle (and fish eggs are virtually never encountered).

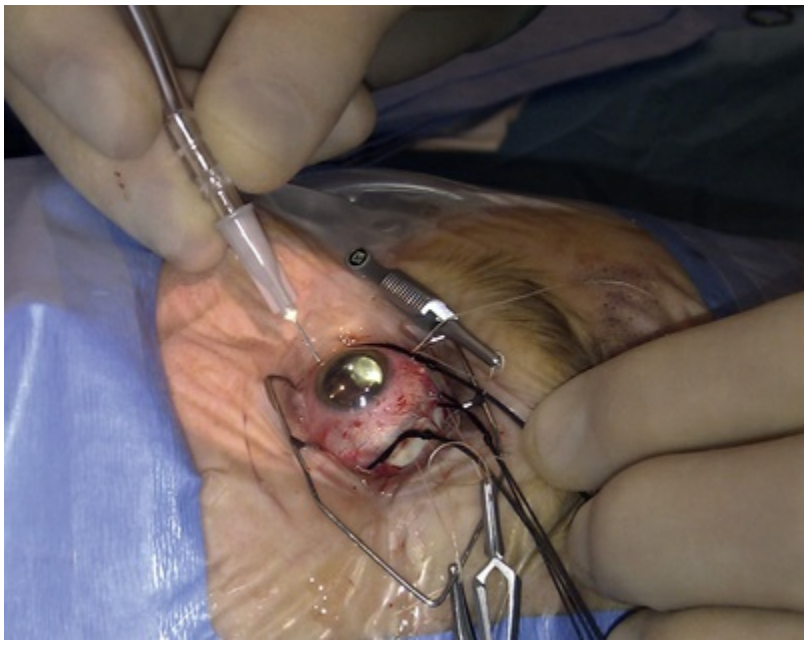

FIG. 104.45 Air injection with an air pump. Note the single bubble despite suboptimal position.

Macular folds are a rare complication of the combination of

subretinal fluid, air injection, and buckling (Fig. 104.46).[61,62] There is some uncertainty about the best way to avoid this devastating complication. Face-down posturing immediately after surgery to displace subretinal fluid away from the macula may be helpful.

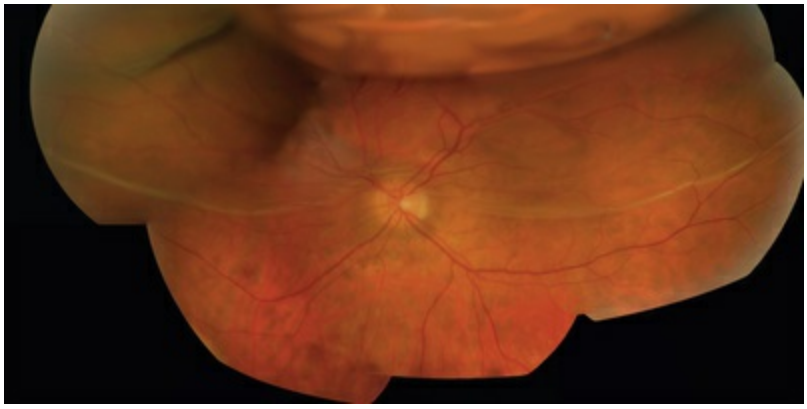

FIG. 104.46 Compression fold following drain, air, and explant. This may be avoided by prone posturing.

Pneumatic retinopexy using expansile gas may be used to treat fishmouthing or to facilitate the closure of breaks that are significantly elevated after buckling.

If general anesthesia is used, nitrous oxide should be discontinued at least 15 minutes before the injection to prevent unpredictable expansion of the bubble.[63] Avoiding the use of nitrous oxide altogether removes this risk.

Encirclement

Segmental buckles provide local support which often fades. This may lead to reopening of breaks if insufficient retinopexy has been applied.[23] Encirclement produces permanent support of the vitreous base retina. Indeed, encirclement has been used without any retinopexy:[64] as the breaks are permanently supported there is no need to seal them.

The indications and evidence for encirclement are reviewed more extensively in Chapter 109 (Optimal procedures for retinal detachment repair). There is little evidence to support the routine use of encirclement in buckling surgery, and the procedure appears to have a significantly greater risk of complications than a segmental buckle. In practice, a case-by-case judgment has to be

made on whether the benefits (the increased chance of success is probably quite modest) justify the risks.

Encirclement has a particular role in certain situations:

- Early PVR
- Very extensive scleromalacia
- Extensive detachment in which breaks are difficult to detect (for example in some pseudophakic eyes with small anterior breaks and capsular phimosis)
- Multiple breaks in three or more quadrants.

Encirclement is produced with a combination of a local silicone tire (confined to the areas of visible the breaks) with a 2-mm band, which lies in the gutter of the tire and encircles the globe before being attached to itself (Fig. 104.47). The 2-mm band is often too narrow to support breaks, and its primary purpose is to maintain the height of the indent from the tire.

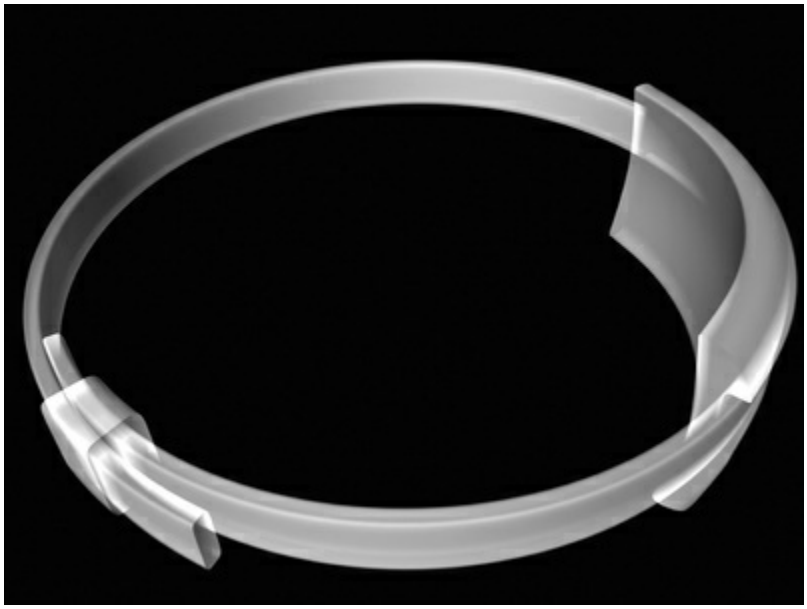

FIG. 104.47 The basic elements of an encirclement: a tire, a band, and a silicone sleeve.

The steps are:

1. A 360° peritomy with slinging of all four rectus muscles.

2. Break localization, retinopexy, and preplacement of the mattress

sutures of the tire. Generally two sutures are required per quadrant.

3. Threading the tire and band together under the recti and mattress sutures. Ensure that both limbs of all the mattress sutures are above the buckle as it is not uncommon to leave one under the encirclement by mistake. Some thought needs to be given to where the ends of the band will be secured at this stage. It is also important to ensure that the band does not become twisted. An oblique trimming of the ends allows the orientation to be checked after the band has been passed around the globe (as a 180° twist will be immediately apparent).

4. Subretinal fluid drainage is required in the majority of cases. The exact stage at which it is performed is variable, but it may be done now to create space for the indent.

5. Tighten the mattress sutures over the tire to create a local indent.

6. Place a small holding stitch over the band in each quadrant where there is no tire to stop it bow stringing forward when tightened. These are placed at the equator (approximately 12 mm behind the limbus).

7. Fasten the ends of the band to each other. A Watzke sleeve is a small silastic tube designed to secure the ends and allow adjustment of the tension in the band. The steps for engaging the ends of the band in the sleeve with a specially designed cross acting ("Watzke") forceps are illustrated in Fig. 104.48.

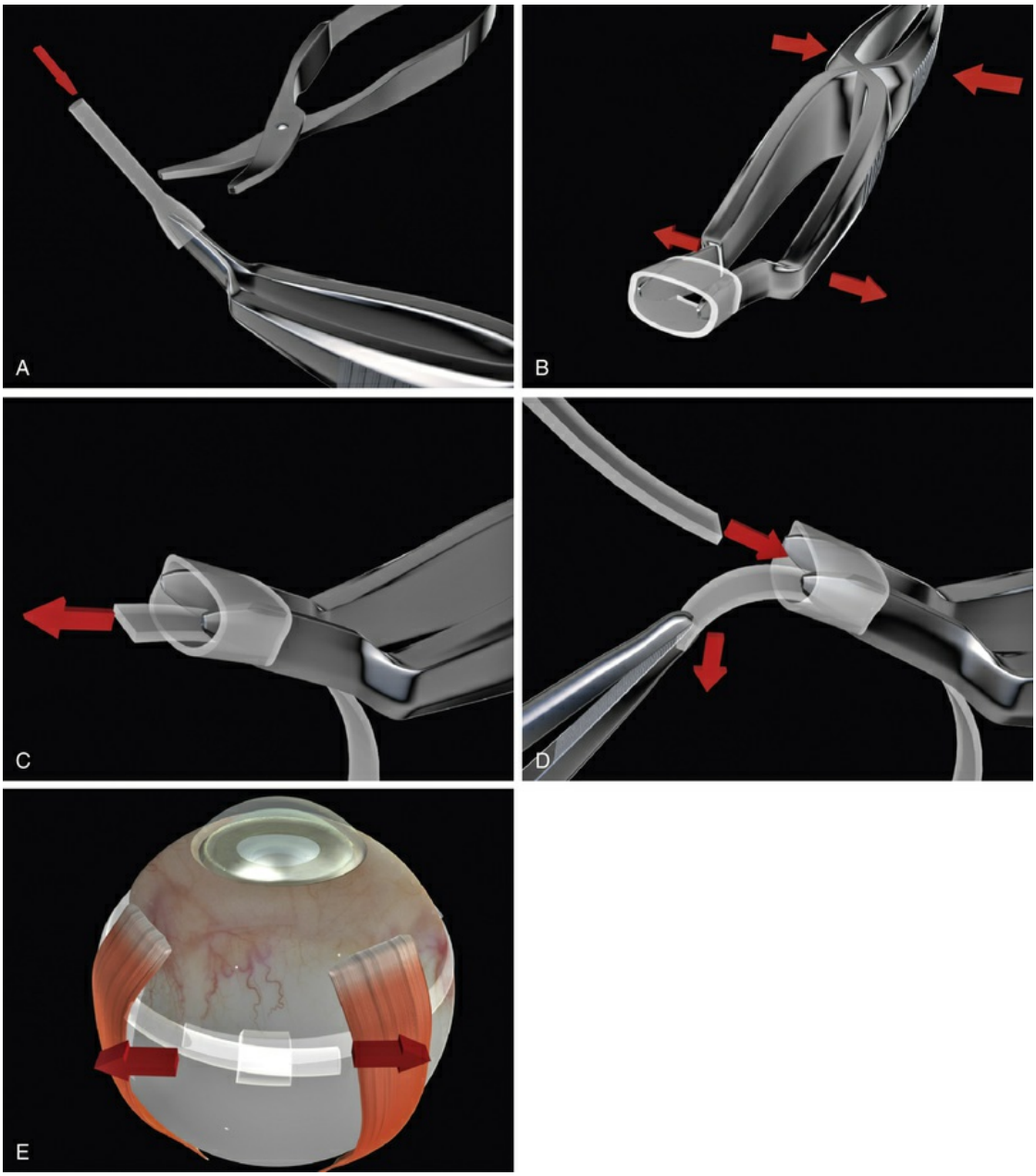

FIG. 104.48 Engaging (A–D) and (E) tightening the band, using a Watzke sleeve and forceps.

8. The ends of the band are pulled to create the encircling indent. A 6-mm shortening will produce approximately a 1-mm indent, irrespective of the size of the globe. The end point of this tightening is best judged ophthalmoscopically; a shallow indent should be just visible. The practice of tightening the band to reform the eye after drainage is dangerous as it may produce a grossly excessive indentation.

9. The optic nerve perfusion should be checked and, if necessary, steps taken to normalize it such as paracentesis, subretinal fluid drainage, or adjusting the buckle.

Final Examination of the Retina

The retina is now examined to determine the adequacy of the buckle and the perfusion of the central retinal artery.

The buckle should be in the correct position and of sufficient height to support all the retinal breaks (Fig. 104.49). Unsupported breaks may be supported by moving existing explants or by placing additional explants as required (e.g., by the addition of more radial sponges under encircling circumferential explants).

FIG. 104.49 Final check: all the retinal breaks (*arrows*) are supported on the buckle.

Judging the correct height of the buckle can be difficult, as even breaks that are not fully closed at the end of surgery may close postoperatively allowing the RPE to pump out the residual subretinal fluid. If the contour of the detached retina follows that of the buckle, the break is likely to close (Fig. 104.50). The height of the buckle may be adjusted by readjusting scleral sutures (if they have been tied on bows) or replacing scleral sutures (usually with wider

bites). Otherwise, the buckle may be replaced. The height of the buckle may also be adjusted by subretinal fluid drainage at this stage. A simpler alternative is adjunctive pneumatic retinopexy.[65]

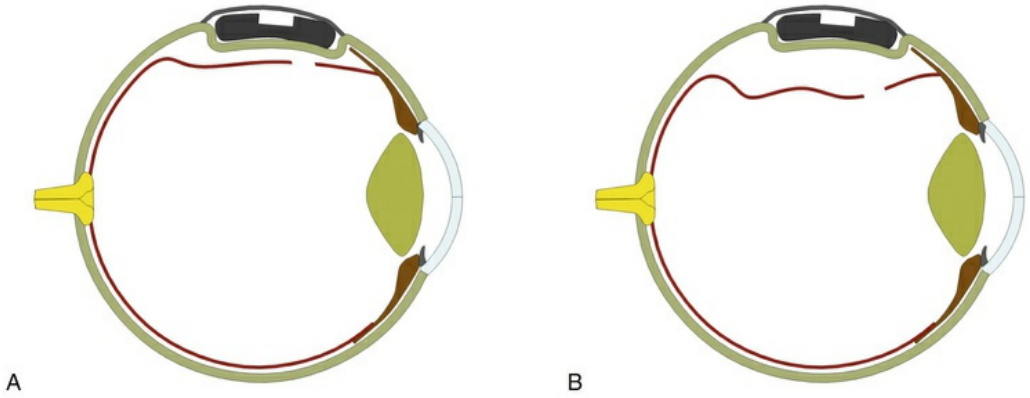

FIG. 104.50 Final check of the retina. If the detachment follows the contour of the buckle: (A) the detachment is likely to settle postoperatively. If it does not, (B) further steps need to be taken – either adjustment of the buckle, drain, pneumatic, or a combination.

A pink disc with large-calibre retinal vessels indicates a pressure below the diastolic closing pressure of the retinal vessels. Spontaneous pulsation of the retinal arteries indicates an intraocular pressure between the systolic and diastolic closing pressure. Intraocular pressure greater than the systolic closing pressure of the retinal arteries causes a pale disc with thready vessels. Reducing the intraocular pressure, typically by paracentesis, is necessary to prevent permanent visual loss. The cornea is often hazy at this point in the operation, making it difficult to judge the patency of the central retinal artery. In this case, it is still usually possible to see vessel pulsation. If arterial pulsation can be induced with pressure on the globe, the intraocular pressure is acceptable (below the retinal artery diastolic pressure).

Closure

The risk of buckle extrusion may be reduced by trimming any protruding edges of sponges (Fig. 104.51), rotating radial mattress

sutures so that the knots lie posteriorly, and ensuring that the buckles are covered by the Tenon capsule. This may entail closure of the Tenon capsule as a separate layer before closure of conjunctiva, particularly with radial sponges where the risk of exposure and extrusion is much greater.[66,67]

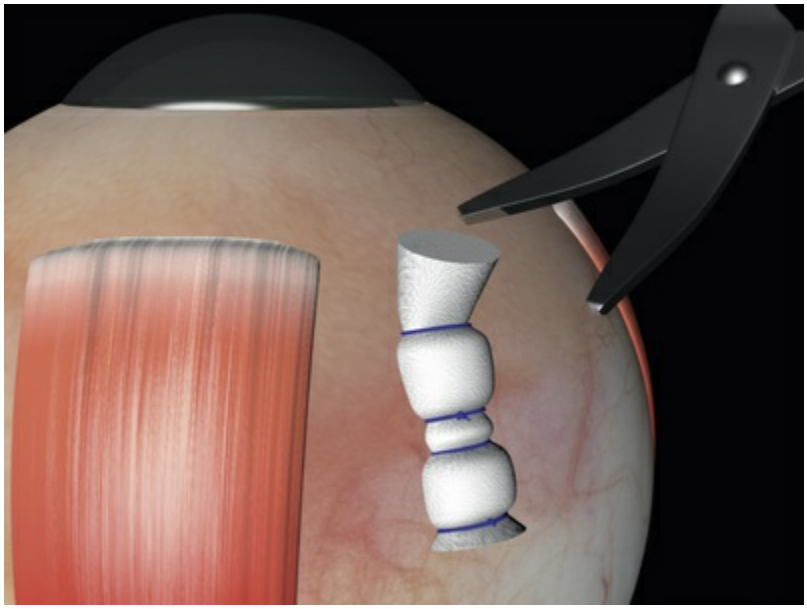

FIG. 104.51 Trimming protruding pieces of explant does not compromise the indent and reduces the risk of extrusion.

An absorbable suture such as 7-0 Vicryl is used to close conjunctiva. The conjunctival edge is identified (taking care not to mistake the edge of the Tenon capsule or plica semilunaris). Accurate realignment is achieved using the "ship to shore" principle: sutures are passed from more mobile flaps of conjunctiva towards the incised edge.

A subconjunctival injection of broad-spectrum antibiotic and steroid may be given.

Documentation

Clear documentation of the surgery, with diagrams to show the position and sutures of all explants (including Watzke sleeves), is very helpful if the eye has to undergo subsequent surgery.

Outcomes

Reported outcomes for primary success with scleral bucking are generally high. In a series of 4325 patients, a success rate of 84% was achieved following a single operation.[68] There is some variation in reported success rates, and many failures are avoidable.[69,70] This underlines the importance of good surgical technique in achieving a satisfactory result.

Functional success with recovery of central vision is somewhat lower than anatomic success[71] and depends on the stage of presentation and the duration of macular detachment. It is important to remember that binocular visual function, ocular cosmesis, and ocular comfort are the most important outcomes for the patient. Measures taken to maximize the anatomic success rate (e.g., the routine use of large encirclements in simple cases) may not therefore be justified if they carry a greater morbidity.[72]

Postoperative Complications

Recurrent Retinal Detachment

Persistent subretinal fluid is often seen in the early postoperative period, particularly if a nondrainage operation has been performed. Resorption of fluid may take much longer (Fig. 104.52), particularly in chronic detachments with subretinal precipitates and demarcation lines.[73] Persistence of subretinal fluid alone is not an indication for revision surgery. Indications for early revision surgery are a visible open retinal break or increasing subretinal fluid.[74]

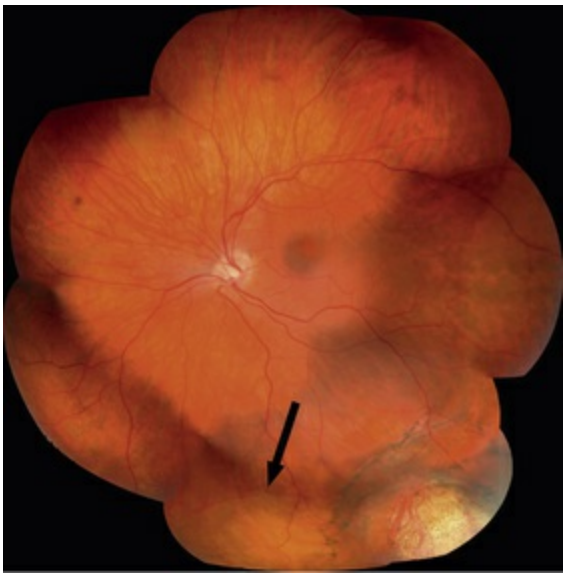

FIG. 104.52 Rarely resorption of subretinal fluid (*arrow*) can take months.

Recurrent detachment is often due to errors in the initial surgery.[9] Successful revision surgery starts with an analysis of the cause of failure. Is there an open break? Are the indents in the right place? Are they high enough to close the breaks? These questions are answered by carefully observing the distribution of subretinal fluid, the presence of subretinal fluid on indents, and visibly open or unsupported breaks.[9]

Example 1: Inadequate buckle – A patient with a shallow inferior detachment due to several atrophic holes underwent a nondrainage procedure with a local circumferential tire. Postoperatively, the distribution of subretinal fluid was unchanged from before the operation, implying that one of the original breaks remained open (Fig. 104.53). There was subretinal fluid on the indent at 6 o'clock communicating with an open break. The height of the buckle was uneven, and at revision surgery no sutures were found near the site of the break. The addition of extra sutures to support this area successfully reattached the retina.

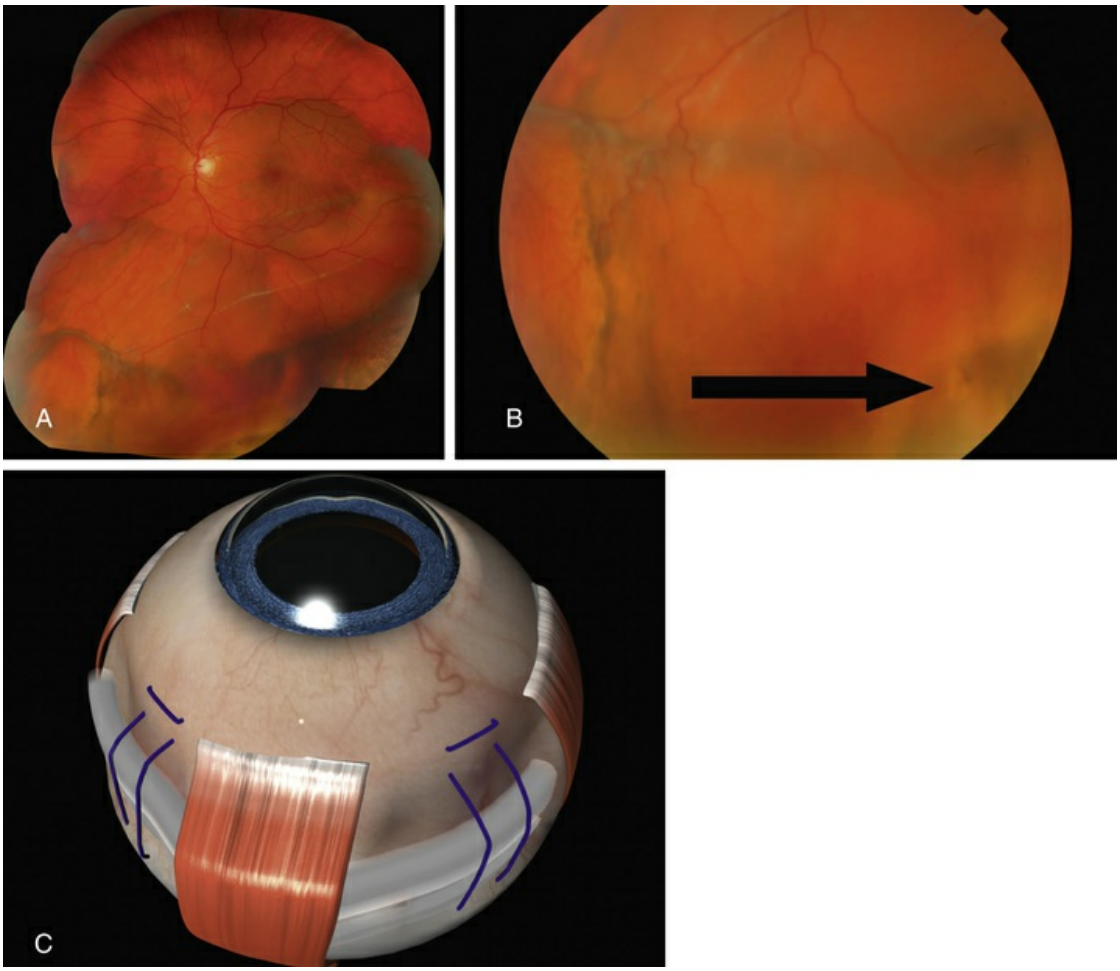

FIG. 104.53 Failed buckle with subretinal fluid on the buckle inferiorly. (A) The indent is high in places but not over the break at 6 o'clock. Magnified view reveals open break (B, *arrow*). At reoperation (C) there is very little indentation inferiorly due to poor placement of the mattress sutures.

Example 2: Missed retinal break – A child presented with an extensive inferior detachment. The operation note stated that no definite breaks were found but cryotherapy and radial sponge were applied to a "thin area with probable hole" inferiorly. The amount and distribution of fluid was unchanged postoperatively. The fluid distribution did not obey Lincoff's laws. This suggested a break had been missed at the original surgery. At repeat surgery, a superonasal retinal dialysis was found (Fig. 104.54).

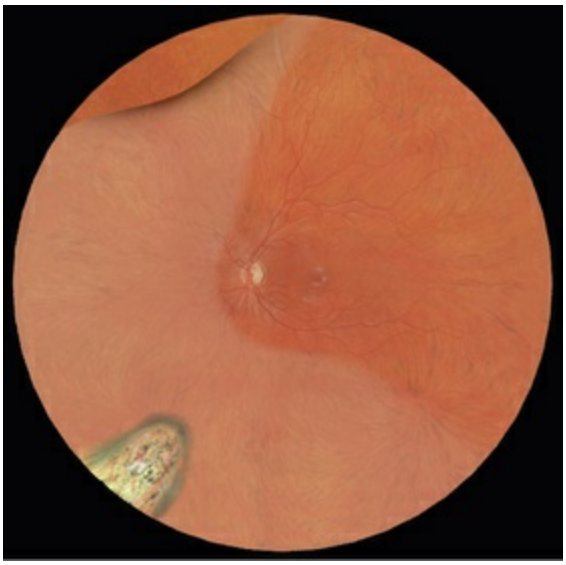

FIG. 104.54 Failed retinal detachment due to a missed dialysis. Lincoff's rules indicate an undetected superonasal break.

Example 3: Misplaced buckle – A patient presented with recurrent retinal detachment following an encircling procedure. There was no subretinal fluid on the indent. Closer examination revealed a small tear behind the indentation (Fig. 104.55). This was managed by locally augmenting the encirclement with a radial explant (Fig. 104.56).

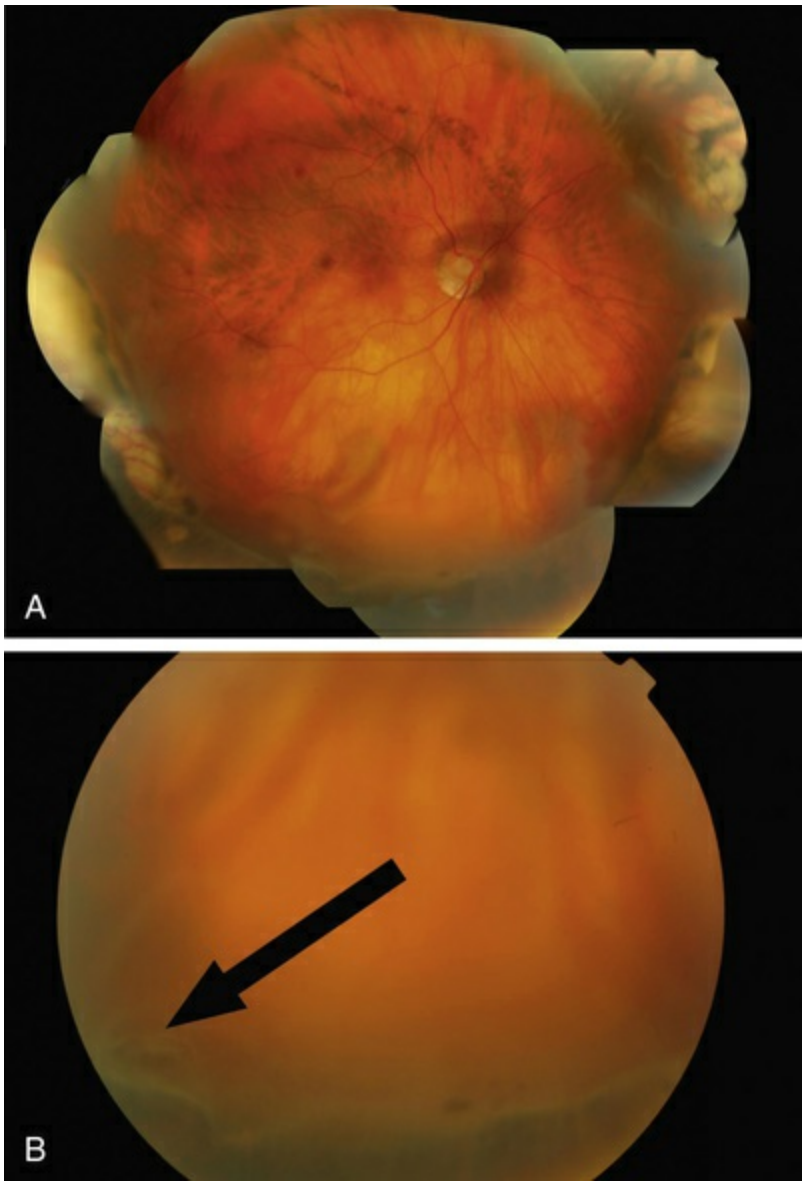

FIG. 104.55 Recurrent retina detachment following encirclement (A). There is no fluid on the buckle. (B) Magnified view showing a break (*arrow*) posterior to the encirclement.

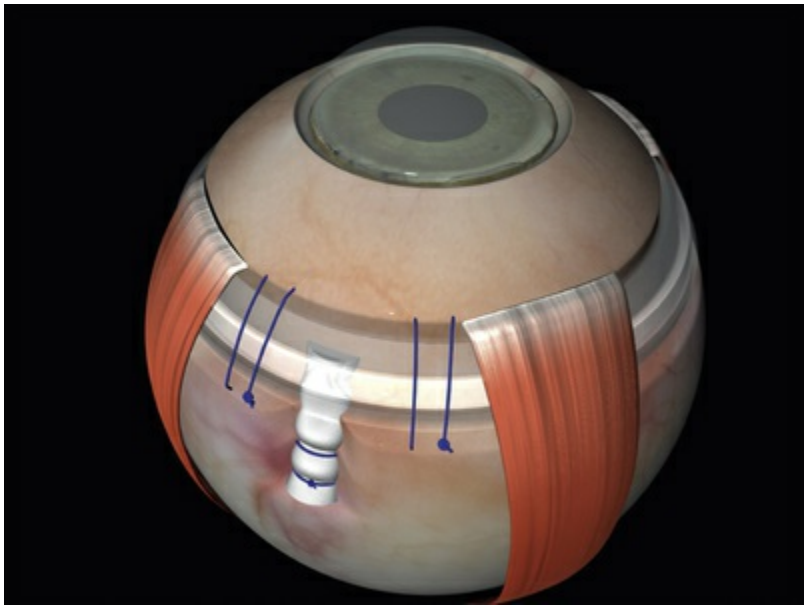

FIG. 104.56 The case in Fig. 104.55 managed by local augmentation of the buckle using a sponge.

Example 4: Fishmouthing – A patient underwent a local circumferential sponge nondrainage operation for a detachment due to several small tractional tears in one quadrant of the retina. Postoperatively, persistent subretinal fluid with folds of retina on the buckle were present (Fig. 104.57). One of these folds was in communication with a retinal tear. A diagnosis of fishmouthing was made.[75] Injection of 0.3 mL 100% SF_6 quickly resolved the problem.[76]

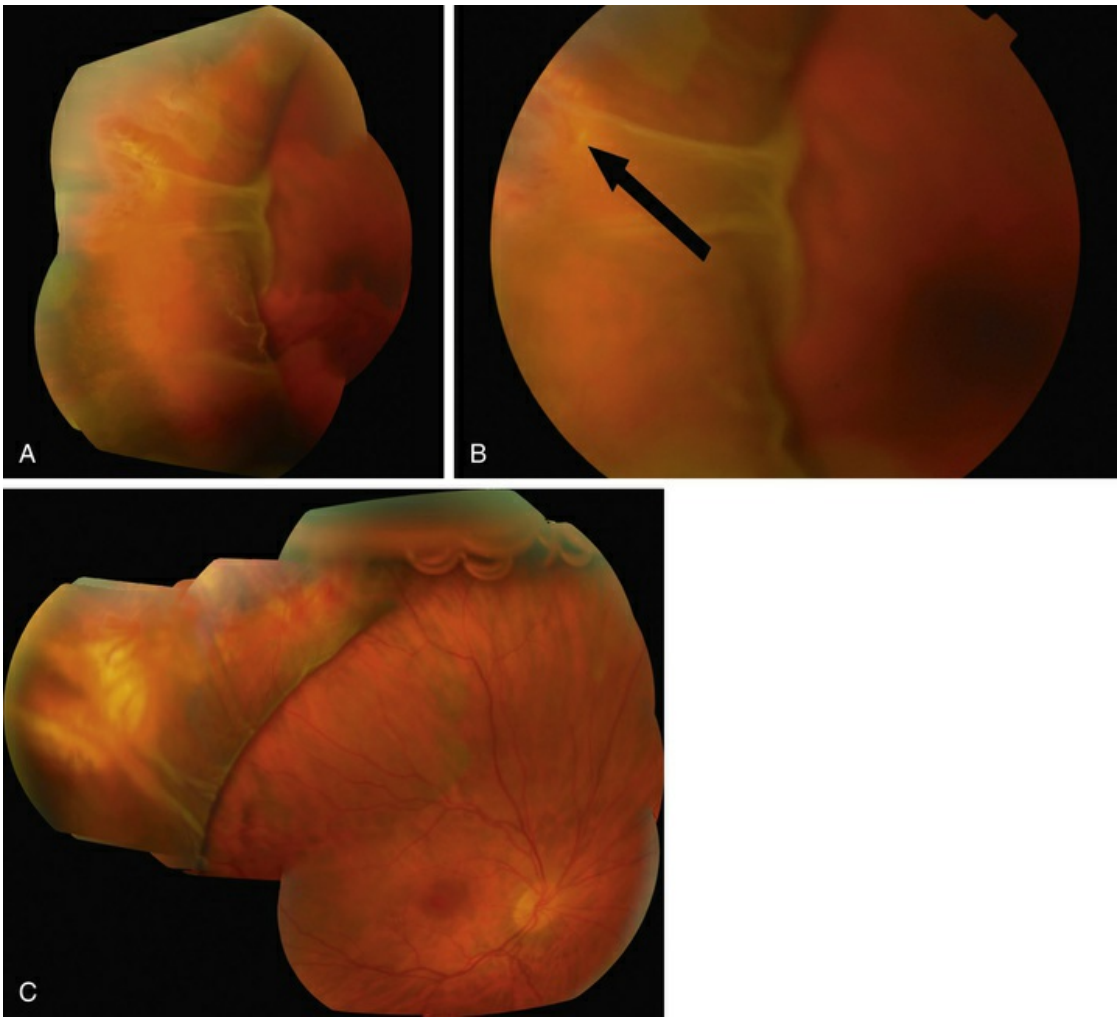

FIG. 104.57 Fishmouthing. Folds on the tire (A) with fishmouthing of the break (*arrow*) apparent in magnified view (B). This was managed successfully by pneumatic retinopexy (C).

Example 5: Misplaced buckle: Radial sponge malposition in the radial meridian – A nondrainage operation with a radial sponge was used for a detachment due to a single tear. The amount and distribution of fluid were unchanged postoperatively (Fig. 104.58). The tear was on the edge of the indentation. Placement of a radial sponge in the correct meridian closed the break.

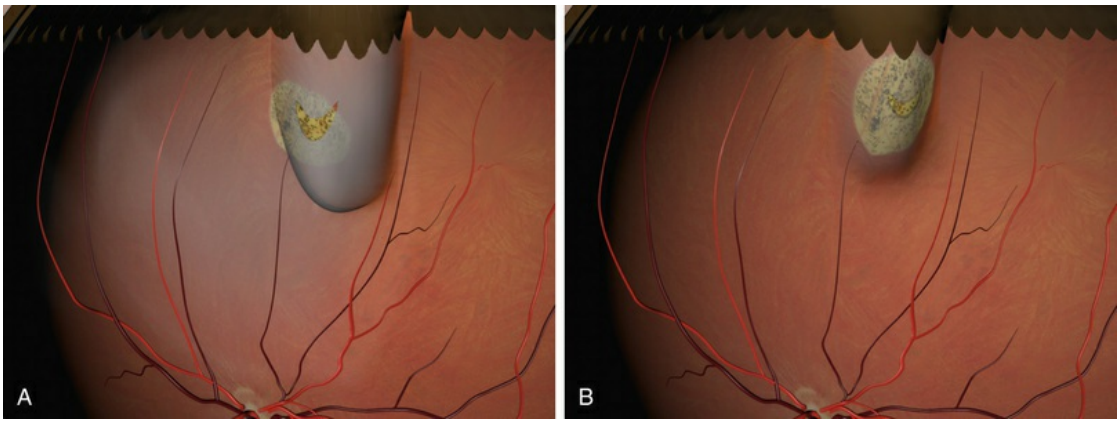

FIG. 104.58 Misplaced sponge. The break is on the edge of the sponge (A), which has to be repositioned to close the break (B). Positioning of the apex of the indent under the tear is critical when using radial sponges.

Proliferative vitreoretinopathy, the most important cause of ultimate failure to reattach the retina, is discussed in Chapter 111 (Proliferative vitreoretinopathy).

Glaucoma

Retinal detachment is associated with glaucoma,[77] so in some cases postoperative glaucoma may have been present preoperatively.

A steroid response is the commonest cause of open angle glaucoma after buckling surgery. Most cases of buckle-related angle closure glaucoma occur without pupil block.[78] The central anterior chamber is shallow due to forward displacement of the ciliary body (Fig. 104.59). This may be due to the combined effects of interrupted choroidal venous drainage and the mass effect of a large explant. This condition does not respond to iridotomy or miosis (which tends to exacerbate it). Most cases resolve after 1 week with conservative measures including steroids, cycloplegia, and ocular hypotensive agents. In intractable cases, the Watzke sleeve may need to be loosened or the band divided.

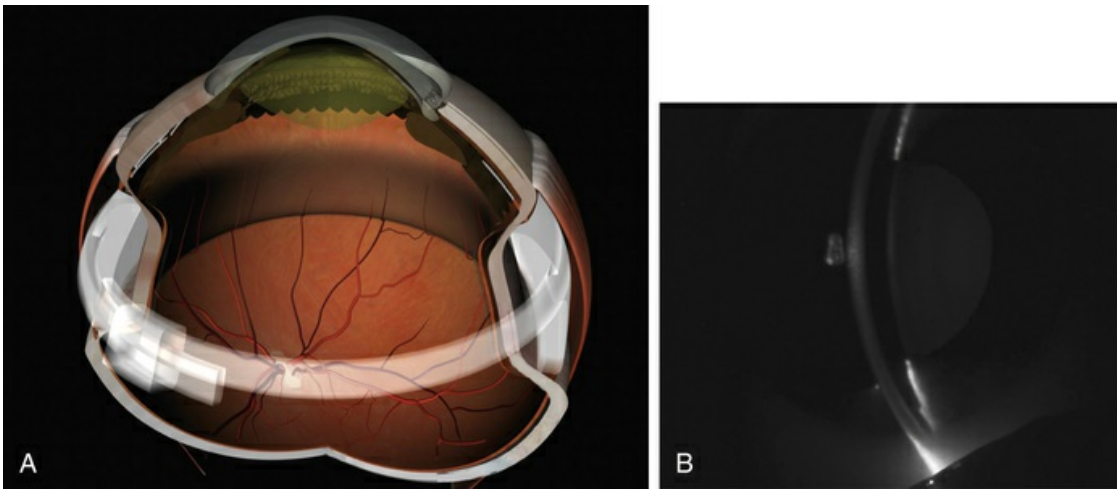

FIG. 104.59 Angle closure without pupil block after buckle. The high encirclement (A) causes choroidal venous congestion, which displaces the ciliary body, and thus the whole lens–iris diaphragm, forward. (B) A slit-lamp photograph shows central and peripheral anterior chamber shallowing (in pupil block the central anterior chamber is deeper).

Epiretinal Membranes

Epiretinal membranes at the macula are the commonest cause of visual loss after successful scleral buckling.[79–81] Their management is discussed in Chapter 120 (Epiretinal membranes, vitreoretinal traction, and cystoid macular edema).

Extrusion/Infection

These typically present several weeks or months postoperatively as an inflamed eye with purulent discharge. Even if exposure of the buckle is not evident, it is often possible to express some pus through associated conjunctival dehiscence. As infection and extrusion are often associated, it can be difficult to establish which comes first. The risk seems to be heavily influenced by the surgical technique used, radial sponges having a greater risk than circumferential ones.[67] This fact, together with the delayed presentation, suggests that in most cases microorganisms gain access to the explants through conjunctival dehiscences over protruding segment of buckle or suture rather than being

introduced at the time of surgery. This highlights the importance of trimming the ends of sutures and explants and covering them well during closure. Closure of the Tenon capsule and conjunctiva in separate layers may be the best way of achieving this, especially if the conjunctiva is particularly thin.

Bacteria produce a biofilm coating on explants which makes it impossible to eradicate them medically.[82] The only definitive treatment is removal of the explant.[83] Provided adequate retinopexy has been performed recurrent retinal detachment is unusual.[84,85] If there is any doubt about this, supplementary retinopexy may be carried out around the breaks before removing the buckle.

Removal of extruding radial sponges is generally easy and can often be done on the slit lamp. Encircling elements are technically more challenging and may require general anesthesia. Occasionally exposed encircling elements with minimal symptoms can be managed conservatively, particularly if the patient is in poor general health or the initial surgery was complex or complicated.

Buckle exposure tends to follow a relatively chronic course, but occasionally patients develop acute sight-threatening complications such as endophthalmitis or scleritis[86,87] requiring urgent removal of all foreign material (explants and sutures) and local and systemic antibiotics.

Band Migration

Encircling bands may intrude or migrate over the surface of the eye, usually anteriorly.

Intrusion is often an incidental finding but may cause vitreous hemorrhage or, less frequently, recurrent detachment many years after buckling surgery. It is usually managed conservatively. Vitreous hemorrhage and retinal detachment may both be managed by vitrectomy without disturbing the band.

Migration anteriorly may affect rectus muscle function and even cause the band to migrate anteriorly and extrude through the limbal conjunctiva.

Diplopia

Diplopia is common after scleral buckling surgery.[88] It tends to

improve with time, and intervention is only indicated for persisting diplopia that does not respond to prisms. Removal of the explant alone may cure the problem.[89] Strabismus surgery can be challenging due to the presence of buckles and adhesions. In patients with very extensive buckles that cannot safely be removed, repeated injections of botulinum toxin may be useful.[90]

Metamorphopsia following detachment of the macula may lead to poor sensory fusion with diplopia. It is important to identify these cases as the diplopia does not respond well to surgical intervention.

Anterior Segment Ischemia

Anterior segment ischemia is now rare, as very high encirclements and rectus disinsertion, both of which compromise the uveal circulation, are rarely used. Patients with sickle-cell disease are at particularly high risk[91] and may benefit from exchange transfusion particularly if an encircling buckle has to be used. Presenting features are corneal edema, pain, anterior chamber flare, and a deep anterior chamber. The intraocular pressure may be high initially but falls as the ciliary body fails. Mild cases may be managed with topical steroids, but severe cases carry a poor prognosis, and loosening or division of the band should be considered.

References

1. Sodhi A, Leung LS, Do DV, et al. Recent trends in the management of rhegmatogenous retinal detachment. *Surv Ophthalmol*. 2008;53:50–67.
2. Lincoff H. Radial buckling in the repair of retinal detachment. *Int Ophthalmol Clin*. 1976;16:127–134.
3. Schepens CL. Management of retinal detachment. *Ophthalmic Surg*. 1994;25:427–431.
4. Schepens CL, Okamura ID, Brockhurst RJ. The scleral buckling procedures. I. Surgical techniques and management. *AMA Arch Ophthalmol*. 1957;58:797–811.
5. Custodis E. Treatment of retinal detachment by circumscribed diathermal coagulation and by scleral

depression in the area of tear caused by imbedding of a plastic implant. *Klin Monbl Augenheilkd Augenarztl Fortbild*. 1956;129:476–495.
6. Lincoff H, McLean JM. Modifications to the Custodis procedure. II. A new silicone implant for large tears. *Am J Ophthalmol*. 1967;64:877–879.
7. Demer JL, Miller JM, Poukens V. Surgical implications of the rectus extraocular muscle pulleys. *J Pediatr Ophthalmol Strabismus*. 1996;33:208–218.
8. White MH, Lambert HM, Kincaid MC, et al. The ora serrata and the spiral of Tillaux. Anatomic relationship and clinical correlation. *Ophthalmology*. 1989;96:508–511.
9. Lincoff H, Kreissig I. Extraocular repeat surgery of retinal detachment. A minimal approach. *Ophthalmology*. 1996;103:1586–1592.
10. Chignell AH, Markham RH. Retinal detachment surgery. Buckling procedures and drainage of subretinal fluid. *Trans Ophthalmol Soc U K*. 1977;97:474–477.
11. Lincoff H, Gieser R. Finding the retinal hole. *Arch Ophthalmol*. 1971;85:565–569.
12. Sasoh M. The frequency of subretinal fluid drainage and the reattachment rate in retinal detachment surgery. *Retina*. 1992;12:113–117.
13. Wilkinson CP. Whatever happened to bilateral patching? *Retina*. 2005;25:393–394.
14. Lai MM, Lai JC, Lee WH, et al. Comparison of retrobulbar and sub-Tenon's capsule injection of local anesthetic in vitreoretinal surgery. *Ophthalmology*. 2005;112:574–579.
15. Mein CE, Flynn HWJ. Augmentation of local anesthesia during retinal detachment surgery. *Arch Ophthalmol*. 1989;107:1084.
16. Bergman L, Backmark I, Ones H, et al. Preoperative sub-Tenon's capsule injection of ropivacaine in conjunction with general anesthesia in retinal detachment surgery. *Ophthalmology*. 2007;114:2055–2060.
17. King LMJ, Schepens CL. Limbal peritomy in retinal detachment surgery. *Arch Ophthalmol*. 1974;91:295–298.
18. Gass JD. Fenestrated muscle hook for retinal detachment

surgery. *Arch Ophthalmol*. 1967;77:676.
19. Yokoyama T, Kanbayashi K, Yamaguchi T. Scleral buckling procedure for paediatric rhegmatogenous retinal detachment. *Clin Ophthalmol*. 2015;9:169–173.
20. Gass JD. Scleral marker for retinal detachment surgery. *Arch Ophthalmol*. 1966;76:700–701.
21. Gilbert C, McLeod D. D-ACE surgical sequence for selected bullous retinal detachments. *Br J Ophthalmol*. 1985;69:733–736.
22. Stanford MR, Chignell AH. Surgical treatment of superior bullous rhegmatogenous retinal detachments. *Br J Ophthalmol*. 1985;69:729–732.
23. Chignell AH, Wong D. The role of induced choroidal retinal adhesion in retinal detachment surgery. *Trans Ophthalmol Soc U K*. 1986;105:580–582.
24. Singh AK, Michels RG, Glaser BM. Scleral indentation following cryotherapy and repeat cryotherapy enhance release of viable retinal pigment epithelial cells. *Retina*. 1986;6:176–178.
25. Johnson RN, Irvine AR, Wood IS. Endolaser, cryopexy, and retinal reattachment in the air-filled eye. A clinicopathologic correlation. *Arch Ophthalmol*. 1987;105:231–234.
26. Campochiaro PA, Kaden IH, Vidaurri-Leal J, et al. Cryotherapy enhances intravitreal dispersion of viable retinal pigment epithelial cells. *Arch Ophthalmol*. 1985;103:434–436.
27. Jaccoma EH, Conway BP, Campochiaro PA. Cryotherapy causes extensive breakdown of the blood–retinal barrier. A comparison with argon laser photocoagulation. *Arch Ophthalmol*. 1985;103:1728–1730.
28. Laqua H, Machemer R. Repair and adhesion mechanisms of the cryotherapy lesion in experimental retinal detachment. *Am J Ophthalmol*. 1976;81:833–846.
29. Haller JA, Blair N, de Juan EJ, et al. Transscleral diode laser retinopexy in retinal detachment surgery: results of a multicenter trial. *Retina*. 1998;18:399–404.
30. Steel DH, West J, Campbell WG. A randomized controlled

study of the use of transscleral diode laser and cryotherapy in the management of rhegmatogenous retinal detachment. *Retina*. 2000;20:346–357.
31. Veckeneer M, Van Overdam K, Bouwens D, et al. Randomized clinical trial of cryotherapy versus laser photocoagulation for retinopexy in conventional retinal detachment surgery. *Am J Ophthalmol*. 2001;132:343–347.
32. Lira RP, Takasaka I, Arieta CE, et al. Cryotherapy vs laser photocoagulation in scleral buckle surgery: a randomized clinical trial. *Arch Ophthalmol*. 2010;128:1519–1522.
33. Lincoff H, Kreissig I. Cryopexy is not as bad as all that. *Retina*. 1998;18:486–488.
34. Baino F. Scleral buckling biomaterials and implants for retinal detachment surgery. *Med Eng Phys*. 2010;32:945–956.
35. Schepens CL, Okamura ID, Brockhurst RJ, et al. Scleral buckling procedures. V. Synthetic sutures and silicone implants. *Arch Ophthalmol*. 1960;64:868–881.
36. Russo CE, Ruiz RS. Silicone sponge rejection. Early and late complications in retinal detachment surgery. *Arch Ophthalmol*. 1971;85:647–650.
37. Aaberg TM, Wiznia RA. The use of solid soft silicone rubber exoplants in retinal detachment surgery. *Ophthalmic Surg*. 1976;7:98–105.
38. Heimann H, Bartz-Schmidt KU, Bornfeld N, et al. Scleral buckling versus primary vitrectomy in rhegmatogenous retinal detachment: a prospective randomized multicenter clinical study. *Ophthalmology*. 2007;114:2142–2154.
39. Stoffelns BM, Richard G. Is buckle surgery still the state of the art for retinal detachments due to retinal dialysis? *J Pediatr Ophthalmol Strabismus*. 2010;47:281–287.
40. Watson PG, Young RD. Scleral structure, organisation and disease. A review. *Exp Eye Res*. 2004;78:609–623.
41. Eisner G. *Eye surgery: an introduction to operative technique*. Springer-Verlag: Berlin; 1990.
42. Lincoff H, Kreissig I. The treatment of retinal detachment without drainage of subretinal fluid. (Modifications of the Custodis procedure. VI). *Trans Am Acad Ophthalmol Otolaryngol*. 1972;76:1121–1133.

43. Ruiz RS, Drouilhet JH, Salmonsen PC. Paracentesis in scleral buckling procedures. *Ophthalmic Surg*. 1979;10:71–73.
44. Hilton GF, Grizzard WS, Avins LR, et al. The drainage of subretinal fluid: a randomized controlled clinical trial. *Retina*. 1981;1:271–280.
45. Brinton D, Wilkinson CP. *Retinal detachment: principles and practice*. 3rd ed. Oxford University Press/American Academy of Ophthalmology: New York; 2009.
46. Johnston GP, Okun E, Boniuk I, et al. Drainage of subretinal fluid: why, when, where and how. *Mod Probl Ophthalmol*. 1975;15:197–206.
47. Pearce IA, Wong D, McGalliard J, et al. Does cryotherapy before drainage increase the risk of intraocular haemorrhage and affect outcome? A prospective, randomised, controlled study using a needle drainage technique and sustained ocular compression. *Br J Ophthalmol*. 1997;81:563–567.
48. Jaffe GJ, Brownlow R, Hines J. Modified external needle drainage procedure for rhegmatogenous retinal detachment. *Retina*. 2003;23:80–85.
49. Freeman HM, Schepens CL. Innovations in the technique for drainage of subretinal fluid, transillumination and choroidal diathermy. *Mod Probl Ophthalmol*. 1975;15:119–126.
50. Saran BR, Brucker AJ, Maguire AM. Drainage of subretinal fluid in retinal detachment surgery with the El-Mofty insulated diathermy electrode. *Retina*. 1994;14:344–347.
51. Ryan EHJ, Arribas NP, Olk RJ, et al. External argon laser drainage of subretinal fluid using the endolaser probe. *Retina*. 1991;11:214–218.
52. Pitts JF, Schwartz SD, Wells J, et al. Indirect argon laser drainage of subretinal fluid. *Eye (Lond)*. 1996;10:465–468.
53. Charles ST. Controlled drainage of subretinal and choroidal fluid. *Retina*. 1985;5:233–234.
54. Burton RL, Cairns JD, Campbell WG, et al. Needle drainage of subretinal fluid. A randomized clinical trial. *Retina*. 1993;13:13–16.
55. Raymond GL, Lavin MJ, Dodd CL, et al. Suture needle

drainage of subretinal fluid. *Br J Ophthalmol*. 1993;77:428–429.
56. Meyer-Schwickerath G, Klein M. Drainage of subretinal fluid with a cathode needle. *Mod Probl Ophthalmol*. 1975;15:154–157.
57. Aylward GW, Orr G, Schwartz SD, et al. Prospective, randomised, controlled trial comparing suture needle drainage and argon laser drainage of subretinal fluid. *Br J Ophthalmol*. 1995;79:724–727.
58. Aaberg TM, Maggiano JM. Choroidal edema associated with retinal detachment repair: experimental and clinical correlation. *Mod Probl Ophthalmol*. 1979;20:6–15.
59. Sarrafizadeh R, Williams GA. Submacular hemorrhage during scleral buckling surgery treated with an intravitreal air bubble. *Retina*. 2000;20:415–417.
60. Rubsamen PE, Flynn HWJ, Civantos JM, et al. Treatment of massive subretinal hemorrhage from complications of scleral buckling procedures. *Am J Ophthalmol*. 1994;118:299–303.
61. Twomey JM, Leaver PK. Retinal compression folds. *Eye (Lond)*. 1988;2:283–287.
62. Elliott AJ, Scott JD. Retinal compression folds after surgery for acute bullous retinal detachment. *Eye (Lond)*. 1989;3:100.
63. Stinson TWR, Donlon JVJ. Interaction of intraocular air and sulfur hexafluoride with nitrous oxide: a computer simulation. *Anesthesiology*. 1982;56:385–388.
64. Figueroa MS, Corte MD, Sbordone S, et al. Scleral buckling technique without retinopexy for treatment of rhegmatogeneous: a pilot study. *Retina*. 2002;22:288–293.
65. Sabates WI, Abrams GW, Swanson DE, et al. The use of intraocular gases: the results of sulfur hexafluoride gas in retinal detachment surgery. *Ophthalmology*. 1981;88:447–454.
66. Arribas NP, Olk RJ, Schertzer M, et al. Preoperative antibiotic soaking of silicone sponges. Does it make a difference? *Ophthalmology*. 1984;91:1684–1689.
67. Brown DM, Beardsley RM, Fish RH, et al. Long-term stability of circumferential silicone sponge scleral buckling exoplants. *Retina*. 2006;26:645–649.

68. Thelen U, Amler S, Osada N, et al. Outcome of surgery after macula-off retinal detachment – results from MUSTARD, one of the largest databases on buckling surgery in Europe. Results from a large German case series. *Acta Ophthalmol*. 2012;90(5):481–486.
69. Smiddy WE, Glaser BM, Michels RG, et al. Scleral buckle revision to treat recurrent rhegmatogenous retinal detachment. *Ophthalmic Surg*. 1990;21:716–720.
70. Rachal WF, Burton TC. Changing concepts of failures after retinal detachment surgery. *Arch Ophthalmol*. 1979;97:480–483.
71. Wilkinson CP. Mysteries regarding the surgically reattached retina. *Trans Am Ophthalmol Soc*. 2009;107:55–57.
72. Kreissig I. [Treatment of primary retinal detachment. Minimal extraocular or intraocular?]. *Ophthalmologe*. 2002;99:474–484.
73. Robertson DM. Delayed absorption of subretinal fluid after scleral buckling procedures. *Am J Ophthalmol*. 1979;87:57–64.
74. Chignell AH, Talbot J. Absorption of subretinal fluid after nondrainage retinal detachment surgery. *Arch Ophthalmol*. 1978;96:635–637.
75. Pruett RC. The fishmouth phenomenon. I. Clinical characteristics and surgical options. *Arch Ophthalmol*. 1977;95:1777–1781.
76. Norton EW. Use of gas in retinal surgery: management of the fishmouth phenomenon. *Trans Ophthalmol Soc U K*. 1980;100:66–68.
77. Phelps CD, Burton TC. Glaucoma and retinal detachment. *Arch Ophthalmol*. 1977;95:418–422.
78. Perez RN, Phelps CD, Burton TC. Angel-closure glaucoma following scleral buckling operations. *Trans Sect Ophthalmol Am Acad Ophthalmol Otolaryngol*. 1976;81:247–252.
79. Tanenbaum HL, Schepens CL, Elzeneiny I, et al. Macular pucker following retinal detachment surgery. *Arch Ophthalmol*. 1970;83:286–293.
80. Wilkinson CP. Visual results following scleral buckling for retinal detachments sparing the macula. *Retina*. 1981;1:113–116.

81. Lobes LAJ, Burton TC. The incidence of macular pucker after retinal detachment surgery. *Am J Ophthalmol*. 1978;85:72–77.
82. Holland SP, Pulido JS, Miller D, et al. Biofilm and scleral buckle-associated infections: a mechanism for persistence. *Ophthalmology*. 1991;98:933–938.
83. Smiddy WE, Miller D, Flynn HWJ. Scleral buckle removal following retinal reattachment surgery: clinical and microbiologic aspects. *Ophthalmic Surg*. 1993;24:440–445.
84. Hilton GF, Wallyn RH. The removal of scleral buckles. *Arch Ophthalmol*. 1978;96:2061–2063.
85. James M, O'Doherty M, Beatty S. Buckle-related complications following surgical repair of retinal dialysis. *Eye (Lond)*. 2008;22:485–490.
86. Folk JC, Cutkomp J, Koontz FP. Bacterial scleral abscesses after retinal buckling operations: pathogenesis, management, and laboratory investigations. *Ophthalmology*. 1987;94:1148–1154.
87. Rich RM, Smiddy WE, Davis JL. Infectious scleritis after retinal surgery. *Am J Ophthalmol*. 2008;145:695–699.
88. Farr AK, Guyton DL. Strabismus after retinal detachment surgery. *Curr Opin Ophthalmol*. 2000;11:207–210.
89. Fison PN, Chignell AH. Diplopia after retinal detachment surgery. *Br J Ophthalmol*. 1987;71:521–525.
90. Scott AB. Botulinum treatment of strabismus following retinal detachment surgery. *Arch Ophthalmol*. 1990;108:509–510.
91. Ryan SJ, Goldberg MF. Anterior segment ischemia following scleral buckling in sickle cell hemoglobinopathy. *Am J Ophthalmol*. 1971;72:35–50.

105

Principles and Techniques of Vitreoretinal Surgery

Steve Charles

Introduction

Vitreoretinal surgery is a complex blend of the most difficult high-technology microsurgery applied to complex pathobiologic systems. This rapidly growing field requires continued research and training and an honest assessment of one's surgical skills, knowledge, and experience. The surgical team must be well-trained, efficient, and technologically competent; the complex equipment must be constantly updated as the technology progresses.

To help deal with the complexity of vitreoretinal surgery, the

author proposes an approach utilizing a surgical algorithm made up of scenarios. The surgical scenarios are similarly composed of smaller elements referred to as tasks, tools, associated analog parameters (pressure, power), and interconnects (fluid–gas exchange, air–silicone exchange). Tasks are common to the surgical approach to different disease states that share common pathoanatomic configurations. Each algorithm contains decision nodes with several alternative scenarios. The decision process requires outcome data, knowledge of physical principles, individual patient factors, and experiential information. This chapter will begin with a description of relevant general pathoanatomy, with specific information left to other chapters on specific disease states. Understanding the mechanics of the tools used will allow discussion of the details of how to perform each task. The chapter concludes with a suggested algorithm for each common disease state, with specific management details again left to other authors.

Vitreoretinal Surgical Anatomy

The vitreous can be considered as a three-dimensional matrix of collagen fibers and hyaluronan gel (Fig. 105.1). In the normal state, the outer surface of the vitreous is in contact with the retina, pars plana, and ciliary body in a roughly spherical shape with an anterior facet abutting the lens. Disease-induced retinal pigment epithelium (RPE) and glial cell migration, attachment of cells to the extracellular matrix, and hypocellular contraction of the collagen matrix take place with the majority of the relevant changes occurring at the cortex surface. The anterior vitreous cortex (AVC) is contiguous with the posterior vitreous cortex (PVC) and, for the most part, is not fenestrated.

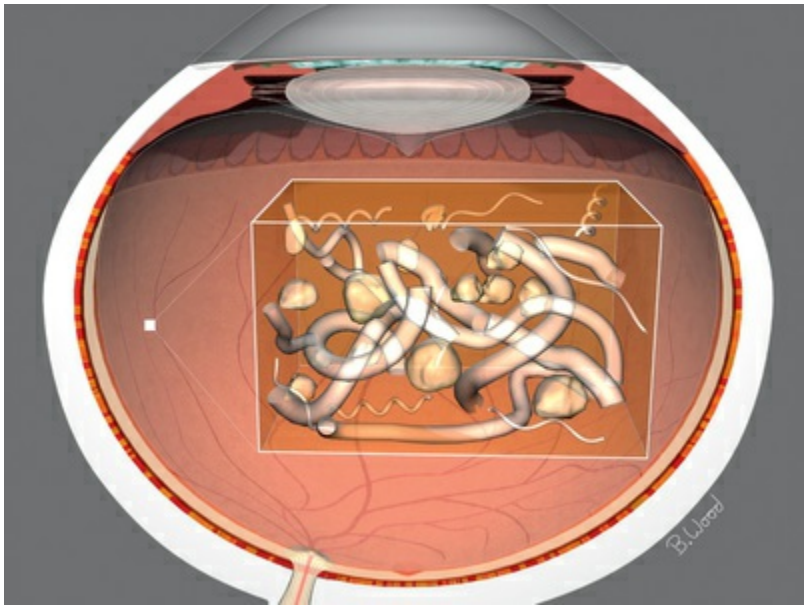

FIG. 105.1 The vitreous is a three-dimensional matrix of collagen fibers and hyaluronan gel.

Activated retinal glial cells, RPE cells, and cells of hematogenous origin migrate along the front and back surfaces of the retina and vitreous. These cells have coated pits lined with fibronectin, allowing them to attach to and contract the collagen matrix.

A detailed understanding of the abnormal vitreoretinal interface and its derivative geometry is requisite to undertaking vitreoretinal surgery. The task involves visualization of vitreous structures and a systematic search for membranes based on observed retinal topology. In general, membranes are white and matte-finish, whereas the retina has a reflective surface luster and appears pale yellow. If a complete posterior vitreous separation has not occurred, there is usually continuity between areas of epiretinal membrane (ERM) and adjacent detached PVC. Because the retina itself does not contract or develop substantial intraretinal proliferation, changes in contour occur because of perpendicular or oblique vitreoretinal traction (funnel, plateau, or ridge-like elevations) or tangential ERM-related traction (star folds, epimacular membranes).

Retinal breaks result in loss of the normal transretinal pressure gradient. Trans-hole flow is related to intraocular pressure, capability of the RPE pump, viscosity of the fluid, and the area and dimensions of the retinal break.

Mechanics of Vitreoretinal Surgery

An understanding of the physical principles of surgical tools enhances the capabilities of the vitreoretinal surgeon. Discussion of the forces available for cutting and thermal effects follows. Cutting may simply be defined as the separation of a tissue into two parts.

Peeling

Force along the axis of a collagen fiber bundle causes nonelastic collagen fibers to slightly stretch and ultimately to fail. Damage to attached structures is a function of the number of fibers and the strength of the attachment and the substrate. Membrane peeling requires force preferably tangential to the retina, which causes failure of the attachment at the vitreoretinal interface by elongation. Because dense, highly adherent membranes such as those associated with diabetic traction retinal detachments are approximately 100 times stronger than the retina, retina surface defects or retinal breaks usually occur before removal of the membrane occurs (Fig. 105.2). For this reason, membrane peeling may be inappropriate in diabetic traction retinal detachment cases.

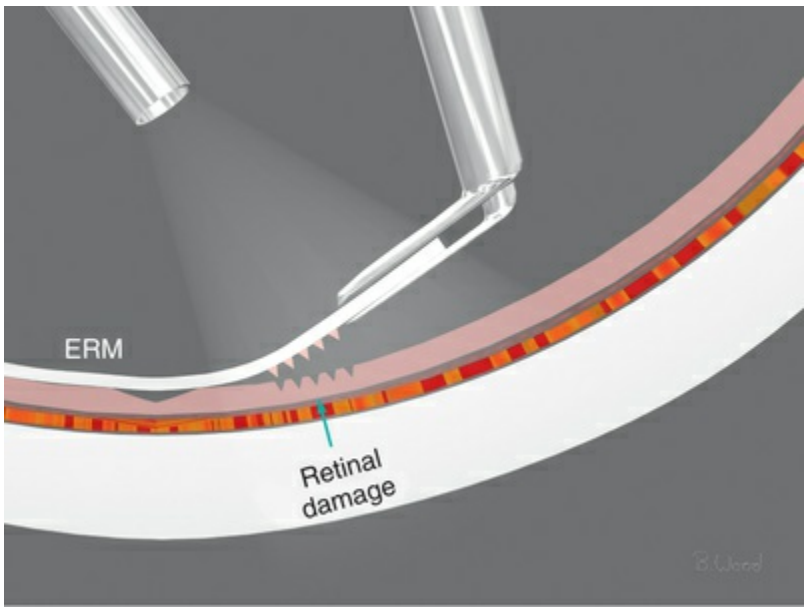

FIG. 105.2 Forceps designed to place one blade under the epiretinal membrane (*ERM*) damage the retinal surface. Similarly, pics and membrane scrapers

damage the retinal surface.

Shear

Shear cutting occurs when force is applied along two opposing right-angle edges moving past each other and forced against each other. Vitreous cutters and scissors use shearing to cut tissue. Inclusive shears such as a vitreous cutter prevent the push-out force that occurs as exclusive shears (scissors) close (Fig. 105.3), pushing the tissue away from the fulcrum, but require elastic deformation of tissue into the port caused by transport pressure gradient, which may cause fluid surge and iatrogenic retinal breaks (Fig. 105.4).

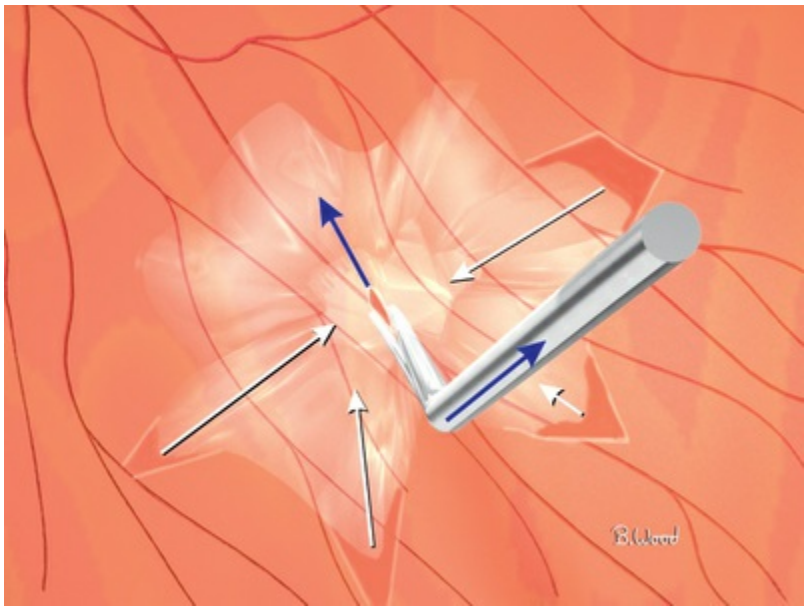

FIG. 105.3 Scissors create a push-out force; if they are inserted open and then closed they tear the retina at the epiretinal membrane attachment points.

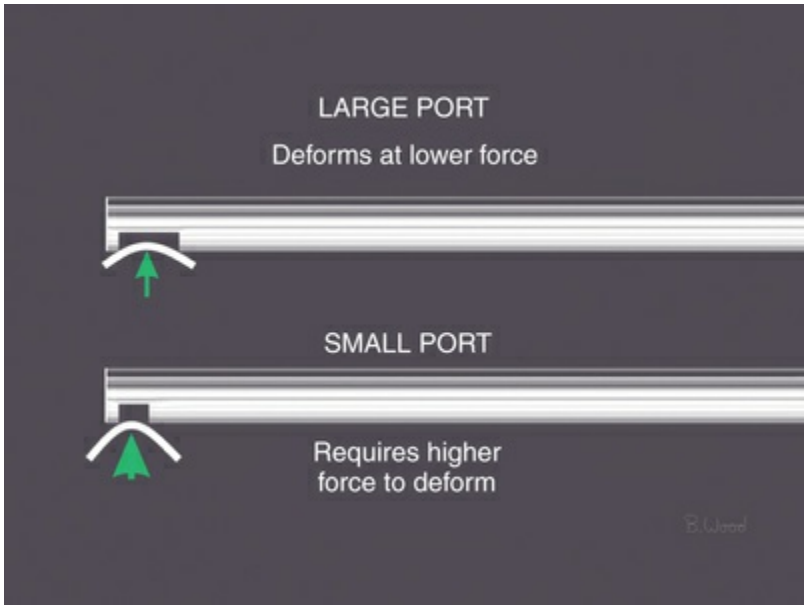

FIG. 105.4 Inclusive shears (vitreous cutters) require elastic deformation of tissue into the port.

Fatigue Failure

Fatigue failure occurs when repetitive motion, elongation, and compression weaken tissue structure and cause failure. Ultrasonic cavitation (fragmentation, phacoemulsification) is an example of this mode of cutting.

Infusion System Management

Vitrectomy surgeons have occasionally experienced excessively low intraocular pressure (IOP) during vitreoretinal surgery throughout the history of vitreoretinal surgery. Gravity-fed infusion systems were simplistic and could only cause low intraocular pressure if the bottle was too low or the infusion fluid was depleted. Sutured 20-gauge (G) vitrectomy resulted in low intraoperative IOP if the cannula was initially positioned into the suprachoroidal space without surgeon recognition or displaced intraoperatively thereby causing suprachoroidal infusion. Digital display of infusion driven by an air pressure source in the machine created the false impression that IOP was controlled when in fact as much as 25 mmHg of difference existed between infusion pressure and IOP with typical flow rates during core vitrectomy and especially

fragmenter use. The fragmenter lumen, unlike the vitreous cutter, is not obstructed by an inner needle or port opening and closing. Low intraoperative IOP is prevented by using a sufficient infusion pressure to compensate for infusion line and cannula resistance-based losses. Ohm's law of fluidic resistance, pressure = flow × resistance, explains pressure drop in the infusion system during flow. There are many causes of excessively low intraocular pressure during vitrectomy, each of which will be discussed. Inadvertent suprachoroidal infusion is a relatively common cause of low pressure as well as other more serious complications during vitrectomy with 23–25–27-gauge surgery as well as the 20G sutured systems used for over three decades. Sutureless 25G vitrectomy initially utilized straight-in trocar cannula trajectories to produce sclerotomies perpendicular to the sclera. When 23G, sutureless surgery was introduced subsequently, oblique trocar-cannula entry was utilized in order to construct a scleral tunnel to reduce wound leakage. Initially, surgeons used a two-plane approach; the initial trocar-cannula insertion segment was approximately 30° relative to the sclera and the second segment trajectory perpendicular to the sclera. Some surgeons even believed that a biplanar incision was constructed, although this is not true because the scleral tunnel was created before changing the trajectory. More recently, surgeons using both 23G and 25G systems have switched to oblique entry in order to create a long scleral tunnel;[1–3] unfortunately some surgeons use excessively steep angles (~10°). Although near tangential entry creates a long scleral tunnel; it increases the chances of infusing into the suprachoroidal or subretinal space (Fig. 105.5). If the cannula is in the suprachoroidal space, the peripheral choroid, which is not observed by the surgeon, expands early in the case, allowing infusion without hypotony, later the choroid can no longer expand and infusion becomes limited, alerting the surgeon to the problem (Fig. 105.6). Thinking that hypotony caused a choroidal effusion leads to incorrect management. A single plane, 30° trajectory is better compromise between the benefits of a long scleral tunnel and the catastrophe of suprachoroidal infusion. Inspecting the infusion cannula with the operating microscope after insertion and before initiating infusion was standard practice with sutured 20G vitrectomy. Many surgeons have discontinued this practice since

23/25G sutureless vitrectomy began; clearly the crucial step of observing the tip of the infusion cannula should not be omitted. It is best practice to insert the infusion port in the cannula with the infusion running to prevent bubbles followed by immediate inspection of the tip of the infusion cannula. The naked eye and endoilluminator provide insufficient magnification to make the determination that the cannula has penetrated the choroid and nonpigmented pars plana epithelium; microscope visualization is essential. Adhesively fastening the infusion cannula tubing and associated stopcock(s) and connectors to the drape is imperative to prevent traction on the infusion cannula and the eye. Unrecognized pulling on the tubing by the assistant or surgeon can easily cause the cannula to partially pull out causing a suprachoroidal infusion. Adhesively fastening the infusion cannula tubing to the drape with eye in the primary position with a short tubing loop can result in a suprachoroidal infusion when the eye is rotated to view the periphery creating tension on the cannula. Scleral depression is another cause of inadvertent suprachoroidal infusion by causing torque on the cannula as the eye is rotated by the depressor. In addition, scleral depression can force blood clots, dense scar tissue, peripheral vitreous, or silicone oil into the infusion cannula and tubing, effectively plugging it, giving the false impression of infusion system failure. Placing the infusion cannula too close to the lower lid rather than just inferior to the horizontal meridian is a common cause of suprachoroidal infusion created when the eye is rotated down to visualize the inferior periphery and the cannula is rotated into the suprachoroidal space. Kinking of the more flexible silicone tubing terminal segment of the infusion cannula can be caused by the surgeon or assistant accidentally pulling on the tubing. This problem is exacerbated by using excessively low infusion pressure settings (10–25 mmHg) insufficient to straighten out the tubing kink. The author has always used 45 mmHg except when operating on children or patients with very low systemic blood pressure, typically under general anesthesia. Some surgeons have recently advocated using infusion settings of 10–20 mmHg because of a completely unfounded belief that occult ischemia is common during vitrectomy. Using infusion settings of 10–20 mmHg causes miosis, bleeding, and corneal astigmatism from

contact lens pressure on the cornea and instrument forces on the sclerotomies as well as scleral infolding often mistakenly thought to be choroidals. Kinking as well as multiple bubbles in the infusion line increase resistance to flow and cause pressure drop, ultimately resulting in excessively low IOP. Surgeon remediation of intraoperative low IOP should be systematic; the first step is to inspect the cannula with the microscope to make sure it extends all the way through the choroid and nonpigmented ciliary epithelium. If not, a 25G MVR blade can be used to incise the tissue covering the cannula while pressing the cannula into the eye with smooth forceps (Fig. 105.7). Another option is to move the infusion system port to the supranasal cannula. The infusion tubing should be examined for kinking or inadvertent disconnection. Kinking is most common when excessively low infusion pressure settings are used and the tubing bends at the fluid–air stopcock/valve. If a suprachoroidal infusion occurs, infusion through a cannula with a 25G needle (if 25G surgery or 27G needle if 27G surgery) into the middle of the eye will compress the choroid against the sclera and cause the suprachoroidal fluid to disappear often via egress around the cannulas (Fig. 105.8). Cut down drainage is almost never necessary. If choroidals are present at the inception of surgery, a 6-mm instead of 4-mm cannula can be used and/or infusion initiated with a 25G needle as described above.

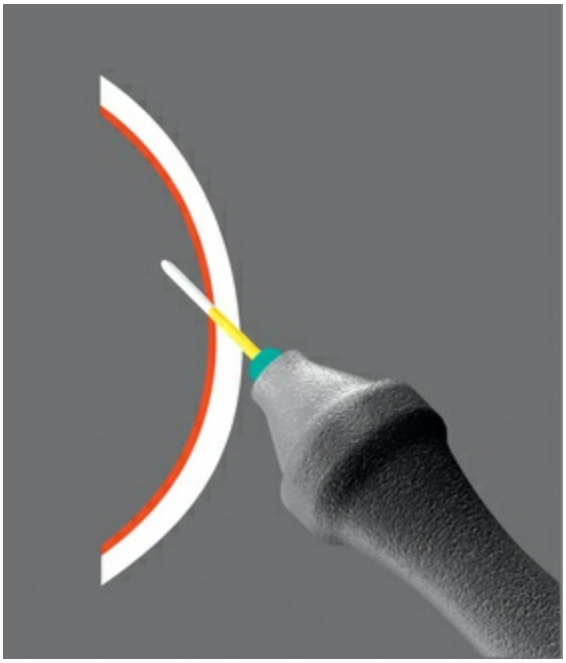

FIG. 105.5 An excessively almost tangential entry angle creates a long scleral tunnel but increases the risk of infusing into the suprachoroidal or subretinal space.

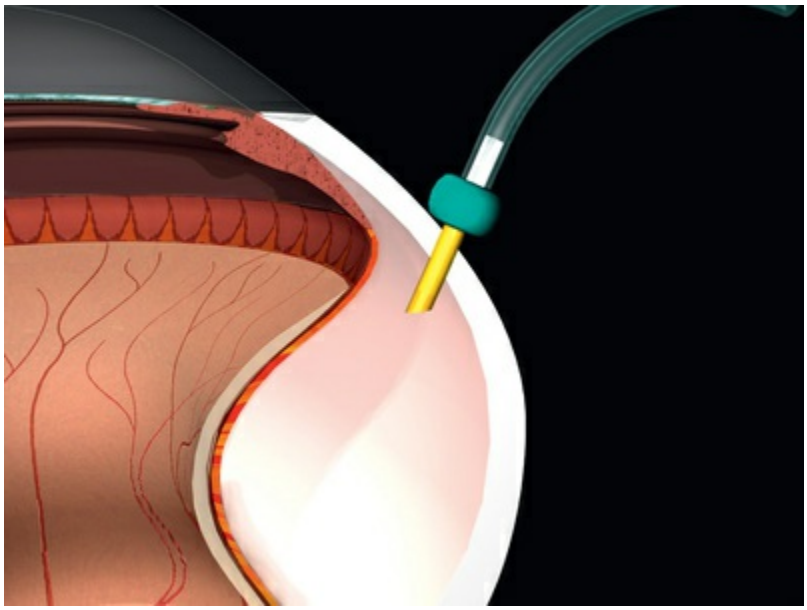

FIG. 105.6 Infusion into the suprachoroidal space causes expansion of the peripheral choroid.

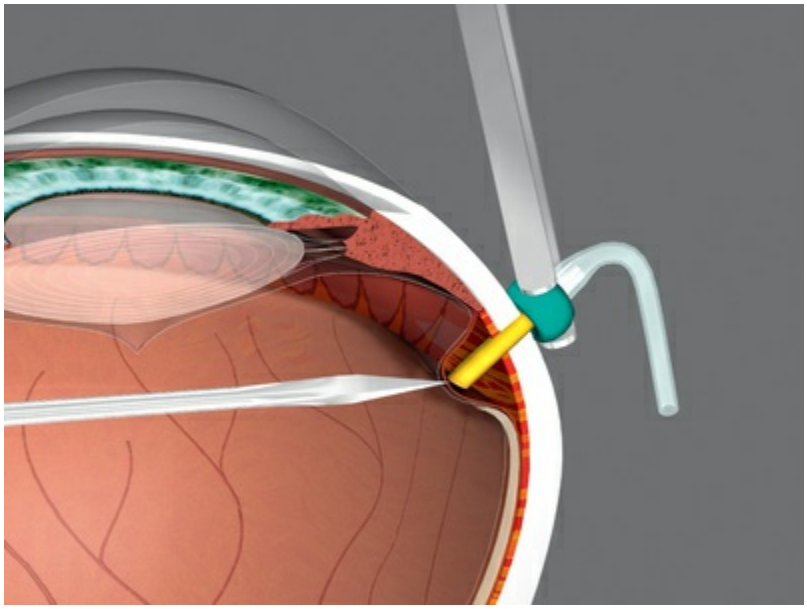

FIG. 105.7 If the infusion cannula does not extend into the vitreous cavity, a 25G MVR blade can be used to incise the tissue covering the tip.

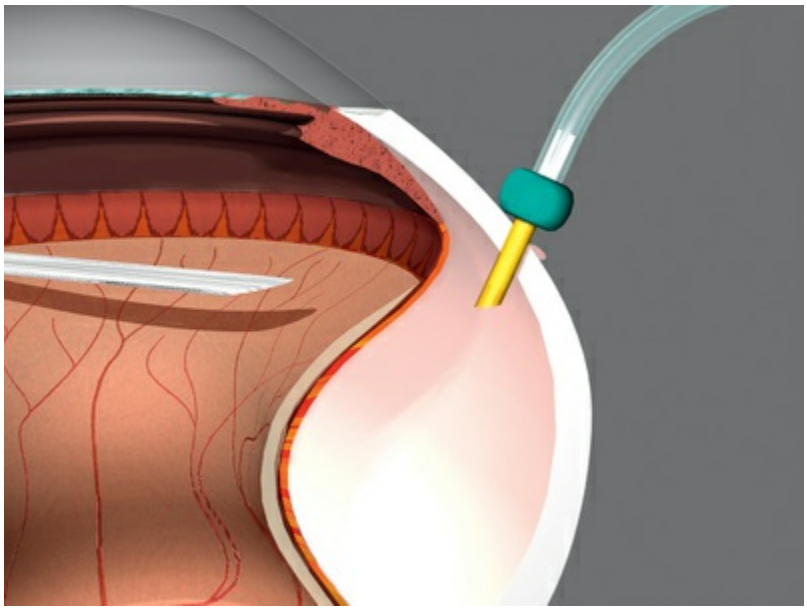

FIG. 105.8 Infusion through a 25G needle will compress the choroid and cause egress of the suprachoroidal fluid around the cannula.

Vitreous Cutter Considerations

All current vitreous cutters utilize suction and inclusive shearing. Ideal tissue cutting is defined as that producing zero displacement of the tissue to be removed and no vitreoretinal traction. It is safest to use the lowest suction force sufficient to imbricate tissue or vitreous into the cutter port. High cutting rates (7500-10,000 cuts/minute) decrease pulsatile fluid flow and pulsatile vitreoretinal traction (Fig. 105.9). Port-based flow limiting via high cutting rates and smaller gauge cutters limits fluid surge after sudden elastic deformation of dense ERM, scar tissue, or lens material through the port, thereby reducing iatrogenic retinal breaks. Dual actuation eliminates the spring, which enables higher cutting rates while maintaining effective duty cycle control (Fig. 105.10). In summary, using the highest available cutting rate is usually the best approach for all tasks and all cases unless all the vitreous has been removed first.

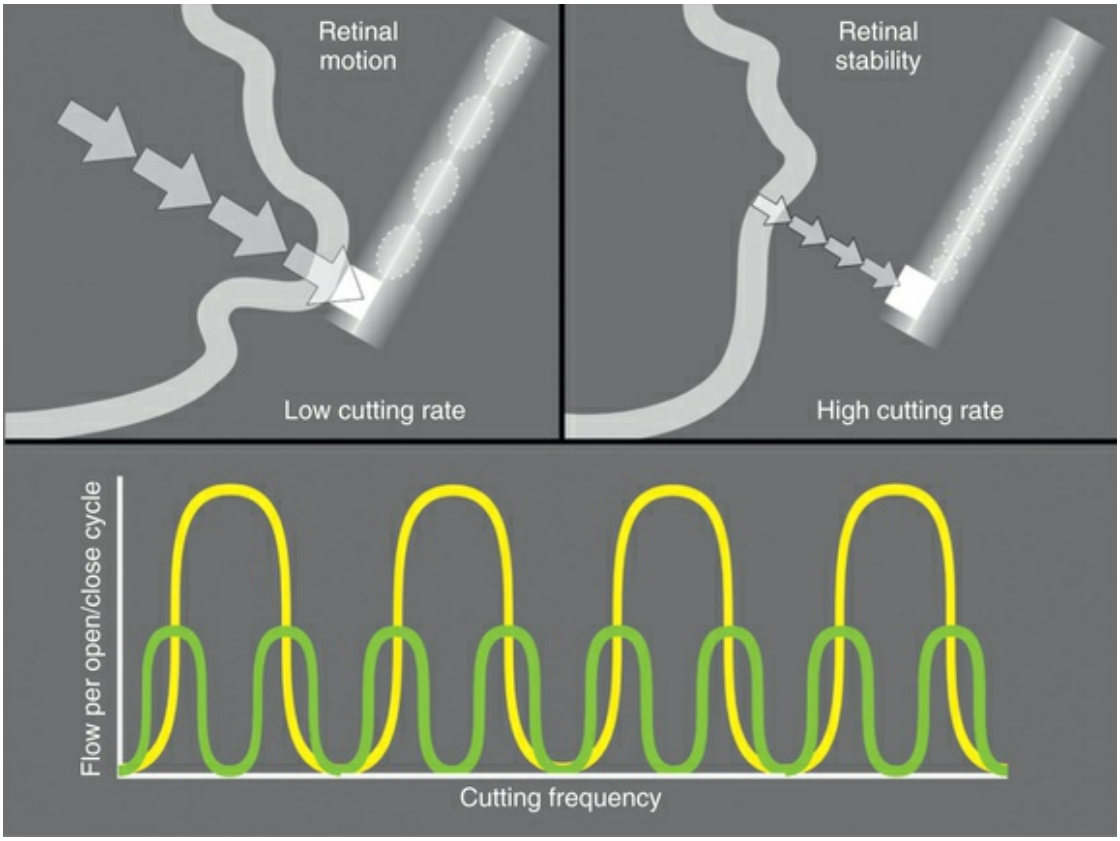

FIG. 105.9 High cutting rates reduce pulsatile vitreoretinal traction.

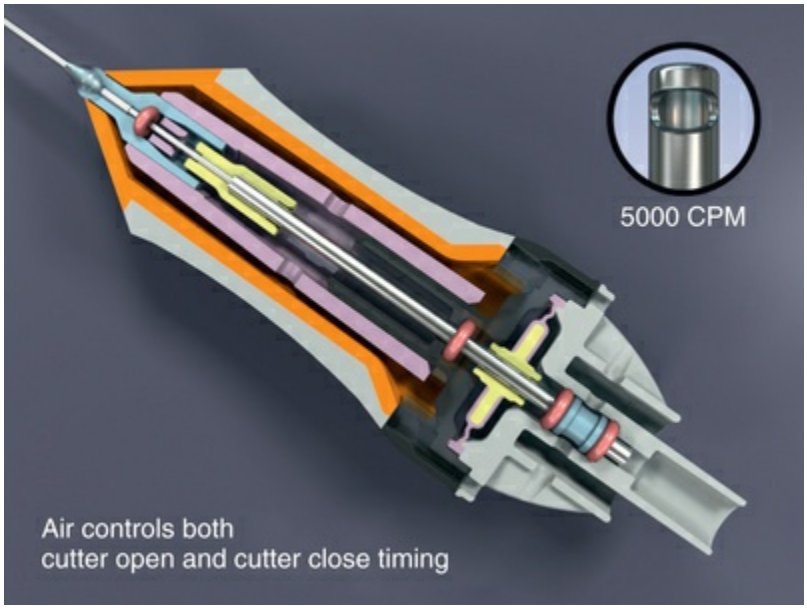

FIG. 105.10 Dual actuated cutters eliminate the return spring and enable higher cutting rates.

Fluidics

Venturi-based, vacuum-controlled aspiration systems are preferred over flow control using peristaltic pumps or piston pumps for all vitreoretinal tasks. Peristaltic pumps produce high transorifice pressure when dense vitreous or ERM transiently occludes the port leading to surge and iatrogenic retinal breaks when the material suddenly deforms through the port. In addition, peristaltic and piston pumps cannot function in an air-filled environment, thereby preventing use of the valuable technique of interface vitrectomy under air.[4,5]

Control Systems

Analog parameters using surgical force such as suction levels, power scissors and forceps, and power injector rate are best controlled by proportional depression of the surgeon's foot (linear control). Switching of valves, pumps, electronic devices, and lasers are ideally controlled by a single integrated system, with functions controlled by the surgeon rather than the circulating nurse or even scrub tech.

Microscope Requirements

A stereo operating microscope with magnification up to ×30 with coaxial illumination is required. The microscope should have a beam splitter to enable stereo-optical viewing by the assistant and television viewing for the operating room team. Illumination on–off should be controllable by the surgeon's foot. So-called heads-up surgery, viewing surgery with a television-based system and flat panel display, significantly reduces resolution and dynamic range and offers no advantage.

Microscope XY positioning must be controlled via surgeon footswitch. Power zoom and focus positioning are required. Physical stability of the microscope and patient's head is required to preserve the dimensional stability of the surgical view for microsurgery. Ceiling-mounted microscopes are less mechanically stable than floor-mounted microscopes because of longer moment arms and inherent lack of ceiling rigidity. The surgeon's hands should be in contact with the patient's head so hand motion can be coordinated with head motion. The goal is to provide a stable mechanical relationship between the microscope, the patient's head, the surgeon's hands, and the OR table resting on the floor.

All power and control sources for surgical tools should be integrated into a single system for greater efficiency. Advanced vitreoretinal surgery systems have a unified human–machine interface combining all surgical functions into an integrated system (Fig. 105.11). Illumination, diathermy, and infusion are referred to as global functions and are always available. Infusion is best controlled by digital, sensor-based, pressurized infusion systems.

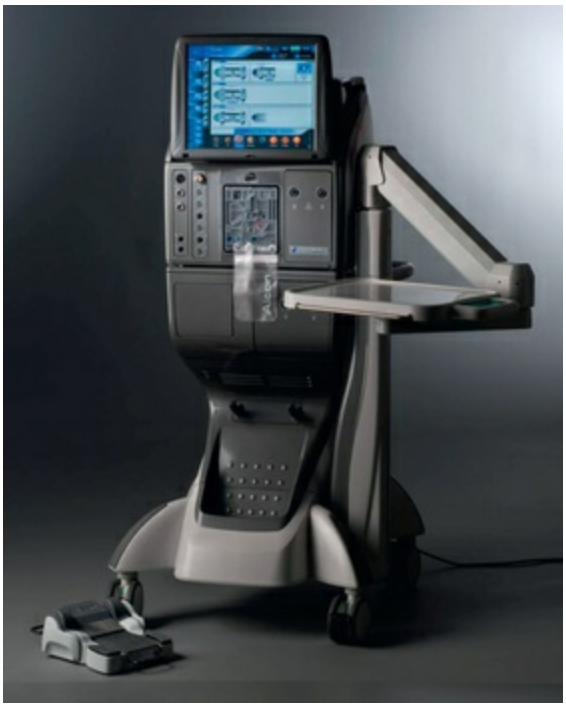

FIG. 105.11 Advanced vitreoretinal surgical systems utilize an intuitive human–machine interface and combine all surgical functions into an integrated system.

Tool Ergonomics

All surgical tools should be as light as possible and held in the surgeon's fingertips. They should be contoured rather than cylindrical to reduce the force required to prevent dropping and constrain grip at a consistent position. They should be no longer than the distance from the fingertips to the point of contact with the hand. Shorter handles reduce the torque produced by the weight and reduce friction as the cables, fibers, and tubing used to connect surgical tools slide on the drape. Minimizing forces required to hold tools increase the surgeon's proprioceptive sense (Weber–Fechner law) and decrease fatigue and tremor. Standardization of tip-to-grip across all tools facilitates so-called muscle memory; the surgeon's cerebellum, motor strip, and frontal lobe trajectory generator knows where the tip is located if view is suddenly lost.

Surgical Steps

Transconjunctival, Small-Gauge Vitrectomy

Transconjunctival, sutureless 23/25/27G vitrectomy systems have improved to the point that there is no longer a need for 20G vitrectomy; referring to 20G vitrectomy as the "gold standard" is arcane. The advantages of 23/25/27G are improved safety because of fewer iatrogenic retinal breaks, reduced operating times, less patient discomfort, and faster visual improvement.[6–8] A single 20G sclerotomy is required to remove intraocular foreign bodies and for a fragmenter to remove dense lens material (Fig. 105.12).

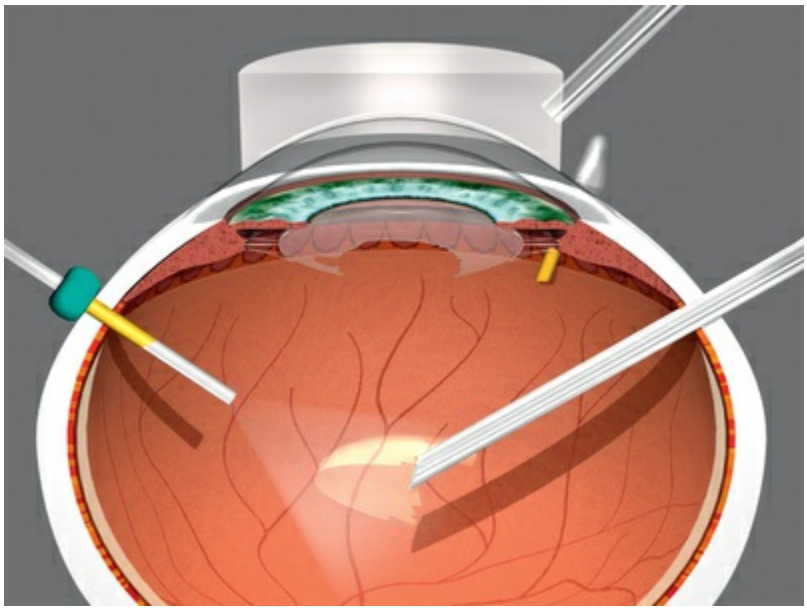

FIG. 105.12 A single 20G sclerotomy can be used to allow fragmenter access or foreign body removal in microincision vitrectomy when using a 25G surgical approach.

There is no solid evidence that combining a scleral buckle with vitrectomy improves retinal detachment outcomes, especially in the absence of severe proliferative vitreoretinopathy (PVR). Elimination of the scleral buckle supports many of the advantages of sutureless, transconjunctival vitrectomy, i.e., no refractive error changes and no strabismus. Elimination of the scleral buckle eliminates the need for conjunctival incisions. Similarly, sutured-on contact lens rings make no sense in the context of transconjunctival, sutureless

vitrectomy.

Sclerotomies

Conjunctival displacement ensures that the conjunctival trocar-cannula wound is not overlying the scleral trocar-cannula wound (Fig. 105.13). Conjunctival displacement is essential for the transconjunctival sutureless technique, to provide containment of vitreous wick as well as prevent access of tear film to the sclerotomies, thereby reducing endophthalmitis risk.

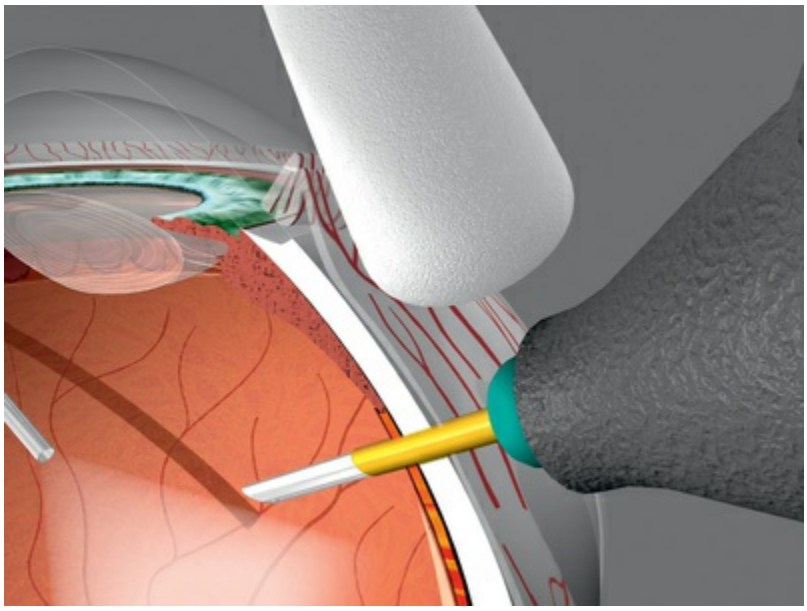

FIG. 105.13 The 25G vitrectomy systems utilize transconjunctival trocars, which eliminate suturing, reduce surgery times, and increase patient comfort. Conjunctival displacement ensures that the conjunctival wound does not overlay the scleral wound.

There is no rule that sclerotomies should be placed at certain hours of the clock or at the borders of the rectus muscles; they should be located to avoid conjunctival scars, filtering blebs, and regions of abnormal pars plana, as well as facilitate the greatest possible solid angle intraocular access (Fig. 105.14). The inferotemporal sclerotomy should be located just below the horizontal meridian to reduce the risk of bumping the lower lid when rotating the eye to view the inferior retina. The superonasal

sclerotomy should be located on a virtual line from the lowest point of the bridge of the nose to the pupillary axis. The superotemporal sclerotomy should be located on a virtual line from the lowest point of the supraorbital rim to the pupillary axis; the cannula hub will then be immediately adjacent to the inferotemporal cannula hub. More anterior or nonstandard locations are required in cases of congenital or pathologic abnormalities of the pars plana.

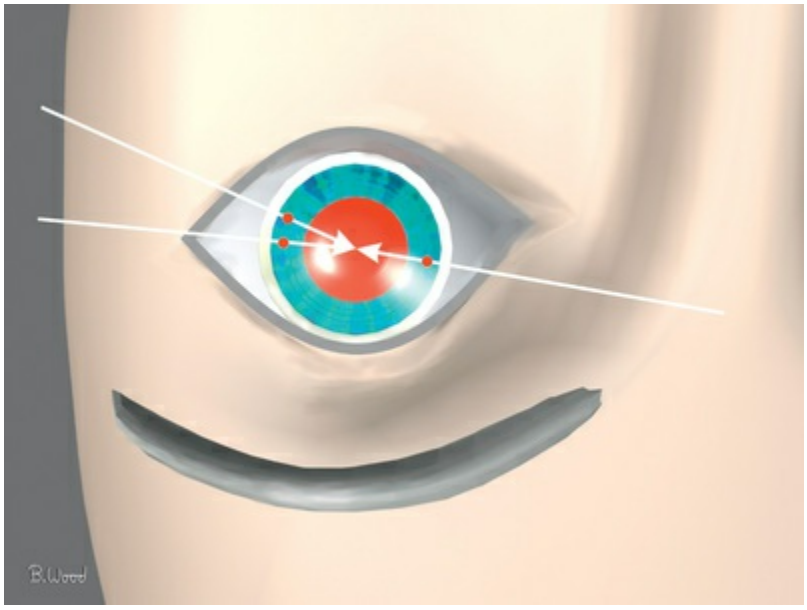

FIG. 105.14 Sclerotomies should be located to avoid conjunctival scars, filtering blebs, regions of abnormal pars plana, and allow the greatest degree of intraocular access.

Vitreous Removal

Conventional algorithms have stressed the sequence: core vitrectomy followed by posterior vitreous detachment (PVD) creation if PVD is not present, then so-called peripheral vitreous shaving and finally management of epiretinal membranes. Cutting technology, surgical techniques, and understanding of pathoanatomy have improved to the point that a linear algorithm no longer suffices; therefore, each algorithm should be selected according to case-specific pathoanatomy. If the AVC is semiopaque, opaque, or taut, it should usually be removed first. If it is clear and

the lens is to be left in place, it should be retained unless there is an element of anterior loop traction (anterior PVR) or compartmentalization requiring removal (see Lens management, below). In the majority of cases, the "core" vitreous requires no specific attention, and the algorithm should proceed to the decision about whether to truncate the PVC or to delaminate ERM first. If the PVC is opaque or semiopaque, it usually requires truncation before the ERM can be peeled or delaminated (Fig. 105.15). When there is a partial PVD and the ERM is continuous with sections of the PVC, delamination should usually precede PVC truncation (Fig. 105.16).

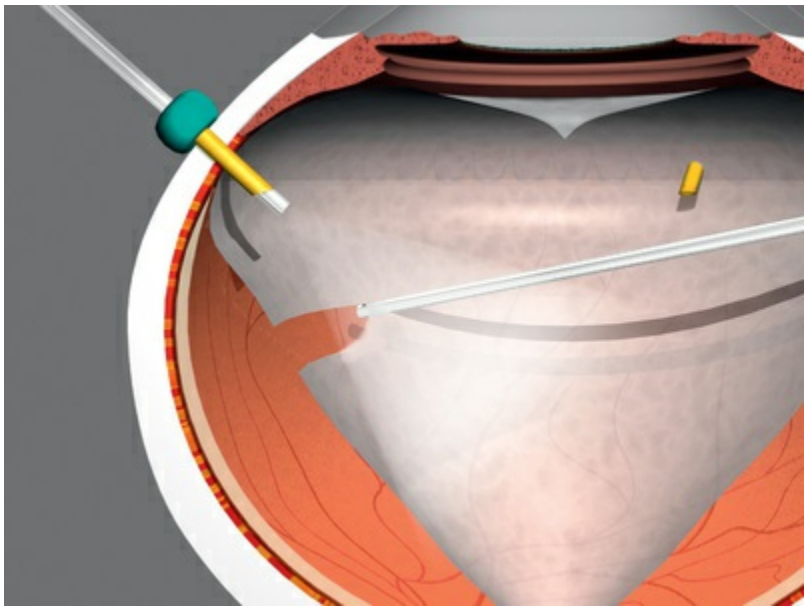

FIG. 105.15 Opaque posterior vitreous cortex should be entered away from the macula and periphery in an area known to be attached or away from the retina. This incision should be extended circumferentially to accomplish truncation.

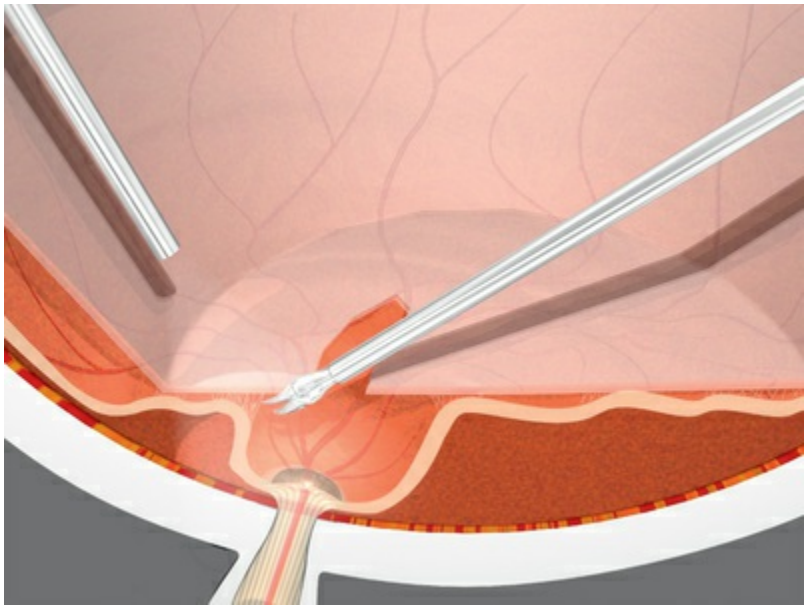

FIG. 105.16 Access segmentation exposes the delamination plane to enable inside-out delamination.

If sub-PVC blood products are encountered while PVC truncation is under way, a soft-tip cannula or vitreous cutter with cutting deactivated should be used to remove blood; this is referred to as extrusion (Fig. 105.17). If, in the process of PVC truncation, regions of PVC are stretched between areas of ERM, they can be sectioned with the cutter only if it can be done without undue traction on the retina. Curved scissors are preferred over vertical scissors for segmentation of these sections of the PVC if there is concern about iatrogenic retinal breaks in atrophic, elevated retina (Fig. 105.18).

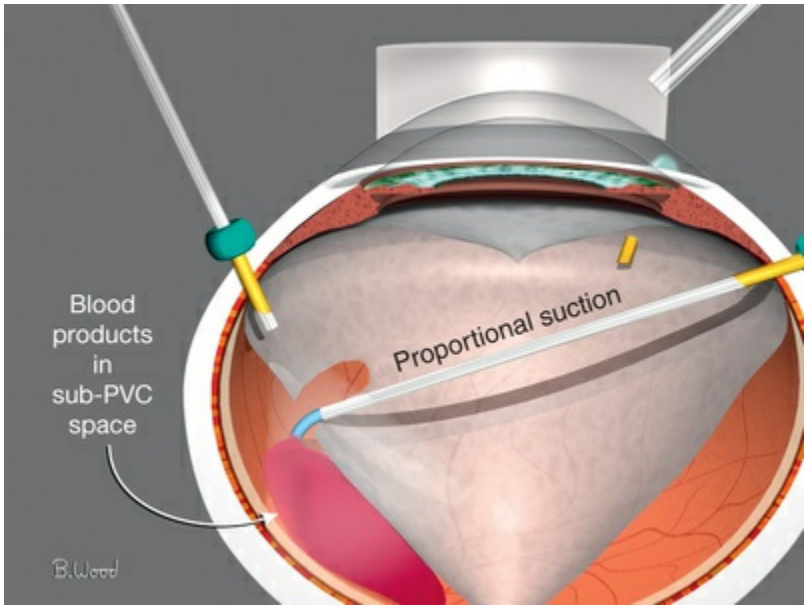

FIG. 105.17 Proportionally controlled suction, rather than a flute needle or cutter, permits safe, nonpulsatile removal of subposterior vitreous detachment blood products.

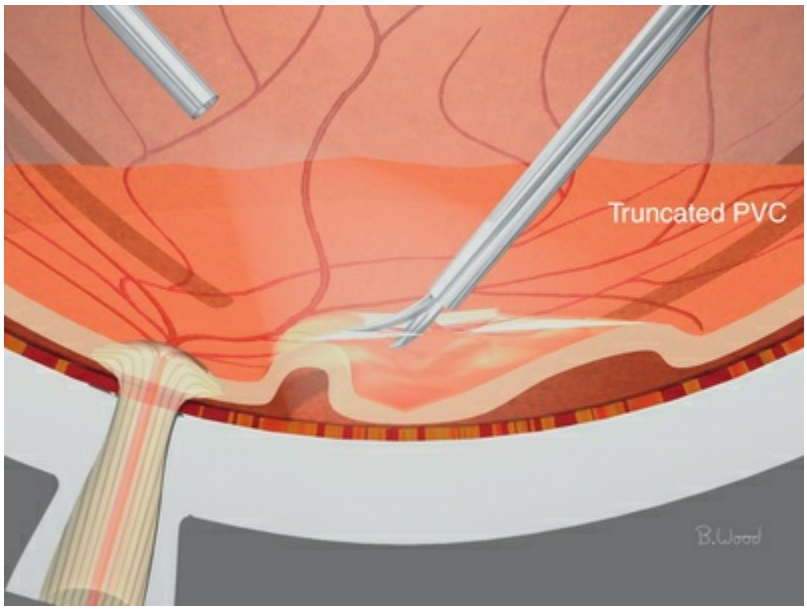

FIG. 105.18 Posterior vitreous cortex (PVC) truncation. Inside-out segmentation and delamination are required for much less common, dense, highly adherent membranes. Curved scissors should be used to segment these sections of the PVC if there is concern about iatrogenic retinal breaks in atrophic, elevated retina.

Anterior loop traction (radial fibers) is a significant feature of anterior proliferative PVR, some trauma cases, and anterior hyaloidal fibrovascular proliferation (retrolenticular neovascularization) in severe proliferative diabetic retinopathy (PDR) cases. Anterior cortical fibers are made taut by hypocellular vitreous contraction extending in the anteroposterior direction from the vitreous base to the pars plana, ciliary body, and even to the posterior iris surface. They can be present typically inferiorly in PVR cases, or in severe cases, this pathoanatomy can extend for 360°. Anterior loop traction is to be differentiated from the "skirt" that is left after core vitrectomy. Anterior loop traction can be visualized with contact-based wide-angle viewing, scleral depression by the surgeon using chandelier illumination, or scleral depression by the assistant. Wide-angle viewing systems are essential for viewing the periphery; contact-based wide-angle viewing provides 10° greater field of view than non-contact systems, eliminates all corneal asphericity, and requires less ocular rotation. Scleral depression is very effective but requires a skilled assistant or chandelier illumination, which reduces the ability to visualize clear vitreous. Anterior loop traction can usually be resected with a 23/25/27G vitreous cutter (Fig. 105.19).

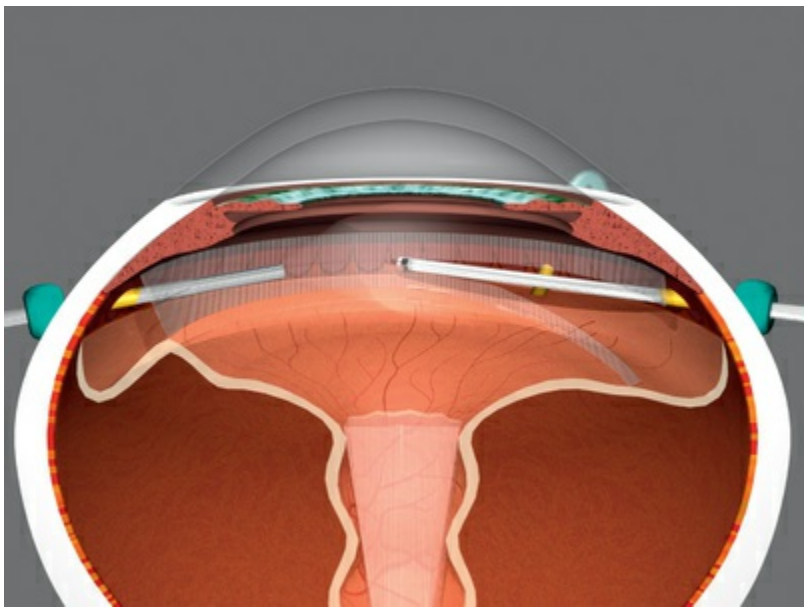

FIG. 105.19 Anterior loop traction can usually be resected with 23G or 25G vitreous cutters.

Lens Management

In addition to its normal optical function for the patient, the lens affects the vitrectomy-based management of retinal detachment. Cells, as well as cytokines, proteins, and inflammatory components, are retained in the vitreous cavity and thus are exposed to the retina longer in the phakic and pseudophakic eye. In cases of severe inflammatory PVR, severe uveitis, and severe trauma, it may be advantageous to remove the lens to accomplish decompartmentalization of the eye (Fig. 105.20). Aphakia also permits better dissection of the anterior vitreous, eliminates concern about subsequent cataract surgery, improves visualization, and facilitates exchanges. In PDR, there is a trade-off in that the presence of the lens reduces neovascular glaucoma now manageable with anti-VEGF agents, but facilitates anterior fibrovascular proliferation (retrolenticular neovascularization) and greatly prolongs the retention time of postoperative hemorrhage. Lens removal in conjunction with vitrectomy is usually best managed with phacovitrectomy and introduction of an acrylic posterior chamber lens.

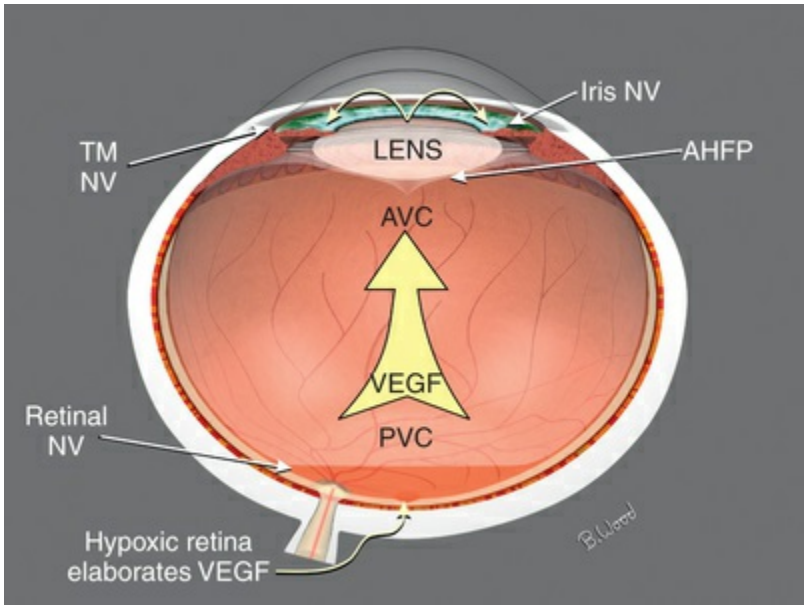

FIG. 105.20 Decompartmentalization of the eye facilitates vascular endothelial growth factor (VEGF) access to the trabecular meshwork (*TM*) and iris but reduces retinal levels. *NV*, neovascularization; *AVC*,

anterior vitreous cortex; *AHFP*, anterior hyaloidal fibrovascular proliferation; *PVC*, posterior vitreous cortex.

Endocapsular lensectomy is an efficient and safe method of lens removal if intraocular lens (IOL) implantation is not planned. The first step is placement and verification of the infusion cannula insertion through the choroid and nonpigmented pars plana epithelium using the operating microscope, not the naked eye. Anterior vitrectomy should be performed before lensectomy to prevent traction on the retina from the fragmenter. The cutter should then be used to make a circular rhexis in the posterior capsule. Hydrodissection and delineation should be performed with a 27–30G blunt cannula. A fluid wave should be seen under the anterior lens capsule (Fig. 105.21). An assistant-held syringe or preferably a machine-controlled fluid injector connected to a short length of tubing facilitates this step. Sculpting of the epinucleus, nucleus, and inner cortex with the fragmenter at moderate power levels is the next step (Fig. 105.22). Simultaneous sonification and aspiration using a 20G fragmenter is better than intermittent suction followed by sonification without aspiration, because it is less likely to cause scleral burns. Constant fluid flow is required to dissipate frictional heat. The cortex should then be aspirated with the vitreous cutter in suction-only mode (Fig. 105.23). The cutter can then be used in cutting mode after the cortex has been displaced from the capsular bag. If severe miosis occurs, scleral depression or injection of 1 : 10,000 epinephrine (adrenaline) without preservative will facilitate the required removal of all peripheral cortex. Proportional (linear) suction should be used with typical suction levels of 100–150 mmHg while in the capsular bag. A capsulotomy to facilitate forceps removal of the capsule should be made with the MVR blade or cutter after all cortex is removed if lens implantation is not planned. The entire capsule should then be removed with textured end-grasping forceps using a circular, zonular rhexis motion (Fig. 105.24). Removal of the complete capsule prevents the inflammation and peripheral proliferation associated with the retention of lens material as well as fibrosis-based closure of peripheral iridectomies.

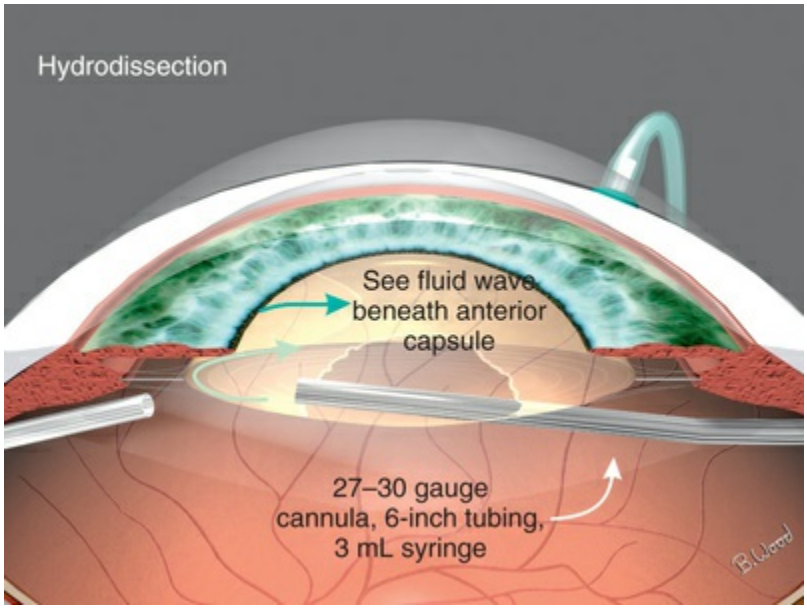

FIG. 105.21 A fluid wave should be seen under the anterior capsule during hydrodissection and delineation.

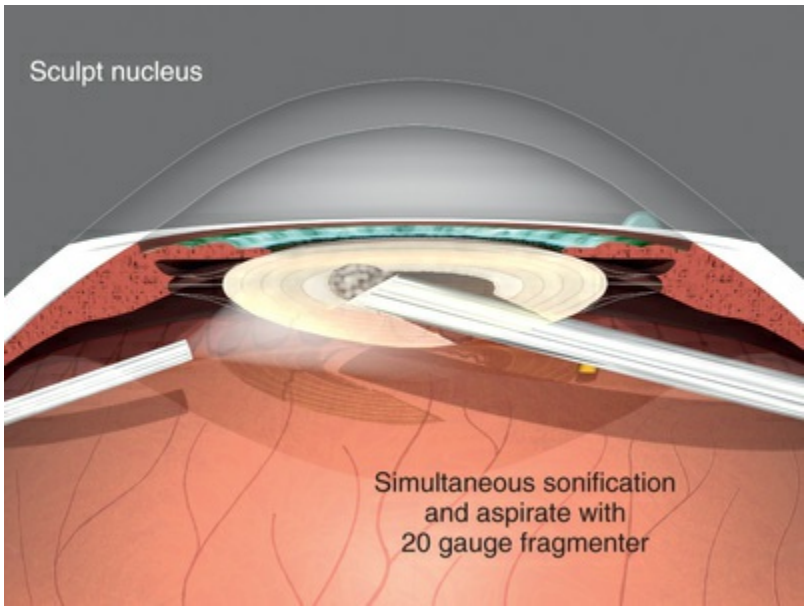

FIG. 105.22 Simultaneous sonification and aspiration with the 20G fragmenter at moderate power is used to sculpt the epinucleus, nucleus, and inner cortex.

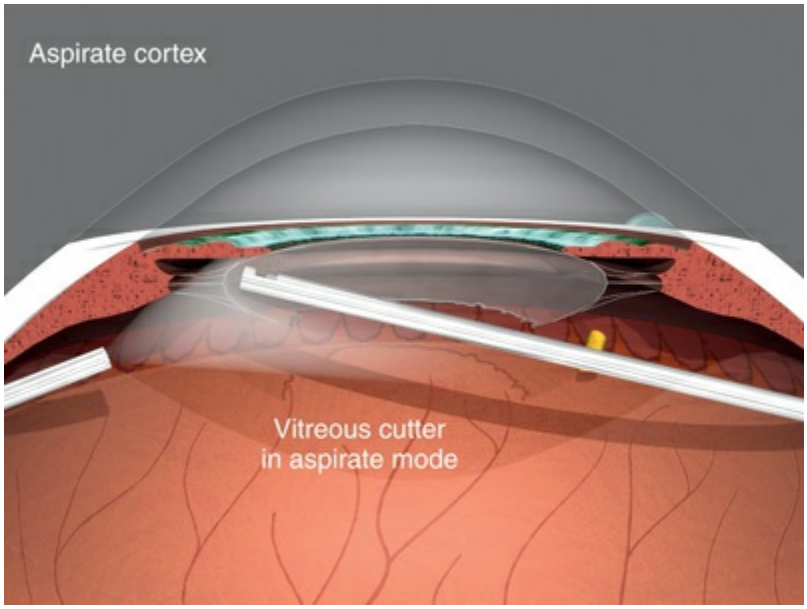

FIG. 105.23 Use the vitreous cutter in suction-only mode to aspirate the cortex, then switch to cutting mode after the cortex has been displaced from the capsule.

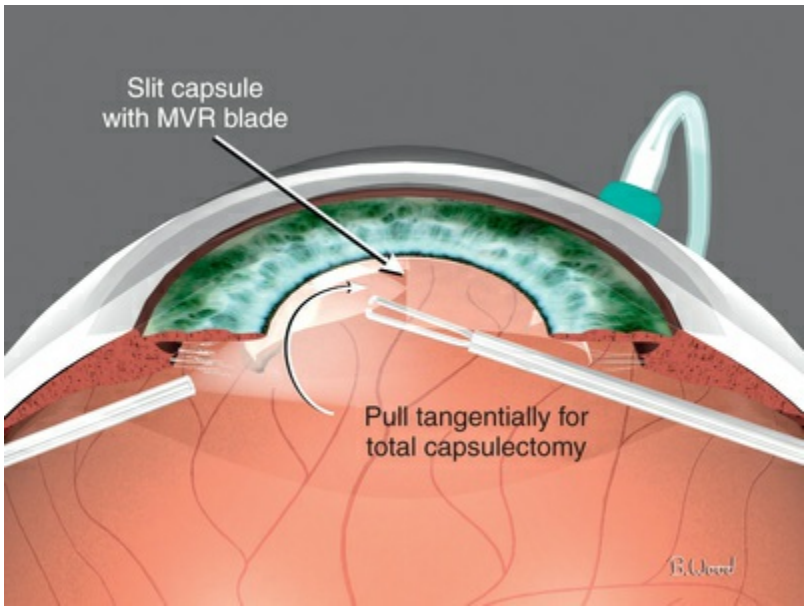

FIG. 105.24 End-grasping or ILM forceps should be used to remove the entire capsule using a circular, zonular rhexis technique.

Combining phacoemulsification with vitrectomy is now common practice; phacovitrectomy is ideal for rhegmatogenous retinal detachment, traction retinal detachment, and PVR cases with

significant cataract. Many surgeons incorrectly believe that vitrectomy always causes cataract; this is simply not literally true. Vitrectomy virtually always causes progression of preexisting nuclear sclerosis but not de novo cataract. Removal of clear lenses because of the false assumption that cataract is inevitable is overdone. Patients expect emmetropia after cataract surgery, and this is very difficult to achieve with phacovitrectomy because of axial length measurement error and surgeon variables. A better practice is to have a cataract surgeon perform phaco several weeks before vitreomacular surgery if preoperative examination indicates that the cataract will interfere with optimal visualization during vitrectomy. If moderate nuclear sclerosis is present, phaco and intraocular (IOL) implantation can be delayed for a month after vitreomacular surgery when the cataract progresses; this approach produces better refractive outcomes.

IOLs should be removed for most severe uveitis, AVC fibrovascular proliferation, and fibrin syndrome cases. Removal should be accomplished by making a cataract surgery-type incision and using specialized scissors to cut the implant into smaller segments, thereby reducing wound size. The wound should be closed with multiple X-type 10–0 monofilament sutures to prevent wound leaks and intraoperative iris prolapse. Residual capsule, cortex, and associated fibrous proliferation should be completely removed to reduce inflammation and peripheral proliferation.

Epiretinal Membrane Management

The decision node in ERM management has three branches. ERM can be managed by peeling, segmentation, or delamination. If the membrane is segmented to release tangential force, the epicenters are retained. Choices are disease-dependent, in that diabetic traction retinal detachments usually require delamination often preceded by access segmentation. PVR requires peeling in most early, less adherent cases, with segmentation or delamination used in a small number of late-stage, dense, highly adherent membrane situations.

Disposable, 25G or 27G, end-grasping ILM forceps are the author's preferred instruments for peeling PVR membranes, as well

as epimacular membranes and internal limiting membrane (ILM) peeling (Fig. 105.25). End-grasping forceps membrane peeling eliminates the need for pics, membrane scrapers, and MVR blades, all of which can damage the retinal surface.

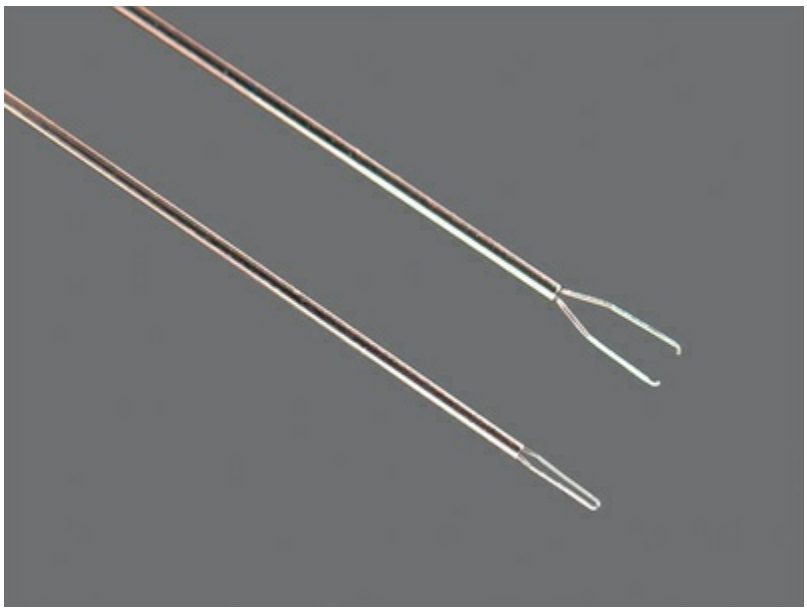

FIG. 105.25 Internal limiting membrane (ILM) forceps are ideal for both epimacular membrane and internal limiting membrane peeling.

The preferred tool for delamination and access segmentation is 25G or 27G curved scissors (Fig. 105.26). Because the radius of curvature is similar to the retinal contour, the chance of making iatrogenic retinal breaks is reduced compared with the 135° ("right-angle") scissors. Curved scissors are also preferred over vertical scissors for segmentation because blade thickness is much less than blade width (Fig. 105.27); iatrogenic retinal breaks are less likely when the bottom blade is inserted in the potential space between ERM and retina. In addition, transition from access segmentation to delamination does not require tool exchange, only small-angle tool rotation to place both blades under the ERM and begin delamination.

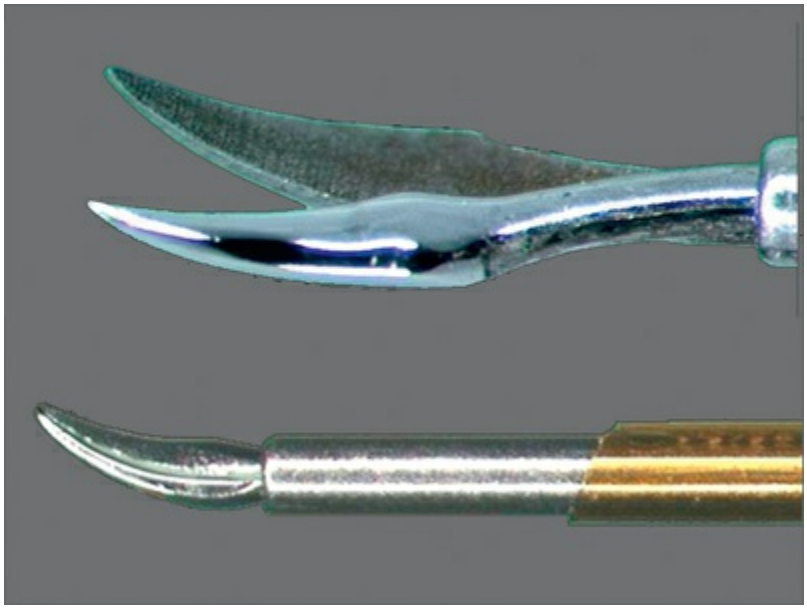

FIG. 105.26 The 25G curved scissors have a radius similar to retinal curvature, reducing the chance of making iatrogenic retinal breaks.

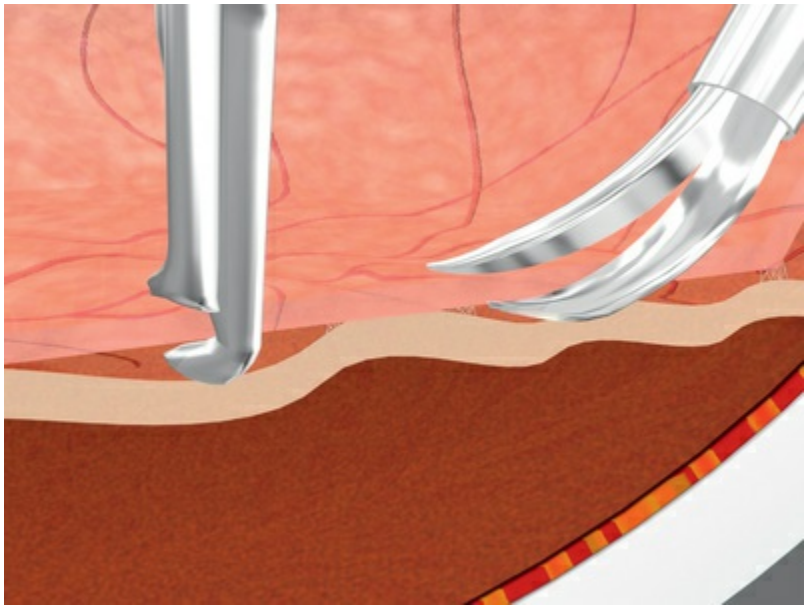

FIG. 105.27 Blade thickness of curved scissors is much less than blade width of vertical scissors facilitating access to the space between the epiretinal membrane and retina while decreasing the likelihood of retinal breaks.

The goal from a biologic perspective is to minimize trauma to the retina, eliminate all tangential force from the retina, and reduce

reproliferation due to bleeding resulting in fibrin bridges between epicenters of retained ERM.

When peeling the ILM, both indocyanine green (ICG) and triamcinolone should be employed with caution. In many reports, ICG has been shown to be toxic to the retina and RPE, and triamcinolone particles may get trapped within a macular hole or in the subretinal space. The author uses only end-grasping ILM forceps with or without the use of brilliant blue staining for all cases that require ILM peeling. In macular hole cases requiring surgery, ILM peeling removes tangential traction on the surface of the macula, guarantees that ERMs are successfully removed, and increases retinal elasticity, all of which increase the likelihood of successful hole closure. While never used as a primary approach, performing an arcuate retinotomy has shown some success in achieving closure of large, otherwise inoperable macular holes.[9]

Management of Subretinal Proliferation

Subretinal proliferation can be placoid, band-like, or annular in configuration (Fig. 105.28). Because the biologic behavior seems to be less likely to result in reproliferation, subretinal membrane removal is dictated by geometric considerations. If the retina cannot be reattached with an undistorted macula due to subretinal proliferation, subretinal surgery is indicated.

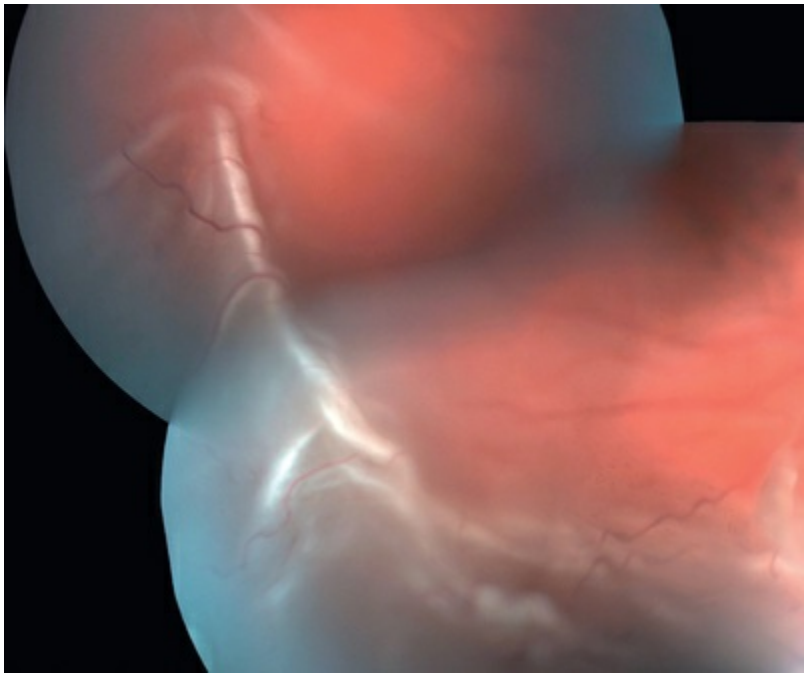

FIG. 105.28 Subretinal proliferation can be placoid, band-like, or annular in configuration.

Subretinal surgery can be categorized as peeling or scissors segmentation. If a retinal break is appropriately positioned, forceps can be passed through the break and used to grasp and remove long dendrites with a sequential regrasping technique (Fig. 105.29). If a convenient break is not present, punch-through retinotomy with the closed forceps tip is the preferred technique (Fig. 105.30). If the membrane is placoid, forceps removal should be used. Occasionally, subretinal bands are fibrovascular and require scissors segmentation rather than forceps removal.

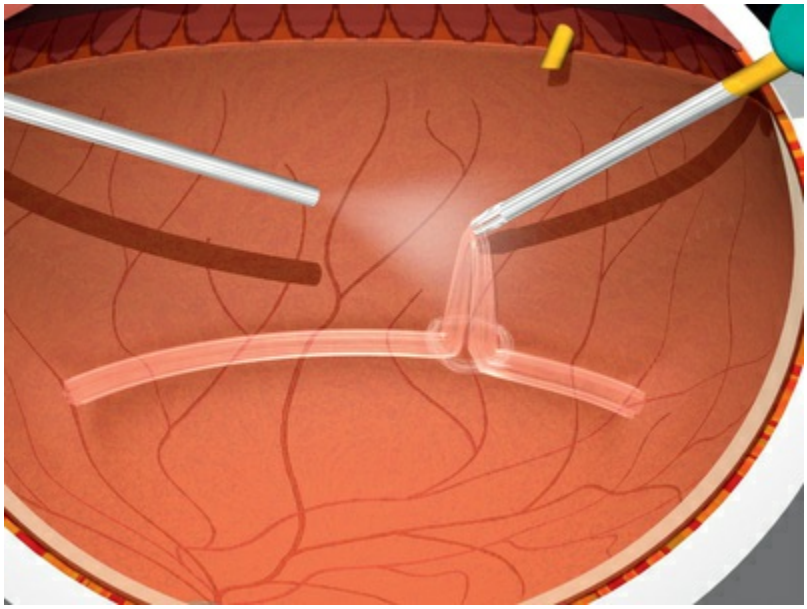

FIG. 105.29 Subretinal bands can be removed utilizing a sequential regrasping technique.

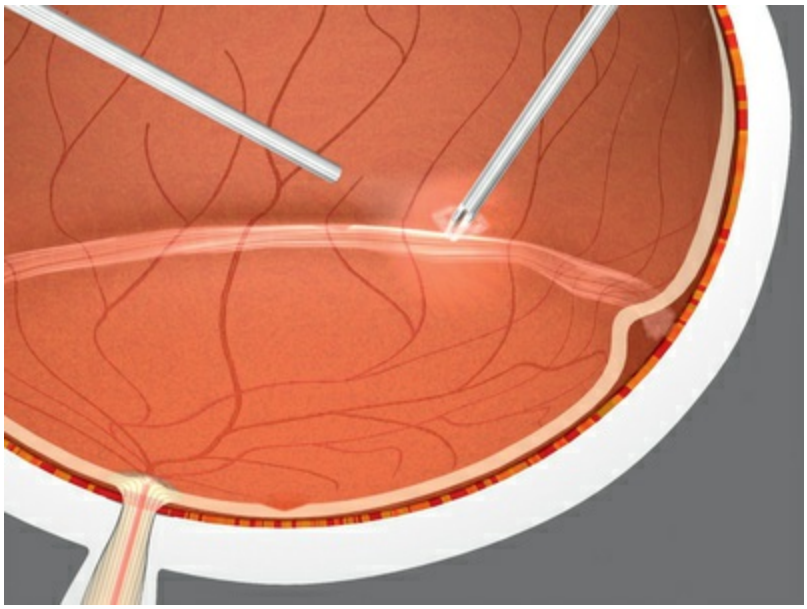

FIG. 105.30 End-grasping forceps can be passed through an existing break or punch-through retinotomy to remove subretinal proliferation.

Extrusion Techniques

Soft-tip cannulas (Fig. 105.31) can be used to remove material from

the eye using footpedal-controlled machine-driven aspiration; this is called extrusion. Soft-tip 25–27G cannulas with low suction levels are ideal for removing free blood products, PFO (perfluoro-n-octane), oil droplets, or small pieces of lens material from the retinal surface or vitreous cavity after the vitreous is removed with the cutter. Extrusion is preferable to using the flute cannula because inadvertent tip movement due to covering the egress hole on the handle, and extrusion provides more precise aspiration control as well as footpedal-controlled precision reflux.

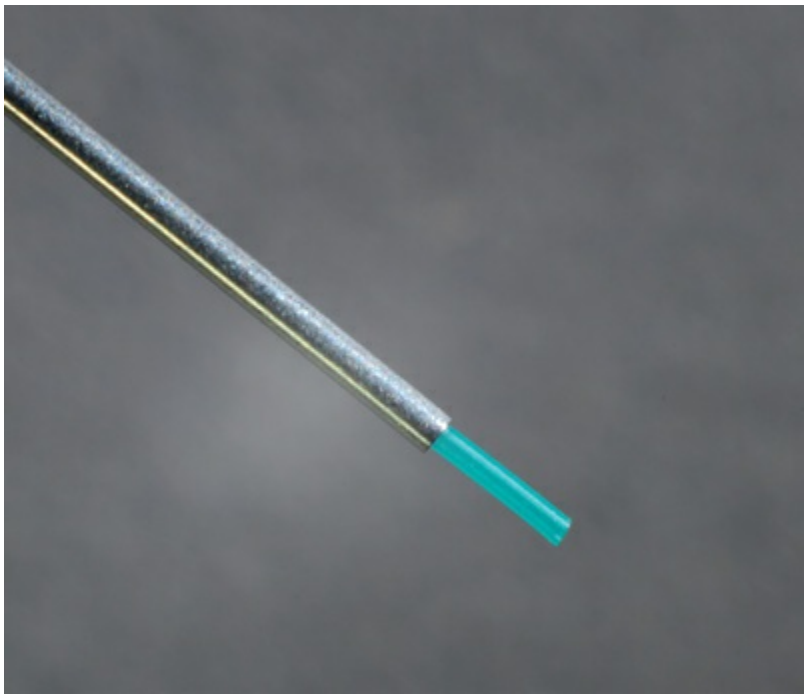

FIG. 105.31 Soft-tip cannulas are preferred for internal drainage of subretinal fluid, PFO (perfluoro-n-octane) removal, fluid–air exchange, and air–gas exchange.

Flexible cannulas are preferred for internal drainage of subretinal fluid (SRF) because they can be angulated into the subretinal space (Fig. 105.32) and are less likely to damage the choroid and cause bleeding with patient movement or suboptimal positioning due to poor visualization. The algorithm for internal drainage of SRF begins with drainage, then fluid–air exchange with continued or repetitive internal drainage of SRF. If fluid–air exchange is performed before internal drainage of subretinal fluid, the SRF is forced posteriorly, creating the need for drainage retinotomy,

potentially detaching an attached macula, and causing postoperative macular folds.

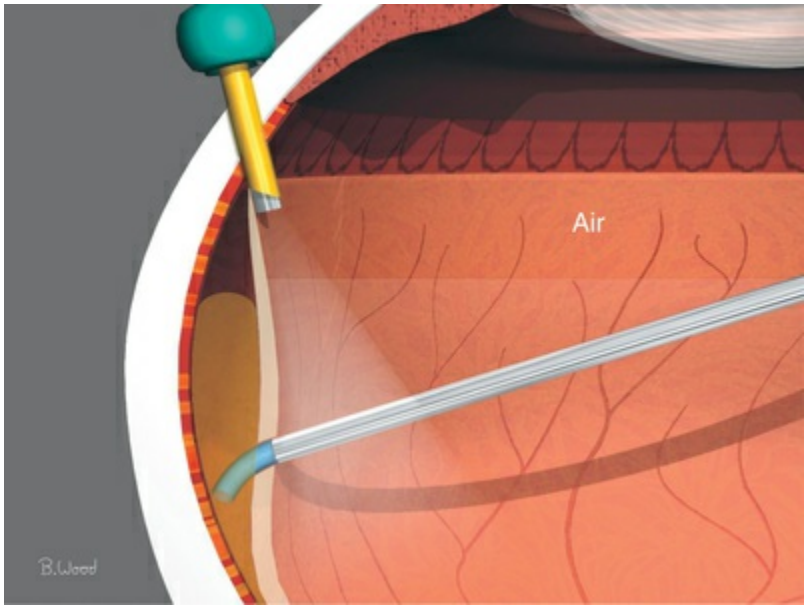

FIG. 105.32 A soft-tip cannula held near the retinal pigment epithelium and controlled by proportional aspiration allows safe internal drainage of subretinal fluid.

Interfacial Surface Tension Management

Air (gas) interface with aqueous (72 dyne/cm^2) provides greater interfacial surface tension than the silicone–aqueous interface (40 dyne/cm^2) (Fig. 105.33). Viscoelastics and lipoproteins from blood or inflammation lower the interfacial tension of the silicone–aqueous interface causing emulsification.

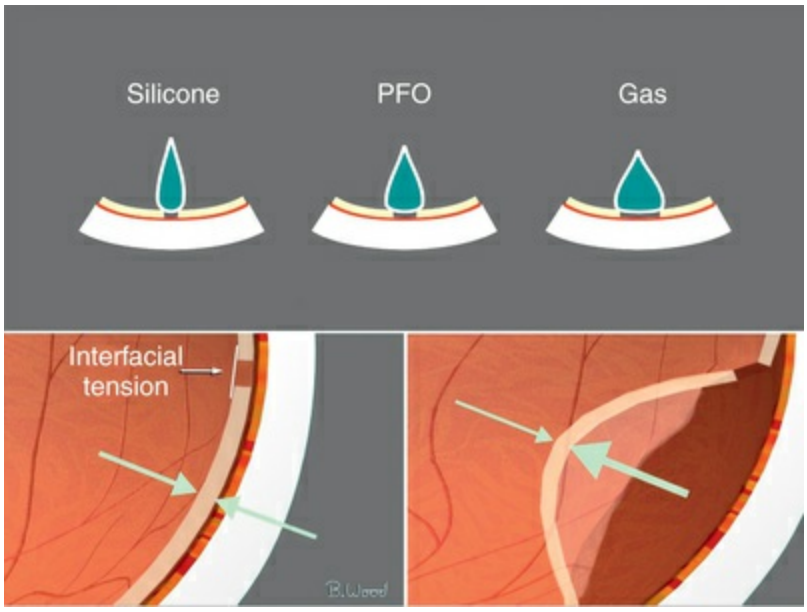

FIG. 105.33 The interfacial surface tension between air/gas and aqueous is greater than that of the silicone/aqueous or PFO (perfluoro-n-octane)/aqueous interface.

Force due to interfacial surface tension is far more significant than buoyancy effects provided by air, gas, or silicone. The purpose of these agents is to eliminate trans-hole fluid flow, thus restoring a transretinal pressure gradient. This effect is termed rhegmatogenous confinement when using long-term silicone oil; it addresses missed breaks, breaks from subsequent surface proliferation, and the opportunity for retinopexy avoidance in inflamed eyes. Silicone oil is also useful for retinopexy avoidance to reduce the reproliferation that is associated with excessive retinopexy to large area breaks or retinectomies. Retinopexy can be performed weeks or months later when retinal edema, subretinal fluid, and inflammation have subsided.

Silicones and gases may contribute to reproliferation by sequestering cytokines, proteins, and cells at the retinal surface (Fig. 105.34). The best silicone oils are those with the highest electrical resistance, lowest vapor pressure, and 1000 cSt (centi-Stokes) viscosity. There is little scientific evidence that 5000 cSt oil has lower emulsification rates than 1000 cSt and 5000 cSt oil takes five times as long to inject and remove as 1000 cSt.

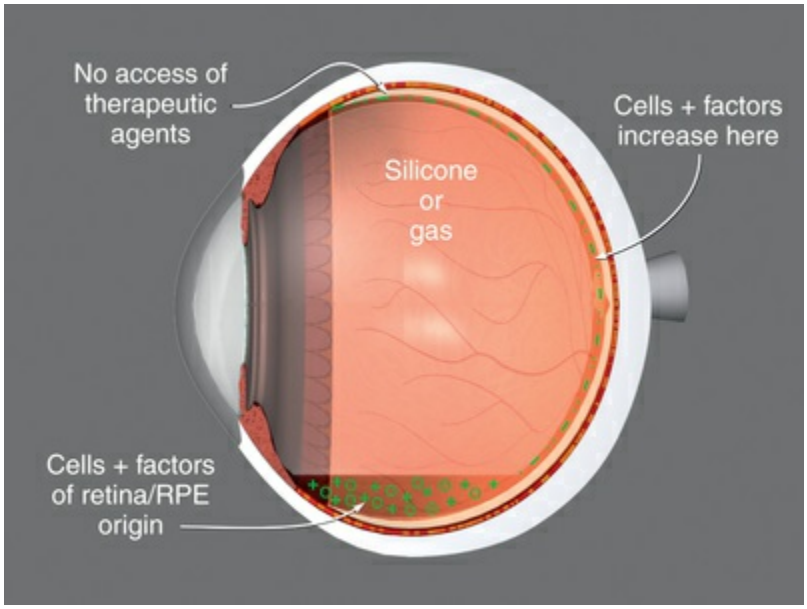

FIG. 105.34 Silicone and gases may increase reproliferation by sequestering cells and factors at the retinal surface, and decrease access of therapeutic agents to the retina.

An inferior peripheral iridectomy in aphakic eyes or eyes with decentered intraocular lenses and capsular defects allows aqueous to enter the anterior chamber from below and reduces the chance of silicone oil contact with the cornea. Fewer than 5% of long-term silicone cases develop corneal problems because of the iridectomy and higher-quality silicone oil available today. Emulsification glaucoma is relatively uncommon if proper precautions are taken. With the improvements in silicone oil, the incidence of emulsification glaucoma is now less than 20%, as previously reported.[10] Nevertheless, silicone oil should be removed after the retina has been attached in most cases, especially if the patient is young because of initially subclinical emulsification in the trabecular meshwork and macular edema that often occurs with silicone oil.

Eyes filled with silicone oil requiring additional surgery (for epimacular membrane, proliferative vitreoretinopathy, recurrent retinal detachment, etc.) can safely be operated on "under" oil.[11,12] Utilizing a two-port approach, silicone oil is intermittently infused after subretinal fluid is aspirated to maintain a stable intraocular pressure. This technique avoids the excessive manipulation, complexity, operating time, and cost that are associated with

complete silicone oil removal then replacement.

Fluid–Air Exchange

Air, for surface tension management, should be injected through the infusion cannula while simultaneously removing infusion fluid and SRF (Fig. 105.35), as described earlier (proportional suction, extrusion). Constant-pressure air pumps control intraocular pressure, are nonpulsatile, and can provide large flow rates to compensate for wound leaks. Incremental retinectomy and further vitreoretinal traction removal, forceps membrane peeling, segmentation, or delamination can be performed under air if persistent traction is identified.[13–15]

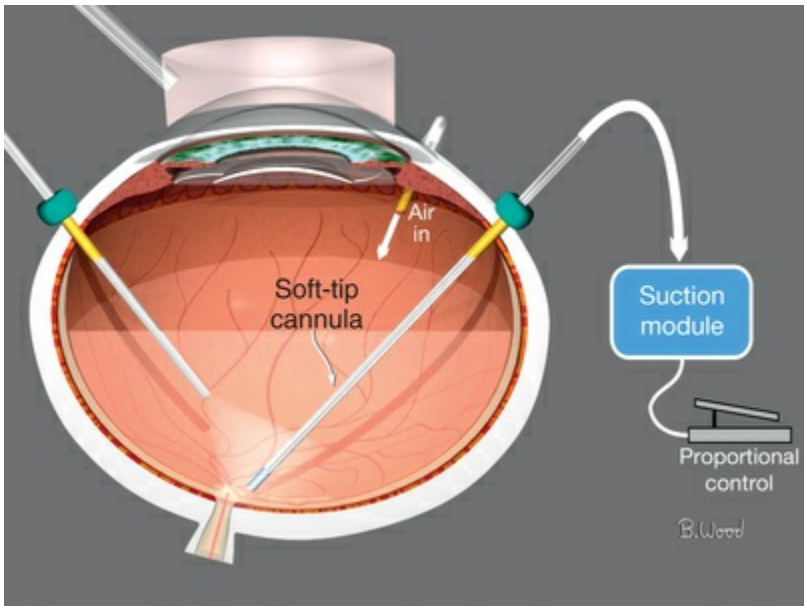

FIG. 105.35 An air pump infuses air through the infusion cannula and maintains intraocular pressure while intraocular and subretinal fluid is removed with a proportionally controlled soft-tip cannula.

Air–Gas Exchange

If a long-acting gas is chosen to maintain surface tension until retinopexy "seals" retinal defects, it should be injected in an isoexpansive concentration (25% SF_6 or 18% C_3F_8) through the

infusion cannula after fluid–air exchange and endolaser retinopexy has been completed (Fig. 105.36).[16–23] The air is aspirated with constant low suction near the optic nerve to ensure complete exchange and accurate gas concentration. Injecting aliquots of gas into an air-filled eye provides poor control of gas concentration and subsequent bubble size because of unknown ocular volume. This technique increases the likelihood of excessive intraocular pressure, potentially resulting in central artery occlusion or insufficient gas fills.

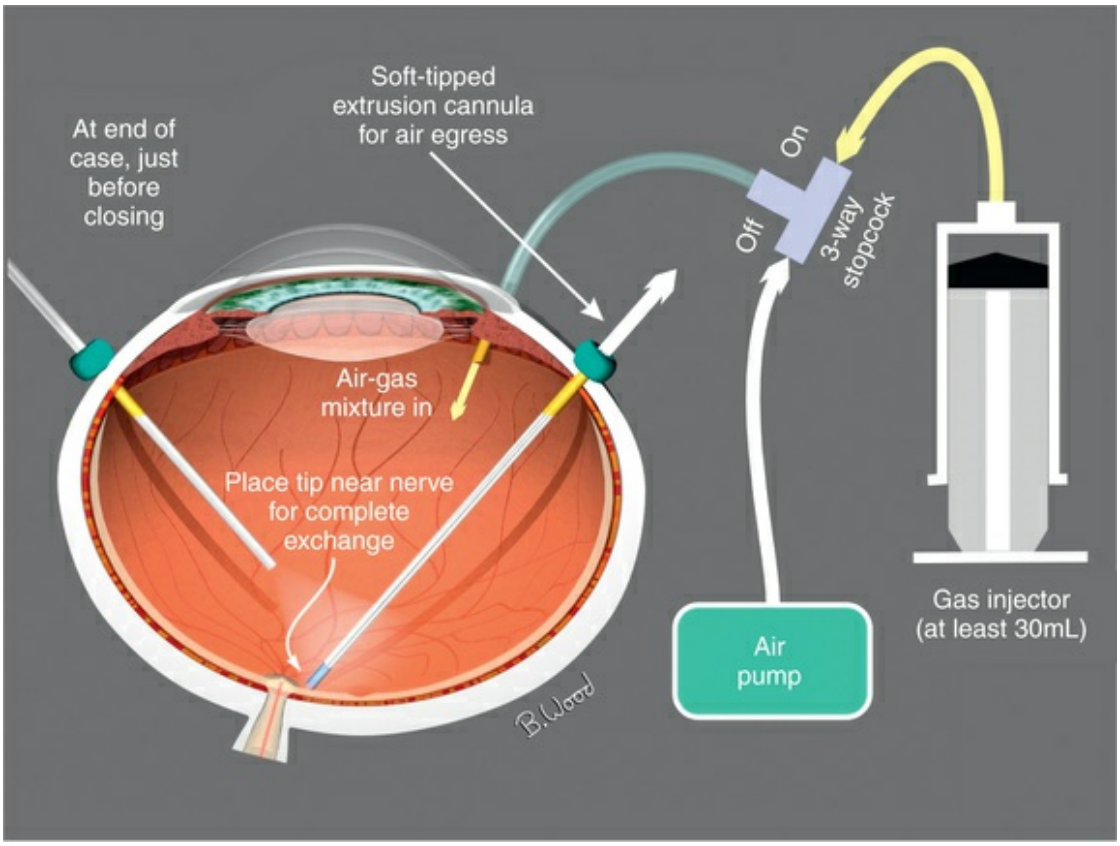

FIG. 105.36 Air–gas exchange using an isoexpansive gas concentration produces predictable postoperative bubbles without causing increased intraocular pressure.

Liquid Perfluorocarbon

Liquid perfluorocarbon such as perfluoro-n-octane (PFO) is essential for repositioning giant retinal breaks and can be used for

removal of subretinal fluid as well as stabilization of the retina to offset membrane peeling forces (Fig. 105.37).[24–27] Additionally, the use of medium-term PFO in cases of inferior retinal detachments can allow for upright positioning after surgery.[28–30] A foreign body response has been noted to occur in approximately 30% of eyes with PFO after 7–10 days.[31] This response is associated with longer duration of PFO, but was not associated with age, ethnicity, visual outcome, or persistent IOP elevation.

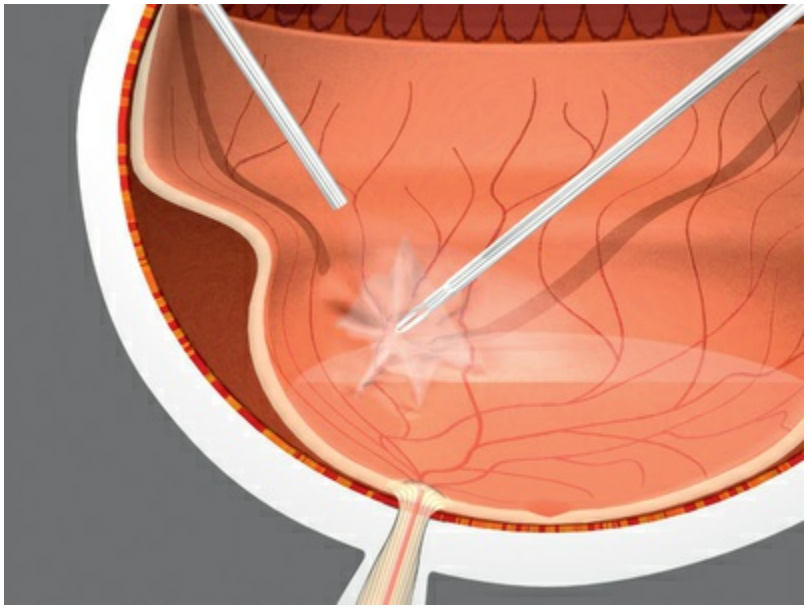

FIG. 105.37 PFO (perfluoro-n-octane) can be used to stabilize the retina and offset membrane peeling forces.

Fogging of the posterior surface of IOLs occurs because the room temperature infusion fluid cools the IOL and the infused air is saturated with water vapor (Fig. 105.38). A capsule defect as well as discontinuity in anterior vitreous cortex is necessary for fogging to occur. Fogging can occur with polymethylmethacrylate (PMMA) and acrylic IOLs, although it is more common with silicone IOLs because of higher posterior capsule opacification (PCO) rates and greater thermal mass. If fogging occurs, the best practice is to return to balanced salt solution infusion, remove the air, reattach the retina with PFO, and treat all retinal breaks with endolaser before performing PFO–gas exchange with isoexpansive SF_6 or C_3F_8. PFO can be used in all retinal detachment cases, but fluid–air exchange

and internal drainage of subretinal fluid is effective and does not add cost. PFO should be used with caution in PVR cases because of the not uncommon occurrence of subfoveal PFO due to retinal breaks combined with rigid retina.[32]

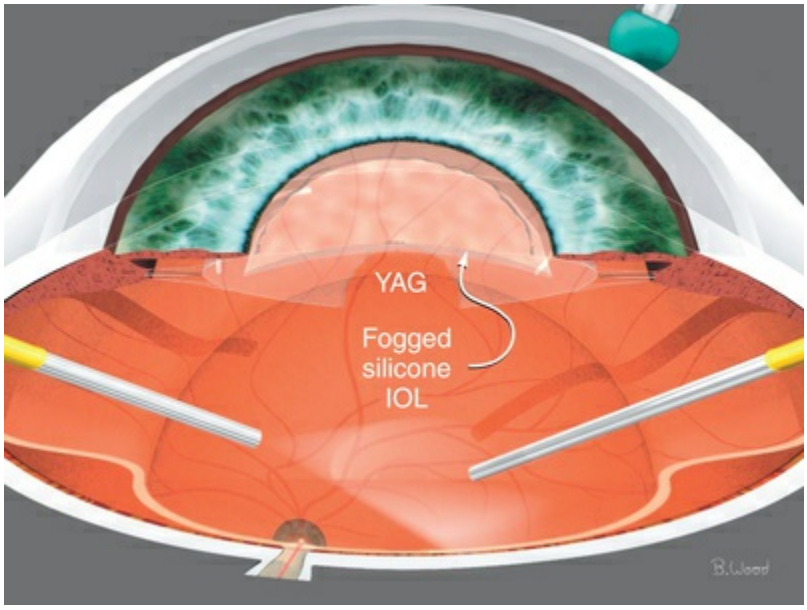

FIG. 105.38 Fogging can occur when humid air contacts an intraocular lens (*IOL*) that has been cooled by infusion fluid. Fogging only occurs if there is not an intact posterior capsule and anterior vitreous cortex.

PFO should be injected under direct visualization by first injecting a small bubble at the optic nerve head with a 25G dual-bore cannula. This bubble is enlarged by injecting, using a power injector with 10 psi proportional injection pressure withdrawing the dual-bore cannula during the injection maintaining contact between the tip and the top of the PFO bubble. The proximal fluid egress port always stays above the PFO to avoid loss of PFO but allows fluid egress and a normotensive process (Fig. 105.39). PFO–air exchange in non-giant break cases is the inverse; the soft-tip cannula is always positioned at the periphery of the fluid–PFO interface and advanced posteriorly so all the fluid is removed and replaced with air before PFO is removed.

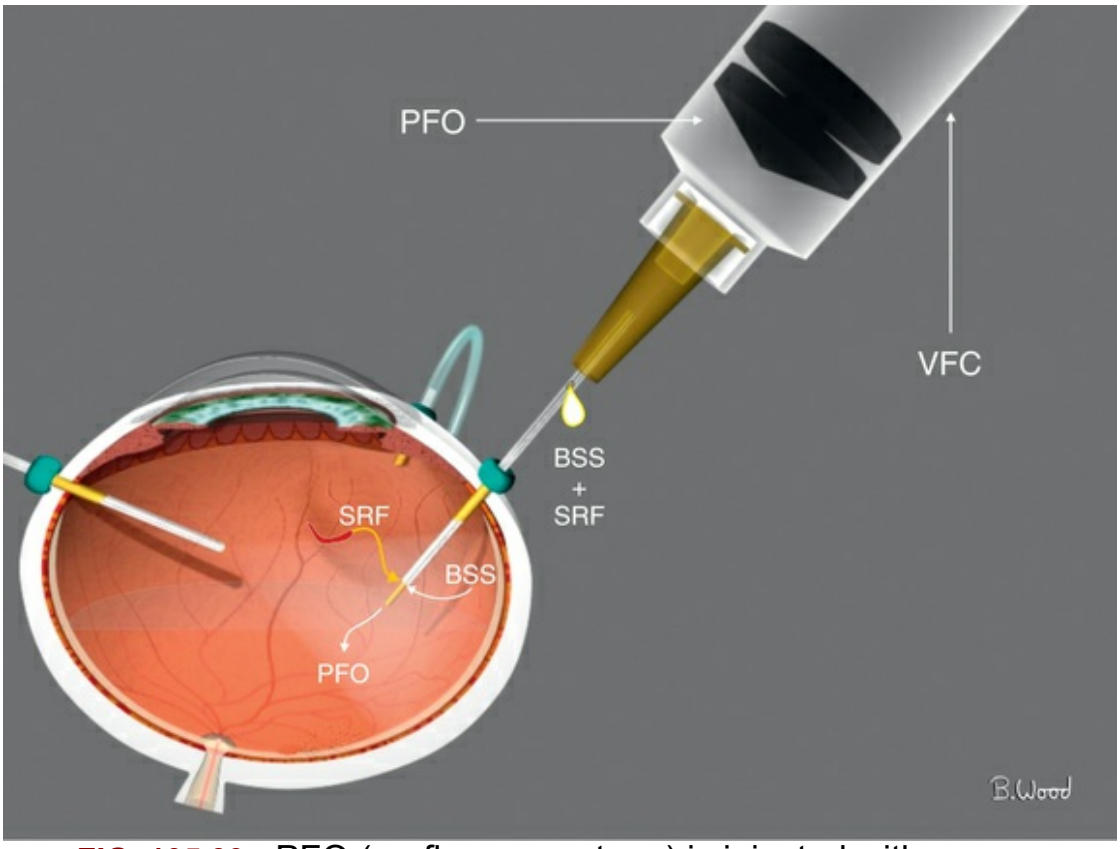

FIG. 105.39 PFO (perfluoro-n-octane) is injected with a power injector at 10 psi, and a dual-bore cannula allows simultaneous fluid egress. *VFC*, viscous fluid control (Alcon Laboratories, Inc.); *BSS*, balanced salt solution; *SRF*, subretinal fluid.

Air–Silicone Exchange

Because air has a higher interfacial tension than silicone oil, fluid–air exchange with internal drainage of SRF to reattach the retina should precede silicone infusion. Silicone should be injected with a pressure-controlled power injector through a short 23/25G straight cannula through the superotemporal cannula; not through the infusion cannula (Fig. 105.40). The air will egress through the open superonasal cannula until the silicone oil reaches the pupillary plane. Devices are required to hold valved cannulas open. Viscoelastics should be used to reform the anterior chamber if it becomes flat or if oil enters the anterior chamber.

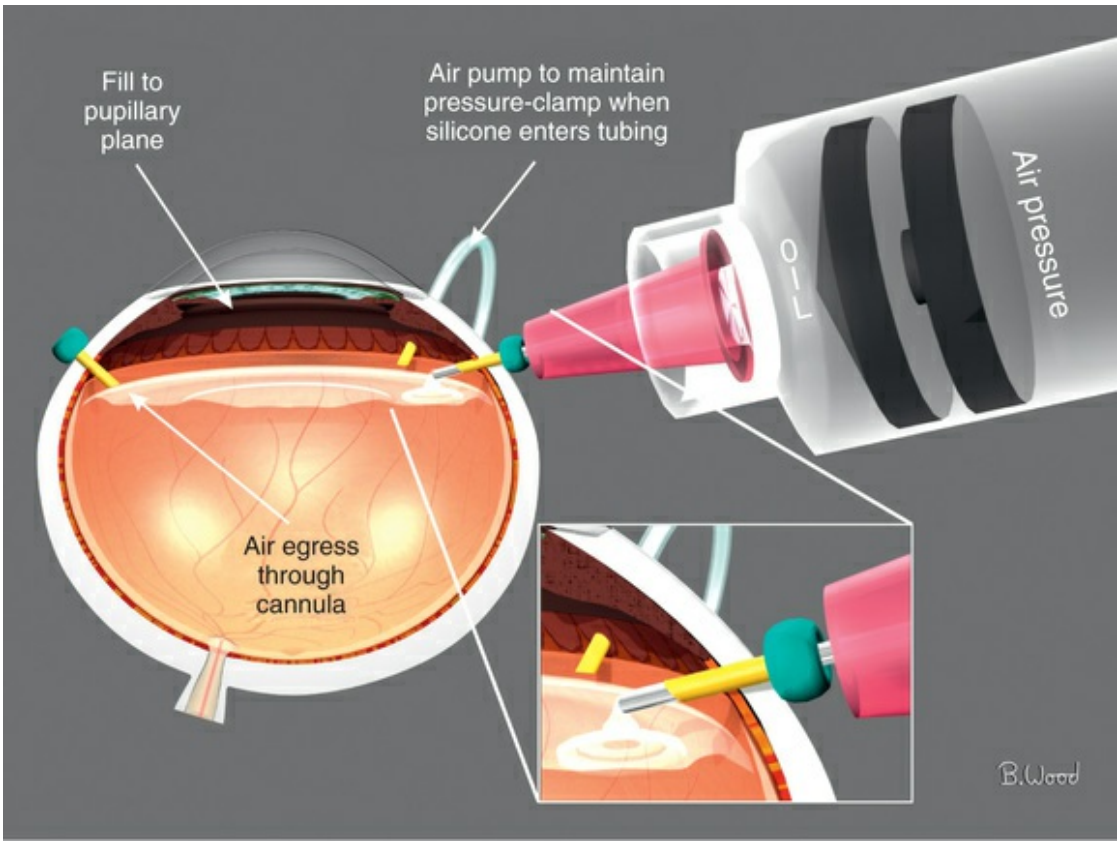

FIG. 105.40 Inject silicone through a short, thin wall, 23/25G cannula; air flows out through the superonasal cannula to enable normotensive air–silicone exchange.

Perfluorocarbon–Silicone Oil Exchange

Direct perfluorocarbon–silicone exchange can be used instead of an intermediate step of fluid–air exchange followed by air–perfluorocarbon exchange in giant retinal break cases. The rationale for this approach is reduced chance of posterior slippage of the giant break. The goal is a full PFO fill and elimination of all subretinal fluid, infusion fluid, and liquid vitreous. The soft-tip cannula is used to remove PFO as the power injector is used to inject oil through a special infusion cannula (Fig. 105.41). If a standard cannula is used for oil injection, each of the surgeon's hands are in use therefore requiring a chandelier for illumination.

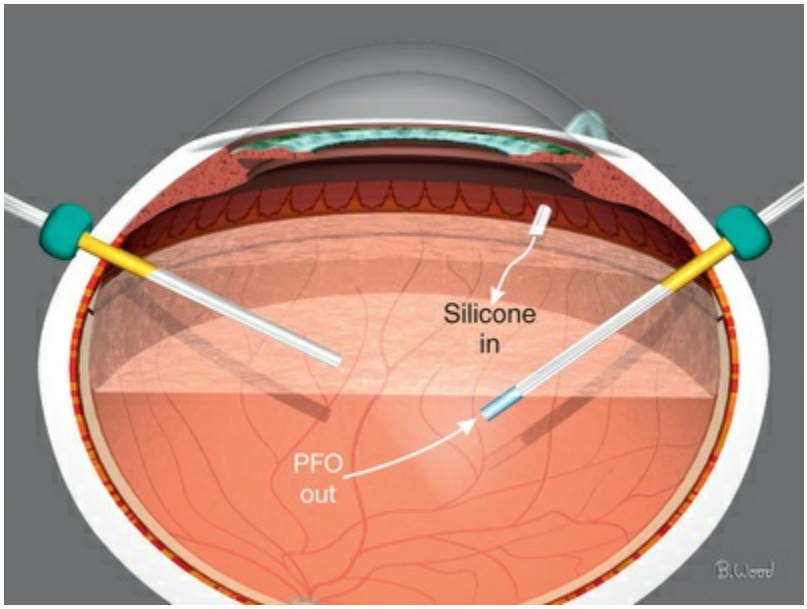

FIG. 105.41 Simultaneous PFO(perfluoro-n-octane)–silicone exchange reduces the incidence of posterior slippage of giant breaks.

Retinectomy

Retinectomy is preferred over relaxing retinotomy because removal of all tissue anterior to the cut reduces hypotony and recurrent PVR. Retinectomy should be performed in conjunction with fluid–air exchange and internal drainage of SRF (Fig. 105.42) (see also Chapter 112, Retinotomies and retinectomies). If subretinal air appears as internal drainage of SRF is slowly proceeding, the subretinal air location indicates residual retinal traction. Further vitrectomy, forceps membrane peeling, scissors segmentation/delamination, subretinal surgery, or retinectomy is required to achieve reattachment. Retinectomy should proceed incrementally with the vitreous cutter until the retina is reattached. Retinectomy performed under fluid is more difficult and may result in excessive or insufficient retinectomy. Large vessels should be precoagulated with bipolar diathermy.

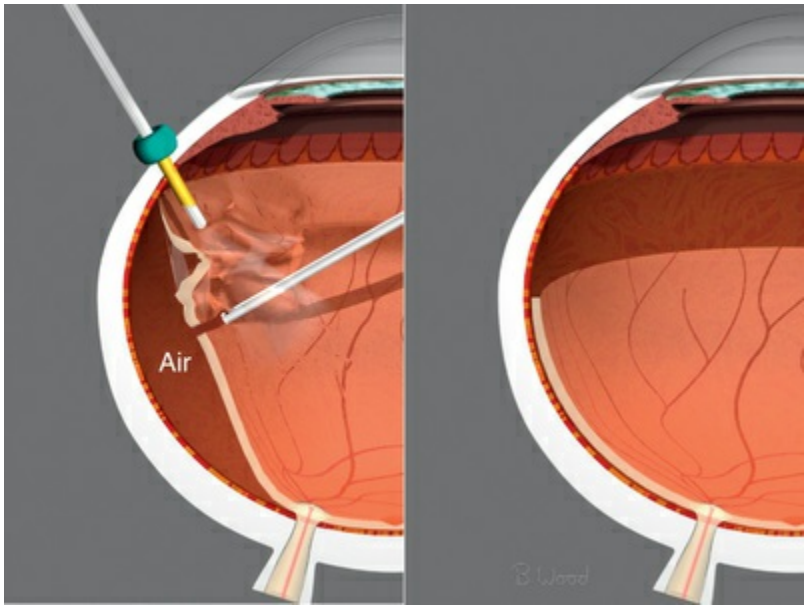

FIG. 105.42 Incremental retinectomy to manage retinal foreshortening or residual traction should be performed under air after fluid–air exchange and initial drainage of subretinal fluid.

Hemostasis

Transient (approximately 5 minutes) elevation of intraocular pressure, preferably with a footpedal-controlled system, is the initial means of controlling intraoperative bleeding. Rapid elevation of intraocular pressure when bleeding is first noted will prevent the formation of extensive, tenacious preretinal blood clots. Holding the intraocular pressure between capillary and diastolic arterial pressure can be used while dissecting vascular ERM attachment points. The intraocular pressure should be normalized in a few minutes after clotting occurs. Any vessels that are still bleeding should be treated with endophotocoagulation, which is preferable to bipolar endodiathermy. Diathermy causes a larger area of retinal necrosis than laser, which can result in late, so-called, atrophic holes. Extensive pretreatment of vascular areas with diathermy or laser results in retinal necrosis and unnecessary coagulation of the tissue to be removed. Systemic blood pressure elevation should be very closely monitored in cases with a high potential for bleeding.

Retinopexy

All forms of retinopexy create tissue destruction and reproliferation and therefore should be used as little as possible. Continuous (painting) laser endophotocoagulation surrounding retinal breaks and retinectomies is preferable to rows of spots because it results in more uniform tissue destruction and greater tensile strength (Fig. 105.43). Panretinal photocoagulation should be used only for neovascular retinopathies, never for PVR. Cryopexy causes more proliferation than laser or diathermy, and in my opinion, it should be avoided in vitrectomy surgery.

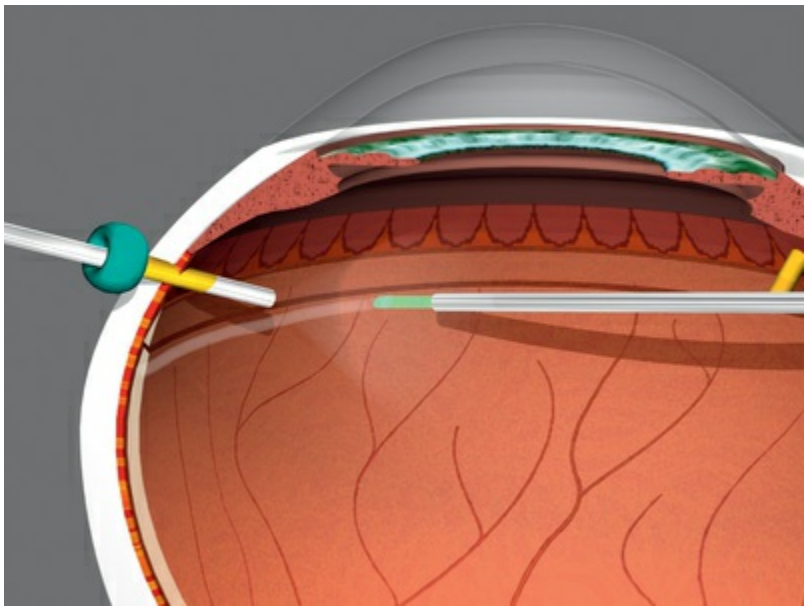

FIG. 105.43 Confluent laser endophotocoagulation (painting) results in less tissue destruction, more uniform retinopexy, and stronger tensile strength of retinal–retinal pigment epithelium adherence than multiple rows of individual spots.

Panretinal Photocoagulation

Panretinal photocoagulation reduces VEGF (vascular endothelial growth factor) production, causes the RPE to release an antiangiogenesis cytokine, RPE-derived growth factor, and increases choroidal oxygen transport to the retina. Diode-pumped,

frequency-doubled YAG (532 nm) lasers are preferable to near-IR diode lasers because they cause less damage to the choroid and are effective for hemostasis.

Subconjunctival Pharmacotherapeutics

Subconjunctival antimicrobials for gram-negative and gram-positive bacteria and penicillinase-producing *Staphylococcus* can be considered after vitrectomy. Topical antibiotics do not reach a level above the minimal inhibitory concentration (MIC) in the vitreous cavity of phakic or pseudophakic eyes. A subconjunctival steroid injection such as dexamethasone should be considered unless the patient is known to have corticosteroid-induced glaucoma or has an immune deficiency.

Surgical Algorithms

Earlier sections of this chapter provided an intellectual framework of physical, biologic, and surgical principles. Each of the surgical scenarios has been illustrated graphically and described. The combination of these scenarios into a surgical algorithm depends on the disease state, and indications and specific management of disease states are discussed in other chapters.

Conclusion

Conservative indications, aggressive use of the best techniques and technologies, and careful follow-up are required for optimal results in vitreoretinal surgery. Continued improvements in instrumentation and biotherapeutics are needed for vitreoretinal surgeons to achieve better results in managing the diseases that potentially have high recurrence rates and occasionally poor outcomes.

References

1. Rizzo S, Genovesi-Ebert F, Vento A, et al. Modified incision in 25-gauge vitrectomy in the creation of a tunneled airtight sclerotomy: an ultrabiomicroscopic study. *Graefes Arch Clin Exp Ophthalmol*. 2007;245:1281–1288.
2. Inoue M, Shinoda K, Shinoda H, et al. Two-step oblique incision during 25-gauge vitrectomy reduces incidence of postoperative hypotony. *Clin Experiment Ophthalmol*. 2007;35:693–696.
3. López-Guajardo L, Vleming-Pinilla E, Pareja-Esteban J, et al. Ultrasound biomicroscopy study of direct and oblique 25-gauge vitrectomy sclerotomies. *Am J Ophthalmol*. 2007;143:881–883.
4. Sigler EJ, Charles S, Calzada JI. Interface vitrectomy. *Retina*. 2014;34:616–617.
5. Charles S. Fluidics and cutter dynamics. *Dev Ophthalmol*. 2014;54:31–37.
6. Asheesh T, Shah GK, Fang A. Visual outcomes with 23-gauge transconjunctival sutureless vitrectomy. *Retina*. 2008;28:258–262.
7. Fujii GY, De Juan E Jr, Humayun MS, et al. A new 25-gauge instrument system for transconjunctival sutureless vitrectomy surgery. *Ophthalmology*. 2002;109:1807–1813 [Erratum in: Ophthalmology 2003;110:9.].
8. Lakhanpal RR, Humayun MS, de Juan E Jr, et al. Outcomes of 140 consecutive cases of 25-gauge transconjunctival surgery for posterior segment disease. *Ophthalmology*. 2005;112:817–824.
9. Charles S, Randolph JC, Neekhra A, et al. Arcuate retinotomy for the repair of large macular holes. *Ophthalmic Surg Lasers Imaging Retina*. 2013;44(1):69–72.
10. Barr CC, Lai MY, Lean JS, et al. Postoperative intraocular pressure abnormalities in the Silicone Study. Silicone Study Report 4. *Ophthalmology*. 1993;100:1629–1635.
11. Charles S, Randolph JC, Sigler EJ. Pars plana vitrectomy reoperation without removing silicone oil. *Retina*. 2012;32:1664–1665.
12. Sigler EJ, Randolph JC, Calzada JI, et al. Anatomical and visual outcomes after two-port pars plana vitrectomy

reoperation under silicone oil for epimacular membrane or recurrent retinal detachment. *Retina*. 2014;34:1939–1944.
13. Charles S. Fluid–gas exchange in the vitreous cavity. *Ocutome Newslett*. 1977;2:1.
14. Charles S. Controlled drainage of subretinal and choroidal fluid. *Retina*. 1985;5:233.
15. McCuen BW, Bessler M, Hickingbotham D, et al. Automated fluid–gas exchange. *Am J Ophthalmol*. 1983;95:717.
16. Abrams GW, Edelhauser HF, Aaberg TM, et al. Dynamics of intravitreal sulfur hexafluoride gas. *Invest Ophthalmol*. 1974;13:863–868.
17. Fineberg E, Machemer R, Sullivan P. SF_6 for retinal detachment surgery, a preliminary report. *Mod Probl Ophthalmol*. 1974;12:173.
18. Fineberg E, Machemer R, Sullivan P, et al. Sulfur hexafluoride in owl monkey vitreous cavity. *Am J Ophthalmol*. 1975;79:67.
19. Chang S, Lincoff H, Coleman J, et al. Perfluorocarbon gases in vitreous surgery. *Ophthalmology*. 1985;92:651.
20. Lincoff A, Haft D, Liggett P, et al. Intravitreal expansion of perfluorocarbon bubbles. *Arch Ophthalmol*. 1980;98:1646.
21. Lincoff H, Coleman J, Kreissig J, et al. The perfluorocarbon gases in the treatment of retinal detachment. *Ophthalmology*. 1983;90:546.
22. Lincoff H, Mardirossian J, Lincoff A, et al. Intravitreal longevity of three perfluorocarbon gases. *Arch Ophthalmol*. 1980;98:1610.
23. Aaberg TM, Abrams GW, Edelhauser HF. *Intraocular sulfur hexafluoride: experimental and clinical correlation. International Symposium on New and Controversial Aspects of Vitreoretinal Surgery, Texas Medical Center, Houston, Texas*. Mosby: St. Louis; 1977:393–397.
24. Chang S, Ozmert E, Zimmerman NJ. Intraoperative perfluorocarbon liquids in the management of proliferative vitreoretinopathy. *Am J Ophthalmol*. 1988;106:668–674.
25. Chang S, Reppucci V, Zimmerman NJ, et al. Perfluorocarbon liquids in the management of traumatic retinal detachments. *Ophthalmology*. 1989;96:785–791.

26. Chang S, Lincoff H, Zimmerman NJ, et al. Giant retinal tears. surgical techniques and results using perfluorocarbon liquids. *Arch Ophthalmol*. 1989;107:761–766.
27. Randolph JC, Diaz RI, Sigler EJ, et al. 25-gauge pars plana vitrectomy with medium-term postoperative perfluoro-n-octane for the repair of giant retinal tears. *Graefes Arch Clin Exp Ophthalmol*. 2016;254(2):253–257.
28. Sigler EJ, Randolph JC, Calzada JI, et al. 25-gauge pars plana vitrectomy with medium-term postoperative perfluoro-n-octane tamponade for inferior retinal detachment. *Ophthalmic Surg Lasers Imaging Retina*. 2012;1–8.
29. Sigler EJ, Randolph JC, Calzada JI, et al. 25-gauge pars plana vitrectomy with medium-term postoperative perfluoro-n-octane tamponade for inferior retinal detachment. *Ophthalmic Surg Lasers Imaging Retina*. 2013;44:34–40.
30. Sigler EJ, Randolph JC, Calzada JI, et al. Pars plana vitrectomy with medium-term postoperative perfluoro-N-octane for recurrent inferior retinal detachment complicated by advanced proliferative vitreoretinopathy. *Retina*. 2013;33:791–797.
31. Sigler EJ, Randolph JC, Charles S. Foreign body response within postoperative perfluoro-N-octane for retinal detachment repair: clinical features, grading system, and histopathology. *Retina*. 2014;34:237–246.
32. Sigler EJ, Randolph JC, Rafieetary MR, et al. Spectral domain optical coherence tomography characteristics of retained subretinal perfluoro-n-octane. *Retin Cases Brief Rep*. 2013;7:164–168.

106

Primary Vitrectomy in Rhegmatogenous Retinal Detachment

Young Hee Yoon, Shwu-Jiuan Sheu, Hiroko Terasaki

Introduction

Currently, rhegmatogenous retinal detachment (RRD) continues to be an important cause of visual loss. The fundamental principles involved in reattachment of a retina include identification of all retinal breaks and relief of the vitreous traction. Traditionally, scleral buckling (SB) was viewed as the gold standard treatment for uncomplicated RRD. Pars plana vitrectomy (PPV) was traditionally reserved for treatment of eyes with complications, such as those showing giant retinal tears or exhibiting significant proliferative vitreoretinopathy (PVR). In the 1980s, the indications for PPV in RRD patients were broadened to include less complicated instances and the term "primary vitrectomy" was introduced by Klöti[1] (Videos 106.1 and 106.2 online).

As the necessary instrumentation for, and safety of, PPV continue to improve with developments in microscope technology, intensified endoillumination, and wide-angle viewing systems, the indications for vitrectomy in RRD have been further expanded to include most patients with RRD. Indeed, PPV is more useful than SB in eyes requiring simultaneous cataract extraction or those of pseudophakic status.[2–6]

Compared to SB, PPV offers several advantages. The view of the retinal periphery is enhanced, identification of retinal breaks is rendered easier, achievement of complete intraoperative retinal

attachment is possible, the risks of hemorrhage or retinal incarceration inherent to the external drainage procedure applied during SB is eliminated, and the technique is less likely to cause a refractive change. In addition, the introduction of small-gauge vitrectomy has shifted the paradigm of standard vitreous surgery to microincision vitrectomy surgery (MIVS) that is less invasive, affords fast recovery, and is sutureless. As a result of these advances, vitreoretinal surgeons now have more procedural choices when treating RRD patients. Further, recently trained vitreoretinal surgeons may be more familiar with application of PPV (compared to SB) in challenging situations.

In this chapter, the use of primary vitrectomy for treatment of RRD, and the advantages and disadvantages of employing different gauges of vitrectomy system, will be explained and evaluated.

Pathogenesis of Rhegmatogenous Retinal Detachment

The vitreous is firmly attached to the vitreous base, an area 3–6 mm in diameter that straddles the ora serrata surrounding the retina. The posterior border of the vitreous base is located farther posteriorly in older individuals and temporally. Therefore, retinal tears may occur at a higher frequency at the temporal periphery in such patients, following posterior vitreous detachment (PVD).

Three factors predispose to development of RRD: (1) the existence of a liquefied vitreous gel; (2) tractional forces that precipitate a retinal break; and (3) the presence of a retinal break through which fluid may access the subretinal space.

Liquefaction of the vitreous occurs naturally upon aging, developing more rapidly in eyes with significant myopia, surgical or nonsurgical trauma, and/or intraocular inflammation. Apart from liquefaction, alterations in the extracellular matrix of the vitreous facilitate detachment of the posterior vitreous from the underlying retina. PVD usually presents as an acute event, and is more prevalent in patients older than 50 years, with frequencies as high as 53%.[7] PVD often precipitates RRD, and the reported incidence of retinal tears in patients with acute symptomatic PVD

varies from 8% to 46%.[8] Risk factors for progression included fresh, symptomatic, horseshoe-shaped tears; breaks suggestive of the presence of subclinical retinal detachment (RD); and pseudophakia/aphakia.

Categories of Rhegmatogenous Retinal Detachment

Retinal breaks are traditionally classified as round holes, tears, or resulting from retinal dialysis. Accordingly, RRD can be categorized as (1) round hole retinal detachment; (2) retinal detachment occurring secondary to retinal tears; and (3) retinal detachment attributable to retinal dialysis. This categorization, and the status of the vitreous, are important when exploring management options, in particular whether SB or vitrectomy should be employed.

Retinal holes are full-thickness retinal defects that usually occur as a result of localized atrophic intraretinal abnormalities or lattice degeneration, and are not associated with vitreoretinal traction. Typical RD patients with round holes show one or more areas of limited retinal detachment and may thus be optimally treated with either laser demarcation or segmental SB, rather than vitrectomy.

Retinal tears are usually produced by PVD and subsequent vitreoretinal traction. As persistent vitreous traction at an edge usually causes detachment to progress, the vast majority of RD patients in this category require surgical treatment. Among the various methods available, release of traction via PPV is preferred by many vitreoretinal surgeons.

Retinal dialysis is most often associated with blunt ocular trauma and rarely occurs spontaneously. Dialyses are most common in the inferotemporal quadrant. The vitreous remains firmly attached to the entire peripheral retina, and vitreoretinal traction caused by gravity results in slow retinal detachment. Vitrectomy in an eye with an attached vitreous gel can be technically difficult and may introduce unnecessary surgical complexity. Therefore, vitrectomy is less desirable than are other treatment options, e.g., a circumferential buckle.

The number of aphakic/pseudophakic patients with RRD has increased significantly over the past decades. After cataract surgery, vitreous liquefaction accelerates, causing premature PVD and subsequent RD. Aphakic/pseudophakic eyes tend to have small (and sometimes multiple) anterior breaks. The status of the posterior capsule also influences the speed of vitreous liquefaction. One study found that Nd : YAG laser posterior capsulotomy increased the risk of RD after cataract extraction up to 4.9-fold.[9] Because of the characteristics of the breaks and the status of the vitreous in aphakic/pseudophakic eyes, vitrectomy is preferred by many surgeons and has a good success rate.[10]

Patient Selection for Primary Vitrectomy

SB and/or pneumatic retinopexy serve as the first treatment option(s) in patients with localized detachment in one quadrant together with single neighboring breaks. Young age and anteriorly located small holes in phakic patients encourage the use of SB. The success rates of final reattachment are 90–95%.[11]

PPV is indicated for patients with wide and bullous RD, and for older patients with a liquefied vitreous. The presence of RD with marked traction with different anterior posterior depth of breaks, the presence of breaks in multiple quadrants, or the absence of an apparent retinal break in a pseudophakic patient are all good candidates for the use of PPV. RD of preoperative PVR grade C, giant tear-induced RD, and macular hole RD are all commonly treated using PPV.

Recent developments in vitrectomy instruments, including small-gauge systems, wide-angle viewing systems, and endoilluminators, as well as adjuvants including triamcinolone acetonide suspension, perfluorocarbon liquids, and intraocular tamponades, led the choice of surgical technique for the treatment of RRD with medium complexity to shift more and more towards PPV.[12,13] Several trials comparing PPV to SB in patients undergoing RRD surgery have been reported.[14–18] In general, PPV was favored for treatment of pseudophakic eyes with unseen breaks, eyes featuring ocular

hypotony, or eyes showing prolonged macular detachment. The results to date suggest that SB or PPV is a good treatment option for primary phakic RRD, whereas PPV may be preferable to SB when pseudophakic RRD is to be treated.[14] It is important to consider individual patient factors, surgeon preference, and availability of equipment to make an optimal treatment decision.

Principles of Vitrectomy

Abnormal vitreoretinal traction (either perpendicular or tangential) increases vitreous mobility caused by PVD, and atypical posterior extension of the anterior vitreous base predisposes to formation of retinal tears. Therefore, removal of the vitreous gel and any abnormal preretinal structure releases the tractional force causing retinal breaks and detachment.

After release of abnormal vitreoretinal traction, the detached retina must be reattached. To stabilize and flatten the detached retina, a heavy liquid is initially applied; this is subsequently replaced by sterile air. If the retina is mobile and becomes flattened in air, a nonexpansive gas–air mixture is used to achieve a postoperative gas tamponade. Although silicone oil is not routinely used in instances of uncomplicated RRD, use of silicone oil should be considered if eyes have multiple inferior breaks, if PVR is present, or if the eye is an only seeing eye. Retinopexy has been used to create permanent retinal–RPE adherence. Both forms of retinopexy (cryopexy and the laser photocoagulation) cause tissue destruction and cellular proliferation and should be used as little as possible.

Surgical Techniques

Primary vitrectomy is commonly performed using a wide-angle viewing system attached to an operating microscope. The surgical steps of primary vitrectomy using sutureless MIVS are described below (Figs. 106.1–106.4).

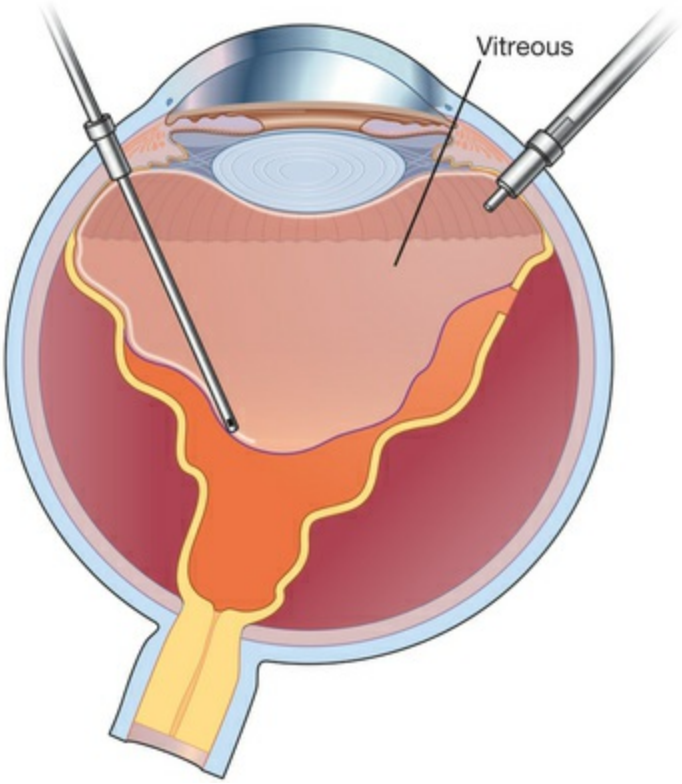

FIG. 106.1 Detached retina with posterior vitreous detachment is shown. Core vitrectomy is performed.

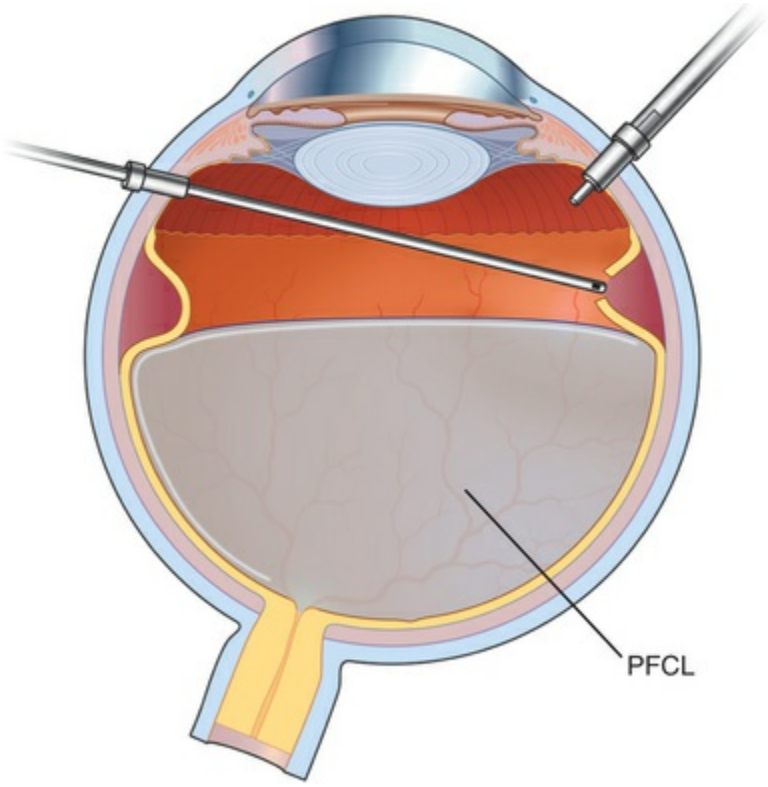

FIG. 106.2 A bubble of perfluorocarbon liquid (PFCL) has been injected to displace posterior subretinal fluid. While holding down the detached posterior retina, peripheral vitreous base is safely shaved and the flap of the retinal break is cut to release the vitreoretinal traction.

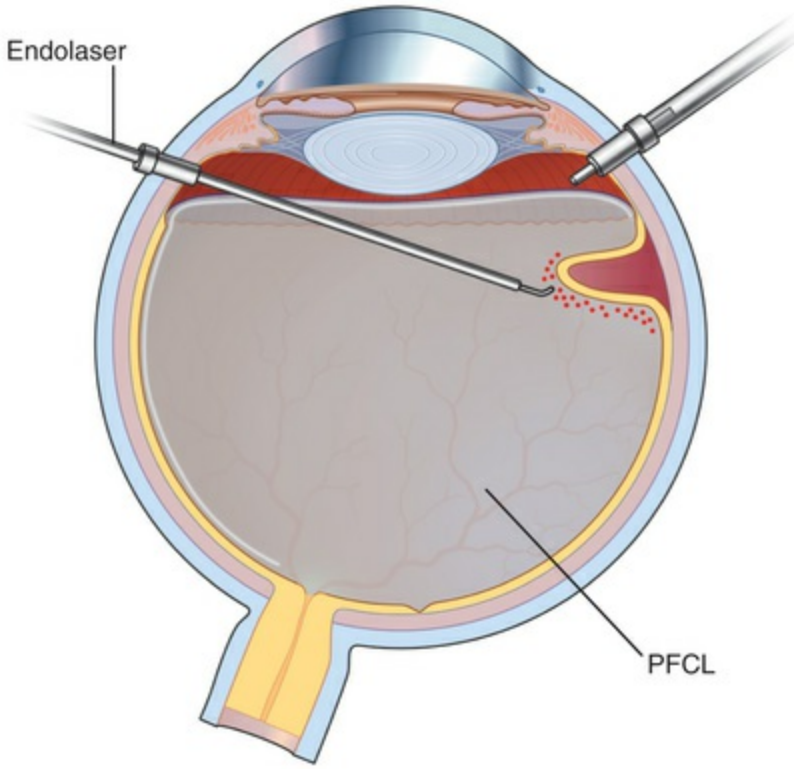

FIG. 106.3 Endolaser retinopexy is applied around the retinal break under the perfluorocarbon liquid (PFCL) bubble.

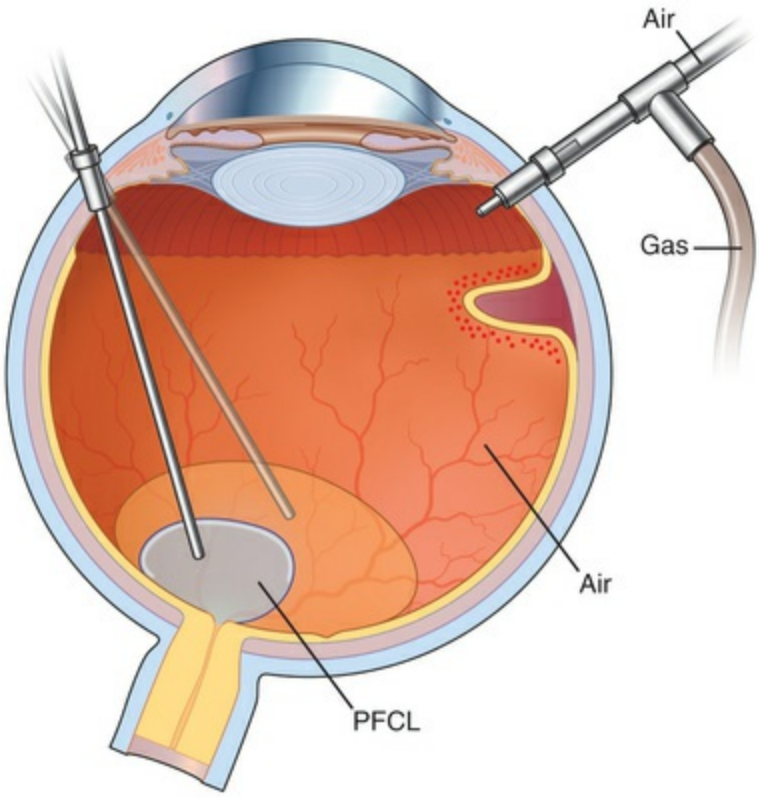

FIG. 106.4 Air–perfluorocarbon liquid (PFCL) exchange is performed, and air is replaced with SF_6, C_2F_6 gas.

Anesthesia

The choice between general anesthesia and local anesthesia for primary vitrectomy depends on several factors, including patient age, surgeon preference, and the anticipated difficulty and duration of operation. Although general anesthesia is still preferred for complex surgery or young patients, local anesthesia for vitrectomy surgery has steadily increased because of several advantages: presumed reduced cardiopulmonary risk to patients, shorter turnover time, and cost-effectiveness.[19]

Create Three Ports Through the Pars Plana

Firmly insert the infusion cannula. Irrigation pressure is set around 20–35 mmHg, depending on the choice of operating system gauge. Confirm that the infusion cannula is in the vitreous cavity by examining its position using an exterior light pipe.

Core Vitrectomy

First, the central vitreous is removed (Fig. 106.1). When PVD is absent, or even when PVD has occurred, triamcinolone acetonide can be injected to afford better visualization of the vitreous gel, to facilitate PVD, and to completely remove the residual vitreous. The posterior vitreous membrane can be removed using a diamond-dusted scraper; this prevents secondary macular pucker (Fig. 106.5).

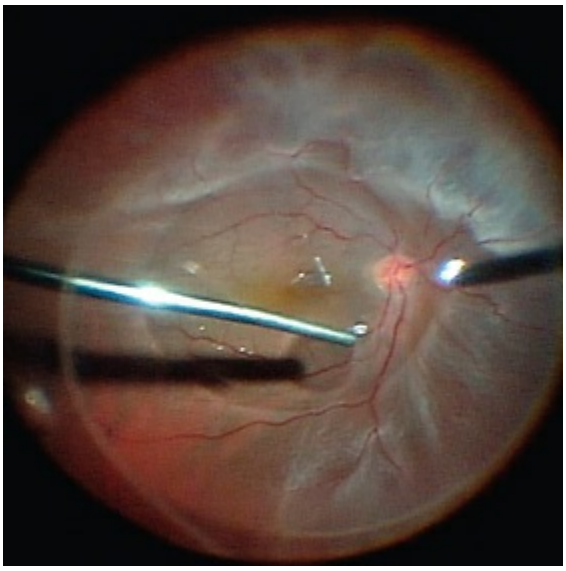

FIG. 106.5 Core vitrectomy has been performed, and a small bubble of PFCL was injected to hold down the posterior retina.

Peripheral Vitrectomy

After core vitrectomy, PVD is further extended using a wide-angle viewing system. Usually PVD is already present, up to the positions of the retinal breaks. However, abnormal attachment may be noted in other locations. If retinal breaks are located posterior to the equatorial zone, the vitreous bridge between the tears and the ora serrata must be separated and removed. If the breaks are peripheral to the equatorial zone, the vitreous on the flap should be shaved away, with scleral indentation. In case of bullous RD, perfluorocarbon liquid (PFCL) may be injected to flatten the detached retina so that the peripheral vitreous can be safely shaved

without creating an iatrogenic tear (Fig. 106.2).

Fluid–Air Exchange

Subretinal fluid is removed through the original breaks using a backflush needle in the presence of air irrigation. PFCL may be injected, up to the level of the posterior edge of the break; the PFCL bubble displaces posterior subretinal fluid through the break. Next, air–fluid exchange at the top of the PFCL bubble may displace peripheral subretinal fluid through the break. PFCL is not indicated for all eyes. The preferable indications are bullous RD or RD that is associated with retinal breaks anterior to the equatorial zone; the subretinal fluid can thus be removed without creating a drainage retinotomy (Fig. 106.4).

Photocoagulation/Cryopexy of the Retinal Tear

Whenever retinal breaks are found, endodiathermy may be used to mark the breaks. Once retinal reattachment is complete, endophotocoagulation is performed under air or a PFCL bubble. Two-to-three rows of laser burns can be applied around each break and site of lattice degeneration (Fig. 106.3). Strong photocoagulation should be avoided on the thin retina detached by the residual subretinal fluid. Alternatively, cryopexy may be utilized if a break is located at the far periphery of phakic RD eyes.

Tamponade

If the retina is flattened under air, nonexpandable gas–air exchange is performed in order to achieve postoperative gas tamponade. The maximum concentrations to be used are 20% for SF_6, 14% for C_3F_8, and 17% for C_2F_6; these levels ensure that eye pressure is not increased. RD in the inferior quadrant alone, or associated multiple breaks in various quadrants, is an indication for use of a long-acting gas such as C_3F_8. In a few exceptional instances, such as the occurrence of RD in the only seeing eye, the use of silicone oil should be considered.

Positioning After Surgery

Face-down positioning should be commenced as early as possible after surgery to ensure that the macula is attached first and to prevent any shift of the reattached retina. Adjustable head positioning depending on the location of retinal breaks can be an effective and safe option after gas tamponade.[20]

In some cases, primary vitrectomy may be combined with additional surgical procedures such as encircling buckling or phacoemulsification.

Vitrectomy With Encircling Buckling

The placement of an encircling band depends on the preference of the individual surgeon. A circumferential band can be placed in the preequatorial region to support the residual vitreous base, preventing recurrent detachment if peripheral breaks develop postoperatively. However, such bands are being placed less frequently because recent technologic advances, including high-speed cutters, intraoperative use of triamcinolone, wide-angle viewing systems, and chandelier illumination, allow surgeons to completely relieve vitreous base traction.

Vitrectomy With Phacoemulsification and Intraocular Lens Implantation

A small incision (2–2.75 mm) is made in the peripheral corneal region or the limbus, and standard phacoemulsification is performed. An intraocular lens (IOL) may be inserted before or after vitrectomy, depending on the surgeon's preference. Currently, acrylic foldable IOLs with relatively hard haptics are preferred. As silicone oil adheres to a silicone IOL, such implants are not recommended.

Sutureless Microincision Vitrectomy Surgery

Transconjunctival sutureless MIVS using 25-gauge (25G) instrumentation provides several advantages over conventional 20G surgery, including a shorter surgical time, less surgically

induced inflammation, and a reduced risk of postoperative corneal astigmatism. These factors ultimately lead to improved patient comfort and faster visual recovery. The 2009 Preferences and Trends (PAT) surveys conducted by the American Society of Retinal Specialists reported that nearly 80% of respondents commonly employ small-gauge MIVS systems.[21]

The original MIVS procedure, introduced in 2002,[22] had some limitations. The excessive flexibility of the first 25G instruments rendered it difficult for surgeons to adequately dissect the peripheral vitreous, to shave the vitreous base, and to rotate the eye. These limitations were particularly troublesome when operating on eyes with RRD. In addition, postoperative leakage of gas or silicone oil from the sclerotomies in the subconjunctival space was a further concern.

The introduction of 23G instruments solved several of these problems. The greater rigidity of such instruments, better illumination, and improved fluidics have facilitated manipulation of the peripheral retina, which is important when RRD is to be treated. MIVS technology continues to develop. Newly introduced 25G instruments, the 25G+ system, are substantially more rigid than their earlier counterparts. Further, an increase in instrument inner diameter has improved both infusion flow rates and illumination. In addition, a new trocar entry system and continued development of instrumentation have enhanced the performance of both 23G and 25G systems. Most recently a 27G vitrectomy system was shown to be a feasible option for repair of primary RRD.[23] Figs. 106.6–106.8 show a surgical view of transscleral sutureless vitrectomy using the 25G+ system and a wide-angle viewing system.

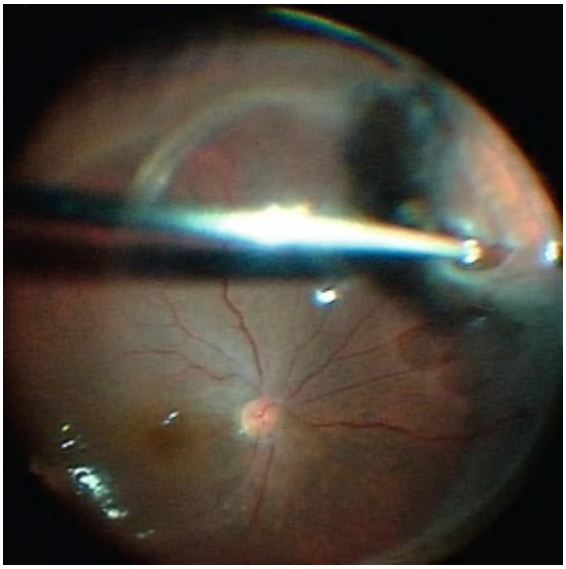

FIG. 106.6 After peripheral vitreous base dissection, more perfluorocarbon liquid (PFCL) has been injected to the level of the peripheral tear. Subretinal fluid was first displaced anteriorly by PFCL and then aspirated through the peripheral retinal break.

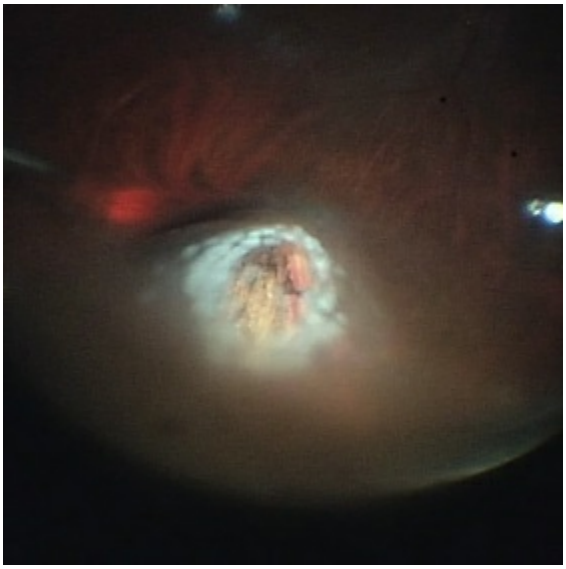

FIG. 106.7 Endolaser retinopexy was applied around the retinal breaks under the perfluorocarbon liquid (PFCL) bubble.

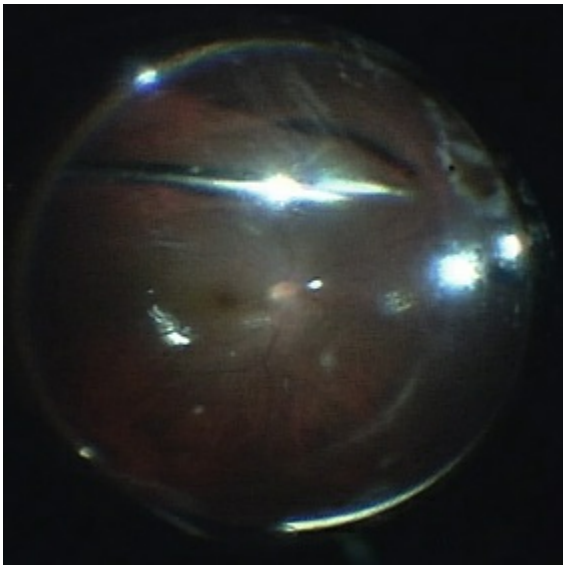

FIG. 106.8 Air–perfluorocarbon liquid (PFCL) exchange was performed while draining subretinal fluid through the peripheral retinal break.

The most recent vitrectomy system features a pneumatic dual-drive cutter with an ultrahigh cut rate of 7,500 cpm (cuts per minute) that effectively reduces vitreoretinal traction.[23–25] In this instrument, the port is also 50% closer to the tip than is the case with conventional cutters and the inner lumen diameter is enlarged. Therefore, surgeons may work remarkably close to a detached retina, with minimal movement of mobile tissue. Other features include IOP compensation via direct control of infusion pressure, and direct control of the duty cycle (this controls the proportion of time during which the port is open, in terms of the total time of the cutting cycle). These features afford excellent control of flow rate with a constant cut rate, thus increasing precision without sacrificing speed.

A new scleral entry system uses an MVR-style blade that features a trailing edge so that the cannula can be inserted via a linear incision. Such incisions are associated with a need for less force during trocar insertion, and retain shape well, resulting in less postoperative leakage than is the case when chevron incisions are made.[23–25]

Another advance in the field has been the wide-angle viewing systems that provide a better field of view compared to that afforded by contact lenses, improving surgeon recognition of peripheral fundus pathology and allowing lesions to be treated

safely and efficiently. A wide view of the fundus has become increasingly important during treatment of eyes with RRD employing 23G to 25G MIVS, because it is difficult to rotate the globe and indent the peripheral sclera during vitrectomy. Additionally, wide-angle viewing systems afford a relatively good view of the fundus in eyes with small pupils or mild corneal opacity. Further, surgeons do not need to change the contact lens during fluid–air exchange at the end of vitrectomy.

Several groups have reported good surgical outcomes when RRD was treated with transconjunctival MIVS, either the 25G or 23G systems (Table 106.1).[5,6,12,26–30] Although a few reports found that such MIVS afforded a lower single-operation success rate (SOSR) than did 20G vitrectomy,[5,27] most authors attained success rates (91.7–97.4%) similar to that of 20G surgery.[6,26,28,29] The major reported advantages of MIVS include no or mild pain on the first postoperative day in the majority of patients,[27] a shorter operation time,[6] and faster postoperative visual recovery.[31] Although some instances of transient hypotony have been reported following MIVS, no patient experienced significant postoperative leakage or endophthalmitis.[5,6,12,27–31]

TABLE 106.1

Surgical Outcomes of Microincision Vitrectomy Surgery for Treatment of RRD

Author	Year	Study Design	Type of MIVS	Patients (*n*)	SOSR	Final Success	Complications	Comm
Tsang et al.[26]	2008	Prospective	23G	24	91.7%	100%	1: hypotony	29.2% inferic breaks
Lai et al.[27]	2008	Retrospective noncomparative	25G	53	74.0%	100%		79.1% mild p postop day 1
Von Fricken et al.[28]	2009	Retrospective comparative	25G	64	90.6%	100%	2: hypotony (25G)	
			20G	61	91.8%	100%		
Bourla et al.[29]	2010	Retrospective	25G	42	97.4%		36.4%: intraoperative suturing sclerotomy	
Kunikata et al.[6]	2010	Retrospective consecutive	25G	84	95.2%	100%	6%: increased IOP 0%:	

							intraoperative suturing	
Colyer et al.[5]	2010	Retrospective consecutive	25G	30	83.3%		20%: transient hypotony	
			20G	48	89.6%			
Acar et al.[30]	2008	Prospective	25G (oblique sclerotomy)	22	95.5%	100%	9%: transient hypotony	
Lewis et al.[12]	2011	Retrospective	25G	100	93.3%	100%		All Ps local anesth
			23G		88.9%			
			20G		89.3%			

G, gauge; IOP, intraocular pressure; MIVS, microincision vitrectomy surgery; PsRD, pseudophakic RD; RRD, rhegmatogenous retinal detachment; SOSR, single-operation success rate.

Surgical Outcomes

After the occurrence of any type of RD, approximately 40% of patients will not achieve reading ability, 10–40% will need more than one surgical procedure, and approximately 5% will suffer permanent anatomic and functional failure. The reported primary success rates for RRD repair by PPV range from 64% to 96%.[2,3,14,17]

In the time since the first report of the use of PPV without concomitant SB to treat retinal detachment in 1985,[32] numerous case series have been reported (Table 106.2). Although primary vitrectomy had historically been indicated principally for treatment of pseudophakic RD with superior retinal breaks, several studies found that the technique was also useful in phakic RD patients and in those with inferior breaks.[17,33] In general, the SOSR and the improvement in visual acuity appear to be comparable to those achieved using SB. Exploiting the recent advances in surgical technology including MIVS, several recent case series reported that the SOSR improved to over 90% and that the final average visual acuity was 20/40 or better.

TABLE 106.2

Selected Case Series Using Pars Plana Vitrectomy to Treat RRD

Author	Year	Patients (*n*)	SOSR	VA Outcome	Comments
Escoffery et al.[32]	1985	29	79%	>20/50 in 81%	Phakic RD and PsRD
Sharma et al.[17]	2004	48	81%	Mean 20/66	Inferior breaks

Martinez-Castillo et al.[33]	2005	15	93%	Mean 20/30	PsRD, inferior breaks, air tamponade
Heimann et al.[14]	2006	512	70%	>20/50 in 48%	Some PPV/SB
Johansson et al.[34]	2006	131	87%	Mean 20/80	Phakic RD and PsRD
Mendrinos et al.[4]	2008	100	92%	Mean 20/50	Lens opacity 68% of phakic eyes
Schneider et al.[35]	2012	93	96%	>20/40 in 77.4%	Noncomplex RD
Figueroa et al.[36]	2013	133	96%	Mean 20/30	Phakic RD and PsRD

PPV/SB, combined pars plana vitrectomy/scleral buckling; PsRD, pseudophakic RD; RRD, rhegmatogenous retinal detachment; SOSR, single-operation success rate; VA, visual acuity.

Several retrospective series and prospective clinical trials comparing SB, PPV, and/or combined SB/PPV found no statistically significant difference in SOSR among the various procedures (Table 106.3).[3,14,15,17,18,37–43] However, a few studies reported that PPV was superior in terms of either anatomic or visual outcome in comparison with SB alone.[14,15,17,40,44] In addition, several reports comparing PPV and combined PPV/SB also found that the use of a combined procedure did not significantly influence anatomical or visual outcomes.[38,39,41]

TABLE 106.3

Selected Comparative Trials: Scleral Buckling Versus Primary Vitrectomy in RRD

Study	Year	Patients (*n*)			SOSR
		SB	PPV	PPV/SB	
Tewari et al.[18]	2003	20	0	20	Equivalent SOSR (70% SB, 80% SB/PPV), equivalent VA (median 20/120 SB, 20/200 SB/PPV)
Afrashi et al.[37]	2004	30	0	22	Higher SOSR (80% SB, 90% SB/PPV)
Stangos et al.[38]	2004	0	45	26	Equivalent SOSR (98% PPV, 92% SB/PPV), equivalent VA (improve ≥3 lines in 60% PPV, 69% SB/PPV)
Sharma et al.[17]	2005	25	25	0	All PsRD, equivalent SOSR (76% SB, 84% PPV), better VA with PPV (20/105 SB, 20/71 PPV)
Brazitikos et al.[15]	2005	75	75	0	All PsRD, higher SOSR for PPV (83% SB, 94% PPV), equivalent vision (20/50 SB, 20/43 PPV)
Halberstadt et al.[39]	2005	190	0	53	Phakic RD 88.9% SB, 82.1% SB/PPV
					PsRD 87.7% SB, 77.6% SB/PPV
Heimann et al.[14]	2007	342	339	0	Phakic RD 63.6% SB , 63.8% PPV
					PsRD 53.4% SB, 72% PPV
					No difference in VA
Azad et al.[40]	2007	31	30	0	80.6% SB, 80% PPV
Pastor et al.[3]	2008	108	278	160	Global SOSR 94.7%, equivalent (phakic RD/PsRD)
Orlin et al.[41]	2014	0	52	22	83% PPV, 86% PPV/SB

Wong et al.[42]	2014	308	415		84.6% SB, 84.6% PPV or PPV/SB
Falkner-Radler et al.[43]	2015	0	30	30	93.3% PPV, 93.3% PPV/SB

PPV, pars plana vitrectomy; PPV/SB, combined pars plana vitrectomy/scleral buckling; PsRD, pseudophakic RD; RRD, rhegmatogenous retinal detachment; SB, scleral buckling; SOSR, single-operation success rate; VA, visual acuity.

A meta-analysis of 29 studies on patients with pseudophakic RD found that both PPV and combined PPV/SB were associated with a higher SOSR and better visual acuity outcomes than was SB alone;[45] another review of nine reports comparing PPV to SB found no statistically significant difference with respect to SOSR or visual outcomes.[46]

Although the data are not entirely consistent, most surgeons agree that PPV without buckling effectively treats pseudophakic RD and results in better long-term outcomes than does conventional SB.[4] The rationale for use of primary PPV alone to treat pseudophakic RD patients is that visualization of the peripheral retina is good, the causative retinal breaks can be properly identified and treated, buckling-related complications are absent, and the risk of PPV-induced cataracts is absent. When it is considered that the need for reoperation is a (negative) indicator of the quality and efficacy of surgical techniques, the SPR study showed that the risk of such surgery was significantly reduced when PPV was used, compared to SB, in pseudophakic eyes, but not in phakic eyes. The results also showed that the prognostic factors differed between the pseudophakic and phakic subgroups.[47,48]

Prognostic Factors

Identification of patients at high risk of failure at the time of initial presentation would allow surgeons to individually tailor patient management. Reported risk factors for surgical failure after PPV in the repair of RRD include duration of symptoms, older age, the extent of RD, macular detachment, involvement of inferior quadrants, absence of detectable retinal breaks, high myopia, hypotony, and PVR-related risk factors such as pseudophakia/aphakia, uveitis, vitreous hemorrhage, and preoperative PVR.[4,17,45–52] A recent study highlighted the role of

genetic factors as a useful tool for the identification of patients at high risk of suffering PVR and indicated that reduced apoptosis could be implicated as a possible new target in PVR prophylaxis after RD.[53]

The extent of RD can be considered to serve as a surrogate marker of RD duration, although the location of retinal breaks may affect the speed of detachment after onset. Nevertheless, such patients may have a higher level of retinal glial upregulation and RPE cell dispersion and may also develop PVR, which is an important risk factor in terms of surgical failure.[54]

A number of studies have found that previous lens extraction was a risk factor for development of PVR and was associated with worse outcomes.[55] The association between pseudophakia/aphakia and surgical failure may be related to the observations that (1) pseudophakic/aphakic patients often have small, sometimes multiple anterior breaks, which may be missed at the time or surgery; or (2) such patients tend to develop new retinal breaks after vitrectomy, caused by residual vitreous base traction. Many features of pseudophakic eyes, including anterior or posterior capsular fibrosis, the presence of cortical remnants, poor pupillary dilation, vitreous opacity, and optic aberrations secondary to IOL placement, *per se* may seriously compromise the surgical view, resulting in poor outcomes.

Macular detachment and subsequent structural change detected by OCT appear to cumulatively reduce final visual acuity.[50,51] An experimental study showed that rapid retinal reattachment reversed the retinal degeneration associated with detachment.[56] As complete intraoperative attachment of the macula is achieved in most patients during vitrectomy, visual recovery after surgery is faster. The recent development of intraoperative OCT allows the surgeon to detect any preretinal membranes at the macular area that may not have been visible preoperatively and to achieve good postoperative morphologic recovery of macular retina (Figs. 106.9 and 106.10). Delayed or incomplete visual recovery after SB for macula-off RD may be associated with macular subretinal fluid persistence, which can also be assessed using OCT.[57]

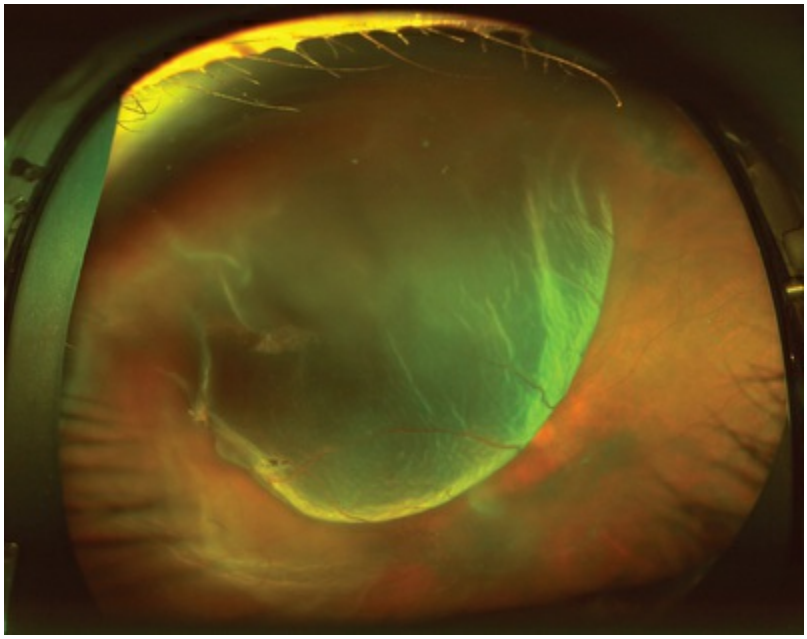

FIG. 106.9 Preoperative wide-angle fundus photography showing a bullous retinal detachment involving the macula. Optical coherence tomography imagery could not be obtained.

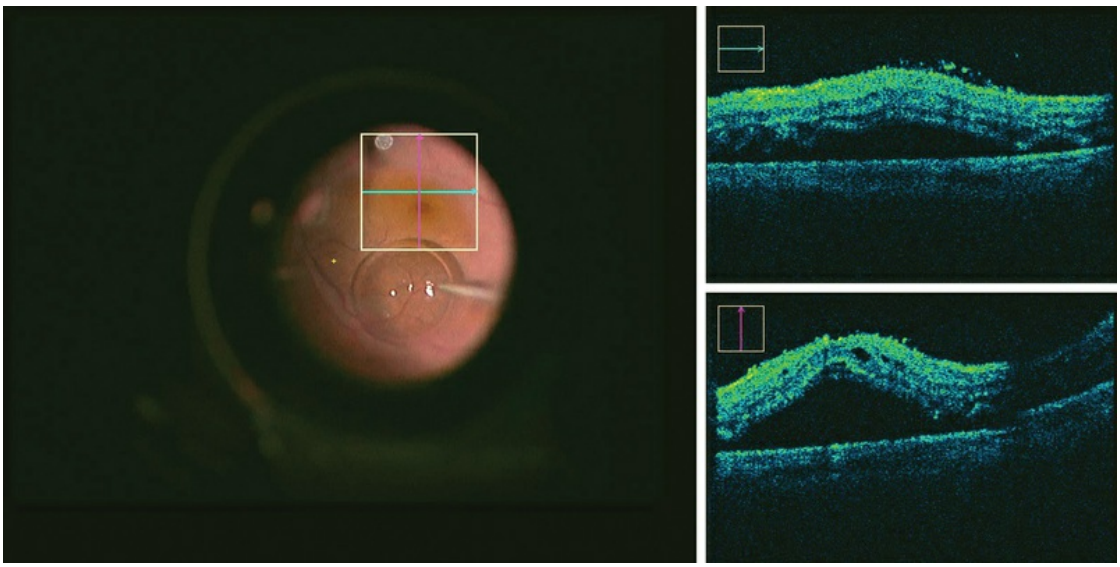

FIG. 106.10 Intraoperative optical coherence tomography with a bubble of perfluorocarbon liquid (PFCL) revealed a fine epiretinal membrane on the macula, which was removed with a diamond-dusted eraser.

Inferior breaks have also been reported to be associated with

surgical failure following PPV for RRD.[2,17,30,58] The functional study of the SPR group showed that inferior detachment with breaks below the 4 and 8 o'clock positions was a significant risk factor in a pseudophakic/aphakic subtrial.[49] However, other studies have failed to show any advantage of combined PPV with SB, compared with PPV alone, in treatment of inferior retinal breaks.[50]

Complications

The most frequent intraoperative complications are relatively high rates of iatrogenic retinal breakage (0.78–24%)[4,15,17,18,37,38,40,59] and crystalline lens damage (0.03–9%).[16,37,59,60] Several less serious complications include retinal incarceration at retinotomy sites (0.6–2.9%), corneal abrasion (0.6%), and choroidal effusion (0.5%), as reported in one national audit.[61]

Transient or persistent intraocular pressure increases have been reported in 15–24% of patients.[4,36–38,40,59–61] Phakic patients are at significant risk of developing nuclear cataracts; this is especially true of patients older than 50 years (21–86%).[14,37,40,60,61] Other anterior segment problems, occurring less frequently, include hemorrhage, subluxation or capture of intraocular lenses, posterior capsular opacification, and synechia.[2,4,14,29,36–38,40,59–61]

Major postoperative complications include retinal redetachment, with or without PVR, usually by new or missed breaks, or reopening of former breaks. In selected cases of redetachment, pneumatic retinopexy can be utilized as a rescue procedure.[62] As discussed above in terms of surgical outcomes, recent advances in surgical technology, including the development of MIVS and wide-angle viewing systems, have reduced the frequency of anatomic failures. Apart from recurrent detachment, several posterior segment complications may occur; these include cystoid macular edema and macular pucker.[2,4,37,60,61] Although very rare, endophthalmitis has been reported,[61] as has sympathetic ophthalmia. The incubation period for the latter condition after vitrectomy varies from 4 weeks to 2 years.[63,64]

Recently, as MIVS has become more popular, the risks of postoperative hypotony and endophthalmitis have become of concern. However, recent case series have found that

endophthalmitis did not occur more frequently than after conventional vitrectomy, and postoperative hypotony following MIVS was transient and resolved spontaneously in most patients.[5,6,17,18,26,28–30]

Perspectives

Future studies should evaluate surgical interventions from multiple perspectives, not only clinical but also socioeconomic. In addition to final anatomic and functional outcomes, the rate of recovery and the need for secondary procedures should be considered. As the paradigm of vitrectomy has shifted from conventional 20G PPV to sutureless MIVS using either 25G or 23G, it is now imperative to assess patient outcomes including postoperative pain and discomfort, time away from work, and quality of life. Relevant societal outcomes include procedural cost and cost-effectiveness; these issues cannot be ignored as technology advances rapidly.

References

1. Klöti R. Amotio-Chirurgie ohne Skleraeindellung. Primäre Vitrektomie. *Klin Monatsbl Augenheilkd*. 1983;182:474–478.
2. Heimann H, Zou X, Jandeck C, et al. Primary vitrectomy for rhegmatogenous retinal detachment: an analysis of 512 cases. *Graefes Arch Clin Exp Ophthalmol*. 2006;244:69–78.
3. Pastor JC, Fernandez I, Rodriguez de la RE, et al. Surgical outcomes for primary rhegmatogenous retinal detachments in phakic and pseudophakic patients: the Retina 1 Project – report 2. *Br J Ophthalmol*. 2008;92:378–382.
4. Mendrinos E, Dang-Burgener NP, Stangos AN, et al. Primary vitrectomy without scleral buckling for pseudophakic rhegmatogenous retinal detachment. *Am J Ophthalmol*. 2008;145:1063–1070.
5. Colyer MH, Barazi MK, von Fricken MA. Retrospective comparison of 25-gauge transconjunctival sutureless vitrectomy to 20-gauge vitrectomy for the repair of pseudophakic primary inferior rhegmatogenous retinal detachment. *Retina*. 2010;30:1678–1684.

6. Kunikata H, Nishida K. Visual outcome and complications of 25-gauge vitrectomy for rhegmatogenous retinal detachment; 84 consecutive cases. *Eye (Lond)*. 2010;24:1071–1077.
7. Pischel DK. Detachment of the vitreous as seen by slitlamp examination; with notes on the technique of slitlamp microscopy of the vitreous cavity. *Am J Ophthalmol*. 1953;36:1497–1507.
8. Boldrey EE. Risk of retinal tears in patients with vitreous floaters. *Am J Ophthalmol*. 1983;96:783–787.
9. Sheu SJ, Ger LP, Ho WL. Late increased risk of retinal detachment after cataract extraction. *Am J Ophthalmol*. 2010;149:113–119.
10. Minihan M, Tanner V, Williamson TH. Primary rhegmatogenous retinal detachment: 20 years of change. *Br J Ophthalmol*. 2001;85:546–548.
11. Ah-Fat FG, Sharma MC, Majid MA, et al. Trends in vitreoretinal surgery at a tertiary referral centre: 1987 to 1996. *Br J Ophthalmol*. 1999;83:396–398.
12. Lewis SA, Miller DM, Riemann CD, et al. Comparison of 20-, 23-, and 25-gauge pars plana vitrectomy in pseudophakic rhegmatogenous retinal detachment repair. *Ophthalmic Surg Lasers Imaging*. 2011;42:107–113.
13. Albrieux M, Rouberol F, Bernheim D, et al. Comparative study of 23-gauge vitrectomy versus 20-gauge vitrectomy for the treatment of rhegmatogenous retinal detachment. *Graefes Arch Clin Exp Ophthalmol*. 2011;249:1459–1468.
14. Heimann H, Bartz-Schmidt KU, Bornfeld N, et al. Scleral buckling versus primary vitrectomy in rhegmatogenous retinal detachment: a prospective randomized multicenter clinical study. *Ophthalmology*. 2007;114:2142–2154.
15. Brazitikos PD, Androudi S, Christen WG, et al. Primary pars plana vitrectomy versus scleral buckle surgery for the treatment of pseudophakic retinal detachment: a randomized clinical trial. *Retina*. 2005;25:957–964.
16. Ahmadieh H, Moradian S, Faghihi H, et al. Anatomic and visual outcomes of scleral buckling versus primary vitrectomy in pseudophakic and aphakic retinal

detachment. Six-month follow-up results of a single operation – report no. 1. *Ophthalmology*. 2005;112:1421–1429.
17. Sharma YR, Karunanithi S, Azad RV, et al. Functional and anatomic outcome of scleral buckling versus primary vitrectomy in pseudophakic retinal detachment. *Acta Ophthalmol Scand*. 2005;83:293–297.
18. Tewari HK, Kedar S, Kumar A, et al. Comparison of sclera buckling with combined scleral buckling and pars plana vitrectomy in the management of rhegmatogenous retinal detachment with unseen retinal breaks. *Clin Experiment Ophthalmol*. 2003;31:403–407.
19. Sallam AA, Donachie PH, Williamson TH, et al. The Royal College of Ophthalmologists' National Ophthalmology Database Study of vitreoretinal surgery: report 5, anaesthetic techniques. *Br J Ophthalmol*. 2016;100(2):246–252.
20. Chen X, Yan Y, Hong L, et al. A comparison of strict face-down positioning with adjustable positioning after pars plana vitrectomy and gas tamponade for rhegmatogenous retinal detachment. *Retina*. 2015;35(5):892–898.
21. American Society of Retina Specialists. *Annual Preferences and Trends Survey 2009*. http://www.asrs.org [access for members only].
22. Fujii GY, De Juan E Jr, Humayun MS, et al. A new 25-gauge instrument system for transconjunctival sutureless vitrectomy surgery. *Ophthalmology*. 2002;109:1807–1812.
23. Romano MR, Scotti F, Vinciguerra P. 27-gauge vitrectomy for primary rhegmatogenous retinal detachment: is it feasible? *Ann Acad Med Singapore*. 2015;45(5):185–187.
24. Hariprasad SM. Microincision vitrectomy surgery for the repair of retinal detachment. *Retinal Physician*. 2009;Nov:103654.
25. Rizzo S, Genovesi-Ebert F, Belting C, et al. Comparative study between a standard 25-gauge vitrectomy system and a new ultrahigh-speed 25-gauge system with duty cycle control in the treatment of various vitreoretinal diseases. *Retina*. 2011;31:2007–2013.
26. Tsang CW, Cheung BT, Lam RF, et al. Primary 23-gauge transconjunctival sutureless vitrectomy for

rhegmatogenous retinal detachment. *Retina*. 2008;28:1075–1081.
27. Lai MM, Ruby AJ, Sarrafizadeh R, et al. Repair of primary rhegmatogenous retinal detachment using 25-gauge transconjunctival sutureless vitrectomy. *Retina*. 2008;28:729–734.
28. Von Fricken MA, Kunjukunju N, Weber C, et al. 25-Gauge sutureless vitrectomy versus 20-gauge vitrectomy for the repair of primary rhegmatogenous retinal detachment. *Retina*. 2009;29:444–450.
29. Bourla DH, Bor E, Axer-Siegel R, et al. Outcomes and complications of rhegmatogenous retinal detachment repair with selective sutureless 25-gauge pars plana vitrectomy. *Am J Ophthalmol*. 2010;149:630–634.
30. Acar N, Kapran Z, Altan T, et al. Primary 25-gauge sutureless vitrectomy with oblique sclerotomies in pseudophakic retinal detachment. *Retina*. 2008;28:1068–1074.
31. Nam Y, Chung H, Lee JY, et al. Comparison of 25- and 23-gauge sutureless microincision vitrectomy surgery in the treatment of various vitreoretinal diseases. *Eye (Lond)*. 2010;24:869–874.
32. Escoffery RF, Olk RJ, Grand MG, et al. Vitrectomy without scleral buckling for primary rhegmatogenous retinal detachment. *Am J Ophthalmol*. 1985;99:275–281.
33. Martinez-Castillo V, Verdugo A, Boixadera A, et al. Management of inferior breaks in pseudophakic rhegmatogenous retinal detachment with pars plana vitrectomy and air. *Arch Ophthalmol*. 2005;123:1078–1081.
34. Johansson K, Malmsjo M, Ghosh F. Tailored vitrectomy and laser photocoagulation without scleral buckling for all primary rhegmatogenous retinal detachments. *Br J Ophthalmol*. 2006;90:1286–1291.
35. Schneider EW, Geraets RL, Johnson MW. Pars plana vitrectomy without adjuvant procedures for repair of primary rhegmatogenous retinal detachment. *Retina*. 2012;32:213–219.
36. Figueroa MS, Contreraso I, Noval S, et al. Anatomic and

visual outcomes of 23-G vitrectomy without scleral buckling for primary rhegmatogenous retinal detachment. *Eur J Ophthalmol*. 2013;23:417–422.
37. Afrashi F, Erakgun T, Akkin C, et al. Conventional buckling surgery or primary vitrectomy with silicone oil tamponade in rhegmatogenous retinal detachment with multiple breaks. *Graefes Arch Clin Exp Ophthalmol*. 2004;242:295–300.
38. Stangos AN, Petropoulos IK, Brozou CG, et al. Pars-plana vitrectomy alone vs vitrectomy with scleral buckling for primary rhegmatogenous pseudophakic retinal detachment. *Am J Ophthalmol*. 2004;138:952–958.
39. Halberstadt M, Chatterjee-Sanz N, Brandenberg L, et al. Primary retinal reattachment surgery: anatomical and functional outcome in phakic and pseudophakic eyes. *Eye (Lond)*. 2005;19:891–898.
40. Azad RV, Chanana B, Sharma YR, et al. Primary vitrectomy versus conventional retinal detachment surgery in phakic rhegmatogenous retinal detachment. *Acta Ophthalmol Scand*. 2007;85:540–545.
41. Orlin A, Hewing NJ, Nissen M, et al. Pars plana vitrectomy compared with pars plana vitrectomy combined with scleral buckle in the primary management of noncomplex rhegmatogenous retinal detachment. *Retina*. 2014;34:1069–1075.
42. Wong CW, Yeo IY, Loh BK, et al. Scleral buckling versus vitrectomy in the management of macula-off primary rhegmatogenous retinal detachment: a comparison of visual outcomes. *Retina*. 2015;35:2552–2557.
43. Falkner-Radler CI, Graf A, Binder S. Vitrectomy combined with endolaser or an encircling scleral buckle in primary retinal detachment surgery: a pilot study. *Acta Ophthalmol*. 2015;93:464–469.
44. Huang CM, Fu T, Zhang TH, et al. Scleral buckling versus vitrectomy for macula-off rhegmatogenous retinal detachment as accessed with spectral-domain optical coherence tomography: a retrospective observational case series. *BMC Ophthalmol*. 2013;13:12.
45. Arya AV, Emerson JW, Engelbert M, et al. Surgical

management of pseudophakic retinal detachments: a meta-analysis. *Ophthalmology*. 2006;113:1724–1733.
46. Saw SM, Gazzard G, Wagle AM, et al. An evidence-based analysis of surgical interventions for uncomplicated rhegmatogenous retinal detachment. *Acta Ophthalmol Scand*. 2006;84:606–612.
47. Heussen N, Hilgers RD, Heimann H, et al. Scleral buckling versus primary vitrectomy in rhegmatogenous retinal detachment study (SPR Study): multiple-event analysis of risk factors for reoperations. SPR Study Report No. 4. *Acta Ophthalmol*. 2009;89:622–628.
48. Feltgen N, Heimann H, Hoerauf H, et al. Scleral buckling versus primary vitrectomy in rhegmatogenous retinal detachment study (SPR study): risk assessment of anatomical outcome. SPR Study Report No. 7. *Acta Ophthalmol*. 2013;91:282–287.
49. Heussen N, Feltgen N, Walter P, et al. Scleral buckling versus primary vitrectomy in rhegmatogenous retinal detachment study (SPR Study): predictive factors for functional outcome. Study Report No. 6. *Graefes Arch Clin Exp Ophthalmol*. 2011;249:1129–1136.
50. Wickham L, Ho-Yen GO, Bunce C, et al. Surgical failure following primary retinal detachment surgery by vitrectomy: risk factors and functional outcomes. *Br J Ophthalmol*. 2010;95:1234–1238.
51. Joe SG, Kim YJ, Chae JB, et al. Structural recovery of the detached macula after retinal detachment repair as assessed by optical coherence tomography. *Korean J Ophthalmol*. 2013;27:178–185.
52. Adelman RA, Parnes AJ, Michalewska Z, et al. European Vitreo-Retinal Society Retinal Detachment Study G. Clinical variables associated with failure of retinal detachment repair: the European Vitreo-retinal Society Retinal Detachment Study Report No. 4. *Ophthalmology*. 2014;121:1715–1719.
53. Pastor-Idoate S, Rodriguez-Hernandez I, Rojas J, et al. BAX and BCL-2 polymorphisms, as predictors of proliferative vitreoretinopathy development in patients suffering retinal

detachment: the Retina 4 project. *Acta Ophthalmol*. 2015;93:e541–9.
54. Sethi CS, Lewis GP, Fisher SK, et al. Glial remodeling and neural plasticity in human retinal detachment with proliferative vitreoretinopathy. *Invest Ophthalmol Vis Sci*. 2005;46:329–342.
55. Kon CH, Asaria RH, Occleston NL, et al. Risk factors for proliferative vitreoretinopathy after primary vitrectomy: a prospective study. *Br J Ophthalmol*. 2000;84:506–511.
56. Lewis GP, Charteris DG, Sethi CS, et al. The ability of rapid retinal reattachment to stop or reverse the cellular and molecular events initiated by detachment. *Invest Ophthalmol Vis Sci*. 2002;43:2412–2420.
57. Wolfensberger TJ. Foveal reattachment after macula-off retinal detachment occurs faster after vitrectomy than after buckle surgery. *Ophthalmology*. 2004;111:1340–1343.
58. Goto T, Nakagomi T, Iijima H. A comparison of the anatomic successes of primary vitrectomy for rhegmatogenous retinal detachment with superior and inferior breaks. *Acta Ophthalmol*. 2013;91:552–556.
59. Lv Z, Li Y, Wu Y, et al. Surgical complications of primary rhegmatogenous retinal detachment: a meta-analysis. *PLoS ONE*. 2015;10(3):e0116493.
60. Day S, Grossman DS, Mruthyunjaya P, et al. One-year outcomes after retinal detachment surgery among medicare beneficiaries. *Am J Ophthalmol*. 2010;150:338–345.
61. Thompson JA, Snead MP, Billington BM, et al. National audit of the outcome of primary surgery for rhegmatogenous retinal detachment. II. Clinical outcomes. *Eye (Lond)*. 2002;16:771–777.
62. Petrushkin HJ, Elgohary MA, Sullivan PM. Rescue pneumatic retinopexy in patients with failed primary retinal detachment surgery. *Retina*. 2015;35(9):1851–1859.
63. Abu El-Asrar AM, Al Kuraya H, Al-Ghamdi A. Sympathetic ophthalmia after successful retinal reattachment surgery with vitrectomy. *Eur J Ophthalmol*. 2006;16:891–894.
64. Haruta M, Mukuno H, Nishijima K, et al. Sympathetic ophthalmia after 23-gauge transconjunctival sutureless

vitrectomy. *Clin Ophthalmol*. 2010;4:1347–1349.

107

Pneumatic Retinopexy

Daniel A. Brinton, Allen Chiang

Introduction

For more than a half century, the operation most favored for primary retinal detachment had been scleral buckling (SB). Between 75% and 88% of cases attain permanent reattachment with one operation with this procedure.[1–3] However, it frequently results in

tissue trauma, complications,[4] relatively high expense, and use of a hospital or surgicenter operating room.

In recent decades, pars plana vitrectomy has become the most frequently used procedure in industrialized countries for primary retinal detachments, as well as for complex and secondary retinal detachments, particularly in pseudophakic eyes. This technique also presents potential complications and requires an operating room with similar high expense.

Pneumatic retinopexy (PR) was developed in an attempt to minimize these problems in selected patients. This outpatient procedure for retinal reattachment consists of an intravitreal gas injection with transconjunctival cryopexy or laser photocoagulation, followed by a period of appropriate head positioning.[5] No incisions are required. PR is substantially less expensive than scleral buckling or vitrectomy and has become widely accepted as the treatment of choice for selected retinal detachments, with the vast majority of vitreoretinal surgeons employing this procedure.[6,7]

A multicenter, randomized controlled clinical trial has demonstrated that in selected cases the anatomic success rate of PR is comparable to SB, with less morbidity and with significantly better visual results than with SB.[8] Cataract surgery is required more often following SB than following PR[9] and is required substantially more frequently following vitrectomy. PR should be considered in patients who do not have detached inferior breaks, extensive retinal breaks, or significant proliferative vitreoretinopathy.

History

Ohm[10] performed the first intravitreal air injection for retinal detachment in 1911. In 1938 Rosengren[11] reported the use of intravitreal air with drainage of subretinal fluid in a series of 256 retinal detachments. In 1973 Norton[12] reported intravitreal sulfur hexafluoride (SF_6) injection used with SB or vitrectomy for various surgical problems, such as giant breaks, large posterior breaks, and fishmouthing. Blodi and Folk[13] treated detachments due to a macular hole using intravitreal gas. Retinal detachments treated with “repeated insufflations of expansive gas” were described by

Dominguez et al.[14,15] In 1985 Hilton and Grizzard[5] introduced the term "pneumatic retinopexy," a procedure using only transconjunctival cryotherapy and gas injection without conjunctival incision.

Unlike SB or vitrectomy, PR affords no permanent relief of vitreoretinal traction. The fact that detachments can be cured without permanently relieving traction, demonstrated decades before by Ohm[10] and by Rosengren,[11] was reconfirmed in 1979 by Lincoff et al.,[16] who introduced the use of a balloon to achieve temporary scleral buckling. The efficacy of this procedure was demonstrated, but it never caught on, and the orbital balloon is not commercially available. However, retinal detachment repair without permanently relieving vitreoretinal traction, well proven by Lincoff's technique, combined with the demonstrated safety of intravitreal gas, formed the basis for PR.

In 1989 Tornambe and Hilton[8] co-directed a multicenter, randomized controlled clinical trial comparing PR with SB. Tornambe[17] reviewed over 200 studies on PR, including statistical reports on over 1300 cases. The single-operation success rate in these combined series was 80%, increasing to 98% after reoperations[18] – results that have been subsequently replicated.[19] Chan et al.[20] reviewed all published reports on PR cases from 1986 to 2007, totaling 4138 eyes. Single-operation success was 74.4%, and success with one or more operations was 96.1%.

Basic Principles

Intraocular Gases

Sulfur hexafluoride (SF_6) and perfluoropropane (C_3F_8) are the gases most frequently used with PR. Success has also been reported with sterile room air.[21] In 1993 the United States Food and Drug Administration approved certain SF_6 and C_3F_8 products for use in PR.

The value of the intraocular bubble is based on three features: buoyancy, surface tension, and isolation of retinal tears from intraocular currents.[22,23] Buoyancy applies upward pressure on the detached retina. The surface tension of the bubble closes the retinal

break and prevents the bubble from passing into the subretinal space. With the break closed, the retinal pigment epithelial pump removes the subretinal fluid.

Because of their low solubility in water, SF_6 and especially C_3F_8 tend to diffuse from the eye very slowly. However, the nitrogen and oxygen that are in solution in the surrounding tissues of the eye are much more soluble and pass relatively quickly into the gas bubble, following the law of partial pressures. The net result is the initial expansion of a bubble of pure SF_6 or C_3F_8 within the vitreous, followed by gradual resorption. Characteristics of gas expansion and resorption for SF_6, C_3F_8, and air are listed in Table 107.1.

TABLE 107.1

Intravitreal Gas Duration and Expansion

Gas	Typical Dose	Average Duration	Largest Size	Average Expansion
Air	0.8 mL	4 days	Immediate	No expansion
SF_6	0.5 mL	12 days	36 hours	Doubles
C_3F_8	0.3 mL	38 days	3 days	Quadruples

C_3F_8, perfluoropropane; SF_6, sulfur hexafluoride.

SF_6 and C_3F_8 are chemically inert, colorless, odorless, and nontoxic.[24] SF_6 has been studied extensively in experimental animals and has been found to be nontoxic as judged by electrophysiologic testing and electron microscopy.[25] One study of rabbits concluded that "eyes only partially filled with C_3F_8 showed no permanent damage, with a total recovery of the cortical matrix, gel, and liquid vitreous."[26] Early concerns[27] regarding PVR from intravitreal gas injection have not been substantiated. A 0.22-μm Millipore™ filter is sufficient to render gas sterile.[25]

Lincoff et al.[28] noted that gas bubble contact with the crystalline lens can produce cataract after several days, but this is avoidable by appropriate positioning. Mougharbel et al.[29] have demonstrated with Scheimpflug photography that PR does not cause cataract.

Retina–Gas Interface

Larger areas of tamponade require disproportionate increases in

bubble volume. A 0.3 mL gas bubble in humans covers more than a 45° arc of the retina, but it takes approximately a 1.2 mL bubble to cover 80–90°.[5] Because surface tension causes the gas to take on a relatively spherical contour, particularly with smaller bubbles, the extent of retina–gas contact is significantly less than that published from studies of model eyes.[30] To cover the same arc of the retina, a highly myopic eye requires a larger volume of gas than an emmetropic eye. These factors are considered in deciding how much gas to inject.

Case Selection

The multicenter clinical trial excluded cases with the following characteristics:[8]

1. Detached breaks larger than 1 clock-hour or multiple breaks extending over more than 1 clock-hour of the retina.

2. Detached breaks in the inferior 4 clock-hours of the retina.

3. Presence of PVR grade C or D (Retina Society Terminology Committee, 1983).[31]

4. Physical disability or mental incompetence precluding maintenance of the required positioning.

5. Severe or uncontrolled glaucoma.

6. Cloudy media precluding full assessment of the retina.

A review of 1000 consecutive detachments[5] revealed that 41% qualified for PR under these limiting criteria. Subsequent experience has demonstrated that selected cases that do not strictly meet these criteria can also be successfully treated with PR.[32,33] In our hands, about half of all primary retinal detachments are treated with PR using expanded criteria as described below.

Extent of Breaks

Detached breaks spanning more than 1 clock-hour can be treated

with PR. Single or multiple detached tears spanning 2 or even 3 clock-hours pose no particular problem. Detached tears 6 clock-hours apart are difficult to fix with PR, although alternating positioning has been used successfully. Even detachments with giant retinal tears have been cured with PR.[34] However, scleral buckling or vitrectomy is usually preferred for detachments with widely separated or giant tears. Attached breaks can generally be ignored in deciding whether a case is amenable to PR, and postoperative positioning does not need to be planned to close them with the gas bubble. Attached break(s) should generally be treated with laser before the gas injection. Care should then be taken, such as by using the steamroller technique, if necessary, to prevent the bubble from pushing the subretinal fluid into the attached break and causing it to detach. By following these two steps, multiple attached breaks may be ignored in the calculation of bubble size and in positioning.

Inferior Breaks

Most cases involving detached breaks in the inferior 4 clock-hours of the eye (from 4:00 to 8:00) have been difficult to treat with PR, despite various attempts.[33] Even for flexible patients, it can be difficult to tilt the head below the horizontal plane for extended periods, although this worked well in two series,[35,36] and another showed success positioning for only 8 hours.[37] Hilton et al.[38] treated retinal detachment with inferior breaks by augmenting PR with in-office partial vitrectomy, allowing injection of a large enough gas bubble to close the breaks with side positioning. We believe a detached break in the inferior 4 clock-hours represents a contraindication to PR in most cases, although breaks from 4:00 to 4:30 or from 7:30 to 8:00 may be attempted in a motivated patient using sideways positioning with an additional downward head tilt. Attached inferior breaks do not necessarily contraindicate PR if treated as described above, taking care to avoid iatrogenic detachment of an attached break caused by the gas bubble.

Proliferative Vitreoretinopathy

Because PR does not relieve traction like vitrectomy or SB, significant preoperative tangential traction on a retinal tear (as in

periretinal proliferation) is a contraindication to the pneumatic procedure. When a tear is adjacent to a star fold, PR is not generally the procedure of choice. Mild to moderate proliferative vitreoretinopathy (PVR) (such as a star fold) that is distant from any retinal break generally does not contraindicate PR. More severe PVR requires vitrectomy or possibly SB, or both.

Inability to Maintain Positioning

Failure to maintain the appropriate position faithfully is an important cause of failure of PR. It is important to ask patients about back or neck problems and to assess mental competence before deciding on PR. Some positions are quite easy to maintain, whereas others are more difficult. Positioning is easiest with tears between 11 and 1 o'clock. Positioning is probably easier for horizontally oriented tears (between 2 and 4 or between 8 and 10 o'clock) than it is for obliquely oriented tears (between 1 and 2 or between 10 and 11 o'clock).

Glaucoma

The majority of patients with primary open angle glaucoma can be treated with PR without a problem. Performing paracentesis prior to gas injection may be prudent in patients with severe glaucoma (e.g., splitting of the macular field as a result of glaucoma) since they might suffer noticeable damage even from brief elevations in intraocular pressure. In glaucomatous eyes that have had trabeculectomy or may need it in the future, PR has advantages over SB in that it minimizes scarring of the conjunctiva. Except in cases of severely impaired trabecular outflow facility, serial measurements of intraocular pressure after gas injection are not necessary.

Cloudy Media

For PR to be successful, all detached retinal breaks need to be identified and treated. Opacities that preclude an adequate view of the peripheral retina, such as peripheral vitreous hemorrhage or pseudophakic lens capsular opacification, represent relative contraindications to PR. However, there is no contraindication if the

extent of detached peripheral retina can be identified, treated with cryopexy, and then covered by gas. Because evidence suggests that PR does not jeopardize an eye for future vitrectomy or SB if needed,[8,17] we will frequently use the pneumatic procedure even when opacities obscure parts of the detached retina that cannot be covered by gas, but the chance of success may be lower.

Lattice Degeneration

Many studies have shown no detrimental effect on single-operation success from lattice degeneration,[17,39] particularly if under 3 clock-hours in extent. Extensive lattice may indicate increased risk for vitreoretinal traction, and these cases may benefit from vitrectomy or SB.

Aphakia and Pseudophakia

Retinal detachments in aphakic or pseudophakic eyes have a poorer prognosis than phakic eyes, no matter what surgery is performed.[9] In some series, aphakic eyes did poorly with PR,[40] especially if the posterior capsule was open,[41] but in other reports this was not the case.[8,9] Aphakic and pseudophakic eyes are prone to multiple, tiny, far-peripheral breaks and require an especially careful preoperative examination. In pseudophakic eyes, the view of the peripheral retina can be quite limited if much peripheral capsular opacity is present. PR should probably not be performed in these cases unless retinal detachment is rather limited. In our opinion, if the peripheral retina can be adequately examined, aphakia or pseudophakia is not a contraindication to PR.

Posterior Vitreous Detachment

Phakic eyes with complete posterior vitreous detachment tend to have a higher success rate with PR than those with partial vitreous detachment.[42]

Cases Where PR Presents a Particular Advantage

Compared with vitrectomy, PR is especially advantageous in the

management of the following three situations:

1. Phakic eyes. PR avoids the induced cataract to which vitrectomy is prone.

2. Impending macular detachment. Because PR can be performed promptly in the office without the delays required to prepare a patient for the operating room, a macula at imminent risk of detachment may be best served by PR, using the steamroller maneuver (see below) to move subretinal fluid away from the macula.

3. Limited operating room access. Financial and logistical difficulties may preclude use of the operating room and favor a procedure that can be done in the office.

Compared with SB, PR is especially advantageous in the management of the following five situations:

1. Macular breaks and other posterior retinal breaks. Posterior retinal breaks are difficult to treat with SB, so PR is the procedure of choice in many of these cases, especially in phakic eyes. It also has been reported as an effective option in the treatment of optic pits with macular detachment.[43,44]

2. Redetachment or persistent detachment after scleral buckling. When subretinal fluid accumulates or persists because of a superior break after SB, PR may be much easier to perform than buckle revision.[45] This is especially effective if the break is located on or anterior to the buckle.[46]

3. Isolated tears under the superior rectus. Placing a segmental buckle under a vertically acting muscle runs the risk of iatrogenic diplopia; this is eliminated with PR.

4. Filtering blebs. If a functioning filtering bleb is present, or if a filtering procedure may be necessary in the future, PR or vitrectomy should be considered instead of SB.

5. Bullous detachment. When retinal detachment is highly bullous,

retinal tears can be difficult to localize and treat with SB, a problem that is avoided by two-session PR.

Preoperative Counseling

The details of the procedure should be explained to the patient and the potential risks and complications reviewed. Required postoperative positioning is described, and the patient's ability to comply is evaluated. The possibility of recurrence or persistence of detachment, with potential need for additional surgery, is explained. The patient is informed that infection inside the eye is a very rare but potentially devastating complication. Restrictions on air travel and travel to significantly higher altitudes while gas is in the eye is explained.

Surgical Technique

Anesthesia

Topical anesthesia, usually with subconjunctival anesthesia or application of lidocaine-soaked pledgets, may be adequate, but in sensitive patients or if extensive cryopexy is planned, retrobulbar anesthesia is often helpful.

If subsequent general anesthesia is used in a patient who has an intraocular gas bubble, nitrous oxide should not be administered. When gas is to be introduced into an eye during surgery, nitrous oxide should be turned off at least 15 minutes before gas injection.

One-Session vs. Two-Session Procedure

See Box 107.1 for indications for the one-session and two-session procedures.

Box 107.1

Indications for One-Session Versus Two-Session Procedure

Indications for a One-Session Procedure With Cryopexy

- Issues of convenience or logistics

- Small or hard-to-find breaks
- Media opacities preventing laser
- Pigment atrophy preventing adequate laser burns
- Appropriate laser not available

Indications for a Two-Session Procedure With Laser

- Use of the "steamroller" procedure
- Large or extensive breaks (to minimize retinal pigment epithelial dispersion)
- Bullous detachment precluding accurate cryopexy
- Tear overlying a scleral buckle
- Recently operated eye (incision not healed)
- Very posterior breaks

Indications for a Two-Session Procedure With Cryopexy

- Initially bullous detachment but cryopexy preferred
- New media opacities preventing intended laser treatment
- Persistent subretinal fluid precluding adequate laser burns

PR can be done in one session, with cryopexy applied to the retinal breaks just before gas injection, or as a two-session procedure, with initial gas injection followed by laser photocoagulation 1 or 2 days later, when the retina is reattached. One-session procedures always involve cryopexy since the laser cannot be applied to detached retina. Two-session procedures are usually, but not always, done with the laser.

The chance of dispersing retinal pigment epithelial (RPE) cells into the vitreous may be minimized by a two-session procedure,

flattening the retina with gas before later applying retinopexy, particularly if large retinal breaks are present or if the "steamroller" technique is used (see page 1950). Also, if a tear is so bullously detached that a cryopexy ice ball will not reach the retina, it may be difficult to place the cryopexy spots with sufficient accuracy, so a two-session procedure may be preferable. Small or hard-to-find breaks may become impossible to locate once the retina is reattached, so cryopexy treatment before gas injection in a one-session procedure maximizes the chance of all tears being treated. Whenever a two-session procedure is selected, it is important to make a careful preoperative drawing of the location of the breaks relative to vascular and other landmarks. For these reasons, pneumatic retinopexy is most commonly performed in a single session.

Cryopexy vs. Laser

Cryopexy may be necessary if vitreous hemorrhage or other media opacities make laser treatment difficult. Laser application may be ineffective for tears that develop in areas of pigmentary atrophy. Cryopexy may be easier to apply than laser in some patients who have difficulty keeping their eyes still. In some cases, even after a few days of positioning, enough subretinal fluid remains that laser cannot be applied, and cryopexy may be necessary.

If a laser indirect ophthalmoscope (LIO) is not available, tears in the far periphery may not be treatable with laser delivered by slit lamp, necessitating cryopexy. The LIO is ideal for PR because it allows treatment of the far periphery and facilitates maneuvering of the gas bubble out of the way.[35] Although most tears can be treated with laser through a slit-lamp delivery system by tilting the patient's head as necessary to move the bubble away from the tear, this is difficult with tears from 11 to 1 o'clock. Although it is often possible to apply laser treatment through a large gas bubble as can be achieved with vitrectomy, it can be very difficult with the smaller bubble utilized with PR because of optical factors. Application of laser through gas causes concentration of heat due to the insulating effect of gas, and excessively hot burns may result.

Certain circumstances might indicate use of laser instead of

cryopexy. Laser is required if a tear develops overlying a previously placed scleral buckle, since cryopexy cannot penetrate the silicone. In eyes with a recent surgical incision (within the past 4–6 weeks), laser may be safer than cryopexy because the scleral depression of the cryoprobe elevates the intraocular pressure. Very posterior breaks are easier to treat with laser than with cryopexy, although a small conjunctival incision in the cul-de-sac allows passing of the cryoprobe posteriorly.

Chorioretinal adhesion may be quicker and firmer using laser rather than cryopexy.[47,48] In addition, some authors believe that cryopexy is associated with a higher incidence of proliferative vitreoretinopathy and other complications,[49,50] although others could find no such association.[51] Laser also has the advantage of less morbidity compared with cryopexy, especially if multiple or large breaks are present.

Although laser generally cannot be applied to detached retina, if the detachment is very shallow, it may be possible to apply laser using firm scleral depression to flatten the retina combined with increased laser power. However, this technique may cause retinal breaks as a result of excessive laser intensity, and it must be used with caution.

Applying Retinopexy

Transconjunctival cryopexy consists of multiple contiguous applications that entirely surround the retinal tear and is monitored with binocular indirect ophthalmoscopy. Cryopexy to bare RPE in the middle of the hole should be avoided if possible. The RPE is pushed into apposition with the overlying retina, if possible, causing a visible white reaction in the retina. In very bullous detachments when the RPE cannot be brought into contact with the detached retina, the endpoint for cryopexy is the appearance of a dull, orange glow at the level of the pigment epithelium. Following treatment, do not attempt to move the cryoprobe until the freeze at the tip has thawed.

Laser application begins at a low intensity and is gradually increased until a dull, gray-white burn is achieved. If a red or infrared wavelength is used, an even less-intense burn is desired. Multiple rows of almost contiguous burns are applied to surround

all tears completely, with generous treatment along the anterior aspect of a horseshoe-shaped tear where it is most likely to extend.

Amount and Type of Gas to Inject

PR usually requires a gas bubble large enough to cover all detached breaks simultaneously for about 5 days. The size of the gas bubble should reflect the extent of the break(s). Generally, the injected gas bubble before expansion must be moderately larger than the largest retinal break to prevent subretinal gas. In most cases, we prefer to have a bubble volume of 1.0 mL or more, which requires an injection of at least 0.5 mL of pure SF_6.

If filtered room air is injected, we recommend at least 0.8 mL. If it is desired to inject more than 0.6 mL, multiple paracenteses (one before and one or more after the gas injection) or multiple gas injections may be needed.

We believe that it is optimal for the gas bubble to cover the break(s) for 5 days and then disappear as soon as possible. However, successful reattachment has been reported after as little as 6–8 hours of tamponade, as with inverted positioning for inferior tears.[37]

The longevity of an air bubble is probably sufficient for most cases, but occasionally the chorioretinal adhesion may not be sufficiently mature when the air has resorbed. The use of air also forfeits the advantage of postinjection bubble expansion within the eye, necessitating injection of a larger volume, but it offers the advantages of decreased expense and universal availability.

In most cases the prolonged longevity of a perfluoropropane (C_3F_8) bubble is a disadvantage. Air travel is contraindicated for a much longer period of time with C_3F_8, and patients are instructed not to sleep on their back until the bubble disappears to prevent prolonged contact between the gas bubble and the lens. However, the use of C_3F_8 may eliminate the need to reinject gas if a new break develops, and C_3F_8 allows the injection of a smaller amount of gas initially, thereby reducing the need for paracentesis. We recommend C_3F_8 only when an unusually large gas bubble is needed.

Our usual procedure is to perform a preinjection paracentesis, followed by injection of 0.5–0.6 mL of pure SF_6. The amount of fluid removed by paracentesis helps determine how much gas to inject. One can usually inject that amount of gas plus 0.15–0.2 mL without needing a second paracentesis, particularly if the eye was initially softened by cryopexy. Note that it takes more than 0.05 mL to fill the hub of the needle before fluid comes into the measuring chamber of the syringe. For example, if the paracentesis syringe fills to 0.40 mL, >0.45 mL has been removed from the eye. In that instance, 0.55 mL of gas can probably be injected into the eye without closing the central retinal artery. It may be possible to inject up to 0.60 mL, especially if the eye was substantially softened by firm depression during cryopexy.

Sterilizing Ocular Surface

Meticulous attention to sterile technique is mandatory. Sterilization of the ocular surface requires topical antiseptics; antibiotics are inadequate. We recommend povidone–iodine solution,[52] and we do not recommend other preparations that contain detergent or alcohol.

A sterile lid speculum is utilized. Several drops of povidone–iodine solution are instilled directly onto the conjunctiva and left in contact with the eye while the gas is prepared. The injection site is then dried with a sterile cotton-tipped applicator, and the eye is ready for paracentesis and injection of gas. With these precautions, the occurrence of endophthalmitis after PR is extremely uncommon, with very few reported cases in the literature.[53,54]

Preparing the Gas

A pressure-reducing system is attached to the gas cylinder to allow drawing of the gas from a low-pressure system. High pressure can blow out the Millipore filter and render it useless in sterilizing the gas.[55] A condom catheter can be attached to the cylinder, as shown in Fig. 107.1, or a step-down valve system can be used. Alternatively, the gas can be drawn into a large syringe and then transferred to a small syringe.

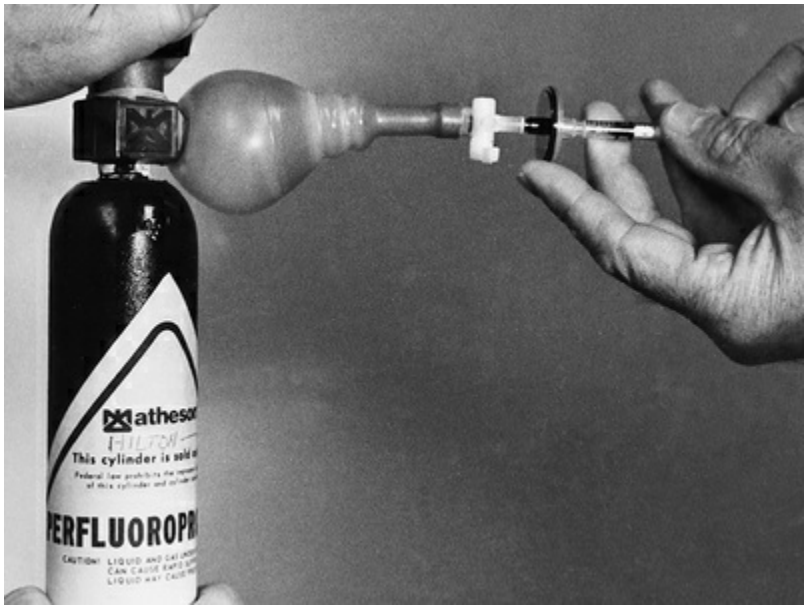

FIG. 107.1 The gas is transferred from the high-pressure tank into a low-pressure balloon made from an external urinary catheter. Gas is then easily withdrawn. Pressure in the balloon pushes gas through the Millipore filter into the syringe. To avoid dilution with air, gas in the syringe is expelled and refilled twice. (Reprinted from Hilton GF, Grizzard WS. Pneumatic retinopexy. A two-step outpatient operation without conjunctival incision. Ophthalmology 1986;93:626–41. ©1986, with permission from the American Academy of Ophthalmology.)

The selected gas passes through a Millipore filter into a 3-mL syringe in sterile fashion. The tube connecting the gas cylinder with the syringe, including the filter, is flushed through with gas to ensure no dilution with room air. The syringe is filled with a few milliliters of gas, and the gas is discarded. The syringe is then refilled. Passive filling of the syringe ensures that room air is not drawn in. A disposable 30-gauge (12-mm, half-inch) needle is then placed tightly on the syringe, and excess gas is expelled to leave the exact amount intended for injection. The gas should not be stored in the syringe for more than a few minutes before injection because room air infiltrates the syringe and dilutes the gas sample.[56]

Performing a Paracentesis

Although gas can be injected before paracentesis, we generally recommend a paracentesis first. Paracentesis performed after gas

injection can result in gas in the anterior chamber. Preinjection paracentesis helps determine how much gas to inject and avoids marked intraocular pressure elevations. Dehiscence of a recent clear corneal cataract incision has been reported following PR when preinjection paracentesis was not performed.[57]

For a paracentesis, we use a 30-gauge needle mounted on a 1-mL syringe without a plunger. After sterilization of the ocular surface, the needle is passed obliquely through the limbus into the anterior chamber, with the needle tip kept over the peripheral iris to avoid touching the lens.

The intraocular pressure quickly drops, so pressure must be applied externally to the eye in order for fluid to continue to pass into the syringe. Gentle pressure can be applied to the center of the cornea with a sterile cotton-tipped applicator, thereby forcing aqueous into the angle (Fig. 107.2). However, care must be taken to avoid contact between the cornea and the lens. Instead we prefer applying pressure with the cotton-tipped applicator at the equator of the eye, facilitating passage of fluid into the anterior chamber and allowing more firm and prolonged pressure on the eye.

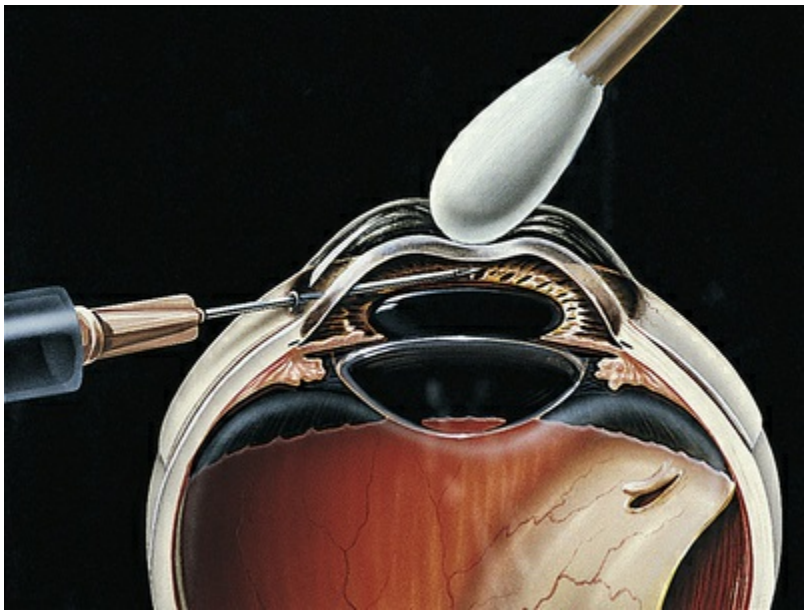

FIG. 107.2 Paracentesis of the anterior chamber with a 30-gauge disposable needle on a 1-mL syringe without a plunger. The lumen is open toward the cornea and positioned over the peripheral iris. Gentle pressure on the cornea with a cotton-tipped applicator forces

aqueous into the periphery of the anterior chamber near the needle tip, thereby facilitating more complete drainage. (Reproduced with permission from Hilton GF, Tornambe PE, and the Retinal Detachment Study Group. Pneumatic retinopexy: an analysis of intraoperative and postoperative complications. Retina 1991;11:285–94.)

Patience is called for when performing the paracentesis. Fluid will initially flow freely into the syringe, but will then slow. By continuing to press on the eye and very gradually withdrawing the needle over several minutes, one can usually remove another 0.05–0.2 mL from the eye, which will often be necessary in order to inject a 0.5–0.6-mL bubble. Highly myopic eyes tend to have more ample anterior chambers, but they also call for a larger intraocular gas bubble.

Paracentesis through the limbus may be done in phakic eyes and in pseudophakic eyes if the posterior capsule is intact or if a small capsulotomy is firmly closed against the intraocular lens (IOL); otherwise, paracentesis should usually be performed through the pars plana to prevent vitreous strands from incarcerating in the limbus. When performing paracentesis through the pars plana in a pseudophakic eye, the plunger is left in the syringe to prevent occlusion of the needle with vitreous. The needle is directed anteriorly into the anterior chamber through the pupil adjacent to the IOL. Paracentesis of the anterior chamber is contraindicated in the presence of an iris-supported anterior chamber IOL because of the possibility of the implant touching the endothelium.

Injecting Gas

With the needle attached, gas is expelled from the syringe down to the amount it is intended to inject into the eye. With the ocular surface still sterile and the patient supine, the head and the eye are turned a total of approximately 45° to one side to place the pars plana injection site uppermost. The gas usually is injected temporally unless the pars plana epithelium is detached or large retinal breaks are present in that area, in which case another site is selected. The injection is made 3–4 mm posterior to the limbus with a 30-gauge needle. The needle is directed toward the center of the vitreous and inserted to a depth of 7 or 8 mm to ensure penetration

of the pars plana epithelium and the anterior hyaloid face. It is then partially withdrawn so that approximately 9 mm of the needle shaft is seen outside the eye, leaving only 3 mm of the needle tip inside the globe. With the injection site uppermost and the needle vertical, the gas is injected evenly and moderately briskly, but not too forcefully. We estimate that the injection should take place over 0.5–1.0 seconds. This technique creates one single bubble at the needle tip (Fig. 107.3C) rather than multiple small bubbles, often referred to as "fish eggs" (see below).

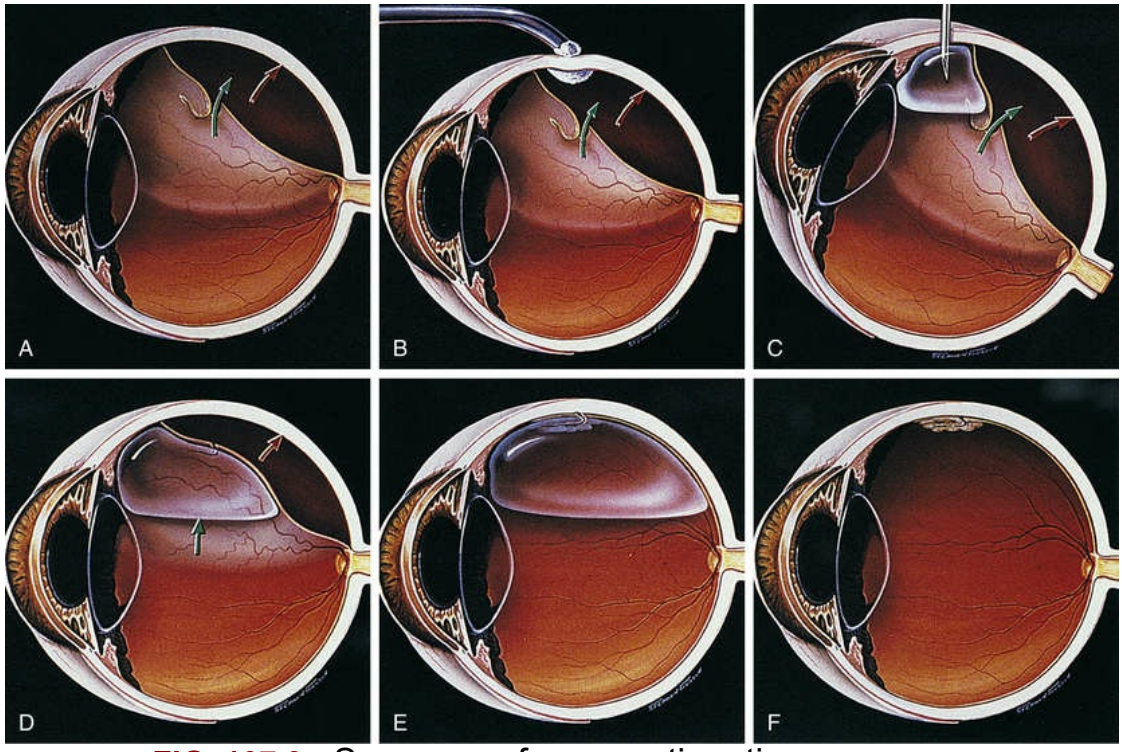

FIG. 107.3 Summary of pneumatic retinopexy procedure. (A) The volume of the subretinal fluid is determined by the inflow of fluid vitreous (*green arrow*) and the outflow through the retinal pigment epithelial pump into the choroid (*red arrow*). (B) The area of the retinal break is treated with multiple contiguous applications of transconjunctival cryotherapy. (C) With the pars plana injection site uppermost, the needle vertical, and the needle tip placed shallowly within the vitreous, the gas is injected moderately briskly through a 30-gauge needle. For purposes of illustration, the artist has drawn the injection in the same meridian as the retinal break, but usually this meridian is avoided.

(D) The head is positioned so that the intravitreal gas bubble closes the retinal break. (E) With the break closed, the retina usually is reattached by the first postoperative day. (F) The gas bubble is spontaneously absorbed. (Reprinted from Hilton GF, Kelly NE, Salzano TC, et al. Pneumatic retinopexy. A collaborative report of the first 100 cases. Ophthalmology 1987;94:307–14. ©1987, with permission from the American Academy of Ophthalmology.)

It is not necessary to visualize the needle tip within the vitreous with the ophthalmoscope. As the needle is withdrawn from the eye, the needle tract is immediately covered with a sterile cotton-tipped applicator by rolling it onto the needle shaft simultaneously as the needle is withdrawn to prevent the loss of gas. The head is then rotated to the opposite side, moving the gas bubble away from the injection site, and the cotton-tipped applicator is then removed. Alternatively, the head can be rotated prior to removing the needle. Within seconds the needle tract swells closed, preventing further leakage.

Assessing Intraocular Pressure

Despite preinjection paracentesis, the central retinal artery sometimes closes after gas injection. Several studies suggest that the retina can tolerate 60 minutes without blood flow as a result of elevated pressure.[26,58–62] If the artery does not reopen within about 10 minutes, intraocular pressure should be lowered by repeat paracentesis.

While waiting for the central retinal artery to reopen, intermittent ocular compression can hasten the return to normal intraocular pressure. A scleral depressor is pressed against the lateral aspect of the eye so that the eye is compressed against the medial orbital wall. This raises the intraocular pressure, augmenting fluid egress and stretching the scleral wall.[63] This is not recommended in eyes that have had recent surgery or penetrating trauma, or in eyes with severe glaucoma.

The patency of the central retinal artery is evaluated with ophthalmoscopy. If it is difficult to tell whether the artery is patent, the eye is compressed with gradually increasing force while

monitoring with an indirect ophthalmoscope. If pulsation of the central retinal artery cannot be induced in this manner, it is probably closed. In addition to ensuring patency of the central retinal artery, the ophthalmoscope is used to rule out the possible complications of anterior gas entrapment or fish egg bubbles.

Once patency of the central retinal artery has been reestablished, the outflow of aqueous is more than adequate to compensate for the expansion of the gas bubble in nonglaucomatous eyes. Accordingly, we no longer check postoperative pressures unless severe glaucoma is present.

Instructing the Patient

The eye is irrigated to rinse out the povidone-iodine, an antibiotic-steroid ointment is instilled, and the eye is patched. Most patients require no pain medication. The axis of the retinal break is marked with an arrow on the bandage, and the head is tilted so that the arrow points toward the ceiling. Alternatively, a commercially produced "pneumo-level" disc can be attached to the forehead to indicate the required head tilt. Using a mirror to demonstrate, the patient is carefully instructed to position the head so that the break is uppermost. The patient is instructed not to lie on their back facing upward for three reasons: first, the gas will likely not be in position against the retinal breaks; second, prolonged gas contact with the lens may cause a cataract in a phakic patient; and third, egress of fluid from the eye may be blocked, resulting in a rise in intraocular pressure. The appropriate position, with the retinal break uppermost, should be maintained (at least during waking hours) for 5 days. If possible, maintaining the position during sleep is helpful, especially until the retina is reattached. Successful retinal reattachment has been described with positioning for shorter than 5 days, and positioning for 3 days or fewer may often be adequate.[37]

Special Procedures

Fish Eggs

Multiple small intravitreal gas bubbles, or "fish eggs"[18] (Fig. 107.4),

can result in gas getting under the retina, particularly in the presence of large retinal breaks. This occurrence is generally preventable by performing the following steps (Fig. 107.5):

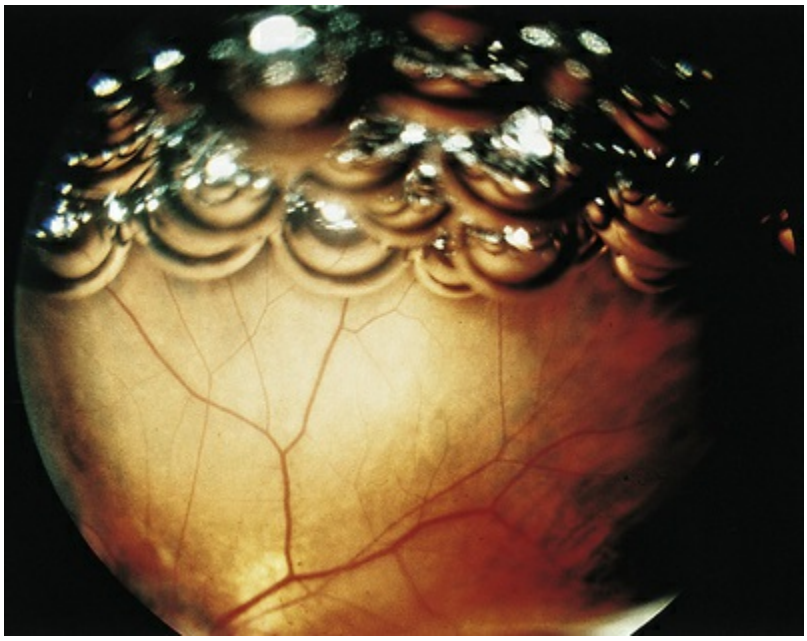

FIG. 107.4 Fish eggs – multiple, small intravitreal gas bubbles, generally caused by faulty injection technique – can result in gas getting under the retina. (Reproduced with permission from Hilton GF, Tornambe PE, and the Retinal Detachment Study Group. Pneumatic retinopexy: an analysis of intraoperative and postoperative complications. Retina 1991;11:285–94.)

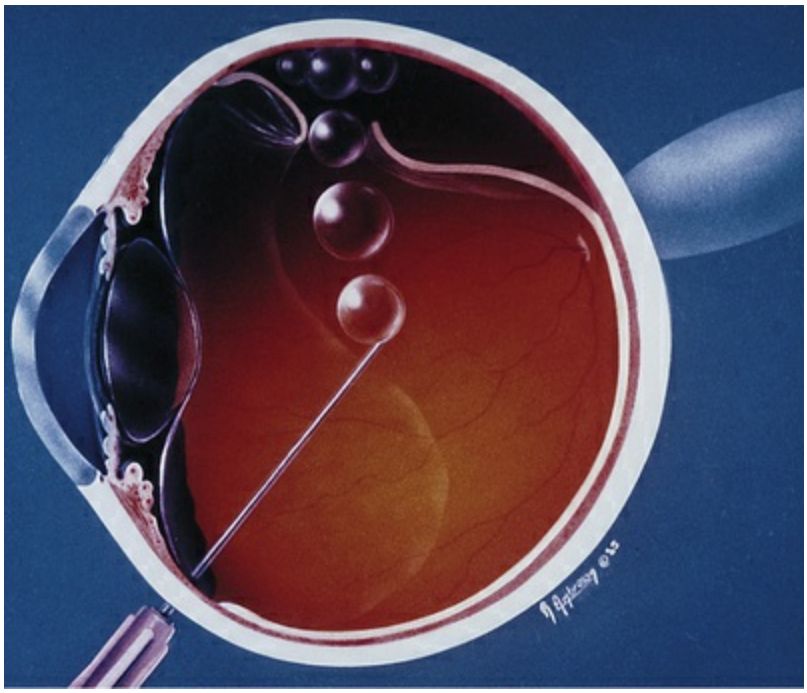

FIG. 107.5 How not to inject gas in the presence of detached retinal breaks. (Reproduced with permission from Hilton GF, Tornambe PE, and the Retinal Detachment Study Group. Pneumatic retinopexy: an analysis of intraoperative and postoperative complications. Retina 1991;11:285–94.)

1. Make sure that the needle tip is placed shallowly within the vitreous at the time of injection.

2. Make sure that the injection site is uppermost.

3. Inject moderately briskly (0.5–1.0 seconds).

4. Inject with the needle vertical.

If fish eggs do occur, the patient is strictly positioned to keep the bubbles away from retinal breaks. If all retinal breaks are small, this may not be necessary, but keep in mind that breaks can stretch a little. The bubbles usually coalesce spontaneously within 24 hours, and then the patient can adopt a position with the retinal break(s) uppermost.

Alternatively, the bubbles usually can be caused to coalesce by flicking the eye with a sterile cotton-tipped applicator or gloved finger. The eye is turned so that sclera without underlying retinal

breaks is uppermost, and then this site is flicked moderately firmly. Since it may not be possible to keep fish eggs away from superior breaks, this maneuver is especially important if large breaks are present in the superior several clock-hours. Impending macular detachment might also indicate this procedure or indicate a face-down position until the bubbles coalesce.

Gas Entrapment at the Injection Site

After gas injection, the head is turned to the opposite side and mobility of the gas is confirmed ophthalmoscopically. If the gas bubble remains trapped at the injection site, it is probably trapped in the canal of Petit (between the anterior hyaloid, the lens and zonules, and the pars plana epithelium). Typically, the gas trapped in this canal is visible peripherally behind the lens, forming a partial ring, variously described as the "bagel," "donut," or "sausage" sign (Fig. 107.6).

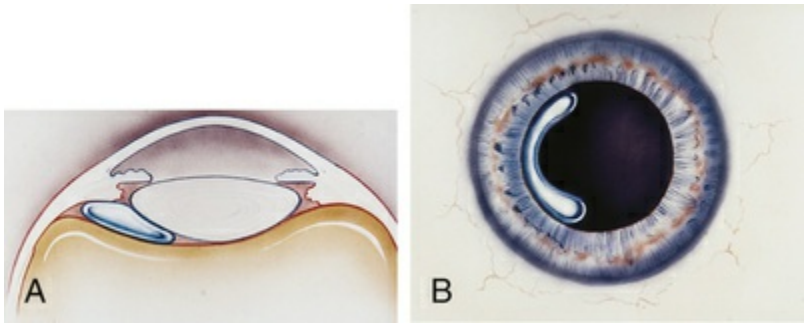

FIG. 107.6 Gas entrapment at the injection site. (A) Gas trapped in the canal of Petit (between the anterior hyaloid, the lens and zonules, and the pars plana epithelium). (B) Gas is visible peripherally behind the lens, forming a partial ring (the "sausage sign").

(Reproduced with permission from Hilton GF, Tornambe PE, and the Retinal Detachment Study Group. Pneumatic retinopexy: an analysis of intraoperative and postoperative complications. Retina 1991;11:285–94.)

If only a small amount of gas is trapped, no treatment is necessary. If most of the gas is trapped, the patient is advised to follow face-down positioning for 1 day. As the gas subsequently expands, it will generally break through and float up to the macula. Thereafter, the patient assumes the desired position with the retinal

break uppermost.

Waiting for trapped gas to break free may jeopardize an attached macula imminently threatened by detachment. A trapped bubble can be removed by passing a 27-gauge needle back through the injection site. This needle is mounted on a syringe without the plunger, containing a small amount of sterile saline solution. The entry site is positioned uppermost, and the needle passed vertically into the bubble. Sometimes it takes a little manipulation to break the surface tension of the bubble and get it to pass into the needle. Most of the gas will escape, bubbling up through the fluid in the syringe. At another site, the gas is reinjected deeper into the vitreous, with 4–5 mm of the needle in the globe. This procedure also may be indicated if trapped gas does not become mobile after face-down positioning, which may constitute the rare and potentially painful occurrence of gas trapped beneath the pars plana epithelium or in the choroid.[64,65]

Steamroller Technique

If bullous subretinal fluid extends almost to an attached macula, placement of a bubble against the bullous detachment peripherally may push fluid into the macula and cause it to detach.[66] This complication, as well as the impending threat of spontaneous macular detachment, usually can be avoided by the "steamroller" technique (Fig. 107.7).[67]

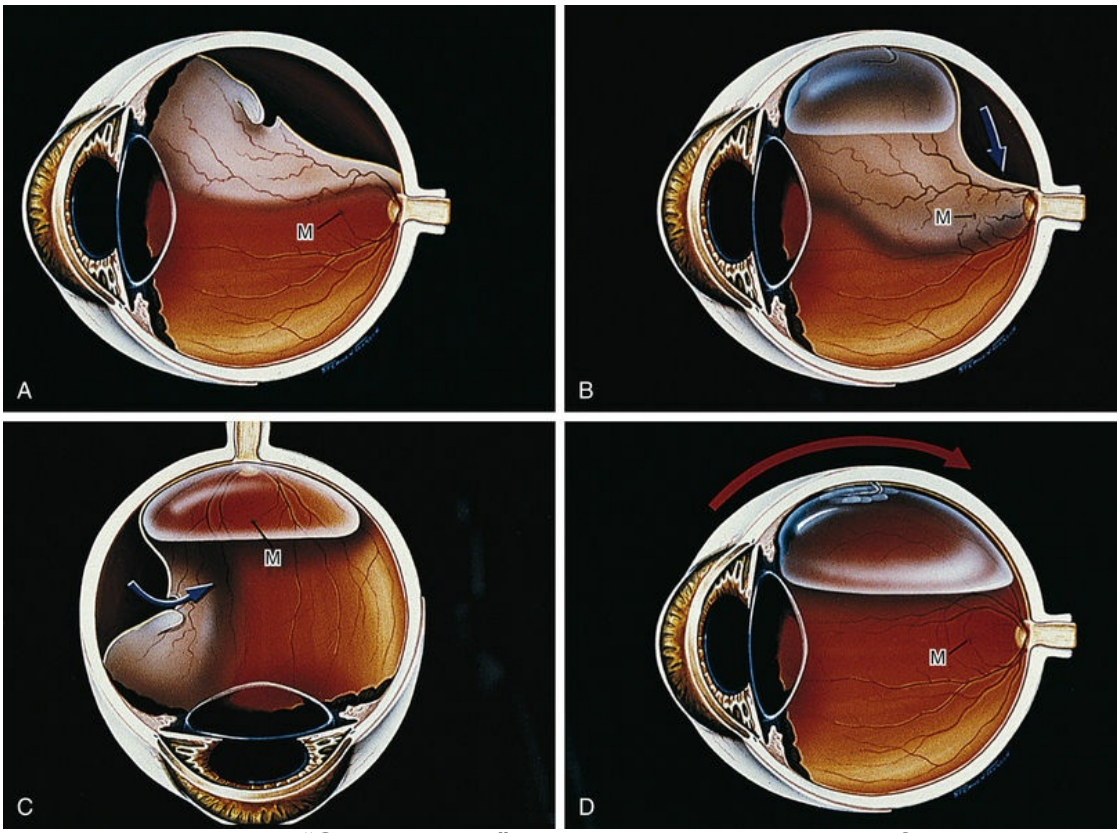

FIG. 107.7 "Steamroller" maneuver: prevention of iatrogenic macular detachment. (A) Bullous retinal detachment near an attached macula (*M*), indicating the "steamroller" maneuver. (B) What to avoid – the gas bubble may force subretinal fluid posteriorly (*arrow*), causing iatrogenic detachment of the macula. (C) Steamroller step 1 – iatrogenic macular detachment is prevented by placing the patient in a face-down position immediately following gas injection, making sure that the gas bubble traverses attached retina on its way to the macula. This frequently causes some subretinal fluid to pass through the break into the vitreous (*arrow*). (D) Steamroller step 2: over 1–10 minutes, the patient's head position is very gradually moved along the meridian between the macula and the retinal break (*arrow*) until the retinal break is uppermost. This causes the bubble to roll toward the retinal break, pushing the subretinal fluid away from the macula and back into the vitreous and flattening the retina. Cryopexy should generally not be performed before a steamroller maneuver. (Reprinted from Hilton GF, Kelly NE, Salzano TC, et al. Pneumatic retinopexy. A collaborative report of the first 100 cases. Ophthalmology 1987;94:307–14. ©1987, with permission from the American Academy of Ophthalmology.)

An injection site is selected in a meridian where the retina is attached. After injection of the gas bubble, the patient's head is placed face-down by turning the patient in a direction planned to ensure that the bubble traverses only attached retina en route to the macula. Over 1–10 minutes, the patient's head position is then gradually changed until the retinal break is uppermost, causing the bubble to roll from the macula toward the retinal break, pushing the subretinal fluid away from the macula and back into the vitreous, and flattening the retina. Because cryopexy causes liberation of pigment epithelial cells, which may cause PVR if they enter the vitreous cavity, cryopexy should generally not be performed before steamrolling.

Whether steamrolling is necessary to prevent macular detachment depends on several factors:

1. How close the detachment is to the macula (only detachments well within the arcades usually need steamrolling);

2. How bullous the detachment is; and

3. How large the gas bubble is.

Possible indications for steamrolling include the following:

1. Prevention of iatrogenic macular detachment.

2. Prevention of iatrogenic detachment of an attached retinal break.

3. Reduction of a bullous detachment overhanging the optic nerve, preventing visualization of the central retinal artery during the procedure.

4. Reduction of subretinal fluid to encourage more rapid resolution of retinal detachment (possibly of use in cases where all retinal breaks cannot be covered at one time by the gas bubble).

5. Avoidance of posterior gaping of the tear and subretinal gas in the presence of large retinal breaks (the extreme example of this being a somersault maneuver performed to unroll the inverted flap

of a giant retinal tear).

The movement of subretinal fluid into the vitreous has raised theoretical concerns about the production of PVR. However, two studies[68,69] showed no increase in PVR in steamrolled cases.

Summary of Procedure

The following constitutes the sequence of a typical pneumatic retinopexy procedure (see Fig. 107.3):

1. Anesthetic: topical/subconjunctival or retrobulbar.

2. Cryopexy to retinal tears: if one-session procedure, in lieu of laser.

3. Sterilization of ocular surface: povidone–iodine solution.

4. Paracentesis: limbal, or via pars plana if capsule is open.

5. Intravitreal gas injection: 0.4–0.6 mL of SF_6.

6. Second paracentesis and/or ocular compression: if needed to open central retinal artery.

7. Special procedures: e.g., steamroller if needed (cryopexy should not be performed before steamroller)Irrigate, apply antibiotic and patch: draw arrow.

8. Laser to retinal tears: next day or when retina is reattached (in lieu of cryopexy, as two-session procedure), with 360° peripheral laser if desired.

Postoperative Management

The patient is usually examined in the office on the first or second postoperative day, at which time the retina is usually reattached (Fig. 107.3E), although an occasional case may take an extra day or two. If the fluid is not reabsorbing, there may be a new or missed

break, traction may be keeping the break open, the bubble may be too small, or the patient may not have maintained proper positioning. The importance of proper positioning should be reemphasized.

Inferior subretinal fluid or loculated pockets of subretinal fluid on rare occasion will persist for weeks or months. As long as the fluid is not increasing, there are no detached retinal breaks, and the macula is attached, reoperation is not necessary.

As a general guideline, the patient is examined on about postoperative days 1 or 2, 5–7, and 14–21 and periodically thereafter, looking especially for new retinal breaks. If close follow-up results in early detection and treatment, these breaks do not jeopardize the final outcome.[8] At least half of these can be cured with an office procedure without resorting to vitrectomy or SB.

The gas bubble will reabsorb spontaneously (Fig. 107.3F). Until it does, the patient is advised against air travel because the lower atmospheric pressure in flight can cause expansion of the gas bubble with a marked increase in intraocular pressure. We recommend that activity be limited until the gas bubble is small. For example, jarring activities (such as jogging) and rapid head tilting (as with somersaults) are best avoided.

Results

In 1991 a compilation of 26 statistical series from seven countries including 1274 eyes treated with PR showed a single-operation success rate of 80%, with 98% cured with one or more operations.[18] More recently, Chan et al.[20] reviewed 81 published PR series from 1986 to 2007, totaling 4138 eyes. Single-operation success was 74.4%, and success with one or more operations was 96.1%. New retinal breaks occurred in 11.7% of eyes, and PVR occurred in 5.2% (Table 107.2).

TABLE 107.2

Summary of 81 Published Statistical Reports on Pneumatic Retinopexy, 1986–2007: Anatomic Results and Two Postoperative Complications

Reports (*n*)	Eyes (*n*)	Reattached	Complications		
		One Operation[a]	Reoperations	New Retinal Breaks	PVR
81	4138	74.4%	96.1%	11.7%	5.2%

[a]Some series included postoperative supplemental laser photocoagulation or cryotherapy.

PVR, postoperative proliferative vitreoretinopathy.

Reproduced with permission from Chan CK, Lin SG, Nuthi AS, et al. Pneumatic retinopexy for the repair of retinal detachments: a comprehensive review (1986–2007). Surv Ophthalmol 2008;53:443–78.

Tornambe[17] reviewed the causes of failure and concluded that pseudophakia/aphakia, detachment of >50% of the retina, and multiple retinal breaks adversely influence single-operation success. Several studies[9,70] have shown that initial failure with PR, subsequently requiring vitrectomy or SB, does not adversely affect the final visual outcome compared with vitrectomy or SB alone. Unsuccessful initial PR, SB, or vitrectomy can often be safely and effectively rescued with a subsequent PR procedure.[71]

Comparison of PR With Scleral Buckle

The multicenter, randomized controlled clinical trial compared PR and SB in 198 eyes, establishing two statistically similar groups with similar preoperative visual acuity. The conclusions of the study include the following:[8]

1. Postoperative morbidity was less and had a shorter duration in the PR group.

2. Postoperative visual acuity was significantly better with PR than with SB for eyes in which the macula was detached for up to 2 weeks (p=.05). In this group, 80% of the PR patients regained 20/50 or better vision, compared with only 56% of SB patients.

3. With one operation and with occasional postoperative cryotherapy or laser supplementation, retinal reattachment was 84% in the SB group and 81% in the PR group. This difference was not statistically significant. However, subsequent studies have confirmed a modestly higher single-operation success rate with SB.[72]

4. With reoperations, the final reattachment rate was 98% in the SB group and 99% in the PR group, also not a statistically significant difference. Subsequent studies have confirmed comparable final reattachment rates.[72]

5. Complications were similar, based on a score system that weighted heavily the need for postoperative laser or cryotherapy.

6. Cataract surgery was required four times more often after SB than after PR.

7. New and missed retinal breaks occurred more frequently after PR but did not usually produce an unfavorable outcome. New and missed retinal breaks after SB had the worst prognosis, requiring more extensive reoperation with decreased visual results.

8. An open or absent posterior capsule was associated with an equally lower single-operation success rate in both groups.

9. Postoperative proliferative vitreoretinopathy occurred in 5% in the SB group and 3% in the PR group (not a statistically significant difference).

Comparison of PR With Vitrectomy

Unfortunately, similar prospective data for a direct comparison of PR to primary vitrectomy are unavailable. As SB has declined in favor among retinal surgeons, vitrectomy for primary rhegmatogenous retinal detachment has gained tremendous popularity in recent years,[73,74] driven by continual advances in vitreoretinal instrumentation, microincisional techniques, endoillumination, and wide-field viewing systems. Similar to PR, vitrectomy avoids some of the morbidity more frequently associated with SB, such as induced myopia. Unlike PR, it tends to induce cataract and demands the time and expense associated with an operating room procedure.

Vitrectomy presents advantages in some circumstances where PR is inadequate. It is the procedure of choice in dealing with significant PVR and vitreoretinal traction, and it may be ideal when

vitreous or capsular opacity causes poor visualization. By facilitating placement of a large gas bubble, vitrectomy shares with SB the ability to treat inferior and widely spread breaks.

Because vitrectomy tends to induce cataract, it is used most commonly in pseudophakic eyes. Tiny breaks, common in pseudophakic eyes, may be most readily identified by internal search during vitrectomy. In a multicenter clinical trial of SB versus primary vitrectomy for rhegmatogenous retinal detachment,[75] vitrectomy yielded significantly better single-operation success rates than SB in pseudophakic eyes, but no difference in final vision. In phakic eyes, vitrectomy yielded poorer visual results than SB with no benefit in single-operation success.

In the more simple cases appropriate for PR, especially in phakic patients, PR may be preferable to vitrectomy or SB.

Complications

Fish eggs, gas entrapment, and iatrogenic macular detachment are discussed under "Special procedures" above. Other intraoperative complications of PR are minimal. A number of postoperative complications have been noted in the literature, but most of these occur with an incidence of less than 2% (Table 107.3). The two major concerns are PVR and new or missed retinal breaks. The management of subretinal gas also warrants discussion.

TABLE 107.3

Postoperative Complications[a] in 565 Eyes in 10 Series[b]

	Eyes	
	n	(%)
OPERATIVE		
Incarceration of vitreous	8	1.4
Subconjunctival gas	6	1.1
POSTOPERATIVE		
New or missed breaks	75	13.3
PVR	26	4.6
Redetachment	17	3.0
Mild macular pucker	10	1.8
Persistent subretinal fluid	12	2.1
Minimal epiretinal membrane	8	1.4
Reopening of original break	6	1.1

Vitreous haze, 3–8 days	6	1.1

[a]Complications of 0.3–1.0% omitted: choroidal detachment, anterior gas entrapment, vitreous hemorrhage, subretinal gas, shift of subretinal fluid, and macular hole. Complications, one case each (0.2%): peripheral subretinal hemorrhage, hyphema, pars plana detachment, cataract, malignant glaucoma, and endophthalmitis.

[b]See references 5, 8, 33, 35, 40, 41, 67, 76–78.

PVR, postoperative proliferative vitreoretinopathy.

Proliferative Vitreoretinopathy

PVR is the major complication for all types of retinal reattachment surgery. A review of the PR literature revealed an incidence of 4% (Table 107.2). PVR developed in 3% of eyes managed with PR compared with 5% in the SB control group in the multicenter clinical trial.[8] Evidence does not support the concern that intravitreal gas might stimulate PVR.

New or Missed Retinal Breaks

The incidence of new and missed retinal breaks in a compilation of 81 series including 4138 eyes treated with PR was 11.7% (Table 107.2). Remarkably, this is less than the 14% figure reported in a study of 171 eyes with retinal breaks without significant retinal detachment, treated with laser photocoagulation or cryopexy but without gas injection.[79] This and other evidence suggests that intravitreal gas plays little role in causing new retinal breaks and underscores that the natural history of the disease includes the rather frequent development of additional breaks. The most common cause of detachment requiring reoperation following pneumatic retinopexy appears to be development of a new retinal break with new rather than persistent retinal detachment.[80]

In long-term follow-up, the need for reoperation is evident within the first 3 months in 89% of cases.[19] With or without gas, the majority of new breaks appear within the first postoperative month, suggesting that incomplete posterior vitreous detachment may be responsible for some postoperative breaks.[8,79] In phakic eyes with complete rather than partial posterior vitreous detachment, as determined by B-scan ultrasonography, Rezende et al.[42] reported a higher rate of single-operation retinal reattachment, particularly in

eyes treated with PR.

Since PR failures are sometimes caused by new retinal breaks in untreated areas of the retina, Tornambe has recommended that 360° laser retinopexy be applied between the insertion of the vitreous base and the ora serrata.[17] He reported a significant improvement in single-operation success with this approach, but only about 1 in 12 PR surgeons employs this technique.[81]

New retinal breaks following pneumatic retinopexy do not portend a poor outcome. Some 96% of such eyes were successfully treated in the multicenter trial.[9] New retinal detachments following pneumatic retinopexy do not necessarily require vitrectomy or scleral buckling and can often be treated by a repeat pneumatic procedure alone.

Subretinal Gas

Subretinal gas is usually a preventable complication, as described above (see under "Fish eggs"). However, if gas does get under the retina, the bubble can generally be teased back through the break if the break is larger than the gas bubble or if the diagnosis is made promptly before gas expansion. Under indirect ophthalmoscopic visualization, scleral depression is used to maneuver the bubble to the break and force it through.

If this fails but the amount of subretinal gas is small relative to the intravitreal gas, it may not be necessary to remove the subretinal gas. In this instance, strict prolonged positioning may still resolve the detachment since the intravitreal gas will outlast the subretinal gas. Larger amounts of subretinal gas can be removed with a needle passed through the sclera and into the subretinal space, similar to the technique described above in the section "Gas entrapment at the injection site." Rarely, vitrectomy may be indicated to remove the gas.

Utilization of Pneumatic Retinopexy

In a 2002 survey of the American Society of Retinal Specialists (then called the "Vitreous Society"), 72% of respondents selected PR for a phakic macula-on detachment with a 12 : 00 tear, and PR was also

the most commonly selected option if the eye was pseudophakic (45% for PR versus 13% for primary vitrectomy).[81] However, acceptance of PR in Europe has lagged far behind that in the United States.[82,83] Gains in popularity of vitrectomy have been mostly at the expense of scleral buckling. A 2010 analysis of Medicare claims showed that vitrectomies for primary retinal detachment increased 72% from 1997 to 2007, while SB decreased 69% and PR remained relatively unchanged.[73] According to a 2015 survey, microincisional vitrectomy is now performed more frequently than PR or SB in pseudophakic eyes.[84]

While treatment of retinal detachment is extremely cost-effective regardless of treatment modality,[85] significant cost savings could be achieved while maintaining anatomic and visual outcomes by increasing utilization of PR.[86]

Algorithm for Choosing PR Versus Other Procedures for Retinal Detachments

In *Retinal Detachment: Principles and Practice*, Brinton and Wilkinson[1] presented an algorithm (Fig. 107.8) intended to organize the decision of type of surgery to use for a given retinal detachment case. This algorithm does not reflect all factors that may influence a decision. The individual circumstances of each specific patient, as well as the experience of the surgeon and the availability of equipment, should also be taken into account. This algorithm provides guidelines reflecting the opinion of the authors and is not intended to establish the standard of care for a given case.

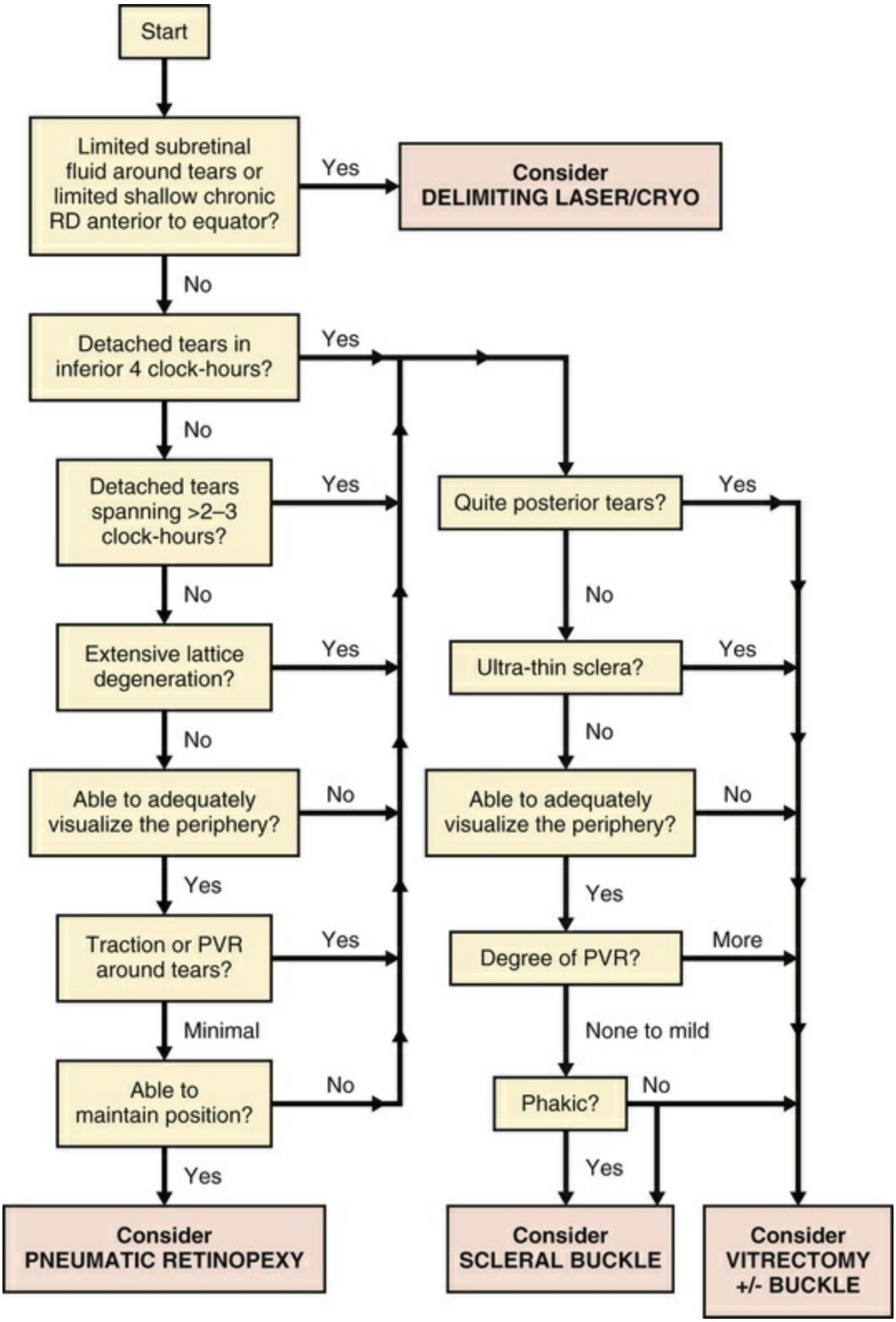

FIG. 107.8 Algorithm demonstrating an approach to selection of an appropriate retinal reattachment procedure. *PVR,* proliferative vitreoretinopathy; *RD,* retinal detachment. (Reprinted from Brinton DA, Wilkinson CP. Retinal detachment: principles and practice. 3rd ed. New York: Oxford University Press/American Academy of Ophthalmology ©2009, with permission from Oxford

Conclusion

Pneumatic retinopexy (PR) may be the procedure of choice for selected uncomplicated retinal detachments without inferior or extensive retinal breaks or significant proliferative vitreoretinopathy. New retinal breaks or detachments following PR can also frequently be managed just by laser or repeat pneumatic techniques. PR requires thorough preoperative evaluation, skillful case selection, diligent postoperative positioning, and close follow-up.

Evidence shows that in selected cases, PR gives better visual results and minimizes morbidity at considerably decreased expense compared with vitrectomy and/or scleral buckling. PR yields a modestly lower single-operation success rate than these procedures, but PR failure does not jeopardize success if subsequent procedures are needed.

References

1. Brinton DA, Wilkinson CP. *Retinal detachment: principles and practice*. 3rd ed. Oxford University Press/American Academy of Ophthalmology: New York; 2009.
2. Lincoff H, Kreissig I, Goldbaum M. Reasons for failure in non-drainage operations. *Mod Probl Ophthalmol*. 1974;12:40–48.
3. Rachal WF, Burton TC. Changing concepts of failures after retinal detachment surgery. *Arch Ophthalmol*. 1979;97:480–483.
4. Wilkinson CP. Surgery for retinal detachment. Iliff NT. *Complications in ophthalmic surgery*. Churchill Livingstone: New York; 1983.
5. Hilton GF, Grizzard WS. Pneumatic retinopexy: a two-step outpatient operation without conjunctival incision. *Ophthalmology*. 1986;93:626–641.
6. Ai E, Gardner TW. Current patterns of intraocular gas use

in North America. *Arch Ophthalmol*. 1993;111:331–332.
7. Benson WE, Chan P, Sharma S, et al. Current popularity of pneumatic retinopexy. *Retina*. 1999;19:238–241.
8. Tornambe PE, Hilton GF, the Retinal Detachment Study Group. Pneumatic retinopexy: a multicenter, randomized, controlled clinical trial comparing pneumatic retinopexy with scleral buckling. *Ophthalmology*. 1989;96:772–783.
9. Tornambe PE, Hilton GF, Brinton DA, et al. Pneumatic retinopexy: a two-year follow-up study of the multicenter clinical trial comparing pneumatic retinopexy with scleral buckling. *Ophthalmology*. 1991;98:1115–1123.
10. Ohm J. Uber die Behandlung der Netzhautablosung durch operative Entleerung der subretinalen Flussigkeit und Einspritzung von Luft in den Glaskoper. *Graefes Arch Clin Exp Ophthalmol*. 1911;79:442–450.
11. Rosengren B. Results of treatment of detachment of the retina with diathermy and injection of air into the vitreous. *Acta Ophthalmol*. 1938;16:573–579.
12. Norton EW. Intraocular gas in the management of selected retinal detachments. *Trans Am Acad Ophthalmol Otolaryngol*. 1973;77:85–98.
13. Blodi CF, Folk JC. Treatment of macular hole retinal detachments with intravitreal gas. *Am J Ophthalmol*. 1984;98:811.
14. Dominguez DA, Boyd BF, Gordon S. Repeated insufflation of expansive gas. *Highlights Ophthalmol Lett*. 1986;14:1–14.
15. Dominguez DA, Fonseca A, Gomez-Montana J. *Gas tamponade for ambulatory treatment of retinal detachment*. [In: Proceedings of the 25th International Congress of Ophthalmology, Rome, May 4–10, 1986. Amsterdam: Kugler and Ghedini] 1987.
16. Lincoff H, Kreissig I, Hahn YS. A temporary balloon buckle for the treatment of small retinal detachments. *Ophthalmology*. 1979;86:586–592.
17. Tornambe P. Pneumatic retinopexy: the evolution of case selection and surgical technique – a 12-year study of 302 eyes. *Trans Am Ophthalmol Soc*. 1997;95:551–578.
18. Hilton GF, Tornambe PE, the Retinal Detachment Study

Group. Pneumatic retinopexy: an analysis of intraoperative and postoperative complications. *Retina*. 1991;11:285–294.
19. Eter N, Böker T, Spitznas M. Long-term results of pneumaticretinopexy. *Graefes Arch Clin Exp Ophthalmol*. 2000;238:677–681.
20. Chan CK, Lin SG, Nuthi AS, et al. Pneumatic retinopexy for the repair of retinal detachments: a comprehensive review (1986–2007). *Surv Ophthalmol*. 2008;53:443–478.
21. Sebag J, Tang M. Pneumatic retinopexy using only air. *Retina*. 1993;13:8–12.
22. DeJuan E Jr, McCuen B, Tiedeman J. Intraocular tamponade and surface tension. *Surv Ophthalmol*. 1985;30:47–51.
23. Machemer R. The importance of fluid absorption, traction, intraocular currents, and chorioretinal scars in the therapy of rhegmatogenous retinal detachments. *Am J Ophthalmol*. 1984;98:681–693.
24. Braker W, Mossman AL. *Matheson gas book*. Matheson Gas Products: Secaucus, NJ; 1980.
25. Fineberg B, Machemer R, Sullivan P, et al. Sulfur hexafluoride in the owl monkey vitreous cavity. *Am J Ophthalmol*. 1975;79:67–76.
26. Panessa-Warren B, Maisel JM, Warren J. Alterations in rabbit vitreal fine structure following C3F8 injection. *Graefes Arch Klin Exp Ophthalmol*. 1990;228:541–551.
27. Lincoff H. Results and complications of pneumatic retinopexy. [discussion of Chen JC, Robertson JE, et al] *Ophthalmology*. 1988;95:601–608.
28. Lincoff H, Coleman J, Kreissig I, et al. The perfluorocarbon gases in the treatment of retinal detachment. *Ophthalmology*. 1983;90:546–551.
29. Mougharbel M, Koch FHJ, Boker T, et al. No cataract two years after pneumatic retinopexy. *Ophthalmology*. 1994;101:1191–1194.
30. Parver LM, Lincoff H. Geometry of intraocular gas used in retinal surgery. *Mod Probl Ophthalmol*. 1977;18:338–343.
31. Retina Society Terminology Committee. The classification of retinal detachment with proliferative vitreoretinopathy. *Ophthalmology*. 1983;90:121–125.

32. McAllister IL, Zegarra H, Meyers SM, et al. Treatment of retinal detachments with multiple breaks by pneumatic retinopexy. *Arch Ophthalmol*. 1987;105:913–916.
33. Tornambe PE, Hilton GF, Kelley NF, et al. Expanded indications for pneumatic retinopexy. *Ophthalmology*. 1988;95:597–600.
34. Irvine AR, Lahey JM. Pneumatic retinopexy for giant retinal tears. *Ophthalmology*. 1994;101:524–528.
35. Friberg TR, Eller AW. Pneumatic repair of primary and secondary detachments using a binocular indirect ophthalmoscope laser delivery system. *Ophthalmology*. 1988;95:187–193.
36. Hwang JF, Chen SN, Lin CJ. Treatment of inferior rhegmatogenous retinal detachment by pneumatic retinopexy technique. *Retina*. 2011;31:257–261.
37. Chang TS, Pelzek CD, Nguyen RL, et al. Inverted pneumatic retinopexy: A method of treating retinal detachments associated with inferior retinal breaks. *Ophthalmology*. 2003;110:589–594.
38. Hilton GH, Josephberg RG, Halperin LS, et al. Office-based sutureless transconjunctival pars plana vitrectomy. *Retina*. 2002;22:725–732.
39. Kulkarni KM, Roth DB, Prenner JL. Current visual and anatomic outcomes of pneumatic retinopexy. *Retina*. 2007;27:1065–1070.
40. Chen JC, Robertson JE, Coonan P, et al. Results and complications of pneumatic retinopexy. *Ophthalmology*. 1988;95:601–608.
41. McAllister IL, Meyers SM, Zegarra H, et al. Comparison of pneumatic retinopexy with alternative surgical techniques. *Ophthalmology*. 1988;95:877–883.
42. Rezende FA, Kapusta MA, Burnier MN Jr, et al. Preoperative B-scan ultrasonography of the vitreoretinal interface in phakic patients undergoing rhegmatogenous retinal detachment repair and its prognostic significance. *Graefes Arch Clin Exp Ophthalmol*. 2007;245:1295–1301.
43. Hendrikse F. Pneumatic retinopexy to treat optic nerve pits and retinal detachments. *Vitreoretinal Surg Technol*. 1991;3:1–

2.
44. McDonald HR, Schatz H, Johnson RN. Treatment of bullous rhegmatogenous retinal detachment associated with optic pits. *Int Ophthalmol Clin*. 1992;32:35–42.
45. Friberg TR, Eller AW. Laser pneumatic retinopexy for repair of recurrent retinal detachment after failed scleral buckle – ten years experience. *Ophthalmic Surg Lasers*. 2001;32:13–18.
46. Sharma T, Badrinath SS, Mukesh BN, et al. A multivariate analysis of anatomic success of recurrent retinal detachment treated with pneumatic retinopexy. *Ophthalmology*. 1997;104:2014–2017.
47. Friberg TR. *Laser photocoagulation to produce chorioretinal adhesion*. [Paper presented at the Second International Conference on Pneumatic Retinopexy, Tampa, FL, October 6] 1989.
48. Folk JC, Sneed SR, Folberg R, et al. Early retinal adhesion from laser photocoagulation. *Ophthalmology*. 1989;96:1523–1525.
49. Campochiaro PA, Kaden IH, Vidaurri-Leal J, et al. Cryotherapy enhances intravitreal dispersion of viable retinal pigment epithelial cells. *Arch Ophthalmol*. 1985;103:434–436.
50. Cowley M, Conway BP, Campochiaro PA, et al. Clinical risk factors for proliferative vitreoretinopathy. *Arch Ophthalmol*. 1989;107:1147–1151.
51. Grizzard WS, Hilton GF, Hammer ME, et al. A multivariant analysis of anatomic success of retinal detachments treated with scleral buckling. *Graefes Arch Clin Exp Ophthalmol*. 1994;232:1–7.
52. Speaker MG, Menikoff JA. Prophylaxis of endophthalmitis with topical povidone-iodine. *Ophthalmology*. 1991;98:1769–1775.
53. Eckardt C. Staphylococcus epidermidis endophthalmitis after pneumatic retinopexy. *Am J Ophthalmol*. 1987;103:720–721.
54. Sharma T. Post-pneumatic retinopexy endophthalmitis: management of infection and persistent retinal detachment. *Ophthalmic Surg Lasers Imaging*. 2010;9:1–2.

55. Packo KH. *Gas injection techniques*. [Paper presented at the Second International Conference on Pneumatic Retinopexy, Tampa, FL, October 6] 1989.
56. Humayun MS, Yeo JH, Koski WS, et al. The rate of sulfur hexafluoride escape from a plastic syringe. *Arch Ophthalmol*. 1989;107:853–854.
57. Jun AS, Pieramici DJ, Bridges WZ. Clear corneal cataract wound dehiscence during pneumatic retinopexy. *Arch Ophthalmol*. 2000;118:847–848.
58. Bock J, Bornschein H, Hommer K. Die Wiederbelebungszeit der menschlichen Netzhaut: eine elektroretinographische Studie. *Graefes Arch Klin Exp Ophthalmol*. 1963;165:437–451.
59. Foulds WS, Johnson NF. Rabbit electroretinogram during recovery from induced ischaemia. *Trans Ophthalmol Soc U K*. 1974;94:383–393.
60. Fujino T, Hamasaki DI. Effect of intraocular pressure on the electroretinogram. *Arch Ophthalmol*. 1967;78:757–765.
61. Popp C. Die Retinafunktion nach intraocularer Ischamie. *Graefes Arch Klin Exp Ophthalmol*. 1955;156:395–403.
62. Vassileva PL, Dabov SB. Changes in the glycogen content and the electroretinogram in retinal ischaemia experimentally induced in rabbits. Cant JS. *Vision and circulation: Proceedings of the Third William Mackenzie Memorial Symposium*. Kimpton: London; 1976.
63. Shaffer RN. *Paper presented in discussion at the American Ophthalmological Society*. [Hot Springs, VA, March 19–22] 1985.
64. Baker SR, Hainsworth DP. Suprachoroidal gas as a complication of pneumatic retinopexy. *Retina*. 2000;20:224–225.
65. Jabaly-Habib HY, et al. Prolonged pain following unintentional injection of gas into the suprachoroidal space during pneumatic retinopexy. *Retina*. 2003;23:722–723.
66. Yeo JH, Vidaurri-Leal J, Glaser BM. Extension of retinal detachments as a complication of pneumatic retinopexy. *Arch Ophthalmol*. 1986;104:1161–1163.
67. Hilton GF, Kelly NE, Salzano TC, et al. Pneumatic retinopexy: a collaborative report of the first 100 cases.

Ophthalmology. 1987;94:307–314.
68. Tornambe PE, Hilton GF. The steamroller maneuver and proliferative vitreoretinopathy (Correspondence). *Arch Ophthalmol*. 1992;110:15.
69. Yanyali A, Horozoglu F, Bayrak YI, et al. Steamroller versus basic technique in pneumatic retinopexy for primary rhegmatogenous retinal detachment. *Retina*. 2007;27:74–82.
70. Ambler JS, Meyers SM, Zegarra H, et al. Reoperations and visual results after failed pneumatic retinopexy. *Ophthalmology*. 1990;97:786–790.
71. Petrushkin HJ, Elgohary MA, Sullivan PM. Rescue pneumatic retinopexy in patients with failed primary retinal detachment surgery. *Retina*. 2015;35(9):1851–1859.
72. Saw SM, Gazzard G, Wagle AM, et al. An evidence-based analysis of surgical interventions for uncomplicated rhegmatogenous retinal detachment. *Acta Ophthalmol Scand*. 2006;84:606–612.
73. Ramulu PY, Do DV, Corcoran KJ, et al. Use of retinal procedures in Medicare beneficiaries from 1997 to 2007. *Arch Ophthalmol*. 2010;128:1335–1340.
74. Minihan M, Tanner V, Williamson TH. Primary rhegmatogenous retinal detachment: 20 years of change. *Br J Ophthalmol*. 2001;85:546–548.
75. Heimann H, Bartz-Schmidt KU, Bornfeld N, et al. Scleral buckling versus primary vitrectomy in rhegmatogenous retinal detachment: a prospective randomized multicenter clinical study. *Ophthalmology*. 2007;114:2142–2154.
76. Algvere P, Hallnas K, Palmquist BM. Success and complications of pneumatic retinopexy. *Am J Ophthalmol*. 1988;106:400–404.
77. Lowe MA, McDonald HR, Campo RV, et al. Pneumatic retinopexy: surgical results. *Arch Ophthalmol*. 1988;106:1672–1676.
78. van Effenterre G, Abi-Rached J, Vachet JM, et al. Utilisation exclusive d'une injection de gaz dans le traitement de certain decollements de retine. *Ophtalmologie*. 1987;2:209–212.
79. Smiddy WE, Flynn HW, Nicholson DH, et al. Results and

complications in treated retinal breaks. *Am J Ophthalmol*. 1991;112:623–631.
80. Mudvari SS, Ravage ZB, Rezaei KA. Retinal detachment after primary pneumatic retinopexy. *Retina*. 2009;29:1474–1478.
81. Pollack JS, Packo KH. *American Society of Retina Specialists Preferences and Trends Survey*. http://www.asrs.org/http://www.asrs.org; 2002.
82. Laqua H, Honnicke K. Is scleral buckling still current? *Ophthalmology*. 2001;98:881–885.
83. Assi AC, Charteris DG, Gregor ZJ. Practice patterns of pneumatic retinopexy in the United Kingdom. *Br J Ophthalmol*. 2001;85:244.
84. Stone TW. *American Society of Retina Specialists Preferences and Trends Membership Survey*. [editor] http://www.asrs.org; 2015.
85. Chang JS, Smiddy WE. Cost-effectiveness of retinal detachment repair. *Ophthalmology*. 2014;121(4):946–951.
86. Goldman DR, Shah CP, Heier JS. Expanded criteria for pneumatic retinopexy and potential cost savings. *Ophthalmology*. 2014;121(1):318–326.

108

Special Adjuncts to Treatment

Ian Y. Wong, David Wong

Introduction

The first use of intraocular gas in treating retinal detachment dates back a century.[1] At that time, the causal relationship between retinal break and detachment was not fully appreciated. It was only later, when the importance of localization and sealing of retinal breaks was recognized, that the concept of air injection was introduced.[2] Rosengren described his technique of internal tamponade with air after subretinal fluid (SRF) drainage, coupled with external diathermy to create adhesion, and demonstrated an increase in success rate in retina detachment repair.[2] The technique of scleral buckling was introduced in the 1950s and in the 1960s, complicated retinal detachments were treated with a combination of scleral

buckling and intraocular gas injection.[3] As air is absorbed quickly, other longer-lasting gases were sought.[4] Sulfur hexafluoride and the perfluorocarbons have proved themselves to be the most popular intraocular gases. In the 1980s, pneumatic retinopexy was first introduced by Lincoff, and later popularized by Hilton and Grizzard.[5] It was made possible with the use of expansile gases and this procedure obviated the need for scleral buckling for some patients. More significantly, pneumatic retinopexy transformed retinal detachment surgery from an inpatient operation to an office-based procedure that has a reasonably high reattachment rate in selected patients. With the advent of vitrectomy,[6] the use of intraocular gas became indispensable. The combination of closed three-port pars plana microsurgical approach with long-acting gases improved the success rates especially for the more complicated situations such as proliferating vitreoretinopathy and giant tears. Indication for intraocular gas extended to macular hole repair and pneumatic displacement of submacular hemorrhage. There are surgeons who would argue that vitrectomy and gas are used in cases that might equally be treated with scleral buckling. The findings of randomized trials do little to change this trend.[7]

Physical Properties of Intraocular Gases

The properties of an ideal intraocular gas are listed in Box 108.1. In reality, no single gaseous product has all the desired properties. A variety of gaseous products have been investigated for intraocular use.[8–12] It is good to understand the different characteristics of the available products so that we as surgeons can make rational choices. Of interest to the clinician are the longevity inside the eye, expansion ratio in pure form, and the nonexpansile concentration. Gases could be used in their pure forms, or as a mixture with air. The expansile property could be adjusted by mixing the pure form with air in different proportions (Table 108.1). In daily practice, air, sulfur hexafluoride (SF_6), perfluoroethane (C_2F_6), and perfluoropropane (C_3F_8) are most commonly used. Table 108.2 highlights the physical properties of these gases. Historically, xenon was used for its shortest intraocular longevity.

Box 108.1

Properties of an Ideal Intraocular Gas

Availability

- Readily available
- Cheap/not expensive

Biocompatibility and safety

- Nontoxic
- Odorless
- Colorless
- Inflammable
- Not cause lens opacity

Variability in terms of longevity and expansile property

- Water soluble

Stable when mixed with air

TABLE 108.1
Gases Investigated for Intraocular Use

Nonexpansile	Expansile
Air	Sulfur hexafluoride (SF_6)
Xenon (Xe)	Perfluoromethane (CF_4)
Nitrogen (N_2)	Perfluoroethane (C_2F_6)
Helium (He)	Perfluoropropane (C_3F_8)
Oxygen (O_2)	Perfluorobutane (C_4F_{10})
Argon (Ar)	Perfluoropentane (C_5F_{12})
Krypton (Kr)	Octafluorocyclobutane (C_4F_8)

Carbon dioxide (CO_2)	

TABLE 108.2
Physical Properties of Commonly Used Intraocular Gases

	Chemical Formula	Molecular Weight (g/mol)	Odorless	Colorless	Inflammable	Inert	Expansion (Times Original Size)
Air	–	29	Yes	Yes	Yes	Yes	–
Xenon	Xe	131	Yes	Yes	Yes	Yes	–
Sulfur hexafluoride	SF_6	146	Yes	Yes	Yes	Yes	2.0
Perfluoroethane	C_2F_6	138	Yes	Yes	Yes	Yes	3.3
Perfluoropropane	C_3F_8	188	Yes	Yes	Yes	Yes	4.0

Air was the initial gas to be tried in retinal surgeries. If the vitreous cavity is entirely filled with air, then the bubble does not dissolve or disappear for 5–7 days. It is nonexpansile for all intent and purposes. This is not a drawback but rather an advantage. In Europe, air is often used in conventional scleral buckling surgery. SRF is drained first, followed by the injection of air. This effectively restores the anatomy, in that the retina becomes reapposed to the underlying retinal pigment epithelium and choroid. Cryotherapy can then be applied. The application can be precise and limited as there is no need for a large ice-ball or to freeze through a depth of SRF. Equally, localization of the retina break can be precise. The scleral buckle need only be as low profile as the retinal break/breaks, as the retina is already attached.[13] Air injection is useful in three specific ways. First, the intraocular pressure (IOP) is restored after air injection. Secondly, the surface tension of the air bubble enables the retina to be kept opposed and attached (had saline been injected instead, the liquid might go through the retinal breaks and the retina might redetach again). Thirdly, air is nonexpansile. This eliminates the concern about causing traction to the inferior retina and new break formation. This last point is not often appreciated. The use of air combined with scleral buckling is highly popular in Europe. There are many complications, including the break-up of the air bubble into "fish eggs" by poor injection techniques. Inferior breaks, however, is not one of the complications noted, despite a large number of publications on this

technique.[14] This is in contrast to pneumatic retinopexy. The fact that the bubble expands may cause further collapse of the gel with trans-gel traction. Because the gas bubble floats, this trans-gel traction is transmitted to the vitreous base inferiorly to give rise to inferior retinal breaks.[15] The fact that air does not expand makes it uniquely safe when combined with scleral buckling in nonvitrectomized eyes. Air has also enjoyed a resurgence of popularity when combined with vitrectomy. The success of retinal detachment relies on identification of all offending retinal breaks and sealing them. With the increasing use of endolaser, it is generally acknowledged that adhesion can develop much more quickly. Hence, there is therefore reduced need for prolonged tamponade. The duration of tamponade from a gaseous bubble only needs to be long enough for chorioretinal adhesion to develop. In the absence of any risk factors for developing proliferative vitreoretinopathy and when the causative retinal breaks are confined to 1 or 2 clock-hours, air is a perfectly acceptable tamponade.[16] The rapid absorption is an advantage. It simply means that the patients can be rehabilitated quicker and that they can travel by air sooner.

When the retinal breaks are multiple and their locations widely separated (in terms of clock-hours), then it would be desirable to have a large postoperative bubble. Long duration of tamponade is not particularly needed if proliferative vitreoretinopathy (PVR) is not anticipated. Sulphur hexafluoride (SF_6) in these cases might be suitable. The nonexpansile concentration of SF_6 is 20%. As a rule of thumb, if the vitreous cavity were totally filled, a bubble of 20% SF_6/air would last for about 2 weeks.[17] The bubble would be relatively large in the first few days to give a sufficiently large area of tamponade to widely separated retinal breaks. SF_6 is seldom used neat. It is inert, nontoxic, colorless, and is five times heavier than air. Hydrolysis only occurs at high temperatures (>500 °C). We will discuss the choice of tamponade agents later in this chapter.

The perfluorocarbon gases have the generic chemical formula (C_xF_{2x+2}, where x can be 1 to 4). These are inert gases with no odor or color. Water solubility varies according to the carbon chain length. The longer the carbon chain, the lower the solubility in water, hence

the longer is the intraocular longevity. For instance as a rough guide, 1 mL of pure C_2F_6 expands 3.3 times when injected into the eye, and stays in the eye for 4–5 weeks; but for 1 mL of C_3F_8, the same volume expands four times, and stays for 6–8 weeks.

When a gas bubble is injected into the eye, two forces act on the gas bubble. There is a downward force caused by gravity, and there is an upward force generated by buoyancy. Gravity equals the weight of the intraocular gas. Archimedes' Principle states that any floating object displaces its own weight of fluid. For instance, 1 mL of C_3F_8 weighs 0.001 g. Hence 1 mL of C_3F_8 displaces 1 mL of fluid, which weighs 1 g (specific gravity of water is 1.0). Therefore buoyancy is 1 g upwards (1 g equals 0.0098 Newton; gram is used here for ease of understanding). Net weight acting on the C_3F_8 bubble is therefore 0.999 g (i.e., 1 g buoyancy minus 0.001 g gravity). This force is pushing the bubble upwards. In terms of magnitude, this upward force is large compared with that of a silicone oil (SO) bubble. This upward force is the same order of magnitude as the downward force associated with perfluorocarbon liquids, with a specific gravity close to 2 g/mL. The orthodoxy is that perfluorocarbon liquid (PFCL) is too heavy to be left in the eye, as this may cause retinal damage.[18] It is interesting that no one speaks of gas bubbles pressing too hard and causing toxic changes to the upper retina.[19]

The classical concept of tamponade is that the bubble makes contact with the retina and prevents water from gaining access to the subretinal space via the retinal breaks. The interfacial tension between water and gas is high. The bubble therefore wants to stay as one bubble, and it would not go through a small aperture such as a retinal break. To do so, it would need to deform. The bubble would need to assume a smaller radius, and this would require higher surface energy.

In practice, an air or gas bubble would seldom have a chance to go through retinal breaks, except when they were associated with fixed retinal folds. If a retinal detachment were mobile, as soon as a bubble was injected, the bubble would float to the uppermost position of the vitreous cavity. Any SRF would be displaced inferior to the bubble. The upper retina would be opposed to the underlying retinal pigment epithelium, including any retinal breaks

that might be situated in that upper part of the retina. Furthermore, there are those who believed that direct contact between the retina break or bubble might not be necessary. Clinical studies have shown that inferior retinal breaks can be successfully treated with vitrectomy, gas tamponade, and no scleral buckling.[20] One school of thought is that gas bubbles (for that matter oil bubbles) act inside the eye as splints, thereby reducing intraocular currents. In the absence of traction, the lack of intraocular currents would allow the retina to settle back. There may or may not be a need for direct contact between the bubble and the retinal breaks.[20]

If, however, contact were important, then the shape of the bubble would determine the effectiveness of tamponade. When buoyancy was large, the bubble would take on the shape of the vitreous cavity and assume a flat bottom. This way, most of the volume would contribute to making contact with the retina. Thinking about it in another way, very little volume would be wasted in forming the meniscus. If the buoyancy were small, as would be the case with SO, the shape of the bubble would be rounded. In other words, very little of the volume would contribute to making contact with the retina; much of the bubble would go to form the meniscus, which would make no contact with the retina. The extreme case would be a spherical bubble inside a spherical cavity. Unless the fill is 100%, the contact would go from nil to total. In practice, total tamponade is probably unachievable. Most surgeons use the so-called nonexpansile concentration of gases. By definition, the volume of the bubble decreases in the postoperative phase. Those who use "slightly expansile" concentration are risking high IOP. In a normal eye, any increase in IOP would result in an increase in outflow that in turn would lower the IOP pressure. If the vitreous cavity was totally filled with gas, the only aqueous available to increase the outflow would be that in the anterior chamber (AC). The AC would then be shallow. If the iris lens diaphragm was lax, then secondary angle closure might ensue. In practice, we could not know, for a given individual, precisely what the nonexpansile concentration of each gas might be. Using expansile concentration would therefore be unnecessarily risky.

Functions of Gas

The main functions of a gas bubble inside the eye are to: (1) provide internal tamponade; (2) flatten folded retina; (3) enable visualization; (4) replace globe volume; (5) reduce intraocular currents.

Internal Tamponade

Providing internal tamponade for retinal detachments has been the main indication of intraocular gas use.[21] The purpose is to oppose the break by utilizing the surface tension of the bubble. The surface tension of gas is high compared with liquid tamponade agents such as SO. The interaction between buoyancy, weight, shapes of intraocular gas bubbles and contact have been alluded to previously.

It is worthwhile mentioning that the shape of a gas bubble varies with its volume. When a small gas bubble is injected, it takes on a rounded shape. This is observed routinely when pneumatic retinopexy is performed. For example, where 0.3 mL of C_3F_8 is injected the bubble stays relatively rounded until it expands in size over the next 24–48 hours. It then clearly adopts a flattened shape (this shape is referred to as a "spherical cap"). When a gas bubble is small, its shape is mainly determined by its surface tension. Because the surface tension is high, the bubble is rounded. When the bubble expands, buoyancy becomes important. Every molecule of the bubble wants to float upwards, which is why the bottom of the bubble has a flattened shape. Lincoff made this observation many years ago and went on to suggest a means of assessing the size of intraocular gas bubble by observing this flattened bottom surface of the gas bubble.[22] In terms of upward force, it is greatest at the apex of the bubble, whereas it is near zero at the bottom. Table 108.3 gives an estimation of the volume of the gas injected and the effective arc of tamponade. It has been shown by using a model eye constructed of surface modified polymethylmethacrylate to mimic the hydrophilic retinal surface. The efficiency curve plots the arc of contact against the percentage fill. It was shown that the curve was sigmoidal. Initially, the plot was exponential. It showed that a relatively small bubble would provide a large arc of contact. The plot was linear; the fill and contact was proportional, and towards the end, the plot was exponential again. This time, a slight underfill

would leave a large arc of retina out of contact with the bubble.[23]

TABLE 108.3

Changes in Arc of Contact With Gas Bubble Volume (Assume a Vitreous Cavity Diameter of 21 mm)

Arc of Contact (°)	Gas Bubble Volume (mL)
90	0.28
120	0.75
150	1.49
180	2.40

The tamponade bubble also acts to seal off the break, such that cellular elements can no longer escape from the subretinal space into the vitreous cavity. This was considered important in preventing proliferative vitreoretinopathy (PVR). However, cellular elements that have already gone into the vitreous cavity tend to concentrate in the thin film of fluid just beneath the bubble. This accounts for why postoperative PVR is more commonly found inferiorly.[24,25]

Unfolding and Folding of the Retina

The surface tension and buoyancy force of the bubble can help to unfold the retina. Circumferential folds sometimes occur with high radial buckles. If SRF was drained and air was injected, these folds would be less prominent. The so-called retinal redundancy would be minimized, as the retina would be made to follow closely the contour of the indent. Equally, if SRF drainage was incomplete and a large bubble was injected, retinal fold could occur. When these folds involve the macula, the patients would be very symptomatic, complaining of distortion and poor vision.[26] This complication could be prevented by achieving a more complete drainage of SRF before injection and judicious posturing of the patients immediately postoperatively. This posturing might involve "steam-rolling," with the patient lying first with the retina break lowest most, then turning slowly to position the bubble to the posterior pole, followed by posturing on the correct side.[27] This type of maneuver aims to use the bubble to express the SRF out through the retinal break and to protect the macula from being affected by retinal folds.[28,29]

Postoperative Visualization

In the postoperative period, after vitrectomy and gas tamponade, the view of the fundus may be obscured by vitreous hemorrhage. It is usually possible to have a glimpse of the upper fundus by looking through the gas bubble. The observer, however, needs to be positioned lower than the patient. Specifically, the aim is to look through the lower flat bottom surface of the gas bubble. Asking the patient to stand, while the physician remains seated, can work well. If other parts of the fundus are to be viewed, the patient can be asked to lie on their side. Again, if the vantage point is lower than the fluid level, the ophthalmologist can easily see the lower nasal or temporal half of the fundus. If the bubble is small, then fundoscopy is difficult. It would be better to rely on B-mode ultrasonography. One additional point should be made, i.e., looking through the bubble, the retina often appears to be attached, even in the presence of residual fluid. This may simply be due to the buoyancy of the bubble displacing SRF laterally and posteriorly.

Replace Globe Volume

Air is used in conventional scleral buckling surgery after the drainage of SRF. The air prevents SRF being recruited again. The air also restores the IOP. At this stage, effectively a flat retinal tear would be treated. Without the presence of SRF, cryotherapy would be limited and break localization would be more accurate. The fact that the IOP is normal also means that suture can be applied to the sclera more safely. In this way, air serves a role as an intraoperative tool.

Dynamics of the Gas Bubble Inside the Eye

Different Phases of Gas Resorption

After injection, the gas bubble inside the eye undergoes three phases before complete resorption. The three phases are expansion, equilibration, and dissolution. This occurs when pure expansile gases (i.e., SF_6, C_2F_6, and C_3F_8) are injected. Air does not expand, and this will be discussed later. Due to lower water-solubility than nitrogen, pure SF_6, C_2F_6, and C_3F_8 will expand when injected into

the eye. This is because nitrogen diffusion rate into the bubble is higher than the rate of gas dissolving into the surrounding tissue fluid compartment. Expansion is most rapid in the initial 6–8 hours, and is similar for all gases. This is because the rate is mostly affected by the convection currents in the surrounding vitreous fluid.[30] The bubble reaches its maximum size when the gaseous diffusion in and out of the bubble equilibrates. For SF_6, this occurs around 1–2 days after injection; for C_3F_8, it takes 3–4 days to reach maximum expansion.[31] This has practical implications, as IOP may rise if the outflow facility cannot cope with the rapid increase in intraocular volume. It has been found that the eye can accommodate up to 1.2 mL of pure expansile gas injection without significant IOP change.[12,31] This equals 20–25% of the vitreous cavity volume. In eyes with occludable angles, pure expansile gas should therefore be avoided, or prophylactic IOP-lowering agents should be used.

The equilibration phase begins when the partial pressure of nitrogen in the bubble equals that in the surrounding fluid compartment. During this phase, there is a small net diffusion of expansile gas into the fluid compartment. This can be explained by the higher solubility of nitrogen, such that nitrogen equilibration is reached at a faster rate than other gases. Hence, the bubble diminishes slightly in volume during this phase. Duration of this phase differs for different expansile gases and is dependent on solubility. For C_3F_8, this phase lasts 2–3 days.[31]

When partial pressure of all gases within the bubble equals that in the fluid compartment, the dissolution phase begins. The gas compartment gradually decreases in size as gases dissolve into the fluid compartment. The decrease in volume follows first-order exponential decay.[32] This phase is the longest among all three phases. Despite the fact that it may take up to 6–8 weeks for a bubble to completely resorb, internal tamponade is often only effective during the initial 25% of the bubble's lifespan. This is because it requires at least 50% of the initial size to provide an effective tamponade. If the bubble is smaller than 50% or it breaks into a few smaller bubbles (i.e., fish eggs), internal tamponade is ineffective and no therapeutic effect can be achieved, even though it may still remain in the eye for a long time. Fig. 108.1 illustrates

gaseous transfers in and out of the bubble during the three phases.

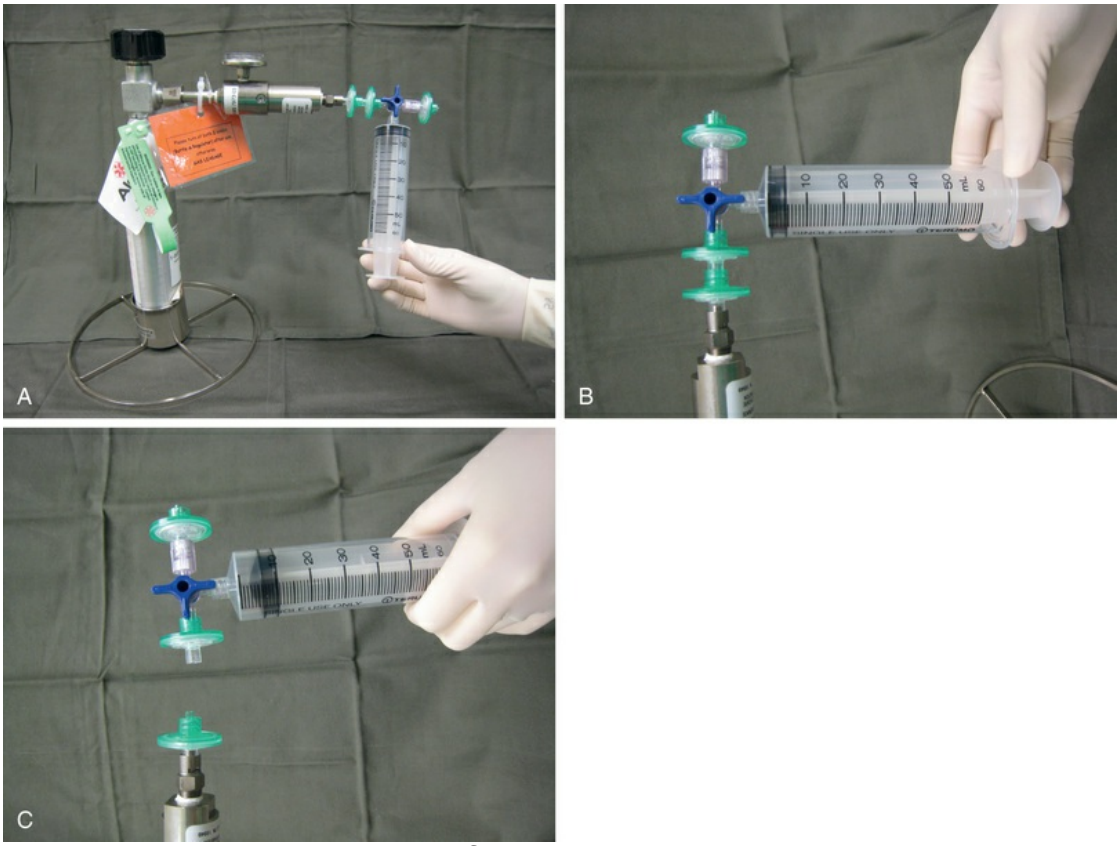

FIG. 108.1 Preparation for gas injection. (A) Pure gas is stored in a cylinder with a regulatory valve. Two sterile filters should be connected between the cylinder and the syringe in use. (B) As physiologic dead space exists within the system, accuracy may be affected by the air contained within these spaces. Pure gas should then be drawn from the cylinder and the syringe flushed a few times to ensure complete evacuation of air from the dead space. The appropriate amount of pure gas is then drawn into the syringe. (C) The syringe with one filter is then disconnected. The three-way tap is then turned to the other unused filter, and air is drawn in to achieve the appropriate concentration of air–gas mixture.

Air, which is already a mixture of gases, does not expand and enters the dissolution phase immediately after injection. This is because the partial pressure of nitrogen, oxygen, and carbon dioxide roughly equal that in the blood. Since equilibrium has

already been reached during gaseous exchange in the lung, dissolution phase begins immediately after injection.

In clinical practice, expansile gas is often mixed with air to give a "nonexpansile" concentration. This can be interpreted as injecting two separate gas compartments into the eye, one being pure expansile gas, the other being pure air. The reduction in volume of the air compartment compensates for the increase in volume of the expansile gas compartment. When the appropriate ratio of these two compartments is met, the overall gas compartment volume remains constant. The percentages of gas/air mixtures to produce a nonexpansile volume are outlined in Table 108.2.

The time taken for complete resorption of the bubble also depends on other factors such as lens status, aqueous turnover, presence of vitreous, presence of periretinal membranes, ocular blood flow, and ocular elasticity.[32] The lifespan of SF_6 and C_3F_8 may be more than twice as long in phakic nonvitrectomized eyes than in aphakic vitrectomized eyes.[33]

Special Considerations When Under General Anesthesia

During general anesthesia, the anesthetic gases inhaled may interfere with intraocular gas volume. Nitrous oxide (N_2O) is, respectively, 34 times and 117 times more water-soluble than nitrogen and SF_6.[33] Therefore, when there is a gas bubble in the eye, nitrous oxide quickly diffuses from the fluid compartment into the bubble and increases the bubble volume. If SF_6 is used, the bubble may increase up to three times its original size during anesthesia with nitrous oxide. Because of its high solubility, maximum IOP rise may occur after 15–20 minutes of nitrous oxide use; and IOP decreases once it is discontinued, as it diffuses out of the body through ventilation. It has been found that the concentration of nitrous oxide in the lung alveolars is reduced by 90% after it has been stopped for 10 minutes. Therefore, in practice, nitrous oxide should be discontinued for at least 15 minutes prior to intraocular gas injection to avoid interference in the desired bubble volume. If it has been continued during gas injection, the resultant bubble will be smaller than expected.

Special attention is required for patients undergoing general anesthesia for nonocular purposes while they still have an intraocular gas in situ. Severe visual loss resulting from central retinal artery occlusion and choroidal ischemia have been reported.[34,35] This was thought to be due to the uncompensated rapid rise in IOP during surgery as a result of nitrous oxide diffusion into the bubble. For this reason, every patient with an intraocular gas bubble should be given a wristband to wear, indicating clearly the type and time of intraocular gas injection. It should be worn throughout the lifespan of the bubble.

Response to Changes in Altitude

Assuming most patients remain at a similar altitude after intraocular gas injection, the bubble size would not change significantly. However, when there is a change in altitude, significant changes in bubble size may occur. This is especially important for patients undertaking air travel shortly after surgery, because airplane cabin pressure is only equal to atmosphere pressure at an altitude of 8000 feet. Climb rate occurs at roughly 2000–3000 feet per minute during airplane ascent, and the rapid expansion in bubble size may be translated into IOP rise.[36] Central retinal arterial occlusion may result. It has been reported in animal studies that a bubble equivalent to 10% of the vitreous cavity or 0.6 mL may be safe for air travel. Up to 1.0 mL of gas was reported to be tolerable without significant IOP change.[36] However, this is entirely dependent on outflow facility, and some surgeons feel that no volume is safe for air travel.[17]

For the same reason, air bubble size may change during scuba diving.[37] During scuba diving, gaseous equilibrium under atmospheric conditions may be affected by inhalation of oxygen from compressed air tanks. When the diver returns to the surface, the bubble expands inside the eye and gives rise to an increase in IOP.

Preparation for Injection

Gases of highest purity from either a disposable or reusable cylinder should be used. Prior to obtaining gas from the cylinder,

gas pressure within the cylinder should be checked to ensure no gas leakage has occurred, which may affect the concentration of the gas inside. Silicone tubing is first connected to the cylinder at one end, and to two 0.22-μm Millipore filters (Millex-GS) at the external end. A 50-mL syringe is then connected to the filters. The syringe is then flushed two to three times to remove air trapped within the tubing and filters. Pure gas is then drawn into the syringe to the desired volume. For pure gas injection, the syringe could then be connected to either a needle or the infusion for use. For air–gas mixtures, the syringe should be disconnected from the cylinder at the junction between the two filters, having one filter still connected on the syringe. Sterile air is then drawn into the syringe to achieve the desired concentration of air–gas mixture. The filter is disconnected and syringe connected to a needle of the infusion for use. The gas or gas mixture should be used immediately to avoid inaccuracy in the concentration as a result of air influx from the surroundings. Fig. 108.2 illustrates how gas is prepared for injection.

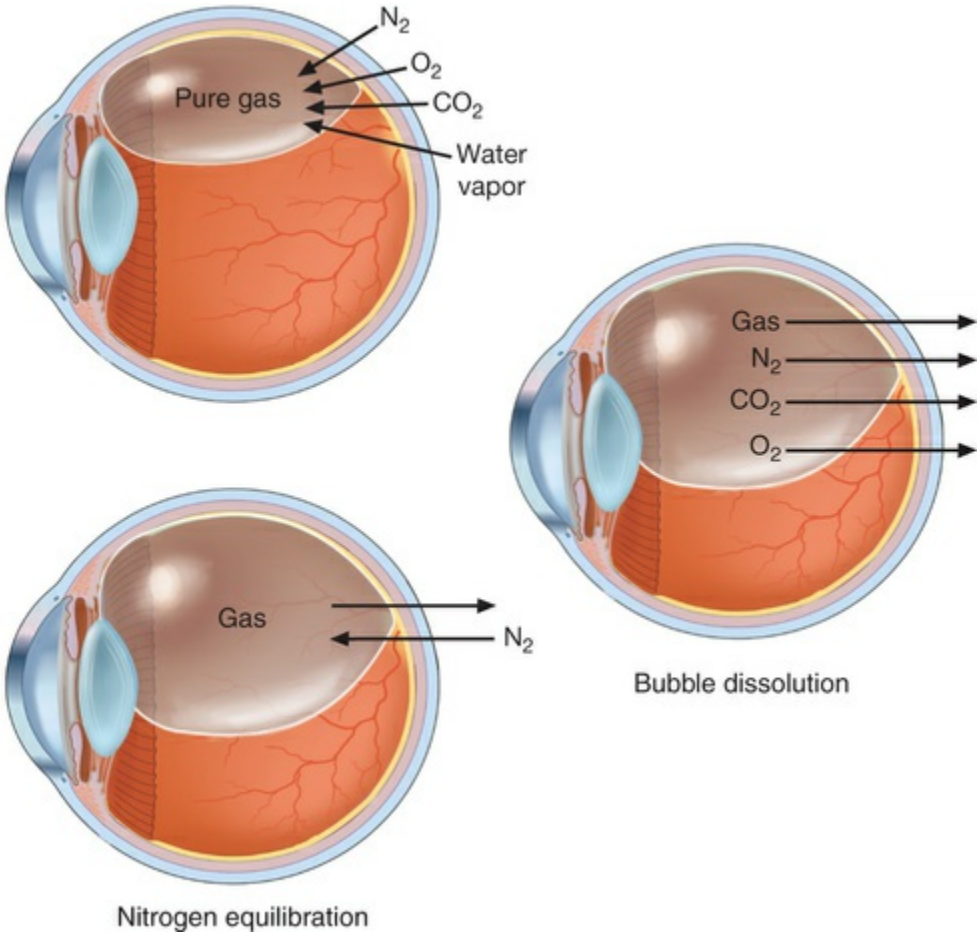

FIG. 108.2 The three phases of gas transfer after injection of pure expansile gas.

Human error can occur in the process of gas preparation. It is therefore imperative that all operating theater staff are acquainted with the techniques of gas preparation. It is also vital that they do not confuse the different gases for use, and proper labeling is done to ensure the correct gas is injected into the correct eye. When mixing pure gas with air, it also especially important to ensure that the correct concentration is produced. This is because an expansile bubble in an eye intended for a nonexpansile bubble could have devastating consequences.

Clinical Applications and Surgical Techniques

The most common indications for intraocular gas injection are to assist: (1) retinal detachment surgery with vitrectomy; (2) pneumatic retinopexy; (3) retinal detachment surgery with scleral buckle; (4) macular hole surgery; (5) displacement of subretinal hemorrhage; and (6) postvitrectomy gas exchange in vitrectomized eyes. The techniques discussed below are based on the authors' personal surgical experiences and preferences, and may not necessarily be applicable in all cases.

In Vitrectomy for Retinal Detachments

This is the one of the most common indications for intraocular gas injection. After full vitrectomy and relieving of tractions, fluid–air exchange is used to flatten the retina. Residual traction is indicated by persistence of SRF and inability of retina to flatten out. Fluid has to be reinstilled, and all traction must be relieved prior to proceeding. When the retina is flat, and air is in situ, endolaser can be performed. The advantage of performing laser under air is that the peripheral retina is easier to visualize. In cases where PFCL is required to flatten the retina or to assist drainage of SRF, endolaser can be performed under PFCL, and PFCL–air exchange should be performed afterwards. Direct PFCL–gas exchange is generally not advised as (1) residual traction could be seen on extraction of PFCL,

fluid has to be reinstilled for further intervention, and gas injected would be wasted, and (2) closure of the wound after gas injection could potentially cause gas leakage and postoperative hypotony.

When the eye is filled with air, air–gas exchange can be performed. The infusion line should be kept in place, and IOP controlled by the air-insufflation pump of the vitrectomy machine. The other two sclerotomy wounds should then be closed. This should be done with suturing in a 20-gauge (G) system or the trocars be removed in a 23G system, and air-tightness ensured. The syringe holding the desired gas or gas/air mixture should then be connected to the infusion line, at a site as close to the eye as possible. This is to minimize dead space in the tubings that may interfere with the desired concentration of the gas. A 27G needle connected to an empty syringe, with plunger removed, is then inserted through the sclerotomies, or through the sclera at the same plane as the sclerotomies, to allow exit passage for the air inside. The gas or gas/air mixture is then flushed into the eye through the infusion line. Flushing the eye with a minimum of 25 mL of gas or gas/air mixture is required to achieve an identical concentration to that in the original syringe. The infusion line is then pulled and the last sclerotomy closed. Another method is to inject the gas or gas/air mixture directly into the eye through the sclera or sclerotomy and allow air inside to exit via the infusion line, which is opened to atmosphere on the other end. In both techniques, the needle tip, be it for exit passageway or for injection, has to be clearly visualized through the cornea before any air–gas exchange is performed. This is to avoid the inadvertent insertion of the needle in the suprachoroidal space. If gas has leaked during the sclerotomy closure, additional gas could be injected directly to maintain a normal IOP at the end of surgery. Conversely, if IOP is high, gas could be released by either depressing the sclerotomy wound or by inserting a syringe into the eye to relieve part of the gas. Fig. 108.3 shows how this is performed.

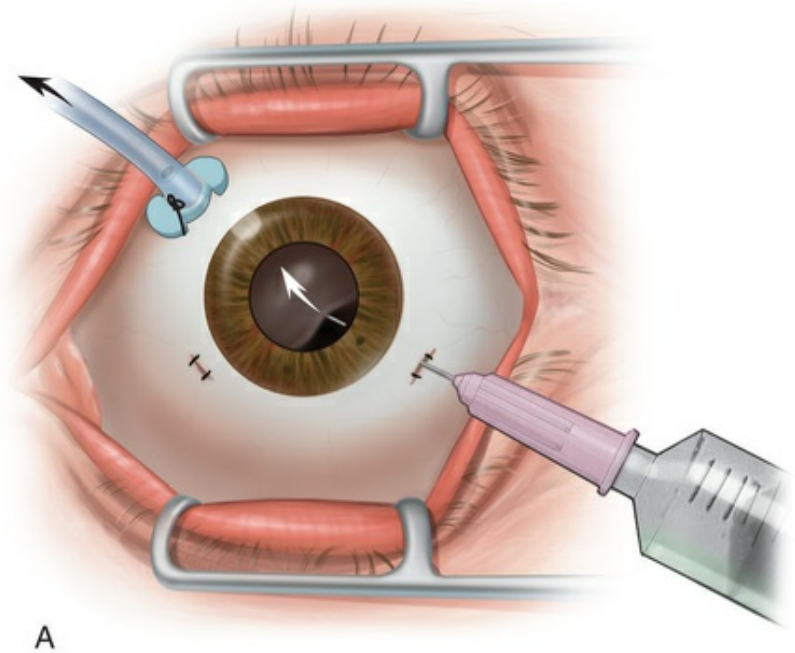

A

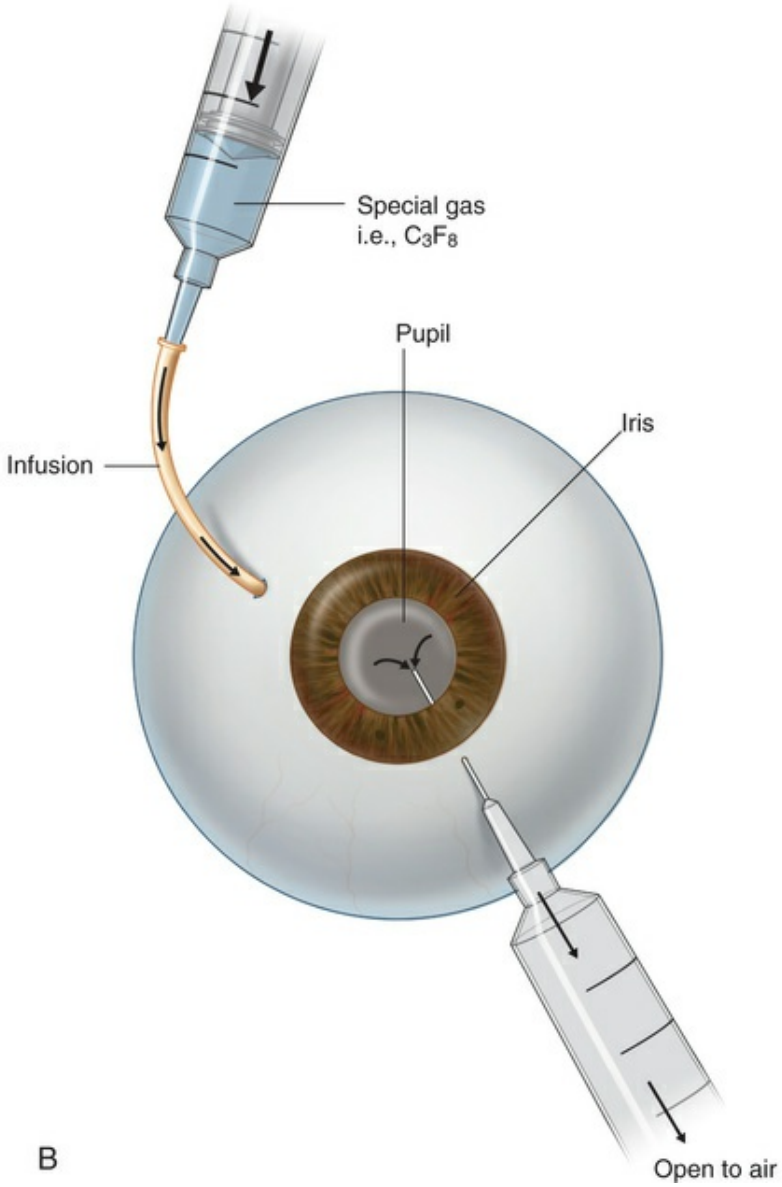

B

FIG. 108.3 Technique of air–gas exchange in a vitrectomized eye. (A) Injection of gas through a syringe connected to a needle. Air inside the eye is flushed out through infusion, which is disconnected externally. (B) Injection of gas is done through a syringe connected to the infusion, and gas is flushed into the eye. Air is allowed to exit the eye through the needle inserted with the plunger of the syringe removed.

The choice of gas is sometimes based on the availability of gases, and the surgeon's experience and preferences. In general, the choice of gas is dependent on the intended duration of tamponade. For simple cases where duration required is short, air could be used.[16,38] In more complicated cases where longer tamponade is desired, nonexpansile concentration of gas/air mixture (18% SF_6 or 14% C_3F_8) should be used.[33,39] When a larger bubble is needed, a gas/air mixture with an expansile concentration should be used. This is especially important for inferior breaks where a larger bubble could provide better tamponade. A larger bubble also has the advantage of being able to unroll folded retina. In the Silicone Study, C_3F_8 has been found to be more effective than SF_6 in cases with PVR.[14,40,41]

In Pneumatic Retinopexy

As mentioned earlier, careful patient selection is important, as failure of opposing the retina may subject the patient to further operations. Up to 63% success with this as the only procedure has been reported.[42] Before gas is injected, there are several prerequisites: (1) the retinal detachment has to be in the superior half of the retina; (2) the break or hole is ideally solitary or grouped within 1–2 clock-hours; (3) there are no inferior breaks or retinal thinning; and (4) preferably the presence of posterior vitreous detachment (PVD). This can be an office procedure, and local anesthesia is usually sufficient in experienced hands. In contrast to buckled cases, internal traction is not counteracted therefore opposition of the retina to choroid has to be provided by the bubble initially, and later by the chorioretinal adhesion induced by

cryotherapy.

Gas is injected only after adequate cryotherapy. Pure expansile gas should be used.[43] In practice, 0.3 mL of 100% C_3F_8 is used most commonly. The same volume of SF_6 can also be used. First, the injection should be on the side of the break. If the break is located at 12 o'clock, then the injection is at the midline. Gas is then injected through a 27G needle, 3.5–4 mm behind the limbus. Normally 0.3 mL 100% C_3F_8 is used. To avoid "fish-egg" formation (small bubbles instead of one large bubble), the injection site should be rotated such that it is in the uppermost part. The needle should be inserted just deep enough to penetrate all layers, and the injection force should be swift and constant, aiming at creating a single bubble. After injection, the injection site should be rotated laterally before pulling the needle out of the eye. This is to ensure the bubble moves away from the opening before the needle is retrieved, to prevent leakage. If fish-egg has formed, the sclera can be gently tapped a few times to promote fusion of the small bubbles. Fig. 108.4 illustrates how this is performed. After injecting gas, AC paracentesis can be performed to counter the increase in intraocular volume. The patient's head is then rolled 180°, to the face-down position. This serves to unroll any folded retina associated with the break. The patient is then instructed to assume this position as much as possible, until complete dissolution of the bubble has occurred. Careful monitoring is required during the postoperative period for proper opposition of the retina, resolution of SRF, and any new break formation inferiorly. In cases where opposition is doubtful, SRF persists, or new breaks are found, a reoperation with either scleral buckling or a vitrectomy approach has to be performed.

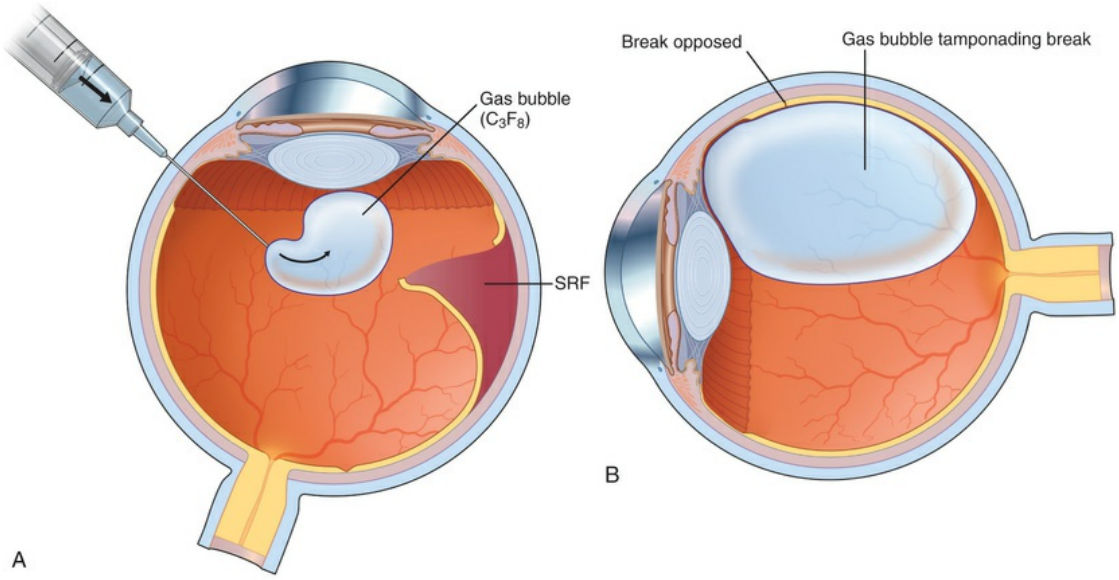

FIG. 108.4 Injecting gas in pneumatic retinopexy or postscleral buckle cases. (A) Detachment is located superiorly. Injection of gas is done via a needle, with the patient lying supine. (B) When the patient assumes an upright position, the bubble tamponades the break and displaces subretinal fluid (*SRF*). Detached retina is opposed to the original position.

In Scleral Buckling for Retinal Detachments

Intraocular gas injection is generally not required, provided adequate drainage of SRF and relieving of traction with the buckle has been achieved. However, its use is still invaluable in certain cases, for example when fishmouthing of the break on a circumferential buckle is seen and is insufficiently opposed by the buckle, or as a "salvage" procedure to save the patient from a reoperation.

For intraoperative use, we prefer injecting the gas towards the end of operation. This is mainly because the view of the fundus will be obscured by the bubble after injection. The injection technique is identical to that in pneumatic retinopexy. It should be stressed that the major therapeutic component under these circumstances is still the sclera buckle, whereas gas bubbles only act as an adjunct, and should not be relied on totally to treat the detachment.

The "salvage" procedure for postscleral buckled cases is an invaluable tool to save the patient from a reoperation. When after

sclera buckling surgery a persistent layer of SRF remains underneath the break, or meridional folds are present, or there is fishmouthing of the break, injecting gas could be of help. The technique is identical to pneumatic retinopexy; 0.3 mL gas should be injected followed by AC paracentesis. Depending on the location of the break and likelihood of redetachment, different gases could be used. For instance, for superior breaks with minimal SRF, air could be used. For inferior breaks with fishmouthing breaks, an expansile bubble of 0.3 mL 100% C_3F_8 would be desired, although a reoperation would likely be required.

In Macular Hole Surgery

When first described, macular hole surgery was not complete without the injection of intraocular gas tamponade followed by face-down posture for 1 week. This provides a mechanical effect by the buoyancy force of the bubble, over the macular hole, in hope of assisting closure. The injecting technique is identical to that in retinal detachment surgery with vitrectomy approach. The duration of postoperative posturing has been a topic of debate in recent years. Similar closure rate was found between air and 20% SF_6, and that between 20% SF_6 and 12% C_3F_8.[44] The choice of gas is generally based on the surgeon's preference and experience. The authors' choice of gas is 12% C_3F_8 followed by face-down posturing until dissolution of the bubble.

In Displacement of Subretinal Blood

Pneumatic displacement of subretinal blood clot has been found to be therapeutic in treating polypoidal choroidal vasculopathy, macroaneurysm, choroidal neovascularization, and trauma. It has been shown to allow speedier recovery of vision, and may potentially reduce the harmful effect of blood on the photoreceptors. The original procedure was to treat within 1 week from onset of hemorrhage, coupled with tissue plasminogen activator (TPA) injection. There are recent reports showing improvement in vision and reduction in scar area following the use of TPA.[45,46]

Prior to injection, careful patient selection should be done.

Distinction between subretinal blood and intraretinal blood should be made. Injecting gas for intraretinal blood will not displace the clot, but rather increases the chances of blood dispersing into the vitreous. When there is retinal thinning or lattice formation, particularly inferiorly, or when there is no PVD, the risk of inducing retinal breaks cannot be omitted, and close monitoring should be performed.

The injection technique is identical to that in pneumatic retinopexy, where 0.3 mL 100% C_3F_8 should be used, with or without the injection of TPA. This is followed by a strict face-down posture for a few days.

In Postvitrectomy Gas Exchange

This technique is invaluable for recurrent detachment, and can avoid the need for reoperation.[47] Success rate is highest when there is no evidence of PVR. If PVR has already set in, gas injection may be complicated by formation of new retinal breaks or extension of existing breaks, which usually occur at the edge of laser marks. A fluid–gas exchange could be performed at the slit lamp, via a 30G needle connected to a syringe filled with the desired gas of injection. The needle is inserted at 3.5–4 mm posterior to the limbus, at the inferotemporal quadrant, from a dependent angle, aiming towards the center of the globe. Fluid–gas exchange is then performed via a push–pull technique. When the plunger is pushed, gas is injected into the eye. This is followed by aspiration of intraocular fluid by pulling the plunger. This cycle is repeated until the bubble has reached the desired size. Special note has to be taken to visualize the needle tip prior to any movement of the plunger. This is to avoid any inadvertent entry of the needle into the suprachoroidal space. If the patient is aphakic, the procedure could be performed by inserting the needle into the AC through the cornea, instead of the pars plana approach. The choice of gas is dependent on the condition of the redetachment. If a larger bubble is desired, expansile gas should be injected; whereas if a smaller bubble is needed, air or nonexpansile concentration of gas/air mixture could be used. Fig. 108.5 shows how this could be done at the slit lamp.

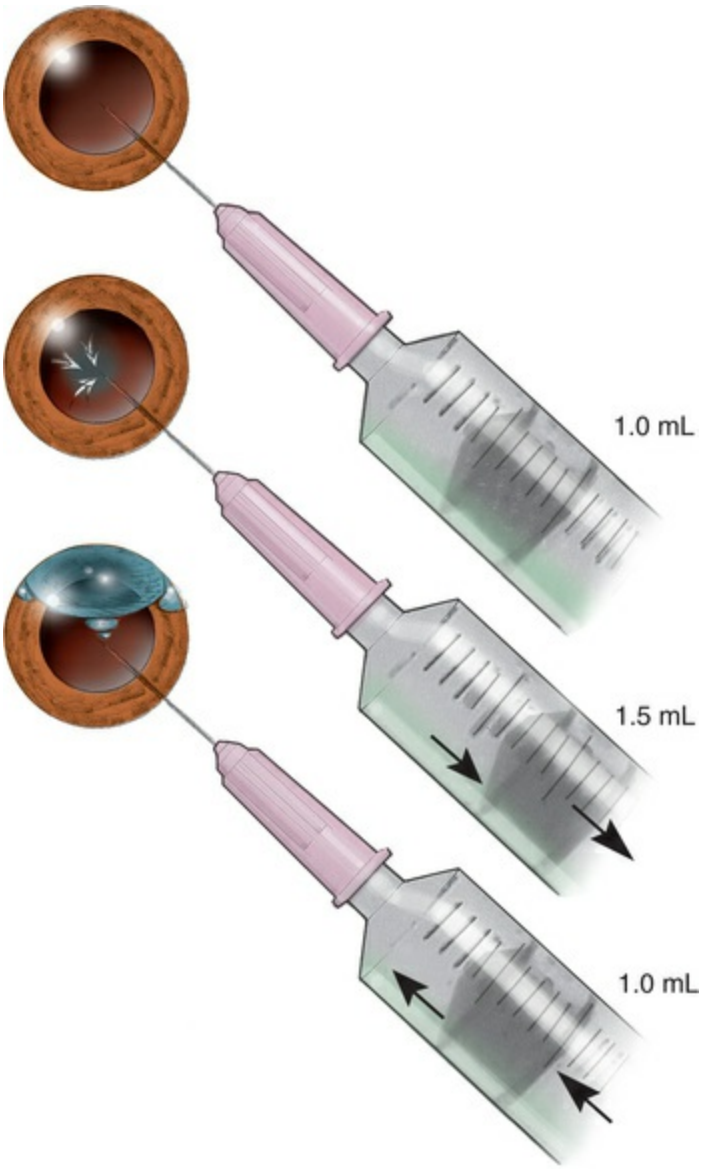

FIG. 108.5 Technique of postoperative gas exchange at the slit lamp.

Gas–gas exchange is sometimes required. For instance, when a patient is required to undergo air travel before the expected dissolution of the bubble, another gas of shorter longevity (i.e., air or xenon) could be exchanged. This could be done using the same technique described above, with the needle connected to two syringes via a three-way stopper. The bubble in the eye is aspirated into one syringe, which is followed by injection of the desired gas into the eye from the second syringe. It should be noted that it is difficult to ascertain an accurate concentration of the second bubble with this method.

Postoperative Care

Head Posture After Intraocular Gas Injection

Proper opposition of the break is only ensured by proper posturing of the head. This is done such that the break is located at the uppermost part of the eye, and be in direct contact with the bubble. Face-down posturing with the use of expansile gas has another advantage of preventing pupil block glaucoma or optic capture. Another potential advantage is that in a phakic patient this reduces the contact between the posterior surface of the lens and the gas bubble, and reduces the risk of cataract development. This should be done by assuming a face-down or prone posture immediately after surgery. If face-down or prone posture is difficult, or the patient needs to take rest from prolonged face-down position, lying laterally on the opposite side of the break is also accepted (i.e., lying on the left for a right-side break). This could be facilitated with the use of pillows designed for posturing purposes. As chorioretinal adhesion from laser or cryotherapy takes 2–3 days to become effective, the initial tamponade by bubble is the main force to keeping the retina attached. This should be conveyed to the patient and compliance should be checked every visit or over the phone. If the patient has good compliance to face-down posturing, precipitates could be noted on the central corneal endothelium, which are sometimes referred as "positioning spots." This is due to gravitational deposition of intraocular inflammatory elements, which is usually more obvious in combined phacovitrectomy cases. In nonvitrectomized cases, it is especially important for the patient to assume proper posturing. Movement of the bubble may cause traction in the vitreous gel and may induce new breaks. This is problematic if inferior breaks are induced, since the bubble cannot provide tamponade for these breaks and reoperation is likely. Posturing is needed until complete dissolution of the bubble has occurred. As the bubble gets smaller, patients with good visual prognosis may report seeing the bubble inferiorly. Fundal exam and sometimes history taking can tell when the bubble has completely dissolved. The wristband indicating an in situ bubble can only be removed at this time.

Fundal Exam in the Postoperative Period

Examining the fundus with an in situ bubble can be difficult in inexperienced hands. When there is a near complete fill, examination through the bubble is relatively easy. As the bubble gets smaller, the retina is easier to see through the gas compartment. This is due to reflections from the gas–fluid interface. To visualize the whole fundus, the head has to be tilted sideways, to allow the bubble to cover different areas for inspection. When the gas compartment is smaller than the fluid compartment, examining the patient when lying supine helps to bring the bubble behind the pupil and reduces glare.

Intraocular Pressure Measurements

Maximum expansion of the bubble occurs within the first postoperative day. During this period, monitoring of intraocular pressure (IOP) is important, as an overfilled expansile bubble may predispose to central retinal arterial occlusion. Measurement with applanation tonometry has been found to be more accurate than other measures, including dynamic contour tonometry.[48,49] Risk of having an IOP rise is lower with air injection or nonexpansile gases. For high-risk cases, prophylaxis with oral acetazolamide and topical timolol should be given, especially in cases having preexisting glaucoma.

Laser Photocoagulation

When more photocoagulation is deemed necessary, it can be done through the bubble. Hypotony may cause corneal striae when contact lenses are applied on the eye for photocoagulation. This can be overcome by temporarily injecting air into the eye to increase the IOP, which could then be released afterwards with a needle and syringe. The peripheral fundus may not be easily visualized with a wide-angle contact lens, and photocoagulation via laser indirect ophthalmoscopy (LIO) may be necessary. In cases where LIO is not possible, cryotherapy should be used. It has been reported that up to 85.7% of redetachment can be flattened with the use of fluid–gas exchange coupled with supplementary photocoagulation.[50]

It should be emphasized preoperatively to the patient that vision

will drop after injecting gas. This is vital in cases of macular-on retinal detachments, where preoperative vision may be normal. Vision is usually poor during the lifespan of the bubble, mainly due to diffraction and glare. After dissolution of the bubble, vision may slowly return, provided the patient has good visual prognosis.

Changes in Altitude

As mentioned above, the gas bubble changes in size at different altitudes. It is therefore important to advise the patient to refrain from changing altitudes. If the change in altitude is gradual and could be compensated for by outflow facility, IOP change may not be apparent and would not cause significant problems. However, rapid changes in altitude may cause a sudden expansion in bubble volume and IOP, which may not be compensated for in time, and central arterial occlusion may occur. The use of scleral buckles reduces the capacity of deformation of the sclera, hence may further predispose the patient to significant IOP changes during air travel.[17] Air travel should therefore only be permitted after complete dissolution of the bubble(s).[51]

Complications and Management

Cataract Formation

Gas-induced cataract is usually in the form of feathery posterior subcapsular cataracts. It can also appear as vacuoles at the superior portion of the lens. Incidence is higher if the eye is two-thirds or more filled with gas. It is also more likely to occur if the gas of choice is of higher purity and longer longevity.[11,52] Assuming a prone position, as well as leaving a thin layer of anterior hyaloid help prevent this from occurring. These help to isolate the bubble from the lens. If in mild form, gas-cataracts tend to resolve without treatment. For persistent opacities, which are more likely to occur with gases of longer longevity, surgical removal may sometimes be required, especially when view of the fundus is compromised. If cataract extraction has to be performed when the bubble is still in situ, aspirating the gas before cataract extraction is needed. Otherwise, the bubble will push the posterior capsule upwards and increase the risks of complications.

Raised Intraocular Pressure

Expansile gases or gas/air mixtures of high purity tend to cause IOP rise more frequently. Various risk factors include the combined use of encircling band, the agent of tamponade, and the combination of cataract extraction. In a recent series, a risk of up to 37.9% for raised IOP was seen in cases with gas tamponade.[53] It is usually due to overfill or expansion of the bubble, which cannot be compensated for by the outflow facility. This is usually short-lived and can be managed without difficulty using antiglaucoma medications. Refractory cases may be due to outflow compromise. For cases with peripheral anterior synechiae (PAS), preexisting angle closure glaucoma, or neovascular glaucoma, care must be taken when choosing the gas for injection. In general, air or a nonexpansile gas/air mixture should be used in these cases, to reduce the risk of postoperative IOP rise. Other than medical treatment, excess gas could be partially aspirated to reduce the volume and hence IOP.

Secondary glaucoma with intraocular gas use is infrequently seen. It can occur with angle disruption from forwardly displaced lens–iris diaphragm, by a large bubble. This is more frequently seen in patients who cannot adopt a prone posture after surgery. Therefore in patients with cervical spine problems or who cannot assume a face-down posture, nonexpansile gas or air should be used, and a complete fill should be avoided.

Hypotony

The bubble can leak from sclerotomies either at the end of operation during wound maneuvers, or postoperatively, through a leaky wound. This results in hypotony. This should not be overlooked, as choroidal effusion or hemorrhage may occur with prolonged hypotony. Observation is enough for mild cases, but when hypotony is prolonged or if the risk for choroidal hemorrhage is high, reinjecting the eye with more gas is indicated. This could be performed using the pars plana approach at the slit lamp.

Subretinal Gas

Migration of gas into the subretinal space can occur both intraoperatively, or in the postoperative period. It can occur either

because the bubble is smaller than the tear, or when persistent traction elevates the retina and allows passage for gas into the subretinal space. If noted during surgery, the bubble can be displaced with the help of scleral depression externally. During the postoperative period, if the bubble has gone into the subretinal space, it can affect proper attachment of the break and may lead to redetachment. If away from the break and it does not affect break attachment, it can be left alone and will usually be absorbed within a few days. If break adherence is affected, reoperation may be required, and presence of residual traction should be inspected and released prior to reinjection of gas.

Gas in the Anterior Chamber and Corneal Decompensation

This may occur in aphakic eyes or in pseudophakic eyes with a nonintact posterior capsule. View of the fundus is often compromised if this happens. If noted intraoperatively, AC could be filled with viscoelastics prior to proceeding. If found postoperatively, it can usually be left alone and will be absorbed within a few days. Reoperation is seldom required. However, prolonged contact of the bubble in aphakic eyes with the use of expansile gases may predispose the corneal endothelium to hypoxia and decompensation.[54] This is mainly due to the interruption of aqueous flow to the endothelium, which in turn reduces the oxygen supply. Avoiding lying supine may reduce bubble–endothelium contact and potentially reduce the risk of corneal decompensation in such cases. In patients with cervical spine problems that prevent them from posturing, a large bubble should be avoided.

Intraocular Lens Capture

With combined phacovitrectomy and intraocular gas injection, the intraocular lens (IOL) may be pushed forward into the AC, causing optic capture. This could be prevented by limiting the anterior capsulorrhexis to a size smaller than the optic of the IOL. The patient should also be advised to avoid a faceup posture. The condition may be left alone if there is no tilting of the IOL and disturbance to vision is minimal. However, repositioning of the IOL

may be needed if dislocation has occurred or pigment dispersion is significant.

Conclusion

Intraocular gas has grown into an indispensable part of vitreoretinal surgery. Its use has been extended to indications other than retinal detachment. The high surface tension and buoyant force is highest among the vitreous substitutes available. The versatility of types and concentration of gases available enables the surgeon to manipulate procedure according to clinical scenarios, and has hugely improved operative success rates. A clear understanding of the properties of available gases is essential to making the right choice for different circumstances.

Perfluorocarbon Liquid in Vitreoretinal Surgery

Introduction

Perfluorocarbon liquid (PFCL) was initially designed for use as a blood substitute.[55] Clark and Gollan first used it as an oxygen transporter in a mouse model.[55] In humans, its use was involved in coronary angioplasty to deliver oxygen to ischemic myocardial tissue. PFCL has a high oxygen-carrying capacity and is also chemically inert. In 1982, Haidt and associates first examined its use as a vitreous substitute.[56] Clark later examined its possibility as an intraoperative tool, as well as postoperative vitreous substitute.[57]

In 1987, Chang pioneered its use in humans.[58] He investigated the possibility of PFCL as an intraoperative tool to assist the manipulation of the retina in complicated retinal detachments (RD). This was acknowledged by many as a major advancement. The use of PFCL has greatly improved retinal attachment rates, especially in complicated RD. This chapter will cover the physical and chemical properties of PFCL, surgical techniques, and the potential complications that may arise with its use.

Types and Properties of Perfluorocarbon Liquid

PFCL is a synthetic fluorinated hydrocarbon containing carbon–fluorine bonds. Some also contain other elements such as hydrogen, bromide, and nitrogen. Their chemical structures can be either straight chains or cyclical. Straight chain compounds contain carbon chains from C_5 to C_9, whereas cyclic compounds are made up of carbon chains from C_5 to C_{17}. For compounds with a carbon chain shorter than C_5, e.g., perfluoropropane (C_3F_8) and perfluoroethane (C_2F_6), they exist in gaseous form at room temperature. In general, all PFCLs are odorless, colorless, low viscosity, and have higher specific gravity and density than water. They are stable under high temperatures and do not absorb wavelengths of commonly used lasers. A few low-density PFCLs have been investigated for potential use in ophthalmology. This includes perfluoro-n-octane (C_8F_{18}),[59] perfluoroethylcyclohexane (C_8F_{16}),[60] perfluorodecalin ($C_{10}F_{18}$),[61] perfluoro-octylbromide ($C_8F_{17}Br$),[62] perfluorophenanthrene ($C_{14}F_{24}$),[18,62] perfluorotributylamine ($C_{12}F_{27}N$),[63] and perfluorotri-n-propylamine ($C_9F_{21}N$).[64] Details are listed in Table 108.4. Chemical and physical properties vary according to chemical structures. Of these, C_8F_{18} was found to possess higher efficacy and was approved by the US Food and Drug Administration for intraocular use.

TABLE 108.4

Characteristics of Perfluorocarbon Liquids Being Investigated for Intraocular Use

Chemical Formula	Molecular Weight (g/mol)	Specific Gravity	Surface Tension (dyn/cm at 25 °C)	Refractive Index	Vapor Pressure (mmHg at 37 °C)	Viscosity (cSt at 25 °C)
C_8F_{18}	438	1.76	14	1.27	50	0.8
$C_{10}F_{18}$	462	1.94	16	1.31	13.5	2.7
$C_{14}F_{24}$	624	2.03	16	1.33	<1	8.03
C_2F_6	138	1.83	n/a	1.29	55	0.94
$C_6F_{13}C_8H_{18}$	433	1.35	20	1.34	n/a	2.5
$C_{12}F_{27}N$	671	1.89	16	1.29	1.14	2.6
$C_8F_{17}Br$	499	1.93	18.2	1.30	1.1	2.3

cSt, centistokes.

There are several advantages that have made PFCL popular: (1) optical clarity allows manipulations under PFCL possible; (2) high density and specific gravity allows flattening of the retina and unrolling of folds, and also avoids the need for a posterior retinotomy to drain SRF; (3) different refractive indexes from saline allow a visible PFCL–fluid interface, which aids intraocular maneuvers, and ease of removal; (4) that it has a higher boiling point than water and no interference to laser wavelengths allows endophotocoagulation under PFCL;[59] (5) low surface tension and high interfacial tension tends to hold it in a big bubble, and reduce the risk of PFCL migration into subretinal space through the break; (6) low viscosity allows easy injection and aspiration even with small-gauge vitrectomies; (7) immiscibility with water resists incursion by saline and blood and allows a clear operating field despite intraoperative bleeding; (8) immiscibility with silicone oil allows PFCL–SO exchange, which is helpful when treating giant retinal tears by reducing risk of slippage.

Technique of Perfluorocarbon Liquid Injection

Viscosity of commonly used PFCLs ranges from 0.8 to 2.7 milliPascal-seconds (mPa · s) at 25 °C (Table 108.4). When using a 20G vitrectomy system, a dual-bore cannula should be used to inject PFCL. Under standard three-port vitrectomy conditions, all the ports will be occupied by the infusion, the light-pipe, and the PFCL injection cannula. If a single-bore cannula is used, IOP will elevate during the process, and resistance to injection will increase. A dual-bore injection cannula provides an exit passageway for intraocular fluid and reduces resistance during injection. High resistance plus forceful injection may dislodge the cannula from the syringe, and serious complications if the cannula is impacted into the retina and choroid. Therefore, a syringe with a Luer-lock is preferred. When a chandelier endoillumination source is used, any vacant port should be plugged prior to injecting PFCL. Escape currents through the vacant port may cause mobile retina to incarcerate into it.

When using the 23- or 25G system, if there was a separate light-infusion, PFCL should be injected with a single-bore cannula, while fluid is aspirated using a cutter. This system gives more control over the exchange procedure. Another complication is that vitreous can be forced to incarcerate by this high injection pressure, either into the infusion port or at any one of the remaining sclerotomies. Blockage of the infusion port can give rise to hypotony and intraocular hemorrhage, if the surgeon is unaware of the condition.

The injection speed should be sustained and gradual. This allows time for SRF to be displaced, retina unfolded and flattened. If a dual-bore cannula was to be used, injection must be gradual and a Luer-lock-enabled syringe must be used. This will prevent dislodgement of the needle from the syringe due to the build-up of injection pressure inside the syringe. If traction has not been completely cleared and injection was too forceful, PFCL may go through breaks into the subretinal space. The interface with fluid should also be observed and injection stopped when it has reached the desired level. During the injection process, the tip of the cannula should always be submerged in the formed PFCL bubble. This prevents formation of small bubbles of PFCL, which can also migrate under the retina.

With a 20G system, especially when the ports are free flowing, removing instruments from one of the ports can cause a jet of infusion fluid into the vitreous. Such a jet of fluid can give rise to disruption of the PFCL into tiny droplets. With the modern 23- or 25G system, some of the cannulas are guarded to prevent free flow of infusion fluid out of the sclerotomies. Equally, some vitrectomy machines are designed to match the flow of intraocular pressure. Nonetheless, surgeons' awareness of this potential complication can prevent its occurrence. Ideally, PFCL should be injected once and then removed. However, with complex manipulations of the retina, sometimes it is necessary to remove the PFCL and reinject. This again is a major cause for dispersion into droplets.

Technique of Perfluorocarbon Liquid Removal

After PFCL has served its function, it should be removed

completely from the vitreous cavity. Depending on the indication of PFCL use, PFCL–fluid, PFCL–air, or PFCL–SO exchange could be performed. A flute needle or a soft-tip needle should be used in this regard. Technique varies under different scenarios and will be discussed below.

An air-insufflation pump with IOP control should be used. As the level of PFCL lowers, the tip of the aspirating needle should be placed at the edge of the PFCL bubble. With the eye in the primary position, the PFCL bubble would have a dome upper surface. In order to aspirate all the vitreous fluid before removing the PFCL, a wide-angle optical viewing system is necessary to get access to the recess between the PFCL and the retina. Rotation of the eye should be avoided. Any vitreous fluid would be less accessible when the eye is rotated.

For PFCL–SO exchange there are two pathways where SO can be infused. The first option is to use a chandelier endoillumination and an automated SO injection through one of the sclerotomies. This frees a port for the passive extrusion of PFCL. The second option is to infuse SO through the infusion port. With both options, the SO injection cannula should first be inserted into the eye and positioned for injection. A flute needle is then inserted and placed within the PFCL bubble. Aspiration of PFCL is usually passive, and it starts once SO infusion begins. As SO is lighter than PFCL, it floats on top of PFCL, and fills the eye from anterior to posterior (Fig. 108.6).

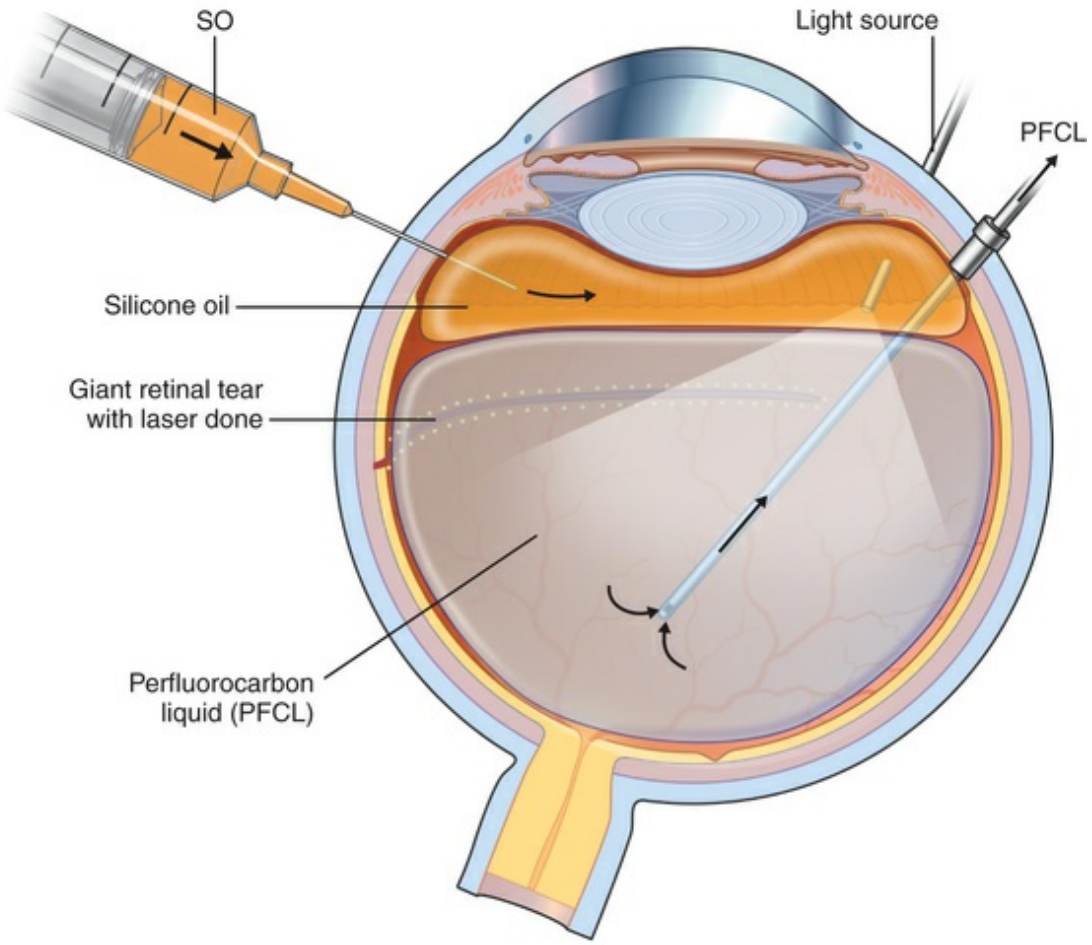

FIG. 108.6 Perfluorocarbon liquid (PFCL)–silicone oil (SO) exchange. SO is filled progressively superiorly, while PFCL is being extruded through the flute needle placed within the PFCL bubble. The giant retinal tear is kept constantly flat by the tamponade agents to avoid slippage.

To avoid slippage, the draining needle should be passed through the incoming SO bubble, into the PFCL bubble, several times. This has the effect of making the PFCL bubble join up with the SO bubble. As both bubbles are hydrophobic, they will preferentially stay in contact with each other and form a single bubble. Any aqueous would be excluded from the interface, and displaced either laterally or superiorly. This way, slippage is avoided. Slippage is the posterior displacement of vitreous fluid underneath the retina to the posterior pole, by the incoming SO bubble. By joining the SO bubble with the PFCL bubble, such posterior displacement is much less likely to occur.[65]

An additional maneuver to ensure that there is no aqueous in the

eye is to overfill the eye with PFCL all the way back to the three-way tap, before commencing the PFCL–SO exchange process. This method expels all aqueous from the eye, as well as the infusion tubings, and reduces the risk of slippage when SO is filled in progressively.[66]

Indications for Use

Proliferative Vitreoretinopathy

The use of PFCL has changed the management of proliferative vitreoretinopathy (PVR). Before the introduction of PFCL, PVR would be dealt with from anterior to posterior. After PFCL was introduced, dissection of membranes starting from the posterior pole was made possible (Fig. 108.7).[67] This is a safer approach as it reduces the risk of iatrogenic tears and the trauma to the retina. The success rate for severe PVR has been reported to range from 84% to 96%. Its use also shortens operative time, and allows more thorough removal of membranes.[68]

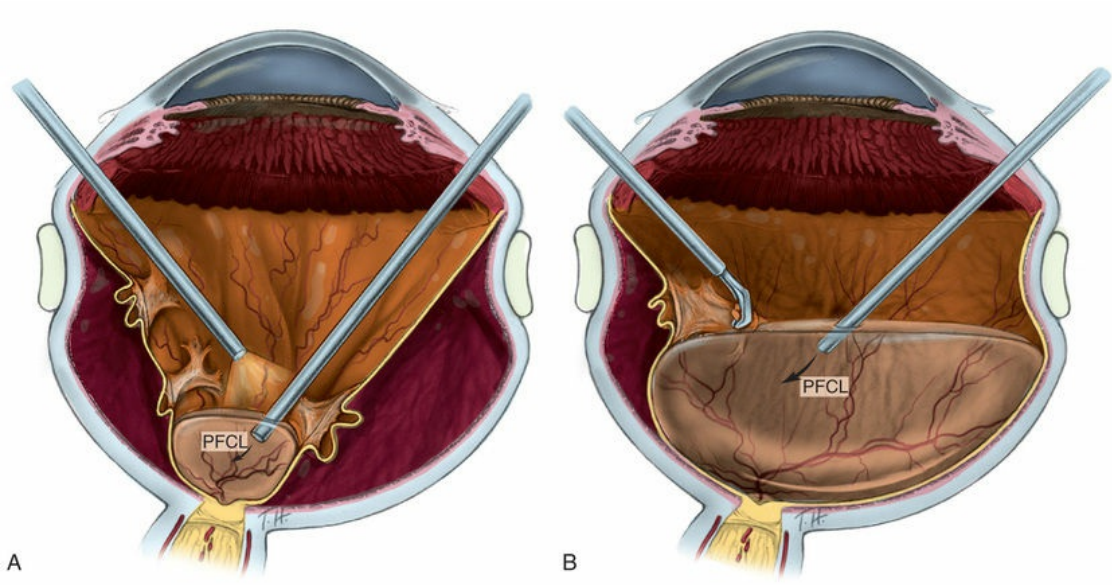

FIG. 108.7 Use of perfluorocarbon liquid (PFCL) facilitating the removal of membranes.

For cases with PVR, some surgeons prefer to insert an encircling buckle prior to performing vitrectomy. This provides additional relief of traction anteriorly and maximizes anatomic success rate.

Following core vitrectomy and initial anterior dissection, PFCL is injected over the disc to open up the funnel-shaped detachment. Usually PVD has already occurred, but if not, this helps to dissect the posterior hyaloid from the disc and retina. By doing so, the peripapillary retina is flattened and provides an initial platform for later dissections. As dissection proceeds anteriorly, more PFCL is injected to aid visualization of residual membranes.[67,69] This delineates areas that require further peeling. As the peeling process progresses anteriorly, more PFCL is injected to stabilize the retina and aid visualization of the membranes. The procedure is complete only when the whole retina is flattened under PFCL and no residual traction is left up to the vitreous base anteriorly. Scleral depression with vitreous base shaving is advisable in severe PVR to reduce the risk of reproliferations.[70] A bimanual dissection technique using a lighted pic and membrane forceps has been reported to reduce the likelihood of creating iatrogenic breaks. In severe PVR, where fibrotic membranes cannot be completely removed, retinotomies are created to relieve traction.[71] PFCL should only be filled posterior to the retinotomies to avoid any subretinal migration. When all traction has been relieved, PFCL could be added to tamponade the retina over the retinotomy. Risk of subretinal migration is low if all traction has been relieved and PFCL remains in one single bubble. Endophotocoagulation could be performed under PFCL at this point.

Depending on the extent and duration of internal tamponade required, PFCL–air or PFCL–SO exchange can be performed at this time. For less severe cases and those not requiring retinotomies, a PFCL–air exchange followed by internal tamponade with an expansile gas/air mixture (e.g., perfluoropropane-C_3F_8), may be sufficient. This could be done with the technique described above. For more severe cases where extended tamponade is required, a PFCL–SO exchange needs to be done. This has the advantage of having tamponade over the entire retina throughout the process, keeping the retina stabilized and preventing slippage from occurring. Endophotocoagulation could also be performed after PFCL exchange, either under air or through SO.

In recent series, the possibility of using PFCL as a short- to mid-term tamponade agent, to keep the retina flat postoperatively in

complex retinal detachments, has been explored.[72–74] Successful reattachment of the retina has been reported in up to 80% to 92.4% of eyes. Main problems reported were cataract formation, transient IOP rise, and a foreign body response in the eye.[73]

In general, PFCL has improved the outcomes in terms of anatomic success rate and visual outcomes in PVR surgeries.[72–76] PFCL provides the best available internal tamponade during membrane dissection. It has proved to be an indispensable tool when dealing with PVR cases.

Vitreous Base Shaving

The dissection of vitreous base is difficult even in the presence of PFCL. The reason is that the retina has already been stretched out to length. Additionally, the vitreous base cannot be separated from the retina. Most surgeons feel, in the case of PVR, meticulous dissection of the vitreous base is important as well as a close shaving of the vitreous base. The challenge of vitreous base shaving is to visualize the vitreous. The PFCL displaces the vitreous anteriorly, and the high refractive index shows a clear interface between PFCL and vitreous fluid. The contrast between vitreous fluid and gel, however, is poor because they have similar refractive indexes. It has been proposed that triamcinolone be used in combination with transscleral illumination to increase the light scatter. Particles of triamcinolone caught up in the peripheral gel can easily be seen especially when light is shone perpendicular to the line of sight. The technique of vitreous base shaving using PFCL and triamcinolone was described by Veckeneer and Wong.[77]

In all instances, vitreous base shaving should be a bimanual technique with the surgeon in control of the indentation. The use of an additional one or more fiberoptics inserted at the pars plana can make the procedure highly controllable. The availability of PFCL to stabilize the retina greatly reduces the risk of iatrogenic retinotomies. This is because the retina is less likely to engage the cutter accidentally when under the tamponade by PFCL.

Vitreous base shaving is needed in PVR cases, not only for a more complete removal of anterior traction systems; it is also desirable to ensure a more complete removal of vitreous gel. This in turn would result in a more complete SO fill. Fawcett and associates have

shown in the past that a slight underfill with SO would give rise to large area of retina unsupported.[23] If there was substantial residual gel left after a vitrectomy, it would be compressed and dehydrated by the silicone bubble, thus increasing the capacity of the eye and resulting in an underfill. When injecting PFCL, care must be taken not to overfill the vitreous cavity before adequate relieve of traction. Otherwise, there would be a substantial risk of the PFCL migrating into the subretinal space.

Giant Tears

In many parts of the world, before PFCL was available, giant tear repair involved using the Stryker table as described by Peyman.[78] This involved rolling the patient intraoperatively into a prone position and unfolding the retina with the help of an intraocular gas bubble. This proved to be difficult and yielded low success rates.[79] The introduction of PFCL allows the entire surgery to be performed with the patient lying supine. In eyes without PVR, the folded flap can be slowly repositioned by injecting PFCL slowly over the optic disc. This allows manipulation of the retina in a gentle manner and assures that endophotocoagulation is performed with the retina attached to the underlying retinal pigment epithelium (Fig. 108.8). This method hugely improved the anatomic success rate to over 88%, even without the use of a scleral buckle.[80]

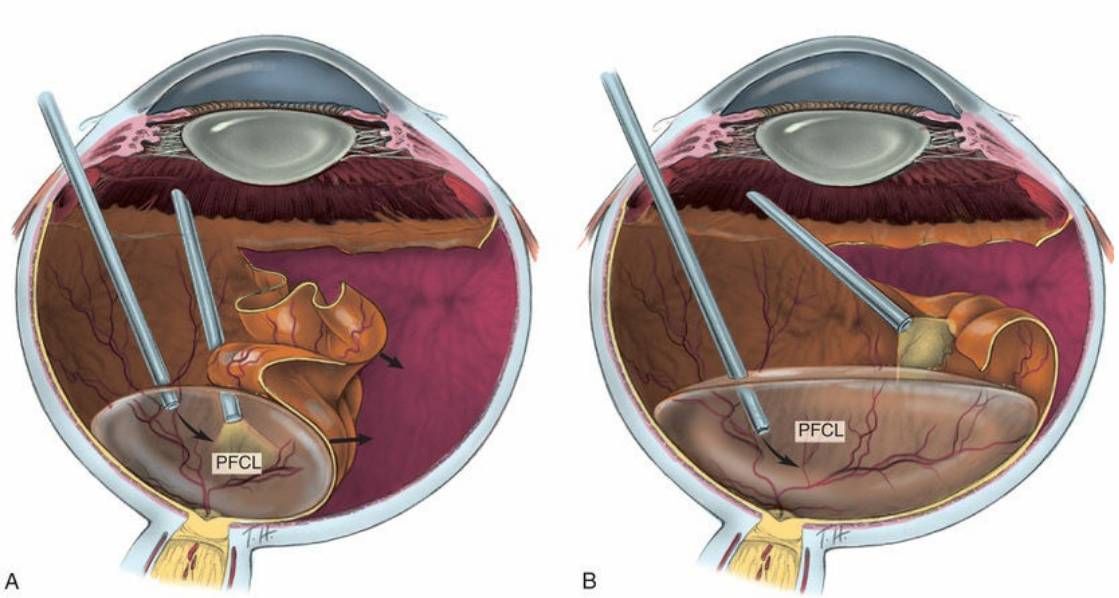

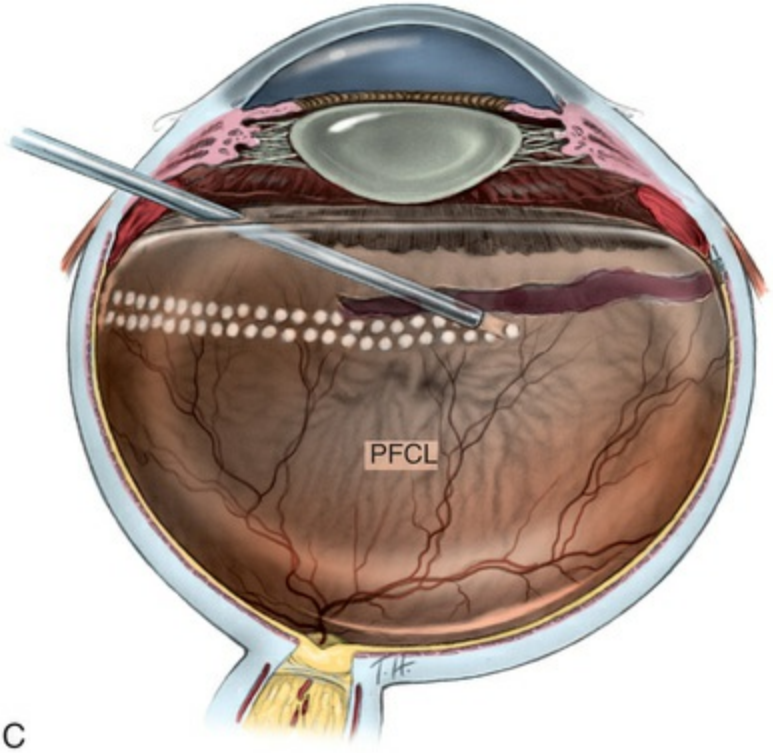

FIG. 108.8 Perfluorocarbon liquid (PFCL) could be used to unroll folded retina in cases of giant tears. (A) When the posterior flap of a giant retinal tear is inverted, the flap is elevated to allow delivery of PFCL into the preretinal space. (B) Additional PFCL is injected, and the retina is repositioned. (C) Endphotocoagulation can be applied through the PFCL bubble as the retina is stabilized by the posterior tamponade force of the heavy liquid.

For cases with immobile inverted flaps and PVR, thorough dissection of membranes is critical to reattaching the retina. Using PFCL, a high success rate of up to 90% can be expected.[70] Additional encircling buckle is favored by some. Endophotocoagulation is performed under PFCL, as the heavy tamponade opposes the retina to the underlying RPE, ensuring good uptake of laser energy. Two to three rows of confluent laser spots are created at the edge of the tear. Additional 360° endophotocoagulation can be done on the indentation created by the buckle. It is, however, controversial as to whether this should be done routinely. The majority of surgeons will do this, believing that it can reduce the risk of redetachment. Heavy 360° endophotocoagulation is associated with brisk uveitis

postoperatively. Similarly, heavy treatment at 3 and 9 o'clock might damage the anterior ciliary nerves and result in a permanently dilated pupil and reduced accommodative ability.

To prevent slippage of the retina during PFCL–SO exchange, a modified PFCL injection technique was recommended by Li and Wong.[66] First, the infusion is opened to the external atmosphere at the three-way tap, and the eye is filled with PFCL until it overflows into the infusion tubing. More PFCL is filled such that all aqueous is expelled from the three-way tap opening. This is done until PFCL is dripping out of the three-way tap. This ensures complete aqueous evacuation during PFCL injection. During subsequent PFCL–air or PFCL–SO exchange, risk of slippage is lower, as there is no residual fluid in the system (Fig. 108.9).

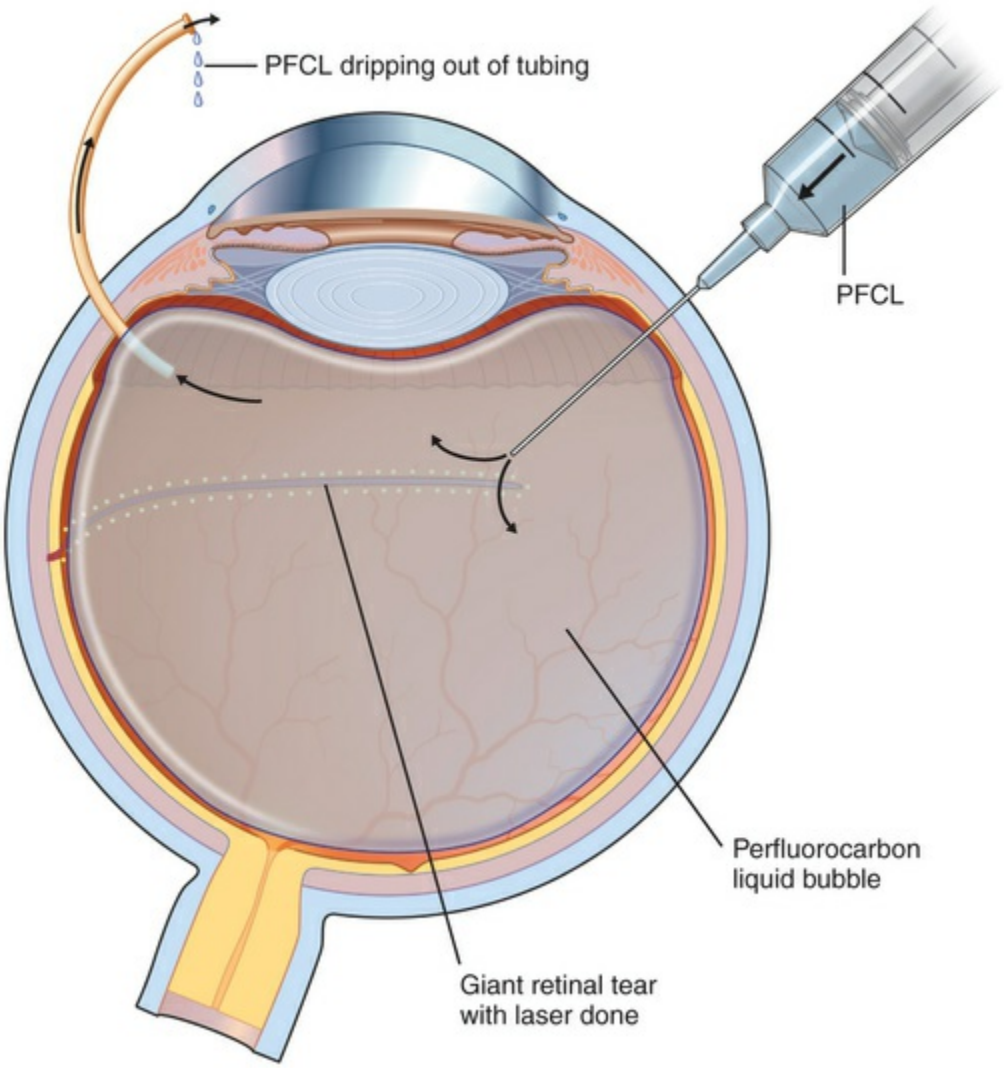

FIG. 108.9 Complete perfluorocarbon liquid (PFCL) fill to prevent slippage. PFCL is filled progressively into the eye. The external end of the infusion is disconnected, and excess PFCL is allowed to drip out from the external end of the infusion. This ensures the whole system is filled with PFCL and prevents slippage due to residual aqueous in the system.

Previously, there have been reports of using PFCL for prolonged internal tamponade.[69,81] Different PFCL and duration have been tried. In a study using perfluoroperhydrophenanthrene, it was left in situ for a mean of 20.5 days.[69] In another study using perfluorophenanthrene (Vitreon), it was left in situ for up to 4 weeks.[81] However, due to potential intraocular toxicity and other complications such as cataract formation, extended tamponade with PFCL is seldom used nowadays. Surgeons in Australia, in particular, are choosing PFCL to treat giant retinal tear. The PFCL is usually left in situ for 1–2 weeks. A second operation is then carried out, during which the PFCL is removed and further assessment of the retina is made. If the retina was deemed to be stable, gas is then used, otherwise further manipulation including photocoagulation and epiretinal membrane dissection are carried out, followed by the use of SO as a prolonged tamponade.

The rationale for the use of PFCL was to avoid slippage during air–PFCL exchange or a SO–PFCL exchange. Using the technique described by Li and Wong, a low rate of slippage was reported.[66] If PFCL is to be used for giant retinal tear and prolonged tamponade, it might be advisable for the patient to remain relatively still during convalescence. The rationale is that less dispersion might occur. Correspondingly, less inflammation might ensue. Complications related to PFCL use will be discussed below.

Ocular Trauma

Traumatic retinal detachments can be managed with the help of PFCL.[82] Coexisting intraocular hemorrhage is common and the hemorrhage may be situated in the suprachoroidal space, choroid, retina, and vitreous cavity. Most patients do not have established PVD. And in the case of laceration or rupture, vitreous incarceration is a feature. Management of these cases poses great

challenges. The use of PFCL has several advantages under these circumstances, it can: (1) stabilize the retina during vitrectomy; (2) assist separating the posterior hyaloid and retina; (3) displace preretinal, subretinal, or suprachoroidal blood; (4) assist removal of incarcerated vitreous or retina; (5) facilitate the removal of dislocated lens, intraocular lens implant (IOL), or intraocular foreign bodies (IOFB), and (6) maintain a clear media for visualization.

Traumatic incarceration of the retina through sclera can be repositioned with the help of PFCL.[83] Any incarcerated vitreous must first be completely removed. PFCL is then instilled in the vitreous cavity, to tamponade the posterior retina. This produces a tamponade effect on the posterior retina, to pull the incarcerated retina back into the eye. With this method, the incarcerated retina can sometimes be retrieved without damage. Where the retina cannot be freed, a limited retinotomy to circumscribe the incarcerated site is considered important to prevent subsequent entry-site proliferation, PVR, and recurrent detachment. The use of PFCL ensures a clear media through which such manipulation is made possible, while at the same time stabilizing the retina.

PFCL is also valuable in the removal of intraocular foreign body (IOFB). Organic or nonmetallic IOFBs can usually float on PFCL, and hence could be retrieved through the sclerotomy, or from an anterior approach. For metallic or sinking IOFBs, filling PFCL over it helps to stabilize and make grasping easier. If the foreign body is impacted in the retina, then the PFCL provides a counter pressure to any pulling force used to extract the foreign body. Large foreign bodies that float can be levitated by the PFCL to facilitate extraction through either the pars plana or a corneal wound. Extraction of impacted IOFB might lead to subretinal hemorrhage postoperatively. A small bubble of PFCL placed over the macula would ensure that this bleeding does not spread to the submacular region.

Dislocated Lens

PFCL has helped in the management of dislocated crystalline lens, dropped cataract fragments,[84] and intraocular lens (IOL) implant.[76] It is generally advisable to carry out a thorough vitrectomy,

including the separation of posterior hyaloid face, before PFCL is injected.

Small fragments can be removed successfully without the use of the heavy liquid. The technique generally involves either using a vitreous cutter or an ultrasound fragmentation. Lens fragments should be purchased using aspiration, and then levitated to the midvitreous cavity before activation of pulsed ultrasound fragmentation. Some surgeons instill a small bubble of PFCL in the posterior pole as a "cushion" against transmitted ultrasound energy causing damage to the vital structures such as the macula, optic disc, and major vessels. Others feel that PFCL hinders fragment removal rather than helps it, as it tends to displace the fragments to the edge of the bubble where they are less easily accessible. For large fragments, including the whole crystalline lens, PFCL is used as a way of lifting the whole lens to the midvitreous cavity, where it could be safely broken up and removed either by a cutter or by ultrasound fragmentation. PFCL can also be used to float the whole lens to the anterior segment in an aphakic eye, where it can be delivered through a scleral or corneal wound. If such a maneuver is attempted, some PFCL could leak through the corneal or scleral wound, such that the lens seems to drop back further into the vitreous cavity. Practically for some surgeons, there is never "enough" PFCL to float the lens clean out of the eye. One way is to perform an "expression" of the lens, much like the technique used in the extracapsular cataract extraction. The lips of the wounds are held open, and indentation of the sclera would cause the lens to be "expressed" and delivered outside the eye. PFCL is particularly useful when the dropped lens is associated with retinal detachment, where subretinal migration of fragments is prevented.[76.84]

In the case of dropped IOLs, PFCL is used to float up the IOL. It can then be grasped from an anterior approach and delivered through the limbus, or repositioned in the sulcus if there is enough capsule remnant (Fig. 108.10). Whether it is IOL or crystalline lens, if PFCL is to be used, the lenses are often displaced laterally. The upper surface of a PFCL bubble inside the eye is convex. Therefore, the crystalline lens or IOL cannot be expected to stay in the middle where convexity is highest. Instead, the lens slides off to the periphery and often becomes engaged with any residual vitreous.

Therefore, a moderately thorough shaving of the vitreous base should be carried out prior to any attempts to float the lens.

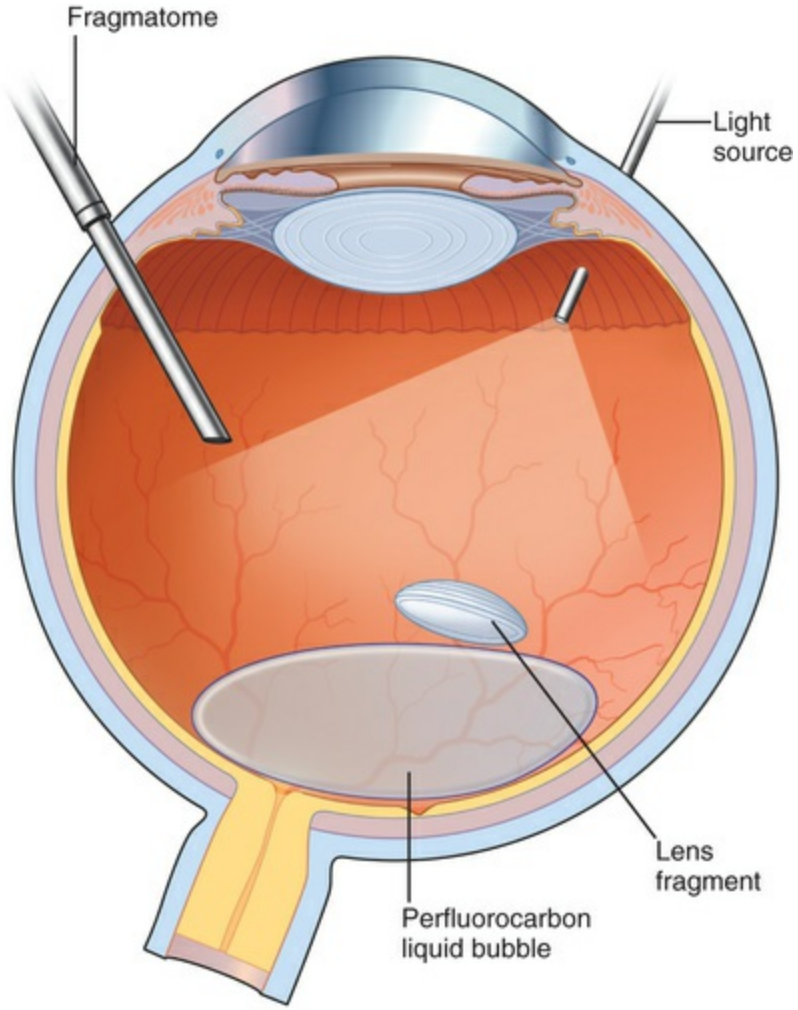

FIG. 108.10 Perfluorocarbon liquid could be used to float the nucleus fragment out through the pupil in cases of dropped nucleus after complicated cataract surgery. Perfluorocarbon liquid is used to float the nucleus fragment away from the surface of the retina. This allows easier manipulation of the lens fragment during phacofragmentation and reduces the risk of injuring the retina.

Suprachoroidal Hemorrhage

Suprachoroidal blood may not necessarily require drainage. This particularly applies to small suprachoroidal hemorrhages that do not involve the posterior pole or the macula. B-mode ultrasound is

used to assess the degree of liquefaction of the suprachoroidal hemorrhage before drainage is attempted. Such liquefaction is recognized by a "Brownian"-type movement of speckled ultrasound signals. The simple fashioning of the sclerotomy is sometimes associated with significant drainage of the altered dark-colored blood. Therefore, a scleral cut-down over the posterior choroid is unnecessary, except when there is a large posteriorly loculated hemorrhage, in which case, the injection of PFCL may be attempted. The liquefied blood would be lighter than PFCL, and as such, be displaced anteriorly towards the port. Otherwise, a sclerotomy, specially fashioned for drainage purposes, can be used. Complete drainage of suprachoroidal blood is seldom achievable. Partial drainage may be sufficient to relieve patients of pain associated with suprachoroidal hemorrhage or to prevent kissing choroidals, and the retina developing a fixed retinal fold.

However, PFCL can be of help in some cases. Following vitrectomy, 3-mm circumferential sclerotomies are created 4 mm posterior to the limbus, in the superior, nasal, and temporal quadrants. The eye is then filled with PFCL, which exerts an internal tamponade, to facilitate the evacuation of blood through the sclerotomies (Fig. 108.11).[85] Air or gas tamponade have also been tried but the evacuation with PFCL was found to be more complete.[86]

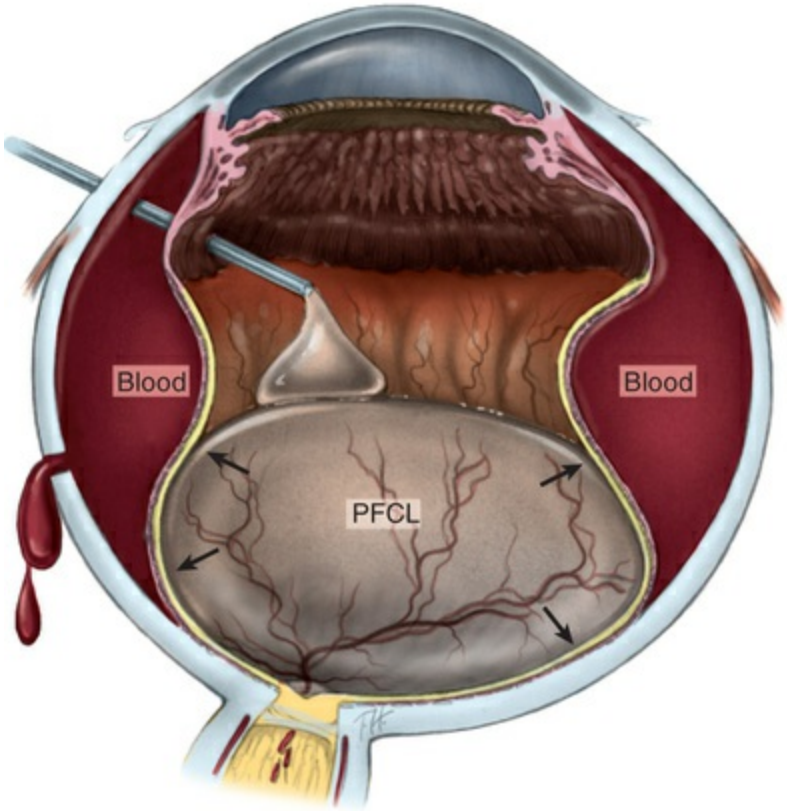

FIG. 108.11 Displacement of suprachoroidal blood clot through an external sclerotomy, with the help of perfluorocarbon liquid (PFCL) internally.

Other Indications

PFCL has also been reported to be useful in a certain number of conditions.[87] These include retinal detachment associated with diabetic retinopathy,[68] detachment associated with disc coloboma,[88] detachment from retinopathy of prematurity,[89] vitrectomy for endophthalmitis,[90] displacement of submacular hemorrhage during surgical drainage,[91] and the excision of subretinal membranes. Surgical principles are the same. It helps stabilize the retina, displaces subretinal blood, reveals preretinal membranes, and assists drainage of SRF. With these numerous advantages, PFCL has become an indispensable operative tool.

Complications and Management

Although PFCL is primarily used as an intraoperative tool with good safety profile, toxicity from extended intraocular use has been

reported in animal as well as human reports.[66,92] Although toxicity has not been observed when PFCL is retained in rabbit eyes for up to 48 hours, white precipitates appear when it is left for longer periods. In humans, Elsing and associates reported the appearance of white flake-like deposits on intraocular structures and showed inflammatory response featuring macrophages.[93] Hence, complete removal of PFCL from the eye towards the end of surgery is therefore recommended. Complications related to the use of PFCL can be divided into those seen during surgery, or after surgery, due to the effect of retained PFCL.

Subretinal PFCL

PFCL may go into the subretinal space during surgery or may be seen under the retina postoperatively. During surgery, predisposing factors for PFCL going under the retina include: (1) PFCL breaking into globules; (2) giant retinal tears; and (3) incomplete relief of tractional membranes on the retina.

PFCL bubbles have high interfacial tension against water, therefore tend to hold themselves together. If the injection process is too forceful or rapid, it may, however, break into smaller bubbles. These bubbles usually fuse together to form a large bubble fairly quickly. However, if the tear is too large, or the retina is elevated due to traction, small PFCL globules may go into the subretinal space. Therefore, injection speed should be gradual and monitored, with the injecting needle tip buried in the PFCL bubble already formed, to avoid small globule formation. A small bubble also invariably occurs if the PFCL has been injected, aspirated, and reinjected. Ideally, therefore, PFCL should be injected once and removed. However, with complicated surgical maneuvers, injection, aspiration, and reinjection repeatedly might be unavoidable. The use of dual-bore cannula for small-gauge vitrectomy is now the trend. A recently published new dual-bore cannula with four vent ports have been shown to be able to create a broad fan-like egress of fluid that is perpendicular to the axial direction of the needle.[94] This new cannula may avoid the risk of traumatizing the retina due to the jet of PFCL, and also the risk of PFCL going under the retina due to this. Some surgeons use PFCL to test the relief of traction. The understanding is that a detached

retina with no epiretinal membrane would be reattached readily with PFCL injection. This maneuver can be hazardous when injecting PFCL in the presence of one or more retinal breaks. The first sign that the traction relief was inadequate might be the migration of PFCL into the subretinal space. Small bubbles of PFCL in the subretinal space far away from the macula might be ignored. A large bubble, especially when situated above the macula, should be removed, as it could migrate and involve the fovea.

If PFCL has accidentally gone under the retina, it should be removed with every effort during the surgery, as it eventually migrates under the fovea with time even if it was located peripherally initially. It may reduce retinal function, and may cause central scotomas.[95] Retinal hole formation has also been reported in long-standing subretinal PFCL.[96] In recent reports damaged retinal function is partially recovered following removal of PFCL surgically.[97] This can either be done through a small drainage retinotomy adjacent to the PFCL bubble, or by creating a peripheral retinotomy and inserting a flute needle directly under the retina for drainage. The former technique used a small-gauge cannula (39–50G), inserted through the retina adjacent to the bubble for direct aspiration.[98,99] The latter method should be performed if a large amount of PFCL has gone under the retina. At least a 90° peripheral retinotomy has to be created to allow insertion of a flute needle under the retina for direct drainage, which is followed by gas or SO infusion. If subretinal PFCL is only noted postoperatively, drainage should be performed, as retinal sensitivity is regained after PFCL drainage.[97] A recent report utilizes intraoperative optical coherence tomography to aid visualization of the remaining PFCL during surgery, to ensure complete removal of the residual subretinal PFCL.[100]

The latter approach could be modified. Following partially detaching the retina, the PFCL bubble would then be surrounded by fluid and be round in shape. The bubble can then be removed via a retinotomy and a flute needle passed through the retinal opening to gain access to the subretinal PFCL. Equally, it is possible to displace the PFCL by simply injecting a gas bubble into the eye. This has the effect of displacing the PFCL bubble to the most dependent part of the limited retinal detachment. This is probably

the least traumatic procedure and may be suitable for bubbles of PFCL under the macula, or just above it. This strategy is essentially only displacing the bubble to an extramacular and inferior location, rather than removing the PFCL entirely.

Intraocular Toxicity

Most toxicities are related to incomplete removal of PFCL at the end of surgery, which has a reported incidence of 0.9–11.1%.[98,101] Risk is higher when peripheral retinotomy is large, especially for those where a 360° retinotomy was performed.[101] Residual PFCL can either be seen during fundal examination, appearing as fluid level inferiorly, or when it permeates into the AC, appearing as fluid level inferiorly, or as small PFCL bubbles resting in the inferior angle (Fig. 108.12). The presence of PFCL in the AC does not necessary mean that there is extensive PFCL in the vitreous cavity. This is because once it permeates into the AC, it is prevented from flowing back by the iris, as one assumes an upright posture most of the time.

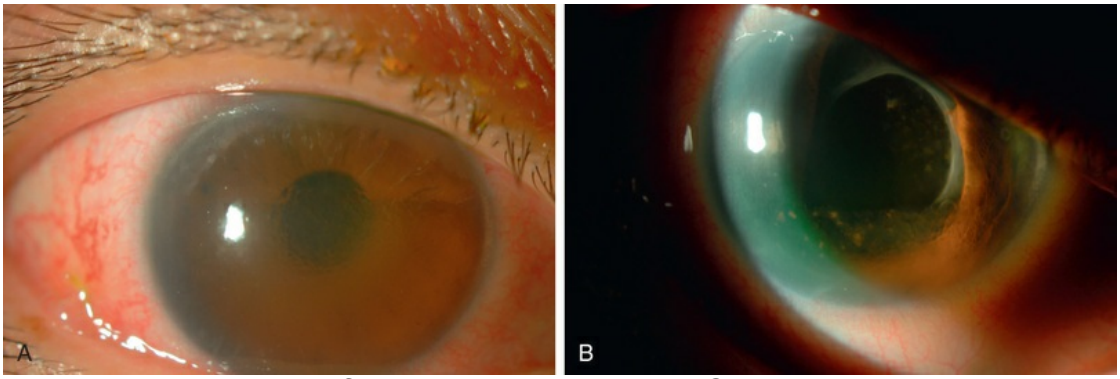

FIG. 108.12 Perfluorocarbon liquid (PFCL) globules in the anterior chamber. (A) Slit-lamp photos showing globules of PFCL in the anterior chamber. (B) Presence of keratic precipitates can be seen on the corneal endothelium. This signifies the presence of inflammation in the anterior chamber as a result of retained PFCL.

Toxicity to ocular tissues may be chemical or mechanical. Chemical toxicity is related to the both the high oxygen carrying capacity and the presence of polar impurities.[102] High oxygen

carrying capacity of PFCL might induce damage to the retina and blood vessels in two ways.[102] First, a high partial pressure of oxygen in the residual PFCL bubble causes vasoconstriction of the retinal blood vessel.[102,103] Second, direct oxygen toxicity is also capable of inducing damage to the retinal vessels, as shown in histologic reports.[102,104] The damage included loss of pericytes and endothelial cells of the retinal vessels.[104] Impurities may alter the PFCL interface, making it less resistant to absorbing lipoproteins, which is considered important in the formation of fibrotic membranes.[105] Of the various PFCLs, perfluoro-n-octane is preferred by some, as it is FDA-approved. It is also available in its purest form. It has been found to be free from toxicity when left in rabbit eyes for up to 1 week.[64]

Mechanical toxicity is due to the extended compression of inferior retina by retained PFCL, due to its higher specific gravity. Histologic changes in the retina as a result of prolonged compression include loss of the outer plexiform layer, displacement of photoreceptor nuclei into the outer segments, and atrophy of the retinal pigment epithelium.[63] We have also postulated that the trophic changes observed in the retina might be due to the exclusion of water from the surface of the retina, thus, disrupting the potassium siphoning mechanism of the Müller cells. This in turn may lead to excitotoxicity. The weight of the PFCL cannot account for similar histologic changes observed in the superior retina when SO is used. The buoyancy of a SO bubble and the force exerted on the superior retina is several folds smaller, but the changes to the retina are similar.[106]

PFCL in the Anterior Chamber

If present in the AC, PFCL may cause visual disturbance, corneal endothelial loss, as well as rise in IOP.[93] If the level of PFCL is high enough, it may block visual axis and cause disturbance of vision.

PFCL has been found to cause secondary open angle glaucoma in rabbits by causing inflammation and trabecular damage.[85,107] Pupil block glaucoma has also been reported following the use of PFCL.[107] PFCL removal is indicated under these circumstances and can be done at the slit lamp. After sterilization, a fine needle connected to a syringe is inserted into the AC, through the limbus from inferiorly.

PFCL is slowly aspirated into the syringe (Fig. 108.13). This could be repeated several times as needed, over a few hours, giving sufficient time for the AC depth to replenish. Occasionally drainage with revision vitrectomy may be required.

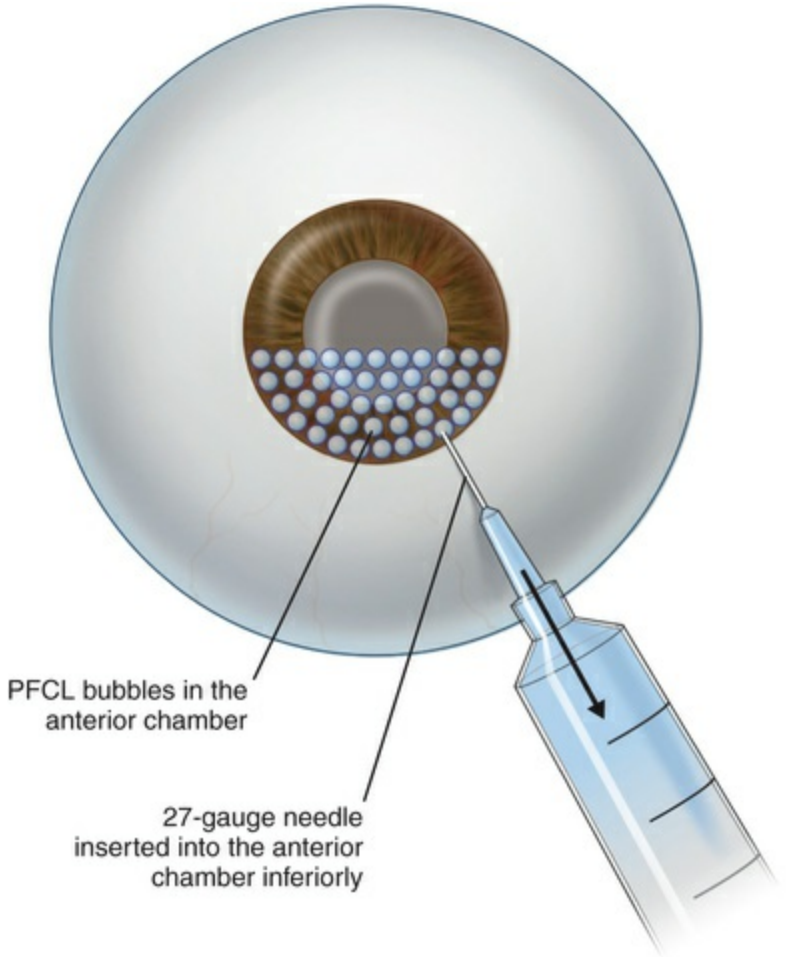

FIG. 108.13 Aspiration of perfluorocarbon liquid (PFCL) from the anterior chamber at the slit lamp. A 27-gauge needle connected to a syringe with plunger removed is inserted into the anterior chamber at near 6 o'clock position. PFCL will then be drained through the needle due to gravity.

A recent report has described a new technique using a Rycroft cannula mounted on the tip of a tuberculin syringe with continued irrigation by means of an anterior chamber maintainer.[108] This may represent a novel attempt to remove PFCL from the AC. However, this requires more intervention as an AC maintainer has to be used.

Conclusion

The perfluorocarbon liquids have proved to be an invaluable tool for the retinal surgeon in tackling challenging cases. Its use has greatly improved the outcomes of retinal detachments associated with proliferative vitreoretinopathy and use of PFCL was also proved to be helpful in assisting removal of dislocated lens, giant tears, drainage of suprachoroidal blood, and trauma cases. We anticipate that the indication for PFCL may increase, as newer techniques are developed.

Silicone Oil in Vitreoretinal Surgery

Introduction

Silicone oil (SO) was first introduced as an internal tamponade agent in the early 1960s.[109] It has since grown into an invaluable tool to the retinal surgeon in managing complex rhegmatogenous retinal detachments, especially those with severe PVR. Indications of SO have been extended to include the treatment of giant retinal tears, viral retinitis, traumatic retinal detachments, proliferative diabetic retinopathy (PDR), complicated pediatric retinal detachments, macular hole surgeries, and endophthalmitis. (This list is not exhaustive.) The use of SO has its advocates and its doubters. Here, we review the physical and chemical properties of SO, current indications of use, the surgical techniques involved, as well as the potential complications and their management.

Background

Clinical usage of SO in treating retinal detachment was first introduced by Paul Cibis in the 1960s,[109] before the introduction of pars plana vitrectomy. SO was initially injected into nonvitrectomized eyes as an aid to overcome tractional forces and the dissection of preretinal membranes.[110] This was met by initial enthusiasm, but its use later declined owing to the encountered complications and possible toxic effects reported from histologic studies.[111] As a result, many surgeons discontinued its use, especially in the United States. Despite that, some persisted in its

usage and, later, combined it with vitrectomy.[112] This achieved higher anatomic success, especially in cases of PVR that were previously thought untreatable. Through the perseverance of some surgeons, higher anatomic success rates were gradually achieved.

By the 1980s, SO had successfully re-established its role as an internal tamponade agent in many European countries. Long-acting intraocular gas was introduced and gained popularity in the United States. The divergence in the choice of tamponade agents led invariably to a head-to-head comparison: the Silicone Study. The Silicone Study was a series of randomized controlled trials comparing the efficacy and safety of SO against intraocular gases, sulfur hexafluoride (SF_6), and perfluoropropane (C_3F_8), in the management of retinal detachments with PVR.[21,113] Results showed that the differences between SO and intraocular gases were not as significant as expected. There are observations to show that the agent of choice is different between those in Europe, and those in the United States,[114] both SO and long-acting gases have their own advantages and disadvantages. To this day, the indication for SO remains controversial.

Chemical Properties of Silicone Oil

Silicone is made up of repeating units of siloxane. In fact, the term silicone is a generic term referring to all materials made up of siloxane, including silicone in its fluid form (e.g., SO), as well as silicone in its solid form (e.g., encircling band, gutters, and tires). Siloxane consists of a silicone and an oxygen molecule, with the chemical formula [−Si-O−]. Since silicone is capable of forming two additional bonds on its sides, different organic or inorganic side chains could be attached to the silicone molecule to form polymers with different properties.

Silicone oil is described as being either lighter, or heavier than water. Heavier-than-water SO is in fact a solution of a mixture of polymethylsiloxane and semifluorinated alkanes or alkenes. Lighter-than-water silicone oils (i.e., conventional SOs) vary with regards to their viscosities (Table 108.5). Heavier-than-water SOs are designed for inferior tamponade purposes. For instance, the most common SO consists of polydimethylsiloxane (siloxane with

two attached methyl side chains), also known as PDMS. PDMS has a specific gravity of 0.97, which is lighter-than-water. On the other hand, a methyl and a trifluoropropyl side chain could be added to the siloxane unit to form polytrifluoropropylmethylsiloxane, also known as fluorosilicone oils.[115] Fluorosilicone oils have a specific gravity of 1.25–1.3, hence its heavier-than-water properties.

TABLE 108.5

Chemical Properties of Silicone Oil and Other Commonly Used Intraocular Tamponade Agents

Tamponade Agent	Chemical Composition	Specific Gravity (g/cm^3 at 25 °C)	Viscosity (cSt at 25 °C)	Surface Tension (mN/m)
Silicone oil (1000 cSt)	PDMS – 100%	0.97	1000	21
Silicone oil (2000 cSt)	PDMS – 100%	0.97	2000	21
Silicone oil (5000 cSt)	PDMS – 100%	0.97	5000	21
C_8F_{10}	C_8F_{10} – 100%	1.94	0.69	14
$C_{10}F_{18}$	$C_{10}F_{18}$ – 100%	1.76	2.7	16
F_6H_8	F_6H_8 – 100%	1.35	3.44	19.7
Densiron 68	F_6H_8 – 30.5% PDMS (5000 cSt) – 69.5%	1.06	1349	19.13
Oxane HD	RMN3 – 11.9% Oxane 5700– 88.1%	1.02	3300	N/A
HWS 46–3000	F_4H_5 – 55% PDMS (100, 000 cSt) – 45%	1.118	2903	18.8
Air	N/A	<0.0001	N/A	70
C_3F_8	N/A	<0.0001	N/A	70
SF_6	N/A	<0.0001	N/A	70

cSt, centistokes; PDMS, polydimethylsiloxane; F_4H_5, perfluorobutylpentane; F_6H_8, perfluorohexyloctane; C_8F_{18}, perfluoro-n-octane; $C_{10}F_{18}$, perfluorodecalin.

Silicone oil is also described as being highly purified. This refers to the removal of impurities that are usually present, which can impact on the chemical properties of the end-product. For instance, unpolymerized residual monomers, low-molecular-weight oligomeric chains, high-molecular-weight polymeric chains, cyclic forms of siloxane, and siloxane chains with a methyl group at its end, are usually present.[116] Other than having polymer chains of undesired lengths, other impurities such as residual catalysts from

the manufacturing process may be present. Catalysts are involved in the ionic ring-opening polymerization of cyclic siloxane, to yield polysiloxane chains of different lengths. Catalysts, such as tetramethylammonium siloxanolate, are often highly toxic.[117] At the moment, albeit some SOs have obtained Food and Drug Administration approval for ophthalmic use, there is still no International Standard for the manufacturing process and the purity gradings of SO products available commercially.[118] Commercially sold SO is classified according to the average viscosities. The lower-molecular-weight SOs tend to promote emulsification. Highly purified SO refers to SO that has had impurities and the lower molecular weight components removed. Molecular weights of polymer chains are determinants of viscosity and are in proportional relationship. Hence, overall viscosity may be higher than expected if more high-molecular-weight polymers are produced and low if more low-molecular-weight polymers are produced. While the product is essentially a mixture of compounds, viscosity is judged by measuring the overall average value as a whole.[119] Therefore, commercially available SOs are sold and classified according to the average viscosities (which is a representation of the averaged molecular weights).

Physical Properties of Silicone Oil

Specific Gravity

Aqueous has specific gravity of around 1.01. Hence, we can assume it is about the same as water (1.00). Polydimethylsiloxanes (PDMS) all have a specific gravity of 0.97. It must be noted that for all PDMS, specific gravity remains the same regardless of its chain length or molecular weight. This is because the molecular density of the repeating unit of dimethylsiloxane is independent of the chain length. Hence, all PDMS have identical specific gravities of 0.97, and they all float in the presence of water or aqueous. Specific gravities of heavier-than-water SOs and heavy tamponades are discussed later in this chapter.

Buoyancy

Details of the physics involved are discussed above. The area in

contact with the retina, and the bubble's size and shape determines the effectiveness of tamponade by a bubble. This is governed mainly by buoyancy. When buoyancy is large, as in gas bubbles, the bubble takes on the shape of a spherical cap. A spherical cap is a sphere with a flat bottom. Conversely, when buoyancy is small, the bubble assumes a relative spherical shape, as in the case of SO. For this reason, a gas bubble makes a larger area of contact against the retinal surface than an equivalent volume of SO bubble. It has been demonstrated that a SO bubble virtually makes no contact with the retina until the eye is near 50% filled. In contrast, a small gas bubble (as small as 0.28 mL) already tamponades up to 90° of arc on the retina (Fig. 108.14).[120] Scleral buckles cause an indent into an otherwise near-spherical vitreous cavity. SO has been shown not to make contact with the retina on either side of the indent. Hence, SO retains a spherical shape, and it does not fill the recesses created by the indent. Therefore, when SO use is intended, it is important to achieve a near 100% fill, in order to achieve a good tamponade effect.

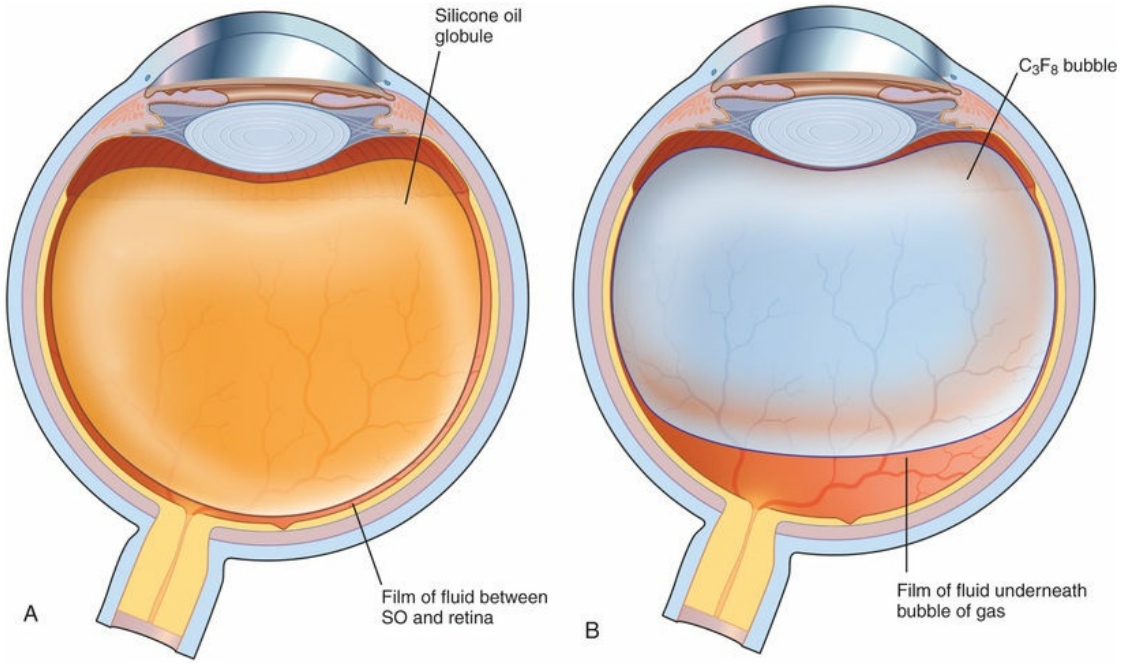

FIG. 108.14 Slight underfill predisposes to formation of a fluid film between silicone oil (SO) bubble and retina.

This reduces the tamponade effect because the buoyancy of SO is less than that of intraocular gas. (A) Due to the lower buoyancy, the SO globule assumes a

round shape when injected into the eye, leaving a film of fluid between it and the retina. This happens even with only a slight underfill. (B) When the eye is slightly underfilled with C_3F_8, the tamponade effect is relatively better with only a film of fluid underneath the bubble.

Surface Tension and Interfacial Tension

Surface tension refers to the Van de Waal forces between molecules. In a drop of liquid in air, the molecules in the center are attracted equally to every other molecule. A molecule on the surface, however, is only attracted to its neighbors. As a result, the surface energy always acts to try to reduce the surface for a given volume. Interfacial tension is a more general term relating to the surface tension between two immiscible liquids. Surface tension specifically refers to the surface energy when one of the two liquids is air. The forces reach equilibrium when free energy at the interface is kept at a minimum. This is usually reached when all like-molecules reside on one side and unlike molecules settle on the other side. Hence an interface is formed, which acts like a taught membrane across two phases.

Here, interfacial tension refers to the force that tends to keep a bubble as a whole.[121] It has been found that an oil bubble remains intact as long as the interfacial tension is above 6 mN/m (milli-Newton/meter). This is important as a single bubble enhances effectiveness of the tamponade. When SO (1000 cSt) comes in contact with pure water, interfacial tension was found to be 40 mN/m. This value was reduced to 33 mN/m when it is physiologic fluid. Presence of impurities such as proteins and lipids, or simply blood, can also alter the interfacial tension. For example, it was found that in the presence of blood the interfacial tension can be further reduced to 14 mN/m.[122]

Viscosity

Viscosity is a measure of the resistance of a fluid towards being deformed when under shear stress. Hence, it is also known as shear viscosity. It is caused by the attractive forces between molecules in close contact and the friction between molecular chains. Higher

energy is required to deform a highly viscous liquid, while lower energy is needed when deforming a less viscous fluid. Generally, SOs with longer chain lengths have higher viscosity. This has practical implications, as ease of injection and removal is directly proportional to viscosity.

Two kinds of viscosities are involved, namely "shear" and "extensional" viscosities. It has been shown that the lower the shear viscosity, the greater the propensity for dispersion; this has been demonstrated up to a viscosity of 12, 500 cSt. It has also been shown that the presence of low-molecular-weight components also increases the readiness of the oil to disperse. The second type of viscosity that is important refers to extensional viscosity. This is a measure of the resistance of the SO to break up when a globule is drawn into a strand. When the strand breaks, satellite droplets tend to form (Fig. 108.15). Williams and associates added these high-molecular-weight polymers to low-viscosity SO (1000 cSt) and successfully increased the extensional viscosity to a level equal to that of SO of 5000 cSt.[123] By adding 5% or 10% of 423 kD to 1000 cSt SO, the shear viscosity of the mixture can be increased to 2000 cSt and 5000 cSt, respectively. At the same time, the extensional viscosity can be increased, especially when the liquid is subjected to shear stress. Whether these silicone oils are more stable when used in the eye is yet to be proven in clinical trials.

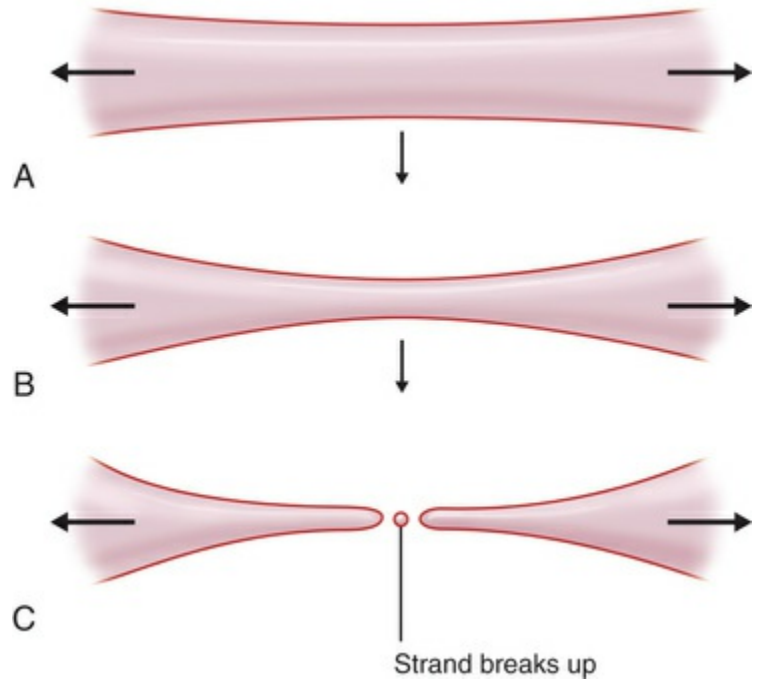

FIG. 108.15 Demonstration of how a thin strand of silicone oil breaks up when pulled apart.

"Dispersion" and "emulsification" are terms sometimes used interchangeably. Technically, dispersion refers to the break-up of a large bubble of oil into smaller droplets. These droplets naturally have higher surface energy and will tend to coalescence back into a single bubble. Emulsification only occurs when this surface energy is reduced by the presence of surfactants. The droplets are therefore stabilized and tend not to reform into a single bubble.

Indications

Usage of SO as described by Cibis was without vitrectomy.[109] Reports of complications associated with its use have led to slow adoption by many surgeons.[124,125] It was only after the introduction of the vitrectomy system that usage of SO became more popular, especially after the Silicone Study.

Retinal Detachments With Proliferative Vitreoretinopathy

The Silicone Study[21,113] defined the role of SO in the management of retinal detachments. It was a multicenter prospective randomized

clinical trial comparing the effect of SO with long-acting intraocular gases (SF_6 and C_3F_8) in the management of complex retinal detachments associated with PVR grade C_3 or above (i.e., full retinal thickness retinal folds in three or more quadrants; Retinal Society Classification). In general, SO was found to be as effective as C_3F_8, and better than SF_6, in reattaching the retina.[21] Both SO and C_3F_8 were equivalent in terms of improving visual function and low complication rates.[21] Regarding postoperative complications, in particular hypotony and keratopathy, SO did better than SF_6.[21]

Despite having equivalent results, subgroup analyses revealed relative superiority in SO under certain circumstances. Subjects were divided into Group 1 (no history of previous vitreous surgery) and Group 2 (had at least one vitrectomy with gas use). Among Group 1 eyes that required retinotomy to flatten the retina, use of SO initially increased the likelihood of visual recovery and reduced risk of hypotony at 6 months. However, at 24 months, a deteriorating trend was observed among eyes that used SO; whereas an improving trend was seen in eyes that used intraocular gas. Risk of recurrent detachment after SO removal was also studied. In a matched-pair cohort comparing SO-removed eyes with SO-in-situ eyes, risk of recurrent detachment was increased if SO was removed. However, if the retina remained attached, despite SO removal, visual acuity tended to be better and complication rates were lower.

In a recent meta-analysis published by the Cochrane Collaboration,[126] the reviewers concluded that the Silicone Study remained the only well-conducted randomized controlled trial comparing the effect of SO in treating retinal detachments. The evidence from the Silicone Study did not reveal any significant differences between SO and C_3F_8. While SF_6 was found to be inferior to both within the first year of the study, the differences diminished towards the end of the second year of follow-up. The reviewers pointed out that at the time of the Silicone Study, only SO of 1000 cSt was used, while currently, SO of other viscosities (i.e., 1300/5000/5500, etc.), is available. Perfluorocarbon liquids (PFCLs) were only introduced later during the Silicone Study, hence most subjects in the studies had surgery performed without the use of

PFCL.

Some relative indications for SO use in detachments with PVR remain controversial. In addition to the surgeon's preference, the patient's ability to comply with postoperative posturing, and the need for air travel shortly after surgery, are used as justifications for the use of SO. Relative contraindications for SO use include a deficient iris diaphragm (e.g., aniridia) that might predispose to keratopathy.

Giant Retinal Tears

In giant retinal tears, the posterior flap of retina is independently mobile. It is because the edge of the posterior flap does not have any vitreous attaching to it. Therefore it has a tendency to slip posteriorly, especially when the extent of the tear is >90°. Traditionally, the role of SO in managing giant retinal tears is twofold: (1) to unroll folded retina and (2) to act as an extended internal tamponade agent. With the introduction of PFCLs,[58] unfolding the retina is easier.

The principle of surgical repair is to reattach the retinal detachment without slippage or exposing a large area of RPE. With the help of PFCLs, folded retinal flaps are unrolled and repositioned. Endophotocoagulation is then performed along both edges of the tear. This is followed by either a PFCL–SO exchange,[127] or a PFCL–air exchange and air–SO exchange. It has been shown that PFCL–SO exchange reduces the risk of slippage during the exchange process.

The use of SO in giant tears without PVR remains controversial. In Europe, SO remains the agent of choice, while in the United States some still prefer intraocular gas. Good anatomic success with either SO or gas has been reported.[128] In particular, a 100% success rate with SO was reported by Leaver and Lean.[129] To date, there are still no randomized controlled trials to compare the outcomes between SO and gas. The authors prefer SO to gas when the patient cannot posture or when the tear is more than 90° in size, especially when it involves the inferior retina.

Severe Proliferative Diabetic Retinopathy

In Europe, SO tamponade is frequently used at the primary

vitrectomy for traction retinal detachment associated with severe proliferative diabetic retinopathy (PDR).[130] However, there are still no randomized controlled trials in this regard to address its efficacy and outcomes. While the main drawback is the need for a second operation to remove it from the eye, SO has several theoretical advantages if used as a tamponade agent following vitrectomy. It enables rapid visual recovery; it reduces postoperative vitreous hemorrhage and allows clear visualization of the fundus during examination; it may provide better tamponade for those who cannot posture after operation.[131] Because SO occupies most of the vitreous cavity, it potentially confines all dissolved oxygen in the anterior segment. It also prevents vascular proliferative factors in the posterior segment from coming anteriorly. This can be beneficial in cases of severe PDR where anterior segment neovascularization is prominent, especially during the postoperative period.[132,133] In a series of 18 patients with anterior proliferation and anterior segment neovascularization, vitrectomy with SO infusion stabilized the neovascularization in 83% of eyes, and achieved retinal attachment in 56%.[133] As a general rule, injection of SO should only commence after hemostasis has been achieved and most, if not all, preretinal blood has been aspirated. This reduces the risk of proliferative changes after the surgery.

Macular Hole

Traditionally, vitrectomy with or without internal limiting membrane (ILM) peeling, followed by internal tamponade with either gas or SO, combined with postoperative face-down posturing has been the treatment of choice for idiopathic macular holes. It was believed by some that mechanical force generated by the tamponade agent and posturing would be helpful in closing the hole. In an early study by Goldbaum and associates, an 80% closure rate on first operation was achieved with vitrectomy and SO tamponade. This figure went up to 92.5% with two operations.[134] However, a later trial by Lai comparing the efficacy in closure rate with either gas or SO as tamponade after vitrectomy revealed a lower closure rate with SO.[135] Due to the differences in results, gas has grown in popularity as the agent of choice.

The current focus has shifted to looking at the efficacy of ILM

peeling, choice and duration of gas tamponade, and need for postoperative posturing.[136–139] A recent study using spectral-domain optical coherence tomography (OCT) to capture hole closure showed that following vitrectomy with ILM peeling and gas tamponade, 77% closure rate was achieved as fast as on postoperative day 1.[140] Another similar study yielded a 90% closure rate on postoperative day 1.[141] This supports the idea of using a gas with shorter intraocular longevity such as air, and obviates the need for posturing. A recent meta-analysis failed to show any significant benefit for extended posturing after surgery, in terms of closure rates.[142] One of the determinants of success rate seems to be hole size. For holes smaller than 400 μm, the lesser algorithm can be applied, namely shorter-acting gases, no posturing, and no need to peel the ILM. With the success of gas tamponade and posturing in the repair of idiopathic macular holes, the role of SO has diminished. Nevertheless, it could still be considered for those who need to travel by air shortly after surgery.

The situation regarding reoperation is less clear. Virtually all series report a reasonable success rate (range 70–80% closure rates) with gas. Some reported up to 100% with the use of heavy tamponade agents,[143] while others have shown less consistent results.[144] It has been shown in a large series that closure rate after reoperation for holes that never closed was far worse than for holes that reopened. It is recommended, for holes that are large and which failed to close with the first operation, that a thorough discussion with the patient is needed, regarding visual expectation and the likelihood of success with further operations.[145]

For retinal detachments associated with macular holes in pathologic myopia, the current trend is to perform vitrectomy with an intraocular gas tamponade. Satisfactory anatomic successes have been achieved with this approach.[146] We performed a prospective case–control study with a double-peel technique, employing triamcinolone (TA) and trypan blue (TB) to assist removal of the adherent cortical vitreous and ILM, respectively. Reattachment rate of 70% was achieved in the study eyes, compared with 44% in the controls, where no staining was used.[147] There has been more evidence to support the use of SO as a primary tamponade agent for macular hole detachments associated with high myopia. Chen

compared the results of 57 cases performed with either gas or SO as tamponade agent. The reattachment rate was in favor of using SO.[148] In another study by Nishimura and associates, 100% reattachment rate was achieved with SO, as primary tamponade following vitrectomy.[149] A prospective randomized controlled trial should be conducted to compare the efficacies of gas versus SO in these cases.

Viral Retinitis

The nature of retinal detachment associated with viral retinitis tends to be diffuse, relentless, and have a high redetachment rate.[150] These are commonly due to cytomegalovirus (CMV) retinitis, as seen in immunocompromised patients, or due to acute retinal necrosis (ARN) associated with herpes simplex type 1.[151] Necrosis of the retina gives rise to large areas of retinal defects that lead to the detachments. Under these circumstances, SO offers long-term, sometimes permanent, internal tamponade, and reduces the risk of redetachment. Azen and associates conducted a prospective observational multicenter study to evaluate the first operational anatomic success rates of using vitrectomy and SO tamponade for CMV-related retinal detachments. At 6 months after surgery, 78% remained attached with this method.[152] In a series with detachment related to ARN, vitrectomy and SO tamponade yielded 100% anatomic success rates.[153] These are anecdotal cases. There are variations in individual presentations, and speed of progression. Response also depends on how promptly intervention is given.

Most patients with CMV retinitis are immunocompromised, usually associated with acquired immunodeficiency syndrome (AIDS). These patients tend to be relatively young and they usually have clear crystalline lens at the time of retinal detachments. Tanna conducted a retrospective cohort study to investigate the incidence of cataract among those that required vitrectomy and SO tamponade. Results showed an estimated median time to cataract formation of 1.8 months after retinal detachment repair with SO. Adjusted relative risk when compared with eyes that did not require retinal detachment repair was 6.74 (<.001). Following phacoemulsification for cataracts, subjects developed posterior capsular opacification at a median time of 7 days only.[154] Results

suggested that clear lens extraction in these patients at the time of retinal detachment repair with SO tamponade may be beneficial. This was later supported by a study by Engstrom et al., who carried out combined clear lens extraction and intraocular lens implantation with vitrectomy, and SO tamponade was performed on 12 patients with retinal detachment associated with CMV retinitis. Retinal attachment rate was 83% and median best corrected visual acuity raised from 20/75 before surgery to 20/50 after surgery.[155] Such a combined approach may be considered in cases of CMV retinitis.

When the eye is filled with SO after surgery, intravitreal injection of ganciclovir would be concentrated in the thin layer of fluid film between the SO and retina. Normal concentration of intravitreal injections would therefore be inappropriately increased. This would cause retinal toxicity and create undesirable effects.[156] An appropriate method is to insert a ganciclovir implant.[157] Ganciclovir implant has been proven to give comparable concentrations in both vitrectomized and nonvitrectomized eyes.[158] A recent study showed that by combining vitrectomy, SO tamponade, and ganciclovir implant insertion, 100% reattachment rate was achieved and 80% showed no CMV retinitis progression.[159] This would be a reasonable option in selected patients where retinitis is still active in the presence of retinal detachment. Otherwise, antiviral treatment would have to be given via the systemic route.

Complicated Pediatric Retinal Detachments

Main indications of SO tamponade in the pediatric population are mainly retinal detachments associated with trauma, retinopathy of prematurity, congenital anomaly such as coloboma or optic disc pit, and myopia (see Chapter 119, Surgery for Pediatric Vitreoretinal Disorders).

Wong and colleagues have published a method in which sequential use of conventional SO and Densiron, a heavier-than-water SO, has helped reduce the number of reoperations. Mean LogMAR visual acuity before surgery was 1.57 among 10 cases, and mean postoperative visual acuity was 0.82. In our series, visual outcomes were favorable despite the need to undergo multiple operations.[160]

Retinal Detachments Associated With Choroidal Coloboma

Coloboma of the choroid is a congenital condition characterized by an area, usually inferonasal to the disc, devoid of retina, retinal pigment epithelium, and choroid. Retinal detachment in these eyes has a reported incidence of 23–42%.[161,162] As the area of detachment is adjacent to the disc, difficulties in exposure translates into poor surgical outcomes with scleral buckling approach.[161,162] In the past, radial explants to both the nasal and temporal edges have been applied. This sometimes resembles the Chinese character for "eight," and has been referred to as such. Anatomic success rates of less than 60% only were reported.[161,162] With modern vitrectomy and SO tamponade, Pal and associates reported a long-term attachment rate of 88.1% at 6 months.[163] In their series, out of the 21 cases that underwent SO removals, only two experienced redetachment. This shows the effectiveness of vitrectomy and SO tamponade in managing these cases. The retinal breaks can overlie bare sclera, and achieving chorioretinal adhesion is not possible simply because there are no choroids for the retina to adhere to. Therefore the retinal breaks overlying the coloboma stay open. Some surgeons attempt to form a barrier by lasering the edge of the coloboma. This laser needs to be applied to the whole extent of the coloboma and may or may not be effective. For this reason, a number of children ended up with permanent SO. Lastly, with use of SO, hyperopic shift after surgery is very amblyogenic. Virtually all will need patching from the early postoperative period.

Trauma

In severely traumatized eyes, internal tamponade with SO may help to flatten the retina and prevent hemorrhage, which is known to increase the risk of PVR formation.[164] In a series of 435 eyes with ocular injury, Spiegel and associates performed vitrectomy and SO tamponade as primary surgery within 24 hours in 13 eyes (3%).[165] These eyes had either retinal lacerations larger than 4 disc diameters, or persistent intraoperative bleeding, with or without retinal detachments. Mean follow-up was 28.7 months and 11 out of the 13 eyes achieved visual acuity 20/200 or better, with the highest

being 20/25. Removal of SO was performed in 11 of the 13 eyes at an average of 6 months and of those, two had recurrent PVRs. While standardization of trauma cases is difficult, the results of this study show that SO tamponade at primary repair of the injury is feasible and relatively reasonable visual outcome is achievable.

In a recent retrospective case series with 88 patients who suffered ocular injury with retinal detachment, Nashed and associates performed primary vitrectomy and SO tamponade within 8 hours of injury.[166] Proliferative vitreoretinopathy occurred in 44% of cases and redetachment was noted in 38% of all cases. Visual outcome was worst with globe rupture cases. Endophthalmitis occurred in 3.4% of cases. Nashed went on to conclude that frequency of endophthalmitis was relatively low and the development of postoperative PVR was avoided in most cases. This might have been the effect of SO in situ. In any case, the great variability in degree of injury makes it difficult to draw conclusions on the role and necessity of SO in these series.

Endophthalmitis

Apart from acting as an internal tamponade agent, SO has been suggested to possess antimicrobial activity. Azad and associates performed a prospective randomized controlled trial, comparing the effect of vitrectomy with or without SO tamponade for posttraumatic endophthalmitis cases.[167] In cases where SO was used, vision achieved a level of 20/200 or better in 58% of cases (seven out of 12), versus only 8% (one out of 12) among those where SO was not used. In another study, Yan and associates performed vitrectomy and SO tamponade in 18 posttraumatic endophthalmitis eyes. Postoperative visual acuity increased in 83% of eyes.[168] In another recent case series, 108 consecutive eyes with bacterial endophthalmitis were randomly assigned to receive ether vitrectomy and intravitreal antibiotic alone, or with silicone oil as tamponade. The overall success rate with silicone oil was significantly higher than those without (67.3% vs. 43.4%, p=.01).[169]

In the presence of SO, it is difficult to be certain of the correct concentration of antibiotic used. Using magnetic resonance imaging, we have shown that an aqueous bolus of antibiotic gets outside the oil bubble relatively quickly and joins the retro-oil

aqueous film. This film of aqueous is usually very small. Hence the concentration of the antibiotic would be higher than expected. One way to ensure correct dosing is to carry out a fluid–air exchange at the end of vitrectomy. Antibiotics of the correct concentration are then used to fill the air-filled vitreous cavity, before SO is injected. This maneuver ensures that a toxic dose of drugs is not administered.

Surgical Techniques of Silicone Oil Infusion

General Considerations

Although surgical techniques involved in SO infusion varies considerably between surgeons, the principles behind how SO behaves as a tamponade agent remain constant. Physical properties of SO such as interfacial tension, specific gravity, and viscosity, which dictate how SO behaves, should be considered.

Commercially available SO has viscosities ranging from 1000 cSt to 5700 cSt. The lower viscosity SO (i.e., 1000 cSt) was used in the Silicone Study, while the 5000 cSt SO is the only SO approved by the Food and Drug Administration for intraocular use in the United States. Practical differences between SO of different viscosities are threefold: (1) difficulty in injection is higher as the viscosity goes up; (2) ease of removal is higher as the viscosity goes down; and (3) risk of emulsification. The tamponade effect appears to be similar among SO with different viscosities.[170]

It must be noted that the interfacial tension between SO and water is lower than that of gas to water. Hence, when the retina appears flat under air before SO infusion, the retina may still be elevated when SO is infused, and SO may migrate subretinally where traction is still present.[171]

Owing to the high viscosity of SO, high pressure is required to infuse it into the eye from its container (i.e., syringe). Generally, 5–10 mL of SO is sterilized and stored in a 20 mL syringe. The infusion could be made through either of the two open sclerotomies. The syringe is first connected to an injection cannula, which can be either metal or plastic. Syringes with a Luer-lock are preferred, as they are more secure under high injection pressures. Short metal injection cannulas can be used as they are, while

plastics ones should be cut short for use. As flow is inversely proportional to its length, injection can also be done via the infusion cannula. The cannula should also be short and rounded to avoid leakage or breakdown during injection.

Injection can be done either with an automated pneumatic pump or manually. Most surgeons now prefer using an automated infusion pump, connected to the SO-containing syringe. This has the advantage of being faster and allows more surgeon-control through a foot pedal-controlled system. The disadvantage of this system is that there is no pressure-feedback mechanism, hence a risk of over- or underfill exists and is dependent on the surgeon's experience. Surgeons are advised to monitor the intraocular pressure digitally during the process. An IOP of around 10 mmHg is desirable at the end of the surgery. Fluid is incompressible, and the sclera is relatively inelastic. A slight overfill can give rise to an exponential rise in IOP. Rupture of the globe, collapse of the AC in the presence of a phaco wound or prolapse of the iris can result from an accidental overfill.

Considerations of Lens Status

In phakic eyes, practical concerns regarding the lens arise when SO tamponade is required. These include whether to remove the lens, and whether to implant an IOL. If the primary pathology is posterior, the lens can be left alone. Some believe that leaving the eye phakic would enhance the tamponade effect of the oil to the superior and inferior retina. Cataract invariably occurs following SO tamponade, even if SO is removed shortly after surgery (i.e., 6 weeks).[172] In this regard, many surgeons prefer removing the lens at the same sitting. Rendering the eye pseudophakic facilitates vitreous base dissection and shaving. Phacovitrectomy is commonly the standard approach by retinal surgeons in most countries except in the United States, where the referral pattern discourages retinal specialists from carrying out phacoemulsification themselves. A combined effort between cataract and retinal surgeons is sometimes practiced. Alternatively, some retinal surgeons still use lensectomy, perhaps preserving the anterior capsule for subsequent secondary lens implantation. Rendering the patient totally aphakic is unacceptable as it would

increase the risk of oil keratopathy even if an inferior peripheral iridectomy was performed. Retention of the anterior lens capsule has also been reported to reduce complications related to either gas or SO use, and can maintain a normal iris appearance.[173]

An IOL made up of polymethyl methacrylate (PMMA) or acrylic should be used to avoid the risk of undesirable adhesions of SO to the IOL. When this happens, the patient becomes very symptomatic. The adherent oil droplet gives rise to often high refractive error. High and irregular astigmatism cannot be fully corrected by spectacles. Monocular diplopia, polyopia, blurred and distorted vision will render the patient symptomatic.

Silicone Oil Infusion in Small-Gauge Vitrectomy Systems

With the advent of sutureless small-gauge vitrectomy systems, such as the 23G or 25G systems, the possibility of SO tamponade in conjunction with these systems has been explored.[174–178] Kapran and associates reported the use of a 25G transconjunctival sutureless system in removing silicone oil. Mean removal time required was 8.93±0.85 minutes.[175] In another series by Lewis, no different was noted when using 20G, 23G, and 25G systems.[176] For the 25G vitrectomy system, Riemann and associates reported their success in infusing both 1000 cSt and 5000 cSt SO in 35 patients who underwent 25G vitrectomy.[177] Due to the unavailability of a 25G cannula at the time of the study, SO infusion was done using a 24G angiocatheter. In their series, SO of both 1000 cSt and 5000 cSt were used and the authors trimmed the angiocatheter to 4 mm in cases where 5000 cSt SO was used, to speed up the injection process. No difficulties were encountered, and this was supported by a later study by Altan et al.[178] Altan and associates injected 1000 cSt in 14 patients undergoing 25G vitrectomy, using a 25G cannula designed for SO infusion (Polytip-VFI, MedOne, Sarasota, FL). No difficulties were encountered during the infusion process. With the increase in popularity of small-gauge vitrectomy systems, and the advent in instrumentation correspondingly, the future trend is to combine the use of SO with these systems. All these injection techniques involve using short cannulas. The time taken for injection would be longer because the flow is inversely proportional to the 4th power of the

radius of the cannula.

The newly introduced SO with high-molecular-weight additives (HMWA) have been shown to be easier to inject and remove. The reason is physical. For instance, Siluron 2000 is a mixture of 1000 cSt SO with 5% 423 kD PDMS. The HMWA increased the shear as well as extensional viscosities. The shear viscosity is around 2000 cSt, however, under extensional flow (i.e., when forced to flow through a narrow cannula), the PDMS macromolecule unfolds and lines up with the flow. In this state, the flow rate is increased. Effectively, when it comes to injection or removal, Siluron 2000 behaves much like SO with 1000 cSt.

Air–Silicone Oil Exchange

This is commonly done towards the end of surgery, when air–fluid exchange has been performed. At this point, the retina should be flat under air, with no or minimal SRF. The presence of fluid inside the vitreous cavity predisposes to underfilling of SO. Endolaser photocoagulation should have been performed to seal all retinal breaks. Injection of SO is then carried out, with the injection cannula inserted through either of the two open sclerotomies. The illumination should be withdrawn after the initial gush of SO has been infused. This allows air inside the eye to escape through the vacant sclerotomy, as SO is being filled progressively. To ensure a good fill of SO, the vacant sclerotomy should be maneuvered to the most independent position such that no bubbles will be trapped when SO fills up to the sclerotomy internally. The endpoint of SO infusion is either when it fills up to the vacant sclerotomy – SO is seen filling the infusion tube from internally – or when it reaches the iris plane in aphakic eyes. In pseudophakic eyes a sign that signifies near complete fill is when the enlarging SO bubble touches the undersurface of the posterior capsule, which can be seen easily under the microscope (Fig. 108.16). The IOP should be normal, or at around 10 mmHg at the end of surgery, otherwise overfill is likely. Overfill prevents the normal egress of aqueous from the posterior chamber anteriorly and predisposes to shallow AC and intractable IOP rise. Therefore, if IOP tends to be on the high side, some SO should be expressed through the sclerotomies passively until the pressure is normalized to around 10 mmHg.

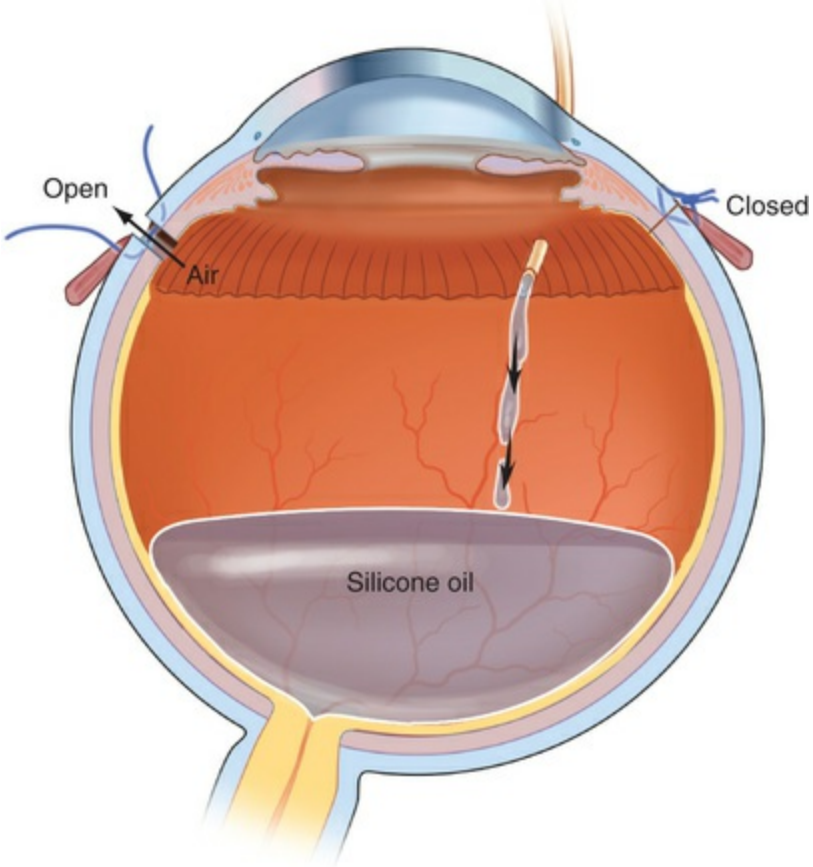

FIG. 108.16 Silicone oil (SO)–air exchange. This is the most commonly performed technique. Air–fluid exchange has to be performed prior to this procedure. Adequate drainage of subretinal fluid has to be ensured prior to instilling SO.

In pseudophakic eyes with a posterior capsulotomy or zonular dehiscence, migration of SO into the AC is frequent, and can sometimes be troublesome. Droplets of SO can be aspirated using an irrigation and aspiration cannula, and if this fails, viscoelastic materials can be injected into the AC to displace the SO posteriorly. In aphakic eyes, an inferior peripheral iridectomy (Ando's PI) needs to be done.[179] This prevents pupil block by the SO droplet and allows a passageway for aqueous to egress through the pupil plane (Fig. 108.17). This is easily performed by first placing the tip of the vitreous cutter under the iris at the desired position, followed by active suction. This creates a dimple on the iris. If positioning is correct, the cutter is activated to create an opening. If the position needs adjustments, suction is released and suction at another site is applied.

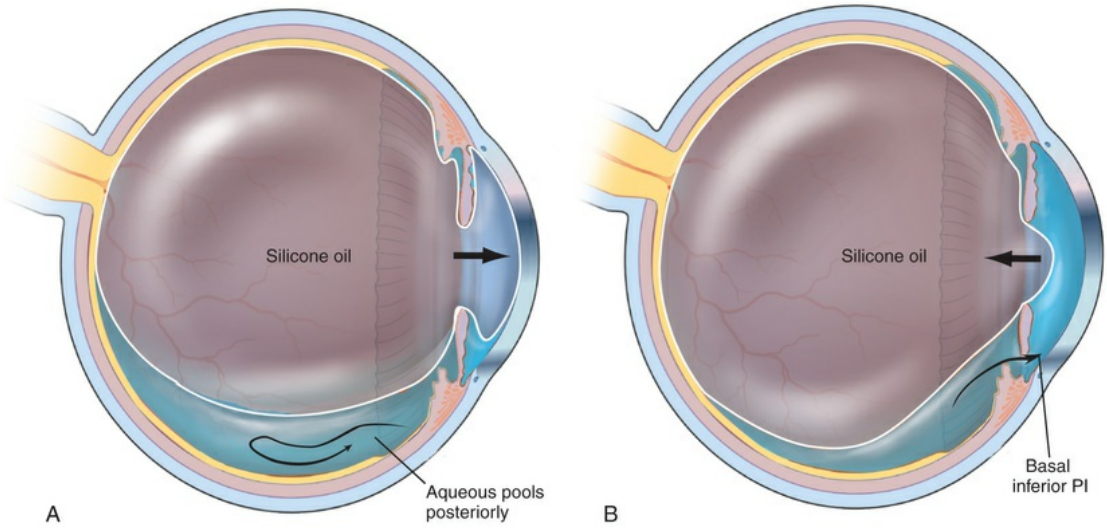

FIG. 108.17 Mechanism by which an inferiorly placed peripheral iridectomy can prevent pupil block glaucoma and silicone oil migration into the anterior chamber. *PI*, peripheral iridectomy.

Perfluorocarbon Liquid–Silicone Oil Exchange

This technique is useful in cases where there is significant risk of slippage.[58,180] Slippage occurs when aqueous is displaced posteriorly by an incoming air bubble. To prevent this, the objective is to get rid of any residual aqueous in the vitreous cavity. First, a PFCL–fluid exchange has to be done. PFCL is injected via one of the ports, while the other port is left vacant, until the eye is almost full. With the PFCL cannula still inside the eye, the infusion of balanced salt solution (BSS) is switched off. This is done by disconnecting the infusion at the three-way tap so that the infusion is now opened to the atmosphere. Then, more PFCL is injected to maintain a normal IOP. As the infusion is open to the atmosphere, any excessive PFCL would displace the aqueous in the infusion tubing between the eye and the three-way tap. Next, a flute needle is inserted via the open port to extract every last drop of aqueous. The whole eye, including the infusion line, is now free of aqueous, and filled with PFCL. The three-way tap can then be switched to continuous air infusion.[66] Following this, a leisurely direct PFCL–air exchange can now be carried out in full confidence that slippage cannot occur, as there simply is no aqueous in the whole system. This could be followed by SO infusion into the air-filled eye, with the technique mentioned

above.

Equally, a direct PFCL–SO exchange could be done. A flute needle is held in one hand, while the other takes the syringe containing the SO. An independent light source is required, because both sclerotomies will be occupied. This could be achieved using an illuminated infusion, or a separate chandelier illumination system.[181–187] Alternatively, SO could be infused through the infusion, such that both sclerotomies are occupied by the light-pipe and flute needle. When active infusion of SO begins, PFCL will be extruded passively through the flute needle (Fig. 108.18). The PFCL–SO interface could be visualized as the PFCL bubble shrinks in size. The tip of the flute needle has to be buried in the PFCL bubble during the whole process. As the PFCL bubble gets progressively smaller, it is often difficult to maintain the tip of the flute needle in the PFCL bubble. If this occurs, SO can block the flute needle. If SO is continuously being infused with the flute needle being blocked, IOP can rise quickly. Therefore it is vital to also monitor the perfusion of the central retinal artery during the process. When all PFCL has been aspirated from the eye, proper filling of the eye with SO should be judged, and the wound closed according to the principles described above.

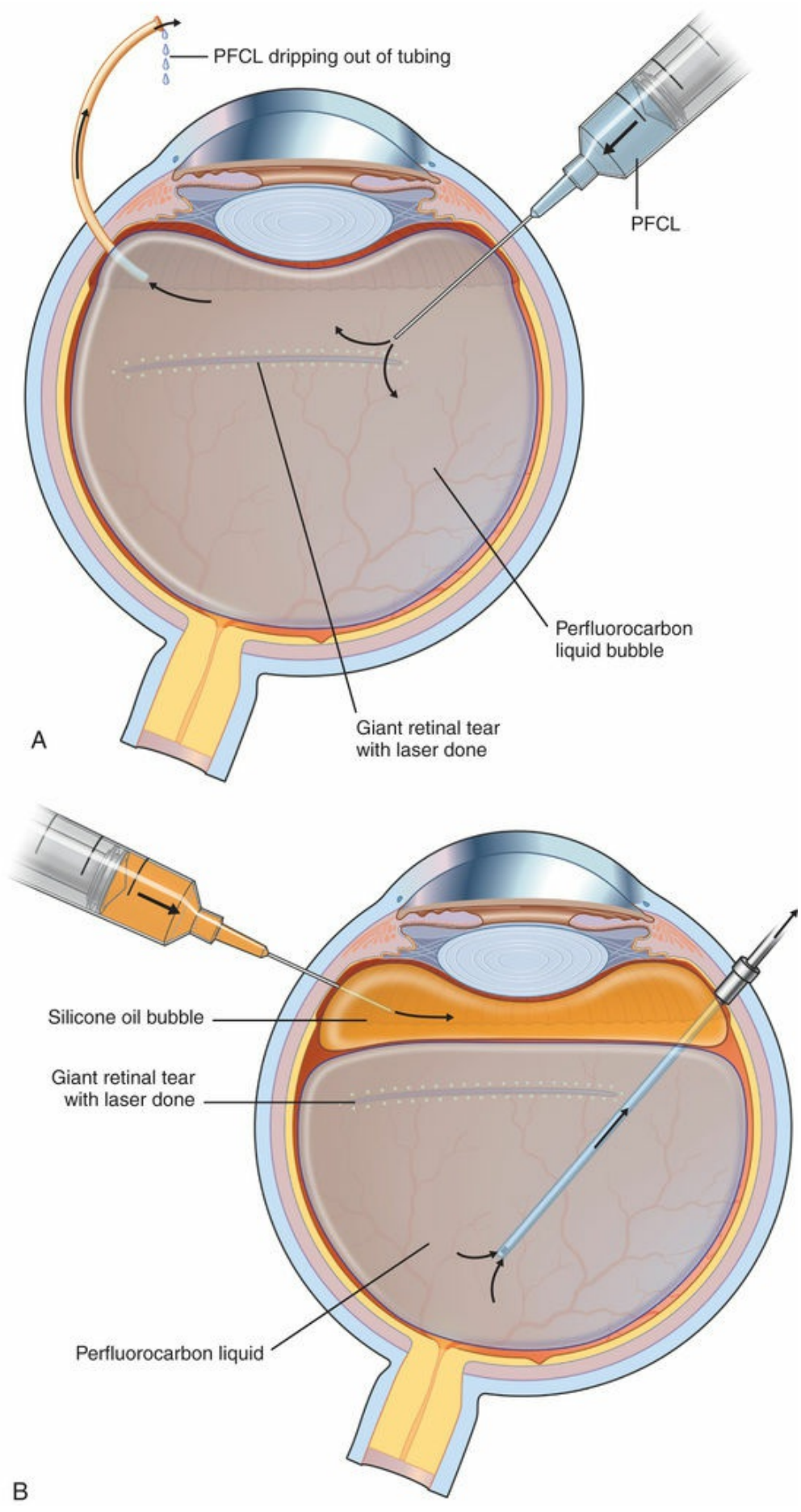
PFCL dripping out of tubing
PFCL
Perfluorocarbon liquid bubble
Giant retinal tear with laser done
A
Silicone oil bubble
Giant retinal tear with laser done
Perfluorocarbon liquid
B

FIG. 108.18 Silicone oil (SO)–perfluorocarbon (PFCL) exchange. This method is particularly useful when the risk of slippage is high. Technique of "over-filling" of perfluorocarbon liquid during PFCL–SO exchange. This method effectively eliminates all aqueous from the system. The "sandwich" technique is used to squeeze subretinal fluid into the vitreous cavity for drainage. (A) Overfilling of the entire eye with PFCL ensures removal of all aqueous and prevents slippage. (B) After overfilling of PFCL has been achieved, the eye is filled with silicone oil from anteriorly. A flute needle aspirates PFCL as more SO is being injected. This prevents slippage of retina.

It has been shown that for giant retinal tear or 360° retinotomy, a direct SO–PFCL exchange is less likely to cause slippage.[66] Both SO and PFCL are hydrophobic and prefer to be in contact with one and other. Once joined, the two liquids form a single bubble and exclude aqueous from the interface. This bubble initially would have a specific gravity greater than water. For example, if 1 mL of SO was used to join with 4 mL of PFCL, the resultant bubble would have a specific gravity of $(1 \times 0.97 + 4 \times 1.94)/5 = 1.75$ (assuming that the PFCL used has a specific gravity of 1.94). Importantly, the aqueous is displaced anteriorly and laterally towards the sclerotomies, where it might be expelled out of the vitreous cavity.

The important features of this technique are: (1) PFCL is filled as full as possible to expel as much aqueous before the exchange; (2) as oil is injected, an instrument should be passed from the SO into the PFCL to promote contact between the two liquids such that they join to form a single bubble. Slippage does not occur because during the initial stage of the exchange, the single bubble formed by the SO and PFCL is effectively a heavier-than-water bubble.

Complications

Silicone Oil in the Anterior Chamber

This occurs in cases where the barrier at the level of the lens–iris diaphragm is inadequate to stop SO from migrating into the AC.

This can be due to aphakia, loose zonular support, blockage of the inferior peripheral iridectomy, or a break in the posterior capsule. SO in the AC can occur either during surgery or in the postoperative period. When the AC is completely filled with SO, it can be undetected, because there is no fluid meniscus present. Confirmatory signs of an AC completely filled with SO include a slightly posterior bulging iris, shimmering reflex on the iris crypts, and absence of aqueous flare in the AC. The pupil can also appear mid-dilated with a raised IOP. The cornea is often perfectly clear, because the AC is totally filled with SO, and hydration of the cornea is not possible. Corneal edema may ensure if SO is later removed and significant damage to the corneal endothelium has occurred.

The SO can be displaced back into the vitreous cavity at the end of the surgery with air or viscoelastic agents. An inferior peripheral iridectomy needs to be done, and the patient should be postured upright or slightly face-down. Any small bubble of SO in the AC would empty itself into the large bubble behind in the vitreous cavity, if they were allowed to join. This is because Laplace's Law states that smaller bubbles have higher surface energy compared with larger bubbles. If a small bubble in the AC fails to reunite with the larger bubble behind and is not causing any complications, it can be left in situ.

SO can egress into the AC in a pseudophakic or phakic eye during surgery. This signifies the inadequacy in the barrier effect of the lens–iris diaphragm, zonular dehiscence, or a defect in the posterior capsule. This can sometimes occur as a result of overfilling of the eye with SO. It is therefore important to leave the eye normotensive to avoid overfilling. Attempts could be made to displace the SO droplets back into the vitreous cavity using viscoelastic agents. Routine inferior peripheral iridectomy in pseudophakic eyes is unnecessary.

During the postoperative period, SO migration into the AC sometimes occurs. This is due to either an inadequate lens–iris diaphragm, or a nonpatent inferior peripheral iridectomy. Blockage of the peripheral iridectomy frequently occurs if there was extensive surgery involving retinotomies, 360° photocoagulation, and extensive cryotherapy. If left alone, it can cause visual disturbance, induce corneal endothelial cell loss, and trabecular

damage. YAG laser is usually ineffective in reopening the iridectomy. Some surgical maneuver is usually needed. If the amount of SO is small, it could be displaced posteriorly through the pupil by injecting viscoelastic agents into the AC. Viscoelastic agents could also be injected through the iridectomy to keep it patent. Occasionally, the patient needs to be taken back to the theater for SO removal and reinjection.

Late migration of SO into the AC is commonly due to recurrent detachment or hypotony. Hypotony is usually caused by a combination of ciliary body shutdown and overdrainage by the uveal–scleral pathway (especially where large retinotomies have been done). Conservative management is appropriate. Heroic surgeries to dissect the vitreous base seldom yield satisfactory outcomes.

Glaucoma

Rise in IOP after surgery with SO can be grossly divided into: (1) pupil block glaucoma; (2) overfill of SO; (3) secondary open angle glaucoma; (4) migration of SO into the AC; (5) secondary angle closure glaucoma.

Pupil block glaucoma occurs in an aphakic eye, usually during the early postoperative period, where the peripheral iridectomy is nonfunctioning. This could be due to closure of the peripheral iridectomy, which has a reported incidence of up to 33%,[184] or due to blockage by inflammatory products such as fibrin or blood. When the peripheral iridectomy is nonfunctioning, aqueous accumulates behind the iris and forces the SO bubble through the pupil. Pupil block results when this phenomenon progresses. Treatment involves reopening the peripheral iridectomy, either with a YAG laser or surgically.[179,185] If the cause is a blockage by fibrin or clot, injection of tissue plasminogen activator (tPA) into the AC has been reported with successes.[186]

If the cause of IOP rise is due to overfill of the eye with SO, the AC will appear shallow. In the aphakic eye, the AC can be so shallow that there could be secondary angle closure. In the pseudophakic or phakic eye, an overfill can result in oil coming in front of the crystalline or intraocular lens, and herniating through the pupil.[187] In the aphakic eye, overfill can be treated with removal

of oil via a corneal or pars plana incision. Care must be taken to ensure that the peripheral iridectomy is patent. In the pseudophakic or phakic eye, removal of the oil from the posterior segment may not be sufficient once the oil is trapped between the lens or intraocular lens and the iris. Its evacuation is difficult, and the patient may need to be taken back to theater for complete evacuation of the oil and reinjection. To avoid overfilling, pressure should be normal at the end of surgery. This applies especially if encircling or scleral buckling is applied after SO injection. The explant or the suture may store elastic energy, creating intractable glaucoma, unless the oil is removed. To avoid overfilling, pressure at the end of surgery should be at its most normal.

Secondary angle closure glaucoma is a diagnosis of exclusion. Care must be taken to ensure that the peripheral iridectomy is patent, and there is no oil in the AC, and no oil is trapped between the iris or crystalline lens and the iris. Some patients may have raised IOP in the fellow eye or a tendency to have glaucoma in the affected eye. They may present with normal IOP in the presence of a retinal detachment. However, when the retina is reattached, angle closure glaucoma may become apparent. The cause of secondary open angle glaucoma associated with SO could be due to mechanical blockage of the trabecular meshwork, or trabeculitis induced by emulsified SO (Fig. 108.19).[188] Medication comprises the initial treatment. If IOP continues to rise, glaucoma surgery in the form of drainage device is preferable over trabeculectomy. One of the reasons why trabeculectomy gives rise to failure is thought to be fibrosis; SO under the conjunctiva is known to cause periocular fibrosis involving foreign body giant cell reaction (Fig. 108.20). A simple unguarded trabeculectomy or drainage device without a valve, or even an ill-fitted valvular implant, can easily overdrain in these cases, in the absence of vitreous, instead of showing simply a shallow AC. The absence of vitreous in the posterior segment means that the whole eye can collapse. Massive suprachoroidal hemorrhage is a devastating complication. In the Silicone Study, 8% of cases that underwent SO tamponade experienced glaucoma at the 36-month follow-up (2% for intraocular gas; $p < .05$).[189] In a series by Al-Jazzaf and associates, the incidence of secondary glaucoma was 11% among 450 eyes that underwent vitrectomy and SO

tamponade. Among the 51 eyes that developed secondary glaucoma, 78% (40 eyes) were successfully treated with medication only, while 22% (11 eyes) required a glaucoma drainage device (Ahmed glaucoma valves were used).[190] Effectiveness of drainage devices in lowering IOP in this regard has been well documented,[191] although failure rates were found to be higher in these cases when compared with cases without history of vitrectomy and SO tamponade.[192]

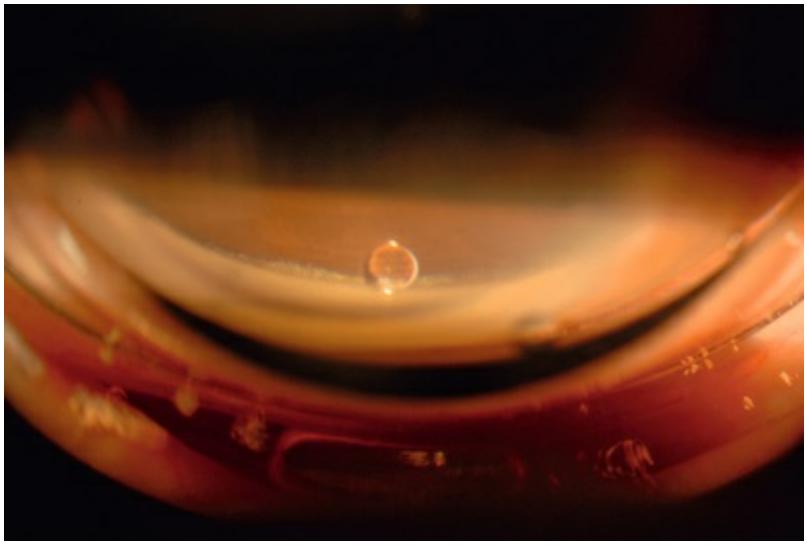

FIG. 108.19 Gonioscopic picture of emulsified silicone oil at the superior angle.

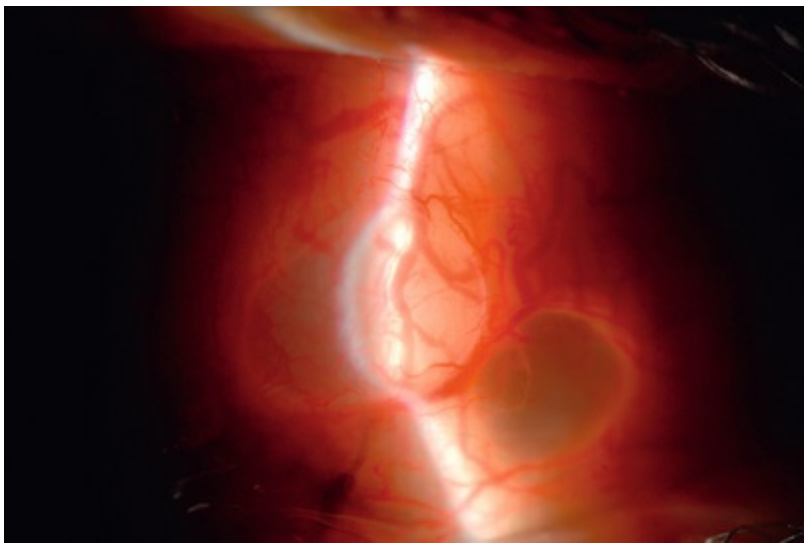

FIG. 108.20 Silicone oil globules trapped under the

conjunctiva.

Some also suggested that simply removing the in situ SO would be beneficial in terms of IOP.[193] Budenz and associates compared the surgical outcomes among 51 cases of secondary glaucoma due to SO tamponade.[194] In their series, three options of surgical approaches were adopted: removal of SO alone, glaucoma drainage device alone, and combined glaucoma drainage device with SO removal. Results showed that all three approaches were effective in lowering IOP, but risk of reoperation due to uncontrolled IOP was more likely among those who had SO removal alone; and when combining SO removal and glaucoma drainage device, risk of postoperative hypotony was more likely. Jonas concluded that this type of secondary glaucoma is reversible upon removal of the in situ SO, based on results from their series.[195] Flaxel and associates, on the other hand, reported that IOP remains elevated in all eyes even with SO removal.[196] In our experience, IOP remains elevated in most patients, even with SO removal. This may be due to the problem of incomplete removal of SO from the eye, especially those trapped within the trabecular meshwork. If damage has already been made to the trabecular meshwork, and scarring has already set in, removal of SO at a later stage may not bring about an IOP-lowering effect.

In refractory cases, transscleral cyclodiode photocoagulation (TSCP) could be used to lower IOP. Ghazi-Nouri and associates achieved sustained IOP-lowering effects up to at least 1 year with this treatment.[197] This was in accordance with a similar study by Han.[198] Some advocate TSCP as a first-line treatment in all cases of open angle glaucoma associated with SO use.[199] Until recently, there have been reports suggesting that the IOP-lowering effect of TSCP may not be sustainable.[200] While the controversy goes on, TSCP remains a reasonable option in refractory cases, especially those that have low visual prognosis and have already tried other options.

Chronic Hypotony

This complication usually occurs during the late postoperative period. It is defined as having IOP ≤5 mmHg in the Silicone

Study.[189] This cutoff level is arbitrary. There are patients with IOP of <5 mmHg, yet the eye is relatively normal and healthy. Equally, there are patients with IOP above this level in which the eye is complicated with swollen optic disc, macular edema, and epiretinal membrane formation. The different clinical picture may be due to different mechanisms giving rise to hypotony. It is assumed that a low IOP may be a combination of increased aqueous uveal–scleral outflow and reduced production.

Large retinectomies are thought to be the cause of increased aqueous uveal–scleral outflow. Ciliary body alterations are thought to be the cause of reduced aqueous production. Nehemy and associates imaged the ciliary body with ultrasound biomicroscopy (UBM), in 44 eyes with chronic hypotony following vitrectomy and SO tamponade.[201] A total of 20 eyes with normal IOP after vitrectomy were used as controls. Results showed that none of the control eyes had ciliary body pathologies, whereas 98% (43 out of 44 eyes) of the study eyes had UBM-detectable ciliary body abnormalities. These include traction ciliary body detachments (n=16); exudative ciliary body detachments (n=11); combined traction detachment and atrophy of the ciliary body (n=7); hypotrophy of the ciliary body (n=5); combined traction and exudative detachment of the ciliary body (n=3); and ciliary body edema (n=1).[201] In the Silicone Study, prevalence of chronic hypotony following vitrectomy with SO tamponade was 18% at 36 months.[189] Prognostic factors included presence of preoperative hypotony, diffuse contraction of retina anterior to the equator, presence of rubeosis, and large retinal breaks.

Treatment of this condition has been disappointing so far. As suggested by findings on ultrasound biomicroscopy, residual membranes on the ciliary processes and ciliary body may cause hyposecretion of aqueous, as a result of traction and fibrosis. Reoperation with further excision and dissection of membranes over the ciliary body has been suggested as a treatment option.[202] The results are usually disappointing. Removal of SO risks the progression to phthisis, hence hypotony with IOP <10 mmHg is a relatively contraindication to SO removal. Finally the measurement of IOP in patients with uveal–scleral outflow should be done with care. With applanation tonometry, the IOP can appear to be high

initially. The act of applanation and indentation causes an increase in uveal outflow. With repeated measurements, the IOP can come down to zero. These eyes are in effect hypotonic. Removal of SO would further increase the access of aqueous to the uveal–scleral pathway and promote phthisis. Hence, in these cases, the SO is preferably left in situ.

Cataract Formation

Formation of cataract in phakic eyes undergoing vitrectomy and SO tamponade is multifactorial. Apart from the SO, cataract can also form as a result of vitrectomy or surgical trauma. Many early studies have provided evidences to suggest an association between long-term SO tamponade and cataract formation. The exact mechanism remains uncertain, although the possibility of impaired metabolic exchange across the posterior capsule and direct toxicity has been speculated. As with the case of gas tamponade, posterior subcapsular feathery lens opacity can be seen in the early postoperative period. A more specific early feature of SO-induced cataract is formation of lens vacuoles in the posterior part of the lens. Early posterior lens opacities may resolve and give way to nucleus-sclerosis. As with cataract formation associated with vitrectomy, nucleus-sclerosis associated with SO can occur with little or no brunescence. Finally, rapid progression to hypermaturity can occur with white cataracts. The lens swells up quickly over a matter of days, with leakage of protein into the AC and brisk uveitis. However, this usually resolves spontaneously with time. If SO is kept in situ for long-term tamponade purposes, cataract inevitably forms, which could be in the form of posterior subcapsular cataract or nucleus sclerosis. Although early removal of SO has been suggested to be beneficial in minimizing the risk of cataract formation, there are reports of cataract formation even with SO removal as early as 6 weeks following the surgery.[203] A practical question presenting to the surgeon is whether to remove the cataract, and if so, when to do so.

Cataract formation is inevitable when SO is used. Leaver and associates showed that in relatively young patients, cataract occurs with a follow-up of 2 years, despite early removal of SO. Some surgeons therefore prefer routine combined phacovitrectomy when

SO use is intended. The advantage is that a more complete vitrectomy, and therefore a better fill with SO, can be achieved. In phakic SO-filled eyes, a combined phacoemulsification with planned continuous capsulorrhexis of the posterior capsule, with in-the-bag implantation of the intraocular lens, can be an elegant and satisfactory approach.

Intraocular lens power calculations can be difficult without prior planning. It is recommended that, routinely, all patients undergoing vitrectomy and SO infusion should have B-mode axial length measurements done prior to surgery. SO in contact with the posterior surface of the intraocular lens would greatly reduce the refractive power. Most intraocular lenses have biconvex configuration. There are intraocular lenses specifically designed for the use of SO, with a concave posterior surface, such that the intended final correction will be correct even with SO in situ.[204]

With the introduction of PMMA and acrylic IOLs, the use of silicone IOLs has become less popular. Risk associated with silicone IOLs in eyes that have SO in situ is the formation of intractable adhesion of SO onto the surface of IOLs.[205] SO adherent to intraocular lens implant can give rise to blurred vision, polyopia, and distortion. To understand this, surgeons need to appreciate that the refractive power can be as high as –60 diopters in some cases. The astigmatism present is often irregular and cannot be corrected by glasses. This occurs where there is a breach in the posterior capsule, such that SO comes into direct contact with the IOL. Adherent SO droplets can cause visual disturbance to the patient.[206] Removing these droplets has proved to be difficult.[207] Various techniques and solvents have been described to aid removal of these SO droplets.[207–211] In a recent laboratory study by Stappler and colleagues, F_4H_5, a hydrophobic semifluorinated alkane, was used to dissolve adherent SO droplets on IOLs.[209] With a simple immersion, over 91.4% of SO droplets were successfully washed off the surface of IOLs. Removal rate surged to over 93.7% with immersion time of over 1 minute. Following treatment with F_4H_5, the IOLs remained optically clear. Currently, F_4H_5 is not available on the market. So effective is it in removing SO, undoubtedly it may represent a new treatment method for SO-related glaucoma. Other options using PFCL, methylcellulose, and mechanical scrubbing

with sponges are all clumsy and traumatic compared with the use of an appropriate solvent. Furthermore, intraocular lens exchange seems unnecessary when the droplets can be washed away with F_4H_5. In a recent in vivo study of 72 patients undergoing vitrectomy for macular holes requiring the use of silicone oil, Stalmans and colleagues compared the outcome of removal of silicone oil from the eye either with or without the use of F_4H_5. There were no major complications encountered, and the group that used F_4H_5 had marginally less silicon oil droplets left.[212]

With ultrasound biometry, measurements of axial lengths in SO-filled eyes may be affected by differences in the speed of sound wave in vitreous and SO. The speed of sound wave in SO is 986 meters per second (m/s), and that in vitreous fluid is 1552 m/s. Hence, if an eye is filled with SO, the time taken for the sound wave to return to the receiving sensor is longer than when the same eye is filled with vitreous. The resulting axial length may be falsely long, which would cause a hyperopic shift if the uncorrected measurement were used for IOL power calculation. Care must be taken, as specific SO-formulae are used when the eye is filled with SO. Furthermore, impurities within the SO bubble, and underfilling of SO may cause disturbances to the signal when using ultrasound biometry.[213] In a recent study, immersion B-scan guided ultrasound biometry has been found to perform better as compared to contact A-scan biometry in SO-filled eyes.[214] A "conversion factor" of 0.71 has been found to give good accuracy with a mean of only 0.74 diopters difference between the predicted and actual postoperative refraction.[215] While ultrasound biometry with special formulae are still the "gold standard" to measure axial lengths in SO-filled eyes, interests in using partial coherence laser interferometry (PCI) has grown.[216–219] A recent study by Parravano and associates showed that measurements of axial lengths were not significantly different before and after SO removal.[219,220] Unlike ultrasound, the speed of light is constant, and therefore unaffected by SO. Using infrared partial coherence interferometry, measurements in axial length could also be done. An additional consideration is that a myopic shift has been reported with the use of combined phacovitrectomy and intraocular lens implantation, with or without tamponade. The precise cause of this myopic shift is uncertain. Some feel that it is

important to slightly undercorrect the patient. However, its measurements are limited by the presence of corneal opacities or media opacities, such as band keratopathy and cataract, which are frequently present in SO-filled eyes. Further studies comparing the outcomes of measurements using ultrasound biometry and PCI need to be done.

Recurrent Retinal Detachment

Silicone oil is not a panacea. Successful retinal detachment repairs rely on identification and closure of all causative retinal breaks. Missed retinal breaks give rise to recurrent retinal detachments, even in the absence of PVR, either with SO in situ or after SO removal. It is highly doubtful whether there is a state of total tamponade that can be achieved with SO fill; the evidence points to the contrary. A slight underfill with SO leaves a large area of the retina unsupported.[23]

Results from the Silicone Study showed that the rates of redetachment were not significantly different when comparing eyes randomized to SO or to gas use. Therefore, redetachment in this regard may not have a direct relationship with whether SO was used or not. Jonas and associates identified risk factors associated with redetachment after SO removal among 225 patients.[221] These include the number of previously unsuccessful retinal detachment surgeries, preoperative visual acuity, incomplete removal of the vitreous base, and absence of an encircling band. Method of SO removal and duration of SO endotamponade were independent of the rate of redetachment. In another study, Jonas found that the mean time taken from SO removal to occurrence of redetachment was 1.3 months.[222] If retina remains flat 3–5 months after SO removal, redetachment becomes unlikely. Preoperative examination to identify all breaks and meticulous removal of all tractional membranes and retinectomy if necessary, are the keys to ultimate anatomic success and the reduction of redetachment in this regard.

In a prospective randomized trial, Avitabile and associates examined the potential benefit of prophylactic 360° laser in cases where there is a need for SO tamponade. Prophylactic 360° laser was done in 151 study eyes, while no laser was done in 152 control eyes. Redetachment occurred in 8.63% among the study eyes, as

compared with 20.93% among the control eyes (p=.007).[223] This was supported by a retrospective study by Falkner-Radler and associates, where a comparable redetachment rate of only 9% was seen when prophylactic 360° laser was done.[224] Another study by Laidlaw and colleagues showed that 360° laser can be performed before SO removal, which may probably reduce the risk of redetachment.[225] Hence, 360° laser as prophylaxis in high-risk patients could be considered, as an adjunct to enhance the chance of anatomic success after SO removal.

Emulsification

Emulsification of SO is an inherent problem. Dispersion of SO is the breaking-up of large bubbles into smaller droplets. The surface energy of these smaller droplets is higher, and therefore they have a tendency to coalesce to form a larger bubble. Emulsification only occurs when surface energy of the droplets is reduced in the presence of surfactants. Surfactants may include phospholipid, protein, lipoprotein, or even solid cellular debris. Dispersion requires shear force between the oil and the retinal surface and is dependent on rate of eye movement. Normal saccadic velocity reaches 300–400/second. All intraocular fluid remains relatively stationary, while the eye moves. The peak shear velocity therefore approximates closely to the saccadic velocity of the eye. The shear force depends on this relative velocity, and also the thickness of the film of aqueous between the SO, and the surface of the retina. Although the thickness of this film of water has not been measured in vivo, when the SO fill of the eye is near complete, this film of fluid can be very thin. Correspondingly, the shear force to disperse SO would be very high.

It has been found that higher viscosity SOs tend to be more difficult to disperse. In vitro, the reason may be purely physical. The higher the shear viscosity, the higher the extensional viscosity (extensional viscosity is usually three times that of shear viscosity, depending on the shear strength). There is, however, little evidence that using oil beyond 5000 cSt, shear viscosity would be of any benefit. The reason is that there are many confounding factors, including the degree of blood–ocular barrier breakdown, the degree of inflammation, and the completeness of the oil fill. These factors

are individual to a particular patient, such that, occasionally, we see very early marked emulsification in an otherwise normal eye. There is, however, consensus that if SO is to be used as a permanent tamponade, SO of 5000 cSt should be used.

Emulsification can lead to glaucoma, inflammation, and PVR formation.[152,226] Emulsification can occur as quickly as 1 week after surgery, but the most common timeframe is a few months after surgery.[227] It was thought to be the combined result of friction between SO and other intraocular fluids, and a reduction in the interfacial tension as a result of absorption of active components from other intraocular fluid, that causes the emulsification process. Likelihood of emulsification of SO is inversely proportional to its viscosity.[228]

However, with the advent of small-gauge vitrectomy systems, the use of SO with lower viscosity has increased, mainly due to its ease in injection and removal through a smaller-gauge trocar. Williams and associates showed that by adding very-high-molecular-weight polymers to low-viscosity SO (1000 cSt), the rate of emulsification was successfully reduced.[123]

In a recent study on patients with macular holes requiring silicone oil tamponade, Siluron 2000 appeared to be equally effective and safe, when compared to the more stable alternative Siluron 5000. The result in terms of emulsification was rather similar but allowed for better handling with the potential for reducing procedure time.[212]

Keratopathy

Prolonged use of SO is associated with keratopathy, either in the form of band keratopathy, which is more commonly seen in early stages, and bullous keratopathy in the late stages. Rate of keratopathy observed in the Silicone Study was 27% at the 24-month follow-up.[229] This was identical to the rate seen in eyes randomized to C_3F_8. Risk factors identified in the Silicone Study include: being pseudophakic or aphakic before surgery; the presence of iris neovascularization before surgery; postoperative aqueous flare, and the need for reoperation. Contact between SO and the corneal endothelium has been thought of as a major contributor to the development of keratopathy. Strategies in

minimizing the risk of keratopathy mainly involve reducing the chance of SO migration into the AC. This includes ensuring a patent peripheral iridectomy and removing the SO as soon as practical.

The increasing use of primary vitrectomy with intraocular lens implant ensures a more effective barrier to the egress of oil into the AC. Some surgeons feel that lensectomy and leaving the eye even temporarily aphakic is not such a good option. Efforts should be made to preserve an intact posterior capsule, until such time as when the oil is to be removed.

Unexplained Visual Loss Following Silicone Oil Tamponade

The precise mechanism is unclear. The characteristic is that optical coherence tomography and angiography reveal no obvious explanation. Multifocal electroretinogram has showed only the foveal segment is involved. It can be speculated that it may be the sudden change in physiologic environment affecting ionic exchange. In a recent report, Scheerlinck investigated the contents in retro-oil fluid and paired serum from 16 patients undergoing oil removal. Results showed that the mean potassium levels in retro-oil fluid and vitreous humor were similar. However, the levels of magnesium and chloride were lower in retro-oil fluid compared with vitreous humour. Lactate dehydrogenase levels (LDL) were, on the other hand, higher in retro-oil fluid. This may make the potassium accumulation theory less likely. However, the differences in magnesium levels and LDL across the reto-oil fluid and vitreous humor may give hints to further research to find out the ultimate cause.[230] Moreover, during SO removal, the oil bubble, being spherical, may form a strong condensing lens, focusing the light from the microscope, albeit briefly. In fact, the mechanism is still obscure.

Silicone Oil Removal

In practice, deciding when to remove SO is difficult. Theoretically, chorioretinal adhesion would have formed certainly by 1 month. However, SO is retained often longer than this, the rationale being that the presence of the oil and the tamponade force might resist

any traction caused by reproliferation. The precise duration of the reproliferating process is therefore less certain if the retina remains attached. The assumption is that the cellular process of PVR would naturally resolve. However, traction may not be clinically manifested. Hiscott and associates introduced the concept of isotonic and isometric contraction; when the retina is attached, epiretinal membrane can cause "isometric" traction, without any surface wrinkling of the retina to indicate the presence of such membranes.[231] It is only when the oil is removed and such traction causes detachment of the retina that this "isometric" contraction becomes manifested as fixed or star-folds. Deciding when to remove the SO and whether it is safe is very much a judgment call.

Removal should be performed when the SO bubble has served its purpose, and when further retention may increase the risk of complications related to its use.[232] In the Silicone Study, SO removal was allowed after a minimum of 8 weeks after surgery. Removal within the first 6 months after surgery is generally recommended. Various techniques have been described for the removal of SO from the eye.[233–237]

In general, an infusion must first be secured at the pars plana to allow saline to replace globe volume as SO is being aspirated. In an aphakic eye, either passive or active egress of SO through a corneal wound could be done. In a phakic or pseudophakic eye, some prefer a two-port system. While one port is used for the infusion, the other port is used for aspiration of SO. The port through which SO is egressed should be placed in the uppermost position because SO floats on top of the infusate (Fig. 108.21). After the removal of the oil, the same port can be used for internal search using a light-pipe combined with scleral indentation using wide-angle optics. Some surgeons feel it is important to do additional maneuvers. These may include removal of epiretinal membranes that might be present or a repeated fluid–air exchange to encourage a more complete removal of the SO. Aspiration of the SO should always be active. It should be understood that the maximum suction that can be generated is not limitless. Even if there were a total vacuum, the difference in pressure in driving the flow of oil out of the eye would be the atmospheric pressure plus the infusion pressure. Therefore, if passive aspiration were used, the aspirating pressure would be

the height of the infusion bottle (for instance 30 mmHg). However, if active aspiration was used, the vacuum driving the flow would be much higher (760 mmHg + bottle height of infusate). This is assuming that a perfect vacuum can be achieved. In fact, for most vitrectomy machines, a maximum aspiration of 600 mmHg is achievable. Another important consideration is the length of the aspirating cannula. Linear extrusion using a length of tubing between the machine and the eye simply does not work. Active aspiration has to be achieved close to the eye with a minimum length provided by a short cannula. In practice, SO injecting syringe drivers or manual aspiration can be used.

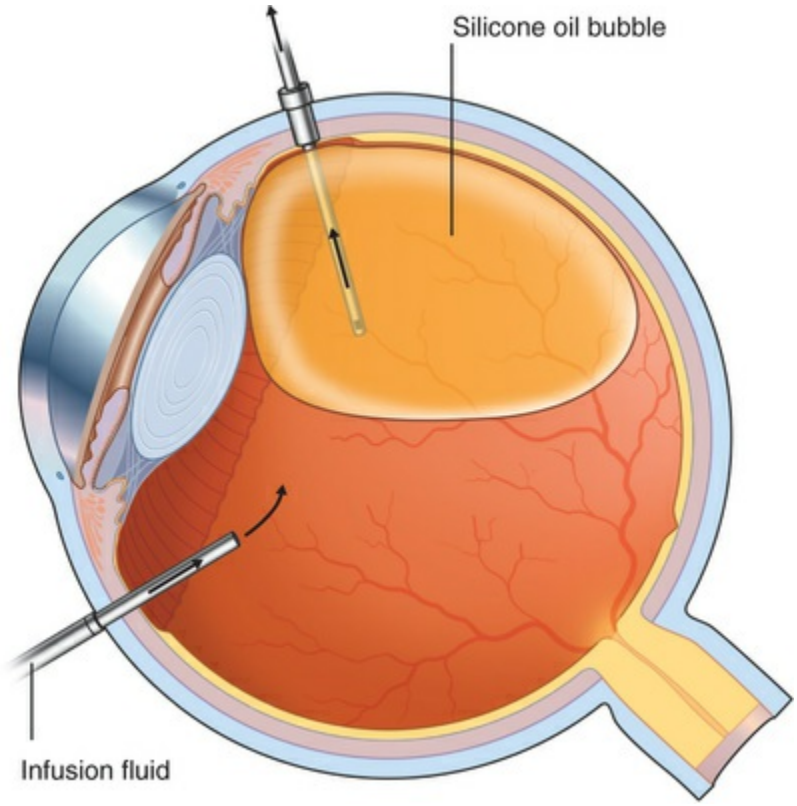

FIG. 108.21 Technique of silicone oil removal with machine-assisted active suction. The draining sclerotomy has to be positioned in the most independent position.

Complete removal of SO is in fact seldom complete. Emulsified droplets adhere to the ciliary processes, zonules, and posterior aspects of the iris. They may only become obvious postoperatively and cause the patient to complain that when they put their head

down, these bubbles come near the line of sight. Emulsified droplets can sometimes adhere to cellular debris such that they are almost density neutral. They may often drift in the visual field giving the sensation of floaters. Multiple air–fluid exchanges has been suggested.[233] The idea is that any residual droplets would be forced to coalesce to form an "oil slick" on the surface of the fluid. However, whether this is effective remains in doubt.

During the removal of SO, it is important that the cannula stays within the main bubble. With aspiration, one could see a "vortex" developing within the oil. If the cannula comes out of the SO bubble, the individual bubble of oil can be isolated and left behind. Therefore, during surgery, the vortex should be closely observed, and the cannula manipulated such that it does not aspirate infusion fluid or come out of the oil.

It is common to use plastic cannulas for aspiration. Plastic, in general, has a greater infinity for SO. Silicone oil bubbles tend to adhere to the outside of the cannula, where they cannot be removed. The adherent oil can be scraped off the outside of the shaft of the cannula, and become free floating in the vitreous cavity, where it becomes difficult to catch. In these instances, a fluid–air exchange would allow easier removal of these droplets.

In cases where phacoemulsification is to be done at the same setting, a posterior capsulotomy could be made for SO removal. This is similar to the technique used in aphakic eyes. Pars plana infusion could be replaced by an AC-maintainer in this case, but the infusion bottle height has to be higher when an AC maintainer is used. In-the-bag intraocular lens implantation could be performed following removal of SO.

Permanent Silicone Oil Tamponade

The decision to remove in situ SO can be affected by factors other than retinal attachment. In eyes that have low or no visual prognosis, when the risk of progression to phthisis cannot be ignored, or when the fellow eye is functioning well, SO could be kept in situ, given that no symptomatic complications have arisen. However, the pros and cons have to be discussed thoroughly between the surgeon and the patient, before arriving at such a decision. SO is used in the eye permanently for more than one

reason. Most frequently, it is because the motivation to remove the SO is not there. This applies to patients with poor visual prognosis. In other circumstances, low IOP deters both the surgeon and the patient. In many instances, patients are simply exhausted by having multiple surgeries. Some surgeons are persuaded against it by patients having only one eye and a bad history of redetachments and therefore, a long-term SO tamponade may be justified. However, close and long-term follow-up is mandatory in these patients.

Conclusion

Silicone oil has proven itself to be an effective endotamponade agent, especially in the management of complex retinal detachments associated with proliferative vitreoretinopathy. SO is, however, not a cure-all. There are still many unanswered questions, including whether 5000 cSt SO is better than 1000 cSt SO; whether heavy SO has a role to play; whether high-molecular-weight additives can reduce the risk of emulsification; what is the mechanism for visual loss following SO use, and how long is the SO needed? Despite the fact that nearly three decades have elapsed since the Silicone Study, it remains the main evidence-based study that guides our practice today. The efficacy of SO has been proven in the Silicone Study, and it has been found to be equally effective when compared with C_3F_8. Despite its shortcomings, SO remains a very important and indispensable tool to the retinal surgeon. Both SO and C_3F_8 have their relative advantages and disadvantages, and in the selection of tamponade agent for extended use, the decision should be made on a case-by-case basis. Fundamentally, anatomic success is reliant on the completeness of removal of tractional membranes, and the tamponade agent serves best as an adjunct to it, regardless whether it is SO or intraocular gas.

The Concept of Heavy Tamponade

Background

Conventional SOs all have a specific gravity of 0.97 at 25 °C, which is lower than that of water, hence they float. This results in a good tamponade effect to the superior retina, when the patient is in an upright position. However, tamponade effect to inferior retina is often less than ideal. A slight underfilled SO bubble would leave a large area of retina unsupported.[23] PVR has a predilection for the inferior retina. In this regard, a heavier-than-water tamponade agent has long been sought.

Fluorinated SOs developed in the 1980s, were associated with high rates of complications, which included the development of PVR and intraocular inflammation.[238,239] The use of perfluorocarbon liquids (PFCL) is now confined to short- or medium-term tamponade in selected cases, such as that in giant retinal tears.[240] In particular, the use of PFCL as intraocular tamponade has general acceptance in Australia. The main motivation for its use is said to be for the prevention of slippage. PFCL is usually left in the eye for 2 weeks, after which it is exchanged for either gas or SO. However, PFCL causes inflammation and emulsification when left in situ for any length of time, it is not universally accepted as a tamponade agent.[241] Yet another approach, known as the "doublefilling," combining the use of SO and fluorosilicone oil,[242] SO and PFCL,[243] or SO with perfluorohexyloctane (F_6H_8)[244,245] have also been tried. This whole approach is deeply flawed. These liquids are all relatively hydrophobic, and they join to form a single bubble and exclude aqueous fluid from the interface between them. Effectively, they are simply heavier-than-water bubbles. They could not provide simultaneous superior and inferior tamponade. Instead, doublefilling would simple create a new aqueous compartment laterally and superiorly.[242,246] The rationale for their use remains controversial.

Whether retinal toxicity could be caused by the weight of heavy tamponade agents has also been a subject of controversy. In the case of PFCL, it has been suggested that perfluorocarbon liquid is

unsuitable as an endotamponade agent simply because of their high specific gravities. The orthodoxy says that it is the downward force on the retina that gives rise to the histologic changes observed. We have shown that force exerted by the heaviest PFCL amounts to 2–3 mmHg; it is the same order of magnitude as the diurnal variation in intraocular pressure. More importantly, in terms of force acting on the retina, the downward force by PFCL on the lower retina is no more than the upward force of any gas bubble acting on the upper retina.[19]

The semifluorinated alkanes and alkenes have a specific gravity of around 1.35 at 25 °C. F_6H_8 was initially designed as a solvent for SO. The numbers 6 and 8 refer to the number of carbon atoms with fluorine attached (6) as opposed to the number of carbon atoms with hydrogen attached (8). F_6H_8 was found to be well tolerated in rabbits, and it was later tested as a long-term internal tamponade in humans for inferior retinal breaks. Clinically, they have been used for up to 3 months as internal tamponade, but the marked emulsification, inflammation, and PVR were worrying complications.[247] Not all of the semifluorinated alkanes, however, are the same. Mackiewicz et al. have shown that some of the semifluorinated alkanes are more inert than others in rabbit eyes. They speculated that the ratio of the number of carbon atoms with attached hydrogen relative to the number of carbon atoms with attached fluorine might be an important determinant of toxicity.[248] Used on their own, semifluorinated alkanes with their low viscosities, readily disperse into small bubbles.[247,249–251] The authors speculate that these droplets could stimulate macrophage and foreign body giant cell reaction. The inflammation could in turn promote PVR.[252]

Semifluorinated alkanes or alkenes are amphiphilic. For example, F_6H_8 has a straight backbone of carbon. The fluorinated end would be hydrophilic and the alkylated end would be hydrophobic, which means they could partially dissolve in SO. The solubility depends on the individual agent used; the amount that can be dissolved also depends on the temperature, the mixing method and the viscosity of the SO used. The resultant solutions are "heavier-than-water" and are sometimes referred to as "heavy silicone oils."[248] Their viscosity could be above 1000 cSt, and as such they are much less

likely to disperse and emulsify as compared with the semifluorinated alkanes and alkenes used on their own. This might be one of the reasons that they are relatively well tolerated. The precise nature of the solution has not been fully elucidated. It could be that the fluorinated part of the molecule is on the surface of the solution and in contact with the surrounding aqueous whilst the alkylated part of the molecule is internalized in the silicone. It could be that the F_6H_8 forms micelles inside the oil. Whether it is the higher viscosity or whether it is the molecular arrangement of the F_6H_8, the fact is that heavy SO is much better tolerated than F_6H_8 when used on it own.

There are a number of agents in the market. These include Densiron 68, Oxane HD, and HWS 46–3000. Table 108.6 shows the comparison of physical properties between the newer heavy tamponade agents with some older tamponade agents. This sections aims to provide the reader with a general overview of the current development in heavy tamponade agents.

TABLE 108.6

Physical Properties of the Newer Generation of Heavy Tamponade Agents in Comparison With Other Older Heavy Tamponades

	Component by Weight	Specific Gravity	Viscosity (cSt at 25 °C)	Surface Tension (mN/m)	Interfacial Tension vs. Water (mN/m)
Densiron 68	F_6H_8 – 30.5% PDMS (5000 cSt) – 69.5%	1.06	1349	19.13	40.82
Oxane HD	RMN_3 – 11.9% Oxane 5700 – 88.1%	1.02	3300	n/a	44.9
HWS 46–3000	F_4H_5 – 55% PDMS (100 000 cSt) – 45%	1.118	2903	18.8	41.3
F_6H_8	F_6H_8 – 100%	1.35	3.44	19.7	45.3
C_8F_{18}	C_8F_{18} – 100%	1.76	0.69	14	n/a
$C_{10}F_{18}$	$C_{10}F_{18}$ – 100%	1.94	2.7	16	n/a

cSt, centistokes; F_6H_8, perfluorohexyloctane; F_4H_6, perfluorobutylhexane; C_8F_{18}, perfluoro-n-octane; $C_{10}F_{18}$, perfluorodecalin.

Newer Generation of Heavy Tamponades

One of the commercially available heavy tamponades, Densiron 68, is a solution of SO (5000 cSt) and F_6H_8. The clinical experience with this agent is extensively reported. It has a specific gravity of 1.06 (higher than water), and a viscosity of 1350 cSt. Wong and associates conducted a pilot study on 42 consecutive patients with retinal detachments from inferior breaks associated with PVR.[253] Anatomic success (after all tamponade was removed) with one operation was 81%, and this increased to 93% with further surgery.[253] The tamponade agent was removed in 90% of cases at the end of the study. Visual acuity significantly improved from a mean of 1.41 to 0.94 (LogMAR chart). This result was supported by a later study by Herbrig et al., with a similar anatomic success rate of 87.6%.[254]

Another commercially available heavy tamponade, Oxane HD, is a mixture of SO (Oxane 5700) and RMN_3, a partially fluorinated and hydrocarbonated olefin. It has a specific gravity of 1.02 and a viscosity of 3300 cSt. Wolf and associates first reported a study using Oxane HD for extended tamponade in 33 patients with inferior retinal detachments. Complete retinal attachment was achieved immediately after surgery and macula remained attached at least 12 months postoperatively.[115] In another study, Rizzo and associates used Oxane HD in 28 eyes with inferior detachments. Oxane HD was removed on an average of 88 days, and attachment was achieved in 15 eyes.[255]

RMN_3 has a low solubility, and the mixture can separate into its original constituents when temperature is below 23 °C. This can occur during transportation or storage. A study looking at the product using nuclear magnetic resonance showed that Oxane HD is not homogenous.[256] Lai and associates have shown that when Oxane HD emulsifies, the droplets tend to float.[257] The authors have serious doubt whether Oxane HD stays as a solution.

Another heavy tamponade, HWS 46–3000, has been tested in a clinical trial by Rizzo and associates.[258] HWS 46–3000 is a mixture of 45% ultrapurified SO 100 000 cSt and 55% perfluorobutylhexane (F_4H_6), a new semifluorinated alkane with viscosity 1.28 cSt; specific gravity 1.254 at 25 °C). The mixture has a viscosity of 3109 cSt and a specific gravity of 1.105 at 25 °C. Among the 36 eyes in their series, retinal reattachment was initially achieved in all. HWS 46–3000 was

removed after 45–96 days, and retinal attachment rate was 84.6% at 6 months with one operation, and 100% with a second operation.[258]

In view of the promising results, there is a need to compare the efficacy of conventional lighter-than-water SO and heavy tamponade, in the treatment of detachments associated with inferior breaks. The heavy tamponade study (HSO Study) was initiated by Joussen and colleagues.[259] The hypothesis was that heavy SO would displace any aqueous (containing proliferative cytokines and activated cells) to the superior retina where there were no retinal breaks. This was a prospective, multicentered, randomized controlled trial, comparing the effect of heavy tamponade (Densiron 68) and conventional SO, in eyes with inferior and posterior PVR grade C or above. Eyes were randomized to receive either Densiron 68 or conventional SO of either 1000 cSt or 5000 cSt. All tamponade agents were removed from the eye at 2–3 months after initial surgery. Interim results from the 12-month visit of 93 recruited cases – 46 patients treated with HSO compared with 47 patients treated with standard SO, showed that there was no significant difference between both groups regarding anatomic success as well as visual outcomes.[260] No significant adverse effects were observed during the course of the study, including emulsification of SO.

The investigators concluded that the use of heavy tamponade did not show any significant benefits over conventional SO in cases of inferior and posterior PVR. They also concluded that the results could not be generalized to cases of simple primary inferior rhegmatogenous detachments. Whether heavy tamponade is better than conventional SO as a primary tamponade agent requires further investigation.[261]

The specific gravity of these agents varies according to the molecular density, but all are above 1.0. Higher specific gravity has led to the debate as to whether extended tamponade with these agents will incur damage on the retina. Stolba and associates have shown retinal damage, when the eye is filled with perfluorophenanthrene (having specific gravity almost double that of vitreous) (Fig. 108.22).[262] However, a recent study by Mackiewicz failed to show such findings.[263] In their study, Mackiewicz infused either perfluorohexyloctane (F_6H_8) or perfluorodecalin, or a mixture

of both, into vitrectomized eyes of rabbits for a period of 3 months. Histologic results failed to show any damages related to the high specific gravity of these fluids.[261] The changes in the retina might also be caused by exclusion of aqueous from the retinal surface.[19] Winter et al. measured the thickness of the fluid film between the SO bubble and the retina using optical coherence tomography, and they found that the fluid film was so thin that there might not be enough aqueous for ionic exchange.[106]

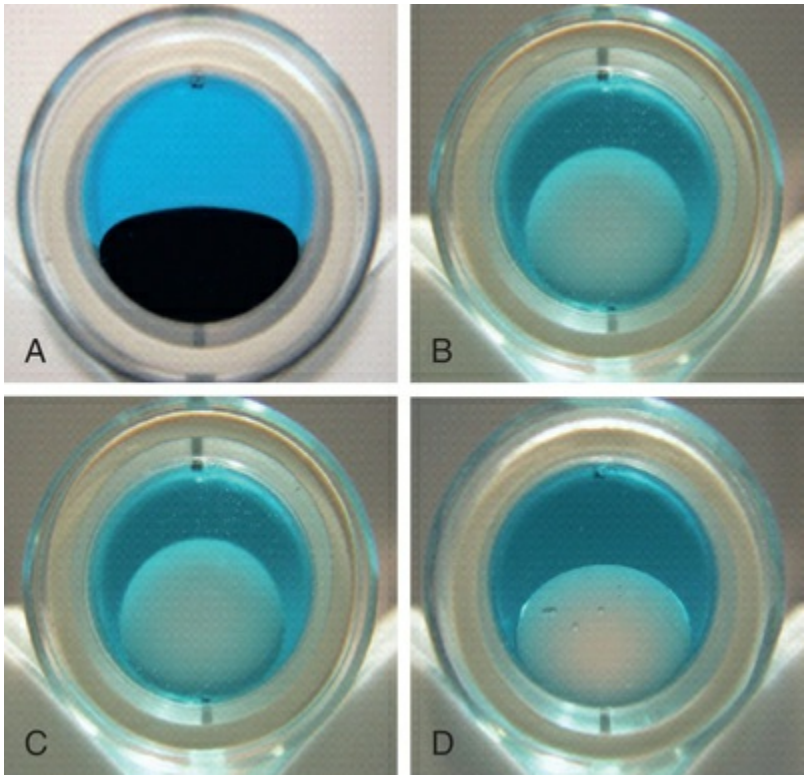

FIG. 108.22 Shape of heavy tamponade bubbles in a model eye chamber. (A) Shows a bubble of perfluorodecalin with specific gravity of 1.94. The bubble assumes a more oval shape (the bubble here appeared in black because it was stained with Sudan Black stain). Bubble in (B) has a specific gravity 1.02. Bubble in (C) has a specific gravity of 1.03. Bubble in (D) has a specific gravity of 1.06. The progressive increase in specific gravities from (B) to (D) shows how the shape of the bubble changes as specific gravity increases.

In a laboratory-based study, Williams et al. have produced

another new agent, produced by adding aerosol silica to a phenyl trimethicone, and mixed via a roller, overhead stirring, and ultrasonics. The product, 11% silica, has greater ease of injection than Densiron 68 or Oxane HD. In vivo testings in rabbit eyes showed no apparent toxicity. This product also has good optical clarity, and better tamponade efficiency than Oxane HD and Densiron 68.[264]

Technique

Heavy SO can be injected following an air–fluid exchange or PFCL/heavy silicone exchange.[247,253,255,260,265,266] In this respect, heavy SO is used much like conventional SO. Heavy SO can also be injected directly. In a giant retinal tear without PVR, it can be injected in the posterior pole. As the bubble gets bigger, the retina unfolds and goes out to length.

It has to be pointed out that some feel that the contact between a heavy tamponade agent and PFCL has the potential of "contaminating" the heavy oil. This might increase the risks of emulsification, inflammation, and sticky SO formation.[267–269] Special note has to be taken when filling an aphakic eye with heavy tamponade. Following complete filling of the vitreous cavity, a superiorly placed peripheral iridectomy should be done.

Conventionally, removal of SO was achieved through active aspiration via a long 18G needle over the optic disc (Fig. 108.23A). Because the oil naturally sinks, this is thought to be necessary. For an 18G cannula, the sclerotomy needs to be suitably large. We have since shown that aspiration over the optic disc is unnecessary (see below).

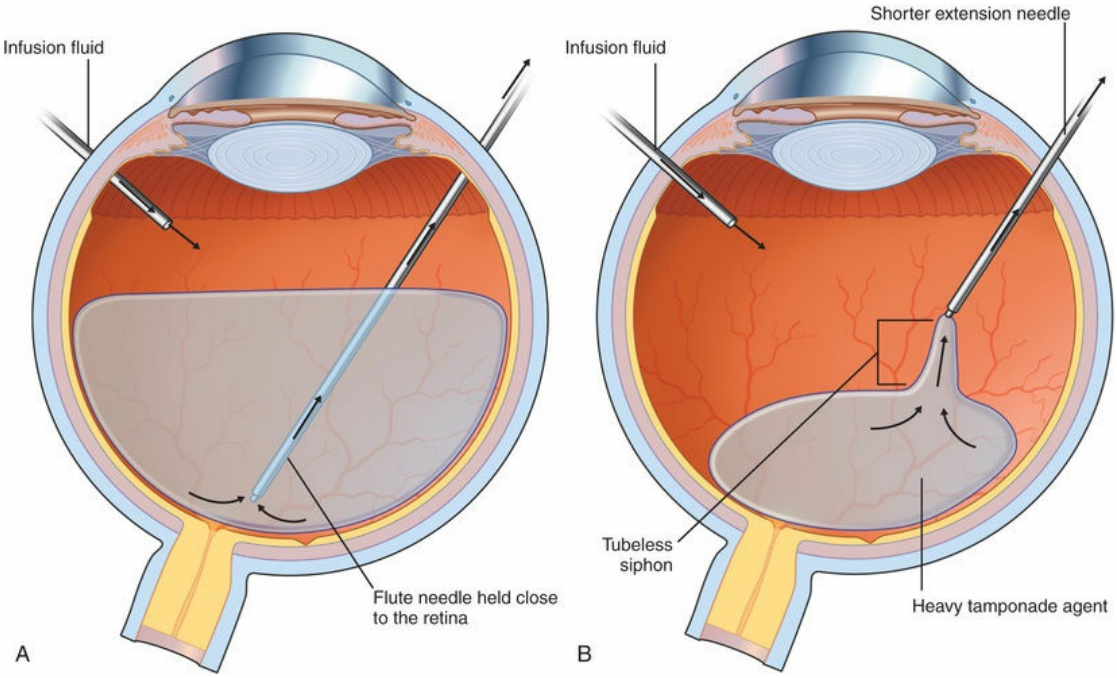

FIG. 108.23 How tubeless siphoning enables removal of heavy tamponade agent through a shorter cannula. (A) How conventional removal is done with the extrusion needle held close to the retina. (B) How a shorter needle can successfully remove heavy tamponade agent using the "tubeless siphoning" phenomenon.

As with all removal of silicone, linear extraction using long tubing is not practical. It may work briefly and initially, but once the tubing starts filling with oil, the flow slows to a halt. Poiseuille's Law dictates that flow is inversely and linearly proportion to the length of the tubing. To minimize this length, no tubing should be used. The suction needs to be generated in a syringe connected directly to the aspirating cannula.

Stappler and colleagues have demonstrated that it is possible to remove heavy tamponade using a short small-gauge cannula.[252] With a 20G polyurethane cannula (Venflon), cut to 7 mm in length, it was shown that it was possible to extract heavy oil and it was unnecessary to reach down to the optic disc. The explanation was attributed to the phenomenon of "tubeless siphoning" (Fig. 108.23B). Heavy SO as well as normal SO are viscoelastic fluids. Under aspiration, extensional flow takes place. The bubble of heavy oil could assume a conical shape while being aspirated such that it was possible to remove all the oil in one go using a short cannula.[252]

Using this method, Romano et al. have shown that it is possible to remove heavy oil even with a 23G cannula.[270]

Removing heavy oil using short 20- or 23G cannulas obviates the need to use large sclerotomies. The risk of accidental trauma to the retina from using high suction and a long cannula close to the retinal surface can be avoided. When using a short cannula, it is important for the tip of the needle not to come out of the heavy oil bubble at any stage. Should this happen, a longer cannula needs to be used to reach the bubble.

Consideration should also be given as to the type cannula used. Plastic cannulas are more hydrophobic than metal ones. SO often tenaciously sticks to the outside of a plastic cannula such that it can be difficult to remove the last drop of oil. Removal of the cannula from the vitreous cavity can cause a bit of oil stuck to the cannula to be scraped off and for that tiny amount of oil to remain in the vitreous cavity. Fortunately, with heavy oil, any oil left tends to round up as a droplet and sinks to the posterior pole where it can be visualized and aspirated by passive or active suction.

Complications

Concerns about inflammation and emulsification have led to slow adoption of heavy tamponade agents.[250,271] Even with the advent of heavy SOs there is conservatism, as there is genuine skepticism as to whether a heavier-than-water tamponade is really safe or indeed necessary. Densiron 68 and, to a certain extent, Oxane HD have been found to be well tolerated in patients, and their use was associated with few complications even when left in the eye for long durations.[253,258]

Densiron 68 shares some of the problems commonly encountered with conventional SO.[238] For instance, it would not conform to the contour of the vitreous cavity; it could not be expected to fit into the nooks and crannies.[23,272] In the presence of high buckles, heavy SO would make contact with the peak of the indent, but leave the retina on the slopes of the indent unsupported.

It is our recommendation that Oxane HD be avoided. It was shown that the olefin RMN3 could come out of solution.[256] The lack of homogeneity of Oxane HD, in the opinion of the authors, should

rule out its use as a heavy tamponade.

Corneal Toxicity

Corneal damage has been reported with the use of F_6H_8.[250,271,273,274] Gerding and Kolck reported in their series of 17 patients, where stromal and epithelial edema was seen in 35% of cases following F_6H_8 use.[271] Similar problems were also reported by Roider et al.,[250] Schatz et al.,[274] and Vote et al.[273] However, in another report by Kirchhof and associates, where 23 eyes were operated on with F_6H_8 kept in situ for a mean of 76 days, no corneal damage was seen.[202] To date, there has been no report on corneal toxicity from the use of Densiron 68, Oxane HD, or HWS 46–3000. However, there is no reason to believe that heavy SO might not cause oil keratopathy should the AC be filled with heavy oil.

Cataract Formation

Cataract formation following vitrectomy with heavy oil tamponade can be multifactorial. It can be the effect of surgical trauma, of the vitrectomy *per se*, of the use of tamponade agent, or a combination of all the above factors. Heavy silicone oil is still an oil and therefore, the chance of cataract formation is 100%, as it has been found that the use of conventional SO leads invariably to cataract formation.[275] Wong and associates identified, in their pilot study of Densiron 68, that all patients developed mild nuclear sclerosis with posterior subcapsular changes during the early postoperative period.[253] Similar observation was also reported by Lappas and colleagues.[276] Kirchhof et al. noted feathery posterior subcapsular opacification in 90% of their patients following the use of F_6H_8.[247] Cataract formation was also observed following the use of Oxane HD and HWS 46–3000.[255,258] Cataract formation was thought to be related to the increase in cellular proliferation in the lens and the change in metabolism of the lens when in contact with the heavy oil.[273,277] In addition to the formation of cataract, progression of posterior capsular opacification has also been seen with the use of heavy tamponade.[278]

As cataract formation with the use of heavy or conventional SO seemed inevitable, some surgeons prefer phacovitrectomy and

intraocular lens implantation at the initial surgery. This has the advantage of facilitating the dissection of membranes at the anterior vitreous. Other surgeons prefer to leave the eye phakic at the time of heavy tamponade injection. There may be valid theoretical reasons to suggest that the tamponade to the posterior retina might be better if the crystalline lens was retained.[279]

Intraocular Inflammation

Severe intraocular inflammation was one of the main reasons for discontinuation of early heavy tamponade agents. High rates of fibrinous reaction and retropupillary membrane formation had led to the cessation of agents such as O62.[260,271,273,280,281] It was thought that the use of heavy tamponade agents would aggravate PVR by inducing an augmented inflammatory response.[271]

For anterior segment inflammation, Theelen and associates observed keratic precipitates in 37% of eyes in their series of 19 patients who received Oxane HD as heavy tamponade.[267] Among these patients, the reaction was granulomatous and some seemed unresponsive to topical steroid. However, excessive inflammation was not observed in the cases series of Wolf et al. (33 eyes)[115] and in a similar study by Rizzo et al. (28 eyes);[255] only minimal inflammatory reaction was noted in these cases. In the case of Densiron 68, Wong and colleagues observed moderate inflammatory reaction at 1 week after surgery.[253] This was in keeping with the observation by Sandner and Engelmann, where similar reaction was seen in 10 of 48 eyes (21%) of their cases.[282] In the series by Sandner and Engelmann, six cases that had inflammatory reaction eventually progressed to sterile hypopyon formation, which in all of whom resolved with the use of topical steroid eyedrops. Majid and associates reported one case of severe AC uveitis out of 40 eyes.[283] For HWS 46–3000, there are so far no reports of severe intraocular inflammation.[258]

Inflammation can be noted in the posterior segment. In a series of 23 cases with F_6H_8 as the tamponade agent, Kirchhof et al. noted pigment clumps were seen on the back of the posterior capsule in 17% of cases.[247] Membranes with prominent inflammatory cells have also been noted.[277] Some have suggested that risk factors for inflammation in the posterior segment include emulsification of the

tamponade agent;[277] contamination of the tamponade agent by PFCL during the surgery;[267] and mechanical trauma from the movement of the of low viscosity tamponade agents within the eye.[273] These risk factors apply mainly to the semifluorinated alkanes and alkenes. With heavy silicone oils, there are to date no reports of severe posterior segment inflammation.[115,253,255,258,262,284,285]

Emulsification

Emulsification is an inherent problem with all liquid tamponade agents. Heavy SO can manifest with: (1) overt emulsification – this may settle as a hypopyon-like fluid level when heavy tamponade agent is used; (2) inflammation – there is some suggestions that heavy SO might give rise to more inflammation although this was not shown in the randomized controlled Heavy Silicone Oil Study; (3) PVR – inflammation could promote PVR. Although, when retinal detachment recurs, it is difficult to know whether PVR is caused by the tamponade agent, or is actually a part of the natural history of the disease process; (4) glaucoma – mechanical blockage of the trabecular meshwork was considered a possible cause of open angle glaucoma in some cases.

In the series with infusion of O62 by Hoerauf and colleagues, 100% emulsification was seen starting from 2 weeks after instillation of the agent.[281] With F_6H_8, Gerding and Kolck also noted a 100% emulsification rate on removal of the agent from the eye, although only 59% were clinically noticeable, with some as early as postoperative day 1.[271] F_6H_8 has relatively low viscosity of around 1–2 cSt. The heavy SO Densiron 68 has a viscosity of around 1350 cSt. The rate of emulsification reported varies tremendously. With Oxane HD, no emulsification was noted in the series by Rizzo et al.[245] and Wolf et al.[115] In other series, a rate (8–20%) has been reported.[253,266,267,282,283]

The rate of emulsification is dependent on the components that make up the heavy tamponade agent. Viscosity is important. The higher the shear viscosity, the more energy is needed to disperse a large bubble into droplets. Dispersed droplets, however, will tend to coalesce back into one single bubble unless they are stabilized by surfactants. There are individual patient factors, including the extent of blood–ocular barrier breakdown, inflammation, presence

of phospholipids and other potential surfactants that might influence the rate of emulsification.

In a recent report by Chan et al. with a model eye, various factors that may influence shear rate were studied. The authors concluded that indentation within an eye, such as that created by scleral buckling, may have the greatest influence in reducing shear force induced by eye movements.[286] Hence, putting in an encircling band may be equally, if not more, effective in preventing emulsification of the heavy SO. However, this was done on a model eye, and whether this can be entirely applied in in-vivo scenarios requires further testing.

At the present time, it is not possible to identify beforehand which patient will have severe emulsification. We can only conclude that emulsification to a greater or lesser extent is inherent with SO use in all patients.

Sticky Silicone Oil

Silicone oil can stick to the retina surface, posterior surface of the capsule, and undersurface of ciliary body and iris.[238,239,258] It has been speculated that SO adheres to the surface of the retina because of the incomplete removal of the posterior hyaloids.[238] Sticky SO might also be related to the use of PFCL, as a small amount of the PFCL might change the physical property of the heavy SOs.[268,269] Sim and Hero reported a case of sticky SO in a phakic patient, after the use of Oxane HD.[278] There are so far only anecdotal reports of such a problem with the use of Densiron 68 and HWS 46–3000.

Adherent Silicone Oil on Intraocular Lens

It was shown that the SO solvent perfluorobutylpentane (F_4H_5) was very effective at removing SO droplets adherent to the posterior surface of the intraocular lens. It is one of the semifluorinated alkanes that is miscible with SO in all proportions. Liang et al. used F_4H_5 on 11 patients and successful removal of all remnants with F_4H_5 was achieved in all cases.[208] In an experimental study, Stappler et al. showed that F_4H_5 was successful in removing virtually all the SO adhering to intraocular lens made from three different materials (silicone, PMMA, and acrylic). By simply rinsing and no mechanical

scrubbing, up to 100% by weight of SO was removed from the surface of PMMA lens (93.7% with silicone lens, and 98.8% with acrylic lens).[209] They, however, also showed that the surface properties of the lenses in terms of hydrophobicity were irreversible, despite virtually complete removal of the oil. Clearly, there was still SO adherent to the lens, even though the layer of oil might only be just a few molecules in thickness.

Hypotony

Hypotony is one of the most difficult to manage complications. This problem is not unique to the use of heavy tamponade and may be related to the severity of the PVR and the extent of surgical retinectomy. With F_6H_8, Gerding and Kolck observed a high rate of hypotony in their series of 16 cases.[271] Others reported rates were only 7% to 11%.[274,279] The rates of hypotony following use of Oxane HD, Densiron 68, and HWS 46–3000 were reported to range from 0–8%.[115,253,255,279,282]

Raised Intraocular Pressure

The mechanism of an acute rise in intraocular pressure as seen with the use of heavy tamponade agents is theoretically identical to that seen with conventional SO. Pupil block glaucoma could occur in aphakic eyes. Avoiding overfill and performing a superiorly placed peripheral iridectomy might be effective in preventing this complication.

Overfilling of heavy tamponade agent could unwittingly occur when an encircling band is applied after the vitreous cavity has already been filled with silicone. Tightening of the band could raise the IOP, which cannot be compensated for by the outflow of aqueous. Therefore, when an encircling band is to be placed, this should be applied before SO injection.

For chronically raised IOP, the mechanism may include (1) intraocular inflammation; (2) emulsification and blockage of the trabecular meshwork by emulsified droplets; (3) steroid response. Rates of chronically raised IOP following the use of Oxane HD have been reported to be from zero to 18%.[115,255,267] Rates for Densiron 68 were from 8% to 19%.[253,282,284] With HWS 46–3000, only one eye out

of 32 had a chronically raised intraocular pressure.[258] In a report with 100 eyes that received vitreoretinal surgery using heavy SO, the mean IOP before surgery was 13.3±5.6 mmHg. This rose to 23.3±8.5 mmHg after surgery and went back down to 13.7±7.2 mmHg following removal.[287] In general, mild to moderate cases of chronically raised intraocular pressure can be managed with the help of antiglaucoma eyedrops. For severe cases, removal or washout of the remnants or droplets in the AC may be tried but the condition sometimes persists, and may eventually require glaucoma surgery.

Redetachment and Proliferative Vitreoretinopathy

Redetachment following the use of heavy tamponade agents usually occurs in the superior half of the retina.[253,255,271,281] Inferior retinal detachment can also occur.[282] Redetachment can occur while the agent is in situ, or after its removal.[253,255,260,265,271]

With the tamponade agent in situ, total redetachment is uncommon. More often, the inferior retina and the posterior pole remain attached, while the superior retina redetaches because of PVR.[253,255,265,271] Wong and associates suggested that a heavy tamponade might be used in cases of conventional SO failure. They suggested that sequential filling with heavy tamponade followed by conventional tamponade (or vice-versa) might lead to long-term anatomic success.[160] In their series, 10 patients underwent sequential "light" SO and "heavy" (Densiron 68) tamponade. Nine patients had light tamponade first, followed by heavy tamponade, whereas the remaining one patient had the reverse. The retina remained attached in all 10 patients after the removal of all tamponade agents, be it heavy or light. The mean logMAR vision improved from 1.57 before surgery, to 0.82 at the latest follow-up (mean follow-up was 19.5 months).[160] Wong et al. concluded that sequential use of light–heavy tamponades might be a strategy in reducing the number of reoperations in complicated retinal detachments. If retinal redetachment was to occur after heavy SO, then a long-acting gas such as C_3F_8 could be used at the reoperation. This would have the advantage of the gas being absorbed spontaneously, which would obviate the need for a further oil removal surgery.

It has been reported that macular-off redetachments occur less frequently with heavy tamponades than with conventional SO.[160,253] This is perhaps explained by the fact that there is a better tamponade effect of the posterior retina when the patient is supine than when the patient is asleep. The shape of the intraocular bubble between Densiron 68 and conventional SO is very similar. Therefore, there are no theoretical reasons to believe that Densiron 68 is a better tamponade agent than conventional SO.[272]

Conclusion

Early heavy tamponade agents such as fluorosilicone oil, perfluorocarbon liquids, and F_6H_8, showed relatively high complication rates and were not acceptable. Of the newer generation of heavy tamponade agents, namely Densiron 68, Oxane HD, and HWS 46–3000, lower complication rates and better in vivo tolerability have been shown, and are comparable with conventional SO in this regard. As mentioned above, Oxane HD is not a homogenous solution, and therefore the authors do not recommend its use. Clinical trials of Densiron so far have shown diversified results. While some noncomparative studies have reported good results,[253,258] others (including the recent multicenter randomized controlled "Heavy Silicone Oil Study"[261]) have demonstrated results that were not superior to conventional SO.[115,282,284] There is sufficient clinical experience with Densiron 68 to indicate that it is well tolerated. Heavy SOs do add to the authors' surgical repertoire, and there are keen advocates for their use. Ultimately, we believe the key to anatomic success lies in careful preoperative evaluation to identify retinal breaks, meticulous planning before surgery and skillful surgery to remove traction and to seal retinal breaks. The tamponade agent, be it heavy or light, is only a minor consideration in the overall approach to patients with retinal detachment.

Drugs for the Prevention of Proliferative Vitreoretinopathy

Introduction

With the advancement of surgical instrumentation, reattachment rates have improved over the years. A group of us have reported success rates of 84% with one operation, and 97.9% at 6 months with multiple operations.[288] This is a significant improvement compared with two decades ago, when vitrectomy for retinal detachment was first introduced. Redetachment occurs for various reasons. Missed retinal breaks are seldom eluded to, while PVR is often quoted as being the main reason for redetachment. The incidence of PVR has been reported to range from 5.2% to 11.7%.[164,289]

Different pathogenic mechanisms are involved in the PVR process accordingly, and multiple targets have been tested either in an animal model of PVR or in human clinical trials. The detailed pathogenesis and surgical treatment of PVR are discussed elsewhere in this book (see Chapter 101, Pathogenesis of proliferative vitreoretinopathy, and Chapter 111, Proliferative vitreoretinopathy). This section intends to summarize some the pharmacologic agents that have been tested for the prevention of PVR formation.

Pharmacologic Agents That Have Been Tested in Clinical Trials

Corticosteroids

Corticosteroid is being tested for use as an inhibitory agent for intraocular proliferations. It exerts its effect though the inhibition of intraocular inflammation and maintains the integrity of the blood–ocular barrier. Steroids also inhibit fibroblast-like activities. In early animal studies, intravitreal injection of dexamethasone or triamcinolone has been shown to effectively reduce the rate of traction retinal detachment (TRD).[290–294] Methylprednisolone has also been shown to reduce the rate of PVR when injected periocularly (Fig. 108.24).[295]

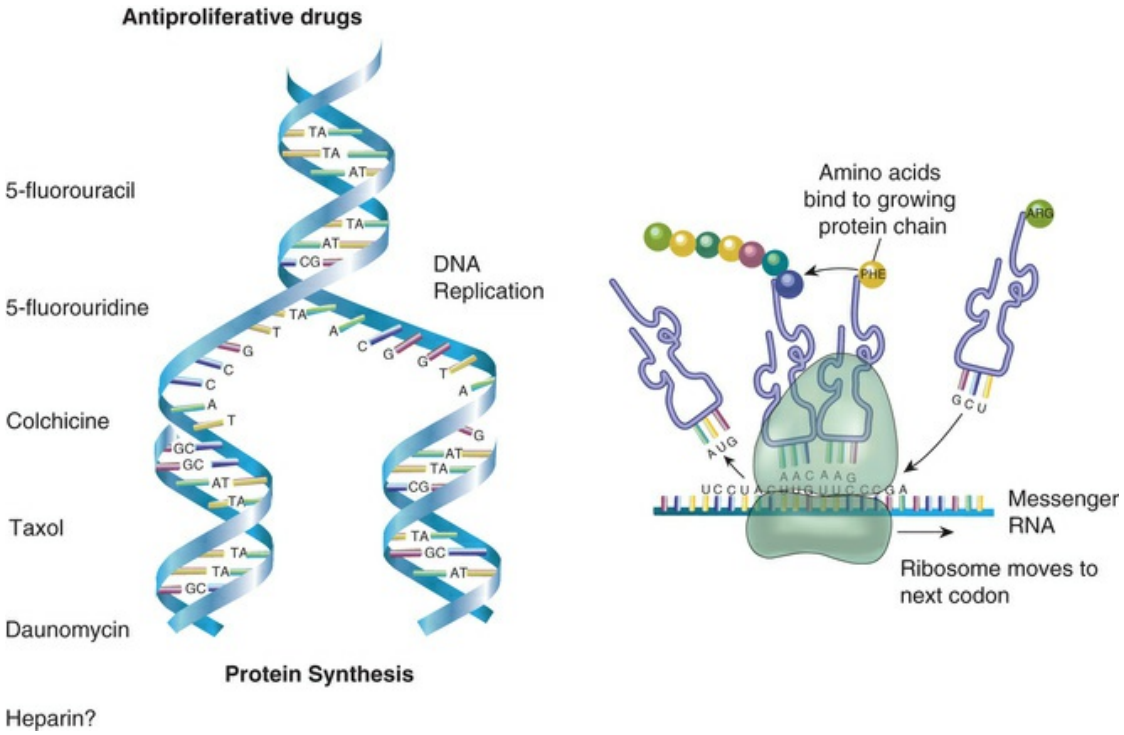

FIG. 108.24 Structural presentation of DNA and the site of action of various chemicals in the prevention of proliferative vitreoretinopathy. The upper portion of the diagram demonstrates the association between purine and pyrimidine pairs contributing to the double-helical structure of DNA. Antimetabolites such as daunomycin intercalate directly into the DNA structure, hence interference with its replication. Others interfere with DNA synthesis by limiting the availability of necessary precursors (fluoropyrimidines) or through their effects on regulatory proteins necessary for the completion of S phase and mitosis (Taxol, colchicine).

The systemic side-effects are such that in the absence of good clinical evidence of their efficacy, the routine use of systemic steroids for the prevention or treatment of PVR does not seem justified. In recent years, however, intravitreal triamcinolone has become part and parcel of vitrectomy. It is not used so much for its pharmacologic effect, but instead, it is used as an intraoperative tool for identification of cortical vitreous or even as a "dye" to assist internal limiting membrane peel. Many of the crystals are left in the vitreous cavity and sometimes purposely, to reduce postoperative inflammation.[290–294]

In a recent retrospective comparative trial, the role of

triamcinolone was being investigated in assisting vitrectomy for pseudophakic retinal detachments associated with PVR.[294] Although the difference between triamcinolone-assisted and nontriamcinolone-assisted cases was not statistically significant, it did point towards a lower redetachment rate among cases where triamcinolone was used, and highlighted the potential for future prospective studies using triamcinolone. Whether the reduction in redetachment is due to the surgery that could be achieved with triamcinolone, or whether it is due to the pharmacologic effect of the drug, remains speculative.

Fluoropyrimidines

The fluoropyrimidines, most notably 5-fluorouracil (5-FU), are the first antimetabolites to be investigated for intraocular use to inhibit PVR formation.[296,297] Its relatively low intraocular toxicity and high potency in inhibiting cellular proliferation made it ideal for this purpose. 5-FU exerts its effect on rapidly growing cells through inhibition of proliferation and contraction. There is more than one pathway in which 5-FU acts to serve its purpose. It inhibits protein synthesis by incorporating into ribonucleic acid (RNA), which in turn affects mitosis and cytoskeleton function.

In animal studies, the inhibitory effect of 5-FU has been widely studied. In a rabbit PVR model, a single intravitreal injection of 1 mg 5-FU successfully prevented PVR formation in 41% of animals at 28 days.[298] In another study, 1 mg 5-FU was loaded onto a biodegradable polymer and implanted into the vitreous and maintained for 14 days. Incidence of TRD was significantly reduced in treated animals.[299] Other than being used alone, its use in combination with other drugs have been investigated. 5-FU in combination with triamcinolone or low-molecular-weight-heparin (LMWH) has been injected into rabbit models of PVR.[300,301] Results showed significant reduction in terms of TRD and severity of the PVR.[300,301] As far as toxicity is concerned, no demonstrable damage was seen in the animal eyes.

Blumenkranz and colleagues pioneered its use in humans in the early 1980s. In a study involving 22 patients with PVR, 5-FU injected intravitreally did not seem to cause any toxic effect, and was thought to be potentially effective in preventing PVR

recurrence after surgery.[296] Subsequently, Asaria et al. published the first randomized controlled trial regarding the use of 5-FU in the prevention of postoperative PVR formation.[302] In the study, 200 μg/mL 5-FU and 5 IU/mL low-molecular-weight heparin (LMWH) were added to the intravitreal infusate during surgery. The outcomes of the 174 patients, when divided into the treatment arm and the placebo arm, showed a significantly lower incidence of PVR in the treated group (12.6% vs. 26.4%) at 6 months.[302] The primary success rate between the two groups was not significantly different and, importantly, the rate of complications was not statistically different between the two groups. It seemed that the so-called "British Cocktail" of 5-FU and heparin is safe and efficacious. Both treated and control groups had a similar number of redetachments. It is not known whether the redetachments were caused by PVR or by missed breaks. Nonetheless, when patients with redetachments presented, the control group had twice the rate of PVR as indicated above. It should be further pointed out that all the patients in this group had high-risk characteristics for PVR. Whether patients were at high risk of developing PVR was calculated using a regression formula. This formula was based on a study by the same investigators of patients previously treated. In this regression formula, the number of quadrants of retinal detachment, the presence of early PVR grades A and B, previous cryotherapy, and the presence of uveitis were all important determinants.

Although the study had a randomized design, the unequivocal result was disappointing. The rationale for a PVR treatment is to reduce the redetachment rate, and this was not the result. Perhaps the basic premise was wrong, i.e., that PVR was not the most important cause of redetachment. If it were due to undetected or untreated retinal breaks, no pharmacologic adjunct would be effective. Also, the external validity of the study was an important consideration. The patients were carefully selected according to strict criteria and a regression formula, but what we needed to know was whether the cocktail was effective in cases with established PVR.

In another study by the same group on cases with established PVR, 174 patients undergoing vitrectomy were recruited. Inclusion criteria were as follows: eyes with PVR grade C: anterior or

posterior with at least 1 clock-hour involvement; types 1, 2, 4, or 5. The primary outcome measure was defined as posterior retinal reattachment after removal of SO without any reoperations at 6 months. Secondary outcome measures recorded were posterior retinal reattachment, localized/tractional retinal detachment, visual acuity, macular pucker, hypotony, glaucoma, keratopathy, and cataract. Removal of SO and reoperations were also recorded. At 6 months, 84% of patients had full retinal reattachment and 94% had stable posterior retinal reattachment. There was no significant difference in success in the primary outcome measure (56%, treatment group; 51%, placebo group; p=.59) or in secondary outcome measures or rates of complications. Secondary macular pucker occurred less often in the treatment group (6% vs. 17% at 6 months; p=.068). The investigators concluded that perioperative infusion of combined 5-fluorouracil and LMWH did not significantly increase the success rate of vitreoretinal surgery for established PVR.

The fact that the drug combination worked in reducing PVR in high-risk groups but not in established PVR might be interesting. In established PVR, the epiretinal membranes would already be maturing. Proliferation might not be such an important feature. In late PVR, the epiretinal membrane might be hypocellular. There may also be a question whether the drugs could penetrate dense membranes. Although the drug combination targeted more than one pathway, it could be that the modulation of the cellular response was the most important. It might also be reasonable to conclude that the cocktail was only effective when given early in the natural history of retinal detachment and by the time that PVR was established, the drugs might not be as effective. This led to the mounting of the third and the largest of the three trials.

The study involved 615 patients with primary rhegmatogenous retinal detachments.[288] The same dosage of 5-FU/LMWH infusate was used. At 6 months, no statistical difference was found between the treated group and placebo, in terms of PVR occurrence. The number of patients who failed due to the development of PVR was not statistically significant: 23 in the treatment group (7.0%) and 14 in the placebo group (4.9%) (p=.309). There was no significant difference in the mean visual acuity at 6 months in the placebo

group (0.48) versus the treatment group (0.53; p=.072). Of more concern were the visual results of patients who presented with macular-on detachments. The visual acuity at 6 months of patients presenting with a macula-sparing retinal detachment was significantly worse in the treatment group (p=.0091). There was no significant difference between the two groups in patients who presented with a macula involving retinal detachment (p=.896). The visual results suggested that the drug combination might be slightly retinotoxic. In the past, high doses of 5-FU were used and considered to be safe. They have, however, always been used in patients with poor prognosis. If there was a slight diminution to the visual outcome, this might not have been detected. For the first time, the drug combination was used on some patients with good visual prognosis.

For a summary of the results of all three trials, refer to the recent report from the Cochrane Eyes and Vision Group. Sundaram et al. suggested that no definite conclusion could be drawn from these studies so far, and that further research should therefore be carried out in high-risk patients only.[303] Due to the lack of supporting evidence at present, 5-FU should therefore not be routinely used in the surgical repair of retinal detachments to prevent PVR formation, until evidence from further research, with favorable results, is available.

Daunorubicin

Daunorubicin is an anthracycline antibiotic, and its mechanism of action in the inhibition of PVR formation is thought to be independent of the cell cycle. It has a significant inhibitory effect on proliferation and migration of cells, but the effect on cellular contraction is limited. It has been shown in animal studies to be capable of reducing the PVR rate.[304,305] It has been shown to be more toxic than 5-FU, but a dosage of up to 7.5 μg/mL when infused into the eye during surgery, has been found to be well tolerated.[304]

The first study was performed on patients undergoing vitrectomy for trauma. In 15 patients, there was only one case of proliferation, and there was no sign of toxicity.[304] Results from a later study involving treatment of advanced PVR with daunorubicin and SO agreed on the beneficial effect, in terms of redetachment and vision

improvement.[306]

An RCT was later conducted to investigate the efficacy of daunorubicin in the prevention of PVR.[307] Wiedemann and associates conducted a multicenter RCT on patients with established PVR, where daunorubicin was infused into the vitreous cavity for 10 minutes during vitrectomy, with an aim to reduce postoperative PVR formation. Six months after standardized surgery, complete retinal reattachment without additional vitreoretinal surgery was achieved in 62.7% (89/142) of eyes in the daunorubicin group versus 54.1% (73/135) in the control group (p=.07, one-sided). However, in the daunorubicin group, significantly fewer vitreoretinal reoperations were performed within 1 year postoperatively (p=.005, one-sided) to achieve the same overall 1-year retinal reattachment rate (80.2% [105/131] vs. 81.8% [103/126]). The rate of patients with no vitreoretinal reoperations was 65.5% (95/145) in the daunorubicin group versus 53.9% (76/141) in the control group. There was no difference in the best corrected visual acuity.[307]

Retinoids

In the eye, retinoids play an important role in the metabolism and turnover of visual pigments. It was thought to have an effect on proliferation and cell-mediated contraction of myofibroblasts, as seen in PVR. Laboratory studies involving treatment of human RPE cells with vitamin A showed significant reduction in cellular proliferation and migration.[308] In rabbits, intravitreal injection of retinoic acid (RA) has successfully reduced the occurrence of PVR.[309] In humans, 13-*cis* RA, an isoform of all-transretinoic acid, was found to have an inhibitory effect on excised membranes from PVR patients and did not show toxic effects.[310]

Fekrat and colleagues, in a small group of patients with PVR, conducted the first pilot study. Subjects were given an oral dose of 13-*cis* RA (80 mg/day) for 4 weeks after surgery. Results showed a decreased rate of PVR and an increased rate of retinal attachment.[311] A recent prospective RCT in 35 patients seemed to concur with the results and points towards a protective effect of retinoids against PVR formation. In this study, the treatment arm subjects were given a dose of 20 mg/day for 8 weeks after surgery for retinal

detachment. Results at 1 year showed that in the treatment arm, the retinal attachment rate was significantly higher than in the placebo arm (93.8% vs. 63.2%, p=.047).[312] The rate of macular pucker formation was also significantly lower and vision was significantly better in the treatment arm. This was an encouraging result, since this drug has been in wide use in other diseases already and has shown a good safety profile (in acne vulgaris,[313] and in the prevention of second primary tumor in squamous cell carcinoma of the head and neck).[314] Results regarding this drug have so far been promising. Further studies should be conducted to delineate the efficacy profile before it can be incorporated into routine use.

Heparin and Low-Molecular-Weight Heparin

Heparin, a glucose aminoglycan derived from heparin sulfate, is well known for its anticoagulation ability. It acts by binding to and altering the properties of antithrombin, and inactivating thrombin in the end. Other than its anticoagulation properties, heparin also has several other abilities. It binds to a number of growth factors, including fibroblast growth factor, platelet-derived growth factor, and endothelial cell growth factor. It reduces cell aggregation by inhibiting fibroblast adhesion to fibronectin-coated substrates, and gives rise to a change in the cytoskeleton of smooth muscles and pericytes.[315] It also inhibits the polymerization of type I collagen, and reduces the hypocellular gel contraction by fibroblast and RPE cells. It also inhibits the proliferation of scleral fibroblasts and RPE cells.[316]

Despite the numerous functions described, the anticoagulation feature of heparin often causes excessive bleeding, which has limited its clinical use. In view of this, heparin has been broken down into fragments, which have a mean molecular weight of ≤5000. These LMWH fragments have increased bioavailability and a longer half-life.[317] They retain the antithrombotic effect of heparin but produce less hemorrhage. This may be due to the fact that LMWH has reduced ability to inhibit platelet aggregation, and some have suggested that, while LMWH can still inhibit factor Xa like heparin, it loses the ability to inhibit activation of thrombin directly.[318] LMWH has been shown to reduce fibrin formation after vitrectomy.[319] LMWH became a better alternative to heparin, while

retaining many of the advantages that heparin confers, especially with respect to prevention of PVR formation. In early animal studies, inclusion of LMWH in the infusate during vitrectomy has successfully reduced the rate of PVR-induced traction retinal detachment.[320] In addition to the effect described, LMWH also reduced the amount of fibrin in the eye after vitrectomy in the rabbit and increased corneal clarity after surgery.[319] More importantly, the rate of postoperative vitreous hemorrhage did not seem to increase.[319]

The mechanism of action of LMWH appears to differ from that of antimetabolites and corticosteroid, with regard to inhibition of PVR formation. Therefore, in clinical studies, LMWH was used in combination with other agents, most commonly with 5-FU or with steroid.[321–323] In a pilot study on 62 patients with severe PVR, vitrectomy with infusate enriched with heparin and dexamethasone did not reduce rate of reproliferation, but rather increased significantly the rate of postoperative hemorrhage.[324] Since the results of this study, the interest in using LMWH instead of the unfractionated heparin has grown. Kumar et al. provide another study that showed some beneficial effect with LMWH-added infusate.[321] However, a recent review by the Cochrane Library looked at two randomized controlled trials with a total of 789 participants using LMWH with 5-FU infusion for the prevention of PVR.[325] However, the authors found inconsistent evidence regarding the efficacy of this regimen in the prevention of PVR.

Anti-Vascular Endothelial Growth Factor

The ophthalmology world has seen tremendous advances in the use of anti-vascular endothelial growth factor (VEGF) in the treatment of various eye diseases, such as age-related macular degeneration,[326] diabetic retinopathy,[327,328] and retinal vein occlusion.[329] It has also been suggested to be tried as a prophylaxis for PVR inhibition.[330] Platelet-derived growth factor receptor α, a receptor tyrosine kinase that is key to the pathogenesis of experimental PVR, maybe engaged by growth factors, including vascular endothelial growth factor (VEGF) A, in the process of PVR formation.[325,331,332] Therefore, by inhibiting VEGF, PVR may potentially be prevented.

Ghasemi et al. have performed a study to evaluate the role of bevacizumab in the prevention of PVR, when injected into the silicone oil at the end of the retinal detachment surgery.[333] In their series, 38 eyes with grade C PVR or more were included, and were divided into two groups, one receiving bevacizumab, and the other without. However, their results have shown that the use of bevacizumab did not eliminate the risk of postoperative PVR formation.[333] In another similar trial by Hsu et al., where 20 eyes that had PVR received serial bevacizumab injections into the silicone oil after vitrectomy were compared to historic controls in terms of re-detachment rates, final visual acuity, and epiretinal membrane formation.[334] The authors failed to detect significant improvement in any of the parameters measured, when bevacizumab was being given serially after vitrectomy. Hence, the theory regarding PVR prevention by antagonizing VEGF requires further testing.

Chemicals yet to Be Tested in Clinical Trials

Many other chemicals have also been proposed for inhibiting PVR formation. These include: taxol,[335] colchicine,[336] immunotoxins,[337] matrix metalloproteinases (MMP),[338] thiotepa,[339] VP16,[339] and vincristine.[339] Although the list is by no means exhaustive, to date none of these has been implemented in clinical practice, either due to toxicity issues or limited efficacy. Details of these chemicals are outlined in Table 108.7.

TABLE 108.7

Various Chemicals Tried in Experimental Models of Proliferative Vitreoretinopathy

Chemical Name	Category	Concentration/Dose	Mechanism of Action	Animal Model
Paclitaxel (Taxol)[335]	Plant-derived mitosis inhibitor	0.0005 mg	Inhibit contraction of collagen gel	Reduced tractional retinal detachment in two rabbit models
Colchicine[336]	Plant-derived alkaloid	1.3–1.7 × 10^8 mol/L	Inhibit mitosis and cell motility	Inhibition of cell proliferation in a cell culture using cells harvested from pig eyes

Immunotoxin (transferrin-ricin A chain)[337]	Monoclonal antibody	0.002 mg	Inhibit protein synthesis by ribosomal inactivation	Reduced tractional retinal detachment in a rabbit model
Matrix metalloproteinases (Prinomastat)[338]	Enzymes responsible for extracellular matrix remodeling	0.5 mg	Inhibit extracellular collagen remodeling and contraction	Reduced tractional retinal detachment in a posttraumatic proliferative vitreoretinopathy rabbit model

Summary

The results of pharmacologic adjunct for the treatment of PVR have so far been disappointing. There are three fundamental problems: first, there is a divergence between what basic scientists are aiming for and what the surgeons want. Surgeons want agents that can improve the primary success rate of retinal repair surgery. We may be deluding ourselves in thinking that PVR is the main cause of retinal detachment. At times, it may only be one of the contributing factors. There are other factors that must be taken into consideration, including the surgeon's training, skill and ability, and the technology that we have at our disposal to help identify all causative retinal breaks and to close them. Nonetheless, the clinicians tell the scientists that what we need is an elixir that could suppress PVR. As a result, the elixir may or may not give us what we want; a high primary success rate. Secondly, PVR may be a poor proxy for success and failure of retinal detachment repair surgery. Conversely, if epiretinal membranes were distant from retinal breaks, their contraction and traction might not open retinal breaks and cause retinal redetachment. Equally, if there were no epiretinal membranes, the retinal redetachment might still occur if breaks were not identified and closed during the initial surgery. Thirdly, our obsession with the anatomic success rate of retinal detachment repair might also entirely miss the point. The fact is that even though we have reached over 90% with multiple operations, the visual outcomes in general of macula-off detachments are still disappointing. The poor visual result seems disproportionate to the number of photoreceptors lost through apoptosis. There is a need for greater understanding of why visual recovery is so poor. Recent evidence from spectral domain OCT indicates that some cellular

recovery and remodeling can take place.[340,341] Photoreceptor regeneration or rearrangement could be potentially estimated from the integrity of the inner/outer-segment junction on OCT.[342] If we were to improve the visual prognosis, perhaps pharmacologic agents that confer neuroprotection might be just as important as targeting the process of PVR. After all, visual recovery is ultimately what patients and surgeons desire.

References

1. Ohm J. Über die Behandlung der Netzhautablösung durch operative Entleerung der subretinalen Flüssigkeit und Einspritzung von Luft in den Glaskörper. *Graefes Arch Klin Ophthalmol*. 1911;79:442–450.
2. Rosengren B. Results of treatment of detachment of the retina with diathermy and injection of air into the vitreous. *Acta Ophthalmol*. 1938;16:573–579.
3. Norton EWD, Aaberg T, Fung W, et al. Giant retinal tears. I. Clinical management with intravitreal air. *Am J Ophthalmol*. 1969;68:1011–1021.
4. Machemer R. Intravitreous injection in sulfur hexafluoride gas (SF_6). Freeman HM, Hirose T, Schepens CL. *Vitreous surgery and advances in fundus diagnosis and treatment*. Appleton–Century–Crofts: New York; 1977.
5. Hilton GF, Grizzard WS. Pneumatic retinopexy: a two-step outpatient operation without conjunctival incision. *Ophthalmology*. 1986;93:626–641.
6. Machemer R, Buettner H, Norton EW, et al. Vitrectomy: a pars plana approach. *Trans Am Acad Ophthalmol Otolaryngol*. 1971;75:813–820.
7. Heimann H, Bartz-Schmidt KU, Scleral Buckling versus Primary Vitrectomy in Rhegmatogenous Retinal Detachment Study Group, et al. Scleral buckling versus primary vitrectomy in rhegmatogenous retinal detachment: a prospective randomized multicenter clinical study. *Ophthalmology*. 2007;114:2142–2154.
8. Lincoff A, Lincoff H, Iwamoto T, et al. Perfluoro-butane – a gas for a maximum duration retinal tamponade. *Arch*

Ophthalmol. 1983;101:460–462.
9. Lincoff A, Lincoff H, Solorzano C, et al. Selection of xenon gas for rapidly disappearing retinal tamponade. *Arch Ophthalmol*. 1982;100:996–997.
10. Vygantas CM, Peyman GA, Daily MJ, et al. Octafluorocyclobutane and other gases for vitreous replacement. *Arch Ophthalmol*. 1973;90:235–236.
11. Fineberg E, Machemer R, Sullivan P, et al. Sulphur hexafluoride in owl monkey vitreous cavity. *Am J Ophthalmol*. 1975;79:67–76.
12. Killey MP, Edelhauser HF, Aaberg TM. Intraocular sulfur hexafluoride and octafluorocyclobutane. *Arch Ophthalmol*. 1978;96:511–515.
13. Gilbert C, McLeod D. D-ACE surgical sequence for selected bullous retinal detachments. *Br J Ophthalmol*. 1985;69:733–736.
14. Tornambe PE. Pneumatic retinopexy: the evolution of case selection and surgical technique. A twelve-year study of 302 eyes. *Trans Am Ophthalmol Soc*. 1997;95:551–578.
15. Mandelcorn ED, Mandelcorn MS, Manusow JS. Update on pneumatic retinopexy. *Curr Opin Ophthalmol*. 2015;26(3):194–199.
16. Zhou C, Qiu Q, Zheng Z. Air versus gas tamponade in rhegmatogenous retinal detachment with inferior breaks after 23-gauge pars plana vitrectomy: a prospective, randomized comparative interventional study. *Retina*. 2015;35(5):886–891.
17. Noble J, Kanchanaranya N, Devenyi RG, et al. Evaluating the safety of air travel for patients with scleral buckles and small volumes of intraocular gas. *Br J Ophthalmol*. 2014;98(9):1226–1229.
18. Stolba U, Krepler K, Pflug R, et al. Experimental vitreous and aqueous replacement with perfluorophenanthrene: clinical, histologic, and electrophysiologic results. *Retina*. 1997;17:146–153.
19. Wong D, Williams R, Stappler T, et al. What pressure is exerted on the retina by heavy tamponade agents? *Graefes Arch Clin Exp Ophthalmol*. 2005;243:474–477.

20. Sharma A, Grigoropoulos V, Williamson TH. Management of primary rhegmatogenous retinal detachment with inferior breaks. *Br J Ophthalmol*. 2004;88:1372–1375.
21. McCuen BW 2nd, Azen SP, Stern W, et al. Vitrectomy with silicone oil or perfluoropropane gas in eyes with severe proliferative vitreoretinopathy. Silicone Study Report 3. *Retina*. 1993;13:279–284.
22. Chang S. Intraocular gases. Ryan SJ. *Retina*. 4th ed. Elsevier: Oxford; 2006.
23. Fawcett IM, Williams RL, Wong D. Contact angles of substances used for internal tamponade in retinal detachment surgery. *Graefes Arch Clin Exp Ophthalmol*. 1994;232:438–444.
24. Khan MA, Brady CJ, Kaiser RS. Clinical management of proliferative vitreoretinopathy: an update. *Retina*. 2015;35(2):165–175.
25. Pastor JC, Rojas J, Pastor-Idoate S, et al. Proliferative vitreoretinopathy: a new concept of disease pathogenesis and practical consequences. *Progr Retinal Eye Res.*2016;51:125–155.
26. van Meurs JC, Humalda D, Mertens DA, et al. Retinal folds through the macula. *Doc Ophthalmol*. 1991;78(3–4):335–340.
27. Hilton GF, Kelly NE, Salzano TC, et al. Pneumatic retinopexy: a collaborative report of the first 100 cases. *Ophthalmology*. 1987;94:307–314.
28. Heimann H, Bopp S. Retinal folds following retinal detachment surgery. *Int J Ophthalmol*. 2011;(Suppl. 1):18–26.
29. Zacharias LC, Nobrega PF, Takahashi WY. Surgical correction of retinal folds involving the fovea. *Ophthalmic Surg Lasers Imaging Retina.*2014;45(1):50–53.
30. Crittenden JJ, de Juan E, Tiedeman J. Expansion of long-acting gas bubbles for intraocular use. *Arch Ophthalmol*. 1985;103:831–834.
31. Peters MA, Abrams GW, Hamilton LH, et al. The nonexpansile, equilibrated concentration of perfluoropropane gas in the eye. *Am J Ophthalmol*. 1985;100:831–839.
32. Thompson JT. Kinetics of intraocular gases: disappearance

of air, sulfur hexafluoride, and perfluoropropane after pars plana vitrectomy. *Arch Ophthalmol*. 1989;107:687–691.
33. McCarthy D. The effect of nitrous oxide on intra-ocular pressure. *Anaesthesia*. 2012;67(6):680–681.
34. Seaberg R, Freeman WR, Goldbaum MH, et al. Permanent postoperative vision loss associated with expansion of intraocular gas in the presence of a nitrous oxide-containing anesthetic. *Anesthesiology*. 2002;97:1309–1310.
35. Fu AD, McDonald HR, Eliott D, et al. Complications of general anesthesia using nitrous oxide in patients with preexisting gas bubbles. *Retina*. 2002;22:569–574.
36. Lincoff H, Weinberger D. Stergiu P. Air travel with intraocular gas. II. Clinical considerations. *Arch Ophthalmol*. 1989;107:907–910.
37. Jackman SV, Thompson JT. Effects of hyperbaric exposure on eyes with intraocular gas bubbles. *Retina*. 1995;15:160–166.
38. Tan HS, Oberstein SY, Mura M, et al. Air versus gas tamponade in retinal detachment surgery. *Br J Ophthalmol*. 2013;97(1):80–82.
39. Kreissig I, Stanowsky A, Lincoff H, et al. The treatment of difficult retinal detachments with an expanding gas bubble without vitrectomy. *Graefes Arch Clin Exp Ophthalmol*. 1986;224:51–54.
40. Chang S, Coleman DJ, Lincoff H, et al. Perfluoropropane gas in the management of proliferative vitreoretinopathy. *Am J Ophthalmol*. 1984;98:180–188.
41. The Silicone Study Group. Vitrectomy with silicone oil or sulfur hexafluoride gas in eyes with severe proliferative vitreoretinopathy: results of a randomized clinical trial. Silicone Study report 1. *Arch Ophthalmol*. 1992;110:770–779.
42. Modi YS, Epstein A, Flynn HW Jr, et al. Outcomes and complications of pneumatic retinopexy over a 12-year period. *Ophthalmic Surg Lasers Imaging Retina.*2014;45(2):132–137.
43. Noohi P, Abdekhodaie MJ, Cheng YL. Computational modeling of intraocular gas dynamics. *Physical Biol*. 2015;12(6):066019.

44. Kim SS, Smiddy WE, Feuer WJ, et al. Outcomes of sulfur hexafluoride (SF_6) versus perfluoropropane (C_3F_8) gas tamponade for macular hole surgery. *Retina*. 2008;28:1408–1415.
45. Fassbender JM, Sherman MP, Barr CC, et al. Tissue plasminogen activator for subfoveal hemorrhage due to age-related macular degeneration: comparison of 3 treatment modalities. *Retina*. 2016;36(10):1860–1865.
46. Chang W, Garg SJ, Maturi R, et al. Management of thick submacular hemorrhage with subretinal tissue plasminogen activator and pneumatic displacement for age-related macular degeneration. *Am J Ophthalmol*. 2014;157(6):1250–1257.
47. Landers MB, Robinson D, Olsen KR, et al. Slit-lamp fluid gas exchange and other office procedures following vitreoretinal surgery. *Arch Ophthalmol*. 1985;103:967–972.
48. Moon CH, Choi KS, Rhee MR, et al. Intraoperative assessment of intraocular pressure in vitrectomized air-filled and fluid-filled eyes. *Acta Ophthalmol*. 2013;91(7):e524–8.
49. Mamas N, Fuest M, Koutsonas A, et al. Goldmann applanation tonometry versus dynamic contour tonometry after vitrectomy. *J Glaucoma*. 2016;25(8):663–668.
50. Jang JH, Kim YC, Kim KS. The efficacy of fluid–gas exchange for the treatment of postvitrectomy retinal detachment. Korean journal of ophthalmology. *Korean J Ophthalmol*. 2009;23(4):253–258.
51. Houston S, Graf J, Sharkey J. Commercial air travel after intraocular gas injection. *Aviat Space Environ Med*. 2012;83(8):809–810.
52. Thompson JT. The role of patient age and intraocular gas use in cataract progression after vitrectomy for macular holes and epiretinal membranes. *Am J Ophthalmol*. 2004;137(2):250–257.
53. Muether PS, Hoerster R, Kirchhof B, et al. Course of intraocular pressure after vitreoretinal surgery: is early postoperative intraocular pressure elevation predictable? *Retina*. 2011;31(8):1545–1552.

54. Lee DA, Wilson MR, Yoshizumi MO, et al. The ocular effects of gases when injected into the anterior chamber of rabbit eyes. *Arch Ophthalmol*. 1991;109:571–575.
55. Clark LC Jr, Gollan F. Survival of mammals breathing organic fluids equilibrated with oxygen at atmospheric pressure. *Science*. 1966;152:1755–1756.
56. Haidt SJ, Clark LC Jr, Ginsberg J. Liquid perfluorocarbon replacement of the eye. *Invest Ophthalmol Vis Sci*. 1982;22:233.
57. Clark LC Jr. *Description*. [U.S. Patent No. 4,490,351. Dec. 25] 1984.
58. Chang S. Low viscosity liquid fluorochemicals in vitreous surgery. *Am J Ophthalmol*. 1987;103:38–43.
59. Bourke RD, Simpson RN, Cooling RJ, et al. The stability of perfluoro-n-octane during vitreoretinal procedures. *Arch Ophthalmol*. 1996;114:537.
60. Sparrow JR, Matthews GP, Iwamoto T, et al. Retinal tolerance to intravitreal perfluoroethylcyclohexane liquid in the rabbit. *Retina*. 1993;13:56–62.
61. Azzolini C, Brancato R, Trabucchi G, et al. Endophotocoagulation through perfluorodecalin in rabbit eyes. *Int Ophthalmol*. 1994;18:33.
62. Batman C, Cekic O. Effects of the long-term use of perfluorophenanthrene on the retina. *Ophthalmic Surg Lasers*. 1998;29:144–146.
63. Chang S, Zimmerman NJ, Iwamoto T, et al. Experimental vitreous replacement with perfluorotributylamine. *Am J Ophthalmol*. 1987;103:29–37.
64. Bryan JS, Friedman SM, Mames RN, et al. Experimental vitreous replacement with perfluorotri-n-propylamine. *Arch Ophthalmol*. 1994;112:1098.
65. Wong D, Williams RL, German MJ. Exchange of perfluorodecalin for gas or oil: a model for avoiding slippage. *Graefes Arch Clin Exp Ophthalmol*. 1998;236:234–237.
66. Li KK, Wong D. Avoiding retinal slippage during macular translocation surgery with 360 retinotomy. *Graefes Arch Clin Exp Ophthalmol*. 2008;246:649–651.

67. Schulman JA, Peyman GA, Blinder KJ, et al. Management of giant retinal tears with perfluoroperhydrophenanthrene (Vitreon). *Jpn J Ophthalmol*. 1993;7:70–77.
68. Wang ZY, Zhao KK, Zhao DS, et al. Dissection under perfluorocarbon liquid: a modified vitrectomy technique for diabetic tractional retinal detachment. *Retina*. 2012;32(4):848–852.
69. Foster RE, Smiddy WS, Alfonso ED, et al. Secondary glaucoma associated with retained perfluorophenanthrene. *Am J Ophthalmol*. 1994;118:253–255.
70. Glaser BM, Carter JB, Kuppermann BD, et al. Perfluoro-octane in the treatment of giant retinal tears with proliferative vitreoretinopathy. *Ophthalmology*. 1991;98:1613–1621.
71. Morse LS, McCuen BW II, Machemer R. Relaxing retinotomies: analysis of anatomic and visual resuhs. *Ophthalmology*. 1990;97:642–648.
72. Imaizumi A, Kusaka S, Noguchi H, et al. Efficacy of short-term postoperative perfluoro-n-octane tamponade for pediatric complex retinal detachment. *Am J Ophthalmol*. 2014;157(2) [384–9.e2].
73. Randolph JC, Diaz RI, Sigler EJ, et al. 25-gauge pars plana vitrectomy with medium-term postoperative perfluoro-n-octane for the repair of giant retinal tears. *Graefes Arch Clin Exp Ophthalmol*. 2016;254(2):253–257.
74. Rush R, Sheth S, Surka S, et al. Postoperative perfluoro-N-octane tamponade for primary retinal detachment repair. *Retina*. 2012;32(6):1114–1120.
75. Scott IU, Flynn HW Jr, Murray TG, et al. Outcomes of surgery for retinal detachment associated with proliferative vitreoretinopathy using perfluoro-n-octane: a multicenter study. *Am J Ophthalmol*. 2003;136(3):454–463.
76. Millar ER, Steel DH. Small-gauge transconjunctival vitrectomy with phacoemulsification in the pupillary plane of dense retained lens matter on perfluorocarbon liquids after complicated cataract surgery. *Graefes Arch Klin Exper Ophthalmol*. 2013;251(7):1757–1762.
77. Veckeneer M, Wong D. Visualising vitreous through

modified trans-scleral illumination by maximising the Tyndall effect. *Br J Ophthalmol*. 2009;93:268–270.
78. Peyman GA. A new operating table for the management of giant retinal breaks. *Arch Ophthalmol*. 1981;99:498–499.
79. Cairns JD, Campbell WG. Vitrectomy techniques in the treatment of giant retinal tears: a flexible approach. *Aust N Z J Ophthalmol*. 1988;16:209–214.
80. Kreiger AE, Lewis H. Management of giant retinal tears without scleral buckling: use of radical dissection of the vitreous base and perfluoro-n-octane and intraocular tamponade. *Ophthalmology*. 1992;99:491–497.
81. Millsap CM, Peyman GA, Mehta NJ, et al. Perfluoroperhydrophenanthrene (Vitreon®) in the management of giant retinal tears: results of a collaborative study. *Ophthalmic Surg*. 1993;24:759–763.
82. Alfaro DV, Liggett PF. Perfluorocarbon liquid in the management of traumatic retinal detachment: advantages of PFCs in traumatic retinal detachment. *Vitreoretinal Surg Technol*. 1993;15:1–2.
83. Peyman GA, Alturki WA, Nelson NC Jr. Surgical management of incarcerated retina in the sclerotomy. *Ophthalmic Surg*. 1992;23:628–629.
84. Oh SY, Lee SJ, Park JM. Comparision of surgical outcomes of intraocular lens refixation and intraocular lens exchange with perfluorocarbon liquid and fibrin glue-assisted sutureless scleral fixation. *Eye (Lond)*. 2015;29(6):757–763.
85. Lakhanpal V, Schocket SS, Elman MJ, et al. A new modified vitreoretinal surgical approach in the management of massive suprachoroidal hemorrhage. *Ophthalmology*. 1989;96:793–800.
86. Desai UR, Peyman GA, Chen CJ. Use of perfluoroperhydrophenanthrene in the management of suprachoroidal hemorrhages. *Ophthalmology*. 1992;99:1542–1547.
87. Yu Q, Liu K, Su L, et al. Perfluorocarbon liquid: its application in vitreoretinal surgery and related ocular inflammation. *Biomed Res Int*. 2014;2014:250323.
88. Lee KJ, Peyman GA, Paris CL, et al. Management of retinal

detachment associated with choroidal coloboma using pertluoroperhydrophenanthrene (Vitreon). *Ophthalmic Surg*. 1992;23:563–564.
89. Millsap CM, Peyman GA, Ma PE, et al. The surgical management of retinopathy of prematurity using a perfluorocarbon liquid. *lnt Ophthalmol*. 1994;18:97–100.
90. Forlini C, Del Fiume E, Cicognani A, et al. Use of PFCL in the surgical management of endophthalmitis: new indicators. *J Vitreo Retina*. 1992;1:55–63.
91. Lambert HM, Capone A Jr, Aaberg TM, et al. Surgical excision of subfoveal neovascular membranes in age related macular degeneration. *Am J Ophthalmol*. 1992;13:257–262.
92. Inoue M, Iriyama A, Kadonosono K, et al. Effects of perfluorocarbon liquid and silicone oil on human retinal pigment epithelial cells and retinal ganglion cells. *Retina*. 2009;29:677–681.
93. Elsing SH, Fekrat S, Green WR, et al. Clinicopathologic findings in eyes with retained perfluoro-n-octane liquid. *Ophthalmology*. 2001;108:45–48.
94. Toygar O, Berrocal MH, Charles M, et al. Next-generation dual-bore cannula for injection of vital dyes and heavy liquids during pars plana vitrectomy. *Retina*. 2016;36(3):582–587.
95. Le Tien V, Pierre-Kahn V, Azan F, et al. Displacement of retained subfoveal perfluorocarbon liquid after vitreoretinal surgery. *Arch Ophthalmol*. 2008;126:98–101.
96. Cohen SY, Dubois L, Elmaleh C, et al. Retinal hole as a complication of long-standing subretinal perfluorocarbon liquid. *Retina*. 2006;26:843–844.
97. Tewari A, Eliott D, Singh CN, et al. Changes in retinal sensitivity from retained subretinal perfluorocarbon liquid. *Retina*. 2009;29:248–250.
98. Roth DB, Sears JE, Lewis H. Removal of retained subfoveal perfluoro-n-octane liquid. *Am J Ophthalmol*. 2004;138:287–289.
99. García-Arumí J, Castillo P, López M, et al. Removal of retained subretinal perfluorocarbon liquid. *Br J Ophthalmol*. 2008;92:1693–1694.

100. Smith AG, Cost BM, Ehlers JP. Intraoperative OCT-assisted subretinal perfluorocarbon liquid removal in the DISCOVER Study. *Ophthalmic Surg Lasers Imaging Retina*. 2015;46(9):964–966.
101. Garcia-Valenzuela E, Ito Y, Abrams GW. Risk factors for retention of subretinal perfluorocarbon liquid in vitreoretinal surgery. *Retina*. 2004;24:746–752.
102. Kobuch K, Menz DH, Dresp JH, et al. New substances for intraocular tamponades: perfluorocarbon liquid, hydrofluorocarbon liquid and hydrofluorocarbon-oligomers in vitreoretinal surgery. *Graefes Arch Clin Exp Ophthalmol*. 2001;239:635–642.
103. Kobuch K, Fuchs B, Tomi A, et al. The influence of O_2 and CO_2 concentrations in perfluorocarbon liquid as vitreous substitutes on the retinal perfusion. *Invest Ophthalmol Vis Sci*. 1999;40:4052.
104. Kobuch K, El Batarny A, Ueda N, et al. Perfluorophenanthrene causes vascular and neural damage in the rabbit eye. *Invest Ophthalmol Vis Sci*. 1997;38:3111.
105. Sparrow JR, Ortiz R, MacLeish PR, et al. Fibroblast behavior at aqueous interfaces with perfluorocarbon, silicone, and fluorosilicone liquid. *Invest Ophthalmol Vis Sci*. 1990;31:638–646.
106. Winter M, Eberhardt W, Scholz C, et al. Failure of potassium siphoning by Müller cells: a new hypothesis of perfluorocarbon liquid-induced retinopathy. *Invest Ophthalmol Vis Sci*. 2000;41:256–261.
107. Toffoli D, Arbour JD, Harasymowycz P. Retained perfluoron postvitreoretinal surgery causing secondary open-angle glaucoma. *Can J Ophthalmol*. 2008;43:372.
108. Keles S, Ates O, Baykal O. Better surgical method for removing perfluorocarbon liquids from the anterior chamber. *Cornea*. 2013;32(11):1514–1515.
109. Cibis PA, Becker B, Okun E, et al. The use of liquid silicone in retinal detachment surgery. *Arch Ophthalmol*. 1962;68:590–599.
110. Machemer R, Laqua H. Pigment epithelium proliferation in retinal detachment (massive periretinal proliferation). *Am J*

Ophthalmol. 1975;80:1–23.
111. Dufour R. *Experience with intraocular silicone injection: new and controversial aspects of retinal detachment surgery*. Harper & Row: New York; 1968:377.
112. Scott JD. Silicone oil as an instrument. Mosby: St. Louis; 1994. Ryan S. *Retina*. vol. 2 [Ch. 135].
113. Silicone Study Group. Vitrectomy with silicone oil or sulfur hexafluoride gas in eyes with severe proliferative vitreoretinopathy: results of a randomized clinical trial: Silicone Study report 1. *Arch Ophthalmol*. 1992;110:770–779.
114. D'Amico DJ. Different preferences between United States and European vitreoretinal surgeons: personal observations. *Curr Opin Ophthalmol*. 2016;27(3):196–200.
115. Wolf S, Schön V, Meier P, et al. Silicone oil–RMN3 mixture ("heavy silicone oil") as internal tamponade for complicated retinal detachment. *Retina*. 2003;23:335–342.
116. Pankratov MM, Sebag J, Refojo MF, et al. Biochemical effects of intraocular silicone oil in the squirrel monkey. *Invest Ophthalmol Vis Sci*. 1987;28:S210.
117. Noll W. *Chemistry and technology of silicones*. Academic Press: New York; 1968.
118. Pacela EJ, Pacela AF. *The guide to biomedical standards*. 3rd ed. Quest: Brea, CA; 1973.
119. Ference M, Lemon HB, et al. *Analytical experimental physics*. 2nd ed. University of Chicago Press: Chicago, IL; 1956:141–168.
120. Parver LM, Lincoff H. Mechanics of intraocular gas. *Invest Ophthalmol Vis Sci*. 1978;17:77–79.
121. Feynman RP, Leighton RB, Sands M. *The Feynman lectures on physics*. 7th ed. Addison–Wesley: Reading, MA; 1972 [vol. I, chs 40, 43; vol II, chs 40, 41].
122. Yamanaka A, Matsuda T, Nakamae K, Interfacial aspects of liquid silicone as an artificial vitreous body. Presented in part at the Fifth Vail Vitreoretinal Seminar, Vail, CO, March 1986.
123. Williams RL, Day M, Garvey MJ, et al. Increasing the extensional viscosity of silicone reduces the tendency for emulsification. *Retina*. 2010;30:300–304.

124. Jalkh AE, McMeel JW, Kozlowski IM, et al. Silicone oil retinopathy. *Arch Ophthalmol*. 1986;104:178–179.
125. Abrams GW, Topping T, Machemer R. An improved method for practice vitrectomy. *Arch Ophthalmol*. 1978;96:521–525.
126. Schwartz SG, Flynn HW Jr, Lee WH, et al. Tamponade in surgery for retinal detachment associated with proliferative vitreoretinopathy. *Cochrane Database Syst Rev*. 2014;(2) [CD006126].
127. Mathis A, Pagot V, Gazagne C, et al. Giant retinal tears: surgical techniques and results using perfluorodecalin and silicone oil tamponade. *Retina*. 1992;12:x7–10.
128. Unlu N, Kocaoglan H, Acar MA, et al. The management of giant retinal tears with silicone oil. *Eur J Ophthalmol*. 2003;13:192–195.
129. Leaver PK, Lean JS. Management of giant retinal tears using vitrectomy and silicone oil/fluid exchange: a preliminary report. *Trans Ophthalmol Soc U K*. 1981;101:189–195.
130. Heimann K, Dahl B, Dimopoulos S, et al. Pars plana vitrectomy and silicone oil injection in proliferative diabetic retinopathy. *Graefes Arch Clin Exp Ophthalmol*. 1989;227:152–156.
131. McLeod D. Microsurgical management of neovascularization secondary to posterior segment ischemia. *Eye (Lond)*. 1991;5(Pt 2):252–259.
132. Castellarin A, Grogorian R, Bhagat N, et al. Vitrecctomy with silicone oil infusion in severe diabetic retinopathy. *Br J Ophthalmol*. 2003;87:318–321.
133. McCuen BW II, Linkoff JS. Silicone oil for progressive anterior ocular neovascularization after failed diabetic vitrectomy. *Arch Ophthalmol*. 1989;107:677–682.
134. Goldbaum MH, McCuen BW, et al. Silicone oil tamponade for idiopathic macular hole surgery. *Ophthalmology*. 1998;105:2140–2147.
135. Lai JC, Stinnett SS, McCuen BW II. Comparison of silicone oil vs. gas tamponade in the treatment of idiopathic full-thickness macular hole. *Ophthalmology*. 2003;110:1170–1177.
136. Bainbridge J, Herbert E, Gregor Z. Macular holes:

vitreoretinal relationships and surgical approaches. *Eye (Lond)*. 2008;22:1301–1309.
137. Gupta D. Facedown posturing after macular hole surgery: a review. *Retina*. 2009;29:430–443.
138. Dhawahir-Scala FE, Maino A, Saha K, et al. To posture or not to posture after macular hole surgery. *Retina*. 2008;28:60–65.
139. Rubinstein A, Ang A, Patel CK. Vitrectomy without postoperative posturing for idiopathic macular holes. *Clin Exp Ophthalmol*. 2007;35:458–461.
140. Masuyama K, Yamakiri K, Arimura N, et al. Posturing time after macular hole surgery modified by optical coherence tomography images: a pilot study. *Am J Ophthalmol*. 2009;147 [481–8.e2].
141. Muqit MM, Akram I, Turner GS, et al. Fourier-domain optical coherence tomography imaging of gas tamponade following macular hole surgery. *Ophthalmic Surg Lasers Imaging*. 2010;41 Online:e1–6.
142. Tatham A, Banerjee S. Facedown posturing after macular hole surgery: a meta-analysis. *Br J Ophthalmol*. 2010;94:626–631.
143. Lappas A, Foerster AM, Kirchhof B. Use of heavy silicone oil (Densiron-68) in the treatment of persistent macular holes. *Acta Ophthalmol*. 2009;87:866–870.
144. Saeed MU, Heimann H, Wong D, et al. Heavy silicone oil tamponade after failed macular hole surgery with perfluoropropane (C_3F_8): a report of five cases. *Graefes Arch Clin Exp Ophthalmol*. 2009;247:707–709.
145. Valldeperas X, Wong D. Is it worth reoperating on macular holes? *Ophthalmology*. 2008;115:158–163.
146. Yu J, Wang F, Cao H, et al. Combination of internal limiting membrane peeling and endophotocoagulation for retinal detachment related to high myopia in patients with macular hole. *Ophthalmic Surg Lasers Imaging*. 2010;41:215–221.
147. Li KK, Tang EW, Li PS, et al. Double peel using triamcinolone acetonide and trypan blue in the management of myopic macular hole with retinal detachment: a case–control study. *Clin Exp Ophthalmol*.

2010;38:664–668.
148. Chen YP, Chen TL, Yang KR, et al. Treatment of retinal detachment resulting from posterior staphyloma-associated macular hole in highly myopic eyes. *Retina*. 2006;26:25–31.
149. Nishimura A, Kimura M, Saito Y, et al. Efficacy of primary silicone oil tamponade for the treatment of retinal detachment caused by macular hole in high myopia. *Am J Ophthalmol*. 2011;151:148–155.
150. Morrison VL, Labree LD, Azen SP, et al. Results of silicone oil removal in patients with cytomegalovirus retinitis related retinal detachments. *Am J Ophthalmol*. 2005;140:786–793.
151. Davis JL, Serfass MS, Lai MY, et al. Silicone oil in repair of retinal detachments caused by necrotizing retinitis in HIV infections. *Arch Ophthalmol*. 1995;113:1401–1409.
152. Azen SP, Scott IU, Flynn HW Jr, et al. Silicone oil in the repair of complex retinal detachments: a prospective observational multicenter study. *Ophthalmology*. 1998;105:1587–1597.
153. Matsuo T. Vitrectomy and silicone oil tamponade as an initial surgery for retinal detachment after acute retinal necrosis syndrome. *Ocul Immunol Inflamm*. 2005;13:91–94.
154. Tanna AP, Kempen JH, Dunn JP, et al. Incidence and management of cataract after retinal detachment repair with silicone oil in immune compromised patients with cytomegalovirus retinitis. *Am J Ophthalmol*. 2003;136:1009–1015.
155. Engstrom RE Jr, Goldenberg DT, Parnell JR, et al. Clear lens extraction with intraocular lens implantation during retinal detachment repair in patients with Acquired Immune Deficiency Syndrome (AIDS) [correction of autoimmune deficiency syndrome] and cytomegalovirus retinitis. *Ophthalmology*. 2002;109:666–673 [Erratum in: Ophthalmology 2002;109:1588].
156. Hegazy HM, Kivilcim M, Peyman GA, et al. Evaluation of toxicity of intravitreal ceftazidime, vancomycin, and ganciclovir in a silicone oil-filled eye. *Retina*. 1999;19:553–557.

157. McGuire DE, McAulife P, Heinemann MH, et al. Efficacy of the ganciclovir implant in the setting of silicone oil vitreous substitute. *Retina*. 2000;20:520–523.
158. Perkins SL, Yang CH, Ashton PA, et al. Pharmacokinetics of the ganciclovir implant in the silicone-filled eye. *Retina*. 2001;21:10–14.
159. Martidis A, Danis RP, Ciulla TA. Treating cytomegalovirus retinitis-related retinal detachment by combining silicone oil tamponade and ganciclovir implant. *Ophthalmic Surg Lasers*. 2002;33:135–139.
160. Wong D, Cazabon S, Ali H, et al. Can the sequential use of conventional silicone oil and heavy oil be a strategy for the management of proliferative vitreoretinopathy? *Ann Acad Med Singapore*. 2006;35:181–184.
161. Jesberg DO, Schepens CL. Retinal detachment associated with coloboma of the choroids. *Arch Ophthalmol*. 1961;65:163.
162. Patnaik B, Kalsi R. Retinal detachment with coloboma of the choroids. *Ind J Ophthalmol*. 1981;29:345.
163. Pal N, Azad RV, Sharma YR. Long-term anatomical and visual outcome of vitreous surgery for retinal detachment with choroidal coloboma. *Indian J Ophthalmol*. 2006;54:85–88.
164. Girard P, Mimoun G, Karpouzas I, et al. Clinical risk factors for proliferative vitreoretinopathy after retinal detachment surgery. *Retina*. 1994;14:417–424.
165. Spiegel D, Nasermann J, Nawrocki J, et al. Severe ocular trauma managed with primary pars plana vitrectomy and silicone oil. *Retina*. 1997;17:275–285.
166. Nashed A, Saikia P, Herrmann WA, et al. The outcome of early surgical repair with vitrectomy and silicone oil in open-globe injuries with retinal detachment. *Am J Ophthalmol*. 2011;151:522–528.
167. Azad R, Ravi K, Talwar D, et al. Pars plana vitrectomy with or without silicone oil endotamponade in posttraumatic endophthalmitis. *Graefes Arch Clin Exp Ophthalmol*. 2003;241:478–483.
168. Yan H, Lu Y, Yu J, et al. Silicone oil in the surgical treatment

of traumatic endophthalmitis. *Eur J Ophthalmol*. 2008;18:680–684.
169. Do T, Hon do N, Aung T, et al. Bacterial endogenous endophthalmitis in Vietnam: a randomized controlled trial comparing vitrectomy with silicone oil versus vitrectomy alone. *Clin Ophthalmol*. 2014;8:1633–1640.
170. de Juan E, McCuen BW II, Tiedeman J. Intraocular tamponade and surface tension. *Surv Ophthalmol*. 1985;30:47–51.
171. Zauberman H, de Guillebon H, Holly FJ. Retinal traction in vitro: biophysical aspects. *Invest Ophthalmol*. 1972;11:46–55.
172. Parikh HA, Kalbag NS, Zarbin MA, et al. Characteristics, demographics, outcomes, and complications of diabetic traction retinal detachments treated with silicone oil tamponade. *Eur J Ophthalmol*. 2016;25(5):497–502.
173. MacCumber MW, Packo KH, Civantos JM, et al. Preservation of anterior capsule during vitrectomy and lensectomy for retinal detachment with proliferative vitreoretinopathy. *Ophthalmology*. 2002;109:329–333.
174. Kapran Z, Acar N. Active removal of silicone oil with 25-gauge sutureless system. *Retina*. 2007;27(8):1133–1135.
175. Kapran Z, Acar N, Unver YB, et al. Passive removal of silicone oil with a 25-gauge sutureless system. *Japn J Ophthalmol*.2008;52(1):63–66.
176. Lewis SA, Miller DM, Riemann CD, et al. Comparison of 20-, 23-, and 25-gauge pars plana vitrectomy in pseudophakic rhegmatogenous retinal detachment repair. *Ophthalmic Surg Lasers Imaging*. 2011;42(2):107–113.
177. Riemann CD, Miller DM, Foster RE, et al. Outcomes of transconjunctival sutureless 25-gauge vitrectomy with silicone oil infusion. *Retina*. 2007;27:296–303.
178. Altan T, Acar N, Kapran Z, et al. Transconjunctival 25-gauge sutureless vitrectomy and silicone oil injection in diabetic tractional retinal detachment. *Retina*. 2008;28:1201–1206.
179. Ando F. Intraocular hypertension resulting from pupillary block by silicone oil. *Am J Ophthalmol*. 1985;99:87–88.
180. Thompson JT. Use of perfluorocarbon liquids in

vitreoretinal surgery. Saunders: St. Louis; 1994:2191–2201. Glaser BM, Michels RG. *Retina*. vol. 3.
181. Oshima Y, Awh CC, Tano Y. Self-retaining 27-gauge transconjunctival chandelier endoillumination for panoramic viewing during vitreous surgery. *Am J Ophthalmol*. 2007;143:166–167.
182. Eckardt C, Eckert T, Eckardt U. 27-gauge Twinlight chandelier illumination system for bimanual transconjunctival vitrectomy. *Retina*. 2008;28:518–519.
183. Oshima Y, Chow DR, Awh CC, et al. Novel mercury vapor illuminator combined with a 27/29-gauge chandelier light fiber for vitreous surgery. *Retina*. 2008;28:171–173.
184. Madreperla SA, McCuen BW II. Inferior peripheral iridectomy in patients receiving silicone oil. *Retina*. 1995;15:87–90.
185. Bartov E, Huna R, Ashkenazi I, et al. Identification, prevention and treatment of silicone oil pupillary block after an inferior iridectomy. *Am J Ophthalmol*. 1991;111:501–504.
186. MacCumber MW, McCuen BW II, Toth CA, et al. Tissue plasminogen activator for preserving inferior peripheral iridectomy patency in eyes with silicone oil. *Ophthalmology*. 1996;103:269–273.
187. Jackson TL, Thiagarajan M, Murthy R, et al. Pupil block glaucoma in phakic and pseudophakic patients after vitrectomy with silicone oil injection. *Am J Ophthalmol*. 2001;132:414–416.
188. Champion R, Faulborn J, Bowald S, et al. Peritoneal reaction to liquid silicone: an experimental study. *Graefes Arch Clin Exp Ophthalmol*. 1987;225:141–145.
189. Silicone Study Group. Silicone Study Report 4. Postoperative intraocular pressure abnormalities in the Silicone Study: results of a randomized clinical trial. *Ophthalmology*. 1993;100:1629–1635.
190. Al-Jazzaf AM, Netland PA, Charles S. Incidence and management of elevated intraocular pressure after silicone oil injection. *J Glaucoma*. 2005;14:40–46.
191. Gedde SJ. Management of glaucoma after retinal

detachment surgery. *Curr Opin Ophthalmol*. 2002;13:103–109.
192. Ishida K, Ahmed II, Netland PA. Ahmed glaucoma valve surgical outcomes in eyes with and without silicone oil endotamponade. *J Glaucoma*. 2009;18:325–330.
193. Han L, Cairns JD, Campbell WG, et al. Use of silicone oil in the treatment of complicated retinal detachment: results from 1981–1994. *Aust N Z J Ophthalmol*. 1998;26:299–304.
194. Budenz DL, Taba KE, Feuer WJ, et al. Surgical management of secondary glaucoma after pars plana vitrectomy and silicone oil injection for complex retinal detachment. *Ophthalmology*. 2001;108:1628–1632.
195. Jonas JB, Knorr HL, Rank RM, et al. Intraocular pressure and silicone oil endotamponade. *J Glaucoma*. 2001;10:102–108.
196. Flaxel CJ, Mitchell SM, Aylward GW. Visual outcome after silicone oil removal and recurrent retinal detachment repair. *Eye*. 2000;14:834–838.
197. Ghazi-Nouri SM, Vakalis AN, Bloom PA, et al. Long-term results of the management of silicone oil-induced raised intraocular pressure by diode laser cycloablation. *Eye (Lond)*. 2005;19:765–769.
198. Han SK, Park KH, Kim DM, et al. Effect of diode laser trans-scleral cyclophotocoagulation in the management of glaucoma after intravitreal silicone oil injection for complicated retinal detachments. *Br J Ophthalmol*. 1999;83:713–717.
199. Kumar A, Dada T, Singh RP, et al. Diode laser trans-scleral cyclophotocoagulation for glaucoma following silicone oil removal. *Clin Exp Ophthalmol*. 2001;29:220–224.
200. Gangwani R, Liu DT, Congdon N, et al. Effectiveness of diode laser trans-scleral cyclophotocoagulation in patients following silicone oil-induced ocular hypertension in Chinese eyes. *Indian J Ophthalmol*. 2011;59:64–66.
201. Nehemy MB, Zisman M, Marigo FA, et al. Ultrasound biomicroscopy after vitrectomy in eyes with normal intraocular pressure and in eyes with chronic hypotony. *Eur J Ophthalmol*. 2008;18:614–618.
202. Zarbin MA, Micels RG, Green WR. Dissection of epiciliary

tissue to treat chronic hypotony after surgery for retinal detachment with proliferative vitreoretinopathy. *Retina*. 1991;1:208–213.
203. Gonvers M. Temporary silicone oil tamponade in the management of retinal detachment with proliferative vitreoretinopathy. *Am J Ophthalmol*. 1985;100:239–245.
204. Baraki H, Petersen J. How can the shift of refraction due to vitreous substitutes be avoided?: Posterior chamber intraocular lens for patients suffering from diabetic retinopathy. *Ophthalmologe*. 2011;108:683–686.
205. Khawly J, Lambert RJ, Jaffe GJ. Intraocular lens changes after short- and long-term exposure to intraocular silicone oil. An in vivo study. *Ophthalmology*. 1998;105:1227–1233.
206. Sims JC, Kent DG, Hamburger HA, et al. Irreversible silicone oil adhesion to silicone intraocular lenses; a clinicopathologic analysis. *Ophthalmology*. 1996;103:1555–1562.
207. Horgan SE, Cooling RJ. Irreversible silicone oil adhesion (Letter). *Ophthalmology*. 1997;104:898–899.
208. Liang Y, Kociok N, Leszczuk M, et al. A cleaning solution for silicone intraocular lenses: "sticky silicone oil". *Br J Ophthalmol*. 2008;92:1522–1527.
209. Stappler T, Williams R, Wong D. F_4H_5: a novel substance for the removal of silicone oil from intraocular lenses. *Br J Ophthalmol*. 2010;94:364–367.
210. Wong SC, Ramkissoon YD, Lopez M, et al. Use of hydroxypropylmethylcellulose 2% for removing adherent silicone oil from silicone intraocular lenses. *Br J Ophthalmol*. 2009;93:1085–1088.
211. Kageyama T, Yaguchi S. Removing silicone oil droplets from the posterior surface of silicone intraocular lenses. *J Cataract Refract Surg*. 2000;26:957–959.
212. Stalmans P, Pinxten AM, Wong DS. Cohort safety and efficacy study of siluron2000 emulsification-resistant silicone oil and f4h5 in the treatment of full-thickness macular hole. *Retina*. 2015;35(12):2558–2566.
213. Ghoraba HH, El-Dorghamy AA, Atia AF, et al. The problems of biometry in combined silicone oil removal and

cataract extraction: a clinical trial. *Retina*. 2002;22:589–596.
214. Abu El Einen KG, Shalaby MH, El Shiwy HT. Immersion B-guided versus contact A-mode biometry for accurate measurement of axial length and intraocular lens power calculation in siliconized eyes. *Retina*. 2011;31:262–265.
215. Murray DC, Durrani OM, Good P, et al. Biometry of the silicone oil-filled eye: II. *Eye (Lond)*. 2002;16:727–730.
216. Lege BAM, Haigis W. Laser interference biometry versus ultrasound biometry in certain clinical conditions. *Graefes Arch Clin Exp Ophthalmol*. 2004;242:8–12.
217. Dietlein TS, Roessler G, Lueke C, et al. Signal quality of optical biometry in silicone oil-filled eyes using partial coherence laser interferometry. *J Cataract Refract Surg*. 2005;31:1006–1010.
218. Roessler GF, Huth JK, Dietlein TS, et al. Accuracy and reproducibility of axial length measurement in eyes with silicone oil endotamponade. *Br J Ophthalmol*. 2009;93:1492–1494.
219. Parravano M, Oddone F, Sampalmieri M, et al. Reliability of the IOLMaster in axial length evaluation in silicone oil-filled eyes. *Eye*. 2007;21:909–911.
220. Ehmann D, García R. Investigating a possible cause of the myopic shift after combined cataract extraction, intraocular lens implantation, and vitrectomy for treatment of a macular hole. *Can J Ophthalmol*. 2009;44:594–597.
221. Jonas JB, Knorr HL, Rank RM, et al. Retinal redetachment after removal of intraocular silicone oil tamponade. *Br J Ophthalmol*. 2001;85:1203–1207.
222. Jonas JB, Budde WM, Knorr HL. Timing of retinal redetachment after removal of intraocular silicone oil tamponade. *Am J Ophthalmol*. 1999;128:628–631.
223. Avitabile T, Longo A, Lentini G, et al. Retinal detachment after silicone oil removal is prevented by 360 degrees laser treatment. *Br J Ophthalmol*. 2008;92:1479–1482.
224. Falkner-Radler CI, Smretschnig E, Graf A, et al. Outcome after silicone oil removal and simultaneous 360° endolaser treatment. *Acta Ophthalmol*. 2011;89:e46–51.
225. Laidlaw DA, Karia N, Bunce C, et al. Is prophylactic 360-

degree laser retinopexy protective? Risk factors for retinal redetachment after removal of silicone oil. *Ophthalmology*. 2002;109:153–158.
226. Avitabile T, Bonfiglio V, Cicero A, et al. Correlation between quantity of silicone oil emulsified in the anterior chamber and high pressure in vitrectomized eyes. *Retina*. 2002;22:443–448.
227. Gabel VP, Kampik A, Gabel C, et al. Silicone oil with high specific gravity for intraocular use. *Br J Ophthalmol*. 1987;71:262–267.
228. Crisp A, de Juan E Jr, Tiedeman J. Effect of silicone oil viscosity on emulsification. *Arch Ophthalmol*. 1987;105:546–550.
229. Silicone Study Group. The incidence of corneal abnormalities in the silicone study: results of a randomized clinical trial. Silicone Study report 7. *Arch Ophthalmol*. 1995;113:764–769.
230. Scheerlinck LM, Kuiper JJ, Liem AT, et al. Electrolyte composition of retro-oil fluid and silicone oil-related visual loss. *Acta Ophthalmol*. 2016;94(5):449–453.
231. Hiscott P, Wong D, Grierson I. Challenges in ophthalmic pathology: the vitreoretinal membrane biopsy. *Eye (Lond)*. 2000;14(Pt 4):549–559.
232. Casswell AG, Gregor ZJ. Silicone oil removal: 1. The effect on the complications of silicone oil. *Br J Ophthalmol*. 1987;71:893–897.
233. Dabil H, Akduman L, Olk RJ, et al. Comparison of silicone oil removal with passive drainage alone versus passive drainage combined with air–fluid exchange. *Retina*. 2002;22:597–601.
234. Frau E, Lautier-Frau M, Labetoulle M, et al. Phacoemulsification combined with silicone oil removal through the posterior capsulorhexis tear. *Retina*. 2002;22:158–162.
235. Jonas JB, Hugger P, Sauder G. Topical anesthesia for transpupillary silicone oil removal combined with cataract surgery. *J Cataract Refract Surg*. 2005;31:1781–1782.
236. Kapran Z, Acar N. Removal of silicone oil with 25-gauge

transconjunctival sutureless vitrectomy system. *Retina*. 2007;27:1059–1064.
237. Clark C, Habib MS, Steel DH. Combined phacoemulsification and transpupillary removal of heavy silicone oil. *J Cataract Refract Surg*. 2008;34:1640–1643.
238. Joussen AM, Wong D. The concept of heavy tamponades-chances and limitations. *Graefes Arch Clin Exp Ophthalmol*. 2008;246:1217–1224.
239. Heimann H, Stappler T, Wong D. Heavy tamponade 1: a review of indications, use, and complications. *Eye (Lond)*. 2008;22:1342–1359.
240. Wong D, Lois N. Perfluorocarbons and semifluorinated alkanes. *Semin Ophthalmol*. 2000;15:25–35.
241. Chang S, Sparrow JR, Iwamoto T, et al. Experimental studies of tolerance to intravitreal perfluoro-n-octane liquid. *Retina*. 1991;11:367–374.
242. Bottoni F, Arpa P, Vinciguerra P, et al. Combined silicone and fluorosilicone oil tamponade (double filling) in the management of complicated retinal detachment. *Ophthalmologica*. 2000;204:77–81.
243. Geh VS, Dabbs TR, Ansari E. Perfluorodecalin and silicone oil used to achieve retinal tamponade left in an eye for 6 months. *Br J Ophthalmol*. 1997;81:252–253.
244. Herbert E, Stappler T, Wetterqvist C, et al. Tamponade properties of double-filling with perfluorohexyloctane and silicone oil in a model eye chamber. *Graefes Arch Clin Exp Ophthalmol*. 2004;242:250–254.
245. Rizzo S, Genovesi-Ebert F, Belting C. The combined use of perfluorohexyloctane (F_6H_8) and silicone oil as an intraocular tamponade in the treatment of severe retinal detachment. *Graefes Arch Clin Exp Ophthalmol*. 2006;244:709–716.
246. De Molfetta V, Bottoni F, Arpa P, et al. The effect of simultaneous internal tamponade on fluid compartmentalization and its relationship to cell proliferation. *Retina*. 1992;12(3 Suppl.):S40–5.
247. Kirchhof B, Wong D, Van Meurs J, et al. Use of perfluorohexyloctane as a long-term internal tamponade

agent in complicated retinal detachment surgery. *Am J Ophthalmol*. 2002;133:95–101.
248. Mackiewicz J, Mühling B, Hiebl W, et al. In vivo retinal tolerance of various heavy silicone oils. *Invest Ophthalmol Vis Sci*. 2007;48:1873–1883.
249. Langefeld S, Kirchhof B, Meinert H, et al. A new way of removing silicone oil from the surface of silicone intraocular lenses. *Graefes Arch Clin Exp Ophthalmol*. 1999;23:201–206.
250. Roider J, Hoerauf H, Kobuch K, et al. Clinical findings on the use of long-term heavy tamponades (semifluorinated alkanes and their oligomers) in complicated retinal detachment surgery. *Graefes Arch Clin Exp Ophthalmol*. 2002;240:965–971.
251. Meinert H, Roy T. Semifluorinated alkanes – a new class of compounds with outstanding properties for use in ophthalmology. *Eur J Ophthalmol*. 2000;10:189–197.
252. Stappler T, Williams R, Gibran SK, et al. A guide to the removal of heavy silicone oil. *Br J Ophthalmol*. 2008;92:844–847.
253. Wong D, Van Meurs JC, Stappler T, et al. A pilot study on the use of a perfluorohexyloctane/silicone oil solution as a heavier than water internal tamponade agent. *Br J Ophthalmol*. 2005;89:662–665.
254. Herbrig E, Sandner D, Engelmann K. Anatomical and functional results of endotamponade with heavy silicone oil – Densiron 68® – in complicated retinal detachment. *Ophthalmic Res*. 2007;39:198–206.
255. Rizzo S, Genovesi-Ebert F, Belting C, et al. A pilot study on the use of silicone oil-RMN3 as heavier-than-water endotamponade agent. *Graefes Arch Clin Exp Ophthalmol*. 2005;243:1153–1157.
256. Tomlins PJ, Woodcock MG, Spencer N, et al. Nuclear magnetic resonance analysis of emulsified silicone oil RMN-3 (Oxane HD). *Br J Ophthalmol*. 2007;91:1379–1381.
257. Lai WW, Wong D, Li KK, et al. Emulsification and inverted hypopyon formation of oxane HD in the anterior chamber. *Graefes Arch Clin Exp Ophthalmol*. 2008;246:1633–1635.
258. Rizzo S, Genovesi-Ebert F, Vento A, et al. A new heavy

silicone oil (HWS 46–3000) used as a prolonged internal tamponade agent in complicated vitreoretinal surgery: a pilot study. *Retina*. 2007;27:613–620.
259. Joussen AM, Kirchhof B, Schrage N, et al. Heavy silicone oil versus standard silicone oil as vitreous tamponade in inferior PVR (HSO Study): design issues and implications. *Acta Ophthalmol Scand*. 2007;85:623–630.
260. Tognetto D, Minutola D, Sanguinetti G, et al. Anatomical and functional outcomes after heavy silicone oil tamponade in vitreoretinal surgery for complicated retinal detachment: a pilot study. *Ophthalmology*. 2005;112:1574.
261. Joussen AM, Rizzo S, Kirchhof B, et al. Heavy silicone oil versus standard silicone oil in as vitreous tamponade in inferior PVR (HSO Study): interim analysis. *Acta Ophthalmol*. 2011;89:e483–9.
262. Stolba U, Krepler K, Velikay-Parel M, et al. The effect of specific gravity of perfluorocarbon liquid on the retina after experimental vitreous substitution. *Graefes Arch Clin Exp Ophthalmol*. 2004;242:931–936.
263. Mackiewicz J, Maaijwee K, Lüke C, et al. Effect of gravity in long-term vitreous tamponade: in vivo investigation using perfluorocarbon liquids and semi-fluorinated alkanes. *Graefes Arch Clin Exp Ophthalmol*. 2007;245:665–675.
264. Williams RL, Kearns VR, Lo AC, et al. Novel heavy tamponade for vitreoretinal surgery. *Invest Ophthalmol Vis Sci*. 2013;54(12):7284–7292.
265. Rizzo S, Genovesi-Ebert F, Belting C, et al. Long-term vitreous replacement with perfluorohexyloctane and silicone oil: preliminary reports of a multicentric study. *Ophthalmologica*. 2005;219:147–153.
266. Cheung BT, Lai TY, Yuen CY, et al. Results of high-density silicone oil as a tamponade agent in macular hole retinal detachment in patients with high myopia. *Br J Ophthalmol*. 2007;91:719–721.
267. Theelen T, Tilanus MA, Klevering BJ. Intraocular inflammation following endotamponade with high-density silicone oil. *Graefes Arch Clin Exp Ophthalmol*. 2004;242:617–620.

268. Dresp JH, Menz DH. Interaction of different ocular endotamponades as a risk factor for silicone oil emulsification. *Retina*. 2005;25:902–910.
269. Dresp JH, Menz DH. The phenomenon of "sticky" silicone oil. *Graefes Arch Clin Exp Ophthalmol*. 2007;245:863–868.
270. Romano MR, Groenwald C, Das R, et al. Removal of Densiron-68 with a 23-gauge transconjunctival vitrectomy system. *Eye (Lond)*. 2009;23:715–717.
271. Gerding H, Kolck A. Perfluorohexyloctane as internal tamponade in patients with complicated retinal detachment. Results after 6 months. *Ophthalmologe*. 2004;101:255–262.
272. Wetterqvist C, Wong D, Williams R, et al. Tamponade efficiency of perfluorohexyloctane and silicone oil solutions in a model eye chamber. *Br J Ophthalmol*. 2004;88:692–696.
273. Vote B, Wheen L, Cluroe A, et al. Further evidence for proinflammatory nature of perfluorohexyloctane in the eye. *Clin Exp Ophthalmol*. 2003;31:408–414.
274. Schatz B, El-Shabrawi Y, Haas A, et al. Adverse side effects with perfluorohexyloctane as a long-term tamponade agent in complicated vitreoretinal surgery. *Retina*. 2004;24:567–573.
275. Helbig H, Kellner U, Bornfeld N, et al. Cataract surgery and YAG-laser capsulotomy following vitrectomy for diabetic retinopathy. *Ger J Ophthalmol*. 1996;5:408–414.
276. Lappas A, Kirchhof B, Konen W. Effects of the long-term tamponade with Densiron on the lens. *Klin Monatsbl Augenheilkd*. 2007;224:434–437.
277. Hiscott P, Magee RM, Colthurst M, et al. Clinicopathological correlation of epiretinal membranes and posterior lens opacification following perfluorohexyloctane tamponade. *Br J Ophthalmol*. 2001;85:179–183.
278. Sim KT, Hero M. Adhesion of heavy oil to posterior lens capsule. *Retina*. 2006;26:964–965.
279. Stefaniotou MI, Aspiotis MV, Kitsos GD, et al. Our experience with perfluorohexyloctane (F_6H_8) as a temporary endotamponade in vitreoretinal surgery. *Eur J Ophthalmol*.

2002;12:518–522.
280. Bottoni F, Sborgia M, Arpa P, et al. Perfluorocarbon liquids as postoperative short-term vitreous substitutes in complicated retinal detachment. *Graefes Arch Clin Exp Ophthalmol*. 1993;231:619–628.
281. Hoerauf H, Roider J, Kobuch K, et al. Perfluorohexylethan (O62) as ocular endotamponade in complex vitreoretinal surgery. *Retina*. 2005;25:479–488.
282. Sandner D, Engelmann K. First experiences with high density silicone oil (Densiron) as an intraocular tamponade in complex retinal detachment. *Graefes Arch Clin Exp Ophthalmol*. 2006;244:609–619.
283. Majid MA, Hussin HM, Biswas S, et al. Emulsification of Densiron-68 used in inferior retinal detachment surgery. *Eye*. 2007;22:152–157.
284. Sandner D, Herbrig E, Engelmann K. High-density silicone oil (Densiron) as a primary intraocular tamponade: 12-month follow up. *Graefes Arch Clin Exp Ophthalmol*. 2007;245:1097–1105.
285. Morescalchi F, Costagliola C, Duse S, et al. Heavy silicone oil and intraocular inflammation. *Biomed Res Int*. 2014;2014:574825.
286. Chan YK, Cheung N, Wong D. Factors influencing the shear rate acting on silicone oil to cause silicone oil emulsification. *Invest Ophthalmol Vis Sci*. 2014;55(11):7451–7456.
287. Schwarzer H, Mazinani B, Plange N, et al. Clinical observations and occurrence of complications following heavy silicone oil surgery. *Biomed Res Int*. 2014;2014:706809.
288. Wickham L, Bunce C, Wong D, et al. Randomized controlled trial of combined 5-fluorouracil and low-molecular-weight heparin in the management of unselected rhegmatogenous retinal detachments undergoing primary vitrectomy. *Ophthalmology*. 2007;114:698–704.
289. Gartry DS, Chignell AH, Franks WA, et al. Pars plana vitrectomy for the treatment of rhegmatogenous retinal detachment uncomplicated by advanced proliferative vitreoretinopathy. *Br J Ophthalmol*. 1993;77:199–203.
290. Furino C, Micelli Ferrari T, Boscia F, et al. Triamcinolone-

assisted pars plana vitrectomy for proliferative vitreoretinopathy. *Retina*. 2003;23:771–776.
291. Sakamoto T, Miyazaki M, Hisatomi T, et al. Triamcinolone-assisted pars plana vitrectomy improves the surgical procedures and decreases the postoperative blood–ocular barrier breakdown. *Graefes Arch Clin Exp Ophthalmol*. 2002;240:423–429.
292. Ueno A, Enaida H, Hata Y, et al. Long-term clinical outcomes and therapeutic benefits of triamcinolone-assisted pars plana vitrectomy for proliferative vitreoretinopathy: a case study. *Eur J Ophthalmol*. 2007;17:392–398.
293. Cheema RA, Peyman GA, Fang T, et al. Triamcinolone acetonide as an adjuvant in the surgical treatment of retinal detachment with proliferative vitreoretinopathy. *Ophthalmic Surg Lasers Imaging*. 2007;38:365–370.
294. Acar N, Kapran Z, Altan T, et al. Pars plana vitrectomy with and without triamcinolone acetonide assistance in pseudophakic retinal detachment complicated with proliferative vitreoretinopathy. *Jpn J Ophthalmol*. 2010;54:331–337.
295. Rubsamen PE, Cousins S. Therapeutic effect of periocular corticosteroids in experimental proliferative vitreoretinopathy. *Retina*. 1997;17:44–50.
296. Blumenkranz MS, Ophir A, Claflin A, et al. Fluorouracil for the treatment of massive periretinal proliferation. *Am J Ophthalmol*. 1982;94:458–467.
297. Blumenkranz M, Hernandez E, Ophir A, et al. 5-Fluorouracil: new applications in complicated retinal detachment for an established antimetabolite. *Ophthalmology*. 1984;91:122–130.
298. Ward T, Hartzer M, Blumenkranz M, et al. A comparison of 5-fluorouridine and 5-fluorouracil in an experimental model for the treatment of vitreoretinal scarring. *Curr Eye Res*. 1993;12:397–401.
299. Rubsamen PE, Davis P, Hernandez E, et al. Prevention of experimental proliferative vitreoretinopathy with a biodegradable intravitreal implant for the sustained release of fluorouracil. *Arch Ophthalmol*. 1994;112:407–413.

300. Yang CS, Khawley JA, Hainsworth DP, et al. An intravitreal sustained-release triamcinolone and 5-fluorouracil codrug in the treatment of experimental proliferative vitreoretinopathy. *Arch Ophthalmol*. 1998;116:69–77.
301. Pimentel S, Hartzer M, El-Rayes E, et al. Effect of 5-fluorouracil and low molecular weight heparin on an improved proliferative vitreoretinopathy model in the rabbit. *Invest Ophthalmol Vis Sci*. 1996;37(Suppl.):1822.
302. Asaria RH, Kon CH, Bunce C, et al. Adjuvant 5-fluorouracil and heparin prevents proliferative vitreoretinopathy: results from a randomized, double-blind, controlled clinical trial. *Ophthalmology*. 2001;108:1179–1183.
303. Sundaram V, Barsam A, Virgili G. Intravitreal low molecular weight heparin and 5-Fluorouracil for the prevention of proliferative vitreoretinopathy following retinal reattachment surgery. *Cochrane Database Syst Rev*. 2010;(7) [CD006421].
304. Wiedemann P, Lemmen K, Schmiedl R, et al. Intraocular daunorubicin for the treatment and prophylaxis of traumatic proliferative vitreoretinopathy. *Am J Ophthalmol*. 1987;104:10–14.
305. Khawly JA, Saloupis P, Hatchell D, et al. Daunorubicin treatment in a refined experimental model of proliferative vitreoretinopathy. *Graefes Arch Clin Exp Ophthalmol*. 1991;229:464–467.
306. Wiedemann P, Leinung C, Hilgers RD, et al. Daunomycin and silicone oil for the treatment of proliferative vitreoretinopathy. *Graefes Arch Clin Exp Ophthalmol*. 1991;229:150–152.
307. Wiedemann P, Hilgers RD, Bauer P, et al. Adjunctive daunorubicin in the treatment of proliferative vitreoretinopathy: results of a multicenter clinical trial. *Am J Ophthalmol*. 1998;126:550–559.
308. Verstraeten T, Hartzer M, Wilcox DK, et al. Effects of vitamin A on retinal pigment epithelial cells in vitro. *Invest Ophthalmol Vis Sci*. 1992;33:2830–2838.
309. Araiz JJ, Refojo MF, Arroyo MH, et al. Antiproliferative effect of retinoic acid in intravitreous silicone oil in an

animal model of proliferative vitreoretinopathy. *Invest Ophthalmol Vis Sci*. 1993;34:522–530.
310. Wu WC, Hu DN, Mehta S, et al. Effects of retinoic acid on retinal pigment epithelium from excised membranes from proliferative vitreoretinopathy. *J Ocul Pharmacol Ther*. 2005;21:44–54.
311. Fekrat S, de Juan E, Campochairo PA. The effect of oral 13-cis-retinoic acid on retinal redetachment after surgical repair in eyes with proliferative vitreoretinopathy. *Ophthalmology*. 1995;102:412–418.
312. Chang YC, Hu DN, Wu WC. Effect of oral 13-cis-retinoic acid treatment on postoperative clinical outcome of eyes with proliferative vitreoretinopathy. *Am J Ophthalmol*. 2008;146:440–446.
313. Goulden V, Clark SM, McGeown C, et al. Treatment of acne with intermittent isotretinoin. *Br J Dermatol*. 1997;137:106–108.
314. Hong WK, Lippman SM, Itri LM, et al. Prevention of second primary tumors with isotretinoin in squamous-cell carcinoma of the head and neck. *N Engl J Med*. 1990;323:795–801.
315. Klebe RJ, Escobedo LV, Bentley KL, et al. Regulation of cell motility, morphology and growth by sulfated glycosaminoglycans. *Cell Motil Cytoskeleton*. 1986;6:273–281.
316. Del Vecchio PJ, Bizios R, Holleran LA, et al. Inhibition of human scleral fibroblast proliferation with heparin. *Invest Ophthalmol Vis Sci*. 1988;29:1272–1276.
317. Bratt G, Tornebohm E, Lockner D, et al. A human pharmacological study comparing conventional heparin and a low molecular weight heparin fragment. *Thromb Haemost*. 1985;53:208–211.
318. Andersson L, Barrowcliffe T, Holmer E, et al. Molecular weight dependency of the heparin-potentiated inhibition of thrombin and activated factor X: effect of heparin neutralization in plasma. *Thromb Res*. 1979;15:531–541.
319. Iverson DA, Katsura H, Hartzer MK, et al. Inhibition of intraocular fibrin formation following infusion of low-molecular-weight heparin during vitrectomy. *Arch*

Ophthalmol. 1991;109:405–409.
320. Chapman C, Iverson D, Hartzer M, et al. The effect of low molecular weight heparin on proliferative vitreoretinopathy induced in the rabbit eye. *Invest Ophthalmol Vis Sci*. 1992;33:818.
321. Kumar A, Nainiwal S, Sreenivas B. Intravitreal low molecular weight heparin in PVR surgery. *Indian J Ophthalmol*. 2003;51:67–70.
322. Garcia RA, Sanchez JG, Arevalo JF. Combined 5-fluorouracil, low-molecular-weight heparin, and silicone oil in the management of complicated retinal detachment with proliferative vitreoretinopathy grade C. *Ophthalmic Surg Lasers Imaging*. 2007;38:276–282.
323. Charteris DG, Aylward GW, Wong D, et al. A randomized controlled trial of combined 5-fluorouracil and low-molecular-weight heparin in management of established proliferative vitreoretinopathy. *Ophthalmology*. 2004;111:2240–2245.
324. Williams RG, Chang S, Comaratta MR, et al. Does the presence of heparin and dexamethasone in the vitrectomy infusate reduce reproliferation in proliferative vitreoretinopathy? *Graefes Arch Clin Exp Ophthalmol*. 1996;234:496–503.
325. Sundaram V, Barsam A, Virgili G. Intravitreal low molecular weight heparin and 5-Fluorouracil for the prevention of proliferative vitreoretinopathy following retinal reattachment surgery. *Cochrane Database Syst Rev*. 2013;(1) [CD006421].
326. Solomon SD, Lindsley K, Vedula SS, Krzystolik MG, Hawkins BS. Anti-vascular endothelial growth factor for neovascular age-related macular degeneration. *Cochrane Database Syst Rev*. 2014;(8) [CD005139].
327. Cheung N, Wong IY, Wong TY. Ocular anti-VEGF therapy for diabetic retinopathy: overview of clinical efficacy and evolving applications. *Diabetes Care*. 2014;37(4):900–905.
328. Wells JA, Glassman AR, Ayala AR, et al. Aflibercept, bevacizumab, or ranibizumab for diabetic macular edema. *N Engl J Med*. 2015;372(13):1193–1203.

329. Braithwaite T, Nanji AA, Lindsley K, et al. Anti-vascular endothelial growth factor for macular oedema secondary to central retinal vein occlusion. *Cochrane Database Syst Rev*. 2014;(5) [CD007325].
330. Pennock S, Haddock LJ, Eliott D, et al. Is neutralizing vitreal growth factors a viable strategy to prevent proliferative vitreoretinopathy? *Progr Retinal Eye Res.*2014;40:16–34.
331. Pennock S, Haddock LJ, Mukai S, et al. Vascular endothelial growth factor acts primarily via platelet-derived growth factor receptor alpha to promote proliferative vitreoretinopathy. *Am J Pathol*. 2014;184(11):3052–3068.
332. Pennock S, Kim D, Mukai S, et al. Ranibizumab is a potential prophylaxis for proliferative vitreoretinopathy, a nonangiogenic blinding disease. *Am J Pathol*. 2013;182(5):1659–1670.
333. Ghasemi Falavarjani K, Hashemi M, Modarres M, et al. Intrasilicone oil injection of bevacizumab at the end of retinal reattachment surgery for severe proliferative vitreoretinopathy. *Eye (Lond)*. 2014;28(5):576–580.
334. Hsu J, Khan MA, Shieh WS, et al. Effect of serial intrasilicone oil bevacizumab injections in eyes with recurrent proliferative vitreoretinopathy retinal detachment. *Am J Ophthalmol*. 2016;161:65–70.e2.
335. Van Bockxmeer FM, Martin CE, Thompson DE, et al. Taxol for the treatment of proliferative vitreoretinopathy. *Invest Ophthalmol Vis Sci*. 1985;26:1140–1147.
336. Lemor M, Yeo JH, Glaser BM. Oral colchicine for the treatment of experimental traction retinal detachment. *Arch Ophthalmol*. 1986;104:1226–1229.
337. Davis AA, Whidby DE, Privette T, et al. Selective inhibition of growing pigment epithelial cells by a receptor-directed immunotoxin. *Invest Ophthalmol Vis Sci*. 1990;31:2514–2519.
338. Kon CH, Occleston NL, Charteris D, et al. A prospective study of matrix metalloproteinases in proliferative vitreoretinopathy. *Invest Ophthalmol Vis Sci*. 1998;39:1524–1529.
339. Barrada A, Peyman GA, Case J, et al. Evaluation of intravitreal 5-fluorouracil, vincristine, VP16, doxorubicin,

and thiotepa in primate eyes. *Ophthalmic Surg*. 1984;15:767–769.
340. Wakabayashi T, Oshima Y, Fujimoto H, et al. Foveal microstructure and visual acuity after retinal detachment repair: imaging analysis by Fourier-domain optical coherence tomography. *Ophthalmology*. 2009;116:519–528.
341. Lai WW, Leung GY, Chan CW, et al. Simultaneous spectral domain OCT and fundus autofluorescence imaging of the macula and microperimetric correspondence after successful repair of rhegmatogenous retinal detachment. *Br J Ophthalmol*. 2010;94:311–318.
342. Wong IY, Iu LP, Koizumi H, et al. The inner segment/outer segment junction: what have we learnt so far? *Curr Opin Ophthalmol*. 2012;23(3):210–218.

109

Optimal Procedures for Retinal Detachment Repair

Louisa Wickham, G.W. Aylward

Introduction

Reports of the primary success rate of rhegmatogenous retinal detachment (RRD) repair can range from 64% to 91%,[1–6] a significant improvement from success rates first reported in 1912, where the estimated success rate of therapy was 1 in 1000.[7] The etiology of RRD is now better understood, and most surgeons agree that retinal breaks should be first closed, and then permanently sealed with retinopexy. With advances in vitreoretinal surgical techniques, a broader range of treatment strategies is now available to surgeons to achieve retinal reattachment, allowing them to tailor their approach to improve primary success rates and visual outcomes. This can be seen by the enormous variation between surgeons in their choice of procedure for particular detachments.[8] Factors such as familiarity with the technique, grade of surgeon, and severity of detachment are also important to consider when assessing which procedure to use for any given type of retinal

detachment.

At present there is no large-scale prospective trial showing statistically different outcomes between all the different treatment options for patients presenting with noncomplex RRD. The highest level of evidence exists for horseshoe tear (HST) detachments where the outcomes of vitrectomy versus scleral buckling were compared.[9] The cost of running such trials is likely to be prohibitive given the high success rate of primary surgery, and therefore the numbers required to show a significant difference in success rate. Therefore this chapter aims to examine procedures currently in use, and assist the reader in choosing between them, for eyes with noncomplex RRD.

Round Hole Retinal Detachment

Introduction

In eyes with round hole retinal detachment, the causative breaks are small, round holes, often associated with lattice degeneration. Patients affected are typically young, low myopes, presenting with blurring of vision and a visual field defect. Some patients are asymptomatic and picked up on routine examination (Figs. 109.1 and 109.2). Round hole detachments are relatively uncommon, and in a large series of RRD reported by Tillery and Lucier, only 2.8% of cases were found to be secondary to round holes.[10] Other series have reported a higher frequency, with 13.9% being reported by Morse and Scheie,[11] and 21% in a series from Japan.[12] An important clinical finding in these patients is that the posterior hyaloid is usually attached. For example, in a large series of 110 round hole detachments requiring treatment, only eight (7%) of the eyes had a detached vitreous, and in these cases, the associated clinical findings suggested that the retinal detachment predated the posterior vitreous detachment (PVD).[13]

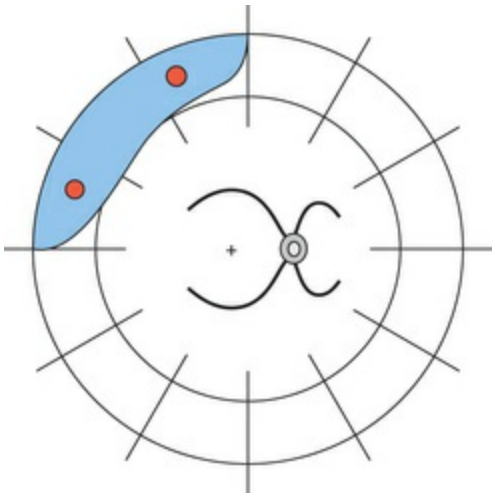

FIG. 109.1 Typical limited retinal detachment associated with round holes. The patient was asymptomatic and was treated with laser demarcation.

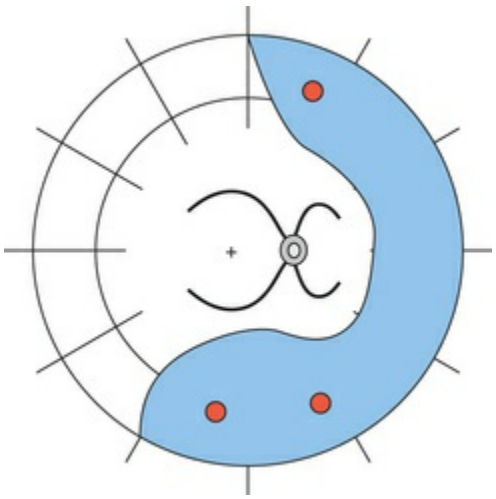

FIG. 109.2 Extensive retinal detachment associated with round holes. Although the patient was asymptomatic prior to detection of the detachment by her optometrist, she was thenceforth conscious of the temporal field defect and requested treatment. She responded well to scleral buckling surgery.

Natural History

Much of our understanding of the natural history of round hole detachments comes from the painstaking work of Norman Byer. In a long-term follow-up of patients with asymptomatic retinal

lesions, there were 17 eyes with 18 areas of round hole retinal detachment.[14] The majority (75%) of the patients were followed-up for more than 5 years, and some for up to 12 years. There was no change in 13 of the 18 areas of detachment, and only a minor change in three areas (18%). In a later report, Byer reported on 19 eyes with up to 33 years of follow-up.[15] There were 22 areas of subclinical detachment in the 19 eyes, seven of which showed some form of progression, and only two of which required treatment, which was successful in both. Therefore, it can be stated that none of the patients in this series lost vision as a result of the initial decision to defer surgery.

A common misconception is that a pigment line, or "tide mark" or "demarcation line" posterior to the area of detachment, will prevent progression. This is not the case, though such a line does imply stability of the extent of the detachment for at least some months. Benson studied 66 retinal detachments with demarcation lines (a subset of a larger series all requiring surgery), 20 of which were detected on routine examination. Most of these patients were young (median age 33) and had detachments secondary to round holes. The demarcation line had failed to prevent progression in 51 of the 66 cases.[16]

Brod et al. observed 28 patients (31 eyes) for 0.5–12.1 years (a mean follow-up of 3.4 years). The patients' age range was 17–82 years, with a mean of 49 years. The majority of eyes were myopic, with 76% of patients having refractive errors of −2 diopters or more. A demarcation line was present in 23 eyes (74%). Only one patient progressed to develop symptoms with associated detachment of the macula, and reduction of visual acuity to 20/30, 3.3 years later. Vision returned to 20/20 following successful surgery. Another patient developed a new detachment from a subsequent PVD and a retinal "U" (horseshoe) tear.[17]

Jarrett reported on 16 patients with retinal detachments in whom surgery was delayed or did not occur. Eleven of these patients had round holes or dialyses. Eight patients had buckling surgery up to 8 years after detection, the delay being for a variety of reasons, including reluctance on behalf of asymptomatic patients to undergo eye surgery. Seven eyes progressed, but only one patient who delayed surgery presented later with a detached macula.[17]

Conservative Management

Conservative management can be considered for patients with peripheral or asymptomatic detachments not threatening the macula. The acceptability of this approach is not dependent solely on the characteristics of the detachment, but rather on patient factors such as the powers of observation of the patient and their ability to attend urgently should they experience symptoms of progression. Many surgeons advocate routine examination at regular intervals, for example every 6 months or annually.[18] However, progression is more likely to occur between follow-up examinations, and if the patient is unable to detect a change, then there is still a risk of the macula detaching before treatment can be applied and the patient suffering long-term visual sequelae. This risk has to be balanced against the possibility of surgical complications in a patient who has presented with an asymptomatic retinal detachment where the risk of progression is small. A patient who develops chronic discomfort, diplopia, or visual loss following surgery for an asymptomatic problem is not surprisingly dissatisfied.

Treatment

Laser Demarcation

The use of laser demarcation treatment to create a band of effective chorioretinal adhesion, which completely surrounds the area of detachment, is often recommended in patients with peripheral or small areas of retinal detachment. The area of chorioretinal adhesion acts like a barrier limiting further progression of subretinal fluid[19] but does not resolve the existing detachment, leaving the patient with a scotoma in this area. This may be appropriate in patients with asymptomatic retinal detachments, or those with very minimal symptoms.

Laser treatment is usually applied from ora to ora, just posterior to the edge of subretinal fluid (Fig. 109.3). Although cryotherapy could be used, laser photocoagulation is preferred as it causes less tissue damage and less inflammatory reaction to the external eye. There is evidence that an adhesion stronger than normal appears

within 24 hours of the application of treatment,[20] but maximum strength is achieved between 3 and 14 days later.[21] Therefore, laser demarcation is not suitable for rapidly progressive detachments.

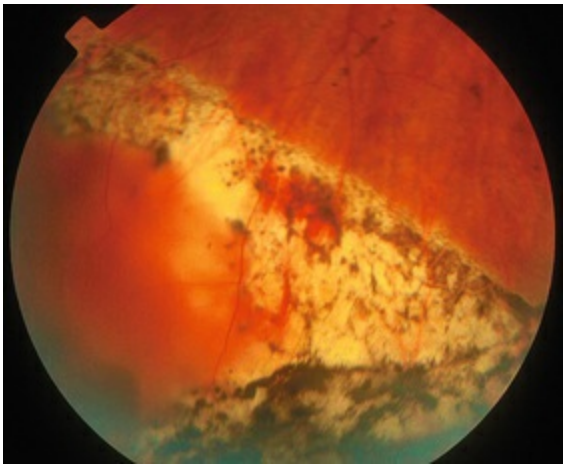

FIG. 109.3 Localized peripheral detachment secondary to round holes. This was treated with a broad band of laser photocoagulation from ora to ora to "wall off" the fluid and prevent it progressing posteriorly to threaten the macula.

The evidence base supporting laser demarcation for retinal detachment is limited, often being retrospective or consisting of small cohorts. Okun et al. discussed demarcation in 1968. The authors treated 48 eyes, and 42 (88%) were stable after 0.5–6 years' follow-up. Of the remaining six eyes, three developed additional areas of detachment from new breaks, and three were judged at the time of laser to need surgical treatment.[22] Gratton treated 42 phakic patients with limited retinal detachments and attached maculas. Most patients (54%) were myopes. Follow-up was for 1–4 years, during which time only one case progressed. In this patient, surgery was successful in reattaching the retina with no visual loss or complications.[23] In a similar study by Vrabec and Baumal, only one case of progression was reported following inadequate laser reaction, in a cohort of 34 eyes.[24]

Extensive round hole detachments can still be considered for laser demarcation; however, following confluent laser retinopexy, the area of affected retina, and hence the area of visual field defect, will increase. This may result in symptoms where they previously

did not occur. Equally, patients with symptomatic retinal detachments may become more troubled by their symptoms. In patients where subretinal fluid extends posteriorly towards the arcade, the interface between attached and detached retina may become more difficult to determine. In these cases slit-lamp laser treatment may be less technically challenging for the most posterior aspect of the retinal detachment prior to converting to indirect laser for more anterior segments as required.

Scleral Buckling

The primary success rate of scleral buckling in round hole detachments is very high, but there is a risk of ocular morbidity. Tillery and Lucier reported results of buckling surgery in cases with detachments secondary to round holes in lattice (some of whom were asymptomatic). The reattachment rate with scleral buckling was 98%. However, 15% had[10] worse vision postoperatively, and the proportion of eyes with worse postoperative vision in the subgroup of those eyes with 20/40 or better preoperatively was 31%.[10] It should be noted, however, that in this cohort scleral buckles were placed under a scleral flap and supplemented with an encircling band which may have led to greater postoperative morbidity.

Greven et al. reported results of 28 eyes of 27 patients with subclinical detachments. In 16 eyes (57%), the detachment was detected on a routine examination, and in eight patients, the fellow eye had a previous symptomatic detachment. All eyes were treated with segmental scleral buckling, and two were encircled. The initial reattachment rate was 100%, but one eye developed another retinal detachment associated with new breaks after 14 months. One eye lost vision from 20/20 to 20/30 "without obvious cause," but no mention was made of any other complications.[25]

Ung et al. from Cambridge reported excellent results from scleral buckling in a large series of retinal detachments secondary to round holes. All but one of 110 detachments were repaired with a single procedure, a success rate of 99%.[13]

Vitrectomy

Vitrectomy is not usually recommended for the treatment of round hole retinal detachments due to the potential difficulties in inducing a posterior vitreous detachment over detached retina. However, the increasing use of vitrectomy in some centers combined with the relative reduction in scleral buckling has led to some advocating vitrectomy for round hole detachments. To date no large-scale studies showing the success rates and complications of this indication have been published.

Detachment Due to Retinal Dialyses

Introduction

Retinal dialysis denotes a circumferential tear of the retina from its insertion at the ora serrata. Some dialyses are secondary to trauma, and are most commonly found in the inferotemporal quadrant.[26] Nontraumatic idiopathic dialyses may also occur, and tend to be bilateral and inferotemporal,[27,28] and some such cases may be inherited.[29] Retinal dialyses account for a small proportion of retinal detachments presenting to a vitreoretinal unit, approximately 4–17%.[30–32] The majority of patients are young (mean age ~30), with a slight male to female preponderance of 1.3 :1.[30,31] Although trauma is often thought to be the most common precipitating event, a recent retrospective study found that only 22% had a history of significant ocular trauma or findings of ocular trauma on clinical investigation.[33–35] This may also reflect differences in the definition of trauma, with some studies including trauma to the head rather than just direct blows to the globe. The posterior vitreous face is attached in the vast majority of cases with a PVD being present in 2–3% of cases.[31,36]

Natural History

There is often a long interval between the creation of the dialysis and the development of a symptomatic retinal detachment. In the series of traumatic retinal detachments described by Cox et al., the time from trauma to retinal detachment was up to 40 years, though in 80% of cases, was less than 2 years.[37] In another series of 50

patients, 41% of the detachments due to traumatic dialysis were diagnosed more than 1 year after injury.[34] Late presentation may be explained by slow progression of the detachment, and this may be related to the lack of vitreous detachment. If the detachment is not detected until the macula becomes involved, then the final visual acuity can be compromised. In Ross's series, 84% of eyes had detached maculas prior to surgery.[34] In a report from Northern Ireland on patients with traumatic retinal detachments, patients with delayed diagnosis were found to have a less favorable visual outcome than those who were diagnosed within 6 weeks of the trauma.[38] It is also important to note that patients may present with more than one retinal dialysis; in a series of 63 patients, 29% had more than one dialysis, illustrating the importance of inspecting all quadrants thoroughly.[31]

Conservative Management

The considerations and options for the management of patients with limited detachment secondary to dialysis are identical to those for patients with round hole detachments. Cases with signs of chronicity, such as tidemarks and retinal cysts, have probably been stable for some time, consequently with a relatively low risk of progression. In one series of 71 detachments secondary to dialysis, three patients had such signs of chronicity and were followed-up without incident.[30]

Treatment

Laser Demarcation

Limited detachments secondary to dialysis respond well to laser demarcation. This is particularly true for the majority of detachments from dialyses that are in the inferotemporal quadrant. Walling off of the affected area here results in a permanent field defect superonasally, which is likely to be less important to the patient, than inferotemporal field loss. In Kennedy's series of 71 patients, five were successfully treated with retinopexy in order to demarcate a local detachment.[30]

Scleral Buckling

Dialyses respond well to segmental scleral buckling procedures. In a series of traumatic retinal detachments including 49 cases of dialysis, the primary success rate was 96%.[38] In another series, from France, of 48 cases of retinal detachment secondary to dialysis, the primary success rate was 100%.[36] Ross described a series of 50 eyes with a primary success rate of 94% and a final success rate of 98%.[34] The primary success rate for surgery in Kennedy's series was 97%.[30] The presence of PVR is rare in patients with retinal dialyses; however, in patients with PVR at the time of surgery, the surgical success rate is reduced.[31,32]

Retinal Detachment Secondary to "U" (Horseshoe) Tears

Introduction

This category represents the most common group of rhegmatogenous retinal detachments.[32] The detachment is secondary to one or more traction "U" tears, which in turn follow PVD (Fig. 109.4). A typical patient will present with visual loss, a symptomatic field defect, and a history of floaters and flashing lights some weeks previously.

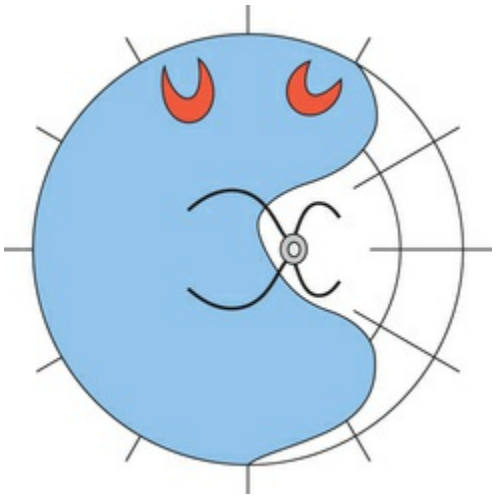

FIG. 109.4 Extensive detachment secondary to traction tears. At 2 weeks after noticing flashing lights and

floaters, this patient suddenly lost vision “like a curtain coming up from below.” There are two large posterior tears, and the detachment is bullous. It was treated successfully using a vitrectomy and SF_6.

Natural History

Retinal detachments associated with HST tend to progress rapidly as a result of continuing vitreous traction on the flap, encouraging further recruitment of subretinal fluid. Fluid currents within the eye also play a significant role in the development and progression of the detachment, as described by Machemer in his Jackson Memorial Lecture in 1988.[39] Subretinal fluid from superior tears spreads more rapidly than that from inferior ones, and this needs to be borne in mind when planning the timing of intervention in eyes with an attached macula. The speed of onset means that patients often complain of PVD symptoms just prior to the onset of visual field loss or at around the same time. However, in pseudophakic patients, there is evidence that chronic traction from a preexisting PVD may lead to new, often small, anterior breaks.[40,41]

The rapid progression of most detachments in this category means that there is an increased risk of macular involvement prior to presentation in these patients. In Burton's series of 953 primary retinal detachments, 69.5% of cases had detached maculas preoperatively.[42] More recently the Scottish Retinal Detachment study reported that 49.4% patients with HST retinal detachments presented with macular involvement compared with 41% round hole detachments.[32] Left untreated, retinal detachment results in severe loss of vision as well as a significant rate of discomfort and cosmetic problems.[43]

Conservative Management

Conservative management for limited detachments is adopted less commonly than in RRD due to round holes or dialyses. This is because patients usually present with symptoms associated with the PVD, and there are rarely signs of the fluid being longstanding. There is therefore much less confidence that the fluid will remain

stationary or progress slowly. Furthermore, the continuing vitreous traction is an additional factor leading to faster progression.

Occasionally, a small, asymptomatic peripheral detachment from a "U" tear might appear stable, with subsequent development of a tide mark, in which case, careful observation might be appropriate (Fig. 109.5). Since these detachments tend to occur in an older age group, there are also cases whereby severe medical comorbidity precludes any form of treatment.

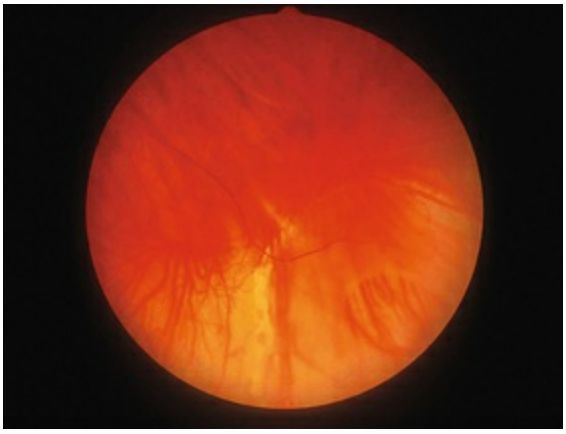

FIG. 109.5 Long-standing retinal detachment secondary to a "U" tear. There is a tidemark indicating chronicity. This patient was treated with laser demarcation to reduce the risk of progression.

Treatment

Laser Demarcation

Although laser photocoagulation creates an instant adhesion, this is not up to full strength for up to 14 days.[21] Rapidly progressing fluid may extend through the area of demarcation before a strong enough adhesion develops. The distinction between a HST with a cuff of subretinal fluid and an early HST retinal detachment is not always clear in the acute stages following posterior vitreous detachment. The rate of subretinal fluid accumulation and hence retinal detachment progression may be determined by the patient history, location, size, and number of breaks. The presence of a large superior break with a short history is more likely to progress

prior to the formation of adequate adhesion in response to laser, and in these cases laser should be used with caution. In patients where laser treatment is used, sufficient margin should be left between the detachment edge and the placement of laser burns to allow for some progression of subretinal fluid prior to an adhesion developing.

Pneumatic Retinopexy

Modern pneumatic retinopexy (see Chapter 107, Pneumatic retinopexy) was introduced by Hilton and Grizzard in 1986.[44] Expanding gas is injected into the vitreous cavity, followed by application of cryotherapy or laser photocoagulation. The technique can be applied in an outpatient setting under local anesthesia. Postoperatively the patient positions their head so that the gas bubble is opposed to the break or breaks. This limits the flow of fluid into the subretinal space and allows reabsorption of the existing fluid by the retinal pigment epithelium. The technique is most appropriate for detachments with breaks limited to one quadrant, usually superiorly. Complications of pneumatic retinopexy include raised intraocular pressure, and subretinal gas.[45] The expanding gas may also exert traction inferiorly leading to the creation of new, inferior breaks, particularly in the presence of inferior lattice degeneration.[46] New or missed breaks are a common cause of failure following pneumatic retinopexy, accounting for half the failures in one series.[47]

Pneumatic retinopexy was found to have a comparable success rate to vitrectomy with cryotherapy and gas in a prospective randomized control trial in 120 cases.[48] A large multicenter randomized trial compared pneumatic retinopexy with scleral buckling in 198 patients. There was a higher rate of primary reattachment in the scleral buckling group (82% vs. 73%), but this difference did not achieve statistical significance (p>.05). There was no difference in the final reattachment rate (98% vs. 99%). However, the patients with pneumatic retinopexy had less morbidity and better final visual acuity.[49] In a more recent study of 422 patients, the primary success rate was 61% with a final success rate of 99.5%.[50]

A recent Cochrane review comparing pneumatic retinopexy to

primary scleral buckling reported that there was some evidence that scleral buckling had a higher primary success rate; however, the reviewers conceded that they could not rule out that there was no difference between the two procedures.[51] Most studies have indicated no difference in the final success rate between the two, and more importantly, no difference in the final visual acuity. There is evidence, however, that pneumatic retinopexy is less effective in aphakic and pseudophakic eyes. In a series of 56 eyes, the primary success rate was 81% in a subgroup of phakic eyes but only 43% in eyes which were aphakic or pseudophakic.[52]

Given that pneumatic retinopexy is a relatively quick and simple procedure, with less morbidity than scleral buckling, it is worth considering as an initial procedure. This is particularly the case for patients who have "classic" indications, as the success rate appears higher in this group. In a subgroup of patients with phakic eyes, single breaks, and fluid confined to one superior quadrant, the primary success rate was 97%.[53] Even if treatment fails, a good final result can be expected following further surgery. Despite this, a recent survey by the American Society of Retinal Specialists showed that preferences toward pneumatic retinopexy as a primary procedure have declined over the past 8 years, commenting that this may reflect a greater confidence in vitrectomy surgery.[54]

Most surgeons who use pneumatic retinopexy apply it as a primary procedure and then employ scleral buckling if it fails. However, pneumatic retinopexy can also be used as an effective method of treating detachments after failed scleral buckling. In most of these cases, there is persistent elevation of the retinal break above the buckle and retinopexy has already been applied. All that is necessary is temporary reduction in fluid flow through the break to allow the retina to settle. In a series of 36 eyes with failed scleral buckling surgery, injection of gas was successful in reattaching the retina in 25 (69.4%).[55] In a more recent study of 42 consecutive cases, secondary pneumatic retinopexy after either scleral buckling surgery or vitrectomy, resulted in a reattachment rate of 100% in the scleral buckle group and 90% in the vitrectomy group.[56]

Scleral Buckling

The aim of buckling surgery is to create an indentation of the sclera

beneath the retinal break. The possible mechanisms of action are well described elsewhere in this volume (see Chapter 104, Techniques of scleral buckling), but the effect is to reduce the rate of flow of fluid into the subretinal space, leading to resolution of the detachment. It is important to understand that buckling achieves only closure, and not sealing of the retinal break, the latter being the role of retinopexy. The implication of this is that buckling alone has the same initial success rate whether retinopexy is applied or not, but if the indentation fades or the buckle is removed, the retinal redetachment will recur. This notion has been confirmed by Chignell, who reported success in 26 of 29 cases of retinal detachment treated with scleral buckling and no retinopexy. Follow-up varied from 6 months to 2 years, and no redetachments were reported,[57] although no buckles needed to be removed during that period. When these cases were followed-up in the long term, late detachments were found in 4 of 46 patients. In all these cases, redetachment occurred because of reopening of the original retinal break, and was associated with progressive reduction of the height of the scleral buckle.[58] In another, larger series of scleral buckling without retinopexy, initial success was achieved in 143 of 175 cases (82%) and final success in 158 cases (90%). Causes of initial failure were all related to malposition of the buckle or the development of new breaks, rather than anything to do with retinopexy. Follow-up was only 6 months, so the long-term effect of buckle fade in these patients is not known.[59]

There is a lack of consensus concerning the best type of buckle to use in any particular circumstance. Limited retinal detachments with single breaks can be treated with a radial element, or a small segmental buckle. Many surgeons supplement the segmental buckle with an encircling band. This has the advantage of helping to maintain the buckle height in the long term. However, if retinopexy has been applied to all the breaks, then this is theoretically unnecessary. Several nonrandomized series have produced good results without encirclement and good long-term follow-up.[60] By contrast, encirclement is associated with a higher risk of motility disturbance and refractive changes, and can also lead to long-term problems, such as erosion of the buckle through the sclera.[61] Singh investigated the role of encirclement in aphakic

patients in a prospective, randomized controlled trial. A total of 84 patients with aphakic retinal detachments were randomized to either local scleral buckling or encirclement. The primary success rate was 90% and 91% in the two groups, respectively.[62] Ho et al. reported no difference in success rates between three different buckling methods in a nonrandomized study of 128 eyes. However, there were more complications in the group of eyes that were encircled.[63]

Vitrectomy

Conventional Indications.

Conventional indications for vitrectomy are those where scleral buckling could be technically challenging. Vitrectomy may offer a more successful approach for simple detachments with significant vitreous opacity, or for those with posterior breaks that would otherwise require a large scleral buckle. Other agreed indications include eyes with thin sclera which would make scleral buckling difficult or dangerous (Video 109.1 online).

As surgeons became more comfortable with vitrectomy techniques to manage cases of vitreous pathology and complex retinal detachments, it became clear that the advantages of an internal approach could also be useful for simpler cases. There is now considerable overlap with current indications for scleral buckling surgery, such that vitrectomy is increasingly used in preference to scleral buckling surgery in many units.[8,54,64] In an analysis of Medicare beneficiaries from 1997 to 2007, the use of vitrectomy (with or without scleral buckle) for the treatment of primary RRD had increased by 72% over the study period.

Currently, controversy surrounds the management of medium complexity, bullous, retinal detachments, which represent the majority of cases (Fig. 109.6). Some centers have moved away from scleral buckling towards vitrectomy for the primary management.[8,65] Proponents of vitrectomy argue that it can directly eliminate vitreous traction, remove media opacities, and allow better detection and localization of retinal pathology, particularly when using wide-angle viewing systems. Vitrectomy eliminates the risks of buckle-related complications, such as drainage problems,[66]

choroidal effusions,[67] diplopia,[68] and extrusion of the explant.[69] However, the use of vitrectomy introduces a new set of potential complications, including entry site breaks,[70] postoperative nuclear sclerosis,[71] and proliferative vitreoretinopathy.[72]

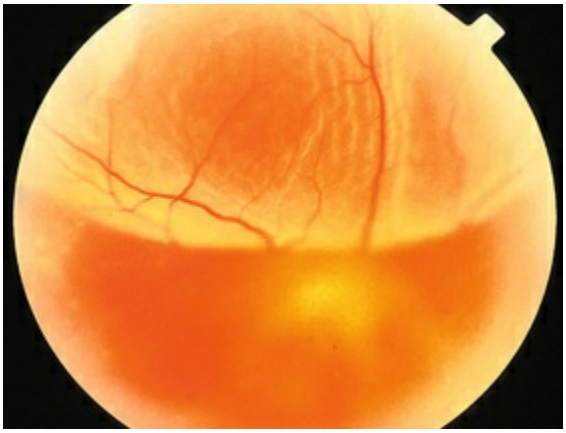

FIG. 109.6 Superior bullous retinal detachment secondary to a posterior vitreous detachment and "U" tears. This type of detachment is difficult to manage by buckling techniques and was treated with a vitrectomy.

Many case series of primary vitrectomy for RRD have been reported. The primary reattachment rate varies between 64% and 100%.[73] A large study from Japan compared 225 phakic eyes with superior retinal detachments associated with "U" tears. Scleral buckling was used in 138 eyes, and 87 eyes were treated with vitrectomy, according to surgeon preference. Primary and final anatomic success rates were identical between the two groups at 92% and 100%, respectively.[74] It is relatively easy to compare reattachment rates between scleral buckling and vitrectomy, and when this is done, the results are similar. However, a valid comparison should also include assessment of the complications, and this is where difficulties occur. This is because the complications are qualitatively different, and there is no scientific method of comparing, e.g., diplopia from a scleral buckle with nuclear cataract from a vitrectomy.

The Scleral Buckling versus Primary Vitrectomy in Rhegmatogenous Retinal Detachment Study (SPR Study) was the first large prospective randomized clinical trial to compare outcomes of two different surgical methods in retinal detachment.[9]

A total of 45 surgeons in 25 centers recruited a total of 681 patients with "medium complexity" detachments. Medium complexity cases were primary RRDs with breaks of size from one to two clock-hours, multiple breaks, superior bullous detachment, central extension of breaks, or marked vitreous traction. Cases were divided into phakic and aphakic/pseudophakic groups before being randomized into scleral buckling or PPV. The protocol allowed the use of a supplementary buckle in cases undergoing PPV at the discretion of the operating surgeon. Surgeons had carried out at least 100 cases using each method before participating in the study. The primary outcome measure was defined as the change in best corrected visual acuity (BCVA) between the initial examination and the final follow-up at 12 months. Secondary outcome measures were the rate of PVR and primary anatomic success. The latter was defined as attachment of the retina central to the equator at the final follow-up visit without additional retinal procedures. With this definition, cases having supplemental laser or treatment of macular pucker would be classified as failures, so it is important to realize that the primary anatomic success rate is not equivalent to what many surgeons might understand as primary reattachment rate, which can be derived from the data for retinal redetachment provided in the study. The key results of the study are shown in Table 109.1, and in summary, there was a better improvement of BCVA with scleral buckling in phakic eyes, and a high primary success rate using vitrectomy in aphakic/pseudophakic eyes.

TABLE 109.1

Summary of the Main Results From the SPR Study

Outcome	Scleral Buckling	Vitrectomy
PHAKIC		
Improvement in BCVA	−0.71*	−0.56
Primary success	63.6%	63.8%
Primary reattachment	73.7%	74.9%
APHAKIC/PSEUDOPHAKIC		
Improvement in BCVA	−0.56	−0.65
Primary success	53.4%	72.0%*
Primary reattachment	60.1%	79.5%*

*Difference statistically significant ($p<.05$).

BCVA, best corrected visual acuity; SPR Study, Scleral Buckling versus Primary Vitrectomy in Rhegmatogenous Retinal Detachment Study.

The SPR Study is a very important contribution to the evidence base of retinal detachment surgery. Since the study was planned, attention has been focused on the "surgeon factor" in surgical trials, because most surgeons have a preferred technique with which they may get better outcomes. Traditional randomization results in only half the patients having a surgeon using their preferred operation, and a better study design for future trials might be expertise-based.[75] However, analysis of the results by surgeon in the SPR Study has found that the majority of surgeons had similar success rates for both operations.[76]

Supplementary Buckle.

Some vitreous remains after vitrectomy, even when shaving of the vitreous base is performed, which may continue to exert traction on retinal breaks, and form a scaffold for later development of PVR. Inferior retinal breaks depend on patient positioning to maintain contact with the tamponade agent. For both these reasons, many surgeons have advocated supplementary scleral buckles. Gartry presented a series of 114 eyes treated with vitrectomy for retinal detachments uncomplicated by PVR. The indication for vitrectomy in the majority was media opacity or large posterior breaks. Supplementary buckles were used for cases that had been operated on previously, and for those with breaks below one clock-hour above the horizontal meridian.[77]

However, a large series of 275 pseudophakic eyes treated with vitrectomy and no buckling showed no evidence of failure resulting from factors associated with lack of a scleral buckle. The anatomic success rate after one operation was 241 (88%), and the final success rate was 265 (96%). No details are given about the distribution of fluid and the position of retinal breaks in this series. However, since the patients were consecutive, it can reasonably be assumed that many of them had inferior breaks. Of the 34 eyes that were not attached with one operation, 17 were associated with new breaks or opening of old ones. Sixteen had PVR and one had a suprachoroidal hemorrhage. Subsequent surgery included a scleral buckle in 12 eyes.[6] A retrospective study of retinal detachments with breaks between 4 and 8 o'clock specifically looked for an advantage of supplementary buckles but failed to find an increased success rate.[78]

In the SPR Study, the use of a buckle in cases randomized to the vitrectomy group was allowed at the discretion of the surgeon. Ancillary analysis found that the use of a supplementary buckle was associated with better success rates in the pseudophakic/aphakic group, but not in the phakic group.[9] A supplementary scleral buckle has the disadvantage of introducing additional risks and complications. Although there may be theoretic advantages in selected cases, there is no evidence base to support its widespread use.

Laser Versus Cryotherapy.

All techniques for retinal reattachment require some form of retinopexy to create a chorioretinal adhesion to seal retinal breaks or wall off areas of detachment. Gonin used thermocautery to achieve this, but today only laser photocoagulation and cryotherapy are widely used. Debate continues about the relative merits of each technique.

Cryotherapy is applied using an external probe, while visualizing the treatment area with the indirect ophthalmoscope or wide-angle viewing system. One practical advantage is that it can be used with moderate degrees of media opacity, and because retinal breaks "light up," the surgeon has increased confidence that hard-to-see breaks have been treated. Many surgeons prefer the use of laser, either endolaser as part of an internal approach, or the indirect laser ophthalmoscope during scleral buckling surgery. Endolaser is easy to apply, but the use of the indirect laser can be difficult with moderate media opacity, or in the presence of shallow subretinal fluid. This problem can be addressed for scleral buckling by applying indirect laser to the tear postoperatively, once the retina has reattached.

Cryotherapy has been shown to promote dispersion of viable retinal pigment epithelial cells and to cause breakdown of the blood–retinal barrier. Ryan reported two cases of cystoid macula edema, which occurred following uncomplicated scleral buckling procedures for macular-on retinal detachment.[79] Cystoid macular edema, and wrinkling of the inner limiting membrane, has also been reported following cryotherapy alone.[80] It must be remembered, however, that macula pathology, particularly

epiretinal membranes, also occur following PVD without tears, and the association with cryotherapy is not necessarily causative.

Cryotherapy has been shown to cause breakdown of the blood–retinal barrier. In rabbit eyes treated with confluent laser in one eye and equivalent cryotherapy in the other, there was a significantly greater increase in vitreous fluorophotometry readings in the cryotherapy-treated eyes. However, both eyes returned to normal readings after 14 days.[81] Similar findings in man were demonstrated in a randomized trial of cryotherapy and laser photocoagulation in conventional retinal detachment surgery. Patients were treated either with cryotherapy at the time of surgery or with laser photocoagulation 4 weeks postoperatively. Postoperative flare was measured using laser flare photometry and was significantly higher in the cryotherapy group than the laser group. In addition visual recovery was slower in the cryotherapy group. However, at 10 weeks postoperatively, there was no difference in visual acuity between the two groups.[82] Cryotherapy produces more extensive retinal edema and necrosis in treated areas than laser. Lesions are similar at 14 days with atrophy of the retina and choroid, and a pigmented chorioretinal scar.[83]

Many studies have examined risk factors for the development of PVR, but results are contradictory. In a large retrospective study of 65 eyes with PVR and 325 controls, Cowley et al. found that the amount of cryotherapy applied and the use of vitrectomy were independent risk factors for PVR.[72] In another retrospective study comparing laser and cryotherapy, no difference in the rate of postoperative PVR was found in those eyes with round hole detachments or traction tears with no preoperative PVR. However, in eyes with traction tears and some preoperative PVR ("curled posterior edges"), cryotherapy was found to be associated with a higher risk of PVR (13/88, 14.7%) compared with 1/56 (1.7%) in the laser group. Unfortunately, the size and number of the retinal breaks was not included in the multivariate analysis.[84] The importance of including confounding factors was illustrated by the results of another multivariate analysis, which was a prospective study with good data collection, looking at factors associated with success of scleral buckling in a large number of eyes with rhegmatogenous retinal detachment. The vast majority of failures

were due to PVR. While the number of applications of cryotherapy was found to be associated with failure after univariate analysis, it was not found to be a significant factor when the other variables, such as the size and number of breaks, were included.[85] A prospective study looking at PVR in a subgroup of 140 patients undergoing vitrectomy for retinal detachment found that cryotherapy was not an independent risk factor for PVR formation.[86]

In summary, there is no strong evidence to suggest that the use of cryotherapy is inferior to laser photocoagulation. Both techniques have their place, and their selection is largely a matter of surgeon preference.

Sutureless Vitrectomy.

The use of transconjunctival vitrectomy using smaller gauge instruments, 25- and 23-gauge (25G, 23G), has become increasingly popular, but there has been some controversy about the use of these systems in the management of RRD.[87] Most surgeons consider that removal of peripheral vitreous is important, and that indentation of the periphery is helpful in locating retinal breaks. Both these steps are more difficult in 25G surgery, and there were early reports of high redetachment rates. In a series of 53 eyes managed by 25G vitrectomy, the primary success rate was only 74%, the reasons for failure being either new retinal breaks or PVR. In addition, three eyes (6%) in this series developed postoperative choroidal hemorrhage.[88] The authors speculated that the lower flow rate associated with 25G might leave higher concentrations of cytokines in the eye. However, more recently studies have shown success rates with 23G and 25G systems comparable to those reported with scleral buckling and 20G surgery.[89–92] In a study of 133 eyes using 23G instrumentation, the primary success rate was 96.2%.[89] Similarly, recent studies have also reported comparable success rates (primary success over 90%) for 25G vitrectomy and gas, without the use of a supplementary buckle.[91–93]

Variations in Practice.

The same case of retinal detachment might be treated in several different ways depending on which country, or which retinal

surgeon, they present to. Not only are there geographic variations in techniques, but these also change rapidly over time.

The success rate of retinal detachment surgery has improved since the pioneering work of Gonin. A report from a single center in the UK reported three cycles of audit over a 10-year period showing a significant increase in primary reattachment rates, which rose from 67% in Audit 1 (1987–1989) to 87% in Audit 3 (1995–1997) (p=.0004).[94] In this audit the increased success rate was attributed to a reorganization of the department whereby retinal detachment surgery was performed solely by vitreoretinal specialists.

The influence of subspecialization in improvement of success rates was also highlighted in a national audit of primary surgery for RRD performed in the UK. Of the surgeons who responded, 38% performed retinal detachment surgery. Of these, 105 (41%) declared a special interest in retinal surgery and were therefore defined as "specialists" for the purposes of the audit.[95] Detachments were graded for severity ranging from 1–4 according to the distribution of retinal breaks and area of retinal detachment, for example, grade 2 detachments were defined as those with breaks within the same quadrant, and/or less that two quadrants of retinal detachment. In grade two detachments, the success rate of specialists was 87% compared with only 70% for nonspecialists (p=.001).[4] The primary success rate overall (specialists and nonspecialists) was 77%.[4]

There is an increasing trend towards using vitrectomy as the preferred method of primary retinal detachment repair.[54,96,97] In the 1995 UK audit of primary surgery for RRD, scleral buckling was used in 83% of the sample and the remaining 17% had vitrectomy.[98] Interestingly, no patients in this survey had pneumatic retinopexy, reflecting a significant difference in practice between the UK and the United States. More recently, however, the National Database in the United Kingdom reported that the procedure of choice for primary retinal detachment was vitrectomy in 79.1% cases, scleral buckle in 12.1%, and vitrectomy with scleral buckle in 8.7%.[97] Similar trends have also been reported in the United States, with 53% preferring to treat a RRD secondary to a superior tear with a vitrectomy, 25% a pneumatic retinopexy and 21% a scleral buckle. This survey also observed that use of pneumatic retinopexy as a primary procedure had declined over the past 8 years, commenting

that this may reflect a greater confidence in vitrectomy surgery.[54]

Changes in preferred technique may also reflect a change in the range of pathology, mostly because of the aging population, and the increasing number of patients undergoing cataract surgery. Among patients with RRDs, the proportion with aphakic/pseudophakic eyes increased to 30% over the 10 years to 1999.[64] These findings were confirmed in a similar study from London. More cases were pseudophakic and fewer aphakic in 1999 than in 1979–1980. Vitrectomy was a primary procedure in 63% of cases in 1999 but in only 1% in 1979–1980. Anatomic success rates were statistically similar: 79.8% primary and 88.8% final success in 1979–1980, compared with 84% primary and 93.6% final success in 1999.[65]

Conclusion

The treatment of rhegmatogenous retinal detachment has advanced considerably since the pioneering work of Gonin. Both primary and final success rates are now high, and it is only a small minority of cases whose retinas remain detached after one or more operations. There is broad agreement about the best method for some categories of detachment, but for the majority of cases, there is both lack of agreement and lack of an evidence base to make rational choices of technique. The current evidence base suggests that many surgical techniques can achieve similar success rates in specialist units, and that perhaps familiarity and surgeon preference are the more compelling reasons for choosing a particular approach. Despite the contribution of the SPR Study, there remains a need for further evidence from well-conducted trials, and when setting up such trials, it is important to consider factors other than success rate. The goal of treatment should be to choose a method for any particular case that has the best chance of anatomic success, but with the lowest risk of introducing further ocular morbidity. Costs of the respective treatments to both the health care economy and the patient might also be considered. As Wilkinson put it: "The best method of repairing a particular detachment will remain a matter of speculation and bias until more appropriate data are acquired."[99]

Acknowledgment

Thank you to Maninder Bhogal MBBS, MD for shooting and editing the video demonstrating surgical techniques used in the treatment of primary retinal detachment with vitrectomy attached to this chapter.

References

1. Heimann H, Bornfeld N, Friedrichs W, et al. Primary vitrectomy without scleral buckling for rhegmatogenous retinal detachment. *Graefes Arch Clin Exp Ophthalmol*. 1996;234:561–568.
2. Halberstadt M, Brandenburg L, Sans N, Koerner-Stiefbold U, Koerner F, Garweg JG. Analysis of risk factors for the outcome of primary retinal reattachment surgery in phakic and pseudophakic eyes. *Klin Monatsbl Augenheilkd*. 2003;220:116–121.
3. Schmidt JC, Rodrigues EB, Hoerle S, Meyer CH, Kroll P. Primary vitrectomy in complicated rhegmatogenous retinal detachment – a survey of 205 eyes. *Ophthalmologica*. 2003;217:387–392.
4. Thompson JA, Snead MP, Billington BM, Barrie T, Thompson JR, Sparrow JM. National audit of the outcome of primary surgery for rhegmatogenous retinal detachment. II. Clinical outcomes. *Eye (Lond)*. 2002;16:771–777.
5. Girard P, Karpouzas I. Pseudophakic retinal detachment: anatomic and visual results. *Graefes Arch Clin Exp Ophthalmol*. 1995;233:324–330.
6. Campo RV, Sipperley JO, Sneed SR, et al. Pars plana vitrectomy without sceral buckle for pseudophakic retinal detachments. *Ophthalmology*. 1999;106:1811–1816.
7. Vail D. An inquiry into results of the established treatment of detachment of the retina and a new theory. *Trans Am Acad Ophthalmol Otolaryngol*. 1912;17:29.
8. Ramulu PY, Do DV, Corcoran KJ, Corcoran SL, Robin AL. Use of retinal procedures in medicare beneficiaries from 1997 to 2007. *Arch Ophthalmol*. 2010;128:1335–1340.

9. Heimann H, Bartz-Schmidt KU, Bornfeld N, Weiss C, Hilgers RD, Foerster MH. Scleral buckling versus primary vitrectomy in rhegmatogenous retinal detachment: a prospective randomized multicenter clinical study. *Ophthalmology*. 2007;114:2142–2154.
10. Tillery WV, Lucier AC. Round atrophic holes in lattice degeneration – an important cause of phakic retinal detachment. *Trans Sect Ophthalmol Am Acad Ophthalmol Otolaryngol*. 1976;81:509–518.
11. Morse PH, Scheie HG. Prophylactic cryoretinopexy of retinal breaks. *Arch Ophthalmol*. 1974;92:204–207.
12. Murakami-Nagasako F, Ohba N. Phakic retinal detachment associated with atrophic hole of lattice degeneration of the retina. *Graefes Arch Clin Exp Ophthalmol*. 1983;220:175–178.
13. Ung T, Comer MB, Ang AJ, et al. Clinical features and surgical management of retinal detachment secondary to round retinal holes. *Eye (Lond)*. 2005;19:665–669.
14. Byer NE. The natural history of asymptomatic retinal breaks. *Ophthalmology*. 1982;89:1033–1039.
15. Byer NE. What happens to untreated asymptomatic retinal breaks, and are they affected by posterior vitreous detachment? *Ophthalmology*. 1998;105:1045–1049 [discussion 1049-1050].
16. Benson WE, Nantawan P, Morse PH. Characteristics and prognosis of retinal detachments with demarcation lines. *Am J Ophthalmol*. 1977;84:641–644.
17. Brod RD, Flynn HW Jr, Lightman DA. Asymptomatic rhegmatogenous retinal detachments. *Arch Ophthalmol*. 1995;113:1030–1032.
18. Ahmad N, West J. Current opinion on treatment of asymptomatic retinal detachments. *Eye (Lond)*. 2007;21:1179–1185.
19. Greenberg PB, Baumal CR. Laser therapy for rhegmatogenous retinal detachment. *Curr Opin Ophthalmol*. 2001;12:171–174.
20. Folk JC, Sneed SR, Folberg R, Coonan P, Pulido JS. Early retinal adhesion from laser photocoagulation. *Ophthalmology*. 1989;96:1523–1525.

21. Yoon YH, Marmor MF. Rapid enhancement of retinal adhesion by laser photocoagulation. *Ophthalmology*. 1988;95:1385–1388.
22. Okun E, Cibis PA. Photocoagulation in "limited" retinal detachment and breaks without detachment. McPherson A. *New and controversial aspects of retinal detachment*. Harper and Row: New York; 1968:164–172.
23. Gratton I, Gazocchi M, Simonini F, Fattori CM, Citroni M. Argon laser photocoagulation in the management of retinal detachment and predisposing lesions. *Lasers Surg Med*. 1984;4:337–344.
24. Vrabec TR, Baumal CR. Demarcation laser photocoagulation of selected macula-sparing rhegmatogenous retinal detachments. *Ophthalmology*. 2000;107:1063–1067.
25. Greven CM, Wall AB, Slusher MM. Anatomic and visual results in asymptomatic clinical rhegmatogenous retinal detachment repaired by scleral buckling. *Am J Ophthalmol*. 1999;128:618–620.
26. Dumas JJ. Retinal detachment following contusion of the eye. *Int Ophthalmol Clin*. 1967;7:19–38.
27. Smiddy WE, Green WR. Retinal dialysis: pathology and pathogenesis. *Retina*. 1982;2:94–116.
28. Zion VM, Burton TC. Retinal dialysis. *Arch Ophthalmol*. 1980;98:1971–1974.
29. Brown GC, Tasman WS. Familial retinal dialysis. *Can J Ophthalmol*. 1980;15:193–195.
30. Kennedy CJ, Parker CE, McAllister IL. Retinal detachment caused by retinal dialysis. *Aust N Z J Ophthalmol*. 1997;25:25–30.
31. Qiang Kwong T, Shunmugam M, Williamson TH. Characteristics of rhegmatogenous retinal detachments secondary to retinal dialyses. *Can J Ophthalmol*. 2014;49:196–199.
32. Mitry D, Singh J, Yorston D, et al. The predisposing pathology and clinical characteristics in the Scottish retinal detachment study. *Ophthalmology*. 2011;118:1429–1434.
33. Williamson JB, Lewis G, Grippo AJ, et al. Autonomic predictors of recovery following surgery: a comparative

study. *Auton Neurosci*. 2010;156:60–66.
34. Ross WH. Traumatic retinal dialyses. *Arch Ophthalmol*. 1981;99:1371–1374.
35. Vote BJ, Casswell AG. Retinal dialysis: are we missing diagnostic opportunities? *Eye (Lond)*. 2004;18:709–713.
36. Bonnet M, Moyenin P, Pecoldowa C, Grange JD. Retinal detachment caused by a tear at the ora serrata.*J Fr Ophtalmol*. 1986;9:231–242.
37. Cox MS, Schepens CL, Freeman HM. Retinal detachment due to ocular contusion. *Arch Ophthalmol*. 1966;76:678–685.
38. Johnston PB. Traumatic retinal detachment. *Br J Ophthalmol*. 1991;75:18–21.
39. Machemer R. The importance of fluid absorption, traction, intraocular currents, and chorioretinal scars in the therapy of rhegmatogenous retinal detachments. XLI Edward Jackson memorial lecture. *Am J Ophthalmol*. 1984;98:681–693.
40. Bradford JD, Wilkinson CP, Fransen SR. Pseudophakic retinal detachments: the relationships between retinal tears and the time following cataract surgery at which they occur. *Retina*. 1989;9:181–186.
41. Wilkinson CP. Phakic retinal detachments in the elderly. *Retina*. 1995;15:220–223.
42. Burton TC. Recovery of visual acuity after retinal detachment involving the macula. *Trans Am Ophthalmol Soc*. 1982;80:475–497.
43. Ivanisevic M. The natural history of untreated rhegmatogenous retinal detachment. *Ophthalmologica*. 1997;211:90–92.
44. Hilton GF, Grizzard WS. Pneumatic retinopexy: a two-step outpatient operation without conjunctival incision. *Ophthalmology*. 1986;93:626–641.
45. Wirostko WJ, Han DP, Perkins SL. Complications of pneumatic retinopexy. *Curr Opin Ophthalmol*. 2000;11:195–200.
46. Poliner LS, Grand MG, Schoch LH, et al. New retinal detachment after pneumatic retinopexy. *Ophthalmology*. 1987;94:315–318.
47. Grizzard JS, Hilton GF, Hammer ME, Taren D, Brinton DA.

Pneumatic retinopexy failures: cause, prevention, timing and management. *Ophthalmology*. 1995;102:929–936.
48. van Effenterre G, Haut J, Larricart P, Abi-Rached J, Vachet JM. Gas tamponade as a single technique in the treatment of retinal detachment: is vitrectomy needed? A comparative study of 120 cases. *Graefes Arch Clin Exp Ophthalmol*. 1987;225:254–258.
49. Tornambe PE, Hilton GF. Pneumatic retinopexy. A multicenter randomized controlled clinical trial comparing pneumatic retinopexy with scleral buckling. The Retinal Detachment Study Group. *Ophthalmology*. 1989;96:772–783 [discussion 784].
50. Gilca M, Duval R, Goodyear E, Olivier S, Cordahi G. Factors associated with outcomes of pneumatic retinopexy for rhegmatogenous retinal detachments: a retrospective review of 422 cases. *Retina*. 2014;34:693–699.
51. Hatef E, Sena DF, Fallano KA, Crews J, Do DV. Pneumatic retinopexy versus scleral buckle for repairing simple rhegmatogenous retinal detachments. *Cochrane Database Syst Rev*. 2015;(5) [CD008350].
52. McAllister IL, Meyers SM, Zegarra H, Gutman FA, Zakov ZN, Beck GJ. Comparison of pneumatic retinopexy with alternative surgical techniques. *Ophthalmology*. 1988;95:877–883.
53. Tornambe PE. Pneumatic retinopexy: the evolution of case selection and surgical technique: a twelve-year study of 302 eyes. *Trans Am Ophthalmol Soc*. 1997;95:551–578.
54. Williams PD, Hariprasad SM. Evolving trends in primary retinal detachment repair: microincisional vitrectomy and the role of OCT. *Ophthalmic Surg Lasers Imaging Retina*. 2014;45:268–272.
55. Sharma T, Badrinath SS, Mukesh BN, et al. A multivariate analysis of anatomic success of recurrent retinal detachment treated with pneumatic retinopexy. *Ophthalmology*. 1997;104:2014–2017.
56. Petrushkin HJ, Elgohary MA, Sullivan PM. Rescue pneumatic retinopexy in patients with failed primary retinal detachment surgery. *Retina*. 2015;35(9):1851–1859.

57. Chignell AH. Retinal detachment surgery without cryotherapy. *Trans Ophthalmol Soc U K*. 1977;97:30–32.
58. Chignell AH, Wong D. The role of induced choroidal retinal adhesion in retinal detachment surgery. *Trans Ophthalmol Soc U K*. 1986;105(Pt 5):580–582.
59. Fetkenhour CL, Hauch TL. Scleral buckling without thermal adhesion. *Am J Ophthalmol*. 1980;89:662–666.
60. Kreissig I, Simader E, Fahle M, Lincoff H. Visual acuity after segmental buckling and non-drainage: a 15-year follow-up. *Eur J Ophthalmol*. 1995;5:240–246.
61. Deramo VA, Haupert CL, Fekrat S, Postel EA. Hypotony caused by scleral buckle erosion in Marfan syndrome. *Am J Ophthalmol*. 2001;132:429–431.
62. Singh M. Surgery of aphakic retinal detachment. *Br J Ophthalmol*. 1988;72:820–822.
63. Ho CL, Chen KJ, See LC. Selection of scleral buckling for primary retinal detachment. *Ophthalmologica*. 2002;216:33–39.
64. Ah-Fat FG, Sharma MC, Majid MA. Trends in vitreoretinal surgery at a tertiary referral centre: 1987 to 1996. *Br J Ophthalmol*. 1999;83:396–398.
65. Minihan M, Tanner V, Williamson TH. Primary rhegmatogenous retinal detachment: 20 years of change. *Br J Ophthalmol*. 2001;85:546–548.
66. Wilkinson CP, Bradford RH Jr. Complications of draining subretinal fluid. *Retina*. 1984;4:1–4.
67. Packer AJ, Maggiano JM, Aaberg TM, Meredith TA, Reeser FH, Kingham JD. Serous choroidal detachment after retinal detachment surgery. *Arch Ophthalmol*. 1983;101:1221–1224.
68. Smiddy WE, Loupe D, Michels RG, Enger C, Glaser BM, deBustros S. Extraocular muscle imbalance after scleral buckling surgery. *Ophthalmology*. 1989;96:1485–1489 [discussion 1489-1490].
69. Hilton GF, Wallyn RH. The removal of scleral buckles. *Arch Ophthalmol*. 1978;96:2061–2063.
70. Carter JB, Michels RG, Glaser BM, De Bustros S. Iatrogenic retinal breaks complicating pars plana vitrectomy. *Ophthalmology*. 1990;97:848–853 [discussion 854].

71. de Bustros S, Thompson JT, Michels RG, Enger C, Rice TA, Glaser BM. Nuclear sclerosis after vitrectomy for idiopathic epiretinal membranes. *Am J Ophthalmol*. 1988;105:160–164.
72. Cowley M, Conway BP, Campochiaro PA, Kaiser D, Gaskin H. Clinical risk factors for proliferative vitreoretinopathy. *Arch Ophthalmol*. 1989;107:1147–1151.
73. Brazitikos PD, D'Amico DJ, Tsinopoulos IT, Stangos NT. Primary vitrectomy with perfluoro-n-octane use in the treatment of pseudophakic retinal detachment with undetected retinal breaks. *Retina*. 1999;19:103–109.
74. Miki D, Hida T, Hotta K, Shinoda K, Hirakata A. Comparison of scleral buckling and vitrectomy for retinal detachment resulting from flap tears in superior quadrants. *Jpn J Ophthalmol*. 2001;45:187–191.
75. Devereaux PJ, Bhandari M, Clarke M, et al. Need for expertise based randomised controlled trials. *BMJ*. 2005;330:88.
76. Heimann H, Bornfeld N, Bartz-Schmidt UK, Hilgers RD, Heussen N. Anaylsis of the surgeon factor in the treatment results of rhegmatogenous retinal detachment in the "Scleral Buckling versus Primary Vitrectomy in Rhegmatogenous Retinal Detachment Study".*Klin Monatsbl Augenheilkd*. 2009;226:991–998.
77. Gartry DS, Chignell AH, Franks WA, Wong D. Pars plana vitrectomy for the treatment of rhegmatogenous retinal detachment uncomplicated by advanced proliferative vitreoretinopathy. *Br J Ophthalmol*. 1993;77:199–203.
78. Wickham L, Connor M, Aylward GW. Vitrectomy and gas for inferior break retinal detachments: are the results comparable to vitrectomy, gas, and scleral buckle? *Br J Ophthalmol*. 2004;88:1376–1379.
79. Ryan SJ Jr. Cystoid maculopathy in phakic retinal detachment procedures. *Am J Ophthalmol*. 1973;76:519–522.
80. Kimball RW, Morse PH, Benson WE. Cystoid macular edema after cryotherapy. *Am J Ophthalmol*. 1978;86:572–573.
81. Jaccoma EH, Conway BP, Campochiaro PA. Cryotherapy causes extensive breakdown of the blood–retinal barrier: a comparison with argon laser photocoagulation. *Arch*

Ophthalmol. 1985;103:1728–1730.
82. Veckeneer M, Van Overdam K, Bouwens D, et al. Randomized clinical trial of cryotherapy versus laser photocoagulation for retinopexy in conventional retinal detachment surgery. *Am J Ophthalmol*. 2001;132:343–347.
83. Curtin VT, Fujino T, Norton EW. Comparative histopathology of cryosurgery and photocoagulation. Observations on the advantages of cryosurgery in retinal detachment operations. *Arch Ophthalmol*. 1966;75:674–682.
84. Bonnet M, Fleury J, Guenoun S, Yaniali A, Dumas C, Hajjar C. Cryopexy in primary rhegmatogenous retinal detachment: a risk factor for postoperative proliferative vitreoretinopathy? *Graefes Arch Clin Exp Ophthalmol*. 1996;234:739–743.
85. Grizzard WS, Hilton GF, Hammer ME, Taren D. A multivariate analysis of anatomic success of retinal detachments treated with scleral buckling. *Graefes Arch Clin Exp Ophthalmol*. 1994;232:1–7.
86. Kon CH, Asaria RH, Occleston NL, Khaw PT, Aylward GW. Risk factors for proliferative vitreoretinopathy after primary vitrectomy: a prospective study. *Br J Ophthalmol*. 2000;84:506–511.
87. Heimann H. Primary 25- and 23-gauge vitrectomy in the treatment of rhegmatogenous retinal detachment – advancement of surgical technique or erroneous trend. *Klin Monatsbl Augenheilkd*. 2008;225:947–956.
88. Lai MM, Ruby AJ, Sarrafizadeh R, et al. Repair of primary rhegmatogenous retinal detachment using 25-gauge transconjunctival sutureless vitrectomy. *Retina*. 2008;28:729–734.
89. Figueroa MS, Contreras I, Noval S, Group PS. Anatomic and visual outcomes of 23-G vitrectomy without scleral buckling for primary rhegmatogenous retinal detachment. *Eur J Ophthalmol*. 2013;23:417–422.
90. Hikichi T, Kosaka S, Takami K, et al. Surgical outcomes of 23- and 20-gauge vitrectomies for rhegmatogenous retinal detachment associated with posterior vitreous detachment. *Ophthalmic Surg Lasers Imaging*. 2011;42:376–382.

91. Dell'Omo R, Barca F, Tan HS, Bijl HM, Oberstein SY, Mura M. Pars plana vitrectomy for the repair of primary, inferior rhegmatogenous retinal detachment associated to inferior breaks. A comparison of a 25-gauge versus a 20-gauge system. *Graefes Arch Clin Exp Ophthalmol*. 2013;251:485–490.
92. Miller DM, Riemann CD, Foster RE, Petersen MR. Primary repair of retinal detachment with 25-gauge pars plana vitrectomy. *Retina*. 2008;28:931–936.
93. Mura M, Tan SH, De Smet MD. Use of 25-gauge vitrectomy in the management of primary rhegmatogenous retinal detachment. *Retina*. 2009;29:1299–1304.
94. Johnson Z, Ramsay A, Cottrell D, Mitchell K, Stannard K. Triple cycle audit of primary retinal detachment surgery. *Eye (Lond)*. 2002;16:513–518.
95. Thompson JA, Snead MP, Billington BM, Barrie T, Thompson JR, Sparrow JM. National audit of the outcome of primary surgery for rhegmatogenous retinal detachment. I. Sample and methods. *Eye (Lond)*. 2002;16:766–770.
96. Wong CW, Wong WL, Yeo IY, et al. Trends and factors related to outcomes for primary rhegmatogenous retinal detachment surgery in a large asian tertiary eye center. *Retina*. 2014;34:684–692.
97. Jackson TL, Donachie PH, Sallam A, Sparrow JM, Johnston RL. United Kingdom National Ophthalmology Database study of vitreoretinal surgery: report 3, retinal detachment. *Ophthalmology*. 2014;121:643–648.
98. Borhani H, Peyman GA, Rahimy MH, Thompson H. Suppression of experimental proliferative vitreoretinopathy by sustained intraocular delivery of 5-FU. *Int Ophthalmol*. 1995;19:43–49.
99. Wilkinson CP. Wanted: optimal data regarding surgery for retinal detachment. *Retina*. 1998;18:199–201.

110

Prevention of Retinal Detachment

C.P. Wilkinson

Introduction

Rhegmatogenous retinal detachment continues to be an important cause of reduced visual acuity and blindness. In consecutive series, initial surgical attempts to reattach the retina currently fail in

approximately 10–20% of cases, and reoperations are unsuccessful in as many as 5% of cases.[1–3] Anatomic success is significantly less common in consecutive series of eyes with features suggesting an increased risk of proliferative vitreoretinopathy (PVR).[4] Following anatomically successful surgery, visual acuity returns to 20/50 or better in only approximately 50% of cases.[5] Thus, the prevention of retinal detachment is a worthy goal, and a variety of prophylactic methods have been investigated since the 1920s, when Jules Gonin first described the pathogenesis and treatment of this previously incurable disorder. However, despite a long-standing interest in the ophthalmologic community regarding prophylactic therapy, there have been no optimal clinical trials to test the legitimate value of any form of preventive treatment.[6–9]

Vitreous liquefaction and a retinal break are prerequisites for rhegmatogenous retinal detachment, and the usual pathologic sequence is vitreous liquefaction followed by some degree of posterior vitreous detachment (PVD). Although PVDs were usually considered to be "total" when they occurred, it is now apparent that from a quarter to a half of symptomatic patients may have subtotal PVDs with a continued risk of tears even after the symptomatic event.[10,11] Regardless, vitreoretinal traction at the site of a vitreoretinal adhesion results in the production of a retinal tear (Fig. 110.1). Alternatively, traction may be exerted upon areas of lattice degeneration containing atrophic retinal holes. Continued vitreoretinal traction near retinal breaks appears to be necessary to cause the vast majority of clinical retinal detachments. Thus, retinal detachment might be avoided by (1) preventing vitreous liquefaction and associated PVD; (2) relieving vitreoretinal traction; or (3) creating a chorioretinal adhesion around vitreoretinal adhesions and retinal breaks.

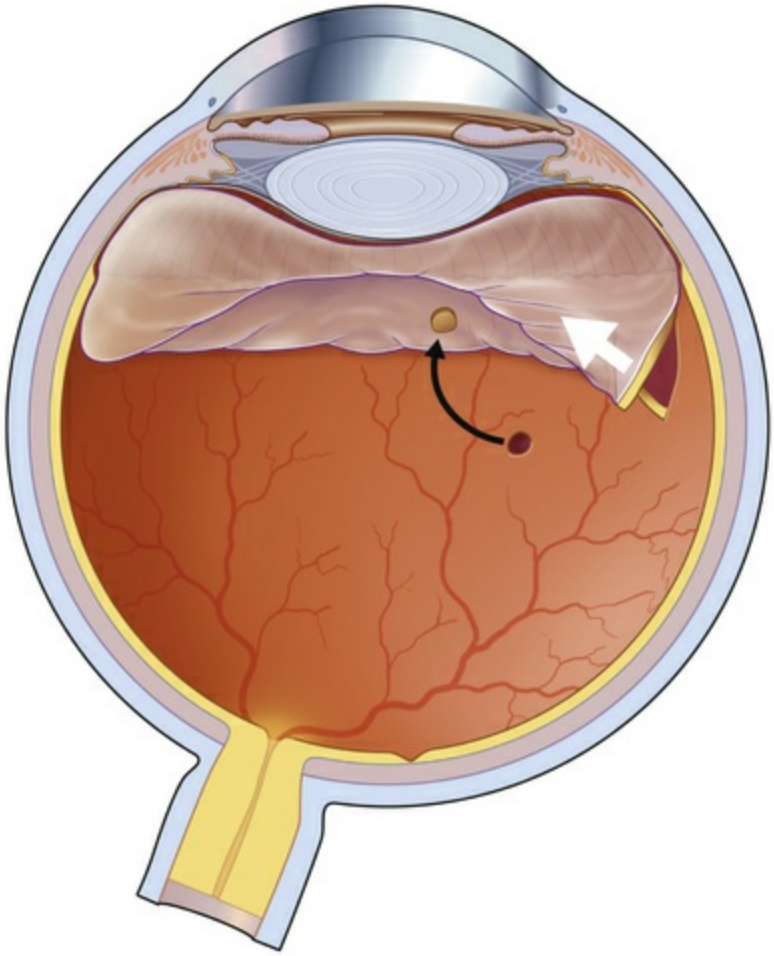

FIG. 110.1 Traction on the retina (*white arrow*) at a site of abnormal vitreoretinal adhesion has created a retinal tear. If left untreated, liquid vitreous posterior to the vitreous gel will pass through this retinal break into the subretinal space, creating a retinal detachment. Operculated tears typically no longer have traction forces upon them (*black arrow*) unless there is a nearby vitreoretinal adhesion. (Reprinted from Brinton D, Wilkinson CP. Retinal detachment: Principles and practice. 3rd ed. New York: Oxford University Press with the cooperation of the American Academy of Ophthalmology. © 2009, with permission from Oxford University Press.)

No means are available to prevent vitreous liquefaction and later PVD in most eyes, although maintaining an intact posterior lens capsule after extracapsular cataract surgery may reduce or delay these changes.[12] Vitreoretinal traction can be relieved by vitrectomy or by scleral buckling. However, prophylactic vitrectomy is not performed because there are technical difficulties in completely removing the peripheral vitreous gel, and it is relatively hazardous.

Scleral buckling is only rarely employed, such as in particularly high-risk cases in which a nontraumatic giant retinal tear has already occurred in a fellow eye[13] or in cases of posterior segment open-globe injuries.[14] Thus, the primary method of preventing retinal detachment involves the use of laser photocoagulation or cryotherapy to create a chorioretinal adhesion around visible sites of vitreoretinal adhesion and retinal breaks, or alternatively around 360° of the peripheral retina including "normal" zones. Although this is frequently successful in sealing the treated lesion and preventing it from causing a clinical retinal detachment, the genuine value of such therapy related to simple observation remains unclear in most situations since most visible asymptomatic retinal breaks and vitreoretinal degenerative lesions do not cause retinal detachments. Instead, breaks causing detachment more frequently occur in regions of the peripheral retina that appear normal before PVD.[6,7] In addition, relatively extensive prophylactic therapy may cause vitreous changes that increase the chances of subsequent vitreoretinal traction and retinal detachment.[6,15]

Risk Factors for Retinal Detachment

In any eye with visible retinal breaks or vitreoretinal adhesive lesions that predispose to retinal detachment, a number of additional factors are considered to be associated with a relatively high risk of subsequent retinal detachment (Table 110.1). Symptoms and signs of acute PVD place an eye at particularly high risk. Additional factors include a variety of hereditary, congenital, acquired, and iatrogenic problems.

TABLE 110.1

Risk Factors for Rhegmatogenous Retinal Detachment

Hereditary/congenital/developmental/degenerative
Male gender
Hereditary vitreoretinopathies
Myopia
Lattice degeneration
Cystic retinal tuft
Degenerative retinoschisis
Retinal breaks
Prior ocular surgery

• Aphakia/pseudophakia • Nd:YAG posterior capsulotomy • Other surgery involving vitreous gel
Prior ocular trauma
Inflammatory
• CMV retinitis • Acute retinal necrosis
Other
• Fellow-eye nontraumatic retinal detachment

In evaluating the natural history or risk of retinal detachment in these cases, particular attention must be paid to the way in which both natural history and postoperative data, regarding a variety of retinal lesions, have been collected.[16] The risk of retinal detachment is substantially different among subgroups of eyes, a fact that influences interpretation of both natural history data and treatment results. For example, since an acute PVD is the primary cause of most retinal detachments, and since most retinal tears occur during or soon after PVD, it is likely that eyes without a PVD have a higher risk of later retinal detachment than eyes with a history of prior PVD and no subsequent retinal breaks, regardless of additional risk factors.[17] Similarly, vitreous liquefaction and PVD occur with greater frequency in older patients and in myopic and pseudophakic eyes.[18,19] Thus, data regarding lesions in otherwise normal, young, nonmyopic eyes are not comparable with data from cases with other risk factors that greatly increase the likelihood of PVD. Since more than one factor is often present, data analysis is difficult if all features are not recorded. For example, myopic pseudophakic eyes with lattice degeneration and with a history of retinal detachment in the fellow eye have a substantially greater risk of retinal detachment than otherwise normal eyes with lattice degeneration. No prospective randomized trials of therapy to prevent retinal detachment have been performed.[6–9] The few published studies of treated and untreated comparable eyes have been retrospective, and most reports regarding prophylactic therapy have simply described results of a treatment series.

This chapter briefly discusses published outcomes regarding both the natural course of lesions that predispose an eye to retinal detachment and results of prophylactic therapy for these retinal breaks and vitreoretinal adhesive lesions. The topic of "subclinical retinal detachment" (for one definition, see Fig. 110.4) will not be

discussed as a separate entity because of the nonspecific nature of the term. This chapter distinguishes symptomatic from asymptomatic cases and is organized according to the type of retinal break or vitreoretinal adhesive disorder and also according to the presence of other high-risk factors. A brief discussion of treatment methods precedes the review of treatment results and complications.

Symptomatic Eyes

Patients are considered symptomatic if they describe increased vitreous floaters and/or photopsia, which are typically associated with an acute posterior vitreous detachment. Approximately 15% of eyes with a symptomatic PVD develop retinal tears of various types.[20–22] The risk of retinal tears is directly related to the amount of vitreous hemorrhage associated with symptoms, and the finding of pigmented cells in the vitreous is a sign associated with a particularly high chance of associated retinal tear(s).[23] In symptomatic eyes, retinal tears associated with persistent vitreoretinal traction are especially likely to cause retinal detachment, and the likelihood is even higher in cases with additional high-risk factors.

Retinal tears resulting from a symptomatic PVD should be distinguished from preexisting retinal breaks detected after the PVD but not caused by it. Thus, atrophic retinal holes within areas of lattice degeneration are not considered "symptomatic," even if they were first observed during an examination prompted by symptoms of an acute PVD. Symptomatic retinal tears are subdivided into those with persistent vitreoretinal traction and those in which all traction in the region of the retinal defect has disappeared (Fig. 110.1).

Tears With Persistent Vitreoretinal Traction

Most symptomatic tears with persistent vitreoretinal traction are horseshoe-shaped and have a high risk of causing clinical retinal detachment. Rarely, a retinal tear with a free operculum may have persistent vitreoretinal traction as a result of a residual vitreoretinal

adhesion near the retinal break, most frequently at the location of a retinal blood vessel (Fig. 110.2).

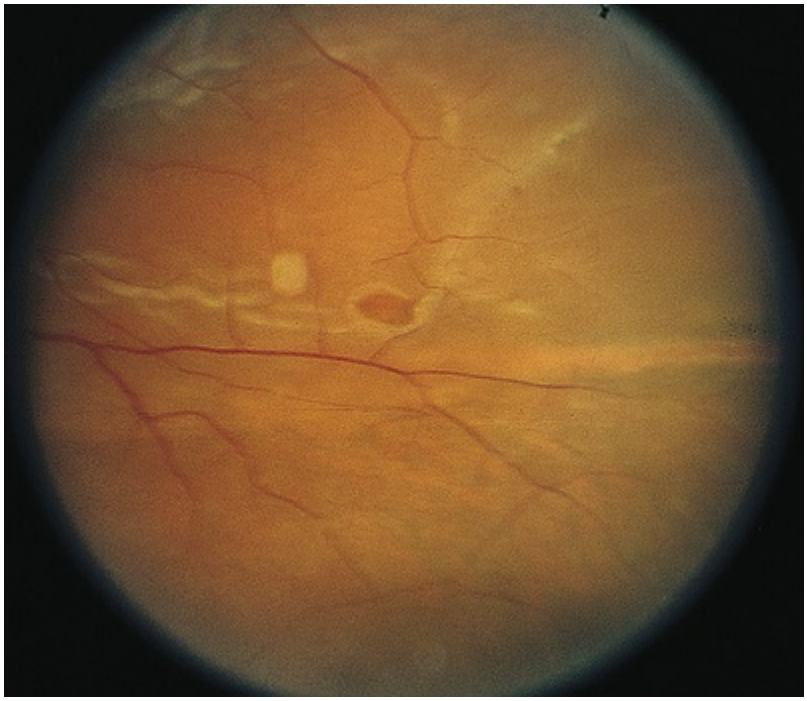

FIG. 110.2 Superior temporal retinal detachment, left eye, resulting from a single operculated retinal break. The minimal movement of the operculum during major ocular saccades indicated that persistent vitreoretinal adhesions were present in the vicinity of the retinal hole.

Horseshoe-Shaped Tears

Untreated symptomatic retinal tears with persistent vitreoretinal traction have been reported to cause retinal detachment in at least 33–55% of cases (Table 110.2).[24,27] Treatment of this type of break substantially reduces the risk of retinal detachment (Table 110.2),[24] and immediate therapy for these lesions is indicated to prevent an accumulation of subretinal fluid.[7,9,25–30] A chorioretinal adhesion is created in flat retina immediately adjacent to localized subretinal fluid (Fig. 110.3). Reviews of treatment techniques have been provided elsewhere in the literature,[31] and these are briefly discussed later in this chapter.

TABLE 110.2

Progression of Symptomatic Retinal Breaks to Retinal Detachment (RD)

Type of Break	Authors	Cases (*n*)	RD (%)
Treated horseshoe-shaped tears	Shea et al. 1974[24]	48	4.2
	Robertson and Priluck 1979[15]	88	7.8
	Verdaguer and Vaismon 1979[25]	74	5.4
	Pollack and Oliver 1981[26]	74	1.4
Untreated horseshoe-shaped tears	Colyear and Pischel 1960[27]	20	55
	Shea et al. 1974[24]	21	48
Treated operculated breaks	Robertson et al. 1981[28]	47	0
Untreated operculated breaks	Colyear and Pischel 1960[27]	22	4.5[a]
	Davis 1973[29]	6	17[a]

[a]A single break in each series exhibited persistent vitreoretinal traction upon a nearby retinal vessel and caused a subsequent retinal detachment.

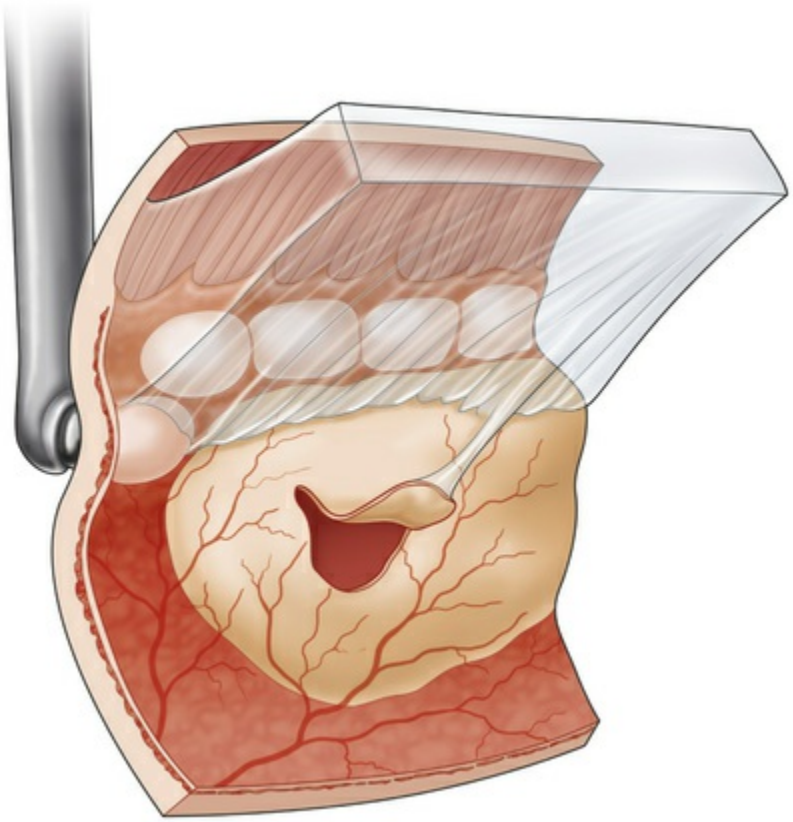

FIG. 110.3 Cryotherapy is placed to surround and demarcate a peripheral, symptomatic, horseshoe-shaped tear with a subclinical retinal detachment. Photocoagulation can often be applied around the posterior portion of the detachment, but cryotherapy

may be needed anteriorly if laser treatment cannot be extended into the vitreous base. (From Brinton D, Wilkinson CP. Retinal detachment: Principles and practice. 3rd ed. New York: Oxford University Press with the cooperation of the American Academy of Ophthalmology. © 2009, with permission from Oxford University Press.)

Round Tears

The percentage of operculated retinal tears that are associated with persistent vitreoretinal traction in the vicinity of the retinal break is unknown, but it is quite low. Only two symptomatic operculated retinal breaks have been reported to progress to retinal detachment, and both were associated with persistent vitreoretinal traction on a nearby retinal vessel.[27,29] In unusual cases in which an operculated retinal hole is the only retinal break associated with a clinical retinal detachment, it is presumed that anomalous persistent vitreoretinal adhesions are located in the vicinity of the retinal tear (see Fig. 110.2). Failures following treatment of operculated retinal holes have not been reported (Table 110.2).

Tears Unassociated With Persistent Vitreoretinal Traction

Retinal breaks and vitreoretinal adhesions unassociated with vitreoretinal traction are unlikely to progress to retinal detachment.

Retinal Tears

Symptomatic operculated retinal tears unassociated with persistent vitreoretinal traction in the vicinity of the retinal break have not been reported to progress to clinical retinal detachment (Table 110.2). Similarly, although large numbers of these breaks have been treated prophylactically, there are no reports in the literature of a treatment failure (Table 110.2). Treatment of this type of retinal break appears to be unnecessary unless the possibility of persistent vitreoretinal traction cannot be excluded.[9]

Retinal Holes and Precursors of Retinal Detachment

Eyes with symptoms and signs of acute PVD frequently contain

atrophic retinal breaks that are not due to acute vitreoretinal traction. For the purposes of this discussion, these lesions are considered to be preexisting and not symptomatic.[21] Similarly, precursors of retinal detachment, including lattice degeneration, cystic retinal tufts, and age-related retinoschisis, are managed as if they were originally discovered in asymptomatic eyes.

Asymptomatic Eyes Without High-Risk Factors

Nonmyopic phakic eyes in patients without a family history of retinal detachment and without previous nontraumatic retinal detachment in the fellow eye are unlikely to develop retinal detachment, regardless of the presence of vitreoretinal pathology. Nevertheless, prophylactic therapy has sometimes been recommended to treat visible precursors of retinal detachment and also asymptomatic retinal breaks.

Vitreoretinal Precursors of Retinal Breaks

Important precursors of retinal breaks and detachment include lattice degeneration, cystic retinal tufts, and degenerative retinoschisis. Of these, lattice degeneration is clearly the most important. Both lattice degeneration and cystic retinal tufts can be sites of retinal tears resulting from vitreoretinal traction at the time of PVD. Atrophic retinal holes commonly occur within areas of lattice degeneration and also in the outer layers of degenerative retinoschisis. However, these holes are a relatively infrequent cause of progressive retinal detachment.

Lattice Degeneration

Lattice degeneration is present in approximately 30% of retinal detachments, and approximately 94% of these detachments occur in primary (nonfellow) eyes.[6]

Because lattice lesions are visible and occur in approximately 8% of the population, they have commonly been considered as candidates for prophylactic therapy. However, Byer's natural

history study of 276 patients and 423 involved eyes, followed for an average of almost 11 years, indicated that lattice lesions in phakic nonfellow eyes were not particularly dangerous.[32] At the end of the follow-up period, atrophic retinal holes were present in 150 (35%) eyes. Subclinical retinal detachments, defined as subretinal fluid extending more than one disc diameter (DD) from the break but not posterior to the equator (Fig. 110.4), were observed in 10 of the eyes with holes. In six of these eyes, the subclinical detachment developed during the observation period, whereas four eyes exhibited the changes at the initial examination. Only one subclinical detachment was considered in need of treatment after a small asymptomatic posterior extension of subretinal fluid.

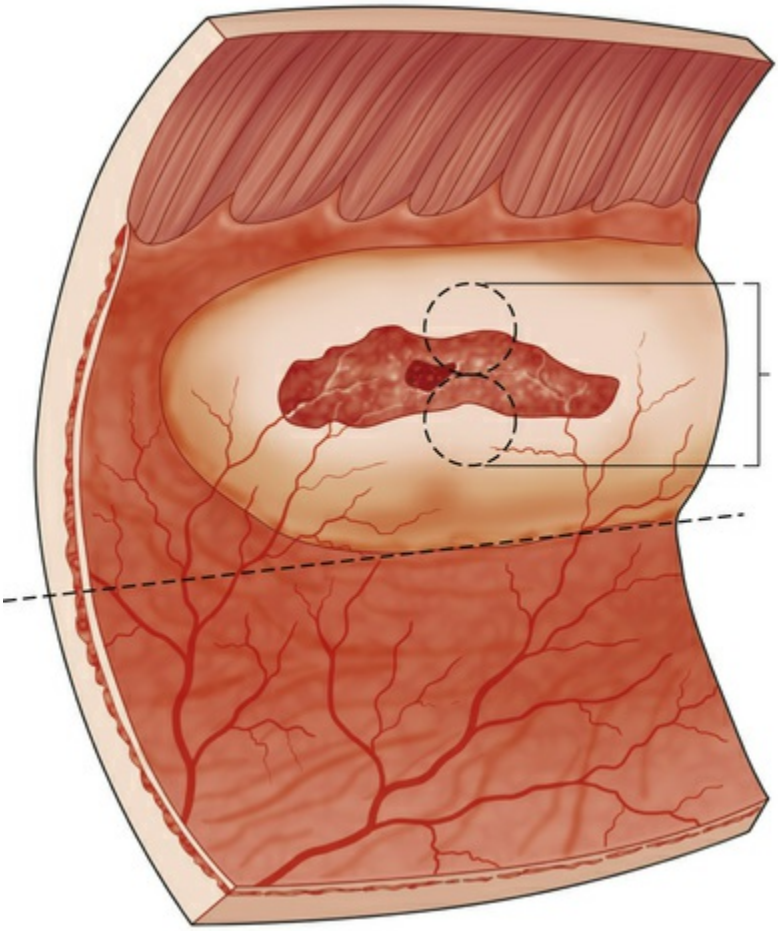

FIG. 110.4 Subclinical detachments are defined as those with fluid extending more than one disc diameter on all sides of the retinal break, but the detachment does not extend posterior to the equator. (From Brinton D, Wilkinson CP. Retinal detachment: Principles and practice. 3rd ed. New York:

Four asymptomatic tractional retinal tears were observed in three of these 423 eyes at the initial examination, and symptomatic tractional tears without clinical detachment developed in five additional eyes during follow-up periods of 1.5–18 years.[32] Three of five symptomatic and all asymptomatic breaks occurred adjacent to lattice lesions. All symptomatic breaks were successfully treated; no asymptomatic tractional tears were treated, and none changed over follow-up periods of 7, 10, and 15 years.

Clinical retinal detachments developed in three of the 423 eyes.[32] Two were due to round retinal holes in lattice lesions of patients in their mid-20s, and one was due to a symptomatic tractional tear. These figures clearly indicate that patients with lattice degeneration in a phakic nonfellow eye should not be treated prophylactically unless symptoms occur.[9] However, retinal detachments associated with vitreoretinal traction upon lattice lesions containing atrophic retinal holes are relatively common in eyes with significant amounts of myopia.[33–35] Importantly, a discussion regarding self-examination of peripheral visual fields and periodic follow-up examinations are in order in myopic patients to reduce chances of macular involvement by slowly progressive detachments resulting from round holes in lattice lesions.

Cystic Retinal Tufts

Retinal tears at sites of cystic retinal tufts may be responsible for as many as 10% of clinical retinal detachments associated with posterior vitreous detachment,[36] and they are also associated with asymptomatic small horseshoe-shaped tears and minimal subretinal fluid in the absence of PVD.[37] Byer[36] calculated the chances of clinical retinal detachment in eyes with cystic retinal tufts to be one in 357, and these lesions are not worthy of prophylactic therapy in otherwise normal eyes.

Degenerative Retinoschisis

Clinical retinal detachments occur in association with degenerative retinoschisis in less than 2%[38] to up to 6%[39] of consecutive retinal

detachment cases, whereas the reported prevalence of retinoschisis ranges from 1.65% to 7% among persons age 40 years and older.[38] However, since most cases are asymptomatic and require extensive examination of the peripheral retina, literal retinoschisis is frequently missed on routine examination. However, particularly when it extends posterior to the equator, it is confused with a retinal detachment, and the topic is discussed in detail in Chapter 100.

The presence of retinoschisis, especially when associated with outer layer breaks, has sometimes been considered an indication for prophylactic therapy. However, a natural course study of 218 eyes in 123 patients demonstrated no clinical retinal detachments during a follow-up period averaging 9.1 years,[39] and in a more recent report[40] this complication developed in only 2.2% of cases followed for approximately 14 years. The vast majority of small subclinical detachments that develop in association with outer layer breaks remain small, and prophylactic therapy appears to be indicated only in selected cases in which there is obvious significant progression of subretinal fluid posterior to the equator.[41]

Asymptomatic Retinal Breaks

In phakic nonfellow eyes, asymptomatic retinal breaks that are routinely discovered during an evaluation of the peripheral retina are extremely unlikely to lead to clinical retinal detachment, even if they are flap tears and even if posterior vitreous detachment occurs.[42] During a follow-up period averaging 11 years, asymptomatic retinal breaks in 235 eyes of 196 patients were studied and horseshoe-shaped tears were present in 45 cases.[42] Acute PVD occurred in nine eyes without adversely affecting the preexisting breaks, although new horseshoe-shaped tears developed in three cases, and these were promptly treated. Subclinical retinal detachments were observed in 19 (8%) eyes. Modest extension of subretinal fluid required therapy in two of these cases, and in a third case a peripheral clinical retinal detachment slowly developed after 14 years of observation.

Prophylactic therapy for asymptomatic retinal breaks in phakic nonfellow eyes is usually not recommended.[9] An occasionally

observed exception to this rule is an inferior retinal dialysis.

These breaks can cause slowly progressive retinal detachments that frequently become symptomatic only after macular involvement.[43]

Asymptomatic Nonfellow Eyes With High-Risk Factors

Myopia and previous cataract extraction are considered as additional risk factors in patients with vitreoretinal lesions believed to predispose a nonfellow eye to retinal detachment. In addition, a positive family history for retinal detachment is considered important by some authors. The existence of any of these factors in nonfellow eyes has been associated with an increased enthusiasm for prophylactic therapy, despite the absence of appropriate supporting data.

Myopic Nonfellow Eyes

Myopia is obviously associated with an increased risk of retinal detachment, and there is a direct correlation between amount of myopia and rate of retinal detachment.[38,44] Lattice degeneration associated with retinal holes did not correlate with degree of myopia in the natural course study of Byer,[32] although most slowly progressive clinical retinal detachments associated with lattice degeneration and an absence of extensive posterior vitreous detachment occur in young myopic patients,[33–35,38] as noted above. There appears to be no increased value for treatment of myopic eyes with lattice degeneration in nonfellow eyes, and it is noteworthy that the small favorable effect of preventive treatment of lattice lesions in phakic fellow eyes could not be demonstrated if the degree of myopia exceeded 6 diopters.[45]

Cystic retinal tufts and degenerative retinoschisis are not more common in myopic eyes, and prophylactic therapy is not recommended in the absence of a progressive subclinical detachment.

Asymptomatic retinal breaks are more common in myopic eyes

than in emmetropic or hyperopic cases.[5] However, clinical retinal detachments in these cases are rare in the absence of new symptoms, and prophylactic treatment is usually not advised in nonfellow eyes.

Aphakic and Pseudophakic Nonfellow Eyes

Removal of the crystalline lens is associated with a substantial increase in the rate of later retinal tears and detachments,[46] regardless of the method of cataract surgery, and this probably is due to vitreous changes in the operated eye, especially the increased incidence of PVD.[19,47,48] An intact posterior lens capsule appears to be associated with a relatively reduced rate of retinal detachment following cataract surgery, whereas Nd:YAG capsulotomy is clearly associated with an increased risk of subsequent detachment.[12]

The natural course of lattice degeneration in nonphakic nonfellow eyes is not well documented, and results of preventive treatment in these particular cases are not available. Similarly, meaningful information regarding cystic retinal tufts and degenerative retinoschisis has not been published. Treatment of these lesions in nonfellow eyes is not advised.

Asymptomatic retinal breaks in nonfellow nonphakic eyes or eyes undergoing cataract surgery have sometimes been regarded as an indication for prophylactic therapy. However, Friedman et al.[49] followed 18 retinal breaks in nonmyopic aphakic eyes for 3–7 years, and none detached. Hyams et al.[50] studied 103 myopic aphakic eyes and discovered 25 asymptomatic retinal breaks in 19 eyes. Although six of the 25 were horseshoe-shaped tears, later retinal detachment occurred in no cases. More thorough reviews of the literature regarding the natural course of asymptomatic nonphakic retinal breaks and therapy for them have been published elsewhere,[6,31] and there are not sufficient data to provide firm guidelines for management of asymptomatic retinal breaks in nonfellow eyes that are nonphakic or scheduled for cataract surgery. Treatment of horseshoe-shaped tears in these cases appears to be frequently recommended despite the lack of appropriate information in the literature.[7,9]

Family History of Retinal Detachment

Heredity clearly influences the chances of retinal detachment, particularly in families with vitreoretinal degenerative disorders such as Stickler syndrome. Prophylactic therapy is frequently considered in these cases, particularly if retinal detachment has occurred in the primary eye. However, no studies have properly stratified the several high-risk factors associated with retinal detachment and evaluated the natural course and the effects of prophylactic therapy in patients with a familial predisposition to retinal detachment and no detachment in either eye.

Asymptomatic Patients With Retinal Detachment in the Fellow Eye

Pathologic vitreoretinal changes often occur bilaterally, and patients with retinal detachment in one eye have a significantly increased risk of retinal detachment in the other eye.[51] This risk has been estimated as ranging from as low as 9% to as high as 40%.[31] Thus attempts to prevent retinal detachment in the second eye have received considerable attention, particularly if the outcome of reattachment surgery was poor in the first. Prospective randomized studies have not been performed, but retrospective data regarding precursors of retinal detachments and asymptomatic retinal breaks have been published.[7] These can be further categorized as phakic and nonphakic fellow eyes.

Asymptomatic Phakic Fellow Eyes

As noted before, phakic fellow eyes have a lower risk of subsequent retinal detachment than comparable pseudophakic eyes. Treatment has been considered for both vitreoretinal precursors of retinal detachment and asymptomatic retinal breaks.

Precursors of Retinal Breaks

Lattice degeneration is three times more common in eyes in which a retinal detachment associated with lattice degeneration has occurred than it is in the general population,[6] and this entity has

been the most frequently studied indication for prophylactic therapy in fellow eyes. The widely quoted study of Folk et al.[45] retrospectively studied 388 consecutive cases in which phakic retinal detachment associated with lattice degeneration occurred in one eye and lattice degeneration with and without retinal holes was present in the second eye. During an average follow-up period of over 7 years, new retinal breaks or detachments occurred in 31 (20%) untreated eyes (Table 110.3). New tears with retinal detachment developed in nine eyes (5.1%), and new tears without detachment developed in 10 cases. In 10 eyes, new holes developed within areas of lattice degeneration, and atrophic retinal breaks occurred in areas distant from lattice lesions in the remaining two cases.

TABLE 110.3

Outcomes for Phakic Fellow Eyes With Lattice Degeneration

Group	Eyes (*n*)	Detachment (%)	New Tears (%)
Untreated	151	5.9	12.6
Partial treatment	73	6.8	16.4
Full treatment	164	1.8	4.9

Reproduced with permission from Folk JC, Arrindell EL, Klugman MR. The fellow eye of patients with phakic lattice detachment. Ophthalmology 1989;96:72–9.

Folk and coworkers[45] reported a reduction in the incidence of new retinal tears and detachments in eyes receiving prophylactic therapy for all lattice lesions (Table 110.3). New tears without detachment occurred in five (3.0%) of these fully treated eyes. Retinal detachment occurred in three additional cases (1.8%), compared with 5.1% in the 151 untreated phakic fellow eyes. The small beneficial effect of treating all lattice lesions was apparent when follow-up periods of 3, 5, and 7 years were analyzed separately. Importantly, the beneficial effect was statistically significant for all patient subgroups, *except* in eyes with myopia of 6 diopters or more and in eyes with both high myopia and more than 6 clock-hours of lattice degeneration. In these subgroups, treatment did not reduce the risk of retinal tears or detachment. Conversely, no detachments occurred after full treatment in eyes with less than 6 clock-hours of lattice degeneration or with less than 1.25 diopters of myopia.

In a subsequent evaluation of the same data, Folk et al[52] reported that new horseshoe-shaped tears developed in areas unassociated with lattice degeneration in approximately 30% of treated cases, and Byer[6] has estimated that as many as 58% of retinal detachments in eyes with lattice degeneration arise in areas that exhibit no visible vitreoretinal abnormalities (Fig. 110.5). Because of this reality, some surgeons have recommended prophylactic therapy featuring the production of laser or cryotherapy burns over 360° of the peripheral retina (Figs. 110.6 and 110.7).[6,31] However, the precise indications, intraocular findings, long-term results, and complications of this form of therapy have not been thoroughly described, and remarkably different success rates have been reported. Haut et al.[53] described 109 phakic fellow eyes followed for a minimum of 5 years, and only one retinal detachment and two additional tears occurred posterior to the circumferential chorioretinal adhesion. However, in another study,[54] retinal detachment occurred in five of 10 cases of Stickler syndrome within 15 months of 360° prophylactic therapy. Byer[6] tabulated and reviewed data from 15 reports advocating such treatment, and he concluded that this form of treatment appeared to be both ineffective in preventing subsequent detachment and dangerous in apparently aggravating vitreoretinal traction. The value of this form of therapy to prevent giant retinal tears and tears following vitrectomy and other procedures will be discussed in a separate section below.

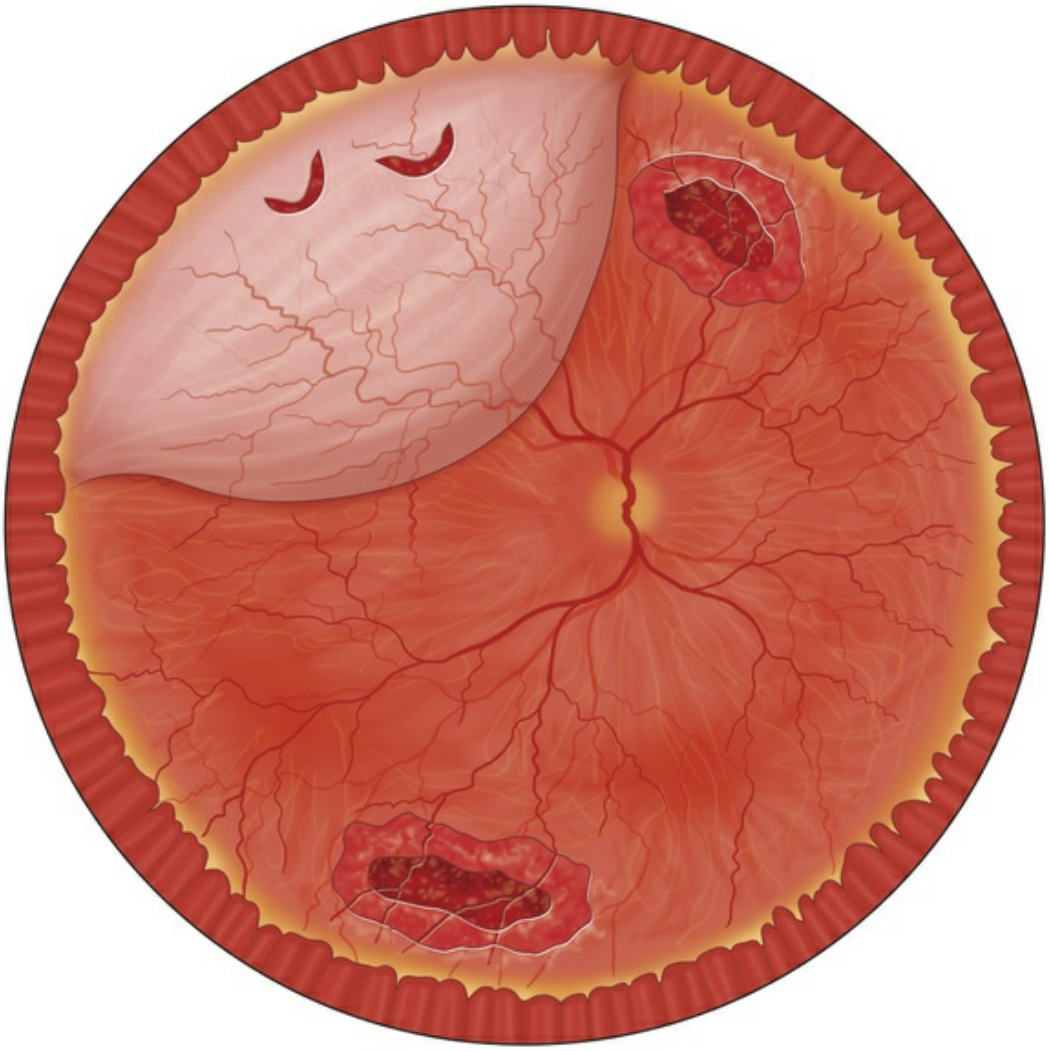

FIG. 110.5 Acute rhegmatogenous retinal detachment occurring despite earlier prophylactic laser photocoagulation for lattice degeneration. Acute horseshoe-shaped tears causing the detachment occurred in an area that previously appeared normal.

(From Brinton D, Wilkinson CP. Retinal detachment: Principles and practice. 3rd ed. New York: Oxford University Press with the cooperation of the American Academy of Ophthalmology. © 2009, with permission from Oxford University Press.)

FIG. 110.6 Nearly confluent ring of prophylactic laser photocoagulation in the equatorial and preequatorial zone. This type of treatment, popular in some locations, extends to the posterior margin of the vitreous base. (From Brinton D, Wilkinson CP. Retinal detachment: Principles and practice. 3rd ed. New York: Oxford University Press with the cooperation of the American Academy of Ophthalmology. © 2009, with permission from Oxford University Press.)

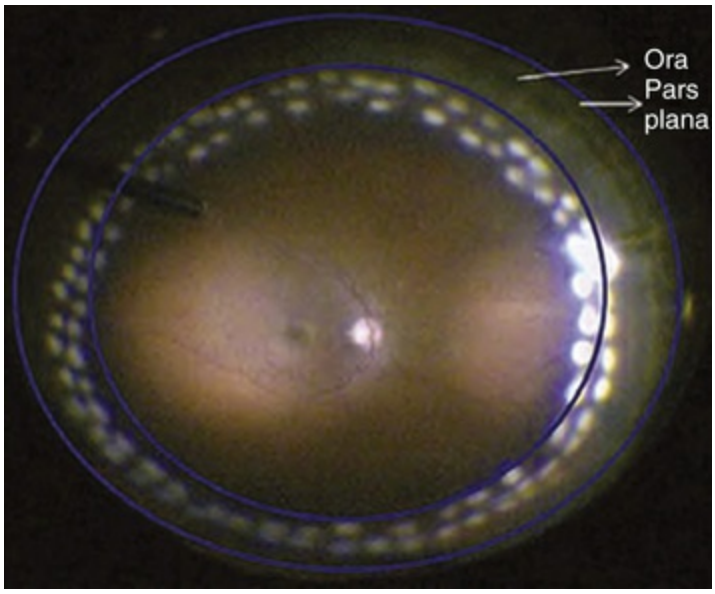

FIG. 110.7 360-degree laser retinopexy to prevent retinal detachment after vitrectomy for macular hole.
(Courtesy of Chalam KV).

Studies of prophylactic therapy of lattice degeneration, with and without holes in phakic fellow eyes, have been of limited value because they have not been prospective and because important information has been missing from available retrospective analyses.[9] In particular, the outcomes have not been studied as a function of the presence of a posterior vitreous detachment. Davis[29] demonstrated that retinal detachments were unusual in phakic fellow eyes if a PVD was present at the time of the initial examination. Retinal detachments occurred in none of 33 such cases. However, if a PVD was not present, retinal detachment subsequently developed in 14 (13%) of 112 phakic fellow eyes with lattice lesions.

Appropriate prospective trials will be required to assess properly the value of treating lattice degeneration in phakic fellow eyes. The relatively low incidence of retinal detachment in untreated cases, the frequency of new tears in normal-appearing retina, the apparent ineffectiveness of therapy in eyes with extensive lattice degeneration and high myopia, and the known success rate following treatment of symptomatic retinal tears and detachments indicate that prophylactic treatment is of limited value. The apparently modest treatment benefit following treatment of all lattice lesions may be of value in selected patients, such as those

with a poor surgical result in the first eye, others who are incapable of recognizing symptoms of vitreous and/or retinal detachment, and patients who live in areas with limited access to ophthalmologic care. In addition, as noted above, patients with atrophic holes in lattice lesions should be evaluated periodically and counseled about loss of peripheral vision because slowly progressive retinal detachments can occur.

Cystic retinal tufts are bilateral in only 6% of cases, so they are not a common cause of bilateral retinal detachment, and there are no data supporting the value of prophylactic therapy.

Degenerative retinoschisis is an unusual cause of progressive retinal detachment, but retinoschisis is both common and frequently bilateral.[40] Thus, patients with both retinal detachment and retinoschisis in one eye frequently have retinoschisis in the fellow eye. An evaluation of the literature regarding prophylactic therapy for retinoschisis in phakic fellow eyes is very difficult because of a lack of complete information regarding the cases.[31] Still, in the unusual case in which outer layer retinal breaks have been responsible for retinal detachment in the first eye, and outer layer breaks and retinoschisis are present in the fellow eye, prophylactic therapy is frequently recommended by some authors.

Retinal Breaks

Asymptomatic retinal breaks in phakic second eyes of patients with previous retinal detachment are frequently cited as an indication for prophylactic therapy.[31] Flap tears appear to be much more likely to cause retinal detachment than round or operculated retinal holes (see Fig. 110.1).[11,29,55] Merin et al.[55] discovered retinal breaks in 186 (19%) of 966 fellow eyes, 28 of which (15%) later developed retinal detachment. Horseshoe-shaped tears were the cause of the detachment in 20 (71%) of the 28 eyes, whereas only 19% of breaks were flap tears in the 158 eyes that did not progress to retinal detachment. However, Hyams et al.[50] followed 10 untreated asymptomatic horseshoe-shaped tears in phakic fellow eyes, and no retinal detachments occurred. Deficiencies in prior reports have made it difficult to assess both the natural course of asymptomatic retinal breaks that are discovered on an examination of a fellow eye and the results of treatment of these lesions. Most of these breaks

are round and located within areas of lattice degeneration, and these cases were discussed earlier. Data regarding therapy for asymptomatic horseshoe-shaped tears in fellow eyes suffer from a lack of details, including the status of the vitreous gel and the relationship between the original retinal break and the cause of subsequent retinal detachment. An aggressive national program of routine treatment of all retinal breaks in fellow eyes did not reduce the prevalence of retinal detachment in Israel.[56] Still, treatment of horseshoe-shaped tears that are discovered in asymptomatic fellow eyes is sometimes recommended despite the absence of optimal supportive data.

Giant Retinal Tears

Prophylactic treatment is frequently recommended in phakic fellow eyes in which a nontraumatic giant retinal tear has occurred in the first eye. Freeman[13] followed 321 cases for 12 months to 29 years. New giant retinal tears occurred in 14 (4.4%) untreated eyes, 13 of which were highly myopic and had developed "high-risk features" of increased vitreous liquefaction, and "white with pressure" that increased in extent. In a report by Wolfensberger et al.,[57] 48 patients were evaluated following repair of a giant retinal tear in one eye and 360° cryotherapy of the second eye for a mean of 84 months. During the follow-up period, retinal detachment developed in three patients and a retinal tear alone was observed in a fourth.

Ang et al.[58] subsequently described 360° cryotherapy to prevent giant retinal tear in Type 1 Stickler syndrome in a retrospective study (Fig. 110.8). Most of the cases were phakic, and the results indicated that such treatment significantly reduced the risk of later retinal detachment. However, the results of this study were subsequently criticized[59] because of methodology issues. More recently, a larger cohort of 487 cases in the trial were reported, and more convincing favorable outcome data were apparent.[60] Depending on the matched comparison group, the untreated eyes had an increased risk of retinal detachment, ranging from 5 to 10.3 times.

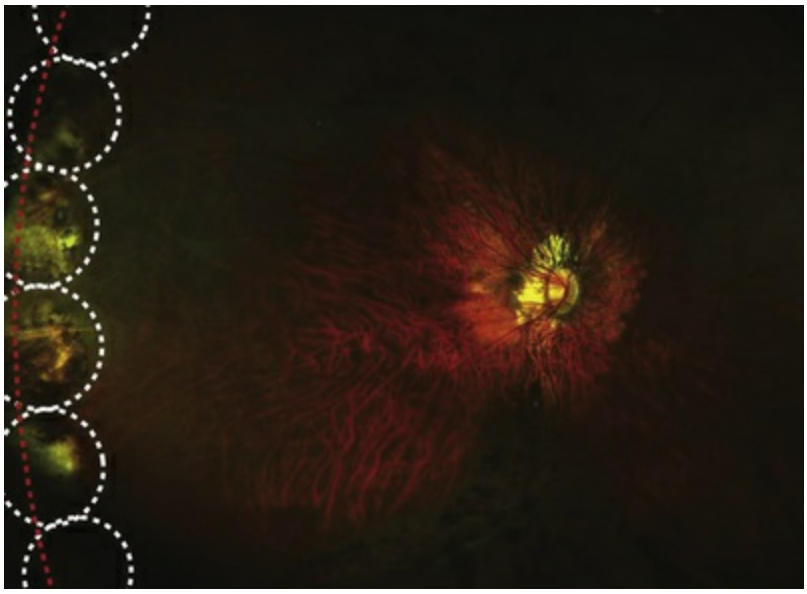

FIG. 110.8 Treatment scheme for 360-degree cryotherapy prophylaxis in Stickler syndrome. (Reproduced from Fincham GS, Pasea L, Carroll C, et al. Prevention of retinal detachment in Stickler syndrome. The Cambridge prophylactic cryotherapy protocol. Ophthalmology 2014;121:1588-97. © 2014 with permission of the American Academy of Ophthalmology.)

Asymptomatic Aphakic and Pseudophakic Fellow Eyes

All eyes have an increased risk of retinal detachment after cataract extraction.[31] The chances of detachment would be expected to be higher if secondary YAG capsulotomy were required.[9,12] Thus, prophylactic therapy has frequently been recommended for vitreoretinal lesions in fellow eyes that are no longer phakic or that are scheduled to undergo cataract extraction.

Precursors of Retinal Breaks

Of the precursors of retinal tears that have been considered for prophylactic therapy before or after cataract extraction, only lattice degeneration has been extensively studied, and reviews of the literature have been published.[6,31] However, no prospective randomized studies have compared the natural course in these cases with outcomes following preventive treatment.[7] As is true of phakic fellow eyes, a major problem in treating only visible

pathology is the frequency of new retinal tears that develop in areas of the peripheral retina that appear normal prior to PVD (Table 110.4, see Fig. 110.5). Although treatment of visible lesions appears to reduce the chances of retinal tears occurring at the treated site, the retinal detachments that frequently develop in these fellow eyes are not prevented by this focal therapy.[8,61–63]

TABLE 110.4
Treatment for Aphakic Fellow Eyes

Eyes	Detachment		Tear in Normal Retina		Tear at Lesion Site	
	n	(%)	*n*	(%)	*n*	(%)
Initially aphakic (*n* = 90)						
Treated (*n* = 13)	0	0	–		–	
No treatment (*n* = 77)	12	16	10	83	2	17
Cataract surgery during the study (n = 34)						
Treated (*n* = 11)	2	18	2	100	–	
No treatment (*n* = 23)	7	30	7	100	–	

Reproduced with permission from Benson WE, Grand MG, Okun E. Aphakic retinal detachment: management of the fellow eye. Arch Ophthalmol 1975;93:245–9.

Studies of prophylactic treatment of lattice degeneration in fellow nonphakic eyes have not been stratified on the basis of posterior vitreous detachment. Hovland[17] demonstrated the critical importance of this variable by studying aphakic eyes of patients with aphakic retinal detachment in the primary eye. Retinal detachment subsequently occurred in one (2.3%) of 43 eyes with a PVD in the fellow eye. In the 40 eyes without a previous PVD, retinal detachment later occurred in eight eyes (21%). Similarly, Davis[29] reported that retinal detachments occurred in five (24%) of 21 aphakic fellow eyes without an apparent PVD (absence of Weiss ring or clearly visible posterior cortical vitreous surface) at the initial examination, but detachments did not occur in 15 additional cases in which a PVD was initially present.

However, as noted earlier, the risk–benefit ratio of this form of treatment in unoperated eyes remains unknown. Treatment of lattice lesions in nonphakic fellow eyes is frequently recommended,[30] despite the lack of supportive data. In eyes in which a PVD has previously occurred, it is doubtful if therapy is particularly effective or necessary. The value of various forms of

prophylactic treatment in eyes without PVD will remain debatable until appropriate trials are conducted.

Cystic retinal tufts and degenerative retinoschisis are unusual causes of bilateral retinal detachment, and data discussing the importance of these entities following cataract surgery are not available. They are managed as discussed under "Asymptomatic phakic fellow eyes" above.

Retinal Breaks

Retinal breaks in nonphakic eyes of patients with a previous retinal detachment in the other eye appear to be followed by a higher rate of detachment.[31] Davis[29] described asymptomatic retinal breaks in 10 aphakic fellow eyes. Subsequent retinal detachments occurred in five of these cases. Four of the five breaks causing retinal detachment were horseshoe-shaped tears, and the type of the fifth break was not reported. The literature regarding the value of treating round holes unassociated with lattice lesions is particularly unclear. Treatment can be expected to prevent retinal detachment resulting from the identified break but not detachment resulting from breaks in other areas of the retina. Treatment of asymptomatic horseshoe-shaped tears in aphakic fellow eyes and in fellow eyes scheduled to undergo cataract extraction is recommended despite the absence of optimal supportive data.[30]

Giant Retinal Tears

Aphakic fellow eyes in nontraumatic giant retinal tear cases have a high risk of retinal detachment. Prophylactic therapy has been recommended for fellow eyes of these patients if significant vitreous liquefaction and progressive "white with pressure" are observed[12] or, alternatively, in all such cases. In the unusual circumstance of a nonphakic eye of a Stickler patient who suffered a detachment due to a giant tear in the first eye, there are compelling data that prophylactic treatment is of value, as noted earlier.[60]

Prophylactic Therapy in Eyes Undergoing Vitreoretinal Surgery

As noted previously, because of the tendency for new retinal breaks to develop in areas of the retina that appear normal, 360° treatment (see Figs. 110.6–110.8) has been advocated during various forms of vitreoretinal surgery.[64]

During Silicone Oil Removal in Previously Operated Eyes

In a nonrandomized retrospective study of eyes following vitrectomy and silicone oil installation, 360° laser therapy appeared to be of value following removal of the oil,[65] and a more recent prospective study[66] demonstrated similar results in apparently comparable eyes following oil removal.

During Primary Vitrectomy for Nonretinal Detachment

In a study of eyes undergoing primary vitrectomy for macular disorders, Koh and coworkers[67] evaluated a consecutive series of 220 eyes in a retrospective analysis. Peripheral 360° laser therapy had been applied in 115 cases, and they were compared with 105 allegedly comparable eyes that had not received treatment. Postoperative retinal detachment subsequently developed in 11.4% of the untreated cases and in 3.5% of those that were treated. However, the eyes were not stratified on the basis of a preexisting vitreous detachment, and 56 cases were lost to follow-up before 6 months.

Another report[68] compared 76 eyes undergoing vitrectomy for macular hole followed by 360° laser therapy with 68 "control" cases in which laser was not employed. At the 1-year postoperative follow-up retinal detachments had occurred respectively in 1.31% and 8.62% of eyes. But again, the data were retrospective, and the validity of matching control cases remains in question. These comments can also be applied to a more recent manuscript on the topic, one that demonstrated a benefit of 360° treatment.[64]

During Pneumatic Retinopexy

Tornambe[69] has advocated 360° laser therapy to prevent later retinal detachment in cases undergoing primary pneumatic retinopexy for retinal detachment, and other authors have described this technique at meetings and in non-peer-reviewed publications. Treated cases have had a lower incidence of subsequent retinal detachments due to new breaks. Still, optimal prospective studies have not been performed.

Summary Regarding Therapy During Vitreoretinal Surgery

The rationale of preventing later retinal detachment by creating a 360° adhesive bond in peripheral regions of the retina, where persistent vitreoretinal traction would be expected to occur following PVD and a variety of vitreoretinal surgical procedures, is attractive. However, the genuine value of such therapy will remain uncertain until better studies are performed.

Treatment Methods

Treatment to prevent retinal detachment can be applied in several ways. Usually, chorioretinal adhesions are created around retinal tears or specific vitreoretinal abnormalities that are judged likely to be the site(s) of future retinal breaks. This can be combined with scleral buckling to further reduce vitreoretinal traction, although buckling is rarely used in the prevention of retinal detachment.

The three methods currently available for creating chorioretinal adhesions are diathermy, photocoagulation, and cryotherapy. Diathermy is best applied with scleral dissection, a surgical technique that currently is very rarely employed to prevent retinal detachment, and it can be used to treat localized subclinical detachments when combined with scleral buckling. Nevertheless, contemporary treatment to prevent retinal detachment usually entails a choice between cryotherapy and laser photocoagulation. Photocoagulation was first performed using a xenon arc light source, but this has been replaced by laser treatment. Cryotherapy and laser photocoagulation cause chorioretinal adhesions that seem equally effective in preventing retinal detachment, and choice of a

treatment method depends on individual features of the case. Sometimes both methods are used in the same eye because parts of one or more lesions can be treated best with one modality and other portions are treated best with the other (see Fig. 110.3).

Cryotherapy

Cryotherapy is usually applied in a transconjunctival fashion, although it is sometimes necessary to open the conjunctiva and insert the probe in the episcleral space when treating posterior lesions. And in the unusual circumstance when 360° prophylactic treatment appears to be indicated, peritomies are frequently performed, especially in younger patients (see Fig. 110.8).[60] Visualization is provided by indirect ophthalmoscopy, and this combination is particularly effective in treating far anterior lesions (see Fig. 110.3) and treating eyes with partial opacities of the ocular media, such as cataract changes or mild vitreous hemorrhage.

Cryotherapy also has certain disadvantages, some of which are theoretical concerns. First, treatment with cryotherapy is difficult for far posterior lesions, unless an incision is created in the conjunctiva. Second, cryotherapy applications do not create an immediately and easily visible effect; therefore, it may be difficult to be certain where the treatment was applied. This can result in areas that are skipped or in refreezing the same area. Third, cryotherapy may cause dispersion of viable pigment epithelial cells through the retinal break into the vitreous cavity, and the dispersion of cells may be further increased if the same area is retreated. Therefore, applications should avoid the centers of relatively large retinal breaks. Cryotherapy also causes breakdown of the blood–retinal barrier, with leakage of serum proteins into the intraocular fluids, and some of the serum components are capable of causing later cellular migration. Cryotherapy applied over the long posterior ciliary nerves can impair accommodation for weeks or months. Finally, chorioretinal adhesions induced by cryotherapy are not as rapidly clinically effective as those that follow laser treatment.[70]

Laser Photocoagulation

Laser photocoagulation has several advantages, as well as certain

limitations and possible disadvantages. Laser applications cause an immediate visible reaction, which aids both in judging the biologic intensity of each application and in documenting the area of treatment. Each application is precisely focused so that the margins of the break and the surrounding retina can be treated without affecting the pigment epithelium within the open break. The laser applications produce a coagulative effect that seems to cause some immediate adhesion between the retina and pigment epithelium.[70]

Laser photocoagulation is usually applied with either a slit-lamp delivery system using a fundus contact lens or an indirect ophthalmoscopic delivery system. Treatment at the slit lamp is best for posterior lesions. Treatment in the far periphery is considerably more difficult, depending on factors such as the amount of pupillary dilation, and it is sometimes impossible to photocoagulate lesions adequately in this region. Laser delivery systems coupled with binocular indirect ophthalmoscopy have significantly improved the ability to treat the peripheral retina. Routine scleral depression can be employed as laser burns are applied to the crest of the indented area. Considerable practice is necessary to produce burns that are as consistent in size and intensity as those that are created with a slit lamp and contact lens. These techniques are routinely employed in the production of 360° preventive laser therapy (see Fig. 110.7).[71]

The major disadvantages of laser treatment include the requirement for relatively clear media and adequate visualization of the lesion. Therefore, eyes with a small pupil or media opacities, such as partial cataract or mild vitreous hemorrhage, are not good candidates for laser treatment. The laser energy can also cause specific complications. Anterior segment burns involving the cornea and lens are probably more common during treatment with binocular indirect ophthalmoscopic laser delivery systems than when energy is applied via a slit lamp and contact lens. Excessive energy delivered in any fashion can cause rupture of Bruch's membrane, choroidal hemorrhage, or even retinal hole formation. Laser treatment also causes some breakdown of the blood–retinal barrier, but this is not as significant as with cryotherapy.

Surgical Techniques

Treatment techniques vary according to the method selected and individual features of each case. However, the general objective is to create a zone of chorioretinal adhesion around each retinal break or area of vitreoretinal abnormality with minimal application of energy and with precise control under direct visualization. The treatment should cause little or no discomfort and minimize potential complications.

Cryotherapy

Cryotherapy is usually applied transconjunctivally using a combination of topical and subconjunctival anesthetic injection, reducing the risk of mechanical damage to the globe or optic nerve with a retrobulbar injection. Also, transconjunctival cryotherapy is easiest when the patient can rotate the eye on command to assist in visualization and to counteract the pressure applied to the globe by the cryoprobe.

The probe tip is properly oriented before being applied to the globe so that the active surface is in direct contact with the eye wall. This prevents accidental freezing in the adjacent meridian. The eye is usually rotated toward the meridian to be treated as the probe is applied, and the probe is moved to indent the sclera beneath the retinal break or vitreoretinal abnormality. If the lesion is located posteriorly or the conjunctival fornix is shallow, the eye is rotated in the opposite direction, thereby permitting placement of the probe in a more posterior location.

The cryoprobe is activated after being positioned beneath or adjacent to the retinal lesion. The freezing effect is permitted to progress until the retina just becomes involved, and then the application is terminated. With experience, the size and intensity of each freezing effect can be anticipated. The probe is moved to an adjacent location, and the freezing mechanism is reactivated. Usually the probe is moved to contiguous locations within the same field of view to minimize the risk of skipping an area or refreezing the same tissue.

Some retinal lesions can be treated with a single application, whereas others require multiple burns. Large retinal breaks are surrounded by contiguous applications while avoiding freezing of the exposed pigment epithelium within the open break, thus

preventing further dispersion of pigment epithelial cells into the vitreous cavity. Areas of lattice degeneration are also surrounded by multiple applications, with each burn straddling the posterior and lateral margins of the lattice lesions where acute retinal tears are most likely. The area anterior to all retinal breaks with persistent vitreous traction is also treated since progressive traction may cause anterior extension of the break (see Fig. 110.3).

If relatively far posterior lesions must be treated, an incision in the conjunctival fornix is made. A supplemental subconjunctival anesthetic injection is given, the conjunctiva is incised with scissors, and dissection is performed in the episcleral space in that meridian. The posterior edge of the incision is grasped with forceps as the cryoprobe is introduced and positioned beneath the lesion. Closure of the conjunctival incision is usually unnecessary, but it can be closed with an absorbable suture. The patient is told that local swelling and subconjunctival hemorrhage are common after transconjunctival cryotherapy and not to be concerned about the external appearance of the eye.

Patient postoperative activity is determined by the type of lesion treated. Normal activity is permitted after treatment of lattice degeneration without retinal breaks. Marked restriction of activity, sometimes including bed rest and bilateral eye patches, may be appropriate after treatment of an acute retinal tear with localized detachment since an effective chorioretinal reaction may not be present for about 5 days.

Laser Photocoagulation

Laser photocoagulation is usually performed with topical anesthesia. The ability of the patient to move the eye on command is also helpful during photocoagulation to assist in visualization. The greatest difficulty may be in identifying the lesion to be treated when viewing through the slit lamp and fundus contact lens. With the slit lamp, a spot size of 200–500 μm is preferred, although a smaller spot size is used if diffraction caused by the ocular media results in significant divergence of the beam. With an indirect laser system, spot size at the laser source is predetermined, although the burn size in the retina can be modified with variations in employment of the condensing lens. A low-power setting is

selected and gradually increased until a coagulation effect of the desired intensity is obtained. Applications are usually limited to 0.1–0.15 seconds since longer applications often cause pain.

The exact treatment technique varies among surgeons. Some prefer a grid pattern around retinal breaks and other lesions, but most use contiguous applications forming a zone 500–1000 μm wide. All sides of each lesion are treated, with special emphasis on the retina anterior to horseshoe-shaped tears and areas of lattice degeneration where progressive vitreoretinal traction may cause anterior extension of a retinal tear.

Discomfort is usually minimal after laser treatment, but a systemic analgesic can be given during the first several hours if treatment was extensive. Activity restrictions depend on the nature of the lesion treated, as described previously for cryotherapy. The coagulative effect of laser treatment seems to cause an effective adhesion more quickly than cryotherapy,[70] although patient activity might still be limited for a few days if substantial subretinal fluid is present.

Scleral Buckling

A scleral buckling operation is rarely necessary as a prophylactic procedure, although it can be performed if there is prominent vitreoretinal traction and significant subretinal fluid and if a chorioretinal adhesion alone is thought to be insufficient in preventing subsequent clinical retinal detachment. Prophylactic scleral buckling is most commonly used to treat progressive subclinical detachments, and a radial scleral buckle is employed in most of these cases. When scleral buckling is used for only prophylactic purposes for extensive vitreoretinal pathology, an encircling buckle is usually required. This procedure is combined with a broad zone of cryotherapy or diathermy treatment extending from near the ora serrata to a location posterior to the posterior margin of the vitreous base or posterior to other specific areas of chorioretinal traction.

The encircling buckling effect can be produced with a band 2.5–4 mm wide, or a band can be combined with a broader, grooved element. Sutures or scleral tunnels are used to secure the band to the sclera in the middle of each quadrant. Volume reduction can be

difficult in these cases because the eye cannot be softened by drainage of subretinal fluid. Multiple anterior chamber paracenteses are often necessary, and the patient may also be given intravenous acetazolamide and hyperosmotic agents.

Results and Complications of Prophylactic Therapy

As noted in previous sections, no prospective randomized clinical trial has been performed to evaluate treatment of precursors of retinal tears and retinal breaks, and interpretation of existing treatment results is difficult because the natural course of the respective lesions is uncertain.[7,9,30,67,68] In addition, available studies have not appropriately stratified important variables for comparison of subgroups. However, the most thorough natural course studies of lattice degeneration,[32] degenerative retinoschisis,[39,40] and asymptomatic retinal breaks[6] demonstrate that these conditions rarely cause acute retinal detachment in patients without a previous retinal detachment in the fellow eye.

Of all vitreoretinal lesions causing clinical retinal detachment, the natural course of symptomatic retinal tears with persistent vitreoretinal traction is best known, and there is agreement that prompt treatment of symptomatic horseshoe-shaped tears is indicated.[9,30] The value of treating other types of retinal breaks and visible vitreoretinal adhesions remains unclear, although effective preventive therapy would be particularly desirable in the second eye of patients with previous retinal detachment in the first eye.

Complications of treatment are also difficult to assess. These may include both failure to prevent retinal detachment and pathologic changes caused by the treatment. Some problems that follow therapy may be due to the pathobiology of retinal detachment rather than to genuine treatment complications. Results and selected complications of therapy have been categorized on the basis of the lesion or lesions treated, whereas additional complications have been studied as nonspecific problems.

Results of Prophylactic Therapy

Results of treatment to prevent retinal detachment are presented in Tables 110.2–110.4. The studies are all somewhat incomplete, as most do not describe information about important variables, including the refractive error, the status of the crystalline lens, the status of the posterior vitreous surface, the type of retinal breaks, and whether there had been a detachment in the fellow eye. In addition, longer-term (e.g., 5–10 years) follow-up information is lacking in most reports. In a 1991 study, Smiddy et al.[72] demonstrated that new retinal breaks continued to occur long after initial prophylactic therapy. In symptomatic eyes that were treated, new retinal breaks were observed in 13% 3 months after therapy and in 21% 2 years postoperatively. The outcomes in this report were not stratified as a function of the type of initial retinal break, so the data are not included in the tables. Another study demonstrated that most detachments that occurred after prophylactic therapy were associated with progression of an incomplete initial PVD,[71] and new tears occur both in "normal" peripheral retina and adjacent to previous chorioretinal burns.[8,10]

Flap Tears

Horseshoe-shaped tears are mostly responsible for clinical retinal detachment. Symptomatic horseshoe-shaped tears are much more likely to cause retinal detachment than are asymptomatic tears,[30] but many studies have not distinguished between these groups. However, failure of treatment is more common following therapy of symptomatic cases.[30] Early failures are usually due to vitreoretinal traction forces that cause an accumulation of subretinal fluid before establishment of an adequate chorioretinal adhesion or to incomplete or inadequate therapy. Treatment should be placed in flat retina immediately adjacent to the location of subretinal fluid, and treatment should extend well anterior to the "horns" of the tear and into the vitreous base (Fig. 110.3).[9,30] However, even optimal therapy may be unsuccessful because of extension of subretinal fluid before an effective chorioretinal adhesion develops. This may be more common following cryotherapy than after laser photocoagulation because the adhesion forms more quickly after application of the latter method.[70]

Lattice Degeneration

There are many difficulties in analyzing results of treatment of lattice degeneration, as mentioned earlier. Results of one study of fellow eyes are listed in Table 110.3. Most new tears following therapy occur in areas not previously treated.

Retinal Holes

The prognosis for round holes after treatment is substantially better than that for flap tears with persistent vitreoretinal traction. As noted earlier, round holes unassociated with persistent vitreoretinal traction or with lattice degeneration are usually not treated.

Patients With Previous Retinal Detachment in the Fellow Eye

Fellow eyes of patients with retinal detachment in a first eye have a substantial risk of retinal detachment, and the risk is even higher after cataract extraction. Smiddy et al.[72] demonstrated that aphakia and pseudophakia are statistically significant risk factors for failure after prophylactic therapy for retinal breaks. Results of treatment of aphakic fellow eyes in one report are listed in Table 110.4. It is important to note that treatment of the visible lesions in untreated eyes would have prevented few retinal detachments.[61]

Complications of Prophylactic Treatment

Complications of preventive therapy include failure to prevent retinal detachment, iatrogenic problems increasing the risk of retinal detachment, and other problems caused by treatment, and they have been reviewed in detail elsewhere.[31] Costs of unnecessary surgery are also a concern. Retinal detachments that occur despite prophylactic therapy are a result of either an inadequate adhesion around a retinal break or a new retinal break. Extension of the detachment is considered a complication of therapy if the treatment is inadequate in extent or intensity, and a particularly common cause of failure in treating horseshoe-shaped tears is an absence of an adequate chorioretinal adhesion surrounding the anterior margins of the break, where vitreoretinal traction persists.[9,30] New

retinal breaks are a complication of prophylactic therapy if the treatment causes excessive damage to the retina, resulting in a break at that location, or if it aggravates vitreous degenerative changes and vitreoretinal traction, causing a tear elsewhere.

Epiretinal proliferation that causes macular pucker has been considered an important complication of prophylactic therapy, but the association between treatment and membrane formation is uncertain. Symptomatic retinal tears are almost always due to a posterior vitreous detachment, and a PVD is present in more than 90% of eyes with idiopathic epimacular proliferation.[18] Also, when vitreoretinal traction causes a retinal tear, pigment epithelial cells are usually liberated into the vitreous cavity, and these may be a source of subsequent epimacular proliferation. The method of creating a chorioretinal adhesion appears to be unrelated to the incidence of postoperative macular pucker.[73]

Conclusion

Although prevention of retinal detachment is an important goal, the genuine value of prophylactic therapy for most vitreoretinal lesions remains unknown because of a lack of appropriate trials. Treatment of symptomatic flap tears is an accepted method of preventing clinical retinal detachments because the natural course of these breaks and the results of therapy are well documented. In most other instances, treatment of visible abnormal vitreoretinal lesions is of limited value, even in eyes with additional risk features such as high myopia, aphakia, or a history of retinal detachment in the fellow eye. The guidelines offered in this chapter represent an attempt to summarize the literature on this topic, and specific decisions regarding prophylaxis for a given eye should be made on the basis of the features of the case and expanding medical knowledge. In the meantime, patients with high-risk features should be made aware of symptoms of posterior vitreous detachment and loss of visual field, and any patient with such symptoms should be promptly evaluated. In addition, periodic follow-up evaluations at the discretion of the examiner may be indicated.

References

1. Comer B, Newman DK, George ND, et al. Who should manage primary retinal detachments? *Eye(Lond)*. 2000;14:572–578.
2. Minihan M, Tanner V, Williamson TH. Primary retinal detachment: 20 years of change. *Br J Ophthalmol*. 2001;85:546–548.
3. Jackson TL, Donache PH, Sallam A, et al. United Kingdom National Ophthalmology Database study of vitreoretinal surgery: report 3, retinal detachment. *Ophthalmology*. 2014;121:643–648.
4. Asaria RH, Gregor ZJ. Simple retinal detachments: identifying the at-risk case. *Eye(Lond)*. 2002;16:404–410.
5. Wilkinson CP, Rice TA. *Michels retinal detachment*. 2nd ed. Mosby: St.Louis; 1997:935–977.
6. Byer NE. Rethinking prophylactic therapy of retinal detachment. Stirpe M. *Advances in vitreoretinal surgery*. Ophthalmic Communications Society: New York; 1992:399–411.
7. Wilkinson CP. Interventions for asymptomatic retinal breaks and lattice degeneration for preventing retinal detachment. *Cochrane Database Syst Rev*. 2014;(9) [CD003170].
8. Kreis AJ, Aylward GW, Wolfensberger TJ. Prophylaxis for retinal detachment. Evidence or eminence based? *Retina*. 2007;27:466–472.
9. American Academy of Ophthalmology. *Preferred Practice Pattern. Posterior vitreous detachment, retinal breaks, and lattice degeneration*. American Academy of Ophthalmology: San Francisco; 2014.
10. Carrero JL. Incomplete posterior vitreous detachment: prevalence and clinical relevance. *Am J Ophthalmol*. 2012;153:497–503.
11. Kuhn F, Aylward B. Rhegmatogenous retinal detachment: a reappraisal of its pathophysiology and treatment. *Ophthalmic Res*. 2014;51:15–31.
12. Tielsch JM, Legro MW, Cassard SD, et al. Risk factors for

retinal detachment after cataract surgery: a population-based case–control study. *Ophthalmology*. 1996;103:1537–1545.
13. Freeman HM. Fellow eye of nontraumatic giant retinal tears. Lewis H, Ryan SJ. *Medical and surgical retina*. Mosby: St. Louis; 1994:222–225.
14. Arroyo JG, Postel EA, Stone T, et al. A matched study of primary buckle placement during repair of posterior segment open globe injuries. *Br J Ophthalmol*. 2003;87:75–78.
15. Robertson DM. Priluck IA. 360-degree prophylactic cryo-retinopexy: a clinical and experimental study. *Arch Ophthalmol*. 1979;97:2130–2134.
16. Blindbaek S, Grausland J. Prophylactic treatment of retinal breaks – a systemic review. *Acta Ophthalmol*. 2015;93:3–8.
17. Hovland KR. Vitreous findings in fellow eyes of aphakic retinal detachment. *Am J Ophthalmol*. 1978;86:350–353.
18. Sebag J. Myopia effects upon vitreous-significance in retinal detachments. Stirpe M. *Anterior and posterior segment surgery: mutual problems and common interests*. Ophthalmic Communications Society: New York; 1998.
19. Bjerrum SS, Mikkelsen KL, La Cour M. Risk of pseudophakic retinal detachment in 202,226 patients using the fellow nonoperated eye as reference. *Ophthalmology*. 2013;120:2573–2579.
20. Brod RD, Lightman DA, Packer AJ, et al. Correlation between vitreous pigment granules and retinal breaks in eyes with acute posterior vitreous detachment. *Ophthalmology*. 1991;98:1366–1369.
21. Byer NE. Natural history of posterior vitreous detachment with early management as the premier line of defense against retinal detachment. *Ophthalmology*. 1994;101:1503–1513.
22. Tasman WS. Posterior vitreous detachment and peripheral retinal breaks. *Trans Am Acad Ophthalmol Otolaryngol*. 1968;72:217–224.
23. Tanner V, Harle D, Tan J, et al. Acute posterior vitreous detachment: the predictive value of vitreous pigment and symptomatology. *Br J Ophthalmol*. 2000;84:1264–1268.

24. Shea M, Davis MD, Kamel I. Retinal breaks without detachment, treated and untreated. *Mod Probl Ophthalmol*. 1974;12:97–102.
25. Verdaguer JT, Vaismon M. Treatment of symptomatic retinal breaks. *Am J Ophthalmol*. 1979;87:783–788.
26. Pollack A, Oliver M. Argon photocoagulation of symptomatic flap tears and retinal breaks of fellow eyes. *Br J Ophthalmol*. 1981;65:469–472.
27. Colyear BH, Pischel DK. Preventative treatment of retinal detachment by means of light coagulation. *Trans Pac Coast Otoophthalmol Soc Annu Meet*. 1960;41:193–215.
28. Robertson DM, Norton EWD. Long-term follow-up of treated retinal breaks. *Am J Ophthalmol*. 1973;75:393–404.
29. Davis MD. The natural history of retinal breaks without detachment. *Trans Am Ophthalmol Soc*. 1973;71:343–372.
30. Khan AA, Gupta A, Bennett H. Risk stratifying retinal breaks. *Can J Ophthalmol*. 2013;48:546–548.
31. Wilkinson CP, Rice TA. *Michels retinal detachment*. 2nd ed. Mosby: St. Louis; 1997:1081–1133.
32. Byer NE. Long-term natural history of lattice degeneration of the retina. *Ophthalmology*. 1989;96:1396–1401.
33. Burton TC. The influence of refractive error and lattice degeneration on the incidence of retinal detachment. *Trans Am Ophthalmol Soc*. 1989;87:143–155.
34. Stirpe M, Heimann K. Vitreous changes and retinal detachment in highly myopic eyes. *Eur J Ophthalmol*. 1996;6:50–58.
35. Williams KM, Dogramaci M, Williamson TH. Retrospective study of rhegmatogenous retinal detachments secondary to round holes. *Eur J Ophthalmol*. 2012;22:635–640.
36. Byer NE. Cystic retinal tufts and their relationship to retinal detachment. *Arch Ophthalmol*. 1981;99:1788–1790.
37. Byer NE. Posterior vitreous detachment as a risk factor for retinal detachment. *Ophthalmology*. 1995;102:528–532.
38. Mitry D, Singh J, Yorson D, et al. The predisposing pathology and clinical characteristics in the Scottish Retinal Detachment Study. *Ophthalmology*. 2011;118:1429–1434.
39. Byer NE. Long-term natural history study of senile

retinoschisis with implications for management. *Ophthalmology*. 1986;93:1127–1137.
40. Buch H, Vindling T, Nielsen NV. Prevalence and long-term natural course of retinoschisis among elderly individuals. The Copenhagen City Eye Study. *Ophthalmology*. 2007;114:751–755.
41. Watzke RC, Folk JC, Lauer AK. Foveal involvement by acquired retinoschisis. Long-term visual outcomes. *Retina*. 2013;33:606–612.
42. Byer NE. What happens to untreated asymptomatic retinal breaks and are they affected by posterior vitreous detachment? *Ophthalmology*. 1998;105:1045–1049.
43. Sigelman J. Vitreous base classification of retinal tears: clinical application. *Surv Ophthalmol*. 1980;25:59–74.
44. The Eye Disease Case–Control Study Group. Risk factors for idiopathic rhegmatogenous retinal detachment. *Am J Epidemiol*. 1993;137:749–757.
45. Folk JC, Arrindell EL, Klugman MR. The fellow eye of patients with phakic lattice retinal detachment. *Ophthalmology*. 1989;96:72–79.
46. Norregaard JC, Thoning H, Andersen TF, et al. Risk of retinal detachment following cataract extraction: results from the International Cataract Surgery Outcomes Study. *Br J Ophthalmol*. 1996;80:689–693.
47. Ripandelli G, Coppe AM, Parisi V, et al. Posterior vitreous detachment and retinal detachment after cataract surgery. *Ophthalmology*. 2007;114:692–697.
48. Kikichi T. Time course of development of posterior vitreous detachments after phacoemulsification surgery. *Ophthalmology*. 2012;119:2102–2107.
49. Friedman Z, Neumann E, Hyams SW. Vitreous and peripheral retina in aphakia: a study of 200 non-myopic aphakic eyes. *Br J Ophthalmol*. 1973;57:52–57.
50. Hyams SW, Neumann E, Friedman Z. Myopia-aphakia. II. Vitreous and peripheral retina. *Br J Ophthalmol*. 1975;59:483–485.
51. Mitry D, Singh J, Yorston D. The fellow eye in retinal detachment. Findings from the Scottish Retinal Detachment

Study. *Br J Ophthalmol*. 2012;96:110–113.
52. Folk JC, Bennet SR, Klugman MR, et al. Prophylactic treatment to the fellow eye of patients with phakic lattice retinal detachment: analysis of failures and risks of treatment. *Retina*. 1990;10:165–169.
53. Haut J, Ladjimi A, Van Effenterre G, et al. Preventative treatment of retinal detachment of the contralateral eye: results of 5 years of follow-up of 109 eyes. *J Fr Ophtalmol*. 1991;14:397–404.
54. Monin C, Van Effenterre G, Andre-Sereys P, et al. Prevention of retinal detachment in Wagner–Stickler disease: comparative study of different methods. *J Fr Ophtalmol*. 1994;17:167–174.
55. Merin S, Feiler V, Hyams S, et al. The fate of the fellow eye in retinal detachment. *Am J Ophthalmol*. 1971;71:477–481.
56. Michaelson IC, Stein R, Neumann E, et al. A national cooperative study in the prevention of retinal detachment. Pruett RC, Regan CD. *Retina congress*. Appleton–Century–Crofts: New York; 1974.
57. Wolfensberger TJ, Aylward GW, Leaver PK. Prophylactic 360 degree cryotherapy in fellow eyes of patients with spontaneous giant retinal tears. *Ophthalmology*. 2003;110:1175–1177.
58. Ang A, Poulsob AV, Goodburn SF, et al. Retinal detachment and prophylaxis in type 1 Stickler syndrome. *Ophthalmology*. 2008;115:164–168.
59. Aylward GW, daCruz L, Sullivan P, et al. Stickler syndrome. *Ophthalmology*. 2008;115:1636–1637.
60. Fincham GS, Pasea L, Carroll C, et al. Prevention of retinal detachment in Stickler syndrome. The Cambridge prophylactic cryotherapy protocol. *Ophthalmology*. 2014;121:1588–1597.
61. Benson WE, Grand MG, Okun E. Aphakic retinal detachment: management of the fellow eye. *Arch Ophthalmol*. 1975;93:245–249.
62. Le Mesurier R, Chignell AH. Prophylaxis of aphakic retinal detachment. *Trans Ophthalmol Soc U K*. 1981;101:212–213.
63. Hudson JR, Kanski JJ. Prevention of aphakic retinal

detachment by circumferential cryotherapy. *Mod Probl Ophthalmol*. 1977;18:530–537.
64. Young-Joon J, Coveson BC. Effect of 360-degree laser therapy for prevention of retinal detachment after phacovitrectomy (peripheral 360-degree laser treatment for prevention of retinal detachment). *BMC Ophthalmol*. 2013;13:77.
65. Laidlaw DA, Karia N, Bunce C, et al. Is prophylactic 360-degree laser retinopexy protective? Risk factors for retinal detachment after removal of silicone oil. *Ophthalmology*. 2002;109:153–158.
66. Avitabile T, Longo A, Lentmig G, et al. Retinal detachment after silicone oil removal is prevented by 360 degrees laser treatment. *Br J Ophthalmol*. 2008;92:1479–1482.
67. Koh HK, Cheng L, Kosobucki B, et al. Prophylactic intraoperative 360 degree laser retinopexy for prevention of retinal detachment. *Retina*. 2007;27:744–749.
68. Cheam KV, Murthy RK, Gupta SK, et al. Prophylactic circumferential intraoperative laser retinopexy decreases the risk of retinal detachment after macular hole surgery. *Eur J Ophthalmol*. 2012;22:790–802.
69. Tornambe PE. Pneumatic retinopexy: the evolution of case selection and surgical technique: a twelve-year study of 302 eyes. *Trans Am Ophthalmol Soc*. 1997;95:551–578.
70. Folk JC, Sneed SR, Folberg R, et al. Early retinal adhesion from laser photocoagulation. *Ophthalmology*. 1989;96:1523–1525.
71. Mastropasqua L, Carpineto P, Ciancaglini M, et al. Treatment of retinal tears and lattice degeneration in fellow eyes in high risk patients suffering retinal detachment: a prospective study. *Br J Ophthalmol*. 1999;83:1046–1049.
72. Smiddy WE, Flynn HW, Nicholson DH, et al. Results and complications in treated retinal breaks. *Am J Ophthalmol*. 1991;112:623–631.
73. Saran BR, Brucker AJ. Macular epiretinal membrane formation and treated retinal breaks. *Am J Ophthalmol*. 1995;120:480–485.

SECTION 3

Complicated Forms of Retinal Detachment

OUTLINE

111

Proliferative Vitreoretinopathy

Ian J. Constable, Manish Nagpal

Introduction

Proliferative vitreoretinopathy (PVR) is the clinical syndrome associated with retinal traction and detachment in which cells with proliferative potential multiply and contract on retinal surfaces and in the vitreous compartment.[1–4] PVR presents with a spectrum of

severity ranging from subtle retinal wrinkling, to fixed folds and tears with rolled edges and to total rigid retinal detachment, retinal shortening, and advanced periretinal proliferation (Figs. 111.1 and 111.2). PVR is the most common cause of failure in retinal detachment surgery. It can occur in untreated eyes with retinal detachment, especially with vitreous hemorrhage, or after cryotherapy or even laser retinopexy, pneumatic retinopexy, scleral buckling, or vitrectomy, and after a variety of surgical complications. It is common after penetrating injuries and a variety of conditions associated with prolonged inflammation. Although surgical reattachment of retinas associated with PVR can now be achieved in most cases, visual results remain disappointing. Therefore, prevention through early recognition of risk factors and subtle signs of PVR and appropriate modification of standard surgical techniques for retinal detachment remain all-important. Some degree of PVR is found in up to 10% of retinal detachments.[5–7] If PVR is progressive and macula reattachment delayed, then despite complex surgery, low vision is the result in the majority of eyes.

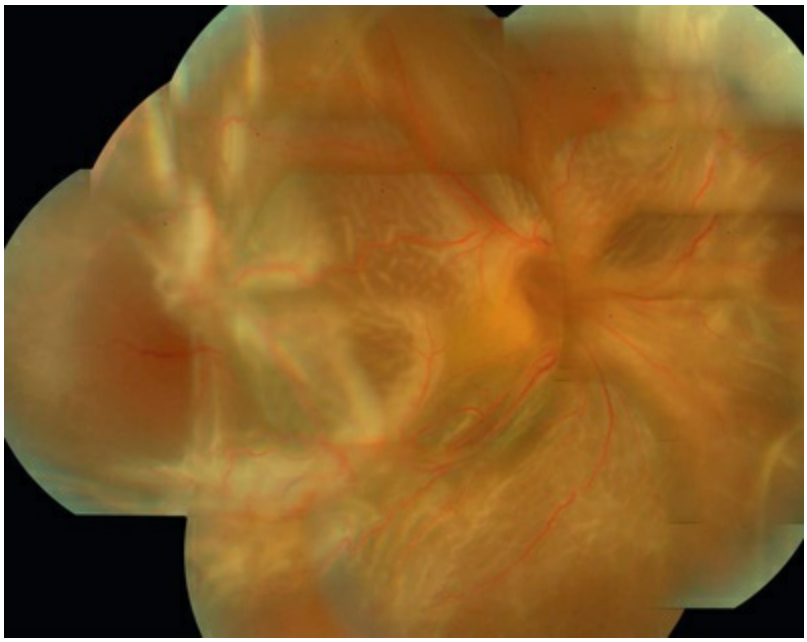

FIG. 111.1 Retinal detachment with advanced proliferative vitreoretinopathy. Fixed folds are present in all four quadrants (Grade D-2).

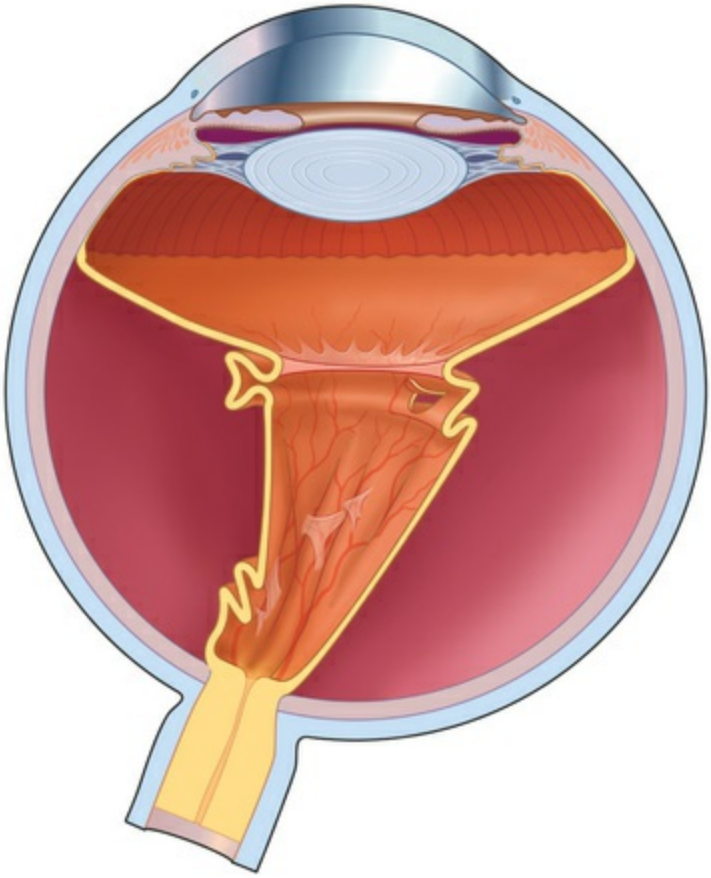

FIG. 111.2 Cross-section of a funnel-shaped retinal detachment with fixed folds posteriorly and a contracted equatorial membrane (Grade D-3).

Pathophysiology

The pathophysiology of PVR is discussed in detail in Chapter 101 (Pathogenesis of proliferative vitreoretinopathy).

PVR is characterized by proliferation of cells derived from retinal pigment epithelium, glia, or inflammatory recruitment on the retinal surfaces and within the vitreous gel.[8,9] These metaplastic cells transdifferentiate and assume contractile properties through internal cellular contractile proteins and by laying down extracellular collagen.[10] They multiply and grow along available scaffolding, either the retinal surfaces or elements of residual vitreous gel. Mass contraction leads to retinal wrinkles, folds, tears, and traction retinal detachment. The vitreous compartment is normally almost devoid of cellular content with just a few

hyalocytes. It is protected from outside invasion by the internal limiting membrane of the retina and from cytokines and other chemoattractants by the blood–retinal barrier. The process of PVR can start when there is an interruption to the surface lining such as can occur with a posterior vitreous detachment and local preretinal membrane formation or retinal tears in the periphery. Retinal tears with surrounding detachment may encourage inflow of freed-up pigment epithelial cells through the break into the vitreous and onto the retinal surface or onto residual contracted vitreous strands and the vitreous base. Simultaneous breakdown of the blood–retinal barrier with retinal detachment or any cause of intraocular inflammation, including cryotherapy, laser, and the trauma associated with scleral buckling, can all lead to the influx of circulating inflammatory cells and a whole range of proteins associated with inflammation.[11] The process is more likely to be triggered in patients with posterior segment trauma, uveitis, choroidal detachment, or severe diabetic retinopathy in the presence of retinal tears. The PVR process is self-propagating and can be considered an inappropriate excess wound-healing response. Cellular proliferation and contraction increases the breakdown of the blood–ocular barrier, in turn causing more traction and more influx of inflammatory cytokines and inflammatory cells. Macular pucker after retinal detachment repair can be considered a mild form of PVR. PVR most frequently develops in the inferior retinal quadrants, probably because the retinal pigment epithelial and inflammatory cells liberated into the vitreous cavity through retinal tears or those associated with vitreous hemorrhage settle inferiorly with gravity.[12] The PVR process usually takes 4–12 weeks to develop a critical mass of cells and significant retinal traction after retinal detachment surgery or other ocular interference such as trauma. As in normal wound healing, the proliferating cells go through a life cycle, and as they progressively lay down collagen, the membranes become hypocellular leaving contracted collagen sheets, membranes, and cords in the vitreous cavity, or on the retinal surfaces and sometimes under the retina. Contraction of equatorial membranes may lead to a funnel-shaped retinal detachment while shortening of the inferior retina may lead to large, inoperable posterior retinal breaks. Severe PVR may also be

superimposed on diabetic tractional retinal detachment when associated with retinal tears. PVR also may occur in other vascular retinopathies such as Eales disease in the presence of retinal breaks and especially in penetrating ocular trauma. The proliferative/inflammatory process underlying PVR complicating retinal detachment is typically associated with loss of central vision even after successful surgery, and this may be due to inflammation-induced apoptosis of the receptor cells at the macula[13] or degeneration of the receptors associated with prolonged retinal detachment.[14] The cellular and biochemical processes underlying PVR are complex and are explored in detail in Chapter 101 (Pathogenesis of proliferative vitreoretinopathy).

Risk Factors for Development of PVR

The most common clinical setting is the development of clinically significant PVR a few weeks after previous retinal detachment repair, whether by scleral buckling, primary vitrectomy, or both (Fig. 111.3). A few eyes develop PVR spontaneously with retinal detachment prior to surgery.[6] Previous trauma, prolonged inflammation of the posterior segment, viral infections of the posterior segment, and prolonged chorioretinitis are also associated with spontaneous PVR. The risks in the presence of retinal detachment are increased with large retinal breaks or giant tears, vitreous hemorrhage associated with retinal tears, multiple previous eye surgery, previous trauma to the posterior segment, and preexisting signs of localized PVR such as fixed folds.[15–17] The risk is increased in retinal detachments with more than two quadrants involved and those with coexisting choroidal detachment. The risk is also increased in retinal detachments associated with a variety of systemic conditions such as Wagner's disease, Stickler syndrome, Marfan syndrome, and familial exudative vitreoretinopathy. A high rate of PVR is reported following a range of novel complex surgical procedures, including macular translocation, retinal prosthesis implantation, and endoresection of ocular tumors. Surgical problems that increase the risk of PVR include vitreous and subretinal bleeding, choroidal detachment,[18] failure to close retinal breaks resulting in prolonged

retinal detachment, incarceration of retina in an external subretinal fluid drainage site, and heavy or excessive cryotherapy.[19–21] Seeding of pigment epithelial cells onto the retinal surface at the time of drainage of subretinal fluid through an internal retinotomy or retinal break may increase the risk. Prolonged inflammation after retinal detachment surgery increases the risk of PVR, especially if associated with postoperative uveitis, residual intraocular blood, or failure to remove all traction off the retina and failure to support it with a scleral buckle. The greatest risk period is 4–12 weeks after detachment surgery. A patient with any of the above predisposing risk factors, either preoperatively or as a result of surgery, should be followed more frequently in the postoperative period to ensure early detection of PVR and recurrence of retinal detachment.

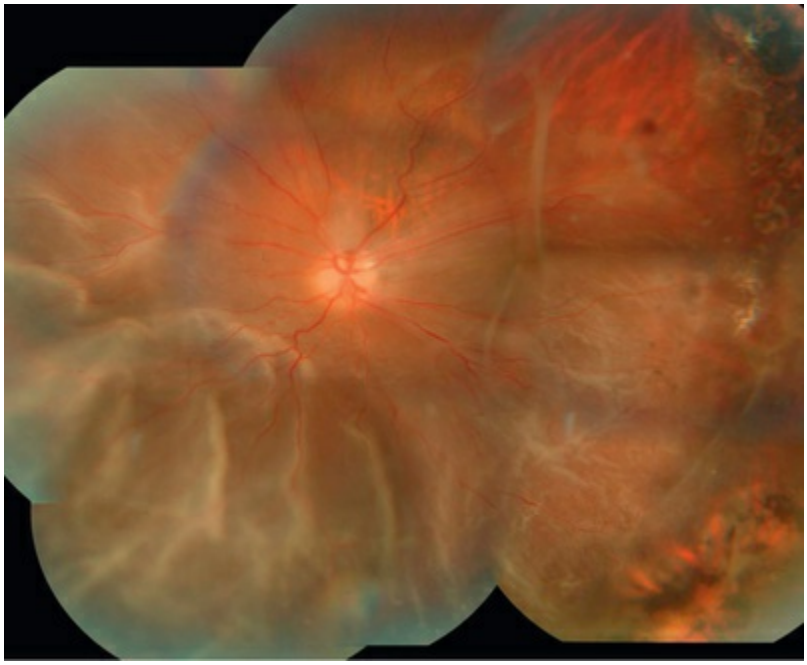

FIG. 111.3 Recurrent retinal detachment due to proliferative vitreoretinopathy. In this case reoperation may include an encircling silicone buckle, repeat vitrectomy with peeling of membranes and clearance of the vitreous base, aspiration of subretinal fluid, fluid air exchange, endolaser, and silicone oil tamponade.

Clinical Signs and Diagnosis of PVR

The early signs of PVR are subtle and include cellular dispersion in the vitreous and on the retinal surface and localized fibrocellular membranes, which appear as a white opacification of the retinal surface and small wrinkles or fixed folds (Figs. 111.4 and 111.5). Cellular proliferation at the edge of a retinal tear can lead to local contraction and a rolled posterior edge (Fig. 111.6). More extensive PVR has fixed folds with retinal detachment, especially inferiorly, and fine membranes bridging the valleys between folds, as well as decreased mobility of the detached retina. Advanced PVR with posterior vitreous detachment results in the eventual formation of a funnel-shaped detachment with a contracted equatorial membrane (Figs. 111.1 and 111.2). In some cases, anterior traction at the vitreous base draws retina forward towards the ciliary body or detaches the ora serrata. Diagnosis of established PVR in the presence of rhegmatogenous retinal detachment is made by indirect ophthalmoscopy and slit-lamp biomicroscopy with a +78 or +90 diopter lens or corneal contact lens. In eyes with opaque media, B-scan ultrasonography outlines immobile retinal folds of detachment and prominent vitreous membranes (Fig. 111.7). Early and subtle signs of PVR should always be looked for and noted in the preoperative assessment of retinal detachment as it may result in modification of the choice of surgical techniques outlined below during primary repair. Early recognition of signs of impending PVR following reattachment of a retina in the 1–3-month period following surgery allows more timely intervention. In many cases of early PVR, timely intervention can avoid the substantial visual loss that almost invariably occurs with macula detachment in patients with delayed diagnosis and reoperation.

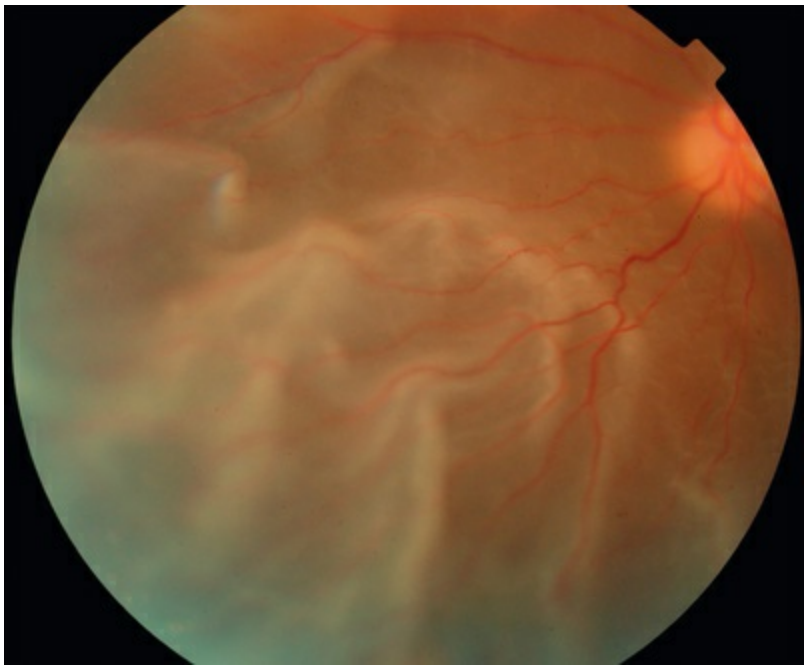

FIG. 111.4 Rhegmatogenous retinal detachment with multiple surface wrinkles and folds – an early sign of proliferative vitreoretinopathy, which is associated with retinal stiffness and decreased mobility on eye movement.

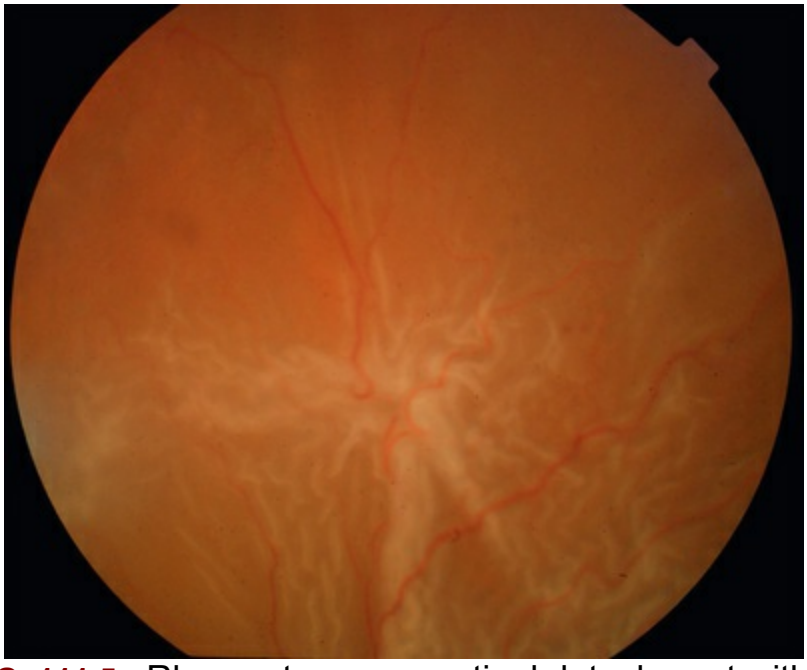

FIG. 111.5 Rhegmatogenous retinal detachment with a fixed star-shaped retinal fold.

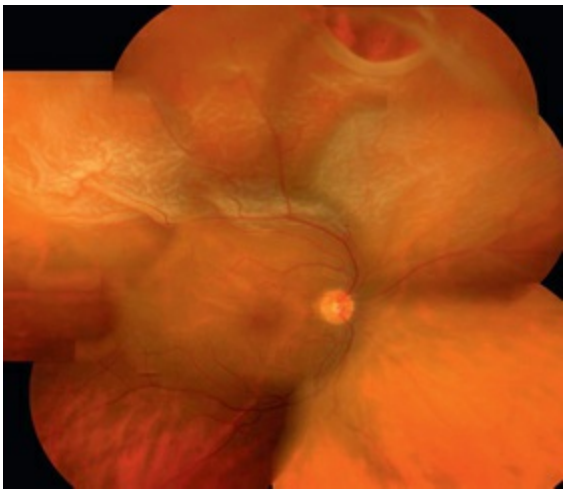

FIG. 111.6 Rhegmatogenous retinal detachment with a superior retinal break with a rolled posterior edge. This an early sign of proliferative vitreoretinopathy.

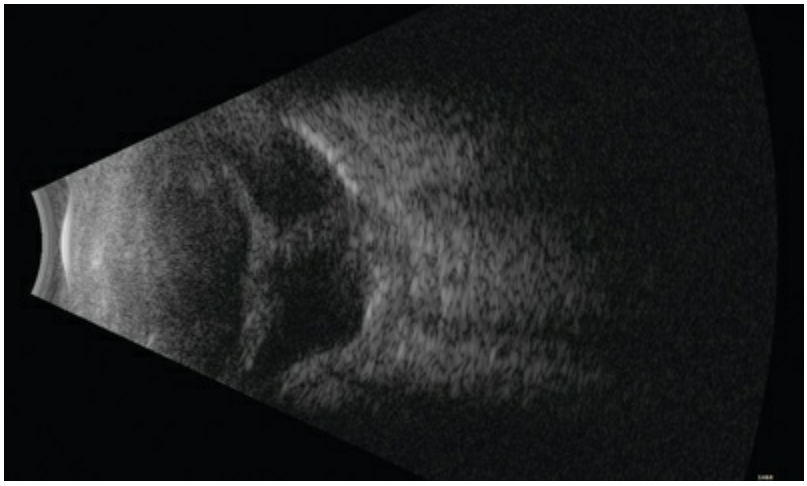

FIG. 111.7 B-scan ultrasound of an eye with rhegmatogenous retinal detachment and proliferative vitreoretinopathy (PVR). A high-intensity echo with a V or funnel shape emanating from the optic disc and lack of mobility of the detached retina are characteristic of advanced PVR.

Classification of PVR

There is benefit in classifying and recording the extent of PVR in all eyes with retinal detachment. This active process prompts a thorough search for the signs in all patients before surgery and in

the postoperative period. It allows cross-comparison of severity of disease in any clinical series that may be audited or published and is the basis for assessing the effect of various therapies through clinical trials. The most commonly used classification system remains that published by the Retina Society Terminology Committee in 1983.[3] It classifies the appearance of PVR on the basis of clinical signs and geographic distribution into four grades (Table 111.1). A major drawback is that it ignores anteroposterior epiretinal proliferation and hence the importance of anterior traction in PVR. It is also a static classification that says nothing about the degree of cellular proliferative activity at the time of the grading. An inactive Grade D PVR affecting all quadrants may have a better prognosis with surgery than a very cellular, active, proliferating PVR affecting only two or three quadrants as in Grade C. The revised classification of PVR of 1991[4] took into account more detailed information about the location, extent, and severity of PVR in an individual eye and hence is more useful especially for clinical trials (Tables 111.2 and 111.3). Further modifications of the classification of PVR were proposed as part of the multicenter controlled trial of silicone oil (SO) as an adjunct treatment for PVR,[22] but the added complexity was found to be less reproducible between different examiners than the more simplified classifications. An analysis of the actual use of these classifications in publications on PVR over the last 15 years confirm their deficiencies as they omit information on cellular activity, do not record intraretinal fibrosis and retinal shortening and do not correlate well with anatomical success for surgery or visual prognosis.[23] A updated classification has not so far been published. Nevertheless, the description of PVR and accompanying preoperative retinal drawing should always be sufficiently detailed to allow any eye to be graded for clinical research and auditing of results of surgery. Wide-field digital imaging is also useful for this purpose.

TABLE 111.1

Retina Society Proliferative Vitreoretinopathy Classification (1983)

Grade (Stage)	Characteristics

A	Vitreous haze, vitreous pigment clumps
B	Wrinkling of the inner retinal surface, rolled edge of retinal break, retinal stiffness, vessel tortuosity
C	Full-thickness retinal folds in
C-1	One quadrant
C-2	Two quadrants
C-3	Three quadrants
D	Fixed retinal folds in four quadrants
D-1	Wide funnel shape
D-2	Narrow funnel shape (anterior end of funnel visible by indirect ophthalmoscopy with 20 diopter lens)
D-3	Closed funnel (optic nerve not visible)

Reprinted from Retina Society Terminology Committee. The classification of retinal detachment with proliferative vitreoretinopathy. Ophthalmology 1983;90:121–5. ©1983, with permission from the American Academy of Ophthalmology.

TABLE 111.2

Updated Proliferative Vitreoretinopathy Grade Classification (1991)

Grade	Features
A	Vitreous haze, vitreous pigment clumps, pigment clusters on inferior retina
B	Wrinkling of the inner retinal surface, retinal stiffness, vessel tortuosity, rolled and irregular edge of retinal break, decreased mobility of vitreous
CP 1–12	Posterior to equator, focal, diffuse or circumferential full-thickness folds, subretinal strands[a]
CA 1–12	Anterior to equator, focal, diffuse, or circumferential full-thickness folds, subretinal strands[a], anterior displacement[a], condensed vitreous strands[a]

[a]Expressed in the total number of clock-hours involved.

Reproduced with permission from Machemer R, Aaberg TM, Freeman HM, et al. An updated classification of retinal detachment with proliferative vitreoretinopathy. Am J Ophthalmol 1991;112:159–65.

TABLE 111.3

Updated Proliferative Vitreoretinopathy Contraction Type Classification (1991)

Type	Location (in Relation to Equator)	Features
Focal	Posterior	Star fold posterior to vitreous base
Diffuse	Posterior	Confluent star folds posterior to vitreous base; optic disc may not be visible
Subretinal	Posterior/anterior	Proliferation under the retina; annular strand near disc; linear strands; motheaten-appearing sheets
Circumferential	Anterior	Contraction along posterior edge of vitreous base with central displacement of the retina; peripheral retina

		stretched; posterior retina in radial folds
Anterior	Anterior	Vitreous base pulled anteriorly by proliferative tissue; peripheral retinal trough; displacement ciliary processes may be stretched, may be covered by membrane; iris may be retracted

Reproduced with permission from Machemer R, Aaberg TM, Freeman HM, et al. An updated classification of retinal detachment with proliferative vitreoretinopathy. Am J Ophthalmol 1991;112:159–65.

Prevention of PVR

Prevention of PVR relies mainly on an understanding of which eyes with or without retinal detachment are at greater risk of development of PVR and a recognition of the early signs of the condition. Increased awareness allows the surgeon to modify the treatment plan and, in most cases, prevent this devastating complication. Eyes with large or multiple retinal breaks or giant tears are more likely to develop PVR as mobilized pigment epithelial cells spill into the vitreous and onto the retinal surface in increased numbers. Likewise, eyes with previous or current penetrating trauma with or without retinal detachment may present with increased cellular content in the vitreous and an enhanced inflammatory response. Eyes with chronic retinal detachment, choroidal detachment, uveitis, viral retinitis, and chorioretinitis associated with detachment all have an increased risk of PVR, particularly if associated with a retinal break. Retinal detachment following cataract surgery with retained lens fragments in the vitreous, or following multiple anterior segment surgeries where there may be an enhanced inflammatory response, are at higher risk of PVR. Most eyes with PVR, however, have undergone a repair of rhegmatogenous retinal detachment in the last 1–3 months, and many of these eyes may have developed PVR regardless of the technique used for initial repair. Intraoperative complications including choroidal hemorrhage, retained vitreous hemorrhage, and intense photocoagulation or especially heavy cryotherapy increase the risks. Laser probably causes less breakdown of the blood–retinal barrier than cryopexy and mobilizes less pigment epithelial cells because of the size of each application and the fact that it is only applied to attached retina. Any eyes with the more

subtle early stages of PVR, including pigment particles in the vitreous, localized fixed folds, retinal breaks with rolled edges, visible vitreous membranes, detached segment of the pars plana ciliaris and ora serrata, and decreased mobility of retinal detachment folds on eye movement during examination, usually require vitrectomy to decrease the chance of progression to the full syndrome. The signs of early PVR may indicate the need for combined vitrectomy and scleral buckling rather than one or the other and also vitreous substitution with long-acting gas or SO.

Surgery for PVR

There has been substantial improvement in the success rate of surgery for PVR progressively over the past four decades.[24–27] The clinical severity of PVR is very variable, and therefore the extent of surgery is planned accordingly. PVR varies from a single inactive fixed star fold on the retinal surface to a rigid total retinal detachment with a funnel shape and dense equatorial fixed membranes. There may be fixed folds involving only the posterior retina or fibrotic organization of the vitreous base with both circumferential and anterior loop traction dragging the retina forward or detaching the pars plana ciliaris. Fixed folds may tent the retina and be relatively easily divided or peeled to relieve traction, or there may be extensive surface retinal fibrosis and consequent shortening of the retina in the anterior/posterior plane requiring a relaxing retinotomy. The severity of PVR may also differ markedly in terms of current inflammation and cellular proliferative activity or take the form of fixed, quiescent acellular membranes which are unlikely to recur if divided or peeled. These factors may affect the timing of repeat vitreoretinal surgery. It is urgent if the macula is still attached or salvageable. It may sometimes be better to wait a few days and quieten the eye down with corticosteroids if the macular vision is not salvageable until the inflammatory activity is less intense. On the other hand, leaving an eye with a retinal detachment and early PVR almost always will lead to further progression and eventual inoperability, so that most eyes deemed to be operable should be operated on as soon as possible. The objects of vitreoretinal surgery for PVR are to

permanently support the retina from any ongoing traction and to close any open retinal breaks. These goals are achieved by an encircling scleral buckle, meticulous relief of all retinal traction with vitrectomy, and temporary or long-term tamponade of the retina with long-acting gas or SO. These steps must be achieved without causing prolonged ocular inflammation or further cellular access to the retinal surface, or else recurrence is frequent.

Scleral Buckling and PVR

Although complete vitrectomy and vitreous replacement have become the core procedures for PVR, a 360° encircling scleral buckle remains a fundamental requirement for most eyes with established PVR in the view of many vitreoretinal surgeons. That is because the vitreous base, particularly inferiorly, becomes fibrocellular in PVR and continues to contract even after a formal vitrectomy, since it is virtually impossible to remove the whole vitreous base. A high encircling scleral buckle supports the vitreous base against further traction and against leakage from new or missed small retinal breaks in peripheral thin retina. Eyes with localized or relatively inactive PVR may be successfully reattached with an encircling scleral buckle, drainage of subretinal fluid, and peripheral laser photocoagulation alone. Most, however, require a vitrectomy and internal tamponade with SO or long-acting gas. To achieve chorioretinal adhesion, laser photocoagulation is preferable to cryotherapy, but laser is not always possible due to residual subretinal fluid after drainage or an atrophic white background associated with previous surgery.

Vitrectomy and PVR

A comprehensive vitrectomy is essential in the management of PVR. Some surgeons rely on a meticulous vitrectomy and SO tamponade without scleral buckling and report comparable results with a combined procedure.[28] In any event, almost all eyes with retinal detachment and PVR also require a vitrectomy to remove all vitreous gel, cellular and inflammatory material, blood, and fibroblastic membranes. It is necessary to relieve all traction by division and peeling or delamination of fixed membranes and to

remove as much as possible of the vitreous base. It is also important to divide any membranes causing anterior loop traction and to release the tractional effect on scarred shortened retina. This surgery is greatly facilitated by the extraordinary advances in the technology now available. Wide-angle viewing systems are either indirect and attached to the operating microscope, or consist of an operating corneal contact lens and a microscope image inverter. Contact lenses provide a crisper image and easier visual access to the far inferior periphery but need frequent repositioning and replenishing with viscoelastic. Indirect viewing systems provide a less panoramic view, and the view is dependent on precise eye positioning, making angulation more difficult. Wide-field illumination is achieved with a range of fiberoptic light sources or a chandelier arrangement inserted into the eye through a separate pars plana entry site. Vitreous cutting and suction probes (vitrectors) have vastly improved, and the surgeon has a choice of 25-, 23-, and the traditional 20-gauge (G) instruments. Air-driven vitrectors can cycle at up to 5000 cycles per minute and have a variable duty cycle controlled by electronic sensors. This allows faster removal of core vitreous and opacities, but also safer cutting and aspiration close to the retinal surface. Another major advance has been the intraoperative use of heavier-than-water perfluorocarbon fluid which displaces subretinal fluid anteriorly and flattens the bullous posterior retina. This highlights tractional membranes and facilitates peeling and dissection by stabilizing the posterior retina. Sometimes relaxing retinotomy is required to fully relieve traction caused by densely adherent fixed folds or shortened fibrosed retina. Rarely subretinal membranes need to be removed or divided through a small deliberate retinotomy. Internal drainage of subretinal fluid and fluid–air exchange of the vitreous compartment allows the testing of release of all retinal traction. Any persistent retinal elevation after fluid–air exchange means that complete release of traction or retinal shortening has not been achieved. Reattached retina and open retinal breaks are sealed with endolaser photocoagulation or cryotherapy and a decision made as to whether temporary tamponade with perfluoropropane (C_3F_8) gas will be sufficient or SO–air exchange is necessary. Although a controlled trial showed the eventual outcomes to be similar, many

surgeons prefer SO to gas because it results in less postoperative inflammation, quicker rehabilitation, and fewer reoperations. The use of heavier-than-water SO can also improve inferior retinal tamponade in severe cases of PVR and is being increasingly used.

Surgical Steps for Established PVR

Modern surgery for PVR is greatly facilitated by a wide-angle microscopic viewing system and a fully integrated, electronically controlled, surgical system. Vastly improved fluidics and a range of inbuilt modalities improve the efficiency, duration, and predictability of vitreoretinal surgery. High-speed 23G or 25G cutters able to trim vitreous and membranes off the retinal surface at up to 5000 cuts/minute have greatly improved the ability to remove residual vitreous and membranes, particularly around the vitreous base, while avoiding retinal incarceration with the cutter and the creation of iatrogenic retinal breaks (see Video 111.1 online). Illuminated picks or chandelier endoillumination allow bimanual dissection of intraocular tissue. Endodiathermy probes and small extrusion/suction needles allow the creation of a controlled microretinotomy for endodrainage of subretinal fluid. Flexible endolaser probes facilitate 360° peripheral laser photocoagulation and treatment of any retinal breaks. Laser is superior to cryotherapy in this situation, as it can seal flattened retinal breaks and allow 360° photocoagulation with less postoperative inflammation, and stimulation of repeat cellular proliferation. An integrated fluid–air exchange pump with self-monitoring of intraocular pressure (IOP) facilitates fluid–air exchange and formal checking that the retina is totally mobilized and retinal breaks are completely flat. Difficult visualization still makes cryotherapy necessary in some cases. Soft silicone-tipped fluid extrusion needles (23G or 25G) with active suction facilitate complete drainage of subretinal fluid through a retinal break or intentional posterior retinotomy. 23G and 25G vitreous forceps and scissors have improved the ability to peel, delaminate, and relieve retinal traction in a controlled manner. An integrated pump for the delivery of SO to the vitreous and fluorinated heavy silicone to tamponade the inferior, flattened retina are important additions.

The use of these tools in a stepwise logical manner means that up to 90% of eyes with advanced PVR may be successfully reattached. Advances in instrumentation for phacoemulsification of the lens have also resulted in a shift by many surgeons from posterior lensectomy to formal anterior lens extraction and insertion of an intraocular lens. Planned extracapsular lens removal still enables surgery at the vitreous base, while retaining a barrier to the anterior segment for SO or gas. Eyes left aphakic after pars plana phacofragmentation that are filled with SO risk corneal endothelial damage and secondary glaucoma from emulsified SO bubbles in the anterior chamber or pupil block.

Anesthesia

As with any vitreoretinal surgery either general or local peribulbar anesthesia is acceptable. If general anesthesia is planned, the anesthetist must be informed if long-acting gas is to be used so as to avoid nitrous oxide. Most cases of PVR can be operated with local anesthesia. The surgery can be prolonged and uncomfortable for the patient, particularly if there is an inadequate deep sub-Tenon block. The block can be supplemented during the operation with further injection and by the attending anesthesiologist with intravenous sedation and analgesia. If a scleral buckle is already in place and the surgery is wholly intraocular, it is not usually painful.

Operative Technique

The surgery should begin with a well-prepared preoperative plan, which can be modified often during the operation, depending on the findings. Preoperative retinal and biomicroscopic diagrams aid this process by ensuring that all aspects of the pathologic findings are, in fact, examined and taken into account. The conjunctiva is opened by limbal peritomy unless an encircling 360° buckle exists already or is not planned. Any preoperative scar tissue is gently dissected under and around the rectus muscles, which are looped with 4/0 black silk traction sutures. A 360° scleral band is then placed and sutured in position with permanent scleral sutures such as 5/0 polyester. The choice of scleral buckle width depends upon the extent of vitreous base contraction and size of any peripheral

retinal tears. It may vary from a broad 7.0-mm, Style 277 or 276 encircling tire and 40 band through a solid encircling 5.0-mm wide scleral band down to a 2.5-mm wide style 240 encircling band. The trend is towards narrower bands to permanently support the vitreous base and any small peripheral retinal tears. Larger, more posterior tears can be supported by an extra meridional explant placed under the tear at the end of the operation, but in most cases after complete relief of traction, they are closed by an internal tamponade and sealed permanently with laser. The scleral sutures are placed at two-thirds scleral thickness, at least 1 mm anterior and posterior to the encircling buckle, one or sometimes two in each quadrant. The sutures are not tied and the buckle not tightened until the end of the procedure and after vitrectomy. If only an encircling band is employed, some surgeons prefer to anchor it with sclera "belt loops." If an adequate encircling scleral buckle is already present from previous surgery, then the above steps may be omitted and surgery proceeds with transconjunctival insertion of three 23G or 25G entry cannulas. Some surgeons still prefer a 20G system, which requires intraoperative sutured ports. The three entry ports are placed in the inferotemporal, superotemporal, and superonasal quadrants with an angled entry to diminish the risk of leakage of air or fluid from the entry site postoperatively. The first port is placed near the horizontal in the inferotemporal quadrant so as not to impede rotation of the eye downwards during surgery to remove inferior vitreous base. The second and third ports are for the fiberoptic probe and vitrector or other instruments such as endodiathermy, endolaser, vitreous scissors, vitreous forceps, and extrusion needle. If a chandelier is to be used, it is inserted through a fourth port. The entry cannulas are placed 3.5 mm from the limbus above the midline almost opposite each other, again to facilitate superior and inferior rotation of the globe for peripheral visualization during surgery. Care must be taken to check that the pars plana ciliaris is not detached and that the indwelling ports have passed into the vitreous to avoid subretinal or suprachoroidal infusion during vitrectomy. At this point, a decision is made as to the adequacy of visualization of the retina, especially the periphery and vitreous base by switching microscopic illumination to an indirect, non-contact wide-angle viewing system, or by placement

of a wide-angle corneal contact lens. If the pupil is small or the iris stuck down to the lens capsule, the anterior chamber is entered and aqueous replaced with viscoelastic sodium hyaluronate. Synechiae may be broken down by this injection and the pupil dilated, or else it is mechanically dilated using soft disposable iris hooks placed through clear cornea in each quadrant.

Management of the Lens in PVR

In most cases, wide-angle viewing systems provide an adequate view of the periphery and the lens is preserved. It always becomes cataractous with SO and is conveniently replaced after phacoemulsification at the time of SO removal or when it becomes visually significant. If lens opacities are sufficient to impede the view of the posterior segment, then the cataract must be removed. Most surgeons now favor a formal phacoemulsification procedure, as this allows insertion of an intraocular lens during the operation. Some surgeons still favor fragmentation of the lens via the pars plana sclerotomy and removal of the whole capsule or retention of the anterior capsule. In this case, the eye is rendered aphakic. If the capsule is totally removed, then there is risk from SO contact to the corneal endothelium in the longer term. An inferior iridotomy reduces this risk.[29] If the anterior capsule is left intact, then it always becomes opaque in the presence of SO and subsequent YAG laser capsulotomy or formal capsulotomy with a sharp instrument is carried out at the time of insertion of an intraocular lens in the sulcus 2–3 months later.

Core Vitrectomy and Removal of the Vitreous Base

During vitrectomy, the cornea is kept clear by a viscoelastic coating of methyl cellulose and the wide-angle view contact lens if used. The microscope is refocused for internal viewing and after insertion of a fiberoptic light probe and the vitrector. The three available probe sizes are all acceptable. The 25G has the smallest opening and is the safest. It is also the slowest. Because it is more flexible it can be difficult to rotate the eye superiorly enough to comfortably

remove vitreous off a superior retinal break with a mobile detached retina. The 20G probe has the largest opening and most efficient fluidics but the ports need suturing. The 23G probe is the most popular compromise. Most eyes with established PVR already have a posterior vitreous detachment. Any remaining central gel is removed completely and then peripheral vitreous is removed meticulously and as completely as possible, particularly inferiorly where pigment and inflammatory cells tend to gravitate. This process is facilitated by the modern, high-speed, vitrectomy cutters with the port close to the tip. With these cutters, it is possible to shave the attached vitreous off the surface, without engaging the retina. A bimanual technique with an illuminated probe or pic held in the second hand, can also be helpful in protecting the retina. Removal of the inferior vitreous base is also facilitated by having an assistant indent with a scleral depressor, squint hook, or cotton-tipped stick (Fig. 111.8). Formed vitreous attached to the peripheral retina is also very difficult to remove if the retina is detached and mobile, in which case it can be stabilized at this stage by partly filling the vitreous compartment with heavy fluorocarbon liquid (Fig. 111.9, see Video 111.1 online).[30,31] This has the dual effect of flattening the retina by displacing subretinal fluid anteriorly and breaking down invisible microscopic retinal bridges of scar tissue. In cases where vitreous remains attached to the retinal surface posteriorly as well as at the vitreous base, the process of removal may be facilitated by an intravitreal injection of triamcinolone. The white suspension sticks to vitreous membranes and residual vitreous gel, making them both more visible (see Video 111.1 online).[32–34]

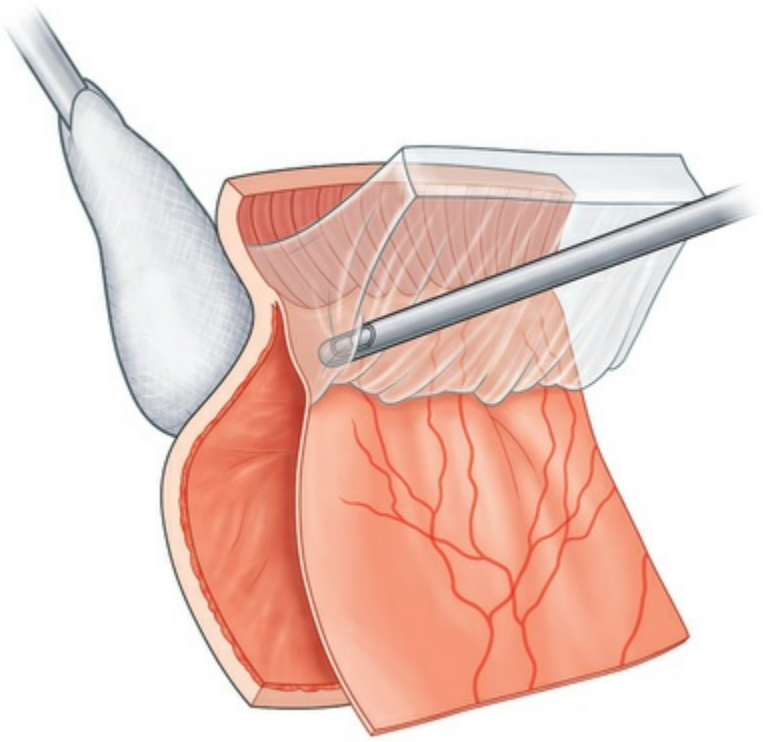

FIG. 111.8 Anterior vitreous and tractional membranes are removed with the high-speed vitreous cutter and low suction. This process may be helped by scleral indentation. Formed vitreous is shaved from the retinal surface to reduce the risk of further postoperative traction.

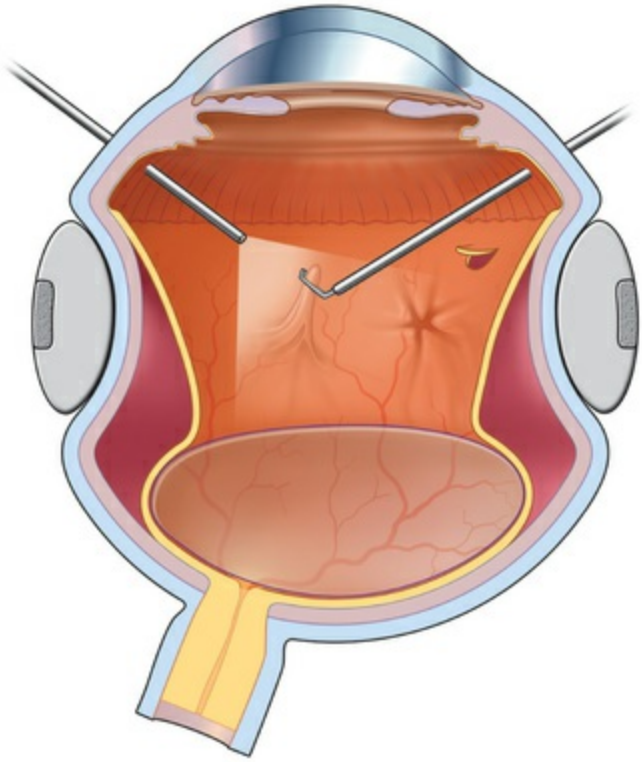

FIG. 111.9 Removal of more anterior membranes and vitreous is facilitated by perfluorocarbon heavy fluid injection into the vitreous compartment. This squeezes subretinal fluid forward and stabilizes the posterior retina while the vitrector, a blunt spatula, or forceps are used. Care must always be taken to avoid heavy fluid passing through a retinal break and under the retina.

Removal of Epiretinal Membranes and Use of Perfluorocarbon Heavy Fluid

After a meticulous vitrectomy, which is as complete as possible, any fixed folds or retinal contraction due to epiretinal membranes must be dealt with. Membranes are peeled from the retinal surface from the posterior pole outwards. If an edge is found, it can be peeled preferably with vitreous forceps. If not, a blunt vitreous spatula or pick may help find a plane and elevate the membrane (Fig. 111.10). Care must be taken to avoid creating iatrogenic retinal breaks. Special attention is given to any fixed folds where contracted membrane tends to fold the retina over underlying valleys. Any membrane involving the macula must be peeled. Some surgeons

advocate the injection of vital dye such as methylene blue at this point to stain and allow peeling of the contracted internal limiting membrane, particularly if the retinal surface at the posterior pole is still stiff or shiny. The degree of adherence of epiretinal membranes to the retinal surface varies so that some may be peeled easily in a single sheet, while many others have to be freed up in a piecemeal fashion or delaminated. Peeling of surface retinal membranes and internal limiting membrane is much easier over attached retina. In many cases, drainage of subretinal fluid through an open retinal break, or if necessary through a small retinotomy away from areas of surface scar tissue, or more often, flattening the posterior retina by the injection of the heavy liquid fluorocarbon facilitates this process (Video 111.1 online).[30] Care must always be taken to avoid the risk of heavy fluid passing through a retinal break under the retina. This can occur if tractional membranes are still elevating a retinal tear. The heavy liquid fill is stopped short of any such retinal break until it is dissected, mobilized, and flattened.

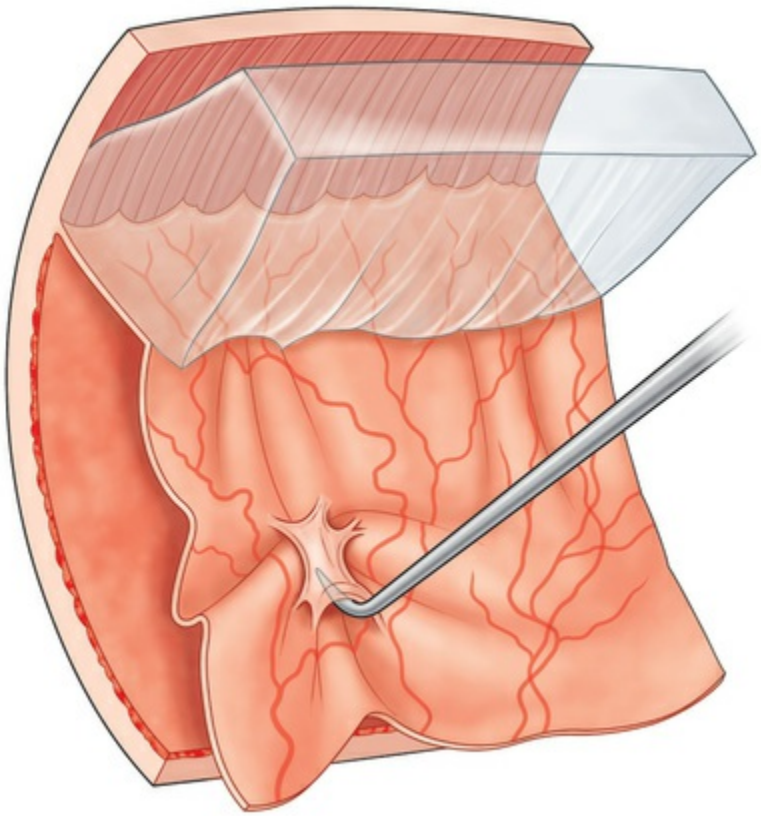

FIG. 111.10 Elevation of an epiretinal membrane

causing a fixed star fold in the retina using a vitreoretinal pick. Peeling of surface membranes is better carried out with blunt end-on vitreous forceps or a blunt spatula to minimize the risk of creating retinal tears.

Removal of Anterior Tractional Membranes

Fibroblastic organization of the vitreous base can cause elevation of peripheral retina and anterior loop traction. This must be sectioned to fully mobilize the retina (Fig. 111.8). As much formed gel as possible must be removed anteriorly also to decrease the risk of recurrence of PVR. High-speed vitreous cutters (23G or 25G) have also greatly facilitated this aspect of surgery so that vertical action scissors are often not needed. Bimanual instrumentation and external scleral depression (Fig. 111.8) may help and wide-angle viewing is very important. Heavy perfluorocarbon liquid is usually needed to stabilize the posterior retina during dissection. If extensive anterior traction is noted preoperatively, then planned lens extraction can also facilitate this dissection, but with modern instrumentation and viewing systems this is no longer usually necessary.

Testing Adequacy of Relief of Traction and Relaxing Retinotomy

At this point, the adequacy of retinal mobilization can be tested by a complete fluid–air exchange. An extrusion needle is placed through the sclerotomy site, and all vitreous fluid or heavy fluid and any residual subretinal fluid is aspirated by positive suction. Drainage of subretinal fluid is facilitated by a silicone soft tubing extension on the needle. If residual traction is present or the retina shortened by surface or intraretinal gliosis, it fails to flatten completely and air may even pass under the retina. This test informs the surgeon that adequate mobilization of the retina has not been achieved. It may require additional dissection around a retinal tear or a limited peripheral relaxing retinotomy or even a circumferential or radial retinotomy with either vitreous scissors or,

more conveniently, with the vitrector (Fig. 111.11).[35–37] Badly fibrosed, contracted retina may also require local retinectomy to allow reattachment under perfluorocarbon heavy fluid (Video 111.1 online, see also Chapter 112, Retinectomy). Endodiathermy is required to prevent or seal retinal bleeding at the cut edge. The endpoint of this step is a total flattening of the retina under air or heavy fluid. The edges are then thoroughly sealed with endolaser (Fig. 111.12). Failure to relieve all traction prevents the retina from apposing the pigment epithelial surface. This is the most frequent cause of a poor anatomic result. On the other hand, a relaxing retinotomy should not be undertaken lightly. After a large circumferential retinotomy the posterior free edge may contract under SO almost back to the disc and macula and compromise the visual outcome. A radial retinotomy may sometimes relieve residual traction and avoid this posterior retraction of the cut retinal edge.[38–41]

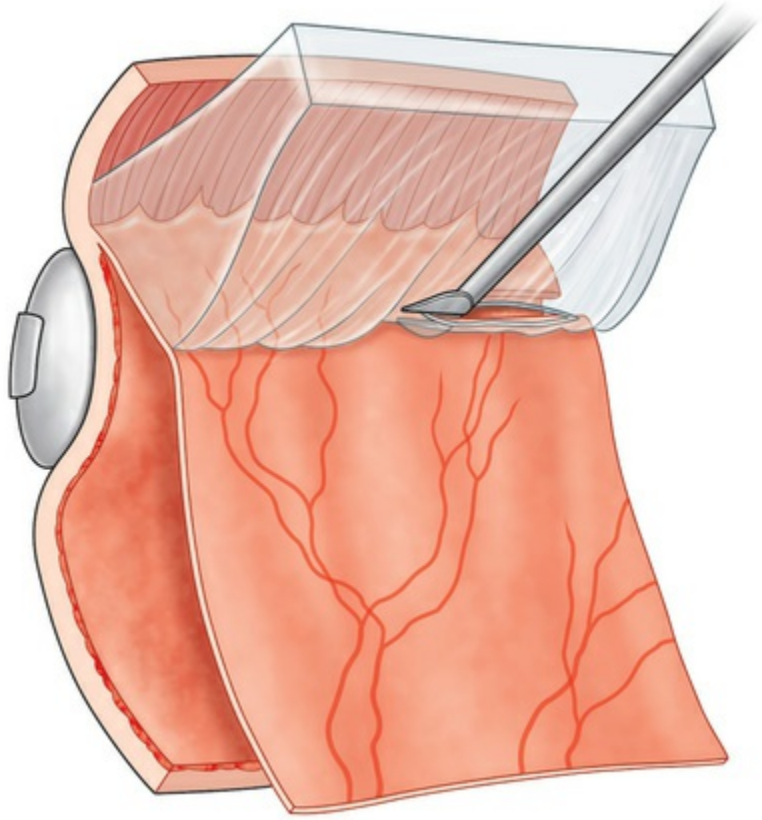

FIG. 111.11 In severe cases of anterior proliferative vitreoretinopathy retinal shortening occurs. This

prevents the retina being flattened unless the traction is relieved by retinotomy. If extensive retinal scar tissue is present, retinectomy must also be performed.

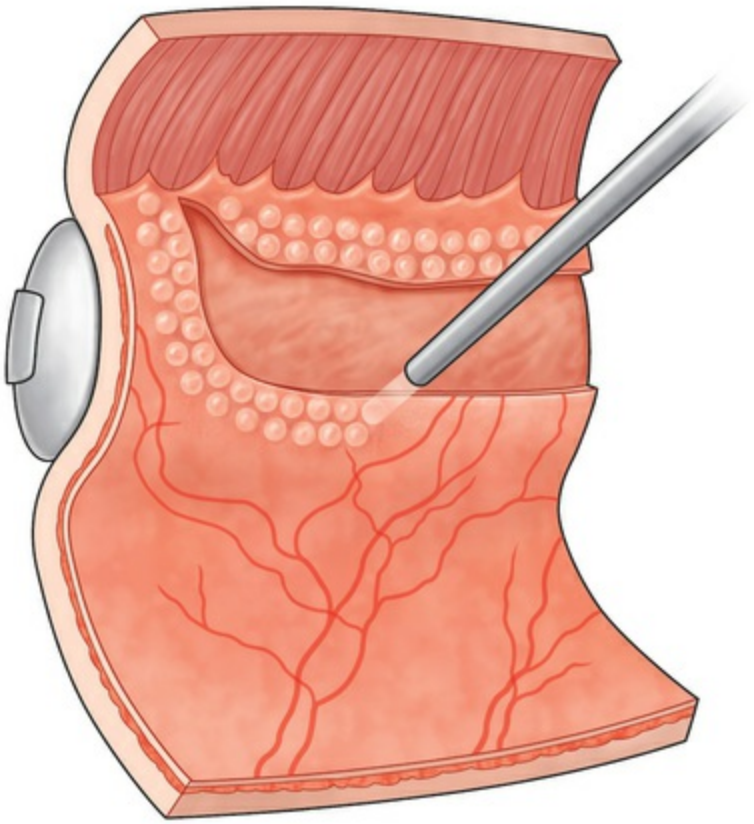

FIG. 111.12 After the retinotomy, traction is relieved and the retina flattens with the help of heavy fluorocarbon liquid and/or fluid–air exchange and active aspiration of subretinal fluid. The edges of the retinotomy and any other retinal breaks are then treated with extensive laser photocoagulation.

Removal of Subretinal Membranes

In a small proportion of eyes, particularly with long-standing PVR and/or excessive prior inflammation, subretinal bands may develop and contract causing tenting of the retina.[42] If these prevent retinal reattachment, then they are removed prior to the fluid–air exchange by creating a small retinotomy with scissors over the tort

membrane, grasping the membrane through the retinotomy with 25G vitreous forceps, and pulling it through the retinotomy into the vitreous compartment.[43,44] It then may be transected or pulled out completely (Fig. 111.13 and Video 111.1 online).

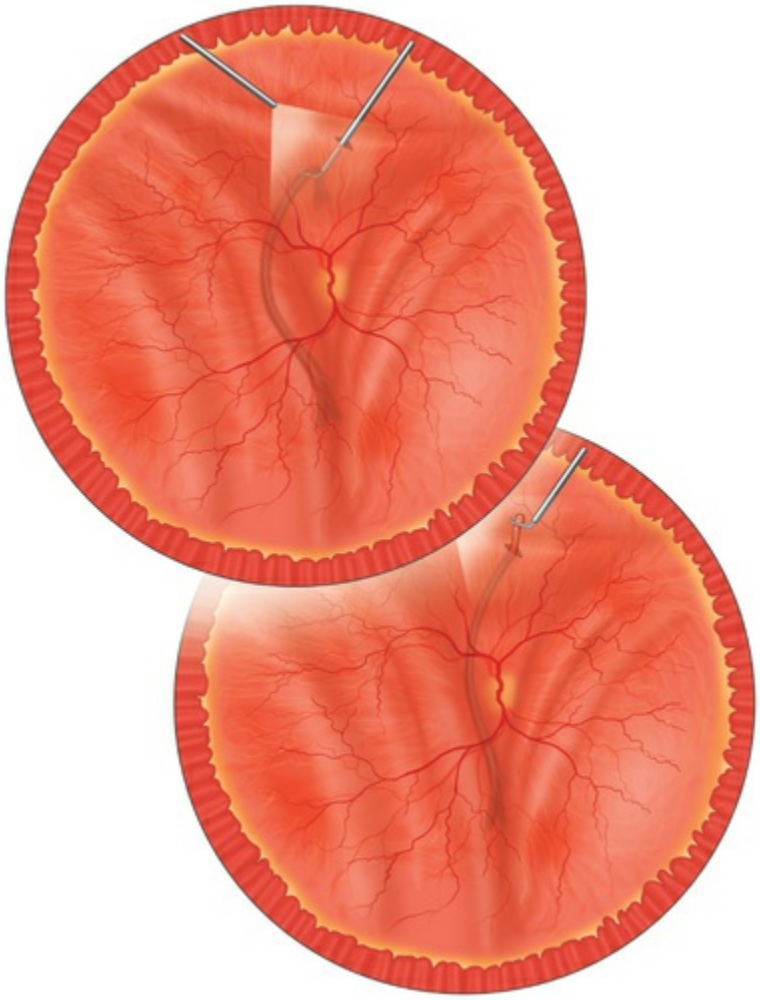

FIG. 111.13 Subretinal bands are removed if they will prevent retinal reattachment. A small retinotomy is made over the subretinal band and forceps are used to pull it through the retinotomy. It may then be simply sectioned and allowed to retract or pulled free of the pigment epithelium and removed in one piece.

Fluid–Air Exchange

After complete mobilization of the retina and relief of all traction, fluid–air exchange is done to achieve a totally flat retina. All

subretinal fluid, heavy fluid, vitreous fluid, and residual opacities such as blood are aspirated through a 25G or 23G extrusion cannula, while maintaining a constant IOP with continuous air infusion (Fig. 111.14). Subretinal fluid drainage may be completed in the presence of heavy fluid by suction through an anterior retinal break, or in the case of fluid–air exchange, a small posterior retinotomy may be required. A planned drainage retinotomy is made by first placing a small white diathermy mark on a spot chosen nasal to the disc, away from any fixed fold but over detached retina and avoiding retinal vessels. The 25G or 23G suction cannula is then used to make a small hole in the weakened spot. Care is taken to continuously aspirate the egressing subretinal fluid and to avoid spreading the mobilized pigment cells onto the retinal surface. A soft flexible silicone tip on the aspirator can be passed under the retina either through the retinotomy or a preexisting retinal tear (Video 111.1 online).

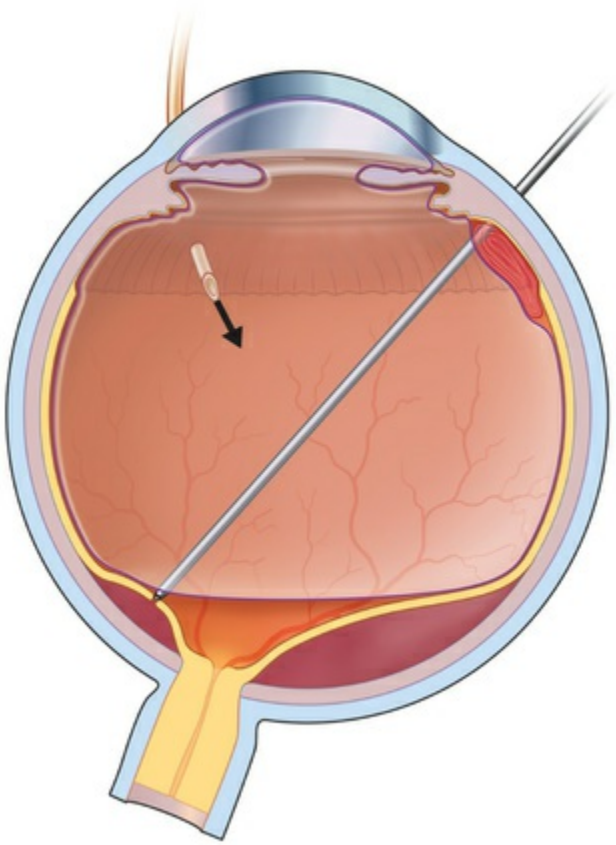

FIG. 111.14 In order to reattach the mobilized retina after vitrectomy and membrane dissection, subretinal

fluid is drained either posteriorly through a deliberate retinotomy or, if present, through a preexisting retinal break. A silicone-tipped extrusion cannula and positive suction facilitates this process as does simultaneous air–fluid exchange. Subretinal fluid is aspirated first to reattach the retina, then remaining intravitreal fluid is replaced by gas. An alternative method if anterior breaks are present is to instil heavy perfluorocarbon liquid and displace subretinal fluid forward where it is aspirated through an open retinal break. (Reproduced with permission from Wilkinson CP, Rice TA. Michels' retinal detachment. 2nd ed. St. Louis: Mosby; 1997.)

Creating Chorioretinal Adhesion and Scleral Indentation

Following complete mobilization of the retina and flattening with air–fluid exchange, extensive endolaser photocoagulation is carried out (Fig. 111.12).[45] All retinal breaks or retinotomies are surrounded with visible retinal burns, and a band of laser is usually extended 360° around the peripheral retina overlying the vitreous base and extending back towards the equator. Endolaser is applied posteriorly almost back to the vascular arcades if an extensive retinotomy or retinectomy has been necessary to flatten scarred contracted inferior retina. Some surgeons prefer to apply laser using an indirect ophthalmoscopic delivery system with scleral depression, particularly if 360°. The settings used tend to be of longer duration (0.3–0.5 seconds) than that used in the clinic with a slit lamp, but care must be made not to increase the energy density excessively, as this may result in choroidal hemorrhage and rupture of Bruch's membrane. Laser photocoagulation is preferable to cryotherapy as it causes less postoperative inflammation and probably is associated with less subsequent complications, namely further breakdown of the blood–vitreous barrier, cellular proliferation, and recurrence of PVR. In some cases, however, cryotherapy is still necessary due to difficulty in dissecting all the membranes in some areas and persisting shallow subretinal fluid under the retina in the far anterior area to be covered by the scleral buckle. Cryotherapy is also necessary if the peripheral view is

compromised. Care should be taken not to overtreat with cryotherapy. If visible laser burns cannot be achieved by endolaser or indirect applications, it usually means that the retina is slightly elevated in the area with persisting shallow subretinal fluid. Once extensive laser photocoagulation and, in some cases, localized cryotherapy is applied, the preplaced scleral buckle is secured by tying each of the preplaced scleral sutures. Indentation is achieved by tightening the encircling element, which is tethered either by a Watzke sleeve or a knotted polyester suture. The resulting scleral buckle should be relatively high to ensure permanent support of the vitreous base. If the eye is left with a low scleral indentation, further proliferation and contraction of residual vitreous base elements can lead to new or reopened retinal tears and recurrence of the detachment. Any large more posterior retinal break should be closed by the buckle if possible. This sometimes requires an additional meridional piece of silicone or even a piece of silicone sponge under the encircling element.

Intraocular Tamponade

The next step is to decide whether short-term tamponade with a long-acting intraocular gas mixture[46]or more extended or permanent tamponade with SO is preferable.[47] A controlled trial suggested that short-term tamponade for 2 weeks with sulfur hexafluoride (SF_6) was inadequate but that longer-acting gas tamponade with octafluorocyclobutane (C_3F_8) for up to 4 weeks was adequate for many eyes. Results were in general comparable in long-term outlook to those in which SO was inserted.[48,49] In practice, however, most surgeons prefer SO (Table 111.4). This is because the majority of these eyes have already had one or more previous surgeries and SO tends to quieten the eye down much quicker and ensure control of a very difficult clinical situation. A further recurrence with long-acting gas tamponade requires another procedure with SO. It also restricts patients' activities for longer. Long-acting gas prevents airplane flights and useful vision for up to 4 weeks. If octafluorocyclobutane gas exchange is selected, a concentration between 15% and 18% is usually used.[50] This is mildly expansile, running the risk of postoperative ocular

hypertension, but creates an effective gas bubble for tamponade with positioning postoperatively and occupies more than half the vitreous compartment for up to 3 weeks. The gas may be instilled via a modern integrated vitrectomy machine or drawn up separately in a 50-ml syringe and diluted to the appropriate concentration with filtered air. Intraocular gas can be replenished postoperatively if the vitreous fill is inadequate or absorbing too quickly as an outpatient procedure using a push/pull fluid–gas exchange technique.[51] In eyes in which the conjunctiva has been dissected, or if there is thin sclera, myopia or a previous vitrectomy and especially with 23G or 20G vitrectomy, it is usual to suture the sclerotomies (7/0 virgin silk) to avoid early postoperative loss of the vitreous gas or SO. Even 25G vitrectomy ports may leak, and if there is any doubt, they should be sutured.

TABLE 111.4

Comparison of Perfluoropropane Gas Versus Silicone Tamponade for Proliferative Vitreoretinopathy

	Advantages	Disadvantages
Perfluoropropane gas	Absorbs spontaneously, giving temporary tamponade to retina	Does not last long enough to provide tamponade needed for eyes with epiretinal reproliferation 6–8 weeks after surgery
	Can control duration of tamponade from intermediate to long duration by adjusting concentration of C_3F_8 with air	Air travel prohibited until bubble absorbed
	Visual rehabilitation occurs more rapidly in eyes with PVR treated with gas	Cataract formation if prone positioning not maintained
	Relatively few long-term complications associated with use	Some short-term complications, such as elevated intraocular pressure
		Hypotony more likely postoperatively
Silicone oil	Provides extended tamponade for months or years, allowing surgeon to determine if and when to remove silicone oil	Does not prevent reproliferation in inferior retina
	The best tamponade for eyes with numerous retinal tears or large retinectomies	Visual acuity slow to improve and causes substantial changes in refraction
	Better in achieving partial retinal reattachment in eyes with residual traction or reproliferation	Corneal toxicity
	No restrictions on air travel	Cataract formation in phakic eyes
	Better tamponade for eyes with	Silicone oil emulsification

	hypotony	Elevated intraocular pressure
		Must be removed by a second surgical procedure to achieve best acuity

Silicone Oil

If SO is selected for longer-duration tamponade, as is usually the case, it is injected directly into the air-filled vitreous cavity (Fig. 111.15). If perfluorocarbon heavy liquid has been used during the procedure, some surgeons will do a direct perfluorocarbon–SO exchange, but most prefer the intermediate step of fluid–air exchange before instilling the SO. This is because residual subretinal fluid may be trapped anteriorly by the heavy fluid and it becomes obvious as it migrates posteriorly again with air towards the posterior pole. A specially designed rigid syringe is provided with SO for its injection under pressure from an air pump in the integrated vitrectomy machine. Oil is injected through the surgical vitrectomy port or through the infusion line of 23G or 20G diameter. It is possible, with modern equipment, to force it through a 23G or 25G short needle or cannula,[52] but some still enlarge the sclerotomy to 20G. The oil syringe is then connected to a short plastic catheter fashioned from the range of intravenous disposable trocar/cannulas available, cut to about 1 cm length, and beveled for easy insertion. At this point, most surgeons still cut a basal iridectomy at 6 o'clock in the inferior iris in aphakic eyes using the vitrector under air to prevent postoperative ciliary block and secondary glaucoma.[29] This step is not necessary if the lens/iris barrier is intact. The SO is injected under direct view with the wide-angle viewing system, while air infusion is still connected to the eye. During injection, air passes out of the air infuser port (Fig. 111.15). The infusion pressure is now lowered to 10–15 mmHg as silicone enters the vitreous compartment from the superior site, thus maintaining IOP. Once air infusion stops as the level of the sclerotomy port is reached by the oil, IOP may rise precipitously. At this point, the air infusion cannula is removed and SO injection continued until the residual air is expelled. Care is taken to monitor the IOP during this maneuver with a cotton-tipped stick. Many surgeons would close one of the sclerotomies prior to injecting the SO and then the remaining two are closed. The final aim is to

achieve a complete fill of the vitreous cavity with SO but an IOP that is towards the lower range of normal, between 10 and 15 mmHg (Fig. 111.16). Silicone oil is available in a less viscous form of 1000 or 1300 cSt (centistokes) or the more viscous 5000 cSt variety. Most vitreoretinal surgeons prefer the 1000–1300 cSt oil because of its relative ease of removal. More viscous SO is said to be less likely to pass through retinal breaks, but any oil will pass through if the hole is not properly flattened after relief of traction or supported by the indentation of a scleral buckle.

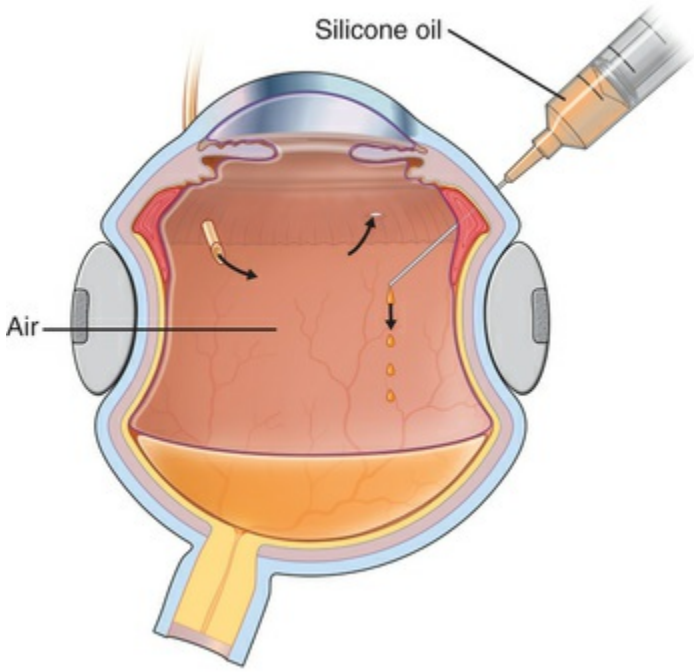

FIG. 111.15 Silicone oil (SO) is injected via a pars plana sclerotomy site through a specially designed 10-mL reinforced syringe attached to a 19G, 20G, or 23G intravenous catheter that has been cut to about 1 cm in length. The oil is pumped in under pressure, and as it flows into the eye, air is pushed either through an open sclerotomy site or, with more control, back up the air infusion line. This helps maintain a normal intraocular pressure during SO injection. Once the oil level reaches the infusion cannula, pressure may rise precipitously. This is avoided by removing the air infusion cannula at this stage and gently continuing the SO injection until all the air is expressed out the sclerotomy sites.

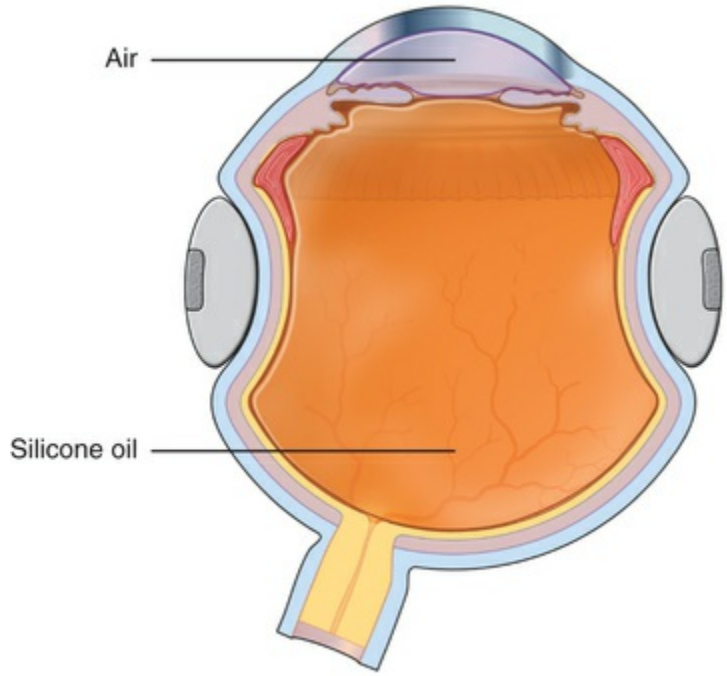

FIG. 111.16 Silicone oil (SO) fills the whole posterior segment after complete vitrectomy, dissection of fibrous tissue membranes, and relief of all retinal traction. The retinal breaks are tamponaded internally with the SO and externally with an encircling silicone buckle. If the eye is aphakic, the anterior segment is temporarily protected from SO by air. SO may have to be left in the eye permanently but is often removed 3–6 months later.

Heavy Silicone Oil

An additional choice for retinal tamponade is that of heavier-than-water, fluorinated silicone liquid. Standard SO is lighter than water, and therefore once the patient is mobile or sitting upright, there tends to be a small gap between the apposition of the fluid bubble and the inferior peripheral retina. This leads to an accumulation of cellular debris and inflammatory proteins in this pool of aqueous between SO and retina. In combination with the lack of inferior tamponade, this often leads to continued retinal surface proliferation and a recurrence of local traction detachment inferiorly.[53,54] This can be avoided or treated when it occurs

postoperatively with the use of heavy fluorinated SO, which tamponades the inferior retina when the patient is upright (Figs. 111.17 and 111.18). It has been used in combination with light SO but more often as an alternative, particularly after inferior relaxing retinotomy.[54–68]

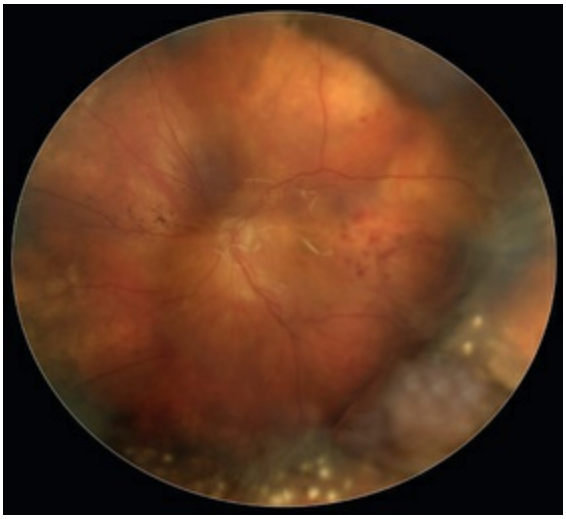

FIG. 111.17 Reattached retina 1 week after proliferative vitreoretinopathy surgery with an encircling scleral band, vitrectomy, membrane peeling, endolaser photocoagulation, and tamponade of inferior retina with heavy silicone oil.

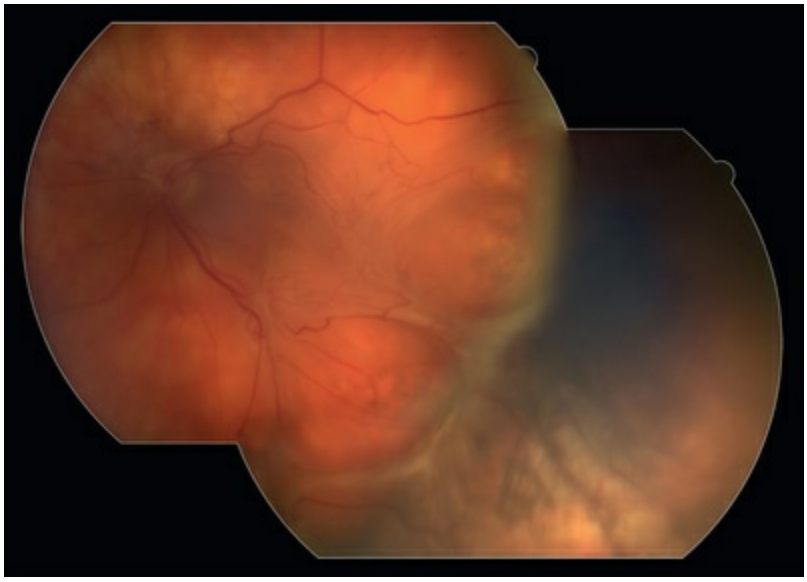

FIG. 111.18 Same eye as in Fig. 111.17, 2 months

later. The retina remains attached, but there has been proliferation of scar tissue posterior to the buckle causing a sharp fold. The retina is weighed down on either side by the heavy silicone oil.

First-generation (fluorinated silicone and perfluorocarbon liquids) and second-generation (partially fluorinated alkanes) heavy tamponades had frequent complications including intraocular inflammation, raised IOP, and emulsification. Three examples of third-generation heavy SO tamponades are reported to have a complication profile similar to light SO.[65] They provide better tamponade of the inferior retina and posterior pole. The toxic effects of long-term retention in the eye are not yet known, and emulsification is frequent.[53–68] Therefore, heavy oil is usually currently removed after 3 months.

Finally, the orbit is rinsed with balanced salt and a long-acting local anesthetic for postoperative pain management. Dilute antibiotics such as gentamicin or a cephalosporin are also added to the sub-Tenon space. The conjunctiva is closed if a peritomy was done, with absorbable 7/0 sutures and an injection of long-acting Celestone or triamcinolone given in the sub-Tenon space.

Operating Under Silicone Oil

Many eyes with PVR continue to develop surface retinal membranes after successful surgery to reattach the retina.[69] These contract and cause complications ranging from premacular pucker to inferior retinal detachment, retinal tears, and retinal shortening. Although some surgeons prefer to remove the SO and peel the scar tissue or relieve the effects of traction with peripheral retinectomy under perfluorocarbon heavy liquid, it is usually possible to operate under the oil.

An infusion port is connected to air to maintain IOP. Membranes are peeled with vitreous forceps off the macula (Figs. 111.19A–B). A secondary retinal tear requires complete relief of traction and further laser. Retinal shortening usually needs a high scleral buckle and/ or peripheral retinectomy. Any residual subretinal and preretinal fluid (in the case of light SO) is drained by active suction, and the SO is topped up as required.

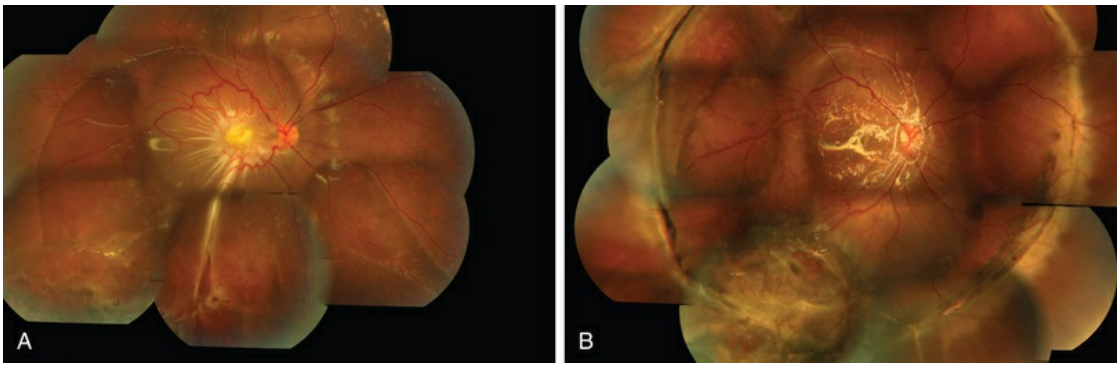

FIG. 111.19 (A,B) Dense preretinal membrane causing macular and inferior retinal traction after proliferative vitreoretinopathy and retinal reattachment with silicone oil. The secondary macular membrane was peeled with vitreous forceps under the silicone oil without first removing it.

Removal of Silicone Oil

Both types of liquid silicone are usually associated with poor vision due to the markedly different refractive index even if, as is usually not the case with PVR, there is reasonable macula visual potential.[70] Migration of SO bubbles and slow neuronal degeneration have long been recognized. The wound-healing sequence of PVR matures like any other scar tissue over 3 months, and therefore SO is left in for at least that length of time. The eye is carefully monitored for recurrent traction and retinal breaks, but if the eye is quiet and all peripheral retinal pathology well supported by a high scleral buckle and all retinal breaks closed, silicone liquid may be removed after approximately 3 months. Delayed removal up to 18 months does not improve functional outcomes.[71] However, there is also a significant risk of retinal redetachment after SO removal.[72,73] Additional 360° laser posterior to the encircling buckle may decrease the risk. Many eyes, however, have relatively poor visual potential despite a flat macula, but evidence of persistent peripheral scar tissue or localized retinal detachment. They may have had numerous retinal breaks or extensive retinectomy. Most have had multiple surgeries by this stage, and in all these circumstances it is generally wiser to leave the SO in situ. Depending on the range of severity of PVR for which the surgeon chooses to use SO, the rate of removal will vary from about 50% to 85% of cases. Cataract occurs

invariably after liquid silicone tamponade of the retina, usually within 6–18 months. Combined phacoemulsification of the lens, insertion of an intraocular lens, and removal of the SO is then carried out at the same time. Late glaucoma is common with or without emulsified silicone bubbles in the anterior chamber and is usually an indication to remove all the oil (Fig. 111.20). Band keratopathy may occur in young people in the presence of SO, even if confined in the vitreous. Removal may slow the progression. SO is usually removed in the operating room through a 20G sclerotomy site using a shortened, bevelled intravenous 21G catheter attached to a 10-mL syringe and active suction. A preplaced infusion cannula in the inferotemporal quadrant maintains IOP during the procedure. The last of the silicone is removed by rotating the eye so that the residual bubble floats out. Controlled active suction through a 23G or 25G cannula is a convenient alternative with modern vitrectomy equipment.[74] Many surgeons do one or two fluid–air exchanges to ensure residual small bubbles are removed. This step may also detect small untreated retinal breaks masked by SO tamponade. They can cause local redetachment during the exchanges and can then be treated with laser under air. Heavy fluorinated silicone is more difficult to remove. An automated aspiration system is now available on integrated vitrectomy machines to aid in this procedure. Using a short 23G or25G cannula continuous suction is applied to draw the heavy SO up to the port. The heavy SO falls back if the suction is interrupted. It then needs to be aspirated with a longer intravenous plastic catheter connected to the aspiration tubing and placed over the optic disc. The vitreous compartment may be left filled with air for a brief postoperative tamponade after removal of SO, or else with saline.

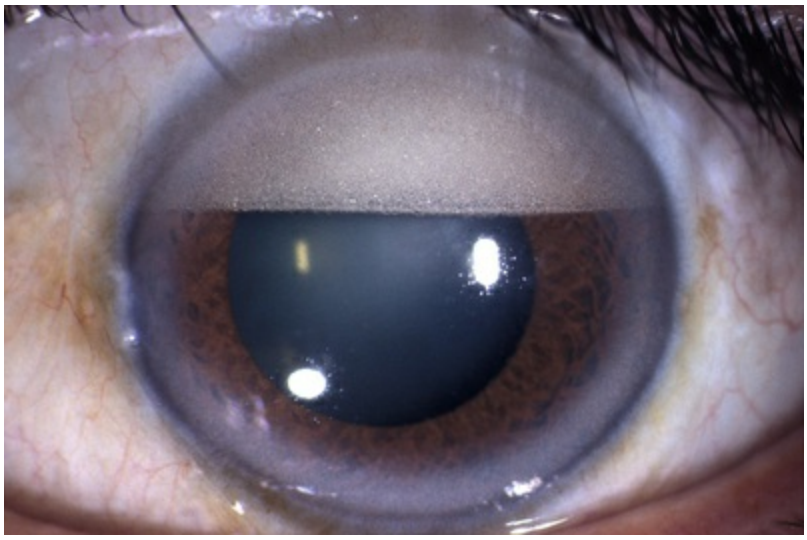

FIG. 111.20 Emulsified silicone oil (SO) bubbles in the anterior chamber and central corneal stromal haze associated with SO keratopathy. Removal is indicated to prevent secondary glaucoma and further corneal degeneration. It is necessary to remove posterior SO as well in this situation or further emulsified bubbles may pass to the anterior chamber causing the situation to recur. If continued SO tamponade of the retina is necessary, fresh SO is injected in the vitreous compartment.

Postoperative Management

The postoperative management following surgery for PVR is particularly important. The patient should be nursed face-down in the prone position for at least the first 24 hours after gas or light SO exchange to allow the pigment epithelium to pump out any remaining subretinal fluid and to facilitate initial adhesion at the sites of photocoagulation or cryotherapy. Some surgeons insist on prone positioning for a much longer duration, up to 7–10 days, if there are inferior retinal breaks.

If heavy SO is used, the patient lies supine for 1–2 days and is then mobilized. A rise in IOP is quite frequent after a high encircling scleral buckle and SO injection or gas and it is important that this is monitored regularly. Most surgeons ask the patients to avoid sleeping on their back as this encourages light SO to move forward away from the retinal surface and possibly into the anterior

chamber. Shallowing of the anterior chamber may also occur. Corticosteroid, mydriatic/cycloplegic drops are usually used four times a day for 3–4 weeks, and the patient may in addition require antihypertensive drops and acetazolamide tablets for postoperative ocular hypertension. A rising IOP that persists despite medical therapy usually implies an overfill of the vitreous cavity, and a small amount may even need to be aspirated back in the operating room. If orbital swelling and pain in the absence of a high IOP occurs, oral prednisolone should also be considered in addition to operative sub-Tenon steroid and routine analgesics.

Complications After PVR Surgery

PVR is a very serious complication of retinal detachment, and patients should be informed preoperatively of the possibility of substantial visual loss despite anatomically successful surgery. There are also risks of significant intraoperative problems and late complications.[75] It is difficult preoperatively to determine how adherent preretinal membranes are to the retinal surface. In some cases, therefore, the membranes cannot be fully dissected and the retina mobilized, and in others, in doing so, retinal breaks can be created. It is now recognized, however, that it is better to relieve retinal traction effectively, even if creation of retinal breaks is inevitable. A deliberate relaxing retinotomy for relief of traction was required in 29% of eyes treated in the Silicone Study.[35] With increasing use of heavy fluids as a surgical aid and for postoperative tamponade, the trend is towards increasingly aggressive intraocular surgery to relieve traction.

Intraoperative Complications

Intraoperative bleeding may occur during dissection of dense membranes and in creating a retinotomy, and this is controlled by raising the infusion pressure temporarily and, if necessary, endodiathermy. The view may also become obscured by intraoperative corneal edema, pupillary constriction, or lens clouding. The corneal epithelium can be scraped clear or the pupil redilated either with 1 : 10,000 epinephrine in the vitrectomy

infusion, flexible iris retractors, or rarely iridectomy/sphincterotomy using the vitrector. Lens clouding during the operation would necessitate a 20G fragmatome lensectomy via the pars plana. Failure to flatten the retina with internal drainage and fluid–air exchange can be treated either by instillation of heavy fluid to push the subretinal fluid forward to the retinal break or by a discrete retinotomy away from any fibrous tissue and preferably in the superior half of the retina near the optic disc. It may also mean that further relief of traction is required. During surgery, air or heavy fluid or SO may pass through a retinal break and under the retina. Further relief of retinal traction usually allows this to be aspirated and the retina to be reattached again, but it may require a large retinotomy. Choroidal hemorrhagic detachment may occur intraoperatively by laceration of a choroidal vessel when placing scleral sutures, spontaneously in a susceptible eye or if prolonged hypotony occurs. This complication if too large to leave is treated by the temporary insertion of heavy liquid hydrocarbon in the vitreous followed by external drainage of blood through a radial sclerotomy. Sometimes such a choroidal detachment cannot be drained during the surgery and requires a repeat visit to the operating room a few days later. Serous choroidal detachment may occur but is usually due to a misplaced infusion cannula under the retina or in the suprachoroidal space. This is managed by transferring the infusion to another port. The intraocular swelling then subsides, and the offending cannula can be adjusted or replaced. Perfluorocarbon heavy fluid may pass through a retinal break and sink back to the posterior pole if the eye is filled beyond the edge of an open retinal break. A retinotomy may be required to remove it with fluid–air exchange. SO can also pass under the retina if it is not fully relieved of traction. This requires more extensive retinotomy and further exchanges to flatten the retina after complete mobilization.

Early Postoperative Complications

Multiple early postoperative complications may occur following this complex surgery. Elevated IOP is the most common, occurring in 10–15% of eyes.[48] A rise to about 25 mmHg is treated

conservatively with ocular hypotensive drops and oral acetazolamide. If higher than this, it is often due to angle closure with a forward shift of the iris diaphragm or overfill of the eye with gas or SO. In aphakic eyes filled with silicone, a pressure rise may be due to an incomplete inferior iridectomy or subsequent blocking of it with lens capsule. An overfill of intraocular gas can be readily dealt with in the clinic or at the bedside under topical anesthetic, with removal of 0.2 ml or so through the pars plana with a 30G needle and syringe. Removal of SO is more difficult and requires a trip back to the operating room and aspiration, plus deepening of the anterior chamber. Postoperative inflammation is common following extensive vitreoretinal surgery and fibrin may occlude the pupil or coat the posterior surface of the intraocular lens. This is treated with intensive topical, and sometimes systemic, steroids. Tissue plasminogen activator injection may also be used to break down fibrin in the anterior chamber but is usually not necessary. A common complication where gas is used is an incomplete fill due to mixing errors or leakage through a sclerotomy site. Gas may be topped up or if the subretinal fluid persists, replaced with SO. An incomplete fill of SO with associated fluid inferiorly may require reoperation with top-up of the oil and internal drainage of the residual fluid or possibly supplementation with an injection of heavy silicone liquid. A persistent corneal epithelial defect particularly after the epithelium has been removed from a cloudy cornea during surgery may require extended patching and antibiotic ointment. Endophthalmitis is very rare, but this is a prolonged operation with multiple insertion of instruments, and must always be considered a possibility. The standard injection of intravitreal antibiotics is complicated by the presence of intravitreal gas or silicone. This could be removed and antibiotics instilled in the vitreous, or the surgeon can rely on high-dose systemic antibiotics as a vitreous substitute will exclude entry of inflammatory byproducts into the vitreous cavity and concentrate antibiotic outside the silicone barrier.

Late Postoperative Complications

There are numerous late complications of surgery for PVR, usually

leading to a disappointing outcome in terms of visual rehabilitation. The commonest is regrowth of surface retinal membranes leading to retinal detachment and tractional retinal tears or, if milder, to macular pucker. Between one-quarter to one-half of eyes undergoing PVR surgery develop recurrent retinal detachment.[72,73] This high incidence has probably improved significantly with the advent of better instrumentation, visualization, and surgical techniques, particularly the intraoperative use of perfluorocarbon heavy fluid as an aid to surgical relief of traction. The commonest situation is inferior recurrence of retinal detachment with or without a new or reopened retinal break inferiorly in association with light SO. Even with a clinically complete fill of silicone, a small meniscus of vitreous fluid remains inferiorly when the patient is upright and the silicone bubble rises slightly superiorly. This is because the shape of the internal eye is not an exact circle like the bubble. The combination of protein, inflammatory, and metaplastic cells and lack of tamponade in this area can lead to further proliferation on the retinal surface in 50–60% of eyes (Fig. 111.21).[75,76] This has been called perisilicone proliferation.[77] It is sometimes advisable to leave this alone and either wall off the local detachment with laser and accept it if the macula stays attached,[78] or alternatively, it can be treated by the supplementation of the silicone with heavy silicone liquid which will press inferiorly with gravity and tamponade the retina (Figs. 110.17 and 110.18). If the fluid is extending towards the posterior pole and threatening useful macula function, then reoperation should be considered. If a retinal break is present, then further dissection of membranes around the edge and indentation with a supplementary radial segment of scleral explant under the encircling band may close it and stop progression. Macular pucker and discrete tractional membranes can be peeled or divided behind SO, without removing it (Figs. 111.19A–B). Macular pucker occurs in PVR eyes subjected to vitreoretinal surgery in 5–15%.[79,80] Peeling is considered if there is significant visual potential and is not difficult under SO.[80] Anterior surface proliferation may gradually interfere with the ciliary body secretory function and lead to hypotony[81] (Fig. 111.22). This is very difficult to treat and, in selected cases, may occasionally justify further surgery to peel membranes off the ciliary body surface

followed by tamponade with SO.[82] Following relaxing retinotomy and retinectomy, the cut edge may fibrose and retract back to the posterior pole (Fig. 111.23). This situation may still allow useful vision. Heavy perfluorocarbon liquid that has passed through a retinal break undetected during surgery localizes under the macula or inferiorly with gravity postoperatively. This can be removed with an additional surgery by suction through a 39G flexible subretinal cannula.[83] Heavy fluid may be left in the vitreous cavity if small in volume, but needs to be aspirated from the anterior chamber.[84]

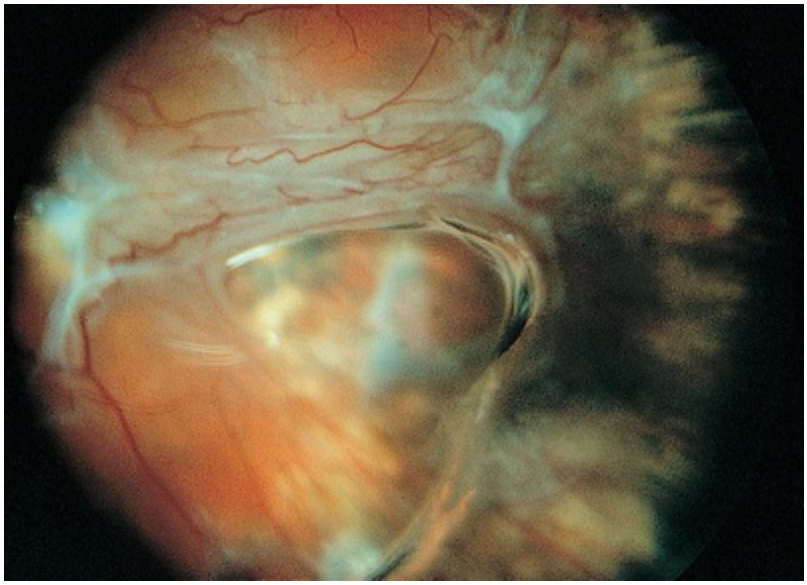

FIG. 111.21 Progressive proliferation of scar tissue and inferior retinal shortening behind silicone oil (SO) incompletely filling the vitreous compartment. Progressive retinal shortening may be accompanied by the late development of large inferior retinal breaks and passage of the SO under the retina. Heavy SO formulations show promise of decreasing the occurrence of this condition sometimes called "perisilicone proliferation."

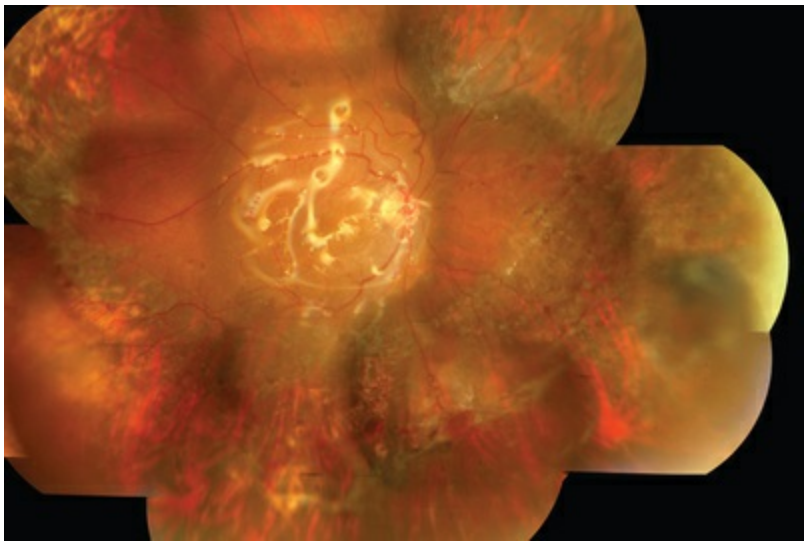

FIG. 111.22 Reattached retina after proliferative vitreoretinopathy surgery with inferior relaxing circumferential retinotomy, extensive laser, and silicone oil with no encircling scleral buckle.

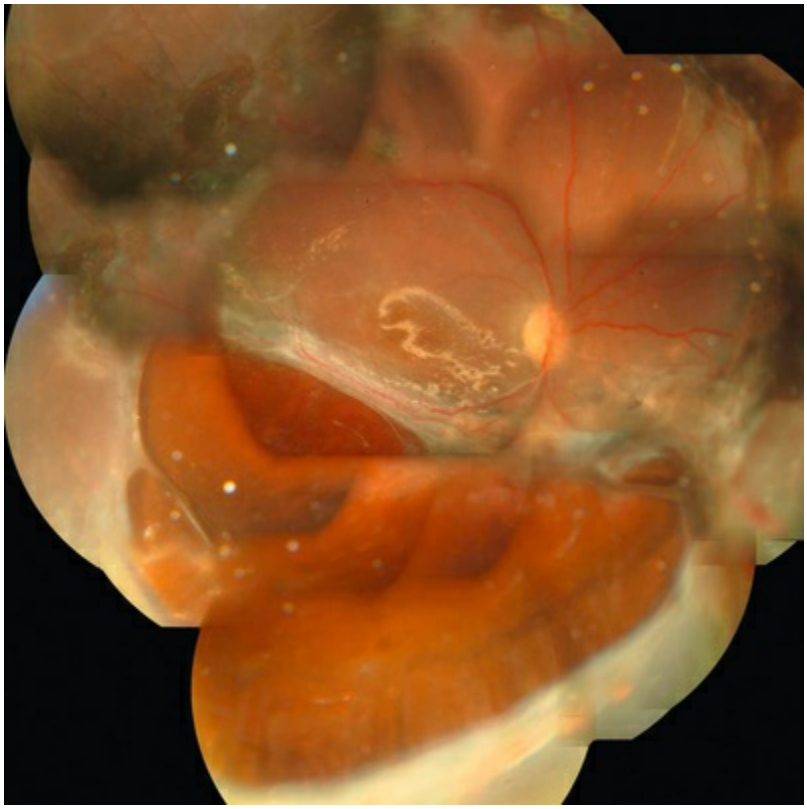

FIG. 111.23 Contraction of cut posterior edge of retinectomy almost back to the macula. Despite this, the macula remains attached under silicone oil with potential for useful vision.

There are many complications of prolonged intraocular SO. Emulsification into fine bubbles is very common, particularly with the lower-viscosity (1000 cSt) material and especially if it has been mixed with inflammatory proteins or blood and in eyes that are aphakic with an incomplete fill where there is a constant fluid/oil surface interaction. If limited in extent and confined to the posterior segment, they can be left alone. Tiny emulsified SO bubbles may pass through the zonules into the anterior chamber (Fig. 111.19) and have also been found in various intraocular and orbital tissues. In particular they can block the angle and lead to late secondary glaucoma. SO in the anterior chamber can also damage corneal endothelial function. If the anterior chamber is full of SO, the cornea does not swell but rapidly does so after removal of the oil if the corneal endothelial function has been damaged. Keratopathy developed in 27% of eyes treated successfully in the Silicone Study,[84] but most of these eyes were aphakic. This incidence is far less in eyes with an inserted intraocular lens and circular capsulorrhexis. Band keratopathy with a degenerative cornea and dystrophic calcification is commonly seen particularly in young people in the presence of long-term SO in the eye even without direct contact to the cornea. Band keratopathy is difficult to treat although the calcium may be temporarily removed by scraping the cornea and applying the chelating agent EDTA. Attempts to remove emulsified SO droplets in the anterior chamber by irrigation and aspiration can be frustrating as further oil tends to flow through from the vitreous cavity. This may be stopped in some cases by replacement of the anterior chamber fluid with viscous sodium hyaluronate and management of any rise in IOP afterwards by intermittent release through a preplaced limbal incision. Otherwise the SO usually needs to be removed completely and, if still required, replaced with fresh SO.

Cataract is universal in phakic eyes following vitrectomy and extended silicone tamponade. Late phacoemulsification of cataract and intracapsular lens implantation presents no special difficulties, and the silicone liquid can be removed at the same time or left in the eye permanently. Some surgeons advocate phacoemulsification and replacement of the lens routinely at the time of surgery for PVR, as this may facilitate dissection of the vitreous base and

anterior loop traction of the retina. With modern systems this is no longer usually necessary and the lens is spared until cataract develops later. Rubeosis of the iris is occasionally seen following surgery for retinal detachment and PVR but is uncommon unless the patient already has coexisting diabetic retinopathy.[85] It is more likely where there is recurrent persisting retinal detachment and intraocular inflammation. Modern SO has fewer impurities and the incidence has decreased. Treatment for rubeosis iridis, if active, rather than low grade and chronic, involves injection of a vascular endothelial growth factor blocker and consideration for subsequent glaucoma surgery if salvageable vision is still present.

Other complications for PVR surgery include late cystoid macular edema with or without preretinal membranes.[79] This can be readily analyzed with spectral domain optical coherence tomography (OCT). Treatment is with topical steroid and nonsteroidal drops, intravitreal triamcinolone injection, and, in special circumstances where vision might be salvageable, peeling of the internal limiting membrane over the macula. Sympathetic ophthalmia must also be considered as a rare complication after multiple vitreoretinal surgeries.

The other group of complications of PVR surgery involves those associated with a scleral buckle. Surface scarring around the muscles may lead to squint and double vision. The scleral buckle may erode through the conjunctiva and lead to chronic low-grade infection. Attempts are often made to retain a scleral buckle rather than remove it in this circumstance. It may be possible to treat the chronic discharge with excision of a local section of the buckle, leaving the band intact and removing the local offending suture, but usually the material all has to be removed. If the buckle does have to be removed, preoperative 360° prophylactic laser immediately posterior to the buckle may be carried out. If persistent membranes are present on the retina and silicone has not been injected previously, then silicone replacement of the vitreous is an additional option to ensure recurrent retinal detachment does not occur. If retinal detachment does recur after removal of an exposed or infected scleral buckle, then SO tamponade is usually the most practical option.

Medical Adjunctive Therapy for PVR

The devastating effect of PVR on visual prognosis and the expense and difficulty of multiple surgeries has led to sustained efforts to find pharmacologic therapies that may decrease the risk and recurrence after retinal detachment surgery. Systemic prednisolone and sub-Tenon injection of long-acting Celestone or triamcinolone have long been used to dampen down inflammation and its sequelae that predispose to PVR. The very complex cellular and protein factors activated and upregulated in PVR are outlined in detail in Chapter 101 (Pathogenesis of proliferative vitreoretinopathy). Intravitreal triamcinolone acetamide is the most favored agent of those studied, and it is increasingly used as an adjunct during surgery to delaminate fine tissue planes and pockets of formed vitreous and membranes that may not be visible with normal operative systems of illumination. Hopefully, a beneficial dose persists after vitreous replacement. Triamcinolone can also be injected into the SO for slow release.[86,87] As with other steroids, it is thought to have a wide-ranging effect on factors in the inflammatory cascade and hence diminish the stimulus to cellular proliferation and contraction. Antiproliferative agents including 5-fluorouracil[88,89] and daunomycin[90] have been evaluated, but unfortunately the therapeutic window between inhibition of fibroblastic tissue proliferation and toxicity to surrounding sensitive neuronal cells has not been sufficient to demonstrate a clinical benefit in humans.[91] The many biologic signals of PVR found with laboratory investigation of the cell biology and proteomics, for example, with platelet-derived growth factor and connective tissue growth factor,[92,93] will hopefully one day provide a suitable target for a more specific intervention in the process. Early evidence along these lines has been reported with anti-VEGF injections (bevacizumab) into silicone oil.[94] Genetic variations in patients with PVR are starting to emerge, for example, an association with the gene linked to tumor necrosis factor.[95] Hopefully, clinical trials to block specific biologics using humanized antibodies, RNA interference, or gene therapy will emerge.[96]

Results of Surgery for PVR

The anatomic success, which is defined as retinal reattachment for at least 6 months, has progressively improved over the last 40 years, along with the steady improvement in instrumentation and surgical techniques.[97–122] A summary list of published results is shown in Tables 111.5 and 111.6. It is important to note that it is difficult to compare results in case series that may include eyes of different severity and do not define or control enrollment parameters. A scleral buckle without vitrectomy successfully reattached up to 50% of milder cases 30 years ago, while at present, with all the surgical techniques at our disposal, up to 90% of all cases of PVR can be anatomically reattached.[26] However, many eyes need more than one operation because of continuing cellular proliferation and retinal traction. An example of moderate severity successfully reattached and maintained with extensive laser is shown in Fig. 111.24. Another case requiring extensive retinectomy and long-term SO is shown in Fig. 111.25. Functional success defined as improved visual acuity is more problematic, as any macula detached for more than a few days is unlikely to recover more than 10–20% of central vision[14] which, in the context of the other eye, may be more or less clinically significant. In addition, as outlined in Chapter 101 (Pathogenesis of proliferative vitreoretinopathy), the substantial and multifactorial inflammatory events associated with PVR lead to apoptosis of retinal cells as well as activation and a breakdown in the function of retinal glial cells. If this process is prolonged or particularly severe, then most visual potential is lost. In the multicenter and largely controlled Silicone Study, now almost 25 years old, about half the eyes overall, whether with gas or SO, obtained 5/200 vision or better.[48,121,122] If the process was not so severe that SO was able to be removed, eyes after removal of oil were 19 times more likely to experience a visual acuity improvement of ≥3 lines. However, removal of SO resulted in recurrent retinal detachment in 19% of eyes, and this was twice the risk of retinal detachment in eyes in which the SO was not removed. The visual results were relatively stable in those eyes that obtained retinal reattachment 6 years after surgery. Visual results were better in those that required only one surgery. There was no statistically significant difference in the

anatomic reattachment rate or visual acuity between 14% perfluoropropane gas tamponade or SO after long-term follow-up of up to 6 years.[122]

TABLE 111.5

Results of Vitreous Surgery for Proliferative Vitreoretinopathy (1978–2003)

Reference	Eyes (*n*)	Anatomic Results: Retina Reattached (%)	Functional Results	Comments
Machemer and Laqua (1978)[97]	47	36	Not stated	Air or 40% sulfur hexafluoride gas
Grey and Leaver (1979)[98]	105	64	55% "improved vision"	Silicone oil injected in retrohyaloid space without vitrectomy
Lean et al. (1982)[99]	49	68	Not stated	Vitrectomy and silicone oil tamponade
de Bustros and Michels (1984)[100]	82	66	32% >20/200	Air or sulfur hexafluoride tamponade
Jalkh et al. (1984)[101]	410	59	25% >20/400	Air tamponade
Sternberg and Machemer (1985)[102]	72	33	19% >5/200	Air or sulfur hexafluoride tamponade
Gonvers (1982)[103]	146	62	57% >20/400	Silicone oil used in all eyes; results 6 months after oil removal
McCuen et al. (1985)[104]	44	64	57% 5/200 or better	All eyes had prior failed PVR surgery, silicone oil tamponade
Cox et al. (1986)[105]	51	65	25% >20/400	Results using silicone oil; oil removed in 30%
Stern et al. (1986)[106]	19	68	Not stated	Results similar for silicone oil and sulfur hexafluoride
Glaser (1986)[107]	19	95	44% 5/200 or better	All eyes had giant tears and PVR; silicone oil used in all eyes
Yeo et al. (1987)[108]	30	67	53% 5/200 or better	Silicone oil used in all eyes
Aaberg (1988)[109]	80	70 (posterior PVR), 57 (anterior PVR)	54% 5/200 or better (posterior PVR), 47% 5/200 or better (anterior PVR)	Gas and silicone oil used
Fisher et al. (1988)[110]	76	82	69% >20/400	Perfluoropropane gas
Hanneken and Michels (1988)[111]	95	80	88% reattached retinas 5/200 or better	Gas 84% eyes; silicone oil 16% eyes
Lewis et al.	20	65	20% 5/200 or better	Eyes with PVR that

(1989)[44]				required removal of subretinal membranes
Silicone Study Group (1992)[76]	265	61–73	33–45% 5/200 or better	Gas or silicone oil used
Körner and Böhnke (1995)[112]	501	85 stage C PVR, 70 stage D PVR	78% stage C, 65% stage D 5/200 or better	Silicone oil used in 69% of eyes
Coll et al. (1995)[29]	223	78 with one surgery, 96 with multiple surgeries	74% were 20/400 or better	Perfluoro-n-octane used in all eyes, 92% gas, 8% silicone oil tamponade
Scott et al. (2003)[113]	555	78 at 6 months	60% improved acuity at the final exam, perfluoro-n-octane used in all eyes	Proliferative vitreoretinopathy

TABLE 111.6

Results of Vitreous Surgery for Proliferative Vitreoretinopathy (2004–2015)

Reference	Eyes (*n*)	Anatomic Results: Retina Reattached (%)	Functional Results	Comments
Charteris et al. (2004)[114]	157	84	Not stated	5-fluorouracil and low-MW heparin made no difference
Tseng et al. (2005)[115]	38	97	Not stated	Relaxing retinotomy, silicone oil
Quiram et al. (2006)[116]	56	93	70% improved or stabilized	Inferior retinotomy, silicone oil removed in 58% and superior to gas
Grigoropoulos et al. (2007)[118]	304	72	VA improved 45%, unchanged in 24%, worse in 29%	Retinectomy
Berker et al. (2007)[55]	21	81	43% improved	Temporary heavy silicone oil tamponade
Lam et al. (2008)[72]	147	82	Correlated with reattachment	Silicone oil removed at 12.4 ± 9.8 months
de Silva et al. (2008)[119]	145	68	49% 20/400 or better; 51% <20/400	Retinectomy
Lim et al. (2009)[38]	30	93	67% improved; 27% same	Combined large radial retinotomy/retinectomy
Chen et al. (2011)[86]	36	97	84%	Silicone oil and triamcinolone 2 mg injected into oil
Stopa and Kociek (2011)[39]	25	96	2.3 logMAR preop improved to 1.00	Retinectomy
Hussain and Banerjee (2011)[66]	12	91	36% 2-4 lines 27% same	Heavy SO
Joussen et al. (2011)[67]	93	48 SO vs 28 HSO	1.24 SO vs 1.27 HSO	First prospective randomized Comparison SO vs HSO

Garnier et al. (2013)[40]	20	70	20% had 20/200 or better	360 degree retinotomy
Hocaoglu et al. (2015)[41]	40	75-79	25% had 20/200 or better	360 degree retinotomy, anterior flap retinectomy and radial retinotomy
Mancino et al. (2015)[120]	33	97	Median 1.28 preop improved to 0.74	previous scleral buckle better outcome

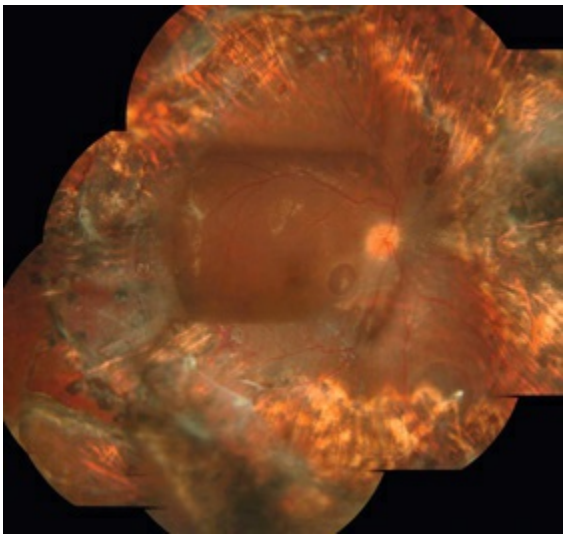

FIG. 111.24 Reattached retina after extensive proliferative vitreoretinopathy surgery. A wide band of laser 360° decreases the risk of recurrent detachment after removal of silicone oil.

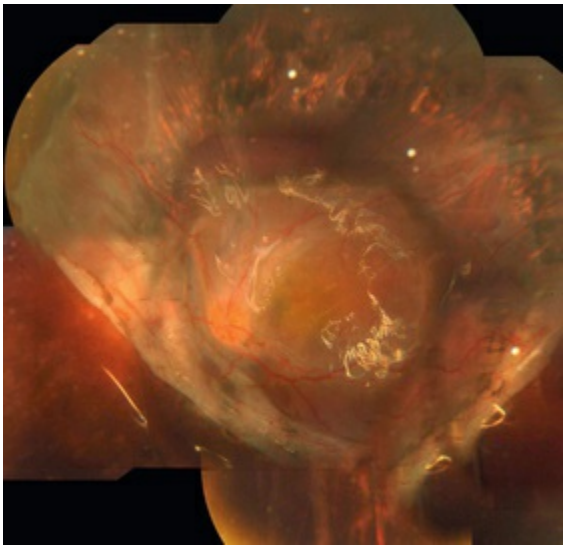

FIG. 111.25 Reattached retina after proliferative vitreoretinopathy surgery requiring extensive inferior

retinectomy. Although there is a large bare area devoid of retina inferiorly, the retinal edge is held flat with a combination of silicone oil tamponade and laser applications.

When is Surgery for PVR Not Justified?

Analysis of fellow eyes in 249 patients with PVR showed that more than 50% of fellow eyes have some vision-threatening pathology. Prophylactic laser to any retinal tears or other predetachment changes such as lattice degeneration in the second eye. Therefore, in the opinion of some authorities the most important action to take in this clinical setting, since most patients at this time with PVR achieve what is really only peripheral vision that is often distorted or inducive of diplopia. Judgment is required as to when not to intervene. One cost–utility analysis of surgery for PVR reasoned that it was cost-effective compared with many other medical interventions in ophthalmology and this would be especially so where there is pathology and low vision in the second eye.[123] If the PVR has occurred in the second eye and the first is already afflicted with low vision or blindness, then the complete range of surgical intervention and multiple procedures is justifiable, as a large majority can be expected to recover reasonable mobility vision. Even if retinectomy is required, vision can improve in up to almost half of the eyes and anatomic reattachment in about 70%.[117,118] If the second eye has normal vision and is safe after prophylactic retinal laser, then eyes at the severe end of the spectrum with chronic retinal detachment and no hope of macular redemption, with extensive intraretinal gliosis and inferior retinal shortening, with very large or posterior retinal breaks, or with failure after SO injection, could all be justifiably left alone and further surgery advised against. Eyes with preexisting PVR require a mean of 3.7 operations compared with 1.8 for those with retinal detachment and no PVR in one study.[124] The decision-making process, however, must be flexible and is dependent on the patient and their relatives having a thorough understanding of the expectations and of the

possible outcomes, so that a joint decision-making process can occur. It is to be hoped that the rapidly evolving understanding of the molecular biology and cellular biology of PVR will soon change the outlook beyond the extraordinary therapeutic advances achieved by fine instrumentation, surgical techniques, and current adjunctive therapy (Figs. 111.19 and 111.22).

References

1. Scott JD. Treatment of massive vitreous retraction. *Trans Ophthalmol Soc U K*. 1975;95:429–432.
2. Machemer R. Pathogenesis and classification of massive periretinal proliferation. *Br J Ophthalmol*. 1978;62:737–747.
3. The classification of retinal detachment with proliferative vitreoretinopathy. *Ophthalmology*. 1983;90:121–125.
4. Machemer R, Aaberg TM, Freeman HM, et al. An updated classification of retinal detachment with proliferative vitreoretinopathy. *Am J Ophthalmol*. 1991;112:159–165.
5. Charteris DG, Sethi CS, Lewis GP, et al. Proliferative vitreoretinopathy: developments in adjunctive treatment and retinal pathology. *Eye (Lond)*. 2002;16:369–374.
6. Tseng W, Cortez RT, Ramirez G, et al. Prevalence and risk factors for proliferative vitreoretinopathy in eyes with rhegmatogenous retinal detachment but no previous vitreoretinal surgery. *Am J Ophthalmol*. 2004;137:1105–1115.
7. Heimann H, Bartz-Schmidt KU, Bornfeld N, et al. Scleral buckling versus primary vitrectomy in rhegmatogenous retinal detachment: a prospective randomized multicenter clinical study. *Ophthalmology*. 2007;114:2142–2154.
8. Glaser BM, Cardin A, Biscoe B. Proliferative vitreoretinopathy. The mechanism of development of vitreoretinal traction. *Ophthalmology*. 1987;94:327–332.
9. Campochiaro PA. Pathogenic mechanisms in proliferative vitreoretinopathy. *Arch Ophthalmol*. 1997;115:237–241.
10. Guidry C. The role of Müller cells in fibrocontractive retinal disorders. *Prog Retin Eye Res*. 2005;24:75–86.
11. Hui Y, Shi Y, Zhang X, et al. TNF-alpha, IL-8 and IL-6 in the early inflammatory stage of experimental PVR model

induced by macrophages.*Zhonghua Yan Ke Za Zhi*. 1999;35:140–143.
12. Singh AK, Glaser BM, Lemor M, et al. Gravity-dependent distribution of retinal pigment epithelial cells dispersed into the vitreous cavity. *Retina*. 1986;6:77–80.
13. El Ghrably I, Powe DG, Orr G, et al. Apoptosis in proliferative vitreoretinopathy. *Invest Ophthalmol Vis Sci*. 2004;45:1473–1479.
14. Doyle E, Herbert EN, Bunce C, et al. How effective is macula-off retinal detachment surgery. Might good outcome be predicted? *Eye (Lond)*. 2007;21:534–540.
15. Girard P, Mimoun G, Karpouzas I, et al. Clinical risk factors for proliferative vitreoretinopathy after retinal detachment surgery. *Retina*. 1994;14:417–424.
16. Duquesne N, Bonnet M, Adeleine P. Preoperative vitreous hemorrhage associated with rhegmatogenous retinal detachment: a risk factor for postoperative proliferative vitreoretinopathy? *Graefes Arch Clin Exp Ophthalmol*. 1996;234:677–682.
17. Yanyali A, Bonnet M. Risk factors of postoperative proliferative vitreoretinopathy in giant tears. *J Fr Ophtalmol*. 1996;19:175–180.
18. Dumas C, Bonnet M. Choroidal detachment associated with rhegmatogenous retinal detachment: a risk factor for postoperative PVR? *J Fr Ophtalmol*. 1996;19(6–7):455–463.
19. Campochiaro PA, Kaden IH, Vidaurri-Leal J, et al. Cryotherapy enhances intravitreal dispersion of viable retinal pigment epithelial cells. *Arch Ophthalmol*. 1985;103:434–436.
20. Bonnet M, Guenoun S. Surgical risk factors for severe postoperative proliferative vitreoretinopathy (PVR) in retinal detachment with grade B PVR. *Graefes Arch Clin Exp Ophthalmol*. 1995;233:789–791.
21. Bonnet M, Fleury J, Guenoun S, et al. Cryopexy in primary rhegmatogenous retinal detachment: a risk factor for postoperative proliferative vitreoretinopathy? *Graefes Arch Clin Exp Ophthalmol*. 1996;234:739–743.
22. Lean J, Azen SP, Lopez PF, et al. The prognostic utility of the

Silicone Study Classification System. Silicone Study Report 9. Silicone Study Group. *Arch Ophthalmol*. 1996;114:286–292.
23. Di Lauro S, Kadhim MR, Charteris DG, et al. Classifications for proliferative vitreoretinopathy (PVR): an analysis of their use in publications over the last 15 years. *J Ophthalmol*. 2016;2016:7807596.
24. Michels RG. Surgery of retinal detachment with proliferative vitreoretinopathy. *Retina*. 1984;4:63–83.
25. Aaberg TM Sr. Surgery as the primary management of proliferative vitreoretinopathy: a history reflecting my experiences and biases. *Arch Ophthalmol*. 2010;128:1068–1070.
26. Khan MA, Brady CJ, Kaiser RS. Clinical management of proliferative vitreoretinopathy: an update. *Retina*. 2015;35(2):165–175.
27. Claes C, Lafetá AP. Proliferative vitreoretinopathy. *Dev Ophthalmol*. 2014;54:188–195.
28. Oyagi T, Emi K. Vitrectomy without scleral buckling for proliferative vitreoretinopathy. *Retina*. 2004;24:215–218.
29. Beekhuis WH, Ando F, Zivojnovic R, et al. Basal iridectomy at 6 o'clock in the aphakic eye treated with silicone oil: prevention of keratopathy and secondary glaucoma. *Br J Ophthalmol*. 1987;71:197–200.
30. Coll GE, Chang S, Sun J, et al. Perfluorocarbon liquid in the management of retinal detachment with proliferative vitreoretinopathy. *Ophthalmology*. 1995;102:630–638 [discussion 638–639].
31. Barthelmes D, Chandra J. Perfluoro-n-octane as a temporary intraocular tamponade in a staged approach to manage complex retinal detachments. *Clin Ophthalmol*. 2015;9:413–418.
32. Furino C, Micelli Ferrari T, Boscia F, et al. Triamcinolone-assisted pars plana vitrectomy for proliferative vitreoretinopathy. *Retina*. 2003;23:771–776.
33. Jonas JB, Sofker A, Hayler J, et al. Intravitreal crystalline triamcinolone acetonide as an additional tool in pars plana vitrectomy for complicated proliferative vitreoretinopathy? *Acta Ophthalmol Scand*. 2003;81:663–665.

34. Tognetto D, Zenoni S, Sanguinetti G, et al. Staining of the internal limiting membrane with intravitreal triamcinolone acetonide. *Retina*. 2005;25:462–467.
35. Blumenkranz MS, Azen SP, Aaberg T, et al. Relaxing retinotomy with silicone oil or long-acting gas in eyes with severe proliferative vitreoretinopathy. Silicone Study Report 5. The Silicone Study Group. *Am J Ophthalmol*. 1993;116:557–564.
36. Bovey EH, De Ancos E, Gonvers M. Retinotomies of 180 degrees or more. *Retina*. 1995;15:394–398.
37. Metge F, Massin P, Gaudric A. Retinectomies in the treatment of retinal detachments with vitreoretinal proliferation. *J Fr Ophtalmol*. 1997;20:345–349.
38. Lim AK, Alexander SM, Lim KS. Combined large radial retinotomy and circumferential retinectomy in the management of advanced proliferative vitreoretinopathy. *Retina*. 2009;29:112–116.
39. Stopa M, Kociecki J. Anatomy and function of the macula in patients after retinectomy for retinal detachment complicated by proliferative vitreoretinopathy. *Eur J Ophthalmol*. 2011;21(4):468–472.
40. Garnier S, Rahmi A, Grasswil C, et al. Three hundred and sixty degree retinotomy for retinal detachments with severe proliferative vitreoretinopathy. *Graefes Arch Clin Exp Ophthalmol*. 2013;251(9):2081–2085.
41. Hocaoglu M, Karacorlu M, Muslubas IS, et al. Peripheral 360 degree retinotomy, anterior flap retinectomy, and radial retinotomy in the management of complex retinal detachment. *Am J Ophthalmol*. 2015;163:115–121.
42. Wallyn RH, Hilton GF. Subretinal fibrosis in retinal detachment. *Arch Ophthalmol*. 1979;97:2128–2129.
43. Machemer R. Surgical approaches to subretinal strands. *Am J Ophthalmol*. 1980;90:81–85.
44. Lewis H, Aaberg TM, Abrams GW, et al. Subretinal membranes in proliferative vitreoretinopathy. *Ophthalmology*. 1989;96:1403–1414 [discussion 1414–1415].
45. Parke DW 2nd, Aaberg TM. Intraocular argon laser photocoagulation in the management of severe proliferative

vitreoretinopathy. *Am J Ophthalmol*. 1984;97:434–443.
46. Chang S, Coleman DJ, Lincoff H, et al. Perfluoropropane gas in the management of proliferative vitreoretinopathy. *Am J Ophthalmol*. 1984;98:180–188.
47. Gonvers M. Temporary silicone oil tamponade in the management of retinal detachment with proliferative vitreoretinopathy. *Am J Ophthalmol*. 1985;100:239–245.
48. Vitrectomy with silicone oil or sulfur hexafluoride gas in eyes with severe proliferative vitreoretinopathy: results of a randomized clinical trial. Silicone Study Report 1. *Arch Ophthalmol*. 1992;110:770–779.
49. Schwartz SG, Flynn HW Jr, Lee WH, et al. Tamponade in surgery for retinal detachment associated with proliferative vitreoretinopathy. *Cochrane Database Syst Rev*. 2009;(4) [CD006126].
50. Thompson JT. The absorption of mixtures of air and perfluoropropane after pars plana vitrectomy. *Arch Ophthalmol*. 1992;110:1594–1597.
51. Blumenkranz M, Gardner T, Blankenship G. Fluid–gas exchange and photocoagulation after vitrectomy: indications, technique, and results. *Arch Ophthalmol*. 1986;104:291–296.
52. Oliveira LB, Reis PA. Silicone oil tamponade in 23-gauge transconjunctival sutureless vitrectomy. *Retina*. 2007;27:1054–1058.
53. Heimann H, Stappler T, Wong D. Heavy tamponade 1: a review of indications, use, and complications. *Eye (Lond)*. 2008;22:1342–1359.
54. Asaria RH, Kon CH, Bunce C, et al. Silicone oil concentrates fibrogenic growth factors in the retro-oil fluid. *Br J Ophthalmol*. 2004;88:1439–1442.
55. Berker N, Batman C, Ozdamar Y, et al. Long-term outcomes of heavy silicone oil tamponade for complicated retinal detachment. *Eur J Ophthalmol*. 2007;17:797–803.
56. Auriol S, Pagot-Mathis V, Mahieu L, et al. Efficacy and safety of heavy silicone oil Densiron 68 in the treatment of complicated retinal detachment with large inferior retinectomy. *Graefes Arch Clin Exp Ophthalmol*.

2008;246:1383–1389.
57. Duan A, She H, Qi Y. Complications after heavy silicone oil tamponade in complicated retinal detachment. *Retina*. 2011;31:547–552.
58. Majid MA, Hussin HM, Biswas S, et al. Emulsification of Densiron-68 used in inferior retinal detachment surgery. *Eye (Lond)*. 2008;22:152–157.
59. Wolf S, Schon V, Meier P, et al. Silicone oil-RMN3 mixture ("heavy silicone oil") as internal tamponade for complicated retinal detachment. *Retina*. 2003;23:335–342.
60. Wong D, Van Meurs JC, Stappler T, et al. A pilot study on the use of a perfluorohexyloctane/silicone oil solution as a heavier than water internal tamponade agent. *Br J Ophthalmol*. 2005;89:662–665.
61. Rizzo S, Genovesi-Ebert F, Vento A, et al. A new heavy silicone oil (HWS 46–3000) used as a prolonged internal tamponade agent in complicated vitreoretinal surgery: a pilot study. *Retina*. 2007;27:613–620.
62. Sandner D, Herbrig E, Engelmann K. High-density silicone oil (Densiron) as a primary intraocular tamponade: 12-month follow up. *Graefes Arch Clin Exp Ophthalmol*. 2007;245:1097–1105.
63. Stappler T, Heimann H, Gibran SK, et al. Densiron-68 heavy silicone oil in cases of PVR. Anatomic and functional outcomes.*Ophthalmologe*. 2009;106:320–326.
64. Li W, Zheng J, Zheng Q, et al. Clinical complications of Densiron 68 intraocular tamponade for complicated retinal detachment. *Eye (Lond)*. 2010;24:21–28.
65. Morescalchi F, Costagliola C, Duse S, et al. Heavy silicone oil and intraocular inflammation. *Biomed Res Int*. 2014;2014:574825.
66. Hussain RN, Banerjee S. Densiron 68 as an intraocular tamponade for complex inferior retinal detachments. *Clin Ophthalmol*. 2011;5:603–607.
67. Joussen AM, Rizzo S, Kirchhof B, et al. HSO -Study Group. Heavy silicone oil versus standard silicone oil in as vitreous tamponade in inferior PVR (HSO Study): interim analysis. *Acta Ophthalmol*. 2011;89(6):483–489.

68. Regler R, Sachs HG, Hillenkamp J, et al. Long-term evaluation of anatomic and functional results after complicated retinal detachment treated with pars plana vitrectomy and heavy silicone oil tamponade. *Klin Monatsbl Augenheilkd*. 2009;226(9):707–712.
69. Wickham L, Ho-Yen GO, Bunce C, et al. Surgical failure following primary retinal detachment surgery by vitrectomy: risk factors and functional outcomes. *Br J Ophthalmol*. 2011;95(9):1234–1238.
70. La Cour M, Lux A, Heegaard S. Visual loss under silicone oil. *Klin Monbl Augenheilkd*. 2010;227:181–184.
71. Halberstadt M, Domig D, Kodjikian L, et al. PVR recurrence and the timing of silicone oil removal. *Klin Monatsbl Augenheilkd*. 2006;223:361–366.
72. Lam RF, Cheung BT, Yuen CY, et al. Retinal redetachment after silicone oil removal in proliferative vitreoretinopathy: a prognostic factor analysis. *Am J Ophthalmol*. 2008;145:527–533.
73. Mondal S, Hussain N, Natarajan S. Retinal redetachment after silicone oil removal in proliferative vitreoretinopathy: a prognostic factor analysis. *Am J Ophthalmol*. 2008;146:145 [author reply 145].
74. Song ZM, Chen D, Ke ZS, et al. A new approach for active removal of 5,000 centistokes silicone oil through 23-gauge cannula. *Retina*. 2010;30:1302–1307.
75. Lewis H, Aaberg TM, Abrams GW. Causes of failure after initial vitreoretinal surgery for severe proliferative vitreoretinopathy. *Am J Ophthalmol*. 1991;111:8–14.
76. Silicone Study Group. Vitrectomy with silicone oil or perfluoropropane gas in eyes with severe proliferative vitreoretinopathy: results of a randomized clinical trial. Silicone Study Report 2. *Arch Ophthalmol*. 1992;110:780–792.
77. Lewis H, Burke JM, Abrams GW, et al. Perisilicone proliferation after vitrectomy for proliferative vitreoretinopathy. *Ophthalmology*. 1988;95:583–591.
78. Steel DH, Weir P, James CR. Silicone assisted, argon laser confinement of recurrent proliferative vitreoretinopathy related retinal detachment: a technique to allow silicone oil

removal in problem eyes. *Br J Ophthalmol*. 1997;81:765–770.
79. Bonnet M. Macular changes and fluorescein angiographic findings after repair of proliferative vitreoretinopathy. *Retina*. 1994;14:404–410.
80. Cox MS, Azen SP, Barr CC, et al. Macular pucker after successful surgery for proliferative vitreoretinopathy. Silicone Study Report 8. *Ophthalmology*. 1995;102:1884–1891.
81. Lewis H, Verdaguer JI. Surgical treatment for chronic hypotony and anterior proliferative vitreoretinopathy. *Am J Ophthalmol*. 1996;122:228–235.
82. Lee GD, Goldberg RA, Heier JS. Endoscopy-assisted vitrectomy and membrane dissection of anterior proliferative vitreoretinopathy for chronic hypotony after previous retinal detachment repair. *Retina*. 2015;36(6):1058–1063.
83. Roth DB, Sears JE, Lewis H. Removal of retained subfoveal perfluoro-n-octane liquid. *Am J Ophthalmol*. 2004;138:287–289.
84. Abrams GW, Azen SP, Barr CC, et al. The incidence of corneal abnormalities in the Silicone Study. Silicone Study Report 7. *Arch Ophthalmol*. 1995;113:764–769.
85. van Meurs JC, Bolt BJ, Mertens DA, et al. Rubeosis of the iris in proliferative vitreoretinopathy. *Retina*. 1996;16:292–295.
86. Chen W, Chen H, Hou P, et al. Midterm results of low-dose intravitreal triamcinolone as adjunctive treatment for proliferative vitreoretinopathy. *Retina*. 2011;31:1137–1142.
87. Shi H, Guo T, Liu PC, et al. Steroids as an adjunct for reducing the incidence of proliferative vitreoretinopathy after rhegmatogenous retinal detachment surgery: a systematic review and meta-analysis. *Drug Des Devel Ther*. 2015;9:139–312.
88. Blumenkranz M, Hernandez E, Ophir A, et al. 5-fluorouracil: new applications in complicated retinal detachment for an established antimetabolite. *Ophthalmology*. 1984;91:122–130.
89. Asaria RH, Kon CH, Bunce C, et al. Adjuvant 5-fluorouracil and heparin prevents proliferative vitreoretinopathy: Results from a randomized, double-blind, controlled clinical trial. *Ophthalmology*. 2001;108:1179–1183.

90. Wiedemann P, Sorgente N, Bekhor C, et al. Daunomycin in the treatment of experimental proliferative vitreoretinopathy: effective doses in vitro and in vivo. *Invest Ophthalmol Vis Sci*. 1985;26:719–725.
91. Sundaram V, Barsam A, Virgili G. Intravitreal low molecular weight heparin and 5-Fluorouracil for the prevention of proliferative vitreoretinopathy following retinal reattachment surgery. *Cochrane Database Syst Rev*. 2010;(7) [CD006421].
92. Yamada H, Yamada E, Ando A, et al. Platelet-derived growth factor-A-induced retinal gliosis protects against ischemic retinopathy. *Am J Pathol*. 2000;156:477–487.
93. He S, Chen Y, Khankan R, et al. Connective tissue growth factor as a mediator of intraocular fibrosis. *Invest Ophthalmol Vis Sci*. 2008;49:4078–4088.
94. Hsu J, Khan MA, Shieh WS, et al. Effect of serial intrasilicone oil bevacizumab injections in eyes with recurrent proliferative vitreoretinopathy retinal detachment. *Am J Ophthalmol*. 2016;161:65–70.
95. Rojas J, Fernandez I, Pastor JC, et al. A strong genetic association between the tumor necrosis factor locus and proliferative vitreoretinopathy: the Retina 4 project. *Ophthalmology*. 2010;117:2417–2423 [e1–2].
96. Sakamoto T, Kimura H, Scuric Z, et al. Inhibition of experimental proliferative vitreoretinopathy by retroviral vector-mediated transfer of suicide gene. Can proliferative vitreoretinopathy be a target of gene therapy? *Ophthalmology*. 1995;102:1417–1424.
97. Machemer R, Laqua H. A logical approach to the treatment of massive periretinal proliferation. *Ophthalmology*. 1978;85:584–593.
98. Grey RH, Leaver PK. Silicone oil in the treatment of massive preretinal retraction. I. Results in 105 eyes. *Br J Ophthalmol*. 1979;63:355–360.
99. Lean JS, Leaver PK, Cooling RJ, et al. Management of complex retinal detachments by vitrectomy and fluid/silicone exchange. *Trans Ophthalmol Soc U K*. 1982;102(Pt 1):203–205.

100. de Bustros S, Michels RG. Surgical treatment of retinal detachments complicated by proliferative vitreoretinopathy. *Am J Ophthalmol*. 1984;98:694–699.
101. Jalkh AE, Avila MP, Schepens CL, et al. Surgical treatments of proliferative vitreoretinopathy. *Arch Ophthalmol*. 1984;102:1135–1139.
102. Sternberg P Jr, Machemer R. Results of conventional vitreous surgery for proliferative vitreoretinopathy. *Am J Ophthalmol*. 1985;100:141–146.
103. Gonvers M. Temporary use of intraocular silicone oil in the treatment of detachment with massive periretinal proliferation. Preliminary report. *Ophthalmologica*. 1982;184:210–218.
104. McCuen BW 2nd, Landers MB 3rd, Machemer R. The use of silicone oil following failed vitrectomy for retinal detachment with advanced proliferative vitreoretinopathy. *Ophthalmology*. 1985;92:1029–1034.
105. Cox MS, Trese MT, Murphy PL. Silicone oil for advanced proliferative vitreoretinopathy. *Ophthalmology*. 1986;93:646–650.
106. Stern WH, Johnson RN, Irvine AR, et al. Extended retinal tamponade in the treatment of retinal detachment with proliferative vitreoretinopathy. *Br J Ophthalmol*. 1986;70:911–917.
107. Glaser BM. Treatment of giant retinal tears combined with proliferative vitreoretinopathy. *Ophthalmology*. 1986;93:1193–1197.
108. Yeo JH, Glaser BM, Michels RG. Silicone oil in the treatment of complicated retinal detachments. *Ophthalmology*. 1987;94:1109–1113.
109. Aaberg TM. Management of anterior and posterior proliferative vitreoretinopathy. XLV. Edward Jackson memorial lecture. *Am J Ophthalmol*. 1988;106:519–532.
110. Fisher YL, Shakin JL, Slakter JS, et al. Perfluoropropane gas, modified panretinal photocoagulation, and vitrectomy in the management of severe proliferative vitreoretinopathy. *Arch Ophthalmol*. 1988;106:1255–1260.
111. Hanneken AM, Michels RG. Vitrectomy and scleral

buckling methods for proliferative vitreoretinopathy. *Ophthalmology*. 1988;95:865–869.
112. Körner F, Böhnke M. Vitrectomy in proliferative vitreoretinopathy: anatomical and functional results in 501 patients. *Klin Monatsbl Augenheilkd*. 1995;206:239–245.
113. Scott IU, Flynn HW Jr, Murray TG, et al. Outcomes of surgery for retinal detachment associated with proliferative vitreoretinopathy using perfluoro-n-octane: a multicenter study. *Am J Ophthalmol*. 2003;136:454–463.
114. Charteris DG, Aylward GW, Wong D, et al. A randomized controlled trial of combined 5-fluorouracil and low-molecular-weight heparin in management of established proliferative vitreoretinopathy. *Ophthalmology*. 2004;111:2240–2245.
115. Tseng JJ, Barile GR, Schiff WM, et al. Influence of relaxing retinotomy on surgical outcomes in proliferative vitreoretinopathy. *Am J Ophthalmol*. 2005;140:628–636.
116. Quiram PA, Gonzales CR, Hu W, et al. Outcomes of vitrectomy with inferior retinectomy in patients with recurrent rhegmatogenous retinal detachments and proliferative vitreoretinopathy. *Ophthalmology*. 2006;113:2041–2047.
117. Gupta B, Mokete B, Laidlaw DA, et al. Severe folding of the inferior retina after relaxing retinectomy for proliferative vitreoretinopathy. *Eye (Lond)*. 2008;22(12):1517–1519.
118. Grigoropoulos VG, Benson S, Bunce C, et al. Functional outcome and prognostic factors in 304 eyes managed by retinectomy. *Graefes Arch Clin Exp Ophthalmol*. 2007;245:641–649.
119. de Silva DJ, Kwan A, Bunce C, et al. Predicting visual outcome following retinectomy for retinal detachment. *Br J Ophthalmol*. 2008;92:954–958.
120. Mancino R, Aiello F, Ciuffoletti E, et al. Inferior retinotomy and silicone oil tamponade for recurrent inferior retinal detachment and grade C PVR in eyes previously treated with pars plana vitrectomy or scleral buckle. *BMC Ophthalmol*. 2015;15(1):173.
121. McCuen BW 2nd, Azen SP, Stern W, et al. Vitrectomy with

silicone oil or perfluoropropane gas in eyes with severe proliferative vitreoretinopathy. Silicone Study Report 3. *Retina*. 1993;13:279–284.
122. Abrams GW, Azen SP, McCuen BW 2nd, et al. Vitrectomy with silicone oil or long-acting gas in eyes with severe proliferative vitreoretinopathy: results of additional and long-term follow-up. Silicone Study Report 11. *Arch Ophthalmol*. 1997;115:335–344.
123. Brown GC, Brown MM, Sharma S, et al. A cost-utility analysis of interventions for severe proliferative vitreoretinopathy. *Am J Ophthalmol*. 2002;133:365–372.
124. Patel NN, Bunce C, Asaria RH, et al. Resources involved in managing retinal detachment complicated by proliferative vitreoretinopathy. *Retina*. 2004;24:883–887.

112

Retinotomies and Retinectomies

Gary W. Abrams, Enrique Garcia-Valenzuela, Sumit K. Nanda

Introduction

The term retinotomy denotes cutting the retina, whereas retinectomy means excision of retina. A retinotomy may vary from a small hole created for drainage of subretinal fluid or removal of a subretinal membrane to a 360° cut to release massive peripheral

traction. Retinectomy may mean limited excision of the fixed edge of a retinal flap or total excision of peripheral fibrotic retina. Subjects discussed in this chapter include the indications and techniques for retinotomy and retinectomy, the results and complications of the procedures, and the techniques for managing the retina after a retinotomy or retinectomy.

Drainage Retinotomy

A drainage retinotomy is a retinal hole created to allow removal of subretinal fluid.[1,2] A drainage retinotomy is most often used in conjunction with treatment of a retinal detachment with vitrectomy techniques. Because of the potential for complications and the availability of other techniques, posterior drainage retinotomy is less frequently used today; if a drainage retinotomy is needed, a peripheral drainage retinotomy can sometimes be used. A drainage retinotomy may be necessary in proliferative vitreoretinopathy (PVR), other complicated retinal detachments, proliferative vascular retinopathy, and primary rhegmatogenous retinal detachment treated with vitrectomy. The drainage retinotomy can be used when a preexisting retinal tear is not present or not adequate for drainage or egress of the subretinal fluid.

General Principles

The drainage retinotomy is made after as complete removal as possible of periretinal membranes, and should not be created in an area with residual membranes or traction. The drainage retinotomy is most easily created with endodiathermy.[3] Taking care not to close large vessels, the unimanual, bipolar endodiathermy probe is set on a continuous mode and held against the retina in the selected area. A necrotic retinal hole with a well-marked white edge is usually produced. The advantages of creating the retinotomy with diathermy are (1) complete hemostasis of the retinal blood vessels; and (2) whitening of the edge of the hole, which allows easy identification of the retinotomy for laser treatment when the hole is flat against the retinal pigment epithelium. If the diathermy probe does not perforate the necrotic area, the central necrotic area is

perforated with a sharp blade or by suction with the blunt tip of the vacuum needle.

Surgical Technique in Conjunction With Perfluorocarbon Liquid

The preferred technique for retinal reattachment is to use perfluorocarbon liquid (PFCL). PFCL, heavier than water or saline, can be used to reattach the retina from posteriorly to anteriorly.[4] In addition, PFCL can fixate and stabilize the posterior retina, thereby facilitate removal of peripheral vitreous and membranes.[5] A peripheral retinal break is necessary to allow egress of subretinal fluid when PFCL is injected over the posterior pole. A preexisting retinal break is usually present, but if the break is not located anteriorly enough, subretinal fluid may become loculated beneath peripheral retina, anterior to the anterior-most retinal break (Figs. 112.1A–B). Anterior subretinal fluid can usually be drained through posteriorly located retinal breaks during PFCL–air exchange. However, most surgeons prefer to do laser treatment through PFCL rather than air, so it is desirable to flatten the retina with PFCL. If anteriorly loculated subretinal fluid is present, one of several approaches can be taken to remove it. With PFCL filling the eye to just posterior to the most anteriorly located retinal break, a partial fluid–air exchange can be done to remove the subretinal fluid through the break. Then, if the desire is to do laser treatment through the PFCL, additional PFCL is injected to bring the level anteriorly; anterior air can then be replaced with infusion fluid in order to have a clear view. There is a risk of corneal striate keratopathy or pupillary constriction associated with the air in the aphakic eye that can reduce visualization and interfere with laser treatment and subsequent fluid–air exchange. In the phakic eye, there is the possibility of posterior subcapsular lens opacity induced by the air that could interfere with visualization.

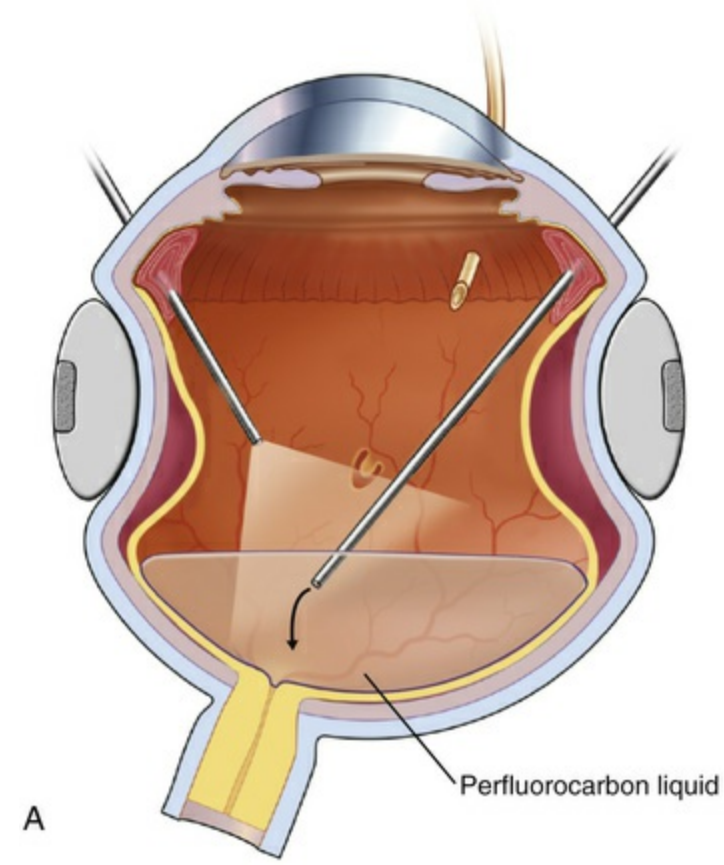
Perfluorocarbon liquid
A

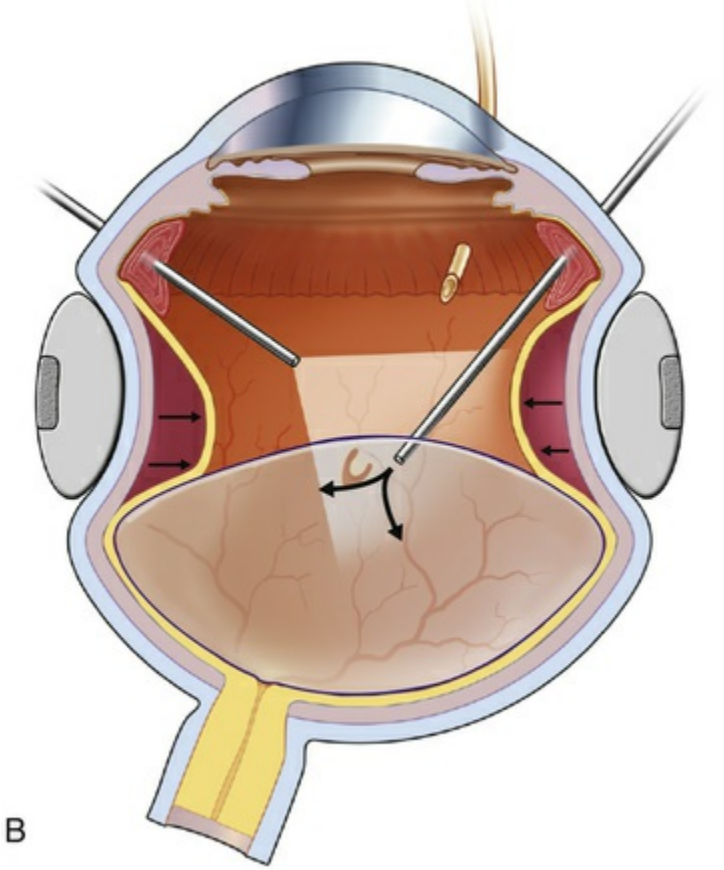
B

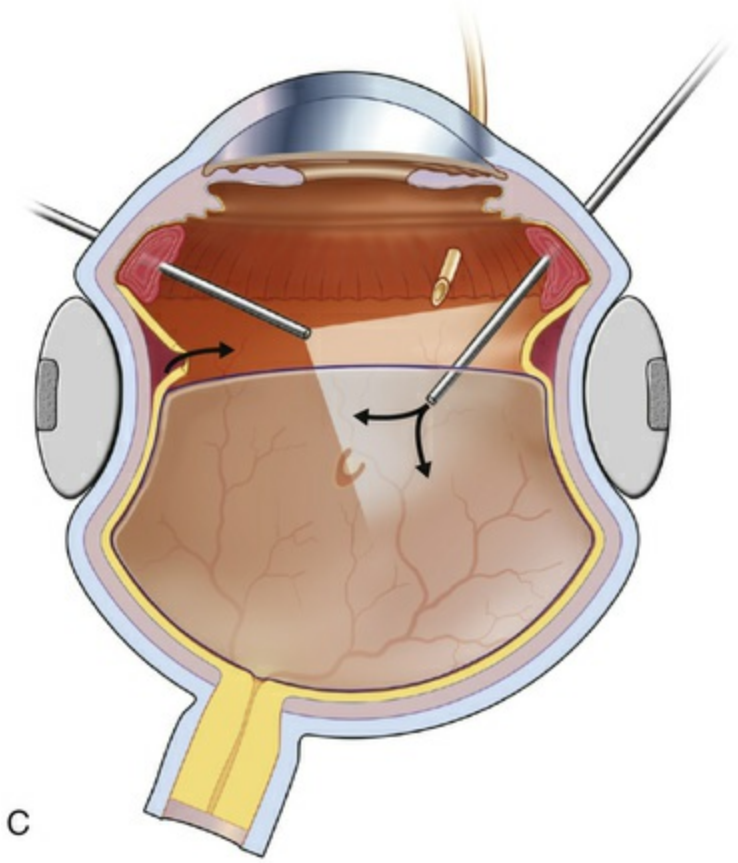

FIG. 112.1 Retinal reattachment using perfluorocarbon liquid (PFCL). Drainage retinotomy to allow egress of anteriorly loculated subretinal fluid. (A) Detached retina with midperipheral retinal break. PFCL is injected over the posterior pole, and subretinal fluid egresses through the retinal break (*arrow*). (B) Retinal break closed by PFCL. Subretinal fluid loculated beneath anterior retina is unable to escape subretinal space. (C) Anterior drainage retinotomy over anterior scleral buckle allows egress of subretinal fluid and retinal flattening as more PFCL is injected.

An alternative approach that is less time-consuming and more likely to maintain good visualization is to create an anterior drainage retinotomy with endodiathermy in the area where subretinal fluid is loculated in order to allow egress of the fluid into the vitreous cavity (Fig. 112.1C). If a scleral buckle is not present and will not be used, the retinotomy can be made just posterior to the ora serrata. If a scleral buckle is present, the retinotomy should be made in an area of retina supported by the buckle rather than anterior or posterior to the scleral buckle. It is usually preferable to

perform the retinotomy in an area of superior, rather than inferior, retina. This minimizes the risk of a redetachment caused by complicating fibrosis in the vicinity of the retinotomy. After the drainage retinotomy is created, PFCL is injected to reattach the retina. If the retinotomy is made in an area under traction, there is a risk that the PFCL could go through the retinal break and course beneath the retina; however, if no traction is present, the level of the PFCL can safely be brought anterior to the break to allow laser treatment. The PFCL is usually removed by performing a PFCL–air exchange. Alternatively, a direct PFCL–silicone oil exchange can be done. It is preferable to drain any residual subretinal fluid, if present, through the anterior-most retinal break or retinotomy during the early portion of the exchange. This will prevent trapping of subretinal fluid that can be forced posteriorly as the eye is filled with air or silicone oil.

Surgical Technique Without PFCL

Posterior Drainage Retinotomy

Fluid–air exchange was the most commonly used technique to reattach the retina during vitrectomy before introduction of PFCL and is often employed today if PFCL is not used. In the absence of a posterior retinal break or easily accessible peripheral tear for internal drainage of subretinal fluid, a posterior drainage retinotomy can be created. The posterior drainage retinotomy is usually made with diathermy, taking care to make it in a superior quadrant at least 1.5 disc diameters from the optic nerve and avoiding the macula and large blood vessels in order to avoid complications. Our preferred location of the drainage retinotomy, with the least visual impact, is an area 5 disc diameters superotemporal to the center of the macula, just outside the superotemporal vascular arcade. The retina is reattached by suctioning subretinal fluid through the retinotomy while the eye is filled with air supplied by a continuous infusion air pump (Fig. 112.2A). For fluid–air exchange through a drainage retinotomy, intraocular air pressure is usually set at approximately 30 mmHg. Before air is insufflated, fluid–fluid exchange (internal drainage of fluid through a retinal break or retinotomy in a fluid-filled eye) will

sometimes partially flatten the retina. Air is then insufflated and the air bubble is enlarged to fill the anterior vitreous cavity. In an eye that is partially filled with air, the view is minimized, and it is necessary to refocus the operating microscope on the drainage retinotomy. Place the end of a silicone-tip needle just inside the orifice of the drainage retinotomy and gently aspirate subretinal fluid to reattach the retina. As the retina flattens against the retinal pigment epithelium, fluid ceases to flow into the cannula. Do not push the needle tip forcibly against the retinal pigment epithelium (RPE) because damage to Bruch's membrane and/or choroidal hemorrhage may occur. More fluid often collects in the vitreous cavity, and it is necessary to aspirate fluid from the retinotomy and over the optic disc several times to make sure all fluid is removed. Residual fluid is removed by “dipping” the silicone tip into the fluid meniscus over the optic nerve. A bright reflex appears as the needle tip enters the fluid meniscus; this reflex disappears as the fluid level drops below the needle tip during aspiration. The dipping maneuver is repeated until all of the fluid is removed. Fluid tends to accumulate posteriorly in the vitreous cavity, so the dipping procedure over the optic disc is repeated after several minutes. It is crucial to avoid damage to the optic nerve by not compressing the nerve during this maneuver. When no fluid remains, the margins of the drainage retinotomy are treated with laser endophotocoagulation. Usually one confluent row of laser burns surrounding the margins of the retinotomy is adequate for adhesion.

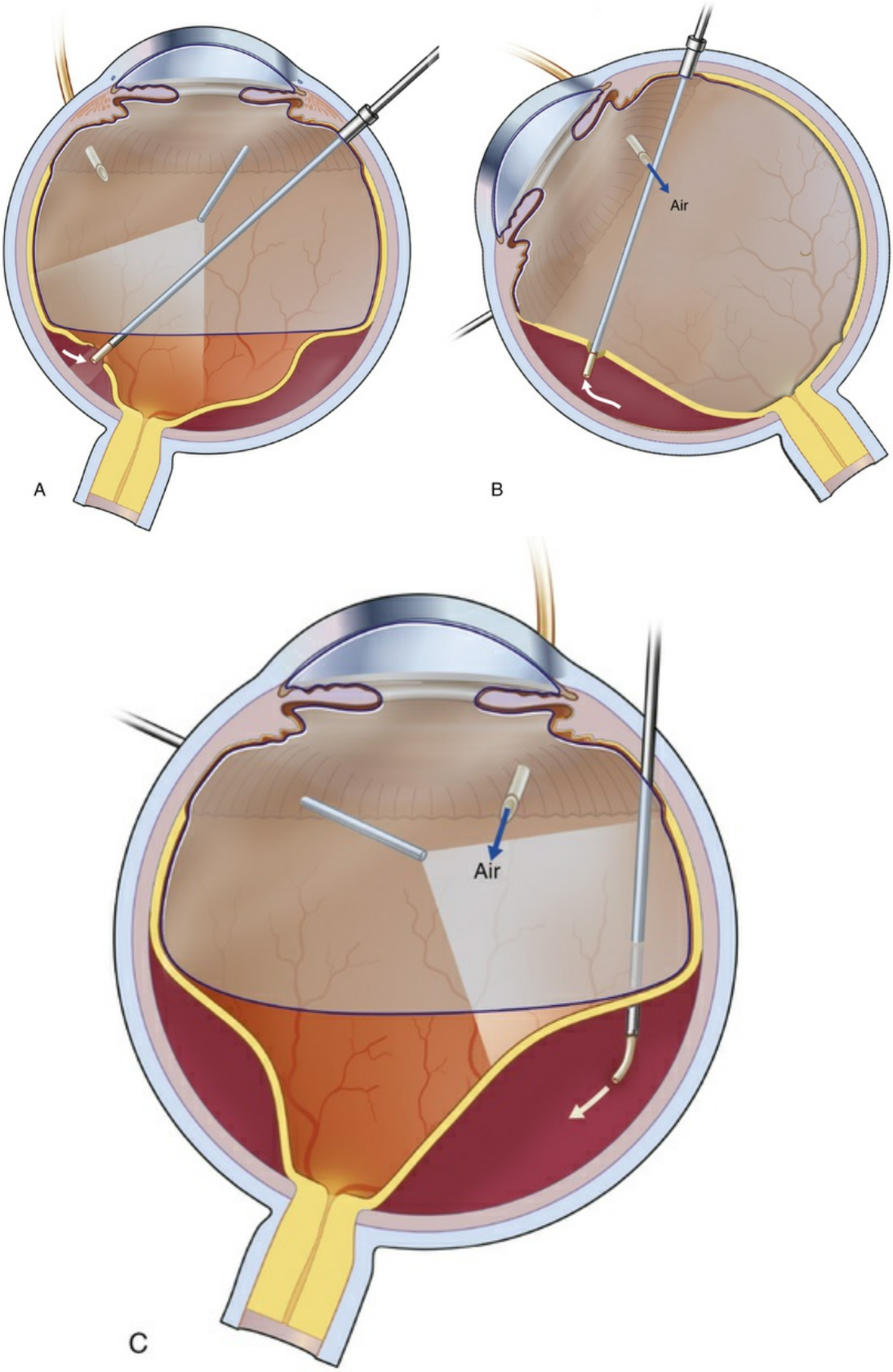

FIG. 112.2 (A) Fluid–air exchange through posterior drainage retinotomy. Silicone-tip cannula attached to variable suction through the vitrectomy console is

placed immediately anterior to or into the retinotomy, and the subretinal fluid is aspirated as the eye fills with air from the continuous infusion air pump. After retina is attached and retinotomy is flat against retinal pigment epithelium, retinotomy is treated with laser endophotocoagulation. (B) Fluid–air exchange through peripheral drainage retinotomy. The head is tilted or turned to place the drainage retinotomy at a dependent position in the retinal detachment to remove subretinal fluid as completely as possible. (C) Fluid–air exchange through peripheral drainage retinotomy. A flexible silicone tube from a cannulated extrusion needle inserted through peripheral retinotomy toward posterior retina. Subretinal fluid aspirated during fluid–air exchange (*lower arrow*). Level of fluid in vitreous cavity is below level of retinotomy, and retina is flat over proximal portion of subretinal cannula.

Peripheral Drainage Retinotomy

A posterior drainage retinotomy can be associated with significant complications, including hemorrhage, fibrosis with traction, choroidal neovascularization (CNV), and visual field loss.[6] In some instances, a peripheral drainage retinotomy can be used instead of a posterior retinotomy to reattach the retina (Fig. 112.2B). Although the same complications can occur in the periphery, peripheral complications are usually less visually significant than posterior complications. Yamaguchi and colleagues reported a 93% single operation success rate in 112 eyes with primary retinal detachments without advanced PVR by draining subretinal fluid through original breaks without the use of posterior drainage retinotomies or PFCL.[7] The essence of their technique, using a non-contact wide-angle viewing system, was to turn the head to make the drainage break as dependent as possible. They were able to internally drain all of the subretinal fluid in 45% of the cases and enough subretinal fluid in the remainder of the cases to be able to treat the breaks with endolaser photocoagulation or cryotherapy.

If the retinal break is in a location where it cannot be placed in a dependent position for drainage, an alternative technique is to make a drainage retinotomy with endodiathermy in a peripheral

dependent position in the area of retinal detachment to maximize subretinal fluid drainage. A risk of incomplete peripheral drainage of subretinal fluid is that residual subretinal fluid can be forced posteriorly to create a retinal fold in the macula.[8] This most commonly happens when the border of a subtotal retinal detachment is near the center of the macula. A posterior retinal fold is less likely to occur when perfluorocarbon liquid is used to reattach the retina or when fluid is drained through a posterior drainage retinotomy; however, it should be possible to prevent a posterior retinal fold during fluid–air exchange. Techniques to avoid a macular fold include first-day positioning on the temporal side (operated eye down) to place the gas bubble against the nasal retina so as not to force fluid into the macula or initial temporal side positioning followed by rolling the patient to a prone position to move the fluid away from the macula and flatten the macula (steamroller maneuver).

An alternative technique for more complete drainage through a peripheral retinotomy or break is to use a soft-tipped cannulated sliding extrusion needle (Universal Soft Tip, Synergetics, Inc., St. Louis, MO) that has a 20- or 23-gauge (G) metal cylinder, a sliding silicone tube within the cylinder, and a handle with a lever for moving the silicone tube in and out of the metal cannula. This technique was originally described by Flynn et al.[9] The instrument can be used with active suction or by extrusion as a fluted needle. The soft silicone tip can be extended through the peripheral retinotomy or break to drain subretinal fluid posterior to the break (Fig. 112.2C). When the retina flattens posteriorly over the silicone tube, the tube is slowly withdrawn from the subretinal space while gently aspirating subretinal fluid. A modified silicone tube has multiple fenestrations near the tip of the tube that reduces the likelihood of retinal incarceration in the tube during aspiration of subretinal fluid.[10] At this point all or most of the subretinal fluid has been removed. Vitreous cavity fluid can be aspirated over the optic nerve to complete the fluid–air exchange; then endolaser photocoagulation is applied to the edge of the retinotomy.

Drainage during fluid–silicone oil exchange is similar to that during fluid–air exchange. For fluid–silicone oil exchange, less viscous 1000 cSt oil is easier to use than 5000 cSt oil, but the former

oil may result in more emulsification. Silicone oil can be pumped through either a 20G or smaller infusion cannula. It is necessary to use a fluted needle to remove the intraocular fluid. A vacuum needle cannot be used because it will collapse the eye during the silicone oil infusion. The silicone oil infusion forces the fluid out of the eye through the fluted needle. The vitreous cavity is filled with silicone oil as completely as possible before the subretinal space is entered. Most of the subretinal fluid can be removed at the orifice of the peripheral retinotomy, and less subretinal penetration by the silicone cannula is necessary compared with that necessary for fluid–air exchange. By repeatedly removing fluid at the retinotomy, then going back and using the dipping maneuver over the optic disc, one can remove most of the subretinal fluid.

Complications

Intraoperative complications are hemorrhage from the retina or the choroid or enlargement of the retinotomy. By producing the retinotomy with diathermy and by avoiding larger vessels, retinal hemorrhages can usually be avoided. Incarceration of retina beyond the diathermized edge of the retinotomy with the drainage needle tip can sometimes lead to hemorrhage. Hemostasis with diathermy should be obtained as soon as possible.

Choroidal hemorrhage may result from impact of the instruments on the choroid. Silicone-tipped cannulas should be used as they are less likely to damage the choroid than metal-tipped instruments. If the silicone tube does not easily slip into the subretinal space, it should not be forced.

Enlargement of the retinotomy may follow excessive diathermy. The area of diathermy becomes necrotic, and if a wide area is treated with diathermy, the retinotomy may enlarge during fluid–air exchange. Enlargement can also occur due to incarceration of the retina at the edge of the retinotomy in the drainage needle tip during fluid–air exchange.

Postoperative complications of drainage retinotomies are few. McDonald et al.[6] first described cellular proliferation and CNV from drainage retinotomies. Richards and Maberley[11] found that subretinal neovascularization was associated with the retinotomy

site in 1% of 287 cases and focal PVR was associated with the retinotomy site in 2%. Retinal detachment from the retinotomy site is extremely rare. The retinotomy site may even remain attached if the rest of the retina detaches postoperatively. Cellular proliferation from the retinotomy site may lead to periretinal proliferation. In gas-filled eyes, the proliferation usually remains in the local area of the retinotomy site and rarely leads to complications. In silicone-oil-filled eyes, the proliferation may be more extensive and lead to tractional complications. CNV probably results from damage to the underlying choroid and RPE.

An extensive visual field defect may result from a large retinotomy too close to the optic disc or macula. Bourke et al.[12] found visual field defects within 30° of fixation in 12 of 14 eyes with drainage retinotomies. Visual field defects were found in all eyes in which the retinotomy was created within 5 disc diameters of fixation. The researchers recommended that retinotomies be placed more than 5 disc diameters from the fovea and in the superotemporal quadrant to minimize visual field loss.

Inner Retinal Fenestration for Optic Pit Maculopathy

Spaide and coworkers described successful treatment of a case of optic pit maculopathy by creating a partial-thickness retinotomy (fenestration) in the retina just temporal to the optic disc with the bent tip of 25G needle.[13] They theorized that fluid from the optic pit entered the peripapillary retina under pressure and that a small partial thickness hole would allow egress of the fluid into the vitreous cavity. In a subsequent paper, Ooto et al. reported 18 patients treated with inner retinal fenestration, with complete resolution of intraretinal and subretinal fluid in 17.[14] They did not remove cortical vitreous in 12 of the eyes and did not peel the internal limiting membrane (ILM) or treat with laser in any eyes. Only 1 eye was left with an air bubble in the vitreous cavity at the conclusion of surgery.

Retinotomy to Gain Access to the

Subretinal Space

It is sometimes necessary to create a retinotomy to gain access to the subretinal space. A retinotomy or retinectomy may be necessary to remove a subretinal band or membrane, a subretinal hemorrhage, a subretinal neovascular membrane, a subretinal foreign body, or, rarely, a subretinal mass such as a disciform scar, abscess, or retinal or subretinal tumor.

Subretinal Membranes

Subretinal bands or membranes complicating PVR are frequent indications for retinotomies and retinectomies. They should be removed or sectioned only if they exert significant traction, preventing retinal reattachment after removal of epiretinal membranes. Subretinal membranes and bands will sometimes relax enough to allow retinal reattachment, so in most cases an attempt to flatten the retina with PFCL or air may be warranted to determine if removal of the membranes is necessary. Details on management of subretinal membranes can be found in Chapter 111 (Proliferative vitreoretinopathy).

Choroidal Neovascularization and Subretinal Hemorrhage

An indication that has decreased greatly in numbers since the advent of anti-VEGF medications is retinotomy to remove a choroidal neovascular membrane. However, displacement of submacular hemorrhages remains one of the more frequent reasons for a retinotomy. Since both are discussed in Chapter 122 (Surgical management of choroidal neovascularization and subretinal hemorrhage), we will only briefly describe the technique here.

Removal of Subretinal Neovascular Membrane

A small retinotomy is made adjacent to the neovascular membrane, and the subretinal new vessel membrane is separated from the underlying tissue and retina and extracted with subretinal forceps.

Displacement of Subretinal Hemorrhage

Subretinal hemorrhages can be caused by trauma or retinal arterial macroaneurysms, but they are much more frequently encountered as a complication of choroidal neovascularization. When the hemorrhage is large and central enough, surgical displacement is warranted. Although multiple techniques have been described, most rely on performing a small-gauge retinotomy adjacent to the subretinal clot to inject beneath the retina 12–50 μg of tPA in 0.05–0.1 mL of saline solution. Intravitreal air or gas tamponade is used to exert pressure on the dissolved blood to displace it away from the macula.

Macular Translocation Surgery

Macular translocation surgery is still used in some centers for advanced age-related macular degeneration not responsive to medical therapy. Briefly, after detaching the retina by transretinal injection of a balanced saline solution, a 360° peripheral retinotomy is created. When the retina is reattached with PFCL, it is rotated to relocate the macula to a more normal area of retinal pigment epithelium (see Chapter 123, 360-degree macular translocation).

Subretinal Foreign Body

A rare indication for retinotomy is removal of a subretinal foreign body. A subretinal foreign body may result from perforation of the retina from the vitreal side or, rarely, from perforation of the sclera at an oblique angle, with lodging of the foreign body between the retina and the choroid. If the foreign body is nonmobile and anteriorly located, external extraction through the sclera and the choroid may work quite well. If the foreign body is located posteriorly, or if it is mobile beneath a detached retina, a posterior external extraction is quite difficult. In the latter case, a vitrectomy with retinotomy may be the best approach. If the retina is not detached, the foreign body will usually lie at or near the retinal perforation site. After the vitrectomy, laser endophotocoagulation is applied to surround the foreign body. The retina overlying the foreign body is treated with diathermy, after which a membrane pick is used to remove retina, fibrin, or other material from the

surface of the foreign body. An inflammatory capsule is often present around the foreign body, and this should be opened with the membrane pick and the foreign body dislodged from its capsule if possible. The foreign body can then be grasped and removed with foreign-body forceps or a rare-earth magnet.

If the retina is detached, the foreign body may be mobile. In this case, after vitrectomy, a retinotomy is made with endodiathermy. The retinotomy is made in an area where forceps or the rare-earth magnet will have access to the foreign body. The posterior pole or areas of fibrous proliferation should be avoided when the retinotomy is made. It is often possible to manipulate a subretinal foreign body to the area of the retinotomy before the foreign body is grasped. Joondeph and Flynn described moving the foreign body to the retinotomy site with the soft flexible tip of the cannulated extrusion needle.[15] The foreign body is then grasped and pulled into the vitreous cavity through the retinotomy. Regardless of the method to free-up and grasp the foreign body, it is quite important to be certain that the sclerotomy site for removal is sufficiently large.

Removal of Subretinal PFCL

An occasional indication for retinotomy is the removal of subretinal PFCL. This indication may arise intraoperatively or postoperatively, subsequent to vitrectomy with use of PFCL. Insufficient release of retinal traction or misdirected injection of preretinal PFCL into a retinal break can result in intraoperative subretinal PFCL. Postoperative retention of subretinal PFCL occurs in up to 12% of cases and is most often associated with large peripheral retinectomies.[16]

Small extramacular bubbles of subretinal PFCL are usually visually insignificant and should not be removed unless they show migration toward the subfoveal region. Migration is more likely to occur with bubbles trapped subretinally superior to the macula, and in the presence of epiretinal membranes. If the PFCL bubble is located subfoveally, or is found migrating in that direction, repeat vitrectomy with small retinotomy is indicated, given PFCL's known toxicity to the photoreceptors and pigment epithelium.[16] Subretinal

PFCL has been found to produce a dense scotoma on microperimetry.[17] Once PFCL is removed, the affected retina tends to regain partial function; the degree of recovery is probably dependent on the duration of its subretinal presence. Large amounts of subretinal PFCL, either intra- or postoperatively, should be removed regardless of location. If the retina is attached, a PFCL bubble can be removed through a small retinotomy given its high fluidity.

A recently reported technique for removal of a subfoveal PFCL bubble is to create a small retinotomy with a sharp needle tip in the thin tissue over the retained subfoveal PFCL, creating a therapeutic macular hole.[18] The retinotomy is created after injecting PFCL into the vitreous cavity overlying the macula; preretinal and subfoveal PFCL are then removed with a silicone-tip backflush needle. After removing the PFCL bubble, the macular hole is closed with complete gas tamponade of the vitreous cavity.[18] Another reported technique is perifoveal insertion of a small-gauge cannula into the subfoveal PFCL bubble and removal of the bubble with active suction.[19–22] When the PFCL is subfoveal, the small-gauge cannula can be inserted through an extrafoveal retinotomy to infuse BSS beneath the fovea in order to move the PFCL bubble to an extrafoveal location where manipulation and suction are safer.

Retinal or Subretinal Mass

Pars plana vitrectomy and retinectomy have been used to remove a retinal vasoproliferative tumor to treat recurrent hemorrhages and exudation and provide a specimen for histopathologic diagnosis.[23] Gaudric et al. reported retinectomy to treat nine eyes with retinal capillary hemangiomas in von Hippel–Landau disease.[24]

Removal of a subretinal mass is an uncommon indication for retinotomy, although retinotomy can be used for removal of a subretinal mass such as a disciform scar.[25,26] The surgical results of disciform scar removal have been disappointing. Biopsy of choroidal melanomas is now commonly done, sometimes with vitrectomy (see Chapter 127, Vitreous, retinal, and choroidal biopsy). Surgical resection of choroidal melanomas with vitrectomy has been popularized in some centers (see Chapter 151, Surgical

resection of choroidal melanoma). Harris et al. described successfully using extensive retinectomy to remove a subretinal abscess due to *Klebsiella*.[27]

Retinectomies to Obtain Abnormal Retinal Tissue: Retinal Biopsy

Retinal and choroidal biopsies use retinectomies and choroidectomies to obtain tissue for pathologic diagnosis in difficult diagnostic problems, such as retinitis, uveitis, and neoplastic diseases. (This topic is covered in Chapter 127, Vitreous, retinal, and choroidal biopsy.)

Retinectomy for Treatment of Intractable Glaucoma

The pressure-lowering effect of anterior retinectomy has been advocated for treatment of intractable glaucoma.[28,29] Of 44 eyes treated by Joussen et al, with at least 5 years' follow-up, 52.3% had long-term control of intraocular pressure without complications. Among the remaining eyes, complications were frequent, with a high rate of PVR, hypotony, and phthisis bulbi. Eyes with neovascular glaucoma due to central retinal vein occlusion and eyes with uveitis had a particularly poor prognosis. Because the complication rate was much higher than for more traditional methods to lower the intraocular pressure, others have challenged the use of retinectomy to treat glaucoma.[30]

Relaxing Retinotomy and Retinectomy

Relaxing retinotomies and retinectomies are used in the presence of retinal shortening that results from retinal incarceration or fibrous proliferation and contraction that prevents contact of the retina with the RPE.[31–36] Usually, the peripheral retina is cut or removed to preserve function of the more visually significant posterior retina. If the retina is cut and not removed, the procedure is technically a

retinotomy; however, in discussing relaxing retinotomies and retinectomies, we will refer here to all retinotomies and retinectomies as "retinectomies."

The indications for relaxing retinectomies are listed in Box 112.1. Except for retinal incarceration in traumatic or surgical wounds and excision of the inner wall of congenital retinoschisis, all the indications involve PVR or proliferative vascular retinopathy, with fibrous proliferation causing contraction and shortening of the retina. Relaxing retinectomies should only be done if other methods have failed or have no chance of success. A scleral buckle will sometimes adequately relieve traction to avoid cutting the retina. Michels et al.[37] described how a scleral buckle will change the vector force of contraction of proliferative membranes so the force is no longer applied to pull the retina away from the pigment epithelium. A buckle should be considered in the presence of [illegible] contraction.

Box 112.1

Indications for Relaxing Retinotomies and Retinectomies

- Retinal incarceration in traumatic or surgical wound
- Proliferative vitreoretinopathy
- Focal contraction (star fold)
- Diffuse contraction
- Circumferential contraction
- Intrinsic retinal contraction
- Anterior retinal displacement
- Extensive fibrous periretinal proliferation
- Contraction and fibrosis of flap of giant retinal tear

- Proliferative vascular retinopathy
- Inner wall of congenital retinoschisis

Factors influencing the decision to perform a retinectomy or to place or revise a scleral buckle include the location and extent of the traction and the difficulty of revising or placing the buckle. Traction that can be easily and efficiently relieved with a scleral buckle (traction usually anterior in location and focal in extent) should be managed in such a manner; however, with extensive traction and fixed folds, a buckle is often not adequate. In addition, the extensive dissection and time required to revise a scleral buckle may sometimes be more harmful to the eye than internally relieving traction with a retinectomy.

Membrane dissection at vitrectomy will relieve most traction. Because posterior membranes can almost always be removed, posterior relaxing retinectomies are rarely indicated. However, peripheral membrane dissection is often more difficult, and if traction cannot be adequately relieved, a retinectomy may be required to reattach the retina.

General Surgical Principles and Techniques

The relaxing retinectomy can be performed after either 20G or smaller-gauge vitrectomy. Newer instrumentation and the ability to inject silicone oil into eyes using microincisional vitrectomy system (MIVS) technology makes the use of smaller-gauge technology possible.[38] The retinectomy should only be performed after complete membrane removal. If the retina is cut or excised before complete membrane removal, further membrane removal will be more difficult and may result in unnecessarily large retinal defects or residual membranes that may lead to redetachment of the retina. Larger peripheral retinectomies are less functionally significant than are smaller posterior retinectomies. Although a large peripheral retinectomy may be more difficult to manage at the end of the operation, the greater preservation of retinal function obtained is usually worthwhile. Circumferential relaxing retinectomies are usually preferred to radial retinectomies. In the

face of circumferential traction, a radial retinectomy that adequately relieves traction may extend too far posteriorly into the central retina.

It is useful to be able to see the full extent of the retina to be cut or excised during creation of a retinectomy. With full visualization, it is easier to assess the best location and the necessary extent of the retinectomy. A wide-angle viewing system is ideal for visualization of the retina during this maneuver. Either a contact or non-contact system can be used. Use of a wide-angle system may reduce the time necessary to do the procedure, improve the ability to apply laser photocoagulation, and reduce the need for scleral depression.[39] Before a relaxing retinectomy is created, diathermy should be applied to the entire area to be cut (Fig. 112.3A). Blood vessels in the area should be occluded. The retina can be cut with scissors or a vitrectomy instrument. Scissors will make the most precise, controlled cut, but 23G and 25G vitreous cutters can be well controlled and are much more precise than 20G instruments. Use of the vitreous cutter is faster than using scissors. The vitreous cutter is used for excising the anterior flap of the retinectomy. For folded retina, sequential cutting and reapplication of diathermy, as described later for release of retinal incarceration, is the preferred method. PFCL may be useful to stabilize the retina posterior to the retinectomy.[5] As a general principle, for maximal relaxation of traction, the retinectomy should extend into normal retina on each end of the area of contraction. With shorter retinectomies, the extension into normal retina needs to be only a few degrees in length. With very large retinectomies, extension into the normal retina may need to be up to 30°. If the normal retina to be cut is attached, care must be taken not to damage the choroid during retinectomy, because bleeding may occur. After diathermy, the retina should be gently pulled away from the pigment epithelium by the scissors tips, a soft silicone tip cannula with or without suction, or a pick before cutting.

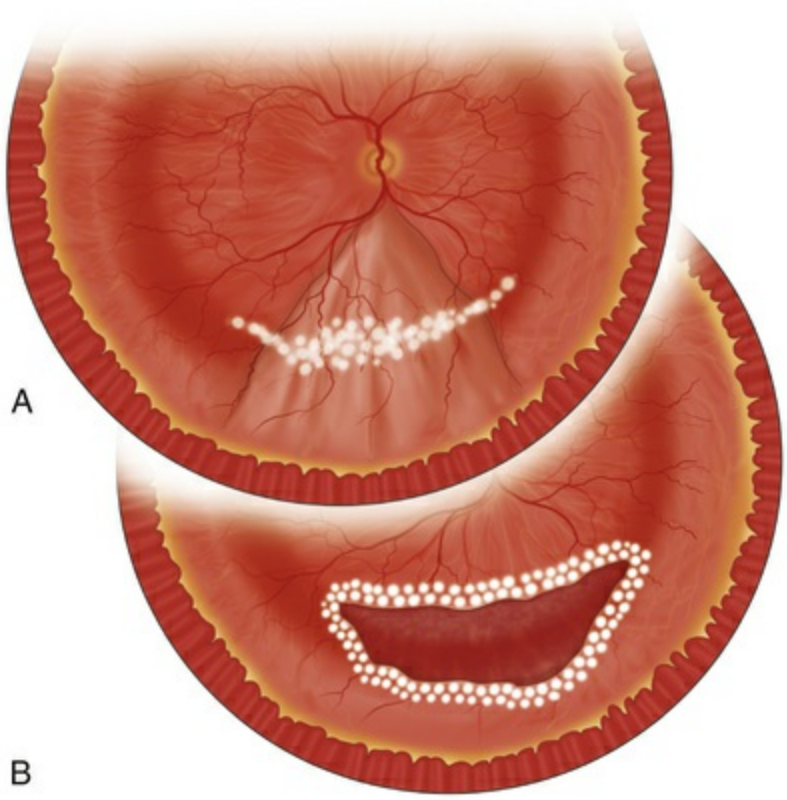

FIG. 112.3 Persistent retinal contraction and shortening after membrane removal. (A) Diathermy applied heavily to vessels and lightly to the remainder of the retina in the area of proposed retinotomy. (B) After retinectomy and reattachment of the retina, the retinal defect is greatest centrally and least at the ends.

The surgeon should pay attention to the pattern of retinal contraction in designing a retinectomy. After retinal reattachment, a circumferential relaxing retinectomy will have an oval configuration (Fig. 112.3B). Relaxation is greatest in the central area where the retinal defect spreads apart the most and least at each end of the retinectomy. For a smaller retinectomy, without extensive traction toward the ends, a simple circumferential cut is usually adequate. For larger retinectomies, especially those with traction toward the ends, the surgical principle of the Z-plasty is useful. By angling the cut anteriorly to the ora serrata or sometimes the pars plana epithelium oblique to the circumferential direction of the relaxing retinectomy, one can relieve residual traction at the ends of the retinectomy (Fig. 112.4).[33] The combination of

circumferential retinectomy to relieve anteroposterior shortening and oblique extension at each end into normal retina to relieve circumferential shortening achieves the greatest retinal relaxation in the face of extensive retinal shortening.

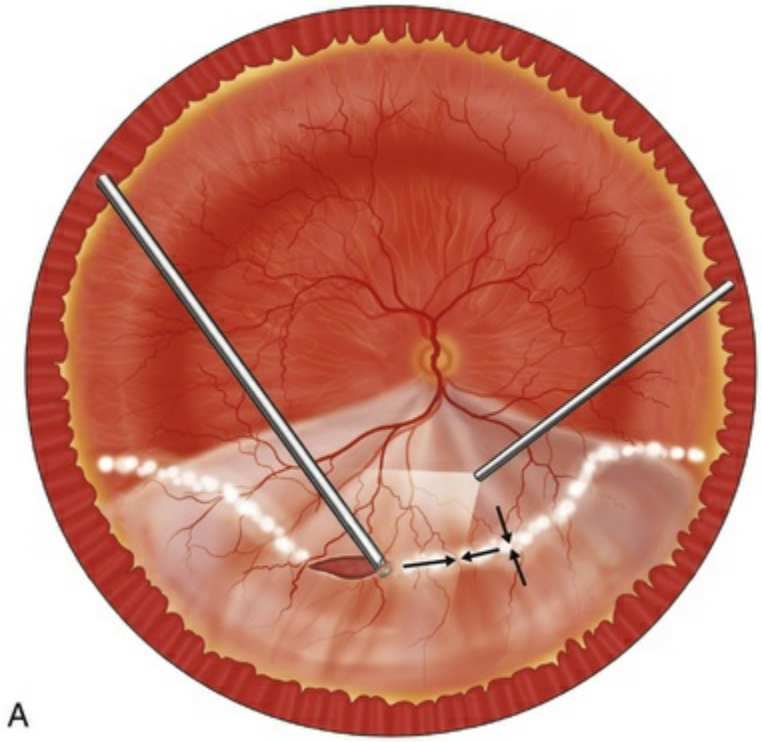

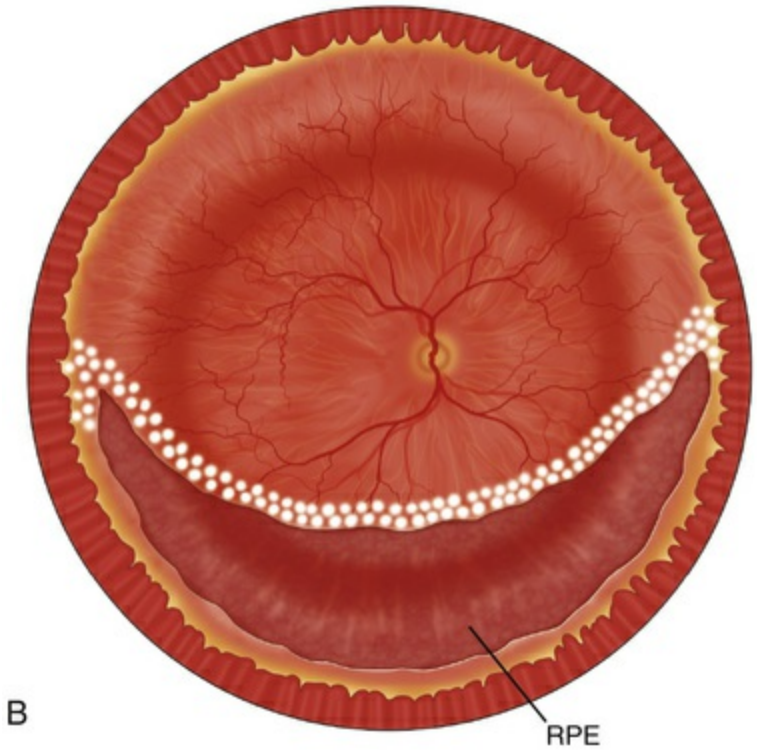

FIG. 112.4 Extensive retinal shortening persists after membrane removal. (A) *Arrows* indicate both circumferential and radial retinal shortening. Diathermy is applied to the retina and vessels in the proposed retinotomy site. The retinectomy is extended obliquely anteriorly into the uninvolved retina to maximize relaxation. (B) Retina flat following fluid–air exchange. The anterior flap of the functionless retina was excised, which reduces the likelihood of recurrent traction in the area of retinotomy. Note the bare retinal pigment epithelium (*RPE*) anterior to the retinectomy.

The anterior flap of the retinectomy is avascular and nonfunctional. We recommend excision of the retina anterior to a large retinectomy so that fibrin and cellular proliferation do not rejoin the cut edges of the retina or proliferation from the anterior flap does not produce traction on the ciliary body. Excision of the anterior flap is especially important at the ends of the circumferential retinectomy. Failure to extend the retinectomy into normal retina or to excise the anterior flap may allow recurrent proliferation and contraction to redetach the retina (Fig. 112.5).

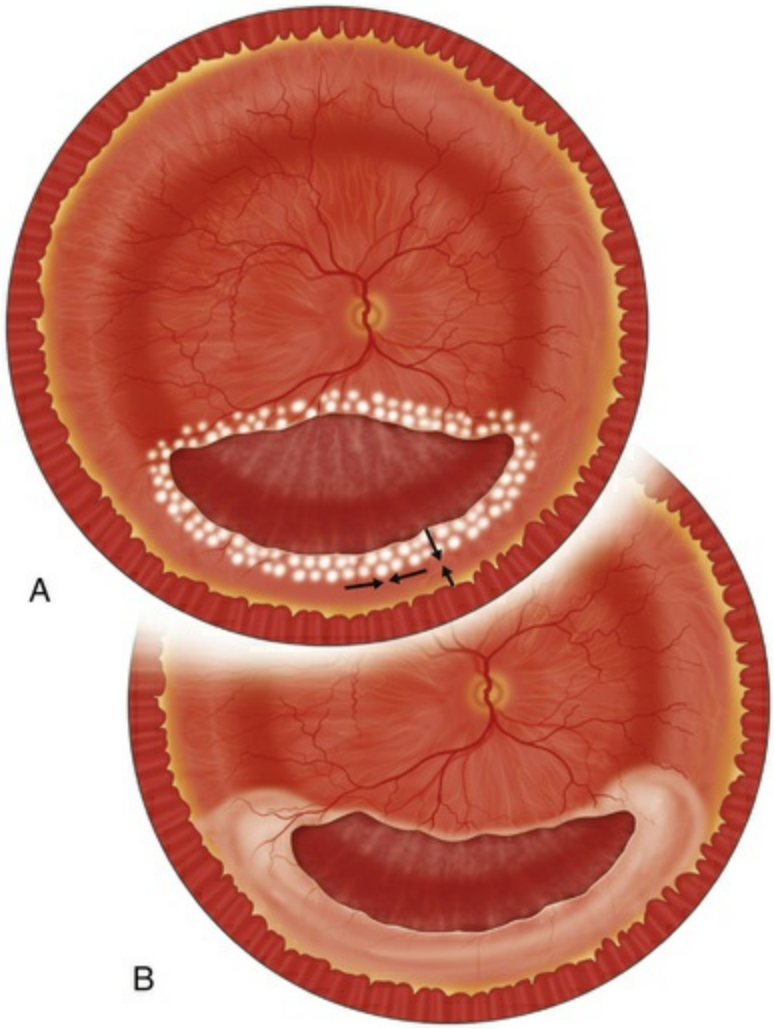

FIG. 112.5 (A) Eye in which retinectomy is not extended anteriorly. *Arrows* indicate forces of recurrent traction, which redetach retina at the ends of the retinectomy. (B) Retinal redetachment around inadequate retinectomy. A larger, more extensive retinectomy is less likely to detach.

If a circumferential retinectomy extends more than 270°, it is usually best to extend it to 360°. Similarly, if a small isthmus of intact retina separates two large retinectomies, it is usually best to cut the intact retina to join the two areas of retinectomy. These small areas of intact retina are of little functional use and may become areas of contraction that elevate the edges of the retinectomy.

Retinal Incarceration in Traumatic or

Surgical Wounds

A retinectomy is sometimes necessary for relief of traction that results from traumatic scleral perforation with retinal incarceration.[33,40] Retinal incarceration may result from several mechanisms. Focal (limited) retinal incarceration occurs when local retina is forced or drawn into a penetrating wound. Retina may actually be acutely extruded at the time of injury as vitreous is extruded, or the fibrosis of healing after a penetrating injury may progressively draw retina towards the injury site. In both situations, the final result is overall shortening of the retina with folds radiating toward the central wound (Fig. 112.6). Alternatively, retina may be incarcerated in a sclerotomy site after drainage of subretinal fluid during retinal detachment surgery. Another mechanism of retinal incarceration involves incarceration of retina distant from the penetrating wound (Fig. 112.7). This results from acute extrusion of vitreous out of the wound associated with collapse of the eye during injury. Distant retina attached to the vitreous is pulled into the wound as the vitreous is extruded. The most extreme example of the latter mechanism is total extrusion of the vitreous through a wound with complete avulsion of the anterior retinal insertion. The retina is found in a tight funnel configuration extending from the posterior optic nerve connection to the anterior wound. Incarceration of the retina in an anterior wound such as a cataract surgery wound can result from a massive suprachoroidal hemorrhage in which the vitreous and retina are extruded through the wound by the enlarging choroidal detachment. As the hemorrhage is surgically drained or resolves on its own, the retina may be left incarcerated in the wound.

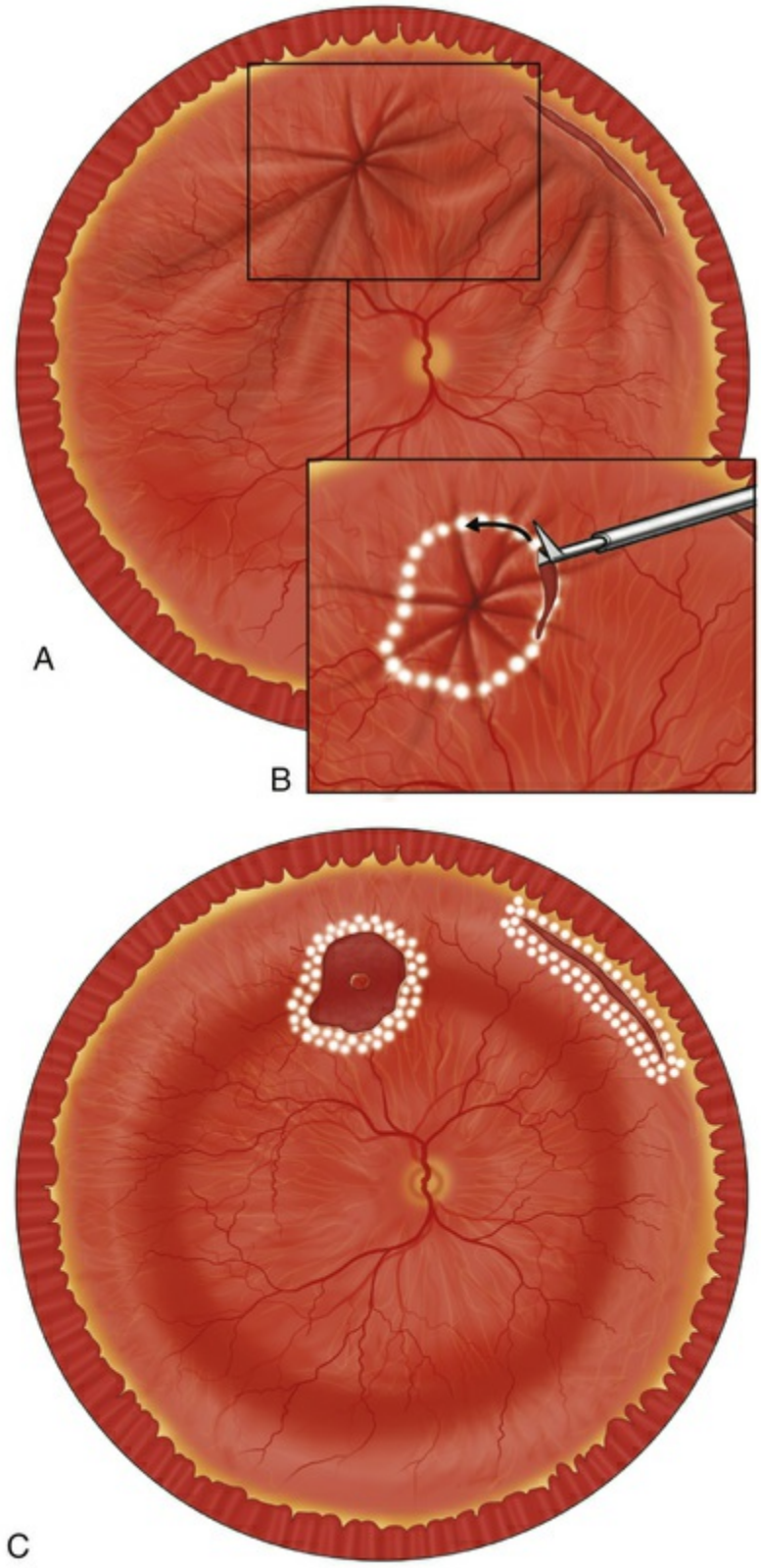

FIG. 112.6 Release of focal retinal incarceration. (A) Superior traumatic penetrating injury with retinal incarceration and retinal detachment with peripheral dialysis. (B) Endodiathermy applied to retina surrounding incarceration. The retina is cut in layers,

and diathermy is reapplied as deeper retina is uncovered. The retina is cut 360° around the incarceration site. (C) Postoperative appearance. The retinectomy is enlarged after flattening of retina. Laser endophotocoagulation was applied to the edges of the retinectomy.

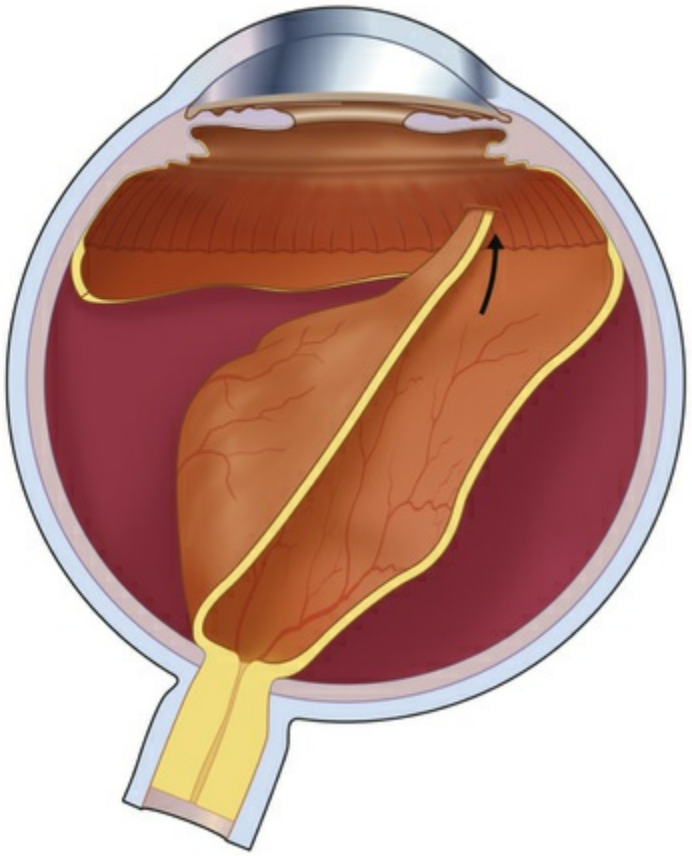

A

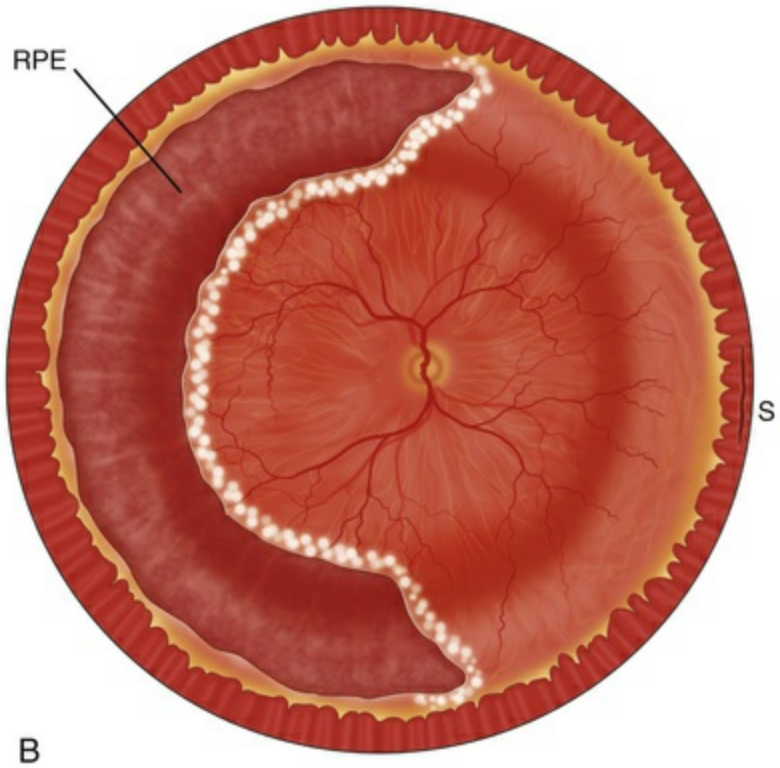

FIG. 112.7 Distant retinal incarceration. (A) Torn retina incarcerated in wound on the opposite side of the eye. (B) After excision of the retina from the wound, the retina is flattened. *RPE*, area of bare retinal pigment epithelium after retinal reattachment. Note the scar at the previous incarceration site (*S*).

In limited incarcerations, the retina has a focal morning-glory configuration at the point of incarceration (Fig. 112.6A). Surrounding retina is usually detached with fixed folds radiating from the area of incarceration. The degree of retinal shortening and contraction is determined by the size of the scleral wound, the amount of retina incarcerated, and the degree and chronicity of fibrous proliferation at the incarceration site. A retinotomy should be performed only if contraction and folds from the incarceration site prevent retinal reattachment.

Surgical Technique

Vitrectomy should be completed and hemorrhage and membranes within the vitreous and on the retinal surface should be removed before retinectomy is considered. If the retina is extruded into an anterior wound, it may be difficult to place the instruments through

the pars plana in the normal position; the surgeon should be careful to avoid placement of the infusion cannula into the subretinal space. In a fresh wound, the retina may sometimes be teased out of the incarceration site with forceps or reposited by the injection of a viscoelastic substance. Injection of PFCL over retina posterior to the incarceration may pull retina out of the incarceration. A retinotomy is required if the retina cannot be dislodged from a fresh wound or if it is incarcerated in a fibrotic, older wound. Retina must also be cut if significant shortening and fixed folds persist after a complete vitrectomy and membrane peeling.

Initially, diathermy is applied to the retina at the margin of the incarceration to ensure that all blood vessels are closed (Fig. 112.6B). There may be large vessels within the incarceration site, so it is preferable to cut just peripheral to the incarceration site rather than directly into it. The retina is usually cut with the vertically cutting vitreoretinal scissors 360° around the incarceration site (Fig. 112.6B). Bullous retina posterior to the incarceration site can be flattened and stabilized with PFCL during the retinectomy.[5] If PFCL is used, the retina posterior to the incarceration site should be free of membranes. There should be no open retinal breaks under traction in the area to be covered by the PFCL. The PFCL is injected over the posterior pole and the level of the PFCL brought just posterior to the incarceration.

The retina may be thickened, and parts of the retina may be hidden between folds, making hemostasis with diathermy difficult. It may be necessary to cut the retina in layers, reapplying diathermy as the untreated tissue is uncovered.[33] When the retina is circumcised around an area of incarceration, the defect in the retina will be larger than would initially appear (Fig. 112.6C). Therefore, the closer the cut is made to the area of incarceration, the smaller the potential defect will be. In areas where the retina is closely apposed to the RPE, there is risk of damage to the choroid by the scissors, with resultant hemorrhage. After diathermy, the scissors blade or a membrane pick can usually be placed tangentially through the necrotic retina into the subretinal space. The retina should be lifted away from the RPE before cutting. The retinal defect created by the retinectomy should be treated with laser endophotocoagulation and tamponaded with gas or silicone oil

(Fig. 112.6C).

Management of distant retinal incarceration is a special problem. Very large defects are created when the retina is excised from the wound (Fig. 112.7). These eyes may require up to a 360° retinectomy to separate the retina from the wound. PFCLs may be useful in managing extensive distant retinal incarcerations. PFCL might be useful to stabilize the retina during the retinectomy, open the closed funnel of the retinal detachment, and to reattach the resultant giant retinal tear (Fig. 112.8).[4,5]

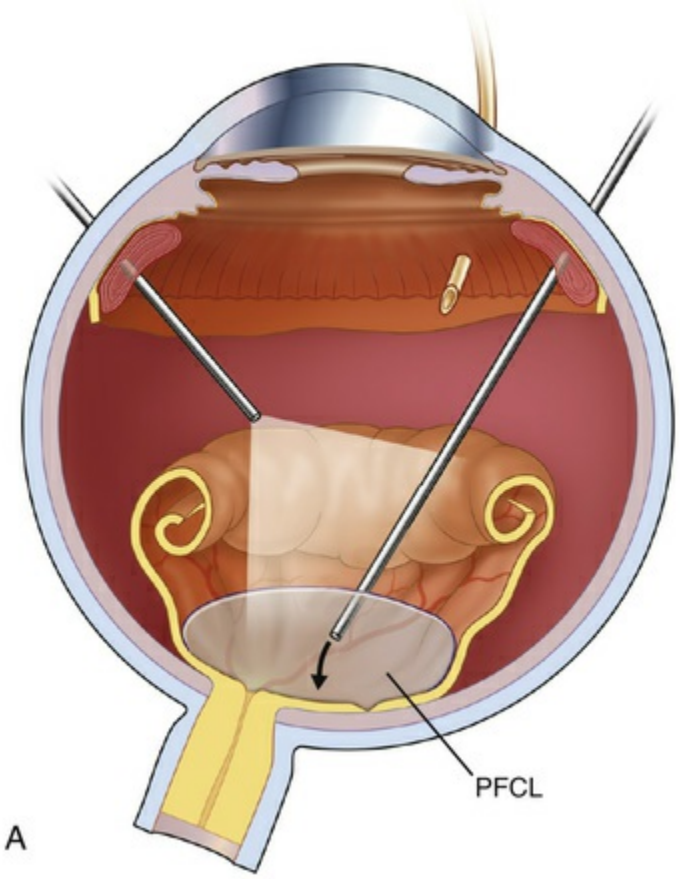

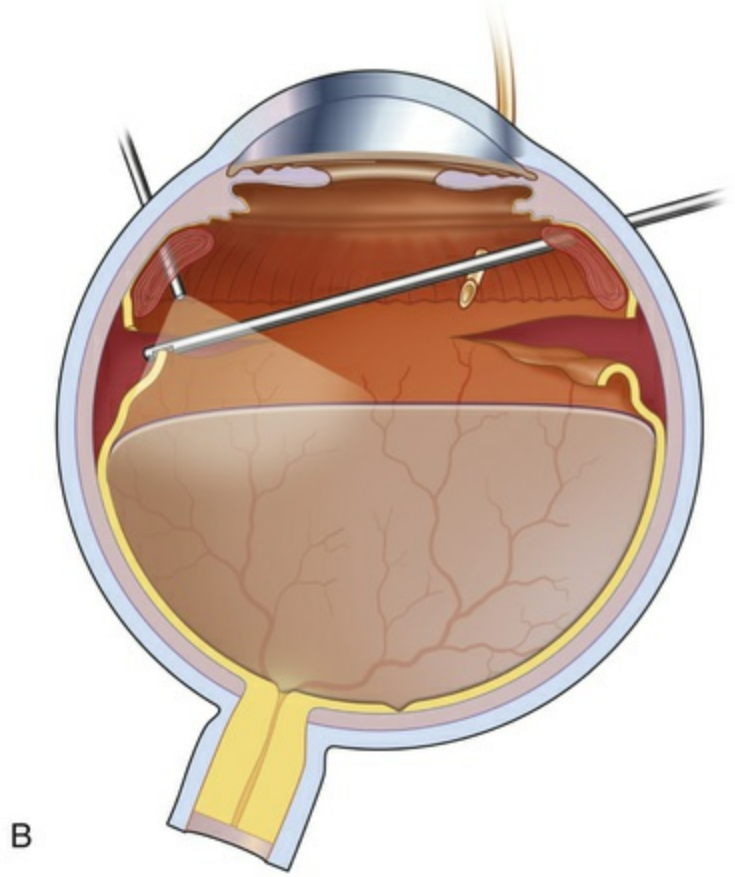

B

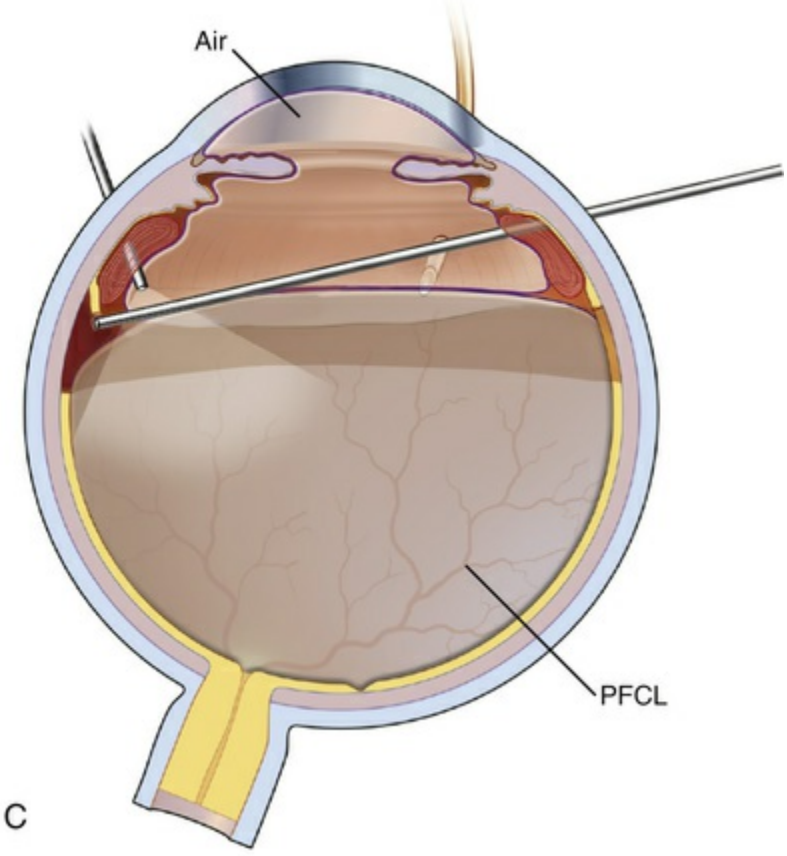

C

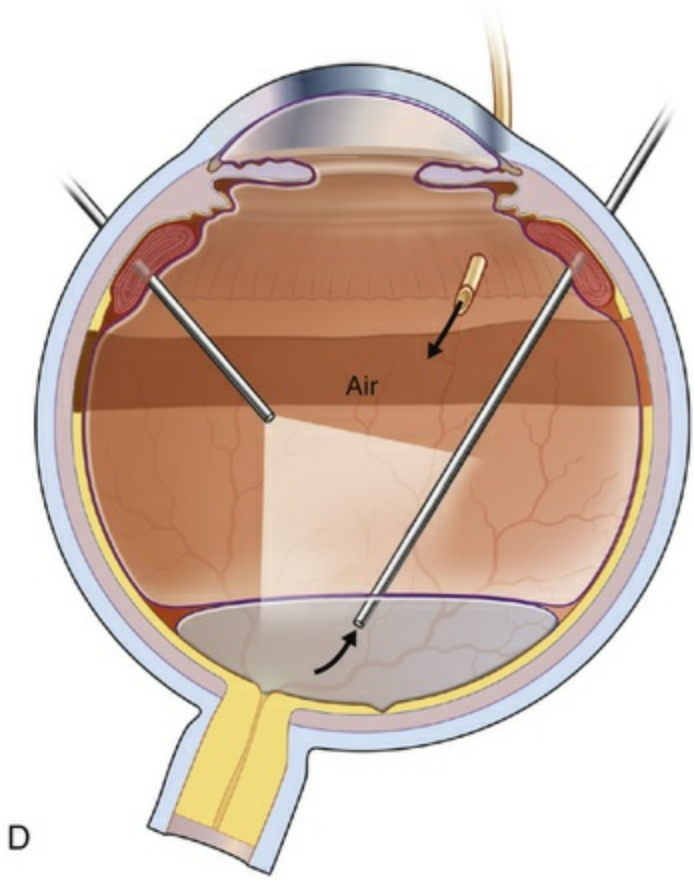

FIG. 112.8 Management of giant retinal tear or retinectomy with perfluorocarbon liquid (PFCL). (A) Folded-over giant tear/retinectomy with marked folding of the peripheral retina. PFCL injected over posterior pole after posterior epiretinal membrane removal. (B) Posterior retina reattached. Organized, folded edge of giant tear treated with diathermy, then excised with vitrectomy instrument. (C) Retina completely reattached with PFCL. "Drying" anterior edge of giant tear during initial phase of fluid–air exchange by applying suction with soft-tip needle beneath anterior edge of retina. (D) Continuing fluid–air exchange to remove residual PFCL. No retinal slippage has occurred.

Retinal Shortening (Contraction) Because of PVR

Retinal shortening in PVR is divided into seven categories (Box 112.1). In the revised Retina Society Classification of PVR,

contraction posterior to the equator was classified as posterior PVR, whereas contraction at the equator and anteriorly was classified as anterior PVR.[41] The first two categories, focal contraction and diffuse contraction, are similar; both result from contraction of epiretinal membranes and vary mainly in the extent of retinal involvement (see Chapter 112, Proliferative vitreoretinopathy, for further information on classification of PVR).

Surgical Technique

The surgical goals and techniques of performing retinectomies for the various subtypes of PVR are similar. Some modifications in technique are necessary for eyes with the various subgroups of PVR. In all forms of PVR, a complete vitrectomy and aggressive membrane removal are essential to relieve contraction. A scleral buckle may relieve lesser degrees of contraction, but with extensive shortening, a retinectomy is necessary. The size, location, orientation, and configuration of a retinectomy will vary according to the indication.

Focal or Diffuse Retinal Contraction

It is usually unnecessary to cut the retina to manage focal or diffuse contraction. Occasionally when the retina is atrophic, the membranes will not strip from the retina without extensive retinal tearing. Focal retinectomy in areas where membranes cannot be removed is sometimes necessary (Fig. 112.9). Diathermy is applied to the retina surrounding the area to be excised, particularly to the retinal vessels. If the retina is detached, the retinectomy can usually safely be done with a small-gauge vitreous cutter; however, if the retina is partially or completely attached in the area of contraction, the retina is most safely excised with scissors.

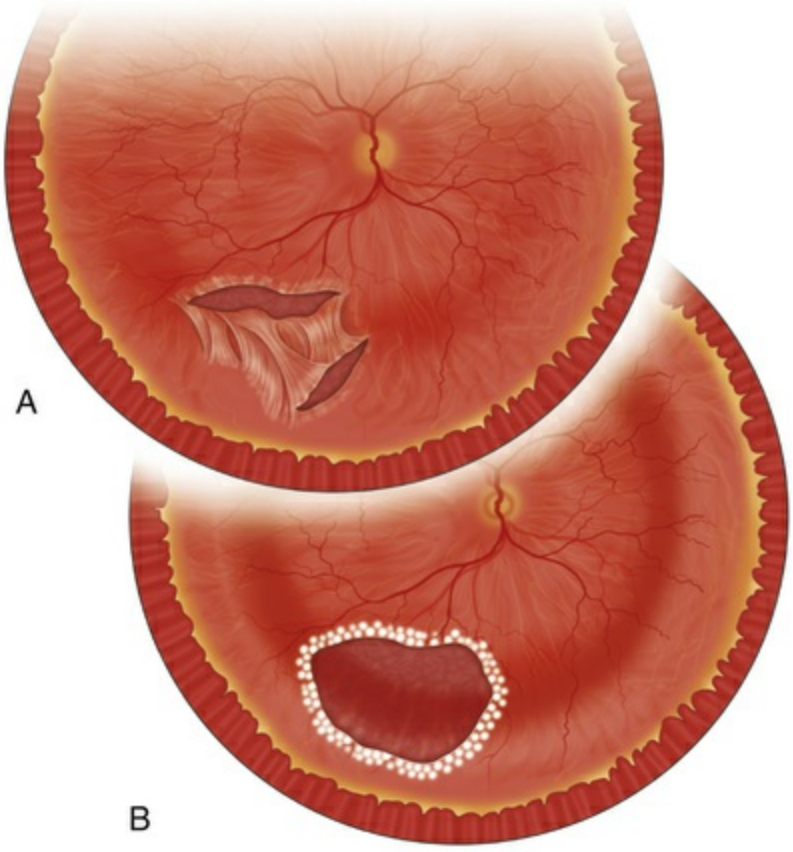

FIG. 112.9 (A) Diffuse contraction associated with large retinal breaks. Remove all membranes. If all membranes cannot be removed, local retinectomy is performed. (B) Large defect after retinectomy. Traction is relieved, and the retina is reattached. The edge of the break is treated with laser endophotocoagulation.

Circumferential Contraction

Extensive circumferential contraction may occur because of marked membrane contraction at the posterior aspect of the vitreous base. In the revised Retina Society Classification of PVR, circumferential contraction is a form of anterior PVR.[41] Coronal contraction of the posterior hyaloid pulls the retina centrally into a funnel shape, and circumferential contraction creates tight retinal folds that extend posteriorly in a radial fashion (Fig. 112.10A). Even with excision of the posterior hyaloid and stripping and sectioning of membranes, a ridge of equatorial retina may sometimes remain in a circular contracted state. It is usually visually apparent if circumferential

contraction has not been adequately relieved by membrane peeling and sectioning. If dissection does not release traction, a circumferential retinectomy should be made just posterior to the area of contraction (usually the posterior aspect of the vitreous base) (Fig. 112.4). The relaxing retinectomy is best made with PFCL stabilizing the retina posterior to the area of contraction (Fig. 112.11). With the posterior retina held in place by the PFCL, the retinectomy is extended circumferentially into normal-appearing retina on each end of the retinectomy, and then extended anteriorly to the ora serrata (or the ciliary body if the pars plana is involved with traction) (Figs. 112.4 and 112.11). The retina anterior to the retinectomy should be excised with the vitrectomy instrument. Once all traction is released by the retinectomy, the PFCL can be brought anterior to the level of the retinectomy to reattach the remaining retina without fear of subretinal PFCL.

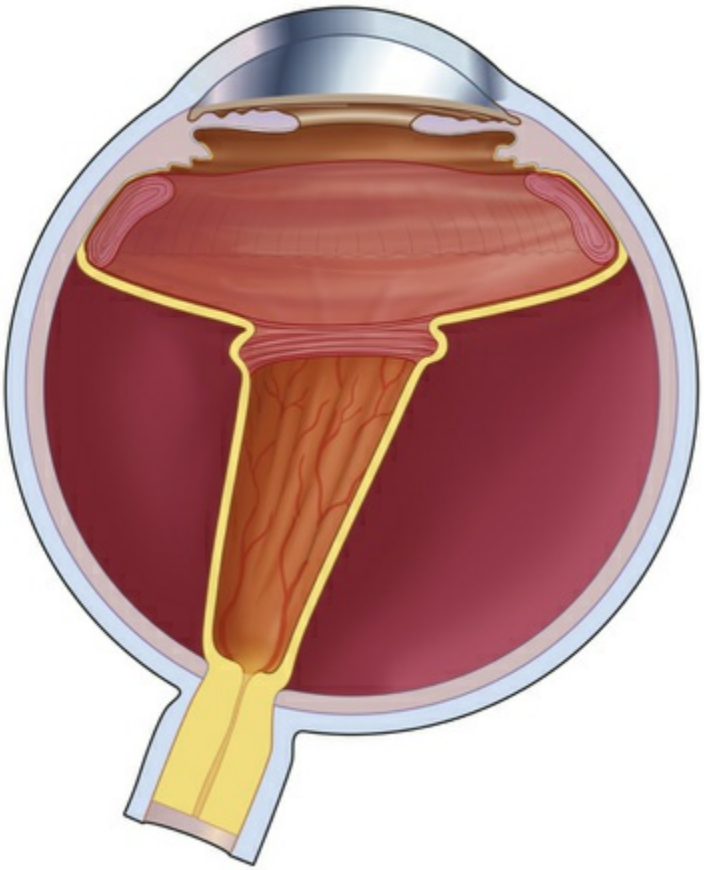

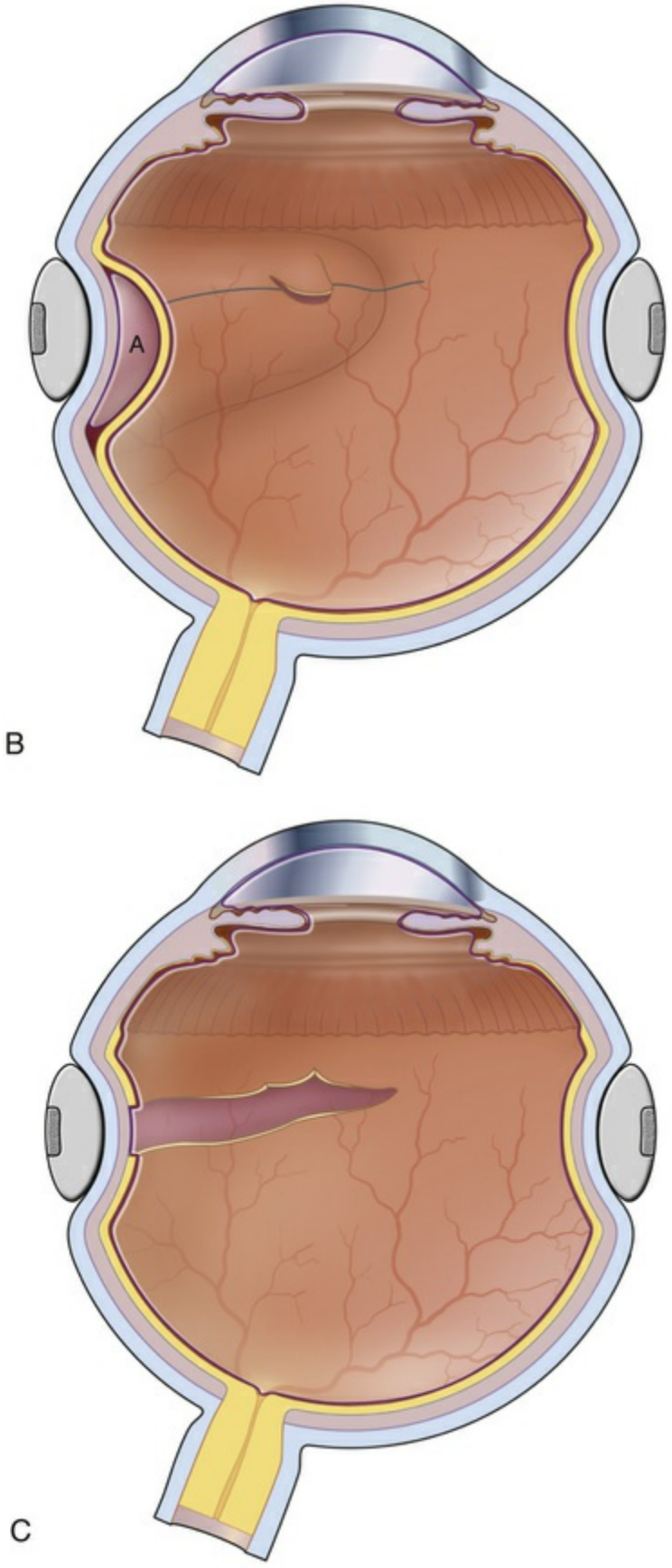

FIG. 112.10 Contraction of posterior aspect of vitreous base. (A) Retina pulled into funnel configuration.

Circumferential contraction of posterior vitreous base with radial folds in retina. (B) After vitrectomy, membrane removal, scleral buckle, and fluid–air exchange, air (*A*) courses subretinally through the retinal break. Dashed line indicates location of proposed retinectomy. (C) Circumferential retinectomy is performed under air, and the retina flattens. Extend retinectomy into attached retina on each end.

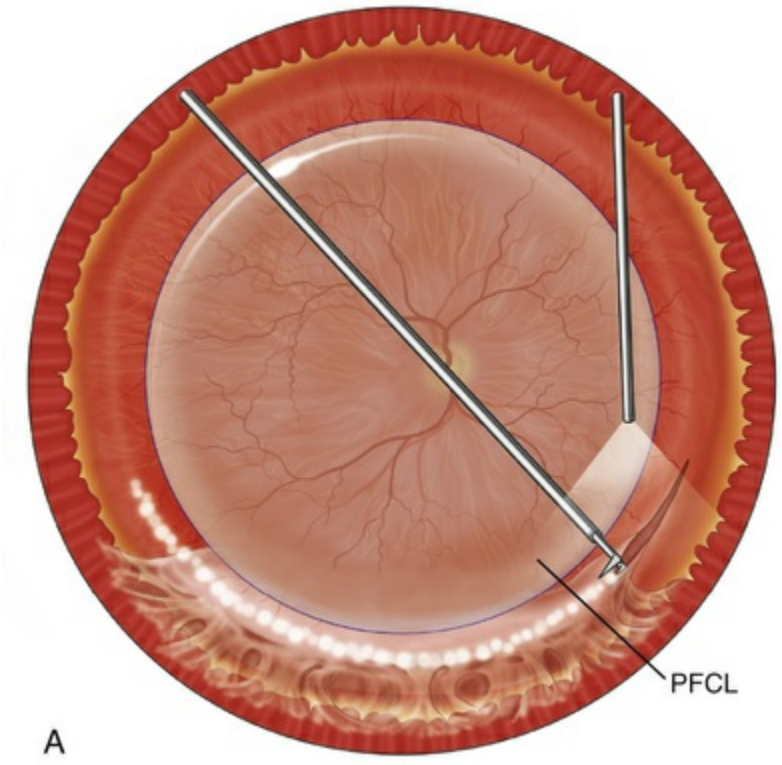

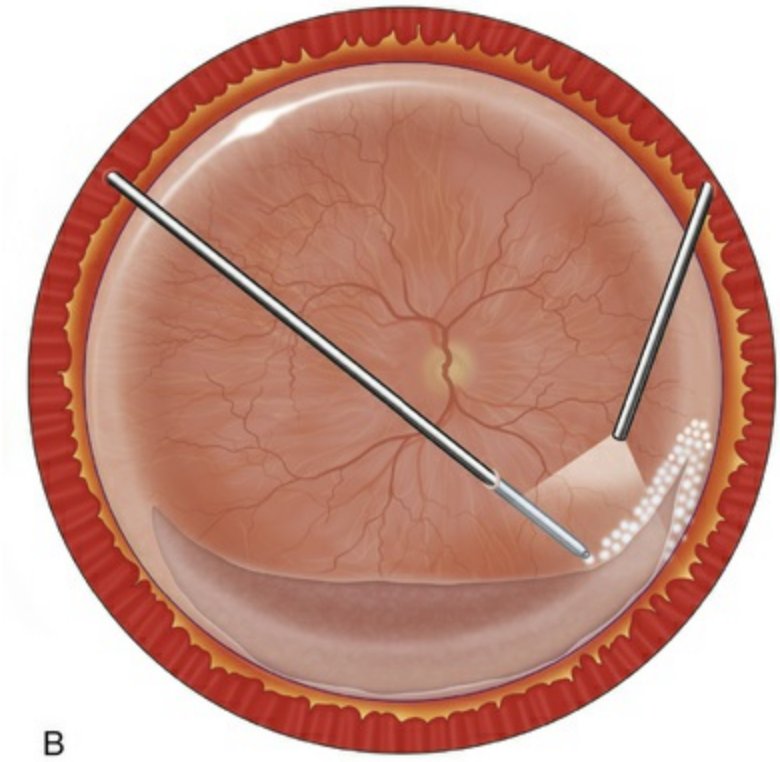

FIG. 112.11 (A) Anterior proliferative vitreoretinopathy extends from 5 to 8 o'clock. The posterior retina is held in place by perfluorocarbon liquid (PFCL). Retinectomy anterior to the PFCL extends into unaffected retina at each end of the retinectomy. (B) The full extent of the retinectomy is now flattened by PFCL and is large because of excision of anterior flap. Laser endophotocoagulation is applied to the margin of retinectomy.

Alternatively, the need for a relaxing retinectomy at the posterior aspect of the vitreous base may be noted during injection of PFCL or after fluid–air exchange. The surgeon may notice persistent circumferential tenting of the retina or the air or PFCL may course subretinally through retinal breaks elevated by traction. It is best to try to determine if contraction has been adequately relieved before air or PFCL goes subretinally, as both situations further complicate surgery. If PFCL goes under the retina, it will be necessary to retrieve it with a fluted needle or suction cannula, often requiring folding the retina over in order to visualize the subretinal PFCL. If air has gone under the retina, the air may delineate most of the area of residual traction (Fig. 112.10B). It is important to extend the relaxing retinectomy well beyond the point that allows the retina to

flatten because the surface tension of the air may overcome residual traction that might redetach the retina as the gas bubble resolves. Subretinal air will coalesce with air in the vitreous cavity when the retinectomy is made and the retina will reattach (Fig. 112.10C).

Anterior Retinal Displacement

Anterior retinal displacement is an important cause of retinal detachment with PVR and is primarily found in patients who have undergone a previous vitrectomy.[41–43] In these cases, fibrous proliferation and contraction of membranes at the vitreous base pull peripheral retina anteriorly to the pars plana, pars ciliaris, or even to the posterior iris. This may lead to anterior retinal detachment, recurrent posterior retinal detachment, or to ciliary body detachment and hypotony (Fig. 112.12).

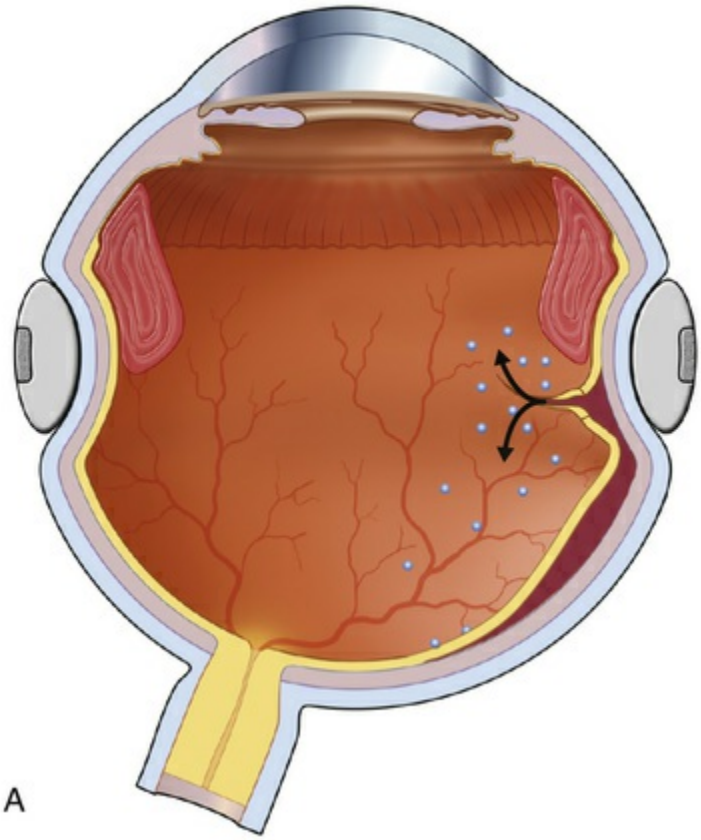

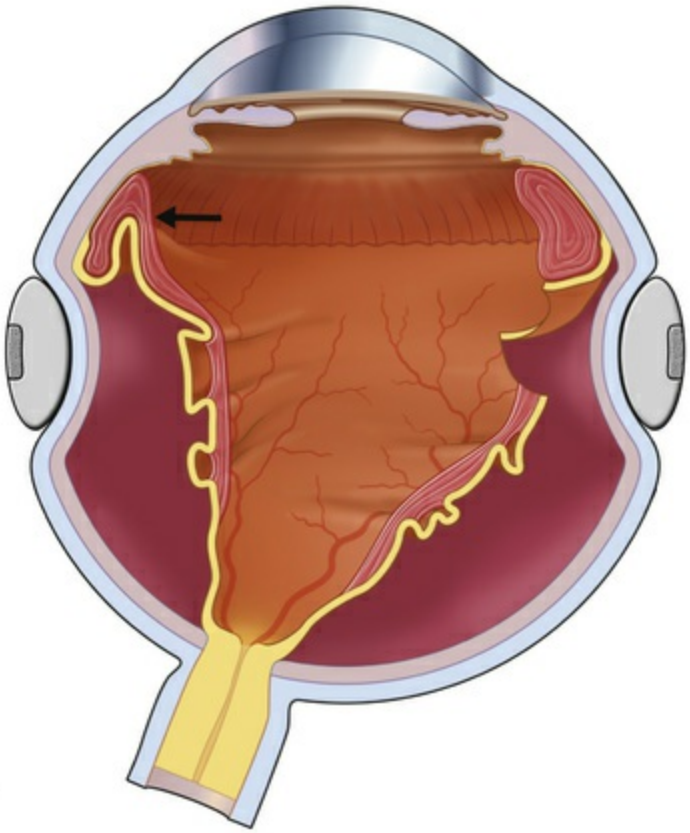

B

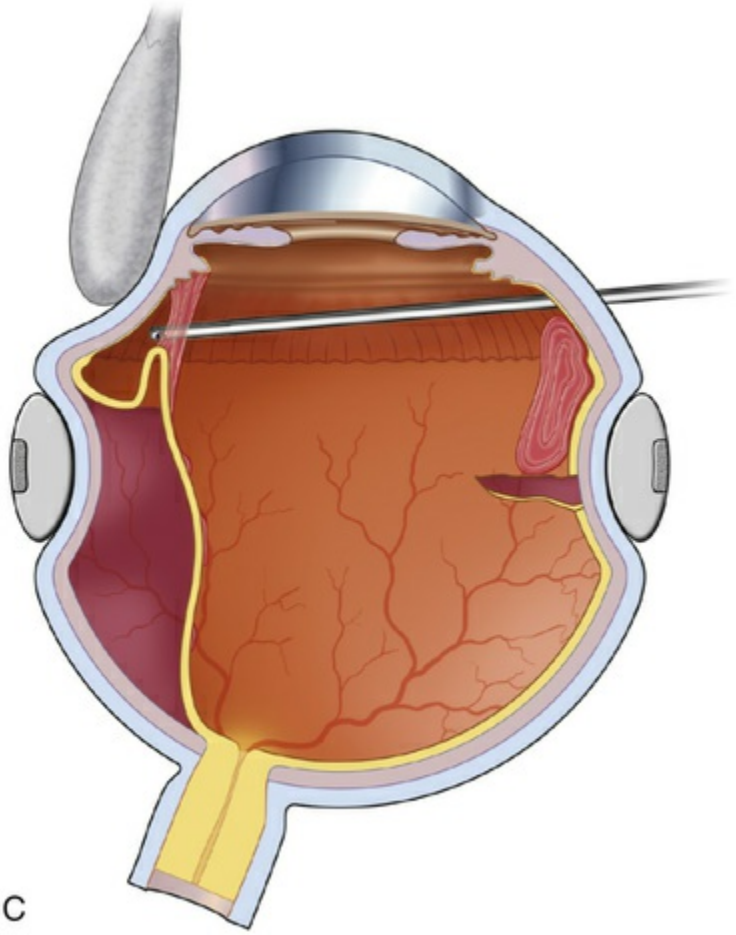

C

FIG. 112.12 Anterior retinal displacement (ARD) after previous vitrectomy and scleral buckle. (A) Proliferation of cells onto the retina and residual peripheral vitreous. (B) Recurrent retinal detachment after contraction of proliferative membranes. Note ARD (*arrow*) with peripheral retina pulled in a fold toward the ciliary body by contracting vitreous base. (C) Release of ARD with scissors by cutting membrane.

If excessive traction persists after membrane dissection, an anterior retinectomy is necessary (Figs. 112.11 and 112.13). The retinectomy is performed after all posterior membranes have been removed and is made just posterior to the anterior retinal traction. The retinectomy is performed in a manner similar to that described for extensive equatorial contraction.

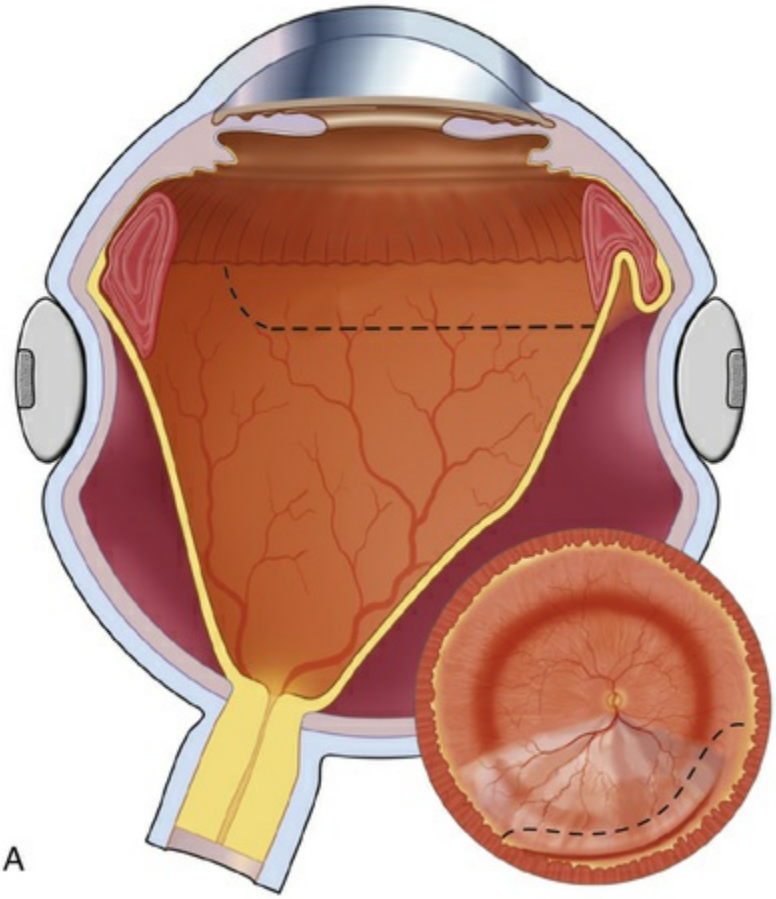

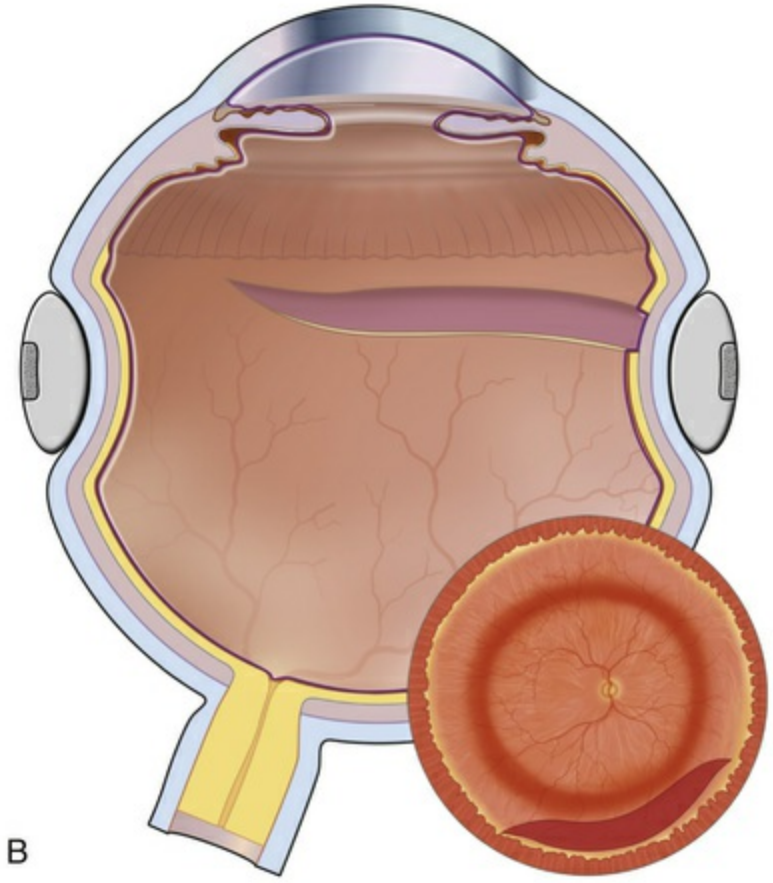

FIG. 112.13 Relaxing retinectomy for localized anterior retinal displacement. (A) Area of contraction not released by membrane dissection. *Dashed line* indicates proposed retinectomy. Extend anteriorly into unaffected retina. (B) After retinal reattachment. Retinectomy with anterior flap excised.

Intrinsic Retinal Contraction

Intrinsic retinal contraction is retinal contraction in the absence of epiretinal or subretinal membranes and is most often found in eyes with chronic retinal detachments. Retinectomy for intrinsic retinal contraction is similar to retinectomy for other forms of contraction, but intrinsic retinal contraction is often only recognized after injection of PFCL or insufflation of air. If the area of intrinsic retinal contraction is in the peripheral retina, a circumferential retinectomy is made posterior to the area of contraction. With intrinsic retinal contraction, the area of involvement is often extensive, so the retinectomy may need to be quite large. The retinectomy should be

extended circumferentially into normal retina at each end and anteriorly to the ora serrata.

Intrinsic retinal contraction involving the posterior retina is more difficult to manage. When there is annular contraction involving the posterior retina, if no subretinal membrane is found as a cause, a retinectomy is necessary to relieve traction. A circumferential retinectomy in the posterior pole is problematic because of loss of visual field. Several radial cuts in retina will sometimes adequately relieve the traction; however, these cuts may extend too far posteriorly toward the optic nerve. Excision of a section of nasal retina may adequately relieve traction and allow the more visually significant temporal retina to be reattached.

Extensive Periretinal Fibrous Proliferation

Extensive periretinal fibrous proliferation may occur in eyes after extensive traumatic retinal contusion or necrosis. The retina may be replaced by fibrous tissue with further fibrous proliferation on the anterior and/or the posterior surface of the retina. With longstanding PVR and chronic retinal detachment with severe fibrous proliferation, the retina may become very thin and atrophic in areas of fibrous proliferation, making membrane removal impossible. Perisilicone proliferation may involve widespread fibrous proliferation, especially at the margin of a previous retinectomy. The peripheral retina may become so encased in fibrous tissue that the tissue cannot be separated from the retina.

In all these instances, the dense, white fibrous tissue cannot be separated from the retina. The retina in these areas becomes nonfunctional and should be excised if it prevents retinal reattachment. These membranes are often quite contracted, causing marked folding and shortening of the retina. The involved areas may be vascularized, although sometimes they are avascular. Diathermy should be applied along the posterior edge of the area to be excised, and then excision is carried out with the vitreous cutting instrument in a technique similar to that described for diffuse retinal contraction (Fig. 112.9).

Prophylactic Removal of Anterior Flap of

Horseshoe Tears

One of the most common forms of retinectomy is the removal of the anterior flap of a horseshoe tear. These flaps always have strong vitreoretinal adhesions, and the flap is removed because of the possibility of progressive traction on the edge of the tear by vitreous contraction in the postoperative period. Traction may lead to lifting of the retina away from the pigment epithelium and/or anterior extension of the horseshoe tear. The tear should be left in a rounded shape, which is more likely to withstand vitreous traction without experiencing extension or elevation. If present, the operculum of a retinal tear is also commonly excised as part of the necessary peripheral vitrectomy. Sometimes retinal vessels bridge the operculum or flap of the tear. Diathermy should be applied to the vessels prior to removal of the flap or operculum with the vitreous cutting instrument.

Contraction and Fibrosis of Flap of Giant Retinal Tear

The posterior flap of most giant retinal breaks shows inward curling of the edge because of the normal contractility of the retina. With chronicity and the onset of PVR, this folding may become permanent and prevent reattachment of the edge of the flap (Fig. 112.14A). The inwardly folded retina may become fixed with proliferative membranes, and the edge may be thickened, fibrous, and taut. Even after removal of membranes, the edge may remain folded, requiring retinectomy to allow complete flattening of the flap of the giant break.

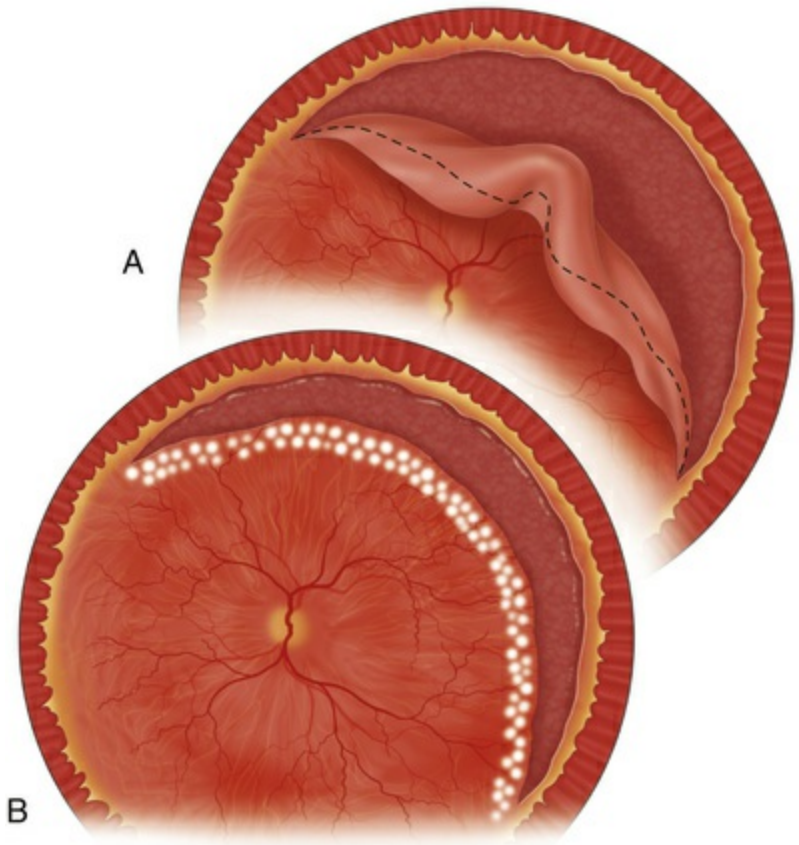

FIG. 112.14 (A) A 180° giant retinal tear with folded rolled edge, which prevents complete unfolding. The *dashed line* indicates the limit of the edge to be excised. (B) Retina relaxed and reattached.

There is often both anteroposterior shortening because of inward rolling of the edge of the break and circumferential shortening as a result of fibrous contraction. Membranes are removed on both the anterior and posterior surfaces of the retina. The flap is unfolded mechanically using two instruments. If the flap will not unfold, it is often best to excise the folded edge of the flap.[44] Alternatively, a series of radial cuts may be placed approximately every 30° along the margin of the flap to allow unfolding.[44] However, the irregular edge created by this series of cuts is more difficult to manage, and excision of the edge is the preferred approach (Fig. 112.14B).

After removal of posterior membranes, PFCL is injected over the posterior pole and the level is brought to a level posterior to the fibrotic edge of the giant tear (Fig. 112.8B).[4] The PFCL fixes the retina and makes excision of the organized edge easier. Diathermy is applied to the edge of the flap throughout the extent to be

excised. Excision is usually with the vitreous cutting instrument, being careful to apply low suction so that excessive retina is not excised. If radial cuts are to be made, diathermy is applied only locally in the area to be cut.

Inner-Wall Retinectomy for Complications of Congenital Retinoschisis

Congenital retinoschisis can be complicated by combined schisis–traction retinal detachment, combined schisis–rhegmatogenous retinal detachment, vitreous hemorrhage, and obscuration of the macula by the overhanging inner wall of a schisis cavity. Ferrone et al. reported pars plana vitrectomy with excision of the inner wall of the peripheral schisis cavity in nine eyes with various complications of congenital retinoschisis.[45] The retina was attached postoperatively in eight of nine eyes; six had improvement in visual acuity (VA), and one had stabilization of VA. Two eyes had a decrease in VA. An alternate technique with posterior hyaloid dissection, a small retinotomy, fluid drainage with a 42G cannula, laser photocoagulation, and silicone oil injection was successful in one reported case.[46]

Retinal Shortening Because of Proliferative Vascular Retinopathy

Retinectomy is sometimes indicated for the repair of longstanding traction retinal detachment associated with diabetic retinopathy and other proliferative vascular retinopathies such as branch retinal vein occlusion, proliferative sickle-cell retinopathy, and retinopathy of prematurity.[47] The indications and techniques for relaxing retinectomy are similar to the indications and techniques for PVR.

Management of Retinectomy

Production of a relaxing retinectomy can create problems in closing the tear and managing what may be a giant retinal break that can invert or retract posteriorly. Small retinectomies can usually be

flattened with air and treated with laser endophotocoagulation without slippage or inversion of the posterior flap. Larger circumferential retinectomies need to be treated as a giant tear.

PFCL is the best method for managing a large circumferential retinectomy. The PFCL is injected over the optic disc and reattaches the retina from posteriorly to anteriorly. The anterior edge of the retina should be carefully monitored during PFCL injection. If the retina is completely mobile, the level of the PFCL can be safely brought anterior to the edge of the retinectomy. However, if traction remains on the anterior retina, the PFCL may go beneath the retina. Therefore, if traction remains, the anterior edge of the flap should be excised before further PFCL injection. With traction relieved, the meniscus of the PFCL can safely be brought anterior to the flap of the tear to completely reattach the retina. The PFCL interface should not be brought in contact with the infusion cannula because small bubbles of PFCL will be created that can migrate under the edge of the retina if the edge is still elevated. The use of valved cannulas will reduce overall fluid flow and decrease production of PFCL bubbles.

Laser photocoagulation can be applied to the edge of the retina either before or after exchanging the perfluorocarbon for air or silicone oil. The view is usually superior through PFCL than through either air or silicone oil. The fluid anterior to the PFCL maintains good corneal clarity and pupillary dilation, whereas air sometimes causes striate keratopathy, pupillary miosis, and a minimized view. Small bubbles suspended in silicone oil can sometimes interfere with visualization through silicone oil. If the anterior edge of the retinectomy has been completely flattened by PFCL, it is easier to apply laser through the PFCL than through air or silicone oil. However, if it is not possible to flatten the edge of the tear completely with PFCL, laser treatment should be delayed until after exchanging the PFCL for air or silicone oil. Alternatively, an anterior drainage retinotomy can be made to allow egress of loculated anterior subretinal fluid into the vitreous cavity (Fig. 112.1).

Exchange of the PFCL for air or silicone oil is an important step that can lead to problems if not performed correctly. There is often a small amount of subretinal fluid beneath the anterior edge of the

retina, and there can be small bubbles of PFCL beneath the retinal edge. Unless this fluid is removed, it will be forced posteriorly during the exchange and can lead to posterior slippage of the retina and/or to accumulation of subretinal PFCL. During PFCL–air exchange, the fluid anterior to the PFCL should first be replaced with air. "Drying" of the anterior edge of the retina is accomplished with either a backflush brush or other soft-tipped extrusion or suction cannula placed just anterior to the retinal flap (Fig. 112.8C). The exchange is completed (Fig. 112.8D) after all subretinal fluid is removed and the anterior edge is thoroughly "dried."

Posterior retinal slippage can occur during PFCL–air exchange for giant tears or retinectomies. Slippage most commonly occurs in large, highly myopic eyes and is due to fluid behind the anterior edge of the retina being forced posteriorly during the exchange. Inadequate removal of that fluid (inadequate drying of the anterior edge of the retina) is the most important cause of posterior slippage. Sometimes it is possible to manipulate the anterior edge of the retina with the backflush brush to pull the retina to its proper position. However, if the retina cannot be brought to its normal position, the air should be removed and the retina once more flattened with PFCL. Thorough drying of the anterior edge of the retina during exchange usually prevents further retinal slippage. Laser treatment to the retinal edge prior to PFCL removal anecdotally appears to exert a small immediate protective effect against slippage, perhaps by dehydrating the retina-RPE interface. Exchange with silicone oil rather than air is less likely to cause slippage of the retina.

Results

In the Silicone Study,[48] group 2 eyes (previous vitrectomy) were twice as likely to undergo retinectomy as group 1 eyes (no previous vitrectomy) (42% vs. 20%; $p<.0001$). Variables identified with stepwise logistic regression analysis that were associated with the need for retinectomy were (1) membership in group 2 and (2) the presence of >6 clock-hours of anterior retinal displacement. Group 1 eyes undergoing retinectomy had a significantly poorer anatomic prognosis than eyes not undergoing retinectomy (50% attached vs.

69% attached at 6 months, p =.03; 38% vs. 69% at 24 months, p =.01) regardless of whether perfluoropropane gas or silicone oil was used. In group 2, this difference was only significant at 24 months (52% attached with retinectomy vs. 70% attached without retinectomy; p =.052). Group 1 eyes (but not group 2 eyes) undergoing retinectomy were more likely to have visual acuity less than 5/200 than eyes not undergoing retinectomy (32% vs. 59%, p <.01 at 6 months; 28% vs. 55%, p = .03 at 24 months), regardless of tamponade modality. In group 1 (but not in group 2), hypotony (intraocular pressure ≤5 mmHg) was about twice as prevalent in eyes that had a retinectomy than in those that did not (35% vs. 17% at 6 months, p<.05; 24% vs. 14% at 12 months, not significant) regardless of tamponade. It is probable that eyes with poorer anatomic and visual prognosis underwent retinectomy, which might explain some of the results.

More recent series report better anatomic and visual results than those reported in the Silicone Study and lower rates of hypotony. Bovey et al.[49] reported excellent anatomic and visual results following peripheral retinectomies of 180° or more. Of 33 eyes reported (all managed with silicone oil), silicone oil was permanently removed from 24. The final VA was 5/200 or better in 85% and 20/200 or better in 51%. Only one eye had hypotony (intraocular pressure ≤5 mmHg) at the last follow-up examination, although two eyes required reinstillation of silicone oil because of hypotony.

Eckardt et al.[50] reported silicone oil removal from 32 eyes that had peripheral relaxing retinectomies for proliferative vitreoretinopathy. Only three eyes developed retinal detachments following silicone oil removal and 28 eyes obtained a VA of 0.1 or better and 15 eyes 0.2 or better. One eye was hypotonus and 11 eyes were treated for glaucoma.

Tseng et al.[51] looked at the influence of relaxing retinectomy on surgical outcomes in PVR. They found that silicone oil was significantly superior to gas for long-term tamponade in eyes with a relaxing retinectomy, confirming the results of the Silicone Study.

Quiram et al.[52] reported complete reattachment in 93% of 56 eyes with recurrent retinal detachment with PVR treated with retinectomy. Patients undergoing radical anterior vitreous base

dissection and lensectomy at the time of first retinectomy had a higher success rate than those who did not. Hypotony was present in 5.4% at the last follow-up.

Grigoropoulos et al.[53] reported the results of 304 eyes managed with retinectomy. The cause of retinal detachment was rhegmatogenous retinal detachment with PVR (78%), posterior trauma (17%), and vasoproliferative diseases, acute retinal necrosis, and endophthalmitis in the rest. A total of 51% were completely reattached with one operation and 72% with more than one operation. A final VA of 6/24 or better was significantly associated with better preoperative vision, shorter duration of silicone oil tamponade, silicone oil removal, and smaller size of retinectomy.

Of 145 patients managed with retinectomy, de Silva et al.[54] reported visual acuity of 20/60 or better in 16%, between 20/60 and 20/400 in 33%, and <20/400 in 51%. There was complete retinal reattachment in 68%. They found with each stepwise increase in the grade of preoperative PVR, there was an approximately 15% increased risk of final visual acuity of <20/40. They found that the use of 360° prophylactic laser retinopexy prior to removal of silicone oil was associated with a higher rate of final retinal reattachment.

Tan et al.[55] advocate retinectomy without a scleral buckle for eyes with anterior PVR without an existing scleral buckle. Of 123 eyes, the single operation success rate was 77% with a final reattachment rate of 96% after one or two additional procedures. They demonstrated significant improvement in visual acuity, and hypotony was present in only 4.1%.

There are several reports of the results of 360° retinectomy. Faude et al.[56] reported 30 eyes with advanced PVR or proliferative diabetic retinopathy treated with 360° retinectomy. Silicone oil tamponade was used in all eyes. At 10 months, VA had improved in 47% and the retina was attached in 83%. Hypotony was present in six eyes.

Zhang and Jiang[57] reported 26 cases with more than 6 months follow-up after 360° retinectomy following severe ocular trauma. The retina was reattached in 77%, and visual acuity was 4/200 or better in 70%, 20/400 or better in 35%, and 20/200 or better in 11.5%. In a mixed series of 30 eyes with more than half secondary to ocular trauma, Kolomeyer et al.[58] reported the retina attached at 6 months

in 83% of 30 eyes with 360° retinectomies, but only 11% with ambulatory vision. Garnier et al. reported similar results in 20 eyes.[59] Only 10% recovered visual acuity of 20/200 or better.

Williamson and Gupta reported a technique of planned delayed retinectomy for PVR in 27/87 eyes operated on for advanced PVR.[60] In the first operation, they partially reattached the retina with vitrectomy and silicone oil, then returned to surgery at a later date to do a relaxing retinectomy and completely reattach the retina. Following silicone oil removal, 24/27 eyes (89%) had complete retinal reattachment.

Stopa and coworkers, in a nonrandomized study, compared the anatomic and visual results of 25 adult patients and 20 pediatric patients, each group managed with vitrectomy and retinectomy for retinal detachment.[61] Reattachment rate was higher in adults than children (88% vs. 60%, p=.041), and visual acuity was better in the adult group. Children required more reoperations (p=.008) and postoperative PVR was significantly more frequent in pediatric eyes (p=.003).

Complications

Relaxing retinectomies can have several potentially serious complications. Because these complications can sometimes lead to surgical failure, retinectomy should not be taken lightly and other methods should be used if possible. The major complications of retinectomy are hemorrhage, inability to unfold and reattach the retina, visual field loss, hypotony, fibrous proliferation from the retinectomy site, and persistent traction leading to retinal detachment when the retinectomy is too small.

Hemorrhage may result from inadequate diathermy of the vessels. Relatively heavy diathermy should be applied to close the blood vessels within the area of retinectomy. Although the retina between the vessels may not bleed in some cases, there may be oozing from smaller vessels in other cases. Optimal control of systemic blood pressure might reduce the chances of hemorrhage.

Because of the potential for hemorrhage, we prefer to treat the retina with a row of diathermy before cutting. Fibrotic retina may have many blood vessels requiring more extensive diathermy.

Raising the infusion bottle temporarily, causing an increase in intraocular pressure, can usually control intraoperative hemorrhage. Use of a combination diathermy and fiberoptic light source (fiberoptic tissue manipulator, Alcon Laboratories, Fort Worth, TX) will allow readily available diathermy in the event of hemorrhage during a retinectomy.[62] This manipulator, currently only available in 20-gauge, has infusion capability, so a small stream of fluid can be injected and directed toward the bleeding site to uncover the bleeding vessel and allow precise placement of diathermy.

Complete hemostasis is essential because inadequately diathermized vessels may reopen later, causing a significant postoperative hemorrhage. Postoperative hemorrhage under silicone oil can lead to severe fibrous proliferation. In gas-filled eyes, recurrent hemorrhage can sometimes be removed with repeat postoperative fluid–gas exchange.

Inability to unfold and reattach the retina may occur after retinectomy when the retina retracts posteriorly and resists unfolding because of retinal contraction in longstanding PVR or other conditions such as retinopathy of prematurity. Most flaps can be manipulated and unfolded with PFCL. Only rarely does one encounter an eye in which contraction is so severe that the retina cannot be unfolded with any method.

Anterior retinal neovascularization, probably secondary to ischemia in avascular retina anterior to the retinectomy, is a possible late complication that can result in hemorrhage.[63] Complete removal of residual anterior retina or its ablation with laser is necessary to avoid this adverse event.

Hypotony is seen in some eyes after large retinectomies. In the report by Morse et al.,[64] hypotony (intraocular pressure ≤5 mmHg) developed in 43% of reattached eyes. In the Silicone Study,[48] the incidence of hypotony following retinectomy was 24% at 12 months. More recent series have reported a much lower incidence of hypotony following retinectomy.[49–52,55] This complication is probably most often related to the PVR process with fibrosis and detachment of the ciliary body associated with anterior proliferation. Another possible etiology of hypotony is increased absorption of intraocular fluid from the large area of exposed RPE.

Whether the latter is a significant factor in the production of hypotony is unknown.

Subretinal retention of PFCLs occurs in up to 12% of cases, usually associated with large peripheral retinectomies.[16] Posterior small to medium-size retinotomies rarely lead to this complication. Saline wash after removal of PFCLs may have a preventive role in both preretinal and subretinal retention. As discussed above, the need to remove retained postoperative subretinal PFCL depends upon the amount and location.

Visual field loss may occur if a retinotomy or retinectomy is made too close to the optic nerve or macula.[12] Relaxing retinectomies should be made in the periphery, and it is better to make a larger peripheral retinectomy, even to the extent necessary to fold the retina over to gain access to more posterior pathologic processes, than to make a posterior retinectomy that may produce marked loss of visual field.

Retinal pigment epithelial and choroidal damage can occur during retinectomy because of trauma due to scissors, vitrectomy instruments, endolaser probes, or other devices. This complication is most likely to happen if the retina is attached or only shallowly detached, such as in retinectomies near the ora serrata during macular translocation. It may lead to immediate choroidal hemorrhage that needs to be controlled by raising intraocular pressure or cauterization. Sometimes damage to Bruch's membrane will lead to development of choroidal neovascularization in the postoperative period.[65]

Fibrous proliferation from the retinectomy site most commonly follows the use of silicone oil. Reproliferation often occurs if there is hemorrhage beneath the silicone oil. The fibrous proliferation may bridge between the edge of the cut retina and more anterior structures, and occasionally retraction of fibrous tissue will redetach the retina. In patients with diabetes, the membranes may be vascular and cover a large section of retina. There may also be a release of cells from a large bed of exposed RPE, leading to fibrous proliferation elsewhere. The surgeon should try to avoid reproliferation by meticulous control of hemorrhage.

Postoperative fibrin may be a matrix for reproliferation, so accumulation or deposition of fibrin should be prevented if

possible. Preoperative and postoperative corticosteroids and nonsteroidal antiinflammatory agents may play a role in preventing deposition of fibrin. Tissue plasminogen activator will lyse postoperative fibrin.[66] If significant reproliferation and traction are seen, early reoperation with removal of the membranes may be successful in stabilizing the eye.

Persistent traction leading to retinal detachment when the retinectomy is too small is not a complication of the retinectomy but rather a complication of inadequate retinectomy. It is important to extend the retinectomy into more normal retina beyond each end of the area of traction. Extension of a large circumferential retinectomy obliquely anteriorly to the ora serrata on each end of the retinectomy and excision of anterior retina should allow maximal release of traction.

One of the major limiting factors in visual recovery following vitrectomy with retinectomy is abnormal macular status following surgery. Stopa and Kociecki[67] found optical coherence tomography evidence of macular abnormalities in 75% of 25 patients following retinectomy including retinal pigment epithelium irregularities, cystoid macular edema, epiretinal membranes, subretinal fluid, and subretinal PFCL. Fluorescein angiographic studies of the retina in eyes with healed retinectomies showed that the attached retina had very little change as a result of the retinectomy.[65] An intact blood–retinal barrier was found in areas of uncovered RPE. Complications noted on angiography included occasional choroidal neovascular membranes at the retinotomy site, cystoid macular edema, optic atrophy, pigment fallout, depigmented tracks, and choroidal folds. Most complications were believed to be nonspecific findings following vitrectomy and retinal detachment surgery.

In a nonrandomized comparative study, Odrobina et al. compared two groups, each with vitrectomy and retinectomy ≥180 degrees.[68] Group A had peeling of the ILM in the posterior pole and group B did not have the ILM peeled. Although visual results were similar, the group with ILM peel had significantly less macular pucker formation (0/33, 0% vs. 9/51,17.6%, p=.008).

References

1. Charles S. Vitrectomy for retinal detachment. *Trans Ophthalmol Soc U K*. 1980;100:542–549.
2. Charles S. *Vitreous microsurgery*. Williams & Wilkins: Baltimore, MD; 1981:81.
3. Doft BH. Intentional retinotomy for internal drainage of subretinal fluid. *Arch Ophthalmol*. 1986;104:807–810.
4. Chang S, Lincoff G, Zimmerman NJ, et al. Giant retinal tears: surgical techniques and results using perfluorocarbon liquids. *Arch Ophthalmol*. 1989;107:761–766.
5. Chang S, Ozmert E, Zimmerman NJ. Intraoperative perfluorocarbon liquids in the management of proliferative vitreoretinopathy. *Am J Ophthalmol*. 1988;106:668–674.
6. McDonald HR, Lewis H, Aaberg TM, et al. Complications of endodrainage retinotomies created during vitreous surgery for complicated retinal detachment. *Ophthalmology*. 1989;96:358–396.
7. Yamaguchi M, Ataka S, Shiraki K. Subretinal fluid drainage via original retinal breaks for rhegmatogenous retinal detachment. *Can J Ophthalmol*. 2014;49:256–260.
8. Larrison WI, Frederick AR Jr, Peterson TJ, et al. Posterior retinal folds following vitreoretinal surgery. *Arch Ophthalmol*. 1993;111:621–625.
9. Flynn HW Jr, Blumenkranz MS, Parel JM, et al. Cannulated subretinal fluid aspirator for vitreoretinal microsurgery. *Am J Ophthalmol*. 1987;103:106–110.
10. Nishimura A, Segawa Y, Shirao Y, et al. Less traumatic internal drainage instrument for subretinal fluid. *Retina*. 2000;20:693.
11. Richards SC, Maberley AL. Complications of retinotomies or subretinal fluid drainage. *Can J Ophthalmol*. 1993;28:24–28.
12. Bourke RD, Dowler JG, Milliken AB, et al. Perimetric and angiographic effects of retinotomy. *Aust N Z J Ophthalmol*. 1996;24:245–249.
13. Spaide RF, Fisher Y, Ober M, et al. Surgical hypothesis: inner retinal fenestration as a treatment for optic disc pit maculopathy. *Retina*. 2006;26:89–91.
14. Ooto S, Mittra RA, Ridley ME, et al. Vitrectomy with inner retinal fenestration for optic pit maculopathy.

Ophthalmology. 2014;121:1727–1733.
15. Joondeph BC, Flynn HW Jr. Management of subretinal foreign bodies with a cannulated extrusion needle. *Am J Ophthalmol*. 1990;110:250–253.
16. Garcia-Valenzuela E, Ito Y, Abrams GW. Risk factors for retention of subretinal perfluorocarbon liquid in vitreoretinal surgery. *Retina*. 2004;24:746–752.
17. Tewari A, Eliott D, Singh CN, et al. Changes in retinal sensitivity from retained subretinal perfluorocarbon liquid. *Retina*. 2009;29:248–250.
18. Kim JM, Woo SJ, Park KH, et al. Surgical removal of retained subfoveal perfluorocarbon liquid through a therapeutic macular hole with intravitreal PFCL injection and gas tamponade. *Korean J Ophthalmol*. 2013;27:392–395.
19. Escalada Gutierrez F, Mateo Garcia C. [Extraction of subfoveal liquid perfluorocarbon]. *Arch Soc Esp Oftalmol*. 2002;77:519–577.
20. Lai JC, Postel EA, McCuen BW 2nd. Recovery of visual function after removal of chronic subfoveal perfluorocarbon liquid. *Retina*. 2003;23:868–870.
21. Lesnoni G, Rossi T, Gelso A. Subfoveal liquid perfluorocarbon. *Retina*. 2004;24:172–176.
22. García-Arumí J, Castillo P, López M, et al. Removal of retained subretinal perfluorocarbon liquid. *Br J Ophthalmol*. 2008;92:1693–1694.
23. Yeh S, Wilson DJ. Pars plana vitrectomy and endoresection of a retinal vasoproliferative tumor. *Arch Ophthalmol*. 2010;128:1196–1199.
24. Gaudric A, Krivosic V, Duguid G, et al. Vitreoretinal surgery for severe retinal capillary hemangiomas in von Hippel–Lindau disease. *Ophthalmology*. 2011;118:142–149.
25. de Juan E Jr, Machemer R. Vitreous surgery for hemorrhagic and fibrous complications of age-related macular degeneration. *Am J Ophthalmol*. 1988;105:25–29.
26. Zivojnovic R. *Silicone oil in vitreoretinal surgery*. Martinus Nijhoff/Dr W Junk: Dordrecht; 1987:104.
27. Harris EW, D'Amico DJ, Bhisitkul R, et al. Bacterial subretinal abscess: a case report and review of the

literature. *Am J Ophthalmol*. 2000;129:778–856.
28. Kirchhof B. Retinectomy lowers intraocular pressure in otherwise intractable glaucoma: preliminary results. *Ophthalmic Surg*. 1994;25:262–267.
29. Joussen AM, Walter P, Jonescu-Cuypers CP, et al. Retinectomy for treatment of intractable glaucoma: long term results. *Br J Ophthalmol*. 2003;87:1094–1102.
30. Wong VWY, Lai TYY, Lam DSC. Comment on: retinectomy for intractable glaucoma. *Br J Ophthalmol*. 2004;88:1352–1353.
31. Machemer R. Schneiden der netzhaut: eine behandlungsmoglichkeit zur weideranlegung der netzhaut. *Klin Monatsbl Augenheilkd*. 1979;175:597–601.
32. Machemer R. Retinotomy. *Am J Ophthalmol*. 1981;92:768–792.
33. Machemer R, McCuen BW II, deJuan E Jr. Relaxing retinotomies and retinectomies. *Am J Ophthalmol*. 1986;102:7–12.
34. Zivojnovic R, Mertens DAE, Peperkamp E. Das flussige silikon in dermotiochirurgie (II). Bericht uber 280 falle-weitere entwicklung der technik. *Klin Monbl Augenheilkd*. 1982;181:444–452.
35. Zivojnovic R. *Silicone oil in vitreoretinal surgery*. Martinus Nijhoff/Dr W Junk: Dordrecht; 1987:19.
36. Parke DW II, Aaberg TM. Intraocular argon laser photocoagulation in the management of severe proliferative vitreoretinopathy. *Am J Ophthalmol*. 1984;97:434–443.
37. Michels RG, Thompson JT, Rice TA, et al. Effect of scleral buckling on vector forces caused by epiretinal membranes. *Am J Ophthalmol*. 1986;102:449–451.
38. Siqueira RC, Gil AD, Jorge R. Retinal detachment surgery with silicone oil injection in transconjunctival sutureless 23-gauge vitrectomy. *Arq Bras Oftalmol*. 2007;70:905–970.
39. Lesnoni G, Billi B, Rossi T, et al. The use of panoramic viewing system in relaxing retinotomy and retinectomy. *Retina*. 1997;17:186–190.
40. Han DP, Mieler WF, Abrams GW, et al. Management of traumatic retinal incarceration with vitrectomy. *Arch Ophthalmol*. 1988;106:640–645.

41. Machemer R, Aaberg TM, Freeman HM, et al. An updated classification of retinal detachment with proliferative vitreoretinopathy. *Am J Ophthalmol*. 1991;112:159–165.
42. Charles S. *Vitreous microsurgery*. Williams & Wilkins: Baltimore, MD; 1981:124.
43. Lewis H, Aaberg TM. Anterior proliferative vitreoretinopathy. *Am J Ophthalmol*. 1988;105:277–284.
44. Zivojnovic R. *Silicone oil in vitreoretinal surgery*. Martinus Nijhoff/Dr W Junk: Dordrecht; 1987:64.
45. Ferrone PJ, Trese MT, Lewis H. Vitreoretinal surgery for complications of congenital retinoschisis. *Am J Ophthalmol*. 1997;123:742–747.
46. Garcia-Arumi J, Corcostegui IA, Navarro R, et al. Vitreoretinal surgery without schisis cavity excision for the management of juvenile X-linked retinoschisis. *Br J Ophthalmol*. 2008;92:1558–1560.
47. Zivojnovic R. *Silicone oil in vitreoretinal surgery*. Martinus Nijhoff/Dr W Junk: Dordrecht; 1987:98.
48. Blumenkranz MS, Aaberg TM, Azen SP, et al. Relaxing retinotomy with silicone oil or long-acting gas in eyes with severe proliferative vitreoretinopathy: Silicone Study report 5. *Am J Ophthalmol*. 1993;116:557–564.
49. Bovey EH, De Ancos E, Gonvers M. Retinotomies of 180 degrees or more. *Retina*. 1995;15:394–398.
50. Eckardt C, Behrendt S, Zwick A. Results of silicone oil removal from eyes treated with retinectomies. *Ger J Ophthalmol*. 1992;1:2–6.
51. Tseng JJ, Barile GR, Schiff WM, et al. Influence of relaxing retinotomy on surgical outcomes in proliferative vitreoretinopathy. *Am J Ophthalmol*. 2005;140:628–636.
52. Quiram PA, Gonzales CR, Hu W, et al. Outcomes of vitrectomy with inferior retinectomy in patients with recurrent rhegmatogenous retinal detachments and proliferative vitreoretinopathy. *Ophthalmology*. 2006;113:2041–2047.
53. Grigoropoulos VG, Benson S, Bunce C, et al. Functional outcome and prognostic factors in 304 eyes managed by retinectomy. *Graefes Arch Clin Exp Ophthalmol*. 2007;245:641–

649.
54. de Silva DJ, Kwan A, Bunce C, et al. Predicting visual outcome following retinectomy for retinal detachment. *Br J Ophthalmol*. 2008;92:954–992.
55. Tan HS, Mura M, Oberstein SY, et al. Primary retinectomy in proliferative vitreoretinopathy. *Am J Ophthalmol*. 2010;149:447–452.
56. Faude F, Lambert A, Wiedemann P. 360 degree retinectomy in severe anterior PVR and PDR. *Int Ophthalmol*. 1998-1999;22:119–123.
57. Zhang MN, Jiang CH. 360-degree retinectomy for severe ocular rupture. *Chin J Traumatol*. 2005;8:323–327.
58. Kolomeyer AM, Grigorian RA, Mostafavi D, et al. 360° retinectomy for the treatment of complex retinal detachment. *Retina*. 2011;31:266–274.
59. Garnier S, Rahmi A, Grasswil C, et al. Three hundred and sixty degree retinotomy for retinal detachments with severe proliferative vitreoretinopathy. *Graefes Arch Clin Exp Ophthalmol*. 2013;251:2081–2085.
60. Williamson TH, Gupta B. Planned delayed relaxing retinotomy for proliferative vitreoretinopathy. *Ophthalmic Surg Lasers Imaging*. 2010;41:31–34.
61. Stopa M, Kociecki J, Rakowicz P, et al. Comparison of anatomic and functional results after retinotomy for retinal detachment in pediatric and adult patients. *Eur J Ophthalmol*. 2013;23:410–416.
62. McCuen BW II, Hickingbotham D. A fiberoptic diathermy tissue manipulator for use in vitreous surgery. *Am J Ophthalmol*. 1984;98:803–804.
63. Bourke RD, Cooling RJ. Vascular consequences of retinectomy. *Arch Ophthalmol*. 1996;2:155–160.
64. Morse LS, McCuen BW II, Machemer R. Relaxing retinotomies: analysis of anatomic and visual results. *Ophthalmology*. 1990;97:642–648.
65. Bopp S, Laqua H, Lucke K. Fluoreszenzangiographische befunde nach retinotomien und retinektomien. *Klin Monatsbl Augenheilkd*. 1991;199:170–176.
66. Williams GA, Lambrou FH, Jaffe GA, et al. Treatment of

postvitrectomy fibrin formation with intraocular tissue plasminogen activator. *Arch Ophthalmol*. 1988;106:1055–1058.
67. Stopa M, Kociecki J. Anatomy and function of the macula in patients after retinectomy for retinal detachment complicated by proliferative vitreoretinopathy. *Eur J Ophthalmol*. 2011;21:468–472.
68. Odrobina D, Bednarski M, Cisiecki S, et al. Internal limiting membrane peeling as prophylaxis of macular pucker formation in eyes undergoing retinectomy for severe proliferative vitreoretinopathy. *Retina*. 2012;32:226–231.

113

Giant Retinal Tear

Lingam Gopal, Tarun Sharma, Pramod S. Bhende, Muna Bhende

Introduction

Giant retinal tear by definition is a retinal tear of more than 90° circumferential extent.[1] Since the posterior vitreous is detached, the vitreous gel is adherent to the anterior flap. Hence the posterior flap has a tendency to fold over. In contrast, in a giant retinal dialysis the retina is either torn at the ora serrata or there is a break in ciliary epithelium, with the vitreous being adherent to the posterior

retina.[2] Thus the posterior flap does not have the tendency to fold over, since it is supported by the vitreous gel.

The management of fresh giant retinal tear is an emergency. The delay in surgical intervention could lead to significant proliferative vitreoretinopathy (PVR) changes jeopardizing reattachment of the retina and eventual visual gain. Before the introduction of perfluorocarbon liquids by Stanley Chang,[3] the management of giant retinal tear was challenging and resulted in limited success. The present day management of giant retinal tear is reasonably straightforward with predictably good success rate.[4]

Etiology

Most giant retinal tears are idiopathic in origin with males being at higher risk. Traumatic giant retinal tears are commonly located in the upper nasal and lower temporal quadrants and are again commoner in males. In a population-based study in the United Kingdom, Ang et al. have reported an annual incidence of 0.091 patients per 100,000 population.[5] Most of the cases were idiopathic (54.8%) and males predominated (71.7%).[5]

The association with high myopia is well established.[6] Of all retinal detachments in Marfan syndrome, 11.3% have been reportedly caused by giant retinal tears.[7] Retinal detachment, especially due to giant retinal tear, has been identified as an important complication of Stickler syndrome.[8,9] Other diseases associated with occurrence of giant retinal tear include the Ehler–Danlos syndrome,[10] lens coloboma,[11] and aniridia.[12] Giant retinal tears can also occur following acute retinal necrosis[13]

Iatrogenic Giant Retinal Tear

Special mention should be made of the occurrence of giant retinal tear during/after intraocular surgery.

1. During a cataract surgery misadventure.[14] If attempts are made to fish around for the dislocated nucleus, giant retinal tear can easily occur due to the uncontrolled vitreous traction.

2. During vitreoretinal surgery.[15,16] Circumstances that predispose to such an occurrence are:

a) Inadvertently large leaky sclerotomies with prolapsing vitreous gel.

b) During extraction of a foreign body, especially a large one with irregular surface that can engage the gel vitreous in the vitreous base area.

c) Too frequent exchange of instruments prior to good vitrectomy.

Use of minimally invasive vitrectomy and wide-angle visualization have definitely reduced the incidence of the iatrogenic giant retinal tears.

1. Giant retinal tear has also been reported after pneumatic retinopexy and has been attributed to partly detached vitreous that exerted traction following the expansion of the bubble of expansile gas.[17,18]

2. Shinoda et al. have reported the occurrence of giant retinal tear due to jamming of the 25G instruments in the cannula, while operating on eyes with vitreous hemorrhage.[19]

3. Giant retinal tear has also been described after refractive surgery in the form of LASIK[20] and phakic IOLs,[21] although the cause and effect relationship remains debatable.

4. Barrage laser for subclinical retinal detachments in rare instances may lead to giant retinal tear along the line of treatment.[22] The occurrence of giant retinal tear has been attributed to a combination of thin retina due to high myopia and heavy treatment.

5. During surgery for retinal detachment with PVR, giant retinal tear may be the result of a deliberate relaxing retinotomy.

Pathogenesis

Schepens first described the important role played by the vitreous in giant retinal tear. Central vitreous liquefaction is associated with condensation in the peripheral vitreous base that leads to traction on the peripheral retina.[1] As traction progresses, it is evident clinically as spreading white without pressure. Later, transvitreal contraction of the cortical gel occurs, tearing the retina along the vitreous base in a zipper fashion. Sometimes, multiple horseshoe-shaped tears may form along the posterior vitreous base and coalesce to form a giant retinal tear. Radial extensions (horns) can occur at the two ends of the giant retinal tear. Eyes with radial extension invariably have some amount of vitreous hemorrhage since the tears cut across larger blood vessels posteriorly.

A giant retinal tear nearing 180° in circumferential extent has a tendency to fold over. The size of the giant retinal tear also has an effect on the amount of retinal pigment epithelium (RPE) that gains access to the vitreous cavity, thus increasing the risk of PVR. Giant retinal tear occurring after penetrating injuries has high risk of PVR while giant dialysis tends to progress very slowly.

History of Management of Giant Retinal Tear

The management of giant retinal tear can be divided conveniently into pre- and post- perfluorocarbon liquids (PFCL) eras. Most techniques used in the pre-PFCL era are of historic importance. However, a brief mention of these techniques is relevant in the overall understanding of the management of giant retinal tear. The primary problem faced by the surgeon was the gravity-driven tendency of the flap of the retinal tear to fold and fall back. Scleral buckles have been done for tears of smaller extent (around 90°). A relatively shallow but broad buckle was aimed at so that the tendency for the flap to slip back is reduced and the inevitable central sagging of the flap is accommodated on the broad buckle.[23] Attempts were also made to rotate the patient and reposition the retinal flap with the help of an air bubble.[24] Vitreoretinal surgery

helped mobilize the inverted flaps of large giant retinal tears, but the surgeon still faced difficulty in unrolling the same and fixing it in position. One strategy was to divide the giant retinal tear into smaller segments by pinning the edge of the tear down to the RPE/choroid complex using retinal tacks[25,26] or sutures.[27] This enabled routine fluid–air exchange to fix the retina without slippage of the retinal flap. Another technique involved fluid–air exchange in prone position. After a vitrectomy (and sometimes placement of buckle), the sclerotomies were closed and the patient was turned prone. Without contaminating the operative field, fluid–air exchange was then performed, with the air injection being done in front of the optic disc and fluid being evacuated from the anterior chamber.[28] The air progressively attached the retina posteroanteriorly. The patient was repositioned in the supine position, and internal tamponading agent was injected – gas or silicone oil as the case may be. Among all these techniques, perhaps the best attachment of the retina with no folds or slippage was seen with prone fluid–air exchange following vitrectomy.

However, with the use of PFCLs the surgery has become much simpler.

Preoperative Evaluation and Planning

A thorough evaluation of both the anterior and posterior segments is important to plan the surgery properly. Corneal and lens status must be noted. Perforating injury-related retinal detachments with vitreous incarceration and giant retinal tear can have associated corneal problems such as generalized haze due to edema, opacity, Descemet membrane folds, etc. The lens could be subluxated due to the blunt trauma and could be also cataractous.

Pseudophakic eyes can also have specific problems. The IOL could be tilted or subluxated (especially in eyes that had capsular dehiscence and vitreous disturbance during cataract surgery). Deposits on the IOL and posterior capsule opacification can interfere with surgery. A decision as to the need to remove the IOL should be taken based on this evaluation. There is, however, no justification to remove a well-placed IOL.

The intraocular pressure (IOP) could be low, normal, or high. A

low to very low IOP is seen in relatively recent giant retinal tears and often associated with choroidal detachment. One may chose to treat such cases with a course of systemic steroids for a few (3–5) days before performing the surgery. High intraocular pressure is rare at the time of presentation with acute giant retinal tear even in eyes with preexisting glaucoma. However, eyes with traumatic dialysis can have persistent high pressures despite presence of retinal detachment. Following reattachment of the retina, one should anticipate an acute rise in intraocular pressure. Hence arrangements for frequent IOP monitoring must be in place. It is only rarely that a glaucoma surgery needs to be combined with the retinal reattachment surgery.

The posterior vitreous will be found to be detached in cases of giant retinal tear, unlike in dialysis. In eyes that had blunt injury, the vitreous base can be avulsed and is seen as a rope-like structure near the pars plana. In eyes with perforating injury or following cataract surgery misadventure, the vitreous could be incarcerated in the wound and is seen as a transvitreal membrane. The giant tear or dialysis is seen usually in the opposite quadrant.[14]

The extent of retinal detachment can vary. A dialysis can be associated with chronic partial detachments of the retina with high-water marks, while giant retinal tear is usually associated with a more rapidly spreading retinal detachment. Eyes with around 90° tears are characterized by sagging of the center of the tear posteriorly but do not show inversion of flap. However, if the two ends of the giant retinal tear trail significantly posteriorly (horns), the retinal flap that is enclosed in between can fold back. Retinal tears that are nearing 180° circumferentially will show a tendency to fold back. The inverted flap can sometimes obscure the disc (Fig. 113.1). The edge of the tear usually is scrolled inwards despite lack of obvious PVR elsewhere. The pars plana epithelium can be detached in the area of tear and sometimes beyond, due to the vitreous base traction. The anterior flap of the retina can harbor lattice degeneration. Additional horseshoe tears can be seen in other quadrants near the posterior vitreous base. A macular hole can coexist – especially in eyes that are highly myopic or where the giant retinal tear is a result of blunt injury. Significant pigment dispersal is seen in the vitreous cavity, and pigment is often seen

adherent to the surface of the retina. A traumatic dialysis is often associated with evidence of damage to the RPE and choroid at the site of the ora serrata.

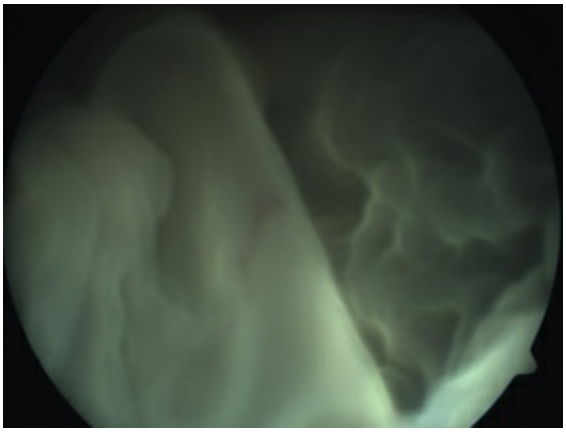

FIG. 113.1 Fundus photograph showing giant retinal tear with inverted flap that is obscuring the optic disc. Note the retinal blood vessels seen through the thickness of the edematous inverted retina.

Ultrasonographic Diagnosis of Giant Retinal Tear[29]

In eyes with opaque media, giant retinal tear can be suspected on ultrasonography. A suggestive feature is a discontinuity in the retinal echo anteriorly and extending more than one quadrant. Double linear echo would be seen near the disc due to the close proximity of the two layers of the retina – one representing the flap of the giant retinal tear and hence discontinuous with the globe contour and the other representing the detached retina and hence continuous with the globe contour (Fig. 113.2).

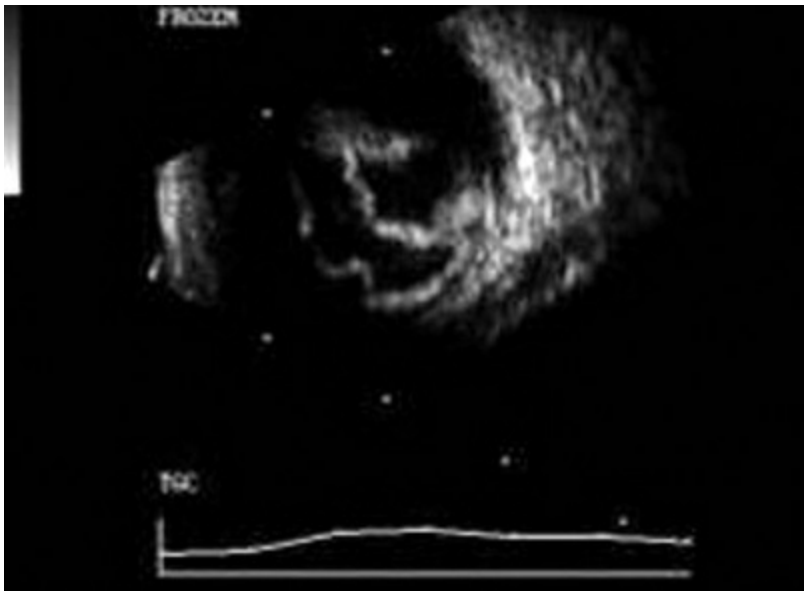

FIG. 113.2 Ultrasonography in an eye with giant retinal tear. Note double linear echo close to the optic disc: the inner layer is discontinuous while the outer layer is continuous with the globe contour.

Proliferative Vitreoretinopathy (PVR)

The vitreous base can contract circumferentially and anteroposteriorly causing a significant anterior loop, evident in the peripheral retina that is not involved in the giant retinal tear. The inverted flap of the retina can get adherent to the opposite detached retina, especially when vitreous is incarcerated in a wound. Extensive membranes can form on both sides of the retina – both focally and diffusely. In badly traumatized eyes, the anatomy can be fairly distorted and the true nature of the detachment and the presence of giant retinal tear will be evident more during the surgery than preoperatively. A 360° retinal tear with PVR has the worst-looking configuration. The entire retina can be seen to be lying posteriorly, crumpled around the disc, and wrapped around by fibrotic tissue. It is not possible in all such cases to assess the operability or otherwise of the retina preoperatively.

Eyes with acute retinal necrosis can develop giant retinal tear at the posterior edge of the retinitis patch. There will be tell-tale signs of the previous retinitis anteriorly, characterized by very thin, atrophic, parchment-like retina in the involved area.

Role of Nonsurgical Treatment

Laser Barrage Photocoagulation

Very occasionally one may get an opportunity to barrage the dialysis/tear with laser photocoagulation if the lesion is detected before it has resulted in clinical retinal detachment. Such an event is more likely with a dialysis where clinical retinal detachment takes some time to develop. Laser treatment would involve production of 2–3 rows of retinal burns along the posterior limit of the dialysis/tear and continuing the treatment anteriorly to meet the ora on the either side. Indirect delivery of laser assisted by scleral indentation would be needed to complete the treatment satisfactorily. Cryopexy is also an option but is best avoided in view of increased risk of PVR.

Outpatient Fluid–Gas Exchange Followed by Cryopexy or Laser Photocoagulation

Fresh giant retinal tears noted following a vitreoretinal surgery can sometimes be managed by outpatient fluid–air exchange followed by retinopexy with laser or cryo, thus avoiding a major resurgery. A push–pull technique or a two-needle technique can be used to inject 12–14% C_3F_8 gas while removing the vitreous fluid. A two-needle technique has the advantage of not permitting gross fluctuations in the intraocular pressure and has less risk of the uncut vitreous gel or the giant retinal tear flap getting caught in the needle. Following the fluid–gas exchange, laser would be possible by the next day, by which time the retina is well attached and the gas has formed a single bubble (without frog eggs).

Role of Simple Scleral Buckling

In the present era, where vitreous surgery has become the desired approach to fix even simple retinal detachments with horseshoe tears, most surgeons would not perform simple scleral buckling for giant retinal tear of any degree. The role of scleral buckling is perhaps restricted to cases of giant retinal dialysis. In the absence of

a vitreous detachment and in these usually younger patients, a vitrectomy approach may not be ideal in cases with dialysis. Scleral buckling would suffice in most such cases.

Technique of Simple Scleral Buckling

After the recti muscles are tagged, the two ends of the dialysis are localized. It is expected that the center of the dialysis will sag to some extent, hence a broader than anticipated tire is used to accommodate the expected sag in the center. The surgeon should aim for a shallow buckle. Cryo is done to the posterior edge of the dialysis and is connected to the ora serrata at both ends. Most dialysis-related retinal detachments tend to be chronic in nature and are best drained. The drainage is done as posteriorly as possible to avoid the vitreous tracking into the perforation site through the open dialysis. It is also useful to indent anteriorly with a cotton-tipped applicator, so as to effectively approximate the dialysis edge to the underlying RPE while permitting the posteriorly trapped SRF to exit without danger of vitreous finding its way to the perforation site.

A similar technique can be potentially adopted with a giant retinal tear of about 90°. The risk of central sag of the retina is even more than with the dialysis. Gas injection would help smooth the folds on the buckle. Cryopexy of the edge of the giant retinal tear could also pose a problem if it is lifted significantly away from the RPE. The risk of excessive treatment of the bare RPE/choroid exists.

Vitreous Surgery

In the current scenario, most cases of giant retinal tear would be managed by a vitreoretinal approach.

Role of Encircling Band With Vitreoretinal Surgery

Many surgeons feel comfortable placing an encircling band even in eyes undergoing vitreoretinal surgery.[30] An encircling band is expected to support the vitreous base and reduce the risk of

recurrent detachment taking place from the quadrants where there is no retinal tear. However, there are reports that the success rate of surgery for fresh giant retinal tear is not reduced by not placing the buckle.[31] In addition, minimally invasive sutureless vitreous surgery is possible if one is not placing the buckle.[32] The trick is in the use of a wide-angle system of visualization and radical vitreous base removal.[33] In the presence of some degree of PVR, placement of an encircling band is desirable.

Lens Management

The options for lens management are (1) leave it untouched; (2) lensectomy and leaving the eye aphakic; (3) lens removal and keeping the posterior capsule intact for future IOL placement; and (4) lens removal and IOL placement same time. The exact approach would depend on the individual case, the surgeon's choice, and the ability to be reasonably certain of the power of the IOL to be implanted. In general, IOL placement would be avoided in eyes with severe PVR. In fresh giant retinal tears, IOL placement is possible, especially if a buckle is not being placed. Guidance from previous refractive status and fellow eye measurements would be needed to calculate the IOL power. In eyes with gross subluxation of the lens, scleral fixation of IOL is an option, but is best deferred to a later date. In eyes where silicone oil is being used as a tamponading agent, one can leave the eye aphakic at the first sitting and implant the IOL at time of silicone oil removal.

Management of Intraocular Lens

A well-positioned IOL is not an issue in the management of giant retinal tear. However, IOL can be associated with problems such as deposits of pigment and inflammatory precipitates on the IOL surface, posterior capsule opacification, tilt, and displacement of IOL (especially if the cataract surgery had been eventful). As long as the visualization is not hampered, the IOL need not be disturbed. Simple maneuvers, such as creating an opening in the posterior capsule or gently scraping the precipitates on the IOL surface under viscoelastic fill of the anterior chamber, can greatly improve the visualization. Silicone IOLs can be associated with problems when

silicone oil is injected, especially if there is posterior capsule opening. The oil tends to stick to the posterior exposed surface of the IOL, and at the time of silicone oil removal, a film of oil remains permanently adherent to the IOL surface. This, however, is not an absolute indication to remove the IOL.

Explanting the IOL is best done through a scleral tunnel rather than a clear corneal wound. With scleral entry, there is much better maintenance of corneal clarity during the subsequent vitreoretinal surgery. A scleral wound is also less prone to leak even when the eye is distorted, e.g., during scleral indentation.

Visualization

With the advent of wide-angle viewing systems, the management of giant retinal tear has considerably improved. It is a tremendous advantage to be able to visualize the periphery without losing view of the posterior pole, especially while exchanging the PFCL with gas or silicone oil. Landers lens system even with prism lenses would be a poor substitute. However, a Landers lens or similar contact lens would be useful for internal limiting membrane (ILM) peeling, if there is associated macular hole.

Handheld illumination and three-port vitrectomy will suffice in cases of fresh giant retinal tear. In badly traumatized eyes with giant retinal tear (especially when the tear is 360°), and in eyes with severe PVR, bimanual surgery would be required. The choice is between using a combined instrument such as an illuminated pic or making a fourth sclerotomy and placing a chandelier light pipe.

Vitrectomy

Vitreous removal is perhaps the easiest of the steps in giant retinal tear surgery. With a total PVD that is most often associated with a giant retinal tear, all the vitreous lies anteriorly and can be easily removed. In fresh giant retinal tear, the flap tends to be mobile and care should be exercised to prevent accidental unnecessary nibbling of the flap. While placing the infusion cannula one should be aware that some eyes with profuse hypotony can have significant ciliochoroidal edema/detachment. Placement of a 6-mm infusion cannula can reduce the risk of suprachoroidal infusion, but the

surgeon must ensure that the tip is seen inside the vitreous cavity before switching on the infusion. If the cannula tip is not seen, a MVR blade introduced through one of the upper sclerotomies can be used to cut the tissue overlying the tip of the infusion cannula. A loose pars plana epithelium can also drape round the infusion cannula but can be easily removed with the cutter.

In eyes with vitreous in the anterior segment wound and a giant retinal tear, the first step would be to excise the incarcerated vitreous and allow the retina to fall back before performing the rest of the vitrectomy.

Radical Excision of the Vitreous Base

The vitreous base is debulked to the maximum extent possible. However, to be able to perform this step adequately, the posterior pole and the retinal flap should be kept down with a bubble of PFCL. Otherwise the retinal flap will keep getting sucked into the port even while working in the opposite quadrant. Even in phakic eyes, a good amount of debulking is possible without lens sacrifice by having the assistant indent the sclera.

Mobilizing the Retina and Management of Anterior Retinal Flap

The anterior retinal flap to which the vitreous is adherent should be excised as much as possible. If the same is left behind, it can get fibrosed and also exert traction on the ciliary body. As mentioned, the edge of the giant retinal tear tends to scroll in, and this does not necessarily indicate fibrosis along the edge. However, if the edge is stiff, it can be excised. Inspection of the retina should include the assessment of PVR and the location of the fibrosis – pre- and subretinal. In cases of fresh giant retinal tear, the retina will be freely mobile and the inverted flap can be lifted up with the intraocular instruments. Despite absence of frank PVR, one very often sees pigment deposition on the surface of the retina, especially inferiorly. The pigment clumps can be relatively adherent to the surface of the retina and could indicate early attempts at proliferation. One may have to use fine instruments such as a

membrane scratcher (rake) to remove these immature membranes. Loose pigment can be removed with a brush needle. Meticulous removal of such immature membranes can reduce the risk of recurrent retinal detachment.

Eyes With PVR

In eyes with PVR, the anatomy could be varied depending on the severity. Some description on the pathoanatomy has been given in the section on preoperative evaluation. In general, the posterior pole is cleared first, a bubble of PFCL is placed to stabilize the posterior pole, and then the rest of the dissection is carried out. A combination of spatula, scratcher, and forceps would be needed. As one proceeds with the dissection, more membranes become evident, especially by placing the retina on stretch with additional PFCL. Injecting too much PFCL in the initial stages without adequate relief of posterior traction will result in the bubble finding its way into the subretinal space. The subretinal PFCL may need to be removed before further dissection. Subretinal fibrosis is identifiable once most of the preretinal traction is relieved. In the presence of giant retinal tear, removal of the subretinal membranes should not be difficult. The ease of attaining complete relief of traction would depend on the severity of the PVR. Anterior circumferential traction would usually need bimanual dissection while keeping the posterior pole down with PFCL.

In eyes presenting with 360° giant retinal tear and PVR, picking up the membranes with forceps could become difficult, since the retina does not offer any resistance and moves with the forceps. With bimanual surgery, the dissection can be done comfortably. Appearances can be deceptive and what looks like an apparently inoperable bunched up retina lying in the posterior pole can open up to reveal a relatively healthy posterior retina. Delay in performing surgery after penetrating injury greatly increases the risk of the retina becoming contracted and inoperable.

Conversion to 360-Degree Tear

If peripheral traction relief is not adequate, it is best to excise the peripheral retina along with the fibrosis, rather than trying to

compromise, by placing a buckle underneath an area of unrelieved peripheral traction. Converting a giant tear to a 360° tear does not worsen the prognosis.

While excising the peripheral retina, it may be worthwhile to leave behind tags of attachment to the ora, till PFCL is placed up to the arcade. Then the residual tags can be cut to convert it into a 360° tear. This may sometimes permit proper orientation of the macula. In view of the extreme distortion of the retina due to the PVR, there can be tendency for the macula to be shifted to abnormal locations, necessitating manipulation of the retina under the PFCL. On occasions, areas of residual traction are identified after reattaching the retina with PFCL. Some of these membranes can be removed under PFCL. If not, one should not hesitate to remove the PFCL to facilitate removal of the newly identified membranes and then reinject the PFCL. The edge of the giant retinal tear can be folded under the PFCL. As long as there is no fibrosis, these edges are easily smoothed with the help of a spatula. A silicone brush can also be used to stroke the edge into position. Fibrosed edges must be excised.

Perfluorocarbon Liquids

Several properties make these liquids well suited for vitreoretinal surgery, namely the specific gravity (greater than water), transparency (can see and treat the retina underneath), low viscosity (easy to inject and easy to remove), excellent tamponading effect (good retinal flattening), and a refractive index that is different from the infusion fluid (visible interface). PFCLs are useful at several stages of the surgery: (1) during membrane dissection to stabilize the posterior pole; (2) for facilitating internal limiting membrane removal around macular hole in detached retina; (3) for reattachment of the mobilized retina without fear of posterior slippage; (4) for medium-term tamponade.

Injection of PFCL

Wide-field visualization is very useful in this step. The initial bubble of PFCL is injected over the optic disc to unfurl the folded retina. Further injection is done into the main bubble to prevent

formation of multiple bubbles. Forceful injection should be avoided since the jet of the liquid can tear through retina and can even cause choroidal bleed. The PFCL bubble is injected till it flattens the edge of the giant retinal tear. One should be cognizant of the fact that there is subretinal fluid anterior to the bubble in the areas where the retina is not torn from the ora serrata.

In eyes with 360° retinal tear and some intrinsic contracture of the retina, injection of the PFCL may not result immediately in a smoothly attached retina. There will be tendency for the retina to form circumferentially oriented folds around the disc. If the contracture is not severe, the folds can be smoothed with help of a blunt instrument – used to massage the retina gently. A flat retinal spatula, a knob spatula, or even the tip of the vitreous cutter can be used for this purpose. In eyes with severe retinal contracture, there will be a tendency for the PFCL bubble to roll off the retina, leaving it bunched up around the disc. At this stage one may have to accept the inability to reattach the retina.

Retinopexy

Endolaser is the preferred modality of retinopexy. By tilting the eye to the same side, the edge of the giant retinal tear can be kept entirely under PFCL, thus facilitating the application of the laser along its edge. In general, about 3–4 rows of burns are applied along the margin. It is best to treat 360° including the peripheral retina, beyond the area of the giant retinal tear.[34]

The peripheral retina beyond the giant tear will still have subretinal fluid anterior to the PFCL bubble, and this would make it difficult at this stage of surgery to produce burns till the ora serrata in this area. Treatment of this anterior retina is easier done once the PFCL is exchanged with silicone oil or gas and the residual anterior subretinal fluid is removed. In phakic eyes, anterior treatment is done with laser delivery by indirect ophthalmoscope (LIO). Only very rarely is cryo resorted to.

Internal Tamponade

The choice of internal tamponade is between long-acting gases such as 12–14% C_3F_8 or silicone oil. SF_6 and air are not suited, in view of

the large extent of the tear and the need for extended period of support.

PFCL–Air Exchange

This is the step when slippage of the retinal flap can potentially occur. The edge of the tear should be dried frequently before removing the main PFCL bubble. In view of the relatively rapid sequence of events (unlike with silicone oil), there is a tendency for fluid pockets to be trapped anteriorly and then getting pushed under the retina as the PFCL is removed – leading to retinal slippage characterized by circumferentially oriented folds in the quadrant of the tear. Depending on the extent of the tear and the amount of residual subretinal fluid, the extent of slippage varies. The macula can be involved in these folds in cases of temporal tears. Attempts at drying the edge of the tear at this stage does not usually succeed since the air keeps the fluid trapped posteriorly. Some surgeons suggest leaving behind some vitreous fluid and then positioning the patient prone to permit postoperative smoothing of the folds. Posterior retinotomy is not recommended. It is perhaps best to reinject the PFCL and perform the exchange with gas more carefully or opt for silicone oil–PFCL exchange.

PFCL–Silicone Oil Exchange

Directly exchanging PFCL with silicone oil has the least chance of retinal slippage. One should understand the fluid dynamics during this process to obtain best results with least complications.

1. As the silicone oil is being injected it forms initially a circular bubble. Once it comes in contact with the central part of the upper meniscus of the PFCL, further injection flattens the anterior surface of the PFCL bubble, thus spreading it over a larger surface of the retina.

2. The balanced salt solution (BSS) will slowly be pushed into a circumferential ring all round, sandwiched between the oil and PFCL. One should not forget the rim of subretinal fluid that is trapped anterior to the PFCL in the area outside the giant retinal tear (Fig. 113.3).

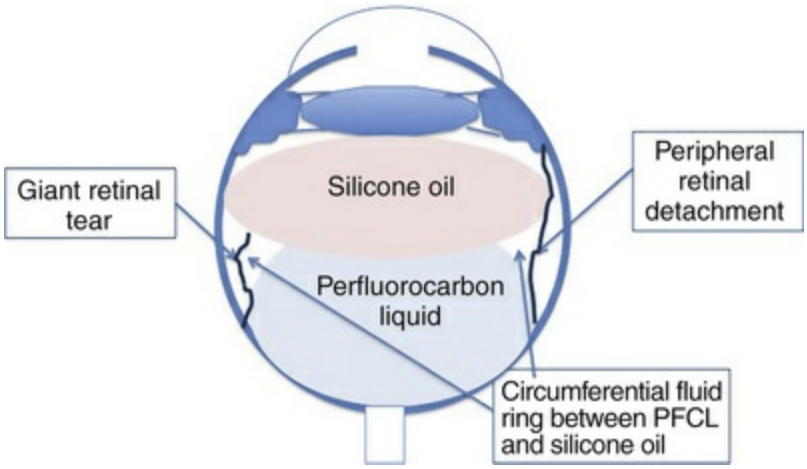

FIG. 113.3 Drawing demonstrating the concept of circumferential ring of fluid trapped between silicone oil and perfluorocarbon liquids (PFCL). Unless this fluid is completely removed before removing the PFCL, slippage of the giant retinal tear flap can occur.

3. BSS, subretinal fluid, as well as PFCL can be easily sucked with both active and passive suction devices. Silicone oil will tend to block the suction device. Hence while injecting silicone oil, sudden rise in IOP can occur if suction port is located within the silicone oil bubble. Failure to notice the raising IOP can result in some unpleasant consequences such as (1) the edge of retinal flap getting sucked into the port of the suction device, (2) snapping of corneal sutures in eyes with recently repaired corneal wounds, or (3) iris prolapse through a gaping scleral or corneal wound that has been made for IOL explantation.

4. Intermittent injection of silicone oil coupled with careful positioning of the suction tip at the edge of the giant retinal tear and just beyond the PFCL bubble margin will result in slow evacuation of the circumferential ring of BSS. Even the fluid located in the opposite quadrant will find its way to the site of suction and the subretinal space becomes totally dry. It is easy to distinguish between the residual fluid and silicone oil by the ease with which it finds its way into the suction port. Once all the fluid is removed, the PFCL bubble can be removed. Intermittently one can go back to the edge of the giant retinal tear to make sure that it is dry. Slow injection of the silicone oil will permit controlled removal of the

PFCL, and the endpoint is clearly visualized.

5. If the suction port is blocked with silicone oil, the IOP will rapidly rise as evidenced by appearance of central retinal artery pulsations and rapidly developing corneal edema. If the suction port is now shifted to the PFCL bubble, the block reopens as the PFCL washes the silicone oil out and one can clearly see the perfusion returning.

Figs. 113.4 and 113.5 show pre- and postoperative photographs of a case of giant retinal tear. Note the postoperative photograph shows early PVR inferiorly.

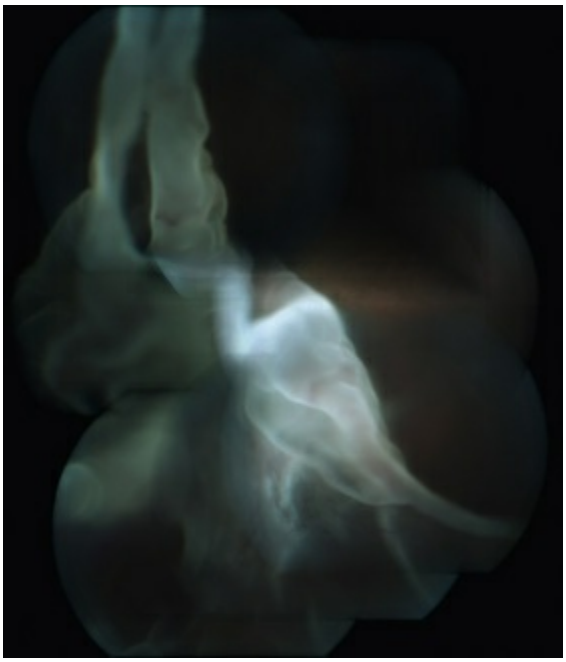

FIG. 113.4 Preoperative photograph of an eye with 180° giant tear and folded flap.

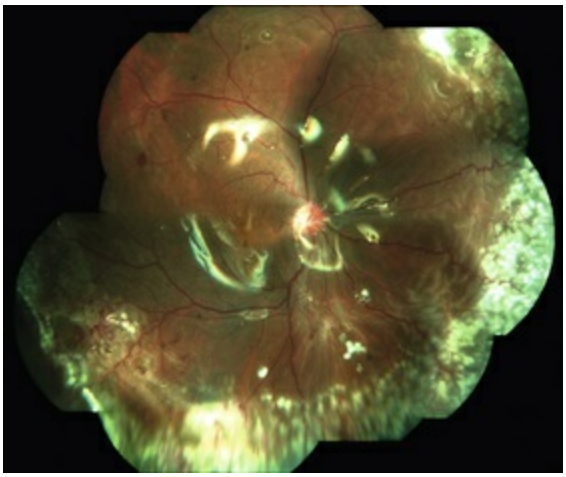

FIG. 113.5 Postoperative photograph of the eye in Fig. 113.4 showing attached retina and early proliferative vitreoretinopathy (PVR) inferiorly. Note the reflexes due to silicone oil.

Alternative Techniques

1. *PFCL as medium-term tamponade:* In this technique, PFCL are injected during the first stage and retained for 5–10 days, during which period the patient is encouraged to lie supine. A second procedure is then performed to exchange the PFCL with gas or silicone oil.[35,36]

2. *Air–PFCL exchange followed by air–silicone oil exchange*: Some surgeons are not comfortable with direct silicone oil–PFCL exchange and perform first air–PFCL exchange followed by silicone oil–air exchange. This, however, retains the risk of retinal slippage during the first step of the procedure.

3. *Use of heavy silicone oil:* Densiron is heavier than water and is made up of perfluorohexyl octane (F_6H_6) and conventional silicone oil. This mixture has a specific gravity of 1.06 and a viscosity of 1480 mPas. It can be used both to settle the retina (since it is heavier than water) and can serve as internal tamponade. Unlike silicone oil, the inferior retina is better supported. There have been conflicting reports of its utility. The major concern appears to be that of significant emulsification that has been reported with Densiron even within 12 weeks of injection, leading potentially to

inflammation and membrane formation.[37,38]

Additional Steps

1. Once the whole retina is reattached following PFCL–air or silicone oil exchange, the untreated anterior retina can be treated comfortably.

2. In aphakic eyes, a peripheral iridectomy is done inferiorly to reduce the risk of pupillary block. This step is best done before exchanging the PFCL with silicone oil. In oil-filled aphakic eyes, iridectomy can still be done by filling the anterior chamber first with BSS and then nibbling away the iris at 6 o'clock by placing the cutter behind the iris.

3. Where phacoemulsification has been done at the beginning of the surgery and IOL implantation is planned, this step is best done just before PFCL–air or silicone oil exchange. Alternatively, one can implant the IOL as the first step of the surgery along with the phacoemulsification and then proceed with the vitreoretinal surgery. However, the additional optical interfaces are avoided if the IOL is placed subsequent to reattachment of the retina.

4. *Management of associated macular hole:* Macular hole not uncommonly coexists with giant retinal tear, especially in traumatized eyes and highly myopic eyes. Once the retina is mobilized, internal limiting membrane can be peeled around the macular hole. A small bubble of PFCL placed on the macular area helps achieve this goal. Staining of the ILM can be done with brilliant blue under the PFCL bubble. By injecting small quantities of the dye with the PFCL bubble in place, one can avoid the migration of the dye into the subretinal space. Some eyes with high myopia and extensive chorioretinal atrophy in the macular area may develop large macular holes. In these eyes, the aim of treatment would be to seal the hole with laser since there are high chances of recurrence of retinal detachment.

Results

In the previtrectomy era, Schepens and Freeman could achieve successful reattachment in only 2 out of 14 eyes.[39] Machemer et al. have reported a final success rate of 43% following vitrectomy with prone fluid–gas exchange and use of SF_6 gas, although intraoperative success was achieved in 12 of the 14 cases.[40] Aylward et al. reported a success rate of 89% in traumatic giant retinal tears using vitrectomy and silicone oil tamponade.[41] Batman et al. have reported no difference in success rate between silicone oil and long-acting gas tamponade.[42]

The routine use of encirclage continues to be debated, with Goezinne et al. reporting higher failure rate in the absence of encirclage,[30] while Kreiger et al.[31] (11 eyes) and Hoffman[43] (6 eyes) have reported success without buckle. Loewenstein et al. compared perfluoro-perhydro-phenanthrene and perfluoro-octane and found no statistically significant difference between the two groups.[44] The overall success was 71.7% and 78.3% respectively in the two groups. But the authors found greater incidence of retained perfluorophenanthrene compared to perfluoro-octane. This was attributed to its (perflurophenanthrene) greater specific gravity, lesser vapor pressure, and less prominent interface with BSS. Al-Khairi et al. analyzed the prognostic factors associated with surgical results and identified phakic/clear lens at presentation, unfolded flap of the giant retinal tear, absence of postoperative cataract, and absence of postoperative PVR to be associated with better than 20/200 vision.[45] They also found that placement of encircling band and silicone oil tamponade were associated with higher anatomic reattachment with one procedure. In a series of 24 eyes with giant retinal tear greater than 180° Dabour used the technique of direct PFCL–silicone oil exchange in addition to encirclage. There was no incidence of slippage, and the final anatomic success was achieved in 83.3%.[46]

In unpublished data of management of 36 children (age group 4–16 years) with giant retinal tear, 41.7% were found to have severe PVR at presentation, suggesting a delay in diagnosis.[47] Nearly 50% of them had an abnormal fellow eye (phthisis in 16.8%, anophthalmic socket in 8.3%, history of repair of retinal detachment

in 19.4%, and history of giant retinal tear-related retinal detachment in 5.7%). Twenty-five percent needed more than one surgery to achieve anatomic success. The final rate of reattachment was 91.6%, but visual acuity of >20/200 was achieved in only 58.3% of the eyes.

Management of the Fellow Eye

In a study of the natural history of the fellow eyes, Freeman has reported a 14% incidence of giant retinal tear and 36% incidence of other retinal tears.[10,48] High-risk fellow eyes include high myopia, eyes with progressively increasing white without pressure areas with sharp posterior margin and increased vitreous condensation, and patients with Wagner–Stickler syndrome. In a series of 204 patients with Type 1 Stickler syndrome, Ang et al. reported a risk reduction from 73% to 6.5% by performing prophylactic 360° cryopexy posterior to the ora serrata. Posterior lesions were not treated in this study.[8] Wolfensberger et al. have reported a series of 48 eyes with giant retinal tear wherein the fellow eye was prophylactically treated with 360° crypexy.[49] They found an 8% (4 eyes) incidence of retinal breaks (3 with retinal detachment) over a 84-month follow-up period, of whom 1 patient had giant retinal tear posterior to the treated area. Based on their data, the authors believe that there is justification for prophylactic treatment.

While Freeman advocated prophylactic buckling along with cryopexy,[48] most surgeons have resorted to only cryopexy or laser photocoagulation without scleral buckling.[45,49,50] Laser has the advantage of being an outpatient procedure and can be spaced over two or more sittings in an attempt to reduce the inflammation caused by the treatment.

Despite these publications, one has to admit that there is still no consensus on (1) the need for prophylaxis; (2) modality of treatment (cryo or laser); (3) where to treat (ora or equator); and (4) what to treat (visible lattice degenerations/visible areas of white without pressure or just 360° treatment). In a review of literature on interventions for prevention of giant retinal tear in the fellow eye, Ang et al. did not find conclusive evidence to support or refute the value of prophylaxis.[51] In Stickler syndrome, however, the evidence is more strongly in favor of offering prophylaxis for the fellow eye.[8]

References

1. Freeman HM, Schepens CL, Couvillion GC. Current management of giant retinal breaks. II. *Trans Am Acad Ophthalmol Otolaryngol*. 1970;74:59–74.
2. Smiddy WE, Gree WR. Retinal dialysis: pathology and pathogenesis. *Retina*. 1982;2:94–116.
3. Chang S. Low viscosity liquid fluorochemicals in vitreous surgery. *Am J Ophthalmol*. 1987;103:38–43.
4. Shunmugam M, Ang GS, Lois N. Giant retinal tears. *Surv Ophthalmol*. 2014;59:192–216.
5. Ang GS, Townend J, Noemi L. Epidemiology of giant retinal tears in the United Kingdom: the British giant retinal tear epidemiology eye study (BGEES). *Inv Ophthalmol Vis Sci*. 2010;51:4781–4787.
6. Schepens CL, Dobble JG, McMeel JW. Retinal detachments with giant breaks: preliminary report. *Trans Am Acad Ophthalmol Otolaryngol*. 1962;66:471–479.
7. Sharma T, Gopal L, Shanmugam MP, et al. Retinal detachment in Marfan's syndrome: clinical characteristics and outcome. *Retina*. 2002;22:423–428.
8. Ang A, Poulson AV, Goodburn SF, et al. Retinal detachment and prophylaxis in Type 1 Stickler syndrome. *Ophthalmology*. 2008;115:164–168.
9. Yonekawa Y, Haddock LJ, Eliott D. A 360° giant retinal tear in Stickler syndrome. *JAMA Ophthalmol*. 2015;133:e141812.
10. Freeman HM. Fellow eyes of giant retinal breaks. *Trans Am Ophthalmol Soc*. 1978;76:343–382.
11. Hovland KR, Schepens CL, Freeman HM. Developmental giant retinal tears associated with lens coloboma. *Arch Ophthalmol*. 1968;80:325–331.
12. Dowler JG, Lyons CJ, Cooling RJ. Retinal detachment and giant retinal tears in aniridia. *Eye*. 1995;9:268–270.
13. Topilow HW, Nussbaum JJ, Freeman HM, et al. Bilateral acute retinal necrosis: clinical and ultrastructural study. *Arch Ophthalmol*. 1982;100:1901–1908.
14. Aaberg TM Jr, Rubsamen PE, Flynn HW Jr, et al. Giant retinal tear as a complication of attempted removal of

intravitreal lens fragments during cataract surgery. *Am J Ophthalmol*. 1997;124:222–226.
15. Abu el-Asrar AM. Giant retinal tears after pars plana vitrectomy. *Eye*. 1997;11:325–327.
16. Gonzalez MA, Flynn HW, Smiddy WE, et al. Giant retinal tears after prior pars plana vitrectomy: management strategies and outcomes. *Clin Ophthalmol*. 2013;7:1687–1691.
17. Yam JC, Liu DTL, Lee VYW, et al. Giant retinal tear after pneumatic retinopexy. *Acta Ophthalmol*. 2008;86:232–233.
18. Sinker SN, Simon SJ, Gilhotra JG. Giant retinal tear after pneumatic retinopexy. *Retinal Cases Brief Reports*. 2012;6:151–152.
19. Shinoda H, Nakajima T, Shinoda K, et al. Jamming of 25-gauge instruments in the cannula during vitrectomy for vitreous hemorrhage. *Acta Ophthalmol*. 2008;86:160–164.
20. Al Rashaed S, Abboud E, Al-Dhibi H. Bilateral retinal detachment after laser in situ keratomileusis. *Ophthalmic Surg Lasers Imaging*. 2009;40:180–184.
21. Georgalas I, Petrou P, Papaconstantinou D, et al. Bilateral giant tear – associated retinal detachment following Artisan phakic intraocular lens implantation for correction of moderate myopia. *Acta Ophthalmol*. 2010;88:43–44.
22. Quezada X, Pieramici DJ, Matsui R, et al. Demarcation laser photocoagulation induced retinal necrosis and rupture resulting in large retinal tear formation. *Photodiagn Photodyn Ther*. 2015;12:314–316.
23. Mehta MC, Hirose T, Schepens CL. Giant retinal tears. Schepens CL, Hartnett ME, Hirose T. *Schepens' Retinal detachment and allied diseases*. 2nd ed. Butterworth–Heinemann: Boston; 2000:421–433.
24. Norton EWD, Aabert T, Fung W, et al. Giant retinal tears: I Clinical management with intravitreal air. *Am J Ophthalmol*. 1969;68:1011.
25. Ando F, Kando J. A plastic tack for the treatment of retinal detachment with giant tear. *Am J Ophthalmol*. 1983;95:260–261.
26. Javey G, Schwartz SG, Flynn HW Jr, et al. Lack of toxicity of stainless steel retinal tacks 21 years of follow up. *Ophthalmic*

Surg Lasers Imaging. 2009;40:75–76.
27. Federman JL, Shakin JL, Lanning RC. The microsurgical management of giant retinal tears with trans-scleral retinal sutures. *Ophthalmology*. 1982;89:832–838.
28. Freeman HM, Castillejos ME. Current management of giant retinal breaks: results with vitrectomy and total fluid air exchange in 95 eyes. *Trans Am Ophthalm Soc*. 1981;79:89–102.
29. Jalkh AE, Jabbour N, Avila MP, et al. Ultrasonographic findings in eyes with giant retinal tears and opaque media. *Retina*. 1983;3:154–158.
30. Goezinned F, Heij EC, Berendschot TT, et al. Low redetachment rate due to encircling scleral buckle in giant retinal tears treated with vitrectomy and silicone oil. *Retina*. 2008;28:485–492.
31. Kreiger AE, Lewis H. Management of giant retinal tears without scleral buckling. Use of radical dissection of the vitreous base and perfluoro-octane and intraocular tamponade. *Ophthalmology*. 1992;99:491–497.
32. Oliveira LB, Reis PA. Silicone oil tamponade in 23-gauge transconjunctival sutureless vitrectomy. *Retina*. 2007;27:1054–1058.
33. Kunikata H. Management of giant retinal tears using microincision vitrectomy surgery. *Dev Ophthalmol*. 2014;54:182–187.
34. Ambresin A, Wolfensberger TJ, Bovey EH. Management of giant retinal tears with vitrectomy, internal tamponade, and peripheral 360 degree retinal photocoagulation. *Retina*. 2003;23:622–628.
35. Ventrua MC, Melo C, Diniz JR, et al. Perfluoro-ocatane liquid as a short-term vitreous–retinal tamponade in the postoperative period in patients with retinal detachment due to giant tears. *Arq Bras Oftalmol*. 2007;70:495–500.
36. Sirmaharaj M, Balachnadran C, Chan WC, et al. Vitrectomy with short term postoperative tamponade using perfluorocarbon liquid for giant retinal tears. *Br J Ophthalmol*. 2005;89:1176–1179.
37. Majid MA, Hussin HM, Biswas S, et al. Emulsification of Densiron-68 used in inferior retinal detachment surgery.

Eye. 2008;22:152–157.
38. Gerding H, Timmernann H, Hefner L, et al. Heavy internal tamponade for cases with complicated retinal detachment. *Klin Monatsbl Augerheilkd*. 2011;228:273–276.
39. Schepens CL, Freeman HM. Current management of giant retinal breaks. *Ophthalmology*. 1967;71:474–487.
40. Machemer R. Retinal tears 180 degrees and greater-management with vitrectomy and intravitreal gas. *Arch Ophthalmol*. 1976;94:1340.
41. Aylward GW, Cooling RJ, Leaver PK. Trauma induced retinal detachment associated with giant retinal tears. *Retina*. 1993;13:136–141.
42. Batman C, Cekic O. Vitrectomy with silicone oil or long acting gas in eyes with giant retinal tear. *Retina*. 1999;19:175–180.
43. Hoffman ME, Sorr EM. Management of giant retinal tear without scleral buckling. *Retina*. 1986;6:197–204.
44. Loewenstein A, Humayun MS, de Juan E Jr, et al. Perfluoroperhydrophenanthrene versus perfluoro-n-octane in vitreoretinal surgery. *Ophthalmology*. 2000;107:1078–1082.
45. Al-Khairi AM, Al-Kahtani E, Kangave D, et al. Prognostic factors associated with outcomes after giant retinal tear management using perfluorocarbon liquids. *Eur J Ophthalmol*. 2008;18:270–277.
46. Dabour SA. The outcome of surgical management for giant retinal tear more than 180. *BMC Ophthalmol*. 2014;14:86.
47. Muna Bhende. Personal communication of unpublished data.
48. Freeman HM. Fellow eyes of giant retina breaks. *Mod Probl Ophthalmol*. 1979;20:267–274.
49. Wolfensberger TJ, Aylward GW, Leaver PK. Prophylactic 360° cryotherapy in fellow eyes of patients with spontaneous giant retinal tears. *Ophthalmology*. 2003;110:1175–1177.
50. Pollack A, Milstein A, Oliver M, et al. Circumferential argon laser photocoagulation for prevention of retinal detachment. *Eye*. 1994;8:419–422.
51. Ang GS, Townend J, Lois N. Interventions for prevention of

giant retinal tear in the fellow eye. *Cochrane Database Syst Rev*. 2009;(2) [CD006909].

114

Surgery for Ocular Trauma

Principles and Techniques of Treatment

Franco M. Recchia, Paul Sternberg Jr.

Extent of Ocular Injuries

It is estimated that 1.6 million blinding ocular injuries occur worldwide each year, with an additional 2.3 million people sustaining bilateral low vision from trauma, and almost 19 million with unilateral blindness or low vision.[1] Ocular trauma is second only to cataract as the most common cause of visual impairment in the United States. Of 2.4 million eye injuries sustained each year, up to 50,000 people are left with significant impairment.[2] Nearly 1 million Americans are visually impaired due to ocular trauma, of whom 7% have severe impairment and about 5% are blind in one eye. The annual cost of ocular trauma in the United States is estimated at between US$175 million and US$200 million for hospital care alone.[3] Based on data published in the United States from 2000 to 2010, the estimated total economic cost attributable to military eye injuries exceeded $25 billion during that decade. This figure included direct costs of medical care and vision rehabilitation, federal disability benefits, and projected costs over the remaining lifetimes of visually disabled service members.[4]

According to trauma registries in the United States and abroad, ocular injuries are more common among younger people, males, and those with less education and wealth.[5] Statistics from the

National Institute for Occupational Safety and Health on work-related diseases and injuries indicate that more than 800 ,000 work-related ocular injuries are reported annually in the United States. The impact of these injuries is compounded by the personal and national financial burden incurred. Total costs (direct workers' compensation claims and indirect costs such as time lost by noninjured workers and production slowdowns) exceed US$4 billion.[2,6]

Ocular Trauma Classification

In 1996, Kuhn et al. published a terminology for ocular trauma, with the intention of establishing a standardized and unambiguous language for ocular traumatology (Table 114.1).[7] In 1997, the Ocular Trauma Classification Group incorporated this new terminology into a more extensive classification scheme designed to improve consistency and accuracy in clinical practice and research.[8] In this "classification system for mechanical injuries of the globe," the group incorporated anatomic and physiologic variables that had been shown to be prognostic of visual outcome after ocular injury. In addition to mechanism and extent of injury, these variables included visual acuity, presence or absence of a relative afferent pupillary defect, and zone of injury (external, anterior segment, or posterior segment). These classification schemes have improved communication between physicians and have been incorporated into many subsequent retrospective studies.

TABLE 114.1

New Standardized Classification of Ocular Trauma Terminology

Term	Definition
Eyewall	Sclera and cornea
Closed-globe injury	The eyewall does not have a full-thickness wound
Open-globe injury	The eyewall does have a full-thickness wound
Rupture	Full-thickness eyewall wound caused by a blunt object; the impact results in momentary increase of the intraocular pressure and an inside-out injury mechanism
Laceration	Full-thickness wound of the eyewall, usually caused by a sharp object; the wound occurs at the impact site by an outside-in mechanism

Penetrating injury	Single laceration of the eyewall, usually caused by a sharp object
Intraocular foreign body (IOFB)	Retained foreign object(s) causing body injury and entrance laceration(s)
Perforating injury	Two full-thickness lacerations (entrance + exit) of the eyewall, usually caused by a sharp object or missile

Closed-Globe Injuries

Hyphema

Traumatic hyphema, or anterior chamber hemorrhage, can often manifest after blunt trauma. Most hyphemas clear spontaneously and do not cause residual visual impairment. However, permanent visual impairment can arise from complications of hyphema. These complications include (1) corneal blood staining;[9] (2) ghost cell glaucoma as a result of blocked outflow from clogging of the trabecular meshwork by erythrocytes;[10] or (3) central retinal artery occlusion from elevated intraocular pressure.[11] All these complications are more common when secondary bleeding occurs, usually 48–72 hours after the injury.

The laboratory workup for traumatic hyphema is tailored to the specific patient. While laboratory evaluation is not indicated in most patients with a hyphema, blood coagulation tests should be considered in patients with a known bleeding diathesis or pertinent review of systems. African American patients should be questioned about a family or personal history of sickle-cell disease or trait. If unknown, a sickle preparation or hemoglobin electrophoresis should be obtained. Patients with sickle-cell hemoglobinopathies and traumatic hyphema present special problems because of their decreased ability to tolerate modest rises in intraocular pressure. Optic atrophy may result in this setting due to decreased perfusion pressure, sludging and sickling of erythrocytes, and subsequent infarction.[12] In addition, because of its lower likelihood to cause systemic acidosis that promotes sickling, methazolamide (Neptazane) rather than acetazolamide (Diamox) should be used to decrease intraocular pressure in these patients. Mannitol should be used once only to avoid hemoconcentration.

Primary management of traumatic hyphema is directed at

prevention of rebleeding, which can complicate up to 35% of cases.[13] Previous clinical studies have demonstrated the benefits of shielding the injured eye to prevent accidental repeat trauma, using atropine for cycloplegia, and daily checking of visual acuity, corneal status, and intraocular pressure.[14] On the other hand, no benefit in the prevention of rebleeding has been proven for hospitalization with enforced bed rest or for bilateral patching to reduce eye movement.[15]

Several pharmacologic measures have been used to prevent rebleeding. Corticosteroids, both topical (prednisolone acetate 1% q.i.d.) and systemic (prednisone 0.5–1.0 mg/kg per day), reduce iritis and ciliary spasm, increase patient comfort, and theoretically stabilize the clot formation, thereby decreasing the rate of rebleed. Clinical trials have demonstrated the efficacy of oral epsilon-aminocaproic acid, both systemic (Amicar, Lederle Laboratories, Pearl River, NY, given 50 mg/kg every 4 hours for 5 days) and topical (Caprogel, ISTA Pharmaceuticals Irvine, CA, given every 6 hours for 5 days) and tranexamic acid (Cyklokapron, Pfizer, New York, NY) in reducing the incidence of secondary bleeding.[16,17] These antifibrinolytic agents reduce clot degradation from traumatized blood vessels by inhibiting the conversion of plasminogen to plasmin, the protein responsible for clot breakdown.

A recent review and meta-analysis examined the use of antifibrinolytic agents, corticosteroids, cycloplegics, miotics, aspirin, conjugated estrogens, traditional Chinese medicine, unilateral or bilateral patching, elevation of the head, and bed rest. In this review, traumatic hyphema in the absence of other intraocular injury uncommonly led to permanent loss of vision. No intervention had a significant effect on visual acuity, whether measured at ≤2 weeks after the trauma or at later time points. Systemic aminocaproic acid reduced the incidence of recurrent hemorrhage but prolonged the time needed for the hyphema to clear and was associated with increased nausea, vomiting, and other adverse events compared with placebo. The evidence to support an associated reduction in the risk of complications from secondary hemorrhage (i.e., corneal blood staining, peripheral anterior synechiae, elevated intraocular pressure, and development

of optic atrophy) by antifibrinolytics was limited by the small number of these events.[18] Since no solid evidence was found to support the use of cycloplegics, corticosteroids, or nonpharmacologic interventions such as eye patching, head elevation, or bed rest, these measures should be individualized to patient needs and circumstances.

In most cases the hyphema improves with medical management. However, empiric criteria for surgical evaluation have been developed:[14,19,20] (1) intractably elevated intraocular pressure (IOP) despite medical therapy (>60 mmHg for 2 days in sickle-negative patients; or >24 mmHg for more than 1 day in sickle-positive patients); (2) total hyphema for more than 5 days with IOP >25 mmHg; (3) corneal bloodstaining; (4) persistence of hyphema occupying at least one-half of the anterior chamber volume. Several surgical techniques have been suggested to manage this problem, including paracentesis, anterior chamber washout with a one-needle irrigation or irrigation–aspiration technique,[21] washout with a two-needle technique, clot evacuation with a forceps or cryoprobe through a large limbal incision,[22] or clot evacuation associated with a trabeculectomy filtering operation.[23]

The concerns of shallowing of the anterior chamber with concomitant intraoperative fluctuations in intraocular pressure and renewed bleeding can be mitigated by the use of an anterior chamber maintainer (ACM). In this technique, an inferotemporal corneal paracentesis is made to accommodate the ACM connected to balance saline solution. A second paracentesis is then made in the superior cornea to allow evacuation of clot and blood.[24]

A two-instrument bimanual technique using vitrectomy instrumentation inserted through limbal incisions permits controlled removal of anterior chamber hemorrhage (Fig. 114.1).[25,26] The surgeon inserts through one incision a blunt infusion cannula (20-gauge (G), or smaller) or a bent needle (typically 23G) connected to balanced salt solution and a vitreous cutter through the second incision. Using both the aspiration and cutting functions of the cutter, as much of the clot and free blood is removed as possible. Care is taken to avoid damaging the crystalline lens and corneal endothelium. It is not uncommon to leave some residual blood at the end of the procedure. The incisions are closed with "X-

type" sutures using 9–0 or 10–0 monofilament nylon with knots buried in the incision. With the newer small-gauge (23G or 25G) vitrectomy instruments, self-sealing incisions may be feasible.

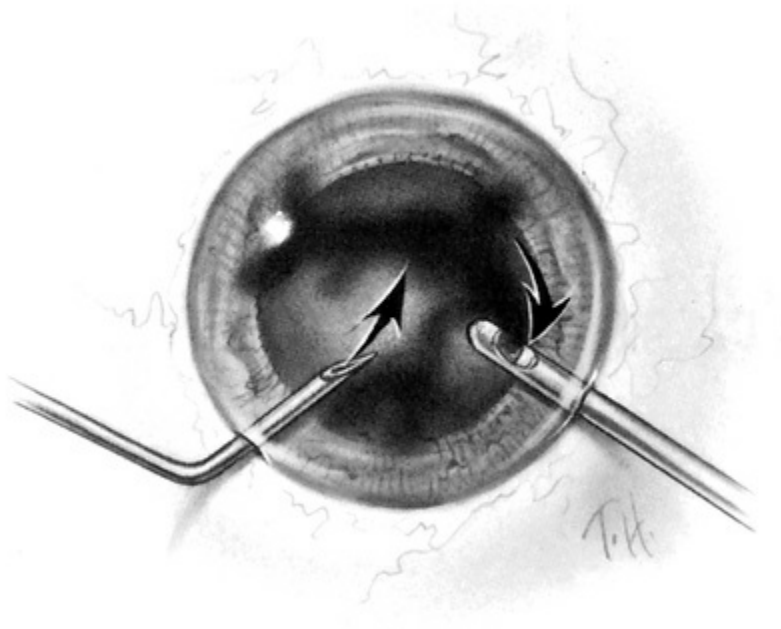

FIG. 114.1 A two-instrument bimanual technique permits controlled removal of anterior chamber hemorrhage. An angled, blunt, 20G infusion cannula is inserted through a nasal limbal incision, and the vitrectomy instrument is inserted temporally. Careful aspiration and cutting are used to evacuate the clot. The instruments can be transposed to reach hemorrhage inaccessible in the primary position. Alternatively, smaller gauge infusion and vitrectomy instrumentation can be used for the same procedure.

Lens Subluxation and Dislocation

Blunt trauma can lead to either subluxation or dislocation of the crystalline lens. In lens subluxation, zonular filaments are broken, and the lens is no longer held securely in place but remains in the pupillary aperture. Lens dislocation occurs following complete disruption of the zonular filaments and displacement of the lens from the pupil. Trauma is the leading cause of lens dislocation.[27]

The dislocation or subluxation is not a problem in itself. Patients

can have normal visual acuity with a totally dislocated lens and aphakic correction. However, the contusive impact can lead to cataract formation. Special considerations and techniques are required when extracting a subluxated or dislocated cataractous lens.

In the evaluation of a patient with a cataractous lens after blunt trauma, it is important to remember that the lens may be subluxated. During the slit-lamp examination, evidence of iridodonesis or phacodonesis must be sought. This usually is more apparent in the undilated state, when the remaining intact zonular filaments are under less tension. Phacodonesis can be detected by having the patient look quickly from side to side or up and down, or by jarring the slit-lamp table. If an associated iridodialysis is present, the absence of zonular fibers can be identified by looking through the area of absent iris (Fig. 114.2). Presence of vitreous in the anterior chamber is proof of zonular rupture and probable lens subluxation.

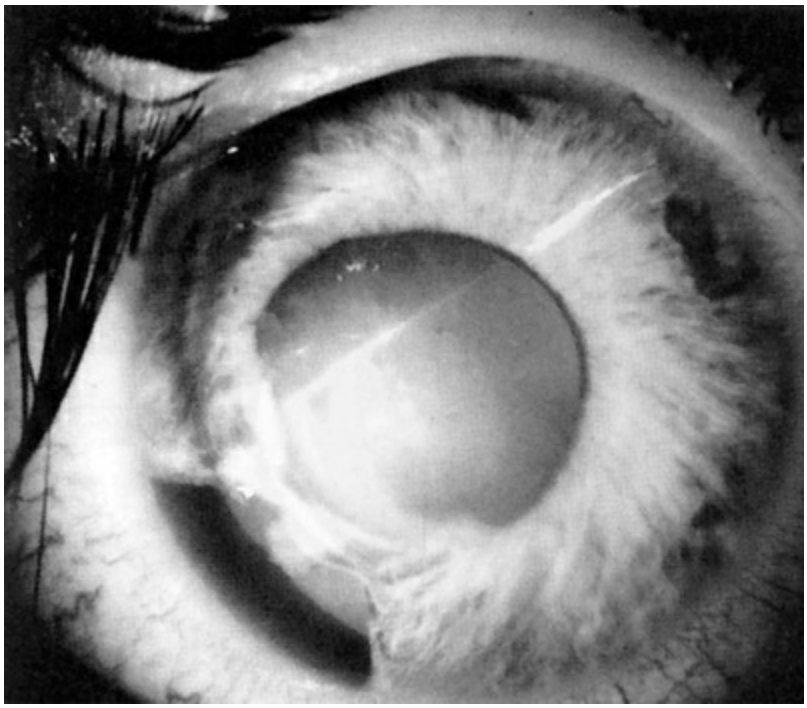

FIG. 114.2 This 13-year-old boy suffered an iridodialysis and subluxated lens with zonular rupture from a nonpenetrating BB pellet injury. A cataract developed within 2 weeks of the injury.

Extraction of a subluxated or dislocated cataractous lens should be considered only when the cataract is causing significant visual impairment. Urgent intervention is indicated for cases of pupillary block glaucoma, intractable uveitis, or lens–corneal touch leading to corneal decompensation. In children, the possibility of amblyopia may necessitate surgery. Lens extraction also may be necessary if visualization of the fundus is impaired and ultrasonography is equivocal with regard to retinal status. When surgery is planned for a subluxated or dislocated cataractous lens, vitreous loss is likely, and the success of surgery most likely depends on the care with which the vitreous is managed.

For cases with minimal lens instability, the traditional phacoemulsification techniques through a corneal limbal or scleral tunnel incision may be used, with a thorough hydrodissection and care taken to minimize the stress on the zonule and vitreous. A capsular support device, such as a capsular tension ring, may increase the safety and ease of phacoemulsification by stabilizing the capsular bag. Alternatively, a larger capsulorhexis may be used, and the lens may be prolapsed into the anterior chamber for phacoemulsification. Of great concern is vitreous prolapse through the cataract wound, and if vitreous is pulled on, traction transmitted to the vitreous base can cause retinal tears, giant retinal tear, and retinal detachment.[28] Consequently, the surgeon must recognize that vitreous prolapse through the wound is probable and be prepared for its management.

A pars plana approach using vitreoretinal instrumentation avoids many of the risks associated with limbal extraction (Fig. 114.3). Using a two- or three-port system, a myringotomy blade or a bent 21G or 23G butterfly intravenous needle connected to irrigation is inserted through the pars plana into the lens for fixation, and either a vitrectomy or a phacofragmentation instrument is inserted through the opposite pars plana to digest the lens. If the lens is soft, as in children and young adults (the most frequent victims of trauma), the entire lensectomy can be performed with the vitreous cutter. Vitreous around the lens can be managed with high-speed cutting and low vacuum to prevent traction on the vitreous base. Should the lens nucleus be harder and require phacofragmentation, care should be taken to perform either a limited vitrectomy around

the lens before introduction of the phacofragmatome or to use the phacofragmatome only when inside the lens capsule. This avoids unintentional aspiration pressure on the vitreous that could lead to retinal damage.

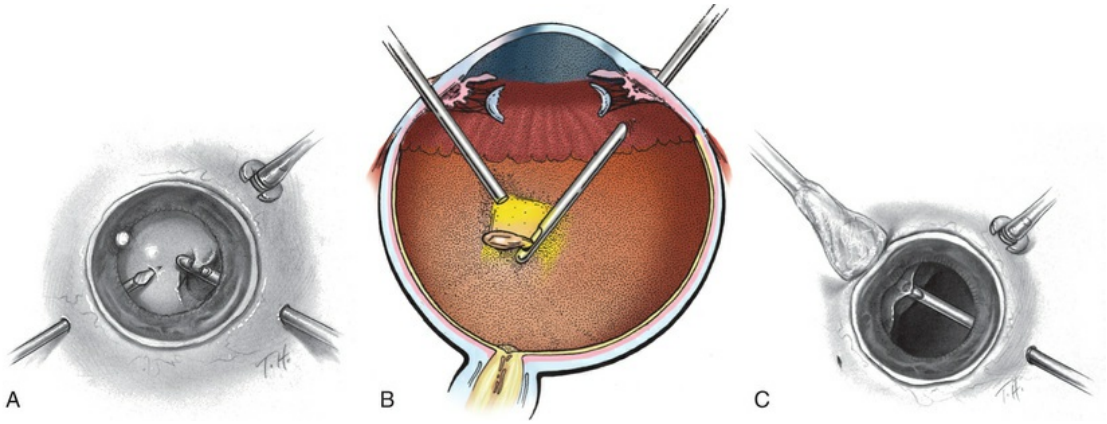

FIG. 114.3 Technique for pars plana lensectomy for subluxated cataractous lens. (A) A pars plana infusion cannula is sutured in place in the inferotemporal quadrant, and the lens is fixated with a myringotomy blade inserted through a pars plana sclerotomy. A vitrectomy instrument (if the lens is soft) or phacofragmentation instrument (if the lens nucleus is harder) is inserted into the lens through the opposite pars plana. (B) If any lens material falls posteriorly, a fiberoptic probe is inserted in place of the myringotomy blade, and the lens material is removed using standard two-hand vitrectomy techniques. (C) Residual peripheral lens material is removed with the use of careful scleral indentation to bring the pars plicata area into view.

If any lens fragments fall posteriorly, a fiberoptic probe can be inserted through a sclerotomy and the lens material can be removed using standard vitrectomy techniques. In order to minimize vitreous traction during manipulation, all vitreous surrounding the lens must first be carefully removed. Lens material on the retinal surface should then be brought into the middle or anterior vitreous cavity before fragmentation. Removal of residual peripheral lens material can be facilitated by gentle scleral depression to bring the pars plicata area into view. Vitrectomy (including mechanical

dissection of the posterior hyaloid) should be as complete as possible in order to decrease the chance of postoperative retinal detachment, posterior hyaloid contraction, or vitreomacular traction. However, even though the induction of a posterior vitreous detachment (PVD) is ideal, the surgeon should not risk iatrogenic retinal damage in an attempt to create a vitreous separation.

If enough zonular filaments remain intact to support a sulcus-fixated intraocular lens (IOL), primary placement of an IOL can be considered. If minimal capsular support remains, the residual capsule should be removed, as this may increase the risk of late postoperative anterior fibrous proliferation and traction on the ciliary body and retina. Complete capsular removal is most easily performed using a two-handed technique: in one hand, an end-grasping microforceps engages the capsule, gently pulling it centrally, and in the other hand, a vitrector aspirates and cuts the residual capsule and zonular filaments. In these cases, the resulting refractive error can be corrected either by use of an aphakic contact lens following surgery or by implantation of an intraocular lens at the time of lensectomy. Options for lens implantation include an open-loop flexible anterior chamber intraocular lens (AC-IOL), iris-fixated lens, or a posterior-chamber lens (PC-IOL) secured in the ciliary sulcus or pars plana by a variety of means (suture, fibrin glue, or sutureless scleral fixation).[29,30]

Pars plana vitrectomy and pars plana lensectomy (PPV/PPL) with implantation of IOL can be used for cases of subluxated traumatic cataract with extensive zonular damage. Kazemi et al. reported on nine such eyes, in which an anterior chamber IOL was placed. Best corrected visual acuity of better than 20/40 was achieved in six of the nine eyes.[31]

Kodjikian et al. reported on nine consecutive cases of traumatic cataract with zonular dialysis of at least 180° and visual acuity of 20/100 or worse. Following PPV/PPL and implantation of an iris-fixated Artisan IOL, all patients achieved best corrected visual acuity of 20/30 or better.[32] Other authors have reported similar results using PPV/PPL and sutured sulcus IOLs.[33] A consistent finding in these studies is that the primary determinant of postoperative visual acuity is posterior segment pathology related

to the original injury[34]

An iridodialysis can be repaired at the end of the case using a 10–0 Prolene suture introduced through the cornea in a modification of the technique described by McCannel[35] to fixate IOLs to the pars plana (Fig. 114.4). At the end of the procedure, the peripheral retina should be carefully inspected with scleral depression to identify retinal breaks, dialyses, or areas of retinal detachment. Inspection can be performed either with binocular indirect ophthalmoscopy or through the microscope equipped with wide-field viewing. Should retinal breaks or detachment be present, they should be treated immediately with retinopexy and, if necessary, scleral buckling and endotamponade.

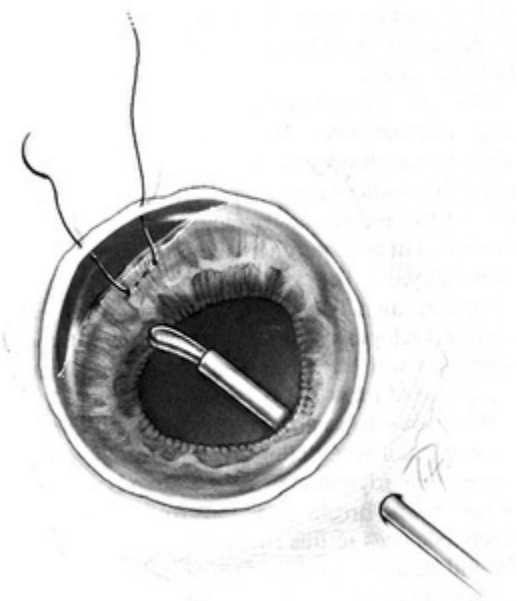

FIG. 114.4 An iridodialysis can be repaired with a modification of the McCannel suture technique. A curved needle attached to a 10–0 Prolene suture is introduced through the limbus. With the iris grasped with a microforceps and pushed back into place, the needle is passed through the iris and back out through the limbus. The needle is then tied, reapproximating the iris in its original position.

Vitreous Hemorrhage

Vitreous hemorrhage may result from damage to blood vessels in

the ciliary body, retina, or choroid. Vitreous hemorrhage from blunt trauma may be associated with a retinal tear, and meticulous indirect ophthalmoscopy with scleral depression should be performed to identify retinal abnormalities. Fundus visualization is usually best at the initial exam, as diffusion of hemorrhage or further bleeding may compromise later examinations. If occult scleral rupture is suspected, then scleral depression should be deferred.

Ultrasonography is critical in decision-making in cases of fundus-obscuring hemorrhage. With combined contact A-scan and B-scan techniques, many details of the posterior segment can be determined, including presence of retinal detachment, PVD, occult scleral rupture, hemorrhagic or serous choroidal detachment, and giant retinal tear (Fig. 114.5). For example, if ultrasound demonstrates vitreous strands emanating from an equatorial location, an occult scleral rupture with vitreous incarcerated in the wound can be inferred, requiring conjunctival peritomy and exploration.

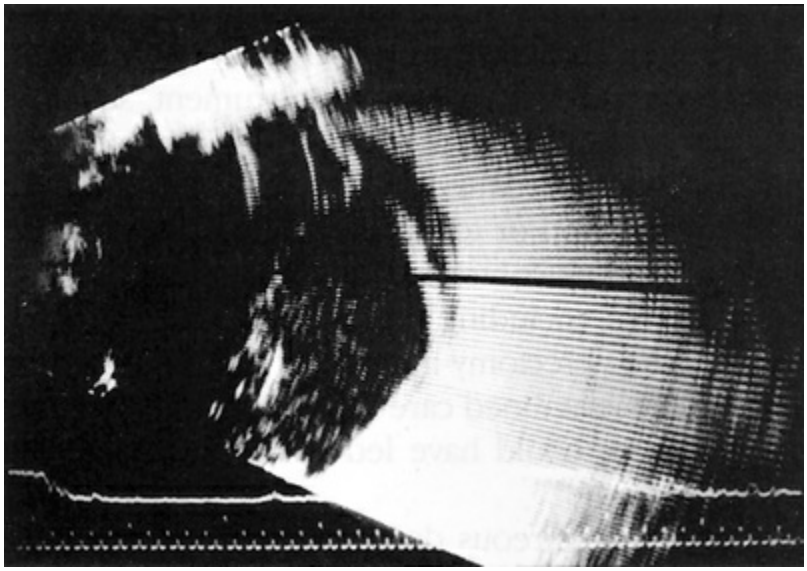

FIG. 114.5 In the presence of vitreous hemorrhage, contact B-scan ultrasonography can demonstrate a retinal detachment and can sometimes also identify the causative retinal tear.

In general, patients with a nonpenetrating ocular injury and a vitreous hemorrhage without associated retinal tear or detachment

should be observed. In cases of minimal diffuse hemorrhage, indirect ophthalmoscopy may be sufficient to establish retinal attachment. However, if the blood does not settle, the patient should be followed every few weeks with ultrasonography repeated to confirm retinal attachment. If retinal detachment is seen or suspected on ultrasonography, pars plana vitrectomy should be performed.

If pars plana vitrectomy is performed for a nonclearing vitreous hemorrhage caused by nonpenetrating trauma, we recommend a standard three-port technique. After the infusion cannula is secured in place and confirmed to be in the vitreous cavity, a core vitrectomy should be performed to remove hemorrhagic vitreous. In most cases a PVD will have developed in the time between injury and surgery. After one cuts through the detached posterior hyaloid face with the vitrectomy instrument, subhyaloid blood can be aspirated from the preretinal space. A blunt cannula connected either to the vitrectomy system for powered extrusion or to a fluted handle for passive extrusion will allow controlled removal of the blood. Residual vitreous, including posterior hyaloid, is then excised with the vitrectomy instrument. The retinal periphery should be examined carefully to identify retinal tears or dialyses that could have led to the original vitreous hemorrhage.

If a PVD is not present, the surgeon should attempt to induce one. We have found that induction of a PVD can be made significantly easier and safer with the instillation of triamcinolone (either full-strength or diluted 20% in balanced salt solution) after a brief core vitrectomy. With this method, residual adherent cortical vitreous is marked by the triamcinolone particles and can be clearly visualized. The posterior hyaloid can then be engaged over the optic nerve with gentle suction from the vitrector or a powered soft-tip extrusion cannula and carefully stripped from the retinal surface. Other techniques for initiating posterior vitreous separation include incising the posterior hyaloid with a vitreoretinal pick, myringotomy blade, or diamond-dusted scraper over the periphery of the optic nerve. The vitreous detachment can be extended using an illuminated vitreoretinal pick while the hyaloid is elevated with either the extrusion cannula or vitrectomy instrument. If the posterior hyaloid remains adherent in certain locations, it should be

freed from surrounding vitreous so that all localized vitreoretinal traction is relieved. If traction persists, it may be necessary to place a local scleral buckle. Areas of persistent vitreoretinal traction should be scrutinized carefully because they may represent sites of occult scleral rupture and vitreous incarceration.

Smaller-gauge vitrectomy instrumentation can be used successfully for cases of traumatic vitreous hemorrhage, even those with associated retinal detachment and proliferative vitreoretinopathy. The surgeon should remember several aspects of transconjunctival small-gauge surgery that are especially relevant to traumatized eyes. First, since the infusion cannula is not sutured in place, it may slip backward into the suprachoroidal space, even after being well-visualized at initial placement. This risk is higher in eyes with choroidal hemorrhage, choroidal congestion, or dense accumulation of blood or fibrin at the anterior vitreous base. This risk can be minimized by preoperative ultrasonographic confirmation of an absence of choroidal detachment, by choosing a quadrant of the eye with a relatively clearer periphery, and by selecting the longest infusion cannula available. Second, smaller-gauge vitreous cutters (especially earlier-generation 25G cutters and 27G cutters) may become clogged with dense hemorrhage or vitreous debris. Third, additional instrumentation (such as intraocular forceps, scissors, lighted instruments, or equipment for oil infusion) may be required for treatment of associated vitreoretinal pathology. The surgeon must have as much information as possible regarding the ocular anatomy and have readily available the requisite surgical instruments.

The visual prognosis for eyes with vitreous hemorrhage associated with nonpenetrating trauma depends on associated macular damage (from choroidal rupture, traumatic macular hole, Berlin's edema, or macular contusion), retinal dysfunction from associated retinal detachment, and occlusional amblyopia in young children. In a study of 33 eyes with severe vitreous hemorrhage associated with closed-globe injury, best corrected visual acuity following resolution and/or treatment of hemorrhage was <20/200 in 54%. The most common cause of poor visual outcome was macular scar. Poor prognostic factors included presenting visual acuity of light perception or worse, hyphema, traumatic cataract,

and age 55 years or younger.[36]

"Commotio Retinae," Avulsion of the Vitreous Base, and Retinal Tears

Blunt trauma can damage the retina in many ways, ranging from retinal edema to retinal detachment. "Commotio retinae" is commonly seen after a contusive injury to the globe and appears ophthalmoscopically as retinal whitening (Fig. 114.6A). Edema involving the macula (termed Berlin's edema) can impart an appearance similar to a cherry-red spot. Experimental and histopathologic studies suggest that disruption of the photoreceptor cell outer segments and damage to the retinal pigment epithelium account for the retinal whitening.[37] Vision can be markedly decreased with commotio retinae, but vision most often improves as the swelling resolves over several weeks. Long term, however, vision can remain decreased as the macula develops an atrophic appearance with granular hyperpigmentation or if cystoid areas coalesce to form a macular hole (Fig. 114.6C).

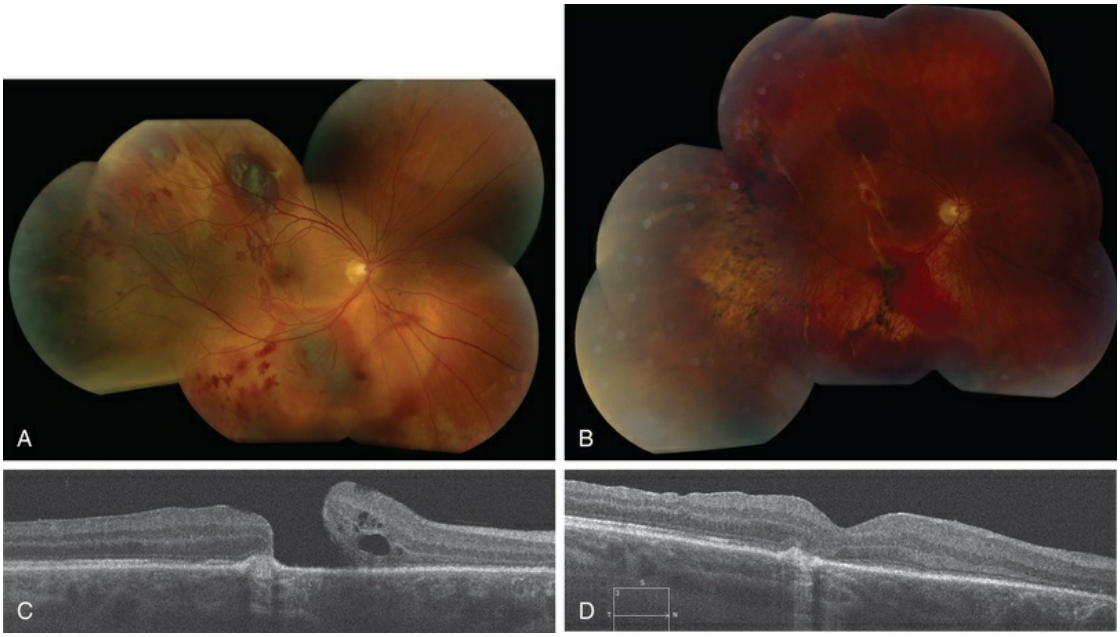

FIG. 114.6 This 40-year-old helicopter pilot suffered closed-globe trauma to the left eye when struck with an air-pressure hose. (A) Color fundus montage at presentation shows dispersed vitreous hemorrhage,

intraretinal and subretinal hemorrhage, and diffuse retinal whitening (commotio retinae). Visual acuity was counting fingers. (B, C) Color fundus montage and spectral domain optical coherence tomography (SD-OCT) 2 months later shows resolution of retinal whitening and reduction in intraocular hemorrhage, but the patient has now developed a full-thickness macular hole, with best corrected visual acuity of 20/400. Given the lack of spontaneous closure of the macular hole after 6 weeks, the patient underwent pars plana vitrectomy, removal of the internal limiting membrane, gas-air exchange with 14% perfluoropropane, and 3 days of prone positioning. (D) SD-OCT taken 6 weeks postoperatively shows complete closure of the macular hole. Visual acuity was 20/60 with eccentric fixation and will likely remain limited by disruption of outer retinal anatomy.

Blunt trauma can lead to large areas of irregular, jagged retinal holes. These breaks have been observed almost immediately after the contusive injury and are believed to be the result of mechanical disruption and fragmentation of the retina. Similar-appearing breaks have been produced in an experimental model of concussive injury to the globe.[38] This syndrome has been given a variety of names, including "acute retinal necrosis"[38] and "chorioretinitis sclopetaria."[39] We prefer the term "contusive or traumatic retinopathy," as it more precisely describes the etiology and mechanism of the clinical finding and avoids confusion with the acute retinal necrosis inflammatory syndrome of herpetic viral origin.

In eyes with chorioretinitis sclopetaria, it is tempting to intervene in some way because of the frightening size and often posterior location of the retinal breaks (Fig. 114.7). However, the retina rarely detaches in this situation, presumably because inflammation at the edges of the necrotic retina leads to a firm chorioretinal adhesion. Therefore, we do not recommend routine prophylactic retinopexy to areas of chorioretinitis sclopetaria. If a retinal detachment occurs, it is usually from another site and typically within the first few weeks of injury.[40] Patients with this condition often have poor visual acuity because of the effects of the severe blunt force on the

macula.

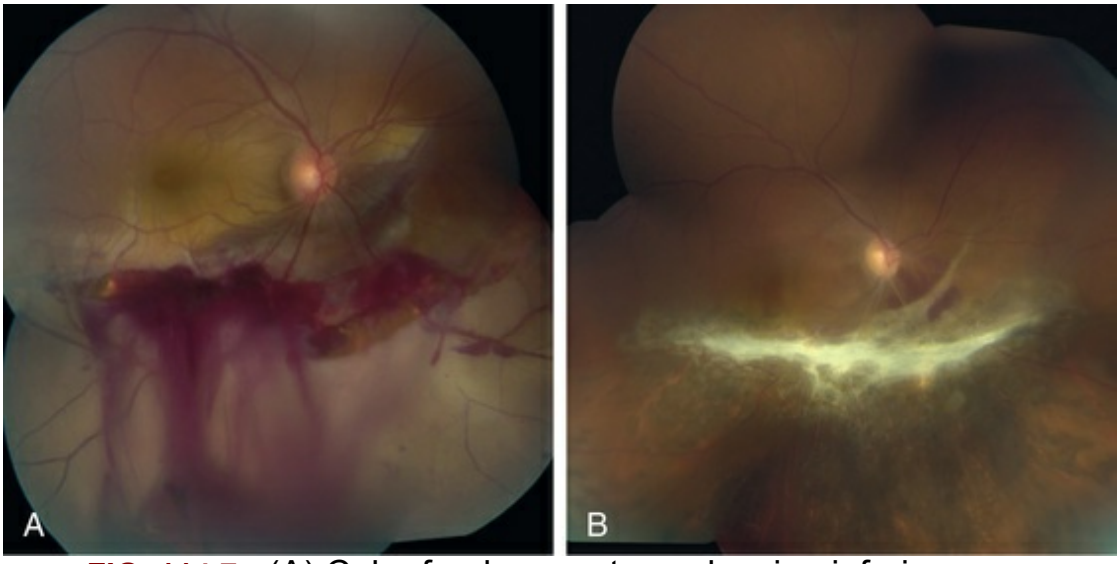

FIG. 114.7 (A) Color fundus montage showing inferior retinal detachment caused by a giant retinal tear (GRT) along the inferior arcade with overlying vitreous hemorrhage. The inferior peripheral retina is white from presumed infarction arising from arteriolar transection. Posterior segment injuries often result from contrecoup forces and vitreoretinal traction. As the vitreous was forcefully separated from the retina, abnormally strong perivascular vitreous traction over the postequatorial retina may have contributed to the unique location of the GRT in this case. (B) Color montage taken 10 months following vitrectomy, scleral buckling, endolaser, and gas endotamponade.

Blunt trauma can also cause retinal breaks by transmission of the force to the vitreous base, leading to acute severe vitreoretinal traction. Rapid displacement of the vitreous can tear the retina in various ways, including retinal dialysis with or without avulsion of the vitreous base, operculated retinal tear, macular hole, and horseshoe-shaped retinal tears at the posterior margin of the vitreous base, at the edge of a meridional fold, or at the equator.[41,42] A study by Cox[38] concluded that the different forms of retinal abnormalities are a result of the point of impact of blunt trauma.

A retinal break that commonly follows trauma (and considered pathognomonic for blunt ocular trauma) is a retinal dialysis. This is

seen most commonly in the superonasal and inferotemporal quadrants because of blunt trauma frequently striking the globe inferotemporally.[43] The blunt force causes equatorial stretching of the globe, leading to traction on the vitreous base at the site of impact and diametrically opposite. Cox et al.[41] reviewed 160 patients with retinal detachment caused by contusion. In that series, retinal dialyses larger than one oral bay were found to be the most common retinal break.

It is important to perform careful indirect ophthalmoscopy with scleral depression on all patients with a history of blunt trauma. The authors recommend prophylactic cryopexy or photocoagulation to any retinal dialyses or tears that are identified, in the hope of decreasing the likelihood of subsequent retinal detachment.

Retinal Detachment and Macular Hole

It is uncommon for a patient to develop an acute rhegmatogenous retinal detachment after blunt trauma. Most trauma victims are young with solid vitreous, providing internal tamponade to the retina despite retinal tears or dialyses. However, with time the vitreous liquefies, allowing fluid to form in the vitreous cavity, which can pass through the retinal breaks and detach the retina. By careful examination of the retina shortly after the injury and treatment of areas of retinal damage, detachment can be prevented in many cases.

Most traumatic retinal detachments can be treated with conventional scleral buckling techniques. Because of the potential for retinal damage 180° from the impact site, an encircling element is recommended. The selection of chorioretinal adhesive procedure and determination of the need to drain subretinal fluid should be made by the surgeon using the same principles as for nontraumatic detachments. Johnston[44] reported 77 eyes with retinal breaks after contusive injury; 65 developed rhegmatogenous detachment. Surgical treatment restored or maintained retinal apposition in 96% of the eyes.

In rare cases, blunt trauma may cause a rhegmatogenous retinal detachment from a macular hole or giant retinal tear (a tear greater

than 3 clock-hours). Although these detachments have been repaired successfully in the past with a variety of scleral buckling techniques, modern vitreoretinal surgery has significantly increased the rate of anatomic reattachment. Vitreous surgery allows mobilization of the flap by excising adherent vitreous. With the aid of surgical adjuvants, such as perfluorocarbon liquids, and current surgical techniques (as described in Chapter 109, Optimal procedures for retinal detachment repair), the rate of successful retinal reattachment for such cases has greatly improved.

Traumatic macular hole formation is uncommon. Like idiopathic macular holes, traumatic holes can be rehabilitated with vitrectomy. However, a significant number of traumatic macular holes may close spontaneously. In a consecutive series of 18 such cases, spontaneous closure and accompanying visual improvement were seen in eight (44%) and occurred between 1 week and 4 months following injury.[45] In a retrospective study of 27 patients with traumatic macular hole observed for at least 6 months, multivariate regression analysis was performed to identify factors predictive of spontaneous closure. Holes with smaller inner diameter (mean of 245 μm) and fewer intraretinal cysts were more likely to close without surgery.[46] Although the visual outcome may be limited by associated macular damage (such as a macular choroidal rupture), there are encouraging reports of successful anatomic and functional outcomes with vitrectomy. Since patients with traumatic macular hole are typically younger and phakic, we elect to use long-acting gas endotamponade with 14% perfluoropropane to optimize the chance of hole closure (Fig. 114.6D). It has been suggested that surgical adjuvants such as autologous plasmin enzyme[47] or removal of internal limiting membrane[48,49] may improve the rate of anatomic success. Improvement in visual acuity of at least 2 Snellen lines has been reported in 69–94% of cases.[48–50]

Open-Globe Injuries

Preoperative Evaluation

It is important to obtain a history from any patient being evaluated for a possible eye injury. Although many trauma patients will be

poor historians because of associated shock, intoxication, or neurologic problems, the history can give important clues about the ocular damage. For instance, if a patient felt something flying into the eye while hammering a nail but did not note any visual disturbance, the physician must carefully search for evidence of an intraocular foreign body (IOFB), even if there is no evidence of obvious ocular laceration. Furthermore, since many of the medical malpractice cases brought against vitreoretinal specialists involve trauma, careful documentation of the details surrounding the injury may prove valuable in case of future litigation.[51]

Careful evaluation can also aid in prognostication of visual outcome when used according to the ocular trauma score (OTS). The OTS was developed by Kuhn et al.[52] following review of over 2500 registered cases of ocular trauma and has since been validated in adult and pediatric populations.[53,54] The OTS provides a single probability estimate that an eye trauma patient will obtain visual acuity within a specific range by 6 months after injury.[52] In the OTS, a numeric score is derived by adding or subtracting points on the basis of initial visual acuity, presence of rupture, endophthalmitis, globe perforation, retinal detachment, or afferent pupillary defect. Higher OTS scores are associated with better visual prognosis.[52] The OTS can thus be used as an aid in patient counseling and in identifying ocular injuries with a poor visual prognosis.

The initial step in examination is determination of visual acuity (VA) with either a near vision card or a Snellen acuity chart. When a retrospective review of penetrating injury patients was subjected to multivariate analysis, VA was the most important determinant of final visual outcome. Patients with initial VA of 5/200 or better had a 28 times greater chance of salvaging acuity at this level than those with vision worse than 5/200.[55] Two subsequent prospective studies of penetrating injuries have confirmed this finding. In the first of these series, 94% of patients with initial VA of 20/200 or better achieved a final VA of 20/200 or better.[56] In the second series, multivariate analysis revealed that presenting visual acuity of 5/200 or worse was the most important factor contributing to poor visual outcome; statistically insignificant factors were time since injury, cataract, and presence of IOFB.[57] In one review of 167 open-globe injuries, only 3% of eyes presenting with vision better than light

perception ultimately underwent enucleation, as compared with 39% of eyes presenting with light perception and 89% of eyes presenting with no light perception.[58]

The presence or absence of an afferent pupillary defect (APD) is a strong predictor of outcome.[59,60] A multivariate analysis of 240 traumatized eyes found 69% of eyes without an APD obtained a final VA of 20/200 or better, as compared with 34% of eyes with an APD (p<.00001).[59]

On rare occasions, the surgeon may contemplate primary enucleation when encountering a totally disorganized globe with prolapse of intraocular contents, including retina. In these cases it is important to determine carefully whether the patient can perceive light. This is best done with the uninjured eye covered, with the indirect ophthalmoscope light at maximal intensity, and with the light held at sufficient distance so that the patient cannot perceive the heat of the ophthalmoscope light. Unfortunately, since many patients with injuries of this severity often are either intoxicated or have other injuries affecting their mental status, determination of light perception is questionable. Additionally, there are several reports of eyes with preoperative measurement of no light perception achieving visual acuity of light perception or better following reconstructive ocular surgery.[61–63] For these reasons, primary enucleation is rarely performed.

It is important to perform an examination sufficient to determine the extent of injury but not so extensive as to cause further damage to the globe. Pressure on the globe that could cause further prolapse of ocular contents must be avoided. Lid retractors may be used with care when lid swelling precludes visualization of the globe. If the history is highly suggestive of a penetrating injury and the examination is inconclusive, possibly because of poor cooperation, an examination under anesthesia should be performed, at which time repair can be performed if needed.

Occasionally, a scleral rupture can be occult (hidden under conjunctiva, Tenon capsule, or rectus muscles). Diffuse chemosis or subconjunctival hemorrhage suggests the presence of occult rupture. An open globe often has low IOP, but normal or elevated IOP does not rule out the possibility of a rupture. On occasion, slit-lamp biomicroscopy or ultrasonography of the anterior vitreous can

demonstrate vitreous strands directed toward a hidden scleral rupture site (Fig. 114.8). Computed tomography (CT) can also show occult rupture, with flattening of the posterior contour of the sclera ("flat tire" sign).[64]

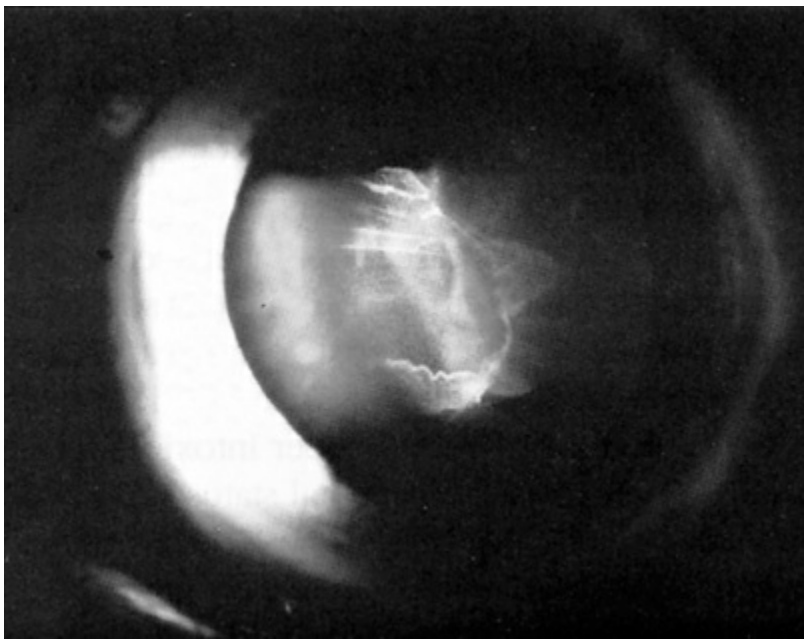

FIG. 114.8 In cases of occult scleral rupture, slit-lamp biomicroscopy can demonstrate vitreous strands directed toward the rupture site.

Confirming the presence or absence of a retained IOFB is critical to management. An IOFB can often be identified by slit-lamp biomicroscopy or indirect ophthalmoscopy (Fig. 114.9). However, if the ocular media are clouded by corneal damage, hyphema, cataract, or vitreous hemorrhage, ancillary techniques (typically ultrasonography and CT) are necessary. Ultrasonography can accurately localize foreign bodies, particularly with a systematic approach providing transverse and longitudinal views in all meridians (Fig. 114.10). When the globe is open, however, the resolution of ultrasound may be limited, as the examination often must be performed gently through closed lids. The usefulness of echography is also limited by shadowing caused by highly reflective surfaces such as air, reverberation artifacts created by some IOFBs, and by the user's skill and familiarity with ocular pathology.[65]

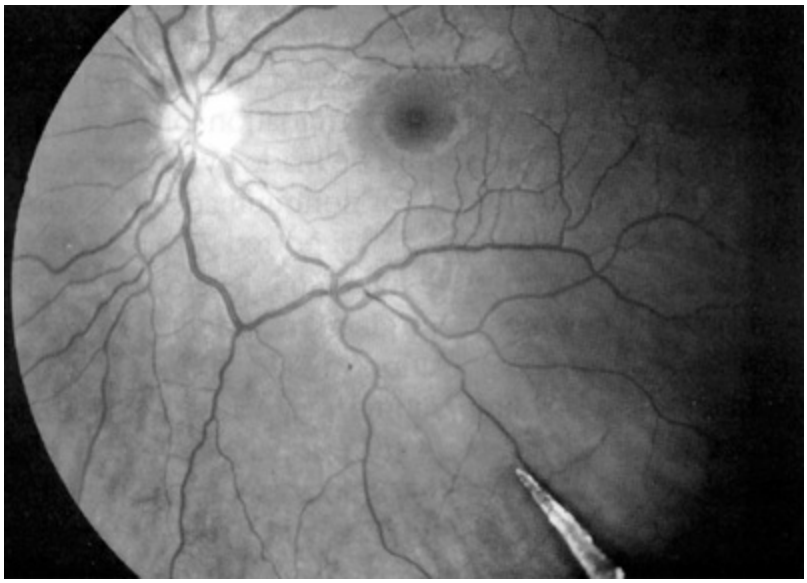

FIG. 114.9 This patient suffered an intravitreal foreign body while shooting at a rifle range. The intraocular foreign body was nonmagnetic and was successfully removed via vitrectomy with foreign body forceps.

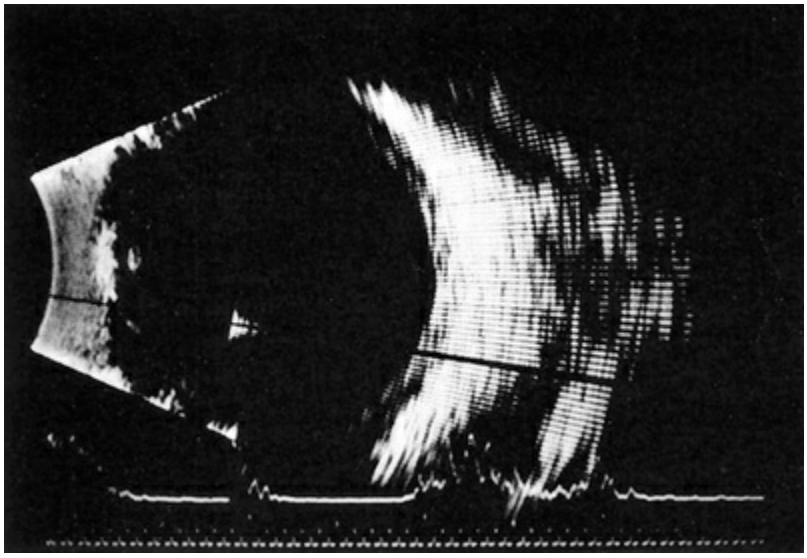

FIG. 114.10 Contact B-scan ultrasonography can demonstrate a metallic intraocular foreign body. The foreign body has a characteristic triangular shape because of its absorbance of the sound waves and the resultant trail of artifact behind it. The foreign body is highly reflective and remains visible even at low gain.

CT has emerged as the imaging technique of choice in the evaluation of IOFBs, as it requires minimal patient cooperation and

can image radiolucent and radiopaque foreign bodies (Fig. 114.11). By assembling many consecutive orbital slices that demonstrate the ocular anatomy, and by using computer-generated reconstructions in three dimensions, the location of an IOFB can be determined. In an experimental study to determine the size of CT cuts required to detect small IOFBs, Dass et al. concluded that with modern spiral CT scanning both 3-mm and 1-mm cuts were effective (100% sensitivity) in detecting a 0.5-mm metallic, glass, or stone IOFB.[66] The absorption characteristics of the foreign body are quantitated in Hounsfield units and can be compared with the absorptions of various known materials. Zinreich et al.[67] have shown that wood is the least dense of the nonmetallic foreign bodies, followed by plastic and then glass. Unfortunately, all metallic foreign bodies have the same absorptions and are impossible to differentiate. CT scanning does have limitations, in that metallic IOFBs often create significant scattering artifact that may obscure their precise location. This can be particularly bothersome when attempting to determine whether a foreign body is intraretinal or intrascleral. In addition, identifying some of the lower-density foreign bodies, such as wood, may be difficult with CT scanning.[68]

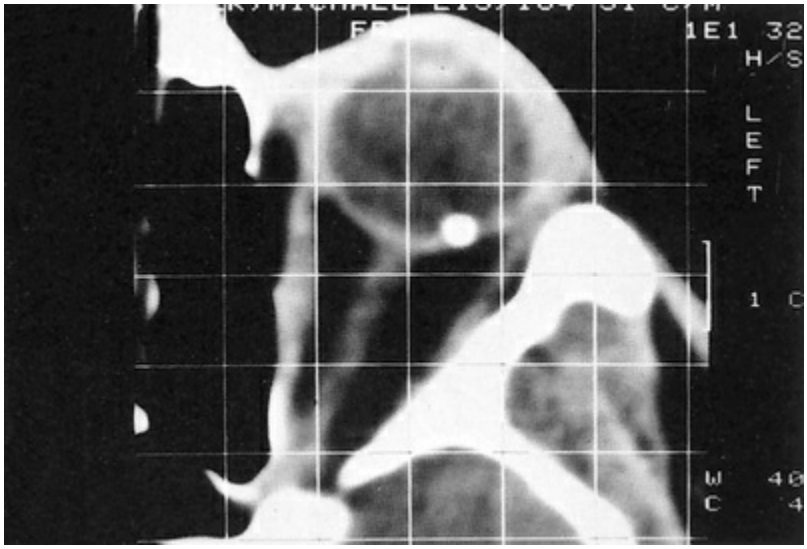

FIG. 114.11 This computed tomography (CT) scan demonstrates an intraretinal shotgun pellet in the patient's left eye.

Magnetic resonance imaging (MRI) is useful for imaging

intraocular tumors and other lesions. However, the magnetic fields and heat generated during MRI scanning preclude examination of patients with suspected intraocular or intraorbital metallic foreign bodies, as these objects can move within the suprachoroidal or vitreous spaces when subjected to the torsional forces of MRI.[69] Another disadvantage of MRI is its inability to image bone. MRI's principal advantage over CT is its detection of wood and plastic IOFBs.

The possibility of intraocular infection must also be addressed during the initial evaluation. Endophthalmitis is a devastating complication of penetrating injuries, and its prognosis is related to a number of factors, including time to diagnosis. Classically, eyes with endophthalmitis will be painful and have swollen conjunctiva and marked intraocular inflammation, including hypopyon. However, since these signs may be more difficult to identify in an already traumatized globe, infection can be diagnosed only if the physician remembers it as a possibility. Traumatic endophthalmitis is discussed in greater detail later in this chapter.

In many parts of the world, even in developed countries, there are limited numbers of emergency departments and medical centers with the requisite personnel and resources to provide complete care for the patient with ocular trauma. Thus, many patients will require transfer to a separate, specialized center after initial evaluation. At least one study has suggested that, with appropriate education as to key examination criteria, emergency physicians and general surgeons can determine the need for ophthalmic intervention with accuracy comparable to that of a general ophthalmologist.[70] The vitreoretinal specialist can be invaluable in advising the initial evaluation and streamlining the timely delivery of definitive treatment. We recommend, for example, in cases of suspected open-globe injury, that when feasible the evaluating physicians confirm the patient's medical and neurologic stability, shield the injured eye, evaluate for additional injuries, check toxicology screen, administer broad-spectrum systemic antibiotics with high intravitreal penetration (preferably fourth-generation fluoroquinolone), administer tetanus toxoid, and perform noncontrast CT of head and orbits to detect foreign body and determine any deformation of the globe. In parallel with this

initial evaluation, the ocular trauma surgeon can plan appropriate treatment and mobilize appropriate surgical personnel and services. If this initial evaluation cannot be performed with adequate quality or timeliness, then we recommend direct and immediate transfer of the patient.

Repair of Laceration

Principles guiding the repair of a laceration or rupture of the globe are the same whether confronting a straightforward corneal laceration or a complex corneoscleral laceration with prolapse of ocular contents. First, the structural integrity of the globe must be restored, providing a watertight closure of all wounds and restoration of normal IOP. Second, iatrogenic damage to the eye must be avoided. Efforts should be made to protect the visual axis but not if this sacrifices the previous principles.

Before repair of a laceration, it is critical to determine the extent of the injury. If a corneal laceration extends to the limbus, a limited conjunctival peritomy is necessary to evaluate for any scleral extension. After establishing the extent of injury, the presence or absence of iris or vitreous incarceration must be determined.

A simple corneal laceration without tissue incarceration should be closed with interrupted 10–0 nylon sutures. Tissue bites should be placed roughly two-thirds deep into corneal stroma on either side of the laceration. Closure can be attained by starting at one end and working to the other, starting at both ends and working toward the center, or starting at the middle and continually bisecting the laceration until the wound is watertight. We prefer the last approach. It is often necessary to replace some of the earlier sutures if they become loose as the wound is pulled together more tightly. In some cases it may be helpful to use larger sutures during initial approximation of the wound, similar to the way cardinal sutures are used for penetrating keratoplasty surgery. Placement of cardinal sutures may be particularly helpful in repair of jagged lacerations. If the edges of the corneal wound are edematous, the suture bites need to be placed at a greater distance from the wound edge. After tying the knots, the surgeon should try to bury them, but this may not be possible when the cornea is edematous.

A watertight closure can be difficult to achieve with stellate lacerations. In some cases the wound leaks even with multiple sutures crisscrossing the laceration, and a purse-string closure may be necessary. The suture is placed in a circle through the various portions of the cornea involved in the laceration and then tied to itself with the knot buried in the laceration. If this technique does not work, corneal tissue may have been lost, and tissue adhesive can seal the leakage site. When there is too much tissue loss for glue to work, a corneal patch graft can be used.

When iris is incarcerated in the corneal wound, it can be reposited in most cases. We advocate excision of uveal tissue only if it looks extremely necrotic, usually having been externalized for more than 24 hours. Reposition of incarcerated iris usually can be accomplished with introduction of an iris or cyclodialysis spatula or a 27G cannula connected to viscoelastic through a limbal stab incision made about 90° away from the laceration. This maneuver is best done after the corneal integrity has been partially restored by the first few sutures and the anterior chamber has been reformed with balanced salt solution, air, or viscoelastic substance. When there is positive pressure or in the presence of a hyphema, the surgeon may be helped by having the assistant reposit incarcerated iris while the surgeon places the suture. The success of subsequent surgical iridoplasty and pupillary reconstruction is directly related to the amount of iris that is preserved at the time of primary repair. The surgeon, therefore, should be meticulous in salvaging as much iris tissue as possible, resisting the understandable urge simply to excise all prolapsed tissue.

Whereas the location and extent of corneal lacerations are obvious, scleral lacerations require deliberate exploration. Therefore, good exposure is important. Lid sutures can be useful for lid retraction without putting excessive pressure on the globe. A conjunctival peritomy should be performed for 360°, followed by sharp dissection of the conjunctiva and Tenon fascia from the sclera in the four quadrants to avoid undue pressure on the globe.

Scleral lacerations should be repaired with 8–0 or 7–0 nonabsorbable sutures. We prefer spatulated needles similar to those used for placement of sutures for scleral buckling. In general, we use interrupted sutures to close the laceration, working from

anterior to posterior. If a scleral laceration is well delineated, a running shoestring suture can provide a watertight closure.

In some cases a scleral laceration may either be located under the rectus muscles or extend under the muscles. In these cases the area under the muscle can be exposed by gently passing a muscle hook under the muscle and using the hook to lift it out of the way. If this is unsuccessful or is causing too much pressure on the globe, the muscle should be isolated on a 6–0 Vicryl suture and cut from the globe. After repair of the laceration, the muscle is resutured to its original insertion. If a scleral rupture has resulted in extensive loss of tissue, such as with large missile injuries, it may be necessary to use a scleral patch graft.

Uveal tissue often extrudes through scleral lacerations. In most cases this tissue can be reposited by the assistant while the surgeon closes the overlying sclera. Even when the tissue appears necrotic, cutting the tissue can cause significant bleeding; rarely should extruded tissue be excised if the repair is performed within 24 hours of the injury.

Vitreous that has prolapsed through the laceration must be removed to decrease the chance of incarceration and subsequent vitreoretinal traction. Typically, extruded vitreous is cut with sharp scissors placed flush against the sclera. Alternatively, a vitreous cutter at high cutting speed and low vacuum can be used. This approach, if available, is preferable because of the reduction in traction placed on the vitreous and transmitted to the retina. The vitreous cutter should not be inserted into the eye through a scleral laceration to remove extruded vitreous because of the potential for damaging the choroid or retina. If the surgeon suspects extrusion of retina, every attempt should be made to reposit the retina, avoiding excision or incarceration if possible.

In some cases, the scleral laceration extends posterior to the ora serrata and may have an associated retinal laceration. Because of associated vitreous hemorrhage, it is rare to identify a retinal laceration during primary repair. Cryopexy should not be performed prophylactically unless a specific retinal tear can be visualized, since cryotherapy may cause excessive inflammation that may promote the development of later traction retinal detachment.[71]

In cases of lacerations involving both the cornea and sclera, the extent of the laceration must be determined first. To restore structural integrity, the limbus is the best place to start, as it provides a recognizable anatomic landmark. Limbal wounds are closed using 9–0 nylon sutures (Fig. 114.12). After the limbal portion of the laceration is closed, it is easier to repair the corneal laceration first, then the scleral laceration. The same techniques and principles described for lacerations limited to the cornea or sclera should be employed.

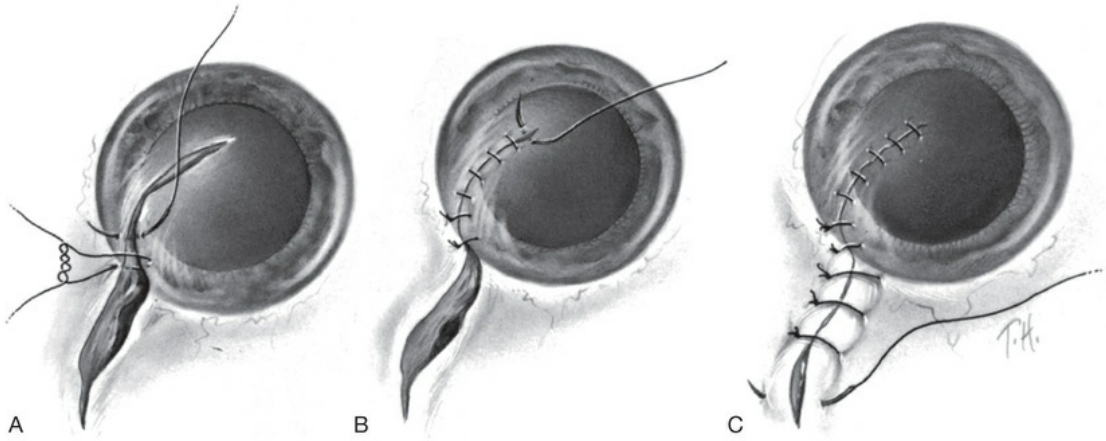

FIG. 114.12 Repair of a complex corneoscleral laceration begins with exploration of the globe to determine the extent of the injury. (A) The limbus is then reapproximated with 9–0 nylon sutures. (B) The corneal laceration is then repaired with 10–0 nylon sutures. (C) Subsequently, the scleral portion is sutured with nonabsorbable interrupted sutures.

In some cases, a hyphema or cataract is identified at the time of laceration repair. Because of the possibility of causing additional damage to the eye by attempting significant intraocular manipulations at the time of primary repair, we generally advocate deferring the anterior chamber washout or lensectomy to a secondary procedure. These issues are discussed in greater detail below.

The value of scleral buckling at the time of primary open-globe repair has been examined by several retrospective studies.[72–74] The justification for prophylactic scleral buckling (typically only considered in eyes with lacerations extending >5 mm posterior to

the limbus) is that support of the vitreous base may reduce vitreoretinal traction and subsequent retinal tears or detachment, which occurs in up to two-thirds of cases.[75] Placement of a buckling element at the time of primary repair is easier because the rectus muscles are often already isolated during exploration of the open globe, and there is no scarring of the wound, Tenon fascia, or conjunctiva. A matched cohort study from two US institutions[73] and a recent retrospective case–control study of 38 patients in Israel[74] have addressed this question. According to these studies, as with our experience, in selected high-risk eyes treated with scleral buckling at the time of globe repair, there was a significantly lower rate of proliferative vitreoretinopathy and a trend toward a lower incidence of later retinal detachment.

Management of Intraocular Foreign Body

Conventional wisdom has held that an IOFB be removed at the time of repair of the entry site or soon afterward. This recommendation was based on several concerns: (1) because of the inflammation caused by IOFBs, they often are rapidly surrounded by a fibrous capsule that can make delayed surgical removal more difficult; (2) metallic foreign bodies containing copper or iron may cause inflammatory damage to intraocular structures; (3) traumatic endophthalmitis, particularly associated with the *Bacillus cereus*, is more commonly seen with IOFBs than with other forms of penetrating injuries,[76] and IOFB removal within 24 hours of injury has been advocated because of the increased risk of endophthalmitis.[76,77] In these series, however, it was not clear that systemic antibiotics were administered.

On the other hand, in certain cases, IOFB removal must be delayed because of inaccessibility to appropriate specialized resources, surgeon inexperience with foreign body removal, or because of systemic medical instability. In a recent report of military soldiers sustaining ocular trauma with IOFB, none of 79 eyes developed endophthalmitis despite a median delay of 38 days in IOFB removal. Since 97% of patients received antibiotics (most commonly by systemic administration, and most commonly levofloxacin), the authors contended that prompt antibiotic use was

helpful in reducing the chance of endophthalmitis.[78] It is reasonable, therefore, to consider for some patients that IOFB removal be intentionally delayed, especially in cases without access to adequate equipment or personnel at the time of primary repair. Such a paradigm of deliberately staged procedures may be considered in patients presenting immediately after injury with no signs of endophthalmitis, in whom appropriate systemic and/or intravitreal antibiotics can be administered, and in whom compliance and timely follow-up are assured. In cases involving an IOFB, it helps to determine preoperatively whether the object is magnetic. If it is not known whether the IOFB is magnetic, the surgeon may attempt to extract the foreign body with the magnet. If the foreign body does not move when the magnet is turned on, an alternative approach must be used.

Three instruments are commonly available for IOFB extraction: external magnets, intraocular forceps, and intraocular magnets. External magnets are best reserved for cases in which extraction can be performed immediately (success rates fall when the IOFB becomes encapsulated[79]) and when there is good fundus visualization with minimal associated posterior segment injury. (In a study of eyes with comparable damage, significantly better anatomic and functional results were achieved in eyes managed with vitrectomy and intraocular magnet.[80])

Our surgical approach to IOFBs is summarized in Table 114.2. When a magnetic intravitreal foreign body can be well visualized, extraction with an external electromagnet is usually effective (Fig. 114.13). This should be done through a pars plana sclerotomy after repair of the entry site. It is important to make the sclerotomy large enough so that the foreign body can pass out of the globe without becoming incarcerated in the pars plana. If the scleral laceration site is used for extraction, then it should be enlarged, since the elastic sclera and ocular tissues will have stretched after initial IOFB entry and made the wound smaller than the longest dimension of the IOFB. A magnetic extraction is best performed with an assistant holding the magnet over the sclerotomy while the surgeon visualizes the IOFB with indirect ophthalmoscopy and controls the magnet's foot pedal. If a large sclerotomy is needed, it is helpful to pre-place a mattress suture so that it can be closed quickly after

removal of the IOFB to decrease the period of hypotony. We do not advocate prophylactic cryopexy or scleral buckle in these patients.

TABLE 114.2
Management of Intraocular Foreign Bodies

	Well Visualized	Poorly Visualized
INTRAVITREAL		
Magnetic	External magnet	Vitrectomy, forceps/REM
Nonmagnetic	Vitrectomy/forceps	Vitrectomy/forceps
INTRARETINAL		
Magnetic	Transscleral trapdoor or vitrectomy, forceps/REM	Vitrectomy, forceps/REM
Nonmagnetic	Transscleral trapdoor or vitrectomy, forceps	Vitrectomy/forceps

REM, rare earth magnet.

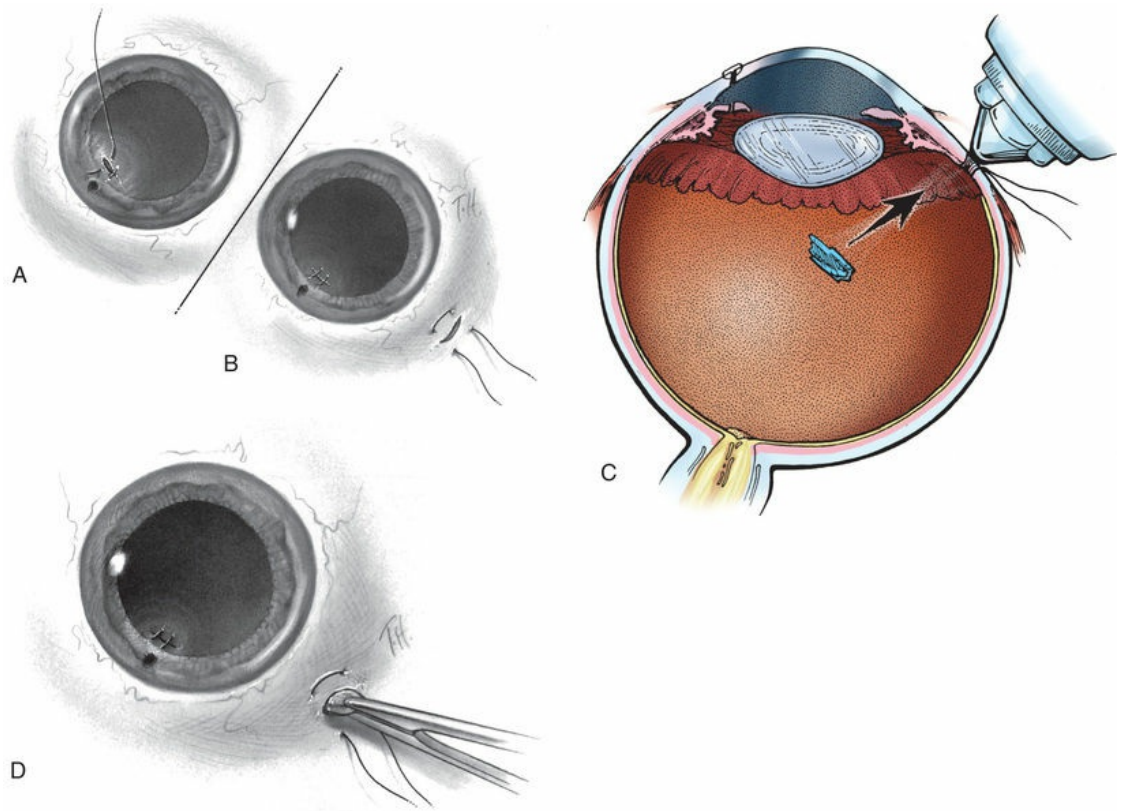

FIG. 114.13 Management of magnetic intravitreal foreign body. (A) Suturing of entry site. (B) Creation of a pars plana sclerotomy with a preplaced mattress suture. (C) The external magnet is held over the sclerotomy while the surgeon visualizes the foreign body with indirect ophthalmoscopy and controls the magnet's foot pedal. (D) Occasionally, the foreign body

must be grasped at the sclerotomy site with a forceps and pulled out.

When the magnetic intravitreal foreign body is poorly visualized because of cataract or vitreous hemorrhage, one must perform a pars plana vitrectomy and/or lensectomy (Fig. 114.14). The foreign body can then be removed by a number of techniques. The IOFB can be removed with greatest control using IOFB forceps inserted through the pars plana sclerotomy or with the rare earth intraocular magnet. If the intraocular magnet is used to grasp the foreign body and bring it into the anterior vitreous, it often helps to transfer the IOFB to foreign body forceps to pull it through the sclerotomy.

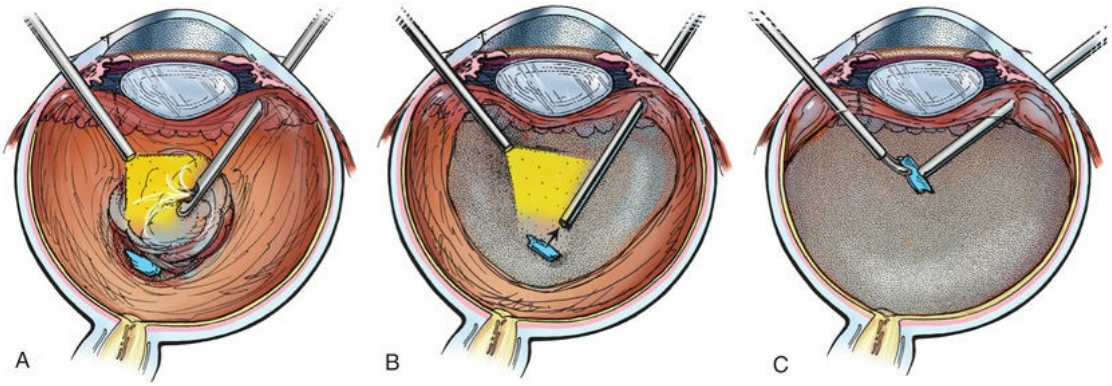

FIG. 114.14 Management of magnetic intraocular foreign body in the presence of vitreous hemorrhage. (A) A pars plana vitrectomy is performed to remove the vitreous hemorrhage in order to visualize and mobilize the foreign body. (B) The foreign body is grasped with the intraocular rare earth magnet and brought into the anterior vitreous. (C) The foreign body is transferred to a foreign body forceps and removed through a sclerotomy.

The surgeon must have the foreign body grasped firmly when removing it through the sclerotomy. If the foreign body is dropped, it will likely strike the macula. Injection of liquid perfluorocarbon has been recommended as a means to protect the macula in this setting. However, experimental studies suggest that these heavier-than-water agents will not support a metallic foreign body.

Removal of intraretinal foreign bodies is more difficult and more hazardous because of the risk of retinal detachment (Fig. 114.15). If

the ocular media are clear and the IOFB can be localized by indirect ophthalmoscopy, it can be removed by a transscleral approach (Fig. 114.16). A trapdoor scleral flap is created, the choroidal bed is treated with external diathermy, the choroid is incised, and the foreign body is removed with either forceps or an external magnet. If retinal incarceration occurs, then scleral buckling should be performed. The choice of buckling element is determined by the extent and location of vitreoretinal traction. For example, if a vitrectomy has been performed and all traction in the transvitreal vector has been relieved, then a localized segmental element over the area of incarceration is sufficient. If transvitreal traction has not been sufficiently eliminated, then an encircling element should be placed in order to reduce traction that may develop on the retina diametrically opposite the site of incarceration. Because the surrounding area has already been treated with diathermy, it is unnecessary to add cryopexy.

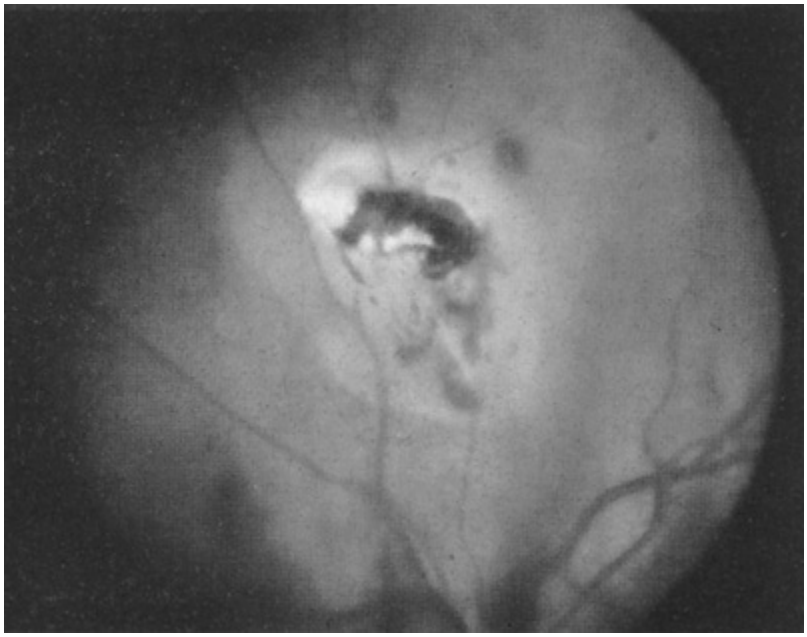

FIG. 114.15 This patient was striking a chisel with a hammer when he suffered a penetrating ocular injury. The metallic intraocular foreign body is located within the retina. Inflammatory retinal whitening developed within 6 hours of the injury.

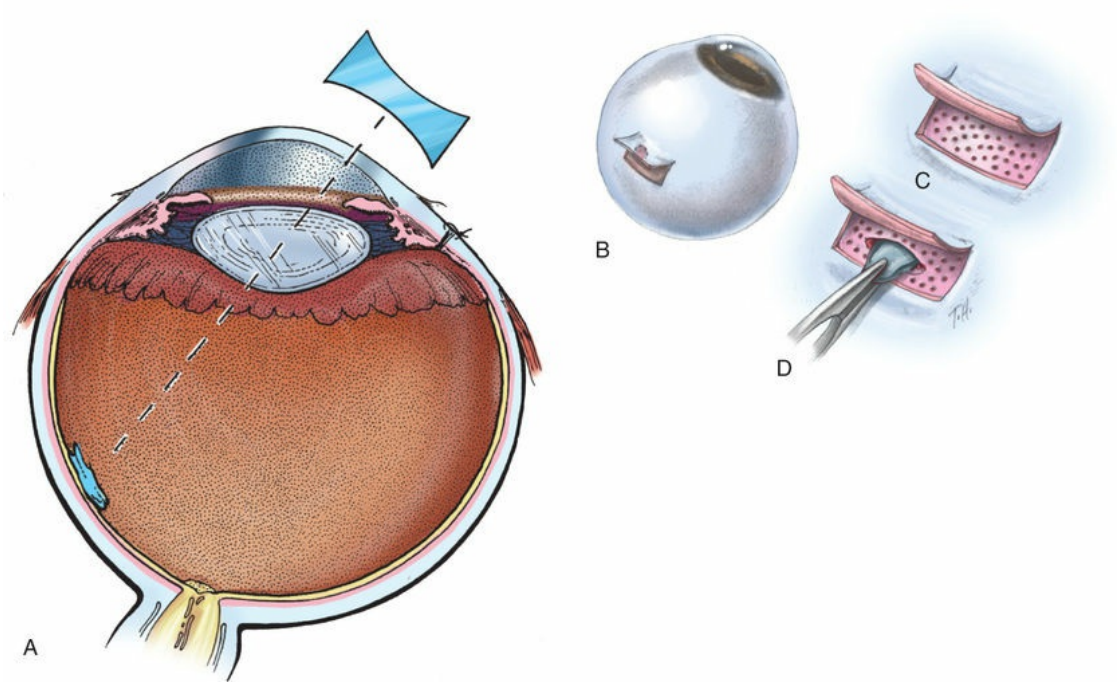

FIG. 114.16 Transscleral approach to intraretinal foreign bodies. (A) The foreign body is localized with indirect ophthalmoscopy. (B) A trapdoor scleral flap is created. (C) The choroidal bed is treated with external diathermy and the choroid incised. (D) The foreign body is removed with either forceps or an external magnet.

Intraretinal foreign bodies can also be removed via a transvitreal approach, particularly when they cannot be well visualized (Fig. 114.17). After a pars plana vitrectomy is performed, the foreign body should be gently mobilized with the foreign body forceps. In many cases the foreign body will be somewhat adherent to the retina or choroid. If the IOFB has been surrounded by a fibrous capsule, the capsule may be incised with a myringotomy blade before removal. All these manipulations are made to avoid further tearing of the retina. After the IOFB is freed, it can then be removed with either the forceps or intraocular magnet using the method described above.

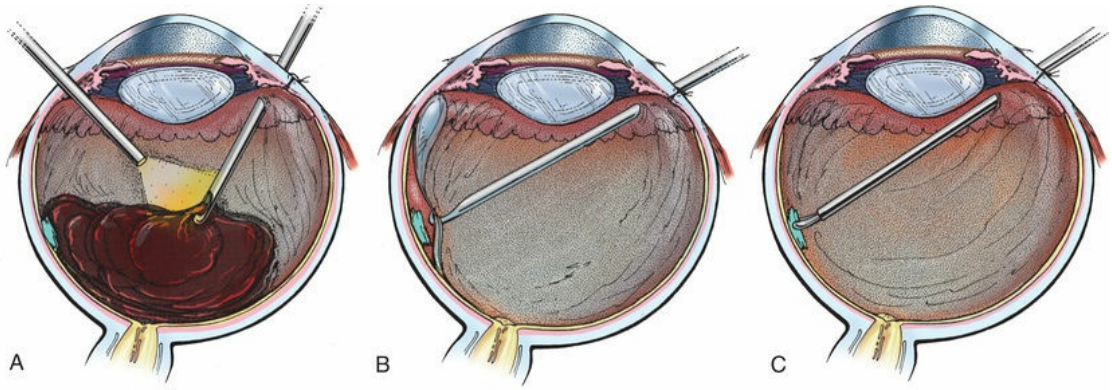

FIG. 114.17 Management of an intraretinal foreign body in the presence of vitreous hemorrhage. (A) A pars plana vitrectomy is performed removing vitreous blood. (B) If a posterior vitreous detachment is not present, one is created by gently aspirating the posterior hyaloid with suction or a vitreoretinal pick. (C) The foreign body is grasped with the foreign body forceps and removed from the eye.

When it is necessary to perform a vitrectomy to remove an intraretinal foreign body, it is important to remove the posterior hyaloid overlying the incarceration site. In some cases a PVD will be present; otherwise one must be created. Residual posterior hyaloid may lead to the postoperative development of vitreoretinal traction or formation of epiretinal membrane (Fig. 114.18). In an early report describing the use of pars plana surgical techniques for removal of intraretinal foreign bodies, 90% of eyes developed either macular pucker or proliferative vitreoretinopathy.[81] The authors believe the frequency of this complication can be decreased by careful attention to removal of the posterior hyaloid. In a more recent series of 34 eyes undergoing vitrectomy for removal of intraretinal foreign body, macular pucker and/or scarring developed in one-fourth of eyes and sclerotomy-associated retinal breaks were seen in one-third. Postoperative visual acuity was 20/200 or better in two-thirds of eyes and was unrelated to the size, shape, or type of foreign body.[82]

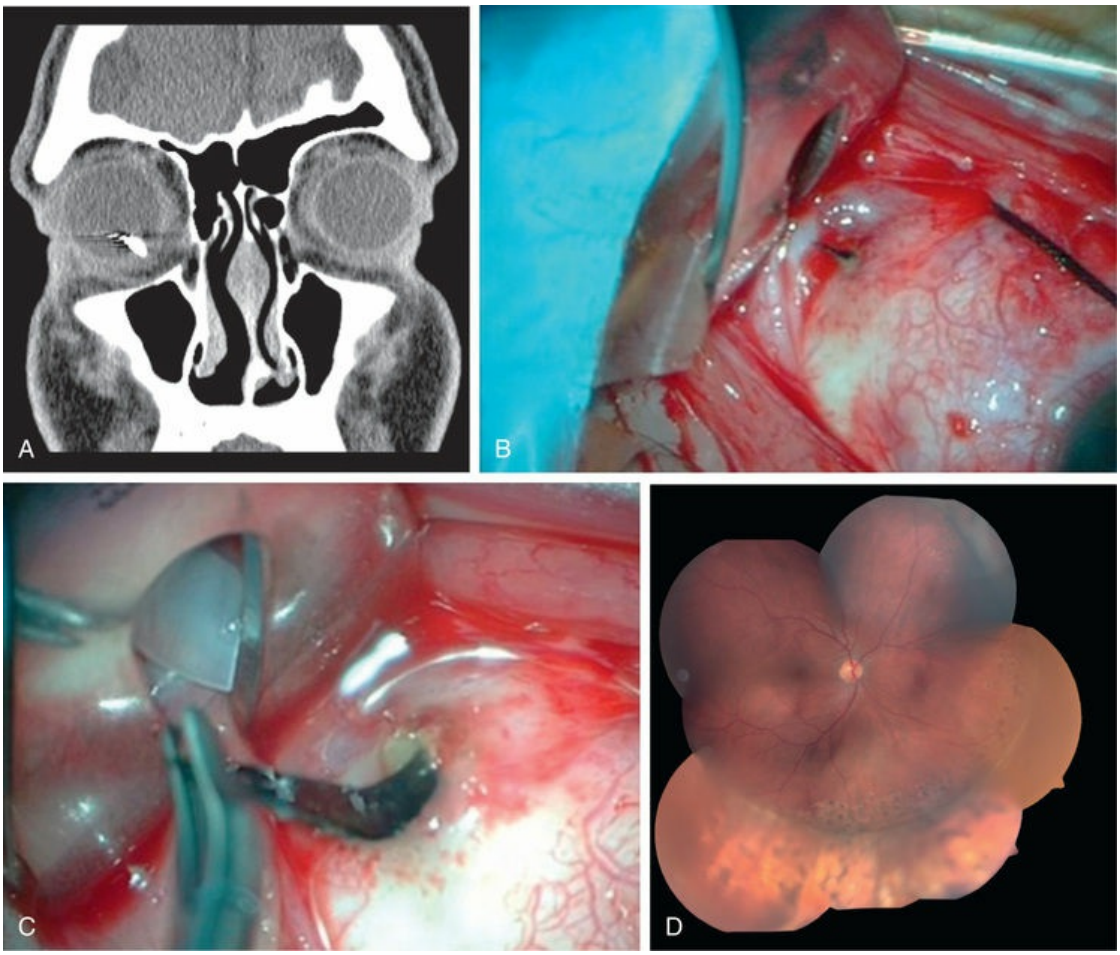

FIG. 114.18 This 19-year-old man suffered a penetrating injury from hammering metal. A metallic intraocular foreign body was lodged in the inferior sclera (A). Following placement of an encircling band, the foreign body was extracted from the exit wound (B,C), which was then closed and supported by the scleral buckle. Vitrectomy, endolaser photocoagulation, and silicone oil infusion were then performed to repair the inferior retinal detachment. Postoperative photograph taken 3 months later following removal of silicone oil shows retinal reattachment and the old exit wound inferiorly (D).

There has also been controversy over the optimal management of a retinal tear caused by the foreign body. Some surgeons emphasize the necessity of creating a chorioretinal adhesion at this site with either cryopexy or photocoagulation. In our experience the inflammation caused by the foreign body impaction has been adequate to prevent retinal detachment, particularly if the surgeon pays close attention to proper management of the posterior hyaloid.

There has also been discussion of the need to place photocoagulation around the intraretinal foreign body preoperatively to decrease the risk of retinal detachment at the time of foreign body removal. Again, it has been our experience that this is unnecessary. Ambler and Meyers[83] reported five eyes with intraretinal foreign bodies managed without retinopexy or fluid–air exchange without developing retinal detachment or preretinal fibrosis. If, however, a retinal detachment does occur at the time of extraction, it is particularly important to attempt removal of adherent posterior cortical vitreous before fluid–gas exchange to reattach the retina. In these cases, endophotocoagulation should be placed around the retinal break. If the surgeon is unable to remove all adherent vitreous, then the retinal tear should be supported on a scleral buckle. We perform prophylactic encircling scleral buckles in all eyes receiving vitrectomy for management of penetrating injuries, as discussed later in this chapter.

Nonmagnetic intravitreal foreign bodies require extraction with intraocular forceps whether they are well visualized or partially hidden by vitreous hemorrhage or cataract.[84,85] In these cases, we perform a vitrectomy with or without a lensectomy, depending on the lens clarity. The foreign body is grasped with the IOFB forceps and removed through the pars plana sclerotomy site. Inert nonmagnetic foreign bodies such as glass or plastic can be observed without immediate removal. However, since it is difficult to know whether they are infected, we advocate treatment with systemic antibiotics prior to IOFB removal.

Extremely large foreign bodies can pose great difficulty for the surgeon attempting removal via a pars plana approach. The foreign body forceps designed to pass through the 20G or 19G sclerotomy sites is unable to grasp large IOFBs, such as BB gun pellets. When they can be grasped, they are too large to be removed through the sclerotomy and must be removed through a second incision created at the limbus. When one suspects that a foreign body cannot be removed by way of pars plana surgery, a scleral tunnel, a limbal opening, or even an open-sky approach should be considered. In many of these cases, there is severe corneal damage with a stellate laceration that makes visualization of the posterior structures difficult. By removing a corneal button and performing an open-sky

vitrectomy, one can identify and remove the foreign body.

Intralenticular foreign bodies usually must be removed in concert with lens extraction. However, if the anterior capsule tear is small and the foreign body is composed of a nontoxic material, the capsular wound may fibrose, resulting in a localized, visually insignificant cataract that can be observed.[86] If cataract formation has occurred, or if the object is metallic, then lens and foreign body extraction should be performed using standard extracapsular cataract extraction methods. We also recommend lensectomy for small capsular defects when endophthalmitis is suspected or if the foreign body was dirty (e.g., rural trauma).

Overall, patients with IOFBs can have an excellent outcome, with approximately one-half of eyes achieving visual acuity of 20/50 or better.[87] Worse outcomes are typically associated with IOFBs of greater mass, uveal prolapse, and injury with a BB or other pellet.[88,89]

Perforating Injury

Perforating injuries represent a small subset of ocular trauma, occurring in only 4.4% of lacerated globes.[90] Until the introduction of vitreoretinal surgery, these eyes had a uniformly poor prognosis because of ingrowth of fibrovascular tissue through the posterior exit site, leading to severe retinal detachment. Our current management of this type of injury is guided by experimental studies of Topping et al.[91] Scleral wounds had self-sealed by day 7 following injury, after which the degree of transvitreal proliferation (and subsequent risk of traction retinal detachment) increased dramatically.

Ideally, vitrectomy would be performed early enough to prevent transvitreal proliferation,[92] but it is impossible unless the scleral rupture sites are sealed. The entry site can be repaired by the surgeon using standard techniques described earlier in this chapter. However, attempts to close posterior rupture sites can be difficult, as well as hazardous, causing excessive traction on the globe and optic nerve and possibly leading to extrusion of intraocular contents. Having learned from the experimental studies that the scleral wounds seal by day 7, we routinely delay vitrectomy until

this time or later. We do advocate suturing the anterior “entry site” promptly after injury (see Chapter 102, Pathophysiology of ocular trauma).

We employ the standard three-port technique for vitrectomy, proceeding from anterior to posterior, clearing vitreous opacities (Fig. 114.19). As in vitrectomies for penetrating injuries, it is important to identify the posterior hyaloid and, if it is still adherent to the retina, create a PVD. The stump of proliferation growing through the exit site should be reduced but not eliminated, so that the posterior exit site is not reopened. When planning surgery and choosing one's vitrectomy setup, the surgeon should remember that this fibrovascular ingrowth can often be exceedingly thick and difficult to cut with smaller-gauge vitreous cutters. Thus, in the eventuality that fibrous ingrowth may be encountered, the surgeon is well served to have access to a cutter or scissors strong enough to transect and trim stiff fibrous tissue. Retinal breaks are managed with air–fluid exchange and endophotocoagulation or scleral buckling with cryopexy. We advocate an encircling scleral buckle, even in eyes without retinal detachment.

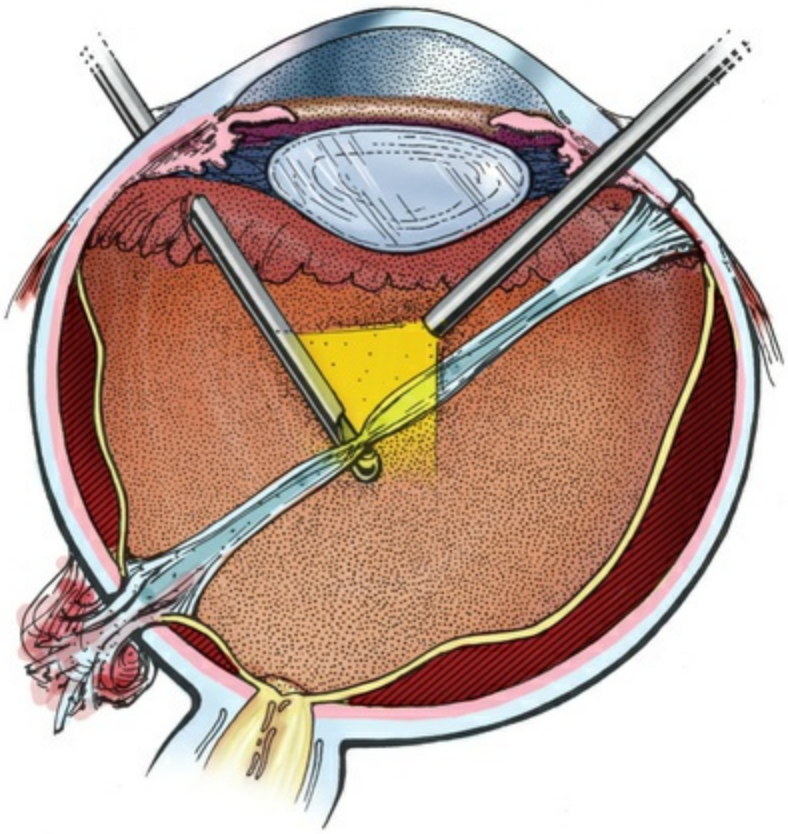

FIG. 114.19 Perforating injuries are managed with primary repair of the entry site. At 7–10 days later, pars plana vitrectomy is performed with removal of the posterior hyaloid. The proliferation growing through the exit site should be reduced to a stump but not eliminated.

Overall, the prognosis for these eyes appears to be improved by this management (Fig. 114.20). In a case–control study of penetrating injuries, a beneficial trend was demonstrated for those eyes managed with vitrectomy.[93] Martin et al.[94] achieved anatomic success in 41 of 51 eyes, with functional success (visual acuity better than 5/200) in 32 eyes (63%). The location of the exit site has profound influence on the final visual acuity. If the exit site is through the macula or optic nerve, the final vision is obviously limited. The location of the exit site also affects the success of hyaloid removal. Complete removal is more easily achieved when the exit site is located posterior to the vitreous base.

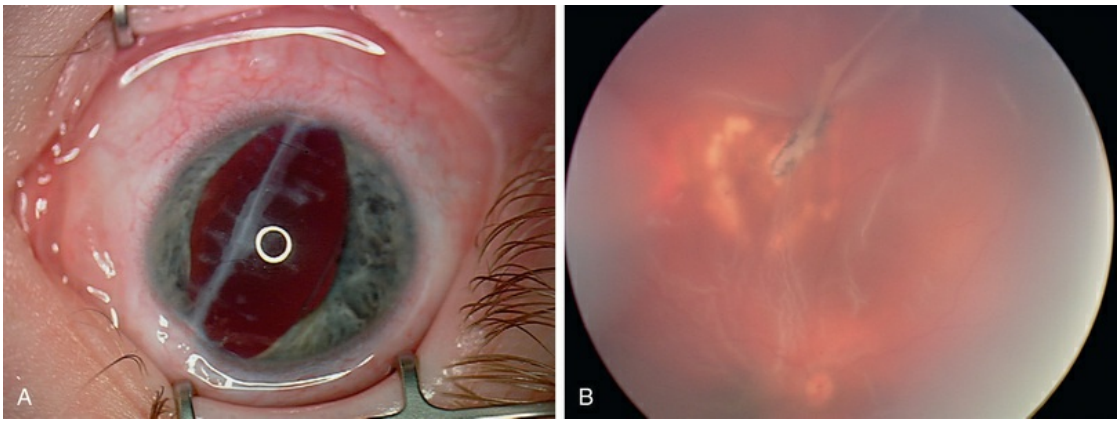

FIG. 114.20 This child suffered a perforating injury with a whittling knife. Following emergent repair of the corneal laceration (A), lensectomy and vitrectomy were subsequently performed. He returned 2 months later with (B) traction retinal detachment associated with fibrous ingrowth at the exit site.

More recently, it has been demonstrated that chorioretinectomy (removal of the choroid and/or retina at the impact or perforation site) may improve final visual acuity and increase the chance of globe salvage.[95] In this technique, first advanced by Zivojnovic nearly three decades ago,[96] any retinal or uveal tissue incarcerated into the perforation site is removed with the vitrector, with diathermy destruction of the retina/choroid in a 1-mm ring around the exit wound/impact site. High cutting speeds (up to 7500 cpm) with low vacuum are typically used. Bleeding, though uncommon from necrotic incarcerated tissue, is controlled with endodiathermy or transient elevation of infusion pressure. In a small pilot series of such a "proactive technique" reported by Kuhn et al. in 2004, chorioretinectomy was performed in five consecutive eyes within 100 hours of perforating globe injury. Their strategy involved limited vitrectomy (performed while looking through the binocular indirect ophthalmoscope) at the time of primary repair, intensive topical corticosteroid therapy, and followed 3 days later by complete vitrectomy, localized retinectomy, evacuation of subretinal blood, laser retinopexy, and placement of silicone oil.[97] Two retrospective series comparing eyes with perforating injury treated with early vitrectomy and chorioretinectomy and those treated with later vitrectomy alone have since been reported.[98,99] In eyes treated with chorioretinectomy, higher rates of globe survival

and retinal reattachment and lower rates of proliferative vitreoretinopathy were observed. This technique should only be considered, however, by surgeons with the requisite experience and in cases with adequate visualization of the posterior segment and confirmation that there is minimal retinal or choroidal detachment.

Vitreous Hemorrhage and Retinal Detachment

Despite advances in the management of eyes with penetrating injuries, a large group of patients still have a poor prognosis. These more severe injuries most often have posterior segment involvement. A seminal study evaluating the outcome of penetrating ocular injuries identified several factors other than initial visual acuity that correlate with a poor final visual outcome. These include presence of an afferent pupillary defect, wounds involving the sclera or extending posterior to the insertion of rectus muscles, wounds >10 mm, and vitreous hemorrhage.[55] The study emphasized that the prognosis following penetrating injury is strongly influenced by the nature of the injury and the location and extent of initial damage. Functional loss of these eyes is caused by either inoperable retinal detachment or damage to ciliary body function, arising from intravitreal fibrovascular and fibroglial proliferation. This proliferation seems to occur more commonly in injuries with lacerations of the ciliary body and retina and in injuries with vitreous hemorrhage. These initial conclusions were corroborated in a prospective observational study of 69 eyes with penetrating injury.[57]

In a study of retinal detachment following open-globe injury, Stryjeski et al. reported the clinical course of 893 cases of open-globe injury repaired emergently at the Massachusetts Eye and Ear Infirmary. The overall incidence of retinal detachment in this cohort was 29%. Of these, roughly one-fourth were identified within 24 hours of injury, roughly one-half were identified within one week of injury, and roughly three-fourths were identified within one month of injury.[100] (In most cases, especially within the first week, the diagnosis was made by ultrasonography.) By multivariable regression analysis, the factors associated with occurrence of retinal

detachment (at any timepoint) were poorer visual acuity at presentation following injury, higher zone of injury, and presence of vitreous hemorrhage. The authors constructed a useful model (the RD-OGI, or Retinal Detachment after Open Globe Injury, score) that incorporates these three clinical variables to estimate the probability of retinal detachment.[100]

The importance of vitreous hemorrhage in the pathophysiology of retinal detachment following penetrating ocular injury has been recognized for decades. Additionally, early case series suggested the efficacy of vitreous surgery in management of severe penetrating ocular injury.[101–103] Vitrectomy for penetrating ocular trauma was first advocated by Coles and Haik[104] in 1972 when, on examining several eyes enucleated after trauma, they noted fibroblastic tissue in areas of vitreous hemorrhage within several hours of injury. Beginning in 1979, Cleary and Ryan[105] published a series of papers in which they described an experimental model for penetrating ocular injury with vitreous hemorrhage. Invariably, a traction retinal detachment resulted. In subsequent animal studies, they demonstrated that vitrectomy performed 1–14 days after injury could significantly reduce the risk of traction retinal detachment.[106] These elegant translational studies support collective clinical impressions that vitrectomy may reduce the incidence of severe visual loss after penetrating injuries by removing the scaffold for intraocular fibrocellular proliferation and by lowering circulating levels of profibrotic chemokines.

Vitreous surgery should be performed in all eyes with light perception vision, lacerations involving the sclera, and moderate to severe vitreous hemorrhage. Growing clinical experience also supports the utility of secondary vitreoretinal surgery in eyes with no light perception at presentation. In several series of such patients treated with vitreoretinal surgery (typically performed after the initial repair), light perception was restored in 23–83% of patients and visual acuity of 20/200 or better was attained in 7%. By contrast, eyes in which secondary vitrectomy was deferred almost uniformly progressed to phthisis or enucleation.[62,63,107–109] In eyes undergoing secondary vitrectomy, favorable outcome (i.e., an anatomically restored eye with at least light perception) was associated with recovery of light perception after initial globe repair and vitrectomy

within 14 days of initial repair. Eyes with unfavorable outcome (NLP, phthisis, enucleation) were more likely to have sustained globe rupture (rather than laceration), zone III injury, ciliary body damage, choroidal detachment, and/or closed funnel retinal detachment.[107,108]

While there may be general consensus on the indications for vitrectomy in patients with penetrating injuries, the appropriate timing of vitrectomy has not been clarified.[110] Some experienced surgeons favor operating within the first 48–72 hours, and others prefer delaying surgery up to 14 days after injury.

Advantages of earlier intervention include prompt visualization of the fundus and immediate retinal surgery when indicated; reduction in complications related to vitreous incarceration in the laceration; and eliminating the need for a second operation by combining vitrectomy with primary repair.

Delaying vitreous surgery beyond 72 hours after the injury permits further diagnostic evaluation, including ultrasonography and electrophysiology, which may assist the surgeon in determining prognosis, counseling the patient about realistic expectations, and formulating a surgical plan. It also permits the operation to be performed under conditions more favorable than emergency circumstances. Furthermore, excision of the posterior cortical vitreous (a critical step in the vitrectomy) may be easier when vitrectomy has been delayed.

In addition, there is a concern of severe hemorrhage when attempting early vitrectomy, presumably secondary to uveal congestion associated with acute injury. Hemorrhagic choroidal detachment can cause extreme difficulty with insertion of an infusion cannula or other vitrectomy instruments without damaging the retina. Delaying surgery may decrease the risk of uncontrollable intraoperative hemorrhage, as well as allow choroidal hemorrhage to recede or to be drained more easily.

Most authors agree, however, that vitrectomy for severe penetrating injuries should not be delayed beyond 14 days.[103] First, if the vitrectomy is unsuccessful, these eyes may be at risk for developing sympathetic ophthalmia and require enucleation to prevent its development. The risk of sympathetic ophthalmia may be reduced if enucleation is performed within 14 days of injury.

Second, histologic studies of penetrating eye injuries show intraocular cellular proliferation within 1 week of injury with membrane formation already occurring by 2 weeks.[111]

Once the decision has been made to perform a vitrectomy, the surgeon has the following goals: (1) to clear the ocular media through removal of cataractous lens or vitreous hemorrhage; (2) to remove the vitreous scaffold from the scleral laceration site; (3) to remove the posterior hyaloid that could provide a future scaffold for epiretinal membrane formation and vitreoretinal traction; and (4) to identify and treat retinal breaks and detachment.

In most cases, general anesthesia with endotracheal intubation is employed for vitrectomy following trauma. Peribulbar or retrobulbar anesthesia has the risk of increasing orbital pressure leading to extrusion of intraocular contents, but has been used successfully in selected patients, typically those with short corneal or limbal wounds and a formed anterior chamber.[112] Historically, succinylcholine chloride has been avoided during induction. However, in an experimental study, succinylcholine administration resulted only in forward displacement of the iris and lens without extrusion of intraocular contents, suggesting that some of the historical fears of its use may be unwarranted.[113] In most cases, the wound will have been closed prior to vitrectomy, but the globe should still be inspected, with open or leaking wounds resutured to make the eye watertight.

At the onset of surgery, the surgeon must make several critical decisions that can profoundly influence the success of the procedure. First, the presence or absence of hemorrhagic choroidal detachment must be determined. This is best done by preoperative ultrasonography. If present, the blood can often be drained through scleral incisions while simultaneously infusing air or balanced salt solution into the eye. Infusion maintains normal IOP and can be done through a cannula or short needle inserted either through the limbus (in aphakic eyes) or through the pars plana (in phakic eyes) (Fig. 114.21). After drainage of the choroidal hemorrhage, a long pars plana infusion cannula (6 mm) may be inserted, but infusion should not be turned on until the cannula tip can be visualized in the vitreous cavity.

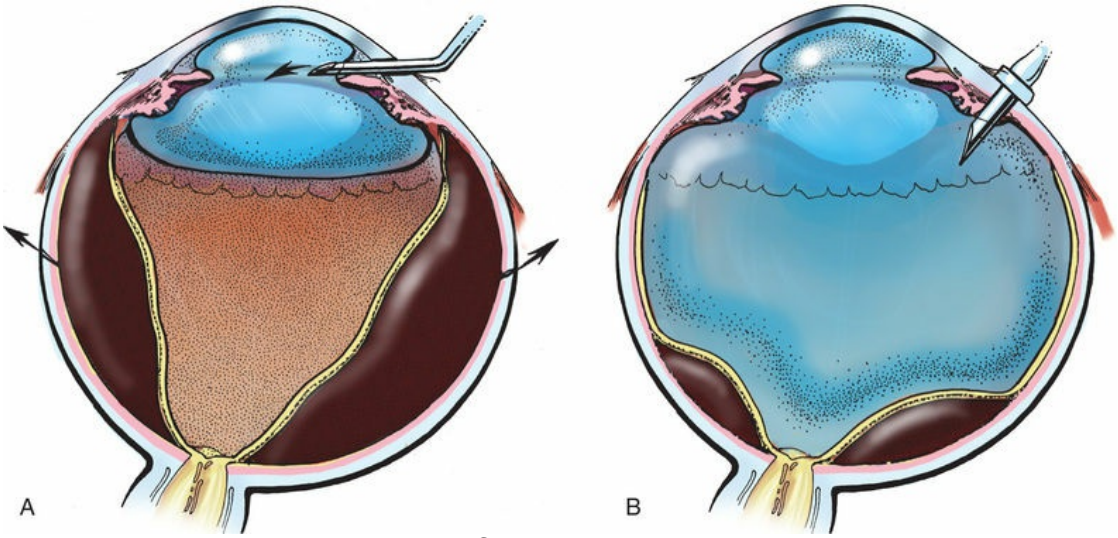

FIG. 114.21 Vitrectomy for vitreous hemorrhage with hemorrhagic choroidal detachment after penetrating injury. (A) Scleral cutdown incisions are made to drain choroidal blood while air is infused into the eye through a cannula inserted through the limbus. (B) After drainage, a 6 mm pars plana infusion cannula is inserted and infusion started only when the cannula can be visualized within the vitreous cavity.

Second, the surgeon must decide whether surgery can begin through the pars plana or whether it must be started through limbal incisions. For instance, in the presence of total hyphema, where the status of the retina is unknown, the hyphema can be evacuated through a limbal incision with an irrigating infusion needle inserted through a second incision (Fig. 114.22). The same problem can be managed in aphakic eyes by inserting a long irrigating infusion needle through a pars plana incision and into the anterior chamber where it can be visualized and then turned on. Similarly, the vitrectomy instrument can be inserted through a pars plana sclerotomy and brought anteriorly to evacuate the hyphema. It is essential that all sclerotomies be deep enough to ensure penetration through the uveal tissue into the vitreous cavity. Recent improvements in the stiffness of smaller gauge (23G and 25G) vitrectomy instrumentation, and the accompanying expansion of available instrumentation, allow the surgeon to use these systems successfully in the treatment of traumatized eyes. One must be cognizant, however, that in the preparation of sclerotomies, the insertion of a 25G trocar imparts significantly more force on the

globe than a 20G blade. The correspondingly high IOP may cause leakage of freshly sutured rupture sites. To avoid the potential for leakage or hypotony, therefore, one can use a 25G MVR blade to create the initial sclerotomy prior to placing the small-gauge cannula or inserting instruments.

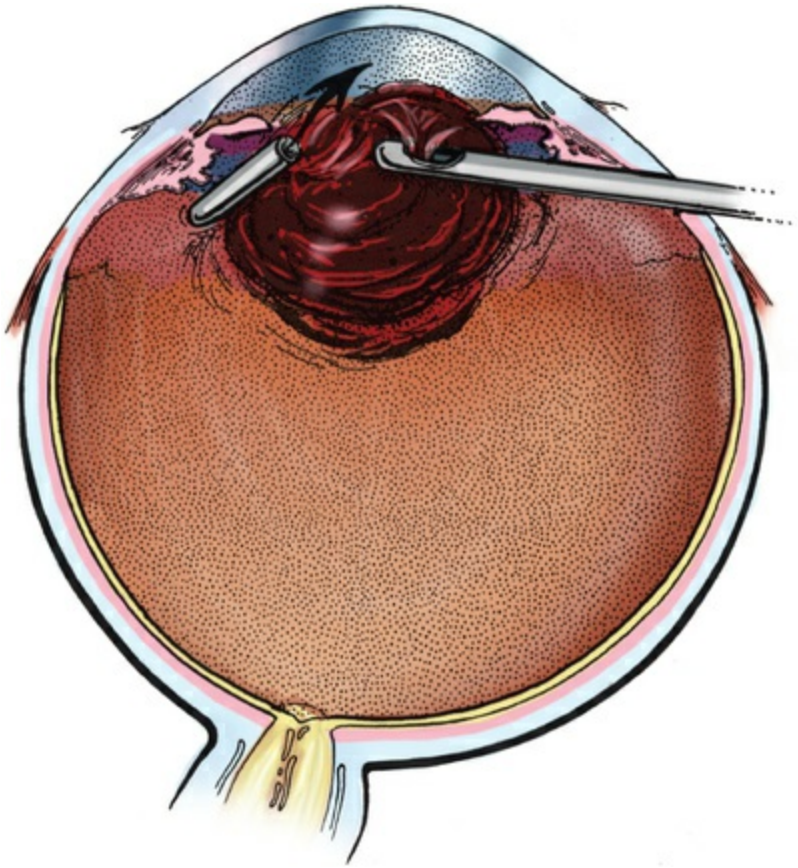

FIG. 114.22 When anterior chamber hemorrhage precludes visualization of the infusion cannula at the beginning of a vitrectomy for vitreous hemorrhage after penetrating injury, a blunt 20G infusion needle can be inserted through the pars plana, maneuvered into the anterior chamber where it can be visualized through the cornea, and infusion turned on. The vitrectomy instrument can be brought into the anterior chamber in a similar manner to remove the hyphema and begin the vitrectomy. When the anterior chamber hemorrhage has been cleared to adequately visualize the pars plana infusion cannula, the blunt infusion needle can be removed and replaced with a fiberoptic probe.

Third, a decision must be made on the necessity of lens removal. Often, the lens has been lost at the time of the injury. In other instances, the lens will have become opacified, subluxed, or dislocated and will need to be removed. If the lens interferes with visualization of the posterior segment because of cataract or blood on its anterior or posterior surface, then it must be removed. In cases with cyclitic membranes, transvitreal sheets extending to an anterior injury site or to anterior hyaloid hemorrhage, the lens must be removed to achieve the objectives of the procedure. In most cases the lens is removed through the pars plana using either the vitrectomy probe or an ultrasonic fragmenting device.

After the anterior segment is cleared, the vitrectomy can be performed, proceeding from anterior to posterior. It is critical to remove the posterior cortical vitreous (Fig. 114.23). The peripheral retina is then carefully inspected for retinal tears and detachment. We routinely place a 3.5-mm or 4-mm encircling band to support the vitreous base and decrease the risk of subsequent retinal detachment.

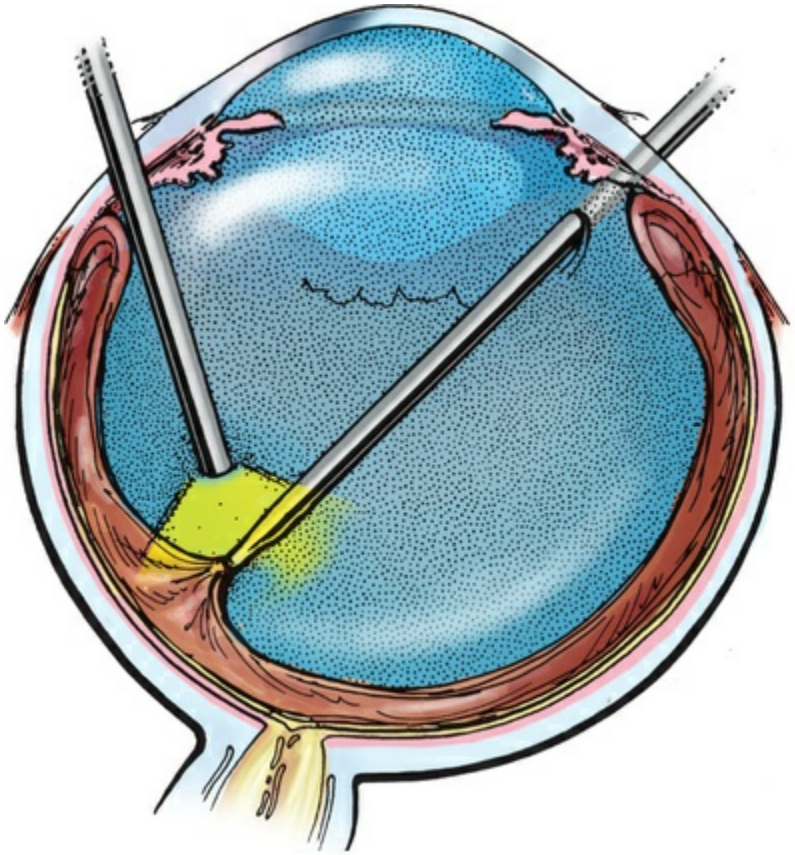

FIG. 114.23 When a vitrectomy is performed for ocular trauma, it is critical to remove the posterior cortical vitreous. When a posterior vitreous detachment is not present, one can be created by either suction, a vitreoretinal pick, or carefully incising the posterior hyaloid with a myringotomy blade and then lifting it with the pick.

When retinal tears are identified, they are treated by endophotocoagulation. Cryopexy should be avoided due to concern about the increased inflammatory response and release of profibrotic cytokines. Placement of a posterior radial scleral buckle is recommended in cases with persistent traction adjacent to a posterior retinal tear.

When retinal detachment is present, it is essential that all tangential and anteroposterior vitreoretinal traction on the retinal break be relieved either by membrane peeling, delamination, or segmentation. If this traction cannot be relieved, it will be necessary to place a scleral buckle of adequate size to alleviate traction or to perform a relaxing retinectomy. Subretinal fluid usually is drained transvitreally during a fluid–gas exchange either through a posterior retinal break or through a posterior retinotomy created in an area free of traction, ideally superonasal to the optic nerve. In some cases, extrusion can be used to flatten the retina by drainage of posterior subretinal fluid through a peripheral retinal break. Long-acting gases, such as sulfur hexafluoride or perfluoropropane, or silicone oil can be injected to provide a longer-lasting internal tamponade.[114]

Retinal incarceration in the scleral laceration site can produce complicated retinal detachments. In many cases this situation can be managed with vitrectomy and scleral buckling, particularly when the incarceration is located anteriorly. However, when the incarceration is more posterior, scleral buckling is more difficult and retinotomy may be necessary. Han et al.[115] reviewed their experience with this problem and recommended retinectomy when a scleral buckle is insufficient to relieve the traction or when the incarceration is located too posteriorly to be treated with a scleral buckle. In the former situation, they performed a circumferential relaxing retinectomy. In the latter situation, they performed

retinotomies circumscribing the retinal incarceration site. Endodiathermy was placed to provide hemostasis before the retinotomy. With these techniques, they achieved anatomic success in 11 of 15 eyes (73%), but only six eyes regained visual acuity of 5/200 or better. Eyes with traumatic retinal detachment associated with retinal incarceration appear to carry a poor prognosis even when managed aggressively.

Intraocular bleeding is a frequent intraoperative hazard of vitrectomy for penetrating injuries and, if massive and uncontrolled, can preclude successful vitrectomy. Intraoperative bleeding can be managed by a number of maneuvers, including raising the infusion pressure to increase the IOP, endodiathermy or endophotocoagulation to areas of active hemorrhage, fluid–air exchange, injection of viscoelastic substance (i.e., sodium hyaluronate), or injection of heavy liquids (i.e., fluorinated hydrocarbons such as perfluoro-n-octane or perfluorodecalin). Control of bleeding by infusion of a thrombin solution at a concentration of 100 U/mL has been reported.[116]

Visualization of the posterior structures must be preserved. When the cornea becomes cloudy because of epithelial edema, the epithelium can be carefully removed with a surgical blade. Folds in Descemet's membrane can be overcome by coating the corneal endothelial surface with sodium hyaluronate.[117] In some cases, visualization through a scarred cornea can be improved with the use of a wide-angle viewing system. In cases in which the cornea is grossly edematous, markedly distorted by a stellate laceration with multiple sutures, or damaged with tissue loss requiring a patch graft, vitreoretinal surgery can be performed with a temporary keratoprosthesis or with endoscopic visualization. The first temporary keratoprosthesis, the Landers–Foulks device, is a clear cylindrical polymethylmethacrylate lens that fits into a trephinated corneal bed and permits excellent visualization of the vitreous and retina without an additional contact lens.[118] Though a great advance, this keratoprosthesis has a concave lens that minimizes the retinal image and a long optical cylinder that obstructs visualization of the anterior retina and vitreous base where much of the significant pathology in traumatized eyes exists. Our preference is the Eckardt temporary keratoprosthesis,[119] which is made of clear

silicone rubber and has normal magnification and a short optical cylinder, allowing visualization for anterior vitreoretinal dissections, as well as posterior segment pathology. In a series of 11 traumatized eyes surgically rehabilitated with the aid of an Eckardt keratoprosthesis, five (45%) obtained a visual acuity of 20/400 or better.[120]

Penetrating keratoplasty (PKP) can be combined with vitrectomy and temporary keratoprosthesis to reconstruct severely traumatized eyes. However, functional outcomes are usually disappointing, often due to graft failure and hypotony from ciliary body dysfunction. In a recent series of 34 eyes managed with combined PKP and vitrectomy, fewer than one-third achieved vision of better than hand motions at any time postoperatively and fewer than 15% of grafts remained clear more than 1 year postoperatively.[121]

An alternative to temporary keratoprosthesis in eyes with impaired visualization due to corneal opacity is endoscopy.[122] This approach may be particularly useful in cases in which a donor graft or corneal surgeon may not be readily available or in cases in which silicone oil placement is planned and there is concern of corneal graft failure. Disadvantages of endoscopy include the need for specialized equipment, mandatory additional surgery for corneal transplantation, and a steep learning curve.

No prospective controlled study has evaluated the efficacy of vitrectomy in penetrating ocular injury. Large series of patients treated with vitrectomy have been published, with the comment that favorable results would not have been possible without vitreoretinal surgical techniques. The frequency of obtaining functional visual acuity of 5/200 or better ranged from 52% to 78%. A 1984 case–control study matched eyes managed with vitrectomy with similar eyes that did not undergo vitrectomy.[93] A trend toward benefit with vitrectomy was demonstrated in severe injuries in which initial visual acuity was worse than 5/200. In a more recent retrospective series of 36 eyes treated with immediate vitrectomy and silicone oil endotamponade for coexisting penetrating injury and retinal detachment, ambulatory vision was achieved postoperatively in 64%. Patients were most likely to attain ambulatory vision if they presented preoperatively with ambulatory vision and without macular detachment.[123]

Endophthalmitis

Endophthalmitis is a potentially devastating complication of penetrating injury. The reported incidence has ranged from 1–16% of penetrating injuries.[124–126] but there has been a steady decline over the past few decades.[127]

Ocular signs associated with traumatic endophthalmitis are similar to those with a postoperative infection: aqueous cell and flare, hypopyon, and vitreous cell and flare exceeding that expected from the injury itself. Aqueous or vitreous fluff balls are characteristic of fungal infections. However, the initial diagnosis of posttraumatic endophthalmitis can be difficult because the considerable postoperative inflammation and pain that commonly occur in these eyes can obscure infectious endophthalmitis. Delay in diagnosis, compounded by the virulent bacteria involved in these cases, makes the prognosis for recovery particularly grim.

In one retrospective investigation, risk factors for endophthalmitis after penetrating ocular trauma were subjected to univariate and multivariate analysis.[128] Factors such as scleral wounds, hyphema, uveal prolapse, retinal detachment, suprachoroidal and vitreous hemorrhage, lens rupture, and IOFB were investigated. Only lens rupture was independently significant for the development of endophthalmitis, carrying a relative risk of infection of 15.8. In a more recent comparative cohort study, patients developing posttraumatic endophthalmitis were ascertained prospectively and compared with historical controls of patients with open-globe injury. Delay in primary repair, ruptured lens capsule, and dirty wound were each independently associated with the development of posttraumatic endophthalmitis.[129] The presence of an IOFB had a relative risk of infection of 1.9, but this did not reach statistical significance. In the National Eye Trauma Study, conducted between 1985 and 1991, there was a statistically significant increased incidence of endophthalmitis for eyes with retained IOFBs, particularly if surgical intervention occurred more than 24 hours after the injury (13.4% versus 3.5%, $p<.0001$).[130,131] One must not infer from this study, however, that prompt IOFB removal is always the preferred treatment, since it was not clear which patients (if any) received prompt systemic antibiotics, and the study was conducted before the widespread availability of antibiotics

with high vitreous penetration.

Three more recent series have reported lower rates of endophthalmitis, and the authors attributed this reduction in part to the systematic use of antibiotics.[78,125,126] In one of these series, intravenous vancomycin (or clindamycin if allergic) and ceftazidime (or a fluoroquinolone if allergic) were administered promptly and continued for at least 48 hours.[125]

While the majority of cases of postoperative endophthalmitis are caused by less virulent coagulase-negative staphylococci (especially in injuries associated with metallic foreign bodies), posttraumatic endophthalmitis is frequently caused by virulent organisms such as *Bacillus*, *Streptococcus*, and Gram-negative organisms.[132] *Bacillus cereus* is most commonly associated with penetrating ocular injuries that occur in rural areas and, while rarely seen in postoperative endophthalmitis, accounts for 25–46% of cases of posttraumatic endophthalmitis.[126] The multiple enzymes and exotoxins elaborated by this organism lead to blindness or enucleation in the vast majority of eyes,[126] although several cases of successful management and retained useful vision have been reported.[133] Gram-negative bacteria are responsible for up to 20% of cases of posttraumatic endophthalmitis.[75] These cases also carry a poor prognosis, with one-third of eyes ending in no light perception or enucleation.[134]

Management of traumatic endophthalmitis parallels that described for postoperative endophthalmitis. Cultures of the aqueous and vitreous are obtained, any retained foreign body is removed, and antibiotic therapy is administered. Cultures should include blood agar, chocolate agar, thioglycolate broth incubated at 37°C for bacteria, and Sabouraud agar incubated at 25°C for fungi. Gram stains should also be obtained and may provide useful information for antibiotic selection. The patient's history of immunization against tetanus should be evaluated, especially in injuries involving contact with soil or rust, and appropriate booster or vaccination should be given.

We recommend antibiotic delivery via systemic, subconjunctival, intraocular, and topical routes. Although the Endophthalmitis Vitrectomy Study (EVS) did not show a benefit to using intravenous ceftazidime or aminoglycosides, it should be noted that

the EVS studied only patients with acute endophthalmitis following cataract extraction or lens exchange.[135] In posttraumatic endophthalmitis, we still consider systemic antibiotic use the standard of care. We prefer a third- or fourth-generation fluoroquinolone (levofloxacin 500–750 mg or moxifloxacin 400 mg daily for 7 days) because of its broad coverage of common pathogens and its excellent vitreous penetration following intravenous or oral administration.

Intraocular antibiotics in cases of suspected endophthalmitis should target a broad range of gram-positive and gram-negative organisms, and intraocular toxicity must be negligible. Vancomycin is active against gram-positive bacteria, is bactericidal, rarely promotes resistance, and is well tolerated by the eye in efficacious dosages (1.0 mg/0.1 mL). Ceftazidime (2.25 mg/0.01 mL) is a β-lactamase third-generation cephalosporin with excellent activity against most gram-negative bacteria and some gram-positive bacteria, including penicillinase-producing *Staphylococcus aureus*. Alternative intraocular antibiotics include clindamycin phosphate (1 mg/0.1 mL) and amikacin (400 μg/0.1 mL).

Prophylactic intraocular injection of antibiotics to prevent endophthalmitis in patients with penetrating injury is controversial. However, when there is high suspicion of injury from a contaminated foreign body, or early signs of endophthalmitis are present (e.g., significant anterior chamber cells, perivascular retinal sheathing), prophylactic treatment with intravitreal antibiotics should be considered. In a prospective study of eyes with penetrating injury, patients were randomized to receive either intraocular injection of antibiotics (40 μg of gentamicin sulfate and 45 μg of clindamycin sulfate) or balanced saline solution. The rate of endophthalmitis within 2 weeks was significantly lower in the group treated with antibiotics (2.3% versus 0.3%), but this difference was driven by the high incidence of infection in eyes with IOFB (28% in the control group versus 0% in the antibiotic group).[136]

Prognostication for cases of traumatic endophthalmitis is difficult because of the compounding effect of the penetrating injury. Prognosis also relates to the specific organism and to the interval to diagnosis. Overall, Brinton et al.[124] reported 42% of cases obtaining

final VA of 20/300 or better and 26% with 20/30 or better. Affeldt et al.[137] reported only 22% of their patients with 20/400 or better. Lieb et al. reported final VA of 20/400 or better in only 50% of open globes with a positive bacterial culture and overt signs of endophthalmitis.[138]

Cataract

Management of cataract after penetrating injury is controversial. Diagnosis of cataract at presentation can be difficult, as fibrin in the anterior chamber almost immediately after the injury can simultaneously obscure visualization of the lens and give the appearance of a cataract. In such settings, we rarely perform a lensectomy at the time of repair of the corneal laceration. In some cases, however, a rent can be identified in the anterior lens capsule accompanying an opacified lens. It is in this situation that cataract extraction at the time of primary repair of the laceration may be considered to reduce the chance of postoperative inflammation and infection.

After deciding to perform a primary lensectomy, the surgeon should first repair the laceration using the techniques and principles described earlier in this chapter. One must then decide whether the cataract extraction can be performed through a limbal incision or via the pars plana. When the laceration is limited to the cornea and the posterior lens capsule is believed to be intact, a limbal incision should be created and lens aspiration or phacoemulsification performed. If, during the course of the surgery, it becomes apparent that the posterior capsule has been damaged, it is critical to manage the vitreous loss properly, making sure there is no vitreous incarcerated in either the laceration site or the limbal incision. Primary placement of an IOL has been shown to be well tolerated in selected cases and does not appear to increase the risk of endophthalmitis or other postoperative complications. However, the IOL power selection may be inaccurate, and the surgeon may misjudge the intactness of the posterior capsule. Echography with a 20-MHz probe has been shown to be highly accurate in assessing the integrity of the posterior lens capsule in eyes with dense traumatic cataract.[139]

In one series, 64% of patients who underwent lensectomy and IOL implantation at the time of primary repair of a penetrating ocular injury obtained 20/40 or better visual acuity.[140] Therefore, if capsular support allows, one can proceed with IOL placement. If too little capsule remains, an anterior chamber IOL, or sutured posterior chamber IOL, should be deferred as a second procedure. Implantation of an IOL in children has also become an accepted means of visual rehabilitation. In children 4–17 years of age, up to 87% of penetrating ocular injuries primarily managed with lens aspiration and IOL implantation obtained 20/40 or better visual acuity.[141] IOL implantation in infants, however, is still controversial and should probably be deferred to a secondary procedure.

Cataract surgery is more easily performed following primary repair. Deferral of surgery permits clearing of fibrin and intraocular inflammation and allows proper determination of the extent of the cataract, position of the lens, capsular integrity, and IOL power.

When cataract surgery is planned, the choice between a limbal or a pars plana approach depends on the extent of zonular support. If the lens is in place with no signs of iridodonesis or phacodonesis, standard cataract surgery through a limbal or clear corneal incision can be performed. If the lens is believed to be dislocated or subluxated, the surgery should be performed through the pars plana with vitrectomy instrumentation as described for cataracts associated with nonpenetrating injuries. Because of the high incidence of damage to anterior chamber angle structures in eyes with penetrating injuries, we routinely do not advocate anterior chamber IOL implantation when pars plana lensectomy has been performed. However, the evolution of techniques for sulcus fixation of posterior chamber IOLs presents a potentially acceptable alternative to contact lens fitting for the aphakic patient.

Late Complications of Penetrating Injury

Despite excellent repair of corneoscleral lacerations and proper vitreoretinal surgery for vitreous hemorrhage, cataract, and other immediate complications of penetrating injuries, a variety of late complications can arise.

Fibrotic membranes result from organization of residual lens

material after a traumatic cataract. In this situation, the material is often quite difficult to cut with the vitrectomy instrument alone (Fig. 114.24). However, after segmentation with a myringotomy blade or scissors, the material may be more easily removed with the vitrectomy probe. When this fails, the segments of tissue can be grasped with intraocular microforceps, cut with microscissors, and removed from the eye through the sclerotomy. If the tissue has become vascularized, it may be necessary to use endodiathermy for hemostasis. With these techniques, a clear pupillary space can be achieved in nearly all cases. Final visual acuity depends on the anatomy of the posterior segment and, in children, the presence of amblyopia.

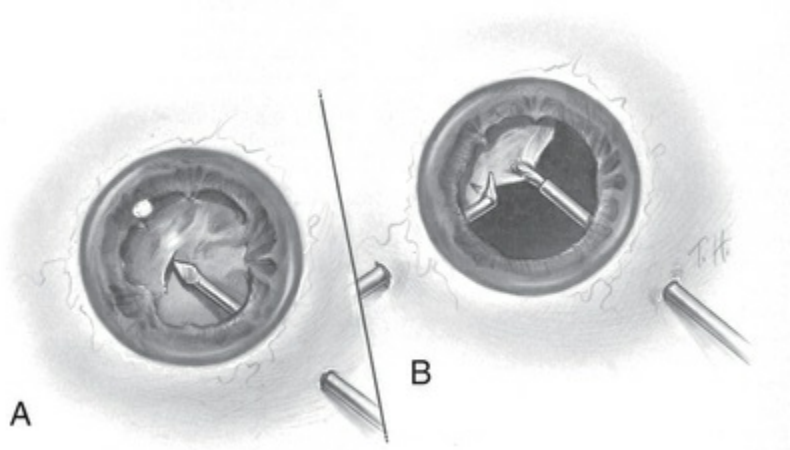

FIG. 114.24 Residual lens material can cause an opaque pupil. This material can be difficult to remove with vitrectomy instrumentation. In these cases the material is incised (A) and then grasped with a microforceps held in one hand and cut with an intraocular scissors (B) or vitrectomy instrument held in the other hand.

Some aphakic eyes develop an occluded pupil (Fig. 114.25). This often is caused by residual lens material but can also result from contraction of a vitreous sheet incarcerated in a corneal or limbal laceration. In the latter situation, the pupillary space can be recreated by freeing the vitreous from the wound and excising it, although cutting of the iris with the vitrectomy instrument may be necessary in some instances.

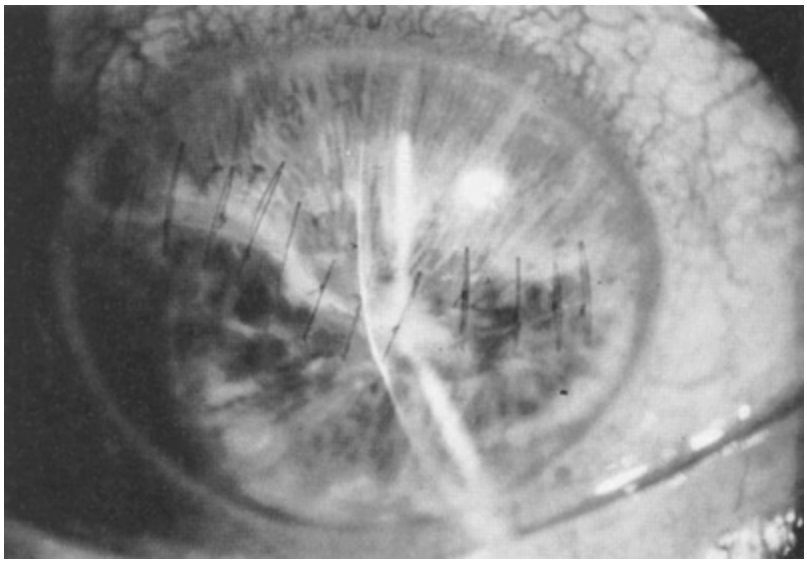

FIG. 114.25 This patient developed an occluded pupil after an extensive corneal laceration with extrusion of the lens.

Pupillary membranes can occur after penetrating injury in the absence of residual lens material. These presumably develop either from proliferation through an anterior scleral laceration that grows in the retropupillary space or from proliferation of tissues as a result of the inflammation associated with a penetrating injury. Although some of these membranes simply impair visualization of posterior structures, more advanced cyclitic membranes can cause ciliary body detachment and hypotony.

In general, we advocate surgery through the pars plana for these membranes, using techniques similar to those described for residual lens material. However, if one suspects a cyclitic membrane, care must be taken to avoid infusing into the subretinal or suprachoroidal space. Surgery should be performed with a bent infusing needle until the sutured pars plana infusion cannula can be visualized. The use of a smaller-gauge vitrectomy instrument may be contemplated in these cases; however, the larger 20G probe may be necessary for effective cutting and ingestion of the often thick cyclitic membranes.

Macular pucker can develop after penetrating injuries and is managed in a manner identical to that for idiopathic macular pucker. Retinal detachment, either traction or rhegmatogenous, can also be a late complication of a penetrating injury[142] and can be managed similarly to nontraumatic detachments. However,

additional care should be taken when one is performing the conjunctival peritomy and isolating the rectus muscle because of the possibility of areas of scleral thinning associated with the laceration.

Sympathetic Ophthalmia

Sympathetic ophthalmia is a bilateral inflammation of the uveal tract characterized by nodular or diffuse infiltration with lymphocytes and epithelioid cells. Its onset is insidious, and its course is characterized by exacerbations and remissions. Although the cause is unknown, almost all reported cases are associated with a penetrating injury to the globe.[143] The risk of sympathetic ophthalmia following nonsurgical trauma is estimated at 0.3% to 1.9%.[144] In a prospective surveillance study for sympathetic ophthalmia performed in the UK and Ireland, an incidence of 0.03/100,000 was calculated. Interestingly, the most common cause in the 23 cases reported was retinal surgery.[145]

The inflammation appears in the injured (exciting) eye usually within 4–8 weeks. The injured eye does not quiet readily, remaining injected with a persistent, low-grade uveitis. The iris is thickened, is unresponsive to light, and can have nodules at the pupillary margin. Keratic precipitates can be seen. Eventually, phthisis bulbi may develop.

The sympathizing eye becomes involved simultaneously or shortly thereafter. It usually develops mild uveitis with pain, photophobia, and keratic precipitates. The iris will become thickened and immobile with posterior synechiae, leading to a vascularized pupillary membrane and possible secondary glaucoma. In some cases, the disease begins in the posterior segment with small whitish choroidal lesions (histopathologically termed “Dalen–Fuchs nodules”), retinal and choroidal swelling, and possibly exudative retinal detachment.

Evidence suggests that the risk of sympathetic ophthalmia is extremely low if the injured eye is enucleated within 2 weeks of the injury. Thus, we recommend secondary vitreoretinal surgery within this timeframe to allow determination of whether an injured eye is salvageable. If it is believed that the eye has no visual potential after

vitrectomy, enucleation (rather than evisceration) is performed. However, isolated cases of inflammation in the sympathizing eye isolated cases have been reported at 5, 8, and 10 days after injury.[146]

Once the diagnosis of sympathetic ophthalmia has been made, enucleation of the exciting eye should seldom be done because this eye may turn out to be the better of the two. However, if there is little or no vision, enucleation may be beneficial, particularly if it is performed within 2 weeks of the onset of symptoms.

Corticosteroids remain the treatment of choice for sympathetic ophthalmia, though steroid-sparing immunomodulating agents, such as infliximab, may be necessary because of side-effects of corticosteroids or the need for long-term use. High doses of prednisone (up to 200 mg/day) over the first 7–10 days may be particularly critical to the patient's prognosis. Frequent topical corticosteroids should be used in cases with anterior segment inflammation. In patients whose disease does not appear to respond to corticosteroids, cytotoxic agents may be effective. Use of corticosteroids beginning at the time of injury does not appear to prevent development of sympathetic ophthalmia.[147]

Although there is little consensus on the optimal method of treatment, it is generally agreed that prompt recognition and treatment of sympathetic ophthalmia are crucial for preservation of vision. Kilmartin et al. reported 1-year visual acuity of 20/40 or better in 12 of 16 patients treated initially with systemic corticosteroids, although 11 received additional immunosuppression.[145] In a larger series of 85 patients drawn from three tertiary-care uveitis centers, 59% maintained visual acuity of 20/50 or better in the sympathizing eye and 75% maintained visual acuity of 20/200 or better.[148]

Application of Online Resources and Newer Technology to Ocular Trauma

Numerous online resources regarding the incidence, scope, and prevention of eye trauma are available to patients and general medical practitioners. We recommend the following two sites, sponsored by the American Academies of Ophthalmology and

Pediatrics, respectively: (1) http://www.geteyesmart.org/eyesmart/living/eye-injuries/preventing.cfm; and (2) https://www.healthychildren.org/English/tips-tools/Symptom-Checker/Pages/Eye-Injury.aspx.

The advent of smartphone technology has allowed the concept of ophthalmic telemedicine to approach realization. In this scenario, smartphone-based ophthalmic examination devices (such as a funduscope or portable slit lamp) are used to perform ocular examination. Image data are sent wirelessly for real-time analysis (either by trained readers or by artificial-intelligence algorithms) and stored for later complete analysis by specialists as needed. The Professional Eye Exam Kit (www.peek.org) is a smartphone-based platform through which a variety of vision tests and ocular imaging can be performed. Such a paradigm allows real-time examinations in remote settings in which access to necessary diagnostic services is impossible. In the context of ocular trauma, for example, real-time telemedical evaluation would assist onsite field personnel to determine the relative urgency of referral and the appropriate destination for definitive treatment.

Prevention

As the vast majority of ocular trauma is preventable, physicians should reinforce the importance of eye protection for all occupational or recreational activities that may lead to eye injury. The primary occupational risks include metalworking and use of powered tools. Sports with a higher risk of injury included basketball, baseball, pool sports, and racquet sports.[149] In a joint policy statement, the American Academy of Ophthalmology and the American Academy of Pediatrics recommend the mandatory use of protective eyewear for all young athletes with best-corrected vision worse than 20/40 in one eye or those who have undergone eye surgery.[150] Various styles of goggles, face shields, face guards, and masks tailored to individual sports are readily available. Sports eyewear should conform to the requirements of the American Society for Testing and Materials (ASTM), which provides standards of protection appropriate for specific sports. In the

United States, the Protective Eyewear Certification Council (PECC) has begun certifying protectors that comply with the ASTM requirements. Lenses made of polycarbonate material (or CR-39, an allyl/resin plastic, for stronger prescriptions) are recommended.

Legislation in a given country has a major impact on the incidence of serious eye injuries caused by a particular object. For example, the rate of injury from firearms, BB guns, and fireworks is 10-fold greater in the United States (where their use is legal) than in Hungary, where their use by individuals is illegal.[151] Similarly, a mandate in 2011 by the National Federation of State High School Associations to require high school field hockey players to wear protective eyewear led to a threefold reduction in orbital and eye injuries among players.[152] Thus, legislation directed at regulation of behaviors or restriction of items known to be associated with ocular injury may reduce incidence and severity of ocular trauma.

References

1. Negrel AD, Thylefors B. The global impact of eye injuries. *Ophthalmic Epidemiol*. 1998;5:143–169.
2. Prevent Blindness America. *The scope of the eye injury problem (brochure)*. [Chicago, IL] 2010.
3. Anon. Leads from the MMWR: leading work-related diseases and injuries – United States. *JAMA*. 1984;251:2503–2504.
4. http://www.eyeresearch.org/pdf/costofmilitaryblindness.pd
5. Morris DS, Willis S, Minassian D, et al. The incidence of serious eye injury in Scotland: a prospective study. *Eye (Lond)*. 2014;28(1):34–40.
6. Centers for Disease Control and Prevention. *National Institute for Occupational Safety and Health*. http://www.cdc.gov/niosh/nioshtic-2/20038281.html [updated 10.03.15].
7. Kuhn F, Morris R, Witherspoon CD, et al. A standardized classification of ocular trauma. *Ophthalmology*. 1996;103:240–243.
8. Pieramici DJ, Sternberg P Jr, Aaberg TM Sr, et al. A system

for classifying mechanical injuries of the eye (globe). The Ocular Trauma Classification Group. *Am J Ophthalmol*. 1997;123(6):820–831.
9. Broadrick JD. Corneal blood staining after hyphema. *Br J Ophthalmol*. 1972;56:589–592.
10. Campbell DG. Ghost cell glaucoma following trauma. *Ophthalmology*. 1981;38:1151–1158.
11. Radius RL, Finkelstein D. Central retinal artery occlusion (reversible) in sickle trait with glaucoma. *Br J Ophthalmol*. 1976;60:428–430.
12. Goldberg MF. Sickled erythrocytes, hyphema, and secondary glaucoma. I. The diagnosis and treatment of sickled erythrocytes in human hyphemas. *Ophthalmic Surg*. 1979;10:17–31.
13. Kearns P. Traumatic hyphema: a retrospective study of 314 cases. *Br J Ophthalmol*. 1991;75:137–141.
14. Read J, Goldberg MF. Comparison of medical treatment for traumatic hyphema. *Trans Am Acad Ophthalmol Otolaryngol*. 1974;78:799–806.
15. Spoor TC, Hammer M, Belloso H. Traumatic hyphema: failure of steroids to alter its course. *Arch Ophthalmol*. 1980;98:116–119.
16. Palmer DJ, Goldberg MF, Frenkel M, et al. A comparison of two dose regimens of epsilon aminocaproic acid in the prevention and management of secondary traumatic hyphemas. *Ophthalmology*. 1986;93:102–108.
17. Rahmani B, Jahadi HR. Comparison of tranexamic acid and prednisolone in the treatment of traumatic hyphema: a randomized clinical trial. *Ophthalmology*. 1999;106:375–379.
18. Gharaibeh A, Savage HI, Scherer RW, et al. Medical interventions for traumatic hyphema. *Cochrane Database Syst Rev*. 2013;(12) [CD005431].
19. Read J. Traumatic hyphema: surgical versus medical management. *Ann Ophthalmol*. 1975;7:659–670.
20. Deutsch TA, Weinreb RN, Goldberg MF. Indications for surgical management of hyphema in patients with sickle cell trait. *Arch Ophthalmol*. 1984;102:566–569.
21. Belcher CD, Brown SVL, Simmons RJ. Anterior chamber

washout for traumatic hyphema. *Ophthalmology*. 1979;16:475–479.
22. Sears ML. Surgical management of blackball hyphema. *Trans Am Acad Ophthalmol Otolaryngol*. 1970;74:820–826.
23. Weiss JS, Parrish RK, Anderson DR. Surgical therapy of traumatic hyphema. *Ophthalmic Surg*. 1983;14:343–345.
24. Yu T, Dahan E, Yin ZQ, et al. Use of an anterior chamber maintainer in the surgical management of traumatic hyphaemas. *Clin Experiment Ophthalmol*. 2008;36(3):206–208.
25. McCuen BW, Fung WE. The role of vitrectomy instrumentation in the treatment of severe traumatic hyphema. *Am J Ophthalmol*. 1979;88:930–934.
26. Stern WH, Monclal KM. Vitrectomy instrumentation for surgical evacuation of total anterior chamber hyphema and control of recurrent anterior chamber hemorrhage. *Ophthalmic Surg*. 1979;10:34–37.
27. Jarrett WH. Dislocation of the lens: a study of 166 hospitalized cases. *Arch Ophthalmol*. 1979;78:289–296.
28. Aaberg TM Jr, Rubsamen PE, Flynn HW Jr, et al. Giant retinal tear as a complication of attempted removal of intravitreal lens fragments during cataract surgery. *Am J Ophthalmol*. 1997;24:222–226.
29. Gabor SG, Pavlidis MM. Sutureless intrascleral posterior chamber intraocular lens fixation. *J Cataract Refract Surg*. 2007;33(11):1851–1854.
30. Kumar DA, Agarwal A. Glued intraocular lens: a major review on surgical technique and results. *Curr Opin Ophthalmol*. 2013;24(1):21–29.
31. Kazemi S, Wirostko WJ, Sinha S, et al. Combined pars plana lensectomy-vitrectomy with open-loop flexible anterior chamber intraocular lens (AC IOL) implantation for subluxated lenses. *Trans Am Ophthalmol Soc*. 2000;98:247–251 [discussion 251–253].
32. Kodjikian L, Beby F, Spire M, et al. Combined pars plana phacofragmentation, vitrectomy, and Artisan lens implantation for traumatic subluxated cataracts. *Retina*. 2006;26:909–916.
33. Chaudhry NA, Belfort A, Flynn HW Jr. Combined

lensectomy, vitrectomy and scleral fixation of intraocular lens implant after closed-globe injury. *Ophthalmic Surg Lasers*. 1999;30:375–381.
34. Greven CM, Collins AS, Slusher MM, et al. Visual results, prognostic indicators, and posterior segment findings following surgery for cataract/lens subluxation-dislocation secondary to ocular contusion injuries. *Retina*. 2002;22:575–580.
35. McCannel MA. A retrievable suture idea for anterior uveal problems. *Ophthalmic Surg*. 1976;7:98–103.
36. Yeung L, Chen TL, Kuo YH, et al. Severe vitreous hemorrhage associated with closed-globe injury. *Graefes Arch Clin Exp Ophthalmol*. 2006;244:52–57.
37. Mansour AM, Green WR, Hogge C. Histopathology of commotio retinae. *Retina*. 1992;12:24–28.
38. Cox MS. Retinal breaks caused by blunt nonperforating trauma at the point of impact. *Trans Am Ophthalmol Soc*. 1980;78:414–465.
39. Richards RD. Chorioretinitis sclopetaria. *Trans Am Ophthalmol Soc*. 1966;66:214–232.
40. Papakostas TD, Yonekawa Y, Wu D, et al. Retinal detachment associated with traumatic chorioretinal rupture. *Ophthalmic Surg Lasers Imaging Retina*. 2014;45(5):451–455.
41. Cox MS, Schepens CL, Freeman HM. Retinal detachment due to ocular contusion. *Arch Ophthalmol*. 1966;76:678–685.
42. Weidenthal DT, Schepens CL. Peripheral fundus changes associated with ocular contusion. *Am J Ophthalmol*. 1966;62:465–477.
43. Ross WH. Traumatic retinal dialysis. *Arch Ophthalmol*. 1981;99:1371–1374.
44. Johnston PB. Traumatic retinal detachment. *Br J Ophthalmol*. 1991;75:18–21.
45. Yamashita T, Uemara A, Uchino E, et al. Spontaneous closure of traumatic macular hole. *Am J Ophthalmol*. 2002;133:230–235.
46. Chen H, Chen W, Zheng K, et al. Prediction of spontaneous closure of traumatic macular hole with spectral domain

optical coherence tomography. *Sci Rep*. 2015;5:12343.
47. Wu W, Drenser KA, Capone A, et al. Pediatric traumatic macular hole: results of autologous plasmin enzyme-assisted vitrectomy. *Am J Ophthalmol*. 2007;144:668–672.
48. Johnson RN, McDonald HR, Lewis H, et al. Traumatic macular hole: observations, pathogenesis, and results of vitrectomy surgery. *Ophthalmology*. 2001;108:853–857.
49. Kuhn F, Morris R, Mester V, et al. Internal limiting membrane removal for traumatic macular hole. *Ophthalmic Surg Lasers*. 2001;32:308–315.
50. Chow DR, Williams GA, Trese MT, et al. Successful closure of traumatic macular holes. *Retina*. 1999;19:405–409.
51. Kraushar MF. Medical malpractice experiences of vitreoretinal specialists: risk prevention strategies. *Retina*. 2003;23:523–529.
52. Kuhn F, Maisiak R, Mann L, et al. The ocular trauma score (OTS). *Ophthalmol Clin North Am*. 2002;15:163–165.
53. Hossain A, Hussain E, Ferdausi N, et al. Prognostic value of ocular trauma score in evaluating visual outcome of pediatric (4–16 years) open globe injuries. *Asia Pac J Ophthalmol (Phila)*. 2014;3(4):226–229.
54. Schörkhuber MM, Wackernagel W, Riedl R, et al. Ocular trauma scores in paediatric open globe injuries. *Br J Ophthalmol*. 2014;98(5):664–668.
55. Sternberg P Jr, de Juan E, Michels RG. Multivariate analysis of prognostic factors in penetrating ocular injuries. *Am J Ophthalmol*. 1984;98:467–472.
56. Gilbert CM, Soong HK, Hirst LW. A two-year prospective study of penetrating ocular trauma at the Wilmer Ophthalmological Institute. *Ann Ophthalmol*. 1987;19:104–106.
57. Rao LG, Ninan A, Rao KA. Descriptive study on ocular survival, visual outcome and prognostic factors in open globe injuries. *Indian J Ophthalmol*. 2010;58:321–323.
58. Esmaeli B, Elner SG, Schork MA, et al. Visual outcome and ocular survival after penetrating trauma: a clinicopathologic study. *Ophthalmology*. 1995;102:393–400.
59. Ahmadieh H, Soheilian M, Sajjadi H, et al. Vitrectomy in

ocular trauma: factors influencing final visual outcome. *Retina*. 1993;13:107–113.
60. De Juan E, Sternberg P Jr, Michels RG. Penetrating injuries: types of injuries and visual results. *Ophthalmology*. 1983;90:1318–1322.
61. Weichel ED, Colyer MH, Ludlow SE, et al. Combat ocular trauma visual outcomes during operations Iraqi and enduring freedom. *Ophthalmology*. 2008;115:2235–2245.
62. Soni NG, Bauza AM, Son JH, et al. Open globe ocular trauma: functional outcome of eyes with no light perception at initial presentation. *Retina*. 2013;33(2):380–386.
63. Salehi-Had H, Andreoli CM, Andreoli MT, et al. Visual outcomes of vitreoretinal surgery in eyes with severe open-globe injury presenting with no-light-perception vision. *Graefes Arch Clin Exp Ophthalmol*. 2009;247(4):477–483.
64. Sevel D, Krausz H, Ponder T, et al. Value of computed tomography for the diagnosis of a ruptured eye. *J Comput Assist Tomogr*. 1983;7:870–875.
65. Kramer M, Hart L, Miller JW. Ultrasonography in the management of penetrating ocular trauma. *Int Ophthalmol Clin*. 1995;35:181–192.
66. Dass AB, Ferrone PJ, Chu RY, et al. Sensitivity of spiral computed tomography scanning for detecting intraocular foreign bodies. *Ophthalmology*. 2001;108:2326–2328.
67. Zinreich SJ, Miller NR, Aguayo JB, et al. Computed tomographic three-dimensional localization and compositional evaluation of intraocular and orbital foreign bodies. *Arch Ophthalmol*. 1986;104:1477–1482.
68. Topilow HW, Ackerman AL, Zimmerman RD. Limitations of computerized tomography in the localization of intraocular foreign bodies. *Arch Ophthalmol*. 1986;104:1477–1482.
69. Gunenc U, Maden A, Kayak S, et al. Magnetic resonance imaging and computed tomography in the detection and location of intraocular foreign bodies. *Doc Ophthalmol*. 1992;81:369–378.
70. Shams-Vahdati S, Gholipour C, Jalilzadeh-Binazar M, et al. Clinical findings provide criteria to evaluate priorities of

ophthalmologic intervention in conscious multiple trauma patients. *Injury*. 2015;46(7):1238–1240.
71. Campochiaro PA, Kaden IH, Vidaurri-Leal J, et al. Cryotherapy enhances intravitreal dispersion of viable retinal pigment epithelial cells. *Arch Ophthalmol*. 1985;103:434–436.
72. Stone TW, Siddiqui N, Arroyo JG, et al. Primary scleral buckling in open-globe injury involving the posterior segment. *Ophthalmology*. 2000;107:1923–1926.
73. Arroyo JG, Postel EA, Stone T, et al. A matched study of primary scleral buckle placement during repair of posterior segment open globe injuries. *Br J Ophthalmol*. 2003;87:75–78.
74. Cohen D, Levy J, Lifshitz T, et al. The outcomes of primary scleral buckling during repair of posterior segment open-globe injuries. *Biomed Res Int*. 2014;2014:613434.
75. Brinton GS, Aaberg TM, Reeser FH, et al. Surgical results in ocular trauma involving the posterior segment. *Am J Ophthalmol*. 1982;94:271–278.
76. Thompson JT, Parver LM, Enger CL, et al. Infectious endophthalmitis after penetrating injuries with retained intraocular foreign bodies. National Eye Trauma System. *Ophthalmology*. 1993;100:1468–1474.
77. Chaudhry IA, Shamsi FA, Al-Harthi E, et al. Incidence and visual outcome of endophthalmitis associated with intraocular foreign bodies. *Graefes Arch Clin Exp Ophthalmol*. 2008;246:181–186.
78. Colyer MH, Weber ED, Weichel ED, et al. Delayed intraocular foreign body removal without endophthalmitis during Operations Iraqi Freedom and Enduring Freedom. *Ophthalmology*. 2007;114:1439–1447.
79. Percival SPB. Late complications from posterior segment intraocular foreign bodies. *Br J Ophthalmol*. 1972;56:462–468.
80. Mester V, Kuhn F. Ferrous intraocular foreign bodies retained in the posterior segment: management options and results. *Int Ophthalmol*. 1998;22:355–362.
81. Slusher MM, Sarin LK, Federman JL. Management of intraretinal foreign bodies. *Ophthalmology*. 1982;89:369–373.
82. Feghhi M, Dehghan MH, Farrahi F, et al. Intraretinal foreign

bodies: surgical techniques and outcomes. *J Ophthalmic Vis Res*. 2013;8(4):330–336.
83. Ambler JS, Meyers SM. Management of intraretinal metallic foreign bodies without retinopexy in the absence of retinal detachment. *Ophthalmology*. 1991;98:391–394.
84. Hutton WL, Snyder WB, Vaiser A. Surgical removal of nonmagnetic foreign bodies. *Am J Ophthalmol*. 1975;80:838–843.
85. Michels RG. Surgical management of nonmagnetic intraocular foreign bodies. *Arch Ophthalmol*. 1975;93:1003–1006.
86. Pieramici DJ, Capone A Jr, Rubsamen PE, et al. Lens preservation after intraocular foreign body injury. *Ophthalmology*. 1996;103:1563–1567.
87. Valmaggia C, Baty F, Lang C, et al. Ocular injuries with a metallic foreign body in the posterior segment as a result of hammering: the visual outcome and prognostic factors. *Retina*. 2014;34(6):1116–1122.
88. Woodcock MG, Scott RA, Huntbach J, et al. Mass and shape as factors in intraocular foreign body injuries. *Ophthalmology*. 2006;113:2262–2269.
89. Ehlers JP, Kunimoto DY, Ittoop S, et al. Metallic intraocular foreign bodies: characteristics, interventions, and prognostic factors for visual outcome and globe survival. *Am J Ophthalmol*. 2008;146:427–433.
90. Muller-Jensen K. Doppelt perforierende augenverletzungen. *Klin Monatsbl Augenheilkd*. 1964;145:754–758.
91. Topping TM, Abrams GW, Machemer R. Experimental double perforating injury of the posterior segment in rabbit eyes. *Arch Ophthalmol*. 1979;97:735–742.
92. Abrams GW, Topping TM, Machemer R. Vitrectomy for injury. *Arch Ophthalmol*. 1979;97:743–748.
93. De Juan E, Sternberg P Jr, Michels RG. Evaluation of vitrectomy in penetrating ocular trauma: a case control study. *Arch Ophthalmol*. 1984;102:1160–1163.
94. Martin DF, Meredith TA, Topping TM, et al. Perforating (through-and-through) injuries of the globe: surgical results with vitrectomy. *Arch Ophthalmol*. 1991;109:951–956.

95. Weichel ED, Bower KS, Colyer MH. Chorioretinectomy for perforating or severe intraocular foreign body injuries. *Graefes Arch Clin Exp Ophthalmol*. 2010;248:319–330.
96. Zivojnovic R. *Silicone oil in vitreoretinal surgery. Chapter 5: Surgical techniques*. Marinus Nijhoff: Dordrecht; 1987:45–103.
97. Kuhn F, Mester V, Morris R. A proactive treatment approach for eyes with perforating injury. *Klin Monbl Augenheilkd*. 2004;221:622–628.
98. Weichel ED, Bower KS, Colyer MH. Chorioretinectomy for perforating or severe intraocular foreign body injuries. *Graefes Arch Clin Exp Ophthalmol*. 2010;248(3):319–330.
99. Ferreira N, Monteiro S, Meireles A, et al. Outcome of vitrectomy and chorioretinectomy in perforating eye injuries. *Ophthalmic Res*. 2015;53(4):200–206.
100. Stryjewski TP, Andreoli CM, Eliott D. Retinal detachment after open globe injury. *Ophthalmology*. 2014;121(1):327–333.
101. Benson WE, Machemer R. Severe perforating injuries treated with pars plana vitrectomy. *Am J Ophthalmol*. 1976;81:728–732.
102. Meredith TA, Gordon PA. Pars plana vitrectomy for severe penetrating injury with posterior segment involvement. *Am J Ophthalmol*. 1987;103:549–554.
103. Ryan SJ, Allen AW. Pars plana vitrectomy in ocular trauma. *Am J Ophthalmol*. 1979;88:483–491.
104. Coles WH, Haik GM. Vitrectomy in intraocular trauma. *Arch Ophthalmol*. 1972;87:621–628.
105. Cleary PE, Ryan SJ. Method of production and natural history of experimental posterior penetrating eye injury in the rhesus monkey. *Am J Ophthalmol*. 1979;88:212–220.
106. Cleary PE, Ryan SJ. Vitrectomy in penetrating eye injury: results of a controlled trial of vitrectomy in an experimental posterior penetrating eye injury in the rhesus monkey. *Arch Ophthalmol*. 1981;99:287–292.
107. Feng K, Shen L, Pang X, et al. Case–control study of risk factors for no light perception after open-globe injury: eye injury vitrectomy study. *Retina*. 2011;31(10):1988–1996.
108. Feng K, Hu YT, Ma Z. Prognostic indicators for no light perception after open-globe injury: eye injury vitrectomy

study. *Am J Ophthalmol*. 2011;152(4):654–662.
109. Heidari E, Taheri N. Surgical treatment of severely traumatized eyes with no light perception. *Retina*. 2010;30(2):294–299.
110. Kuhn F. The timing of reconstruction in severe mechanical trauma. *Ophthalmic Res*. 2014;51(2):67–72.
111. Winthrop SR, Cleary PE, Minckler DS, et al. Penetrating eye injuries: a histopathological review. *Br J Ophthalmol*. 1980;64:809–817.
112. Scott IU, Gayer S, Voo I, et al. Regional anesthesia with monitored anesthesia care for surgical repair of selected open globe injuries. *Ophthalmic Surg Lasers Imaging*. 2005;36:122–128.
113. Moreno RJ, Kloess P, Carlson DW. Effect of succinylcholine on the intraocular contents of open globes. *Ophthalmology*. 1991;98:636–638.
114. Spiegel D, Nasemann J, Nawrocki J, et al. Severe ocular trauma managed with primary pars plana vitrectomy and silicone oil. *Retina*. 1997;17:275–285.
115. Han DP, Mieler WF, Abrams GL, et al. Management of traumatic retinal incarceration with vitrectomy. *Arch Ophthalmol*. 1988;106:640–645.
116. De Bustros S, Glaser BM, Johnson MA. Thrombin infusion for the control of intraocular bleeding during vitreous surgery. *Arch Ophthalmol*. 1985;103:837–839.
117. Landers MBIII. Sodium hyaluronate (Healon) as an aide to intravitreal fluid/gas exchange. *Am J Ophthalmol*. 1982;94:557–559.
118. Landers MB III, Foulks GN, Landers DM, et al. Temporary keratoprosthesis for use during pars plana vitrectomy. *Am J Ophthalmol*. 1981;91:615–619.
119. Eckardt C. A new temporary keratoprosthesis for pars plana vitrectomy. *Retina*. 1987;7:34–37.
120. Gallemore RP, Bokosky JE. Penetrating keratoplasty with vitreoretinal surgery using the Eckardt temporary keratoprosthesis: modified technique allowing use of larger corneal grafts. *Cornea*. 1995;14:33–38.
121. Roters S, Szurman P, Hermes S, et al. Outcome of combined

penetrating keratoplasty with vitreoretinal surgery for management of severe ocular injuries. *Retina*. 2003;23:48–56.
122. Sabti KA, Raizada S. Endoscope-assisted pars plana vitrectomy in severe ocular trauma. *Br J Ophthalmol*. 2012;96(11):1399–1403.
123. Nashed A, Aikia P, Herrmann WA, et al. The outcome of early surgical repair with vitrectomy and silicone oil in open-globe injuries with retinal detachment. *Am J Ophthalmol*. 2010;151(3):522–528.
124. Brinton GS, Topping TM, Hyndiuk RA, et al. Posttraumatic endophthalmitis. *Arch Ophthalmol*. 1984;102:547–550.
125. Andreoli CM, Andreoli MT, Kloek CE, et al. Low rate of endophthalmitis in a large series of open globe injuries. *Am J Ophthalmol*. 2009;147:601–608.
126. Boldt HC, Pulido JS, Blodi CF, et al. Rural endophthalmitis. *Ophthalmology*. 1989;96:1722–1726.
127. Ahmed Y, Schimel AM, Pathengay A, et al. Endophthalmitis following open-globe injuries. *Eye (Lond)*. 2012;26(2):212–217.
128. Thompson WS, Rubsamen PE, Flynn HW, et al. Endophthalmitis after penetrating trauma: risk factors and visual acuity outcomes. *Ophthalmology*. 1995;102:1696–1701.
129. Essex RW, Yi Q, Charles PG, et al. Post-traumatic endophthalmitis. *Ophthalmology*. 2004;111:2015–2022.
130. Dannenberg AL, Parver LM, Brechner RJ, et al. Penetrating eye injuries in the workplace: the National Eye Trauma System Registry. *Arch Ophthalmol*. 1992;110:843–848.
131. Dannenberg AL, Parver LM, Fowler CJ. Penetrating eye injuries related to assault: the National Eye Trauma System Registry. *Arch Ophthalmol*. 1992;110:849–852.
132. Long C, Liu B, Xu C, et al. Causative organisms of post-traumatic endophthalmitis: a 20-year retrospective study. *BMC Ophthalmol*. 2014;14:34.
133. Foster RE, Martinez JA, Murray TG, et al. Useful visual outcomes after treatment of *Bacillus cereus* endophthalmitis. *Ophthalmology*. 1996;103:390–397.
134. Irvine WD, Flynn HW Jr, Miller D, et al. Endophthalmitis caused by gram-negative organisms. *Arch Ophthalmol*.

1992;110:1450–1454.
135. Endophthalmitis Vitrectomy Study Group. Results of the Endophthalmitis Vitrectomy Study. A randomized trial of immediate vitrectomy and of intravenous antibiotics for the treatment of postoperative bacterial endophthalmitis. *Arch Ophthalmol*. 1995;113:1479–1496.
136. Soheilian M, Rafati N, Mohebbi MR, et al. Prophylaxis of acute posttraumatic bacterial endophthalmitis: a multicenter, randomized clinical trial of intraocular antibiotic injection, report 2. *Arch Ophthalmol*. 2007;125:460–465.
137. Affeldt JC, Flynn HW Jr, Forster RK, et al. Microbial endophthalmitis resulting from ocular trauma. *Ophthalmology*. 1987;94:407–413.
138. Lieb DF, Scott IU, Flynn HW Jr, et al. Open globe injuries with positive intraocular cultures: factors influencing final visual acuity outcomes. *Ophthalmology*. 2003;110:1560–1566.
139. Tabatabaei A, Kiarudi MY, Ghassemi F, et al. Evaluation of posterior lens capsule by 20-MHz ultrasound probe in traumatic cataract. *Am J Ophthalmol*. 2012;153(1):51–54.
140. Rubsamen PE, Irvin WD, McCuen BW II, et al. Primary intraocular lens implantation in the setting of penetrating ocular trauma. *Ophthalmology*. 1995;102:101–107.
141. Koenig SB, Ruttum MS, Lewandowski MF, et al. Pseudophakia for traumatic cataracts in children. *Ophthalmology*. 1993;100:1218–1224.
142. Cox MS, Freeman HM. Retinal detachment due to ocular penetration. I. Clinical characteristics and surgical results. *Arch Ophthalmol*. 1978;96:1354–1361.
143. Lewis ML, Gass JDM, Spencer WH. Sympathetic uveitis after trauma and vitrectomy. *Arch Ophthalmol*. 1978;96:263–267.
144. Gasch AT, Foster CS, Grosskreutz CL, et al. Postoperative sympathetic ophthalmia. *Int Ophthalmol Clin*. 2000;40:69–84.
145. Kilmartin DJ, Dick AD, Forrester JV. Prospective surveillance of sympathetic ophthalmia in the UK and Republic of Ireland. *Br J Ophthalmol*. 2000;84:259–263.
146. Lubin JR, Albert DM, Weinstein M. Sixty-five years of

sympathetic ophthalmia: a clinicopathologic review of 105 cases (1913–1978). *Ophthalmology*. 1980;87:109–121.
147. Kay ML, Yanoff M, Katowitz JA. Development of sympathetic uveitis in spite of corticosteroid therapy. *Am J Ophthalmol*. 1974;78:90–94.
148. Galor A, Davis JL, Flynn HW Jr, et al. Sympathetic ophthalmia: incidence of ocular complications and vision loss in the sympathizing eye. *Am J Ophthalmol*. 2009;148(5):704–710.
149. Larrison WI, Hersh PS, Kunzweiler T, et al. Sports-related ocular trauma. *Ophthalmology*. 1990;97:1265–1269.
150. American Academy of Pediatrics Committee on Sports Medicine and Fitness. Protective eyewear for young athletes. *Pediatrics*. 2004;113:619–622.
151. Kuhn F, Morris R, Witherspoon CD, et al. Serious fireworks-related eye injuries. *Ophthalmic Epidemiol*. 2000;7:139–148.
152. Kriz PK, Zurakowski RD, Almquist JL, et al. Eye protection and risk of eye injuries in high school field hockey. *Pediatrics*. 2015;136(3):521–527.

115

Surgery for Proliferative Diabetic Retinopathy

Simon Brunner, Susanne Binder

Introduction

Surgery for non-life-threatening diseases always has to be carefully balanced against conservative treatments. Similarly, the decision to recommend surgery for complications of diabetic retinopathy

depends on many factors. The present and possible future visual function has to be determined and compared with the patient's expectations and needs. All potential surgical benefits and unwanted side-effects, as well as consequences of alternative strategies including observation, must be discussed in detail with each patient.

Pars plana vitrectomy was originally developed by Machemer in 1971 as a closed system, allowing for a safe intraocular manipulation and constant viewing of the retina.[1] At that time, indications were mainly nonclearing vitreous hemorrhages of greater than 1-year duration and complicated retinal detachments with macular involvement. However, in the past decades, improvements in technique and instrumentation have broadened the use of vitrectomy.[2–5] Today, it has an established role in the management of many severe complications of diabetic retinopathy, together with many other surgical procedures.[6,7] The principal underlying pathology in this disease is retinal ischemia, which may finally lead to the development of fibrovascular proliferations and membranes with the risk of secondary glaucoma, vitreous hemorrhage, and/or retinal detachment. The principles and techniques described in this chapter may be applied to the medical and surgical treatment of other proliferative vascular retinopathies as well, e.g., retinal vein occlusions, Coats disease, or retinopathy of prematurity (ROP).

Following the pathogenetic evolution of proliferative diabetic retinopathy, the cornerstones are progressive retinal microvascular closures with ischemia (see also Chapter 50, Nonproliferative diabetic retinopathy and diabetic macular edema, and Chapter 51, Diabetic proliferative retinopathy). They are the main causes of tissue hypoxia with subsequent development of macular edema and/or retinal and iris neovascularizations. These processes are triggered by diverse local proangiogenic factors, as insulin-like growth factor 1 (IGF-1), basic fibroblast growth factor (bFGF), and others.[8–12]

The conversion from nonproliferative to proliferative diabetic retinopathy was assumed to involve recruitment and proliferation of retinal vascular endothelial cells, eventually promoted by locally activated cytokines, as vascular endothelial growth factor (VEGF).

This cytokine provokes endothelial cell growth and permeability,[8–12] being associated with higher white blood cell counts and other inflammatory markers. The VEGF protein was found to be expressed in glial cells of the retina and optic nerve, retinal astrocytes, pigment epithelial cells, vascular endothelial cells, and ganglion cells.[12] VEGF is also suspected to mobilize and augment endothelial progenitor cells (EPC) from bone marrow by acting as a chemoattractant protein.[13–16] Circulating EPCs then are assumed to directly go to the sites of ischemia or neovascularizations to initiate new vessel and tissue formation.[13,14] The new (fibro-)vascular tissue may then proliferate in the space between retina and vitreous. With further ingrowth it may contract, potentially resulting in vitreous hemorrhage, which may stimulate further fibrosis and vitreous contraction, leading to retinal breaks or tractional detachment.[12]

Indications and Timing of Surgery

Cataract

Extracapsular cataract surgery with intraocular lens (IOL) implantation is usually well tolerated in advanced diabetic retinopathy, when there are no anterior segment neovascularizations.[17,18] The removal of an opacified lens allows for a better fundus evaluation and visualization, e.g., for panretinal photocoagulation. In the past, a higher incidences of iris neovascularizations, secondary glaucoma, and vitreous hemorrhage were reported after intracapsular cataract extraction in association with proliferative diabetic retinopathy, notably by Aiello et al.[19] However, in recent times, as small incision cataract surgery, photocoagulation, and anti-VEGF drugs are widely used, anxiety has shifted from iris and retinal neovascularizations to diabetic macular edema (DME). Progression may be lower when grid/focal lasers are applied before cataract surgery, or when panretinal photocoagulation is applied after lens extraction instead of before.[20] In general, proliferative diabetic retinopathy should be treated with panretinal photocoagulation with/without intravitreal anti-VEGF medication before cataract surgery whenever possible, but panretinal photocoagulation may also be applied at time of surgery

or shortly thereafter.[21] Along with improvements in vitrectomy surgery techniques, an increasing trend for simultaneous vitrectomy and cataract surgery has been observed in recent decades; lensectomy may be particularly helpful in revision vitrectomy surgery or in eyes with much reduced prognosis.[22,23] The advantages of any cataract extraction are a better intraoperative view and access to the vitreous base, which is of utmost importance in cases of fibrovascular proliferations in diabetic retinopathy or proliferative vitreoretinopathy; there is also evidence from Schiff et al. that reoperation rates seem to decrease when the lens has been removed during vitrectomy.[24] Similarly, fear of iris neovascularizations after combined surgery has been reduced by careful application of panretinal photocoagulation and anti-VEGF drugs during surgery.[24] In younger patients with clear lenses, the loss of accommodation has to be weighed against possible intra- and postoperative complications, such as earlier cataract formation requiring another surgery.[17,24]

High-Risk Retinal Neovascularization

Fibrovascular Proliferations

Severe fibrovascular proliferations in proliferative diabetic retinopathy can produce a major threat of profound loss of vision without surgical intervention. A progressive proliferation of fibrovascular preretinal tissue may occur, despite panretinal photocoagulation, as described by Hutton, Smiddy, and Ho (Figs. 115.1–115.3).[17,18,25]

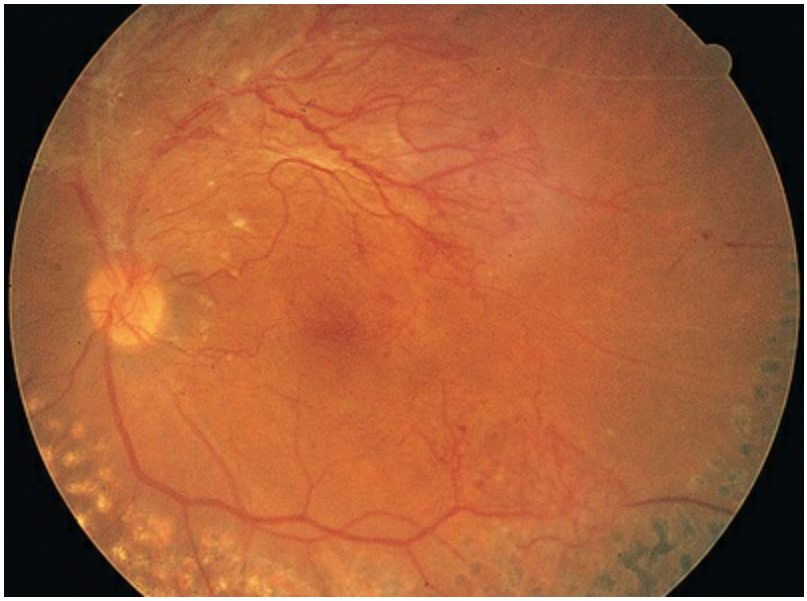

FIG. 115.1 Proliferative diabetic retinopathy with extensive neovascularization.

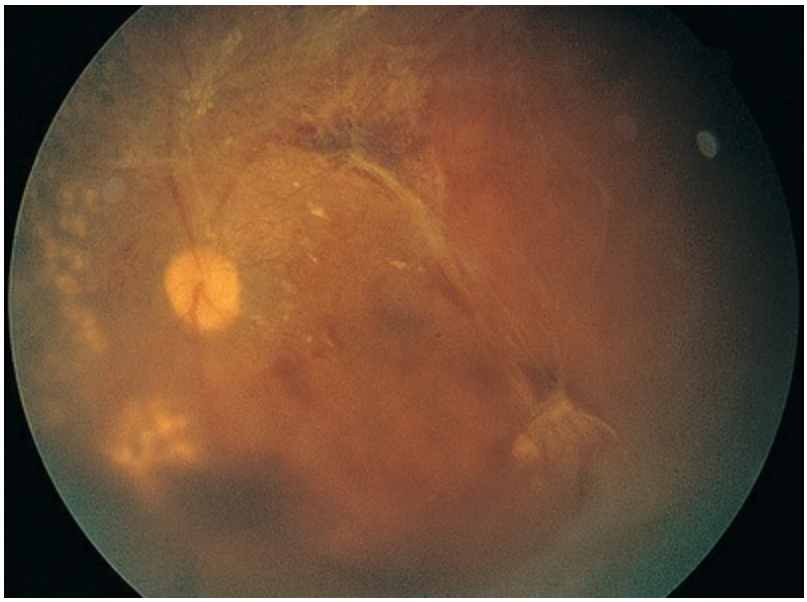

FIG. 115.2 Progression of fibrovascular proliferation and vitreous hemorrhage despite panretinal photocoagulation.

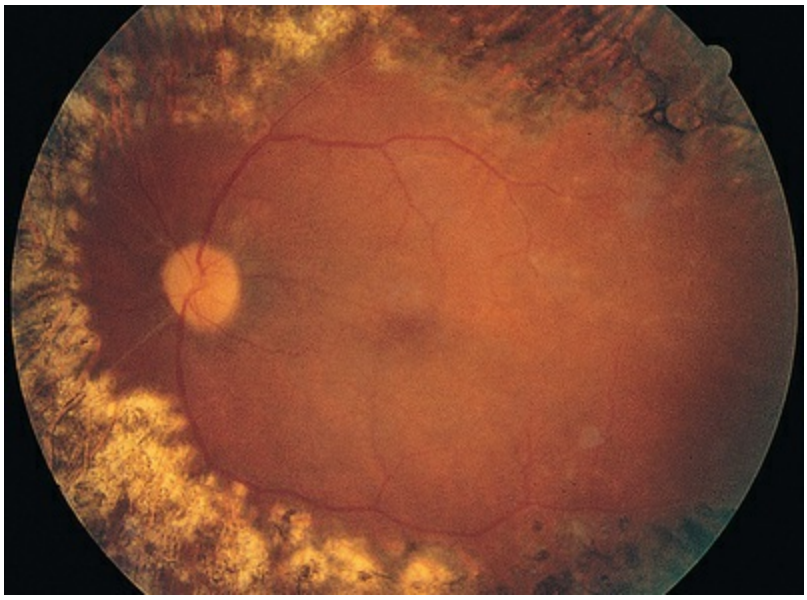

FIG. 115.3 Postoperative appearance after vitrectomy for severe fibrovascular proliferation.

The Diabetic Retinopathy Vitrectomy Study (DRVS)[26,27] established the definition of "advanced, active, neovascular, or fibrovascular proliferation" based on a review of studies of the natural history. The term "severe" for new vessels or fibrovascular proliferations was defined in the DRVS according to standard photographs and size definitions.[26] Basically, the benefit of surgery tends to increase with increasing severity of neovascularization. Eyes most suitable for early vitrectomy are those with both severe fibrovascular proliferations and at least moderately severe neovascularizations despite extensive panretinal photocoagulation.[6,27] More recent papers reported similar favorable surgical results for severe diabetic fibrovascular proliferations.[28,29]

Stable or improved visual function may be achieved in 78% of cases on average. Good prognostic factors include younger age at baseline (<40 years), preoperative panretinal photocoagulation, better visual acuity (>5/200), no iris neovascularizations, and no iatrogenic breaks at surgery.[26,30] Therefore, extensive panretinal photocoagulation and/or anti-VEGF medications are recommended prior to early vitrectomy to improve the patient's outcome.[25,31–33] In patients with relatively asymptomatic pathologies, intensive counseling is essential, as some eyes lose vision despite careful surgery.

Vitreous Hemorrhage

Nonclearing vitreous hemorrhage in diabetic retinopathy was the earliest indication for vitrectomy in the 1970s, representing 70% of cases at that time.[2] Today, it is still one of the most common indications for vitrectomy, although surgery may be avoided or at least postponed in many cases. Waiting, head elevation, or intravitreal injection of hyaluronidase may lead to spontaneous blood clearing, thus allowing for panretinal photocoagulation to induce regression of active retinal neovascularizations.[34,35] Diode laser systems, eventually delivered by indirect ophthalmoscopy, might be more effective than argon laser in some cases.[25] Early vitrectomy, defined by the DRVS as within 1–4 months from onset, results in earlier recovery of vision and better functional outcome after 2 and 4 years.[27] The benefit is greater in patients with type 1 diabetes mellitus, compared to type 2. This difference might be influenced by a greater incidence of maculopathy and posterior vitreous detachment in elderly type 2 diabetic patients.[36]

In proliferative diabetic retinopathy with dense premacular (subhyaloidal) vitreous hemorrhage, blood is trapped between the posterior hyaloid interface and the internal limiting membrane. The hemorrhage is usually well demarcated, resulting in significant visual loss. It may be associated with fibrovascular proliferations, preretinal membrane formation, or tractional macular detachment, which are common indications for an early vitrectomy (Figs. 115.4 and 115.5).[26] Less-invasive treatment methods include observation, laser membranotomy, or intravitreal injections with recombinant tissue plasminogen activator (r-tPA) or gas. When those methods are not successful, vitrectomy may improve functional recovery or decrease the risk of complications.[26,32,37] Again, a longer delay than a few months for surgery is not recommended, as the proliferative process may advance and surgical dissection become more difficult[25,38] Another relatively urgent indication for vitrectomy in nonclearing vitreous hemorrhage is rubeosis iridis and/or severe progressive proliferation of the fellow eye, especially when no panretinal photocoagulation has been applied.[25,27]

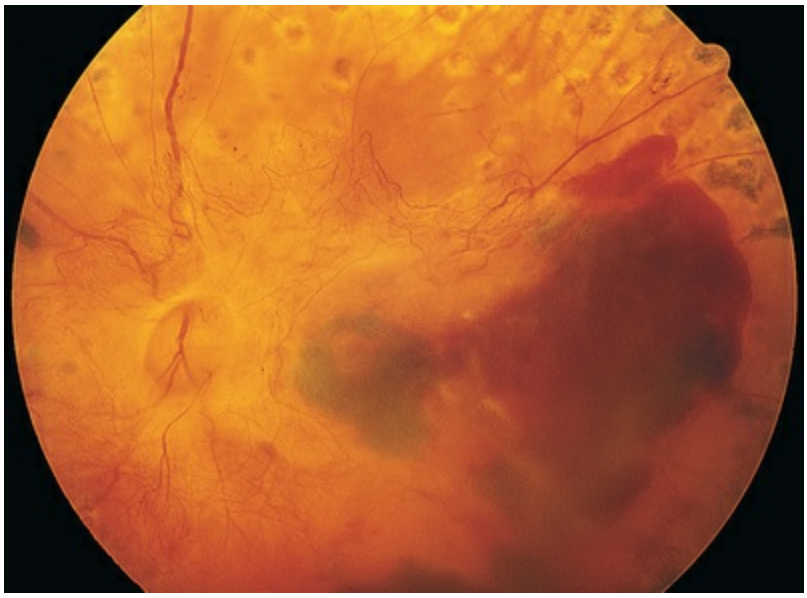

FIG. 115.4 Dense premacular hemorrhage. Note extensive fibrovascular proliferation, contraction, and distortion of retinal vessels.

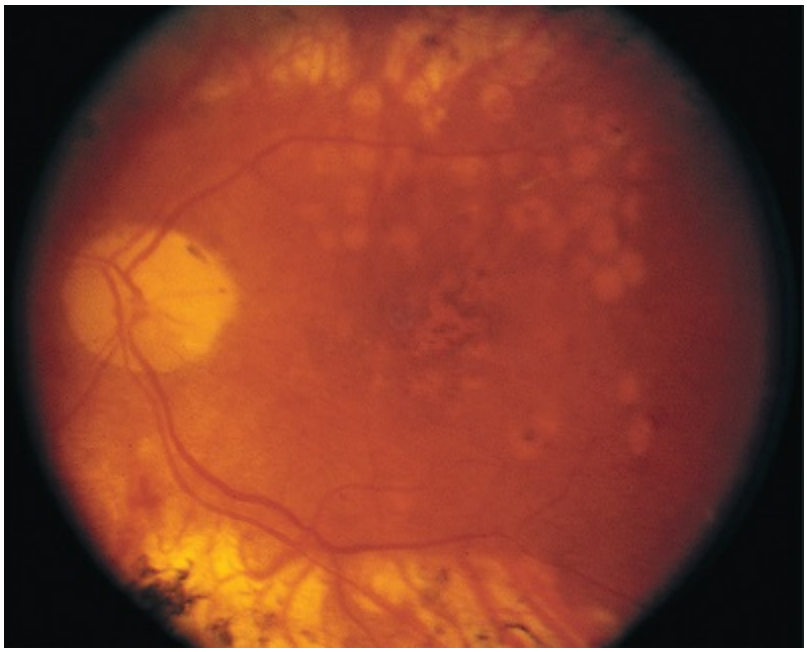

FIG. 115.5 Postoperative appearance after vitrectomy, membranectomy, and removal of preretinal hemorrhage.

Macular Traction and Macular Edema

Vitreomacular traction syndrome, vitreopapillary traction, diabetic macular edema, epiretinal membrane, or macular hole formation in patients with proliferative diabetic retinopathy have specific features in their presentation and management, representing newer indications for vitrectomy.[39–43] Opacification of posterior vitreous cortex or preretinal membrane formation alone results in substantial visual loss, sometimes associated with metamorphopsia or diplopia.[31,44] These changes may occur after premacular hemorrhage or extensive panretinal photocoagulation.[26] Vitreomacular traction may be associated with more complex vitreoretinal adhesions than in nondiabetic patients, eventually resulting in tractional retinoschisis.[45] Vitreopapillary traction is a relatively new, controversial indication for vitrectomy, with limited evidence for functional improvement.[46] In eyes with coexistent macular edema, a causative role of vitreopapillary traction has been suggested.[47] Diabetic epiretinal membranes are more likely to have more focal attachments to the macula and more proliferative activity than idiopathic epiretinal membranes.[41,42] In cases of diabetic macular edema, tangential traction, or former intravitreal surgery, macular holes may develop.[39,40,48] To avoid progression of diabetic macular edema, panretinal photocoagulation may be divided into smaller sessions or be applied after intravitreal injections of anti-VEGF drugs.[49,50]

All these pathologies are relative indications for early, extensive, and meticulous surgical treatment, usually featuring vitrectomy combined with central membrane peeling.[51] Generally, the functional outcome is negatively associated with preoperative visual acuity and the degree of maculopathy.[39,52]

Retinal Detachment

Traction Retinal Detachment

As neovascular membranes in proliferative diabetic retinopathy grow within the cortical vitreous gel attached to the retina, they may produce firm vitreoretinal adhesions and contract over time,[43,53] resulting in tractional retinal detachment.[54] Diabetic tractional macular detachment, therefore, has been the most common indication for vitrectomy.[25] However, the management of

peripheral retinal tractional detachment seems to have changed in recent times. Traditionally, those cases were observed for a while as the risk of complicated vitrectomy seemed to exceed the low progression rates.[55] As anatomic and functional results after vitrectomy substantially improved, an earlier surgical approach in cases with peripheral tractional detachment seemed reasonable.[56,57] Still, functional results after successful vitrectomy in severe macular tractional detachment remain rather poor (Figs. 115.6 and 115.7).[57] Also, chronic cases of diabetic tractional detachment may be a lesser indication for surgery, as the retina under tractional fibrovascular proliferations usually becomes atrophic.[6,18,57] In general, vitrectomy reoperation rates in diabetic tractional detachment are between 24% and 47%.[58–60]

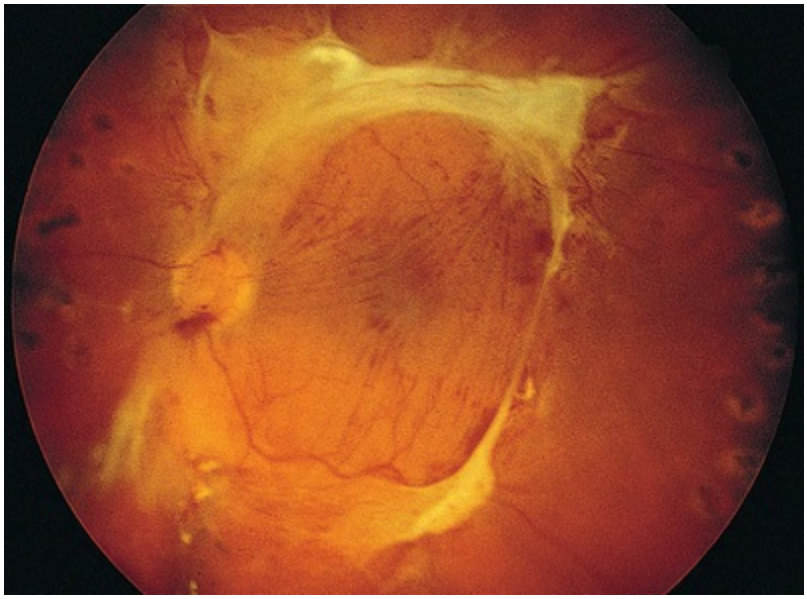

FIG. 115.6 Tractional retinal detachment involving the entire macula. This patient had severe fibrovascular proliferation and traction along the arcades with recent extension of the detachment to involve the macula.

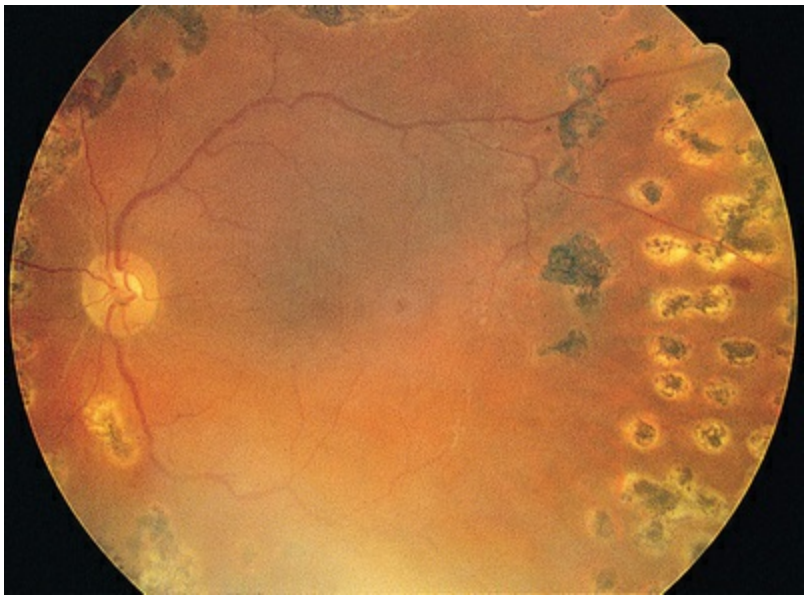

FIG. 115.7 Postoperative appearance after vitrectomy, membranectomy, and retinal reattachment.

Factors with a more favorable outcome in the literature are age <50 years; preoperative panretinal photocoagulation; visual acuity >5/200; no or few iris neovascularizations or retinal proliferations; macular detachments <30 days; and no iatrogenic breaks.[6,25,61]

Combined Tractional–Rhegmatogenous Retinal Detachment

Severe fibrovascular proliferations in proliferative diabetic retinopathy may result in progressive traction and membrane contraction leading to the development of posterior retinal breaks. The shape of the retina appears convex in contrast to tractional detachment, and the dimensions of detachment are often greater, extending over the ora serrata.[43,62,63] The retinal surface often shows white hydration lines, which are diagnostic of retinal breaks. These are often small, located posteriorly, paravascular or immediately adjacent to vitreoretinal tractions and retinal elevations.[63,64] Sometimes, subretinal hemorrhage may be present.[65] Vitrectomy combined with silicone oil tamponade is frequently indicated in particularly severe cases, especially when the second eye shows a poor visual function (Figs. 115.8 and 115.9).[63,66] Reports of silicone oil surgery generally show a high rate of reattachments with just a moderate chance of functional improvements (see below). Silicone oil finally helps to reduce the incidence of further complications

such as neovascular glaucoma and phthisis in those desperate cases.[63,66]

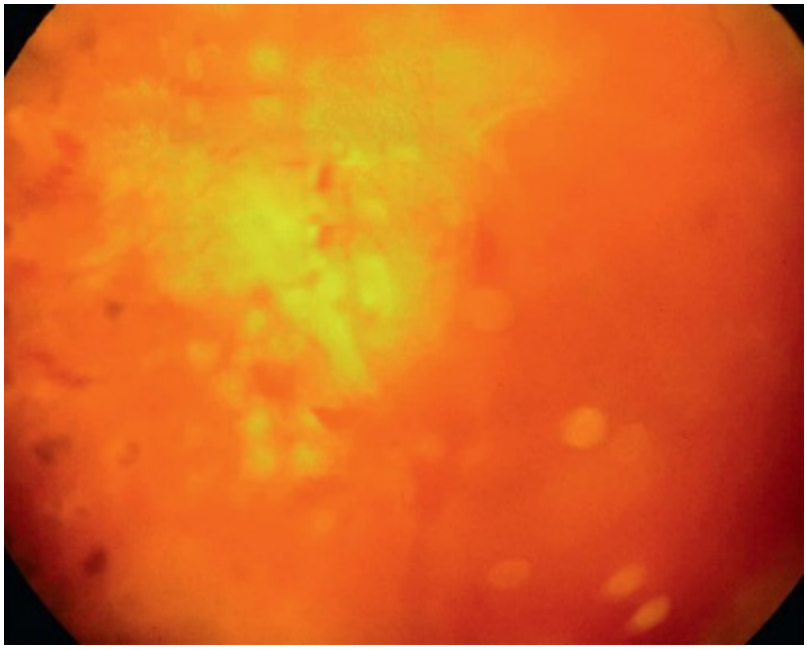

FIG. 115.8 Combined tractional–rhegmatogenous detachment with dense fibrovascular proliferations over optic nerve and arcades.

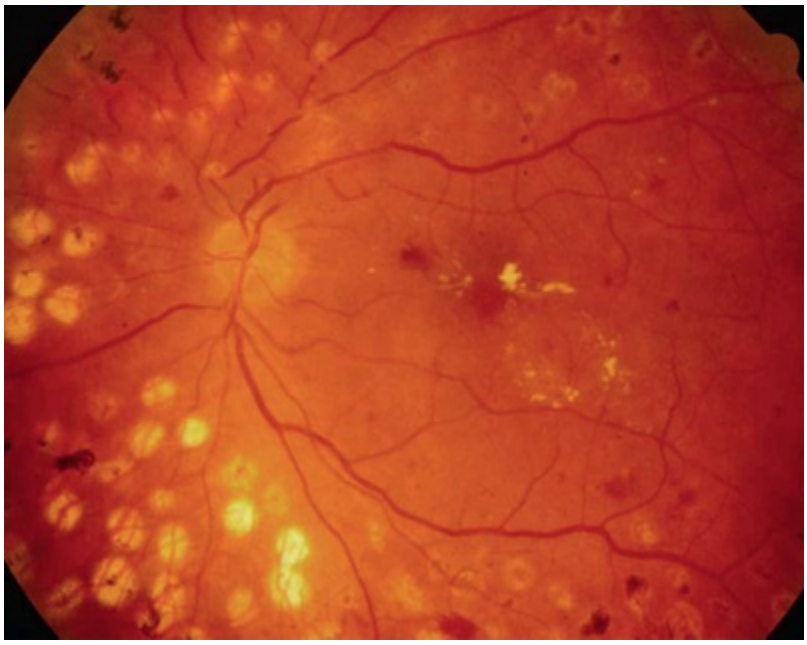

FIG. 115.9 Postoperative appearance after successful vitrectomy, membranectomy, endophotocoagulation,

and silicone oil tamponade/removal.

Neovascular Glaucoma

Neovascular glaucoma is a very severe complication in proliferative diabetic retinopathy. It is assumed that the ischemic retina is the source of vasoproliferative growth factors that may diffuse into the anterior segment. Consequently, growth of neovascularizations and fibrovascular membranes in the chamber angle obstruct aqueous outflow and intraocular pressure rises; different stages of neovascular glaucoma have been described.[67,68] Therefore, the first therapeutic target should be the cause of the neovascular stimulus, indicating extensive panretinal photocoagulation or cryotherapy.[69] Intravitreal or intracameral anti-VEGF medications, such as bevacizumab, may be helpful as short-term adjunct to panretinal photocoagulation or when panretinal photocoagulation fails to cause regression of rubeosis.[70–72] This treatment alone usually induces regression of neovascularizations; however, fibrovascular proliferations in the chamber angle may contract and the pressure remain high.[62]

In cases of opaque optical media, as vitreous hemorrhage or cataract, controlled panretinal photocoagulation can only be performed after vitrectomy and/or cataract extraction, which has been shown to reduce rubeosis and improve neovascular glaucoma.[73,74] In addition, silicone oil tamponade prevents recurrent vitreous hemorrhage and may induce regression of rubeosis.[75]

Vitrectomy may be combined with endocyclophotocoagulation of ciliary processes or partial retinectomy to improve perfusion and reduce intraocular pressure.[76,77] Patients with higher-stage neovascular glaucoma with synechial angle closure almost always need some sort of glaucoma surgery.

Filtering surgery in diabetic neovascular glaucoma has significantly lower success rates than surgery for primary or secondary open angle glaucoma.[78] The intraoperative use of antimetabolites, such as 5-fluorouracil and mitomycin C, is strongly recommended; in addition, intensive perioperative antiinflammatory and antiproliferative treatments, as well as anti-VEGF injections and panretinal photocoagulation, can improve the

outcome.[71,79]

The implantation of glaucoma-drainage tubes (as Molteno, Baerveldt, or Ahmed implants) is also very common, although the drainage capacity can be compromised by epibulbar scarring or recurrent intracameral or intravitreal hemorrhages.[80,81] Nonpenetrating glaucoma surgery, as well as argon laser trabeculoplasty, is generally not recommended in diabetic neovascular glaucoma, as angle closure due to the rubeotic process can deteriorate postoperatively.[78]

Additional vitrectomy surgery should be considered at earlier stages of proliferative diabetic retinopathy and not be reserved for only advanced neovascular glaucoma.[82] It should be combined with panretinal photocoagulation ab interno; in addition, a pars plana glaucoma drainage implant may be considered to stabilize the glaucoma.[80]

Cyclodestruction, with transscleral cryo- or diode-laser cyclocoagulation, is a helpful, widely used method in advanced neovascular glaucoma. However, this treatment is usually reserved for eyes with low visual function at presentation.[83,84] Blind, painful eyes may still need retrobulbar alcohol injections or, in the worst case, evisceration or enucleation.[85]

Preoperative Evaluation and Informed Consent

As the presence of advanced diabetic retinopathy may indicate significant macro- and microvascular disease, all patients should be referred to an internist or endocrinologist before surgery. It is important to evaluate the patient's medical and glycemic status, as well as coexistent problems such as hypertension, hyperlipidemia, or cardiovascular or renal disease. Those findings will influence the decision for the extent, timing, and prognosis of surgery.[86,87] Optimal blood glucose management may be protective against perioperative infection.[88] Patients should be well informed about adjustments of medications, especially those for blood glucose and blood pressure control. Anticoagulants, as well as antiplatelet medications, may be stopped or substituted at the surgeon's

suggestion. Another issue is that of patients needing renal dialysis. In those cases, surgery has to be arranged between dialysis sessions. In any case, an optimal medical control will optimize surgical success and reduce intra- and postoperative complications in diabetic patients.

Every patient must undergo a thorough ophthalmic evaluation before surgery to determine all anatomic abnormalities, as well as actual and possible future visual function. It is important to correlate the history of visual decrease with possible anatomic changes, which can be discovered by anamnesis or the referring ophthalmologists. This correlation is a major prognostic factor for surgical success. A complete ophthalmic status, with best corrected distance and near acuity, pupillary function, intraocular pressure, and visual field tests, is essential. Slit-lamp biomicroscopy of all anatomic abnormalities, and, if possible, fundus examination with indirect binocular lenses, provides further important information to plan the surgical approach.[89,90]

Silicone IOL implants should be avoided, as intraocular silicone oil tamponades would firmly adhere to silicone lenses, thereby affecting intra- and postoperative fundus visualization and visual function.[91,92] If applicable, fluorescein angiography and optical coherence tomography (OCT) may add further details, as the presence and extent of retinal or iris neovascularizations, macular or retinal ischemia, macular edema, vitreoretinal tractions, and epiretinal membrane formation.[87,89,93]

In cases with opacified media preventing fundus visualization such as cataract or intracameral or intravitreal hemorrhage, ophthalmic echography should be performed; it can provide most relevant information, as the presence or absence of vitreoretinal adhesions, vitreoschisis, retinal detachment, or other subretinal opacities and tumors.[90,94]

Preoperative electrophysiologic testing (visually evoked potentials, VEP, or electroretinography, ERG) is another tool to evaluate function in those cases. However, in clinical practice it is not routinely used, as results in predicting postoperative outcome are sometimes contradictory.[95]

Prior to surgery, possible infections of the lid, conjunctiva, cornea, or ocular adnexae must be treated. Antibiotic prophylaxis

may be reasonable when the risk for endophthalmitis is increased, although there is no evidence-based general recommendation.[43,96] The presence of iris neovascularizations or massive fibrovascular proliferations is an indicator for an early surgical intervention, with preoperative intravitreal or intracameral application of anti-VEG medications and panretinal photocoagulation, if possible.[97,98] Especially in severe proliferative diabetic retinopathy in type 1 diabetic patients, there is strong evidence of the value of performing adequate panretinal photocoagulation, especially in the anterior periphery to minimize the risk of further anterior neovascularizations or fibrovascular proliferations.[6,31,99,100]

Before any treatment, the patient, his/her family, and/or responsible persons should be thoroughly informed about the nature of the disease and the scheduled surgery, as well as possible alternative treatments or nontreatment. This important decision-making process is dependent on the physician's knowledge of all general and ocular conditions, as well as on the patient's understanding of the impact of surgery. A promising final decision can only be made on the basis of all the patient's needs and expectations. It is always necessary to obtain a written informed consent, which should include a detailed description of all information. Preprinted forms may be used, favorably including some additional graphic illustrations.

Surgery

Education and Training

Surgery for complications of diabetic retinopathy, notably vitrectomy, requires advanced surgical judgment and skills and the use of highly developed instruments and equipment. Technical advances in the development of instruments and surgical techniques require regular and frequent trainings of surgical skills of all operating personnel, as well as modernization and proper maintenance of all surgical equipment and instrumentation.[87] Wet laboratories using animal models play an important role in modern ophthalmology surgical residency training. In recent times, new virtual reality simulators can be used as a gated, quantifiable

performance goal to expert-level benchmarks (Fig. 115.10).[101,102]

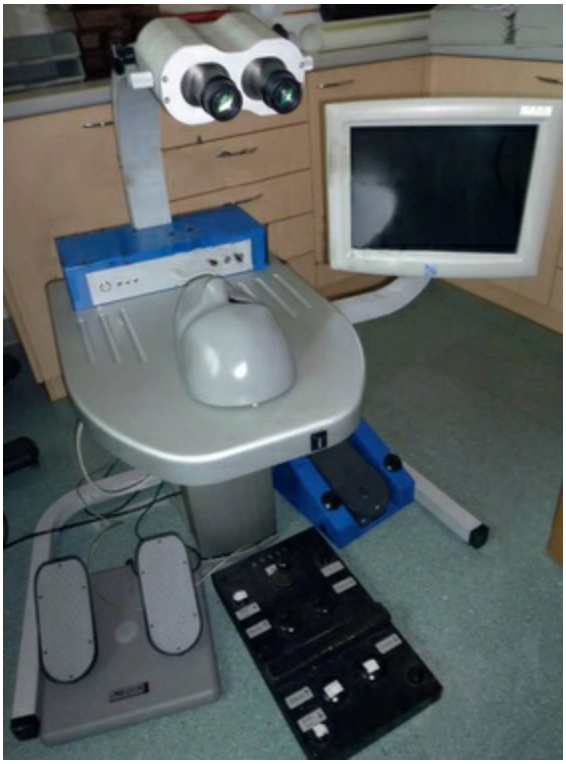

FIG. 115.10 An EYESI simulator, for training of intraocular surgery in a virtual reality system. The simulator is equipped with a binocular microscope and an eye phantom model to train or improve skills as visual coordination and digital micromanipulations.

Anesthesia

Surgery in proliferative diabetic retinopathy can be performed under local or general anesthesia, sedoanalgesia, or a combination of those. The adequate form of anesthesia depends on many factors, as the extent and duration of surgery, the patient's mental or physical condition, or simply the patient's and surgeon's choice. It also depends on geographic and economic factors, as there are diverging anesthesia standards in different countries. The patient's vital signs should be continuously monitored by experienced operating staff members, even during local anesthesia. The advantage of local anesthesia is a minimal disturbance of the diabetic metabolism; however, the patient may feel some pain or

move during surgery. Local anesthesia can also be applied during sedoanalgesia or general anesthesia to minimize the patient's postoperative discomfort.[103] General anesthesia or sedoanalgesia should be performed only by an anesthesiologist, who can stabilize the patient or help to medically reduce the intraocular pressure. Nitrous-containing agents should be terminated before an intraocular gas bubble is injected.[87,103]

Preoperative Preparation

To provide adequate intraocular visualization, wide pupillary dilatation is necessary. A combination of different mydriatic, sympathomimetic, and cycloplegic drops should be instilled repeatedly before surgery to allow for a maximal pupillary dilatation.[87] Additional topical medications, as antibiotic or antiphlogistic drops, may be added, as well as systemic sedative or diuretic medications for optimal preparation of the patient. If general anesthesia is scheduled, additional preoperative medication or modification of the patient's medications should be discussed with the anesthesiologist.

In the operating room, a 5% povidone iodine solution must be applied on the eyelids and a 5% solution in the conjunctival sac, respectively, and should dry out for at least 3 minutes to guarantee adequate disinfection.[104] The eye is then covered with a sterile plastic sheet, equipped with 1–2 side bags, and a lid speculum is inserted (Fig. 115.11).

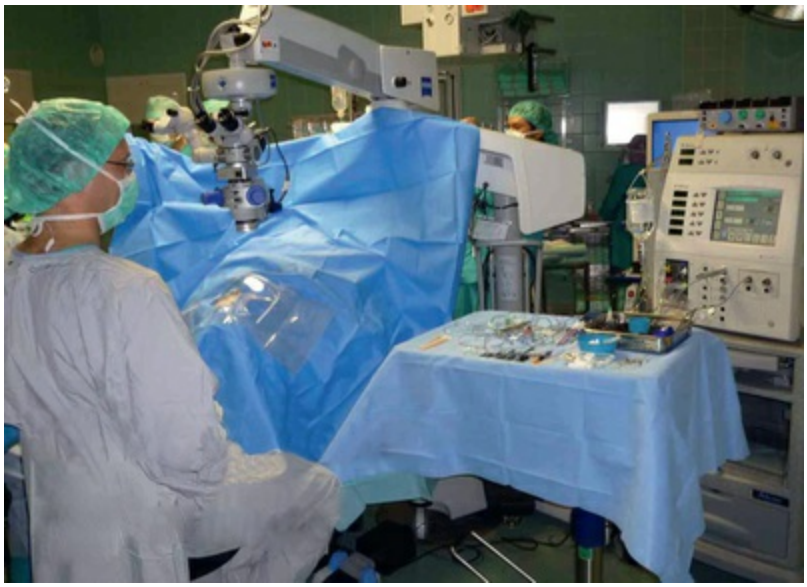

FIG. 115.11 Preoperative situs before vitrectomy. The eye was covered with a blue plastic sheet, equipped with two side bags, and a lid speculum was inserted. Sterile hand grips were attached on the binocular microscope and all necessary instruments, as well as a modern phacovitrectomy unit, prepared.

Surgical Equipment

Microscope and Lenses

As prerequisite, a modern binocular surgical (stereo-) microscope is required with coaxial illumination that should allow a magnification of 10–30-fold. It should be equipped with a motorized power zoom, power focusing, and X–Y-positioning via foot pedals. The microscope must be fitted with the corresponding laser filters to permit photocoagulation. A light-splitter is necessary for covisualization of the operating personnel and for the integration of a video system or other imaging features, as intraoperative OCT.[105]

For fundus visualization, different lens systems are available to neutralize the cornea's refractive power. The initial visualization of the central retina was performed using hand-held, planoconcave lenses or various contact lenses centered by the assistant or a sclera-fixated metal ring. For a better visualization of the fundus periphery, especially in gas-filled phakic eyes, biconcave lenses with 20–35° angle were developed.[106,107]

Today, 130° wide-angle viewing systems are available, and the inverted image is corrected through a stereoscopic diagonal inverter. Non-contact wide-angle systems (BIOM, EIBOS) are widely in use and can be managed by the surgeon alone.[105,108] They offer a greater depth of field and better visualization through media opacities. Also, a lower incidence of postoperative epithelial defects or retinal detachments has been reported.[109,110] To protect the corneal epithelium and guarantee for optimal fundus visualization, a corneal tear film must be maintained. The adjunctive use of carboxymethylcellulose gel or similar substances at surgery will promote corneal clarity.

Microinstruments and Illumination

Various types of surgical instruments have been developed and modified over the years. The instruments vary in the number of functions provided. Currently, a trend is towards single-use instruments or parts of them, providing maximal aseptic conditions. Twenty-gauge systems had become the long-time standard and are still used in rare situations, offering the greatest number of supplementary instruments with minimal flex.[87,111]

Small-Gauge Systems.

In more recent years, 23-, 25-, and 27-gauge instruments have been developed to provide nonsuturing vitrectomy, thereby minimizing inflammation and postoperative discomfort to the patient (Fig. 115.12).[112–115] However, their efficiency in complex cases, such as advanced diabetic retinopathy, is still a matter of debate, as a higher rate of postoperative hypotony has been reported.[116] In the recent literature, 23- and 25-gauge systems showed more stable and reproducible results even in severe proliferative diabetic retinopathy, compared with 27-gauge.[112,117,118]

FIG. 115.12 Comparison of 20-, 23-, 25- and 27-gauge vitrectomy cutter handpieces. Notably, the ports of the thinner handpieces are closer to the probe tip.

Basic Equipment.

The standard equipment for vitrectomy consists of a vitrectomy cutter, combined with a suction unit, a fiberoptic light pipe, an infusion of balanced salt solution (BSS), and an air pump. A modern vitrectomy unit provides all those base functions, in different combinations with diathermy, endolaser coagulation, gas filling, or phacoemulsification modules (Fig. 115.13).

FIG. 115.13 Front view of a new Constellation© vitrectomy unit, providing phacoemulsification, vitrectomy, photocoagulation, diathermy, and air/gas/silicone tamponades in one machine.

Vitrectomy Cutter.

The vitrectomy probe serves to cut and dissect membranes or fibrovascular proliferations in addition to vitreous gel. Shaving of peripheral vitreous or membranous fibrovascular proliferations has become significantly safer with the newer probes, in which the port is closer to the probe tip.

Illumination.

Handheld illuminators range from single-function illumination probes to multipurpose illuminated scissors, forceps, or vitrectomy probes. The use of "chandelier" light illuminators inserted manually or through additional sclerotomies allows for bimanual dissection.[119–121]

Membrane Dissecting Instruments.

A wide variety of tissue scissors, forceps, spatulas, picks, or cannulas are available to peel or remove epiretinal membranes;

similarly, the vitrectomy probe can be used with lower suction rates at the decision of the surgeon. Vertical scissors may be used for segmentation of tissues in complex fibrovascular proliferations, whereas horizontal scissors are beneficial to delaminate the vitreous cortex from the retina.[122,123]

Retinopexy Instrumentation.

Different endolaser probes for all incision sizes are available to perform panretinal photocoagulation or retinopexy. Scleral depression with an indentator may be used for peripheral treatment. Endodiathermy is useful for stopping bleeding during surgery or for preparing retinotomy sites.

Dyes and Tamponades

Various dyes are used to identify vitreous and epiretinal structures. Corticosteroid crystals may be used for easier identification of the vitreous cortex, especially in retinal detachment surgery; e.g., triamcinolone acetonide marks otherwise invisible remnants or patches of vitreous on the retina.[104,124–126] In addition, it may help to prevent fibrin exudation in proliferative diabetic retinopathy due to its antiinflammatory potential. No retinal toxicity was described for intravitreal doses of 2–4 mg of triamcinolone acetonide.[105,127] Epiretinal membranes or fibrovascular proliferations must be carefully removed to prevent recurrent proliferative vitreoretinopathy or tractional detachment. Dyes as trypan blue are helpful to stain epiretinal membranes; indocyanine green, infracyanine green, and brilliant blue are more specific for internal limiting membrane identification; epiretinal structures appear in negative contrast with those substances.[128–131] There is divided opinion on whether infracyanine or indocyanine green might have toxic retinal effects, provoking (peripheral) visual field defects. However, this effect could be time- and dose-dependent.[131,132]

For internal tamponade of the vitreous cavity, various gases and liquids are in use. As a short-term intraoperative instrument, perfluorocarbon liquid is most commonly employed. It is helpful to reattach the retina or to protect the retina against damage from endophacoemulsification, intraocular foreign bodies, or lens fragments.[133–136] Filtered air may serve as a short-term, nontoxic

tamponade; for a more prolonged tamponade in cases of retinal detachment or proliferative diabetic retinopathy, different gases such as SF_6, C_2F_6, or C_3F_8 are in use, providing tamponade times from 2 to 8 weeks. Gases are preferred for superior or posterior pathologies, in patients where positioning is possible, or when surgical removal would not be possible.[137–139]

Silicone oil is still the instrument of choice for longer tamponades in most severe cases. Different silicone oil types from 1000 to 10, 000 centistokes are available. They can also serve as protective shield to inhibit neovascular growth factors and cytokines from dissolving in ocular tissues. Silicone oils usually should be removed after a short time, usually 3–6 months, to avoid silicone-related complications.[140–144]

Additional Equipment

To improve the efficacy and outcome of surgery in proliferative diabetic retinopathy, different helpful adjuncts have been developed in the past years. A peri- or intraoperative injection of antiangiogenic drugs might decrease the risk of recurrent intravitreal hemorrhage or neovascular glaucoma with rubeosis iridis. Preoperative injections 7 days prior to surgery have shown to improve the outcome and facilitate surgical manipulations in diabetic tractional detachment.[145,146] To facilitate posterior vitreous detachment and to shorten operating time, pharmacologic vitreolysis with plasmin, microplasmin, and/or hyaluronidase was developed. Such agents may reduce intraoperative complications, such as retinal tears.[147,148] When there is a need for visualization of the ciliary body in cases of severe anterior hyaloidal fibrovascular proliferation or extreme corneal opacification or capsule fibrosis, endoscopy provides a novel, elegant approach. The endoscope is inserted through the pars plana, providing a direct visualization of the entire vitreoretinal anatomy.[149,150]

Surgical Procedure

Cataract Surgery

Patients undergoing vitrectomy surgery for proliferative diabetic

retinopathy may have concomitant cataract. Surgical management options include cataract surgery followed by vitrectomy surgery later, or combined operations in a single procedure.[151] Further variations include cataract extraction, followed by vitrectomy and lens implantation at the end of surgery, or alternatively, cataract extraction with primary lens implantation, followed by vitrectomy. Cataract and vitrectomy surgery may be both performed by one surgeon or two different surgeons, depending on geographic and cultural differences.[151]

As cataract surgery has become safer over the years and small incision phacoemulsification is now available, combined phacoemulsification with simultaneous implantation of a posterior chamber lens is performed by our group in patients over 60 years and with signs of cataract. Performing a capsulorhexis without red reflex in an eye with vitreous hemorrhage can be challenging. Here, the vitreous surgeon also has to be an experienced cataract surgeon, or this part of the surgery is provided by an anterior segment surgeon. In any case, the dying of the anterior capsule is recommended. In 20-gauge vitrectomy, the infusion line is preplaced but not connected before the lens surgery to avoid pressure created during infusion placement and sutures. In small incision vitrectomy, all three sclerotomies are performed and trocars inserted before cataract surgery for the same reason.

The advantage of any cataract extraction procedure is a much better intraoperative access to the vitreous base, which is of utmost importance in cases of fibrovascular proliferations in diabetic retinopathy or proliferative vitreoretinopathy; there is also evidence that reoperation rates seem to decrease when the lens has been removed during vitrectomy.[24]

Progression of coexisting diabetic macular edema may be lower when grid/focal laser is applied before cataract surgery, or when panretinal photocoagulation is applied after lens extraction instead of before.[20] All cases with proliferative diabetic retinopathy should be treated with panretinal photocoagulation, if possible, and/or anti-VEGF injections before cataract surgery, to avoid a higher incidence of postoperative iris neovascularizations; panretinal photocoagulation may also be applied at time of surgery or shortly thereafter.[21,24] In younger patients with less cataract formation, the

loss of accommodation after cataract extraction has to be weighed against possible serious intra- and postoperative complications when the lens was not removed. The patient should be informed that an earlier cataract formation is common after vitrectomy.[17,24] Likewise, it has been reported that in eyes without a crystalline lens, a more complete panretinal photocoagulation and resection of proliferations was possible.[24]

Glaucoma Surgery

Aqueous Shunt Procedures

Diabetic patients with refractory advanced open angle glaucoma or neovascular glaucoma with different stages of angle closure almost always need glaucoma surgery, depending on the prognosis for visual function.

Nonpenetrating procedures, as canaloplasty or viscocanalostomy, are usually not indicated, especially when the chamber angle is closed.[152] Similarly, filtering surgery such as trabeculectomy in neovascular glaucoma has significantly lower success rates than surgery for primary or secondary open angle glaucoma.[78] The reason is an excessive risk for inflammation and hemorrhage in these eyes. To improve the outcome, it is advisable to use intraoperative antimetabolites, such as 5-fluorouracil and mitomycin C, as well as perioperative anti-VEGF injections and panretinal photocoagulation.[71,79]

It has recently been shown that an intravitreal injection of bevacizumab, followed by panretinal photocoagulation and glaucoma surgery 1–2 weeks later, may produce a much better pressure control.[153] Alternatively, glaucoma-drainage tubes, as Molteno, Baerveldt, or Ahmed implants, may be implanted. They can be used either after or at the same time as vitrectomy with endophotocoagulation. The tube may be placed in the anterior chamber or in the sulcus ciliaris or through the pars plana, if the chamber angle is closed.[152]

Postoperative results are inferior to standard trabeculectomy procedures in nondiabetic patients, as the drainage capacity can be compromised by scarring of epibulbar tissue, bleb formation, or recurrent intracameral or intravitreal hemorrhages.[80,81]

Furthermore, other long-term complications, such as exposure of tube material or decompensation of the corneal endothelium, have been described.[153–155] Bevacizumab has been reported to improve the outcome after glaucoma implant surgery as well; however, more trials are needed to clarify the role of anti-VEGF medications in surgery for diabetic glaucoma.

In addition, vitrectomy surgery may be considered even at earlier stages of glaucoma in proliferative diabetic retinopathy, as it can be easily combined with full scatter panretinal photocoagulation ab interno.[74,75,82] Furthermore, a pars plana glaucoma drainage implant may be considered to stabilize the intraocular pressure.[80]

Cyclodestructive Therapy

In eyes with extensive retinal ischemia or optic nerve damage in advanced neovascular glaucoma, in which visual outcome is expected to be very poor, the efforts and risks of incisional trabeculectomy or glaucoma implant surgery may not be accepted.[152] In those eyes, cyclodestruction procedures, such as transscleral cryo- or diode-laser cyclocoagulation, can be helpful methods, depending on the grade of angle closure.[83,84] In the right indication, it has proven as effectively as trabeculectomy or drainage implant surgery.[156,157]

Before transscleral cyclophotocoagulation, a retrobulbar injection with lidocaine 2% is usually given and a lid speculum should be used. The handpiece of the diode laser features a footplate designed for this procedure.[152] The footplate is placed along the limbus so that the fiberoptic tip sits on the surface directly over the ciliary body to concentrate the laser energy in the target tissue. Power settings of between 1500 and 2500 mW with a pulse delivering time between 1.5 and 2.0 seconds are commonly used. A total of 15–30 applications of the laser are applied to the full circumference; only the horizontal meridians should be spared.[152,158] After surgery, topical prednisolone, diclofenac, and atropine, eventually subconjunctival prednisolone–hydrogen succinate, are given. The intraocular pressure will be reduced postoperatively for 6–8 weeks on average, providing effective pressure control in about 67% of patients.[152,158] The treatment may be repeated after several months. Cyclocryocoagulation of the ciliary body in a similar fashion or

cryocoagulation of the peripheral retina by indirect ophthalmoscopy may be an alternative; however, "blind" cryocoagulation bears the risk of overtreatment and induction of choroidal neovascularization.[73,159]

Blind, refractory, painful eyes may be treated with retrobulbar alcohol injections or finally by evisceration or enucleation.[85]

Pars Plana Vitrectomy

Preparation of Entry Sites

Three-port vitrectomy remains the most used technique, in which two sclerotomies are prepared superotemporally and superonasally, and a third inferotemporal pars plana incision permits intraocular infusion. Incisions are chosen in 3.5–4.0-mm distances from the limbus. Transconjunctival trocar-guided systems are used with increasing frequency in diabetes-related indications in smaller gauges (23-, 25- and 27-gauge) to provide higher comfort for the patients and reduce surgical trauma.[112]

To avoid intra- or postoperative wound dehiscence, sclerotomy blades should be oriented parallel to the limbus and trocars should be inserted 20–30° oblique to the scleral surface (Fig. 115.14).

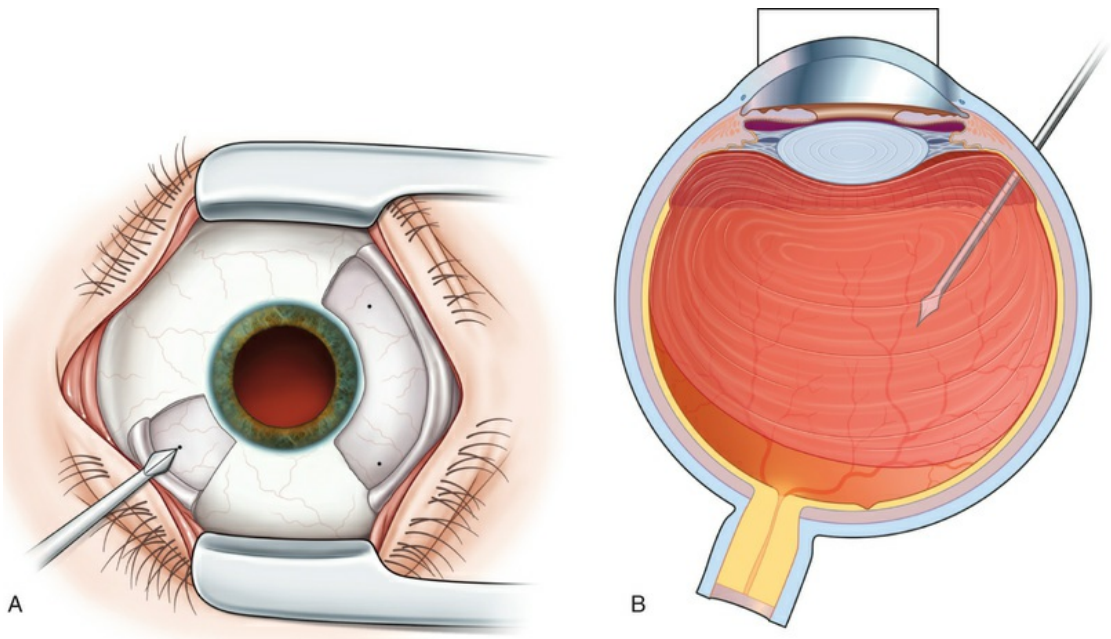

FIG. 115.14 The blade or trocar is directed toward the center of the vitreous cavity to avoid contact with the

lens or retina.

However, 27- and 25-gauge systems might be more preferred in easier diabetic cases such as nonclearing vitreous hemorrhage or macular edema.[111,118] In eyes with complex pathologies where silicone oil injection is likely, 23- or even 20-gauge incisions provide the surgeon with a higher range of instrumentation and an easier silicone oil tamponade.[111,116,118] Suturing of sclerotomies is recommended in silicone oil use because silicone oil can evade through unsutured wounds subconjunctivally. Precise infusion cannula placement is critical to avoid suprachoroidal infusion and choroidal detachment (Fig. 115.15).

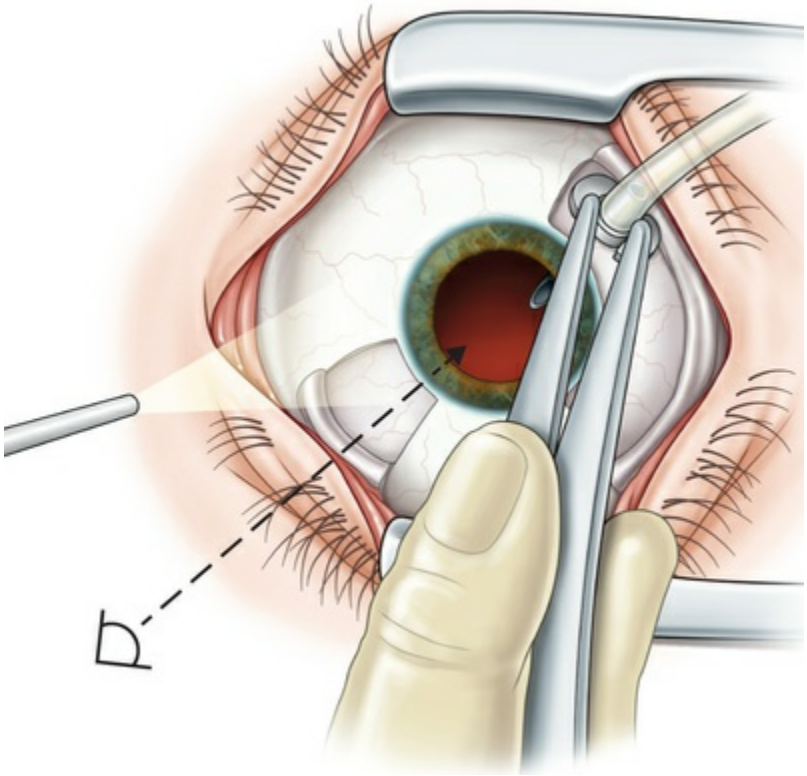

FIG. 115.15 The infusion cannula is inserted and secured with a suture in the inferotemporal pars plana sclerotomy. Indentation of the infusion cannula allows visualization of the unobstructed tip in the vitreous cavity behind the pupil.

A 6-mm cannula can be used instead of the routinely used 4-mm infusion cannula in eyes with anterior displacement of the retina or fibrotic tissue strongly connected with the retina. Sometimes both

hands are needed for dissection of epiretinal tissue with forceps and scissors. Then, a four-port vitrectomy is needed in which a (chandelier-) light probe is fixed either in the nasal inferior quadrant or at 12 o'clock between the two superior sclerotomies.

Vitrectomy

Light probe and vitrector are inserted through the trocars/sclerotomies, and vitreous removal is started behind the crystalline or intraocular lens (Fig. 115.16). The infusion is turned on only when the cutter is in the eye and vitreous removal can be started simultaneously. Otherwise, the infusion pressure will move the lens implant anteriorly and iris incarceration into the wound can occur. The anterior part of the vitreous is removed under microscopic view, then a wide-angle viewing system (e.g., BIOM) is inserted and central vitreous removal performed.

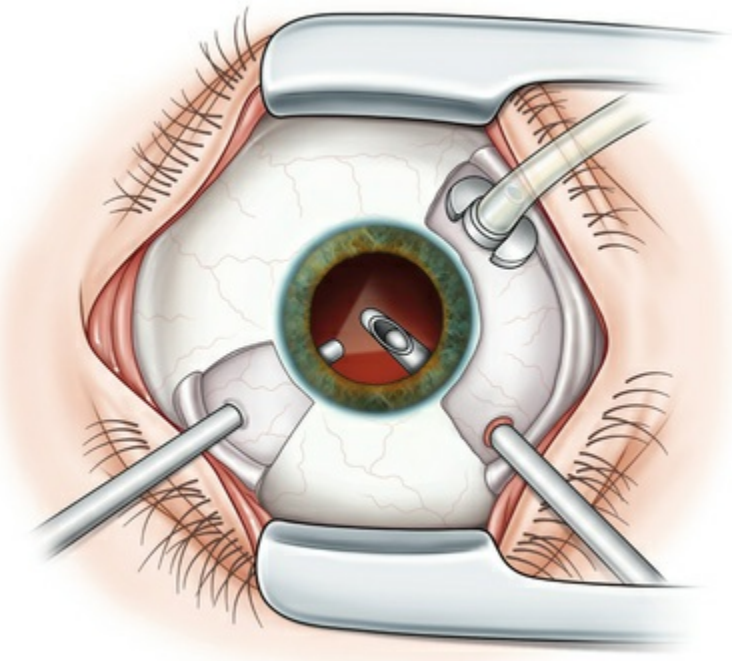

FIG. 115.16 The vitreous cutter and fiberoptic illuminator are positioned in the anterior vitreous cavity and visualized through the pupil.

To facilitate identification of the vitreous cortex, triamcinolone acetonide may mark otherwise invisible remnants or patches of vitreous on the retina.[125,126] Due to its antiinflammatory potential it

may also help to prevent fibrin exudation in proliferative diabetic retinopathy. Intravitreal doses of 2–4 mg of triamcinolone acetonide will offer sufficient staining with no retinal toxicity.[105,127]

Eyes With Complete Posterior Hyaloid Separation.

If a nearly complete separation of the posterior hyaloid is present after anterior and central vitreous removal, the posterior hyaloid membrane is incised and the opening enlarged circumferentially to allow adequate visualization of the retinal area (Fig. 115.17).[12] While cutting rate is usually highest (3000–7000 cuts/min), aspiration might be increased in the midportion of the vitreous, but should be decreased again during posterior hyaloid removal to avoid unnecessary traction. Blood might be pooled at the posterior pole, usually unclotted, and it can be aspirated with a soft-tipped fluid needle (Fig. 115.18). As precise visualization of the retina is achieved, areas of neovascularizations or small bleeding sources can be identified. Diathermy should be used for bleeding sources, and then the vitreous is removed out to the periphery. Indentation is used to remove all anteriorly located blood and vitreous. Otherwise this can be a source for rebleeding, tissue contraction, and rubeosis iridis. Full-scatter endophotocoagulation is now performed up to the peripheral retina for the same reason.

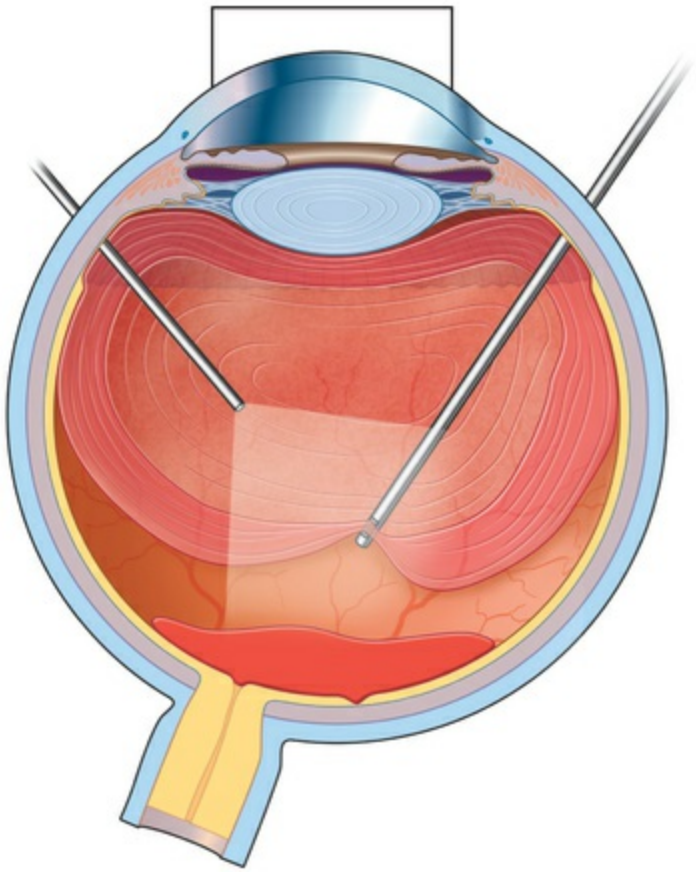

FIG. 115.17 The vitreous cutter easily incises the posterior hyaloid face since a complete posterior vitreous detachment is present.

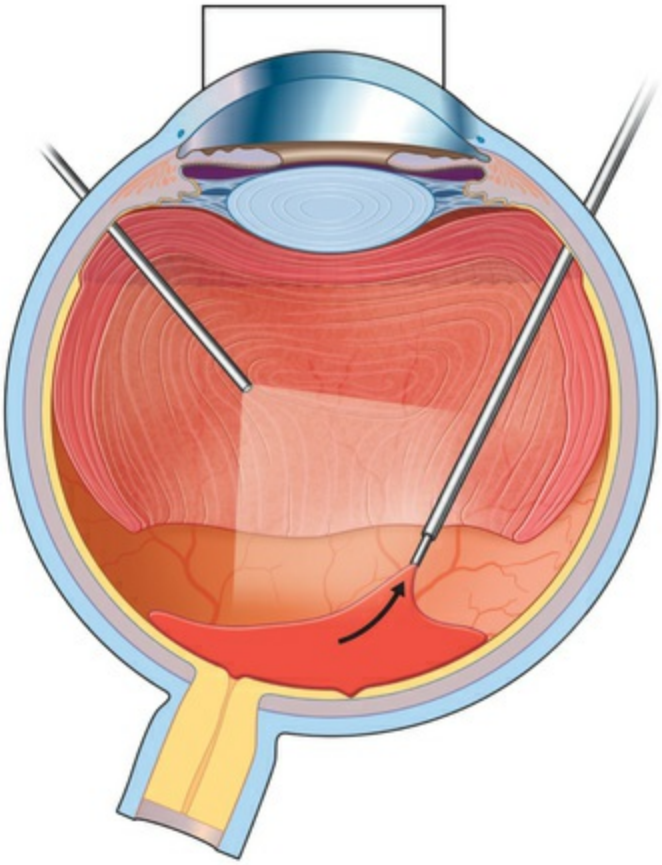

FIG. 115.18 Removal of layered hemorrhage using a soft-tipped cannula.

If a glistening reflex over the fovea is visible, dyes or an intraoperative OCT system (Fig. 115.19) can be used to look for residual preretinal membranes; as well, the internal limiting membrane can be removed. However, it remains uncertain if removal of the internal limiting membrane improves the final visual outcome.

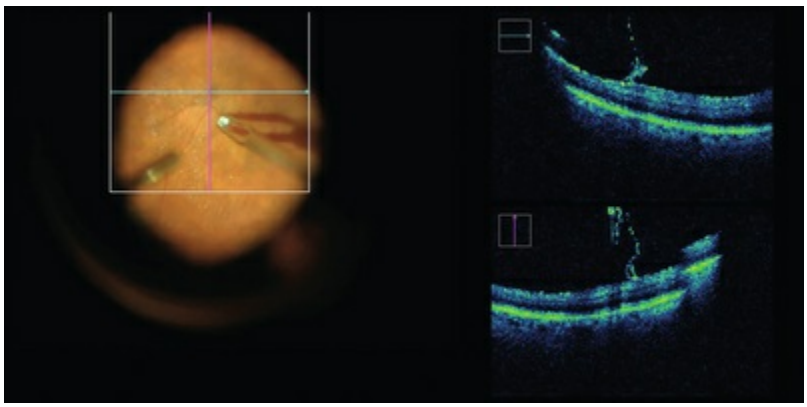

FIG. 115.19 Intraoperative optical coherence

tomography to visualize epiretinal membrane formation and removal.

In contrast, it was reported from a pilot study that peeling of the internal limiting membrane in proliferative diabetic retinopathy with fibrovascular proliferations might reduce postoperative epiretinal membrane formation; similarly, this was reported for primary retinal detachment (RD) repair surgery[51,160]

Finally, an air tamponade can be used to avoid both hypotony and hemorrhage in small incision vitrectomy. In phakic eyes, anterior vitrectomy can be performed using indentation, but usually more residual vitreous will remain than in pseudophakic eyes.

Eyes With Incomplete Posterior Hyaloid Separation.

If incomplete separation of the posterior hyaloid is present, which is usually the case in these eyes, surgery can be difficult and should remain in experienced hands. Usually a core vitrectomy is performed at the beginning to gain sufficient view over the areas of adhesion and the connections between them. If there is a wide separation between the formed vitreous and the retina, circumferential release of anterior–posterior traction can be achieved with the vitreous cutter. However, if the posterior vitreous is closely overlying the retina in certain areas, care must be taken not to injure the retina (Fig. 115.20). If the retina is attached, gentle suction with the vitrector might be sufficient to further separate the vitreous from the retina to provide safe dissection. If the retina is detached or holes do exist, separation of tissue might be achieved with the use of some viscoelastic to provide higher safety.[161–163] In any case, careful separation, usually with scissors, has to be done. Several surgical techniques for membrane removal have been developed. The first were delamination and segmentation.[164] In segmentation, tractions between centers of adhesions are removed (Figs. 115.21 and 115.22),[12,55,165] while in delamination, the connections between the posterior hyaloid and/or fibrovascular tissue and the internal limiting membrane are cut (Fig. 115.23).[165–167] The later developed "en bloc" technique includes removal of the vitreous and associated vitreoretinal membranes as a single unit

(Fig. 115.24).[168] If only one or few focal adhesions do exist, vitrectomy might be started with a core vitrectomy, followed by excision of the posterior hyaloid over 360° in order to separate small islands of adhesions. If extensive, firm adhesions are present, the "en bloc" technique might facilitate surgery: a core vitrectomy is performed and the posterior hyaloid opened in an area close to or over the optic nerve. The fibrovascular tissue is now grasped with an end-gripping forceps and the tissue separated. Gentle traction is exercised to avoid bleeding or hole formation. If it is possible to loosen the connected tissue over the posterior pole in one piece, then the remaining hyaloid of the peripheral vitreous will lift the residual vitreous and membranes into the midvitreous cavity, where it can be removed safely (Fig. 115.25). As tempting as it might sound to remove everything in one big piece, two things need to be mentioned: first, complete removal of membranes and vitreous together in cases with adhesions of different strength is rarely possible. Second, bleeding from several sources might create a less controllable situation. If confronted with a firm adhesion during the "en bloc" technique, a change to delamination or segmentation is advisable. The newer cutters of the 23- and 25-gauge systems have an opening nearer to the end tip and do allow segmentation of tissue without additional scissors or picks (Fig. 115.26). The use of some perfluorocarbon to prevent bleeding into the foveal area can be helpful if a bridging membrane has been removed, but further dissection needs to be done in the midperipheral retina. If the retina is cleaned from all fibrovascular tissue up to the periphery and bleeding sources are cauterized, circular photocoagulation treatment is performed up to the ora serrata under indentation.

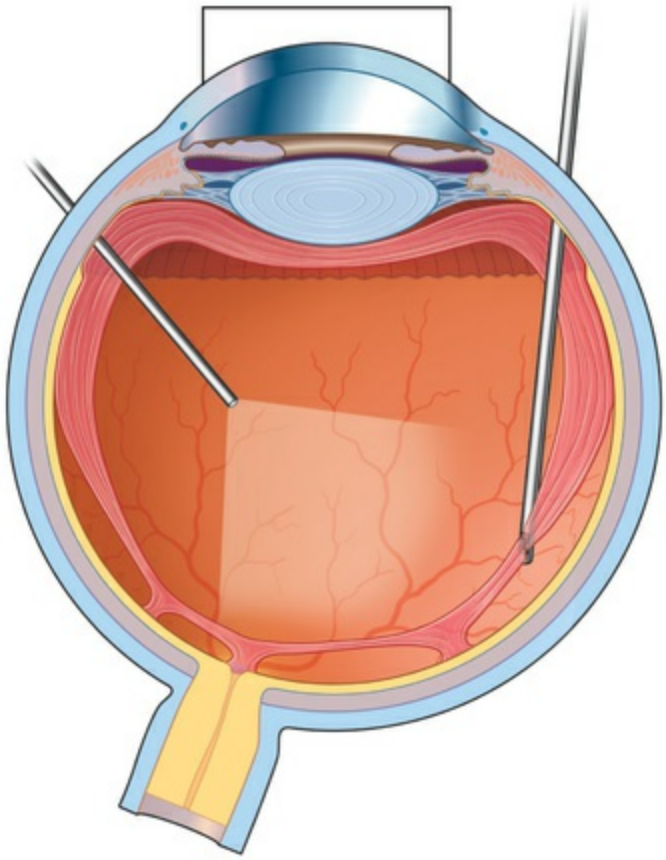

FIG. 115.20 Incomplete posterior vitreous detachment with multiple focal vitreoretinal adhesions. An opening is made in the outer cortical vitreous into the subhyaloidal space in an area of vitreoretinal separation. The cutting port is against the cortical vitreous and away from the retina.

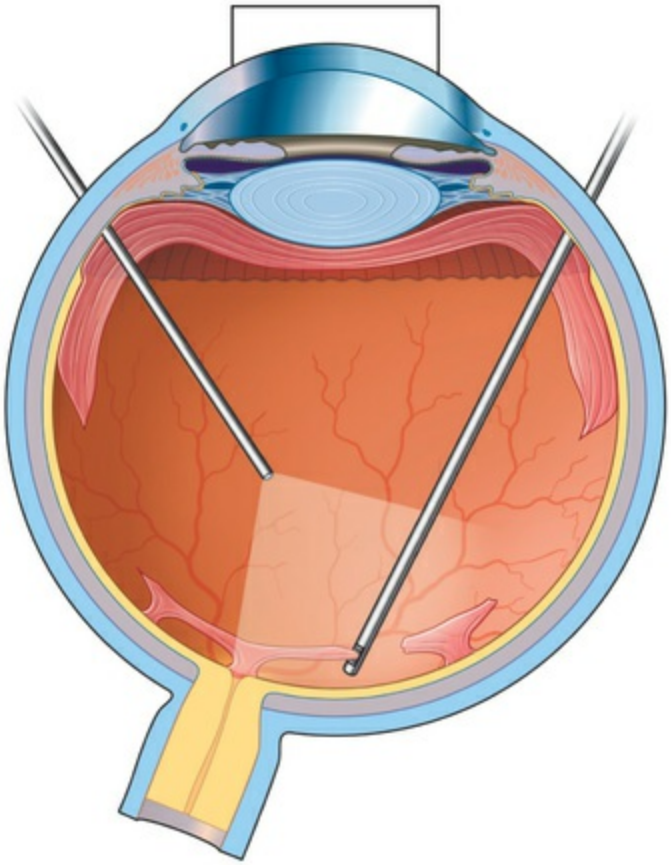

FIG. 115.21 Tangential traction is released with the vitreous cutter by excising the remaining posterior hyaloid and fibrovascular tissue between areas of vitreoretinal adhesions.

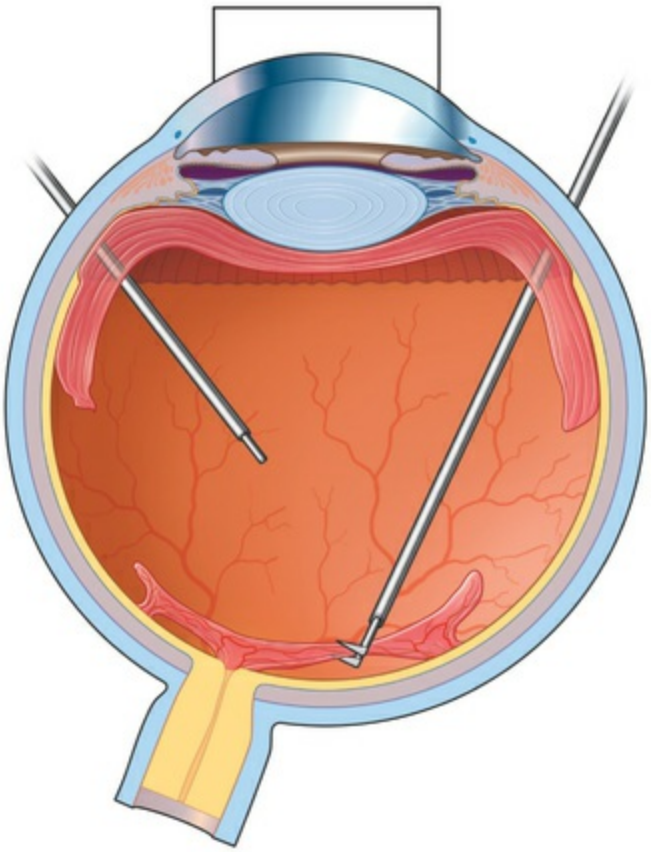

FIG. 115.22 When posterior vitreous separation is inadequate to accommodate the vitreous cutter, a plane between the posterior hyaloid and retina can be created with vertical membrane peeler–cutter scissors.

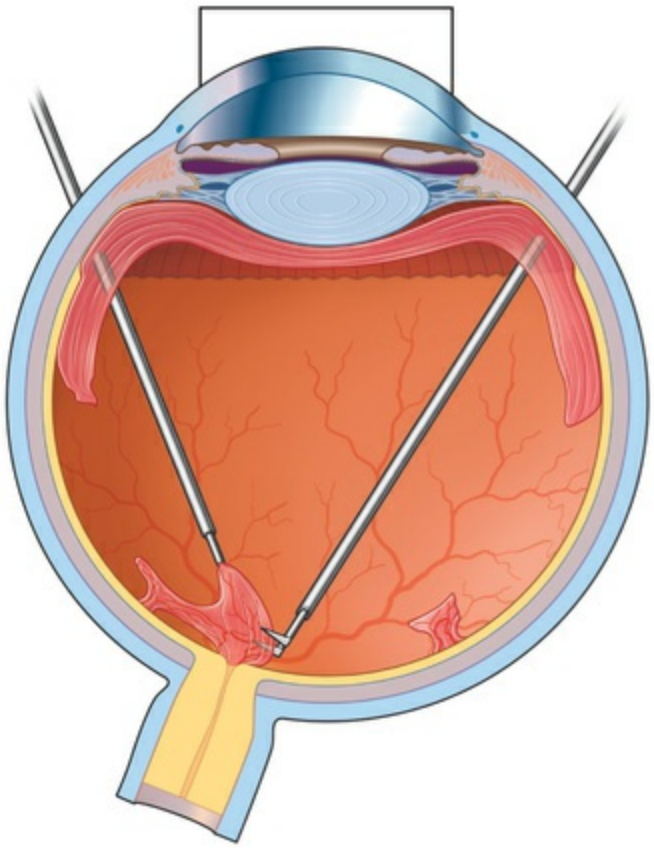

FIG. 115.23 In delamination, fibrovascular adhesions to the posterior hyaloid are excised parallel to the retinal surface with horizontal scissors.

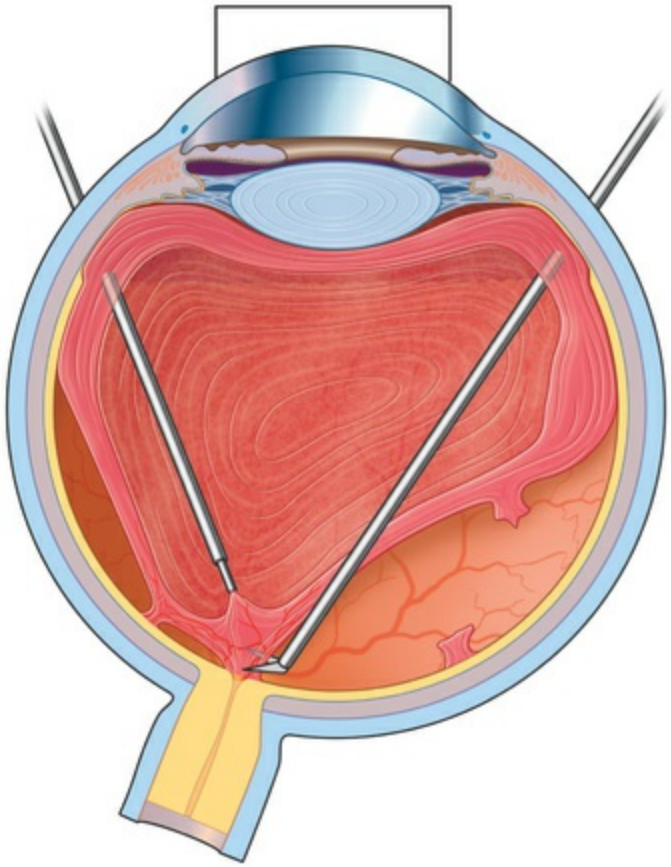

FIG. 115.24 En bloc vitrectomy. After an opening is made in the posterior hyaloid adjacent to vascular epicenters, membrane peeler–cutter scissors enter the subhyaloidal space. The unremoved formed vitreous provides anterior traction that helps separate the vitreous and fibrovascular tissue from the retina and helps identify sites of adhesion.

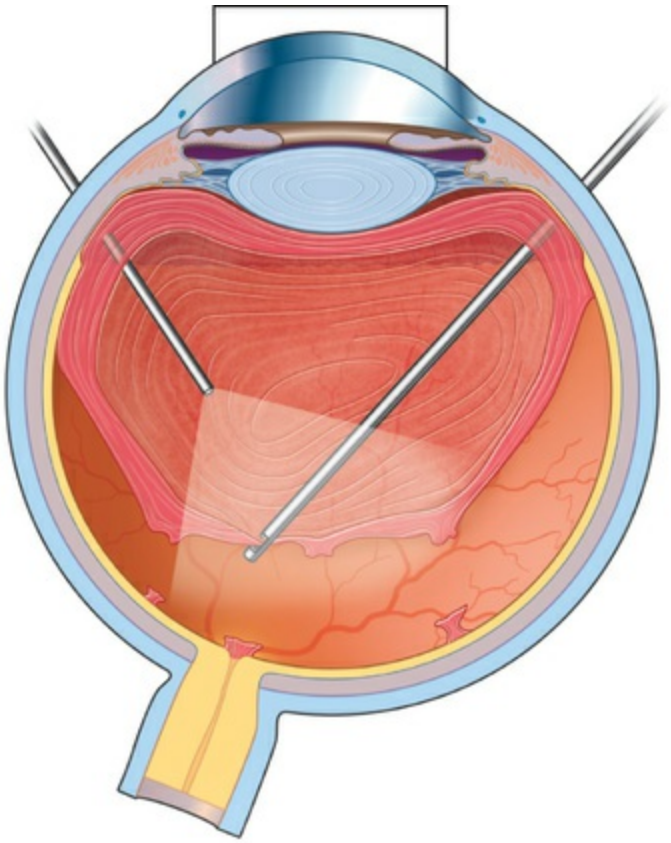

FIG. 115.25 After all posterior adhesions have been released, the vitreous cutter is used to excise the detached formed vitreous and associated fibrovascular membranes en bloc.

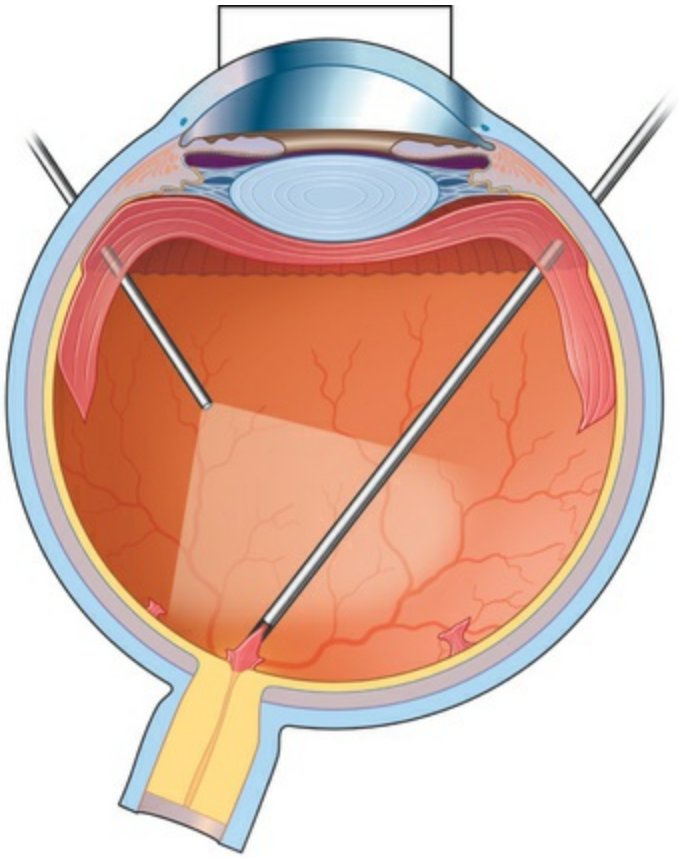

FIG. 115.26 Fibrovascular tissue that is firmly attached to the disc is reduced with the vitreous cutter.

Eyes With Subtotal Posterior Vitreous Adhesion.

If the posterior hyaloid is almost completely attached to the retina, access to the subhyaloidal space is difficult. After a core vitrectomy is performed, gentle suction can be used to find areas where the vitreous is less adherent. Usually, these are areas of subhyaloidal hemorrhage. As it is not possible to incise this tissue with the vitrector, a sharp blade or subretinal pick is used to create an opening into the subhyaloidal space. The safest areas for such maneuvers are around the optic disc. Once part of the hyaloid is lifted, a patient separation of the fibrovascular tissue is needed.

Usually, dissection is performed centripetally. Again, bleeding sources need to be cauterized immediately, and it is mandatory to maintain a controlled situation. If retinal holes are detected under proliferating tissue or created during preparation, the surrounding tissue must be excised without residual traction. Also here, some perfluorocarbon might be helpful to flatten out a localized retinal

detachment and facilitate sufficient laser treatment of the holes. As already mentioned above, careful panretinal laser treatment is performed once the retina is cleaned. The tamponade of choice can be either a longer-acting gas tamponade or silicone oil.

When identifying the posterior vitreous cortex in diabetic patients, surgeons should be aware of posterior vitreoschisis, simulating posterior vitreous separation (Fig. 115.27).[94,169] If this phenomenon is unrecognized, only the inner wall of the vitreoschisis will be removed, leaving much traction unrelieved.[12]

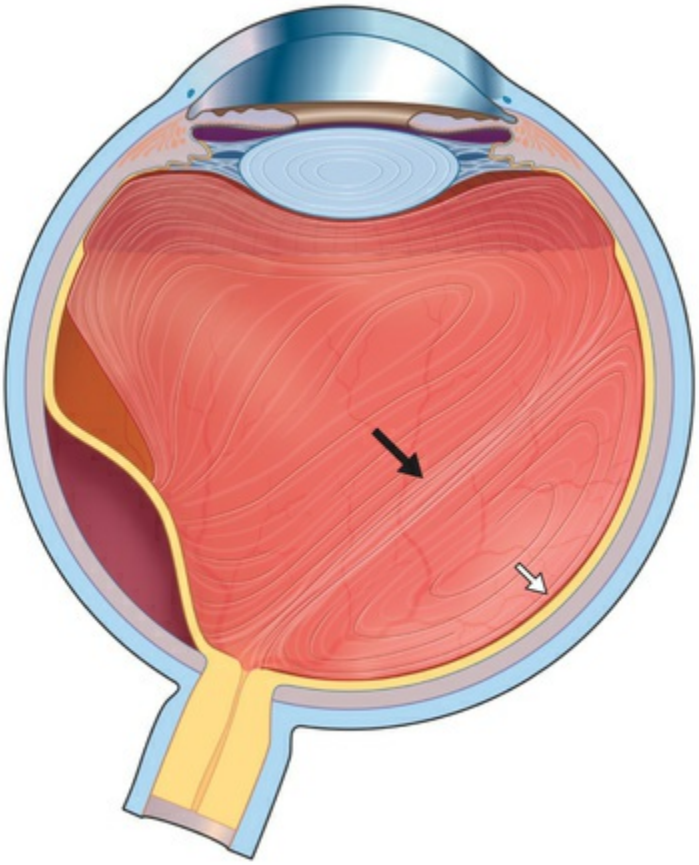

FIG. 115.27 Posterior vitreoschisis. Split hyaloid with partial vitreous separation. Although there is unseparated posterior hyaloid (*white arrow*), there is a pseudohyaloidal membrane (*black arrow*), giving the illusion of vitreous separation. The pseudohyaloidal membrane may be the result of condensed vitreous collagen that is often found after a hemorrhage in formed vitreous.

Eyes With Combined Tractional and Rhegmatogenous Detachment.

In eyes in which rhegmatogenous retinal detachment is present in addition to tractional detachment, great care has to be taken to avoid aspiration and inadvertent cutting of the retina. Core vitrectomy is performed with lesser suction than usual, and the tissue is carefully inspected before cutting. Once a clear overview of the retinal situation is created, dissection of tissue is started usually in an area distant from the detached retina. Still, preparation of tissue from the center to the periphery is advisable. Perfluorocarbon can be used to stabilize the posterior retina, while further tissue removal in the periphery is performed. However, if an atrophic retinal detachment is present, the use of perfluorocarbon can be dangerous because the retina is inelastic and shortened. A primarily small retinal hole can turn into a large retinal hole, and perfluorocarbon may glide in the subretinal space. A similar situation can occur when silicone oil tamponade is used too early and the retina is still under traction. Careful inspection of the periphery under indentation is needed, and anteriorly dislocated retina is either freed from fibrotic tissue or cut. Retinectomies and retinotomies should be used only in selected cases and performed as a last resort (see also Chapter 112, Retinotomies and retinectomies). They cannot replace careful membrane dissection. Usually peripheral retinectomies are needed in eyes where reoperations become necessary and severe anterior hyaloid fibrovascular proliferation has developed. Before the retina is cut, diathermy is applied to the anterior and posterior margin of the retina and the vessels to be excised. The extension of the retinotomy should reach normal retinal area around the area of traction. The retina can be cut either with the cutter or scissors. If not already detached, a shallow detachment must be created in order to cut without traumatizing the choroid or creating hemorrhage. It is mandatory in diabetic vitrectomy to release all tractions around retinal holes before tamponades can be used. The anterior part of the retina is also trimmed and cauterized in retinectomies to avoid secondary fibrosis of residual anterior retina and traction on surrounding tissue and/or the ciliary body. Smaller posterior retinotomies can also become necessary if persistent traction

around an old tear exists. Silicone oil is the tamponade of choice for diabetic eyes requiring retinectomies. Eyes requiring retinectomies have a poorer outcome and visual prognosis than those not requiring them.[170] Placement of a scleral buckle can be added to complex surgery in diabetic vitrectomy. It is usually performed in reoperations or as a primary surgery in younger diabetic patients where massive activity and fibrovascular proliferation and detachment exist, but visual acuity is still useful.

In primary procedures, the retina is usually more elastic and an additional encircling band might make a large retinectomy unnecessary. Usually, the surgery is started with episcleral surgery. The conjunctiva is dissected over 360° at 1–2 mm distance from the limbus, and Tenon capsule peritomy performed. Four-0 sutures are placed under each rectus muscle and four 5-0 nylon mattress sutures prepared in each quadrant to secure the band. The anterior suture is placed 2–4 mm behind the insertion of the rectus muscles; the posterior suture depends on the size of the band. For a 4-mm band, at least a 6-mm distance between sutures has to be chosen in order to create indentation. Alternatively, scleral tunnels can be created for this purpose. When the silicone band is placed under the muscles and the sutures (or tunnels), sutures are fixed and the ends of the band secured with a variety of choices.

The buckle should be relatively shallow and mainly support the vitreous base. A paracentesis can be performed to reduce pressure during buckle placement. Certainly fixation of the cerclage can be postponed until after vitrectomy, but this makes a change from internal surgery to external surgery necessary. In eyes where lens surgery is planned, an inferior sclerotomy is placed to allow some liquefied vitreous to escape. Then the infusion line is prepared but not turned on. If the eye pressure is too high, a second or third paracentesis is performed. If the anterior chamber is deep enough to allow cataract surgery, a small limbal incision is performed and the anterior chamber filled with viscoelastic. Routine phacoemulsification and IOL implantation follows as the next surgical step. A permanent or transient 10-0 nylon suture to seal the cataract wound is advisable in complex diabetic vitrectomy, where changes in intraocular pressure can be expected during and after surgery.

Photocoagulation

Panretinal photocoagulation with an endophotocoagulation probe is always performed during diabetic vitrectomy to achieve regression of neovascularizations and to create adhesions around retinal breaks, retinotomies, and retinectomies.[6,43,163,171] Although preexisting panretinal photocoagulation might be present, additional photocoagulation is usually applied, especially to the retinal periphery, and in areas around neovascularizations.

The adequate coagulation effect requires apposition of the retina to the retinal pigment epithelium, which eventually requires the use of intraoperative internal tamponades, as gas or perfluorocarbon liquids.[172] The power of the laser beam is continuously adjusted, depending on the clarity of media, the density of subretinal pigmentation, and the distance to the retina. The angle of the instrument in relation to the retinal plane will also influence intensity of the coagulates. Whitish laser effects should be visible; however, hard hyperintense treatment should be avoided.[43,173]

Endocryocoagulation is rarely applied to the retinal periphery today because endophotocoagulation with flexible probes is available, which makes a treatment up to the ora serrata possible, eventually with the help of scleral depression.[174] Moreover, cryocoagulation usually causes more inflammation than standard panretinal photocoagulation, and the effect is less predictable.[43]

Tamponades

Various gases and liquids are in use to provide internal tamponade of the vitreous cavity. As a short-term intraoperative instrument, heavy perfluorocarbon liquid is most commonly used. It is helpful to reattach the retina, permitting panretinal photocoagulation or membrane dissection. Perfluorocarbon must be completely removed before the end of surgery due to retinotoxic effects.[133–136] Filtered air serves as short-term tamponade for a few days. For a fluid–air exchange, infusion is turned off and air is supplied through the infusion port with a continuous air pump. A silicone-tipped fluid needle or cannula is then used to aspirate the fluid from the vitreous cavity. If subretinal fluid is present, it can be aspirated through a preexisting or iatrogenic retinal break.[12]

For a more prolonged tamponade in cases of retinal breaks with

traction, retinal detachments, or diffuse hemorrhage, different gases such as SF_6, C_2F_6, or C_3F_8 are in use, providing tamponade times from 2 to 8 weeks. Gases are preferred tamponades for superior or posterior pathologies or in patients where positioning is possible.[137–139] After fluid–air exchange, the intraocular air is usually exchanged for long-acting gases. The eye is flushed with gases in the desired nonexpansive concentration, usually 18% for SF_6, 16% for C_2F_6, and 14% for C_3F_8, to guarantee for a maximal duration with no risk of pressure elevation. If nitrous oxide is used in general anesthesia, it must be discontinued 20 minutes before gas injection to prevent high nitrogen in the gas bubble, resulting in an undesirably small postoperative gas bubble.[12]

Finally, silicone oil is the instrument of choice in reoperations or severe cases, if a longer tamponade is required, if positioning is difficult, or if air travel is necessary. Silicone oil may be instilled directly or after fluid–air exchange. In aphakic eyes, an inferior ("Ando"-) iridectomy should be created to prevent silicone oil from entering the anterior chamber. If possible, silicone oils should be removed after several (3–6) months to avoid late silicone-related complications, as cataract, secondary glaucoma, keratopathy, or optic disc atrophy.[134,140,141,143,144]

Wound Closure

Sclerotomy closure prevents leakage of vitreous cavity fluid, gas, or silicone oil and helps to maintain a normal intraocular pressure. During closure of the superior sclerotomies, the infusion maintains a stable intraocular pressure; if self-sealing incisions were used, the intraocular pressure should be slightly lowered before removal of the cannulas. In 20-gauge vitrectomy, sclerotomies are sutured carefully with partial-thickness 7-0 or 8-0 Vicryl sutures. In 25- or 23-gauge transconjunctival small incision vitrectomy, wounds can remain unsutured. Here, the trocar cannulas will be removed and the eye may be pressurized with a gas bubble. If silicone oil is used, careful wound closure is recommended to avoid subconjunctival silicone escape. In addition, one should keep in mind that delayed wound healing is present in diabetic patients, simultaneously with a higher likelihood of infections, and therefore decide on the

necessity of suturing even smaller incisions. Injections of antibiotics and/or steroids in the Tenon capsule or the bulbar conjunctiva may prevent infection and postoperative inflammation. At the end of surgery a paracentesis may be necessary to normalize an increased intraocular pressure. Topical antibiotics, cycloplegics, and steroids are applied together with a sterile dressing and/or a protective shield.

Postoperative Care

Examinations

Regular ophthalmic examinations are scheduled according to the individual case; however, they should usually be performed on a daily basis in the first postoperative days. Additional unscheduled examinations are necessary when the patient complains of abnormal or increasing pain, especially in cases with a history of glaucoma or when expanding gas bubbles were used. It is reasonable to perform further evaluations on a weekly basis in the first month and on a monthly basis until the eye has stabilized and/or local or systemic medications are stopped.[87] Finally, periodical routine examinations every 3–6 months are recommended, according to the severity of diabetic retinopathy. In the routine evaluation, the anterior segment must be checked for unexpected inflammation, media opacities, or signs for neovascular glaucoma, such as rubeosis iridis. Intraocular pressure is monitored and normalized to prevent pain or eventual visual field loss. The posterior segment must always be carefully examined to observe the healing process and identify possible complications. Macular edema or tractional detachment may take time to resolve and can be monitored by optical coherence tomography. Written instructions, such as medical prescriptions or visits, are always preferred.[43,87,175]

Hospitalization and Convalescence

The length of any hospitalization is determined by the rules for admission, extent of surgery, and the condition of the patient.

Cataract surgery is usually performed on an outpatient basis, whereas after vitrectomy or complicated surgery, hospitalization is routine in many countries. The management of patients with pain or elevated intraocular pressure, who need more frequent examinations and adaptations of their medication, is always more efficient in hospital.[87] Furthermore, good diabetic and general medical control is necessary (see below).

When surgery on outpatient basis is performed, it is important to carefully instruct the patient for further behavior, medications, and visits. For confused or disoriented patients, it is important that responsible persons always accompany them. Postoperative positioning is of great importance when intraocular gases were used, depending on the location of retinal breaks, and this may be facilitated with pillows and tables.[43] Normally, adhesion of the retina to the retinal pigment epithelium occurs in 1–4 days after laser retinopexy.[176,177] Face-up positioning might accelerate cataract formation in phakic eyes, iris capture in pseudophakia, or loss of anterior chamber in aphakia.[178,179] If additional laser treatment is needed when a gas bubble is in the eye, the surgeon should be aware of unintentional retinal damage from laser beam reflection at the fluid/gas interface.[180] In cases with intraocular silicone oil tamponade, positioning is less critical. However, silicone oil changes the refractive power of the eye and interferes with diagnostic ultrasound, possibly hampering follow-up examinations or axial length measurements.[181,182] Despite the need for early silicone oil removal due to complications, silicone oil is usually removed after 3–4 months at the decision of the surgeon. Recurrent retinal detachment is unusual after silicone oil removal and appears to be independent of the duration of silicone oil tamponade.[183,184] In most severe cases, silicone oil might be also used as long-term tamponade to prevent phthisis of the eye.[144,185]

Medications

The common preference for few topical medications in ophthalmology might differ after surgery for proliferative diabetic retinopathy, especially in more complex cases. Patients will rarely feel heavy pain after vitrectomy, but it can happen more frequently

after additional buckling surgery.[87] Oral analgesics are usually sufficient, but sometimes additional intravenous analgesics are needed. The use of patches did not appear to be helpful in controlling pain from corneal abrasions; however, pain from corneal epithelial defects might be more common due to diabetic neuropathy.[186,187] An increase of intraocular pressure needs topical or systemic pressure lowering medications. Topical cycloplegic drops provide pupillary dilatation, immobilization of the ciliary body, reduction of inflammation, and the risk of synechia formation.[87] In addition, topical antibiotics, steroids, and antiinflammatory drops are prescribed in the first postoperative days or weeks to minimize inflammation and prevent infection. Steroids may be administered periorbitally during or after surgery. In severe cases, systemic antiinflammatory drugs or corticosteroids might be added, but they can interfere with the patient's antidiabetic medication. A sudden, increasing inflammation raises suspicion of endophthalmitis and needs urgent intravitreal antibiotic injection, vitreous culture, and vitrectomy.

Further Surgery

After cataract surgery, proliferative diabetic retinopathy must be sufficiently treated or re-treated with panretinal photocoagulation if it was not performed at time of cataract surgery.[21] Similarly, diabetic macular edema progression may be slightly lower when grid/focal laser and/or anti-VEGF medications are applied after lens extraction instead of before.[20] In patients who had vitrectomy surgery with silicone oil instillation, recurrent retinal detachment after silicone oil removal is unusual and seems not to be related to the duration of silicone oil tamponade.[183,184] In most severe cases, silicone oil might be used as a long-term tamponade to prevent phthisis.[144,185] In cases of secondary or neovascular glaucoma in the absence of preoperative panretinal photocoagulation, adjunctive treatments with panretinal photocoagulation, anti-VEGF injections, or glaucoma filtering surgery might be useful.[24,152,188]

Diabetes Control

The challenge for the primary care physician and the diabetologist

in managing all patients with diabetic retinopathy is to attain excellent glycemic control, aggressive control of blood pressure, and normalization of lipids.[189] After surgery for proliferative diabetic retinopathy, diabetic patients are at increased risk for adverse outcomes, which are related to preexisting complications of diabetes, especially atherosclerotic disease, nephropathy, and peripheral and autonomic neuropathy; similarly, hyperglycemia is associated with a higher risk for poorer wound healing or infections,[190] and a possible loss of nutrients through glycosuria.[191] The use of insulin offers great flexibility of timing and dose in the postoperative management of most diabetic patients. Short-acting insulin analogs have been shown to work well as premeal medication or as rapid counteraction against pronounced hyperglycemia for outpatients as well as hospitalized patients.[191]

On the other hand, rapid-acting insulin analogs may be associated with an increased risk for hypoglycemia, especially if the delay to the next meal is too long.[192] Accordingly, oral sulfonylurea and other insulin secretagogues lower blood glucose levels acutely; however, the risk for hypoglycemia is smaller with nonsulfonylurea agents.[191] In general, hospitalization provides a chance to organize long-term diabetes management issues: advice and information on optimum nutrition, exact glycemic control, management of hypertension or dyslipidemia, as well as basic guidelines for foot care should be given during this time. Finally, an appropriate diabetes education for newly diagnosed or poorly controlled diabetic patients, arrangements for medical nutrition, and regular medical follow-up visits are important to attain the best possible long-term surgical and medical outcomes.[191,192]

Complications

Intraoperative Complications

New technologies and improved understanding of the disease process have reduced both numbers and severity of complications in diabetic vitrectomy. Nevertheless, complications do occur and proper management is essential to achieve a successful completion of the surgery.

Cornea, Anterior Chamber, Lens

Reduced Visualization.

Corneal edema, a narrow pupil, and lens opacification are the main reasons for reduced intraocular visualization during vitrectomy in diabetic patients.[12] From these three, corneal edema still remains the most problematic.

Corneal Edema.

Reduced epithelial adherence and epithelial basement membrane abnormalities in diabetic patients predispose these eyes to develop corneal edema during surgery.[12,193,194] Clear visualization of details is hindered because of the edema, and this might occur during the most important steps during surgery. The occurrence of corneal edema might be related to intraocular pressure, dryness, duration of surgery, or trauma to the epithelium or endothelium.[194,195] Mechanical abrasion of the epithelium, performed almost routinely in diabetic patients in earlier years, should be avoided if possible. Gently wiping the cornea with a cotton-tip to reduce the water content might help for a short period. In addition, viscoelastic placed in the anterior chamber can improve visualization. The use of corneal lubricants as methylcellulose in different compositions maintains a longer corneal integrity and clarity during vitrectomy surgery, reducing the need for intraoperative debridement.[196] If an epithelial debridement is unavoidable, the patient should be provided with a medical contact lens at the end of surgery to provide painless and quick healing of the epithelial defect. It has been shown that the debridement rate for infusion lenses was 23.8% compared with 13.0% for sew-on lenses and 15.6% for non-contact wide-angle (e.g., BIOM) lenses.[197] Folds in Descemet's membrane may develop during fluid–air exchange, resulting in distortion of intraocular structures. This issue can be improved by viscoelastic, placed under the corneal endothelium.[12]

Pupillary Constriction.

Intraoperative miosis reduces peripheral fundus visualization. It usually occurs after prolonged surgery, ocular hypotony, or direct surgical trauma during cataract extraction. As wide-angle systems

are now used in almost all vitrectomies, better visualization is provided also if the pupil becomes medium-sized during surgery. Dilating medications, such as mydriatic agents or viscoelastic substances, might be used either topically or injected into the anterior chamber via a paracentesis. Alternatively, flexible iris hooks can be used temporarily to achieve better visualization of the periphery.[198,199]

Lens Touch, Cataract Formation.

Lens opacities may develop from direct instrument contact during surgery, after prolonged surgery in phakic patients, or, less frequently, if the patient's serum glucose is much higher than in the infusion fluid.[12,200] The overall incidence of postoperative cataract formation after vitrectomy in diabetic eyes was reported to occur in 17–37%.[17] Touching a clear lens with instrumentation must be avoided. As diabetic vitrectomies combined with lens surgery and IOL implantations are increasing in numbers, this problem has become rare. However, if lens opacification does occur during vitrectomy, immediate lens removal is advisable if the surgery would be otherwise incomplete. If lens opacification is so discrete that vitrectomy can be finalized, proper cataract surgery can be delayed. A careful dissection, especially in the horizontal meridian, may protect from lens touch; alternatively, a small amount of vitreous gel can be left behind the lens capsule to protect the lens from infusion fluid or mechanical damage.[194,200]

Intraocular Hemorrhage

Intraocular hemorrhage is frequently observed in proliferative diabetic retinopathy, representing a potential serious complication. Bleeding during surgery mainly occurs from inadvertent cutting of vessels. If not controlled immediately, it can prevent successful completion of surgery, with untimely silicone tamponade in an uncontrolled situation. As a general rule, even if a small hemorrhage occurs, the source needs to be identified and controlled. Systemic blood pressure should be immediately evaluated and treated aggressively if it is too high. Sometimes transient intraocular pressure elevation might be sufficient to control bleeding, but mainly diathermy should be used to cauterize

sclerotomy sites, iris vessels, choroid, or retina. Modern vitrectomy machines allow an automatic pressurization of the infusion system so that the intraocular pressure can be controlled faster and more exactly. The elevated pressure should then be normalized as soon as possible to prevent ischemic damage to ocular structures.[12] Combined instruments providing infusion and cauterization are useful because they eliminate the need to exchange instruments. For small hemorrhage, viscoelastic or perfluorocarbon can be used to prevent pooling of blood over the posterior pole; for a larger hemorrhage, thrombin was reported to control bleeding.[201,202] Pre- or intraoperative intravitreal application of anti-VEGF medication might reduce intraoperative complications and improve the surgical outcome in severe proliferative diabetic retinopathy.[203,204] Finally, blood clots should be carefully removed from the eye without provoking new hemorrhage. It is advisable to let a small plug of fibrin on the site that has bled to support hemostasis.[121] Reducing the intraocular pressure at the end of surgery may identify potential bleeding sites that can be treated before closing the eye.[12]

Retinal Breaks and Detachment

Retinal breaks are a typical, severe complication during or after any vitrectomy; however, in proliferative diabetic retinopathy they are observed more frequently.[161,205] Occult preexisting retinal breaks may be sometimes detected under fibrovascular tissue, or may occur during tissue manipulation. Usually they are located in the posterior pole and can be treated once all traction around the breaks is relieved. They mainly occur in eyes with long-standing tractional retinal detachment where the retina is atrophic and vulnerable. Although creation of holes should be avoided, small iatrogenic breaks are preferable to an unclean separation of the posterior hyaloid, resulting in persistent or recurrent traction. If a localized retinal detachment develops, perfluorocarbon is usually used to flatten the retina and to facilitate photocoagulation of the tear. A gas tamponade might also be sufficient to seal tears and retinal detachment.[161] Because fluid dynamics are now better controlled with newer vitreous machines, incarceration of the retina and tear formation at the entry sites have become rare. Trocar systems for

small-gauge vitrectomy can prevent excessive incarceration of tissue. However, entry site retinal detachments, related to postoperative shrinking of residual fibrovascular tissue around the sclerotomies, may still occur postoperatively. Posterior or central retinal breaks most frequently occur in eyes with chronic tractional detachments, massive vitreoretinal adhesions, or tractional fibrovascular proliferations.[205,206] For posterior breaks, diathermy can be used to recognize the breaks when performing laser coagulation under air or gas.

Subretinal Perfluorocarbon or Silicone Oil

As mentioned above, perfluorocarbon and silicone oil can glide under the retina if the retina is atrophic and under tension. In any case, removal is necessary. With subretinal perfluorocarbon, a more posteriorly located retinotomy can be created if the primary retinal defect is in the periphery and aspiration via a fluid needle or with an active aspiration cannula cannot be achieved. For subretinal silicone oil, aspiration via a fluid needle is rarely possible. A retinectomy might be the last resort to remove the subretinal substances. If perfluorocarbon or silicone oil can be removed successfully, further preparation of tissue is mandatory to relax the retina even if this means to enlarge a retinectomy. While maintaining a rather low intraocular pressure, perfluorocarbon is injected again slowly over the optic disc and additional photocoagulation is performed around the retinotomies and retinectomies. Carefully, perfluorocarbon is then exchanged with silicone oil.

Postoperative Complications

The most frequent postoperative complications after vitrectomy for diabetic retinopathy are elevated intraocular pressure, corneal erosion, fibrin formation, bleeding, and retinal detachment.

Anterior Segment

Conjunctival Complications.

Wound dehiscence and stitch abscess may eventually progress to

conjunctivitis, scleritis, or endophthalmitis. It is commonly treated by local or systemic antibiotic therapy after taking a swab from the infectious site; treatment should be continued until resorption of all sutures. Careful stitching or buried knots may prevent incision sites or scleral implants from exposure. Subconjunctival silicone oil granuloma is prevented by exact closure of sclerotomies.[193]

Corneal Complications.

Corneal epithelial defects after vitrectomy in diabetic patients are common. They may be caused by prolonged operating time or iatrogenic debridement, and are often the consequence of diabetic neuropathy and a pathologic basement membrane. Large corneal erosions heal slowly in diabetic patients and need immediate treatment to prevent scarring and additional visual loss. A curative contact lens might prevent pain and can be supplemented with a combination of liquefying drops as well as antibiotics.[194–196,207]

Uveitis.

Postoperative iritis and uveitis are usually mild following diabetic vitrectomy. Pronounced inflammation or fibrin deposition combined with pain is uncommon and should raise suspicion of beginning endophthalmitis. White deposits of triamcinolone after an intravitreal injection can simulate inflammation or hypopyon ("pseudoendophthalmitis") but are recognized by the chalk-white appearance of multiple crystals.[43,208]

Iris Neovascularization and Neovascular Glaucoma.

See below, Results of surgery by evidence-based trials.

Cataract Formation.

See below, Results of surgery by evidence-based trials.

Intraocular Pressure Elevation

Elevated intraocular pressure represents one of the most common issues in the early postoperative period after vitrectomy for proliferative diabetic retinopathy.[209–212] Moreover, diabetic eyes are especially vulnerable to pressure rise due to long-standing retinal

ischemia. In the literature, the incidence of significant pressure elevation of ≥30 mmHg is about 36% in the first 48 hours after surgery.[210] Elevation of intraocular pressure can occur as a result of inflammation after surgery, bleeding, or be related to tamponade use. In addition to antiinflammatory medication and mydriatics, topical antiglaucomatous treatment is primarily used. This can be supplemented with oral acetazolamide for the first postoperative days or weeks. If the pressure remains high but inflammation or blood have resolved, transscleral laser treatment might be indicated. In some cases, filtering surgery becomes necessary. For eyes with intraocular gas tamponade, the gas bubble may provoke angle closure from anterior displacement of the iris diaphragm.[213,214]

Face-down positioning may allow an accumulation of intraocular fluid in the anterior chamber; an additional paracentesis of the chamber can relieve excessive fluid. An expanding large intraocular gas bubble might as well be removed by fluid needle through the pars plana or through the limbus in aphakic eyes. For eyes with an additional scleral buckle, angle closure may result from choroidal detachment or swelling that can be treated by topical cycloplegics and corticosteroids.[12]

Fibrinoid Syndrome

As vitrectomy surgery in diabetic patients may lead to the breakdown of the blood–retina barrier, this can result in intraocular fibrin deposition.[12] In some patients, fibrin in the anterior chamber will provoke a pupillary block. In young patients with massive retinal ischemia, massive fibrin formation in the vitreous cavity (the fibrinoid syndrome) may cause tractional retinal detachment, a pupillary block, ciliary body detachment, hypotony, or finally rubeosis iridis with neovascular glaucoma.[215,216] Other risk factors include lensectomy, extensive dissection, intensive panretinal photocoagulation, or scleral buckle surgery. The incidence of the fibrinoid syndrome associated with retinal detachment was reported to be 5%.[215] Those eyes have a bad prognosis with recurrent fibrin deposition, intraocular hemorrhage, and tractional detachment.[217] Prophylactic treatment consists of a subconjunctival dexamethasone injection at the end of surgery. Postoperative fibrin formation is primarily treated with topical corticosteroids, applied

frequently during the day. If there is massive fibrin also in the vitreous, recombinant tissue plasminogen activator (r-tPA) can be injected into the anterior chamber.[218,219] In eyes in which a corneal erosion is present, peribulbar or subconjunctival injection of a corticosteroid might be preferable to topical treatment, to avoid delay of wound healing. When substantial fibrin deposition occurs, eyes are best managed with repeated vitrectomy, fibrin removal, and silicone oil injection.[12]

Vitreous Hemorrhage

Postoperative vitreous hemorrhage after vitrectomy is common. A single postoperative vitreous hemorrhage occurs in about 65% of patients, whereas 35% will suffer two or more recurrences of vitreous hemorrhage.[64,175,209,220] However, the vast majority of immediate postoperative vitreous hemorrhages are mild and do not impair fundus visualization; 80% of them will occur in the first postoperative year.[220] Vitreous hemorrhages may also occur in association with iris or angle neovascularizations, retinal fibrovascular proliferations, or an anterior hyaloidal fibrovascular proliferation (AHFVP).[12] A careful control of intraoperative hemorrhages may prevent or reduce postoperative vitreous hemorrhage (see above). The management of postoperative vitreous hemorrhage includes observation, vitreous cavity lavage, or repeated vitrectomy. A slight hemorrhage might occur in eyes where silicone oil has not been used. If it clears within 1–3 weeks, no further treatment is necessary. If the hemorrhage is massive, a washout procedure might be indicated after 3 weeks in eyes where the retina is attached. Serial ultrasound tests are mandatory in eyes without fundus visualization. If the retinal situation is unclear, repeated vitrectomy is necessary. Only 4–10% of cases will require another vitrectomy, which includes removal of blood and probable residual fibrovascular tissue, additional photocoagulation treatment, and most likely silicone oil tamponade.[25,32,167,221,222]

Anterior Hyaloidal Fibrovascular Proliferation

AHFVP is a most severe complication following diabetic vitrectomy, occurring in up to 13% of cases with severe proliferative diabetic retinopathy (Figs. 115.28 and 115.29).[43,223] The presentation

of AHFVP includes the growth of neovascular tissue onto the vitreous base, the anterior retina, ciliary body, lens capsule, and iris. Therefore patients may present with rubeosis iridis, vitreous hemorrhage, peripheral tractional retinal detachment, or hypotony.[43] Risk factors for AHFVP include male gender, type I diabetes, phakic patients, insufficient panretinal photocoagulation, severe ischemia with recurrent neovascularizations, and previous surgery with placement of a scleral buckle.[223] The origin of the disease may be at the sclerotomy sites or at the peripheral retina.[43,100] For treatment, cataract extraction, lensectomy, scleral buckling, extensive laser or cryopexy, and anterior dissection with eventual retinectomy might become necessary.[223] As membranes are highly vascularized, preoperative injections of bevacizumab can be helpful for short-term regression during vitrectomy.[224] The functional prognosis is always poor; therefore, all efforts for prevention and early detection of AHFVP should be made.[43]

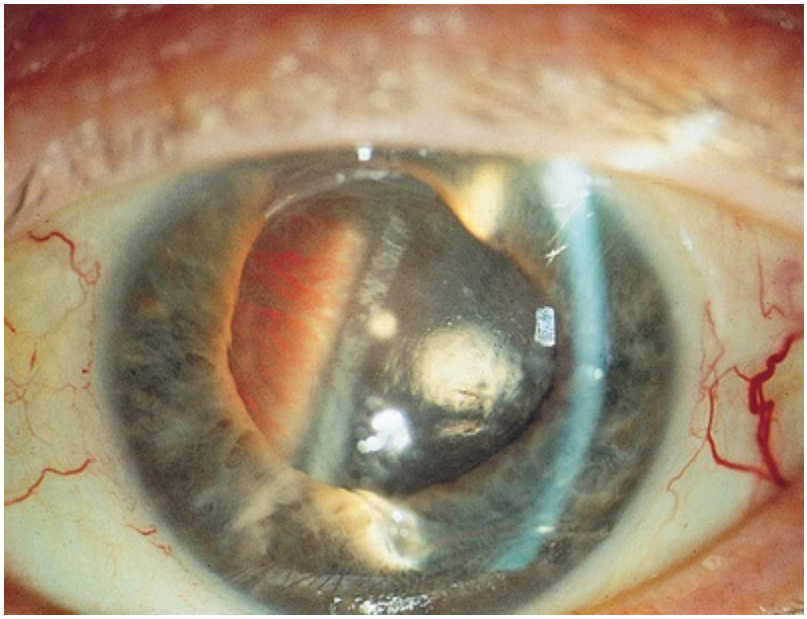

FIG. 115.28 Anterior hyaloid fibrovascular proliferation. Peripheral retinal fibrovascular proliferation is seen extending on the posterior lens capsule.

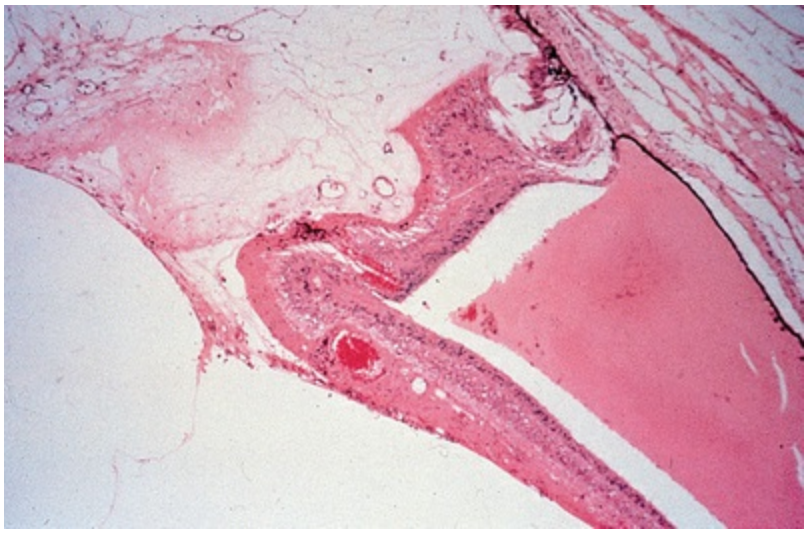

FIG. 115.29 Microscopic features of anterior hyaloid fibrovascular proliferation. The peripheral retina is detached and displaced anteriorly by fibrovascular tissue originating in the retina and extending along the anterior hyaloid towards the posterior lens capsule (hematoxylin and eosin, ×30).

Results of Surgery as Indicated by Evidence-Based Trials

Cataract

There is a frequent coexistence of cataract and proliferative diabetic retinopathy.[225,226] Improvement in acuity after cataract surgery may be achieved in >55% of patients,[227,228] but long-term results are generally inferior to patients without diabetes.[229,230] The Early Treatment for Diabetic Retinopathy Study (ETDRS) reported a gain of ≥2 lines in 64.5% of eyes with early and 59.3% of eyes with delayed panretinal photocoagulation one year after cataract surgery.[189,231] However, the literature regarding optimal timing of cataract surgery and panretinal photocoagulation, with respect to maximal visual gain and minimal risk of diabetic macular edema, is scarce.[73] There were reports about progression of untreated proliferative diabetic retinopathy after extracapsular cataract surgery or development of vitreous hemorrhage in 20% of patients after intracapsular surgery.[19,20,232] Another randomized study

reported that panretinal photocoagulation treatment shortly after cataract surgery was associated with less macular edema and less acuity loss than with panretinal photocoagulation right before cataract surgery.[73] As levels of intraocular VEGF and other cytokines are elevated after cataract surgery, intraocular injections of triamcinolone acetonide or anti-VEGF agents are indicated to stabilize the eye if panretinal photocoagulation cannot be adequately applied before cataract surgery.[233–237]

Similarly, those agents may be helpful in cases of diabetic macular edema with the risk of deterioration after cataract extraction.[238] Cataract surgery before or during vitrectomy was reported to produce faster visual recovery and less vitrectomy reoperations.[239–243] Disadvantages are a poor red reflex in eyes with vitreous hemorrhage and a higher rate of postoperative inflammation or synechia formation.[244–247] Inflammation has shown to be lower in two separate procedures or in combined vitrectomy with pars plana lensectomy procedures, especially in complicated tractional detachment cases requiring silicone oil tamponade.[22,245,248–252]

In all cases with combined surgery, independent of timing, additional complications may occur: capsular tears, zonulolysis (10%), anterior capsule opacification and traction, hypotony, or ciliary body effusion.[245,253–255] The risk of rubeosis iridis and neovascular glaucoma, on the other hand, is diminished to <1% with appropriate application of panretinal photocoagulation.[6,243,256] Visual outcome is related to the severity of diabetic retinopathy, according to the ETDRS.[256] Therefore, patients with proliferative diabetic retinopathy are far less likely to achieve a 20/40 or better acuity than patients with nonproliferative diabetic retinopathy.[227,256] In summary, the general effect of cataract surgery on the progression of diabetic retinopathy, diabetic macular edema, or proliferative diabetic retinopathy is still a matter of debate. Although literature is insufficient, it seems that if diabetic macular edema or proliferative diabetic retinopathy is sufficiently treated with laser and/or anti-VEGF medications before cataract surgery, no significant progression of diabetic retinopathy should occur.[256–258]

Vitreous Hemorrhage

In diabetic eyes with nonclearing vitreous hemorrhage, the benefit of early vitrectomy, defined as 1–4 months from onset, was clearly demonstrated by the DRVS.[27] Patients with visual acuity <5/200 and vitreous hemorrhage for 1–6 months were enrolled and randomized into an early and late surgery group, where vitrectomy was delayed for 12 months. Recovery of vision was significantly better for early surgery, compared to late surgery, at 3 months (50% vs. 17%) and 2 years (25% vs. 15%). Slightly better results for the early surgery group were reported at the 4 years-visit as well. Benefits were much higher for patients with type 1 (36% vs. 12%) than for those with type 2 diabetes mellitus (16% vs. 18%), probably because of the more severe course of proliferative diabetic retinopathy in type 1 diabetic patients.[27] Also, the poorer results for type 2 diabetics could be a consequence of a higher rate of maculopathy or posterior vitreous detachment in those cases. In addition, it should be noted that the DRVS preceded the use of the most contemporary equipment, including intraocular and indirect laser systems. Other retrospective studies for diabetic vitreous hemorrhage reported an improvement of acuity in >80% of operated cases, with a final vision of 20/200 or better in 48–72% of eyes, with a proportion of 20/40 or better in up to 38%.[32,221] Good prognostic factors are a preoperative vision >5/200, no neovascular glaucoma or rubeosis, no or minimal cataract, and preexisting panretinal photocoagulation in at least one quadrant.[32,221] Cases of associated anterior segment neovascularization (rubeosis iridis or manifest neovascular glaucoma) and/or severe progressive proliferation of the fellow eye are indications for an early vitrectomy.[25,27] Postoperative vitreous hemorrhage after vitrectomy is common; however, only 4–10% of cases will require another vitrectomy, according to the literature.[25,32,167,221,222,259,260]

Diabetic Maculopathy and Macular Traction

The benefits of early vitrectomy in cases with advanced proliferative diabetic retinopathy and macular traction, despite hemorrhage or retinal detachment, have been known since the DRVS:[7,261] in eyes after early vitrectomy, a final acuity of 10/20 or

better after 4 years could be reached in 44% compared with 28% of the nonoperated eyes (p<0.005).[7,73,261] Other authors reported improved vision after vitrectomy for macular traction detachments in 59–80% of cases, with a postoperative acuity of ≥20/200 in 21–58% of cases.[66,262–264] Starting in the 1990s, several authors reported good anatomic and functional effects of vitrectomy in persistent diabetic macular edema;[265–270] the procedure of surgically induced vitreomacular separation based on the finding that a posterior vitreous detachment was less frequent in patients with diffuse diabetic macular edema than in diabetic controls without edema.[271–274] Similarly, one trial reported about a resorption of diabetic macular edema in 55% of patients with posterior vitreous detachment, in contrast to only 25% of patients without.[274] Consequently, a large number of mostly retrospective case series and trials have been conducted, performing vitrectomy for diabetic macular edema in eyes with taut hyaloid adherent to the macula;[266–268,275,276] in eyes with attached, but nonthickened hyaloid;[277–280] in eyes with persistent diabetic macular edema despite previous laser or anti-VEGF therapy;[281–283] or as primary therapy in eyes with severe diabetic macular edema irrespective of posterior vitreous detachment.[284–288] One trial in eyes with diabetic macular edema unresponsive to laser therapy and a taut, adherent hyaloid reported a functional improvement of two lines in 49% and a reduction in diabetic macular edema in 94.5% of patients.[73,268]

However, the majority of those trials lack homogenous inclusion criteria or even an accurate definition of such criteria (as "taut hyaloid" or "macular thickening").[288] Similarly, the effect of internal limiting membrane peeling is still controversially discussed; potential benefits in releasing traction have to be weighed against surgical complications, such as possible toxic effects of indocyanine green staining.[289–291] Other open questions include different intraoperative steps that could affect diabetic macular edema: enzymatic adjuncts, panretinal photocoagulation or focal laser treatment, cataract extraction, or concomitant injection of anti-VEGF medications.[286,287,289,292–294] Interestingly, the effect of vitrectomy was found to be independent of preexisting posterior vitreous detachment in one case series, indicating other causative factors for diabetic macular edema, as different cytokines.[287,295]

Finally, results show a large variety of outcomes following vitrectomy. Even in those trials reporting both morphologic and functional improvements, the effects on morphology have been always more pronounced than the acuity gain. This could be the consequence of ischemia, more subretinal exudates, longer duration of diabetic macular edema, or damage of previous therapies.[296–299] Therefore, at least some agreement exists about which conditions may negatively affect the outcome after vitrectomy for diabetic macular edema: previous focal/grid laser therapy, presence of submacular fluid, longer duration of diabetic macular edema, significant ischemia, or subretinal fibrosis.[298,300–303] In sum, for best ophthalmic treatment, it is not only necessary to know the different techniques, risks, and benefits of vitrectomy in diabetic maculopathy; the most important clinical issue is whether to attempt focal/grid laser therapy or intravitreal antiangiogenic injections prior to surgery to treat the nontractional component of diabetic macular edema.[288,304]

For the future, large controlled, randomized, multicenter studies will hopefully provide a better definition of the role and efficacy of vitrectomy in diabetic macular edema, e.g., pharmacologic vitreolysis may be used adjunctively with small-gauge vitrectomy surgery, and precise nearly tractionless cutting of membranes seems possible with a new pulsed electron knife.[305,306]

Retinal Detachment, Tractional Detachment, and Proliferative Vitreoretinopathy

Outcomes of vitrectomy for retinal detachment in proliferative diabetic retinopathy are worse than for diabetic vitreous hemorrhage alone.[6,307] For diabetic tractional detachment, visual improvements of ≥2 lines have been reported in 60–75% of cases, with a mean postoperative acuity of ≥20/200 in 47–57% of patients, or ≥5/200 in 69–77% (Table 115.1).[57,58,168,309–312] An overall persistent reattachment rate of 82% was reported within 6 months,[304,313] with successful anatomic reattachment of the macula in 80–100%.[57,59,312,314,315] In contrast, for cases with complete tractional detachment, average reattachment rates were approximately 56%.[58] Results for combined rhegmatogenous and tractional detachments

or long detachments including the macula were even worse than for cases with tractional detachment alone. These subgroups reach visual improvements in 20–53%, a final acuity of ≥20/200 in 25–36%, and a final acuity of ≥5/200 in 55–68% of all eyes, on average.[61,262,307,313] Retinal reattachment was reached in 47–82%. With the use of encircling bands and silicone oil, attachment rates of 73–93% could be reached.[43] Improvement in vision increased to 64–81%, with a final acuity of ≥5/200 in 55–68% of eyes.[43,66,307,316–318] In a parallel fashion, the incidence of phthisis decreased from 10% to nearly 0%.

TABLE 115.1

Literature Overview of Vitrectomy for Diabetic Tractional Retinal Detachment

Author(s)	*n*	Scl. Buckl.	Lensect.	% Gas/Silicone	Outcome					
					Ret. Attached	≥5/200	≥20/200	Reop.	Improv.	Ph
Tolentino et al. (1980)[264]	140	±	4%	None	75%	67%	51%	NR	65%	9%
Rice et al. (1983)[262]	197	>35%	47%	± Gas; no Sil	57%	59%	NR	29%	57%	9%
Thompson et al. (1987)[263]	360	22%	29%	Gas 42; no Sil	69%	64%	NR	24%	48%	11
Oldendoerp and Spitznas (1989)[308]	100	39%	None	Gas 65; Sil 9	81%	77%	47%	9%	71%	4%
Williams et al. (1989)[59]	69	17%	7%	Gas 51; no Sil	83%	71%	NR	47%	NR	6%
Han et al. (1994)[60]	30	17%	3%	Gas 40; no Sil	97%	77%	54%	27%	NR	Nc
Steinmetz et al. (2002)[57]	67	24%	6%	Gas 64; Sil 1	93%	70%	57%	33%	72%	Nc

Improv., percentage of functional (visual) improvement; Lensect., lensectomy; *n*, number of cases in trials; NR, not reported; % Gas/Silicone, percentage of fluid–gas exchange or silicone oil instillation; Phthisis, percentage of postoperative phthisis bulbi; Ret., retina; Reop., reoperations rate; Scl. buckl., scleral buckling procedure.

Functional results are often disappointing, although a good anatomic success is achieved; this may be the consequence of (long-standing) retinal or macular ischemia, optic disc atrophy, or retinal thinning. Other conditions that negatively influence the outcome

are preoperative rubeosis iridis, neovascular glaucoma, age >50 years, visual acuity <5/200, ischemic maculopathy, vitreopapillary traction, lack of panretinal photocoagulation, vitreous hemorrhage, fibrinoid syndrome, or AHFVP.[6,55,58,61,73,248] As anatomic and functional results after vitrectomy have substantially improved, so too has the management of peripheral retinal tractional detachment in recent times.[318] Generally, there is a better prognosis, with a risk of only approximately 14% of severe visual loss per year.[55,73,319] Nevertheless, an earlier surgical approach in those cases seems reasonable to avoid the risk of macular involvement with poorer prognosis.[56–58,244] The need for vitrectomy reoperation generally ranges from 24% to 47% after diabetic tractional detachment, and from 29–90% after combined rhegmatogenous and tractional detachment, excluding laser treatment.[57,59,61,66,185,288,307]

Secondary Glaucoma (Neovascular Glaucoma)

At earlier stages of neovascular glaucoma with rubeosis and normal or moderately elevated intraocular pressure, panretinal photocoagulation alone can normalize pressure in 33–88% of patients.[320] Regression of rubeosis can be achieved in 33–94% of patients, depending on how many quadrants of anterior synechia are present.[152,321] In more advanced, refractory neovascular glaucoma, glaucoma filtering surgery is still the most promising approach; however, long-term success rates have been relatively poor, with an effective 5-year-control of intraocular pressure in only 25–30% of operated eyes. Similar results are reported for glaucoma implants, using Ahmed, Molteno, or Baerveldt valves.[152,322–324] A better control of intraocular pressure has recently been shown by panretinal photocoagulation and glaucoma implant surgery 1–2 weeks after an intravitreal injection of bevacizumab.[153,325] Success rates were 85% for patients who received adjunctive bevacizumab plus panretinal photocoagulation, compared with 70% for those who were given photocoagulation alone.[152,326,327] As an alternative treatment option, vitrectomy with photocoagulation may help to treat or prevent rubeosis iridis.[74,75] In earlier reports, a substantial risk of development or progression of iris neovascularizations after

vitrectomy in 8–26% of phakic and 31–55% of aphakic eyes was described;[15,328] however, recent series do not support this hypothesis any-more, quantifying the risk to <5%.[152,308] The risk may be somewhat higher (OR = 1.7) in the absence of preoperative panretinal photocoagulation.[64] In eyes with advanced neovascular glaucoma and low visual function, transscleral cryo- or diode-laser cyclocoagulation have proven as effective as trabeculectomy or drainage implant surgery.[156,157]

Conclusion

Modern vitrectomy techniques have significantly reduced the rate of severe visual loss in diabetic patients. The main surgical principles are removal of intravitreal hemorrhages, relief of vitreoretinal tractions by excising the posterior cortical vitreous surface, laser treatment of ischemic retinal areas, and application of tamponades or antiangiogenic substances. Prerequisites are complete, up-to-date technical equipment; refined skills; and, last but by no means least, well-trained and experienced surgeons.

Online Resources and Apps

http://www.mayoclinic.org/diseases-conditions/diabetic-retinopathy/basics/definition/con-20023311.
https://nei.nih.gov/health/diabetic/retinopathy.
https://en.wikipedia.org/wiki/Diabetic_retinopathy.
http://www.facharztzentrum-votivpark.at/augenkrankheiten/diabetische-augenerkrankung/.

References

1. Machemer R, Buettner H, Norton EW, et al. Vitrectomy: a pars plana approach. *Trans Am Acad Ophthalmol Otolaryngol*. 1971;75(4):813–820.
2. Aaberg TM, Abrams GW. Changing indications and techniques for vitrectomy in management of complications

of diabetic retinopathy. *Ophthalmology*. 1987;94(7):775–779.
3. Michels RG. Vitrectomy for complications of diabetic retinopathy. *Arch Ophthalmol*. 1978;96(2):237–246.
4. Michels RG, Ryan SJ Jr. Results and complications of 100 consecutive cases of pars plana vitrectomy. *Am J Ophthalmol*. 1975;80(1):24–29.
5. Machemer R, Parel JM, Norton EW. Vitrectomy: a pars plana approach. Technical improvements and further results. *Trans Am Acad Ophthalmol Otolaryngol*. 1972;76(2):462–466.
6. Flynn HW Jr, Chew EY, Simons BD, et al. Pars plana vitrectomy in the Early Treatment Diabetic Retinopathy Study. ETDRS report number 17. The Early Treatment Diabetic Retinopathy Study Research Group. *Ophthalmology*. 1992;99(9):1351–1357.
7. The Diabetic Retinopathy Vitrectomy Study Research Group. Early vitrectomy for severe proliferative diabetic retinopathy in eyes with useful vision. Results of a randomized trial – Diabetic Retinopathy Vitrectomy Study report 3. *Ophthalmology*. 1988;95(10):1307–1320.
8. Fong DS, Aiello LP, Ferris FL 3rd, et al. Diabetic retinopathy. *Diabetes Care*. 2004;27:2540–2553 [Review].
9. Ciulla TA, Amador AG, Zinman B. Diabetic retinopathy and diabetic macular edema: pathophysiology, screening and novel therapies. *Diabetes Care*. 2003;26:2653–2664.
10. Calles-Escandon J, Cipolla M. Diabetes and endothelial dysfunction: a clinical perspective. *Endocr Rev*. 2001;22:36–52.
11. Clermont AC, Aiello LP, Mori F, et al. Vascular endothelial growth factor and severity of nonproliferative diabetic retinopathy mediate retinal hemodynamics in vivo: a potential role for vascular endothelial growth factor in the progression of nonproliferative diabetic retinopathy. *Am J Ophthalmol*. 1997;124:433–446.
12. Eliott D, Lee MS, Abrams GW. Proliferative diabetic retinopathy: principles and techniques of surgical treatment. 4th ed. Mosby: Philadelphia; 2006:2413–2449. Ryan SJ, Hinton DR, Schachat AP, et al. *Retina*. vol. 142.

13. Kalka C, Masuda H, Takahashi T, et al. Vascular endothelial growth factor(165) gene transfer augments circulating endothelial progenitor cells in human subjects. *Circ Res*. 2000;86(12):1198–1202.
14. Asahara T, Masuda H, Takahashi T, et al. Bone marrow origin of endothelial progenitor cells responsible for postnatal vasculogenesis in physiological and pathological neovascularization. *Circ Res*. 1999;85(3):221–228.
15. Brunner S, Schernthaner GH, Satler M, et al. Correlation of different circulating endothelial progenitor cells to stages of diabetic retinopathy: first in vivo data. *Invest Ophthalmol Vis Sci*. 2009;50(1):392–398.
16. Brunner S, Hoellerl F, Schmid-Kubista KE, et al. Circulating angiopoietic cells and diabetic retinopathy in type 2 diabetes mellitus, with or without macrovascular disease. *Invest Ophthalmol Vis Sci*. 2011;52:4.
17. Hutton WL, Pesicka GA, Fuller DG. Cataract extraction in the diabetic eye after vitrectomy. *Am J Ophthalmol*. 1987;104(1):1–4.
18. Smiddy WE, Stark WJ, Michels RG, et al. Cataract extraction after vitrectomy. *Ophthalmology*. 1987;94(5):483–487.
19. Aiello LM, Wand M, Liang G. Neovascular glaucoma and vitreous hemorrhage following cataract surgery in patients with diabetes mellitus. *Ophthalmology*. 1983;90(7):814–820.
20. Suto C, Hori S, Kato S. Management of type 2 diabetics requiring panretinal photocoagulation and cataract surgery. *J Cataract Refract Surg*. 2008;34(6):1001–1006.
21. Menchini U, Cappelli S, Virgili G. Cataract surgery and diabetic retinopathy. *Semin Ophthalmol*. 2003;18:103–108 [Review].
22. Blankenship GW, Flynn HW Jr, Kokame GT. Posterior chamber intraocular lens insertion during pars plana lensectomy and vitrectomy for complications of proliferative diabetic retinopathy. *Am J Ophthalmol*. 1989;108(1):1–5.
23. Demetriades AM, Gottsch JD, Thomsen R, et al. Combined phacoemulsification, intraocular lens implantation, and vitrectomy for eyes with coexisting cataract and

vitreoretinal pathology. *Am J Ophthalmol*. 2003;135(3):291–296.
24. Schiff WM, Barile GR, Hwang JC, et al. Diabetic vitrectomy: influence of lens status upon anatomic and visual outcomes. *Ophthalmology*. 2007;114(3):544–550.
25. Ho T, Smiddy WE, Flynn HW Jr. Vitrectomy in the management of diabetic eye disease. *Surv Ophthalmol*. 1992;37(3):190–202 [Review].
26. Two-year course of visual acuity in severe proliferative diabetic retinopathy with conventional management. Diabetic Retinopathy Vitrectomy Study (DRVS) report. *Ophthalmology*. 1985;92(4):492–502.
27. The Diabetic Retinopathy Vitrectomy Study Research Group. Early vitrectomy for severe vitreous hemorrhage in diabetic retinopathy. Two-year results of a randomized trial. Diabetic Retinopathy Vitrectomy Study report 2. *Arch Ophthalmol*. 1985;103(11):1644–1652.
28. Gupta B, Wong R, Sivaprasad S, et al. Surgical and visual outcome following 20-gauge vitrectomy in proliferative diabetic retinopathy over a 10-year period, evidence for change in practice. *Eye*. 2012;26(4):576–582.
29. Tao Y, Jiang YR, Li XX, et al. Long-term results of vitrectomy without endotamponade in proliferative diabetic retinopathy with tractional retinal detachment. *Retina*. 2010;30(3):447–451.
30. Case reports to accompany Early Treatment Diabetic Retinopathy Study Reports 3 and 4. The Early Treatment Diabetic Retinopathy Study Research Group. *Int Ophthalmol Clin*. 1987;27(4):273–333.
31. de Bustros S, Thompson JT, Michels RG, et al. Vitrectomy for progressive proliferative diabetic retinopathy. *Arch Ophthalmol*. 1987;105(2):196–199.
32. Thompson JT, de Bustros S, Michels RG, et al. Results of vitrectomy for proliferative diabetic retinopathy. *Ophthalmology*. 1986;93:1571–1574.
33. Favard C, Guyot-Argenton C, Assouline M, et al. Full panretinal photocoagulation and early vitrectomy improve prognosis of florid diabetic retinopathy. *Ophthalmology*.

1996;103(4):561–574.
34. Wilkinson CP. What ever happened to bilateral patching? *Retina*. 2005;25(4):393–394.
35. Kuppermann BD, Thomas EL, de Smet MD, et al. Safety results of two phase III trials of an intravitreous injection of highly purified ovine hyaluronidase (Vitrase) for the management of vitreous hemorrhage. *Am J Ophthalmol*. 2005;140(4):585–597.
36. Ono R, Kakehashi A, Yamagami H, et al. Prospective assessment of proliferative diabetic retinopathy with observations of posterior vitreous detachment. *Int Ophthalmol*. 2005;26(1–2):15–19.
37. O'Hanley GP, Canny CL. Diabetic dense premacular hemorrhage: a possible indication for prompt vitrectomy. *Ophthalmology*. 1985;92(4):507–511.
38. Ramsay RC, Knobloch WH, Cantrill HL. Timing of vitrectomy for active proliferative diabetic retinopathy. *Ophthalmology*. 1986;93(3):283–289.
39. Kurihara T, Noda K, Ishida S, et al. Pars plana vitrectomy with internal limiting membrane removal for macular hole associated with proliferative diabetic retinopathy. *Graefes Arch Clin Exp Ophthalmol*. 2005;243(7):724–726.
40. Cooper BA, Shah GK, Sheidow TG, et al. Outcome of macular hole surgery in diabetic patients with nonproliferative retinopathy. *Retina*. 2004;24(3):360–362.
41. Heidenkummer HP, Kampik A, Petrovski B. Proliferative activity in epiretinal membranes. The use of the monoclonal antibody Ki-67 in proliferative vitreoretinal diseases. *Retina*. 1992;12(1):52–58.
42. Mori K, Gehlbach PL, Sano A, et al. Comparison of epiretinal membranes of differing pathogenesis using optical coherence tomography. *Retina*. 2004;24(1):57–62.
43. Pautler SE. Treatment of proliferative diabetic retinopathy. Browning DJ. *Diabetic retinopathy – evidence-based management*. Springer: New York; 2010:227–304.
44. Packer AJ. Vitrectomy for progressive macular traction associated with proliferative diabetic retinopathy. *Arch Ophthalmol*. 1987;105(12):1679–1682.

45. Faulborn J, Ardjomand N. Tractional retinoschisis in proliferative diabetic retinopathy: a histopathol study. *Graefes Arch Clin Exp Ophthalmol*. 2000;238(1):40–44.
46. Meyer CH, Schmidt JC, Mennel S, et al. Functional and anatomical results of vitreopapillary traction after vitrectomy. *Acta Ophthalmol Scand*. 2007;85(2):221–222.
47. Karatas M, Ramirez JA, Ophir A. Diabetic vitreopapillary traction and macular oedema. *Eye*. 2005;19(6):676–682.
48. Brazitikos PD, Stangos NT. Macular hole formation in diabetic retinopathy: the role of coexisting macular edema. *Doc Ophthalmol*. 1999;97(3–4):273–278.
49. Shimura M, Yasuda K, Nakazawa T, et al. Visual dysfunction after panretinal photocoagulation in patients with severe diabetic retinopathy and good vision. *Am J Ophthalmol*. 2005;140(1):8–15.
50. Mason JO 3rd, Yunker JJ, Vail R, et al. Intravitreal bevacizumab (Avastin) prevention of panretinal photocoagulation-induced complications in patients with severe proliferative diabetic retinopathy. *Retina*. 2008;28(9):1319–1324.
51. Chang PY, Yang CM, Yang CH, et al. Pars plana vitrectomy for diabetic fibrovascular proliferation with and without internal limiting membrane peeling. *Eye (Lond)*. 2009;23(4):960–965.
52. Sakimoto S, Saito Y, Nakata K, et al. Surgical outcomes of epiretinal membrane removal after successful pars plana vitrectomy for retinal diseases. *Jpn J Ophthalmol*. 2008;52(3):227–230.
53. Walshe R, Esser P, Wiedemann P, et al. Proliferative retinal diseases: myofibroblasts cause chronic vitreoretinal traction. *Br J Ophthalmol*. 1992;76(9):550–552.
54. Ryan SJ. Traction retinal detachment. XLIX Edward Jackson memorial lecture. *Am J Ophthalmol*. 1993;115(1):1–20 [Review].
55. Charles S, Flinn CE. The natural history of diabetic extramacular traction retinal detachment. *Arch Ophthalmol*. 1981;99(1):66–68.
56. Oshima Y, Shima C, Wakabayashi T, et al. Microincision

vitrectomy surgery and intravitreal bevacizumab as a surgical adjunct to treat diabetic traction retinal detachment. *Ophthalmology*. 2009;116(5):927–938.
57. Steinmetz RL, Grizzard WS, Hammer ME. Vitrectomy for diabetic traction retinal detachment using the multiport illumination system. *Ophthalmology*. 2002;109(12):2303–2307.
58. La Heij EC, Tecim S, Kessels AG, et al. Clinical variables and their relation to visual outcome after vitrectomy in eyes with diabetic retinal traction detachment. *Graefes Arch Clin Exp Ophthalmol*. 2004;242(3):210–217.
59. Williams DF, Williams GA, Hartz A, et al. Results of vitrectomy for diabetic traction retinal detachments using the en bloc excision technique. *Ophthalmology*. 1989;96(6):752–758.
60. Han DP, Murphy ML, Mieler WF. A modified en bloc excision technique during vitrectomy for diabetic traction retinal detachment: results and complications. *Ophthalmology*. 1994;101(5):803–808.
61. Thompson JT, de Bustros S, Michels RG, et al. Results and prognostic factors in vitrectomy for diabetic traction-rhegmatogenous retinal detachment. *Arch Ophthalmol*. 1987;105(4):503–507.
62. Kakehashi A, Trempe CL, Fujio N, et al. Retinal breaks in diabetic retinopathy: vitreoretinal relationships. *Ophthalmic Surg*. 1994;25:695–699.
63. Yang CM, Su PY, Yeh PT, et al. Combined rhegmatogenous and traction retinal detachment in proliferative diabetic retinopathy: clinical manifestations and surgical outcome. *Can J Ophthalmol*. 2008;43:192–198.
64. Rice TA, Michels RG, Rice EF. Vitrectomy for diabetic rhegmatogenous retinal detachment. *Am J Ophthalmol*. 1983;95:34–44.
65. Morse LS, Chapman CB, Eliott D, et al. Subretinal hemorrhages in proliferative diabetic retinopathy. *Retina*. 1997;17:87–93.
66. Douglas MJ, Scott IU, Flynn HW Jr. Pars plana lensectomy, pars plana vitrectomy, and silicone oil tamponade as initial management of cataract and combined

traction/rhegmatogenous retinal detachment involving the macula associated with severe proliferative diabetic retinopathy. *Ophthalmic Surg Lasers Imaging*. 2003;34:270–278.
67. Allen RC, Bellows A, Hutchinson BT, et al. Filtration surgery in the treatment of neovascular glaucoma. *Ophthalmology*. 1982;89:1181–1187.
68. Helbig H. Proliferative diabetic retinopathy: a surgical approach to proliferative diabetic retinopathy. Joussen AM, Gardner TW, Kirchhof B, et al. *Retinal vascular disease*. Springer: Berlin-Heidelberg; 2007:330–341.
69. Pauleikhoff D, Gerke E. Photocoagulation in diabetic rubeosis iridis and neovascular glaucoma. *Klin Monatsbl Augenheilkd*. 1987;190:11–16 [in German].
70. Avery RL, Pearlman J, Pieramici DJ, et al. Intravitreal bevacizumab (Avastin) in the treatment of proliferative diabetic retinopathy. *Ophthalmology*. 2006;113:1695–1705.
71. Spiteri CK, Ramamurthi S, Saidkasimova S, et al. Intravitreal bevacizumab and augmented trabeculectomy for neovascular glaucoma in young diabetic patients. *Eye*. 2008;23:979–981.
72. Chalam KV, Gupta SK, Grover S, et al. Intracameral Avastin dramatically resolves iris neovascularization and reverses neovascular glaucoma. *Eur J Ophthalmol*. 2008;18:255–262.
73. Joussen AM, Joeres S. Benefits and limitations in vitreoretinal surgery for proliferative diabetic retinopathy and macular edema. *Dev Ophthalmol*. 2007;39:69–87.
74. Helbig H, Kellner U, Bornfeld N, et al. Rubeosis iridis after vitrectomy for diabetic retinopathy. *Graefes Arch Clin Exp Ophthalmol*. 1998;236:730–733.
75. Bartz-Schmidt KU, Thumann G, Psichias A, et al. Pars plana vitrectomy, endolaser coagulation of the retina and the ciliary body combined with silicone oil endotamponade in the treatment of uncontrolled neovascular glaucoma. *Graefes Arch Clin Exp Ophthalmol*. 1999;237:969–975.
76. Kirchhof B. The contribution of vitreoretinal surgery to the management of refractory glaucomas. *Curr Opin Ophthalmol*. 1999;10:117–120.

77. Joussen AM, Walter P, Jonescu-Cuypers CP, et al. Retinectomy for treatment of intractable glaucoma: long-term results. *Br J Ophthalmol*. 2003;89:1094–1103.
78. Iliev ME, Wolf S. Management of neovascular glaucoma. Grieshaber LC, Orgül S, Flammer J. *Glaucoma therapy – state of the art*. Grieshaber: Basel; 2009:165–170.
79. Miki A, Oshima Y, Otori Y, et al. Efficacy of intravitreal bevacizumab as adjunctive treatment with pars plana vitrectomy, endolaser photocoagulation and trabeculectomy for neovascular glaucoma. *Br J Ophthalmol*. 2008;92:1431–1433.
80. Schlote T, Ziemssen F, Bartz-Schmidt KU. Pars plana-modified Ahmed glaucoma valve for treatment of refractory glaucoma: a pilot study. *Graefes Arch Clin Exp Ophthalmol*. 2006;244:336–341.
81. Sivak-Callcott JA, O'Day DM, Gass JD, et al. Evidence-based recommendations for the diagnosis and treatment of neovascular glaucoma. *Ophthalmology*. 2001;108:1767–1776 [quiz1777, 1800; Review].
82. Singh H, Grand MG. Treatment of blood-induced glaucoma by trans pars plana vitrectomy. *Retina*. 1981;1:255–257.
83. Iliev ME, Gerber S. Long-term outcome of trans-scleral diode laser cyclophotocoagulation in refractory glaucoma. *Br J Ophthalmol*. 2007;91:1631–1635.
84. Murphy CC, Burnett CA, Spry PG, et al. A two centre study of the dose-response relation for transscleral diode laser cyclophotocoagulation in refractory glaucoma. *Br J Ophthalmol*. 2003;87:1252–1257.
85. Ehlers JP, Shah CP, Fenton GL, et al. *The Wills eye manual: office and emergency room diagnosis and treatment of eye disease*. 5th ed. Lippincott Williams & Wilkins: Philadelphia; 2008:214–217.
86. Thompson JT, Auer CL, de Bustros S, et al. Prognostic indicators of success and failure in vitrectomy for diabetic retinopathy. *Ophthalmology*. 1986;93:290–295.
87. Blankenship GW. Proliferative diabetic retinopathy: principles and techniques of surgical treatment. Ryan SJ. *Retina*. Elsevier Mosby: The Netherlands; 2001:515–539.

88. Moitra VK, Meiler SE. The diabetic surgical patient. *Curr Opin Anaesthesiol*. 2006;19:339–345.
89. Iwasaki T, Miura M, Matsushima C, et al. Three-dimensional optical coherence tomography of proliferative diabetic retinopathy. *Br J Ophthalmol*. 2008;92:713.
90. Blankenship GW. Preoperative prognostic factors in diabetic pars plana vitrectomy. *Ophthalmology*. 1982;89:1246–1249.
91. Kusaka S, Kodama T, Ohashi Y. Condensation of silicone oil on the posterior surface of a silicone intraocular lens during vitrectomy. *Am J Ophthalmol*. 1996;121:574–575.
92. Khawly JA, Lambert RJ, Jaffe GJ. Intraocular lens changes after short- and long-term exposure to intraocular silicone oil: an in vivo study. *Ophthalmology*. 1998;105:1227–1233.
93. Pavan PR, Folk JC, Weingeist TA, et al. Diabetic rubeosis and panretinal photocoagulation. *Arch Ophthalmol*. 1983;101:882–884.
94. Chu TG, Lopez PF, Cano MR, et al. Posterior vitreoschisis: an echographic finding in proliferative diabetic retinopathy. *Ophthalmology*. 1996;103:315–322.
95. Tzekov R, Arden GB. The electroretinogram in diabetic retinopathy. *Surv Ophthalmol*. 1999;44(1):53–60 [Review].
96. Starr MB, Lally JM. Antimicrobial prophylaxis for ophthalmic surgery. *Surv Ophthalmol*. 1995;39:485–501 [Review].
97. Jonas JB, Hayler JK, Söfker A, et al. Regression of neovascular iris vessels by intravitreal injection of crystalline cortisone. *J Glaucoma*. 2001;10:284–287.
98. Grisanti S, Biester S, Peters S, et al. Intracameral bevacizumab for iris rubeosis. *Am J Ophthalmol*. 2006;142:158–160.
99. Liggett PE, Lean JS, Barlow WE, et al. Intraoperative argon endophotocoagulation for recurrent vitreous hemorrhage after vitrectomy for diabetic retinopathy. *Am J Ophthalmol*. 1987;103:146–149.
100. West JF, Gregor ZJ. Fibrovascular ingrowth and recurrent haemorrhage following diabetic vitrectomy. *Br J Ophthalmol*. 2000;84:822–825.
101. Henderson BA, Grimes KJ, Fintelmann RE, et al. Stepwise

approach to establishing an ophthalmology wet laboratory. *J Cataract Refract Surg*. 2009;35:1121–1128.
102. Le TD, Adatia FA, Lam WC. Virtual reality ophthalmic surgical simulation as a feasible training and assessment tool: results of a multicentre study. *Can J Ophthalmol*. 2011;46:56–60.
103. Benatar-Haserfaty J, Puig Flores JA. Locoregional anesthesia in ophthalmology: update. *Rev Esp Anestesiol Reanim*. 2003;50:284–298.
104. Scott WJ. Povidone-iodine antisepsis for cataract surgery and ophthalmic procedures. *Am J Ophthalmol*. 2011;151:914 [author reply, 914–5].
105. Joussen AM, Kirchhof B. Vitrectomy in retinal vascular disease: surgical principles. Joussen AM, Gardner TW, Kirchhof B, et al. *Retinal vascular disease*. Springer-Verlag: Berlin, Heidelberg; 2007:260–273.
106. Chalam KV, Gupta SK, Agarwal S. Lightweight autoclavable wide-angle contact lens for vitreous surgery. *Ophthalmic Surg Lasers Imaging*. 2007;38:523–524.
107. Emi K, Oyagi T, Futamura H. New biconcave prism contact lens for vitreous surgery in gas-filled eyes. *Nippon Ganka Gakkai Zasshi*. 2005;109:400–405 [in Japanese].
108. Spitznas M. A binocular indirect ophthalmomicroscope (BIOM) for non-contact wide-angle vitreous surgery. *Graefes Arch Klin Exp Ophthalmol*. 1987;225:13–15.
109. Virata SR, Kylstra JA, Singh HT. Corneal epithelial defects following vitrectomy surgery using hand-held, sew-on, and noncontact viewing lenses. *Retina*. 1999;19:287–290.
110. Virata SR, Kylstra JA. Postoperative complications following vitrectomy for proliferative diabetic retinopathy with sew-on and noncontact wide-angle viewing lenses. *Ophthalmic Surg Lasers*. 2001;32:193–197.
111. Williams GA. 25-, 23-, or 20-gauge instrumentation for vitreous surgery? *Eye (Lond)*. 2008;22:1263–1266.
112. Kellner L, Wimpissinger B, Stolba U, et al. 25-gauge vs 20-gauge system for pars plana vitrectomy: a prospective randomised clinical trial. *Br J Ophthalmol*. 2007;91:945–948.
113. Ibarra MS, Hermel M, Prenner JL, et al. Longer-term

outcomes of transconjunctival sutureless 25-gauge vitrectomy. *Am J Ophthalmol*. 2005;139:831–836.
114. Oshima Y, Wakabayashi T, Sato T, et al. A 27-gauge instrument system for transconjunctival sutureless microincision vitrectomy surgery. *Ophthalmology*. 2010;117:93–102.
115. Hubschman JP, Gupta A, Bourla DH, et al. 20-, 23-, and 25-gauge vitreous cutters: performance and characteristics evaluation. *Retina*. 2008;28:249–257.
116. Byeon SH, Lew YJ, Kim M, et al. Wound leakage and hypotony after 25-gauge sutureless vitrectomy: factors affecting postoperative intraocular pressure. *Ophthalmic Surg Lasers Imaging*. 2008;39:94–99.
117. Shinoda H, Nakajima T, Shinoda K, et al. Jamming of 25-gauge instruments in the cannula during vitrectomy for vitreous haemorrhage. *Acta Ophthalmol*. 2008;86:160–164.
118. Eckardt C. Transconjunctival sutureless 23-gauge vitrectomy. *Retina*. 2005;25:208–211.
119. Chalam KV, Shah GY, Agarwal S, et al. Illuminated curved 25-gauge vitrectomy probe for removal of subsclerotomy vitreous in vitreoretinal surgery. *Indian J Ophthalmol*. 2008;56:331–334.
120. Oshima Y, Awh CC, Tano Y. Self-retaining 27-gauge transconjunctival chandelier endoillumination for panoramic viewing during vitreous surgery. *Am J Ophthalmol*. 2007;143:166–167.
121. Williamson TH. Diabetic retinopathy and other vascular disorders. *Vitreoretinal surgery*. Springer-Verlag: Berlin, Heidelberg; 2008:141–160.
122. Peyman GA, Lee KJ. New forceps for preretinal membrane removal. *Retina*. 1994;14:88–89.
123. Johnson TM, Glaser BM. Intraocular rake for removal of epiretinal membranes. *Am J Ophthalmol*. 2006;141:381–383.
124. Kampougeris G, Cheema R, McPherson R, et al. Safety of triamcinolone acetonide (TA)-assisted pars plana vitrectomy in macular hole surgery. *Eye (Lond)*. 2007;21:591–594.
125. Yamaguchi T, Inoue M, Ishida S, et al. Detecting

vitreomacular adhesions in eyes with asteroid hyalosis with triamcinolone acetonide. *Graefes Arch Clin Exp Ophthalmol*. 2007;245:305–308.
126. Rodrigues EB, Meyer CH, Kroll P. Chromovitrectomy: a new field in vitreoretinal surgery. *Graefes Arch Clin Exp Ophthalmol*. 2005;243:291–293.
127. McCuen BW 2nd, Bessler M, Tano Y, et al. The lack of toxicity of intravitreally administered triamcinolone acetonide. *Am J Ophthalmol*. 1981;91:785–788.
128. Farah ME, Maia M, Rodrigues EB. Dyes in ocular surgery: principles for use in chromovitrectomy. *Am J Ophthalmol*. 2009;148:332–340 [Review].
129. Bardak Y, Cekiç O, Tiğ SU. Comparison of ICG-assisted ILM peeling and triamcinolone-assisted posterior vitreous removal in diffuse diabetic macular oedema. *Eye (Lond)*. 2006;20:1357–1359.
130. Mennel S, Meyer CH, Schmidt JC, et al. Trityl dyes patent blue V and brilliant blue G – clinical relevance and in vitro analysis of the function of the outer blood-retinal barrier. *Dev Ophthalmol*. 2008;42:101–114.
131. Schmid-Kubista KE, Lamar PD, Schenk A, et al. Comparison of macular function and visual fields after membrane blue or infracyanine green staining in vitreoretinal surgery. *Graefes Arch Clin Exp Ophthalmol*. 2010;248:381–388.
132. von Jagow B, Höing A, Gandorfer A, et al. Functional outcome of indocyanine green-assisted macular surgery: 7-year follow-up. *Retina*. 2009;29:1249–1256.
133. Kobuch K, Menz IH, Hoerauf H, et al. New substances for intraocular tamponades: perfluorocarbon liquids, hydrofluorocarbon liquids and hydrofluorocarbon-oligomers in vitreoretinal surgery. *Graefes Arch Clin Exp Ophthalmol*. 2001;239(9):635–642.
134. Chang S, Lincoff HA, Coleman DJ, et al. Perfluorocarbon gases in vitreous surgery. *Ophthalmology*. 1985;92(5):651–656.
135. Stolba U, Binder S, Velikay M, et al. Use of perfluorocarbon liquids in proliferative vitreoretinopathy: results and

complications. *Br J Ophthalmol*. 1995;79(12):1106–1110.
136. Ruiz-Moreno JM, Barile S, Montero JA. Phacoemulsification in the vitreous cavity for retained nuclear lens fragments. *Eur J Ophthalmol*. 2006;16:40–45.
137. Chang TS, Pelzek CD, Nguyen RL, et al. Inverted pneumatic retinopexy: a method of treating retinal detachments associated with inferior retinal breaks. *Ophthalmology*. 2003;110:589–594.
138. Yang CM, Yeh PT, Yang CH. Intravitreal long-acting gas in the prevention of early postoperative vitreous hemorrhage in diabetic vitrectomy. *Ophthalmology*. 2007;114:710–715.
139. Yamane S, Kadonosono K, Inoue M, et al. Effect of intravitreal gas tamponade for sutureless vitrectomy wounds: three-dimensional corneal and anterior segment optical coherence tomography study. *Retina*. 2011;31(4):702–706.
140. Cibis PA, Becker B, Okun E, et al. The use of liquid silicone in retinal detachment surgery. *Arch Ophthalmol*. 1962;68:590–599.
141. Heimann K, Dahl B, Dimopoulos S, et al. Pars plana vitrectomy and silicone oil injection in proliferative diabetic retinopathy. *Graefes Arch Clin Exp Ophthalmol*. 1989;227(2):152–156.
142. Scott IU, Flynn HW Jr, Murray TG, et al. Outcomes of complex retinal detachment repair using 1000- vs 5000-centistoke silicone oil. *Arch Ophthalmol*. 2005;123(4):473–478.
143. Wong D, Van Meurs JC, Stappler T, et al. A pilot study on the use of a perfluorohexyloctane/silicone oil solution as a heavier than water internal tamponade agent. *Br J Ophthalmol*. 2005;89(6):662–665.
144. Brunner S, Izay B, Weidinger B, et al. Chemical impurities and contaminants in different silicone oils in human eyes before and after prolonged use. *Graefes Arch Clin Exp Ophthalmol*. 2011;249:29–36.
145. Figueroa MS, Contreras I, Noval S. Anti-angiogenic drugs as an adjunctive therapy in the surgical treatment of diabetic retinopathy. *Curr Diabetes Rev*. 2009;5:52–56.
146. di Lauro R, De Ruggiero P, di Lauro R, et al. Intravitreal

bevacizumab for surgical treatment of severe proliferative diabetic retinopathy. *Graefes Arch Clin Exp Ophthalmol*. 2010;248:785–791.
147. Gandorfer A, Kampik A. Pharmacologic vitreolysis combining the two enzymes plasmin and hyaluronidase. *Retina*. 2005;25:674.
148. Hirata A, Takano A, Inomata Y, et al. Plasmin-assisted vitrectomy for management of proliferative membrane in proliferative diabetic retinopathy: a pilot study. *Retina*. 2007;27:1074–1078.
149. Ciardella AP, Fisher YL, Carvalho C, et al. Endoscopic vitreoretinal surgery for complicated proliferative diabetic retinopathy. *Retina*. 2001;21:20–27.
150. Sabti KA, Raizada S, Kandari JA, et al. Applications of endoscopy in vitreoretinal surgery. *Retina*. 2008;28:159–166.
151. Browning DJ. Cataract surgery and diabetic retinopathy. Browning DJ. *Diabetic retinopathy – evidence-based management*. Springer: New York; 2010:305–323.
152. Browning DJ, Rotberg MH. The relationship of diabetic retinopathy and glaucoma. Browning DJ. *Diabetic retinopathy – evidence-based management*. Springer: New York; 2010:325–346.
153. Kitnarong N, Chindasub P, Metheetrairut A. Surgical outcome of intravitreal bevacizumab and filtration surgery in neovascular glaucoma. *Adv Ther*. 2008;25:438–443.
154. Chen H, Zhang SX, Liu L, et al. Intermediate-term and long-term clinical evaluation of the Ahmed glaucoma valve implantation. *Zhonghua Yan Ke Za Zhi*. 2005;41:796–802 [in Chinese].
155. Hille K, Hille A, Ruprecht KW. Drainage systems in glaucoma surgery. *Ophthalmologe*. 2002;99:902–916 [Review; in German].
156. Faghihi H, Hajizadeh F, Mohammadi SF, et al. Pars plana Ahmed valve implant and vitrectomy in the management of neovascular glaucoma. *Ophthalmic Surg Lasers Imaging*. 2007;38:292–300.
157. Luttrull JK, Avery RL. Pars plana implant and vitrectomy for treatment of neovascular glaucoma. *Retina*. 1995;15:379–

387.
158. Smith MF, Doyle JW, Fanous MM. Modified aqueous drainage implants in the treatment of complicated glaucomas in eyes with pre-existing episcleral bands. *Ophthalmology*. 1998;105:2237–2242.
159. Kirchhof B. Retinectomy lowers intraocular pressure in otherwise intractable glaucoma: preliminary results. *Ophthalmic Surg*. 1994;25:262–267.
160. Nam KY, Kim JY. Effect of internal limiting membrane peeling on the development of epiretinal membrane after pars plana vitrectomy for primary rhegmatogenous retinal detachment. *Retina*. 2015;35:880–885.
161. Stirpe M, Orciuolo M. Pneumatic syringe used in fibrovascular membrane surgery. *Am J Ophthalmol*. 1985;99:729.
162. McLeod D, James CR. Viscodelamination at the vitreoretinal juncture in severe diabetic eye disease. *Br J Ophthalmol*. 1988;72:413–419.
163. Stenkula S. Photocoagulation in diabetic retinopathy: a multicentre study in Sweden. *Acta Ophthalmol Suppl*. 1984;162:1–100.
164. Charles S. Vitrectomy for retinal detachment. *Trans Ophthalmol Soc U K*. 1980;100:542–549.
165. Meredith TA, Kaplan HJ, Aaberg TM. Pars plana vitrectomy techniques for relief of epiretinal traction by membrane segmentation. *Am J Ophthalmol*. 1980;89:408–413.
166. Han DP, Pulido JS, Mieler WF, et al. Vitrectomy for proliferative diabetic retinopathy with severe equatorial fibrovascular proliferation. *Am J Ophthalmol*. 1995;119:563–570.
167. Mason JO 3rd, Colagross CT, Haleman T, et al. Visual outcome and risk factors for light perception and no light perception vision after vitrectomy for diabetic retinopathy. *Am J Ophthalmol*. 2005;140:231–235.
168. Abrams GW, Williams GA. "En bloc" excision of diabetic membranes. *Am J Ophthalmol*. 1987;103:302–308.
169. Schwatz SD, Alexander R, Hiscott P, et al. Recognition of vitreoschisis in proliferative diabetic retinopathy: a useful

landmark in vitrectomy for diabetic traction retinal detachment. *Ophthalmology*. 1996;103:323–328.
170. Han DP, Lewis MT, Kuhn EM, et al. Relaxing retinotomies and retinectomies: surgical results and predictors of visual outcome. *Arch Ophthalmol*. 1990;108:694–697.
171. Chaudhry NA, Lim ES, Saito Y, et al. Early vitrectomy and endolaser photocoagulation in patients with type I diabetes with severe vitreous hemorrhage. *Ophthalmology*. 1995;102:1164–1169.
172. Imamura Y, Minami M, Ueki M, et al. Use of perfluorocarbon liquid during vitrectomy for severe proliferative diabetic retinopathy. *Br J Ophthalmol*. 2003;87:563–566.
173. Singerman LJ. Red krypton laser therapy of macular and retinal vascular diseases. *Retina*. 1982;2:15–28.
174. Fisher YL, Friedman R. Scleral depression to facilitate endophotocoagulation. *Arch Ophthalmol*. 1988;106:721.
175. Blankenship GW, Machemer R. Long-term diabetic vitrectomy results: report of 10 year follow-up. *Ophthalmology*. 1985;92:503–506.
176. Yoon YH, Marmor MF. Rapid enhancement of retinal adhesion by laser photocoagulation. *Ophthalmology*. 1988;95:1385–1388.
177. Folk JC, Sneed SR, Folberg R, et al. Early retinal adhesion from laser photocoagulation. *Ophthalmology*. 1989;96:1523–1525.
178. Hilton GF, Tornambe PE, Brinton DA, et al. The complication of pneumatic retinopexy. *Trans Am Ophthalmol Soc*. 1990;88:191–207 [discussion 207–210].
179. Abecia E, Pinilla I, Olivan JM, et al. Anatomic results and complications in a long-term follow-up of pneumatic retinopexy cases. *Retina*. 2000;20:156–161.
180. Whitacre MM, Mainster MA. Hazards of laser beam reflections in eyes containing gas. *Am J Ophthalmol*. 1990;110:33–38.
181. Shugar JK, de Juan E Jr, McCuen BW 2nd, et al. Ultrasonic examination of the silicone-filled eye: theoretical and practical considerations. *Graefes Arch Klin Exp Ophthalmol*.

1986;224:361–367.
182. Dietlein TS, Roessler G, Lüke C, et al. Signal quality of biometry in silicone oil-filled eyes using partial coherence laser interferometry. *J Cataract Refract Surg*. 2005;31:1006–1010.
183. Kampik A, Höing C, Heidenkummer HP. Problems and timing in the removal of silicone oil. *Retina*. 1992;12:S11–16.
184. Falkner CI, Binder S, Kruger A. Outcome after silicone oil removal. *Br J Ophthalmol*. 2001;85:1324–1327.
185. Shen YD, Yang CM. Extended silicone oil tamponade in primary vitrectomy for complex retinal detachment in proliferative diabetic retinopathy: a long-term follow-up study. *Eur J Ophthalmol*. 2007;17:954–960.
186. Turner A, Rabiu M. Patching for corneal abrasion. *Cochrane Database Syst Rev*. 2006;(2) [CD004764].
187. Alberti MM, Bouat CG, Allaire CM, et al. Combined indomethacin/gentamicin eyedrops to reduce pain after traumatic corneal abrasion. *Eur J Ophthalmol*. 2001;11:233–239.
188. Rice TA, Michels RG, Maguire MG, et al. The effect of lensectomy on the incidence of iris neovascularization and neovascular glaucoma after vitrectomy for diabetic retinopathy. *Am J Ophthalmol*. 1983;95:1–11.
189. Fong DS, Ferris FL 3rd, Davis MD, et al. Causes of severe visual loss in the early treatment diabetic retinopathy study: ETDRS report no. 24. Early Treatment Diabetic Retinopathy Study Research Group. *Am J Ophthalmol*. 1999;127:137–141.
190. Browning AC, Alibhai A, McIntosh RS, et al. Effect of diabetes mellitus and hyperglycemia on the proliferation of human Tenon's capsule fibroblasts: implications for wound healing after glaucoma drainage surgery. *Wound Repair Regen*. 2005;13:295–302.
191. Hoogwerf BJ. Postoperative management of the diabetic patient. *Med Clin North Am*. 2001;85:1213–1228 [Review].
192. Kansagara D, Fu R, Freeman M, et al. Intensive insulin therapy in hospitalized patients: a systematic review. *Ann Intern Med*. 2011;154:268–282 [Review].
193. Oyakawa RT, Schachat AP, Michels RG, et al.

Complications of vitreous surgery for diabetic retinopathy. I. Intraoperative complications. *Ophthalmology*. 1983;90:517–521.
194. Perry HD, Foulks GN, Thoft RA, et al. Corneal complications after closed vitrectomy through the pars plana. *Arch Ophthalmol*. 1978;96:1401–1403.
195. Hiraoka M, Amano S, Oshika T, et al. Factors contributing to corneal complications after vitrectomy in diabetic patients. *Jpn J Ophthalmol*. 2001;45:492–495.
196. Garcia-Valenzuela E, Abdelsalam A, Eliott D, et al. Reduced need for corneal epithelial debridement during vitreo-retinal surgery using two different viscous surface lubricants. *Am J Ophthalmol*. 2003;136:1062–1066.
197. Friberg TR, Ohji M, Scherer JJ, et al. Frequency of epithelial debridement during diabetic vitrectomy. *Am J Ophthalmol*. 2003;135:553–554.
198. Fuller DG, Wilson DL. Translimbal iris hook for pupillary dilation during vitreous surgery. *Am J Ophthalmol*. 1990;110:577.
199. Chong LP. A disposable iris retractor for vitrectomy. *Am J Ophthalmol*. 1991;112:731–732.
200. Haimann MH, Abrams GW. Prevention of lens opacification during diabetic vitrectomy. *Ophthalmology*. 1984;91:116–121.
201. Thompson JT, Glaser BM, Michels RG, et al. The use of intravitreal thrombin to control hemorrhage during vitrectomy. *Ophthalmology*. 1986;93:279–282.
202. Packer AJ, McCuen BW 2nd, Hutton WL, et al. Procoagulant effects of intraocular sodium hyaluronate (Healon) after phakic diabetic vitrectomy: a prospective, randomized study. *Ophthalmology*. 1989;96:1491–1494.
203. Smith JM, Steel DH. Anti-vascular endothelial growth factor for prevention of postoperative vitreous cavity haemorrhage after vitrectomy for proliferative diabetic retinopathy. *Cochrane Database Syst Rev*. 2011;(5) [CD008214].
204. Yeh PT, Yang CM, Lin YC, et al. Bevacizumab pretreatment in vitrectomy with silicone oil for severe diabetic retinopathy. *Retina*. 2009;29:768–774.

205. Carter JB, Michels RG, Glaser BM, et al. Iatrogenic retinal breaks complicating pars plana vitrectomy. *Ophthalmology*. 1990;97:848–853.
206. Ramkissoon YD, Aslam SA, Shah SP, et al. Risk of iatrogenic peripheral retinal breaks in 20-G pars plana vitrectomy. *Ophthalmology*. 2010;117:1825–1830.
207. Schulze SD, Sekundo W, Kroll P. Autologous serum for the treatment of corneal epithelial abrasions in diabetic patients undergoing vitrectomy. *Am J Ophthalmol*. 2006;142:207–211.
208. Roth DB, Flynn HW Jr. Distinguishing between infectious and non-infectious endophthalmitis after intravitreal triamcinolone injection. *Am J Ophthalmol*. 2008;146:346–347.
209. Schachat AP, Oyakawa RT, Michels RG, et al. Complications of vitreous surgery for diabetic retinopathy. II. Postoperative complications. *Ophthalmology*. 1983;90:522–530.
210. Han DP, Lewis H, Lambrou FH Jr, et al. Mechanisms of intraocular pressure elevation after pars plana vitrectomy. *Ophthalmology*. 1989;96:1357–1362.
211. Kangas TA, Bennett SR, Flynn HW Jr, et al. Reversible loss of light perception after vitreoretinal surgery. *Am J Ophthalmol*. 1995;120:751–756.
212. Anderson NG, Fineman MS, Brown GC. Incidence of intraocular pressure spike and other adverse events after vitreoretinal surgery. *Ophthalmology*. 2006;113:42–47.
213. Thompson JT. Kinetics of intraocular gases: disappearance of air, sulfur hexafluoride, and perfluoropropane after pars plana vitrectomy. *Arch Ophthalmol*. 1989;107:687–691.
214. Barondes MJ, Davis MD, Myers FL. Acute glaucoma following fluid–gas exchange in a phakic patient. *Am J Ophthalmol*. 1989;108:738–740.
215. Sebestyen JG. Fibrinoid syndrome: a severe complication of vitrectomy surgery in diabetics. *Ann Ophthalmol*. 1982;14:853–856.
216. Jaffe GJ, Schwartz D, Han DP, et al. Risk factors for postvitrectomy fibrin formation. *Am J Ophthalmol*. 1990;109:661–667.
217. Dabbs CK, Aaberg TM, Aguilar HE, et al. Complications of

tissue plasminogen activator therapy after vitrectomy for diabetes. *Am J Ophthalmol*. 1990;110:354–360.
218. Williams DF, Bennett SR, Abrams GW, et al. Low-dose intraocular tissue plasminogen activator for treatment of postvitrectomy fibrin formation. *Am J Ophthalmol*. 1990;109:606–607.
219. Jaffe GJ, Abrams GW, Williams GA, et al. Tissue plasminogen activator for postvitrectomy fibrin formation. *Ophthalmology*. 1990;97:184–189.
220. Novak MA, Rice TA, Michels RG, et al. Vitreous hemorrhage after vitrectomy for diabetic retinopathy. *Ophthalmology*. 1984;91:1485–1489.
221. Kato S, Fukada Y, Hori S, et al. Influence of phacoemulsification and intraocular lens implantation on the course of diabetic retinopathy. *J Cataract Refract Surg*. 1999;25:788–793.
222. Brown GC, Tasman WS, Benson WE, et al. Reoperation following diabetic vitrectomy. *Arch Ophthalmol*. 1992;110:506–510.
223. Lewis H, Abrams GW, Williams GA. Anterior hyaloidal fibrovascular proliferation after diabetic vitrectomy. *Am J Ophthalmol*. 1987;104:607–613.
224. Eren E, Küçükerdönmez C, Yilmaz G, et al. Regression of neovascular posterior capsule vessels by intravitreal bevacizumab. *J Cataract Refract Surg*. 2007;33:1113–1115.
225. Klein BE, Klein R, Lee KE. Diabetes, cardiovascular disease, selected cardiovascular disease risk factors, and the 5-year incidence of age-related cataract and progression of lens opacities: the Beaver Dam Eye Study. *Am J Ophthalmol*. 1998;126:782–790.
226. Ederer F, Hiller R, Taylor HR. Senile lens changes and diabetes in two population studies. *Am J Ophthalmol*. 1981;91:381–395.
227. Chew EY, Benson WE, Remaley NA, et al. Results after lens extraction in patients with diabetic retinopathy: early treatment diabetic retinopathy study report number 25. *Arch Ophthalmol*. 1999;117:1600–1606.
228. Gallego-Pinazo R, Dolz-Marco R, Berrocal M, Pan-American

Collaborative Retina Study Group (PACORES), et al. Outcomes of cataract surgery in diabetic patients: results of the Pan American Collaborative Retina Study Group. *Arq Bras Oftalmol*. 2014;77:355–359.
229. Samanta A, Kumar P, Machhua S, Rao GN, Pal A. Incidence of cystoid macular oedema in diabetic patients after phacoemulsification and free radical link to its pathogenesis. *Br J Ophthalmol*. 2014;98:1266–1272.
230. Bhushan B, Sen A, Mitra A. Re: Role of combined cataract surgery and ranibizumab injection in postoperative macula edema in non-proliferative diabetic retinopathy. *Retina*. 2015;35:e18.
231. Ferris FL 3rd. Results after lens extraction in patients with diabetic retinopathy: Early Treatment Diabetic Retinopathy Study report number 25. *Arch Ophthalmol*. 1999;117:1600–1606.
232. Pollack A, Dotan S, Oliver M. Progression of diabetic retinopathy after cataract extraction. *Br J Ophthalmol*. 1991;75:547–551.
233. Kutschan A, Heinz P, Wiegand W. Extracapsular cataract surgery with posterior chamber lens implantation in patients with diabetes mellitus – retrospective study on 145 patients. *Klin Monatsbl Augenheilkd*. 2002;219:117–124 [in German].
234. Patel JI, Hykin PG, Cree IA. Diabetic cataract removal: postoperative progression of maculopathy – growth factor and clinical analysis. *Br J Ophthalmol*. 2006;90:697–701.
235. Shimura M, Yasuda K, Shiono T. Posterior sub-Tenon's capsule injection of triamcinolone acetonide prevents panretinal photocoagulation-induced visual dysfunction in patients with severe diabetic retinopathy and good vision. *Ophthalmology*. 2006;113:381–387.
236. Tonello M, Costa RA, Almeida FP, et al. Panretinal photocoagulation versus PRP plus intravitreal bevacizumab for high-risk proliferative diabetic retinopathy (IBeHi study). *Acta Ophthalmol*. 2008;86:385–389.
237. Cho WB, Oh SB, Moon JW, et al. Panretinal photocoagulation combined with intravitreal bevacizumab

in high-risk proliferative diabetic retinopathy. *Retina*. 2009;29:516–522.
238. Munir WM, Pulido JS, Sharma MC, et al. Intravitreal triamcinolone for treatment of complicated proliferative diabetic retinopathy and proliferative vitreoretinopathy. *Can J Ophthalmol*. 2005;40:598–604.
239. Krepler K, Biowski R, Schrey S, et al. Cataract surgery in patients with diabetic retinopathy: visual outcome, progression of diabetic retinopathy, and incidence of diabetic macular oedema. *Graefes Arch Clin Exp Ophthalmol*. 2002;240:735–738.
240. Benson WE, Brown GC. Combined extracapsular cataract extraction, posterior chamber lens implantation and pars plana vitrectomy. *Trans Pa Acad Ophthalmol Otolaryngol*. 1989;41:814–817.
241. Lahey JM, Francis RR, Kearney JJ, et al. Combining phacoemulsification and vitrectomy in patients with proliferative diabetic retinopathy. *Curr Opin Ophthalmol*. 2004;15:192–196 [Review].
242. Smiddy WE, Feuer W. Incidence of cataract extraction after diabetic vitrectomy. *Retina*. 2004;24:574–581.
243. Bhatnagar P, Schiff WM, Barile GR. Diabetic vitrectomy: the influence of lens status upon surgical outcomes. *Curr Opin Ophthalmol*. 2008;19:243–247.
244. Lahey JM, Francis RR, Kearney JJ. Combining phacoemulsification with pars plana vitrectomy in patients with proliferative diabetic retinopathy: a series of 223 cases. *Ophthalmology*. 2003;110:1335–1339.
245. Scharwey K, Pavlovic S, Jacobi KW. Early posterior capsule fibrosis after combined cataract and vitreoretinal surgery with intraocular air/SF_6 gas tamponade. *Klin Monatsbl Augenheilkd*. 1998;212:149–153 [in German].
246. Treumer F, Bunse A, Rudolf M, et al. Pars plana vitrectomy, phacoemulsification and intraocular lens implantation. Comparison of clinical complications in a combined versus two-step surgical approach. *Graefes Arch Clin Exp Ophthalmol*. 2006;244:808–815.
247. Kadonosono K, Matsumoto S, Uchio E, et al. Iris

neovascularization after vitrectomy combined with phacoemulsification and intraocular lens implantation for proliferative diabetic retinopathy. *Ophthalmic Surg Lasers*. 2001;32:19–24.
248. Shinoda K, O'hira A, Ishida S, et al. Posterior synechia of the iris after combined pars plana vitrectomy, phacoemulsification, and intraocular lens implantation. *Jpn J Ophthalmol*. 2001;45:276–280.
249. Pagot V, Gazagne C, Galiana A, et al. Extracapsular cataract extraction and implantation in the capsular sac during vitrectomy in diabetics. *J Fr Ophtalmol*. 1991;14:523–528 [in French].
250. Ryan EH Jr, Gilbert HD. Lensectomy, vitrectomy indications, and techniques in cataract surgery. *Curr Opin Ophthalmol*. 1996;7:69–74.
251. Romero P, Salvat M, Almena M, et al. Combined surgery for lens extraction, vitrectomy, and implantation in the diabetic patient using phacoemulsification versus phacofragmentation. *J Fr Ophtalmol*. 2006;29:533–541 [in French].
252. Hsu SY, Wu WC. Comparison of phacoemulsification and planned extracapsular cataract extraction in combined pars plana vitrectomy and posterior chamber intraocular lens implantation. *Ophthalmic Surg Lasers Imaging*. 2005;36:108–113.
253. MacCumber MW, Packo KH, Civantos JM, et al. Preservation of anterior capsule during vitrectomy and lensectomy for retinal detachment with proliferative vitreoretinopathy. *Ophthalmology*. 2002;109:329–333.
254. Salzmann J, Khaw PT, Laidlaw A. Choroidal effusions and hypotony caused by severe anterior lens capsule contraction after cataract surgery. *Am J Ophthalmol*. 2000;129:253–254.
255. Geyer O, Lazar M. Ciliary body detachment caused by capsule contraction. *J Cataract Refract Surg*. 2000;26:305–306.
256. Chang MA, Parides MK, Chang S, et al. Outcome of phacoemulsification after pars plana vitrectomy. *Ophthalmology*. 2002;109:948–954.

257. Somaiya MD, Burns JD, Mintz R, et al. Factors affecting visual outcomes after small-incision phacoemulsification in diabetic patients. *J Cataract Refract Surg*. 2002;28:1364–1371.
258. Borrillo JL, Mittra RA, Dev S, et al. Retinopathy progression and visual outcomes after phacoemulsification in patients with diabetes mellitus. *Trans Am Ophthalmol Soc*. 1999;97:435–445 [discussion 445–449].
259. Gupta B, Wong R, Sivaprasad S, Williamson TH. Surgical and visual outcome following 20-gauge vitrectomy in proliferative diabetic retinopathy over a 10-year period, evidence for change in practice. *Eye (Lond)*. 2012;26:576–582.
260. Li JK, Jin XH, Fang W, et al. Preretinal hemorrhage and prognosis following vitrectomy and silicone oil tamponade for severe proliferative diabetic retinopathy. *Zhejiang Da Xue Xue Bao Yi Xue Ban*. 2015;44:167–173 [in Chinese].
261. The Diabetic Retinopathy Vitrectomy Study Research Group. Early vitrectomy for severe proliferative diabetic retinopathy in eyes with useful vision. Clinical application of results of a randomized trial – Diabetic Retinopathy Vitrectomy Study report 4. *Ophthalmology*. 1988;95:1321–1334.
262. Rice TA, Michels RG, Rice EF. Vitrectomy for diabetic traction retinal detachment involving the macula. *Am J Ophthalmol*. 1983;95:22–33.
263. Thompson JT, de Bustros S, Michels RG, et al. Results and prognostic factors in vitrectomy for diabetic traction retinal detachment of the macula. *Arch Ophthalmol*. 1987;105:497–502.
264. Tolentino FI, Freeman HM, Tolentino FL. Closed vitrectomy in the management of diabetic traction retinal detachment. *Ophthalmology*. 1980;87:1078–1089.
265. Lewis H, Abrams GW, Blumenkranz MS, et al. Vitrectomy for diabetic macular traction and edema associated with posterior hyaloidal traction. *Ophthalmology*. 1992;99:753–759.
266. Harbour JW, Smiddy WE, Flynn HW Jr, et al. Vitrectomy for diabetic macular edema associated with a thickened and taut posterior hyaloid membrane. *Am J Ophthalmol*. 1996;121:405–413.

267. Gandorfer A, Messmer EM, Ulbig MW, et al. Resolution of diabetic macular edema after surgical removal of the posterior hyaloid and the inner limiting membrane. *Retina*. 2000;20:126–133.
268. Pendergast SD, Hassan TS, Williams GA, et al. Vitrectomy for diffuse diabetic macular edema associated with a taut premacular posterior hyaloid. *Am J Ophthalmol*. 2000;130:178–186.
269. Stolba U, Binder S, Gruber D, et al. Vitrectomy for persistent diffuse diabetic macular edema. *Am J Ophthalmol*. 2005;140:295–301.
270. Kumar A, Sinha S, Azad R, et al. Comparative evaluation of vitrectomy and dye-enhanced ILM peel with grid laser in diffuse diabetic macular edema. *Graefes Arch Clin Exp Ophthalmol*. 2007;245:360–368.
271. Nasrallah FP, Van de Velde F, Jalkh AE, et al. Importance of the vitreous in young diabetics with macular edema. *Ophthalmology*. 1989;96:1511–1516.
272. Nasrallah FP, Jalkh AE, Van Coppenolle F, et al. The role of the vitreous in diabetic macular edema. *Ophthalmology*. 1988;95:1335–1339.
273. Lewis H. The role of vitrectomy in the treatment of diabetic macular edema. *Am J Ophthalmol*. 2001;131:123–125.
274. Hikichi T, Fujio N, Akiba J, et al. Association between the short-term natural history of diabetic macular edema and the vitreomacular relationship in type II diabetes mellitus. *Ophthalmology*. 1997;104:473–478.
275. Kaiser PK, Riemann CD, Sears JE, et al. Macular traction detachment and diabetic macular edema associated with posterior hyaloidal traction. *Am J Ophthalmol*. 2001;131:44–49.
276. Massin P, Duguid G, Erginay A, et al. Optical coherence tomography for evaluating diabetic macular edema before and after vitrectomy. *Am J Ophthalmol*. 2003;135:169–177.
277. Browning DJ, McOwen MD, Bowen RM Jr, et al. Comparison of the clinical diagnosis of diabetic macular edema with diagnosis by optical coherence tomography. *Ophthalmology*. 2004;111:712–715.

278. Ikeda T, Sato K, Katano T, et al. Improved visual acuity following pars plana vitrectomy for diabetic cystoid macular edema and detached posterior hyaloid. *Retina*. 2000;20:220–222.
279. La Heij EC, Hendrikse F, Kessels AG, et al. Vitrectomy results in diabetic macular oedema without evident vitreomacular traction. *Graefes Arch Clin Exp Ophthalmol*. 2001;239:264–270.
280. Tachi N, Ogino N. Vitrectomy for diffuse macular edema in cases of diabetic retinopathy. *Am J Ophthalmol*. 1996;122:258–260.
281. Rosenblatt BJ, Shah GK, Sharma S, et al. Pars plana vitrectomy with internal limiting membranectomy for refractory diabetic macular edema without a taut posterior hyaloid. *Graefes Arch Clin Exp Ophthalmol*. 2005;243:20–25.
282. Yanyali A, Horozoglu F, Celik E, et al. Pars plana vitrectomy and removal of the internal limiting membrane in diabetic macular edema unresponsive to grid laser photocoagulation. *Eur J Ophthalmol*. 2006;16:573–581.
283. Recchia FM, Ruby AJ, Carvalho Recchia CA. Pars plana vitrectomy with removal of the internal limiting membrane in the treatment of persistent diabetic macular edema. *Am J Ophthalmol*. 2005;139:447–454.
284. Terasaki H, Kojima T, Niwa H, et al. Changes in focal macular electroretinograms and foveal thickness after vitrectomy for diabetic macular edema. *Invest Ophthalmol Vis Sci*. 2003;44:4465–4472.
285. Yanyali A, Nohutcu AF, Horozoglu F, et al. Modified grid laser photocoagulation versus pars plana vitrectomy with internal limiting membrane removal in diabetic macular edema. *Am J Ophthalmol*. 2005;139:795–801.
286. Asami T, Terasaki H, Kachi S, et al. Ultrastructure of internal limiting membrane removed during plasmin-assisted vitrectomy from eyes with diabetic macular edema. *Ophthalmology*. 2004;111:231–237.
287. Yamamoto T, Hitani K, Tsukahara I, et al. Early postoperative retinal thickness changes and complications after vitrectomy for diabetic macular edema. *Am J*

Ophthalmol. 2003;135:14–19.
288. Browning DJ. Diabetic macular edema. Browning DJ. *Diabetic retinopathy – evidence-based management*. Springer: New York; 2010:141–202.
289. Radetzky S, Walter P, Fauser S, et al. Visual outcome of patients with macular edema after pars plana vitrectomy and indocyanine green-assisted peeling of the internal limiting membrane. *Graefes Arch Clin Exp Ophthalmol*. 2004;242:273–278.
290. Ando F, Yasui O, Hirose H, et al. Optic nerve atrophy after vitrectomy with indocyanine green-assisted internal limiting membrane peeling in diffuse diabetic macular edema. Adverse effect of ICG-assisted ILM peeling. *Graefes Arch Clin Exp Ophthalmol*. 2004;242:995–999.
291. Gandorfer A, Haritoglou C, Kampik A. Toxicity of indocyanine green in vitreoretinal surgery. *Dev Ophthalmol*. 2008;42:69–81 [Review].
292. Matsumoto H, Yamanaka I, Hisatomi T, et al. Triamcinolone acetonide-assisted pars plana vitrectomy improves residual posterior vitreous hyaloid removal: ultrastructural analysis of the inner limiting membrane. *Retina*. 2007;27:174–179.
293. Okamoto Y, Okamoto F, Hiraoka T, et al. Vision-related quality of life and visual function following intravitreal bevacizumab injection for persistent diabetic macular edema after vitrectomy. *Jpn J Ophthalmol*. 2014;58:369–374.
294. Diabetic Retinopathy Clinical Research Network Authors/Writing Committee, Baker CW, Almukhtar T, et al. Macular edema after cataract surgery in eyes without preoperative central-involved diabetic macular edema. *JAMA Ophthalmol*. 2013;13:870–879.
295. Yamamoto T, Akabane N, Takeuchi S. Vitrectomy for diabetic macular edema: the role of posterior vitreous detachment and epimacular membrane. *Am J Ophthalmol*. 2001;132:369–377.
296. Patel JI, Tombran-Tink J, Hykin PG, et al. Vitreous and aqueous concentrations of proangiogenic, antiangiogenic factors and other cytokines in diabetic retinopathy patients with macular edema: implications for structural differences

in macular profiles. *Exp Eye Res*. 2006;82:798–806.
297. Browning DJ, Fraser CM, Powers ME. Comparison of the magnitude and time course of macular thinning induced by different interventions for diabetic macular edema: implications for sequence of application. *Ophthalmology*. 2006;113:1713–1719.
298. Parolini B, Panozzo G, Gusson E, et al. Diode laser, vitrectomy and intravitreal triamcinolone: a comparative study for the treatment of diffuse non tractional diabetic macular edema. *Semin Ophthalmol*. 2004;19:1–12.
299. Higuchi A, Ogata N, Jo N, et al. Pars plana vitrectomy with removal of posterior hyaloid face in treatment of refractory diabetic macular edema resistant to triamcinolone acetonide. *Jpn J Ophthalmol*. 2006;50:529–531.
300. Fong DS, Segal PP, Myers F, et al. Subretinal fibrosis in diabetic macular edema. ETDRS report 23. Early Treatment Diabetic Retinopathy Study Research Group. *Arch Ophthalmol*. 1997;115:873–877.
301. Diabetic Retinopathy Clinical Research Network Writing Committee, Haller JA, Qin H, et al. Vitrectomy outcomes in eyes with diabetic macular edema and vitreomacular traction. *Ophthalmology*. 2010;117:1087–1093.
302. Flaxel CJ, Edwards AR, Aiello LP, et al. Factors associated with visual acuity outcomes after vitrectomy for diabetic macular edema: diabetic retinopathy clinical research network. *Retina*. 2010;30:1488–1495.
303. Gaudric A. Macular cysts, holes and cavitations : 2006 Jules Gonin lecture of the Retina Research Foundation. *Graefes Arch Clin Exp Ophthalmol*. 2008;246:1071–1079.
304. Helbig H. Diabetic tractional retinal detachment. *Klin Monatsbl Augenheilkd*. 2002;219:186–190 [in German].
305. Hirata A, Takano A, Inomata Y, et al. Plasmin-assisted vitrectomy for management of proliferative membrane in proliferative diabetic retinopathy: a pilot study. *Retina*. 2007;27(8):1074–1078.
306. Priglinger SG, Haritoglou C, Mueller A, et al. Pulsed electron avalanche knife in vitreoretinal surgery. *Retina*. 2005;25(7):889–896.

307. Sima P, Zoran T. Long-term results of vitreous surgery for proliferative diabetic retinopathy. *Doc Ophthalmol*. 1994;87:223–232.
308. Oldendoerp J, Spitznas M. Factors influencing the results of vitreous surgery in diabetic retinopathy. I. Iris rubeosis and/or active neovascularization at the fundus. *Graefes Arch Klin Exp Ophthalmol*. 1989;227:1–8.
309. Smiddy WE, Flynn HW. Vitrectomy for diabetic retinopathy. Flynn HW, Smiddy WE. *Diabetes and ocular disease: past, present and future therapies*. 2000:155–179 [The Foundation of the American Academy of Ophthalmology; 14].
310. Wu WC, Lin JC. The experience to use a modified en bloc excision technique in vitrectomy for diabetic traction retinal detachment. *Kaohsiung J Med Sci*. 1999;15:461–467.
311. Hutton WL, Bernstein I, Fuller D. Diabetic traction retinal detachment: factors influencing final visual acuity. *Ophthalmology*. 1980;87:1071–1077.
312. Meier P, Wiedemann P. Vitrectomy for traction macular detachment in diabetic retinopathy. *Graefes Arch Klin Exp Ophthalmol*. 1997;235:569–574.
313. Helbig H, Kellner U, Bornfeld N, et al. Limits and possibilities of vitreous body surgery in diabetic retinopathy. *Ophthalmologe*. 1996;93:647–654 [in German].
314. Arevalo JF, Serrano MA, Arias JD. Perfluorocarbon in vitreoretinal surgery and preoperative bevacizumab in diabetic tractional retinal detachment. *World J Diabetes*. 2014;5:724–729.
315. Rahimy E, Pitcher JD 3rd, Gee CJ, et al. Diabetic tractional retinal detachment repair by vitreoretinal fellows in a county health system. *Retina*. 2015;35:303–309.
316. Stoffelns BM, Dick B. Pars-plana vitrectomy in diabetic traction retinal detachments with holes. *Klin Monatsbl Augenheilkd*. 2000;216:286–289 [in German].
317. Tao Y, Jiang YR, Li XX, et al. Long-term results of vitrectomy without endotamponade in proliferative diabetic retinopathy with tractional retinal detachment. *Retina*. 2010;30:447–451.

318. Hsu YJ, Hsieh YT, Yeh PT, et al. Combined tractional and rhegmatogenous retinal detachment in proliferative diabetic retinopathy in the anti-VEGF era. *J Ophthalmol*. 2014;2014:917375.
319. The Diabetes Control and Complications Trial Research Group. The effect of intensive treatment of diabetes on the development and progression of long-term complications in insulin-dependent diabetes mellitus. *N Engl J Med*. 1993;329:977–986.
320. Tasman W, Magargal LE, Augsburger JJ. Effects of argon laser photocoagulation on rubeosis iridis and angle neovascularization. *Ophthalmology*. 1980;87:400–402.
321. Teich SA, Walsh JB. A grading system for iris neovascularization. Prognostic implications for treatment. *Ophthalmology*. 1981;88:1102–1106.
322. Shen CC, Salim S, Du H, et al. Trabeculectomy versus Ahmed glaucoma valve implantation in neovascular glaucoma. *Clin Ophthalmol*. 2011;5:281–286.
323. Al Obeidan SA, Osman EA, Al-Amro SA, et al. Full preoperative panretinal photocoagulation improves the outcome of trabeculectomy with mitomycin C for neovascular glaucoma. *Eur J Ophthalmol*. 2008;18:758–764.
324. Cheng Y, Liu XH, Shen X, et al. Ahmed valve implantation for neovascular glaucoma after 23-gauge vitrectomy in eyes with proliferative diabetic retinopathy. *Int J Ophthalmol*. 2013;6:316–320.
325. Hou XR, Miao H, Tao Y, et al. Expression of cytokines on the iris of patients with neovascular glaucoma. *Acta Ophthalmol*. 2015;93:e100–4.
326. Every SG, Molteno AC, Bevin TH, et al. Long-term results of Molteno implant insertion in cases of neovascular glaucoma. *Arch Ophthalmol*. 2006;124:355–360.
327. Lloyd MA, Sedlak T, Heuer DK, et al. Clinical experience with the single-plate Molteno implant in complicated glaucomas. Update of a pilot study. *Ophthalmology*. 1992;99:679–687.
328. Kono T, Shiga S, Takesue Y, et al. Long-term results of pars plana vitrectomy combined with filtering surgery for

neovascular glaucoma. *Ophthalmic Surg Lasers Imaging*. 2005;36:211–216.

116

Management of Combined Inflammatory and Rhegmatogenous Retinal Detachment

Marc D. de Smet, Karina Julian

Introduction

Retinal detachments (RD) are infrequent in the setting of intraocular inflammation but present a particular challenge both to the vitreoretinal surgeon and to the uveitis specialist. They occur most frequently during or following an episode of intraocular infection and are most commonly seen in eyes having suffered from a viral retinitis. Whether not related to ocular infection, the diagnostic and therapeutic approach may be difficult since different forms of retinal involvement suppose different treatments and prognosis. Serous retinal detachments (SRD) are the form most commonly associated with active, purely inflammatory conditions and, often, their presence helps to establish the diagnosis, as in the case of Vogt–Koyanagi–Harada disease (see Chapter 78, Vogt–Koyanagi–Harada disease). At times, it may be misdiagnosed for a rhegmatogenous retinal detachment (RRD), but the management of SRD is pharmacologic, aimed at controlling the intraocular inflammation, though on a rare occasion, surgery may be needed to drain the subretinal fluid.[1] Visual prognosis in most cases of SRD is excellent provided that the immunosuppressive agents have been introduced at a sufficient dose to lead to rapid resolution, and tapering is done slowly.

Rhegmatogenous retinal detachment (RRD) is fortunately rare in active uveitis, but when present, the visual prognosis is guarded even with modern vitreoretinal surgical techniques. Tractional retinal detachments (TRD) are observed in both infectious and noninfectious uveitis, whenever vitreous organization develops in an eye without posterior vitreous detachment (PVD), or when proliferative vitreoretinopathy (PVR) complicates the course of

intraocular inflammation. Combined forms of RD are also possible. Establishing the exact cause, and the mechanisms involved in each individual case, is needed to ascertain the appropriate therapeutic approach and ensure visual recovery.

Epidemiology

A systematic review of population-based studies on RRD published between 1970 and 2009 found a reported incidence between 6.3 and 17.9 for 100, 000 people/year, with significant geographic variations.[2] It is widely accepted that RRD occurrence varies with ethnicity and is strongly associated with aging, myopia, vitreoretinal degeneration, and pseudophakia.[3,4] Uveitis itself is not considered a predisposing factor for developing RRD. However, a retrospective study conducted in The Netherlands found a prevalence of RRD of 3.1% among 1387 uveitic patients, suggesting inflammation as an independent risk factor for its development.[5]

Not all types of uveitis carry the same risk of RRD; this complication is most commonly seen in posterior uveitis from infectious etiology, with the highest risk in viral retinitis cases. Acute retinal necrosis (ARN) (see Chapter 91, Acute retinal necrosis syndrome) evolves to RRD in more than 50% of cases, in a median time of 53 days after presentation.[6] This risk is even higher for progressive outer retinal necrosis (PORN), in which almost 70% of affected eyes will develop RRD soon after presentation.[7] For cytomegalovirus (CMV) retinitis (see Chapter 84, HIV-associated infections), even though the course of the disease has positively changed with the introduction of highly active antiretroviral therapy (HAART), the rate of RRD remains as high as 2.3/100 eye-years.[8]

Parasitic infections can lead to RD when a choroidal process extends to the retina and vitreous or when a retinal process causes overlying vitreous to condense and contract. Toxoplasmic retinochoroiditis (see Chapter 88, Ocular toxoplasmosis) presents a risk of RRD of 3.5–6%.[9–11] In a subset of toxoplasmosis patients addressed for vitreoretinal surgery, Adan et al. found 53.3% of cases of RD, most of which had pure RRD, with a few cases having combined tractional and RRD.[12] Exudative detachments are rarely

associated with ocular toxoplasmosis but have been described in the literature.[13,14] Vision-threatening features in ocular toxocariasis (OT) (see Chapter 89, Helminthic disease) are mainly severe vitritis, cystoid macular edema, and tractional detachment of the macula. A retrospective series on OT found a prevalence of macular traction of about 30% regardless of the site where the choroidal granuloma was located. In peripheral lesions with retinal traction, TRD occurs in about 40% of cases.[5,15]

Acute syphilitic panuveitis may be complicated by retinal detachment: while SRD are well known to occur in these cases, RRD have been recently reported in 11 patients following a literature review. Seventy-five percent of these were HIV-positive. The detachment occurred in the convalescent period following a severe vitreous inflammatory response.[16]

Among noninfectious uveitis, the risk of RRD is less than 1%. Most patients developing retinal tears and detachments appear to do so as a result of concomitant retinal pathology, often in areas unrelated to sites of inflammation. However, inflammatory processes affecting the vitreous base may present an exception to this rule. In the healing phase, following severe inflammation, vitreous contraction can lead to important tractional forces on the retina. Hence, pars planitis, when untreated for a prolonged period of time or if severe, is known to develop TRD[17] and retinoschisis.[18] The differentiation between true retinoschisis and TRD may sometimes be difficult, especially for those lesions situated in the far periphery.[19] Sarcoidosis is also known to develop various forms of RD (see Chapter 81, Sarcoidosis), though this complication is rare. Serous RD,[20] RRD,[21] retinal pigment epithelium (RPE) detachments,[22] and even a rare case of necrotizing retinitis with subsequent RRD[23] were described in the context of ocular sarcoidosis, but mostly as isolated cases. RRD may be also part of the spectrum of posterior segment complications of Behçet's disease, both in the active stage or in the convalescent period. Detailed fundoscopy should be performed periodically in these patients, particularly in cases with healed retinitis or in the presence of vitreous shrinkage.[24] A case of RRD secondary to a macular hole in a young patient with Behçet uveitis has also been reported, stressing the role of recurrent vitritis and vitreous traction in the

pathogenesis of this severe complication (see Chapter 80, Autoimmune retinopathies).[25]

Pathophysiology

The nature of the inflammatory or infectious process determines the mechanism by which the detachment occurs and provides an indication as to the means by which it can be resolved. SRD is usually the result of an immune-mediated assault on the choroid, RPE, and retinal vasculature. Its follows from loss of the tight junctions between retinal endothelial cells, leading to increased outward flow of fluid from the retinal vasculature, loss of tight junctions between RPE cells, and a failure of the compensatory pump function of RPE cells. Disruption of the normal oncotic gradient between the vitreous cavity and the choroid may also compromise passive transfer mechanisms responsible for a good portion of normal fluid flow to the choroid. Inflammatory mediators modulate vascular permeability and modulate the type and expression of aquaporins within the retina (mainly Müller cells) and the RPE, as well as of chloride receptors such as CLIC4 necessary for retinal attachment.[26–28] Resolution of a serous detachment requires one to reestablish the status quo by inhibiting both humoral and cellular inflammatory mechanisms through appropriate systemic or local immunosuppression (Fig. 116.1).

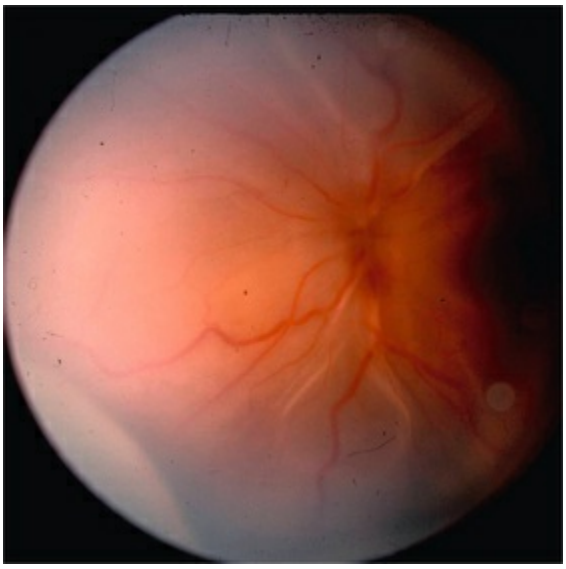

FIG. 116.1 Serous retinal detachment in a patient with Vogt–Koyanagi–Harada disease. Detachments are usually bullous, with shifting fluid but without undulating retinal surface. Hyperemia of the optic nerve head is often present.

In the case of both RRD and TRD, vitreous body traction plays a predominant role. In RRD associated with toxoplasmosis, active toxoplasmic retinochoroiditis often precedes or is concurrent with the development of the RRD.[9] Inflammation not only enhances vitreous liquefaction but also leads to crosslinking between collagen fibrils, particularly those close to the retinal interface, leading to the formation of an anomalous PVD and retinal tears[29–31] Vitreal strands between the optic disc and the ocular toxocariasis granuloma are present in nearly 50% of patients (Fig. 116.2). These strands are often the source of retinal traction and detachment. Contraction of the vitreous base, particularly seen in chronic longstanding uveitis, leads to the development of fibrous or fibrovascular bands, which can be very adherent to the underlying retina.[30,32] Their removal can be quite challenging at the time of surgery (Fig. 116.3).

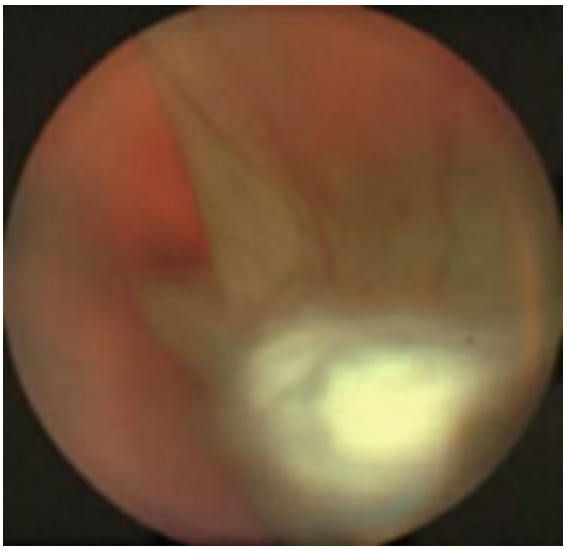

FIG. 116.2 Fundus photograph from an ocular toxocariasis case. A peripheral granuloma causes a tractional retinal detachment in the central retina.

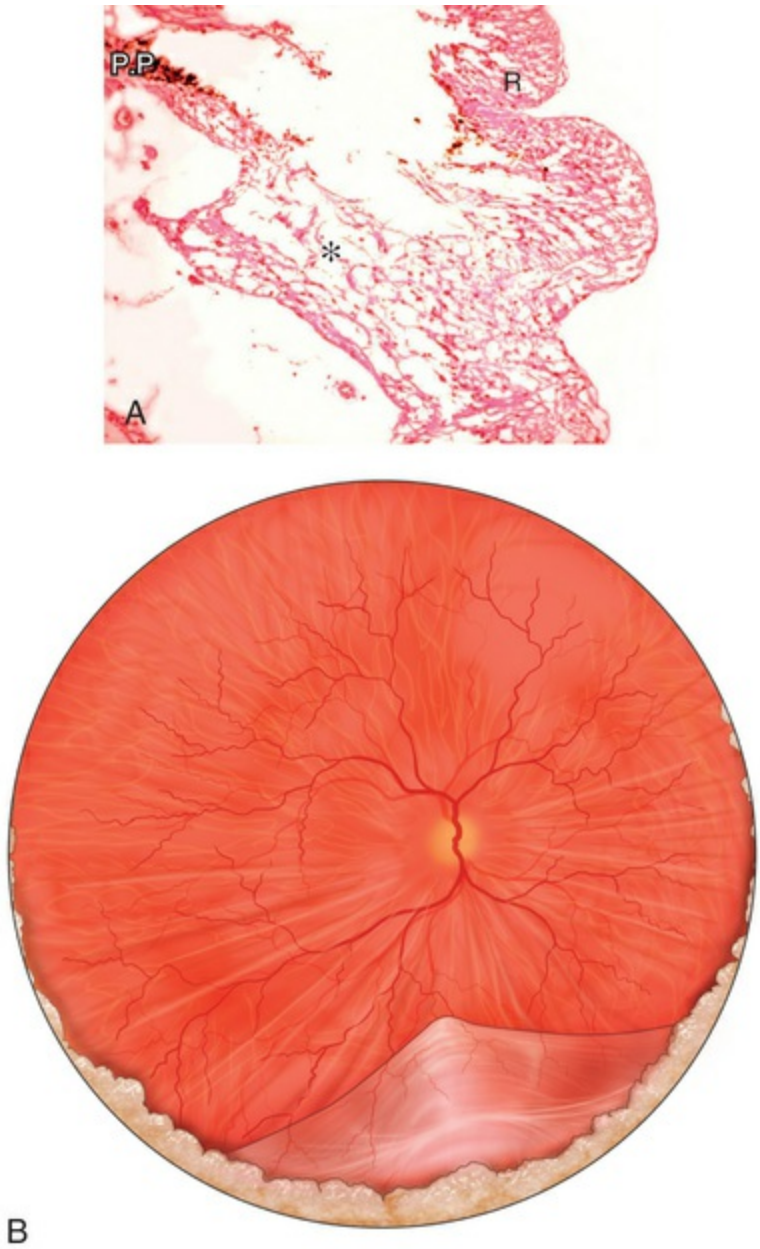

FIG. 116.3 (A) Histopathologic section in a patient with pars planitis. Fibrous proliferation (*) leads to vitreous contraction between the pars plana (*PP*) and the retina (*R*). This tissue may be particularly difficult to remove surgically (hematoxylin and eosin, ×110). (B) Artist rendition of the pars plana exudation leading to vitreous base fibrosis and traction on the peripheral retina. (Panel A courtesy of Dr. Chi-Chao Chan, National Eye Institute, Bethesda, United States.)

High levels of s-ICAM1 (type 1 soluble intercellular adhesion molecule) are found in vitreous from uveitic eyes complicated by RD similar to what has been observed in cases of proliferative

vitreoretinopathy (PVR) where it is felt to perpetuate a cytokine-mediated vascular reaction that may contribute to PVR formation.[33–35] It correlates positively with vitreous levels of tumor necrosis factor-alpha (TNF-α), a cytokine with a key role in the initiation of the inflammatory cascade and the pathogenesis of uveitis.[36] Though the exact role is not known in this context, it is probably a marker of disease severity, an important predisposition to the development of any RD.

The cause of RD following viral retinitis is somewhat different. Herpetic retinal infections (CMV, HSV, VZV) are characterized by retinal necrosis leaving in its wake a diaphanous glial membrane (Fig. 116.4). Any traction on these areas can easily lead to retinal tears and a detachment. Depending on the interplay between the virus and the host immune system, it is associated with moderate to severe vitreous inflammation. Cytomegalovirus retinitis is quintessentially seen in the context of AIDS or severe immunosuppression. It still today remains an AIDS-defining infection but is also seen in patients who fail to respond, become intolerant of, or stop responding to HAART. Traditionally, it was not associated with vitreous inflammation, and therefore detachments were rarely complicated by proliferative vitreoretinopathy. In the HAART era the frequency of an inflammatory response, late detachments, and PVR has increased, with some series reporting up to 30% of CMV retinitis cases complicated by PVR.[37] The incidence of RD is highest among newly diagnosed patients (within 45 days of diagnosing a CMV retinitis) at 4.9/100 eye-years, while the overall rate among AIDS patients with CMV retinitis is 2.3/100 eye-years.[8] Additional risk factors for RD include large lesion size, anterior lesion location, associated retinal pathology (e.g., myopia), and older age.[38,39] Local and systemic therapy might reduce slightly the risk of RD, possibly due to a more rapid resolution of retinitis.[40] Most detachments occur once the initial infection has subsided. The healed retinitis leaves a thin glial sheet above which an epiretinal membrane, possibly containing condensed vitreous, can be found (Fig. 116.5).[41] Vitreoretinal gliosis is often present at the interface between normal and abnormal retina on optical coherence tomography (OCT) images but is difficult to visualize clinically. It is possible that the

gliosis contributes to the formation of retinal detachments in these patients.

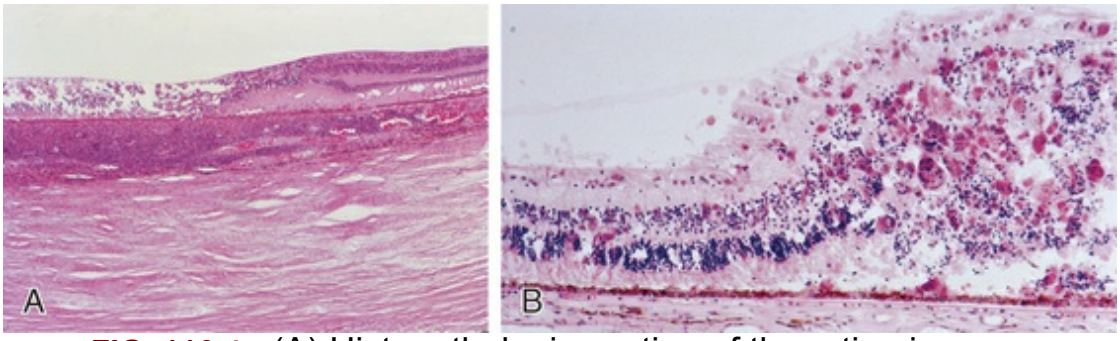

FIG. 116.4 (A) Histopathologic section of the retina in acute retinal necrosis showing a sharp border between healed and affected tissue. (B) Histopathologic section of the retina in cytomegalovirus retinitis, showing also a sharp border in the healed phase.

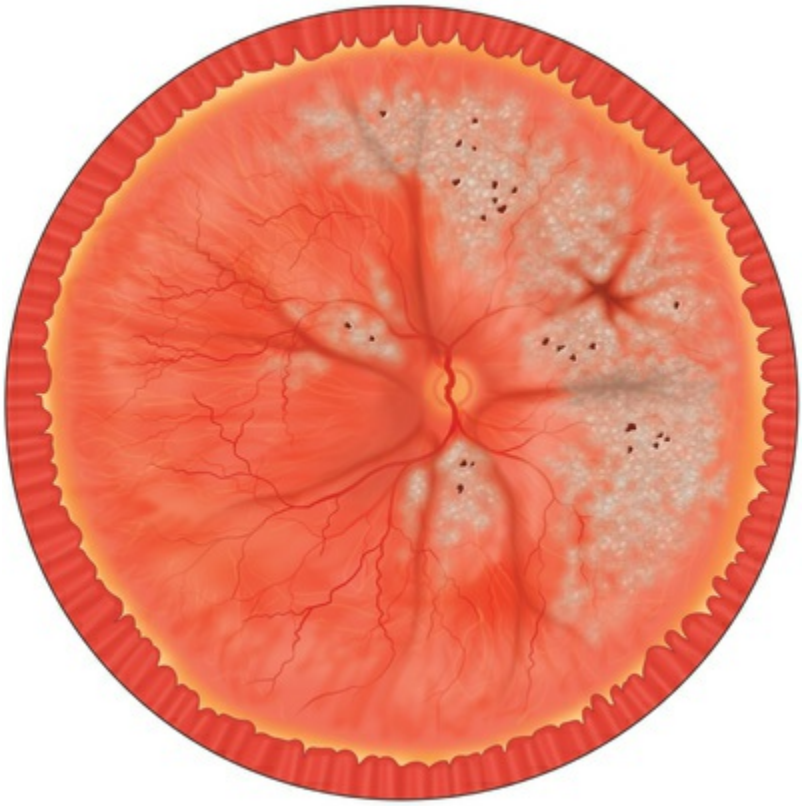

FIG. 116.5 Artist's rendition of a retinal detachment following cytomegalovirus retinitis. Atrophic scars of healed retinitis often harbor retinal breaks.

Acute retinal necrosis (Fig. 116.6A) is characterized by large, peripheral, often confluent zones of retinitis.[42–44] Pathologically, it is characterized by full-thickness retinal necrosis and occlusive vasculitis (Fig. 116.4B).[45] Vitreous involvement, often not present initially, develops within days and can obliterate the view of the posterior pole. A more aggressive form starting at the posterior pole, called progressive outer retinal necrosis (PORN, Fig. 116.6B), also affects all retinal layers and represents an ophthalmic emergency since it may lead to complete blindness within hours if not treated aggressively.[46–48] In both cases, detachments occur due to vitreous traction on the atrophic retina, often as a PVD develops. When severe inflammation is present, they may occur even before resolution of the active retinitis. Retinal detachments in ARN are frequently complicated by an anterior vitreous contraction along the vitreous base. Retinal breaks are usually multiple and located at the juncture between normal and gliotic retina. Vitreoretinal adhesions are common, and the retinal detachment has both tractional and rhegmatogenous components (Fig. 116.7).

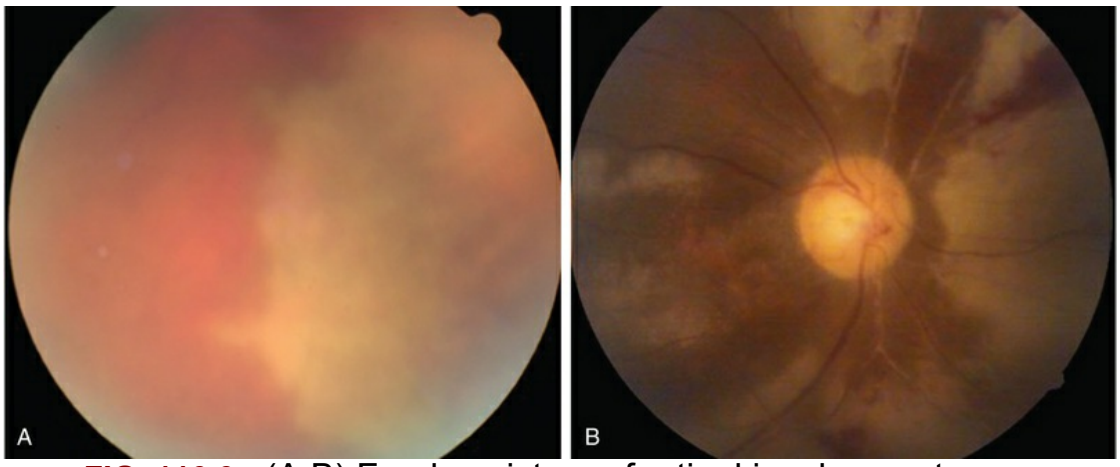

FIG. 116.6 (A,B) Fundus picture of retinal involvement in viral posterior uveitis. (A) A large peripheral area of retinal whitening with diffuse borders and hazy view, due to important vitritis, in a case of herpes simplex-associated acute retinal necrosis. (B) Several areas of retinal whitening surrounding the optic nerve head, clearly viewed through a noninflammatory vitreous, in an immunosuppressed patient suffering from varicella-zoster-associated progressive outer retinal necrosis.

(Panel A courtesy of Alvaro Fernández-Mendy, MD, Instituto de la Visión, Buenos Aires, Argentina. Panel B courtesy of Eric Campos, MD, Universidad Nacional de Trujillo, Perú.)

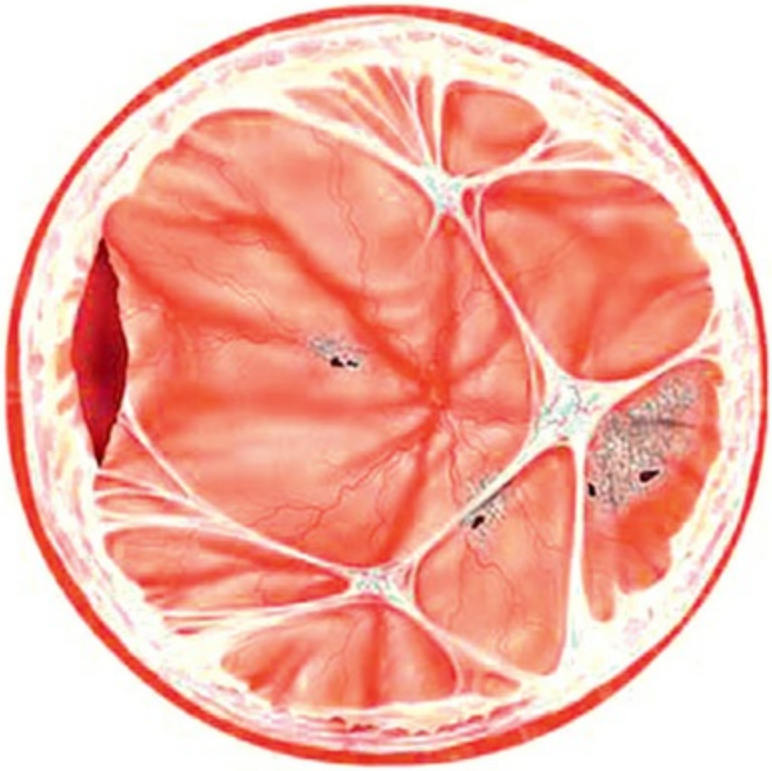

FIG. 116.7 Artist's rendition of a retinal detachment associated with acute retinal necrosis showing vitreous strands, vitreous base fibrosis, and retinal thinning, tears, and preretinal fibrosis. Large tears form in areas of retinal gliosis. The more extensive the area of gliosis, the more probable is the development of a detachment.

Clinical Examination and Findings

As stated above, RDs in uveitis can arise in a number of ways. Not infrequently, TRD, even schisis cavities, can be misdiagnosed as RRD (Fig. 116.8).[18] As part of the initial workup, it is important to establish the nature of the detachment, the etiology, severity, and stage of ocular inflammation or infection, and the status of the

retina and vitreous. In particular, it is important to determine the relationship between the detached retina and the area of retinal inflammation or infection, the presence or absence of a PVD, and the presence of peripheral vitreous base fibrosis and foreshortening. These observations and workup are often hampered by poor visualization resulting from posterior synechiae, cataract, vitreous haze, or cellular infiltration. In infectious cases, particularly ARN, vitreous inflammation may increase shortly after initiating treatment to the point where it is impossible to visualize the fundus. Analogous to trauma cases, it is important in these cases to document, as early as possible, findings in the vitreous and retina.

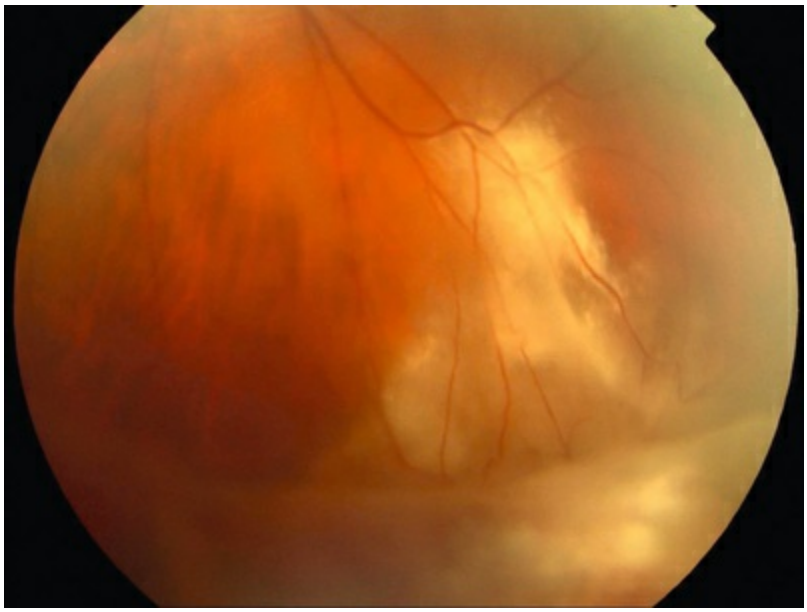

FIG. 116.8 Peripheral traction due to vitreous bands and contraction in a patient with pars planitis and neovascularization of the vitreous base causing exudation into the subretinal space. One of the vitreous bands is visible on the retina surface.

When visualization becomes inadequate, ancillary tests may be required. To evaluate the macular area through a small pupil, a nonmydriatic camera, SLO (scanning laser ophthalmoscopy), or OCT may be useful. Unfortunately, they do not give any information on the condition of the peripheral retina. B-scan ultrasonography (both 10 and 50 MHz) is probably the most useful tool to evaluate the peripheral fundus. Uveitis-related RD often has

a highly reflective posterior hyaloid when detached (which can even mimic a RD).[49] Occasionally, during active inflammation, fine echoes within the retrohyaloid space are visible, corresponding to inflammatory cells within the vitreous. If visualization of the vitreoretinal interface becomes difficult and therapy with intravitreal steroids is envisaged, triamcinolone will improve the ultrasound signal and facilitate visualization of posterior structures.[50] The presence of a thickened choroid (≥2 mm thickness) and the asymmetry between the two eyes can help confirm the diagnosis of a choroidal inflammation in the involved eye.[49] Choroidal detachments are not infrequent, and their anterior extent needs to be defined.

Ciliary body detachments may develop as a result of uveitis, causing or predisposing to hypotony. Ultrabiomicroscopy (UBM) is the preferred tool to visualize the ciliary body. It is also possible to assess the state of the peripheral vitreous, in particular, if it has become adherent to the posterior iris surface causing posterior displacement of the iris plane (an indirect sign of vitreous base fibrosis and likely foreshortening of the retina) (Fig. 116.9).[51,52]

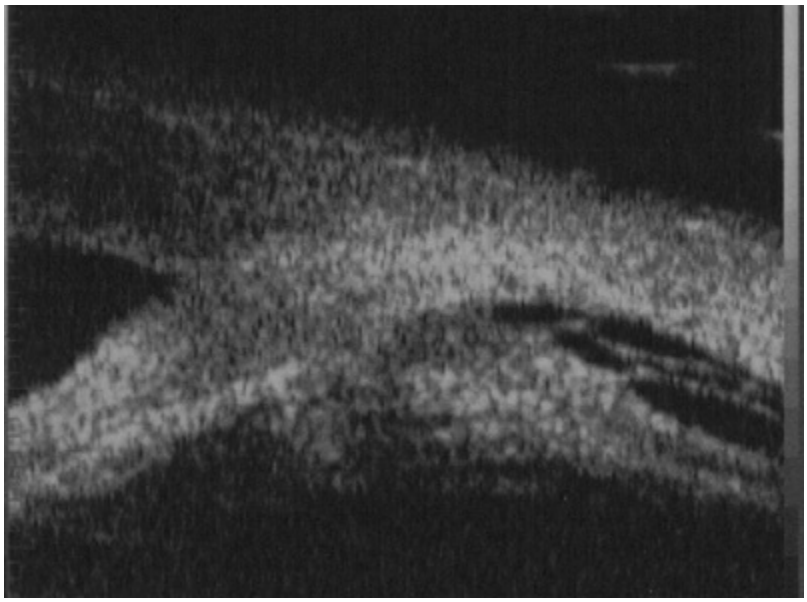

FIG. 116.9 Ultrasound biomicroscopy of the pars plana region of a patient with sarcoidosis. Vitreous condensation and contraction onto the posterior iris surface has also led to traction and detachment on the ciliary processes.

Tears in inflammatory retinal detachments are usually found and localized using the same rules as for standard detachments. In postherpetic detachments, tears are often located at the margin of the atrophic scar or at the insertion of the posterior hyaloid onto the retinal surface.

Management

As in all retinal detachment repairs, the decision and mode of intervention is based on an analysis of the potential risks contrasted with the probability of anatomic success and vision improvement. In the absence of active inflammation, most cases respond as if they were uncomplicated retinal detachments, and thus the benefit outweighs the surgical risk. With active inflammation, or in AIDS patients, vision recovery is likely to be more limited, and there is a higher risk of recurrence or PVR. Here, timing may need to be modified and a more aggressive approach adopted.

As in every case of intraocular surgery on uveitis patients, results are best if inflammation is absent. It should be under control and as low as possible prior to the intervention. Preoperative, intraoperative, and postoperative systemic and local medications (corticosteroids, antivirals, and antibiotics) should be adapted for each particular case.

Rhegmatogenous Retinal Detachment With Active Inflammation

Results of surgery performed on retinal detachments during active inflammation have generally been poor.[5,53,54] Inflammation leads to poor postoperative visualization and development of fresh membranes on the retinal surface and in the retrolenticular space. It is crucial to adequately and aggressively manage the inflammatory component with a combination of systemic and local therapy. Systemic therapy should be initiated prior to surgery. The choice will depend on the nature of inflammation and previous response to treatment. If the iris requires manipulation during surgery, prostaglandin inhibitors should be added topically as well as systemically starting the day prior to surgery. This is commonly

done in uveitis patients undergoing cataract surgery as it can significantly reduce postoperative anterior segment inflammation.[55] At the end of surgery, periocular and intraocular steroids should be considered. The use of a long-acting (or slow release) steroid preparation will reduce the severity of any recurrence developing in the postoperative period.

In general, better surgical success is obtained when a more aggressive approach is taken. The lens, if present, is removed, the decision whether to implant an intraocular lens (IOL) or not will depend on the degree of inflammation and the underlying diagnosis. In case implantation is chosen, in-the-bag fixation with a hydrophobic acrylic or polymethyl methacrylate IOL is preferred (since the use of silicone oil tamponade in these cases is almost the rule, as will be further discussed). Lens extraction should be considered, even in the presence of a clear lens, in all cases requiring vitreous base shaving or when a significant postoperative fibrinous response is expected. It is very difficult to achieve an adequate ablation of anterior vitreous over 360° without removal of the lens. Anterior displacement of the lens by draining the anterior chamber is frequently not sufficient.

Following a core pars plana vitrectomy, which preferably is performed with small-gauge instruments, a posterior vitreous detachment is induced and carried out to the vitreous base (Fig. 116.10A). This can be facilitated by the use of intravitreal triamcinolone or a coloring agent. If it is not possible to remove the posterior hyaloid completely, the vitreous is shaven down to the retinal surface (Fig. 116.10B). This is particularly important at the vitreous base (Fig. 116.10C), as there will be a tendency for any remaining scaffold to contract and pull on the ciliary body and peripheral retina potentially leading to hypotony and/or recurrent detachments (Fig. 116.9). Membranes present on the retinal surface are peeled; given their tenacity, this is often best done using a bimanual technique with a pic and a forceps (Fig. 116.10D).

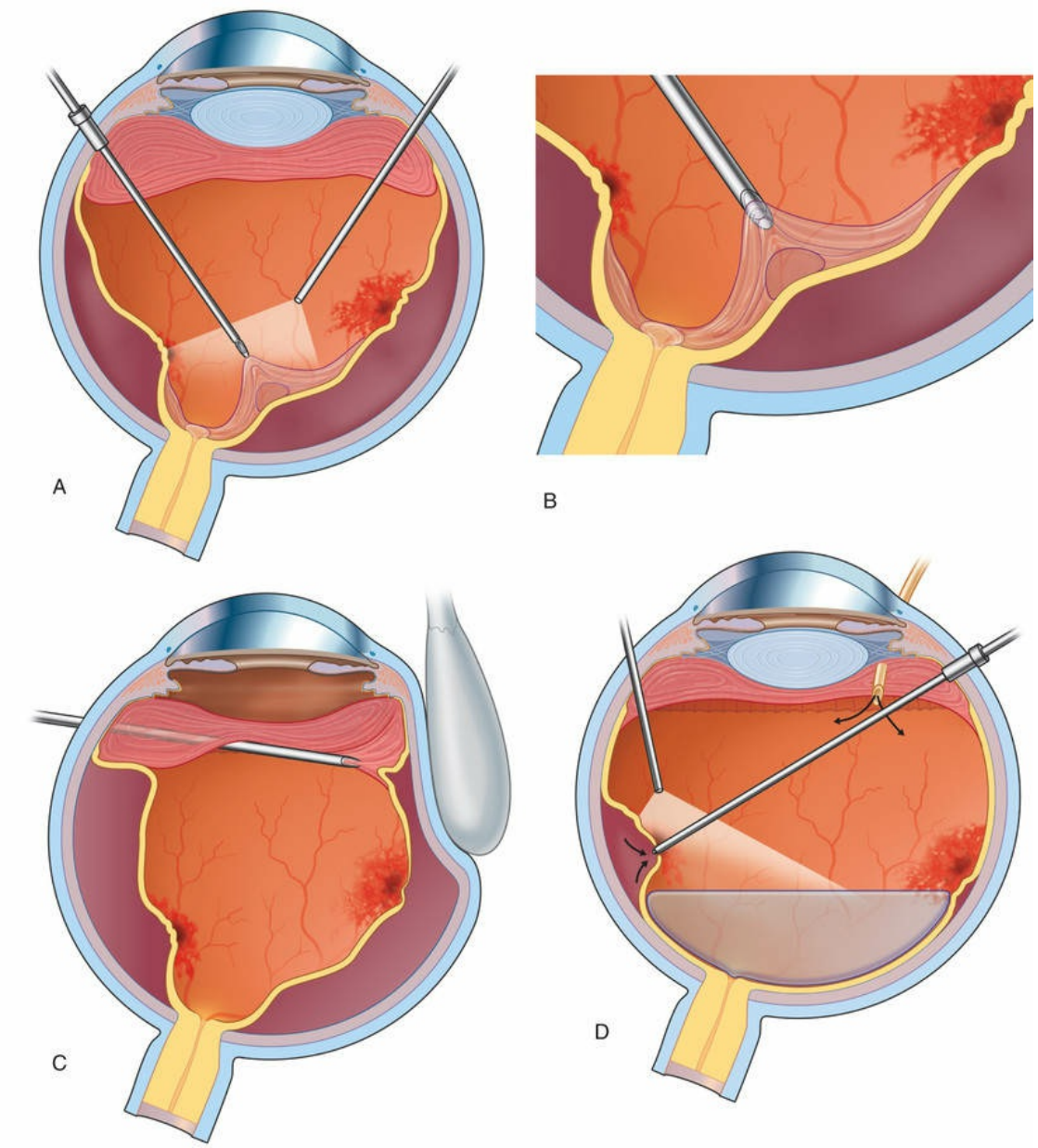

FIG. 116.10 Vitrectomy for retinal detachment in patients with active uveitis. (A) A standard pars plana vitrectomy is carried out, followed by the induction of a posterior vitreous detachment. The vitrectomy is usually initiated after removal of the crystalline lens and its replacement with an intraocular lens. (B) When the posterior hyaloid cannot be easily detached even with the use of a coloring agent, the vitreous is resected up to the surface of the retina. (C) Resection of the vitreous is carried out over the vitreous base, where the vitreous remnants are shaven down to the retina surface. (D) Dissection of membranes present on the retinal surface is best achieved using a bimanual technique, the use of perfluorocarbon, and a

chandelier lighting system.

Illumination is provided by a chandelier or transscleral illumination system. Peeling is facilitated by using perfluorocarbon, which acts as a “third” harm, providing posterior stabilization to the membranes being peeled. Once the retina is fully reattached under perfluorocarbon, the edges of the tears are treated by photocoagulation. Cryotherapy should be avoided, as it enhances breakdown of the blood–ocular barrier and can increase postoperative inflammation.[56] Silicone oil is the preferred tamponading agent, as it will allow continued visualization of the retinal structures while the inflammation is brought under control (Fig. 116.11). It is also thought to limit the accumulation of proinflammatory cytokines in the vitreous cavity.[57] The oil can be removed when the retina has completed healed, and the inflammation is brought fully under control. This may take 6 or more months to occur.

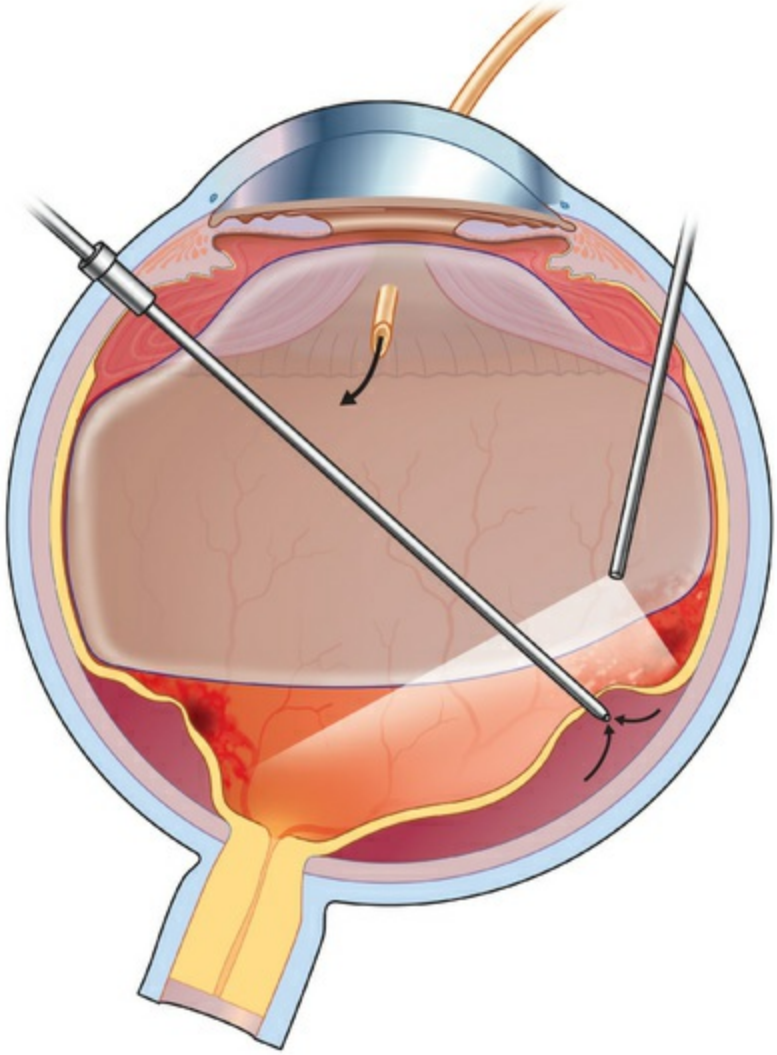

FIG. 116.11 Once the retina is mobilized, an air–fluid exchange is performed to reattach the retina. Retinotomies are done if traction is not fully relieved. Alternatively, silicone oil–perfluorocarbon exchange can be undergone.

Persistent Inflammatory Serous Retinal Detachment

When inflammation has already been controlled and SRD persists after at least 3 months of corticosteroid and/or immunosuppressive treatment, surgical drainage may be considered to hasten recovery in cases with macular involvement and decreased vision. Galor et al.[1] reported on five cases of persistent SRD surgically drained through a technique involving a complete vitrectomy, a

peripherally and superior drainage retinotomy, use of perfluorocarbon to assist drainage followed by endolaser, and a gas tamponade. In all cases a scleral buckle was used to provide peripheral support in the area of drainage. In our own experience the buckle is not required, provided tamponade can be achieved until the laser forms a firm adhesion between the retina and choroid. As indicated by the authors, this approach is meant to drain persistent subretinal fluid in patients with quiescent inflammation. If inflammation persists, the subretinal fluid will reaccumulate.

Retinal Detachment With Retinal Necrosis

Cytomegalovirus Retinitis

In selected cases of CMV-associated retinal detachments, photocoagulation may be effective in delimiting or demarcating the affected area.[58–60] This approach can lead to a significant delay in macular detachment. Delaying intraocular surgery in these patients is a valid strategy, since successful surgical reattachment, as several studies have suggested, is often associated with some degree of central loss of vision, possibly related to microangiopathy, optic neuropathy, or silicone-oil-related toxicity.[61–65] Once a surgical option is chosen, retinal detachments due to CMV, whether or not associated with PVR, should be approached in a standardized fashion. The risk of recurrence or progression of CMV should be assessed in conjunction with the treating internist, as it will determine the choice of tamponade and the need for concurrent cataract extraction.

The surgery begins with a standard three-port vitrectomy (Fig. 116.10). When preexisting vitreous separation is present, the posterior hyaloid is identified and resected up to the posterior margin of the vitreous base. In some cases, however, the vitreous has not detached posteriorly. If it can be mechanically engaged and easily elevated from the retina, this is done to create a posterior vitreous separation. In some cases, this technical separation cannot be safely accomplished. An attempt should be made to resect the vitreous as close to the surface of the retina as possible, without inducing a vitreous detachment. In cases in which CMV has caused

necrosis of a large area of retina, an en bloc dissection of diaphanous retina and vitreous is possible but should in most cases follow separation of the vitreous from surrounding healthy retina, or at least after it has been shaven off the retinal surface. The edges of retinal breaks or the area of resection are marked with intraocular diathermy (Fig. 116.12). This makes later identification easier. Internal drainage of subretinal fluid in conjunction with air–fluid or fluid–silicone exchange is performed to flatten the retina (Fig. 116.11). The retinal breaks are surrounded with endophotocoagulation (Fig. 116.13).

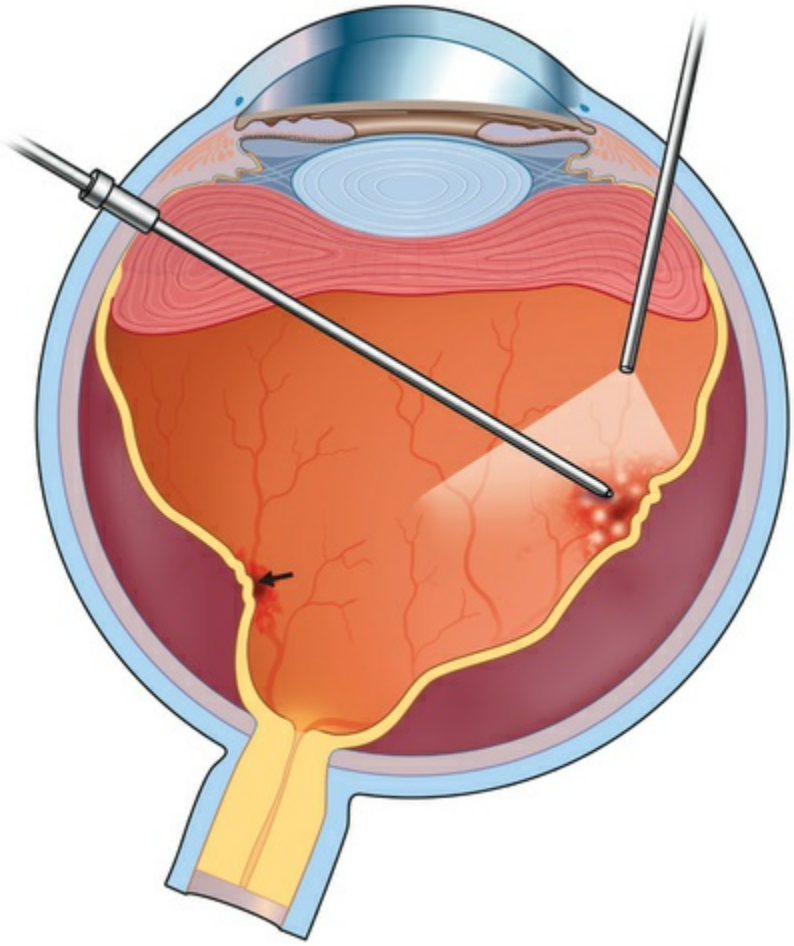

FIG. 116.12 The retinal breaks are identified and marked with diathermy, particularly if a gas exchange is chosen to flatten the retina.

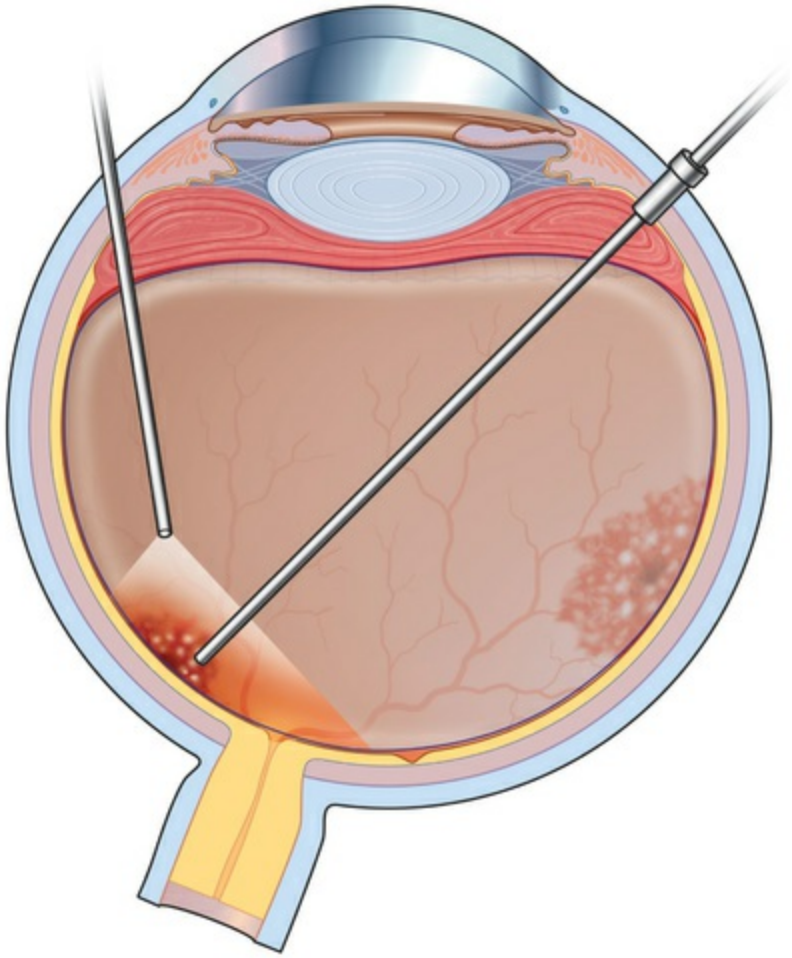

FIG. 116.13 Once attached under air, perfluorocarbon, or silicone oil, the edges of all tears and retinotomies are treated with endolaser.

Many surgeons advocate demarcating the atrophic areas with laser, as well as those regions that are likely to harbor retinal breaks. In certain circumstances, scatter photocoagulation applied to the lower hemisphere up to the edge of the inferior vascular arcade can help mitigate the appearance of a later detachment, particularly if CMV progression in this area is expected in the following months. A silicone–air exchange or air–gas exchange is performed at this point. The choice will depend on the configuration of the detachment and the likelihood of recurrent activity. If progression is likely, silicone oil is a better and more permanent choice. Postoperatively, the patient is kept face down for 12 hours, after which time special positioning is not necessary. Postoperative follow-up is aimed at identifying evidence of silicone oil toxicity, reactivation of the viral infection, and to detect

recurrent retinal detachment.[39,61,62,64–69]

Redetachment of the retina may occur at any time postoperatively and may be caused by new retinal breaks or reopening of previously treated breaks. Typically, the recurrent retinal detachment is shallow and located inferiorly, where the silicone bubble may not be entirely in contact with the retina. If the redetachment is localized and extramacular, observation is usually the best strategy. If the macula is threatened or detached in an eye with previously good vision, then reoperation may be warranted. Often, drainage of subretinal fluid combined with injection of more silicone with additional photocoagulation is the treatment of choice. If visualization is poor, the oil must be removed and the retina reattached, as described above, before the oil is reinjected.

Lensectomy may be necessary, preferably with the implantation of an intraocular lens, maintaining the posterior capsule. Later capsular opacification is common, however, and one should consider primary capsulotomy in selected cases.[70] An inferior iridectomy must be performed in aphakic eyes and should be considered in pseudophakic eyes to prevent pupillary block.

If the lens is extracted, a planoconvex polymethylmethacrylate (PMMA) or hydrophobic acrylic intraocular lens provides the ideal optical correction.[71,72] Engstrom et al. reported satisfactory results with simultaneous lensectomy and intraocular lens implantation at the time of vitrectomy and silicone oil injection.[71] This strategy is used to avoid silicone-oil-induced anisometropia and to obviate the need for later cataract removal, as silicone oil almost always induces cataract formation.[70]

Acute Retinal Necrosis

The operation should be tailored to the severity of the disease. In most cases, traction from a partially detached vitreous on the vascular scaffold remaining in the friable retinal tissue after the infection subsides and leads to the presence of multiple holes, low-lying detachments, and PVR, both anterior and posterior.

A standard three-port vitrectomy is performed (Fig. 116.10). As in CMV cases, the infusion pressure should be kept low since the ischemic optic nerve in these patients does not tolerate standard

infusion pressures. Looking at the nerve to avoid a pulsatile perfusion at the onset of surgery, and periodically during surgery, can avoid further loss of vision from prolonged retina anoxia. A lens extraction is required in nearly all cases to expose the full extent of the vitreous base so that all condensed vitreous and vitreous traction can be eliminated.

In the presence of a RRD, a spontaneous posterior vitreous detachment is present. The vitreous gel must be resected out to the margin between healthy and atrophic retina or to the posterior margin of the vitreous base (Fig. 116.14). Posterior epiretinal membranes overlying healthy retina are identified and removed with pick and forceps. A chandelier lighting system may facilitate this maneuver (Fig. 116.15).

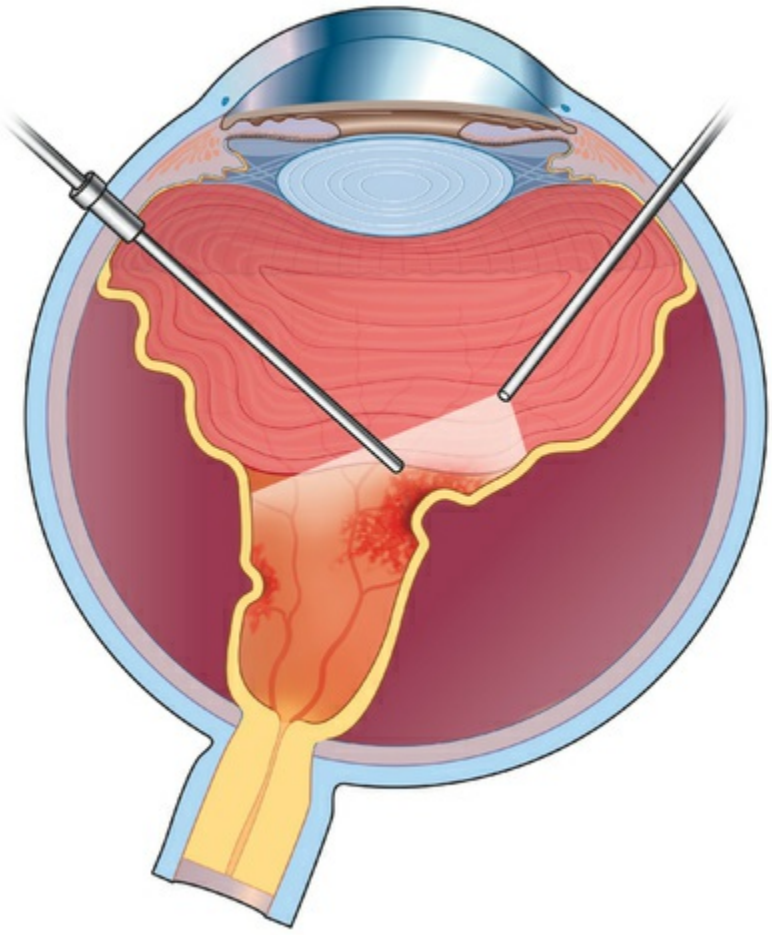

FIG. 116.14 In acute retinal necrosis syndrome, a posterior vitreous detachment is usually present. It is carried out to the vitreous base.

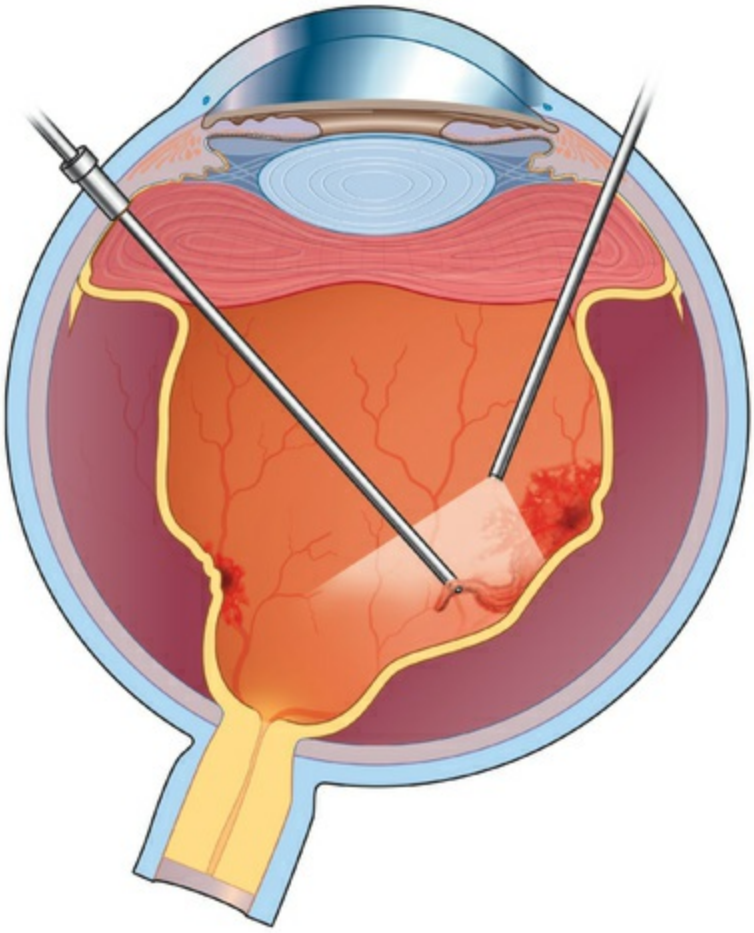

FIG. 116.15 In acute retinal necrosis syndrome, posterior epiretinal membranes are identified and removed with pic and forceps.

Once the posterior healthy retina is free of membranes, perfluorocarbon is used to tamponade this retina out to the edge of atrophic retina. If detached, atrophic retina should be removed en bloc. Its diaphanous nature makes it difficult to peel off membranes, and it does not coagulate well with laser. As this is nonfunctional retinal tissue, it has no physiologic function and can best be removed. Larger vessels, even though these are attenuated, should be treated with diathermy as they may bleed. To facilitate removal, deep scleral depression can be used. This may lead to a 360° retinotomy leaving a fairly central area of viable, healthy retina.

Once the vitreous, preretinal membranes, and detached atrophic

retina have been removed, remaining retinal breaks are identified and marked with endodiathermy. Under perfluorocarbon the edge between healthy and any remaining atrophic retina, as well as the free edge that was created earlier, are treated by endophotocoagulation, placing several rows of laser along the edge of healthy retina.

If peripheral support is necessary, particularly inferiorly, an encircling band or a complete scleral buckle can be placed. However, in many cases it is not needed, and best avoided, as it can lead to choroidal ischemia and compromise residual retinal function.

In most cases silicone oil is used to tamponade the retina. The oil should be ideally removed in 3–6 months to avoid long-term complications related to its presence. Removal should be considered only if the risk of redetachment is believed to be minimal.

In managing PORN-related retinal detachments, the surgical principles are identical to those for ARN. The extent of the necrosis, however, is almost always greater than in patients with ARN-related retinal detachments, so extra care must be taken with vitreous manipulation, and the amount of photocoagulation required is often much more extensive in an effort to surround and preserve the macular region.[46,73]

Prognosis

Visual restoration after SRD is usually good, with most eyes achieving >20/40 after adequate treatment. Visual function after uveitis-associated RRD is frequently guarded, with almost 70% of eyes remaining under 20/200 if the RD was repaired during active inflammation. This poor visual prognosis is related both to the ocular inflammation itself and to the high frequency of proliferative vitreoretinopathy (PVR) appearing after surgery. In order to mitigate the effects of inflammation, it is necessary to anticipate its consequences and hence use silicone oil, even though there may be little evidence of PVR at the time of surgery, or remove a perfectly clear crystalline lens in order to complete the vitreous resection up and over the vitreous base. In viral retinitis, a similar approach is

often required. In addition in these conditions, the surgery should be carried out as much as possible with a low intraocular pressure, as the circulation through the optic nerve may be occluded at even standard infusion pressures. Proliferative retinopathy (PVR) is enhanced by inflammatory cytokines, and chemokines normally present in the anterior chamber and vitreous body of eyes with uveitis. Reducing these molecules can improve the prognosis and implies a concerted local and systemic effort to minimize intraocular inflammation. It is best achieved as a team effort between the vitreoretinal surgeon and the uveitis specialist.

Conclusion

Management of retinal detachments in patients with inflammation or infection demands not only knowledge of surgical options, but also a good grasp of the underlying disease, an estimate of the probable postoperative course as well as the likelihood of recurrence. A multidisciplinary approach is most likely to provide the optimal outcome in most settings. While in the past, visual results after surgery were relatively poor, the advent of better equipment, less traumatic surgical approaches, and a better understanding of the pathophysiologic processes at hand have improved both short-term and long-term outcomes. Both timing and extent of surgery are critical issues, which vary depending on the etiology. Larger series obtained by combining results from several different centers will help to define more precisely these parameters in years to come.

References

1. Galor A, Lowder CY, Kaiser PK, et al. Surgical drainage of chronic serous retinal detachment associated with uveitis. *Retina*. 2008;28:282–288.
2. Mitry D, Charteris DG, Fleck BW, et al. The epidemiology of rhegmatogenous retinal detachment: geographical variation and clinical associations. *Br J Ophthalmol*. 2010;94:678–684.
3. Mitry D, Charteris DG, Yorston D, et al. The epidemiology

and socioeconomic associations of retinal detachment in Scotland: a two-year prospective population-based study. *Invest Ophthalmol Vis Sci*. 2010;51:4963–4968.
4. Mitry D, Singh J, Yorston D, et al. The predisposing pathology and clinical characteristics in the Scottish retinal detachment study. *Ophthalmology*. 2011;118:1429–1434.
5. Kerkhoff FT, Lamberts QJ, van den Biesen PR, et al. Rhegmatogenous retinal detachment and uveitis. *Ophthalmology*. 2003;110:427–431.
6. Carifi G, Onyema L. Acute retinal necrosis. *Ophthalmology*. 2010;117:1659.
7. Holland G. The progressive outer retinal necrosis syndrome. *Int Ophthalmol*. 1994;18:163–165.
8. Jabs DA, Ahuja A, Van Natta M, et al. Course of cytomegalovirus retinitis in the era of highly active antiretroviral therapy: five-year outcomes. *Ophthalmology*. 2010;117:2152–2161.
9. Bosch-Driessen LH, Karimi S, Stilma JS, et al. Retinal detachment in ocular toxoplasmosis. *Ophthalmology*. 2000;107:36–40.
10. Friedman C, Knox D. Variations in recurrent active toxoplasmic retinochoroiditis. *Arch Ophthalmol*. 1969;81:481–493.
11. Mets MB, Holfels E, Boyer KM, et al. Eye manifestations of congenital toxoplasmosis. *Am J Ophthalmol*. 1996;122:309–324.
12. Adan A, Giralt J, Alvarez G, et al. Pars plana vitrectomy for vitreoretinal complications of ocular toxoplasmosis. *Eur J Ophthalmol*. 2009;19:1039–1043.
13. Frezzotti R, Gerengo A, Guerra F. Toxoplasmic Coats' retinitis: a parasitologically proven case. *Am J Ophthalmol*. 1965;59:1099–1102.
14. Rieger H. On the etiology of retinitis exudativa externa centralis. *Graefes Arch Clin Exp Ophthalmol*. 1960;162:178–192.
15. Stewart J, Cubillan L, Cunningham E Jr. Prevalence, clinical features, and causes of vision loss among patients with ocular toxocariasis. *Retina*. 2005;25:1005–1013.

16. Haug SJ, Takakura A, Jumper JM, et al. Rhegmatogenous retinal detachment in patients with acute syphilitic panuveitis. *Ocul Immunol Inflamm*. 2014;24:1–8.
17. Brockhurst RJ. Retinoschisis: complication of peripheral uveitis. *Arch Ophthalmol*. 1981;99:1998–1999.
18. Pollack AL, McDonald HR, Johnson RN, et al. Peripheral retinoschisis and exudative retinal detachment in pars planitis. *Retina*. 2002;22:719–722.
19. Jalil A, Dhawahir-Scala FE, Jones NP. Nonprogressive tractional inferior retinal elevation in intermediate uveitis. *Ocul Immunol Inflamm*. 2010;18:60–63.
20. Watts P, Mantry S, Austin M. Serous retinal detachment at the macula in sarcoidosis. *Am J Ophthalmol*. 2000;129:262–264.
21. Straub W, Strempel I. Retinal detachment and sarcoidosis. *Bull Soc Ophtalmol Fr*. 1989;89:1013–1015.
22. Bourcier T, Lumbroso L, Cassoux N, et al. Retinal pigment epithelial detachment: an unusual presentation of ocular sarcoidosis. *Br J Ophthalmol*. 1998;82:585.
23. Shenoy R, Al Burwani B. Necrotizing retinopathy simulating acute retinal necrosis causing rhegmatogenous retinal detachment in sarcoidosis: a case report. *Eur J Ophthalmol*. 2010;20:218–220.
24. Dabour SA, Ghali MA. Outcome of surgical management for rhegmatogenous retinal detachment in Behçet's disease. *BMC Ophthalmol*. 2014;14:61.
25. Georgalas I, Markomichelakis N, Ladas I. Retinal detachment due to a macular hole in a patient with Behçet disease treated with vitrectomy and silicone oil tamponade. *Eur J Ophthalmol*. 2008;18:1023–1024.
26. Chuang JZ, Chou SY, Sung CH. Chloride intracellular channel 4 is critical for the epithelial morphogenesis of RPE cells and retinal attachment. *Mol Biol Cell*. 2010;21:3017–3028.
27. He G, Ma Y, Chou SY, et al. Role of CLIC4 in the host innate responses to bacterial lipopolysaccharide. *Eur J Immunol*. 2011;41:1221–1230.
28. Eberhardt C, Amann B, Feuchtinger A, et al. Differential

expression of inwardly rectifying K+ channels and aquaporins 4 and 5 in autoimmune uveitis indicates misbalance in Müller glial cell-dependent ion and water homeostasis. *Glia*. 2011;59(5):697–707.
29. Hikichi T, Ueno N, Chakrabarti B, et al. Evidence of cross-link formation of vitreous collagen during experimental ocular inflammation. *Graefes Arch Klin Exp Ophthalmol*. 1996;234:47–54.
30. Hirokawa H, Takahashi M, Trempe CL. Vitreous changes in peripheral uveitis. *Arch Ophthalmol*. 1985;103.
31. de Smet M, Gad El Kareem A, Zwinderman AH. The vitreous, the retinal interface in ocular health and disease. *Ophthalmologica*. 2013;230:165–178.
32. Spencer W. Vitreous. WB Saunders: Philadelphia; 1996:650–654. Spencer WH. *Ophthalmic pathology: an atlas and textbook*. vol. 2.
33. Limb GA, Chignell AH, Cole CJ, et al. Intercellular adhesion molecule-1 in proliferative vitreoretinopathy. *Invest Ophthalmol Vis Sci*. 1997;38:1043–1048.
34. Ricker LJ, Altara R, Goezinne F, et al. Soluble apoptotic factors and adhesion molecules in rhegmatogenous retinal detachment. *Invest Ophthalmol Vis Sci*. 2011;52:4256–4262.
35. Webster L, Stanbury RM, Chignell AH, et al. Vitreous intercellular adhesion molecule 1 in uveitis complicated by retinal detachment. *Br J Ophthalmol*. 1998;82:438–443.
36. Sijssens KM, Rijkers GT, Rothova A, et al. Cytokines, chemokines and soluble adhesion molecules in aqueous humor of children with uveitis. *Exp Eye Res*. 2007;85:443–449.
37. Kunavisarut P, Bijlsma WR, Pathanapitoon K, et al. Proliferative vitreoretinopathy in human immunodeficiency virus-infected patients in the era of highly active antiretroviral therapy. *Am J Ophthalmol*. 2010;150:218–222.
38. Freeman WR, Friedberg DN, Berry C. Risk factors for development of rhegmatogenous retinal detachment in patients with cytomegalovirus retinitis. *Am J Ophthalmol*. 1993;116:713–720.
39. Irvine AR, Lonn L, Schwartz DM, et al. Retinal detachment

in AIDS: long term results after repair with silicone oil. *Br J Ophthalmol*. 1997;81:180–183.
40. Young S, McCluskey PJ, Minassian DC, et al. Retinal detachment in cytomegalovirus retinitis: intravenous versus intravitreal therapy. *Clin Experiment Ophthalmol*. 2003;31:96–102.
41. Brar M, Kozak I, Freeman WR, et al. Vitreoretinal interface abnormalities in healed cytomegalovirus retinitis. *Retina*. 2010;30:1262–1266.
42. Culbertson WW, Atherton SS. Acute retinal necrosis and similar retinitis syndromes. *Int Ophthalmol Clin*. 1993;33:129–143.
43. Fisher JP, Lewis ML, Blumenkranz M, et al. The acute retinal necrosis syndrome. Part 1. Clinical manifestations. *Ophthalmology*. 1982;89:1309–1316.
44. Lau CH, Missotten T, Salzmann J, et al. Acute retinal necrosis: features, management, and outcomes. *Ophthalmology*. 2007;114:756–762.
45. Culbertson W, Blumenkranz M, Haines M, et al. The acute retinal necrosis syndrome. II. Histopathology and etiology. *Ophthalmology*. 1982;89:1317–1325.
46. Engstrom R, Holland G, Margolis T, et al. The progressive outer retinal necrosis syndrome: a variant of necrotizing herpetic retinopathy in patients with AIDS. *Ophthalmology*. 1994;101:1488–1502.
47. Forster DJ, Dugel PU, Frangieh GT, et al. Rapidly progressive outer retinal necrosis in the acquired immunodeficiency syndrome. *Am J Ophthalmol*. 1990;110:341–348.
48. Yin PD, Kurup SK, Fischer SH, et al. Progressive outer retinal necrosis in the era of highly active antiretroviral therapy: successful management with intravitreal injections and monitoring with quantitative PCR. *J Clin Virol*. 2007;38:254–259.
49. Satger D, Pegourie P, Romanet JP, et al. Ultrasound imaging in the management of endophthalmitis. *J Fr Ophtalmol*. 2007;30:1037–1048.
50. Mourtzoukos S, Mangouritsas G, Feretis E. Triamcinolone-

assisted vitreous imaging using B-scan ultrasonography. *Eur J Ophthalmol*. 2008;18:1028–1030.
51. Inazumi K, Gentile RC, Lee KYC, et al. Ultrasound biomicroscopic diagnosis of cyclitic membranes. *Am J Ophthalmol*. 2001;131:446–450.
52. Liu W, Wu Q, Huang S, et al. Ultrasound biomicroscopic features of anterior proliferative vitreoretinopathy. *Retina*. 1999;19:204–212.
53. Hagler WS, Jarrett WH II, Chang M. Rhegmatogenous retinal detachment following chorioretinal inflammatory disease. *Am J Ophthalmol*. 1978;86:373–379.
54. Jarrett WH II. Rhegmatogenous retinal detachment complicated by severe intraocular inflammation, hypotony, and choroidal detachment. *Trans Am Ophthalmol Soc*. 1981;79:664–683.
55. Foster CS, Fong LP, Singh G. Cataract surgery and intraocular lens implantation in patients with uveitis. *Ophthalmology*. 1989;96:281–288.
56. Veckeneer M, van Overdam K, Bouwens D, et al. Randomized clinical trial of cryotherapy versus laser photocoagulation for retinopexy in conventional retinal detachment surgery. *Am J Ophthalmol*. 2001;132:343–347.
57. Aras C, Ozdamar A, Karacorlu M, et al. Silicone oil in the surgical treatment of endophthalmitis associated with retinal detachment. *Int Ophthalmol*. 2002;24:147–150.
58. Davis JL, Hummer J, Feuer WJ. Laser photocoagulation for retinal detachments and retinal tears in cytomegalovirus retinitis. *Ophthalmology*. 1997;104:2053–2060.
59. Meffert SA, Ai E. Laser photocoagulation prophylaxis for CMV retinal detachments. *Ophthalmology*. 1998;105:1353–1355.
60. Vrabed T. Laser photocoagulation repair of macula-sparing cytomegalovirus-related retinal detachment. *Ophthalmology*. 1997;104:2062–2067.
61. Dugel PU, Liggett PE, Lee MB, et al. Repair of retinal detachment caused by cytomegalovirus retinitis in patients with the acquired immunodeficiency syndrome. *Am J Ophthalmol*. 1991;112:235–242.

62. Jabs DA, Enger C, Haller J, et al. Retinal detachments in patients with cytomegalovirus retinitis. *Arch Ophthalmol*. 1991;109:794–799.
63. Kuppermann BD, Flores-Aguilar M, Quiceno JI, et al. A masked prospective evaluation of outcome parameters for cytomegalovirus-related retinal detachment surgery in patients with acquired immune deficiency syndrome. *Ophthalmology*. 1994;101:46–55.
64. Regillo C, Vander J, Duker J, et al. Repair of retinitis-related retinal detachments with silicone oil in patients with acquired immunodeficiency syndrome. *Am J Ophthalmol*. 1992;113:21–27.
65. Sidikaro Y, Silver L, Holland GN, et al. Rhegmatogenous retinal detachments in patients with AIDS and necrotizing retinal infections. *Ophthalmology*. 1991;98:129–135.
66. Canzano JC, Morse LS, Wendel RT. Surgical repair of cytomegalovirus-related retinal detachment without silicone oil in patients with AIDS. *Retina*. 1999;19:274–280.
67. Chuang EL, Davis JL. Management of retinal detachment associated with CMV retinitis in AIDS patients. *Eye (Lond)*. 1992;6:28–34.
68. Freeman WR, Quiceno JI, Crapotta JA, et al. Surgical repair of rhegmatogenous retinal detachment in immunosuppressed patients with cytomegalovirus retinitis. *Ophthalmology*. 1991;99:466–474.
69. Orellana J, Teich SA, Lieberman RM, et al. Treatment of retinal detachments in patients with the acquired immune deficiency syndrome. *Ophthalmology*. 1991;98:939–943.
70. Tanna A, Kempen J, Dunn J, et al. Incidence and management of cataract after retinal detachment repair with silicone oil in immune compromised patients with cytomegalovirus retinitis. *Am J Ophthalmol*. 2003;136:1009–1015.
71. Engstrom R, Goldenberg D, Parnell J, et al. Clear lens extraction with intraocular lens implantation during retinal detachment repair in patients with autoimmune deficiency syndrome and cytomegalovirus retinitis. *Ophthalmology*. 2002;109:666–673.

72. Meldrum M, Aaberg T, Patel A, et al. Cataract extraction after silicone oil repair of retinal detachment due to necrotizing retinitis. *Arch Ophthalmol*. 1996;114:885–892.
73. Dowling J, Towler H, Mitchell S, et al. Retinal detachment and herpesvirus retinitis in patients with AIDS. *Br J Ophthalmol*. 1995;79:575–580.

117

High Myopia and the Vitreoretinal Complications

Yasushi Ikuno, Masahito Ohji

Introduction

The incidence of high myopia varies among ethnic groups, races, and countries, but there is a higher incidence in Asian countries. Some of the incidence rates worldwide range from 1% in Black Americans,[1] 2% in Caucasian Americans,[1] 2.6% in Chinese individuals,[2] to 5.5% in Japanese individuals.[3] The prevalence of myopia seems to be increasing,[4] and it is one of the major causes of visual impairment, especially in Europe and East Asia.[5,6]

The definitions of high myopia vary slightly; however, there is agreement that the spherical equivalent refractive error exceeds −6 diopters (D) and/or the axial length is longer than 26.5 mm. Pathologic myopia is defined as high myopia with any posterior myopia-specific pathology from excess axial elongation. Pathologic myopia is characterized by posterior staphyloma formation and also is associated with specific macular complications such as choroidal neovascularization and chorioretinal atrophy. Myopic foveoschisis and macular holes with or without retinal detachment are also specific to myopia and major indications for surgical

intervention.

Observation of a myopic macular area using a contact or non-contact lens has been challenging because the atrophy lowers the contrast. This has hindered detailed observation and consequent understanding of the pathophysiology, although myopia-specific macular diseases have been well known for a long time. Technologies such as optical coherence tomography (OCT) have facilitated both visualization of the retinal microstructures in pathologic conditions and an understanding of the pathogenesis, interaction, and disease progression. For instance, a recent OCT study showed a more detailed interaction between the vitreous and retina using swept source OCT (Fig. 117.1) and described that even after a Weiss ring was visible, vitreous cortex still remained on the macula,[7] which may play an important role in development of such myopic pathologies as macular holes and retinoschisis. This information has led to revolutionary changes in the disease concept of myopia-specific macular diseases. Pathologic myopia is now a much more accessible disease than it was 20 years ago.

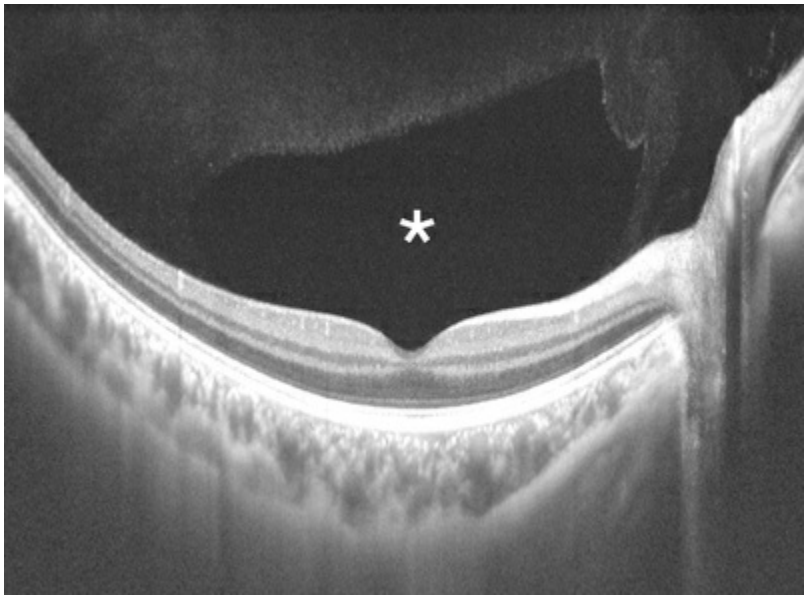

FIG. 117.1 The status of posterior vitreous in normal highly myopic eyes. Swept-source optical coherence tomography (SS-OCT) can visualize vitreous gel and thus shows an interaction between the vitreous and retina. This OCT image clearly shows a cortical vitreous pocket (*asterisk*).

Examiners often have difficulties obtaining clear and high-contrast OCT images in highly myopic eyes. The characteristics of the OCT image in these eyes are (1) a relatively low signal to noise ratio; (2) deep posterior staphyloma in the presence of which the peripheral tissue often drops off from the top edge of the image; (3) poor fixation due to a large central scotoma from chorioretinal atrophy; and (4) critical signs that are mostly outside the fovea. The pearls for the OCT examination are as follows. First, it is much better to use spectral domain (SD-) OCT, which provides much higher sensitivity and scanning speed than time domain (TD-) OCT. Second, the pathology of interest must be located near the top of the OCT image. SD-OCT has the strongest signal at the top and the weakest at the bottom because of the so-called signal decay. This procedure maximizes the signal and enhances the contrast of the pathology being targeted. Third, large internal fixation or external fixation must be used to avoid unnecessary ocular movement in cases with a large central scotoma. Finally, attention must be paid to pathologies outside the fovea. For instance, a small macular hole is sometimes outside the fovea, and other micropathologies such as retinal vascular microfolds, internal limiting membrane detachments, and paravascular microholes are far outside the macula. The use of the 5-lines or grid scan has a significantly higher rate of detection of these pathologies than the use of a single B-scan alone.

Imaging technologies have identified myopic foveoschisis, which is a relatively new pathology that was recognized about 15 years ago.[8] It is now generally agreed that this pathology is common in highly myopic eyes, and myopic foveoschisis is regarded as a precondition for development of a macular hole and retinal detachment. OCT studies of myopic foveoschisis have revealed many preclinical and pathologic conditions underlying the myopic macular diseases, as discussed below. This information is also helpful for understanding the process and pathophysiology of macular holes and retinal detachments, which are the most problematic complications for vitreoretinal surgeons. In this chapter, we review the recent studies and shed light on the vitreoretinal complications of high myopia.

Retinal Detachment From Peripheral Breaks

Retinal detachments from peripheral retinal breaks are common in high myopia. The prevalence of any type of retinal detachment increases in association with the degree of negative refractive error.[9] The distribution of high myopia exceeding −6.0 D is about 16% in overall cases, and the lifetime risk is more than 20-fold compared with emmetropia.[9] In addition, the onset of retinal detachment is at a younger age, based on the degree of myopia.[10] The frequency of retinal peripheral degeneration increases along with the axial length.[11] The development of posterior vitreous detachment (PVD) according to the higher liquefaction of the vitreous body occurs at a younger age in eyes with severe high myopia.[12] These facts seem to account for the increased prevalence of retinal detachment.

A rhegmatogenous retinal detachment (RRD) must be treated with a scleral buckling procedure or vitrectomy combined with gas or silicone oil tamponade, as for non-highly myopic retinal detachment. Scleral buckling is the first choice for retinal breaks with non- or minimal vitreous traction and vitrectomy for significant traction from the vitreous. We normally use a 25-gauge system for vitrectomy, and a small-gauge system works well in cases of high myopia.

Epidemiology of Surgical Macular Complications

The incidence rates of myopia-specific macular complications such as myopic foveoschisis and macular holes with or without retinal detachments have not been well documented because these complications are rare. Myopic foveoschisis was identified in 9% of patients with posterior staphyloma.[13] In patients with a macular hole and retinal detachment, 8.5% develop the same pathology in the fellow eye within 4 years.[14]

Rhegmatogenous Retinal Detachment After

Refractive Surgeries

Rhegmatogenous retinal detachment is a major complication after refractive surgeries. The incidence is not as high after laser in situ keratomileusis (LASIK) and was reported to be 0.25%;[15] however, it is much higher after refractive lens exchange, reportedly 7.3% within 3 years.[16] Retinal detachment is a rare but general complication after cataract surgery, with incidence rates of 0.9% in the general population[17] and 1.5–2.2% after phacoemulsification in highly myopic eyes.[18,19] A high likelihood of PVD occurring within 5 years after surgery[20] seems to be associated with a higher incidence.

Etiology and Pathophysiology

Myopic Foveoschisis

Myopic foveoschisis is characterized by retinoschisis with or without localized retinal detachment and is specific to high myopia. OCT can depict the pathology very clearly (Fig. 117.2). Myopic foveoschisis is also referred to as a posterior retinal detachment without a macular hole in highly myopic eyes, described by Phillips in 1958, who reported a case with a retinal detachment within posterior staphyloma but no apparent macular hole.[21] The detailed pathology and its mechanism awaited the development of OCT for decades. Takano and Kishi examined 32 highly myopic eyes with OCT and found retinoschisis in nine eyes and a foveal detachment in one eye, suggesting that retinoschisis and foveal detachment are common in highly myopic eyes.[8] It has been reported that myopic foveoschisis is characterized by variations in the foveal architecture, including a foveal cyst in 47%, a lamellar hole in 29%, and a foveal detachment in 29%.[22]

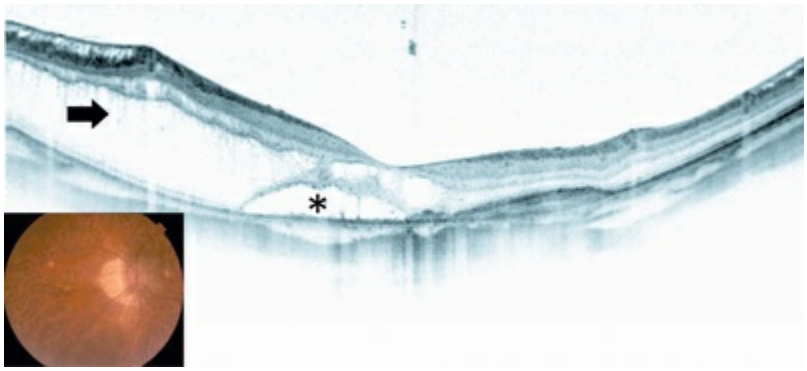

FIG. 117.2 Typical appearance of myopic foveoschisis. The fundus photograph (inset) shows a slightly elevated retina at the posterior pole, although it is not visually apparent. A horizontal optical coherence tomography scan involving the macula shows retinoschisis in multiple retinal layers and a retinal detachment at the fovea (*asterisk*). There is glial tissue bridging the inner and outer layers of the retinoschisis (a so-called column, *arrow*).

The pathogenesis of myopic foveoschisis has been disclosed recently. Various OCT images from these myopic eyes have led to the hypothesis that the inner retina is less flexible than the outer retina.[23] Factors limiting the inner retinal flexibility include the vitreous cortex adhering to the retina, epiretinal membranes (ERMs), internal limiting membrane (ILM), and retinal vessels. Preretinal membranes, which can be hard to recognize clinically and are found only at the microscopic level in highly myopic eyes,[24] cause deterioration in the retinal flexibility.

Histologic studies have shown retinoschisis at multiple levels in the outer plexiform layer, inner plexiform layer, ganglion cell layer, and nerve fiber layer.[25] There also is a preretinal fibrous membrane. An electron microscopic study on excised ILM samples during vitrectomy has shown that collagen fibers and cell debris were present on the inner surface of the ILM in 70% of the myopic foveoschisis, substantially more than that found in idiopathic nonmyopic macular holes (0%).[24] Another study has shown a much higher incidence (61.8%) of preretinal membrane recognized during vitrectomy in high myopia than controls (7.0%).[26]

ILM detachments, sometimes recognized as "inner retinoschisis," are often seen in highly myopic eyes, which explains the underlying traction from the ILM on the other retinal layers (Fig. 117.3).[27] Inner

retinal elevations along with retinal vessels recognized as tent-like lesions on OCT images, so-called retinal vascular microfolds, are observed especially in vertical sections (Fig. 117.4).[28] This finding represents traction from the vessels on the retinal surface. A large OCT study of 200 highly myopic eyes reported a 6% incidence of ILM detachments, a 13.5% incidence of retinoschisis, and a 20% incidence of retinal vascular microfolds.[29] These components generate inward tractional force on the inner retina, which potentially splits the retina, causing retinoschisis, and finally leads to a retinal detachment at the fovea.

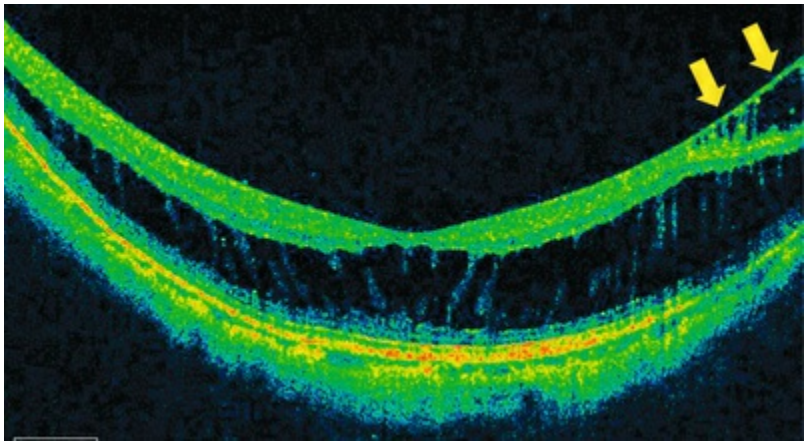

FIG. 117.3 Representative optical coherence tomography appearance of an internal limiting membrane (ILM) detachment (*arrows*) in highly myopic eyes. The ILM layer is detached from the other retinal layers.

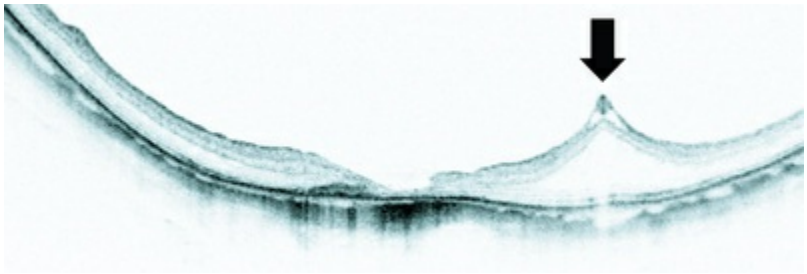

FIG. 117.4 Representative optical coherence tomography appearance of retinal microfolds (*arrow*) in highly myopic eyes. This microfold is associated with the retinal vessels and warrants microvascular traction

on the retina.

Macular Hole With or Without Retinal Detachment

Retinal detachments from a macular hole are a typical complication in highly myopic eyes. The vitreous cortex adhering to the retinal surface around the hole causes tangential traction that generates an inward vector component in deep staphyloma in highly myopic eyes, resulting in a retinal detachment.[30] Releasing the retinal traction is critical to successful reattachment; thus, vitrectomy with vitreous cortex and membrane removal is effective. An OCT study reported that persistent traction at the macular hole edge after opening is critical for initiating a retinal detachment.[31] A macular hole with retinoschisis has a higher likelihood of progressing to a retinal detachment than those with a retinal cyst, resembling idiopathic nonmyopic macular holes (Fig. 117.5).

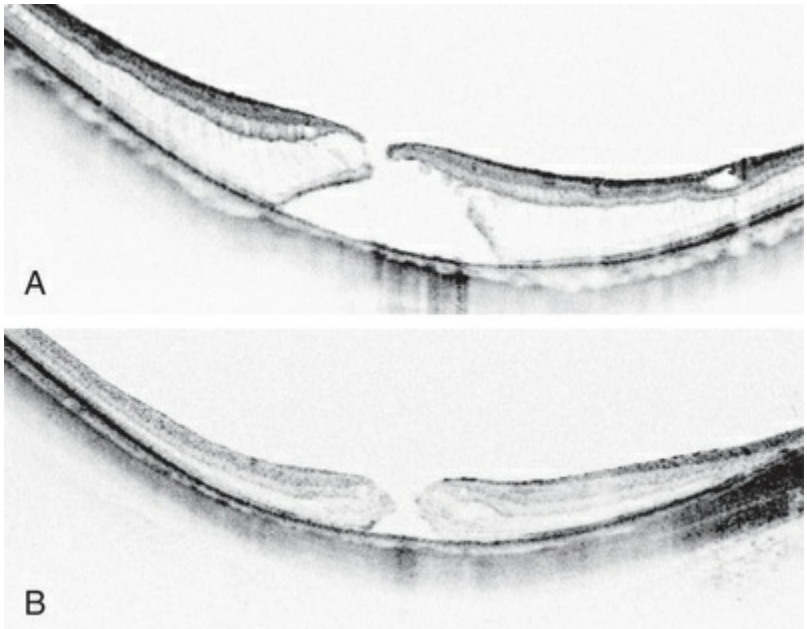

FIG. 117.5 Optical coherence tomography appearance of two distinct subtypes in highly myopic macular holes. (A) A macular hole with surrounding retinoschisis usually presents a higher likelihood of consequent retinal detachment, while (B) a macular hole without retinoschisis has only retinal cysts and is

normally stable.

A macular hole with retinoschisis typically presents with deeper posterior staphyloma, which explains the lower anatomic success rate in this subtype.[31,32] Deep posterior staphyloma generates a larger vector component from the tangential traction exerted by the ERM or the ILM, which acts on the retina as an inward tractional force. In addition, with deep staphyloma it is more difficult to close the macular hole because of excess stretching in the retina. While shallower, posterior staphyloma generates less tractional force and the retina is flat as seen in nonmyopic eyes. This flat configuration exerts less stretching in the retina, and, thus, the macular hole is more likely to close. The type of macular hole is highly dependent on the depth of the posterior staphyloma and underlying tractional force, which affect the anatomic success rate. Thus, preoperative OCT observation of the macular hole edge provides one clue to the prognosis.

In highly myopic eyes, multiple components adhere to the retinal surface in most cases and are often recognized during vitreous surgery. Electron microscopic studies have shown that they are the vitreous cortex, cellular ERMs, and ILMs,[33] suggesting that complete removal of these tractional forces is essential in reattachment surgery.

Posterior Retinal Detachments From Paravascular Microholes

Retinal detachment from a paravascular microhole is also specific to highly myopic eyes (Fig. 117.6). Microholes are typically small, round or oval retinal holes associated with posterior major vessels.[34] There are sometimes multiple holes that are adjacent to the major vessels. An OCT study of highly myopic eyes reported that the incidence rates of retinal cysts and paravascular holes were 50% and 27%, respectively.[35] The vitreoretinal adhesion is often strong at the paravascular region, and traction from the vitreous at the site is believed to be a main cause of retinal rarefaction, resulting in retinal cysts and breaks.[36] Paravascular microholes often colocalize with vascular microfolds and retinoschisis,[28] suggesting a close

relationship with the retinal vascular traction.

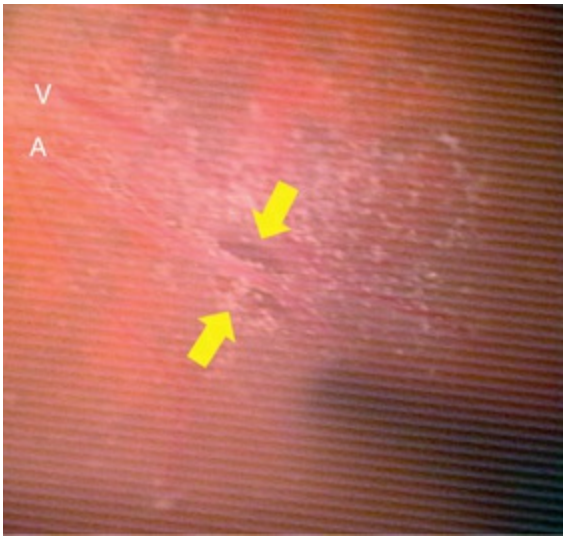

FIG. 117.6 Intraoperative view of paravascular microholes in a highly myopic retinal detachment. Multiple, small and round retinal holes are located along the retinal vessels of the temporal arcade (*arrows*). *A*, Retinal superotemporal artery; *V*, retinal vein.

Symptoms of Myopic Foveoschisis and Macular Holes With or Without Retinal Detachments

Myopic foveoschisis and macular holes with or without retinal detachments typically occur in highly myopic, middle-aged to older women. In the authors' clinic, 44 of 52 patients referred for this disease during the period from 2000 to 2005 were women.[37] Patients are normally aware of central visual distortion if they have only retinoschisis and a relative central scotoma corresponding to the involved area when the retinal detachment starts. Patients may be aware of an absolute scotoma at the center of the relative scotoma when a macular hole opens. Patients also report visual loss at the involved area if an extensive retinal detachment is complicated. Even if patients present with a macular hole, the Watzke–Allen test is usually negative.

Clinical Findings

Myopic foveoschisis can be recognized as a slight elevation of the posterior retina in highly myopic eyes; however, it is difficult to accurately diagnose without OCT, especially in an atrophic fundus. OCT and other imaging tools are essential for complete assessment of the retinal status for surgical decision-making, for example, to determine the presence/absence of retinoschisis and the area of retinoschisis or retinal detachment. This information is essential for surgical planning. For instance, if there is a foveal detachment found on OCT images, macular hole formation is likely to start in the near future, and surgery must be planned soon (normally within 1 or 2 months). However, if the patient presents with only retinoschisis but not a foveal retinal detachment, the surgery is not as urgent. Evolution of macular hole and its diagnosis are difficult in high myopia.[38] OCT also facilitates assessment of the presence/absence of the hole and its size.

Optical Coherence Tomography Features

Myopic foveoschisis presents with retinoschisis in multiple retinal layers. The split retinal layers normally have a bridge between them, the so-called column, which is presumed to be residual Müller cells (Fig. 117.2). In cases with a very atrophic retina, it can be difficult to distinguish retinoschisis from a retinal detachment, and the presence of the column is an important clue for diagnosing retinoschisis but not a detachment. Tracing the junction of the inner/outer-segment (IS/OS) line of the photoreceptors is also useful for differentiating a retinal detachment from retinoschisis as shown in an early OCT study.[39] ILM separation from the other retinal layers also is observed, i.e., a so-called ILM detachment, and is an indicator of the tractional force from the ILM.[27] The tent-like peak of the inner retina is observed on the OCT image. This is coincident with retinal vessels and the so-called retinal microvascular traction.[28] Because the retinal vessels normally run horizontally around the macular area, there is a higher chance of finding this in a vertical than a horizontal section because of the higher chance of observing a cross-section of the retinal vessels. The IS/OS junction

line of the photoreceptors sometimes disappears in the area of the retinal detachment;[40] however, the IS/OS junction line is typically well preserved in the area of retinoschisis, suggesting that the photoreceptor function is well preserved in this subtype.

There are two stages before macular hole formation associated with retinoschisis (Fig. 117.7). The first stage is the development of the so-called retinoschisis type, in which only retinoschisis is present and not a retinal detachment. Several months (sometimes several years) later a retinal detachment begins around the fovea. This stage is the so-called foveal detachment type, and a retinal detachment involving the fovea and retinoschisis around the macula are present. After a while, the inner retina above the detachment is stretched and torn. This is how a macular hole appears as a consequence of retinoschisis with a retinal detachment. Small macular holes are often difficult to visualize in a B-scan image because the fixation point has shifted.

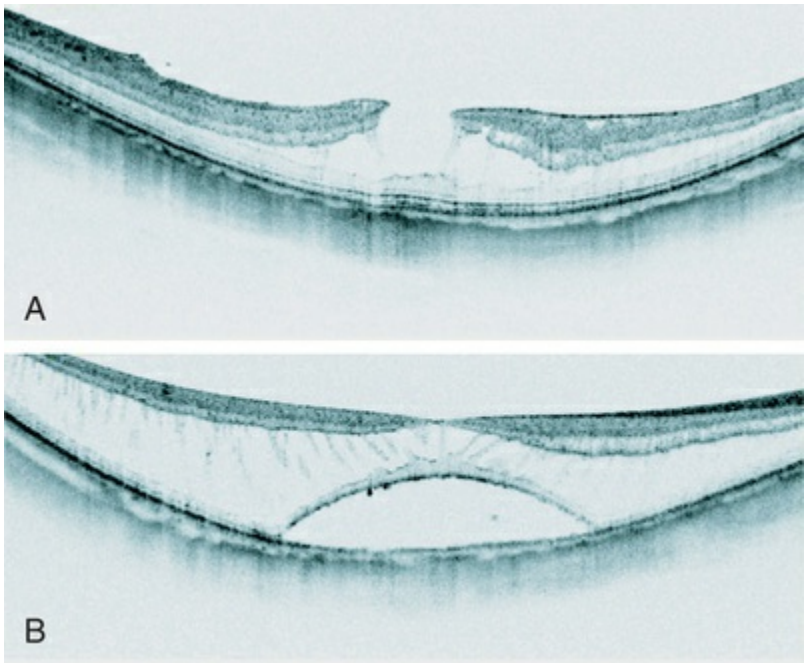

FIG. 117.7 Two distinct subtypes of myopic foveoschisis. (A) The retinoschisis type is characterized by only retinoschisis without a retinal detachment. (B) The foveal detachment type is characterized by a small localized retinal detachment, and the inner/outer segment line is separated from the retinal pigment epithelium. The retinoschisis type

develops before the foveal detachment type.

The edge of a macular hole provides valuable information. As discussed previously, there are two types of macular holes in highly myopic eyes.[31,32] One is similar to an idiopathic macular hole, as normally seen in nonmyopic eyes (Fig. 117.5B). In these, the edge of the hole is thickened with retinal cysts. There is no retinal detachment around the hole clinically, and this type usually does not progress for months or years. The other type has surrounding retinoschisis instead of retinal cysts around the hole (Fig. 117.5A). This type of macular hole results from myopic foveoschisis and can be considered a transition from foveoschisis to a macular hole with a retinal detachment. This type of macular hole typically progresses rapidly and is likely to complicate the retinal detachment because of underlying traction (see Etiology and pathophysiology, above). The typical OCT appearance of this type is characterized by a relatively high and rectilinear wall of the macular hole edge with an acute angle to the RPE line, and a sharp-angled edge of the top of the macular hole.[31] Therefore, observing the macular hole edge is essential for exact diagnosis, which is critical for decision-making and planning of the vitreous surgery.

Fundus Autofluorescence

Fundus autofluorescence (FAF) stimulates emission of light from the lipofuscin accumulated in the RPE and is an indicator of the oxidative stress level[41] and the functioning of the RPE. In the atrophic fundus in myopic eyes, FAF helps distinguish the retinal detachment from the retinoschisis, because loss of the contact between the photoreceptors and the RPE results in hypoautofluorescence.[42] The hypofluorescent area indicates the area of the retinal detachment and is a good indicator for monitoring its progression and the level of RPE damage and consequent visual outcome.[43]

Treatment of Foveoschisis

The natural course of myopic foveoschisis is unfavorable.

Investigators have reported that the vision decreased in 69% of patients, a macular hole developed in 31% after 3 years of follow-up,[44] and in 50% of patients with retinoschisis a macular hole or retinal detachment developed after 2 years.[45] These observations encourage surgery to treat myopic foveoschisis as prophylaxis to prevent macular holes with consequent development of a retinal detachment.

Surgical Indications

Myopic foveoschisis is sometimes asymptomatic, especially in cases with simple retinoschisis and no retinal detachment. Those cases are not good indications for vitreous surgeries. Even though patients are aware of a visual disturbance, turbulence, or visual loss, surgery can be postponed until the vision decreases to about 20/40 because there is still a chance of visual worsening after vitrectomy. The chance of visual improvement after surgery is about 80% in cases with a foveal detachment and 50% with retinoschisis alone.[46] Another study reported a similar trend and showed that 70% of eyes with a foveal detachment had significant visual improvement compared with 42% in the retinoschisis group.[47] The chance of visual improvement is substantially smaller if a macular hole is present before surgery,[46,48] which is partly because macular holes have a poor closure rate after surgery. Appearance of subretinal fluid after macular hole formation indicates a worse prognosis.[49] Hence, surgical intervention before macular hole formation is considered beneficial, although there is not yet strong evidence for this.

A localized retinal detachment in the posterior staphyloma from the macular hole often develops; however, there may be surgical benefits only in selected cases. This type of detachment is sometimes stable and does not progress. The retina is detached from the RPE and follows the minimal distance bridging the posterior staphyloma edge on the opposite site, which maintains balance and compensates for the retinal traction. Surgery can be postponed if the retinal detachment does not extend beyond the border of the staphyloma, and its progress should be monitored with OCT and/or FAF (see Fundus autofluorescence, above). The

surgery should be performed as soon as possible if the situation progresses, because patients are at risk of total visual loss.

A macular hole with an extensive retinal detachment is a good indication for surgery. The surgical goal is to remove the entire component that is generating the tractional force on the retina and causing a detachment, including the vitreous cortex, ERMs, and the ILM. However, sometimes the traction persists from the retinal vessels even after a complete vitrectomy, leading to recurrence of the retinal detachment. Treating the posterior staphyloma is theoretically required for these cases, and placing a macular buckle might be considered. Simple gas injection was attempted in an early case series especially for eyes with a PVD; however, this procedure cannot relieve the traction exerted by ERMs, for instance. Therefore, the expectation for anatomic success is not as high as that associated with vitrectomy with complete removal of any traction.[50]

Surgical Prognosis

The retina usually reattaches to the retinal pigment epithelium (RPE) slowly after the surgery (Fig. 117.8). The visual outcome associated with myopic foveoschisis is favorable if no macular hole develops. We reported that a substantial visual gain was achieved after vitrectomy in either group and that the final vision was similar between the foveal detachment type and the retinoschisis type; however, the visual change was significantly greater in the foveal detachment group than in the retinoschisis group.[46,47] Postoperative macular hole formation is a great concern in myopic foveoschisis. We investigated the incidence of postoperative macular hole formation and explored the risk factors. The incidence of macular holes was 19.8%, and eyes with preoperative discontinuity of the IS/OS line (IS/OS defect) seen on OCT was a predictor of macular hole development. Other factors, such as age, gender, and visual acuity, did not affect the rate of macular hole formation (Fig. 117.9).[51]

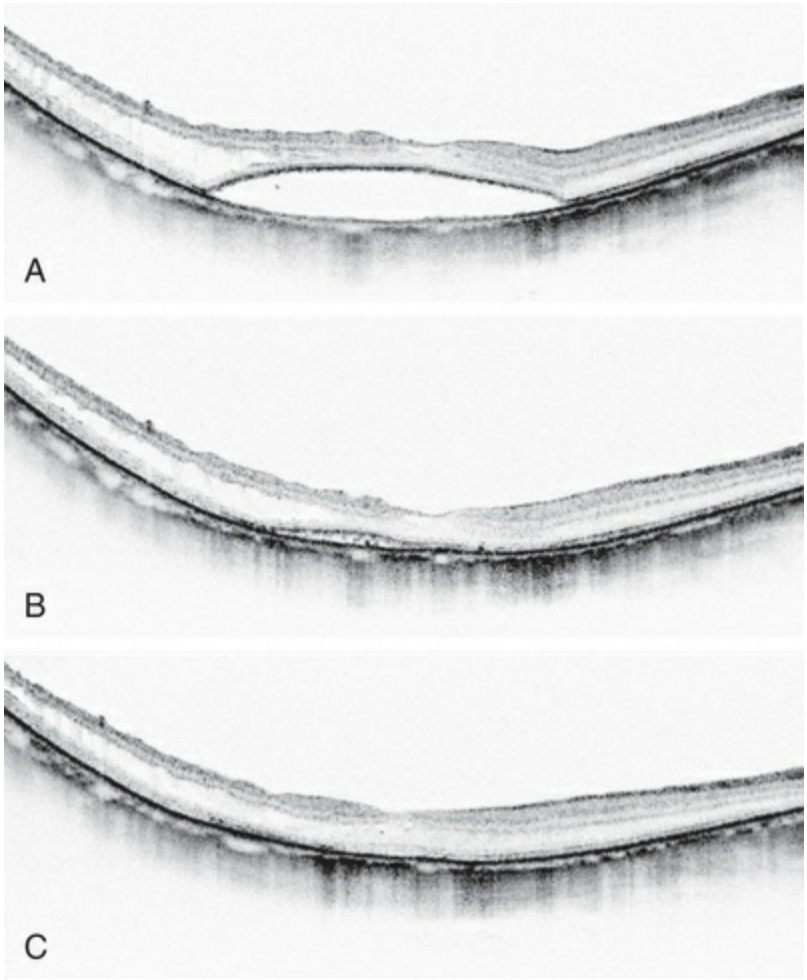

FIG. 117.8 Optical coherence tomography (OCT) appearance of a patient who underwent vitrectomy with internal limiting membrane peeling and gas tamponade for myopic foveoschisis in Fig. 117.7 (lower panel, foveal detachment type). (A) OCT image 2 months after surgery shows flattening of the retina. (B) An OCT image at the same position, 6 months after surgery shows that the retinoschisis has resolved; however, there is still substantial subretinal fluid. (C) An OCT image 12 months after surgery shows complete resolution of the retinal detachment.

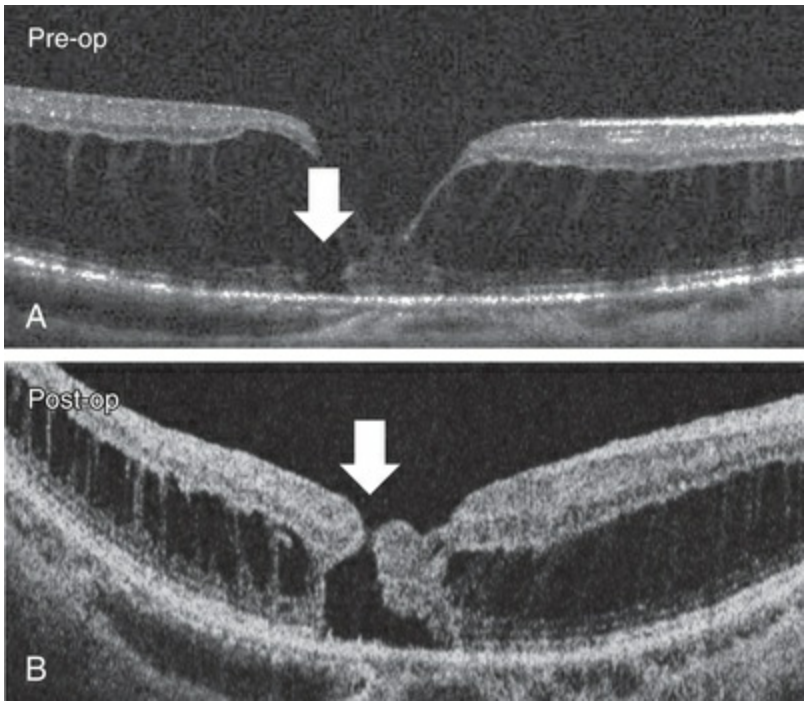

FIG. 117.9 A preoperative photoreceptor inner/outer segment (IS/OS) defect and postoperative macular hole formation after vitrectomy for myopic foveoschisis. (A) A 66-year-old woman had an IS/OS defect at the fovea (*arrow*) and surrounding retinoschisis preoperatively. (B) One month after vitrectomy, including internal limiting membrane peeling, the macular hole was open (*arrow*).

Once a macular hole develops, the hole is hard to close after vitrectomy in highly myopic eyes.[52] Also the visual outcome is not so favorable as nonmyopic eyes.[53] The macular hole closure rate with retinoschisis or retinal detachment is about 40–50% based on OCT images.[54,55] The mean visual acuity after vitrectomy for macular hole with retinal detachment was below 20/200, and the initial reattachment rate was about 50–70% after vitrectomy.[56] A longer axial length is generally a poor prognostic factor.[57,58] Usage of long-term gas tamponade seems to improve the visual outcome.[59] Macular buckling can compensate for any tractional force and showed a slightly higher initial reattachment rate than vitrectomy in macular hole with retinal detachment.[60,61]

Surgical Procedures

Vitreous Separation

A 25-gauge vitrectomy system is the first-line treatment for highly myopic eyes. The vitreous plays an important role; therefore, creating a PVD is critical for reattaching the retina. The vitreous tightly and extensively adheres to the retinal surface in highly myopic eyes. Use of triamcinolone acetonide is essential for visualization and to identify residual cortex. To create posterior vitreous separation, a vitreous cutter and silicone-tipped backflush needle with active suction are normally used. A diamond-dusted membrane scraper[62] is another option for an extremely thin vitreous cortex. The vitreoretinal adhesion is normally tight around the optic nerve disc, and, therefore, the surgeon might consider starting temporally where the adhesion is normally the weakest. Importantly, great care is needed to separate the vitreous at the macula because the macula is tightly adhered to the vitreous; placing stress on the macula may lead to macular hole formation. This procedure is difficult to perform in the detached retina, and a bimanual technique can be considered for a safe separation.

Internal Limiting Membrane Peeling

The necessity for ILM peeling remains controversial in myopic foveoschisis, and one group reported a high success rate even without this procedure.[63] However, the ILM is separated from the other retinal layers on OCT images in most eyes,[27] suggesting that rigidity of the ILM plays a major role in this pathology. Also, a higher recurrence rate of macular detachment was reported in eyes without ILM peeling in the initial surgery.[64] This fact warrants the necessity of ILM peeling for myopic foveoschisis at least in selected cases.

ILM peeling also can enhance macular hole closure and remove any traction on the retina in myopic macular holes with a retinal detachment,[65] and this raises the initial success rate.[66] Indocyanine green was used to stain the ILM in the initial case series; however, it remains in the eye for longer than 6 months postoperatively.[67] Brilliant blue G (BBG) can selectively stain the ILM and is less toxic.[68] However, a recent OCT study of retinal surface has shown an increasing number of dimples within the area of ILM peeling after surgery.[69]

It is hypothesized that traumatic damage at the fovea induced by

ILM peeling may cause full-thickness tissue loss at the fovea in myopic foveoschisis. This idea led us to attempt to leave the foveal ILM. Recently, a nonfoveal ILM peeling technique was introduced in an attempt to avoid macular holes (Fig. 117.10).[70] One study reported a significant reduction of the incidence of postoperative macular holes; however, the visual acuity level was similar even with a higher anatomic success rate.[71]

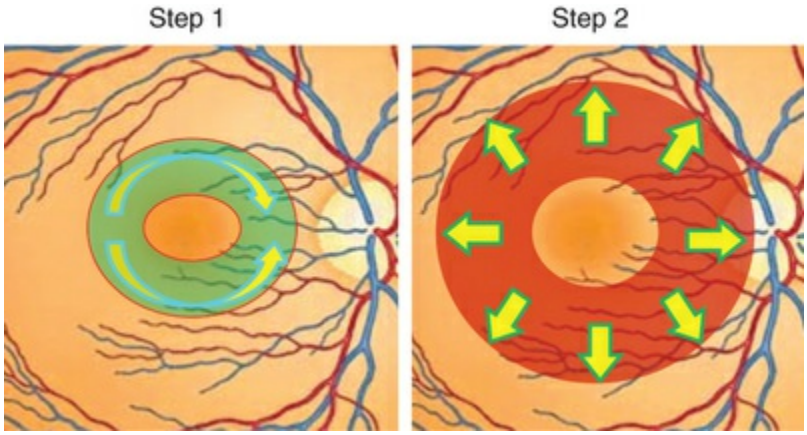

FIG. 117.10 The two-step technique of nonfoveal internal limiting membrane (ILM) peeling for myopic foveoschisis. Step 1: After vitreous separation from the retina, the peeling of the ILM is started at a distance from the fovea. The ILM is peeled in a donut-fashion, and a round strip of ILM remains around the fovea. Step 2: The ILM peeling then is extended toward the periphery to leave the fovea unpeeled.

Macular holes in eyes with high myopia are much less likely to close. This is partly because of higher mechanical tension of the posterior eye wall inside the posterior staphyloma. The inverted ILM flap technique, introduced for idiopathic macular hole cases, was applied for highly myopic cases. The visual benefit has not been proven, especially in cases with retinal detachment;[72] however, the macular hole closure rate seems to be higher than with the conventional ILM peeling technique (Fig. 117.11).[73] Most recently, this technique was modified by use of an autologous blood clot, resulting in a high anatomic success rate of 96%.[74] We also reported in a case series that temporal scleral shortening facilitates retinal reattachment (100%) and macular hole closure (75%).[75]

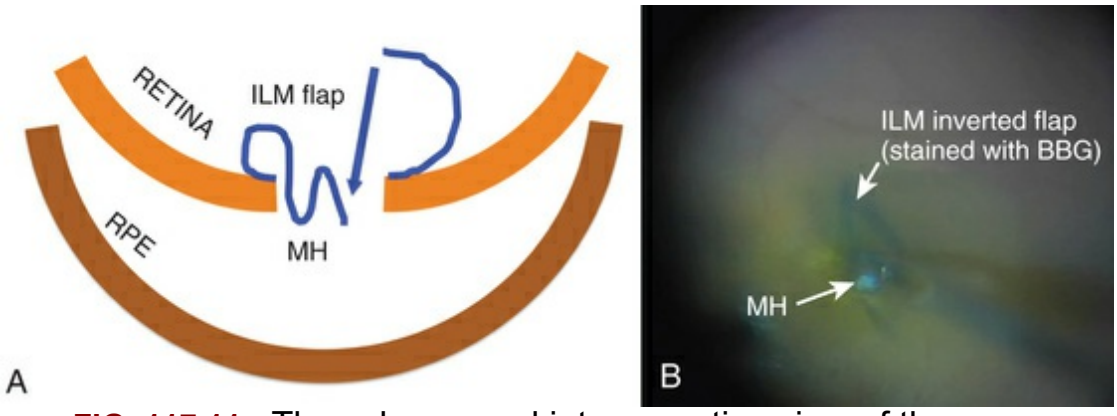

FIG. 117.11 The schema and intraoperative view of the inverted internal limiting membrane (ILM) peeling technique for a retinal detachment that developed from a macular hole in highly myopic eyes. (A) The ILM is peeled in the usual manner; however, the ILM remains attached at the edge of the macular hole. The peeled ILM then is inverted and placed inside the hole. (B) The ILM flap is held with forceps and pushed into the hole during the surgery. After this, vitreous fluid is exchanged with air, and gas tamponade is performed. *ILM*, internal limiting membrane; *MH*, macular hole; *RPE*, retinal pigment epithelium; *BBG*, brilliant blue G.

Tamponade

In cases of macular holes with or without a retinal detachment, gas tamponade must be performed at the end of surgery. Long-acting gas tamponade (i.e., perfluoropropane) must be used because it has a higher anatomic success rate.[59,76] Because there is no coagulation maneuver around the macula, it is critical to support the retina for a long time to recover the integrity between the RPE and photoreceptors in atrophic eyes. Silicone oil tamponade is also an effective option.[55,77]

Macular Buckling

In cases of recurrent retinal detachments, placing a buckle can be considered to fix the dimensional abnormality of the posterior staphyloma. Several case series have been reported with better surgical outcome in eyes with a macular hole and retinal detachment.[60,61] Vitrectomy is more commonly used to treat myopic foveoschisis;[78] however, macular buckling is also considered as

another option.[79,80] Direct macular buckling was attempted in the initial cases, and the modified silver clip[81] method was then developed. Most recently use of silicone sponges with bendable metallic wire inside the sponge has been reported.[82] The superotemporal conjunctiva is cut down and a mattress suture placed to fixate the top of the buckle. The indented part is on the other side. The arm is adjusted to fit the scleral curve so that the tip of the buckle reaches the macula.

Macular buckling reportedly has a higher success rate for retinal reattachment than vitrectomy,[60,61] likely because of the change in the vector force. Tangential traction generates the inward vector force in the posterior staphyloma, which is concave in shape. Macular buckling changes the macular area to a convex shape, and the vector force changes in direction to reattach the retina. Therefore, macular buckling is supposed to provide stronger contact between the neural retina and the RPE.

However, metamorphopsia and disruption of the choroidal circulation with protrusion of the posterior pole are the major concerns after macular buckling surgery. This maneuver is associated with a learning curve for placing the tip at the macula because it is a blinded procedure.

The authors normally perform vitrectomy as the first-line treatment for macular holes and retinal detachments and attempt to remove all tractional force from the vitreous cortex, ERMs, and ILMs, and long-acting gas or silicone tamponade. This technique is associated with a success rate of approximately 70–90%. However, if the retina detaches again because of macular hole reopening, macular buckling is performed, since another vitrectomy would not work well. Thus, the authors regard this procedure as rescue surgery for redetachment cases.

Postoperative Complications

Opening of a macular hole occurs from 10% to 20% of patients who undergo vitrectomy for myopic foveoschisis.[46,47,51] Cases in which ILM peeling was performed in the presence of an extremely thin, stretched fovea are at risk of developing this complication. Attention must be paid to detecting any small macular holes before

vitrectomy because the holes are normally stretched and enlarged postoperatively. Simply using a long-acting gas injection is not well accepted for postoperative macular holes, because this complication results from a shortage of retinal redundancy. Reoperation and removing any residual traction might be useful.

Recurrence of a retinal detachment is a major postoperative complication after vitrectomy performed to treat a macular hole with a retinal detachment. Removing residual vitreous cortex and ERMs is critical during a reoperation. However, it is sometimes difficult to identify the apparent cause of a redetachment. In those cases, persistent traction, such as microvascular traction, is responsible. Macular buckling is essential in those cases.

Conclusion

Thanks to the development of ocular imaging technologies, the pathophysiology of myopic macular diseases has become more understandable. Numerous interesting findings have suggested the presence of underlying traction in highly myopic eyes. We must evaluate the preoperative features of these pathologies carefully. This is useful in deciding upon the most minimally invasive and effective procedures for vitrectomy in patients with myopic macular complications.

References

1. Katz J, Tielsch JM, Sommer A. Prevalence and risk factors for refractive errors in an adult inner city population. *Invest Ophthalmol Vis Sci*. 1997;38:334–340.
2. Xu L, Li J, Cui T, et al. Refractive error in urban and rural adult Chinese in Beijing. *Ophthalmology*. 2005;112:1676–1683.
3. Sawada A, Tomidokoro A, Araie M, et al. Refractive errors in an elderly Japanese population: the Tajimi Study. *Ophthalmology*. 2008;115 [363–70.e3].
4. Williams KM, Bertelsen G, Cumberland P, et al. Increasing prevalence of myopia in Europe and the impact of education. *Ophthalmology*. 2015;122:1489–1497.
5. Klaver CC, Wolfs RC, Vingerling JR, et al. Age-specific

prevalence and causes of blindness and visual impairment in an older population: the Rotterdam Study. *Arch Ophthalmol*. 1998;116:653–658.
6. Iwase A, Araie M, Tomidokoro A, et al. Prevalence and causes of low vision and blindness in a Japanese adult population: the Tajimi Study. *Ophthalmology*. 2006;113:1354–1362.
7. Itakura H, Kishi S, Li D, Nitta K, Akiyama H. Vitreous changes in high myopia observed by swept-source optical coherence tomography. *Invest Ophthalmol Vis Sci*. 2014;55:1447–1452.
8. Takano M, Kishi S. Foveal retinoschisis and retinal detachment in severely myopic eyes with posterior staphyloma. *Am J Ophthalmol*. 1999;128:472–476.
9. Ogawa A, Tanaka M. The relationship between refractive errors and retinal detachment – analysis of 1,166 retinal detachment cases. *Jpn J Ophthalmol*. 1988;32:310–315.
10. Burton TC. The influence of refractive error and lattice degeneration on the incidence of retinal detachment. *Trans Am Ophthalmol Soc*. 1989;87:143–155.
11. Pierro L, Camesasca FI, Mischi M, et al. Peripheral retinal changes and axial myopia. *Retina*. 1992;12:12–17.
12. Akiba J. Prevalence of posterior vitreous detachment in high myopia. *Ophthalmology*. 1993;100:1384–1388.
13. Baba T, Ohno-Matsui K, Futagami S, et al. Prevalence and characteristics of foveal retinal detachment without macular hole in high myopia. *Am J Ophthalmol*. 2003;135:338–342.
14. Oie Y, Emi K. Incidence of fellow eye retinal detachment resulting from macular hole. *Am J Ophthalmol*. 2007;143:203–205.
15. Ruiz-Moreno JM, Pérez-Santonja JJ, Alió JL. Retinal detachment in myopic eyes after laser in situ keratomileusis. *Am J Ophthalmol*. 1999;128:588–594.
16. Barraquer C, Cavelier C, Mejía LF. Incidence of retinal detachment following clear-lens extraction in myopic patients. Retrospective analysis. *Arch Ophthalmol*. 1994;112:336–339.
17. Norregaard JC, Thoning H, Andersen TF, et al. Risk of

retinal detachment following cataract extraction: results from the International Cataract Surgery Outcomes Study. *Br J Ophthalmol*. 1996;80:689–693.
18. Neuhann IM, Neuhann TF, Heimann H, et al. Retinal detachment after phacoemulsification in high myopia: analysis of 2356 cases. *J Cataract Refract Surg*. 2008;34:1644–1657.
19. Jiang T, Chang Q, Wang X, et al. Retinal detachment after phakic intraocular lens implantation in severe myopic eyes. *Graefes Arch Clin Exp Ophthalmol*. 2012;250:1725–1730.
20. Friedman Z, Neumann E. Posterior vitreous detachment after cataract extraction in non-myopic eyes and the resulting retinal lesions. *Br J Ophthalmol*. 1975;59:451–454.
21. Phillips CI. Retinal detachment at the posterior pole. *Br J Ophthalmol*. 1958;42:749–753.
22. Benhamou N, Massin P, Haouchine B, et al. Macular retinoschisis in highly myopic eyes. *Am J Ophthalmol*. 2002;133:794–800.
23. Ikuno Y. Pathogenesis and treatment of myopic foveoschisis. *Nippon Ganka Gakkai Zasshi*. 2006;110:855–863.
24. Bando H, Ikuno Y, Choi JS, et al. Ultrastructure of internal limiting membrane in myopic foveoschisis. *Am J Ophthalmol*. 2005;139:197–199.
25. Tang J, Rivers MB, Moshfeghi AA, et al. Pathology of macular foveoschisis associated with degenerative myopia. *J Ophthalmol*. 2010 [Epub:175613].
26. Wu LL, Ho TC, Yang CH, et al. Vitreo-retinal relationship and post-operative outcome of macular hole repair in eyes with high myopia. *Graefes Arch Clin Exp Ophthalmol*. 2016;254:7–14.
27. Sayanagi K, Ikuno Y, Tano Y. Tractional internal limiting membrane detachment in highly myopic eyes. *Am J Ophthalmol*. 2006;142:850–852.
28. Ikuno Y, Gomi F, Tano Y. Potent retinal arteriolar traction as a possible cause of myopic foveoschisis. *Am J Ophthalmol*. 2005;139:462–467.
29. Forte R, Cennamo G, Pascotto F, et al. En face optical coherence tomography of the posterior pole in high

myopia. *Am J Ophthalmol*. 2008;145:281–288.
30. Stirpe M, Michels RG. Retinal detachment in highly myopic eyes due to macular holes and epiretinal traction. *Retina*. 1990;10:113–114.
31. Jo Y, Ikuno Y, Nishida K. Retinoschisis: a predictive factor in vitrectomy for macular holes without retinal detachment in highly myopic eyes. *Br J Ophthalmol*. 2011;96:197–200.
32. Alkabes M, Pichi F, Nucci P, et al. Anatomical and visual outcomes in high myopic macular hole (HM-MH) without retinal detachment: a review. *Graefes Arch Clin Exp Ophthalmol*. 2014;252:191–199.
33. Sakaguchi H, Ikuno Y, Choi JS, et al. Multiple components of epiretinal tissues detected by triamcinolone and indocyanine green in macular hole and retinal detachment as a result of high myopia. *Am J Ophthalmol*. 2004;138:1079–1081.
34. Favre M. Trous parapapillaires comme cause du décollement de la rétine. *Ophthalmologica (Basel)*. 1954;127:351–356.
35. Shimada N, Ohno-Matsui K, Nishimuta A, et al. Detection of paravascular lamellar holes and other paravascular abnormalities by optical coherence tomography in eyes with high myopia. *Ophthalmology*. 2008;115:708–717.
36. Spencer LM, Foos RY. Paravascular vitreoretinal attachments: role in retinal tears. *Arch Ophthalmol*. 1970;84:557–564.
37. Soga K, Sayanagi K, Ikuno Y, et al. Foveal anatomical profile of myopic foveoschisis in high myopia clinic. *Atarashii Ganka*. 2011;28:739–741.
38. Lin CW, Ho TC, Yang CM. The development and evolution of full thickness macular hole in highly myopic eyes. *Eye (Lond)*. 2015;29:388–396.
39. Ip M, Garza-Karren C, Duker JS, et al. Differentiation of degenerative retinoschisis from retinal detachment using optical coherence tomography. *Ophthalmology*. 1999;106:600–605.
40. Sayanagi K, Ikuno Y, Soga K, et al. Photoreceptor inner and outer segment defects in myopic foveoschisis. *Am J*

Ophthalmol. 2008;145:902–908.
41. Yannuzzi LA, Ober MD, Slakter JS, et al. Ophthalmic fundus imaging: today and beyond. *Am J Ophthalmol*. 2004;137:511–524.
42. Sayanagi K, Ikuno Y, Tano Y. Different fundus autofluorescence patterns of retinoschisis and macular hole retinal detachment in high myopia. *Am J Ophthalmol*. 2007;144:299–301.
43. Arias L, Caminal JM, Rubio MJ, et al. Autofluorescence and axial length as prognostic factors for outcomes of macular hole retinal detachment surgery in high myopia. *Retina*. 2015;5:423–428.
44. Gaucher D, Haouchine B, Tadayoni R, et al. Long-term follow-up of high myopic foveoschisis: natural course and surgical outcome. *Am J Ophthalmol*. 2007;143:455–462.
45. Shimada N, Ohno-Matsui K, Baba T, et al. Natural course of macular retinoschisis in highly myopic eyes without macular hole or retinal detachment. *Am J Ophthalmol*. 2006;142:497–500.
46. Ikuno Y, Sayanagi K, Soga K, et al. Foveal anatomical status and surgical results in vitrectomy for myopic foveoschisis. *Jpn J Ophthalmol*. 2008;52:269–276.
47. Kumagai K, Furukawa M, Ogino N, et al. Factors correlated with postoperative visual acuity after vitrectomy and internal limiting membrane peeling for myopic foveoschisis. *Retina*. 2010;30:874–880.
48. Ikuno Y, Tano Y. Vitrectomy for macular holes associated with myopic foveoschisis. *Am J Ophthalmol*. 2006;141:774–776.
49. Shao Q, Xia H, Heussen FM, et al. Postoperative anatomical and functional outcomes of different stages of high myopia macular hole. *BMC Ophthalmol*. 2015;15:93.
50. Li X, Wang W, Tang S, et al. Gas injection versus vitrectomy with gas for treating retinal detachment owing to macular hole in high myopes. *Ophthalmology*. 2009;116:1182–1187.
51. Gao X, Ikuno Y, Fujimoto S, et al. Risk factors for development of full-thickness macular holes after pars plana vitrectomy for myopic foveoschisis. *Am J Ophthalmol*.

2013;155:1021–1027.
52. Wu TT, Kung YH. Comparison of anatomical and visual outcomes of macular hole surgery in patients with high myopia vs. non-high myopia: a case–control study using optical coherence tomography. *Graefes Arch Clin Exp Ophthalmol*. 2012;250:327–331.
53. Qu J, Zhao M, Jiang Y, et al. Vitrectomy outcomes in eyes with high myopic macular hole without retinal detachment. *Retina*. 2012;32:275–280.
54. Ikuno Y, Sayanagi K, Oshima T, et al. Optical coherence tomographic findings of macular holes and retinal detachment after vitrectomy in highly myopic eyes. *Am J Ophthalmol*. 2003;136:477–481.
55. Nadal J, Verdaguer P, Canut MI. Treatment of retinal detachment secondary to macular hole in high myopia: vitrectomy with dissection of the inner limiting membrane to the edge of the staphyloma and long-term tamponade. *Retina*. 2012;32:1525–1530.
56. Nakanishi H, Kuriyama S, Saito I, et al. Prognostic factor analysis in pars plana vitrectomy for retinal detachment attributable to macular hole in high myopia: a multicenter study. *Am J Ophthalmol*. 2008;146:198–204.
57. Lam RF, Lai WW, Cheung BT, et al. Pars plana vitrectomy and perfluoropropane (C_3F_8) tamponade for retinal detachment due to myopic macular hole: a prognostic factor analysis. *Am J Ophthalmol*. 2006;142:938–944.
58. Conart JB, Selton J, Hubert I, et al. Outcomes of macular hole surgery with short-duration positioning in highly myopic eyes: a case–control study. *Ophthalmology*. 2014;121:1263–1268.
59. Lim LS, Tsai A, Wong D, et al. Prognostic factor analysis of vitrectomy for retinal detachment associated with myopic macular holes. *Ophthalmology*. 2014;121:305–310.
60. Ripandelli G, Coppé AM, Fedeli R, et al. Evaluation of primary surgical procedures for retinal detachment with macular hole in highly myopic eyes: a comparison of vitrectomy versus posterior episcleral buckling surgery. *Ophthalmology*. 2001;108:2258–2264.

61. Alkabes M, Burés-Jelstrup A, Salinas C, et al. Macular buckling for previously untreated and recurrent retinal detachment due to high myopic macular hole: a 12-month comparative study. *Graefes Arch Clin Exp Ophthalmol*. 2014;252:571–581.
62. Lewis JM, Park I, Ohji M, et al. Diamond-dusted silicone cannula for epiretinal membrane separation during vitreous surgery. *Am J Ophthalmol*. 1997;124:552–554.
63. Kwok AK, Lai TY, Yip WW. Vitrectomy and gas tamponade without internal limiting membrane peeling for myopic foveoschisis. *Br J Ophthalmol*. 2005;89:1180–1183.
64. Taniuchi S, Hirakata A, Itoh Y, et al. Vitrectomy with or without internal limiting membrane peeling for each stage of myopic traction maculopathy. *Retina*. 2013;33:2018–2025.
65. Kadonosono K, Yazama F, Itoh N, et al. Treatment of retinal detachment resulting from myopic macular hole with internal limiting membrane removal. *Am J Ophthalmol*. 2001;131:203–207.
66. Uemoto R, Yamamoto S, Tsukahara I, et al. Efficacy of internal limiting membrane removal for retinal detachments resulting from a myopic macular hole. *Retina*. 2004;24:560–566.
67. Sayanagi K, Ikuno Y, Soga K, et al. Residual indocyanine green fluorescence pattern after vitrectomy with internal limiting membrane peeling in high myopia. *Am J Ophthalmol*. 2007;144:600–607.
68. Enaida H, Hisatomi T, Goto Y, et al. Preclinical investigation of internal limiting membrane staining and peeling using intravitreal Brilliant blue G. *Retina*. 2006;26:623–630.
69. Sakimoto S, Ikuno Y, Fujimoto S, et al. Characteristics of the retinal surface after internal limiting membrane peeling in highly myopic eyes. *Am J Ophthalmol*. 2014;158:762–768.
70. Ho TC, Chen MS, Huang JS, et al. Foveola nonpeeling technique in internal limiting membrane peeling of myopic foveoschisis surgery. *Retina*. 2012;32:631–634.
71. Shimada N, Sugamoto Y, Ogawa M, et al. Fovea-sparing internal limiting membrane peeling for myopic traction maculopathy. *Am J Ophthalmol*. 2012;154:693–701.

72. Hayashi H, Kuriyama S. Foveal microstructure in macular holes surgically closed by inverted internal limiting membrane flap technique. *Retina*. 2014;34:2444–2450.
73. Kuriyama S, Hayashi H, Jingami Y, et al. Efficacy of inverted internal limiting membrane flap technique for the treatment of macular hole in high myopia. *Am J Ophthalmol*. 2013;156:125–131.
74. Lai CC, Chen YP, Wang NK, et al. Vitrectomy with internal limiting membrane repositioning and autologous blood for macular hole retinal detachment in highly myopic eyes. *Ophthalmology*. 2015;122(9):1889–1898.
75. Fujikawa M, Kawamura H, Kakinoki M, et al. Scleral imbrication combined with vitrectomy and gas tamponade for refractory macular hole retinal detachment associated with high myopia. *Retina*. 2014;34:2451–2457.
76. Uemoto R, Saito Y, Sato S, et al. Better success of retinal reattachment with long-standing gas tamponade in highly myopic eyes. *Graefes Arch Clin Exp Ophthalmol*. 2003;241:792–796.
77. Nishimura A, Kimura M, Saito Y, et al. Efficacy of primary silicone oil tamponade for the treatment of retinal detachment caused by macular hole in high myopia. *Am J Ophthalmol*. 2011;151:148–155.
78. Gohil R, Sivaprasad S, Han LT, et al. Myopic foveoschisis: a clinical review. *Eye (Lond)*. 2015;29:593–601.
79. Mateo C, Gómez-Resa MV, Burés-Jelstrup A, et al. Surgical outcomes of macular buckling techniques for macular retinoschisis in highly myopic eyes. *Saudi J Ophthalmol*. 2013;27:235–239.
80. Burés-Jelstrup A, Alkabes M, Gómez-Resa M, et al. Visual and anatomical outcome after macular buckling for macular hole with associated foveoschisis in highly myopic eyes. *Br J Ophthalmol*. 2014;98:104–109.
81. Klöti R. Silver clip for central retinal detachments with macular hole. *Mod Probl Ophthalmol*. 1974;12:330–336.
82. Parolini B, Frisina R, Pinackatt S, et al. Indications and results of a new L-shaped macular buckle to support a posterior staphyloma in high myopia. *Retina*. 2015;5:2469–

2482.

118

Surgical Management of Retinopathy of Prematurity

Yoshihiro Yonekawa, Lisa J. Faia, Michael T. Trese

Introduction

Retinopathy of prematurity (ROP) affects thousands of children each year. Fortunately, ROP causes blindness in only a small percentage. ROP was previously called "retrolental fibroplasia." The original work in the 1950s of Kinsey et al.[1] and Patz and Kinsey[2] showed that oxygen contributes to the tissue change described as ROP. It was believed that if the arterial oxygen was

kept within prescribed guidelines, ROP might be eliminated. However, with the ability of neonatologists to keep alive newborns of very low birthweight and very young gestational age, there has been a resurgence of ROP despite tight control of the partial pressure of oxygen.

Oxygen's role in ROP has come under extensive investigation. Many workers have shown in animal models that immature vessels characteristic of ROP can be produced but not retinal detachment.[3–6] Clinical observations by many investigators have shown that ROP can be seen in 85–90% of children of low birthweight when exposed to oxygen.[7] Similar clinical pictures have been seen in full-term infants, in familial exudative vitreoretinopathy, and in infants of mothers who are cocaine users.[8,9]

The role of vascular endothelial growth factor (VEGF) in ROP has been well established. VEGF under control of oxygen concentration or retinal ischemia can overcome the genetic mandate to form normal retinal vasculature and instead contribute to neovascularization or development of abnormal intraretinal vascular patterns in the retinal periphery.[10]

The lesser stages of ROP are so common in the closely observed low birthweight (<1500 g) infants as to suggest that these early changes are a physiologic response of the immature eye to oxygen. Endogenous transforming growth factor-beta (TGF-β) produced at the due date causes the process to regress in a large percentage of eyes but continue to progress to retinal detachment in only a small percentage of cases.

Classification System

In the past, there were several classifications of ROP, which led to much confusion between ophthalmologists, neonatologists, and pediatricians. However, an International Classification of Retinopathy of Prematurity (ICROP) was subsequently adopted.[11] It describes three zones of the eye. Zone I uses the optic nerve as the center of a circle, and the radius is defined as twice the distance between the foveola and the optic nerve. Zone II uses as a radius the distance between the nasal ora serrata in the horizontal meridian and the center of the optic nerve. All of the remaining

retina is zone III (Fig. 118.1); that is, zone III is present in all meridians except at the nasal horizontal meridian.

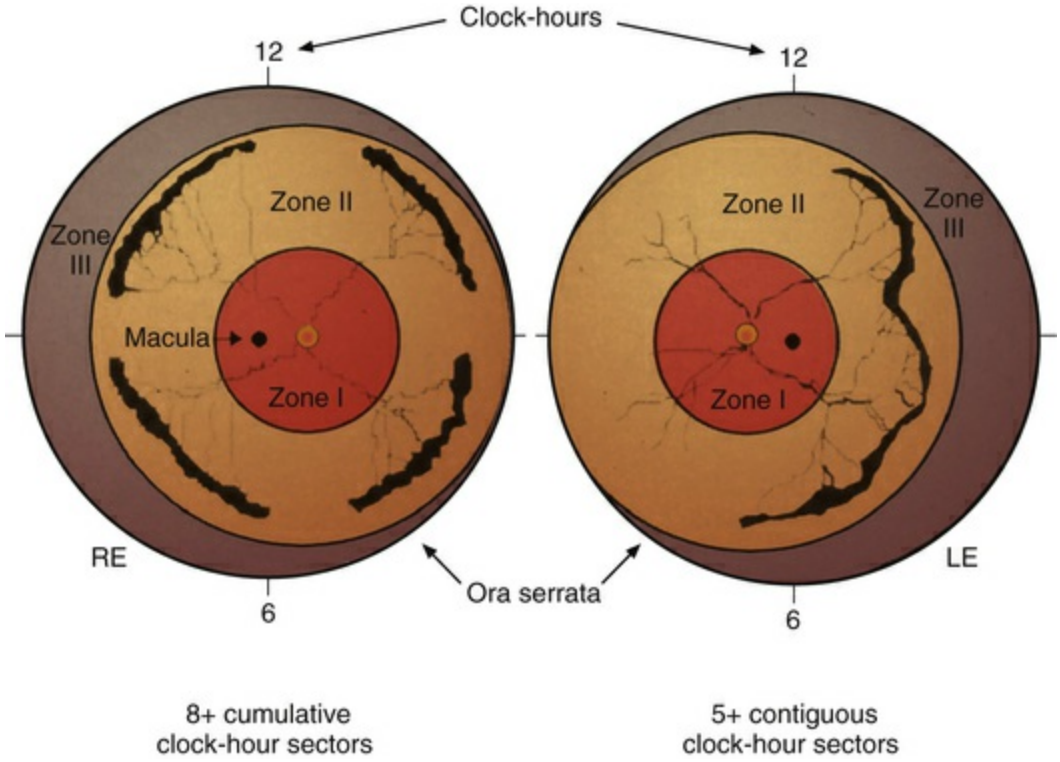

FIG. 118.1 Zones of the retina with the threshold criteria used in the Cryotherapy for Retinopathy of Prematurity (CRYO-ROP) study.

Children who have vessels only in zone I at their first examination tend to have a worse prognosis and may have "aggressive posterior ROP" (AP-ROP), in which the eye has a high risk of progression to retinal detachment. It seems that retinal ischemia may be at least one of the mechanisms of VEGF that support the neovascular process. It makes sense therefore that an eye with zone I vasculature at only 32 weeks postmenstrual age (PMA) and a very large avascular (ischemic) zone concentrically would have the worst prognosis.

The ICROP defines five stages of ROP. The process of ROP begins at the junction between the vascular and avascular retina. ROP is described as stage 1 if a narrow white line is present at the junction. Stage 2 is a ridge of activity that shows thickening of this line (Fig. 118.2). In addition to this thickening, there is sometimes a ruddy appearance due to a vascular shunt within this ridge. Stage 3

involves the growth of vessels from the retina toward the vitreous cavity immediately posterior to and contiguous with the ridge (Fig. 118.3). Stage 4 is a partial retinal detachment and is subclassified as 4A, with the macula attached, and 4B, with the macula detached. Stage 5 implies a total detachment of the vascularized retina (Fig. 118.4) and can be classified further depending on the opening or closure of the anterior and posterior aspects. Even with significant retinal detachment causing a white retrolenticular appearance, the very far peripheral avascular retina often remains attached (Fig. 118.5). The avascular peripheral retina, however, if functioning, can yield only low vision.

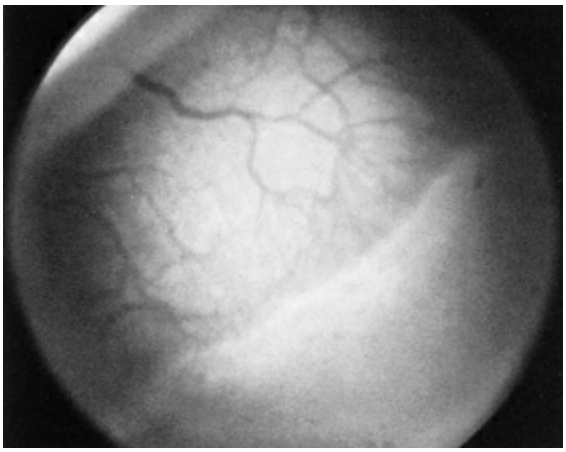

FIG. 118.2 Widened line of stage 2 retinopathy of prematurity at the junction of the vascularized and avascular retina.

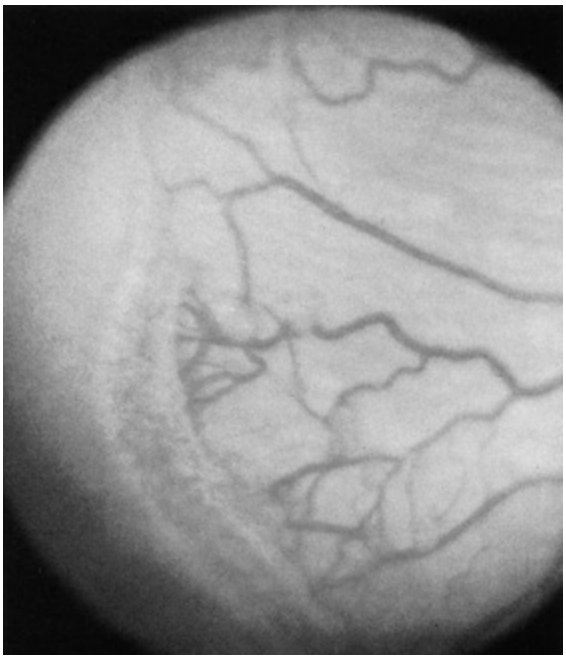

FIG. 118.3 Extraretinal neovascularization immediately posterior to the ridge. Several clock-hours of neovascularization are visible.

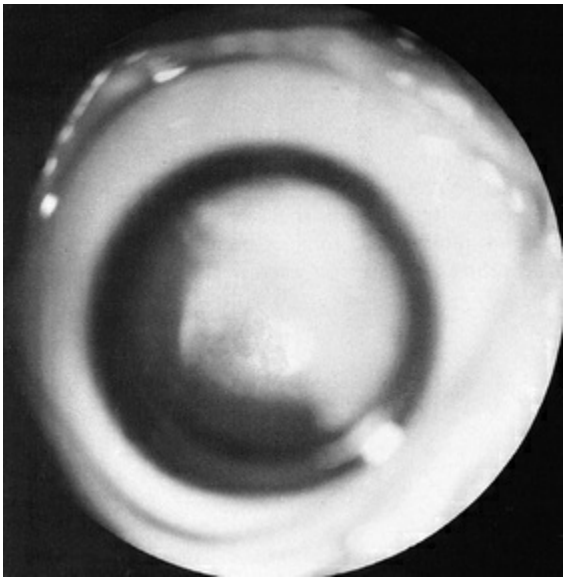

FIG. 118.4 Leukocoric pupil of advanced retinopathy of prematurity.

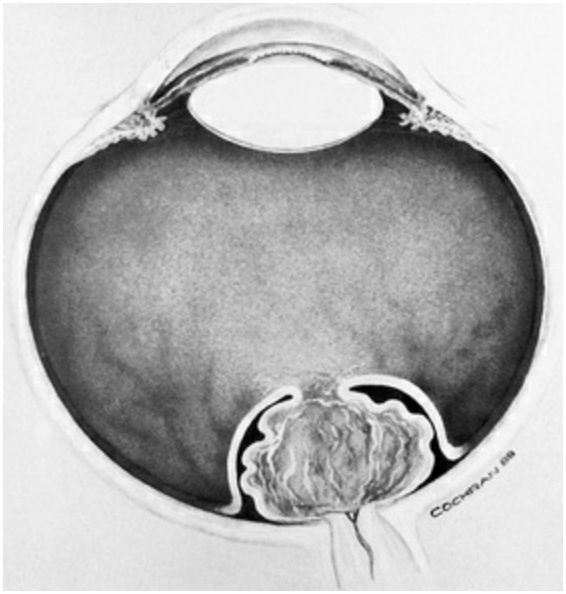

FIG. 118.5 Cross-sectional drawing of a rare configuration of stage 5 retinopathy of prematurity with large areas of attached peripheral retina despite total detachment of the vascularized retina as seen in very posterior zone I disease.

The ICROP also addressed the problem of "plus disease." It is not a disease different from ROP but is a descriptive term for dilated and tortuous vessels of the posterior pole. In addition, the anterior segment in plus disease often shows dilated iris vessels (Fig. 118.6). These iris vessels may not be true neovascularization of the anterior segment but may represent dilation of an existing tunica vasculosa lentis.[11] This anterior segment vessel dilation appears to be a manifestation of a generalized intraocular increased VEGF concentration.

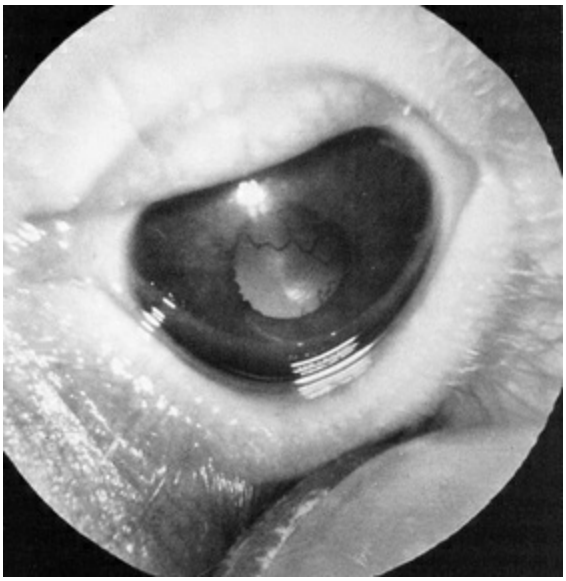

FIG. 118.6 Rubeotic iris vessels. These make the iris appear red and may represent a persistent dilated tunica vasculosa lentis. "Plus disease" refers to the dilated tortuous vessels of the posterior pole and can be seen with or without this anterior segment change.

The ICROP was updated in 2005.[12] As neonatology has progressed, smaller babies are being kept alive, and these babies present with more posterior disease. Three features are worthy of discussion:

- First, ROP presenting completely in zone I or posterior zone II as mentioned above usually has a more aggressive course, and this type of ROP (AP-ROP) may require more aggressive ablative treatment.
- Second, the stage 3 neovascularization of ROP may appear differently depending on the zone of involvement: (1) mid and anterior zone II and zone III neovascularization is always posterior to the ridge tissue and growing into the vitreous cavity; and (2) zone I and posterior zone II can be flat, lying along the retinal surface, without the typical ridge tissue features.
- Third, "plus disease" is a function of an open shunt vessel contained deep within the ridge tissue. As this arteriovenous shunt is established, the vessels become dilated in the periphery. With the advent of wide-angle photography, this image can be easily appreciated. Although plus disease is a posterior pole finding and should remain so, the dilated peripheral vessels have

been referred to as "pre-plus" and suggests that the eye is at higher risk of developing frank "plus disease."

Of these three findings, the aggressive posterior form seems to encompass many features of a very "vascularly active" eye, namely posterior disease, severe plus disease, and absence of ridge tissue, but also marked circumferential shunt vessels and areas of flat neovascularization that can be very large. Eyes such as this suggest eyes with a high degree of vascular activity and a high risk of progression to retinal detachment. These eyes merit consideration for earlier laser treatment. Later in the chapter, the Early Treatment for Retinopathy of Prematurity Study will be discussed.

In order to try to identify eyes at high risk of progression, the authors have adopted a modification of the ICROP system. Namely, we designate the number of clock-hours of vessels that are entirely in zone I by a subscript. For example, if all 12 clock-hours are in zone I, that would be written zone I_{12}. Additionally, if flat neovascularization is present, we use another subscript, "F." Stage 3_F denotes flat neovascularization is present. Since these vessels lie flat on the retina and appear anterior to the shunt vessels, the drawing of the findings show the extent of the clock-hours of the flat stage 3 (Fig. 118.7). This designation is best done by photographic screening, which allows the images to be studied carefully.[13–15]

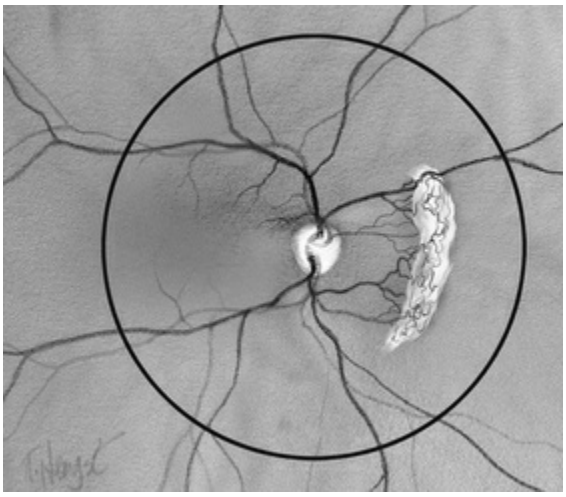

FIG. 118.7 Flat neovascularization.

In our experience, an eye with one clock-hour of vessels in zone I and no flat neovascularization (zone I_1 stage 3) behaves better than an eye with 12 clock-hours of vessels in zone I and flat neovascularization (zone I_{12} stage 3_F). Both of these eyes are less at risk if they do not have plus disease. It is rare that an eye with 12 clock-hours in zone I does not have plus disease. We have found that plus disease is the clinical finding that exemplifies a vascularly active eye (excessive VEGF) and requires treatment. This is particularly true in a child who presents with these findings prior to the due date (40 weeks' postmenstrual age).

Histopathologic Features, Clinically Relevant Cell Biology, and Pathophysiology

Stages 1 and 2

Much work has been done to promote the understanding of the early changes at the junction of the vascular and avascular retina. Foos[8] speaks of a vanguard and rearguard of cells that contribute to the tissue changes.[3,11] These cells have been infrequently studied in their active form because most of these neonates survive and the eyes do not become available for study. Other authors[16] have described the cells in this region as “spindle shaped.” These spindle-shaped cells are found in many proliferative processes, and this descriptive term does not help define the cell biology. Histologic features of the avascular and vascularized retina reveal a difference in the retina's thickness, with the posterior vascular retina being somewhat thicker than the more peripheral avascular retina.

Terry[17] was perhaps the first to note vitreous abnormalities in children with ROP. The vitreous, which is normally firm and dense in the newborn, is syneretic and organized into fluid lacuna and sheets of collagen in ROP. This vitreous abnormality seems to be present in children with lesser stages of ROP and certainly is present in children with more advanced stages. The significance of these vitreous abnormalities may relate to both development of

exudative and tractional detachments and to development of late rhegmatogenous retinal detachments. ROP should properly be thought of as a vascular *vitreo*retinopathy. Stage 1 ROP is the visible white line that separates the vascular from the avascular retina. In stage 2 that line widens and may become a salmon color as the shunt vessel opens.

Stage 3

The classical concept of neovascularization in ROP is that a retinal vasoconstriction secondary to oxygen administration or an increase in oxygen concentration as seen with birth alone is followed by vasodilation and associated vascular budding after oxygen withdrawal. However, some infants show significant vasodilation or plus disease even while receiving supplemental oxygen. No matter what the mechanism, the neovascularization that develops in stage 3 ROP has interesting features. One is that the active vessels are usually present at the posterior ridge of tissue. Also, there is often a directional orientation of the vessels toward the posterior apex of the lens in zones II and III. One of the most curious findings of the more posterior ROP is the lack of ridge tissue seen in eyes with extensive shunts and plus disease. The concept of Foos and spindle cells is based on eyes with changes in mid-zone II, and the absence of ridge tissue is a posterior finding. One suggestion is that angioblasts and astrocytes do not meet until the progenitor cells have progressed from the area of the disc into mid-zone II in the animal models of ROP.[18] This still leaves the difference in appearance of the flat stage 3 neovascularization in zone I. It may be that the secondary vitreous formed by vascularized retina may dictate at least in part the position of the neovascular fronds. The more posterior smaller-volume vitreous cavity may produce enough secondary vitreous to press the frond along the retinal surface. As is known from diabetic retinopathy, these fronds tend to grow on the posterior hyaloid surface. As the vascularized retina expands, the volume of secondary vitreous needed to fill the hemisphere of the vitreous cavity may not keep pace and allow vessels to grow along the anterior surface of the developing secondary vitreous toward the center of the vitreous

cavity or toward the lens. This organization of vitreous collagen or hypocellular gel contraction requires few cells to organize large amounts of collagen, as seen in eye tissue samples with stage 5 ROP (Fig. 118.8). In tissue culture, cells have been identified that have the ability to organize large amounts of collagen (Fig. 118.9). It is believed these cells organize anterior vitreous collagen into a plane that allows the vessels to grow on a surface anteriorly toward the posterior aspect of the lens.

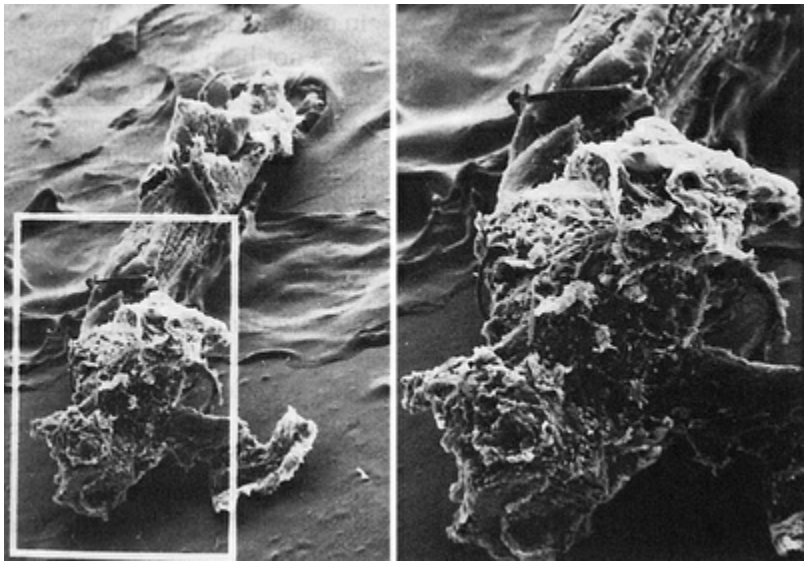

FIG. 118.8 Scanning electron micrograph of the dense core of vitreous collagen removed from an eye with stage 5 retinopathy of prematurity. It is organized into a tight central core with only a few cells and cell processes, as seen on its surface. (Final magnification ×1000; higher magnification of inset ×2500.)

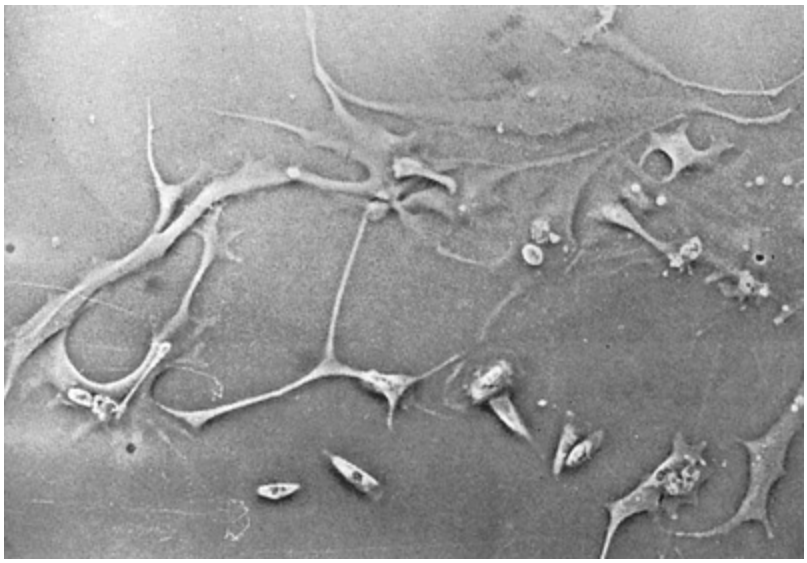

FIG. 118.9 A phase-contrast micrograph of cells with long processes that reach out from their cell body. Antisera immunofluorescent technique determined that these cells were neuroglial in origin.

Distortion of Retinal Vascular Architecture

Machemer[19] suggested that avascular retina is more elastic because it lacks retinal vessels and that this helps explain why the peripheral avascular retina can stretch over large areas of retinal pigment epithelium (RPE). In contrast, we believe that the organization of the cortical vitreous collagen, which is formed by and intimately attached to the vascularized retina, makes this stretching of the vascularized retina difficult. This inelastic cortical vitreous collagen and retinal ridge inhibits stretching of the vascularized retina. It is the absence of the cortical collagen over areas of avascular retina that allows the avascular retina to be stretched over large areas of RPE. Circumferential stretching of the retina is often recognized because of distortion of retinal vessels and is associated with an incomplete retinal ridge.

Stages 4 and 5

ROP has both exudative retinal detachments and traction retinal detachments. In the evolution of retinal detachments of ROP, at least three factors are involved. The first is the existence of permeable, leaky blood vessels, as seen in stage 3 ROP. These

vessels, within the shunt and posterior to the ridge, are capable of supplying large amounts of proteinaceous fluid to both the vitreous cavity and subretinal space. Second, as shown by Ashton and Cook,[20] the neovascularization that is commonly thought of as growing only into the vitreous cavity also can be seen growing into the subretinal space (Hirose, pers. comm.). Third, these blood vessels can bleed into both the vitreous cavity and subretinal space. Foos[21] showed that eyes with vitreous hemorrhage are susceptible to retinal detachment and seem to have a worse prognosis for total retinal detachment.

Okamoto et al.[22] developed a murine model showing that neovascularization into the subretinal space from the retina can occur with increased VEGF expression. Cells from the retinal ridge or regressing hyaloid and tunica vasculosa lentis organize vitreous collagen that is tightly attached to the retina. This creates traction on these permeable vessels and results in additional leakage of fluid or blood from these vessels. In children who develop stage 4 ROP, the retinal ridge is the most common location for retinal detachment to begin. Detachments without traction in the area of the ridge often settle spontaneously.[23]

Most retinal detachments in ROP have a tractional and an exudative component. By attempting to determine the predominate component, one can better select clinical therapy. We suggest that the exudative detachment is caused by leaking vessels and traction on these vessels. The tractional forces aggravate the exudative component. Resolution occurs when the vessels spontaneously involute before significant traction (vitreous organization) has occurred. However, if enough cells have migrated into the vitreous cortex, even if the leaking vessels involute, cell-mediated organization of the vitreous can continue to cause complicated, predominantly traction retinal detachments.

In eyes with ROP, cells that organize the vitreous appear to migrate into the vitreous cortex from the ridge of retina between avascular and vascular retina and from the area of the optic disc. This means that manipulation of these two areas is important to resolve the tractional component of retinal detachment. It also may be that the cells of the primary vitreous or tunica vasculosa lentis, or both, now called “ocular fetal vasculature,” may contribute cells

to this hypocellular gel contraction. The genetically determined apoptosis of the cellular elements of the primary vitreous and tunica vasculosa lentis may be clinically slowed or reversed under the influence of increased VEGF. The higher the concentration of VEGF, the less the apoptosis proceeds, and the more cells are available to organize vitreous collagen and contribute to retinal traction.[24]

We, and colleagues, have grown cells in tissue culture from the retrolenticular membrane of stage 5 ROP eyes. These cells have been studied by immunofluorescent techniques and appear to be predominantly neuroglial in origin. Some cells seemed very immature, perhaps representing multipotent cells that have migrated from the retina into the vitreous cavity. These cells show the ability to organize large amounts of collagen in vitro, as well as the ability to produce collagen. When these cells are tested for collagen organization against cells from both proliferative vitreoretinopathy and tractional diabetic retinal detachment, the cells of ROP are able to organize much more collagen than the proliferative vitreoretinopathy cells.[25,26] This organization of vitreous collagen into sheets is supported by the original observations of Terry[17] in eyes with ROP.

Development of Stage 4A ROP Retinal Detachments

In stage 4A ROP, the detachment begins at the ridge of the retina. Fluid can leak posteriorly under the retina and cause the posterior retina to detach as well. When a primarily exudative retinal detachment develops, the retinal surface is smooth and shows no evidence of epiretinal proliferation or peaked folds. This is a significant observation in our clinical experience. Eyes with smooth anterior retinal surfaces, despite large areas (four disc areas) of retinal detachment, sometimes flatten spontaneously over several months. When the retina flattens, however, the RPE is often disrupted, and many eyes do not have useful vision. As cells migrate into the vitreous cortex along the surface of the vascularized retina, both anteriorly from the ridge and posteriorly from the disc, they can form folds in the retina. These cells can convert a predominantly exudative retinal detachment to a predominantly tractional detachment. Machemer,[19] Charles,[27] and

others often discussed the peripheral retinal “trough,” or anterior loop traction, associated with ROP. The vitreous is organized in a fashion that allows the retina to form a trough in the far periphery. As retinal detachment in ROP evolves, its configuration depends partly on the symmetry of the retinal ridge. A ridge that contracts evenly and is located an equal distance from the disc in all meridians results in a detachment that closes centrally.

Subretinal fluid can have several clinical manifestations. It can be opalescent or red, being either serum or blood in the subretinal space. This fluid may have a toxic effect on the neurosensory retina and RPE, in addition to the expected degenerative effect on the photoreceptors from retinal detachment itself. This subretinal fluid has been found to have high concentrations of hemoglobin and iron, both bound and unbound.[28,29] In addition, cholesterol is often found in the subretinal space, either crystallized or in solution. Opaque subretinal fluid, after even spontaneous reattachment, appears to leave the eye with disrupted RPE and presumably a poor visual result.

Clinical Considerations

Many years ago, examination of an infant's eye for ROP in a teaching institution was often assigned to a resident with limited indirect ophthalmoscopy experience. Now with new information regarding ROP, it is necessary for an experienced physician to examine carefully infants who are at risk photographically and with confirmatory bedside exams.

In the results of the Cryotherapy for Retinopathy of Prematurity Study[30] and the Early Treatment for Retinopathy of Prematurity Study,[31] a positive treatment effect was reported, and it was suggested that infants be examined at the later of either 4 weeks after birth or at 31 weeks PMA, if they are less than 1500 g birth weight or 30 weeks or less gestational age. These infants need to be examined meticulously, including indirect ophthalmoscopy, for vascularization of the anterior segment, pupillary dilation, plus disease, zone of eye involvement, and stage of the disease process. The authors have found that the Alfonso lid speculum (Fig. 118.10A) and Kelge swab (Fig. 118.10B), accompanied by the

indirect small pupil ophthalmoscope and 28 diopter lens, are the best instruments to examine the peripheral retina in the neonate. When bedside examination is needed, we do not use topical anesthesia because this can cause clouding of the cornea.

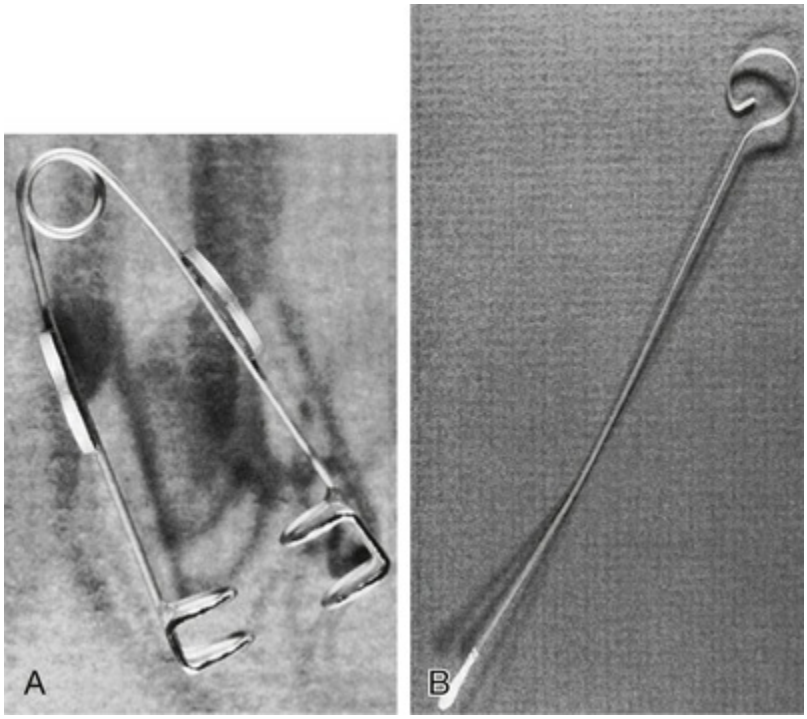

FIG. 118.10 (A) Alfonso lid speculum. (B) Kelge swab used for scleral depression.

This examination is generally well tolerated, even by the intubated neonate. It is important to know that scleral depression can obscure the minimal demarcation line or ridge. Therefore minimal force should be used with scleral depression. It occasionally may cause some hemorrhage along the ridge or sometimes even into the vitreous cavity, but this generally resolves without incident.

Photographic Imaging

The Photo-ROP (Photographic Screening for Retinopathy of Prematurity) study and that of Ells et al. evaluated and confirmed the utility of photographic imaging in ROP screening.[32,33] This photographic imaging allows a very good representation of the posterior pole and the midperiphery of the eyes of premature

infants. Photographic documentation in diabetes, age-related macular degeneration, and other retinal vascular disease is well known,[34–36] and photographic documentation of ROP has been available for several years and is equally valuable. Treatment in ROP in large part is driven by zone I and zone II findings, which are well seen with photography.[32]

The interpretation of these pictures requires they be obtained and managed in a timely fashion and read by a qualified reader. Retinopathy of prematurity is a time-dependent disease, allowing development of stage 1 to stage 5 to occur in as little as 2 weeks.[37–39] FocusROP (FocusROP, LLC, Troy, MI), an internet-based, HIPAA-compliant, secure website using certified and expert readers, has been developed to handle these images. This website (www.FocusROP.com), receives the uploaded digital information obtained by trained individuals in the neonatal care centers and immediately notifies a previously certified local ophthalmologist to read these images. The follow-up algorithm contained in the software program allows an unchangeable examination schedule, which reduces the risk of late treatment.

Though bedside examinations allow a more extensive examination of the periphery, photographic screening has its advantages. Such advantages include an excellent view of the most severe aggressive posterior ROP and the ability to compare, side by side, the current exam with the previous one. The coupling of this remote management by photographic images as well as bedside examinations gives perhaps the ideal screening mechanism for the early stages of retinopathy of prematurity. Implementation of a longitudinal digital-imaging paradigm with remote image interpretation (i.e., a reading center) has the potential to maximize utilization of the physician's time, broaden the availability of high-level ROP diagnostic expertise, and provide excellent patient care. Photographic screening does not replace the bedside examination but can be sufficient for screening to provide care for the patient and protect the hospital and doctor in malpractice cases. In addition, the ROPtool, which gives a numeric value to tortuosity, can aid the examiner as to the development of plus disease.[40]

Cryotherapy

The Cryotherapy for Retinopathy of Prematurity study defined eyes with plus disease showing five contiguous or eight discontiguous clock-hours of stage 3 ROP (Fig. 118.1) as reaching a threshold for cryotherapy. Cryotherapy was defined as use of a cryoprobe to treat the avascular retina but not the ridge.[41] This technique was found to be effective in reducing by 50% the unfavorable outcome of retinal fold and retinal detachment.

As mentioned earlier, eyes with zone I disease tend to have the worst prognosis, and eyes with zone I involvement and extensive plus disease are said to have Rush disease. Rush disease refers to the tempo of ROP, which can go from stage 1 to stage 5 in only 2 weeks.[37–39] Zone I cryotherapy, however, requires extensive treatment and risks occlusion of the central retinal artery for a significant time.

Cryotherapy has the potential to induce future retinal problems in these patients, who have an increased risk for rhegmatogenous retinal detachment as adults, with or without treatment.[30] Trese has seen several eyes that developed cataract, hypotony, and iris depigmentation.[29] These changes were seemingly caused by anterior segment ischemia following peripheral cryotherapy treatment. Cryotherapy is no longer considered the treatment of choice with the advent of the indirect laser.

Indirect Laser Photocoagulation

Numerous reports have shown peripheral ablation by laser (argon blue–green and diode) to be effective in the treatment of ROP. This is not surprising in that peripheral ablation, no matter how performed, should have a similar effect on the course of the disease. Iverson et al.,[42] Landers et al.,[43] and McNamara et al.[44] have shown a positive treatment effect for the use of peripheral laser ablation. This type of treatment can be performed using topical anesthesia and may be performed in the nursery, eliminating the need for the infant to be transported to the operating room. The diode laser has significant physical advantages because of its portable nature.[45] We prefer using the red diode laser because it theoretically causes less lens damage from tunica vasculosa lentis laser uptake.

Most physicians who treat ROP today prefer using indirect laser

to ablate the retinal periphery. It should be noted that cataracts, as well as anterior segment ischemia, can be observed after laser treatment with either argon or diode energy. It is important to recall that the nursery personnel require education regarding laser safety before such treatment is instituted in the nursery area.

The Early Treatment for Retinopathy of Prematurity Study (ETROP)

The ETROP[31] used a risk management program RM-ROP2 to evaluate each eye. If the risk generated by the program exceeded 0.15, the eye was randomized to treatment. The eyes eventually were analyzed, and using an ICROP-based classification system, they were grouped into type 1 and type 2:

Type 1 prethreshold

- Zone I any stage ROP with plus disease
- Zone I stage 3 with or without plus disease
- Zone II stage 2 or 3 with plus disease.

Type 2 prethreshold

- Zone I stage 1 or 2 without plus disease
- Zone II stage 2 or 3 without plus disease.

The ETROP treatment systems yields 9.6% failure rate, which is better than the CRYO-ROP study results.[46]

As with all clinical trials, the results of the CRYO-ROP study and the ETROP study should be considered when the treatment of a child is considered, but physicians should choose the treatment plan in a fashion that best suits the patient's circumstance in their best medical judgment. The results of the ETROP study describe times when treatment should be considered. There may be

circumstances where, with close monitoring of the patient, treatment can be avoided or treatment should be performed earlier. The physician needs to realize what is in the balance. The ETROP study, as did the CRYO-ROP study, shows that plus disease is very important in determining the need for treatment. The eye that is vascularly active is an eye that may need treatment. The ETROP study also points out that eyes with zone I disease are worthy of evaluation for treatment. These eyes again have a very large area of avascular retina and therefore are vascularly active eyes with a high likelihood of progression. As the physician becomes more comfortable with the progression of the disease and its potential tempo, the timing of evaluation and treatment can be adapted to the clinical situation.

Examination is probably the most difficult part of ROP care. The best plan is to have weekly examination coverage done at the same time and scheduled by a neonatal intensive care unit (NICU) employee, and the screener needs to be prepared to see some children even at half-week intervals. Currently, this is usually done by physician examiners but most likely will be photographically screened in the future, as mentioned above.

Currently, laser treatment is the best therapy available. It causes less effusion than cryotherapy and has results at least as good from an anatomic and visual standpoint. In the not too distant future, it may be that pharmacologic therapy may be possible. This would eliminate the need to destroy half to two-thirds of the retina with laser.

Anti-Vascular Endothelial Growth Factor Therapy

Multiple reports and series have demonstrated the use of intravitreal bevacizumab (Avastin; Genentech, South San Francisco, CA), an anti-VEGF agent originally approved by the US Food and Drug Administration (FDA) for the treatment of metastatic colon cancer, for various stages of ROP.[47] Intravitreal bevacizumab has been used as monotherapy, as well as in combination with conventional laser therapy or with vitrectomy.[48–62] Ranibizumab (Lucentis; Genentech), a humanized monoclonal Fab fragment of

bevacizumab and FDA approved for treatment of various adult retinal conditions, has also been reported in several ROP studies.[63,64] However, there are no authoritative studies yet, such as CRYO-ROP or ETROP, that show how anti-VEGF agents should be incorporated into the care of children with treatment-requiring ROP.

The largest study thus far was comprised of 150 infants with zone I or posterior zone II ROP with stage 3 and plus disease, who were randomized to laser or intravitreal bevacizumab.[65] It appeared that bevacizumab was more beneficial for zone I disease, but unfortunately, many design flaws did not allow support of its conclusions and left unanswered many questions. Below are several points of discussion placed in context of recent developments in the field.

First, the study suggested that bevacizumab does not enter the systemic circulation, but numerous studies have shown systemic VEGF suppression and circulating bevacizumab in neonates after bevacizumab injections.[66–68] No long-term studies have been performed yet at the time of writing to determine whether bevacizumab may affect the development of other organ systems.

Second, the study suggested that only one bevacizumab injection is required to manage ROP, but this is a dangerous assumption.[69] Late recurrence of neovascularization is well described after anti-VEGF treatment of ROP.[70,71] As a pediatric retina surgical referral practice, we have also managed numerous infants who were referred for extensive traction retinal detachment after anti-VEGF injections for stage 3 disease.[72] We observed that the majority of these eyes underwent a "crunch" phenomenon, where the fibrovascular proliferation of stage 3 disease quickly progressed to retinal detachment. These detachments are often posterior and assume tight circumferential tractional vectors. Vigilant long-term screening after anti-VEGF treatment and access to a pediatric vitreoretinal surgeon should be readily available.

The study also suggested that bevacizumab allows full retinal vascularization, but numerous other studies have shown with fluorescein angiography that this is not the case, and late reactivation, persistent avascular peripheral retina, and other peripheral vascular abnormalities are common.[70,71] Animal studies

have also suggested that global retinal functioning may be affected with anti-VEGF treatment.[73]

Finally, the laser failure rate of 42% in zone I eyes in the study is very high. The success rates in previously published studies are significantly better.[74–77] Larger studies are underway to hopefully provide a clearer understanding of the role of anti-VEGF agents in ROP care.[78]

Therapeutic Oxygen

Increasing oxygen has been shown to reduce VEGF activity. Because of this effect, the STOP-ROP study was undertaken to increase the oxygen saturation in infants whose transcutaneous oxygen saturation is less than 94% in hopes that the increased oxygen would decrease VEGF activity and allow the genetically driven development of retinal vessels to regain control. The STOP-ROP study did not show a statistically significant effect, while causing increased risk of pulmonary events.[79]

Stages 4 and 5 Preoperative Evaluation

Preoperative evaluation of a child with stage 4 or 5 ROP necessitates special considerations. It may be difficult to determine the visual function of the child. The examiner or parent often forms a clinical impression on the basis of the child's behavior after exposure to a bright light. Many authors[80] have tried to define electrophysiologic criteria for visual acuity in infants. In our experience, the awake visual evoked potential (VEP) or electrical evoked potential (EEP) seems the most reliable. The VEP is perhaps the most easily accessible and reliable piece of clinical information. The VEP is valuable if a child is without clinical light perception vision but does have a recordable VEP. The positive VEP response supports that the child has an objective demonstration of functional retina, and we would proceed with surgery. In the absence of a VEP response and clinical light response in screening children for surgical intervention, these findings indicate less possibility of favorable visual results after surgery. It is possible for children to have a clinical light response and a nonrecordable VEP (false-negative VEP exam).

Preoperatively, it is important to assess corneal clarity and anterior chamber depth, as well as size of the eye and intraocular pressure. Children with ROP can have greatly elevated intraocular pressure (up to 50–70 mm Hg) and not have the clinical symptoms of elevated intraocular pressure and cloudy cornea. Glaucoma may be a cause of vision loss in such cases. We have found that the buphthalmic eye with ROP frequently contains large amounts of subretinal blood. This can often be demonstrated by ultrasound or magnetic resonance imaging showing layered fluid in the subretinal space. These eyes have a poor prognosis.

Ultrasonographic evaluations can be performed when the retrolenticular tissue is opaque or the funnel of retinal detachment is closed and the entire configuration of the retinal detachment cannot be determined clinically. In this circumstance, ultrasound is used to define the configuration of the detachment or composition of the subretinal fluid. If a preoperative ultrasound is needed, the offset water bath ultrasound placed directly on the eye, with the patient either under anesthesia or sedation, seems to be the most helpful. However, because of the convolutions of the redundant retinal architecture and solid and liquid conformations of the vitreous, we frequently find ultrasound to be of little value, though it may allow one to find a surgical space for access.

Surgical Therapy

The choice of surgical techniques depends on the stage of ROP and the specific features of each case.

Scleral Buckling

Scleral buckling has been suggested for stage 4 ROP. In two series it has been demonstrated that scleral buckling for stage 4 eyes has a success rate of 66–70% for stage 4A and 67% for stage 4B retinal detachment.[29,81] Encirclement is performed with or without drainage of subretinal fluid. If subretinal fluid is not drained, a paracentesis must be performed. Although scleral buckling has not to date been studied in a randomized, prospective clinical trial, data from the Cryotherapy for Retinopathy of Prematurity study suggest

that if stage 4 retinal detachment involves eight of 34 ROP sectors of the retina, there is an 88% chance of progression to stage 5 ROP.[82] It would seem from these data that scleral buckling would be a reasonable alternative in a predominantly effusive stage 4 ROP retinal detachment. With the use of laser, predominantly effusive eyes are rare.

Division of the encircling scleral buckling material should be performed after reattachment of the retina, usually at about 3 months after scleral surgery. Originally we believed this was to allow growth of the eye, but have found the buckle can induce a great deal of anisometropia (5–9 diopters). This anisometropia is reduced when the scleral buckle is divided. With the advent of lens-sparing vitrectomy (LSV), we rarely perform scleral buckling for nonrhegmatogenous retinal detachment.

Lens-Sparing Vitrectomy for Stage 4A ROP

In addition to the changes in the appearance of the eyes requiring peripheral ablation over the last 15 years, the appearance of retinal detachment following laser treatment has also changed. With less effusion from laser treatment than cryotherapy, there is less blood in the subretinal space and the eyes are vascularly quieter at an earlier time, allowing vitreous intervention in a vascularly quiet eye where the macula has not detached (stage 4A). This basic principle of retinal detachment repair "that a macula-on retinal detachment is an urgent operation" is also true in ROP. The natural history part of the CRYO-ROP study showed that a child with an 8-sector 4A ROP detachment at their due date (40 weeks PMA) had a high risk of going on to an unfavorable outcome or total retinal detachment (stage 5).[82] Two studies have shown 90% or better anatomic success rates with LSV.[83,84]

The development of the infusion light pipe, miniaturized contact lenses, which can be used on the anterior surface of the eye, and the binocular indirect ophthalmoscopy (BIOM) non-contact system, allowing wide-angle viewing in children with a smaller anterior segment, for visualization in the phakic state are perhaps the most significant changes in pediatric vitreoretinal surgery in the recent past (Fig. 118.11). A wide-view infusion light pipe used with the

BIOM allows visualization and peripheral dissection without the need for scleral indentation, a practice that can create retinal tears in children with redundant retina. These developments also allow us to deal with the tractional detachment of the posterior pole, leaving the lens in position (Fig. 118.12). Children having this type of procedure can retain clear lenses for many years. Current follow-up suggests that lenses can remain clear at least 10–15 years.[85–87]

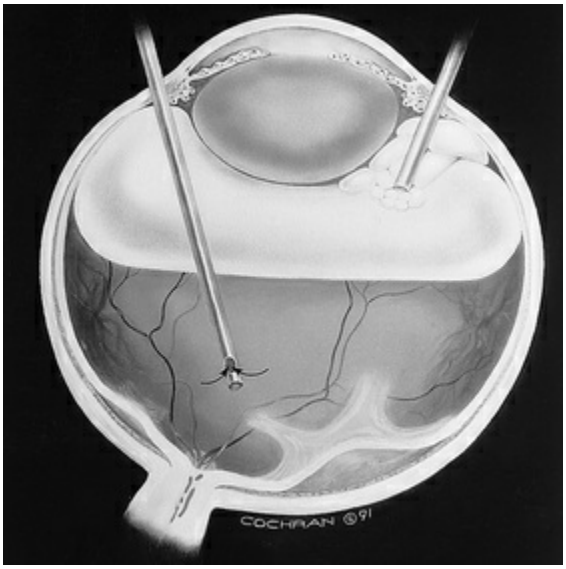

FIG. 118.11 Infusion light pipe at the time of delivering air into the eye during phakic vitrectomy in an infant.

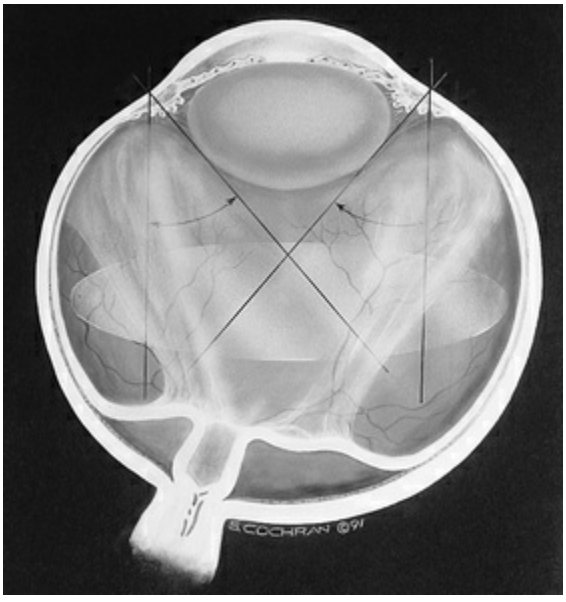

FIG. 118.12 Entry sites and the technique enabling dissection of the entire posterior pole.

In addition, the visual rehabilitation in these children, without the complications of aphakia, allows us to treat unilateral tractional detachment, as well as bilateral tractional detachments, more effectively. This greatly reduces the refractive rehabilitation and increases the cooperation of the patient and family with conventional forms of refractive and amblyopia therapy. Children with this level of tractional detachment and ROP can achieve levels of vision in the 20/100 to 20/60 level, assuming the central nervous system is able to process visual information.[82,88] Children who are operated with a true 4A retinal detachment can achieve visual acuity of 20/20.[84]

Lens-Sparing or Non-Lens-Sparing Vitrectomy for Stage 4B ROP

Results for 4B ROP detachments can also be broken down anatomically and visually. A total of 76% of eyes reattached part or all of the retina. Some 15% achieved 20/60–20/300 vision; 30% achieved 20/60–20/800 vision; 48% achieved 20/60–20/1900 (ambulatory) vision; and 72% of eyes achieved 20/60-LP vision. A total of 28% of eyes had no light perception (NLP), despite surgery.[82] These results compare favorably with the natural history.

Lensectomy, Vitrectomy, and Membrane Peeling for Stage 5 ROP

Perhaps the most important consideration in dealing with surgical therapy of stage 5 ROP is recognition of the configuration of retinal detachment. The funnel is defined as the retina from the ridge to the optic nerve area. Many years ago, it was known that retinal detachment of stage 5 has three basic configurations:

- An open central funnel (Fig. 118.13)

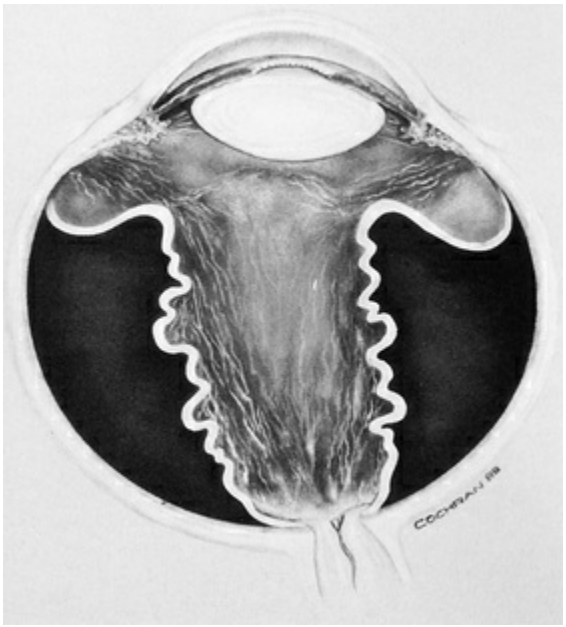

FIG. 118.13 An open funnel retinal detachment with right folding of anterior retinal surface.

- A partially closed central funnel (Fig. 118.14)

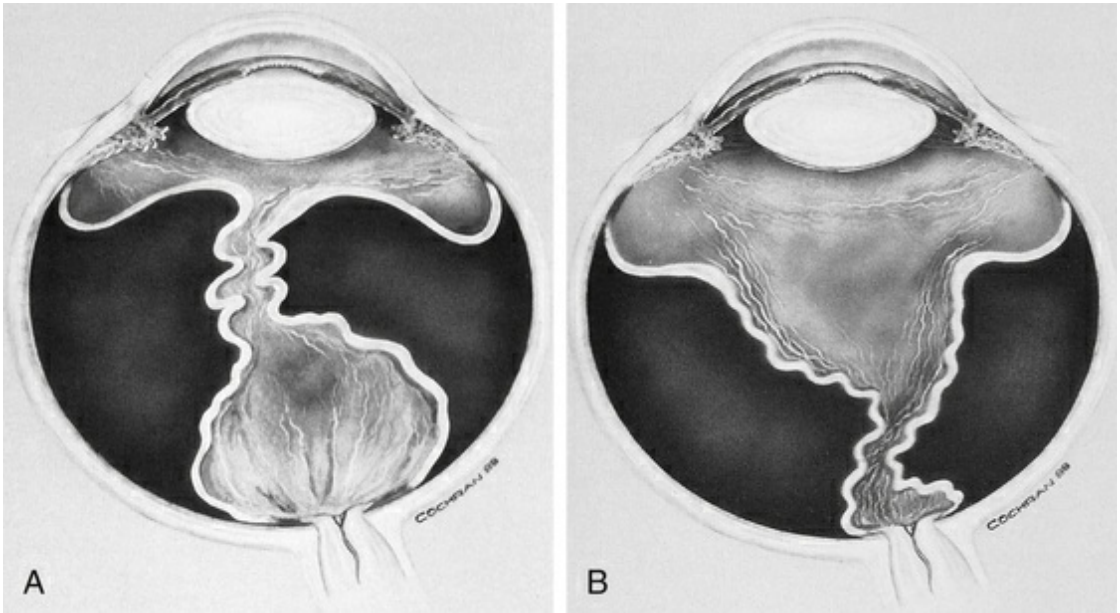

FIG. 118.14 (A) Partially closed retinal detachment with a narrow anterior open posterior configuration. (B) Partially closed retinal detachment, narrow posteriorly. This is the more commonly occurring partially closed configuration.

- A totally closed central funnel[19,80] (Fig. 118.15).

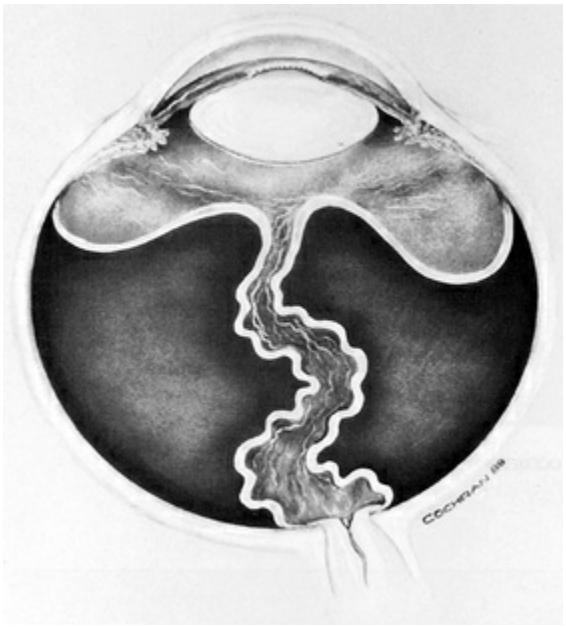

FIG. 118.15 Closed funnel configuration of retinal detachment.

Detachments in eyes with stage 5 have many features not seen in other retinal detachments. The configuration of the retinal detachment can vary greatly between different quadrants of the same eye. The peripheral retinal trough can be shallow or deep (Fig. 118.16). Depending on differential contraction along the ridge, the funnel can be closed tightly centrally or can be eccentrically displaced toward the periphery in a crescent pattern (Fig. 118.17). It is also common to see the retina posterior to the ridge detached in a spiral configuration caused by differential, circumferential traction (Fig. 118.18). This causes confusion to the novice surgeon, who believes that radial division of epiretinal tissue is safe. Radial division when a spiral configuration is present is dangerous, and it is important to follow the spiral back toward the optic nerve.

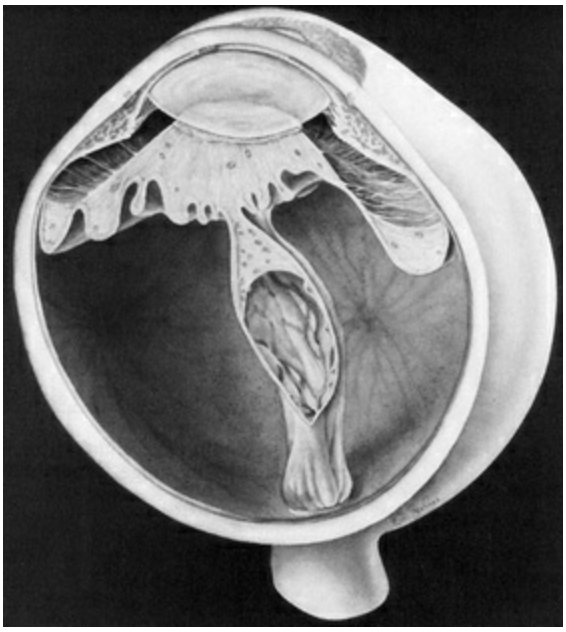

FIG. 118.16 In the same eye the peripheral trough can have a variety of depths. (Courtesy of Eugene de Juan, MD.)

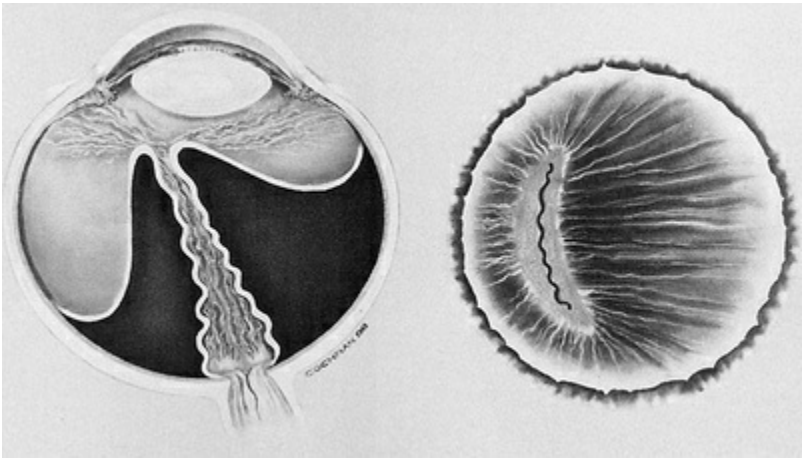

FIG. 118.17 Anterior crescentic appearance that occurs when the ridge is fixed in one area while other areas of the ridge are movable.

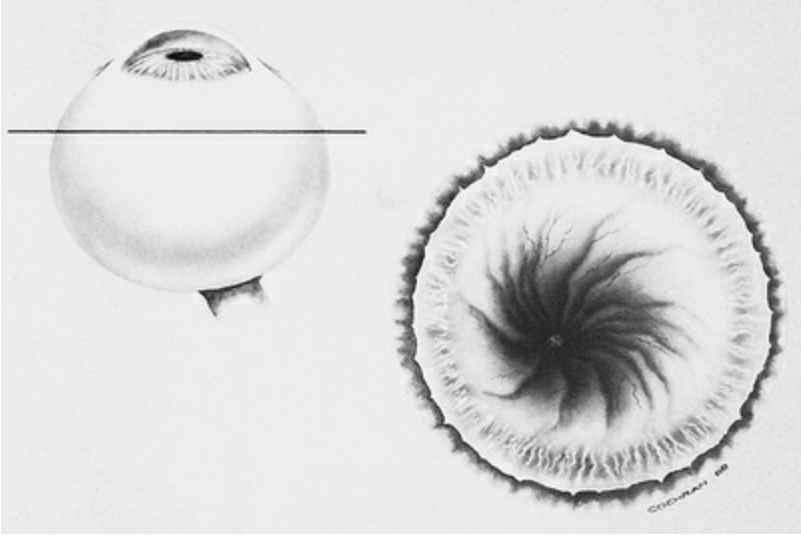

FIG. 118.18 Spiral form of retinal detachment. If the vitreous organization was uniform and the peripheral trough of equal depth for 360°, the retinal ridge would "purse-string," leading to symmetric, radially folded retinal detachment. Most of the time the amount of vitreous organization differs along its retinal surface and can result in a spiral easily seen here in this widely open funnel. However, these can be difficult to recognize as the funnel narrows or if only part of the retina is involved in this differential circumferential traction.

At the posterior pole, the retina most often shows dragging across the optic nerve head, causing a triple layer of retinal tissue (Fig. 118.19). This often interferes with a good view of the optic nerve. Thorough and careful dissection should be carried out to the posterior pole. This configuration can have an exaggerated form of retinal detachment with a large fold of retina dragged over the disc, often in the horizontal meridian (Fig. 118.20). This fold of retina can be dragged along the top of a radial fold, continuing far anteriorly, which can leave large areas of usually avascular retina attached (Fig. 118.21). If the retina surrounding this fold is attached, it is impossible to flatten the retina; however, if the fold of detached retina is over detached retina, surgical flattening is possible.

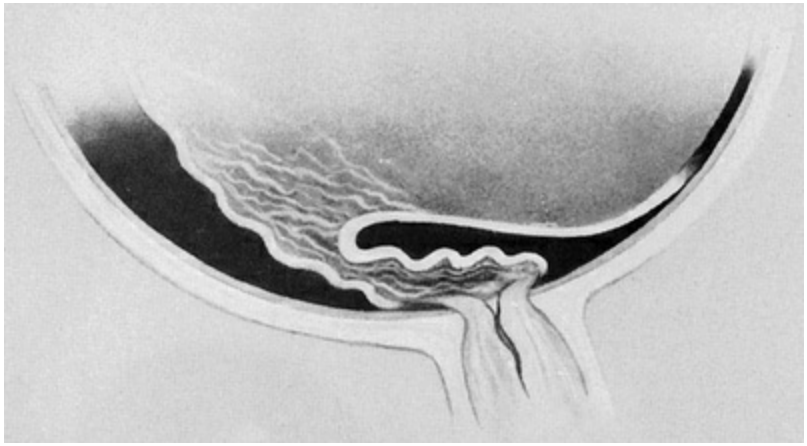

FIG. 118.19 Dragging of the retina across the disc, leaving in some areas a triple thickness of retina.

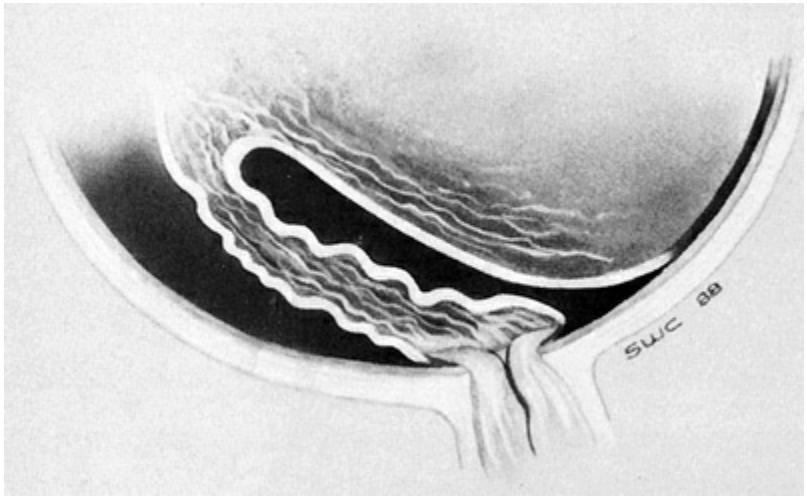

FIG. 118.20 The exaggerated dragging of the retina across the disc. The retina folded across the disc obscures the view of the optic nerve head.

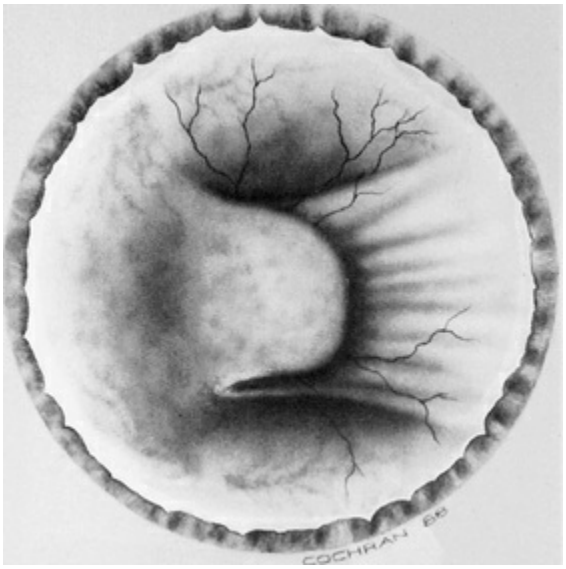

FIG. 118.21 Appearance of the exaggerated form of retinal fold when the fold is superimposed on a radially oriented area of retinal detachment. Naturally, the optic nerve head is not visible, and the seam between the apex of the fold and the radial detachment may be obscured by organized vitreous collagen. A clue to the edges of the fold is the emergence of retinal vessels from beneath the fold and the absence of retinal vessels along the anterior surface of the fold. This configuration may occur when the 360° ridge has several clock-hours very posterior in zone I or zone II and other clock-hours with the ridge are very anterior to zone II or zone III.

Enzymatic Manipulation of the Vitreoretinal Junction

A subset of pediatric vitreoretinal surgery requires successful peeling of preretinal membranes or the posterior hyaloid to achieve repair. The vitreoretinal adhesion is mediated in part by laminin and fibronectin.[89] Autologous plasmin enzyme (APE) cleaves both laminin and fibronectin and produces vitreous liquefaction and posterior vitreous detachment in adult eyes after intravitreal injection.[90] Plasmin enzyme may facilitate the removal of such membranes and reduce the risk of creating an iatrogenic retinal break during membrane peeling.[91,92] In young children who cannot tolerate an intravitreal injection in the clinic, APE is injected into the

vitreous cavity approximately 30 min before the start of surgery.

Jetrea (Thrombogenics Inc., Leuven, Belgium) is a truncated recombinant form of plasmin, which retains the enzymatic activity of autologous plasmin.[93] Clinical trials in adults have shown that microplasmin can safely relieve vitreoretinal traction, and a clinical trial using microplasmin in pediatric vitreoretinal surgical cases is ongoing.[94]

Surgical Approach

The surgical techniques used in stage 5 are confined to closed lensectomy, pars plicata vitrectomy (with membrane peeling accompanied occasionally by external drainage of subretinal fluid), and rarely, scleral buckling. Open-sky vitrectomy with intracapsular lensectomy and membrane peeling has also been used. The bulk of our experience has been in closed vitrectomy, and we reserve the open-sky vitrectomy for those eyes in which the anterior segment is severely clouded and will not allow the use of the closed vitrectomy technique. Open-sky vitrectomy has the advantage of allowing two-handed dissection through the large anterior incision, and it allows surgery in eyes with clouded corneas.[95] However, operating in an unpressurized eye has higher risk of hemorrhagic choroidal detachments and bleeding during dissection of tissues.

The technique we prefer in mild to moderately clouded corneas is a two- to three-staged approach. During the first surgery, we perform a lensectomy and careful removal of the lens capsule. An iridectomy is also performed if there is severe anteriorization of ocular structures. This is to avoid iris–retina adhesion, which is nearly impossible to dissect subsequently. During these maneuvers to debulk the anterior segment, a plane will be formed between the corneal endothelium and underlying iris and/or lens. Healon can be injected into the plane to gently dissect the adherent tissues from the cornea. After completion of the lensectomy, capsulectomy, and synechiolysis, the eye is closed.

The second stage of the surgery is scheduled for several weeks subsequently, depending on the degree of corneal clouding. Not only does this allow the cornea to clear, but the retina moves

posteriorly after release of the traction from the lensectomy. During the second stage, we initiate plaque dissection under the improved view. Rarely, a third staged surgery may be needed to complete the membrane dissection for severe cases. The initial membrane dissection makes the retina more mobile, and the subretinal fluid resorbs between the second and third surgeries, which can allow visualization of more counter-traction for a safer third surgery.

Ab Interno Incision

A modification of the lens-sparing vitrectomy technique, called an "ab interno incision," is used in infants in which the surgical entry space between the lens and the retina is too small for current vitrectomy instrumentation.[86,96] In circumstances where retinal folds, organized vitreous, and/or fibrotic tissue are in close approximation to the lens for several clock-hours, standard lens-sparing entry into the eye may not be possible. In this setting, an ab interno incision is used. With this technique, once the sclera is entered, the microvitreoretinal (MVR) blade is first directed carefully posterior and then inserted into the space or tissue between the retina and posterior lens capsule (Figs. 118.22A–C). Once the MVR blade is located between the posterior lens capsule and retinal tissue, anterior retinal traction is relieved and a posterior relaxation of the retina is immediately apparent. The incision can be extended for many clock-hours by sweeping in the surgical space parallel to the lens capsule using the sclerotomy as a pivot point or by sliding the blade like a saw to release any tractional vectors (Figs. 118.22A,D). Damage to the retina or lens is a possible complication of this technique, and care should be taken to avoid violating the lens equator or causing an unintentional retinal break. This provides standard vitrectomy instrumentation a safe entry to complete the posterior vitrectomy (Figs. 118.22A,E–F) and allows for dissection along the retinal surface once more surgical space is created.

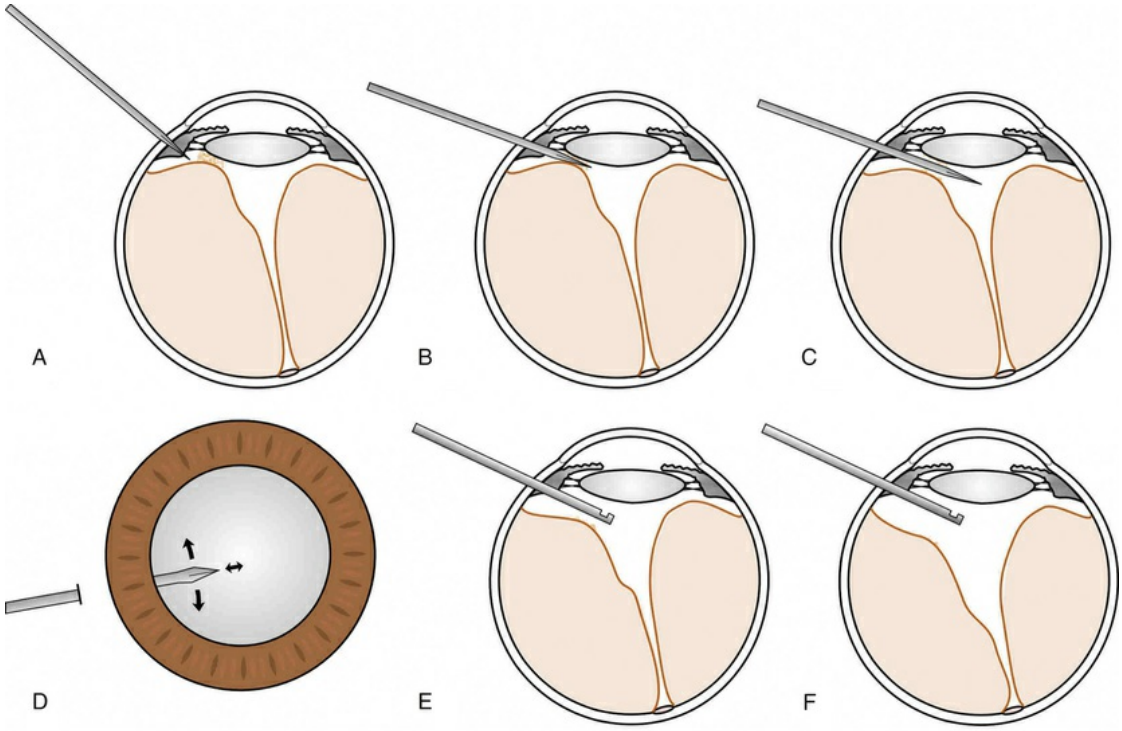

FIG. 118.22 (A) The microvitreoretinal blade is inserted through the pars plicata with great care. (B) The microvitreoretinal blade is advanced into the space between the lens capsule and retinal surface, cutting through any tissue between the retina and the lens. (C) The microvitreoretinal blade is advanced further into the space between the lens capsule and retina, and as anterior retinal traction is relieved, the posterior relaxation of the retina is immediately apparent. (D) The ab interno incision can be extended by sweeping parallel to the lens capsule or by sliding the blade like a saw to release any additional tractional vectors. (E) Standard vitrectomy instrumentation is inserted into the space between the lens capsule and retina. (F) As the vitrectomy proceeds, further relaxation of the retina can be observed, and dissection along the retinal surface can be performed.

Techniques for Closed Lensectomy Pars Plicata Vitrectomy

Because the infant's eye does not have a pars plana, entry into the eye in the closed vitrectomy is through the pars plicata, iris root, or limbus.[27,80,97,98] After entry into the eye, a complete lensectomy is performed, including capsular removal in eyes with open funnel

configuration. The main reason for failure caused by reproliferation and redetachment often can be traced to incomplete removal of lens epithelium. A two-handed cross action opening of the retrolenticular tissue is performed with two disposable no. 26 needles. This causes little peripheral traction. The resulting central vertical slit in the membrane is then extended using intraocular scissors with continuous Healon infusion (Fig. 118.23). Then two-handed dissection with forceps and scissors or spatula lamellar dissection is used to divide the retrolenticular tissue.[99]

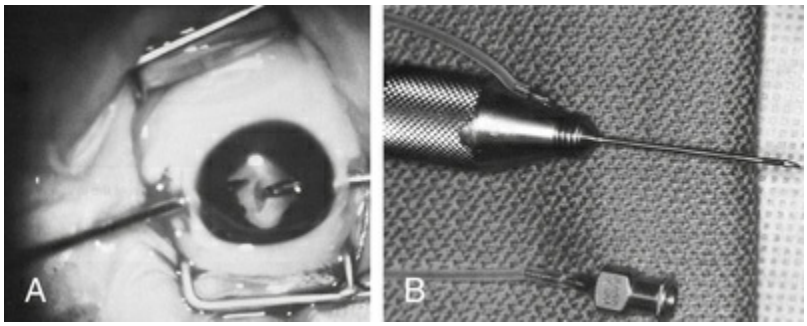

FIG. 118.23 (A) Intraocular scissors being used to expand the vertical slit in the retrolenticular membrane under Healon. (B) The membrane peeler cutter set-up to allow continuous infusion of Healon.

After lensectomy, if the retina is continually pushed into the center of the eye, a fluid–Healon exchange is performed. After the center of the funnel is opened, dissection is continued posteriorly under Healon if the retina is pushed toward the center of the eye. The Healon is added under low pressure to avoid forcing the retina open. This opening of the funnel then allows two-handed dissection of the posterior pole. As previously described, the cells that organize the vitreous collagen and result in traction detachment probably come from the ridge and disc; therefore, careful dissection of tissue at the disc is important.

Because our surgical goal is to flatten the posterior pole, this is one of the most important areas for dissection. Often, the smaller folds across the optic nerve are left alone. After the central funnel of detached retina is opened, the anterior peripheral trough is approached. Two-handed dissection is used to delaminate this tissue at the ridge where possible. Some ridge tissue cannot be

dissected (Fig. 118.24).

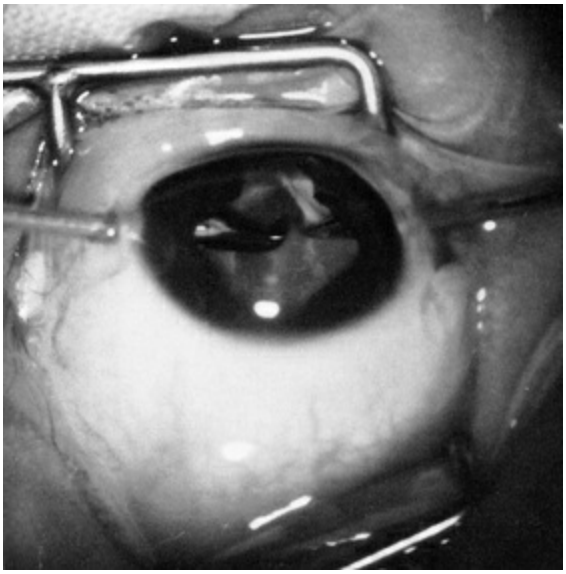

FIG. 118.24 Two-hand dissection technique to allow controlled delamination at the ridge.

After removal of as much proliferative tissue as possible, a Healon–fluid exchange can be performed. Next a fluid–air exchange is performed. If the retina is freely movable, the base of the peripheral trough can be seen, and the fluid is thick and unlikely to reabsorb, then drainage of subretinal fluid is performed. Though sometimes there may be postoperative pressure rises, we often leave Healon as a tamponade.

After surgery the child is placed face down for 24 hours. This is done to flatten the posterior retina quickly and displace the subretinal fluid. The subretinal fluid is often very viscous and contains cholesterol crystals. The bulk of subretinal fluid reabsorbs in 2–4 months; some eyes may still reabsorb subretinal fluid/blood for months and years. As soon as the posterior retina flattens, the child is given spectacles and begins vision training. When both open-sky and closed vitrectomy are used, the anatomic success rate has been 50% for reattachment of zone I of the retina in eyes with stage 5 ROP without peripheral ablation. The reattachment rates vary from 60% to 70% reattachment of zone I with open funnel retinal detachments to 26% reattachment rates for closed funnel detachments (Hirose, pers. comm.).[80,91,100,101] We reserve reoperation

for eyes that have shown visual improvement and later develop redetachment of, or that obscures, the posterior pole.

The long-term anatomic and visual results with a nearly 4-year follow-up showed that appropriate intervention with peripheral ablation and 4B/5 retinal detachment intervention yielded 76% of eyes with attachment of the posterior pole and 15% of eyes with 20/300–20/60 vision; 30% of eyes with 20/800 to 20/60 vision; 48% of eyes with 20/1900–20/60 vision; and 72% of eyes with light perception or better. Some 30% required more than one operation, other than peripheral ablation.[82] With timely laser ablation (success rate 90%) and 4A lens-sparing vitrectomy, 90% anatomic success and function as good as 20/20 can be achieved. This results in only 1% of eyes with poor outcomes. The visual results of stage 5 ROP suggest that timing of intervention is important. Intervening as early as possible after retinal detachment in a vascularly inactive eye is more favorable than waiting for spontaneous vascular involution. The belief is that this period of visual deprivation may be irretrievable in these young infants.[101] The ideal time is when the eye is vascularly quiet and the macula is still attached (stage 4A).

Although ROP remains a challenging form of pediatric retinal detachment, many advances have been made in recent years including (1) the earlier use of laser photocoagulation to achieve peripheral ablation with less in the way of an inflammatory response; (2) the added therapy of lens-sparing vitrectomy techniques, which have given the surgeon a very effective way of dealing with traction retinal detachments involving the posterior pole; and (3) data emerging in regard to the use of vitrectomy for 4A is most encouraging and makes physiologic sense to avoid foveal detachment in the developing visual system. All three of these newer surgical approaches generate better anatomic and visual results.

Although much is left to be done worldwide, great strides have been made in the management of ROP.

References

1. Kinsey VE, Arnold HJ, Kalina RE, et al. PaO_2 levels and retrolental fibroplasia: a report of the cooperative study.

Pediatrics. 1977;60:655–668.
2. Patz A, Kinsey VE. Retrolental fibroplasia: the pediatrician's dilemma. *Pediatrics*. 1971;48:509–510.
3. Ashton N. The pathogenesis of retrolental fibroplasia. *Ophthalmology*. 1979;86:1695–1699.
4. Garner A, Ashton N. Vaso-obliteration and retrolental fibroplasia. *Proc R Soc Med*. 1971;64:774–777.
5. Hammer HM, Noble BA, Harcourt RB, et al. Ophthalmic findings in very low birth weight children. *Trans Ophthalmol Soc U K*. 1985;104:329–331.
6. Phelps DL, Rosenbaum AL. The role of tocopherol in oxygen-induced retinopathy: kitten model. *Pediatrics*. 1977;59:998–1005.
7. Flynn JT, O'Grady GE, Herrera J, et al. Retrolental fibroplasias. I. Clinical observations. *Arch Ophthalmol*. 1977;95:217–223.
8. Foos RY. Acute retrolental fibroplasia. *Graefes Arch Clin Exp Ophthalmol*. 1975;195:87–100.
9. Teske MP, Trese MT. Retinopathy of prematurity-like fundus and persistent hyperplastic primary vitreous associated with maternal cocaine use. *Am J Ophthalmol*. 1987;103:719–720.
10. Pierce EA, Foley ED, Smith LE. Regulation of vascular endothelial growth factor by oxygen in a model of retinopathy of prematurity. *Arch Ophthalmol*. 1996;114:1219–1228.
11. The Committee for the Classification of Retinopathy of Prematurity. An international classification of retinopathy of prematurity. *Arch Ophthalmol*. 1984;102:1130–1134.
12. International Committee for the Classification of Retinopathy of Prematurity. The International Classification of Retinopathy of Prematurity revisited. *Arch Ophthalmol*. 2005;123:991–999.
13. Scott KE, Kim DY, Wang L, et al. Telemedical diagnosis of retinopathy of prematurity intraphysician agreement between ophthalmoscopic examination and image-based interpretation. *Ophthalmology*. 2008;115:1222–1228.
14. Gschließer A, Stifter E, Neumayer T, et al. Inter-expert and

intra-expert agreement on the diagnosis and treatment of retinopathy of prematurity. *Am J Ophthalmol*. 2015;60(3):553–560.
15. Trese MT. Subjectivity in retinopathy of prematurity screening. *Am J Ophthalmol*. 2015;160:406–407.
16. Kretzer FL, Hittner HM, Godio LB. Ultrastructural evaluation of the retina in retinopathy of prematurity and correlations with vitamin E therapy. *Curr Eye Res*. 1984;3:881–882.
17. Terry TL. Fibroblastic overgrowth of persistent tunica vasculosa lentis in infants born prematurely. III. Studies in development and regression of hyaloid artery and tunica vasculosa lentis. *Am J Ophthalmol*. 1942;25:1409.
18. Hughes S, Yang H, Chan-Ling T. Vascularization of the human fetal retina: roles of vasculogenesis and angiogenesis. *Invest Ophthalmol Vis Sci*. 2000;41:1217–1228.
19. Machemer R. Description and pathogenesis of late stages of retinopathy of prematurity. *Ophthalmology*. 1985;92:1000–1004.
20. Ashton N, Cook C. Studies on developing retinal vessels. I. Influence of retinal detachment. *Br J Ophthalmol*. 1955;39:449–456.
21. Foos RY. Chronic retinopathy of prematurity. *Ophthalmology*. 1985;92:563–574.
22. Okamoto N, Tobe T, Hackett SF, et al. Transgenic mice with increased expression of vascular endothelial growth factor in the retina: a new model of intraretinal and subretinal neovascularization. *Am J Pathol*. 1997;151:281–291.
23. Garfinkel RA, Trese MT. Spontaneous resolution of retinal detachment in retinopathy of prematurity (unpublished).
24. Alon T, Hemo I, Itin A, et al. Vascular endothelial growth factor acts as a survival factor for newly formed retinal vessels and has implications for retinopathy of prematurity. *Nat Med*. 1995;1:1024–1028.
25. Mancini MA, Kennedy A, Frank RN, et al. A cell line derived from non-neoplastic human retinal cells. *Invest Ophthalmol Vis Sci*. 1987;28:S290.
26. Trese MT, Lin LR, Blumenkranz MS, et al. Cell biology of

retinopathy of prematurity. *Invest Ophthalmol Vis Sci*. 1987;28:S204.
27. Charles S. *Vitreous surgery for retinopathy of prematurity (ROP)*. [In: Syllabus: Retinopathy of Prematurity Conference, Washington, DC] 1981 [2:858–63].
28. Loh A, Hadziahmetovic M, Dunaief JL. Iron homeostasis and eye disease. *Biochim Biophys Acta*. 2009;1790:637–649.
29. Trese MT. Visual results and prognostic factors for vision following surgery for stage V retinopathy of prematurity. *Ophthalmology*. 1986;93:574–579.
30. Cryotherapy for Retinopathy of Prematurity Cooperative Group. Multicenter trial of cryotherapy for retinopathy of prematurity: preliminary results. *Arch Ophthalmol*. 1988;106:471–479.
31. Early Treatment for Retinopathy of Prematurity Cooperative Group. Revised indications for the treatment of retinopathy of prematurity. Results of the early treatment for retinopathy of prematurity randomized trial. *Arch Ophthalmol*. 2003;121:1684–1696.
32. The Photographic Screening for Retinopathy of Prematurity Cooperative Group. The Photographic Screening for Retinopathy of Prematurity Study: primary outcomes. *Retina*. 2008;28:S47–54.
33. Ells AL, Holmes JM, Astle WF, et al. Telemedicine approach to screening for severe retinopathy of prematurity – a pilot study. *Ophthalmology*. 2003;110:2113–2117.
34. Age-Related Eye Disease Study Research Group. Risk factors associated with age-related macular degeneration. A case–control study in the age-related eye disease study: Age-Related Eye Disease Study report number 3. *Ophthalmology*. 2000;107:2224–2232.
35. Azen SP, Irvine AR, Davis MD, et al. The validity and reliability of photographic documentation of proliferative vitreoretinopathy. *Ophthalmology*. 1989;96:352–357.
36. Pugh JA, Jacobson JM, Van Heuven WA, et al. Screening for diabetic retinopathy: the wide-angle retinal camera. *Diabetes Care*. 1993;16:889–895.
37. International Committee for the Classification of

Retinopathy of Prematurity. The International Classification of Retinopathy of Prematurity revisited. *Arch Ophthalmol*. 2005;123:991–999.
38. Morizane H. Initial sign and clinical course of the most severe form of acute proliferative retrolental fibroplasias (type 1) [in Japanese]. *Nippon Ganka Gakkai Zasshi*. 1976;80:54–61.
39. Quiram PA, Capone A Jr. Current understanding and management of retinopathy of prematurity. *Curr Opin Ophthalmol*. 2007;18:228–234.
40. Abbey AM, Besirli CG, Musch DC, et al. Evaluation of screening for retinopathy of prematurity by ROPtool or a lay reader. *Ophthalmology*. 2016;123:385–390.
41. Tasman W, Brown GC, Naidoff M, et al. Cryotherapy for active retinopathy of prematurity. *Graefes Arch Clin Exp Ophthalmol*. 1987;225:3–4.
42. Iverson DA, Trese MT, Orgel IK, et al. Laser photocoagulation for threshold retinopathy of prematurity (Letter). *Arch Ophthalmol*. 1991;109:1342.
43. Landers MB III, Toth CA, Semple HC, et al. Treatment of retinopathy of prematurity with argon laser photocoagulation. *Arch Ophthalmol*. 1992;110:44–47.
44. McNamara JA, Tasman WS, Brown GC, et al. Laser photocoagulation for stage 3 retinopathy of prematurity. *Ophthalmology*. 1991;98:576–580.
45. Hunter DG, Repka MX. Diode laser photocoagulation for threshold retinopathy of prematurity: a randomized study. *Ophthalmology*. 1993;100:238–244.
46. Gilbert WS, Quinn GE, Dobson V, et al. For the Multicenter Trial of Cryotherapy for Retinopathy of Prematurity Cooperative Group. *Arch Ophthalmol*. 1996;114:1085–1091.
47. Smith LEH. Through the eyes of a child: understanding retinopathy through ROP: the Friedenwald lecture. *Invest Ophthalmol Vis Sci*. 2008;49:5177–5182.
48. Chung EJ, Kim JH, Ahn HS, et al. Combination of laser photocoagulation and intravitreal bevacizumab (Avastin) for aggressive zone I retinopathy of prematurity. *Graefes Arch Clin Exp Ophthalmol*. 2007;245:1727–1730.

49. Travassos A, Teixeira S, Ferreira P, et al. Intravitreal bevacizumab in aggressive posterior retinopathy of prematurity. *Ophthalmic Surg Lasers Imaging*. 2007;38:233–237.
50. Quiroz-Mercado H, Martinez-Castellanos MA, Hernandez-Rojas ML, et al. Antiangiogenic therapy with intravitreal bevacizumab for retinopathy of prematurity. *Retina*. 2008;28(Suppl):S19–25.
51. Honda S, Hirabayashi H, Tsukahara Y, et al. Acute contraction of the proliferative membrane after intravitreal injection of bevacizumab for advanced retinopathy of prematurity. *Graefes Arch Clin Exp Ophthalmol*. 2008;246:1061–1063.
52. Lalwani GA, Berrocal AM, Murray TG, et al. Off-label use of intravitreal bevacizumab (Avastin) for salvage treatment in progressive threshold retinopathy of prematurity. *Retina*. 2008;28:S13–18 [Erratum, Retina 2009;29:127].
53. Kusaka S, Shima C, Wada K, et al. Efficacy of intravitreal injection of bevacizumab for severe retinopathy of prematurity: a pilot study. *Br J Ophthalmol*. 2008;92:1450–1455.
54. Mintz-Hittner HA, Kuffel RR Jr. Intravitreal injection of bevacizumab (Avastin) for treatment of stage 3 retinopathy of prematurity in zone I or posterior zone II. *Retina*. 2008;28:831–838 [Erratum, Retina 2008;28:1374].
55. Zepeda-Romero LC, Liera-Garcia JA, Gutiérrez-Padilla JA, et al. Paradoxical vascular-fibrotic reaction after intravitreal bevacizumab for retinopathy of prematurity. *Eye (Lond)*. 2010;24:931–933.
56. Law JC, Recchia FM, Morrison DG, et al. Intravitreal bevacizumab as adjunctive treatment for retinopathy of prematurity. *J AAPOS*. 2010;14:6–10.
57. Lee JY, Chae JB, Yang SJ, et al. Effects of intravitreal bevacizumab and laser in retinopathy of prematurity therapy on the development of peripheral retinal vessels. *Graefes Arch Clin Exp Ophthalmol*. 2010;248:1257–1262.
58. Altinsoy HI, Mutlu FM, Güngör R, et al. Combination of laser photocoagulation and intravitreal bevacizumab in

aggressive posterior retinopathy of prematurity. *Ophthalmic Surg Lasers Imaging*. 2010;9:1–5.
59. Dorta P, Kychenthal A. Treatment of type 1 retinopathy of prematurity with intravitreal bevacizumab (Avastin). *Retina*. 2010;30(Suppl):S24–31.
60. Ahmed AE, Channa R, Durrani J, et al. Early experience with intravitreal bevacizumab combined with laser treatment for retinopathy of prematurity. *Middle East Afr J Ophthalmol*. 2010;17:264–267.
61. Nazari H, Modarres M, Parvaresh MM, et al. Intravitreal bevacizumab in combination with laser therapy for the treatment of severe retinopathy of prematurity (ROP) associated with vitreous or retinal hemorrhage. *Graefes Arch Clin Exp Ophthalmol*. 2010;248:1713–1718.
62. Wu WC, Yeh PT, Chen SN, et al. Effects and complications of bevacizumab use in patients with retinopathy of prematurity: a multicenter study in Taiwan. *Ophthalmology*. 2011;118:176–183.
63. Castellanos MA, Schwartz S, Garcia-Aguirre G, et al. Short-term outcome after intravitreal ranibizumab injections for the treatment of retinopathy of prematurity. *Br J Ophthalmol*. 2013;97:816–819.
64. Wong RK, Hubschman S, Tsui I. Reactivation of retinopathy of prematurity after ranibizumab treatment. *Retina*. 2015;35:675–680.
65. Mintz-Hittner HA, Kennedy KA, Chuang AZ. for the BEAT-ROP Cooperative Group. Efficacy of intravitreal bevacizumab for stage 3+ retinopathy of prematurity. *N Engl J Med*. 2011;364:603–615 [66].
66. Sato T, Wada K, Arahori H, et al. Serum concentrations of bevacizumab (Avastin) and vascular endothelial growth factor in infants with retinopathy of prematurity. *Am J Ophthalmol*. 2012;153:327–333.
67. Kong L, Bhatt AR, Demny AB, et al. Pharmacokinetics of bevacizumab and its effects on serum VEGF and IGF-1 in infants with retinopathy of prematurity. *Invest Ophthalmol Vis Sci*. 2015;56:956–961.
68. Wu WC, Lien R, Liao PJ, et al. Serum levels of vascular

endothelial growth factor and related factors after intravitreal bevacizumab injection for retinopathy of prematurity. *JAMA Ophthalmol*. 2015;133:391–397.
69. Moshfeghi DM, Berrocal AM. Retinopathy of prematurity in the time of bevacizumab: incorporating the BEAT-ROP results into clinical practice. *Ophthalmology*. 2011;118:1227–1228.
70. Hu J, Blair MP, Shapiro MJ, et al. Reactivation of retinopathy of prematurity after bevacizumab injection. *Arch Ophthalmol*. 2012;130:1000–1006.
71. Lepore D, Quinn GE, Molle F, et al. Intravitreal bevacizumab versus laser treatment in type 1 retinopathy of prematurity: report on fluorescein angiographic findings. *Ophthalmology*. 2014;121:2212–2219.
72. Yonekawa Y, Thomas BJ, Chan RVP, et al. Retinal detachments after intravitreal anti-VEGF injections for retinopathy of prematurity. *Invest Ophthalmol Vis Sci*. 2015;56 [E-Abstract 982].
73. Tokunaga CC, Mitton KP, Dailey W, et al. Effects of anti-VEGF treatment on the recovery of the developing retinal following oxygen-induced retinopathy. *Invest Ophthalmol Vis Sci*. 2014;55:1884–1892.
74. Capone A Jr, Diaz-Rohena R, Sternberg P Jr, et al. Diode-laser photocoagulation for zone 1 threshold retinopathy of prematurity. *Am J Ophthalmol*. 1993;116:444–450.
75. Foroozan R, Connolly BP, Tasman WS. Outcomes after laser therapy for threshold retinopathy of prematurity. *Ophthalmology*. 2001;108:1644–1646.
76. Jalali S, Kesarwani S, Hussain A. Outcomes of a protocol-based management for zone 1 retinopathy of prematurity: the Indian Twin Cities ROP Screening Program report number 2. *Am J Ophthalmol*. 2011;151:719–724.
77. Vinekar A, Jayadev C, Mangalesh S, et al. Comparing the outcome of single versus multiple session laser photoablation of flat neovascularization in zone 1 aggressive posterior retinopathy of prematurity: a prospective randomized study. *Retina*. 2015;35(10):2130–2136.

78. *RAINBOW study: ranibizumab compared with laser therapy for the treatment of infants born prematurely with retinopathy of prematurity*. [Clinicaltrials.gov identifier: NCT02375971] https://clinicaltrials.gov/ct2/show/NCT02375971.
79. The STOP-ROP Multicenter Study Group. Supplemental therapeutic oxygen for prethreshold retinopathy of prematurity (STOP-ROP), a randomized, controlled trial. I. Primary outcomes. *Pediatrics*. 2000;105:295–310.
80. Trese MT. Surgical results of stage V retrolental fibroplasia and timing of surgical repair. *Ophthalmology*. 1984;91:461–466.
81. Greven C, Tasman W. Scleral buckling in stages 4B and 5 retinopathy of prematurity. *Ophthalmology*. 1990;97:817–820.
82. Trese MT, Droste PJ. Long-term postoperative results of a consecutive series of stages 4 and 5 retinopathy of prematurity. *Ophthalmology*. 1998;105:992–997.
83. Capone A Jr, Trese MT. Lens-sparing vitreous surgery for tractional 4A retinopathy of prematurity retinal detachments. *Ophthalmology*. 2001;108:2058–2070.
84. Prenner JL, Capone A Jr, Trese MT. Visual outcomes after lens-sparing vitrectomy for stage 4A retinopathy of prematurity. *Ophthalmology*. 2004;111:2271–2273.
85. Maguire AM, Trese MT. Lens-sparing vitreoretinal surgery in infants. *Arch Ophthalmol*. 1992;110:284–286.
86. Thomas BJ, Yonekawa Y, Trese MT. Complete resolution of large retinal fold with lens contact after lens-sparing vitrectomy for retinopathy of prematurity: 15-year follow up. *Retin Cases Brief Rep*. 2016;10(1):93–95.
87. Nudleman E, Robinson J, Rao P, et al. Long-term outcomes on lens clarity after lens-sparing vitrectomy for retinopathy of prematurity. *Ophthalmology*. 2015;122:755–759.
88. Maguire AM, Trese MT. Visual results of lens-sparing vitreoretinal surgery in infants. *J Pediatr Ophthalmol Strabismus*. 1993;30:28–32.
89. Kohno T, Sorgente N, Ishibashi T, et al. Immunofluorescent studies of fibronectin and laminin in the human eye. *Invest Ophthalmol Vis Sci*. 1987;28:506–514.
90. Liotta LA, Goldfarb RH, Brundage R, et al. Effect of

plasminogen activator (urokinase), plasmin, and thrombin on glycoprotein and collagenous components of basement membrane. *Cancer Res*. 1981;41(11 Pt 1):4629–4636.
91. Margherio AR, Margherio RR, Hartzer M, et al. Plasmin enzyme-assisted vitrectomy in traumatic pediatric macular holes. *Ophthalmology*. 1998;105:1617–1620.
92. Wu WC, Drenser KA, Trese MT, et al. Pediatric traumatic macular hole: results of autologous plasmin enzyme-assisted vitrectomy. *Am J Ophthalmol*. 2007;144:668–672.
93. Gandorfer A, Rohleder M, Sethi C, et al. Posterior vitreous detachment induced by microplasmin. *Invest Ophthalmol Vis Sci*. 2004;45:641–647.
94. Williams GA. *Results from the MIVI III (Microplasmin for Vitreous Injection) trial*. [Hong Kong: World Ophthalmology Congress] 2008.
95. Tasman W, Borrone RN, Bolling J. Open-sky vitrectomy for total retinal detachment in retinopathy of prematurity. *Ophthalmology*. 1987;94:449–452.
96. Trese MT, Capone A Jr. Surgical approaches to infant and childhood retinal diseases: invasive methods. Hartnett ME, Trese MT, Capone A Jr, et al. *Pediatric retina*. Lippincott Williams & Williams: Philadelphia; 2005:359–364.
97. Lightfoot D, Irvine AR. Vitrectomy in infants and children with retinal detachments caused by cicatricial retrolental fibroplasia. *Am J Ophthalmol*. 1982;94:305–312.
98. Lin LR, Hartzer M, Blumenkranz M, et al. Hypo-cellular gel contraction: ultrastructural studies on human epiretinal membranes – comparison with experimentally contracted gels. *Invest Ophthalmol Vis Sci*. 1987;28:S207.
99. Trese MT. Two-hand dissection technique during closed vitrectomy for retinopathy of prematurity. *Am J Ophthalmol*. 1986;101:251–252.
100. Machemer R. Closed vitrectomy for severe retrolental fibroplasia in the infant. *Ophthalmology*. 1983;90:436–441.
101. Trese MT. Surgical therapy for stage V retinopathy of prematurity: a two-step approach. *Graefes Arch Clin Exp Ophthalmol*. 1987;225:266–268.

119

Surgery for Pediatric Vitreoretinal Disorders

Petra Meier, Peter Wiedemann

General Aspects

Development of the Child's Eye and

Surgical Consequences

The development of spatial vision and binocular fusion (sensitive period) begins in the human infant at the age of 3–4 months.[1] A reduction in the visual acuity of one or both eyes with morphologic intactness is termed amblyopia. The child's age at exposure to an amblyopia-inducing condition is the most important determinant for its development. Children up to 8 years of age can develop an amblyopia; development later is rare. The therapy of choice for all forms of amblyopia is an appropriate occlusion therapy which sometimes must be continued until the child is 12 or 13 years old in order to avoid a recurrence.

Untreated anisometropia resulting from vitreoretinal operations induces amblyopia, especially in small children (Table 119.1).[2] Whereas a refractive error averaging −2.75 diopters (D) is induced by an encircling scleral buckle in the adult,[3] the anisomyopia resulting from a cerclage may be greater in pediatric eyes. Myopia occurs as a result of the axial elongation induced by the encircling band, and this has a more pronounced effect on refraction due to the very short axial length of the infant eye. Furthermore, buckling surgery with a cerclage induces forward displacement of the lens, which can cause severe myopia in the infant lens with its relatively high refractivity.[4] Still, this refractive change is generally less than 6 D and amblyopia is rarely manifest, since patients still have sharp near vision.[5] These patients can usually be fitted with spectacles. High axial myopia of −11 to −15 D following buckling surgery in infants with retinopathy of prematurity (ROP) is more difficult to treat. Therefore, once successful reattachment of the retina has been achieved, the encircling band can be cut, thus reducing the refractive error to values around −5 D.[4]

TABLE 119.1

Deprivation Caused by Vitreoretinal Disease[2]

Stimulus Deprivation	Stimulus Deprivation and Suppression
Bilateral deprivation: amblyopia due to media opacity of the same severity, e.g., bilateral congenital cataract or bilateral vitreous hemorrhage	1.All predominantly unilateral stimulus deprivations or bilaterally differing stimulus deprivations
	2.Relative amblyopia: congenital or early manifestation of defects in the foveal region
	3.Uncorrected anisometropia because of blurred

	image and aniseikonia (e.g., anisomyopia due to cerclage anisohyperopia in silicone oil tamponade, cycloplegic eye drops)
	4.Acquired medium opacity

Source: Hanse[2]

A silicone oil tamponade also increases the risk of amblyopia development, since hyperopic refractive correction of +5 to +6 D is required regardless of the lens status. If pediatric eyes filled with silicone oil are not optically corrected, the anisohyperopia causes severe amblyopia. Another result is pronounced refractive anisometropia. The first-line corrective therapy for eyes filled with silicone oil or aphakic eyes is a contact lens. Extended-wear contact lenses are suitable for very young children. Pathologic structures affecting vision (e.g., cataracta congenita, persistent hyperplastic primary vitreous, vitreous hemorrhage) and resulting in amblyopia ex anopsia require treatment. Attention must also be paid to "relative amblyopia," which may be superimposed on an organic lesion (e.g., macular scar). The danger of monocular deprivation must be considered in prolonged postoperative atropinization of the operated eye.

The most obvious and important anatomic consideration in pediatric retinal surgery is the relatively smaller size of the child's globe and orbit compared with that of the adult (Table 119.2). At birth, the average axial eye length is 17.5 mm; which is 70% of the axial length of an adult eye. In the first year of life eyeball length increases by nearly 3.5 mm. From age 3–14, the eye grows very slowly; an average of 0.1 mm/year.[6] The average horizontal and vertical corneal diameters are 9.8 ± 0.33/10.4 ± 0.35 mm (newborn boys) and 10.1±0.33/10.7 ± 0.29 mm (newborn girls). By age 7, the cornea has an average diameter of 11.7 mm.[7] In the newborn, the anterior segment already comprises 80% of its final area, while the surface of the posterior segment comprises only 20% of an adult eye; in the first 6 months of life, the posterior segment surface increases by 50%. The lens of the newborn is spherical and is relatively thicker than the adult lens. As the lens flattens, the power of the lens is reduced by approximately 8 D; in the first 2 years, it is reduced by approximately 11.5 D, and it reaches adult values between 7 and 10 years.[8] Since the cornea flattens, its power is also reduced: in the first 6 weeks of life, the power is reduced from 51 D

to 44 D.[9]

TABLE 119.2
Anatomic Changes With Age

Age	Newborn	1–2 Years	2–3 Years	Young Adult
Globe length (mm)	16.8	20.2	21.4	23.6
Corneal power (D)	51.2	44.9	44.1	43.5
Lens power (D)	34.4	26.4	23.0	18.8
Refractive error	+0.4 ± 1.5	+0.3 ± 0.6	+0.5 ± 0.6	−0.5 ± 1.5

Reproduced with permission from Hairston RJ, Maguire AM, Vitale S, et al. Morphometric analysis of pars plana development in humans. Retina 1997;17:135–8.

A vision-dependent feedback mechanism is necessary for the development of emmetropia.[10] It is assumed that various forms of stimulus deprivation induce a myopic shift during development.[11] Dense hemorrhages persisting in the neonatal vitreous for 4 weeks or longer appear to cause axial myopia and severe amblyopia. Surgical intervention before this time should be considered to avert deprivation amblyopia and to retard axial myopia.[12]

The ciliary body of the eye is divided into the pars plicata ciliaris and the pars plana ciliaris. The pars plicata of the mature newborn is nearly adult in size, whilst the pars plana is relatively small (Table 119.3).[13,14] The pars plana of mature newborns measures 1.6–2.0 mm.[6]

TABLE 119.3
Developmental Morphology of the Pars Plana and Pars Plicata in the Postnatal Phase

	Age (months)				
	<6	6–12	12–24	24–72	Adult
Ciliary Body (mm)					
Nasal	3.06	3.54	3.87	4.28	4.79
Temporal	3.31	3.85	4.14	4.94	5.76
Pars Plana (mm)					
Nasal	2.23	2.69	2.98	3.25	3.64
Temporal	2.48	2.96	3.15	3.85	4.32

Reproduced with permission from Aiello AL, Tran VT, Rao NA. Postnatal development of the ciliary body and pars plana. A morphometric study in childhood. Arch Ophthalmol 1992;110:802–5.

The anterior–posterior extension of the pars plana begins in the

postnatal phase (Fig. 119.1). In a 6-month-old infant, the pars plana is >3.0 mm.[6,14] This means that in infants younger than 6 months, the pars plana width is <3.0 mm. However, the extension of the entire ciliary body is quite variable in individual eyes; its total extension in the age group 24 months ranges from 3.75 to 5.5 mm. A total of 75% of the final length of the ciliary body at adulthood is reached by 24 months.[14] A positive correlation between the anteroposterior diameter of the eye and the distance from the sclerocorneal limbus to the ora serrata was demonstrated in the four meridians.[13]

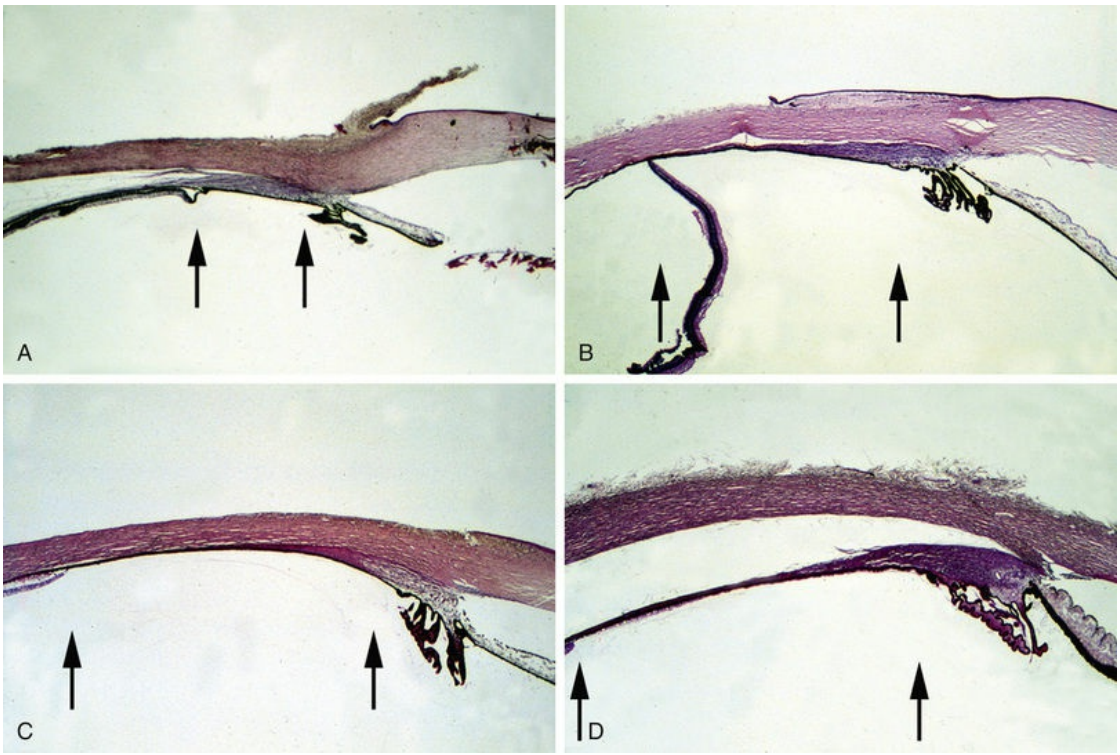

FIG. 119.1 Histologic section of the ciliary body shows the width of the pars plana in: (A) the eye of a mature newborn; (B) in a 6-month-old infant; (C) in a 12-month old child; (D) in a 24-year-old man (hematoxylin and eosin, original magnification ×32).

The results of the morphometric investigations are of great importance for the choice of the vitreoretinal-surgical entrance. The anterior-posterior expansion of the ciliary body corresponds approximately to the distance from the corneoscleral limbus measured externally (in millimeters). For an accurate external

determination of the location of the ora serrata, 0.3–0.4 mm must be added to the measured distance starting from the corneoscleral limbus for the values of the ciliary body extension.[14] Accordingly, in babies, one must select a pars plicata entrance for a vitrectomy. Only then is it ensured that the retina will not be damaged. The disadvantage of this entrance is the direct proximity of the lens, and therefore manipulations and lens-saving operations are often not possible. Because of the relatively larger size of the lens in relation to the anterior segment in children compared with adults, special care is required if the eye is operated on without removing the lens. For a standard three-port vitrectomy, the width of the pars plana should be at least 3 mm[6] so that the earliest age that a pars plana approach can be selected is approximately a 1-year-old child. The measurements mentioned here are based exclusively on histologic slides, i.e., after appropriate fixation of the material. The real dimensions are therefore larger.

Scleral thickness is clearly age-dependent. During the first half-year of life the average scleral thickness is approximately 0.4 mm; by age 2, the thickness has doubled. After that age, the scleral thickness increases very slowly, and the tissue becomes stiffer with age.[15]

The vitreous body is avascular, transparent, and gel-like in consistency, and comprises 80% of the eyeball volume. The vitreous body is attached to the surrounding structures; a firm attachment exists within the area of the vitreous base, and Wiegers ligament forms the firm attachment between the soft crystalline lens and anterior vitreous. The posterior vitreous cortex (posterior vitreous hyaloid) is 100–110 μm thick and consists of closely packed collagen fibrils. In pediatric eyes the posterior vitreous cortex lies adjacent to the retinal surface. This structure is known as the vitreoretinal border region, the vitreoretinal junction, or the vitreoretinal interface. The vitreoretinal interface consists of the internal limiting membrane (ILM) and the posterior hyaloid. In the newborn, the vitreous body appears homogeneous with a fine radial stripe pattern. It is interspersed with so-called transvitreal channels. With increasing age vitreous strands develop, and in the adult eye these form typical concentrically arranged diaphragm-like condensations.[16] The secondary vitreous in the term infant without

ocular disease consists of a very dense collagenous gel. Some authors believe that in term infants there is no hyaluronic acid present until 4 years of age. There are, however, many diseases that are associated with a lack of densely formed vitreous (e.g., myopia, retinitis pigmentosa, ROP, familial exudative vitreoretinopathy [FEVR], Goldmann–Favre disease, and congenital retinoschisis). In pediatric eyes, the attachment between the vitreous cortex and retina is very firm. Formed vitreous and increased scarring seem to be correlated. It is believed that children develop proliferative vitreoretinopathy (PVR) more frequently than adults.

Examination of Pediatric Patients

A child is often referred for one of the following diagnoses: leukocoria, no red reflex, unexplained strabismus, suspected retinal detachment, history of trauma, a change in visual function, or unexplained irritability. The most important component of the diagnostic evaluation of infantile vision loss is the exclusion of malignant tumors and systemic and heritable diseases. The examiner must often rely on physical examination techniques, as pediatric patients are frequently unable to verbalize their visual complaint and are often uncooperative during the examination. Therefore, the examination must be very thorough yet brief enough as to not lose the cooperation of the child. Observing the child interacting with his or her environment may be the most vital piece of information one can obtain. It is always critical to judge the apparent presence or absence of light perception. A past history of the child and family are important. The history should include birthweight; conceptual age (i.e., weeks from conception to the present); gestational age (i.e., weeks from conception to birth); the mother's due date; pregnancy data (e.g., illness, trauma, drug use, human immunodeficiency virus (HIV) status); and familial ocular and systemic diseases. The examination technique varies depending on the child's age. An infant younger than 1 year may be quite tolerant of being swaddled and undergoing scleral depression using an indirect ophthalmoscope and a 30-D lens. The decision to perform an examination under anesthesia should be made if additional information can be gained that can help with the child's

management.

Preoperative Treatment

All patients are given atropine eye drops twice for preoperative pupil dilation. The dosage of atropine (preoperative evening and morning) is determined depending on age (0–3 months: atropine 0.125%; 3–6 months: atropine 0.25%; 6–12 months: atropine 0.5%; >1 year: atropine 1%). The drops are first given in the preoperative evening. Directly before the operation tropicamide-phenylephrine eye drops (tropicamide 0.5%; phenylephrine 1%) three times every 15 minutes are given. If sufficient mydriasis cannot be achieved, healthy children can be given an injection of 0.1 cm^3 epinephrine (adrenaline: 1:10000) into the anterior chamber or applied over the vitrectomy infusion line after consultation with the anesthesiologist.

Surgical Considerations and Techniques

Cornea and Keratoprosthesis

If corneal edema develops during the vitrectomy, 50% glycerin can be used to dehydrate the cornea.

If the cornea does not clear up, the corneal epithelium is removed. If substantial Descemet folds arise, the anterior chamber is filled with Healon.

In the case of extensive corneal opacities with insufficient visibility of the fundus the employment of a temporary intraoperative keratoprosthesis can be considered in order to enable a vitreoretinal operation to be performed for internal reconstruction.

The placement of a temporary keratoprosthesis (e.g., Eckhardt keratoprosthesis, DORC) or Landers keratoprosthesis (Ocular instruments) allows a clear view for vitreoretinal surgery, which is then followed by a corneal transplant. Several retrospective studies have documented acceptable outcomes with combined surgery in adults, but only a few cases with children have been well documented.[17–19] The best outcome was of a 7-year-old boy whose

operation included usage of a keratoprosthesis followed by lensectomy, scleral buckling, vitrectomy, C_3F_8-fluid–gas exchange, and penetrating keratoplasty. At 10 months postoperatively, the best corrected visual acuity was 20/30.[17] In surgical summaries, 10 of 17 corneal grafts in children remained clear in the follow-up period, but in 16 eyes, visual acuity did not exceed finger counting. Phthisis occurred in about 40%.[17–19]

In general, the prognosis of keratoplasty in children is poorer than in adults. There is a greater risk of an immune reaction with development of neovascularization. Perforating keratoplasties in children following trauma have a poorer general prognosis, especially in cases of aphakia and after injuries involving the posterior segment of the eye as opposed to phakic eyes and after isolated injuries to the anterior segment. In a meta-analysis,[20] 55–100% of transplants were not opaque 1 year after keratoplasty in children.

Some special surgical aspects must be considered if using a keratoprosthesis on the pediatric eye. The decreased scleral rigidity relative to that of the adult eye means that children's eyes can collapse more easily with greater risk of intraocular tissue extrusion. It is therefore imperative that a Flieringa scleral fixation ring be sewn on. The keratoplasties heal relatively quickly, but since a higher rate of vascularization has been observed, it is advisable to use only interrupted sutures, which can be removed or replaced.

The corneal sutures in children can be removed much sooner than in adults. Removal should be performed within the time intervals specified in Table 119.4, in order to enable immediate provision of contact lenses, especially in aphakic eyes.[21]

TABLE 119.4

Recommendation for Removal of Corneal Suture by Age

Age	Removal of Corneal Suture
1–6 months	4–6 weeks
6–12 months	6–8 weeks
12–24 months	8–12 weeks
24–48 months	12–16 weeks
5–15 years	4–6 months

Reproduced with permission from Reidy JJ. Penetrating keratoplasty in infancy and early childhood. Curr Opin Ophthalmol 2001;12:258–61.

Lens Management

During the early period of pediatric vitreoretinal surgery, lensectomy was routinely performed. Later, favorable anatomic and functional outcomes were reported with lens-sparing vitrectomy in selected cases of infantile retinal detachment. The instruments are introduced into the eye via a pars plicata or pars plana approach, parallel to the visual axis to avoid lens injury. Many eyes show no evidence of postoperative cataract formation. Lens preservation may optimize optical rehabilitation and stimulation of the developing visual system.

In some cases, especially in eyes with a high risk of developing proliferative vitreoretinopathy, such as after severe open-globe injury and in uveitis, an intraocular lens (IOL) should not be implanted. Opacity of the remaining capsule fragments with optically disadvantageous postcataract membranes is usually inevitable. In addition, remnants of the lens capsule and the zonular fibers lead to development of synechiae with distortion of the pupil which is associated with a reduction in the visibility of the peripheral retina. Surgical treatment of retinal detachment is therefore impeded. For this reason, complete removal of the entire lens, including the complete capsule, should be planned for eyes with a high risk of developing PVR. In addition, one study demonstrated a significantly increased endophthalmitis risk if an intraocular lens was placed in eye immediately after open-globe injury.[22]

The risk of a severe intraocular fibrin reaction is one of the further drawbacks of intraocular lens implantation in children. After operation for a nontraumatic cataract in a pediatric eye, a significantly less pronounced fibrin reaction is observed after pars plana lensectomy than with the limbal approach that is necessary for optimal implantation of an intraocular lens.[23,24] In darkly pigmented eyes, an even more intense fibrin reaction is frequently observed. Further disadvantages of primary intraocular lens implantation are the imprecise biometry and unclear prognosis

concerning eye growth.

A lensectomy during vitrectomy is accomplished by aspiration. Phacoemulsification of the lens in children is unnecessarily traumatic. The soft juvenile lens can be removed solely by means of aspiration, if no vitreous is involved. Furthermore, the use of 23-gauge (G) instruments is sufficient for removal of pediatric lens material with a 23G cutter with a cutting rate of 450 revolutions per minute and relatively low suction power (maximum 450 mmHg).

The empty lens bag is completely removed at the end of the operation, preferably bimanually, with forceps holding the capsule on traction and the cutter removing the zonular fiber attachments. Removal of the capsule with forceps alone should be avoided as aberrant attachments of zonular fibers, the so-called zonular traction tufts, may create peripheral retinal tears. These traction tufts are described as connections of retina to one or more posteriorly inserting zonular fibers. If silicone oil is instilled, an inferior iridectomy is performed.

Optimal visual rehabilitation can be achieved without the need for contact lens wear by IOL implantation. Implantation of an intraocular lens has the advantage of attaining an immediate optical improvement, but is associated with the substantial drawbacks mentioned above.

Secondary lens implantation should only be considered in stable situations, when silicone oil has been removed and the retina is attached.

Postiridial iris claw lenses are our first choice and can be implanted quite easily. The preferred choice of secondary lens implantation should be the implantation of an iris claw lens in the posterior chamber or, as second choice, the suturing of an intraocular lens, a scleral-fixated IOL, or an iris-fixated IOL. The indications for suturing an intraocular lens should be considered carefully.

Posterior-Segment Surgical Techniques

The smaller size of infant eyes results in differences in surgical landmarks, relative instrument size, and fluid dynamics of vitreous surgery (Fig. 119.2) in addition to increased vitreoretinal adhesion.

These specific issues are addressed below.

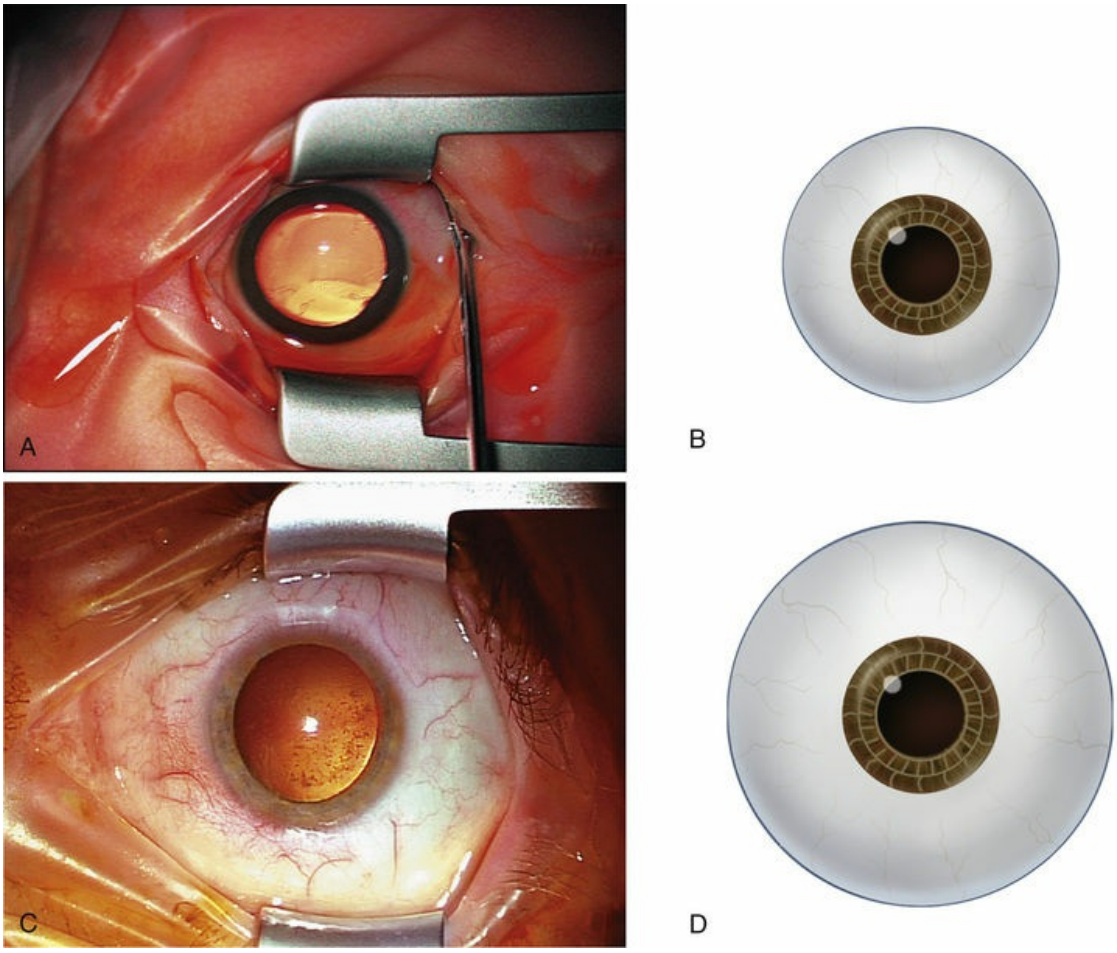

FIG. 119.2 Comparison of a globe from a neonate (A,B) with that of an adult (C,D) shows different proportions.

Buckling surgery (see also Chapter 104, Techniques of scleral buckling): after a peritomy, traction sutures (silk 5/0) are placed beneath the insertion of two to four rectus muscles. Then the retinal holes are located, marked, and a transscleral cryoretinopexy is performed under ophthalmoscopic control. Depending on location of the hole, appropriate radial or circumferential scleral buckles are placed and fixed, if necessary with an additional segmental silicone-rubber sponge. For an encircling procedure, one suture per quadrant is placed, and the ends are secured with a sleeve. Due to spatial considerations, the sleeve is preferably placed in the lower temporal quadrant. The perfusion of the central retinal artery must be checked. Rarely, a paracentesis is necessary. The scleral thickness

is less than in adult eyes, therefore thinner (6/0) suture (polyester fiber, polyamide fiber) should be used for partial-thickness scleral sutures in babies. We also recommend the use of flat spatula needles (0.28 mm diameter).

A child's eyes are more prone to vigorous cellular reproliferation than those of an adult. This can be attributed to the biochemistry of this age group which supports cell growth more actively, or to a longer delay between the time of detachment and the establishing of diagnosis and therapy. For primary detachments, we use a sculpted 3 × 5-mm sponge with an encircling 2.5-mm solid silicone band. It is often assumed that the children's orbits cannot accommodate a large sponge, but this type of exoplant is well tolerated. Drainage of subretinal fluid is controversial. Postoperative complications of scleral buckling in children range from refractive amblyopia to alteration of eye growth. To avoid these complications, the band is cut in all children younger than 3 years, approximately 3 months after the scleral buckling operation, once a stable reattachment has been achieved.[4] We choose to cut rather than to remove the element because we believe that continued support to the retina is provided by the encapsulated exoplant. To reduce amblyopia development in the postoperative period, we prescribe 1% atropine drops for 5 days; if both eyes have good visual potential, we prescribe the drops for both eyes. In addition to amblyopia therapy, a refractive error needs to be treated with adequate prescriptions.

In combination with vitrectomy, we use an encircling band with a width of 2.0 mm in babies; in older children we use a circumferential buckle width of 2.5 mm. While a primary encircling band is fixed in the area of the equator, a cerclage placed during a vitrectomy is fixed somewhat anterior to the equator. Tightening of the band for stronger indentation is done during vitrectomy, after the central vitreous has been removed in order to facilitate visualization of the vitreous base.

Usually a three-port vitrectomy is performed in children. The infusion is preferably placed temporally. The sclerotomies are placed 3.5 mm behind the limbus in infants older than 2 years. In children younger than 2 years, the sclerotomies are performed within the range of the pars plicata and/or pars plana, in accordance

with Table 119.5. In the infant eye, especially in babies, the scleral incisions are made posterior to the limbus with incisions through the pars plicata. Displacement of the conjunctiva for adequate coverage of the sclerotomies necessary for transconjunctival sutureless surgery is not possible.[25] Therefore, conjunctival dissection is preferred before the sclerotomy incisions are made. Because of the very thin sclera in babies and infants, we recommend using trocars beginning at age 2. In preschool children, we recommend placing the trocars perpendicular through the sclera. In young eyes, oblique placement of the trocars is associated with an increased risk of accidental dislocation, since the trocars have only a short path through the pediatric sclera compared to the longer path through an adult sclera. The insertion of a 25G trocar imparts significantly more force on the globe than a 20G blade. A young patient age is a risk factor for intraoperative sclerotomy leakage: in a study of 322 eyes, 61% of patients aged <40 years needed intraoperative suture placement for leaking sclerotomies at the end of 23G transscleral vitrectomy.[26] Others report postoperative hypotony in up to 40% after 25G vitrectomy in children.[27]

TABLE 119.5

Distance of Sclerotomies From the Limbus as a Function of Age

	Age (months)				
	<3	>3–6	>6–12	>12–24	>24
Distance of sclerotomy from limbus (mm)	1.5	2.0	2.5	3.0	3.5

Due to the decreased scleral stiffness and the increased elasticity of young sclera, suturing of sclerotomies in children is necessary to ensure a leakproof closure. Especially if eyes have ocular disorders which are associated with neovascular tissue, the sclera should be sutured to prevent postoperative intraocular hemorrhages from the vascular ridge in case of postoperative hypotony.[28] Furthermore, children often rub their eyes after surgery. For the closure of the conjunctiva, absorbable Vicryl 10/0 can be used.

A complete range of small incision instruments that permit a complete vitrectomy through small (23G and 25G) incisions has been developed. Performing surgical maneuvers with smaller

instruments allows the surgeon to work more precisely and increases the potential for minimizing surgical trauma. We prefer the use of 23G instruments, but case selection remains important. In case of very dense cellular membranes, the 23G or 25G cutter cannot adequately address this tissue, and additional instrumentation may be necessary. In more complicated cases, such as traction retinal detachments, eyes with extensive fibrovascular proliferation, complex retinal detachments requiring scleral buckles for proliferative vitreoretinopathy, and giant retinal tears, surgical maneuvers can be performed with small-gauge instruments, but they are often more easily performed using 20G instrumentation.[29] For cases requiring enhanced panoramic illumination, it is possible to use the 20G shielded bullet light pipe instead of the 23G illumination light pipe. The sclerotomies are made with a 23-MVR blade. In babies, we use a 23G disposable Tornambe infusion cannula (DORC 1272). Larger sclerotomies may allow for better manipulation of the 23G or 25G cutter within the sclerotomy, avoiding unintentional bending of the instrument and potential damage to the lens or retina.[25]

Minimizing infusion pressure may diminish the risk of corneal clouding and retinal incarceration during instrument withdrawal. Occasionally, the anterior chamber is so shallow that is difficult to avoid dragging the iris while creating sclerotomies. This increases the risks of iridodialysis, hemorrhage, and traction on the peripheral retina. Proliferations may develop anteriorly, often along the ciliary body, and dissection of these peripheral proliferations may be necessary to enable the widest possible dilatation. The use of flexible iris retractors has greatly facilitated this goal without significantly complicating the operation.

Vitrectomies are always performed with wide-angle observation systems. In addition, wide-field vitrectomy contact lenses are specifically designed to facilitate pediatric vitreoretinal surgery.[30]

The wide-angle observation systems for vitreous surgery (binocular indirect ophthalmomicroscope, vitreopanfundoscope, and stereoscopic diagonal inverter) have many advantages: (1) wide angle of view; (2) large depth of field; (3) stereopsis; (4) good visualization in hazy media, even with narrow pupil; (5) upright, true-to-side image; (6) magnification with the microscope zoom; (7)

beam splitter for the assistant; (8) good visualization in gas-filled or silicone-filled eyes; (9) free mobility of the eye for peripheral surgery. With these systems, surgery is possible from the posterior pole to the vitreous base and the anterior loop traction, regardless of whether the eye is phakic, pseudophakic, or aphakic. The vitreous body can be removed with a 23G high-speed cutter with a cutting rate of 5000 revolutions/minute and a suction power of 400 mmHg. With the cutter near the peripapillary retina, suction should be applied to separate the posterior hyaloid from the retina in slow circular movements. Special attention is necessary to create a posterior vitreous detachment; "tenting of the retina" is a sign of very strong vitreoretinal adherence and poses a high risk for development of iatrogenic retinal holes. A compromise is a judicious core vitrectomy, leaving as thin a layer of cortical vitreous on the retina as possible. If it is not possible to remove vitreous in the periphery, a thorough shaving is necessary. This can be performed by a small-gauge high-speed cutter; if 20G instruments are used, special 20G shaver-cutters are available. Creation of a posterior vitreous detachment with suction alone to lift the vitreous off of the optic nerve is more difficult with small gauge vitrectomy probes. The smaller port opening decreases the ability to engage and hold the vitreous. Creating a posterior vitreous detachment in a child with adherent posterior hyaloid remains substantially easier with 20G instruments because of larger port sizes and greater flow rates.[29] For small-gauge vitrectomies, higher infusion rate in the range of 35–50 mmHg are necessary to ensure adequate intraocular fluid dynamics. Due to the lower systolic blood pressure of babies and infants, iatrogenic occlusion of the central retinal artery can be induced, and the surgeon has to observe the optic nerve.[31] Retinal breaks should be prevented because they are often difficult to treat. Posterior drainage retinotomies are associated with profound postoperative proliferation. Iatrogenic breaks are best avoided by abandoning peeling in favor of bimanual dissection with forceps and scissors. If a retinotomy is unavoidable, it must be performed as close as possible to the ora serrata and following diathermy coagulation. Retinopexy of retinotomy edges is done with argon laser coagulation. If the extension of the retinotomy is larger than 2 clock-hours, a silicone oil tamponade is used. Diagnostic vitrectomy

can be used to evaluate conditions such as inflammatory conditions and amyloidosis. The cytopathologic analysis of ocular fluids obtained for diagnostic purposes has proven to be effective for establishing and confirming the diagnosis.

Pharmacologic agents have become available to assist in separating the youthful posterior cortical vitreous from the retina. The goals of enzymatic vitrectomy (dispase, plasmin, tissue plasminogen activator, or chondroitinase) are either to disinsert the posterior hyaloid from the retinal surface in an atraumatic, precise, cleavage plane or to try to disinsert the peripheral vitreous from the neurosensory retina. Enzymatic (collagenase or hyaluronidase) manipulation of the central vitreous in terms of liquefaction has been evaluated. At present microplasmin is used in clinical studies.[32,33] This is certainly only the beginning of this type of vitreous surgery, whether adjuvant or alternative.

Silicone Oil and Gas Tamponade

The physical properties of silicone oil include a combination of specific gravity, refractive index, and surface tension. Heavy silicone oil may be of interest for inferior traumatic retinal detachments. Use of 1000 centistokes or 5000 centistokes silicone oil can be considered in the management of pediatric complex retinal detachments associated with multiple etiologies.[34] The choice of viscosity offers an optimal balance between easy injection and a longtime tamponade. Indications and the long-term results of pars plana vitrectomy in children are comparable with those in the adult. Retinal reattachment and preserved visual acuity can be achieved in the majority of eyes using silicone oil retinal tamponade. In complicated retinal detachments, especially after injuries, an approach with primary silicone oil injection and later silicone oil removal has proved useful. In children, who usually have a long life expectancy, timely removal of silicone oil is vital for maintaining the function of the eye.

Intraocular gas has a limited use in children and is complicated by difficulties in adequate positioning, intraocular pressure monitoring, and corneal clouding.

Biostaining of the ILM and intraocular membranes is a technique

that is still evolving, and despite good results in adults, it should be used in children with utmost care. We recommend trypan blue and brilliant blue G[35] as "safe" dyes for staining, assuming they have nontoxic or at least minimal toxic effects.[36] Visualization of the stained posterior hyaloid greatly facilitates complete removal and reduces surgical time. Control staining following membrane removal is possible, preferably by the use of triamcinolone to check if all gel and membranes have been successfully removed.

Injuries

(See also Chapter 102, Pathophysiology of ocular trauma, and Chapter 104, Techniques of scleral buckling.)

Direct Injury

Open-Globe Injury

Some 29–47% of pediatric open-globe injuries involve both the anterior and posterior segments of the eye.[37–40] Whereas the primary surgery typically includes external reconstruction of the globe, internal reconstruction can be performed simultaneously with the primary wound closure or, in most cases, in a second step.

The timing of secondary comprehensive anatomic internal reconstruction is crucial. Various authors have recommended a secondary vitreoretinal operation for internal reconstruction in the period between the 7th and 10th posttraumatic day in adults;[41–43] whereas others recommend 3–10 days after trauma.[42,44] The general rule is to delay comprehensive anatomic reconstruction of the seriously injured eye for approximately 1 week, when the risk of intraoperative hemorrhage is dramatically reduced and a separation of the posterior vitreous begins to develop.[41,42] Kuhn et al. recommend early vitrectomy within 3 days to prevent development of vitreoretinal proliferation.[42]

Immediate intervention is, however, necessary if signs of infection are recognizable or in rare cases of retinal detachment at the time of wound closure.

The value of a prophylactic encircling band in severe globe-opening injuries is controversial. There are no prospective studies

documenting the advantage in children. In adults, the frequency of retinal detachment may be less after applying an encircling band. An encircling buckle procedure is recommended in the presence of a corneoscleral or scleral wound >5 mm with ciliary body involvement with marked vitreous loss and vitreous hemorrhage.[45–47] Despite optimal follow-up, the functional results after combined pediatric anterior and posterior segment injuries are limited: about 12%[34] to 69%[39] of the children attain a visual acuity of 0.1 or better after primary wound closure and secondary surgery for reconstruction of the anterior and posterior segments.

Children may develop more extensive postoperative inflammation, scarring, and severe proliferative vitreoretinopathy than adults, and this affects the anatomic and functional outcomes.[48] The results after pediatric vitreoretinal surgery depend greatly on the extent and severity of the primary damage (Fig. 119.3). A wound size exceeding 10 mm, a lens lesion, and a patient age under 4 years are factors with unfavorable prognoses. Further negative influential factors include severe intravitreal bleeding, poor initial vision, and gunshot injuries. Retinal detachment always correlates with significantly poorer results. Preoperative macular attachment is a crucial prognostic factor for attaining a postoperative vision better than 0.1.[49,50]

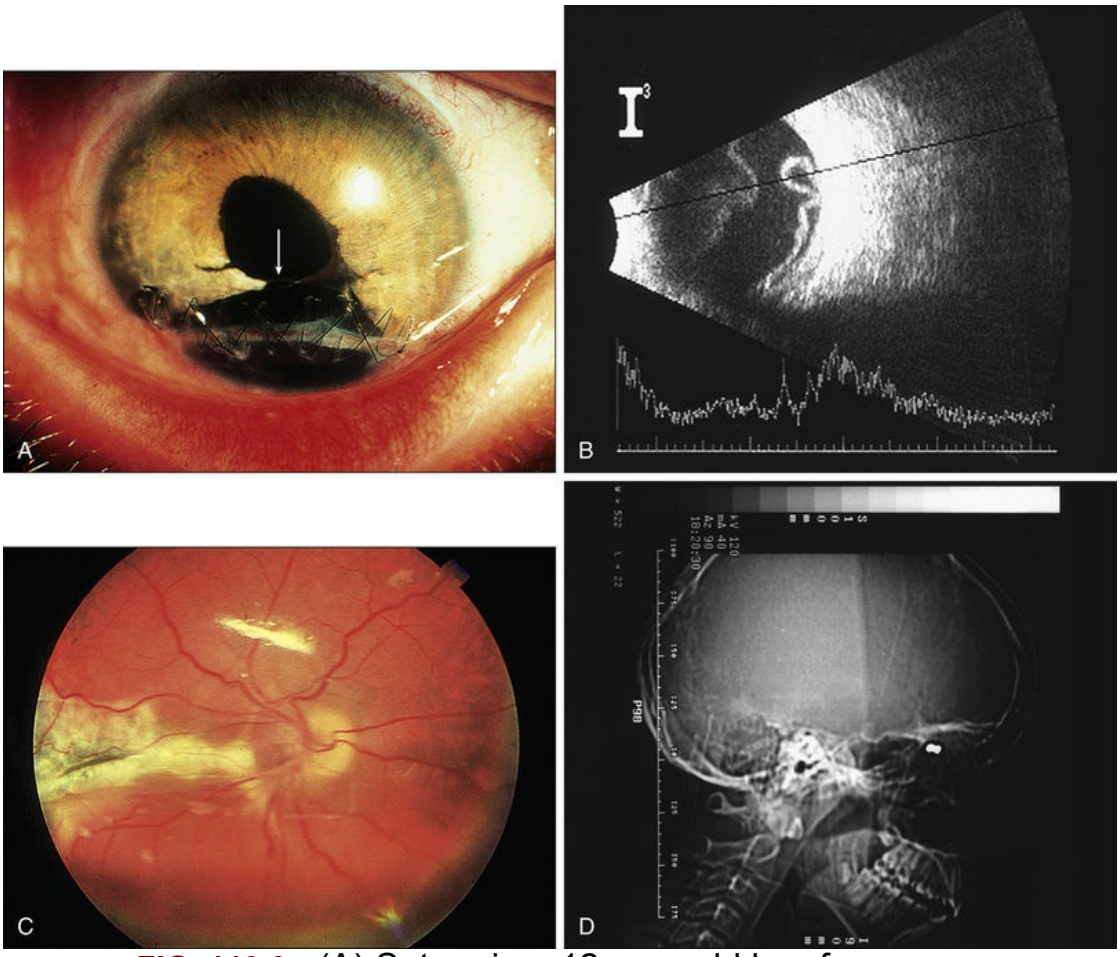

FIG. 119.3 (A) Suture in a 12-year-old boy for a corneal perforation caused by a knife. (B) Vitreous hemorrhage and retinal dialysis were diagnosed in the posterior segment of the same eye. (C) Scarring and pigmentation at the exit site of the eye of a 13-year-old boy, who had sustained a perforating injury from a shotgun pellet (D) and was treated with a pars plana vitrectomy with silicone oil injection.

There is strong support for scleral buckling as the standard primary surgery for treatment of trauma-associated retinal detachment in children. Differently from adults, the vitreous is rarely detached and complete vitrectomy is impossible. Furthermore, remnants of vitreous are responsible for development of severe PVR following vitrectomy. Indications for primary scleral buckling include absence of cataract, minimal vitreous hemorrhage, and clear identification of retinal breaks; significant vitreal opacities and giant or posterior retinal breaks require primary vitrectomy.[40]

Traumatically ruptured globes occur rarely in children.

Predisposition for rupture of pediatric eyes includes diseases associated with thin sclera, e.g., Ehlers–Danlos syndrome and osteogenesis imperfecta. Even blind eyes should be treated, as enucleation can often be prevented.

Closed-Globe Injury

Oradialysis.

A common finding in closed injuries is an oradialysis. An oradialysis is located most often inferotemporally, and it may become symptomatic only years after the trauma. In the absence of cataract, minimal vitreous hemorrhage, or significant haze, treatment consists of a circumferential segmental buckle. The edge of the segmental buckle should exceed the edge of the dialysis by twice.[51] Anatomic reattachment has been achieved in 67–88% of cases, whereas the rate of PVR was (Figs. 119.4A–B).[52,53,54]

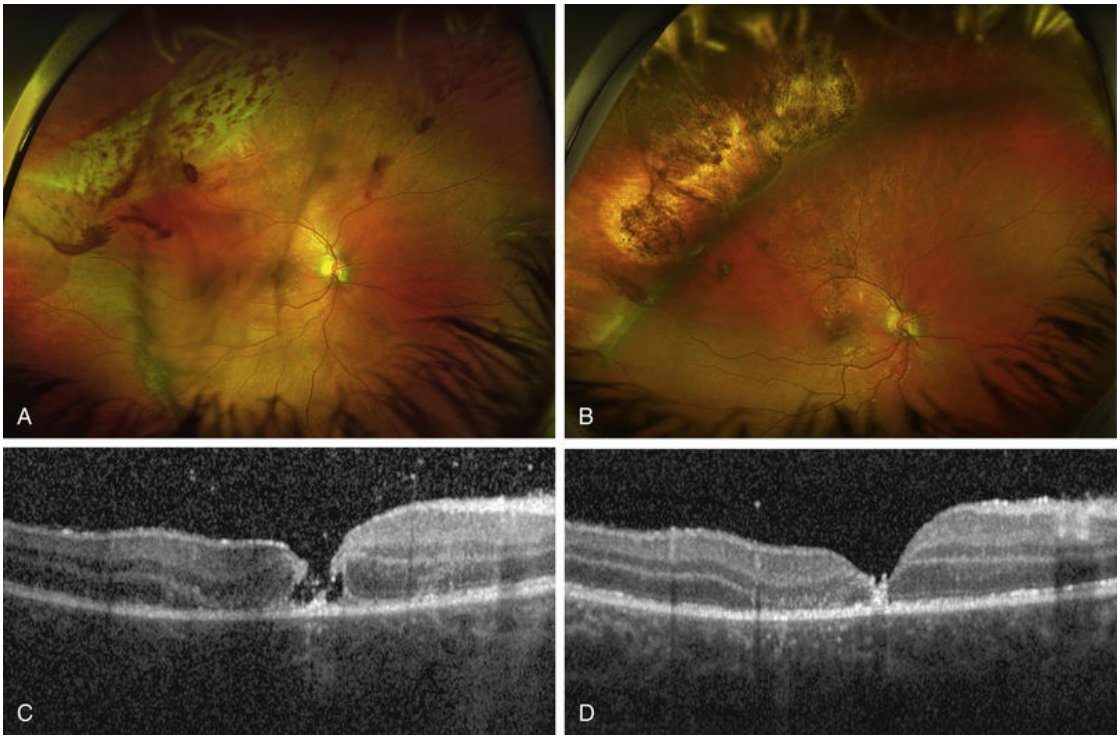

FIG. 119.4 (A) Oradialysis, macular hole, and vitreous hemorrhage in a 12-year-old boy caused by a soccer. (B) 4 weeks postoperatively, after cryoretinopexie, and segmental buckle the retina is attached. (C) The spectral-domain optical coherence tomography

showed the full-thickness traumatic macular hole. (D) The hole resolved spontaneously 6 days after trauma.

Traumatic Macular Hole.

Most traumatic macular holes result from closed-globe contusion injuries, but the formation of a macular hole secondary to a penetrating injury was documented in an 8-year-old boy.[55]

Traumatic macular holes may result from blunt trauma when it causes separation of the vitreous from the retina, contusion necrosis, or subfoveal hemorrhage. The cause of visual deterioration is necrosis resulting from contrecoup forces or tearing of the retina by a sudden separation of the posterior vitreous face from the retinal surface.[56] However, in one report, the posterior vitreous was detached from the macula in only 5% of eyes with traumatic macular holes.[57] This supports the theory that rupture of the macula caused by retinal stretching occurs as a result of either ocular deformity in the equatorial region or from the strong force of impact on the macula.[57]Small, full-thickness traumatic macular holes with a size of 0.1–0.2 disc diameter (DD) can resolve spontaneously in 64–100% of pediatric cases 3–4 months following trauma, and this may be associated with good visual recovery in most cases even as excellent as 20/20.[58–61] In contrast to spontaneous closure of small macular holes (100–200 μm), closure of large holes (400–600 μm) has been rarely described (Figs. 119.4C–D).[62]

In preschool children, the timing of surgery should be based on the fact that traumatic macular holes may be amblyogenic. We therefore recommend vitreous surgery for the treatment of traumatic macular hole after 4 weeks. In elderly children, a period of observation of 3–4 months before vitreoretinal surgery is recommended.[59]

Common features of patients with spontaneous closure of traumatic macular hole are young age (<25 years), small size of the macular hole (0.1–0.2 DD), no posterior vitreous detachment, and no epiretinal membrane.[59]

Vitreous surgery for traumatic macular holes can lead to anatomic success in 92–100% and visual acuity improvement in 92–100% of pediatric patients.[55,59,63] Recent studies recommend surgical

procedures including removal of the posterior hyaloid, the epiretinal membrane, and ILM and expanding gas–air mixture tamponade.[59,63,64] Studies with adjunctive treatments have been published and describe the successful use of platelet concentrate[65] and plasmin (0.4 IU of autologous plasmin) for enzyme-assisted pars plana vitrectomy.[63] In young patients, poor compliance with face-down positioning may be a factor in surgical failure. It is difficult for a child to maintain a face-down position postoperatively, therefore the use of silicone oil is advocated in children who need long-term intraocular tamponade after vitreoretinal surgery. However, additional surgery for silicone oil removal is necessary.

Vitreous Hemorrhage.

Trauma remains the first among all causes of pediatric vitreous hemorrhages, and the differential diagnosis for spontaneous intraocular hemorrhages in infants includes vasculitis, ocular tumors, FEVR, X-chromosomal retinoschisis, retinal breaks, *Toxocara* infection, and systemic disorders (e.g., hematologic disorders, diabetic retinopathy, hepatorenal dysfunction, sepsis).[66] Complications of infantile vitreous hemorrhage include epiretinal membrane formation, pigmentary retinopathy, strabismus, high anisometropic myopia, and occlusion amblyopia.[10] These serious complications occur as early as 5 weeks after the onset of the vitreous hemorrhage. Vitrectomy is an acceptable early therapy for infantile vitreous hemorrhage, and we recommend that this be considered as early as 5 weeks after the onset of a dense, infantile, vitreous hemorrhage in an attempt to avert serious complications of the hemorrhage.[12,67] In suspicious cases of infectious etiology diagnostic vitreous biopsies should be performed, e.g., histopathologic confirmation of tuberculosis.

Furthermore, early removal of severe vitreous blood clots and severe vitreous hemorrhaging is recommended for injured eyes. Traction retinal detachments arise as a result of contracting epiretinal membranes, and vitrectomy appears to reduce the incidence of these traction retinal detachments in open-globe injuries.[41,68] The timing of vitrectomy for the removal of vitreous hemorrhage remains crucial. If retinal and/or choroidal

involvement are not present, serial ultrasonography is necessary to detect complications. In individual cases, vitreous hemorrhage may absorb spontaneously, but because of the danger of amblyopia, vitrectomy may nevertheless be indicated.

Indirect Injury

Terson Syndrome

Terson syndrome is characterized by intraocular hemorrhage secondary to subarachnoidal or subdural hemorrhage. Vitreous hemorrhage in patients surviving subarachnoid hemorrhage appears to be more common than previously thought, underscoring the need for routine funduscopic screening. In the only published prospective case series of nonabuse instances of intracranial hemorrhage in children,[69] 2% had intraocular hemorrhages. The authors estimate the incidence of Terson syndrome in children with intracranial hemorrhage to be less than 8%. There is a low incidence of spontaneous intracranial hemorrhage in infants.

Only a few case reports of Terson syndrome in babies, from 4 weeks to 7 months old, due to a ruptured angiodysplasia or an aneurysm have been published.[70,71] The hemorrhages can occur within the sensory retina, in the subretinal space, and in the vitreous cavity. In approximately one-third of these eyes, a premacular accumulation of blood termed a “hemorrhagic macular cyst (HMC)” may be found.[72] Based on the blood's relation to the ILM, two types of HMC can be distinguished in Terson syndrome. A HMC is preretinal if the blood is located anterior to all layers of the retina and submembranous if the blood has accumulated beneath the ILM.[72] The anterior cyst wall may initially be formed by the posterior hyaloid face and later by proliferation. This newly formed membrane may present even if the blood has cleared from the cyst. Hemorrhagic macular cysts are more often submembranous than preretinal. At the vitreous base and in the equatorial zone, attachment plaques are present between the ILM and the Müller cells. Because attachment plaques are missing in the posterior zone, where the ILM is much thicker, a retinal hemorrhage is capable of detaching the ILM from the retina in that area. The presence of attachment plaques is considered in relation

to centripetal vitreous traction, which is absent in the area of the posterior precortical vitreous pocket (PPVP). The posterior wall of the PPVP therefore probably coincides exactly with the thick part of the ILM in the posterior zone.[73] Most cases of vitreous and retinal hemorrhages in Terson syndrome do not require surgery because of spontaneous resorption. However, young individuals with a healthy vitreous gel may have delayed hemorrhage clearance, but babies and preschool-age infants can develop deep amblyopia within a few weeks. The formation of epiretinal membranes in severe cases is associated with the development of PVR. To prevent this complication, some authors advocate close follow-up and early, extensive treatment in Terson syndrome.[74] Complete cyst removal should be performed, i.e., including contents and anterior wall, to prevent blood-related complications and to allow early rehabilitation of macular function (Fig. 119.5).[72]

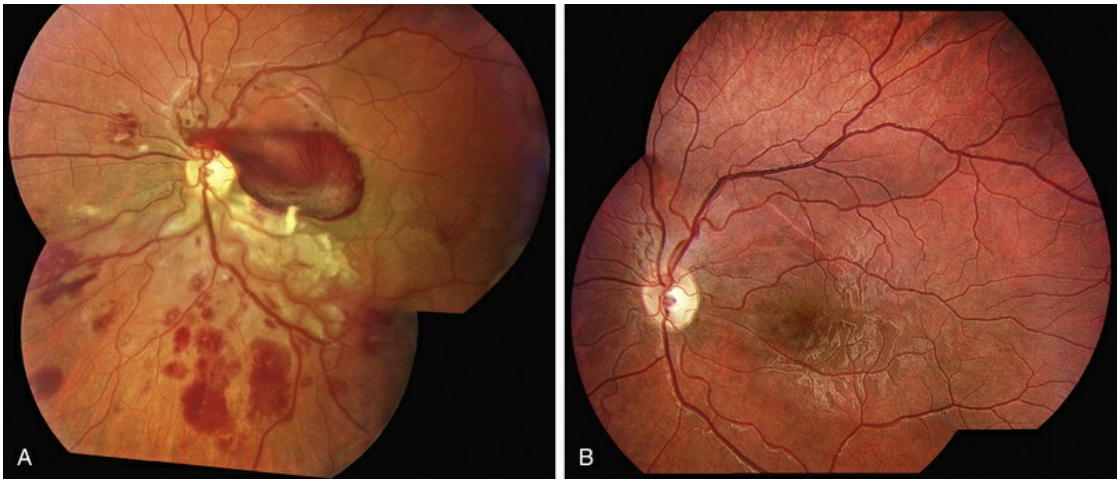

FIG. 119.5 (A) Submembranous hemorrhagic macular cyst (HMC) seen in a 6-year-old child suffering from Terson syndrome caused by a subdural hemorrhage; the striae show stress on the internal limiting membrane. (B) Postoperatively the fundus showed a perimacular light line corresponding to the edge of the HMC.

If a pars plana vitrectomy is performed, the possibility of a hydraulically dissected ILM has to be considered. Indications for vitrectomy therefore include dense vitreous hemorrhage, bilateral hemorrhage, premacular HMC and/or dense vitreous hemorrhage

if spontaneous resorption has failed after 4 weeks, development of esotropia, and/or PVR. Postoperatively, perimacular retinal folds or fibrotic lines may occur.[75] Whereas the prognosis of vitrectomy for Terson syndrome is excellent in adults, it remains relatively poor in visually immature children. Amblyopia, despite early intervention, and permanent brain damage are potentially responsible for this limited visual outcome. We recommend surgical intervention, management of amblyopia, correction of refractive errors, and intensive orthoptic treatment.

Spontaneous Terson syndrome is one of the differential diagnoses for intraocular hemorrhages in infants with suspected abusive head trauma. Distinguishing characteristics are the mild severity and confinement of retinal findings to the posterior pole in spontaneous Terson syndrome, which are in contrast to the usually severe, multilayered intraocular hemorrhages extending to the retinal periphery in abusive head trauma.

Shaken-Baby Syndrome

In shaken-baby syndrome, retinal hemorrhages are the most common fundus finding, and dome-shaped hemorrhages are the most distinctive form of hemorrhage (Fig. 119.6). The dome-shaped hemorrhages are most often seen in the macular area, but can be found in any area of the retina on histopathologic examination. They can be caused by separation of the ILM or a more vision-threatening deep retinoschisis. Studies have shown that handheld spectral domain optical coherence tomography (OCT) is helpful in the evaluation of patients with shaken-baby syndrome to detect vitreoretinal abnormalities, e.g., multilayered retinoschisis, disinsertion of the ILM, and foveal detachment.[76,77] In some cases, the blood breaks through the ILM and/or hyaloid face and causes a vitreous hemorrhage. This can occur immediately after injury or a few days after the cerebrovascular accident from rupture of the ILM over a dome-shaped hemorrhage.

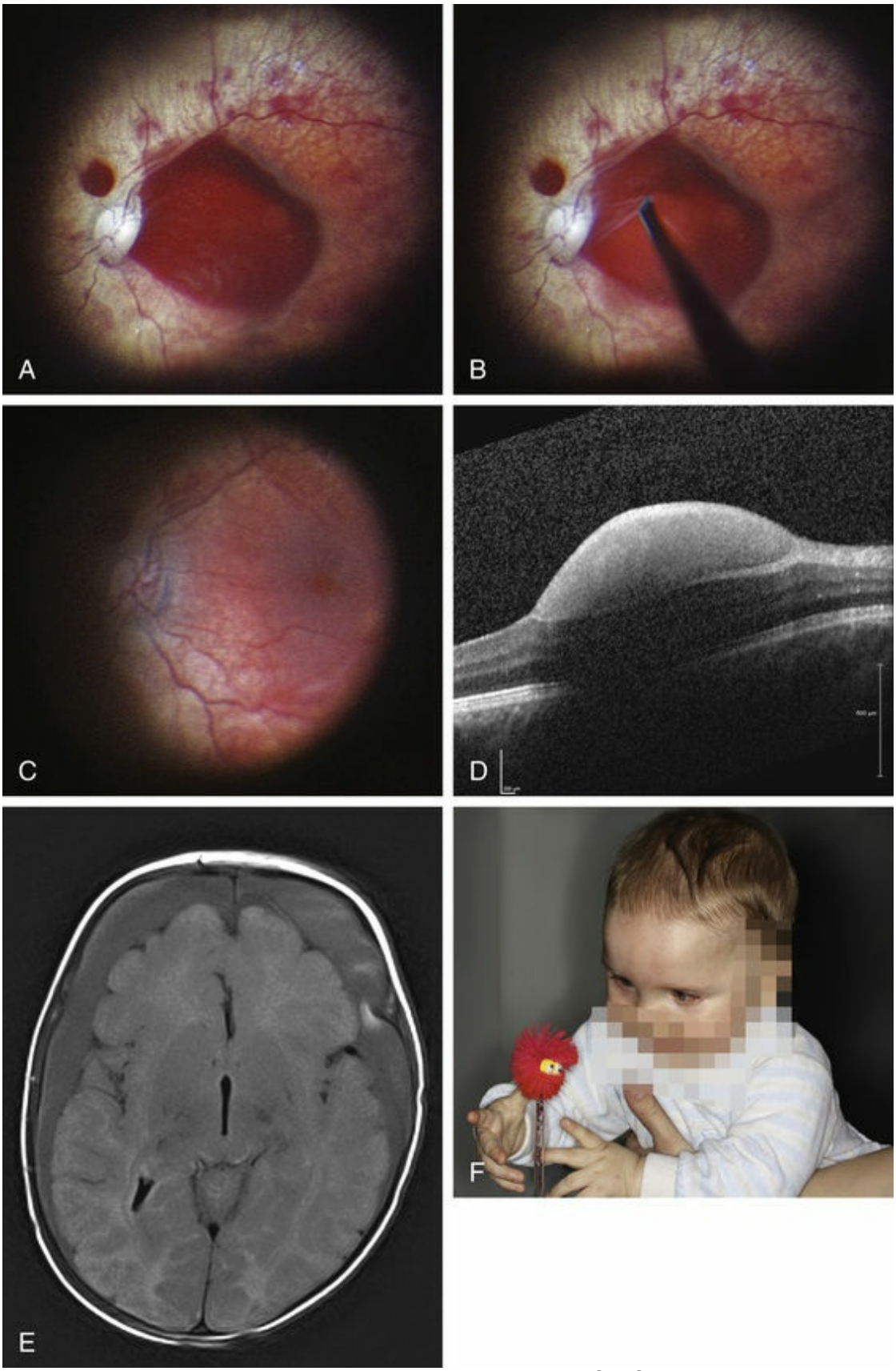

FIG. 119.6 (A) Typical appearance of a fresh submembranous hemorrhagic macular cyst (HMC) seen in shaken-baby syndrome in an 8-month-old

baby. (B) Fundus photograph after opening and (C) removing of the anterior cyst wall of the HMC. (D) Optical coherence tomography shows blood accumulation beneath the internal limiting membrane. (E) Noncontrast computed tomogram of the 8-month-old baby shows a massive hemorrhage due to abusive head trauma. (F) On follow-up 2 weeks later, he was able to fix and follow with both eyes.

In addition to extensive retinal and preretinal hemorrhages, bilateral symmetric white ring-shaped retinal folds are seen encircling the macula outside the vascular arcades. These retinal folds may be a hallmark of shaking injuries in child abuse victims.[78] Short-term follow-up is necessary with large dome-shaped hemorrhages because they can induce severe amblyopia by themselves or can break into the vitreous and linger for months in these visually immature patients. We recommend vitrectomy for large premacular hemorrhage and/or after absence of vitreous hemorrhage clearing after 4 weeks. If esotropia develops, vitrectomy should be performed promptly. During vitrectomy, the hyaloid is peeled and the membrane covering the macula is completely removed, i.e., the ILM is ruptured: following careful incision of the anterior wall of the HMC with a bent microvitreoretinal blade in a selected macular quadrant, the flap is grasped by end-gripping forceps and the membrane is slowly torn in a motion respecting the visible edge of the HMC. In most eyes, this is a nearly circular motion concentric to the fovea. Vitreous surgery for HMC leads to excellent anatomic success,[75] and it offers immediate visual rehabilitation.

All maculas show retinal folds or demarcation lines postoperatively. These correspond to the edge of the HMC, i.e., the edge of the hemorrhagic detachment of the ILM.

Diseases of the Pediatric Retina

Myopia

Myopia is one of the important predisposing factors of nontraumatic rhegmatogenous retinal detachment in childhood.[79] In east Asia, about 40% of children younger than 18 years who

underwent surgery for retinal detachment suffered from high myopia (>−6 diopters).[80] Up to one-third of pediatric retinal detachment is related to myopia. [81] In most cases retinal detachment in pediatric myopic eyes is associated with round holes in the presence of lattice degeneration; horseshoe tears occur rarely.[54,82] According to the results of the scleral buckling versus primary vitrectomy in rhegmatogenous retinal detachment study (SPR-study)[83] and the results of other studies in most phakic pediatric eyes, primary treatment should be performed with a scleral buckling procedure.[54,82] Primary vitrectomy is reserved for posterior tears, severe PVR, or for cases with obscured ocular media. The value of an additional encircling buckle is controversial, but we recommend it for eyes with PVR.

In a study[84] of highly myopic children <10 years of age, the authors found retinal holes in 4%; lattice degeneration in 20%, and white without pressure in 11% of the eyes. The authors recommend performing laser photocoagulation of retinal holes and prophylactic laser photocoagulation of lattice degenerations because children are less likely to report symptoms, thus delaying diagnosis and treatment of retinal detachment.[84] Prophylactic laser photocoagulation remains a controversial issue; to date the database on prophylactic treatment in children is lacking.(See also Chapter 110, Prevention of retinal detachment.)

Subfoveal Membranes

Choroidal neovascularization membranes (CNVMs) in children are rare. The causes of the CNVMs are due to ocular histoplasmosis syndrome, idiopathic membranes, optic nerve coloboma and drusen, ocular toxoplasmosis, *Toxocara canis*, rubella retinopathy, serpiginous choroidopathy, trauma, degenerative myopia, and Best disease. The treatment of CNVM is a controversial topic, and the natural history of idiopathic CNVM is not necessarily associated with a profound loss of vision.[85] Photodynamic therapy is impractical in babies and infants, and surgical excision might have visually threatening risks. Worsening of visual acuity, protracted neurosensory detachment with the development of cystoid macular edema, or subfoveal hemorrhage may be factors that make treatment of CNVM by intravitreal anti-VEGF a favorable option.

Various authors reported children (aged 19 months to 15 years) with CNVM that regressed with documented improvement in visual acuity following treatment with intravitreal anti-VEGF.[86–89] Some authors used bevacizumab in a dose of 1.25 mg/0.05 mL;[86,88,89] others employed ranibizumab, in a dose of 0.25 mg/0.025 mL to 0.5 mg/0.05 mL.[87,89] Most patients required 2–5 injections of the anti-VEGF agent. No ocular or systemic adverse events were observed in any of our treated patients.

Coats Disease

Coats disease is characterized by exudative retinitis and telangiectasias of the retina.[90] Usually (95%) only one eye is affected, and the etiology is unknown.[91] The typical morphologic features of Coats disease are multiple, saccular aneurysmal retinal vascular dilations with exudative features. The angiographic characteristics of Coats disease include areas of nonperfusion, telangiectatic capillaries most prominent in the temporal macula, and "light bulb" aneurysm. Additional findings are vascular leakage, tortuosity, and blockage from overlying exudate.[92,93]

A classification of Coats disease has been proposed by Shields and Shields.[91] Stage 1 is characterized by telangiectasia only and Stage 2 by telangiectasia and exudation**.** In stage 2A, the fovea is not involved by exudation, whereas eyes with stage 2B show foveal exudation. A dense yellow-gray nodule, a macular fibrosis, centered within the foveal exudation is usually associated with a worse visual outcome.[94] Stage 3A disease is characterized by subtotal retinal detachment, and (Fig. 119.7) stage 3B disease by total retinal detachment. Stage 4 disease shows total retinal detachment with glaucoma, and stage 5 disease is defined as a blind, nonpainful eye with a total retinal detachment, often with cataract and phthisis.[91]

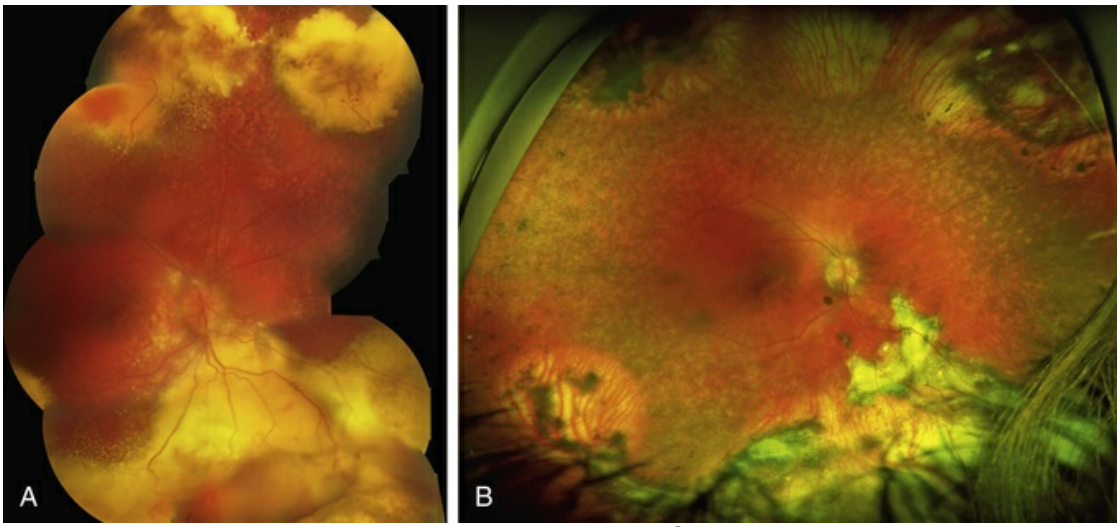

FIG. 119.7 (A) Fundus photograph of a 7-year-old girl with Coats disease shows massive lipid exudation and retinal detachment inferiorly (stage 3A). The retinal telangiectasias are located in the peripheral retina, between the equator and ora serrata in the upper half. (B) Three years after 4× cryocoagulation of the peripheral telangiectasias and injection of bevacizimab, there is a complete resolution of the exudates development of peripheral scars with surrounding pigment changes.

The main goal of treatment of Coats disease should be to eradicate telangiectasias and ischemic retina by photocoagulation with green laser light (532 nm) or cryocoagulation. Preferred method of cryotherapy is a double freeze–thaw technique applied directly to the telangiectasias. But excessive cryotherapy can induce an increase in the extent of retinal detachment. Therefore, in cases with diffuse telangiectasias involving all quadrants, it is advisable to initially treat two quadrants only and the other quadrants 4 weeks later. A second treatment of the same area should be withheld for 3 months because resolution of exudation is a very slow process.[95]

Recent studies[96] have shown that Coats disease is associated with an increased intraocular VEGF level, and therefore intravitreal anti-VEGF injection can be a valuable adjunctive treatment in combination with laser photocoagulation or cryotherapy to reduce leakage and prevent neovascular complications.[88,97] Sigler et al.[92] recommend injection of 1.25 mg/0.05 mL bevacizumab, followed by argon laser photocoagulation in a single session. Alternatively the

use of ranibizumab in a dose of 0.5 mg (0.05 mL) is possible.[98] The authors performed intravitreal injection in nine eyes in patients who suffered from Coats disease in stage 3B and 4 after transscleral subretinal fluid drainage by using a 30G needle; additional photocoagulation (up to 7 times) or cryocoagulation (up to 10 times) were performed and eight eyes achieved retinal reattachment. Another recent study[99] described the treatment of 24 eyes suffering from stage 3 Coats disease via a two-port pars plana nonvitrectomy approach; two incisions were made 3 mm posterior to the corneal limbus, and laser was applied directly on the abnormal blood vessels. Additional subretinal fluid was drained, and 17 eyes received intravitreal anti-VEGF-injections. In 96% of treated eyes the retina reattached. A further study[100] described 14 pediatric eyes with Coats disease in stage 2, 3A, and 3B after primary intravitreal injection of 1.25 mg bevacizumab; partial resorption of subretinal fluid and partial regression of exudates, and telangiectasis were observed, but additional laser photocoagulation or cryocoagulation was performed.

Other authors[101] observed the development of vitreoretinal fibrosis and traction retinal detachment in four of eight eyes with stage 2 to 3B disease treated with bevacizumab and adjuvant modalities, others[102] had seen fibrotic vitreoretinopathy in five of nine eyes after injection of ranibizumab and adjuvant treatment. The development of vitreoretinal fibrosis and traction was a common complication after anti-VEGF and adjuvant treatment.

The optimal time period between injection and coagulation treatment is unclear. Most authors used a dosage for bevacizumab of 1.25 mg/0.1 mL (14–17 years old)[92,100,101] to 2.5 mg/0.1 mL (6 months to 12 years old).[103] Patients received up to three injections.

It is paramount that ophthalmologists maintain a high clinical suspicion for the possibility of retinoblastoma before performing an injection that could spread tumor cells to the subconjunctival space and orbit.[92,104] Unless the retina and the abnormal telangiectatic vessels found in Coats disease can be examined by indirect ophthalmoscopy, no injection should be performed, even with the absence of calcification on B-scan. Furthermore, a diffuse infiltrating retinoblastoma and advanced Coats disease can be indistinguishable from each other on magnetic resonance imaging.

Therefore, enucleation should usually be performed in patients with poor visual potential and when it is impossible to rule out the possibility of retinoblastoma.[105]

Hereditary Vitreoretinopathies

Stickler Syndrome

Hereditary vitreoretinopathies are potentially blinding disorders characterized by an abnormal-appearing vitreous gel with associated retinal changes. Stickler et al.[106,107] described an autosomal dominant disorder with characteristic ophthalmologic and systemic abnormalities, orofacial features, deafness, and arthritis. Abnormalities of vitreous gel architecture are a pathognomonic feature, usually associated with high myopia, which is congenital and nonprogressive, and cataract (Fig. 119.8). Nonocular features show great variation in expression. Stickler syndrome type 1 (STL1) arises due to mutations in *COL2A1* gene and shows membranous vitreous phenotype, while type 2 (STL2) disease arises from mutations in *COL11A1* and affected patients have a fibrillar appearance of the vitreous.[108] Only patients with STL1 or STL2 show ocular changes. An ocular-only variants will have minimal or no associated systemic features; this subgroup exhibits mutations in *COL2A1* too,[109] whereas STL3 and STL 4 patients have no eye problems. More than 80% of affected patients have STL1.[109,110] Retinal features of Stickler syndrome are radial perivascular pigmented retinal degenerations, lattice degeneration, anterior giant retinal tears, and posterior retinal tears. The first retinal detachment (RD) is usually observed between the ages of 10 and 30 years; 8% of affected children have RD between 0 and 9 years, and 26% between the ages of 10 and 19 years.[107,111]

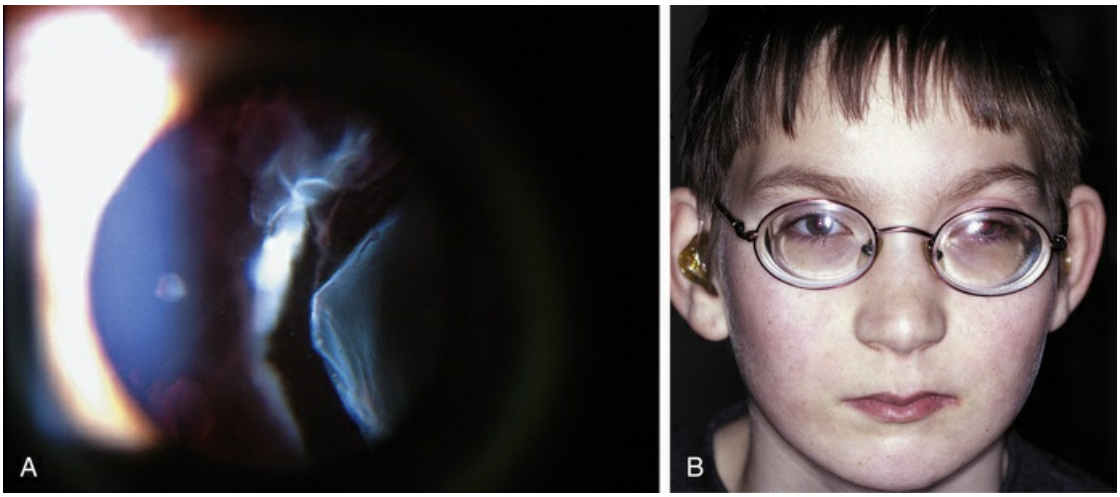

FIG. 119.8 (A) Type 1 vitreous gel anomaly in an 11-year-old girl with Stickler syndrome; within 9 months the patient developed retinal detachment in both eyes. (B) The child suffered from sensorineural hearing deficit and high myopia and at birth showed a midline cleft of the hard and soft palate.

With a high rate of bilateral spontaneous retinal detachment, "unaffected" family members without retinal detachment or other associated symptoms of Stickler syndrome should be approached and offered molecular genetic analysis to rule out the presence and type of Stickler syndrome and should be examined regularly.[112]

Positive effects of prophylactic intervention have been described.[109,110,113,114] In a recent systematic review,[112] two principal retrospective cohort studies with control groups in populations with STL1 were analyzed. One study evaluated 360° cryotherapy (n=204) on the post-oral retina and reported a statistically significant lower rate in the treatment group compared with the untreated STL1 group (n = 22). Leiba et al.[114] performed a subgroup analysis based on age and reported that 0/6 eyes treated prophylactically by laser coagulation (circumferential treatment for eyes with extensive contiguous retinal lesions where lesions were present in at least three quadrants; focal laser treatment for eyes with small localized lesions of lattice degeneration or isolated breaks) in children aged ≤13 years detached compared with 1/4 eyes treated prophylactically in children aged ≥13 years. In the control group, which did not receive any prophylaxis, the retina detached in 46% eyes of children aged ≤13 year and in 60% of adolescents and adults aged ≥13 years in the follow-up of 1–15 years. However,

both studies were subject to a high risk of bias, and the optimal age for prophylaxis is uncertain.[112]

Despite complicated surgery and often multiple procedures, Stickler patients undergoing primary vitrectomy for rhegmatogenous detachment have good anatomic outcomes as well as useful functional visual results in comparison to outcomes of scleral buckling. Vitrectomy may be considered as the operation of choice in the Stickler group.[111] Almost three-quarters of redetachments occur within the first 4 postoperative months. Complications are predominantly redetachment and subsequently multiple surgeries. As such, the use of primary vitrectomy to improve the primary success rate is also likely to reduce the overall complication rate.

Kniest Dysplasia

Kniest dysplasia is inherited in an autosomal dominant manner and presents with kyphoscoliosis, severe short-trunked dwarfism, cleft palate, flat face, hearing defects, and joint contractures.[115–117] Kniest dysplasia is associated with heterozygous (frequently de novo) *COL2A1* mutations. Patients with Kniest dysplasia have severe congenital myopia and vitreoretinal degeneration. The vitreous cavity contains fibrous, clouded, membranous structures floating in the retrolental space (Fig. 119.9). Other eyes have cortical and posterior subcapsular opacity of the lens, and also veil-like vitreous opacities in the periphery. The common retinal changes include perivascular lattice degeneration and white without pressure of various degrees. Bullous retinal detachment with Kniest dysplasia can be treated successfully, especially by vitreous surgery with silicone oil tamponade.[118]

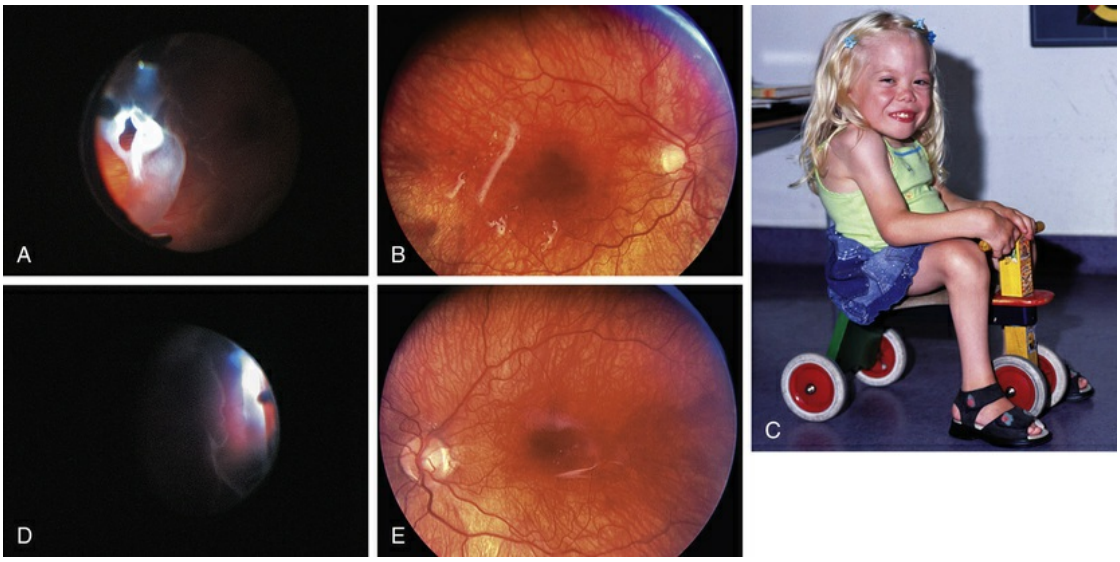

FIG. 119.9 (A,D) A 7-year-old girl with Kniest syndrome presented with a bilateral retinal detachment in both eyes. (C) The patient has characteristic severe short-trunked dwarfism, kyphoscoliosis, flat face, joint contractures, and sensorineural hearing defect; she is not able to walk and uses the vehicle for transport. (B,E) After cerclage, vitrectomy, and silicone oil tamponade, the retinas were reattached.

Familial Exudative Vitreoretinopathy

Familial exudative vitreoretinopathy (FEVR) is a bilateral disorder of aberrant peripheral retinal development, including peripheral avascular retina, abnormal vascularization with retinal neovascularization, subretinal exudation, formation of an abnormal vitreoretinal interface, and retinal detachment (Fig. 119.10). The phenotype of FEVR resembles a form fruste of ROP, occurring in a larger and often term infant. Inheritance is autosomal dominant, autosomal recessive, or X-linked, or can affect individuals with no family history. Five genes have so far been identified that cause FEVR: *NDP*, *FZD4*, *LRP5*, *TSPAN12*, and *ZNF408*.[119] Aberrant vasculogenesis and subsequent abnormal angiogenesis are thought to cause the vitreoretinal abnormalities in FEVR.[120] FEVR patients have a mutation in the Norrie disease gene. This results in dysregulation of the Wnt-receptor/ß-catenin pathway and has been associated with increased levels of vascular endothelial growth factor (VEGF). These can potentially explain the lifelong chronic

nature of FEVR, which is characterized by exacerbations in exudation secondary to upregulated vascular activity. The clinical classification is based on five stages. Wide-field angiography demonstrates aberrant circumferential peripheral vessels, venous and arterial tortuosity, late-phase disc leakage, central and peripheral telangiectasis, capillary anomalies, and capillary agenesis.[121,122]

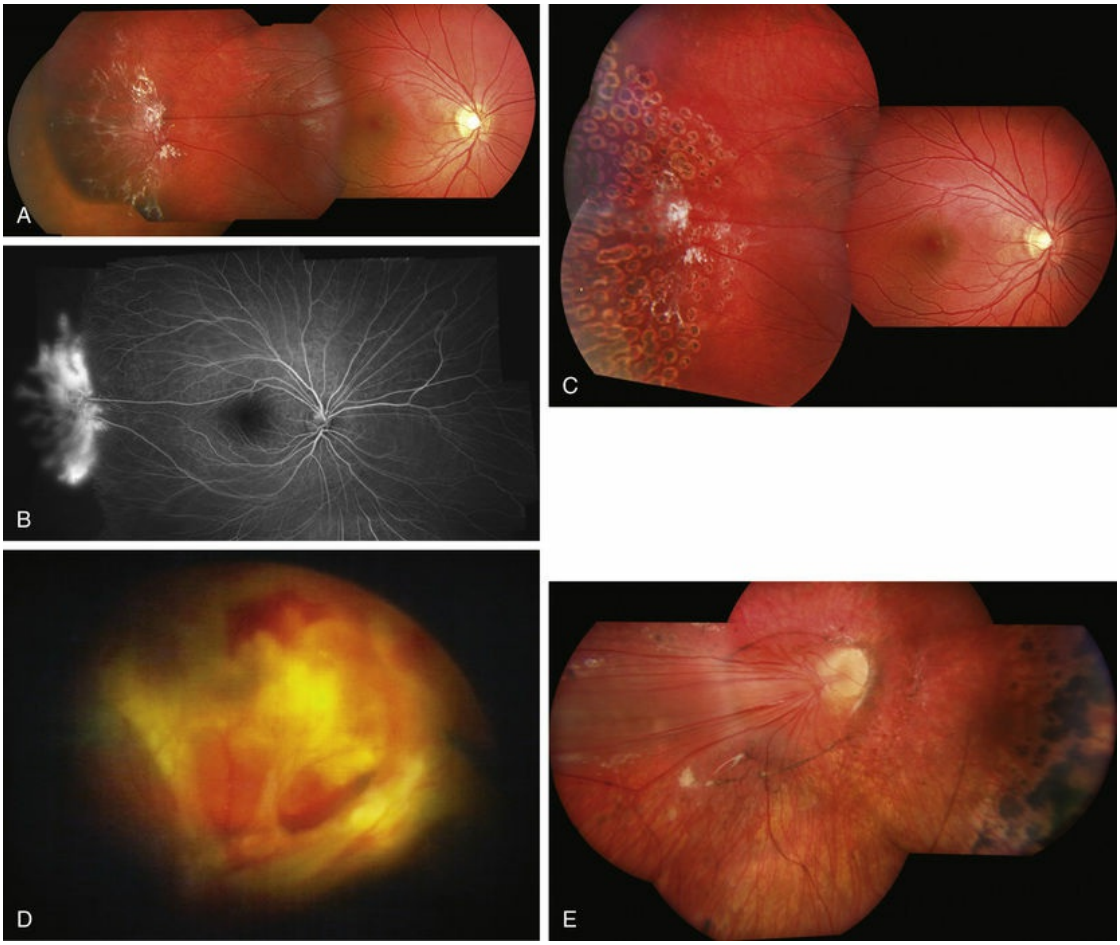

FIG. 119.10 Familial exudative vitreoretinopathy in a 13-year-old girl. (A) V-shaped area of avascular retinal periphery with extraretinal vascularization in stage 2. (B) Angiography shows avascular retinal periphery and leakage of the abnormal vessels. (C) The fundus of the same patient after photocoagulation. (D) A 9-year-old girl with familial exudative vitreoretinopathy with tractional retinal detachment involving the fovea and with subretinal exudates (stage 4) was subjected to pars plana vitrectomy, laser coagulation, and silicone oil injection (E).

Systemic associations are absent. The management of FEVR is similar to that for ROP: in the early stages, peripheral coagulation by laser or cryocoagulation of the avascular retinal periphery is used to reduce subretinal and intraretinal exudation. The presence of angiographic leakage, especially at the site of vascular–avascular junction, warrants prompt laser ablation of the area (green or red laser to the area of leakage and 0.5-disc- to 1-disc-diameter area surrounding it).[122] Anti-VEGF therapy may provide a valuable adjunctive treatment for FEVR. In one study,[123] three children (6–14 years), with persistent vascular activity and increasing exudation, despite aggressive laser photocoagulation and cryocoagulation, were successfully treated by intravitreal injection of pegaptanib sodium (Macugen; 0.3 mg per 0.09 mL). All patients showed a reduction of exudation, but two children developed vitreous hemorrhage due to traction retinal detachment and needed pars plana vitrectomy. After injection of bevacizumab (Avastin; 1.25 mg per 0.05 mL) in an adult patient, rapid regression and accelerated fibrosis of neovascular tissues was observed.[124]

In traction retinal detachment, scleral buckling should be performed in cases with peripheral traction anterior to the equator,[125] and vitreoretinal surgery is indicated to release posterior vitreous traction. The vitreoretinal adhesions are so strong in the peripheral avascular area that iatrogenic retinal breaks occur easily. A bimanual technique with vitreous scissors and forceps is preferred to dissect the vitreous membranes from the retinal surface. Dissection of the vitreous in the peripheral avascular area is very difficult, and if this procedure cannot successfully be performed, the prognosis is poor.[121,126] If an eye is symptomatic in the first 3 years of life, the prognosis is poor. Fibrovascular proliferation has a rich vascular component in patients younger than 3 years, and collagen fibers become more evident with advancing age.[125] Vitreoretinal surgery can preserve some degree of vision in FEVR patients but amblyopia, reproliferation, and vitreous hemorrhage may limit long-term visual improvement.[127] The ultimate goal of prophylactic laser treatment in FEVR is the prevention of retinal detachment or secondary macular exudate.

Marfan Syndrome

Retinal detachment is the most serious eye complication, occurring in up to 25% of patients with Marfan syndrome. A total of 75% of retinal detachments occur before patients are 20 years old.[128] Retinal detachment in Marfan syndrome is bilateral in about one-third of cases. Most Marfan syndrome patients with retinal detachment have a subluxated lens or have undergone previous lens surgery. Therefore, these patients should be checked especially carefully.[129]

Retinal detachment surgery can be complicated by insufficient pupil dilation, ectopia lentis, and multiple retinal breaks.[130] The edge of the clear or cataractous subluxated lens hampers evaluation of the peripheral fundus.

Primary scleral buckling is recommended if the clear lens is in proper position; if the clear subluxated lens is not interfering with visualization of fundus details; or if the retinal breaks are located near or anterior to the equator. The placement of scleral sutures for buckling is challenging due to the thin and collapsible sclera.

Vitreous surgery should be considered in the following situations: failed scleral buckling; proliferative vitreoretinopathy; a posteriorly dislocated lens; a subluxated or cataractous lens not allowing an adequate evaluation of the fundus periphery; and giant retinal tears.[131] Due to the thin sclera, the use of trochars should be avoided.

The results of surgery vary depending on the nature of the retinal tear and the presence of PVR. Generally, the results are comparable with those patients without Marfan syndrome and successful reattachment of the retina is achieved in 86%[131] to 100%[130] of cases. But poorer visual outcome is likely to be encountered when there is concomitant lens dislocation or a history of intraocular surgery.[130] The increased incidence of high myopia and peripheral lattice degeneration predisposes these eyes to retinal breaks. According to some authors the high bilateral rate of retinal detachment may justify prophylactic laser treatment of lattice degenerations in the fellow eye of these patients.[130,132]

Congenital X-Linked Retinoschisis

Congenital X-linked retinoschisis (CX-LRS) is an inherited retinal disease characterized by abnormal Müller cell pillars that allow schisis cavities to form. In 98–100% of the cases, these cavities in the

foveal area, and the peripheral retinoschisis, usually inferotemporal, is present in about 50% of cases and is associated with severe vision-threatening complications, such as vitreous hemorrhage and retinal detachment. The most severe disease form, which manifests as bullous, peripheral retinoschisis cavities, occurs primarily in patients younger than 10 years. The age of onset follows a bimodal distribution with one group of patients presenting in infancy with strabismus and nystagmus and a second group with poor vision and reading difficulties presenting at school age.[133] There are a few case reports on children suffering from retinoschisis in the first year of life. In a series of five children who presented in the first 18 months of life, highly elevated bullous retinoschisis involving the macula was observed. In 9 of 10 eyes of these patients, the bullous retinoschisis cavity flattened, leaving only pigment demarcation lines within an observation time of 1–6.5 years.[134] Surgical intervention for congenital retinoschisis is frequently recommended under certain clinical conditions: rapid progression of the peripheral schisis cavity involving or threatening the macula, obscuration of the macula by the overhanging inner wall of a schisis cavity, dense nonclearing vitreous hemorrhage with a large schisis cavity hemorrhage, schisis combined with rhegmatogenous retinal detachment, and schisis combined with tractional retinal detachment, and macular pucker.[135] Prenner et al.[136] developed a new classification system for CX-LRS based on an improved understanding of the underlying pathologic lesion, and identified better surgical approaches (Table 119.6).

TABLE 119.6
Classification System for CXLRS

CXLS Type	Foveal Cystic Schisis Clinical Examination	Flat or Lamellar Macula Schisis OCT Finding	Peripheral Schisis (Clinical Examination)
Type 1 foveal	+	−	−
Type 2 foveolamellar	+	+	−
Type 3 complex	+	+	+
Type 4 foveoperipheral	+	−	+

CXLRS, congenital X-linked retinoschisis; OCT, optical coherence tomography.

Reproduced with permission from Prenner JL, Capone A Jr, Ciaccia S, et al.

Congenital X-linked retinoschisis classification system. Retina 2006;26:S61–4.

Recent studies advocate vitrectomy for a bullous schisis cavity with or without hemorrhage in children with successful surgically induced posterior vitreous detachment.[135,137,138] García-Arumí et al.[137] performed posterior hyaloid dissection after injection of 0.05 mL of diluted preservative-free triamcinolone acetonide in an 8-month-old child. Trese[139] describes the adjuvant use of autologous plasmin for hyaloid separation. In pediatric eyes is it very difficult to mechanically achieve a complete posterior vitreous detachment. In most cases, the only way to relieve the vitreous traction is to remove the inner wall of the retinoschisis, since there is no effective way to remove the posterior cortical vitreous in children.[140,141] Because the area of retinoschisis corresponds to an absolute scotoma on the visual field, removing the inner wall of retinoschisis has no effect on the patient's visual field,[140] but it results in loss of retinal ganglion cells and interneurons, eliminating any chance for future schisis cavity adhesion. Furthermore, eyes that undergo inner-wall retinotomy are prone to proliferation along the anterior leaflet of the schisis. Trese recommends the application of autologous plasmin, since this method eliminates the need for inner-wall retinectomy in up to 82% of eyes.[139] They performed inner-wall retinectomy on eyes with type 4 CX-LRS only. Incision into the inner wall of the schisis cavity should be performed 2–3 mm anterior to the posterior border of the schisis cavity; some authors describe fluid drainage by use of a 42G cannula.[137] Photocoagulation should applied to the border of the attached retina and the schisis cavity to prevent the progression of retinal splitting. Gas or silicone can be used for postoperative tamponade. Silicone oil is particularly recommended for younger children.

Authors described postoperative retinal reattachment in the pediatric eyes, but the functional results are limited; the visual acuity improved in only 53% of cases, best reported postoperative visual acuity was 20/50 attained by a 6-year-old child.[137,141] In a series of cases, the main indication for unilateral vitrectomy in a 7-year-old and bilaterally in a 17-year-old was foveal retinoschisis, which was associated with peripheral retinoschisis or peripheral inner holes. The vitreous surgery consisted of core vitrectomy, surgically induced posterior vitreous detachment, removal of the

ILM, and a 30% sulfur hexafluoride gas tamponade. Restoration of the foveal depression with flattening of the schisis cavity was achieved in the first surgery in all three eyes, and visual acuity improved in all cases. The anatomic result was normal foveal configuration with small cystoid spaces in the retina layer, but negative b-waves persisted in the affected eyes even 3 years after clinical resolution of the retinoschisis due to the inability of the intraretinal nerve fibers to reconnect despite repositioning of the retinoschisis.[138]

Others[142] reported results of vitrectomy with surgery-induced PVD in 17 eyes in which the premacular vitreous cortex was removed and the ILM of 2 to 3 disc diameters around the fovea was peeled. The authors avoid ILM-peeling over the very weakened retinoschisis area. Finally they used C_3F_8 gas tamponade. In all operated eyes the macular schisis cavity resolved and mean visual acuity increased from 20/125 to 20/55.

Rhegmatogenous retinal detachment in retinoschisis occurs if outer- and inner-wall holes develop in an area of peripheral schisis. The surgical principle is to coagulate outer-wall breaks and perform scleral buckling, if the location and size of the outer-wall breaks allow for support along the element. The reported advantage of scleral buckling is that it is less invasive than vitrectomy and provides support to the vitreous base. If scleral buckling fails, vitrectomy is recommended because it allows improved treatment of the outer-wall break with laser after internal drainage and flattening the retina.[135] An additional indication for vitrectomy is tractional retinal detachment. In such cases, a combination of primary scleral buckling and vitrectomy is usually recommended. The surgical approach is scleral buckling for retinal detachment, particularly in the absence of PVR and in which the outer wall holes are located anterior to the equator and vitrectomy for vitreous hemorrhage or PVR. PVR is the major reason for reoperation, and multiple operations and the use of advanced vitreoretinal techniques to manage PVR-related complications are necessary for ultimate success in certain cases.[143]

Knobloch Syndrome

Knobloch syndrome is a recessive syndrome of hereditary

vitreoretinal degeneration with retinal detachment, high myopia, cataract, telecanthus, hypertelorism, and a high-arched palate.[144] There is also a defect of the anterior midline scalp with involvement of the frontal bone. The presence of a congenital midline scalp defect should alert the clinician to possible underlying central nervous system and/or ocular pathology and should lead to consideration of further diagnostic evaluations and prophylactic measures. It has been reported that fellow eyes should be treated with prophylactic retinal cryotherapy, although the value of such therapy is unproven.[145,146]

Incontinentia Pigmenti

Incontinentia pigmenti is a rare, X-linked, dominant disorder in which affected female infants develop characteristic abnormalities of the skin, central nervous system, hair, teeth, and eyes. Ocular abnormalities occur in about 35% of patients[147,148] and consist of nystagmus, strabismus, microphthalmos, ptosis, blue sclera, pigmentation of the conjunctiva, corneal changes, cataract, optic atrophy, vitreous hemorrhage, myopia, and in 11.5% of cases, fibroblastic retinal detachment secondary to ischemic vasculopathy similar in appearance to retinopathy of prematurity. Fluorescein angiography indicates profound peripheral retinal ischemia and abnormal arteriovenous connections in these eyes. The affected cases develop neovascularizations, followed by preretinal fibrotic tissue at the temporal equator, and in a late stage, an extensive fibrovascular tissue pulls the retina anteriorly behind the lens. It seems likely that most retinal detachments occur within the first year of life, and all retinal detachments occur within the first 3 years of life. Most of the ocular abnormalities are unilateral, and in those with bilateral involvement one eye is usually less affected. Patients with *NEMO* mutation may have an increased risk of retinal pathology.[149] For affected babies, retinal screening should usually be performed under anesthesia as soon as possible after birth, and fluorescein angiography should be performed when areas of avascular peripheral retina are noted by indirect ophthalmoscopy. Therapeutic intervention with indirect laser photocoagulation to the peripheral ischemic retina should usually be performed as soon as the diagnosis is made; some authors describe successful resolution

of the vasculopathy after early laser photocoagulation.[150] Today, the intravitreal injection of anti-VEGF could be a further adjunctive treatment option. Five days after intravitreal injection of 1.25 mg/0.05 mL bevacizumab in an 11-month-old boy, extensive neovascularization transformed into sclerotic ghost vessels, and vitrectomy was facilitated.[151]

Norrie Disease

Norrie disease is a bilateral X-linked recessive syndrome of ocular dysgenesis with progressive auditory and mental impairment. Norrie disease is believed to result from mutations in the 28-kb Norrie disease protein (*NDP*) gene, located on chromosome Xp11.3.[152] The disease is characterized by a retinal falciform fold, retinal detachment, repeated vitreous hemorrhage, retrolental membrane formation, and finally clinical progression from these early retinal and vitreous changes to the more typical retrolental detached retina. There are large areas of avascular retina, but without neovascularization. Walsh et al.[153] hypothesize that the avascular retina is so dysgenic that it does not produce a significant vascular endothelial growth factor response, and they do not perform photo- or cryocoagulation. They recommend early diagnosis and vitrectomy to avoid the dismal natural history of Norrie disease, namely, no light perception (NLP) vision and phthisis. Dysplastic retina can be flattened by vitrectomy; children who achieved light perception were operated at a median age of 3.5 months (1 week to 14 months).[153,154]

Anomalies of the Papilla

Several cavitary anomalies of the optic disc, including optic nerve coloboma, morning glory anomaly, and optic pit, are congenital disc abnormalities secondary to a colobomatous malformation of the optic nerve head. Molecular biology allows detection of the mutations in the *PAX2* gene in approximately 50% of cases. The observation of cavitary anomalies of the optic disc and/or coloboma of the fundus or related abnormality usually stimulates nephrologic investigations to check for renal hypoplasia, a potentially life-threatening disease.[155]

The cavity anomalies of the optic pit can be associated with the

development of a schisis-like thickening and serous macular detachment, most commonly in the second to fourth decades, onset in the early childhood has been reported in rare cases.[156] The unifying anatomic theme of these anomalies is the presence of a scleral (or lamina cribrosa) defect permitting anomalous communications between intraocular and extraocular spaces. These communications enable the critical pathogenic mechanism responsible for dynamic fluctuations in the gradient between intraocular and intracranial pressures that direct the movement of fluid (vitreous humor or cerebrospinal fluid) into and under the retina.[155]

As a result of abnormal anatomic features, the vitreous, subretinal, subarachnoid, and possibly orbital spaces may be variably interconnected through the relatively compliant and porous tissues comprising the excavated disc anomaly.[155]

Morning-glory disc is a unilateral markedly enlarged optic papilla with funnel-shaped excavation involving the optic disc and peripapillary retina. Furthermore it is characterized by a radial arrangement of retinal vessels, glial hyperplasia over the center of the disc, and a rim of elevated peripapillary pigmented tissue.

Morning-glory disc anomaly is a descriptive classification for a characteristic lesion of the optic nerve that is often associated with serous retinal detachment. Systemic associations are present in some patients. A wide range of posterior segment abnormalities can be observed. Retinal detachment occurs in one-third of cases and can be associated with a break at the optic disc margin[157] or within the optic disc cup.[158] Detachment may be limited to the peripapillary retina or be extensive. Retinal detachment is usually seen after the first year of life. The benefit of vitreous surgery with drainage of subretinal fluid, gas tamponade, or silicone oil, and peripapillary photocoagulation has been established.[159]

Congenital pits of the optic nerve vary in size, shape, depth, and location. They often appear as small, hypopigmented, yellow or whitish, oval or round excavated defects, most often within the inferior temporal portion of the optic cup. They are bilateral in 15% of patients, covered or filled with a veil of tissue. Some 40–60% of patients with optic pits develop nonrhegmatogenous serous macular detachments. A tear in the diaphanous tissue overlying the

optic nerve pit may be responsible for the development of this problem,[160] which is consistent with findings in similar conditions, such as retinal detachment, in association with chorioretinal coloboma. These tears may be quite subtle, and careful biomicroscopic examination is required to appreciate them. Initially, conservative management is recommended, as 25% of optic disc pit maculopathies resolve spontaneously (Figs. 119.11A–C).[161] The value of laser photocoagulation alone along the temporal disc margin is not very convincing, since even worse retinal detachments or redetachments have been observed.[155,161]

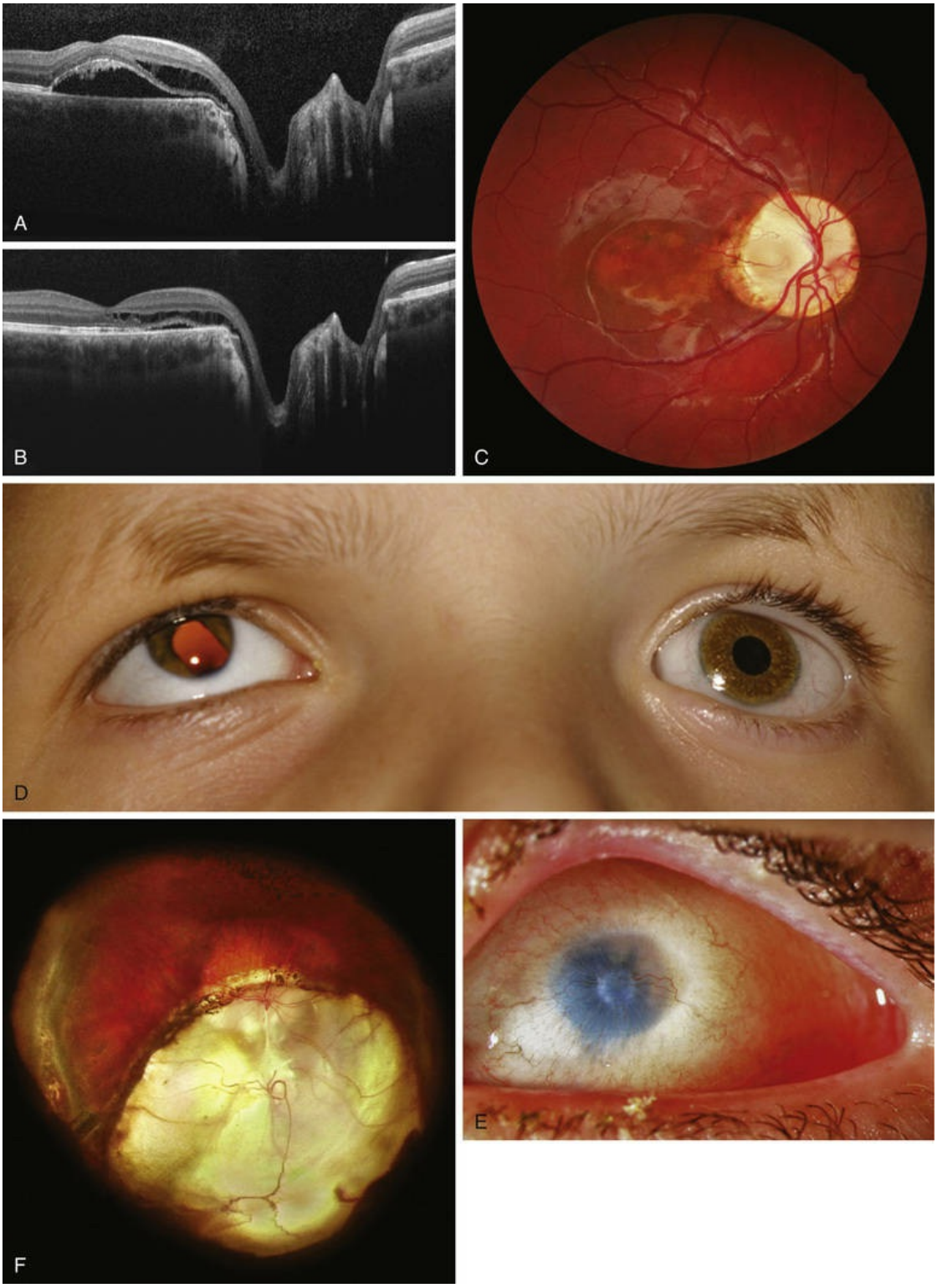

FIG. 119.11 (A) Optical coherence tomography (OCT) of a 12-year-old boy with congenital pit of the optic nerve and serous macular detachment. (B) After 5 months, OCT demonstrates the spontaneous reattachment. (C) Fundus photograph shows the congenital pit of the optic nerve after regression of the

serous maculopathy. (D) A 14-year-old boy suffered from trisomy 22, the “cat-eye syndrome,” uveal coloboma of both eyes was associated on the left eye (E) with microphthalmus. The boy wears a flat glass prosthesis over the microphthalmic eye. (F) Retinal detachment in the right eye was treated by vitrectomy, cerclage, endolaser coagulation, and silicone oil tamponade. Two years after silicone oil removal, the eye shows retinal stability, a laser barrier after gentle laser coagulation seals the junction between the intercalary membrane and extra colobomatous retina.

In recent reviews of results of vitreoretinal surgery for treatment of an optic pit maculopathy, the most widely accepted treatment for both adult patients and children is a pars plana vitrectomy.[155,161,162]

There are several case reports on successfully performed vitrectomies in children aged 7–16 years old.[160–163] The removal of the posterior hyaloid face from the macula is an essential element of successful treatment, but this may be difficult to achieve in pediatric eyes. Georgalas et al.[164] reported that surgical PVD seemed impossible in the case of a 5-year-old boy with optic disc pit maculopathy, and therefore the posterior vitreous was peeled off from the macular area within the retinal arcades and air was used as an endotamponade. ILM peel may not improve outcomes, and no difference between short- or long-acting gas tamponade was observed in one report.[162] Others[165] found that vitrectomy alone without gas tamponade and laser photocoagulation is a safe and effective method for management of serous macular detachment resulting from optic pit.

Some authors[165,166,167] performed laser photocoagulation in the peripapillary area during vitrectomy, but more recent studies[162,168] found that vitrectomy with juxtapapillary laser coagulation had similar functional and anatomic outcomes compared with vitrectomy without juxtapapillary laser coagulation. Some authors[155] recommend a carefully titrated juxtapapillary laser photocoagulation (4 to 5 confluent rows in the temporal juxtapapillary area) with slit-lamp (647 nm) laserlight with a 200 μm spot size performed 1–2 hours before vitrectomy. As an alternative to laser photocoagulation, the successful use of a small plug of autologous sclera to create a barrier to the passage of

vitreous fluid into large optic pits was described in a 11- and 15-year-old patient.[156]

Migration of gas or silicone oil into the subretinal space has been reported as a surgical complication.[169] Furthermore, intracranial migration of silicone oil after vitreoretinal surgery for the treatment of optic disc maculopathy has been described.[170] Therefore, if possible, a gas tamponade should preferably be used.

Coloboma

Coloboma of the fundus is a congenital defect caused by the faulty closure of the embryonal fissure. It occurs in 0.14% of the general population.[171] The literature quotes a 40% occurrence of retinal detachment in these patients, typically in the second decade of life.[172] Near the margin of the coloboma, the retina splits into two layers.[173] The inner layer continues as an intercalary membrane on to the coloboma, while the outer layer turns back, becomes disorganized, and fuses with the retinal pigment epithelium. The choroid is terminated as a distinct pigmented layer peripheral to this point of reversal. The split in the retinal layer has been identified at the level of inner nuclear layer or outer plexiform layer, or both. The junction where this reversal occurs is a locus minoris resistentiae. The intercalary membrane progressively becomes thinner as it is traced centrally. Breaks can occur at the junction and in the intercalary membrane. Peripheral retinal breaks are also observed. The preferred technique for treatment of retinal detachment associated with choroidal coloboma is vitrectomy with either long-acting gas or oil tamponade. The use of silicone oil has the advantage of being a long-term tamponade of the entire colobomatous border.

Breaks in the intercalary membrane can be identified pre- or intraoperatively, whereas the breaks at the locus minoris resistentiae are not identifiable but can be expected to be located along the coloboma border. Treatment of the pigmented fundus just beyond the coloboma with laser should close these breaks and eliminates the need to close the breaks in the intercalary membrane. The diode laser is preferred to the argon laser because it is less likely to damage the nerve fiber layer. Tansu et al. recommend an endolaser barrier of three to four rows along the border of the

coloboma. Near the optic disc and papillomacular bundle we perform a gentle endolaser coagulation as consistent with other authors.[174] If adequate chorioretinal adhesion can be achieved around the coloboma, laser of the papillomacular bundle and optic disc may not be necessary (Figs. 119.11D–F).[175] After vitrectomy and silicone oil removal, OCT showed persistent detachment of the intercalary membrane in most patients. These findings emphasize the importance of sealing the junction between the intercalary membrane and extra colobomatous retina with a laser barrier.[174]

The placement of an encircling band is performed on a purely empirical basis. Several authors observed no difference in the outcome between the buckled and nonbuckled eyes. Peripheral laser photocoagulation along the ora serrata may reduce the risk of recurrent retinal detachment after silicone oil removal.[172,175]

Persistent Hyperplastic Primary Vitreous

Persistent hyperplastic primary vitreous (PHPV), also known as persistent fetal vasculature, is a congenital anomaly of the eye that results from failure of the embryologic, primary vitreous, and the hyaloid vasculature to regress. It typically presents unilaterally, without associated systemic findings in normal full-term infants. In rare cases, bilateral PHPV has also been described.[176] Most cases of PHPV are sporadic, but it can be inherited as an autosomal dominant or recessive trait.[177] PHPV is subclassified into three types: (1) most often an anterior PHPV (retrolental fibrovascular membrane, elongated ciliary processes, cataract, microphthalmia); (2) posterior PHPV (vitreous membrane and stalk, retinal fold, traction retinal detachment, hypoplastic optic nerve and macula, microphthalmia); (3) a combination of anterior and posterior PHPV (Fig. 119.12). Without surgery, most eyes with PHPV will develop severe glaucoma, retinal detachment, intraocular hemorrhage, and/or phthisis early in life. If it is left untreated, enucleation may become necessary. To prevent these complications, many authors recommend vitreoretinal surgery without delay if light perception is present, especially in rare cases of bilateral PHPV.[178] But in eyes with severe PHPV with an unrecordable visual evoked potential, no light perception, and intense afferent pupillary defect, an operation should not be performed.[179] Indications for surgical intervention

include recurrent or severe intravitreal hemorrhage, retinal detachment, progressive shallowing of the anterior chamber, and uncontrolled pressure secondary to anterior chamber angle closure.[180] The vitrectomy port location should be varied according to the age of the child, but in these often microphthalmic eyes, the ora serrata may be anteriorly displaced, the pars plana may be absent, or the anterior retina may insert directly onto the pars plicata ciliary body. It is recommended to place the sclerotomies as anteriorly as possible, especially if retinal detachment is determined by preoperative ultrasonography.[181] Transillumination is occasionally helpful to locate the ora serrata. To avoid manipulations of the vitreous base or peripheral retina, which may be drawn anteriorly, other authors prefer an approach for vitrectomy through the iris root; incisions are made at the limbus, but this is associated with the danger of severe iris lesions. After lensectomy, diathermy should be used when vessels are visible and the retrolental membrane has to be cut from the ciliary processes using the vitreous cutter. In case of nonaxial lens opacification, lens-sparing vitrectomy should be performed, and Shaikh and Trese[182] recommend dividing the stalk immediately on entry. After division of the stalk and hemostasis, with diathermy if necessary, vitrectomy should be carried out with dissection of epiretinal membranes in the posterior pole. The authors presume that the manipulation of the stalk by vitrectomy and diathermy before division result in damage to the lens capsule and resultant cataract formation.

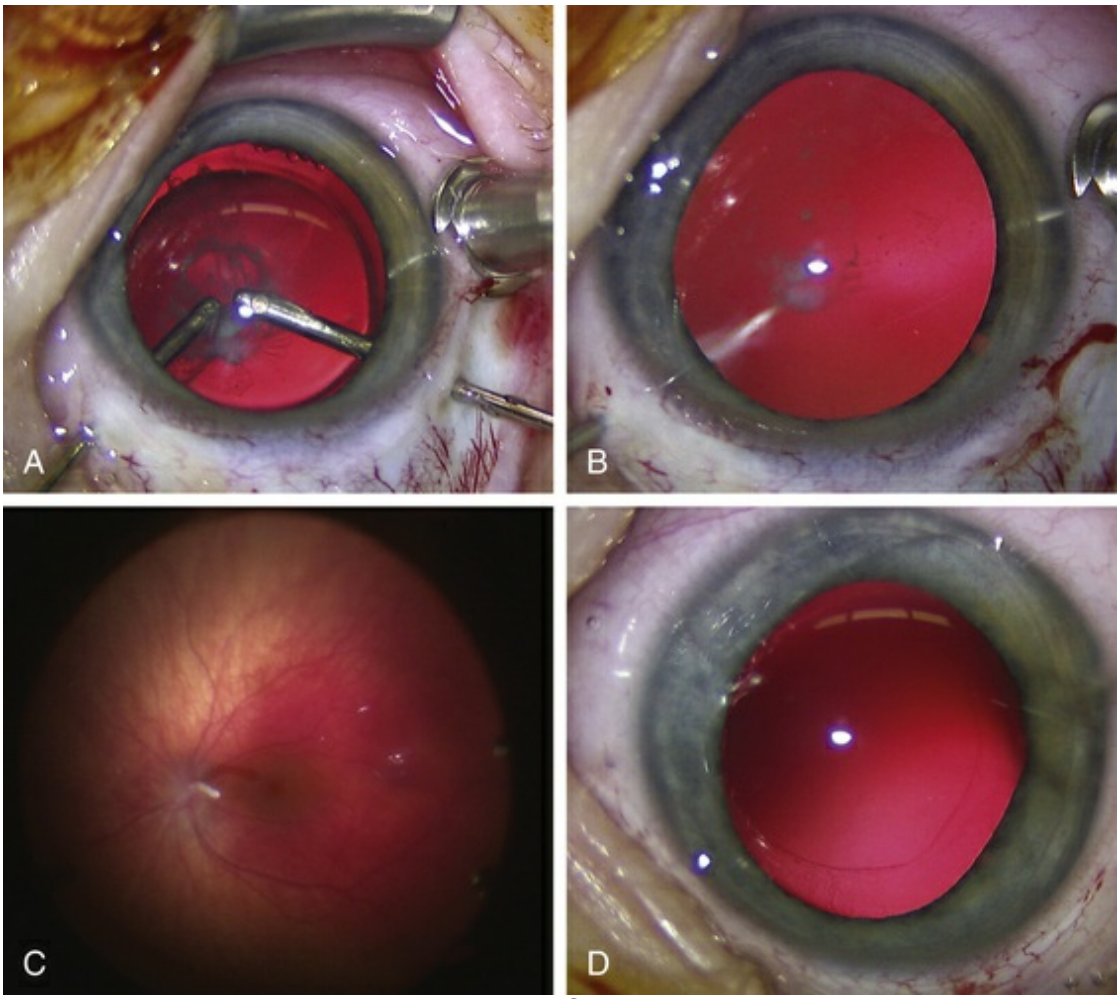

FIG. 119.12 (A) Lensectomy of congenital cataract via pars plan approach. (B) After aspiration of lens material dense capsular opacity and stalk of posterior persistent hyperplastic primary vitreous was visible. (C) The postoperative fundus photograph shows remnants of the central stalk and (D) capsular bag after anterior and posterior capsulorhexis.

Membrane peeling is necessary in cases of traction retinal folds or traction detachment. In the purely anterior form, the cataract should be removed to provide clear media for visual rehabilitation. Eyes with a posterior PHPV have poor visual results due to posterior pole abnormalities. However, despite posterior segment involvement, surgical treatment of PHPV can result in functional visual outcome. The degree of ocular malformation, however, will ultimately limit the amount of visual improvement. A total of 71% of patients undergoing vitrectomy for a combined form of anterior and posterior PHPV achieved 20/300 or better.[181] In another

study,[179] six of 24 eyes operated for PHPV maintained Snellen visual acuity and approximately 50% of patients undergoing surgery for persistent fetal vasculature may achieve useful vision. In a series of patients suffering from the rare condition of bilateral combined anterior and posterior PHPV, Walsh et al.[178] found that vitrectomy with or without lensectomy is beneficial: 69% of patients maintained at least light perception vision in at least one eye at the last follow-up. Of the 28 operated eyes in 16 patients with follow-up data, only 11% of eyes were phthisical at the last follow-up. A more recent study[180] suggested that early intervention at younger than or equal to 13 months of age offers improved visual potential. Their data suggest that a period of retinal "physical plasticity" extends to at least 13 months of age. All 10 patients who received surgical intervention within this time had reattachment of the retina with reversal of retinal dragging and decreased retinal folds. After surgery, every child should have a short trial (2 months) of occlusion therapy. This can be terminated if no visual improvement is noted, to avoid undue psychosocial impairment.[181] Early age at surgery, prompt optical correction with contact lens, and aggressive occlusion therapy are required for successful visual rehabilitation.

Retinopathy of Prematurity (ROP)

ROP is discussed in Chapter 118, Retinopathy of prematurity.

Conclusions

Both the feasibility of surgical intervention and the growing sophistication of genetic counseling have created a renewed interest in the field of pediatric vitrectomy. The result is likely to be improved understanding of elusive truths that surround functional ocular development. The intravitreal use of VEGF inhibitors to treat vasoproliferative retinopathy in children is a new effective tool, but further results on safety and side-effects are needed. In addition, the use of pharmacologic agents to assist in detaching the cortical vitreous from the retina will hopefully improve outcomes in the future. Surgical innovations and disease-specific treatment strategies will improve the results in these patients.

References

1. Birch EE, Stager DR. The critical period for surgical treatment of dense congenital unilateral cataract. *Invest Ophthalmol Vis Sci*. 1996;37:1532–1538.
2. Hanse W. Amblyopie. Kaufmann H. *Strabismus*. Ferdinand Enke: Stuttgart; 1995:285–395.
3. Smiddy WE, Loupe DN, Michels RG, et al. Refractive changes after scleral buckling surgery. *Arch Ophthalmol*. 1989;107:1469–1471.
4. Chow DR, Ferrone PJ, Trese MT. Refractive changes associated with scleral buckling and division in retinopathy of prematurity. *Arch Ophthalmol*. 1998;116:1446–1448.
5. Lang J. *Strabismus, Schielformen, Therapien*. Hans Huber: Berne; 2003.
6. Hairston RJ, Maguire AM, Vitale S, et al. Morphometric analysis of pars plana development in humans. *Retina*. 1997;17:135–138.
7. Möller H. Milestones and normative data. Taylor D. *Pediatric ophthalmology*. Lippincott, Williams & Wilkins: Philadelphia; 1997.
8. Gordon RA, Donzis PB. Refractive development of the human eye. *Arch Ophthalmol*. 1985;103:785–789.
9. Inagaki Y. The rapid change of corneal curvature in the neonatal period and infancy. *Arch Ophthalmol*. 1986;104:1026–1027.
10. Miller-Meeks MJ, Bennett SR, Keech RV, et al. Myopia induced by vitreous hemorrhage. *Am J Ophthalmol*. 1990;109:199–203.
11. Hubel DH, Wiesel TN. The period of susceptibility to the physiological effects of unilateral eye closure in kittens. *J Physiol*. 1970;206:419–436.
12. Mohney BG. Axial myopia associated with dense vitreous hemorrhage of the neonate. *J AAPOS*. 2002;6:348–353.
13. Bonomo PP. Pars plana and ora serrata anatomotopographic study of fetal eyes. *Acta Ophthalmol (Copenh)*. 1989;67:145–150.
14. Aiello AL, Tran VT, Rao NA. Postnatal development of the

ciliary body and pars plana. A morphometric study in childhood. *Arch Ophthalmol*. 1992;110:802–805.
15. Friberg TR, Lace JW. A comparison of the elastic properties of human choroid and sclera. *Exp Eye Res*. 1988;47:429–436.
16. Sebag J. Vitreous pathobiology. Tasman W. *Duane's ophthalmology*. Lippincott Williams & Wilkins: Philadelphia; 2004.
17. Gallemore RP, Bokosky JE. Penetrating keratoplasty with vitreoretinal surgery using the Eckardt temporary keratoprosthesis: modified technique allowing use of larger corneal grafts. *Cornea*. 1995;14:33–38.
18. Garcia-Valenzuela E, Blair NP, Shapiro MJ, et al. Outcome of vitreoretinal surgery and penetrating keratoplasty using temporary keratoprosthesis. *Retina*. 1999;19:424–429.
19. Roters S, Szurman P, Hermes S, et al. Outcome of combined penetrating keratoplasty with vitreoretinal surgery for management of severe ocular injuries. *Retina*. 2003;23:48–56.
20. Vanathi M, Panda A, Vengayil S, et al. Pediatric keratoplasty. *Surv Ophthalmol*. 2009;54:245–271.
21. Reidy JJ. Penetrating keratoplasty in infancy and early childhood. *Curr Opin Ophthalmol*. 2001;12:258–261.
22. Andreoli CM, Andreoli MT, Kloek CE, et al. Low rate of endophthalmitis in a large series of open globe injuries. *Am J Ophthalmol*. 2009;147:601–608.
23. Chen TC, Bhatia LS, Walton DS. Complications of pediatric lensectomy in 193 eyes. *Ophthalmic Surg Lasers Imaging*. 2005;36:6–13.
24. Meier P, Sterker I, Tegetmeyer H, et al. 23-gauge-lentectomy for the treatment of congenital cataract. *Ophthalmologe*. 2010;107:241–245.
25. Gonzales CR, Boshra J, Schwartz SD. 25-Gauge pars plicata vitrectomy for stage 4 and 5 retinopathy of prematurity. *Retina*. 2006;26:S42–6.
26. Woo SJ, Park KH, Hwang JM, et al. Risk factors associated with sclerotomy leakage and postoperative hypotony after 23-gauge transconjunctival sutureless vitrectomy. *Retina*. 2009;29:456–463.
27. Lam DS, Fan DS, Mohamed S, Yu CB, Zhang SB, Chen WQ.

25-gauge transconjunctival sutureless vitrectomy system in the surgical management of children with posterior capsular opacification. *Clin Experiment Ophthalmol*. 2005;33:495–498.
28. Gonzales CR, Singh S, Schwartz SD. 25-Gauge vitrectomy for paediatric vitreoretinal conditions. *Br J Ophthalmol*. 2009;93:787–790.
29. Thompson JT. Advantages and limitations of small gauge vitrectomy. *Surv Ophthalmol*. 2011;56:162–172.
30. Peyman GA, Canakis C, Livir-Rallatos C, et al. Small-size pediatric vitrectomy wide-angle contact lens. *Am J Ophthalmol*. 2003;135:236–237.
31. Recchia FM, Scott IU, Brown GC, et al. Small-gauge pars plana vitrectomy: a report by the American Academy of Ophthalmology. *Ophthalmology*. 2010;117:1851–1857.
32. Benz MS, Packo KH, Gonzalez V, et al. A placebo-controlled trial of microplasmin intravitreous injection to facilitate posterior vitreous detachment before vitrectomy. *Ophthalmology*. 2010;117:791–797.
33. Wong SC, Capone A Jr. Microplasmin (ocriplasmin) in pediatric vitreoretinal surgery: update and review. *Retina*. 2013;33:339–348.
34. Scott IU, Flynn HW Jr, Azen SP, et al. Silicone oil in the repair of pediatric complex retinal detachments: a prospective, observational, multicenter study. *Ophthalmology*. 1999;106:1399–1408.
35. Hisatomi T, Notomi S, Tachibana T, et al. Brilliant blue G double staining enhances successful internal limiting membrane peeling with minimal adverse effect by low cellular permeability into live cells. *Retina*. 2015;35:310–318.
36. Jackson TL, Vote B, Knight BC, et al. Safety testing of infracyanine green using retinal pigment epithelium and glial cell cultures. *Invest Ophthalmol Vis Sci*. 2004;45:3697–3703.
37. Gupta A, Rahman I, Leatherbarrow B. Open globe injuries in children: factors predictive of a poor final visual acuity. *Eye (Lond)*. 2009;23:621–625.
38. Jandeck C, Kellner U, Bornfeld N, et al. Open globe injuries

in children. *Graefes Arch Clin Exp Ophthalmol*. 2000;238:420–426.
39. Lee CH, Lee L, Kao LY, et al. Prognostic indicators of open globe injuries in children. *Am J Emerg Med*. 2009;27:530–535.
40. Choovuthayakorn J, Patikulsila P, Patikulsila D, et al. Characteristics and outcomes of pediatric open globe injury. *Int Ophthalmol*. 2014;34:839–844.
41. Mittra RA, Mieler WF. Controversies in the management of open-globe injuries involving the posterior segment. *Surv Ophthalmol*. 1999;44:215–225.
42. Kuhn F, Mester V, Morris R. A proactive treatment approach for eyes with perforating injury. *Klin Monatsbl Augenheilkd*. 2004;221:622–628.
43. Kuhn F. *Ocular trauma in children and elderly patients*. Springer: Berlin; 2008:417–435.
44. Heimann K. Silicone oil in penetrating eye injuries. Alfaro DV. *Vitreoretinal surgery of the injured eye*. Lippincott-Raven: Philadelphia; 1999:211–224.
45. Boiko E, Shishkin M, Dolgih V. *Indications for the encircling buckle (EB) procedure in severe open-globe eye injury (OGI)*. [Meeting abstract] http://www.egms.de/static/de/meetings/rg2008/08rg024.shtı 2008.
46. Azad RV, Kumar N, Sharma YR, et al. Role of prophylactic scleral buckling in the management of retained intraocular foreign bodies. *Clin Experiment Ophthalmol*. 2004;32:58–61.
47. Ahmadieh H, Soheilian M, Sajjadi H, et al. Vitrectomy in ocular trauma. Factors influencing final visual outcome. *Retina*. 1993;13:107–113.
48. Moisseiev J, Vidne O, Treister G. Vitrectomy and silicone oil injection in pediatric patients. *Retina*. 1998;18:221–227.
49. Sarrazin L, Averbukh E, Halpert M, et al. Traumatic pediatric retinal detachment: a comparison between open and closed globe injuries. *Am J Ophthalmol*. 2004;137:1042–1049.
50. Farr AK, Hairston RJ, Humayun MU, et al. Open globe injuries in children: a retrospective analysis. *J Pediatr Ophthalmol Strabismus*. 2001;38:72–77.

51. Freemann HM. Giant retinal tears. Lippincott Williams & Wilkins: Philadelphia; 1996:1–11. Tasman W. *Duane's clinical ophthalmology*. vol. 6(69).
52. Haring G, Wiechens B. Long-term results after scleral buckling surgery in uncomplicated juvenile retinal detachment without proliferative vitreoretinopathy. *Retina*. 1998;18:501–505.
53. Wang NK, Chen YP, Yeung L, et al. Traumatic pediatric retinal detachment following open globe injury. *Ophthalmologica*. 2007;221:255–263.
54. Errera MH, Liyanage SE, Moya R, et al. Primary scleral buckling for pediatric rhegmatogenous retinal detachment. *Retina*. 2015;35:1441–1449.
55. Chen YJ. Vitrectomy and internal limiting membrane peeling of a traumatic macular hole with retinal folds. *Case Rep Ophthalmol*. 2011;2:78–83.
56. Kuhn F, Morris R, Mester V, et al. Internal limiting membrane removal for traumatic macular holes. *Ophthalmic Surg Lasers*. 2001;32:308–315.
57. Yanagiya N, Akiba J, Takahashi M, et al. Clinical characteristics of traumatic macular holes. *Jpn J Ophthalmol*. 1996;40:544–547.
58. Lai MM, Joshi MM, Trese MT. Spontaneous resolution of traumatic macular hole-related retinal detachment. *Am J Ophthalmol*. 2006;141:1148–1151.
59. Mitamura Y, Saito W, Ishida M, et al. Spontaneous closure of traumatic macular hole. *Retina*. 2001;21:385–389.
60. Kusaka S, Fujikado T, Ikeda T, et al. Spontaneous disappearance of traumatic macular holes in young patients. *Am J Ophthalmol*. 1997;123:837–839.
61. Faghihi H, Ghassemi F, Falavarjani KG, et al. Spontaneous closure of traumatic macular holes. *Can J Ophthalmol*. 2014;49:395–398.
62. Yeshurun I, Guerrero-Naranjo JL, Quiroz-Mercado H. Spontaneous closure of a large traumatic macular hole in a young patient. *Am J Ophthalmol*. 2002;134:602–603.
63. Wu WC, Drenser KA, Trese MT, et al. Pediatric traumatic macular hole: results of autologous plasmin enzyme-

assisted vitrectomy. *Am J Ophthalmol*. 2007;144:668–672.
64. Johnson RN, McDonald HR, Lewis H, et al. Traumatic macular hole: observations, pathogenesis, and results of vitrectomy surgery. *Ophthalmology*. 2001;108:853–857.
65. García-Arumí J, Corcostegui B, Cavero L, et al. The role of vitreoretinal surgery in the treatment of posttraumatic macular hole. *Retina*. 1997;17:372–377.
66. Sudhalkar A, Chhablani J, Jalali S, et al. Spontaneous vitreous hemorrhage in children. *Am J Ophthalmol*. 2013;156:1267–1271.
67. Ferrone PJ, de Juan E Jr. Vitreous hemorrhage in infants. *Arch Ophthalmol*. 1994;112:1185–1189.
68. Cleary PE, Ryan SJ. Vitrectomy in penetrating eye injury. Results of a controlled trial of vitrectomy in an experimental posterior penetrating eye injury in the rhesus monkey. *Arch Ophthalmol*. 1981;99:287–292.
69. Schloff S, Mullaney PB, Armstrong DC, et al. Retinal findings in children with intracranial hemorrhage. *Ophthalmology*. 2002;109:1472–1476.
70. Reddy AR, Clarke M, Long VW. Unilateral retinal hemorrhages with subarachnoid hemorrhage in a 5-week-old infant: is this nonaccidental injury? *Eur J Ophthalmol*. 2010;20:799–801.
71. Scheller J, Doroslovacki P. Ruptured aneurysm and Terson syndrome in a 1-month-old infant. *Pediatr Neurol*. 2015;52:653–654.
72. Morris R, Kuhn F, Witherspoon CD. Hemorrhagic macular cysts. *Ophthalmology*. 1994;101:1.
73. de Vries-Knoppert W. Vitreous findings in a patient with Terson's syndrome. *Doc Ophthalmol*. 1995;90:75–80.
74. Velikay M, Datlinger P, Stolba U, et al. Retinal detachment with severe proliferative vitreoretinopathy in Terson syndrome. *Ophthalmology*. 1994;101:35–37.
75. Meier P, Schmitz F, Wiedemann P. Vitrectomy for pre-macular hemorrhagic cyst in children and young adults. *Graefes Arch Clin Exp Ophthalmol*. 2005;243:824–828.
76. Koozekanani DD, Weinberg DV, Dubis AM, et al. Hemorrhagic retinoschisis in shaken baby syndrome

imaged with spectral domain optical coherence tomography. *Ophthalmic Surg Lasers Imaging*. 2010; 10.3928/15428877-20100215-87.
77. Muni RH, Kohly RP, Sohn EH, et al. Hand-held spectral domain optical coherence tomography fi nding in shaken-baby syndrome. *Retina*. 2010;30:S45–50.
78. Gaynon MW, Koh K, Marmor MF, et al. Retinal folds in the shaken baby syndrome. *Am J Ophthalmol*. 1988;106:423–425.
79. Fivgas GD, Capone A Jr. Pediatric rhegmatogenous retinal detachment. *Retina*. 2001;21:101–106.
80. Wang NK, Tsai CH, Chen YP, et al. Pediatric rhegmatogenous retinal detachment in East Asians. *Ophthalmology*. 2005;112:1890–1895.
81. Lee RW, Mayer EJ, Markham RH. The aetiology of paediatric rhegmatogenous retinal detachment: 15 years experience. *Eye (Lond)*. 2008;22:636–640.
82. Oono Y, Uehara K, Haruta M, Yamakawa R. Characteristics and surgical outcomes of pediatric rhegmatogenous retinal detachment. *Clin Ophthalmol*. 2012;6:939–943.
83. Feltgen N, Weiss C, Wolf S, et al. Scleral buckling versus primary vitrectomy in rhegmatogenous retinal detachment study (SPR Study): recruitment list evaluation. Study report no. 2. *Graefes Arch Clin Exp Ophthalmol*. 2007;245:803–809.
84. Bansal AS, Hubbard GB 3rd. Peripheral retinal findings in highly myopic children < or =10 years of age. *Retina*. 2010;30:S15–19.
85. Ho AC, Yannuzzi LA, Pisicano K, et al. The natural history of idiopathic subfoveal choroidal neovascularization. *Ophthalmology*. 1995;102:782–789.
86. Cakir M, Cekic O, Yilmaz OF. Intravitreal bevacizumab for idiopathic choroidal neovascularization. *J AAPOS*. 2009;13:296–298.
87. Goodwin P, Shields CL, Ramasubramanian A, et al. Ranibizumab for coloboma-related choroidal neovascular membrane in a child. *J AAPOS*. 2009;13:616–617.
88. Cackett P, Wong D, Cheung CM. Combined intravitreal bevacizumab and argon laser treatment for Coats ' disease. *Acta Ophthalmol*. 2010;88:e48–9.

89. Kohly RP, Muni RH, Kertes PJ, et al. Management of pediatric choroidal neovascular membranes with intravitreal anti-VEGF agents: a retrospective consecutive case series. *Can J Ophthalmol*. 2011;46:46–50.
90. Coats G. Forms of retinal disease with massive exudation. *Roy Lond Ophthalmol Hosp Rep*. 1908;17:440–525.
91. Shields JA, Shields CL. Review: Coats disease: the 2001 LuEsther T. Mertz Lecture. *Retina*. 2002;22:80–91.
92. Sigler EJ, Randolph JC, Calzada JI, et al. Current management of Coats disease. *Surv Ophthalmol*. 2014;59:30–46.
93. Sigler EJ, Calzada JI. Retinal angiomatous proliferation with chorioretinal anastomosis in childhood Coats disease: a reappraisal of macular fibrosis using multimodal imaging. *Retina*. 2015;35:537–546.
94. Jumper JM, Pomerleau D, McDonald HR, et al. Macular fibrosis in Coats disease. *Retina*. 2010;30:S9–14.
95. Shields JA, Shields CL, Honavar SG, et al. Classification and management of Coats disease: the 2000 Proctor Lecture. *Am J Ophthalmol*. 2001;131:572–583.
96. Zhao Q, Peng XY, Chen FH, et al. Vascular endothelial growth factor in Coats' disease. [See comment in PubMed Commons.] *Acta Ophthalmol*. 2014;92:225–228.
97. Venkatesh P, Mandal S, Garg S. Management of Coats disease with bevacizumab in 2 patients. *Can J Ophthalmol*. 2008;43:245–246.
98. Gaillard MC, Mataftsi A, Balmer A, et al. Ranibizumab in the management of advanced Coats disease Stages 3B and 4: long-term outcomes. *Retina*. 2014;34:2275–2281.
99. Cai X, Zhao P, Zhang Q, et al. Treatment of stage 3 Coats' disease by endolaser photocoagulation via a two-port pars plana nonvitrectomy approach. *Graefes Arch Clin Exp Ophthalmol*. 2015;253:999–1004.
100. Zheng XX, Jiang YR. The effect of intravitreal bevacizumab injection as the initial treatment for Coats' disease. *Graefes Arch Clin Exp Ophthalmol*. 2014;252:35–42.
101. Ramasubramanian A, Shields CL. Bevacizumab for Coats'disease with exudative retinal detachment and risk

for vitreoretinal traction. *Br J Ophthalmol*. 2012;96:356–359.
102. Stergiou PK, Symeonidis C, Dimitrakos SA. Coats ' disease: treatment with intravitreal bevacizumab and laser photocoagulation. *Acta Ophthalmol*. 2009;87:687–688.
103. Lin CJ, Hwang JF, Chen YT, et al. The effect of intravitreal bevacizumab in the treatment of Coats disease in children. *Retina*. 2010;30:617–622.
104. Murthy R, Honavar SG, Vemuganti GK, et al. Systemic metastasis following hyphema drainage in an unsuspected retinoblastoma. *J Pediatr Ophthalmol Strabismus*. 2007;44:120–123.
105. Grabowska A, Calvo JP, Fernandez-Zubillaga A, et al. A magnetic resonance imaging diagnostic dilemma: diffuse infiltrating retinoblastoma versus coats ' disease. *J Pediatr Ophthalmol Strabismus*. 2010;47:e1–3.
106. Stickler GB, Belau PG, Farrell FJ, et al. Hereditary progressive arthro-ophthalmopathy. *Mayo Clin Proc*. 1965;40:433–455.
107. Stickler GB, Hughes W, Houchin P. Clinical features of hereditary progressive arthro-ophthalmopathy (Stickler syndrome): a survey. *Genet Med*. 2001;3:192–196.
108. Snead MP, Yates JR. Clinical and molecular genetics of Stickler syndrome. *J Med Genet*. 1999;36:353–359.
109. Snead MP, McNinch AM, Poulson AV, et al. Stickler syndrome, ocular-only variants and a key diagnostic role for the ophthalmologist. *Eye (Lond)*. 2011;25:1389–1400.
110. Fincham GS, Pasea L, Carroll C, et al. Prevention of retinal detachment in Stickler syndrome: the Cambridge prophylactic cryotherapy protocol. *Ophthalmology*. 2014;121:1588–1597.
111. Abeysiri P, Bunce C, da Cruz L. Outcomes of surgery for retinal detachment in patients with Stickler syndrome: a comparison of two sequential 20-year cohorts. *Graefes Arch Clin Exp Ophthalmol*. 2007;245:1633–1638.
112. Carroll C, Papaioannou D, Rees A, et al. The clinical effectiveness and safety of prophylactic retinal interventions to reduce the risk of retinal detachment and subsequent vision loss in adults and children with Stickler

syndrome: a systematic review. *Health Technol Assess*. 2011;15:iii–xiv [1 – 62].
113. Pollack A, Milstein A, Oliver M, et al. Circumferential argon laser photocoagulation for prevention of retinal detachment. *Eye (Lond)*. 1994;8(Pt 4):419–422.
114. Leiba H, Oliver M, Pollack A. Prophylactic laser photocoagulation in Stickler syndrome. *Eye (Lond)*. 1996;10(Pt 6):701–708.
115. Snead MP. Hereditary vitreopathy. *Eye (Lond)*. 1996;10(Pt 6):653–663.
116. Subramanian S, Gamanagatti S, Sinha A, et al. Kniest syndrome. *Indian Pediatr*. 2007;44:931–933.
117. Sergouniotis PI, Fincham GS, McNinch AM, et al. Ophthalmic and molecular genetic findings in Kniest dysplasia. *Eye (Lond)*. 2015;29:475–482.
118. Makino I, Watanabe M, Okamoto N, et al. A case of retinal detachment in Kniest dysplasia treated with vitreous surgery. *Nippon Ganka Gakkai Zasshi*. 1997;101:734–737.
119. Gilmour DF. Familial exudative vitreoretinopathy and related retinopathies. *Eye (Lond)*. 2015;29:1–14.
120. Zhao S, Overbeek PA. Elevated TGF-beta signaling inhibits ocular vascular development. *Dev Biol*. 2001;237:45–53.
121. Pendergast SD, Trese MT. Familial exudative vitreoretinopathy. Results of surgical management. *Ophthalmology*. 1998;105:1015–1023.
122. Kashani AH, Learned D, Nudleman E, et al. High prevalence of peripheral retinal vascular anomalies in family members of patients with familial exudative vitreoretinopathy. *Ophthalmology*. 2014;121:262–268.
123. Quiram PA, Drenser KA, Lai MM, et al. Treatment of vascularly active familial exudative vitreoretinopathy with pegaptanib sodium (Macugen). *Retina*. 2008;28:S8–12.
124. Tagami M, Kusuhara S, Honda S, et al. Rapid regression of retinal hemorrhage and neovascularization in a case of familial exudative vitreoretinopathy treated with intravitreal bevacizumab. *Graefes Arch Clin Exp Ophthalmol*. 2008;246:1787–1789.
125. Yamane T, Yokoi T, Nakayama Y, et al. Surgical outcomes

of progressive tractional retinal detachment associated with familial exudative vitreoretinopathy. *Am J Ophthalmol*. 2014;158:1049–1055.
126. Shubert A, Tasman W. Familial exudative vitreoretinopathy: surgical intervention and visual acuity outcomes. *Graefes Arch Clin Exp Ophthalmol*. 1997;235:490–493.
127. Glazer LC, Maguire A, Blumenkranz MS, et al. Improved surgical treatment of familial exudative vitreoretinopathy in children. *Am J Ophthalmol*. 1995;120:471–479.
128. Maumenee IH. The eye in the Marfan syndrome. *Trans Am Ophthalmol Soc*. 1981;79:684–733.
129. Nemet AY, Assia EI, Apple DJ, et al. Current concepts of ocular manifestations in Marfan syndrome. *Surv Ophthalmol*. 2006;51:561–575.
130. Lee SY, Ang CL. Results of retinal detachment surgery in Marfan syndrome in Asians. *Retina*. 2003;23:24–29.
131. Sharma T, Gopal L, Shanmugam MP, et al. Retinal detachment in Marfan syndrome: clinical characteristics and surgical outcome. *Retina*. 2002;22:423–428.
132. Abboud EB. Retinal detachment surgery in Marfan ' s syndrome. *Retina*. 1998;18:405–409.
133. Sikkink SK, Biswas S, Parry NR, et al. X-linked retinoschisis: an update. *J Med Genet*. 2007;44:225–232.
134. George ND, Yates JR, Bradshaw K, et al. Infantile presentation of X linked retinoschisis. *Br J Ophthalmol*. 1995;79:653–657.
135. Wu WC, Drenser KA, Capone A, et al. Plasmin enzyme-assisted vitreoretinal surgery in congenital X-linked retinoschisis: surgical techniques based on a new classification system. *Retina*. 2007;27:1079–1085.
136. Prenner JL, Capone A Jr, Ciaccia S, et al. Congenital X-linked retinoschisis classification system. *Retina*. 2006;26:S61–4.
137. García-Arumí J, Corcóstegui IA, Navarro R, et al. Vitreoretinal surgery without schisis cavity excision for the management of juvenile X linked retinoschisis. *Br J Ophthalmol*. 2008;92:1558–1560.

138. Ikeda F, Iida T, Kishi S. Resolution of retinoschisis after vitreous surgery in X-linked retinoschisis. *Ophthalmology*. 2008;115 [718–22.e1].
139. Trese MT. Enzymatic-assisted vitrectomy. *Eye (Lond)*. 2002;16:365–368.
140. Ferrone PJ, Trese MT, Lewis H. Vitreoretinal surgery for complications of congenital retinoschisis. *Am J Ophthalmol*. 1997;123:742–747.
141. Lee JJ, Kim JH, Kim SY, et al. Infantile vitreous hemorrhage as the initial presentation of X-linked juvenile retinoschisis. *Korean J Ophthalmol*. 2009;23:118–120.
142. Yu H, Li T, Luo Y, et al. Long-term outcomes of vitrectomy for progressive X-linked retinoschisis. *Am J Ophthalmol*. 2012;154:394–402.
143. Rosenfeld PJ, Flynn HW Jr, McDonald HR, et al. Outcomes of vitreoretinal surgery in patients with X-linked retinoschisis. *Ophthalmic Surg Lasers*. 1998;29:190–197.
144. Knobloch WH, Layer JM. Clefting syndromes associated with retinal detachment. *Am J Ophthalmol*. 1972;73:517–530.
145. Seaver LH, Joffe L, Spark RP, et al. Congenital scalp defects and vitreoretinal degeneration: redefining the Knobloch syndrome. *Am J Med Genet*. 1993;46:203–208.
146. Sniderman LC, Koenekoop RK, O'Gorman AM, et al. Knobloch syndrome involving midline scalp defect of the frontal region. *Am J Med Genet*. 2000;90:146–149.
147. Carney RG. Incontinentia pigmenti: a world statistical analysis. *Arch Dermatol*. 1976;112:535–542.
148. Swinney CC, Han DP, Karth PA. Incontinentia pigmenti: a comprehensive review and update. *Ophthalmic Surg Lasers Imaging Retina*. 2015;46:650–657.
149. O'Doherty M, Mc Creery K, Green AJ, et al. Incontinentia pigmenti – ophthalmological observation of a series of cases and review of the literature. *Br J Ophthalmol*. 2011;95:11–16.
150. Sanghi G, Dogra MR, Ray M, et al. Predominant exudative retinopathy in incontinentia pigmenti and clinical course after peripheral laser photocoagulation. *Indian J Ophthalmol*. 2011;59:255–256.
151. Lin KL, Hirose T, Kroll AJ, et al. Prospects for treatment of

pediatric vitreoretinal diseases with vascular endothelial growth factor inhibition. *Semin Ophthalmol*. 2009;24:70–76.
152. Warden SM, Andreoli CM, Mukai S. The Wnt signaling pathway in familial exudative vitreoretinopathy and Norrie disease. *Semin Ophthalmol*. 2007;22:211–217.
153. Walsh MK, Drenser KA, Capone A Jr, et al. Early vitrectomy effective for Norrie disease. *Arch Ophthalmol*. 2010;128:456–460.
154. Shima C, Kusaka S, Kondo H, et al. Lens-sparing vitrectomy effective for reattachment of newly developed falciform retinal detachment in a patient with Norrie disease. *Arch Ophthalmol*. 2009;127:579–580.
155. Jain N, Johnson MW. Pathogenesis and treatment of maculopathy associated with cavitary optic disc anomalies. *Am J Ophthalmol*. 2014;158:423–435.
156. Travassos AS, Regadas I, Alfaiate M, et al. Optic pit: novel surgical management of complicated cases. *Retina*. 2013;33:1708–1714.
157. Ho CL, Wei LC. Rhegmatogenous retinal detachment in morning glory syndrome pathogenesis and treatment. *Int Ophthalmol*. 2001;24:21–24.
158. Coll GE, Chang S, Flynn TE, et al. Communication between the subretinal space and the vitreous cavity in the morning glory syndrome. *Graefes Arch Clin Exp Ophthalmol*. 1995;233:441–443.
159. Jo YJ, Iwase T, Oveson BC, et al. Retinal detachment in morning glory syndrome with large hole in the excavated disc. *Eur J Ophthalmol*. 2011;21:841–844.
160. Postel EA, Pulido JS, McNamara JA, et al. The etiology and treatment of macular detachment associated with optic nerve pits and related anomalies. *Trans Am Ophthalmol Soc*. 1998;96:73–93.
161. Georgalas I, Ladas I, Georgopoulos G, et al. Optic disc pit: a review. *Graefes Arch Clin Exp Ophthalmol*. 2011;249:1113–1249.
162. Rayat JS, Rudnisky CJ, Waite C, et al. Long-term outcomes for optic disk pit maculopathy after vitrectomy. *Retina*. 2015;35:2011–2017.

163. Snead MP, James N, Jacobs PM. Vitrectomy, argon laser, and gas tamponade for serous retinal detachment associated with an optic disc pit: a case report. *Br J Ophthalmol*. 1991;75:381–382.
164. Georgalas I, Kouri A, Ladas I, et al. Optic disc pit maculopathy treated with vitrectomy, internal limiting membrane peeling, and air in a 5-year-old boy. *Can J Ophthalmol*. 2010;45:189–191.
165. Teke MY, Citirik M. 23 gauge vitrectomy, endolaser, and gas tamponade versus vitrectomy alone for serous macular detachment associated with optic disc pit. *Am J Ophthalmol*. 2015;160(4):779–785.
166. Ishikawa K, Terasaki H, Mori M, et al. Optical coherence tomography before and after vitrectomy with internal limiting membrane removal in a child with optic disc pit maculopathy. *Jpn J Ophthalmol*. 2005;49:411–413.
167. Ghosh YK, Banerjee S, Konstantinidis A, et al. Surgical management of optic disc pit associated maculopathy. *Eur J Ophthalmol*. 2008;18:142–146.
168. Abouammoh MA, Alsulaiman SM, Gupta VS, King Khaled Eye Specialist Hospital International Collaborative Retina Study Group, et al. Pars plana vitrectomy with juxtapapillary laser photocoagulation versus vitrectomy without juxtapapillary laser photocoagulation for the treatment of optic disc pit maculopathy: the results of the KKESH International Collaborative Retina Study Group. *Br J Ophthalmol*. 2016;100(4):478–483.
169. Becht C, Senn P, Lange AP. Delayed occurrence of subretinal silicone oil after retinal detachment surgery in an optic disc pit – a case report. *Klin Monatsbl Augenheilkd*. 2009;226:357–358.
170. Kuhn F, Kover F, Szabo I, et al. Intracranial migration of silicone oil from an eye with optic pit. *Graefes Arch Clin Exp Ophthalmol*. 2006;244:1360–1362.
171. Jesberg DO, Schepens CL. Retinal detachment associated with coloboma of the choroid. *Arch Ophthalmol*. 1961;65:163–173.
172. Gopal L, Badrinath SS, Sharma T, et al. Surgical

management of retinal detachments related to coloboma of the choroid. *Ophthalmology*. 1998;105:804–809.
173. Schubert HD. Structural organization of choroidal colobomas of young and adult patients and mechanism of retinal detachment. *Trans Am Ophthalmol Soc*. 2005;103:457–472.
174. Tansu E, Serhad N. Optical coherence tomography after pars plana vitrectomy for retinal detachment related to choroidal coloboma. *Retina*. 2010;30:1078–1083.
175. Teoh SC, Mayer EJ, Haynes RJ, et al. Vitreoretinal surgery for retinal detachment in retinochoroidal colobomata. *Eur J Ophthalmol*. 2008;18:304–308.
176. Sanghvi DA, Sanghvi CA, Purandare NC. Bilateral persistent hyperplastic primary vitreous. *Australas Radiol*. 2005;49:72–74.
177. Shastry BS. Persistent hyperplastic primary vitreous: congenital malformation of the eye. *Clin Experiment Ophthalmol*. 2009;37:884–890.
178. Walsh MK, Drenser KA, Capone A Jr, et al. Early vitrectomy effective for bilateral combined anterior and posterior persistent fetal vasculature syndrome. *Retina*. 2010;30:S2–8.
179. Dass AB, Trese MT. Surgical results of persistent hyperplastic primary vitreous. *Ophthalmology*. 1999;106:280–284.
180. Bosjolie A, Ferrone P. Visual outcome in early vitrectomy for posterior persistent fetal vasculature associated with traction retinal detachment. *Retina*. 2015;35:570–576.
181. Mittra RA, Huynh LT, Ruttum MS, et al. Visual outcomes following lensectomy and vitrectomy for combined anterior and posterior persistent hyperplastic primary vitreous. *Arch Ophthalmol*. 1998;116:1190–1194.
182. Shaikh S, Trese MT. Lens-sparing vitrectomy in predominantly posterior persistent fetal vasculature syndrome in eyes with nonaxial lens opacification. *Retina*. 2003;23:330–334.

SECTION 4

Vitreous Surgery for Macular Disorders

OUTLINE

120

Epiretinal Membranes, Vitreoretinal Traction, and Cystoid Macular Edema

Louisa Wickham, Lazaros Konstantinidis, Thomas J. Wolfensberger

Introduction

Disorders of the vitreomacular interface include a number of conditions such as macular hole, lamellar hole, vitreomacular traction, cystoid macular edema, and epiretinal membrane.[1] It is

increasingly recognized that these conditions lie on a spectrum of disease caused by abnormalities of the vitreomacular interface. Our understanding of these conditions has increased significantly with the introduction of optical coherence tomography (OCT) and has led to a new classification of vitreomacular adhesion, traction and macular hole based on OCT characteristics.[1] Here we look at each of these conditions as discrete entities, but it should be borne in mind that they have commonalities in both etiology and clinical presentation.

Epiretinal Membranes

Epiretinal membrane (ERM) is a term used to describe cellular proliferation on the inner retinal surface. Premacular fibroplasia, macular pucker, cellophane maculopathy, and premacular gliosis have all been used to describe this condition. The variety of names given to this disorder reflects the wide spectrum of presentation and clinical findings as ERMs may range from a benign asymptomatic disorder to a condition associated with debilitating metamorphopsia and central visual loss. Appropriate management of patients presenting with an ERM relies on clinicians distinguishing between those that will benefit from surgery and those that will not.

Prevalence of ERM

Evidence regarding the epidemiology of ERMs predominantly comes from two large population studies, the Beaver Dam Eye Study and the Blue Mountains Eye Study.[2–4] The overall prevalence of ERM in these populations was 7–11.8%, with a 5-year incidence of 5.3%.[2–4] Idiopathic ERMs were bilateral in 19.5–31%, with a 13.5% 5-year incidence of second eye involvement.[2–4]

The age distribution shows a peak between the ages of 70 and 79 (11.6%), with ERMs being uncommon before the age of 60 (1.9%).[4] The increased odds of ERM for persons over the age of 70 compared with those younger than 60 was 7.4.[4] ERMs were more commonly diagnosed in women in the Beaver Dam cohort but not in the Blue Mountains Study, and this difference may merely reflect

the greater survival rate of women in this age group.

The prevalence of ERM appears to vary with ethnicity.[5,6] Higher prevalence was noted in Chinese participants in a multiethnic epidemiologic study (39% in Chinese vs. 27.5% in Caucasians),[6] whereas lower rates have been observed in the Japanese (4%).[5] In the Blue Mountains Study, the prevalence of ERM was significantly increased following cataract surgery (16.8%) and retinal vein occlusion (12.5%);[4] 9.1% of patients with no retinal abnormality at baseline developed an ERM following cataract surgery.[3]

Classification of ERM

The majority of ERMs have no associated ocular abnormality and are termed idiopathic. ERMs may be classed as secondary when a preexisting or coexisting condition has had a significant impact on development, and iatrogenic if they occur following medical or surgical intervention (Table 120.1).[7]

TABLE 120.1

Classification of Epiretinal Membranes

IDIOPATHIC
Secondary
Retinal vascular disease
Vascular occlusion, e.g., BRVO, CRVO
Diabetic retinopathy
Telangiectasias
Macroaneurysm
Sickle-cell retinopathy
Intraocular inflammation
Trauma
Retinal detachment and retinal tears
Intraocular tumors
Retinal angiomas
Hamartomas
Retinal dystrophies
Retinitis pigmentosa
IATROGENIC
Postoperative
Cataract
Retinal detachment
Silicone oil
Retinopexy
Laser or cryotherapy

BRVO, branch retinal vein occlusion; CRVO, central retinal vein occlusion.

Clinical Features

ERM is a spectrum of disease and may present in a number of ways.[8] A clinical grading system was proposed by Gass to describe the different stages of the disease.[9]

In Grade 0 (also termed cellophane maculopathy), a translucent membrane with no underlying retinal distortion is observed. These membranes are asymptomatic, and the diagnosis is often an incidental finding during routine examination (Fig. 120.1).

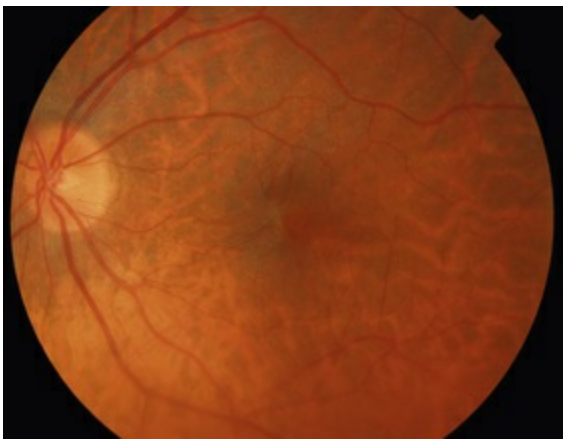

FIG. 120.1 Color fundus photograph of a Grade 0 epiretinal membrane showing mild abnormality of the macular reflex.

An epiretinal membrane associated with irregular wrinkling of the inner retina is classed as Grade 1 (Fig. 120.2). When this involves the fovea, patients often complain of distorted or blurred vision. These symptoms may only be perceptible when the unaffected eye is covered, particularly if the ERM occurs in the nondominant eye. Other symptoms that patients may report include loss of binocularity, central photopsia, and macropsia and, rarely, monocular diplopia.[8] Eccentric Grade 1 ERMs that do not involve the fovea may be asymptomatic (Fig. 120.3).

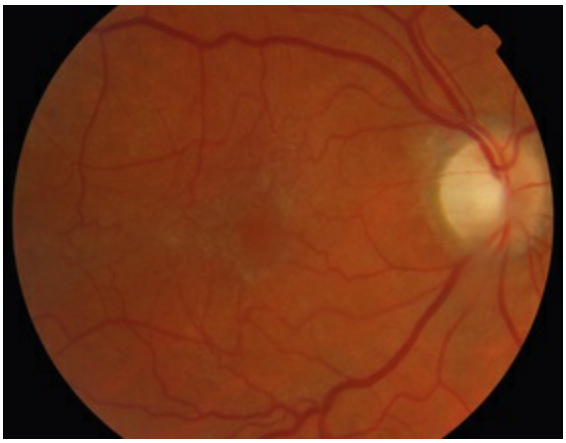

FIG. 120.2 Color fundus photograph of a Grade 1 epiretinal membrane showing vascular tortuosity.

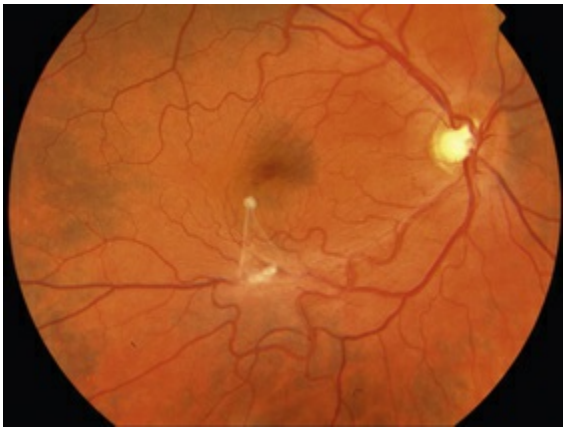

FIG. 120.3 Color fundus photograph of an eccentric Grade 1 epiretinal membrane.

A Grade 2 ERM is characterized by an opaque membrane causing obscuration of underlying vessels and marked full-thickness retinal distortion (Fig. 120.4). Increasing vascular tortuosity and size of vessel involved tend to be a sign of more advanced disease. ERMs with full-thickness retinal distortion may also be associated with cotton-wool spots, exudates, blot hemorrhages, and microaneurysms (Fig. 120.5). Cystoid macular edema (CME) is present in approximately 20–40% of patients (Fig. 120.6).[10–12] Vascularization of the ERM and underlying RPE disturbance are rare but indicate more severe disease. Although symptoms are more commonly associated with increasing severity of ERM, patients may have significant ERMs and remain asymptomatic.[7] Approximately 80% of patients with Grade 2 ERM will have

symptoms of blurred vision or metamorphopsia.[13]

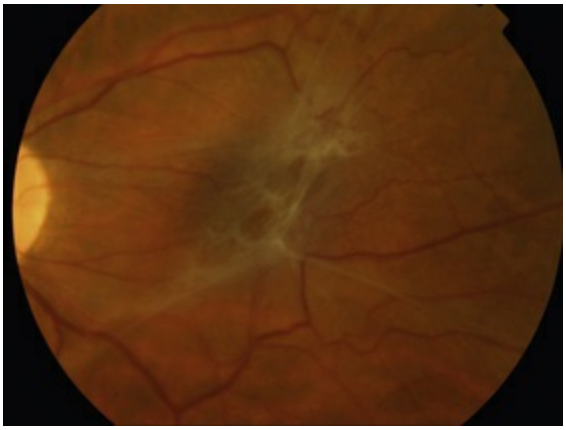

FIG. 120.4 Color fundus photograph of a Grade 2 epiretinal membrane, showing an opaque membrane with underlying vascular tortuosity.

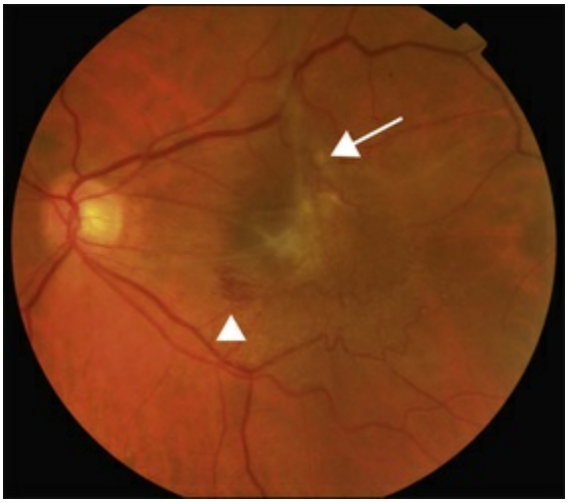

FIG. 120.5 Color fundus photograph of an epiretinal membrane with cotton-wool spots (*arrow*) and intraretinal hemorrhages (*arrowhead*).

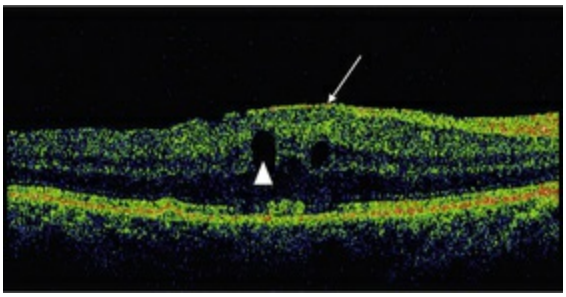

FIG. 120.6 Optical coherence tomography showing presence of intraretinal fluid (*arrowhead*) associated with an epiretinal membrane, which is seen as a hyperreflective layer on the surface (*arrow*).

A posterior vitreous detachment (PVD) is present in approximately 60–90% of patients at the time of diagnosis.[10–12] Those with partial PVD and persistent vitreomacular adhesion (VMA) are more likely to develop CME and present with a lower visual acuity (VA).[12] In cases where a PVD does not exist, the clinical findings may be very similar to those commonly seen in vitreomacular traction syndrome (VMTS). The subsequent evolution of a PVD can result in avulsion of the ERM in ~5% patients, and this may be observed as a "scroll" of tissue at the membrane edge or within the vitreous gel (Fig. 120.7).[14] Avulsion of the ERM is usually accompanied by a reduction in or resolution of symptoms.

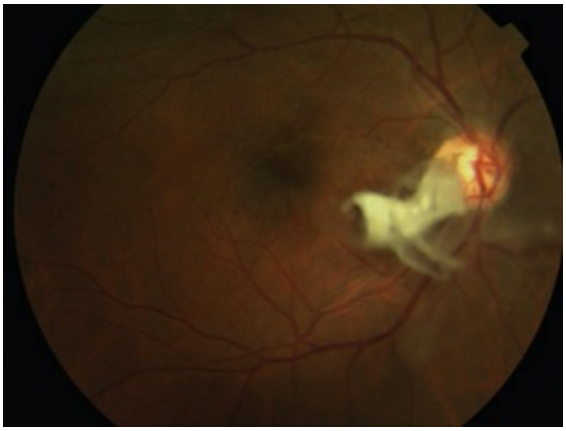

FIG. 120.7 Color fundus photograph of an avulsed epiretinal membrane in the vitreous cavity.

ERMs may also be associated with macular pseudoholes, lamellar holes, and much less commonly, with full-thickness macular holes,

presumably as a result of tangential traction. It is possible that lamellar holes form when retinal cysts associated with the ERM rupture forming inner neural defects. When contraction of the ERM distorts the underlying retina to form a steepened foveal contour that clinically resembles a macular hole, the term pseudohole is used (Fig. 120.8). This has been described in up to 20% of patients.[15]

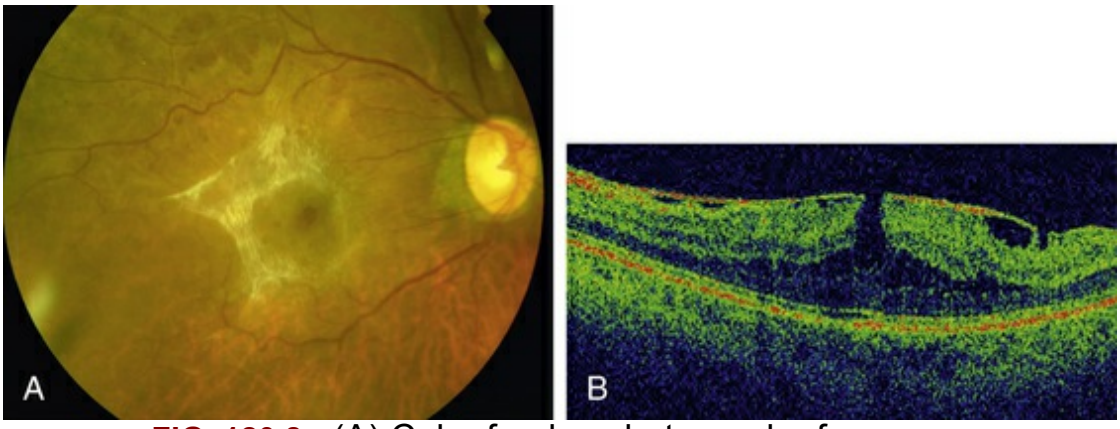

FIG. 120.8 (A) Color fundus photograph of an epiretinal membrane with a pseudohole. (B) Optical coherence tomography showing presence of an epiretinal membrane and a pseudohole.

Although rapid progression of the disease has been described,[16] the usual course is one of stability or slow progression over years with the VA rarely deteriorating below 20/200. In a study by Appiah et al., of 324 idiopathic ERMs with a mean follow-up of 33.6 months, 49.5% maintained a VA within 1 line of the initial acuity, 37.4% showed a reduction in vision, and 13.1% stayed the same.[12] In the Blue Mountains Study, the area of retina occupied by the ERM remained stable in 39%, regressed in 25.7%, and progressed in 28.6% in a 5-year period, where change was defined as a change in area of >25%.

Pathogenesis

The initiating event or factors responsible for the development of ERM have yet to be elucidated fully; however, there is evidence that ERM formation represents a reactive gliosis in response to retinal injury or disease involving inflammatory and glial cells.

In general terms, ERMs have two main components: an extracellular matrix (consisting of collagen, laminin, tenascin, fibronectin, vitronectin, etc.) and cells of retinal and extra retinal origin (such as glial cells, neurites, retinal pigment epithelium [RPE], immune cells, and fibrocytes).[17,18] The relative abundance of these components within the ERM reflects the underlying etiology, severity of disease, or its duration. For example, ERMs secondary to proliferative vitreoretinopathy (PVR) are more heavily pigmented due to a high RPE content when compared with idiopathic ERMs, which are composed predominantly of glial elements (Fig. 120.9).[19,20] Similarly, ERMs that develop in response to retinal ischemia and neovascular proliferation may have a larger vascular component. Growth factors play an important role in the formation, progression, and transformation of membranes with differential expression being observed in membranes according to their etiology.[21,22] A summary of some of the growth factors involved in the development of idiopathic and secondary ERMs is given in Table 120.2.

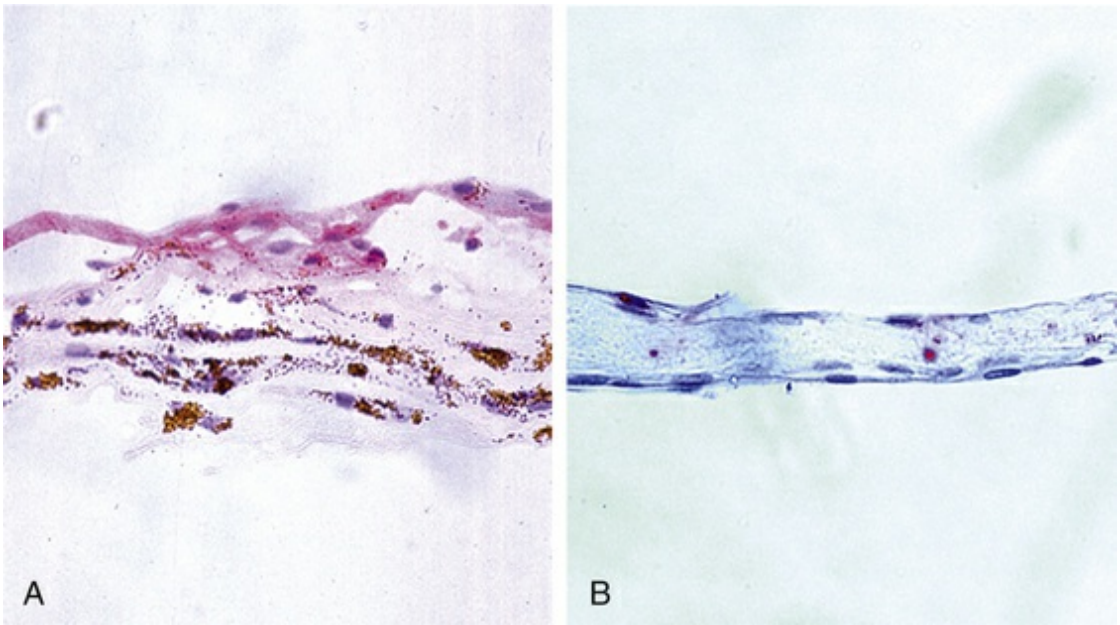

FIG. 120.9 Increased pigmentation observed in proliferative vitreoretinopathy membranes (A) compared with an idiopathic epiretinal membrane (B).

TABLE 120.2

Expression of Cytokines and Growth Factors in Different Types of Epiretinal Membranes

	Idiopathic	PVR	PDR
Vascular endothelial growth factor (VEGF)	✓	✓	✓
Placental growth factor (PGF)	✓		✓
Tumor necrosis factor-alpha (TNF-α)	✓	✓	✓
TRAIL		✓	
Platelet-derived growth factor (PDGF)	✓	✓	✓
Transforming growth factor-beta (TGF-β)		✓	✓
Angiopoietin	✓		✓
Interleukin-6 (IL-6)		✓	✓
Tenascin	✓	✓	✓
Basic fibroblast growth factor (bFGF)	✓	✓	✓
NF-κB	✓	✓	✓

NF-κB, nuclear factor-kappa B; PDR, proliferative diabetic retinopathy; PVR, proliferative vitreoretinopathy; TRAIL, TNF-related apoptosis-inducing ligand.

Data taken from Harada C, Mitamura Y, Harada T. The role of cytokines and trophic factors in epiretinal membranes: involvement of signal transduction in glial cells. Prog Retin Eye Res 2006;25(2):149-64.

Membranes appear to develop predominantly where Müller cells have proliferated and migrated onto the inner surface of the retina and where hypertrophied cell processes extend towards the vitreous cavity. In idiopathic ERMs, it is possible that vitreous separation at the time of PVD exerts traction on the retina and induces Müller cell gliosis, a process of cellular hypertrophy, upregulation of cellular proteins such as vimentin and GFAP (glial fibrillary acidic protein), and transient cellular proliferation. Müller cells are thought to migrate to the epiretinal surface via small defects in the internal limiting membrane (ILM),[17] which may occur naturally, such as those commonly seen near retinal vessels, or as a result of larger paravascular breaks observed following PVD.[23,24] Activation of Müller cells may continue even once the original stimulus has been withdrawn. In retinal detachment, activated Müller cells, that have penetrated the ILM and migrated on to the epiretinal surface, continue to proliferate even once retinal reattachment is achieved.[25] The degree of cellular proliferation may vary according to the underlying etiology of the ERM, with PVR membranes having the highest proliferation index when labeled with K_i-67[22] (see Chapter 31, Cellular effects of detachment and

reattachment on the neural retina and the RPE).

Where ERMs form in the absence of PVD, a period of vitreomacular traction may cause chronic irritation of Müller cells inducing gliosis and vascular leakage. In the absence of a PVD, glial cells appear to grow through the posterior hyaloid, which then in turn becomes incorporated into the membrane.[23] This may explain the mechanism behind spontaneous avulsion of ERMs following PVD.

More advanced ERMs have contractile components that exert traction on the underlying retina and distort the retinal vasculature with or without a breakdown of blood–retina barrier and fluid accumulation in the macula. In these membranes a higher content of contractile actin or myofibroblasts is observed. This is also described in some secondary ERMs such as those found in PVR and proliferative diabetic retinopathy (PDR), and in these cases ERMs may lead to detachment of the underlying retina. As the ERM matures the contractile nature of the membrane may change. This is characterized by an alteration in the expression of surface proteins, for example a reduction in GFAP and increase in α-smooth-muscle actin are associated with increasing contractility.[26]

Clinical Assessment and Differential Diagnosis

Assessment of patients presenting with an ERM should aim to distinguish an idiopathic ERM from one that is secondary or iatrogenic. A good ophthalmic and general medical history will elicit predisposing factors for secondary or iatrogenic ERMs. A VA that is lower than expected for the degree of ERM present may indicate underlying retinal disease and warrants further clinical investigation. Although idiopathic ERMs can present with small intraretinal hemorrhages, exudates, or cotton-wool spots, the presence of such abnormalities should also alert the clinician to the possibility that an underlying vascular abnormality may also be present.

The diagnosis of an ERM is usually straightforward; however, there are some conditions that may closely resemble an ERM and should be considered when making the diagnosis, such as VMT and

CME.

VMT, like ERM, may cause increased retinal thickness, CME, and lamellar or full-thickness macular holes.[27] ERMs may coexist with VMT in 26–83%, and it has been suggested that this is a distinct subgroup of the condition.[28–30] VMT is said to differ from ERM by the degree of vitreous separation in the midperiphery. In VMT with ERM the vitreous in the midperiphery is detached, whereas in ERM without PVD the vitreous is attached.[31]

CME may also have a similar appearance to an ERM, and it is discussed in more detail later in this chapter. CME differs from an ERM in that there is no distortion of the microvasculature, it is always centered on the fovea, and may be seen on fluorescein angiography as a "star pattern" in late pictures.[8] CME may be the final common pathway of many diseases and may also coexist with ERM, e.g., following a retinal vein occlusion, and management will depend on determining which is the primary condition. ERM surgery is considered if it is thought to be responsible for the CME or if more conservative management has failed.

Diagnostic Investigations

Optical Coherence Tomography

Although fluorescein angiography was once the first-line investigation for ERMs, this has now been largely replaced with OCT, detecting ERM in up to 90% of cases.[15,32–34] On OCT, an ERM can be seen as a hyperreflective layer on the surface of the retina. It may be associated with an underlying corrugation of the retinal surface, blunting of the foveal contour (Fig. 120.10), increased retinal thickness, and intraretinal cysts. Idiopathic ERMs tend to be adherent globally to the underlying retina, whereas secondary ERMs are more likely to be characterized by focal retinal adhesion (Fig. 120.11).[35]

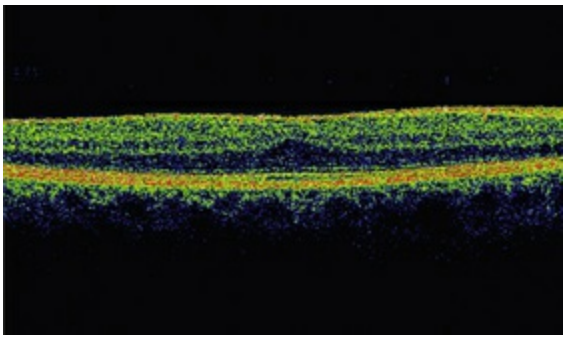

FIG. 120.10 Optical coherence tomography of an epiretinal membrane showing blunting of the foveal contour. The epiretinal membrane is seen as a hyperreflective layer on the retinal surface.

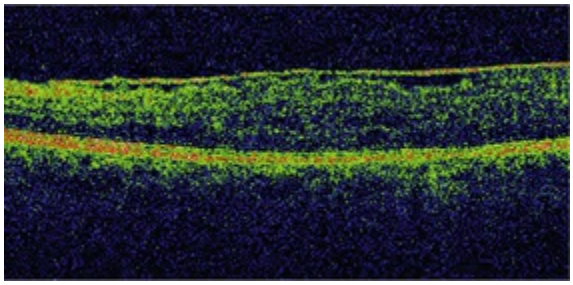

FIG. 120.11 Optical coherence tomography of a secondary epiretinal membrane showing focal areas of adhesion with the underlying retinal surface.

The introduction of spectral domain OCT (SD-OCT), which offers higher axial resolution, has allowed more precise visualization of the effect of ERM on the underlying retinal layers. This has demonstrated that ERMs are also associated with thickening of the outer retina, increased central foveal thickness (CFT), disruption of the photoreceptor inner/outer-segment junction (IS/OS), and disruption of the cone outer-segment tips (COST).[36–40]

OCT may also be a useful tool to monitor the clinical course of ERMs both prior to and following surgery, and intraoperative OCT has been used at the time of surgery with some success.[41] Following successful ERM surgery macular thickness and foveal contour tend to improve on OCT, although neither returns to normal. This does not, however, preclude a gradual improvement in visual function.[15]

Fluorescein Angiography

Despite the advantages of OCT, fluorescein angiography (FA) still remains a useful tool, particularly in cases where an underlying vascular event or choroidal neovascular membrane is suspected. FA can highlight the extent of retinal wrinkling, degree of retinal vascular tortuosity, and presence of macular edema (Fig. 120.12). Wise demonstrated diffuse leakage from retinal capillaries or small veins in the late venous phase; however, some ERMs showed no leakage despite having advanced disease with deep retinal edema.[8] Extensive leakage from retinal capillaries or veins was associated with more rapidly progressing lesions.[8] Displacement or distortion of the foveal capillary network may indicate foveal ectopia.

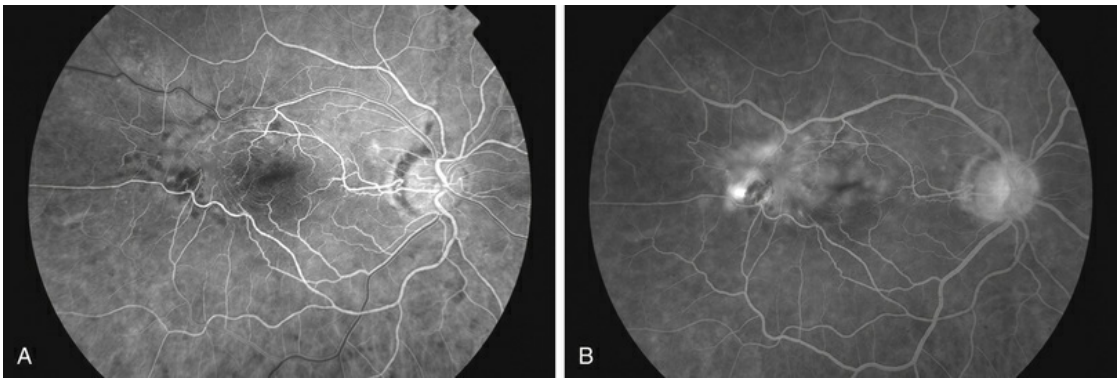

FIG. 120.12 Fluorescein angiogram showing retinal vascular tortuosity as a result of an overlying epiretinal membrane (A). Vascular leakage is seen in the late venous phase due to traction from the overlying epiretinal membrane (B).

Fundus Autofluorescence

The presence of retinal vessel printings on autofluorescence has demonstrated retinal vessel displacement which may be correlated with more severe metamorphopsia.[42]

Surgical Management of ERM

When to Offer Surgery and Prognostic Indicators

The principal indications for ERM surgery are patient-reported symptoms of reduced VA with or without metamorphopsia.

Although surgery is usually reserved for patients with a reduction in acuity to ≤20/60, improvements in surgical techniques have led to patients undergoing surgery with better VA if disturbed by symptoms of metamorphopsia or diplopia and for occupational reasons.

Following surgery there is often a period of several weeks without any noticeable visual improvement. Patients can expect a visual improvement of two or more lines in 60–85% of cases 6–12 months after surgery, with 44–55% achieving a VA of 20/50 or better.[13,15,43,44] A poor presenting VA is associated with a greater visual improvement following surgery, in one series a mean improvement of 4.1 lines was achieved in those with preoperative acuity of 20/200 or worse.[43] However, multiple regression analysis has shown that a higher preoperative VA is associated with a higher final acuity at 6 and 12 months, even though the percentage improvement may be less.[45,46] Both idiopathic and secondary ERMs appear to benefit to an equal extent from surgery; however, in some cases a preexisting macular pathology may limit the visual recovery.[43]

Other parameters of visual function such as contrast sensitivity have been shown to improve significantly following surgery, even when VA does not.[47] Contrast sensitivity appears more closely correlated with improvements in Quality of Life measures than VA and may therefore be a better indicator of the benefits of surgery.[48] Stereopsis has also been shown to be significantly worse in patients presenting with ERM as compared with controls.[49] Successful surgery may result in a significant improvement but does not return to normal levels within 6 months. There are conflicting reports that the degree to which stereopsis is affected may be related to changes in microstructure on SD-OCT such as CFT, macular volume, and mean inner nuclear layer (INL) thickness.[49–51]

The variability in visual results following successful surgery has led to a search for favorable prognostic factors. The available studies are largely retrospective and must therefore be interpreted with caution. A systematic review of the current published literature found only 19 studies of adequate quality.[44] Preoperative VA was the only variable consistently associated with postoperative acuity. There is also evidence that integrity of the

IS/OS junction, severity of metamorphopsia, COST integrity, and fundus autofluorescence (FAF) may also impact postoperative outcomes.[44]

CFT was found to be significant in studies using time domain OCT but not in SD-OCT. More robust studies are required to determine prognostic factors before a prediction model can be developed.

Surgical Techniques

Epiretinal membrane surgery usually starts with a standard pars plana vitrectomy, the degree of vitreous clearance is surgeon-dependent but should avoid any risk of lens trauma or retinal breaks. In most cases a PVD will be present at the start of surgery. In those where the posterior hyaloid is attached, removal should be as atraumatic as possible due to the presence of ILM attachments through the vitreous. In cases where the posterior hyaloid is attached, triamcinolone may be used to assist visualization and removal, particularly over the macular area. Following vitrectomy vital dyes are commonly used to assist visualization of the ERM, as noted below.

Nonvitrectomizing surgery has also been reported for ERM, particularly with the introduction of small-gauge instrumentation. This has the potential benefit of reducing cataract formation postoperatively. The benefit of this technique may be limited by the continued presence of floaters and vitreous debris compared with standard ERM techniques.[52,53]

Use of Vital Dyes to Assist in ERM Peeling

Vital dyes are a useful adjunct to ERM surgery, and there is some evidence that they may improve visual outcomes.[54–56] A number of dyes are in use with different affinities for intraocular collagen and cellular elements. Commonly used dyes in clinical practice include indocyanine green (ICG), trypan blue (TB), and brilliant blue.

Although ICG has been associated with toxicity in macular hole surgery, a study comparing ILM peeling with or without ICG in idiopathic ERM found no difference in outcomes.[57–59] ICG has greater affinity for ILM than ERM and may be more useful when viewed as a negative stain, i.e., the ERM will be seen as an area free

of stain while the surrounding ILM will be clearly visible.[60,61] A number of studies reporting ICG toxicity have been published with varying incubation times, osmolarity, and concentrations. In general, RPE toxicity has been more commonly demonstrated with a solution that has an osmolarity <270 mOsm, a concentration above 0.5%, and incubation time >30 seconds.[62] Additional factors that may be associated with RPE toxicity include application technique and duration of light exposure.[62] A similar approach of negative staining can be employed using brilliant blue (0.25 mg/mL). Brilliant blue stains ILM but does not appear to have the concerns regarding toxicity of ICG and thus may be a good alternative.[62]

Trypan blue highlights ERMs due to its strong affinity for glial cells, allowing good visualization of the extent of the membrane and thus aiding peeling. The facilitation of peeling with dyes does not appear to correlate with improvement in visual outcomes although there is a trend favoring the use of trypan blue.[54–56] Providing that the dye does not enter the subretinal space, there has been no evidence of RPE toxicity.[63–65]

Techniques for Engaging and Peeling ERMs

Once the ERM is visualized adequately, there are a number of techniques that may be used to engage the ERM. In some cases, the edge of the ERM is clearly visible and can be engaged directly with end-grabbing forceps. Where an edge cannot be clearly identified, it may be created prior to peeling using a surgical pick, a bent-tipped microvitreoretinal (MVR) blade, or a diamond-dusted scraper. When using a pick or an MVR blade, gentle traction at the edge of the ERM may also elevate it from the retinal surface, facilitating the subsequent peeling with a membrane forceps.

An alternative technique is to directly seize the surface of the ERM with a pair of fine end-grabbing forceps. The forceps are opened slightly and gently pressed onto the surface of the ERM, closed, and then raised by applying tangential traction, which is less likely to cause a retinal tear. However, the limited view of the underlying retina with this technique may increase the risk of trauma to the retina and RPE. This risk may be reduced by slightly reopening the forceps when the initial tractional force is applied and then regripping, allowing any retina trapped within the forceps

to be released.

In some cases, the membrane may be very adherent with no clearly defined tissue planes, and this may result in strands of white glial tissue adhering to the membrane leaving areas of retinal whitening underneath. When such an area of adherent ERM is encountered, the ERM peel may be completed by finding an alternative edge and peeling this toward the adherent area. This may be repeated until only the adherent area remains, allowing it to be gently peeled without exerting traction on surrounding areas of retina.

Benefit of Peeling Internal Limiting Membrane in ERM Surgery

Although patches of ILM are often removed at the time of ERM surgery,[66] there is debate as to the potential benefit of completing an ILM peel following the removal of ERM. It has been proposed that removal of ILM at the time of surgery removes the scaffold for myofibroblast proliferation and any residual microscopic ERM, thus reducing the risk of recurrence as well as improving visual outcomes.[66–69] Conversely, there are concerns that loss of retinal tissue and damage to Müller cell footplates may adversely affect visual function and that rates of recurrence are not affected.[70,71] Although there may be variations in VA initially, postoperatively, these do not appear to be sustained at 12 months.[68,69] There is currently no high-level evidence to inform this debate with published series being either small in number, retrospective, or with variable staining and peeling techniques.

Complications of ERM Surgery

Intraoperative Complications

Small petechial hemorrhages from the perifoveal capillary bed have been reported in 19% of cases, but these do not appear to be associated with reduced visual outcome.[72] Preretinal hemorrhages are usually self-limiting and do not require any treatment.

Peripheral retinal breaks are observed intraoperatively in 4–9% of patients following 20-gauge vitrectomy.[43,73] More recent data suggest that the incidence of entry site breaks is reduced further

with 23-gauge systems to as low as 1%.[74,75] If present, such retinal breaks are treated at the time of surgery with cryotherapy or laser, according to their position, followed by gas or air tamponade.

Lens touch may occur in approximately 0.9% of patients during surgery.[76] In most cases, this will not prevent successful removal of the ERM; however, if the view is significantly impaired, a lensectomy may be required. Patients with a lens touch cataract will show rapid progression postoperatively and may exhibit more postoperative inflammation. Removal of cataract in these patients is also more technically challenging with an increased risk of posterior capsular rupture.

Postoperative Complications

Cataract.

The most common complication following ERM surgery is the formation or progression of cataract. This is true of all vitrectomy surgery and has been reported to occur with an incidence of 6–100% depending on the underlying condition, duration of follow-up, and method of measuring cataract formation.[43,77] The incidence of cataract within the first year ranges from 30% to 65% and increases with increasing length of follow-up.[73]

The combination of cataract progression with delayed visual recovery following ERM surgery often means that patients do not achieve their target vision until the cataract has been removed. Increasingly surgeons are electing to perform cataract surgery at the time of ERM peeling.[76] Both techniques appear to produce equivalent outcomes.[78]

Retinal Detachment.

Retinal detachment following ERM surgery occurs in 2–14% of eyes.[43,79] The most common source of detachment is unidentified entry site breaks at the time of surgery. This emphasizes the importance of careful search for retinal tears using scleral indentation at the end of surgery.

Recurrence.

Recurrence of ERM occurs in less than 20% of patients and is rarely

visually significant and results in further ERM surgery in approximately 5% of cases.[68] Recurrences tend to occur approximately 20 months postoperatively (range 3–96 months).[68] Rates of recurrence appear to be higher in younger patients (25%).[7]

Other rarer complications include endophthalmitis, retinal toxicity from the use of vital dyes, phototoxicity, visual field defects, and subretinal neovascularization.

Vitreomacular Traction and Cystoid Macular Edema

Macular edema contributes to vision loss by altering the functional cell relationship in the retina and promoting an inflammatory reparative response.[80,81] Macular edema associated with vitreous traction, first described over 50 years ago,[82] represents a particular tissue reaction due to the mechanical distortion of the retina. However, it is often difficult to differentiate whether edema is linked to the fact that the vitreous is pulling actively on the retina or to the fact that it is simply adherent. In certain circumstances the changes at the vitreoretinal interface may represent the cause and in some others, the effect of vitreoretinal traction.[83]

Anatomy of Macular Edema With Vitreoretinal Traction

The central area of the retina is predisposed to develop edema due to its unique anatomy, which is characterized by an extremely high cell count with increased metabolic activity and a central avascular zone creating a watershed arrangement between the choroidal and retinal circulation which decreases resorption of extracellular fluid.[84–87] In the foveal region, the fibers of the Henle layer demonstrate a loose arrangement allowing accumulation of fluid leaking from perifoveal capillaries. However, it has been shown that the cystoid spaces can also form in the outer nuclear, inner nuclear (INL), inner plexiform, and even the ganglion cell layer (GCL).[88] The presence of cystoid spaces in the GCL might be explained with the assumption that epiretinal membranes,

thickened internal limiting membrane (ILM), and/or adherence of the vitreal cortex to the retina disturb the fluid movement between the vitreous and retina.[89]

Pathophysiology of Macular Edema With Vitreoretinal Traction

In a normal steady state several mechanisms maintain a balance of osmotic forces, hydrostatic forces, capillary permeability, and tissue compliance, with the result that the rate of capillary filtration equals the rate of fluid removal from the extracellular retinal tissue.[81,90]

The vitreous has been implicated as a cause of macular edema via several mechanisms. One of the most constructive hypothesis on how vitreomacular traction (VMT) may result in macular edema was given by Schubert in 1989 and was summarized by Bringmann and Wiedemann in 2009.[17,91] Vitreous fibers, which adhere to Müller cell end-feet at sites of vitreoretinal attachments after partial detachment of the vitreous, exert tractional forces onto the cells; this activates Müller cells and results in cell hypertrophy, proliferation, and vascular leakage.[17,91] Furthermore, long-lasting mechanical stress of astrocytes and Müller cells induced by vitreal fibers adhering to the cells can stimulate the release of inflammatory factors such as basic fibroblast growth factor (bFGF), inducing local inflammation and blood–retinal barrier (BRB) breakdown promoting vascular leakage and macular edema.[92] Vitreoretinal traction can also exert forces at the level of the RPE, which can eventually result in morphologic RPE changes.[93,94] Furthermore, VMT has been shown to induce pigment epithelial detachment and RPE tearing.[95] It is a well-known phenomenon in many retinal vascular diseases that direct traction on the macula or on the RPE may induce not only induce local inflammation but also increase of vascular endothelial growth factor (VEGF) locally with subsequent macular edema formation.[96–98] Mechanical traction can also cause macular edema by direct distortion of the surrounding intraretinal vessels resulting in leakage due to disturbance of the macular microcirculation with reduced capillary blood flow and a loss of apposition between the retina and the RPE pump.[99]

It is less well known that the vitreous may also play an important

role in the pathophysiology of macular edema through other mechanisms than the obvious direct tractional components. Sebag and others have found enzyme-mediated vitreous crosslinking and nonenzymatic glycation in the diabetic vitreous, and they have suggested that the abnormal crosslinking might affect the collagen structure and destabilize the attached vitreous gel strengthening the adhesion of the posterior vitreous cortex to the ILM, which in turn produces stronger vitreoretinal attachment with subsequent macular edema.[100,101]

Furthermore, the vitreous in various pathologic conditions may act as a sink for factors influencing macular edema themselves. The breakdown of the BRB, for example, usually leads to an increased concentration of intravitreal serum-derived chemoattractants, which may provide a stimulus for cellular migration into the attached premacular posterior hyaloid. Cellular contraction may potentially lead to tangential traction with consequent leakage and macular edema.[102,103] In turn, leakage from the vascular bed aggravates chemoattractant outflow, thus creating an inexorable vicious circle.

It has also been shown that several growth factors such as VEGF, interleukin (IL)-6, platelet-derived growth factor (PDGF), and others are secreted in large amounts into the vitreous during proliferative vasculopathies such as diabetic retinopathy or retinal vein occlusion,[104–106] and these factors may increase vasopermeability and promote macular edema. Furthermore, during aging, VEGF is increasingly bound by altered vitreous collagen fibrils at the interface between retina and posterior vitreous cortex potentiating the effects of these growth factors.[107]

Clinical Signs of Cystoid Macular Edema With Vitreoretinal Traction

Clinically, macular edema can be best detected using the slit lamp and either a handheld, non-contact lens (e.g., +78 D), or a contact lens (e.g., Goldmann flat lens). These changes may be better visible using green light, while retroillumination can help to delineate the polycystic spaces. A thorough examination of the anterior segment should always complement the clinical evaluation as incarcerated

vitreous or an intraocular lens irritating the iris or ciliary body may be the underlying cause of macular edema.[89] Clinical symptoms range from loss in distance VA, contrast sensitivity, color vision, and reading acuity to a reduction in reading speed as well as metamorphopsia and micropsia.[108–111]

Imaging of Cystoid Macular Edema With Vitreoretinal Traction

Angiography

Fluorescein angiography has for many years been one of the most useful tests in detecting macular edema of various etiologies showing cystoid spaces located in the outer plexiform layer (Henle's layer) displayed as the classic petaloid staining pattern in the macula or a honeycomb-like appearance in the more peripheral regions.[86,112–114] Reasons for so-called “silent” angiograms may be very long-standing changes within the retina, such as intraretinal cysts, which have become impermeable to the fluorescein dye diffusion. Macular edema can also occur without vascular leakage, when the fluid clearance through glial and RPE cells is impaired.[90]

Optical Coherence Tomography (OCT)

Optical coherence tomography (OCT) is able to accurately measure the retinal thickness allowing a more precise and reproducible assessment than fluorescein angiography[115–117] with a particular efficacy in the volumetric analysis of macular edema and the characterization of the vitreoretinal interface. Several authors have proposed different patterns and classifications of macular edema according to the underlying pathology based on OCT findings.[28,113,118–122]

OCT and Diabetic Macular Edema.

In diabetic macular edema, there are several broad nonexclusive categories: diffuse retinal thickening, cystoid macular edema, serous retinal detachment, and OCT identified vitreomacular interface abnormality, which includes the presence of epiretinal membranes, and/or vitreomacular traction.[123] Vitreomacular

traction is identified by a hyperreflective band that is in apposition with the inner surface of the retina at discrete site(s) and elevated above the surface of the retina elsewhere.[118,121] Ghazi et al.[124] demonstrated that in eyes with persistent diabetic macular edema vitreomacular interface abnormalities may be found in up to 52–67% on OCT and concluded that OCT was nearly twice as sensitive as traditional techniques in detecting vitreomacular interface abnormalities.

Kim et al.[118] proposed five different morphologic patterns at OCT evaluation of diabetic macular edema in relation to vitreoretinal traction: *Pattern I* is a diffuse increased retinal thickening, with areas of reduced intraretinal reflectivity; *Pattern II* is macular edema as described above; *Pattern III* shows posterior hyaloidal traction, which appears as a highly reflective band over the retinal surface; *Pattern IV* exhibits serous retinal detachment not associated with posterior hyaloidal traction, which appears as a dark accumulation of subretinal fluid beneath a highly reflective dome-like elevation of detached retina; *Pattern V* shows posterior hyaloidal traction and traction retinal detachment, which appear as a peak-shaped detachment with a highly reflective signal arising from the inner retinal surface and with an area of low signal beneath the highly reflective border of detached retina (Table 120.3). More recent reports have also shown unequivocal proof of proliferative changes on the retinal and vitreal surface of the diabetic ILM[125] while others have quantified the frequency of vitreomacular interface pathologies in diabetic macular edema in general[126] and in particular in the presence of an incomplete posterior vitreous detachment and vitreopapillary adhesion.[127]

TABLE 120.3

Morphologic Subtypes of Diabetic Macular Edema on Optical Coherence Tomographic Imaging

Morphologic Subtype	Number of Scans (%)	Mean Thickness (μm)	Range (μm)
DRT	97	409.3	215–772
DME	55	485.1	235–772
SRD without PHT	7	551.6	376–760
PHT without TRD	12.7	576.8	376–759
PHT with TRD	2.9	459.1	255–765

DME, diabetic macular edema; DRT, diffuse retinal thickening; PHT, posterior

hyaloidal traction; SRD, serous retinal detachment; TRD, traction retinal detachment.

Reproduced with permission from Kim BY, Smith SD, Kaiser PK. Optical coherence tomographic patterns of diabetic macular edema. Am J Ophthalmol 2006;142:405–412.

OCT in Vitreoretinal Traction Syndrome.

Vitreoretinal traction syndrome can be characterized most easily using OCT, which frequently shows a perifoveal vitreous detachment, a thickened hyperreflective posterior hyaloid, as well as an epiretinal membrane (Fig. 120.13). Koizumi et al.[122] described two different OCT patterns of vitreous attachment in VMT using spectral-domain OCT: foveal cavitation defined as the formation of cystoid cavity located in the inner part of the central fovea secondary to mechanical forces and CME that was defined as intraretinal cyst-like cavities extending beyond the foveal region. Sometimes a neurosensory retinal detachment occurs while the macular traction may resolve in the formation of a lamellar-macular hole.[114]

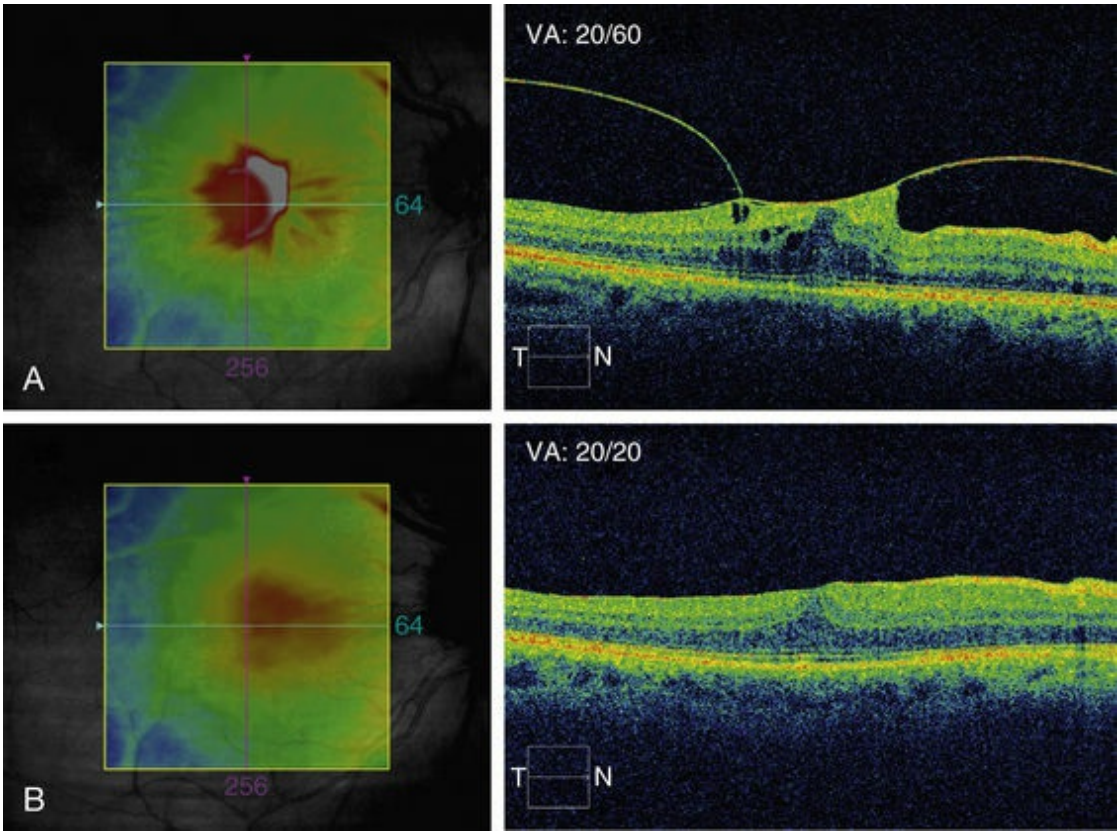

FIG. 120.13 (A) Preoperative optical coherence

tomography (OCT) image of the right eye of a 43-year-old male patient suffering from vitreomacular traction syndrome. Best corrected visual acuity (BCVA) was 20/60. (B) Postoperative OCT image 6 weeks after 23-gauge vitrectomy and peeling of the posterior hyaloid and internal limiting membrane. BCVA has increased to 20/20 with an associated important reduction in macular thickness.

Odrobina et al. (28) also advocated that vitreous surface adhesion and persistence of ERM on OCT may be the prognostic factors for the natural course of the vitreomacular traction. They observed spontaneous resolution of vitreomacular traction in eyes with less vitreous surface adhesion and without ERMs while eyes with higher vitreous surface adhesion or coexisting ERM suggested a surgical intervention.[28] Similar observations have been made on vitreomacular traction in retinal vein occlusion.[128]

OCT for Vitreomacular Traction in Age-Related Macular Degeneration.

With the advent of OCT, the theory that vitreomacular traction may be pathophysiologically related to age-related macular degeneration (AMD) has gained more and more momentum.

The initial observations were made using B-scan ultrasound, which showed that AMD patients have a high rate of persisting vitreous attachment using ultrasound[129] and other means of diagnosis.[130–132] But more recently, using high-resolution OCT, vitreomacular adhesions and traction have confirmed the high incidence of attached vitreous of up to 79%.[98] The main remaining questions are: what role if any is the vitreous playing? Is it a causative role, or is it simply aiding progression of the AMD? The answers to these questions are still to be elucidated.

Surgical Treatment of Traction Macular Edema

Rationale for Vitrectomy

Tractional Origin of Macular Edema.

The initial rationale for using vitrectomy in cases of macular edema was entirely structural, i.e., aimed at the removal of vitreous traction on the macula.[133,134] As Newton's third law states: To any action there is always an equal reaction in the opposite direction. The force of vitreoretinal traction will thus be met by an equal and opposite force in the retina, resulting in the manifold pathologic reactions described previously. Vitrectomy may thus conceptually relieve traction on Müller and RPE cells that had resulted in vascular leakage, but it may also suppress the release of inflammatory factors previously induced by the mechanical stress on these cells. Additionally, vitrectomy may reduce the tractional disturbance of the macular microcirculation, and it may restore the apposition between the retina and the RPE pump.[135]

Nontractional Origin of Macular Edema.

Recent discoveries have shown that vitrectomy may not only be beneficial in the presence of macular traction, but also in cases where no particular deformation of the macula can be identified. This is particularly true for macular edema of vascular origin, such as diabetes or retinal vein occlusion. The beneficial effect of vitrectomy is thought to be based – at least in part – on two mechanisms. Firstly, it has been found that oxygenation of the posterior segment of the eye is increased after vitrectomy.[136–139] Others have shown that pharmacologic vitreolysis also improves vitreal O_2 levels and that it increases the rate of O_2 exchange within the vitreous cavity.[140,141] This may also be the mechanism behind the observation that vitrectomy may reduce the extent of the foveal avascular zone as seen on fluorescein angiography.[142] Secondly, it has been shown that several growth factors such as VEGF, IL-6, platelet-derived growth factor, and others are secreted in large amounts into the vitreous during proliferative vasculopathies such as diabetic retinopathy or retinal vein occlusion,[105,106,143,144] and it is conceivable that a complete vitrectomy will remove this excess of growth factors mechanically with the desired effect of a restitution of the BRB.[93] The rapid clearance of VEGF and other cytokines may thus help to prevent macular edema and retinal neovascularization in ischemic retinopathies, such as diabetic retinopathy and retinal vein occlusions. Vitreous clearance of growth factors may indeed

have the same effect as the presence of, for example, VEGF antibodies in the vitreous cavity.[135,145,146]

Rationale for Internal Limiting Membrane Peeling

ILM may thicken due to an increased content of extracellular matrices and cellular proliferation on the vitreous surface in cases of diabetic macular edema.[147] It has been hypothesized that ILM changes contribute to the structural and functional disturbance of water movement between the vitreous and the retina[147] and eventually retain proteins in the interstitial space avoiding diffusion of proteins to the vitreous space leading to macular edema.[148] Additionally, the diffusion of oxygen from the fluid in the vitreous cavity into the retina would be retarded by a thickened ILM.[149] Also, the absence of the vitreous gel would increase the transport of cytokines, such as VEGF, from the retina into the vitreous cavity, and the absence of ILM would further speed up this clearance of cytokines from the retina.[135] The efficacy of ILM delamination may be caused by the removal of a growth factor reservoir, which may have accumulated in the ILM and in cellular elements on its vitreous side. Vitreous remnants may be present even after surgical vitreous separation[150] and ILM delamination allows a more complete removal of vitreous elements.[147,150] In uveitis and in vitreomacular traction complicating AMD it has been speculated that intraocular inflammation, through the release of chemokines and cytokines into the vitreous, may result in a firmer attachment of the posterior hyaloid to the macula and/or contraction of the ILM creating tangential traction on the retina and the development of macular edema. In such cases, macular edema may be refractive to medical treatment and it may only be relieved by vitrectomy with separation of the posterior hyaloid and/or peeling of the ILM (Fig. 120.14).[151]

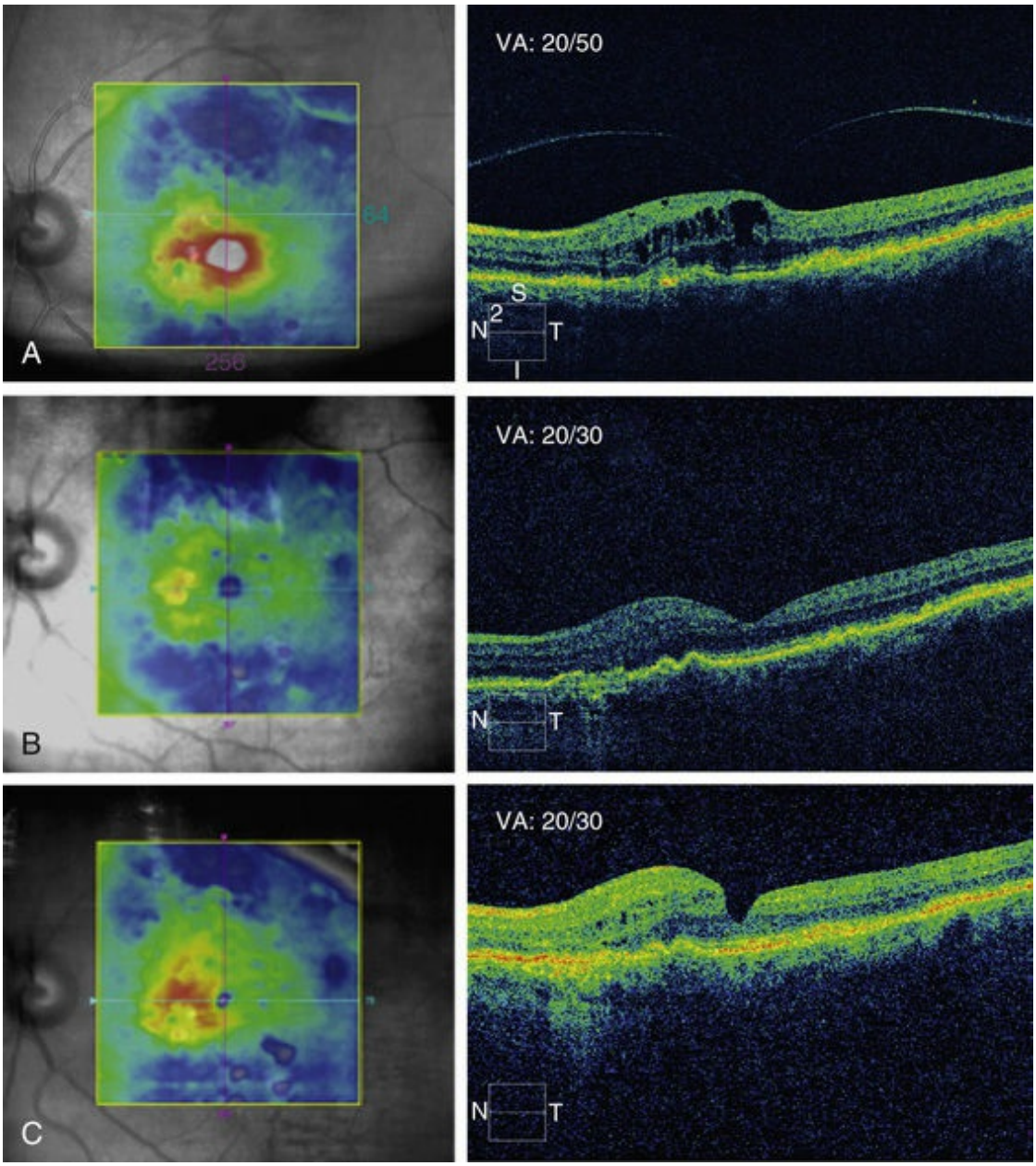

FIG. 120.14 (A) Preoperative optical coherence tomography (OCT) image of the left eye of an 86-year-old woman suffering from exudative age-related macular degeneration (AMD) with initial response to anti-VEGF therapy. Prior to referral the patient had become refractory to the injections and a possible tractional component of the macular edema was suspected. Best corrected visual acuity (BCVA) was 20/50. (B) Postoperative OCT image 3 weeks after 23-gauge vitrectomy and peeling of the posterior hyaloid, BCVA has increased to 20/30 with an associated important reduction in macular thickness. (C) Postoperative OCT image of the left eye 1 year after surgery and after seven additional intraocular anti-

VEGF injections showing a stable BCVA of 20/30.

Clinical Entities With Macular Edema Associated With Vitreomacular Traction

Diabetic Macular Edema

Role of Vitrectomy in DME.

It has been shown that the risk of developing diffuse diabetic macular edema (DME) may be 3.4-fold lower in the group of eyes with complete PVD or complete vitreoretinal separation compared to the eyes with incomplete PVD.[152] Moreover, a small prospective study by Hikichi and colleagues strongly suggested that vitreomacular separation can cause spontaneous resolution of diabetic macular edema.[153] This evidence suggests that surgical separation of the VMA is imperative in certain cases to treat DME. In 1992 Lewis et al. were the first to report the resolution of macular edema in 80% of cases after vitrectomy for diabetic edema associated with posterior hyaloidal traction.[133] Other studies have also suggested a beneficial result of vitrectomy for traction DME.[154,155] The functional prognosis was considered to be better when vitrectomy is performed at an early stage.[156] In 2010 the Diabetic Retinopathy Clinical Research Network evaluated vitrectomy for diabetic macular edema in eyes with at least moderate vision loss and vitreomacular traction. They found retinal thickening to be reduced in most eyes postoperatively. The median change in VA increased on average at 6 months after surgery by 3 letters, with VA improving by more than or equal to 10 letters from baseline to 6 months in 38% and worsening by more than or equal to 10 letters in 22%. Reduction in central macular thickness as shown by OCT to be less than 250 μm occurred in almost half, and most eyes had a thickness reduction of more than or equal to 50%.[157] Since 1990, several other authors have confirmed that vitrectomy is beneficial for diffuse DME combined with a taut thickened posterior hyaloids, presumably with tangential hyaloidal traction.[158] Pendergast et al.[159] reported stability or improvement in 91% of eyes and complete disappearance in 92% of patients after vitrectomy for

diffuse DME associated with a taut posterior hyaloid. Studies on vitrectomy for DME in the absence of traction have reported mixed results. Some studies suggested positive outcomes, others have shown anatomic but not visual improvement after surgery, while some studies suggested that vitrectomy is not beneficial in eyes with DME without traction.[155–157]

Role of Internal Limiting Membrane Peel in DME.

Despite several clinical studies over the past few years, the role of ILM peeling in DME is still far from clear. Some studies have reported a favorable outcome following vitrectomy and ILM peeling opposed to the natural course of diabetic macular edema.[160,161] In contrast, others found good anatomic but less impressive visual results.[162,163] Kumar et al. compared the effectiveness of vitrectomy and ILM peeling with grid laser photocoagulation in patients with diffuse diabetic macular edema and found that vitrectomy with ILM peeling was beneficial by inducing a statistically significant reduction of macular thickness and macular volume. However, the comparative VA outcome analysis between the two groups was not significantly different.[164] Gentile et al. have advocated that a taut ILM on its own can still cause diffuse diabetic macular edema after vitrectomy, and that its removal can restore the normal foveal contour and improve VA.[165] In a recent randomized controlled study, Hoerauf et al.[149] demonstrated a favorable anatomic effect of additional ILM removal in vitrectomy for cystoid diabetic macular edema without evident vitreomacular traction although the visual improvement was not significant.

Surgical Technique for Vitreomacular Traction in DME

Pars Plana Vitrectomy.

A standard three-port pars plana vitrectomy is performed. A PVD is induced, if not present, by suction over the optic nerve disc until the Weiss ring is identified. Simple suction may not result in complete PVD in cases of taut posterior hyaloid, and the membrane on the retinal surface needs to be engaged initially with a pick or a bent MVR blade and formally removed using membrane forceps.

Occasionally, a diamond-dusted scraper may also have to be used to create an edge for the cutter to engage the vitreous. Following this, the peripheral vitrectomy is completed and fibrovascular membranes, if present, needs to be delaminated.[166]

Role of Triamcinolone.

The injection of intravitreal triamcinolone can be used to better visualize the posterior hyaloid and thus facilitate PVD induction. Furthermore, triamcinolone acetate has been shown to facilitate fluid absorption from the edematous retinal tissue both by stimulating endogenous adenosine signaling in Müller cells[167] and by downregulating vascular endothelial growth factor (VEGF) production.[168] It can thus be used as an adjuvant also at the end of the surgery to reduce macular edema and postsurgical inflammation in general.

Internal Limiting Membrane Peel.

The ILM peel may be initiated with a slight incision of the ILM temporal to the fovea, or the ILM may be grasped directly with the forceps. In this area it is less likely to slice nerve fibers and cause small paracentral scotoma. Alternatively, a diamond-dusted brush can be used. Once the ILM is lifted, it is peeled tangentially and circumferentially like a capsulorhexis.[169] Visibility of the ILM can be greatly improved using brilliant blue G.[170]

Retinal Vein Occlusion

Role of Vitrectomy in Retinal Vein Occlusion.

Pars plana vitrectomy with complete adherent hyaloid removal has been reported as a potential treatment for macular edema related to both central (CRVO) and branch retinal vein occlusion (BRVO).[171] Several studies found improvement of VA after vitrectomy with complete posterior hyaloid removal in patients with ischemic CRVO.[172,173] It appears that the vitreous level of VEGF is significantly higher in CRVO patients with less improvement of best corrected visual acuity (BCVA) after vitrectomy.[172] It is thought that high VEGF levels may be associated with permanent photoreceptor cell damage due to macular ischemia. Soluble ICAM-

1 and pigment epithelium-derived factor (PEDF) may also influence the visual prognosis and the response of macular edema after vitrectomy.[174] Yamasaki et al. also reported both a significant improvement of VA and retinal thickness after vitrectomy for BRVO-related macular edema and a significant positive correlation between the vitreous levels of VEGF and improvement of macular edema.[175] A more recent retrospective study has characterized extrafoveal vitreoretinal traction in a large proportion of retinal vein occlusions causing macular edema and macular detachment. Evidence of traction was defined as (a) areas where the retina was elevated or thickened and where there was deformity at the traction site and (b) where the posterior hyaloid or vitreous strands changed angle. Conversely, vitreous adherence without traction was defined as vitreous attachment not associated with inner retinal deformity.[176]

Role of ILM Peel in Retinal Vein Occlusion.

Vitrectomy and ILM peeling for macular edema secondary to central retinal vein occlusion and hemiretinal vein occlusion have shown anatomic improvement, which persists up to 5 years, and VA improvement, at least in perfused CRVO and HRVO.[177] Others have reported that vitrectomy, ILM peel, and panretinal photocoagulation for macular edema secondary to central retinal vein occlusion reduced foveal thickness at final follow-up; however, anatomic improvement did not correlate with a statistically significant improvement in VA.[178]

Uveitic Macular Edema

Role of Vitrectomy in Uveitic Macular Edema.

The value of vitreous surgery in uveitic macular edema is based on the assumption that many inflammatory mediators accumulate in the vitreous and particularly in the posterior hyaloid, and a removal of these mediators may have a beneficial effect on macular edema. In addition, inflammation often results in the formation of epiretinal membranes (ERM), and vitrectomy associated with an ERM peel is thought to be of benefit.[179] There have been few reports on the outcome of pars plana vitrectomy in uveitis cases

unresponsive to medical treatment.[180–188] Dugel et al.[186] investigated the efficacy of vitrectomy in 11 eyes of nine patients with intraocular inflammation-related CME that was unresponsive to corticosteroids and reported improvement of VA and regression of macular edema. Wiechens et al.[189] investigated the role of vitrectomy in refractive uveitic CME and found that the response to vitrectomy was variable according to the type of underlying form of uveitis. Stavrou et al.[190] studied the effect of vitrectomy without ILM peel in 37 eyes with intermediate uveitis and reported resolution of CME in 32.4% of the cases, which allowed discontinuation of immunosuppressive treatment in 16% patients. Kiryu et al.[183] reported visual improvement of 2 or more Snellen lines in 56% of 18 studied eyes within 12 months after vitrectomy for CME secondary to sarcoid uveitis. Tranos et al.[180] found angiographic improvement in one-third of the patients that underwent vitrectomy for macular edema secondary to chronic uveitis in a randomized controlled pilot study. Vitrectomy may thus be a useful therapeutic alternative in selective cases which include unresponsiveness to medical treatment, significant inflammatory vitreous debris which compromises clinical assessment, and cases associated with epiretinal membranes and/or an obvious tractional component.[191]

Role of ILM Peel in Uveitic CME.

The role of ILM peel is not well defined. Only a handful of small studies have shown mixed results, with both good results in terms of macular edema and VA[151] and a more mitigated outcome.[192]

Postoperative Macular Edema

Role of Vitrectomy in Postoperative Macular Edema.

Postoperative CME is thought to be an inflammatory process[193] and is the most frequent cause of decreased vision in patients following cataract surgery.[194] Clinically significant CME has a reported incidence of 1–2% after cataract surgery,[195] while angiographic CME is more common and has been reported to occur after about 20% of cataract surgeries.[196,197] Its incidence is higher when associated with complicated surgery that may include capsule rupture, vitreous

loss, vitreous wick with potential traction, and retained lens fragments.

Vitrectomy has been used especially in cases refractory to medical treatment, which either show traction through vitreous incarceration in the corneal wound or have persistent residual lens fragments. The Vitrectomy–Aphakic–Cystoid Macular Edema Study, a prospective multicenter study of patients with vitreous adherent to the corneoscleral wound and with chronic aphakic cystoid macular edema, showed significant improvement in VA following vitrectomy.[134,198] Harbour et al. reported vitrectomy results of 24 eyes with chronic pseudophakic macular edema, unresponsive to medical treatment, and evidence of either vitreous adhesions to anterior segment structures or iris capture of the intraocular lens. VA improved in all patients, with 71% of subjects experiencing postoperative visual improvement of three or more lines.[199] Visual outcome was better when a complete vitrectomy was performed compared to a limited anterior vitrectomy. Pendergast et al.[200] reported a significant improvement in VA after vitrectomy in cases of pseudophakic CME even without vitreous incarceration in the wound.

In summary, the beneficial role of vitrectomy has been clearly demonstrated for CME associated with aphakia and vitreous incarceration in the wound. In cases of CME associated with pseudophakia, the current results suggest that vitrectomy is most likely beneficial in cases of traction from vitreous incarceration in the corneal wound after complicated cataract surgery and in cases of residual lens fragments. Vitrectomy may also be considered in cases of chronic CME that is unresponsive to topical antiinflammatory medications and after failure of other therapeutic alternatives such as periocular and intraocular steroids.

Vitreomacular Traction Syndrome and Epiretinal Membrane

Role of Vitrectomy in VMTS.

Vitrectomy with peeling of any tangential tractional components usually results in resolution of retinal thickening and visual improvement in patients with VMTS.[83] Hikichi et al.,[201] in a study

regarding the natural history of vitreomacular traction in the pre-OCT era, reported that 64% of the eyes lost 2 lines of vision over the course of follow-up. Since a report by Smiddy et al.[202] described an equally successful surgery for nondiabetic eyes with macular traction and visual decrease, many surgeons have elected to operate rather than to follow patients with evident vitreomacular traction and significant visual impairment.[157] Davis et al.[203] in a recent study reported improvement of more than 2 lines in 50% of eyes after vitrectomy for vitreofoveal traction syndrome and complete resolution of traction on OCT in all eyes while cystic changes improved markedly or resolved in 86% of eyes. Patients with symptoms for less than a 6-month duration (p=.048) were more likely to obtain a VA of 20/40 or better postoperatively. Vitrectomy surgery with peeling of the ERM and the posterior hyaloid is able to relieve all of the traction and has been shown to be associated with good visual outcome and resolution of the CME.[204–206] Konstantinidis et al.[207] reported that the concomitant administration of intravitreal triamcinolone acetonide after pars plana vitrectomy may speed up and improve the anatomic and functional outcome considerably. A more recent meta-analysis of pars plana vitrectomy for VMTS confirmed that this surgical procedure yields good VA recovery.[208]

Vitreomacular Traction in Age-Related Macular Degeneration

Role of Vitrectomy for AMD.

There have been several hypotheses linking vitreomacular traction with AMD, although it is still debated whether this relationship is causal or not. Chronic traction on the retina may cause degeneration or alteration of the RPE or Bruch membrane, and traction has also been shown to induce low-grade inflammation and VEGF release, which in turn may influence the progression of AMD. Furthermore, an adhesion between the vitreous and the retina may create anatomic structures, which facilitate a sustained contact of free radicals or other angiogenic cytokines in the vitreous gel with the retina, thus promoting the evolution of AMD. In addition, an attached posterior vitreous face may also prevent

oxygen diffusion or nutrient exchange.[209] It has also been shown that VMA in exudative AMD may lead to a decreased response to anti-VEGF therapy causing either increased numbers of intravitreal injections[210] or poorer visual outcomes.[211]

In some recent publications it has thus been proposed that vitrectomy for vitreous adhesion and traction on the macula in patients with exudative ARMD has a therapeutic effect on the neovascular portion of the disease (Fig. 120.14). In a series of 12 eyes of 11 patients and a follow-up of 6 months, 6 eyes showed regression of choroidal neovascularization (CNV). In 2 eyes the CNV disappeared completely. VA improved vision in 4 eyes, was unchanged in 4 eyes, and there was worsening of vision in 4 eyes.[212] Roller et al.[213] found in a pilot study that vitrectomy was associated with a reduced progression of geographic atrophy or CNV. In summary, the role of vitreous in AMD remains at present speculative and the role of vitrectomy in AMD remains currently unclear.

Vitreomacular Traction in Retinitis Pigmentosa

Garcia-Arumi et al.[214] has evaluated the role of vitrectomy accompanied by ILM peeling in 12 eyes with retinitis pigmentosa and CME refractory to medical therapy and reported anatomic and functional improvement. Their results showed a decrease in macular thickness of >40% in 10 eyes (83.3%) while the mean VA increased from 20/115 to 20/45, with an average of 3 lines of improvement. These positive results were not confirmed in a case report by Hagiwara et al.[215]

Pharmacologic Vitreolysis

Pharmacologic vitreolysis can potentially relieve vitreoretinal traction and increase vitreal O_2 levels and the rate of O_2 exchange within the vitreous cavity.[141,216] Different substances have been investigated, including chondroitinase, dispase, hyaluronidase, plasmin, and microplasmin.[217] When used as an adjunct to vitrectomy, plasmin showed promising results in diabetic macular edema facilitating PVD induction.[218] The main drawback of plasmin is that it is not easily available for clinical use. Autologous

plasminogen has to be isolated from the patient's own blood and then converted in vitro to plasmin by streptokinase. This procedure has to be done immediately before surgery as it yields a highly unstable product.[219] Microplasmin is currently the agent that shows the greatest clinical potential. It is a recombinant product that contains only the catalytic domain of human plasmin and shares all of its catalytic properties. It is much more stable than the original molecule, which greatly simplifies storage and administration.[219] Phase II trials have shown that intravitreal microplasmin is well tolerated in patients with diabetic macular edema and vitreomacular traction maculopathy,[220] and the ease of PVD induction during surgery was found to be dose- and time-dependent.[221] Further trials by the MIVI-TRUST (Traction Release without Surgical Treatment) showed an overall release rate of the VMA in 26.5% at 28 days compared to 10.1% in the placebo group.[222] The release rate was improved to around 35% in young phakic patients with no epiretinal membrane and a width of the vitreoretinal adhesion below 1,500 μm.[222] Closure of macular holes was achieved in 37% if the diameter was below 400 μm and in 58% if the hole diameter was below 250 μm.[222] The latest results have confirmed that the most likely candidates in whom the resolution of the VMA was achieved after 1 month are phakic patients younger than 65 years, without an epiretinal membrane, and with a VMA that measures less than 1,500 μm in diameter.[223] Ocriplasmin has also been used to treat VMA associated with AMD, achieving a PVD in 24% in treated eyes compared to 12% in the sham injected eyes, which was associated with a reduction of the numbers of intravitreal anti-VEGF injections from 6 to 4 in the patients who responded to ocriplasmin.[224]

The rate of nonresponse to this enzymatic therapy may be explained by the fact that the treatment decision is based primarily on an anatomic assessment, whereas the biological strength of the adhesion is not known and may not be related to the anatomic situation.[223,225] It has been argued that a prolonged observation time, or watchful waiting, may be enough to see an increased rate of spontaneous VMA resolution. In a recent observational study of patients, who were included using to the MIVI criteria detailed above, up to 44% of cases showed spontaneous VMA release during

a 24 month follow-up.[226] Others have observed that spontaneous separation of vitreomacular traction may occur much more often if there is isolated inner retinal distortion on OCT.[227]

Several authors have described potential side-effects associated with ocriplasmin use, such as photopsia, blurred vision, dyschromatopsia, and visual field loss, and further functional and anatomic evaluations have shown a transient disruption in the ellipsoid layer on OCT.[228–230] Significant electroretinogram (ERG) abnormalities have also been reported after ocriplasmin injection for vitreomacular traction and macular holes.[229,231,232] Although the cone-mediated changes appear to be transient, the rod-mediated ERG trace is depressed for a much longer period and the changes in the ellipsoid layer on OCT and the ERG appear to be linked. The massive ERG changes only concerned two patients, in whom the macular hole was closed after ocriplasmin injection. One patient with no treatment response showed only very moderate ERG changes, whereas the five other patients had no therapy response and no ERG changes.[232] It is not yet known why certain patients are more susceptible to show such retinal changes than others.

Other pharmacologic agents, which interfere with integrins, a family of proteins facilitating the attachments between cells and the extracellular matrix, have been investigated to induce vitreoretinal separation. Luminate®, for example, is an integrin peptide antagonist that interferes both with the process of neovascularization and in the maintenance of the vitreoretinal adhesion by inhibiting the integrin $\alpha 5\beta 1$.[233,234] In recent not yet published phase I and II studies Luminate® has been shown to induce a full or partial PVD in 55–65% of patients with diabetic macular edema at 90 days after injection versus 10% in the placebo group.

Treatment of Vitreomacular Traction Syndrome With Intravitreal Gas Injection

It has been reported that a single intravitreal injection of fluid can induce a posterior vitreous detachment in up to 25% of patients,[235] and in view of the high costs of ocriplasmin, cost options to treat VMTS have been investigated by several authors. McHugh et al.

proposed, for example, the injection of 0.3 mL of pure C_3F_8 gas to induce a PVD detachment as the gas bubble expands. This technique was successful in a series of patients with diabetic maculopathy resulting in a PVD associated with an improvement of vision and the reduction of macular thickness on OCT in all patients.[236] These results compare well with another study, which also showed separation of VMT in 40% of patients at 1 month and 60% at 3 months following injection of C_3F_8.[237] More recently, Day et al. injected 0.3 mL of pure SF_6 gas intravitreally in nine eyes with VMTS. In five patients (55.6%) the expansile gas was able to detach the posterior hyaloid from the macula, resulting in a resolution of the VMTS or the closure of small macular holes at 1 month after injection.[238]

Conclusion

An understanding of the factors responsible for the development of vitreomacular interface disorders together with prognostic factors, and potential complications of surgery will allow clinicians to inform and educate patients while making a choice between continuing follow-up and the appropriate timing of a surgical intervention. OCT has become an invaluable tool in the early diagnosis of these disorders. Further the increased number of therapeutic interventions available have led to an excellent prognosis of this retinal pathology.

References

1. Duker JS, Kaiser PK, Binder S, et al. The International Vitreomacular Traction Study Group classification of vitreomacular adhesion, traction, and macular hole. *Ophthalmology*. 2013;120(12):2611–2619.
2. Klein R, Klein BE, Wang Q, Moss SE. The epidemiology of epiretinal membranes. *Trans Am Ophthalmol Soc*. 1994;92:403–430.
3. Fraser-Bell S, Guzowski M, Rochtchina E, Wang JJ, Mitchell P. Five-year cumulative incidence and progression of

epiretinal membranes: the Blue Mountains Eye Study. *Ophthalmology*. 2003;110(1):34–40.
4. Mitchell P, Smith W, Chey T, Wang JJ, Chang A. Prevalence and associations of epiretinal membranes. The Blue Mountains Eye Study, Australia. *Ophthalmology*. 1997;104(6):1033–1040.
5. Miyazaki M, Nakamura H, Kubo M, et al. Prevalence and risk factors for epiretinal membranes in a Japanese population: the Hisayama study. *Graefes Arch Clin Exp Ophthalmol*. 2003;241(8):642–646.
6. Ng CH, Cheung N, Wang JJ, et al. Prevalence and risk factors for epiretinal membranes in a multi-ethnic United States population. *Ophthalmology*. 2011;118(4):694–699.
7. McLeod D, Hiscott PS, Grierson I. Age-related cellular proliferation at the vitreoretinal juncture. *Eye*. 1987;1:263–281.
8. Wise G. Clinical features of idiopathic preretinal macular fibrosis. *Am J Ophthalmol*. 1975;79(3):349–357.
9. Gass JDM. *Stereoscopic atlas of macular diseases: diagnosis and treatment*. 3rd ed. Mosby: St. Louis; 1987.
10. Appiah AP, Hirose T. Secondary causes of premacular fibrosis. *Ophthalmology*. 1989;96(3):389–392.
11. Hirokawa H, Jalkh AE, Takahashi M, Trempe CL, Schepens CL. Role of the vitreous in idiopathic preretinal macular fibrosis. *Am J Ophthalmol*. 1986;101(2):166–169.
12. Appiah AP, Hirose T, Kado M. A review of 324 cases of idiopathic premacular gliosis. *Am J Ophthalmol*. 1988;106(5):533–535.
13. Pesin SR, Olk RJ, Grand MG, et al. Vitrectomy for premacular fibroplasia. Prognostic factors, long-term follow-up, and time course of visual improvement. *Ophthalmology*. 1991;98(7):1109–1114.
14. Yang HS, Hong JW, Kim YJ, Kim JG, Joe SG. Characteristics of spontaneous idiopathic epiretinal membrane separation in spectral domain optical coherence tomography. *Retina*. 2014;34(10):2079–2087.
15. Massin P, Allouch C, Haouchine B, et al. Optical coherence tomography of idiopathic macular epiretinal membranes

before and after surgery. *Am J Ophthalmol*. 2000;130(6):732–739.
16. Sheard RM, Sethi C, Gregor Z. Acute macular pucker. *Ophthalmology*. 2003;110(6):1178–1184.
17. Bringmann A, Wiedemann P. Involvement of Müller glial cells in epiretinal membrane formation. *Graefes Arch Clin Exp Ophthalmol*. 2009;247(7):865–883.
18. Lesnik Oberstein SY, Lewis GP, Dutra T, Fisher SK. Evidence that neurites in human epiretinal membranes express melanopsin, calretinin, rod opsin and neurofilament protein. *Br J Ophthalmol*. 2011;95(2):266–272.
19. Wickham LJ, Asaria RH, Alexander R, Luthert P, Charteris DG. Immunopathology of intraocular silicone oil: retina and epiretinal membranes. *Br J Ophthalmol*. 2007;91(2):258–262.
20. Morino I, Hiscott P, McKechnie N, Grierson I. Variation in epiretinal membrane components with clinical duration of the proliferative tissue. *Br J Ophthalmol*. 1990;74(7):393–399.
21. Harada C, Mitamura Y, Harada T. The role of cytokines and trophic factors in epiretinal membranes: involvement of signal transduction in glial cells. *Prog Retin Eye Res*. 2006;25(2):149–164.
22. Oberstein SY, Byun J, Herrera D, Chapin EA, Fisher SK, Lewis GP. Cell proliferation in human epiretinal membranes: characterization of cell types and correlation with disease condition and duration. *Mol Vis*. 2011;17:1794–1805.
23. Foos RY. Vitreoretinal juncture; epiretinal membranes and vitreous. *Invest Ophthalmol Vis Sci*. 1977;16(5):416–422.
24. Gandorfer A, Schumann R, Scheler R, Haritoglou C, Kampik A. Pores of the inner limiting membrane in flat-mounted surgical specimens. *Retina*. 2011;31(5):977–981.
25. Lewis GP, Charteris DG, Sethi CS, Leitner WP, Linberg KA, Fisher SK. The ability of rapid retinal reattachment to stop or reverse the cellular and molecular events initiated by detachment. *Invest Ophthalmol Vis Sci*. 2002;43:2412–2420.
26. Sramek SJ, Wallow IH, Stevens TS, Nork TM. Immunostaining of preretinal membranes for actin,

fibronectin, and glial fibrillary acidic protein. *Ophthalmology*. 1989;96(6):835–841.
27. Jaffe NS. Vitreous traction at the posterior pole of the fundus due to alterations in the vitreous posterior. *Trans Am Acad Ophthalmol Otolaryngol*. 1967;71(4):642–652.
28. Odrobina D, Michalewska Z, Michalewski J, Dziegielewski K, Nawrocki J. Long-term evaluation of vitreomacular traction disorder in spectral-domain optical coherence tomography. *Retina*. 2011;31(2):324–331.
29. Koizumi H, Spaide RF, Fisher YL, Freund KB, Klancnik JM Jr, Yannuzzi LA. Three-dimensional evaluation of vitreomacular traction and epiretinal membrane using spectral-domain optical coherence tomography. *Am J Ophthalmol*. 2008;145(3):509–517.
30. Gandorfer A, Rohleder M, Kampik A. Epiretinal pathology of vitreomacular traction syndrome. *Br J Ophthalmol*. 2002;86(8):902–909.
31. Heilskov TW, Massicotte SJ, Folk JC. Epiretinal macular membranes in eyes with attached posterior cortical vitreous. *Retina*. 1996;16(4):279–284.
32. Wilkins JR, Puliafito CA, Hee MR, et al. Characterization of epiretinal membranes using optical coherence tomography. *Ophthalmology*. 1996;103(12):2142–2151.
33. Witkin AJ, Ko TH, Fujimoto JG, et al. Redefining lamellar holes and the vitreomacular interface: an ultrahigh-resolution optical coherence tomography study. *Ophthalmology*. 2006;113(3):388–397.
34. Nigam N, Bartsch DU, Cheng L, et al. Spectral domain optical coherence tomography for imaging ERM, retinal edema, and vitreomacular interface. *Retina*. 2010;30(2):246–253.
35. Mori K, Gehlbach PL, Sano A, Deguchi T, Yoneya S. Comparison of epiretinal membranes of differing pathogenesis using optical coherence tomography. *Retina*. 2004;24(1):57–62.
36. Michalewski J, Michalewska Z, Cisiecki S, Nawrocki J. Morphologically functional correlations of macular pathology connected with epiretinal membrane formation

in spectral optical coherence tomography (SOCT). *Graefes Arch Clin Exp Ophthalmol*. 2007;245(11):1623–1631.
37. Watanabe A, Arimoto S, Nishi O. Correlation between metamorphopsia and epiretinal membrane optical coherence tomography findings. *Ophthalmology*. 2009;116(9):1788–1793.
38. Ooto S, Hangai M, Takayama K, et al. High-resolution imaging of the photoreceptor layer in epiretinal membrane using adaptive optics scanning laser ophthalmoscopy. *Ophthalmology*. 2011;118(5):873–881.
39. Inoue M, Morita S, Watanabe Y, et al. Inner segment/outer segment junction assessed by spectral-domain optical coherence tomography in patients with idiopathic epiretinal membrane. *Am J Ophthalmol*. 2010;150(6):834–839.
40. Okamoto F, Sugiura Y, Okamoto Y, Hiraoka T, Oshika T. Inner nuclear layer thickness as a prognostic factor for metamorphopsia after epiretinal membrane surgery. *Retina*. 2015;35(10):2107–2114.
41. Falkner-Radler CI, Glittenberg C, Gabriel M, Binder S. Intrasurgical microscope-integrated spectral domain optical coherence tomography-assisted membrane peeling. *Retina*. 2015;35(10):2100–2106.
42. Dell'omo R, Cifariello F, Dell'omo E, et al. Influence of retinal vessel printings on metamorphopsia and retinal architectural abnormalities in eyes with idiopathic macular epiretinal membrane. *Invest Ophthalmol Vis Sci*. 2013;54(12):7803–7811.
43. Wong JG, Sachdev N, Beaumont PE, Chang AA. Visual outcomes following vitrectomy and peeling of epiretinal membrane. *Clin Exp Ophthalmol*. 2005;33(4):373–378.
44. Scheerlinck LM, van der Valk R, van Leeuwen R. Predictive factors for postoperative visual acuity in idiopathic epiretinal membrane: a systematic review. *Acta Ophthalmol*. 2015;93(3):203–212.
45. Inoue M, Morita S, Watanabe Y, et al. Preoperative inner segment/outer segment junction in spectral-domain optical coherence tomography as a prognostic factor in epiretinal membrane surgery. *Retina*. 2011;31(7):1366–1372.

46. Shiono A, Kogo J, Klose G, et al. Photoreceptor outer segment length: a prognostic factor for idiopathic epiretinal membrane surgery. *Ophthalmology*. 2013;120(4):788–794.
47. Sugiura Y, Okamoto F, Okamoto Y, Hiraoka T, Oshika T. Contrast sensitivity and foveal microstructure following vitrectomy for epiretinal membrane. *Invest Ophthalmol Vis Sci*. 2014;55(11):7594–7600.
48. Ghazi-Nouri SM, Tranos PG, Rubin GS, Adams ZC, Charteris DG. Visual function and quality of life following vitrectomy and epiretinal membrane peel surgery. *Br J Ophthalmol*. 2006;90(5):559–562.
49. Okamoto F, Sugiura Y, Okamoto Y, Hiraoka T, Oshika T. Stereopsis and optical coherence tomography findings after epiretinal membrane surgery. *Retina*. 2015;35(7):1415–1421.
50. Kinoshita T, Imaizumi H, Miyamoto H, et al. Changes in metamorphopsia in daily life after successful epiretinal membrane surgery and correlation with M-CHARTS score. *Clin Ophthalmol*. 2015;9:225–233.
51. Falkner-Radler CI, Glittenberg C, Hagen S, Benesch T, Binder S. Spectral-domain optical coherence tomography for monitoring epiretinal membrane surgery. *Ophthalmology*. 2010;117(4):798–805.
52. Reibaldi M, Longo A, Avitabile T, et al. Transconjunctival nonvitrecomizing vitreous surgery versus 25-gauge vitrectomy in patients with epiretinal membrane: a prospective randomized study. *Retina*. 2015;35(5):873–879.
53. Saito Y, Lewis JM, Park I, et al. Nonvitrectomizing vitreous surgery: a strategy to prevent postoperative nuclear sclerosis. *Ophthalmology*. 1999;106(8):1541–1545.
54. Haritoglou C, Eibl K, Schaumberger M, et al. Functional outcome after trypan blue-assisted vitrectomy for macular pucker: a prospective, randomized, comparative trial. *Am J Ophthalmol*. 2004;138(1):1–5.
55. Haritoglou C, Gandorfer A, Schaumberger M, et al. Trypan blue in macular pucker surgery: an evaluation of histology and functional outcome. *Retina*. 2004;24(4):582–590.
56. Kwok AK, Lai TY, Li WW, Yew DT, Wong VW. Trypan blue- and indocyanine green-assisted epiretinal membrane

surgery: clinical and histopathological studies. *Eye*. 2004;18(9):882–888.
57. Hillenkamp J, Saikia P, Gora F, et al. Macular function and morphology after peeling of idiopathic epiretinal membrane with and without the assistance of indocyanine green. *Br J Ophthalmol*. 2005;89(4):437–443.
58. Hillenkamp J, Saikia P, Herrmann WA, Framme C, Gabel VP, Sachs HG. Surgical removal of idiopathic epiretinal membrane with or without the assistance of indocyanine green: a randomised controlled clinical trial. *Graefes Arch Clin Exp Ophthalmol*. 2007;245(7):973–979.
59. Koestinger A, Bovey EH. Visual acuity after vitrectomy and epiretinal membrane peeling with or without premacular indocyanine green injection. *Eur J Ophthalmol*. 2005;15(6):795–799.
60. Foster RE, Petersen MR, Da Mata AP, Burk SE, Rosa RH Jr, Riemann CD. Negative indocyanine green staining of epiretinal membranes. *Retina*. 2002;22(1):106–108.
61. Sakamoto H, Yamanaka I, Kubota T, Ishibashi T. Indocyanine green-assisted peeling of the epiretinal membrane in proliferative vitreoretinopathy. *Graefes Arch Clin Exp Ophthalmol*. 2003;241(3):204–207.
62. Rodrigues EB, Costa EF, Penha FM, et al. The use of vital dyes in ocular surgery. *Surv Ophthalmol*. 2009;54(5):576–617.
63. Balayre S, Boissonnot M, Fernandez B, Quellard N, Babin P, Dighiero P. [Ultrastructural study of epiretinal membrane stained by trypan blue: 15 case reports.]. *J Fr Ophthalmol*. 2005;28(2):159–167.
64. Uno F, Malerbi F, Maia M, Farah ME, Maia A, Magalhaes O Jr. Subretinal trypan blue migration during epiretinal membrane peeling. *Retina*. 2006;26(2):237–239.
65. Balayre S, Boissonnot M, Curutchet L, Dighiero P. Role of trypan blue in epiretinal membrane surgery. *J Fr Ophthalmol*. 2005;28(3):290–297.
66. Bovey EH, Uffer S, Achache F. Surgery for epimacular membrane: impact of retinal internal limiting membrane removal on functional outcome. *Retina*. 2004;24(5):728–735.
67. Park DW, Dugel PU, Garda J, et al. Macular pucker removal

with and without internal limiting membrane peeling: pilot study. *Ophthalmology*. 2003;110(1):62–64.
68. Sandali O, El Sanharawi M, Basli E, et al. Epiretinal membrane recurrence: incidence, characteristics, evolution, and preventive and risk factors. *Retina*. 2013;33(10):2032–2038.
69. Ahn SJ, Ahn J, Woo SJ, Park KH. Photoreceptor change and visual outcome after idiopathic epiretinal membrane removal with or without additional internal limiting membrane peeling. *Retina*. 2014;34(1):172–181.
70. Lim JW, Cho JH, Kim HK. Assessment of macular function by multifocal electroretinography following epiretinal membrane surgery with internal limiting membrane peeling. *Clin Ophthalmol*.2010;4:689–694.
71. Kifuku K, Hata Y, Kohno RI, et al. Residual internal limiting membrane in epiretinal membrane surgery. *Br J Ophthalmol*. 2009;93(8):1016–1019.
72. Donati G, Kapetanios AD, Pournaras CJ. Complications of surgery for epiretinal membranes. Graefe's archive for clinical and experimental ophthalmology. *Graefes Arch Clin Exp Ophthalmol*. 1998;236(10):739–746.
73. Pournaras CJ, Donati G, Brazitikos PD, Kapetanios AD, Dereklis DL, Stangos NT. Macular epiretinal membranes. *Semin Ophthalmol*. 2000;15(2):100–107.
74. Issa SA, Connor A, Habib M, Steel DH. Comparison of retinal breaks observed during 23 gauge transconjunctival vitrectomy versus conventional 20-gauge surgery for proliferative diabetic retinopathy. *Clin Ophthalmol*.2011;5:109–114.
75. Nakano T, Uemura A, Sakamoto T. Incidence of iatrogenic peripheral retinal breaks in 23-gauge vitrectomy for macular diseases. *Retina*. 2011;31(10):1997–2001.
76. Jackson TL, Donachie PH, Williamson TH, Sparrow JM, Johnston RL. The Royal College of Ophthalmologists' national ophthalmology data base study of vitreoretinal surgery: report 4, epiretinal membrane. *Retina*. 2015;35(8):1615–1621.
77. Do DV, Hawkins B, Gichuhi S, Vedula SS. Surgery for post-

vitrectomy cataract. *Cochrane Database Syst Rev*. 2008;(3) [CD006366].
78. Dugas B, Ouled-Moussa R, Lafontaine PO, et al. Idiopathic epiretinal macular membrane and cataract extraction: combined versus consecutive surgery. *Am J Ophthalmol*. 2010;149(2):302–306.
79. Poliner LS, Olk RJ, Grand MG, Escoffery RF, Okun E, Boniuk I. Surgical management of premacular fibroplasia. *Arch Ophthalmol*. 1988;106(6):761–764.
80. Coscas G, Cunha-Vaz J, Soubrane G. Macular edema: definition and basic concepts. *Dev Ophthalmol*. 2010;47:1–9.
81. Scholl S, Kirchhof J, Augustin AJ. Pathophysiology of macular edema. *Ophthalmologica*. 2010;224(Suppl. 1):8–15.
82. Irvine SR. A newly defined vitreous syndrome following cataract surgery. *Am J Ophthalmol*. 1953;36(5):599–619.
83. Johnson MW. Etiology and treatment of macular edema. *Am J Ophthalmol*. 2009;147(1):11–21.e1.
84. Fine BS, Brucker AJ. Macular edema and cystoid macular edema. *Am J Ophthalmol*. 1981;92(4):466–481.
85. Yanoff M, Fine BS, Brucker AJ, Eagle RC Jr. Pathology of human cystoid macular edema. *Surv Ophthalmol*. 1984;28(Suppl.):505–511.
86. Gass JD, Anderson DR, Davis EB. A clinical, fluorescein angiographic, and electron microscopic correlation of cystoid macular edema. *Am J Ophthalmol*. 1985;100(1):82–86.
87. Scholl S, Augustin A, Loewenstein A, Rizzo S, Kupperman B. General pathophysiology of macular edema. *Eur J Ophthalmol*. 2010;21(S6):10–19.
88. Tso MO. Pathology of cystoid macular edema. *Ophthalmology*. 1982;89(8):902–915.
89. Antcliff RJ, Hussain AA, Marshall J. Hydraulic conductivity of fixed retinal tissue after sequential excimer laser ablation: barriers limiting fluid distribution and implications for cystoid macular edema. *Arch Ophthalmol*. 2001;119(4):539–544.
90. Bringmann A, Reichenbach A, Wiedemann P. Pathomechanisms of cystoid macular edema. *Ophthalmic Res*. 2004;36(5):241–249.

91. Schubert HD. Cystoid macular edema: the apparent role of mechanical factors. *Prog Clin Biol Res*. 1989;312:277–291.
92. Lindqvist N, Liu Q, Zajadacz J, Franze K, Reichenbach A. Retinal glial (Müller) cells: sensing and responding to tissue stretch. *Invest Ophthalmol Vis Sci*. 2010;51(3):1683–1690.
93. Wolfensberger TJ, Gregor ZJ. Macular edema – rationale for therapy. *Dev Ophthalmol*. 2010;47:49–58.
94. Smiddy WE, Green WR, Michels RG, de la Cruz Z. Ultrastructural studies of vitreomacular traction syndrome. *Am J Ophthalmol*. 1989;107(2):177–185.
95. Meyer CH, Toth CA. Retinal pigment epithelial tear with vitreomacular attachment: a novel pathogenic feature. *Graefes Arch Clin Exp Ophthalmol*. 2001;239(5):325–333.
96. Kuiper EJ, de Smet MD, van Meurs JC, et al. Association of connective tissue growth factor with fibrosis in vitreoretinal disorders in the human eye. *Arch Ophthalmol*. 2006;124(10):1457–1462.
97. Donoso LA, Kim D, Frost A, Callahan A, Hageman G. The role of inflammation in the pathogenesis of age-related macular degeneration. *Surv Ophthalmol*. 2006;51(2):137–152.
98. Krebs I, Brannath W, Glittenberg C, Zeiler F, Sebag J, Binder S. Posterior vitreomacular adhesion: a potential risk factor for exudative age-related macular degeneration? *Am J Ophthalmol*. 2007;144(5):741–746.
99. Augustin A, Loewenstein A, Kuppermann BD. Macular edema. General pathophysiology. *Dev Ophthalmol*. 2010;47:10–26.
100. Bhagat N, Grigorian RA, Tutela A, Zarbin MA. Diabetic macular edema: pathogenesis and treatment. *Surv Ophthalmol*. 2009;54(1):1–32.
101. Sebag J, Buckingham B, Charles MA, Reiser K. Biochemical abnormalities in vitreous of humans with proliferative diabetic retinopathy. *Arch Ophthalmol*. 1992;110(10):1472–1476.
102. Jumper JM, Embabi SN, Toth CA, McCuen BW II, Hatchell DL. Electron immunocytochemical analysis of posterior hyaloid associated with diabetic macular edema. *Retina*. 2000;20(1):63–68.

103. Lewis H. The role of vitrectomy in the treatment of diabetic macular edema. *Am J Ophthalmol*. 2001;131(1):123–125.
104. Praidou A, Papakonstantinou E, Androudi S, Georgiadis N, Karakiulakis G, Dimitrakos S. Vitreous and serum levels of vascular endothelial growth factor and platelet-derived growth factor and their correlation in patients with non-proliferative diabetic retinopathy and clinically significant macula oedema. *Acta Ophthalmol*. 2011;89(3):248–254.
105. Praidou A, Klangas I, Papakonstantinou E, et al. Vitreous and serum levels of platelet-derived growth factor and their correlation in patients with proliferative diabetic retinopathy. *Curr Eye Res*. 2009;34(2):152–161.
106. Noma H, Funatsu H, Mimura T, Harino S, Hori S. Vitreous levels of interleukin-6 and vascular endothelial growth factor in macular edema with central retinal vein occlusion. *Ophthalmology*. 2009;116(1):87–93.
107. Adamis AP, Shima DT. The role of vascular endothelial growth factor in ocular health and disease. *Retina*. 2005;25(2):111–118.
108. Kiss CG, Barisani-Asenbauer T, Maca S, Richter-Mueksch S, Radner W. Reading performance of patients with uveitis-associated cystoid macular edema. *Am J Ophthalmol*. 2006;142(4):620–624.
109. Valentincic NV, Berendschot TT, Hawlina M, Kraut A, Rothova A. Effect of tinted optical filters on visual acuity and contrast sensitivity in patients with inflammatory cystoid macular edema. *Retina*. 2007;27(4):483–489.
110. Pinckers A, van Aarem A, Keunen JE. Colour vision in retinitis pigmentosa. Influence of cystoid macular edema. *Int Ophthalmol*. 1993;17(3):143–146.
111. Kiss CG, Barisani-Asenbauer T, Simader C, Maca S, Schmidt-Erfurth U. Central visual field impairment during and following cystoid macular oedema. *Br J Ophthalmol*. 2008;92(1):84–88.
112. Cunha-Vaz J, Coscas G. Diagnosis of macular edema. *Ophthalmologica*. 2010;224(Suppl. 1):2–7.
113. Staurenghi G, Invernizzi A, de Polo L, Pellegrini M. Macular edema. Diagnosis and detection. *Dev Ophthalmol*.

2010;47:27–48.
114. Tranos PG, Wickremasinghe SS, Stangos NT, Topouzis F, Tsinopoulos I, Pavesio CE. Macular edema. *Surv Ophthalmol*. 2004;49(5):470–490.
115. Hee MR, Puliafito CA, Duker JS, et al. Topography of diabetic macular edema with optical coherence tomography. *Ophthalmology*. 1998;105(2):360–370.
116. Abouzeid H, Wolfensberger T. Optical coherence tomography assessment of macular oedema. Holz FG, Spaide RF. *Medical retina. Essentials in ophthalmology*. Springer: Berlin, Heidelberg, New York; 2005:1–16.
117. Antcliff RJ, Stanford MR, Chauhan DS, et al. Comparison between optical coherence tomography and fundus fluorescein angiography for the detection of cystoid macular edema in patients with uveitis. *Ophthalmology*. 2000;107(3):593–599.
118. Kim BY, Smith SD, Kaiser PK. Optical coherence tomographic patterns of diabetic macular edema. *Am J Ophthalmol*. 2006;142(3):405–412.
119. Markomichelakis NN, Halkiadakis I, Pantelia E, et al. Patterns of macular edema in patients with uveitis: qualitative and quantitative assessment using optical coherence tomography. *Ophthalmology*. 2004;111(5):946–953.
120. Soliman W, Sander B, Jorgensen TM. Enhanced optical coherence patterns of diabetic macular oedema and their correlation with the pathophysiology. *Acta Ophthalmol Scand*. 2007;85(6):613–617.
121. Baskin DE. Optical coherence tomography in diabetic macular edema. *Curr Opin Ophthalmol*. 2010;21(3):172–177.
122. Koizumi H, Spaide RF, Fisher YL, Freund KB, Klancnik JM Jr, Yannuzzi LA. Three-dimensional evaluation of vitreomacular traction and epiretinal membrane using spectral-domain optical coherence tomography. *Am J Ophthalmol*. 2008;145(3):509–517.
123. Barthelmes D, Sutter FK, Gillies MC. Differential optical densities of intraretinal spaces. *Invest Ophthalmol Vis Sci*. 2008;49(8):3529–3534.
124. Ghazi NG, Ciralsky JB, Shah SM, Campochiaro PA, Haller

JA. Optical coherence tomography findings in persistent diabetic macular edema: the vitreomacular interface. *Am J Ophthalmol*. 2007;144(5):747–754.
125. Kenawy N, Wong D, Stappler T, et al. Does the presence of an epiretinal membrane alter the cleavage plane during internal limiting membrane peeling? *Ophthalmology*. 2010;117(2) [320–3.e1].
126. Thomas D, Bunce C, Moorman C, Laidlaw AH. Frequency and associations of a taut thickened posterior hyaloid, partial vitreomacular separation, and subretinal fluid in patients with diabetic macular edema. *Retina*. 2005;25(7):883–888.
127. Ophir A, Martinez MR. Epiretinal membranes and incomplete posterior vitreous detachment in diabetic macular edema using spectral-domain optical coherence tomography. *Invest Ophthalmol Vis Sci*. 2011;52(9):6414–6420.
128. Ophir A, Trevino A, Martinez MR. Extrafoveal vitreous traction associated with branch retinal vein occlusion. *Eur J Ophthalmol*. 2010;20(4):733–739.
129. Weber-Krause B, Eckardt U. Incidence of posterior vitreous detachment in eyes with and without age-related macular degeneration. An ultrasonic study. *Ophthalmologe*. 1996;93(6):660–665.
130. Ondes F, Yilmaz G, Acar MA, Unlu N, Kocaoglan H, Arsan AK. Role of the vitreous in age-related macular degeneration. *Jpn J Ophthalmol*. 2000;44(1):91–93.
131. Hayreh SS, Jonas JB. Posterior vitreous detachment: clinical correlations. *Ophthalmologica*. 2004;218(5):333–343.
132. Lambert HM. The management of subfoveal choroidal neovascular membranes and hemorrhage. *Semin Ophthalmol*. 2000;15(2):92–99.
133. Lewis H, Abrams GW, Blumenkranz MS, Campo RV. Vitrectomy for diabetic macular traction and edema associated with posterior hyaloidal traction. *Ophthalmology*. 1992;99(5):753–759.
134. Fung WE. Vitrectomy for chronic aphakic cystoid macular edema. Results of a national, collaborative, prospective, randomized investigation. *Ophthalmology*. 1985;92(8):1102–

1111.
135. Stefansson E. Physiology of vitreous surgery. *Graefes Arch Clin Exp Ophthalmol*. 2009;247(2):147–163.
136. Williamson TH, Grewal J, Gupta B, Mokete B, Lim M, Fry CH. Measurement of PO2 during vitrectomy for central retinal vein occlusion, a pilot study. *Graefes Arch Clin Exp Ophthalmol*. 2009;247(8):1019–1023.
137. Stefansson E, Novack RL, Hatchell DL. Vitrectomy prevents retinal hypoxia in branch retinal vein occlusion. *Invest Ophthalmol Vis Sci*. 1990;31(2):284–289.
138. Holekamp NM, Shui YB, Beebe DC. Vitrectomy surgery increases oxygen exposure to the lens: a possible mechanism for nuclear cataract formation. *Am J Ophthalmol*. 2005;139(2):302–310.
139. Siegfried CJ, Shui YB, Holekamp NM, Bai F, Beebe DC. Oxygen distribution in the human eye: relevance to the etiology of open-angle glaucoma after vitrectomy. *Invest Ophthalmol Vis Sci*. 2010;51(11):5731–5738.
140. Giblin FJ, Quiram PA, Leverenz VR, Baker RM, Dang L, Trese MT. Enzyme-induced posterior vitreous detachment in the rat produces increased lens nuclear pO2 levels. *Exp Eye Res*. 2009;88(2):286–292.
141. Quiram PA, Leverenz VR, Baker RM, Dang L, Giblin FJ, Trese MT. Microplasmin-induced posterior vitreous detachment affects vitreous oxygen levels. *Retina*. 2007;27(8):1090–1096.
142. Kadonosono K, Itoh N, Ohno S. Perifoveal microcirculation before and after vitrectomy for diabetic cystoid macular edema. *Am J Ophthalmol*. 2000;130(6):740–744.
143. Noma H, Funatsu H, Mimura T, Harino S, Eguchi S, Hori S. Pigment epithelium-derived factor and vascular endothelial growth factor in branch retinal vein occlusion with macular edema. *Graefes Arch Clin Exp Ophthalmol*. 2010;248(11):1559–1565.
144. Matsunaga N, Chikaraishi Y, Izuta H, et al. Role of soluble vascular endothelial growth factor receptor-1 in the vitreous in proliferative diabetic retinopathy. *Ophthalmology*. 2008;115(11):1916–1922.

145. Stefansson E. The therapeutic effects of retinal laser treatment and vitrectomy. A theory based on oxygen and vascular physiology. *Acta Ophthalmol Scand*. 2001;79(5):435–440.
146. Stefansson E. Ocular oxygenation and the treatment of diabetic retinopathy. *Surv Ophthalmol*. 2006;51(4):364–380.
147. Matsunaga N, Ozeki H, Hirabayashi Y, Shimada S, Ogura Y. Histopathologic evaluation of the internal limiting membrane surgically excised from eyes with diabetic maculopathy. *Retina*. 2005;25(3):311–316.
148. Saravia M. Persistent diffuse diabetic macular edema. The role of the internal limiting membrane as a selective membrane: the oncotic theory. *Med Hypotheses*. 2010;76(6):858–860.
149. Hoerauf H, Bruggemann A, Muecke M, et al. Pars plana vitrectomy for diabetic macular edema. Internal limiting membrane delamination vs posterior hyaloid removal: a prospective randomized trial. *Graefes Arch Clin Exp Ophthalmol*. 2011;249(7):997–1008.
150. Gandorfer A, Rohleder M, Grosselfinger S, Haritoglou C, Ulbig M, Kampik A. Epiretinal pathology of diffuse diabetic macular edema associated with vitreomacular traction. *Am J Ophthalmol*. 2005;139(4):638–652.
151. Schaal S, Tezel TH, Kaplan HJ. Surgical intervention in refractory CME –-role of posterior hyaloid separation and internal limiting membrane peeling. *Ocul Immunol Inflamm*. 2008;16(5):209–210.
152. Lopes de Faria JM, Jalkh AE, Trempe CL, McMeel JW. Diabetic macular edema: risk factors and concomitants. *Acta Ophthalmol Scand*. 1999;77(2):170–175.
153. Hikichi T, Fujio N, Akiba J, Azuma Y, Takahashi M, Yoshida A. Association between the short-term natural history of diabetic macular edema and the vitreomacular relationship in type II diabetes mellitus. *Ophthalmology*. 1997;104(3):473–478.
154. Harbour JW, Smiddy WE, Flynn HW Jr, Rubsamen PE. Vitrectomy for diabetic macular edema associated with a thickened and taut posterior hyaloid membrane. *Am J*

Ophthalmol. 1996;121(4):405–413.
155. Massin P, Duguid G, Erginay A, Haouchine B, Gaudric A. Optical coherence tomography for evaluating diabetic macular edema before and after vitrectomy. *Am J Ophthalmol*. 2003;135(2):169–177.
156. Bandello F, Battaglia Parodi M, Lanzetta P, et al. Diabetic macular edema. *Dev Ophthalmol*. 2010;47:73–110.
157. Diabetic Retinopathy Clinical Research Network Writing C, Haller JA, Qin H, et al. Vitrectomy outcomes in eyes with diabetic macular edema and vitreomacular traction. *Ophthalmology*. 2010;117(6) [1087–93.e3].
158. Capone A Jr, Panozzo G. Vitrectomy for refractory diabetic macular edema. *Semin Ophthalmol*. 2000;15(2):78–80.
159. Pendergast SD, Hassan TS, Williams GA, et al. Vitrectomy for diffuse diabetic macular edema associated with a taut premacular posterior hyaloid. *Am J Ophthalmol*. 2000;130(2):178–186.
160. Stolba U, Binder S, Gruber D, Krebs I, Aggermann T, Neumaier B. Vitrectomy for persistent diffuse diabetic macular edema. *Am J Ophthalmol*. 2005;140(2):295–301.
161. Stefaniotou M, Aspiotis M, Kalogeropoulos C, et al. Vitrectomy results for diffuse diabetic macular edema with and without inner limiting membrane removal. *Eur J Ophthalmol*. 2004;14(2):137–143.
162. Bahadir M, Ertan A, Mertoglu O. Visual acuity comparison of vitrectomy with and without internal limiting membrane removal in the treatment of diabetic macular edema. *Int Ophthalmol*. 2005;26(1–2):3–8.
163. Patel JI, Hykin PG, Schadt M, Luong V, Fitzke F, Gregor ZJ. Pars plana vitrectomy with and without peeling of the inner limiting membrane for diabetic macular edema. *Retina*. 2006;26(1):5–13.
164. Kumar A, Sinha S, Azad R, Sharma YR, Vohra R. Comparative evaluation of vitrectomy and dye-enhanced ILM peel with grid laser in diffuse diabetic macular edema. *Graefes Arch Clin Exp Ophthalmol*. 2007;245(3):360–368.
165. Gentile RC, Milman T, Eliott D, Romero JM, McCormick SA. Taut internal limiting membrane causing diffuse diabetic

macular edema after vitrectomy: clinicopathological correlation. *Ophthalmologica*. 2011;226(2):64–70.
166. Lyndon da Cruz ZJG. Surgery in the treatment of cystoid macular edema. Ryan SJ. *Retina*. 4th ed. Mosby; 2005.
167. Reichenbach A, Wurm A, Pannicke T, Iandiev I, Wiedemann P, Bringmann A. Müller cells as players in retinal degeneration and edema. *Graefes Arch Clin Exp Ophthalmol*. 2007;245(5):627–636.
168. Zhang X, Bao S, Lai D, Rapkins RW, Gillies MC. Intravitreal triamcinolone acetonide inhibits breakdown of the blood-retinal barrier through differential regulation of VEGF-A and its receptors in early diabetic rat retinas. *Diabetes*. 2008;57(4):1026–1033.
169. Williamson T Macular disorders. Vitreoretinal surgery: Springer-Verlag Berlin Heidelberg; 2008. p. 120.
170. Haritoglou C, Schumann RG, Kampik A, Gandorfer A. Heavy brilliant blue G for internal limiting membrane staining. *Retina*. 2011;31(2):405–407.
171. Aref AA, Scott IU. Management of macular edema secondary to central retinal vein occlusion: an evidence-based. *Adv Ther*. 2011;28(1):40–50.
172. Noma H, Funatsu H, Mimura T, Shimada K. Visual acuity and foveal thickness after vitrectomy for macular edema. *Ophthalmologica*. 2010;224(6):367–373.
173. Leizaola-Fernandez C, Suarez-Tata L, Quiroz-Mercado H, et al. Vitrectomy with complete posterior hyaloid removal for ischemic central retinal vein occlusion: series of cases. *BMC Ophthalmol*. 2005;5:10.
174. Noma H, Funatsu H, Mimura T, Eguchi S, Shimada K. Visual prognosis and vitreous molecules after vitrectomy for macular edema with branch retinal vein occlusion. *Clin Ophthalmol.*2011;5:223–229.
175. Yamasaki M, Noma H, Funatsu H, et al. Changes in foveal thickness after vitrectomy for macular edema with branch retinal vein occlusion and intravitreal vascular endothelial growth factor. *Int Ophthalmol*. 2009;29(3):161–167.
176. Martinez MR, Ophir A. Extrafoveal traction in retinal vein occlusion using spectral domain optical coherence

tomography. *Graefes Arch Clin Exp Ophthalmol*. 2011;249(6):811–820.
177. Park DH, Kim IT. Long-term effects of vitrectomy and internal limiting membrane peeling for macular edema secondary to central retinal vein occlusion and hemiretinal vein occlusion. *Retina*. 2010;30(1):117–124.
178. DeCroos FC, Shuler RK Jr, Stinnett S, Fekrat S. Pars plana vitrectomy, internal limiting membrane peeling, and panretinal endophotocoagulation for macular edema secondary to central retinal vein occlusion. *Am J Ophthalmol*. 2009;147(4) [627–33.e1].
179. Ossewaarde-van Norel A, Rothova A. Clinical review: Update on treatment of inflammatory macular edema. *Ocul Immunol Inflamm*. 2011;19(1):75–83.
180. Tranos P, Scott R, Zambarakji H, Ayliffe W, Pavesio C, Charteris DG. The effect of pars plana vitrectomy on cystoid macular oedema associated with chronic uveitis: a randomised, controlled pilot study. *Br J Ophthalmol*. 2006;90(9):1107–1110.
181. Aylward GW. The place of vitreoretinal surgery in the treatment of macular oedema. *Doc Ophthalmol*. 1999;97(3–4):433–438.
182. Radetzky S, Walter P, Fauser S, Koizumi K, Kirchhof B, Joussen AM. Visual outcome of patients with macular edema after pars plana vitrectomy and indocyanine green-assisted peeling of the internal limiting membrane. *Graefes Arch Clin Exp Ophthalmol*. 2004;242(4):273–278.
183. Kiryu J, Kita M, Tanabe T, Yamashiro K, Miyamoto N, Ieki Y. Pars plana vitrectomy for cystoid macular edema secondary to sarcoid uveitis. *Ophthalmology*. 2001;108(6):1140–1144.
184. Androudi S, Ahmed M, Fiore T, Brazitikos P, Foster CS. Combined pars plana vitrectomy and phacoemulsification to restore visual acuity in patients with chronic uveitis. *J Cataract Refract Surg*. 2005;31(3):472–478.
185. Wiechens B, Nolle B, Reichelt JA. Pars-plana vitrectomy in cystoid macular edema associated with intermediate uveitis. *Graefes Arch Clin Exp Ophthalmol*. 2001;239(7):474–

481.
186. Dugel PU, Rao NA, Ozler S, Liggett PE, Smith RE. Pars plana vitrectomy for intraocular inflammation-related cystoid macular edema unresponsive to corticosteroids. A preliminary study. *Ophthalmology*. 1992;99(10):1535–1541.
187. Heiligenhaus A, Bornfeld N, Foerster MH, Wessing A. Long-term results of pars plana vitrectomy in the management of complicated uveitis. *Br J Ophthalmol*. 1994;78(7):549–554.
188. Heiligenhaus A, Bornfeld N, Wessing A. Long-term results of pars plana vitrectomy in the management of intermediate uveitis. *Curr Opin Ophthalmol*. 1996;7(3):77–79.
189. Wiechens B, Reichelt JA, Urbat C, Nolle B. Pars plana vitrectomy in cystoid macular edema of different forms of chronic uveitis. *Ophthalmologe*. 2003;100(1):33–43.
190. Stavrou P, Baltatzis S, Letko E, Samson CM, Christen W, Foster CS. Pars plana vitrectomy in patients with intermediate uveitis. *Ocul Immunol Inflamm*. 2001;9(3):141–151.
191. Konstantinidis L, Wolfensberger TJ. Inflammatory macular edema. Gupta A, Gupta V, Herbort C, et al. *Uveitis text and imaging*. Jaypee Brothers Medical Publishers; 2009:809–822.
192. Gutfleisch M, Spital G, Mingels A, Pauleikhoff D, Lommatzsch A, Heiligenhaus A. Pars plana vitrectomy with intravitreal triamcinolone: effect on uveitic cystoid macular oedema and treatment limitations. *Br J Ophthalmol*. 2007;91(3):345–348.
193. Henderson BA, Kim JY, Ament CS, Ferrufino-Ponce ZK, Grabowska A, Cremers SL. Clinical pseudophakic cystoid macular edema. Risk factors for development and duration after treatment. *J Cataract Refract Surg*. 2007;33(9):1550–1558.
194. Rossetti L, Autelitano A. Cystoid macular edema following cataract surgery. *Curr Opin Ophthalmol*. 2000;11(1):65–72.
195. Ray S, D'Amico DJ. Pseudophakic cystoid macular edema. *Semin Ophthalmol*. 2002;17(3–4):167–180.
196. Wright PL, Wilkinson CP, Balyeat HD, Popham J, Reinke M. Angiographic cystoid macular edema after posterior chamber lens implantation. *Arch Ophthalmol*.

1988;106(6):740–744.
197. Ursell PG, Spalton DJ, Whitcup SM, Nussenblatt RB. Cystoid macular edema after phacoemulsification: relationship to blood-aqueous barrier damage and visual acuity. *J Cataract Refract Surg*. 1999;25(11):1492–1497.
198. Fung WE. The national, prospective, randomized vitrectomy study for chronic aphakic cystoid macular edema. Progress report and comparison between the control and nonrandomized groups. *Surv Ophthalmol*. 1984;28(Suppl.):569–575.
199. Harbour JW, Smiddy WE, Rubsamen PE, Murray TG, Davis JL, Flynn HW Jr. Pars plana vitrectomy for chronic pseudophakic cystoid macular edema. *Am J Ophthalmol*. 1995;120(3):302–307.
200. Pendergast SD, Margherio RR, Williams GA, Cox MS Jr. Vitrectomy for chronic pseudophakic cystoid macular edema. *Am J Ophthalmol*. 1999;128(3):317–323.
201. Hikichi T, Yoshida A, Trempe CL. Course of vitreomacular traction syndrome. *Am J Ophthalmol*. 1995;119(1):55–61.
202. Smiddy WE, Michels RG, Glaser BM. deBustros S. Vitrectomy for macular traction caused by incomplete vitreous separation. *Arch Ophthalmol*. 1988;106(5):624–628.
203. Davis RP, Smiddy WE, Flynn HW Jr, Puliafito CA. Surgical management of vitreofoveal traction syndrome: optical coherence tomographic evaluation and clinical outcomes. *Ophthalmic Surg Lasers Imaging*. 2010;41(2):150–156.
204. Fine HF, Iranmanesh R, Iturralde D, Spaide RF. Outcomes of 77 consecutive cases of 23-gauge transconjunctival vitrectomy surgery for posterior segment disease. *Ophthalmology*. 2007;114(6):1197–1200.
205. Tewari A, Shah GK, Fang A. Visual outcomes with 23-gauge transconjunctival sutureless vitrectomy. *Retina*. 2008;28(2):258–262.
206. Kinoshita T, Kovacs KD, Wagley S, Arroyo JG. Morphologic differences in epiretinal membranes on ocular coherence tomography as a predictive factor for surgical outcome. *Retina*. 2011;31(8):1692–1698.
207. Konstantinidis L, Berguiga M, Beknazar E, Wolfensberger

TJ. Anatomic and functional outcome after 23-gauge vitrectomy, peeling, and intravitreal triamcinolone for idiopathic macular epiretinal membrane. *Retina*. 2009;29(8):1119–1127.
208. Jackson TL, Nicod E, Angelis A, et al. Pars plana vitrectomy for vitreomacular traction syndrome: a systematic review and metaanalysis of safety and efficacy. *Retina*. 2013;33(10):2012–2017.
209. Green-Simms AE, Bakri SJ. Vitreomacular traction and age-related macular degeneration. *Semin Ophthalmol*. 2011;26(3):137–138.
210. Ciulla TA, Ying GS, Maguire MG, et al. Influence of the vitreomacular interface on treatment outcomes in the comparison of age-related macular degeneration treatments trials. *Ophthalmology*. 2015;122(6):1203–1211.
211. Krishnan R, Arora R, De Salvo G, et al. Vitreomacular traction affects anti-vascular endothelial growth factor treatment outcomes for exudative age-related macular degeneration. *Retina*. 2015;35(9):1750–1756.
212. Ikeda T, Sawa H, Koizumi K, Yasuhara T, Yamasaki T. Pars plana vitrectomy for regression of choroidal neovascularization with age-related macular degeneration. *Acta Ophthalmol Scand*. 2000;78(4):460–464.
213. Roller AB, Mahajan VB, Boldt HC, Abramoff MD, Russell SR, Folk JC. Effects of vitrectomy on age-related macular degeneration. *Ophthalmology*. 2010;117(7):1381–1386.
214. Garcia-Arumi J, Martinez V, Sararols L, Corcostegui B. Vitreoretinal surgery for cystoid macular edema associated with retinitis pigmentosa. *Ophthalmology*. 2003;110(6):1164–1169.
215. Hagiwara A, Yamamoto S, Ogata K, et al. Macular abnormalities in patients with retinitis pigmentosa: prevalence on OCT examination and outcomes of vitreoretinal surgery. *Acta Ophthalmol*. 2011;89(2):e122–5.
216. Stefansson E. Microplasmin-induced posterior vitreous detachment affects vitreous oxygen levels. *Retina*. 2008;28(8):1175–1176 [author reply 6].
217. Gandorfer A, Ulbig M, Kampik A. Plasmin-assisted

vitrectomy eliminates cortical vitreous remnants. *Eye (Lond)*. 2002;16(1):95–97.
218. Sakuma T, Tanaka M, Inoue J, Mizota A, Souri M, Ichinose A. Use of autologous plasmin during vitrectomy for diabetic maculopathy. *Eur J Ophthalmol*. 2006;16(1):138–140.
219. Rheaume MA, Vavvas D. Pharmacologic vitreolysis. *Semin Ophthalmol*. 2010;25(5–6):295–302.
220. de Smet MD, Gandorfer A, Stalmans P, et al. Microplasmin intravitreal administration in patients with vitreomacular traction scheduled for vitrectomy: the MIVI I trial. *Ophthalmology*. 2009;116(7):1349–1355 [1355.e1–2].
221. Stalmans P, Delaey C, de Smet MD, van Dijkman E, Pakola S. Intravitreal injection of microplasmin for treatment of vitreomacular adhesion: results of a prospective, randomized, sham-controlled phase II trial (the MIVI-IIT trial). *Retina*. 2010;30(7):1122–1127.
222. Stalmans P, Benz MS, Gandorfer A, et al. Enzymatic vitreolysis with ocriplasmin for vitreomacular traction and macular holes. *N Engl J Med*. 2012;367(7):606–615.
223. Haller JA, Stalmans P, Benz MS, et al. Efficacy of intravitreal ocriplasmin for treatment of vitreomacular adhesion: subgroup analyses from two randomized trials. *Ophthalmology*. 2015;122(1):117–122.
224. Novack RL, Staurenghi G, Girach A, Narendran N, Tolentino M. Safety of intravitreal ocriplasmin for focal vitreomacular adhesion in patients with exudative age-related macular degeneration. *Ophthalmology*. 2015;122(4):796–802.
225. Schumann RG, Wolf A, Mayer WJ, et al. Pathology of internal limiting membrane specimens following intravitreal injection of ocriplasmin. *Am J Ophthalmol*. 2015;160(4):767–778.
226. Dimopoulos S, Bartz-Schmidt KU, Gelisken F, Januschowski K, Ziemssen F. Rate and timing of spontaneous resolution in a vitreomacular traction group: should the role of watchful waiting be re-evaluated as an alternative to ocriplasmin therapy? *Br J Ophthalmol*. 2015;99(3):350–353.
227. Almeida DR, Chin EK, Rahim K, Folk JC, Russell SR.

Factors associated with spontaneous release of vitreomacular traction. *Retina*. 2015;35(3):492–497.
228. Quezada Ruiz C, Pieramici DJ, Nasir M, Rabena M, Avery RL. Severe acute vision loss, dyschromatopsia, and changes in the ellipsoid zone on SD-OCT associated with intravitreal ocriplasmin injection. *Retinal Cases Brief Rep*. 2015;9(2):145–148.
229. Tibbetts MD, Reichel E, Witkin AJ. Vision loss after intravitreal ocriplasmin: correlation of spectral-domain optical coherence tomography and electroretinography. *JAMA Ophthalmol*. 2014;132(4):487–490.
230. Hermel M, Dailey W, Hartzer MK. Efficacy of plasmin, microplasmin, and streptokinase-plasmin complex for the in vitro degradation of fibronectin and laminin-implications for vitreoretinal surgery. *Curr Eye Res*. 2010;35(5):419–424.
231. Fahim AT, Khan NW, Johnson MW. Acute panretinal structural and functional abnormalities after intravitreous ocriplasmin injection. *JAMA Ophthalmol*. 2014;132(4):484–486.
232. Small KW, Shaya FS, La Fontaine M. Post-market experience with ocriplasmin including chronic electrophysiologic changes. *Ophthalmic Surg Lasers Imaging retina*. 2015;46(9):956–962.
233. Oliveira LB, Meyer CH, Kumar J, et al. RGD peptide-assisted vitrectomy to facilitate induction of a posterior vitreous detachment: a new principle in pharmacological vitreolysis. *Curr Eye Res*. 2002;25(6):333–340.
234. Ramakrishnan V, Bhaskar V, Law DA, et al. Preclinical evaluation of an anti-alpha5beta1 integrin antibody as a novel anti-angiogenic agent. *J Exp Ther Oncol*. 2006;5(4):273–286.
235. Geck U, Pustolla N, Baraki H, Atili A, Feltgen N, Hoerauf H. Posterior vitreous detachment following intravitreal drug injection. *Graefes Arch Clin Exp Ophthalmol*. 2013;251(7):1691–1695.
236. McHugh D, Gupta B, Saeed M. Intravitreal gas injection for the treatment of diabetic macular edema. *Clin*

*Ophthalmol.*2011;5:1543–1548.
237. Rodrigues IA, Stangos AN, McHugh DA, Jackson TL. Intravitreal injection of expansile perfluoropropane (c(3)f(8)) for the treatment of vitreomacular traction. *Am J Ophthalmol*. 2013;155(2) [270–6.e2].
238. Day S, Martinez JA, Nixon PA, et al. Intravitreal sulfur hexafluoride injection for the treatment of vitreomacular traction syndrome. *Retina*. 2016;36(4):733–737.

121

Macular Hole

Alain Gaudric, Ramin Tadayoni

Introduction

Macular hole (MH) is a round full-thickness opening in the foveal center. In most cases it is primary, i.e., due to abnormal vitreofoveal traction. The role of the vitreous cortex in the pathogenesis of MH started to be better understood with the biomicroscopic

observations of Gass.[1,2] The advent of optical coherence tomography (OCT), which showed the partially detached posterior hyaloid, clarified the understanding of MH formation. Spectral domain OCT (SD-OCT) subsequently provided more detailed views of the initial foveal changes induced by vitreofoveal traction. MH are known since the nineteenth century. However, they only aroused renewed interest after Kelly and Wendel[3] had shown that pars plana vitrectomy (PPV) combined with vitreous cortex detachment and fluid–gas exchange could close MH in a significant proportion of cases, although it was assumed that the retina would be unable to heal. The success rate of MH surgery gradually increased progressively, and this surgery is now one of the most successful vitreoretinal surgery.

History

MH was first described in 1869 by Knapp[4] in a traumatic case. Noyes[5] in 1871 gave a detailed ophthalmoscopic description of a traumatic case, and in 1900 Ogilvie[6] was the first to use the term of "hole at the macula." Early in the 20th century Kuhnt (1900)[7] and Coats (1908)[8] suggested that the origin of MH was degenerative, although Zeeman[9] (1912) and Lister[10] (1924) attributed it to a vitreoretinal tractional mechanism. The modern history of MH started with Gass, who proposed a staging system ranging from impending to full-thickness MH, on the basis of his biomicroscopic observations.[11–13] Kelly and Wendel[3] performed the first successful surgery of MH, and Hee et al.[14] were the first to describe the stages of MH on OCT scans (see Frangieh[15] and Ho,[16] for review)

Epidemiology and Risk Factors for Primary Full-Thickness Macular Holes

Prevalence

The prevalence of MH reported in the literature varies greatly. It was 3.3 per 1000 in the Baltimore Eye Study,[17] 0.2 per 1000 in the Blue Mountains Study,[18] 0.9 per 1000 in the Beijing study,[19] and 1.7

per 1000 in a study in Southern India.[20] In the Beaver Dam Study the prevalence was 4 per 1000 in a population of subjects aged 63–102 years.[21] The incidence of MH was studied in the United States in a county of Minnesota and had been found to occur in 7.8 persons per 100,000 and per year, with a female-to-male ratio of 3.3 to 1. MH was bilateral in 11.7% of patients.[22]

Incidence in the Fellow Eye

The data on the incidence of bilateral MH vary considerably from 5 to 16 %. In a retrospective study of 84 cases followed up for 39 months in average, Akiba[23] found that 16.6% of patients had an MH in the fellow eye, and that the proportion rose to 36.8% when that eye presented with a foveal cyst or a central yellow spot. However, no MH occurred in the fellow eye when the vitreous was detached.[23] In a retrospective study by Lewis[24] the incidence was 13% in 4 years; it was 15.6% at 5 years in a prospective study of 144 patients by Ezra,[25] and 7.6% at 6 years in another prospective study of 122 patients.[26] In 2004 Chan et al.[27] proposed the concept of stage zero MH to designate fellow eyes with a normal macular profile on OCT but a posterior hyaloid still attached to the foveal center. In their prospective study of 94 fellow eyes, MH occurred only in 4.5% of cases without visible vitreofoveal adhesion and in 42% of cases with a stage zero MH. However, Chan et al.'s study was limited by the use of OCT1, which at this time did not allowed sufficiently accurate assessment of vitreofoveal adhesion. In 2011, Takahashi[28] selected 42 fellow eyes of 176 patients with MH, examined with OCT3, and presented with persistent vitreofoveal adhesion and early stage 1 intrafoveal lesions. MH occurred in 11.9% of these eyes during the 5-year follow-up period. In a cohort of 43 fellow eyes, the same author has identified five eyes with intrafoveal microstructural changes, including foveolar detachment, two of which evolved to a MH over a 6-month follow-up period.[29]

Risk Factors

Age 65 or older and female gender are the only two relevant systemic risk factors yet identified. Several authors have found that these factors were present in 67–72% of MH cases.[21,30–32] In a cohort

of 1045 patients undergoing MH surgery, the age at presentation was 70.3 years with a 2.2 : 1 female preponderance.[33]

Pathogenesis, From Posterior Vitreous Detachment to Impending Macular Hole

History of Theories on the Pathogenesis of Macular Hole

Vitreomacular Traction

Vitreomacular traction (VMT) has long been suspected to be a cause of MH formation, but until the advent of OCT it was difficult to visualize the vitreofoveal interface routinely. However, various indications of the role of the vitreous had been given in the literature. Thus, in 1952 Grignolo provided histologic evidence of strong vitreomacular adherence to the fovea.[34] In particular cases, biomicroscopic observations strengthened the hypothesis that anteroposterior traction of vitreous fibers on the fovea played a role in the formation of MH.[35–40] The biomicroscopic observation of opercula also strengthened the possibility that anteroposterior traction is the cause of MH.[36,41]

Foveal Cyst

The existence of a foveal cyst in the fellow eye of an eye with MH was shown histologically by Kornzweig in 1950[42] and by Frangieh and Green in 1981.[15] Also in 1981, Bronstein,[43] and in 1982 McDonnell et al.,[44] analyzed a series including fellow eyes and eyes with MH. They concluded that idiopathic macular cysts and holes were part of the same disorder and described the role of the vitreous body in their formation. On the basis of scanning laser ophthalmoscope observations Kishi et al.[45] deduced, in 1995, that foveal cyst formation due to vitreous traction was the first step in MH formation. In 1998, Folk et al.,[46] who used laser slit-lamp photography, were able to obtain a direct image of the foveal cysts which they considered to be a prehole condition. This was

confirmed in the same year by Hee et al.[14] using OCT, which showed, for the first time, the vitreous cortex attached on the roof of a foveal cyst. Foveal cyst appeared then to be an initial change in the foveal structure that predisposes to the risk of progression to MH.[47,48]

Contraction of the Premacular Vitreous Cortex

In 1988 Gass revised the biomicroscopic description of MH and proposed a new interpretation of the role of the vitreous in the pathogenesis of MH. He also proposed a system of MH staging, from impending to full-thickness MH. In his initial description in 1988, Gass postulated that the tangential contraction of the prefoveal "posterior hyaloid membrane" resulted in the detachment of the central photoreceptors and then in the opening of the fovea.[2] The process of MH formation was divided in four stages that are still used today, despite the changes in their interpretation due to OCT findings. Lastly, Gass proposed the use of a surgical approach design to prevent impending MH from evolving into full-thickness MH by peeling off or dissecting the posterior hyaloids.[2]

Update on the Pathogenesis of Macular Hole Based on SD-OCT

For the first time, OCT has shown routinely the status of the posterior hyaloid or vitreous cortex, making it possible to combine in a single explanation, oblique anteroposterior vitreous traction, and the occurrence of intrafoveal microstructural changes even before the occurrence of a foveal cyst. SD-OCT has now refined the description of the initial stages of impending MH by showing discrete changes in the foveal tissue such as discrete elevation of the interdigitation zone (IdgZ), minute foveolar detachment, subtle vertical line across the foveal center, or paracentral foveal splits.[28,29,49,50]

Early Stages of Posterior Vitreous Detachment

The process of posterior vitreous detachment (PVD) is not yet clear, but its understanding has progressed thanks to the images obtained with OCT of the posterior hyaloid in normal eyes, and in fellow eyes of eyes with MH. It was usually thought that PVD occurred suddenly after a long period of vitreous gel liquefaction, intravitreal lacunae formation, and posterior hyaloid erosion by one of these lacunae, thus suddenly giving the liquefied vitreous access to the preretinal space.[51–54] However, contrary to this belief, both OCT studies[55] and ultrasonographic observations[56] have established that in normal individuals, the process of PVD starts gradually at the posterior pole, around the fovea, and occurs relatively early in life, long before detachment of the Weiss ring.[57] This aspect is also known as vitreous macular adhesion and is normal in the process of PVD[58] (Fig. 121.1A).

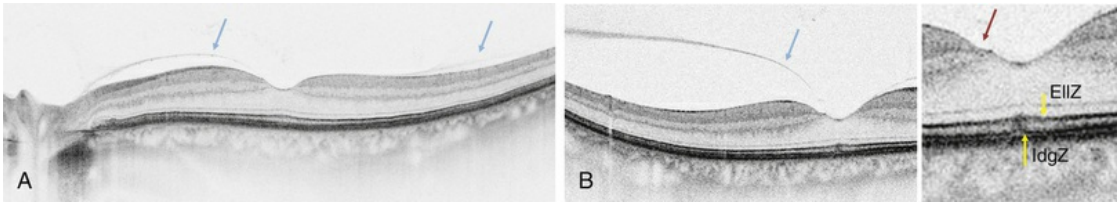

FIG. 121.1 Vitreomacular adhesion and vitreomacular traction in fellow eyes of macular holes. (A) Vitreomacular adhesion: horizontal optical coherence tomography (OCT) B-scan showing the posterior hyaloid (*arrows*) slightly detached from the macular surface but still adherent to the fovea. The foveal curvature and structure are normal. (B) Horizontal OCT scan showing most of the posterior hyaloid (*blue arrow*) detached from the macular surface, except at the edge of the foveal pit to which it still adheres. (Inset) Detail of panel B: Change in the inner foveal curvature at the point of traction exerted by the posterior hyaloid (*red arrow*). The ellipsoid zone (EllZ, *yellow arrow*) is intact, but a small section of the interdigitation zone (IdgZ) is detached (*yellow arrow*).

The attachments of the posterior hyaloid to the foveal center and optic disc are the last to be released. The reason for posterior hyaloid detachment from the retina remains unclear. It might be due to the action of oblique anteroposterior forces that follows the

direction of the collagen fibers of the vitreous body. An alternative explanation, which takes into account the presence of the precortical vitreous pocket,[59–61] might be the passage of liquefied vitreous behind the thinned posterior hyaloid which, combined with ocular movements, would extend its detachment. Both mechanisms might lead to the creation of oblique tractional forces on the foveal floor.

Impending Macular Hole

Early Changes in Foveal Tissue (Figs. 121.1B and 121.2)

Based on the observation that in patients with macular hole OCT of the fellow eye often showed PVD around the fovea,[14,47,48] Chan et al.[27] have found that cases with partial perifoveal vitreous detachment, but no foveal cyst, were at risk of developing MH. At present, in such cases, SD-OCT shows, even in asymptomatic eyes, a variety of changes in the foveolar structure and impending MH are considered as a special circumstance of VMT occurring in the fellow eye of a MH.[58] SD-OCT is able to detect a slight focal elevation of the inner curvature of the foveal center due to the traction exerted by the posterior hyaloids.[49] Minor changes in the interdigitation zone[62] and foveolar detachment may correspond to the central yellow spot observed by Gass in impending MH.[29] Subtle changes in the reflectivity of the center of the foveola, along an anteroposterior axis extending from the internal limiting membrane (ILM) to the ellipsoid zone, may also be detected by high-definition SD-OCT scans. In other cases, the foveal floor is elevated by the traction exerted by the posterior hyaloid, which is detached around the foveola but still attached at its center (Fig. 121.3 online).[47,48] Some dissociated Henle fibers are often visible inside the cyst, but the retinal outer layers may be intact.[28,48] In such cases the photoreceptor ellipsoid zone may be normal or elevated or even disrupted at the foveal center (Fig. 121.4). Finally, these various anomalies may be combined and include a disruption of the outer part of the photoreceptors and of the Henle fiber layer, only the ILM remaining intact. These cases may be considered as occult MH and correspond to what has been described as stage 1B

MH[13,28,29,47,48,63] (Fig. 121.5).

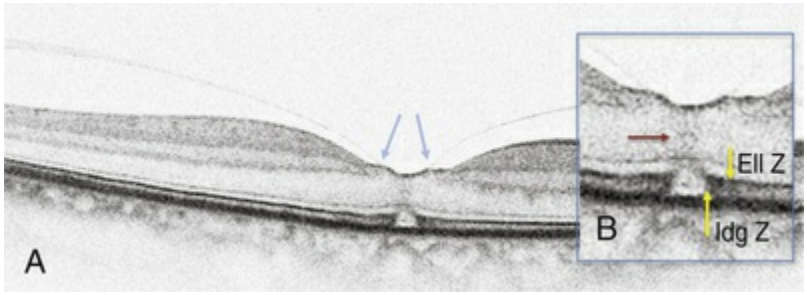

FIG. 121.2 Vitreomacular traction in a fellow eye of macular hole. Partial detachment of the posterior hyaloid, which still adheres to the foveal floor, creating two small elevations of the foveal pit contour (*blue arrows*). (Inset) Detail of panel A: Foveal elevation of the EllZ and IdgZ. A hyperreflective columnar structure links the internal and external limiting membranes. The eye is asymptomatic, and vision is 20/20.

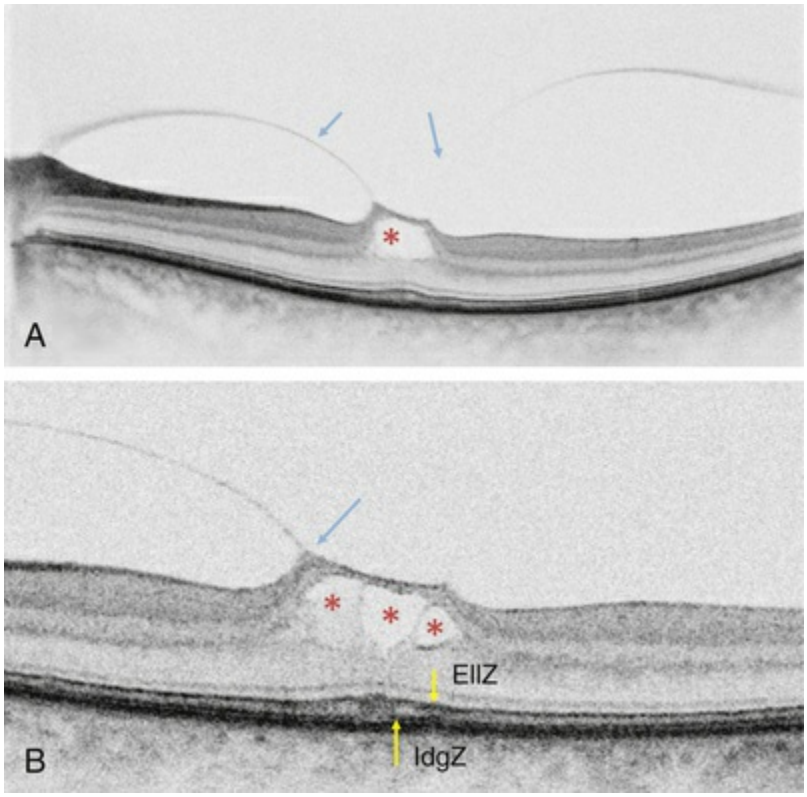

FIG. 121.4 Impending macular hole with vitreomacular traction. (A) Horizontal 9-mm optical coherence tomography scan showing a cyst in the inner part of

the fovea (*asterisk*) due to the traction exerted by the incompletely detached posterior hyaloid (*arrows*). (B) Magnification of panel A showing that the central cyst is divided into several cystic spaces (*asterisks*) by septa. The ellipsoid zone (EllZ) is intact, but the interdigitation zone (IdgZ) is elevated at the foveal center.

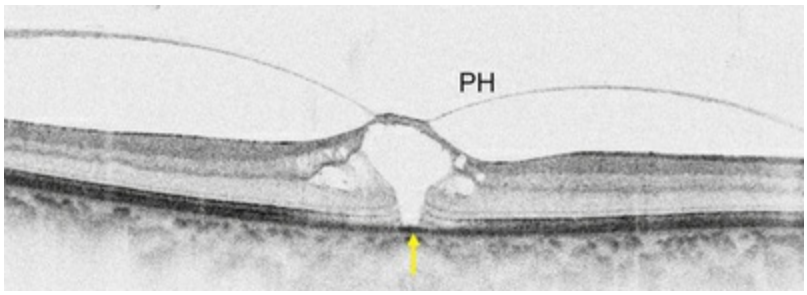

FIG. 121.5 Impending macular hole with vitreomacular traction. The posterior hyaloid (*PH*) is still attached to the roof of the cyst. The cystic space extends posteriorly, and there is a break in the photoreceptor layer. Note also the cystic cavities around the central defect. This impending macular hole is an occult macular hole.

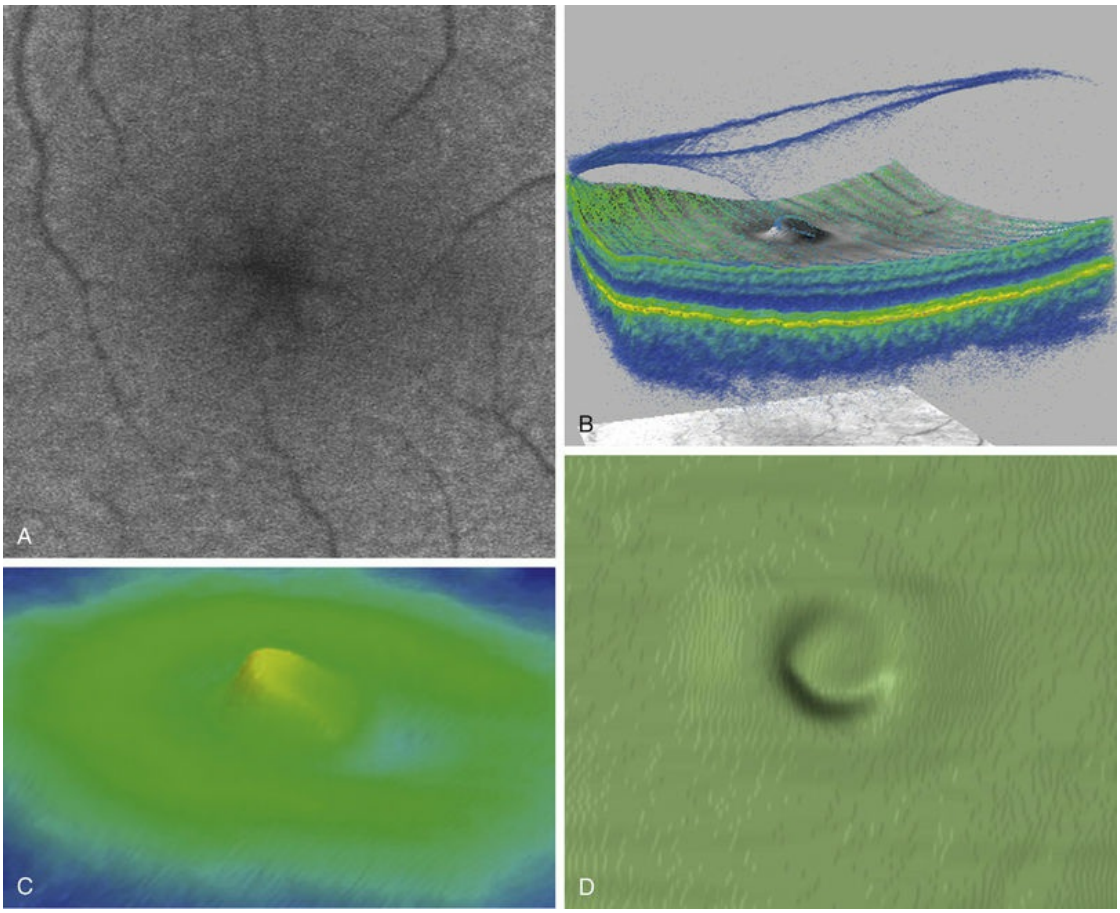

FIG. 121.3 Impending macular hole with vitreomacular traction (same case as in Fig. 121.4). (A) Autofluorescence photograph of the macula showing that the clear spaces of the cystic spaces encroach on the xanthophyll. (B) Reconstruction of the volume of the vitreoretinal interface showing the cone of the posterior hyaloid (*PH*) adherent to the top of the foveal pit (*arrow*). (C) and (D) Three-dimensional views of the foveal surface showing the elevation of the roof of the foveal cyst into the foveal pit.

At any stage, complete normalization of the fovea may occur after vitreofoveal separation.

Clinical and Imaging Features of Full-Thickness Macular Holes

Biomicroscopy Observations of Full-Thickness Macular Hole

A classification of MH based on biomicroscopy has been provided by Gass in 1988 and updated in 1995.[13,64] Stage 2 MH was described as an eccentric oval, crescent, or horseshoe-shaped retinal defect on the edge of the yellow ring. This was interpreted as a tear in the contracted prefoveolar vitreous tissue bridging the round retinal hole, with no loss of foveolar retina.[13] According to the Gass definition, the Stage 3 MH was a central round retinal defect of more than 400 μm in diameter, with a rim of elevated retina, with or without prefoveolar pseudo-operculum (Fig. 121.6) and without a Weiss ring. OCT has now changed the understanding and staging of MH.

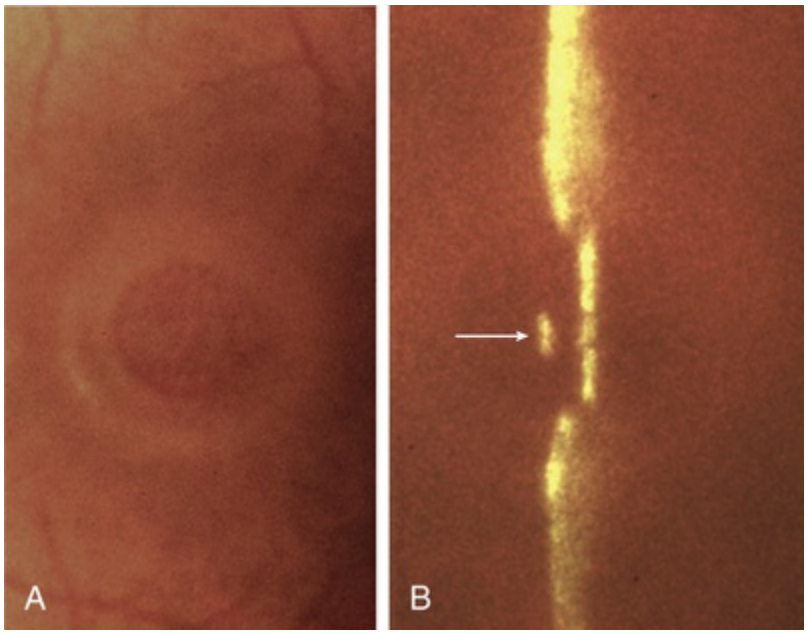

FIG. 121.6 Full-thickness macular hole. (A) Color photograph showing the hole and its rim of detached and thickened retina. (B) Laser slit-lamp photograph showing the thickened edge of the macular hole and the operculum in front of the hole (*arrow*); the posterior hyaloid is not visible by slit-lamp photography.

OCT Classification of Macular Hole

OCT has now replaced biomicroscopy for the diagnosis of MH, and a new classification has been proposed based on both the MH diameter and the status of the vitreous attachment at the hole edge.

It has indeed been shown that the hole size was correlated with the need for ILM peeling,[65] face-down positioning,[66,67] or the indications of enzymatic vitreolysis.[68] The presence of a vitreoretinal attachment is also the target of enzymatic vitreolysis, although its presence is not related to the hole size.[58,69]

When the vitreous is still attached to the hole edge, the incompletely detached operculum is pulled in an oblique direction by the posterior hyaloid.[14,47] Recent observations by Takahashi[29,50] showed that neuronal elements formed a constitutive part of the operculum at least in some cases, which supports the histologic findings of Ezra showing the presence of cone constituents in two-thirds of the opercula he examined[70] (Fig. 121.7).

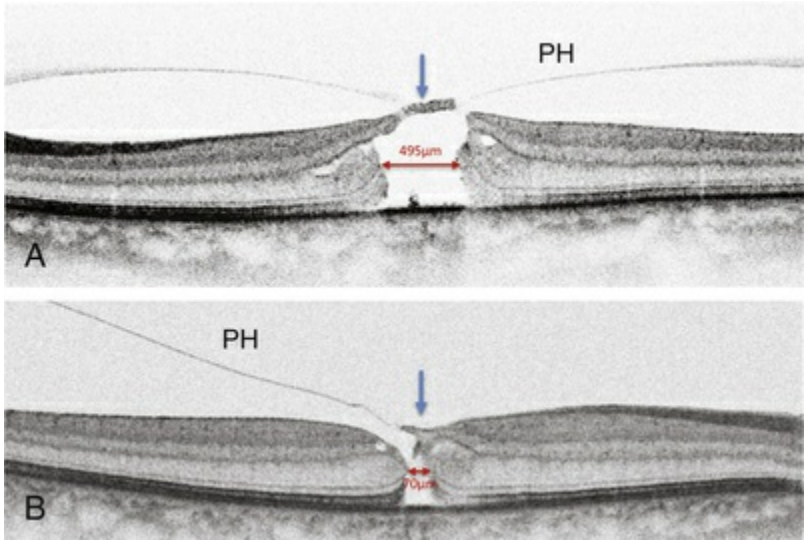

FIG. 121.7 Full-thickness macular holes with vitreomacular traction. (VMT). (A) Large macular hole with VMT. The posterior hyaloid (*PH*) is still attached to the operculum (*arrow*). The operculum is only partially detached from the hole edge. The hole diameter is 495 µm. (B) Small macular hole with VMT. The posterior hyaloid (*PH*) is detached from the temporal part of the macula only and adheres to the operculum (*arrow*). The hole diameter is small, 70 µm.

At a later stage in the course of MH, the posterior hyaloid is completely detached from the retinal surface over the posterior pole and not connected to the hole edge whereas it remains attached to the optic disc (Fig. 121.8). Finally, the PVD becomes complete with

a Weiss ring visible on biomicroscopy.

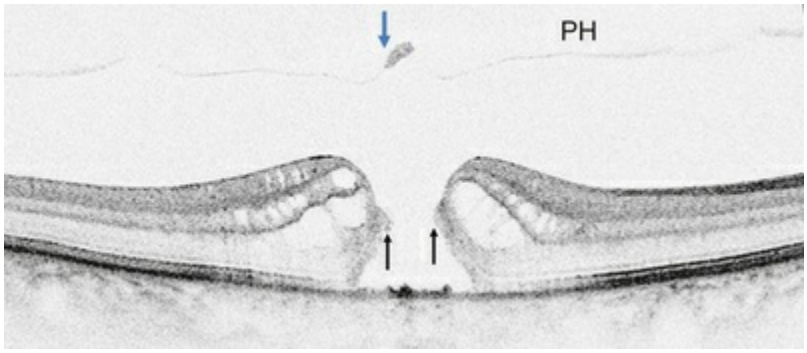

FIG. 121.8 Full-thickness macular hole with the posterior hyaloid (*PH*) detached from the macular surface and containing an operculum (*blue arrow*). The edge of the hole is thickened by cystic spaces, and the photoreceptors are elevated (*black arrows* mark the end of the outer segments of the elevated photoreceptors).

Measurement of the Macular Hole Diameter

The aperture size is measured using the caliper function on SD-OCT devices. The minimum hole width is measured at the narrowest hole point in the mid retina, using the OCT caliper function, as a line parallel to the retinal pigment epithelium.[58] Empirically it corresponds to a line drawn between the terminations of the detached photoreceptor outer segments (Fig. 121.6). Other methods have also been described,[71,72] but the minimum hole width tends to be a standard.

International Vitreomacular Traction Study Group Classification

An OCT-based FTMH classification system was based on the hole size, the presence or the absence of a VMT, and the cause of the hole. The VMT was defined as present or absent. The hole size (diameter) was defined as small, medium, or large. Small holes have an aperture size less than 250 μm. These small holes usually represent less than 10% of operated MH. A medium hole is defined by an aperture size ranging between 250 and 400 μm. Almost half

of FTMHs are large (diameter >400 μm) at the time of diagnosis[58] (Tables 121.1 and 121.2).

TABLE 121.1
Classification of Macular Holes

Classification Commonly Used for Full-Thickness MH	International VMT Study
Stage 2: small hole	Small or medium FTMH with VMT
Stage 3: large hole	Medium or large FTMH with VMT
Stage 4: FTMH with PVD	Small, medium, or large FTMH without VMT

FTMH, full-thickness macular hole; PVD, posterior vitreous detachment; VMT, vitreomacular traction.

Adapted from Duker JS, Kaiser PK, Binder S, et al. The International Vitreomacular Traction Study Group classification of vitreomacular adhesion, traction, and macular hole. Ophthalmology 2013; 120:2611-2619.

TABLE 121.2
Correspondence of the Macular Hole Classification

Stage	Biomicroscopy (Gass)[13]	Interpretation (Gass)[13]	OCT[27,29,47,48]	International VMT Classification[58]
Stage 0 MH			Perifoveolar detachment of posterior hyaloid with normal fovea contour[27,28]	VMA
Stage 1A Impending MH	Central yellow spot, loss of foveolar depression, no vitreofoveolar separation	Early serous detachment of foveolar retina	Perifoveolar detachment of posterior hyaloid. Foveal cyst in the inner foveola, and/or foveolar detachment of the cone outer segment tip line[28]	VMT
Stage 1B Impending MH	Yellow ring with bridging interface, loss of foveolar depression, no vitreofoveolar separation	Serous foveolar detachment with lateral displacement of xanthophyll, or Central occult foveolar hole with bridging contracted prefoveolar cortex	Perifoveolar detachment of posterior hyaloid. Foveal cyst extending in the outer retina, causing a break in the photoreceptor layer. "Occult Macular Hole"	VMT
Stage 2 Macular	Eccentric oval, crescent, or	Hole (tear) in contracted	Hole of various size. Partial opening of the roof of the cyst,	Small or medium

hole	horseshoe retinal defect Inside edge of yellow ring	prefoveolar vitreous bridging round retinal hole, no loss of foveolar retina	the operculum staying still attached to the edge of the hole. Partial detachment of the posterior hyaloid, which is still attached at the operculum. The operculum contains retinal elements	FTMH with VMT
	Central round retinal defect retina, with or without prefoveolar opacity	Hole with pseudo-operculum, rim of retinal detachment		Small or medium FTMH with VMT
Stage 3 Macular hole	Central round ≥400 μm diameter retinal defect, no Weiss ring, rim of elevated retina, with or without prefoveolar opacity	Hole with pseudo-operculum, no posterior vitreous detachment	Hole of various size. Posterior hyaloid detached from the macular surface, but still attached to the optic disc, most often containing an operculum	Medium or large FTMH with VMT
Stage 4 Macular hole	Central round defect, rim of elevated retina. Weiss ring with prefoveolar opacity	Hole with pseudo-operculum and posterior vitreous detachment from optic disc and macula	Hole of various size, with complete PVD on biomicroscopy. The posterior hyaloid is not visible on OCT	Small, medium, or large FTMH without VMT

FTMH, full-thickness macular hole; MH, macular hole; OCT, optical coherence tomography; PVD, posterior vitreous detachment; VMA, vitreomacular adhesion; VMT, vitreomacular traction.

This classification does not take into account the possible presence of an epiretinal membrane (ERM) around the hole, which is more frequent in large MH.

Macular Hole and Epiretinal Membrane (Fig. 121.9)

A noncontractile ERM may cover the macular surface around the hole. It is especially well visualized on blue reflectance photographs.[73] The frequency of the formation of an ERM increases with the hole stage, duration, and size.[73–75] They are mainly composed of glial cells and hyalocytes and do not show any sign of contraction in small MH.[76,77] Their presence does not affect the surgical outcome once the membrane has been peeled off during

surgery.

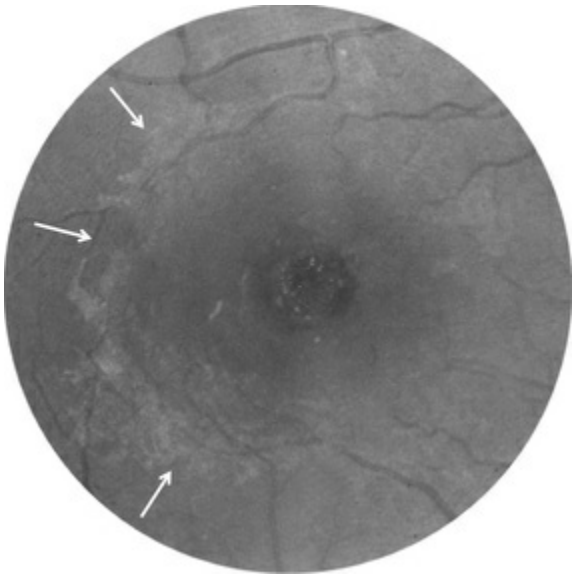

FIG. 121.9 Stage 3 full-thickness macular hole, blue reflectance photograph. The contours of a noncontractile epiretinal membrane are visible around the hole (*arrows*).

Differential Diagnosis

Differentiating a full-thickness MH from other roundish anomalies of the fovea is no longer a problem since the advent of OCT, which clearly shows the characteristic profiles of lamellar MH and macular pseudoholes, as well as foveal cysts of various origins.

Lamellar Macular Hole

The term lamellar macular hole (LMH) was coined by Gass in 1975 to characterize a macular lesion resulting from the opening of the central cyst of a cystoid macular edema. On biomicroscopy, LMH differ from FTMH because they are rarely round but rather bi- or trilobulated. Their center is reddish like that of FTMH, but their edge is thin, whereas the FTMH edge is thick and elevated. The term lamellar hole was used to describe both the endstage of a cystoid macular edema[15] and the aborted process of formation of a

MH.[78] With the advent of high resolution or SD-OCT, the irregular thickness of the foveal center due to the contraction of an ERM was also referred to as a LMH.[79]

Histology of Lamellar Macular Hole

Frangieh et al.[15] described the histology of 17 cases of LMH of various etiologies. The cases were characterized by thinning of the foveal tissue leaving the RPE and photoreceptor layers intact, but causing partial loss of the inner nuclear layer. A cleft between the inner and outer retina was present at the edges of the LMH, as well as cystic changes. In some cases remnants of vitreous bands adhered to the lamellar hole edge. An ERM was found in several cases around the lamellar hole edge[15,80] and was thought to be the cause of certain LMH.[80,81]

Optical Coherence Tomography (Fig. 121.10)

LMH, i.e., defects in the inner fovea due to the avulsion of the roof of a foveal cyst (either tractional or due to cystoid macular edema), is characterized on OCT by irregular thinning of the foveal floor, a cleavage between the inner and outer retina at the lamellar hole edge, and the absence of a contractile ERM.[78,82] An epiretinal proliferation is present in about 30% of cases but differs from conventional ERMs. It looks like an amorphous material of medium reflectivity with no evidence of traction, especially on en face OCT images, where no retinal folds are seen.[82,83] Moreover, this proliferation has a dense yellow appearance with a fluffy consistency and histology shows that, unlike conventional ERMs, this proliferation does not contain myofibroblasts.[84,85]

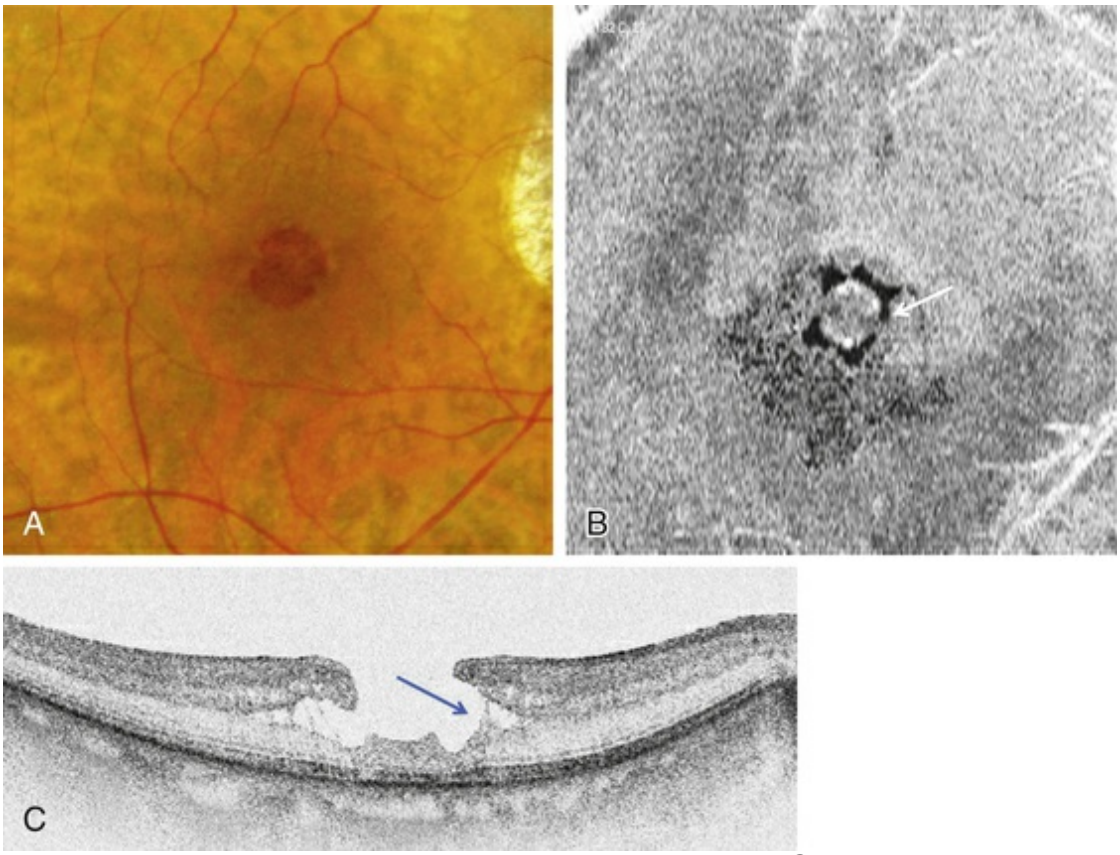

FIG. 121.10 Lamellar macular hole. (A) Color photograph showing a roundish, lobulated, red central area corresponding to the thinning of the fovea after avulsion of the roof of a foveal cyst. (B) En face optical coherence tomography (OCT) image of the same case. The dark area (*white arrow*) indicates the extent of the central defect and corresponds to the cleft between the inner and outer retina inside the edge of the lamellar hole. (C) OCT scan showing the irregular base of the lamellar hole and the cleft between the inner and outer retina inside the edge of the lamellar hole (*blue arrow*).

Macular Pseudoholes

The term of macular pseudohole was coined by Allen and Gass[86] in 1976 to designate a roundish centrofoveal image seen on biomicroscopy, which was due to the centripetal contraction of an ERM. This contraction induces the verticalization of the edge of the foveal pit. Vision may remain relatively good, and there are no microscotomas.

Optical Coherence Tomography (Fig. 121.11 online)

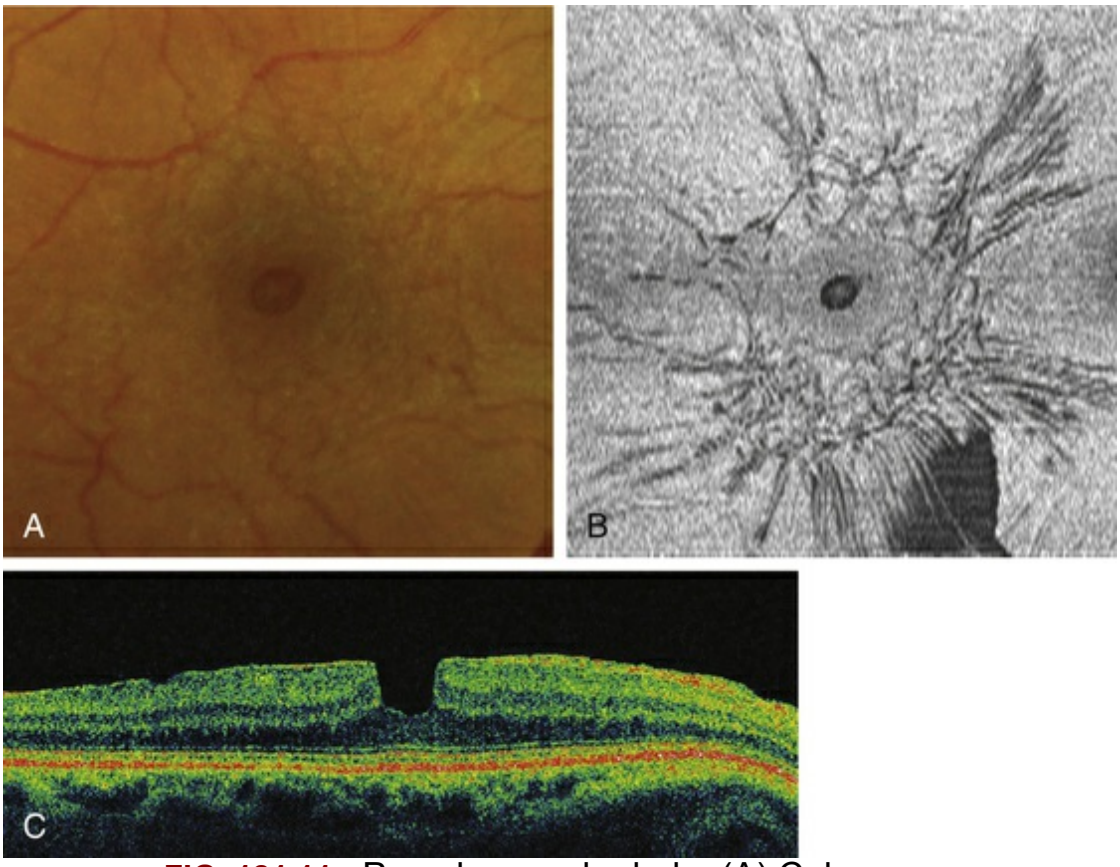

FIG. 121.11 Pseudo macular hole. (A) Color photograph showing a roundish, red, central area surrounded by the reflex of an epiretinal membrane (ERM). (B) En face optical coherence tomography (OCT) image focused on the retinal surface showing the retinal folds induced by the ERM. (C) A horizontal OCT scan shows the typical appearance of a U-shaped foveal pit with vertical edges, due to the contraction of the ERM (*arrows*).

OCT examination makes diagnosis of macular pseudoholes easy, by showing the thickening of the macula contracted by an ERM, and the U or V shape of the fovea. There is no loss of retinal tissue at the umbo of the fovea.[78] Some aspects of macular pseudoholes have been mistaken for LMH because of a stretching of the Henle fibers on the edge of the fovea.[79] However, en face OCT and surgical outcome show that these aspects are a peculiar form of macular pseudohole,[82] and histopathology confirmed the presence of

myofibroblasts in ERMs while they were absent in LMHs.[84]

Secondary Macular Hole

Orbital Trauma and High Myopia (Fig. 121.12 online)

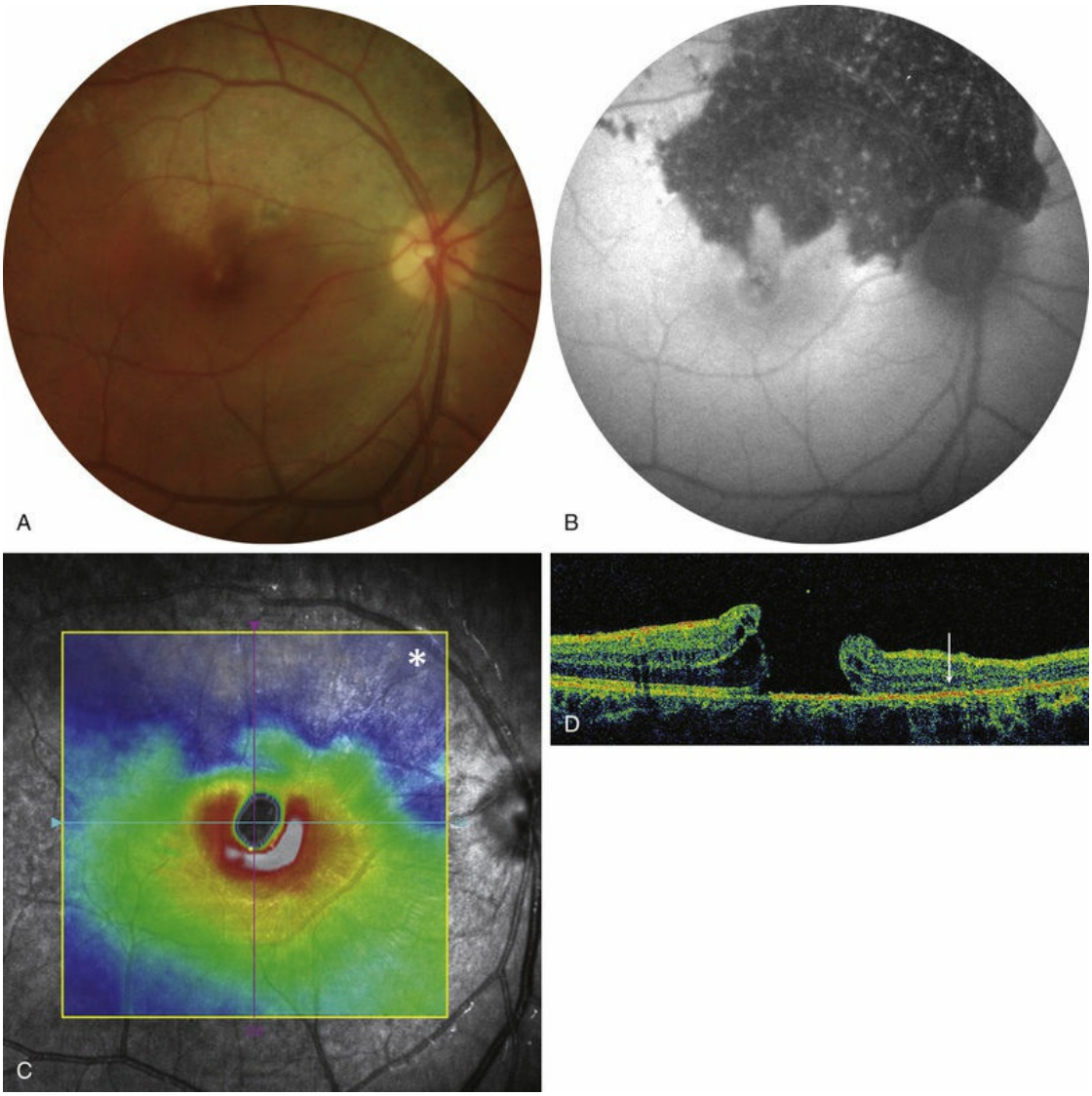

FIG. 121.12 Posttraumatic macular hole. (A) Color photograph showing the macular hole, and in the upper part of the posterior pole, a greyish area resulting from the trauma. (B) Autofluorescence of the same case showing, in the upper part of the posterior pole, deep hypoautofluorescence due to damage to the retinal pigment epithelium, as well as loss of

photoreceptors in the contused area. The vertical line indicates the orientation of the OCT scan. (C) On the optical coherence tomography (OCT) map, the upper part of the macular area is atrophic (deep blue, *asterisk*). (D) The edge of the macular hole is asymmetric, i.e., thicker in its lower than upper part. The upper limit of the hole is adjacent to the area of retinal atrophy. The limit between the relatively normal and atrophic area of the outer retina is about 500 μm from the hole edge (*white arrow*).

These MH usually occur in children and young male adults as accidents at work in the home, or during ball games.[87,88] They are due to sudden axial compression of the eye resulting in equatorial expansion and retinal rupture of the fovea. The hole may be combined with other fundus lesions such as choroidal or Bruch's membrane disruption, commotio retinae, sclopetaria, or peripheral breaks. The visual prognosis depends not only on the closure of the hole but also on the topography of the other lesions. If a choroidal disruption passes through the fovea, or if the postcontusive RPE atrophy includes the foveal center, the visual prognosis will be poor. Unlike what occurs in idiopathic MH, the vitreous is not detached at all from the posterior pole. Surgery is usually successful, but a traumatic MH may also sometimes close spontaneously within the first weeks of its occurrence.[89–91]

High Myopia

MH are one of the complications of high myopia together with posterior staphyloma and choroidal atrophy. Their pathogenesis may be different from that of nonmyopic eyes because the vitreous cortex often remains adherent to the retinal surface. Some of these MH occur after a progressive decrease in vision due to the worsening of foveoschisis.[92] Others may be asymptomatic and may only be disclosed by OCT examination of the fundus.[93] Despite progress in vitreous cortex and ILM removal, the anatomic and visual postoperative prognosis for MH in high myopia remains lower than for idiopathic MH[94,95] (see Chapter 117, High myopia and the vitreoretinal complications).

Other Rare Causes

Many other rare causes of secondary MH have been described, of which the most significant are listed in Box 121.1.

Box 121.1

Rare Causes of Secondary Macular Holes

Alport syndrome[96]

Behçet disease[97]

Best macular dystrophy[98]

Cat scratch disease[99]

Central retinal artery occlusion[100]

Drusen[101]

Electrical shock injury[102]

Fungal endophthalmitis[103]

Idiopathic parafoveal telangiectasia[93]

Laser pointer[104]

Nd:YAG laser injury[105]

Nd:YAG posterior capsulotomy[106]

Retinal arterial macroaneurysm[107]

Retinitis pigmentosa[108]

Stargardt disease[109]

Syphilis[110]

Toxoplasmic choroiditis[111]

Valsalva retinopathy[112]

Vitrectomy[113]

Vogt–Koyanagi–Harada disease[114]

X-linked juvenile retinoschisis[115]

Surgery for Macular Hole

Introduction

Kelly and Wendel first initiated successful surgery for MH and reported their results for 52 cases in 1990.[3] Their success rate was 58% with a technique combining extensive vitrectomy, detachment of the posterior vitreous cortex, peeling of any ERM around the hole, thorough fluid–gas exchange, and postoperative face-down positioning. Two years later in a larger series of 170 eyes, the closure rate reached 73%.[116] The technique of posterior vitreous cortex removal had benefitted from the attempt made by de Bustros et al. to prevent surgically the progression of impending hole to full-thickness hole.[117]

How Do Vitrectomy and Gas Work to Close the Hole?

Releasing Vitreous Traction on the Hole Edge

OCT has shown that the posterior vitreous cortex remained attached to the hole edge only in a minority of cases[118] regardless of the hole size. The role of vitreous traction release has been shown in certain cases of spontaneous closure of small MH[119] and after vitreoretinal separation provoked by vitreolysis[120] in MH smaller than 400 μm. Surgery also acts in releasing VMT in these cases. However, in a majority of cases the MH edge is already no longer under the traction of the vitreous because the vitreous cortex is separated from the posterior pole or even from the optic disc. The role of vitrectomy is then rather to enable maneuvers such as ERM or ILM peeling and mainly to make room for gas.

The role of gas in MH closure has been extensively debated. The more likely role is that the gas bubble acts first by dehydrating the

hole edge and then by preventing fluid currents from hampering the healing process. (See Discussion by Berger and Brucker[121].) However, even gas tamponade is not always essential for hole closure since for small MH the mere release of vitreous attachment by vitreolysis may result in hole closure with a rate of almost 60% in MH smaller than 250 μm,[120] although gas tamponade raises the success rate in these small holes to 98% or more. In large holes (more than 400 μm), an effective gas tamponade is mandatory to obtain a success rate of over 90%, where nonsurgical vitreolysis does not close any hole.[68]

The Healing Process, Histology, Animal Models, and Early OCT (Fig. 121.13)

It has been shown, both in man and in animal models, that MH closure is due to the proliferation of glial cells, which close the break caused by vitreous traction on the foveal center. Histopathologic studies of four eyes with surgically closed MH all showed that the hole was sealed by the proliferation of Müller cells, but that a residual defect persisted in the photoreceptor layer, which measured 16 to 250 μm.[122–124]

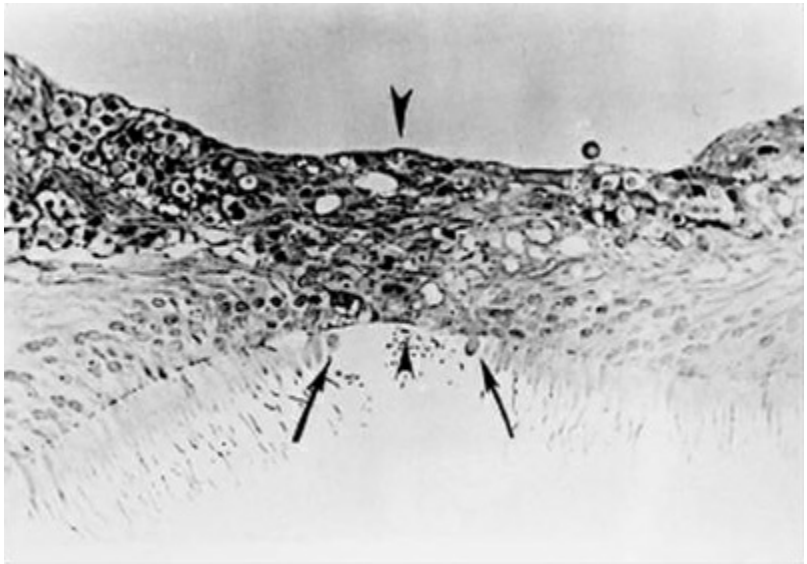

FIG. 121.13 Postmortem photomicrograph of a healed macular hole, obtained 3 years after vitreous surgery. A glial scar seals the hole (*between arrowheads*). The broken part of the photoreceptor line is only 50 μm

long, between the arrows (paraphenylenediamine; phase contrast, x 218). (Reproduced from Funata M et al. Clinicopathologic study of bilateral macular holes treated with pars plana vitrectomy and gas tamponade. Retina 1992;12:289-298. With permission from Masuyama K, Yamakiri K, Arimura N, et al. Posturing time after macular hole surgery modified by optical coherence tomography images: a pilot study. Am J Ophthalmol 2009;147(3):481-8 e2.)

A rabbit model of retinal hole closure was constructed, which enabled the steps involved to be followed histologically.[125] By the fourth day after gas tamponade, glial cell proliferation had occurred at the hole edge, and by the seventh day, the hole had been closed by glial tissue.

Optical coherence tomography has also occasionally been performed through silicone oil[126] or through the gas bubble.[127,128] These OCT observations showed that on the day after surgery the hole edge had flattened and that the hole had become smaller or had closed. Another observation made with SD-OCT is that MH closed within 1–3 days depending on the hole size.[129]

Principles and Techniques of Macular Hole Surgery

MH surgery has greatly benefitted from the advent of small-gauge transconjunctival sutureless vitrectomy, especially 25-G incisions.

Posterior Hyaloid Detachment (Fig. 121.14 and Video 121.1 online)

Detachment of the posterior hyaloid (PH) is a crucial step in MH with VMT, in which the vitreous still adheres to the hole edge and optic disc, but also in MH in which the vitreous still adheres to the optic disc. The concept of detaching the posterior vitreous cortex after completing core vitrectomy was introduced in the late 1980s by the group headed by Ron Michels (S de Brustos, personal communication). Histopathology showed that the substance that was separated from the retinal surface exactly corresponded to the vitreous cortex.[130] Various tools have been used for this separation, including an aspirating cannula with a rigid or soft tip, a microvitreoretinal blade[131] or an aspirating forceps,[132] and the

vitreous probe. The 23- and even 25- or 27-G vitreous probes, whose aspirating port is narrower and closer to the tip of the probe, are now very effective for firm aspiration and detachment of the posterior hyaloid. Direct aspiration of the vitreous fibers attached to the Weiss ring appears to be the most effective way of lifting the vitreous cortex en bloc and gradually extending its detachment to the equator in all the quadrants of the fundus. Before starting PH detachment, it is also possible to inject diluted triamcinolone or brilliant blue G in front of the posterior pole for clearer visualization of the vitreous cortex.

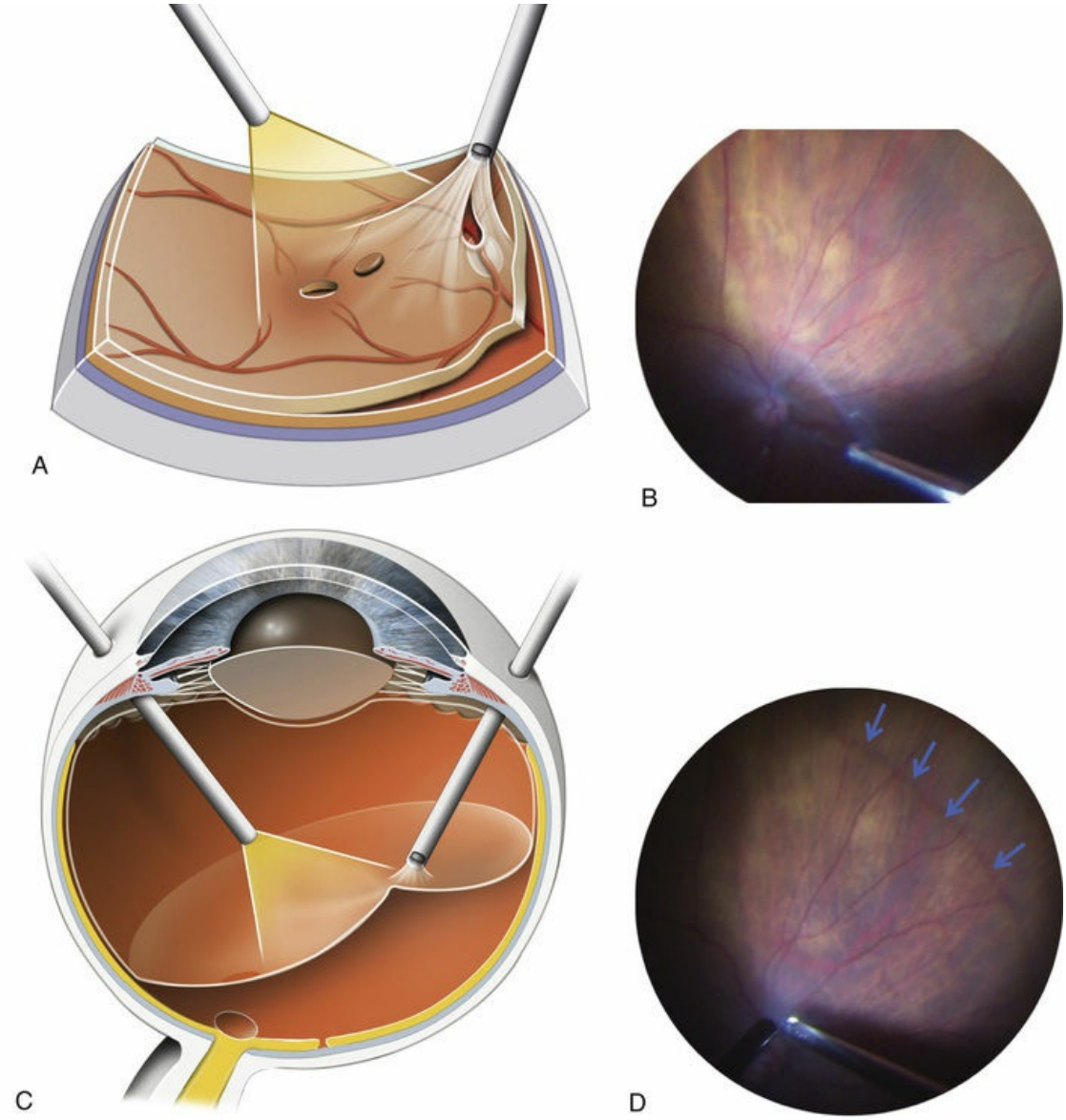

FIG. 121.14 Steps in hyaloid detachment in stage 2

and 3 macular holes. (A) Schematic representation: detachment of the Weiss ring by aspiration over the optic disc with the vitreous probe. (B) Peroperative photograph: the Weiss ring (*arrow*) is almost completely detached by the vitreous probe. (C) Enlargement of the vitreous detachment by the gradual exertion of traction on the posterior hyaloid using aspiration by the vitreous probe. (D) Peroperative view: The limit of the detachment of the posterior hyaloid appears as an arcuate line (*arrows*). (See Video 121.1 online.)

Extensive Vitrectomy

Although there is no way of proving that extensive vitrectomy is better than partial vitrectomy, there are several arguments in favor of the most extensive vitrectomy possible. Extensive vitrectomy means detachment of the PH up to the equator, followed by shaving of the vitreous base. The removal of as much vitreous as possible allows more gas mixture to be injected into the eye and subsequently prolongs the effect of the gas tamponade. Shaving the vitreous base, especially in the lower periphery, also reduces the risk of postoperative lower retinal breaks and detachment by preventing the gas bubble from exerting traction on the remaining vitreous fibers.[133,134]

Epiretinal Membrane Peeling (Fig. 121.15 and Video 121.2 online)

When present, the ERM around the hole should be peeled off.[73,74] ERM are usually soft and friable. They can be removed by brushing the retinal surface with the soft tip of a back-flush cannula, which is more efficient than forceps. These ERM adhere firmly to the thickness of the hole edge. If a dye that stains the ILM, such as brilliant blue, is used before removing the ERM, the ERM is not stained and appears as a “negative” at the surface at the ILM. The ERM can also be removed en bloc together with the ILM.

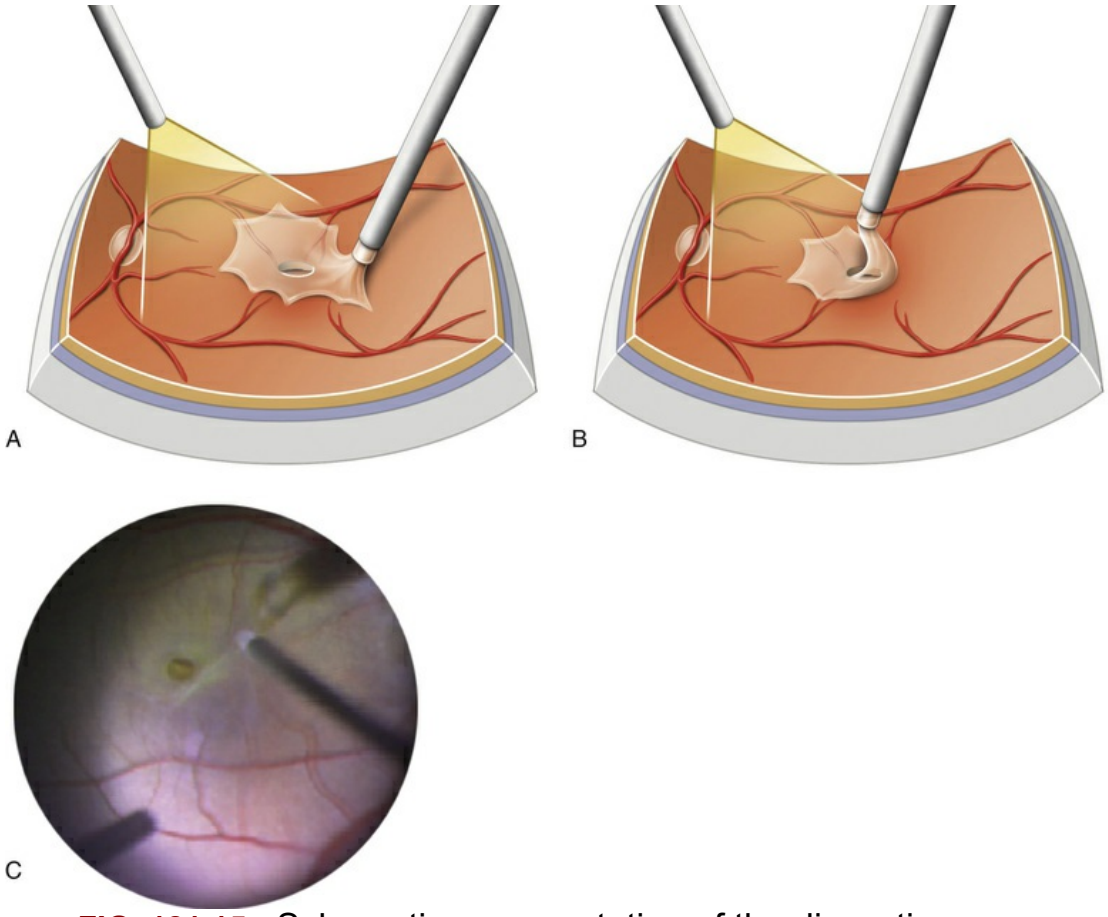

FIG. 121.15 Schematic representation of the dissection of an epiretinal membrane around a macular hole. (A) This soft epiretinal membrane is being detached from the retinal surface to which it is slightly adherent, by gently brushing the surface with the soft tip of a back-flush cannula. (B) The membrane has gradually been detached around the hole. It often adheres firmly to the hole edge. (C) Peroperative view of the dissection of an epiretinal membrane around a macular hole. (See Video 121.2 online.)

Internal Limiting Membrane Peeling (Fig. 121.16 and Video 121.3 online)

ILM peeling as a method of improving the MH closure rate was first described by Eckardt et al. in 1997.[135] The technique has evolved, and the use of dyes has greatly helped ILM visualization. End-gripping forceps are used to pinch and tear a flap of ILM without touching the optic nerve fibers. The ILM is then peeled off in a circular movement, thus creating a "maculorrhexis."[136] The use

of a diamond-dusted scraper has been proposed to initiate and complete ILM peeling[137] or to disrupt the ILM,[138] but this instrument could be more dangerous for the optic nerve fibers than a forceps.[139,140] More recently Michalewska et al. have proposed not to remove the dissected ILM from the eye but to cover the hole with an ILM flap, especially in myopic eyes and large or refractory MH.[141,142]

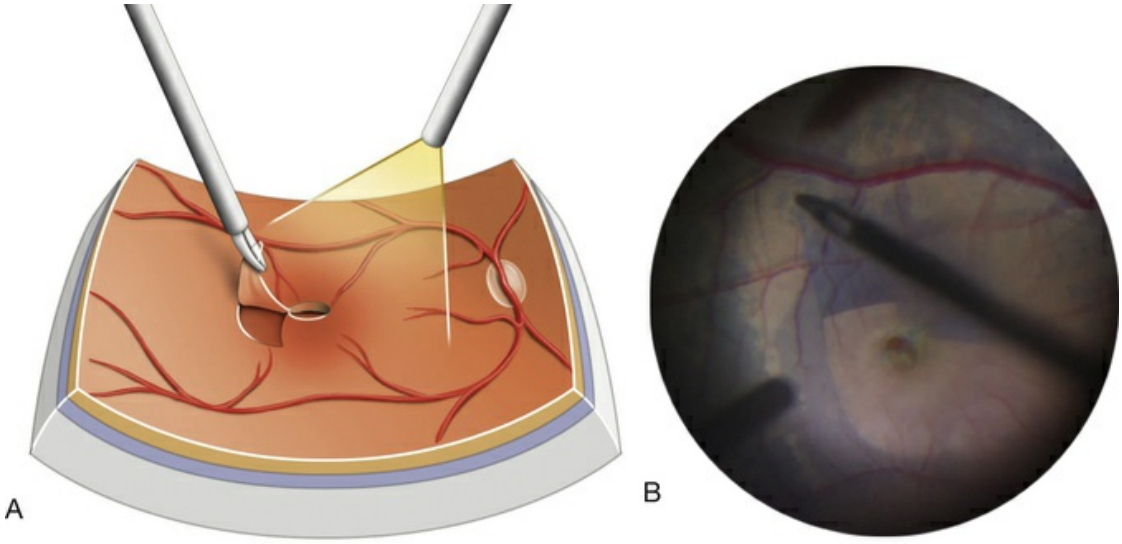

FIG. 121.16 Internal limiting membrane (ILM) peeling. (A) Schematic drawing: a flap of ILM is torn off with an end-gripping forceps. (B) Peroperative view of the ILM dissection: after staining with brilliant blue, a flap of the ILM is progressively detached around the hole in a circular direction to create a maculorhexis. (See Video 121.3)

Vital Dyes

The use of dyes to stain the ERM and ILM, also known as chromovitrectomy,[143] has made the peeling of the retinal surface more precise, more complete, and less traumatic. (Please refer to Chapter 126, Diagnostic and therapeutic vitrectomy for uveitis.)

Indocyanine Green and Infracyanine.

Indocyanine green (ICG) was introduced by Kadodonoso[144] in 2000 for ILM staining and is still widely used, despite concern in some

quarters regarding its safety. ICG has a selective affinity for the ILM and was initially used at the concentration of 0.5%, but on account of changes in the RPE and visual field defects , this concentration has been reduced to 0.125% and even 0.05%, which makes the staining paler but still useful. Nevertheless, Engelbrecht et al. using an ICG concentration at 0.12% concentration observed RPE changes in half their cases.[145] A meta-analysis of ILM peeling in 837 cases showed worse functional results after the use of ICG at the higher concentration of 0.5%.[146] The osmolarity of the ICG solution might have a harmful effect on the retina. Initially a 0.5% ICG solution was used, which had an osmolarity of 250 mOsm. The use of a concentration of 0.05%, whose osmolarity is 290 mOsm, combined with a brief contact time not exceeding 30 sec, with the retina, seems to give no sign of RPE toxicity.[147] Infracyanine, an iodine-free product, diluted in 5% glucose, results in an iso-osmolar solution that might be safer for the retina.[148] However, infracyanine also enters the RPE cells, which it may stain for months after surgery, and like ICG[149] also stains the axons of the retinal ganglion cells.[150,151]

Finally, as exposure to light seems to increase the risk of damage to the retina, the light should be turned off during the short time of ICG contact with the retina.[152] Opinion among vitreoretinal surgeons remains divided on the possible toxicity of ICG application to the retina. ICG should therefore only be used at the minimal concentrations of 0.025–0.05% (0.25–0.5 mg/ml) and for a short time.

Trypan Blue.

Trypan blue (TB) stains well the ERM but poorly the ILM. Nevertheless, it remains an alternative to ICG. To improve TB staining of the ILM, it must be used after fluid–gas exchange. Alternatively, it is easier to mix the dye isovolumetrically in 10% glucose to create heavy TB, which falls onto the posterior pole and results in an acceptable staining after a 2-min contact.[153] However, it has been suggested that this may also increase its osmolarity to toxic levels.[154,155] Alternatively, ready-to-use solutions combining TB with a viscosity- and density-increasing agent or another dye are also available in some countries. In most studies, TB showed no

signs of toxicity to the RPE or neuronal tissue.[156]

Brilliant Blue.

Brilliant blue (BB) has a selective affinity for the ILM and gives a good staining in an iso-osmolar solution of 0.25 mg/ml (0.025%). The staining occurs after a brief contact with the dye injected onto the retinal surface. In animal experiments, the safety profile of BB was good,[157] and it seems the best alternative to ICG. (For a review of the use of dyes in vitreoretinal surgery, see Rodrigues[158] and Farah.[159])

Type of Gas to Use in Macular Hole Surgery.

Various gases have been used for MH surgery, including C_3F_8, C_2F_6, SF_6, and air. The rationale for preferring one gas to another is based on the expected duration of the gas bubble. If we assume that most MH close within 3–7 days of tamponade, a bubble large enough to insulate the macula from intraocular fluid during this period will be sufficient. This, for instance, is the case for a 17% C_2F_6–air mixture, provided the vitrectomy is large enough to create a large gas bubble. With this mixture, the gas bubble still covers the macula 1 week after surgery if the head is in the upright position, and still fills more than 70% of the vitreous cavity. The essential characteristic of the gas mixture is not so much to persist for a long time in the eye as to decrease slowly in quantity during the first postoperative week. If the hole is small and a 3-day tamponade is assumed to be sufficient, 20% SF_6–air, or even air alone, might be enough, but it may be preferable for the patient to remain face-down during that time.

Use of Silicone Oil in Macular Hole Surgery.

Silicone oil has been used to avoid the need for positioning in patients unable to maintain the face-down position, to allow air travel after surgery, or to ensure prolonged tamponade in case of failure of the initial surgery. In such cases, some authors stressed the advantages of the use of silicone oil, which gave good results.[160–163] Others noted that the anatomic results were no better with silicone oil than with gas, or that the visual results were

worse.[164–166] Consequently, silicone oil should be used sparingly in MH surgery.[167]

Use of Healing Adjuvants.

Soon after MH surgery was introduced, attempts were made to improve MH closure by applying healing adjuvants. Bovine transforming growth factor-beta (TGF-ß) was used at first and gave favorable results in a randomized study,[168] but these results were not reproduced with recombinant TGF-ß.[169] Autologous serum has not proved effective in improving MH closure,[170] but autologous platelet concentrates successfully increased the closure rate of MH in a randomized study,[171] although they are not used routinely. Recently, however, autologous blood[172] or autologous platelets[173] have been used again in high myopic eyes or chronic MH or after failure of a first operation.

Peroperative Complications

Specific peroperative complications are rare. Those that do occur are usually due to vitreous detachment and ILM peeling. In stage 2 and 3 MH, the posterior hyaloid has to be detached from the optic disc and the retina, which may result in retinal breaks at the equator or, very occasionally, paravascular breaks.[174,175] If extensive vitrectomy is accompanied by shaving of the vitreous base, intrabasal vitreous breaks may also occur, although today they are less frequent thanks to the high cutting speed and improved fluidics of the new vitrectomy machines.[176] Nevertheless, rates of 10–20% are currently reported for peripheral retinal breaks that occur during vitrectomy for MH.[175] This highlights the imperative need to check the retinal periphery before performing fluid–gas exchange, in order to treat any peripheral breaks by laser or cryotherapy and avoid the risk of retinal detachment.[133,175]

Complications of ILM peeling such as punctuate damage to the RPE by retinal compression at the ILM gripping point, or fascicular defects due to pinching of the optic nerve fibers, should be avoided by a very cautious approach to the retinal surface. Appropriate staining of the ILM makes its removal safer. Nevertheless, retinal petechiae are common, and bleeding may sometimes occur during

the tangential traction exerted during ILM peeling.

Postoperative Positioning (Fig. 121.17)

Although Kelly and Wendel considered that strict face-down positioning for at least a week was essential to the success of vitrectomy for MH,[3] attempts to reduce or suppress the burden of positioning started as early as 1997 with a pilot study by Tornambe et al.[177] The authors of this study postulated that the most important function of the gas bubble was to isolate the hole from vitreous fluid and argued that if the bubble was large enough to cover the hole, successful closure would be possible regardless of the patient's position. The same authors discussed the negative effect of the long duration of the hole on the success rate. It is clearer today that the indication for an alleviated position should take into account the hole diameter[67] and be kept for small holes.

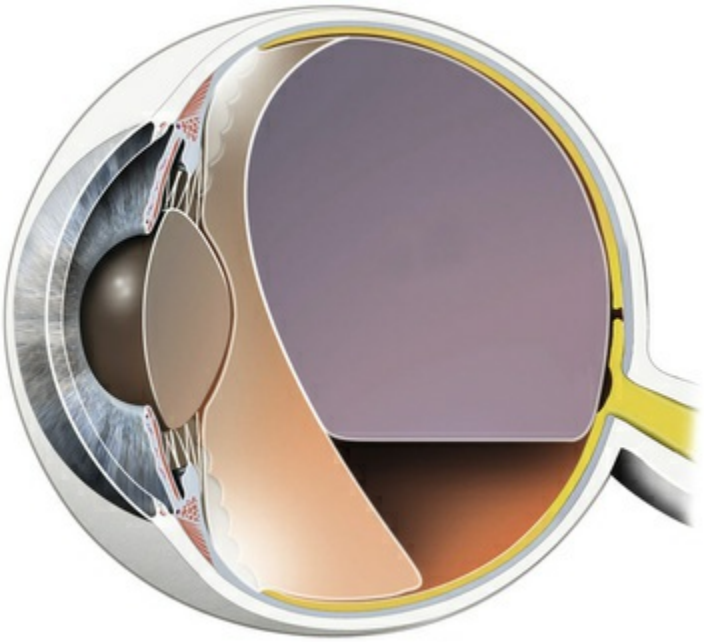

FIG. 121.17 Schematic drawing of the vitreous cavity filled by gas mixture when the head is in the upright position. The gas bubble should cover the macula until the hole is closed.

As regards the positioning itself, it should be borne in mind that the aim of positioning is to keep the MH insulated from liquid

currents until the healing process has started to close the hole. The upright position allows the gas bubble to cover the macula for a period of time that depends on the extent of the vitrectomy, the surgery of the lens, the way in which the vitreous cavity is filled with air, the tightness of the sclerotomies, and how fast the gas mixture is resorbed. The time for which a tamponade is needed depends on the duration of the healing process, which is certainly related to hole diameter. In actual fact, if the gas mixture injected is able to cover the macula for a week, even in the upright position, MH with a diameter of up to 400 μm may be candidates for non-face-down positioning. In such cases, the patient will only be advised to avoid the supine position, even during the night. At least two meta-analyses have now confirmed the absence of benefit of the positioning in MH smaller than 400 μm.[178,179]

Results of Surgery

Anatomic Results

As stated above, in the initial series of 52 cases published by Kelly and Wendel in 1990[3] the successful closure rate for MH surgery was 58%, but in the series of 170 eyes published a year later the rate rose to 73%.[116] However, in 1996, a randomized prospective study of vitrectomy for stage 3 and 4 MH versus observation only achieved a success rate of 69% in the vitrectomy group,[180] thus showing that at the time surgery for MH was still in the learning curve phase. Today the closure rate is currently 90–95% or more.[167,181,182]

Results According to Hole Size

The concept that the success rate for MH surgery depends on hole diameter emerged in 2002 with the publications by Ip[183] and Ulrich.[184] Ip showed that the closure rate was 92% for MH smaller than 400 μm but only 56% for MH of 400 μm or more, as measured on OCT.[183] Subsequent observations confirmed the importance of the size of the hole for its closure. In a series of MH, which had closed spontaneously, mean hole diameter at baseline was less than 200 μm.[119] In a randomized study in which the MH closure rates were compared after intravitreal injection of ocriplasmin and after

placebo, MH smaller than 250 μm had a closure rate of 58.3%.[120]

These findings highlighted the prognostic value of MH diameter for the efficacy of treatment and opened the way to the introduction of the idea of individual treatments tailored to the initial size of the hole.

Results According to Internal Limiting Membrane Peeling

Since the publication by Eckardt[135] showing that the MH closure rate might improve if the ILM was peeled off, many publications, all of them retrospective, have reported closure rates of 87–100% in relatively large series of cases after peeling of the ILM.[185–188] Some of these studies also have compared ILM peeling and nonpeeling in large series of eyes and gave success rates comprised between 77 and 89% without peeling compared to 92–97% with peeling.[188–190] For instance, in a retrospective study Kugamai obtained 92% MH closure after ILM peeling in 175 MH compared to 81% closure without ILM peeling in 417 MH. An interesting observation by this author was that the initial success rate for holes measuring more than 400 μm was significantly less than that for holes measuring less than 400 μm.[189] So far, however, only three prospective randomized studies of ILM peeling versus nonpeeling in MH surgery have been published. Success rates in the peeling groups ranged from 84 to 92% compared to only 32–48% in the nonpeeling groups.[191–193] These results for nonpeeling are far below the success rate of 58% initially obtained by Kelly and Wendel in 1991.[3] The discrepancy between the results for the control groups in the above randomized studies and those of other retrospective studies seems to indicate that other conditions, in addition to ILM peeling, are necessary for MH closure.

On the other hand, it appears that the need for ILM peeling may depend on the size of the hole. In a retrospective study Tadayoni et al.[65] showed that ILM peeling had a positive effect on MH closure in a series of 84 eyes (100% MH closure with peeling vs. 83.3% without). However, this effect did not apply to MH smaller than 400 μm (100% closure in both group). For MH larger than 400 μm, the difference between the effects of peeling and nonpeeling increased (100% closure with peeling vs. 73.3% without). This

tendency was confirmed by a multicenter randomized trial in which the results for ILM peeling were compared to those for nonpeeling in a series of 80 MH larger than 400 μm, and in which the success rate for peeling was 94.9% compared to 73.2 without peeling.[194]

Results According to Postoperative Positioning

From the beginning of MH surgery, face-down positioning for at least a week has been considered of crucial importance for MH closure. However, as early as 1997 Tornambe obtained a reasonable success rate of 79% for hole closure without any face-down positioning.[177] Several other studies that only included a few patients variously combined phacoemulsification, ILM peeling, the use of air or gas mixtures, brief face-down positioning (1–3 days), or none, and obtained success rates of 87–90%. In a randomized prospective trial comparing face-down and seated positioning, face-down positioning was found to give a better closure rate. However, there was no difference between the rates for the two positions when MH were smaller than 400 μm in diameter.[181] Another prospective randomized study compared face-down positioning and an alleviated position for MH not larger than 400 μm in diameter after surgery without ILM peeling and found an equally high success rate of over 90% for both positions.[67] Another study has also compared the results between face-down positioning and nonsupine positioning in MH larger than 400 μm after surgery, including ILM peeling: a similar success rate of at least 90% was found in both groups.[66] It therefore appears in a meta-analysis[178] that face-down positioning after MH surgery is not essential, provided that the gas bubble stays in contact with the macula until the healing process has started to close the hole, and the needed duration depends on the hole size.[195] For this purpose, various gas mixtures can be used, as long as the volume of the gas bubble remains large enough for 3-5 days to make an effective tamponade of the macula in the upright position. Holes larger than 600 μm may, on the contrary, require longer face-down positioning and a longer - acting gas mixture.

Visual Outcome

Overall Results

There are few recent prospective studies in which visual acuity has been recorded in a controlled procedure. Moreover, due to the high rate of postoperative cataract, visual acuity (VA) measurement gives pertinent information concerning the value of MH surgery only once the cataract has been operated on, or after combined cataract and MH surgery. In a retrospective study of 74 eyes operated on successfully for a MH, Scott et al.[196] found that after cataract surgery median VA was 20/40 and that 58% of eyes had a VA of 20/40 or more. Among 99 patients with closed MH, 91% of whom were pseudophakic at the end of follow-up, Haritoglou et al.[197] also found that VA improved from a median of 20/100 to 20/40. Three other series showed that VA improved with time and that mean VA reached 20/32 or more 1 and 2 years after surgery.[198–200] After MH closure, preferred retinal locus shifts from an eccentric location on the edge of the hole to a more central position, but the new location is not always in the middle of the hole. A relative or absolute microscotoma detected by microperimetry persists in some cases.[201,202] Visual acuity improves mainly because of the improvement in fixation stability.[203]

Visual and Anatomic Closure Correlation (Fig. 121.18)

Long-lasting and large size are MH characteristics that are considered poor prognostic factors for MH surgery.[183,184,204,205] Today, however, this may not always be the case, because ILM peeling has improved the anatomic prognosis for large holes, which is nearly the same as for smaller ones, and even long-standing MH may benefit from surgery.[206] However, the hole size affects visual outcome because the closure of large holes may leave a larger glial scar than the closure of smaller ones.[199] In this connection it has indeed been shown on OCT that the morphology and thickness of the foveal photoreceptor layer correlated with final visual acuity.[207,208] The length of the defect in the interdigitation zone[209] or external limiting membrane or ellipsoid zone[210] has been found to correlate postoperatively with the final VA.[211,212]

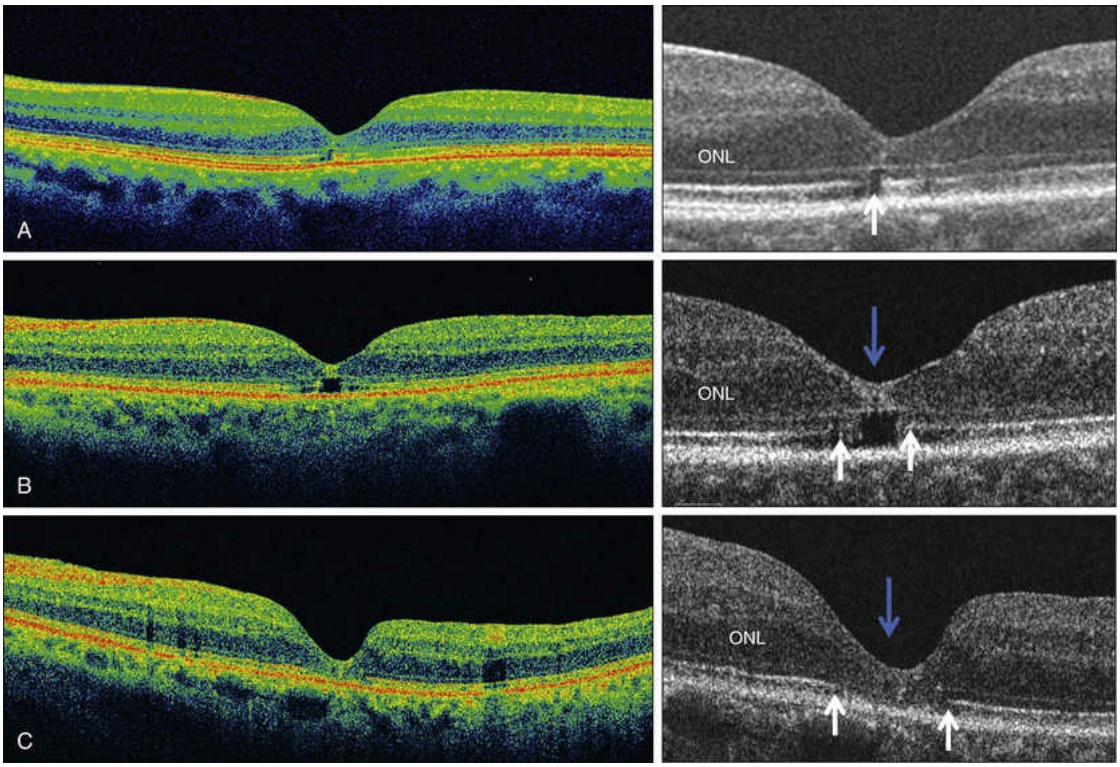

FIG. 121.18 Macular holes closed after surgery with various degrees of photoreceptor loss. (A) Left: Horizontal optical coherence tomography (OCT) scan showing a good macular profile after closure of the hole. Right: Detail showing a very small disruption of the ellipsoid zone (*white arrow*). The outer nuclear layer (ONL) is almost continuous at the foveal center. (B) Left: Horizontal OCT scan showing a macular profile thinner than normal after closure of the hole. Right: Detail showing disruption of the ellipsoid zone (*between white arrows*). A central outer cavitation persists in the outer retina. In the foveal center, the ONL has been replaced by scar tissue (*blue arrow*). (C) Left: Horizontal OCT scan showing an abnormal macular profile with a deep foveal pit after closure of the hole. Right: Detail showing great disruption of the ellipsoid zone (*between white arrows*). At the foveal center, most of the ONL has been replaced by a hyperreflective scar (*blue arrow*).

Visual Outcome and ILM Dye-Assisted Peeling

Although ILM peeling has been proved to improve the closure rate at least of MH larger than 400 μm, it may also have harmful effects

on optic fiber and ganglion cell layers, either through a mechanical effect or the use of ICG to stain the ILM. Several studies have compared visual outcome of eyes in which ILM was stained by ICG or brilliant blue G (BBG) and shown a significantly better outcome in visual acuity with BBG than with surgery using ICG.[213–215] A trend for a lower VA improvement when ICG was used has also been found in a meta-analysis.[216]

Postoperative Complications of Surgery

Retinal Detachment

Retinal detachment (RD) may complicate MH surgery as it does for other vitrectomy procedures. At the beginning of MH surgery an especially high proportion of RD (up to 14%) was reported,[217] mainly due to postoperative inferior breaks. These breaks have been attributed to the traction exerted by the gas bubble on the inferior vitreous in the upright position. In more recent publications the rate of retinal detachment tended to decrease to 5% in a meta-analysis of randomized studies[218] and even under 2% for more recent studies,[67,219,220] probably due to a more efficient search for retinal breaks during surgery and to more thorough removal of the inferior peripheral vitreous. However, some other authors still find a higher rate of retinal detachment after MH surgery than after ERM surgery.[133]

Adverse Anatomic Effects of Internal Limiting Membrane Peeling

ILM peeling results in corrugations of the retinal surface, called dissociated optic nerve fiber layer (DONFL), first observed on blue light reflectance retinographies.[221] The damage to the optic nerve fiber layer could be more important when the cleavage plane is created with a diamond-dusted scraper than with a forceps.[140] OCT B-scan has further shown that this aspect corresponded to dimples in the retinal nerve fiber layer,[222] which are clearly shown on en face

OCT segmented at the retinal surface.[223] DONFL were first thought to have no adverse effect on visual function. However, it has been shown that they were often associated with ganglion cell layer defects[224,225] and microperimetric loss of retinal sensitivity[226,227] (Fig. 121.19).

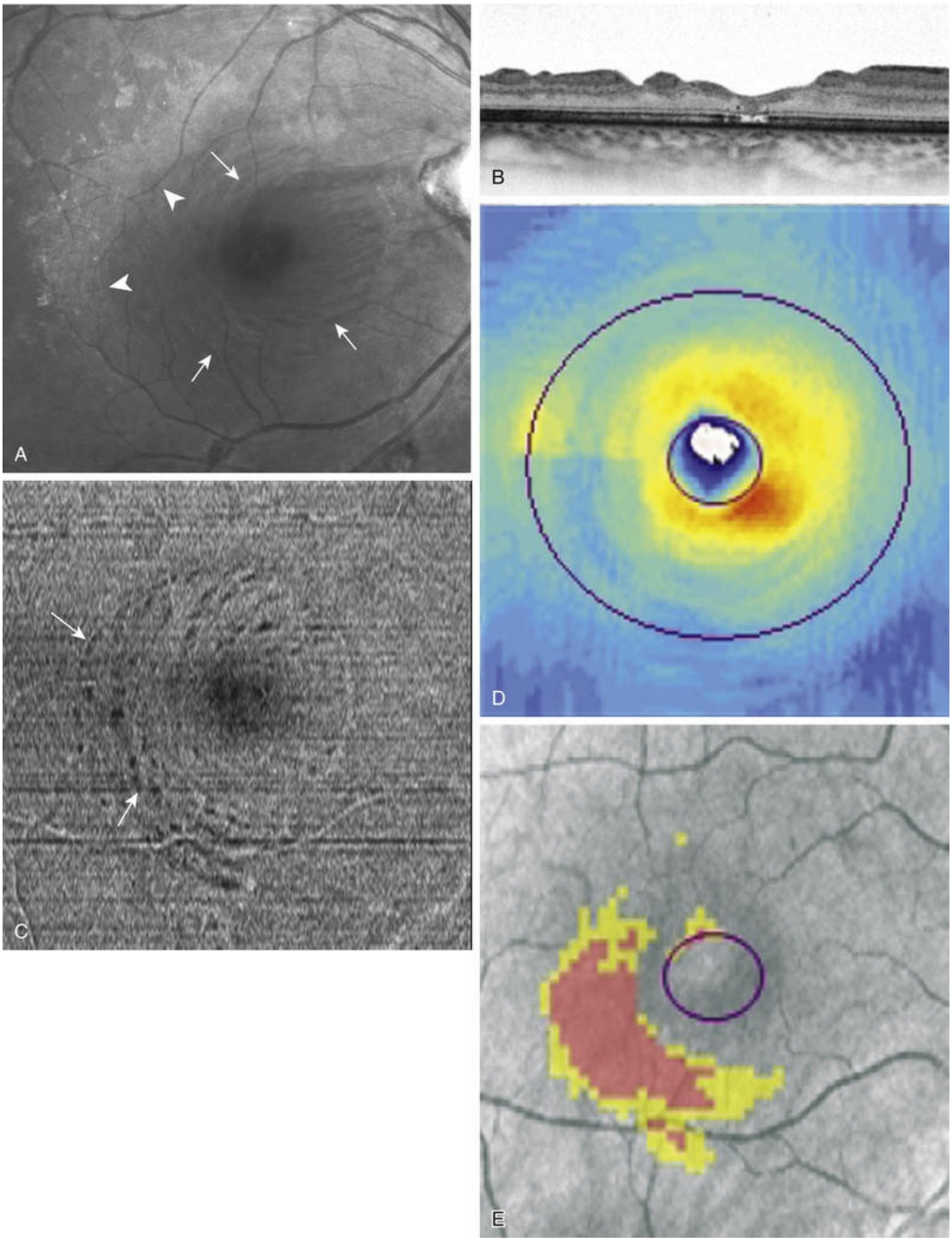

FIG. 121.19 Macular holes closed after surgery with dissociated optic nerve fiber layer (DONFL). (A) Blue light reflectance photo showing the arcuate striae of the DONFL (*arrows).* Limit of the area of internal limiting membrane peeling (*arrowheads*). (B) Horizontal B-scan showing more or less deep dimples in the optic nerve fiber layer corresponding to the DONFL. (C) DONFL seen on en face OCT mode,

segmented at the inner retinal surface (*arrows*). (D) Ganglion cell layer thickness map showing a defect in the temporal part of the macula. (E) Ganglion cell layer thickness deviation from normal: note the loss of ganglion cell (in red) in the temporal part of the macula, where the DONFL are maximum.

ILM peeling may also affect ganglion cell layer thickness, especially in the temporal part of the macular area, mostly in cases in which ICG has been used to stain the ILM,[225,228] although another study using brilliant blue-assisted ILM peeling did not find any reduction in ganglion cell layer thickness.[229]

Visual Field Defects

Inferotemporal sectorial visual field defects were first described in young patients who had undergone pars plana vitrectomy with fluid–gas exchange,[230] and were attributed to retinal nerve fiber layer damage to the nasal portion of the optic nerve rim, probably due to traction during cortical vitreous peeling.[231] Another hypothesis was that injury to the nerve fiber layer by dehydration during the fluid-air exchange might cause visual field defects.[232] In a prospective study in 1997, visual field defects were observed in 23% of cases,[233] but in another series published in 2001, this incidence was only 1%.[234] In any case, sectorial field defects do not significantly affect the outcome of MH surgery.

Reopening of Macular Hole

Late reopening of MH after successful surgery, i.e., reopening of the hole several months or years after its closure, has been attested on OCT in 5–7% of cases before the era of ILM peeling.[235,236] The reason for reopening remains unclear, but in most cases it might be the proliferation of a secondary ERM around the hole,[74] rather than a side-effect of cataract surgery, as sometimes suggested. Systematic ILM peeling seems to lower the risk of MH reopening to less than 2%.[197,237,238] Reopening might be a complication specific to large MH,[186] which are precisely those whose initial closure rate is improved by ILM peeling. Once a MH reopens, reoperation, with

peeling of the ILM and any ERM, if this was not done during the first operation, usually results in hole closure and visual improvement. If ILM has already been removed, the presence of a tangential traction at the limit of ILM ablation should be investigated and removed. It may also be suggested to dissect a patch of ILM in the posterior pole and to cover the MH, or to use healing adjuvants, but none of these methods has been validated. Otherwise, a simple fluid–gas exchange may be enough to close the hole again.

Cataract

Cataract is a common complication of pars plana vitrectomy after the age of 60, which explains the high rate of its occurrence after MH surgery. The postoperative rate of pseudophakia at 3 or 5 years is commonly 85–98%.[196,239] This observation has led many surgeons to propose performing combined cataract and MH surgery. In a comparative retrospective study, Muselier et al.[240] have shown that visual results and complications were no different, whether the cataract had been removed after or during MH surgery, but that combined surgery shortened the period required for visual recovery.

Vitreolysis as a Nonsurgical Treatment for Macular Hole

Ocriplasmin (ThromboGenics NV, Leuven, Belgium) is a recombinant containing the catalytic domain of plasmin and has the same catalytic properties as the human plasmin used for vitreolysis. It has been used in several clinical trials to create a posterior vitreous detachment.[241] The authors of one phase III study compared the respective effects at one month of a single intravitreal injection of ocriplasmin and placebo, on the closure rate of stage 2 MH smaller than 400 μm. The overall success rate for the ocriplasmin group was 40.6% compared to 10.6% in the placebo group. For MH with a diameter of 250 μm or less, the success rate rose to 58.3%, but for holes with a diameter of 250–400 μm, it was

only 24.6%.[120] The proportion of small holes with persistent VMT being small, the indications of enzymatic vitreolysis remain limited so far.

References

1. Aaberg TM, Blair CJ, Gass JDM. Macular holes. *Am J Ophthalmol*. 1970;69(4):555–562.
2. Gass JD. Idiopathic senile macular hole: its early stages and pathogenesis. *Arch Ophthalmol*. 1988;106(5):629–639.
3. Kelly NE, Wendel RT. Vitreous surgery for idiopathic macular holes: results of a pilot study. *Arch Ophthalmol*. 1991;109(5):654–659.
4. Knapp H. Uber isolirte zerreissungen der aderhaut in folge von traumen auf dem augopfel. *Arch Augenhetlkd*. 1869;1:6–29.
5. Noyes HD. Detachement of the retina with laceration at the macula lutea. *Trans Am Ophthalmol Soc*. 1871;1:128–129.
6. Ogilvie FM. On one of the results of concussion injuries of the eye ("holes" at the macula). *Trans Am Ophthamol Soc*. 1900;20:202–229.
7. Kuhnt H. Ueber eine Eigenthümliche Veränderung der Netzhaut ad Maculam (retinitis Atrophicans sive rareficans centralis). *Z Augenheilkd*. 1900;3:105–112.
8. Coats G. The pathology of macular holes. *Royal London Ophthal Hosp Rep*. 1907;17:69–97.
9. Zeeman WPC. Uber Loch-und cystenbildung der fovea centralis. *Graefes Arch Klin Exp Ophthalmol*. 1912;80:259–269.
10. Lister W. Holes in the retina and their clinical significance. *Br J Ophthalmol*. 1924;8:1–20.
11. Gass JDM. *Stereoscopic atlas of macular diseases: diagnosis and treatment*. 3rd ed. Mosby: St. Louis; 1987:2 [684-93].
12. Gass JD, Joondeph BC. Observations concerning patients with suspected impending macular holes. *Am J Ophthalmol*. 1990;109(6):638–646.
13. Gass JD. Reappraisal of biomicroscopic classification of stages of development of a macular hole. *Am J Ophthalmol*. 1995;119(6):752–759.

14. Hee MR, Puliafito CA, Wong C, et al. Optical coherence tomography of macular holes. *Ophthalmology*. 1995;102(5):748–756.
15. Frangieh GT, Green WR, Engel HM. A histopathologic study of macular cysts and holes. *Retina*. 1981;1:311–336.
16. Ho AC, Guyer DR, Fine SL. Macular hole. *Surv Ophthalmol*. 1998;42(5):393–416.
17. Rahmani B, Tielsch JM, Katz J, et al. The cause-specific prevalence of visual impairment in an urban population. The Baltimore Eye Survey. *Ophthalmology*. 1996;103(11):1721–1726.
18. Mitchell P, Smith W, Chey T, et al. Prevalence and associations of epiretinal membranes. The Blue Mountains Eye Study. *Australia Ophthalmology*. 1997;104(6):1033–1040.
19. Wang S, Xu L, Jonas JB. Prevalence of full-thickness macular holes in urban and rural adult Chinese: the Beijing Eye Study. *Am J Ophthalmol*. 2006;141(3):589–591.
20. Sen P, Bhargava A, Vijaya L, et al. Prevalence of idiopathic macular hole in adult rural and urban south Indian population. *Clin Exp Ophthalmol*. 2008;36(3):257–260.
21. Meuer SM, Myers CE, Klein BE, et al. The epidemiology of vitreoretinal interface abnormalities as detected by spectral-domain optical coherence tomography: the Beaver Dam Eye Study. *Ophthalmology*. 2015;122(4):787–795.
22. McCannel CA, Ensminger JL, Diehl NN, Hodge DN. Population-based incidence of macular holes. *Ophthalmology*. 2009;116(7):1366–1369.
23. Akiba J, Kakehashi A, Arzabe CW, et al. Fellow eyes in idiopathic macular hole cases. *Ophthalmic Surg*. 1992;23(9):594–597.
24. Lewis ML, Cohen SM, Smiddy WE, et al. Bilaterality of idiopathic macular holes. *Graefes Arch Klin Exp Ophthalmol*. 1996;234(4):241–245.
25. Ezra E, Wells JA, Gray RH, et al. Incidence of idiopathic full-thickness macular holes in fellow eyes: a 5-year prospective natural history study. *Ophthalmology*. 1998;105(2):353–359.
26. Chew EY, Sperduto RD, Hiller R, et al. Clinical course of macular holes: the Eye Disease Case–Control Study. *Arch*

Ophthalmol. 1999;117(2):242–246.
27. Chan A, Duker JS, Schuman JS, Fujimoto JG. Stage 0 macular holes: observations by optical coherence tomography. *Ophthalmology*. 2004;111(11):2027–2032.
28. Takahashi A, Yoshida A, Nagaoka T, et al. Macular hole formation in fellow eyes with a perifoveal posterior vitreous detachment of patients with a unilateral macular hole. *Am J Ophthalmol*. 2011;151(6):981–989.
29. Takahashi A, Nagaoka T, Yoshida A. STAGE 1-A macular hole: a prospective spectral-domain optical coherence tomography study. *Retina*. 2011;31(1):127–147.
30. Shah SP, Bunce C, Johnston RL, et al. Are biometric parameters a risk factor for idiopathic macular hole formation? Results of a matched case-control series. *Br J Ophthalmol*. 2006;90(1):117–118.
31. Evans JR, Schwartz SD, McHugh JD, et al. Systemic risk factors for idiopathic macular holes: a case–control study. *Eye*. 1998;12(Pt 2):256–259.
32. The Eye Disease Case–Control Study Group. Risk factors for idiopathic macular holes. The Eye Disease Case–Control Study Group. *Am J Ophthalmol*. 1994;118(6):754–761.
33. Jackson TL, Donachie PH, Sparrow JM, et al. United Kingdom National Ophthalmology Database study of vitreoretinal surgery: report 2, macular hole. *Ophthalmology*. 2013;120(3):629–634.
34. Grignolo A. Fibrous components of the vitreous body. *Arch Ophthalmol*. 1952;47:760–774.
35. Avila MP, Jalkh AE, Murakami K, et al. Biomicroscopic study of the vitreous in macular breaks. *Ophthalmology*. 1983;90(11):1277–1283.
36. Kakehashi A, Schepens CL, Trempe CL. Vitreomacular observations. II. Data on the pathogenesis of idiopathic macular breaks. *Graefes Arch Clin Exp Ophthalmol*. 1996;234(7):425–433.
37. Maumenee AE. Further advances in the study of the macula. *Arch Ophthalmol*. 1967;78:151–165.
38. Reese AB, Jones IS, Cooper WC. Macular changes secondary to vitreous traction. *Am J Ophthalmol*. 1967;64:544–549.

39. Schepens CL. Fundus changes caused by alterations of the vitreous body. *Am J Ophthalmol*. 1955;39(5):631–633.
40. Schepens CL. Macular holes and PVD. *Ophthalmology*. 1996;103(3):349–350.
41. Akiba J, Quiroz MA, Trempe CL. Role of posterior vitreous detachment in idiopathic macular holes. *Ophthalmology*. 1990;97(12):1610–1613.
42. Kornzweig AL, Feldstein M. Studies of the eye in old age. II. Hole in the macula: a clinico-pathologic study. *Am J Ophthalmol*. 1950;33:243–247.
43. Bronstein MA, Trempe CL, Freeman H. Fellow eyes of eyes with macular holes. *Am J Ophthalmol*. 1981;92(6):757–761.
44. McDonnell PJ, Fine SL, Hillis AI. Clinical features of idiopathic macular cysts and holes. *Am J Ophthalmol*. 1982;93(6):777–786.
45. Kishi S, Kamei Y, Shimizu K. Tractional elevation of Henle's fiber layer in idiopathic macular holes. *Am J Ophthalmol*. 1995;120(4):486–496.
46. Folk JC, Boldt HC, Keenum DG. Foveal cysts: a premacular hole condition associated with vitreous traction. *Arch Ophthalmol*. 1998;116(9):1177–1183.
47. Gaudric A, Haouchine B, Massin P, et al. Macular hole formation: new data provided by optical coherence tomography. *Arch Ophthalmol*. 1999;117(6):744–751.
48. Haouchine B, Massin P, Gaudric A. Foveal pseudocyst as the first step in macular hole formation: a prospective study by optical coherence tomography. *Ophthalmology*. 2001;108(1):15–22.
49. Kumagai K, Hangai M, Larson E, et al. Vitreoretinal interface and foveal deformation in asymptomatic fellow eyes of patients with unilateral macular holes. *Ophthalmology*. 2011;118(8):1638–1644.
50. Takahashi A, Nagaoka T, Ishiko S, et al. Foveal anatomic changes in a progressing stage. 1. Macular hole documented by spectral-domain optical coherence tomography. *Ophthalmology*. 2010;117(4):806–810.
51. Eisner G. Posterior vitreous detachment. *Klin Monatsbl Augenheilkd*. 1989;194:389–392.

52. Jaffe NS. Complications of acute posterior vitreous detachment. *Arch Ophthalmol*. 1968;79:568–571.
53. Sebag J. *The vitreous: structure, function, and pathobiology. The vitreous: structure, function, and pathobiology*. Springer-Verlag: New York; 1989:80–95.
54. Wilkinson CPR, Michels R. *Retinal detachment*. 2nd ed. Mosby: St Louis; 1990:30–34.
55. Uchino E, Uemura A, Ohba N. Initial stages of posterior vitreous detachment in healthy eyes of older persons evaluated by optical coherence tomography. *Arch Ophthalmol*. 2001;119(10):1475–1479.
56. Johnson MW, Van Newkirk MR, Meyer KA. Perifoveal vitreous detachment is the primary pathogenic event in idiopathic macular hole formation. *Arch Ophthalmol*. 2001;119(2):215–222.
57. Johnson MW. Posterior vitreous detachment: evolution and complications of its early stages. *Am J Ophthalmol*. 2010;149(3):371–382.
58. Duker JS, Kaiser PK, Binder S, et al. The international vitreomacular traction study group classification of vitreomacular adhesion, traction, and macular hole. *Ophthalmology*. 2013;120(12):2611–2619.
59. Kishi S, Hagimura N, Shimizu K. The role of the premacular liquefied pocket and premacular vitreous cortex in idiopathic macular hole development. *Am J Ophthalmol*. 1996;122(5):622–628.
60. Spaide RF. Measurement of the posterior precortical vitreous pocket in fellow eyes with posterior vitreous detachment and macular holes. *Retina*. 2003;23(4):481–485.
61. Worst JG. Cisternal systems of the fully developed vitreous body in the young adult. *Trans Ophthalmol Soc U K*. 1977;97(4):550–554.
62. Srinivasan VJ, Monson BK, Wojtkowski M, et al. Characterization of outer retinal morphology with high-speed, ultrahigh-resolution optical coherence tomography. *Invest Ophthalmol Vis Sci*. 2008;49(4):1571–1579.
63. Michalewski J, Michalewska Z, Dziegielewski K, et al. Evolution from macular pseudohole to lamellar macular

hole – spectral domain OCT study. *Graefes Arch Clin Exp Ophthalmol*. 2011;249(2):175–178.
64. Johnson RN, Gass JD. Idiopathic macular holes. Observations, stages of formation, and implications for surgical intervention. *Ophthalmology*. 1988;95(7):917–924.
65. Tadayoni R, Gaudric A, Haouchine B, et al. Relationship between macular hole size and the potential benefit of internal limiting membrane peeling. *Br J Ophthalmol*. 2006;90(10):1239–1241.
66. Alberti M, la Cour M. Nonsupine positioning in macular hole surgery: a noninferiority randomized clinical trial. *Retina*. 2016;36(11):2072.
67. Tadayoni R, Vicaut E, Devin F, et al. A randomized controlled trial of alleviated positioning after small macular hole surgery. *Ophthalmology*. 2011;118(1):150–155.
68. Haller JA, Stalmans P, Benz MS, et al. Efficacy of intravitreal ocriplasmin for treatment of vitreomacular adhesion: subgroup analyses from two randomized trials. *Ophthalmology*. 2015;122(1):117–122.
69. Philipakis E, Amouyal F, Couturier A, et al. Size and vitreomacular attachment of full thickness macualar hole. *Invest Ophthalmol Vis Sci*. 2015;56(7):1221.
70. Ezra E, Fariss RN, Possin DE, et al. Immunocytochemical characterization of macular hole opercula. *Arch Ophthalmol*. 2001;119(2):223–231.
71. Xu D, Yuan A, Kaiser PK, et al. A novel segmentation algorithm for volumetric analysis of macular hole boundaries identified with optical coherence tomography. *Invest Ophthalmol Vis Sci*. 2013;54(1):163–169.
72. Wakely L, Rahman R, Stephenson J. A comparison of several methods of macular hole measurement using optical coherence tomography, and their value in predicting anatomical and visual outcomes. *Br J Ophthalmol*. 2012;96(7):1003–1007.
73. Blain P, Paques M, Massin P, et al. Epiretinal membranes surrounding idiopathic macular holes. *Retina*. 1998;18(4):316–321.
74. Cheng L, Azen SP, El-Bradey MH, et al. Effects of

preoperative and postoperative epiretinal membranes on macular hole closure and visual restoration. *Ophthalmology*. 2002;109(8):1514–1520.
75. Cheng L, Freeman WR, Ozerdem U, et al. Prevalence, correlates, and natural history of epiretinal membranes surrounding idiopathic macular holes. Vitrectomy for Macular Hole Study Group. *Ophthalmology*. 2000;107(5):853–859.
76. Schumann RG, Hagenau F, Haritoglou C, et al. Cells at the vitreoretinal interface in small full-thickness macular holes. *Retina*. 2015;35(6):1158–1165.
77. Schumann RG, Eibl KH, Zhao F, et al. Immunocytochemical and ultrastructural evidence of glial cells and hyalocytes in internal limiting membrane specimens of idiopathic macular holes. *Invest Ophthalmol Vis Sci*. 2011;52(11):7822–7834.
78. Haouchine B, Massin P, Tadayoni R, et al. Diagnosis of macular pseudoholes and lamellar macular holes by optical coherence tomography. *Am J Ophthalmol*. 2004;138(5):732–739.
79. Witkin AJ, Ko TH, Fujimoto JG, et al. Redefining lamellar holes and the vitreomacular interface: an ultrahigh-resolution optical coherence tomography study. *Ophthalmology*. 2006;113(3):388–397.
80. Guyer DR, Green WR, de Bustros S, et al. Histopathologic features of idiopathic macular holes and cysts. *Ophthalmology*. 1990;97(8):1045–1051.
81. Johnson RN, McDonald HR, Lewis H, et al. Traumatic macular hole: observations, pathogenesis, and results of vitrectomy surgery. *Ophthalmology*. 2001;108(5):853–857.
82. Gaudric A, Aloulou Y, Tadayoni R, et al. Macular pseudoholes with lamellar cleavage of their edge remain pseudoholes. *Am J Ophthalmol*. 2013;155(4):733–742 [742.e1–4].
83. Pang CE, Spaide RF, Freund KB. Comparing functional and morphologic characteristics of lamellar macular holes with and without lamellar hole-associated epiretinal proliferation. *Retina*. 2015;35(4):720–726.

84. Compera D, Entchev E, Haritoglou C, et al. Lamellar hole-associated epiretinal proliferation in comparison to epiretinal membranes of macular pseudoholes. *Am J Ophthalmol*. 2015;160(2) [373–84.e1].
85. Parolini B, Schumann RG, Cereda MG, et al. Lamellar macular hole: a clinicopathologic correlation of surgically excised epiretinal membranes. *Invest Ophthalmol Vis Sci*. 2011;52(12):9074–9083.
86. Allen AW Jr, Gass JD. Contraction of a perifoveal epiretinal membrane simulating a macular hole. *Am J Ophthalmol*. 1976;82(5):684–691.
87. Atmaca LS, Yilmaz M. Changes in the fundus caused by blunt ocular trauma. *Ann Ophthalmol*. 1993;25(12):447–452.
88. Shakin JL, Yannuzzi LA. Posterior segment manifestations of orbital trauma. *Adv Ophthalmic Plast Reconstr Surg*. 1987;6(115):115–135.
89. Barreau E, Massin P, Paques M, et al. Surgical treatment of post-traumatic macular holes. *J Fr Ophtalmol*. 1997;20(6):423–429.
90. Kusaka S, Fujikado T, Ikeda T, et al. Spontaneous disappearance of traumatic macular holes in young patients. *Am J Ophthalmol*. 1997;123(6):837–839.
91. Parmar DN, Stanga PE, Reck AC, et al. Imaging of a traumatic macular hole with spontaneous closure. *Retina*. 1999;19(5):470–472.
92. Shimada N, Ohno-Matsui K, Yoshida T, et al. Progression from macular retinoschisis to retinal detachment in highly myopic eyes is associated with outer lamellar hole formation. *Br J Ophthalmol*. 2008;92(6):762–764.
93. Coppe AM, Ripandelli G, Parisi V, et al. Prevalence of asymptomatic macular holes in highly myopic eyes. *Ophthalmology*. 2005;112(12):2103–2109.
94. Patel SC, Loo RH, Thompson JT, et al. Macular hole surgery in high myopia. *Ophthalmology*. 2001;108(2):377–380.
95. Okuda T, Higashide T, Kobayashi K, et al. Macular Hole closure over residual subretinal fluid by an inverted internal limiting membrane flap technique in patients with macular hole retinal detachment in high myopia. *Retin Cases*

Brief Rep. 2016;10(2):140–144.
96. Sakarya Y, Sakarya R, Kara S, et al. Giant macular hole in Alport syndrome. *Ophthalmic Genet*. 2011;32(1):64.
97. Georgalas I, Markomichelakis N, Ladas I. Retinal detachment due to a macular hole in a patient with Behçet disease treated with vitrectomy and silicone oil tamponade. *Eur J Ophthalmol*. 2008;18(6):1023–1024.
98. Mehta M, Katsumi O, Tetsuka S, et al. Best's macular dystrophy with a macular hole. *Acta Ophthalmol (Copenh)*. 1991;69(1):131–134.
99. Albini TA, Lakhanpal RR, Foroozan R, et al. Macular hole in cat scratch disease. *Am J Ophthalmol*. 2005;140(1):149–151.
100. Levison AL, Schachat AP. Macular hole from a central retinal artery occlusion. *JAMA Ophthalmol*. 2014;132(12):1493.
101. Chaudhry NA, Flynn HW Jr, Smiddy WE, et al. Macular hole surgery in the presence of prominent macular drusen. *Arch Ophthalmol*. 2000;118(1):131–132.
102. Rajagopal J, Shetty SB, Kamath AG, et al. Macular hole following electrical shock injury. *Canad J Ophthalmol*. 2010;45(2):187–188.
103. Kusaka S, Hayashi N, Ohji M, et al. Macular hole secondary to fungal endophthalmitis. *Arch Ophthalmol*. 2003;121(5):732–733.
104. Petrou P, Patwary S, Banerjee PJ, et al. Bilateral macular hole from a handheld laser pointer. *Lancet*. 2014;383(9930):1780.
105. Thach AB, Lopez PF, Snady-McCoy LC, et al. Accidental Nd:YAG laser injuries to the macula. *Am J Ophthalmol*. 1995;119(6):767–773.
106. Munteanu M, Petrovic Z, Stanca H, et al. Accidental macular hole following neodymium:YAG posterior capsulotomy. *Srp Arh Celok Lek*. 2014;142(7–8):468–471.
107. Uemoto R, Mizuki N. Spontaneous closure of a macular hole caused by a ruptured retinal arterial macroaneurysm. *Eur J Ophthalmol*. 2008;18(3):462–465.
108. Jin ZB, Gan DK, Xu GZ, et al. Macular hole formation in patients with retinitis pigmentosa and prognosis of pars

plana vitrectomy. *Retina*. 2008;28(4):610–614.
109. Sodi A, Bini A, Passerini I, et al. Occurrence of full-thickness macular hole complicating Stargardt disease with ABCR mutation. *Eur J Ophthalmol*. 2006;16(2):335–338.
110. Manschot WA, Von Winning CHOM. Hole in the macula due to syphilis. *Am J Ophthalmol*. 1953;36:261–262.
111. Panos GD, Papageorgiou E, Kozeis N, et al. Macular hole formation after toxoplasmic retinochoroiditis. *BMJ Case Rep*. 2013;2013.
112. Xie ZG, Yu SQ, Chen X, et al. Macular hole secondary to Valsalva retinopathy after doing push-up exercise. *BMC Ophthalmol*. 2014;14:98.
113. Lee SH, Park KH, Kim JH, et al. Secondary macular hole formation after vitrectomy. *Retina*. 2010;30(7):1072–1077.
114. Kobayashi I, Inoue M, Okada AA, et al. Vitreous surgery for macular hole in patients with Vogt–Koyanagi–Harada disease. *Clin Exp Ophthalmol*. 2008;36(9):861–864.
115. Brasil OF, da Cunha AL, de Castro MB, et al. Macular hole secondary to X-linked juvenile retinoschisis. *Ophthalmic Surg Lasers Imaging*. 2011;42 Online:e4–5.
116. Wendel RT, Patel AC, Kelly NE, et al. Vitreous surgery for macular holes. *Ophthalmology*. 1993;100(11):1671–1676.
117. de Bustros S. Early stages of macular holes: to treat or not to treat. *Arch Ophthalmol*. 1990;108(8):1085–1086.
118. Philippakis E. The development and evolution of full thickness macular hole in highly myopic eyes. *Invest Ophthalmol Vis Sci*. 2015.
119. Privat E, Tadayoni R, Gaucher D, et al. Residual defect in the foveal photoreceptor layer detected by optical coherence tomography in eyes with spontaneously closed macular holes. *Am J Ophthalmol*. 2007;143(5):814–819.
120. Dugel PU, MIVI-TRUST Study Group. A single injection of ocriplasmin for the treatment of symptomatic vitreomacular adhesion (sVMA): results of the phase III MIVI-TRUST Program. *Invest Ophthalmol Vis Sci*. 2011;52(6):6628.
121. Berger JW, Brucker AJ. The magnitude of the bubble buoyant pressure: implications for macular hole surgery. *Retina*. 1998;18(1):84–86 [discussion 6-8].

122. Funata M, Wendel RT, de la Cruz Z, et al. Clinicopathologic study of bilateral macular holes treated with pars plana vitrectomy and gas tamponade. *Retina*. 1992;12(4):289–298.
123. Madreperla SA, Geiger GL, Funata M, et al. Clinicopathologic correlation of a macular hole treated by cortical vitreous peeling and gas tamponade. *Ophthalmology*. 1994;101(4):682–686.
124. Rosa RH Jr, Glaser BM, de la Cruz Z, et al. Clinicopathologic correlation of an untreated macular hole and a macular hole treated by vitrectomy, transforming growth factor-beta 2, and gas tamponade. *Am J Ophthalmol*. 1996;122(6):853–863.
125. Yamana T, Kita M, Ozaki S, et al. The process of closure of experimental retinal holes in rabbit eyes. *Graefes Arch Clin Exp Ophthalmol*. 2000;238(1):81–87.
126. Jumper JM, Gallemore RP, McCuen BW, et al. Features of macular hole closure in the early postoperative period using optical coherence tomography. *Retina*. 2000;20(3):232–237.
127. Masuyama K, Yamakiri K, Arimura N, et al. Posturing time after macular hole surgery modified by optical coherence tomography images: a pilot study. *Am J Ophthalmol*. 2009;147(3) [481–8.e2].
128. Sato H, Kawasaki R, Yamashita H. Observation of idiopathic full-thickness macular hole closure in early postoperative period as evaluated by optical coherence tomography. *Am J Ophthalmol*. 2003;136(1):185–187.
129. Kikushima W, Imai A, Toriyama Y, et al. Dynamics of macular hole closure in gas-filled eyes within 24 h of surgery observed with swept source optical coherence tomography. *Ophthalmic Res*. 2014;53(1):48–54.
130. Smiddy WE, Michels RG, de Bustros S, et al. Histopathology of tissue removed during vitrectomy for impending idiopathic macular holes. *Am J Ophthalmol*. 1989;108(4):360–364.
131. Han DP, Abrams GW, Aaberg TM. Surgical excision of the attached posterior hyaloid. *Arch Ophthalmol*. 1988;106(7):998–1000.
132. Gaudric A, Massin P, Qinyuan C. An aspirating forceps to

remove the posterior hyaloid in the surgery of full-thickness macular holes. *Retina*. 1996;16(3):261–263.
133. Guillaubey A, Malvitte L, Lafontaine PO, et al. Incidence of retinal detachment after macular surgery: a retrospective study of 634 cases. *Br J Ophthalmol*. 2007;91(10):1327–1330.
134. Yagi F, Takagi S, Tomita G. Incidence and causes of iatrogenic retinal breaks in idiopathic macular hole and epiretinal membrane. *Semin Ophthalmol*. 2014;29(2):66–69.
135. Eckardt C, Eckardt U, Groos S, et al. Removal of the internal limiting membrane in macular holes. Clinical and morphological findings. *Ophthalmologe*. 1997;94(8):545–551.
136. Park DW, Lee JH, Min WK. The use of internal limiting membrane maculorrhexis in treatment of idiopathic macular holes. *Korean J Ophthalmol*. 1998;12(2):92–97.
137. Hirakata A, Inoue M, Oshitari K, et al. Histopathological examination of internal limiting membrane surface after scraping with diamond-dusted membrane scraper. *Acta Ophthalmol*. 2010;88(7):e293–4.
138. Mahajan VB, Chin EK, Tarantola RM, et al. Macular hole closure with internal limiting membrane abrasion technique. *JAMA Ophthalmol*. 2015;133(6):635–641.
139. Kuhn F, Mester V, Berta A. The Tano diamond dusted membrane scraper: indications and contraindications. *Acta Ophthalmol Scand*. 1998;76(6):754–755.
140. Steel DH, Dinah C, Habib M, et al. ILM peeling technique influences the degree of a dissociated optic nerve fibre layer appearance after macular hole surgery. *Graefes Arch Clin Exp Ophthalmol*. 2015;253(5):691–698.
141. Michalewska Z, Michalewski J, Adelman RA, et al. Inverted internal limiting membrane flap technique for large macular holes. *Ophthalmology*. 2010;117(10):2018–2025.
142. Michalewska Z, Michalewski J, Dulczewska-Cichecka K, et al. Temporal inverted internal limiting membrane flap technique versus classic inverted internal limiting membrane flap technique: a comparative study. *Retina*. 2015;35(9):1844–1850.
143. Rodrigues EB, Meyer CH, Mennel S, et al. Mechanisms of intravitreal toxicity of indocyanine green dye: implications

for chromovitrectomy. *Retina*. 2007;27(7):958–970.
144. Kadonosono K, Itoh N, Uchio E, et al. Staining of internal limiting membrane in macular hole surgery. *Arch Ophthalmol*. 2000;118(8):1116–1118.
145. Engelbrecht NE, Freeman J, Sternberg P, et al. Retinal pigment epithelial changes after macular hole surgery with indocyanine green-assisted internal limiting membrane peeling. *Am J Ophthalmol*. 2002;133(1):89–94.
146. Rodrigues EB, Meyer CH. Meta-analysis of chromovitrectomy with indocyanine green in macular hole surgery. *Ophthalmologica*. 2008;222(2):123–129.
147. Stalmans P, Van Aken EH, Veckeneer M, et al. Toxic effect of indocyanine green on retinal pigment epithelium related to osmotic effects of the solvent. *Am J Ophthalmol*. 2002;134(2):282–285.
148. Haritoglou C, Gandorfer A, Gass CA, et al. Histology of the vitreoretinal interface after staining of the internal limiting membrane using glucose 5% diluted indocyanine and infracyanine green. *Am J Ophthalmol*. 2004;137(2):345–348.
149. Weinberger AW, Kirchhof B, Mazinani BE, et al. Persistent indocyanine green (ICG) fluorescence 6 weeks after intraocular ICG administration for macular hole surgery. *Graefes Arch Clin Exp Ophthalmol*. 2001;239(5):388–390.
150. Tadayoni R, Paques M, Girmens JF, et al. Persistence of fundus fluorescence after use of indocyanine green for macular surgery. *Ophthalmology*. 2003;110(3):604–608.
151. Paques M, Genevois O, Regnier A, et al. Axon-tracing properties of indocyanine green. *Arch Ophthalmol*. 2003;121(3):367–370.
152. Yip HK, Lai TY, So KF, et al. Retinal ganglion cells toxicity caused by photosensitising effects of intravitreal indocyanine green with illumination in rat eyes. *Br J Ophthalmol*. 2006;90(1):99–102.
153. Lesnik Oberstein SY, de Smet MD. Use of heavy Trypan blue in macular hole surgery. *Eye*. 2010;24(7):1177–1181.
154. Costa Ede P, Rodrigues EB, Farah ME, et al. Vital dyes and light sources for chromovitrectomy: comparative assessment of osmolarity, pH, and spectrophotometry.

Invest Ophthalmol Vis Sci. 2009;50(1):385–391.
155. Mohr A, Bruinsma M, Oellerich S, et al. Dyes for eyes: hydrodynamics, biocompatibility and efficacy of 'heavy' (dual) dyes for chromovitrectomy. *Ophthalmologica*. 2013;230(Suppl. 2):51–58.
156. Grisanti S, Szurman P, Tatar O, et al. Histopathological analysis in experimental macular surgery with trypan blue. *Br J Ophthalmol*. 2004;88(9):1206–1208.
157. Enaida H, Hisatomi T, Hata Y, et al. Brilliant blue G selectively stains the internal limiting membrane/brilliant blue G-assisted membrane peeling. *Retina*. 2006;26(6):631–636.
158. Rodrigues EB, Costa EF, Penha FM, et al. The use of vital dyes in ocular surgery. *Surv Ophthalmol*. 2009;54(5):576–617.
159. Farah ME, Maia M, Rodrigues EB. Dyes in ocular surgery: principles for use in chromovitrectomy. *Am J Ophthalmol*. 2009;148(3):332–340.
160. Goldbaum MH, McCuen BW, Hanneken AM, et al. Silicone oil tamponade to seal macular holes without position restrictions. *Ophthalmology*. 1998;105(11):2140–2147 [discussion 7-8].
161. Lappas A, Heinrich Foerster AM, Kirchhof B. Use of heavy silicone oil (Densiron-68) in the treatment of persistent macular holes. *Acta Ophthalmol*. 2009;87(8):866–870.
162. Saeed MU, Heimann H, Wong D, et al. Heavy silicone oil tamponade after failed macular hole surgery with perfluoropropane (C3F8): a report of five cases. *Graefes Arch Clin Exp Ophthalmol*. 2009;247(5):707–709.
163. Schurmans A, Van Calster J, Stalmans P. Macular hole surgery with inner limiting membrane peeling, endodrainage, and heavy silicone oil tamponade. *Am J Ophthalmol*. 2009;147(3):495–500.
164. Karia N, Laidlaw A, West J, et al. Macular hole surgery using silicone oil tamponade. *Br J Ophthalmol*. 2001;85(11):1320–1323.
165. Lai JC, Stinnett SS, McCuen BW. Comparison of silicone oil versus gas tamponade in the treatment of idiopathic full-thickness macular hole. *Ophthalmology*. 2003;110(6):1170–

1174.
166. Tafoya ME, Lambert HM, Vu L, et al. Visual outcomes of silicone oil versus gas tamponade for macular hole surgery. *Semin Ophthalmol*. 2003;18(3):127–131.
167. Gaudric A. Macula hole surgery: simple or complex? *Am J Ophthalmol*. 2009;147(3):381–383.
168. Glaser BM, Michels RG, Kuppermann BD, et al. Transforming growth factor-beta 2 for the treatment of full-thickness macular holes: a prospective randomized study. *Ophthalmology*. 1992;99(7):1162–1172.
169. Thompson JT, Smiddy WE, Williams GA, et al. Comparison of recombinant transforming growth factor-beta-2 and placebo as an adjunctive agent for macular hole surgery. *Ophthalmology*. 1998;105(4):700–706.
170. Ezra E, Gregor ZJ. Surgery for idiopathic full-thickness macular hole: two-year results of a randomized clinical trial comparing natural history, vitrectomy, and vitrectomy plus autologous serum: Morfields Macular Hole Study Group RAeport no. 1. *Arch Ophthalmol*. 2004;122(2):224–236.
171. Paques M, Chastang C, Mathis A, et al. Effect of autologous platelet concentrate in surgery for idiopathic macular hole: results of a multicenter, double-masked, randomized trial. Platelets in Macular Hole Surgery Group. *Ophthalmology*. 1999;106(5):932–938.
172. Lai CC, Chen YP, Wang NK, et al. Vitrectomy with internal limiting membrane repositioning and autologous blood for macular hole retinal detachment in highly myopic eyes. *Ophthalmology*. 2015;122(9):1889–1898.
173. Kapoor KG, Khan AN, Tieu BC, et al. Revisiting autologous platelets as an adjuvant in macular hole repair: chronic macular holes without prone positioning. *Ophthalmic Surg Lasers Imaging*. 2012;43(4):291–295.
174. Carter JB, Michels RG, Glaser BM, et al. Iatrogenic retinal breaks complicating pars plana vitrectomy. *Ophthalmology*. 1990;97(7):848–853 [discussion 54].
175. Chung SE, Kim KH, Kang SW. Retinal breaks associated with the induction of posterior vitreous detachment. *Am J Ophthalmol*. 2009;147(6):1012–1016.

176. Scartozzi R, Bessa AS, Gupta OP, et al. Intraoperative sclerotomy-related retinal breaks for macular surgery, 20- vs 25-gauge vitrectomy systems. *Am J Ophthalmol*. 2007;143(1):155–156.
177. Tornambe PE, Poliner LS, Grote K. Macular hole surgery without face-down positioning: a pilot study. *Retina*. 1997;17(3):179–185.
178. Hu Z, Xie P, Ding Y, et al. Face-down or no face-down posturing following macular hole surgery: a meta-analysis. *Acta Ophthalmol*. 2016;94(4):326–333.
179. Solebo AL, Lange CA, Bunce C, et al. Face-down positioning or posturing after macular hole surgery. The Cochrane Library. *Cochrane Database Syst Rev*. 2011;(12) [CD008228].
180. Freeman WR, Azen SP, Kim JW, et al. Vitrectomy for the treatment of full-thickness stage 3 or 4 macular holes. Results of a multicentered randomized clinical trial. The Vitrectomy for Treatment of Macular Hole Study Group. *Arch Ophthalmol*. 1997;115(1):11–21.
181. Guillaubey A, Malvitte L, Lafontaine PO, et al. Comparison of face-down and seated position after idiopathic macular hole surgery: a randomized clinical trial. *Am J Ophthalmol*. 2008;146(1):128–134.
182. American Academy of Ophthalmology Retina Vitreous Panel. *Idiopathic macular hole*. Preferred Practice Pattern Guidelines. 2014.
183. Ip MS, Baker BJ, Duker JS, et al. Anatomical outcomes of surgery for idiopathic macular hole as determined by optical coherence tomography. *Arch Ophthalmol*. 2002;120(1):29–35.
184. Ullrich S, Haritoglou C, Gass C, et al. Macular hole size as a prognostic factor in macular hole surgery. *Br J Ophthalmol*. 2002;86(4):390–393.
185. Rice T. Internal limiting membrane removal in surgery for full-thickness macular holes. Madreparia SM. *Macular hole pathogenesis diagnosis and treatment*. Butterworth Heinemann: Boston; 1999:125–146.
186. Brooks HLJ. Macular hole surgery with and without

internal limiting membrane peeling. *Ophthalmology*. 2000;107(10):1939–1948 [discussion 48-9].
187. Haritoglou C, Gass CA, Schaumberger M, et al. Macular changes after peeling of the internal limiting membrane in macular hole surgery. *Am J Ophthalmol*. 2001;132(3):363–368.
188. Sheidow TG, Blinder KJ, Holekamp N, et al. Outcome results in macular hole surgery: an evaluation of internal limiting membrane peeling with and without indocyanine green. *Ophthalmology*. 2003;110(9):1697–1701.
189. Kumagai K, Furukawa M, Ogino N, et al. Vitreous surgery with and without internal limiting membrane peeling for macular hole repair. *Retina*. 2004;24(5):721–727.
190. Tognetto D, Grandin R, Sanguinetti G, et al. Internal limiting membrane removal during macular hole surgery: results of a multicenter retrospective study. *Ophthalmology*. 2006;113(8):1401–1410.
191. Kwok AK, Lai TY, Wong VW. Idiopathic macular hole surgery in Chinese patients: a randomised study to compare indocyanine green-assisted internal limiting membrane peeling with no internal limiting membrane peeling. *Hong Kong Med J*. 2005;11(4):259–266.
192. Christensen UC, Kroyer K, Sander B, et al. Value of internal limiting membrane peeling in surgery for idiopathic macular hole stage 2 and 3: a randomised clinical trial. *Br J Ophthalmol*. 2009;93(8):1005–1015.
193. Lois N, Burr J, Norrie J, et al. Internal limiting membrane peeling versus no peeling for idiopathic full-thickness macular hole: a pragmatic randomized controlled trial. *Invest Ophthalmol Vis Sci*. 2011;52(3):1586–1592.
194. Tadayoni R, Creuzot-Garcher C, Korobelnik J-F, et al. Internal limiting membrane peeling for large macular holes: a randomized, multicentric, and controlled clinical trial. *Invest Ophthalmol Vis Sci*. 2009;50(5):5206.
195. Yamashita T, Sakamoto T, Yamashita T, et al. Individualized, spectral domain-optical coherence tomography-guided facedown posturing after macular hole surgery: minimizing treatment burden and maximizing outcome. *Retina*. 2014;34(7):1367–1375.

196. Scott IU, Moraczewski AL, Smiddy WE, et al. Long-term anatomic and visual acuity outcomes after initial anatomic success with macular hole surgery. *Am J Ophthalmol*. 2003;135(5):633–640.
197. Haritoglou C, Gass CA, Schaumberger M, et al. Long-term follow-up after macular hole surgery with internal limiting membrane peeling. *Am J Ophthalmol*. 2002;134(5):661–666.
198. Purtskhvanidze K, Treumer F, Junge O, et al. The long-term course of functional and anatomical recovery after macular hole surgery. *Invest Ophthalmol Vis Sci*. 2013;54(7):4882–4891.
199. Bonnabel A, Bron AM, Isaico R, et al. Long-term anatomical and functional outcomes of idiopathic macular hole surgery: the yield of spectral-domain OCT combined with microperimetry. *Graefes Arch Clin Exp Ophthalmol*. 2013;251(11):2505–2511.
200. Scupola A, Mastrocola A, Sasso P, et al. Assessment of retinal function before and after idiopathic macular hole surgery. *Am J Ophthalmol*. 2013;156(1) [132–9.e1].
201. Guez JE, Le Gargasson JF, Massin P, et al. Functional assessment of macular hole surgery by scanning laser ophthalmoscopy. *Ophthalmology*. 1998;105(4):694–699.
202. Haritoglou C, Ehrt O, Gass CA, et al. Paracentral scotomata: a new finding after vitrectomy for idiopathic macular hole. *Br J Ophthalmol*. 2001;85(2):231–233.
203. Tarita-Nistor L, Gonzalez EG, Mandelcorn MS, et al. Fixation stability, fixation location, and visual acuity after successful macular hole surgery. *Invest Ophthalmol Vis Sci*. 2009;50(1):84–89.
204. Ryan EH Jr, Gilbert HD. Results of surgical treatment of recent-onset full-thickness idiopathic macular holes. *Arch Ophthalmol*. 1994;112(12):1545–1553.
205. Kang SW, Ahn K, Ham DI. Types of macular hole closure and their clinical implications. *Br J Ophthalmol*. 2003;87(8):1015–1019.
206. Scott RA, Ezra E, West JF, Gregor ZJ. Visual and anatomical results of surgery for long standing macular holes. *Br J Ophthalmol*. 2000;84(2):150–153.

207. Villate N, Lee JE, Venkatraman A, et al. Photoreceptor layer features in eyes with closed macular holes: optical coherence tomography findings and correlation with visual outcomes. *Am J Ophthalmol*. 2005;139(2):280–289.
208. Christensen UC, Kroyer K, Sander B, et al. Prognostic significance of delayed structural recovery after macular hole surgery. *Ophthalmology*. 2009;116(12):2430–2436.
209. Itoh Y, Inoue M, Rii T, et al. Correlation between length of foveal cone outer segment tips line defect and visual acuity after macular hole closure. *Ophthalmology*. 2012;119(7):1438–1446.
210. Chawla A, Barua A, Patton N. Long-term structural and functional outcomes after macular hole surgery. *Retina*. 2016;36(2):321–324.
211. Ruiz-Moreno JM, Arias L, Araiz J, et al. Spectral-domain optical coherence tomography study of macular structure as prognostic and determining factor for macular hole surgery outcome. *Retina*. 2013;33(6):1117–1122.
212. Chang YC, Lin WN, Chen KJ, et al. Correlation between the dynamic postoperative visual outcome and the restoration of foveal microstructures after macular hole surgery. *Am J Ophthalmol*. 2015;160(1) [100–6.e1].
213. Mochizuki N, Yamamoto T, Enaida H, et al. Long-term outcomes of 3 surgical adjuvants used for internal limiting membrane peeling in idiopathic macular hole surgery. *Jpn J Ophthalmol*. 2014;58(6):455–461.
214. Machida S, Toba Y, Nishimura T, et al. Comparisons of cone electroretinograms after indocyanine green-, brilliant blue G-, or triamcinolone acetonide-assisted macular hole surgery. *Graefes Arch Clin Exp Ophthalmol*. 2014;252(9):1423–1433.
215. Williamson TH, Lee E. Idiopathic macular hole: analysis of visual outcomes and the use of indocyanine green or brilliant blue for internal limiting membrane peel. Graefes Arch Clin Exp Ophthalmol. *Graefes Arch Clin Exp Ophthalmol*. 2014;252(3):395–400.
216. Wu Y, Zhu W, Xu D, et al. Indocyanine green-assisted internal limiting membrane peeling in macular hole

surgery: a meta-analysis. *PLoS ONE*. 2012;7(11):e48405.
217. Park SS, Marcus DM, Duker JS, et al. Posterior segment complications after vitrectomy for macular hole. *Ophthalmology*. 1995;102(5):775–781.
218. Parravano M, Giansanti F, Eandi CM, et al. Vitrectomy for idiopathic macular hole. *Cochrane Database Syst Rev*. 2015;(5) [CD009080].
219. Rizzo S, Belting C, Genovesi-Ebert F, et al. Incidence of retinal detachment after small-incision, sutureless pars plana vitrectomy compared with conventional 20-gauge vitrectomy in macular hole and epiretinal membrane surgery. *Retina*. 2010;30(7):1065–1071.
220. Tabandeh H, Chaudhry NA, Smiddy WE. Retinal detachment associated with macular hole surgery: characteristics, mechanism, and outcomes. *Retina*. 1999;19(4):281–286.
221. Tadayoni R, Paques M, Massin P, et al. Dissociated optic nerve fiber layer appearance of the fundus after idiopathic epiretinal membrane removal. *Ophthalmology*. 2001;108(12):2279–2283.
222. Mitamura Y, Suzuki T, Kinoshita T, et al. Optical coherence tomographic findings of dissociated optic nerve fiber layer appearance. *Am J Ophthalmol*. 2004;137(6):1155–1156.
223. Kishimoto H, Kusuhara S, Matsumiya W, et al. Retinal surface imaging provided by Cirrus high-definition optical coherence tomography prominently visualizes a dissociated optic nerve fiber layer appearance after macular hole surgery. *Int Ophthalmol*. 2011;31(5):385–392.
224. Spaide RF. "Dissociated optic nerve fiber layer appearance" after internal limiting membrane removal is inner retinal dimpling. *Retina*. 2012;32(9):1719–1726.
225. Baba T, Yamamoto S, Kimoto R, et al. Reduction of thickness of ganglion cell complex after internal limiting membrane peeling during vitrectomy for idiopathic macular hole. *Eye (Lond)*. 2012;26(9):1173–1180.
226. Tadayoni R, Svorenova I, Erginay A, et al. Decreased retinal sensitivity after internal limiting membrane peeling for macular hole surgery. *Br J Ophthalmol*. 2012;96(12):1513–

1516.
227. Imai H, Ohta K. Microperimetric determination of retinal sensitivity in areas of dissociated optic nerve fiber layer following internal limiting membrane peeling. *Jpn J Ophthalmol*. 2010;54(5):435–440.
228. Seo KH, Yu SY, Kwak HW. Topographic changes in macular ganglion cell-inner plexiform layer thickness after vitrectomy with indocyanine green-guided internal limiting membrane peeling for idiopathic macular hole. *Retina*. 2015;35(9):1828–1835.
229. Sevim MS, Sanisoglu H. Analysis of retinal ganglion cell complex thickness after Brilliant Blue-assisted vitrectomy for idiopathic macular holes. *Curr Eye Res*. 2013;38(1):180–184.
230. Melberg NS, Thomas MA. Visual field loss after pars plana vitrectomy with air/fluid exchange. *Am J Ophthalmol*. 1995;120(3):386–388.
231. Ezra E, Arden GB, Riordan-Eva P, et al. Visual field loss following vitrectomy for stage 2 and 3 macular holes. *Br J Ophthalmol*. 1996;80(6):519–525.
232. Welch JC. Dehydration injury as a possible cause of visual field defect after pars plana vitrectomy for macular hole. *Am J Ophthalmol*. 1997;124(5):698–699.
233. Paques M, Massin P, Santiago PY, et al. Visual field loss after vitrectomy for full-thickness macular holes. *Am J Ophthalmol*. 1997;124(1):88–94.
234. Gass CA, Haritoglou C, Messmer EM, et al. Peripheral visual field defects after macular hole surgery: a complication with decreasing incidence. *Br J Ophthalmol*. 2001;85(5):549–551.
235. Paques M, Massin P, Santiago PY, et al. Late reopening of successfully treated macular holes. *Br J Ophthalmol*. 1997;81(8):658–662.
236. Christmas NJ, Smiddy WE, Flynn HW Jr. Reopening of macular holes after initially successful repair. *Ophthalmology*. 1998;105(10):1835–1838.
237. Passemard M, Yakoubi Y, Muselier A, et al. Long-term outcome of idiopathic macular hole surgery. *Am J*

Ophthalmol. 2010;149(1):120–126.
238. Rahimy E, McCannel CA. Impact of internal limiting membrane peeling on macular hole reopening: a systematic review and meta-analysis. *Retina*. 2016;36(4):679–687.
239. Leonard RE 2nd, Smiddy WE, Flynn HW Jr, et al. Long-term visual outcomes in patients with successful macular hole surgery. *Ophthalmology*. 1997;104(10):1648–1652.
240. Muselier A, Dugas B, Burelle X, et al. Macular hole surgery and cataract extraction: combined vs consecutive surgery. *Am J Ophthalmol*. 2010;150(3):387–391.
241. de Smet MD, Gandorfer A, Stalmans P, et al. Microplasmin intravitreal administration in patients with vitreomacular traction scheduled for vitrectomy: the MIVI I trial. *Ophthalmology*. 2009;116(7):1349–1355 [1355.e1–2].

122

Surgical Management of Choroidal Neovascularization and Subretinal Hemorrhage

Enchun M. Liu, Mathew W. Aschbrenner, Matthew A. Thomas

Choroidal Neovascular Membranes

Introduction

The growth of choroidal neovascular membranes (CNV) beneath the macula usually causes significant disturbance of central visual function. Prior to the advent of photodynamic therapy and anti-vascular endothelial growth factor (anti-VEGF) agents, the only therapy of proven benefit compared with observation was thermal photocoagulation of the CNV.[1] During that era, surgical removal of subfoveal CNV of various etiologies was an alternative method of eradicating the CNV and improved visual function was achieved in a variety of etiologic settings. Even with current anti-VEGF agents, on occasion extensive submacular hemorrhage (SMH) occurs and surgical intervention may be warranted (Fig. 122.1A). Rarely, surgical removal of CNV without hemorrhage is indicated. This chapter presents current concepts regarding the use of vitreoretinal

surgical techniques as treatment of CNV with or without SMH.

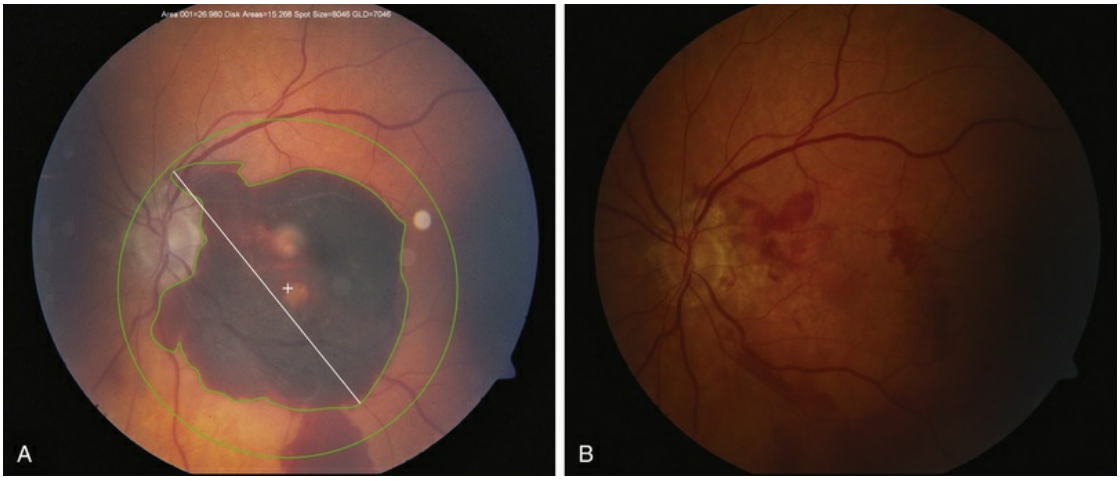

FIG. 122.1 (A) Thick fovea-involving submacular hemorrhage of 1-day duration in the left eye of an 82-year-old man with exudative macular degeneration who was treated with vitrectomy, subretinal tPA, and sulfur hexafluoride pneumatic displacement. Color fundus photograph on the day of presentation; visual acuity was 3/200, and the area of the hemorrhage was 26.98 mm^2. (B) Color fundus photograph at 2 weeks after surgery with complete displacement of hemorrhage inferiorly. Visual acuity was 20/400 at postoperative month 1 and 20/80 at 1 year postoperatively after two total anti-VEGF injections.

Surgical Technique

De Juan and Machemer first reported vitrectomy for the removal of macular CNV through large temporal retinal incisions.[2] Thomas and Kaplan subsequently modified the technique to utilize an eccentric, small retinotomy. Fluid was injected through the retinotomy, and manipulation and extraction of the CNV were achieved.[3,4] Face-down positioning overnight proved adequate to close the small retinotomies without laser photocoagulation.[5] Complications with this technique were minimal.

Early Results

These surgical techniques were applied to macular CNV, and favorable visual outcomes were reported for CNV of a variety of etiologies.[6–17] It was soon recognized that although some eyes regained excellent central visual function following removal of subfoveal CNV, others did not. Gass hypothesized that some CNV proliferate within Bruch's membrane and beneath the retinal pigment epithelium (RPE), as well as beneath the neurosensory retina (type I CNV – typical of AMD). Removal of such CNV would be expected to leave defects in the RPE and thus poor vision. In other eyes, he postulated that CNV grow through relatively discrete defects in Bruch's membrane and proliferate anterior to native RPE in the subneurosensory retinal space (type II CNV – typical of presumed ocular histoplasmosis syndrome [POHS]).[18] Eyes with CNV associated with POHS, other chorioretinal inflammatory conditions, and idiopathic CNV indeed often demonstrate preserved central RPE and good foveal function after surgical extraction. Eccentricity of the choroidal ingrowth site was found to be an important prognostic factor for good vision in these cases with focal ingrowth sites.[19] Recurrent CNV proved to be a major obstacle to good vision following surgery, as is the case with essentially all other therapies for choroidal neovascularization.[20]

Submacular Surgery Trials

The Submacular Surgery Trials (SST) were four NIH-sponsored, multicenter, randomized, prospective trials conducted to compare outcomes of submacular surgery versus then-current standard therapy.[21] The SST Pilot Trial found no advantage to surgery over laser photocoagulation for recurrent choroidal neovascularization secondary to age-related macular degeneration (AMD).[22]

The SST Group N enrolled 454 patients with new subfoveal choroidal neovascularization secondary to AMD and randomly assigned patients to surgery or observation. Both groups declined in visual acuity (VA) from 20/100 at baseline to 20/400 by month 24, and the investigators concluded that surgery should not be recommended for these patients.[23]

The SST Group H enrolled 225 patients, 18 years or older with new or recurrent subfoveal choroidal neovascularization that was

either idiopathic or associated with POHS. At all time points, median VA was better in the surgery group than in the observation group, but the difference did not reach statistical significance. At 24 months, median VA was 20/250 for observation eyes and 20/160 for surgery eyes. Only those eyes with acuity worse than 20/100 at baseline achieved a significantly better outcome with surgery than observation at 24 months. The study concluded that submacular surgery may be considered in similar eyes with poor vision (worse than 20/100).[24]

Current Indications for Surgical Removal of CNV

In the era of anti-VEGF therapy, surgical removal of CNV is rarely necessary. Possible indications would include large peripapillary CNV unresponsive to anti-VEGF agents and/or photodynamic therapy and too large for thermal laser photocoagulation.[25] In such extrafoveal lesions, the CNV can be removed to produce a small, quiet, atrophic scar around the nerve. If the fovea is involved in the neovascular process, then surgical extraction results in loss of foveal RPE and a poor visual outcome. However, in CNV due to POHS, central RPE and reasonable VA may be preserved.[26–31]

Submacular Hemorrhage

Introduction

Subretinal hemorrhage, defined as blood located in the potential space between the neurosensory retina and the RPE, is a common manifestation of several diseases of the retina and choroid. The natural history of untreated, thick SMH is generally poor due to a combination of iron toxicity, blockage of nutrient exchange between photoreceptors and the RPE, and mechanical shearing forces of clot retraction.[32] Over the past two decades, a variety of treatment options have been proposed for the treatment of fovea-involving SMH. However, data from large randomized comparative studies are lacking, and the ideal management of SMH remains controversial.

Etiology

Subretinal hemorrhage involving the macula is most often caused by CNV. Therefore any macular condition that causes growth of CNV can lead to SMH. In a series of 47 consecutive cases of SMH reported by Ibanez et al., over 80% of cases were due to AMD. The remainder of cases were due to CNV from POHS, angioid streaks, and idiopathic SMH.[33] Pathologic myopia and polypoidal choroidal vasculopathy (PCV) have also been reported as causes of SMH.[34,35] Trauma is another possible cause of SMH, and this may occur either at the time of trauma due to localized choroidal rupture or remotely due to the development of CNV at the edge of the rupture site.[36] Aside from ruptured retinal arterial macroaneurysms, other non-CNV related sources of subretinal hemorrhage in the macula are rare.

Natural History

The natural history of untreated SMH has been described by several authors. Bennet et al.[36] described 29 eyes with SMH and found that the etiology was the most important factor in predicting the final visual outcome. In this series of 12 patients with AMD as the cause of the hemorrhage, 67% of the patients had unimproved or worsened VA at the end of the follow-up period. The final mean VA was 20/1700. Another study, by Scupola et al.,[37] examined 60 eyes with SMH due to AMD and confirmed this poor prognosis, with 80% of the eyes having a worse mean VA of 20/1250. In contrast to this, in Bennet's series, the five patients with traumatic choroidal rupture with SMH fared much better. All five eyes improved, with mean VA of 20/35.[36] Likewise, in a case series of 11 patients with SMH due to Best disease, 10 of the 11 patients experienced improvement, with a final mean VA of 20/50.[38]

The largest natural history study of AMD-associated SMH to date is the observation arm of the Submacular Surgery Trials Group B in which 168 eyes with subfoveal choroidal neovascular lesions composed of at least 50% blood involving the foveal center and with initial VA between 20/100 and light perception (LP) were followed for 2–3 years. Only 19% of eyes gained 2 or more lines of vision during follow-up, while loss of 2 or more lines occurred in

59%, and 36% experienced severe vision loss of 6 lines or more. At 2 years, only 10% of eyes had VA of 20/200 or better.[39]

These natural history studies demonstrate that thicker hemorrhages portend a poorer prognosis due to scar tissue formation and photoreceptor loss and are less likely to clear spontaneously. Duration of the SMH is also an important factor, and most studies recommend intervention within the first 2 weeks, if intervention is undertaken. In the rabbit eye, Glatt and Machemer demonstrated that subretinal blood caused irreversible photoreceptor loss in less than 24 hours.[40] In this animal model, severe damage to the outer retina was seen at 7 days, with scant photoreceptors detected on electron microscopy, and the photoreceptor and outer nuclear layers were completely absent at 2 weeks after injection of autologous blood into the subretinal space.

Management Options

Given the generally poor natural history of SMH, especially when caused by AMD, various treatment modalities have been explored.

Surgical Removal of Blood and CNV

Although small retrospective reviews of surgical extraction of clots and associated CNV appeared encouraging compared to the poor natural history of SMH, these early attempts were limited by intraoperative and postoperative complications, including retinal detachment, proliferative vitreoretinopathy (PVR), and recurrent hemorrhage.[33,39,41–43] The SST Group B was a randomized, prospective, multicenter trial comparing surgical extraction of the clot and CNV to observation for patients with hemorrhagic lesions (AMD-associated lesions >3.5 MPS [Macular Photocoagulation Study] disc areas in size in which blood comprised >50% of the lesion).[39] Surgery entailed vitrectomy, optional use of subretinal tissue plasminogen activator, and manual extraction of the clot and any apparent CNV beneath the foveal center through a single retinotomy. Of 168 eyes randomized to surgery, only 18% had VA of 20/200 or better after 2 years and there was no statistically significant difference between the surgery and observation arms in terms of stabilization of vision at any point during 24–36 months'

follow-up. However, at 2 years, fewer surgery eyes (21%) compared with observation eyes (36%) had experienced severe vision loss of 6 lines or more (p=.004). This benefit of surgery was most evident in eyes with relatively better vision at presentation (20/100 to 20/160). A high rate of retinal detachment was seen in the surgical arm (16% of all eyes), and these were more common in eyes with very poor vision and very large hemorrhagic lesions on presentation. Progression of cataract was the most common complication of surgery. The study concluded that surgical removal of hemorrhagic AMD lesions was generally not beneficial, although the data would support considering the procedure for lesions that were neither very large nor had very poor vision.[39]

Vitrectomy, Injection of Subretinal Tissue Plasminogen Activator, and Aspiration of Liquefied Blood

The disappointing results obtained with direct surgical extraction of clot led investigators to study possible adjuvants to assist in the removal of subretinal blood. Experimental models of subretinal hemorrhage in animals suggested that the subretinal injection of tissue plasminogen activator (tPA) was safe in doses up to 50 μg/mL.[44] Proponents of subretinal tPA injection hypothesized that it could decrease the thickness of hemorrhage,[45] improve the rate of clearance,[44] and potentially reduce outer retinal damage during surgical removal of subretinal clots.[46]

In 1991, Peyman et al. first reported their experience with five patients treated for SMH using a standard pars plana vitrectomy, followed by tPA (12.5 μg/mL) injected into the subretinal space. After dissolution of the clot, the subretinal hemorrhage was removed with presumed minimal trauma via gentle irrigation of balanced salt solution.[41] Despite this approach, VA results in cases of AMD were disappointing. In 1994, Lew[42] published a pilot study involving 24 consecutive eyes with recent SMH secondary to AMD treated with tPA followed by surgical drainage. This study demonstrated improved final visual outcome when causative CNV was eccentric to the fovea. Factors predictive of good postoperative VA in this study included duration of hemorrhage <7 days, hemorrhage limited to the temporal arcades, and the absence of sub-RPE hemorrhage. In 1995, Lim et al.[43] reported retrospectively

18 patients managed with a similar surgical technique and final VA improved 2 or more lines in only 28% of patients.

Intravitreal Tissue Plasminogen Activator With Pneumatic Displacement

In 1997, Heriot initially described a novel method for the management of SMH using intravitreal tPA injection and pneumatic displacement of blood.[47] The potential benefits of this treatment modality are that it is minimally invasive and can be performed in the office.

Hesse et al. reported their experience with this technique in 11 eyes with SMH due to AMD.[48] The method described by these investigators involved intravitreal injection of 50 μg or 100 μg of tPA and injection of a long-acting gas bubble (C_3F_8 or SF_6), either immediately or 24 hours after the tPA injection, followed by 24-hour face-down positioning. A typical clinical outcome with this technique was partial but not total displacement of SMH, leading to asymptomatic exudative inferior retinal detachment. Complications included breakthrough vitreous hemorrhage, which occurred in all four eyes treated with 100 μg of tPA and only one of the seven eyes (14.3%) treated with the 50 μg dose.[48] Hassan et al. reported similar results in their case series of 15 patients, with 10 of 15 patients having improved final VA. Vitreous hemorrhage was the common complication, and there was one case of postoperative endophthalmitis in this group.[49] In a large series of 43 consecutive eyes treated with this in-office technique, Hattenbach et al. found that 30% of eyes gained 2 or more lines of VA at the final visit and that SMHs of ≤14 days duration had the most favorable outcomes.[50]

Animal models show conflicting data on whether tPA injected intravitreally penetrates into the subretinal space in a concentration sufficient for dissolution of a subretinal blood clot.[51–53] At a molecular weight of 70 kD, tPA is similar in size to albumin (68 kD), which has been shown to diffuse across intact retina into the subretinal space.[54] However, in the rabbit eye model, Kamei and coauthors demonstrated that intravitreal radiolabeled tPA did not diffuse through intact retina compared to radiolabeled dextran (20 kD) at a dose of 50 μg/0.1 mL.[53] They found that the fluorescence-labeled tPA accumulated at the internal limiting membrane,

vitreous cortex, or both. Based on their findings, the authors concluded that there was no scientific rationale for giving intravitreal tPA for SMH. Other authors have modified this in-office technique to include pneumatic displacement without the use of intravitreal tPA.[55] Ohji et al. reported a series of five patients with SMH treated with this modified approach, and anatomic and visual improvement were noted in all eyes in their small series. Because subretinal hemorrhage will undergo some degree of gradual spontaneous liquefaction 7–10 days after onset, maximum displacement of SMH using this technique may be achieved with the use of a long-acting gas bubble such as C_3F_8 and repeated overnight sessions of prone positioning for 7–10 days for as long as the gas bubble persists.

Subretinal Injection of Tissue Plasminogen Activator With Pneumatic Displacement

A novel surgical procedure of vitrectomy with subretinal tPA injection and pneumatic displacement without clot extraction was first described by Haupert et al. in 2001.[56] Using a bent 36-gauge needle, the authors injected tPA (25–50 μg/mL) into the subretinal space. Instead of waiting for clot lysis and attempting to remove the hemorrhage as in previous subretinal techniques, the authors performed a fluid–air exchange followed by air–gas exchange for nonexpansile 20% sulfur hexafluoride (SF_6). Postoperatively the patients were instructed to maintain a prone position. In their series of 11 patients with thick SMH secondary to AMD, anatomic inferior displacement of the clot was achieved in all eyes, while final postoperative VA was improved in eight (73%) cases.[56]

This technique was then slightly modified by Olivier et al. and others.[57] Using a 39- or 40-gauge cannula, they injected tPA into the subretinal space at a concentration of 12.5 μg/0.1 mL. The tPA was slowly injected at a steady infusion rate to "balloon up" the retina, creating a neurosensory retinal detachment in the macula and bathing the entire subretinal hemorrhage. The subretinal blood collected in this potential space and was pushed inferiorly by an intraocular air bubble injected at the end of the vitrectomy surgery. Following postoperative prone positioning, the macula was

generally cleared of subretinal hemorrhage (Fig. 122.1B), permitting fluorescein angiography and possible treatment of the underlying CNV. They reported total subfoveal blood displacement in 86% of 29 eyes treated with this technique, and 59% of patients gained 2 or more lines of vision at 3 months after surgery.[57] In a large retrospective series, Chang et al. reported complete displacement of hemorrhage from the fovea in 83 of 101 eyes (82%) using this technique.[58] Furthermore, 40% of patients in that study continued to receive anti-VEGF therapy after vitrectomy and maintained improved VA for 6 months compared to those who did not receive postvitrectomy anti-VEGF treatment and experienced a regression in treatment effect.

The advantages of this technique are maximal chemical lysis of the clot via subretinal injection of tPA, which minimizes the risk of mechanical trauma to the retina and RPE from manual clot extraction. In addition, vitrectomy surgery allows for a larger gas bubble to be placed in the vitreous cavity compared to in-office gas injection, allowing for more complete displacement of blood from the submacular space. Sandhu et al. reported that vitrectomy with subretinal tPA and air–fluid exchange displaced subretinal hemorrhage in three of four patients who failed expansile gas injection in the office.[59] Also, Hillenkamp et al. compared vitrectomy with intravitreal tPA injection to vitrectomy with subretinal tPA injection, with both groups receiving nonexpansile SF_6. Hemorrhage was displaced completely in only 22% of the intravitreal tPA group compared to 55% of the subretinal tPA group.[60]

Subretinal tPA Plus Subretinal Air and/or Subretinal Anti-VEGF

As vitreoretinal instrumentation and surgical techniques continue to improve, novel procedures involving additional subretinal injections of anti-VEGF and/or subretinal air have been reported.

Shah et al. reported the successful displacement of AMD-related SMH in two patients treated with vitrectomy and subretinal injection of both tPA and an anti-VEGF agent followed by intraocular SF_6.[61] Both patients received continued intravitreal anti-

VEGF treatments after surgery and maintained functional VA (20/70 to 20/80) during 1-year follow-up. In a larger retrospective series, Treumer et al. reported successful complete displacement of SMH in 35 of 41 eyes treated with vitrectomy, combined subretinal tPA, and subretinal bevacizumab, and intraocular SF_6.[62] Twenty-six patients with at least 12 months follow-up received postoperatively an average of 4.5 intravitreal bevacizumab injections, and BCVA improved in 22 patients. Although the optimal concentration and pharmacokinetics of subretinally injected anti-VEGF agents are unknown, neither study found any evidence of toxicity to the retina or RPE.

Martel and Mahmoud first reported the successful displacement of SMH using injection of subretinal air in addition to subretinal tPA and bevacizumab.[63] The authors used a 41-gauge extendable cannula to inject a combination of 0.4 mL of tPA at a concentration of 12.5 μg/0.1 mL (50 μg total), 0.1 mL of bevacizumab (2.5 mg), and 0.2 mL of filtered air. At the end of the vitrectomy, 20% SF_6 is injected to about 50% of the vitreous cavity to keep the subretinal air within the macular space, and the patient is positioned upright in the postoperative period. The authors hypothesize that based on Archimedes' principal, the addition of subretinal air dramatically lowers the buoyancy force of red blood cells in the subretinal space and allows for a more effective and immediate inferior displacement of the hemorrhage.[63] In another recent case series, Kadonosono et al.[64] described a similar procedure in which 0.4 mL of tPA at a concentration of 62.5 μg/0.1 mL (250 μg total) was injected into the subretinal space followed by 0.4 mL of filtered air. Following additional subretinal air injection to displace the dissolved clot inferiorly, there was no fluid–air exchange. The eyes in this study also did not receive subretinal anti-VEGF injection. Although they reported total blood displacement in all 13 eyes, this study was limited by its short 3-month follow-up and also included hemorrhages due to PCV.

Anti-VEGF Agents

Intravitreal anti-VEGF injections have become the standard of care for patients with exudative AMD following several large randomized clinical trials. However, patients with predominantly

hemorrhagic lesions were excluded from these landmark trials, and it is therefore difficult to apply the results of these studies to patients with AMD-related SMH. A recent report on a subgroup of patients in the CATT trial with hemorrhage comprising >50% of lesion size[65] found a similar percentage of 3-line gainers at 2 years between the predominantly hemorrhagic and nonhemorrhagic groups (33.3% vs. 29.4%, respectively). However, the baseline VA in the hemorrhagic group was 20/80, and only 59.5% of those patients had subfoveal hemorrhage. Other studies have also reported on the outcomes of treating AMD-related SMH with anti-VEGF monotherapy alone.[66–71] Stifter et al. reported a ≥3 line VA gain at 4 months in 9.5% of 21 eyes with SMH treated with bevacizumab monotherapy.[67] In a small prospective series of 7 eyes, Chang et al. reported that nearly half of ranibizumab-treated eyes gained 2 or more lines of VA with a median gain of 7 ETDRS letters at 12 months.[66] In a recent retrospective study by Shienbaum et al.,[69] 19 eyes with AMD-related SMH received an average of 4.7 anti-VEGF injections over 12 months, at which time 60% gained ≥3 lines of VA.[69] In a large retrospective study using anti-VEGF monotherapy for SMH, Kim et al.[70] reported 91 eyes with fovea-involving SMH treated with ranibizumab only, bevacizumab only, or a combination of the two drugs. However, only 26% of their patient population had typical neovascular AMD, whereas 48% had polypoidal choroidal vasculopathy (PCV) on indocyanine green angiography, and the remainder could not be definitively classified due to the large hemorrhage. In their study, 59.3% of eyes had ≥3 lines of VA improvement at 6 months and 64.8% improved ≥3 lines at 12 months. Unlike typical neovascular AMD, PCV has relatively good visual prognosis with higher rates of spontaneous hemorrhage resolution.[34,70] In a prospective study of ranibizumab monotherapy in 23 patients with AMD-related SMH, Iacono et al. found that only 34.7% of their patients gained ≥3 lines of VA at 12 months of follow-up.[71] However, only 26% of hemorrhages in this study involved the fovea, and similar to the other anti-VEGF monotherapy studies, their cohort had a better baseline VA compared to studies using intravitreal or subretinal tPA.

One retrospective study compared patients with combination anti-VEGF and expansile gas versus anti-VEGF monotherapy and

found that vision improved in 80% of patients with both agents compared to 60% with the anti-VEGF agent alone. This study was retrospective, and the duration of hemorrhage was not well matched between the groups.[72] To date, there are no prospective data to guide the clinician in the use of anti-VEGF agents alone or in combination with expansile gas displacement or with vitrectomy and tPA injection.

Conclusion

SMH is a potentially devastating complication of many macular disorders. The natural history is especially poor in patients with the underlying diagnosis of AMD. Other factors that portend a poor visual prognosis include increasing size, thickness, and duration of submacular blood.

In an attempt to improve upon the natural history of the disease, several investigators have attempted to remove the blood from the submacular space. Initial efforts and those of the SST showed disappointing visual results with limited complications. The use of anti-VEGF agents either alone or in combination with expansile gas or with vitrectomy and tPA use seems more promising than the natural history. However, there is no large randomized study comparing anti-VEGF monotherapy to intravitreal or subretinal tPA for the treatment of SMH, and there is no consensus on the preferred management strategy. Although there are no set criteria for which patients would benefit from tPA-assisted displacement of SMH versus anti-VEGF monotherapy, the authors believe that eyes with thicker hemorrhages of less than 7 days' duration, located within the vascular arcades, and without a large hemorrhagic pigment epithelial detachment, benefit the most from displacement of SMH out of the macula. Because successful displacement has been reported with both intravitreal injection of tPA and expansile gas, and vitrectomy and subretinal tPA injection with intraocular gas, the technique chosen will ultimately depend on the surgeon's comfort level and experience with the procedure. After either procedure, face-down positioning should be strongly encouraged to help facilitate displacement of the hemorrhage out of the macula, and close follow-up with continued anti-VEGF treatment of the

underlying CNV is ideal. Regardless of which treatment modality is used, the functional outcome in AMD-driven SMH will largely depend on the location and extent of the underlying CNV.

References

1. Macular Photocoagulation Study Group. Laser photocoagulation of subfoveal neovascular lesions in age-related macular degeneration: results of a randomized clinical trial. *Arch Ophthalmol*. 1991;109:1220–1231.
2. de Juan E Jr, Machemer R. Vitreous surgery for hemorrhagic and fibrous complications of age-related macular degeneration. *Am J Ophthalmol*. 1989;105:25–29.
3. Thomas MA, Kaplan HJ. Surgical removal of subfoveal neovascularization in the presumed ocular histoplasmosis syndrome. *Am J Ophthalmol*. 1991;111:1–7.
4. Thomas MA, Ibanez HE. Instruments for submacular surgery. *Retina*. 1994;14:84–87.
5. Cooper BA, Thomas MA, Holekamp NM. Open retinotomy after submacular surgery. *Am J Ophthalmol*. 2000;130:838–839.
6. Thomas MA, Grand MG, Williams DF, et al. Surgical management of subfoveal choroidal neovascularization. *Ophthalmology*. 1992;99:952–968.
7. Berger AS, Kaplan HJ. Clinical experience with the surgical removal of subfoveal neovascular membranes: short-term post-operative results. *Ophthalmology*. 1992;99:969–976.
8. Lambert HM, Capone A Jr, Aaberg TM, et al. Surgical excision of subfoveal neovascular membranes in age-related macular degeneration. *Am J Ophthalmol*. 1992;113:257–262.
9. Mandelcorn MS, Menezes AV. Surgical removal of subretinal hemorrhage and choroidal neovascular membranes in acute hemorrhagic age-related macular degeneration. *Can J Ophthalmol*. 1993;28:19–23.
10. Thomas MA, Dickinson JD, Melberg NS, et al. Visual results after surgical removal of subfoveal choroidal neovascular membranes. *Ophthalmology*. 1994;101:1384–1396.
11. Ormerod LD, Puklin JE, Frank RN. Long-term outcomes

after the surgical removal of advanced subfoveal neovascular membranes in age-related macular degeneration. *Ophthalmology*. 1994;101:1201–1210.
12. Holekamp NM, Thomas MA, Dickinson JD, et al. Surgical removal of subfoveal choroidal neovascularization in presumed ocular histoplasmosis: stability of early visual results. *Ophthalmology*. 1997;104:22–26.
13. Berger AS, Conway M, Del Priore LV, et al. Submacular surgery for subfoveal choroidal neovascular membranes in patients with presumed ocular histoplasmosis. *Arch Ophthalmol*. 1997;115:991–996.
14. Cooper BA, Thomas MA. Submacular surgery to remove choroidal neovascularization associated with central serous chorioretinopathy. *Am J Ophthalmol*. 2000;130:187–191.
15. Uemura A, Thomas MA. Subretinal surgery for choroidal neovascularization in patients with high myopia. *Arch Ophthalmol*. 2000;118:344–350.
16. Uemura A, Thomas MA. Visual outcome after surgical removal of choroidal neovascularization in pediatric patients. *Arch Ophthalmol*. 2000;118:1373–1378.
17. Joseph DP, Uemura A, Thomas MA. Subretinal surgery for juxtafoveal choroidal neovascularization. *Retina*. 2003;23:463–468.
18. Gass JDM. Biomicroscopic and histopathologic considerations regarding the feasibility of surgical excision of subfoveal neovascular membranes. *Am J Ophthalmol*. 1994;118:285–289.
19. Melberg NS, Thomas MA, Burgess DB. The surgical removal of subfoveal choroidal neovascularization: ingrowth site as a predictor of visual outcome. *Retina*. 1996;16:190–195.
20. Melberg NS, Thomas MA, Dickinson JD, et al. Managing recurrent neovascularization after subfoveal surgery in presumed ocular histoplasmosis syndrome. *Ophthalmology*. 1996;103:1064–1068.
21. Submacular Surgery Trials Research Group. *Submacular Surgery trials (SST) manual of procedures*. [NTIS accession No. PB98–166648. Springfield: National Technical Information Services, US Department of Commerce; June] 1998.

22. Submacular Surgery Trials Pilot Study Investigators. Submacular Surgery Trials randomized pilot trial of laser photocoagulation versus surgery for recurrent choroidal neovascularization secondary to age-related macular degeneration: I. Ophthalmic outcomes. SST pilot study report no. 1. *Am J Ophthalmol*. 2000;130:387–407.
23. Submacular Surgery Trials Research Group. Surgery for subfoveal choroidal neovascularization in age-related macular degeneration: ophthalmic findings. SST report no. 11. *Ophthalmology*. 2004;111:1967–1980.
24. Submacular Surgery Trials Research Group. Surgical removal vs. observation for subfoveal choroidal neovascularization, either associated with the ocular histoplasmosis syndrome or idiopathic: I. ophthalmic findings from a randomized clinical trial: SST Group H Trial: report no. 9. *Arch Ophthalmol*. 2004;122:1597–1611.
25. Atebara N, Thomas MA, Holekamp NM, et al. Surgical removal of extensive peripapillary choroidal neovascularization associated with presumed ocular histoplasmosis syndrome. *Ophthalmology*. 1998;105:1598–1605.
26. Bains HS, Patel MR, Singh H, et al. Surgical treatment of extensive peripapillary choroidal neovascularization in elderly patients. *Retina*. 2003;23:469–474.
27. Kertes PJ. Massive peripapillary subretinal neovascularization: an indication for submacular surgery. *Retina*. 2004;24:219–225.
28. Blinder KJ, Shah GK, Thomas MA, et al. Surgical removal of peripapillary choroidal neovascularization associated with age-related macular degeneration. *Ophthalmic Surg Lasers Imaging*. 2005;36:358–364.
29. Kokame GT, Yamaoka S. Subretinal surgery for peripapillary subretinal neovascular membranes. *Retina*. 2005;25:564–569.
30. Aisenbrey S, Gelisken F, Szurman P, et al. Surgical treatment of peripapillary choroidal neovascularization. *Br J Ophthalmol*. 2007;91:1027–1030.
31. Almony A, Thomas MA, Atebara NH, et al. Long-term

follow-up of surgical removal of extensive peripapillary choroidal neovascularization in presumed ocular histoplasmosis syndrome. *Ophthalmology*. 2008;115:540–545.
32. Cohen SY, Creuzot-Garcher C, Darmon J, et al. Types of choroidal neovascularization in newly diagnosed exudative age-related macular degeneration. *Br J Ophthalmol*. 2007;91:1173–1176.
33. Ibanez HE, Williams DF, Thomas MA, et al. Surgical management of submacular hemorrhage: a series of 47 consecutive cases. *Arch Ophthalmol*. 1995;113:62–69.
34. Hayasaka S, Uchida M, Setogawa T. Subretinal hemorrhages with or without choroidal neovascularization in the maculas of patients with pathologic myopia. *Graefes Arch Clin Exp Ophthalmol*. 1995;228:277–280.
35. Shiraga F, Matsuo T, Yokoe S, et al. Surgical treatment of submacular hemorrhage associated with idiopathic polypoidal choroidal vasculopathy. *Am J Ophthalmol*. 1999;128:147–154.
36. Bennet SR, Folk JC, Blodi CF, et al. Factors prognostic of visual outcome in patients with subretinal hemorrhage. *Am J Ophthalmol*. 1990;109:33–37.
37. Scupola A, Coscas G, Soubrane G, et al. Natural history of macular subretinal hemorrhage in age-related macular degeneration. *Ophthalmologica*. 1999;213:97–102.
38. Chung MM, Oh KT, Streb LM, et al. Visual outcome following subretinal hemorrhage in Best's disease. *Retina*. 2001;21:575–580.
39. Submacular Surgery Trials Research Group. Surgery for predominantly hemorrhagic choroidal neovascular lesions of age-related macular degeneration: ophthalmic findings. SST report No. 13. *Ophthalmology*. 2004;111:1993–2006.
40. Glatt H, Machemer R. Experimental subretinal hemorrhage in rabbits. *Am J Ophthalmol*. 1982;94:762–773.
41. Peyman GA, Nelson NC Jr, Alturki W, et al. Tissue plasminogen activating factor assisted removal of subretinal hemorrhage. *Ophthalmic Surg*. 1991;22:575–582.
42. Lewis H. Intraoperative fibrinolysis of submacular hemorrhage with tissue plasminogen activator and surgical

drainage. *Am J Ophthalmol*. 1994;118:559–568.
43. Lim JI, Drews-Botsch C, Sternberg P Jr, et al. Submacular hemorrhage removal. *Ophthalmology*. 1995;102:1393–1399.
44. Lewis H, Resnick SC, Flannery JG, et al. Tissue plasminogen activator treatment of experimental subretinal hemorrhage. *Am J Ophthalmol*. 1991;111:197–204.
45. Johnson MW, Olsen KR, Hernandez E. Tissue plasminogen activator treatment of experimental subretinal hemorrhage. *Ophthalmology*. 1992;99:515–521.
46. Benner JD, Hay A, Lander MB III, et al. Fibrinolytic-assisted removal of experimental subretinal hemorrhage within seven days reduces outer retinal degeneration. *Ophthalmology*. 1994;101:672–681.
47. Heriot WJ. *Further experience in management of submacular hemorrhage with intravitreal tPA*. [Vitreoretinal update 1997, American Academy of Ophthalmology, Retina Subspecialty Day. San Francisco] 1997:82–84.
48. Hesse L, Schmidt J, Kroll P. Management of acute submacular hemorrhage using recombinant tissue plasminogen activator and gas. *Graefes Arch Clin Exp Ophthalmol*. 1999;237:273–277.
49. Hassan AS, Johnson MW, Schneiderman TE, et al. Management of submacular hemorrhage with intravitreous tissue plasminogen activator injection and pneumatic displacement. *Ophthalmology*. 1999;106:1900–1907.
50. Hattenbach LO, Klais C, Koch FH, Gumbel HO. Intravitreous injection of tissue plasminogen activator and gas in the treatment of submacular hemorrhage under various conditions. *Ophthalmology*. 2001;108(8):1485–1492.
51. Coll GE, Sparrow JR, Marinovic A, et al. Effect of intravitreal tissue plasminogen activator on experimental subretinal hemorrhage. *Retina*. 1995;15:319–326.
52. Boone DE, Boldt HC, Ross RD, et al. The use of intravitreal tissue plasminogen activator in the treatment of experimental subretinal hemorrhage in the pig model. *Retina*. 1996;16:518–524.
53. Kamei M, Misono K, Lewis H. A study of the ability of tissue plasminogen activator to diffuse into the subretinal space

after intravitreal injection in rabbits. *Am J Ophthalmol*. 1999;128:739–746.
54. Takeuchi A, Kricorian G, Yao XY, et al. The rate and source of albumin entry into saline-filled experimental retinal detachments. *Invest Ophthalmol Vis Sci*. 1994;35:3792–3798.
55. Ohji M, Saito Y, Hayaski A, et al. Pneumatic displacement of subretinal hemorrhage without tissue plasminogen activator. *Arch Ophthalmol*. 1998;116:1326–1332.
56. Haupert CL, McCuen BW Jr, Jaffe GJ, et al. Pars plana vitrectomy, subretinal injection of tissue plasminogen activator, and gas/fluid exchange for displacement of thick submacular hemorrhage in age-related macular degeneration. *Am J Ophthalmol*. 2001;131:208–215.
57. Olivier S, Chow DR, Packo KH, et al. Subretinal recombinant tissue plasminogen activator injection and pneumatic displacement of thick submacular hemorrhage in age-related macular degeneration. *Ophthalmology*. 2004;111:1201–1208.
58. Chang W, Garg SJ, Maturi R, et al. Management of thick submacular hemorrhage with subretinal tissue plasminogen activator and pneumatic displacement for age-related macular degeneration. *Am J Ophthalmol*. 2014;157(6):1250–1257.
59. Sandhu SS, Manvikar S, Steel DHW. Displacement of submacular hemorrhage associated with age-related macular degeneration using vitrectomy and submacular tPA injection followed by intravitreal ranibizumab. *Clin Ophthalmol*. 2010;4:637–642.
60. Hillenkamp J, Surguch V, Framme C, et al. Management of submacular hemorrhage with intravitreal versus subretinal injection of recombinant tissue plasminogen activator. *Graefes Arch Clin Exp Ophthalmol*. 2010;248:5–11.
61. Shah SP, Hubschman JP, Gonzales CR, et al. Submacular combination treatment for management of acute, massive submacular hemorrhage in age-related macular degeneration. *Ophthalmic Surg Lasers Imaging*. 2009;40:308–315.
62. Treumer F, Roider J, Hillenkamp J. Long-term outcome of

subretinal coapplication of rtPA and bevacizumab followed by repeated intravitreal anti-VEGF injections for neovascular AMD with submacular hemorrhage. *Br J Ophthalmol*. 2012;96:708–713.
63. Martel JN, Mahmoud TH. Subretinal pneumatic displacement of subretinal hemorrhage. *JAMA Ophthalmol*. 2013;131:1632–1635.
64. Kadanosono K, Arakawa A, Yamane S, et al. Displacement of submacular hemorrhages in age-related macular degeneration with subretinal tissue plasminogen activator and air. *Ophthalmology*. 2015;122:123–128.
65. Altaweel M, Ebenezer D, Martin D, et al. Outcomes of eyes with lesions composed of >50% blood in the comparison of age-related macular degeneration treatment trials (CATT). *Ophthalmology*. 2015;122(2):391–398.
66. Chang MA, Do DV, Bressler SB, et al. Prospective one-year study of ranibizumab for predominantly hemorrhagic choroidal neovascular lesions in age-related macular degeneration. *Retina*. 2010;30:1171–1176.
67. Stifter E, Michels S, Prager F, et al. Intravitreal bevacizumab therapy for neovascular age-related macular degeneration with large submacular hemorrhage. *Am J Ophthalmol*. 2007;144:886–892.
68. McKibbin M, Papastefanou V, Matthews B, et al. Ranibizumab monotherapy for sub-foveal haemorrhage secondary to choroidal neovascularization in age-related macular degeneration. *Eye (Lond)*. 2010;24:994–998.
69. Shienbaum G, Garcia Filho CA, Flynn HW Jr, et al. Management of submacular hemorrhage secondary to neovascular age-related macular degeneration with anti-vascular endothelial growth factor monotherapy. *Am J Ophthalmol*. 2013;155:1009–1013.
70. Kim JH, Chang YS, Kim JW, et al. Intravitreal anti-vascular endothelial growth factor for submacular hemorrhage from choroidal neovascularization. *Ophthalmology*. 2013;121(4):926–935.
71. Iacono P, Parodi MB, Introini U, et al. Intravitreal ranibizumab for choroidal neovascularization with large

submacular hemorrhage in age-related macular degeneration. *Retina*. 2014;34(2):281–287.
72. Sacu S, Stifter E, Vecsei-Marlovits PV, et al. Management of extensive subfoveal haemorrhage secondary to neovascular age-related macular degeneration. *Eye (Lond)*. 2009;23:1404–1410.

123

360-Degree Macular Translocation

Justis P. Ehlers, Cynthia A. Toth

Background and Rationale

Preservation of the integrity and function of the foveal photoreceptors is vital to visual outcome in patients with macular disease, including diseases such as age-related macular degeneration (AMD), myopic degeneration, and pattern dystrophies. Many of these disorders initially affect subretinal layers, including the retinal pigment epithelium (RPE), Bruch's membrane, and the choriocapillaris. These layers provide critical support for overlying outer retina, including the foveal photoreceptors.[1] Ultimately, disruption of these tissues results in structural and functional deterioration of the photoreceptors with subsequent vision loss. Macular translocation surgery moves the fovea from over a severely diseased subretinal bed to a new location with healthier subretinal tissues to allow for improved function and ideally restoration of functional central vision.

Animal Studies

Machemer and Steinhorst utilized a rabbit model to demonstrate the feasibility of purposeful retinal detachment with subretinal infusion via a transscleral approach.[2] Electron microscopy confirmed preservation of photoreceptor nuclei and mitochondria in the inner segments with some disruption of the outer segments, suggesting this technique was reasonably atraumatic and may be well tolerated. In addition, successful retinal translocation around the axis of the optic nerve following 360-degree (360°) peripheral retinectomy was also demonstrated. Additionally, maximal shaving of the vitreous base was found to be critical for creation of the retinectomy. Residual vitreous resulted in increased difficulty and less predictability during creation of the retinectomy.[2]

The rabbit model has also been used to demonstrate the utility of calcium- and magnesium-free infusate in reducing retinal adhesion to the RPE without creating cellular toxicity.[3,4] Collateral damage to photoreceptor outer segments was also reduced by using calcium- and magnesium-free solutions. Although transient electroretinogram (ERG) depression of b-wave amplitude was noted on postoperative day 1, subsequent recovery was observed.[3] Animal studies have also revealed that dark adaptation results in easier retinal detachment with reduced retinal damage. In model surgery, a red-free intraocular light source was used during the surgical procedure to prevent reversal of dark adaptation.[4]

Historical Perspective and Evolution of Technique

In 1983 Lindsey first proposed translocation of the retina.[5] Tiedeman et al. published their proposal for retinal translocation in 1985.[6] Machemer published the first human surgical cases in 1993. All three subjects had AMD and were treated with 360° peripheral retinectomy and translocation (MTS360, MT360).[7] The original MTS360 technique involved pars plana vitrectomy with transscleral injection of subretinal fluid with 360° retinectomy, removal of subretinal blood and choroidal neovascularization (CNV), partial fill with silicone oil, retinal translocation, complete silicone oil fill, and finally laser retinopexy. All surgeries were performed under general anesthesia. One of the original patients had significant

improvement in central acuity (1/200–20/80).[7]

The original procedure has gone through multiple evolutionary iterations with major developments by Eckardt et al., Toth and Freedman, and Tano.[8–10] Changes to technique have focused on facilitating retinal detachment, effectively translocating the macula, reducing complications (e.g., proliferative vitreoretinopathy [PVR]), and decreasing the duration of surgery.[8–18] Because retinal rotation results in significant cyclotorsion,[8,9,12,14,17,19] extraocular muscle surgery to counter-rotate the globe is used routinely to manage the cyclotropia.[8] Attempts at reducing the extent of the retinectomy (e.g., <360°) have not been widely adopted due to very high rates of PVR.[10,11,20,21]

Variations on MTS360 also included the development of limited macular translocation, which shifted the macula a shorter distance than with MTS360. De Juan developed a technique to shorten the sclera following detachment of the superotemporal retina across the macula. This resulted in redundant retina that allowed the foveal center to be relocated downward by gravity after surgery, by positioning the patient upright with a partially gas-filled eye. Because of the variable and limited distance of macular displacement, this procedure has become much less popular.[22–24]

Macular translocation has been used to describe all of these surgical displacement procedures. The terms retinal rotation, full macular translocation, macular translocation surgery with 360° peripheral retinectomy, MTS360, and MT360 have been used to describe the Machemer technique.

Principles of Foveal Relocation

The primary goal of macular translocation surgery is to relocate the fovea to a new location of healthier subretinal tissues in order to preserve and maintain foveal function to maximize visual acuity. Thus the fovea should be relocated to an area outside that of the subfoveal lesion.[1] The distance from the preoperative foveal center to the edge of the lesion is the minimum desired translocation. The distances of postoperative foveal displacement versus the minimum desired translocation have been found to be predictors of anatomic success following macular translocation.[25] The distance of

translocation is limited by the resistance of retinal tissue to twist around the optic nerve, by potential for both axonal injury and retinal folds with extreme rotation around the nerve, and by the maximum amount of ocular counter-rotation that is possible.

Characteristics of the underlying lesion (e.g., shape, size) determine the minimum desired translocation. Most surgeons move the retina further than the minimum distance in order to have a reasonable margin between the lesion edge and the new foveal location. Lesion location is also critical to required translocation distance. Central larger lesions may require the same displacement distance as smaller eccentric lesions (Fig. 123.1). The postoperative foveal location in MTS360 is highly predictable since the new foveal location is determined intraoperatively and the retina is reattached at the new location. MTS360 has an average foveal displacement of 3500 μm and the capacity to translocate the macula upward or downward.[8–11]

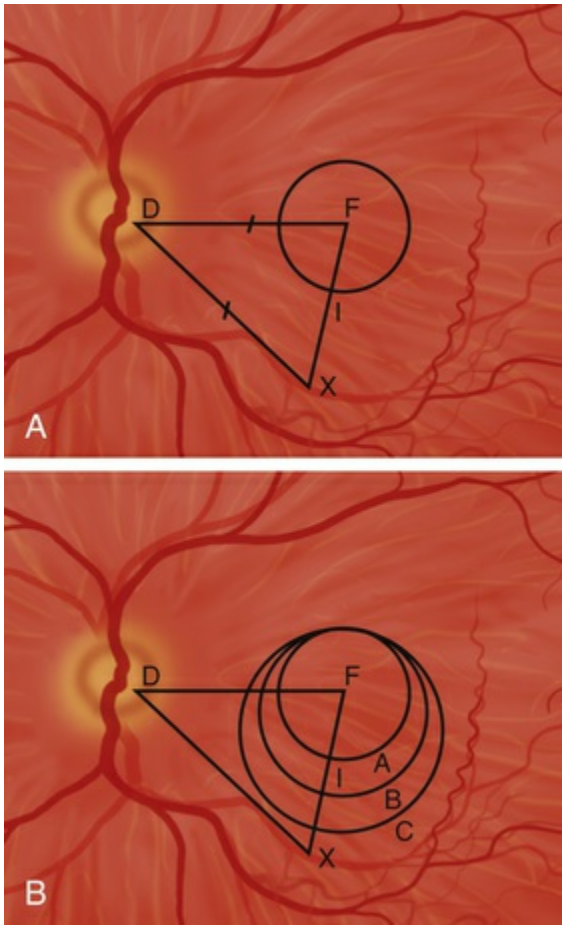

FIG. 123.1 Schematic diagram of left fundus where *F*

is the foveal center, *D* is a point on the temporal edge of the optic disc, and *I* is a point on the superior border of the subfoveal lesion such that *DF* = *DI*. (A) The distance *FI* is the minimum desired translocation for a superior translocation. (B) The minimum desired translocation for a superior translocation is the same for three subfoveal lesions of different sizes (A–C). The typical translocation would be to point *X*, which leaves a reasonable distance between the old subfoveal lesion and the new foveal location.

In MTS360, advantages to translocating the macula upward off the subretinal abnormality are to position the blind spot from the subretinal lesion site in the superior visual field; to position the macula in an optimal superior location for silicone oil tamponade; to avoid placing the macula over RPE that has been in an area of chronic exudate or hemorrhage, which is more likely inferior to the macula; and to allow for the most effective surgery for the cyclotropia since advancing the inferior oblique produces more torsional effect than advancing the superior oblique.

Preoperative Considerations

Indications

Although clear guidelines for the indications for macular translocation are not established, there are several generally agreed upon principles. Anti-vascular endothelial growth factor (VEGF) therapy is clearly the first-line treatment for subfoveal neovascular disease.[26,27] Because of the potential to induce postoperative torsional diplopia even after extraocular muscle surgery for correction, MTS360 surgery is only considered in patients who already also have central vision loss or low vision in the other eye. The surgical eye is typically the eye with better visual potential, more recent vision loss, and greater preservation of retinal architecture. MTS360 may be considered in nonresponders to anti-VEGF treatment, eyes with extensive subretinal fibrosis, selected cases of massive subretinal hemorrhage, retinal pigment epithelial tears, or submacular diseases that are not VEGF-driven.[8,9,12,15,17,28–35] Although macular translocation has been reported in numerous

diseases including neovascular AMD, non-neovascular AMD with geographic atrophy, myopic degeneration with CNV, ocular histoplasmosis with CNV, adult-onset foveomacular vitelliform dystrophy, punctate inner choroidopathy with subfoveal CNV, angioid streaks with CNV, North Carolina macular dystrophy, and central serous chorioretinopathy, there are cases in which it has a lower likelihood of success.[8,9,12,15,17,28,29,32–35] In cases of central geographic atrophy with AMD, the atrophy has often recurred in the new foveal location, and many would consider this a contraindication to surgery.[32,36,37] Underlying ocular inflammatory diagnoses (e.g., punctate inner choroidopathy, ocular histoplasmosis) may also be associated with worse outcome.[29] General inclusion and exclusion criteria for patients being assessed for MT-360 are outlined in Box 123.1.

Box 123.1

Inclusion and Exclusion Criteria for Macular Translocation With 360° Peripheral Retinectomy

Inclusion Criteria

Bilateral disease

Severe loss of central vision in second affected eye for no more than 6 months[a]

Best corrected Snellen visual acuity between 20/50 and 20/400 in the surgically treated eye

May have a previous photodynamic therapy, anti-VEGF therapy, or intravitreal steroid

Caution if there was previous extrafoveal or juxtafoveal thermal laser treatment with retinal thinning on optical coherence tomography or retinal angiomatous proliferation or choroidal anastomosis

Exclusion Criteria

Surgical eye characteristics:

No light perception visual acuity

Previous thermal laser treatment of fovea

Other ocular disease such as:

Diabetic retinopathy

Retinal vascular occlusive disease

Uncontrolled glaucoma

Optic neuropathy

Fellow eye characteristics:

Visual acuity of no light perception

Other ocular disease causing severe peripheral visual field loss

[a]Duration of vision loss determined by patients' reports of when they were unable to perform vision-related daily activities such as reading and driving.

History and Ocular Examination

Information regarding the history of progression and duration of vision loss is useful before surgery. The longer the duration of vision loss, the greater the likelihood of atrophy or scarring of the neurosensory retina with permanent dysfunction, and thus the lower likelihood of benefitting from MTS360. Unfortunately, the duration of significant vision loss may be difficult to ascertain. Other critical components of the ocular history include previous

strabismus surgery or previous vitreoretinal procedures. Both posterior and peripheral retinal examination are critical prior to performing macular translocation surgery. The posterior examination considers extent of macular chorioretinal scarring, active CNV, retinal atrophy and RPE atrophy, and whether any of these may extend into the site of proposed translocation. Identifying retinal angiomatous lesions and chorioretinal anastomoses aids in planning for dissection of the retina from the subretinal lesion. The peripheral retinal examination with scleral depression is important to identify pathology that may pose issues during the procedure (e.g., peripheral holes, chorioretinal scars that may inhibit retinal detachment). Peripheral retinal vascular disease such as diabetic retinopathy could lead to anterior segment ischemia and neovascularization of the iris after surgery on multiple extraocular muscles. The lens status of the patient is also important. Phakic patients typically undergo phacoemulsification and posterior chamber lens placement prior to or at the time of macular translocation surgery. If the patient is pseudophakic, the type of intraocular lens and the status of the posterior capsule are important given the planned infusion of silicone oil.

Diagnostic Testing

Preoperative evaluation for macular translocation may include fundus photography, fluorescein angiography, optical coherence tomography (OCT), fundus autofluorescence (FAF), fixation capability, and microperimetry. These tests may be useful to identify eyes that are poor candidates for MTS360, such as eyes with severe macular chorioretinal scarring, extensive neurosensory retinal atrophy, widespread RPE atrophy, CNV in the site of proposed translocation, retinal angiomatous lesions, chorioretinal anastomoses, or unexpected retinal vascular disease. Unfortunately, overall these tests, including fixation and microperimetry, have been shown to be poor predictors of 1 year visual outcomes in patients who were considered eligible for MTS360.[38] As noted in ocular examination above, however, these details have been very useful in surgical planning.

Spectral domain or swept source (SD- or SS-) OCT imaging of the

ultrastructure of the retina can be helpful in identifying outer retinal atrophy, which may limit the utility of macular translocation. Histologic evidence has shown significant photoreceptor atrophy overlying disciform scars.[39] If outer retinal atrophy is present in the entire macula on OCT, patients are probably unlikely to realize improvement in visual function after macular translocation. Surprisingly, a thinner retina on time domain OCT before surgery was associated with good visual outcomes in one study.[38] However, time domain OCT lacks the resolution of SD-OCT imaging; therefore, resolution was not sufficient to identify photoreceptor layer details. In some cases, perhaps the more compact retina was healthier than the edematous retina before MTS360. Additionally, OCT may be helpful in identifying other structural abnormalities that are important to preoperative planning (e.g., large intraretinal cysts, areas of adhesion).

Fluorescein and/or indocyanine green angiography are utilized to assess the extent, location, and activity of the CNV and/or submacular disease process. Additionally, preoperative fluorescein angiography can be helpful in identifying retinal angiomatous proliferation or chorioretinal anastomosis, which should be considered in surgical planning, as these can result in a retinal tear or significant intraoperative hemorrhage during the separation of the retina from the RPE and choroid.[40,41] Additionally, the RPE integrity and perfusion status of the choroid and retina can be assessed. FAF can be useful for evaluation of the RPE health of the future subfoveal RPE bed. Hyper- or hypofluorescence in the area of the future foveal location should be considered before committing to surgery.

Surgical Technique for Macular Translocation

MTS360

MTS360 is performed under general or local anesthesia. If the patient has the muscle surgery at the start of the translocation surgery, then this is typically under general anesthesia. If a patient

is phakic, cataract extraction and intraocular lens placement are performed at the time of macular translocation. Complete pars plana vitrectomy with elevation of the posterior hyaloid, if attached, is the first step of MTS360. Careful, close shaving of the vitreous base with the vitreous cutter and 360° of scleral depression is performed. Retinal detachment is induced with subretinal fluid injection through a retinotomy that is typically located peripherally within the vitreous base. Posterior retinotomies have been associated with greater epiretinal membrane formation. Different specialized cannulas have been utilized to infuse the subretinal fluid to detach the retina.[8–11,14,15] Fluid is typically either infused into the subretinal space through a 41-gauge cannula posteriorly,[42] or at the ora serrata through a silicone-tipped cannula larger than a very small retinotomy made with the vitreous cutter, and marked using endodiathermy (Fig. 123.2A).[9] A fluid–air exchange facilitates subretinal fluid displacement from areas of detached retina to areas of attached retina. Although animal models have shown that calcium- and magnesium-free solutions may facilitate retinal detachment, prolonged use of these solutions in humans may result in higher postoperative keratopathy and the use of these solutions is not common.

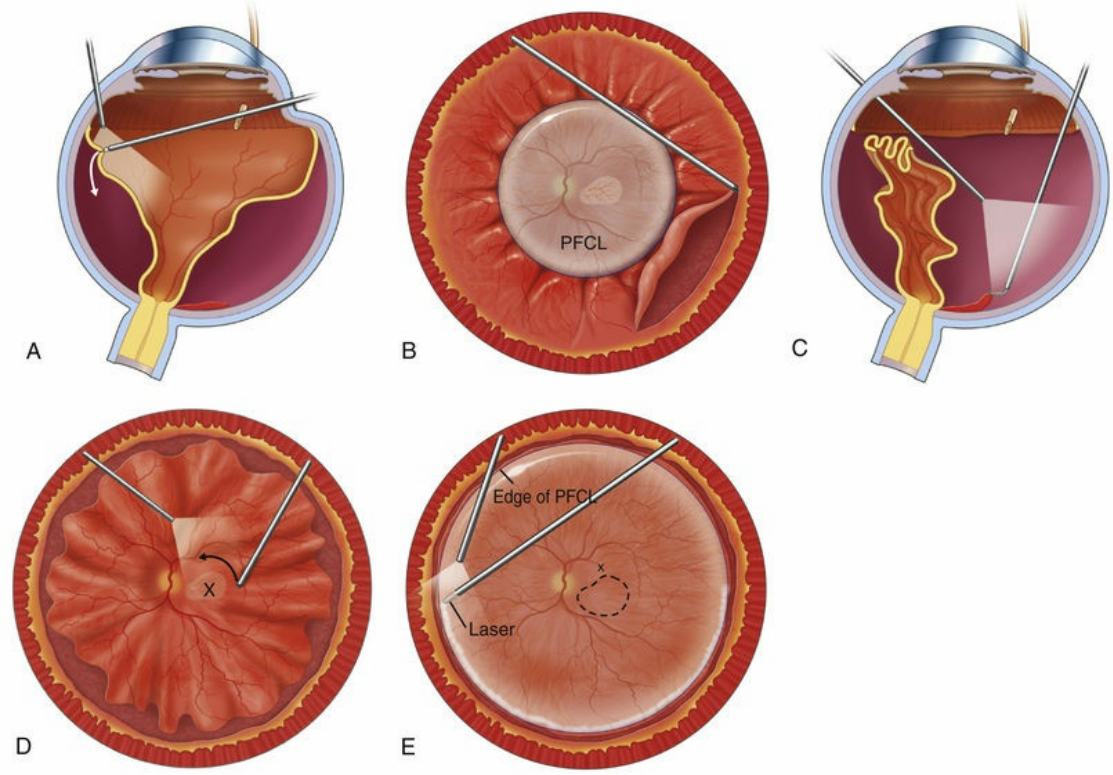

FIG. 123.2 Diagrams showing the steps involved in macular translocation with 360° peripheral retinectomy. (A) The retina is detached by subretinal injection of fluid through a retinotomy that may be located posteriorly or peripherally. (B) After the retina is totally detached, it is then cut at the ora serrata using the vitreous cutter (retinectomy) or retinal scissors (retinotomy). (C) When the retina has been completely cut free at the ora serrata, it is reflected and the subretinal lesion is removed. (D) The neurosensory retina is then translocated off the subfoveal abnormality usually in a superior direction. While a number of instruments can be used to manipulate the retina, a modified diamond-dusted silicone-tipped needle that is connected via short tubing to a syringe containing perfluorocarbon is shown here. (E) At completion of the surgery the retina is typically rotated 40–45° displacing the fovea (*X*) off the bed of choroidal neovascularization (*dotted line*). *PFCL,* perfluorocarbon liquid.

Once the retina is totally detached, the retina is cut at the ora serrata with the vitreous cutter (peripheral retinectomy)[9–11] or retinal scissors (peripheral retinotomy) (Fig. 123.2B).[8,10,11,15]

Perfluorocarbon liquid (PFCL) is temporarily placed over the posterior pole of the retina to stabilize the retina if performing a peripheral retinectomy; once the retina is completely free from the periphery, the PFC is removed. The retina is reflected allowing removal of the subfoveal lesion, if present, and diathermy of feeding vessels as required (Fig. 123.2C). The retina is then translocated into the new position. Most commonly, the retina is translocated superiorly (Fig. 123.2D). A small bubble of preretinal PFCL is utilized to stabilize the retina while the translocation is performed. Multiple instruments have been utilized for the retinal manipulation during translocation, including retinal forceps[8,10,11] and a silicone-tipped needle,[14] although the diamond-dusted silicone-tipped needle is excellent for atraumatically snagging the retinal surface with very gentle pressure over an arcade, and then sliding the retina. The tip may be connected to a syringe containing PFCL.[9] Once appropriate displacement has been achieved (typically approximately 45° off the CNV bed, which equates to positioning the center of the old CNV bed under the inferotemporal arcade), additional PFCL is added to reattach the retina in the manner of a giant retinal tear. Laser photocoagulation is then applied to the retinectomy margins under PFCL tamponade. A direct PFCL/silicone oil exchange is performed to avoid retinal slippage (Fig. 123.2E).

Early Postoperative Management

Positioning

Positioning following MTS360 is based on the surgeon's preferences. Approaches include face-down positioning or alternating side-to-side positioning thought to diminish pooling of factors for PVR in aqueous medium at the 6 o'clock position.

Extraocular Muscle Surgery for Macular Translocation

Given the extensive translocation that occurs during MTS360, often 30–45° in an upward direction, the amount of torsion exceeds the

maximum amplitude of cyclofusion (typically around 15°).[43] Translocation results in both horizontal and vertical strabismus. In order to alleviate the symptoms associated with excess cyclotorsion, extraocular muscle surgery is performed to strengthen the inferior oblique and weaken the superior oblique. Rectus muscle transposition is also often performed to increase excyclorotation.[8,43] Two major techniques have been described.

The Freedman technique involves performing the extraocular muscle surgery 8 weeks after the MTS360 procedure. Because of separate and thus shorter procedures, general anesthesia is not needed for the extraocular muscle surgery or the MTS360. The number of operated muscles is determined by the measured posttranslocation torsion. The inferior oblique is advanced to the temporal border of the superior rectus muscle with the anterior and posterior edges 13 and 15 mm posterior to the limbus, respectively, and a complete superior oblique tenotomy is performed. If an eye has between 20 and 35° of torsion, superior transposition of the lateral rectus muscle is also performed adjacent to the superior rectus, 7 mm from the limbus. For the majority of cases, more than 35° of torsion is present and thus the medial rectus is also transposed to the nasal edge of the inferior rectus muscle (Fig. 123.3).[43]

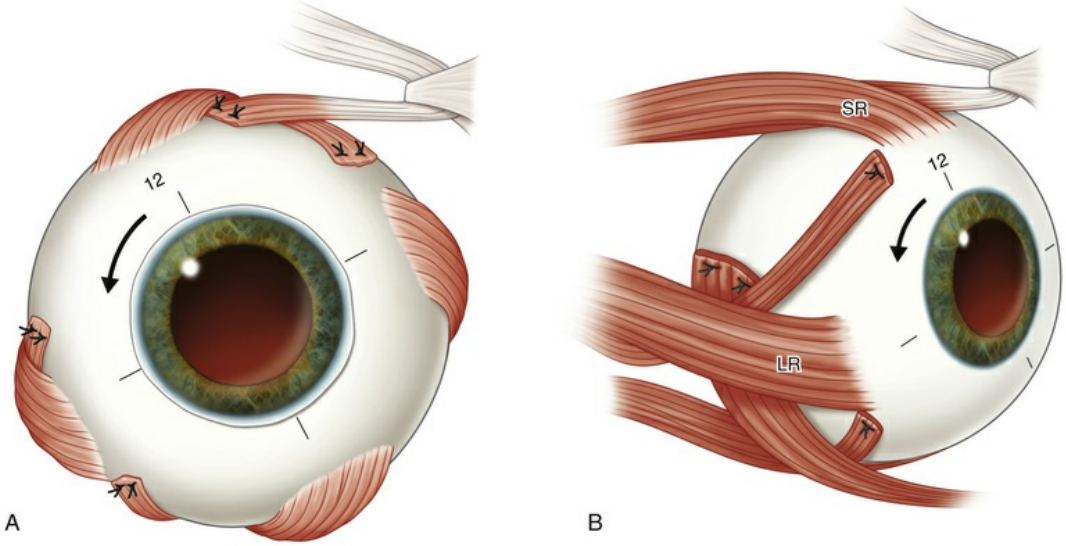

FIG. 123.3 Drawing of torsional muscle surgery to create an excyclotropia in the right eye using the Eckardt technique. (A) The anterior part of the inferior

oblique muscle is advanced 12 mm and the posterior part, 9 mm, while the anterior and posterior parts of the superior oblique muscles are recessed the same distances. In addition, muscle strips from two opposing rectus muscles are passed beneath the original muscles and transposed in a clockwise direction and attached at the insertion of the adjoining rectus muscles. (B) If more counter-rotation of the eye is required, opposing strips from all four rectus muscles can be moved after the oblique muscle surgery previously described. *LR*, lateral rectus; *SR*, superior rectus.

Simultaneous extraocular muscle surgery may also be performed during the initial MTS360 procedure as demonstrated by Eckardt.[8] General anesthesia is typically utilized when the muscle surgery is combined with MTS360. The muscle surgery may be either the above-described Freedman technique or the Eckardt technique. In the latter, strengthening of the inferior oblique is achieved by advancement or through a 12-mm tuck, and the superior oblique is weakened by recession or tenotomy. Each rectus muscle is split by about one-quarter of the width of the entire muscle for a radial length of 15–17 mm. Each strip is passed under the remaining portion of the rectus, transposing them clockwise (right eye) or counter-clockwise (left eye) to the margins of the adjacent rectus muscle (windmill technique) producing excyclorotation (Fig. 123.4).[8]

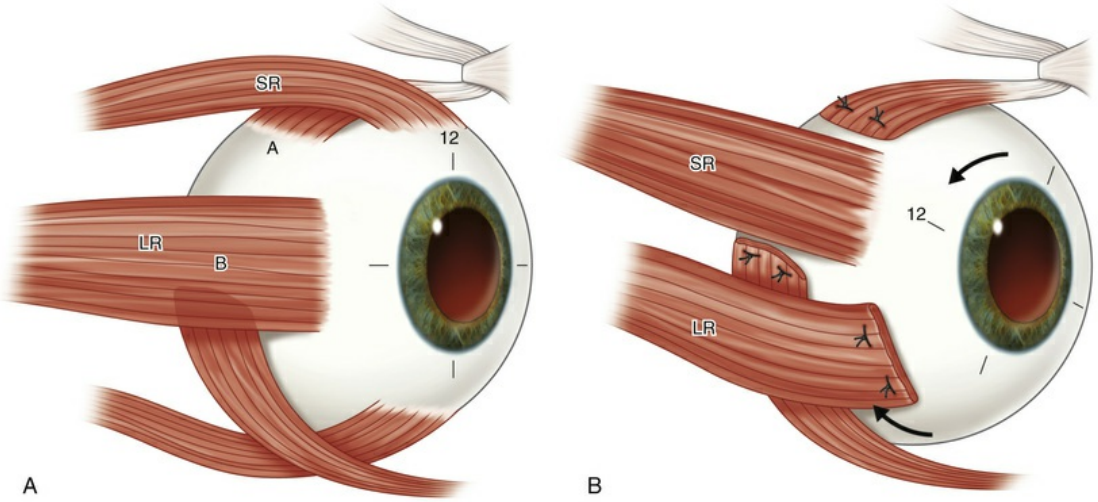

FIG. 123.4 Drawing of torsional muscle surgery to create an excyclotropia in the right eye from the surgeon's view superiorly, using the Freedman technique. (A) The first step is advancement of the inferior oblique muscle. Pen marks on the limbus denote the 6 and 12 o'clock positions of the eye, made prior to beginning strabismus surgery. A muscle hook has been placed beneath the superior rectus insertion. The superior oblique tendon has been transected (not shown). The medial and lateral rectus muscles have each been secured on a 6–0 Vicryl suture and detached from their respective insertions on the globe. The inferior oblique muscle, located on a clamp, is being advanced towards the site on the sclera where partial-thickness scleral bites have been taken with the same 5–0 Dacron suture, which is attached to the inferior oblique behind the clamp. (B) The final positions of the medial and lateral rectus and inferior oblique muscles during strabismus surgery are shown. The lateral rectus muscle has been reattached adjacent to the lateral border of the superior rectus muscle. The inferior oblique muscle, having been advanced as shown previously, is just visible in the superior temporal fornix. The medial rectus muscle has been reattached adjacent to the medial border of the inferior rectus muscle. The pen markings at the limbus demonstrate the excyclorotation of the globe, which has been affected by the surgery. *LR*, lateral rectus; *SR*, superior rectus.

Postoperative Management of Choroidal Neovascularization

Following MTS360, the previous subfoveal CNV is likely extrafoveal in location (if it has not been removed intraoperatively). If the CNV is active, anti-VEGF therapy, laser photocoagulation, or photodynamic therapy may be used individually or combined to reduce the risk of CNV growth into the new foveal location and to reduce the risk of further vision loss from hemorrhage. Because of the risk of recurrent CNV, postoperative care should include home monitoring and diagnostic testing and examination should seek

evidence of recurrence.

Functional Outcomes for Macular Translocation Surgery

Neovascular AMD

Multiple reports have documented functional outcomes after MTS360 for neovascular AMD (Table 123.1).[8–12,14–18,42,44–47] In a prospective randomized clinical trial of MTS360 versus photodynamic therapy with follow-up through 2 years, MTS360 produced superior vision recovery at both 1 and 2 years, with a gain of 0.3 letters in distance acuity and 7 letters in near acuity after MTS360 versus a loss of 12.6 letters in distance acuity and of 9.6 letters in near acuity in the PDT group.[45,48] The subsequent success of anti-VEGF inhibitors in the treatment of CNV has diminished the need for macular translocation surgery and changed the context of these analyses.[26,27]

TABLE 123.1

Visual Acuity Results of Macular Translocation With 360° Peripheral Retinectomy for Age-Related Macular Degeneration

First Author	Ohji[11]	Pertile[15]	Eckardt[8]	Toth[9]	Aisenbrey[14]	Fujikado[16]	A-Meguid[17]	Mruthyunj
No. of study eyes	36	50	30	16	90	21	39	64
Study design	Retro	Retro	Pro	Pro	Pro	Pro	Pro	Pro
Follow-up (mth)	15.0	21.0	10.7	14.0	12.0	9.6	12.0	12.0
PREOPERATIVE VISUAL ACUITY								
Mean or median	NA	NA	20/125	20/125	20/200	20/125	20/260	20/125
>20/40	0 (0.0)	0 (0.0)[b]	0 (0.0)	0 (0.0)	NA	0 (0.0)	0 (0.0)	0 (0.0)
20/40–20/80	NA[a]	2 (4.0)[b]	12 (40.0)	9 (56.2)	NA	8 (38.1)	7 (18.0)	23 (38)
20/100–20/200	29 (80.5)	30 (60.0)[b]	13 (43.3)	4 (25.0)	NA	10 (47.6)	13 (33.3)	27 (44)
<20/200	7 (19.4)	18 (36.0)[b]	5 (16.7)	3 (18.8)	NA	3 (14.3)	19 (48.7)	11 (18)

Postoperative Visual Acuity								
Mean or median	NA	NA	20/100	20/250	20/200	20/160	20/260	20/80
>20/40	3 (8.3)	9 (18.0)[b]	4 (13.3)	0 (0.0)	NA	2 (9.5)	1 (2.6)	5 (8)
20/40–20/80	NA[a]	11 (22.0)[b]	13 (43.3)	3 (18.8)	NA	6 (28.6)	2 (5.2)	27 (44)
20/100–20/200	20 (55.6)	21 (42.0)[b]	7 (23.4)	6 (37.5)	NA	6 (28.6)	14 (35.9)	21 (34)
<20/200	13 (36.1)	8 (16.0)[b]	6 (20.0)	7 (43.7)	NA	7 (33.3)	22 (56.3)	8 (13)
Any improvement	7 (19.4)	33 (66.0)[c]	16 (53.3)	4 (25.0)	24 (26.6)[d]	9 (42.9)	17 (43.6)	32 (52.5)
No change	19 (52.8)	14 (28.0)[c]	6 (20.0)	0 (0.0)	37 (41.2)[d]	2 (9.5)	17 (43.6)	11 (18.0)
Any worsening	10 (27.8)	3 (6.0)[c]	8 (26.7)	12 (75.0)	29 (32.2)[d]	10 (47.6)	5 (12.8)	18 (29.5)
Improved by ≥3 lines	NA	NA	4 (13.3)	2 (12.5)	24 (26.6)	5 (23.8)	14 (35.9)	18 (29.5)
Worsened by ≥3 lines	NA	NA	2 (6.6)	9 (56.2)	29 (32.2)	6 (28.6)	9 (23.1)	7 (11.5)

[a]Visual acuity groups included >20/40, 20/40–20/200, <20/200.

[b]Visual acuity groups included >20/50, 20/50 to <20/80, 20/80–20/200, <20/200.

[c]Improvement denotes increase in visual acuity by two or more lines, no change denotes stable visual acuity ± 1 line, and worsening denotes reduction in visual acuity by two or more lines.

[d]Improvement denotes increase in visual acuity by 3 or more lines, no change denotes stable visual acuity or a change in visual acuity of less than 3 lines, and worsening denotes reduction in visual acuity by 3 or more lines.

[e]Prospective randomized trial of macular translocation versus photodynamic therapy with 25 participants in each subgroup.

NA, Information not available; Pro, prospective; Retro, retrospective.

Numerous reviews of the data from clinical series after MTS360 show benefit of treatment and document the potential complications of this surgery.[8–12,14–18,42,44,45,47,49] Duration of follow-up has ranged from 9.6 months to 83 months. Mean preoperative visual acuity varied from 20/125 to 20/260. Mean postoperative visual acuity ranged from 20/80 to 20/260, and some patients achieved a distance visual acuity of 20/40 or better. The percentage of patients with postoperative improvement in distance visual acuity has ranged from 43% to 66%.[8,15,18,44] Gains in visual acuity of three lines or more varied from 13% to 69%, while the percentage of patients in each study who lost three or more lines of visual acuity after MTS360 ranged from 4% to 56.2% (Fig. 123.5).[8–12,14–18,42,44,45,47]

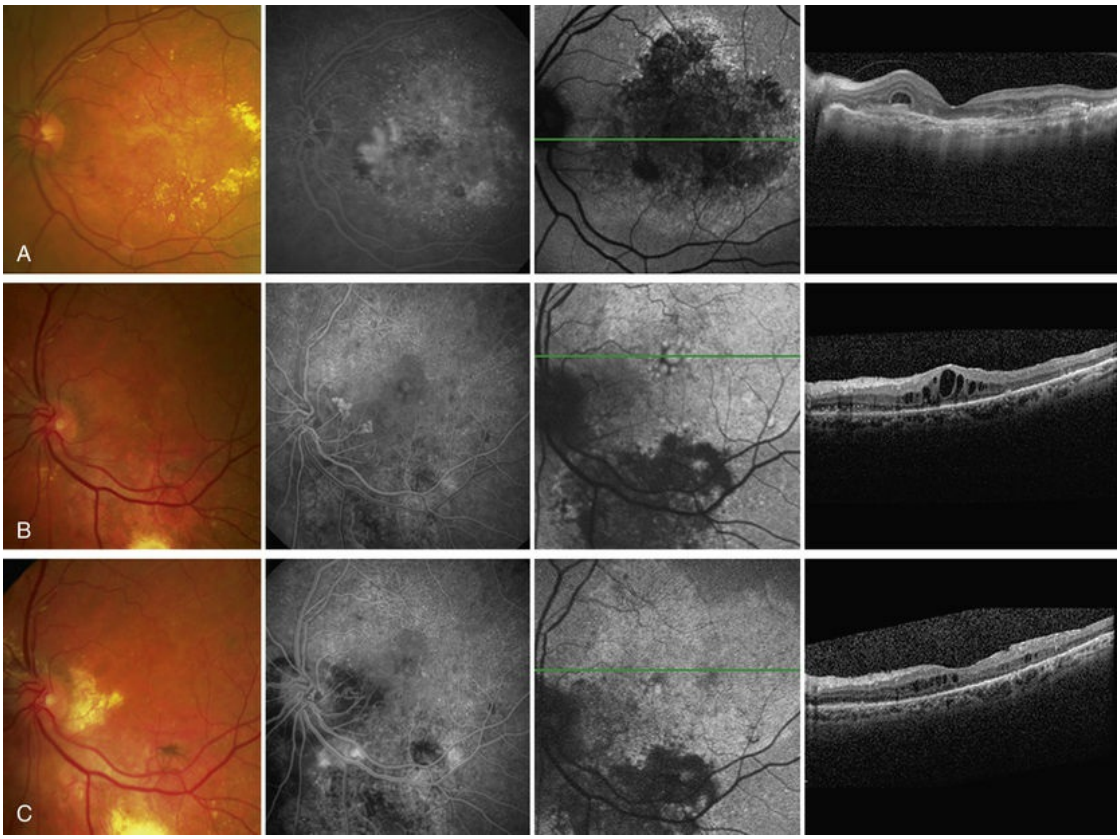

FIG. 123.5 Color fundus photograph, fluorescein angiogram, fundus autofluorescence, and spectral domain optical coherence tomography (from left to right) documenting macular translocation with 360° retinectomy (MTS360). (A) One month before MTS360 with visual acuity of 20/100, active choroidal neovascularization (CNV), diffuse cystoid macular edema (CME), and atrophy of the retinal pigment epithelium; (B) postoperative year 1 after MT360 with recurrent neovascularization at the edge of the old CNV lesion and CME in the translocated fovea; (C) postoperative year 3 after MT360 with improving visual acuity of 20/80 and regression of CNV and CME after laser and intravitreal antiangiogenic therapy.

MTS360 has also been utilized following photodynamic therapy (PDT) and other nonsurgical treatments. Prior to the anti-VEGF era, eyes treated with a single prior PDT session improved after MTS360 from mean visual acuity of 20/160 to postoperative mean acuity of 20/100, while eyes with more than one previous PDT session generally worsened from 20/200 before MTS360 to a mean postoperative visual acuity of 20/250.[50] In the anti-VEGF era, a study of 43 patients with anti-VEGF therapy or PDT or both,

sustained significant improvement in all measures of visual function at 1 year after MTS360 (mean gain of >9 letters).[38] An additional study examined 38 consecutive patients in the anti-VEGF era and showed that MTS360 resulted in improved visual acuity, particular in those patients with submacular hemorrhage and CNV, secondary to pathologic myopia.[51,52]

Numerous studies have also reported changes in near visual acuity, with near acuity sometimes improving greater than distance acuity.[13,18,45,48] Reported mean preoperative near visual acuity ranged from 20/100 to 20/160, with a significant improvement in mean near visual acuity to 20/63 and 20/55, postoperatively.[8,18] MTS360 has been shown to have better improvement in near visual acuity when compared to PDT (+7 letters versus −9.6 letters).[53] In several studies, over 20% of patients achieved postoperative near visual acuity OF 20/40 or better.[8,18,40,54]

The impact of MTS360 on other visual functions, including reading speed, contrast sensitivity, and color vision, have also been reported. Significant improvements in reading speed have been found following MTS360 with a mean increase of 26–45 words/minute.[18,40,54,55] MTS360 has been shown to not only improve reading speed and fixation quality but also to improve saccades during reading activities.[56] Improved contrast sensitivity has also been documented following MTS360, while color vision has been minimally affected following MTS360.[38,55]

Goldman perimetry studies have shown peripheral field loss but overall good preservation of the visual field following MTS360.[57] Microperimetry studies have shown recovery of central visual sensitivity following MTS360 (Fig. 123.6)[38,56,58] and a new focal scotoma in the superotemporal field due to the translocated CNV bed.[58] Reduction in photopic and scotopic electroretinograms have been documented following MTS360 for up to 5 months after surgery. The mechanism for ERG reduction is not clear, but it may be related to length of surgery, composition of subretinal infusate, and duration of detachment.[59–61] In addition to ERG, electro-oculogram findings have shown a decreased dark trough following MTS360, although the Arden ratio was within normal limits.[62]

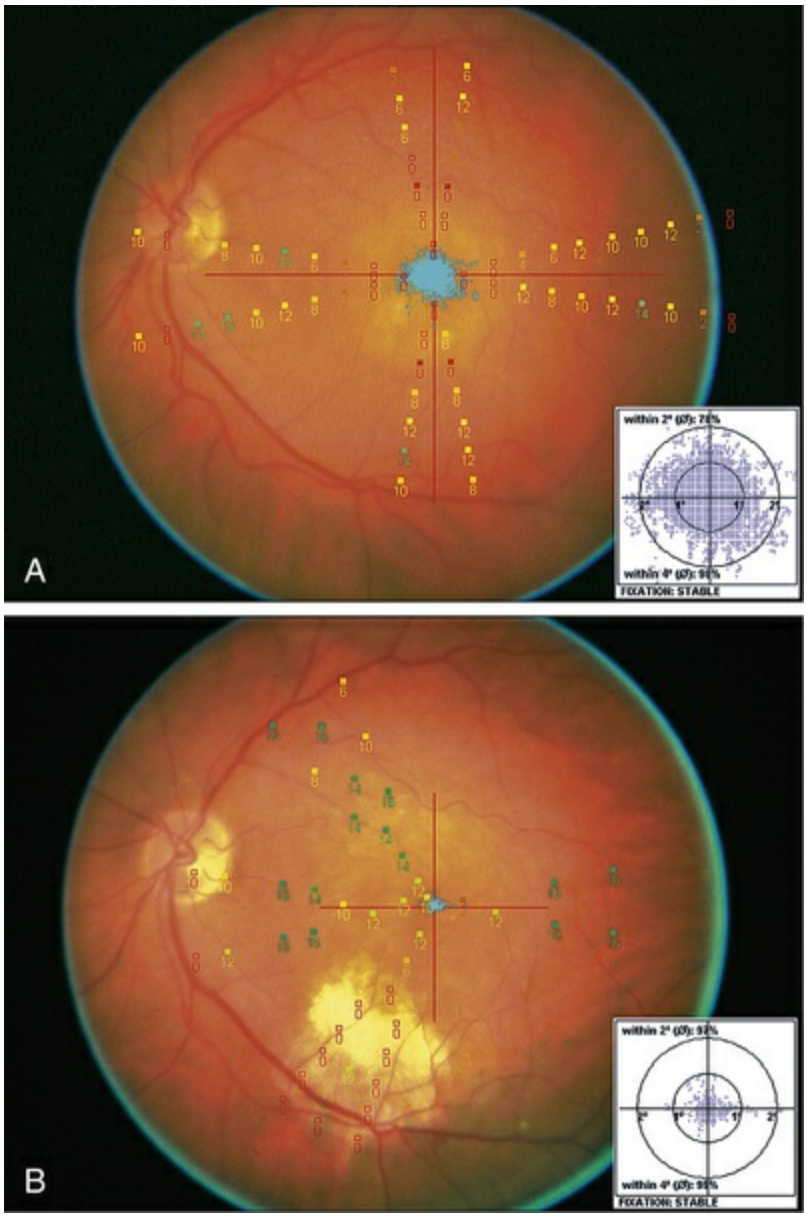

FIG. 123.6 Fundus photographs with superimposed microperimetry (Nidek MP-1) of the left eye of a 76-year-old female with bilateral age-related macular degeneration who had a 4-month history of progressive vision loss in her second affected eye. Photodynamic therapy with Visudyne had been performed 3 months before for predominantly classic subfoveal neovascularization. Microperimetry was performed using a Goldmann III equivalent target and 4–2 threshold testing strategy. Zero (0) signifies the highest-intensity stimulus and 16 the lowest. *Open square*, no response; *filled square*, response to stimulus. (A) Preoperatively best corrected visual acuity on ETDRS testing was 20/250. Microperimetry showed a central dense scotoma with no response to

the brightest stimulus centrally, unstable fixation (inset), and a good response to peripherally stimuli. (B) At 1 year postoperatively, best corrected distance visual acuity on ETDRS testing was 20/64 with resolution of central scotoma, stable fixation (inset), and development of a new peripheral scotoma over the displaced choroidal neovascular membrane bed.

Vision-related quality of life (QOL) has been found to significantly reduce in patients with bilateral severe AMD.[63] Following MTS360, vision-related QOL has been reported to have significant improvement, particularly in relation to distance acuity, near acuity, and reading speed. Near acuity was found to have the greatest impact in vision-related QOL. A 1-line change in near acuity resulted in a 13.7 point change in QOL score, compared with a 1.4–2.1 point change for a 1-line change in distance acuity or an increase in reading speed of 15 words/minute.[63] Vision-related QOL showed significant improvement in vision-related subscores following MTS360 in a prospective randomized study.[53] MTS360 showed significantly higher improvement in QOL scores for general vision, mental health, and dependency compared with treatment with PDT.[53]

Non-Neovascular AMD

Macular translocation has also been utilized in geographic atrophy (GA) secondary to AMD. Multiple reports have discussed MTS360 for these cases.[32,33,36,37] The first study published included eight eyes undergoing MTS360. Five of eight eyes had visual improvement, one remained stable, and two eyes had worsening visual acuity.[32] A more recent study included four eyes with GA, and in this study the mean preoperative and postoperative visual acuity were unchanged.[36] Recurrent RPE atrophy is a significant concern in patients treated with macular translocation and GA secondary to AMD.[32,36,37]

Non-AMD Diagnoses

In addition to AMD, multiple other submacular diseases can result in bilateral vision loss. In cases of severe functional limitation,

consideration may be given to macular translocation when other treatment modalities are not effective or a viable option (e.g., anti-VEGF therapy, photodynamic therapy, focal laser photocoagulation). Some of these conditions may not be VEGF-driven and may not respond to intravitreal therapy. Although limited in number, macular translocation has been utilized in many of these non-AMD conditions.[29] One recent study examined 16 subjects treated with MTS360 for conditions other than AMD. Conditions included in this report were adult-onset foveomacular vitelliform dystrophy (AOFVD), myopic degeneration, ocular histoplasmosis, punctate inner choroidopathy (PIC), Best disease, angioid streaks, North Carolina macular dystrophy, and central serous.[29] Of all of these conditions, myopic degeneration has been the most widely studied for macular translocation. A large study of MTS360 for myopic degeneration included 52 eyes with a final visual acuity of 20/40 or better in 39% of subjects.[64] In general, eyes with myopic degeneration had smaller CNVs (e.g., 0.4–1.2 disc diameters) and required less retinal rotation than eyes with neovascular AMD. A study of 15 eyes undergoing MTS360 for myopic degeneration reported that 73% of eyes showed visual improvement, with only 10% of eyes losing vision.[16,34,54] A smaller series of three eyes with myopic degeneration showed a final visual acuity of 20/60 or better in 3/3 eyes, with 2/3 eyes improving ≥3 lines.[29] An additional series of 17 eyes examined long-term follow-up (5 years or greater) for MTS360 for myopic CNV. Mean preoperative visual acuity was approximately 20/200 and improved to a mean postoperative visual acuity of approximately 20/100.[47] Long-term follow-up has also been reported for an additional group with 60 eyes with myopic CNV and a mean follow-up of 76.3 months. This series reported baseline best corrected visual acuity of approximately 20/125 with improvement to approximately 20/70 that remained stable >5 years after initial intervention.[65]

A case study of MTS360 for idiopathic CNV reported worsening visual acuity from 20/63 preoperatively to 20/100 postoperatively.[16] Comparing inflammatory preoperative diagnoses (e.g., presumed ocular histoplasmosis syndrome [POHS], PIC) with noninflammatory diagnoses (e.g., myopic degeneration, AOFVD, Best disease, North Carolina macular dystrophy, angioid streaks,

and central serous), only 20% of eyes with a preoperative inflammatory diagnosis maintained a visual acuity of 20/100 or better, and the mean final visual acuity in those eyes was 20/209.[29] Three of 5 (60%) eyes with inflammatory disease lost ≤3 lines of visual acuity, and the mean line change in visual acuity was a loss of 1.4 lines.[29] In eyes with a noninflammatory diagnosis the mean final visual acuity was 20/83 with 73% of eyes maintaining a final visual acuity of ≥20/100. Five of 11 eyes maintained a final visual acuity of ≥20/50. The mean line change was +1.0 lines.[29] Though this study was retrospective and small, this suggests that increased caution should be used prior to proceeding with MTS360 for inflammatory diagnoses. The most likely cause of worsening final visual acuity appeared to be an increase in postoperative complications for this group.[29] Polypoidal choroidal vasculopathy (PCV) has also been treated with MTS360, with two reported cases showing visual improvement following MTS360.[35]

Postoperative Surgical Complications Following Macular Translocation

Surgical complications following MTS360 for neovascular AMD are summarized in Table 123.2.[8–12,14–18,42,44,48] Retinal detachment is among the most common complications, with a prevalence of 7.8–42.8%. The higher rates of retinal detachment were reported in studies of early experience of surgeons with MTS360. Recurrence of CNV is also a common complication following MTS360. The prevalence of this complication ranges from 0.0% to 27.8%. Often due to the typical extrafoveal location of the CNV, thermal laser with or without anti-VEGF therapy can be employed. Cystoid macular edema (CME) and epiretinal membrane (ERM) formation are also two frequently reported complications. CME has not been consistently reported; however, studies have given a range of 0.0–44%. Many of these studies were prior to the widespread use of optical coherence tomography (OCT), and subclinical CME may go unrecognized. The studies reporting the highest rate of CME used OCT to examine every patient postoperatively.[18,48] ERM formation has been reported to occur in 6.6–28.2% of patients postoperatively.

However, the lack of uniform definition of ERM and the lack of widespread OCT use should lend caution to the interpretation of these numbers. Other complications such as macular hole, keratopathy, and hypotony tended to be less frequent.

TABLE 123.2

Surgical Complications After Macular Translocation With 360° Peripheral Retinectomy for Age-Related Macular Degeneration

First Author	Ohji[11]	Pertile[15]	Eckardt[8]	Toth[9]	Aisenbrey[14]	Fujikado[16]	A-Meguid[17]	Mruthyunjay
No. of patients	36	50	30	16	90	21.0	39	64
Follow-up (mth)	15.0	21.0	10.7	14.0	12.0	9.6	12.0	12.0
Retinal detachment	15 (41.6)	9 (18.0)	5 (16.6)	5 (31.2)	17 (18.9)	6 (19.3)[a]	10 (25.6)	5 (7.8)
Recurrent CNV	10 (27.8)[b]	5 (10.0)	3 (10.0)	3 (18.7)	3 (3.3)	2 (9.5)	3 (7.6)	13 (20.3)
CME	NA	NA	4 (13.3)	1 (6.2)	26 (28.9)	NA	NA	25 (39.1)
ERM	4 (11.1)	NA	2 (6.6)	2 (12.5)	12 (13.3)[c]	3 (9.7)[a]	11 (28.2)	14 (21.9)
Macular hole/tear	2 (6.0)	1 (2.0)	1 (3.3)	0 (0.0)	1 (1.1)	2 (6.4)[a]	3 (7.6)	0 (0.0)
Hypotony	1 (2.8)	0 (0.0)	0 (0.0)	0 (0.0)	2 (2.2)	NA	11 (28.2)	2 (3.1)
Keratopathy	1 (2.8)	NA	1 (3.3)	1 (6.2)	1 (1.1)	NA	2 (5.1)	0 (0.0)

[a]Complications recorded as proportion of 31 patients.

[b]Includes enlargement of CNV that was not removed and recurrence of CNV that was removed.

[c]Includes macular and peripheral epiretinal membranes.

[d]Five patients with recurrent CNV at 24 months follow-up; 10 patients with CME; 1 patient with an epiretinal membrane.

CME, cystoid macular edema; CNV, choroidal neovascularization; ERM, epiretinal membrane; NA, information not available.

Complications following MTS360 for non-AMD diagnoses have also been reported. For myopic degeneration, MTS360 has been reported to have a retinal detachment rate of 34% and recurrent CNV rate of 6%. A small study examining MTS360 for multiple non-AMD conditions showed that eyes with an underlying inflammatory diagnosis had a significantly higher complication rate compared with noninflammatory diagnoses.[29] In that report, the

overall complication rates were 50% for ERM (including mild ERM on OCT); 31% for CME; 13% for retinal detachment; and 13% for CNV. A total of 38% needed an office-based procedure due to a complication (e.g., sub-Tenon injection, laser). Surgical intervention was required in 19% of eyes. In eyes with an underlying inflammatory diagnosis, 100% (5/5) of eyes required some type of intervention for a complication, compared with only 36% (4/11) of eyes with a noninflammatory diagnosis. In eyes with an underlying inflammatory diagnosis, the CNV recurrence rate was 40%.[29]

Given the extensive rotation associated with MTS360, binocular vision is often not recovered and extraocular muscle surgery is required. Almost all patients have a central scotoma in the fellow eye preoperatively, but their peripheral vision is well maintained. The findings regarding binocularity are variable. Using Bagolini glasses, five studies reported findings of postoperative binocular vision in 6.6–28.5% of eyes.[8,10,11,14,17,66] However, one study reported a 0% rate of binocular function in patients.[67]

Retinal and RPE Changes After Macular Translocation

The positioning of the previously dysfunctional macula over new underlying RPE provides a unique opportunity to study the relationship between photoreceptor and RPE function in humans with macular disease. The status of these tissues has been examined through numerous imaging techniques after MTS360. This has included angiography, autofluorescence imaging, spectral domain optical coherence tomography, and color fundus photography.

A striking finding in patients with GA treated with macular translocation is the recurrence of the RPE atrophy in the new foveal bed, which has now been reported in multiple studies.[32,36,37] In one study, recurrent RPE changes were seen in 75% of eyes treated with MTS360.[36] Similar findings of new RPE atrophy are quite rare in patients with neovascular AMD treated with MTS360.[36] The precipitating factor for RPE atrophy is not clear. Given the rarity of similar findings in MTS360 for neovascular AMD, surgical trauma seems to be an unlikely cause. RPE atrophy may be the primary event, particularly if the increased metabolic activity of the

overlying foveal photoreceptors results in increased stress to the fragile RPE. Alternatively, apoptotic photoreceptors may result in secondary RPE atrophy in the new foveal bed. Additional research is needed to further elucidate the mechanisms involved in this phenomenon.

The reports of recurrence of GA were in the era before more routine autofluorescence imaging. The FAF techniques are useful to monitor the health of the new RPE under the macula. In patients with neovascular AMD and with non-AMD diseases such as myopia, the RPE under the new macula demonstrates hyperautofluorescence that persists with little change over months to years.[42,47,68] This finding is often compatible with good visual acuity. The phenomenon of increased autofluorescence in the area of the new macular location after macular translocation is thought to be related to an unmasking of autofluorescence due to thinning of retina from loss of photoreceptors, though it may also be due to an increase in fluorophores in the RPE due to the metabolic demand of the concentrated central macular photoreceptors.[69] In addition, the RPE that was in the shadow of retinal vessels for the lifetime of the patient, and is now exposed for imaging after translocation, shows increased autofluorescence relative to adjacent RPE, whether after intentional MTS360 or after inadvertent translocation in retinal detachment repair.[70]

Both angiography and OCT imaging are used to monitor for evidence of recurrent CNV, while OCT imaging is also useful to evaluate the photoreceptor layer in the macula after translocation. OCT imaging is also useful for assessment of postoperative CME, which may be chronic and responsive to anti-VEGF therapy or antiinflammatory therapy, including intravitreal steroids.[42]

Unintentional Macular Translocation Following Retinal Detachment Repair

Translocation of the macula is a feared complication during rhegmatogenous retinal detachment repair. Shifting of the retina during surgery may occur during multiple time points. Intraoperatively, as the retina is reattached (e.g., during perfluorocarbon liquid infusion, air–fluid exchange), there is some

risk of shift. However, postoperative positioning is the most likely reason for translocation. Residual subretinal fluid combined with gravitational forces may shift the retina inferiorly (when the patient is upright) or nasally (when the patient is positioned with the nasal side of the surgical eye down). When the detachment involves the superior retina through the macula, this retinal shift can produce a limited macular translocation, resulting in a retinal fold.[71,72] The location of the fold in cases of upright positioning would depend on the location of the inferior border of the detached retina.

In one study, patients with gas-filled eyes after vitrectomy for retinal reattachment were positioned upright for several minutes prior to face-down positioning.[70] This upright positioning was carried out to determine if subtle shifts in the retina occurred inferiorly. Fundus autofluorescence found hyperfluorescent changes corresponding to the preoperative location of the retinal vessels, suggesting an inferior rotation of the retina in 63% (27/43) of eyes. In those eyes with hyperfluorescent changes, a synoptophore measurement revealed that 59% of eyes had excyclotorsion and 49% of eyes had a vertical deviation. Interestingly, none of these eyes had symptomatic diplopia. Risk factors associated with retinal translocation included macula off status and increased size of retinal detachment. The use of perfluorocarbon liquid had no association with risk of retinal rotation.[70]

An increase in cases of partial macular translocation with macular fold was reported after a shift to outpatient surgery, and the fold was associated with patients failing to position face down after leaving the surgical center.[73] Because it is often difficult to assure postoperative prone positioning without inadvertent upright positioning, placing the patient initially on their side with the temporal retina dependent in the early period after surgery may reduce the risk of inadvertent translocation.

Advantages of Macular Translocation and Future Directions

In the anti-VEGF era, the landscape for macular translocation has

changed significantly. The good results achieved with anti-VEGF therapy for neovascular AMD have shifted primary treatment of AMD away from surgical intervention.[26,27] As Zeimssen and Gelisken[74] point out, "Generally, in the presence of highly effective anti-VEGF drugs, FMT can be discussed for second-line treatment, if the fellow eye has poor function and no additional risk factors of the affected eye are known."

Numerous researchers note that MTS360 may well have a role in the management of bilateral submacular diseases, including AMD. This may be particularly true in cases with early subretinal fibrosis with preservation of the outer retina. If the fellow eye has lost significant visual acuity and anti-VEGF therapy or other modalities have been unsuccessful, consideration may be given to proceeding with macular translocation. Without surgical removal, progressive enlargement of CNV may occur resulting in enlargement of the area of photoreceptor damage.[75,76] Central acuity may not recover even with arrest of CNV leakage, due to underlying fibrosis and loss of RPE. MTS360 may allow recovery of function through the translocation of the foveal photoreceptors off the scarred underlying tissues to an area with improved vitality.[1] Cases of extensive subretinal hemorrhage may also be amenable to MTS360, as the procedure allows for removal of the subretinal blood during the translocation process.[7]

Given that macular translocation is a type of autotransplantation, macular translocation not only provides a service to patients through potentially restoring central vision but has provided the proof that RPE transplants could support central vision and the impetus for surgical trials of transplantation of autologous patches of RPE-choroid beneath the macula (see Chapter 124, Retinal pigment epithelium and choroid translocation in patients with age-related macular degeneration).[77] In the future, MTS360 could provide a future scenario of neurosensory retina with damaged macular photoreceptors translocated over healthier RPE–Bruch's–choriocapillaris along with additional growth factors or stem cells to support photoreceptor recovery. Meanwhile, this autotransplantation provides a unique look at the pathophysiology of many submacular diseases that we treat. Findings such as recurrent atrophy in the new RPE bed following macular

translocation for GA but not neovascular AMD provide a window into the possible mechanisms involved in AMD and other disorders. In the future, continued research will hopefully help to answer multiple questions, including photoreceptor damage reversibility, the interactions between photoreceptors and RPE in disease pathogenesis, and the possible role of novel therapies such as growth factors or stem cells in the recovery of function in a new RPE bed.

References

1. Toth CA, Machemer R. Macular translocation. Fine S, Berger J, Maguire M. *Age-related macular degeneration*. Mosby: St Louis; 1999:353–362.
2. Machemer R, Steinhorst UH. Retinal separation, retinotomy, and macular relocation: I Experimental studies in the rabbit eye. *Graefes Arch Clin Exp Ophthalmol*. 1993;231:629–634.
3. Fang XY, Hayashi A, Cekic O, et al. Effect of Ca2+-free and Mg2+-free BSS Plus solution on the retinal pigment epithelium and retina in rabbits. *Am J Ophthalmol*. 2001;131:481–488.
4. Faude F, Wendt S, Biedermann B, et al. Facilitation of artificial retinal detachment for macular translocation surgery tested in rabbit. *Invest Ophthalmol Vis Sci*. 2001;42:1328–1337.
5. Lindsey P, Finkelstein D, D'Anna S. Experimental retinal relocation. *Invest Ophthalmol Vis Sci*. 1983;24:S242.
6. Tiedeman JS, de Juan E Jr, Machemer R, et al. Surgical rotation of the macula. *Invest Ophthalmol Vis Sci*. 1985;26:S59.
7. Machemer R, Steinhorst UH. Retinal separation, retinotomy, and macular relocation: II. A surgical approach for age-related macular degeneration? *Graefes Arch Clin Exp Ophthalmol*. 1993;231:635–641.
8. Eckardt C, Eckardt U, Conrad HG. Macular rotation with and without counter-rotation of the globe in patients with age-related macular degeneration. *Graefes Arch Clin Exp*

Ophthalmol. 1999;237:313–325.
9. Toth CA, Freedman SF. Macular translocation with 360-degree peripheral retinectomy impact of technique and surgical experience on visual outcomes. *Retina*. 2001;21:293–303.
10. Tano Y. Pathologic myopia: where are we now? *Am J Ophthalmol*. 2002;134:645–660.
11. Ohji M, Fujikado T, Kusaka S, et al. Comparison of three techniques of foveal translocation in patients with subfoveal choroidal neovascularization resulting from age-related macular degeneration. *Am J Ophthalmol*. 2001;132:888–896.
12. Wolf S, Lappas A, Weinberger AW, et al. Macular translocation for surgical management of subfoveal choroidal neovascularizations in patients with AMD: first results. *Graefes Arch Clin Exp Ophthalmol*. 1999;237:51–57.
13. Lai JC, Lapolice DJ, Stinnett SS, et al. Visual outcomes following macular translocation with 360-degree peripheral retinectomy. *Arch Ophthalmol*. 2002;120:1317–1324.
14. Aisenbrey S, Lafaut BA, Szurman P, et al. Macular translocation with 360 degrees retinotomy for exudative age-related macular degeneration. *Arch Ophthalmol*. 2002;120:451–459.
15. Pertile G, Claes C. Macular translocation with 360 degree retinotomy for management of age-related macular degeneration with subfoveal choroidal neovascularization. *Am J Ophthalmol*. 2002;134:560–565.
16. Fujikado T, Shimojyo H, Hosohata J, et al. Effect of simultaneous oblique muscle surgery in foveal translocation by 360 degrees retinotomy. *Graefes Arch Clin Exp Ophthalmol*. 2002;240:21–30.
17. Abdel-Meguid A, Lappas A, Hartmann K, et al. One year follow up of macular translocation with 360 degree retinotomy in patients with age related macular degeneration. *Br J Ophthalmol*. 2003;87:615–621.
18. Mruthyunjaya P, Stinnett SS, Toth CA. Change in visual function after macular translocation surgery with 360 degree peripheral retinectomy for neovascular age-related macular degeneration. *Ophthalmology*. 2004;111:1715–1724.

19. Seaber JH, Machemer R. Adaptation to monocular torsion after macular translocation. *Graefes Arch Clin Exp Ophthalmol*. 1997;235:76–81.
20. Ninomiya Y, Lewis JM, Hasegawa T, et al. Retinotomy and foveal translocation for surgical management of subfoveal choroidal neovascular membranes. *Am J Ophthalmol*. 1996;122:613–621.
21. Akduman L, Karavellas MP, MacDonald JC, et al. Macular translocation with retinotomy and retinal rotation for exudative age-related macular degeneration. *Retina*. 1999;19:418–423.
22. de Juan E Jr, Loewenstein A, Bressler NM, et al. Translocation of the retina for management of subfoveal choroidal neovascularization II: a preliminary report in humans. *Am J Ophthalmol*. 1998;125:635–646.
23. Imai K, Loewenstein A, de Juan E Jr. Translocation of the retina for management of subfoveal choroidal neovascularization I: experimental studies in the rabbit eye. *Am J Ophthalmol*. 1998;125:627–634.
24. Imai K, de Juan E Jr. Experimental surgical macular relocation by scleral shortening. ARVO abstracts. *Invest Ophthalmol Vis Sci*. 1996;37:S116.
25. Au Eong KG, Pieramici DJ, Fujii GY, et al. Macular translocation: unifying concepts, terminology, and classification. *Am J Ophthalmol*. 2001;131:244–253.
26. Brown DM, Kaiser PK, Michels M, et al. Ranibizumab versus verteporfin for neovascular age-related macular degeneration. *N Engl J Med*. 2006;355:1432–1444.
27. Rosenfeld PJ, Brown DM, Heier JS, et al. Ranibizumab for neovascular age-related macular degeneration. *N Engl J Med*. 2006;355:1419–1431.
28. Lewis H, Kaiser PK, Lewis S, et al. Macular translocation for subfoveal choroidal neovascularization in age-related macular degeneration: a prospective study. *Am J Ophthalmol*. 1999;128:135–146.
29. Ehlers JP, Maldonado R, Sarin N, et al. Treatment of non-age-related macular degeneration submacular diseases with macular translocation surgery. *Retina*. 2011;31:1337–1346.

30. Polito A, Cereda M, Romanelli F, et al. Macular translocation with 360 degrees retinotomy for management of retinal pigment epithelial tear: long-term results. *Br J Ophthalmol*. 2011;95:74–78.
31. Steel DH, Sandhu SS. Submacular haemorrhages associated with neovascular age-related macular degeneration. *Br J Ophthalmol*. 2011;95:1051–1057.
32. Eckardt C, Eckardt U. Macular translocation in nonexudative age-related macular degeneration. *Retina*. 2002;22:786–794.
33. Cahill MT, Freedman SF, Toth CA. Macular translocation with 360 degrees peripheral retinectomy for geographic atrophy. *Arch Ophthalmol*. 2003;121:132–133.
34. Fujikado T, Ohji M, Kusaka S, et al. Visual function after foveal translocation with 360-degree retinotomy and simultaneous torsional muscle surgery in patients with myopic neovascular maculopathy. *Am J Ophthalmol*. 2001;131:101–110.
35. Terasaki H, Miyake Y, Suzuki T, et al. Polypoidal choroidal vasculopathy treated with macular translocation: clinical pathological correlation. *Br J Ophthalmol*. 2002;86:321–327.
36. Cahill MT, Mruthyunjaya P, Bowes Rickman C, et al. Recurrence of retinal pigment epithelial changes after macular translocation with 360 degrees peripheral retinectomy for geographic atrophy. *Arch Ophthalmol*. 2005;123:935–938.
37. Khurana RN, Fujii GY, Walsh AC, et al. Rapid recurrence of geographic atrophy after full macular translocation for nonexudative age-related macular degeneration. *Ophthalmology*. 2005;112:1586–1591.
38. Mettu PS, Sarin N, Stinnett SS, et al. Recovery of the neurosensory retina after macular translocation surgery is independent of peroperative macular sensitivity in neovascular age-related macular degeneration. *Retina*. 2011;31:1637–1649.
39. Kim SY, Sadda S, Pearlman J, et al. Morphometric analysis of the macula in eyes with disciform age-related macular degeneration. *Retina*. 2002;22:471–477.

40. Lafaut BA, Aisenbrey S, Vanden Broecke C, et al. Clinicopathological correlation of deep retinal vascular anomalous complex in age related macular degeneration. *Br J Ophthalmol*. 2000;84:1269–1274.
41. Kuhn D, Meunier I, Soubrane G, et al. Imaging of chorioretinal anastomoses in vascularized retinal pigment epithelium detachments. *Arch Ophthalmol*. 1995;113:1392–1398.
42. van Romunde S, Polito A, Bertazzi L, et al. Long-term results of full macular translocation for choroidal neovascularization in age-related macular degeneration. *Ophthalmology*. 2015;122:1366–1374.
43. Freedman SF, Holgado S, Enyedi LB, et al. Management of ocular torsion and diplopia after macular translocation for age-related macular degeneration: prospective clinical study. *Am J Ophthalmol*. 2003;136:640–648.
44. Chen FK, Patel PJ, Uppal GS, et al. Long-term outcomes following full macular translocation surgery in neovascular age-related macular degeneration. *Br J Ophthalmol*. 2010;94:1337–1343.
45. Lüke M, Ziemssen F, Völker M, et al. Full macular translocation (FMT) versus photodynamic therapy (PDT) with verteporfin in the treatment of neovascular age-related macular degeneration: 2-year results of a prospective, controlled, randomised pilot trial (FMT-PDT). *Graefes Arch Clin Exp Ophthalmol*. 2009;247:745–754.
46. Skaf AR, Mahmoud T. Surgical treatment of age-related macular degeneration. *Semin Ophthalmol*. 2011;26:181–191.
47. Takeuchi K, Kachi S, Iwata E, et al. Visual function 5 years or more after macular translocation surgery for myopic choroidal neovascularization and age-related macular degeneration. *Eye (Lond)*. 2012;26:51–60.
48. Gelisken F, Voelker M, Schwabe R, et al. Full macular translocation versus photodynamic therapy with verteporfin in the treatment of neovascular age-related macular degeneration: 1-year results of a prospective, controlled, randomised pilot trial (FMT-PDT). *Graefes Arch Clin Exp Ophthalmol*. 2007;245:1085–1095.

49. Eandi CM, Giansanti F, Virgili G. Macular translocation for neovascular age-related macular degeneration. *Cochrane Database Syst Rev*. 2008;(4) [CD006928].
50. Park CH, Toth CA. Macular translocation surgery with 360-degree peripheral retinectomy following ocular photodynamic therapy of choroidal neovascularization. *Am J Ophthalmol*. 2003;136:830–835.
51. Yamada Y, Miyamura N, Suzuma K, et al. Long-term follow-up of full macular translocation for choroidal neovascularization. *Am J Ophthalmol*. 2010;149:453–457.
52. Haverbeke GM, Claes C. Full macular translocation for choroidal neovascularization in the era of intravitreal pharmacological therapy. *Retina*. 2010;30:1739–1743.
53. Lüke M, Ziemssen F, Bartz-Schmidt KU, et al. Quality of life in a prospective, randomised pilot-trial of photodynamic therapy versus full macular translocation in treatment of neovascular age-related macular degeneration – a report of 1 year results. *Graefes Arch Clin Exp Ophthalmol*. 2007;245:1831–1836.
54. Fujikado T, Asonuma S, Ohji M, et al. Reading ability after macular translocation surgery with 360-degree retinotomy. *Am J Ophthalmol*. 2002;134:849–856.
55. Toth CA, Lapolice DJ, Banks AD, et al. Improvement in near visual function after macular translocation with 360-degree peripheral retinectomy. *Graefes Arch Clin Exp Ophthalmol*. 2004;242:541–548.
56. Uppal G, Feely M, Crossland M, et al. Assessment of reading behaviour with an infrared eyetracker following 360 degree macular translocation for age related macular degeneration. *Invest Ophthalmol Vis Sci*. 2011;52:6486–6496.
57. Kubota A, Ohji M, Kusaka S, et al. Evaluation of the peripheral visual field after foveal translocation. *Am J Ophthalmol*. 2001;132:581–584.
58. Chieh JJ, Stinnett SS, Toth CA. Central and pericentral retinal sensitivity after macular translocation surgery. *Retina*. 2008;28:1522–1529.
59. Luke C, Aisenbrey S, Luke M, et al. Electrophysiological changes after 360 degrees retinotomy and macular

translocation for subfoveal choroidal neovascularisation in age related macular degeneration. *Br J Ophthalmol*. 2001;85:928–932.
60. Terasaki H, Miyake Y, Suzuki T, et al. Change in full-field ERGs after macular translocation surgery with 360 degrees retinotomy. *Invest Ophthalmol Vis Sci*. 2002;43:452–457.
61. Sickel W. Retinal metabolism in dark and light. Fuortes MG. *Handbook of sensory physiology*. Springer: Berlin; 1972:667–727.
62. Luke C, Alteheld N, Aisenbrey S, et al. Electro-oculographic findings after 360 degrees retinotomy and macular translocation for subfoveal choroidal neovascularisation in age-related macular degeneration. *Graefes Arch Clin Exp Ophthalmol*. 2003;241:710–715.
63. Cahill MT, Stinnett SS, Banks AD, et al. Quality of life after macular translocation with 360-degree peripheral retinectomy for age-related macular degeneration. *Ophthalmology*. 2005;112:152–158.
64. Chan WM, Ohji M, Lai TY, et al. Choroidal neovascularisation in pathological myopia: an update in management. *Br J Ophthalmol*. 2005;89:1522–1528.
65. Sakimoto S, Hirokazu S, Ohji M, et al. Consecutive case series with long-term follow-up of full macular translocation for myopic choroidal neovascularization. *Br J Ophthalmol*. 2014;98:1221–1225.
66. Fricke J, Neugebauer A, Nobis H, et al. Counterrotation of the globe in macular translocation. *Graefes Arch Clin Exp Ophthalmol*. 2000;238:664–668.
67. Freedman SF, Holgado S, Enyedi LB, et al. Management of ocular torsion and diplopia after macular translocation for age-related macular degeneration: prospective clinical study. *Am J Ophthalmol*. 2003;136:640–648.
68. Sawa M, Gomi F, Ohji M, et al. Fundus autofluorescence after full macular translocation surgery for myopic choroidal neovascularization. *Graefes Arch Clin Exp Ophthalmol*. 2008;246:1087–1095.
69. Chen FK, Patel PJ, Coffey PJ, et al. Increased fundus autofluorescence associated with outer segment shortening

in macular translocation model of neovascular age-related macular degeneration. *Invest Ophthalmol Vis Sci*. 2010;51(8):4207–4212.
70. Shiragami C, Shiraga F, Yamaji H, et al. Unintentional displacement of the retina after standard vitrectomy for rhegmatogenous retinal detachment. *Ophthalmology*. 2010;117:86–92.
71. Van Meurs JC, Humalda D, Mertens DAE, et al. Retinal folds through the macula. *Doc Ophthalmol*. 1991;78:335–340.
72. Heimann H, Bopp S. Retinal folds following retinal detachment surgery. *Ophthalmologica*. 2011;226:18–26.
73. Isaico R, Malvitte L, Bron AM, et al. Macular folds after retinal detachment surgery: the possible impact of outpatient surgery. *Graefes Arch Clin Exp Ophthalmol*. 2013;251:383–384.
74. Ziemssen F, Gelisken F. Macular translocation – a therapeutic approach for neovascular macular degeneration in the era of anti-VEGF therapy? *Klin Monatsbl Augenheilkd*. 2009;226:31–37.
75. TAP: Treatment of Age-Related Macular Degeneration with Photodynamic Therapy Study Group. Photodynamic therapy of subfoveal choroidal neovascularization in age-related macular degeneration with verteporfin: one-year results of 2 randomized clinical trials – TAP report. *Arch Ophthalmol*. 1999;117:1329–1345.
76. Bressler NM, Treatment of Age-Related Macular Degeneration with Photodynamic Therapy (TAP) Study Group. Photodynamic therapy of subfoveal choroidal neovascularization in age-related macular degeneration with verteporfin: two-year results of 2 randomized clinical trials – TAP report 2. *Arch Ophthalmol*. 2001;119:198–207.
77. Chen FK, Patel PJ, Uppal GS, et al. A comparison of macular translocation with patch graft in neovascular age-related macular degeneration. *Invest Ophthalmol Vis Sci*. 2009;50(4):1848–1855.

124

Retinal Pigment Epithelium and Choroid Translocation in Patients With Age-Related Macular Degeneration

Jan C. van Meurs, Bernd Kirchhof, Robert MacLaren

Epidemiology

In industrialized countries the endstage of age-related maculopathy (ARM) is the principal cause of legal blindness in persons older than 60 years.[1–3] Severe age-related macular degeneration (AMD) occurs in an atrophic (two-thirds) and an exudative form (one-third). While we currently have an effective treatment to manage exudative AMD, there is no equally effective treatment in sight for

geographic atrophy (GA). This situation is likely to increase the relative proportion of blindness through GA compared with exudative AMD in the future, and increasing life expectancy will similarly lead to an increase in the prevalence of GA. (Epidemiology is discussed further in Chapter 66, Epidemiology and risk factors for age-related macular degeneration.)

Alternative Treatments for AMD

Exudative AMD

The current 2015 approved treatment for many patients with exudative AMD is anti-vascular endothelial growth factor injections. (This is discussed further in Chapter 69, Neovascular (exudative or "wet") age-related macular degeneration.)

However, for patients with a retinal pigment epithelium (RPE) tear[4,5] or a large submacular hemorrhage, anti-VEGF therapy is generally less effective in restoring or improving visual acuity (VA), because the underlying anatomy of the outer retina is disrupted. In addition, even with the established anti-VEGF treatments, a substantial percentage of patients fail to respond, especially long term. In the original MARINA study, 10% of patients receiving ranibizumab had lost ≥15 letters and overall, 15% of patients on ranibizumab were 20/200 or worse by year 2.[6] A recent retrospective analysis of those patients who responded poorly to ranibizumab in both the MARINA and ANCHOR studies by year 2 revealed that these patients may have had disruption of retinal anatomy rather than highly active choroidal neovascularization (CNV).[7] The SEVEN-UP study looked at the long-term (7–8 years) outcomes of patients in the above trials and found a mean loss of VA of 8.6 letters at 7.3 years, with a third (34%) losing vision by 15 lines or more.[8] This highlights the need to consider alternative strategies, such as surgery, to improve the anatomy of the retina–RPE interface in selected patients.

Dry AMD

Geographic atrophy (GA) is an untreatable advanced form of dry

age-related macular degeneration. However, a number of clinical and animal model studies have evaluated medical treatment approaches, e.g.,

- Growth factors (ciliary neurotrophic factor (see http://www.clinicaltrials.gov, NCT00447954, for details)
- Modulation of gene expression (DICER protein)[9]
- Modulation of the visual cycle to decrease toxic by-products (see http://www.clinicaltrials.gov, NCT01002950, for details)
- Modulation of inflammation (see http://www.clinicaltrials.gov, NCT00766649, for details)
- Plasma filtration (see http://www.clinicaltrials.gov, NCT00460967, for details).

Nevertheless, to date, there is no approved treatment regimen for GA.

Surgical Treatment

As an alternative treatment, five surgical treatment modalities have been described for exudative AMD and to a lesser extent for dry AMD.

1. Removal of the submacular choroidal membrane and/or hemorrhage. This was shown to be of little benefit in the Submacular Surgery Trials (SST), although the percentage of patients with more than 6 lines VA loss was statistically smaller in the subgroup of patients with large submacular hemorrhage (group B) when compared to natural history[10]

2. Macular translocation after 360° retinectomy. This method was first reported by Machemer et al. in 1993.[11] A tilted image in successful cases, complex and time-consuming surgery, and a high percentage of vision-threatening complications such as proliferative vitreoretinopathy (PVR), particularly in the earlier studies, remain drawbacks of this technique[12] (described in more detail in Chapter 123, Macular translocation). In a randomized controlled trial (RCT) in Tübingen in 50 patients, however, with photodynamic therapy (PDT) treatment in the control arm, vision gain was significantly

greater in the surgical arm.[13] The limit to the extent of retinal rotation possible makes it most effective for smaller lesions, particularly classic CNV, but this clinical presentation is also particularly well suited to anti-VEGF treatments, making this surgery less easy to justify in the modern era. Nevertheless, in highly skilled hands, good long-term results can be obtained.[14]

3. Minimal macular translocation by scleral infolding and the induction of retinal detachment (RD) was described by de Juan in 1998.[15] The macular translocation achieved, however, was less than one disc diameter.[16] This has indeed limited its use since the advent of treatments that were particularly effective for small lesions, such as PDT and anti-VEGF (see Chapter 123, Macular translocation).

4. The displacement of an acute hemorrhage by gas and recombinant tissue plasminogen activator, with or without vitrectomy, with subsequent treatment with PDT or anti-VEGF.[17,18] Several case series suggest a clear benefit over natural history.[19–21]

5. Transplantation of an autologous graft of RPE, Bruch's membrane, choriocapillaris, and choroid. This method was first described in a case report by Peyman et al. in 1991.[22] Initially, the graft was harvested from the edge of the macular RPE defect.[23] Later studies utilized midperipheral tissue.[24–29] The most frequent complications of this transplantation technique were recurrent CNV, RD, PVR, failure of the graft to revascularize, macular pucker, and postoperative hemorrhages.

Both macular translocation surgery and the transplantation of a free autologous graft of RPE and choroid will probably achieve a better VA than no intervention. Though macular translocation surgery might produce better outcomes,[30] it has a greater risk of complications and there is a physical limit to the amount of rotation possible (even after 360° retinectomy), which makes it less suited to large CNV.

This chapter focuses on the transplantation of free autologous grafts of retinal pigment epithelium and choroid. It will discuss its history, surgery, published results in patients with exudative and atrophic AMD, and conclude with potential developments.

Rationale for Reconstitution of Retinal Pigment Epithelium

The spectacular functional restoration achieved in some patients with exudative AMD after macular translocation by rotation proved the principle of reopposing a reversibly compromised fovea to a fresh undersurface of functioning RPE cells.[11,31] Other key discoveries in the concept of restoring the underlayer of the macula have included:

- Showing that functioning RPE cells are essential for the preservation of Bruch's membrane and the underlying choriocapillaris in rabbits.[32]
- Demonstrating that human RPE cells secrete VEGF on their basal side and that the adjoining underlying choriocapillaris has VEGF-receptors.[33]
- Proving the principle that healthy RPE cells can postpone photoreceptor death after subretinal transplantation in a rat model of RPE dysfunction.[34]

Consequently many different surgical approaches to recreate a functioning RPE underlayer of the macula have been tried. These approaches may broadly be defined by several complementary techniques: autografts versus allografts; cells in suspension versus cell sheets or patches; RPE versus iris pigment epithelium (IPE) cells (Table 124.1).

TABLE 124.1

Reconstitution of RPE: Cell Suspension or Cell Sheets; Allograft or Autograft; RPE or IPE

	Author, Year of Publication (No. of Patients)
Autograft IPE suspension	Thumann et al., 2000 (12),[35] Lappas et al., 2000 (12)[36]
Autograft IPE patch graft	Navea Tejerina, 1998[37]
Autograft RPE suspension	Binder, 2002 (14),[38] Binder et al., 2004 (53),[39] van Meurs et al., 2004 (8),[40] Falkner-Radler et al., 2011 (7)[41]
Autograft RPE patch	Peyman et al., 1991 (1),[22] Stanga et al., 2002 (9),[23] van Meurs and Van Den Biesen, 2003 (6),[24] Bindewald et al., 2004,[42] MacLaren, 2005 (9),[43] Joussen et al., 2006 (45),[25]

graft	Maaijwee et al., 2007 (84),[28] Treumer et al., 2007 (10),[27] MacLaren et al., 2007 (12),[26] Joussen et al., 2007 (12[a]),[44] Chen et al., 2009 (12),[30] Chen et al., 2009 (24),[45] Gibran et al., 2009 (4[b]),[46] Ma et al., 2009 (21[b,c]),[43] Caramoy et al., 2010 (10[a]),[47] Cereda, 2010 (13[b]),[48] Falkner-Radler et al., 2011 (7),[41] van Zeeburg et al., 2012 (134),[29] van Zeeburg, 2015 (10)[49]
Allograft RPE suspension	Valtink et al., 1999,[50] Valtink et al., 1999[51]
Allograft RPE patch graft	Peyman, 1991 (1),[22] Algvere, 1994 (5),[52] Algvere, 1997 (5),[53] Del Priore, 2001 (12)[54]

[a]Geographic atrophy.

[b]Flapover technique.

[c]Partial-thickness graft.

IPE, iris pigment epithelium; RPE, retinal pigment epithelium.

Transplantation of a Full-Thickness Patch From the Midperiphery

With the current lack of demonstrable presence or function of RPE or IPE suspension transplants,[38,40,41] the authors decided to pursue the use of a sheet of autologous RPE on its own substratum. Peyman reported a case history on the use of a full-thickness flap with a pedicle. Follow-up was 6 months and stabilization of vision at 20/400 was reported.[22] Aylward, in nine patients, used a full-thickness patch, cut out from a location adjacent to the removed subfoveal membrane. In four patients, some function on microperimetry could be shown over the patch; but the preoperative vision was too low to assess vision in detail using the techniques available at the time.[23] Fibrosis of the patch, however, developed in the second year of follow-up in most patients, and previously documented function on the graft had disappeared.[55] In Aylward's patients the grafted paramacular choriocapillaris appeared sclerotic and damaged by the surgery, and we speculated that it was therefore less likely to be successfully revascularized. Van Meurs[24] sought to improve on Aylward's technique by harvesting a relatively healthy midperipheral full-thickness RPE and choroid patch with the advantage of having easy access to cut out the patch and direct control of bleeding from the donor site. Surgeons in Cologne, Kiel, Liverpool, Vienna, Verona, Beijing,

London, and Rotterdam have published further reports, some with a different surgical approach with a flapover technique to expose the subretinal space. Surgeons have also reported the use of a split-thickness graft, removing most of the choroid with an excimer laser[42] or with a spatula,[43] or using a spontaneously occurring free RPE sheet in patients with a pigment epithelium detachment.[56] The possibility of finding a surgical dissection plane between (layers of) Bruch's membrane and RPE is likely largely dependent on the specific type of exudative AMD. In patients with choroidal polyps, the new vessels grow in that plane and separation along that plane may occur while injecting balanced salt solution (BSS) to detach the retina (personal observation, van Meurs, Jakarta October 2013). This approach, pioneered by Zhizong Ma,[43] is particularly interesting in view of the recent development of free RPE sheets, grown from embryonic stem cells (see below), because this anatomic separation would be most favorable for transplanting an RPE monolayer directly onto host choriocapillaris.

Surgery

Keyhole Approach

After the induction of a posterior vitreous detachment, a complete vitrectomy is performed (see video under http://www.eyemoviepedia.com/videos/3971697493/153). The macular retina can be separated from the RPE and/or blood and/or CNV membrane by injecting a balanced salt solution into the subretinal space through a 28-gauge subretinal cannula. A paramacular temporal retinotomy is made, through which the CNV membrane and/or subretinal hemorrhage is removed from the subretinal space with Thomas subretinal forceps. Remaining hemorrhage is flushed out by irrigation with a 135° bent 32-gauge needle connected by tubing to a syringe filled with BSS and operated by an assistant.

Initially, a small retinotomy was made in the raphe; in later surgeries a radial cut was made along the raphe, from the retinotomy located peripherally. However, a vertical retinotomy temporal to the macula (Fig. 124.1) was found to work best for two

reasons: (1) less tendency to enlarge in the direction of the fovea and (2) easier for later introduction of the flat graft (François Devin, Marseille, personal communication). After circular heavy diathermy or laser in the midperiphery at the 6 or 12 o'clock position, vitreous scissors are used to cut a full-thickness graft of retina, RPE, Bruch's membrane, and choroid of approximately 2.5–3×2.5–4 mm. Initially, the graft was loaded onto an aspiration-reflux spatula. Subsequently the technique was changed so that the graft could be grasped from the choroidal side by fine forceps. The retina is removed from the graft just before it is repositioned under the macula through the existing paramacular retinotomy (Fig. 124.2). Perfluorocarbon liquid is injected over the macula to hold the graft in position during retraction of the instrument. A vibration device attached to the forceps facilitates the release.[57] The midperipheral donor site is then surrounded with laser photocoagulation, followed by silicone oil tamponade.

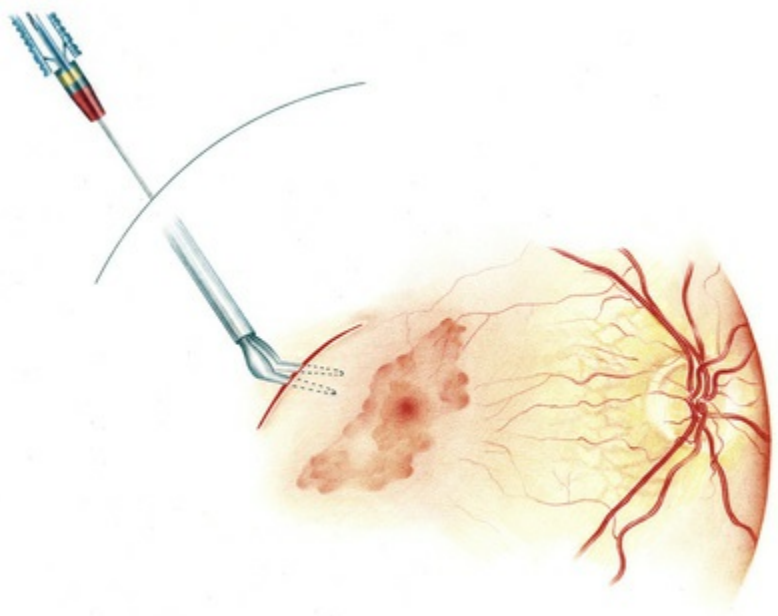

FIG. 124.1 A vertical retinectomy (as suggested by F. Devin) is currently preferred because this retinotomy has less tendency to enlarge towards the fovea and the graft is inserted more easily.

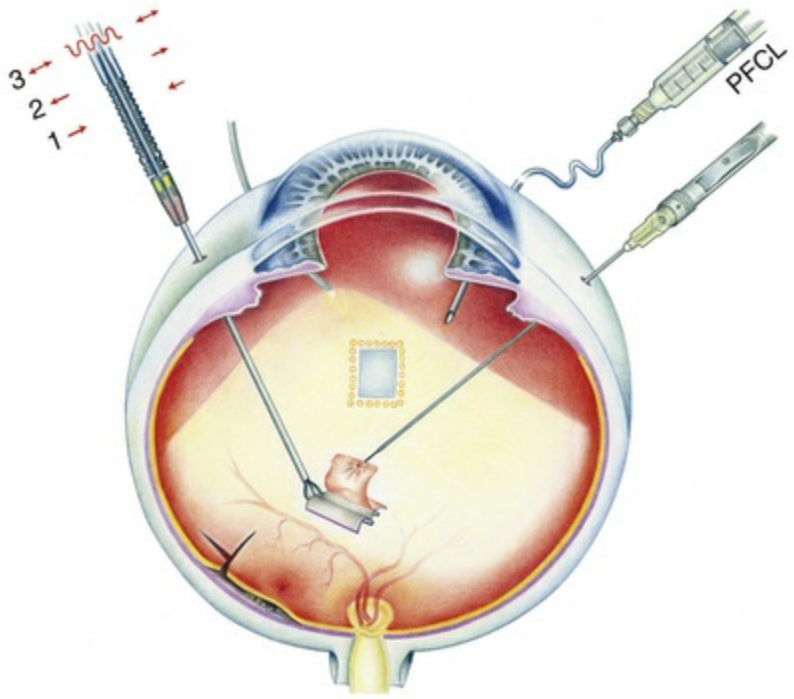

FIG. 124.2 Technique of a free retinal pigment epithelium–choroid transplantation using the keyhole technique. *PFCL*, perfluorocarbon liquid.

In a second procedure, approximately 3 months later, the silicone oil can be removed and the inner limiting membrane (ILM) peeled, which may reduce the risk of macular pucker. In phakic patients, lensectomy and intraocular lens (IOL) insertion can be performed during the first or second procedure.

Peroperative Course

Bleeding from the choroidal extraction site may pose a serious problem. This can be countered by increasing the infusion pressure up to 180 mmHg and repeated rinsing out of the hemorrhage with a submacular cannula connected to a syringe (operated by an assistant), with or without a perfluorocarbon liquid (PFCL) bubble over the macula. The area of damaged RPE resulting from membrane and hemorrhage removal is generally much larger than the RPE and choroid graft.

Finding a Cleavage Plane Between Sclera and Choroid

When trying to place the harvested patch under the fovea, remnants of the fibrous connecting tissue between choroid and sclera may jeopardize a clean release. Before cutting out the patch, the authors try to separate the patch from the sclera by introducing and sweeping a sharp spatula in the suprachoroidal space. When we cut out the graft, we leave a slight connection of choroidal tissue at the edge facing the macula, acting as a hinge to fold over and expose the choroidal side. In this manner, the graft is tethered internally so that we can remove loose connective fibers bimanually with intraocular forceps and scissors.

Positioning the Graft on the Spatula

When all four sides of the rectangular 1.5–3×2.5–4 mm graft are cut clear of the adjoining tissue and the collagenous connections of the choroid to the sclera have been swept away, the graft has the tendency to roll up in a half cylinder with the RPE on the convex side, usually with the half cylinder limbus parallel.

This occurs in BSS (possibly due to the inherent elastic tension of the choroid), and the free floating patch may subsequently become difficult to grasp. Moreover, the infusion bottle should be quite low to minimize turbulence and to prevent the patch being trapped or expelled through a sclerotomy when changing instruments. It is helpful to use a chandelier-style illumination so that the patch can be manipulated bimanually and steadied when changing instruments.

Preparation of the patch under PFCL may help to keep the patch flat on the spatula; while it allows us to keep the bottle raised, thereby decreasing the risk of bleeding from the choroidal or retinal vessels. A concern exists, however, about whether or not a remaining PFCL film/thin layer may interfere with later function. The approach we favor, however, makes use of the observation that an excised choroid-RPE–retina transplant has no tendency at all to curl: the attached retina counteracts any curling forces of the choroid. Thus, while the choroid–RPE plus retina graft is steadied from the choroidal side with horizontal forceps, we peel off the neurosensory retina by means of suction of a flute needle, just before insertion under the macula.

Positioning of the Graft Under the Fovea

Positioning of the graft under the fovea with a standard vitreoretinal spatula may be difficult. Horizontal forceps, even when designed not to close entirely, proved to be unsuitable because the patch frequently cannot be released easily due to adherence to the forceps. A better instrument to hold and release the patch turned out to be a cannulated spatula with one opening, with an assistant applying aspiration to hold the patch or reflux to release the patch. A single opening appeared better than more openings, since once occlusion is lost over one opening, release can no longer be effected by refluxing. Most recently, the authors rely once more on a wide-opening horizontal forceps, attached to a vibrating device, to facilitate mechanical release of the tissue.[58]

Tamponade

We have used silicone oil to facilitate examination of the patients in the early postoperative period. A gas tamponade might be possible too in selected cases. It may be speculated that in patients with an inferior donor site, the use of a heavier than water tamponade would decrease the risk of retinal detachment and PVR. This was not confirmed in a study analyzing the occurrence of PVR in 235 patients with either a superior or an inferior donor site with lighter than oil tamponade for all.[59] Indeed, in a prospective randomized study with heavy silicone oil (Densiron, Fluoron, Neu-Ulm, Germany) versus standard silicone oil the rate of PVR was overall unchanged, but the PVR-membranes were shifted from the inferior circumference to the upper.[60]

Flapover Approach

To obviate the need for a parafoveal and midperipheral retinotomy, to enable better control of choroidal bleeding and to enable the surgeon to fashion the size of the graft to the RPE defect, a technique from macular translocation by retinal rotation can be used.[61] Moreover, this technique allows surgery in patients with more massive hemorrhages.

A temporal retinal detachment is created by subretinal infusion

of BSS through a 41-gauge needle, followed by a retinectomy near the ora serrata in the temporal 13 clock-hours with subsequent folding over of the retina over the disc to expose the temporal subretinal space. While working under BSS for membrane removal and later under PFCL for preparation of the graft, more direct control of obtaining a correctly sized patch is possible. It may be the approach of choice in large lesions and allows direct control of bleeding from the stalk of the CNV. This technique is currently favored by more surgeons, and the best results so far reported are by Pertile in Verona.[48] A specific concern here is that the detached temporal retina may incarcerate in the nasal sclerotomy. Measures to prevent this occurring are the meticulous removal of vitreous base remnants, a low infusion pressure, and a retinectomy that should not be extended too far to the nasal sclerectomy. When incarceration occurs, the incarcerated retina can be manipulated out of the sclerotomy with a ring forceps, after closing the infusion (Gracia Pertile, May 2011, personal communication). With the advent of valved pars plana cannulas, however, the risk of incarceration is much smaller.

Instruments

Instruments for the keyhole technique were designed and manufactured in close collaboration with Ger Vijfvinkel of the Dutch Ophthalmic Research Center (DORC), Zuidland, The Netherlands. For the flapover technique, standard instruments proved to be adequate.

Choroidal Rotation

As a further refinement to avoid creating a double layer of choriocapillaris, Lee and colleagues[62] described a novel technique in the nonhuman primates of rotating the choroid beneath the retina. The blood supply to the rotated choroid came from the lateral long posterior ciliary artery (LPCA), at the base of the choroidal flap, which was lasered in a circle extending from the temporal disc to the ora, before being cut and rotated by 180° (Fig. 124.3A). The overlying neurosensory retina was folded over in a similar manner to the “flapover” technique described above, in order to gain access

to the choroid from the transvitreal approach (Fig. 124.3B).

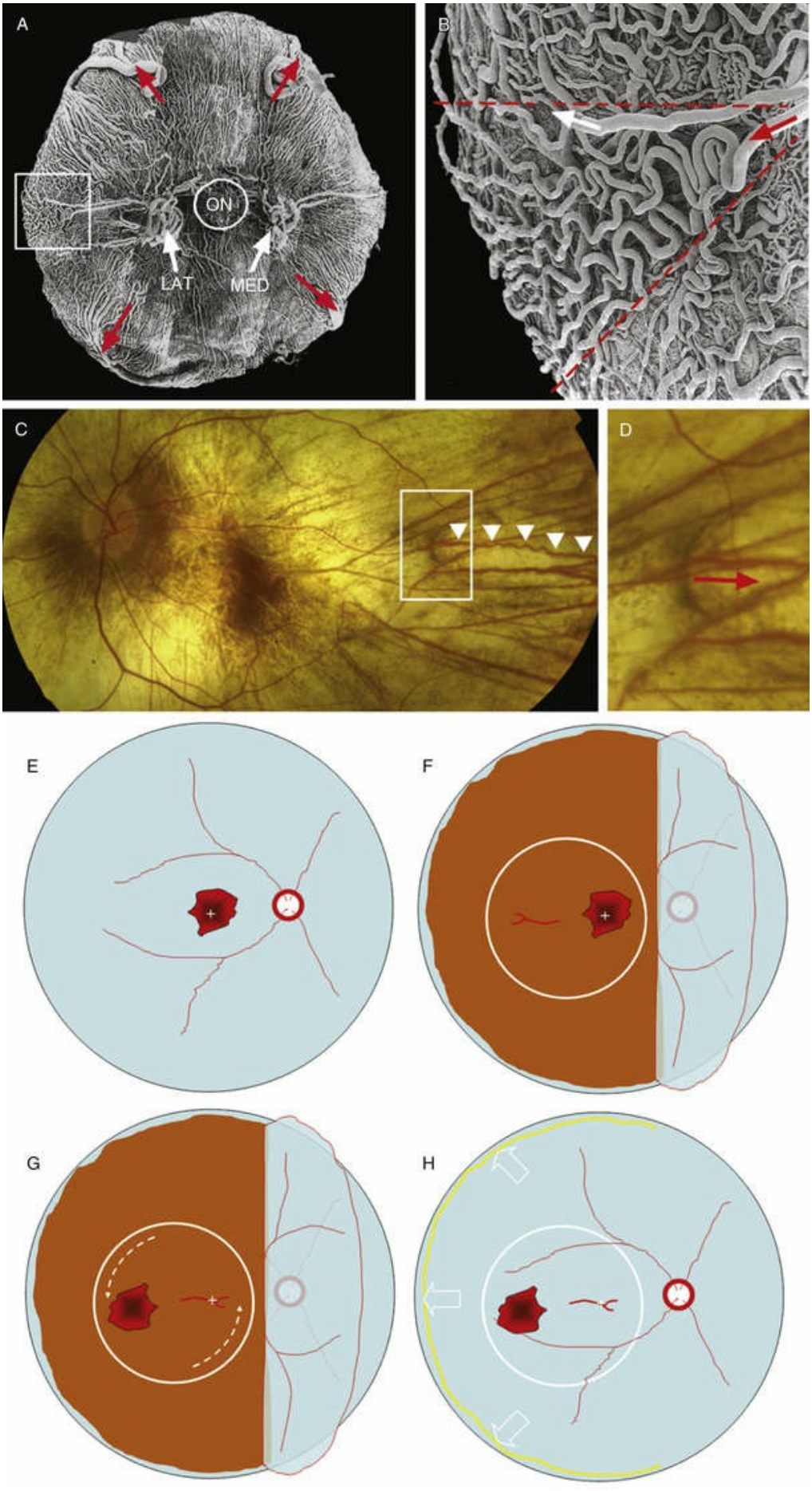
A
ON
LAT
MED
B
C
D
E
F
G
H

FIG. 124.3A (A) Technique of rotation of autologous translocation using a pedicle of full-thickness choroid. A cast of the human choroidal circulation is shown in panels A and B. *ON*, optic nerve head; *LAT*/*MED*, lateral and medial posterior choroidal arteries. The location of the lateral long posterior ciliary artery (LPCA) is shown by the *white arrows* in C and the *red line* in D, in a patient with choroideremia in whom the choroidal atrophy has revealed the underlying perforating vessels. (E) An imaginary choroidal new vessel (CNV) complex is seen in red under the fovea. In the era before anti-VEGF treatments, this patient may have been considered for retinal translocation surgery. (F) A peripheral retinectomy allows folding of the retina nasally to expose the underlying choroid. Care is taken to avoid damage to the papillomacular bundle and perfluorocarbon (heavy liquid) is used to stabilise the retina. Under heavy liquid, a circle in the choroid is circumscribed with heavy laser to cauterise choroidal vessels and the choroid is then cut along this line with scissors. The choroid is easily mobilised from the underlying sclera but care is taken to preserve the perforating lateral posterior ciliary vessel which courses laterally across the posterior choroid (red). (G) The mobilised choroidal pedicle is then rotated about 180 degrees to displace the diseased area into the temporal periphery and bring the healthy temporal choroid into the subfoveal zone. (H) The retina is reattached with heavy liquid and peripheral laser applied (yellow). The operation is completed with a heavy liquid silicone oil exchange. (Panels A and B courtesy of Jane Olver MD. Panels E–H reproduced with permission from Lee E, Singh MS, Jones HE, et al. Assessment of 180 degrees rotation of the choroid as a novel surgical treatment for age-related macular degeneration. Invest Ophthalmol Vis Sci 2012;53(6):2523-2532.)

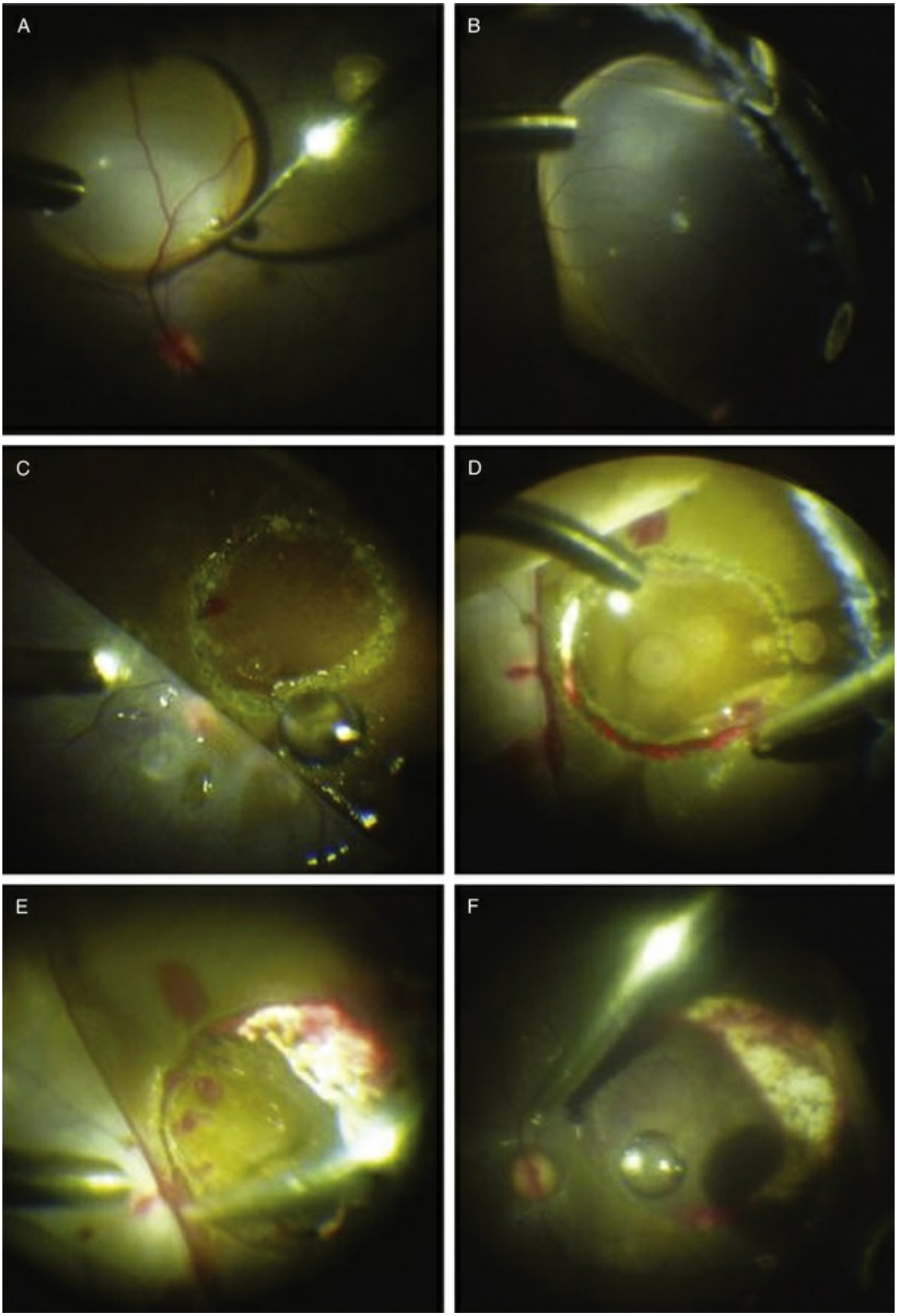

FIG. 124.3B Choroidal rotation surgery under the retina in the nonhuman primate (*Macaca mulatta*). (A) The retina is detached with balanced salt solution (here using a metal 34 gauge cannula). (B) The detached retina is cut along the periphery, along a

preplaced laser track to reduce retinal bleeding. (C) The retina is folded over under heavy liquid and the circular choroidal laser track can be seen. (D) The choroid is cut along the track to expose the underlying sclera. Note that there is only minimal bleeding under heavy liquid. (E) The choroidal pedicle is rotated carefully around the perforating lateral posterior choroidal artery pedicle. Some shrinkage of the graft is seen, which exposes sclera temporally. This occurs because the free choroid is an elastic structure. (F) After heavy liquid/oil exchange, the retina is reattached over the choroidal pedicle with no significant subretinal hemorrhage. (Reproduced with permission from Lee E, Singh MS, Jones HE, et al. Assessment of 180 degrees rotation of the choroid as a novel surgical treatment for age-related macular degeneration. Invest Ophthalmol Vis Sci 2012;53(6):2523-2532.)

Although the technique was shown to be technically feasible, the revascularization of the rotated choroid was poor, despite the arterial pedicle being present. The choroid has a unique dual blood supply, because while the arteries enter at predefined points penetrating the sclera posteriorly, the veins drain to separate structures (the vortex veins) anteriorly. In a typical vascularized rotational skin graft, the pedicle has both arterial and venous components within it and blood supply is maintained throughout. In the case of the choroidal rotation, however, only the arterial supply is in the pedicle and the venous drainage needs to be reestablished by peripheral vascular networks reconnecting. The researchers speculated that the elastic nature of the choroidal tissue caused peripheral retraction and prevented the venous circulation from being reestablished.[62] These experiments highlight the complex nature of the choroidal circulation, which needs to be explored before progressing to surgical trials in humans.

Results in Exudative AMD

Reports of free RPE grafts generally have been reported on small groups of patients and have had a follow-up of only 6 months to 3 or 4 years (Table 124.1). MacLaren and Aylward have presented patients with a 5- and 6-year follow-up, but for only four of nine

operated patients.[63]

A recent report followed a cohort of 132 consecutive patients (134 eyes) who underwent RPE–choroid graft surgery; in some patients VA and/or microperimetry results of 4–7 years after surgery were documented (Fig. 124.4).[64] In several patients, clear evidence of retained retinal function on the graft proved in principle the longevity of this technique and at timepoints not yet reached with anti-VEGF treatments (Figs. 124.5 and 124.6).

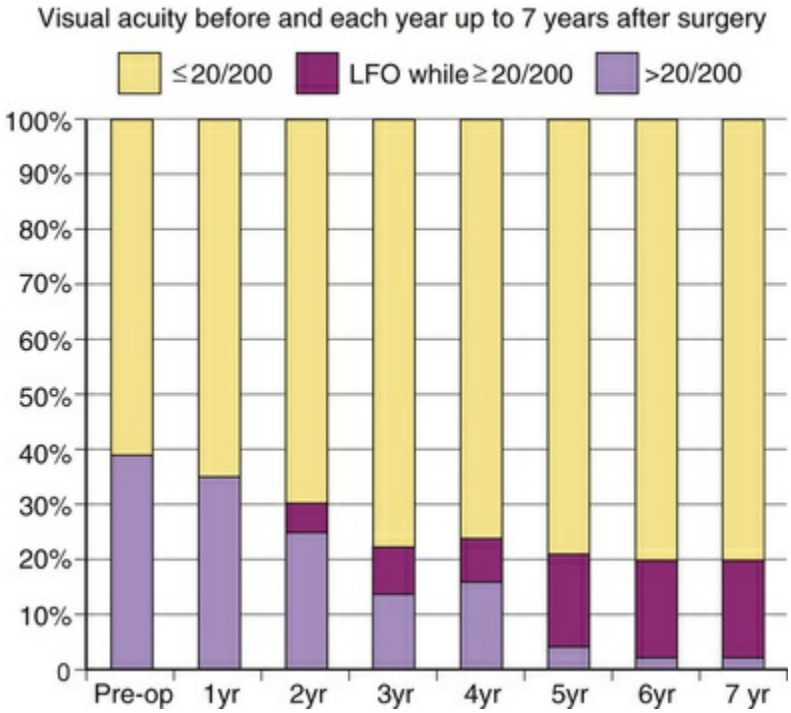

FIG. 124.4 Visual acuity (VA) before surgery (preoperative) and each year up to 7 years thereafter. Three groups are depicted. Groups 1 and 2 comprise percentages of patients with a VA of >20/200 or ≤20/200. The third group comprises percentages of patients whose last measured VA had been >20/200 before they were lost to follow-up (LFO), and patients who had not able to reach their next yearly follow-up visit yet, while VA was >20/200 at last measurement (LFO while >20/200). The data of this third group have been carried forward in this figure.

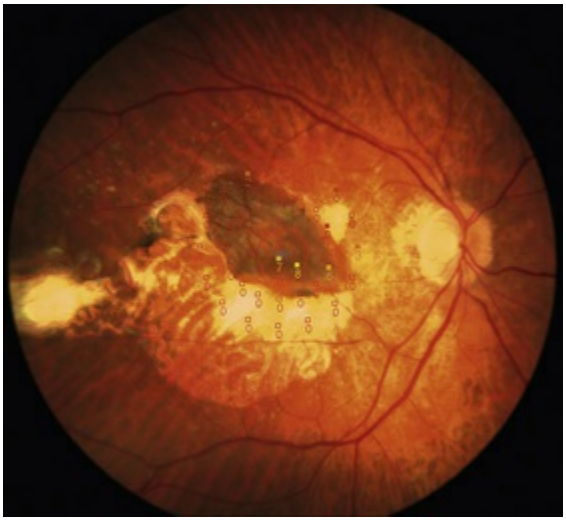

FIG. 124.5 A 78-year-old male. Preoperative visual acuity (VA) 20/100, minimally classic choroidal neovascularization. NIDEK MP-1, 5 years postoperatively, with VA 5 20/40.

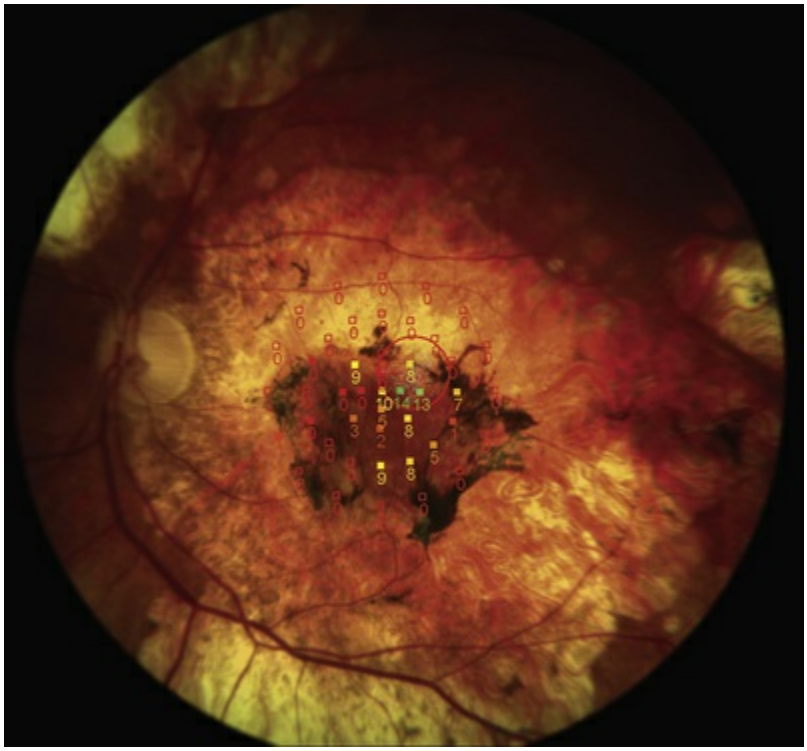

FIG. 124.6 Twelve years after RPE and choroid graft transplantation for a 12-week-old submacular hemorrhage with only counting fingers vision in a now 85-year-old woman. Visual acuity 20/40 with preserved retinal sensitivity over the graft on microperimetry (NIDEK MP-2).

The number of patients with preserved macular function remains modest, however, due to several factors: preexisting and surgical damage to the retina; ischemic and surgical trauma to the RPE–choroid graft; revascularization delay; and potential revascularization injury of the graft. Comparison with the results of the submacular surgery trials, however, suggested that it is the RPE graft, rather than simply the removal of the submacular choroidal neovascular scar and blood, that was responsible for the preservation of reasonably good macular function in some patients.[29]

Recently, it was shown that spectral domain optical coherence tomography (SD-OCT), a noninvasive technique, allows the monitoring of revascularization of a RPE–choroid graft (Fig. 124.7A).[29] Indeed, the revascularization steps strongly suggested by SD-OCT[29] have been confirmed by Doppler-OCT, in which flow was demonstrated in the graft's vasculature.[65]

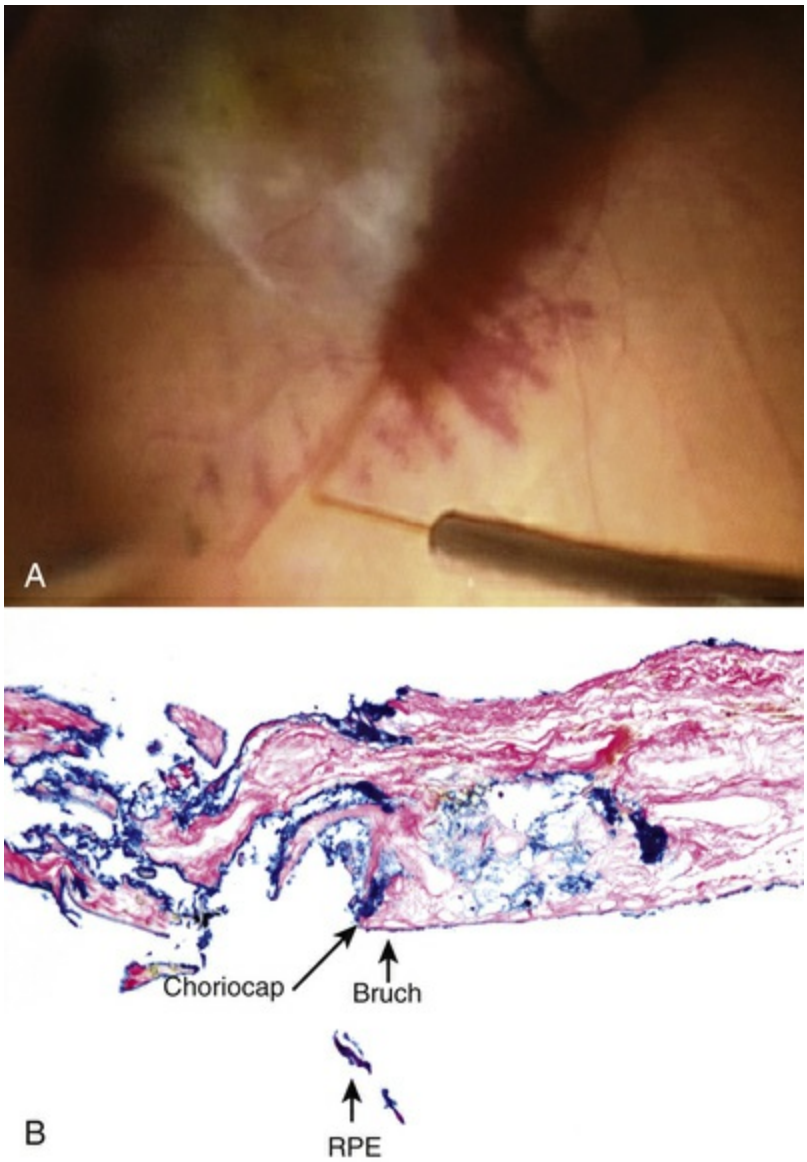

FIG. 124.7 (A) A rapid and rare fibrotic reaction to a RPE graft in an 83-year-old woman. We removed this graft 8 weeks after its insertion and replaced it with a second one. (B) Microscopic tissue section of the graft removed in Fig. 124.6 (×100 magnification, Syrian Red staining for collagen), highlighting the thick fibrotic capsule under the retinal pigment epithelium (RPE) and choroid graft; almost no RPE cells are visible, possibly partly due to preparation artifact. *Bruch,* Bruch's membrane; *Choriocap,* choriocapillaris; *RPE,* retinal pigment epithelium. (Courtesy of Rob Verdijk, MD, PhD.)

SD-OCT may also prove to be an important tool to select patients with a potentially functional retina, by selecting patients with preserved outer retina structures.

Continuing Concerns

The major concerns with autologous retinal pigment epithelium transplantation that we encounter include the too-frequent development of RD and PVR, and the common fibrosis around or (fortunately rare, three patients out of more than 350) over the graft (Fig. 124.7B). At this moment, in the absence of proven pharmacologic preventive measures, surgery that is as atraumatic as possible remains the key factor. This is exemplified by the low incidence of PVR in a recent report from Verona.[14]

Although an autologous RPE graft is not "foreign," the surgical procedures to remove the submacular scar and cutting out of the graft certainly produce tissue trauma and elicit an inflammatory reaction with many features of immune involvement (the "danger" model[66,67]).

It is likely that both challenges will remain in future surgery even if RPE grafts are eventually produced in the laboratory from stem cells.

Retinal Pigment Epithelium Transplantation in Dry AMD

Full macular translocation is usually complicated by rapid onset of RPE atrophy at the new location of the macula.[68] Two prospective nonrandomized studies are available looking at the prognosis after patch translocation in GA.[44,47] A follow-up of more than 2 years is required to be able to discern a therapeutic effect compared to the slow progressive natural course.[47]

Surgical Aspects in Dry AMD

In patients with dry AMD, several surgical steps are slightly different from those for exudative AMD (see video under http://www.eyemoviepedia.com/videos/4166636950/67). After a three-port pars plana vitrectomy, BSS was injected subretinally temporal and adjacent to the macula. In almost all eyes, the macula did not detach, but this was not the case for the retina around the

macula. Additional mechanical separation of the macula proved necessary. An angulated infusion needle was used as spatula and fluid jet. At the same time Bruch's membrane was scratched to create breaks in Bruch's membrane, allowing choroidal vessels to connect to the transplant later on, as graft nonperfusion was observed in our first patients (Cologne, Rotterdam) (Fig. 124.8) when this step was omitted. Access to the subretinal space was through a temporal retinotomy. The excision site of the graft was chosen in the inferior retinal periphery after demarcation by laser photocoagulation. After removal of the overlaying retina, the graft was mobilized from the sclera, grasped with angulated forceps from the choroidal side, and inserted under the macula through the temporal retinotomy.[69] Heavy silicone (Densiron, Fluron, Ulm) was used as vitreous tamponade for 3 months.

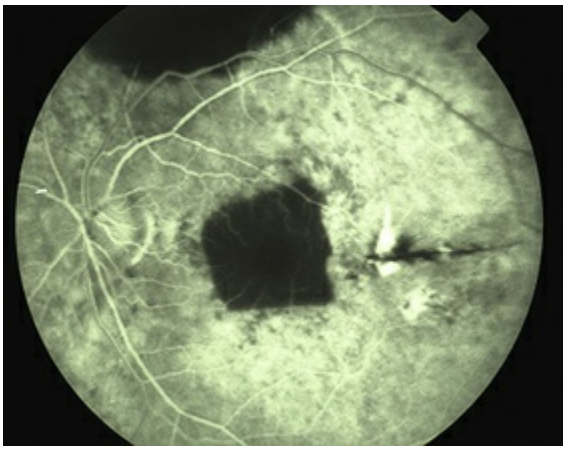

FIG. 124.8 One of the first patients with dry age-related macular degeneration (AMD) and a free retinal pigment epithelium–choroid graft, in whom Bruch's membrane was left untouched and no revascularization occurred.

Functional outcomes of 10 patients were as follows: prior to surgery, seven of the 10 patients were able to read compared with five patients being able to read 2–3 years postoperatively. Microperimetry showed central fixation in five eyes prior to surgery and in two eyes 2–3 years after surgery. In all but one eye revascularization of the graft was confirmed by indocyanine green angiography beginning as early as 3 weeks after translocation.

Autofluorescence was present in all eyes throughout the follow-up period, including the patient with no revascularization of the graft and more obvious retinal thinning over the graft than the others.

Recurrent CNV appeared in three eyes at the edge of the graft, not affecting the fovea. Macular pucker was noted in three eyes. PVR retinal detachment outside the posterior pole occurred in three eyes.

Conclusions for Patient Benefit in Geographic Atrophy

In terms of timing of surgery, the insidious onset of changes in the choroid and RPE in atrophic AMD with subsequent atrophic changes in the overlying retina compare unfavorably with the relatively acute-onset changes in RPE and choroid in patients with exudative AMD, with more often some degree of preservation of the overlying retina.

None of our patients with atrophic AMD improved in VA. Stabilization or further visual loss is a more likely long-term outcome. Retinal atrophy could not be reversed by RPE–choroidal grafting. Eccentric preoperative fixation will persist. Tight adhesion of the central neurosensory retina to the choroid is characteristic of GA. This may explain a higher risk of surgical damage to photoreceptors compared to exudative AMD, in addition to preexisting retinal atrophy as part of dry AMD. Only a very small selection of patients with preserved central fixation and an intact junction of inner/outer-segment photoreceptor junction on OCT may profit from grafting, at a considerable risk, however, of losing central vision.

Of interest, we observed no recurrence of RPE atrophy on the graft, as opposed to its rapid recurrence after full macular translocation.

Retinal Pigment Epithelium–Choroid Translocation and Future Stem Cell

Treatments for AMD

A stem cell is a dividing self-renewing cell also capable of differentiating into a variety of adult differentiated cell types to renew various tissues. While it has always been appreciated that embryonic stem (ES) cells are pluripotent, in that they give rise to a whole embryo and any one of the approximately 220 different cell types that define the adult mammalian organism, it was not until the cloning of Dolly the sheep in 1997 that it became apparent that adult differentiated cells could also have a similar potential. In the case of Dolly, the DNA from a mammary gland cell taken from her genetic mother was extracted and injected into a newly fertilized oocyte, from which the original gamete-fused nucleus was removed.[70] This process, known as somatic cell nuclear transfer (SCNT), led to the development of a clone of ES cells, which was subsequently able to differentiate into the sheep, which was born after implantation into a surrogate mother.

The fact that the sheep was normal proved the principle that any adult somatic cell could potentially be reprogrammed by undefined factors within a newly fertilized oocyte cytoplasm to become an ES cell, and this was subsequently confirmed in primates.[71] Somatic cell nuclear transfer requires a newly fertilized oocyte and so brings with it some ethical considerations and practical limitations. However, a decade after the successful cloning of Dolly the sheep it was discovered that adult differentiated cells could be reprogrammed without the oocyte by manipulating the histones, which are the protein switches that inactivate specific genes, particularly histone H3, or by direct methylation of the DNA promoter sequences.[72,73] Both of these approaches switch specific genes on and off and effectively reprogram the cell to become, for instance, a stem cell.[74] This research identified the transcription factors that facilitate reprogramming of skin cells that were then reimplanted to become a fully differentiated mouse embryo and the reprogramming part (without implantation) has subsequently been achieved in human cells.[75] Hence, current talk about stem cells is not discussing fetal cells or even cells modified via the oocyte; it is believed that induced stem cells may hold the key to regeneration of diseased tissues in future. These could be obtained potentially

from any patient and manipulated into the desired cell type prior to transplantation – referred to as induced pluripotent (iPS) stem cells.

It should be immediately apparent at this stage that since an iPS cell could potentially give rise to a normal mammalian organism, it should by definition be able to give rise to any of the cell types present in that organism. This includes of course the RPE, photoreceptors, retinal ganglion cells, and other components of the visual system. This raises the possibility that we may be able to take adult skin cells from a patient with AMD and reprogram these into RPE cells prior to transplantation. This sounds like an exciting concept, but we need to consider some of the observations learned through two decades of AMD surgery research. We know from the studies mentioned above that suspensions of healthy RPE cells isolated from the retinal periphery in AMD patients are unable to reform a physiologic monolayer underneath the macula. This may in part be due to the fact that these cells need to be fused with the underlying Bruch's membrane and the latter is almost certainly diseased and compromised in the later stages of AMD.[76] The choriocapillaris that gives rise to Bruch's membrane may be derived from the mesoderm germ layer, whereas the RPE originates from the neuroectoderm.[77] This is highly relevant because in studies to date, that have derived RPE cells from both ES cells and iPS cells, it has become apparent that the RPE cell differentiation does not include the creation of a choriocapillaris or Bruch's membrane.[78,79] The key challenge of the application of iPS-derived RPE cells will be to generate these cells not as a suspension, but fused to an underlying substrate of Bruch's membrane, or similar, that can facilitate polarization and hence balanced homeostasis of RPE cells once transplanted into the subretinal space.[80] To address this problem, a trial at the UCL Institute of Ophthalmology in London has recently started that includes support for the transplanted stem cell-derived RPE on a polyester membrane (NCT01691261). In that study, the researchers are also limiting transplantation to AMD patients who have rapid loss of vision, primarily due to tears in the subfoveal RPE. This is helpful as these patients generally do poorly with anti-VEGF treatments and the prospect of a temporarily compromised but otherwise anatomically intact fovea raises the possibility for assessing restored vision on the transplanted

monolayer.

It can therefore be seen that the techniques described above, particularly in relation to RPE–choroid patch graft surgery, are highly relevant to any future stem cell approach because it is almost certain that a very similar surgical technique would be employed to deliver reengineered tissue into the subretinal space. In cases where the retinal degeneration has progressed to the point of photoreceptor loss, any stem cell strategy to transplant photoreceptors back into the fovea would need to be combined with restoration of the underlying RPE, because otherwise the transplanted cells would not survive.[81] It may therefore be possible to use iPS cell-derived RPE engineered on a suitable Bruch's substrate via a standard surgical procedure to restore submacular RPE as the first step, followed by reintroduction of photoreceptors via an alternative stem cell approach at a later stage.[82] It is, however, worth noting that the RPE–choroid patch graft results, described in detail in the section above, suggest that there is no intrinsic problem in using autologous cells harvested from the retinal equator for subfoveal RPE replacement. This would also solve the Bruch's membrane substrate problem because RPE cells would remain adherent to the choriocapillaris throughout the transplantation procedure. While there is no doubt that photoreceptors would almost certainly need to be derived from an alternative possibly stem cell source, the idea of using stem cells or iPS cells to replace the RPE is less clear because the problem of recreating the Bruch's membrane substrate still remains (Fig. 124.9). Furthermore, the concept of introducing genetically modified and potentially teratogenic cells brings with it additional risks that would delay clinical application,[83] whereas autologous grafting techniques are already established in the clinical arena. A clinical trial using iPS cell-derived RPE in a cultured monolayer started in 2014 at the RIKEN Institute in Japan, and one patient has so far been implanted.[84] The trial was, however, suspended in 2015 prior to the second planned surgery due to concerns about possible oncogene activation during the reprogramming process of the harvested autologous cells.

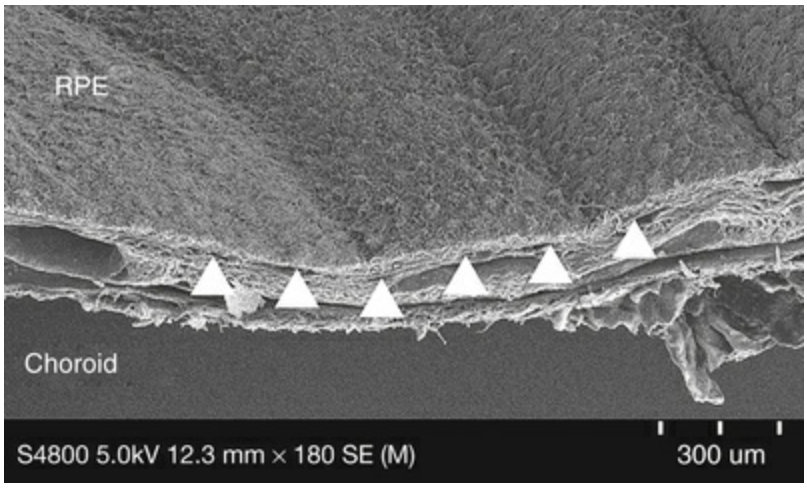

FIG. 124.9 Ultrastructure of a full-thickness RPE–choroid graft. Scanning electron micrograph showing the regular alignment of retinal pigment epithelium (*RPE*), choriocapillaris, and the continuous Bruch's membrane between (*arrowheads*). The challenge of any stem cell approach will be to recreate a structure similar to this, particularly as autologous tissue can be harvested with minimal risk from the anterior region of the eye and supports foveal vision up to at least 20/30.

(Reproduced with permission from MacLaren RE, Pearson RA. Stem cell therapy and the retina. Eye 2007;21:1352–9.)

Recently, a phase I clinical trial has shown safety and reported some promising early results transplanting human embryonic stem cells in nine patients with Stargardt disease and nine with AMD.[85,86] This concept has many challenges, not least of which because many patients with Stargardt disease lose vision prior to disruption of the underlying RPE, presumably due to photoreceptor dysfunction.[87] Similarly, it is not clear if these transplanted RPE cells have any capacity to adhere to or polarize on the underlying Bruch's membrane in these patients. Nevertheless, it is likely that observations on the behavior of these ES cell-derived RPE cells will provide useful information on the viability or not of this as a potential future treatment, and there is good evidence from the reports that the transplanted stem cell-derived RPE cells survive after cessation of immune suppression. Moreover, many of the technical challenges relating to surgery with these cells will be overcome, at least in part, as a result of what we have learned to date with the surgical approaches using autologous RPE–choroid grafts.

References

1. Augood CA, Vingerling JR, de Jong PT, et al. Prevalence of age-related maculopathy in older Europeans: the European Eye Study (EUREYE). *Arch Ophthalmol*. 2006;124:529–535.
2. Resnikoff S, Pascolini D, Etya'ale D, et al. Global data on visual impairment in the year 2002. *Bull World Health Organ*. 2004;82:844–851.
3. Owen CG, Fletcher AE, Donoghue M, et al. How big is the burden of visual loss caused by age related macular degeneration in the United Kingdom? *Br J Ophthalmol*. 2003;87:312–317.
4. Gelisken F, Ziemssen F, Voelker M, et al. Retinal pigment epithelial tears after single administration of intravitreal bevacizumab for neovascular age-related macular degeneration. *Eye (Lond)*. 2009;23:694–702.
5. Smith BT, Kraus CL, Apte RS. Retinal pigment epithelial tears in ranibizumab-treated eyes. *Retina*. 2009;29:335–339.
6. Rosenfeld PJ, Rich RM, Lalwani GA. Ranibizumab: phase III clinical trial results. *Ophthalmol Clin North Am*. 2006;19:361–372.
7. Rosenfeld PJ, Shapiro H, Tuomi L, et al. Characteristics of patients losing vision after 2 years of monthly dosing in the phase III ranibizumab clinical trials. *Ophthalmology*. 2011;118:523–530.
8. Rofagha S, Bhisitkul RB, Boyer DS, et al. Seven-year outcomes in ranibizumab-treated patients in ANCHOR, MARINA, and HORIZON: a multicenter cohort study (SEVEN-UP). *Ophthalmology*. 2013;120(11):2292–2299.
9. Kaneko H, Dridi S, Tarallo V, et al. DICER1 deficit induces Alu RNA toxicity in age-related macular degeneration. *Nature*. 2011;471:325–330.
10. Hawkins BS, Bressler NM, Miskala PH, et al. Surgery for subfoveal choroidal neovascularization in age-related macular degeneration: ophthalmic findings: SST report no. 11. *Ophthalmology*. 2004;111:1967–1980.
11. Machemer R, Steinhorst UH. Retinal separation, retinotomy, and macular relocation: II. A surgical approach for age-

related macular degeneration? *Graefes Arch Clin Exp Ophthalmol*. 1993;231:635–641.
12. Aisenbrey S, Lafaut BA, Szurman P, et al. Macular translocation with 360 degrees retinotomy for exudative age-related macular degeneration. *Arch Ophthalmol*. 2002;120:451–459.
13. Luke M, Ziemssen F, Volker M, et al. Full macular translocation (FMT) versus photodynamic therapy (PDT) with verteporfin in the treatment of neovascular age-related macular degeneration: 2-year results of a prospective, controlled, randomised pilot trial (FMT-PDT). *Graefes Arch Clin Exp Ophthalmol*. 2009;247:745–754.
14. van Romunde SH, Polito A, Bertazzi L, et al. Long-term results of full macular translocation for choroidal neovascularization in age-related macular degeneration. *Ophthalmology*. 2015;122(7):1366–1374.
15. Au Eong KG, Pieramici DJ, Fujii GY, et al. Macular translocation: unifying concepts, terminology, and classification. *Am J Ophthalmol*. 2001;131:244–253.
16. Buffenn AN, de Juan E, Fujii G, et al. Diplopia after limited macular translocation surgery. *J AAPOS*. 2001;5:388–394.
17. Chen CY, Hooper C, Chiu D, et al. Management of submacular hemorrhage with intravitreal injection of tissue plasminogen activator and expansile gas. *Retina*. 2007;27:321–328.
18. Hillenkamp J, Surguch V, Framme C, et al. Management of submacular hemorrhage with intravitreal versus subretinal injection of recombinant tissue plasminogen activator. *Graefes Arch Clin Exp Ophthalmol*. 2010;248:5–11.
19. van Zeeburg EJ, Van Meurs JC. Literature review of recombinant tissue plasminogen activator used for recent-onset submacular hemorrhage displacement in age-related macular degeneration. *Ophthalmologica*. 2013;229(1):1–14.
20. Arias L, Mones J. Transconjunctival sutureless vitrectomy with tissue plasminogen activator, gas and intravitreal bevacizumab in the management of predominantly hemorrhagic age-related macular degeneration. *Clin Ophthalmol*. 2010;4:67–72.

21. Sacu S, Stifter E, Vecsei-Marlovits PV, et al. Management of extensive subfoveal haemorrhage secondary to neovascular age-related macular degeneration. *Eye (Lond)*. 2009;23:1404–1410.
22. Peyman GA, Blinder KJ, Paris CL, et al. A technique for retinal pigment epithelium transplantation for age-related macular degeneration secondary to extensive subfoveal scarring. *Ophthalmic Surg*. 1991;22:102–108.
23. Stanga PE, Kychenthal A, Fitzke FW, et al. Retinal pigment epithelium translocation after choroidal neovascular membrane removal in age-related macular degeneration. *Ophthalmology*. 2002;109:1492–1498.
24. Van Meurs JC, Van Den Biesen PR. Autologous retinal pigment epithelium and choroid translocation in patients with exudative age-related macular degeneration: short-term follow-up. *Am J Ophthalmol*. 2003;136:688–695.
25. Joussen AM, Heussen FM, Joeres S, et al. Autologous translocation of the choroid and retinal pigment epithelium in age-related macular degeneration. *Am J Ophthalmol*. 2006;142:17–30.
26. MacLaren RE, Uppal GS, Balaggan KS, et al. Autologous transplantation of the retinal pigment epithelium and choroid in the treatment of neovascular age-related macular degeneration. *Ophthalmology*. 2007;114:561–570.
27. Treumer F, Bunse A, Klatt C, et al. Autologous retinal pigment epithelium-choroid sheet transplantation in age related macular degeneration: morphological and functional results. *Br J Ophthalmol*. 2007;91:349–353.
28. Maaijwee K, Heimann H, Missotten T, et al. Retinal pigment epithelium and choroid translocation in patients with exudative age-related macular degeneration: long-term results. *Graefes Arch Clin Exp Ophthalmol*. 2007;245:1681–1689.
29. van Zeeburg EJT, Maaijwee K, Missotten TOAR, et al. A free retinal pigment epithelium-choroid graft in patients with exudative macular degeneration; results up to seven years. *Am J Ophthalmol*. 2012;153:120–127.
30. Chen FK, Uppal GS, MacLaren RE, et al. Long-term visual

and microperimetry outcomes following autologous retinal pigment epithelium choroid graft for neovascular age-related macular degeneration. *Clin Experiment Ophthalmol*. 2009;37:275–285.
31. Eckardt C, Eckardt U, Conrad HG. Macular rotation with and without counter-rotation of the globe in patients with age-related macular degeneration. *Graefes Arch Clin Exp Ophthalmol*. 1999;237:313–325.
32. Korte GE, Reppucci V, Henkind P. RPE destruction causes choriocapillary atrophy. *Invest Ophthalmol Vis Sci*. 1984;25:1135–1145.
33. Blaauwgeers HG, Holtkamp GM, Rutten H, et al. Polarized vascular endothelial growth factor secretion by human retinal pigment epithelium and localization of vascular endothelial growth factor receptors on the inner choriocapillaris. Evidence for a trophic paracrine relation. *Am J Pathol*. 1999;155:421–428.
34. Lavail MM, Li L, Turner JE, et al. Retinal pigment epithelial cell transplantation in RCS rats: normal metabolism in rescued photoreceptors. *Exp Eye Res*. 1992;55:555–562.
35. Thumann G, Aisenbrey S, Schraermeyer U, et al. Transplantation of autologous iris pigment epithelium after removal of choroidal neovascular membranes. *Arch Ophthalmol*. 2000;118:1350–1355.
36. Lappas A, Weinberger AW, Foerster AM, et al. Iris pigment epithelial cell translocation in exudative age-related macular degeneration: a pilot study in patients. *Graefes Arch Clin Exp Ophthalmol*. 2000;238:631–641.
37. Navea Tejerina A. Autotrasplante del epitelio pigmentario del iris a la retina macular. Navea Tejerina A. *Trasplante de retina: epitelio pigmentario. 74 Congreso de la Sociedad Española de Oftalmología*. 1–1–1998:67–77.
38. Binder S, Stolba U, Krebs I, et al. Transplantation of autologous retinal pigment epithelium in eyes with foveal neovascularization resulting from age-related macular degeneration: a pilot study. *Am J Ophthalmol*. 2002;133:215–225.
39. Binder S, Krebs I, Hilgers RD, et al. Outcome of

transplantation of autologous retinal pigment epithelium in age-related macular degeneration: a prospective trial. *Invest Ophthalmol Vis Sci*. 2004;45:4151–4160.
40. Van Meurs JC, ter Averst E, Hofland LJ, et al. Autologous peripheral retinal pigment epithelium translocation in patients with subfoveal neovascular membranes. *Br J Ophthalmol*. 2004;88:110–113.
41. Falkner-Radler CI, Krebs I, Glittenberg C, et al. Human retinal pigment epithelium (RPE) transplantation: outcome after autologous RPE-choroid sheet and RPE cell-suspension in a randomised clinical study. *Br J Ophthalmol*. 2011;95:370–375.
42. Bindewald A, Roth F, Van Meurs J, et al. Transplantation of retinal pigment epithelium (RPE) following CNV removal in patients with AMD. Techniques, results, outlook. *Ophthalmologe*. 2004;101:886–894.
43. Ma Z, Han L, Wang C, et al. Autologous transplantation of retinal pigment epithelium-Bruch's membrane complex for hemorrhagic age-related macular degeneration. *Invest Ophthalmol Vis Sci*. 2009;50:2975–2981.
44. Joussen AM, Joeres S, Fawzy N, et al. Autologous translocation of the choroid and retinal pigment epithelium in patients with geographic atrophy. *Ophthalmology*. 2007;114:551–560.
45. Chen FK, Patel PJ, Uppal GS, et al. A comparison of macular translocation with patch graft in neovascular age-related macular degeneration. *Invest Ophthalmol Vis Sci*. 2009;50:1848–1855.
46. Gibran SK, Romano MR, Wong D. Perfluorocarbon liquid assisted large retinal epithelium patching in sub-macular hemorrhage secondary to age related macular degeneration. *Graefes Arch Clin Exp Ophthalmol*. 2009;247:187–191.
47. Caramoy A, Liakopoulos S, Menrath E, et al. Autologous translocation of choroid and retinal pigment epithelium in geographic atrophy: long-term functional and anatomical outcome. *Br J Ophthalmol*. 2010;94:1040–1044.
48. Cereda MG, Parolini B, Bellesini E, et al. Surgery for CNV and autologous choroidal RPE patch transplantation:

exposing the submacular space. *Graefes Arch Clin Exp Ophthalmol*. 2010;248:37–47.
49. van Zeeburg EJ, Cereda MG, Amarakoon S, et al. Prospective, randomized intervention study comparing retinal pigment epithelium-choroid graft surgery and anti-VEGF therapy in patients with exudative age-related macular degeneration. *Ophthalmologica*. 2015;33(3–4):134–145.
50. Valtink M, Engelmann K, Strauss O, et al. Physiological features of primary cultures and subcultures of human retinal pigment epithelial cells before and after cryopreservation for cell transplantation. *Graefes Arch Clin Exp Ophthalmol*. 1999;237:1001–1006.
51. Valtink M, Engelmann K, Kruger R, et al. Structure of a cell bank for transplantation of HLA-typed, cryopreserved human adult retinal pigment epithelial cells. *Ophthalmologe*. 1999;96:648–652.
52. Algvere PV, Berglin L, Gouras P, et al. Transplantation of fetal retinal pigment epithelium in age-related macular degeneration with subfoveal neovascularization. *Graefes Arch Clin Exp Ophthalmol*. 1994;232:707–716.
53. Algvere PV, Berglin L, Gouras P, et al. Transplantation of RPE in age-related macular degeneration: observations in disciform lesions and dry RPE atrophy. *Graefes Arch Clin Exp Ophthalmol*. 1997;235:149–158.
54. Del Priore LV, Kaplan HJ, Tezel TH, et al. Retinal pigment epithelial cell transplantation after subfoveal membranectomy in age-related macular degeneration: clinicopathologic correlation. *Am J Ophthalmol*. 2001;131:472–480.
55. MacLaren RE, Bird AC, Sathia PJ, et al. Long-term results of submacular surgery combined with macular translocation of the retinal pigment epithelium in neovascular age-related macular degeneration. *Ophthalmology*. 2005;112:2081–2087.
56. Kimura H, Li X, Torii K, et al. Glucocorticoid enhances hypoxia and/or transforming growth factor-beta-induced plasminogen activator inhibitor-1 production in human proximal renal tubular cells. *Clin Exp Nephrol*. 2011;15:34–

40.
57. Maaijwee K, Missotten T, Mulder P, et al. Influence of intraoperative course on visual outcome after an RPE-choroid translocation. *Invest Ophthalmol Vis Sci*. 2008;49:758–761.
58. Maaijwee K, Koolen T, Rosenbrand D, et al. Threshold amplitude and frequency for ocular tissue release from a vibrating instrument: an experimental study. *Invest Ophthalmol Vis Sci*. 2008;49:1629–1632.
59. van Zeeburg EJ, Maaijwee K, van Meurs JC. There is no relation between the occurrence of proliferative vitreoretinopathy and the location of the donor site after transplantation of a free autologous retinal pigment epithelium-choroid graft. *Acta Ophthalmol*. 2014;92(3):228–231.
60. Joussen AM, Rizzo S, Kirchhof B, et al. Heavy silicone oil versus standard silicone oil in gas vitreous tamponade in inferior PVR (HSO Study): interim analysis. *Acta Ophthalmol*. 2011;89(6):e483–9.
61. Kirchhof B. *RPE symposium*. [Cologne; September 12] 2003.
62. Lee E, Singh MS, Jones HE, et al. Assessment of 180 degrees rotation of the choroid as a novel surgical treatment for age-related macular degeneration. *Invest Ophthalmol Vis Sci*. 2012;53(6):2523–2532.
63. MacLaren RE, Aylward GW. Delayed atrophy of the retinal pigment epithelium after submacular surgery. *Eur J Ophthalmol*. 2005;15:170–172.
64. van Zeeburg ETJ, Cereda MG, van der Schoot J, et al. Early perfusion of a free RPE-choroid graft in patients with exudative macular degeneration can be imaged with spectral domain-OCT. *Invest Ophthalmol Vis Sci*. 2011;52:5881–5886.
65. van Zeeburg EJ, Braaf B, Cereda MG, et al. Direct blood flow measurements in a free RPE-choroid graft with phase-resolved Doppler OCT. *Transl Vis Sci Technol*. 2015;4(1):2.
66. Matzinger P. The danger model: a renewed sense of self. *Science*. 2002;296(5566):301–305.
67. Matzinger P. The evolution of the danger theory. Interview

by Lauren Constable, Commissioning Editor. *Expert Rev Clin Immunol*. 2012;8(4):311–317.
68. Cahill MT, Mruthyunjaya P, Bowes RC, et al. Recurrence of retinal pigment epithelial changes after macular translocation with 360 degrees peripheral retinectomy for geographic atrophy. *Arch Ophthalmol*. 2005;123:935–938.
69. Kirchhof B. *RPE and choroid translocation in geographic atrophy*. http://www.eyemoviepedia.com/videos/4166636950/67; 2009.
70. Wilmut I, Schnieke AE, McWhir J, et al. Viable offspring derived from fetal and adult mammalian cells. *Cloning Stem Cells*. 2007;9:3–7.
71. Byrne JA, Pedersen DA, Clepper LL, et al. Producing primate embryonic stem cells by somatic cell nuclear transfer. *Nature*. 2007;450:497–502.
72. Takahashi K, Yamanaka S. Induction of pluripotent stem cells from mouse embryonic and adult fibroblast cultures by defined factors. *Cell*. 2006;126:663–676.
73. Wernig M, Meissner A, Foreman R, et al. In vitro reprogramming of fibroblasts into a pluripotent ES-cell-like state. *Nature*. 2007;448:318–324.
74. Strahl BD, Allis CD. The language of covalent histone modifications. *Nature*. 2000;403:41–45.
75. Takahashi K, Tanabe K, Ohnuki M, et al. Induction of pluripotent stem cells from adult human fibroblasts by defined factors. *Cell*. 2007;131:861–872.
76. Gullapalli VK, Sugino IK, Van Patten Y, et al. Impaired RPE survival on aged submacular human Bruch's membrane. *Exp Eye Res*. 2005;80:235–248.
77. Sellheyer K, Spitznas M. The fine structure of the developing human choriocapillaris during the first trimester. *Graefes Arch Clin Exp Ophthalmol*. 1988;226:65–74.
78. Buchholz DE, Hikita ST, Rowland TJ, et al. Derivation of functional retinal pigmented epithelium from induced pluripotent stem cells. *Stem Cells*. 2009;27:2427–2434.
79. Carr AJ, Vugler AA, Hikita ST, et al. Protective effects of human iPS-derived retinal pigment epithelium cell

transplantation in the retinal dystrophic rat. *PLoS ONE*. 2009;4:e8152.
80. Kokkinaki M, Sahibzada N, Golestaneh N. Human induced pluripotent stem-derived retinal pigment epithelium (RPE) cells exhibit ion transport, membrane potential, polarized vascular endothelial growth factor secretion, and gene expression pattern similar to native RPE. *Stem Cells*. 2011;29:825–835.
81. Lee E, MacLaren RE. Sources of retinal pigment epithelium (RPE) for replacement therapy. *Br J Ophthalmol*. 2011;95:445–449.
82. MacLaren RE, Pearson RA. Stem cell therapy and the retina. *Eye (Lond)*. 2007;21:1352–1359.
83. Wobus AM. The Janus face of pluripotent stem cells – connection between pluripotency and tumorigenicity. *Bioessays*. 2010;32:993–1002.
84. Reardon S, Cyranoski D. Japan stem-cell trial stirs envy. *Nature*. 2014;513(7518):287–288.
85. Advanced Cell Technology, Inc. *Advanced Cell Technology receives FDA clearance for the first clinical trial using embryonic stem cells to treat macular degeneration*. [Santa Monica: ACT] http://www.advancedcell.com/news-and-media/press-releases/advanced-cell-technology-receives-fda-clearance-for-the-first-clinical-trial-using-embryonic-stem-cel/.
86. Schwartz SD, Regillo CD, Lam BL, et al. Human embryonic stem cell-derived retinal pigment epithelium in patients with age-related macular degeneration and Stargardt's macular dystrophy: follow-up of two open-label phase 1/2 studies. *Lancet*. 2015;385(9967):509–516.
87. Chen Y, Ratnam K, Sundquist SM, et al. Cone photoreceptor abnormalities correlate with vision loss in patients with Stargardt disease. *Invest Ophthalmol Vis Sci*. 2011;52:3281–3292.

SECTION 5

Vitreous Surgery: Additional Considerations

OUTLINE

125

Infectious Endophthalmitis

Travis A. Meredith, J. Niklas Ulrich

Introduction

Infectious endophthalmitis is a condition in which the internal structures of the eye are invaded by replicating microorganisms, resulting in an inflammatory response that ultimately may involve all tissues of the eye. Exogenous endophthalmitis occurs when the outer wall of the eye sustains a break as a result of surgical intervention or trauma; only rarely do microorganisms invade through the cornea or sclera without an overt disruption of these tissues. Endogenous endophthalmitis is less common and occurs when the microorganisms spread to the eye from a source

elsewhere in the body, usually through the bloodstream. The most common causative agents are bacteria, but fungi and parasites can also cause endophthalmitis. The time course of the disease may be acute, subacute, or chronic.

The majority of endophthalmitis cases occur after surgery, and over 90% of all cases are caused by bacteria. Each clinical setting of infection has its own characteristics, and as knowledge is refined, various constellations of findings have emerged. In certain clinical settings there is an increased likelihood of infection by certain groups of bacteria. In turn, the clinical condition that is present at the onset of infection and the pathogenicity of the bacteria involved are the primary determinants of the outcome. For example, endophthalmitis following cataract surgery is most often caused by *Staphylococcus epidermidis*, and these eyes have a reasonably good prognosis. Injured eyes, on the other hand, have an increased likelihood of infection with gram-positive *Bacillus* spp., which has a markedly worse prognosis.

Organisms That Cause Endophthalmitis

Bacteria, fungi, protozoa, and parasites are all capable of producing endophthalmitis (Box 125.1).

Box 125.1

Infective Agents That Commonly Cause Endophthalmitis

Bacteria

Gram-Positive Cocci

- *Staphylococcus*
- *Staph. aureus*
- *Staph. epidermidis* and related species
- *Streptococcus*

- *Strep. pneumoniae*
- Viridans group
- *Strep. faecalis*

Gram-Positive Bacilli

- *Bacillus*
- *B. cereus*
- *B. subtilis*
- *Corynebacterium*
- *Listeria monocytogenes*
- *Clostridium* spp.
- *Propionibacterium acnes*

Gram-Negative Cocci

- *Neisseria*
- *Moraxella*

Gram-Negative Bacilli

- *Acinetobacter* spp.
- *Haemophilus influenzae*
- *Pseudomonas*
- *P. aeruginosa*

- *Pseudomonas* spp.
- Enterobacteriaceae
- *Escherichia coli*
- *Klebsiella*
- *Proteus*
- *Serratia*
- *Enterobacter*

Higher Bacteria

- *Nocardia* spp.
- *Actinomyces israelii*
- *Mycobacterium*

Fungi

- *Candida*
- *Aspergillus*
- *Histoplasma capsulatum*
- *Blastomyces dermatitidis*

Helminths

- *Onchocerca volvulus*
- *Taenia solium* (*Cysticercus cellulosae*)

- *Toxocara canis* and *T. cati*

Protozoa

- *Toxoplasma gondii*

Ectoparasites

- Maggots (myiasis)

Bacteria

Bacteria are the most common group of organisms causing endophthalmitis. Gram-positive organisms are responsible for 60–80% of acute infections in all large series. These organisms vary widely in their virulence and, therefore, in their effect on the eye.

Gram-Positive Cocci

Staphylococci.

Staphylococci are gram-positive organisms that grow singly, in pairs, in chains, or in clusters. They are members of the family Micrococcaceae, and the individual organisms have a diameter of 0.2–1.2 μm. The main groups of staphylococci producing endophthalmitis are *Staphylococcus aureus* and coagulase-negative staphylococci.

Staph. aureus is a nonspore-forming facultative anaerobic organism that colonizes human skin and mucous membranes intermittently. It is often cultured from conjunctiva in asymptomatic persons. *Staph. aureus* is identified by positive reactions to catalase, coagulase, deoxyribonuclease test, and mannitol fermentation. *Staph. aureus* produces many enzymes, including catalase, which correlates with pathogenicity. β-Lactamases (which play a role in antimicrobial resistance), coagulase, and hyaluronidase are also bacterial products. Toxins produced by *Staph. aureus* include exfoliatins, which produce dramatic epidermal changes in skin infections; toxins associated with toxic shock syndrome; and enterotoxins, which are a major cause of food poisoning.

Staph. aureus is the second most commonly isolated organism in clinical cases of postoperative bacterial endophthalmitis and usually produces a virulent, rapidly progressive intraocular infection.

Coagulase-negative staphylococci have at least 11 different subspecies, including *Staph. epidermidis*, *Staph. capitis*, *Staph. haemolyticus*, and *Staph. hominis*. Only *Staph. epidermidis* is consistently pathogenic for humans. *Staph. epidermidis* is a prevalent and persistent species colonizing human skin and mucous membranes.

Staph. epidermidis has been increasingly identified as a cause of human infection often associated with foreign bodies, such as implanted catheters, and has become the most common cause of postoperative endophthalmitis.[1–9] Hospitals may not subspeciate coagulase-negative staphylococci, reporting them all as *Staph. epidermidis*.

Production of an exopolysaccharide (or "slime") may be one factor allowing adherence of *Staph. epidermidis* to plastic surfaces, permitting resistance to phagocytosis and failure of antimicrobial therapy. Virtually all *Staph. epidermidis* infections are hospital-acquired, whereas *Staph. saprophyticus* infections almost always involve the urinary tract and are acquired outside hospital. *Staph. epidermidis* is often resistant to multiple antibiotics, particularly methicillin, and should be considered cross-resistant to all β-lactam antibiotics. Almost all are susceptible, however, to vancomycin and rifampin.

Streptococci.

Streptococci are facultative anaerobic organisms or obligate anaerobes that are spherical or ovoid and found in pairs or chains. They are gram-positive, nonspore-forming, catalase-negative, and nonmotile organisms. The genus *Streptococcus* has more than 20 species, and its classification is complex. The viridans group of *Streptococcus* includes *Strep. mitis*, *Strep. mutans*, and *Strep. pneumoniae* (previously called *Diplococcus pneumoniae*). If the Gram stain is positive, the quellung reaction may be used to identify pneumococcus. The viridans-group streptococci are predominantly respiratory tract pathogens found in short chains. They have been

subtyped by surface antigens into 84 known serotypes. In the laboratory they exhibit fastidious growth, replicating best on complex media and often requiring carbon dioxide. They are thought to produce toxins that increase their pathogenicity. The drug of choice for these organisms is penicillin, but they are also sensitive to vancomycin.

Group D streptococci are separated into enterococcal species, including *Strep. faecalis*, *Strep. faecium*, and *Strep. durans*, and nonenterococcal species (*Strep. bovis* and *Strep. equinus*). *Strep. faecalis* and *Strep. faecium* are found in the gastrointestinal tract in humans and in human feces. Group A streptococci (*Strep. pyogenes*) make up some of the most important human pathogens, accounting for both acute rheumatic fever and poststreptococcal acute glomerulonephritis. In the laboratory, they produce β-hemolysis on blood agar plates, with discoloration around the colonies. These organisms grow in pairs or chains and are gram-positive, nonmotile, nonspore-forming, and catalase-negative. They are facultatively anaerobic, nutritionally fastidious, and usually grow on complex media when supplemented with blood or serum. They may produce extracellular products, including hemolysins, pyrogenic exotoxin, streptokinase, and hyaluronidase.

Group B streptococci (*Strep. agalactiae*) are facultative gram-positive diplococci that are usually easily grown. They have a narrow zone of β-hemolysis on blood agar plates. They are usually isolated from the lower gastrointestinal tract or genital tract of pregnant women and can produce infection in both neonates and adults. These organisms are universally susceptible to penicillin and also ampicillin, vancomycin, and first-, third-, and fourth-generation cephalosporins and ciprofloxacin.

A study of 48 cases of streptococcal endophthalmitis showed that all were sensitive to vancomycin, while nine (19%) were resistant to cefazolin or cephaloridine, and 16 (33%) were resistant to gentamicin.[10]

Gram-Positive Bacilli

Bacillus.

The genus *Bacillus* has more than 13 members, the most widely

known of which is *B. anthrax*. The most common intraocular pathogen is *B. cereus*, with *B. subtilis* also identified as a cause of endophthalmitis.[11] *Bacillus* is an aerobic spore-forming rod that is gram-positive or gram-variable in stain. The size varies from 3 × 0.4 μm to 9 × 2 μm. These organisms grow singly, in chains, or in diplobacillary form. In nature they are usually found in decaying organic matter, dust, soil, vegetables, water, and human flora. *B. cereus* is an important cause of food poisoning and may cause bacteremia as a result of wound or burn infections. It produces multiple extracellular products, including antimicrobial substances, enzymes, and toxins. The enterotoxins are diarrheal and emetic in action, and there are two additional toxins that may be correlated with virulence. Some toxins have produced severe inflammation when injected into the eye.[12] Identification by the laboratory is usually as a cultural contaminant.

Risk factors for *Bacillus* infection include intravenous (IV) drug use, sickle-cell disease, foreign bodies, including IV catheters, immunosuppression from malignancy, neutropenia, corticosteroid use, and acquired immunodeficiency syndrome (AIDS). *Bacillus* is now the most commonly identified organism in traumatic endophthalmitis.[13–17] The infection is particularly virulent and may destroy the eye in 12–24 hours. It is unique in inducing fever and leukocytosis in endophthalmitis.

Vancomycin is the drug of choice against *Bacillus* spp. because β-lactam antibiotics are rarely effective in vitro against *B. cereus*. Strains other than *B. cereus* are susceptible to penicillin, cephalosporins, ciprofloxacin, and gentamicin.

Corynebacterium diphtheriae.

Corynebacterium diphtheriae is a gram-positive bacillus that is nonsporulating, noncapsulated, nonmotile, and pleomorphic. Humans are the only known reservoir for *C. diphtheriae* and spread is by airborne respiratory droplets or by direct contact. Occasionally *C. diphtheriae* resides on skin. The main cause of virulence is a potent exotoxin producing diphtheria and skin infection. The choice for primary treatment of this organism is penicillin or erythromycin.

Listeria monocytogenes.

There are seven species of *Listeria* that have been identified, but only *L. monocytogenes* is pathogenic for humans. *Listeria* organisms are gram-positive, nonspore-forming aerobic rods that are motile at room temperature and hemolytic on colony growth. They appear coccoid-shaped in smears. In nature these organisms are found in soil, dust, animal feed, water, sewage, and colonizing animals and humans. *L. monocytogenes* causes a wide variety of infections, including dermatitis and conjunctivitis, but it is a fairly rare infection and the prevalence of symptomatic disease is therefore difficult to estimate. Because of its rarity, there are no good control studies defining the most efficacious drugs, but ampicillin or penicillin are most likely the drugs of choice.

Clostridium Species.

The genus *Clostridium* includes all anaerobic gram-positive spore-forming bacilli. There are 60 recognized species, 30 of which cause clinical disease. These organisms are ubiquitous, found in soil, decaying vegetation, marine sediment, and the gastrointestinal tract of humans, vertebrates, and insects. They are often isolated as part of polymicrobial isolates from infected sites. *C. perfringens* is well known for its ability to cause gas gangrene, a rare infection. It may also produce exotoxin and food poisoning. Penicillin G is the drug of choice, although vancomycin is an appropriate choice for *C. difficile*.

Propionibacterium.

Propionibacterium organisms are gram-positive or gram-variable rods that are often pleomorphic, anaerobic, and nonsporulating. Propionibacteria are a predominant component of skin flora and are also found on mucosal surfaces of the mouth, intestines, urethra, and vagina. They are the most common clinical isolate of gram-positive, nonsporulating bacteria. They are found in acne, prosthetic joints, cerebrospinal fluid shunts, endocarditis, and osteomyelitis. They have been identified as a cause of postoperative endophthalmitis of a chronic granulomatous nature, almost exclusively found in patients with intraocular lenses (IOLs).[18–23] *P. acnes* is almost always the clinical isolate.

Gram-Negative Cocci

Neisseria.

Neisseria organisms are gram-negative diplococci. *N. meningitidis* has fastidious growth requirements, growing best in a moist environment at 35–37°C under carbon dioxide. It has been serotyped on the basis of capsulopolysaccharides into at least 13 serogroups. The carrier state for *N. meningitidis* is the human nasopharynx. Paradoxically, however, despite the fact that it is frequently found in asymptomatic patients, the primary disease manifestations are meningococcal meningitis and sepsis, which tend to occur in epidemics. Both *N. meningitidis* and *N. gonorrhoeae* have been demonstrated to cause endophthalmitis on rare occasions. The disease is almost always endogenous in origin.

Moraxella.

Moraxella organisms are gram-negative cocci in the family Neisseriaceae. They were previously known as diplococcus of Morax-Axenfeld. Moraxellae are normal inhabitants of the upper respiratory tract and are also found on the skin and in the urogenital tract. They are strictly anaerobic, nonsaccharolytic, nonmotile, and grow on routine media. They are best known clinically as a cause of external eye disease and rarely cause systemic disease. The classic infection of *M. lacunata* is chronic angular blepharoconjunctivitis, which occurs in rare epidemics. *M. liquefaciens* is a variant of *M. lacunata* and is occasionally a cause of serious systemic disease. Moraxellae are almost universally sensitive to penicillin, but β-lactamase-producing strains are now found.

Gram-Negative Bacilli

Actinobacter.

A member or the family Neisseriaceae, *Actinobacter* is a ubiquitous saprophyte. It has low virulence and is usually the source of nosocomial infections sometimes found in immunosuppressed hosts.

Haemophilus influenzae.

Haemophilus influenzae is a small, nonspore-forming bacterium that is a strict parasite of humans. It is found principally in the upper respiratory tract but is also found in the conjunctiva and in the genital tract. It requires growth factors for isolation and takes up dye inconsistently on staining. Noncapsulated strains are normal inhabitants of the nasopharynx, but invasive diseases such as meningitis, septic arthritis, epiglottitis, and bacteremia tend to be caused by encapsulated strains. Contiguous spread to areas adjacent to the nasopharynx, including otitis media and conjunctivitis, is more often caused by noncapsulated strains. Other *Haemophilus* spp., such as *H. ducreyi* and *H. hemolyticus*, have similar distribution and growth characteristics but a significantly lower pathogenicity. In treatment of meningitis, the drug of choice is a combination of chloramphenicol and ampicillin.

Pseudomonas.

The genus *Pseudomonas* comprises a group of nonmotile, gram-negative, strictly aerobic organisms found in soil, water, and marine environments. They are straight or slightly curved bacilli that are motile, catalase-positive, and grow well over a wide range of temperatures. The nonfastidious growth requirements of *Pseudomonas* allow a wide distribution in nature. They may be part of normal human flora but are predominantly isolated as a result of nosocomial opportunistic infection. There are five major groups based on ribosomal RNA and DNA homology. The pathogenesis of disease created by *Pseudomonas* is complex and includes the production of extracellular proteases and other toxic proteins, as well as hemolysin, endotoxin, and exotoxin A.

Pseudomonas produces a wide variety of clinical syndromes, including endocarditis on prosthetic valves and in IV drug users, lower respiratory infections in persons with compromised defense mechanisms, bacteremia in immunocompromised patients, meningitis and brain abscesses, corneal ulcers, keratitis, ophthalmia neonatorum, scleral abscess, and conjunctivitis. *Pseudomonas* is the most common cause of gram-negative endophthalmitis. Most cases of endophthalmitis are produced by *P. aeruginosa*, but other species have also been isolated in clinical cases.[13,24] Sensitivities include

aminoglycosides and ceftazidime.[24,25]

Enterobacteriaceae.

The family Enterobacteriaceae comprises a large heterogeneous group of gram-negative, nonspore-forming facultative anaerobes; they are among the most important human pathogens. They are widely distributed in soil and plants and are colonizers of the gastrointestinal tract of humans and animals. Although they are uncommonly found outside the gastrointestinal tract, they are a leading cause of nosocomial disease. *Escherichia coli* is the best-studied free-living organism. It is a cause of urinary tract infection and traveler's diarrhea and is the most common cause of nosocomial bacteremia.

The tribe Klebsiellae consists of four genera: *Klebsiella*, *Enterobacter*, *Serratia*, and *Hafnia*. They are all colonizers of the human gastrointestinal tract and are rarely associated with disease in normal hosts; however, they are major causes of nosocomial and opportunistic infections, inducing a wide variety of clinical syndromes.

Klebsiella.

The genus *Klebsiella* contains a group of three species of bacteria, including *K. pneumoniae*. They are a relatively common isolate in gram-negative endophthalmitis[26] and are characteristically resistant to multiple antibiotics. Enterobacter organisms are opportunistic pathogens that rarely produce human disease. When they function as opportunistic pathogens, however, they may be resistant to first-generation cephalosporins. *Serratia* spp. are opportunistic pathogens that have only been recognized as capable of producing human disease since the 1960s. They are more likely to colonize the respiratory and urinary tracts of hospitalized patients than other Enterobacteriaceae. Most hospital infections are caused by catheterization and instrumentation of the urinary and respiratory tracts. These organisms have multiple drug resistances but are most often sensitive to amikacin.

Higher Bacteria

The order Actinomycetales has three major families of pathogens:

the Mycobacteriaceae, Actinomycetaceae, and Nocardiaceae. Actinomycetales comprises a heterogeneous group only partially defined as a collection of microorganisms. They are facultatively anaerobic and are prokaryotic filamentous bacteria. These organisms are slow-growing and gram-positive. They exhibit true branching and form mycelia-type colonies with branching filaments that grow from an ill-defined center. Reproduction, however, is by bacterial fission, and their growth is inhibited by antibiotics.

Actinomyces.

The genus *Actinomyces* includes *A. israelii*, the primary cause of human actinomycosis. *A. israelii* grows best anaerobically and may be isolated in 30–50% of all cultures taken from the mouth. It is not highly virulent but is an endogenous oral pathogen. Actinomycosis presents as a slow-growing cutaneous or soft-tissue swelling of the head, face, or neck. *A. israelii* is susceptible to penicillin, cefazolin, ampicillin, and erythromycin, in addition to other antibiotics.

Nocardia.

Nocardia spp. are aerobic actinomycetes that reproduce by fragmenting into bacillary and coccoid elements, distinguished by filamentous growth with true branching. *N. asteroides* is a predominant human pathogen. These organisms grow in a wide range of temperatures on simple media but may grow slowly in mixed cultures. They are weakly gram-positive or stain irregularly. They are also acid-fast. *Nocardia* spp. have a wide distribution in nature. They may be a respiratory saprophyte in humans, as well as being isolated from the skin. Most human infections begin in the respiratory tract. They are found most often in humans in debilitated states or in immunosuppressed patients, and the infections evade the bactericidal mechanisms of the host. In humans they produce a suppurative necrosis and abscess formation typical of pyogenic infection. They usually enter the eye as a result of a traumatic injury or from hematogenous spread. They respond to sulfanilamides, trimethoprim–sulfamethoxazole, and minocycline.

Fungi

Fungi are typically divided into yeasts and molds, although some, such as *Candida*, may grow in both forms. Yeasts are typically round or oval and reproduce by budding. Characteristic yeasts include *Candida*, *Cryptococcus neoformans*, *Blastomyces dermatitidis*, and *Coccidioides immitis*. Molds are composed of tubular structures called hyphae. They grow by branching in a longitudinal extension. Classic molds include *Aspergillus* and the agents of mucormycosis. Organisms that grow in the host as yeast-like forms, but at room temperature in vitro as molds, are called dimorphic fungi and include *Histoplasma capsulatum*, *Blastomyces*, and *C. immitis*. Most fungi reproduce asexually by forming spores through mitosis, although sexual reproduction can occur. Fungi that are pathogenic for humans are typically nonmotile and have rigid cell walls that can be stained with Gomori methenamine-silver and, when the organisms are viable, by periodic acid–Schiff. Only *Candida* can be seen well on Gram stain. Inside the fungal cell wall are sterol-containing cytoplasmic membranes, which are the site of action of polyene macrolide antibiotics, including amphotericin B and nystatin.

Candida

Candida is predominantly a unicellular organism that is small, thin-walled, ovoid, and reproduces by budding. Yeast forms, hyphae, and pseudohyphae may all be identified in clinical specimens; their identification is facilitated by staining with KCl 10%. On culture, it grows as a smooth, creamy-white colony that usually must be identified by physiologic rather than morphologic means. *Candida* is widespread in soil, hospital environments, inanimate objects, food, and as a commensal of humans, being isolated from diseased skin, the gastrointestinal tract, female genitalia, and the urine of patients with Foley catheters. The incidence of *Candida* infections has increased with the use of immunosuppression, indwelling catheters, and with increased IV drug use.[27,28] *Candida* typically causes endophthalmitis as a complication of candidemia[29] or as a result of epidemics of contaminated irrigating solutions used in intraocular surgery.[30] It typically responds to amphotericin, triazoles,[31] and 5-fluorocytosine.

Aspergillus spp.

Aspergillus spp. have been increasingly identified in endophthalmitis. *Aspergillus* is a ubiquitous mold with many species, the most common of which are *A. fumigatus* and *A. flavus*. *Aspergillus* grows well in soil, decaying vegetation, hay, dung, compost piles, hospital air-conditioner filters, and potted plants, and may be isolated from the air. Intravenous drug users are not uncommonly found to have *Aspergillus* fungemia, thought to be caused by contamination of the injected material during its preparation. Exposure to *Aspergillus* is nearly universal, but disease from *Aspergillus* is uncommon, suggesting that host factors are important.

Aspergillus creates corneal ulcers after trauma, and endophthalmitis is seen after hematogenous spread, especially in immunosuppressed patients or those abusing IV drugs. Amphotericin is the drug of choice, at times combined with 5-fluorocytosine. Invasive *Aspergillus* in the soft tissues may require surgical treatment for successful eradication.

Histoplasma capsulatum

Histoplasma capsulatum is a dimorphic fungus found in soil, particularly in areas where avian and bat excrement collect, including blackbird and pigeon roosts and chicken houses. Old buildings where bats and pigeons have roosted are frequent sources of *H. capsulatum*. The mycelial form consists of septate-branching, hyphae-bearing spores, while the yeast form is oval. Reproduction occurs through budding. Within the viable tissues, *H. capsulatum* is found almost entirely within macrophages. It is best stained with methenamine-silver but may also be identified with hematoxylin and eosin. Infection begins in *H. capsulatum* with inhalation of spores. Immunity is based on cellular immune mechanisms, and *H. capsulatum* is killed by activated macrophages after living as an intracellular parasite.

Histoplasmosis is the most common human fungus infection in the United States. Virtually all persons in the Ohio river valley and along the lower Mississippi river have been infected. Two eye syndromes are produced by *H. capsulatum*. The presumed ocular histoplasmosis syndrome consists of a morphologic triad of fundus

scarring consisting of peripheral punched-out spots, macular disciform scars, and peripapillary scarring. This is thought to be a late effect of *H. capsulatum* after hematogenous spread has created earlier choroidal infections. Organisms have not been identified in this form of the disease. Endophthalmitis associated with disseminated histoplasmosis has been described in an immunocompromised host.[32] Amphotericin is the drug of choice in active disease but is not indicated in presumed ocular histoplasmosis syndrome.

Blastomyces dermatitidis

Blastomyces dermatitidis is a dimorphic fungus that grows in a mycelial form at room temperature, and as a yeast at 37°C. These organisms have not been well studied but probably exist in nature in warm, moist soil of wooded areas rich in organic debris. *B. dermatitidis* is commonly found in outdoorsmen and hunters. It is thought to enter the lung, subsequently producing a widespread pyogranulomatous infection through hematogenous spread involving the lungs, skin, bone, and genitourinary tract. It is a relatively uncommon cause of endophthalmitis. Amphotericin is the treatment of choice.

Helminths, Protozoa, and Ectoparasites

Protozoa (as represented by *Toxoplasma gondii*), helminths (including *Onchocerca volvulus*, *Taenia solium*, and *Toxocara canis*), and ectoparasites all produce infestations that may cause a chronic intraocular infection.

Helminths

Helminths are worms of sufficient size to be visible to the naked eye. Helminths may be the most prevalent infective causative agents in human disease. They are divided into three groups: (1) nematodes, or roundworms; (2) trematodes, or flukes; and (3) cestodes, or tapeworms. Onchocerciasis is produced by *O. volvulus* and is the leading cause of blindness in the world, with over 30 million humans affected. *Onchocerca* is transmitted to humans by bites of blackflies. The larvae then make their way through the skin

and lodge in connective tissue, where adult worms tend to collect in nodules of tissue. Within the eye they produce chronic infestation. The microfilariae, swimming in the anterior chamber, may be identified by slit-lamp examination. A single dose of ivermectin is capable of killing the microfilariae but not the adult worms.

Taenia solium, a trematode, is the pork tapeworm for which humans are the only definitive host. Ingestion of the organism allows the development of the intermediate-stage *Cysticercus cellulosae*. This organism may invade almost any area of the body, including the vitreous cavity. Other helminths of ocular importance are *Toxocara canis* and *T. cati*. The predominant hosts for these organisms are dogs and cats, respectively. There are a large number of viable eggs, particularly from *T. canis*, in the environment. Eggs are spread by direct ingestion or, in the case of dogs, by eating infected meat. *T. canis* in children produces a chronic inflammatory granulomatous disease involving the vitreous and retina.[33]

Protozoa

Toxoplasmosis is the most common protozoon causing eye disease.[34] *Toxoplasma gondii* is an obligate intracellular protozoon that is ubiquitous in nature, infecting all herbivorous, carnivorous, and omnivorous animals. The definitive host is the cat. The ingestion of raw or uncooked meat allows tissue cysts to enter the gastrointestinal tract where they are broken down. They then invade the walls of the gastrointestinal tract and spread throughout the body to many tissues. The organisms remain viable for the life of the host. Although most humans are asymptomatic for the infection, a recurrent panuveitis may be an ocular manifestation of infestation.

Ectoparasites

Ectoparasites are organisms that live on the skin of a host, from which they derive their sustenance. The phylum Arthropoda includes the two-winged, or dipterous, flies. The larvae or maggots of these flies may invade living or necrotic tissue of animals and humans, producing myiasis. Multiple dipterous flies are thought to be capable of producing ocular myiasis. It is thought that the larvae

are imbedded in the eye, that they burrow directly through the sclera and then under the retina. Typically, they leave asymptomatic tracks throughout the fundus, but a number of cases of destructive endophthalmitis have been reported, particularly from Scandinavia.

Experimental Endophthalmitis

Experimental models of endophthalmitis have been produced with gram-positive and gram-negative organisms and with fungi; most models have been used to evaluate various forms of treatment.

Meyers-Elliott and Dethlefs[35] injected *Klebsiella oxytoca* organisms into the vitreous cavity of the phakic rabbit. Pathologic evaluation demonstrated widespread polymorphonuclear leukocyte invasion throughout ocular tissues within 24 hours and significant photoreceptor degeneration within 48 hours. Peak numbers of organisms could be cultured from the eye at 24 hours, but they declined spontaneously, with no organisms being recovered after 72 hours. Pathologic signs continued to increase once the cavity was sterile, however, implicating endotoxins as important to ongoing tissue damage. Davey and colleagues[36] injected *K. pneumoniae* and *P. aeruginosa* into the vitreous of the phakic rabbit and noted that bacterial growth peaked at 48 hours, with the number of organisms falling spontaneously after this. Measurable changes in biochemical parameters of the vitreous did not seem to account for this phenomenon; the authors postulated that it might be a characteristic of gram-negative infections. Meredith and coworkers[37] created an experimental model of *Staph. epidermidis* endophthalmitis by injecting various numbers of organisms into the vitreous cavity of the aphakic rabbit. Low numbers of organisms produced mild disease with slow progression; some infections appeared to be self-limited. Larger numbers of organisms produced infections of greater intensity, which were almost uniformly steadily progressive. Organisms could not be recovered from the vitreous cavity after 96 hours, however, regardless of the size of the initial inoculum. This fact suggests that progressive inflammatory signs were related to factors other than continuing active infection. Other models of *Staph. epidermidis* have yielded organisms from the

phakic eye as long as 7 days after their injection into the vitreous. Peyman[38] produced endophthalmitis with *Staph. aureus* in phakic rabbits to compare various treatment regimens, reporting uniformly poor results with loss of the eye in untreated animals.

Beyer et al.[39] studied the role of the posterior capsule in the development of *Staph. aureus* endophthalmitis in the primate. Nine monkeys had bilateral lens extraction; in one eye a large capsulotomy was performed, while in the other the capsule was intact. Inoculation of 10^5 *Staph. epidermidis* organisms was made into the anterior chamber, and the vitreous was cultured after 72 hours. Only one culture was positive with the capsule intact, but all nine cultures were positive when the capsule was opened. The experiment was repeated with a posterior-chamber lens implanted. None of ten eyes with an intact capsule and IOL was culture-positive, whereas 40% of the eyes with the capsule open and a lens in place were culture-positive and an additional 20% showed histopathologic signs of vitreous inflammation. An intact posterior capsule thus appeared to inhibit the spread of infection from the anterior chamber into the vitreous cavity, an effect that was not compromised by the addition of a posterior-chamber IOL.

Anaerobic organisms have also been used to produce clinical disease in the rabbit. The injection of 1000 organisms of *Fusobacterium necrophorum* into the vitreous cavity of the phakic rabbit produced clinical infection in 100% of eyes. *P. acnes* was studied in the aphakic rabbit with and without a posterior-chamber IOL. Injection of 10^8 organisms into the anterior chamber produced a severe infection, while inoculation of 2.5×10^6 produced clinical inflammation that peaked at 3 days but persisted for up to 24 days. The presence of an IOL appeared to favor the development of chronic, low-grade inflammation.

Clinical Findings

Postoperative Infection

Postoperative infection is the cause of roughly two-thirds of all cases of endophthalmitis in most clinical series. Although infectious endophthalmitis may follow any operative procedure performed on

the eye, most cases follow cataract extraction, and almost all are bacterial in origin. Studies from a single institution suggest that the incidence of endophthalmitis over the past several decades has been declining. At the Bascom Palmer Eye Institute, the incidence from 1984 to 1994 was 0.09%, dropping to 0.04% from 2000 to 2004.[40] Studies indicate that causative organisms in infection after cataract surgery are usually genetically identical to the patient's own flora.[41,42] In 75–95% of the reported cases, the causative organisms are gram-positive. A significant percentage of cases of apparent infectious endophthalmitis proved to be culture-negative.[2,3,43]

Cataract Extraction

Allen[44] reviewed 30, 000 intracapsular cataract procedures performed at the Massachusetts Eye and Ear Infirmary from 1964 to 1977 and found an incidence of endophthalmitis of 0.057%. A review of 23, 625 cases of extracapsular cataract extraction from Bascom Palmer Eye Institute revealed an incidence of 0.072%.[5] More recent figures from two studies in the phacoemulsification era suggest an incidence of 0.03%[45] to 0.04%.[38,46,47] National registries in Sweden[48] and Norway[49] identified rates of 0.04% and 0.11–0.16%, respectively. A large study from Saudi Arabia revealed an incidence of 0.08%.[50]

Symptomatically, typically the patient notes a sudden increase in pain 1–7 days after surgery. Examination demonstrates conjunctival chemosis and increased injection, often with a significant amount of yellowish exudate in the conjunctival cul-de-sac. The upper lid becomes edematous and may be difficult to open to complete a thorough examination. The cornea demonstrates variable degrees of edema, and pigmented cells may accumulate on its posterior surface. The surgical wound may show signs of dehiscence, and in advanced cases exudate can stream from the wound. The anterior chamber shows heavy flare and cells, and hypopyon is often present in the inferior angle, sometimes mixed with a tinge of red blood. In more extreme cases, the anterior chamber is filled with exudate and the cornea is white. When an IOL is in place, a fibrin membrane is usually present over both surfaces.

Heavy cellular debris is present in the vitreous, and there may be focal accumulations of whitish material or sheets of opacification within the vitreous. The intraocular pressure may be low, normal, or high. The pupil often dilates poorly, making examination with an indirect ophthalmoscope difficult. Retinal periphlebitis[51] has been reported as an early sign, but in most cases the retinal vessels are seen poorly, if at all. With more severe disease, large areas of opacity are seen within the vitreous; there may be a red reflex, or only a dark appearance to the posterior cavity.

Infection caused by *Staph. epidermidis* and other species of coagulase-negative staphylococci may have the clinical onset delayed by 5 days or more after surgery. Even then, the clinical signs and symptoms may be mild and may be difficult to distinguish from a noninfectious inflammatory process.[1,4,52,53] There was no hypopyon or pain in 25% of confirmed cases in the Endophthalmitis Vitrectomy Study (EVS).[54] In this study a number of clinical features at initial presentation were associated with microbiologic factors. More severe initial findings suggest infection with gram-negative bacteria, *Streptococcus* or *Staph. aureus*. Factors noted at initial diagnosis correlating with gram-negative and gram-positive organisms other than gram-positive coagulase micrococci included corneal infiltrate, cataract wound abnormalities, afferent pupillary defect, loss of red reflex, initial light perception only vision, and symptom onset within 2 days of surgery. Gram-negative organisms were not identified in those eyes in which retinal vessels were visualized preoperatively; 61.9% of those eyes had equivocal or no growth. Diabetes mellitus was associated with a higher yield of gram-positive, coagulase-negative micrococci, while there was a shift toward other gram-positive organisms in eyes undergoing secondary IOL implantation compared with those that had initial cataract surgery.[55,56]

Late-onset disease may occur with predisposing anatomic problems such as a persistent conjunctival filtering bleb or the presence of a vitreous wick.[57] Chronic, low-grade inflammation that ultimately proves to be of an infectious origin may occur in rare instances and has been termed chronic postoperative endophthalmitis or delayed-onset endophthalmitis.[19,58] This may occur secondary to coagulase-negative gram-positive organisms

(such as *Staph. epidermidis*)[19,58] and also results from infections with the anaerobic species *P. acnes*.[18–23] In reviews of cases of endophthalmitis after cataract extraction, a significant incidence of intraoperative complications has been found.[19–21,59–61] Postoperative filtering blebs, wound leaks,[59] and vitreous wick are also found more frequently in infected eyes.[2] Infection can also result after the cutting of sutures holding the cataract wound or after an invasive procedure to incise the posterior capsule.[2,62]

The type of cataract incision has recently attracted attention as a possible contributor to the incidence of postoperative infection. A case–control study demonstrated a threefold greater risk of endophthalmitis with clear corneal incisions than with scleral tunnel incision.[63] However, this has not been confirmed by newer studies.[64,65] Temporal incisions were noted to have a higher incidence of infection than superior incisions in another study.[66] A case–control study of secondary IOL implantation showed endophthalmitis to be associated with diabetes mellitus, transscleral suture fixation of posterior-chamber IOLs, polypropylene haptics, preoperative eyelid abnormalities, reentry of the eye through a previous wound, and postoperative wound defects.[67]

Gram-positive organisms are found in 75–90% of culture-positive cases.[3,55] Most common is *Staph. epidermidis*, followed by *Staph. aureus* and *Streptococcus* spp. Gram-negative organisms accounted for only 6% of the culture-positive cases in the EVS.[3,55] Fungi are rare, with the exception of epidemics such as those of *Candida parapsilosis*[68] and *Paecilomyces lilacinus*,[69] which were traced to infected irrigating solutions. Bacterial epidemics have also been traced to an infected phacoemulsifier (*Pseudomonas*)[70] and to infected viscoelastic material (*Bacillus* spp.).[71] Culture-negative cases account for 25–35% of cases of pseudophakic endophthalmitis.[2,3,55,72]

To this day there is no standardized approach to the perioperative use of antibiotics during cataract surgery. A recent review paper reported a preventative effect of intracameral antibiotics while topical antibiotics did not appear to be effective in reducing the rate of postoperative endophthalmitis.[73]

Corneal Transplantation

Since endophthalmitis after corneal transplantation is rarely seen, its characteristics are less well defined. In three large series of corneal transplants, an incidence of 0.65%, 0.11%, and 0.08% of postoperative endophthalmitis was reported.[46,74,75] In a review of over 90 ,000 cases between 1972 and 2002, the incidence after PKP was 0.38%.[76] Guss et al.[74] studied 445 corneal transplant cases and demonstrated that, in addition to three acute cases, there were eight other cases, six of which occurred after an ulcerative process in the graft. Endophthalmitis of delayed or late onset can also result from suture abscess formation or from bacterial access to the anterior chamber associated with a loose suture.[77] In an ulcerative process, entry may occur because of disruption of continuity of the graft, or the bacteria may invade through an intact but thinned cornea. Endophthalmitis following corneal transplantation has also been associated with a vitreous wick. Unlike endophthalmitis following cataract surgery, the onset of the disease may be relatively pain-free and is heralded by an increased anterior-chamber reaction, hypopyon, and loss of red reflex. The bacteria usually involved in these cases are gram-positive, with *Staphylococcus* spp. and *Streptococcus* spp. being equally represented; fungal and gram-negative cases are least common. In the series of Leveille et al.,[78] three of four acute cases were associated with a contaminated donor rim; this was not noted in any of the cases reported by Guss et al.[74] The prognosis in postcorneal transplantation cases is poor; 9 of the 11 cases reported by Guss et al.[74] had final vision of light perception or no light perception.

Glaucoma Filtration Surgery

The risk of developing endophthalmitis after filtering surgery is similar to the risk following cataract extraction,[5,46,79–82] but most of these cases occur months to years after the original procedure. A prodrome of browache, headache, or eye pain is not uncommon.[83] There may be an antecedent conjunctivitis, but often the abrupt onset of pain and redness constitutes the presenting signs and symptoms. An inferior location to the bleb and use of antifibrotic agents increase the likelihood of subsequent infection.[84–86] The blebs may appear intact in these cases, although some may be Seidel-

positive.[57,86] Thin, avascular, and leaking blebs appear to be at increased risk of infection.[83] The material within the bleb is white or yellow, giving a "white-on-red" appearance against the conjunctival erythema. Eyes with glaucoma drainage devices are also at risk for infection.[81] The spectrum of bacteria isolated from culture-positive bleb infection is quite different from that of endophthalmitis following cataract surgery, with 31–57% demonstrating *Streptococcus* spp. as the causative organism.[57,83,85,87–89] More recent series have found more cases caused by *Staphylococcus* spp. and *Enterococcus* spp. than older reports. Gram-negative species are also more common than after acute postcataract infections.[89] Visual outcomes remain generally poor in these cases, even with modern therapy. In two large series, 50% of eyes had final visual acuity of 20/400 or better,[88,89] in part because of the influence of *Streptococcus* spp. infections on the outcome.

Pars Plana Vitrectomy

The incidence of endophthalmitis after pars plana vitrectomy appears to be about the same as that after other intraocular procedures.[46,90] The diagnosis is most difficult to make because the normal postoperative pain and intraocular inflammation after vitrectomy may mask the symptoms. The diagnosis rests on findings that are more severe than usual; appearance of hypopyon is often rapid and should cause particular concern.[90,91] In one case with intraocular silicone, findings were limited to a whitish material collecting between the silicone and the retina.[92] The spectrum of bacteria in these cases is similar to other acute postoperative infections. In spite of this, the prognosis is uniformly poor, and retention of vision is rare.

The first large, multicenter studies in the era of small-gauge vitrectomy suggested a significant higher rate of endophthalmitis with 25-gauge sutureless vitrectomy (0.23% and 0.84%).[93,94] Since then, several large series have not confirmed these findings.[95–98] Optimized wound construction, modifications in case selection, and a lower threshold for suturing appear to reduce the incidence of endophthalmitis in small-gauge cases to the level of standard 20-gauge cases.

Intraocular Injection

Introduction of organisms into the eye may occur during a pars plana injection of intraocular gas for pneumatic retinopexy.[99] In recent years intraocular injection of medications to treat age-related macular degeneration, diabetic macular edema, retinal vein occlusions, cytomegalovirus retinitis, and uveitis have increased in frequency dramatically, resulting in increased numbers of cases of endophthalmitis. The reported incidence of endophthalmitis following intravitreal injections varies significantly. A recent review paper described a rate of endophthalmitis from 0.014% up to 0.87% per injection. The overall incidence was 0.051% (50/98 962).[100] A similar incidence of 0.06% (11 of 11,509) was recently reported by investigators of the "Comparison of Age-related macular degeneration Treatments Trials (CATT).[101] A large French multicenter study found an incidence of 0.021% (65 of 316,576).[102] Injection technique used varied from study to study. To this day there is no clear consensus on a "standard" injection protocol as for the use of a sterile drape, gloves, surgical mask, or topical antibiotics. So far, only the use of povidone iodine and a lid speculum is routinely recommended.[103] Cultures most frequently showed coagulase-negative staphylococci as causative organism, with atypical organisms being more common after the use of triamcinolone.[100] With triamcinolone, the typical clinical signs of endophthalmitis may be masked by antiinflammatory effects and the presentation may be difficult to differentiate from a pseudohypopyon without infection, which can occur after triamcinolone injection caused by deposition of the injected material in the anterior chamber.[104]

Scleral Buckling Procedure

Most infections after retinal detachment repair by scleral buckling are confined to the extrascleral implant. In past years these have resulted in endophthalmitis, but this is now an exceedingly rare occurrence because scleral flaps, diathermy, and polyethylene implants are only rarely used. Organisms may be introduced into the eye during an inadvertent perforation of the sclera by a suture or during the drainage procedure. Since these maneuvers introduce

organisms present in the tear film or adjacent skin and lashes, staphylococcal species are most commonly reported. It has been suggested that the diagnosis, like that after pars plana vitrectomy, rests on findings of pain and inflammation in the early postoperative course that are more severe than expected.

Strabismus Surgery

Endophthalmitis is a rare but devastating complication of strabismus surgery. True endophthalmitis probably always occurs after an inadvertent suture perforation, although a scleral abscess at the site of a suture could possibly lead to an intraocular infection. Lethargy, asymmetric eye redness, eyelid swelling, and fever have been reported as presenting signs, but diagnosis may be delayed.[105] Prognosis is poor in these eyes, possibly because delays in diagnosis are common.[105,106]

Other

Endophthalmitis has also been reported after paracentesis,[107,108] keratoprosthesis surgery,[109] especially in patients with Stevens–Johnson syndrome, and ocular cicatricial pemphigoid,[110,111] and radial keratotomy.[112]

Posttraumatic Endophthalmitis

After postoperative cases, posttraumatic endophthalmitis is the second largest category, accounting for 20–30% of the cases in large mixed series.[43,113–116] The incidence of endophthalmitis after penetrating trauma ranges from as low as 2% to as high as 17%.[13,117] In rural injuries, infections have been reported in 30% of the eyes.[13] Eyes with intraocular foreign bodies have a risk of infection about twice as high as those without a foreign body.[118,119] Other independent risk factors of traumatic endophthalmitis include dirty wound, lens capsule rupture, age greater than 50 years, and delayed presentation of more than 24 hours after the injury.[120]

Of those eyes with open-globe injury which are culture-positive at primary trauma repair, not all develop endophthalmitis.[119,121] Eyes with more virulent organisms were at greater risk of developing clinical infection in one study.[121] The onset of infection

after injury varies with the virulence of the organism and is usually accompanied by increasing pain, intraocular inflammation, hypopyon, and vitreous opacities. As with postoperative endophthalmitis, about two-thirds to three-quarters of the cases are due to gram-positive organisms, with about 10–15% being caused by gram-negative organisms. An important difference, however, is that in recent series, approximately one-quarter of the infections were due to *Bacillus* spp., making this the second most common pathogen in most series of posttraumatic endophthalmitis. Most *Bacillus* infections are associated with intraocular foreign bodies.[13–16,43,118,122,123] Unfortunately, infection caused by *Bacillus* has a particularly poor prognosis, and only two of 25 eyes reported in the literature had a final vision better than being able to count fingers. Fungal infections are also important in series of traumatic endophthalmitis, accounting for 10–15% of the cases; they should be particularly suspected in soil-contaminated injuries. Overall, the reported results of therapy for traumatic endophthalmitis are not as satisfactory as for postoperative endophthalmitis.[124] This is most likely due to a higher proportion of cases caused by virulent organisms, the influence of the initial injury on the final visual outcome, as well as potential delay in diagnosis due to posttraumatic inflammation. Although recent series report vision of 20/400 or better for 42–73% of cases of postoperative endophthalmitis, comparable vision following traumatic endophthalmitis is achieved in only 9–50% of cases.[43,113,115,118,124,125]

Endogenous Endophthalmitis

Endogenous endophthalmitis accounts for 5–7% of cases in large mixed series of endophthalmitis. Although cases occur in otherwise healthy patients, most occur in patients with systemic disease, including chronic immune-compromising illness such as diabetes mellitus or renal therapy, immunosuppressive disease and therapy, IV drug use, or systemic septicemia.[126–129] Patients may present with mild symptoms of decreased vision, redness, pain, and photophobia. The initial diagnosis is not made at the first presentation in 50% of patients.[126,128] Bilaterality is common. A search for a systemic focus of infection is indicated when

endogenous endophthalmitis is suspected; blood cultures are frequently positive. Assistance of an internist or infectious disease specialist is often sought due to the systemic implications of the condition. Fungal causes are found in 50–62% of cases,[126,129] with *Candida* spp. being the most common isolate in some series and *Aspergillus* in others.[25] In cases of bacterial cause, both gram-positive and gram-negative organisms are identified, with the proportions depending on the location of the series.[130] Visual outcomes are often poor.[128–130] More alarming is the mortality rate, which has been reported to vary from 5%[116] to 29%.[129]

Therapy

In the past, antibiotics administered topically, subconjunctivally, by IV infusion, and by intramuscular injection were the mainstays of therapy for endophthalmitis. It was not until the 1980s that intravitreal antibiotics were accepted and recommended in bacterial disease.[131]

When pars plana vitrectomy became available, a number of potential advantages were recognized.[132,133] A significant amount of material may be obtained for culture purposes. Removal of infected vitreous allows the classic principles of incision and drainage to be applied to the eye for the first time. Removing infected material reduces not only the number of living bacteria but also the toxins. Media opacities are cleared more rapidly in those eyes that survive the infection, allowing more rapid restoration of visual function. Maylath and Leopold[134] have previously shown that organisms are more effectively cleared from the anterior chamber than from the posterior chamber, and removal of the vitreous allows the vitreous chamber and anterior chamber to become joined in the aphakic eye. Furthermore, it has been suggested that vitreous removal may have a beneficial effect on antibiotic distribution within the eye.[132]

Antimicrobial Therapy

Although detailed consideration of antimicrobial therapy is beyond the scope of this chapter, several principles deserve emphasis. The target area for microbial therapy in endophthalmitis is the vitreous

cavity. Intravitreal therapy is the cornerstone of antimicrobial administration, whereas the role of subconjunctival and systemic antibiotics is more controversial.

Choice of Antimicrobial Agent

Because most cases of endophthalmitis manifest as acute fulminant infections, the initial antibiotic administration is usually made without culture results to identify the organism definitively. The choice of agent administered initially is therefore empiric. Broad-spectrum coverage is important, and the choice depends in part on the microbes expected in a given clinical setting. Gram-positive bacteria predominate in all types of acute endophthalmitis, but specific organisms and their frequency vary.

Microbes causing acute postoperative endophthalmitis are most often the patient's own bacterial flora. Staphylococcal species account for more than two-thirds of all cases, but gram-negative organisms are also encountered.[3,55] In acute traumatic endophthalmitis, gram-positive organisms are the most commonly identified, but this includes a high incidence of *Bacillus* species. In traumatic endophthalmitis, the microbes reflect not only the patient's flora but also contaminants from the scene of the trauma. Gram-negative infections and mixed infections are encountered more often than in acute postoperative cases.[11,13,16,118,106] In delayed postoperative endophthalmitis, *P. acnes*,[19–23,135] nonvirulent staphylococci,[19,58] and fungi[19,61] are most often the causative agents. When the infection is associated with a filtering bleb, *Streptococcus* species are identified in a high percentage of cases.[57,136]

Characteristics for ideal drugs for the treatment of bacterial endophthalmitis include the following:

1. Bactericidal properties. Because the eye is an immune-privileged site, like the central nervous system, a bactericidal drug rather than bacteriostatic agent is preferred.

2. Broad spectrum of coverage. Coverage must include gram-positive organisms, especially methicillin-resistant staphylococci and *Bacillus* species in trauma cases, and gram-negative organisms.

3. Excellent therapeutic ratio (activity/toxicity) after intravitreal injection. Toxicity has not been well studied for most antibiotics after intravitreal injections. Toxicity is often defined by histologic studies, electron microscopic studies, and electroretinography (ERG) testing. Most antibiotics are tested in rabbits, which are a limited model because of the relative avascularity of rabbit retinas. This relative avascularity may have contributed to the delayed recognition of the vascular occlusive potential of intravitreal aminoglycosides[137,138] because of the lack of toxicity studies in primates. Toxicity may be increased by repeat injections of certain antibiotics.

4. Good therapeutic ratio after intravenous injections. Most antimicrobials penetrate the vitreous cavity poorly after IV injection because of the blood–eye barrier. Intravitreal antimicrobial levels are only rarely reported to reach levels above the minimum inhibitory concentration (MIC) for organisms usually seen in endophthalmitis after IV or oral administration.[139–146] Hydrophilic antibiotics (including aminoglycosides and β-lactam antibiotics) have less potential for penetration into the eye than lipid-soluble compounds. On the other hand, there is significant systemic toxicity to the antimicrobials commonly used in treating endophthalmitis, particularly the aminoglycosides and amphotericin.[147] Furthermore, some combinations of antibiotics have a favorable spectrum of coverage (e.g., vancomycin and aminoglycosides), but their toxicities are additive when used simultaneously.

5. Favorable pharmacokinetic properties. Intraocular inflammation enhances penetration of certain antibiotics.[139,148–150] Vitrectomy has been shown to enhance the penetration of cefazolin,[144] vancomycin,[150] and ceftazidime[148] into the eye. Repeated IV dosing may contribute to increased penetration into the vitreous cavity after IV administration, particularly in inflamed and previously operated eyes.[148–150] After intravitreal administration, antibiotics are eliminated through either an anterior or posterior route.[151,152] Aminoglycosides are eliminated anteriorly, and the β-lactam antibiotics are removed posteriorly. Vitreous removal shortens the half-life of all antimicrobial agents studied in animal models.[151–153] Lens removal decreases the half-life of antibiotics eliminated

anteriorly.[152] Inflammation may increase the half-life of antimicrobials excreted posteriorly, such as cefazolin;[153] blocking agents such as probenecid may also increase the half-life of these drugs. The half-life for anteriorly excreted drugs such as gentamicin and amikacin is decreased by inflammation.[154,155] A higher initial dose is preferred whenever possible to allow the drug to remain at levels greater than the MICs of common pathogens for a longer period. Known activity of the drug is also an important consideration in the choice of the antibiotics. If drugs are given in equivalent concentrations, the one with higher activity against suspected organisms should be chosen.

Route of Administration

Intraocular administration of antibiotics is widely accepted as standard care in endophthalmitis (Box 125.2). The major limitation of intraocular antimicrobials is the short duration of action. Most antibiotics studied have a drug level greater than the MICs for the common organisms, producing endophthalmitis for only 36–48 hours. Toxicity is also a significant problem. Injected antibiotics may create vascular shutdown (aminoglycosides),[138,156,157] retinal damage, and retinal necrosis.[158,159] Repeated injections of antibiotics are occasionally administered but may increase the potential for toxicity, as demonstrated by the combination of vancomycin and amikacin.[158,159]

Box 125.2

Dosing of Intravitreal Antibiotics in Endophthalmitis

1. Vancomycin 1 mg/0.1 mL

2. Cefazolin 2.25 mg/0.1 mL

3. Amikacin 0.2–0.4 mg/0.1 mL

4. Ceftazidime 2 mg/0.1 mL

In select cases with severe vitreous inflammation consider:

- Dexamethasone 4 mg/0.1 mL

In traumatic endophthalmitis with vegetable matter consider:

- Amphotericin B 5 μL/0.1 mL

Systemic antibiotics are recognized to be largely ineffective when used as the only route of administration with the exception of some cases of endogenous endophthalmitis. There is controversy over whether systemic antibiotics should be used, because of their poor penetration into the eye. One study demonstrated cures of endophthalmitis caused by *Staphylococcus* species and other more virulent organisms with use of IV antibiotics only.[160] In the EVS, patients given IV antibiotics in conjunction with intraocular antibiotics did not have a better visual outcome than patients given intravitreal antimicrobials alone.[3] Another recent study demonstrated that in an animal model of *Staph. aureus* endophthalmitis intravitreal vancomycin and amikacin were superior to intravenous imipenem alone, and combination treatment provided no additional benefit to intravitreal administration.[161] The IV antibiotic given for gram-positive coverage was amikacin, which has very poor penetration into the vitreous cavity after IV injection.[162] Other antimicrobial drugs, such as vancomycin and cefazolin, gatifloxacin, or moxifloxacin, which demonstrate better penetration, may be beneficial in some circumstances.[144,146,148,163]

Subconjunctival antibiotics, formerly recommended in endophthalmitis treatment,[164] are currently used as postsurgical prophylaxis. The levels achieved in the vitreous after subconjunctival injection, however, are insignificant in comparison to intravitreal injection and rarely reach therapeutic levels when given alone.[140,165]

Antibiotic administration as part of the infusion fluid has been recommended as part of vitrectomy procedure. This has the advantage of initiating antibiotic exposure to the organisms somewhat earlier than injection into the vitreous cavity at the close of the surgical procedure. Despite some concerns of retinal toxicity, one recommendation is to place gentamicin (8 mg/mL) into the infusion.[166] Because this is approximately one-third of the concentration achieved by injecting 100 mg into a 4-mL eye (25

mg/mL), the peak dosage and effective duration of action are significantly reduced.

Antimicrobial Agents

Four groups of antimicrobials are commonly prescribed in endophthalmitis: (1) cephalosporins; (2) aminoglycosides; (3) fluoroquinolones; and (4) antifungal agents.

Cephalosporins.

The cephalosporins are synthetic penicillins active against the bacterial cell wall. They are well tolerated systemically, and cefazolin has been established to be a relatively safe drug when 2.25 mg is injected intravitreally. All the cephalosporins have good broad-spectrum coverage for gram-positive and some gram-negative organisms, but the first-generation drugs are weak against enterococcus and methicillin-resistant staphylococcal organisms. Injection of cefazolin (2.25 mg) into the aphakic eye produces levels greater than the MICs for approximately 48 hours.[153] Penetration in inflamed vitrectomized eyes can be achieved after repeated IV dosages, and cefazolin reaches levels well above the MICs for sensitive organisms.[144] Ceftazidime is a promising antibiotic for gram-negative coverage in endophthalmitis therapy because it has good cerebrospinal fluid penetration and excellent *Pseudomonas* coverage. In a study of 37 gram-negative isolates from cases of endophthalmitis, 80% were susceptible to ceftazidime.[25] Initial reports indicate an excellent therapeutic ratio after intraocular injection.[167,168]

Vancomycin.

Vancomycin has been recommended as the antibiotic of choice for gram-positive coverage.[169–171] In a study of 246 gram-positive isolates from cases of human endophthalmitis, 100% were susceptible to vancomycin.[25] Its coverage is purely gram-positive, but its spectrum includes all of the staphylococcal species, *Bacillus*, and *P. acnes*. The mechanism of vancomycin is inhibition of cell wall assembly, in addition to damaging protoplasts and inhibiting RNA synthesis. The intraocular therapeutic ratio for vancomycin is good, although the half-life suggests that therapeutic concentrations will

be maintained for only about 48 hours after intravitreal injections.[172,173] Vitreous sampling after intraocular injection in human infection has suggested that potentially therapeutic levels may persist for 3–4 days after initial injection depending on the initial dose.[80,174] Systemic toxicity is seen after high IV dosages and is unfortunately additive with IV aminoglycosides. Penetration into the vitreous cavity of inflamed eyes after IV injection is sufficient to be above the MIC for most pertinent pathogens after repeated dosing in animal models,[150] but produces variable concentrations in humans after a single dose.[175]

Aminoglycosides.

Aminoglycosides have a spectrum that includes both gram-positive and gram-negative organisms. They are chosen particularly for their gram-negative coverage in endophthalmitis. The mechanism of action for aminoglycosides is to inhibit protein synthesis. Unfortunately, the intraocular therapeutic ratio after intraocular injection is a source of problems.[135,138,156,157] Retinal vascular infarction has been frequently reported after gentamicin,[33] and it has also been noted after amikacin administration.[137] Tolerated dosages may be higher for amikacin than for gentamicin, but all of the aminoglycosides cause retinal changes after higher intravitreal dosages.[176–178] The half-life of amikacin is approximately 8 hours in inflamed, vitrectomized eyes.[155] Because of the limitations in the amount given for the initial dosage, the concentration of these antibiotics remains above the MIC for only 24–36 hours after administration. The therapeutic ratio for treatment of ocular disease after IV administration is also unfavorable because of systemic toxicity. Penetration of gentamicin into the eye after IV administration has been studied in both rabbits[179] and humans.[180] It does not reach therapeutic levels in traumatized rabbit eyes,[162] normal rabbit eyes, or human eyes with various ocular diseases after single doses.[180]

Fluoroquinolones.

The quinolones are broad-spectrum antibiotics with both gram-positive and gram-negative coverage. Their mechanism of action is thought to be inhibition of DNA synthesis. The second-generation

drugs are ciprofloxacin and ofloxacin, while levofloxacin is a third-generation agent. The fourth-generation drugs, gatifloxacin and moxifloxacin, have significant potential in the prophylaxis and treatment of endophthalmitis. Initial reports of the therapeutic ratio of ciprofloxacin after intraocular injection suggest that intraocular toxicity occurs at low dosage levels.[181,182] Fluoroquinolones penetrate the blood–ocular barrier more readily than do several of the other classes of antimicrobials. Ciprofloxacin has reasonable penetration after oral administration, but many ocular pathogens have developed resistance to it.[25] After two doses of oral administration, levofloxacin achieves concentrations in the aqueous and vitreous above the MIC (90) for many gram-positive and gram-negative pathogens but not for *Pseudomonas aeruginosa*.[181] Studies of penetration of gatifloxacin and moxifloxacin into noninflamed eyes undergoing vitreous surgery after oral administration of two doses demonstrated that the percentages of serum concentrations achieved in the vitreous and aqueous were 26.17% and 21.01%, respectively. These levels are above the MIC (90) for most of the pathogens producing human disease. These include *Staph. epidermidis*, *Staph. aureus*, *Strep. pneumoniae*, *Strep. pyogenes*, *Enterococcus faecalis*, *Proteus mirabilis*, *E. coli*, and *P. acnes*, among others. Notably, however, neither agent achieved vitreous MIC (90) for *P. aeruginosa* and moxifloxacin did not reach the MIC (90) for *Bacteroides fragilis*.[120,142,146] Because two genetic alterations in the target bacteria must occur for resistance to emerge to the fourth-generation drugs, the rapid development of resistance noted for ciprofloxacin may be avoided.

Antifungal Agents

Amphotericin has been considered the gold standard in antifungal therapy. Its mechanism of action is the alteration of membrane permeability by combination with sterols and fungal cytoplasmic membranes. The intraocular therapeutic ratio has not been well studied, but the usual recommended dosage is 5 μg/mL.[183] After IV administration, there are significant systemic complications, including renal toxicity. Penetration into the eye is also relatively poor. After intraocular injection, the half-life has been reported to

be 9.1 days. The half-life is further decreased by inflammation and vitreous removal.[183] Vitrectomy and oral fluconazole have been reported to treat *Candida* endophthalmitis successfully, with fewer side-effects.[31] Fluconazole has significant penetration into the noninflamed eye after oral administration.[184] Voriconazole is a triazole antifungal agent that is a second-generation synthetic derivative of fluconazole. It demonstrates a broad spectrum of action, including *Aspergillus* species, *Candida* species, and *Paecilomyces*, and has a low MIC (90) for many organisms. After oral administration, potentially therapeutic levels are achieved in aqueous and vitreous in noninflamed eyes.[143] Uses of intravitreal voriconazole for fungal endophthalmitis have been reported.[185,186]

Pars Plana Vitrectomy

Pars plana vitrectomy plays a role in many phases of endophthalmitis therapy. As initial therapy it is validated by the EVS results only for acute postcataract extraction infections in eyes presenting with vision of hand motions or less. This recommendation should not be generalized to infection associated with filtering blebs, endogenous endophthalmitis, posttraumatic endophthalmitis, or even chronic or delayed-onset endophthalmitis in which the clinical circumstances, and, most importantly, the causative organisms, are likely to be different.[187] In addition to use as initial therapy in many of these clinical settings, pars plana vitrectomy should also be considered for eyes not responding to an original tap-and-inject strategy, and may be necessary to clear vitreous opacities in eyes cured of infection when spontaneous clearing does not occur.

Acute Postoperative Endophthalmitis After Cataract Surgery

Early in the development of pars plana vitrectomy, treatment of acute postoperative endophthalmitis was identified as a potential application. Although there was general agreement that the most severe cases might benefit from vitreous surgery, there was no clear indication about when surgery should be undertaken in acute cases of infection.

The EVS was designed to address the issue of the relative efficacy of vitrectomy and intraocular antibiotic injection in the treatment of acute endophthalmitis after cataract surgery compared with initial diagnostic tap and injection of antibiotics alone.[3,188] In this study, patients with acute postoperative endophthalmitis were randomized to one of the two strategies for initial management. Patients with a progressive downhill course after tap and injection were allowed to have a vitrectomy procedure. As a second randomization, patients in each group were assigned to either IV antibiotic therapy or no IV antibiotic therapy. A total of 420 patients with clinical evidence of endophthalmitis within 6 weeks of cataract surgery or secondary IOL implantation were included. Visual acuity was evaluated 9 months after the initial intervention.[3]

In this study, 30.7% of the eyes were culture-negative. Of the 291 culture-positive cases, the isolates identified were as follows: gram-positive, coagulase-negative micrococci 70%; *Staph. aureus* 9%; *Streptococcus* species 9%; *Enterococcus* species 2.2%; gram-negative species 5.9%.[47,48] The initial vision was an important determinant of outcome. In eyes presenting with vision of hand motions or better there was no difference in visual outcome regardless of whether an immediate vitrectomy was performed. In patients with initial vision of light perception, eyes treated by immediate vitrectomy had a threefold increase in the frequency of achieving 20/40 or better acuity (33% vs. 11%), approximately a twofold chance of achieving 20/100 or better (56% vs. 30%), and a 50% decrease in the frequency of severe visual loss (20% vs. 47%) compared with an initial tap-and-inject strategy. Eyes treated with systemic antibiotics did not show improved outcomes compared with those not receiving them. Thus the study recommended that vitrectomy be reserved as an initial treatment strategy for those eyes presenting with light perception vision.[3] Subsequent evaluation of the data suggested that patients with diabetes mellitus had a better outcome with an initial strategy of vitrectomy and antibiotic injection regardless of presenting vision. The conclusions of this retrospective analysis did not reach a level of statistical significance to allow the authors to make a firm recommendation that surgery should be the initial intervention in all diabetic patients.[189] Since small-gauge vitrectomy has become the standard for most retina surgeons, vitrectomy

usage is higher than that recommended from the EVS; however, there has not been evidence of increased benefit.[190]

Traumatic Endophthalmitis

Traumatic endophthalmitis accounts for approximately 25% of all cases of intraocular infection. These cases create difficult therapeutic problems because of the effects of the injury and the wider, more virulent spectrum of bacteria that are involved in more traumatic infections than in postoperative endophthalmitis.[11,13–16,118,124]

Bacillus species are commonly identified after injuries involving farm materials and may be the causative organism in approximately 25% of cases, depending on the environment of the injury.[13] Rates of infection after trauma vary from 2–3% after penetrating injuries to 11–17% with industrial foreign bodies[118,119] to 30% in injuries occurring in rural environments.[13] Vitrectomy has been recommended because of the severity of the injuries, severity of infection, and the more adverse outcome reported in these cases.[124] Vitrectomy allows treatment of the residual intraocular effects of the trauma, such as retained lens cortex, vitreous hemorrhage, and retinal breaks, as well as allowing removal of infected vitreous, bacteria, and toxins.

Chronic Postoperative Endophthalmitis

The syndrome of chronic or delayed-onset postoperative endophthalmitis has been increasingly recognized. Causative organisms of these cases include *P. acnes*,[18,20–23,135] fungal cases (particularly *Candida parapsilosis*),[19,69] and nonvirulent forms of *Staph. epidermidis*.[19,58] The onset is usually days to weeks after surgery, and the clinical manifestation is one of chronic, indolent inflammation, often initially responding to suppression by topical corticosteroid therapy. *P. acnes* often produces a granulomatous inflammation, usually beginning 4–8 weeks after surgery. It characteristically manifests as a white plaque on the lens capsule. Fungal cases have less specific findings, and the diagnosis is often made by Gram stain, Giemsa stain, and culture. Cooperation with the microbiology department is important in these cases so that appropriate measures can be taken for the proper identification of

the organisms. Cultures should be kept for at least 2 weeks, particularly for *P. acnes* because these organisms may grow slowly. Surgery is recommended in these cases because the slow growth of the organisms makes sterilization more likely after their surgical removal than intraocular antibiotic injection alone.

It is thought to be necessary to remove the white plaque on the lens capsule in cases of *P. acnes*, and in some cases the capsule itself along with the IOL.[18,19,22] High rates of recurrence are noted when only intraocular antibiotics are injected, and persistent disease occurs in a significant percentage of patients even when the capsule is removed. Complete capsulectomy and IOL exchange is almost always successful in eradicating infection either as the initial intervention or as a secondary procedure.[18,19,22] Recurrent inflammation and persistent infection are not uncommon, and secondary procedures are often necessary in both *P. acnes* and fungal infection some weeks after the initial surgery. Recommended antimicrobial therapy includes vancomycin for *P. acnes* and intraocular amphotericin for fungi; imidazoles, including ketoconazole, fluconazole, or voriconazole may be of benefit.[18,19,143]

Bleb-Associated Endophthalmitis

Bleb-associated endophthalmitis may be seen after cataract extraction or after filtering procedures.[18,57,83,89,136] It typically occurs long after the initial surgery and is preceded by a period of irritation and redness of the eye. The classic initial finding is "white on red" because the white bleb filled with inflammatory material is highlighted against the redness of the conjunctiva. *Streptococcus* is the infecting organism in as many as 60% of these cases. In general, bleb-associated endophthalmitis has a poor visual outcome, leading to a recommendation for initial vitrectomy in these cases.[57,136] However, in some cases, particularly in phakic eyes, the initial infection may be confined to the anterior segment ("blebitis"), so systemic and intensive topical antibiotics may achieve good therapeutic levels in the anterior chamber and aqueous, thus curing the condition without vitrectomy surgery or intravitreal antimicrobial injection.[191,192]

Endogenous Endophthalmitis

Endogenous endophthalmitis is often associated with significant systemic illness or IV drug use. In these cases it is important to search for the cause of the endophthalmitis because it is secondary to infection elsewhere and may be associated with a life-threatening condition. Repeated blood cultures and a multidisciplinary approach are often helpful for locating the source of infection.[126,128–130,193] Systemic therapy may be sufficient in some cases if the vitreous cavity is not heavily involved. Vitrectomy has the advantage of both obtaining a reasonable amount of material for cytologic and microbiologic studies to make the diagnosis and allowing removal of the offending organisms. IV medication may penetrate at the site of invasion through the eye wall, but when organisms proliferate within the vitreous cavity, vitrectomy is more often needed. A literature review by Jackson et al. reported a three times better chance of retaining useful vision and avoiding evisceration or enucleation if vitrectomy is performed.[194]

If fungal disease is strongly suspected, most authors[43,132,195] concur that therapeutic vitrectomy is the treatment of choice if the vitreous is significantly involved, although systemic therapy may be sufficient in early endogenous disease. Vitrectomy has also been employed in chronic progressive inflammatory disorders that ultimately prove to be caused by fungus, such as *Cryptococcus*.[196] In these instances the indications are diagnostic, as well as therapeutic.

Parasitic diseases may produce a chronic endophthalmitis with both acute components and secondary complications, such as retinal detachment, vitreous opacity, and cataract. In these instances the acute or active stages of the infection have been the indications for surgical intervention for some authors,[197] although the chronic sequelae are more common indications for surgery in *T. canis* and toxoplasmosis-related endophthalmitis.

Preoperative Evaluation

A careful and extensive history should be taken. Clinical details such as systemic infectious disease, type of eye injury, or previous surgery may hold important clues to the identity of the infecting organism. Particular attention should be paid to the length of time from the surgical insult or trauma to the onset of symptoms and to the time that has passed since symptoms began. Previous antibiotic

or corticosteroid therapy should be noted. A thorough ocular examination should include a careful search for any possible route of entry for the infecting organism. The effects of the inflammation should also be noted: corneal clarity and thickness, condition of any surgical wound, degree of anterior-chamber reaction, hypopyon, clarity of the vitreous, visibility of the retina, and presence or absence of a red reflex. Standardized ultrasonography can define the degree of condensation of the vitreous, determine whether the retina is attached, and identify choroidal swelling.[198] Preoperative ERG findings may have a predictive value for postoperative visual result, but this has not yet been well defined.[116,198]

Surgical Techniques

If an extensive procedure is contemplated, general anesthesia is preferred because of the difficulty of obtaining adequate local anesthesia for an inflamed, painful eye. Local anesthesia may be adequate for shorter procedures or if the patient's medical condition warrants this approach.

Since the introduction of small-gauge vitrectomy, the use of 23G, 25G, and 27G transconjunctival instruments has become more popular in the treatment of infectious endophthalmitis.

The first technical problem that confronts the surgeon is placement of the infusion cannula. Because the media is almost always too cloudy for the surgeon to be able to visualize a pars plana port, this infusion cannot be used for the initial stages of the operation. Because the incision and placement of the infusion port are easier in a firm eye, it is often worthwhile placing an inferotemporal port, reserving its use for later in the procedure, once the location of the tip in the vitreous cavity can be verified.

The clarity of the cornea and anterior chamber and the presence of the crystalline lens or a pseudophakos will determine the incisions into the eye after infusion cannula placement. If the anterior vitreous can be easily seen, two trochars are placed 3.5 mm from the limbus. The anterior chamber often contains significant amounts of fibrin and hypopyon. Because the cornea invariably has some combination of epithelial edema, folds, and cells deposited on the posterior surface, the iris and central anterior vitreous are often impossible to visualize adequately. Initial incisions may be made in

the limbus at approximately the 9.30 and 2.30 clock positions, modifying the location as necessary depending on the condition of the previous surgical wound and on the presence of a filtering bleb. Fluid is infused into the anterior chamber through a secondary infusion on a blunt needle as inflammatory debris is removed with the vitrector handpiece (Fig. 125.1).

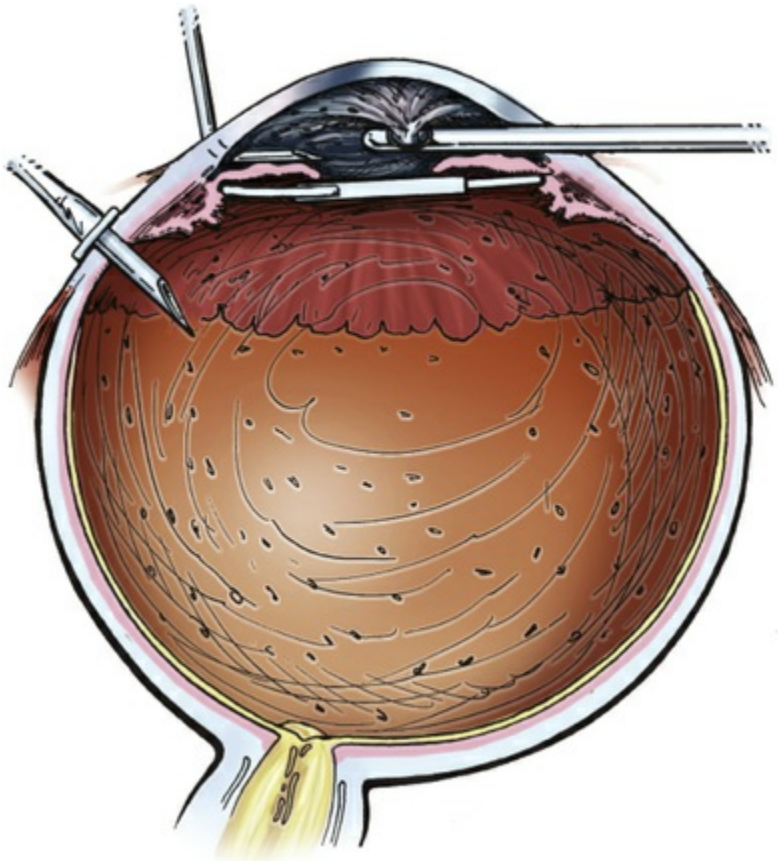

FIG. 125.1 Opaque material being removed from the anterior chamber; active infusion into the anterior chamber.

An inflammatory membrane usually extends continuously over the lens or pseudophakos and on to the surface of the iris. When a pseudophakos is present, the lens need not be removed; attempting to do so may increase the risk of bleeding. The inflammatory membrane, however, should be removed from its surface for better visualization of the posterior segment. It may be initially incised with a myringotomy blade or other sharp needle and then elevated for removal with a cutting instrument or intraocular forceps (Fig.

125.2). Removal of an inflammatory membrane from the crystalline lens should begin over the iris, close to the pupillary border, if it is believed that the lens can be spared. Often, because of poor dilation of the pupil and poor visualization of the internal structures, the lens in phakic eyes must be removed. The fastest way to accomplish this is with fragmentation through pars plana incisions, although young, soft lenses can often be removed with cutting instruments.

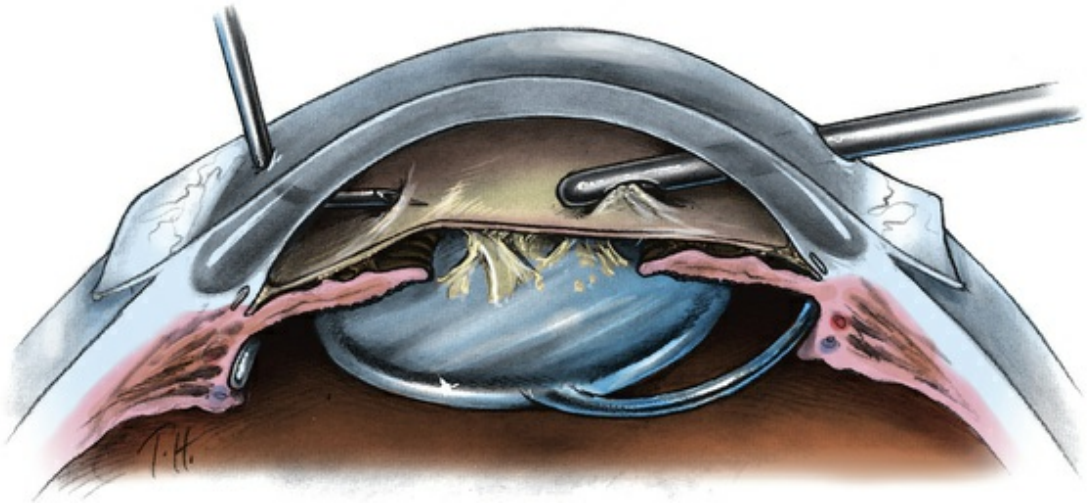

FIG. 125.2 Elevation of fibrin membrane from lens and iris to mobilize for cutting.

In severe cases the cornea and anterior chamber may be totally opaque. In theses eyes, a temporary keratoprosthesis can be used, followed by a penetrating keratoplastic. Alternatively, the initial approach may be to remove a central corneal button and to then proceed with an open-sky vitrectomy, removing as much as possible of the vitreous and then suturing a donor button into position.

Material for culture and stain should be removed from the eye early in the case. Because anterior-chamber samples frequently do not render positive culture results, attention should be directed to obtaining an adequate vitreous sample. In most surgical setups, the tubing that comes from the suction–cutting portion of the instrument can be opened. Alternatively, a very short piece of tubing is attached to the egress port of the vitrectomy probe (Fig. 125.3). A sterile syringe is connected, and the vitreous is withdrawn with manual suction. Approximately 0.2 mL is removed before

starting infusion into the eye to obtain an undiluted sample. The material is then immediately sent to the laboratory for Gram and Giemsa stain, as well as cultures on blood agar, chocolate agar, brain–heart infusion, and Sabouraud's media or broth and in thioglycolate broth. It is important to obtain the specimens for culture before any antibiotics are injected into the eye.

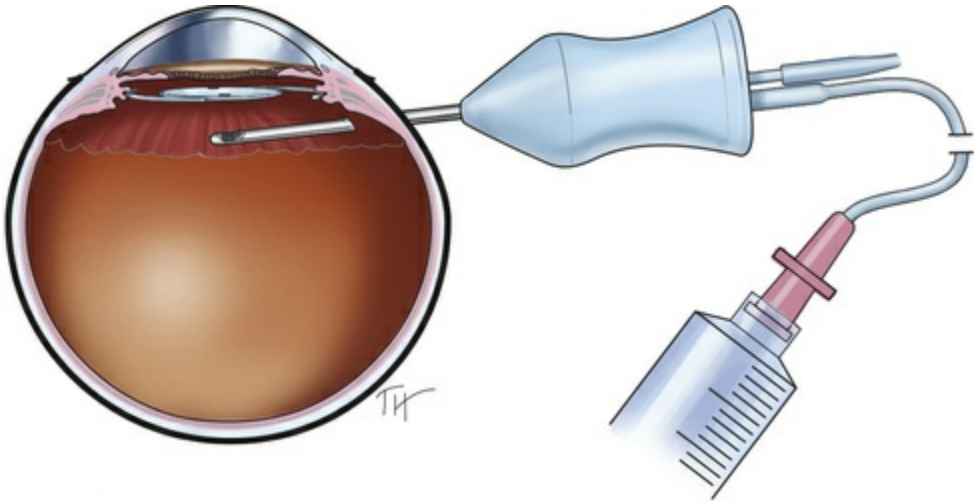

FIG. 125.3 A short piece of tubing connects a syringe to the vitrectomy probe to obtain an undiluted vitreous sample.

The vitrectomy is now progressively carried posteriorly. The vitreous removal is performed initially in the center of the vitreous cavity. Pockets of more heavily infiltrated vitreous are sometimes located near the vitreous base; in the aphakic eye, peripheral depression may be used to bring these into view. Aggressive removal of all infiltrated vitreous in the basal area should not be attempted because this often results in retinal tears. The presence of a posterior vitreous detachment, on the other hand, allows more complete vitreous removal. If the vitreous is still attached, a judgment must be made about the amount of vitreous to be removed. The cutting of vitreous adjacent to inflamed or necrotic retina will often cause retinal breaks; these are difficult to seal and may result in failure of the case. In eyes with posterior vitreous detachment, a white mound of inflammatory debris may be visible over the posterior pole. This should be approached with care and may be gently aspirated into the cutting port. If the mound proves

to be solid and adherent, small amounts can usually be removed, but in most cases it is unwise to attempt to remove large portions. In some instances the material is flocculent and equivalent to an unorganized hypopyon; this can be gently sucked up with vacuum techniques (Fig. 125.4).

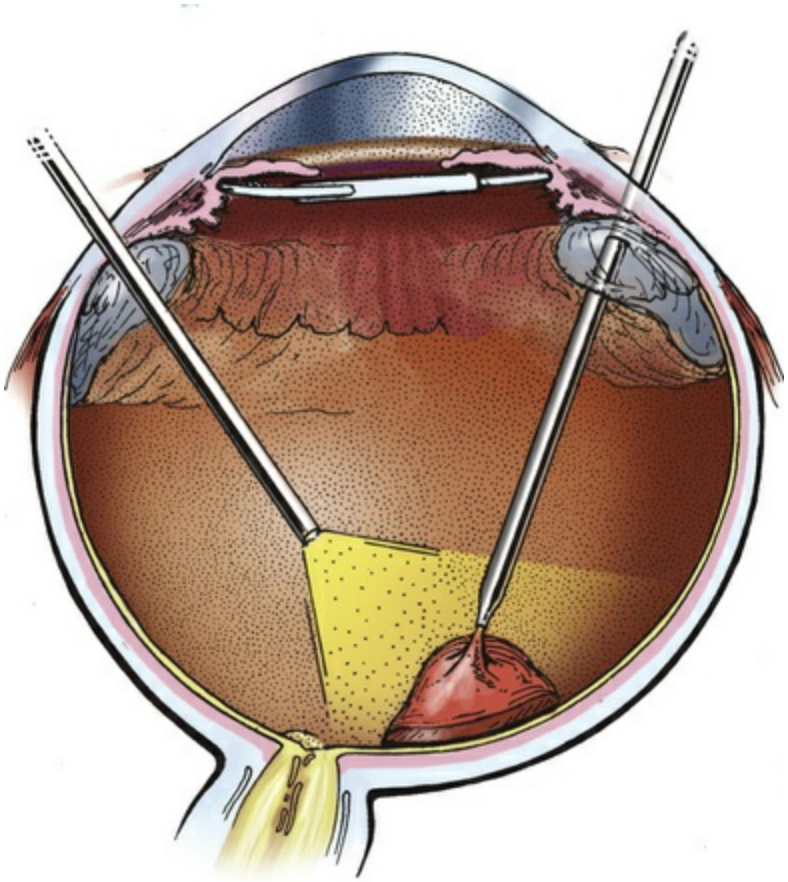

FIG. 125.4 Vacuuming removal of "hypopyon" from macular area.

If visibility is so poor that the vitreous posterior to the central area cannot be adequately defined, repeated attempts should be made to clear the anterior chamber. Membranes can also be present on the posterior surface of the lens, and these should be removed. If good visibility cannot be obtained, it is better to discontinue the procedure than to risk retinal damage by cutting posteriorly with inadequate visualization.

The procedure is completed by closing all incisions in a watertight manner and injecting intraocular antibiotics. After closure of the conjunctival incisions, subconjunctival antibiotics are

often injected.

The major intraoperative complications to be feared are hemorrhage and retinal detachment. Anterior hemorrhages can occur from the surgical wound site, the iris root, or the iris surface. These may be controlled initially by raising the intraocular pressure, usually by raising the height of the infusion bottle. Visible hemorrhage from a point source can also be controlled with intraocular diathermy. Retinal breaks are a major problem. If vitreous is not attached to the breaks, they can be treated with intraocular argon laser or cryotherapy. Posterior breaks can then be managed with gas tamponade alone, but this makes intraocular antibiotic injection problematic. Consideration should be given to a scleral buckle if anterior breaks are present. If vitreous remains attached to the break, attempts to remove it can be made, but such manipulation may result in further tearing. If this occurs, external buckling must then be provided. A choroidal hemorrhage may be devastating and can destroy the eye. The best way to avoid this complication is to keep intraocular pressure at a constant level during the entire procedure, thereby preventing hypotony. If choroidal hemorrhage does develop, intraocular pressure should be immediately raised to high levels in an attempt to close the bleeding vessel.

Breakdown of the original surgical wound is also occasionally encountered. Resuturing the wound with broader bites may be necessary. Despite the use of transconjunctival vitrectomy techniques, many surgeons still choose to routinely suture all sclerotomies at the end of endophthalmitis cases.

Postoperative Management

If treatment is proceeding well, patients usually have a dramatic improvement in ocular pain by the first postoperative day. Nonetheless, some form of analgesic, including narcotics, is often required. Resolution of the disease can be monitored in part by the progressive reduction in pain.

Antibiotics given intravitreally at the time of surgery maintain high therapeutic levels for 24–48 hours. In bacterial disease, the necessity for repeat intravitreal injection is not known with certainty; levels exceeding minimal bactericidal levels are present

for at least 24–36 hours after most intravitreal injections. Drops may also be prepared by the hospital pharmacy in highly concentrated doses; administered between 4 times a day to hourly, they may have a booster effect but probably do not significantly increase intraocular concentrations. Not all infections are cured by a single dose of injected antimicrobial.[3,199–205] If the inflammation appears to worsen or does not respond as well as expected, particularly if it is associated with persistent pain, the physician should suspect that the infectious process remains active. The index of suspicion should be highest for streptococcal species and gram-negative organisms; gram-positive coagulase-negative micrococci usually respond to initial therapy. A repeat tap and injection of antibiotics, chosen on the basis of the culture results, should be considered; if the media appears significantly opaque, or if the initial therapy was only injection of antibiotics, a vitrectomy may be considered, particularly if most of the vitreous was not removed during the initial procedure. If the initial culture sensitivities show that the organism is resistant to the antibiotic originally injected, injection of an appropriate antibiotic is strongly recommended. In the EVS 8% of eyes were subjected to early secondary intervention.[3]

IV aminoglycosides have not been demonstrated to be effective in improving outcome, but other antimicrobials with better penetration into the vitreous cavity after IV administration may be considered in some cases. Vancomycin,[150] ceftazidime,[146,148] cefazolin,[143,148] or a fluoroquinolone[142,146,150] may be useful when a longer duration of antimicrobial effect is desired than the 24–48 hours provided by intravitreal injection.

Second operations are frequent in patients with endophthalmitis. In the EVS, 35% of all eyes needed some secondary procedure.[3,148] Opacities in the vitreous cavity may continue to interfere with vision, even if the eye responds well in terms of inflammatory signs. The retina should be monitored at regular intervals with ultrasound if the surgeon cannot be sure by indirect ophthalmoscopy that it remains attached. Removal of these opacities may be undertaken with a repeat vitrectomy as an elective procedure once the eye becomes quiet.

Control of Inflammation

In addition to eradication of viable organisms from the eye and sterilization of the vitreous cavity, control of intraocular inflammation is an important therapeutic goal. Inflammation can increase even when microbes are no longer viable. Corticosteroid administration has long been recognized as important to this goal. Subconjunctival administration at the close of the surgical procedure can achieve intraocular levels of medication within the first hours after surgery but has not been rigorously tested in clinical or animal trials. Topical corticosteroids are usually given in frequent dosages after either surgery or vitreous tap and antibiotic injection.

Corticosteroid administration by other routes is often chosen as part of the therapeutic plan. All patients in the EVS received systemic prednisone 30 mg twice daily for 5–10 days.[3] Systemically administered corticosteroids have been demonstrated to reduce inflammation independently of the effects of surgery in animal models of treatment of *Staph. epidermidis* endophthalmitis.[206,207] Intraocular corticosteroid administration was first advocated by Peyman and others[208–210] in treatment of animal models of endophthalmitis. In treatment of a rabbit model of *Staph. epidermidis* endophthalmitis, Meredith et al.[207] demonstrated a beneficial effect of intraocular corticosteroid administration that was equivalent but not superior to systemic administration. Histopathologic studies of treatment of a similar model by Maxwell et al.[211] also demonstrated a beneficial effect of intraocular corticosteroid administration. When intraocular corticosteroids were administered after vitrectomy and intraocular antibiotic injection in a model of *Staph. aureus* endophthalmitis, however, there was an increase in inflammatory scores, corneal opacity, and the number of eyes developing retinal necrosis.[200] These results suggest caution in intraocular corticosteroid use because a beneficial effect may not result in all cases of endophthalmitis. There are a number of prospective, randomized[212–214] and retrospective[215,216] human series that demonstrate earlier reduction of intraocular inflammation after injection of intravitreal dexamethasone but there appears to be no lasting benefit on visual outcome compared to controls. However, one retrospective series found a significantly reduced likelihood of achieving a three-line improvement in visual acuity among patients

receiving intravitreal corticosteroids.[215]

Complications

The cornea is often edematous in the early postoperative period. Epithelial edema usually clears within the first week if the endothelium has not undergone major damage; stromal edema will also slowly clear. Persistent epithelial defects may occasionally be seen, and their healing can be compromised by the frequent use of topical medications. Pigmented cells may remain on the posterior surface of the cornea for months. If epithelial edema does not clear and the eye seems otherwise salvageable, a corneal graft may be considered.

The intraocular pressure may be elevated or decreased in the postoperative period. Elevated pressure usually responds to medical management and improves as the inflammatory process resolves. Persistent hypotony, which not only contributes to poor corneal clearing but is also usually associated with persistent inflammation and a progressive downhill course, even in the presence of a sterile vitreous cavity, should raise the suspicion of a leaking wound site. Ultrasonography may reveal choroidal detachment; the only management currently available is a vigorous attempt to control the inflammatory process medically.

Inflammatory signs (usually more flare than cells) can persist for many weeks after surgery, especially if the initial disease was severe. Bacterial products such as endotoxins in gram-negative infections and exotoxins in gram-positive infections may persist, even after successful vitrectomy, resulting in a recurrence of vitreous cavity fibrin and cells 24 hours after an adequate vitrectomy. If there is no sign of slow but steady improvement, the ultimate outcome is almost uniformly poor, and phthisis is the usual result.

Cataract may also develop in the postoperative period if the crystalline lens has been left in place. Cataract removal can also be performed electively when the eye becomes quiet. If the ultrasound or clinical examination indicates the presence of significant vitreous opacities associated with the lens change, a pars plana approach may be used for fragmentation of the lens and removal of the vitreous opacities during the same procedure.

Retinal detachment is a feared complication of vitrectomy for endophthalmitis. Retinal detachment occurred in 8.3% of eyes in the EVS.[217] Tears that occur at the time of surgery are managed as outlined earlier. Unrecognized intraoperative tears, such as entry-site tears, can result in a detachment soon after surgery. Necrotic retina may also break down, creating an atrophic retinal break. Standard buckling procedures may help in many cases, but these may be difficult to perform because of the inability to see the fundus clearly on account of corneal opacity, poor dilation of the pupil, persistent opacity of the media, haze on the surface of an IOL, or opacification of the vitreous base. These retinal detachments can sometimes be repaired successfully, but they are reportedly the major cause of failure in most series.[218] Anatomic success was achieved in 78% of the cases in the EVS, but the occurrence of detachment was correlated with a poor visual outcome.[217] Proliferative vitreoretinopathy is a major risk in eyes with detachment; sympathetic ophthalmia has also been reported.[32]

Despite anatomic success, some eyes see poorly. A rough correlation exists between poor visual results and an abnormal ERG, suggesting that these eyes have sustained extensive damage to the retina.[116]

Postoperatively a small percentage of eyes injected with aminoglycosides at surgery develop whitening of the macular area with intraretinal hemorrhages in the posterior pole. Fluorescein angiography demonstrates shutdown of the capillaries and arterioles supplying the macula and vision is frequently poor.[138,156] Histologic examination of similar-appearing lesions produced experimentally in primates by injection of gentamicin shows extensive destruction of the nerve fiber layer.[176]

Results

The outcome of treatment for postoperative endophthalmitis began to improve dramatically during the 1980s. Factors in this improved outcome include (1) higher incidence of endophthalmitis produced by less virulent organisms;[3,5,219] (2) earlier diagnosis and treatment; (3) widespread acceptance of intravitreal antibiotic therapy; (4) employment of vitrectomy surgery; and (5) control of the

inflammation with corticosteroids.

At this time, the visual outcome after treatment of postoperative endophthalmitis is better than in other forms of the disease. Nine months after therapeutic intervention in the EVS, 53% of the patients achieved visual acuity of 20/40 or better and 74% achieved 20/100 or better; 15% of eyes were equal to or worse than 5/200 and 5% had no light perception. A significantly greater percentage of patients in the vitrectomy group had clear media by the 3-month follow-up visit (86% vs. 75%).[3,5] There was a significant difference in outcome depending on the infecting organism. The rates of achieving final visual acuity of 20/100 or better were as follows: gram-positive, coagulase-negative micrococci, 84%; gram-negative organisms, 14%; *Staph. aureus*, 50%; *Streptococci*, 30%; and *Enterococci*, 14%. Both a positive Gram stain and infection with species other than gram-positive coagulase-negative micrococci were associated with a significantly worse outcome.[3,55]

The specific factors in the outcome of endophthalmitis treatment are difficult to analyze in other series because a number of variables are always involved. Most series report a mixture of case etiologies, including postoperative, traumatic, and endogenous. Traumatic endophthalmitis, bleb-related infections, and many endogenous cases do not in general have outcomes as favorable as postoperative cases. The indications for surgery, timing of surgery, antibiotics administered, dosage and route of antibiotic administration, and corticosteroid therapy are not uniform from one case to the next. Standards for defining success vary from one report to another. However, it appears that the achievement of 20/200 posttreatment vision is becoming a common standard.

A number of prognostic factors have been proposed, the most important of which is probably the virulence of the infecting organism, as demonstrated in the EVS. The percentage of eyes achieving at least 20/400 vision is relatively high in cases in which the culture obtained is negative (53–94%),[1–4,7,55,72,125,220] when *Staph. epidermidis* is the infecting organism (65–91%),[2,10,26,116,136] or if *P. acnes* or a fungus is the infecting organism. In endophthalmitis caused by gram-negative organisms and streptococci, vision of 20/400 or better is reported in 40–50% of cases. When *P. aeruginosa* or *Bacillus* organisms are the infecting microbes, salvage of useful vision is

almost never reported.[14,15,24,113] Delay of therapy for more than 36 hours after onset of symptoms has been reported to be associated with poor visual outcome in one series, whereas delay of more than 24 hours after onset of symptoms in eyes in which vitrectomy was performed was associated with a worse outcome in others.[123,221] In animal experiments administration of antibiotics in a model of *Pseudomonas* endophthalmitis 24 hours after bacterial injection produced sterilization of the vitreous cavity, whereas later injection did not.[201]

Visual acuity at initial manifestation has also been correlated with outcome. In one series, initial vision of light perception infrequently improved to acuity of 20/400 or better (21% of cases), whereas 87% of cases with initial acuity of 20/400 or better had this level of vision after therapy. In the EVS, 33% of eyes with initial vision of light perception achieved 20/40 when treated with immediate vitrectomy.[3] Cases associated with other ocular diseases such as damage from trauma and proliferative vitreoretinopathy tend to have less frequent achievement of 20/400 vision postoperatively.[113]

Future Directions

In the future, improved antibiotic therapy will undoubtedly play a role in improved results. Defining better drugs for broad-spectrum coverage and identifying antimicrobials with improved penetration into the inflamed postsurgical eye after systemic administration are important goals. Further studies of ocular toxicity of new antibiotics will also allow selection of drugs with better therapeutic ratios for intraocular injection. Drug delivery to the vitreous cavity should be further improved by devising systems for either continuous delivery or better noninvasive delivery. The necessity for reinjection, potential toxicity of reinjection of various antibiotics, and proper timing of reinjection also need further study.

Advances in vitrectomy, as the recently described addition of 0.025% povidone iodine to the saline solution, may help to further reduce the bacterial load during surgery.[222]

Further, the invention of new molecular diagnostic methods may enhance the results of standard microbial culture and allow for

quicker adjustment of antimicrobial therapy.[223]

Improved control of inflammation initiated by the infection will be critical to improve the visual outcome. This will include expanded understanding of the role of corticosteroids in endophthalmitis treatment and a definition of the best route of administration. Other means of reducing intraocular inflammation, particularly in *Bacillus* and *Pseudomonas* infections, must be devised and may include repeat surgery or lavage. Blockage of toxins that mediate intraocular damage may be developed clinically.[203] Finally, rapid diagnostic systems that allow immediate identification of bacteria and more specifically targeted antimicrobial therapy should further increase the efficacy of treatment.

Conclusion

Endophthalmitis remains a devastating complication of intraocular surgery and penetrating ocular trauma despite recent advances in diagnosis and treatment. Two-thirds of cases are postoperative, and 20–25% occur after penetrating trauma. Gram-positive organisms predominate in incidence and usually fare better than gram-negative infections, with *Staph. epidermidis* having a better prognosis than *Staph. aureus*. Fungal endophthalmitis accounts for 5–10% of all cases.

Intraocular antibiotics are well established as the mainstay of treatment for endophthalmitis because of the poor penetration of antibiotics into the vitreous cavity when administered by other routes because of the blood–retina barrier. Antibiotics are sometimes injected into the vitreous cavity as the only intravitreal therapy, whereas on other occasions they are combined with pars plana vitrectomy.

Pars plana vitrectomy has the advantage of removing bacteria and their toxins and clearing the ocular media, allowing a more rapid visual recovery. The eye is sterilized more quickly and reliably. Most authors recommend vitrectomy as the initial therapy for fungal infections and for the secondary structural changes, such as vitreous opacification, occurring after chronic infections such as *T. canis*. Most authors recommend vitrectomy for *P. acnes* infections and for traumatic endophthalmitis. In bacterial infections,

immediate vitrectomy is recommended for the most severe infections, including clinical settings such as filtering blebs, which are known to have a high incidence of virulent organisms. Vitrectomy is then followed by intraocular antibiotic injection. Although severity of infection is difficult to define precisely, mild to moderate infections are managed with immediate vitrectomy by some authors, but others recommend initial intraocular antibiotic injection, followed by vitrectomy only if the disease worsens. The EVS demonstrated that vision with only light perception was an indication for immediate vitrectomy based on improved results in these eyes compared with a strategy of vitreous tap and injection of antibiotics.

Results of therapy for endophthalmitis have improved in the last decade. Reasonable return of vision is often achieved in cases with negative culture results and infections with *Staph. epidermidis* and some fungi. Smaller percentages of eyes infected with *Staph. aureus* and even fewer with gram-negative organisms survive with recovery of ambulatory vision. Infections after trauma have a poorer prognosis than postoperative cases after cataract extraction; postoperative pars plana vitrectomy eyes and eyes with filtering blebs do poorly. The length of time from onset of infection to initiation of therapy and differences in virulence from one strain of bacteria to another are other important factors in outcome.

References

1. Bode DD Jr, Gelender H, Forster RK. A retrospective review of endophthalmitis due to coagulase-negative staphylococci. *Br J Ophthalmol*. 1985;69:915–919.
2. Driebe WT Jr, Mandelbaum S, Forster RK, et al. Pseudophakic endophthalmitis: diagnosis and management. *Ophthalmology*. 1986;93:442–448.
3. Endophthalmitis Vitrectomy Study Group. Results of the Endophthalmitis Vitrectomy Study. A randomized trial of immediate vitrectomy and of intravenous antibiotics for the treatment of postoperative bacterial endophthalmitis. Endophthalmitis Vitrectomy Study Group. *Arch Ophthalmol*. 1995;113:1479–1496.

4. Ficker LA, Meredith TA, Wilson LA, et al. The role of vitrectomy in Staphylococcus epidermidis endophthalmitis. *Br J Ophthalmol*. 1987;72:386–389.
5. Kattan HM, Flynn HW, Pflugfelder SC, et al. Nosocomial endophthalmitis survey: current incidence of infection following intraocular surgery. *Ophthalmology*. 1991;98:227–238.
6. Valenton MJ, Brubaker RF, Allen HF. Staphylococcus epidermidis (albus) endophthalmitis. *Arch Ophthalmol*. 1973;89:94–96.
7. Weber DJ, Hoffman KL, Thoft RA, et al. Endophthalmitis following intraocular lens implantation: report of 30 cases and review of the literature. *Rev Infect Dis*. 1986;8:12–20.
8. Moloney TP, Park J. Microbiological isolates and antibiotic sensitivities in culture-proven endophthalmitis: a 15-year review. *Br J Ophthalmol*. 2014;98(11):1492–1497.
9. Schimel AM, Miller D, Flynn HW Jr. Endophthalmitis isolates and antibiotic susceptibilities: a 10-year review of culture-proven cases. *Am J Ophthalmol*. 2013;156(1) [50–2.e1].
10. Mao LK, Flynn HW Jr, Miller D, et al. Endophthalmitis caused by streptococcal species. *Arch Ophthalmol*. 1992;110:798–801.
11. Hamady R, Zaltas M, Paton B. Bacillus-induced endophthalmitis: new series of 10 cases and review of the literature. *Br J Ophthalmol*. 1990;74:26–29.
12. Beecher DJ, Pulido JS, Barney NP, et al. Extracellular virulence factors in Bacillus cereus endophthalmitis: methods and implication of involvement of hemolysin BL. *Infect Immun*. 1995;63:632–639.
13. Boldt HC, Pulido JS, Blodi CS, et al. Rural endophthalmitis. *Ophthalmology*. 1989;96:1722–1726.
14. Davey RT, Tauber WB. Posttraumatic endophthalmitis: the emerging role of Bacillus cereus infection. *Rev Infect Dis*. 1987;9:110–123.
15. O'Day DM, Smith RS, Gregg CR, et al. The problem of Bacillus species infection with special emphasis on the virulence of Bacillus cereus. *Ophthalmology*. 1981;88:833–838.

16. Schemmer GB, Driebe WT. Post-traumatic Bacillus cereus endophthalmitis. *Arch Ophthalmol*. 1987;105:342–344.
17. Miller JJ, Scott IU, Flynn HW Jr, et al. Endophthalmitis caused by Bacillus species. *Am J Ophthalmol*. 2008;145(5):883–888.
18. Aldave AJ, Stein JD, Deramo VA, et al. Treatment strategies for postoperative Propionibacterium acnes endophthalmitis. *Ophthalmology*. 1999;106:2395–2401.
19. Fox GM, Jooneph BC, Flynn HW. Delayed-onset pseudophakic endophthalmitis. *Am J Ophthalmol*. 1991;111:163–173.
20. Meisler DM, Palestine AG, Vastine DW. Chronic Propionibacterium endophthalmitis after extracapsular cataract extraction and intraocular lens implantation. *Am J Ophthalmol*. 1986;102:733–739.
21. Meisler DM, Zakov ZN, Bruner WE, et al. Endophthalmitis associated with sequestered intraocular Propionibacterium acnes. *Am J Ophthalmol*. 1987;104:428–429.
22. Winward KE, Pflugfelder SC, Flynn HW, et al. Postoperative Propionibacterium endophthalmitis. Treatment strategies and long-term results. *Ophthalmology*. 1993;100:447–451.
23. Zambrano W, Flynn HW Jr, Pflugfelder SC, et al. Management options for Propionibacterium acnes endophthalmitis. *Ophthalmology*. 1989;96:1100–1105.
24. Eifrig CW, Scott IU, Flynn HW Jr, et al. Endophthalmitis caused by Pseudomonas aeruginosa. *Ophthalmology*. 2003;110:1714–1717.
25. Benz MS, Scott IU, Flynn HW, et al. Endophthalmitis isolates and antibiotic sensitivities: a 6-year review of culture-proven cases. *Am J Ophthalmol*. 2004;137:38–42.
26. Irvine WD, Flynn HW Jr, Miller D, et al. Endophthalmitis caused by Gram-negative organisms. *Arch Ophthalmol*. 1992;110:1450–1454.
27. Aguilar GL, Blumenkrantz MS, Egbert PR, et al. Candida endophthalmitis after intravenous drug abuse. *Arch Ophthalmol*. 1979;97:96–100.
28. Elliot JH, O'Day DM, Gutow GS. Mycotic endophthalmitis in drug abusers. *Am J Ophthalmol*. 1979;88:66–72.

29. Parke DW II, Jones DB, Gentry LO. Endogenous endophthalmitis among patients with candidemia. *Ophthalmology*. 1982;89:789–795.
30. Stern WH, Tamura E, Jacobs RA, et al. Epidemic postsurgical Candida parapsilosis endophthalmitis: clinical findings and management of 15 consecutive cases. *Ophthalmology*. 1985;92:1701–1709.
31. Christmas NJ, Smiddy WE. Vitrectomy and systemic fluconazole for treatment of endogenous fungal endophthalmitis. *Ophthalmic Surg Lasers*. 1996;27:1012–1018.
32. Croxatto JO, Galentine P, Cupples HP, et al. Sympathetic ophthalmia after pars plana vitrectomy–lensectomy for endogenous bacterial endophthalmitis. *Am J Ophthalmol*. 1981;91:342–346.
33. Hagler WS, Pollard Z, Jarrett WH, et al. Results of surgery for ocular Toxocara canis. *Ophthalmology*. 1981;88:1081–1086.
34. Bonfioli AA, Orefice F. Toxoplasmosis. *Semin Ophthalmol*. 2005;20(3):129–141.
35. Meyers-Elliott RH, Dethlefs BA. Experimental Klebsiella-induced endophthalmitis in the rabbit. *Arch Ophthalmol*. 1982;100:1959–1963.
36. Davey P, Barza M, Peckman C. Spontaneous inhibition of bacterial growth in experimental Gram-negative endophthalmitis. *Invest Ophthalmol Vis Sci*. 1987;28:867–873.
37. Meredith TA, Trabelsi A, Miller MJ, et al. Spontaneous sterilization of experimental Staphylococcus epidermidis endophthalmitis. *Invest Ophthalmol Vis Sci*. 1990;31:181–186.
38. Peyman GA. Antibiotic administration in the treatment of bacterial endophthalmitis. II. Intravitreal injections. *Surv Ophthalmol*. 1977;21:332–346.
39. Beyer TL, O'Donnell FE, Gonclaves V, et al. Role of the posterior capsule in the prevention of postoperative bacterial endophthalmitis. *Br J Ophthalmol*. 1985;69:841–846.
40. Miller JJ, Scott IU, Flynn HW Jr, et al. Acute-onset endophthalmitis after cataract surgery (2000–2004): incidence, clinical settings, and visual acuity outcomes after treatment. *Am J Ophthalmol*. 2005;139(6):983–987.

41. Bannerman TL, Rhoden DL, McAllister SK, et al. The source of coagulase-negative staphylococci in the Endophthalmitis Vitrectomy Study. A comparison of eyelid and intraocular isolates using pulsed-field gel electrophoresis. *Arch Ophthalmol*. 1997;115:357–361.
42. Speaker MG, Milch FA, Shah MK. Role of external bacterial flora in the pathogenesis of acute postoperative endophthalmitis. *Ophthalmology*. 1991;98:639–649.
43. Forster RK, Abbott RL, Gelender H. Management of infectious endophthalmitis. *Ophthalmology*. 1980;87:313–318.
44. Allen HF. Symposium: postoperative endophthalmitis. Introduction: incidence and etiology. *Ophthalmology*. 1978;85:317–319.
45. Bohigian G. A study of the incidence of culture-positive endophthalmitis after cataract surgery in an ambulatory care center. *Ophthalmic Surg Lasers*. 1999;30:295–298.
46. Eifrig CW, Flynn HW Jr, Scott IU, et al. Acute-onset postoperative endophthalmitis: review of incidence and visual outcomes (1995–2001). *Ophthalmic Surg Lasers*. 2002;33:373–378.
47. Lalwani GA, Flynn HW Jr, Scott IU, et al. Acute-onset endophthalmitis after clear corneal cataract surgery (1996–2005). Clinical features, causative organisms, and visual acuity outcomes. *Ophthalmology*. 2008;115(3):473–476.
48. Behndig A, Montan P, Stenevi U, et al. One million cataract surgeries: Swedish National Cataract Register 1992–2009. *J Cataract Refract Surg*. 2011;37(8):1539–1545.
49. Sandvig KU, Dannevig L. Postoperative endophthalmitis: establishment and results of a national registry. *J Cataract Refract Surg*. 2003;29:1273–1280.
50. Khandekar R, Al-Motowa S, Alkatan HM, et al. Incidence and determinants of endophthalmitis within 6 months of surgeries over a 2-year period at King Khaled Eye Specialist Hospital, Saudi Arabia: a review. *Middle East Afr J Ophthalmol*. 2015;22(2):198–202.
51. Packer AJ, Weingeist TA, Abrams GW. Retinal periphlebitis as an early sign of bacterial endophthalmitis. *Am J Ophthalmol*. 1983;96:66–71.

52. Mandelbaum S, Forster RK. Postoperative endophthalmitis. *Int Ophthalmol Clin*. 1987;27:95–106.
53. Ormerod LD, Becker LE, Cruise RJ, et al. Endophthalmitis caused by the coagulase-negative staphylococci 2. Factors influencing presentation after cataract surgery. *Ophthalmology*. 1993;100:724–729.
54. Wisniewski SR, Capone A, Kelsey SF, et al. Characteristics after cataract extraction or secondary lens implantation among patients screened for the Endophthalmitis Vitrectomy Study. *Ophthalmology*. 2000;107:1274–1282.
55. Endophthalmitis Vitrectomy Study Group. Microbiologic factors and visual outcome in the endophthalmitis vitrectomy study. *Am J Ophthalmol*. 1996;122:830–846.
56. Han DP, Wisniewski SR, Wilson LA, et al. Spectrum and susceptibilities of microbiologic isolates in the Endophthalmitis Vitrectomy Study. *Am J Ophthalmol*. 1996;122:1–17.
57. Mandelbaum S, Forster RK, Gelender H, et al. Late onset endophthalmitis associated with filtering blebs. *Ophthalmology*. 1985;92:964–972.
58. Ficker L, Meredith TA, Wilson LA, et al. Chronic bacterial endophthalmitis. *Am J Ophthalmol*. 1987;103:745–748.
59. Beatty RF, Robin JB, Trousdale MD, et al. Anaerobic endophthalmitis caused by Propionibacterium acnes. *Ophthalmology*. 1986;101:114–116.
60. Wallin T, Parker J, Jin Y, et al. Cohort study of 27 cases of endophthalmitis at a single institution. *J Cataract Refract Surg*. 2005;31:735–741.
61. Ormerod LD, Ho DD, Becker LE, et al. Endophthalmitis caused by the coagulase-negative staphylococci. 1. Disease spectrum and outcome. *Ophthalmology*. 1993;100:715–723.
62. Gelender H. Bacterial endophthalmitis following cutting of sutures after cataract surgery. *Am J Ophthalmol*. 1982;94:528–533.
63. Cooper BA, Holekamp NM, Bohigian G, et al. Case–control study of endophthalmitis after cataract surgery comparing scleral tunnel and clear corneal wounds. *Am J Ophthalmol*. 2003;136:300–305.

64. Oshika T, Hatano H, Kuwayama Y, et al. Incidence of endophthalmitis after cataract surgery in Japan. *Acta Ophthalmol Scand*. 2007;85(8):848–851.
65. Miller JJ, Scott IU, Flynn HW Jr, et al. Acute-onset endophthalmitis after cataract surgery (2000–2004): incidence, clinical settings, and visual acuity outcomes after treatment. *Am J Ophthalmol*. 2005;139(6):983–987.
66. Nagaki Y, Hayasaka S, Kadoi C, et al. Bacterial endophthalmitis after small-incision cataract surgery: effect of incision placement and intraocular lens type. *J Cataract Refract Surg*. 2003;29:20–26.
67. Scott IU, Flynn HW, Feuer WJ. Endophthalmitis after secondary intraocular lens implantation. *Ophthalmology*. 1995;102:1925–1931.
68. McCray E, Rampell N, Solomon SL, et al. Outbreak of Candida parapsilosis endophthalmitis after cataract extraction and intraocular lens implantation. *J Clin Microbiol*. 1986;24:625–628.
69. Pettit TH, Olson RJ, Foos RY, et al. Fungal endophthalmitis following intraocular lens implantation: a surgical epidemic. *Arch Ophthalmol*. 1980;98:1025–1039.
70. Hoffmann KK, Weber DJ, Gergen MF, et al. Pseudomonas aeruginosa-related postoperative endophthalmitis linked to a contaminated phacoemulsifier. *Arch Ophthalmol*. 2002;120:90–93.
71. Chen JC, Roy M. Epidemic Bacillus endophthalmitis after cataract surgery II: chronic and recurrent presentation and outcome. *Ophthalmology*. 2000;107:1038–1041.
72. Olson JC, Flynn WH Jr, Forster RK, et al. Results in the treatment of postoperative endophthalmitis. *Ophthalmology*. 1983;90:692–699.
73. Kessel L, Flesner P, Andresen J, et al. Antibiotic prevention of postcataract endophthalmitis: a systematic review and meta-analysis. *Acta Ophthalmol*. 2015;93(4):303–317.
74. Guss RB, Koenig S, De La Pena W, et al. Endophthalmitis after penetrating keratoplasty. *Am J Ophthalmol*. 1983;95:651–658.
75. Chen JY, Jones MN, Srinivasan S, NHSBT Ocular Tissue

Advisory Group and Contributing Ophthalmologists (OTAG Audit Study 18). Endophthalmitis after penetrating keratoplasty. *Ophthalmology*. 2015;22(1):25–30.
76. Taban M, Behrens A, Newcomb RL, et al. Incidence of acute endophthalmitis following penetrating keratoplasty: a systematic review. *Arch Ophthalmol*. 2005;123(5):605–609.
77. Confino J, Brown SI. Bacterial endophthalmitis associated with exposed monofilament sutures following corneal transplantation. *Am J Ophthalmol*. 1985;99:111–113.
78. Leveille AS, McMullan FD, Cavanagh HD. Endophthalmitis following penetrating keratoplasty. *Ophthalmology*. 1983;90:38–39.
79. Katz LJ, Cantor LB, Spaeth GL. Complications of surgery in glaucoma: early and late bacterial endophthalmitis following glaucoma filtering surgery. *Ophthalmology*. 1985;92:959–963.
80. Gan IM, van Dissel JT, Beekhuis WH, et al. Intravitreal vancomycin and gentamicin concentrations in patients with postoperative endophthalmitis. *Br J Ophthalmol*. 2001;85:1289–1293.
81. Gedde SJ, Scott IU, Tabandeh H, et al. Late endophthalmitis associated with glaucoma drainage implants. *Ophthalmology*. 2001;108:1323–1327.
82. Stein JD, Ruiz D Jr, Belsky D, et al. Longitudinal rates of postoperative adverse outcomes after glaucoma surgery among Mdicare beneficiaries 1994 to 2005. *Ophthalmology*. 2008;115(7) [1109–16.e7].
83. Poulsen EJ, Allingham RR. Characteristics and risk factors of infections after glaucoma filtering surgery. *J Glaucoma*. 2000;9:438–443.
84. Greenfield DS, Suner IJ, Schiffman J. Endophthalmitis after filtering surgery with mitomycin. *Arch Ophthalmol*. 1996;114:943–949.
85. Higginbotham EJ, Stevens RK, Musch DC. Bleb-related endophthalmitis after trabeculectomy with mitomycin C. *Ophthalmology*. 1996;103:650–656.
86. Wolner B, Liebmann JM, Sassani JW. Late bleb-related endophthalmitis after trabeculectomy with adjunctive 5-

fluorouracil. *Ophthalmology*. 1991;98:1053–1060.
87. Ciulla TA, Beck AD, Topping TM, et al. Blebitis, early endophthalmitis, and late endophthalmitis after glaucoma-filtering surgery. *Ophthalmology*. 1997;104:986–995.
88. Kangas TA, Greenfield DS, Flynn HW, et al. Delayed-onset endophthalmitis associated with conjunctival filtering blebs. *Ophthalmology*. 1997;104:746–752.
89. Song A, Scott IU, Flynn HW Jr, et al. Delayed-onset bleb-associated endophthalmitis: clinical features and visual acuity outcomes. *Ophthalmology*. 2002;109:985–991.
90. Ho PC, Tolentino FI. Bacterial endophthalmitis after closed vitrectomy. *Arch Ophthalmol*. 1984;102:207–210.
91. Blankenship GW. Endophthalmitis after pars plana vitrectomy. *Am J Ophthalmol*. 1977;84:815–817.
92. Chong LP, de Juan E Jr, McCuen BW, et al. Endophthalmitis in a silicone oil-filled eye. *Am J Ophthalmol*. 1986;102:660–661.
93. Kunimoto DY, Kaiser RS, Wills Eye Retina Service. Incidence of endophthalmitis after 20- and 25-gauge vitrectomy. *Ophthalmology*. 2007;114:2133–2137.
94. Scott IU, Flynn HW Jr, Dev S, et al. Endophthalmitis after 25-gauge and 20-gauge pars plana vitrectomy: incidence and outcomes. *Retina*. 2008;28:138–142.
95. Hu AY, Bourges JL, Shah SP, et al. Endophthalmitis after pars plana vitrectomy: a 20- and 25-gauge comparison. *Ophthalmology*. 2009;116:1360–1365.
96. Mason IIIJO, Yunker JJ, Vail RS, et al. Incidence of endophthalmitis following 20-gauge and 25-gauge vitrectomy. *Retina*. 2008;28:1352–1354.
97. Shimada H, Nakashizuka H, Hattori T, et al. Incidence of endophthalmitis after 20- and 25-gauge vitrectomy: causes and prevention. *Ophthalmology*. 2008;115:2215–2220.
98. Wu L, Berrocal MH, Arévalo JF, et al. Endophthalmitis after pars plana vitrectomy: results of the Pan American Collaborative Retina Study Group. *Retina*. 2011;31(4):673–678.
99. Eckardt C. Staphylococcus epidermidis endophthalmitis after pneumatic retinopexy. *Am J Ophthalmol*. 1987;103:720–

721.
100. Schwartz SG, Flynn HW, Scott IU. Endophthalmitis after intravitreal injections. *Expert Opin Pharmacother*. 2009;10(13):2119–2126.
101. Meredith TA, McCannel CA, Barr C, et al. Comparison of Age-Related Macular Degeneration Treatments Trials Research Group. Postinjection endophthalmitis in the comparison of age-related macular degeneration treatments trials (CATT). *Ophthalmology*. 2015;122(4):817–821.
102. Dossarps D, Bron AM, Koehrer P, et al. FRCR net (FRenCh Retina specialists net). Endophthalmitis after intravitreal injections: incidence, presentation, management, and visual outcome. *Am J Ophthalmol*. 2015;160(1):17–25.e1.
103. Aiello LP, Brucker AJ, Chang S, et al. Evolving guidelines for intravitreous injections. *Retina*. 2004;24:S3–19.
104. Moshfeghi DM, Kaiser PK, Scott IU, et al. Acute endophthalmitis following intravitreal triamcinolone acetonide injection. *Am J Ophthalmol*. 2003;136:791–796.
105. Recchia FM, Baumal CR, Sivalingam A, et al. Endophthalmitis after pediatric strabismus surgery. *Arch Ophthalmol*. 2000;118:939–944.
106. Salamon SM, Friberg TR, Luxenberg MN. Endophthalmitis after strabismus surgery. *Am J Ophthalmol*. 1982;93:39–41.
107. Apt L. Purulent anterior segment endophthalmitis following paracentesis. *Ophthalmic Surg*. 1986;17:526.
108. Joondeph BC, Joondeph HC. Purulent anterior segment endophthalmitis following paracentesis. *Ophthalmic Surg*. 1986;17:91–93.
109. Lee WB, Shtein RM, Kaufman SC, et al. Boston keratoprosthesis: outcomes and complications: a report by the American Academy of Ophthalmology. *Ophthalmology*. 2015;122(7):1504–1511.
110. Aquavella JV, Rao GN, Brown AC, et al. Keratoprosthesis: results, complications, and management. *Ophthalmology*. 1982;89:655–660.
111. Nouri M, Terada H, Alfonso EC, et al. Endophthalmitis after keratoprosthesis: incidence, bacterial causes, and risk factors. *Arch Ophthalmol*. 2001;119:484–489.

112. Gelender H, Flynn HW Jr, Mandelbaum SH. Bacterial endophthalmitis resulting from radial keratotomy. *Am J Ophthalmol*. 1982;94:528–533.
113. Bohigian GM, Olk RJ. Factors associated with a poor visual result in endophthalmitis. *Am J Ophthalmol*. 1986;101:332–341.
114. Forster RK, Zachary IG, Cottingham AJ Jr, et al. Further observations on the diagnosis, cause, and treatment of endophthalmitis. *Am J Ophthalmol*. 1976;81:52–56.
115. Rowsey JJ, Newson DL, Sexton DJ, et al. Endophthalmitis: current approaches. *Ophthalmology*. 1982;89:1055–1066.
116. Azad R, Ravi K, Talwar D, et al. Pars plana vitrectomy with or without silicone oil endotamponade in post-traumatic endophthalmitis. *Graefes Arch Clin Exp Ophthalmol*. 2003;241(6):478–483.
117. Gilbert CM, Soong HK, Hirst LW. A two-year prospective study of penetrating ocular trauma at the Wilmer Ophthalmological Institute. *Ann Ophthalmol*. 1987;19:104–106.
118. Brinton GS, Topping TM, Hyndiuk RA, et al. Posttraumatic endophthalmitis. *Arch Ophthalmol*. 1984;102:547–550.
119. Williams DF, Mieler WF, Abrams GW, et al. Results and prognostic factors in penetrating ocular injuries with retained intraocular foreign bodies. *Ophthalmology*. 1988;95:911–916.
120. Lemley CA, Han DP. Endophthalmitis: a review of current evaluation and management. *Retina*. 2007;27(6):662–680.
121. Lieb DF, Scott IU, Flynn HW Jr, et al. Open globe injuries with positive intraocular cultures: factors influencing final visual acuity outcomes. *Ophthalmology*. 2003;110:1560–1566.
122. Peyman GA, Carroll CP, Raichand M. Prevention and management of traumatic endophthalmitis. *Ophthalmology*. 1980;87:320–324.
123. Puliafito CA, Baker AS, Haaf J, et al. Infectious endophthalmitis: a review of 36 cases. *Ophthalmology*. 1982;89:921–929.
124. Affeldt JC, Flynn HW Jr, Forster RK, et al. Microbial endophthalmitis resulting from ocular trauma.

Ophthalmology. 1987;94:407–413.
125. Nobe JR, Gomez DS, Liggett P, et al. Post-traumatic and postoperative endophthalmitis: a comparison of visual outcomes. *Br J Ophthalmol*. 1987;71:614–617.
126. Binder MI, Chua J, Kaiser PK, et al. Endogenous endophthalmitis: an 18-year review of culture-positive cases at a tertiary care center. *Medicine (Baltimore)*. 2003;82:97–105.
127. Essman TF, Flynn HW Jr, Smiddy WE, et al. Treatment outcomes in a 10-year study of endogenous fungal endophthalmitis. *Ophthalmic Surg Lasers*. 1997;28:185–194.
128. Okada AA, Johnson RP, Liles WC, et al. Endogenous bacterial endophthalmitis. Report of a ten-year retrospective study. *Ophthalmology*. 1994;101:832–838.
129. Schiedler V, Scott IU, Flynn HW Jr, et al. Culture-proven endogenous endophthalmitis: clinical features and visual acuity outcomes. *Am J Ophthalmol*. 2004;137:725–731.
130. Jackson TL, Eykyn SJ, Graham EM, et al. Endogenous bacterial endophthalmitis: a 17-year prospective series and review of 267 reported cases. *Surv Ophthalmol*. 2003;48:403–423.
131. Baum J, Peyman GA, Barza M. Intravitreal administration of antibiotic in the treatment of bacterial endophthalmitis. III. Consensus. *Surv Ophthalmol*. 1982;26:204–206.
132. Irvine AR. The role of vitrectomy in endophthalmitis. *Trans Pac Coast Otoophthalmol Soc*. 1977;58:185–188.
133. Peyman GA, Raichand M, Bennett TO. Management of endophthalmitis with pars plana vitrectomy. *Br J Ophthalmol*. 1980;64:472–475.
134. Maylath FR, Leopold IH. Study of experimental intraocular infection. I. The recoverability of organisms, inoculated into ocular tissues and fluids. II. The influence of antibiotics and cortisone, alone and combined, on intraocular growth of these organisms. *Am J Ophthalmol*. 1955;40:86–101.
135. Rousell TJ, Culbertson WW, Jaffe NS. Chronic postoperative endophthalmitis associated with Propionibacterium acnes. *Arch Ophthalmol*. 1987;105:1199–1201.
136. Mandelbaum S, Forster RK. Endophthalmitis associated with filtering blebs. *Int Ophthalmol Clin*. 1987;27:107–111.

137. Campochiaro PA, Conway BP. Aminoglycoside toxicity: a survey of retinal specialists. *Arch Ophthalmol*. 1991;109:946–950.
138. Conway BP, Campochiaro PA. Macular infarction after endophthalmitis treated with vitrectomy and intravitreal gentamicin. *Arch Ophthalmol*. 1986;104:367–371.
139. Barza M. Factors affecting the intraocular penetration of antibiotics. The influence of route, inflammation, animal species and tissue pigmentation. *Scand J Infect Dis*. 1978;14:S151–9.
140. Barza M, Kane A, Baum J. Oxacillin for bacterial endophthalmitis: subconjunctival, intravenous, both, or neither? *Invest Ophthalmol Vis Sci*. 1980;19:1348–1354.
141. El Baba FZ, Trousdale MD, Gauderman WJ, et al. Intravitreal penetration of oral ciprofloxacin in humans. *Ophthalmology*. 1992;99:483–486.
142. Hariprasad SM, Mieler WF, Holz ER. Vitreous and aqueous penetration of orally administered gatifloxacin in humans. *Arch Ophthalmol*. 2003;121:345–350.
143. Hariprasad SM, Mieler WF, Holz ER, et al. Determination of vitreous, aqueous, and plasma concentration of orally administered voriconazole in humans. *Arch Ophthalmol*. 2004;122:42–47.
144. Martin DF, Ficker LA, Aguilar HA, et al. Vitreous cefazolin levels after intravenous injection. Effects of inflammation, repeated antibiotic doses, and surgery. *Arch Ophthalmol*. 1990;108:411–414.
145. O'Day DM, Head WS, Robinson RD, et al. Intraocular penetration of systemically administered antifungal agents. *Curr Eye Res*. 1985;4:131–134.
146. Hariprasad SM, Shah GK, Mieler WF, et al. Vitreous and aqueous penetration of orally administered moxifloxacin in humans. *Arch Ophthalmol*. 2006;124(2):178–182.
147. Wilson L. Endophthalmitis. *Trans Ophthalmol Soc U K*. 1986;105:56–59.
148. Aguilar HE, Meredith TA, Shaarawy A, et al. Vitreous cavity penetration of ceftazidime after intravenous administration. *Retina*. 1995;15:154–159.

149. Meredith TA, Mandell BA, Aguilar EA, et al. Amikacin levels after intravitreal injection: effects of inflammation and surgery. *Invest Ophthalmol Vis Sci*. 1992;33:747.
150. Meredith TA, Aguilar HE, Shaarawy A, et al. Vancomycin levels in the vitreous cavity after intravenous administration. *Am J Ophthalmol*. 1995;119:774–778.
151. Barza M, Kane A, Baum J. Pharmacokinetics of intravitreal carbenicillin, cefazolin, and gentamicin in rhesus monkeys. *Invest Ophthalmol Vis Sci*. 1983;24:1602–1606.
152. Meredith TA. Antimicrobial pharmacokinetics in endophthalmitis treatment; studies of ceftazidime. *Trans Am Ophthalmol Soc*. 1993;91:653–699.
153. Ficker L, Meredith TA, Gardner S, et al. Cefazolin levels after intravitreal injection: effects of inflammation and surgery. *Invest Ophthalmol Vis Sci*. 1990;31:502–505.
154. Kane A, Barza M, Baum J. Intravitreal injection of gentamicin in rabbits: effect of inflammation and pigmentation on half-life and ocular distribution. *Invest Ophthalmol Vis Sci*. 1981;20:593–597.
155. Mandell BA, Meredith TA, Aguilar E, et al. Effects of inflammation and surgery on amikacin levels in the vitreous cavity. *Am J Ophthalmol*. 1993;115:770–774.
156. Campochiaro PA, Lin JI, Aminoglycoside Study Group. Aminoglycoside toxicity in the treatment of endophthalmitis. *Arch Ophthalmol*. 1994;112:48–53.
157. Conway BP, Tabatabay CA, Campochiaro PA, et al. Gentamicin toxicity in the primate retina. *Arch Ophthalmol*. 1989;107:107–112.
158. Oum BP, D'Amico DJ, Kwak HW, et al. Intravitreal antibiotic therapy with vancomycin and aminoglycoside: examination of the retinal toxicity of repetitive injections after vitreous and lens surgery. *Graefes Arch Clin Exp Ophthalmol*. 1992;230:56–61.
159. Oum BS, D'Amico DJ, Wong KW. Intravitreal antibiotic therapy with vancomycin and aminoglycoside: an experimental study of combination and repetitive injections. *Arch Ophthalmol*. 1989;107:1055–1060.
160. O'Day DM, Jones DB, Patrinely J, et al. Staphylococcus

epidermidis endophthalmitis: visual outcome following noninvasive therapy. *Ophthalmology*. 1982;89:354–360.
161. Engelbert M, Miño de Kaspar H, Thiel M, et al. Intravitreal vancomycin and amikacin versus intravenous imipenem in the treatment of experimental Staphylococcus aureus endophthalmitis. *Graefes Arch Clin Exp Ophthalmol*. 2004;242(4):313–320.
162. El-Massry A, Meredith TA, Aguilar HE, et al. Aminoglycoside concentrations in the vitreous cavity after intravenous administration. *Am J Ophthalmol*. 1996;121:684–689.
163. Hariprasad SM, Mieler WF, Holz ER. Vitreous penetration of orally administered gatifloxacin in humans. *Trans Am Ophthalmol Soc*. 2002;100:153–159.
164. Baum JL. Antibiotic administration in the treatment of bacterial endophthalmitis. I. Periocular injections. *Surv Ophthalmol*. 1977;21:332–346.
165. Barza M, Kane A, Baum J. Ocular penetration of subconjunctival oxacillin, methicillin, and cefazolin in rabbits with staphylococcal endophthalmitis. *J Infect Dis*. 1982;145:899–903.
166. Peyman GA. Aminoglycoside toxicity. *Arch Ophthalmol*. 1992;110:1683–1685.
167. Campochiaro PA, Green WR. Toxicity of intravitreal ceftazidime in primate retina. *Arch Ophthalmol*. 1992;110:1625–1629.
168. Meredith TA, Abdala C, Aguilar HE, et al. Toxicity of intravitreal ceftazidime and vancomycin. *Invest Ophthalmol Vis Sci*. 1995;36:3647.
169. Davis JL, Koidou-Tsiligianni A, Pflugfelder SC, et al. Coagulase-negative staphylococcal endophthalmitis: increase in antimicrobial resistance. *Ophthalmology*. 1988;95:1404–1410.
170. Flynn HW Jr, Pulido JS, Pflugfelder SC. Endophthalmitis therapy: changing antibiotic sensitivity patterns and current therapeutic recommendations (Letter). *Arch Ophthalmol*. 1991;109:175–176.
171. Smith MA, Sorenson JA, D'Aversa G, et al. Treatment of

experimental methicillin-resistant Staphylococcus epidermidis endophthalmitis with intravitreal vancomycin and intravitreal dexamethasone. *J Infect Dis*. 1997;175:462–466.
172. Aguilar HE, Meredith TA, el Massry A, et al. Vancomycin levels after intravitreal injection. Effects of inflammation and surgery. *Retina*. 1995;15:428–432.
173. Pflugfelder SC, Hernandez E, Fleisler SJ, et al. Intravitreal vancomycin. *Arch Ophthalmol*. 1987;105:831–837.
174. Haider SA, Hassett P, Bron AJ. Intraocular vancomycin levels after intravitreal injection in post cataract extraction endophthalmitis. *Retina*. 2001;21:210–213.
175. Ferencz JR, Assia EI, Diamantstein L, et al. Vancomycin concentration in the vitreous after intravenous and intravitreal administration for postoperative endophthalmitis. *Arch Ophthalmol*. 1999;117:1023–1027.
176. D'Amico DJ, Libert J, Kenyon KR, et al. Retinal toxicity of intravitreal gentamicin: an electron microscopic study. *Invest Ophthalmol Vis Sci*. 1984;25:564–572.
177. D'Amico DJ, Caspers-Velu L, Libert J, et al. Comparative toxicity of intravitreal aminoglycoside antibiotics. *Am J Ophthalmol*. 1985;100:264–275.
178. Talamo JH, D'Amico J, Kenyon KR. Intravitreal amikacin in the treatment of bacterial endophthalmitis. *Arch Ophthalmol*. 1986;104:1483–1485.
179. Yoshizumi MO, Leinwand MJ, Kim J. Topical and intravenous gentamicin in traumatically lacerated eyes. *Graefes Arch Clin Exp Ophthalmol*. 1992;230:175–177.
180. Rubinstein E, Goldfarb J, Keren G, et al. The penetration of gentamicin into the vitreous humor in man. *Invest Ophthalmol Vis Sci*. 1983;24:637–639.
181. Slana VS, Marchese AL, Jay WM. Ocular toxicity of intravitreal ciprofloxacin injection in pigmented rabbit eyes. *Invest Ophthalmol Vis Sci*. 1992;33:727.
182. Fiscella RG, Shapiro MJ, Solomon MJ, et al. Ofloxacin penetration into the eye after intravenous and topical administration. *Retina*. 1997;17:535–539.
183. Doft BH, Weiskopf J, Nillson-Ehle I, et al. Amphotericin

clearance in vitrectomized versus non-vitrectomized eyes. *Ophthalmology*. 1985;92:1601–1605.
184. O'Day DM, Foulds G, Williams TE, et al. Ocular uptake of fluconazole following oral administration. *Arch Ophthalmol*. 1990;108:1006–1008.
185. Breit SM, Hariprasad SM, Mieler WF, et al. Management of endogenous fungal endophthalmitis with voriconazole and caspofungin. *Am J Ophthalmol*. 2005;139(1):135–140.
186. Gao H, Pennesi ME, Shah K, et al. Intravitreal voriconazole: an electroretinographic and histopathologic study. *Arch Ophthalmol*. 2004;122(11):1687–1692 [Erratum in: Arch Ophthalmol 2005;123(1):130.].
187. Sternberg P Jr, Martin DF. Management of endophthalmitis in the post-endophthalmitis vitrectomy study era. *Arch Ophthalmol*. 2001;119:754–755.
188. Doft BH. The Endophthalmitis Vitrectomy Study. *Arch Ophthalmol*. 1991;109:487–489.
189. Doft BH, Wisniewski SR, Kelsey SF, et al. Diabetes and postoperative endophthalmitis in the Endophthalmitis Vitrectomy Study. *Arch Ophthalmol*. 2001;119:650–656.
190. Gower EW, Keay LJ, Stare DE, et al. Characteristics of endophthalmitis after cataract surgery in the United States Medicare population. *Ophthalmology*. 2015;122(8):1625–1632.
191. Brown RH, Yang LH, Walker SD, et al. Treatment of bleb infection after glaucoma surgery. *Arch Ophthalmol*. 1994;112:57–61.
192. Reynolds AC, Skuta GL, Monlux R, et al. Management of blebitis by members of the American Glaucoma Society: a survey. *J Glaucoma*. 2001;10:340–347.
193. Greenwald MJ, Wohl LG, Sell CH. Metastatic bacterial endophthalmitis: a contemporary reappraisal. *Surv Ophthalmol*. 1986;31:81–101.
194. Jackson TL, Eykyn SJ, Graham EM, et al. Endogenous bacterial endophthalmitis: a 17-year prospective series and review of 267 reported cases. *Surv Ophthalmol*. 2003;48(4):403–423 [Review].
195. Verbraeken H, Van Laethem J. Treatment of endophthalmitis with and without pars plana vitrectomy.

Ophthalmologica. 1985;191:1–3.
196. Henderly DE, Liggett PE, Rao NA. Cryptococcal chorioretinitis endophthalmitis. *Retina*. 1987;7:75–79.
197. Rodriguez A. Early pars plana vitrectomy in chronic endophthalmitis of toxocariasis. *Graefes Arch Clin Exp Ophthalmol*. 1986;224:218–220.
198. Diamond JG. Intraocular management of endophthalmitis: a systematic approach. *Arch Ophthalmol*. 1981;99:96–99.
199. Mao LK, Flynn HW, Miller D, et al. Endophthalmitis caused by Staphylococcus aureus. *Am J Ophthalmol*. 1993;116:584–589.
200. Aguilar HE, Meredith TA, Drews CD, et al. Treatment of experimental S. aureus endophthalmitis with vancomycin, cefazolin and corticosteroids. *Invest Ophthalmol Vis Sci*. 1990;31:S140.
201. Davey PG, Barza M, Stuart M. Dose response of experimental Pseudomonas endophthalmitis to ciprofloxacin, gentamicin, and imipenem: evidence of resistance to "late" treatment of infections. *J Infect Dis*. 1987;155:518–523.
202. Forster RK. Experimental postoperative endophthalmitis. *Trans Am Ophthalmol Soc*. 1992;505–559.
203. Jett BD, Jensen HG, Atkuri RV, et al. Evaluation of therapeutic measures for treating endophthalmitis caused by isogenic toxin-producing and toxin-nonproducing Enterococcus faecalis strains. *Invest Ophthalmol Vis Sci*. 1995;36:9–15.
204. Shaarawy A, Grand MG, Meredith TA, et al. Persistent infection after intravitreal antibimicrobial therapy. *Ophthalmology*. 1995;102:382–387.
205. Stern GA, Engel HM, Driebe WT. Recurrent postoperative endophthalmitis. *Cornea*. 1990;9:102–107.
206. Baum JL, Barza M, Lugar J, et al. The effect of corticosteroids in the treatment of experimental bacterial endophthalmitis. *Am J Ophthalmol*. 1975;80:513–517.
207. Meredith TA, Aguilar HE, Miller MJ, et al. Comparative treatment of experimental staphylococcus epidermidis endophthalmitis. *Arch Ophthalmol*. 1990;108:857–860.

208. Coats ML, Peyman GA. Intravitreal corticosteroids in the treatment of exogenous fungal endophthalmitis. *Retina*. 1992;12:46–51.
209. Graham RO, Peyman GA. Intravitreal injection of dexamethasone: treatment of experimentally induced endophthalmitis. *Arch Ophthalmol*. 1974;92:149–154.
210. Peyman GA, Herbst R. Bacterial endophthalmitis: treatment with intraocular injection of gentamicin and dexamethasone. *Arch Ophthalmol*. 1974;91:416–418.
211. Maxwell DP Jr, Brent BD, Diamond JG, et al. Effect of intravitreal dexamethasone on ocular histopathology in a rabbit model of endophthalmitis. *Ophthalmology*. 1991;98:1370–1375.
212. Das T, Jalali S, Gothwal VK, et al. Intravitreal dexamethasone in exogenous bacterial endophthalmitis: results of a prospective randomised study. *Br J Ophthalmol*. 1999;83:1050–1055.
213. Gan IM, Ugahary LC, van Dissel JT, et al. Effect of intravitreal dexamethasone on vitreous vancomycin concentrations in patients with suspected postoperative bacterial endophthalmitis. *Graefes Arch Clin Exp Ophthalmol*. 2005;243(11):1186–1189.
214. Albrecht E, Richards JC, Pollock T, et al. Adjunctive use of intravitreal dexamethasone in presumed bacterial endophthalmitis: a randomised trial. *Br J Ophthalmol*. 2011;95:1385–1388.
215. Shah GK, Stein JD, Sharma S, et al. Visual outcomes following the use of intravitreal steroids in the treatment of postoperative endophthalmitis. *Ophthalmology*. 2000;107:486–489.
216. Hall EF, Scott GR, Musch DC, et al. Adjunctive intravitreal dexamethasone in the treatment of acute endophthalmitis following cataract surgery. *Clin Ophthalmol*. 2008;2(1):139–145.
217. Doft BM, Kelsey SF, Wisniewski SR. Retinal detachment in the endophthalmitis vitrectomy study. *Arch Ophthalmol*. 2000;118:1661–1665.
218. Nelsen PT, Marcus DA, Bovino JA. Retinal detachment

following endophthalmitis. *Ophthalmology*. 1985;92:1112–1117.
219. Leopold IH. Management of intraocular infection. *Trans Ophthalmol Soc U K*. 1971;91:575–610.
220. Rowsey JJ, Stonecipher KG, Jensen H, et al. Culture and sensitivities of infectious endophthalmitis: a microbiological analysis of 302 intravitreal biopsies. *Invest Ophthalmol Vis Sci*. 1992;33:S745.
221. Laatikainen L, Tarkkanen A. Early vitrectomy in treatment of postoperative purulent endophthalmitis. *Acta Ophthalmol*. 1987;65:455–460.
222. Nakashizuka H, Shimada H, Hattori T, et al. Vitrectomy using 0.025% povidone-iodine in balanced salt solution plus for the treatment of postoperative endophthalmitis. *Retina*. 2015;35(6):1087–1094.
223. Hong BK, Lee CS, Van Gelder RN, et al. Emerging techniques for pathogen discovery in endophthalmitis. *Curr Opin Ophthalmol*. 2015;26(3):221–225.

126

Diagnostic and Therapeutic Vitrectomy for Uveitis

Hyeong Gon Yu, Tae Wan Kim

Introduction

Uveitis is a type of intraocular inflammation that can affect vision and may lead to legal blindness. Uveitis is classified into autoimmune, infectious, and malignant forms based on the underlying pathogenic mechanism. The diagnosis of different forms of uveitis is primarily based on a combination of the patient history and clinical manifestation rather than laboratory findings.[1] A patient's medical history, the course of uveitis, the typical appearance of the ocular involvement, and therapeutic response are also important in making a diagnosis. Regardless of cause, accurate diagnosis and appropriate pharmacotherapy are critical for positive visual outcomes. Diagnostic vitrectomy can be helpful in discriminating between different causes of uveitis. For example, few oncologists would agree to treat a patient with presumed intraocular lymphoma without an adequate biopsy result. However, histopathologic diagnosis of biopsy specimens is not common due to the difficulty of obtaining and manipulating ocular specimens.

The vitreous, which constitutes most of the ocular volume, can be a valuable tool for an accurate diagnosis, and considering specimen volume requirements, evaluating vitreous samples is of greater value than using aqueous humor samples.[2] In addition, vitrectomy can be beneficial for managing vitreoretinal complications in uveitis patients. This chapter, which is divided into diagnostic and therapeutic vitrectomy sections, covers the surgical indications, principles, and techniques for management of uveitis. Novel advances in laboratory techniques are also discussed.

Diagnostic Vitrectomy

Indications

The efficacy of evaluating vitreous cytology has been well documented. However, diagnostic vitrectomy is usually performed as a final diagnostic option due to the increasing risk of vitrectomy-related ocular complications. Recently, advances in surgical techniques such as small-gauge vitrectomy and wide-viewing systems have expanded the use of diagnostic vitrectomy. Diagnostic vitrectomy is indicated in an inflamed eye when the course or appearance of uveitis is not typical for an autoimmune disease and the presence of an infectious agent or malignant process is suspected. Diagnostic vitrectomy is usually indicated in rapidly progressive disease with inconclusive noninvasive workup. If the disease fails to respond to therapy in an expected manner, the physician should reconsider the original diagnosis; in such cases, other diagnoses need to be considered. Indications for diagnostic vitrectomy are shown in Box 126.1. Since many etiologies should be considered, multiple tests such as culture, cytology, and polymerase chain reaction (PCR) are generally recommended; therefore, clinicians should get as much vitreous sample as they can.

Box 126.1

Indications of Diagnostic Vitrectomy

Infectious Uveitis

Endophthalmitis:[3] bacterial, fungal, parasitic, or viral

Traumatic endophthalmitis including intraocular foreign body

Postsurgical endophthalmitis

Endogenous endophthalmitis

Sterile endophthalmitis

Vitritis

Retinitis

Choroiditis

Retinal vasculitis

Noninfectious Uveitis

Autoimmune uveitis[4]

Primary intraocular lymphoma[5]

Carcinoma metastasis[6] including leukemia infiltration

Choroidal melanoma[7]

Surgical Principles and Techniques

Preoperative Preparation

Patients should be evaluated for concurrent diseases, including systemic infection, primary CNS lymphoma, or systemic lymphoma/leukemia. Because extraocular lymphoma is sometimes diagnosed late, patients should be evaluated systemically with caution. Sequential extraocular lymphoma is considered to have the highest specificity in confirming the diagnosis of an intraocular lymphoma.

Informed consent for diagnostic vitrectomy should be obtained

after discussing with the patient the necessity of performing the surgery and its potential for vision-threatening complications such as retinal tear or detachment, cataract formation, proliferative vitreoretinopathy, or postoperative endophthalmitis. Advances in surgical and laboratory techniques have expanded the indications for diagnostic vitrectomies. Laboratory tests of intraocular fluid or vitreous samples should be tailored according to the preliminary preoperative diagnosis. In addition, proper transportation of vitreous samples, judicious selection of ancillary tests, interpretation by experienced pathologists, and preoperative communication between the clinician and the pathologist are crucial for high diagnostic yields.

From a technical viewpoint, cutting with a vitrector does not appear to cause more cellular degeneration compared to simple aspiration. Vitreous tap can be performed in the outpatient department under local anesthesia, but three-port vitrectomy is typically considered to be the standard procedure. Further studies have yet to determine if the use of 23-, 25-, or 27-gauge (G) sutureless vitrectomy affects diagnostic yield compared with conventional 20G vitrectomy. In general, small-gauge vitrectomy is considered not to affect cellular integrity. 20G, 23G, or 25G vitrectomy are known to produce sufficient amounts of vitreous samples with good preservation of cellular integrity necessary for a cytologic evaluation.[5,8–11] More recently, 27G cutters have been introduced and will likely provide another option for diagnostic vitrectomy though the technique requires further clinical studies. Some authors advocate a lower cutting rate and higher duty cycle because larger and more intact pieces of the aspirated vitreous may have a better yield.[12] Cell viability was found to begin to decrease at 600 cpm and was lowest at a high cutting rate.[13] However, these settings have not yet proven to be more advantageous compared to traditional sampling techniques.[14] Because of the limited volume of vitreous samples, clinicians should be aware of the minimum sample requirement for microbiologic and malignancy workup and ensure that an adequate amount of vitreous is sampled accordingly.

Vitreous Sampling

Adequate sampling of the vitreous is still challenging despite

advances in vitrectomy system technology. Vitreous biopsy can be a vitreous tap or diagnostic vitrectomy. Vitreous tap is performed in the outpatient department under local anesthesia. Subconjunctival injection of 0.1 mL of 2% lidocaine can be given at the site of entry into vitreous cavity. The 23- to 25G needle is inserted in the vitreous cavity under visualization with a surgical microscope. The empty syringe withdraws the vitreous in the eye. After withdrawal, a similar quantity of antibiotics or balanced salt solution (BSS) is usually injected into the vitreous cavity. Obtaining vitreous samples by tap is easier, but the quantity of obtained samples is small and is associated with a high rate of false-negative results.[15,16]

In contrast, three-port vitrectomy enables the operators to obtain the vitreous samples in the area with active disease such as the vitreous opacity or fungus ball under direct visualization. This can be also performed using the single-port technique,[17] but as single-port vitrectomy has no direct visualization, its use can have a lower diagnostic yield. Obtaining vitreous samples by three-port vitrectomy is more difficult and should be done in an operating room, but the amount of recovered material is usually sufficient and can have higher diagnostic yields compared to a vitreous tap. But as the purpose of diagnostic vitrectomy is to obtain maximal tolerable amounts of undiluted tissue from which a diagnosis can be made, small amounts of collected samples with few inflammatory cells and without adequate preparation of samples can reduce the diagnostic yield.

The standard technique for performing three-port pars plana vitrectomy (PPV) involves keeping the cutter tip within the vitreous. The undiluted vitreous humor is collected through the suction line with a 3-or 5-mL syringe directly connected to the vitreous cutter. This syringe is manually aspirated by an assistant while the operator visualizes the diseased area in the vitreous cavity. The operator can compress the eyeball with his/her fingers or a cotton swab to prevent eyeball collapse (Fig. 126.1). When the eye visibly softens, the infusion is turned on.[18] In our experience, up to 1.5 mL of undiluted vitreous can be safely obtained using this technique. Other techniques, such as using continuous air or perfluorocarbon liquid (PFCL) infusion, can yield large volumes of undiluted vitreous without compressing the eyeball. Air substitutes

the vitreous removed from the eyeball, and this can yield vitreous samples ranging in volume from 0.6 to 1.5 mL.[12] Perfluorocarbon-perfused vitrectomy, in which BSS is replaced with PFCL during vitreous aspiration, can be a good option for preventing complications of hypotony such as suprachoroidal hemorrhage.[19] Using this technique, an average of 2.24 mL of undiluted vitreous could be obtained. However, a major disadvantage, in addition to the high cost of perfluorocarbon, is that samples obtained using this technique need to be frozen to completely remove the perfluorocarbon.

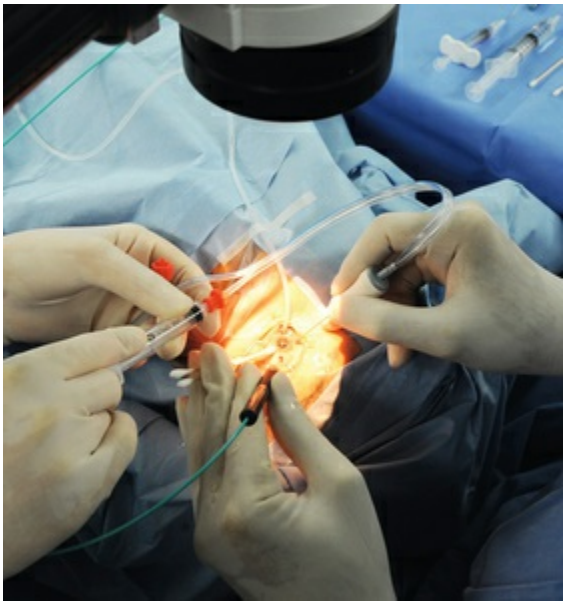

FIG. 126.1 Undiluted vitreous specimen is obtained using the vitreous cutter directly connected to a 3- or 5-mL syringe. In the case of a standard three-port vitrectomy, an assistant manually acquires the vitreous aspirate with a syringe while the operator compresses the eyeball with cotton swabs. The infusion is turned off until the eye visibly softens.

The undiluted vitreous sample is then typically referred to for cytologic analysis with either Papanicolaou (Pap) or hematoxylin–eosin staining, viral culture, or immunohistochemical staining. The supernatant of the undiluted sample is sent for cytokine analysis and determination of antibody levels. The diluted vitreous wash is typically used for Gram staining, DNA gene rearrangement studies,

flow cytometry, PCR testing, and filtered for bacterial and fungal cultures. Cytologic analysis may also be performed with the diluted specimen after centrifugation in a pathology laboratory. Vitreous cells and bacterial or fungal cultures are transported at room temperature.

Handling and Preparation of Vitreous Samples

Careful handling of ocular specimens obtained for diagnostic purposes is essential. Advanced planning and notification of the pending procedure to laboratories are useful in ensuring that the specimen will be processed correctly. In addition, it is essential to coordinate the diagnostic vitrectomy with the microbiology laboratory so that the samples can be placed in appropriate culture media; handling errors may result in false negatives. Attention should be paid to adequate preparation of microbiologic culture media, accurate cell culture procedures, and molecular analysis. Some authors recommend that the vitreous sample be collected in a tube containing RPMI-1640 medium to improve the cytologic diagnosis of intraocular lymphoma from vitreous fluid.[20]

When an infectious cause is suspected, immediate sampling and transfer of the vitreous specimen to a sterile, airtight test tube with a screw cap is strongly recommended for cultivating pathogens. To maximize the chance of pathogen detection, it is recommended that the aqueous humor be also obtained. Considering that the specimen volume is usually insufficient for culture in all types of culture media, appropriate culture media should be selected according to the initial diagnosis.

Overall range for diagnostic yields from vitrectomy is wide according to various reports. Generally, the number of tests that can be carried out on a vitreous specimen depends on the amount of material retrieved. In addition, patient selection, surgical technique, and vitreous specimen analysis are factors that may contribute to this variation. Ideally, cytologic analysis and microbiologic cultures should be performed with undiluted vitreous specimen as soon as it is collected from the eye. Cytokine, chemokine, and flow cytometry analysis can also be performed using the aqueous humor that is

obtained. It is nevertheless important to realize that a negative cytologic diagnosis or microbiologic culture does not prove the absence of malignancy or infection. PCR analysis is recommended in cases where viral infection is suspected because the quantity of organisms shed into the vitreous cavity is minute and viral culture more often than not is likely to fail; as an example, a positive detection of human herpesviruses with PCR from the vitreous of patients with uveitis has been identified.[21,22]

Retinal or Choroidal Biopsy

If a vitreous biopsy does not yield a diagnosis, chorioretinal biopsy of the involved eye can be considered, depending on the location of lesions and response to therapy. Chorioretinal biopsy increases the probability of achieving a correct diagnosis. Retinal or choroidal biopsy is considered when the inflammatory process is localized primarily in the sensory retina or the retinal pigment epithelium (see Chapter 127, Vitreous, retinal, and choroidal biopsy). In such cases, if the disease only involves the retina or choroid, pathogens may not spill into the vitreous. For example, cytomegalovirus, which is difficult to culture from the vitreous fluid, can be cultured from the retina or seen on the electron microscopic examination of the retina.

An endoretinal biopsy can be helpful in diagnosing tuberculosis, sarcoidosis, and lymphoma.[23] Accurate biopsy results will lead to a specific treatment for uveitis of suspected infectious or malignant origin. Histologic examination of chorioretinal biopsies provides some advantages over cytologic examination of vitreous specimens. In the biopsy, more material is available for immunohistochemistry; this allows for more precise classification and differentiation of the pathology of the lesion. Despite these advantages, choroidal and retinal biopsies are used as a last resort considering the severe complications that may accompany the procedure.

Retinal or choroidal biopsy can be performed under retrobulbar block or topical anesthesia. Standard three-port vitrectomy is the preferred technique. The surgical technique for performing a chorioretinal biopsy can either be transscleral or transvitreal depending on the location of the lesion. In patients with panuveitis,

a choroidal mass, and a detached retina, it is recommended that transvitreal endoretinal biopsy be performed at the junction of the attached and detached retina. Upon completion of the vitrectomy, the area with active disease can be identified more accurately; this area can then be biopsied. However, a biopsy specimen obtained from a retinal area in which the disease is quiescent will rarely provide diagnostic information.

Retinochoroidal tissue is taken after dissecting using intraocular scissors and forceps. The preferred location for this surgical procedure is the superior and nasal retina. Intense endolaser or heavy endodiathermy at the margin of the biopsy is performed prior to long-acting gas or silicone oil tamponade.[24] In cases in which the retina is still attached, a cannula is used to inject saline under the sensory retina to create a small bleb. The advancing edge of the lesion should be included if retinitis is suspected, since actively replicating microorganisms are most likely to be found in this location.

The retinal or chorioretinal biopsy specimen should be divided in order to permit culture, histologic examination, and monoclonal antibody studies. PCR can be performed on the retinal tissue as well. However, it has been reported that retinochoroidal biopsies may be associated with the risk of retinal detachment and that false-negative results often occur in these specimens.[25] In addition, proper positioning is essential to maintain retinal tamponade after endoretinal biopsy.

Potential complications include vitreous hemorrhage, retinal detachment, and the potential for intraocular or extraocular dissemination. However, diagnostic vitrectomy using the vitrector to obtain tumor cells has resulted in no intraocular dissemination or increased metastasis to date.

Diagnostic Techniques for Vitrectomy Specimens

Ancillary tests have been invaluable in addressing the diagnostic limitations of traditional histopathologic and microbiologic analyses. Flow cytometry, gene rearrangement studies, and cytokine measurements are useful adjuncts to cytologic analysis for

diagnosis of malignancy, in particular, primary intraocular lymphoma (PIOL). Selecting one or more of these tests depends on the preoperative diagnosis. Due to the limited volume of samples obtained, the number of diagnostic tests that can be performed is limiting. Differences in reported yields have been attributed to patient selection with higher diagnostic yields for clinical suspicion of infection or lymphoma. Clinicians should be aware of the sensitivity, specificity, and overall positive and negative predictive values of the diagnostic test to avoid misinterpreting the results.

Cytologic Evaluation

Cytologic evaluation helps to differentiate infectious, noninfectious, and malignant etiologies. Cytologic examination reveals the phenotypes of infiltrating cells into the vitreous in malignancy and microbe or fungal hyphae in infectious etiology. Noninfectious etiologic diagnosis is based on presence of nonspecific inflammatory cells. Vitreous humor fluid obtained by PPV is centrifuged, and the cells are smeared onto glass slides and then either immersed in 95% ethanol for Papanicolaou staining or left to dry for subsequent Giemsa staining. The diagnosis of a PIOL depends primarily on cytologic examination of the vitreous sample. It might be difficult to differentiate retinal cells from malignant lymphoma cells by the Pap stain because they appear as mostly round cells by the Pap stain. However, cellular processes can be clearly differentiated using the Giemsa stain. Therefore, Giemsa stain is recommended when performing intraocular cytology. The characteristic feature, from either Giemsa or Diff Quick staining, is the presence of large B-cell lymphoblasts and atypical lymphocytes with high nuclear/cytoplasm ratios amongst small round lymphocytes.[26] However, diagnosis of PIOL is difficult, resulting in a high false-negative rate due to the small sample volumes with low number of malignant cells, inadequate preparation of samples or carrying media, and previous administration of corticosteroids.

In chronic endogenous uveitis, cytology reveals classic degenerative inflammatory cells with poor morphology, although cytologic examination of the vitreous specimen can be difficult because there may be a relative lack of inflammatory cells. Cytologic examination can also be helpful in diagnosing

sarcoidosis. Kinoshita et al. showed multinucleated giant cells in 85.7% of cases and lymphocytes and epitheloid cells in all cases of intraocular sarcoidosis.[4]

Histopathologic Evaluation

It is recommended that the biopsy tissue be immediately processed by an ophthalmic pathologist. The biopsy specimen is generally divided into three portions: one-third is fixed for routine histopathologic evaluation, including light and electron microscopic examinations. The second portion is frozen in optimal cutting temperature embedding compound for immunopathologic and molecular characterization. The third portion is sent for culture of viruses and other microorganisms or for tissue culture. If the biopsy specimen is not sufficient for all three aforementioned procedures, the tissue should be processed for frozen sections, as these can undergo routine histopathology, immunohistochemistry, and molecular analysis. Svozilkova et al. reported that the highest percentage of positive results was achieved by histopathologic evaluation in uveitis.[2]

One interesting indication for histologic evaluation is ocular toxocariasis, which has a variable presentation, from localized peripheral or macular granulomas to chronic endophthalmitis. Histologic analysis reveals peripheral granuloma with fibrous membrane. Histologic evaluation can also be helpful in the diagnosis of ocular tuberculosis. In specimens from patients with ocular tuberculosis, microscopy reveals necrotizing granulomatous inflammation with the presence of a giant cell near the area of necrosis.

Microbiologic Culture

Microbiologic culture plays a crucial role in the diagnosis of infectious diseases. However, microbial culture collections are challenging due to difficulty in obtaining and manipulating the vitreous samples. When an infectious cause is suspected, different types of microbial culture media are recommended for isolation of the causative agent: for bacterial infections, blood agar, MacConkey agar, and *Brucella* agar are used; for infections caused by pathogenic fungi and yeast, Sabouraud dextrose agar is used; for viral

infections, shell vial culture is used, in which the final pathogen is identified on the basis of the cytopathic effects.

To diagnose infection, vitreous samples are routinely sent for Gram staining, culture, and antibiotic sensitivity tests. Currently, microbiologic culture is still the gold standard for diagnosing infectious uveitis (Fig. 126.2). Microbiologic cultures are recommended to be performed with undiluted vitreous specimen as soon as it is collected from the eye. Some authors advocate that the vitreous wash fluid that is collected in the vitrector cassette can be used for additional filtered microbiologic cultures. Diluted samples are passed through a Millipore filter and the filter, which contains the microorganisms and cellular elements on the surface, is then cut and used for culture. It should be kept in mind that a negative microbiologic culture does not prove the absence of infection. If the first trial fails, clinicians are recommended to repeat the microbiologic culture. Vitreous tapping can be performed in the outpatient clinic in vitrectomized eyes.

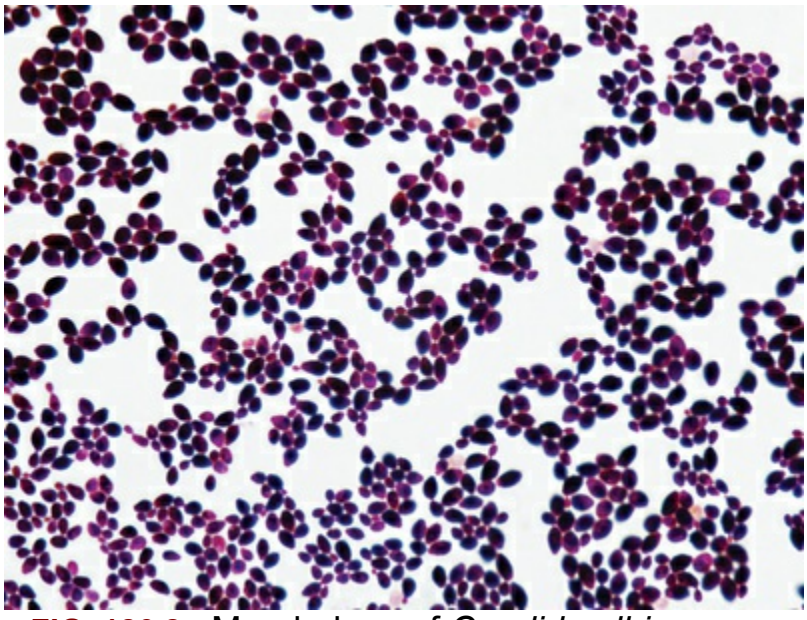

FIG. 126.2 Morphology of *Candida albicans* on Sabouraud Dextrose Agar (SDA) agar at incubation time of 24 hours and incubation temperature of 30 °C. Gram stain showing gram-positive, 2–8-μm sized, oval, budding yeast cell. Magnification ×1000.

Some experts advocate immediate culture inoculation by the

surgeon in the appropriate media in order to maximize organism recovery.[18] However, in viral retinitis it should be noted that viral cultures of the vitreous can reveal false-negative results because of neutralizing antibodies or low viral shedding. In addition, communication with the microbiologists to hold long-term cultures, sometimes for a month, is important to avoid missing slower-growing organisms such as *Propionibacterium acnes* and fungi.[27–29]

Molecular Analysis

The most obvious reason for performing a molecular analysis is to rule out lymphoma as the cause of a masquerade syndrome and to identify the causative agents of infections. For PIOL, molecular analysis of vitreous specimens is primarily used to study the genotypic classification of PIOL with the goal of identifying prognostic factors. As an example, with *bcl-2* gene translocation, it has been reported that patients were significantly younger than those who lacked the translocation, suggesting the need for aggressive treatment based on this molecular signature.[30] PCR is also used to detect monoclonality within the variable region of the third complementary determining region (CD3) in the immunoglobulin heavy chain gene of malignant B-cells. Single-band detection of immunoglobulin heavy chain rearrangement can also be useful in PIOL.[31]

For infections, it is important to detect the DNA of microorganisms in the aqueous or vitreous humor and this is done by PCR, as it amplifies minute quantities of nucleic acid from infectious organisms and viruses into analytic amounts.[32] A PCR diagnosis is very useful since only a small quantity of ocular samples is required for the detection of a causative agent. For example, the addition of PCR to identify bacterial DNA has increased the diagnostic sensitivity from 48% to more than 80%.[33] Recently, some authors attempted to use various approaches for DNA extraction with PCR to enhance PCR sensitivity.[34] Samples were first analyzed by multiplex quantitative real-time PCR for various viral pathogens. Subsequently, samples were examined by broad-range real-time PCR for bacterial and fungal pathogens. Their results indicate that a comprehensive PCR system can be used to diagnose infectious uveitis with high positive results. PCR can

also be used to screen vitrectomy samples for a variety of pathogens, such as *Propionibacterium acnes* or *Mycobacterium tuberculosis*, in unresponsive or atypical uveitis cases.[35] Microbial DNA amplification by PCR and intraocular antibody measurement is particularly helpful in detecting infection by organisms that are difficult to culture. Moreover, prior short-term use of intravitreal antibiotics does not seem to affect the ability of PCR-based DNA amplification.

Flow Cytometry

Flow cytometry allows concurrent analysis of several different cell surface markers. This technique involves centrifuging diluted vitreous and resuspension in cell culture medium. Cells are counted and stained with antibodies to detect cellular surface markers that identify leukocytes. In addition, flow cytometry has been shown to be useful in the diagnosis of intraocular lymphoma.[36] The test relies on the fact that most PIOLs are composed of monoclonal populations of B-cell lineage origin that stain positive for B-cell markers. Combined analysis by cytologic examination and flow cytometry appears to be more confirmatory for lymphoma than using either test alone. Both techniques require a sufficient number of cells and an experienced cytopathologist.

Cytokine Measurement

Cytokine assay measurement can provide polymorphonuclear cellular activity. B-cell malignancies can secrete high levels of interleukin (IL)-10, an immunosuppressive cytokine, while inflammatory conditions are associated with high levels of IL-6, a proinflammatory cytokine. Some authors have shown that PIOLs can produce high IL-10 levels, with IL-10/IL-6 ratios of greater than 1.[37] Cytokine levels and IL-10/IL-6 ratios by themselves are not diagnostic of PIOL, but they can be useful adjunctive tests in corroborating the diagnosis of PIOL and determining whether there is a significant response to treatment. In contrast to a molecular analysis, the measurement of cytokine levels via ELISA (enzyme-linked immunosorbent assay) is much easier. Therefore, measurement of IL-10 and IL-6 levels is recommended for patients with suspected PIOL in hospitals where a cytopathologist is not

present.

The use of the cytokine analysis is now widely accepted in clinical practice to facilitate differentiating the cause of endogenous uveitis. For ocular sarcoidosis, Kojima et al. demonstrated that the CD4/CD8 ratio of vitreous-infiltrating T lymphocytes has high diagnostic value, and this was demonstrated by a combination of PCR, cytology, and flow cytometry.[38] We have also shown that the intraocular cytokine or chemokine environment can vary between patients; therefore, the underlying immunopathogenesis may be different between endogenous uveitis cases.[39,40] Because the vitreous is considered to be a reservoir of proinflammatory mediators that contribute to the development of many inflammatory diseases of the eye, vitreous samples can be a valuable tool for accurate diagnosis of the pathogenic mechanism.

Future Directions

Diagnostic yields of vitrectomy specimens depend on initial patient selection, number and types of tests used, and the vitrectomy technique employed. Considering that a diagnostic vitrectomy may be performed after treatment with antibiotics or antiinflammatory medications, microbial load and malignant cell counts may be suppressed, thus yielding false-negative results. More sensitive diagnostic techniques are needed to overcome this problem. Commercially available laboratory approaches such as a comprehensive PCR system can be used for ocular infectious diseases in the near future. An additional factor that can affect the diagnostic outcome is the lag time between collecting and processing the specimen. For a prompt identification of causative agents, a rapid and accurate diagnostic system is required. Moreover, future studies will be aimed at exploring the genotypic classification of PIOLs based on the quantitative molecular framework of gene expression profiling with the goal of providing useful adjuncts to the pathologic diagnosis of this complex disease.

Therapeutic Vitrectomy

In the past, vitrectomy was reluctantly recommended for uveitis

patients due to the high incidence of complications, including uncontrolled inflammation, retinal tears or detachment, proliferative vitreoretinopathy, cataract, and hypotony. Recently, rapid advances in microsurgical techniques have contributed to safer surgical intervention for ocular inflammation. In general, therapeutic vitrectomy aims at improving vision by clearing the visual axis, reducing inflammation in active disease and thereby treating nonresolving cystoid macular edema. Vitrectomy facilitates postoperative control of inflammation by immune-suppressive drugs, perhaps by removing a depot of activated lymphocytes, and cytokines and increasing the effectiveness of drugs or by improving penetration of drugs into the eye.

Indications

Therapeutic vitrectomy for uveitis is conventionally indicated for (1) media opacity causing significant visual loss;[41] (2) intractable cystoid macular edema (CME);[42] (3) cyclitic membrane removal for the treatment of nonresponding hypotony; and (4) other vitreoretinal complications, including traction retinal detachment, rhegmatogenous retinal detachment, macular pucker, hemophthalmos, hypotony,[43] or macular hole.[44] Recent advances in vitrectomy techniques have expanded the indications for therapeutic vitrectomy. Vitrectomy can be used as an adjunctive procedure with intravitreal applications of antiinfectious, cytostatic drugs, or intravitreal sustained-release drug implants.[45–47]

The risks and benefits of therapeutic vitrectomy for uveitic disease seem to be similar to those described for diagnostic vitrectomy; patients should be informed before surgery so that the patient's expectations can be adjusted accordingly.

Surgical Principles and Techniques

It is well recognized that chronic inflammation, even a low-grade one, can irreversibly damage the retina and optic nerve. As such, inflammatory control, both pre- and postoperatively, is vital. Preoperative rigorous control of inflammation is critical for a good surgical outcome. With a few exceptions, such as rhegmatogenous retinal detachment and infectious endophthalmitis, surgery should

be performed when inflammation is quiescent. It is certainly advisable to adequately suppress inflammatory activity utilizing topical, regional, and systemic steroids for a minimum of 3 months prior to surgery. Previous studies consistently demonstrate the importance of perioperative control of inflammation. Systemic corticosteroids are still the best drugs for controlling inflammation during the perioperative period. We prefer administering steroids one day before surgical intervention; typically, 1 mg/kg per day of steroid treatment is adequate. However, when diagnostic vitreous biopsy is also planned, ensuring that patients with suspected PIOL are not receiving corticosteroid medication at the time of vitrectomy improves the diagnostic yield for lymphoma, since lymphoma cells degenerate in response to corticosteroid treatment.[48]

A standard 20G, 23G, 25G, or 27G three-port PPV are currently used. Special attention needs to be given to the removal of peripheral vitreous base and posterior cortical vitreous. Since the largest accumulation of vitreous opacities is often found in the vitreous base and remnant posterior cortical vitreous, providing a platform for fibroglial proliferation, near-complete vitreous removal is of high importance. The peripheral retina becomes usually thin and fragile due to the long-standing intraocular inflammation, making it vulnerable to tearing and subsequent detachment. During peripheral vitrectomy, careful shaving of the vitreous base using scleral depression techniques and high cutting rate with low aspiration is essential to avoid iatrogenic tears. Wide-angle viewing systems have allowed for much better visualization of the peripheral retina so that nearly complete removal of the vitreous base is possible. Triamcinolone acetonide has been used during vitrectomy as an aid to visualize residual vitreous cortex and peripheral vitreous.[49] The use of surgical adjuvants is now widely accepted in clinical practice to facilitate peeling of the internal limiting membrane (ILM) during vitrectomy because membranes in uveitic eyes are very fragile and adhere to the retina. Indocyanine green (ICG) can also be used to visualize the ILM during PPV and ILM peeling.[50] The ILM can also be selectively stained by brilliant blue G, which is less toxic to the retina than ICG.

Giant retinal tears that may complicate viral retinitis, such as acute retinal necrosis or cytomegalovirus retinitis, are managed by

vitrectomy with or without scleral buckling. In viral retinitis, the retina becomes necrotic with possible ischemic areas. The use of a high buckle might increase this ischemia, leading to retinal neovascularization, so a broad low buckling is recommended. An alternative option is to perform a PPV and to reattach the retina with gas or silicone oil tamponade, with laser photocoagulation. However, laser photocoagulation should be performed very carefully and at the physician's discretion because it promotes postoperative inflammation.

Cataract extraction is often combined with vitrectomy since cataracts are a common complication of intraocular inflammation as well as a complication of long-term corticosteroid therapy. The operator should take special care to avoid contact with the iris during the procedure. An intraocular lens (IOL) can be implanted in the bag during combined cataract extraction with vitrectomy though it was not recommended in the past. The use of disposable iris retractors will provide the surgeon with an adequate view in patients with posterior synechia and small pupil. The pupillary aperture can also be enlarged with the vitrectomy probe or vitreous scissors. In patients with synechia, in-the-bag implantation of the IOL is important because postoperative recurrence of synechia can cause serious complications.

Intravitreal administration of drugs at the end of therapeutic PPV may alone be sufficient to decrease inflammatory activity. Administration of intravitreal triamcinolone acetonide at the end of vitrectomy can effectively reduce immediate postoperative inflammation, which has been demonstrated in patients with retinal vascular diseases and proliferative vitreoretinopathy.[51,52] Antimicrobial medications can be administered at the end of vitrectomy in patients with viral, bacterial or fungal endophthalmitis. In patients with fungal endophthalmitis, intravitreal application of amphotericin B alone inhibited uveitis activity, and no exacerbation was observed during the postoperative period.[2]

Outcomes

Vitrectomy can be safe and effective for management of

vitreoretinal complications in patients with persistent panuveitis.[44,53,54] Retinal detachment, vitreous hemorrhage or macular hole can be successfully managed with vitrectomy. Visual improvement has also been reported in most patients who underwent vitrectomy in uveitis cases.[55] It has been suggested by several authors that PPV reduces or eliminates recurrences of inflammation because it reduces the antigen load, inflammatory mediators or toxic elements from the vitreous. Moreover, a clear vitreous cavity facilitates diffusion of intravitreally injected drugs and permits better examination of the eye postoperatively. However, although the removal of the vitreous can decrease accumulation of cells and haze during an episode of inflammation, vision can be affected by new inflammatory episodes.

Some retrospective studies suggested that PPV can reduce the overall inflammatory activity of disease, and improve refractory uveitic CME.[56] Vitrectomy may also modulate the natural history of inflammation in patients with intermediate uveitis. A prospective randomized pilot study also reported the comparison of PPV with immunomodulatory therapy for patients with intermediate uveitis.[57] A higher percentage of patients treated with PPV achieved resolution of uveitis compared to those given immunomodulatory therapy, although there was no statistically significant difference in visual outcome for either group during the 18-month follow-up.

Visual improvement has been reported for vitrectomy treatments for epiretinal membranes associated with pars planitis and sarcoidosis. Epiretinal membrane peeling usually results in significant visual improvement and restoration of normal foveal contour in patients with uveitis,[58] even though the efficacy of ILM peeling seems to be controversial (Fig. 126.3). However, there is a possibility of poor visual outcome associated with CME or recurrence of the membrane with persistent inflammation. Moreover, associated vascularization or scarring of the underlying retina is more common with epiretinal membranes associated with uveitis, which can limit positive visual outcome. Outcomes of PPV with silicone oil tamponade were reported in patients with chronic hypotony due to uveitis.[43] Eyes with posterior inflammation contained a dense anterior hyaloid that may be associated with ciliary body traction. If ciliary atrophy was present, intraocular

pressure was restored only in eyes that received silicone oil tamponade treatment.

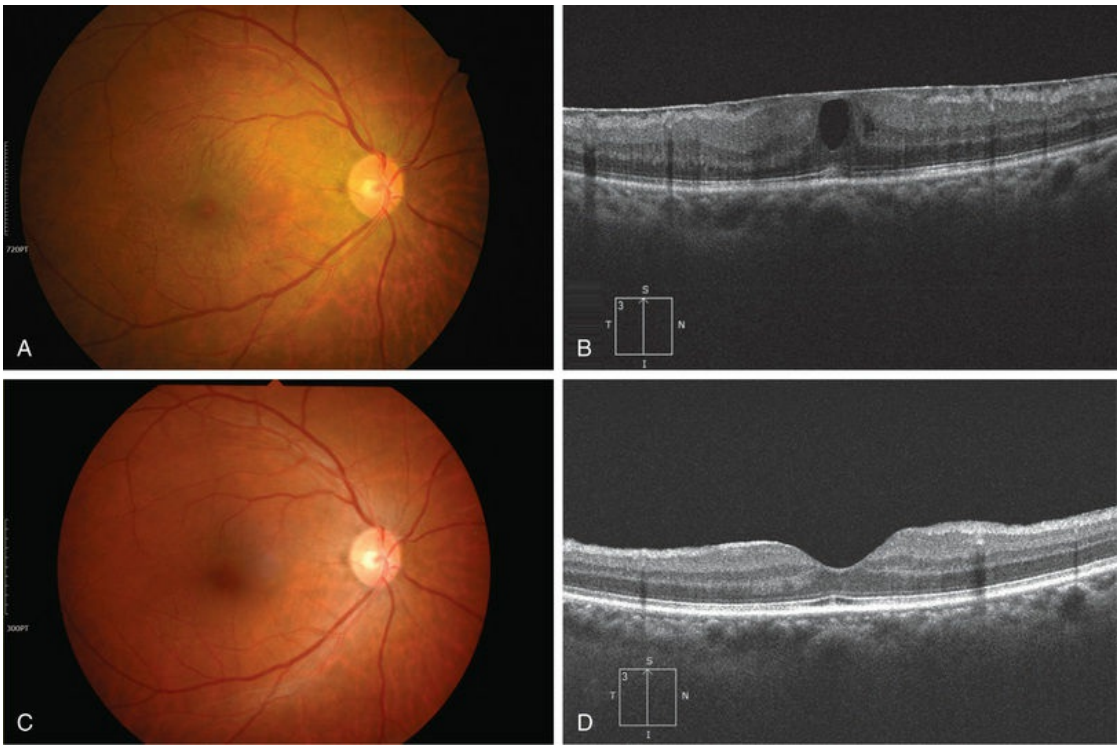

FIG. 126.3 (A) Epiretinal membrane is present in a 57-year-old patient with intermediate uveitis. (B) On spectral domain optical coherence tomography (OCT), epiretinal membrane with macular edema could be visualized. (C) Postoperative photograph revealed smooth macula without epiretinal membrane. (D) Postoperative OCT revealed normal foveal contour.

Postoperative complications such as hypotony, retinal detachment, and vitreous hemorrhage should be kept in mind after vitrectomy in uveitis. Hypotony generally responds to topical, systemic, or periocular/intraocular corticosteroids. Recurrence of uveitis following vitrectomy can also occur. Vitreous cells are sparser and affect vision less because the vitreous gel is absent. There may be a false sense that the inflammation is entirely under control in the absence of vitreous cellular reaction.

Some issues still remain controversial, including whether vitrectomy reduces the activity of disease and the number of recurrences, and whether vitrectomy actually reduces CME. A

large, prospective, randomized clinical trial is needed to draw a firm conclusion on the subject. In addition, clinicians should keep in mind that vitrectomy improves visual acuity and inflammatory control in some patients, but postoperative complications such as retinal detachment, vitreous hemorrhage, and high intraocular pressure can limit the visual outcome.[2]

Future Directions

The complexity of performing a prospective study for vitrectomy in uveitis is at the present very difficult. No randomized clinical trials or comparative interventional case series have tested the hypothesis that vitrectomy has an antiinflammatory effect independent of its role in correcting uveitic complications or clearing the ocular media. A large, randomized, prospective clinical trial is required to test this hypothesis. In addition, biologic plausibility of vitrectomy in uveitis is still lacking, including topics such as postvitrectomy reduction in intraocular inflammatory mediators and changes in the vitreoretinal interface influencing CME. Further work is needed to verify these hypotheses. Improved applications of antibiotic therapies and control of inflammation should be pursued. In addition, blocking the products of inflammatory reactions is a worthwhile therapeutic goal. A more systematic investigation would support the perceived importance of vitrectomy in the management of uveitis.

Conclusion

The major indications for performing vitrectomy in uveitis cases are to analyze vitreous fluid for diagnostic purposes and to treat complications. Vitreous biopsies are routinely used to help diagnose patients with posterior uveitis of uncertain etiology. Vitreous biopsy for uveitis can be both diagnostic and therapeutic for patients who have life-threatening but treatable illnesses. It is important that the procedure be safe, yield a large volume of high-quality sample, and, ideally, be cost-efficient. When performed appropriately, diagnostic vitrectomy with carefully selected ancillary testing is a valuable tool for the assessment and diagnosis

of uveitis in a large proportion of patients. Key factors that can improve diagnostic yield include obtaining sufficient volume of cells from the vitreous or subretinal space, choosing appropriate tests for specimen analysis, informing the laboratory of the suspected clinical diagnosis, promptly delivering the samples, and having the diagnostic tests performed by experienced personnel. Moreover, with the advent of modern vitreoretinal microsurgical techniques, the spectrum for surgical intervention in various forms of uveitis has been notably expanded and the visual outcomes have been improved. Removal of optically relevant vitreous opacities, improvement of CME, peeling of epiretinal membranes, and release of traction in the presence of abnormal vitreoretinal adhesions are the most common indications for vitreoretinal procedures in the management of uveitis patients.

References

1. Durani OM, Meads CA, Murray PI. Uveitis: a potentially blinding disease. *Ophthalmologica*. 2004;218:223–236.
2. Svozilkova P, Hessingerova J, Brichova M, et al. The role of pars plana vitrectomy in the diagnosis and treatment of uveitis. *Eur J Ophthalmol*. 2011;21:89–97.
3. Endophthalmitis Vitrectomy Study. Microbiologic factors and visual outcome in the endophthalmitis vitrectomy study. *Am J Ophthalmol*. 1996;122:830–846.
4. Kinoshita Y, Takasu K, Adachi Y, et al. Diagnostic utility of vitreous humor fluid cytology for intraocular sarcoidosis: a clinicopathologic study of 7 cases. *Diagn Cytopathol*. 2012;40(3):210–213.
5. Kanavi MR, Soheilian M, Bijanzadeh B, et al. Diagnostic vitrectomy (25-gauge) in a case with intraocular lymphoma masquerading as bilateral granulomatous panuveitis. *Eur J Ophthalmol*. 2010;20:796–798.
6. Lee EJ, Kim TW, Heo JW, et al. Natural killer/T-cell lymphoma of nasal type with intraocular involvement: case report. *Eur J Ophthalmol*. 2010;20:215–217.
7. Abi-Ayad N, Grange JD, Salle M, et al. Transretinal uveal melanoma biopsy with 25-gauge vitrectomy system. *Acta*

Ophthalmol. 2013;91(3):279–281.
8. Margolis R, Brasil OF, Lowder CY, et al. Vitrectomy for the diagnosis and management of uveitis of unknown cause. *Ophthalmology*. 2007;114:1893–1897.
9. Yeh S, Weichel ED, Faia LJ, et al. 25-Gauge transconjunctival sutureless vitrectomy for the diagnosis of intraocular lymphoma. *Br J Ophthalmol*. 2010;94:633–638.
10. Margolis R, Brasil OF, Lowder CY, et al. Vitrectomy for the diagnosis and management of uveitis of unknown cause. *Ophthalmology*. 2007;114:1893–1897.
11. Kanavi MR, Soheilian M, Hosseini SB, et al. 25-gauge transconjunctival diagnostic vitrectomy in suspected cases of intraocular lymphoma: a case series and review of the literature. *Int J Ophthalmol*. 2014;7:577–581.
12. Tsui I, Schwartz SD, Hubschman JP. A current method to collect an undiluted vitrectomy sample. *Retina*. 2010;30:830–831.
13. Jiang T, Zhao Z, Chang Q. Evaluation of cytologic specimens obtained during experimental vitreous biopsy using B-cell lymphoma line. *Eur J Ophthalmol*. 2014;24:911–917.
14. Hubschman JP, Bourges JL, Tsui I, et al. Effect of cutting phases on flow rate in 20-, 23-, and 25-gauge vitreous cutters. *Retina*. 2009;29:1289–1293.
15. Wakefield D, Zierhut M. Intraocular lymphoma: more questions than answers. *Ocul Immunol Inflamm*. 2009;17:6–10.
16. Sen HN, Bodaghi B, Hoang PL, et al. Primary intraocular lymphoma: diagnosis and differential diagnosis. *Ocul Immunol Inflamm*. 2009;17:133–141.
17. Murthy SI, Pappuru RR, Latha KM, et al. Surgical management in uveitis. *Indian J Ophthalmol*. 2013;61:284–290.
18. Margolis R. Diagnostic vitrectomy for the diagnosis and management of posterior uveitis of unknown etiology. *Curr Opin Ophthalmol*. 2008;19:218–224.
19. Quiroz-Mercado H, Rivera-Sempertegui J, Macky TA, et al. Performing vitreous biopsy by perfluorocarbon-perfused vitrectomy. *Am J Ophthalmol*. 2005;140:1161–1163.

20. Ranty ML, Laurent C, Aziza J, et al. Improving the cytological diagnosis of intraocular lymphoma from vitreous fluid. *Histopathology*. 2015;67:48–61.
21. Lau CH, Missotten T, Salzmann J, et al. Acute retinal necrosis features, management, and outcomes. *Ophthalmology*. 2007;114:756–762.
22. Sugita S, Shimizu N, Watanabe K, et al. Use of multiplex PCR and real-time PCR to detect human herpes virus genome in ocular fluids of patients with uveitis. *Br J Ophthalmol*. 2008;92:928–932.
23. Cassoux N, Charlotte F, Rao NA, et al. Endoretinal biopsy in establishing the diagnosis of uveitis: a clinicopathologic report of three cases. *Ocul Immunol Inflamm*. 2005;13:79–83.
24. Cole CJ, Kwan AS, Laidlaw DA, et al. A new technique of combined retinal and choroidal biopsy. *Br J Ophthalmol*. 2008;92:1357–1360.
25. Eide N, Walaas L. Fine-needle aspiration biopsy and other biopsies in suspected intraocular malignant disease: a review. *Acta Ophthalmol*. 2009;83:588–601.
26. Intzedy L, Teoh SC, Hogan A, et al. Cytopathological analysis of vitreous in intraocular lymphoma. *Eye (Lond)*. 2008;22:289–293.
27. Mruthyunjaya P, Jumper JM, McCallum R, et al. Diagnostic yield of vitrectomy in eyes with suspected posterior segment infection or malignancy. *Ophthalmology*. 2002;109:1123–1129.
28. Davis JL, Miller DM, Ruiz P. Diagnostic testing of vitrectomy specimens. *Am J Ophthalmol*. 2005;140:822–829.
29. Margolis R, Brasil OF, Lowder CY, et al. Vitrectomy for the diagnosis and management of uveitis of unknown cause. *Ophthalmology*. 2007;114:1893–1897.
30. Wallace DJ, Shen D, Reed GF, et al. Detection of the bcl-2 gene t(14;18) translocation and proto-oncogene expression in primary intraocular lymphoma. *Invest Ophthalmol Vis Sci*. 2006;47:2750–2756.
31. Intzedy L, Teoh SC, Hogan A, et al. Cytopathological analysis of vitreous in intraocular lymphoma. *Eye (Lond)*. 2008;22:289–293.

32. Van Gelder RN. CME review: polymerase chain reaction diagnostics for posterior segment diseases. *Retina*. 2003;23:445–452.
33. Garweg JG, Wanner D, Sarra GM, et al. The diagnostic yield of vitrectomy specimen analysis in chronic idiopathic endogenous uveitis. *Eur J Ophthalmol*. 2006;16:588–594.
34. Sugita S, Ogawa M, Shimizu N, et al. Use of a comprehensive polymerase chain reaction system for diagnosis of ocular infectious diseases. *Ophthalmology*. 2013;120:1761–1768.
35. Lohmann CP, Linde HJ, Reischl U. Improved detection of microorganisms by polymerase chain reaction in delayed endophthalmitis after cataract surgery. *Ophthalmology*. 2000;107:1047–1051.
36. Zaldivar RA, Martin DF, Holden JT, et al. Primary intraocular lymphoma: clinical, cytologic, and flow cytometric analysis. *Ophthalmology*. 2004;111:1762–1767.
37. Ohta K, Sano K, Imai H, et al. Cytokine and molecular analysis of intraocular lymphoma. *Ocul Immunol Inflamm*. 2009;17:142–147.
38. Kojima K, Maruyama K, Inaba T, et al. The CD4/CD8 ratio in vitreous fluid is of high diagnostic value in sarcoidosis. *Ophthalmology*. 2012;119:2386–2392.
39. Ahn JK, Yu HG, Chung H, et al. Intraocular cytokine environment in active Behçet uveitis. *Am J Ophthalmol*. 2006;142:429–434.
40. Kim TW, Chung H, Yu HG. Chemokine expression of intraocular lymphocytes in patients with Behçet uveitis. *Ophthalmic Res*. 2011;45:5–14.
41. Waters FM, Goodall K, Jones NP, et al. Vitrectomy for vitreous opacification in Fuch's heterochromic uveitis. *Eye (Lond)*. 2000;14:216–218.
42. Kiryu J, Kita M, Tanabe T, et al. Pars plana vitrectomy for cystoid macular edema secondary to sarcoid uveitis. *Ophthalmology*. 2001;108:1140–1144.
43. Kapur R, Birnbaum AD, Goldstein DA, et al. Treating uveitis-associated hypotony with pars plana vitrectomy and silicone oil injection. *Retina*. 2010;30:140–145.

44. Wu TT, Hong MC. Pars plana vitrectomy with internal limiting membrane removal for a macular hole associated with Behçet's disease. *Eye (Lond)*. 2009;23:1606–1607.
45. Jaffe GJ, Ben-Nun J, Guo H, et al. Fluocinolone acetonide sustained drug delivery device to treat severe uveitis. *Ophthalmology*. 2000;107:2024–2033.
46. Rush RB, Goldstein DA, Callanan DG, et al. Outcomes of birdshot chorioretinopathy treated with an intravitreal sustained-release fluocinolone acetonide-containing device. *Am J Ophthalmol*. 2011;151:630–636.
47. Malone PE, Herndon LW, Muir KW, et al. Combined fluocinolone acetonide intravitreal insertion and glaucoma drainage device placement for chronic uveitis and glaucoma. *Am J Ophthalmol*. 2010;149 [800–6.e1].
48. Whitcup SM, Chan CC, Buggage RR, et al. Improving the diagnostic yield of vitrectomy for intraocular lymphoma. *Arch Ophthalmol*. 2000;118:446.
49. Sonoda KH, Sakamoto T, Enaida H, et al. Residual vitreous cortex after surgical posterior vitreous separation visualized by intravitreous triamcinolone acetonide. *Ophthalmology*. 2004;111:226–230.
50. Radetzky S, Walter P, Fauser S, et al. Visual outcome of patients with macular edema after pars plana vitrectomy and indocyanine green-assisted peeling of the internal limiting membrane. *Graefes Arch Clin Exp Ophthalmol*. 2004;242:273–278.
51. Lee GH, Ahn JK, Park YG. Intravitreal triamcinolone reduces the morphologic changes of ciliary body after pars plana vitrectomy for retinal vascular diseases. *Am J Ophthalmol*. 2008;145:1037–1044.
52. Jonas JB, Hayler JK, Panda-Jonas S. Intravitreal injection of crystalline cortisone as adjunctive treatment of proliferative vitreoretinopathy. *Br J Ophthalmol*. 2000;84:1064–1067.
53. Ahn JK, Chung H, Yu HG. Vitrectomy for persistent panuveitis in Behçet's disease. *Ocul Immunol Inflamm*. 2005;13:447–453.
54. Giuliari GP, Chang PY, Thakuria P, et al. Pars plana vitrectomy in the management of paediatric uveitis: the

Massachusetts Eye Research and Surgery Institution experience. *Eye (Lond)*. 2010;24:7–13.
55. Bovey EH, Herbort CP. Vitrectomy in the management of uveitis. *Ocul Immunol Inflamm*. 2000;8:285–291.
56. Tranos P, Scott R, Zambarakji H, et al. The effect of pars plana vitrectomy on cystoid macular oedema associated with chronic uveitis: a randomised, controlled pilot study. *Br J Ophthalmol*. 2006;90:1107–1110.
57. Quinones K, Choi JY, Yilmaz T, et al. Pars plana vitrectomy versus immunomodulatory therapy for intermediate uveitis: a prospective, randomized pilot study. *Ocul Immunol Inflamm*. 2010;18:411–417.
58. Tanawade RG, Tsierkezou L, Bindra ME, et al. Visual outcomes of pars plana vitrectomy with epiretinal membrane peel in patients with uveitis. *Retina*. 2015;35:736–741.

127

Vitreous, Retinal, and Choroidal Biopsy

William R. Rhoades, Andrew J. Baldwin, Quan Dong Nguyen, Diana V. Do

Introduction

The diagnosis of posterior segment infectious or inflammatory disease is based primarily on clinical examination. In the majority of cases, the slit-lamp biomicroscopic and ophthalmoscopic appearance of the vitreous, retina, and choroid is diagnostic of a specific disorder, especially when combined with the findings from ancillary tests such as fluorescein angiography, ocular echography, and radiologic and serologic tests.[1]

However, not all patients have the characteristic clinical features or classic appearance of a specific disease, and the etiology of their disorder can be a diagnostic dilemma. The inability to make a specific diagnosis has been reported in up to 33% of patients who present with intraocular inflammation.[2] Moreover, some infectious and malignant processes are manifested first, or only, in the eye, in which case the diagnostic yield from systemic testing is low. This is often the situation in patients with atypical malignancy in the eye; chronic low-grade endophthalmitis after cataract surgery; intraocular inflammation of atypical viral, bacterial, or fungal origin; and some types of progressive retinitis, choroiditis, and pigment epitheliopathies. In these patients, particularly if they are immunocompromised or if one of the possible diagnoses is malignancy, the disease process may threaten not only vision but also life. Intraocular biopsy provides affected ocular tissue for culture, examination, and other tests to help with therapeutic decision-making.[3] In most of these cases, therapeutic intervention will be either antimicrobial, antineoplastic, or antiinflammatory.[4,5]

A number of factors in recent years have brought about an increased demand for tissue diagnosis in posterior segment

inflammatory disease. One of these is the rise in the number of individuals who have been iatrogenically immunosuppressed as a result of systemic disease, malignancy, or organ transplantation. In addition, the frequent use of intravitreal steroids has also led to the report of opportunistic ocular infections in immunocompetent individuals.[6] The clinical presentation of ocular inflammatory disease may be variable and atypical in these immunocompromised patients; the possible etiologic agents are numerous and diverse, and serologic testing is frequently misleading. Another factor increasing the indication for intraocular biopsy is the common practice in modern cataract surgery to place intraocular lenses directly into intact capsular bags. These capsular bags can rarely serve as small reservoirs and sequester low-virulent organisms which multiply, and subsequently clinicians are confronted with a chronic, smoldering, postoperative endophthalmitis that is due to organisms such as *Candida parapsilosis* or *Propionibacterium acnes* (Figs. 127.1–127.5). These cases often cannot be adequately treated until a tissue diagnosis is made.

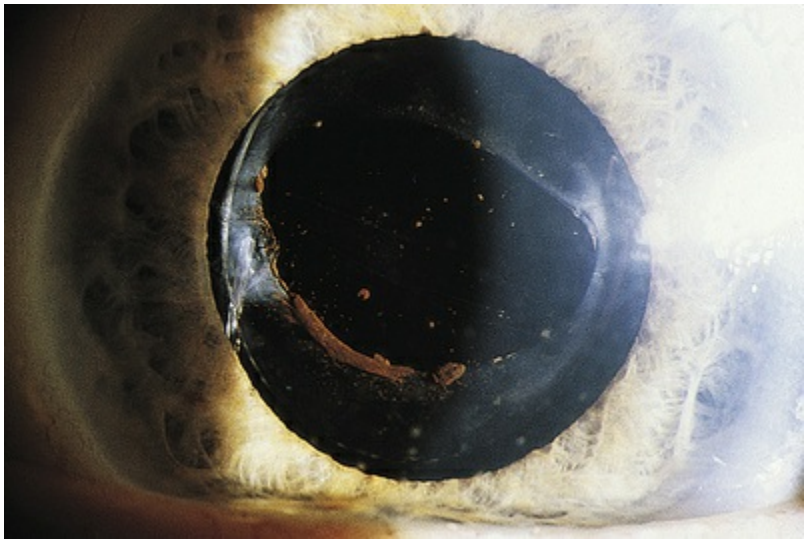

FIG. 127.1 After cataract surgery, inflamed eye of a patient with chronic indolent uveitis is caused by *Candida parapsilosis*.

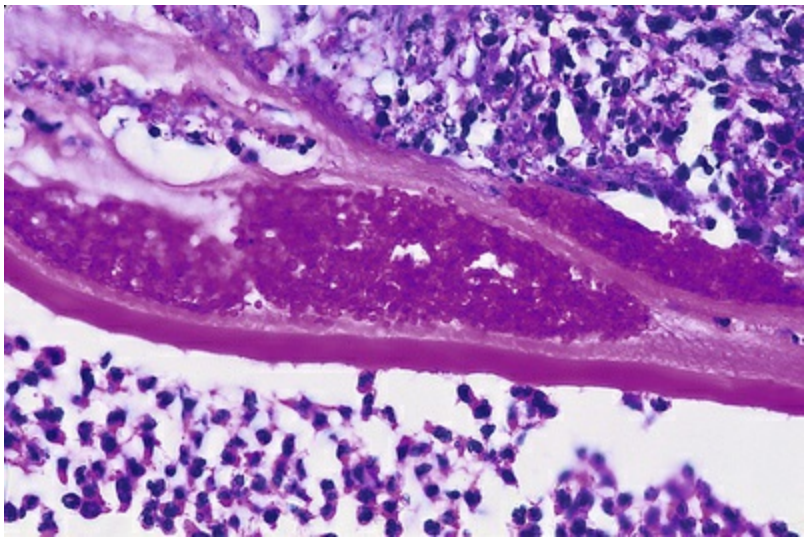

FIG. 127.2 *Candida parapsilosis* organisms crowd this capsular bag, surrounded by an area of dense neutrophilic incursion.

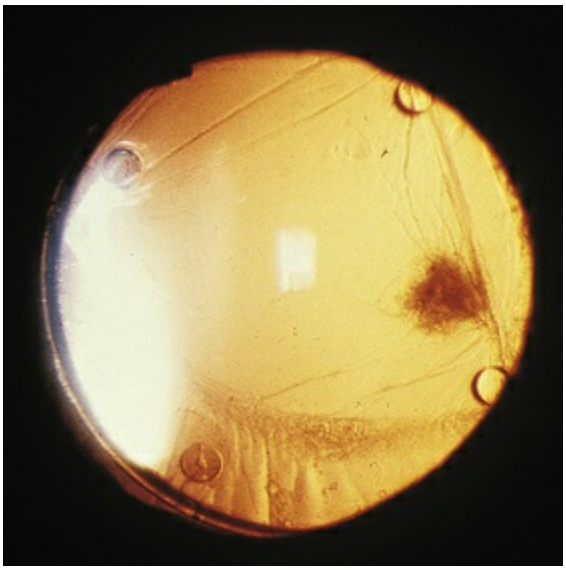

FIG. 127.3 Characteristic posterior capsular plaque seen in a patient with chronic postcataract inflammation caused by *Propionibacterium acnes*.

(Reproduced with permission from Sawusch MR, Michels RG, Stark WJ, et al. Endophthalmitis due to *Propionibacterium acnes* sequestered between IOL optic and posterior capsule. Ophthalmic Surg 1989;20:90–2. By kind permission of Slack Inc.)

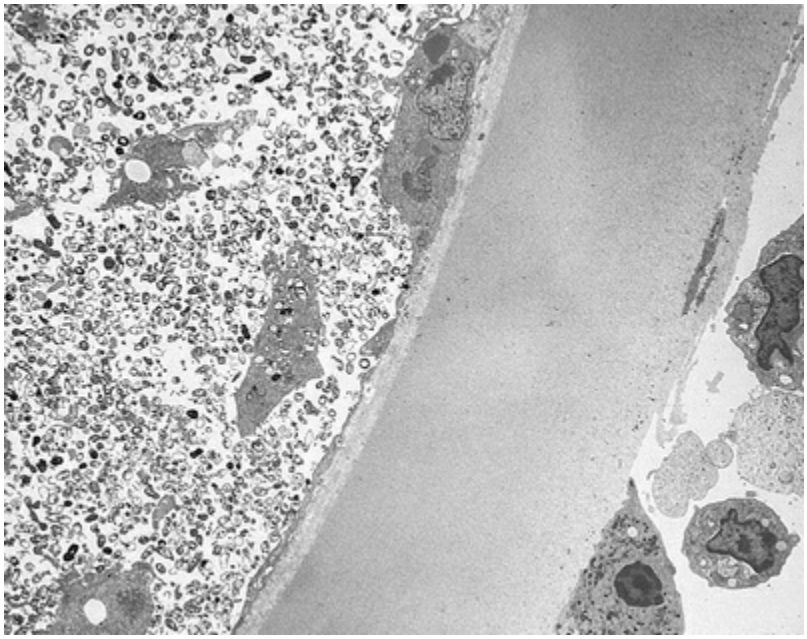

FIG. 127.4 *Propionibacterium acnes* organisms fill the capsular bag in this patient with smoldering endophthalmitis and retinal detachment more than 1 year after cataract surgery.

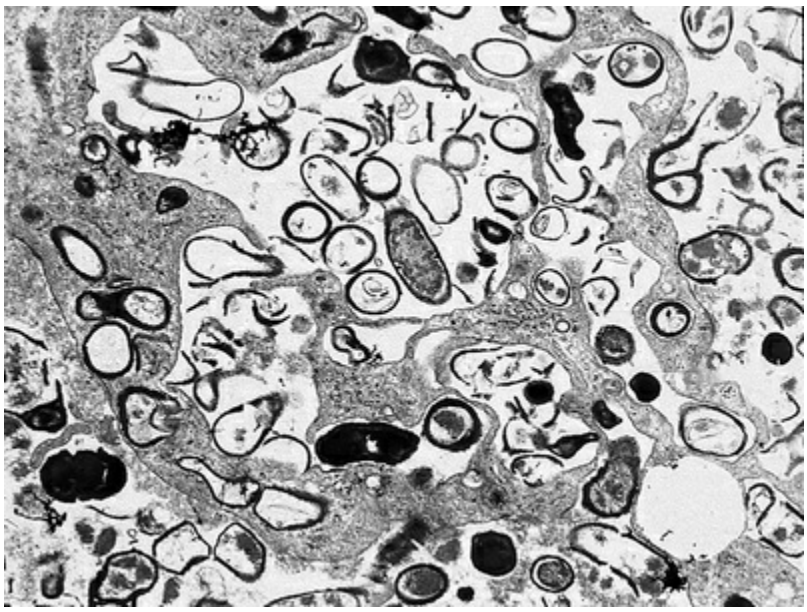

FIG. 127.5 High-power view of the *Propionibacterium acnes* organisms seen in Fig. 127.4.

Ongoing advances in laboratory testing continue to improve the diagnostic yield from biopsied material. For example, polymerase chain reaction (PCR) testing, a biochemical technique, is able to

detect infinitesimally small amounts of specific nucleic acids, which permits identification of genetic components of infectious organisms. In fact, modifications to traditional PCR methods (multiplex, nested PCR) allow for simultaneous testing for numerous pathogens such as herpessimplex virus (HVZ), varicella-zoster virus (VZV), and cytomegalovirus (CMV) without significant loss in sensitivity or specificity.[7] This allows for quick and efficient testing for multiple pathogens. Furthermore, quantitative PCR (qPCR) allows for in situ quantification, thus allowing the clinician an idea of the disease burden.[8]

Finally, advances in vitreoretinal surgical instrumentation and increasing use of 25- and 23-gauge (G) transconjunctival pars plana vitrectomy[9] have allowed for possibly safer access and acquisition of ocular tissue for analyses. Table 127.1 lists common indications for ocular biopsy.

TABLE 127.1

Common Indications for Biopsy

Biopsy Site	Diagnostic Dilemma
Vitreous	Endophthalmitis (bacterial or fungal)
	Intraocular lymphoma
	Retinitis with associated vitritis
Retinal	Retinitis (atypical or not responsive to empiric therapy)
Choroidal	Tumor
	Choroiditis (atypical or not responsive to empiric therapy)

The efficacy of ocular biopsy depends partly on the expertise of the surgeon who obtains the specimen and the laboratory personnel who analyze the specimen(s). Before embarking on surgery, harvesting and handling of the specimen should be carefully mapped out in advance. The pathologist should be familiar with ophthalmic disease processes, aware of the diagnoses being considered, and involved at the outset in planning how the specimen will be handled from the moment it is taken – a step that is critical to the success of the procedure.[4,10,11]

The pathologist's available investigative methods include, among others, light microscopy, electron microscopy, immunohistochemistry, and PCR. PCR can be used to identify unique DNA and RNA sequences specifically from infectious agents and, occasionally, from other disease processes, such as

proliferating monoclonal B lymphocytes in ocular malignant lymphoma.[11–15] The laboratories responsible for culture and identification of bacterial, fungal, and viral disease should receive the specimen as soon as possible. It should be plated on a variety of specific media and maintained under the correct (aerobic, anaerobic, temperature) conditions. Plates may need to be specially treated or held for extra time to reveal growth from some of the more fastidious organisms. Despite disadvantages such as inability to detect certain microbes and relatively low yield compared to more modern testing such as PCR, microbial culture remains the gold standard for the diagnosis of most intraocular infections.

Vitreous Biopsy

With the evolution of modern vitrectomy techniques, including 23G, 25G, and 27G vitrectomy, removal of vitreous from the eye has become a common and relatively safe procedure.[16] A number of different goals are achieved with diagnostic vitrectomy.[5,17] In vitritis with a possible neoplastic, infectious, or inflammatory cause, diagnostic vitrectomy may provide a definitive diagnosis, thereby allowing appropriate therapy to be instituted.[5,10] In some cases of retinitis and choroiditis, a diagnosis can be made from vitreous sampling alone, particularly if marked vitritis is present. The vitrectomy also removes or debulks infectious material within the eye, reduces the intraocular load of inflammatory cells and debris, effectively removes material (e.g., retained lens material and blood) that may be part of the pathogenesis of the ocular disorder, allows clinicopathologic correlation in the active stages of disease for some conditions, and helps to define the pathophysiologic basis of many disorders.[5] Cytopathologic diagnosis has proved valuable in reported series or case reports of patients with endogenous and exogenous bacterial and fungal infections (Fig. 127.6); nematode endophthalmitis; inflammatory pseudotumor of the iris and ciliary body; pars planitis; phacoanaphylaxis; intraocular lymphoma; leukemia; metastatic melanoma; metastatic carcinoma; medulloepithelioma of the ciliary body; secondary glaucoma (including blood-induced, phacolytic, and melanomalytic glaucoma); epithelial ingrowth; proliferative vitreoretinopathy; and

miscellaneous conditions with vitreous opacities (including chronic inflammation in patients with suspected lymphoma, acute retinal necrosis, birdshot chorioretinopathy, toxoplasmosis, Whipple disease, amyloidosis, and asteroid hyalosis).[4,5,18,19] Vitrectomy may also help to clear vitreous opacities, remove scaffolding on which postoperative cicatricial proliferation can grow, relieve traction, and allow for improved intraocular penetration of antibiotics.[5,17] Table 127.2 lists a sample of vitreous findings in major disease categories.

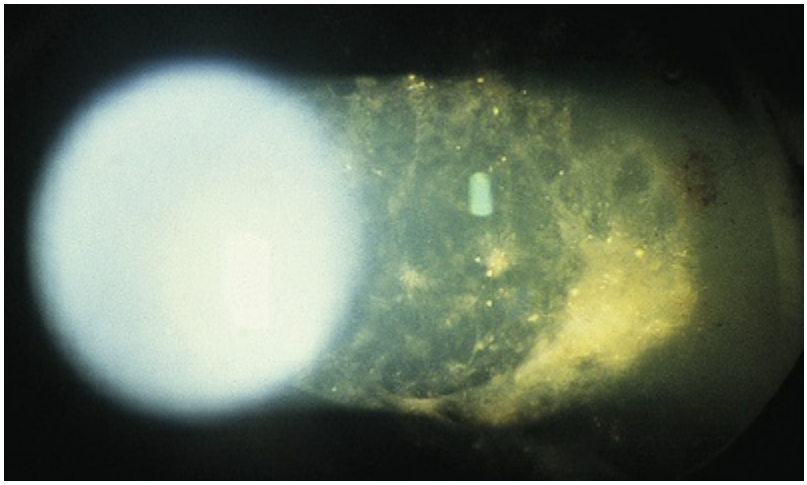

FIG. 127.6 This 61-year-old woman had a history of idiopathic uveitis, quiescent for years, and cataract surgery 10 years previously. She developed a red eye and decreased vision with active anterior segment inflammation, shown here with cellular and fibrinous anterior chamber deposits. A retinal detachment was noted on echography. Examination of smears and culture of the vitrectomy specimen from the time of detachment repair revealed *Cryptococcus* organisms.

TABLE 127.2

Sample of Vitreous Findings in Major Disease Categories

	Noninfectious Uveitis	Infectious Uveitis	Tumor
Cells	Inflammatory	Microbes	Malignant cells
Immunohistochemistry	$CD4^+$ cells	Polymorphonuclear cells	Light chain restriction in lymphoma
Culture	Negative	Positive	Negative
Antibody	Negative	Positive	Negative

Cytokines	IL-1, -2, -6	IL-6	IL-10
Polymerase chain reaction	No gene sequences	Microbial or viral products	CDR3 of IgH gene

Surgical Technique

To obtain an undiluted specimen, a variety of vitrectomy techniques (with either 20-, 23-, 25-, or 27G instrumentation) may be used. If a large sample (>0.5 mL) of vitreous is needed, a standard three-port vitrectomy system should be utilized. A 10-mL Luer–Lok syringe is spliced via a three-way stopcock into the aspiration line (Fig. 127.7). Manual aspiration and specimen collection are carried out for retrieval of an undiluted specimen from the most intensely involved area (usually posteriorly, inferiorly, or over the area of retinitis or chorioretinitis).

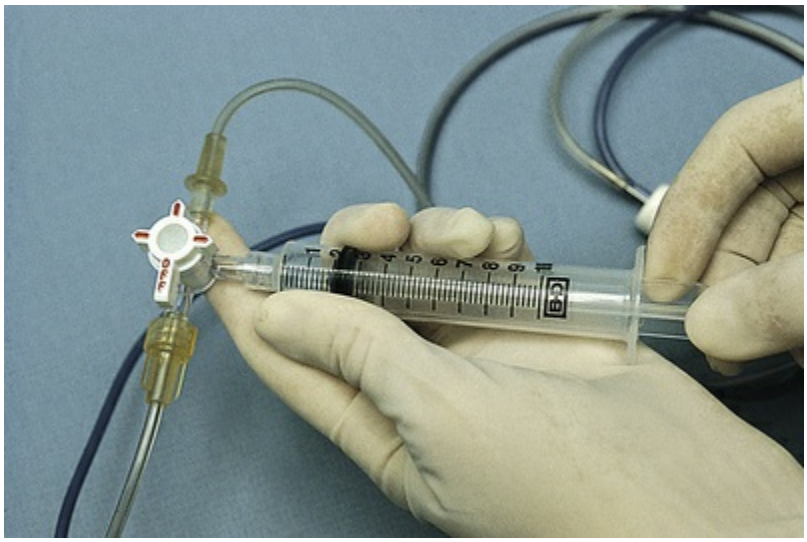

FIG. 127.7 Technique of specimen collection in diagnostic vitrectomy. A 10-mL syringe is spliced into the vitrectomy aspiration tubing, and a choice undiluted specimen is obtained with manual aspiration.

Alternatively, a vitreous "trap" method may also be performed using two 18G needles, a male adaptor, and a sterile red-topped test tube.[20] In the vitreous trap method, the male adaptor is attached to one of the needles and the needles are attached to the ends of the aspiration tubing. The two needles are then inserted into the test tube. The diagnostic vitrectomy is performed, and the pure vitreous

sample is directed into the test tube.

After a sufficient amount of sample is obtained, the infusion is turned on and either fluid or air is infused before large choroidals form and the eye begins to collapse.[16] The vitrector is withdrawn from the eye, and the vitreous specimen is aspirated into the syringe. Vitrectomy can then be completed. At completion of the surgery, the cassette with the dilute residual vitreous is also sent to the pathology laboratory, where the specimen is concentrated, using a micropore filter, or cytospin smears are made.[4,21]

If a small sample (≤0.5 mL) of vitreous is needed, a 27G vitrectomy with a single incision may be utilized.[22,23] In this technique, the 27G vitrector is inserted perpendicular to the pars plana. Using a cut rate of 800 cuts/minute and an aspiration rate of 600 mmHg, a small amount of undiluted vitreous may be safely removed from the eye without the need of an additional infusion line or endoillumination port. The 27G scleral wound is also self-sealing and does not require sutures.

Histologic Technique and Preparations

The number of investigations that can be carried out on an individual specimen depends on the amount of harvested material. Ideally the undiluted vitreous specimen is plated for aerobic and anaerobic bacterial, fungal, and (occasionally) viral culture if an infectious etiology is suspected. An aliquot is collected for immediate Gram stain, periodic acid–Schiff stain, and Giemsa stain, and another one is done for PCR analysis. The remainder is kept for light and electron microscopy or immunohistochemistry.

If primary intraocular lymphoma is suspected, obtaining a sufficient vitreous sample for cytologic testing is essential. Consultation with an experienced cytopathologist is recommended because correct identification of lymphoma cells in the biopsy sample is essential for the diagnosis. In addition to characterizing cells from the vitreous biopsy, testing for immunohistochemical markers for leukocytes (e.g., CD45), B cells (e.g., CD 20), and T cells (e.g., CD45RO) can also aid in the diagnosis.[16,24,25] Other diagnostic modalities that can be useful include flow cytometry, PCR to detect V–J immunoglobulin gene rearrangements, and measurements of

interleukin (IL)-6 and IL-10 in aqueous or vitreous samples.[24–26] Table 127.3 summarizes the key laboratory features of several patients who underwent 25G diagnostic vitrectomy for suspected intraocular lymphoma. Additional information on the diagnosis and management of primary intraocular lymphoma is available in Chapter 159, Leukemias and lymphomas.

TABLE 127.3

Summary of Vitreous Biopsy Results in Series of Patients With Intraocular Lymphoma

Patient	Cytopathology	Flow Cytometry	Gene Rearrangement	Final Diagnosis
1	Scattered lymphocytes, monocytes	CD45 (bright), CD19 (dim), monoclonal κ light chain	IgH gene rearrangement detected	B-cell intraocular lymphoma
3	Atypical lymphoid cells with irregular nuclei, lymphocytes	T-cell leukemia, abnormal CD3 (dim) population	TCR gamma gene rearrangement detected	T-cell intraocular lymphoma
9	Atypical lymphoid cells with irregular nuclei and condensed chromatin	No evidence of lymphoma	IgH gene rearrangement detected	B-cell intraocular lymphoma
12	Atypical lymphoid cells with irregular nuclei	T-cell predominance, no evidence of lymphoma	κ light chain gene rearrangement detected	B-cell intraocular lymphoma

Adapted from Yeh S, Weichel ED, Faia LJ, et al. 25-gauge transconjunctival sutureless vitrectomy for the diagnosis of intraocular lymphoma. Br J Ophthalmol 2010;94:633–8.

Results

In cases of infectious endophthalmitis, vitreous samples can often reveal the presence of microbes. Unfortunately, these may not be found in all infectious cases, principally because of suboptimal sampling, inadequate culturing, or pretreatment with antimicrobials that render microbes nonculturable on routine media.[12] In the Endophthalmitis Vitrectomy Study, confirmed microbiologic growth was demonstrated in intraocular specimens from 291 of 420 patients (69.3%).[27] More recently, PCR testing has been applied to identify bacterial causes of endophthalmitis. Very little tissue is needed for PCR. Usually 50–100 μL samples are sufficient, but even a sample as small as 1 μL can be processed for PCR testing.[28] Numerous studies have demonstrated PCR to be

sensitive and specific in diagnosing bacterial and fungal endophthalmitis, even when corresponding cultures where negative.[29–31] Furthermore, PCR has also been shown to be a useful tool in the diagnosis and management of challenging cases of infectious viral chorioretinitis.[32]

Several studies have shown that PCR has sensitivities exceeding 90% for varicella-zoster virus (VZV), herpessimplex virus (HSV), and cytomegalovirus (CMV), with specificities in excess of 95% for these organisms.[28] Sensitivity approaches 95% in detecting untreated CMV retinitis, dropping to 48% in treated eyes.[33–35] Moreover, false-positive rates are low.[36] In addition, PCR can aid in detecting antiviral-resistant strains of CMV, which have mutations in the UL97 polymerase gene.[28] Information on possible antiviral resistance is essential in the management of viral retinitis and may influence the choice of agent for a particular patient. Of note, PCR inhibitor has been detected in normal aqueous and vitreous fluids, but it can be removed by diluting the specimen, by chloroform extraction, or by thermostable DNA polymerases.[37]

The clinical indications for diagnostic vitrectomy and associated results were reported by Palexas and colleagues,[38] who published on 405 consecutive vitreous biopsy cases studied at the Wilmer Eye Pathology laboratory. Vitrectomy had been performed in six categories of eye disease: posttraumatic infections (8.4%); postoperative endophthalmitis (38.5%); endogenous endophthalmitis (6.2%); idiopathic inflammation (25.4%); intraocular neoplasm (14.3%); and miscellaneous (7.2%). Diagnostic vitrectomy was performed in 215 cases (53%) for suspected endophthalmitis. Of these cases, 60 (28.8%) had microbial organisms present, while only 36 (16.7%) were culture-positive. Of note, Gram-positive bacteria were most common in the postoperative endophthalmitis group (74%) while fungal infections were most common in patients with endogenous infections. Neoplasms were diagnosed in 58 (14%) of the 405 vitrectomy specimens, the most common being ocular lymphoma in 42 (72%) (Fig. 127.8). Other malignancies diagnosed cytopathologically included metastatic squamous cell carcinoma and acute lymphoblastic leukemia.

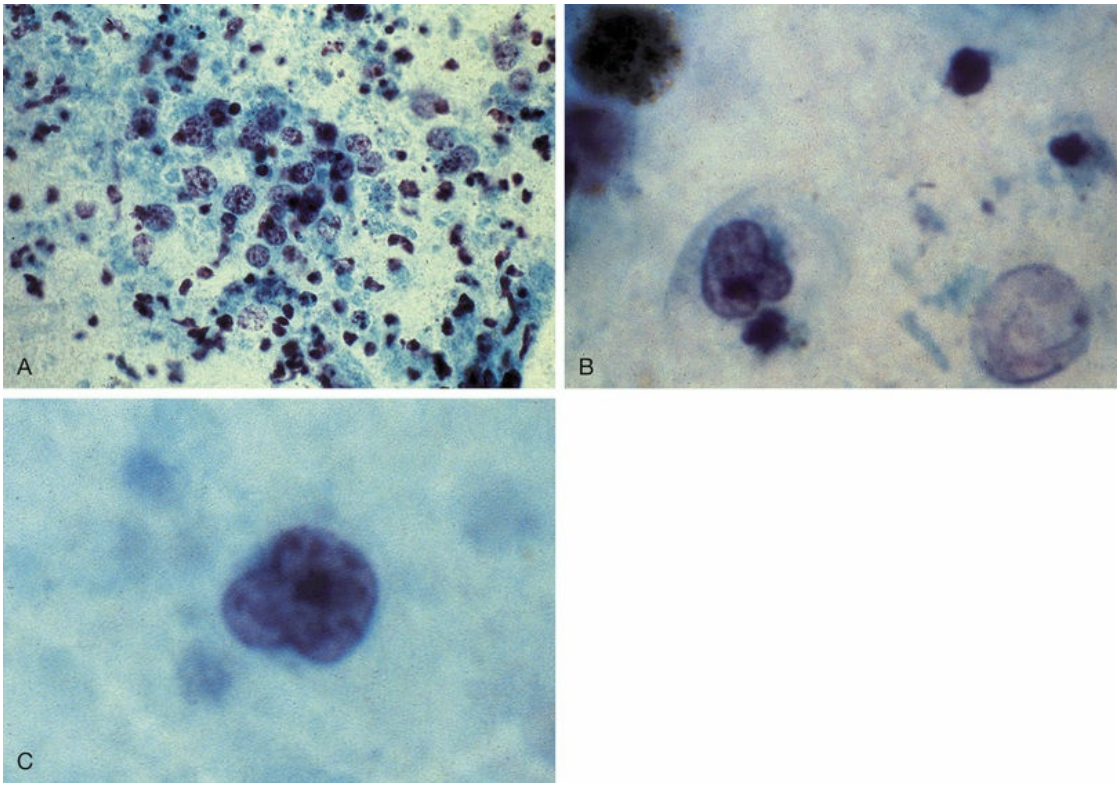

FIG. 127.8 (A–C) Examples of tumor cells with large, round nuclei with numerous micronucleoli or prominent nucleoli and nuclear membrane infoldings. Millipore filter, modified Papanicolaou stain. (A, ×1500; B,C, ×1900.)

Atypical toxoplasmic chorioretinitis that mimics viral retinitis can also be diagnosed by vitreous biopsy.[39] In a series of 22 patients with widespread chorioretinitis, 16 individuals were diagnosed with toxoplasmosis using PCR, culture, antibody detection, histopathologic examination, or a combination of the aforementioned techniques. Bottos and colleagues have also demonstrated the utility of PCR in diagnosing an atypical strain of *Toxoplasma gondii* as the causative agent in an unusual bilateral retinochoroiditis.[40] The correct diagnosis is important in challenging cases since treatment with proper medicines may help avoid vision loss.

In addition to advances in surgical technique and laboratory testing, the development of imaging modalities such as wide-field fluorescein angiography has also provided the clinician with increased information when managing complicated posterior uveitic conditions. For the first time, clinicians are able to obtain high-quality fluorescein images of the peripheral vasculature and

identify pathologic changes.[41,42]

Case 127.1

A 29-year-old white woman with history of acute myeloid leukemia, status post allogeneic bone marrow transplant 2 months prior, was referred for evaluation of blurred vision OD. She had recently been diagnosed with CMV colitis, but ganciclovir had been discontinued because of thrombocytopenia. Visual acuity was 20/320 OD. A serous retinal detachment of the macula was present with white flocculent material beneath it (Fig. 127.9). A chest radiograph examination at this time revealed a right lower lobe infiltrate interpreted as pulmonary aspergillosis. She was treated with systemic antibiotics, including amphotericin B and flucytosine, but 3 days later the ocular lesion was substantially larger (Fig. 127.10). A diagnostic vitrectomy was performed, and 5 μg of intravitreal amphotericin B was given at the end of surgery. The vitreous specimen revealed branching septate hyphae and vitreous culture grew *Aspergillus flavus*.

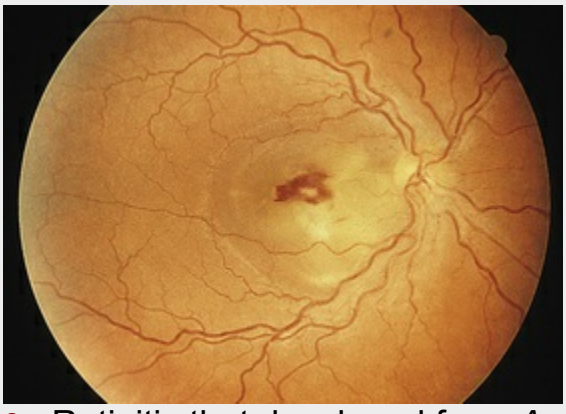

FIG. 127.9 Retinitis that developed from *Aspergillus* infection after bone marrow transplantation. (Reproduced with permission from Coskuncan NM, Jabs DA, Dunn JP, et al. The eye in bone marrow transplantation. VI. Retinal complications. Arch Ophthalmol 1994;112:372 – 9. © (1994) American Medical Association. All rights reserved.)

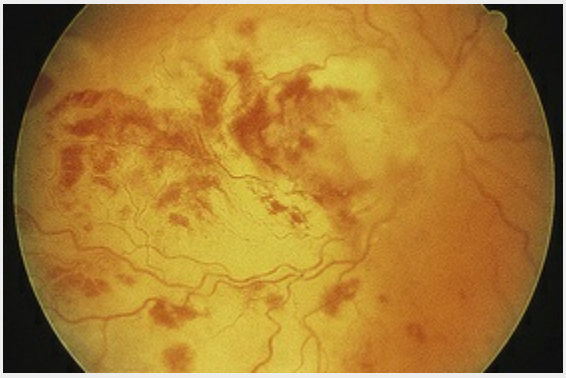

FIG. 127.10 Same eye as in Fig. 124.9, shown 3 days later, despite intravenous amphotericin B and systemic flucytosine, with progressive fulminant infection. Histopathologic study of the vitreous biopsy disclosed branching, septate hyphae, and culture positivity for *Aspergillus flavus*. (Reproduced with permission from Coskuncan NM, Jabs DA, Dunn JP, et al. The eye in bone marrow transplantation. VI. Retinal complications. Arch Ophthalmol 1994;112:372–9.© (1994) American Medical Association. All rights reserved.)

Case 127.2

A 36-year-old white man was seen with a 2-week history of blurred vision in the left eye. Past history was positive for systemic lymphoma stage IIIA, which was treated with total nodal irradiation and chemotherapy. A relapse was successfully treated with chemotherapy, resulting in remission for 3 years, until a bone marrow biopsy showed Burkitt's lymphoma. He was treated with chemotherapy, including seven intrathecal methotrexate injections for central nervous system relapse, and was referred for bone marrow transplantation. He had undergone bone marrow harvesting and had started cytoreductive therapy before transplantation. Vision was counting fingers. Fundus examination disclosed a retinitis involving the macula and optic nerve head with white vitreous opacities (Fig. 127.11). Diagnostic vitrectomy revealed atypical lymphocytes characteristic of lymphoma. The patient was treated with ocular irradiation, and his vision improved to 20/30 one month later (Fig. 127.12).

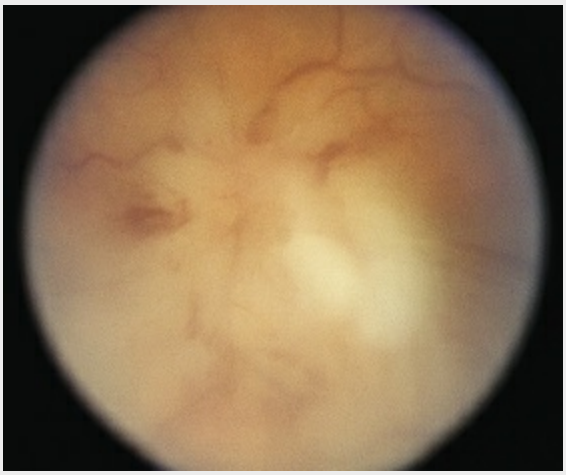

FIG. 127.11 Ocular recurrence of lymphoma that developed after cytoreductive therapy and before bone marrow transplantation in a patient with previous chemotherapy and radiation. Vitreous biopsy revealed atypical lymphocytes consistent with a B-cell lymphoma. (Reproduced with permission from Coskuncan NM, Jabs DA, Dunn JP, et al. The eye in bone marrow transplantation. VI. Retinal complications. Arch Ophthalmol 1994;112:372–9.© (1994) American Medical Association. All rights reserved.)

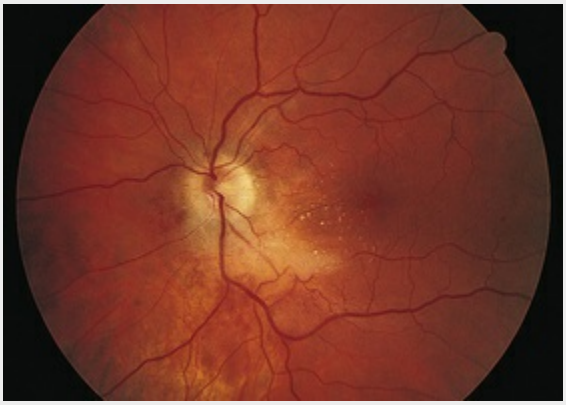

FIG. 127.12 Same eye as in Fig. 124.11, shown 1 month later. After ocular irradiation and bone marrow transplantation, the infiltrates have almost entirely resolved, and vision is 20/30.

Case 127.3

A 53-year-old white male was referred for evaluation of bilateral anterior uveitis in the setting of recent branch retinal artery

occlusion (BRAO). The anterior uveitis was noted OU 3 days following the BRAO. Despite topical steroid eyedrops, the inflammation worsened and he was referred for evaluation. Examination revealed panuveitis with occlusive vasculitis in both eyes and possible acute retinal necrosis. Wide-field imaging allowed for accurate assessment of the degree of vascular nonperfusion (Figs. 127.13 and 127.14). He was empirically treated for possible infection with herpetic virus due to a high serum IgG positivity for herpes zoster virus. The patient's condition continued to progress despite empiric treatment, and a diagnostic vitrectomy was performed, which was negative for an infectious etiology by PCR and culture. Because of the negative vitrectomy, an infectious etiology was thought to be less likely and aggressive steroid therapy was initiated with significant clinical improvement.

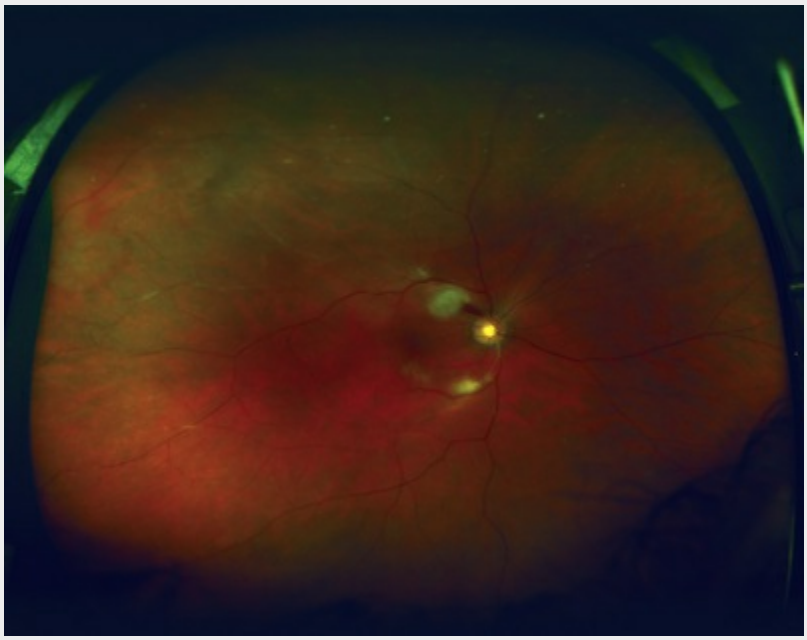

FIG. 127.13 Optos ultrawide-field imaging of right eye demonstrating superior/inferior arcade infarctions with peripheral ghost vessels and sheathing.

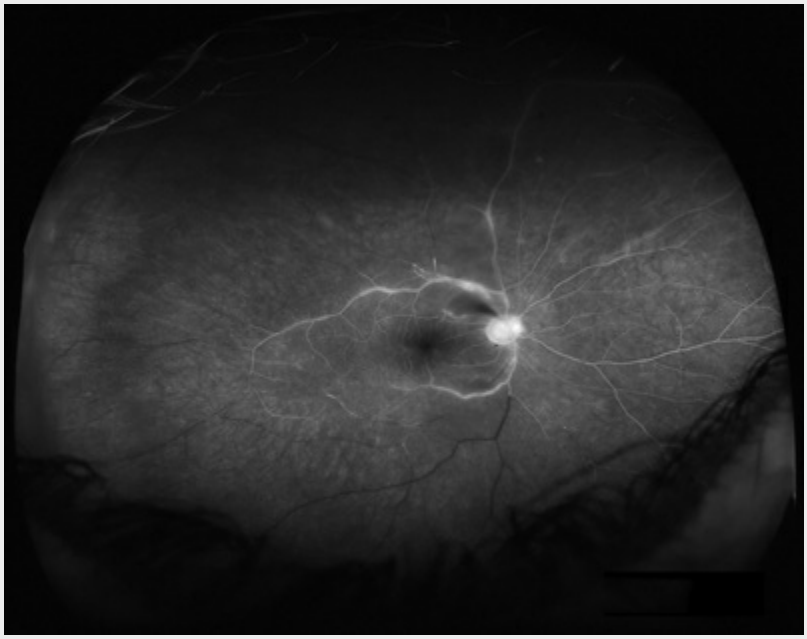

FIG. 127.14 Ultrawide-field fluorescein angiography demonstrating disc leakage, large vessel leakage, and nonperfusion of inferior retina.

Transvitreal Retinal Biopsy

Vitreous biopsy is limited by its dependency on the spillover of cells from the diseased tissue in question into the vitreous cavity to allow a diagnosis. Some ocular pathologic processes are primarily confined to the retina, choroid, or both, and only histologic examination of these areas can yield a diagnosis. The transvitreal approach to retinal biopsy is of particular value in lesions located posterior to the equator, although more peripheral lesions are also accessible, particularly in pseudophakic and aphakic eyes. This approach also allows concomitant vitreous sampling.[43–47]

Surgical Technique

A three-port vitrectomy with either 20G, 23G, or 25G instrumentation is performed, and the cortical vitreous is removed. A chandelier illumination system can be placed as a fourth port to allow for bimanual vitrectomy and retinal biopsy. An appropriate site is chosen for the retinal biopsy, preferably in the superior and nasal retina, at the junction of infected and uninfected retina, as

peripheral as possible, and in a relatively avascular area.

The specimen should include the advancing edge of the retinitis because this is where actively replicating, viable organisms are most likely to be found. Central areas of the lesion may contain only necrotic tissue. Cautery at the area of the biopsy site is occasionally needed if large vessels are present. The tissue is excised with scissors, leaving a small area of anchoring attachment (Fig. 127.15). The biopsied retina is grasped securely with forceps so that as little as possible of the specimen is crushed and is removed from the eye (Fig. 127.16). Laser is not necessary at the biopsy edges involved by inflammation, but it is placed at the edges of normal retina. An air–fluid exchange is performed, and occasionally a long-acting gas is injected.

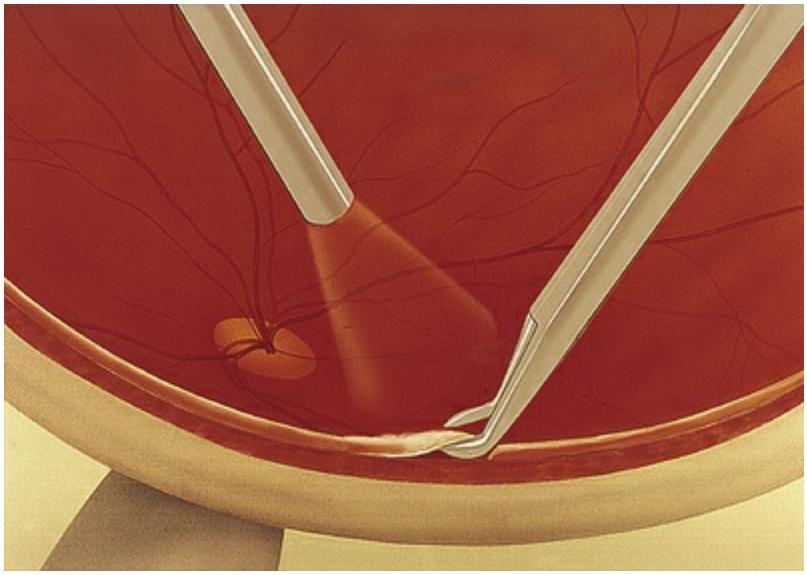

FIG. 127.15 After cortical vitreous is removed, the retina is engaged with automated scissors and a specimen is excised, leaving a tiny tissue bridge to anchor the biopsy to the eye wall.

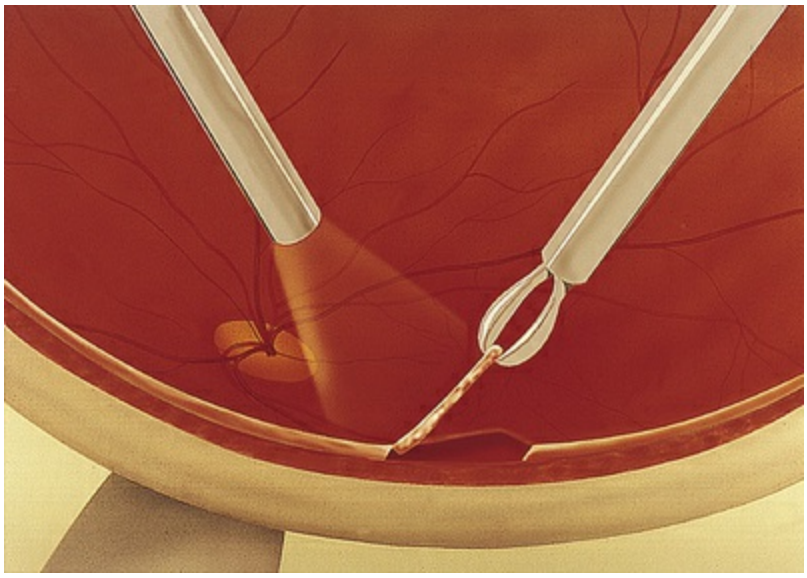

FIG. 127.16 Technique of transvitreal retinal biopsy. Forceps are introduced into the eye, and the specimen is grasped securely but carefully so that as little as possible is crushed and removed from the eye. The cut edges of retina are then photocoagulated, and a fluid–gas exchange performed.

Histologic Technique and Preparation

After the tissue sample is removed from the eye, it is immediately placed in glutaraldehyde/formaldehyde fixative. If orientation is important, the sample may be placed on a piece of filter paper or other material and the correct localization marked on the paper. This is an important point of discussion for the surgeon and the pathologist before the surgical procedure. Depending on the size of the specimen, it is processed for light and electron microscopy and immunohistochemistry.

Results

Rutzen et al.[48] reported a series of 24 transvitreal retinal biopsies, 19 from eyes with clinical signs suggestive of viral retinitis. The clinical diagnosis was confirmed by electron microscopy, immunohistochemical staining, in situ DNA hybridization, and/or PCR in 10 of the 19 eyes (53%). Virus was identified in seven of 10 cases of suspected CMV retinitis, in one of seven cases of acute

retinal necrosis, and in two of two cases of progressive outer retinal necrosis. The remaining five biopsies disclosed *Candida* organisms in one specimen, subretinal fibrosis in one, and chronic inflammation in three.

Johnston and colleagues[49] performed a retrospective review of retinal and choroidal biopsies undertaken in cases of unclear uveitis of suspected infectious or malignant origin. In this series, 13 patients underwent either a retinal or choroidal biopsy. The pathologic diagnosis differed from the initial clinical diagnosis in five (38%) cases and helped to direct treatment in seven (54%) cases. Retinal biopsies were invaluable in making the proper diagnosis in

Case 127.4

A 65-year-old white man had metamorphopsia and a gray scotoma. His history was positive for non-Hodgkin lymphoma and two courses of chemotherapy, followed by autologous bone marrow transplantation 7 months previously. Vision was 20/400, and white macular retinitis was seen with minimal vitreous inflammation (Fig. 127.17). A retinal biopsy disclosed intracytoplasmic nucleocapsids measuring 120–140 nm and several intracytoplasmic spherical election-dense bodies measuring 120–350 nm, consistent with CMV retinitis (Fig. 127.18). The PCR analysis of the vitreous was also positive for CMV. The infection responded well to ganciclovir (Fig. 127.19).

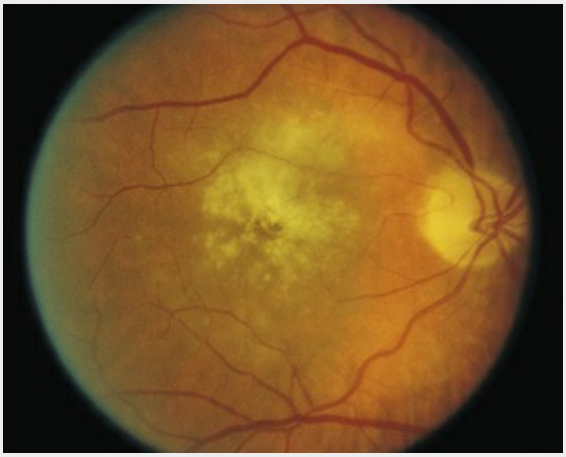

FIG. 127.17 Macular retinitis after bone marrow transplantation in a 65-year-old man.

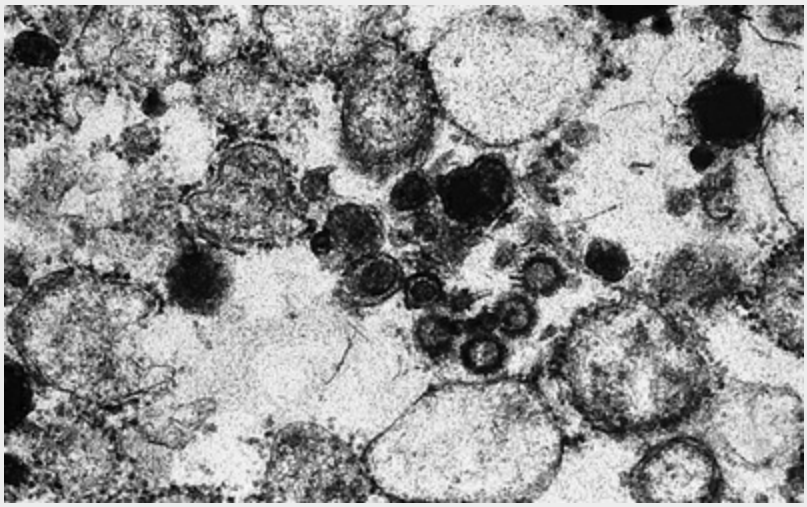

FIG. 127.18 Same eye as in Fig. 127.17. Retinal biopsy disclosed cytomegalovirus cells, with cytoplasmic particles typical of herpes virus. Polymerase chain reaction was positive for cytomegalovirus.

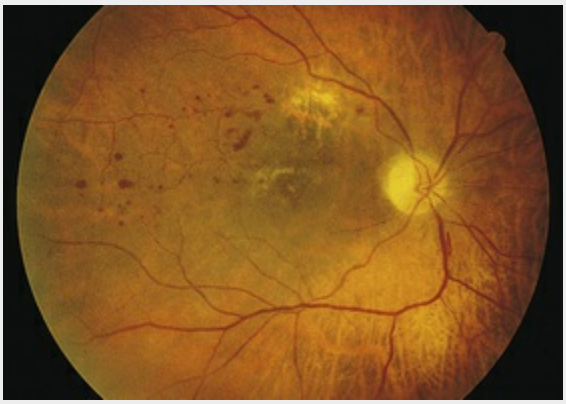

FIG. 127.19 Same eye as in Fig. 127.17, 1 month after the biopsy. With the patient undergoing ganciclovir treatment, the retinitis is resolving well. Note the healed biopsy site just below the superotemporal arcade.

Case 127.5

A 34-year-old white man developed blurred vision and floaters in his left eye. He had a history of bone marrow transplantation, with graft-versus-host disease requiring persistent immunosuppression. At first the white peripheral retinitis was thought to represent

CMV infection, and he was unsuccessfully treated with ganciclovir (Fig. 127.20). Because of the atypical clinical picture (including no old toxoplasmic scars on earlier ophthalmologic evaluation), a retinal biopsy was performed, disclosing *Toxoplasma* organisms (Fig. 127.21).

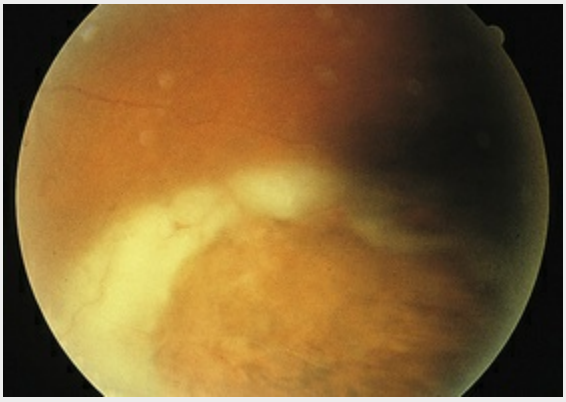

FIG. 127.20 Atypical retinitis featuring active borders with central scarring. Retinal biopsy confirmed *Toxoplasma* infection. (Reproduced with permission from Coskuncan NM, Jabs DA, Dunn JP, et al. The eye in bone marrow transplantation. VI. Retinal complications. Arch Ophthalmol 1994;112:372–9.© (1994) American Medical Association. All rights reserved.)

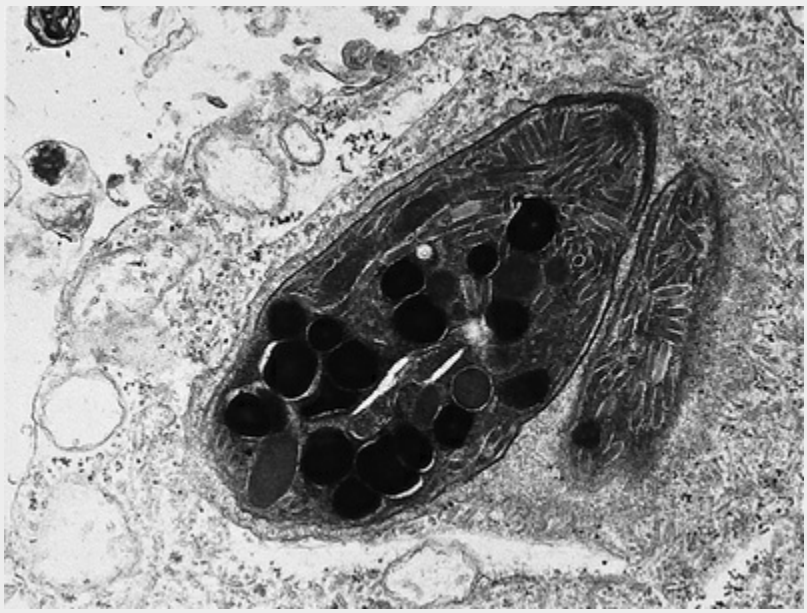

FIG. 127.21 Same eye as in Fig. 127.20. Characteristic *Toxoplasma gondii* organisms in the retinal biopsy

specimen.

Transvitreal and Transscleral Choroidal Biopsy

In certain ocular disease processes, the pathologic evidence is primarily located at the level of the choroid. In such cases, the cells recovered by vitrectomy may be nonspecifically inflammatory in nature and not representative of the actual disorder.[50,51] Therefore the biopsy of the choroid (and retina) may be informative and useful.[8,43,52] Choroidal and chorioretinal biopsies have been performed to investigate nonspecific uveitis, acute retinal necrosis, tuberculous choroiditis, and retinal pigment epitheliopathies and to identify malignant incursion into the choroid.[8,43]

Transscleral chorioretinal biopsy was pioneered by Foulds, Peyman, and others who developed procedures that allow choroidal tissue sampling but minimize associated complications, particularly retinal detachment.[53–59] Cole and colleagues have reported on the success of transvitreal chorioretinal biopsy using 20G instrumentation and vertical-cutting scissors to remove a large specimen (at least 2 × 2 mm) from the biopsy site.[60,61] Among the nine eyes that underwent biopsy, a positive histologic diagnosis was made in five cases (55.6%).

Surgical Technique

Transvitreal Biopsy

A standard three-port pars plana vitrectomy is performed and endolaser is applied around the margins of the intended biopsy site, which should measure at least 2 × 2 mm.[60,61] Vertical cutting intraocular scissors are used to isolate the retinal and choroidal biopsy specimen by cutting within the margins of the laser burns. The blade of the scissor should penetrate the choroid until clear white sclera is visible. In order to prevent intraocular hemorrhage, the infusion bottle should be raised to elevate the intraocular pressure. After obtaining the specimen, the sclerostomy site should

be enlarged to allow for removal of the specimen from the eye. The specimen should be immediately sent for processing and analysis. After fluid/gas exchange, 20% SF_6 gas can be injected into the eye to tamponade the retina.

Recently, a surgical technique using a newly developed instrument, the Essen biopsy forceps, was reported to be effective in the diagnosis of choroidal tumors in 20 patients.[62] After performing a standard 23G vitrectomy, Akgul and colleagues used a modified version of a CE-certified intraocular forceps, which was redesigned to capture and hold a sufficient tissue sample, to grasp a biopsy of the tumor. Laser is applied prophylactically to the retinotomy site, but no fluid–gas exchange was performed.

Transscleral Biopsy

The conjunctiva is incised, and the rectus muscles in the involved quadrant are isolated with silk sutures.[63] In biopsies of the choroid and retinal pigment epithelium, the retina tends to bulge into the biopsy site with a risk of retinal tear or incarceration. This risk is reduced by performing a pars plana vitrectomy first.[59] If visualization is adequate, a heavy barrier of photocoagulation, cryotherapy, or diathermy is applied some days preoperatively around the planned biopsy area. Otherwise, endolaser therapy or cryotherapy is applied at the time of vitrectomy. The biopsy site is marked on the sclera, and a 6 × 6 mm scleral flap, nearly full-thickness and hinged (usually posteriorly), is dissected beginning about 5–6 mm posterior to the limbus, depending on the lesion site. The flap is retracted, exposing a near-bare choroid with a few remaining thin fibers of overlying sclera. Diathermy or cautery is done along the outer margin of the inner choroidal bed. A sharp blade is used to make an incision, or two parallel incisions, through the choroid (and retina, if retina is to be removed). One blade of a 0.12 forceps is placed through the incision, and the biopsy specimen is grasped at one edge. The block excision is then completed with Vannas scissors (Fig. 127.22). During removal of the specimen, particular attention is directed at grasping the tissue only once and ensuring that the entire specimen is delivered in one piece. If the retina is not being removed, it is carefully separated from the choroid and left intact. The biopsy specimen is then placed in

fixative or handled as planned with the pathologist. Any prolapsed vitreous is then removed from the wound, and the scleral flap is sutured with interrupted 9–0 nylon or 7–0 Vicryl. Fluid–gas exchange is performed.

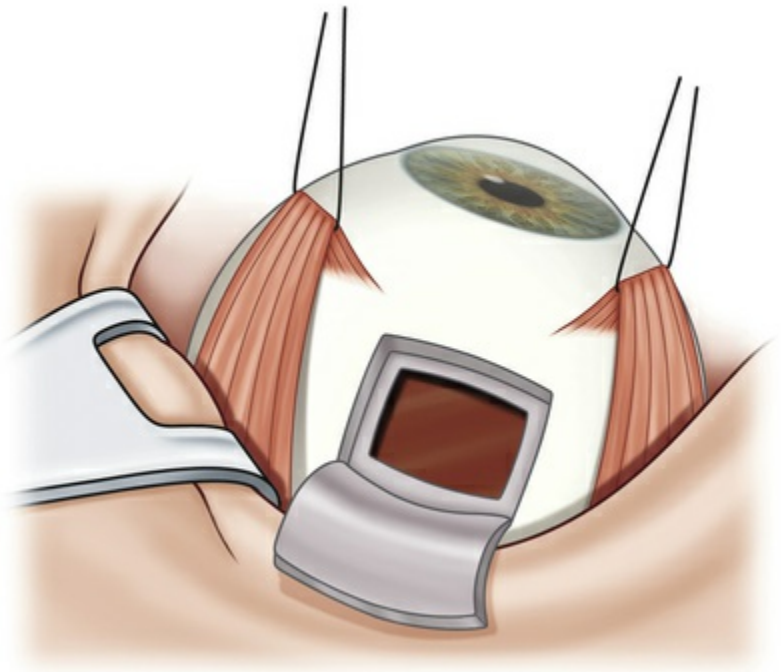

FIG. 127.22 Technique of transscleral choroidal biopsy. After the area planned for biopsy is delimited by photocoagulation or cryotherapy and a pars plana vitrectomy is performed, the biopsy site is carefully marked on the sclera and a scleral flap (usually hinged posteriorly) is developed. The near full-thickness scleral flap is retracted, and the choroidal tissue and overlying thin scleral lamellae are incised with a sharp blade. Scissors may be used to complete the dissection.

Another technique for obtaining a specimen of sclera, choroid, retinal pigment epithelium, and retina from the eye is to use a corneal trephine and to reconstitute the eye wall with a full-thickness donor scleral graft. In this situation, hemostasis may be improved by systemic hypotensive anesthesia.[53,54,64]

Cyanoacrylate tissue glue can be used to stabilize the choroidal specimen before its removal from the eye.[53,54] A drop of

cyanoacrylate glue is applied to the exposed choroid, forming a dense plaque that can be grasped or glued to an arrowhead sponge.

Histologic Technique and Preparations

Handling of the choroidal or chorioretinal biopsy specimen depends greatly on the amount of tissue harvested. Consultation with the pathologist is important to prioritize the tests that can be performed. Ideally, the tissue can be divided into three parts in a sterile manner under a dissecting microscope for microbiology, tissue culture, routine light histologic and immunopathologic studies, and electron microscopy.[1]

Results

Martin et al.[63] reported their results with chorioretinal biopsy performed on seven eyes with progressive chorioretinal lesions of unknown cause. Chorioretinal biopsy provided useful information for determining the diagnosis (multifocal choroiditis with subretinal fibrosis, sarcoidosis, and viral retinitis) and led to change of therapy in five patients. Final visual acuity was unchanged or improved in five eyes.

Foulds and colleagues[10,43,53,54] reported on 34 transscleral biopsies of the choroid and retina for the diagnosis of choroidal melanoma, acute retinal necrosis, chronic uveitis, and progressive retinal pigment epitheliopathy. An adverse event occurred in only one case: a retinal break developed, with associated vitreous hemorrhage and resultant proliferative vitreoretinopathy. Initial vitrectomy might have prevented this complication.[10,43,53,54]

Case 127.6

A 58-year-old man with a history of prostate cancer, thought to be in remission, had an amelanotic intraocular mass OS at presentation. Echographic study showed a plaque on the surface of the mass similar to a previously reported benign fibrous tumor. Needle aspiration biopsy was nondiagnostic. Because of tumor enlargement, choroidal biopsy was performed and disclosed features diagnostic of metastatic carcinoma of the prostate (Fig. 127.23).

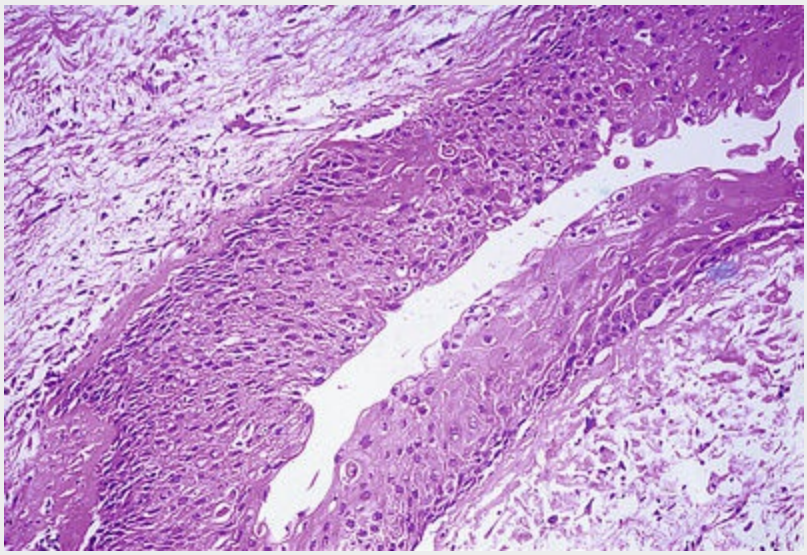

FIG. 127.23 Biopsy of an amelanotic choroidal mass in this 59-year-old man with prostatic carcinoma without known metastases revealed stratified squamous epithelium that was later determined to be squamous metaplasia of prostate carcinoma under the influence of estrogen therapy. The cells stained positive for prostate-specific antigen phosphatase and prostate-specific antigen, which is diagnostic of prostatic carcinoma, with the mass infiltrating the choroidal tissue.

Fine-Needle Biopsy

Fine-needle aspiration biopsy techniques have been used extensively in the diagnostic evaluation of many human tumors, including tumors of the orbit and eye.[65] With an ever-increasing knowledge of gene expression profiling, clinicians have the ability to provided prognostication in such entities as choroidal melanoma with these minimally invasive techniques.[66,67] Furthermore, imaging modalities such as spectral domain optical coherence tomography can be utilized to assist in location and wound architecture of the fine-needle biopsy.[68] Although there is a theoretical risk of tumor dissemination along the needle track, no such occurrence has been documented with a needle of 25G or finer; nor has vitreous hemorrhage or retinal detachment been a problem.[69,70]

Surgical Technique

The technique involves 22G–30G disposable needles for intraocular aspiration.[71,72] The length of the needle selected depends on the intraocular location of the tumor and the planned biopsy route. The biopsy needle is connected to a 10-mL plastic disposable aspirating syringe via a standard plastic tubing. The connector tubing is used so that there will be no induced movement in the needle tip during the biopsy as the assistant exerts suction in the line for aspiration (Fig. 127.24).

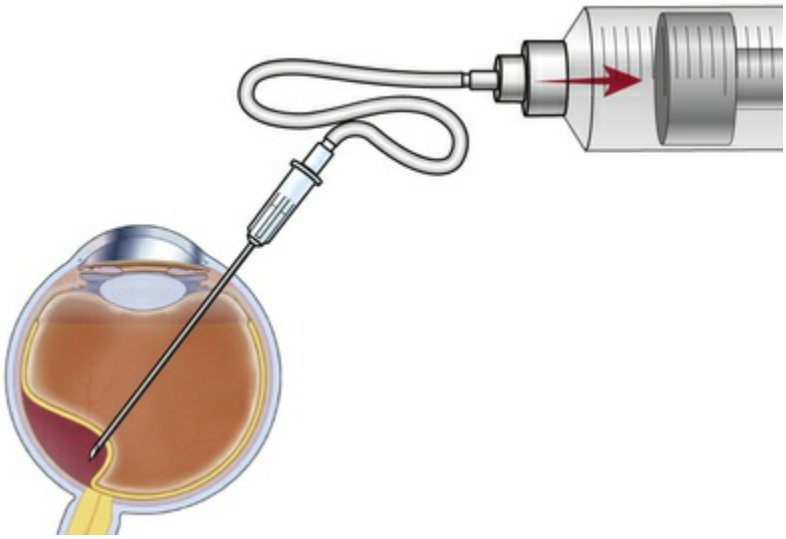

FIG. 127.24 Technique of fine-needle aspiration biopsy. A 25-gauge, 1½-inch needle is inserted through the pars plana in this eye and into the tumor, which is located posteriorly. Once the needle is within the lesion to be biopsied, an assistant exerts forceful suction on a 10-mL syringe connected to the needle via tubing.

Results

Transscleral fine-needle aspiration biopsy can be feasible in diagnosing choroidal melanoma. In addition, aspiration biopsy may assist in assessing cytogenetics of these tumors. In a prospective, interventional case series, 30G fine-needle aspiration biopsy diagnosed macular choroidal melanoma in 17 of 24 (71%) eyes.[65] Adverse events such as submacular hemorrhage (nine eyes) and

vitreous hemorrhage (five eyes) resolved spontaneously within 1 month of the biopsy. In addition, four eyes had retinal perforation, but this did not require treatment and did not result in retinal detachment. Examples of cellular specimens obtained by needle aspiration biopsy are seen in Fig. 127.25.

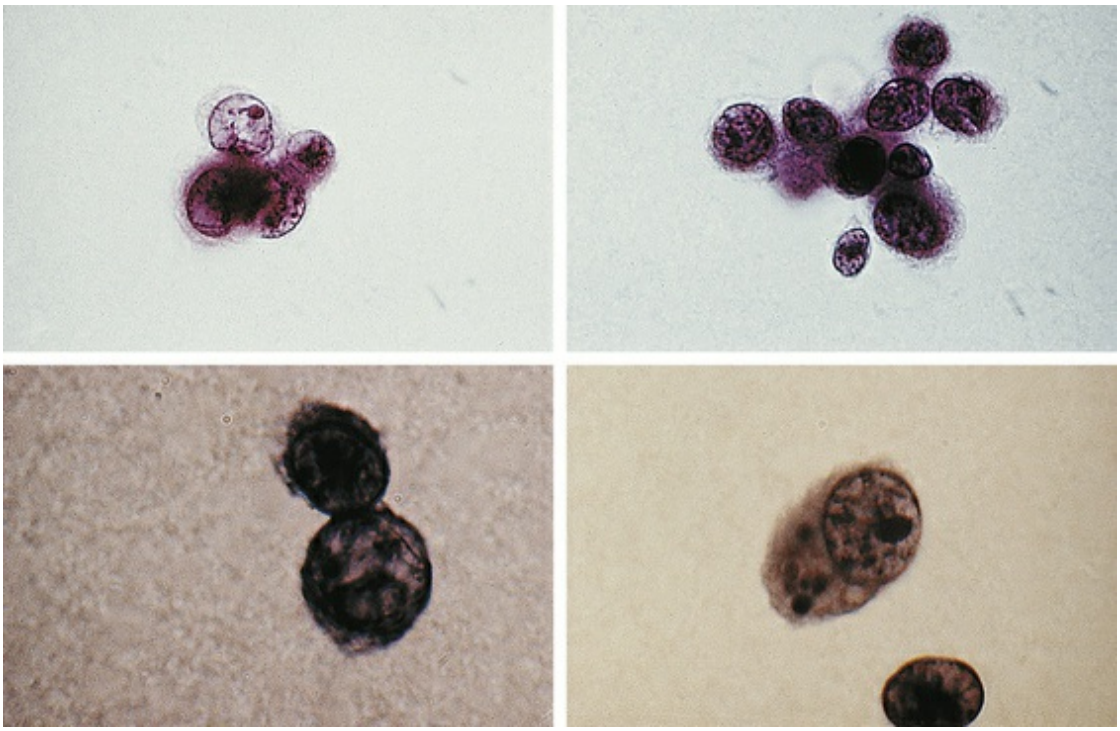

FIG. 127.25 Examples of tumor cells obtained by needle aspiration biopsy. The large tumor cell in the lower right box has pigment in the cytoplasm and a large round nucleus with prominent nucleolus, characteristic of malignant melanoma.

Complications of Intraocular Biopsy

The risks of intraocular biopsy are those of vitreoretinal surgery in general. These include increased intraocular pressure, cataract progression, peripheral retinal tears, retinal detachment, choroidal hemorrhage, vitreous hemorrhage, endophthalmitis, exacerbation of the underlying inflammatory disease, and proliferative vitreoretinopathy.[65] The most hazardous of the biopsy procedures is the transscleral choroidal or retinochoroidal resection.

Conclusion

Vitreous, retinal, and choroidal biopsy have roles in the management of disorders of the posterior segment of the eye. Noninvasive means of establishing a diagnosis are exhausted before surgical procedures are considered. In some patients, however, the clinical appearance and serologic and other laboratory investigations are nondiagnostic, and a biopsy is recommended if there is substantial likelihood that the results will improve patient management. Advancements in surgical instrumentation and diagnostic studies have increased the yield from vitreous, retinal, and choroidal biopsies, and these procedures can be safely performed by retina surgeons who are faced with diagnostic dilemmas.

References

1. Nussenblatt RB, Davis JL, Palestine AG. Chorioretinal biopsy for diagnostic purposes in cases of intraocular inflammatory disease. *Dev Ophthalmol*. 1992;23:133–138.
2. Henderly DE, Genstler AJ, Smith RE, et al. Changing patterns of uveitis. *Am J Ophthalmol*. 1987;103:131–136.
3. Park SS, D'Amico DJ, Foster CS. The role of invasive diagnostic testing in inflammatory eye diseases. *Int Ophthalmol Clin*. 1994;34:229–238.
4. Green WR. Diagnostic cytopathology of ocular fluid specimens. *Ophthalmology*. 1984;91:726–749.
5. Michels RG, Green WR, Engel HM, et al. Diagnostic vitrectomy. Jakobiec FA, Sigelman J. *Techniques in ocular surgery*. WB Saunders: Philadelphia; 1984.
6. Vertes D, Snyers B, De Potter P. Cytomegalovirus retinitis after low-dose intravitreous triamcinolone acetonide in an immunocompetent patient: a warning for the widespread use of intravitreous corticosteroids. *Int Ophthalmol*. 2010;5:595–597.
7. Bharathi MJ, Murugan N, Rameshkumar G, et al. Comparative evaluation of uniplex, nested, semi-nested, multiplex and nested multiplex PCR methods in the

identification of microbial etiology of clinically suspected infectious endophthalmitis. *Curr Eye Res*. 2013;38:550–562.
8. Ogawa M, Sugita S, Shimizu N, et al. Broad-range real-time PCR assay for detection of bacterial DNA in ocular samples from infectious endophthalmitis. *Jpn J Ophthalmol*. 2012;56:529–535.
9. Parolini B, Prigione G, Romanelli F, et al. Postoperative complications and intraocular pressure in 943 consecutive cases of 23-gauge transconjunctival pars plana vitrectomy with 1-year follow-up. *Retina*. 2010;107–111.
10. Foulds WS. The uses and limitations of intraocular biopsy. *Eye*. 1992;6:11–27.
11. Stoflet ES, Koeberl DD, Sarkar G, et al. Genomic amplification with transcript sequencing. *Science*. 1988;239:491–494.
12. Hykin PG, Tobal K, McIntyre G, et al. The diagnosis of delayed post-operative endophthalmitis by polymerase chain reaction of bacterial DNA in vitreous samples. *J Med Microbiol*. 1994;40:408–415.
13. Katai N, Nuriowa S, Fujimori K, et al. Diagnosis of intraocular lymphoma by polymerase chain reaction. *Graefes Arch Clin Exp Ophthalmol*. 1997;235:431–436.
14. Lohmann CP, Linde HJ, Reischl U. Rapid diagnosis of infectious endophthalmitis using polymerase chain reaction (PCR) as supplement to conventional microbiological diagnostic methods. *Klin Monatsbl Augenheilkd*. 1997;211:22–27.
15. Norose K, Tokushima T, Yano A. Quantitative polymerase chain reaction in diagnosing ocular toxoplasmosis. *Am J Ophthalmol*. 1996;121:441–442.
16. Yeh S, Weichel ED, Faia LJ, et al. 25-gauge transconjunctival sutureless vitrectomy for the diagnosis of intraocular lymphoma. *Br J Ophthalmol*. 2010;94:633–638.
17. Engel HM, Green WR, Michels RG, et al. Diagnostic vitrectomy. *Retina*. 1981;1:121–149.
18. Michels RG, Knox DL. Reticulum cell sarcoma: diagnosis by pars plana vitrectomy. *Arch Ophthalmol*. 1975;93:1331–1335.
19. Piro P, Pappas HR, Erozan YE, et al. Diagnostic vitrectomy

in metastatic breast carcinoma in the vitreous. *Retina*. 1982;2:182–188.
20. Malinowski SM. The vitreous trap: a simple, surgeon-controlled technique for obtaining undiluted vitreous and subretinal specimens during pars plana vitrectomy. *Retina*. 2010;30:828–829.
21. Engel H, de la Cruz Z, Jimenez-Abalahin LD, et al. Cytopreparatory techniques for eye fluid specimens obtained by vitrectomy. *Acta Cytol*. 1982;26:551–560.
22. Oshima Y, Wakabayashi T, Ohguro N, et al. A 27-gauge sharp-tip short-shaft pneumatic vitreous cutter for transconjunctival sutureless vitreous biopsy. *Retina*. 2011;31:419–421.
23. Oshima Y, Wakabayashi T, Sato T, et al. A 27-gauge instrument system for transconjunctival sutureless microincision vitrectomy surgery. *Ophthalmology*. 2010;117:93–102.
24. Rajagopal R, Harbour JW. Diagnostic testing and treatment choices in primary vitreoretinal lymphoma. *Retina*. 2011;31:435–440.
25. Intzedy L, Teoh SC, Hoga A, et al. Cytopathological analysis of vitreous in intraocular lymphoma. *Eye*. 2008;22:289–293.
26. Grimm SA, McCannel CA, Omuro AM, et al. Primary CNV lymphoma with intraocular involvement: International PCNSL Collaborative Group Report. *Neurology*. 2008;71:1355–1360.
27. Endophthalmitis Vitrectomy Study Group. Results of the Endophthalmitis Vitrectomy Study. *Arch Ophthalmol*. 1995;113:1479–1496.
28. Van Gelder RN. Polymerase chain reaction diagnostics for posterior segment disease. *Retina*. 2003;23:445–452.
29. Melo GB, Bispo PJ, Campos Pignatari AC, et al. Real-time polymerase chain reaction test to discriminate between contamination and intraocular infection after cataract surgery. *J Cataract Refract Surg*. 2011;37:1244–1250.
30. Lohmann CP, Linde HJ, Reischl U. Improved detection of microorganisms by polymerase chain reaction in delayed endophthalmitis after cataract surgery. *Ophthalmology*.

2000;107:1047–1051.
31. Salman AG, Mansour DE, Radwan AA, et al. Polymerase chain reaction in pediatric post-traumatic fungal endophthalmitis among Egyptian children. *Ocul Immunol Inflamm*. 2010;18:127–132.
32. Harper TW, Miller D, Schiffman JC, et al. Polymerase chain reaction analysis of aqueous and vitreous specimens in the diagnosis of posterior segment infectious uveitis. *Am J Ophthalmol*. 2009;147:140–147.
33. Garweg J, Fenner T, Bohnke M, et al. An improved technique for the diagnosis of viral retinitis from samples of aqueous humor and vitreous. *Graefes Arch Clin Exp Ophthalmol*. 1993;231:508–513.
34. Mitchell SM, Fox JD. Aqueous and vitreous humor samples for the diagnosis of cytomegalovirus retinitis. *Am J Ophthalmol*. 1995;120:252–253.
35. Mitchell SM, Fox JD, Tedder RX, et al. Vitreous fluid sampling and viral genome detection for the diagnosis of viral retinitis in patients with AIDS. *J Med Virol*. 1994;43:336–340.
36. McCann JD, Margolis TP, Wong MG, et al. A sensitive and specific polymerase chain reaction-based assay for the diagnosis of cytomegalovirus retinitis. *Am J Ophthalmol*. 1995;120:219–226.
37. Wiedbrauk DL, Werner JC, Drevon AM. Inhibition of PCR by aqueous and vitreous fluids. *J Clin Microbiol*. 1995;33:2643–2646.
38. Palexas GN, Green WR, Goldberg MF, et al. Diagnostic pars plana vitrectomy: report of a 21-year retrospective study. *Trans Am Ophthalmol Soc*. 1995;93:623–684.
39. Moshfeghi DM, Dodds EM, Couto CA, et al. Diagnostic approaches to severe, atypical toxoplasmosis mimicking acute retinal necrosis. *Ophthalmology*. 2004;111:716–725.
40. Bottos J, Miller RH, Belfort RN, UNIFESP Toxoplasmosis Group, et al. Bilateral retinochoroiditis caused by an atypical strain of *Toxoplasma gondii*. *Br J Ophthalmol*. 2009;93:1546–1550.
41. Hong BK, Nazari Khanamiri H, Rao NA. Role of ultra-

widefield fluorescein angiography in the management of uveitis. *Can J Ophthalmol*. 2013;48(6):489–493.
42. Karampelas M, Sim DA, Chu C, et al. Quantitative analysis of peripheral vasculitis, ischemia, and vascular leakage in uveitis using ultra-widefield fluorescein angiography. *Am J Ophthalmol*. 2015;159(6):1161–1168.
43. Foulds WS, Lee WR, Roxburg STD, et al. Can chorioretinal biopsy be justified? *Trans Ophthalmol Soc U K*. 1985;104:866–868.
44. Freeman WR, Stern WH, Gross JG, et al. Pathologic observations made by retinal biopsy. *Retina*. 1990;10:195–204.
45. Freeman WR, Thomas AEL, Rao NA. Demonstration of herpes group virus in acute retinal necrosis syndrome. *Am J Ophthalmol*. 1986;102:701–709.
46. Freeman WR, Wiley CA, Cross JG, et al. Endoretinal biopsy in immunosuppressed and healthy patients with retinitis: indications, utility, and techniques. *Ophthalmology*. 1989;96:1559–1565.
47. Warren K, Goldstein E, Hung VS, et al. Use of retinal biopsy to diagnose *Bartonella* (formerly *Rochalimaea*) *henselae* retinitis in an HIV-infected patient. *Arch Ophthalmol*. 1998;116:937–940.
48. Rutzen AR, Ortega-Larrocea G, Dugel PU, et al. Clinicopathologic study of retinal and choroidal biopsies in intraocular inflammation. *Am J Ophthalmol*. 1995;119:597–611.
49. Johnston RL, Tufail A, Lightman S, et al. Retinal and choroidal biopsies are helpful in unclear uveitis or suspected infectious or malignant origin. *Ophthalmology*. 2004;111:522–528.
50. Lopez JS, Chan CC, Burnier M. Immunohistochemistry findings in primary intraocular lymphoma. (Letter). *Am J Ophthalmol*. 1991;112:472–474.
51. Ridley ME, McDonald HR, Sternberg P Jr. Retinal manifestations of ocular lymphoma (reticulum cell sarcoma). *Ophthalmology*. 1992;99:1153–1161.
52. Barondes MJ, Sponsel WE, Stevens TS, et al. Tuberculous

choroiditis diagnosed by chorio-retinal endobiopsy. *Am J Ophthalmol*. 1991;112:460–461.
53. Foulds WS. The local excision of choroidal melanomata. *Trans Ophthalmol Soc U K*. 1973;93:343–346.
54. Foulds WS, Damato BE, Burton RL. Local resection of choroidal melanoma. Bornfeld N, Gragoudas ES, Hopping W. *Tumors of the eye*. Kugler: Amsterdam; 1991.
55. Peyman GA. Internal retinal biopsy: surgical technique and results. *Int Ophthalmol*. 1990;14:101–104.
56. Peyman GA, Fishman GA, Sanders DR, et al. Biopsy of human chorioretinal tissues. *Invest Ophthalmol Vis Sci*. 1975;14:707–710.
57. Peyman GA, Juarez CP, Diamond JG, et al. Ten years' experience with eye wall resection for uveal malignant melanomas. *Ophthalmology*. 1984;91:1720–1725.
58. Peyman GA, Maisel SH, Batko KA, et al. An experimental approach to the tissue diagnosis and study of choroidal and retinal lesions. *Invest Ophthalmol Vis Sci*. 1975;14:484–487.
59. Peyman GA, Raichand M. Full thickness eye wall resection of choroidal neoplasms. *Ophthalmology*. 1978;6:1024–1036.
60. Cole CJ, Kwan AS, Laidlaw DAH, et al. A new technique of combined retinal and choroidal biopsy. *Br J Ophthalmol*. 2008;92:1357–1360.
61. Westerfeld C, Mukai S. Retinal and choroidal biopsy. *Int Ophthalmol Clin*. 2009;49:145–154.
62. Akgul H, Otterbach F, Bornfeld N, et al. Intraocular biopsy using special forceps: a new instrument and refined surgical technique. *Br J Ophthalmol*. 2011;95:79–82.
63. Martin DF, Chi-Chao C, de Smet MD, et al. The role of chorioretinal biopsy in the management of posterior uveitis. *Ophthalmology*. 1993;100:705–714.
64. Constable IG, Chester GH, Horne R, et al. Human chorioretinal biopsy under controlled systemic hypotensive anaesthesia. *Br J Ophthalmol*. 1980;64:659–664.
65. Young TA, Burgess BL, Rao NP, et al. Transscleral fine-needle aspiration biopsy of macular choroidal melanoma. *Am J Ophthalmol*. 2008;145:297–302.
66. Bagger M, Andersen MT, Heegaard S, et al. Transvitreal

retinochoroidal biopsy provides a representative sample from choroidal melanoma for detection of chromosome 3 aberrations. *Invest Ophthalmol Vis Sci*. 2015;56:5917–5924.
67. McCannel TA. Fine-needle aspiration biopsy in the management of choroidal melanoma. *Curr Opin Ophthalmol*. 2013;24:262–266.
68. Murray TG, Gold AS, Markoe AM, et al. Spectral-domain optical coherence tomography evaluation of choroidal melanoma and nevus fine-needle aspiration biopsy incision sites. *Ophthalmic Surg Lasers Imaging Retina*. 2014;45:165–168.
69. Henkes HE, Manschott WA. The danger of diagnostic biopsy in eyes suspected of an intraocular tumour. *Ophthalmologica*. 1963;145:467–469.
70. Reese AB. *Tumors of the eye*. 3rd ed. Harper & Row: Hagerstown; 1976.
71. Augsburger JJ, Shields JA. Fine-needle aspiration biopsy of solid intraocular tumors: indications, instrumentation and techniques. *Ophthalmic Surg*. 1984;15:34–40.
72. Czerniak B, Woyke S, Domagala W. Fine needle aspiration cytology of intraocular malignant melanoma. *Acta Cytol*. 1983;27:157–165.

128

Transplantation Frontiers

Vamsi K. Gullapalli, Mohamad A. Khodair, Anton M. Kolomeyer, Ilene K. Sugino, Steven Madreperla, Marco A. Zarbin

Introduction

In 1959, Paris Royo and Wilbur Quay reported experiments that were among the earliest steps taken in intraocular retinal cell transplantation.[1] Using a paradigm originally developed by Van Dooremaal,[2] Royo and Quay transplanted rat fetal retina into the

anterior chamber of maternal rat eyes. Prolonged graft survival and a normal rate of graft development and differentiation were noted. Expanding on this work, del Cerro and his colleagues[3] transplanted embryonic rat retina into the anterior chamber of adult eyes from various rat strains with similar results. After Gouras and coworkers[4] successfully transplanted cultured human retinal pigment epithelium (RPE) cells to monkey Bruch's membrane from which the retina had been removed, Li and Turner, in 1988, reported prevention of photoreceptor cell degeneration by RPE transplants in the Royal College of Surgeons (RCS) rat, an animal with an inherited defect causing impaired RPE phagocytosis of outer segments and progressive RPE and photoreceptor death.[5,6] Li and Turner's work, which has been replicated by many investigators, was the first successful treatment of retinal degeneration with cellular transplantation.

In principle, successful transplantation requires graft survival and integration with the host. Graft survival depends on a number of factors, both immunologic and non-immunologic,[7] that will be discussed in this chapter. Regarding graft–host integration, RPE cell transplants integrate readily with host photoreceptors through the extension of apical villous RPE processes around photoreceptor outer segments. In contrast, synapse formation between retinal grafts and host retina is much more complex. Experiments in the central nervous system, however, have established the possibility that synapse formation between donor and host neural tissue can occur. For example, Lund and others[8,9] demonstrated that embryonic retina transplanted into neonatal and adult rat tectum develops the proper layering of the normal retina and extends neuronal projections only to the normal retinorecipient structures, i.e., the superior colliculus, the pretectum, and the dorsal lateral geniculate nucleus. Similarly, intraocular retinal transplants establish with their targets functional connections that elicit light-driven visual response[10] and mediate visual behaviors.[11,12] These and other studies[13,14] have stimulated interest in transplantation as a treatment for retinal disease. The background and rationale for transplantation, results of transplants in experimental animals and humans, immune response to transplanted tissue, nonimmunologic causes of graft failure, and future directions for development of

transplantation for RPE and photoreceptor grafts will be considered in this chapter.

Background and Rationale for RPE Transplantation in Age-Related Macular Degeneration

Late complications of age-related macular degeneration (AMD) are major causes of irreversible loss of central vision among the elderly.[15,16] Severe visual loss in AMD occurs due to growth of abnormal blood vessels (choroidal new vessels, CNVs) under the RPE and retina with secondary exudative retinal detachment, subretinal hemorrhage and lipid exudation, and outer retinal degeneration.[17] It can also result from atrophy of RPE with consequent atrophy of overlying photoreceptors and underlying choriocapillaris (geographic atrophy, GA). The prevalence of AMD-associated CNV or GA is approximately 1.47%, increasing to 10% in people older than 80 years.[18] There is no fully effective therapy for either CNVs or GA. Blocking the effects of vascular endothelial growth factor (VEGF) by frequent intravitreal injection of antibodies is the best currently available treatment for CNVs, but only 30–40% of the patients experience a moderate visual improvement.[19–21] Cell-based therapy, which involves placing cells in the subretinal space, potentially offers a better option compared to pharmacologic monotherapy with anti-VEGF agents. Advantages of such an approach would include long-term therapy without frequent minor surgical injections with medications; since cells like RPE produce numerous factors that help maintain the normal retinal and choroidal anatomy and physiology,[19,22–26] transplantation of such cells could provide a richer and more effective therapy that is less susceptible to treatment resistance;[27] cell transplantation could potentially restore the subretinal anatomy that is altered by growth (and surgical removal) of CNVs or by atrophy of RPE. Another indication for transplantation of RPE in AMD might be in patients who develop RPE tears[28] while receiving anti-VEGF therapy,[29] which have a poor visual prognosis. RPE transplantation in patients with exudative macular degeneration might require

prior removal of CNVs, which would result in loss of adjacent native RPE and the subjacent RPE basement membrane,[30,31] causing a more complex graft bed than normal. On the other hand, in GA, transplantation of cells would involve resurfacing of the atrophic areas with less surgical manipulation with the goal of restoring the normal structure and function of the photoreceptor–RPE–choriocapillaris complex.

A number of preclinical experiments in animal models have demonstrated that transplantation of cells, e.g., RPE or stem cells or cells secreting growth factors, into the subretinal space can prevent photoreceptor degeneration and preserve function.[32–38] The RCS rat is used commonly for these studies. A recessive mutation in merTK tyrosine kinase receptor in RPE[6] causes a failure of outer segment phagocytosis by the RPE. Consequently, debris accumulates in the subretinal space, and there is eventual loss of photoreceptors causing blindness. Transplantation of RPE into the subretinal space of RCS rats causes a decrease in the amount of subretinal debris,[34] prevents loss of photoreceptors,[5] maintains synaptic connections of rescued photoreceptors,[39] maintains electroretinography responses in areas of rescued retina,[40] and preserves pupillary light reflexes,[41] cortical visual functions,[32,35] and visual acuity.[35,42,43]

Results of macular translocation surgery may mean that establishment of a healthy subfoveal RPE monolayer in AMD eyes can restore macular function. In macular translocation, the retina is moved so that the fovea is relocated to an area away from submacular disease. This maneuver can result in improved visual acuity.[44,45] However, after translocation, the fovea rests on previously extrafoveal RPE, Bruch's membrane, and choriocapillaris. Thus, the procedure is not completely analogous to an RPE transplant per se. In addition, the recurrence of GA in the new location of the fovea following macular translocation[46] suggests that at least some cases of GA may not be treated successfully with RPE transplantation solely.

Cell Selection for RPE Transplantation

Stem Cell-Derived RPE

Stem cells are undifferentiated cells that have the capacity for self-renewal (i.e., can divide indefinitely to produce more karyotypically stable stem cells) and pluripotency (i.e., produce cells that are destined to differentiate into more than one type of cell).[47–49] (See Chapter 37, Stem cells and cellular therapy.) During the course of differentiation, stem cells form intermediate populations of increasingly committed progenitor cells that have a decreasing proliferative capacity. Embryonic stem cells (ESCs) are derived from the inner cell mass of the blastocyst and are capable of differentiating into cells of all three germ layers.[50,51] Embryonic and fetal tissues (e.g., retina) contain cells that vary in their differentiation status, ranging from progenitor cells, that can proliferate but have a restricted differentiation potential compared to embryonic stem cells, to committed but still immature rods and cones isolated from fetal retina. In adults, multipotent stem cells exist that can differentiate to replace lost or injured cells. Such cells have been isolated from various organs,[52,53] including the eye.[54–56] Stem cells isolated from a particular tissue can be induced to differentiate into cells of an unrelated tissue. Bone marrow cells, for example, can undergo metaplasia to form skeletal muscle;[57] neural stem cells can develop into muscle[58] (Table 128.1). It seems that stem cells exhibit plastic behavior depending upon their environment and signals from damaged tissues.[59] The central nervous system contains neural progenitor cells. They exist in both embryonic and adult tissues and can differentiate into glial and neuronal lineages. The capacities for self-renewal and pluripotency render stem cells candidates to replace lost or injured cells. In summary, potential sources for replacement of RPE include non-eye-derived embryonic stem cells from the blastocyst, bone marrow-derived stem cells, neural progenitor cells, and eye-derived progenitor cells.

TABLE 128.1

Potential Sources of Cells for Retinal Cell Replacement

Cell Type	Potential Developmental Capacity
Totipotent stem cell	Can develop into cells derived from all lineages, i.e.,

(mammalian zygote, blastomeres)	ectoderm, mesoderm, and endoderm, as well as supporting tissues like placenta
Pluripotent stem cell (e.g., embryonic stem cell from inner cell mass)	Can develop into cells derived from all three germ layers (ectoderm, mesoderm, endoderm)
Multipotent stem cell (e.g., retinal progenitor cell)	Can develop into different cell types derived from one lineage
Reprogrammed cell (induced pluripotent cell)	Somatic cell reprogrammed by nuclear transfer, limited transfer of transcription factors, or cell fusion to enhance potency
Immature postmitotic rod precursor cell	Rod photoreceptors
Neural retina and retinal pigment epithelium	Rods, cones, Müller cells, or committed retinal neurons

Modified from Jaenisch R, Young R. Stem cells, the molecular circuitry of pluripotency and nuclear reprogramming. Cell 2008;132:567–82 and Zarbin MA. Retinal pigment epithelium-retina transplantation for retinal degenerative disease. Am J Ophthalmol 2008;146:151–3.

During development, the various retinal cells are derived from a common population of multipotent retinal progenitor cells (RPCs).[60] Embryonic retina can be a potential source of such cells. Such cells exist in adults in lower species like fish and amphibians in the ciliary margin zone (CMZ), located in the retinal periphery, surrounded by a pigmented ciliary margin.[61–63] These cells can regenerate the neural retina throughout the life of the organism.[64] Progenitor cells from chick CMZ can regenerate retina if there is ectopic expression of fibroblastic growth factor and sonic hedgehog.[65] More importantly, retinal progenitor cells have been isolated from mouse eyes and from fetal and adult human eyes.[55,66–69] Efforts to induce RPCs to differentiate into RPE continue,[70,71] and there is evidence that the human eye harbors stem cells that can differentiate into RPE cells.[72]

Due to ethical considerations associated with the use of stem cells from human embryos, methods have been developed to establish stem cell lines without destruction of the embryo.[73,74] It is also possible to generate embryonic stem cells by somatic nuclear transfer, nucleus transfer from an adult, neonatal, or fetal somatic cell into an unfertilized oocyte, whose nucleus has been removed.[75–77] The oocyte would then reprogram the donor nuclear DNA and develop in a normal embryonic pattern and form embryonic stem cells (NT-ESCs). The result of such reprogrammed cells could be the creation of genetically matched cell lines for autologous transplants.[78] However, mitochondrial DNA (mtDNA)

primarily derived from the oocyte can still elicit an immune response. In a humanized mouse study, genetically matched NT-ESCs were rejected based on mtDNA mismatch, but it was possible to induce immunologic tolerance to the allogeneic mitochondrial peptides.[79] However, ethical considerations remain.

Alternatively, adult fibroblasts can be manipulated by transferring into these cells transcription factors like Oct4, Sox2, Klf4, and c-Myc that can reactivate developmentally regulated genes, thus inducing the cells to become an induced pluripotent stem cells (iPSCs).[80,81] Nuclear transfer may be more effective at establishing the ground state of pluripotency than factor-based reprogramming, which can leave an epigenetic memory of the tissue of origin that may influence efforts at directed differentiation for applications in disease modeling or treatment.[82,83] Although iPSCs are pluripotent stem cells, iPSCs and ESCs do differ in some important ways. iPSCs have the theoretical advantage of not being rejected by the patient from whom they are derived (versus ESCs, unless the ESCs were harvested from the patient as an embryo). Abnormal gene expression in some cells differentiated from iPSCs (both via a retroviral and episomal approach), however, can induce a T-cell-dependent immune response in a syngeneic recipient.[84] This response is likely due to the abnormal expression of antigens (e.g., Zg16, Hormad1) not expressed during normal development or differentiation of ESCs, leading to loss of tolerance.[84] Expression of these antigens is a reflection of epigenetic differences (e.g., DNA methylation) between iPSCs and ESCs.[85,86] These differences may not be relevant in terminally differentiated iPSCs, as immunogenicity of autologous differentiated iPSCs may depend on the terminal cell type. In a humanized mouse study, differentiated autologous iPSC-RPE were not immunogenic while differentiated iPSC-smooth muscle cells (iPSC-SMC) were highly immunogenic.[87]

RPE can be derived easily from embryonic stem cells (perhaps because RPE develop early during embryogenesis)[42,70,88–90] as well as from iPSCs.[91–95] Stem cell-derived RPE have been shown to express RPE properties such as ion transport, membrane potential, transepithelial resistance, polarized vascular endothelial growth factor secretion, neurotrophic factor secretion, visual pigment recycling, pigmentation, and gene expression profiles similar to

those of native RPE.[96–103] Rodent models of retinal degeneration have demonstrated the ability of iPSC-RPE and ESC-RPE to perform some RPE functions in vivo (e.g., trophic factor secretion, photoreceptor rescue, preservation of visual function, visual pigment recycling).[24,38,42,97,99,104]

With stem cells, there is a risk of dedifferentiation in the subretinal space and potentially developing into a teratoma. Indeed, in one study, when embryonic stem cell-derived neural cell precursors were injected into mouse subretinal space, 50% of the eyes developed teratomata within 8 weeks.[105] However, in another study, a more stringent selection of 18 different human embryonic stem cell lines did not result in teratoma formation.[42] In yet another study, 7 iPSC and 5 ESC mouse lines were compared to assess teratoma rates in C57BL/6 wild-type mice. Both stem cells showed a high incidence of teratoma formation with no statistically significant differences between ESC and iPSC lines.[106] Tumorigenicity of ESC and iPSC lines may thus be cell line-dependent. Regardless, iPSCs are more prone to genetic instability than ESCs. With iPSCs, there is a risk of insertional mutagenesis due to the use of viral vectors, and risk of teratoma formation due to the use of oncogenic factors such as c-Myc, during cell production. Newer techniques of iPSC production using nonintegrating reprogramming methods[107–109] lessen such concerns. In a study comparing integrating (lentiviral) and nonintegrating (episomal or Sendai virus vectors) reprogramming for iPSC generation, nonintegrating reprogramming was found to yield a more stable genome, using the parental cell line genotype for comparison.[109] Genomic stability is critical to prevent genetic aberrations associated with cancer. The inherent tumorigenicity risk of undifferentiated stem cells, particularly iPSCs, emphasizes the importance of monitoring genomic stability and assessing the purity of iPSC-RPE cultures for patient use. With ESC-RPE, the risk may not be as great; an ESC-RPE preparation currently in use in clinical trials showed no tumor formation in mice undergoing subretinal injections of ESC-RPE containing up to 1% undifferentiated ESCs. ESCs alone formed teratomata by 2 months post-subretinal injection.[110] These studies suggest that a critical number of undifferentiated stem cells must be present for tumor

formation. iPSC-RPE preparations, using the method generated for a clinical study, showed no tumor formation after subretinal injection in albino nude rats, RCS rats, and nonhuman primates.[99,111] In these studies of iPSC-RPE, a highly sensitive qRT-PCR method was used to detect residual iPSCs to establish purity of iPSC-RPE cultures.[112]

Recently, in situ RPE (native) were found to contain a small population of multipotent cells (RPESC) that can be expanded in culture and redifferentiated into RPE.[56] In addition to offering the possibility of a more efficient way to generate RPE, RPESCs have limited differentiation potential and therefore may be safer than iPSC-RPE for patient transplantation.[113–115] One potential disadvantage of RPESCs is their limited expansion capability.

Autologous bone marrow-derived stem cells (BMSCs) are another potential source of stem cells. BMSCs can be enriched by selecting for cells with RPE differentiation potential by cell sorting based on surface markers ($C35^{+}C38^{-}$); these cells can then be induced to differentiate into RPE by co-culturing with mitomycin C-inactivated RPE cells.[116,117] Although BMSC-RPE tested positive for some RPE markers and were shown to phagocytose outer segments, it is not clear that fully functional RPE cells can be generated with this approach. Thus far, studies have described the differentiated cells at early time points only, and full characterization has not been reported.[117] RPE derived from mouse BMSCs that have been transplanted into subretinal space of RCS rats rescue photoreceptors.[118] Additional experiments are needed to determine whether one source is preferable or whether several different sources might be equivalent in their potential to provide RPE cells for clinical use. To be useful for cell-based replacement therapy, stem cells must have the following properties:

1. Proliferate extensively to generate sufficient quantities of material to serve as a “universal donor” and maintain genetic stability after expansion.

2. Differentiate into the desired cell type(s). ESC-derived RPE can spontaneously dedifferentiate to non-RPE-like cells and spontaneously redifferentiate into RPE-like cells, indicating phenotypic instability.[119] The cultures may not retain a stable

phenotype after 5–8 passages. ESCs and iPSCs vary in their tendency to differentiate into cells of a given lineage.[82,119] As mentioned above, a number of different criteria should be applied to define a "differentiated" RPE[48] and photoreceptor cell.[120] The retinal and subretinal microenvironment can influence the differentiation and functionality of transplanted cells, including expression of developmental markers and markers of proliferation.[121,122]

3. Survive in the recipient after transplantation.

4. Integrate into the surrounding tissue after transplantation.

5. Function appropriately for the duration of the recipient's life.

RPE cell transplants are an attractive starting-point for cell-based combination replacement and rescue therapy in the eye because: (1) ESCs and iPSCs can be induced to differentiate into RPE relatively easily, and, at least in the case of ESC–RPE, one can generate large quantities of cells with stable genotype and appropriate phenotype; (2) RPE cells integrate easily with host photoreceptors; (3) RPE cells elaborate trophic substances that support photoreceptors;[24,35,103] (4) there is abundant evidence for transplant efficacy in pre-clinical models; (5) diseases in which RPE cells appear to be targeted primarily include Best disease[123,124] and some forms of retinitis pigmentosa,[125–127] and secondarily include Stargardt macular dystrophy[128,129] and AMD.[130,131] However, abnormalities in Bruch's membrane may prevent transplanted stem cell-derived RPE from surviving and differentiating long-term in AMD eyes.[24] Since Bruch's membrane is derived from mesoderm, there is no expectation that ESC- or iPSC-derived RPE will manufacture Bruch's membrane.

Non-RPE Subretinal Cell Transplants

Non-RPE cell-based therapy for AMD involves subretinal transplantation of cells that can perform some, if not all, RPE functions and may offer an advantage over transplantation of stem cell-derived RPE. At a minimum, non-RPE cells must be able to

survive in the subretinal space following transplantation without tumor formation and support the photoreceptors and/or RPE. Neural progenitor cells (NPCs) derived from iPSCs (iPSC-NPCs)[132] or ESCs (ESC-NPCs)[133] and human central nervous system stem cells (HuCNS-SCs)[134,135] rescue photoreceptors in the RCS rat. After subretinal injection, iPSC-NPCs, ESC-NPCs, and HuCNS-SCs migrated out from the injection site, survived long-term in the subretinal space, preserved native RPE and photoreceptors, preserved visual function, and showed no tumor formation. Importantly, iPSC-NPCs and HuCNS-SCs ingested and degraded photoreceptor outer segments.[132,135] NPCs have the capacity to migrate to damaged sites, secrete a host of factors, including immune mediators and trophic factors, and remain undifferentiated after transplantation.[136,137] Because of the migration potential of NPCs and HuCNS-SCs, cells can be transplanted outside areas of diseased/atrophic RPE. By 40 days after transplantation, HuCNS-SCs cover a 7-mm^2 area.[134] The fovea occupies a 1.8-mm^2 area. Thus, one may be able to transplant these cells in an extrafoveal location with the expectation that they will migrate under the fovea and rescue cones, thus preserving high-acuity vision. Normally, delivery of cells to a subfoveal location requires foveal detachment, which may compromise the patient's vision, particularly in the setting of retinal degenerative disease.[138] Safety of NPCs has been demonstrated in clinical trials for ALS,[139] cerebral palsy,[140] and spinal cord injury.[141] The safety of subretinal HuCNS-SCs transplants has been demonstrated in phase I/II clinical trials to treat AMD patients (http://www.stemcellsinc.com/Clinical-Programs/AMD).

Additional cell preparations under consideration for subretinal transplantation are bone marrow mesenchymal stem cells (BMSCs) and umbilical cord mesenchymal stem cells (UCMSCs). Both cell preparations offer the possibility of autologous cell transplantation and have been shown to rescue photoreceptors in RCS rats.[142–144] Intravenously injected BMSCs can home into areas of chemically induced RPE loss in mice.[145]

Cell Delivery Strategies

Cell Suspension vs. Polarized Sheet

Delivery of a cell suspension to the subretinal space has the advantage of simplicity, i.e., injection through a small retinotomy after a relatively small retinal detachment is created. However, there is a greater chance of cell efflux into the vitreous cavity following bolus injection relative to cell sheet placement. Injection of a polarized cell sheet, with or without a support, will require a larger retinal detachment, larger retinotomy, and specialized instruments to assure placement of the polarized RPE in the correct orientation and location. Theoretically, cell suspension delivery could cover a larger area while sheet delivery is limited to the size of a sheet that can be manipulated for successful placement. Potential advantages to transplanting sheets of cells on a scaffold are threefold. First, one can transplant cells that are differentiated and organized anatomically, resembling the in situ configuration. Highly differentiated transplanted cells may be better suited for subfoveal RPE transplantation, for example, than RPE suspensions. Once the foveal photoreceptors are detached, they begin to degenerate. Clinically, this process is stopped by reapposition of the retina against functional RPE cells. When RPE cells are delivered as a suspension, time is required for them to attach to Bruch's membrane and to reacquire features of differentiation. In principle, this time interval (up to 1–2 weeks) can be eliminated by use of a scaffold delivering differentiated RPE cells. A second potential advantage is that scaffold delivery may be associated with a lower antigen load. Fewer cells are delivered with scaffolds than with cell suspensions. There may be an advantage to reducing the antigen load with regard to stimulating immune surveillance of the transplanted cells. Third, it may be possible to integrate growth factors, immunomodulatory molecules, or other useful moieties into the scaffold, thus prolonging RPE graft survival as well as photoreceptor survival. In cell culture studies, polarized sheets were found to be less prone to oxidative stress-induced cell death than nonpolarized and subconfluent ESC-RPE.[146] In preclinical animal studies, Schwartz et al.[110] found ESC-RPE integrated into the host RPE layer following bolus injection into the subretinal space of NIH III mice. In a preclinical nonhuman primate study, Kamao et al.[99] found injected iPSC-RPE tended to accumulate in the lower

bleb margin 7 days after cell suspension delivery while iPSC-RPE sheets maintained their position. In the same study, Kamao et al. compared bolus vs. sheet iPSC-RPE transplantation in the RCS rat and found similar extent of photoreceptor preservation and ERG responses. Using a mouse model, Carido et al.[147] found ESC-RPE primarily formed clusters on top of the existing RPE monolayer while in eyes devoid of RPE (killed by iodoacetate); transplanted ESC-RPE formed a monolayer. iPSC-NPCs were primarily layered between the native RPE and photoreceptors after bolus injection into the subretinal space of RCS rats.[132] HuCNS-SC behaved similarly with some integration into the host inner retina in long-term survival animals.[134] Overall, it is difficult to predict how cell suspensions will behave in the human subretinal space, particularly when examining results of rodent studies, since the number of cells injected are relatively high in the small rodent eye. In AMD patients, it is likely that cell survival will be impaired in areas devoid of RPE (i.e., areas of GA), exposing diseased Bruch's membrane (unlike the iodoacetate model used in preclinical studies, where Bruch's membrane is not diseased).[148]

RPE on Scaffold Supports

Transplantation of a monolayer of differentiated, functional RPE on a scaffold support would allow placement of an RPE graft in the right orientation and might even prevent the age-related changes in Bruch's membrane from damaging the transplanted RPE cells.[91,92] In addition to supporting a polarized monolayer of functional RPE, an ideal scaffold would be biocompatible or biodegradable, would have transport and diffusion properties resembling normal Bruch's membrane, would not migrate in subretinal space after surgical delivery, and must have handling properties that would enable tissue delivery without damaging the cells. In addition to natural materials such as gelatin, collagen, and silk, various polymers including parylene, polyester, poly (L-lactide-co-caprolactone), and others have been used with RPE, stem cell-derived RPE, and Schwann cells (reviewed in reference[149]). Advances in biomedical engineering have allowed the manufacture of scaffolds with specific physical properties, thereby enabling the creation of an artificial

Bruch's membrane. As noted above, in addition to the advantage of delivery of a functional RPE monolayer to the subretinal space, scaffold delivery may permit the incorporation of drugs that might retard graft rejection and foster graft integration and/or retinal preservation. A study comparing survival of ESC-RPE cell suspensions with ESC-RPE monolayers on parylene scaffolds following transplantation in immunocompromised nude rats reported that cells on the scaffold survived longer than cell suspensions.[150] To date three substrates have been approved for clinical trials (Table 128.2). In one clinical study, ESC-RPE on a polyester membrane will be introduced into the subretinal space of patients with wet AMD (www.clinical trials.gov). Polyester membranes are a component of transwell culture plates and are used routinely in RPE culture.[151] Aside from the challenges of creating scaffolds with the previously mentioned properties, an instrument must be designed and manufactured to allow precise insertion and placement in the subretinal space without damage to cells and undue damage to the overlying retina.[152]

TABLE 128.2

Stem Cell Studies Approved for Clinical Trials to Treat Macular Degeneration

Sponsor	Cell Designation/Description	Delivery	Disease Target	Study Locations
Chinese Academy of Sciences	ESC-RPE	Subretinal	Dry AMD	Henan and Beijing China
Southwest Hospital, Shapingba District, China	ESC-RPE	Subretinal	AMD, SMD	Chongqing, China
Astellas Institute for Regenerative Medicine (formerly Ocata Therapeutics)	MAO9-hRPE/ESC-RPE	Subretinal	Dry AMD, SMD	Los Angeles CA, Miami FL, Boston MA, Philadelphia PA, Edinburgh and Newcastle upon Tyne, United Kingdom
CHABiotech CO., Korea	MAO9-hRPE/ESC-RPE	Subretinal	Dry AMD	Gyeonggi-do, Korea
Cell Cure Neurosciences	OpRegen/ESC-RPE	Subretinal	Dry AMD	Jerusalem, Petah Tikva, Rehovot, and Tel Aviv, Israel
Pfizer	PF-05206388/ESC-RPE	Subretinal	Wet AMD	London, United Kingdom

	on polyester membrane			
Federal University of Sao Paulo	ESC-RPE in suspension and on polymeric scaffold	Subretinal	AMD, SMD	Sao Paulo, Brazil
Regenerative Patch Technologies	CPCB-RPE1/ESC-RPE on parylene membrane	Subretinal	Dry AMD	Beverly Hills and Los Angeles CA
StemCells, Inc.	HuCNS-SC/neural stem cells	Subretinal	Dry AMD	Beverly Hills, Campbell, Mountain View, Los Angeles, and Palo Alto CA, Chicago IL, Royal Oak, MI, New York NY, Abilene, Austin, and Dallas TX, Salt Lake City, UT
Janssen R&D	CNTO2476/umbilical cord stem cells	Subretinal	Dry AMD	Arcadia, Rapid City, and Santa Barbara CA, Philadelphia PA, Chicago IL, Lexington KY, Boston MA, Royal Oak MI, St. Louis MO, Durham NC, Cincinnati, OH, Dallas TX, Vancouver and Toronto Canada, Chiyoda, Hirakata, Kagoshima, Mitaka, Nagakute, Nagoya, Tokyo, and Yokohama, Japan
RIKEN	iPSC-RPE sheets	Subretinal	Wet AMD	Kobe, Japan
Kobe City Medical Center	Allogeneic iPSC-RPE	Subretinal	Wet AMD	Kobe, Japan
Federal University of Sao Paulo	AMDCELL/autologous bone-marrow derived stem cells	Intravitreal	AMD, SMD	Sao Jose do Rio Petro, Brazil
Al-Azhar University	Autologous bone marrow derived stem cells	Intravitreal	Dry AMD	Cairo and Nasr City, Egypt
MD Stem Cells	Autologous bone marrow derived stem cells	Retrobulbar, subtenon, intravenous, intravitreal, intraocular	AMD, SMD	Margate FL, Dubai, United Arab Emirates
University of California, Davis	CD34+ bone marrow derived stem cells	Intravitreal	Dry AMD, hereditary macular degeneration	Sacramento CA

Abbreviations: AMD, age-related macular degeneration; ESC, embryonic stem cells; iPSC, induced-pluripotent stem cell; SMD, Stargardt Macular Dystrophy.

With permission from ClinicalTrials.gov and WHO International Clinical Trials Registry Platform (http://apps.who.int/trialsearch/).

Results of RPE Transplants in Humans

RPE Transplants

The first human RPE transplant in AMD was reported by Peyman and coworkers in 1991.[153] Since then, numerous reports have described the results of allogeneic and autologous RPE transplantation.[154–167] These surgeries have involved removal of CNV and placement of suspended allogeneic RPE cells,[153] autologous RPE cells,[157,163] patches of RPE,[155,164] or autografts of RPE-choroid.[157,160,161,163,165,166] Thus far, RPE transplantation has not been successful in the majority of patients undergoing surgery, although a few patients show improvement of two or more lines of visual acuity following autografts.[157,159,160,162,163,165] Allogeneic RPE transplants in AMD patients that have undergone CNV excision have failed with poor visual outcome and, in patients who are not immune-suppressed, subretinal fibrosis and chronic fluid leakage in the dissection bed.[154,155,167] In autologous transplants, graft failure has resulted from intra- and postoperative subretinal hemorrhage, failure of graft revascularization, fibrous encapsulation of the graft, and development of epiretinal membrane, proliferative vitreoretinopathy, and retinal detachment.[159,160,162] Optical coherence tomography (OCT) studies indicate the presence of outer retinal atrophy in the majority of patients undergoing autologous RPE transplants, whether as cell suspensions or as sheets of RPE–Bruch's membrane–choroid.[163,168] Immune rejection and graft failure may underlie these results. The allogeneic RPE transplants may not have survived in the subretinal space independent of immune rejection. Tezel and coworkers showed that if RPE cells cannot adhere to their basement membrane (or comparable surface) within 24 hours, they undergo apoptosis.[169] All previous demonstrations of successful RPE transplants in laboratory animals have involved transplantation onto normal Bruch's membrane (Fig. 128.1) or onto native RPE.[4,5,33,34,170–173] In AMD, Bruch's membrane is itself abnormal.[130,174–176] Uncultured RPE isolated from adult human donor eyes show very limited adherence to aged submacular human Bruch's membrane in vitro.[177] In organ culture experiments,

even cultured fetal RPE, which exhibit robust attachment to Bruch's membrane, cannot survive for more than 1–2 weeks on aged or AMD submacular human Bruch's membrane,[24,148,178–180] presumably due to age- and AMD-related changes in this substrate. Histopathology of an immune-suppressed patient who underwent CNV excision plus uncultured adult RPE transplantation indicates that the cells were not organized as a monolayer, and there was photoreceptor atrophy over the transplant (Fig. 128.2).[164] These results are consistent with the observations of RPE behavior on human submacular Bruch's membrane in organ culture.

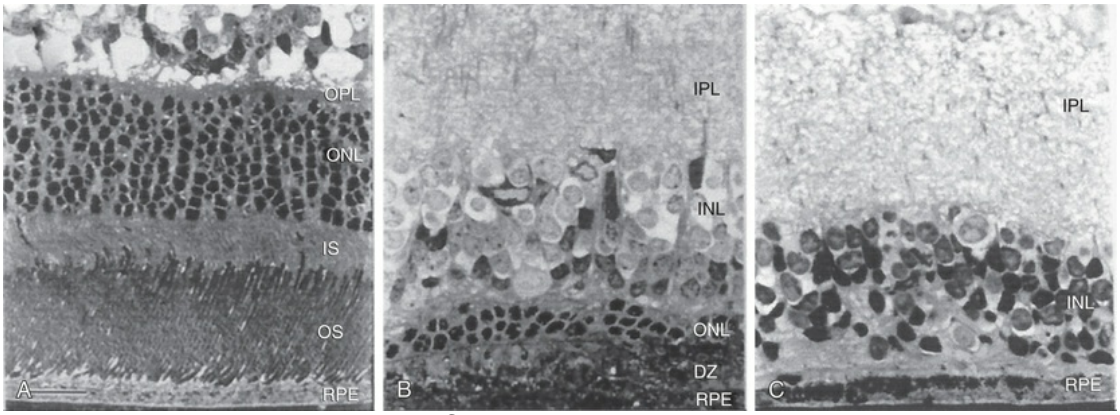

FIG. 128.1 Rescue of photoreceptors by subretinal retinal pigment epithelium (RPE) transplants in dystrophic retina. Toluidine blue-stained semi-thin sections of nondystrophic (A), and dystrophic (B,C) Royal College of Surgeons rat retina. (A) Six-month-old nondystrophic rat retina shows intact outer nuclear layer, 8–10 cells thick. (B) Retina of a 6-month-old dystrophic rat that received a well-characterized, nontumorigenic, SV40 T-transformed human RPE cell line (h1RPE7) 5 months prior to sacrifice. This section is about 1400 μm from the site of injection and shows 2–3-cell-thick outer nuclear layer (ONL). Areas closer to the injection site had up to 6-cell-thick ONL. (C) A 6-month-old dystrophic rat that underwent sham-surgery 5 months prior to sacrifice received only the carrier medium without any cells. No photoreceptor nuclei are seen. *DZ*, debris zone; *INL*, inner nuclear layer; *IPL*, inner plexiform layer; *IS*, photoreceptor inner segments; *ONL*, outer nuclear layer; *OPL*, outer plexiform layer; *OS*, photoreceptor outer segments.

(Republished with permission of National Academy of Sciences from Lund RD, Adamson P, Sauve Y, et al. Subretinal transplantation of genetically modified human cell lines attenuates loss of visual function in dystrophic rats. Proc Natl Acad Sci USA 2001;98:9942–7.)

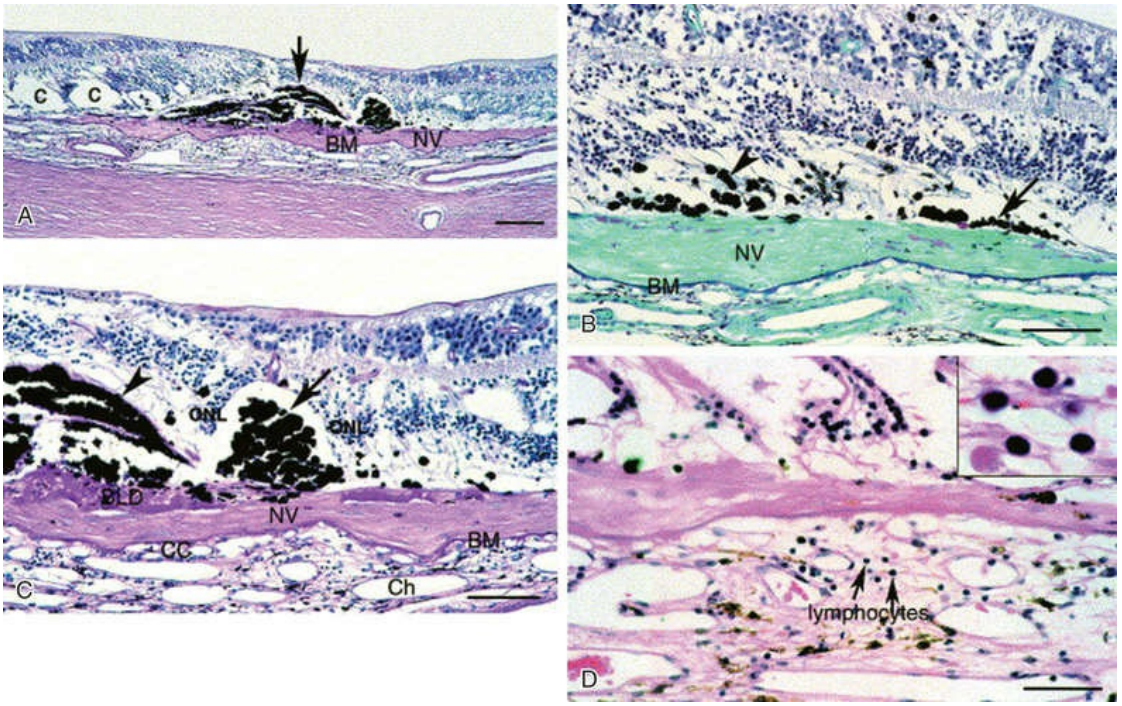

FIG. 128.2 Histopathology of retinal pigment epithelium transplant under the fovea. (A) Transplant site (*arrow*) contains multiple layers of pigment-laden cells. Residual neovascular scar (*NV*) is present between transplant and Bruch's membrane (*BM*). Large cysts (*C*) are present in the outer retina. (B) There is photoreceptor degeneration over an area containing a thin layer (*arrow*) of pigmented cells. Pigmented cells that are not attached to Bruch's membrane are in the subretinal space (*arrowhead*). Residual disciform scar with neovascularization (*NV*) is present internal to Bruch's membrane (*BM*). (C) The outer nuclear layer (*ONL*) is disrupted over a mound of pigmented cells (*arrow*) present in center of transplant site. A bilayer of pigmented cells (*arrowhead*) is visible. Choriocapillaris (*CC*) and choroidal (*Ch*) vessels are patent external to Bruch's membrane (*BM*). Basal laminar deposit (*BLD*) is present internal to residual neovascularization (*NV*). (D) Occasional lymphocytes (*arrows and inset*) are present in the choroid away from the transplant bed.

Scale bars: 200 μm (top left), 100 μm (bottom left, top right), 50 μm (bottom right). (With permission from Del Priore LV, Kaplan HJ, Tezel TH, et al. Retinal pigment epithelial cell transplantation after subfoveal membranectomy in age-related macular degeneration: clinicopathologic correlation. Am J Ophthalmol 2001;131:472-480.)

ESC-RPE and iPSC-RPE Transplants

The first clinical trials of stem cell-derived RPE utilized ESC-RPE to treat patients with Stargardt macular dystrophy (SMD) and atrophic AMD.[110,181] ESC-RPE (50,000–150,000 cells/eye) were transplanted as a bolus injection with the goal of delivering cells in the area of transition between atrophic and clinically intact-appearing RPE. (In the areas where RPE appeared intact clinically, they likely were diseased.) Placing the donor cells in this junctional locus might be similar to transplanting cells in eyes with earlier stages of AMD, where this therapy might be most useful. Patients were immunosuppressed with low-dose tacrolimus and mycophenolate mofetil 1 week prior to surgery, which was to be continued for several months postoperatively. ESC-RPE showed no signs of tumor formation, and the transplants appeared to be well tolerated up to 37 months after surgery (longest patient follow-up in this report). Pigmented cells, presumably ESC-RPE, appeared to expand outward or migrate away from the injection site and accumulated along the edge of areas of RPE atrophy in both SMD and AMD patients (Fig. 128.3). Identification of the pigmented cells seen in fundus photos as transplanted ESC-RPE is not certain, as noted by the investigators of this study. It is possible that other cells such as macrophages that have engulfed released pigment could account for pigmented cells observed in the subretinal space. Some visual improvement in most patients was reported at 1 year,[181] but some concern has been expressed regarding the interpretation of the visual results.[182] Another study, using the same ESC-RPE preparation and similar immunosuppressive regime, reported similar findings at 1-year follow-up of four Asian patients, two with atrophic AMD and two with SMD.[183]

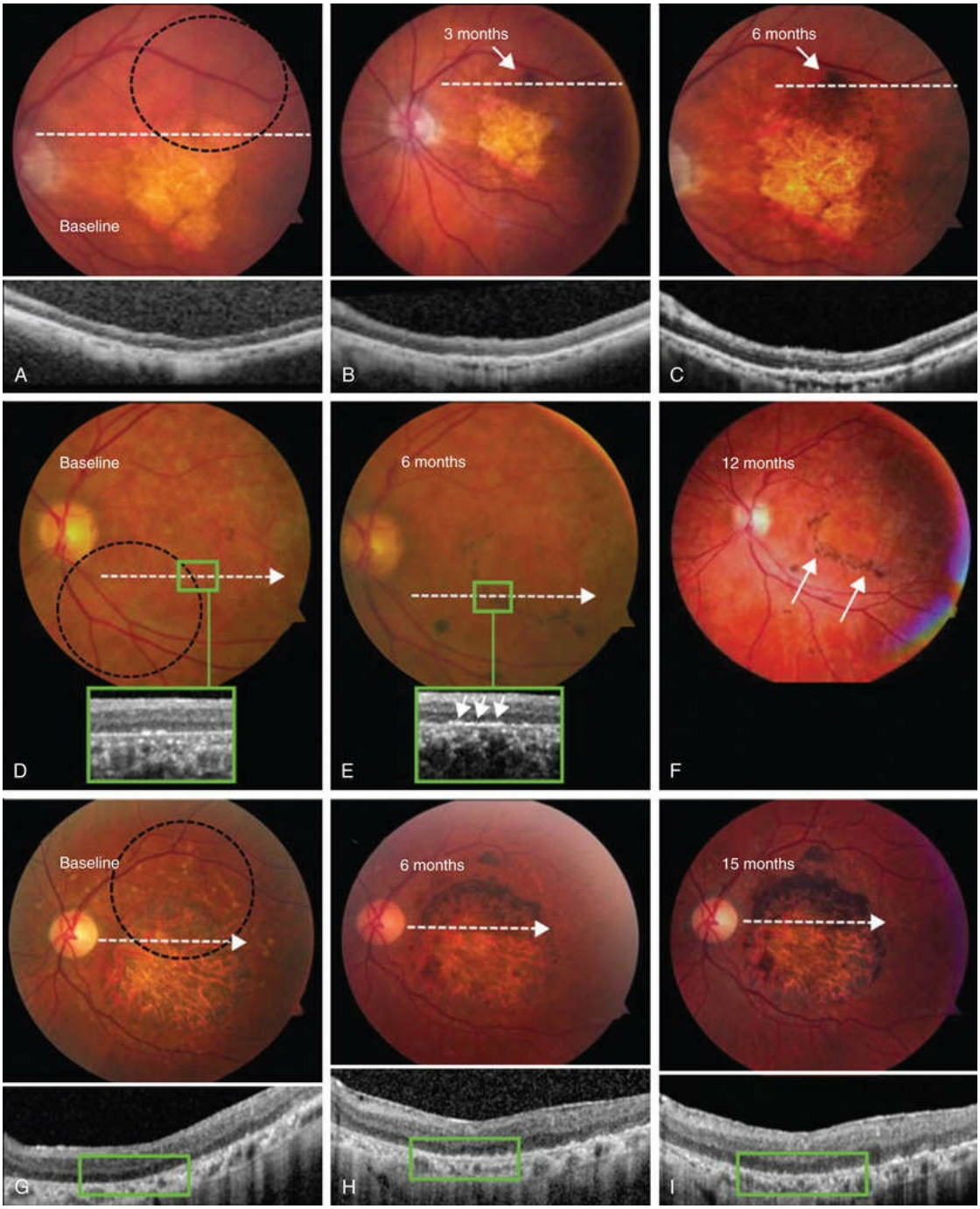

FIG. 128.3 Fundus images of eyes with pigmentation after transplantation with human embryonic stem cells-retinal pigment epithelium (hESC-RPE) (A–C). Colour fundus photographs and spectral domain optical coherence tomography (SD-OCT) images at baseline of an eye from a patient with age-related macular degeneration (dotted circle shows an outline of the transplanted area), 3 months, and 6 months. Note the presence of a pigmented patch of transplanted cells (B,C, *arrows*) that becomes larger and more

pigmented by 6 months. OCTs (inset) show the presence of cells on the inner aspects of Bruch's membrane at 6 months compared with baseline. (D–F) Colour fundus photographs and SD-OCT images at baseline of an eye from a patient with Stargardt macular dystrophy (dotted circle shows an outline of the transplanted area), 6 months, and 1 year. Note the absence of pigment in the preoperative photograph (D). Patches of pigmented cells are evident around the border of baseline atrophy in retinal pigment epithelium (E) that become more prominent at 1 year (F, *arrows*). SD-OCT images at baseline (D) and 6 months (E) show increasing pigmentation is at the level of the retinal pigment epithelium, normal monolayer retinal pigment epithelium engraftment, and survival at 6 months (E, *arrows*) adjacent to a region of bare Bruch's membrane devoid of native retinal pigment epithelium. (G–I) Colour fundus photographs of a patient with Stargardt macular dystrophy (dotted circle shows an outline of the transplanted area). A large central area of atrophy is visible on the preoperative photograph (G). An area of transplanted retinal pigment epithelium cells is visible at the superior half of the atrophic lesion at 6 months (H) that becomes larger and more pigmented at 15 months (I). (With permission from Schwartz SD, Regillo CD, Lam BL, et al. Human embryonic stem cell-derived retinal pigment epithelium in patients with age-related macular degeneration and Stargardt's macular dystrophy: follow-up of two open-label phase 1/2 studies. Lancet 2015; 385:509–516.)

The first autologous iPSC-RPE transplant was done in a patient with exudative AMD in a clinical study performed in Japan in 2014. The iPSC-RPE were introduced as a sheet containing mature, functional RPE with no scaffold support. The sheets were harvested from a porcine collagen I gel substrate using collagenase I to release the sheet from the substrate. (Immunocytochemistry evidence indicates there is no collagen I remaining on the basal surface of the cell sheet.[99]) The first patient was reported to be “faring well”, one year after transplantation.[184] Transplantation surgery for the second patient was halted in 2015 after the discovery of six gene mutations that were not present in the patient's fibroblasts from which the iPSCs were derived. Three mutations were gene deletions; three

were nucleotide changes (single nucleotide polymorphism, SNP). One SNP was in a low-risk oncogene.[185] The mutations are thought to have been the result of the reprogramming method.

Immune Response to RPE Transplants

Immune Privileged Sites and Immune Privileged Tissue

An immune privileged site (e.g., the ocular anterior chamber) accepts allografts for prolonged periods compared to a nonimmune privileged site (e.g., the subconjunctival space). Immune privileged tissue can survive for prolonged periods in a nonimmune privileged site compared to nonimmune privileged tissue. Thus, resistance of an allograft to immune rejection can be due to properties of both the transplantation site and the transplanted tissue.

Immune privilege in the eye is the result of multiple anatomic and physiologic factors acting on both the innate and adaptive immune systems.[186,187] Streilein et al.[187] noted that among the factors and mechanisms responsible for ocular immune privilege are (1) the blood–ocular barrier, which minimizes contact of allografts with the cells and molecules of the systemic immune system, thus blunting the immune response to alloantigens; (2) deficient lymphatic drainage of the eye, which leads to initial alloantigen presentation in the spleen (versus regional lymph nodes) and, therefore, relatively less inflammatory immune responses; (3) an unusual distribution and functional properties of bone marrow-derived antigen-presenting cells; and (4) an ocular microenvironment rich in soluble or cell membrane-associated immunomodulatory factors. Examples of such factors include transforming growth factor (TGF)-β2, α-melanocyte-stimulating hormone, vasoactive intestinal peptide, calcitonin gene-related peptide, macrophage migration inhibitory factor, interleukin (IL)-1 receptor antagonist, Fas ligand, CD46, CD59, and free cortisol.[188–195] These molecules help to create an immune-suppressive

microenvironment by affecting the function of immune cells that come in contact with transplanted tissue or inhibiting complement activation. Ocular sympathetic innervation is necessary for maintenance of high ocular levels of TGF-β, and denervation leads to loss of immune privilege.[196]

Ocular immune privilege is a dynamic state of immune regulation that results in the induction of an antigen-specific "deviant" systemic immune response characterized by (1) active downregulation of donor-specific delayed hypersensitivity reactions; (2) activation of regulatory cytotoxic $CD8^+$ T cells that suppress delayed hypersensitivity as well as suppress B-cells producing complement-fixing antibodies; (3) activation of regulatory $CD4^+$ cells that block terminal differentiation of delayed hypersensitivity effector cells; and (4) enhancement of B-cells that produce noncomplement-fixing antibodies. Initial descriptions of this response were based on experiments in which alloantigens were placed in the ocular anterior chamber, which led to the acronym ACAID, anterior chamber-associated immune deviation.[188,189,197,198]

Immune privilege exists in the subretinal space, but it is not absolute. Subretinal allografts resist immune rejection and induce the development of systemic tolerance in the form of a suppressed antigen-specific delayed hypersensitivity reaction.[198,199] RPE cells may create a local immune suppressive microenvironment through the production of immunomodulatory factors such as TGF-β[200–202] and through suppression of T-cell activation[203,204] and the induction of activated-T-cell apoptosis.[205,206] In addition, RPE expresses ligands for T-cell inhibitory receptor programmed cell death-1 (PD-1) receptors on T cells. These ligands (PDL1 and PDL2), whose expression is upregulated by interferon-γ, bind to PD-1 and suppress T cells.[207,208] RPE also expresses a novel immunosuppressive factor, cathepsin L inhibitor, CTLA-2α, that converts exposed T cells to regulatory T cells.[209]

The RPE can behave as immune privileged tissue. Neonatal RPE sheets resist immune rejection at heterotopic sites (i.e., anatomic locations in which the transplanted tissue is not found normally) when compared to nonprivileged tissue.[210] It is not known whether adult RPE, as a sheet or single cell suspension, is immune

privileged. Constitutive expression of Fas ligand on the RPE may contribute to its status as immune privileged tissue.[210,211] This status does not mean, however, that the RPE is incapable of sensitizing its host. Allogeneic neonatal RPE grafts can sensitize recipient mice if the grafts are placed at a nonimmune privileged site.[210]

RPE cells express transplantation antigens. Low levels of major histocompatibility (MHC) class I antigens are present on the surface of fetal RPE cells.[212] Also, RPE cells may express minor histocompatibility antigens. They do not seem to express MHC class II antigens normally although they can do so if exposed to interferon (IFN)-γ.[213] Culturing RPE cells also can induce MHC antigen expression.[214] In addition, RPE cells can process antigen prior to antigen presentation.[215] Higher levels of IFN-γ-induced MHC class II antigen expression on RPE cells leads to increased activation of antigen-specific T cells as manifested by the production of proinflammatory tumor necrosis factor-α.[216] This activation does not include T-cell proliferation or production of IL-2, however, as is the norm for T-cell activation.

Implantation of neonatal allogeneic RPE cells into ocular immune privileged sites (e.g., the subretinal space) suppresses typical delayed hypersensitivity in the recipients, and the capacity to do so appears to be related to the immune privileged status of the graft site rather than to the immune privileged status of the graft.[210] Thus, it may be that if RPE transplantation is done in a setting in which the immune privilege of the recipient site is compromised (e.g., breakdown of the blood–ocular barrier due to removal of native RPE), then allogeneic RPE grafts will be rejected despite their immune privileged status. If native RPE cells are compromised with sodium iodate, for example, tumor cells or ovalbumin injected into the subretinal space do not induce immune deviation.[198] Immune deviation appears to be impaired persistently (i.e., after restoration of the blood–retinal barrier is complete) following iodate treatment and may be due to entry of plasma proteins into the subretinal space.[198]

In patients receiving RPE transplants after CNV excision, the outer blood–retinal barrier will be compromised both by the presence of CNVs preoperatively and by the iatrogenic RPE defect in the transplant bed postoperatively. Experimental studies indicate

that the outer blood–retinal barrier is disrupted for approximately 1 week after hydraulic debridement of the native RPE.[217,218] Experiments in mice indicate that breakdown of the outer blood–retinal barrier for approximately 14 days (beginning a few days before antigen inoculation) abolished immune privilege and abrogated immune deviation to cell-associated and soluble antigens in the subretinal space.[198] It should be noted that placement of alloantigen in the eye in ocular immune privilege experiments involves disruption of the blood–ocular barrier. That immune privilege is extended despite this disruption indicates the importance of the factors in the microenvironment. Persistent loss of the blood–retinal barrier (e.g., due to CNVs) may result in dilution or absence of immunomodulatory factors in the microenvironment in addition to increased access to subretinal space by systemic immune cells. Also, the role of age-related changes in the RPE *vis-à-vis* subretinal immune privilege is unexplored. Finally, the extent to which immunologic abnormalities associated with AMD,[131] even in the absence of CNVs, compromise the normal immune suppressive environment of the subretinal space is unknown.

In summary, immune privilege may promote allograft survival in the subretinal space, but the changes due to disease and surgical intervention may significantly affect the degree of privilege.

Are RPE Transplants Rejected?

It is not clear that orthotopic (i.e., transplants placed in an anatomic location in which they are found normally) allogeneic RPE transplants are rejected. Some clinical and experimental evidence indicates that they are rejected.[154,155,167,173,219–224] In contrast, other studies indicate that RPE transplants, including iPSC-RPE, may not be rejected.[87,99,170,225] In still other studies, it is not clear whether rejection occurred or not.[226] Interpretation of many early studies, however, is complicated by the fact that it was difficult to identify unambiguously the transplanted RPE cells due to lack of a unique histologic or clinical marker. Another confounding factor in comparing the animal studies involving transplant rejection (reviewed in reference[227]) is that the transplantation surgery in some

studies resulted in damage to the blood retinal barrier, which may have promoted transplant rejection. In a rodent study by Lu et al.,[228] after excluding animals in which the blood–retina barrier was compromised following bone marrow-derived somatic cell subretinal transplantation, it was noted that immunosuppression was not necessary since there was no statistical difference in rejection rates and outcome in immunosuppressed vs. nonimmunosuppressed animals. For stem cell-derived RPE, undifferentiated cells present as a contaminant in the cell preparation could lead to rejection. As discussed previously, nondifferentiated iPSCs are likely to be immunogenic; even with nonintegrating methods, some degree of immunogenicity is induced.[229] Terminally differentiated cells are less likely to be immunogenic.[87]

In a pilot study, transplanted allogeneic uncultured adult human RPE did not appear to be rejected in AMD patients who had undergone CNV excision and were treated with systemic azathioprine, prednisone, and cyclosporine, which suggests that immune suppression might prevent RPE transplant rejection in this setting.[164] However, these elderly patients were not able to tolerate systemic triple immune suppressive therapy for an extended time. Local immune suppression is somewhat effective in laboratory experiments involving intravitreal injection of cyclosporine,[230] but it has not been reported in human RPE transplants. In clinical trials using subretinally transplanted ESC-RPE to treat patients with SMD and atrophic AMD, patients were treated with oral systemic immunosuppression (low-dose tacrolimus and mycophenolate mofetil (MMF)) 1 week prior to surgery and for 6 weeks after surgery. At week 6, the protocol required discontinuation of tacrolimus and continuation of MMF for an additional 6 weeks or longer. However, three of the patients did not tolerate the full immunosuppressive regimen, and the regimen was modified for an additional seven patients who continued the MMF for up to >66 weeks. No signs of acute graft rejection were noted in the 18 patients of this study, indicating that immune suppression following allogeneic cell transplantation is possible.[231] Autologous RPE transplants (e.g., transplants of uncultured peripheral RPE cells to the submacular space of the same eye) should not undergo

graft rejection. Methods for harvesting RPE cells for autologous transplants exist,[159,232] but in vitro data indicate that harvested aged human RPE do not adhere well to aged submacular Bruch's membrane, even in the presence of native RPE basement membrane.[177] This result may explain why patients undergoing autologous RPE transplants after CNV excision have generally shown very limited visual improvement.[159,163] Also, aged autologous adult RPE may exhibit aging and AMD changes that render them unsuitable for transplantation.[233,234]

RPE Graft Failure

As noted above, RPE transplants in humans may have failed independently of immune rejection of the graft. Attachment of RPE to Bruch's membrane after transplantation is crucial as RPE undergo apoptosis otherwise.[235] In vitro studies indicate that trypsin-harvested, cultured fetal human RPE can adhere to adult submacular Bruch's membrane even on surfaces lacking native RPE basement membrane.[24,178,179,236] In contrast, uncultured collagenase IV-harvested adult RPE adhere poorly to aged human submacular Bruch's membrane even in the presence of native RPE basement membrane.[177] Del Priore and coworkers have shown higher attachment rates with cultured RPE from older donors when seeded onto peripheral Bruch's membrane of older persons.[237–240] This higher attachment rate might reflect a difference in integrin expression of primary isolated RPE cells versus cultured cells.[178,241] It also might reflect differences in extracellular matrix composition of peripheral versus submacular Bruch's membrane.[174,242] Histology of excised CNVs,[30,31,243] histopathology of eyes following CNV excision,[244,245] and postoperative clinical findings[30,246] all suggest that CNV dissection exposes both the superficial and deeper layers of the inner collagenous layer of Bruch's membrane, which will constitute much of the surface to which transplanted RPE must adhere and on which they must survive if transplants are done after CNV excision. Cultured fetal human RPE can adhere to the superficial and deep inner collagenous layers of aged human submacular Bruch's membrane, but long-term survival is impaired.[24,179,241] An additional age-related change in Bruch's

membrane that could contribute to poor graft survival and function is the increased deposition of cholesterol.[247] It is not known if the lipid deposits, which may contribute to the decreased hydraulic conductivity of aged Bruch's membrane,[242] might affect RPE transplant function or survival by masking extracellular matrix ligands. In vitro studies show that fetal RPE can attach to a high degree on the surface of the inner collagenous layer and that the majority of cell death occurs after 7 days in culture, indicating that poor cell survival is a post-attachment event.[24] The poor visual results associated with autologous iris pigment epithelium (IPE) transplants might be due to graft failure and, perhaps less likely, from limitations in the ability of IPE to replace RPE.[248–250]

In a SMD patient receiving an ESC-RPE transplant, pigmented autofluorescent cells were observed in the atrophic lesion following transplantation into this area. With time, the pigmented cells and autofluorescent signal disappeared, indicating either graft failure or loss of cell pigmentation (Fig.128.4). An in vitro study examining similarly prepared ESC-RPE on aged and AMD Bruch's membrane predicted graft failure with time in culture as the majority of transplanted ESC-RPE were dead or dying after 21-day culture.[24] These studies point out the need for a method to improve graft survival on AMD Bruch's membrane, since Bruch's membrane in atrophic lesions has not supported transplanted cell survival.

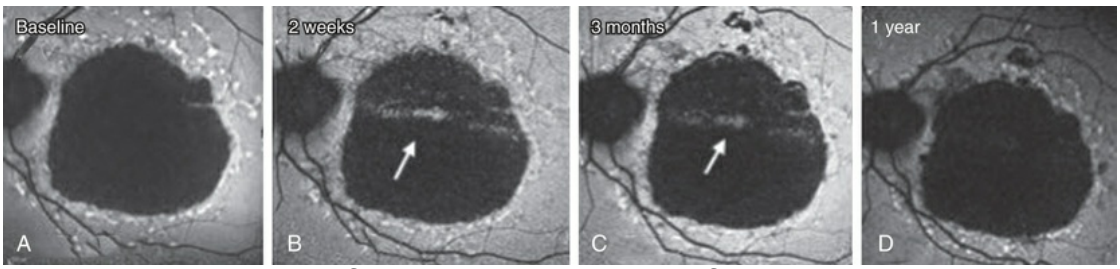

FIG. 128.4 Autofluorescence images of a patient with increasing pigmentation consistent with transplanted human embryonic stem cells-retinal pigment epithelium (hESC-RPE). Autofluorescence images (A–D) of a Stargardt macular dystrophy patient, which correspond to the color fundus photographs in Figs. 128.3G–I. Preoperative autofluorescence imaging shows hypoautofluorescence centrally with small satellite lesions of hypo-autofluorescence, and a surrounding

rim of hyperautofluorescence (A). Two weeks (B) and 3 months (C) after surgery. There is speckled hyperautofluorescence in the upper half of the central atrophic lesion (B,C, *arrows*) that diminishes by 1 year (D). (From Schwartz SD, Regillo CD, Lam BL, et al. Human embryonic stem cell-derived retinal pigment epithelium in patients with age-related macular degeneration and Stargardt's macular dystrophy: follow-up of two open-label phase 1/2 studies. Lancet 2015;385:509-516.)

RPE Replacement: Future Directions

The seminal work by Advanced Cell Technology, Inc., now Astellas Institute for Regenerative Medicine (AIRM), paved the way for RPE transplantation clinical trials by demonstrating the safety of ESC-RPE transplants in AMD and SMD patients. Halting of the autologous iPSC-RPE transplantation study to treat patients with exudative AMD in Japan emphasizes the necessity of careful assessment of donor tissue to assure safety of the transplants. As yet undetermined from these early clinical trials is whether significant long-term visual improvement can be achieved through stem cell-derived RPE transplants. The results of current and future clinical trials (Table 128.2) will drive the future of cell transplantation therapy for patients with AMD and SMD. It is likely that cell selection, preparation, and delivery strategy will vary, depending upon the target disease and the stage of disease progression.

Histocompatibility Leukocyte Antigen (HLA) Matching

Autologous iPSC-RPE transplantation theoretically should circumvent the need for immunosuppressive therapy. Aside from the possibility of the stem cell-derived RPE containing the same genetic defects that led to RPE atrophy in the patient, autologous iPSC-RPE transplantation may not be practical as a large-scale therapeutic for other reasons. Currently, most methods to generate RPE from stem cells are labor-intensive and time-consuming. New protocols have been developed to increase the efficiency, reduce the

need for laborious hand picking of pigmented colonies, and/or reduce the time to differentiate into RPE,[102,251–254] but the high costs of creating clinical grade cells remain. Regardless of the method of differentiation, rigorous testing at all stages of clinical grade cell production must take place beginning with the procurement of the starting cells through the final product to assure purity, safety, stability, and functionality of transplanted cells. These requirements increase the costs of cell production.

An alternative to autologous transplantation is the creation of iPSC lines with a range of HLA types to allow for HLA matching to minimize the need for immunosuppressive therapy. As formidable as this approach seems, it is possible to generate an iPSC haplobank for a given population within a geographic region as HLA alleles and haplotypes are conserved within populations.[255] For example, one estimate is that an iPSC bank from 150 homozygous HLA-typed individuals could match 93% of the United Kingdom population and, due to limited diversity of the Japanese population, as few as 50 such lines could potentially match 90% of the population.[229]

Immune Rejection

Many different strategies can be pursued to prevent graft rejection, including systemic or local drug therapy with established (e.g., prednisone, azathioprine, cyclosporine) or new (e.g., recombinant cytokines) compounds or via other techniques, e.g., diminishing MHC class-II-positive cells in the transplant.[256] Cyclosporine does not appear to interfere with the ability of allogeneic neonatal retinal grafts to induce ACAID, nor does prolonged treatment with systemic cyclosporine interfere with persistence of allospecific suppressor cells for 35 days after transplantation.[257] Nonetheless, retina grafts in the anterior chamber do deteriorate in 35-day grafts suggesting that graft destruction is the result either of immune mechanisms not inhibited by cyclosporine and/or nonimmunologic factors. Independent of its effectiveness, systemic immune suppression can be complicated by side-effects such as nephrotoxicity, hypertension, risk of malignancy, susceptibility to infection, hepatotoxicity, seizures, and even anaphylaxis,

depending on the medications used.[258] Thus, local immune suppression has been considered. In one study, local immune suppression of rabbit eyes with cyclosporine prolonged cultured human fetal RPE xenograft survival in the subretinal space, but by 25 weeks, only ~10% of the green fluorescence protein-labeled grafted cells could be identified.[230] It may be that the viral vector used to introduce green fluorescence protein induced an inflammatory response. Sustained slow-release cyclosporine delivery was as effective at promoting transplant survival as repeated intravitreal injections of much higher doses. Thus, it is not clear that intraocular immune suppression with cyclosporine alone will prevent allogeneic RPE transplant rejection. High-dose dexamethasone therapy is known to be effective in preventing acute allograft rejection[259,260] although lymphocyte resistance to prednisolone can develop.[261] Repeated intravitreous injections of dexamethasone can be well tolerated by the retina,[262] which suggests that sustained intravitreal dexamethasone delivery may not be complicated by retinal damage. Use of the sustained dexamethasone delivery system has prevented allogeneic corneal transplant rejection in rats.[263] Currently, there are several intravitreal sustained-release steroid formulations that could be considered in human transplants.[264,265] Thus, if immune suppression of RPE grafts is necessary, this approach may also be effective in preventing RPE transplant rejection. Donor iPSC banks are being created and are targeted for individuals homozygous at some of the MHC loci.[266–270] Because disparities at minor histocompatibility loci can provoke immune rejection,[271] it is not clear how useful this approach will be. Supplementing MHC matching with immune suppression might be associated with an increased risk of ESC-derived tumor formation. Another strategy is to induce tolerance (i.e., absence of a destructive immune response to transplanted tissue without immune suppression).[272] Tolerance can be achieved via mixed chimerism or by inducing anergy through blockade of costimulatory signals that activate T cells (e.g., with belatacept). The combination of the immune privileged site of the transplant (i.e., the subretinal space) and the immune privileged tissue that is transplanted might result in the induction of ignorance (i.e., failure of the immune system to recognize transplanted tissue).

Photoreceptors, for example, have low MHC class I expression and express MHC class 1b antigens (HLA-G and HLA-E) that bind CD94-NKG2 and block NK cell-mediated lysis,[272] and RPE cells express Fas ligand.[273]

Transplanted RPE Survival and Differentiation on Aged Bruch's Membrane

There is no fully validated animal model of AMD at present. In vivo and in vitro RPE wound healing and transplantation models exist, but they do not appear to be directly relevant to AMD patients. Previously reported successful in vivo RPE transplants involve attachment to normal Bruch's membrane or native RPE as noted above. Experiments using aged submacular human Bruch's membrane in organ culture indicate that aged human RPE do not adhere well to this surface unless they are cultured.[177,178] Cultured fetal RPE appear to adhere to aged submacular Bruch's membrane better than cultured aged RPE, but even in this case the cells do not appear to survive and differentiate well at 7 days in organ culture. It appears that aging changes in Bruch's membrane are responsible for this deleterious effect on the cells.[180,274,275] Thus, one approach to improving RPE transplantation success is to identify and manage these Bruch's membrane changes. Experiments in vitro have included “cleaning” Bruch's membrane with Triton X-100 (a detergent) and/or resurfacing the Bruch's membrane with extracellular matrix molecules, singly or in combination,[276,277] or resurfacing the Bruch's membrane with a cell-secreted matrix.[180] The latter has shown promise, but translation to clinical application remains a challenge. Another approach has included enhancing the expression of cell-matrix adhesion molecules, i.e., integrins, to improve RPE adhesion and survival.[241,278] Finally, it may be possible to enhance graft success through stimulation of the transplanted cells, for example, via trophic factors, to enhance long-term survival following transplantation onto diseased Bruch's membrane.[148]

As previously mentioned, cells introduced into the subretinal space on a scaffold could conceivably prevent deleterious effects from Bruch's membrane affecting the graft. Because cell-scaffold placement may require a larger retinotomy and a larger retinal

detachment, it may create more surgical damage than dispersed cell subretinal injections. In the case of patients undergoing CNV excision, however, scaffold-based cell delivery may be best because of the damage to Bruch's membrane generated by CNV removal. Tissue engineering and scaffold development is a rapidly evolving field, with sophisticated scaffolds manufactured that can reproduce properties of normal Bruch's membrane, allowing control over porosity and mechanical properties.[152] Pending and future clinical trials utilizing a variety of scaffolds will determine whether this approach is feasible.

Native RPE Resurfacing of Aged Bruch's Membrane

An alternative to RPE transplantation is to stimulate RPE ingrowth from the edge of the dissection bed. Human pathologic studies indicate that RPE ingrowth following CNV excision in AMD patients is incomplete and aberrant.[30,244,279] Previously described cell culture RPE wound-healing models are associated with complete wound resurfacing, in contrast to the situation in AMD patients undergoing CNV excision.[280–282] In vivo RPE wound-healing models (e.g., rabbit, pig) are associated with complete resurfacing of the RPE defect[283,284] or involve administration of compounds (e.g., mitomycin C) that complicate further experimental study or have unclear relevance to resurfacing Bruch's membrane in AMD patients.[217,285,286] Experiments from a Bruch's membrane organ culture model indicate that resurfacing of ~65–85% of a ~3-mm-diameter circular RPE defect in aged submacular human Bruch's membrane occurs by approximately 10 days if RPE basement membrane or the superficial inner collagenous layer is present. If deeper defects are created, exposing deeper regions of the inner collagenous layer, significantly less resurfacing is observed (~54%) at day-10 indicating that one should expect less resurfacing with greater damage to Bruch's membrane.[287,288] However, these experiments were performed on aged (non-AMD) Bruch's membrane and therefore may be more relevant to cases in which the RPE are relatively healthy. Additional experiments are needed to determine whether one can alter the denuded Bruch's membrane

surface (or the RPE cells at the edge of the defect) so that resurfacing of the RPE defect occurs in situ.

Human clinical studies indicate that periods of macular detachment up to 2 weeks are compatible with recovery of visual acuity of 20/50 or better in a substantial number of patients.[289] Monkey and cat experiments indicate that many photoreceptors survive during retinal detachment periods of several weeks' duration, although some photoreceptors definitely die.[290,291] Approximately 80% of the cat outer nuclear layer survives during 3 days of detachment.[292] The numbers of photoreceptor nuclei in detached cat retina do not begin to decline significantly (i.e., >20% decline in density) until detachment periods longer than 13 days.[293] Data from cat retinal detachment studies indicate that 14-day detachments followed by 30-day reattachment is associated with rod and cone outer segment length similar to that observed after 5-day detachments.[291] The cat retina, however, is rod-dominated. Cones are more prone to apoptosis with detachment (versus rods)[294] although in one study, approximately 75% of S- and M-cones survived a 1-day detachment (followed by retinal reattachment) in the ground squirrel.[295] Thus, at this time, published experimental data do not indicate clearly what the exact survival of cones is after 2-week periods of retinal detachment, but clinical data indicate that it is good enough to warrant developing methods to promote RPE resurfacing. In addition to duration of detachment, the height of detachment influences photoreceptor survival.[295,296] The macular detachments that would arise from CNV excision are quite shallow (<1–2 mm height), which also favors photoreceptor survival during a 2-week RPE resurfacing period. Thus, we believe that the RPE resurfacing approach is feasible despite its possible association with photoreceptor death during the resurfacing process.

Background and Rationale for Photoreceptor Transplantation in Retinal Dystrophies

Retinitis pigmentosa (RP) is a group of heterogeneous hereditary disorders with an estimated prevalence between 1 : 3000 and 1 :

5000, affecting 50, 000 to 100, 000 individuals in the United States and approximately 1.5 million people worldwide.[297] In the vast majority of cases, the condition results from mutations in photoreceptor cell genes encoding a myriad of structural and phototransduction proteins, and, to a lesser extent, from mutations in genes of the RPE.[297] Blindness ultimately results from rod and cone photoreceptor cell death.[298] Inner retinal layers remain relatively preserved, especially early in the course of the disease.[299,300] As degeneration progresses, however, extensive synaptic rewiring of the inner retina occurs.[298,301,302]

A variety of approaches to restore vision are under study, including gene therapy,[303–307] pharmacotherapy,[308,309] visual prostheses,[310] endogenous regeneration,[311] and transplantation.[312–318] The goal of retinal transplantation is to restore and/or maintain visual function by transplanting healthy donor photoreceptors that replace lost photoreceptors by integrating with the host inner retina to reconstruct a functional, neural retinal network. As noted above, this approach to sight restoration is termed "replacement." Retinal transplantation may also slow down the progression of the disease by means of graft-released trophic substances that rescue residual host photoreceptors,[319–322] an approach termed "rescue." A trophic effect would be most useful, however, only while the critical number of foveal cones required to support useful vision is present.[323] In late stages of the disease, when most photoreceptors have degenerated, replacement of lost photoreceptors probably would be more effective.

Results of Photoreceptor Transplants in Experimental Animals

Animal Models of Retinal Degeneration

Early studies of retinal transplantation utilized normal animals as hosts. Subsequently, investigators turned to animal models of retinal degeneration. Animal models became available either by discovery of naturally occurring genetic mutants, such as the retinal degeneration (*rd*) mouse,[324] the retinal degeneration slow (*rds*) mouse,[325] the RCS rat,[6] and the rod–cone dysplasia (*Rdy*) Abyssinian

cat,[326] or by experimentally induced degenerations such as photoreceptor degeneration induced by phototoxicity[327] and by intravitreal injection of a concentrated solution of human hemoglobin.[328] In addition, genetically engineered models of homologous human RP mutations such as the transgenic rhodopsin (Pro23His) mutant mouse[329] and the transgenic rhodopsin (Pro347His) mutant pig[330] were developed. The advantages of these models include the rapid and nearly total loss of target cells such as RPE or rod photoreceptor cells as well as their similarity (in some cases, equivalence) to human disease, allowing for the efficient study of retinal transplantation under more clinically relevant conditions. Most work to date has employed rodent models such as the light-damaged rat retina,[14,331,332] the *rd* mouse,[314,333–337] the P23H rhodopsin transgenic mouse,[338] and the RCS rat.[339] The small eye and large lens of the rodent favor transscleral rather than transvitreal graft delivery. Transvitreal delivery is a less traumatic and more pertinent technique to human retinal transplantation than the transscleral approach. Furthermore, the rod to cone ratio in rodent retina[340] differs from that of the relatively cone-rich human retina. To overcome these problems, animal models using larger eyes, such as the chemically ablated rabbit retina[328] and the Abyssinian *Rdy* cat,[341,342] have been employed as well as normal rabbits,[328,343,344] pigs,[345,346] and primates.[347] The pig may prove to be a valuable animal model because the anatomy and size of the porcine eye are closer to that of the human,[348,349] and the pig retina is well endowed with cones, has an area centralis, and is holangiotic.[350] In addition, Pro347His mutant pig[330] carries a mutation similar to that found in a form of human RP and is an animal model closest to human RP, especially with regard to refining surgical procedures.[351] However, the pig retina does not have a fovea.

Graft Implantation Sites and Preparations

Retinal transplants have been placed in a surgically induced retinal lesion, in the vitreous cavity (i.e., epiretinally),[13,352] and into the host subretinal space.[14,353] Grafts from donors of the same species (i.e., allogeneic grafts) and from a different species (i.e., xenogeneic grafts)[347,354,355] have been transplanted with or without host immune

suppression.

Photoreceptor microaggregates, which are retinal fragments in which tissue integrity is disrupted by gentle trituration with cells remaining attached to each other in small clusters (<0.2 mm^2), have been used in retinal transplantation.[13] Isolated cell suspensions obtained by mechanical and/or enzymatic dissociation of the retina also have been used.[333,335,353,356] Compared to microaggregates, isolated photoreceptors usually are more traumatized, frequently lose their outer segments, display less organization, and often are not properly oriented.[313,356] Both preparations often form spherical structures or rosettes, with photoreceptors oriented towards a central lumen similar to those seen in retinoblastomas and retinal dysplasias.[13,352,354] Outer segments of misoriented photoreceptors as well as those found in rosettes rapidly degenerate due to their failure to contact RPE cells.[357] In addition, both retinal microaggregates and cell suspensions frequently are contaminated with nonphotoreceptor retinal cells. Rosette formation prevents the reconstruction of the normal retinal anatomy and interferes with establishing contacts between graft photoreceptor terminals and host second-order neurons.[35]

To avoid these problems, Silverman and Hughes[14] introduced the photoreceptor sheet preparation, created by vibratome-sectioning of adult mammalian retina. Sheet preparations preserve the organization and polarity of grafted photoreceptors and maintain the densely packed arrangement of photoreceptors found in situ and thought to be critical for good visual acuity.[358] Furthermore, the inner retina, which could interfere with synaptic interactions between grafted photoreceptors and host second-order neurons, is removed. Sheets can be placed between the host retina and RPE in the proper orientation, and they show a much lower frequency of rosette formation.[14,320,328,334] This technique has been modified further to obtain photoreceptor sheets using both vibratome-sectioning and excimer laser ablation of the inner retina.[359,360] A similar approach has been used to transplant sheets of adult full-thickness retina, intact embryonic or fetal retinal sheets,[332,339,344] and vibratome-sectioned fetal retina. Aramant and coworkers introduced the approach of cotransplanting fetal neural retina with the adjacent RPE.[339] This approach might be advantageous in cases

of advanced disease where both retinal cell types have degenerated.[316]

Age is an important variable in the choice of donor tissue. Studies in neural retinal transplantation have utilized tissue from embryonic, early postnatal, late postnatal, and adult donors as well as transplantation of homo- and heterotypic neural progenitor cells (stem cells, see below). There are several advantages to transplanting embryonic or fetal retinal grafts.[312] Immature retinal tissue has a high potential for plasticity,[361] lacks immunogenicity,[186] and survives and differentiates well in the host.[332] However, it is extremely fragile, difficult to handle, and is undifferentiated, which makes obtaining pure photoreceptor sheets difficult or impossible. In one study, attempts to obtain photoreceptor sheets from embryonic retina using vibratome-sectioning resulted in abnormal morphology and poor survival.[344] Excimer laser was used to obtain a monolayer of human fetal cones, but the ultrastructure of their synaptic pedicles was disorganized.[362] Also, embryonic or fetal retinal grafts often are associated with rosette formation. Finally, obtaining embryonic or fetal tissue for transplantation has many logistical and ethical constraints. Adult retinal grafts seem to show normal morphology and organization in the host retina and are associated with minimal rosette formation, which might allow for better restoration of retinal anatomy,[328,334,347] especially if the outer blood–retina barrier remains intact.[198] Adult retinal graft preparations have been shown to yield good survival rates.[328,334,347] Furthermore, mature retinal tissue is easier to handle and, because it is fully differentiated, reliably yields pure photoreceptor sheets and can be obtained readily from eye banks.[363] Also, it seems that differentiated photoreceptors can integrate with host retina,[313] although the best integration seems to occur with cells that are developmentally committed to becoming photoreceptors but which have not yet matured morphologically (see below).

Transplantation Aimed at Photoreceptor Cell Rescue

A wide variety of cells, including rod photoreceptors, RPE, IPE, and

even nonocular cells such as Schwann cells and olfactory ensheathing cells, as well as progenitor stem cells, have been used in transplantation paradigms aimed at rescuing host residual photoreceptors and retarding the progression of retinal degenerative diseases. The strategies employed, including the type of cells used, in these paradigms depend on the primary derangement that causes photoreceptor cell death. For example, Schwann cells, derived from peripheral nerves, have been used as autologous grafts to rescue photoreceptors. Schwann cells are known to produce growth factors such as ciliary neurotrophic factor (CNTF), glial cell line-derived neurotrophic factor (GDNF), and brain-derived neurotrophic factor (BDNF) and are therefore a source for sustained growth factor release. Schwann cells, however, do not phagocytose photoreceptor outer segments. Nevertheless, subretinal Schwann cell transplants have been shown to limit photoreceptor cell loss in RCS rats for as long as 9 months[37,364] and for up to 2 months in rhodopsin knockout mice (Fig. 128.5).[365] In addition, Schwann cells engineered to secrete GDNF or BDNF promote photoreceptor rescue in RCS rats to an even greater degree than that observed with parent Schwann cells.[36] Similar to Schwann cells, a mixture of adult olfactory ensheathing cells and olfactory nerve fibroblasts have been shown to produce nerve growth factor, basic fibroblast growth factor (bFGF), and BDNF, as well as restore recoverin expression and maintain ERG b-wave after subretinal transplantation in the RCS rat. However, in contrast to Schwann cells, olfactory ensheathing cells were shown to phagocytose porcine retinal outer segments in an in vitro assay.[366] Additional cell preparations considered for retina rescue therapy, particularly to treat patients with AMD, are discussed above (see Cell Selection for RPE Transplantation, Non-RPE Subretinal Cell Transplants).

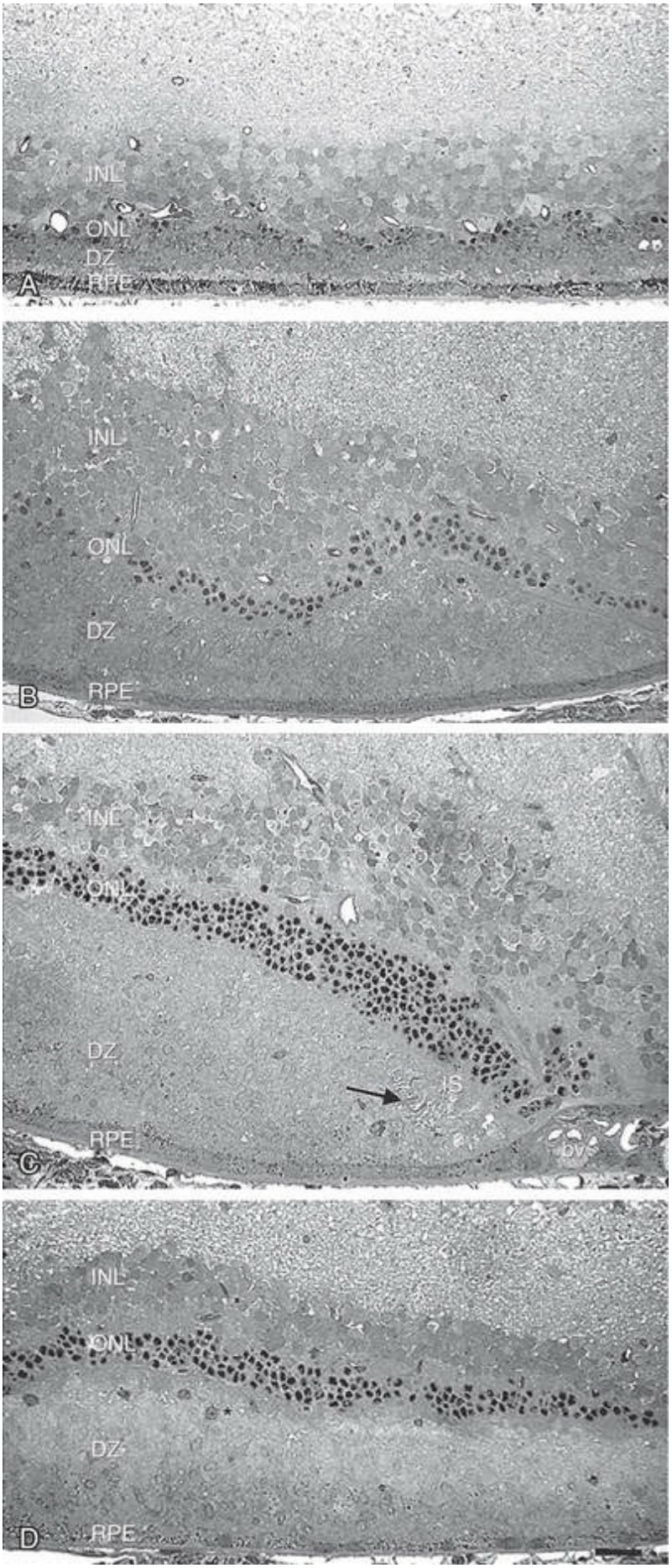
INL
ONL
DZ
RPE
A
INL
ONL
DZ
RPE
B
INL
ONL
DZ
IS
RPE
OVS
C
INL
ONL
DZ
RPE
D

FIG. 128.5 Subretinal transplants of Schwann cells rescue photoreceptors in dystrophic Royal College of Surgeons (RCS) rats, the degree of rescue being greater with cells modified to secrete brain-derived neurotrophic factor (BDNF) or glial-cell-derived neurotrophic factor (GDNF). Toluidine blue-stained semi-thin sections of 16-week-old dystrophic RCS rats that had undergone sham surgery (A) or Schwann cell transplants (B–D) at the age of 4 weeks. (A) Retina after a sham surgery shows only occasional outer nuclear layer (ONL) nuclei. (B) Dystrophic rats that received Schwann cell transplants showed discontinuous regions of 2–3-cell-thick ONL. (C) Schwann cells secreting BDNF in the subretinal space resulted in more extensive preservation of ONL with some outer segment (*arrow*) and inner segment preservation. However, the debris zone is also quite extensive. (D) GDNF-secreting Schwann cells also led to anatomic rescue of photoreceptors greater than that caused by the parent Schwann cell line. *bv*, blood vessel; *DZ*, debris zone; *INL*, inner nuclear layer; *IPL*, inner plexiform layer; *IS*, photoreceptor inner segments; *ONL*, outer nuclear layer; *OPL*, outer plexiform layer; *RPE*, retinal pigment epithelium.
(Republished with permission of the Association for Research in Vision and Ophthalmology from Lawrence JM, Keegan DJ, Muir EM, et al. Transplantation of Schwann cell line clones secreting GDNF or BDNF into the retinas of dystrophic Royal College of Surgeons rats. Invest Ophthalmol Vis Sci 2004;45:267–74.)

Transplantation of rod photoreceptors with the goal of cone photoreceptor "rescue" has been undertaken because, in the vast majority of RP cases and related animal models, the disease-causing mutations are expressed exclusively in rods. Transplanted rods might rescue existing cones that would be lost secondary to rod degeneration.[367] Subretinal rod photoreceptor transplants have been shown to exert a protective effect on cone photoreceptors in animal models of retinal dystrophies, delaying photoreceptor degeneration and limiting cell death. Mohand-Said and coworkers[320] demonstrated that rod-rich retinal grafts transplanted into the subretinal space of *rd* mice, a strain with a naturally occurring

mutation in the gene encoding the β-subunit of rod cyclic guanosine monophosphate phosphodiesterase (cGMP), preserved cone cells, with cone density 30–40% greater than that of untreated *rd* retinas (Table 128.3). This rescue effect was observed at some distance from the grafted cells, suggesting the existence of diffusible trophic factor release by the transplant. These findings were substantiated by in vitro coculture studies in which significantly greater numbers of surviving cones were seen in mouse dystrophic retinas cultured with retinas containing normal rods compared to dystrophic retinas cultured in medium alone or with rod-deprived retinas.[319] Molecules mediating this paracrine effect have been identified.[321,322] Several growth factors, neurotrophic factors, and cytokines such as bFGF, acidic FGF (aFGF), CNTF, GDNF, BDNF, and IL-1β have been shown to exert robust survival-promoting effects in the retina when injected subretinally or intravitreally,[308,368] or when delivered by adenovirus gene therapy[369] in various animal models of retinal degeneration.[370,371] A similar rescue effect has been shown to occur by focal mechanical injury to the retina in light-induced retinal damage[372–374] as well as in sham-operated animals during transplantation studies.[375,376] This effect is probably mediated by injury-induced upregulation of neurotrophic factors.[372,374]

TABLE 128.3

Quantitative Estimates of Effects of Tissue Transplantation on Host Retinal Degeneration (rd) Cone Numbers After 2 Weeks[a]

	Nonoperated Controls (*rd*)		C57 Outer Nuclear Layer		C57 Inner Retina		Entire *rd* Retina		Gelatin (Sham Control)	
	5 Week *rd*	7 Week *rd*	Grafted Eyes	Paired Controls	Grafted Eyes	Paired Controls	Grafted Eyes	Paired Controls	Grafted Eyes	Paired Control
No. of eyes	10	42	12	12	12	12	11	11	7	7
Total no. cones	119, 445	88 ,515	98 ,913	86, 310	90, 846	89 ,180	91, 780	89, 740	86 ,026	89 ,227
SEM	5160	6778	5713	4895	8688	9034	3738	6762	4595	4627

[a]Only rod transplantation leads to significant preservation of cone numbers ($p<.001$).

Transplantation of rod-rich photoreceptors leads to rescue of cone photoreceptors. Five-week-old *rd/rd* mice received gelatin-encased subretinal transplants of one of the following in the right eye: sheets of rod-dominant (97%) photoreceptors from 8-day-old C57BL/6 mice, sheets of inner retina without photoreceptors from 8-day-old C57BL/6 mice, entire retina of 8-week-old *rd* mice, or gelatin sheet alone. The left eye served as unoperated control. Two weeks later, by which time *rd* mice lose 97% of rods, the mice were sacrificed, and the number of surviving cones in the host retina were labeled and counted in an unbiased manner. Five-week-old unoperated *rd* mice were used to determine the baseline rate of degeneration over the same 2-week period, and a loss of 30, 000 cones was noted. Only those eyes receiving an outer nuclear layer transplant showed a statistically significant higher number of surviving cones ($p<.001$).

SEM, standard error of mean.

Clinical trials involving encapsulation and intravitreal delivery of ARPE-19 cells transfected with a human *CNTF* gene (NT-501 cells) in patients with retinal degenerative diseases have been conducted.[377–381] Although reliable long-term intraocular release of CNTF was confirmed and despite several studies suggesting visual improvement in a select subset of patients, sustained long-term improvements in visual acuity, visual field sensitivity, or ERG responses have not been confirmed.

Transplantation Aimed at Photoreceptor Cell Replacement

Various neural retinal transplantation paradigms have been developed in laboratory animals,[312,382,383] some of which have evolved into clinical trials in humans.[316,347,384–387] This work has documented the feasibility of retinal transplantation, with long-term survival of the transplant in both animals[344,357] and humans.[316,347,384–388] There is evidence that some degree of graft–host integration might occur after retinal transplantation,[317] but light and electron microscopy have not demonstrated unambiguous significant direct graft–host synaptic integration in all cases.[13,14,332,334,335,339,344,389] In many of these studies, a glial limiting membrane, derived from Müller cell processes, formed a barrier between graft and host retinas (reviewed in reference[390]). In areas

where this glial barrier was absent, the transplant and host retinas were in close apposition, and their cell processes intermingled indistinguishably.[332] Disruption of the outer limiting membrane seems to improve integration between transplanted photoreceptors and wild-type as well as degenerating retina.[391,392] In a study of rod photoreceptor integration in six different murine models of inherited retinal degenerations, Barber and colleagues found that (1) degree of integration related to disease progression but not severity, (2) integration was possible even in advanced disease, and (3) glial scarring and outer limiting membrane integrity significantly affected photoreceptor integration.[393] In addition, efficiency of integration may be related to tissue age and augmented by soluble factors.[394–396]

Ultrastructural analysis of full-thickness embryonic retinal sheets transplanted into the subretinal space of normal rabbits has shown bundles of nerve fibers containing mature neuronal processes and growth cones on either side of the graft–host interface in close association with intermingled graft and host Müller cell processes, which form a glial barrier.[344] Immunohistochemical analysis of these transplants showed some direct contact between processes of rod bipolar and AII amacrine cells as well as between a few cone bipolar and ganglion cell processes believed to be derived from both transplant and host retinas.[344] Identification of graft versus host cells was made based on location, however, not on specific cell markers. Under similar transplant conditions, a subpopulation of wide-field amacrine cells expressing neuronal nitric oxide synthase was found to extend processes from the graft into the host inner plexiform layer (IPL), but no direct contacts were observed.[397] Synaptic contacts between graft and host retinas are suggested by trans-synaptic tracing studies from the host brain to the transplant. A study conducted by Warre-Cornish et al. attempted to shed light on some of the changes that occur in photoreceptors after transplantation in the mouse retina by conducting a detailed histologic analysis. The sequence of events is as follows: transplanted cells migrate individually through the interphotoreceptor matrix into the host retina, localize to the ONL, form apical attachments, acquire mature rod structure, form synapses with resident neurons, and develop photoreceptor outer

segments.[398]

In an important study, MacLaren et al. showed that if donor cells isolated from retinas at the height of rod development were used for transplantation, integration can occur even if the host has a mature retina.[399] Using *rds*, *rd*, and rhodopsin knockout mouse models, MacLaren and colleagues demonstrated successful integration of postmitotic rod precursors by showing the presence of spherule synapse in donor cells (an essential component to communicate with inner retina), ganglion cell recordings in low light intensities that stimulate rods, and by restoration of pupillary light reflex. However, the cells were not morphologically mature even though they expressed photoreceptor markers. Similarly, when donor tissue was used during the development when retina was rich in rod-committed cells, similar integration into the mature retina was seen after transplantation.[400] As noted above, this integration is improved when outer limiting membrane is disrupted.[391,392] In addition to isolating photoreceptors at specific time points in development, another method that might improve photoreceptor cell integration involves isolating an enriched population of cells with the highest ability to integrate into host retina based on select molecular markers.[401] Gust and Reh have shown that adult photoreceptors can integrate into the host retina but have a higher transplant failure rate compared to less developmentally mature cells (Fig. 128.6).[313] Whether such integration can occur with human tissues is not known. Santos-Ferreira et al.[402] conducted a preclinical study specifically aimed at cone photoreceptor replacement. The team generated cone-like photoreceptors by crossing neural retina leucine zipper-deficient (Nrl($^{-/-}$)) mice with a GFP reporter line resulting in double transgenic mice. The cone-like photoreceptors were enriched by magnetic-activated cell sorting, transplanted into the subretinal space of Nrl($^{-/-}$) adult wild-type mice as well as cone photoreceptor function loss 1 mice, and were shown to integrate into the host retina, acquire photoreceptor morphology, express cone-specific markers, and survive for up to 6 months. Finally, retinal ganglion cell recordings demonstrated photopic responses in retinas with cone cell degeneration, implying restoration of visual function in this model system.[402] The number of integrated cones decreased

significantly during the first 6 months after transplantation, and CD68-positive monocytes/macrophages infiltrated the subretinal space. Lakowski et al.[403] used flow sorting to isolate Crx-expressing cells, which are committed to differentiate into cones and rods. Only embryonic-stage Crx-positive cells integrated within the ONL and differentiated into cones. Postnatal Crx-expressing cells generated primarily rods. Cone integration efficiency seemed to be highest in cone-deficient recipients (Gucy2e$^{-/-}$ mice) compared to Crb1$^{rd8/rd8}$ mice, which demonstrates that the recipient environment can have a profound impact on transplant outcome.

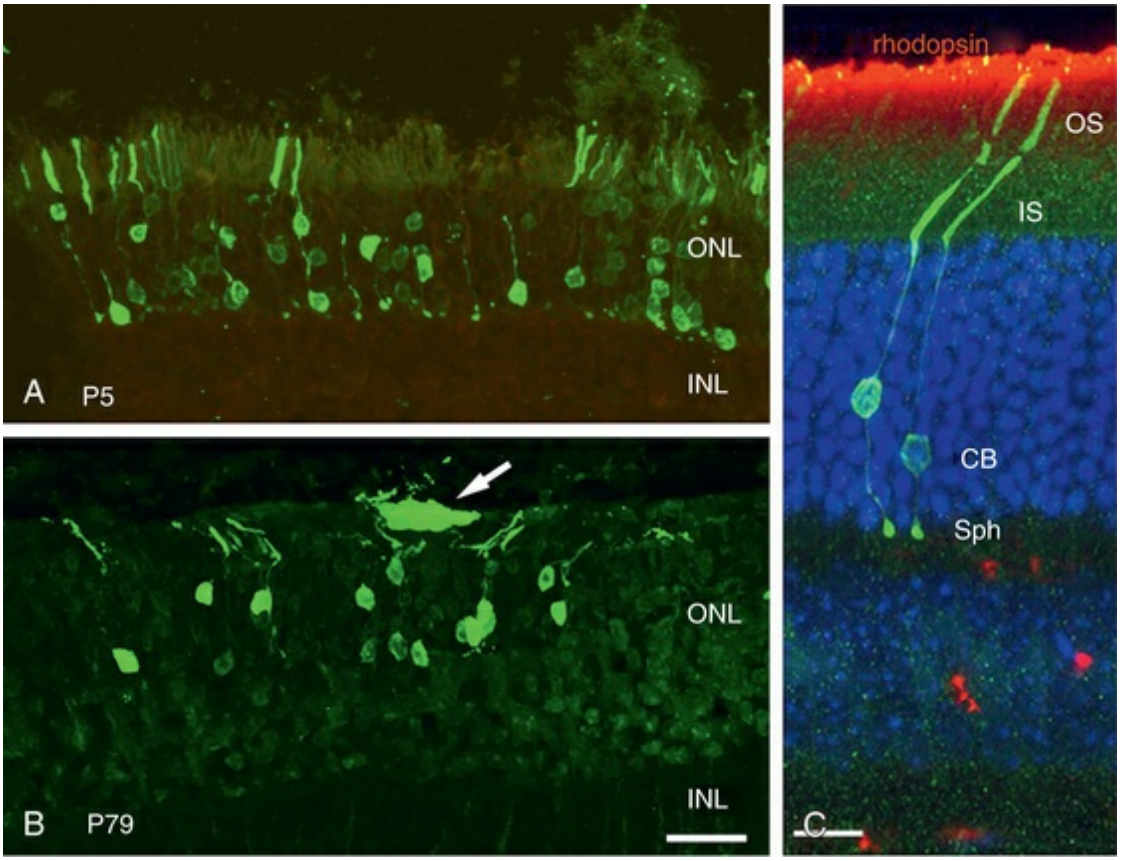

FIG. 128.6 Dissociated retinal cells from green fluorescent protein-positive donor mice of ages postnatal day 5 and day 79 (fully mature adult) were transplanted into the subretinal space of adult wild-type C57/B16 mice. The hosts were sacrificed 2 weeks after transplantation, and the eyes were fixed, embedded in agar, and cut into 60-μm sections. Cells from neonatal (A; P5) and mature (B; P79) donor mice (green) integrate into the unlabeled host outer nuclear layer

(*ONL*). Arrow points to an unintegrated clump of donor cells. Integrated mature rod photoreceptors exhibit complete morphology (C) including outer segment (*OS*); inner segment (*IS*); cell body (*CB*); and a spherule synapse (*Sph*). Outer segments of integrated cells express rhodopsin. Note that in an unintegrated cell, rhodopsin is present throughout the cell. *INL*, inner nuclear layer. Scale bars: 20 μm (A,B); 10 μm (C). (Republished with permission of the Association for Research in Vision and Ophthalmology from Gust J, Reh TA. Adult donor rod photoreceptors integrate into the mature mouse retina. Invest Ophthalmol Vis Sci 2011;52:5266–72.)

Although significant restoration of vision in humans after photoreceptor transplantation has not been documented (see below), there is some indication of improved visual function in laboratory animals.[404,405] Recovery of visual function is the goal of retinal transplantation, but it does not per se constitute evidence of graft–host synaptic connectivity sufficient to reestablish retinal neural circuitry since visual recovery might be due to a "rescue" effect rather than a "replacement" effect. Furthermore, accurate evaluation of visual function is a complex task, particularly in experimental animals. Simple reflexes, electrophysiologic testing, and visually guided behaviors have been used to evaluate visual function in laboratory animals. Silverman and coworkers[334] reported that visually evoked cortical potentials could be recorded over the retinotopic area that corresponded to the transplant. Light-elicited retinal ganglion cell responses and local light-driven electroretinograms (ERGs) have been recorded from host retina overlying transplants.[336] Visual-evoked potentials (VEPs) from areas of the host superior colliculus topographically corresponding to the transplant have also been recorded.[317] Recovery of the pupillary light reflex[334] as well as behavioral correlates, such as light-flash inhibition of the startle reflex[331] and light/dark preference behaviors,[335] have also demonstrated some degree of visual function restoration in animal models of retinal degeneration following photoreceptor transplantation. While the results of these tests are promising, the level of elicited responses was often less than that of normal controls.[334,336] Moreover, it is not clear that synaptic interactions between the transplant and host underlie the observed improvement in all cases.[335] A confounding factor in these

experiments is the possible trophic effect of the transplant,[321,322,337] and, to a lesser extent, of the surgery itself as a form of injury,[372,374,375] both of which have been shown to enhance residual host photoreceptor cell survival. A further difficulty is that the validity of some of these tests as accurate measures of visual function remains controversial. For example, Kovalevsky and coworkers[406] found no correlation between the intensity of the pupillary light reflex and the number of photoreceptor cells present in the host retina. This result limits the validity of the pupillary light reflex as an accurate tool for evaluating the extent of photoreceptor repopulation or the formation of functional contacts sufficient for the recovery of visual function following retinal transplantation. Approximately 120,000 functioning rods are required to generate a reproducible scotopic ERG response in preclinical models of RP.[407] (Restored visual behavior, however, can be detected with only 25,000 functioning photoreceptors in this model.)

Stem Cells in Photoreceptor Transplantation

Stem cells that have been explored for possible retinal transplantation include brain-derived neural progenitor cells, embryonic stem cells, retinal stem cells, bone marrow-derived stem cells, and Müller cell-derived stem cells.

Given that the brain and retina are derived from neuroectoderm and that immature neuronal and progenitor cells are intrinsically capable of migrating and differentiating during neural development, it would appear that brain-derived neural progenitor cells could potentially differentiate into photoreceptors in the subretinal space. Several groups have examined this possibility[408–411] and noted that there was limited integration of neural progenitor cells into adult host retina,[409] but migration of transplanted cells was observed in all layers of a developing immature retina. However, these integrated cells did not express markers of mature retinal cells.[408,411,412] Perhaps this result reflects the fact that the lineage is restricted to brain-derived neural cells.[413]

Alternatively, retinal progenitors isolated from developing retina would not have the above-mentioned lineage restriction. Transplantation of such cells isolated from embryonic retina into young transgenic S334ter rats, an RP model, showed grafted cells forming a multilayered cellular sheet in the subretinal space and expressing retina-specific neuronal differentiation markers, e.g., recoverin and rhodopsin. Similarly, multipotent retinal stem cells isolated from adult mouse retina were able to successfully integrate, assume photoreceptor morphology, form synapses with host retinal neurons, and become functional based on electrophysiologic measurements in *rd1* and *rd7* mutant mice.[414] Human retinal progenitor cells isolated from fetal neural retina were transplanted into the subretinal space of an RCS rat, and 12 weeks later showed significantly better optokinetic response and superior preservation of the ONL thickness, spread distance, and cell count than vehicle controls.[415] In an effort aimed at photoreceptor rescue as well as restoration of retinal function, retinal progenitor cells were incubated with BDNF or GDNF slow-releasing microspheres and transplanted into the degenerating retina of S334ter line 3 rats.[416] In transplanted areas, there were RPE-photoreceptor outer segment interactions, rod and cone opsin immunoreactivity, preservation of amacrine and horizontal cells, and absence of glial hypertrophy allowing host-graft integration. Mouse retinal progenitor cells grown on a biodegradable thin-film polycaprolactone scaffold not only showed differentiation into photoreceptor lineage in vitro, but, when injected into the subretinal space of rhodopsin null mice, the cells localized in the ONL and expressed photoreceptor-specific markers.[417] A modification of the polycaprolactone scaffold by hybridizing it with the interphotoreceptor matrix may prove an even better platform for retinal progenitor cell transplantation.[418] Hyaluronic acid-based hydrogels may serve as a scaffold by which to reliably deliver retinal progenitor cells into the subretinal space.[419] Studies by MacLaren and Bartsch mentioned above also demonstrated survival, integration, and expression of mature photoreceptor markers when cells isolated at the peak of rod development were transplanted into the adult retina.[400,420] However, isolation of such cells from developing human retina would be unethical.[421]

Retinal progenitor cells exist in lower vertebrates in the ciliary margin zone, and similar cells have been isolated from adult human eyes.[67,69] Thus, human donor eyes might be used for isolation of retinal progenitor cells. These cells grow as neurospheres in culture and give rise to both glial and neural cells. Only a small fraction of cells express mature retinal cell types, however, and they do not completely differentiate into functional retinal cells.[422,423] These cells can be induced in culture by retroviral transduction of photoreceptor-specific transcription factors to express molecules such as transducin and recoverin, and they differentiate into light-sensitive rod phenotypes.[424,425] When transplanted into adult normal or degenerate retina, results have varied with some studies showing no differentiation or expression of mature retinal markers[426] and others showing differentiation of the cells with expression of mature retinal markers but without expressing mature retinal cell morphology or integration into host retina.[408,427–429] An additional problem with these cells is that they exhibit limited self-renewal in culture.[422,430] Despite the above mentioned limitations, clinical studies on intravitreal and subretinal injection of retinal progenitor cells in patients with RP are being initiated (NCT02464436, NCT02320812).

Müller cells are another potential source of stem cells.[431] Müller cells from mammalian retina possess stem-cell-like properties of growing in neurospheres and expression of neural stem cell markers, and they differentiate and express mature retinal markers including peripherin and opsin.[432,433] A spontaneously immortalized Müller cell line has been reported by Limb and coworkers.[434] Whether these cells can form fully differentiated retinal neurons is not known although, in contrast to retinal progenitor cells, they do not seem to have limited self-renewal. Transplants of Müller-cell-derived stem cells have shown limited integration,[432] but treatment of the host retina with chondroitinase (to break down proteoglycans prior to transplantation) resulted in better integration.[435] Human Müller glial cells were stimulated to differentiate into photoreceptors (showing upregulation of gene and protein expression of CRX, NR2E3, rhodopsin, and other phototransduction markers) that were transplanted into the subretinal space of the P23H rat. After transplantation, they migrated and integrated into

the ONL and increased the a-wave amplitude as measured by scotopic flash ERG.[436]

Embryonic stem cells can be cultured indefinitely and can be induced to differentiate into cell lineages of the three germ layers. Typically, culture of these cells requires the use of animal serum or coculture with animal-derived cells. Approval of use of such cells would be problematic due to potential contamination.[421] However, human ESCs have been cultured without use of such reagents, and cell lines have been established.[437,438] Efficient protocols for producing retinal cells from ESCs have been developed.[94,95,395,439] Transplants of precursors derived from ESCs via techniques prior to those developed by Lamba or Osakada have been shown to rescue photoreceptors in RCS rats[440] or migrate into rabbit retina and express S-opsin and rhodopsin.[441] Yanai et al.[442] recently reported on higher yield and quicker differentiation of human ESCs into photoreceptor precursor cells using size-controlled embryoid bodies, addition of triiodothyronine and taurine to the culture medium, and negative selection of undifferentiated cells. Hypoxia is another factor that increases photoreceptor differentiation from mouse ESCs.[443] It is not known if the newer techniques of deriving mature human retinal cells create cells that are able to survive, integrate, and function to a greater degree following transplantation. Early experiments in mice have been promising. ESC-derived retinal cells survived and were able to form functional photoreceptors after transplantation in $Crx^{-/-}$ mice,[318] a gene knockout animal model of Leber congenital amaurosis that is characterized by reduction or loss of components of phototransduction cycle including rhodopsin, cone opsin, transducin, cone arrestin, and recoverin. Thus, these mice do not have any ERG response. After transplantation, a small ERG response was detected. Human ESCs also replace photoreceptors in mnd mice[315] and in *rd1* mice.[314] Lakowski and colleagues showed that $CD73(^{+})CD24(^{+})CD133(^{+})CD47(^{+})CD15(^{-})$ photoreceptor precursor cells isolated from three-dimensional self-forming retina differentiated from mouse ESC successfully integrated and matured into rod photoreceptors in adult mouse retina after subretinal transplantation.[444] Similarly, Eberle et al. showed a threefold higher retinal integration of $CD73(^{+})$ magnetic-associate cell sorted

photoreceptor cells versus nonsorted cells when transplanted into the subretinal space of adult wild-type mice, as well as successful generation of photoreceptor outer segments.[445,446] Furthermore, Laver et al. visualized the location of transplanted stem cell-derived photoreceptor precursor cells after transplantation, which may aid our understanding of three-dimensional architecture, engraftment, and survival of such cells.[447]

iPSCs may be a good source of genetically matched stem cells whose isolation may not have the ethical complexity associated with the use of embryonic or fetal tissues. However, the efficiency of production is very poor. iPSCs have been induced to differentiate into photoreceptors and can generate cells that integrate into the host retina, express photoreceptor-specific markers, localize to the ONL, and improve ERG response.[448,449] Zhou and coworkers subjected pig iPSCs to a rod differentiation protocol and culture that resulted in rod-like cells that expressed rhodopsin and rod outer-segment-specific membrane protein 1.[450] These differentiated cells, when transplanted into the subretinal space of pigs treated with iodoacetic acid to eliminate photoreceptors, were noted in the outer nuclear layer, but only a few of the cells expressed projections resembling outer segments at 3 weeks. Similarly, Lamba and coworkers showed that such cells were able to integrate into mouse retina.[448]

Following reports of bone marrow-derived stem cells integrating into the retina and differentiating into photoreceptors in rat eyes,[451] attempts have been made to induce these cells to develop into retinal cells in vitro.[452,453] Injection of bone marrow-derived mesenchymal stem cells into the subretinal space appears to have a rescue effect on photoreceptors.[454,455] However, the outcome may be due to a trophic effect rather than a result of transplanted cells differentiating into photoreceptors. As noted above, intravitreal bone marrow-derived lineage-negative hematopoietic stem cells rescue photoreceptors (primarily cones) in *rd1* and *rd10* mice.[337] Peripheral blood mononuclear cells, a population of cells believed to include a small proportion of pluripotent stem cells, have shown results similar to bone marrow-derived stem cells in terms of survival after subretinal transplantation, intraretinal migration, and expression of photoreceptor-specific markers.[456,457]

Results of Photoreceptor Transplants in Humans

Neural retinal transplantation has been performed in human volunteers with RP and AMD.[316,347,384–387] In these studies pre- and postoperative visual acuity and evaluation of retinal function were done using a variety of psychophysical, electrophysiologic, and clinical tests, including macular perimetry, full-field and focal ERGs, fundus examination, fundus photography, and fluorescein angiography. Kaplan and coworkers[347] reported the transplantation of vibratome-sectioned adult cadaveric photoreceptor sheets into the subretinal space of two patients with advanced RP and visual acuity of no light perception (NLP). The patients were not immune-suppressed and showed no signs of graft rejection (e.g., focal chorioretinitis, macular edema, vitritis) for up to 12 months after surgery. However, no improvement of visual function was attained. Das and coworkers[384] transplanted fetal neuroretinal cells into the subretinal space of one eye in 14 RP patients, temporal or superotemporal to the macula. Patients were followed for as long as 44 months after surgery with no apparent signs of rejection in the absence of immune suppression. Visual improvement was reported in five transplant recipients but was based solely on subjective testing (i.e., improved visual acuity in five patients and a detectable narrow visual field in two patients). Moreover, these patients had some degree of visual perception preoperatively, which may have been underestimated resulting in an apparent increase in visual function after surgery. No improvement of results from more objective tests, such as a full-field ERG or VEPs, was observed. In another study, two patients with advanced RP received subretinal transplants of intact fetal retina.[458] Patients were followed for 12 months after surgery with no clinical signs of rejection. Both patients reported subjective visual improvement (new visual sensations), and one patient showed a transient faint positive response during a multifocal ERG that was later undetectable. The same authors cotransplanted sheets of fetal retina together with the adjacent RPE unilaterally into the subretinal space near the fovea in five RP patients with visual acuity of light perception (LP).[386] After 6 months follow-up, there was no evidence of rejection, but no

visual improvement was observed. Although, in another patient with autosomal dominant RP, cotransplantation of fetal retina with RPE resulted in long-term improvement of visual acuity (from 20/800 to 20/270) and visual field.[459] This group subsequently reported on 10 patients (6 RP, 4 AMD) who received retinal implants in one eye and were followed in a phase II trial conducted in a clinical practice setting.[316] Seven patients (3 RP, 4 AMD) showed improved EDTRS visual acuity scores. Three of these patients (1 RP, 2 AMD) showed improvement in both eyes to the same extent. In 1 RP patient, vision remained the same, but in 2 RP patients, vision decreased. One RP patient maintained an improvement in vision from 20/800 to 20/320 at the 6-year follow-up, while the nonsurgery eye had deteriorated to hand motion vision. This patient also showed a 23% increase in light sensitivity at 5 years compared to microperimetry results at 2 years; the other patients showed no improved sensitivity. Although no HLA match was found between donors and recipients, no rejection of the implanted tissue was observed clinically. Humayun and coworkers[385] transplanted fetal retinal microaggregates into the subretinal space of 8 patients with advanced RP and visual acuity of LP, as well as a fetal retinal sheet plus microaggregates in 1 patient (in two separate locations) with advanced neovascular AMD and visual acuity of NLP. Patients were followed for as long as 13 months after surgery with no signs of rejection in the absence of immune suppression. Three patients showed a decline in visual function, and 3 others showed a transient improvement. The patient with AMD died from an unrelated cause 3 years after receiving the transplant. Ultrastructural and immunocytochemical studies of the eye revealed survival of at least some of the transplanted cells in the subretinal space with no signs of inflammation.[388] Although the host retina and transplant were separated in some areas by a fibrocellular membrane composed of Müller cell processes, cellular debris, and collagen, a few GABA-positive and synaptophysin-positive cell processes extended between the transplant and the host retina. However, no synaptic contacts involving these processes were found. In another study, adult human cadaveric photoreceptor sheets harvested with the excimer laser were transplanted into 8 patients with advanced RP.[387] Subjects were

followed for 12 months, but no improvement in visual function was recorded. Siqueira and coworkers[460] reported the results of a prospective phase I, nonrandomized open-label study of autologous bone marrow-derived mononuclear cell transplants in RP patients with best-corrected ETDRS visual acuity worse than 20/200. Patients (3 with RP, 2 with cone–rod dystrophy) received intravitreal injection of 10^4 autologous bone marrow-derived stem cells/0.1 mL, 3–3.5 mm posterior to the limbus with a 27-gauge needle. No adverse effects occurred (e.g., teratoma, visual loss, intraocular inflammation), but there was no documented benefit (e.g., visual acuity, visual field, ERG, optical coherence tomography) at 10-months follow-up. In a similar study, Park et al.[461] injected a mean of 3.4 million human autologous bone marrow $CD34^+$ stem cells into the vitreous of 2 patients with SMD, 2 patients with AMD, and 1 patient with RP (VA <20/200 in all patients). Although VA improved in 4 (80%) of 5 patients during 6 months of follow-up and no long-term ocular or systemic side-effects were observed, progression of geographic atrophy was evident in both patients with AMD (along with decline in ERG and microperimetry) despite the suggestion of stem cell integration into the host retina as assessed by adaptive optics OCT. While these studies have established the feasibility and safety of retinal transplantation in humans as well as the survival of the transplants, additional work remains to achieve long-term preservation of visual function.

Immune Response to Photoreceptor Transplants

Photoreceptor cells are probably minimally immunogenic due to very low levels of expression of MCH class I molecules.[462] Most neural retinal transplantation studies in animal models have employed allografts and, to a lesser extent, xenografts with or without host immunosuppression. In humans, allografts have been used almost exclusively.[347,384–387,458] The occurrence of cell-mediated delayed hypersensitivity rejection following retinal transplantation was only reported in a few studies involving xenografts.[355] Two distinct aspects of immune privilege may play a role in retinal

transplantation. First, immature neural retina is immune privileged tissue,[463] and second, the subretinal space is an immune privileged site.[188] So far, it is not clear whether adult neural retina also behaves as immune privileged tissue.[186] Neural progenitor cells behave like immune privileged tissue as well.[464] As noted above, however, neural tissue derived from iPSCs may not be immune privileged because abnormal gene expression in some cells differentiated from iPSCs (both via a retroviral and episomal approach) can induce a T-cell-dependent immune response in a syngeneic recipient.[84]

Although the majority of neurons, including retinal neurons, do not express MHC molecules, they may express minor histocompatibility antigens.[186] These antigens are not displayed in the absence of MHC class I expression, but if cells die, minor histocompatibility antigens can be released, phagocytosed by antigen-presenting cells, and presented to T-lymphocytes.[186] Furthermore, retinal glial cells, including Müller cells and astrocytes, constitutively express class I and II MHC molecules.[465,466] Neural retinal microglia may also play a major role in the expression of transplantation antigens. Microglia can localize in the lumen of graft rosettes as well as within and surrounding retinal grafts, especially those undergoing rejection.[467] Ma and Streilein[468] have shown that these cells become activated after transplantation of neural retina into the subretinal space and display upregulated expression of both class I and class II MHC molecules. Donor-derived, activated microglia are thought to act as antigen-presenting cells that initially induce ACAID in their recipients following subretinal transplantation but eventually mediate an atypical delayed hypersensitivity reaction in which slow rejection of the graft takes place instead of the acute graft rejection seen in typical delayed hypersensitivity. In addition, Xu et al.[469] showed that conditioned medium from CD11b(+) interferon-gamma and lipopolysaccharide activated microglia was able to influence retinal progenitor cells to differentiate into neuron-like cells expressing the photoreceptor marker recoverin. These results imply that microglia are an important population of cells that may affect photoreceptor cell survival and may represent an additional target in an effort to optimize retinal cell transplantation and integration.

As noted previously, the immune privilege of the subretinal

space is not absolute. Whereas gross infiltration by lymphocytes is seen rarely after transplantation into the subretinal space and graft survival is prolonged, tissue rejection still may occur.[198,463,470] The underlying mechanism of graft rejection in this immune privileged site is not understood fully. However, it appears to involve an unconventional pattern of immune response that comprises only minimal lymphoreticular cell infiltration with gradual rather than acute graft deterioration.[463] Exposure of the subretinal space to systemic immunity, which occurs if the integrity of the blood–retina barrier is compromised due to surgery and/or disease such as RP or AMD, can contribute to graft rejection.[198] Breach of the host blood–retina barrier may allow MHC-expressing cells, e.g., dendritic cells from the systemic circulation, to invade the subretinal space and present the transplant antigens to T-lymphocytes. Immune suppression may be needed to prolong the survival of the graft.[470]

Photoreceptor Transplantation: Future Directions

Studies in experimental animals and humans indicate that absence or paucity of graft–host synaptic interactions remains an unsolved obstacle to successful neural retinal replacement. The retinal and subretinal microenvironment can influence the differentiation and functionality of transplanted cells. Photoreceptor morphology and the degree of integration can vary depending on the state of the recipient.[395] Although synapse formation between donor and host tissue has been documented as has recovery of visual function (in preclinical models), the overall efficiency of photoreceptor transplantation currently is poor with 0.1–1% of transplanted cells surviving long term after transplantation.[395,471–473]

Reactive glial cells may constitute a barrier between the host retina and the grafted cells.[389] Following retinal transplantation, astrocytes and Müller cells become reactive and upregulate expression of the intermediate filament proteins, glial fibrillary acid protein (GFAP), and vimentin.[345] Reactive gliosis can create a barrier that separates the area of injury from surrounding healthy tissue,[474] which may explain the consistent finding that neuritic

processes extend between the graft and the host only in areas of the transplant where the glial barrier is absent[332,344] or where the host outer limiting membrane, rich in adherens junctions involving Müller cell processes, is disrupted.[389] In an in vitro study, neuronal cell processes extended between two pieces of retina placed adjacent to each other in culture. However, processes did not appear to grow if they encountered glial structures such as the outer or inner limiting membranes.[389] In contrast, robust neurite outgrowth was seen in immature isolated retinal cells transplanted into the subretinal space of mutant mice deficient in GFAP and vimentin.[475] Disruption of the outer limiting membrane, breaking down the glial barrier using matrix metalloproteinase delivered through biodegradable polymers, as well as selecting specific cells based on cell surface markers, has been shown to improve graft migration and integration into host retina.[391,392,401,476]

Alternatively, scarcity of graft–host synaptic integration may involve factors intrinsic to the transplant itself. Retinal neurons, including photoreceptors, display synaptic plasticity during injury or disease[301,477–481] and in culture.[482,483] This potential for structural plasticity can be geared towards enhancing synaptic interactions between the graft and the host after transplantation. Photoreceptor sheets prepared by vibratome-sectioning undergo significant morphologic changes, including rapid retraction of axonal terminals towards their cell bodies in culture.[484] This phenomenon has also been seen in studies of experimental retinal detachment[293,477] and may be due to separation of photoreceptors from adjacent RPE cells. Retraction of photoreceptor terminals is likely to interfere with synaptic integration following transplantation since physical proximity is required for synaptogenesis to occur between pre- and postsynaptic elements. One can prevent retraction by increasing intracellular cAMP levels in photoreceptor sheets[485] or by inhibiting RhoA,[486,487] which may help improve synaptic interactions between pretreated photoreceptor grafts and host bipolar and horizontal cells.

Identification of the optimal parameters for successful retinal transplantation, such as the source of cells (e.g., human ESCs versus iPSCs versus mature dispersed photoreceptors) or the surgical procedure (e.g., sheets on a biodegradable membrane versus

dispersed cells), as well as resolving issues of tissue rejection, are important goals, regardless of whether the objective of surgery is "rescue" or "replacement." We anticipate tremendous progress in generating photoreceptors from stem cells (induced pluripotent, embryonic, bone marrow, or peripheral blood) and identification of which cell is most capable of integrating and differentiating in a diseased microenvironment during the next decade. Additional studies on modification of the host transplantation microenvironment in order to optimize cell integration may also be pursued.[394,396] Restoration of a functional neural retinal network capable of mediating visual perception, which is a goal unique to "replacement" therapy, depends primarily on establishing graft–host synaptic integration sufficient to rectify the damaged neural circuitry resulting from cell loss. Preclinical studies have shown that it may be possible to restore transmission of visual stimuli between damaged retinas and higher-order areas of visual processing (i.e., V1 cerebral cortex) in select animal models of retinal degeneration.[407] To achieve neural reintegration, additional experimental studies (e.g., identification of molecules that foster synapse formation, development of means to unambiguously identify donor and recipient neurons, identifying methods to manage the synaptic rewiring that accompanies photoreceptor degeneration) and clinical studies must be done. Initial efforts to visualize integrating tissue reliably are underway. In addition, more rigorous functional tests must be developed to aid in the accurate, objective assessment of incremental changes in vision (particularly for low levels of visual function) following retinal transplantation. Since photoreceptor death is associated with synaptic remodeling in the local retinal circuitry[298,301,302,478,488] and may cause transneuronal cell death of inner retinal neurons, relatively early intervention (i.e., before foveal cone cell loss is profound) may play a significant role in the success of retinal transplantation.

Conclusions

In principle, RPE and retinal cell transplantation offer the possibility of sight-restoring therapy for blindness due to age-

related macular degeneration, retinitis pigmentosa, and allied diseases. Extensive research has led to the identification of several obstacles to success, namely graft survival and differentiation (in the case of RPE and photoreceptors), graft integration with the host (in the case of photoreceptors), and immune rejection (at least in the case of RPE cells). Additional progress in this new field of ocular surgery will occur through an iterative process comprising the development of suitable in vitro and animal models, refinement of immune-suppressive therapy, development of a noncontroversial source of safe and unlimited donor cells from stem cells, improved in vivo imaging technologies for in situ assessment of the transplant anatomy and function in human patients, and carefully designed clinical experiments. The unique anatomy of the eye, including the laminar organization of retinal neurons, the immune-suppressive environment of the subretinal space, and the immune-privileged nature of RPE cells and retinal neurons, combined with straightforward surgical access to the subretinal space, augur well for the ultimate success of these efforts.

References

1. Royo PE, Quay WB. Retinal transplantation from fetal to maternal mammalian eye. *Growth*. 1959;23:313–336.
2. Van Dooremaal JC. De onwikkeling van levende weefsels op vreemden bodem geent. *Onderz Physiol Lab Rijksuniv Utrechtsche Hoogeschool*. 1873;3:277–290.
3. del Cerro M, Gash DM, Rao GN, et al. Intraocular retinal transplants. *Invest Ophthalmol Vis Sci*. 1985;26:1182–1185.
4. Gouras P, Flood MT, Kjedbye H, et al. Transplantation of cultured human retinal epithelium to Bruch's membrane of the owl monkey's eye. *Curr Eye Res*. 1985;4:253–265.
5. Li LX, Turner JE. Inherited retinal dystrophy in the RCS rat: prevention of photoreceptor degeneration by pigment epithelial cell transplantation. *Exp Eye Res*. 1988;47:911–917.
6. D'Cruz PM, Yasumura D, Weir J, et al. Mutation of the receptor tyrosine kinase gene Mertk in the retinal dystrophic RCS rat. *Hum Mol Genet*. 2000;9:645–651.
7. Zarbin M. Cell-based therapy for degenerative retinal disease. *Trends Mol Med*. 2016;22:115–134.
8. Lund RD, Hauschka SD. Transplanted neural tissue develops connections with host rat brain. *Science*. 1976;193:582–584.
9. Das GD, Hallas BH. Transplantation of brain tissue in the brain of adult rats. *Experientia*. 1978;34:1304–1306.
10. Klassen H, Lund RD. Retinal transplants can drive a pupillary reflex in host rat brains. *Proc Natl Acad Sci USA*. 1987;84:6958–6960.
11. Coffey PJ, Lund RD, Rawlins JN. Detecting the world through a retinal implant. *Prog Brain Res*. 1990;82:269–275.
12. Lund RD, Radel JD, Coffey PJ. The impact of intracerebral retinal transplants on types of behavior exhibited by host rats. *Trends Neurosci*. 1991;14:358–362.
13. Turner JE, Blair JR. Newborn rat retinal cell transplanted into a retinal lesion site in adult host eyes. *Brain Res*. 1986;26:91–104.
14. Silverman MS, Hughes SE. Transplantation of

photoreceptors to light- damaged retina. *Invest Ophthalmol Vis Sci*. 1989;30:1684–1690.
15. Klein R, Klein BE, Linton KL. Prevalence of age-related maculopathy. The Beaver Dam Eye Study. *Ophthalmology*. 1992;99:933–943.
16. Ferris FL 3rd, Fine SL, et al. Age-related macular degeneration and blindness due to neovascular maculopathy. *Arch Ophthalmol*. 1984;102:1640–1642.
17. Klein R, Klein BE, Jensen SC, et al. The five-year incidence and progression of age-related maculopathy: the Beaver Dam Eye Study. *Ophthalmology*. 1997;104:7–21.
18. Friedman DS, O'Colmain BJ, Munoz B, et al. Prevalence of age-related macular degeneration in the United States. *Arch Ophthalmol*. 2004;122:564–572.
19. Rosenfeld PJ, Brown DM, Heier JS, et al. Ranibizumab for neovascular age- related macular degeneration. *N Engl J Med*. 2006;355:1419–1431.
20. Brown DM, Kaiser PK, Michels M, et al. Ranibizumab versus verteporfin for neovascular age-related macular degeneration. *N Engl J Med*. 2006;355:1432–1444.
21. Heier JS, Brown DM, Chong V, et al. Intravitreal aflibercept (VEGF trap-eye) in wet age-related macular degeneration. *Ophthalmology*. 2012;119:2537–2548.
22. Hackett SF, Schoenfeld CL, Freund J, et al. Neurotrophic factors, cytokines and stress increase expression of basic fibroblast growth factor in retinal pigmented epithelial cells. *Exp Eye Res*. 1997;64:865–873.
23. Kanuga N, Winton HL, Beauchene L, et al. Characterization of genetically modified human retinal pigment epithelial cells developed for in vitro and transplantation studies. *Invest Ophthalmol Vis Sci*. 2002;43:546–555.
24. Sugino IK, Sun Q, Wang J, et al. Comparison of FRPE and human embryonic stem cell-derived rpe behavior on aged human Bruch's membrane. *Invest Ophthalmol Vis Sci*. 2011;52:4979–4997.
25. Kolomeyer AM, Sugino IK, Zarbin MA. Characterization of conditioned media collected from cultured adult versus fetal retinal pigment epithelial cells. *Invest Ophthalmol Vis*

Sci. 2011;52:5973–5986.
26. Kolomeyer AM, Sugino IK, Zarbin MA. Characterization of conditioned media collected from aged versus young human eye cups. *Invest Ophthalmol Vis Sci*. 2011;52:5963–5972.
27. Zarbin MA. Retinal pigment epithelium-retina transplantation for retinal degenerative disease. *Am J Ophthalmol*. 2008;146:151–153.
28. Maaijwee K, Joussen AM, Kirchhof B, et al. Retinal pigment epithelium (RPE)-choroid graft translocation in the treatment of an RPE tear: preliminary results. *Br J Ophthalmol*. 2008;92:526–529.
29. Chang LK, Sarraf D. Tears of the retinal pigment epithelium: an old problem in a new era. *Retina*. 2007;27:523–534.
30. Nasir MA, Sugino I, Zarbin MA. Decreased choriocapillaris perfusion following surgical excision of choroidal neovascular membranes in age-related macular degeneration. *Br J Ophthalmol*. 1997;81:481–489.
31. Grossniklaus HE, Hutchinson AK, Capone A, et al. Clinicopathologic features of surgically excised choroidal neovascular membranes. *Ophthalmology*. 1994;101:1099–1111.
32. Coffey PJ, Girman S, Wang SM, et al. Long-term preservation of cortically dependent visual function in RCS rats by transplantation. *Nat Neurosci*. 2002;5:53–56.
33. Li L, Turner JE. Optimal conditions for long-term photoreceptor cell rescue in RCS rats: the necessity for healthy RPE transplants. *Exp Eye Res*. 1991;52:669–679.
34. Little CW, Castillo B, DiLoreto DA, et al. Transplantation of human fetal retinal pigment epithelium rescues photoreceptor cells from degeneration in the Royal College of Surgeons rat retina. *Invest Ophthalmol Vis Sci*. 1996;37:204–211.
35. Lund RD, Adamson P, Sauve Y, et al. Subretinal transplantation of genetically modified human cell lines attenuates loss of visual function in dystrophic rats. *Proc Natl Acad Sci USA*. 2001;98:9942–9947.
36. Lawrence JM, Keegan DJ, Muir EM, et al. Transplantation of

Schwann cell line clones secreting GDNF or BDNF into the retinas of dystrophic Royal College of Surgeons rats. *Invest Ophthalmol Vis Sci*. 2004;45:267–274.
37. Lawrence JM, Sauve Y, Keegan DJ, et al. Schwann cell grafting into the retina of the dystrophic RCS rat limits functional deterioration. *Invest Ophthalmol Vis Sci*. 2000;41:518–528.
38. Lu B, Malcuit C, Wang S, et al. Long-term safety and function of RPE from human embryonic stem cells in preclinical models of macular degeneration. *Stem Cells*. 2009;27:2126–2135.
39. Sheedlo HJ, Li L, Barnstable CJ, et al. Synaptic and photoreceptor components in retinal pigment epithelial cell transplanted retinas of Royal College of Surgeons dystrophic rats. *J Neurosci Res*. 1993;36:423–431.
40. Sauve Y, Lu B, Lund RD. The relationship between full field electroretinogram and perimetry-like visual thresholds in RCS rats during photoreceptor degeneration and rescue by cell transplants. *Vision Res*. 2004;44:9–18.
41. Whiteley SJ, Litchfield TM, Coffey PJ, et al. Improvement of the pupillary light reflex of Royal College of Surgeons rats following RPE cell grafts. *Exp Neurol*. 1996;140:100–104.
42. Lund RD, Wang S, Klimanskaya I, et al. Human embryonic stem cell-derived cells rescue visual function in dystrophic RCS rats. *Cloning Stem Cells*. 2006;8:189–199.
43. McGill TJ, Lund RD, Douglas RM, et al. Preservation of vision following cell-based therapies in a model of retinal degenerative disease. *Vision Res*. 2004;44:2559–2566.
44. Mruthyunjaya P, Stinnett SS, Toth CA. Change in visual function after macular translocation with 360 degrees retinectomy for neovascular age- related macular degeneration. *Ophthalmology*. 2004;111:1715–1724.
45. Pieramici DJ, De Juan E Jr, Fujii GY, et al. Limited inferior macular translocation for the treatment of subfoveal choroidal neovascularization secondary to age-related macular degeneration. *Am J Ophthalmol*. 2000;130:419–428.
46. Cahill MT, Mruthyunjaya P, Bowes Rickman C, Toth CA. Recurrence of retinal pigment epithelial changes after

macular translocation with 360 degrees peripheral retinectomy for geographic atrophy. *Arch Ophthalmol*. 2005;123:935–938.
47. Wobus AM, Boheler KR. Embryonic stem cells: prospects for developmental biology and cell therapy. *Physiol Rev*. 2005;85:635–678.
48. Bharti K, Miller SS, Arnheiter H. The new paradigm: retinal pigment epithelium cells generated from embryonic or induced pluripotent stem cells. *Pigment Cell Melanoma Res*. 2011;24:21–34.
49. Jaenisch R, Young R. Stem cells, the molecular circuitry of pluripotency and nuclear reprogramming. *Cell*. 2008;132:567–582.
50. Thomson JA, Itskovitz-Eldor J, Shapiro SS, et al. Embryonic stem cell lines derived from human blastocysts. *Science*. 1998;282:1145–1147.
51. Reubinoff BE, Pera MF, Fong CY, et al. Embryonic stem cell lines from human blastocysts: somatic differentiation in vitro. *Nat Biotechnol*. 2000;18:399–404.
52. Gage FH. Mammalian neural stem cells. *Science*. 2000;287:1433–1438.
53. Weissman IL. Translating stem and progenitor cell biology to the clinic: barriers and opportunities. *Science*. 2000;287:1442–1446.
54. Ahmad I, Tang L, Pham H. Identification of neural progenitors in the adult mammalian eye. *Biochem Biophys Res Commun*. 2000;270:517–521.
55. Tropepe V, Coles BL, Chiasson BJ, et al. Retinal stem cells in the adult mammalian eye. *Science*. 2000;287:2032–2036.
56. Salero E, Blenkinsop TA, Corneo B, et al. Adult human RPE can be activated into a multipotent stem cell that produces mesenchymal derivatives. *Cell Stem Cell*. 2012;10:88–95.
57. Ferrari G, Cusella-De Angelis G, Coletta M, et al. Muscle regeneration by bone marrow-derived myogenic progenitors. *Science*. 1998;279:1528–1530.
58. Galli R, Borello U, Gritti A, et al. Skeletal myogenic potential of human and mouse neural stem cells. *Nat Neurosci*. 2000;3:986–991.

59. Blau HM, Brazelton TR, Weimann JM. The evolving concept of a stem cell: entity or function? *Cell*. 2001;105:829–841.
60. Marquardt T. Transcriptional control of neuronal diversification in the retina. *Prog Retin Eye Res*. 2003;22:567–577.
61. Fischer AJ, Reh TA. Identification of a proliferating marginal zone of retinal progenitors in postnatal chickens. *Dev Biol*. 2000;220:197–210.
62. Johns PR. Growth of the adult goldfish eye. III. Source of the new retinal cells. *J Comp Neurol*. 1977;176:343–357.
63. Reh TA, Nagy T. Characterization of Rana germinal neuroepithelial cells in normal and regenerating retina. *Neurosci Res Suppl*. 1989;10:S151–61.
64. Raymond PA, Hitchcock PF. Retinal regeneration: common principles but a diversity of mechanisms. *Adv Neurol*. 1997;72:171–184.
65. Spence JR, Madhavan M, Ewing JD, et al. The hedgehog pathway is a modulator of retina regeneration. *Development*. 2004;131:4607–4621.
66. Coles BL, Angenieux B, Inoue T, et al. Facile isolation and the characterization of human retinal stem cells. *Proc Natl Acad Sci USA*. 2004;101:15772–15777.
67. Mayer EJ, Carter DA, Ren Y, et al. Neural progenitor cells from postmortem adult human retina. *Br J Ophthalmol*. 2005;89:102–106.
68. Yang P, Seiler MJ, Aramant RB, et al. In vitro isolation and expansion of human retinal progenitor cells. *Exp Neurol*. 2002;177:326–331.
69. Carter DA, Mayer EJ, Dick AD. The effect of postmortem time, donor age and sex on the generation of neurospheres from adult human retina. *Br J Ophthalmol*. 2007;91:1216–1218.
70. Gong J, Sagiv O, Cai H, et al. Effects of extracellular matrix and neighboring cells on induction of human embryonic stem cells into retinal or retinal pigment epithelial progenitors. *Exp Eye Res*. 2008;86:957–965.
71. Vossmerbaeumer U, Kuehl S, Kern S, et al. Induction of retinal pigment epithelium properties in ciliary margin

progenitor cells. *Clin Experiment Ophthalmol*. 2008;36:358–366.
72. Blenkinsop TA, Salero E, Stern JH, Temple S. The culture and maintenance of functional retinal pigment epithelial monolayers from adult human eye. *Methods Mol Biol*. 2013;945:45–65.
73. Klimanskaya I, Chung Y, Becker S, et al. Human embryonic stem cell lines derived from single blastomeres. *Nature*. 2006;444(7118):481–485.
74. Chung Y, Klimanskaya I, Becker S, et al. Human embryonic stem cell lines generated without embryo destruction. *Cell Stem Cell*. 2008;2:113–117.
75. Tachibana M, Amato P, Sparman M, et al. Human embryonic stem cells derived by somatic cell nuclear transfer. *Cell*. 2013;153:1228–1238.
76. Chung YG, Eum JH, Lee JE, et al. Human somatic cell nuclear transfer using adult cells. *Cell Stem Cell*. 2014;14:777–780.
77. Yamada M, Johannesson B, Sagi I, et al. Human oocytes reprogram adult somatic nuclei of a type 1 diabetic to diploid pluripotent stem cells. *Nature*. 2014;510:533–536.
78. Yabut O, Bernstein HS. The promise of human embryonic stem cells in aging-associated diseases. *Aging*. 2011;3:494–508.
79. Deuse T, Wang D, Stubbendorff M, et al. SCNT-derived ESCs with mismatched mitochondria trigger an immune response in allogeneic hosts. *Cell Stem Cell*. 2015;16:33–38.
80. Park IH, Zhao R, West JA, et al. Reprogramming of human somatic cells to pluripotency with defined factors. *Nature*. 2008;451:141–146.
81. Takahashi K, Tanabe K, Ohnuki M, et al. Induction of pluripotent stem cells from adult human fibroblasts by defined factors. *Cell*. 2007;131:861–872.
82. Kim K, Doi A, Wen B, et al. Epigenetic memory in induced pluripotent stem cells. *Nature*. 2010;467:285–290.
83. Ma H, Morey R, O'Neil RC, et al. Abnormalities in human pluripotent cells due to reprogramming mechanisms. *Nature*. 2014;511:177–183.

84. Zhao T, Zhang ZN, Rong Z, et al. Immunogenicity of induced pluripotent stem cells. *Nature*. 2011;474:212–215.
85. Chin MH, Mason MJ, Xie W, et al. Induced pluripotent stem cells and embryonic stem cells are distinguished by gene expression signatures. *Cell Stem Cell*. 2009;5:111–123.
86. Doi A, Park IH, Wen B, et al. Differential methylation of tissue- and cancer-specific CpG island shores distinguishes human induced pluripotent stem cells, embryonic stem cells and fibroblasts. *Nat Genet*. 2009;41:1350–1353.
87. Zhao T, Zhang ZN, Westenskow PD, et al. Humanized mice reveal differential immunogenicity of cells derived from autologous induced pluripotent stem cells. *Cell Stem Cell*. 2015;17:353–359.
88. Haruta M, Sasai Y, Kawasaki H, et al. In vitro and in vivo characterization of pigment epithelial cells differentiated from primate embryonic stem cells. *Invest Ophthalmol Vis Sci*. 2004;45:1020–1025.
89. Klimanskaya I, Hipp J, Rezai KA, et al. Derivation and comparative assessment of retinal pigment epithelium from human embryonic stem cells using transcriptomics. *Cloning Stem Cells*. 2004;6:217–245.
90. Idelson M, Alper R, Obolensky A, et al. Directed differentiation of human embryonic stem cells into functional retinal pigment epithelium cells. *Cell Stem Cell*. 2009;5:396–408.
91. Lu L, Garcia CA, Mikos AG. Retinal pigment epithelium cell culture on thin biodegradable poly(DL-lactic-co-glycolic acid) films. *J Biomater Sci Polym Ed*. 1998;9:1187–1205.
92. Tomita M, Lavik E, Klassen H, et al. Biodegradable polymer composite grafts promote the survival and differentiation of retinal progenitor cells. *Stem Cells*. 2005;23:1579–1588.
93. Buchholz DE, Hikita ST, Rowland TJ, et al. Derivation of functional retinal pigmented epithelium from induced pluripotent stem cells. *Stem Cells*. 2009;27:2427–2434.
94. Osakada F, Ikeda H, Sasai Y, et al. Stepwise differentiation of pluripotent stem cells into retinal cells. *Nat Protoc*. 2009;4:811–824.
95. Osakada F, Ikeda H, Mandai M, et al. Toward the generation

of rod and cone photoreceptors from mouse, monkey and human embryonic stem cells. *Nat Biotechnol*. 2008;26:215–224.
96. Kokkinaki M, Sahibzada N, Golestaneh N. Human induced pluripotent stem-derived retinal pigment epithelium (RPE) cells exhibit ion transport, membrane potential, polarized vascular endothelial growth factor secretion, and gene expression pattern similar to native RPE. *Stem Cells*. 2011;29:825–835.
97. Maeda T, Lee MJ, Palczewska G, et al. Retinal pigmented epithelial cells obtained from human induced pluripotent stem cells possess functional visual cycle enzymes in vitro and in vivo. *J Biol Chem*. 2013;288:34484–34493.
98. Brandl C, Zimmermann SJ, Milenkovic VM, et al. In-depth characterisation of retinal pigment epithelium (RPE) cells derived from human induced pluripotent stem cells (hiPSC). *Neuromolecular Med*. 2014;16:551–564.
99. Kamao H, Mandai M, Okamoto S, et al. Characterization of human induced pluripotent stem cell-derived retinal pigment epithelium cell sheets aiming for clinical application. *Stem Cell Reports*. 2014;2:205–218.
100. Muniz A, Greene WA, Plamper ML, et al. Retinoid uptake, processing, and secretion in human iPS-RPE support the visual cycle. *Invest Ophthalmol Vis Sci*. 2014;55:198–209.
101. Fields MA, Bowrey HE, Gong J, Ablonczy Z, Del Priore LV. Retinoid processing in induced pluripotent stem cell-derived retinal pigment epithelium cultures. *Prog Mol Biol Transl Sci*. 2015;134:477–490.
102. Leach LL, Clegg DO. Concise review: Making stem cells retinal: methods for deriving retinal pigment epithelium and implications for patients with ocular disease. *Stem Cells*. 2015;33:2363–2373.
103. Sun J, Mandai M, Kamao H, et al. Protective effects of human iPS-derived retinal pigmented epithelial cells in comparison with human mesenchymal stromal cells and human neural stem cells on the degenerating retina in rd1 mice. *Stem Cells*. 2015;33:1543–1553.
104. Li Y, Tsai YT, Hsu CW, et al. Long-term safety and efficacy

of human-induced pluripotent stem cell (iPS) grafts in a preclinical model of retinitis pigmentosa. *Mol Med*. 2012;18:1312–1319.
105. Arnhold S, Klein H, Semkova I, et al. Neurally selected embryonic stem cells induce tumor formation after long-term survival following engraftment into the subretinal space. *Invest Ophthalmol Vis Sci*. 2004;45:4251–4255.
106. Araki R, Uda M, Hoki Y, et al. Negligible immunogenicity of terminally differentiated cells derived from induced pluripotent or embryonic stem cells. *Nature*. 2013;494:100–104.
107. Yu J, Hu K, Smuga-Otto K, et al. Human induced pluripotent stem cells free of vector and transgene sequences. *Science*. 2009;324:797–801.
108. Kaji K, Norrby K, Paca A, et al. Virus-free induction of pluripotency and subsequent excision of reprogramming factors. *Nature*. 2009;458:771–775.
109. Kang X, Yu Q, Huang Y, et al. Effects of integrating and non-integrating reprogramming methods on copy number variation and genomic stability of human induced pluripotent stem cells. *PLoS ONE*. 2015;10:e0131128.
110. Schwartz SD, Hubschman JP, Heilwell G, et al. Embryonic stem cell trials for macular degeneration: a preliminary report. *Lancet*. 2012;379:713–720.
111. Kanemura H, Go MJ, Shikamura M, et al. Tumorigenicity studies of induced pluripotent stem cell (iPSC)-derived retinal pigment epithelium (RPE) for the treatment of age-related macular degeneration. *PLoS ONE*. 2014;9:e85336.
112. Kuroda T, Yasuda S, Sato Y. In vitro detection of residual undifferentiated cells in retinal pigment epithelial cells derived from human induced pluripotent stem cells. *Methods Mol Biol*. 2014;1210:183–192.
113. Stanzel BV, Liu Z, Somboonthanakij S, et al. Human RPE stem cells grown into polarized RPE monolayers on a polyester matrix are maintained after grafting into rabbit subretinal space. *Stem Cell Reports*. 2014;2:64–77.
114. Stern J, Temple S. Stem cells for retinal repair. *Dev Ophthalmol*. 2014;53:70–80.

115. Mariotti C, Lazzarini R, Nicolai M, et al. Comparative study between amniotic-fluid mesenchymal stem cells and retinal pigmented epithelium (RPE) stem cells ability to differentiate towards RPE cells. *Cell Tissue Res*. 2015;362:21–31.
116. Chiou SH, Kao CL, Peng CH, et al. A novel in vitro retinal differentiation model by co-culturing adult human bone marrow stem cells with retinal pigmented epithelium cells. *Biochem Biophys Res Commun*. 2005;326:578–585.
117. Mathivanan I, Trepp C, Brunold C, Baerlocher G, Enzmann V. Retinal differentiation of human bone marrow-derived stem cells by co-culture with retinal pigment epithelium in vitro. *Exp Cell Res*. 2015;333:11–20.
118. Arnhold S, Heiduschka P, Klein H, et al. Adenovirally transduced bone marrow stromal cells differentiate into pigment epithelial cells and induce rescue effects in RCS rats. *Invest Ophthalmol Vis Sci*. 2006;47:4121–4129.
119. Feng Q, Lu SJ, Klimanskaya I, et al. Hemangioblastic derivatives from human induced pluripotent stem cells exhibit limited expansion and early senescence. *Stem Cells*. 2010;28:704–712.
120. Lamba DA, Reh TA. Microarray characterization of human embryonic stem cell-derived retinal cultures. *Invest Ophthalmol Vis Sci*. 2011;52:4897–4906.
121. Banin E, Obolensky A, Idelson M, et al. Retinal incorporation and differentiation of neural precursors derived from human embryonic stem cells. *Stem Cells*. 2006;24:246–257.
122. Vugler A, Carr AJ, Lawrence J, et al. Elucidating the phenomenon of hESC-derived RPE: anatomy of cell genesis, expansion and retinal transplantation. *Exp Neurol*. 2008;214:347–361.
123. Marmorstein AD, Marmorstein LY, Rayborn M, et al. Bestrophin, the product of the Best vitelliform macular dystrophy gene (VMD2), localizes to the basolateral plasma membrane of the retinal pigment epithelium. *Proc Natl Acad Sci USA*. 2000;97:12758–12763.
124. Bakall B, Radu RA, Stanton JB, et al. Enhanced

accumulation of A2E in individuals homozygous or heterozygous for mutations in BEST1 (VMD2). *Exp Eye Res*. 2007;85:34–43.
125. Morimura H, Fishman GA, Grover SA, et al. Mutations in the RPE65 gene in patients with autosomal recessive retinitis pigmentosa or leber congenital amaurosis. *Proc Natl Acad Sci USA*. 1998;95:3088–3093.
126. Maw MA, Kennedy B, Knight A, et al. Mutation of the gene encoding cellular retinaldehyde-binding protein in autosomal recessive retinitis pigmentosa. *Nat Genet*. 1997;17:198–200.
127. Li Y, Chan L, Nguyen HV, et al. Personalized medicine: cell and gene therapy based on patient-specific IPSC-derived retinal pigment epithelium cells. *Adv Exp Med Biol*. 2016;854:549–555.
128. Mata NL, Weng J, Travis GH. Biosynthesis of a major lipofuscin fluorophore in mice and humans with ABCR-mediated retinal and macular degeneration. *Proc Natl Acad Sci USA*. 2000;97:7154–7159.
129. Allikmets R, Singh N, Sun H, et al. A photoreceptor cell-specific ATP- binding transporter gene (ABCR) is mutated in recessive Stargardt macular dystrophy. *Nat Genet*. 1997;15:236–246.
130. Zarbin MA. Current concepts in the pathogenesis of age-related macular degeneration. *Arch Ophthalmol*. 2004;122:598–614.
131. Anderson DH, Radeke MJ, Gallo NB, et al. The pivotal role of the complement system in aging and age-related macular degeneration: hypothesis re-visited. *Prog Retin Eye Res*. 2010;29:95–112.
132. Tsai Y, Lu B, Bakondi B, et al. Human iPSC-derived neural progenitors preserve vision in an AMD-like model. *Stem Cells*. 2015;33:2537–2549.
133. Lu B, Morgans CW, Girman S, et al. Neural stem cells derived by small molecules preserve vision. *Transl Vis Sci Technol*. 2013;2:1.
134. McGill TJ, Cottam B, Lu B, et al. Transplantation of human central nervous system stem cells – neuroprotection in

retinal degeneration. *Eur J Neurosci*. 2012;35:468–477.
135. Cuenca N, Fernandez-Sanchez L, McGill TJ, et al. Phagocytosis of photoreceptor outer segments by transplanted human neural stem cells as a neuroprotective mechanism in retinal degeneration. *Invest Ophthalmol Vis Sci*. 2013;54:6745–6756.
136. Giusto E, Donega M, Cossetti C, Pluchino S. Neuro-immune interactions of neural stem cell transplants: from animal disease models to human trials. *Exp Neurol*. 2014;260:19–32.
137. Ottoboni L, De Feo D, Merlini A, Martino G. Commonalities in immune modulation between mesenchymal stem cells (MSCs) and neural stem/precursor cells (NPCs). *Immunol Lett*. 2015;168:228–239.
138. Jacobson SG, Cideciyan AV, Ratnakaram R, et al. Gene therapy for Leber congenital amaurosis caused by RPE65 mutations: safety and efficacy in 15 children and adults followed up to 3 years. *Arch Ophthalmol*. 2012;130:9–24.
139. Mazzini L, Gelati M, Profico DC, et al. Human neural stem cell transplantation in ALS: initial results from a phase I trial. *J Transl Med*. 2015;13:17.
140. Luan Z, Liu W, Qu S, et al. Effects of neural progenitor cell transplantation in children with severe cerebral palsy. *Cell Transplant*. 2012;21(Suppl. 1):S91–8.
141. Shin JC, Kim KN, Yoo J, et al. Clinical trial of human fetal brain-derived neural stem/progenitor cell transplantation in patients with traumatic cervical spinal cord injury. *Neural Plast*. 2015;2015:630932.
142. Inoue Y, Iriyama A, Ueno S, et al. Subretinal transplantation of bone marrow mesenchymal stem cells delays retinal degeneration in the RCS rat model of retinal degeneration. *Exp Eye Res*. 2007;85:234–241.
143. Lund RD, Wang S, Lu B, et al. Cells isolated from umbilical cord tissue rescue photoreceptors and visual functions in a rodent model of retinal disease. *Stem Cells*. 2007;25:602–611.
144. Tzameret A, Sher I, Belkin M, et al. Transplantation of human bone marrow mesenchymal stem cells as a thin subretinal layer ameliorates retinal degeneration in a rat model of retinal dystrophy. *Exp Eye Res*. 2014;118:135–144.

145. Atmaca-Sonmez P, Li Y, Yamauchi Y, et al. Systemically transferred hematopoietic stem cells home to the subretinal space and express RPE-65 in a mouse model of retinal pigment epithelium damage. *Exp Eye Res*. 2006;83:1295–1302.
146. Hsiung J, Zhu D, Hinton DR. Polarized human embryonic stem cell-derived retinal pigment epithelial cell monolayers have higher resistance to oxidative stress-induced cell death than nonpolarized cultures. *Stem Cells Transl Med*. 2015;4:10–20.
147. Carido M, Zhu Y, Postel K, et al. Characterization of a mouse model with complete RPE loss and its use for RPE cell transplantation. *Invest Ophthalmol Vis Sci*. 2014;55:5431–5444.
148. Sugino IK, Rapista A, Sun Q, et al. A method to enhance cell survival on Bruch's membrane in eyes affected by age and age-related macular degeneration. *Invest Ophthalmol Vis Sci*. 2011;52:9598–9609.
149. Jha BS, Bharti K. Regenerating retinal pigment epithelial cells to cure blindness: a road towards personalized artificial tissue. *Curr Stem Cell Rep*. 2015;1:79–91.
150. Diniz B, Thomas P, Thomas B, et al. Subretinal implantation of retinal pigment epithelial cells derived from human embryonic stem cells: improved survival when implanted as a monolayer. *Invest Ophthalmol Vis Sci*. 2013;54:5087–5096.
151. Stanzel BV, Liu Z, Brinken R, et al. Subretinal delivery of ultrathin rigid-elastic cell carriers using a metallic shooter instrument and biodegradable hydrogel encapsulation. *Invest Ophthalmol Vis Sci*. 2012;53:490–500.
152. Lu B, Tai YC, Humayun MS. Microdevice-based cell therapy for age-related macular degeneration. *Dev Ophthalmol*. 2014;53:155–166.
153. Peyman GA, Blinder KJ, Paris CL, et al. A technique for retinal pigment epithelium transplantation for age- related macular degeneration secondary to extensive subfoveal scarring. *Ophthalmic Surg*. 1991;22:102–108.
154. Algvere PV, Berglin L, Gouras P, et al. Transplantation of fetal retinal pigment epithelium in age-related macular

degeneration with subfoveal neovascularization. *Graefes Arch Clin Exp Ophthalmol*. 1994;232:707–716.
155. Algvere PV, Berglin L, Gouras P, et al. Transplantation of RPE in age-related macular degeneration: observations in disciform lesions and dry RPE atrophy. *Graefes Arch Clin Exp Ophthalmol*. 1997;235:149–158.
156. Stanga PE, Kychenthal A, Fitzke FW, et al. Retinal pigment epithelium translocation after choroidal neovascular membrane removal in age-related macular degeneration. *Ophthalmology*. 2002;109:1492–1498.
157. Binder S, Krebs I, Hilgers RD, et al. Outcome of transplantation of autologous retinal pigment epithelium in age-related macular degeneration: a prospective trial. *Invest Ophthalmol Vis Sci*. 2004;45:4151–4160.
158. Angunawela RI, Williamson TH, Khan MA, et al. Choroidal translocation with a pedicle following excision of a type 1 choroidal neovascular membrane. *Br J Ophthalmol*. 2005;89:386.
159. van Meurs JC, Van Den Biesen PR. Autologous retinal pigment epithelium and choroid translocation in patients with exudative age-related macular degeneration: short-term follow-up. *Am J Ophthalmol*. 2003;136:688–695.
160. MacLaren RE, Uppal GS, Balaggan KS, et al. Autologous transplantation of the retinal pigment epithelium and choroid in the treatment of neovascular age-related macular degeneration. *Ophthalmology*. 2007;114:561–570.
161. Joussen AM, Heussen FM, Joeres S, et al. Autologous translocation of the choroid and retinal pigment epithelium in age-related macular degeneration. *Am J Ophthalmol*. 2006;142:17–30.
162. Treumer F, Bunse A, Klatt C, et al. Autologous retinal pigment epithelium- choroid sheet transplantation in age related macular degeneration: morphological and functional results. *Br J Ophthalmol*. 2007;91:349–353.
163. Falkner-Radler CI, Krebs I, Glittenberg C, et al. Human retinal pigment epithelium (RPE) transplantation: outcome after autologous RPE-choroid sheet and RPE cell-suspension in a randomised clinical study. *Br J Ophthalmol*.

2011;95:370–375.
164. Del Priore LV, Kaplan HJ, Tezel TH, et al. Retinal pigment epithelial cell transplantation after subfoveal membranectomy in age-related macular degeneration: clinicopathologic correlation. *Am J Ophthalmol*. 2001;131:472–480.
165. van Zeeburg EJ, Cereda MG, Amarakoon S, van Meurs JC. Prospective, randomized intervention study comparing retinal pigment epithelium-choroid graft surgery and anti-VEGF therapy in patients with exudative age-related macular degeneration. *Ophthalmologica*. 2015;233:134–145.
166. van Zeeburg EJ, Maaijwee KJ, Missotten TO, et al. A free retinal pigment epithelium-choroid graft in patients with exudative age-related macular degeneration: results up to 7 years. *Am J Ophthalmol*. 2012;153 [120–7.e2].
167. Algvere PV, Gouras P, Dafgard Kopp E. Long-term outcome of RPE allografts in non-immunosuppressed patients with AMD. *Eur J Ophthalmol*. 1999;9:217–230.
168. MacLaren RE, Bird AC, Sathia PJ, et al. Long-term results of submacular surgery combined with macular translocation of the retinal pigment epithelium in neovascular age-related macular degeneration. *Ophthalmology*. 2005;112:2081–2087.
169. Tezel TH, Del Priore LV, Kaplan HJ. Reattachment of harvested retinal pigment epithelium to a substrate prevents apoptosis. *Graefes Arch Clin Exp Ophthalmol*. 1997;235:41–47.
170. Sheng Y, Gouras P, Cao H, et al. Patch transplants of human fetal retinal pigment epithelium in rabbit and monkey retina. *Invest Ophthalmol Vis Sci*. 1995;36:381–390.
171. Li LX, Turner JE. Transplantation of retinal pigment epithelial cells to immature and adult rat hosts: short- and long-term survival characteristics. *Exp Eye Res*. 1988;47:771–785.
172. Lopez R, Gouras P, Kjeldbye H, et al. Transplanted retinal pigment epithelium modifies the retinal degeneration in the RCS rat. *Invest Ophthalmol Vis Sci*. 1989;30:586–588.
173. Lai CC, Gouras P, Doi K, et al. Tracking RPE transplants labeled by retroviral gene transfer with green fluorescent

protein. *Invest Ophthalmol Vis Sci*. 1999;40:2141–2146.
174. Karwatowski WS, Jeffries TE, Duance VC, et al. Preparation of Bruch's membrane and analysis of the age-related changes in the structural collagens. *Br J Ophthalmol*. 1995;79:944–952.
175. Pauleikhoff D, Harper CA, Marshall J, et al. Aging changes in Bruch's membrane. A histochemical and morphologic study. *Ophthalmology*. 1990;97:171–178.
176. Zarbin MA. Age related macular degeneration: review of pathogenesis. *Eur J Ophthalmol*. 1998;8:133–205.
177. Tsukahara I, Ninomiya S, Castellarin A, et al. Early attachment of uncultured retinal pigment epithelium from aged donors onto Bruch's membrane explants. *Exp Eye Res*. 2002;74:255–266.
178. Zarbin MA. Analysis of retinal pigment epithelium integrin expression and adhesion to aged submacular human Bruch's membrane. *Trans Am Ophthalmol Soc*. 2003;101:499–520.
179. Gullapalli VK, Sugino IK, Van Patten Y, et al. Impaired RPE survival on aged submacular human Bruch's membrane. *Exp Eye Res*. 2005;80:235–248.
180. Sugino IK, Gullapalli VK, Sun Q, et al. Cell-deposited matrix improves retinal pigment epithelium survival on aged submacular human Bruch's membrane. *Invest Ophthalmol Vis Sci*. 2011;52:1345–1358.
181. Schwartz SD, Regillo CD, Lam BL, et al. Human embryonic stem cell-derived retinal pigment epithelium in patients with age-related macular degeneration and Stargardt's macular dystrophy: follow-up of two open-label phase 1/2 studies. *Lancet*. 2015;385:509–516.
182. Sunness JS. Stem cells in age-related macular degeneration and Stargardt's macular dystrophy. *Lancet*. 2015;386:29.
183. Song WK, Park KM, Kim HJ, et al. Treatment of macular degeneration using embryonic stem cell-derived retinal pigment epithelium: preliminary results in Asian patients. *Stem Cell Reports*. 2015;4:860–872.
184. *Pilot safety study or iPSC-based intervention for wet-type AMD*. http://www.riken-ibri.jp/AMD/english.

185. Coghlan A. Mutation alert halts stem-cell trial to cure blindness. *New Scientist*. 2015 [31 July] www.newscientist.com/article/dn27986/.
186. Streilein JW. Ocular immune privilege: the eye takes a dim but practical view of immunity and inflammation. *J Leukoc Biol*. 2003;74:179–185.
187. Streilein JW, Ksander BR, Taylor AW. Immune deviation in relation to ocular immune privilege. *J Immunol*. 1997;158:3557–3560.
188. Jiang LQ, Jorquera M, Streilein JW. Subretinal space and vitreous cavity as immunologically privileged sites for retinal allografts. *Invest Ophthalmol Vis Sci*. 1993;34:3347–3354.
189. Ferguson TA. The molecular basis of anterior associated immune deviation (ACAID). *Ocul Immunol Inflamm*. 1997;5:213–215.
190. Takeuchi M, Alard P, Streilein JW. TGF-beta promotes immune deviation by altering accessory signals of antigen-presenting cells. *J Immunol*. 1998;160:1589–1597.
191. Taylor AW, Streilein JW, Cousins SW. Identification of alpha-melanocyte stimulating hormone as a potential immunosuppressive factor in aqueous humor. *Curr Eye Res*. 1992;11:1199–1206.
192. Taylor AW, Streilein JW, Cousins SW. Immunoreactive vasoactive intestinal peptide contributes to the immunosuppressive activity of normal aqueous humor. *J Immunol*. 1994;153:1080–1086.
193. Apte RS, Sinha D, Mayhew E, et al. Cutting edge: role of macrophage migration inhibitory factor in inhibiting NK cell activity and preserving immune privilege. *J Immunol*. 1998;160:5693–5696.
194. Griffith TS, Brunner T, Fletcher SM, et al. Fas ligand-induced apoptosis as a mechanism of immune privilege. *Science*. 1995;270:1189–1192.
195. Bora NS, Gobleman CL, Atkinson JP, et al. Differential expression of the complement regulatory proteins in the human eye. *Invest Ophthalmol Vis Sci*. 1993;34:3579–3584.
196. Vega JL, Keino H, Masli S. Surgical denervation of ocular

sympathetic afferents decreases local transforming growth factor-beta and abolishes immune privilege. *Am J Pathol*. 2009;175:1218–1225.
197. Streilein JW. Unraveling immune privilege. *Science*. 1995;270:1158–1159.
198. Wenkel H, Streilein JW. Analysis of immune deviation elicited by antigens injected into the subretinal space. *Invest Ophthalmol Vis Sci*. 1998;39:1823–1834.
199. Jiang L, Streilein JW. Immunologic privilege evoked by histoincompatible intracameral retinal transplants. *Reg Immunol*. 1991;3:121–130.
200. Liversidge J, Forrester JV. Regulation of immune responses by the retinal pigment epithelium. Marmor MF, Wolfensberger TJ. *The retinal pigment epithelium function and disease*. Oxford University Press: New York; 1998:511–527.
201. Tanihara H, Yoshida M, Matsumoto M, et al. Identification of transforming growth factor B expressed in cultured human retinal pigment epithelial cells. *Invest Ophthalmol Vis Sci*. 1993;34:413–419.
202. Holtkamp GM, de Vos AF, Kijlstra A, et al. Expression of multiple forms of IL-1 receptor antagonist (IL-1ra) by human retinal pigment epithelial cells: identification of a new IL-1ra exon. *Eur J Immunol*. 1999;29:215–224.
203. Ishida K, Panjwani N, Cao Z, et al. Participation of pigment epithelium in ocular immune privilege. 3. Epithelia cultured from iris, ciliary body, and retina suppress T-cell activation by partially non-overlapping mechanisms. *Ocul Immunol Inflamm*. 2003;11:91–105.
204. Kaestel CG, Jorgensen A, Nielsen M, et al. Human retinal pigment epithelial cells inhibit proliferation and IL2R expression of activated T cells. *Exp Eye Res*. 2002;74:627–637.
205. Jorgensen A, Wiencke AK, la Cour M, et al. Human retinal pigment epithelial cell-induced apoptosis in activated T cells. *Invest Ophthalmol Vis Sci*. 1998;39:1590–1599.
206. Rezai KA, Semnani RT, Farrokh-Siar L, et al. Human fetal retinal pigment epithelial cells induce apoptosis in allogenic T-cells in a fas ligand and PGE2 independent pathway. *Curr Eye Res*. 1999;18:430–439.

207. Usui Y, Okunuki Y, Hattori T, et al. Functional expression of B7H1 on retinal pigment epithelial cells. *Exp Eye Res*. 2008;86:52–59.
208. Sugita S, Usui Y, Horie S, et al. T-cell suppression by programmed cell death 1 ligand 1 on retinal pigment epithelium during inflammatory conditions. *Invest Ophthalmol Vis Sci*. 2009;50:2862–2870.
209. Sugita S, Horie S, Nakamura O, et al. Retinal pigment epithelium-derived CTLA-2alpha induces TGFbeta-producing T regulatory cells. *J Immunol*. 2008;181:7525–7536.
210. Wenkel H, Streilein JW. Evidence that retinal pigment epithelium functions as an immune- privileged tissue. *Invest Ophthalmol Vis Sci*. 2000;41:3467–3473.
211. Zamiri P, Zhang Q, Streilein JW. Vulnerability of allogeneic retinal pigment epithelium to immune T-cell-mediated damage in vivo and in vitro. *Invest Ophthalmol Vis Sci*. 2004;45:177–184.
212. Rezai KA, Semnani RT, Patel SC, et al. The immunogenic potential of human fetal retinal pigment epithelium and its relation to transplantation. *Invest Ophthalmol Vis Sci*. 1997;38:2662–2671.
213. Liversidge JM, Sewell HF, Forrester JV. Human retinal pigment epithelial cells differentially express MHC class II (HLA, DP, DR and DQ) antigens in response to in vitro stimulation with lymphokine or purified IFN-gamma. *Clin Exp Immunol*. 1988;73:489–494.
214. Liversidge J, Sewell HF, Thomson AW, et al. Lymphokine-induced MHC class II antigen expression on cultured retinal pigment epithelial cells and the influence of cyclosporin A. *Immunology*. 1988;63:313–317.
215. Percopo CM, Hooks JJ, Shinohara T, et al. Cytokine-mediated activation of a neuronal retinal resident cell provokes antigen presentation. *J Immunol*. 1990;145:4101–4107.
216. Sun D, Enzmann V, Lei S, et al. Retinal pigment epithelial cells activate uveitogenic T cells when they express high levels of MHC class II molecules, but inhibit T cell

activation when they express restricted levels. *J Neuroimmunol*. 2003;144:1–8.
217. Leonard DS, Zhang XG, Panozzo G, et al. Clinicopathologic correlation of localized retinal pigment epithelium debridement. *Invest Ophthalmol Vis Sci*. 1997;38:1094–1109.
218. Del Priore LV, Kaplan HJ, Hornbeck R, et al. Retinal pigment epithelial debridement as a model for the pathogenesis and treatment of macular degeneration. *Am J Ophthalmol*. 1996;122:629–643.
219. Jiang LQ, Streilein JW. Neural retina and retinal pigment epithelium allografts suffer different immunological fates in the eye. *Reg Immunol*. 1994;6:90–94.
220. Grisanti S, Ishioka M, Kosiewicz M, et al. Immunity and immune privilege elicited by cultured retinal pigment epithelial cell transplants. *Invest Ophthalmol Vis Sci*. 1997;38:1619–1626.
221. Zhang X, Bok D. Transplantation of retinal pigment epithelial cells and immune response in the subretinal space. *Invest Ophthalmol Vis Sci*. 1998;39:1021–1027.
222. Weisz JM, Humayun MS, De Juan E, et al. Allogenic fetal retinal pigment epithelial cell transplant in a patient with geographic atrophy. *Retina*. 1999;19:540–545.
223. Kohen L, Enzmann V, Faude F, et al. Mechanisms of graft rejection in the transplantation of retinal pigment epithelial cells. *Ophthalmic Res*. 1997;29:298–304.
224. Sohn EH, Jiao C, Kaalberg E, et al. Allogenic iPSC-derived RPE cell transplants induce immune response in pigs: a pilot study. *Sci Rep*. 2015;5:11791.
225. Berglin L, Gouras P, Sheng Y, et al. Tolerance of human fetal retinal pigment epithelium xenografts in monkey retina. *Graefes Arch Clin Exp Ophthalmol*. 1997;235:103–110.
226. Crafoord S, Algvere P, Seregard S, et al. Long-term outcome of RPE allografts to the subretinal space of rabbits. *Acta Ophthalmol Scand*. 1999;77:247–254.
227. Xian B, Huang B. The immune response of stem cells in subretinal transplantation. *Stem Cell Res Ther*. 2015;6:161.
228. Lu B, Wang S, Girman S, McGill T, Ragaglia V, Lund R. Human adult bone marrow- derived somatic cells rescue

vision in a rodent model of retinal degeneration. *Exp Eye Res*. 2010;91:449–455.
229. Scheiner ZS, Talib S, Feigal EG. The potential for immunogenicity of autologous induced pluripotent stem cell-derived therapies. *J Biol Chem*. 2014;289:4571–4577.
230. Lai CC, Gouras P, Doi K, et al. Local immunosuppression prolongs survival of RPE xenografts labeled by retroviral gene transfer. *Invest Ophthalmol Vis Sci*. 2000;41:3134–3141.
231. Schwartz SD, Anglade E, Lanza R, Macular Disease Investigator Group, et al. Stem cells in age-related macular degeneration and Stargardt's macular dystrophy – Authors' reply. *Lancet*. 2015;386:30.
232. Ishida M, Lui GM, Yamani A, et al. Culture of human retinal pigment epithelial cells from peripheral scleral flap biopsies. *Curr Eye Res*. 1998;17:392–402.
233. Boulton M, Roanowska M, Wess T. Ageing of the retinal pigment epithelium: implications for transplantation. *Graefes Arch Clin Exp Ophthalmol*. 2003;242:76–84.
234. Cahill MT, Mruthyunjaya P, Bowes Rickman C, et al. Recurrence of retinal pigment epithelial changes after macular translocation with 360 degrees peripheral retinectomy for geographic atrophy. *Arch Ophthalmol*. 2005;123:935–938.
235. Tezel TH, Del Priore LV. Reattachment to a substrate prevents apoptosis of human retinal pigment epithelium. *Graefes Arch Clin Exp Ophthalmol*. 1997;235:41–47.
236. Castellarin AA, Sugino IK, Vargas JA, et al. In vitro transplantation of fetal human retinal pigment epithelial cells onto human cadaver Bruch's membrane. *Exp Eye Res*. 1998;66:49–67.
237. Ho TC, Del Priore LV. Reattachment of cultured human retinal pigment epithelium to extracellular matrix and human Bruch's membrane. *Invest Ophthalmol Vis Sci*. 1997;38:1110–1118.
238. Tezel TH, Kaplan HJ, Del Priore LV. Fate of human retinal pigment epithelial cells seeded onto layers of human Bruch's membrane. *Invest Ophthalmol Vis Sci*. 1999;40:467–476.

239. Tezel TH, Del Priore LV. Repopulation of different layers of host human Bruch's membrane by retinal pigment epithelial cell grafts. *Invest Ophthalmol Vis Sci*. 1999;40:767–774.
240. Del Priore LV, Tezel TH. Reattachment rate of human retinal pigment epithelium to layers of human Bruch's membrane. *Arch Ophthalmol*. 1998;116:335–341.
241. Gullapalli VK, Sugino IK, Zarbin MA. Culture-induced increase in alpha integrin subunit expression in retinal pigment epithelium is important for improved resurfacing of aged human Bruch's membrane. *Exp Eye Res*. 2008;86:189–200.
242. Starita C, Hussain AA, Pagliarini S, et al. Hydrodynamics of ageing Bruch's membrane: implications for macular disease. *Exp Eye Res*. 1996;62:565–572.
243. Lopez PF, Grossniklaus HE, Lambert HM, et al. Pathologic features of surgically excised subretinal neovascular membranes in age-related macular degeneration. *Am J Ophthalmol*. 1991;112:647–656.
244. Hsu JK, Thomas MA, Ibanez H, et al. Clinicopathologic studies of an eye after submacular membranectomy for choroidal neovascularization. *Retina*. 1995;15:43–52.
245. Castellarin AA, Nasir MA, Sugino IK, et al. Clinicopathological correlation of primary and recurrent choroidal neovascularisation following surgical excision in age related macular degeneration. *Br J Ophthalmol*. 1998;82:480–487.
246. Ormerod LD, Puklin JE, Frank RN. Long-term outcomes after the surgical removal of advanced subfoveal neovascular membranes in age-related macular degeneration. *Ophthalmology*. 1994;101:1201–1210.
247. Rudolf M, Curcio CA. Esterified cholesterol is highly localized to Bruch's membrane, as revealed by lipid histochemistry in wholemounts of human choroid. *J Histochem Cytochem*. 2009;57:731–739.
248. Thumann G, Bartz-Schmidt KU, El Bakri H, et al. Transplantation of autologous iris pigment epithelium to the subretinal space in rabbits. *Transplantation*. 1999;68:195–

201.
249. Thumann G, Kociok N, Bartz-Schmidt KU, et al. Detection of mRNA for proteins involved in retinol metabolism in iris pigment epithelium. *Graefes Arch Clin Exp Ophthalmol*. 1999;237:1046–1051.
250. Sugano E, Tomita H, Abe T, et al. Comparative study of cathepsins D and S in rat IPE and RPE cells. *Exp Eye Res*. 2003;77:203–209.
251. Zhu Y, Schreiter S, Tanaka EM. Accelerated three-dimensional neuroepithelium formation from human embryonic stem cells and its use for quantitative differentiation to human retinal pigment epithelium. *Methods Mol Biol*. 2016;1307:345–355.
252. Leach LL, Buchholz DE, Nadar VP, Lowenstein SE, Clegg DO. Canonical/beta-catenin Wnt pathway activation improves retinal pigmented epithelium derivation from human embryonic stem cells. *Invest Ophthalmol Vis Sci*. 2015;56:1002–1013.
253. Maruotti J, Sripathi SR, Bharti K, et al. Small-molecule-directed, efficient generation of retinal pigment epithelium from human pluripotent stem cells. *Proc Natl Acad Sci USA*. 2015;112:10950–10955.
254. Westenskow P, Sedillo Z, Barnett A, Friedlander M. Efficient derivation of retinal pigment epithelium cells from stem cells. *J Vis Exp*. 2015;8(97).
255. Barry J, Hyllner J, Stacey G, Taylor CJ, Turner M. Setting up a haplobank: issues and solutions. *Curr Stem Cell Rep*. 2015;1:110–117.
256. Borlongan CV, Stahl CE, Cameron DF, et al. CNS immunological modulation of neural graft rejection and survival. *Neurol Res*. 1996;18:297–304.
257. Ishioka M, Okamoto S, Streilein JW, et al. Effect of cyclosporine on anterior chamber-associated immune deviation with retinal transplantation. *Invest Ophthalmol Vis Sci*. 1997;38:2152–2160.
258. Rao KV, Andersen RC, O'Brien TJ. Successful renal transplantation in a patient with anaphylactic reaction to Solu-Medrol (methylprednisolone sodium succinate). *Am J*

Med. 1982;72:161–163.
259. Mittal R, Agarwal SK, Dash SC, et al. Treatment of acute rejection in live related renal allograft recipients: a comparison of three different protocols. *Nephron*. 1997;77:186–189.
260. Delmonico FL, Tolkoff RN. Treatment of acute rejection in real transplantation. Brenner BM, Stein JH. *Contemporary issues in nephrology*. Churchill Livingstone: Edinburgh; 1989:129–146.
261. Hirano T, Oka K, Takeuchi H, et al. Clinical significance of glucocorticoid pharmacodynamics assessed by antilymphocyte action in kidney transplantation. Marked difference between prednisolone and methylprednisolone. *Transplantation*. 1994;57:1341–1348.
262. Yoshizumi MO, Bhavsar AR, Dessouki A, et al. Safety of repeated intravitreous injections of antibiotics and dexamethasone. *Retina*. 1999;19:437–441.
263. Kagaya F, Usui T, Kamiya K, et al. Intraocular dexamethasone delivery system for corneal transplantation in an animal model. *Cornea*. 2002;21:200–202.
264. Haller JA, Kuppermann BD, Blumenkranz MS, et al. Randomized controlled trial of an intravitreous dexamethasone drug delivery system in patients with diabetic macular edema. *Arch Ophthalmol*. 2010;128:289–296.
265. Jaffe GJ, Martin D, Callanan D, et al. Fluocinolone acetonide implant (Retisert) for noninfectious posterior uveitis: thirty-four-week results of a multicenter randomized clinical study. *Ophthalmology*. 2006;113:1020–1027.
266. Nakatsuji N, Nakajima F, Tokunaga K. HLA-haplotype banking and iPS cells. *Nat Biotechnol*. 2008;26:739–740.
267. Boyd AS, Fairchild PJ. Approaches for immunological tolerance induction to stem cell- derived cell replacement therapies. *Expert Rev Clin Immunol*. 2010;6:435–448.
268. Taylor CJ, Peacock S, Chaudhry AN, et al. Generating an iPSC bank for HLA-matched tissue transplantation based on known donor and recipient HLA types. *Cell Stem Cell*. 2012;11:147–152.
269. Zimmermann A, Preynat-Seauve O, Tiercy JM, Krause KH,

Villard J. Haplotype-based banking of human pluripotent stem cells for transplantation: potential and limitations. *Stem Cells Dev*. 2012;21:2364–2373.
270. Turner M, Leslie S, Martin NG, et al. Toward the development of a global induced pluripotent stem cell library. *Cell Stem Cell*. 2013;13:382–384.
271. Robertson NJ, Brook FA, Gardner RL, et al. Embryonic stem cell-derived tissues are immunogenic but their inherent immune privilege promotes the induction of tolerance. *Proc Natl Acad Sci USA*. 2007;104:20920–20925.
272. Tena A, Sachs DH. Stem cells: immunology and immunomodulation. *Dev Ophthalmol*. 2014;53:122–132.
273. Kaplan HJ, Leibole MA, Tezel T, Ferguson TA. Fas ligand (CD95 ligand) controls angiogenesis beneath the retina. *Nat Med*. 1999;5:292–297.
274. Gullapalli VG. *Paucity of cellular integrin receptors and aging changes in Bruch's membrane contribute to poor resurfacing of aged Bruch's membrane by retinal pigment epithelium*. [PHD thesis, Graduate School of Biomedical Sciences, UMDNJ] 2005.
275. Gullapalli VK, Sugino IK, Van Patten Y, et al. Retinal pigment epithelium resurfacing of aged submacular human Bruch's membrane. *Trans Am Ophthalmol Soc*. 2004;102:123–137 [discussion 37–8].
276. Tezel TH, Del Priore LV, Kaplan HJ. Reengineering of aged Bruch's membrane to enhance retinal pigment epithelium repopulation. *Invest Ophthalmol Vis Sci*. 2004;45:3337–3348.
277. Tezel TH, Oda J, Hornbeck R, et al. RPE repopulation of aged inner collagenous layer (ICL) is inhibited by reversible alterations in Bruch's membrane. *Invest Ophthalmol Vis Sci*. 2001;42 [ARVO abstract 4995].
278. Fang IM, Yang CH, Yang CM, et al. Overexpression of integrin alpha6 and beta4 enhances adhesion and proliferation of human retinal pigment epithelial cells on layers of porcine Bruch's membrane. *Exp Eye Res*. 2009;88:12–21.
279. Castellarin AA, Nasir MA, Sugino IK, et al. Progressive presumed choriocapillaris atrophy after surgery for age-

related macular degeneration. *Retina*. 1998;18:143–149.
280. Hergott GJ, Kalnins VI. Expression of proliferating cell nuclear antigen in migrating retinal pigment epithelial cells during wound healing in organ culture. *Exp Cell Res*. 1991;195:307–314.
281. Kamei M, Lewis JM, Hayashi A, et al. A new wound healing model of retinal pigment epithelial cells in sheet culture. *Curr Eye Res*. 1996;15:714–718.
282. MacDonald IM, Peters C, Chen MH. Effect of retinoic acid on wound healing of laser burns to porcine retinal pigment epithelium. *Can J Ophthalmol*. 1996;31:175–178.
283. Del Priore LV, Hornbeck R, Kaplan HJ, et al. Débridement of the pig retinal pigment epithelium in vivo. *Arch Ophthalmol*. 1995;113:939–944.
284. Lopez PF, Yan Q, Kohen L, et al. Retinal pigment epithelial wound healing in vivo. *Arch Ophthalmol*. 1995;113:1437–1446.
285. Valentino TL, Kaplan HJ, Del Priore LV, et al. Retinal pigment epithelial repopulation in monkeys after submacular surgery. *Arch Ophthalmol*. 1995;113:932–938.
286. Ho TC, Del Priore LV, Hornbeck R. Effect of mitomycin-C on human retinal pigment epithelium in culture. *Curr Eye Res*. 1997;16:572–576.
287. Wang H, Ninomiya Y, Sugino IK, et al. Retinal pigment epithelium wound healing on human Bruch's membrane explants. *Invest Ophthalmol Vis Sci*. 2003;44:2199–2210.
288. Sugino IK, Wang H, Zarbin MA. Age-related macular degeneration and retinal pigment epithelium wound healing. *Mol Neurobiol*. 2003;28:177–194.
289. Burton TC. Recovery of visual acuity after retinal detachment involving the macula. *Trans Am Ophthalmol Soc*. 1982;80:475–497.
290. Machemer R. Experimental retinal detachment in the owl monkey. IV. The reattached retina. *Am J Ophthalmol*. 1968;66:1075–1091.
291. Anderson DH, Guerin CJ, Erickson PA, et al. Morphological recovery in the reattached retina. *Invest Ophthalmol Vis Sci*. 1986;27:168–183.

292. Mervin K, Valter K, Maslim J, et al. Limiting photoreceptor death and deconstruction during experimental retinal detachment: the value of oxygen supplementation. *Am J Ophthalmol*. 1999;128:155–164.
293. Erickson PA, Fisher SK, Anderson DH, et al. Retinal detachment in the cat: the outer nuclear and outer plexiform layers. *Invest Ophthalmol Vis Sci*. 1983;24:927–942.
294. Fisher SK, Stone J, Rex TS, et al. Experimental retinal detachment: a paradigm for understanding the effects of induced photoreceptor degeneration. *Prog Brain Res*. 2001;131:679–698.
295. Sakai T, Calderone JB, Lewis GP, et al. Cone photoreceptor recovery after experimental detachment and reattachment: an immunocytochemical, morphological, and electrophysiological study. *Invest Ophthalmol Vis Sci*. 2003;44:416–425.
296. Sakai T, Lewis GP, Linberg KA, et al. The ability of hyperoxia to limit the effects of experimental detachment in cone-dominated retina. *Invest Ophthalmol Vis Sci*. 2001;42:3264–3273.
297. Berson EL. Retinitis pigmentosa: unfolding its mystery. *Proc Natl Acad Sci USA*. 1996;93:4526–4528.
298. Milam AH, Li ZY, Fariss RN. Histopathology of the human retina in retinitis pigmentosa. *Prog Retin Eye Res*. 1998;17:175–205.
299. Santos A, Humayun MS, de Juan E, et al. Preservation of the inner retina in retinitis pigmentosa. A morphometric analysis. *Arch Ophthalmol*. 1997;115:511–515.
300. Humayun MS, Prince M, de Juan E, et al. Morphometric analysis of the extramacular retina from postmortem eyes with retinitis pigmentosa. *Invest Ophthalmol Vis Sci*. 1999;40:143–148.
301. Li ZY, Kljavin IJ, Milam AH. Rod photoreceptor neurite sprouting in retinitis pigmentosa. *J Neurosci*. 1995;15:5429–5438.
302. Jones BW, Watt CB, Frederick JM, et al. Retinal remodeling triggered by photoreceptor degenerations. *J Comp Neurol*. 2003;464:1–16.

303. Ali RR, Sarra GM, Stephens C, et al. Restoration of photoreceptor ultrastructure and function in retinal degeneration slow mice by gene therapy. *Nat Genet*. 2000;25:306–310.
304. Bennett J, Tanabe T, Sun D, et al. Photoreceptor cell rescue in retinal degeneration (rd) mice by in vivo gene therapy. *Nat Med*. 1996;2:649–654.
305. Vollrath D, Feng W, Duncan JL, et al. Correction of the retinal dystrophy phenotype of the RCS rat by viral gene transfer of Mertk. *Proc Natl Acad Sci USA*. 2001;98:12584–12589.
306. Maguire AM, Simonelli F, Pierce EA, et al. Safety and efficacy of gene transfer for Leber's congenital amaurosis. *N Engl J Med*. 2008;358:2240–2248.
307. Bainbridge JW, Smith AJ, Barker SS, et al. Effect of gene therapy on visual function in Leber's congenital amaurosis. *N Engl J Med*. 2008;358:2231–2239.
308. LaVail MM, Yasumura D, Matthes MT, et al. Protection of mouse photoreceptors by survival factors in retinal degenerations. *Invest Ophthalmol Vis Sci*. 1998;39:592–602.
309. Sieving PA, Caruso RC, Tao W, et al. Ciliary neurotrophic factor (CNTF) for human retinal degeneration: phase I trial of CNTF delivered by encapsulated cell intraocular implants. *Proc Natl Acad Sci USA*. 2006;103:3896–3901.
310. Lakhanpal RR, Yanai D, Weiland JD, et al. Advances in the development of visual prostheses. *Curr Opin Ophthalmol*. 2003;14:122–127.
311. Karl MO, Reh TA. Regenerative medicine for retinal diseases: activating endogenous repair mechanisms. *Trends Mol Med*. 2010;16:193–202.
312. del Cerro M, Lazar ES, Diloreto D Jr. The first decade of continuous progress in retinal transplantation. *Microsc Res Tech*. 1997;36:130–141.
313. Gust J, Reh TA. Adult donor rod photoreceptors integrate into the mature mouse retina. *Invest Ophthalmol Vis Sci*. 2011;52:5266–5272.
314. Meyer JS, Katz ML, Maruniak JA, et al. Neural differentiation of mouse embryonic stem cells in vitro and

after transplantation into eyes of mutant mice with rapid retinal degeneration. *Brain Res*. 2004;1014:131–144.
315. Meyer JS, Katz ML, Maruniak JA, et al. Embryonic stem cell-derived neural progenitors incorporate into degenerating retina and enhance survival of host photoreceptors. *Stem Cells*. 2006;24:274–283.
316. Radtke ND, Aramant RB, Petry HM, et al. Vision improvement in retinal degeneration patients by implantation of retina together with retinal pigment epithelium. *Am J Ophthalmol*. 2008;146:172–182.
317. Seiler MJ, Aramant RB, Thomas BB, et al. Visual restoration and transplant connectivity in degenerate rats implanted with retinal progenitor sheets. *Eur J Neurosci*. 2010;31:508–520.
318. Lamba DA, Gust J, Reh TA. Transplantation of human embryonic stem cell-derived photoreceptors restores some visual function in Crx- deficient mice. *Cell Stem Cell*. 2009;4:73–79.
319. Mohand-Said S, Deudon-Combe A, Hicks D, et al. Normal retina releases a diffusible factor stimulating cone survival in the retinal degeneration mouse. *Proc Natl Acad Sci USA*. 1998;95:8357–8362.
320. Mohand-Said S, Hicks D, Dreyfus H, et al. Selective transplantation of rods delays cone loss in a retinitis pigmentosa model. *Arch Ophthalmol*. 2000;118:807–811.
321. Leveillard T, Mohand-Said S, Lorentz O, et al. Identification and characterization of rod-derived cone viability factor. *Nat Genet*. 2004;36:755–759.
322. Chalmel F, Leveillard T, Jaillard C, et al. Rod-derived Cone Viability Factor-2 is a novel bifunctional-thioredoxin-like protein with therapeutic potential. *BMC Mol Biol*. 2007;8:74.
323. Geller AM, Sieving PA. How many cones are required to "see?": lessons from Stargardt's macular dystrophy and from modeling with degenerate photoreceptor arrays. Hollyfield JG, Anderson RE, La Vail MM. *Retinal degeneration*. Plenum Press: New York; 1993:25–34.
324. Lavail M. Analysis of neurological mutants with inherited retinal degeneration. *Invest Ophthalmol Vis Sci*. 1981;21:638–

657.
325. Sanyal S, De Ruiter A, Hawkins RK. Development and degeneration of retina in rds mutant mice: light microscopy. *J Comp Neurol*. 1980;194:193–207.
326. Narfstrom K, Nilsson SE. Hereditary rod-cone degeneration in a strain of Abyssinian cats. *Prog Clin Biol Res*. 1987;247:349–368.
327. Noell WK, Walker VS, Kang BS, et al. Retinal damage by light in rats. *Invest Ophthalmol*. 1966;5:450–473.
328. Schuschereba ST, Silverman MS. Retinal cell and photoreceptor transplantation between adult New Zealand red rabbit retinas. *Exp Neurol*. 1992;115:95–99.
329. Olsson JE, Gordon JW, Pawlyk BS, et al. Transgenic mice with a rhodopsin mutation (Pro23His): a mouse model of autosomal dominant retinitis pigmentosa. *Neuron*. 1992;9:815–830.
330. Petters RM, Alexander CA, Wells KD, et al. Genetically engineered large animal model for studying cone photoreceptor survival and degeneration in retinitis pigmentosa. *Nat Biotechnol*. 1997;15:965–970.
331. del Cerro M, Ison JR, Bowen GP, et al. Intraretinal grafting restores visual function in light-blinded rats. *Neuroreport*. 1991;2:529–532.
332. Seiler MJ, Aramant RB. Intact sheets of fetal retina transplanted to restore damaged rat retinas. *Invest Ophthalmol Vis Sci*. 1998;39:2121–2131.
333. Gouras P, Du J, Kjeldbye H, et al. Reconstruction of degenerate rd mouse retina by transplantation of transgenic photoreceptors. *Invest Ophthalmol Vis Sci*. 1992;33:2579–2586.
334. Silverman MS, Hughes SE, Valentino TL, et al. Photoreceptor transplantation: Anatomic, electrophysiologic, and behavioral evidence for the functional reconstruction of retinas lacking photoreceptors. *Exp Neurol*. 1992;115:87–94.
335. Kwan AS, Wang S, Lund RD. Photoreceptor layer reconstruction in a rodent model of retinal degeneration. *Exp Neurol*. 1999;159:21–33.
336. Radner W, Sadda SR, Humayun MS, et al. Light-driven

retinal ganglion cell responses in blind rd mice after neural retinal transplantation. *Invest Ophthalmol Vis Sci*. 2001;42:1057–1065.
337. Otani A, Dorrell MI, Kinder K, et al. Rescue of retinal degeneration by intravitreally injected adult bone marrow-derived lineage-negative hematopoietic stem cells. *J Clin Invest*. 2004;114:765–774.
338. Yang Y, Mohand-Said S, Leveillard T, et al. Transplantation of photoreceptor and total neural retina preserves cone function in P23H rhodopsin transgenic rat. *PLoS ONE*. 2010;5:e13469.
339. Aramant RB, Seiler MJ, Ball SL. Successful cotransplantation of intact sheets of fetal retina with retinal pigment epithelium. *Invest Ophthalmol Vis Sci*. 1999;40:1557–1564.
340. Carter-Dawson LD, LaVail MM. Rods and cones in the mouse retina: Structural analysis using light and electron microscopy. *J Comp Neurol*. 1979;188:245–262.
341. Ivert L, Gouras P, Naeser P, et al. Photoreceptor allografts in a feline model of retinal degeneration. *Graefes Arch Clin Exp Ophthalmol*. 1998;236:844–852.
342. Bragadottir R, Narfstrom K. Lens sparing pars plana vitrectomy and retinal transplantation in cats. *Vet Ophthalmol*. 2003;6:135–139.
343. Bergstrom A, Ehinger B, Wilke K, et al. Transplantation of embryonic retina to the subretinal space in rabbits. *Exp Eye Res*. 1992;55:29–37.
344. Ghosh F, Bruun A, Ehinger B. Immunohistochemical markers in full thickness embryonic rabbit retinal transplants. *Ophthalmic Res*. 1999;31:5–15.
345. Ghosh F, Arner K. Transplantation of full-thickness retina in the normal porcine eye: surgical and morphologic aspects. *Retina*. 2002;22:478–486.
346. Klassen H, Kiilgaard JF, Warfvinge K, et al. Photoreceptor differentiation following transplantation of allogeneic retinal progenitor cells to the dystrophic rhodopsin Pro347Leu transgenic pig. *Stem Cells Int*. 2012;2012:939801.
347. Kaplan HJ, Tezel TH, Berger AS, et al. Human photoreceptor transplantation in retinitis pigmentosa. *Arch*

Ophthalmol. 1997;115:1168–1172.
348. Prince JH, Diesem CD, Eglitis I, et al. *Anatomy and histology of the eye and orbit in domestic animals*. Charles C. Thomas: Springfield IL; 1960:260–297.
349. Beauchemin ML. The fine structure of the pig's retina. *Graefes Arch Clin Exp Ophthalmol*. 1974;190:27–45.
350. Simoens P, De Schaepdrijver L, Lauwers H. Morphologic and clinical study of the retinal circulation in the miniature pig. A: Morphology of the retinal microvasculature. *Exp Eye Res*. 1992;54:965–973.
351. Ghosh F, Engelsberg K, English RV, et al. Long-term neuroretinal full- thickness transplants in a large animal model of severe retinitis pigmentosa. *Graefes Arch Clin Exp Ophthalmol*. 2007;245:835–846.
352. Seiler M, Aramant RB, Ehinger B, et al. Transplantation of embryonic retina to adult retina in rabbits. *Exp Eye Res*. 1990;51:225–228.
353. Lazar E, del Cerro M. A new procedure for multiple intraretinal transplantation into mammalian eyes. *J Neurosci Methods*. 1992;43:157–169.
354. del Cerro M, Kordower JH, Lazar E, et al. Photoreceptor differentiation in retinal xenografts of fetal monkey retina. *Brain Res*. 1992;574:1–8.
355. Rauer O, Ghosh F. Survival of full-thickness retinal xenotransplants without immunosuppression. *Graefes Arch Clin Exp Ophthalmol*. 2001;239:145–151.
356. Juliusson B, Bergström A, van Veen T, et al. Cellular organization in retinal transplants using cell suspensions or fragments of embryonic retinal tissue. *Cell Transplant*. 1993;2:411–418.
357. Sharma RK. Dissection and cotransplantation of large pieces of RPE and neural retina; effect of protease K on the development. *Acta Ophthalmol Scand*. 2000;78:3–8.
358. Geller AM, Sieving PA. Assessment of foveal cone photoreceptors in Stargardt's macular dystrophy using a small dot detection task. *Vision Res*. 1993;33:1509–1524.
359. Tezel TH, Kaplan HJ. Harvest and storage of adult human photoreceptor cells: the vibratome compared to the excimer

laser. *Curr Eye Res*. 1998;17:748–756.
360. Clerin E, Yang Y, Forster V, Fontaine V, Sahel JA, Leveillard T. Vibratome sectioning mouse retina to prepare photoreceptor cultures. *J Vis Exp*. 2014;22(94).
361. Aramant R, Seiler M, Turner JE. Donor age influences on the success of retinal grafts to adult rat retina. *Invest Ophthalmol Vis Sci*. 1988;29:498–503.
362. Salchow DJ, Trokel SL, Kjeldbye H, et al. Isolation of human fetal cones. *Curr Eye Res*. 2001;22:85–89.
363. LuŽnik Z, Parekh M, Bertolin M. Biobanking of human retinas: the next big leap for eye banks? *Stem Cells Transl Med*. 2015;4(8):868–872.
364. Pinilla I, Cuenca N, Martinez-Navarrete G, et al. Intraretinal processing following photoreceptor rescue by non-retinal cells. *Vision Res*. 2009;49:2067–2077.
365. Keegan DJ, Kenna P, Humphries MM, et al. Transplantation of syngeneic Schwann cells to the retina of the rhodopsin knockout (rho(−/−)) mouse. *Invest Ophthalmol Vis Sci*. 2003;44:3526–3532.
366. Huo SJ, Li YC, Xie J, et al. Transplanted olfactory ensheathing cells reduce retinal degeneration in Royal College of Surgeons rats. *Curr Eye Res*. 2012;37:749–758.
367. Hicks D, Sahel J. The implications of rod-dependent cone survival for basic and clinical research. *Invest Ophthalmol Vis Sci*. 1999;40:3071–3074.
368. LaVail MM, Unoki K, Yasumura D, et al. Multiple growth factors, cytokines, and neurotrophins rescue photoreceptors from the damaging effects of constant light. *Proc Natl Acad Sci USA*. 1992;89:11249–11253.
369. Cayouette M, Gravel C. Adenovirus-mediated gene transfer of ciliary neurotrophic factor can prevent photoreceptor degeneration in the retinal degeneration (rd) mouse. *Hum Gene Ther*. 1997;8:423–430.
370. Chaum E. Retinal neuroprotection by growth factors: a mechanistic perspective. *J Cell Biochem*. 2003;88:57–75.
371. Wenzel A, Grimm C, Samardzija M, et al. Molecular mechanisms of light-induced photoreceptor apoptosis and neuroprotection for retinal degeneration. *Prog Retin Eye Res*.

2005;24:275–306.
372. Wen R, Song Y, Cheng T, et al. Injury-induced upregulation of bFGF and CNTF mRNAS in the rat retina. *J Neurosci*. 1995;15:7377–7385.
373. Faktorovich EG, Steinberg RH, Yasumura D, et al. Photoreceptor degeneration in inherited retinal dystrophy delayed by basic fibroblast growth factor. *Nature*. 1990;347:83–86.
374. Cao W, Wen R, Li F, et al. Mechanical injury increases bFGF and CNTF mRNA expression in the mouse retina. *Exp Eye Res*. 1997;65:241–248.
375. Silverman MS, Hughes SE. Photoreceptor rescue in the RCS rat without pigment epithelium transplantation. *Curr Eye Res*. 1990;9:183–191.
376. Sharma RK, Ehinger B. Retinal cell transplants: How close to clinical application? *Acta Ophthalmol Scand*. 1997;75:355–356.
377. Sieving PA, Caruso RC, Tao W, et al. Ciliary neurotrophic factor (CNTF) for human retinal degeneration: phase I trial of CNTF delivered by encapsulated cell intraocular implants. *Proc Natl Acad Sci USA*. 2006;103:3896–3901.
378. Talcott KE, Ratnam K, Sundquist SM, et al. Longitudinal study of cone photoreceptors during retinal degeneration and in response to ciliary neurotrophic factor treatment. *Invest Ophthalmol Vis Sci*. 2011;52:2219–2226.
379. Zhang K, Hopkins JJ, Heier JS, et al. Ciliary neurotrophic factor delivered by encapsulated cell intraocular implants for treatment of geographic atrophy in age-related macular degeneration. *Proc Natl Acad Sci USA*. 2011;108:6241–6245.
380. Kauper K, McGovern C, Sherman S, et al. Two-year intraocular delivery of ciliary neurotrophic factor by encapsulated cell technology implants in patients with chronic retinal degenerative diseases. *Invest Ophthalmol Vis Sci*. 2012;53:7484–7491.
381. Birch DG, Weleber RG, Duncan JL, Ciliary Neurotrophic Factor Retinitis Pigmentosa Study Group, et al. Randomized trial of ciliary neurotrophic factor delivered by encapsulated cell intraocular implants for retinitis

pigmentosa. *Am J Ophthalmol*. 2013;156:283–292.e1.
382. Lund RD, Kwan AS, Keegan DJ, et al. Cell transplantation as a treatment for retinal disease. *Prog Retin Eye Res*. 2001;20:415–449.
383. Coffey PJ, Whiteley SJ, Lund RD. Preservation and restoration of vision following transplantation. *Prog Brain Res*. 2000;127:489–499.
384. Das T, del Cerro M, Jalali S, et al. The transplantation of human fetal neuroretinal cells in advanced retinitis pigmentosa patients: results of a long- term safety study. *Exp Neurol*. 1999;157:58–68.
385. Humayun MS, de Juan E Jr, del Cerro M, et al. Human neural retinal transplantation. *Invest Ophthalmol Vis Sci*. 2000;41:3100–3106.
386. Radtke ND, Seiler MJ, Aramant RB, et al. Transplantation of intact sheets of fetal neural retina with its retinal pigment epithelium in retinitis pigmentosa patients. *Am J Ophthalmol*. 2002;133:544–550.
387. Berger AS, Tezel TH, Del Priore LV, et al. Photoreceptor transplantation in retinitis pigmentosa: short-term follow-up. *Ophthalmology*. 2003;110:383–391.
388. del Cerro M, Humayun MS, Sadda SR, et al. Histologic correlation of human neural retinal transplantation. *Invest Ophthalmol Vis Sci*. 2000;41:3142–3148.
389. Zhang Y, Arner K, Ehinger B, et al. Limitation of anatomical integration between subretinal transplants and the host retina. *Invest Ophthalmol Vis Sci*. 2003;44:324–331.
390. Hippert C, Graca AB, Pearson RA. Gliosis can impede integration following photoreceptor transplantation into the diseased retina. *Adv Exp Med Biol*. 2016;854:579–585.
391. West EL, Pearson RA, Tschernutter M, et al. Pharmacological disruption of the outer limiting membrane leads to increased retinal integration of transplanted photoreceptor precursors. *Exp Eye Res*. 2008;86:601–611.
392. Pearson RA, Barber AC, West EL, et al. Targeted disruption of outer limiting membrane junctional proteins (Crb1 and ZO-1) increases integration of transplanted photoreceptor precursors into the adult wild-type and degenerating retina.

Cell Transplant. 2010;19:487–503.
393. Barber AC, Hippert C, Duran Y, et al. Repair of the degenerate retina by photoreceptor transplantation. *Proc Natl Acad Sci USA*. 2013;110:354–359.
394. West EL, Pearson RA, Duran Y, et al. Manipulation of the recipient retinal environment by ectopic expression of neurotrophic growth factors can improve transplanted photoreceptor integration and survival. *Cell Transplant*. 2012;21:871–887.
395. Gonzalez-Cordero A, West EL, Pearson RA, et al. Photoreceptor precursors derived from three-dimensional embryonic stem cell cultures integrate and mature within adult degenerate retina. *Nat Biotechnol*. 2013;31:741–747.
396. Yanai A, Laver CR, Gregory-Evans CY, et al. Enhanced functional integration of human photoreceptor precursors into human and rodent retina in an ex vivo retinal explant model system. *Tissue Eng Part A*. 2015;21:1763–1771.
397. Zhang Y, Sharma RK, Ehinger B, et al. Nitric oxide-producing cells project from retinal grafts to the inner plexiform layer of the host retina. *Invest Ophthalmol Vis Sci*. 1999;40:3062–3066.
398. Warre-Cornish K, Barber AC, Sowden JC, et al. Migration, integration and maturation of photoreceptor precursors following transplantation in the mouse retina. *Stem Cells Dev*. 2014;23:941–954.
399. MacLaren RE, Pearson RA, MacNeil A, et al. Retinal repair by transplantation of photoreceptor precursors. *Nature*. 2006;444:203–207.
400. Bartsch U, Oriyakhel W, Kenna PF, et al. Retinal cells integrate into the outer nuclear layer and differentiate into mature photoreceptors after subretinal transplantation into adult mice. *Exp Eye Res*. 2008;86:691–700.
401. Postel K, Bellmann J, Splith V, Ader M. Analysis of cell surface markers specific for transplantable rod photoreceptors. *Mol Vis*. 2013;19:2058–2067.
402. Santos-Ferreira T, Postel K, Stutzki H, Kurth T, Zeck G, Ader M. Daylight vision repair by cell transplantation. *Stem Cells*. 2015;33:79–90.

403. Lakowski J, Baron M, Bainbridge J, et al. Cone and rod photoreceptor transplantation in models of the childhood retinopathy Leber congenital amaurosis using flow-sorted Crx-positive donor cells. *Hum Mol Genet*. 2010;19:4545–4559.
404. Gamm DM, Wang S, Lu B, et al. Protection of visual functions by human neural progenitors in a rat model of retinal disease. *PLoS ONE*. 2007;2:e338.
405. Singh MS, Charbel Issa P, Butler R, et al. Reversal of end-stage retinal degeneration and restoration of visual function by photoreceptor transplantation. *Proc Natl Acad Sci USA*. 2013;110:1101–1106.
406. Kovalevsky G, DiLoreto D Jr, Wyatt J, et al. The intensity of the pupillary light reflex does not correlate with the number of retinal photoreceptor cells. *Exp Neurol*. 1995;133:43–49.
407. Pearson RA, Barber AC, Rizzi M, et al. Restoration of vision after transplantation of photoreceptors. *Nature*. 2012;485:99–103.
408. Chacko DM, Rogers JA, Turner JE, et al. Survival and differentiation of cultured retinal progenitors transplanted in the subretinal space of the rat. *Biochem Biophys Res Commun*. 2000;268:842–846.
409. Sakaguchi DS, Van Hoffelen SJ, Grozdanic SD, et al. Neural progenitor cell transplants into the developing and mature central nervous system. *Ann N Y Acad Sci*. 2005;1049:118–134.
410. Klassen H, Schwartz PH, Ziaeian B, et al. Neural precursors isolated from the developing cat brain show retinal integration following transplantation to the retina of the dystrophic cat. *Vet Ophthalmol*. 2007;10:245–253.
411. Van Hoffelen SJ, Young MJ, Shatos MA, et al. Incorporation of murine brain progenitor cells into the developing mammalian retina. *Invest Ophthalmol Vis Sci*. 2003;44:426–434.
412. Sam TN, Xiao J, Roehrich H, et al. Engrafted neural progenitor cells express a tissue-restricted reporter gene associated with differentiated retinal photoreceptor cells. *Cell Transplant*. 2006;15:147–160.
413. Klassen H, Sakaguchi DS, Young MJ. Stem cells and retinal

repair. *Prog Retin Eye Res*. 2004;23:149–181.
414. Li T, Lewallen M, Chen S, Yu W, Zhang N, Xie T. Multipotent stem cells isolated from the adult mouse retina are capable of producing functional photoreceptor cells. *Cell Res*. 2013;23:788–802.
415. Luo J, Baranov P, Patel S, et al. Human retinal progenitor cell transplantation preserves vision. *J Biol Chem*. 2014;289:6362–6371.
416. Seiler MJ, Jones BW, Aramant RB, Yang PB, Keirstead HS, Marc RE. Computational molecular phenotyping of retinal sheet transplants to rats with retinal degeneration. *Eur J Neurosci*. 2012;35:1692–1704.
417. Yao J, Ko CW, Baranov PY, et al. Enhanced differentiation and delivery of mouse retinal progenitor cells using a micropatterned biodegradable thin-film polycaprolactone scaffold. *Tissue Eng Part A*. 2015;21:1247–1260.
418. Baranov P, Michaelson A, Kundu J, et al. Interphotoreceptor matrix- poly(-caprolactone) composite scaffolds for human photoreceptor differentiation. *J Tissue Eng*. 2014;5 [2041731414554139].
419. Liu Y, Wang R, Zarembinski TI, et al. The application of hyaluronic acid hydrogels to retinal progenitor cell transplantation. *Tissue Eng Part A*. 2013;19:135–142.
420. Maclaren RE, Pearson RA, Macneil A, et al. Retinal repair by transplantation of photoreceptor precursors. *Nature*. 2006;444(7116):203–207.
421. Gruen L, Grabel L. Concise review: scientific and ethical roadblocks to human embryonic stem cell therapy. *Stem Cells*. 2006;24:2162–2169.
422. MacNeil A, Pearson RA, MacLaren RE, et al. Comparative analysis of progenitor cells isolated from the iris, pars plana, and ciliary body of the adult porcine eye. *Stem Cells*. 2007;25:2430–2438.
423. Kokkinopoulos I, Pearson RA, Macneil A, et al. Isolation and characterisation of neural progenitor cells from the adult Chx10(orJ/orJ) central neural retina. *Mol Cell Neurosci*. 2008;38:359–373.
424. Akagi T, Mandai M, Ooto S, et al. Otx2 homeobox gene

induces photoreceptor-specific phenotypes in cells derived from adult iris and ciliary tissue. *Invest Ophthalmol Vis Sci*. 2004;45:4570–4575.
425. Jomary C, Jones SE. Induction of functional photoreceptor phenotype by exogenous Crx expression in mouse retinal stem cells. *Invest Ophthalmol Vis Sci*. 2008;49:429–437.
426. Yang P, Seiler MJ, Aramant RB, et al. Differential lineage restriction of rat retinal progenitor cells in vitro and in vivo. *J Neurosci Res*. 2002;69:466–476.
427. Canola K, Angenieux B, Tekaya M, et al. Retinal stem cells transplanted into models of late stages of retinitis pigmentosa preferentially adopt a glial or a retinal ganglion cell fate. *Invest Ophthalmol Vis Sci*. 2007;48:446–454.
428. Klassen H, Kiilgaard JF, Zahir T, et al. Progenitor cells from the porcine neural retina express photoreceptor markers after transplantation to the subretinal space of allorecipients. *Stem Cells*. 2007;25:1222–1230.
429. Klassen HJ, Ng TF, Kurimoto Y, et al. Multipotent retinal progenitors express developmental markers, differentiate into retinal neurons, and preserve light-mediated behavior. *Invest Ophthalmol Vis Sci*. 2004;45:4167–4173.
430. Liu IH, Chen SJ, Ku HH, et al. Comparison of the proliferation and differentiation ability between adult rat retinal stem cells and cerebral cortex- derived neural stem cells. *Ophthalmologica*. 2005;219:171–176.
431. Del Debbio CB, Balasubramanian S, Parameswaran S, et al. Notch and Wnt signaling mediated rod photoreceptor regeneration by Muller cells in adult mammalian retina. *PLoS ONE*. 2010;5:e12425.
432. Lawrence JM, Singhal S, Bhatia B, et al. MIO-M1 cells and similar Muller glial cell lines derived from adult human retina exhibit neural stem cell characteristics. *Stem Cells*. 2007;25:2033–2043.
433. Das AV, Mallya KB, Zhao X, et al. Neural stem cell properties of Muller glia in the mammalian retina: regulation by Notch and Wnt signaling. *Dev Biol*. 2006;299:283–302.
434. Limb GA, Salt TE, Munro PM, et al. In vitro characterization

of a spontaneously immortalized human Muller cell line (MIO-M1). *Invest Ophthalmol Vis Sci*. 2002;43:864–869.
435. Singhal S, Lawrence JM, Bhatia B, et al. Chondroitin sulfate proteoglycans and microglia prevent migration and integration of grafted Muller stem cells into degenerating retina. *Stem Cells*. 2008;26:1074–1082.
436. Jayaram H, Jones MF, Eastlake K, et al. Transplantation of photoreceptors derived from human Müller glia restore rod function in the P23H rat. *Stem Cells Transl Med*. 2014;3:323–333.
437. Xu C, Inokuma MS, Denham J, et al. Feeder-free growth of undifferentiated human embryonic stem cells. *Nat Biotechnol*. 2001;19:971–974.
438. Ludwig TE, Bergendahl V, Levenstein ME, et al. Feeder-independent culture of human embryonic stem cells. *Nat Methods*. 2006;3:637–646.
439. Lamba DA, Karl MO, Ware CB, et al. Efficient generation of retinal progenitor cells from human embryonic stem cells. *Proc Natl Acad Sci USA*. 2006;103:12769–12774.
440. Schraermeyer U, Thumann G, Luther T, et al. Subretinally transplanted embryonic stem cells rescue photoreceptor cells from degeneration in the RCS rats. *Cell Transplant*. 2001;10:673–680.
441. Amirpour N, Karamali F, Rabiee F, et al. Differentiation of human embryonic stem cell-derived retinal progenitors into retinal cells by sonic hedgehog and/or retinal pigmented epithelium and transplantation into the subretinal space of sodium iodate-injected rabbits. *Stem Cells Dev*. 2011;21:42–53.
442. Yanai A, Laver C, Joe AW, et al. Efficient production of photoreceptor precursor cells from human embryonic stem cells. *Methods Mol Biol*. 2016;1307:357–369.
443. Garita-Hernandez M, Diaz-Corrales F, Lukovic D, et al. Hypoxia increases the yield of photoreceptors differentiating from mouse embryonic stem cells and improves the modeling of retinogenesis in vitro. *Stem Cells*. 2013;31:966–978.
444. Lakowski J, Gonzalez-Cordero A, West EL, et al.

Transplantation of photoreceptor precursors isolated via a cell surface biomarker panel from embryonic stem cell-derived self-forming retina. *Stem Cells*. 2015;33:2469–2482.
445. Eberle D, Kurth T, Santos-Ferreira T, Wilson J, Corbeil D, Ader M. Outer segment formation of transplanted photoreceptor precursor cells. *PLoS ONE*. 2012;7:e46305.
446. Eberle D, Santos-Ferreira T, Grahl S, Ader M. Subretinal transplantation of MACS purified photoreceptor precursor cells into the adult mouse retina. *J Vis Exp*. 2014;e50932.
447. Laver CR, Metcalfe AL, Szczygiel L, Yanai A, Sarunic MV, Gregory-Evans K. Bimodal in vivo imaging provides early assessment of stem-cell-based photoreceptor engraftment. *Eye (Lond)*. 2015;29:681–690.
448. Lamba DA, McUsic A, Hirata RK, et al. Generation, purification and transplantation of photoreceptors derived from human induced pluripotent stem cells. *PLoS ONE*. 2010;5:e8763.
449. Tucker BA, Park IH, Qi SD, et al. Transplantation of adult mouse iPS cell-derived photoreceptor precursors restores retinal structure and function in degenerative mice. *PLoS ONE*. 2011;6:e18992.
450. Zhou L, Wang W, Liu Y, et al. Differentiation of induced pluripotent stem cells of Swine into rod photoreceptors and their integration into the retina. *Stem Cells*. 2011;29:972–980.
451. Kicic A, Shen WY, Wilson AS, et al. Differentiation of marrow stromal cells into photoreceptors in the rat eye. *J Neurosci*. 2003;23:7742–7749.
452. Sun X, Chen M, Li J, et al. E13.5 retinal progenitors induce mouse bone marrow mesenchymal stromal cells to differentiate into retinal progenitor-like cells. *Cytotherapy*. 2011;13:294–303.
453. Tao YX, Xu HW, Zheng QY, et al. Noggin induces human bone marrow-derived mesenchymal stem cells to differentiate into neural and photoreceptor cells. *Indian J Exp Biol*. 2010;48:444–452.
454. Arnhold S, Absenger Y, Klein H, et al. Transplantation of bone marrow-derived mesenchymal stem cells rescue photoreceptor cells in the dystrophic retina of the

rhodopsin knockout mouse. *Graefes Arch Clin Exp Ophthalmol*. 2007;245:414–422.
455. Inoue Y, Iriyama A, Ueno S, et al. Subretinal transplantation of bone marrow mesenchymal stem cells delays retinal degeneration in the RCS rat model of retinal degeneration. *Exp Eye Res*. 2007;85:234–241.
456. Zhang Y, Luo Y, Li K, et al. Pre-induced adult human peripheral blood mononuclear cells migrate widely into the degenerative retinas of rd1 mice. *Cytotherapy*. 2013;15:1416–1425.
457. Peng Y, Zhang Y, Huang B, et al. Survival and migration of pre-induced adult human peripheral blood mononuclear cells in retinal degeneration slow (rds) mice three months after subretinal transplantation. *Curr Stem Cell Res Ther*. 2014;9:124–133.
458. Radtke ND, Aramant RB, Seiler M, et al. Preliminary report: indications of improved visual function after retinal sheet transplantation in retinitis pigmentosa patients. *Am J Ophthalmol*. 1999;128:384–387.
459. Radtke ND, Aramant RB, Seiler MJ, Petry HM, Pidwell D. Vision change after sheet transplant of fetal retina with retinal pigment epithelium to a patient with retinitis pigmentosa. *Arch Ophthalmol*. 2004;122:1159–1165.
460. Siqueira RC, Messias A, Voltarelli JC, et al. Intravitreal injection of autologous bone marrow-derived mononuclear cells for hereditary retinal dystrophy: a phase I trial. *Retina*. 2011;31:1207–1214.
461. Park SS, Bauer G, Abedi M, et al. Intravitreal autologous bone marrow CD34+ cell therapy for ischemic and degenerative retinal disorders: preliminary phase 1 clinical trial findings. *Invest Ophthalmol Vis Sci*. 2015;56:81–89.
462. Wang HM, Kaplan HJ, Chan WC, et al. The distribution and ontogeny of MHC antigens in murine ocular tissue. *Invest Ophthalmol Vis Sci*. 1987;28:1383–1389.
463. Jiang LQ, Jorquera M, Streilein JW, et al. Unconventional rejection of neural retinal allografts implanted into the immunologically privileged site of the eye. *Transplantation*. 1995;59:1201–1207.

464. Hori J, Ng TF, Shatos M, et al. Neural progenitor cells lack immunogenicity and resist destruction as allografts. *Stem Cells*. 2003;21:405–416.
465. Yang P, Chen L, Zwart R, et al. Immune cells in the porcine retina: distribution, characterization and morphological features. *Invest Ophthalmol Vis Sci*. 2002;43:1488–1492.
466. Provis JM, Penfold PL, Edwards AJ, et al. Human retinal microglia: expression of immune markers and relationship to the glia limitans. *Glia*. 1995;14:243–256.
467. Aramant RB, Seiler MJ. Human embryonic retinal cell transplants in athymic immunodeficient rat hosts. *Cell Transplant*. 1994;3:461–474.
468. Ma J, Xu L, Othersen DK, et al. Cloning and localization of RPE65 mRNA in salamander cone photoreceptor cells1. *Biochim Biophys Acta*. 1998;1443:255–261.
469. Xu Y, Balasubramaniam B, Copland DA, et al. Activated adult microglia influence retinal progenitor cell proliferation and differentiation toward recoverin-expressing neuron-like cells in a co-culture model. *Graefes Arch Clin Exp Ophthalmol*. 2015;253:1085–1096.
470. West EL, Pearson RA, Barker SE, et al. Long-term survival of photoreceptors transplanted into the adult murine neural retina requires immune modulation. *Stem Cells*. 2010;28:1997–2007.
471. MacLaren RE, Pearson RA, MacNeil A, et al. Retinal repair by transplantation of photoreceptor precursors. *Nature*. 2006;444:203–207.
472. Pearson RA. Advances in repairing the degenerate retina by rod photoreceptor transplantation. *Biotechnol Adv*. 2014;32:485–491.
473. Jayakody SA, Gonzalez-Cordero A, Ali RR, et al. Cellular strategies for retinal repair by photoreceptor replacement. *Prog Retin Eye Res*. 2015;46:31–66.
474. Fawcett JW, Asher RA. The glial scar and central nervous system repair. *Brain Res Bull*. 1999;49:377–391.
475. Kinouchi R, Takeda M, Yang L, et al. Robust neural integration from retinal transplants in mice deficient in GFAP and vimentin. *Nat Neurosci*. 2003;6:863–868.

476. Tucker BA, Redenti SM, Jiang C, et al. The use of progenitor cell/biodegradable MMP2-PLGA polymer constructs to enhance cellular integration and retinal repopulation. *Biomaterials*. 2010;31:9–19.
477. Lewis GP, Linberg KA, Fisher SK. Neurite outgrowth from bipolar and horizontal cells after experimental retinal detachment. *Invest Ophthalmol Vis Sci*. 1998;39:424–434.
478. Jansen HG, Hawkins RK, Sanyal S. Synaptic growth in the rod terminals of mice after partial photoreceptor cell loss: a three-dimensional ultrastructural study. *Microsc Res Tech*. 1997;36:96–105.
479. Fei Y. Cone neurite sprouting: an early onset abnormality of the cone photoreceptors in the retinal degeneration mouse. *Mol Vis*. 2002;8:306–314.
480. Fariss RN, Li ZY, Milam AH. Abnormalities in rod photoreceptors, amacrine cells, and horizontal cells in human retinas with retinitis pigmentosa. *Am J Ophthalmol*. 2000;129:215–223.
481. Fisher SK, Lewis GP. Muller cell and neuronal remodeling in retinal detachment and reattachment and their potential consequences for visual recovery: a review and reconsideration of recent data. *Vision Res*. 2003;43:887–897.
482. Nachman-Clewner M, Townes-Anderson E. Injury-induced remodelling and regeneration of the ribbon presynaptic terminal in vitro. *J Neurocytol*. 1996;25:597–613.
483. Mandell JW, MacLeish PR, Townes-Anderson E. Process outgrowth and synaptic varicosity formation by adult photoreceptors in vitro. *J Neurosci*. 1993;13:3533–3548.
484. Khodair MA, Zarbin MA, Townes-Anderson E. Synaptic plasticity in mammalian photoreceptors prepared as sheets for retinal transplantation. *Invest Ophthalmol Vis Sci*. 2003;44:4976–4988.
485. Khodair MA, Zarbin MA, Townes-Anderson E. Cyclic AMP prevents retraction of axon terminals in photoreceptors prepared for transplantation: an in vitro study. *Invest Ophthalmol Vis Sci*. 2005;46:967–973.
486. Fontainhas AM, Townes-Anderson E. RhoA inactivation prevents photoreceptor axon retraction in an in vitro model

of acute retinal detachment. *Invest Ophthalmol Vis Sci*. 2011;52:579–587.
487. Fontainhas AM, Townes-Anderson E. RhoA and its role in synaptic structural plasticity of isolated salamander photoreceptors. *Invest Ophthalmol Vis Sci*. 2008;49:4177–4187.
488. Marc RE, Jones BW, Watt CB, et al. Neural remodeling in retinal degeneration. *Prog Retin Eye Res*. 2003;22:607–655.

129

Artificial Vision

Mark S. Humayun, Hossein Nazari, James Weiland

Introduction

More than 1 million Americans are legally blind, 10% of whom have no light perception.[1] Certain approaches, such as gene and drug therapy (see Chapter 36, Gene therapy for retinal disease), may be preventative or therapeutic options for blindness.[2,3] However, once photoreceptors are nearly completely lost, such as in endstage retinitis pigmentosa (RP) (see Chapter 42, Retinitis pigmentosa and allied disorders) or age-related macular degeneration (AMD) (see Chapter 64, Chapter 65, Chapter 66, Chapter 67 on epidemiology/risk factors for AMD, pathogenesis, and diagnosis and treatment of dry and wet AMD, respectively), very few interventions[4] can restore useful vision to blind patients. Retinitis pigmentosa (RP) is the leading inherited cause of blindness, with 1.5 million people worldwide affected and an incidence of 1 in 3,500 live births.[5] AMD is the leading cause of visual loss among adults older than 65, with 700,000 newly diagnosed patients annually in the United States, 10% of whom become legally blind each year.[6] With an increased average lifespan, particularly in the developing world, the number of people with age-related eye disease and resulting visual impairment is expected to double during the next three decades.[7] Blindness imposes major economic and social consequences on affected persons, their caregivers, and society at large. The mean annual expense for patients with visual impairment and blindness is found to be two times the cost for nonblind patients. Time spent by caregivers to care for the visually impaired and other indirect costs due to productivity losses and premature mortality are additional considerable burdens.[8]

Few treatment options exist for outer retinal degeneration. Anti-VEGF therapy is very effective for the treatment of neovascular-AMD by inhibiting the growth of abnormal new blood vessels. This therapy is capable of preventing visual loss and even returning vision to patients treated in the initial phases.[9–11] Nevertheless, like most new therapies, it has limitations and drawbacks, and there is some evidence that there is disease progression in spite of injections, especially in polypoidal choroidal vasculopathy.[12] Moreover, a number of patients seek consultation when the neovascularization is advanced and irreversible vision loss has already occurred. Non-neovascular AMD can also become

advanced, leading to atrophic AMD (e.g., geographic atrophy). There is no approved therapy for atrophic AMD, albeit many companies are trying to develop a therapy for this slowly progressive variant of AMD. Replacement of atrophic retinal pigmented epithelium (RPE) with stem cell-derived RPE cells is being tested in multiple clinical trials;[13] however, it is not clear if patients with endstage macular degeneration with advanced loss of photoreceptors benefit from this method. Combined stem cell-derived RPE and photoreceptor progenitor cell implantation is proposed for such patients, but the safety and efficacy of such interventions have yet to be proven in clinical trials. Gene therapy has shown some success in Leber congenital amaurosis by targeting a specific mutation of the *RPE65* gene.[14–17] This is a tremendous scientific breakthrough, but the impact is limited, since this specific type of retinal degeneration is rare and the total number of eligible patients is small (approximately 1000). Neither anti-VEGF nor many of the proposed pharmacologic treatments or gene therapy can address lost vision due to photoreceptor loss, since photoreceptors are not regenerated by these approaches. Artificial vision, the novel concept of restoring vision by electrically stimulating the surviving retinal cells in a person who has lost vision due to advanced photoreceptor damage, has created hope for treating blindness.

This chapter will briefly summarize the history and evolution of electronic visual prostheses with an emphasis on retinal implants and will present the current state of the field with remaining challenges that lie ahead.

Background and History of Artificial Vision

The concept of electrically stimulating the nervous system to create artificial vision was first introduced in 1929, when Foerster, a German neurosurgeon, observed that electrical stimulation of the visual cortex caused his patient to detect a spot of light (phosphene). He further demonstrated that the perceived location of this phosphene depended on the location of the stimulating

electrode over the cortex.[18] The first effort towards an electrical artificial vision device was undertaken 50 years ago by Giles Brindley. Brindley's implantation of an 80-electrode device onto the visual cortex of a blind patient revealed the possibilities of electrical stimulation to restore vision and the implementation barriers of a suitable device. Limitations of the available technology prevented the realization of a clinically deployed device, but Brindley's pioneering work influenced all subsequent major efforts in the area of electronic visual prostheses. In the past 50 years, exponential advances in our understanding of electronics, physiology, and medicine have enabled the development of implantable microelectronic systems that overcome the shortcomings of Brindley's large, immobile visual cortex stimulator.[19]

Examples of such advances have been noted in the fields of electrical engineering, computer sciences, and micromachining technology. For instance, very large-scale integration (VLSI) circuits and microelectromechanical systems (MEMS) technology have all contributed to the evolution of the field of visual prostheses by allowing for the creation of both smaller electronics and smaller neural interfaces. These technological advancements, coupled with recent scientific investigations, have transformed the focus of the field from that of whether it is possible to create visual sensations through electrical stimulation to the more important question of how to optimize the perceptions for maximum benefit. Current questions being considered are related to the quality of images created by stimulation of many small areas of neuronal tissue as well as the mechanical and electrical biocompatibility of the microelectronic implants.

Whether a useful vision can be rendered via an artificial visual prosthesis depends in part upon establishing a definition of useful vision that is based on the minimum number of pixels required for people to accomplish activities of daily living. Psychophysical experiments were conducted to estimate the number of the pixels needed for specific tasks. Brindley originally suggested that 600 points of stimulation (pixels) would be sufficient for reading ordinary print.[19] Recent studies have tested humans with normal visual function by pixelating their vision via a portable phosphene simulator, consisting of a small head-mounted video camera and

monitor. Patients then walked through an obstacle course and read pixilated text. In this fashion, it was determined that 625 electrodes implanted in a 1-cm^2 area near the foveal representation in the visual cortex could produce a phosphene image with a visual acuity of approximately 20/30 and reading rates near 170 words/minute with scrolled text and 100 words/minute with fixed text.[20–23] Furthermore, a degree of learning was noted as walking speeds increased fivefold during 3 weeks of training.[22]

Studies simulating electrodes placed over the entire macula rather than concentrated on the fovea have assessed the ability of subjects to recognize faces with artificial vision. Parameters included grid size (10 × 10 to 32 × 32 pixels), pixel size, gap width, pixel dropout rate, and grayscale resolution. The subjects achieved highly significant facial recognition accuracies in both high- and low-contrast tests with a marked learning effect documented. These results suggest that reliable facial recognition is possible even with crude visual prostheses, and possibly makes the task of engineering the implant easier as it would require fewer data/stimulation channels.[23] The ability of subjects to read using a pixilated visual simulator has been evaluated in a separate cohort which demonstrated that most subjects are able to read fonts as small as 36 point (with all at 57 point) using a 16 × 16 pixel array.[24,25]

Visual Prostheses

Visual prostheses are based on neuronal electrical stimulation at different locations along the visual pathway (i.e., cortical, optic nerve, thalamus, epiretinal, subretinal). With the exception of thalamic prosthesis, prototype implants have been tested in humans in each location listed above, with varying results. Each approach has advantages and disadvantages. The main advantage of a cortical implant is that many types of blindness can be treated, including optic nerve disease. The main disadvantage of a cortical implant is that significant neural processing that normally occurs at the retinal and thalamic levels are missed with cortical implants. Retinal implants are applicable only in photoreceptor disease but tap into the visual pathway closer to the photoreceptors, thus most of the neural signal processing is preserved, albeit significant

processing in the retina may need to be replicated. The thalamic approach balances these concerns but is difficult to access surgically. In this chapter, the different types of implants, their position in the visual system, and recent results are discussed, but special emphasis is given to retinal implants.

Cortical Prosthesis

Building upon earlier observations of phosphene perception with cortical stimulation, Brindley and Dobelle began work in the 1960s towards functional, visual cortex prosthesis. They demonstrated the ability to evoke phosphenes and patterned perceptions by electrically stimulating the occipital cortex via permanently implanted electrodes.[19,26–32] Both groups used implanted arrays with over 50 electrodes placed subdurally over the occipital pole, thus providing evidence of the ability to return the sensation of vision to individuals who had a severed visual pathway anterior to the visual cortex. Dobelle's 64-channel platinum electrode surface stimulation prosthesis allowed blind patients to recognize 6-inch characters at 5 feet (approximately 20/1200 visual acuity).[29,31,33] Difficulties encountered in these experiments included the following: (1) controlling the number of phosphenes induced by each electrode; (2) interactions between phosphenes; (3) use of high currents and large electrodes that induced pain from meningeal stimulation; and (4) occasional focal epileptic activity following electrical stimulation.[29,34,35] Patients in these initial experiments complained of not being able to appreciate distinct phosphenes, but rather reported seeing “halos” surrounding each phosphene.[36]

Since most of the visual cortex is deep within the calcarine fissure and inaccessible to cortical surface electrodes, intracortical stimulation via penetrating electrodes was introduced in hopes of remedying the shortcomings of surface cortical stimulation. The intracortical devices employed smaller electrodes closer to the target neurons, thus requiring less current and resulting in a more localized stimulation. The stimulus threshold was 10–100 times lower for intracortical prosthesis as compared to surface stimulation. Further, this approach allowed for closer spacing of electrodes at 500 μm apart and thus possibly higher resolution.

Initial studies, during which the intracortical prosthesis was implanted in humans for a period of 4 months, demonstrated the ability to produce phosphenes that usually had color.[37] Documented advantages of the intracortical versus surface cortical implants included (1) predictable forms of elicited phosphenes; (2) absence of flicker phenomenon; (3) reduction in phosphene interactions; (4) increased number of electrodes; (5) reduced overall power requirement.[35,37–39]

Current models of the intracortical prosthesis include the Utah electrode array. This device consists of multiple silicon spikes organized in a square grid measuring 4.2 mm by 4.2 mm.[38] A platinum electrode is at the tip of each spike. A pneumatic system, which inserts a 100-electrode device into the cortex in about 200 ms, is designed for minimal trauma during insertion of this array.[40]

The cortical visual prosthesis is advantageous over other approaches because it bypasses all diseased visual pathway neurons rostral to the primary visual cortex. As such, this approach has the potential to restore vision to the largest number of blind patients. There are some limitations to the cortical visual prostheses. First, histologic changes for chronically implanted prostheses need to be further investigated.[41–43] In the case of silicon-doped penetrating electrodes, such as Utah electrode array, tissue reaction has ranged from none to a thin capsule around each electrode track to gliosis and buildup of fibrotic tissue between the array and meninges.[44] Second, the organization of the visual field is markedly more complex at the level of the primary cortex than at the retina or optic nerve and is not easily reproducible between various patients.[36] Next, there is a high level of specialization of every area of cortex for various parameters including color, motion, and eye movement, making it unlikely to garner simple phosphenes from stimulation.[45] Finally, surgical complications of this approach carry significant morbidity and mortality for the patient. The future success of the intracortical prosthesis requires further investigation of these areas.

Optic Nerve Prosthesis

Investigators have targeted the optic nerve as a potential site for the

implementation of a visual prosthesis.[46] Veraart et al. was the most recent of such groups attempting this method, employing the concept of a spiral nerve cuff electrode.[47–50] An electrode cuff is surgically implanted circumferentially on the external surface of the optic nerve. As this device does not penetrate the optic nerve sheath, it relies on the principle of retinotopic organization within the optic nerve. A volunteer with retinitis pigmentosa and no residual vision was chronically implanted with an optic nerve electrode connected to an implanted neurostimulator and antenna. An external controller with telemetry was used for electrical activation of the nerve that resulted in phosphene perception. Open-loop stimulation allowed the collection of phosphene attributes and the ability to elicit perception of simple geometric patterns. Low perception thresholds allowed for large current intensity range within safety limits. In a closed-loop paradigm, the volunteer was using a head-worn video camera to explore a projection screen. The volunteer underwent performance evaluation during the course of a training program with 45 simple patterns. Multiple bars (each 320 × 22 mm when projected on a screen) were combined to form letters on a 1 × 1-m screen, with the patient at 0.5 m from the screen. After learning, the volunteer reached a recognition score of 63% with a processing time of 60 seconds. The results were encouraging in that the blind volunteer was able to adequately interact with the environment while demonstrating pattern recognition and a learning effect for processing time and orientation discrimination.[51]

The optic nerve is an appealing site for the implementation of a visual prosthesis, as the entire visual field is represented in this small area. This area can be reached surgically and presents a viable anatomic location for an implant; however, there are several hurdles to overcome regarding this approach. First, the optic nerve is a densely consolidated neural structure with approximately 1.2 million axons in a 3-mm-diameter cylinder. While this allows for the entire visual field to be represented in a relatively small area, it is difficult to achieve focal stimulation of neurons and to replicate the exact retinotopy of the optic nerve. The dense packing of neurons requires a large number of electrode contacts from the prosthesis in a small area, increasing the risk of damage to the

nerve.[52] Surgical manipulation of this area requires dissection of the dura mater, creating possible harmful CNS effects including infection and possible interruption of blood flow to the optic nerve. Intervention at this point within the optic pathway requires intact retinal ganglion cells (RGC) and therefore is limited to the treatment of outer retinal (photoreceptor) degenerations. The optic nerve and RGC represent higher-order structures than the bipolar cells targeted by the retinal prosthesis. As such, the processing power of the bipolar, horizontal, and amacrine cells is lost, and therefore much more image processing must be achieved by the implant rather than relying on intact human physiologic pathways. Last, the nerve fibers from the macula lie most centrally within the optic nerve. Cuff electrodes, thus, are farthest away from macular fibers, and this will dramatically limit the use of this approach, especially for AMD, as the peripheral fibers will get stimulated along with the central macular fibers. Future development of this technology must address the above issues. Investigators have also proposed intraneuronal stimulation devices in order to more accurately target individual neurons within the optic nerve.[53]

Retinal Prostheses

The pathobiology of disorders causing blindness must be considered in discussions of visual prostheses.

Pathology of Retinitis Pigmentosa and Selected Macular Disorders

Potts and Inoue, over 45 years ago, demonstrated the ability to evoke an electrically elicited response (EER) via ocular stimulation using a contact lens as a stimulating electrode.[54–56] This discovery was expounded upon by Knighton, who demonstrated that inner retinal layers could be electrically stimulated to elicit an EER.[57,58]

For a retinal prosthesis to function properly, the retina must not be affected by disease to the point where few viable cells remain to initiate a neural signal. Postmortem morphometric analysis of the retina of patients with endstage RP has revealed that 78.4% of inner nuclear and 29.7% of ganglion layer cells (RGC) were retained compared to only 4.9% of photoreceptors.[59] Also, 93% of RGC were

spared and an increase in inner nuclear layer cells (by 10%) was noted in legally blind neovascular AMD patients.[60,61] Furthermore, no statistical significance was noted in the number of inner nuclear layer cells between non-neovascular eyes with geographic atrophy and age-matched controls.[60,61] This demonstrated limited trans-synaptic neuronal degeneration in the aforementioned retinopathies, and as such, showed that it is theoretically possible to electrically stimulate the remaining retinal neurons to elicit useful visual perceptions. However, it is important to understand the stages of outer retinal degeneration and the associated anatomic and physiologic changes that occur. A comprehensive study by Marc et al. has characterized the three phases of retinal neuronal degeneration and remodeling.[62] In the first two phases, photoreceptor stress and death, and associated loss of trophic transport are observed. Both bipolar and horizontal cells can actually retract dendrites, while the latter can sprout axonal and dendritic processes that can reach the inner plexiform layer. Müller cells can form a dense fibrotic layer and seal off the subretinal space, electrically isolating implants placed there via the choroid. In phase 3, the number of viable cells of all classes is depleted. In this phase, bipolar and amacrine cells migrate up to the ganglion cell layer and undergo neural rewiring.

Such anatomic changes manifest physiologically. Using a patch clamp technique in a retinal degeneration mouse model, it has been shown that rod bipolar cells lose their sensitivity to the excitatory neurotransmitter glutamate while they increase their response to the inhibitory horizontal cell neurotransmitter GABA.[63] In addition, oscillatory fluctuations in membrane potential, originating in AII amacrine cells, have been noted in animal models of retinal degeneration.[64] Thus, the retinal circuitry is altered both anatomically and physiologically by degeneration.

In spite of these well-documented changes in the inner retina after photoreceptor loss, numerous studies have established the safety and efficacy of electrical stimulation of the retina. Early studies by Humayun and colleagues established the feasibility of electrical stimulation of the retina.[59,65,66] In an operating room setting, handheld electrodes were inserted into the eye of blind test subjects. The test subjects reported the appearance of small spots of

light when the electrodes were activated. The apparent location of the spot of light in general corresponded with the retinal area stimulated. Similar experiments were repeated by other groups.[67,68] While these experiments only allowed a few hours of testing in each subject, the critical findings led to the development of a chronic implant system.

Epiretinal Prostheses

Epiretinal implants rely on external cameras to capture images and then transform this visual information to patterns of electrical stimulation to excite remaining retinal neurons. Designs tend to vary in terms of how much required electronic circuitry is contained in an intraocular device versus extraocular elements. Powering and signal transmission may be accomplished by induction coils, penetrating wires, or lasers.

The advantages of the epiretinal approach include the following: (1) the epiretinal placement allows for surgical access that follows standard vitrectomy procedures; (2) a minimal number of microelectronics are incorporated into the implantable portion of the device since image processing is external to the body; (3) the wearable portion of electronics allows for easy upgrades without requiring subsequent surgery; and (4) the electronics allow the user and the doctor full control over every electrode and image processing parameters, allowing the implant to be customized for each patient. The disadvantages to this approach include (1) requirement of techniques that will provide prolonged fixation of the device near the inner retina and (2) further distance of the epiretinal device to the target bipolar cells than the subretinal device requires increased current.

ARGUS I.

The ARGUS I system consists of a 16-channel stimulator, based on a commercial cochlear implant, positioned behind the ear, and attached to a cable that terminates at an electrode array on the epiretinal surface. The electrode array is a 4 × 4 grid of platinum disk electrodes, either 260 μm or 520 μm in diameter. The overall size of the ARGUS I retinal array is 3 × 3 mm. An inductive coil link is used to transmit power and data to the internal portion of the

implant from an external video processing unit (VPU), and a miniature camera that is mounted on a pair of glasses. The video camera captures a portion of the visual field and relays the information to the VPU. The VPU digitizes the signal in real time, applies a series of image processing filters, down-samples the image to a 4 × 4 pixilated grid, and creates a series of stimulus pulses based on pixel grayscale values and conversion tables (from grayscale value to pulse amplitude) customized for each subject. The data are delivered via an inductive RF coil link and the application-specific circuitry to the pulse generator.

The surgical procedure for the ARGUS I system implantation included a botulinum toxin injection 2 weeks prior to the surgery, in the superior, inferior, medial, and lateral rectus muscles, due to the concern that the subject's eye movement might break the cable connecting the intraocular electrode array to the extraocular electronic case. Two weeks post-injection, under general anesthesia, the implant was placed in a recess well created in the temporal skull, similar to cochlear implant surgery.[69] To secure and protect the cable, a shallow groove was created along the temporal skull. The cable was then placed in the groove and delivered through a lateral canthotomy into the periocular space. Next, the cable and electrode array were implanted under the four rectus muscles. A complete pars plana vitrectomy was performed and the array introduced to the eye through a 5-mm scleral incision placed 3 mm posterior to and parallel to the limbus. The array was placed temporal to the fovea, and a single retinal tack was inserted to secure the array in place.[70] A clinical trial of the ARGUS I device began in 2002 and enrolled six RP patients.

Subjects were able to discriminate between different electrodes, identify everyday objects such as a knife, a plate or a cup, and detect the direction of motion. Perceptual thresholds were within safe limits and were stable over time.[71,72] Perceptual thresholds correlated with separation (i.e., lift-off) between the electrode array and the retina.[71,73] In addition, increasing frequency of pulses lowered the charge per pulse in a predictable way.[74]

The best visual acuity using the ARGUS I was the maximum allowable by the spacing of electrodes on the array (i.e., 20/4000), but this was only demonstrated in one test subject.[75] Adverse events

included erosion of the conjunctiva over the cable at the sclerotomy and detachment of one array after one subject incurred blunt ocular trauma (subsequent re-tacking was successful).

ARGUS II.

The ARGUS II system (Fig. 129.1) is the first FDA approved and CE Mark certified artificial vision device for human use. It uses an external camera system very similar to ARGUS I, but the implanted part of the device is completely different. The ARGUS II system comprises an encircling band (sclera buckle), an inductive coil, and a case containing the electronic components attached to the band, and an integrated ribbon cable and electrode array. The electrode array spans 20° of visual field corner-to-corner. All components fit inside the orbit.

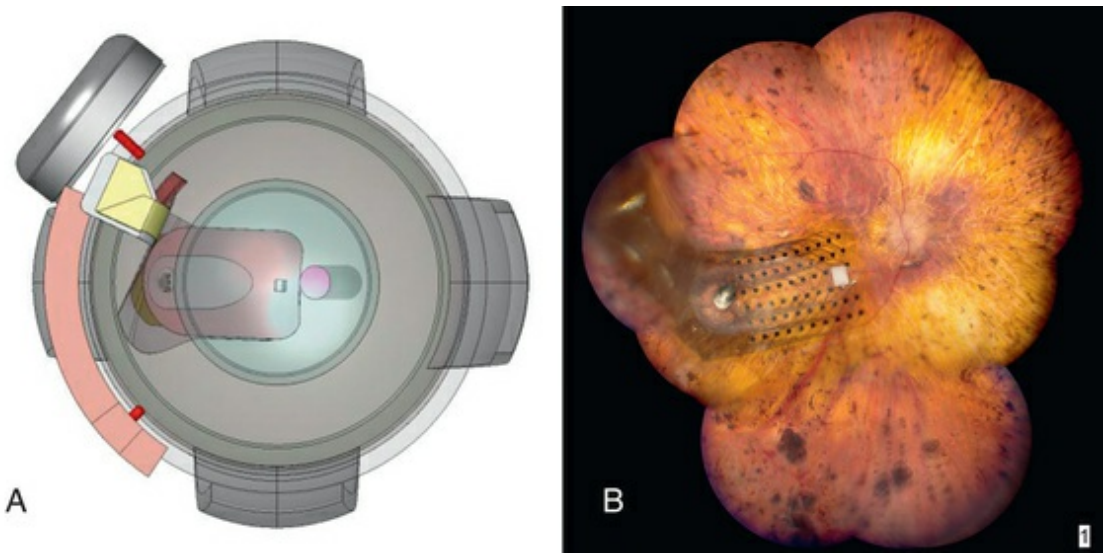

FIG. 129.1 ARGUS II System. (A) Schematics of the ARGUS II system and the eye. (B) ARGUS II 60 electrode array placed in the surface of the retina with tack in place.

The implantation procedure is similar to a pars plana vitrectomy with an encircling buckle. The device is placed under the four rectus muscles, with the implanted electronic components sutured on the superior temporal quadrant, with the anterior edge of the case 7 mm posterior from the limbus, and sutures around the encircling band on the other four quadrants. The cable and array

are then inserted through a 5-mm incision at 3.5 mm posterior to the limbus. The incision is sutured watertight, and then a retinal tack is used to fix the array to the retinal surface. The optimal placement of the array is over the macular area. External components of the system are similar to ARGUS I and the basis of operation is the same.

More than 200 patients worldwide have received the ARGUS II implant.[76–78] Long-term safety and efficacy were evaluated in 30 subjects in a multicenter clinical trial.[77] Of these 30 subjects who were enrolled between June 2007 and August 2009 at 10 clinical centers, 29 had RP (including one with Leber congenital amaurosis) and one patient had choroideremia.[78] All subjects were able to perceive light during electrical stimulation. Experiments documented improvement in object localization. Using a target of a 7-cm white square on a black LCD screen at 30 cm distance, 27 out of 28 subjects (96%) performed better in localizing the object with System on versus off. No subjects performed significantly better with the System off.[74] At 3 years, 89.3% of the subjects continued to demonstrate improved visual task performance with the system on versus system off.[77] Motion detection improved too, but to a lesser extent as this was a more difficult task. Using a target of a white bar moving across a black LCD screen, 63% and 56% of the subjects performed this test better with the System on versus off at the end of year 1 and 3 respectively.[77,78] Some subjects reported the perception of color, which could be reliably produced under certain conditions.

All subjects' acuity was measured at worse than 2.9 logMAR in both eyes before implantation. To date, none of the subjects has been able to reliably score on the visual acuity scale in either eye with the System off. At the end of year 1, seven subjects were able to reliably score on the scale with the System on in at least one follow-up time point. At year 3, 33% of the subjects scored 2.9 logMAR or better with the system on.[77] The best result to date has been 1.8 logMAR (equivalent to Snellen 20/1262).[78] Subjects performed better using their Argus II systems in orientation and mobility functions as measured by door and line recognition tasks. Activities of daily living and quality of life was overwhelmingly rated better with system on.[77]

Letter reading was tested in 22/30 subjects. Six of these subjects were able to identify any letter of the alphabet at a 63.5% success rate (vs. 9.5% with the system off). In all 22 subjects, a small set of eight letters was identified 72.5% correctly, versus 16.8% with the system off. Subjects were free to take as much time as needed to make a judgment. Subjects provided answers after 100 seconds in the full alphabet and 44 seconds in the limited letter set.[76] Seventy percent of the patients could recognize letters with only horizontal and/or vertical components and about half of the patients were able to read letters that had oblique or curved components.[76] Some subjects were able to put the letters together into words and read sentences.[78]

Twenty-nine subjects had functional devices 3 years after implantation. Of the 30 subjects, 19 subjects (61%) had no serious adverse events (SAE) and none had any unanticipated adverse events at the end of 3 years' follow-up. After 3 years of implantation, four subjects experienced conjunctival erosion due to the extraocular device, this being the most common SAE. All but one were successfully repaired. One device was explanted for SAE management, rather than device failure. This patient had recurrent erosions of conjunctiva over the extrascleral elements of the prosthesis and decided to have the device explanted after three attempted repairs. Other SAEs included three cases of presumed endophthalmitis; each was treated with intravitreal antibiotics, and the devices were not explanted and remain functional. There were four cases of hypotony that were resolved with surgical intervention. There was one intraoperative retinal tear treated successfully during surgery with laser retinopexy and two retinal detachments that required subsequent surgery to reattach the retina.[78] Keratitis, corneal opacity, and corneal melt each occurred in one patient and were treated medically.[77]

Based on these results, and manufacturing details provided by Second Sight Medical Products Inc., the ARGUS II received a CE Mark in March 2011 and FDA approval in 2013, making it the first retinal implant to be sold as a medical device in Europe and the United States. This has been a major milestone in the field of artificial vision and would allow more patients to be implanted and allow further postmarket studies.

IRIS Epiretinal Implant.

The IRIS (Intelligent Retinal Implant System) epiretinal implant (Pixium Vision, France) is under clinical trial in multiple centers in Europe at the time of this writing. The device has evolved from the experimental prosthesis developed by Intelligent Medical Implant AG (IMI), a Switzerland-based company. Similar to Argus II, the IRIS epiretinal implant includes three components: (1) an implant with extraocular electronics, an induction coil, a transscleral cable, and an epiretinal array; (2) a body-worn processing unit; and (3) a glasses-mounted camera. In preparation for chronic implant testing, acute stimulation tests of the intraocular array were performed in 20 human subjects with RP.[79] The acute testing surgery was performed under subconjunctival anesthesia. The four rectus muscles were fixed, and a pars plana vitrectomy with complete removal of the vitreous and posterior hyaloid was performed. Afterwards, the electrodes were introduced into the eye using the MESE 12 system (Fig. 129.2), a handheld surgical instrument for controlled positioning of a microcontact film on the surface of the retina. The system must be held by the surgeon during the entire procedure. Most subjects were able to recognize objects as small as a coin at 1 meter.[79]

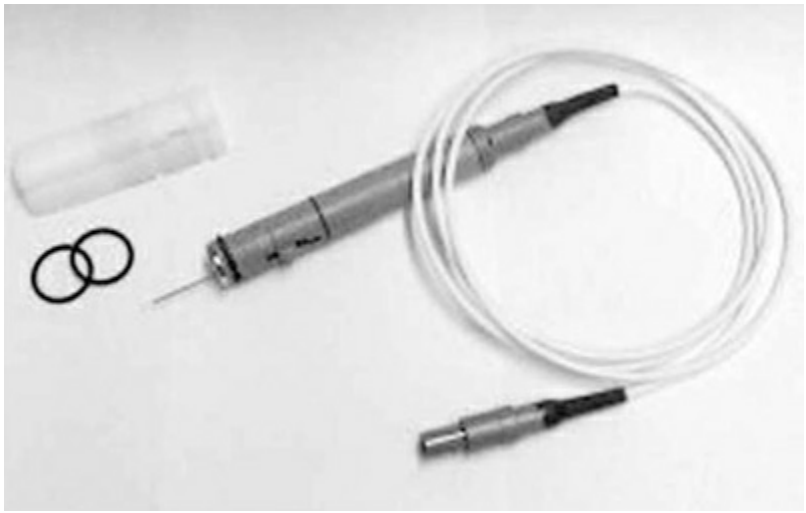

FIG. 129.2 MESE 12 handheld system.

A 49-electrode IRIS epiretinal implant has been tested in eight subjects. Most implants were removed after a few months, but some

have stayed in place for several years. The main findings of the chronic implant clinical trial were low thresholds to elicit visual perceptions and that the implant was reasonably well tolerated by the eye. The device was only activated in the clinic and was directly controlled by computer (i.e., no camera), therefore visual performance results were limited. Thresholds in one subject were measured for an extended period and ranged from 8.0 and 35.9 nC (which corresponds to single μA of current for 1–2 ms) and were reported as stable over an extended period of testing. The subjects reported that the phosphenes had different appearances, point-to-point relative location was possible, and simple shapes such as a horizontal bar were recognized when presented.[80]

In 2014, Pixium Vision (Pixium Vision, SA, Paris, France) acquired IMI's technology to develop the IRIS V1 implant. A multicenter clinical trial involving IRIS V1 is scheduled for completion in June 2017 (www.clinicatrials.gov, NCT01864486). Twenty patients are expected to enroll in the study. The commercial version of the device will have 150 electrodes. A superior image processing system is claimed as the main feature of the IRIS V1 device. The processing unit encompasses the "retina encoder" that modifies each patient's settings until he/she is able to perceive the image. For example, if a square is shown to the patient, the algorithm will adjust the settings until the patient perceives a square.[81] It is shown that less than 100 iterations are necessary to calibrate and personalized the system to the needs of an individual patient.[82] Pixium Vision is also collaborating with Stanford University to develop PRIMA Vision Restoration System, a subretinal implant currently in preclinical phase.

Epi-Ret 3 is the third epiretinal device that was implanted in six test subjects in 2006. This unique implant was designed to fit entirely inside the eye yet had a provision for external power via an inductive wireless link. The electrode array had 25 electrodes that were slightly protruding from the substrate (Fig. 129.3).[83]

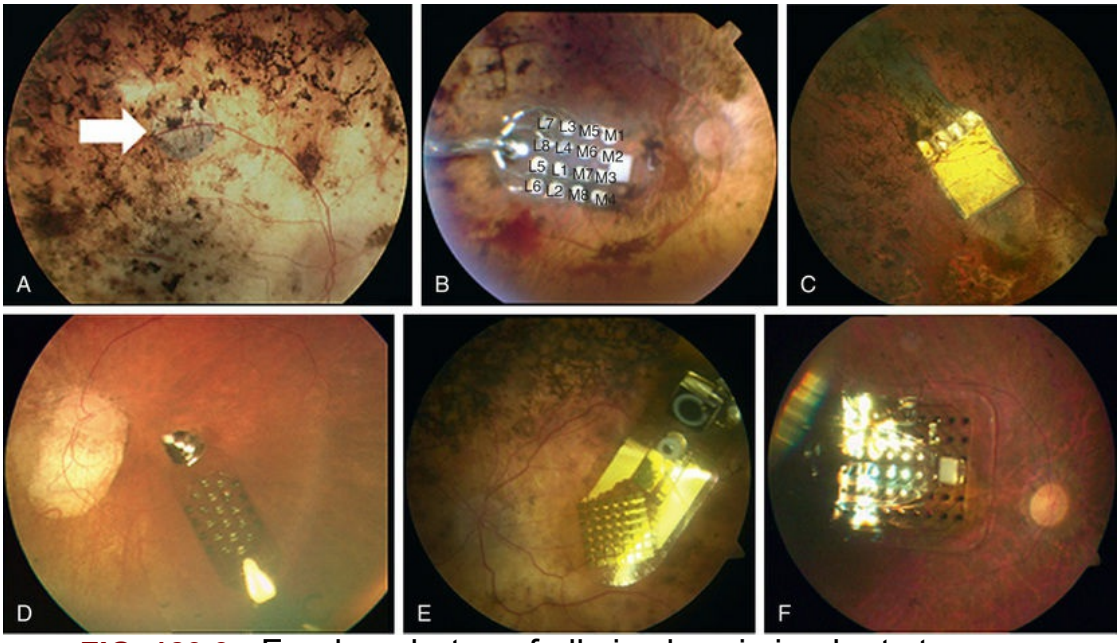

FIG. 129.3 Fundus photos of all six chronic implants to date: (A) Artificial Silicon Retina (*white arrow*); (B) ARGUS I; (C) Active subretinal device; (D) Epi-ret 25 electrode device; (E) 49-electrode epiretinal device; (F) ARGUS II (A, courtesy Optobionics/ASR, Dr John Pollack; B, courtesy Second Sight Medical Products, Inc.; C, courtesy Retina Implant, GmbH, Prof. Eberhart Zrenner; D, courtesy Prof. Peter Walter); E, courtesy Intelligent Medical Implants, Prof. Gisbert Richard); F, courtesy Second Sight Medical Products, Inc.)

The implantation procedure required a pars plana vitrectomy and removal of the lens or intraocular lens (IOL) and the capsular remnants. An 11-mm corneoscleral incision was performed for the insertion of the device, and transscleral 10.0 sutures were utilized for the stabilization and placement of the inductive coil and electronics module right behind the iris, resembling an IOL scleral fixation. A micro cable acted as a substrate for microelectronic components, and its flexibility allowed it to bend and follow the eye curvature. After the corneoscleral incision was closed, the stimulation electrodes were fixed on the surface of the retina with two retinal tacks. The implants were removed after 28 days in the first clinical trial.[83]

Tests during implantation showed that the device remained in position for the entire implant period. Consistent with the other epiretinal implant studies, low perceptual thresholds (i.e., single μA of current) were reported.[83,84] Exams 6 months after explantation

showed only some proliferation around the retinal tacks, which were left in place.[83]

Subretinal Prosthesis

The subretinal approach to the retinal prosthesis involves implanting a microphotodiode array between the bipolar cell layer and retinal pigment epithelium. This is accomplished surgically either via an intraocular approach through a retinotomy site (ab interno) or a transscleral approach (ab externo).

A subretinal prosthesis that uses microphotodiodes (solar cells) to convert light into electrical stimulation signals appears as an elegant solution to replace photoreceptor function.[85] However, several limitations currently hinder this technology from realizing its goal of providing artificial vision. Of primary concern is the inefficiency of current photodiode technology.[86] The illumination levels required in order to achieve adequate electrical current generation are not realistically attainable as the solar cells will need to generate electrical energy many orders of magnitude greater than that which is currently viable.[87–89]

This limitation jeopardizes the passive, all-inclusive nature of the subretinal prosthesis, which more than likely will require an external power source to amplify photocurrent. A device based solely on microphotodiodes (solar cells) is very unlikely to be a prosthesis, since it cannot directly produce phosphenes via electrical stimulation. This section will only focus on subretinal prostheses that have enough power to function as such. A clinical trial of passive subretinal devices is discussed in the section on electrotherapeutics (below).

There are distinct advantages and disadvantages to the subretinal prosthesis approach. Advantages include closer proximity to the next surviving neuron in the visual pathway (i.e., bipolar cell), and therefore less current requirement, and a more stable means of mechanical fixation. The disadvantages include the limited subretinal space to place electronics as well as the close proximity of the retina to the electronics, which would increase the likelihood of thermal injury to the neurons. If the subretinal implant is comprised as an electrode array with the electronics outside the eye (ab externo approach), then the implant will have a cable piercing

the sclera. Issues related to such a surgical approach include long-term tethering effects because of the cable and a transchoroidal incision resulting in a greater likelihood of subretinal hemorrhage as well as possible retinal detachment either total or localized. In the latter case, the subretinal fluid would increase the distance between the underlying electrode and the retinal neurons and therefore increases the current requirements.

Alpha IMS: In 2009, Retina Implant AG (RI), Reutlingen, Germany, started a clinical trial on a prototype subretinal prosthesis, now called Alpha-IMS. The first prototype implant had an intraocular part, comprising the subretinal chip, a flexible substrate to hold the chip and an additional test electrode array, and a cable to connect the chip and array with the supporting electronics (Figs. 129.4A–B). The subretinal chip had 1500 pixels elements, each with a photo diode detector, circuitry to amplify the detected signal, and an electrode to stimulate the retina. The test electrode array had 16 individual electrodes and was included to provide a means for direct stimulation tests via external test equipment (Fig. 129.4A). The chip/array assembly was placed subretinally, and the cable exited the eye through the pars plana and followed an intraorbital, subcutaneous path to a point behind the ear, where the cable crossed the skin. This transcutaneous connection allowed direct access to the subretinal chip for power, measurement, and configuration as well as direct access to the test electrode array (Fig. 129.4B). The implant was designed to give a diamond-shaped visual field of 10° × 10°, diagonally 15°.

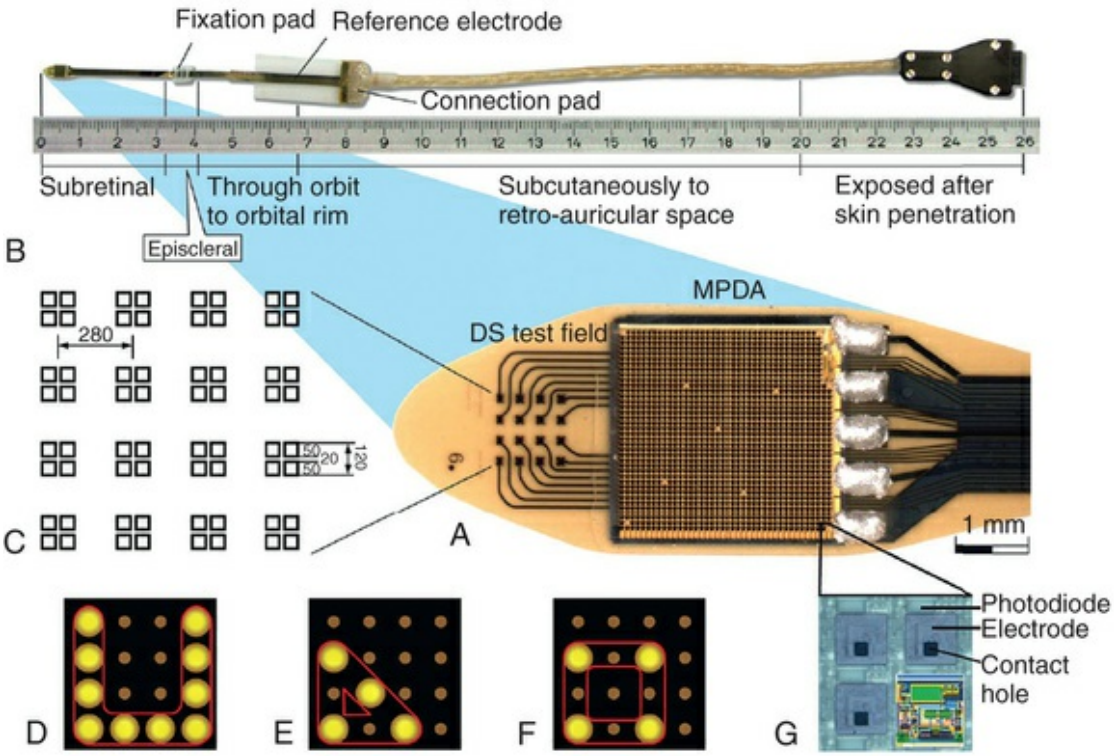

FIG. 129.4 Alpha IMS subretinal implant and cable.

(With permission from Zrenner E, Bartz-Schmidt KU, Benav H, et al. Subretinal electronic chips allow blind patients to read letters and combine them to words. Proc Biol Sci 2011;278:1489–97, with permission from Proc R Soc B, published online November 3, 2010.)

The direct stimulation electrodes with some of the test patterns of stimulation are shown in Figs. 129.4C–F. Also the microphotodiode array is shown magnified, with its rectangular photodiodes above each squared electrode (Fig. 129.4G). The implantation can be theoretically performed through either a pars plana vitrectomy (PPV) and retinotomy (ab interno), or PPV and a transscleral approach (ab externo);[85,90] however, to date, only the ab externo approach has been used in the patients. Multiple publications have detailed the procedure and long-term outcome of Alpha-IMS implantation in humans.[91–95] Hypotensive anesthesia has been used to prevent the risk of excessive choroidal bleeding when a 5-mm incision is made in the sclera and choroid to introduce the array into the subretinal space. A guide was used to help slide the electrode array under the retina, and the placement was controlled with indirect ophthalmoscopy during the surgery. A silicone oil tamponade was used to prevent retinal detachment. Preoperative topographic mapping of the macula was carried out in some

patients to find the optimal macular position.[90] Comparing functional status of the implant in "subfoveal" versus "parafoveal" position showed a remarkable advantage for subfoveal implantation.[95] It should be noted that finding functional fovea can be a challenge in many patients with advanced RP due to extreme retinal atrophy. A fundus photo and the placement of the device on the skull are shown in Fig. 129.5.

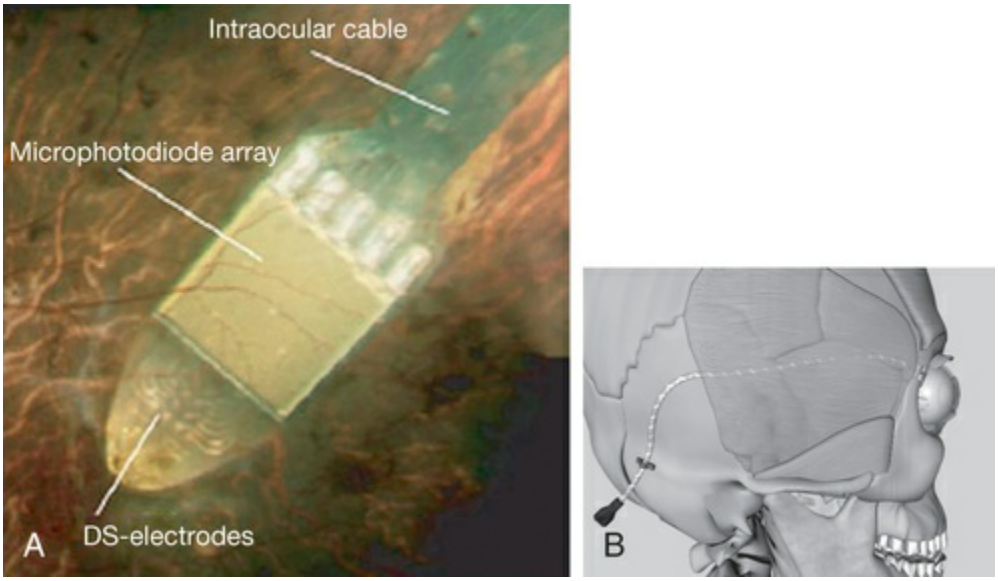

FIG. 129.5 Alpha IMS subretinal implant in a retinitis pigmentosa patient. (A) Electrode placed on the subretinal space. (B) Trajectory of the cable from the eye to the external connector. (Panel A with permission from Zrenner E, Bartz-Schmidt KU, Benav H, et al. Subretinal electronic chips allow blind patients to read letters and combine them to words. Proc Biol Sci 2011;278:1489–97, with permission from Proc R Soc B, published online, November 3, 2010.)

The first set of studies were semichronic, by design and largely due to the infection risk of a transcutaneous cable, with planned explantation several weeks to 3 months later. Twelve subjects were enrolled in this study. Of the first seven subjects, four had electronic hardware problems that precluded further testing of the implanted active chip. For the first nine subjects, implants were removed after 1 month while the last three subjects had longer period of implantation (3 months). One subject refused to have the implant removed. Functional testing of the active subretinal implant

demonstrated the ability to see lines and determine the correct orientation of these lines. A scanning laser ophthalmoscope was used to directly activate the subretinal chip, and a laser spot as small as 100 μm produced a visual perception.[85] Because the device required an external connection to function, it was only operated in a clinic setting and the patients did not use the device outside the clinic.

The group published detailed results from the last three (of 12) subjects in 2011.[85] Having gained experience from the first nine subjects, hardware problems were largely avoided in the last three. Also, placement of the subretinal array was more consistent in the macula. Results from these three subjects showed that one patient could identify the direction of the letter "U" when presented in one of four orientations (20/24 times correct), when using the DS electrodes. Patient two of this group could identify letters and combine these into words. All three patients could detect the orientation of gratings, with patient two achieving a visual acuity of logMAR 1.74. This study was the first to report letter reading, providing strong support for functional vision via electrical stimulation. The short duration of implantation (1 or 3 months) limited the amount of data available from these tests. The robustness of this system needs to be improved. The device experienced technical failures at a rate unacceptable for a clinical implant, although fewer problems were noted in later implants.

The percutaneous connector is eliminated in the newer version of the device by adding a power module which is implanted behind the ear and receives power and controls signals wirelessly.[85,92–95] This change and the addition of a portable, external power supply, allow patients with this device to use it outside the clinic. Other features of the implant are similar to the first prototype described above. A cable connects the power module behind the ear to the subretinal chip. But no direct stimulation electrodes are included in the latest version of the Alpha-IMS. Recent publications reporting long-term outcomes of the Alpha-IMS implant encompass patients implanted with both versions of the device.[94] Of 29 patients included in the 2015 report, 21 subjects (72%) met the primary endpoint of the study at the end of 12 months follow-up. The primary endpoint of the study was significant improvement of

activities of daily living and mobility as determined by daily living tests, recognition tests, or mobility tests. Thirteen participants (45%) reported restoration of visual function to the point to be used in daily life. Twenty-five participants (86%) reached the secondary endpoints of significant improvement of visual acuity/light perception and/or object recognition. One patient achieved Snellen visual acuity of 20/546 using Landolt C charts. Maximal motion perception ranged from 3 to 35 degrees per second. Additionally, detection, localization, and identification of objects were reported significantly better with the implant power switched on in the first 3 months.[94] Four out of 29 patients were never able to perceive any light with the subretinal implant. The inability for light detection in these cases was attributed to (1) intraoperative touch of the optic nerve; (2) retinal edema over the implant; (3) suspected retinal ischemia; and (4) technical failure of the implant. Two SAEs included increased intraocular pressure and retinal detachment immediately after the implantation were reported in this cohort. Both patients were managed with standard methods.[94] An earlier study from the same group focused on the safety of the Alpha-IMS implantation in nine patients implanted in a single center reported a wider range of minor and major SAEs.[92]

The Alpha-IMS's higher photodiode density, subretinal placement, and use of optical properties of the operated eye are main advantages of this subretinal implant. The device harnesses the benefits of eye movements to scan scenes and fixate, and utilizes natural ocular microsaccades for refreshing the perceived images.[93] In addition, visual signal processing by bipolar and amacrine cells may enhance motion and contrast perception in subretinal implants such as the Alpha-IMS. Supported by angiographic and psychophysical evidences, it is proposed that inner retinal function may recover above the baseline after a period of stimulation by subretinal implantation.[95,96]

The Boston Retina Implant Project (BRIP) has been developing a device with more than 200 individually controlled stimulating electrodes.[98] The new-generation implants have the power and data receiver coils that are implanted in the anterior part of the eye, circumferential to the cornea, just posterior to the limbus. The electronics enclosure is made of titanium. The electrode

implantation is in the same quadrant as the electronics facilitating surgical access to the subretinal space via a scleral flap.[10,99] Like the Argus II, the BRIP implant utilizes an external camera to provide wireless, real-time video data to the stimulator. The device is not yet in clinical trial.

Palanker et al. have developed a wireless photovoltaic retinal prosthesis system, in which camera-captured images are projected onto the subretinal implant using pulsed near-infrared (IR) light (~900 nm).[100,101] This architecture seeks to minimize the size and complexity of the implant. To accomplish this goal, the system requires a head-worn display that can display IR light in front of the eye with a subretinal implant. Each pixel in the subretinal implant directly converts pulsed light into local electric current to stimulate the nearby inner retinal neurons. Each single pixel has three photodiodes in series connected between the active central and peripheral return electrodes. Several versions of the subretinal array have been fabricated, with pixel sizes from 100 to 25 μm, corresponding to 640–10,000 pixels on an implant 3 mm in diameter (corresponding to a maximum theoretical visual acuity of 20/80).

This group has evaluated two basic geometries to improve proximity to retinal neural cells: perforated membranes and protruding electrode arrays.[102] In an in vitro experiment placing retinas with the photoreceptor side down in contact with a 13-μm implant with 40-μm apertures, retinal tissue migration was observed in all samples of rat, chicken, and rabbit retinas (Fig. 129.6). Migration occurred through pores >5 μm. Implantation in rat and pig eyes has showed good integration of the implant in the subretinal space ensuring long-term biostability as well as robust cortical responses upon stimulation with pulsed near-IR light.[100,101,103–105] Two different designs of the device each with 5- or 10-μm wide perforations were implanted in rats and pigs. Subretinal placement was verified with optical coherence tomography, and retinal perfusion was studied with fluorescein angiography. Regardless of implant design, retinas of both species showed normal vasculature. Rat retinas showed significant migration of inner nuclear layer (INL) cells through the perforations, INL thinning, and pseudo-rosette formation. Pig retinas maintained photoreceptors, showed no migration, and less

pseudo-rosette formation, but more fibrosis formation in 8 weeks compared with implanted rat retinas.[103] In addition, implantation in rats showed robust cortical responses that could be modulated by irradiance, pulse duration, and frequency, with stimulation thresholds well below the ocular safety limits up to 6 months after implantation.[105] The developers are collaborating with Pixium Vision, France, to rebrand this implant as PRIMA Vision Restoration System. First human trials were planed to start in 2016.

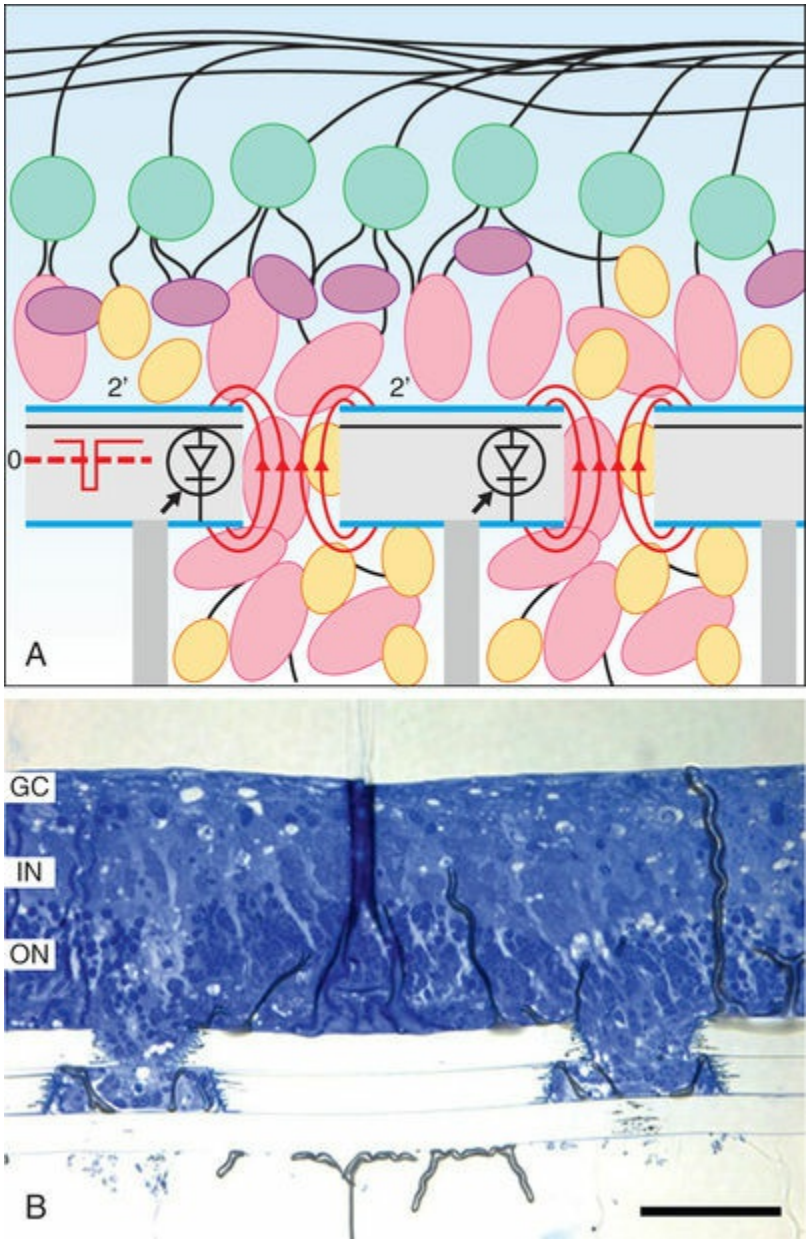

FIG. 129.6 (A) Three-layered membrane with channels on top, inner chambers, and a fenestrated membrane at the bottom. Voltage can be applied across the two

electrodes (*horizontal blue lines*). Current flow between the two electrodes is indicated by the *red lines with arrows*. *2′* indicates electrode interface with inner retina. (B) Rat retina grown on the structure after 7 days in vitro, with migration of retinal cells through the 20- and 35-μm holes into the middle chambers, but not through the 3-μm holes in the lower membrane. *GC*, Ganglion cells; *IN*, inner nuclear layer; *ON*, outer nuclear layer. (Reproduced with permission from Palanker, et al. Attracting retinal cells to electrodes for high-resolution stimulation, Vol. 5314. San Jose, CA: SPIE; 2004.)

Some questions arise from this approach, mainly if the retinal tissue will remain viable after migrating through the pores, if the circuitry will be kept functional given the lack of a proven hermetic coating and lastly, if the migrated tissue will differentiate into fibrous tissue. Another approach consists of subretinal implants with protruding electrodes so that cells can migrate to the spaces between the electrodes, similar to the migration observed in the perforated membrane. In vivo implantation on Royal College of Surgeons (RCS) rats of 70 μm in height with 10 μm in diameter arrays showed penetration of the pillars into the inner plexiform layer and the retina well preserved (Fig. 129.7).[106,107]

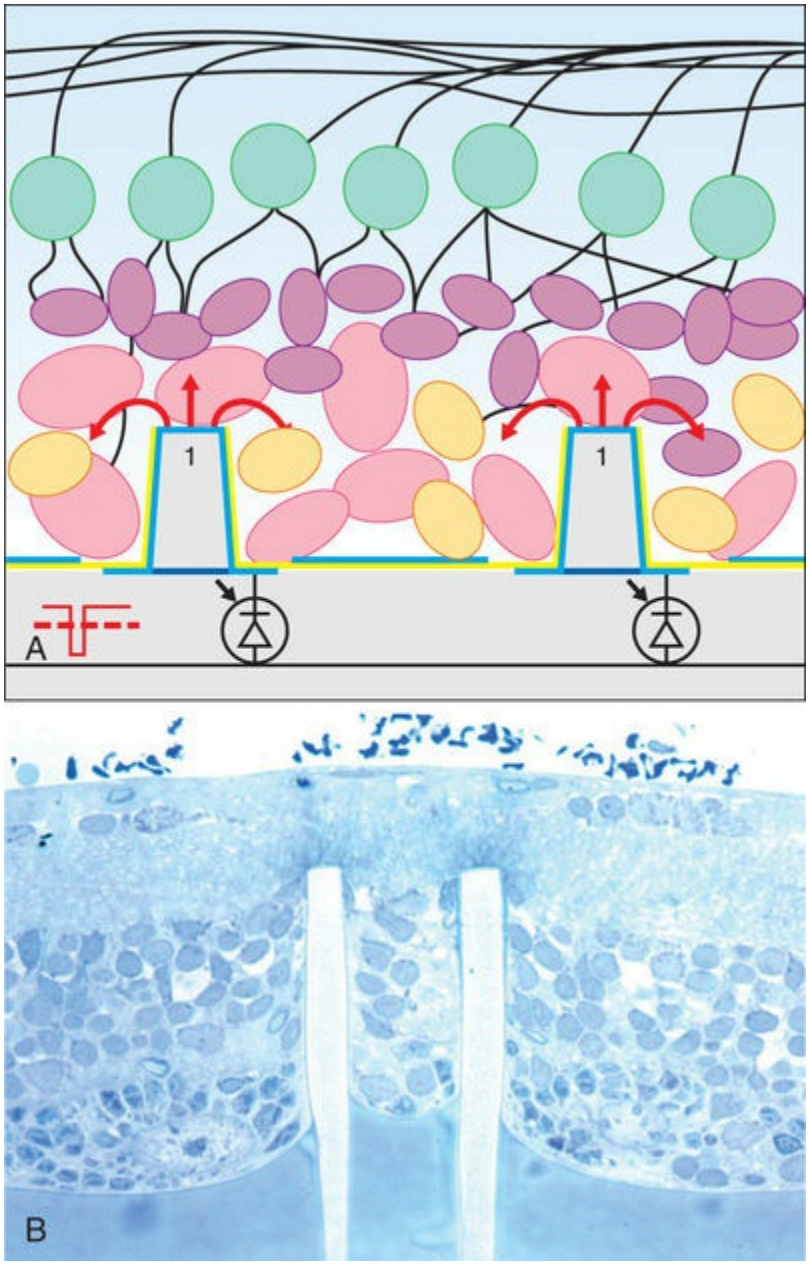

FIG. 129.7 (A) Protruding electrodes (labeled 1) on the subretinal array penetrating the retina after migration of retinal cells into the empty spaces between the pillars. (B) 10-μm pillars protruding into the inner plexiform layer of a Royal College of Surgeons rat after 15 days of implantation. (Reproduced with permission from Palanker, et al. Attracting retinal cells to electrodes for high-resolution stimulation, Vol. 5314. San Jose, CA: SPIE; 2004.)

Suprachoroidal and Transscleral Retinal Prostheses

Two groups of investigators from Japan and Australia have recently moved to in-human trial of a suprachoroidal approach of retinal

stimulation. A suprachoroidal-transretinal stimulation (STS) implant has been developed and tested in human at the Osaka University in collaboration with Nidek Inc., Osaka, Japan (Fig. 129.8). The suprachoroidal approach is based on the premise that placing a stimulating electrode in the suprachoroidal space or in the fenestrated sclera along with a ground electrode in the vitreous cavity may allow for a less-invasive method to achieve visual percepts. The advantages of this approach are multiple. First of all, the surgery is less complicated. Second, the electrodes are less invasive to the retina. Third, the electrodes are relatively easy to remove or replace if damaged.[108,109]

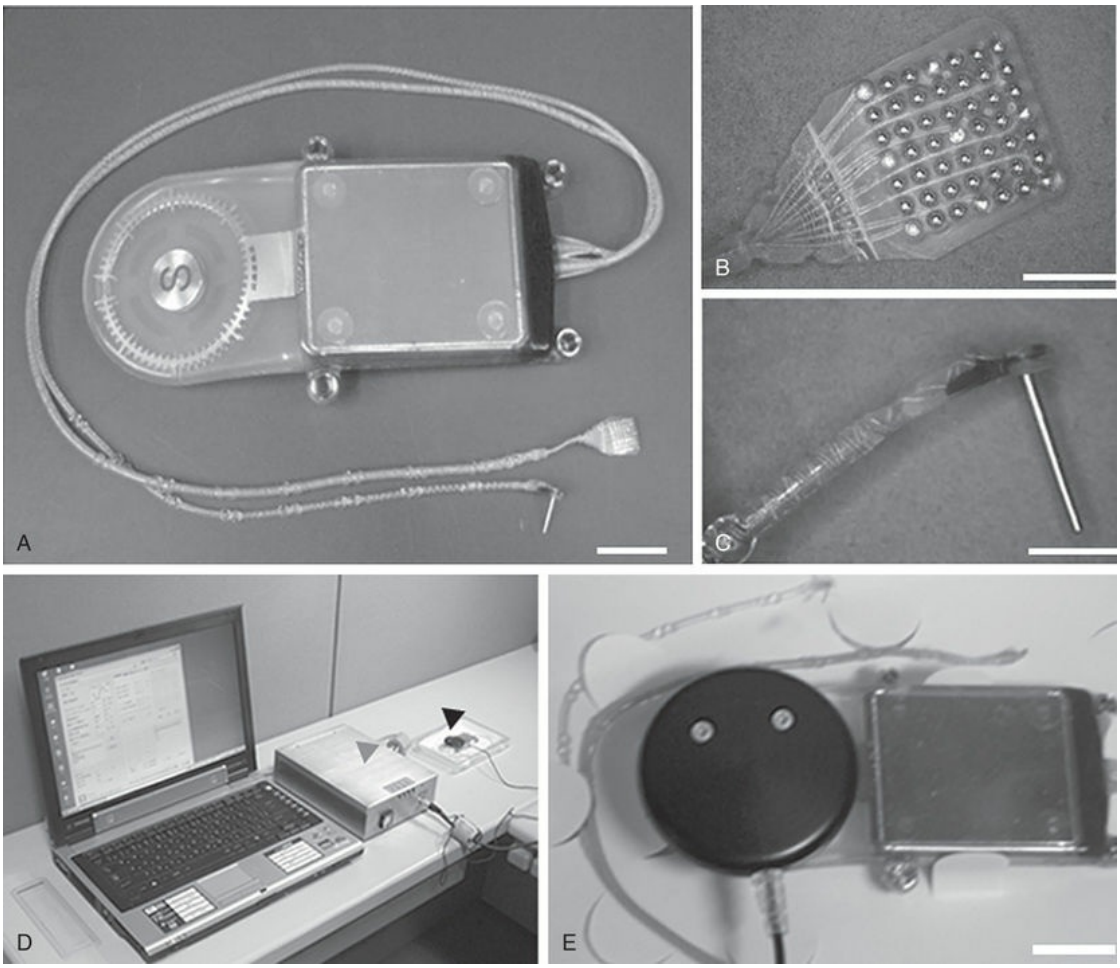

FIG. 129.8 Suprachoroidal-transretinal stimulation (STS) prosthesis. (A) Internal part of the STS system. (B) Electrode array (6 × 6 × 0.5 mm) with 49 platinum electrodes in a 7 × 7 array. (C) Return electrode and extraocular microelectronic simulator. (D) External transmitter and processor of the STS system. (E)

Microstimulator. (Reproduced with permission from Morimoto T, Kamei M, Nishida K, et al. Chronic implantation of newly developed suprachoroidal-transretinal stimulation prosthesis in dogs. Invest Ophthalmol Vis Sci 2011;52:6785–92.)

Because the electrodes are further from the target neurons, they will need to deliver higher currents and the current spread should be greater, therefore limiting the resolution.[108,109] Although no damage was seen at the light microscopic level to the retinal tissue around the area of stimulation in the short term in rabbits implanted with STS devices,[110] this approach remains to be proven safe over long-term implantation.

Initially, STS was investigated in the RCS rats and rabbits. In the RCS rats, the investigators studied threshold intensities of electrically evoked potentials (EEPs) from the superior colliculus (SC). It was found that the response to the STS was recorded in the localized retinotopically corresponding SC areas, suggesting that the focal stimulation to the degenerated retina effectively elicits artificial vision in the RCS rats. Similar findings were noted in rabbits. The threshold intensity of the EEPs was 5–10 nC of electrical charge, suggesting that stimulation via STS may be attained with relatively low stimulating current.[108] However, it should be noted that rabbit sclera and retina are thinner than in humans, thus partially accounting for the relatively low stimulating current in this study.

The results from a long-term implantation in canines were published in 2011.[109] STS microelectrode arrays were implanted in a scleral pocket and were kept in place for 3 months. The electrode array and the return electrode were connected to the extraocular stimulator by a multiwire cable, connected wirelessly to an extracorporeal processor and transmitter. The electrode array measured 6 × 6 × 0.5 mm, with 49 platinum electrodes in a 7 × 7 arrangement fixed in a clear silicone rubber platform coated with Parylene. The stimulating electrode was 0.5 mm in diameter and 0.5 mm in length and the distance between the centers of the electrodes was 0.75 mm, and the return platinum electrode placed in the vitreous cavity was 6.5 mm in length and 0.5 mm in diameter. Nine of the electrodes on the array were electrically active for this experiment, which was performed in three animals. After 3 months,

the devices were safely explanted with no intraoperative complications, the position of the eyes was maintained orthophoric without proptosis during the follow-up period, and all the wounds healed properly with no sign of infections or wound dehiscence. The ERGs had the normal a-wave and b-waves, and the shape did not differ from the ERGs recorded from the unoperated fellow eye 3 months after the implantation in all three animals. Histologic sections from two implanted and control eyes showed no obvious changes in the structure of retina and choroid beneath the electrode array in two dogs; however, pathologic changes were detected in one dog (Fig. 129.9). The retinal and choroidal architecture was destroyed due to the mechanical pressure, according to the authors.[109]

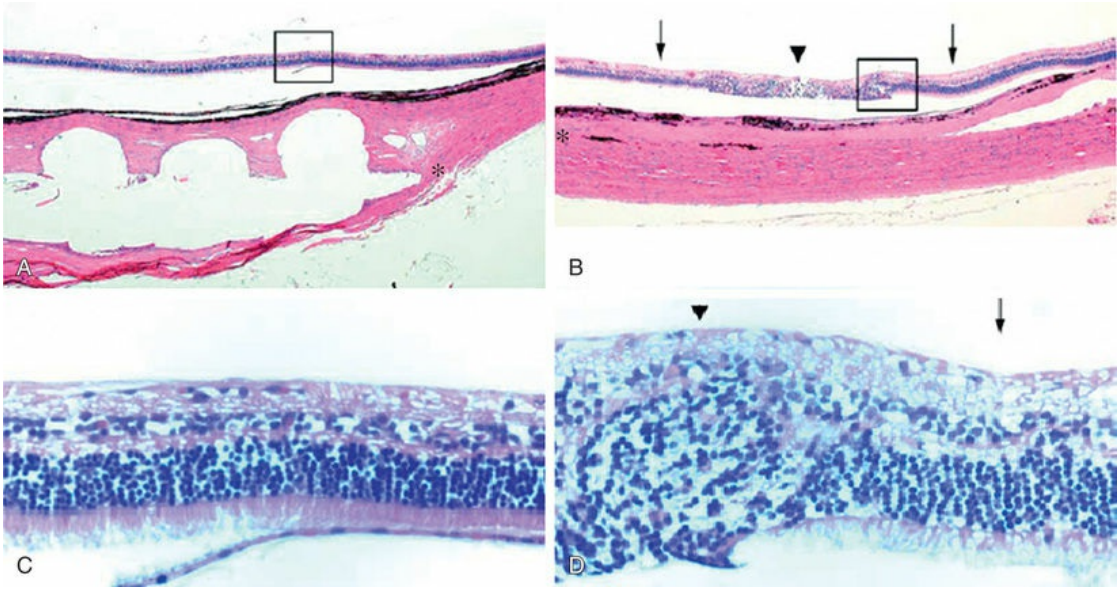

FIG. 129.9 Light microscopic photographs of the retina and sclera from the implanted eyes of two dogs. (A,C) Photographs of the retina and sclera around the electrode array from dog one. No damage of the retina is visualized. (B,D) Photographs of the retina and sclera around the array from dog two. Local damage of the retina and choroid at the site of the implanted electrode array can be seen (*arrowheads*); however, the other area of retina on the array is intact (*arrows*).
(Reproduced with permission from Morimoto T, Kamei M, Nishida K, et al. Chronic implantation of newly developed suprachoroidal-transretinal stimulation prosthesis in dogs. Invest Ophthalmol Vis Sci 2011;52:6785–92.)

In 2011 Fujikado et al. reported results of semi-chronic, suprachoroidal implantation of Nidek Visual Prosthesis in two patients with RP. The visual acuity of the patients before implantation was light perception. A 49-electrode array (5.7 × 4.6 × 0.5 mm) was placed in the suprachoroidal space without causing retinal detachment or vitreous hemorrhage, and the internal electronics of the implant were implanted under the skin on the temporal side of the head. The implants remained functional for the 4 weeks of the study. After 5 and 7 weeks the implants were surgically removed (first and second patient, respectively).[111]

Phosphenes were elicited by currents delivered through six electrodes in patient one and through four electrodes in patient two. The success of discriminating two bars was better than the chance level in both patients. In patient two, the success of a grasping task was better than the chance level, and the success rate of identifying a white bar on a touch panel increased with repeated testing.[111] Chronic implantation of a wide-field implant with the same technology has been tested in middle-size and large mammals.[109,112] However, the group has not yet announced its plan for chronic implantation of human subjects with the wide-field implant.

The Australian group has published in-human feasibility study of a similar approach with suprachoroidal placement of Bionic Vision Australia electrode array (Fig. 129.10).[113,114] Unlike the Japan group's approach for implanting the electrode array within a scleral pocket, the Australian group implanted the device between the choroid and sclera. Preclinical animal studies determined stimulation parameters after acute and chronic implantation of the suprachoroidal array.[115]

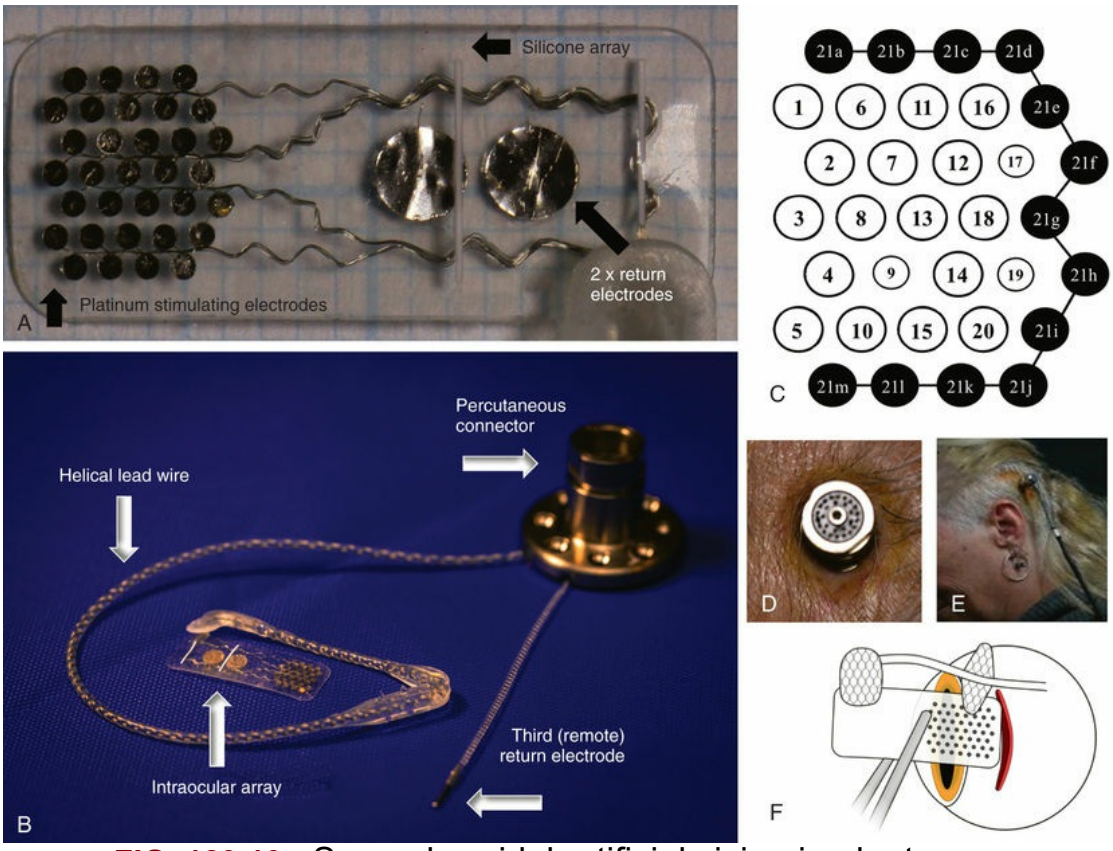

FIG. 129.10 Suprachoroidal artificial vision implant tested by Bionic Vision Australia. The electrode array (A) and the entire device (B). The array is connected to the percutaneous connector via a helical lead wire. The electrodes number 1–20 on the intraocular array (C) perform visual signal transduction and the black electrodes (21a to 21m) are ganged to provide an external ring for common ground and hexagonal stimulation parameter testing. The percutaneous connector protruded through the skin behind the ear (D), allowing direct connection to the neurostimulator via a connecting lead (E). Surgical implantation through scleral incision (F). (Reproduced with permission from Ayton LN, Blamey PJ, Guymer RH, et al. First-in-human trial of a novel suprachoroidal retinal prosthesis. PLoS ONE 2014;9(12):e115239.)

The surgical procedure that was developed in animal and cadaver eyes consisted of lateral canthotomy followed by disinsertion of lateral rectus muscle and creating a full-thickness sclerotomy and exposing the choroid.[113,116,117] A "pocket" was created in the suprachoroidal space for the insertion of a flexible electrode array 15–17 mm toward the posterior pole, beneath the

area centralis. The array was then sutured in place, and platinum ball electrodes (1.5 mm diameter) were placed in the vitreous cavity and in the suprachoroidal space, next to the electrode, to act as return electrodes for electrical stimulation. A "trapdoor" sclerotomy was described to disinsert short posterior ciliary vessels behind the macula in order to avoid hemorrhage during the implantation.[113,117]

Three patients with long-standing RP with 8 to 20 years of light perception vision were included in the clinical trial of Australian suprachoroidal retinal prosthesis.[117] Implantation was carried out as described above and took 3–4 hours. No complications occurred during the surgery. Due to submacular hemorrhage seen in the first patient, the investigators attempted to decrease eye movement immediately after the surgery by injecting botulinum toxin in all four recti muscles at the end of surgery. This proved to be not effective, as patients two and three experienced submacular hemorrhage 3–4 days after the surgery. Patients were assessed for safety and efficacy of surgical procedure and the functional efficacy of suprachoroidal visual prostheses.[117]

The electrode array was easily visible with indirect ophthalmoscopy during the surgery because of the choroidal atrophy. Postoperative period was uneventful. All three subjects experienced a combined subretinal and suprachoroidal hemorrhage 3–4 days postoperatively, which resolved without any complications in two patients. In one patient with a larger hemorrhage than the others, a fibrotic tissue reaction formed at the temporal edge of the implant following hemorrhage resolution. The fibrotic tissue did not affect device efficacy nor caused complications such as retinal detachment. The electrode arrays remained stable during 1-year follow-up. All subjects were able to experience visual percepts within a safe charge limit. In addition, all subjects showed improved light localization with the device on compared to the device off.[117] This proof of concept study served to optimize stimulation parameters and showed that the suprachoroidal anatomic position was a less invasive method with acceptable complication profile, excellent lateral device stability, and successful stimulation of visual percepts. The group is aiming at improving functional efficacy in newer versions of the device.

The transchoroidal systems described above represent a new

approach that has some advantages compared with the subretinal and epiretinal approaches. For example, the ab externo approach through the sclera, potentially less complicated than the ab interno approach, along with a more stable positioning of the electrode on the suprachoroidal space, decrease the risk of retinal detachment. However, given the distance between the retina and sclera (204–490 μm in humans),[118] it is suggested that such prosthesis will not achieve the same resolution as the epiretinal or subretinal prostheses.[119] Also, higher currents are required for stimulation due to the tissue layers interposed between the array and the ganglion/bipolar cells. However, animal studies have shown the ability to evoke cortical potentials using suprachoroidal stimulation of the outer nuclear layer, outer plexiform layer, and inner nuclear layer.[110,120–123] In addition, human trials using suprachoroidal implants have shown functional improvement, indicating adequate stimulation of the retinal ganglion/bipolar cells, with stimulation thresholds well below the safe levels for retina.

The Microfluidic Retinal Prosthesis is an alternative approach that will mimic normal chemical signaling between neurons in the retina and brain.[124–126] The overall hypothesis is that digital images may be transposed into neurochemical signals through a microfluidic chip, implanted in the subretinal space. A neurotransmitter-based visual prosthesis utilizes a multitude of microfluidic orifices that create a two-dimensional array of "chemical pixels," arranged to create an image analogous to an inkjet printer, delivering neurotransmitter to the retina or brain. While conceptually interesting, this approach has not developed into a viable implant, due to the complexity of routing and control of small amounts of neurotransmitter delivered to precise locations in the retina, and due to concerns about potential toxicity of excess neurotransmitters.

Electrotherapeutics

The Optobionics Artificial Silicon Retina (ASR) has shown some efficacy in improving vision, not through direct action of the device, but instead, through a neurotrophic effect. Initially developed as a retinal prosthesis, the ASR was implanted (subretinal and

extramacular) in ten patients in a single-center study and then in 20 subjects in a multicenter study. The 3-mm-diameter implants had 3500 microphotodiodes that generated stimulating current in response to incident light (Fig. 129.3). Results from the first six subjects were published in 2004, reporting that all six described subjective improvements in vision. Three of the six had improved early treatment diabetic retinopathy study (ETDRS) scores, while one in six had an enlarged visual field postoperatively. However, the improved vision included areas of the visual field far from the implant location. The authors concluded that the subretinal ASR implant was not directly mediating artificial vision (i.e., electrical stimulation via the ASR did not directly affect visual perception). Instead, the ASR's presence in the subretinal space was acting via an indirect effect, possibly through release of growth factors, and improving the health of the retina.[127]

The theoretical current output of a subretinal microphotodiode in a sunny environment is <1 nA (nano Ampere) (10^{-9} amperes),[101] or about 1/10,000 of what is required typically for electrical activation of nerves. This estimation explains the lack of direct activation of the retina by a subretinal implant that relies solely on incident light as a power source. The multicenter study provided additional results from visual task performance and more detail on the surgical procedure. Adverse events included three cases of ASR migration, two incidences of fracture of the device during implantation (the damaged device was easily removed), and six visually significant cataracts (versus three in the fellow eyes).[87] The most recent report from the group states that visual improvements are maintained in the original six implant subjects from the single-center trial.[128]

Optogenetics

An alternative to an implanted bioelectronic device is the "optogenetic" approach. Pioneered by Deisseroth,[129–131] the optogenetic technique modifies retinal neurons to express light-sensitive ion channels, the most common being channel rhodopsin 2 (ChR2). When high-intensity light is used, enough ChR2 channels open to depolarize a cell and trigger an action potential. Viral

vectors such as adeno-associated virus are used to introduce ChR2 gene into retinal cell. Bi et al. first demonstrated that this method could be used to modify retinal ganglion cells, showing that light-evoked neural responses were present in a mouse model of retinal degeneration after the mouse RGCs expressed ChR2.[132] Others have extended this initial work to show that behavioral responses were preserved in rd1 mice[133] and that photoreceptor nuclei cell bodies could be modified and initiate a neural response even in the absence of outer segments.[134] Incorporating a second light-sensitive channel (halorhodopsin) into the dendrites of a retinal ganglion cell and ChR2 into the soma, to enable a center-surround response dependent on the wavelength of light, the optogenetic approach has showed significant advantages over the bioelectronic approach. By making each cell light-sensitive, vision can potentially be restored to near normal acuity. Also, using light as the activating signal allows the optics of the eye to be used to focus the image on the retina. In other words, the optogenetic approach can come much closer to restoring natural vision versus artificial vision provided by bioelectronic approaches. However, many potential challenges must be overcome before optogenetic approaches can be clinically viable. The main issue relates to sensitivity. Currently, modified cells require bright blue light to be activated, roughly four orders of magnitude above cone light sensitivity threshold in normally sighted people.[135] It is not clear how such intense light would interact with a diseased retina with minimal light sensitivity. Given that photophobia is sometimes a symptom of RP, a therapy that requires directing a bright light into the photophobic patient's eye is unlikely to provide a benefit. In addition, it is unclear if the modified cells permanently maintain this light sensitivity or if reinjection is required.

Conclusions From Clinical Trials

Both the subretinal and epiretinal artificial vision prostheses have demonstrated feasibility and a reasonable safety profile. Both implants have also demonstrated the ability to restore vision through electrical stimulation of the retina in endstage outer retinal degenerations. However, there are important differences between

the two approaches. The surgical procedure for the subretinal approach is more complex, although it has the potential advantage of stimulating the next layer of neuron after the photoreceptor (i.e., the bipolar cell). However, this advantage may not be present in a severely reorganized retina secondary to chronic endstage outer retinal degeneration. Using a camera to capture visual information is also a theoretical advantage in that it could provide a wider bandwidth of data. On the other hand, using the blind eye's optical system to stimulate subretinal Alpha-IMS implant allows for eye's micro-saccade movement to overcome the "image fading" described as the Troxler phenomenon. ARGUS II implant, that utilizes a glasses-mounted camera to capture the images, obviates the need for clear media and also can overcome image blur caused by nystagmus. Lastly, the size of the clinical trials and the number of years the implants have been in use vary dramatically. The ARGUS II is the largest study of a retinal prosthesis to date with over 200 patients implanted and with the longest follow-up over 8 years as of the writing of this chapter. The Alpha-IMS has fewer cumulative years of testing due to fewer implantations and the limited longevity of the device.

Retinal prostheses have achieved major milestones in recent years. With both ARGUS II and Alpha-IMS retinal implants, we have seen continued improvement in visual acuity with increasing number and density of electrodes. Simulations of artificial vision[19,26] have predicted that 600–1000 individual pixels may be needed to enable face recognition and large font reading (Figs. 129.11 and 129.12). Even though the visual acuity is still poor relative to normal vision, the subjects with either the ARGUS or the Alpha-IMS device can read large letters and do better with daily life activities. Continuing this forward momentum to enable implant recipients' benefit through the use of retinal prostheses in their activities of daily living is the main challenge ahead. Moreover, another major challenge for future implants is to provide color vision for implanted patient. If optogenetic therapies can be made more sensitive, they may provide restoration of near natural vision. The development of retinal prostheses to generate artificial vision for the blind is a complex, long-term, expensive, and interdisciplinary undertaking, but the data from new clinical trials provide hope that

in the near future, doctors can present the long-awaited "good news" to their patients.

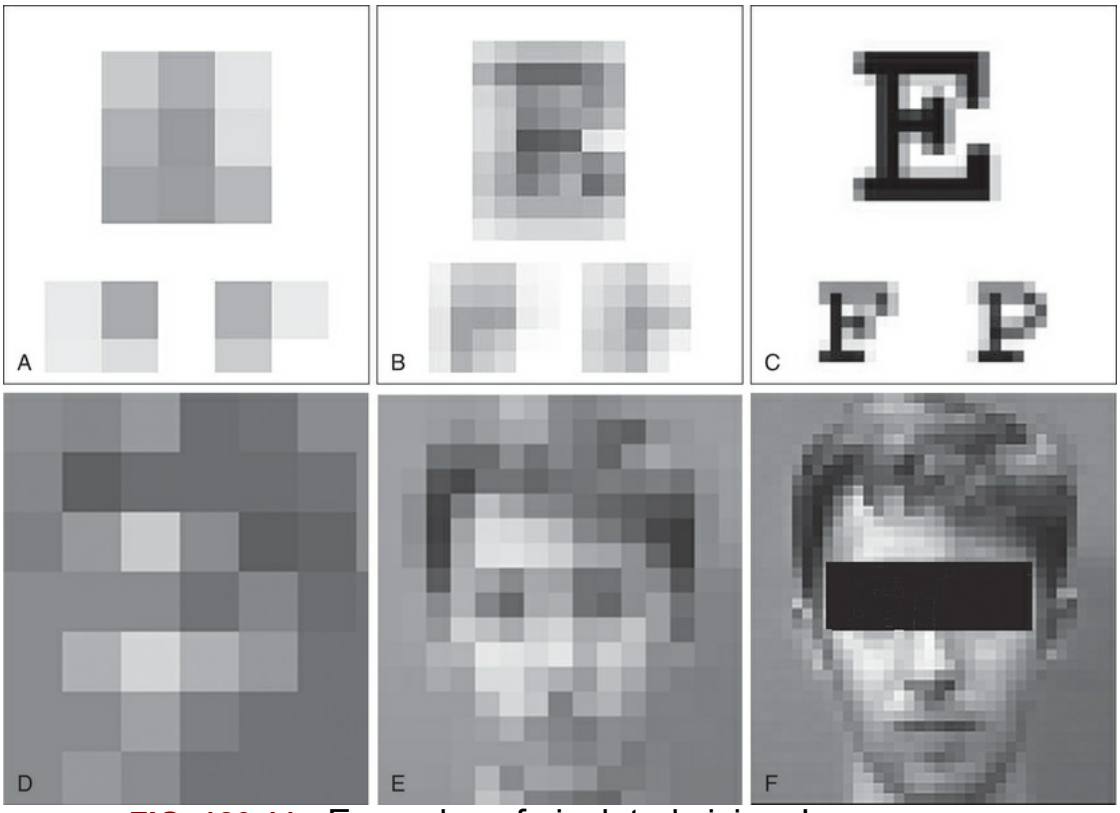

FIG. 129.11 Examples of pixelated vision. Lower resolution may allow crude shape recognition, but increasing resolution can lead to (A–C) reading letters on an eye chart and (D–F) face recognition (rectangle added on last image to protect identity). (Face image courtesy of: http://cswww.essex.ac.uk/mv/allfaces/index.html.)

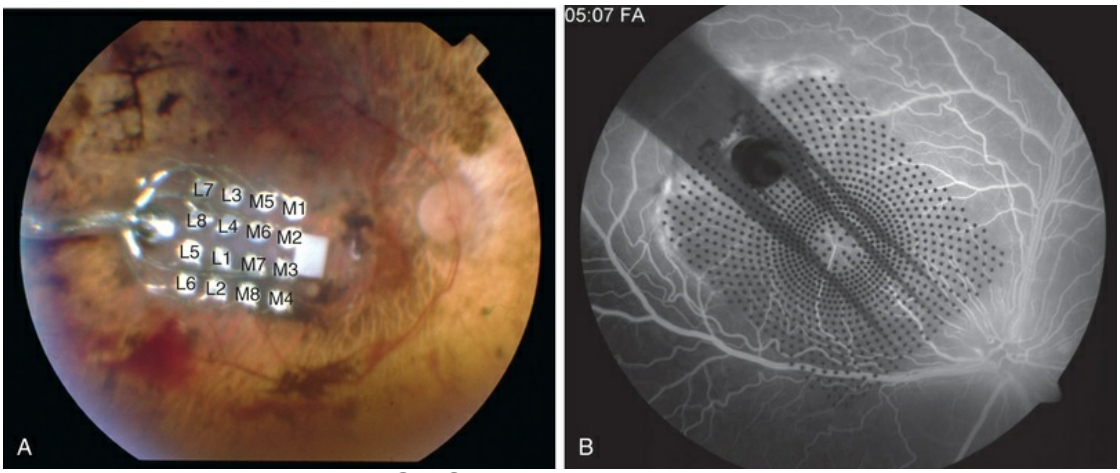

FIG. 129.12 (A) ARGUS I 16-electrode array. (B) 1000 pixels experimental electrode array.

Disclosures

Mark S. Humayun has equity in, is a patent holder for, receives royalties from, and is a consultant to Second Sight Medical Products, Inc. James Weiland received research funding from Second Sight Medical Products, Inc. Hossein Nazari has no disclosures.

References

1. Ross RD. Is perception of light useful to the blind patient? *Arch Ophthalmol*. 1998;116:236–238.
2. Berson EL, Rosner B, Sandberg MA, et al. A randomized trial of vitamin A and vitamin E supplementation for retinitis pigmentosa. *Arch Ophthalmol*. 1993;111:761–772.
3. Sharma RK, Ehinger B. Management of hereditary retinal degenerations: present status and future directions. *Surv Ophthalmol*. 1999;43:427–444.
4. del Cerro M, Gash DM, Rao GN, et al. Retinal transplants into the anterior chamber of the rat eye. *Neuroscience*. 1987;21:707–723.
5. Bunker CH, Berson EL, Bromley WC, Hayes RP, Roderick TH. Prevalence of retinitis pigmentosa in Maine. *Am J Ophthalmol*. 1984;97:357–365.

6. Curcio CA, Medeiros NE, Millican CL. Photoreceptor loss in age-related macular degeneration. *Invest Ophthalmol Vis Sci*. 1996;37:1236–1249.
7. Humayun MS, de Juan E Jr. Artificial vision. *Eye (Lond)*. 1998;12(Pt 3b):605–607.
8. Koberlein J, Beifus K, Schaffert C, Finger RP. The economic burden of visual impairment and blindness: a systematic review. *BMJ Open*. 2013;3:e003471.
9. Brown DM, Kaiser PK, Michels M, et al. Ranibizumab versus verteporfin for neovascular age-related macular degeneration. *N Engl J Med*. 2006;355:1432–1444.
10. Rosenfeld PJ, Brown DM, Heier JS, et al. Ranibizumab for neovascular age-related macular degeneration. *N Engl J Med*. 2006;355:1419–1431.
11. Group CR, Martin DF, Maguire MG, et al. Ranibizumab and bevacizumab for neovascular age-related macular degeneration. *N Engl J Med*. 2011;364:1897–1908.
12. Imamura Y, Engelbert M, Iida T, Freund KB, Yannuzzi LA. Polypoidal choroidal vasculopathy: a review. *Surv Ophthalmol*. 2010;55:501–515.
13. Nazari H, Zhang L, Zhu D, et al. Stem cell based therapies for age-related macular degeneration: the promises and the challenges. *Prog Retin Eye Res*. 2015;48:1–39.
14. Cideciyan AV. Leber congenital amaurosis due to RPE65 mutations and its treatment with gene therapy. *Prog Retin Eye Res*. 2010;29:398–427.
15. Li X, Li W, Dai X, et al. Gene therapy rescues cone structure and function in the 3-month-old rd12 mouse: a model for midcourse RPE65 leber congenital amaurosis. *Invest Ophthalmol Vis Sci*. 2011;52:7–15.
16. Maguire AM, High KA, Auricchio A, et al. Age-dependent effects of RPE65 gene therapy for Leber's congenital amaurosis: a phase 1 dose-escalation trial. *Lancet*. 2009;374:1597–1605.
17. Stein L, Roy K, Lei L, Kaushal S. Clinical gene therapy for the treatment of RPE65-associated Leber congenital amaurosis. *Expert Opin Biol Ther*. 2011;11:429–439.
18. Foerster O. Beitrage zur pathophysiologie der sehbahn und

der spehsphare. *J Psychol Neurol*. 1929;39:435–463.
19. Brindley G. The number of information channels needed for efficient reading. *J Physiol*. 1965;177:44.
20. Hayashi A, Nakae K, Naka H, et al. Cytokine effects on phagocytosis of rod outer segments by retinal pigment epithelial cells of the normal and dystrophic rats. *Curr Eye Res*. 1996;15(5):487–499.
21. Cha K, Horch K, Normann RA. Simulation of a phosphene-based visual field: visual acuity in a pixelized vision system. *Ann Biomed Eng*. 1992;20:439–449.
22. Cha K, Horch KW, Normann RA. Mobility performance with a pixelized vision system. *Vision Res*. 1992;32:1367–1372.
23. Cha K, Horch KW, Normann RA, Boman DK. Reading speed with a pixelized vision system. *J Opt Soc Am A*. 1992;9:673–677.
24. Hayes JS, Yin VT, Piyathaisere D, et al. Visually guided performance of simple tasks using simulated prosthetic vision. *Artif Organs*. 2003;27:1016–1028.
25. Thompson RW Jr, Barnett GD, Humayun MS, Dagnelie G. Facial recognition using simulated prosthetic pixelized vision. *Invest Ophthalmol Vis Sci*. 2003;44:5035–5042.
26. Brindley GS, Rushton D. Implanted stimulators of the visual cortex as visual prosthetic devices. *Trans Am Acad Ophthalmol Otolaryngol*. 1974;78:741–745.
27. Brindley GS. Sensations produced by electrical stimulation of the occipital poles of the cerebral hemispheres, and their use in constructing visual prostheses. *Ann R Coll Surg Engl*. 1970;47:106–108.
28. Brindley GS, Lewin WS. The sensations produced by electrical stimulation of the visual cortex. *J Physiol*. 1968;96:479–493.
29. Dobelle WH, Mladejovsky MG. Phosphenes produced by electrical stimulation of human occipital cortex, and their application to the development of a prosthesis for the blind. *J Physiol*. 1974;243:553–576.
30. Dobelle WH, Turkel J, Henderson DC, Evans JR. Mapping the projection of the visual field onto visual cortex in man

by direct electrical stimulation. *Trans Am Soc Artif Intern Organs*. 1978;24:15–17.
31. Dobelle WH, Mladejovsky MG, Evans JR, Roberts TS, Girvin JP. Braille" reading by a blind volunteer by visual cortex stimulation. *Nature*. 1976;259:111–112.
32. Dobelle WH, Quest DO, Antunes JL, Roberts TS, Girvin JP. Artificial vision for the blind by electrical stimulation of the visual cortex. *Neurosurgery*. 1979;5:521–527.
33. Dobelle WH. Artificial vision for the blind by connecting a television camera to the visual cortex. *ASAIO J*. 2000;46:3–9.
34. Pollen DA. Responses of single neurons to electrical stimulation of the surface of the visual cortex. *Brain Behav Evol*. 1977;14:67–86.
35. Schmidt EM, Bak MJ, Hambrecht FT, et al. Feasibility of a visual prosthesis for the blind based on intracortical microstimulation of the visual cortex. *Brain*. 1996;119(Pt 2):507–522.
36. Maynard EM. Visual prostheses. *Annu Rev Biomed Eng*. 2001;3:145–168.
37. Bak M, Girvin JP, Hambrecht FT, et al. Visual sensations produced by intracortical microstimulation of the human occipital cortex. *Med Biol Eng Comput*. 1990;28:257–259.
38. Maynard EM, Nordhausen CT, Normann RA. The Utah Intracortical Electrode Array: a recording structure for potential brain-computer interfaces. *Electroencephalogr Clin Neurophysiol*. 1997;102:228–239.
39. Uematsu S, Chapanis N, Gucer G, Konigsmark B, Walker AE. Electrical stimulation of the cerebral visual system in man. *Confin Neurol*. 1974;36:113–124.
40. Rousche PJ, Normann RA. Chronic intracortical microstimulation (ICMS) of cat sensory cortex using the Utah Intracortical Electrode Array. *IEEE Trans Rehabil Eng*. 1999;7:56–68.
41. Agnew WF, Yuen TG, McCreery DB, Bullara LA. Histopathologic evaluation of prolonged intracortical electrical stimulation. *Exp Neurol*. 1986;92:162–185.
42. McCreery DB, Yuen TG, Agnew WF, Bullara LA. A characterization of the effects on neuronal excitability due

to prolonged microstimulation with chronically implanted microelectrodes. *IEEE Trans Biomed Eng*. 1997;44:931–939.
43. Weiland JD, Anderson DJ. Chronic neural stimulation with thin-film, iridium oxide electrodes. *IEEE Trans Biomed Eng*. 2000;47:911–918.
44. Normann RA, Maynard EM, Rousche PJ, Warren DJ. A neural interface for a cortical vision prosthesis. *Vision Res*. 1999;39:2577–2587.
45. Margalit E, Maia M, Weiland JD, et al. Retinal prosthesis for the blind. *Surv Ophthalmol*. 2002;47:335–356.
46. Shandurina AN. [Restoration of visual and auditory function using electrostimulation]. *Fiziol Cheloveka*. 1995;21:25–29.
47. Naples GG, Mortimer JT, Scheiner A, Sweeney JD. A spiral nerve cuff electrode for peripheral nerve stimulation. *IEEE Trans Biomed Eng*. 1988;35:905–916.
48. Sweeney JD, Mortimer JT. An asymmetric two electrode cuff for generation of unidirectionally propagated action potentials. *IEEE Trans Biomed Eng*. 1986;33:541–549.
49. Ungar IJ, Mortimer JT, Sweeney JD. Generation of unidirectionally propagating action potentials using a monopolar electrode cuff. *Ann Biomed Eng*. 1986;14:437–450.
50. Veraart C, Raftopoulos C, Mortimer JT, et al. Visual sensations produced by optic nerve stimulation using an implanted self-sizing spiral cuff electrode. *Brain Res*. 1998;813:181–186.
51. Veraart C, Wanet-Defalque MC, Gerard B, Vanlierde A, Delbeke J. Pattern recognition with the optic nerve visual prosthesis. *Artif Organs*. 2003;27:996–1004.
52. Cuoco FA Jr, Durand DM. Measurement of external pressures generated by nerve cuff electrodes. *IEEE Trans Rehabil Eng*. 2000;8:35–41.
53. Branner A, Normann RA. A multielectrode array for intrafascicular recording and stimulation in sciatic nerve of cats. *Brain Res Bull*. 2000;51:293–306.
54. Potts AM, Inoue J. The electrically evoked response (EER) of the visual system. II. Effect of adaptation and retinitis pigmentosa. *Invest Ophthalmol*. 1969;8:605–612.

55. Potts AM, Inoue J. The electrically evoked response of the visual system (EER). 3. Further contribution to the origin of the EER. *Invest Ophthalmol*. 1970;9:814–819.
56. Potts AM, Inoue J, Buffum D. The electrically evoked response of the visual system (EER). *Invest Ophthalmol*. 1968;7:269–278.
57. Knighton RW. An electrically evoked slow potential of the frog's retina. II. Identification with PII component of electroretinogram. *J Neurophysiol*. 1975;38:198–209.
58. Knighton RW. An electrically evoked slow potential of the frog's retina. I. Properties of response. *J Neurophysiol*. 1975;38:185–197.
59. Stone JL, Barlow WE, Humayun MS, de Juan E Jr, Milam AH. Morphometric analysis of macular photoreceptors and ganglion cells in retinas with retinitis pigmentosa. *Arch Ophthalmol*. 1992;110:1634–1639.
60. Kim SY, Sadda S, Humayun MS, et al. Morphometric analysis of the macula in eyes with geographic atrophy due to age-related macular degeneration. *Retina*. 2002;22:464–470.
61. Kim SY, Sadda S, Pearlman J, et al. Morphometric analysis of the macula in eyes with disciform age-related macular degeneration. *Retina*. 2002;22:471–477.
62. Marc RE, Jones BW, Watt CB, Strettoi E. Neural remodeling in retinal degeneration. *Prog Retin Eye Res*. 2003;22:607–655.
63. Varela C, Igartua I, De la Rosa EJ, De la Villa P. Functional modifications in rod bipolar cells in a mouse model of retinitis pigmentosa. *Vision Res*. 2003;43:879–885.
64. Choi H, Zhang L, Cembrowski MS, et al. Intrinsic bursting of AII amacrine cells underlies oscillations in the rd1 mouse retina. *J Neurophysiol*. 2014;112:1491–1504.
65. Humayun MS, Prince M, de Juan E Jr, et al. Morphometric analysis of the extramacular retina from postmortem eyes with retinitis pigmentosa. *Invest Ophthalmol Vis Sci*. 1999;40:143–148.
66. Santos A, Humayun MS, de Juan E Jr, et al. Preservation of the inner retina in retinitis pigmentosa: a morphometric analysis. *Arch Ophthalmol*. 1997;115:511–515.

67. Rizzo JF 3rd, Wyatt J, Loewenstein J, Kelly S, Shire D. Methods and perceptual thresholds for short-term electrical stimulation of human retina with microelectrode arrays. *Invest Ophthalmol Vis Sci*. 2003;44:5355–5361.
68. Rizzo JF 3rd, Wyatt J, Loewenstein J, Kelly S, Shire D. Perceptual efficacy of electrical stimulation of human retina with a microelectrode array during short-term surgical trials. *Invest Ophthalmol Vis Sci*. 2003;44:5362–5369.
69. Webb RL, Pyman BC, Franz BK-HG, et al. The surgery of cochlear prostheses. Clark G, Tong YC, Patrick JF. *Cochlear prostheses*. Churchill Livingstone.: Edinburgh, New York; 1990:vii [264].
70. Humayun MS, Weiland JD, Fujii GY, et al. Visual perception in a blind subject with a chronic microelectronic retinal prosthesis. *Vision Res*. 2003;43:2573–2581.
71. Mahadevappa M, Weiland JD, Yanai D, et al. Perceptual thresholds and electrode impedance in three retinal prosthesis subjects. *IEEE Trans Neural Syst Rehabil Eng*. 2005;13:201–206.
72. Merrill DR, Bikson M, Jefferys JG. Electrical stimulation of excitable tissue: design of efficacious and safe protocols. *J Neurosci Methods*. 2005;141:171–198.
73. de Balthasar C, Patel S, Roy A, et al. Factors affecting perceptual thresholds in epiretinal prostheses. *Invest Ophthalmol Vis Sci*. 2008;49:2303–2314.
74. Ahuja AK, Dorn JD, Caspi A, et al. Blind subjects implanted with the Argus II retinal prosthesis are able to improve performance in a spatial-motor task. *Br J Ophthalmol*. 2011;95:539–543.
75. Caspi A, Dorn JD, McClure KH, et al. Feasibility study of a retinal prosthesis: spatial vision with a 16-electrode implant. *Arch Ophthalmol*. 2009;127:398–401.
76. da Cruz L, Coley BF, Dorn J, et al. The Argus II epiretinal prosthesis system allows letter and word reading and long-term function in patients with profound vision loss. *Br J Ophthalmol*. 2013;97:632–636.
77. Ho AC, Humayun MS, Dorn JD, et al. Long-term results from an epiretinal prosthesis to restore sight to the blind.

Ophthalmology. 2015;122:1547–1554.
78. Humayun MS, Dorn JD, da Cruz L, et al. Interim results from the international trial of Second Sight's visual prosthesis. *Ophthalmology*. 2012;119:779–788.
79. Hornig R, Zehnder T, Velikay-Parel M, et al. The IMI Retinal Implant System. Humayun MS, Weiland JD, Chader G. *Artificial sight : basic research, biomedical engineering, and clinical advances*. Springer: New York; 2007.
80. Richard G, Hornig R, Keserü M, et al. Chronic epiretinal chip implant in blind patients with retinitis pigmentosa: long-term clinical results. *Invest Ophthalmol Vis Sci*. 2007;48:666.
81. Feucht M, Laube T, Bornfeld N, et al. Development of an epiretinal prosthesis for stimulation of the human retina. *Ophthalmologe*. 2005;102:688–691.
82. Matthaei M, Zeitz O, Keseru M, et al. Progress in the development of vision prostheses. *Ophthalmologica*. 2011;225:187–192.
83. Roessler G, Laube T, Brockmann C, et al. Implantation and explantation of a wireless epiretinal retina implant device: observations during the EPIRET3 prospective clinical trial. *Invest Ophthalmol Vis Sci*. 2009;50:3003–3008.
84. Klauke S, Goertz M, Rein S, et al. Stimulation with a wireless intraocular epiretinal implant elicits visual percepts in blind humans. *Invest Ophthalmol Vis Sci*. 2011;52:449–455.
85. Zrenner E, Bartz-Schmidt KU, Benav H, et al. Subretinal electronic chips allow blind patients to read letters and combine them to words. *Proc Biol Sci*. 2011;278:1489–1497.
86. Benav H, Bartz-Schmidt KU, Besch D, et al. Restoration of useful vision up to letter recognition capabilities using subretinal microphotodiodes. *Conf Proc IEEE Eng Med Biol Soc*. 2010;2010:5919–5922.
87. Chow AY, Chow VY, Packo KH, et al. The artificial silicon retina microchip for the treatment of vision loss from retinitis pigmentosa. *Arch Ophthalmol*. 2004;122:460–469.
88. Chow AY, Pardue MT, Perlman JI, et al. Subretinal implantation of semiconductor-based photodiodes: durability of novel implant designs. *J Rehabil Res Dev*.

2002;39:313–321.
89. Peyman G, Chow AY, Liang C, et al. Subretinal semiconductor microphotodiode array. *Ophthalmic Surg Lasers*. 1998;29:234–241.
90. Kusnyerik A, Greppmaier U, Wilke R, et al. Positioning of electronic subretinal implants in blind retinitis pigmentosa patients through multimodal assessment of retinal structures. *Invest Ophthalmol Vis Sci*. 2012;53:3748–3755.
91. Besch D, Sachs H, Szurman P, et al. Extraocular surgery for implantation of an active subretinal visual prosthesis with external connections: feasibility and outcome in seven patients. *Br J Ophthalmol*. 2008;92:1361–1368.
92. Kitiratschky VB, Stingl K, Wilhelm B, et al. Safety evaluation of "retina implant alpha IMS" – a prospective clinical trial. *Graefes Arch Clin Exp Ophthalmol*. 2015;253:381–387.
93. Stingl K, Bartz-Schmidt KU, Besch D, et al. Artificial vision with wirelessly powered subretinal electronic implant alpha-IMS. *Proc Biol Sci*. 2013;280:20130077.
94. Stingl K, Bartz-Schmidt KU, Besch D, et al. Subretinal visual implant Alpha IMS – clinical trial interim report. *Vision Res*. 2015;111:149–160.
95. Stingl K, Bartz-Schmidt KU, Gekeler F, et al. Functional outcome in subretinal electronic implants depends on foveal eccentricity. *Invest Ophthalmol Vis Sci*. 2013;54:7658–7665.
96. Hafed ZM, Stingl K, Bartz-Schmidt KU, Gekeler F, Zrenner E. Oculomotor behavior of blind patients seeing with a subretinal visual implant. *Vision Res*. 2016;118:119–131.
97. Zrenner E. Fighting blindness with microelectronics. *Sci Transl Med*. 2013;5:210ps216.
98. Rizzo JF 3rd. Update on retinal prosthetic research: the Boston Retinal Implant Project. *J Neuroophthalmol*. 2011;31:160–168.
99. Shire DB, Kelly SK, Chen J, et al. Development and implantation of a minimally invasive wireless subretinal neurostimulator. *IEEE Trans Biomed Eng*. 2009;56:2502–2511.
100. Palanker D, Huie P, Vankov A, et al. Migration of retinal cells through a perforated membrane: implications for a

high-resolution prosthesis. *Invest Ophthalmol Vis Sci*. 2004;45:3266–3270.
101. Palanker D, Vankov A, Huie P, Baccus S. Design of a high-resolution optoelectronic retinal prosthesis. *J Neural Eng*. 2005;2:S105–20.
102. Loudin JD, Simanovskii DM, Vijayraghavan K, et al. Optoelectronic retinal prosthesis: system design and performance. *J Neural Eng*. 2007;4:S72–84.
103. Adekunle AN, Adkins A, Wang W, et al. Integration of perforated subretinal prostheses with retinal tissue. *Transl Vis Sci Technol*. 2015;4:5.
104. Lorach H, Goetz G, Mandel Y, et al. Performance of photovoltaic arrays in-vivo and characteristics of prosthetic vision in animals with retinal degeneration. *Vision Res*. 2015;111:142–148.
105. Mandel Y, Goetz G, Lavinsky D, et al. Cortical responses elicited by photovoltaic subretinal prostheses exhibit similarities to visually evoked potentials. *Nat Commun*. 2013;4:1980.
106. Wang L, Mathieson K, Kamins TI, et al. Photovoltaic retinal prosthesis: implant fabrication and performance. *J Neural Eng*. 2012;9:046014.
107. Palanker DV, Huie P, Vankov AB, et al. Attracting retinal cells to electrodes for high-resolution stimulation. *Proc SPIE*. 2004;5314 [undefined].
108. Morimoto T, Miyoshi T, Fujikado T, Tano Y, Fukuda Y. Electrical stimulation enhances the survival of axotomized retinal ganglion cells in vivo. *Neuroreport*. 2002;13:227–230.
109. Morimoto T, Kamei M, Nishida K, et al. Chronic implantation of newly developed suprachoroidal-transretinal stimulation prosthesis in dogs. *Invest Ophthalmol Vis Sci*. 2011;52:6785–6792.
110. Nakauchi K, Fujikado T, Kanda H, et al. Transretinal electrical stimulation by an intrascleral multichannel electrode array in rabbit eyes. *Graefes Arch Clin Exp Ophthalmol*. 2005;243:169–174.
111. Fujikado T, Kamei M, Sakaguchi H, et al. Testing of semichronically implanted retinal prosthesis by

suprachoroidal-transretinal stimulation in patients with retinitis pigmentosa. *Invest Ophthalmol Vis Sci*. 2011;52:4726–4733.
112. Lohmann TK, Kanda H, Morimoto T, et al. Surgical feasibility and biocompatibility of wide-field dual-array suprachoroidal-transretinal stimulation prosthesis in middle-sized animals. *Graefes Arch Clin Exp Ophthalmol*. 2016;25(4):661–673.
113. Ayton LN, Blamey PJ, Guymer RH, et al. First-in-human trial of a novel suprachoroidal retinal prosthesis. *PLoS ONE*. 2014;e115239.
114. Shivdasani MN, Luu CD, Cicione R, et al. Evaluation of stimulus parameters and electrode geometry for an effective suprachoroidal retinal prosthesis. *J Neural Eng*. 2010;7:036008.
115. Villalobos J, Fallon JB, Nayagam DA, et al. Cortical activation following chronic passive implantation of a wide-field suprachoroidal retinal prosthesis. *J Neural Eng*. 2014;11:046017.
116. Nayagam DA, Williams RA, Allen PJ, et al. Chronic electrical stimulation with a suprachoroidal retinal prosthesis: a preclinical safety and efficacy study. *PLoS ONE*. 2014;9:e97182.
117. Saunders AL, Williams CE, Heriot W, et al. Development of a surgical procedure for implantation of a prototype suprachoroidal retinal prosthesis. *Clin Experiment Ophthalmol*. 2014;42:665–674.
118. Brown JS, Flitcroft DI, Ying GS, et al. In vivo human choroidal thickness measurements: evidence for diurnal fluctuations. *Invest Ophthalmol Vis Sci*. 2009;50:5–12.
119. Kanda H, Morimoto T, Fujikado T, et al. Electrophysiological studies of the feasibility of suprachoroidal-transretinal stimulation for artificial vision in normal and RCS rats. *Invest Ophthalmol Vis Sci*. 2004;45:560–566.
120. Nakauchi K, Fujikado T, Kanda H, et al. Threshold suprachoroidal-transretinal stimulation current resulting in retinal damage in rabbits. *J Neural Eng*. 2007;4:S50–7.

121. Wong YT, Chen SC, Kerdraon YA, et al. Efficacy of supra-choroidal, bipolar, electrical stimulation in a vision prosthesis. *Conf Proc IEEE Eng Med Biol Soc*. 2008;2008:1789–1792.
122. Wong YT, Chen SC, Seo JM, et al. Focal activation of the feline retina via a suprachoroidal electrode array. *Vision Res*. 2009;49:825–833.
123. Sakaguchi H, Fujikado T, Fang X, et al. Transretinal electrical stimulation with a suprachoroidal multichannel electrode in rabbit eyes. *Jpn J Ophthalmol*. 2004;48:256–261.
124. Iezzi R, Finlayson P, Xu Y, Katragadda R. Microfluidic neurotransmitter-based neural interfaces for retinal prosthesis. *Conf Proc IEEE Eng Med Biol Soc*. 2009;2009:4563–4565.
125. Peterman MC, Bloom DM, Lee C, et al. Localized neurotransmitter release for use in a prototype retinal interface. *Invest Ophthalmol Vis Sci*. 2003;44:3144–3149.
126. Peterman MC, Mehenti NZ, Bilbao KV, et al. The Artificial Synapse Chip: a flexible retinal interface based on directed retinal cell growth and neurotransmitter stimulation. *Artif Organs*. 2003;27:975–985.
127. Ciavatta VT, Kim M, Wong P, et al. Retinal expression of Fgf2 in RCS rats with subretinal microphotodiode array. *Invest Ophthalmol Vis Sci*. 2009;50:4523–4530.
128. Chow AY, Bittner AK, Pardue MT. The artificial silicon retina in retinitis pigmentosa patients (an American Ophthalmological Association thesis). *Trans Am Ophthalmol Soc*. 2010;108:120–154.
129. Boyden ES, Zhang F, Bamberg E, Nagel G, Deisseroth K. Millisecond-timescale, genetically targeted optical control of neural activity. *Nat Neurosci*. 2005;8:1263–1268.
130. Deisseroth K, Feng G, Majewska AK, et al. Next-generation optical technologies for illuminating genetically targeted brain circuits. *J Neurosci*. 2006;26:10380–10386.
131. Zhang F, Wang LP, Boyden ES, Deisseroth K. Channelrhodopsin-2 and optical control of excitable cells. *Nat Methods*. 2006;3:785–792.
132. Bi A, Cui J, Ma YP, et al. Ectopic expression of a microbial-

type rhodopsin restores visual responses in mice with photoreceptor degeneration. *Neuron*. 2006;50:23–33.
133. Doroudchi MM, Greenberg KP, Liu J, et al. Virally delivered channelrhodopsin-2 safely and effectively restores visual function in multiple mouse models of blindness. *Mol Ther*. 2011;19:1220–1229.
134. Busskamp V, Duebel J, Balya D, et al. Genetic reactivation of cone photoreceptors restores visual responses in retinitis pigmentosa. *Science*. 2010;329:413–417.
135. Rohan JG, Citron YR, Durrell AC, et al. Light-triggered modulation of cellular electrical activity by ruthenium diimine nanoswitches. *ACS Chem Neurosci*. 2013;4:585–593.

130

Pharmacologic Agents and Vitreoretinal Surgery

Christos Haritoglou, Anselm Kampik

Introduction

Within the last years many technical developments in the field of vitreoretinal surgery were introduced. We experienced not only improvements of vitrectomy machines (increased cut rates, improved pumps, improved fluidics, etc.), but also a continuous miniaturization of the surgical instruments such as cutters, forceps, and scissors from 20-gauge to 23- or 25-gauge, and even 27-gauge. In addition, improved illumination and viewing systems allow for a better visualization. All these refinements greatly helped to reduce surgical trauma, facilitate surgical maneuvers, and improve postoperative comfort for the patient. Thus mechanical means of vitrectomy have constantly been optimized during the years. Recent developments have added pharmacologic options to the surgical possibilities in vitreoretinal surgery.

Meanwhile new pharmacologic treatment strategies for many retinal diseases including diabetic retinopathy, age-related macular degeneration, and retinal vein occlusion have been discovered and have opened a perspective of significant visual improvement for many patients. As a consequence of these developments, a pharmacologic option is beginning to be added to the vitreoretinal surgical armamentarium.

In vitreoretinal surgery, pharmacotherapy at the time of surgery formerly mainly played a role in experimental studies addressing the issue of prevention of proliferative vitreoretinopathy, a major sight-threatening complication of vitreoretinal procedures. In addition pharmacotherapy was used routinely when surgery was necessary in cases of severe endophthalmitis. Meanwhile, as pharmacotherapy of retinal diseases has become an essential

standard in the specialty of medical retina, new ideas and concepts regarding this field have also emerged in the field of vitreoretinal surgery.

The following chapter will discuss some of these developments with special emphasis on aspects of relevance as an adjunct for vitreoretinal surgery.

Pharmacologic Vitreolysis

Rationale for Pharmacologic Vitreolysis

Posterior vitreous detachment (PVD) is a progressive physiologic process, involving both syneresis (liquefaction) and synchysis (separation). However, spontaneous PVD is very often incomplete and remnants of the vitreous adhere firmly either to areas in the periphery of the retina or to the macular area. Tractional forces exerted by vitreous collagen fibers and/or cellular proliferations at the vitreoretinal interface also play an important role in the pathogenesis of tractional maculopathies such as macular holes, vitreomacular traction syndrome, or epiretinal membranes. In addition, focal abnormal vitreoretinal adhesions may be implicated in certain types of diabetic macular edema and exudative age-related macular degeneration[1,2] and may have an impact on the effectiveness of the pharmacologic treatment applied in these conditions.[3]

Our present therapeutic approach in these tractional maculopathies is to relieve tractional forces surgically by mechanical means, inducing a more or less complete PVD using suction exerted by the vitrectomy probe followed by a removal of remnants of vitreous collagen fibers and cellular proliferations using an endgripping forceps. As we have learned that cellular proliferations tend to recur using remnants of collagen at the internal limiting membrane (ILM) as a scaffold, most surgeons tend to remove the ILM during the surgical intervention as well, in order to remove all epiretinal tissue. However, it may be hypothesized that direct manipulation in the area of the macula and the removal of the ILM itself may somehow have an impact on function in the macular area or interfere with the morphologic integrity of the

retinal layers, especially when being removed with the aid of visualizing agents.[4] Therefore, although ILM peeling appears safe from a clinical point of view, it may not be the optimum treatment option with regard to the best possible functional results.

Given this background, a pharmacologic liquefaction of the vitreous gel and simultaneous enzymatic separation of vitreous fibrils from the inner aspect of the ILM may result in a resolution of focal vitreomacular adhesions, representing an alternative approach to treat traction-related retinal and macular diseases. Leaving the ILM in place and cleaving the vitreoretinal interface at the vitreal side of the ILM may offer a more complete PVD, and be less traumatic as compared to vitrectomy. This pharmacologic induction of a PVD, if achieved early in the course of retinal or macular diseases, may have also a potential as a prophylactic treatment against advanced stages of potentially sight-threatening conditions such as diabetic retinopathy or age-related macular degeneration (AMD).[3] This concept is referred to as "pharmacologic vitreolysis," and was initially introduced by Sebag in 1998.[5] Additional potential indications theoretically include vitreoretinal procedures for retinal detachment in children, in whom firm adherences of the vitreous often complicate surgery, especially in retinopathy of prematurity (ROP) or ocular trauma with intraocular foreign body. The hope is to make vitreoretinal surgery procedures more safe and effective using the concept of pharmacologic vitreolysis.

The following substances have been evaluated or are currently under investigation.

Enzymatic Vitreolysis – Microplasmin, Plasmin, and Others

A variety of intravitreally applied enzymes has been investigated in animal studies so far and some of them have even progressed to clinical trials in humans. Based on the present published data, plasmin and microplasmin seem to be the most promising substances.

Microplasmin represents a recombinant protein that contains the catalytic domain of human plasmin but is much more stable as compared to the latter; both plasmin and microplasmin are

nonspecific serine proteases cleaving a variety of glycoproteins such as fibronectin, laminin, fibrin, and thrombospondin.[6] These glycoproteins are involved in the adherence of the vitreous cortex to the ILM. Thus cleavage of these enzymes potentially induces a PVD: Experimentally, microplasmin has been shown to increase vitreous diffusion coefficients in vitro using the noninvasive technique of dynamic light scattering[7] and caused simultaneous vitreolysis and posterior vitreous separation in ex vivo and in vivo animal eye models in an apparent dose- and time-dependent fashion[8,9] without morphologic alterations in the retina.[10] In a human, double-masked, phase II trial 60 patients were randomized in four treatment cohorts either receiving increasing doses of microplasmin (75, 125, and 175 μg) or an initial injection of 125 μg followed by an injection of 125 μg if no release of adhesion occurred 1 month later or after sham injection.[11] The study revealed that within 28 days of sham 75, 125, and 175 μg microplasmin administration, a nonsurgical resolution of vitreomacular adhesion was observed in 8, 25, 44, and 27% of patients; when the 125-μg dose was repeated up to three times, adhesion release was observed in 58% of patients 28 days after the final injection.[11] Another phase II, placebo-controlled, double-masked, dose-ranging clinical trial analyzed the effect of a single injection of microplasmin (25, 75, or 125 μg) 7 days prior to scheduled vitrectomy for vitreomacular traction and reported that 125 μg microplasmin was associated with a greater likelihood of induction and progression of PVD than placebo injection.[12] Randomized clinical trials have been published suggesting microplasmin as a monotherapy replacing the need for surgical intervention in some patients with small macular holes less than 250 μm and patients with vitreomacular traction up to 1500 μm[13] (Fig. 130.1). The success of enzymatic vitreolysis in these cases is negatively correlated with the presence of epiretinal membranes.[13,14] It has also been shown that intravitreal injections of microplasmin may increase vitreal O_2 levels, increase the rate of O_2 exchange within the vitreous cavity, and increase vitreous diffusion coefficients in vitro.[15,16] The vitreous detachment induced by microplasmin may lead to a distribution of oxygen to ischemic retinal areas and help to reduce the VEGF concentration at the retinal surface. This may be beneficial in ischemic retinal diseases

such as proliferative diabetic retinopathy or retinal vein occlusion.[17]

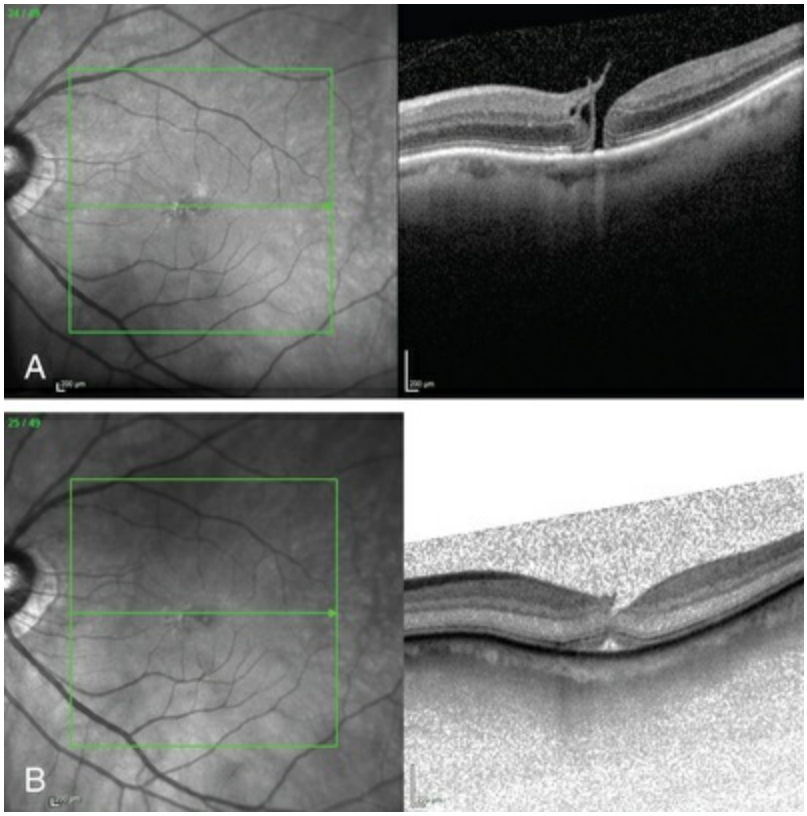

FIG. 130.1 (A) Optical coherence tomography (OCT) demonstrating a small full-thickness macular hole with vitreomacular adhesion visible at the edge of the macular hole. (B) OCT 5 weeks after treatment with 125-µg microplasmin showing the resolution of the vitreomacular adhesion and associated macular hole closure without vitrectomy. Subfoveal fluid is still present, which dissolved over the next few weeks.

Microplasmin has been approved under the generic name "ocriplasmin" since 2012 by the United States Food and Drug Administration as a drug approved to treat symptomatic vitreomacular adhesion (VMA). In Europe the approval by the European Medicines Agency in 2013 included the indications vitreomacular traction, also in association with a macular hole smaller or equal to 400 µm diameter. New data discuss potential side-effects including an assumed ocriplasmin-induced retinopathy.[18] From current surveys it is concluded that further studies are needed to better understand the pathophysiology and

clinical relevance of adverse events after the use of ocriplasmin.[19]

Plasmin was initially used by Verstraten and coworkers to facilitate a PVD during vitrectomy in rabbit eyes. They found a positive effect but also mentioned a transient reduction of the b-wave amplitude in the electroretinogram as a potential adverse effect.[20] This study was followed by other experimental trials confirming the proteolytic activity of plasmin on the vitreoretinal junction. Autologous plasmin was then used in clinical case series investigating the effect of a single injection without vitrectomy as a treatment for refractory diffuse diabetic macular edema,[21] tractional diabetic macular edema,[22] or macular edema associated with branch retinal vein occlusion.[23] The reduction of retinal thickness and improvement of visual acuity in these series supported an effectiveness of plasmin and the need for further trials. Autologous plasmin-assisted vitrectomy was performed for stage 3 macular holes, traumatic macular holes, diabetic macular edema, and stage 5 ROP,[24–29] and all of these trials underlined the potential of plasmin to facilitate vitrectomy and its good safety profile.

Other enzymes investigated included **hyaluronidase** and **dispase**. While the first liquefied vitreous but did not induce a PVD and was therefore not suitable to release traction, the latter showed evidence for retinal bleedings, epimacular membrane formation, abnormalities in the electroretinogram responses, and ultrastructural retinal damage, and it was not further evaluated for clinical use.

Antiproliferative Agents in the Management of Proliferative Vitreoretinopathy

Proliferative vitreoretinopathy (PVR) is a serious and major complication of primary rhegmatogenous retinal detachment, severe diabetic retinopathy, and severe intraocular trauma. The pathophysiology of this disease implies a very complex cascade of events resulting in a subsequent proliferative response within the retina (see Chapter 101, Pathogenesis of proliferative vitreoretinopathy). Experimental studies described an intraretinal

cellular response to retinal detachment which is triggered by serum and growth factors present in the vitreous cavity[30] and includes all types of non-neural cells such as RPE cells, astrocytes, microglia, macrophages, but predominantly Müller cells,[31–34] which is then followed by a fibrocellular growth on the subretinal or epiretinal surface.[35] Both subretinal fibrosis and epiretinal proliferation have an impact on functional results and anatomical failure of retinal detachment surgery.[35,36] The facts that these cellular responses to retinal detachment may occur early in the development of the disease and may continue even in the longer term following (successful) surgical intervention, point to the need for an early pharmacologic intervention and a long-term drug release or pharmacologic effect,[37]

Other contributing factors include a relative hypoxia due to the distance between the neurosensory retina and the choriocapillaris[38] which leads to glial changes and photoreceptor deconstruction. These mechanisms are the target of recent and current approaches for an adjuvant pharmacologic intervention in PVR as these cellular responses cannot be controlled by surgery alone.

Antiproliferative and antiinflammatory agents have been subjects of in vitro investigations including substances such as colchicine, daunomycin, and 5-fluouracil.[39,40] However, none of these agents has become part of any standardized procedure to treat or prevent PVR. Only daunomycin and 5-fluouracil combined with low-molecular heparin were tested in clinical studies, and these revealed no clinically relevant impact on PVR.[41]

Several years ago steroids applied intravitreally were used to suppress the process of PVR in clinical settings and in experimental studies.[42] However, the effect was not sufficiently long-lasting to prevent PVR.

New concepts include other agents such as alkylphosphocholines (APCs), which are synthetic phospholipid derivatives that have been shown to effectively inhibit cellular proliferation.[43] Their mechanism of action involves binding to the membrane-bound G-protein PKC (protein kinase C), which is part of a major intracellular second-messenger system that regulates cell attachment, spreading, migration, and proliferation. As described in the literature, APCs have a potential to inhibit RPE cell spreading

and migration as well as proliferation and cell-mediated membrane contraction at nontoxic concentrations in vitro, and they did not display any toxic effects upon retinal tissue in in vivo animal models.[44] Besides prevention and treatment of PVR, APCs might have the potential for topical application as a single-dose agent to prevent posterior capsule opacification following cataract surgery.[45]

In addition to these above-mentioned substances a variety of other drugs are currently evaluated. However, none so far has reached a clinically relevant potential.

Tissue Plasminogen Activator in Vitreoretinal Surgery

AMD is one of the leading causes of blindness in the Western world. New pharmacologic treatment options have revolutionized the treatment armamentarium and provided true functional improvement in neovascular forms of the disease. However, complications of neovascular AMD such as major subretinal hemorrhages are still associated with a limited visual prognosis that could require vitreoretinal intervention.

This problem may be related to toxic effects of iron released from subretinal hemoglobin as well as an increased physical barrier for retinal diffusion and fibrotic changes.[46–48] Up to now, there is no consensus regarding how to treat subretinal hemorrhages associated with neovascular AMD, and most surgical treatment strategies seem not efficient in restoring or improving vision.[49]

A displacement of the hemorrhage may be achieved by intravitreally applied expansile gas combined with intravitreal injection of recombinant plasminogen activator (rTPA). However, the subretinal lytic effect of intravitreally applied rTPA was challenged by some authors due to its molecular size and the reduced retinal diffusion.[50,51] Therefore, a combination of intravitreal VEGF inhibitors to treat the underlying neovascular process combined with an injection of expansible gas is favored by some authors.[52]

There is clinical evidence that intravitreal rTPA in combination with expansile gas was in the long term more effective if combined

with subsequent anti-VEGF treatment than intravitreal bevacizumab in combination with expansile gas alone.[53] Other groups have suggested triple therapies using using rtPA, bevacizumab or ranibizumab, and have shown a successful management of the disease with this approach.[54] If rTPA and pneumatic displacement combination is contraindicated, an anti-VEGF monotherapy may be performed to prevent further visual loss.[55] However, after intravitreal injection of any agent combined with expansible gas a vitreous hemorrhage may occur, very often due to a displacement of the subretinal blood into the vitreous cavity. In these cases vitrectomy is indicated and may lead to good functional results.

An additional strategy is to perform a vitrectomy and apply rtPA subretinally followed by fluid gas exchange[56] to displace the hemorrhage. This approach led to visual improvement in some cases. The authors also reported that vitrectomy with subretinal injection of rtPA and intravitreal gas tamponade was more effective than vitrectomy with intravitreal injection of rtPA and gas in terms of complete displacement of the submacular blood.[57] Although functional improvement in the majority of patients suggests the absence of direct retinal toxicity of subretinally applied rtPA, vitrectomy and subretinal injection of rtPA carry a greater risk for postoperative complications.[57]

Despite good experiences in clinical use, experimental studies demonstrated dose-dependent negative effects of rtPA as seen by a significant and potentially irreversible reduction of the b-wave amplitude in ERG examination in bovine retinas.[58]

Visualization of the Vitreoretinal Interface

The application of vital dyes to visualize transparent and sometimes barely visible target structures such as the internal limiting membrane (ILM), epimacular membranes or vitreous has become very popular among vitreoretinal surgeons. The ILM is the main target structure for “chromodissection.” This is related to the fact that the ILM has been identified as an important scaffold for

cellular proliferation. In order to remove all cellular proliferations, vitreous collagen remnants, and relieve all relevant tractional forces, the ILM is dissected from the underlying tissue using the retinal surface of the ILM as a cleavage plane. The ILM can be removed without further visualization. A slight whitening of the retinal surface can be used as an indicator where ILM has been successfully peeled. However, this manoeuvre requires a lot of surgical experience and skills. The introduction of visualizing agents has made ILM peeling accessible even to the less experienced surgeon. Several dyes are in clinical use and can be applied to selectively visualize the target structure (Table 130.1).

TABLE 130.1

Dyes in Clinical Use That Can Be Applied to Selectively Visualize the Target Structure[a]

Dye	Epiretinal Membrane	ILM	Vitreous	Application[b]	Comments
Indocyanine green (ICG) (0.5%)	—	Selective +++	—	Usually fluid-filled globe	Question of toxicity, off-label
Brilliant blue G (BBG) (0.025%)	—	Selective ++	—	Fluid filled-globe (if heavy BBG is used)	Approved in Europe
Trypan blue (TB) (0.15%)	+++	(+)	(+)	Fluid- or air-filled globe	Approved in Europe
Bromophenol blue	+++	—	+	In combination with BBG	Approved in Europe
Triamcinolone (TA)	—	Non selective (+)	+++	Fluid filled-globe	No dye, pharmacologic properties
Fluorescein	—	—	+	Intravitreal, intravenous or peroral application	

[a]Several staining substances are available at present. There are differences mainly with regard to their selectivity and biocompatibility.

[b]Surgical techniques may vary depending on individual preference.

The dyes are either injected into the fluid-filled or air-filled globe and different concentrations are used. Fluid–air exchange can especially be avoided if the dye solution is heavier than water, which can be achieved with specific solvent media such as glucose 5% or deuterium oxide.[59]

Current Dyes for Epiretinal Membranes and the Internal Limiting Membrane

Epiretinal membranes can be stained using the anionic disazo dye trypan blue, which is commercially available in a concentration of 0.15% for that purpose. The contrast at the level of the ILM using trypan blue is quite poor. Bromophenol blue[60] is also approved for ERM staining, but is only available as a combination with brilliant blue (see below) as a dual stain. Two other dye classes are currently predominantly used for ILM peeling: The cyanine dye indocyanine green (ICG) and the triarylmethane dye brilliant blue G (BBG). Due to tissue dye interactions and alterations of its collagen structure, the stained ILM can be peeled off more easily and, postulating that the dye used provides a high biocompatibility, with less damage to underlying retinal structures such as the nerve fibres and Müller cell end feet. Both dyes selectively stain the ILM,[61] although the staining effect seen after ICG use appears more pronounced compared to BBG. In contrast to the good biocompatibility of BBG,[62] ICG has revealed toxic effects in some studies which underline the narrow safety margin of this dye.[63] Postoperative visual field defects and less favourable functional outcome have been described in the literature.

In addition, ICG appears not as an ideal candidate for ILM staining as its maximum absorption is in the near infrared and not within the spectral sensitivity of the human eye,[64] meaning that the majority of light absorption of ICG is useless or of low value during vitreoretinal surgery because it is in the invisible NIR and in the bathochromic region of the visible spectrum. As a consequence, relatively high dye concentrations of 0.5% are required and were used to achieve a sufficient contrast on the vitreoretinal interface in contrast to BBG, where concentrations of 0.025% are sufficient for ILM staining.

The availability of different dyes with selective staining properties allows for variable operative techniques and sequential "chromodissection" of the tissue. In theory, one could stain the vitreous using triamcinolone and stain epiretinal membranes using trypan blue, followed by ILM staining using BBG. In epiretinal membrane surgery, where the vitreous is detached already in most

cases, a reasonable approach is to peel the epiretinal membrane without adjuncts first, and then visualize the ILM and peel areas where ILM can be detected (Fig. 130.2). In macular hole surgery, the ILM can be stained without prior removal of epimacular tissue. However, some manufacturers offer combinations of ERM-staining dyes such as trypan blue or bromophenol blue and ILM staining dyes such as BBG suggesting that repeated dye injections can be avoided and potential toxicity can be thereby limited.

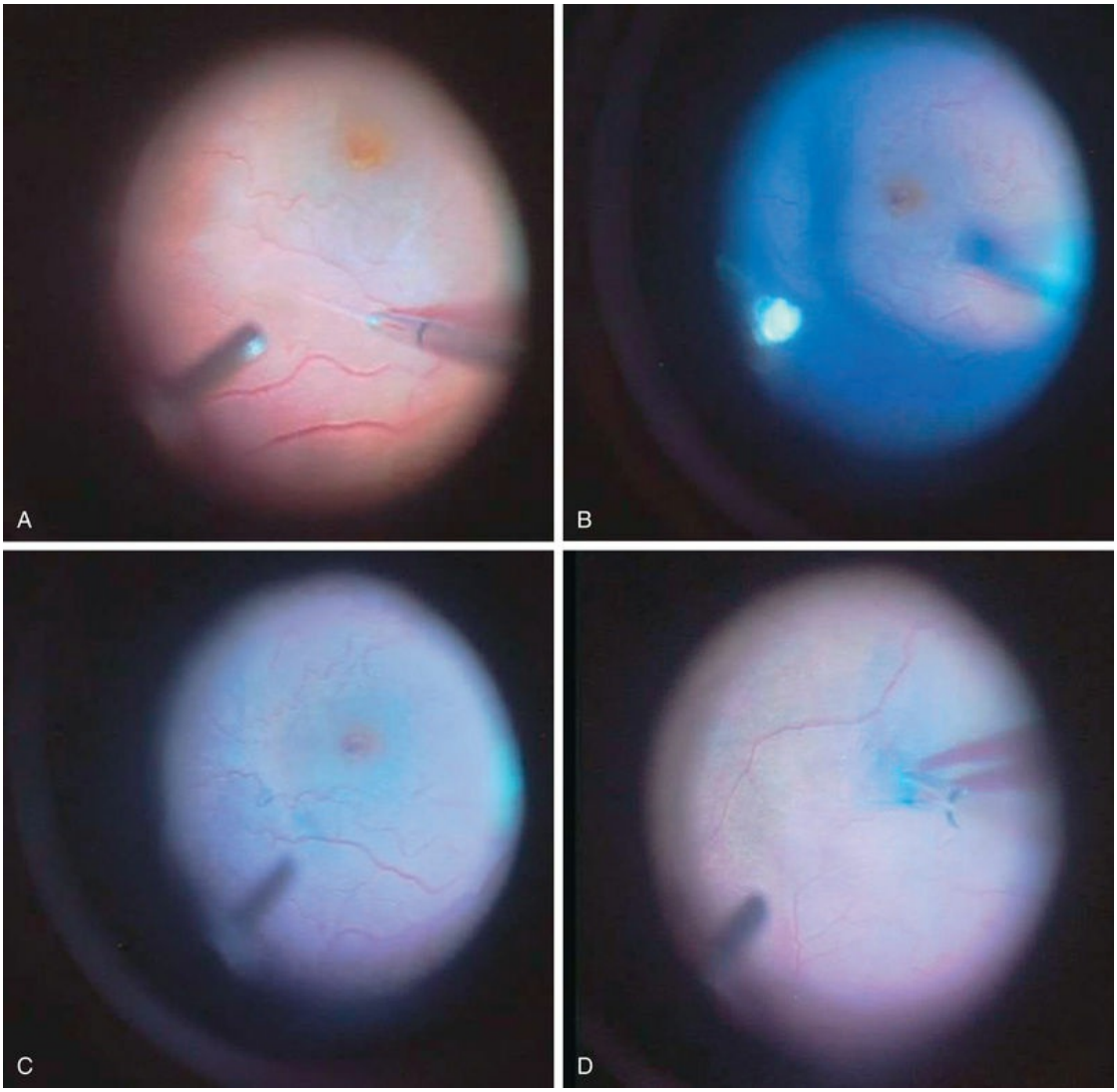

FIG. 130.2 (A) Preoperative fundus picture showing the epimacular membrane which is removed with an end-gripping forceps. (B) Heavy brilliant blue (BBG) is now applied over the macular area. (C) After removal of excessive dye, the internal limiting membrane (ILM) is easily detectable due to the selective staining

properties of BBG. (D) The stained ILM can be peeled off safely.

Perspectives

In general, any dye should be used with care as long as the tissue–dye interactions are not completely understood. There is an ongoing effort to identify better dyes with appropriate staining properties and a high biocompatibility. It seems that an ideal candidate dye would be a dye incorporating the excellent contrast provided by ICG and the high biocompatibility of BBG (i.e., strongly absorbing at visible wavelengths, conveniently binding tissue, non toxic, and physiologically degradable at a practical time scale). This may be reached by synthesizing new cyanine dyes and thereby improving the absorption qualities and the affinity of the dye molecule to the target structure.[65]

These new molecules provide improved absorption and fluorescent qualities and equal staining properties but potentially a better safety profile compared to ICG as it is adapted to the spectral sensitivity of the human eye and to the standard illumination used during surgery. In addition, the contrast is thereby enhanced as it implies both the blue absorption colour and an even stronger purple fluorescence colour. Additionally, several other absorbent dyes have been subjects of experimental in vivo and ex vivo experiments, including among others methyl violet, crystal violet, eosin Y, Sudan black B, methylene blue, toluidine blue, light green, indigo carmine, fast green, Congo red, evans blue, and lutein.[66–68]

VEGF Inhibitors in Vitreoretinal Surgery

Proliferative Diabetic Retinopathy and Macular Edema

The development of diabetic retinopathy is a multifactorial process. Much of the retinal damage that characterizes the disease is understood to result from retinal vascular leakage and

nonperfusion, mediated by numerous growth factors including vascular endothelial growth factor (VEGF).[69] High concentrations of VEGF have been identified in the vitreous of patients with proliferative diabetic retinopathy[70] indicating that VEGF plays a major part in mediating active intraocular neovascularization in patients with ischemic retinal diseases. The upregulation of VEGF is not only associated with a breakdown of the blood–retina barrier resulting in retinal edema, but also with a stimulation of endothelial cell growth and neovascularization.[71] Therefore, the inhibition of VEGF has become a widely used treatment option in these conditions. Available VEGF inhibitors include bevacizumab, ranibizumab, and aflibercept. For intraocular application, the drug is administered via the pars plana using a sterile 27- or 30-gauge needle.

The intravitreal injection of VEGF inhibitors is approved to treat center-involving macular edema associated with retinal ischemic disease such as diabetic macular edema or retinal vein occlusion. Nevertheless, another (at present "off label") indication for the intravitreal application of VEGF inhibitors might be the treatment of proliferative diabetic retinopathy,[72] resulting in a marked regression of neovascularization and possibly a resolution of vitreous hemorrhage within a short period of time in some cases. This treatment effect may be of relevance for patients awaiting vitrectomy for dense vitreous hemorrhage or traction retinal detachment associated with active proliferative vascular diseases (Fig. 130.3). The injection of VEGF inhibitors prior to vitrectomy does help to minimize the risk of perioperative bleeding from active neovascularization and reduces the incidence of postoperative intraocular hemorrhages.[73] It has been shown that the vascular component of proliferation is markedly reduced by day 10 post injection, whereas the contractile components are not yet impacted.[74] Therefore, patients having been treated with intravitreal injections of VEGF inhibitors before surgery should be followed on a daily basis, as an exacerbation of the tractional forces may occur due to fibrotic changes of the neovascularization and require immediate intervention. In clinical practice, vitrectomy could be scheduled 2–7 days after intravitreal injection since in most instances the marked reduction of neovascularization is usually

seen within 48 hours. This holds true for retinal neovascularizations as well as iris neovascularizations.

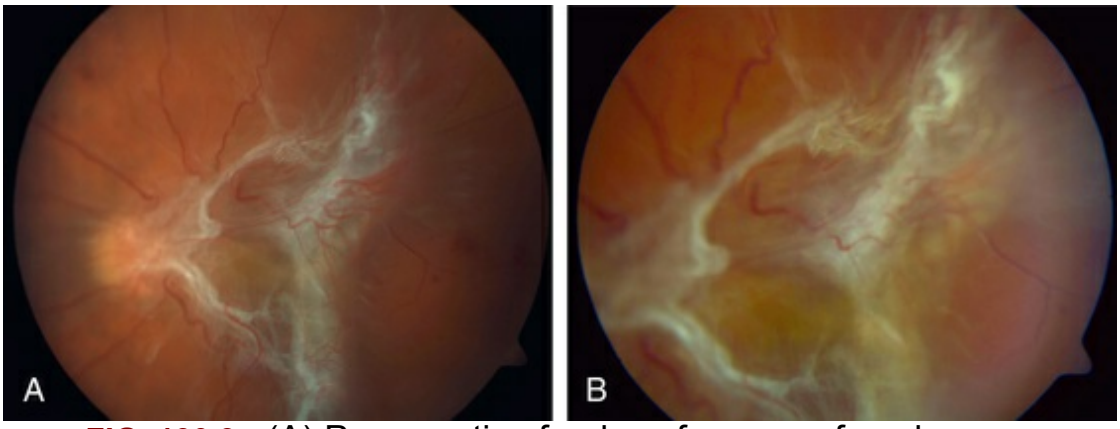

FIG. 130.3 (A) Preoperative fundus of a young female patient with proliferative diabetic retinopathy and massive traction at the posterior pole. Note the intensive vascularization within the fibrovascular membrane. Prior to scheduled vitrectomy bevacizumab (1.25 mg) was injected intravitreally. (B) Two days after intravitreal injection a marked regression of the vascularization was seen and vitrectomy was performed.

With this option of anti-VEGF-assisted vitrectomy, the surgical procedure in patients with active neovascularization at the retina or at the iris becomes safer and more controlled, since the danger of major intraoperative bleeding is markedly reduced.

In addition, some case reports have demonstrated that injection of bevacizumab at the end of vitreous surgery can reduce the recurrence of hemorrhages after vitrectomy.[75]

Retinopathy of Prematurity

Retinopathy of prematurity is a disease of the immature retina affecting children before 31 weeks' gestational age (see Chapter 65, Telescreening for retinopathy of prematurity). It represents one of the three leading causes of legal blindness in childhood in the developed countries. The pathophysiology of the disease implies tissue hypoxia resulting in an upregulation of VEGF and the development of abnormal retinal fibrovascular tissue leading to

tractional retinal detachment and vision loss in progressive stages. The well-established treatment option for this condition is peripheral retinal ablation with conventional (confluent) laser therapy. However, laser photocoagulation is destructive and may cause complications later on. In addition, it does not prevent all vision loss, especially in cases of ROP affecting zone I of the eye.[76] Since the introduction of VEGF inhibitors for the treatment of neovascular diseases, such as AMD, diabetic retinopathy, or retinal vein occlusion, case series described a positive effect of single injections of the VEGF inhibitor bevacizumab in ROP,[77] indicating that this agent may be a useful alternative to laser ablation, especially as it is not destructive to retinal tissue. As a rule this agent is applied only once in this diseases.

A recent prospective, controlled, randomized, multicenter trial compared the effect of a 0.625-mg intravitreal bevacizumab monotherapy for zone I or zone II posterior stage 3+ (i.e., stage 3 with plus disease) to conventional laser therapy.[78] The recurrence of ROP in one or both eyes requiring retreatment before 54 weeks postmenstrual was the primary ocular outcome. The study revealed that intravitreal bevacizumab monotherapy, as compared with conventional laser therapy, in infants with stage 3+ ROP is associated with a significant benefit for zone I but not zone II disease. While development of peripheral retinal vessels continued after treatment with intravitreal bevacizumab, conventional laser therapy led to permanent destruction of the peripheral retina. However, as compared with conventional laser therapy in treating patients with zone I retinopathy of prematurity, intravitreal bevacizumab represents a true breakthrough in disease management of ROP.

Therefore, based on the current literature, the use of VEGF inhibitors in retinopathy of prematurity may provide an advantage compared to laser treatment for acute zone I or zone II posterior stage 3+ disease. A monotherapy using VEGF inhibitors appears advantageous when media opacities such as a tunica vasculosa or hemorrhages in the anterior or posterior segment preclude diode laser photocoagulation.[79] In contrast, the treatment with VEGF inhibitors should be avoided in stage 4 or 5 disease, as fibrotic changes may be accelerated leading to traction retinal detachment.

Whether a combination of anti-VEGF treatment in combination with vitrectomy in stage 4 or 5 disease in ROP has advantages has not yet been examined. Also, it is not known whether the combination of bevacizumab and laser treatment has advantages.

As intravitreal bevacizumab reaches the systemic circulation[80] of the infant there are concerns of negative systemic effects, which have not been demonstrated up to now. However, vigilance is mandatory, and a longer follow-up of patients will help us to outline the best concentration of the agent and the indications (and relative contraindications) for the use of VEGF inhibitors for retinopathy of prematurity.

Neovascular Glaucoma

Another indication for the use of VEGF inhibitors is neovascular glaucoma. Neovascular glaucoma is still a sight-threatening complication of retinal ischemia as seen in a variety of diseases such as diabetic retinopathy or retinal vascular occlusion. Vitrectomy for conditions associated with neovascular glaucoma has been considered, resulting in very bad results. Therefore neovascular glaucoma has to be controlled before vitrectomy. The first-line treatment is laser photocoagulation of ischemic areas of the retina in order to prevent a progression of the neovascularization and to finally stop neovascularization at the iris. In cases where the retina cannot be visualized due to media opacities such as corneal edema or vitreous hemorrhage, transscleral retinal cryotherapy can be performed instead.[81] Vitrectomy and endolaser photocoagulation is indicated in the presence of retinal detachment, progressive disease, or in the presence of vitreous hemorrhage. While filtration surgery often fails in neovascular glaucoma, laser cyclophotocoagulation or cyclocryotherapy are effective means to lower intraocular pressure (IOP) with fewer complications seen after laser cyclophotocoagulation. Vitrectomy with peripheral retinectomy had also been suggested as a treatment for neovascular glaucoma, but retinal complications are frequent.[82] However, despite several treatment modalities being available functional outcome is often unfavourable. Therefore the addition of pharmacotherapy to vitreoretinal surgery in such cases is almost mandatory today.

Again anti-VEGF substances are used.

Several studies[83] have shown that the monoclonal antibody bevacizumab can be used intravitreally as well as intracamerally to reduce not only retinal, but also iris and anterior chamber angle neovascularization (Fig. 130.4). Often, the regression of iris and chamber angle neovascularization is followed by a fast and effective decrease of IOP. However, recurrence of increased IOP is frequent.[84] Therefore, the intracameral application of VEGF inhibitors may extend our therapeutic options in the management of neovascular glaucoma, especially as other options such as photocoagulation of ischemic retinal areas alone may not be sufficient to prevent the progression of neovascular glaucoma, and reduce the need for IOP-lowering drugs. The early treatment effect seen after intracameral application of VEGF inhibitors may also help to bridge the time until the treatment effect of other strategies, such as laser photocoagulation, is noted. Almost as a rule, iris neovascularization is gone within 24 hours after intraocular injection of bevacizumab, and necessary vitreoretinal surgery can be performed one day after injection if needed.

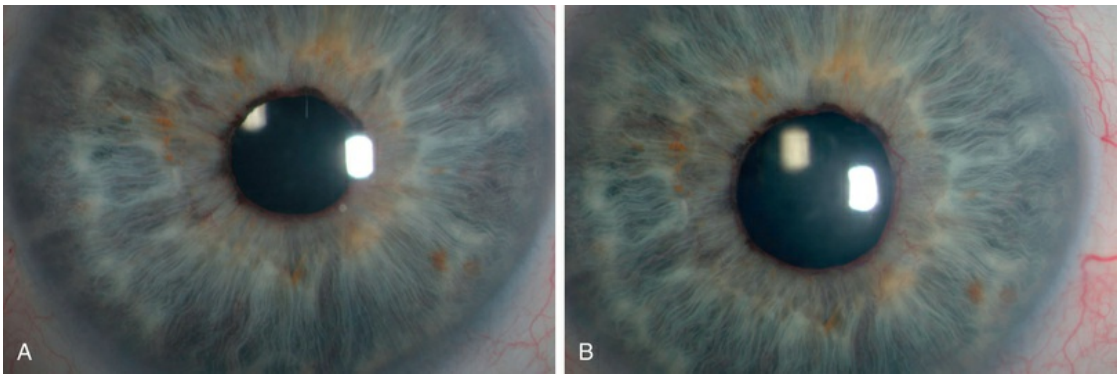

FIG. 130.4 (A) Rubeosis iridis seen in a patient with neovascular glaucoma. (B) Five days after intracameral injection of bevacizumab a marked regression of the neovascularization is seen and a drop of intraocular pressure occurred.

Endophthalmitis

Endophthalmitis is a serious intraocular inflammatory condition

sometimes requiring immediate vitreoretinal intervention. It can be the result of exogenous or endogenous spread of infecting organisms into the eye (see Chapter 125, Infectious endophthalmitis). The prognosis for visual function is often poor independently from the etiology of the disease. Exogenous endophthalmitis is mostly seen after ophthalmic surgical procedures. As cataract surgery is the most frequently performed surgery in ophthalmology, 90% of exogenous endophthalmitis cases are related to this operation.[85] The incidence is reported to range between 0.08% and 0.7%.[86,87]

Endogenous endophthalmitis is less common. It results from secondary hematogenous dissemination and spread from a distant infective source in the body. Therefore, predisposing risk factors should be carefully evaluated when checking the patient's medical history.

Although the incidence of endophthalmitis has decreased over the years due to continuous improvement of preoperative disinfection[88] and perioperative prophylaxis, endophthalmitis is still a very severe disease with indistinct prognosis and requires immediate intervention to maintain at least a possibility of visual recovery. Early diagnosis and treatment with antimicrobial therapy are crucial. Therapy is usually initiated empirically while microbiologic testing of intraocular samples, obtained for example during vitrectomy in severe cases, is being performed. After culturing and identification of the causing organism the spectrum of the antimicrobial therapy may be altered according to the sensitivity of the pathogen. However, unless there is no other unequivocal result from culturing, endophthalmitis therapy should cover both gram-positive organisms, which play a predominant role in exogenous endophthalmitis, and gram-negative organisms, as they are associated with higher virulence and poorer outcome. According to the literature, current antibiotic standard protocols for intravitreal application include the peptide antibiotic vancomycin (1.0 mg/0.1 mL) for gram-positive coverage[89,90] in combination with the β-lactam antibiotic ceftazidime (2.25 mg/0.1 mL) for gram-negative coverage. In patients hypersensitive to β-lactam drugs, amikacin (400 μg/0.1 mL), an aminoglycoside antibiotic, might be considered instead of ceftazidime.[89]

Other antibiotics such as fluoroquinolone, especially the recently developed third- and fourth-generation such as levofloxacin and moxifloxacin, have been discussed as a potential alternative treatment for gram-positive pathogens due to their enhanced activity.[89]

In addition to antibiotics, corticosteroids are commonly used as adjunctive treatment both in bacterial as well in fungal endophthalmitis. The antiinflammatory properties of these drugs may help modulate the inflammatory response to the infection itself and decrease secondary damage. They may be applied topically, under the conjunctiva, intravenously, or intravitreally. However, their use and mode of application in endophthalmitis remains a subject of debate. If surgery is required for such cases in all instances a combination of surgery and intraocular pharmacotherapy is standard of care.

Conclusion

Pharmacologic therapy has become an important field in ophthalmic surgery. Recent developments include microplasmin as an adjunct in vitreoretinal surgery to induce a posterior vitreous detachment and release traction at the vitreoretinal interface, as well as the inhibition of VEGF to prevent vitreal hemorrhages as a result of vitreoretinal surgery in proliferative vitreoretinal diseases, such as diabetic retinopathy, and to prevent progression and sight-threatening complications of retinopathy of prematurity as well as to treat neovascular glaucoma. Tissue plasminogen activator can be used as an adjunct in the treatment of submacular hemorrhages. Recent developments also include the introduction of vital dyes to selectively visualize layers of the vitreoretinal interface in macular surgery. Intravitreal application of antibiotics and steroids have become a standard treatment for intraocular infections such as endophthalmitis. Despite these refinements no effective pharmacologic treatment options are currently available for other blinding conditions such as proliferative vitreoretinopathy.

References

1. Robison CD, Krebs I, Binder S, et al. Vitreomacular adhesion in active and end-stage age-related macular degeneration. *Am J Ophthalmol*. 2009;148(1):79–82.
2. Gandorfer A, Messmer EM, Ulbig MW, et al. Resolution of diabetic macular edema after surgical removal of the posterior hyaloid and the inner limiting membrane. *Retina*. 2000;20:126–133.
3. Mayr-Sponer U, Waldstein SM, Kundi M, et al. Influence of the vitreomacular interface on outcomes of ranibizumab therapy in neovascular age-related macular degeneration. *Ophthalmology*. 2013;120(12):2620–2629.
4. Haritoglou C, Gass CA, Schaumberger M, et al. Macular changes after peeling of the internal limiting membrane in macular hole surgery. *Am J Ophthalmol*. 2001;132:363–369.
5. Sebag J. Pharmacologic vitreolysis. *Retina*. 1998;18(1):1–3.
6. Bishop PN. Vitreous as a substrate for vitreolysis. *Dev Ophthalmol*. 2009;44:7–19.
7. Sebag J, Ansari RR, Suh KI. Pharmacologic vitreolysis with microplasmin increases vitreous diffusion coefficients. *Graefes Arch Clin Exp Ophthalmol*. 2007;245(4):576–580.
8. de Smet MD, Valmaggia C, Zarranz-Ventura J, et al. Microplasmin: ex vivo characterization of its activity in porcine vitreous. *Invest Ophthalmol Vis Sci*. 2009;50(2):814–819.
9. Chen W, Huang X, Ma XW, et al. Enzymatic vitreolysis with recombinant microplasminogen and tissue plasminogen activator. *Eye (Lond)*. 2008;22(2):300–307.
10. Gandorfer A, Rohleder M, Sethi C, et al. Posterior vitreous detachment induced by microplasmin. *Invest Ophthalmol Vis Sci*. 2004;45(2):641–647.
11. Stalmans P, Delaey C, de Smet MD, et al. Intravitreal injection of microplasmin for treatment of vitreomacular adhesion: results of a prospective, randomized, sham-controlled phase II trial (the MIVI-IIT trial). *Retina*. 2010;30(7):1122–1127.
12. Benz MS, Packo KH, Gonzalez V, et al. A placebo-controlled trial of microplasmin intravitreous injection to facilitate posterior vitreous detachment before vitrectomy.

Ophthalmology. 2010;117(4):791–797.
13. Stalmans P, Benz MS, Gandorfer A, et al. MIVI-TRUST Study Group. Enzymatic vitreolysis with ocriplasmin for vitreomacular traction and macular holes. *N Engl J Med*. 2012;367(7):606–615.
14. Schumann RG, Wolf A, Mayer WJ, et al. Pathology of internal limiting membrane specimens following intravitreal injection of ocriplasmin. *Am J Ophthalmol*. 2015;160(4):767–778.
15. Sebag J, Ansari RR, Suh KI. Pharmacologic vitreolysis with microplasmin increases vitreous diffusion coefficients. *Graefes Arch Clin Exp Ophthalmol*. 2007;245(4):576–580.
16. Quiram PA, Leverenz VR, Baker RM, et al. Microplasmin-induced posterior vitreous detachment affects vitreous oxygen levels. *Retina*. 2007;27(8):1090–1096.
17. Stefánsson E. Physiology of vitreous surgery. *Graefes Arch Clin Exp Ophthalmol*. 2009;247(2):147–163.
18. Verstraeten TC, Chapman C, Hartzer M, et al. Pharmacologic induction of posterior vitreous detachment in the rabbit. *Arch Ophthalmol*. 1993;111(6):849–854.
19. Johnson MW, Fahim AT, Rao RC. Acute ocriplasmin retinopathy. *Retina*. 2015;35(6):1055–1058.
20. Shah SP, Jeng-Miller KW, Fine HF, et al. Post-marketing survey of adverse events following ocriplasmin. *Ophthalmic Surg Lasers Imaging Retina*. 2016;47(2):156–160.
21. Diaz-Llopis M, Udaondo P, Arevalo F, et al. Intravitreal plasmin without associated vitrectomy as a treatment for refractory diabetic macular edema. *J Ocul Pharmacol Ther*. 2009;25(4):379–384.
22. Elbendary AM, Elwan MM, Azzam HA, et al. Predictability of vitreous detachment following intravitreal plasmin injection in diabetic macular edema associated with vitreomacular traction. *Curr Eye Res*. 2011;36(6):534–539.
23. Udaondo P, Díaz-Llopis M, García-Delpech S, et al. Intravitreal plasmin without vitrectomy for macular edema secondary to branch retinal vein occlusion. *Arch Ophthalmol*. 2011;129(3):283–287.
24. Wu WC, Drenser KA, Lai M, et al. Plasmin enzyme-assisted

vitrectomy for primary and reoperated eyes with stage 5 retinopathy of prematurity. *Retina*. 2008;28(3 Suppl.):S75–80.
25. Wu WC, Drenser KA, Trese MT, et al. Pediatric traumatic macular hole: results of autologous plasmin enzyme-assisted vitrectomy. *Am J Ophthalmol*. 2007;144(5):668–672.
26. Sakuma T, Tanaka M, Inoue M, et al. Efficacy of autologous plasmin for idiopathic macular hole surgery. *Eur J Ophthalmol*. 2005;15(6):787–794.
27. Margherio AR, Margherio RR, Hartzer M, et al. Plasmin enzyme-assisted vitrectomy in traumatic pediatric macular holes. *Ophthalmology*. 1998;105(9):1617–1620.
28. Hirata A, Takano A, Inomata Y, et al. Plasmin-assisted vitrectomy for management of proliferative membrane in proliferative diabetic retinopathy: a pilot study. *Retina*. 2007;27(8):1074–1078.
29. Rizzo S, Pellegrini G, Benocci F, et al. Autologous plasmin for pharmacologic vitreolysis prepared 1 hour before surgery. *Retina*. 2006;26(7):792–796.
30. Hollborn M, Tenckhoff S, Jahn K, et al. Changes in retinal gene expression in proliferative vitreoretinopathy: glial cell expression of HB-EGF. *Mol Vis*. 2005;11:397–413.
31. Coblentz FE, Radeke MJ, Lewis GP, et al. Evidence that ganglion cells react to retinal detachment. *Exp Eye Res*. 2003;76:333–342.
32. Fisher SK, Lewis GP. Müller cell and neuronal remodelling in retinal detachment and reattachment and their potential consequences for visual recovery: a review and reconsideration of recent data. *Vision Res*. 2003;43:887–897.
33. Francke M, Faude F, Pannicke T, et al. Glial cell-mediated spread of retinal degeneration during detachment: a hypothesis based upon studies in rabbits. *Vision Res*. 2005;45:2256–2267.
34. Fisher SK, Erickson PA, Lewis GP, et al. Intraretinal proliferation induced by retinal detachment. *Invest Ophthalmol Vis Sci*. 1991;32:1739–1748.
35. Anderson DH, Guerin CJ, Erickson PA, et al. Morphological recovery in the reattached retina. *Invest Ophthalmol Vis Sci*.

1986;27:168–183.
36. Charteris DG, Downie J, Aylward GW, et al. Intraretinal and periretinal pathology in anterior proliferative vitreoretinopathy. *Graefes Arch Clin Exp Ophthalmol*. 2007;245:93–100.
37. Lewis GP, Sethi CS, Linberg KA, et al. Experimental retinal reattachment: a new perspective. *Mol Neurobiol*. 2003;28:159–175.
38. Shen WG, Peng WX, Shao Y, et al. Localization and activity of calmodulin is involved in cell–cell adhesion of tumor cells and endothelial cells in response to hypoxic stress. *Cell Biol Toxicol*. 2007;23:323–335.
39. Kirchhof B. Strategies to influence PVR development. *Graefes Arch Clin Exp Ophthalmol*. 2004;242:699–703.
40. Cai J, Wei R, Ma X, et al. Cytotoxic effects of antiproliferative agents on human retinal glial cells in vitro. *Int Ophthalmol*. 2001;24:225–231.
41. Charteris DG, Aylward GW, Wong D, PVR Study Group, et al. A randomised controlled trial of combined 5-fluouracil and low-molecular weight heparin in management of established proliferative vitreoretinopathy. *Ophthalmology*. 2004;111:2240–2245.
42. Chandler DB, Hida T, Rozakis G, et al. The lack of an effect of intraocular steroids on irradiated fibroblasts in experimental proliferative vitreoretinopathy. *Graefes Arch Clin Exp Ophthalmol*. 1992;230(2):188–191.
43. Eibl KH, Lewis GP, Betts K, et al. The effect of alkylphosphocholines on intraretinal proliferation initiated by experimental retinal detachment. *Invest Ophthalmol Vis Sci*. 2007;48:1305–1311.
44. Schuettauf F, Eibl KH, Thaler S, et al. Toxicity study of erucylphosphocholine in a rat model. *Curr Eye Res*. 2005;30:813–820.
45. Eibl KH, Liegl R, Kernt M, et al. Alkylphosphocholines as a potential pharmacologic prophylaxis for posterior capsule opacification. *J Cataract Refract Surg*. 2009;35(5):900–905.
46. Avery RL, Fekrat S, Hawkins BS, et al. Natural history of subfoveal subretinal hemorrhage in age-related macular

degeneration. *Retina*. 1996;16:183–189.
47. Scupola A, Coscas G, Soubrane G, et al. Natural history of macular subretinal hemorrhage in age-related macular degeneration. *Ophthalmologica*. 1999;213:97–102.
48. Toth CA, Morse LS, Hjelmeland LM, et al. Fibrin directs early retinal damage after experimental subretinal hemorrhage. *Arch Ophthalmol*. 1991;109:723–729.
49. Bressler NM, Bressler SB, Childs AL, et al. Surgery for hemorrhagic choroidal neovascular lesions of age-related macular degeneration: ophthalmic findings: SST report no. 13. *Ophthalmology*. 2004;111:1993–2006.
50. Ohji M, Saito Y, Hayashi A, et al. Pneumatic displacement of subretinal hemorrhage without tissue plasminogen activator. *Arch Ophthalmol*. 1998;116:1326–1332.
51. Kamei M, Misono K, Lewis H. A study of the ability of tissue plasminogen activator to diffuse into the subretinal space after intravitreal injection in rabbits. *Am J Ophthalmol*. 1999;128:739–746.
52. Hohn F, Mirshahi A, Hattenbach LO. Combined intravitreal injection of bevacizumab and SF(6) gas for treatment of submacular hemorrhage secondary to age-related macular degeneration. *Ophthalmologe*. 2010;107(4):328–332.
53. Mayer WJ, Hakim I, Haritoglou C, et al. Efficacy and safety of recombinant tissue plasminogen activator and gas versus bevacizumab and gas for subretinal haemorrhage. *Acta Ophthalmol*. 2013;91(3):274–278.
54. Guthoff R, Guthoff T, Meigen T, et al. Intravitreous injection of bevacizumab, tissue plasminogen activator, and gas in the treatment of submacular hemorrhage in age-related macular degeneration. *Retina*. 2011;31:36–40.
55. Sacu S, Stifter E, Vecsei-Marlovits PV, et al. Management of extensive subfoveal haemorrhage secondary to neovascular age-related macular degeneration. *Eye*. 2009;23:1404–1410.
56. Treumer F, Klatt C, Roider J, et al. Subretinal coapplication of recombinant tissue plasminogen activator and bevacizumab for neovascular age-related macular degeneration with submacular haemorrhage. *Br J Ophthalmol*. 2010;94(1):48–53.

57. Hillenkamp J, Surguch V, Framme C, et al. Management of submacular hemorrhage with intravitreal versus subretinal injection of recombinant tissue plasminogen activator. *Graefes Arch Clin Exp Ophthalmol*. 2010;248:5–11.
58. Luke M, Januschowski K, Warga M, et al. The retinal tolerance to bevacizumab in co-application with a recombinant tissue plasminogen activator. *Br J Ophthalmol*. 2007;91:1077–1082.
59. Haritoglou C, Schumann RG, Kampik A, et al. Heavy brilliant blue G for internal limiting membrane staining. *Retina*. 2011;31(2):405–407.
60. Haritoglou C, Schumann RG, Strauss R, et al. Vitreoretinal surgery using bromphenol blue as a vital stain: evaluation of staining characteristics in humans. *Br J Ophthalmol*. 2007;91(9):1125–1128.
61. Henrich PB, Priglinger SG, Haritoglou C, et al. Quantification of contrast recognizability during brilliant blue G (BBG) and indocyanine green (ICG) assisted chromovitrectomy. *Invest Ophthalmol Vis Sci*. 2011;52(7):4345–4349.
62. Lüke M, Januschowski K, Beutel J, et al. Electrophysiological effects of Brilliant Blue G in the model of the isolated perfused vertebrate retina. *Graefes Arch Clin Exp Ophthalmol*. 2008;246(6):817–822.
63. Haritoglou C, Gandorfer A, Gass CA, et al. Indocyanine green-assisted peeling of the internal limiting membrane in macular hole surgery affects visual outcome: a clinicopathologic correlation. *Am J Ophthalmol*. 2002;134(6):836–841.
64. Langhals H, Haritoglou C. Chemical and spectroscopic aspects of the application of dyes in vitreoretinal surgery. *Ophthalmologe*. 2009;106(1):16–20.
65. Langhals H, Varja A, Laubichler P, et al. Cyanine dyes as optical contrast agents for ophthalmological surgery. *J Med Chem*. 2011;54(11):3903–3925.
66. Jackson TL, Griffin L, Vote B, et al. An experimental method for testing novel retinal vital stains. *Exp Eye Res*. 2005;81(4):446–454.

67. Rodrigues EB, Penha FM, de Paula Fiod Costa E, et al. Ability of new vital dyes to stain intraocular membranes and tissues in ocular surgery. *Am J Ophthalmol*. 2010;149(2):265–277.
68. Casaroli-Marano RP, Sousa-Martins D, Martínez-Conesa EM, et al. Dye solutions based on lutein and zeaxanthin: in vitro and in vivo analysis of ocular toxicity profiles. *Curr Eye Res*. 2015;40(7):707–718.
69. Adamis AP, Miller JW, Bernal MT, et al. Increased vascular endothelial growth factor levels in the vitreous of eyes with proliferative diabetic retinopathy. *Am J Ophthalmol*. 1994;118:445–450.
70. Aiello LP, Avery RL, Arrigg PG, et al. Vascular endothelial growth factor in ocular fluid of patients with diabetic retinopathy and other retinal disorders. *N Engl J Med*. 1994;331(22):1480–1487.
71. Frank RN, Amin RH, Eliott D, et al. Basic fibroblast growth factor and vascular endothelial growth factor are present in epiretinal and choroidal neovascular membranes. *Am J Ophthalmol*. 1996;122:393–403.
72. Spaide RF, Fisher YL. Intravitreal bevacizumab (Avastin) treatment of proliferative diabetic retinopathy complicated by vitreous hemorrhage. *Retina*. 2006;26:275–278.
73. Abdelhakim MA, Macky TA, Mansour KA, et al. Bevacizumab (Avastin) as an adjunct to vitrectomy in the management of severe proliferative diabetic retinopathy: a prospective case series. *Ophthalmic Res*. 2011;45(1):23–30.
74. El-Sabagh HA, Abdelghaffar W, Labib AM, et al. Preoperative intravitreal bevacizumab use as an adjuvant to diabetic vitrectomy: histopathologic findings and clinical implications. *Ophthalmology*. 2011;118(4):636–641.
75. Cheema RA, Mushtaq J, Al-Khars W, et al. Role of intravitreal bevacizumab (Avastin) injected at the end of diabetic vitrectomy in preventing postoperative recurrent vitreous hemorrhage. *Retina*. 2010;30(10):1646–1650.
76. Reynolds JD. Bevacizumab for retinopathy of prematurity. *N Engl J Med*. 2011;364:677–678.
77. Lalwani G, Berrocal A, Murray T, et al. Off-label use of

intravitreal bevacizumab (Avastin) for salvage treatment in progressive threshold retinopathy of prematurity. *Retina*. 2008;28:13–18.
78. Mintz-Hittner HA, Kennedy KA, Chuang AZ. BEAT-ROP Cooperative Group. Efficacy of intravitreal bevacizumab for stage 3+ retinopathy of prematurity. *N Engl J Med*. 2011;364(7):603–615.
79. Oberacher-Velten IM, Helbig H. VEGF antibodies as therapy for retinopathy of prematurity. *Klin Monatsbl Augenheilkd*. 2010;227(9):694–700.
80. Bakri SJ, Snyder MR, Reid JM, et al. Pharmacokinetics of intravitreal bevacizumab (Avastin). *Ophthalmology*. 2007;114:855–859.
81. Caprioli J, Strang SL, Spaeth GL, et al. Cyclocryotherapy in the treatment of advanced glaucoma. *Ophthalmology*. 1985;92:947–954.
82. Schlote T, Bartz-Schmidt KU. Treatment of rubeotic secondary glaucoma. Joussen AM, Gardner T, Kirchhof B, et al. *Retinal vascular disease*. Springer: Heidelberg; 2007:274–282.
83. Grisanti S, Biester S, Peters S, et al. Intracameral bevacizumab for iris rubeosis. *Am J Ophthalmol*. 2006;142:158–160.
84. Wolf A, von Jagow B, Ulbig M, et al. Intracameral injection of bevacizumab for the treatment of neovascular glaucoma. *Ophthalmologica*. 2011;226(2):51–56.
85. Essex RW, Yi Q, Charles PG, et al. Post-traumatic endophthalmitis. *Ophthalmology*. 2004;111(11):2015–2022.
86. Javitt JC, Street DA, Tielsch JM, et al. National outcomes of cataract extraction. Retinal detachment and endophthalmitis after outpatient cataract surgery. Cataract Patient Outcomes Research Team. *Ophthalmology*. 1994;101(1):100–105.
87. Mamalis N, Nagpal M, Nagpal K, et al. Endophthalmitis following cataract surgery. *Ophthalmol Clin North Am*. 2001;14(4):661–674.
88. Ta CN, Singh K, Egbert PR, et al. Prospective comparative evaluation of povidone-iodine (10% for 5 minutes versus

5% for 1 minute) as prophylaxis for ophthalmic surgery. *J Cataract Refract Surg*. 2008;34(1):171–172.
89. Kernt M, Kampik A. Endophthalmitis: pathogenesis, clinical presentation, management, and perspectives. *Clin Ophthalmol*. 2010;4:121–135.
90. Results of the Endophthalmitis Vitrectomy Study. A randomized trial of immediate vitrectomy and of intravenous antibiotics for the treatment of postoperative bacterial endophthalmitis. Endophthalmitis Vitrectomy Study Group. *Arch Ophthalmol*. 1995;113(12):1479–1496.

131

Complications in Vitreoretinal Surgery

Kourous A. Rezaei

A complication is an unanticipated event that arises either from the original disease, the treatment, an independent cause, or a combination of above. As surgeons we are trained to predict and treat expected events during surgery. However, unexpected events are the ones that are most dangerous and usually lead to undesirable outcomes. In general, the question is not whether an unexpected event will happen but when it will occur. The early recognition of an impending unexpected event is crucial for its successful management.

The knowledge of how to predict, treat, and prevent unexpected events during surgery is extremely valuable and would make vitreoretinal surgery safer, leading to improved visual outcome for patients. The more one is acquainted with unexpected events the less they are considered "unexpected" since one has already seen these events happen and knows how they were handled and therefore the factor of surprise is eliminated.

In this chapter, experienced surgeons from around the world share with you their unexpected experiences during retinal surgery and show how they handled some of the most unusual surgical cases. Further, they share their surgical pearls on how to predict, prevent, and treat these unusual surgical situations.

Subluxated Intraocular Lens Without Haptics

Renaud Duval

Removal of intraocular foreign bodies usually relies on the use of forceps or magnets (in the case of magnetic objects). Removing a round, smooth optic of an intraocular lens (IOL) that is missing both haptics cannot be done in the usual fashion. Using forceps

would damage the underlying macula. However, a 25-gauge (G) soft-tip cannula placed on the extrusion line can induce sufficient vacuum to lift the IOL to a position where it can be grasped safely. This technique should be kept in mind when dealing with light foreign bodies that lack grasping points.

In Video 131.1, a 72-year-old patient is presented with a history of blunt trauma to the left eye leading to superior iris loss and IOL expulsion from the globe through a superior sclerolimbal rupture. Following primary repair by a general ophthalmologist, the patient was referred for management of aphakia and vitreous hemorrhage. The hemorrhage cleared over the ensuing weeks, and the patient was reoperated for peeling of an epiretinal membrane followed by correction of aphakia with a scleral-fixated IOL.

After removal of the vitreous hemorrhage and indocyanine green-assisted peel of the epiretinal membrane, a three-piece IOL was injected into the eye through a 2.75-mm clear corneal incision and the haptics were externalized through sulcus-based sclerotomies. While attempting to tuck the second haptic into its intrascleral tunnel, sudden motion of the forceps caused by forcing against an overly tight tunnel led to separation of the haptic from the optic. Subsequent maneuvers to cut the IOL and remove it by the "pacman" technique led to the separation of the second haptic and complete dislocation of the now haptic-less optic on the macular surface. Creating a wider scleral pocket and avoiding the use of the haptics to stabilize the IOL while cutting it for explantation may have minimized the risk of haptic separation.

Posterior Synechiae and Small Pupil During Vitrectomy

Ehab El Rayes

Posterior synechiae secondary to inflammation may lead to miotic pupil and limit visualization during vitrectomy surgery. Additional pharmacotherapy may be applied for dilation; however, it has a limited role when posterior synechiae are present. Mechanical stretching of the pupil would be the next option. To safely dilate the pupil one may either use iris hooks or iris

stretching rings such as the Malyugin ring (MicroSurgical Technology (MST), Redmond, WA) or the Morcher ring (FCI Ophthalmics, Pembroke, MA).

In this Video 131.2 a Morcher ring, a 7-mm PMMA ring, is introduced into the anterior chamber by dialing it in through a 2-mm corneal incision. The inferior pupillary margin is engaged first, thus providing a 6-mm opening for visualization. Viscoelastic is injected into the anterior chamber to maintain the depth and to keep the media clear. Removing the cataract can easily be performed through the ring which maintains a dilated pupil (even in cases with floppy iris). Phacoemulsification and IOL implantation are performed. Identifying the tip of the infusion cannula before starting the vitrectomy is important and can now be easily achieved through a dilated pupil and clear media. Vitrectomy is carried out in the usual manner. Once the posterior segment procedure is completed, the Morcher ring will be removed by dislodging it from the pupillary margin and then dialing it clock- or anticlockwise, via the corneal incision, to exit the eye.

Induction of PVD in Retinal Detachment

Andre Gomes

Inducing posterior vitreous detachment (PVD) is a key step during vitrectomy surgery for retinal detachment. Induction of PVD; however, is not always easy and the strong vitreoretinal adherence especially in young patients can make this step challenging.

The patient in Video 131.3 presented with strongly adherent posterior hyaloid and a thin and mobile retina. The induction of PVD was first attempted in the usual manner by applying suction over the peripapillary area followed by suction at more peripheral areas of the fundus. These attempts were followed by using microserrated forceps and end-grasping forceps in an attempt to peel the internal limiting membrane (ILM) while the posterior hyaloid was still attached. To improve the visualization of ILM, brilliant blue dye was injected into the eye. Attention was given to

prevent any subretinal exposure. Inducing openings in the posterior hyaloid/ILM/retina interface allowed fluid to gain access underneath the posterior hyaloid and make the induction of PVD easier. Peeling the ILM in patients with adherent posterior hyaloid can make the induction of PVD easier and safer.

Induction of PVD in High Myopia

Ramin Tadayoni

One surgical challenge during vitrectomy for retinal detachment in high myopia is the induction of posterior vitreous detachment, which is one of the initial steps of the surgery. Missing this step may cause postoperative complications including increased risk for retinal redetachment.

This technical difficulty in high myopia is generally a combination of poor visualization of the posterior hyaloid, presence of vitreoschisis, and the strong adhesion of the posterior hyaloid to the surface of the retina, particularly in younger patients. The strongly adherent posterior hyaloid associated with large pockets of liquefied vitreous may make the usual techniques used for the PVD induction not very successful. Further, in high myopia the presence of vitreoschisis may give the appearance of posterior hyaloid separation while in fact the hyaloid is still attached. Visualizing the vitreous with triamcinolone acetonide suspension may help identifying the posterior hyaloid during surgery. It is usually diluted with balanced salt solution (BSS) to a lower concentration (typically 1/5) before injection into the eye. Further, new imaging technologies such as intraoperative optical coherence tomography (OCT) may help identify the status of the posterior hyaloid during surgery.

In Video 131.4 a complex situation is presented: an attached posterior hyaloid is identified by intraoperative OCT (RESCAN 700®, Carl Zeiss Meditec, Germany) during a 25G vitrectomy (Constellation®, Alcon, TX, USA) for a posterior retinal detachment secondary to macular hole in high myopia. The vitreous cannot be visualized by the surgeon through the microscope (without OCT). Diluted triamcinolone acetonide suspension is injected over the optic nerve to visualize the posterior hyaloid and allow its safe

peeling.

Iatrogenic Retinal Breaks During Peeling

Manish Nagpal

One of the risks involved during membrane peeling is the formation of iatrogenic breaks. Their immediate detection and management is crucial to prevent a negative outcome.

The following tips may help avoid making an iatrogenic break during peeling and also help their management if formed.

1. Use a wide-angle viewing system during vitrectomy surgery to be able to evaluate optimally the periphery of the retina.

2. Peel membranes in a radial fashion and avoid anteroposterior pulling.

3. If iatrogenic breaks are formed, assess the location and extent of the break, mark the edges, and assure adequate endolaser when the retina is reattached.

In Video 131.5 a patient is presented with a semiopen funnel retinal detachment with proliferative vitreoretinopathy (PVR). Core vitrectomy is performed and perfluorocarbon liquid (PFCL [AuroOctane, Aurolab, India]) is injected over the disc to stabilize the retina. A circumferential membrane over the disc is gradually peeled to allow the flattening of the posterior pole under the PFCL liquid.

The residual inferior traction is reassessed, and the responsible epiretinal membrane is peeled to release this traction. During the peel the peripheral inferior retina is stretched and an iatrogenic break is formed. A wide-angle viewing system allowed the immediate detection of the break. The extent of the break and its location is assessed, and diathermy is applied to mark the edges and to control the bleeding. Fluid–air exchange is performed, and subretinal fluid is drained through the break. Once the retina is flattened, laser endophotocoagulation is applied around the break

to assure adequate retinopexy.

Internal Limiting Membrane Peeling

Sjakon Tahija

Creating an edge of the ILM at the beginning of its peeling is the part of the procedure that is associated with the highest risk for retinal bruising and damage. In Video 131.6 the surgeon is performing pars plana vitrectomy for proliferative diabetic retinopathy in a type 1 diabetic patient. After removing the vitreous hemorrhage, endolaser photocoagulation was applied to the retina. Since macular striae were present, it was decided to peel the ILM, which was stained with brilliant blue dye. The ILM appeared very adherent and frequent regrasping of the edge became necessary. When grasping the edge of the ILM nasal to the fovea, one of the retinal folds was pinched, causing retinal bruising and hemorrhage. The intraocular pressure (IOP) was raised to prevent further bleeding and the ILM peeling was completed. The blood clot could not be removed using the back flush technique, so it was gently massaged away from the fovea using the silicone tip of a flute needle.

To avoid this complication, it is best to initiate the ILM peeling inferiorly and further away from the center of the macula. Any visual field defect caused by the peeling would be in the superior field and less noticeable by the patient. Good staining, high magnification, and slow motion peeling would also minimize iatrogenic trauma during ILM peeling.

Subretinal Injection of Brilliant Blue

Arturo Alezzandrini, Francisco Rodriguez

In vitreous surgery, staining of the ILM with vital dyes is widely performed, and surgical outcomes have improved in many vitreoretinal disorders such as macular holes and epiretinal membranes. The dyes currently utilized for different steps during vitrectomy surgery are triamcinolone acetonide for vitreous visualization; indocyanine green (Diagnostic Green LLC, Powell, OH), infracyanine green (SERB Laboratories, Paris, France), and

brilliant blue (DORC, Zuidland, The Netherlands) for ILM staining; and trypan blue (Dutch Ophthalmic USA, Exeter, NH) for epiretinal membrane identification. One of the main complications that is observed during injection is the subretinal injection of the dye.

In Video 131.7 a series of steps are demonstrated to prevent this complication:

1. Dye is injected away from the fovea while the IOP is decreased.

2. A dual-bore cannula with multiple fluid egress vents is used to allow faster pressure relief during injection, eliminating the fluid jet stream.

3. Dye is injected over the light pipe, thus avoiding direct impact of the dye on the macula.

Reopening of Peripheral Retinal Breaks During Surgery for Submacular Hemorrhage

Carl Regillo

Submacular hemorrhage secondary to neovascular age-related macular degeneration (AMD) is a treatment dilemma for physicians and patients.

The patient in Video 131.8, with submacular hemorrhage secondary to neovascular AMD, was managed with subretinal tissue plasminogen activator (tPA) and pneumatic displacement as described by Tamer Mahmoud and colleagues.[1] During the initial core vitrectomy, there was evidence of a previously partially treated horseshoe retinal tear, and the posterior lip of the tear did not appear to have laser marks. We proceeded with submacular tPA injection (25 mcg/0.1 ml tPA [alteplase, Genentech, South San Francisco, CA]). This was followed by injection of filtered subretinal air, resulting in bullous elevation of the retina. In fact, the air made the retina too bullous and actually displaced it temporally towards the tear. When we tried to subsequently laser the break, the detached retina was in the way, making the view extremely

difficult. The air bubbles migrated towards the break and opened it up. The solution to the problem was to go to air and perform an air–fluid exchange, which helped to tamponade the retina so that we were able to aspirate over the break and flatten this area out so that it could be successfully lasered.

There are several potential ways to prevent opening up existing peripheral breaks in such cases. If breaks are found to be present preoperatively, they can be reinforced in the office a week or two ahead of time. Intraoperatively, if extensive subretinal fluid or air injection is being planned, it may be best to inspect the peripheral retina before the injection and, if breaks present, laser the breaks upon identifying them and minimize the volume of fluid or air subsequently injected under the retina.

It should be noted that the use of air in addition to a solution of tPA has not been proven to enhance or aid in the displacement of macular subretinal hemorrhage. A more conservative, safer approach utilizing just the subretinal tPA solution without subretinal air may be preferred approach. Further studies are warranted before routinely adopting the subretinal air technique.

Surgical Management of Hypotony Maculopathy

Jose Garcia Arumi

Low intraocular pressure after vitrectomy surgery (postoperative hypotony) is generally due to the failure of the ciliary body to produce aqueous humor. This may be due to fibrous traction from anterior PVR, cyclodialysis, or ciliary body detachment. A diagnosis can be made with ultrasound biomicroscopy (UBM) that visualizes the ciliary body and tissues around it.

Video 131.9 presents a 54-year-old patient with a history of vitreous hemorrhage after trauma who had undergone a 23G vitrectomy procedure elsewhere. Three months later he developed hypotony maculopathy and was referred for evaluation. Upon examination the best corrected visual acuity was 20/400 and intraocular pressure was 4 mmHg. The UBM suggested a cyclodialysis cleft and ciliary body detachment extending 360°. The

OCT scan indicated increased macular thickness associated with hypotony maculopathy and chorioretinal folds, which were visualized on fluorescein angiography.

The patient underwent a 23G pars plana vitrectomy surgery followed by posterior hyaloid separation, brilliant blue dye staining, and removal of the internal limiting membrane (ILM) in the macular area. Peeling the ILM decreases the rigidity of the retina and eases the opening of the macular folds once the hypotony is resolved. Transconjunctival cryotherapy was applied to the sclera 2.5 mm posterior to the limbus using a curved spherical retinal probe. Eight spots were applied: two spots per quadrant, each with a duration of 10 seconds and a temperature of −80 °C (avoiding the ciliary body). Following cryopexy, fluid–air exchange is performed and 6% C_3F_8 gas was injected into the eye for tamponade. The postoperative course was unremarkable. Two weeks after surgery the best corrected visual acuity improved to 20/25 and IOP was 15 mmHg. Ultrasound biomicroscopy indicated that the ciliary body had reattached to the scleral spur, closing all the clefts.

Key steps in the management of hypotony maculopathy are:

- Performing preoperative UBM.
- Peeling the ILM during the surgery.
- Applying transscleral cryotherapy to the pars plana (avoiding the ciliary body).
- Gas tamponade.

Intraoperative Choroidal Detachment

Homayoun Tabandeh

Intraoperative choroidal detachment may occur as a result of displacement of the infusion cannula into the suprachoroidal space, or it may represent suprachoroidal hemorrhage. Furthermore, continued infusion into the suprachoroidal space from a displaced infusion cannula could result in stretching and subsequent rupture of blood vessels traversing this space causing the additional suprachoroidal hemorrhage. Conversely, intraoperative suprachoroidal hemorrhage may result in displacement of the

infusion cannula into the suprachoroidal space, further exacerbating the choroidal detachment.

Early detection is an important first step. Intraoperative visualization of ora serrata in the absence of scleral depression may be an early warning sign indicating choroidal detachment. Once a choroidal detachment is suspected, surgery should be stopped and the situation assessed, establishing the possible cause. Intraoperative displacement of infusion cannula can be identified by inspection of the infusion cannula internally and externally. Risk factors for infusion cannula displacement include intraoperative manipulations, oblique placement of the cannula, preoperative choroidal detachment, and hypotony. Visualizing the tip of the cannula prior to opening the infusion flow at the beginning of the surgery is an important step that helps in identifying a misplaced cannula in the suprachoroidal space. In eyes with preexisting choroidal detachment, a straight cannula entry aiming towards the center of the vitreous cavity (instead of beveled incision) reduces the chance of suprachoroidal placement of the infusion cannula. Securing the infusion line by a tape helps reduce the chances of cannula displacement during surgical manipulations.

Once a displaced infusion cannula is recognized, the infusion flow should be closed immediately. The infusion line is disconnected from the cannula (leaving the cannula in place) and immediately reinserted through one of the other available cannulas (the tip needs to be visualized prior to reopening the infusion), therefore maintaining the intraocular pressure. The original infusion cannula will be left in the original location to allow drainage of fluid from the suprachoroidal space. Once the choroidal detachment is reduced, an attempt may be made to reposition the displaced cannula. Alternatively the cannula may be removed and a new cannula may be inserted, utilizing a straight entry, aiming towards the center of the vitreous cavity. A modified version of this technique may be used in the management of intraoperative suprachoroidal hemorrhage.

In Video 131.10, a patient with diabetic retinal detachment underwent pars plana vitrectomy. Towards the end of surgery, progressive choroidal detachment was noted. The infusion cannula was inspected and was noted to have been displaced into the

suprachoroidal space. The infusion line was disconnected from the cannula, leaving the displaced cannula in place. The infusion line was immediately reinserted through one of the remaining cannulas, maintaining the IOP. The displaced cannula was left unplugged in the suprachoroidal space to allow drainage of fluid. The posterior segment was inspected. The choroidal detachments were found to have subsided. An attempt was made to reposition the cannula, without success. Subsequently the cannula was removed and a new cannula was inserted with a straight entry, aiming towards the center of the vitreous cavity. The infusion line was relocated, and the surgery was continued uneventfully.

Massive Suprachoroidal Hemorrhage (SCH)

Jose Garcia Arumi

Massive suprachoroidal hemorrhage generally implies the rupture of the short or long posterior ciliary artery branches during intraocular surgery or after penetrating trauma. The incidence of suprachoroidal hemorrhage in vitreoretinal surgery is low. Systemic risk factors include advanced age, hypertension, atherosclerosis, diabetes, and bleeding disorders. Ocular risk factors include high myopia (decreased scleral rigidity and the increased fragility of the choroidal vasculature), prior history of retinal detachment surgery, preoperative hypertension, and intraocular inflammation. Main intraoperative risk factors are elevated blood pressure or heart rate during surgery, prolonged intraocular hypotony, scleral manipulation, and extensive cryopexy.

The goal in the management of suprachoroidal hemorrhage during surgery is to stop the bleeding by increasing the intraocular pressure, closing the surgical wound, and lowering the systemic blood pressure. Emergency drainage sclerotomies may induce transient hypotony and stimulate rebleeding. Further, they increase the risk of retina/uveal tissue incarceration due to the high pressure.

Suprachoroidal blood may not necessarily require drainage. This particularly applies to sectorial hemorrhages that do not involve the posterior pole and the macula. During the follow-up, dynamic B-

scan ultrasound can help in assessing the degree of liquefaction of the suprachoroidal blood clot and indicate the adequate timing for the drainage procedure, which is usually 10–14 days after the incident.

In Video 131.11 a 25G infusion cannula is placed into the anterior chamber through the inferior limbus and the IOP is set at 30 mmHg. A radial sclerotomy is performed parallel to the rectus muscle in the quadrant with the most suprachoroidal hemorrhage. The infusion pressure allows a controlled drainage of the liquefied blood through the sclerotomy. After a partial drainage, 23G cannulas are inserted into the eye through the pars plana and a limited vitrectomy is performed followed by removal of the posterior hyaloid. Injection of PFCL into the vitreous cavity induces an internal tamponade which further displaces the liquefied blood towards the periphery and allows its drainage through the sclerotomy. The eye may then be filled with gas or silicone oil.

Suprachoroidal Hemorrhage During Cataract Surgery

Kazuaki Kadonosono

Suprachoroidal hemorrhage is a rare but severe complication that usually results in poor vision. Intraoperative hypotony is one of the main risk factors resulting in choroidal effusion with subsequent rupture of small arteries traversing the suprachoroidal space. In addition, prolonged hypotony may directly result in rupture of the short or long posterior ciliary arteries or vortex veins. The greatest risk for suprachoroidal hemorrhage during cataract surgery occurs immediately after nucleus removal, when the eye is at greatest risk of prolonged hypotony.

The 73-year-old patient presented in Video 131.12 had had phacoemulsification elsewhere. While aspirating the cortex, the posterior capsule was ruptured with subsequent vitreous loss. Effort was made to implant the IOL into the bag; however, suddenly the choroid became elevated, and suprachoroidal hemorrhage was recognized and surgery was stopped. The patient was referred for evaluation and management to our clinic. One

week after the original surgery, the patient was brought back to the operating room for drainage of the suprachoroidal blood. Iris retractors were placed to have a better visualization of the anterior chamber. An infusion cannula was inserted into the anterior chamber to maintain the IOP. It was noted that patient still had a large blood clot in the suprachoroidal space. A scleral cutdown was performed superotemporally, and tissue plasminogen activator (0.4 ml volume at a concentration of 62.5 μg/0.1 ml [Monteplase, Eisai Co.,Tokyo, Japan]) was injected into the suprachoroidal space to dissolve the clot. The sclera was depressed with a cotton swab to aid its removal. An infusion cannula could now be placed through the pars plana into the vitreous cavity and vitrectomy was performed.

Subretinal Perfluorocarbon Bubble

Maria H. Berrocal

Subretinal perfluorocarbon liquid (PFCL [Alcon Laboratories, Fort Worth TX]) after vitrectomy surgery is one of the most dreaded complications of its use. The risk factors for subretinal migration of PFCL include:

1. Large breaks.

2. Posterior breaks.

3. Residual traction on the breaks.

4. Multiple small bubbles during injection.

5. Turbulence during injection.

6. Injecting directly in the direction of the break.

Although extrafoveal subretinal PFCL bubbles could be monitored (although it has been reported that they can migrate inferiorly and if close to the fovea would need to be removed), submacular PFCL bubbles would have adverse impact on visual acuity and need to be removed.

To decrease the likelihood of getting subretinal/submacular PFCL bubbles, one may relieve all traction on the breaks prior to the injection of PFCL into the eye; use a dual-bore cannula (MedOne Surgical Inc, Sarasota, FL) for PFCL injection or use an aspirating instrument (in the other hand) during the injection (in valved trochar systems); inject with a slow speed over the optic nerve to form a single bubble and inject inside the forming PFCL bubble; use valved cannulas to decrease the amount of turbulence during the injection procedure; and keep the PFCL level below the peripheral breaks. Washing out the residual PFCL bubbles with balanced salt solution (BSS [Alcon Laboratories, Fort Worth TX]) or infusion fluid after the removal of the main bubble may avoid having residual PFCL bubbles inside the vitreous cavity after surgery.

Utilizing a dual-bore cannula that has a side port for injection may prevent damage to the retina from the PFCL jet stream during the injection procedure. This may particularly be an issue when utilizing 25- and 27G vitrectomy systems.

Very small amounts of residual PFCL bubbles inside the vitreous cavity may be tolerated although the patient may complain of seeing the bubble when laying on their back. Larger amounts of PFCL in the vitreous can cause inflammation and may need to be removed.

In Video 131.13 the patient presents with a rhegmatogenous retinal detachment with star fold and inferior PVR. An encircling no. 41 band was placed and tied superonasally; 27G vitrectomy was performed with complete vitreous removal. PFCL was injected into the eye to flatten the retina, and subretinal fluid was drained through the superior retinal tear. The PFCL was injected with a 30G needle. Multiple PFCL bubbles were dispersed inside the vitreous cavity. Air–fluid exchange was performed, and laser endophotocoagulation was applied around the break and the lattice degeneration inferiorly. Residual PFCL bubbles were washed out multiple times and no residual bubbles were visible. Air–gas exchange was performed, and the eye was filled with 14% C_3F_8 gas (Alcon Laboratories, Fort Worth TX).

Postoperatively, a small subretinal PFCL bubble was detected near the peripheral break on the buckle. Laser was applied around the bubble to prevent its migration towards the posterior pole. The

retina has remained attached, and the subretinal PFCL bubble has not moved for over a year.

Perfluorocarbon-Induced Macular Hole

Yusuke Oshima

Perfluorocarbon (PFCL [Alcon Laboratories, Fort Worth TX]) liquid is a very useful tool for flattening the detached retina during vitrectomy, especially in giant retinal tear detachment or detachment associated with proliferative vitreoretinopathy. Special attention should be given to PFCL injection during surgery, especially in small-gauge surgery where resistance to the injection is increased due the narrower size of the injection lumen.

In Video 131.14 PFCL is injected over the macula. A macular hole is formed due to the pressure caused by the injection stream. The surgeon should keep in mind to gently inject PFCL over the optic nerve (or nasal to it) and avoid injecting it directly over the macular area. Further, the injection should be done by the surgeon (rather than an assistant), and a safe distance from the surface of the retina should be kept during the injection procedure (one has the tendency to move closer to the surface of the retina during the injection). If any resistance is felt during the PFCL injection, the cause needs to be evaluated outside the eye instead of applying additional pressure. In this case a standardized macular hole surgical technique was performed including peeling the ILM followed by fluid–air exchange and gas tamponade.

Giant Retinal Tear With Slippage on Encircling Scleral Buckle

Carl Regillo

A combined pars plana vitrectomy (PPV) with encircling scleral buckle (SB) was being performed for a giant retinal tear (GRT) extending approximately 180° in a phakic patient. Despite meticulous drying of the edge of the retina during fluid–air

exchange, when the perfluorocarbon liquid (PFCL) was completely removed, there was posterior slippage of the retina. Another attempt with the same technique, again paying close attention to patiently removing as much fluid over the PFCL as possible, yielded the same results. The scleral buckle was then loosened significantly, and the same technique was attempted. This time, the retina did not slip. We hypothesize that excessive cerclage effect of the encircling scleral buckle promoted posterior slippage which was resolved by loosening the buckle (Video 131.15).

Posterior slippage of the retina in the setting of a GRT-related retinal detachment is generally from anterior fluid (i.e., the layer of fluid between the PFCL and the infused air) displaced posteriorly through the large break. To minimize this effect, it is important to remove all of the anterior fluid in the vitreous cavity before removing the PFCL under air along with any anterior subretinal fluid above the PFCL meniscus by extruding over the break.

In this case, presumably there was the additional factor of excessive 360° of scleral buckle indentation. A "high" indentation may be undesirable and, therefore, best avoided to minimize slippage. Furthermore, there is no proof that encircling significantly enhances the success rate of vitrectomy for retinal detachment repair, with or without GRT. Many surgeons would argue that this combined approach (i.e., PPV plus SB) is not necessary and only adds to the surgical morbidity.

PVR and Subretinal Membrane

Stanislao Rizzo

Subretinal membranes are associated with rhegmatogenous retinal detachment due to proliferative vitreoretinopathy (PVR). Several surgical techniques are available for the removal of subretinal membranes during PVR surgery.

When the subretinal membrane is in the form of branching bands and the extent of the membrane can be visualized through the retina, the membrane can be removed using forceps passed through preexisting retinal breaks or small retinotomies. However, if the membrane is in the form of diffuse sheets or the extent of subretinal membrane cannot be visualized, peripheral retinotomy may

become necessary followed by folding the retina and removal of the subretinal membrane under direct visualization.

In Video 131.16, after performing core vitrectomy and meticulous peripheral vitreous shaving with 360° scleral depression, attention is directed towards the proliferative membranes. Intravitreal triamcinolone acetonide suspension was used to highlight these membranes. Mature preretinal membranes were peeled with forceps and a pick in a bimanual fashion using chandelier light for illumination. The removal of subretinal membranes was attempted through a small access retinotomy. However, the retinal folds still remained, indicating the presence of residual subretinal membranes inducing traction and folding of the retina. The small retinotomy was not sufficient to visualize and remove all the subretinal membranes. It was decided to perform an inferior 180° retinotomy to relieve the traction and to visualize and remove all the residual subretinal membranes. Subsequently perfluoron was injected into the eye to flatten the retina, and endolaser photocoagulation was applied around the edges of the retinotomy. The eye was filled with silicone oil up to the posterior iris plane.

A Problem During 27G Vitrectomy

Carl Claes

Constant monitoring and visualizing the instruments (specially their tips) during surgery is very important to detect any breakage while operating. In Video 131.17 a 27G pars plana vitrectomy is performed with a valved trochar system. A posterior vitreous detachment was induced and core vitrectomy was completed. During the ILM peeling a small retinal hemorrhage was passively aspirated with the 27G silicone-tipped flute needle, after which the ILM peeling continued unremarkably.

Suddenly a foreign body was visualized superior to the optic nerve: a barely visible transparent silicone tip of the flute needle. It probably got stuck in the 27G valved trochar and detached from the flute needle. During consecutive instrument exchange through the trochar, the silicone tip was inadvertently mobilized into the eye and fell on the retina.

An attempt was made to remove the silicone tip by slipping it into the tip of 27 G forceps as a sleeve covering the forceps arm. This maneuver unfortunately widened the diameter of the 27G forceps, and the sleeve got stuck in the valved trochar. To overcome this problem, the silicone tip was regrasped and in a bimanual fashion the silicone tube was pulled over one of the arms of the forceps. The silicone tip was pulled upwards to the shaft of the forceps, allowing the forceps to secure the silicone tip and remove it.

Vitreous Incarceration in the Sclerotomy Sites

Maria H. Berrocal

Vitreous incarceration may occur at the sclerotomy sites and can cause traction and peripheral retinal breaks. There has been a decrease in the incidence of this complication due to a decrease in size of the sclerotomies and the use of trocar cannulas. Nevertheless, it can still occur, particularly if a significant amount of peripheral vitreous remains near the sclerotomy sites. Additional predisposing factors for vitreous incarceration into the sclerotomy sites include elevated intraocular pressure during trocar removal, not using valved cannulas, and removing the trochars without an instrument inside their lumen.

Vitreous incarceration may be avoided by:

1. Thorough removal of the peripheral vitreous around the sclerotomy sites.

2. Careful examination of the peripheral retina around sclerotomy sites using scleral depression.

3. Avoiding increased IOP during trocar removal.

4. Performing a partial air–fluid exchange to have air seal the sclerotomies.

5. Placing the light pipe inside the cannula during its removal

(pushing back incarcerated vitreous).

6. Inspecting the sclerotomy sites for vitreous strands.

7. Suturing the leaking sclerotomies.

Vitreous incarceration does not always cause peripheral breaks or detachments but can potentially be a tract for entry of bacteria into the eye and consequent endophthalmitis as well. During the postoperative period it can only be detected if the peripheral retina is visualized and a peripheral break or detachment occurs. The management is to treat the secondary complications that ensue, namely new breaks, opening of existing breaks, and redetachment.

The 62-year-old female patient in Video 131.18 presented with a pseudophakic total rhegmatogenous retinal detachment with one tear identified at 11 o'clock. Since the patient had to travel by air, she did not want a gas bubble in the eye. It was decided to proceed with a scleral buckling procedure, and an encircling scleral buckle with a no. 41 band was placed around the eye under visualization with microscope. The band was measured and was left with a circumference of 70 mm. A trochar-cannula with a chandelier light was inserted into the eye to serve as light source. The fundus was visualized under the microscope using the wide-angle viewing system. A vitrectomy was not performed.

External drainage was performed by scleral cutdown: applying cautery to the scleral edges and choroidal bed, and puncturing the choroid with a 30G needle under direct visualization with the microscope. The chandelier light was removed, and an illuminated endolaser probe was inserted into the eye through the same cannula to laser around the break. The cannula was removed, the sclerotomy site was not sutured, and the conjunctiva was closed. On the first postoperative day the retina was completely attached. A week later the patient returned with a recurrent retinal detachment and a break near the sclerotomy site (for chandelier light) with vitreous strand visible incarcerating into the sclerotomy. A reoperation was recommended, and pars plana vitrectomy was performed with SF_6 gas (Alcon Laboratories, Fort Worth, TX) and additional laser treatment. The retina has remained attached.

Argus II Array Implantation

J. Fernando Arevalo

In Video 131.19 an Argus II array (Second Sight Medical Products, Inc, Sylmar, CA) was implanted in the usual manner in a retinitis pigmentosa (RP) patient with bare light perception vision. Core and peripheral vitrectomy was performed with the assistance of triamcinolone acetonide. The microelectrode array was then inserted through a temporal sclerotomy (5.2 mm). The array was positioned over the macula and then tacked using a custom retinal tack (Second Sight Medical Products, Inc, Sylmar, CA). However, the retinal tack dislodged from the implant and fell into the vitreous cavity. The retinal tack needed to be removed, similar to an intraocular foreign body (IOFB). The microelectrode array was then placed again over the macula and was stabilized using a new retinal tack without any further issues.

Pearls on how to avoid this complication:

- Open a large inferonasal sclerotomy to tack the array and enlarge it further if necessary (19G).
- Assure that the tack is engaged perpendicular to the tack holder.
- When using bimanual techniques to place the array over the macular area, make sure that the tack does not move from its proper position. If it does, exchange it for a new tack before attempting to tack the array.
- Practice the tacking procedure before the surgery. This is a unique maneuver that is only performed during the Argus II surgery.

Subretinal SF_6 Gas After Retinal Detachment Surgery

Stratos Gotzaridis

Postoperative subretinal SF_6 gas is a rare finding after retinal detachment surgery. It may occur due to the turbulence during the injection of gas near a large retinal break, especially if there is persistent subretinal fluid keeping the break open. The positioning of the patient, location, and size of the break may worsen the

situation during the postoperative period.

The patient in Video 131.20 presented at postoperative day 1 with subretinal gas and total retinal detachment. The patient was brought back to the operating room. A 25G trocar was placed through the corneal limbus into the anterior chamber and was attached to the infusion line. Through a corneal tunnel the endodiathermy probe was introduced into the eye and an anterior retinotomy was made to allow the aspiration of the gas with the vitreous cutter. The infusion fluid pushed the retina back to its original position, allowing the insertion of an infusion cannula through the pars plana.

A new retinotomy was created for further drainage of subretinal gas/ fluid and allow the flattening of retina. Once the retina was flattened, endolaser was applied around the retinotomies, followed by intravitreal gas injection. The patient was asked to maintain a face-down positioning posture for 7 days.

Removal of a Large Glass Intraocular Foreign Body

Grazia Pertile

The patient in Video 131.21 suffered penetrating ocular trauma with a large piece of glass from a broken bottle. During the initial surgery the lens remnants were removed and the corneoscleral wound was sutured with 10-0 nylon sutures, but the foreign body was left behind, and the vitreous hemorrhage prevented the direct visualization of the fundus. Postoperatively, the vitreous cavity and retina were monitored with B-scan ultrasonography. After a couple of weeks a retinal detachment developed. Vitrectomy was performed with the purpose of removing the blood and intraocular foreign body and reattaching the retina. The surgeon who performed the surgery reported that the repeated attempts to remove the glass from the vitreous cavity were unsuccessful due to the very large size of the foreign body, which was irregular in shape and slippery. Different types of intraocular forceps were tried but none were able to grasp the foreign body to remove it.

At this point the patient was referred for second opinion. The

visual acuity was light perception. The cornea was reasonably clear, but there was a large corneoscleral wound involving the center. The temporal half of the iris was missing, and nasally there were points of iris root disinsertion with a mild hyphema. B-scan ultrasonography confirmed the diagnosis of a total retinal detachment.

Twenty-gauge vitrectomy was started by inserting an illuminated infusion cannula. After the removal of the blood, a total retinal detachment with extensive proliferative vitreoretinopathy and multiple posterior retinal breaks was visualized; these perhaps resulted from multiple unsuccessful attempts to remove the large piece of glass. The foreign body was located in the inferonasal quadrant, with an irregular triangular shape. The length was around 15 mm and the width was 9 mm.

A basket (Nitinol Tipless Stone Extractor [G46206] COOK MEDICAL, Bloomington, IN) that is generally utilized by the urologists for the removal of kidney stones was used to remove the foreign body. This retractable instrument with a diameter of 1.1 mm was introduced through an enlarged sclerotomy site. With this device, a thin network made of memory metal was then extruded inside the eye, paying attention not to touch the retina while trying to engage the object with the basket. The large piece of glass is gently moved inside the basket with the help of an illuminated spatula, which permitted us to lift it up from the retina and guide it toward the metal network. The illumination from the spatula allowed us to overcome the shadow that was projected by the large foreign body. (When the object is large, it is crucial to start the maneuver from the most posterior part. In this way, you promote a spontaneous movement inside the basket due to the gravity and prevent it from rotating and getting stuck in the retina.) Finally, the metal network was retracted with the object inside. Once brought behind the iris plane, the large size of the foreign body could be appreciated. The next step was to find the least invasive method of taking the basket with the object inside it out of the eye. In general, when the foreign body is firmly held with an instrument, it is best to enlarge the same sclerotomy with the other hand and remove it through a scleral incision at 3–4 mm posterior to the limbus. However, in this case we would have cut the sclera for more than

one quadrant in addition to the extensive corneal wound and the corneoscleral incision already present in the superonasal quadrant. We chose to reopen the corneoscleral incision used during the previous operation. But this approach was tricky because the slippery foreign body needed to be regrasped. In order to reduce the risk of dropping the foreign body, the basket was directed toward the corneoscleral incision that was kept open with a spatula and then the basket was slowly opened while grasping the piece of glass with forceps in the other hand. The basket was retracted after at least one-third of the foreign body was extruded with forceps. The wound was sutured, the membranes were removed, the retina was flattened, and silicone oil tamponade was injected.

Reference

1. Martel JN, Mahmoud TH. Subretinal pneumatic displacement of subretinal hemorrhage. *JAMA Ophthalmol*. 2013;131:1632–1635.

PART 2

Tumors of the Retina, Choroid, and Vitreous

OUTLINE

SECTION 1

Tumors of the Retina

OUTLINE

132

Retinoblastoma

Jonathan W. Kim, Nancy C. Mansfield, (posthumously), A. Linn Murphree

If most solid tumors of childhood are indeed correctly attributable to mutations in germ and/or somatic cells … then childhood cancer cannot be prevented. … the main effort against childhood cancer must be that of early diagnosis and treatment.

A.G. Knudson Jr.,1976

Introduction

The quote from retinoblastoma pioneer Alfred G. Knudson Jr. is as true today as it was in 1976.[1,2] We now know a great deal more about the molecular basis of the mutations in cancer cells than Knudson knew when he was writing, but we have made distressingly little progress towards Knudson's admonishment to clinicians that early diagnosis and treatment is essential for the successful management of this disease. This chapter on

retinoblastoma (RB) emphasizes the need for pediatricians and other healthcare professionals who must listen and take action when parents report seeing "something in my child's eye." We continue to emphasize what Nancy Mansfield taught us about the importance of recognizing signs and symptoms of classic posttraumatic stress disorder in children undergoing prolonged treatment and multiple anesthesias for intraocular retinoblastoma.

Clinical Advances

Since the fifth edition of this publication in 2012, the most significant addition to the clinical management of children with retinoblastoma is the emergence of local or regional therapies such as intraarterial chemotherapy and intravitreal chemotherapy. Intraarterial ophthalmic artery chemotherapy infusion is a more selective adaptation of the Japanese experience in the use of regional intraarterial chemotherapy.[3,4] Like many other new treatment approaches, the initial excitement of intraarterial chemotherapy has been tempered somewhat as rare but significant complications have been encountered (including choroidal artery occlusion, local orbital recurrence, and metastatic disease).[5–8] Intravitreal chemotherapy has emerged as an effective modality for treating vitreous seeding, and appears to offer a high globe salvage rate and a negligible risk of side-effects as long as the clinician adheres to a strict protocol and dose range.[9–11] The pros and cons of these new approaches to the treatment of retinoblastoma are discussed later in this chapter.

Basic Science Advances

In the previous edition, we cited three advances: (1) the definition of the three-dimensional structure of the retinoblastoma protein (pRB), providing new insights into how it works; (2) the fact that pRb can simultaneously bind to multiple proteins, acting as a coupling factor to recruit proteins to specific genes; and (3) an improved understanding of low-penetrance retinoblastoma.[12]

Genetics of Retinoblastoma

Clinical Genetics

Study of retinoblastoma has been critical to understanding the genetic basis of cancer in general. Although retinoblastoma is rare, occurring in approximately one in every 18,000 live births, the pathogenetic insights gleaned from retinoblastoma have profoundly affected our understanding of common cancers arising from lung, breast, prostate, and virtually every other site. This unique place of retinoblastoma in oncology derives from its very distinct pattern of inheritance and from the fact that the *RB1* gene was not only the first human cancer gene to be cloned but was the first of a whole class of identified human cancer "suppressor" genes.

About 60% of all patients with retinoblastoma have a nonheritable form of the disease with a normal life expectancy if they are cured of the eye cancer. In this group the average age at diagnosis is about 24 months, the eye tumor is always unilateral, and the risk of other cancers is virtually indistinguishable from the normal population.[13] In contrast, the other 40% of patients carry the *RB1* germline mutation and have a heritable cancer predisposition syndrome. The inheritance of a single mutated, inactive allele of the *RB1* gene confers the predisposition to cancer (a dominant trait), but a second inactivating mutation must occur in at least one retinoblast for retinoblastoma to develop. Genetically, because the tumor requires inactivation of both copies of the *RB1* gene, it is considered a recessive trait. However, in pedigrees, the mutation has a dominant phenotype because the chances of at least one retinoblast acquiring the second "hit" is very high. Therefore, a person with the cancer predisposing syndrome genotype ($RB1^{+/-}$) will develop retinoblastoma with a 90–95% probability. Only 7–10% of retinoblastoma patients have a positive family history (someone else in the family with retinoblastoma). Hence, the other patients who carry the *RB1* gene defect, about 30% of patients with retinoblastoma overall, have a new germinal mutation. The average age at diagnosis for germinal retinoblastoma is younger than the nonheritable form – ranging from newborn to 12 months – and they are predisposed to a variety of cancers throughout life.[14] About 85% of germinal retinoblastoma patients develop bilateral eye tumors and the unilateral patients who carry the gene defect tend to

develop multifocal tumors in the one eye. Within the age range of birth to 5 years (typically before age 3), about 5–6% of germinal retinoblastoma patients will develop a midline intracranial tumor usually involving the pineal or suprasellar region, that histologically resembles retinoblastoma and has variably been referred to as a pinealoma, primitive neuroectodermal tumor (PNET). These patients are referred to as having trilateral retinoblastoma, whether the midline intracranial tumor occurs in the sella region or pineal gland. Despite the histologic similarity, it is important to recognize that the intracranial tumor is a primary cancer and not a metastasis from the eye tumor. The intracranial tumor is usually diagnosed before, together with, or within 2 years of the retinoblastoma diagnosis. Germinal retinoblastoma patients also have an elevated risk of osteosarcomas, soft tissue sarcomas, and other mesenchymal tumors through their teenage years; melanomas and brain tumors through middle age; and epithelial malignancies such as lung and bladder cancer into later life.[15,16] This elevated risk is much greater in patients who have received external beam radiotherapy (EBR), particularly in the field of radiation treatment (e.g., head and neck).[14,17]

Genetic Terminology

The genetic terminology used in the retinoblastoma field can be confusing. Clinicians erroneously may use the term unilateral to refer to the nonheritable form of retinoblastoma. However, this nomenclature is inappropriate, since about 12–15% of unilateral cases carry the *RB1* mutation just like bilateral cases.[18] Any patient who carries the *RB1* mutation in cells outside the eye is considered a germinal or heritable case. Patients who have unilateral tumors and no *RB1* mutation outside the eye are considered somatic cases. Epidemiologic studies on second cancers that provide no information about the *RB1* gene status probably overestimate the risk in unilateral, somatic patients. The term sporadic is also commonly misused. Sporadic refers to a lack of family history but is not equivalent to somatic disease since the majority of germinal cases are new mutations. About 90–93% of all retinoblastomas are sporadic with no family history, meaning that they are the result of new mutations that developed either in the sperm or egg. In

contradistinction, virtually all cases in a single family are hereditary.

The term hereditary is often used to indicate the presence of germline *RB1* mutations (i.e., present in virtually all cells in the body, both somatic and germ line), which also includes sporadic, nonfamilial cases. Therefore, a new mutation that develops in the sperm of the father and causes bilateral retinoblastoma would be germinal, hereditary, sporadic, and nonfamilial. The term mosaic refers to the presence of the *RB1* mutation in a subpopulation of cells (somatic, germinal, or both), and is thought to occur from an *RB1* mutation in the developing embryo after conception. The clinical manifestations of a mosaic *RB1* mutation are uncertain in any given patient, but are typically managed clinically like other germinal or hereditary patients. However, the state of *RB1* mosaicism is never inherited and therefore the parents can be ruled out as carriers. However, patients with *RB1* mosaicism can have children with retinoblastoma, although the risk in any individual patient is difficult to predict.

Molecular Genetics of Retinoblastoma

Because of the seemingly autosomal dominant inheritance pattern for retinoblastoma in the clinical setting, the *RB1* gene was assumed for many years to act in a dominant fashion.[13] A major paradigm shift in the genetic understanding of retinoblastoma, and cancer in general, began with the seminal paper published in 1971 by Alfred Knudson, who proposed that retinoblastoma was caused by two mutational events: "In the dominantly inherited form of the disease, one mutation is inherited via the germ line and the second occurs in somatic cells. In the nonhereditary form, both mutations occur in somatic cells."[18] The major implication of this "two-hit theory" was that the *RB1* gene functions in a recessive manner at the cellular level – an unprecedented suggestion at the time. Today, it is known that many cancer-causing mutations are recessive or affect tumor suppressor genes.

The Knudson hypothesis languished for another decade due to a lack of scientific methods for identifying the *RB1* gene. An early clue to the location of the *RB1* gene was the recognition in the 1960s

that a portion of the Group D chromosomes (13, 14, and 15) was occasionally deleted in retinoblastoma. Shortly after the Knudson paper, new chromosome banding techniques allowed chromosome 13 to be identified as the target of these deletions.[19] The smallest deleted region was later mapped to chromosome 13q14.1 to q14.3.[20] An enzyme with a measurable activity, esterase D, had been mapped to chromosome 13 and proved to be critical for linkage analysis in the era before recombinant DNA technology was readily available. Using classic deletion mapping, Sparkes and coworkers studied five patients with retinoblastoma and found that, in all five, esterase D activity was only 50% of normal. These data suggested that the loci for retinoblastoma and esterase D genes were both within the deleted segment of chromosome 13q.[21] Based on the fact that the chromosome 13 deletion and the esterase D locus were tightly linked to retinoblastoma in multiple families with clinically and pathologically indistinguishable disease, Murphree and Benedict argued that there was probably a single *RB1* locus.[22] Further, retinoblastoma tissue from a nonhereditary unilateral patient was also found to contain a 13q14 deletion, suggesting that all forms of retinoblastoma involve the same gene on chromosome 13 at locus 13q14.[23] These investigations led to the consensus that a single retinoblastoma locus, *RB1 at 13q14.2*, is mutated in all forms of retinoblastoma.

Meanwhile, a body of scientific work was accumulating to support the notion that *RB1* is a recessive gene that is lost during tumorigenesis. Benedict and coworkers examined a familial retinoblastoma patient and found a 50% reduction of esterase D in normal cells and a complete absence of the enzyme activity in retinoblastoma cells.[24] Dryja and colleagues used DNA fragments from 13q14 to show that homozygous deletions could occasionally be identified in retinoblastoma tissue.[25] In a landmark paper, Cavenee et al. proved beyond doubt the recessive nature of the *RB1* gene and popularized the use of loss of heterozygosity analysis.[26] By comparing DNA from normal and tumor tissue, they found that the region around the *RB1* gene was frequently "reduced to homozygosity" in retinoblastoma tissue. In other words, one copy of the region around *RB1* was lost during tumorigenesis. Cavenee et al. also showed that in heritable cases, the germline copy of 13q

(carrying the mutant *RB1*) that was passed among affected family members was always the one that was retained in the tumor.[26] The chromosomal mechanisms involved in reduction to homozygosity on 13q14 are shown in Fig. 132.1.

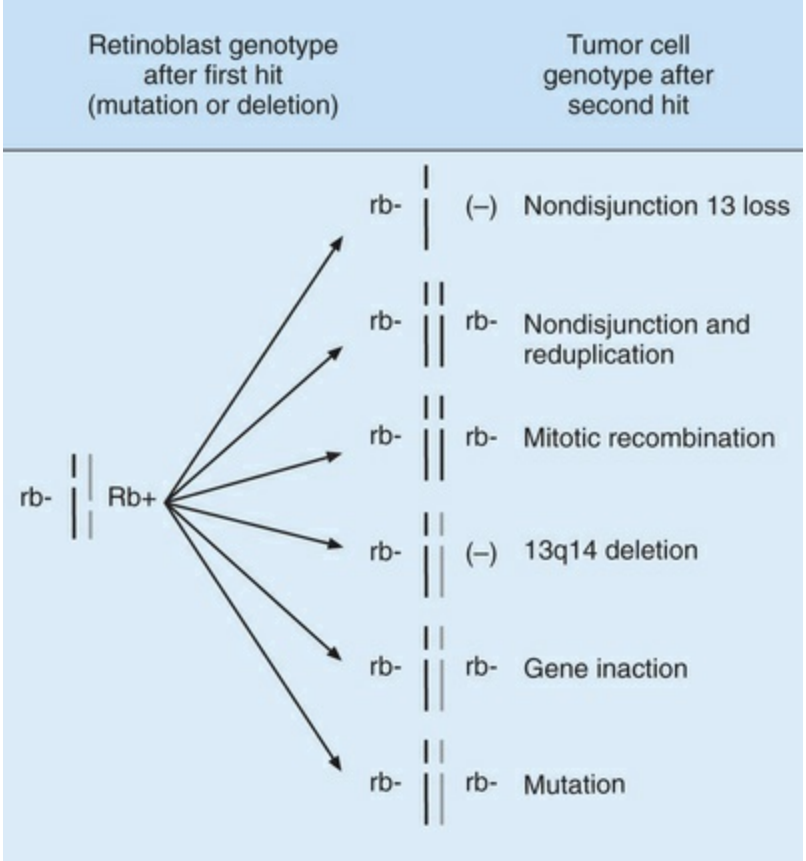

FIG. 132.1 Chromosomal mechanisms for loss of heterozygosity (LOH) that represents the second "hit" and loss of the second *RB1* gene allele in retinoblastoma.

Another breakthrough in the hunt for *RB1* was the cloning of the esterase D gene.[27,28] In the early days of recombinant DNA technology, cloning a gene usually required an activity that could be assayed, and esterase D provided such an activity. Once the esterase D gene was cloned, its DNA sequence was harnessed and could be used to probe adjacent stretches of chromosomal DNA to identify nearby genes. An intensive search ensued for the *RB1* gene, and the esterase D gene proved to be located very nearby to the *RB1* gene. A few short months following the cloning of esterase D, the

search culminated in the discovery of a large gene that contained deletions in many retinoblastomas.[29,30] By the early 1990s, there was a basic molecular understanding of how retinoblastoma is inherited. Transmission of an inactive copy of *RB1* imparts the predisposition to retinoblastoma. Because of the random background mutation rate in the developing retina, inactivation of the second copy then leads to tumor development.

The *RB1* Gene

The *RB1* gene (Fig. 132.2) contains 27 exons spanning over 200 kilobases of DNA. The 5′ end of the gene is oriented toward the centromere of chromosome 13. The promoter region lacks a typical TATA box but contains a CpG-rich region, or CpG island. Germline mutations in the *RB1* gene are distributed throughout the gene with mutational hotspots at CpG dinucleotides.[31,32] Less than 10% of retinoblastoma patients have a constitutional chromosome 13q abnormality (usually a deletion) that can be detected by karyotyping.[33,34] Deletions that are more extensive can be associated with the 13q-syndrome, with features such as growth and mental retardation, facial dysmorphism, microcephaly, skeletal anomalies, and genitourinary abnormalities. About 15–20% of germinal mutations are too small to detect by cytogenetics but can be detected with techniques for analyzing gross DNA rearrangements (e.g., Southern blot). The remainder of *RB1* gene mutations are small alterations involving one or a few nucleotides that can only be detected by high resolution methods and direct sequencing.[35] At our center in 2015, *RB1* gene testing is now performed with next generation sequencing techniques, with results being obtained in 4–6 weeks. The majority of these mutations are frameshift and nonsense mutations, inframe and missense mutations, splicing mutations, and mutations in noncoding regions that result in a truncated, unstable protein product (Table 132.1).[36] A recent review of *RB1* mutations found the following ratios: 37% nonsense, 21% splice, 20% frameshift, 9% large indel, 5% missense, 7% chromosomal deletions, and 1% promoter mutations.[37] The possibility of using truncated pRb protein mutants as the basis for genetic testing to detect germline *RB1* mutations was proposed

several years ago,[31] and recently shown to be feasible.[38] Interestingly, most new germline *RB1* mutations are of paternal origin, suggesting that the gene is more susceptible to mutation during spermatogenesis rather than oogenesis.[39]

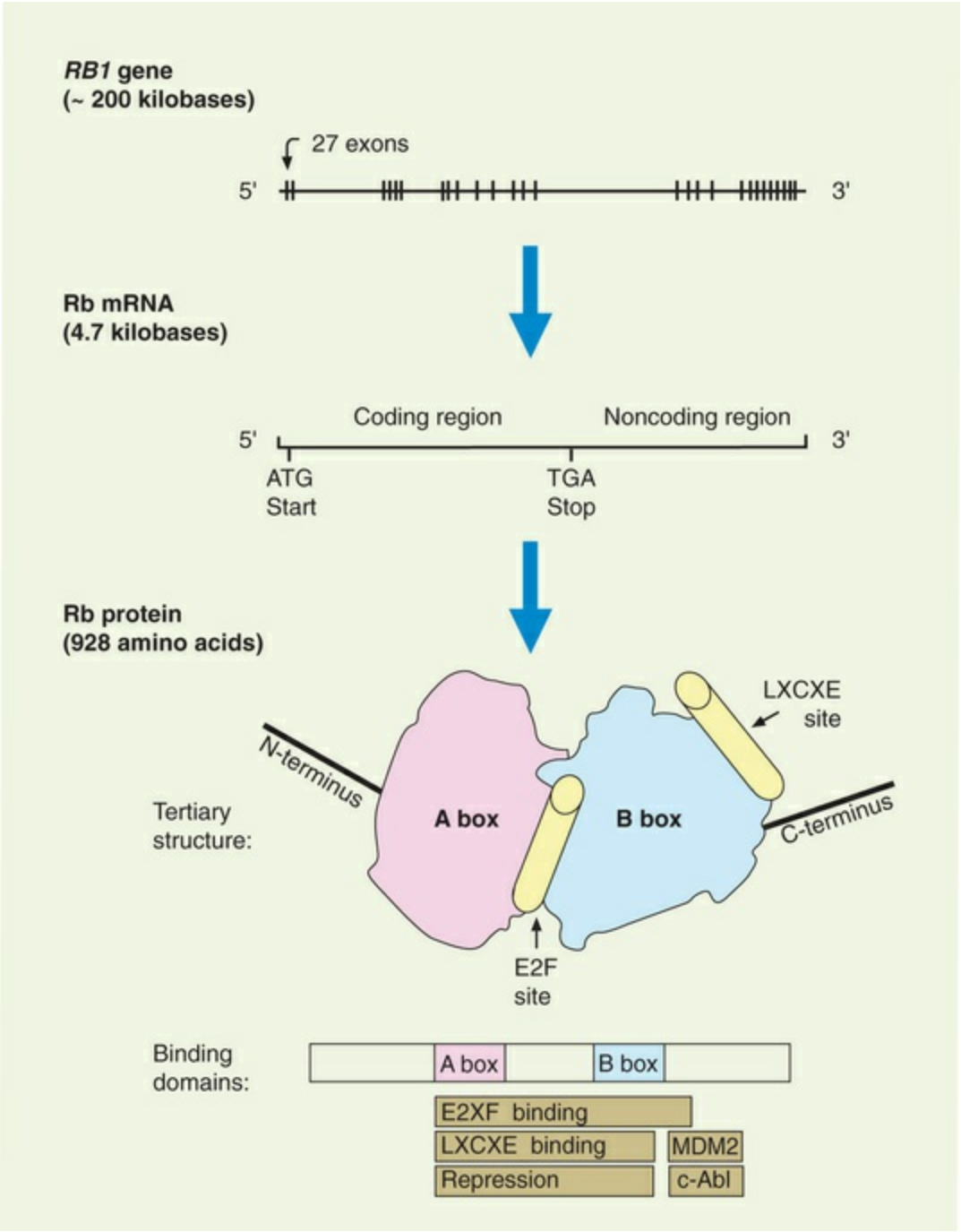

FIG. 132.2 *RB1* gene, mRNA transcript, and protein.

TABLE 132.1

Tumor Regression Patterns Following Primary Chemotherapy

Type	Description	Needs Consolidation
0	Small intraretinal lesion that disappears completely without RPE changes	No
I	Entire lesion calcifies into a mass that looks like "rock-salt." RPE changes at base	Yes (minimal)
II	Homogenous semitranslucent, gray "fish-flesh" lesion	Yes
III	A combination of type I and type II. This is the most common regression pattern	Yes
IV	An entirely flat chorioretinal scar with significant RPE changes, most commonly seen after laser consolidation	Yes
Early retinoma retinocytoma	Looks like type II regression prior to treatment with chemotherapy or radiotherapy and shows no change during or following treatment. May contain cystic or cavitary spaces	Variable

RPE, retinal pigmented epithelium.

Mutation of the second *RB1* allele is typically due to chromosomal aberrations, usually recognized as loss of heterozygosity (LOH) by polymorphism analysis.[40] These mutations occur at a much higher rate than the first, germline mutation (10^{-3} as compared with 10^{-7} for the first mutation).[41] The most common mechanism leading to LOH is mitotic recombination (50%), followed by nondisjunction with or without subsequent reduplication (~40%).[42] Other mechanisms include small deletions and gene conversions. Therapeutic exposure to ionizing radiation induces DNA damage and increases the risk of LOH, and hence tumorigenesis (i.e., second cancers), within the field of radiation.

Advances in rapid genetic testing have allowed for preimplantation genetic diagnosis (PGD) for retinoblastoma.[43] This procedure allows a couple in which one parent has a known germline mutation to undergo in vitro fertilization; prior to implantation, the embryos are tested for the mutation using single cell polymerase chain reaction and rapid DNA sequencing of the exon in question. Only those embryos that are mutation-free are implanted back into the mother. Although expertise and cutting-edge technology are required, PGD for retinoblastoma is currently offered at multiple centers throughout the United States.

Low Penetrance Retinoblastoma

The term penetrance refers to the frequency that a heritable disease

is manifest in the offspring of affected individuals. The word expressivity refers to the variability of clinical manifestations in affected individuals. For example, patients with heritable retinoblastoma who develop only unilateral eye disease manifest reduced expressivity. In general, reduced penetrance and expressivity tend to segregate in the same families. Overall, the penetrance of retinoblastoma is about 80–90%, but this represents a heterogeneous group of high-penetrance and low-penetrance families.[44] The diseased-eye ratio (the ratio of the number of eyes containing tumors to the number of mutation carriers in a family) was devised to quantitatively identify low penetrance retinoblastoma families by taking into account both penetrance and expressivity.[36] Most low penetrance families have diseased-eye ratios <1.5, whereas families with complete penetrance typically have diseased-eye ratios of ≥1.5. Initially, investigators postulated that low penetrance retinoblastoma may be due to immunologic factors, DNA methylation, epigenetic mechanisms, delayed mutation, host resistance factors, a second retinoblastoma locus, or modulator genes.[45,46] However, recent research has shown that most low-penetrance retinoblastoma results from mutations at the *RB1* gene locus that result in an pRb protein with reduced activity.[47–50] One of the most common low penetrance mutations is a missense alteration at codon 661 (exon 20).[47,50] Other reported low penetrance mutations include 3-bp deletion in exon 16 that results in the deletion of Asn480,50 a 4-kb deletion involving exons 24 and 25,54 and a splicing mutation at the last base of exon 21.[49] Insights gained from these low penetrant *RB1* mutants have added much to our understanding of how the retinoblastoma protein works.

RB1 Gene Mutations in Other Tumors

Not surprisingly, *RB1* gene mutations occur frequently in tumors linked to retinoblastoma, such as osteosarcomas, soft tissue sarcomas, and other mesenchymal tumors.[51,52] However, investigators were surprised to find that the *RB1* gene is also mutated frequently in some common adult malignancies such as breast, lung, and prostate cancer.[53–55]As our understanding of the *RB1* gene and its protein product have progressed, it has become

clear that *RB1* is disrupted in most human cancers, either by mutation of the gene or, more commonly, by functional inactivation of the protein.[56]

Retinoblastoma Without the *RB1* Mutation

In 2013 Gallie and colleagues published a landmark paper documenting a small population of unilateral nonhereditary cases with no detectable *RB1* mutations.[57] They analyzed tumor samples from 1068 unilateral tumors, and found no *RB1* mutation in 2.7% of the samples (29 cases). Approximately half of the 29 cases had evidence of MYCN oncogene amplification, ranging from 28 to 121 copies, whereas none of the tested samples with *RB1* mutations had additional copies of MYCN. The authors postulated that in rare cases, retinoblastoma or a tumor resembling retinoblastoma can develop unilaterally in young children without any mutations of *RB1* via the amplification of the MYC oncogene. The clinical profile of these 29 cases revealed a younger age group at presentation than sporadic unilateral retinoblastoma, averaging 4.5 months.[57] Tumors caused by MYCN amplification also demonstrated aggressive histopathologic features, including optic nerve invasion, absence of calcification, and poorly differentiated cells with prominent nucleoli. However, none of the 29 cases developed metastatic disease and the other eye remained normal. Although this is preliminary data, centers should routinely test enucleated globes with unilateral retinoblastoma patients for MYCN amplification. As with all unilateral cases, gene testing should be performed both on the tumor and serum to confirm the nonhereditary status of these patients.

The Role of the Retinoblastoma Protein in Tumor Suppression

The Retinoblastoma Protein

The *RB1* gene encodes a 4.7-kilobase messenger RNA transcript that produces a protein of 110 kD (kilodaltons) and 928 amino acids (Fig. 132.2). The pRb protein is phosphorylated in a cell cycle-dependent manner and localizes to the nucleus.[58–60] The

hypophosphorylated form predominates in quiescent and differentiating cells, whereas the hyperphosphorylated species accumulates in cycling cells as they enter DNA synthesis (S) phase (Fig. 132.3).[61–65] The hypophosphorylated form of pRb binds several viral oncoproteins, including SV40 large T antigen, adenoviral E1a, and human papillomavirus (HPV) E7.[66–68] When bound to pRb, these oncoproteins stimulate cell division. Taken together, these findings provide evidence that hypophosphorylated pRb is important in negatively regulating the cell cycle, and that this inhibitory activity can be thwarted either by phosphorylation or viral oncoprotein binding. Further work has shown that the major cell cycle function of pRb is to inhibit the transition of cells out of gap 1 (G1) phase into S phase.[69]

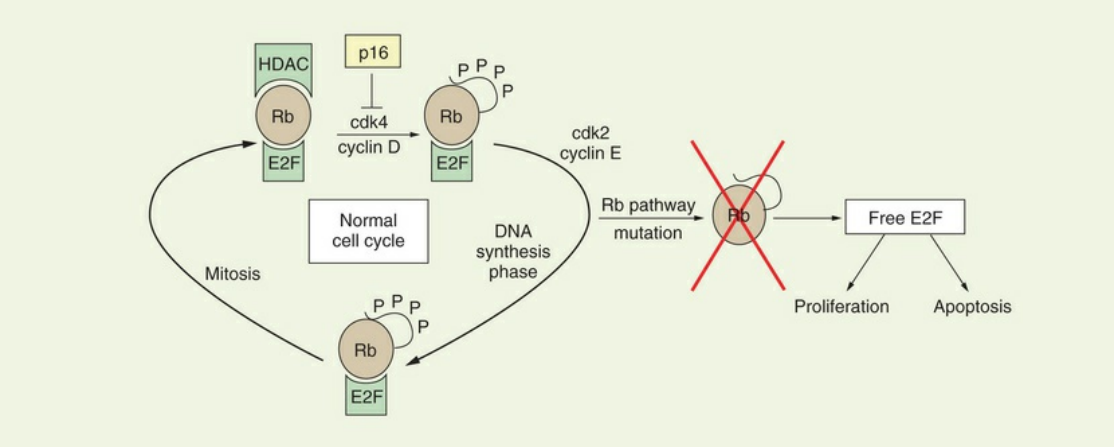

FIG. 132.3 Role of the Rb protein in the cell cycle and apoptosis.

A major breakthrough in understanding how pRb regulates the cell cycle was the observation that pRb binds to members of the E2F transcription factor family (referred to here as E2F).[70–72] Further work has shown that pRb function is largely dependent on interactions with E2F.[73] E2F sites are found in the promoters of many genes that are important for cell cycle progression, and pRb represses transcription of these genes through its interaction with E2F.[74–77] Since E2F (but not pRb) has a DNA binding domain, the pRb-E2F association would explain how pRb is brought to specific DNA elements to exert its effect. Most E2Fs have a transactivation domain that stimulates expression of genes containing E2F binding

sites in their promoters. pRb binds E2F within the transactivation domain, thereby masking its activity.[71,78] Since E2F activates genes involved in cell division, inhibition of E2F provided a mechanistic explanation for how pRb inhibited cell division.[74,79] However, the picture became more complicated with the recognition that pRb has intrinsic or "active" transcriptional repressor activity and is able to block the expression of genes when artificially brought to promoters by proteins other than E2F.[80] These findings suggest a complex relationship between pRb and E2F. In some situations pRb inhibits genes by simply masking the E2F transactivation domain, whereas in other situations E2F serves as a "courier" to deliver pRb to specific genes for active repression.

The importance of active repression by pRb was pointed out in several studies that showed that this activity is required for pRb to inhibit the G1-to-S phase transition of the cell cycle.[81,82] But how does pRb actively represses transcription? In a series of landmark papers several groups showed that pRb binds to and recruits promoters to proteins that alter chromatin structure, such as histone deacetylases,[82–84] SWI-SNF ATPases, DNA methyltransferases, polycomb complexes, and histone methylases.[85–90] Alteration of local chromatin structure into a restricted conformation prevents access by the transcriptional machinery, thereby inhibiting expression, whereas dynamic reorganization of chromatin into an open configuration allows gene transcription. Depending on the nature of the chromatin-remodeling complex that pRb recruits, the cell cycle inhibition can be temporary, as occurs during the quiescent period between cell divisions, or permanent, as occurs during cell differentiation and senescence.[91]

Studies of the tertiary (three-dimensional) structure of the pRb protein have provided insights into how the protein performs these complex functions. The central region of the pRb protein contains the A box and B box, which are highly conserved from human to plants. These regions interact with each other along an extended interdomain interface to form the A–B pocket. The pocket is critical for the tumor suppressor function of pRb, and is disrupted by most germline mutations in hereditary retinoblastoma patients and somatic mutations in tumors.[31,92] The pocket is required for binding to E2F, chromatin remodeling enzymes, viral oncoproteins, and

other molecules. Many pRb-binding proteins contain an LxCxE (leucine – variable amino acid – cysteine – variable amino acid – glutamic acid) binding motif, which has been shown by crystallographic studies to be located in the B box. The B box does not assume an active confirmation unless bound to the A box, thereby providing an explanation for why both boxes of the pocket domain are required for pRb activity. Interestingly, E2F does not contain the LxCxE motif and binds pRb at a distinct site. Recent crystallographic studies confirmed that the E2F binding site, located at the interface between the A and B boxes, is distinct from the LxCxE site.[93] These findings provide a structural explanation for how pRb simultaneously binds E2F and chromatin remodeling proteins, many of which interact with pRb through the LxCxE site.[87] The current molecular view is that pRb orchestrates the assembly of multiprotein complexes, which are then recruited to specific promoters by E2F, where they control access of the transcriptional machinery. Thus, pRb regulates in a dynamic and integrated manner the expression of specific genes involved in cell division, differentiation, and apoptosis.[94]

The carboxy-terminal end of the pRb protein is also critical for its function. This region is required, along with the pocket, for binding to E2F.[95] In addition, most of the phosphorylation sites that seem to be critical for regulating pRb activity are located in the carboxy-terminus.[96] In fact, recent work has shown that phosphorylation of pRb on the C-terminus initiates a novel intramolecular interaction that progressively strips pRb of activity as the cell moves through the cell cycle.[97] The carboxy-terminal region also contains binding sites for the oncoproteins c-abl and MDM2.[98,99] The tyrosine kinase activity of c-abl is blocked when it is complexed with pRb, and this interaction appears to be important for Rb-mediated growth suppression.[100,101] Besides directly blocking c-abl, the C-terminal region also appears to participate in the assembly of multimeric complexes containing pRb, E2F, c-abl, and potentially other proteins.[98] The importance of the pRb-MDM2 interaction is less clear. MDM2 interacts with the p53 tumor suppressor protein and opposes its proapoptotic activity by repressing p53 transcriptional activation and by mediating its degradation.[102,103] While initial results demonstrated that MDM2 blocks pRb function, more recent

studies have shown that pRb can form a trimeric complex with MDM2 and p53 and thereby block the antiapoptotic activity of MDM2 by preventing the degradation of p53.[104]

The function of the amino-terminal end of the pRb protein remains less clear. This region contains phosphorylation sites that may regulate pRb activity. Additionally, this region interacts with several proteins, including a replication-licensing factor (MCM7),[105] a novel G2/M cycle-regulated kinase, and other proteins.[105–107] However, the function of these interactions has not been established. *RB1*$^{+/-}$ mice that develop pituitary tumors due to loss of Rb failed to be "rescued" by expression of a mutant form of pRb that lacked the amino-terminus, although the onset of tumors was delayed.[108] In other experiments tumor suppression by pRb was actually enhanced when the amino-terminal region was removed.[109–111] Thus, the amino-terminus appears to contribute only weakly to the overall tumor suppressor activity of pRb.

Not only was the *RB1* gene the first identified tumor suppressor gene, but the Rb pathway was the first, and still one of the most important, tumor suppressor pathways to be elucidated in human cancer.[56] As described above, the pRb protein is critical for regulation of the cell cycle, as well as senescence, differentiation, and apoptosis, all of which are deregulated during cancer formation.[112–116] While the pRb pathway is deregulated in virtually all cancers, the *RB1* gene is mutated in only a limited spectrum of cancers. In these other cancers the pRb protein is inactivated by maintaining it in a hyperphosphorylated state. This occurs by deregulating the pRb pathway, which controls the phosphorylation state of pRb through kinases and kinase inhibitors.

The *RB1* Tumor Suppressor Pathway

Cell cycle progression normally occurs when pRb is inactivated by phosphorylation that is catalyzed by cyclin-dependent kinases (CDKs) in complex with their cyclin partners.[117,118] pRb contains 16 potential sites for CDK phosphorylation, and it oscillates between hypophosphorylated and hyperphosphorylated forms in cycling cells. At least three different cyclin/CDK complexes phosphorylate pRb during the cell cycle.. Cyclin D-ck4/6 phosphorylates pRb early in G1, cyclin E-CDK2 phosphorylates the protein near the end of

G1, and cyclin A-CDK2 is thought to maintain phosphorylation of pRb during S phase.[56] Phosphorylation of specific sites appears to regulate distinct pRb functions, suggesting complex regulation of pRb by these phosphorylation events. For example, binding of E2F, LxCxE proteins, and c-abl are regulated by distinct sets of phosphorylation sites in the carboxy-terminus.[119,120]

pRb is phosphorylated sequentially by different CDKs during the cell cycle. In fact, successive phosphorylation of pRb by cyclin D-CDK4/6 and cyclin E-CDK2 appears to be necessary to completely hyperphosphorylate pRb.[118] Recently, a mechanistic explanation was suggested for how cyclin D-CDK4/6 and cyclin E-CDK2 may regulate distinct pRb functions.[97] Cyclin D-CDK4/6 appears to phosphorylate specific sites in the carboxy-terminal region of pRb, and this phosphorylation triggers an intramolecular interaction between the phosphorylated C-terminal region and a positively charged "lysine patch" encircling the LxCxE binding site in the B box of the pocket. This interaction displaces LxCxE proteins such as histone deacetylase from the pocket, thereby blocking the ability of pRb to arrest the cell cycle.[81,97] However, pRb can still bind to E2F in this partially phosphorylated state. Under hyperproliferative conditions, the intramolecular interaction between the carboxy-terminal region of pRb and the pocket also can recruit cyclin E/CDK2 to the pocket, where it phosphorylates serine-567, an otherwise inaccessible site buried within the pocket.[106] Ser-567 makes critical contacts between domain A and B,4 and this phosphorylation disrupts the A–B interface and disrupts pRb binding to E2F. The sensitive location of Ser-567 is further illustrated by the fact that it is the only CDK phosphoacceptor site in pRb that is a target of naturally occurring missense mutations in tumors.[121] The more complete inactivation of pRb, indicated by phosphorylation of serine-567, leads to release of E2F and increased apoptosis.[115] Taken together, these findings suggest that the normal cell cycle may be regulated by partial phosphorylation of pRb that is catalyzed by cyclin D-CDK4/6, whereas the more complete phosphorylation that requires cyclin E-CDK2 may serve as a checkpoint for an abnormal hyperproliferative state that would trigger cell death.

Proteins called cyclin dependent kinase inhibitors (CDKIs), which

inhibit the kinases that phosphorylate Rb, represent another layer of complexity in the regulation of pRb. The p16INK4a protein is a CDKI that specifically inhibits CDK4, which catalyzes the early phosphorylation of pRb.[122] A tumor suppressor protein in its own right, p16INK4a is mutated or inactivated in many types of cancer, including cutaneous and uveal melanoma.[123] Loss of p16INK4a allows cyclin D-CDK4 to act unopposed in phosphorylating pRb, which results in constitutive functional inactivation of pRb. Since pRb and p16INK4a act in the same pathway, and mutation of either gene results in a similar deregulation of the cell cycle, both genes are rarely mutated in the same tumor.[124] Other CDKIs, such as p21 and p27 have more broad roles in regulating the cell cycle.[125]

Molecular Pathogenesis of Retinoblastoma

There is now overwhelming evidence that supports the hypothesis that mutational inactivation of the *RB1* gene is the initiating event in retinoblastoma. However, there remain many unanswered questions about the molecular pathogenesis of this tumor. Since pRb is important for regulating normal cell growth and differentiation throughout the body, why does germline mutation of the *RB1* gene predispose primarily to the rare eye tumor? This question was once quite enigmatic but is now becoming clearer. Indeed, carriers of *RB1* mutations are predisposed to a whole range of tumors, but the age of susceptibility is different for each tumor type. Whereas retinoblastomas occur mostly from birth to 5 years of age, mesenchymal tumors tend to occur in the teenage years, and melanomas peak in a slightly older age group. A recent report clearly shows that common epithelial tumors also occur at increased frequency in retinoblastoma survivors, but this effect is only seen in individuals beyond 40 years old.[126] Thus, it seems likely that loss of *RB1* predisposes to a broad range of neoplasms, each requiring different numbers and types of "hits" for tumorigenesis to become manifest; the fewer "hits" required, the earlier in life the tumor begins to appear in patients.

While mutation of the *RB1* gene is clearly necessary for retinoblastoma formation, is inactivation of retinoblastoma alone sufficient for tumorigenesis? Some investigators have argued

additional mutations in other genes must be required based on the following observations. First, deletion of the *RB1* gene in normal cells leads to apoptosis, rather than tumor formation, because loss of pRb triggers a p53-mediated apoptotic response.[127] This presumably explains why most cancers contain mutations in both the pRb and p53 pathways.[91,128] Second, retinoblastomas cannot be produced in mice unless both pRb and p53 are inactivated.[129] This led to a search for mutations in p53 or other proapoptotic genes. Interestingly, however, p53 is rarely mutated in human retinoblastoma, and no other apoptotic genes have been convincingly linked to retinoblastoma.[130] Finally, cytogenetic alterations on other chromosomes (e.g., 6p) are frequently observed in retinoblastomas, potentially suggesting the presence of other retinoblastoma-associated genes located at those chromosomal regions.[131,132]

Recent work has shown that MDM2 and MDMx may play an important role in attenuating the normal apoptotic events that should occur in an $RB1^{-/-}$ state. MDM2 targets p53 for ubiquitin-mediated proteolysis and is also a downstream target of p53. This creates an autofeedback loop that maintains p53 at a low level. Small molecule inhibition of MDM2 has been shown to lead to increased levels of p53 in retinoblastoma cell lines leading to p53-mediated apoptosis.[133,134]

While the existence of a "second RB gene" cannot be confirmed or refuted at this time, the strong autosomal dominant inheritance pattern of retinoblastoma indicates that the *RB1* gene mutations are clearly rate-limiting, so any other necessary events must occur at such a high spontaneous rate that they do not affect the clinical inheritance pattern. The emphasis on mouse models to understand human retinoblastoma may have limitations. Naturally occurring retinoblastomas are virtually nonexistent in mice and other animals, suggesting that the developing human retina may contain molecular, cellular, and anatomic features that make it uniquely susceptible to this tumor.

An alternative explanation for retinoblastoma pathogenesis is simply that retinal progenitor cells pass through a window of susceptibility prior to terminal differentiation in which loss of pRb leads to a differentiation defect, rather than an apoptotic response,

which leads to an accumulation of proliferating embryonic retinal cells. This hypothesis does not require the conjectural existence of additional "retinoblastoma genes" and satisfactorily accounts for developmental and clinical observations. pRb is indeed required in a cell-autonomous manner for appropriate cell cycle exit and differentiation of retinal progenitor cells.[135] Further, the topographic distribution of retinal tumors parallels the pattern of retinal differentiation. The retina differentiates in a posterior-to-anterior wave from the posterior pole to the ora serrata.[136,137] Interestingly, the chronologic development of retinoblastomas follows this same pattern, with earlier tumors occurring posteriorly and later tumors occurring more peripherally.[137] Retinal progenitor cells that retain the capacity to differentiate into photoreceptors, neurons, and glia can be identified in the retina until after birth, suggesting a window of susceptibility from fetal week 12 until 4–5 years of age for the bi-allelic loss of the *RB1* gene to have the possibility of producing retinoblastoma.[138]

Another controversy regards the cell of origin of retinoblastoma. Retinoblastomas derive from cells of the immature neuroepithelial inner layer of the optic cup that have the potential to differentiate into rod and cone photoreceptors and Müller cells.[139] Several studies have documented the presence of cone-specific markers, such as transducin, cone photopigments (red and green opsin), and cone phosphodiesterase in retinoblastoma.[140] However, since cone differentiation may represent a "default" pathway in the absence of normal signaling,[141] it is unclear whether retinoblastomas arise from neuroblasts that are already committed to the cone lineage, or whether retinoblasts that lose pRb are unable to differentiate along their appropriate lineage and are subsequently directed into the cone pathway. Cone cell precursors, but not mature cone cells, express pRb. In addition, cone cell precursors also express MDM2, which is a transcriptional target of Trβ2 that is also transiently expressed in cone cell precursors. Taken together, loss of pRb in a cone cell precursor that is already expressing MDM2 as part of its developmental program could plausibly lead to transformation and would be consistent with this being a potential cell of origin. More specifically, recent work shows that postmitotic human cone precursors possess cell-type circuitry which is uniquely susceptible

to pRB depletion.[142]

Retinoblastoma: the Disease

Terminology

Retinoblastoma can seem like a complicated subject for both medical professionals and affected families. To avoid unnecessary confusion, it is important to use precise terminology when discussing retinoblastoma.

The term "bilateral retinoblastoma" should be used only to describe a phenotype, i.e., a patient who has the clinical disease in both eyes. When the intent is to define a genotype – the whole group or class of patients with a germline mutation, a much clearer term is germinal (or heritable) retinoblastoma. All patients with bilateral disease carry the *RB1* germline mutation but not all people who carry the *RB1* mutation have bilateral disease. The phenotype (clinical presentation of the disease), will depend upon whether the second tumorigenic *RB1* mutation occurs and cancer is initiated in both eyes (bilateral), only one eye (unilateral), or neither eye (unaffected gene carrier).

The term "familial" is correctly used to describe a patient or family in which the germline mutation was passed down from a previous generation. A new sporadic bilateral case of retinoblastoma when neither parent has the *RB1* mutation is more precisely referred to as germinal or "heritable" rather than "hereditary," although many do not make this distinction. A unilaterally affected child who has one parent with a known *RB1* mutation is clearly both heritable and familial but obviously not "bilateral." We consider the terms "heritable" and "germinal" to be interchangeable.

Clinical Overview of Retinoblastoma

Retinoblastoma typically presents between birth and 5 years of age, so the disease predominantly affects young children. The clinical signs that lead to the diagnosis of retinoblastoma are typically noted by one or both parents. In dim light when the pupil dilates

naturally, parents may see light reflected by the tumor causing a "cat's eye" reflection in the pupil (i.e., leukocoria). This whitish pupil reflex may also be noted on pictures, which contrasts with the expected "red eye" on flash photographs (Fig. 132.4). Less commonly, more advanced intraocular retinoblastoma may manifest as the lack of a red pupillary reflex and may appear dark, due to either a vitreous hemorrhage, tumor necrosis, or a complete retinal detachment. When the tumor destroys central vision early in the course of the disease, and binocularity is lost, the presenting sign may be strabismus. Since almost all nonfamilial cases are diagnosed late, patients often have a combination of leukocoria and strabismus at presentation.

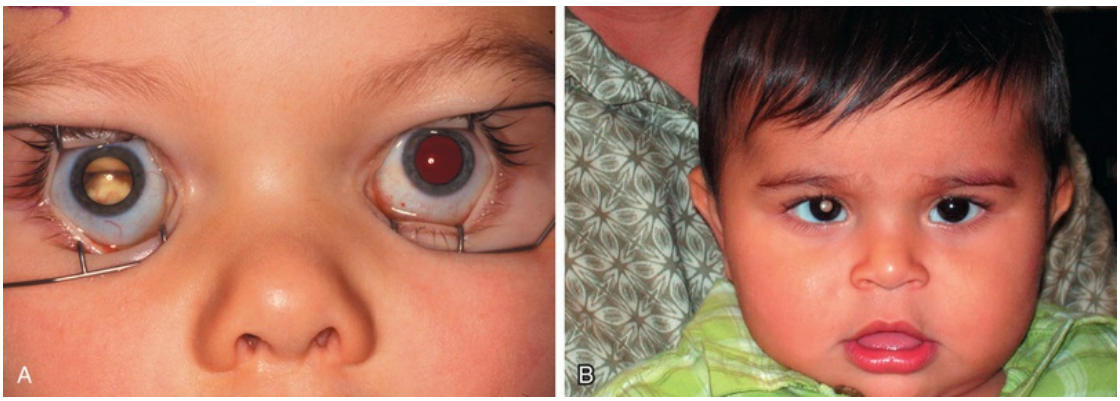

FIG. 132.4 (A) Patient with leukocoria in the right eye and a white mass filling the pupil. (B) "Cat's eye" reflection in the right pupil, noticeable in a flash photograph.

The younger the age of the patient, the more likely the tumors will start in the posterior pole. Early tumors appear as discrete, whitish retinal masses without intrinsic vascularity. As the tumors grow, they increase in both basal diameter and apical height while acquiring more vascularity, eventually fragmenting to cause vitreous or subretinal seeding. Eventually, the expanding mass can cause retinal detachment, neovascular glaucoma and/or intraocular hemorrhage before it spreads beyond the eye, either by contiguous spread through the optic nerve or hematogenously through the choroidal circulation. Very rarely, tumors may spontaneously involute, activating a process that will result in ocular phthisis. If

left untreated, most intraocular retinoblastomas will expand directly into the optic nerve then seed the central nervous system (CNS), or spread via hematogenous dissemination to bone marrow, bone, and other organs. Enucleation was the recommended treatment in James Wardrop's original clinical description of retinoblastoma in 1809 and remains a superb treatment option today, especially for advanced unilateral disease.

Epidemiology

In the United States, retinoblastoma represents approximately 6% of all childhood cancers under age 5, with stable incidence rates over the past 30 years.[143] In developing tropical and subtropical regions of the world, including Central Africa, Southern Asia, and Central America, retinoblastoma is one of the most common solid tumors of childhood.[144–160] While the worldwide incidence of the heritable form of the disease has been relatively constant, this may not be the case for unilateral sporadic nonheritable retinoblastoma. The possibility of an increasing incidence of unilateral nonheritable disease in underdeveloped countries has come to wide attention in part due to the important work of Ian McGrath and colleagues at the International Network of Cancer Treatment and Research (INCTR website at: http://www.inctr.org/). Orjuela and her colleagues at Columbia University in New York and at the Instituto National de Pediatria in Mexico City have suggested deficiencies in maternal diet during pregnancy may increase the risk of sporadic retinoblastoma.[161] Perinatal infection with HPV was suggested as a possible mechanism for increasing the incidence of nonheritable retinoblastoma,[162,163] but this association has not been corroborated by other groups.[164,165]

There are various methods of determining the incidence and prevalence of retinoblastoma in a given population. The overall incidence (heritable and nonheritable cases combined) of retinoblastoma in developed countries is most commonly reported as the number of cases diagnosed in a selected period per live births for that period. Although this index does not reflect the entire population at risk, since children continue to be at risk until 5 years of age and beyond, it does present some uniformity for comparison

of the frequency of the disease across populations. The incidence can also be expressed as the number of cases diagnosed per year for a given population of children in a specified age group.[166]

After 1970, the prevalence of retinoblastoma in the United States (number of cases per number of persons in the at-risk age group) is consistently reported at around 11 cases per million children under 5 years of age, or equivalent to an incidence of 1/18, 000 live births.[167,168] Because there is no complete retinoblastoma registry in North America, the exact incidence is unknown, but it is estimated that there are about 300 new cases per year. These incidence estimates fit closely with studies reported from New Zealand, Sweden, and Australia, which all show incidence rates of 1/17, 000–1/18, 000 live births.[169–171]

As previously mentioned, authors have hypothesized that preconception environmental exposure increases the risk of heritable retinoblastoma and postconception exposure increases the risk of nonheritable retinoblastoma.[172] Bunin and colleagues have demonstrated that some environmental factors, such as gonadal radiation exposure prior to conception and paternal employment in the military or metal industry, were associated with an increased risk of sporadic, heritable retioblastoma.[33,172] However, the incidence of heritable retinoblastoma among the various populations of the world is remarkably constant, providing evidence that environmental influences likely play an insignificant role in the etiology of the hereditary form of this tumor.[171,173] Buckley also provided evidence that environmental factors probably play a very minor role in the hereditary form of cancer in very young children.[174]

One of the few identified risk factors for retinoblastoma is advanced paternal age, which has been unequivocally associated with new sporadic germline mutations and heritable retinoblastoma.[39,175–180] Excess cancer in relatives is also a common finding in solid childhood tumors, particularly retinoblastoma.[181] Some 80–85% of new heritable tumors preferentially retained the paternal allele (i.e., the mutated allele) and lost the normal maternal allele as the result of a chromosomal error at mitosis.[182,183] These data suggest that new germline *RB1* mutations arise more frequently during spermatogenesis than during oogenesis.

Natural History of Intraocular Retinoblastoma

There are many characteristic features of retinoblastoma, but also wide variability in its clinical presentation. In general, patients with bilateral retinoblastoma (heritable disease) present at an earlier age (average 12 months) than patients with unilateral disease (average 24 months). However, it is not uncommon for patients with nonheritable unilateral disease to present before 6 months of age. Approximately 90% of children with retinoblastoma present between birth and 5 years of age,[166] but it is not unusual for retinoblastoma to be diagnosed in utero, or as late as 8 years of age. If it can be assumed that retinoblastoma tumors become ophthalmoscopically apparent in the retina within a short time after the second "hit" at the *RB1* locus, then retinoblastoma may have its initiating genetic event in the retina as late as the 5th birthday. If deficiency of maternal diet can affect the incidence of unilateral nonheritable retinoblastoma, then evidence supports the view that the earliest somatic gene mutations can occur during fetal life. Although more is known about the genetic events that cause retinoblastoma than any other cancer, other unknown factors may be at play that contribute to the variable clinical presentations for retinoblastoma.

Regardless of when the cellular events take place that lead to the formation of retinoblastoma, the earliest physical appearance of the tumor is fixed by the fact that all cells in the tiny tumor focus are identical, i.e., they are daughter cells of the original "founder" cell with the same genes and the same growth rate. A new tumor will expand symmetrically as a round or hemispherical lesion that is homogenous (Fig. 132.5). In its earliest manifestation retinoblastoma resembles bacterial colonies on an agar plate. Because tumor growth begins with a single immortalized retinoblast, all intraocular retinoblastomas are initially confined to the retina. Early tumor formation occurs rapidly, with an estimated tumor doubling time of 15 days.[184] Evidence from optic coherence tomography suggests that the early tumor formation occurs predominantly in the outer retina,[185,186] with eventual full-thickness involvement. Our preliminary experience with optical coherence

tomography (OCT) on small tumors suggests the outer nuclear layer as the site of origin for retinoblastoma, which would support the theory of a cone-precursor origin for the tumor.

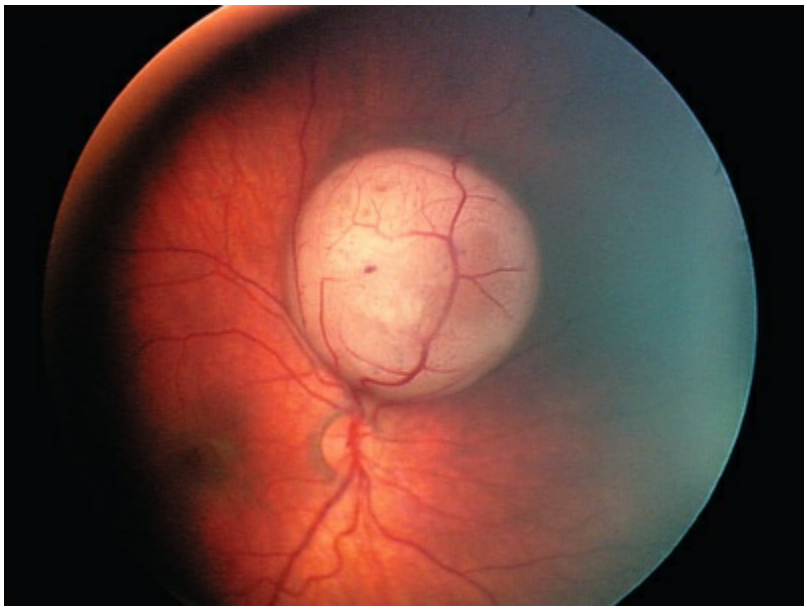

FIG. 132.5 Solitary retinoblastoma that is symmetrically round and homogeneous due to a clone of "founder" cells with identical genes and growth rate.

Tumor angiogenesis is essential if tumors are to expand, and conversely, avascularity severely restricts the potential growth of tumors.[187] Intraretinal retinoblastoma with a diameter less than 2 mm are dependent on diffusion of nutrients and oxygen from the choroid, and this may explain the clinical observation that early small tumors in infants don't respond very well to systemic chemotherapy.[188] Enlarging tumors begin to acquire new blood vessels in response to growth factors generated from upregulated growth factor genes and downregulated angiogenesis inhibitory genes. These new blood vessels can be demonstrated on fluorescein angiography as reticular pattern of fine capillaries in small tumors and large neovascular vessels with bizarre branching patterns and associated hypoperfusion and leakage in larger tumors.[189,190] With the recruitment of new blood vessels, tumors continue to grow toward the vitreous cavity (endophytic growth pattern), or into the subretinal space (exophytic growth pattern). Retinoblastoma tumors remain confined to the retina until new mutations occur,

perhaps due to loss of the suppressor gene PTEN,[191] that allow them to grow without extracellular matrix anchorage dependence. Loss of cell adhesion is likely to be the major cellular event required to enable the emergence of vitreous and subretinal seeding.

Tumor cells that invade the vitreous or subretinal space now enter a low-oxygen, low-nutrient microenvironment. The shape and structure of early vitreous seeds are limited to a thickness of two tumor cells surrounding an inner core of necrotic oxygen-starved tumor. However, large avascular vitreous and subretinal masses eventually form, and represent the continued "progression" of an intraocular malignancy (Fig. 132.6). Tumor cells in these masses can survive and even thrive in this new low-oxygen environment. In advanced group D and E eyes it is common to find large avascular masses either in the vitreous or subretinal space (see discussion of retinoblastoma classification, below).

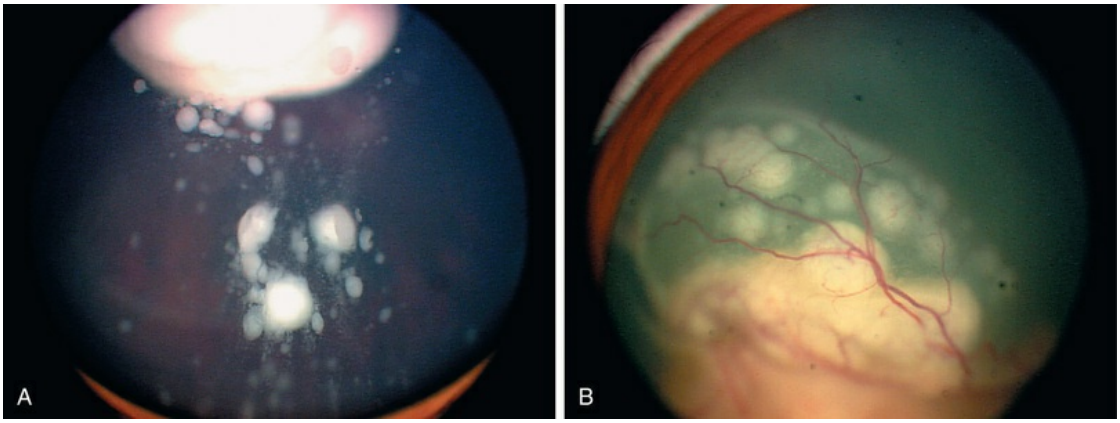

FIG. 132.6 Vitreous (A) and subretinal (B) seeding from the primary tumor. With enough cell divisions and spontaneous mutations there is loss of cellular adhesion.

Continued growth of the tumor leads to total destruction and even replacement of the retina with tumor cells. Angle closure glaucoma is a common endstage manifestation of massive tumor growth, either from pressure of the tumor pushing the iris lens diaphragm forward, from direct occlusion of the chamber angle by tumor cells or red blood cells, or by proliferation of iris neovascularization to involve the anterior chamber angle. Tumor cells will invade the optic nerve and spread into the chiasm and

brain, either by direct contiguous growth or through seeding of the leptomeninges. Less commonly, the tumor will follow vessels and nerves that penetrate the sclera and expand as a mass lesion in the orbit. Retinoblastoma cells that reach the choroid can spread hematogenously to the lung, bone marrow, and other organs.

The ability to metastasize requires the acquisition of a number of cell capabilities that are not present in early descendants of the original "founder" cell. Interruption of the function of the eye and alteration of its normal anatomy are two of the main reasons that most retinoblastomas are diagnosed and treated before they metastasize. Most retinoblastomas attract attention and are treated, long before they have acquired all of the enabling mutations required for metastasis. Simple access to the bloodstream is required but not sufficient for metastasis. To gain access to distant sites via the bloodstream, a tumor cell must have the ability to digest and move through extracellular matrix,[192] and to digest and penetrate the basement membrane, adventitia, and endothelium of the vessel wall. In order to escape the high-flow vascular channels, a tumor cell must be able to adhere to the vascular endothelium at a location outside the eye, digest its way through all layers of the vessel wall, survive in the extravascular environment, recruit a blood supply, and establish its own microenvironment. Because all these abilities are achieved only through a series of spontaneous mutations that require many tumor cell doublings, most patients who develop metastatic disease have had the continued presence of viable tumor cells for an extended period, often with multiple recurrences before the eye was eventually enucleated. For this reason, efforts to salvage an eye that has had multiple episodes of tumor regrowth over a period of more than 6–12 months should raise increasing concerns about the escalating risk of metastatic disease in that child.

Classification of Intraocular Retinoblastoma

The Reese–Ellsworth group classification system specifically predicts the likelihood of ocular salvage following treatment with EBR. It does not function as well in predicting likelihood of salvaging eyes treated with primary chemotherapy and/or focal

consolidation. The introduction of systemic chemotherapy as the main primary modality to salvage intraocular retinoblastoma in most retinoblastoma centers during the 1990s propelled the creation of a new group classification for intraocular retinoblastoma.

Reese–Ellsworth Classification

The Reese–Ellsworth classification system, originally published in 1964, was a major advance in our collective understanding of retinoblastoma.[193,194] It is a group classification system and as such, only deals with organ-confined intraocular disease. In a staging system evaluating the whole child, a group classification would fit entirely within stage I disease. The Reese–Ellsworth classification was developed just as the indirect ophthalmoscope was being introduced into clinical practice. Anterior tumors, which typically occur in the setting of more advanced disease, also cause the eye to be classified in a more advanced group when using the Reese–Ellsworth classification. The classification does not take into account retinal detachment, subretinal tumor seeding, or other ocular findings such as neovascular glaucoma. Also, vitreous seeding of any amount places the eye in group Vb (the last of 10 subgroups), with the poorest prognosis. Today local vitreous seeding can be successfully treated with intravitreal melphalan injections.

International Classification for Intraocular Retinoblastoma

In 1989 Kingston and colleagues began employing the systemic chemotherapy regimen currently in use in most centers (carboplatin, etoposide, vincristine – known as CEV or VEC in North American centers, and JOE in Britain) in combination with EBR as the primary treatment of retinoblastoma for Reese–Ellsworth group Vb eyes.[195] In January 1990 Murphree was the first to use chemotherapy plus local consolidation without EBR for all Reese–Ellsworth groups.[196] Initially the early stage Reese–Ellsworth eyes in Los Angeles were treated with carboplatin alone combined with transpupillary diode laser hyperthermia (chemothermotherapy). Over the next 5 years at many centers,

advanced intraocular disease was treated with CEV systemic chemotherapy combined with sequential aggressive local therapy.[197,198] Authors introduced the term "chemoreduction" to describe the concept of reducing the volume of the tumor with systemic chemotherapy followed by local consolidation.

Efforts at developing a revised classification that reflected the move away from EBR to primary chemotherapy for intraocular retinoblastoma began as early as 1994, when Murphree and Hungerford co-chaired a meeting of retinoblastoma specialists from around the world for a full day of discussions on the development of a new classification system at the International Congress of Ophthalmology in Toronto. The system that grew out of those discussions took into account zone of disease similar to retinopathy of prematurity. Eventually, the ABC classification system was described at the European Congress of Ophthalmology meeting in Istanbul in 2001 and the case for a new group classification was subsequently published.[199]

The International Classification System (Box 132.1) is based both on the natural history of retinoblastoma and on the likelihood of salvaging the eye when systemic chemotherapy is used as the primary treatment. Letters "A" through "E" instead of numbers were chosen to designate each classification group to avoid confusion with the Reese–Ellsworth system. The risk of loss of the eye due to retinoblastoma is graduated from "very low" for group A to "very high" for group E.

Box 132.1

International Classification for Intraocular Retinoblastoma[195]

Group A – Very Low Risk

Small discrete intraretinal tumors away from the fovea and optic disc

- All tumors are ≤3 mm in greatest dimension, confined to the retina
- All tumors are located further than 3 mm from the fovea and 1.5 mm from the optic disc

Group B – Low Risk

All remaining discrete retinal tumors without seeding

- All tumors confined to the retina not in group A
- Any tumor size and location with no vitreous or subretinal seeding
- Small cuff of subretinal fluid allowed (3 mm from tumor border)

Group C – Moderate Risk

Discrete local disease with minimal focal subretinal or vitreous seeding

- Tumor(s) must be discrete
- Subretinal fluid involving up to one quadrant of the fundus
- Local subretinal or vitreous seeding, less than 3 mm from the tumor

Group D – High Risk

Diffuse disease with significant vitreous and/or subretinal seeding

- Tumor(s) are massive or diffuse
- Subretinal fluid, one quadrant of the fundus to total retinal detachment
- Diffuse subretinal seeding, may include subretinal plaques or tumor nodules
- Diffuse or massive vitreous disease may include “greasy” seeds or avascular tumor masses

Group E – Very High Risk

Presence of any one or more of these poor prognosis features

- Neovascular glaucoma and/or buphthalmos

- Tumor anterior to anterior vitreous face involving ciliary body or anterior segment on clinical exam or ultrasound biomicroscopy (i.e., tumor touching the lens)
- Diffuse infiltrating retinoblastoma
- Opaque media from hemorrhage
- Tumor necrosis with aseptic orbital cellulitis
- Phthisis bulbi

In this classification, the letter "A" is assigned to those eyes for which both the likelihood of curing the tumor and retaining excellent vision are both high. In intraocular group A eyes the lesions are small and are away from critical visual structures (fovea and optic nerve). Groups A and B contain all eyes in which the tumor remains confined to the retina. In groups C and D eyes, the tumor has spread into the vitreous and subretinal space. In the case of group C eyes the spread is local. In the case of group D eyes the seeding is diffuse (Fig. 132.7). The definition of local seeding has been further defined as 3 mm or less from the margin of the tumor, whereas subretinal or vitreous seeding more than 3 mm has been defined as being diffuse. Group E eyes have been destroyed by the tumor and are rarely salvageable; these eyes demonstrate neovascular glaucoma, buphthalmos, vitreous hemorrhage, ocular phthisis, or tumor extending anterior to the anterior vitreous face. In this system the morbidity of the treatment increases from group A to group E, and the probability of salvaging the eye and useful vision decreases from A to E. Within limits, when chemotherapy is the primary treatment of retinoblastoma, absolute volume of the tumor is relatively less important than whether the tumor has become dispersed within the eye to either the vitreous or the subretinal fluid or both.

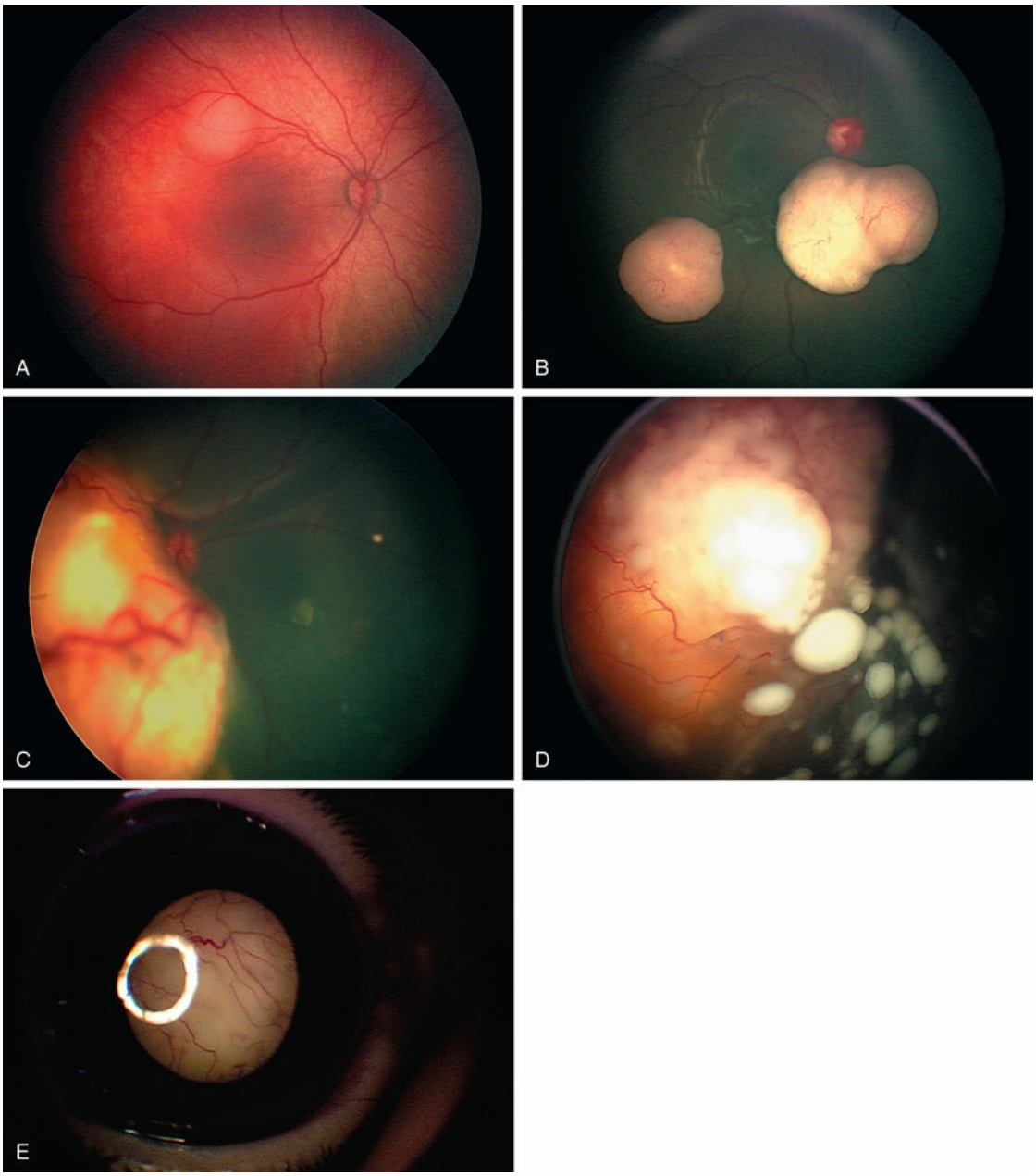

FIG. 132.7 Photographs depicting groups A–E; intraocular retinoblastoma as described in the new group classification (for details see text).

Disease Prognosis

Retinoblastoma Survival Rates

The overall survival rate from retinoblastoma in developed countries is very high, and the deaths in these patients occur from a mixture of causes. In the first 4 years of life mortality is typically from metastatic retinoblastoma or trilateral disease. Later deaths are

increasingly likely to be the result of genetically predisposed second primary tumors such as osteosarcoma or fibrosarcoma, often induced by radiation treatment given during the first two years of life. Thus, the overall survival rate will differ depending upon the time period examined. The survival rate in 1980 from one major retinoblastoma center in the United States was 92%.[200] The similar overall 5-year cumulative survival rate was 91% in SEER (Surveillance, Epidemiology, and End Results) data from 1974 to 1985.[168] However, Abramson and colleagues reported that 86% of bilateral retinoblastoma patients survive 15 years.[200] Five years after diagnosis, more children die of second malignant neoplasms than from retinoblastoma. In the Netherlands the presence of a National Registry shows the striking difference in overall survival between the subgroup of genetically predisposed patients and those who have no genetic predisposition.[201] A major controversy has arisen concerning the percentage of patients who will eventually succumb to second malignant neoplasms (SMNs). Abramson and colleagues had previously reported that as many as 90% of patients carrying the retinoblastoma predisposition allele develop a SMN within 30 years of diagnosis of the original retinoblastoma.[202] In a more recent report of a large number of patients with nearly complete ascertainment from the New York and Boston groups, 6% of bilateral patients had died of SMNs by 40 years after diagnosis if they had not been treated with EBR.[203] In contrast, 35% died of SMNs if EBR had been used in their treatment.

In any given country, the overall survival rate depends upon whether or not there was a delay in receiving medical attention. These delays are likely to be cultural, e.g., if there is no tradition of seeking medical help until a process is far advanced. For example, in a report from Malaysia in 1980, only 6 of 20 patients survived retinoblastoma; all were initially seen with advanced disease and were older children at initial diagnosis.[204] In comparison, in Great Britain where there is a tradition of early access to medical care, only 26 of 317 patients managed at Moorfield's and St Bartholomew's Hospitals in London between 1970 and 1984 developed orbital extension.[205] In Argentina delayed diagnosis was related to lack of access to medical care and initial consultation with a pediatrician instead of an ophthalmologist.[206] In the 1960s Nigeria

had an extremely high mortality rate because of late medical attention and lack of treatment facilities.[207] In Japan 50 years ago, only 50% of patients with unilateral disease and 17% of patients with bilateral disease survived more than 5 years.[208]

Factors Affecting Survival

Traditionally there have been histologic features in enucleated eyes that have seemed to correlate with increased risk of metastatic disease.[209] There are three main histologic findings that are considered to be "high-risk" features when an enucleated globe with retinoblastoma is examined: (1) retrolaminar optic nerve invasion; (2) massive choroidal invasion; (3) scleral invasion.[210] Invasion by the tumor into the optic nerve posterior to the lamina cribrosa either alone or combined with massive invasion of the choroid is considered to be an indication for adjuvant chemotherapy (Fig. 132.8). Patients with isolated massive choroidal invasion represent a controversial group when considering adjuvant therapy, but most centers treat these patients with adjuvant chemotherapy. Patients with scleral invasion always require aggressive adjuvant chemotherapy, sometimes combined with orbital radiation. A review of the estimated risk for each high-risk histopathologic feature in the literature and the current recommendations for adjuvant treatment was published by our group in 2015.[210]

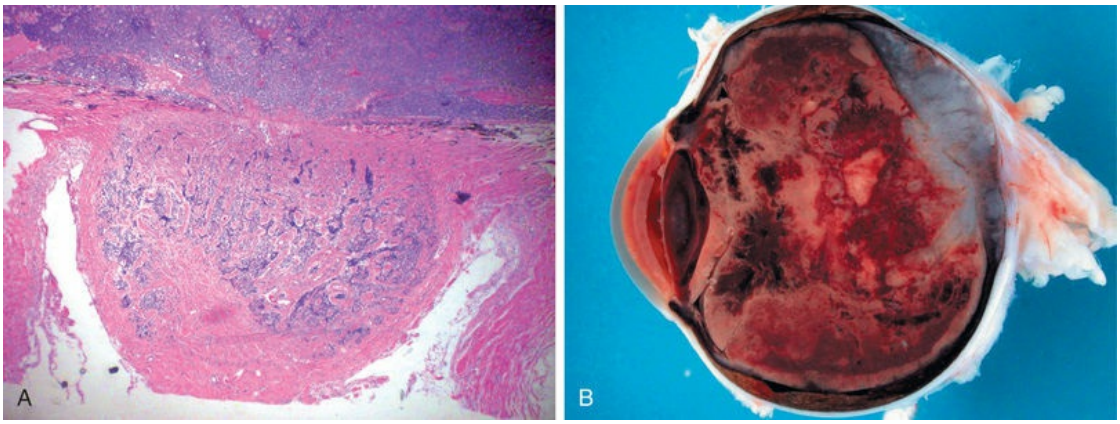

FIG. 132.8 (A) Histopathology showing invasion of the tumor into the optic nerve posterior to the lamina cribrosa. (B) Massive tumor invasion of the choroid.

There appear to be no inherent differences in the risk for metastatic disease between patients that are genetically predisposed to retinoblastoma and those without genetic predisposition, nor for patients with unilateral or bilateral diasease.[40] Delay in diagnosis is a major factor adversely affecting survival of both heritable and nonheritable disease.[211]

Multiple episodes of recurrent disease in an eye is a bad prognostic sign for the survival of the eye and perhaps for the overall survival of the child, particularly if the fundus view is lost and enucleation is delayed. The more cell divisions a tumor cell goes through, the more likely it is that one of the progeny cells will achieve the enabling mutations that allow this clone of cells to survive outside the eye. With each visible recurrence inside the eye, more of those abilities may have been acquired through spontaneous mutations.

Factors Affecting Salvage of Eye and Vision

As suggested by Knudson in 1976, early detection of retinoblastoma when the tumors are small is perhaps the most important factor that increases the likelihood of salvage of the eye.[2] A significant delay in initial diagnosis is associated with a decreased likelihood of retaining the eye. Haik and his colleagues evaluated the cause of the delay in diagnosis.[212] According to these authors, the first delay in diagnosis occurs before the observation of the first symptom by the child's parents or other observer. A second delay occurs between the observation of the first symptom and the visit to the primary care physician. These authors maintain that educating parents on the clinical significance of these signs could possibly reduce this second source of delay. Approximately 50% of the patients without a positive family history and 25% of patients with a positive family history had a delay averaging 4–5 months before the primary care physicians referred them to an ophthalmologist.[212]

When patients are treated with a chemoreduction strategy, there is a direct correlation between prognosis and group classification. In group A, eyes are virtually all preserved with excellent visual acuity with focal modalities alone. Group B eyes have nearly as good a prognosis (90–95%) with the combination of systemic chemotherapy and focal modalities, but the visual outcome varies

from 20/20 to 20/200 depending on whether or not the fovea is destroyed by the tumor. Group C eyes are salvaged at a rate approximating 70–80% with chemoreduction. In contrast, group D eyes with diffuse dissemination and more advanced disease have no greater than a 50% chance of survival without the use of other modalities such as EBR or intravitreal melphalan injections. Only an occasional group E eye is salvaged with chemoreduction, and enucleation is generally recommended.

For patients with macular tumors, posttreatment vision is often 20/200 or worse, but occasionally can be better. In a series of 17 patients with large macular tumors, post-EBR treatment vision ranged from 5/200 to 20/50.[213] The authors pointed out that the ophthalmoscopic appearance and size of the tumors gave little reliable guidelines to visual outcome. In another series of 11 patients following treatment of macular retinoblastomas, two patients eventually recovered 20/20 vision.[214] We have had experience with a patient who had a macular lesion completely filling the space within the vascular arcades. After treatment this tumor mass shrunk away from the disc and the fovea to a site 4 disc diameters temporal to the fovea. Vision returned with excellent central fixation. In this case, and in some other cases, the tumor obviously had mushroomed over the surface of the retina and did not destroy the foveal cones.

Diagnosis of Retinoblastoma

Signs and Symptoms

Leukocoria is the phenomenon created when light entering the eye is reflected back out through the pupil by the yellow or yellow–white tumor. The observer sees this reflex or reflected light diffusely filling the pupil, giving rise to the term “leukocoria” or white pupil. Retinoblastomas in the posterior pole of the globe that have reached 3 mm in basal diameter are sufficiently large to generate a leukocoric reflex. In the United States more than half of all retinoblastomas are diagnosed after observation of leukocoria, in the affected eye, usually by a close family member.

In a retrospective review of 1265 patients with retinoblastoma

from New York Hospital, leukocoria was the presenting sign in 56% of all cases.[215] It is informative to note that in the New York series observation of leukocoria correlated with the presence of advanced (Reese–Ellsworth group Va or Vb) disease. The red-reflex test, as used in a standard manner by pediatricians, will only be positive in the presence of undilated pupils only when advanced or large retinoblastoma is present.

The likelihood of observing leukocoria relates directly to the diameter of the pupil at the time of observation. Family members often see leukocoria in the early evening or in dim light when the pupil dilates naturally. Because their observation is intermittent and due to the variations in pupil size, parents or family members often question their own observation. This tendency to be uncertain about the observation can be reinforced if the pediatrician or primary care physician does not dilate the pupil, does not observe the leukocoria, and assures the family that there is no abnormality.

Flash photography can easily document the presence of leukocoria; however, the camera must be either a model that lacks the "eliminate red eye" feature or have that feature turned off. The flash illuminates the interior of the eye, and the film records the reflected glow from the tumor (leukocoria), before the pupil has a chance to constrict to the bright flash. If an abnormality in the normal red reflex is observed, the parent or family member should immediately take the child and photograph to their pediatrician demonstrating the leukokoria and insist on a referral to an ophthalmologist, preferably one who specializes in pediatrics (for websites where information is available for parents see www.retinoblastoma.net).

Brightly lit rooms and high light intensity on the direct ophthalmoscope are two of the factors that most commonly prevent pediatricians and other primary care physicians from making an early diagnosis of retinoblastoma. The sensitivity of this clinical test for pediatricians can be increased by performing the red reflex examination in a darkened room, and with repeated practice during well-child examinations. Any child who presents with descriptions of leukocoria or any observed abnormality on the red reflex test should be referred to a pediatric ophthalmologist.

The American Academy of Pediatrics (AAP) has published a

policy statement regarding how their members should perform the red reflex test. (Their recommendations can be found on the AAP website at www.aap.org, under Policy Statements; red reflex testing.) This policy statement is a step forward in the effort to assure early detection for all infants and toddlers with intraocular retinoblastoma. However, it should be noted that pupillary dilation is not a part of the general recommendation and is probably underutilized due to concerns regarding side effects of the dilation drops.[216]

Decreased visual acuity caused by destruction of the fovea eventually causes strabismus in young children with retinoblastoma. Strabismus is the initial sign in one of every five patients with retinoblastoma and results from direct infiltration of the macula by the tumor or a serous retinal detachment.[215] Acquired strabismus in any child always requires an immediate dilated fundus examination to rule out the possibility of retinoblastoma.

Other less common signs and symptoms of retinoblastoma include a red, painful eye from neovascular glaucoma, buphthalmos, uveitis, poor visual behavior if bilateral, failed vision screening in older kids, and an aseptic orbital cellulitis in advanced cases (Fig. 132.9). In five cases of retinoblastoma presenting with the clinical picture of aseptic orbital cellulitis, the imaging studies were misinterpreted as showing extraocular extension of the tumor into the optic nerve.[217] We have had similar experiences in patients with advanced intraocular retinoblastoma presenting as orbital cellulitis. Systemic treatment with 3 days of oral corticosteroids will often lead to dramatic reduction of the swelling, leading to a resolution of the orbital findings on MRI scans.

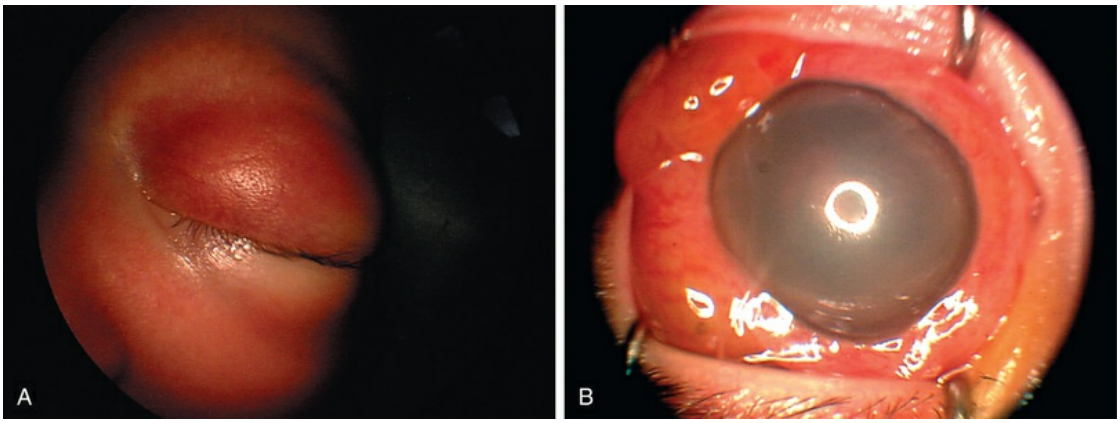

FIG. 132.9 (A) Aseptic orbital cellulitis in a patient with advanced intraocular retinoblastoma. (B) Corneal clouding and conjunctival chemosis in an eye with neovascular glaucoma secondary to advanced intraocular retinoblastoma.

Diseases Simulating Retinoblastoma (Pseudoretinoblastoma)

In 500 consecutive referrals for retinoblastoma, simulating lesions were found in 212 of the 500 patients.[218] There was a total of 23 different conditions that referring pediatricians or ophthalmologists were unable to distinguish from retinoblastoma. The three most common causes of pseudoretinoblastoma were persistent hyperplastic primary vitreous or persistent fetal vasculature (28%), Coats disease (16%), and presumed ocular toxocariasis (16%) (Fig. 132.10). Congenital cataract and retinopathy of prematurity were less frequently mistaken for possible retinoblastoma in this series than in other, earlier reports. Our experience in Los Angeles is similar, in that persistent fetal vasculature is the most common condition referred for leukocoria in infants, while older children referred for leukocoria are often diagnosed with Coats disease or toxocariasis. Other diagnoses that we have seen simulate retinoblastoma include familial exudative vitreoretinopathy (FEVR), Norrie disease, idiopathic vitreous hemorrhage, and congenital retinal folds.

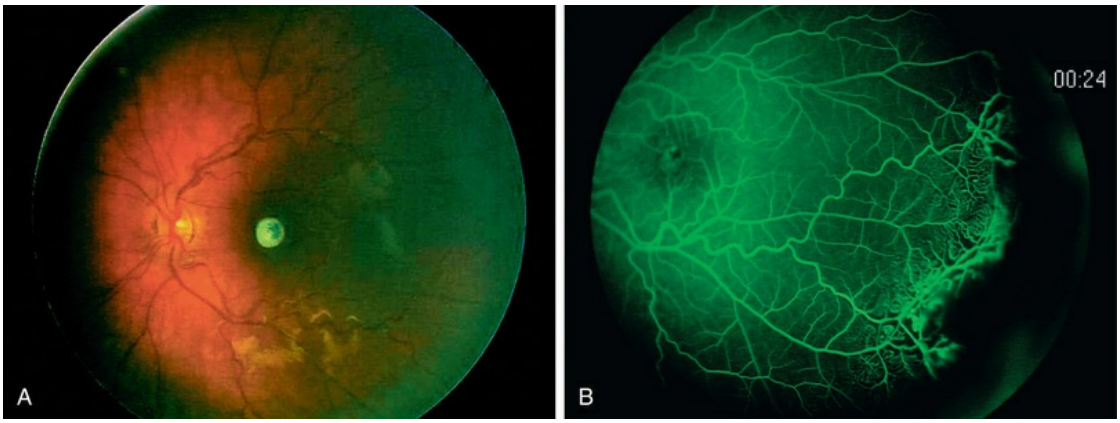

FIG. 132.10 (A) Unusual presentation of Coats disease in a 4-year-old child simulating retinoblastoma. Foveal nodule is the result of chronic lipid from telangiectatic vessels in the periphery seen here by fluorescein angiography (B).

In 1996, de Potter and colleagues evaluated the role of magnetic resonance imaging (MRI) in differentiating solid intraocular tumors from intraocular lesions with primary retinal detachment. They reported that solid intraocular tumors appeared hyperintense on T1-weighted images and hypointense on T2-weighted images.[219] Also, these lesions showed abnormal enhancement on contrast-enhanced T1-weighted images with fat suppression techniques. In secondary serous or exudative retinal detachment from intraocular lesions (Coats disease, persistent hyperplastic primary vitreous, phthisis bulbi, and retinopathy of prematurity), MRI showed hyperintensity of the subretinal space on both T1- and T2-weighted images and no enhancement in the subretinal space on contrast-enhanced sequences.

Meeting the Family and Making a Diagnosis

We, the authors, have developed our own approach to diagnosis and care over a number of years. Obviously, different physicians in different practice settings will develop systems and approaches that work best for their patients. Below, we share our own recommendations.

The first meeting between the ocular oncologist and the family should generally occur in the office as soon as possible after the family's pediatrician or ophthalmologist has seen something in the

child's eye that arouses the suspicion of retinoblastoma. The two major advantages of performing the examination on the same day are that the child's pupils are already dilated and the anxiety and stress level of the family is high. Often the family has been told there is a “mass” or “tumor” in the eye. In our experience, more than 90% have not heard the word “cancer.”

Introduce yourself to the family members and do not approach the child until you have had a discussion with the family. Be reassuring in your mannerisms. The first question to ask the parents is: “What brought you to the pediatrician in the first place?” followed by: “Then what happened when you saw an ophthalmologist?” It is important to ascertain what the family has been told or not told and what their understanding of the information is at the start of the examination. After the discussion with the parents, proceed with the examination of the child. As mentioned earlier, even if the child is an infant in the arms of one of the parents, it is important to explain to the parents what you will do before you do it to lessen anxiety.

After you have determined that you suspect the child may have retinoblastoma and you have fully explained how and why you are leaning toward this diagnosis, you can explain the rest of the diagnostic process, most importantly the need for (1) orbit and brain MRI with and without contrast, and (2) examination of both eyes under anesthesia. If the suspicion for retinoblastoma is low but cannot be ruled out on office examination, the child can delay the MRI until the examination under anesthesia (EUA) has been done. Parents must understand that their child will receive sedation or anesthesia for the next two procedures. Explain that both examinations are part of the protocol used around the world to form a definitive diagnosis for retinoblastoma. Many parents assume, either because they have been on the internet or been in a chat room, that having an MRI means that you suspect that the tumor has progressed to the brain. This is why it is so important to reassure every family you have contact with that this is the accepted protocol and it is the best way to finalize a diagnosis. It is very useful to let the family know that they are in partnership with you and the team of other physicians regarding the diagnosis and treatment plan for the child.

You must tell the family that you will inform them of the results of every examination as soon as you have them. You must also follow through and when you have the results of the MRI you must telephone them with the findings, rather than have them wait until your next appointment to see them. Parents experience so much stress during this process that it can affect their health and ability to care for their family. Provide answers as soon as possible, even if it confirms a diagnosis of retinoblastoma. Parental anxiety will be reduced by the knowledge that you now know what you are dealing with and that they will be an active part of the treatment planning.

The office examination allows the physician to determine the likelihood of this child having retinoblastoma. Another purpose of the office examination is to evaluate the level of visual acuity in each eye. Almost invariably, the parents are not aware of unilateral vision loss. They think that because both eyes move together, that both are seeing normally. Fixation and following behavior on a small toy or other object of interest to the child should be determined for each eye tested separately in a way that the family sees and acknowledges the outcome (often that one eye sees much better than the other). Demonstration of the lack of visual behavior in one eye may go a long way toward helping the parents accept the need for enucleation, should that become a treatment recommendation.

After dilation, the light on the indirect ophthalmoscope should be turned down to a very low level and a very brief 5–10-second view should be sufficient to establish whether or not the mass is typical for retinoblastoma, and whether the involvement is unilateral or bilateral. It may be possible to be certain that the mass in the eye is retinoblastoma. There is usually no need to restrain the child, nor to determine with certainty whether the tumor is unilateral or bilateral at this point. In occasional situations, it may be necessary to examine the child in the office with an eyelid speculum if they are not cooperative or the need for the exam under anesthesia cannot be ascertained any other way.

Diagnostic Workup

At the initial office visit, a B-scan ultrasound examination is also necessary. If the office B-scan examination shows the classic shadowing of intralesional calcium, an eyelid speculum examination is not necessary. Even if the initial indirect ophthalmoscope examination reveals evidence of retinoblastoma, it is still recommended to perform the office ultrasound examination to augment the clinical examination and determine whether one or both eyes are involved.

Regardless of whether calcium can be demonstrated by ocular ultrasound on the child in the office, we routinely order an MRI scan of the brain and orbits (with gadolinium enhancement and fat suppression) for two reasons. First, to evaluate whether there is extraocular extension and optic nerve invasion by the tumor ideally before the staging examination under anesthesia, and second, the MRI of the brain should have specific cuts directed through the region of the pineal gland to eliminate the possibility of the "trilateral" retinoblastoma syndrome first described in 1983,[218,219] and discussed later in this chapter. The MRI scan can demonstrate infiltrative spread into the optic nerve, subarachnoid seeding, and involvement of the brain. MRI and computed tomography (CT) are both useful in determining the extent of recurrent disease, extraocular spread, and defining second primary tumors.[220]

It is preferable to have the results of the MRI before the staging examination in the majority of cases although the EUA can proceed even if the MRI results are not yet available. If the ophthalmologist can confirm that the patient does not have optic nerve tumor extension or trilateral disease, then enucleation can occasionally be performed immediately after the EUA if the eye is particularly advanced and the parents and clinicians are ready to proceed.

Unlike MRI, CT scanning involves exposing the child to a low dose of radiation. This exposure should be avoided if at all possible in cases of heritable retinoblastoma because of the generalized cancer predisposition syndrome. At CHLA, we *never* perform CT scan in any child with confirmed or suspected retinoblastoma. Sometimes a CT scan has already been performed by the emergency department or referring medical center, and it may provide useful information. Exophytic retinoblastoma tends to demonstrate calcification, either in a solid mass or in multifocal locations.[220] Soft

tissue components of retinoblastoma will demonstrate enhancement with contrast material in all cases. It should be kept in mind that calcification can also occur in any of the retinoblastoma-simulating lesions where significant ocular disruption or phthisis is evident, but this dystrophic calcification usually is deposited along the lines of normal structures. We have also seen numerous cases of retinoblastoma without calcification on CT or ultrasound examination, although it is helpful in making the diagnosis if present. It is important to note that ultrasonography performed by a skilled technician is superior to CT scan in detecting intraocular calcification, and CT should never be done after the staging EUA as it adds no useful information.

Metastatic Workup

At centers where retinoblastoma is a relatively rare diagnosis there is often confusion between the workup for intraocular retinoblastoma and metastatic retinoblastoma. There is no place for routine body scans, PET scans, or total body CT scans in patients during the initial workup and treatment of intraocular retinoblastoma. A metastatic work-up can be considered if there is evidence from neuroimaging or pathology of an enucleated eye that the child in question has extraocular (i.e., orbital extension) or metastatic disease.

Until the late 1980s, it was routine for all newly diagnosed retinoblastoma patients in ocular oncology centers to have a bone marrow aspiration and biopsy, as well as a lumbar puncture with analysis of the cerebrospinal fluid (CSF) to look for evidence of CNS spread. Almost uniformly, these tests were normal unless there was evidence clinically or on imaging studies that extraocular spread of the tumor was likely to be present.

Among centers treating retinoblastoma in developed countries, routine bone marrow aspiration and biopsy, as well as lumbar puncture, are not considered necessary in new patients with retinoblastoma when imaging studies show no evidence that tumor has spread outside the eye. These tests add considerable time and expense to the workup and contribute to discomfort for the child, and experience has shown that they are unnecessary in the typical

case of intraocular retinoblastoma. On the other hand, they are essential if the treating physician suspects extraocular or metastatic retinoblastoma when the clinical history or neuroimaging studies suggest a complicated case.

When retinoblastoma presents as aseptic orbital cellulitis as a result of massive intraocular tumor necrosis and hemorrhage, radiologists may diagnose optic nerve invasion on MRI because of the perineural edema. A metastatic workup should be delayed for 2–3 days, while the affected child is treated with a relatively high dose of systemic corticosteroids. This decreases the edema and allows, within 2 or 3 days, a more accurate assessment of the optic nerve signal on the imaging study.

In cases in which there is clear evidence of tumor outside the eye, the full metastatic workup should be pursued. Studies should include a bone scan in addition to a search for tumor cells in the CSF and bone marrow. Aspiration from more than one site may be of value because bone marrow involvement can be uneven. The aspirates are typically taken from the iliac crest in young children under general anesthesia.

Staging Examination Under Anesthesia

Before any treatment for retinoblastoma can be initiated, a staging EUA has to be performed.

During the staging EUA, a complete evaluation and documentation of every feature of the eyes should be undertaken with careful attention given to the examination of the anterior segment, iris, and vitreous cavity. A handheld slit-lamp evaluation of the anterior segment and vitreous should be part of this examination, looking for the presence of vitreous seeding. A Tono-Pen eye pressure should be taken as soon as the child is under anesthesia and before the speculum is inserted. A measurement of the corneal diameter and an ultrasonic measurement of the length of the eye are also helpful to rule out buphthalmos and assess for nanophthalmia, respectively.

The EUA is a good time to carefully examine the child for low-set and posteriorly rotated ears, simian crease in the palms, broad thumbs, hypertelorism, telecanthus, and other minor congenital

anomalies. Systemic findings can suggest other diagnoses that can be helpful in making the diagnosis, such as the 13q deletion retinoblastoma syndrome. A careful retinal drawing with colored pencils should be made of both eyes, with the location of each lesion noted.

Typically, enucleation should be combined with a staging examination only if the MRI has been completed and it shows no extraocular disease and the parents are ready mentally and emotionally to proceed. Parents typically need time to acknowledge and accept the need for enucleation. The affected child, especially if older than 2 years of age, should have a simplified explanation of what will happen during enucleation surgery. Waiting a few days will not significantly increase the risk for metastatic disease, but a long delay before enucleation is not recommended. Our practice is to schedule the enucleation within 7–10 days once a decision has been made. However, there are unique situations when the involved eye is advanced (i.e., buphthalmic), when immediate enucleation at the time of the staging EUA is the best option.

Wide-angle retinal photography or RetCam digital imaging is extremely useful in documenting the size and location of the tumors and confirming the features that allow group classification of the eye. Printed images of the tumor also help the family accept the reality of the diagnosis. Comparison of Retcam images are useful during follow-up examinations under anesthesia to demonstrate to the family the response or lack of response to treatment. In addition, the RetCam also allows the use of fluorescein angiography in the diagnosis and management of retinoblastoma.[190] A fluorescein angiogram is especially useful in confirming the presence of neovascularization of the iris in retinoblastoma eyes with glaucoma and/or chronic retinal detachment (Fig. 132.11). We also find fluorescein angiogram of value if there is a questionable area of recurrent retinoblastoma in a previously treated lesion or scar. In this case an actively growing recurrent lesion will leak, stain with fluorescein, and accumulate dye. Inactive lesions do not stain. The diagnosis of an early "presumed" retinoma may be facilitated by fluorescein angiography. A newly diagnosed, untreated eye that contains a lesion that appears to be type II or type III regression and does not

leak or stain on fluorescein angiography may well be a retinoma (see a more thorough discussion of retinoma later in the chapter).

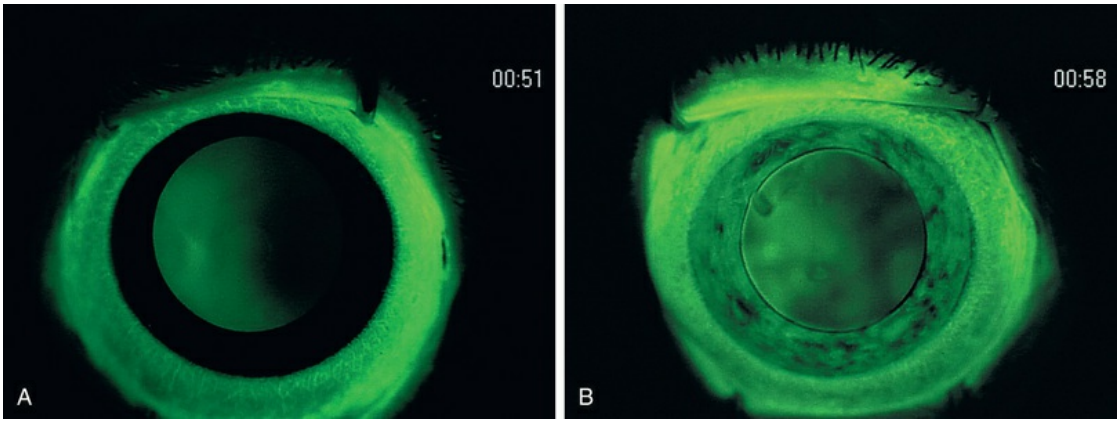

FIG. 132.11 (A) RetCam fluorescein angiography showing normal iris appearance at 51 seconds, compared to (B) abnormal eye with significant rubeosis iridis due to advanced retinoblastoma.

B-scan ultrasonography is useful to measure the height of each discrete tumor in millimeters. Ultrasonography is superior to CT in its ability to detect the presence of calcium within retinoblastoma tumors (Fig. 132.12). In 1973 Coleman described the reliability of ultrasound in retinoblastoma diagnosis.[221,222] In 1975 Sterns et al. reported two configurations, solid and cystic.[223] However, these authors were not always able to differentiate between vitreous hemorrhage and retinoblastoma. In one series of 38 eyes retinoblastoma was the ultrasound diagnosis in 25 and pseudoglioma in 11, and all diagnoses were correct.[224] Ultrasound should be able to detect a tumor as small as 2 mm in diameter.[225]

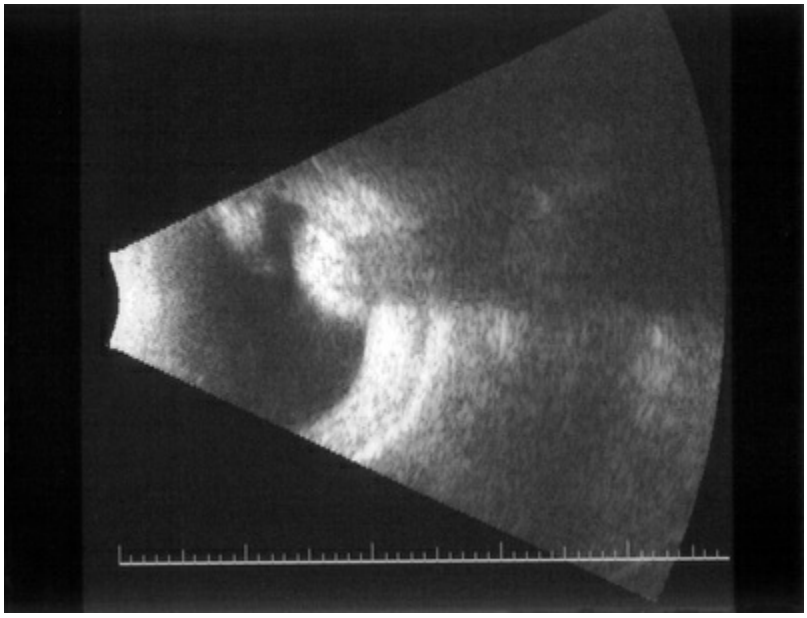

FIG. 132.12 B-scan ultrasonography in retinoblastoma shows an intraocular mass with calcification and shadowing.

Fine-needle aspiration biopsy has been described as a diagnostic tool,[226] but its use is strongly discouraged in any patient suspected to have intraocular retinoblastoma. In 2002 Karcioglu published a survey of major ocular oncology centers that had treated 3651 patients since 1986.[227] During those 17 years, fine-needle biopsy was performed only eight times (once in every 456 patients with retinoblastoma). The biopsy was usually done in older children with a diagnosis of uveitis in which retinoblastoma could not be ruled out. Six of the eight patients were 4 years of age or older. The use of fine-needle biopsy should be limited to those exceptional cases in which a diagnosis cannot be arrived at by any other means, the eye has visual potential, and the procedure is performed by an experienced ocular oncologist. With clinical experience, atypical cases can almost always be diagnosed correctly without the need for introducing a needle into the posterior segment of an eye with possible retinoblastoma.

The Approach to the Child With Cancer

In this section, we discuss some of the less obvious issues involved

in the successful treatment of a child with cancer. The overall treatment approach should consider the child first, rather than focus on the salvage of the eye. Focusing on the eye with retinoblastoma instead of the child may mean the eye is retained (perhaps with little or no vision) but the child/teen/adult has been affected by the morbidity of the treatment and perhaps permanently scarred psychologically. Attempting to salvage an eye with advanced retinoblastoma often means more than 20 EUAs during the treatment course. Children who have undergone treatment for intraocular retinoblastoma may become terrified of medical settings and filled with foreboding and anxiety. In addition, the treatment process becomes very stressful for the parents and siblings as well. If the treating physician understands parental grief behavior, the process becomes easier for everyone involved.

In discussions with the family it is important to stress that preservation of the child's life must be the top priority, with salvage of the eye a secondary goal. In cases with unilateral retinoblastoma, when group D or E disease is present, some parents will insist that enucleation be avoided and treatment with chemotherapy be initiated. That emotional response of not wanting their child to lose an eye is normal. Parents seem to have the most difficulty with their concept of how deforming the removal of an eye will be. The parent's perception is that their previously “perfect child” will never have a social life, never get married or have children because of a disfiguring enucleation as a child.

The management team must patiently counsel the family about the reality of treatment consequences and side-effects. Showing the family photographs of other children with prosthetic eyes may be helpful. Cosmetic outcome is an important concern. The parents may have an image in their mind of an older person who lost an eye and has a less-than-optimal prosthesis.

The parents may think loss of one eye makes the child completely blind. Point out that this eye is not useful to the child now and that any vision he or she has now is due to the remaining eye. In unilateral disease, current vision in the good eye will not be impaired. Finally, be aware of the cultural background of the parents. It is often helpful to have a counselor with the same

cultural background.

Treatment Methods and Techniques

Developing a Customized Treatment Plan

This section discusses the treatment modalities that are available to the retinoblastoma management team in developing an initial customized treatment plan. Potential benefits and complications are discussed in this section because they must be taken into consideration in developing and presenting any treatment plan to the family for consent.

Unilateral Nonheritable Retinoblastoma

The ABC classification of intraocular retinoblastoma helps clinicians decide when to treat unilateral retinoblastoma conservatively. Nearly all centers will attempt to salvage unilateral group A, B, and C eyes. Unilateral group E eyes should always be enucleated.

For group A disease, often detected in newborn members of a pedigree of retinoblastoma, or the contralateral eye of a patient with sporadic, advanced disease in the other eye, photocoagulation or cryotherapy should be employed. Photocoagulation is typically repeated to reduce the risk of recurrence while cryotherapy is only repeated if regrowth is noted during follow-up.

We have found that the majority of unilateral group B disease eyes can be successfully treated with three cycles of three-drug chemotherapy combined with focal consolidation. Many centers use the standard six-cycle three-drug chemotherapy regimen for all group B, C, and D eyes. The exact chemotherapeutic regime varies from center to center with some experts preferring to exclude etoposide (due to its leukemogenic potential) while others use single-agent carboplatin and others use a four-drug regimen using cyclosporin.[228] For group B eyes with a solitary lesion in the periphery, aggressive cryotherapy and/or laser therapy can sometimes be used, or perhaps even a radioactive plaque. However, it should be kept in mind that the vast majority of group B eyes cannot be treated with focal modalities alone and that chemoreduction will produce the best outcomes.

Unilateral group C retinoblastoma, which has local dissemination of tumor into the vitreous or subretinal space, has a high success rate with chemoreduction. Systemic chemotherapy with CEV is the most common regimen administered over six cycles for group C disease.

Unilateral group D eyes represent a very controversial category of patients, given that the rate of salvage for chemoreduction alone is 47%.[229] The success rate can be increased to 78% when failures after chemoreduction are salvaged with EBR, but this may not be advisable in unilateral patients. Therefore, the parents and the clinicians face a difficult decision in giving 6 cycles of 3 drug systemic chemotherapy when the rate of saving the eye is approximately 50%. Factors predictive of a poor visual outcome have been identified in group D eyes, and they include a complete retinal detachment, vitreous seeding of at least three quadrants and tumor involvement of more than half the macula. These eyes have been subclassified as being group D2, and they have a worse visual outcome.[230] Unilateral group D2 eyes may be better served by undergoing primary enucleation. The success rate of treating unilateral group D eyes with intraarterial chemotherapy is being assessed with an ongoing Children's Oncology Group (COG) trial, but retrospective studies from the Memorial Sloan Kettering Cancer Center (MSKCC) group suggest that the success rate with intraarterial chemotherapy alone for advanced disease may be as high as 70–80%.[8] In addition, salvage of active vitreous seeding after chemoreduction with intravitreal melphalan injections can be as high as 87%.[8] The optimal treatment approach for unilateral group D disease will evolve over the next 5–10 years, but it should be kept in mind that enucleation remains an excellent option for those eyes with poor visual potential.

Bilateral Retinoblastoma: Symmetrical and Asymmetric Disease

Bilateral group A disease can follow the treatment strategy stated above: focal modalities only, using laser treatment and/or cryotherapy. For bilateral patients with any combination of group B–D disease, systemic chemoreduction is generally recommended, using the standard six cycles of the three-drug chemotherapy

consisting of carboplatin, etoposide, and vincristine. For patients with group A in one eye and group D or E in the other eye, the treatment approach is tailored to the clinical situation. A successful treatment approach is to enucleate the more advanced eye and treat the other eye with focal modalities (laser and/or cryotherapy). This option avoids systemic chemotherapy and is particularly advantageous for children less than 6 months of age to avoid the potential ototoxicity from carboplatin. The other approach is to treat the patient with six cycles of chemoreduction, with plans to enucleate the more advanced eye after two cycles if there is a suboptimal treatment response.

Advanced Intraocular Disease (Groups D and E)

For group E disease, enucleation is generally recommended. In some centers, if systemic chemotherapy is initiated for the contralateral eye, salvage of a group E is considered. There have been rare case reports of successful salvage of group E eyes with chemoreduction.[231] However, enthusiasm for this approach should be tempered by the finding that up to 39% of group E eyes harbor high-risk histopathologic features.[232,233] There is also evidence that if a group E eye is removed after two cycles of systemic chemotherapy, there is no increased risk of death.[234] However, pre-enucleation chemotherapy can mask high-risk pathology and increase the risk of metastatic disease if enucleation is performed more than 3 months after diagnosis.[234] Therefore, if an attempt is made to salvage a group E eye, enucleation should be strongly considered after two cycles if there is not a dramatic response and the fundus findings cannot be monitored on indirect ophthalmoscopy. As mentioned, pre-enucleation chemotherapy can mask high-risk histopathologic features. Therefore, this approach should only be undertaken if the child is scheduled to receive the full six cycles of chemotherapy (for the other eye) because the regimens for intraocular disease and adjuvant chemotherapy after enucleation are similar.

If the neuroimaging study at diagnosis suggests invasion of the tumor into the optic nerve, there are two approaches. In those cases that have optic nerve enhancement of less than 5 mm, we recommend immediate enucleation of the group E eye, allowing the

socket to heal for 2 weeks, then starting systemic chemotherapy for the contralateral eye or adjuvant therapy if the case is unilateral once pathology confirms the presence of postlaminar optic nerve invasion. For bilateral cases, if the fovea is threatened in the contralateral eye, then systemic chemotherapy can be started immediately, with plans to enucleate the eye with the optic nerve enhancement after 1–2 cycles. Typically the enucleation is scheduled approximately 2 weeks after the cycle of chemotherapy so that the socket can heal for 2 weeks prior to the next cycle of chemotherapy. However, clinicians should be aware that the nadir for thrombocytopenia is about 2 weeks after chemotherapy. If there is optic nerve enhancement of more than 5 mm, there is concern regarding a positive optic nerve margin with upfront enucleation. Therefore, the child will require institution of a more aggressive protocol requiring a full course of high-dose multiagent chemotherapy before enucleation is performed (i.e., neoadjuvant chemotherapy).

Systemic Intravenous Chemotherapy

The introduction of systemic intravenous chemotherapy for the primary treatment of intraocular retinoblastoma by Kingston et al. in 1996 set off a dramatic shift in the management of intraocular retinoblastoma.[195] Although the outcome from the first 14 eyes with Reese–Ellsworth group Vb retinoblastoma treated in London were disappointing, variations on their protocol are widely used today as the most common primary globe-sparing treatment for retinoblastoma throughout the world.

Terminology

The term “chemoreduction” refers to the use of systemic chemotherapy for intraocular retinoblastoma combined with focal modalities such as laser therapy, cryotherapy, and/or brachytherapy. Systemic chemotherapy given to patients with high-risk pathology after enucleation is referred to as “adjuvant” chemotherapy in that it provides prophylactic treatment to patients without any clinical or radiographic evidence of metastatic disease.[210] The term “neoadjuvant” chemotherapy is used to denote

chemotherapy given to patients before a scheduled enucleation, typically for patients with more than 5 mm of optic nerve enhancement on the staging MRI scan. A detailed discussion of the treatment of extraocular disease is beyond the scope of this book and is the domain of the treating ophthalmologist. The usual agents employed for extraocular retinoblastoma include cisplatin, cyclophosphamide, vincristine, and doxorubicin. Pratt et al. described the St. Jude experience with chemotherapy for extraocular retinoblastoma between 1962 and 1984.[235] A total of 11 children received chemotherapy for measurable extraocular disease that had been present at diagnosis (7/11 patients) or developed later (4/11 patients). In this series from 1985, only 2 patients demonstrated complete responses and achieved long-term disease-free survival. In the modern era, the success rate for treating systemic relapse not involving the CNS is approximately 67% with aggressive multimodal therapy and stem cell rescue.[210] For patients with CNS relapse, the survival rate remains dismal despite all measures.

Chemoreduction Regimens

In the majority of centers, systemic chemotherapy remains the most commonly used primary treatment for intraocular retinoblastoma. The chemotherapy agents may vary slightly but most protocols consist of the systemic administration of carboplatin, etoposide, and vincristine, given over a 2-day period every 3 or 4 weeks. The administration of the drugs and the time required for the suppressed bone marrow to recover is considered one cycle. In Los Angeles, we use six cycles of CEV for intraocular group C and D disease and three cycles for intraocular group B disease (Fig. 132.13). The dose of carboplatin used at our center is slightly higher (13 mg/kg per day for 2 consecutive days) versus the dose used at other centers (18.6 mg/kg for 1 day). With this regimen, six cycles of CEV has been well tolerated in our patient population. Almost all children will receive transfusions at some point during the course, and the rate of Grade III neutropenia can range between 10% and 30%.

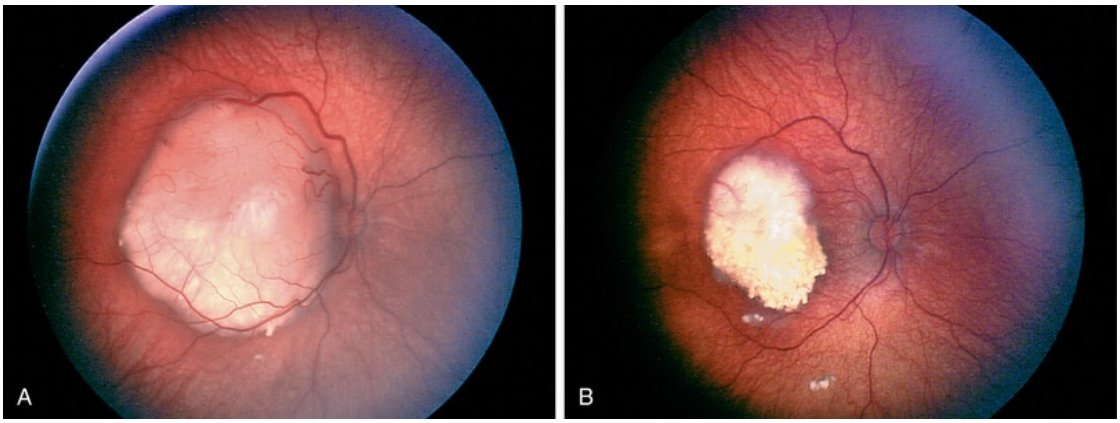

FIG. 132.13 Group B retinoblastoma, before (A) and after (B) primary chemotherapy.

Admittedly, primary intravenous chemotherapy for intraocular retinoblastoma administers a large volume of medication to the entire body to treat a relatively small organ. There is also concern about the possible association of etoposide and secondary acute myelogenous leukemia (AML), which has been reported in a small cohort of children treated for retinoblastoma.[236,237] For this reason, some centers have dropped etoposide from the regimen for less advanced disease (groups A and B). The drug is known to be leukemogenic at higher doses and there has been concern that exposing patients with the *RB1* mutation would increase their risk for secondary AML. Most experts agree that if etoposide poses a risk for second tumors, it remains a small one. Perhaps a bigger concern is the potential risk of hearing loss following carboplatin use. Wilson and colleagues have reported an increase in carboplatin-related ototoxicity at St. Judes.[238] Similar results have not been duplicated elsewhere, although it remains a concern particularly in children less than 6 months of age. The risk of ototoxicity is significant in this patient population when one considers that many retinoblastoma patients are visually disabled relying on other sensory input such as hearing. As with other intravenous forms of chemotherapy, risks of bone marrow suppression, alopecia, and central line infection exist; in rare cases these complications can be severe and life-threatening.

Infants <6 months of age at diagnosis receive a modified dosing regimen with a 50% decrease in all agents for the first cycle. At our institution, vincristine is routinely omitted for patients <2 months of age due to concerns regarding paralytic ileus and irritability. After

the first cycle at 50% dose CEV (or CE), patients are then monitored for intraocular tumor response and Grade III neutropenia (i.e., absolute neutrophil count <1000). If there is adequate tumor response or evidence of systemic toxicity, patients are kept at the 50% dose for the next cycle. If there is inadequate tumor response and no Grade III neutropenia, then the dose is increased to 75%. Patients in this age group can be increased to 100% dose of CEV if all factors are present: (1) older than 3 months of age; (2) no Grade III neutropenia to 75% dose; and (3) inadequate tumor response to 75% dose.

Sub-Tenon Carboplatin

The addition of sub-Tenon carboplatin to augment penetration of systemic carboplatin has been advocated by a number of groups over the past 10 years.[239] However, following sub-Tenon or subconjunctival injections a number of complications have been described including lid swelling, orbital soft tissue scarring and atrophy, and secondary optic neuropathy[240–242]. In particular, severe orbital scarring can lead to strabismus and make subsequent enucleations challenging, and orbital fat atrophy can lead to permanent soft tissue socket deformities. For these reasons, most centers have abandoned the use of sub-Tenon carboplatin injections. For patients with persistent vitreous seeding following chemoreduction, intravitreal melphalan injections have become the treatment of choice (see section on Intravitreal chemotherapy).

Intraarterial Chemotherapy

As far back as 1953, Kupfer described a case of retinoblastoma treated with nitrogen mustard injected directly into the carotid artery.[243] Later, in the 1960s and 1970s, Reese and Ellsworth combined EBR with intracarotid chemotherapeutic agents.[244–246] They later abandoned this approach, not having detected significant benefits of the combined approach over radiotherapy alone. In the 1980s, Kaneko at the National Cancer Institute in Tokyo, Japan developed a new method to administer ocular chemotherapy – he described it as selective ophthalmic arterial infusion (SOAI).[3,247–249] With this approach, developed in a culture

that abhors enucleation, a balloon catheter was inserted in the femoral artery, past the internal carotid and guided just past the origin of the ophthalmic artery. The balloon was then inflated and melphalan injected into the arterial vasculature, allowing it to "backflow" into the ophthalmic artery. Often adjuvant treatments were also administered but more than half of treated eyes were preserved.[4]

In 2008 Abramson and colleagues modified this technique with direct insertion of the cannula into the ophthalmic artery.[6] A phase I/II trial of nine treated patients with group V retinoblastoma salvaged seven eyes that would have otherwise been enucleated; the two enucleated eyes showed no evidence of active disease. While the initial series used melphalan, additional follow-up reports have infused other agents, including carboplatin and topotecan, with promising results. The technique has been used successfully in unilateral and bilateral cases, and as both a primary and salvage approach.[6–8,250–252] Currently, intraarterial chemotherapy (IAC) is the primary modality used to treat unilateral group D retinoblastoma in some centers, rather than chemoreduction. Follow-up electroretinogram (ERG) data suggests improved ERG findings in some very advanced cases as the retina reattaches, but also a small cumulative degradation in eyes receiving multiple treatments.[253,254] Defining an event as "enucleation or need for radiotherapy," cumulative 4-year data from this group demonstrated a 81.7% event-free survival for eyes that received intraarterial chemotherapy as primary treatment, and 58.4% for eyes that had previous treatment failure with intravenous chemotherapy and/or EBR.[8] Although a meaningful comparison with chemoreduction is currently not possible in the literature, there is a general consensus that IAC offers somewhat higher salvage rates for group D eyes, albeit with a higher risk of local and regional side-effects (Fig. 132.14). The Shields group recently published a globe salvage rate of 94% for group D eyes in a small group of patients treated with intraarterial chemotherapy (17 patients).[255] A large-scale retrospective study evaluating the long-term results of group D eyes treated with IA chemo at MSKCC will be published soon. The results of an ongoing COG trial on unilateral group D tumors treated with primary IAC will likely

determine whether this technique will be widely adopted by the ocular oncology community and whether it will replace primary systemic intravenous chemotherapy.

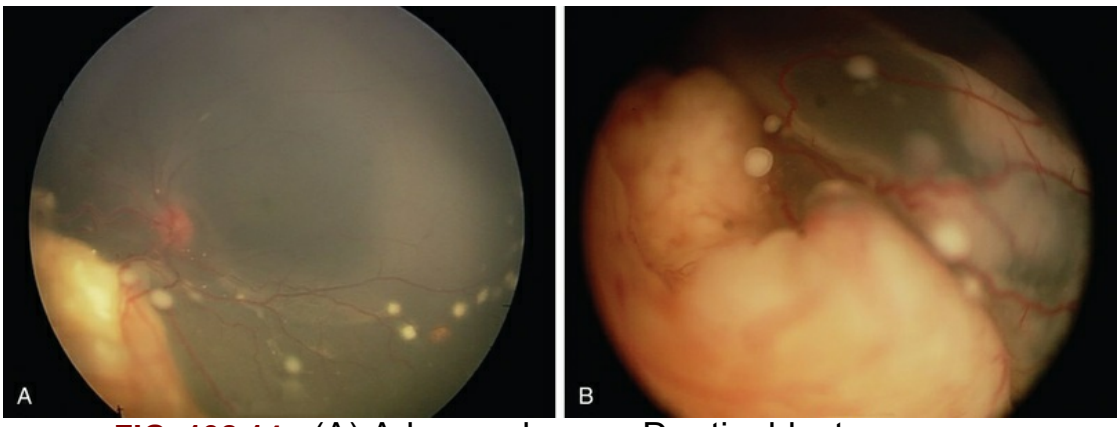

FIG. 132.14 (A) Advanced group D retinoblastoma before and (B) after intraarterial chemotherapy showing dramatic tumor regression.

The technique is technically challenging, requiring significant expertise and experience in pediatric artery catheterization by the neurointerventionalist.[255] The procedure is performed under general anesthesia in the neuroangiography or interventional suite, using a microcatheter inserted into the femoral artery (Fig. 132.15). The microcatheter (500 μm in diameter) is then guided into the internal carotid artery, and fluoroscopy is performed to confirm its placement at the ostium of the ophthalmic artery. Many practitioners have raised concerns regarding the potential for systemic and CNS risks with this approach, including death and stroke, especially in the context of unilateral disease, where enucleation is generally curative. We are aware of one unpublished case of an asymptomatic stroke following IAC, and there are several reports of third nerve palsy, as well as retinal and choroidal vascular occlusion.[5,256,257] Transient side-effects are fairly common following IAC, such as eyelash loss, periorbital edema, and cutaneous hyperemia.[258] One recent study found a reduction in subfoveal choroidal thickness after IAC, suggesting the possibility of permanent choroidal vascular toxicity.[259–261] Concerns have also been raised regarding the small dose of radiation hereditary retinoblastoma patients receive during the fluoroscopy portion of

the procedure, which is necessary to confirm the correct placement of the catheter at the ostium of the ophthalmic artery.[262,263]

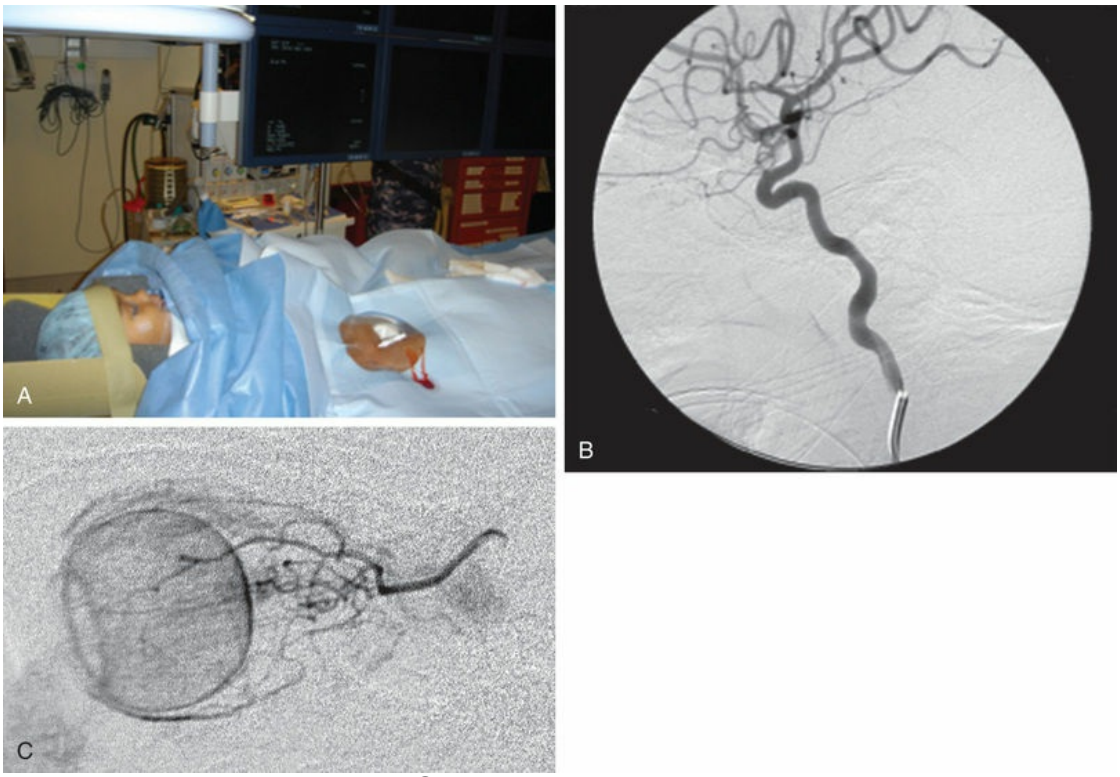

FIG. 132.15 (A) Child undergoing intraarterial chemotherapy in the angiography suite with the catheter inserted into the femoral artery. (B) Cerebral angiogram confirming perfusion of the ophthalmic artery. (C) Angiogram showing vasculature of the globe and orbit with the microcatheter positioned at the ostium of the ophthalmic artery.

The primary drug used in IAC is melphalan, which was identified as the most effective drug against retinoblastoma in vitro.[3] Recommended doses of melphalan per infusion have ranged between 2.5 and 5 mg per infusion, based on weight and age, with an average 3-year-old receiving 5 mg of melphalan.[8] Systemic neutropenia is also observed after IAC, with 29% of cycles being associated with Grade 3 or 4 neutropenia.[264] The risk of neutropenia appears to be the highest when the dose exceeds 0.4 mg/kg of melphalan.[262] The procedure is also technically difficult in children below 6 months of age due to the small size of the ophthalmic artery. The group at MSKCC has reported successful treatment in

children who are at least 3 months of age and 6 kg in weight.[265] In patients who have failed primary therapy and IAC is being used for a recurrence, multiple drugs are often used, using melphalan, carboplatin, and topotecan in combination.[252,266,267]

Intravitreal Chemotherapy Injection

Despite the success of using systemic chemotherapy regimens for the treatment of intraocular retinoblastoma, eye preservation rates for eyes with diffuse vitreous seeding (i.e., group D) have been disappointing, with approximately 50% of eyes avoiding radiation or enucleation.[229] In fact, vitreous seeding is the most common reason for failure with systemic chemoreduction. Using salvage radiotherapy for recurrent vitreous seeding, success rates range between 50% and 70%,[229,268,269] but with the expected short-term and long-term side-effects. The use of intravitreal chemotherapy injections was first reported in Japan, but with some reports of failure, including extraocular spread.[3] Munier modified the protocol to increase its safety, using small needles, paracentesis, and cryotherapy to the injection site.[10,11]

In 2012 intravitreal chemotherapy injection (IVC) emerged as a potential new therapy to treat resistant vitreous seeding in eyes with advanced retinoblastoma, as two clinical series were published in the literature.[10,270] Since then, intravitreal injections of chemotherapeutic drugs have been performed in Europe and the United States as a salvage therapy for eyes with recurrent vitreous seeding from retinoblastoma. In several large series, authors have reported excellent globe salvage rates of 83–100%.[9,10,271,272] The injections have been shown to be safe with no cases of extraocular spread in Europe or the United States.[11,273] In the largest series to date, Munier and colleagues reported on 122 injections in 25 group D eyes with a median follow-up of 22 months (range 9–31 months). They reported an ocular salvage rate of 87% (20 of 23 eyes) for those eyes with resistant vitreous seeding.[9,10] In this series, the eyes developed a "salt and pepper retinopathy" at the injection site in the peripheral retina in 10 cases, but there were no other significant ocular complications and no signs of tumor spread outside the eye.[10] Abramson and colleagues have published clinical data on 16

patients who received weekly intravitreal melphalan injections and found no evidence of systemic spread of the drug.[272] However, there was a small but permanent (and cumulative) degradation of the overall ERG signal in eyes that received intravitreal melphalan injections at a dose of 30 μg.[272] Smith et al. performed a review of 1287 intravitreal chemotherapy injections in 306 eyes with retinoblastoma, and calculated a 3% risk of significant ocular side-effects.[273] There were also no cases of extraocular spread in the United States or Europe in this review.[273] At our center, we are aware of two cases of severe retinal toxicity which presented with a clinical picture resembling a combined retinal artery and retinal vein occlusion. Although parents should be aware of the small risk of significant ocular side-effects with intravitreal melphalan injections, the overall risk is lower than with other modalities such as radiation therapy or intraarterial chemotherapy infusion.

The current protocol for IVC utilized by clinicians was established by Munier in 2012, utilizing small needles, anterior chamber paracentesis, and cryotherapy at the injection site.[10] The schedule used by most centers is 4–6 weekly injections until the vitreous seeding is resolved clinically, with an average of 4.5–6.5 injections per eye.[10,272] An alternative schedule is to use a short course of three injections one week apart, and then waiting 4 weeks and documented clinical relapse before giving an additional injections. Our early results suggest that approximately half the eyes can be cured with the initial three injections. Doses of melphalan used by clinicians have ranged between 10 and 50 μg.[270,272] Currently, most centers use between 20 and 30 μg, keeping in mind that permanent but small ERG changes have been observed at 30 μg.[272] Melphalan is very unstable once reconstituted and injection should be performed within 2 hours to avoid loss of potency.[274] There have also been recent reports combining intravitreal melphalan and topotecan for refractory cases.[270,275] Munier has classified active vitreous seeding into the categories of dust, spheres, and the more extensive cloud (of seeds).[276] Francis and colleagues analyzed the number of injections needed to eradicate each category of seeding, and found eyes with dust required a median of three injections while eyes with clouds with seeding required a median of eight injections and almost 8 months

for complete resolution (Fig. 132.16).[277]

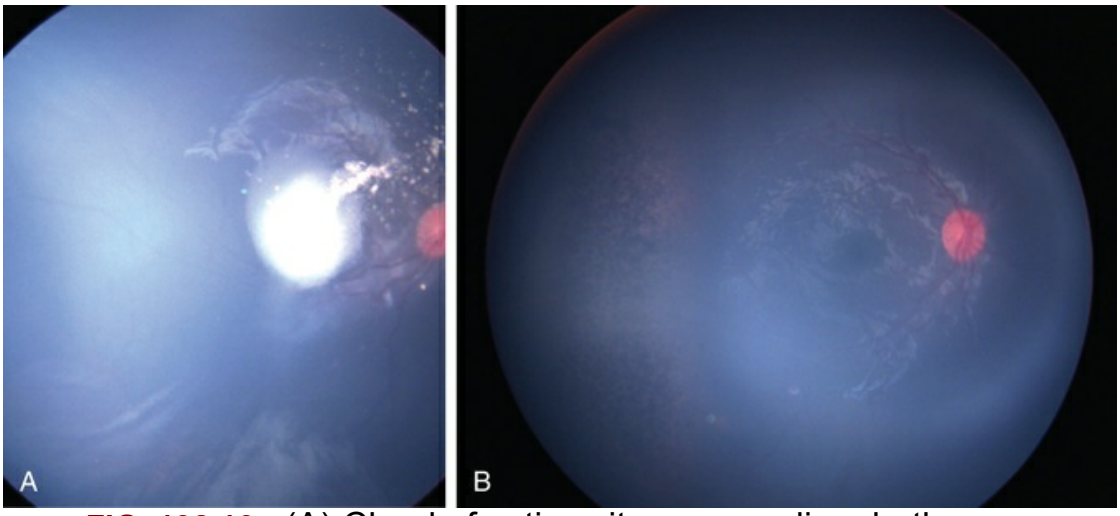

FIG. 132.16 (A) Cloud of active vitreous seeding, both with a large central fragment and diffuse seeding in the inferior vitreous. (B) Resolution of vitreous seeding after seven intravitreal melphalan injections. Note the peripheral retinal atrophy that can be seen after melphalan injections.

Clinicians should keep in mind that intravitreal melphalan should be reserved for eyes with recurrent vitreous seeding after primary therapy has failed. Our clinical experience has demonstrated that intravitreal melphalan injections have no effect on retinal or subretinal tumors. The clinical protocol originally described by Munier should be carefully followed to avoid complications.[10] Although there is the potential for ocular toxicity, the risk of extraocular spread is negligible and the safety profile appears to be better than with other modalities used to treat vitreous seeding.

Laser Treatment

In conjunction with systemic chemotherapy for intraocular retinoblastoma, tumor consolidation with laser therapy is an important component of the chemoreduction protocol. Laser therapy is also commonly used as the sole, primary modality for group A tumors that are less than 2 mm in diameter and thickness.

Two main laser wavelengths are used for retinoblastoma, the green 532-nm argon and the 810-nm diode infrared lasers. The energy of a laser is converted to heat only when it is absorbed, typically by the retinal pigment epithelium (RPE). Therefore, laser treatment is more effective for smaller and flatter tumors. It can be challenging to treat elevated tumors that are more than 2–3 mm away from the RPE and those tumors with an underlying calcium base. In comparing the two lasers, the shorter-wavelength green 532-nm argon is more effective for creating very focal scars, while the diode laser should have deeper penetration into bigger tumors. In addition, the green argon laser is better absorbed by the relatively nonpigmented retinoblastoma, and is typically the choice when treating tumors with a calcified base. The longer wave length 810-nm diode infrared laser provides deeper penetration and probably has a lower risk of causing a hemorrhage.

The technique we find useful with the argon 532 nm is essentially the same for both primary treatment of group A lesions and focal consolidation following primary chemotherapy in groups B–D. In general, focal consolidation begins after the first or second cycle of systemic chemotherapy after the tumor volume has been reduced. The initiation of laser treatment for tumors in the macula is usually delayed until a minimum of 2–3 cycles to allow for more tumor reduction and maximal visual recovery. The goal of the therapy is to completely cover each lesion with 50% overlap during at least three different sessions. We choose initial power setting of 250–300 mW, with a duration of 300 msec. The power and time settings are kept low to prevent tumor disruption, retinal contraction, and possible hemorrhage that may be associated with excessive energy delivery. In general, the first burns are placed at the edge of the lesion with the spot half on and half off the tumor. The power and/or duration can be adjusted to achieve gentle whitening of the tumor. We do not recommend exceeding 600 mW of power with the 532 mm laser. Once the lesion is outlined, then the entire lesion including any type I regression-associated calcium is covered with overlapping rows of burns (Fig. 132.17). A small to moderate-sized lesion may require 200–400 burns for good coverage. The burns over the thicker areas of the tumor may be virtually invisible compared with those placed at the edge of the lesion. Typically, the

power is kept at low levels around the periphery of a larger tumor and increased over the apex of the tumor if a color change is not observed. Repeat the laser coverage at 2–4-week intervals during and/or after the administration of systemic chemotherapy until the entire lesion has been covered on at least three different occasions. It is important that the tumor be reduced to type I regression (calcified) or type IV scars (flat) by the time the last cycle of chemotherapy has been given (Fig. 132.18). If the tumor has a large amount of type II regression ("fish flesh") or active tumor after the last cycle of chemotherapy, regrowth of the tumors off chemotherapy is extremely difficult to control with focal modalities alone.

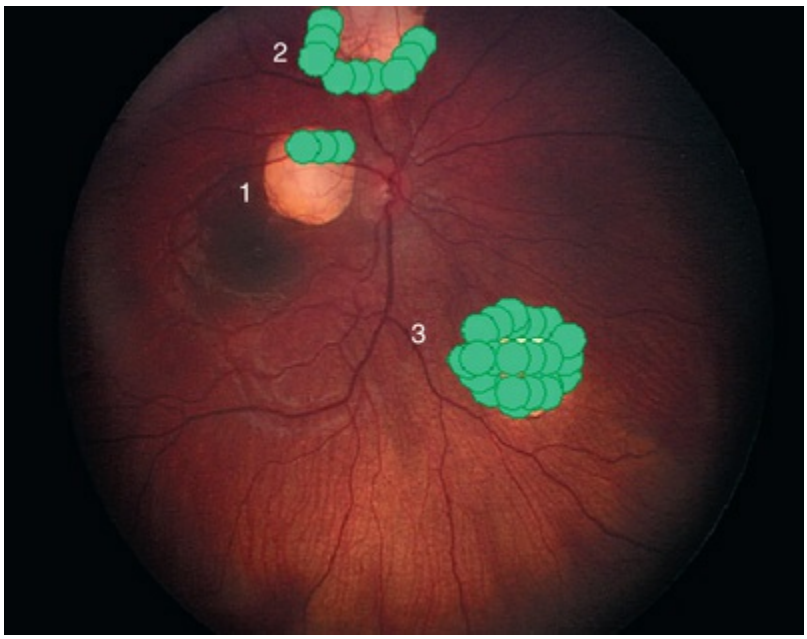

FIG. 132.17 Technique for laser focal consolidation. 1. First burns are placed at the edge of the lesion with the spot half on and half off the tumor. 2. The lesion is then outlined with 50% overlap of the previous spot. 3. The lesion is then covered completely with 50% overlap.

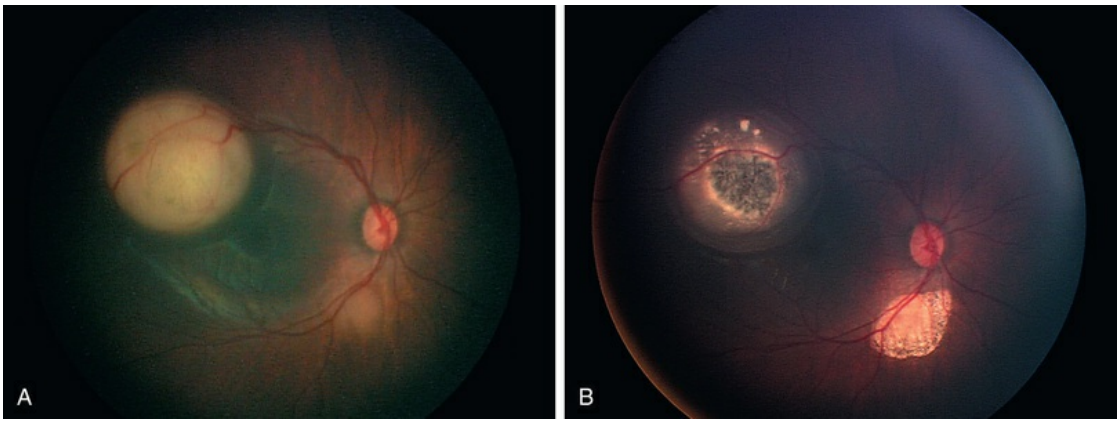

FIG. 132.18 (A) Group B tumor prior to treatment with systemic chemotherapy and focal laser consolidation. (B) After treatment there is significant reduction in tumor volume and appropriate flattening.

Because the infrared 810-nm diode laser has a longer wavelength than the argon laser, it penetrates further and is absorbed mainly by the retinal pigment epithelium. It is useful primarily if RPE is intact under the lesion to be treated. One major advantage of the infrared laser is its larger spot size allowing more rapid coverage of the lesion and offering less opportunity to deliver excessive concentrated energy that might cause bleeding or tumor disruption. The end point of energy application is, like that for the argon laser, a gentle whitening of a spot placed half on and half off the tumor. Because of the larger spot size, the power is generally set initially at 300, and can adjusted upward to 700–800 mW if required. Typically the diode laser used in continuous mode with the duration set at 9000 msec and the interval at 50 msec, with the total time of each laser spot controlled by the surgeon with the pedal. The appearance of punctate hemorrhages within the treated area indicates maximum energy is being delivered.

Complications of focal laser consolidation include burns of the iris at the pupillary margin and focal lens opacities, both of which are very rare in experienced hands. Other complications that are associated with excessive energy delivered to the tumor include subhyaloid and vitreous hemorrhage. We are also aware of several cases in which repeated laser photocoagulation delivered to multiple recurrences of a lesion in the macula was associated with the appearance of an extrascleral nodule of retinoblastoma in the orbit. It is likely that extraocular disease in these rare cases was a

complication of repeated laser applications causing scleral thinning and the creation of a portal of exit for tumor cells into the orbit. Although laser treatment is the safest modality used for intraocular retinoblastoma, any treatment given in excess of what is required to achieve tumor control can lead to significant complications.

Clinicians should also recognize that focal consolidation may lead to decreased vision from RPE scar migration or "creep" in lesions near the foveola. Care must be taken when applying laser on the foveal side of a tumor near fixation. Lee and colleagues demonstrated an increase in the size of laser scars following red diode laser application.[278] It is reasonable to consider close observation after sufficient primary chemotherapy of a small tumor located near the fovea or in the papillomacular bundle that demonstrates complete regression, until documented regrowth is observed. In these rare cases, central vision can be spared by withholding laser treatment if regrowth does not occur.

Cryotherapy

Destruction of the tumor by cryotherapy results from disruption of cellular membranes following the freeze–thaw cycle. It can also have a local vaso-occlusive effect on the tumor and nearby retina/choroid. Cryotherapy is useful for larger peripheral tumors and up to 3.0 mm in diameter and 3.0 mm in thickness.[279–281] The bigger tumors may require more than one treatment although we typically wait to see the effects of the first cryotherapy application before retreating. Cryotherapy can also be used for posterior pole tumors that are not responding to laser treatment, although a limited conjunctival peritomy is necessary so that accurate placement of the probe can be obtained. In addition, because the probe tip position cannot be easily confirmed while the freezing is taking place, it is possible to unintentionally injure the macular or the optic nerve. An important consideration is that cryotherapy routinely destroys a great deal of normal retina surrounding the lesion, thereby increasing the visual deficit from the resulting chorioretinal scar.

After confirming that the cryotherapy unit is working properly, the tip of the probe is used to indent the sclera under the tumor

with indirect ophthalmoscopy. Once the probe is directly beneath the tumor, freezing is initiated, and the ice ball is maintained until it encompasses the entire tumor mass with some overlap over the apex for 1–2 mm. Then the ice ball is allowed to thaw while not moving the tip, and this freeze–thaw cycle is repeated for a total of three applications.

Complications of cryotherapy include vitreous hemorrhage, subretinal fluid, and retinal holes. Rhegmatogenous retinal detachment can result from a combination of atrophic retina and vitreous traction, as cryotherapy results in strong adhesions at the margins of scars.[282,283] We have observed the creation of retinal breaks and rhegmatogenous retinal detachment when the calcium portions of type I regression is included in the ice ball. The presence of subretinal fluid in the region of proposed cryotherapy is a relative contraindication. Extensive cryotherapy can also cause atrophy of the sclera, with formation of a pseudocoloboma of the sclera.

Radiation Therapy

External Beam Radiotherapy (Teletherapy)

EBR was the treatment of choice as primary therapy of intraocular retinoblastoma for much of the 20th century. Verhoeff and Reese pioneered the method in the early 1900s. Retinoblastoma is considered a radiosensitive tumor because a high percentage of tumors respond at doses that the retina and optic nerve will tolerate. For Reese–Ellsworth groups I–IV, tumor control rates and ocular salvage rates are relatively high.[284–286] However, the main limiting factor of EBR is the high risk of SMNs in patients with heritable or germinal retinoblastoma. As a result most centers now use EBR as a salvage technique as a last resort if other treatment options such as intraarterial chemotherapy or intravitreal injections have failed. At our center, we use EBR only if there is a large retinal recurrence which has failed every other therapy and it is the only remaining eye with visual potential. EBR is also still used in cases where extraocular spread is strongly suspected or has developed in the orbit. This group includes patients with a positive cut end of the optic nerve after enucleation.

Newer techniques such as intensity modulated radiotherapy (IMRT) allow for a more focal, conformal treatment to the globe and decreased dose to the orbit. IMRT uses computer-controlled tungsten blades selectively to block areas of the treatment volume for a prescribed fraction of each beam's treatment time to make a radiation field with varying intensities. Fig. 132.19 is a three-dimensional reconstruction of a CT scan done on a retinoblastoma patient with his head positioned using a custom-molded headrest and a custom dental impression and custom bolus material over his retinoblastoma-containing right globe. The green arrows represent the central rays of the eight incident IMRT radiation beams converging on the patient's right retina. Fig. 132.20 compares the radiation dose distributions produced by irradiating the entire globe using the eight-beam IMRT arrangement (A) and a single 20 million volt electron beam (B). The IMRT substantially reduces the dose to the frontal lobe posterior to the orbit. Fig. 132.21 compares the radiation dose distributions produced by irradiating the retina using the eight-beam IMRT arrangement (A) and a single lateral 6 million volt photon beam. Both methods limit the radiation dose to the lens of the eye. The lateral photon beam, however, gives a substantially higher dose to the sphenoid sinus and contralateral orbit.

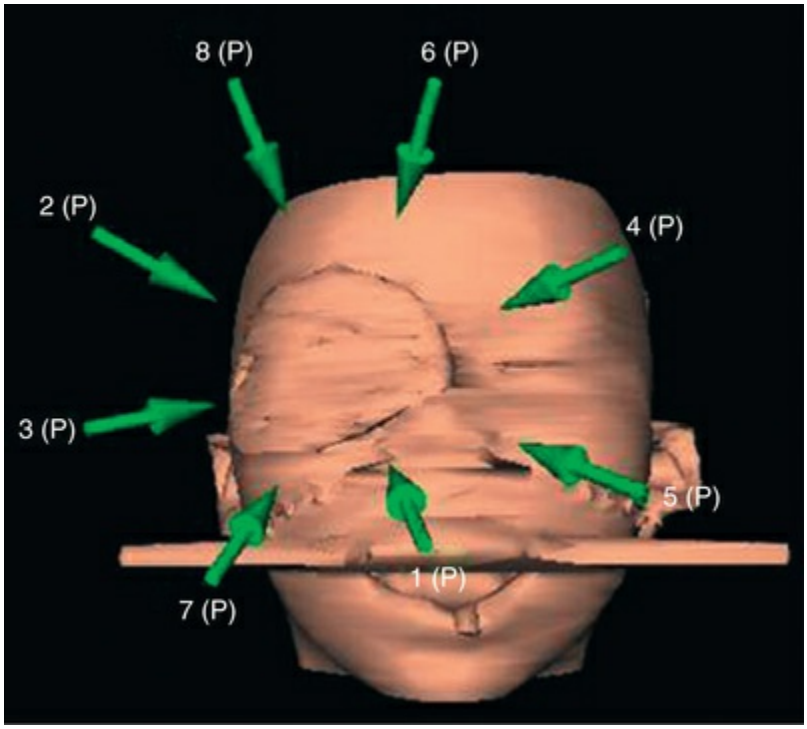

FIG. 132.19 Three-dimensional reconstruction of a computed tomography scan. The *green arrows* represent the central rays of the eight incident intensity-modulated radiation therapy beams converging on the patient's right retina.

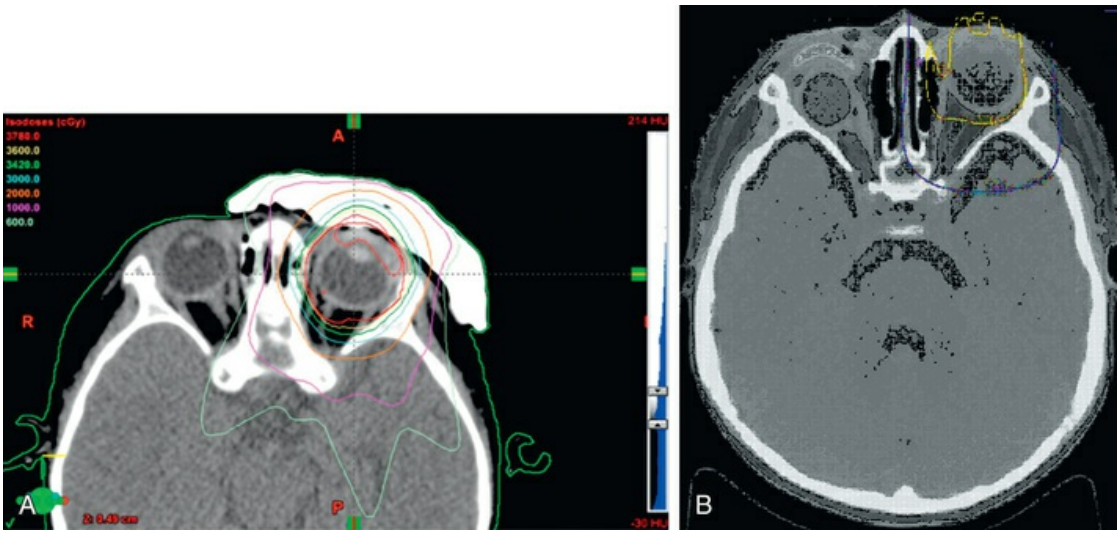

FIG. 132.20 Radiation dose distributions produced by irradiating the entire globe using the eight-beam intensity-modulated radiation therapy (IMRT) arrangement (A) and a single 20-million-volt electron beam (B). The IMRT substantially reduces the dose to

the frontal lobe posterior to the orbit. (Courtesy of Arthur Olch, PhD, FAAPM.)

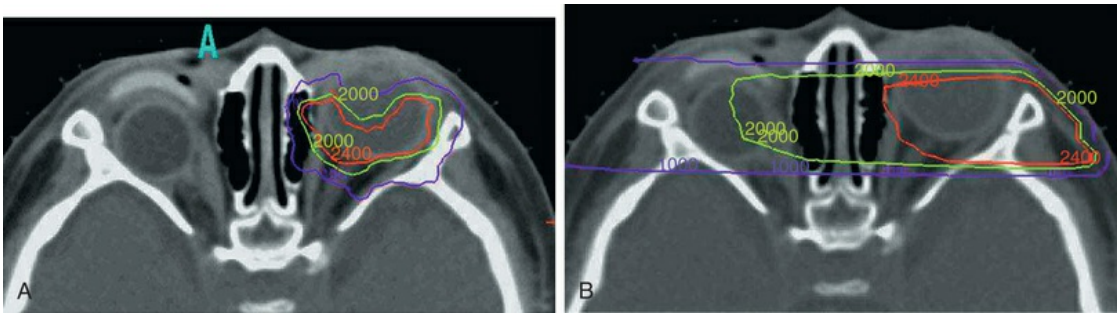

FIG. 132.21 Radiation dose distributions produced by irradiating the retina using (A) the eight-beam intensity-modulated radiation therapy arrangement and (B) a single lateral 6-million-volt photon beam. Both methods limit the radiation dose to the lens of the eye.

The widespread use of IMRT at most centers may reduce the rate of second malignancies long term as well as cataract formation and orbital hypoplasia when compared to standard lateral port EBR. Long-term studies on the use of IMRT for retinoblastoma are not yet available, but it is expected that the side-effect profile will be more favorable than with standard EBR. Total doses to the tumor range between 36 and 42 Gy with IMRT with daily fractions of 200 cGy. Sedation of the patient is necessary to ensure immobilization of the child's head during the daily delivery of radiotherapy. A custom-made head immobilization device is also required to reproduce the position of the patient's head throughout the course of approximately 20 daily treatments. With any EBR technique, the anterior retina (especially the anterior nasal retina) receives a lower total dose due to efforts to spare the lens. For this reason, EBR is much more effective at treating smaller, posterior tumors than larger, anterior tumors. At these doses, the retina and optic nerve typically do not develop late visual complications.

Despite efforts to spare the lens, a significant percentage of patients develop visually significant cataracts following IMRT. In the series reported by Schipper et al., 18 of 54 radiated eyes developed clinically detectable cataract, but only five of the 18 eyes

so affected required cataract surgery.[287] Lens opacity developed only in lenses in which a posterior portion of >1 mm had to be included in the treatment field. The minimum cataractogenic dose in that series was 8 Gy to the lens. Hungerford et al. noted that, by using the Utrecht device (the contact lens) for fixating the eye, the lens and anterior segment can be effectively spared while the whole retina is treated with a full dose of radiation.[288] Our experience at CHLA is that the rate of visually significant cataract is higher than what has been reported in the literature and that the majority of these patients require cataract surgery after IMRT at some point during childhood. We recommend waiting 2 years between the last treatment for retinoblastoma before performing cataract surgery and using a clear cornea approach.

Proton Beam Radiotherapy

Proton beam is a unique type of radiotherapy which utilizes heavy charged particles with a very sharp Bragg peak curve. This results in dosimetric plans that are more focal with less scatter to critical adjacent structures, including the orbital bones, CNS, and pineal region. In particular, the Bragg peak property of protons allows for a reduced dose of radiation to structures behind the tumor, such as the orbit, brain, and skull base. Recent studies have demonstrated the dosimetric superiority of protons over more traditional EBR and even IMRT.[289,290] Furthermore, the Boston group has published preliminary data showing a significant difference in the 10-year rates of second cancers in retinoblastoma patients between protons and photons (0% vs. 14%).[291] Proton beam radiotherapy is also potentially a shorter course of treatment when compared to IMRT, which typically takes at least a month. However, the entrance dose to the cornea is typically higher with proton beam radiotherapy compared to IMRT. A report from Boston described using an oblique or lateral beam to reduce the exposure to the cornea and orbital bones.[292] The same group published a globe salvage rate of 75% for group C and D eyes,[292] but overall globe salvage rates with proton beam appear to be similar to IMRT.[289] The challenge when considering proton beam treatment for retinoblastoma remains the high cost of such equipment and the relatively few centers capable of administering fractionated proton beam treatments under

anesthesia to the pediatric population. Despite the theoretical advantages of proton beam radiotherapy for retinoblastoma, there are not enough documented clinical advantages to recommend this modality over IMRT.

Brachytherapy

The use of brachytherapy in the treatment of retinoblastoma was originally pioneered by Moore and Scott in 1929. Ophthalmic applications were designed using radium and, later, cobalt 60. In 1977, Rosengren and Tengroth reported on the reasonably successful results of such treatment in 20 patients.[293]

Currently, there are two main isotopes in use for intraocular retinoblastoma: iodine-125 in the United States, and ruthenium-106 in Europe. Iodine-125 isotope secured in a gold carrier became a common radiation source used in brachytherapy when cobalt was abandoned decades ago. The gold carrier for the iodine was later modified with deeper wells for the seeds creating a conformal treatment plan (Fig. 132.22).[294] In primary brachytherapy, the calculated dose to the apex of the tumor is generally in the range of 40–45 Gy. These doses are significantly less than what is used for uveal melanoma, but the retina within 3 mm of the plaque margin will still develop significant radiation retinopathy. The isotope ruthenium-106 (a β-emitter), is commonly used in Europe due to the unavailability of iodine sources. The advantage of ruthenium is that the half-life is much longer than iodine so that a single plaque may be reused for up to 1 year. However, with a β-emitter the scleral dose of a ruthenium plaque is higher than a similar plan with iodine-125; as a result, retinoblastoma lesions higher than 5 mm cannot be treated. Also, in ruthenium plaques, the plaque itself contains the radiation sources. Therefore, it is not possible to custom design the location of the radiation seeds in the plaque to conform to the shape of the tumor. However, ruthenium plaques are available in numerous shapes and sizes to address this issue.

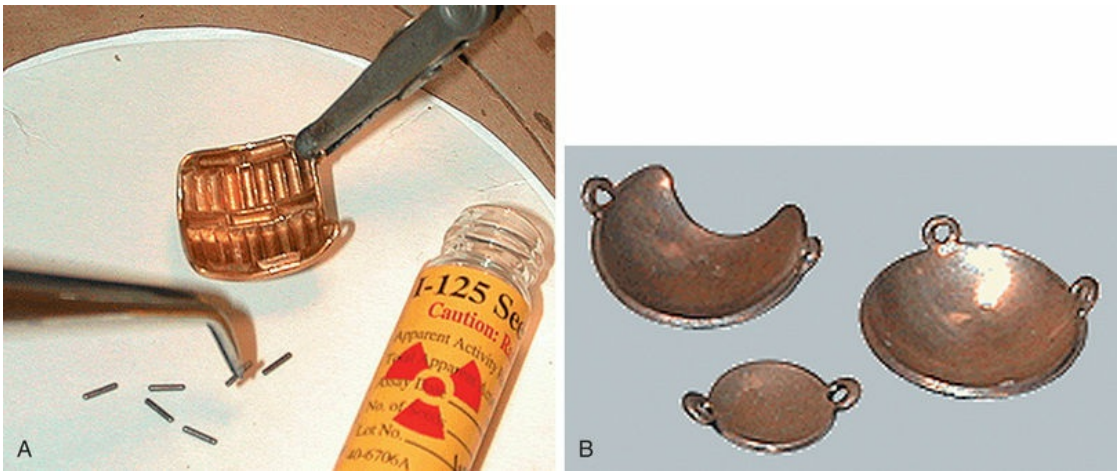

FIG. 132.22 (A) Gold carrier for the iodine was modified with deeper wells for the seeds creating a conformal treatment. The seeds can be loaded specifically depending on location of tumor. (B) The ruthenium plaque itself contains the radiation source. Therefore the possibility of differentially loading radiation seeds in the plaque to conform to the shape of the tumor is avoided with ruthenium.

Primary brachytherapy is an option for some group B patients if the tumor is located away from the posterior pole. Similarly, some group C patients can also be treated with brachytherapy if the tumor is peripheral and there is only a cuff of subretinal fluid. Unlike EBR, brachytherapy does not appear to increase the risk of second cancers in heritable cases, although there are significant ocular side-effects. Shields et al. reported their results of plaque therapy in 103 eyes, used both as primary therapy and for salvage after failure of other modalities.[295] With a mean follow-up of 38 months, 87% of eyes were successfully treated and 13% showed tumor recurrence. Tumor control rates for ruthenium brachytherapy has been reported to be 73%, although similar to iodine-125, its use as salvage therapy is often less successful than primary therapy.[296] The main limiting factor with plaque therapy for posterior pole tumors is the likelihood of permanent visual loss associated with high doses of radiation to the retina and other vital structures. Another limiting factor is the appearance of vitreous seeds after brachytherapy, but intravitreal melphalan injections can now be used to treat residuals seeds which appear during follow-up.

The technique of localizing the plaque when treating retinoblastoma differs somewhat from the localization technique for choroidal melanoma, primarily because of absence of pigment in retinoblastomas. Transillumination techniques used with melanomas are not helpful in localizing retinoblastoma. Surgeons rely on localizing the margins of the tumor with scleral depression and indirect ophthalmoscopy when using COMS plaques, or preoperative computer modeling using Eye Physics plaques.[297,298] With the Bebig Corp. Software, the radiation physicist can tell the surgeon the position in clock-hours for the center of the anterior edge of the plaque, the location of the eyelets, and how many millimeters those points are located posterior to the limbus (Fig. 132.23).[298] When suturing a radioactive plaque in a young child with retinoblastoma, extreme care must be taken not to perforate the thin sclera with the spatulated needle. In general, children are admitted postoperatively to ensure that they can be monitored during brachytherapy. If there is concern regarding the child disrupting the plaque position, sedation may be required. The duration of plaque treatment is generally shorter for retinoblastoma than for melanoma due to the lower total dose, and in most patients the admission time is 2–3 days.

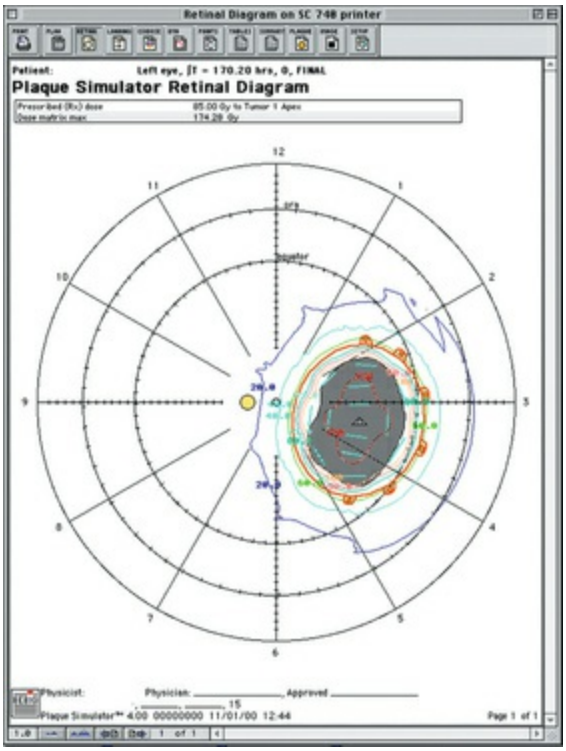

FIG. 132.23 Dosimetry planning is carried out with the help of sophisticated software, such as that available from Bebig Corporation. The position in clock-hours for the center of the anterior edge of the plaque, the location of the eyelets, and how many millimeters those points are located posterior to the limbus are shown.

A child should never receive both brachytherapy and EBR to the same eye due to the very high risk of radiation-related ocular side-effects.[286] Use of brachytherapy for consolidation immediately following primary systemic chemotherapy is also associated with an extremely high risk of aggressive radiation retinopathy. We have observed rapid radiation retinopathy in several eyes when 40 Gy was given to the eye with brachytherapy immediately following completion of CEV chemotherapy. In that situation, other modalities may be used to temporize for several months or a lower total dose to the tumor should be considered.

Enucleation

Enucleation is not only the oldest surgical procedure used to treat intraocular retinoblastoma but often the best option for advanced disease that has compromised the visual potential of the eye.

Despite the progress of various conservative modalities, enucleation remains the most commonly employed technique for treating retinoblastoma worldwide. This chapter will focus on specific technical issues related to performing enucleation for retinoblastoma, including some “surgical pearls” which have been very effective in the authors' experience.

Indications

There are several categories of patients who are considered excellent candidates for enucleation: (1) unilateral advanced tumors (particularly with extensive seeding) with negligible visual potential (group D or E); (2) a blind eye with recurrent disease following chemotherapy and/or radiation; (3) bilateral retinoblastoma with advanced disease and dismal visual potential in one eye and the other eye which can be treated otherwise; and (4) any patients with suspected optic nerve, anterior segment, choroidal, scleral, or extraocular tumor involvement. Finally, patients are also considered candidates for enucleation if they have suspected active tumor in the eye and cannot be followed due to obscured media (e.g., vitreous hemorrhage or phthisis).

If a bilateral patient has advanced disease, which is symmetrical or almost so, then it is reasonable to delay enucleation until response to primary chemotherapy has been evaluated in both eyes. This is because it may not be possible to predict how the tumor(s) in any particular eye will respond to systemic chemotherapy. This approach has been criticized because important pathologic risk factors (e.g., invasion into the optic nerve) might be obscured by systemic chemotherapy. However, this is not a major concern if the child undergoes enucleation of the worse eye and receives the full six cycles of systemic chemotherapy for the contralateral eye. In most centers the adjuvant protocol that would be given if an enucleated eye contained high-risk pathologic features is similar to the traditional three-drug six-cycle primary chemotherapy protocol for intraocular disease (carboplatin, etoposide, and vincristine). When the decision has been made to proceed with enucleation for any patient with retinoblastoma, surgery should ideally be scheduled within 7–10 days. Waiting any longer exposes the child unnecessarily to the risk of metastatic disease (particularly in

untreated patients and any group D), and possibly ocular discomfort if glaucoma or periocular inflammation is present. Prior to enucleation, all patients should be evaluated with a brain and orbit MRI scan to ensure that there is no radiographic evidence of optic nerve or extraocular extension that may require neoadjuvant chemotherapy prior to enucleation to minimize the chances for local and systemic relapse.

Preoperative Counseling

Before performing an enucleation on any child with retinoblastoma, regardless of age, a member of the retinoblastoma management team should thoroughly prepare the child and the extended family. It is also important to discuss with the parents the technical aspects of the surgery and the expected postoperative course. It may be helpful to share with the parents the perspective that enucleating an eye with advanced disease is a reason to celebrate, as it is likely that a relatively simple operation will cure their child with cancer. Greater than 96% of patients who present with intraocular retinoblastoma are cured by enucleation.[299,300] It should also be emphasized to the parents that the involved eye has not had useful vision for a prolonged period and that the child will not experience any functional limitations from enucleation. The adults in the extended family need to see photographs of other children who have had enucleations; if possible they should be able to hold and feel the implant and ocular prosthesis. Finally, it should be explained that the operation is not overly painful and can usually be performed on an outpatient basis. A child as young as 12 months old may be able to understand that his/her eye is sick, and certainly an 18- to 24-month-old child will be able to understand this concept. Therefore, it is very important that the parents be honest with their child about what is about to happen. It is also critical to involve siblings of whatever age in the preoperative discussions. Siblings in the 2- to 6-year-old group may engage in "magical thinking," believing that a previous push or shove of their affected sibling may have caused this problem.

One of the most important considerations when enucleation is part of the treatment plan is the experience of the surgeon with the procedure. Any ophthalmologist without significant experience

doing enucleations for retinoblastoma and harvesting fresh tumor in a manner acceptable to ocular pathology should not assume that these procedures are routine. The implications of technical failures during the surgery may be catastrophic in this subgroup of children. For example, inadvertently opening the globe releases tumor cells into the orbit, greatly increases the risk for metastatic disease. Improper tumor harvesting can compromise *RB1* gene testing, which may have future implications on the child's overall medical care. Finally, a less than ideal cosmetic outcome may have far-reaching social and emotional repercussions for the family and the child. There are also special pediatric anesthesia considerations for children who are undergoing enucleations for retinoblastoma. Presurgical anxiety can be significant, especially in older children, and experienced pediatric anesthesiologists typically use oral Versed (midazolam) in the preoperative holding area. It is often helpful for one of the parents to don a “bunny suit” over their street clothes and carry the child into the operating room. There, while the child is being held in the arms of the parent, mask anesthesia is given until the child can be gently positioned on the operating room table.

Surgical Procedure

Before prepping for surgery, both pupils should be dilated prior to the procedure, so that the presence of the tumor can be confirmed by indirect ophthalmoscopy and the other eye taped and shielded. This step is critical to avoid a tragic error in enucleating the wrong eye. Once the presence of the tumor in the correct eye has been confirmed, the correct eye is prepped and draped. Surgery begins by placing an eyelid speculum for exposure; in general, the widest exposure is preferred, although the tension on the lids may need to be reduced once the globe is removed to allow for closure over the implant. The conjunctiva at the limbus is desiccated with cotton-tipped applicators and outlined with a marking pen to allow for easy identification of the conjunctival edges during final closure. A conjunctival peritomy is started at either the 3 or 9 o'clock positions, and care is taken to preserve as much conjunctiva as possible by “hugging” the limbus with the Westcott scissors. Gentle bipolar cautery may be used on focal points of bleeding from the episclera.

It should be emphasized that meticulous hemostasis maintained from the beginning of the procedure allows the surgery to be precise, and also assures control of postoperative ecchymosis and orbital edema. In addition, care should be taken to avoid undue manipulation and pressure on the globe, and to avoid any maneuvers that may increase the risk of sclera perforation or injury.

Once the conjunctival peritomy has been completed, the Tenon layer is separated from the sclera in the four oblique quadrants, using gentle blunt dissection with the tips of the curved Stevens scissors held parallel with the sclera. Be mindful that vortex veins exit the sclera about 16–18 mm posterior to the limbus. A blunt 20-gauge cannula is then used to infuse local anesthetic (3–4 ml of 1% lidocaine with epinephrine mixed with 0.5% marcaine with epinephrine and Wydase [hyaluronidase]) into the retrobulbar space (typically inferonasally). This maneuver may prevent sudden bradycardia during the rest of the procedure, greatly reduces the amount of bleeding when the optic nerve is transected, and provides postoperative pain control.

The four rectus muscles are then sequentially isolated with muscle hooks, imbricated with a double armed 5-0 Vicryl suture, and transected from the globe at their insertion sites. A suggested sequence of muscle disinsertion follows: (1) inferior rectus, (2) lateral rectus, (3) medial rectus, (4) superior rectus. When passing needles through muscle tissue, the angle of passage should always be parallel or away from the sclera to avoid inadvertent globe perforation. A longer muscle insertion (about 5 mm) is left at the insertion of either the medial rectus or lateral rectus muscles (surgeon's preference) to allow for some traction on the globe (with an Adair clamp) during transection of the optic nerve. As each muscle is disinserted, the ends of the Vicryl suture are secured to the drape with a labeled Steri-Strip to prevent tangling during the rest of the procedure. The superior oblique muscle is then isolated with a muscle hook using a sweeping motion behind the superior rectus insertion, and transected from the globe. The inferior oblique muscle is located in the inferolateral, anterior orbit by sweeping the muscle hook away from the globe toward the orbital rim; this muscle is highly vascular and should be cauterized with bipolar cautery before transection. A visual inspection is then performed of

the anterior and equatorial sclera surfaces to ensure that there are no adhesions remaining between the orbit and sclera (other than the optic nerve).

The scissors chosen to transect the optic nerve varies with the preference of the surgeon. In general, we prefer a pair of slim-profile scissors with long tips that are slightly curved (e.g., long Metz or Metzenbaum scissors). It is our impression that the exaggerated 15-degree curve on the enucleation scissors increases the risk of sclera perforation and reduces the ability to extend the tips into the posterior orbit. Some surgeons utilize an enucleation snare to cut the optic nerve although we do not have a great deal of experience with this instrument because of the induced crush artifact. For similar reasons, we also do not recommend clamping of the optic nerve prior to transection. Another option is to sever the optic nerve under direct visualization through a superior orbital approach, utilizing a small upper lid incision.[301]

Long Optic Nerve Stump.

Certain surgical steps can facilitate obtaining the minimum 15 mm of optic nerve stump recommended in all enucleation cases for retinoblastoma. An Allis Adair artery clamp (same width as the rectus muscle insertion) can be used to exert gentle traction on the globe during this critical step. Our personal experience is that gentle traction applied to the 5 mm of rectus stump will serve to "lengthen" the nerve in the orbit exposed to the scissors. An initial spreading movement adjacent to the optic nerve with the scissors will open the posterior Tenon layer and allow the tips to enter the retrobulbar space. While maintaining tension on the Allis clamp, the scissors tips are mobilized along the medial orbital wall and moved in a vertical motion to palpate the optic nerve. If the surgeon cannot feel the optic nerve with this motion, the nerve may be either below or above the scissors tips due to globe rotation. The surgeon should then find the medial rectus insertion and rotate the globe so that it is located in the correct anatomic position. It should also be kept in mind that the optic nerve follows a temporal to nasal route as it plunges toward the orbital apex. Once the optic nerve is palpated, the tips are opened slightly (with the optic nerve between the tips) and pushed nasally/posterior toward the medial wall. With

the scissors tips pushing toward the posterior belly of the medial rectus muscle, posterior pressure is maintained and the scissors are closed around the optic nerve, transecting the nerve in one decisive motion. The tension on the globe should release at this point, confirming that the optic nerve has been successfully transected. The globe will now move forward and you will note some attachments of orbital fat and soft tissues holding the globe within the orbit. The scissors are then used to gently lyse these attachments fairly close to the globe to avoid cutting any motor nerves within the muscle cone.

After the globe has been removed from the orbit, it is placed on a separate Mayo stand which has been set up with several instruments, including a corneal trephine, small Castro Viejo forceps, and Westcott scissors. Hemostasis within the orbit is obtained with a tonsil ball (i.e., spherical gauze pad) soaked in epinephrine (1 : 1000 concentration) and activated thrombin. An assistant gently holds the tonsil ball within the muscle cone while the globe is prepared for pathologic examination. Another option for hemostasis is to use a test-tube filled with a frozen-slush saline solution to tamponade the orbit. Using the epinephrine soaked tonsil ball (or ice-filled test tube) as a tamponade for approximately 10 minutes results in little postoperative swelling or bruising. There is typically no need for a pressure patch and the dressing can be removed the following day after outpatient surgery.

Harvest of Fresh Tumor for *RB1* Testing or Other Research Uses.

On the Mayo stand, the optic nerve stump should be measured and inspected for any gross pathologic changes. A posterior optic nerve margin is obtained prior to opening the globe to avoid any tumor contamination by artifactual clumps of tumor cells. The posterior stump of optic nerve is prepared by marking the surgical margin with ink, and then transecting the optic nerve with a razor blade 4 mm behind the sclera. This posterior optic nerve margin should be placed into a jar of 10% buffered formaldehyde and submitted separately. The globe is then inspected for any evidence of extraocular tumor extension and the location of the inferior oblique muscle is used to aid in orientation of normal globe landmarks (e.g.,

macula). The location of the base of the tumor is outlined with a marking pen on the sclera, determined either with transillumination or from preoperative fundus drawings. Then, a small sclero-choroidal window is created, adjacent to the tumor base near the equator with a 6- to 8-mm corneal trephine. Once the opening into the vitreous chamber is established, tumor tissue should be gently removed with forceps and scissors. For genetic testing, the sample is sent fresh in saline in a petri dish. Samples of the tumor for research purposes are placed into the appropriate vials and transported immediately to the lab. It is best to leave a hinge on one side of the scleral flap so that it can be closed with one or two suture(s) following the removal of tumor sample. The globe should be placed in a second jar of formalin (separate from the optic nerve stump) and be allowed to fix for at least 24–48 hours before sectioning.

Once the surgeon has completed the handling of the tumor specimen, his/her surgical gloves should be changed before returning to the operating table for the closure. Instruments used to handle the tumor or to open the globe should never be returned to the operative field.

Insertion of Orbital Implant.

A variety of porous and nonporous orbital implants are available to re-establish the orbital volume, including silicone, hydroxyapatite, Medpor, and dermis fat graft. The type of implant chosen depends mainly on the preferences of the surgeon, although there are some important considerations in retinoblastoma patients. Nonporous implants (e.g., silicone spheres) have a lower exposure and extrusion rate, but also have a higher rate of migration in young children than porous implants (e.g., hydroxyapatite, Medpor). Performing an implant exchange later in life is difficult with a porous implant due to the presence of implant ingrowth and therefore a nonporous implant may be a better choice when placing an implant smaller than 18 mm. On the other hand, porous implants such as hydroxyapatite and porous polyethylene (Medpor) offer the potential for better motility, particularly if the implant is pegged later in life to allow coupling with the prosthesis. However, it should be kept in mind that there is no proven motility

advantage for nonpegged porous implants (hydroxyapatite, Medpor) when compared to nonporous implants (silicone). In addition, porous orbital implants have higher rates of implant exposure and infection compared to silicone spheres, as well as higher costs.[302]

We routinely use coated hydroxyapatite implants in our patients as it is easy to work with, has a low rate of migration, and allows the attachment of the extraocular muscles to the anterior surface of the implant. In any child undergoing enucleation, the largest implant that can be reasonably fitted into the orbit should be selected, both to encourage orbital growth and to obviate the need to place a secondary implant when the child grows. In general, an adult-sized 20-mm implant can be placed safely in children older than 2 years of age, while children between 12 and 24 months can be fitted with an 18-mm implant. Children less than 12 months of age may require an 18-mm or 17-mm implant. The implant is soaked in bacitracin solution prior to implantation. The goal is to place the implant as deep into the muscle cone as possible, to minimize postoperative enophthalmos and the risk of anterior implant exposure. This is accomplished by sliding the implant into the muscle cone with the introducer, while applying steady pressure on the surface of the implant.

Attention to Surgical Closure and Prevention of Implant Extrusion.

Once the implant is positioned within the muscle cone and the rectus muscles are attached, the Tenon layer is mobilized over the surface of the implant to ensure that closure can be achieved without undue tension. If the Tenon layer cannot be closed without tension, then the implant is repositioned deeper into the orbit or a smaller implant is chosen. The anterior Tenon capsule is then closed over the implant using buried 5-0 Vicryl sutures (P-3 needle); typically five or six sutures are placed to accomplish a right closure without gaps, which will prevent any postoperative dehiscences of this fascial layer. The conjunctival edges are carefully identified and closed with a running 6-0 plain gut suture. Antibiotic ointment is applied over the socket and a small or medium conformer is then placed to maintain the fornices in the postoperative period. With

the conformer in place, the lids should be able to close. If not, a smaller conformer should be fitted for the patient to prevent discomfort or possible loss of the conformer during the early postoperative period. A double gauze eye patch is adequate as a dressing and we have not found it necessary to place a pressure patch.

Postoperative Care.

Careful attention must be paid to the prevention of nausea, vomiting, and the possibility of an orbital hemorrhage, which will lead to unnecessary discomfort as well as a delay in the healing process. We typically administer intravenous antibiotics, steroids, and a dose of ondansetron (Zofran) or similar agent during surgery. Postoperative pain is controlled for approximately 4 hours by the long-acting local anesthetic infused into the posterior orbit prior to cutting the optic nerve. In addition, appropriate doses of liquid hydrocodone (Lortab) or similar analgesic should be given every 4–6 hours for the first 24–48 hours. We generally discharge the patient after the surgery and see the patient on the first postoperative day for a clinical assessment and dressing change. We instruct the parents to change the patch daily for 7–10 days combined with the application of antibiotic ointment or drops several times per day. We have not found oral postoperative antibiotics to be routinely necessary but some centers advocate their use. Once the postoperative edema has completely resolved 4–6 weeks following enucleation, the patient can be fitted with a prosthesis by the ocularist.

As stated previously, extreme care should be taken to avoid accidental perforation of the globe as this may require additional treatment with associated morbidity. What should the surgeon do if scleral perforation occurs during enucleation of an eye with active retinoblastoma? Surgery should be completed to ensure that the entire globe has been removed, using extreme care to avoid further spillage of the intraocular contents. If the area of tumor exposure is localized, the surgeon should debulk that area of the orbit and send it to pathology as a separate specimen. The socket should then be irrigated with sterile water to encourage hydrolysis of any remaining tumor cells. We would suggest placing a nonporous

implant (e.g., silicone sphere) in case any further socket surgery becomes necessary, although some experts recommend not placing an implant in this situation.[4] The decision to treat the area with local or systemic modalities must be made on a case-by-case basis by the oncology team. If the enucleated globe has high-risk pathology, then systemic adjuvant chemotherapy will be necessary. If the globe does not contain high-risk pathology, the oncology team may still decide to give postoperative chemotherapy to treat any viable cells which may have seeded the orbit. The decision to treat the socket with radiotherapy is controversial and should be considered for those cases with a high risk for orbital recurrence.[303] For example, a patient with a positive optic nerve margin would be expected to have clinically viable disease remaining in the orbit and adjuvant radiotherapy would be indicated. However, surgeons should be aware that orbital radiation given in the first 6 weeks following enucleation will lead to severe socket contracture in all patients and noticeable orbital bone hypoplasia in children less than 18 months of age. There is also concern regarding the association between radiation and second cancers in very young children (<1 year of age) with the germinal form of retinoblastoma. Regardless of the management approach, all of these patients with possible orbital exposure should be carefully monitored with serial MRI scans every 3 months for the first year after enucleation.

Outpatient postoperative care is critical for all children who have undergone enucleation for retinoblastoma, particularly during the first year after surgery. During the first month after surgery, the patient and parents should meet with the oncologist, to discuss the histopathologic findings and their implications. The decision to treat children after enucleation for high-risk pathologic features with adjuvant chemotherapy is controversial. At most centers, 6 months of systemic chemotherapy with a three-drug regimen is recommended for post-laminar optic nerve invasion, massive choroidal invasion, scleral invasion, and anterior segment invasion. The ophthalmologist should be aware that the risk of orbital tumor recurrence is highest during the initial 12 months after enucleation and therefore the prosthesis should be removed and the socket checked for any abnormalities during postoperative visits.[205,299]

Orbital growth following enucleation will be normal if a large

orbital implant is placed in the orbit at the time of surgery and no orbital radiation from an external source is given.[304] However, failure to replace the eye with an orbital implant and failure to maintain the presence of an ocular prosthesis will result in orbital growth deficiency.[305] Imhof and colleagues demonstrated that the growth of irradiated orbits was significantly impaired ($p<.001$) when compared with nonirradiated orbits, and that secondary enucleation did not add to the bony growth retardation triggered by EBR.[306] Not surprisingly, these authors observed the growth-impairing effect of EBR to be most profound when the child is irradiated before 6 months of age ($p<.01$). Orbital growth studies in rabbits show a decrease in orbital growth following enucleation, that was mitigated by an expandable but not static orbital implant.[307] Based on the findings of Fountain et al., growth in enucleated human orbits may be normal if a large but nonexpandable orbital implant is used.[304]

Regression Patterns Following Treatment

The regression patterns following primary chemotherapy are typically formed after two to three cycles of chemoreduction. They are described in Table 132.1 and guidelines about the need for focal consolidation for each type are also given. The patterns of tumor regression following primary chemotherapy are similar to those that result from treatment with EBR, and the nomenclature used by clinicians is identical. Some tumors develop complete calcification with rapid reduction to type I regression. This favorable response can occur in some tumors by the end of the first cycle of systemic chemotherapy, while others may not develop much calcification by the end of the sixth cycle. Pure type II regression ("fish flesh", translucent mass) is an uncommon response following primary chemotherapy in our experience. Type III regression (combination of types I and II) is the most common (Fig. 132.24). Type IV regression is a flat scar, with either atrophic changes, increased pigmentation or a combination of the two. The least common type of regression pattern is type 0 (no visible lesion), but we have observed it in small foveal lesions that were not lasered. As previously mentioned, any active tumor is lasered, with minimum

of three sessions to achieve either a type I or type IV scar. Some type II or III regression patterns may require 15–20 laser sessions to achieve this goal.

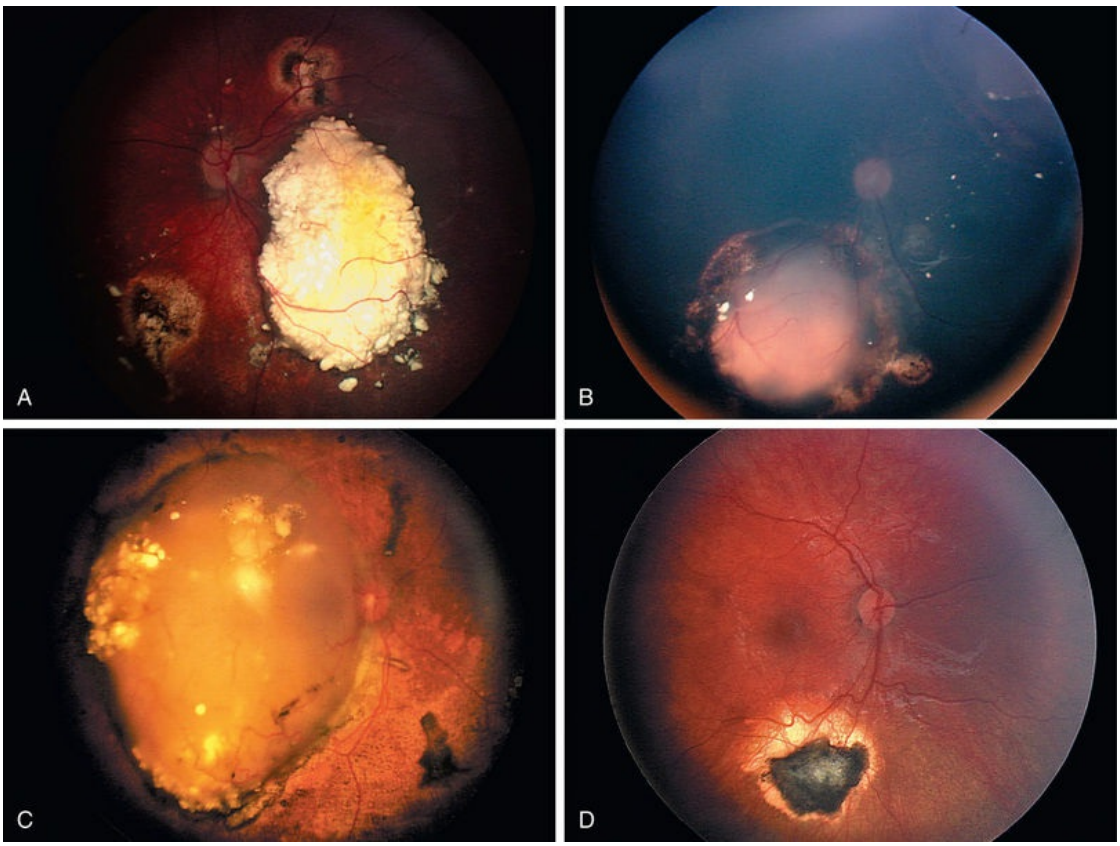

FIG. 132.24 (A–D) Regression patterns I–IV after treatment of retinoblastoma.

Most of the information related to regression patterns in treated retinoblastoma has been reported in eyes treated with EBR. In 1993, Singh and colleagues reported their evaluation of 180 individual tumors in 105 eyes of 83 patients treated at St Bartholomew's Hospital in London with EBR, and found that recurrence of tumor growth was seen in 13/180 tumors (7%), all by 40 months following the end of treatment and none after 4 years.[308] In 1991, the New York experience with 89 tumors in 57 eyes treated only with EBR showed that type II was the most common regression pattern throughout the period of follow-up.[309] The largest tumors showed type I regression and the smallest lesions (1 DD or less) completely disappeared. In 1983, Buys and colleagues from New York reported the regression patterns following cobalt plaque radiotherapy.[310]

They found that type IV regression (a flat scar or bare sclera) in nine of 31 eyes with no recurrence from type IV regression by 6.5 years following treatment. Type I was the most common regression pattern, with fewer type II and III.

Following chemoreduction, Shields et al. reported that type I regression was more common with larger tumors and those closer to the fovea.[311] In our practice, we have not noted a consistent correlation between preoperative factors and the final regression patterns. Shields et al. also noted no differences in recurrence rates between different regression patterns.[312] However, we have noted that the amount of type II regression is a strong predictive factor for future tumor recurrence. Therefore, we perform focal consolidation aggressively to reduce type II or type III regression to type I or type IV; this process should ideally be completed by the end of the six cycles of chemoreduction, but if not, laser treatment is typically continued on a monthly basis until this goal has been achieved.

New Tumors or Tumor Recurrences During Posttreatment Follow-Up

For ophthalmologists following patients with heritable retinoblastoma, the concern always is whether new tumors may appear, either during or after chemotherapy. In a review of 165 tumors in 57 eyes of 34 patients with heritable bilateral retinoblastoma treated with single agent carboplatin and focal consolidation, 63 new tumors appeared in 27 eyes.[313] The mean age of the patient at the time of tumor presentation was 9 months and the mean time to tumor appearance following carboplatin therapy was 4.4 months. Shields et al. reported that in 162 eyes of 106 affected patients, new tumors occurred in 24% of eyes.[314] Most commonly these new tumors appeared in the eyes of children diagnosed at a very young age or who were members of a pedigree with retinoblastoma. Because these newly appearing tumors have no blood supply, the systemically administered chemotherapy should not be expected to prevent their appearance. There is a recent report suggesting that new tumor formation is almost never encountered following intraarterial chemotherapy, possibly due to higher intraocular drug levels after selective arterial infusion.[315]

Another type of new tumor formation is recurrence following initial response, and this can be classified as edge scar recurrence, main tumor recurrence, or new preretinal tumor formation from vitreous seeding. In our experience, focal regrowth or edge scar recurrence is usually seen within 2–6 months following the completion of chemoreduction (Fig. 132.25). Fortunately, most scar recurrences can be treated successfully with aggressive focal consolidation using laser therapy or cryotherapy, if detected early enough. Serial RetCam images are helpful in determining if a suspicious area is regrowth or persistent type II regression. Early focal regrowth usually appears as a slight elevation that will have a pink blush of fine vascularization, and fluorescein angiography can demonstrate the early lacy hyperfluorescence and late leakage. After the last cycle of chemotherapy, we follow children with EUAs at monthly intervals until laser treatment has been completed. Then we follow patients at 6-week intervals for approximately 6 months given that this is the period of time at highest risk for tumor recurrence. After the 6 month monitoring period, children can be followed according to the screening schedule for new tumors: every 1 month below age 1, every 2 months between ages 1 and 2, and every 3 months between ages 2 and 3. After the child has reached age 3–4 years *and* it has been at least 2 years since the last active tumor was observed, follow-up can be transitioned to the office setting. In the office, we examine these children with indirect ophthalmoscopy of the fundus (without a speculum) as well as ultrasound B scan of the peripheral retina. It is unlikely that you will see small tumors in the periphery that are small enough to treat with focal modalities without EUA, but the risk of new tumors is extremely remote when these recommendations are followed.

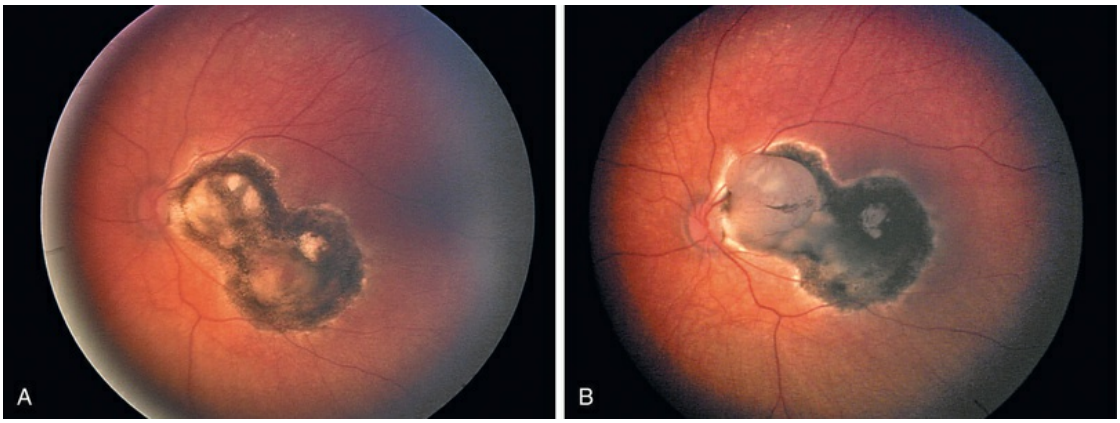

FIG. 132.25 (A) Type IV regression after primary chemotherapy and focal laser consolidation. (B) Edge recurrence seen 3 months later.

Late Effects of Treatment

The late effects of treatment are of major concern to parents and to affected children, as well as to the ophthalmologist who follows these children as they become teenagers and young adults. There are several major studies examining these late effects, which we will summarize. In 1991, 99 German patients treated for retinoblastoma between 1965 and 1982 were reviewed to determine the late effects of treatment.[316] The median age of these 99 patients was 16 years (range 6–27 years) and the median length of follow-up was 15 years (range 6–27 years). In 2001, a series of 21 Israeli retinoblastoma patients treated in Haifa between 1976 and 1994 were described.[317] In this series, the median age of follow-up was 12 years; 13 of the 21 patients were treated with EBR and eight with chemotherapy. In 1996, Imhof and colleagues reported the late orbital effects of radiation in their Dutch series of 68 patients treated with EBR.[306] Radiation alone was given to 77 orbits and both radiation and enucleation to 43. Mean follow-up in the Dutch patients was 5 years 5 months (range 1–20 years). In 2003, an Australian series from Melbourne described 47 eyes treated with EBR between 1965 and 1997, with at least 2 years follow-up.[284]

Bony Hypoplasia of the Midface (Orbit)

The late effects of enucleation combined with EBR, either before or after surgery, create the most significant cosmetic deformities in

retinoblastoma patients, manifesting as deficient growth of the orbital bones and atrophy of the conjunctiva and soft tissues of the socket. The difference in the anatomy as teenagers and adults is striking when growth of irradiated orbits is compared with the growth of nonirradiated orbits.[306] The age of the child when radiation is given influences the extent of the growth retardation, and for this reason any EBR should be avoided if possible in a child less than 12 months of age. Enucleation by itself does not appear to have an additive growth retarding effect on the orbital bones, despite the concern regarding small orbital implants in young children undergoing enucleation. In the German patients, 72 eyes were enucleated without radiation; the cosmetic outcome was significantly better in those eyes than in 28 patients who received EBR plus enucleation.[316] In the Israeli series, 12 of 13 patients treated with EBR had significant hypoplasia of the bony orbit.[317] In the Australian series, growth arrest of the orbital bones was a significant late effect.[284] Orbital reconstruction is difficult in these patients because of the deficiency of a blood supply in the orbital region following radiation. In a report from China, reasonably good results were reported with a hydroxyapatite onlay bone graft substitute covered with a vascularized pedicle flap.[318] Other approaches have been used including free grafts transfer with microvascular anastomoses but with varying success.[319]

Radiation Cataract

Tolerance levels of ocular structures vary greatly. The lacrimal gland, cornea, and conjunctiva can each tolerate up to 50 Gy (5000 rad) of radiation, while the retina tolerates 45 Gy or less. The sclera is the most resistant, tolerating >500 Gy. The most sensitive ocular structure is the lens. Radiation cataract following EBR was discussed in detail by Schipper.[320] The minimum cataractogenic dose was 5.5 Gy and the maximum noncataractogenic dose was 11 Gy in Verhoeff's early treatment using orthovoltage.

A 1996 study compared two different EBR techniques: an anterior lens-sparing electron beam technique and a modified lateral beam technique.[321] The authors reported an overall incidence of cataracts of 22% and no difference in cataract development between the two groups. The system of stabilizing the eye with a vacuum contact

lens developed by Schipper and colleagues reduced the number of eyes that develop surgical radiation cataracts.[287,322] In a series reported from Jerusalem, 20% of irradiated eyes developed cataract.[323] This was similar to the rate of 3/13 eyes (23%) in the Haifa series that developed radiation cataract.[317]

In December 1990 the Wills Eye Hospital experience with the treatment of cataracts and retinoblastoma was reported.[324] A total of 42 eyes in 38 patients had cataract surgery. One eye developed retinal detachment, four had amblyopia, and three developed tumor recurrence, one with extension of retinoblastoma into the subconjunctival space through the sclerotomy. Appropriate timing for cataract removal in retinoblastoma patients has not been documented or verified in the literature. Most centers wait at least 2 years after the eye demonstrates inactive disease to prevent tumor spreading outside the eye as a result of surgery.

Radiation Retinopathy

Radiation retinopathy is a dose-related complication and can present as both retinal and choroidal infarcts.[325] In a series reported from Israel, 12% of radiated eyes developed radiation retinopathy that was first detected 11–72 months (mean 37 months) following treatment.[323] The total dose required to control retinoblastoma is believed to be between 36 and 42 Gy, which is close to the threshold for radiation retinopathy. Other clinical factors may predispose the patient for retinal toxicity, including young age (age <1 year) and concomitant treatment. Although actual data is scarce, the risk of radiation retinopathy is probably increased if brachytherapy or EBR is given immediately following systemic or intraarterial chemotherapy. In a 1996 report from London, 28 eyes were treated with two cycles of CEV chemotherapy followed by 40–44 Gy EBR followed by two additional cycles of triple-drug chemotherapy. There does not seem to have been significant radiation retinopathy in this series.[195] However, we continue to recommend temporizing patients for 2–3 months following chemotherapy before starting EBR to reduce the risk of radiation retinopathy.

Radiation retinopathy has also been described following primary brachytherapy, but tends to occur in proximity to the location of the primary tumor.[326] However, we have also seen widespread

exudative retinopathy causing a complete serous retinal detachment several years following brachytherapy of a macular tumor. Given the extensive treatment that these eyes receive, clinicians should expect a high rate of ocular side-effects with both brachytherapy and EBR in the retinoblastoma population. Management options for radiation retinopathy remain very limited, as anti-VEGF therapy for macular edema is an unproven treatment in this setting, and only an option for those eyes that have been quiescent for a minimum of 2 years.

Second Malignant Neoplasms (SMN)

Long-term studies demonstrate a consistent association between high-dose EBR used to treat intraocular retinoblastoma and the appearance of SMNs in the field of radiation.[202,203] Patients who have bilateral retinoblastoma treated with EBR also develop second malignancies outside the radiation field, such as breast cancer and uterine cancer. Therefore, the single most important factor in determining a patient's lifetime risk of developing a second cancer is a history of radiation treatment in the setting of heritable disease. Another important factor is age of treatment, with the highest risk for those patients who were treated in the first 12 months of life.[327] A third factor is the dose of radiation used, with the highest risk of SMN for those patients who received EBR before the era of dose reduction. There was one report suggesting that the use of older alkylating agents may contribute to the risk for certain SMNs, independent of the history of radiation treatment.[328]

The tissue specificity and relatively short time to radiation-induced solid tumor in hereditary retinoblastoma survivors are, according to Strong and colleagues, consistent with the radiation effect in a predisposed cell.[181,329] François cites more than 300 cases of sarcomas arising in radiated bones, with a latent period of between 3 and 30 years.[330] The tumor types seen in SMNs vary greatly, but up to 80% are osteogenic sarcomas, leiomyosarcoma, and malignant fibrous histiocytoma.[202,203,331] The tumors appearing out of the field include osteosarcomas, breast carcinoma, cutaneous melanoma, and uterine cancers. Other tumor types include renal cell carcinoma, Ewing's sarcoma, carcinoma of the tongue, and medulloblastoma.

All these cases fit the criteria of Cade as radiogenic neoplasms.[332] Approximately 75% of all SMNs in retinoblastoma patients occur in radiated areas. In the July 1993 issue of the *Journal of the National Cancer Institute*, Eng and colleagues provided follow-up on 1000 patients with retinoblastoma treated in New York and Boston.[16] A total of 35% of bilaterally affected retinoblastoma patients treated with EBR will have died of a second malignant neoplasm by 40 years after diagnosis. Only 6% of the bilaterally affected patients not treated with EBR met the same fate. In a review of 215 patients with bilateral retinoblastoma from the Armed Forces Institute of Pathology (AFIP), the 30-year cumulative incidence of SMNs for 137 patients receiving radiotherapy was 35% compared with a cumulative incidence of approximately 6% for 78 patients (5/78) who did not receive radiation.[333] Among those patients who did receive radiation, the incidence rate was 29% inside the radiated field and 8% outside the field. In this study, the incidence rate outside the radiated field was not significantly different from the rate reported for patients who did not receive radiation.

Appropriate surveillance for second primary tumors involves the parents performing weekly examinations of their at-risk children searching for foci of pain, tenderness, or swelling. It has been suggested that susceptible patients have body scans every year. However, bone scans deliver radiation to the patient, and yearly full body MRI scans are costly over a child's lifetime. We have the experience of a child having a completely normal MRI scan only 4 months prior to first symptoms of a SMN. Given the lack of convincing data, routine surveillance scanning for SMN is probably not indicated.

Among patients who eventually develop SMNs, the common finding was that symptoms were present for several months before the diagnosis was suspected. We believe in the importance of educating parents to be aware of nodules, pain in the joints or skull, lumps on the skull, or pain in the extremities that does not resolve in 5–7 days. Such signs or symptoms should prompt a visit to the pediatrician or primary care specialist with an accompanying statement that the child is at high risk for bone cancer and should be examined. Early diagnosis of SMNs can be associated with a good outcome. We have one patient who has survived 17 years

after diagnosis of an osteosarcoma of the greater wing of the sphenoid.

The risk for death from SMNs in patients who are genetically predisposed at 40 years after diagnosis of retinoblastoma has been reported 6% if their retinoblastoma was not treated with EBR and 35% if EBR was used.[16] Data from the Utrecht registry of all cases in the Netherlands from 1945 to 1977 demonstrated that the cumulative risk at 25 years was 22% compared with the 50% risk published by Abramson. Because high doses of EBR were used in earlier studies the incidence of SMN among patients treated in the last 15 years may be smaller.[201]

Metastatic Retinoblastoma

Risk Factors

The risk of extraocular disease after enucleation or globe-conserving treatment is very low in developed countries, ranging between 0% and 4%.[299,334] As previously reviewed, group E eyes have the highest rate of metastatic spread and therefore enucleation is recommended to minimize this risk. Specific clinical features that have been shown to increase the risk of metastasis include the presence of a group E tumor, rubeosis iridis, neovascular glaucoma, and clinical symptoms for greater than 6 months prior to diagnosis.[232] As previously mentioned, there are histopathologic features that have been classified as "high risk" features, and published rates of metastasis have been estimated from the literature.[210] There is consensus that patients with a positive optic nerve margin and scleral invasion require aggressive postenucleation treatment to reduce the risk of metastatic disease. The vast majority of centers also treat patients with tumor invasion of the optic nerve posterior to the lamina cribrosa, although some centers follow these patients and treat the approximately 10% of patients who relapse with aggressive multimodal chemotherapy.[335] Patients with isolated massive choroidal invasion (>3 mm in thickness) represent a very controversial group for adjuvant treatment, as only 6% of patients with this feature will relapse.[210] Patients with massive choroidal invasion combined with any degree of optic nerve invasion should receive adjuvant treatment as

their risk or relapse is greater than 10%.[210]

The onset of metastatic disease is variable, but most cases have been diagnosed by 3 years of age.[336] Metastases are most commonly seen in the bones or bone marrow, paranasal sinuses, salivary glands, lymph nodes, subcutaneous tissue, liver, spleen, lungs, testes, and CNS.[337–340] The prognosis of patients with metastatic disease depends a great deal on whether or not the CNS is involved with metastatic spread.[341] There have been few, if any, survivors once metastatic retinoblastoma involves the CNS. In contrast, if only bone marrow and bone are involved recent reports provide some measure of hope with myeloablative therapy, bone marrow transplant together with focal radiation to bulky disease.[341] Before the introduction of bone marrow rescue techniques, the length of survival after diagnosis of metastatic retinoblastoma varied from 6 to 12 months. However, there have been encouraging reports that high-dose multimodal chemotherapy combined with bone marrow rescue have been associated with long-term survival.[341–345]

Orbital Retinoblastoma

Extraocular disease at presentation is extremely rare in developed countries. When the diagnosis of intraocular retinoblastoma is delayed, the natural history of intraocular retinoblastoma involves eventual extension through the eye wall into the orbit then to regional lymph nodes with eventual metastatic spread. These patients will present with evidence of orbital retinoblastoma at diagnosis, with proptosis, orbital inflammation, and evidence of an orbital mass on imaging studies. We have also seen rare cases of direct CNS extension and CNS metastatic disease at presentation. The risk for extraocular disease strongly depends on the delay in diagnosis in the setting of advanced intraocular disease. In developing countries where primary medical care is not universally available, many retinoblastoma cases present with extraocular disease.[335]

It is important to understand that the majority of patients who present with orbital retinoblastoma have regional or distant metastatic disease, and therefore require a systemic approach as well as aggressive treatment of the orbital component. Chantada and his colleagues from Argentina reported 84% had 5-year event-

free survival when orbital retinoblastoma was treated with primary chemotherapy, limited excision, and orbital radiation.[335,346] We agree with these authors that orbital exenteration is not necessary for these patients, and surgical management has a limited role. We recommend systemic chemotherapy and orbital radiotherapy after an incisional biopsy to confirm the diagnosis. Debulking of large tumors in the orbit may lessen the tumor burden, but often there is dramatic regression with the institution of systemic chemotherapy and orbital radiation.

Retinoma (Retinocytoma)

A benign form of retinoblastoma, initially described by Gallie et al. as a "retinoma," presents as a translucent lesion with some calcification and underlying pigmentary changes.[347,348] The "retinocytoma" has been introduced by other authors.[349,350] Histologic studies have shown that this is a benign variant of retinoblastoma and not a regressed retinoblastoma. Retinomas are typically diagnosed on routine fundus evaluations of healthy patients, or on screening examinations of family members of a patient with retinoblastoma. The typical fundus appearance is a gray translucent mass containing calcified nodules and surrounded by retinal pigment clumping and atrophy. We have seen patients with retinomas and benign vitreous "seeding" that do not change on follow-up exams, and other authors have had similar observations. Lueder and colleagues have described two patients with retinomas and vitreous seeding that were followed for 8 and 33 years, respectively, without evidence of disease progression or transformation.[351] Histopathologic examination shows benign-appearing round blue cells in a bed of well-vascularized ground substance with calcific foci. There are no mitoses, cellular pleomorphism, nuclear atypia, rosettes, or other characteristics of malignancy.

The retinoma or retinocytoma has benign histopathologic features but may rarely retain the ability to undergo malignant transformation into a rapidly growing retinoblastoma.[352] Histologic description of a malignant transformation event was described in a 24-year-old woman from Lausanne.[353] Eagle and colleagues reported a case of a 7-year-old child from Philadelphia who was

seen at age 4 years and found to have a typical retinoma. Three years later the tumor suddenly grew rapidly and seeded the vitreous, leading to loss of the eye.[352] The possibility for malignant transformation underscores the need for close follow-up of these patients. If the retinoma is peripheral, we consider performing careful laser treatment to flatten the lesion, which should reduce the risk of malignant transformation.

There are occasional retinoblastomas which regress into tumors that resemble retinomas, both clinically and histopathologically. In addition, there may be areas of retinoma formation in patients who present with untreated retinoblastoma. These "presumed" retinomas appear gray and translucent, much like the lesion described by Aaby and colleagues.[349] The lesions we have seen resemble type II or III regression, and have translucent portions and cystic spaces (Fig. 132.26). Sequential direct laser photocoagulation can be used to knock the lesions down to a flat scar (type IV regression), but we would recommend documenting progressive growth of these lesions before considering enucleation or radiotherapy.

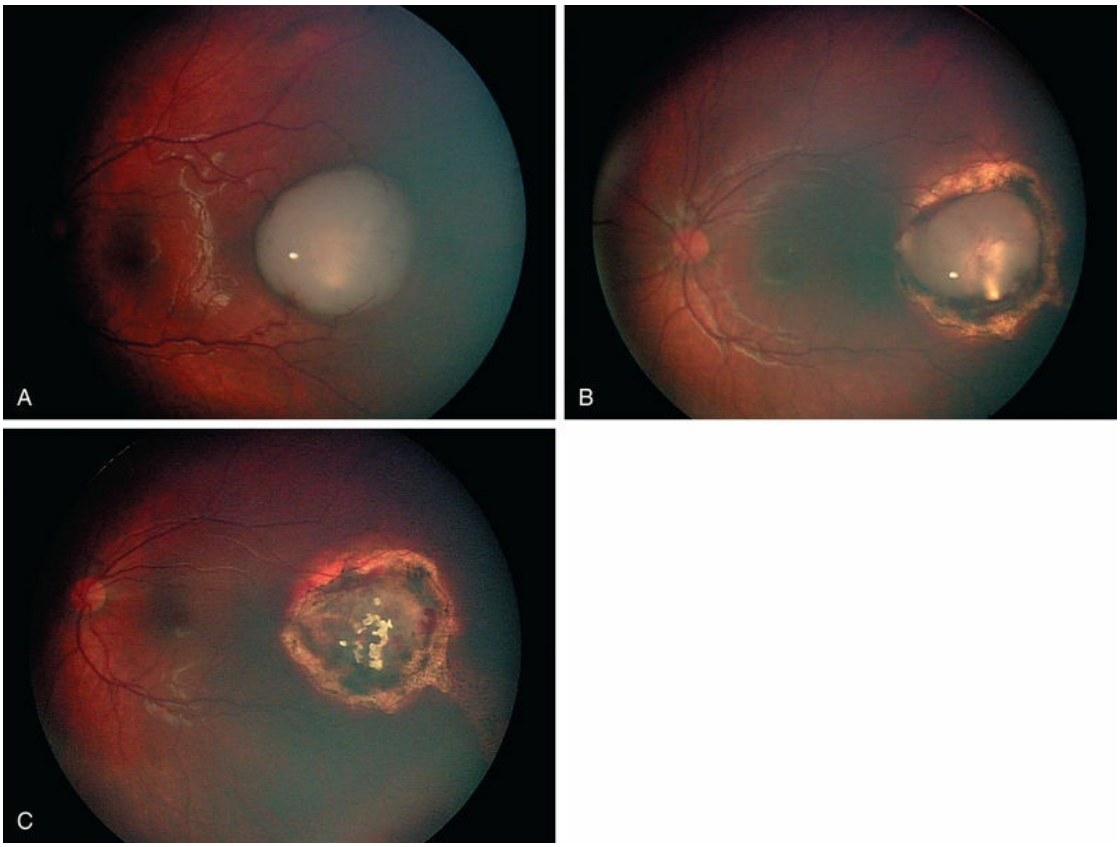

FIG. 132.26 (A) Presumed retinoma. Appearance is similar to type II regression prior to any treatment. (B) After focal laser consolidation it begins to regress. (C) Several laser treatments later the tumor is nearly flat.

Diffuse Infiltrating Retinoblastoma

In the rare and atypical form of retinoblastoma called diffuse infiltrating retinoblastoma, no mass forms in the eye (Fig. 132.27). Instead, the tumor expands by diffusely infiltrating the retina, causing irregular thickening. In this form of atypical retinoblastoma, calcification is not commonly seen. In one review, only four of 28 diffusely infiltrating retinoblastomas demonstrated the presence of intraocular calcium.[354] As a result, neither ocular ultrasound nor CT scanning may be helpful in making this diagnosis as both imaging methods reveal diffusely thickened retina.[355] MRI may provide useful information in some cases.[356]

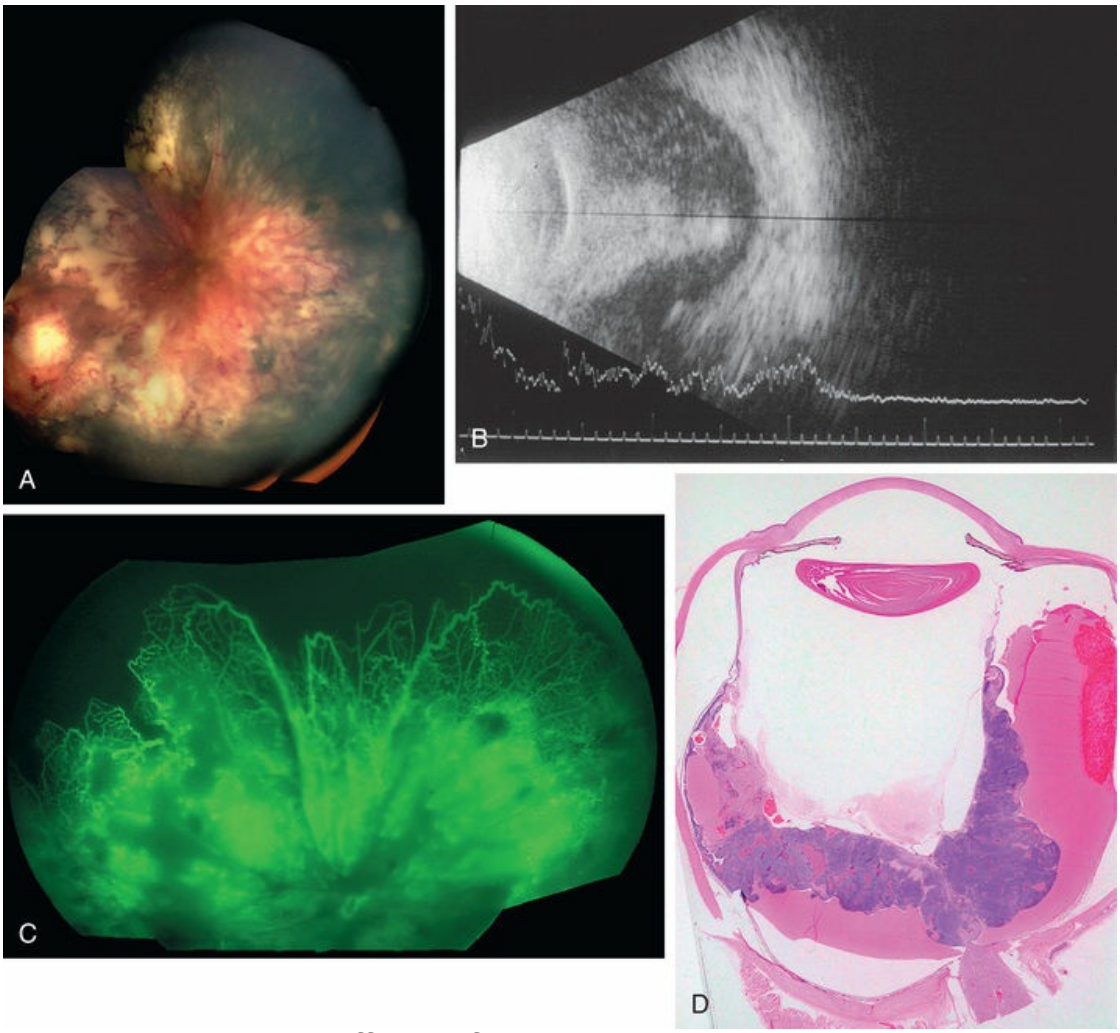

FIG. 132.27 Diffuse infiltrating retinoblastoma. (A) Unusual tractional and exudative retinal detachment in a 4-year-old. (B) B-scan ultrasonography showed no calcium. (C) Fluorescein angiogram resembles Coats disease. (D) Histopathology revealed retinoblastoma involving the entire retina. Subretinal fluid and exudate was present.

Although rare, the diffusely infiltrating retinoblastoma is a frequent cause of misdiagnosis. The classic presentation is unilateral uveitis or retinal detachment in an older child without any previous history, although authors from Taiwan reported one hereditary case.[357] The eye is often red and may present with a pseudohypopyon, nodules on the surface of the iris or in the anterior chamber, and/or endothelial tumor nodules resembling keratic precipitates. The vitreous is frequently hazy, and exudates may cover the peripheral retina. The retina may appear gray, infiltrated, and thickened. This type of retinoblastoma can also

present with a hyphema.[355,357,358] Grossniklaus et al. reported an anterior variant where the only tumor focus was in the anterior retina.[359] Because of the late diagnosis in most of these cases, enucleation is the treatment of choice in the management. Since the lesion grows within and destroys the sensory retina, little is gained by attempts to salvage the eye. Systemic prognosis after enucleation is generally excellent.[360,361]

Retinoblastoma in Older Children

Almost 90% of all cases of retinoblastoma in the United States are diagnosed before the patient is 5 years old.[362] However, newly diagnosed cases have been reported at ages 7–15 years, and in adults.[363–365] In our experience, it is not uncommon for children to be diagnosed with advanced unilateral retinoblastoma between 7 and 8 years of age. The persistence of a rare embryonal retinal cell has been proposed as one explanation for this rare onset of retinoblastoma at an advanced age.[365] An alternative explanation is that a retinoma or retinocytoma that occurs early in life may be unrecognized until it undergoes malignant transformation.[350,352,366] In 400 consecutive retinoblastoma patients, 26 were found to be 5 years of age or older at the time of initial diagnosis.[367] In that series, all of the older children had sporadic, unilateral retinoblastoma.

The clinically important aspect of retinoblastoma presenting in older children is that misdiagnosis is common. Five of the 26 children had vitrectomy prior to the diagnosis of retinoblastoma.[367] The authors suggest that clinicians should consider the possibility of retinoblastoma in children who have unexplained vitreous hemorrhage or atypical endophthalmitis or uveitis. Because of the advanced nature of the unilateral disease in these older children, almost all the cases have group E disease and therefore require enucleation.

Trilateral Retinoblastoma (Primitive Neural Ectodermal Tumors, Pinealoma)

The term trilateral retinoblastoma (TRB) classically refers to the association of bilateral intraocular retinoblastoma with a pineoblastoma, a primitive neuroectodermal tumor that arises in

the pineal gland. The link between intraocular retinoblastoma and an ectopic, intracranial malignancy was first recognized in 1977 by Jakobiec and colleagues.[368] In 1980, Bader et al. reported a series of 10 children with bilateral RB who developed another primary malignancy in the pineal gland, and the term trilateral retinoblastoma was associated with this diagnosis.[369] Histopathologically, the intracranial tumor in TRB resembles PNET, with varying degrees of neuronal and photoreceptor differentiation. One explanation for the development of TRB is that the retina and the pineal gland have a common embryologic origin, and there may be vestigial photoreceptor elements in the pineal gland. In lower animals the pineal gland functions as a photoreceptor organ and is sometimes referred to as the "third eye." In the literature there is some dispute regarding the cell of origin for TRB, and more recent studies suggest that the tumor may arise from the germinal layer of primitive cells (subependymal plate) rather than the pineal gland.[370,371] For that reason, some authors refer to the intracranial tumor in retinoblastoma patients as a pineal neuroblastic tumor (PNT) rather than a pineoblastoma.[372]

Although TRB was classically defined as a patient with bilateral retinoblastoma who develops a tumor in the pineal region, in a minority of TRB cases the intracranial tumors are in suprasellar or parasellar locations. These ectopic tumors at the skull base are referred to as ectopic intracranial neuroblastic tumors (or EINT).[372] When comparing the age of presentation, EINT patients appear to develop earlier than those children with PNT.[372] There are also reports of patients with heritable, unilateral retinoblastoma who have developed midline intracranial tumors. These TRB patients with heritable, unilateral RB appear to be more likely to develop EINT than PNT.[370] There are also rare cases of siblings of patients with retinoblastoma who developed TRB without having clinical evidence of an intraocular tumor.[370] In all cases of TRB, the midline intracranial malignancy appears to represent a focus of multicentric tumorigenesis in patients with the *RB1* cancer predisposition syndrome. There does not appear to be a specific genetic mutation in the retinoblastoma gene that predisposes to the development of TRB. Based on the clinical spectrum of TRB in the literature, it is probably appropriate to refer to TRB as the association of a midline

intracranial malignancy and the heritable form of retinoblastoma.[371]

Incidence

The overall incidence of TRB has been estimated to be 3% of all patients with retinoblastoma, up to 5–6% for patients with bilateral RB, and as high as 10–15% of patients with familial RB.[370,373] TRB used to be a major cause of death from retinoblastoma during the first 5 years of life.[374] In recent years, with the more widespread use of chemoreduction and decreased utilization of external beam radiation for patients with bilateral RB, the incidence of TRB appears to be decreasing. A series of 99 patients with bilateral or familial RB treated with systemic chemotherapy at the Will's Eye Hospital did not develop TRB, with at least 4 years of follow-up.[374] Based on this series, the authors postulated that patients with the genetic form of retinoblastoma who receive systemic chemotherapy for their intraocular disease are protected against the future development of TRB. An alternative explanation is that the reduced use of EBR and its related oncogenic effects in patients with the *RB1* mutation correlates with the decreased incidence of TRB. The majority of TRB patients in the literature prior to 1995 received EBR to one or both eyes,[371,375] while essentially the same patient population with bilateral RB was treated with systemic chemotherapy after the mid-1990s.

Clinical Presentation

The mean age at diagnosis of TRB is between 26 and 40 months, with a range of 1–142 months.[371,372,376] Overall, 89% of TRB patients have bilateral RB, and 11% have unilateral, heritable RB.[371] Among all cases of TRB, 43–68% have a positive family history of retinoblastoma.[372,376] Patients with TRB are usually diagnosed with intraocular retinoblastoma by 5–8 months,[372,373,376] which is earlier than the average age of diagnosis for bilateral RB (i.e., 1 year of age). This may indicate a more clinically and biologically aggressive disease in these patients with TRB, or perhaps indicate a greater percentage of familial cases in the group of patients who develop TRB. Typically, the intracranial tumor is diagnosed asynchronously with the intraocular tumor, with the interval between the diagnosis of bilateral RB and the diagnosis of the brain tumor being an

average of 20–33 months.[371–373,376]

At diagnosis, a minority of TRB patients are asymptomatic, discovered on routine neuroimaging studies,[371] but most have signs of elevated intracranial pressure (ICP). Presenting signs and symptoms of increased ICP include headache, nausea, vomiting, anorexia, lethargy, somnolence, gait disturbances, increased head circumference, and of course papilledema.[371,376] When retinoblastoma patients are diagnosed with an intracranial malignancy, it can occasionally be difficult to distinguish TRB from intracranial metastatic disease, although the latter tends to present with leptomeningeal disease. The critical factor is whether the optic nerve in the most involved eye has evidence of postlaminar infiltration on pathology; if not, then the intracranial lesion is most likely TRB. If a biopsy is performed, there may be certain histopathologic features that may be helpful in identifying TRB. For example, in about one-third of cases of TRB, there can be evidence of tumor differentiation such as Flexner–Wintersteiner or Homer Wright rosettes, which is extremely unusual for metastatic disease.[368] However, CNS metastases and TRB are treated with a similar approach so a diagnostic biopsy is not an absolute necessity if the determination cannot be made on clinical grounds.

Screening

Screening recommendations for TRB are somewhat controversial, mainly because of the low incidence of TRB and the need for anesthesia for performing MRI in this population. Approximately one-quarter of TRB patients are diagnosed on routine screening, typically within the first 3 years after diagnosis of retinoblastoma. Meta-analysis of published TRB cases has found that tumors diagnosed on routine screening tend to be smaller than those found in symptomatic patients.[372,377] Patients diagnosed with TRB on routine screening also tend to survive longer,[370–372,377] although age of death appears to be the same for both symptomatic TRB patients and those found on screening.[372] It has been suggested that this advantage in survival may be due to lead time bias.[378] Given the relatively short interval between the diagnosis of retinoblastoma and the occurrence of TRB, routine screening would likely detect the majority of cases within several years. One review study found

that 89% of TRB patients developed the intracranial tumor within 4 years of the intraocular tumor diagnosis.[370] On the other hand, the clinician has to consider the costs of screening, the necessity of general anesthesia for performing neuroimaging in these young children, and the occasional unnecessary intracranial biopsies performed on benign lesions found on routine neuroimaging.[378] Not infrequently, asymptomatic children with retinoblastoma will have a cystic lesion in the region of the pineal gland identified on routine neuroimaging studies. Neuroradiology expertise is required in assessing the risk of malignancy for these patients with pineal cysts, and neurosurgical consultation should be requested. If the lesion is predominantly cystic and less than 1.5 cm in diameter, neurosurgical biopsy can be avoided in the vast majority of cases and the patient followed carefully with repeat imaging.

In modern retinoblastoma centers, MRI is generally performed at diagnosis to rule out the concurrent presence of orbital or intracranial disease. There is not universal agreement on how often subsequent neuroimaging should occur and when it should be discontinued. The patients at highest risk for TRB are those children with bilateral disease or a positive family history. Therefore, screening programs should be directed at children with bilateral retinoblastoma and those unilateral patients with a positive family history, during the first 3–4 years after the diagnosis of retinoblastoma. A schedule of neuroimaging every 3 months for 2 years, every 4 months the next 2 years, and every 6 months for the next 5 years has been proposed.[371] Another author has suggested screening every 3 months during the first year after diagnosis of retinoblastoma, and at least two times a year for the next 3 years.[372] At our center, we perform neuroimaging every 6 months in bilateral children and unilateral patients with a positive family history until the child is 3–4 years of age as a routine screening protocol. For all children with the *RB1* mutation, CT scans should be avoided to minimize low-dose radiation exposure.[373]

Treatment

The overall prognosis for TRB is poor even with aggressive treatment, as patients usually die of disseminated neuroaxis disease within the first year after diagnosis. The average survival time after

diagnosis of TRB is 6–11 months, regardless of the location of the intracranial tumor.[371,373,377] With an aggressive multimodal treatment approach (chemotherapy, surgery, radiation), a minority of patients can be cured. One series found that treatment appears to prolong survival from 1.3 to 9.7 months.[376] There appears to be no difference in survival time between patients with tumors in the pineal region versus the sella region.[370] Although the location of the intracranial tumor does not affect survival, tumor size greater than 15 mm appears to be a critical size for tumor dissemination. In 1999 Kivela published a meta-analysis of 106 cases of TRB published in the medical literature from 1966 to 1998. Only five patients were event-free survivors at 10–168 months and all of the survivors had tumors less than 15 mm detected via screening.[372]

The mainstay of therapy for TRB is intensive cisplatin-based therapy (with other agents) and autologous stem cell rescue. Aggressive chemotherapy used to be followed by craniospinal irradiation (e.g., 36 Gy with boost to pineal gland to 59 Gy) in many TRB patients.[379] Spinal metastases are very common in TRB, being present in 69–89% of cases at autopsy.[371] However, there are serious long-term toxicities of craniospinal radiation in the very young child. Therefore, current strategies are directed toward avoiding irradiation and using intensive chemotherapy followed by autologous stem cell rescue. In 2010 Dunkel and colleagues published a multicenter series of 13 patients treated with high-dose chemotherapy and autologous hematopoietic stem cell rescue, at a median time from diagnosis of TRB of 5 months (range from 4 to 9 months). In this series, five patients achieved event-free survival with a median follow-up time of 77 months from diagnosis TRB (range 36–104 months). Interestingly, four of the five patients who have achieved event-free survival had tumors that were at least 2 cm in diameter, and none of the event-free survivors received EBR. Surgical resection may play a role in certain cases if the intracranial disease is not disseminated[380] (Fig. 132.28).

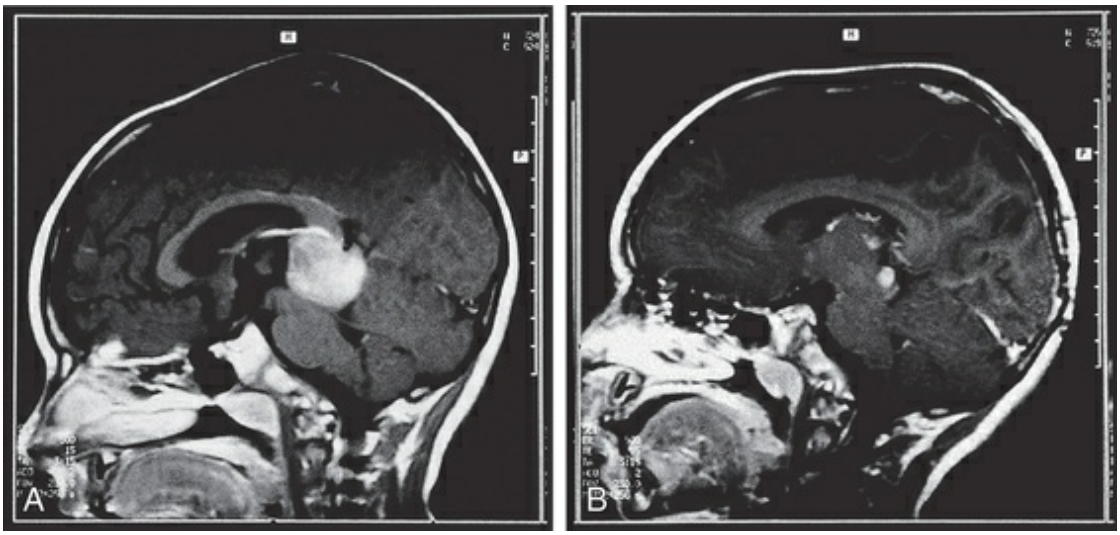

FIG. 132.28 Gadolinium-enhanced magnetic resonance imaging of a 3-year-old boy with trilateral retinoblastoma. (A) Before treatment, showing tumor in pineal region. (B) After tumor excision.

References

1. Knudson AG Jr, Meadows AT, Nichols WW, Hill R. Chromosomal deletion and retinoblastoma. *N Engl J Med*. 1976;295:1120–1123.
2. Knudson AG Jr. Genetics and the etiology of childhood cancer. *Pediatr Res*. 1976;10:513–517.
3. Kaneko A, Suzuki S. Eye-preservation treatment of retinoblastoma with vitreous seeding. *Jpn J Clin Oncol*. 2003;33:601–607.
4. Suzuki S, Yamane T, Mohri M, Kaneko A. Selective ophthalmic arterial injection therapy for intraocular retinoblastoma: the long-term prognosis. *Ophthalmology*. 2011;118:2081–2087.
5. Munier FL, Beck-Popovic M, Balmer A, Gaillard MC, Bovey E, Binaghi S. Occurrence of sectoral choroidal occlusive vasculopathy and retinal arteriolar embolization after superselective ophthalmic artery chemotherapy for advanced intraocular retinoblastoma. *Retina*. 2011;31:566–573.
6. Abramson DH, Dunkel IJ, Brodie SE, Kim JW, Gobin YP. A

phase I/II study of direct intraarterial (ophthalmic artery) chemotherapy with melphalan for intraocular retinoblastoma initial results. *Ophthalmology*. 2008;115:1398–1404 [1404.e1].
7. Peterson EC, Elhammady MS, Quintero-Wolfe S, Murray TG, Aziz-Sultan MA. Selective ophthalmic artery infusion of chemotherapy for advanced intraocular retinoblastoma: initial experience with 17 tumors. *J Neurosurg*. 2011;114:1603–1608.
8. Gobin YP, Dunkel IJ, Marr BP, Brodie SE, Abramson DH. Intra-arterial chemotherapy for the management of retinoblastoma: four-year experience. *Arch Ophthalmol*. 2011;129:732–737.
9. Munier FL, Gaillard MC, Balmer A, Beck-Popovic M. Intravitreal chemotherapy for vitreous seeding in retinoblastoma: recent advances and perspectives. *Saudi J Ophthalmol*. 2013;27:147–150.
10. Munier FL, Gaillard MC, Balmer A, et al. Intravitreal chemotherapy for vitreous disease in retinoblastoma revisited: from prohibition to conditional indications. *Br J Ophthalmol*. 2012;96:1078–1083.
11. Munier FL, Soliman S, Moulin AP, Gaillard MC, Balmer A, Beck-Popovic M. Profiling safety of intravitreal injections for retinoblastoma using an anti-reflux procedure and sterilisation of the needle track. *Br J Ophthalmol*. 2012;96:1084–1087.
12. Harbour JW. Molecular basis of low-penetrance retinoblastoma. *Arch Ophthalmol*. 2001;119:1699–1704.
13. Brantley MA Jr, Harbour JW. The molecular biology of retinoblastoma. *Ocul Immunol Inflamm*. 2001;9:1–8.
14. Wong FL, Boice JD Jr, Abramson DH, et al. Cancer incidence after retinoblastoma. Radiation dose and sarcoma risk. *JAMA*. 1997;278:1262–1267.
15. Woo KI, Harbour JW. Review of 676 second primary tumors in patients with retinoblastoma: association between age at onset and tumor type. *Arch Ophthalmol*. 2010;128:865–870.
16. Eng C, Li FP, Abramson DH, et al. Mortality from second tumors among long-term survivors of retinoblastoma. *J Natl*

Cancer Inst. 1993;85:1121–1128.
17. Kleinerman RA, Tucker MA, Tarone RE, et al. Risk of new cancers after radiotherapy in long-term survivors of retinoblastoma: an extended follow-up. *J Clin Oncol*. 2005;23:2272–2279.
18. Knudson AG Jr. Mutation and cancer: statistical study of retinoblastoma. *Proc Natl Acad Sci USA*. 1971;68:820–823.
19. Francke U. Retinoblastoma and chromosome 13. *Birth Defects Orig Artic Ser*. 1976;12:131–134.
20. Yunis JJ, Ramsay N. Retinoblastoma and subband deletion of chromosome 13. *Am J Dis Child*. 1978;132:161–163.
21. Sparkes RS, Sparkes MC, Wilson MG, et al. Regional assignment of genes for human esterase D and retinoblastoma to chromosome band 13q14. *Science*. 1980;208:1042–1044.
22. Murphree AL, Benedict WF. Retinoblastoma: clues to human oncogenesis. *Science*. 1984;223:1028–1033.
23. Balaban-Malenbaum G, Gilbert F, Nichols WW, Hill R, Shields J, Meadows AT. A deleted chromosome no. 13 in human retinoblastoma cells: relevance to tumorigenesis. *Cancer Genet Cytogenet*. 1981;3:243–250.
24. Benedict WF, Murphree AL, Banerjee A, Spina CA, Sparkes MC, Sparkes RS. Patient with 13 chromosome deletion: evidence that the retinoblastoma gene is a recessive cancer gene. *Science*. 1983;219:973–975.
25. Dryja TP, Friend S, Weinberg RA. Genetic sequences that predispose to retinoblastoma and osteosarcoma. *Symp Fundam Cancer Res*. 1986;39:115–119.
26. Cavenee WK, Hansen MF, Nordenskjold M, et al. Genetic origin of mutations predisposing to retinoblastoma. *Science*. 1985;228:501–503.
27. Lee EY, Lee WH. Molecular cloning of the human esterase D gene, a genetic marker of retinoblastoma. *Proc Natl Acad Sci USA*. 1986;83:6337–6341.
28. Squire J, Dryja TP, Dunn J, et al. Cloning of the esterase D gene: a polymorphic gene probe closely linked to the retinoblastoma locus on chromosome 13. *Proc Natl Acad Sci USA*. 1986;83:6573–6577.

29. Friend SH, Bernards R, Rogelj S, et al. A human DNA segment with properties of the gene that predisposes to retinoblastoma and osteosarcoma. *Nature*. 1986;323:643–646.
30. Fung YK, Murphree AL, T'Ang A, Qian J, Hinrichs SH, Benedict WF. Structural evidence for the authenticity of the human retinoblastoma gene. *Science*. 1987;236:1657–1661.
31. Harbour JW. Overview of RB gene mutations in patients with retinoblastoma: implications for clinical genetic screening. *Ophthalmology*. 1998;105:1442–1447.
32. Mancini D, Singh S, Ainsworth P, Rodenhiser D. Constitutively methylated CpG dinucleotides as mutation hot spots in the retinoblastoma gene (RB1). *Am J Hum Genet*. 1997;61:80–87.
33. Bunin GR, Emanuel BS, Meadows AT, Buckley JD, Woods WG, Hammond GD. Frequency of 13q abnormalities among 203 patients with retinoblastoma. *J Natl Cancer Inst*. 1989;81:370–374.
34. Ejima Y, Sasaki MS, Kaneko A, Tanooka H. Types, rates, origin and expressivity of chromosome mutations involving 13q14 in retinoblastoma patients. *Hum Genet*. 1988;79:118–123.
35. Blanquet V, Gross MS, Turleau C, Senamaud-Beaufort C, Doz F, Besmond C. Three novel germline mutations in exons 8 and 18 of the retinoblastoma gene. *Hum Mol Genet*. 1994;3:1185–1186.
36. Lohmann DR, Brandt B, Hopping W, Passarge E, Horsthemke B. The spectrum of RB1 germ-line mutations in hereditary retinoblastoma. *Am J Hum Genet*. 1996;58:940–949.
37. Dommering CJ, Mol BM, Moll AC, et al. RB1 mutation spectrum in a comprehensive nationwide cohort of retinoblastoma patients. *J Med Genet*. 2014;51:366–374.
38. Tsai T, Fulton L, Smith BJ, et al. Rapid identification of germline mutations in retinoblastoma by protein truncation testing. *Arch Ophthalmol*. 2004;122:239–248.
39. Dryja TP, Mukai S, Petersen R, Rapaport JM, Walton D, Yandell DW. Parental origin of mutations of the retinoblastoma gene. *Nature*. 1989;339:556–558.

40. Cavenee WK, Hansen MF, Nordenskjold M, et al. Genetic origin of mutations predisposing to retinoblastoma. *Science*. 1985;228:501–503.
41. Weinberg RA. Tumor suppressor genes. *Science*. 1991;254:1138–1146.
42. Zhu X, Dunn JM, Goddard AD, et al. Mechanisms of loss of heterozygosity in retinoblastoma. *Cytogenet Cell Genet*. 1992;59:248–252.
43. Xu K, Rosenwaks Z, Beaverson K, Cholst I, Veeck L, Abramson DH. Preimplantation genetic diagnosis for retinoblastoma: the first reported liveborn. *Am J Ophthalmol*. 2004;137:18–23.
44. Bonaiti-Pellie C, Briard-Guillemot ML. Segregation analysis in hereditary retinoblastoma. *Hum Genet*. 1981;57:411–419.
45. Greger V, Passarge E, Hopping W, Messmer E, Horsthemke B. Epigenetic changes may contribute to the formation and spontaneous regression of retinoblastoma. *Hum Genet*. 1989;83:155–158.
46. Matsunaga E. Hereditary retinoblastoma: delayed mutation or host resistance? *Am J Hum Genet*. 1978;30:406–424.
47. Lohmann DR, Brandt B, Hopping W, Passarge E, Horsthemke B. Distinct RB1 gene mutations with low penetrance in hereditary retinoblastoma. *Hum Genet*. 1994;94:349–354.
48. Otterson GA, Chen W, Coxon AB, Khleif SN, Kaye FJ. Incomplete penetrance of familial retinoblastoma linked to germ-line mutations that result in partial loss of RB function. *Proc Natl Acad Sci USA*. 1997;94:12036–12040.
49. Schubert EL, Strong LC, Hansen MF. A splicing mutation in RB1 in low penetrance retinoblastoma. *Hum Genet*. 1997;100:557–563.
50. Onadim Z, Hungerford J, Cowell JK. Follow-up of retinoblastoma patients having prenatal and perinatal predictions for mutant gene carrier status using intragenic polymorphic probes from the RB1 gene. *Br J Cancer*. 1992;65:711–716.
51. Belchis DA, Meece CA, Benko FA, Rogan PK, Williams RA, Gocke CD. Loss of heterozygosity and microsatellite

instability at the retinoblastoma locus in osteosarcomas. *Diagn Mol Pathol*. 1996;5:214–219.
52. Wadayama B, Toguchida J, Shimizu T, et al. Mutation spectrum of the retinoblastoma gene in osteosarcomas. *Cancer Res*. 1994;54:3042–3048.
53. Bookstein R, Rio P, Madreperla SA, et al. Promoter deletion and loss of retinoblastoma gene expression in human prostate carcinoma. *Proc Natl Acad Sci USA*. 1990;87:7762–7766.
54. Harbour JW, Lai SL, Whang-Peng J, Gazdar AF, Minna JD, Kaye FJ. Abnormalities in structure and expression of the human retinoblastoma gene in SCLC. *Science*. 1988;241:353–357.
55. Lee EY, To H, Shew JY, Bookstein R, Scully P, Lee WH. Inactivation of the retinoblastoma susceptibility gene in human breast cancers. *Science*. 1988;241:218–221.
56. Sherr CJ. Cancer cell cycles. *Science*. 1996;274:1672–1677.
57. Rushlow DE, Mol BM, Kennett JY, et al. Characterisation of retinoblastomas without RB1 mutations: genomic, gene expression, and clinical studies. *Lancet Oncol*. 2013;14:327–334.
58. DeCaprio JA, Furukawa Y, Ajchenbaum F, Griffin JD, Livingston DM. The retinoblastoma-susceptibility gene product becomes phosphorylated in multiple stages during cell cycle entry and progression. *Proc Natl Acad Sci USA*. 1992;89:1795–1798.
59. DeCaprio JA, Ludlow JW, Lynch D, et al. The product of the retinoblastoma susceptibility gene has properties of a cell cycle regulatory element. *Cell*. 1989;58:1085–1095.
60. Lee WH, Shew JY, Hong FD, et al. The retinoblastoma susceptibility gene encodes a nuclear phosphoprotein associated with DNA binding activity. *Nature*. 1987;329:642–645.
61. Chen PL, Scully P, Shew JY, Wang JY, Lee WH. Phosphorylation of the retinoblastoma gene product is modulated during the cell cycle and cellular differentiation. *Cell*. 1989;58:1193–1198.
62. Furukawa Y. Cell cycle control during hematopoietic cell

differentiation. *Hum Cell*. 1997;10:159–164.
63. Ikeda MA, Jakoi L, Nevins JR. A unique role for the Rb protein in controlling E2F accumulation during cell growth and differentiation. *Proc Natl Acad Sci USA*. 1996;93:3215–3220.
64. Stein GH, Beeson M, Gordon L. Failure to phosphorylate the retinoblastoma gene product in senescent human fibroblasts. *Science*. 1990;249:666–669.
65. Zacksenhaus E, Jiang Z, Phillips RA, Gallie BL. Dual mechanisms of repression of E2F1 activity by the retinoblastoma gene product. *EMBO J*. 1996;15:5917–5927.
66. DeCaprio JA, Ludlow JW, Figge J, et al. SV40 large tumor antigen forms a specific complex with the product of the retinoblastoma susceptibility gene. *Cell*. 1988;54:275–283.
67. Whyte P, Buchkovich KJ, Horowitz JM, et al. Association between an oncogene and an anti-oncogene: the adenovirus E1A proteins bind to the retinoblastoma gene product. *Nature*. 1988;334:124–129.
68. Dyson N, Howley PM, Munger K, Harlow E. The human papilloma virus-16 E7 oncoprotein is able to bind to the retinoblastoma gene product. *Science*. 1989;243:934–937.
69. Harbour JW, Dean DC. Rb function in cell-cycle regulation and apoptosis. *Nat Cell Biol*. 2000;2:E65–7.
70. Chellappan SP, Hiebert S, Mudryj M, Horowitz JM, Nevins JR. The E2F transcription factor is a cellular target for the RB protein. *Cell*. 1991;65:1053–1061.
71. Helin K, Ed H. The retinoblastoma protein as a transcriptional repressor. *Trends Cell Biol*. 1993;3:43–46.
72. Huber HE, Edwards G, Goodhart PJ, et al. Transcription factor E2F binds DNA as a heterodimer. *Proc Natl Acad Sci USA*. 1993;90:3525–3529.
73. Nevins JR. Toward an understanding of the functional complexity of the E2F and retinoblastoma families. *Cell Growth Differ*. 1998;9:585–593.
74. Blake MC, Azizkhan JC. Transcription factor E2F is required for efficient expression of the hamster dihydrofolate reductase gene in vitro and in vivo. *Mol Cell Biol*. 1989;9:4994–5002.

75. Dalton S. Cell cycle regulation of the human cdc2 gene. *EMBO J*. 1992;11:1797–1804.
76. Ohtani K, DeGregori J, Nevins JR. Regulation of the cyclin E gene by transcription factor E2F1. *Proc Natl Acad Sci USA*. 1995;92:12146–12150.
77. Thalmeier K, Synovzik H, Mertz R, Winnacker EL, Lipp M. Nuclear factor E2F mediates basic transcription and trans-activation by E1a of the human MYC promoter. *Genes Dev*. 1989;3:527–536.
78. Flemington EK, Speck SH, Kaelin WG Jr. E2F-1-mediated transactivation is inhibited by complex formation with the retinoblastoma susceptibility gene product. *Proc Natl Acad Sci USA*. 1993;90:6914–6918.
79. Johnson DG, Schwarz JK, Cress WD, Nevins JR. Expression of transcription factor E2F1 induces quiescent cells to enter S phase. *Nature*. 1993;365:349–352.
80. Chow KN, Dean DC. Domains A and B in the Rb pocket interact to form a transcriptional repressor motif. *Mol Cell Biol*. 1996;16:4862–4868.
81. Zhang HS, Postigo AA, Dean DC. Active transcriptional repression by the Rb-E2F complex mediates G1 arrest triggered by p16INK4a, TGFbeta, and contact inhibition. *Cell*. 1999;97:53–61.
82. Brehm A, Miska EA, McCance DJ, Reid JL, Bannister AJ, Kouzarides T. Retinoblastoma protein recruits histone deacetylase to repress transcription. *Nature*. 1998;391:597–601.
83. Luo RX, Postigo AA, Dean DC. Rb interacts with histone deacetylase to repress transcription. *Cell*. 1998;92:463–473.
84. Magnaghi-Jaulin L, Groisman R, Naguibneva I, et al. Retinoblastoma protein represses transcription by recruiting a histone deacetylase. *Nature*. 1998;391:601–605.
85. Strobeck MW, Knudsen KE, Fribourg AF, et al. BRG-1 is required for RB-mediated cell cycle arrest. *Proc Natl Acad Sci USA*. 2000;97:7748–7753.
86. Trouche D, Le Chalony C, Muchardt C, Yaniv M, Kouzarides T. RB and hbrm cooperate to repress the activation functions of E2F1. *Proc Natl Acad Sci USA*.

1997;94:11268–11273.
87. Zhang HS, Gavin M, Dahiya A, et al. Exit from G1 and S phase of the cell cycle is regulated by repressor complexes containing HDAC-Rb-hSWI/SNF and Rb-hSWI/SNF. *Cell*. 2000;101:79–89.
88. Robertson KD, Ait-Si-Ali S, Yokochi T, Wade PA, Jones PL, Wolffe AP. DNMT1 forms a complex with Rb, E2F1 and HDAC1 and represses transcription from E2F-responsive promoters. *Nat Genet*. 2000;25:338–342.
89. Dahiya A, Wong S, Gonzalo S, Gavin M, Dean DC. Linking the Rb and polycomb pathways. *Mol Cell*. 2001;8:557–569.
90. Nielsen SJ, Schneider R, Bauer UM, et al. Rb targets histone H3 methylation and HP1 to promoters. *Nature*. 2001;412:561–565.
91. Harbour JW, Dean DC. The Rb/E2F pathway: expanding roles and emerging paradigms. *Genes Dev*. 2000;14:2393–2409.
92. Horowitz JM, Park SH, Bogenmann E, et al. Frequent inactivation of the retinoblastoma anti-oncogene is restricted to a subset of human tumor cells. *Proc Natl Acad Sci USA*. 1990;87:2775–2779.
93. Lee C, Chang JH, Lee HS, Cho Y. Structural basis for the recognition of the E2F transactivation domain by the retinoblastoma tumor suppressor. *Genes Dev*. 2002;16:3199–3212.
94. Stevaux O, Dyson NJ. A revised picture of the E2F transcriptional network and RB function. *Curr Opin Cell Biol*. 2002;14:684–691.
95. Hiebert SW. Regions of the retinoblastoma gene product required for its interaction with the E2F transcription factor are necessary for E2 promoter repression and pRb-mediated growth suppression. *Mol Cell Biol*. 1993;13:3384–3391.
96. Hamel PA, Gill RM, Phillips RA, Gallie BL. Regions controlling hyperphosphorylation and conformation of the retinoblastoma gene product are independent of domains required for transcriptional repression. *Oncogene*. 1992;7:693–701.
97. Harbour JW, Luo RX, Dei Santi A, Postigo AA, Dean DC.

Cdk phosphorylation triggers sequential intramolecular interactions that progressively block Rb functions as cells move through G1. *Cell*. 1999;98:859–869.
98. Welch PJ, Wang JY. Disruption of retinoblastoma protein function by coexpression of its C pocket fragment. *Genes Dev*. 1995;9:31–46.
99. Xiao ZX, Chen J, Levine AJ, et al. Interaction between the retinoblastoma protein and the oncoprotein MDM2. *Nature*. 1995;375:694–698.
100. Welch PJ, Wang JY. A C-terminal protein-binding domain in the retinoblastoma protein regulates nuclear c-Abl tyrosine kinase in the cell cycle. *Cell*. 1993;75:779–790.
101. Whitaker LL, Su H, Baskaran R, Knudsen ES, Wang JY. Growth suppression by an E2F-binding-defective retinoblastoma protein (RB): contribution from the RB C pocket. *Mol Cell Biol*. 1998;18:4032–4042.
102. Haupt Y, Maya R, Kazaz A, Oren M. Mdm2 promotes the rapid degradation of p53. *Nature*. 1997;387:296–299.
103. Kubbutat MH, Jones SN, Vousden KH. Regulation of p53 stability by Mdm2. *Nature*. 1997;387:299–303.
104. Hsieh JK, Chan FS, O'Connor DJ, Mittnacht S, Zhong S, Lu X. RB regulates the stability and the apoptotic function of p53 via MDM2. *Mol Cell*. 1999;3:181–193.
105. Sterner JM, Dew-Knight S, Musahl C, Kornbluth S, Horowitz JM. Negative regulation of DNA replication by the retinoblastoma protein is mediated by its association with MCM7. *Mol Cell Biol*. 1998;18:2748–2757.
106. Sterner JM, Murata Y, Kim HG, Kennett SB, Templeton DJ, Horowitz JM. Detection of a novel cell cycle-regulated kinase activity that associates with the amino terminus of the retinoblastoma protein in G2/M phases. *J Biol Chem*. 1995;270:9281–9288.
107. Durfee T, Mancini MA, Jones D, Elledge SJ, Lee WH. The amino-terminal region of the retinoblastoma gene product binds a novel nuclear matrix protein that co-localizes to centers for RNA processing. *J Cell Biol*. 1994;127:609–622.
108. Riley DJ, Liu CY, Lee WH. Mutations of N-terminal regions render the retinoblastoma protein insufficient for functions

in development and tumor suppression. *Mol Cell Biol*. 1997;17:7342–7352.
109. Qin XQ, Chittenden T, Livingston DM, Kaelin WG Jr. Identification of a growth suppression domain within the retinoblastoma gene product. *Genes Dev*. 1992;6:953–964.
110. Chow KN, Starostik P, Dean DC. The Rb family contains a conserved cyclin-dependent-kinase-regulated transcriptional repressor motif. *Mol Cell Biol*. 1996;16:7173–7181.
111. Xu HJ, Xu K, Zhou Y, Li J, Benedict WF, Hu SX. Enhanced tumor cell growth suppression by an N-terminal truncated retinoblastoma protein. *Proc Natl Acad Sci USA*. 1994;91:9837–9841.
112. Hsieh JK, Fredersdorf S, Kouzarides T, Martin K, Lu X. E2F1-induced apoptosis requires DNA binding but not transactivation and is inhibited by the retinoblastoma protein through direct interaction. *Genes Dev*. 1997;11:1840–1852.
113. Lee EY, Hu N, Yuan SS, et al. Dual roles of the retinoblastoma protein in cell cycle regulation and neuron differentiation. *Genes Dev*. 1994;8:2008–2021.
114. Lipinski MM, Jacks T. The retinoblastoma gene family in differentiation and development. *Oncogene*. 1999;18:7873–7882.
115. Ma D, Zhou P, Harbour JW. Distinct mechanisms for regulating the tumor suppressor and antiapoptotic functions of Rb. *J Biol Chem*. 2003;278:19358–19366.
116. Yee AS, Shih HH, Tevosian SG. New perspectives on retinoblastoma family functions in differentiation. *Front Biosci*. 1998;3:D532–47.
117. Hinds PW, Mittnacht S, Dulic V, Arnold A, Reed SI, Weinberg RA. Regulation of retinoblastoma protein functions by ectopic expression of human cyclins. *Cell*. 1992;70:993–1006.
118. Lundberg AS, Weinberg RA. Functional inactivation of the retinoblastoma protein requires sequential modification by at least two distinct cyclin-cdk complexes. *Mol Cell Biol*. 1998;18:753–761.

119. Knudsen ES, Wang JY. Differential regulation of retinoblastoma protein function by specific Cdk phosphorylation sites. *J Biol Chem*. 1996;271:8313–8320.
120. Knudsen ES, Wang JY. Dual mechanisms for the inhibition of E2F binding to RB by cyclin-dependent kinase-mediated RB phosphorylation. *Mol Cell Biol*. 1997;17:5771–5783.
121. Templeton DJ, Park SH, Lanier L, Weinberg RA. Nonfunctional mutants of the retinoblastoma protein are characterized by defects in phosphorylation, viral oncoprotein association, and nuclear tethering. *Proc Natl Acad Sci USA*. 1991;88:3033–3037.
122. Sherr CJ, Roberts JM. Inhibitors of mammalian G1 cyclin-dependent kinases. *Genes Dev*. 1995;9:1149–1163.
123. Merbs SL, Sidransky D. Analysis of p16 (CDKN2/MTS-1/INK4A) alterations in primary sporadic uveal melanoma. *Invest Ophthalmol Vis Sci*. 1999;40:779–783.
124. Otterson GA, Kratzke RA, Coxon A, Kim YW, Kaye FJ. Absence of p16INK4 protein is restricted to the subset of lung cancer lines that retains wildtype RB. *Oncogene*. 1994;9:3375–3378.
125. Sherr CJ, Roberts JM. CDK inhibitors: positive and negative regulators of G1-phase progression. *Genes Dev*. 1999;13:1501–1512.
126. Fletcher O, Easton D, Anderson K, Gilham C, Jay M, Peto J. Lifetime risks of common cancers among retinoblastoma survivors. *J Natl Cancer Inst*. 2004;96:357–363.
127. Morgenbesser SD, Williams BO, Jacks T, DePinho RA. p53-dependent apoptosis produced by Rb-deficiency in the developing mouse lens. *Nature*. 1994;371:72–74.
128. Sherr CJ, McCormick F. The RB and p53 pathways in cancer. *Cancer Cell*. 2002;2:103–112.
129. Howes KA, Ransom N, Papermaster DS, Lasudry JG, Albert DM, Windle JJ. Apoptosis or retinoblastoma: alternative fates of photoreceptors expressing the HPV-16 E7 gene in the presence or absence of p53. *Genes Dev*. 1994;8:1300–1310.
130. Nork TM, Poulsen GL, Millecchia LL, Jantz RG, Nickells RW. p53 regulates apoptosis in human retinoblastoma. *Arch Ophthalmol*. 1997;115:213–219.

131. Squire J, Phillips RA, Boyce S, Godbout R, Rogers B, Gallie BL. Isochromosome 6p, a unique chromosomal abnormality in retinoblastoma: verification by standard staining techniques, new densitometric methods, and somatic cell hybridization. *Hum Genet*. 1984;66:46–53.
132. Gallie BL, Campbell C, Devlin H, Duckett A, Squire JA. Developmental basis of retinal-specific induction of cancer by RB mutation. *Cancer Res*. 1999;59:1731s–1735s.
133. Elison JR, Cobrinik D, Claros N, Abramson DH, Lee TC. Small molecule inhibition of HDM2 leads to p53-mediated cell death in retinoblastoma cells. *Arch Ophthalmol*. 2006;124:1269–1275.
134. Laurie NA, Donovan SL, Shih CS, et al. Inactivation of the p53 pathway in retinoblastoma. *Nature*. 2006;444:61–66.
135. Zhang J, Gray J, Wu L, et al. Rb regulates proliferation and rod photoreceptor development in the mouse retina. *Nat Genet*. 2004;36:351–360.
136. Rugh R. X-rays and the retina of the primate fetus. *Arch Ophthalmol*. 1973;89:221–227.
137. Abramson DH, Gombos DS. The topography of bilateral retinoblastoma lesions. *Retina*. 1996;16:232–239.
138. Turner DL, Cepko CL. A common progenitor for neurons and glia persists in rat retina late in development. *Nature*. 1987;328:131–136.
139. Gonzalez-Fernandez F, Lopes MB, Garcia-Fernandez JM, et al. Expression of developmentally defined retinal phenotypes in the histogenesis of retinoblastoma. *Am J Pathol*. 1992;141:363–375.
140. Hurwitz RL, Bogenmann E, Font RL, Holcombe V, Clark D. Expression of the functional cone phototransduction cascade in retinoblastoma. *J Clin Invest*. 1990;85:1872–1878.
141. Adler R, Hatlee M. Plasticity and differentiation of embryonic retinal cells after terminal mitosis. *Science*. 1989;243:391–393.
142. Xu XL, Singh HP, Wang L, et al. Rb suppresses human cone-precursor-derived retinoblastoma tumours. *Nature*. 2014;514:385–388.
143. Broaddus E, Topham A, Singh AD. Incidence of

retinoblastoma in the USA: 1975–2004. *Br J Ophthalmol*. 2009;93:21–23.
144. Abiose A, Adido J, Agarwal SC. Childhood malignancies of the eye and orbit in northern Nigeria. *Cancer*. 1985;55:2889–2893.
145. BenEzra D, Chirambo MC. Incidence of retinoblastoma in Malawi. *J Pediatr Ophthalmol*. 1976;13:340–343.
146. Klauss V, Chana HS. Ocular tumors in Africa. *Soc Sci Med*. 1983;17:1743–1750.
147. Makata AM, Toriyama K, Kamidigo NO, Eto H, Itakura H. The pattern of pediatric solid malignant tumors in western Kenya, East Africa, 1979–1994: an analysis based on histopathologic study. *Am J Trop Med Hyg*. 1996;54:343–347.
148. Olisa EG, Chandra R, Jackson MA, Kennedy J, Williams AO. Malignant tumors in American black and Nigerian children: a comparative study. *J Natl Cancer Inst*. 1975;55:281–284.
149. Ka AS, Imbert P, Moreira C, et al. [Epidemiology and prognosis of childhood cancers in Dakar, Senegal]. *Med Trop (Mars)*. 2003;63:521–526.
150. Koulibaly M, Kabba IS, Cisse A, et al. Cancer incidence in Conakry, Guinea: first results from the Cancer Registry 1992-1995. *Int J Cancer*. 1997;70:39–45.
151. Nandakumar A, Anantha N, Appaji L, et al. Descriptive epidemiology of childhood cancers in Bangalore, India. *Cancer Causes Control*. 1996;7:405–410.
152. Nguyen QM, Nguyen HC, Kramarova E, Parkin DM. Incidence of childhood cancer in Ho Chi Minh City, Vietnam, 1995-97. *Paediatr Perinat Epidemiol*. 2000;14:240–247.
153. Patil PS, Elem B, Gwavava NJ, Urban MI. The pattern of paediatric malignancy in Zambia (1980–1989): a hospital-based histopathological study. *J Trop Med Hyg*. 1992;95:124–127.
154. Poso MY, Mwanza JC, Kayembe DL. Malignant tumors of the eye and adnexa in Congo-Kinshasa. *J Fr Ophtalmol*. 2000;23:327–332.
155. Tefuarani N, Vince JD, Murthy DP, Sengupta SK, White JC. Childhood malignant tumours in Papua New Guinea. *Ann*

Trop Paediatr. 1988;8:201–206.
156. Thakur SK, Sah SP, Lakhey M, Badhu BP. Primary malignant tumours of eye and adnexa in Eastern Nepal. *Clin Experiment Ophthalmol*. 2003;31:415–417.
157. Tijani SO, Elesha SO, Banjo AA. Morphological patterns of paediatric solid cancer in Lagos, Nigeria. *West Afr J Med*. 1995;14:174–180.
158. Traboulsi EI, Jurdi-Nuwayhid F, Frangieh GT, Der Kaloustian VM. Retinoblastoma in Lebanon. *Ophthalmic Paediatr Genet*. 1986;7:29–34.
159. Welbeck JE, Hesse AA. Pattern of childhood malignancy in Korle Bu Teaching Hospital, Ghana. *West Afr J Med*. 1998;17:81–84.
160. Wessels G, Hesseling PB. Incidence and frequency rates of childhood cancer in Namibia. *S Afr Med J*. 1997;87:885–889.
161. Orjuela MA, Titievsky L, Liu X, et al. Fruit and vegetable intake during pregnancy and risk for development of sporadic retinoblastoma. *Cancer Epidemiol Biomarkers Prev*. 2005;14:1433–1440.
162. Anand B, Ramesh C, Appaji L, et al. Prevalence of high-risk human papillomavirus genotypes in retinoblastoma. *Br J Ophthalmol*. 2011;95:1014–1018.
163. Shetty OA, Naresh KN, Banavali SD, et al. Evidence for the presence of high risk human papillomavirus in retinoblastoma tissue from nonfamilial retinoblastoma in developing countries. *Pediatr Blood Cancer*. 2012;58:185–190.
164. Ryoo NK, Kim JE, Choung HK, Kim N, Lee MJ, Khwarg SI. Human papilloma virus in retinoblastoma tissues from Korean patients. *Korean J Ophthalmol*. 2013;27:368–371.
165. Gillison ML, Chen R, Goshu E, et al. Human retinoblastoma is not caused by known pRb-inactivating human DNA tumor viruses. *Int J Cancer*. 2007;120:1482–1490.
166. Pendergrass TW, Davis S. Incidence of retinoblastoma in the United States. *Arch Ophthalmol*. 1980;98:1204–1210.
167. Devesa SS. The incidence of retinoblastoma. *Am J Ophthalmol*. 1975;80:263–265.
168. Tamboli A, Podgor MJ, Horm JW. The incidence of retinoblastoma in the United States: 1974 through 1985.

Arch Ophthalmol. 1990;108:128–132.
169. O'Day J, Billson FA, Hoyt CS. Retinoblastoma in Victoria. *Med J Aust*. 1977;2:428–432.
170. Kock E, Naeser P. Retinoblastoma in Sweden 1958–1971. A clinical and histopathological study. *Acta Ophthalmol (Copenh)*. 1979;57:344–350.
171. Suckling RD, Fitzgerald PH, Stewart J, Wells E. The incidence and epidemiology of retinoblastoma in New Zealand: a 30-year survey. *Br J Cancer*. 1982;46:729–736.
172. Bunin GR, Petrakova A, Meadows AT, et al. Occupations of parents of children with retinoblastoma: a report from the Children's Cancer Study Group. *Cancer Res*. 1990;50:7129–7133.
173. Matsunaga E. Genetics and epidemiology of retinoblastoma. *Gan No Rinsho*. 1987;33:507–513.
174. Buckley JD. The aetiology of cancer in the very young. *Br J Cancer Suppl*. 1992;18:S8–12.
175. Tunte W. Human mutations and paternal age. *Humangenetik*. 1972;16:77–82.
176. Sivakumaran TA, Ghose S, Kumar H, A S, Kucheria K. Parental age in Indian patients with sporadic hereditary retinoblastoma. *Ophthalmic Epidemiol*. 2000;7:285–291.
177. Moll AC, Imhof SM, Kuik DJ, et al. High parental age is associated with sporadic hereditary retinoblastoma: the Dutch retinoblastoma register 1862–1994. *Hum Genet*. 1996;98:109–112.
178. Matsunaga E, Minoda K, Sasaki MS. Parental age and seasonal variation in the births of children with sporadic retinoblastoma: a mutation-epidemiologic study. *Hum Genet*. 1990;84:155–158.
179. Dockerty JD, Draper G, Vincent T, Rowan SD, Bunch KJ. Case-control study of parental age, parity and socioeconomic level in relation to childhood cancers. *Int J Epidemiol*. 2001;30:1428–1437.
180. DerKinderen DJ, Koten JW, Tan KE, Beemer FA, Van Romunde LK, Den Otter W. Parental age in sporadic hereditary retinoblastoma. *Am J Ophthalmol*. 1990;110:605–609.

181. Strong LC, Herson J, Haas C, et al. Cancer mortality in relatives of retinoblastoma patients. *J Natl Cancer Inst*. 1984;73:303–311.
182. Dryja TP, Morrow JF, Rapaport JM. Quantification of the paternal allele bias for new germline mutations in the retinoblastoma gene. *Hum Genet*. 1997;100:446–449.
183. Zhu XP, Dunn JM, Phillips RA, et al. Preferential germline mutation of the paternal allele in retinoblastoma. *Nature*. 1989;340:312–313.
184. Abramson DH, Schefler AC, Beaverson KL, Rollins IS, Ruddat MS, Kelly CJ. Rapid growth of retinoblastoma in a premature twin. *Arch Ophthalmol*. 2002;120:1232–1233.
185. Shields CL, Manalac J, Das C, Saktanasate J, Shields JA. Review of spectral domain-enhanced depth imaging optical coherence tomography of tumors of the retina and retinal pigment epithelium in children and adults. *Indian J Ophthalmol*. 2015;63:128–132.
186. Saktanasate J, Vongkulsiri S, Khoo CT. Invisible Retinoblastoma. *JAMA Ophthalmol*. 2015;133:e151123.
187. Folkman J. Role of angiogenesis in tumor growth and metastasis. *Semin Oncol*. 2002;29:15–18.
188. Ray A, Gombos DS, Vats TS. Retinoblastoma: an overview. *Indian J Pediatr*. 2012;79:916–921.
189. Shields JA, Sanborn GE, Augsburger JJ, Orlock D, Donoso LA. Fluorescein angiography of retinoblastoma. *Retina*. 1982;2:206–214.
190. Kim JW, Ngai LK, Sadda S, Murakami Y, Lee DK, Murphree AL. RetCam fluorescein angiography findings in eyes with advanced retinoblastoma. *Br J Ophthalmol*. 2014;98:1666–1671.
191. Wu RC, Blumenthal M, Li X, Schonthal AH. Loss of cellular adhesion to matrix induces p53-independent expression of PTEN tumor suppressor. *BMC Mol Biol*. 2002;3:11.
192. Wolf K, Mazo I, Leung H, et al. Compensation mechanism in tumor cell migration: mesenchymal-amoeboid transition after blocking of pericellular proteolysis. *J Cell Biol*. 2003;160:267–277.
193. Ellsworth RM. The practical management of retinoblastoma.

Trans Am Ophthalmol Soc. 1969;67:462–534.
194. Reese AB, Ellsworth RM. Management of retinoblastoma. *Ann N Y Acad Sci*. 1964;114:958–962.
195. Kingston JE, Hungerford JL, Madreperla SA, Plowman PN. Results of combined chemotherapy and radiotherapy for advanced intraocular retinoblastoma. *Arch Ophthalmol*. 1996;114:1339–1343.
196. Murphree AL, Villablanca JG, Deegan WF 3rd, et al. Chemotherapy plus local treatment in the management of intraocular retinoblastoma. *Arch Ophthalmol*. 1996;114:1348–1356.
197. Gallie BL, Budning A, DeBoer G, et al. Chemotherapy with focal therapy can cure intraocular retinoblastoma without radiotherapy. *Arch Ophthalmol*. 1996;114:1321–1328.
198. Shields CL, De Potter P, Himelstein BP, Shields JA, Meadows AT, Maris JM. Chemoreduction in the initial management of intraocular retinoblastoma. *Arch Ophthalmol*. 1996;114:1330–1338.
199. Murphree AL. The case for a new group classification. *Ophthalmol Clin North Am*. 2005;18:41–53.
200. Abramson DH, Ellsworth RM, Grumbach N, Kitchin FD. Retinoblastoma: survival, age at detection and comparison 1914–1958, 1958–1983. *J Pediatr Ophthalmol Strabismus*. 1985;22:246–250.
201. Moll AC, Kuik DJ, Bouter LM, et al. Incidence and survival of retinoblastoma in The Netherlands: a register based study 1862–1995. *Br J Ophthalmol*. 1997;81:559–562.
202. Abramson DH, Ellsworth RM, Kitchin FD, Tung G. Second nonocular tumors in retinoblastoma survivors. Are they radiation-induced? *Ophthalmology*. 1984;91:1351–1355.
203. Abramson DH, Frank CM. Second nonocular tumors in survivors of bilateral retinoblastoma: a possible age effect on radiation-related risk. *Ophthalmology*. 1998;105:573–579 [discussion 579-580].
204. Sinniah D, Narasimha G, Prathap K. Advanced retinoblastoma in Malaysian children. *Acta Ophthalmol (Copenh)*. 1980;58:819–824.
205. Hungerford J, Kingston J, Plowman N. Orbital recurrence of

retinoblastoma. *Ophthalmic Paediatr Genet*. 1987;8:63–68.
206. Chantada G, Fandino A, Manzitti J, Urrutia L, Schvartzman E. Late diagnosis of retinoblastoma in a developing country. *Arch Dis Child*. 1999;80:171–174.
207. Kodilinye HC. Retinoblastoma in Nigeria: problems of treatment. *Am J Ophthalmol*. 1967;63:469–481.
208. Matsunaga E. Hereditary retinoblastoma: penetrance, expressivity and age of onset. *Hum Genet*. 1976;33:1–15.
209. Finger PT, Harbour JW, Karcioglu ZA. Risk factors for metastasis in retinoblastoma. *Surv Ophthalmol*. 2002;47:1–16.
210. Kim JW. Retinoblastoma: evidence for postenucleation adjuvant chemotherapy. *Int Ophthalmol Clin*. 2015;55:77–96.
211. Kao LY, Su WW, Lin YW. Retinoblastoma in Taiwan: survival and clinical characteristics 1978–2000. *Jpn J Ophthalmol*. 2002;46:577–580.
212. Haik BG, Siedlecki A, Ellsworth RM, Sturgis-Buckhout L. Documented delays in the diagnosis of retinoblastoma. *Ann Ophthalmol*. 1985;17:731–732.
213. Buckley EG, Heath H. Visual acuity after successful treatment of large macular retinoblastoma. *J Pediatr Ophthalmol Strabismus*. 1992;29:103–106.
214. Lam BL, Judisch GF, Sobol WM, Blodi CF. Visual prognosis in macular retinoblastomas. *Am J Ophthalmol*. 1990;110:229–232.
215. Abramson DH, Frank CM, Susman M, Whalen MP, Dunkel IJ, Boyd NW 3rd. Presenting signs of retinoblastoma. *J Pediatr*. 1998;132:505–508.
216. Canzano JC, Handa JT. Utility of pupillary dilation for detecting leukocoria in patients with retinoblastoma. *Pediatrics*. 1999;104:e44.
217. Shields JA, Shields CL, Suvarnamani C, Schroeder RP, DePotter P. Retinoblastoma manifesting as orbital cellulitis. *Am J Ophthalmol*. 1991;112:442–449.
218. Shields JA, Parsons HM, Shields CL, Shah P. Lesions simulating retinoblastoma. *J Pediatr Ophthalmol Strabismus*. 1991;28:338–340.
219. De Potter P, Flanders AE, Shields JA, Shields CL. Magnetic resonance imaging of intraocular tumors. *Int Ophthalmol*

Clin. 1993;33:37–45.
220. Tateishi U, Hasegawa T, Miyakawa K, Sumi M, Moriyama N. CT and MRI features of recurrent tumors and second primary neoplasms in pediatric patients with retinoblastoma. *AJR Am J Roentgenol*. 2003;181:879–884.
221. Coleman DJ. Reliability of ocular tumor diagnosis with ultrasound. *Trans Am Acad Ophthalmol Otolaryngol*. 1973;77:OP677–86.
222. Sterns GK, Coleman DJ, Ellsworth RM. The ultrasonographic characteristics of retinoblastoma. *Am J Ophthalmol*. 1974;78:606–611.
223. Sterns GK, Coleman DJ, Ellsworth RM. Characterization and evaluation of retinoblastoma by ultrasonography. *Bibl Ophthalmol*. 1975;125–129.
224. Poujol J, Varene B. Contribution of echography to the diagnosis of retinoblastoma: a homogeneous B-scan study. *Ultrasound Med Biol*. 1985;11:171–175.
225. Oksala A. Ultrasonic diagnosis in melanoma and retinoblastoma. *Acta Ophthalmol Suppl*. 1974;123:136–141.
226. Augsburger JJ, Shields JA, Folberg R, Lang W, O'Hara BJ, Claricci JD. Fine needle aspiration biopsy in the diagnosis of intraocular cancer: cytologic–histologic correlations. *Ophthalmology*. 1985;92:39–49.
227. Karcioglu ZA. Fine needle aspiration biopsy (FNAB) for retinoblastoma. *Retina*. 2002;22:707–710.
228. Chan HS, DeBoer G, Thiessen JJ, et al. Combining cyclosporin with chemotherapy controls intraocular retinoblastoma without requiring radiation. *Clin Cancer Res*. 1996;2:1499–1508.
229. Berry JL, Jubran R, Kim JW, et al. Long-term outcomes of Group D eyes in bilateral retinoblastoma patients treated with chemoreduction and low-dose IMRT salvage. *Pediatr Blood Cancer*. 2013;60:688–693.
230. Berry JL, Jubran R, Wong K, Lee TC, Murphree AL, Kim JW. Factors predictive of long-term visual outcomes of Group D eyes treated with chemoreduction and low-dose IMRT salvage: the Children's Hospital Los Angeles experience. *Br J Ophthalmol*. 2014;98:1061–1065.

231. Shields CL, Ramasubramanian A, Thangappan A, et al. Chemoreduction for group E retinoblastoma: comparison of chemoreduction alone versus chemoreduction plus low-dose external radiotherapy in 76 eyes. *Ophthalmology*. 2009;116:544–551.e1.
232. Kaliki S, Srinivasan V, Gupta A, Mishra DK, Naik MN. Clinical features predictive of high-risk retinoblastoma in 403 Asian Indian patients: a case–control study. *Ophthalmology*. 2015;122:1165–1172.
233. Kaliki S, Shields CL, Rojanaporn D, et al. High-risk retinoblastoma based on international classification of retinoblastoma: analysis of 519 enucleated eyes. *Ophthalmology*. 2013;120:997–1003.
234. Zhao J, Dimaras H, Massey C, et al. Pre-enucleation chemotherapy for eyes severely affected by retinoblastoma masks risk of tumor extension and increases death from metastasis. *J Clin Oncol*. 2011;29:845–851.
235. Pratt CB, Crom DB, Howarth C. The use of chemotherapy for extraocular retinoblastoma. *Med Pediatr Oncol*. 1985;13:330–333.
236. Felice MS, Zubizarreta PA, Chantada GL, et al. Acute myeloid leukemia as a second malignancy: report of 9 pediatric patients in a single institution in Argentina. *Med Pediatr Oncol*. 1998;30:160–164.
237. Gombos DS, Hungerford J, Abramson DH, et al. Secondary acute myelogenous leukemia in patients with retinoblastoma: is chemotherapy a factor? *Ophthalmology*. 2007;114:1378–1383.
238. Bhagat SP, Bass JK, White ST, et al. Monitoring carboplatin ototoxicity with distortion-product otoacoustic emissions in children with retinoblastoma. *Int J Pediatr Otorhinolaryngol*. 2010;74:1156–1163.
239. Abramson DH, Frank CM, Dunkel IJ. A phase I/II study of subconjunctival carboplatin for intraocular retinoblastoma. *Ophthalmology*. 1999;106:1947–1950.
240. Mulvihill A, Budning A, Jay V, et al. Ocular motility changes after subtenon carboplatin chemotherapy for retinoblastoma. *Arch Ophthalmol*. 2003;121:1120–1124.

241. Shah PK, Kalpana N, Narendran V, Ramakrishnan M. Severe aseptic orbital cellulitis with subtenon carboplatin for intraocular retinoblastoma. *Indian J Ophthalmol*. 2011;59:49–51.
242. Kim JW, Yau JW, Moshfeghi D, Fishman M. Orbital fibrosis and intraocular recurrence of retinoblastoma following periocular carboplatin. *J Pediatr Ophthalmol Strabismus*. 2010;47:e1–4 [Online].
243. Kupfer C. Retinoblastoma treated with intravenous nitrogen mustard. *Am J Ophthalmol*. 1953;36:1721–1723.
244. Ellsworth RM. Treatment of retinoblastoma. *Am J Ophthalmol*. 1968;66:49–51.
245. Hyman GA, Ellsworth RM, Feind CR, Tretter P. Combination therapy in retinoblastoma: a 15-year summary of methods and results. *Arch Ophthalmol*. 1968;80:744–746.
246. Hyman GA, Ellsworth RM, Reese AB. The results of combination therapy of retinoblastoma. a nine year study of 250 cases. *Acta Unio Int Contra Cancrum*. 1964;20:407–410.
247. Suzuki S, Kaneko A. Management of intraocular retinoblastoma and ocular prognosis. *Int J Clin Oncol*. 2004;9:1–6.
248. Yamane T, Kaneko A, Mohri M. The technique of ophthalmic arterial infusion therapy for patients with intraocular retinoblastoma. *Int J Clin Oncol*. 2004;9:69–73.
249. Kaneko A. Retinoblastoma. *Nippon Rinsho*. 2000;58:1413–1418.
250. Abramson DH. Super selective ophthalmic artery delivery of chemotherapy for intraocular retinoblastoma: 'chemosurgery' the first Stallard lecture. *Br J Ophthalmol*. 2010;94:396–399.
251. Abramson DH, Dunkel IJ, Brodie SE, Marr B, Gobin YP. Bilateral superselective ophthalmic artery chemotherapy for bilateral retinoblastoma: tandem therapy. *Arch Ophthalmol*. 2010;128:370–372.
252. Francis JH, Gobin YP, Dunkel IJ, et al. Carboplatin$^{+/-}$ topotecan ophthalmic artery chemosurgery for intraocular retinoblastoma. *PLoS ONE*. 2013;8:e72441.
253. Brodie SE, Paulus YM, Patel M, et al. ERG monitoring of

retinal function during systemic chemotherapy for retinoblastoma. *Br J Ophthalmol*. 2012;96:877–880.
254. Brodie SE, Pierre Gobin Y, Dunkel IJ, Kim JW, Abramson DH. Persistence of retinal function after selective ophthalmic artery chemotherapy infusion for retinoblastoma. *Doc Ophthalmol*. 2009;119:13–22.
255. Shields CL, Manjandavida FP, Lally SE, et al. Intra-arterial chemotherapy for retinoblastoma in 70 eyes: outcomes based on the international classification of retinoblastoma. *Ophthalmology*. 2014;121:1453–1460.
256. Shields CL, Bianciotto CG, Jabbour P, et al. Intra-arterial chemotherapy for retinoblastoma. Report No. 2, treatment complications. *Arch Ophthalmol*. 2011;129:1407–1415.
257. Monroy JE, Orbach DB, VanderVeen D. Complications of intra-arterial chemotherapy for retinoblastoma. *Semin Ophthalmol*. 2014;29:429–433.
258. Marr B, Gobin PY, Dunkel IJ, Brodie SE, Abramson DH. Spontaneously resolving periocular erythema and ciliary madarosis following intra-arterial chemotherapy for retinoblastoma. *Middle East Afr J Ophthalmol*. 2010;17:207–209.
259. Maidana DE, Pellegrini M, Shields JA, Shields CL. Choroidal thickness after intraarterial chemotherapy for retinoblastoma. *Retina*. 2014;34:2103–2109.
260. Tse BC, Kaste SC, Brennan R, Orr B, Wilson MW. Enophthalmos and choroidal atrophy after intraophthalmic artery chemotherapy for retinoblastoma. *Ophthalmology*. 2015;122:435–437.
261. Tsimpida M, Thompson DA, Liasis A, et al. Visual outcomes following intraophthalmic artery melphalan for patients with refractory retinoblastoma and age appropriate vision. *Br J Ophthalmol*. 2013;97:1464–1470.
262. Gobin YP, Rosenstein LM, Marr BP, Brodie SE, Abramson DH. Radiation exposure during intra-arterial chemotherapy for retinoblastoma. *Arch Ophthalmol*. 2012;130:403–404 [author reply 404-405].
263. Vijayakrishnan R, Shields CL, Ramasubramanian A, Emrich J, Rosenwasser R, Shields JA. Irradiation toxic effects during

intra-arterial chemotherapy for retinoblastoma: should we be concerned? *Arch Ophthalmol*. 2010;128:1427–1431.
264. Dunkel IJ, Shi W, Salvaggio K, et al. Risk factors for severe neutropenia following intra-arterial chemotherapy for intraocular retinoblastoma. *PLoS ONE*. 2014;9:e108692.
265. Gobin YP, Dunkel IJ, Marr BP, Francis JH, Brodie SE, Abramson DH. Combined, sequential intravenous and intra-arterial chemotherapy (bridge chemotherapy) for young infants with retinoblastoma. *PLoS ONE*. 2012;7:e44322.
266. Francis JH, Abramson DH, Gobin YP, et al. Efficacy and toxicity of second-course ophthalmic artery chemosurgery for retinoblastoma. *Ophthalmology*. 2015;122:1016–1022.
267. Marr BP, Brodie SE, Dunkel IJ, Gobin YP, Abramson DH. Three-drug intra-arterial chemotherapy using simultaneous carboplatin, topotecan and melphalan for intraocular retinoblastoma: preliminary results. *Br J Ophthalmol*. 2012;96:1300–1303.
268. Abramson DH, Jereb B, Ellsworth RM. External beam radiation for retinoblastoma. *Bull N Y Acad Med*. 1981;57:787–803.
269. McCormick B, Ellsworth R, Abramson D, LoSasso T, Grabowski E. Results of external beam radiation for children with retinoblastoma: a comparison of two techniques. *J Pediatr Ophthalmol Strabismus*. 1989;26:239–243.
270. Ghassemi F, Shields CL. Intravitreal melphalan for refractory or recurrent vitreous seeding from retinoblastoma. *Arch Ophthalmol*. 2012;130:1268–1271.
271. Shields CL, Manjandavida FP, Arepalli S, Kaliki S, Lally SE, Shields JA. Intravitreal melphalan for persistent or recurrent retinoblastoma vitreous seeds: preliminary results. *JAMA Ophthalmol*. 2014;132:319–325.
272. Francis JH, Schaiquevich P, Buitrago E, et al. Local and systemic toxicity of intravitreal melphalan for vitreous seeding in retinoblastoma: a preclinical and clinical study. *Ophthalmology*. 2014;121:1810–1817.
273. Smith SJ, Smith BD, Mohney BG. Ocular side effects following intravitreal injection therapy for retinoblastoma: a

systematic review. *Br J Ophthalmol*. 2014;98:292–297.
274. Buitrago E, Lagomarsino E, Mato G, Schaiquevich P. Stability of melphalan solution for intravitreal injection for retinoblastoma. *JAMA Ophthalmol*. 2014;132:1372–1373.
275. Francis JH, Marr BP, Schaiquevich P, Kellick MG, Abramson DH. Properties and clinical utility of topotecan fluorescence: uses for retinoblastoma. *Br J Ophthalmol*. 2015.
276. Munier FL. Classification and management of seeds in retinoblastoma. Ellsworth Lecture Ghent August 24th 2013. *Ophthalmic Genet*. 2014;35:193–207.
277. Francis JH, Abramson DH, Gaillard MC, Marr BP, Beck-Popovic M, Munier FL. The classification of vitreous seeds in retinoblastoma and response to intravitreal melphalan. *Ophthalmology*. 2015;122:1173–1179.
278. Lee TC, Lee SW, Dinkin MJ, Ober MD, Beaverson KL, Abramson DH. Chorioretinal scar growth after 810-nanometer laser treatment for retinoblastoma. *Ophthalmology*. 2004;111:992–996.
279. Shields JA, Parsons H, Shields CL, Giblin ME. The role of cryotherapy in the management of retinoblastoma. *Am J Ophthalmol*. 1989;108:260–264.
280. Shields JA, Shields CL. Treatment of retinoblastoma with cryotherapy. *Trans Pa Acad Ophthalmol Otolaryngol*. 1990;42:977–980.
281. Kim JW, Abramson DH, Dunkel IJ. Current management strategies for intraocular retinoblastoma. *Drugs*. 2007;67:2173–2185.
282. Mullaney PB, Abboud EB, Al-Mesfer SA. Retinal detachment associated with type III retinoblastoma regression after cryotherapy and external-beam radiotherapy. *Am J Ophthalmol*. 1997;123:140–142.
283. Lincoff HA, McLean JM. Cryosurgical treatment of retinal detachment. II. *Am J Ophthalmol*. 1966;61:1227–1234.
284. Phillips C, Sexton M, Wheeler G, McKenzie J. Retinoblastoma: review of 30 years' experience with external beam radiotherapy. *Australas Radiol*. 2003;47:226–230.
285. Sauerwein W, Hopping W, Bornfeld N. Radiotherapy for

retinoblastoma. Treatment strategies. *Front Radiat Ther Oncol*. 1997;30:93–96.
286. Scott IU, Murray TG, Feuer WJ, et al. External beam radiotherapy in retinoblastoma: tumor control and comparison of 2 techniques. *Arch Ophthalmol*. 1999;117:766–770.
287. Schipper J, Imhoff SM, Tan KE. Precision megavoltage external beam radiation therapy for retinoblastoma. *Front Radiat Ther Oncol*. 1997;30:65–80.
288. Hungerford JL, Toma NM, Plowman PN, Kingston JE. External beam radiotherapy for retinoblastoma: I. Whole eye technique. *Br J Ophthalmol*. 1995;79:109–111.
289. Krengli M, Hug EB, Adams JA, Smith AR, Tarbell NJ, Munzenrider JE. Proton radiation therapy for retinoblastoma: comparison of various intraocular tumor locations and beam arrangements. *Int J Radiat Oncol Biol Phys*. 2005;61:583–593.
290. Svitra PP, Budenz D, Albert DM, Koehler AM, Gragoudas E. Proton beam irradiation for treatment of experimental human retinoblastoma. *Eur J Ophthalmol*. 1991;1:57–62.
291. Sethi RV, Shih HA, Yeap BY, et al. Second nonocular tumors among survivors of retinoblastoma treated with contemporary photon and proton radiotherapy. *Cancer*. 2014;120:126–133.
292. Mouw KW, Sethi RV, Yeap BY, et al. Proton radiation therapy for the treatment of retinoblastoma. *Int J Radiat Oncol Biol Phys*. 2014;90:863–869.
293. Rosengren B, Tengroth B. Retinoblastoma treated with a 60CO applicator. *Acta Radiol Ther Phys Biol*. 1977;16:110–116.
294. Astrahan MA, Luxton G, Pu Q, Petrovich Z. Conformal episcleral plaque therapy. *Int J Radiat Oncol Biol Phys*. 1997;39:505–519.
295. Shields CL, Shields JA, Minelli S, et al. Regression of retinoblastoma after plaque radiotherapy. *Am J Ophthalmol*. 1993;115:181–187.
296. Abouzeid H, Moeckli R, Gaillard MC, et al. 106)Ruthenium brachytherapy for retinoblastoma. *Int J Radiat Oncol Biol Phys*. 2008;71:821–828.

297. Astrahan MA, Luxton G, Jozsef G, Liggett PE, Petrovich Z. Optimization of 125I ophthalmic plaque brachytherapy. *Med Phys*. 1990;17:1053–1057.
298. Berry JL, Dandapani SV, Stevanovic M, et al. Outcomes of choroidal melanomas treated with eye physics: a 20-year review. *JAMA Ophthalmol*. 2013;131:1435–1442.
299. Kim JW, Kathpalia V, Dunkel IJ, Wong RK, Riedel E, Abramson DH. Orbital recurrence of retinoblastoma following enucleation. *Br J Ophthalmol*. 2009;93:463–467.
300. Abramson DH, Ellsworth RM. The surgical management of retinoblastoma. *Ophthalmic Surg*. 1980;11:596–598.
301. Tawfik HA. Superomedial lid crease approach to the medial intraconal space. *Ophthal Plast Reconstr Surg*. 2002;18:164 [author reply 164-165].
302. Kim JW, Kikkawa DO, Aboy A, Glasgow BJ. Chronic exposure of hydroxyapatite orbital implants: cilia implantation and epithelial downgrowth. *Ophthal Plast Reconstr Surg*. 2000;16:216–222.
303. Stevenson KE, Hungerford J, Garner A. Local extraocular extension of retinoblastoma following intraocular surgery. *Br J Ophthalmol*. 1989;73:739–742.
304. Fountain TR, Goldberger S, Murphree AL. Orbital development after enucleation in early childhood. *Ophthal Plast Reconstr Surg*. 1999;15:32–36.
305. Yago K, Furuta M. Orbital growth after unilateral enucleation in infancy without an orbital implant. *Jpn J Ophthalmol*. 2001;45:648–652.
306. Imhof SM, Mourits MP, Hofman P, et al. Quantification of orbital and mid-facial growth retardation after megavoltage external beam irradiation in children with retinoblastoma. *Ophthalmology*. 1996;103:263–268.
307. Sarnat BG. Eye and orbital size in the young and adult: some postnatal experimental and clinical relationships. *Ophthalmologica*. 1982;185:74–89.
308. Singh AD, Garway-Heath D, Love S, Plowman PN, Kingston JE, Hungerford JL. Relationship of regression pattern to recurrence in retinoblastoma. *Br J Ophthalmol*. 1993;77:12–16.

309. Abramson DH, Gerardi CM, Ellsworth RM, McCormick B, Sussman D, Turner L. Radiation regression patterns in treated retinoblastoma: 7 to 21 years later. *J Pediatr Ophthalmol Strabismus*. 1991;28:108–112.
310. Buys RJ, Abramson DH, Ellsworth RM, Haik B. Radiation regression patterns after cobalt plaque insertion for retinoblastoma. *Arch Ophthalmol*. 1983;101:1206–1208.
311. Shields CL, Palamar M, Sharma P, et al. Retinoblastoma regression patterns following chemoreduction and adjuvant therapy in 557 tumors. *Arch Ophthalmol*. 2009;127:282–290.
312. Palamar M, Thangappan A, Shields CL. Evolution in regression patterns following chemoreduction for retinoblastoma. *Arch Ophthalmol*. 2011;129:727–730.
313. Lee TC, Hayashi NI, Dunkel IJ, Beaverson K, Novetsky D, Abramson DH. New retinoblastoma tumor formation in children initially treated with systemic carboplatin. *Ophthalmology*. 2003;110:1989–1994 [discussion 1994-1985].
314. Shields CL, Shelil A, Cater J, Meadows AT, Shields JA. Development of new retinoblastomas after 6 cycles of chemoreduction for retinoblastoma in 162 eyes of 106 consecutive patients. *Arch Ophthalmol*. 2003;121:1571–1576.
315. Abramson DH, Francis JH, Dunkel IJ, Marr BP, Brodie SE, Gobin YP. Ophthalmic artery chemosurgery for retinoblastoma prevents new intraocular tumors. *Ophthalmology*. 2013;120:560–565.
316. Messmer EP, Fritze H, Mohr C, et al. Long-term treatment effects in patients with bilateral retinoblastoma: ocular and mid-facial findings. *Graefes Arch Clin Exp Ophthalmol*. 1991;229:309–314.
317. Nahum MP, Gdal-On M, Kuten A, Herzl G, Horovitz Y, Weyl Ben Arush M. Long-term follow-up of children with retinoblastoma. *Pediatr Hematol Oncol*. 2001;18:173–179.
318. Mu X, Dong J, Chang T. Surgical reconstruction of the contracted eye socket and orbitozygomatic hypoplasia in a one-stage operation. *Plast Reconstr Surg*. 1999;103:487–493.
319. Asato H, Harii K, Yamada A, Ueda K. Eye socket reconstruction with free-flap transfer. *Plast Reconstr Surg*. 1993;92:1061–1067.

320. Schipper J, Tan KE, van Peperzeel HA. Treatment of retinoblastoma by precision megavoltage radiation therapy. *Radiother Oncol*. 1985;3:117–132.
321. Blach LE, McCormick B, Abramson DH. External beam radiation therapy and retinoblastoma: long-term results in the comparison of two techniques. *Int J Radiat Oncol Biol Phys*. 1996;35:45–51.
322. Schipper J, Alberti W. Late effects of radiation on surviving retinoblastoma patients. *Ophthalmology*. 1985;92:60A–63A.
323. Anteby I, Ramu N, Gradstein L, Miskin H, Pe'er J, Benezra D. Ocular and orbital complications following the treatment of retinoblastoma. *Eur J Ophthalmol*. 1998;8:106–111.
324. Brooks HL Jr, Meyer D, Shields JA, Balas AG, Nelson LB, Fontanesi J. Removal of radiation-induced cataracts in patients treated for retinoblastoma. *Arch Ophthalmol*. 1990;108:1701–1708.
325. Elmassri A. Radiation chorioretinopathy. *Br J Ophthalmol*. 1986;70:326–329.
326. Archer DB. Doyne Lecture. Responses of retinal and choroidal vessels to ionising radiation. *Eye (Lond)*. 1993;7(Pt 1):1–13.
327. Moll AC, Imhof SM, Schouten-Van Meeteren AY, Kuik DJ, Hofman P, Boers M. Second primary tumors in hereditary retinoblastoma: a register-based study, 1945–1997: is there an age effect on radiation-related risk? *Ophthalmology*. 2001;108:1109–1114.
328. Wong JR, Morton LM, Tucker MA, et al. Risk of subsequent malignant neoplasms in long-term hereditary retinoblastoma survivors after chemotherapy and radiotherapy. *J Clin Oncol*. 2014;32:3284–3290.
329. Strong LC, Knudson AG Jr. Letter: Second cancers in retinoblastoma. *Lancet*. 1973;2:1086.
330. François J. Costenbader Memorial Lecture: Genesis and genetics of retinoblastoma. *Adv Ophthalmol*. 1979;39:181–209.
331. Li FP, Abramson DH, Tarone RE, Kleinerman RA, Fraumeni JF Jr, Boice JD Jr. Hereditary retinoblastoma, lipoma, and second primary cancers. *J Natl Cancer Inst*. 1997;89:83–84.

332. Cade S. Radiation induced cancer in man. *Br J Radiol*. 1957;30:393–402.
333. Roarty JD, McLean IW, Zimmerman LE. Incidence of second neoplasms in patients with bilateral retinoblastoma. *Ophthalmology*. 1988;95:1583–1587.
334. Kaliki S, Shields CL, Shah SU, Eagle RC Jr, Shields JA, Leahey A. Postenucleation adjuvant chemotherapy with vincristine, etoposide, and carboplatin for the treatment of high-risk retinoblastoma. *Arch Ophthalmol*. 2011;129:1422–1427.
335. Chantada GL, Dunkel IJ, de Davila MT, Abramson DH. Retinoblastoma patients with high risk ocular pathological features: who needs adjuvant therapy? *Br J Ophthalmol*. 2004;88:1069–1073.
336. Kopelman JE, McLean IW, Rosenberg SH. Multivariate analysis of risk factors for metastasis in retinoblastoma treated by enucleation. *Ophthalmology*. 1987;94:371–377.
337. Kimball JC, Cangir A. Occurrence of testicular metastasis in a child with bilateral retinoblastoma. *Cancer Treat Rep*. 1979;63:803–804.
338. Pullon PA, Cohen DM. Oral metastasis of retinoblastoma. *Oral Surg Oral Med Oral Pathol*. 1974;37:583–588.
339. Carbajal UM. Metastasis in retinoblastoma. *Am J Ophthalmol*. 1959;48:47–69.
340. Merriam GR Jr. Retinoblastoma; analysis of 17 autopsies. *Arch Ophthal*. 1950;44:71–108.
341. Dunkel IJ, Aledo A, Kernan NA, et al. Successful treatment of metastatic retinoblastoma. *Cancer*. 2000;89:2117–2121.
342. Kingston JE, Hungerford JL, Plowman PN. Chemotherapy in metastatic retinoblastoma. *Ophthalmic Paediatr Genet*. 1987;8:69–72.
343. Petersen RA, Friend SH, Albert DM. Prolonged survival of a child with metastatic retinoblastoma. *J Pediatr Ophthalmol Strabismus*. 1987;24:247–248.
344. Rodriguez-Galindo C, Wilson MW, Haik BG, et al. Treatment of metastatic retinoblastoma. *Ophthalmology*. 2003;110:1237–1240.
345. Caselli D, Tamburini A, La Torre A, et al. High-dose

chemotherapy with autologous stem cell rescue for treatment of retinoblastoma: report of five cases. *Pediatr Transplant*. 2014;18:631–636.
346. Chantada G, Fandino A, Casak S, Manzitti J, Raslawski E, Schvartzman E. Treatment of overt extraocular retinoblastoma. *Med Pediatr Oncol*. 2003;40:158–161.
347. Gallie BL, Ellsworth RM, Abramson DH, Phillips RA. Retinoma: spontaneous regression of retinoblastoma or benign manifestation of the mutation? *Br J Cancer*. 1982;45:513–521.
348. Gallie BL, Phillips RA. Multiple manifestations of the retinoblastoma gene. *Birth Defects Orig Artic Ser*. 1982;18:689–701.
349. Aaby AA, Price RL, Zakov ZN. Spontaneously regressing retinoblastomas, retinoma, or retinoblastoma group 0. *Am J Ophthalmol*. 1983;96:315–320.
350. Margo C, Hidayat A, Kopelman J, Zimmerman LE. Retinocytoma. A benign variant of retinoblastoma. *Arch Ophthalmol*. 1983;101:1519–1531.
351. Lueder GT, Heon E, Gallie BL. Retinoma associated with vitreous seeding. *Am J Ophthalmol*. 1995;119:522–523.
352. Eagle RC Jr, Shields JA, Donoso L, Milner RS. Malignant transformation of spontaneously regressed retinoblastoma, retinoma/retinocytoma variant. *Ophthalmology*. 1989;96:1389–1395.
353. Balmer A, Munier F, Gailloud C. Retinoma. Case studies. *Ophthalmic Paediatr Genet*. 1991;12:131–137.
354. Bhatnagar R, Vine AK. Diffuse infiltrating retinoblastoma. *Ophthalmology*. 1991;98:1657–1661.
355. Mansour AM, Greenwald MJ, O'Grady R. Diffuse infiltrating retinoblastoma. *J Pediatr Ophthalmol Strabismus*. 1989;26:152–154.
356. Brisse HJ, Lumbroso L, Freneaux PC, et al. Sonographic, CT, and MR imaging findings in diffuse infiltrative retinoblastoma: report of two cases with histologic comparison. *AJNR Am J Neuroradiol*. 2001;22:499–504.
357. Kao LY. Diffuse infiltrating retinoblastoma: an inherited case. *Retina*. 2000;20:217–219.

358. Shields JA, Shields CL, Materin M. Diffuse infiltrating retinoblastoma presenting as a spontaneous hyphema. *J Pediatr Ophthalmol Strabismus*. 2000;37:311–312.
359. Grossniklaus HE, Dhaliwal RS, Martin DF. Diffuse anterior retinoblastoma. *Retina*. 1998;18:238–241.
360. Girard B, Brezin A, Gaumond MC, et al. Diffuse retinoblastoma – apropos of a case. *Bull Soc Ophtalmol Fr*. 1989;89:25–30.
361. Shields CL, Ghassemi F, Tuncer S, Thangappan A, Shields JA. Clinical spectrum of diffuse infiltrating retinoblastoma in 34 consecutive eyes. *Ophthalmology*. 2008;115:2253–2258.
362. Rubenfeld M, Abramson DH, Ellsworth RM, Kitchin FD. Unilateral vs. bilateral retinoblastoma. Correlations between age at diagnosis and stage of ocular disease. *Ophthalmology*. 1986;93:1016–1019.
363. Binder PS. Unusual manifestations of retinoblastoma. *Am J Ophthalmol*. 1974;77:674–679.
364. Sheta A. Some aspects on the different clinical characteristics of retinoblastoma. *Bull Ophthalmol Soc Egypt*. 1971;64:413–424.
365. Takahashi T, Tamura S, Inoue M, Isayama Y, Sashikata T. Retinoblastoma in a 26-year-old adult. *Ophthalmology*. 1983;90:179–183.
366. Singh AD, Santos CM, Shields CL, Shields JA, Eagle RC Jr. Observations on 17 patients with retinocytoma. *Arch Ophthalmol*. 2000;118:199–205.
367. Shields CL, Shields JA, Shah P. Retinoblastoma in older children. *Ophthalmology*. 1991;98:395–399.
368. Jakobiec FA, Tso MO, Zimmerman LE, Danis P. Retinoblastoma and intracranial malignancy. *Cancer*. 1977;39:2048–2058.
369. Bader JL, Miller RW, Meadows AT, Zimmerman LE, Champion LA, Voute PA. Trilateral retinoblastoma. *Lancet*. 1980;2:582–583.
370. Paulino AC. Trilateral retinoblastoma: is the location of the intracranial tumor important? *Cancer*. 1999;86:135–141.
371. Marcus DM, Brooks SE, Leff G, et al. Trilateral retinoblastoma: insights into histogenesis and management.

Surv Ophthalmol. 1998;43:59–70.
372. Kivela T. Trilateral retinoblastoma: a meta-analysis of hereditary retinoblastoma associated with primary ectopic intracranial retinoblastoma. *J Clin Oncol*. 1999;17:1829–1837.
373. Blach LE, McCormick B, Abramson DH, Ellsworth RM. Trilateral retinoblastoma–incidence and outcome: a decade of experience. *Int J Radiat Oncol Biol Phys*. 1994;29:729–733.
374. Shields CL, Meadows AT, Shields JA, Carvalho C, Smith AF. Chemoreduction for retinoblastoma may prevent intracranial neuroblastic malignancy (trilateral retinoblastoma). *Arch Ophthalmol*. 2001;119:1269–1272.
375. Bader JL, Meadows AT, Zimmerman LE, et al. Bilateral retinoblastoma with ectopic intracranial retinoblastoma: trilateral retinoblastoma. *Cancer Genet Cytogenet*. 1982;5:203–213.
376. Holladay DA, Holladay A, Montebello JF, Redmond KP. Clinical presentation, treatment, and outcome of trilateral retinoblastoma. *Cancer*. 1991;67:710–715.
377. de Jong MC, Kors WA, de Graaf P, Castelijns JA, Kivela T, Moll AC. Trilateral retinoblastoma: a systematic review and meta-analysis. *Lancet Oncol*. 2014;15:1157–1167.
378. Moll AC, Imhof SM, Schouten-Van Meeteren AY, Boers M. Trilateral retinoblastoma: is the location of the intracranial tumor important? *Cancer*. 2000;88:965–967.
379. Farnia B, Allen PK, Brown PD, et al. Clinical outcomes and patterns of failure in pineoblastoma: a 30-year, single-institution retrospective review. *World Neurosurg*. 2014;82:1232–1241.
380. Dunkel IJ, Jubran RF, Gururangan S, et al. Trilateral retinoblastoma: potentially curable with intensive chemotherapy. *Pediatr Blood Cancer*. 2010;54:384–387.

133

Cavernous Hemangioma

Anita Agarwal, Paul Sternberg Jr.

Introduction

Cavernous hemangioma of the retina is a rare vascular hamartoma. The tumor is composed of clumps of dark intraretinal aneurysms that demonstrate a characteristic "cluster-of-grapes" appearance. It is usually unilateral and rarely increases in size. The hemangioma is almost always asymptomatic, although mild visual disturbance as a result of macular involvement or vitreous hemorrhage has been

reported occasionally. Patients with this hamartoma may also have hemangiomas involving the skin and central nervous system. Several pedigrees with varying manifestations of the retinal and systemic characteristics have been reported consistent with an autosomal dominant pattern of inheritance.

Clinical Findings

Retinal cavernous hemangiomas are composed of clusters of saccular aneurysms filled with dark blood. There is no intervening retinal tissue between the aneurysms. The aneurysms range in size from microaneurysms to a half-disc diameter (DD).[1] The typical tumor is isolated, 1–2 DD in size, and resembles an intraretinal cluster of grapes (Fig. 133.1, see also Fig. 133.2).[2,3] However, the clinical appearance can be quite variable, ranging from a single aneurysm to a wide distribution over the entire fundus or following the course of a major vein (see Fig. 133.3). Commonly, layering of the red blood cells within the aneurysms causes a plasma–erythrocytic separation that has been called a "pseudohypopyon." Often a white or gray fibroglial membrane covers the surface of the tumor (see Fig. 133.3A). The adjacent retinal blood vessels appear unaffected by the tumor, with no evidence of feeder vessels. Although a mild lipid exudate has been reported adjacent to the hemangioma in one case,[4] exudation from the tumor is extremely rare either at presentation or with long-term follow-up. The slow circulation through the aneurysms is responsible for the lack of exudation of lipid or fluid.

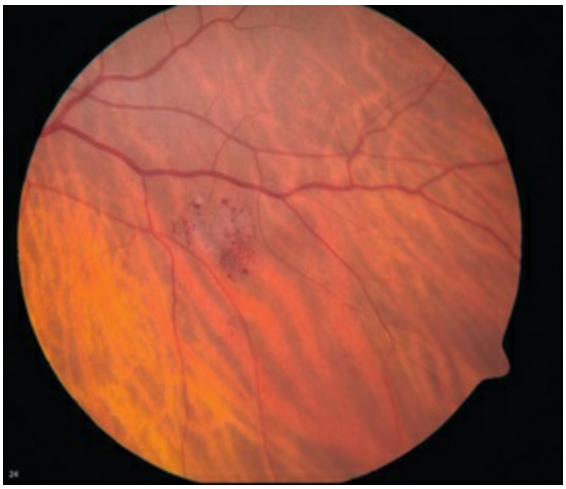

FIG. 133.1 Cavernous hemangioma of the retina. Note the layering of blood within the large aneurysm. Visual acuity is 20/20, and the patient is asymptomatic.

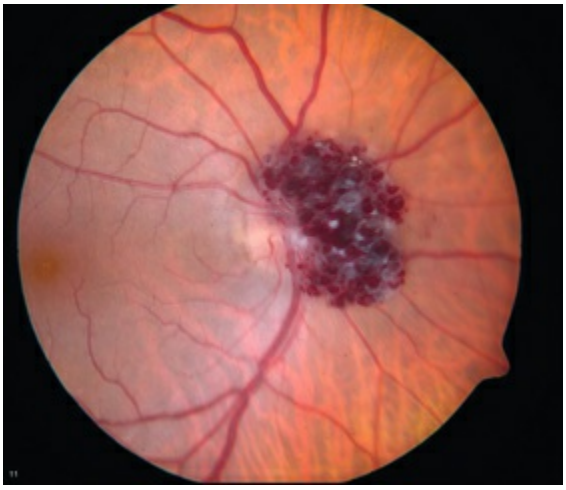

FIG 133.2 Cavernous hemangioma of the optic nerve head. Note the characteristic cluster of grapes appearance. Visual acuity was 20/15.

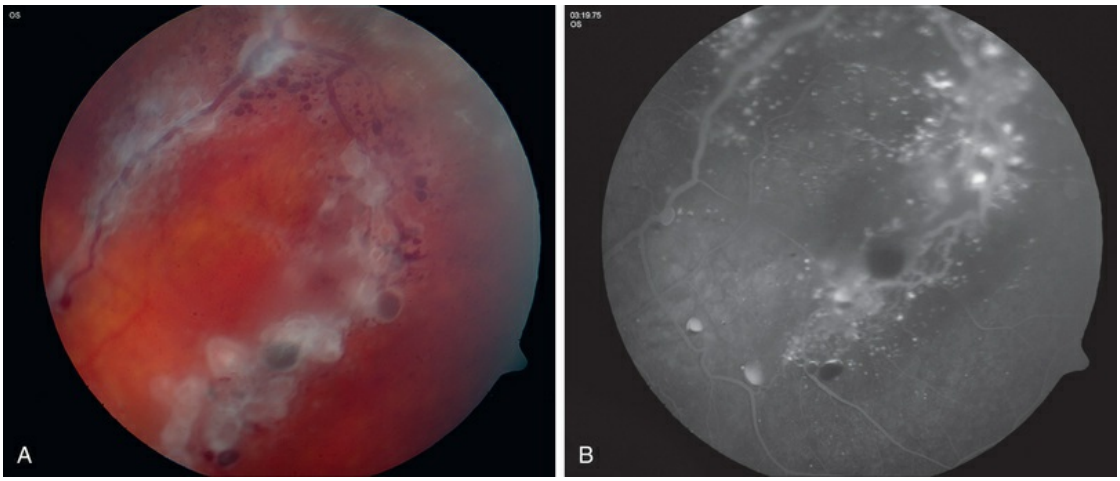

FIG. 133.3 (A) Involvement of the veins in addition to the capillaries. (B) Note extensive empty shells of the cavernomas in the vicinity of the veins that do not fill with fluorescein. (Courtesy of Stephen J. Kim, MD, reproduced with permission from Agarwal A, editor. Gass' atlas of macular diseases, 5th edition. Elsevier Inc. 2012.)

Retinal cavernous hemangiomas are symptomatic when they are located in or adjacent to the macula which has been reported in approximately 10% of the cases in the literature.[1,5,6] In these cases, visual acuity can be decreased on the basis of both tumor location and amblyopia. Visual disturbance can also result from vitreous hemorrhage. Cavernous hemangioma can cause simultaneous subretinal, intraretinal, and preretinal hemorrhage (Fig. 133.4). Although vitreous hemorrhage has been reported in 10% of retinal cavernous hemangiomas, it is usually minimal and unassociated with long-term loss of visual acuity.[1] However, vitreous hemorrhage, if it occurs in a child, may cause amblyopia.[7] One patient who presented at birth with hyphema and vitreous hemorrhage suffered recurrences over 52 years eventually requiring enucleation for glaucoma and pain.[8] The tumor extension into the ciliary body in this case was the cause of the recurrent hyphemas.

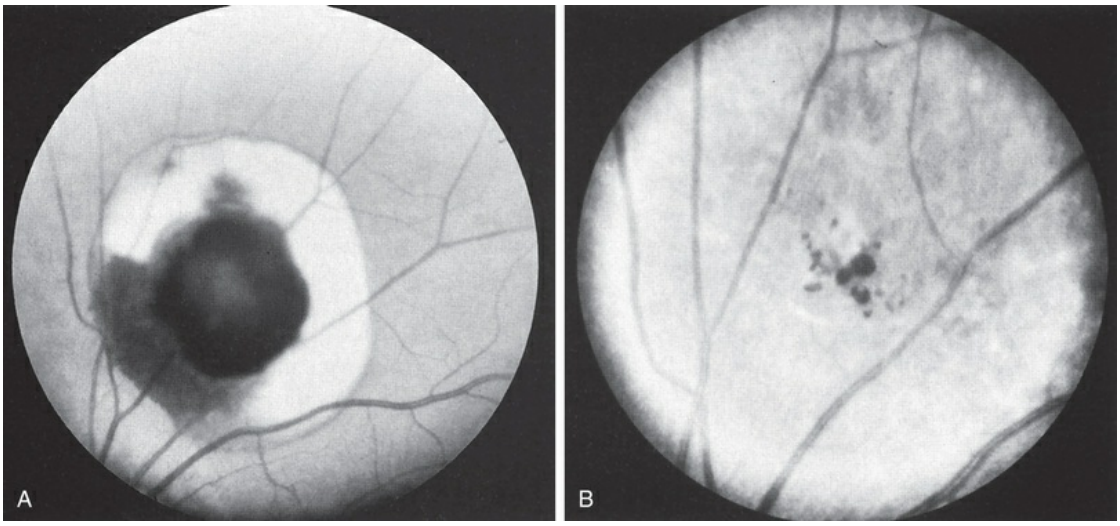

FIG. 133.4 (A) Patient with a combined preretinal, intraretinal, and subretinal hemorrhage. (B) When the blood cleared, a typical cavernous hemangioma of the retina could be seen. (Courtesy of Lawrence Yannuzzi, MD.)

Cavernous hemangiomas have also been reported to be located on the optic nerve head.[9–11] These tumors have a clinical appearance similar to the retinal lesions (Fig. 133.2). An enlarged blind spot may be demonstrated on the visual field, but visual acuity is normal. Gündüz et al.[12] described a patient with a cavernous hemangioma in the superonasal quadrant of the fundus and unilateral decreased visual acuity, with associated red–green color defect. Cone response and 30-Hz flicker responses were nearly absent. More recently, a 22-month-old child with unilateral macular cavernous hemangioma was noted to also have peripheral nonperfusion in both eyes on wide-field angiography. Whether this is a true association or a coincidence was not able to be determined.[13] The present understanding is that cavernous hemangiomas are isolated ocular lesions except in familial cases where they are associated with cavernomas in the brain, and very occasionally in the spinal cord.

Differential Diagnosis

The characteristic appearance of a retinal cavernous hemangioma is rarely confused with other conditions. Retinal telangiectasis can have a similar appearance, and several authors have suggested that

older cases of cavernous hemangioma were mistakenly called Coats' disease or Leber's miliary aneurysms.[3,9,14] The lack of intraretinal exudate distinguishes this tumor from Coats' disease, but the differentiation from Leber's can be more difficult. Gass points out that the retinal telangiectasis of Leber's miliary aneurysms is a progressive condition affecting the integrity and structure of the "intrinsic" vasculature, whereas the cavernous hemangioma is a sessile tumor projecting from and partly isolated from the retinal blood vessels.[8] On the other hand, Giuffre[15] reported a case with a cavernous hemangioma and retinal telangiectasis closely located in the same eye, suggesting a relation between these two developmental conditions. Telangiectatic or microaneurysmal vascular dilation can also be seen as late sequelae in branch vein occlusions and diabetic retinopathy but should be easily differentiated from retinal cavernous hemangioma by the associated features.

Cavernous hemangioma can be distinguished from retinal capillary hemangioma (von Hippel disease) relatively easily. The capillary hemangioma is a discrete tumor with characteristic feeder and draining vessels. It is often accompanied by adjacent lipid exudate or exudative retinal detachment.

Racemose hemangioma (Wyburn Mason syndrome) is another retinal vascular anomaly where dilation of the larger retinal vessels with direct arteriovenous anastomosis is seen, and this lesion should not be confused with cavernous hemangioma.

Ancillary Studies

Fluorescein angiography may show autofluorescence of the gray–white epiretinal membrane overlying the tumor. The aneurysms will fill slowly and often incompletely up to 30 minutes after dye injection. Dye will rarely extravasate from the tumor in the late phase of the angiogram. In addition, the plasma–erythrocytic separation often seen on clinical examination is dramatically demonstrated in the later phases of the angiogram. The fluorescein collects in the superior portion of the aneurysm, with the gravitated blood cells blocking its accumulation in the inferior area (Fig. 133.5 and see Fig. 133.3B). While optical coherence tomography (OCT) is

not typically required to make the diagnosis, which tends to be a clinical one, it may demonstrate associated features such as an epiretinal membrane.[16]

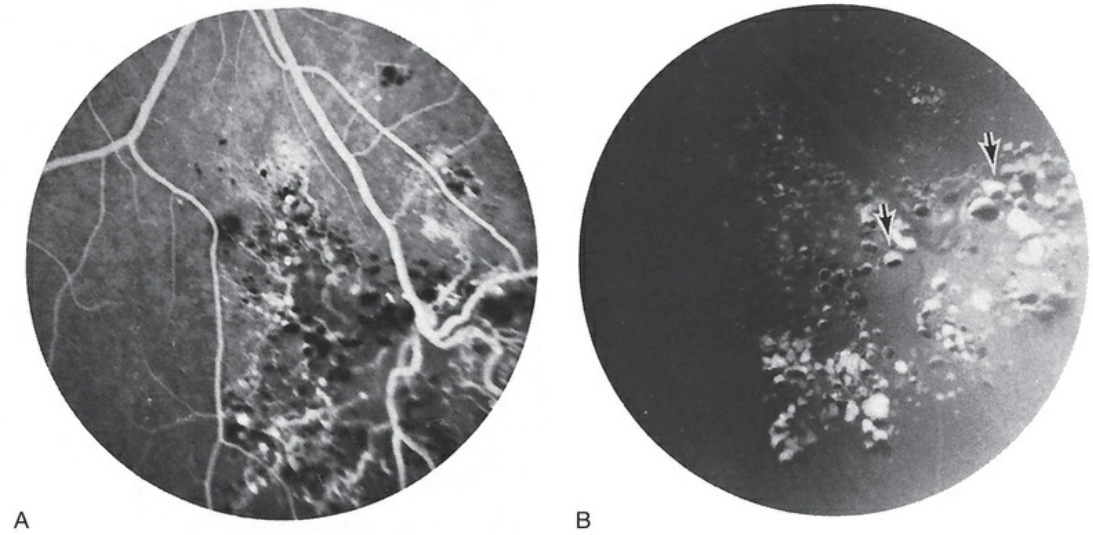

FIG. 133.5 Fluorescein angiography of cavernous hemangioma of the retina. (A) Slow and often incomplete filling of the aneurysms. (B) Plasma–erythrocytic separation in the late phases. (Courtesy of J. Donald M. Gass, MD, reproduced with permission from Agarwal A, editor. Gass' atlas of macular diseases, 5th edition. Elsevier Inc. 2012.)

Although performing echography is rarely necessary, the ultrasonographic features have been described by Shields[3] in cases in which diagnosis was rendered difficult by vitreous hemorrhage. A-scan shows a high initial spike and high internal reflectivity. B-scan shows an irregular surface, large internal acoustic density, and absence of choroidal excavation. Many cavernous hemangiomas are too small to exhibit a characteristic echographic pattern.

Natural History

Growth of a retinal cavernous hemangioma is exceedingly rare. Klein et al.[4] reported the only case of enlargement, and this developed after photocoagulation. Messmer et al.[1] noted enlargement of the fibroglial component, which may represent progressive thrombosis of some of the aneurysms. In a later report,

Kushner et al.[17] monitored two patients over 5–10 years and reported definitive growth.

Visual loss can occur from growth of an associated epiretinal membrane.[18] In addition, macular pucker has been reported separate from the membrane overlying the hemangioma; the membrane and the tumor in this case were probably unrelated.[1] Vitreoretinal or vitreopapillary traction may occur occasionally.[19]

Vitreous hemorrhage is the most common cause of progressive visual disturbance in patients with cavernous hemangioma. Although usually mild due to slow blood flow through the hemangioma, isolated cases of severe hemorrhage have been reported.[20–22] Impairment of visual acuity from vitreous hemorrhage is a very uncommon event.

Treatment

Because cavernous hemangiomas rarely increase in size or cause lipid exudation or severe vitreous hemorrhage, these tumors generally do not require treatment. Photocoagulation or cryotherapy has been advocated if vitreous hemorrhage occurs. However, Gass[9] has reported one case of vitreous hemorrhage following xenon photocoagulation, and Klein et al.[4] described a patient in whom the hemangioma enlarged greatly after xenon treatment. The value of laser treatment or cryopexy remains unproven and periodic observation is standard care. However, for rare cases of nonclearing vitreous hemorrhage, vitrectomy has proved to be effective. Haller and Knox[22] reported a case of dense, nonclearing vitreous hemorrhage due to persistent vitreous traction to a cavernous hemangioma of the optic disc. During vitrectomy, the vitreopapillary traction was relieved and the preretinal portion of the hamartoma was excised. Minimal bleeding occurred and was easily controlled with intraocular diathermy. Vision improved from light perception to 20/40.

Pathology

Histopathologic study of retinal cavernous hemangioma demonstrates a tumor arising from the inner half of the retina (Fig.

133.6).[23] The tumor comprises of multiple endothelial-lined, thin-walled aneurysms. These aneurysms are separated by thin, fibrous septa. There is no evidence of intraretinal or subretinal exudate.

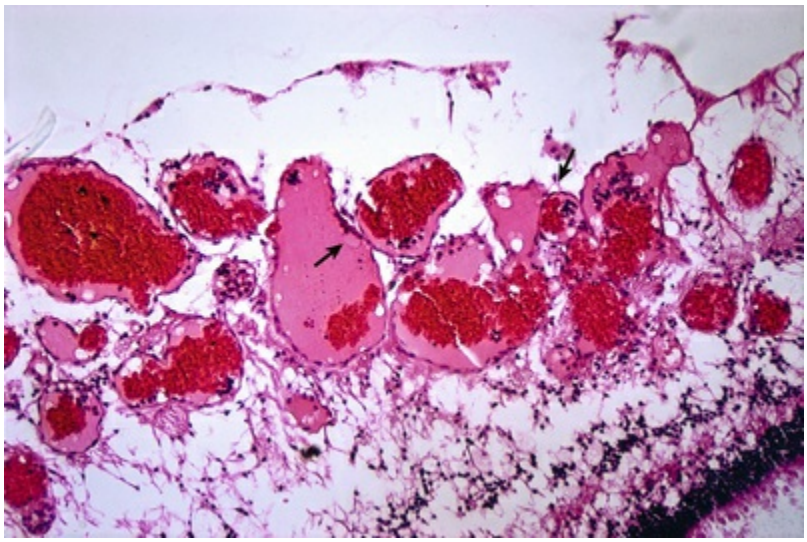

FIG. 133.6 Histologic examination of a cavernous hemangioma of the retina shows multiple endothelial-lined vascular saccules (*arrow*). (Courtesy of J. Donald M. Gass, MD. Reproduced with permission from Agarwal A, editor. Gass' atlas of macular diseases, 5th edition. Elsevier Inc. 2012.)

The cavernous hemangioma is a localized vascular hamartoma arising from the capillaries and is partly isolated from the normal vascular tree as seen on fluorescein angiography.[24] Electron microscopy performed on an eye enucleated for leukocoria in a 6-month-old infant showed the aneurysms to be lined by nonfenestrated, flat endothelial cells with terminal bars on the luminal side and a thin basement membrane.[25] Pericytes were also present. The vessels were surrounded by processes of fibrous astrocytes invested by a basal lamina. These features of normal retinal vessels in association with the slow flow through the vascular abnormality probably account for the lack of exudates and hemorrhage.[24]

A preretinal membrane can overlie the tumor and contains processes of fibrous astrocytes with cytoplasmic filaments. The membrane is attached to the internal limiting membrane (ILM) but is also directly connected to the inner retina through breaks in the

ILM. Immunohistochemistry shows the presence of glial fibrillary acidic protein (GFAP) both intraretinally and in the preretinal membrane. These characteristics support a glial origin for the preretinal membrane.

Systemic and Familial Involvement

Reports of several individuals and pedigrees with retinal cavernous hemangiomas, as well as cutaneous and central nervous system angiomatous lesions, led to the concept that this entity is part of a neuro-oculocutaneous syndrome. Weskamp and Cotlier[26] first reported such a patient with occipital cutaneous angiomas, intracranial calcifications, and seizures who turned out to have a cavernous hemangioma in the pre-Rolandic area of the cerebral cortex diagnosed at the time of craniotomy. Subsequently, several familial cases have been seen, and it is now established that the incidence is higher in Hispanic Americans than non-Hispanic Americans.[6]

A variety of cutaneous lesions have been reported in association with this tumor.[27–30] Most commonly patients have cutaneous capillary malformations on the back of the neck. However, Schwartz et al.[29] reported a patient with cutaneous angiomas on the abdomen, and Mildner discussed a 14-year-old with a cavernous hemangioma of the chest.[28] In addition, Gautier-Smith et al.[27] have reported an association with angioma serpiginosum, a progressive condition with widespread dilation of subpapillary venous plexuses. These cutaneous lesions are associated with motor and sensory loss and have peripheral nerve involvement.[27–30]

Angiomas of the central nervous system are the more consistent association with retinal cavernous hemangiomas. In fact, cerebrocavernous malformations (CCMs) are far more common than retinal cavernomas. The overall incidence of cerebrocavernous hemangioma is between 0.1% and 0.5% in the general population. Only 5% of these patients have an associated retinal hemangioma. Among those with CCMs, the proportion of familial cases has been estimated to be as high as 50% in Hispanic American patients and 10–40% in other populations. In addition to the patient reported by Weskamp and Cotlier,[26] Gass[9] has reported one patient with a

retinal cavernous hemangioma and seizures whose father had cavernous hemangiomas of the midbrain, pons, and cerebellum. He reported another patient with a retinal cavernous hemangioma, a cutaneous angioma, and seizures who had a child who died after excision of the cavernous hemangioma of the third and lateral ventricles.[24] Schwartz et al.[29] reported a patient with a retinal cavernous hemangioma, cutaneous angiomas, and a cerebrovascular lesion consistent with cavernous hemangioma on computed tomography (CT) scan and magnetic resonance imaging (MRI). Subsequently, Pancurak et al.[5] reported a family with two members having CT scans consistent with cavernous hemangioma of the brain. Bell et al.[31] reported a case of bilateral cavernous hemangioma associated with a cavernous hemangioma in the left parietal lobe. Most recent is the report by Sarraf et al.[32] of a family of 12 affected members spanning three generations. The proband had multiple CCMs and a choroidal hemangioma; her son had a retinal cavernous hemangioma; her daughter had CCMs; a sister manifested cutaneous hemangiomas, CCMs, and a choroidal hemangioma; and her father had multiple cutaneous hemangiomas. This is the first association with choroidal hemangioma.[32]

CCMs occur predominantly in the cerebrum and pons, rarely in the spinal cord, and about 60% are symptomatic (Fig. 133.7).[33] They can present with focal or generalized seizures (45%), cerebral hemorrhages (41%), focal neurologic deficits, or headaches.[34] Some 40% of patients with cavernous hemangioma of the brain have calcifications apparent on skull radiographs,[35] but CT is currently the best diagnostic procedure to demonstrate calcium. MRI is most sensitive of all imaging modalities. Gradient echo sequences can identify three times more lesions than turbo spin echo on MRI and is recommended. Four specific MRI patterns have been identified based on the hemangioma characteristics, presence of old or fresh blood, and calcium.[5,36] A perilesional dark halo appearance on MRI is one characteristic feature of CCMs due to hemosiderin laden macrophages around the malformations.[37]

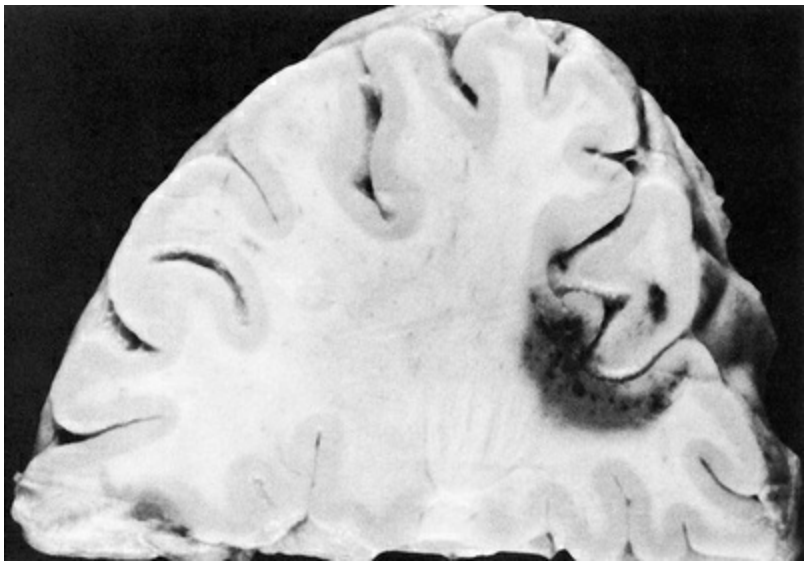

FIG. 133.7 Discrete and confluent cavernous angiomas are present in the cortex and subcortical white matter. The lesions were found incidentally at autopsy. (Reproduced with permission from Rubenstein LJ. Tumors of the central nervous system. Washington, DC: Armed Forces Institute of Pathology; 1972.)

Patients have also been reported with extraocular muscle paresis. Although this may be related to a cavernous hemangioma of the midbrain, Yen and Wu[38] have reported a patient with agenesis of the internal carotid artery associated with retinal cavernous hemangioma and bilateral oculomotor palsies.

Genetics

Several pedigrees have been reported with cavernous hemangioma of the retina in which various family members had retinal, cutaneous, or neurologic lesions. The most extensive pedigree, reported by Goldberg et al.,[19] spanned four generations. One daughter had a retinal cavernous hemangioma, another daughter had seizures and cutaneous lesions, six relatives had seizures, and 14 other relatives had cutaneous vascular lesions. In a family reported by Pancurak et al.[5] the proband had a retinal cavernous hemangioma, his sister had cavernous hemangiomas of both retina and brain, his mother had a cavernous hemangioma of the brain, and a niece had a retinal cavernous hemangioma.

Three separate genes have been identified in association with

familial CCMs: *CCM1/KRIT1*, *CCM2/MGC4607*, and *CCM3/PDCD10*.[34,39–42] *CCM1* is located at chromosome locus 7q11-q22 and was the first one identified with the familial form of CCMs. Linkage studies have shown that a *CCM1* mutation is involved in 40–53% of familial CCMs and nearly half of these patients have neurologic manifestations before 25 years of age.[43,44] The product of *CCM1*, named Krev interaction trapped 1 or KRIT1, is an ankyrin repeat-containing protein that interacts with RAP-1A (Krev-1), which is a member of the RAS family of GTPases.[43,44] *CCM2* is located at 7p15–13; mutations in this gene are involved in up to 25–40% of familial CCMs. Patients with CCM2-associated disease have a lower number of gradient-echo sequence lesions than those with *CCM1* or *CCM3* disease, and the number of lesions increases less rapidly with age than in patients with *CCM1* disease. *CCM3*, localized at 3q25.2-q27, encodes programmed cell death protein 10 (PDCD10) and is the most recently discovered gene involved in familial CCMs.[45]

CCM3 mutation carriers are less common (10%) than *CCM1* or *CCM2* carriers, but they have near 100% penetrance and these patients are more likely to present with hemorrhage and have symptoms before 15 years of age.

References

1. Messmer E, Laqua H, Wessing A, et al. Nine cases of cavernous hemangioma of the retina. *Am J Ophthalmol*. 1983;95:383–390.
2. Colvard DM, Robertson DM, Trautmann JC. Cavernous hemangioma of the retina. *Arch Ophthalmol*. 1978;96:2042–2044.
3. Shields J. *Diagnosis and management of intraocular tumors*. Mosby: St. Louis; 1987.
4. Klein M, Goldberg MF, Cotlier E. Cavernous hemangioma of the retina: report of four cases. *Ann Ophthalmol*. 1975;7:1213–1221.
5. Pancurak J, Goldberg MF, Frenkel M, et al. Cavernous hemangioma of the retina. Genetic and central nervous system involvement. *Retina*. 1985;5:215–220.

6. Naftchi S, la Cour M. A case of central visual loss in a child due to macular cavernous haemangioma of the retina. *Acta Ophthalmol Scand*. 2002;80:550–552.
7. Yamaguchi K, Tamai M. Cavernous hemangioma of the retina in a pediatric patient. *Ophthalmologica*. 1988;197:127–129.
8. Shields JA, Eagle RC Jr, Ewing MQ, et al. Retinal cavernous hemangioma: fifty-two years of clinical follow-up with clinicopathologic correlation. *Retina*. 2014;34(6):1253–1257.
9. Gass JD. Cavernous hemangioma of the retina: a neuro-oculo-cutaneous syndrome. *Am J Ophthalmol*. 1971;71:799–814.
10. Nicholson DH. Tumors of the optic disc. *Trans Sect Ophthalmol Am Acad Ophthalmol Otolaryngol*. 1977;83:751–754.
11. Drummond JW, Hall DL, Steen WH Jr, et al. Cavernous hemangioma of the optic disc. *Ann Ophthalmol*. 1980;12:1017–1018.
12. Gündüz K, Ozbayrak N, Okka M, et al. Cavernous hemangioma with cone dysfunction. *Ophthalmologica*. 1996;210:367–371.
13. Rao P, Abbey AM, Yonekawa Y, et al. Macular cavernous hemangioma associated with peripheral vascular anomalies and nonperfusion. *Ophthalmic Surg Lasers Imaging Retina*. 2015;46(7):764–767.
14. Lewis RA, Cohen MH, Wise GN. Cavernous haemangioma of the retina and optic disc: a report of three cases and a review of the literature. *Br J Ophthalmol*. 1975;59:422–434.
15. Giuffre G. Cavernous hemangioma of the retina and retinal telangiectasis. Distinct or related vascular malformations? *Retina*. 1985;5:221–224.
16. Kavoussi SC, Brinton GS. Epiretinal membrane demonstrated by optical coherence tomography in a patient with retinal cavernous hemangioma. *JAMA Ophthalmol*. 2015;133(8):e151163.
17. Kushner MS, Jampol LM, Haller JA. Cavernous hemangioma of the optic nerve. *Retina*. 1994;14:359–361.
18. Shukla D, Sharan A. Epimacular membrane secondary to an

optic nerve head lesion. *Br J Ophthalmol*. 2012;96(7):1038–1039 [1048].
19. Goldberg RE, Pheasant TR, Shields JA. Cavernous hemangioma of the retina: a four-generation pedigree with neurocutaneous manifestations and an example of bilateral retinal involvement. *Arch Ophthalmol*. 1979;97:2321–2324.
20. Witmer R, Verrey F, Speiser P. Retinal angiomatosis: atypical cases of retinal angiomatosis and telangiectases. *Bibl Ophthalmol*. 1968;76:113–123.
21. Gíslason I, Stenkula S, Alm A, et al. Cavernous haemangioma of the retina. *Acta Ophthalmol (Copenh)*. 1979;57:709–717.
22. Haller JA, Knox DL. Vitrectomy for persistent vitreous hemorrhage from a cavernous hemangioma of the optic disk. *Am J Ophthalmol*. 1993;116:106–107.
23. Agarwal A. *Gass' atlas of macular diseases*. Elsevier: Philadelphia; 2011.
24. Gass J. *Differential diagnosis of intraocular tumors: a stereoscopic presentation*. Mosby: St. Louis; 1974.
25. Messmer E, Font RL, Laqua H, et al. Cavernous hemangioma of the retina. Immunohistochemical and ultrastructural observations. *Arch Ophthalmol*. 1984;102:413–418.
26. Weskamp C, Cotlier I. Angioma del cerebro y de la retina con malformaciones capilares de la piel. *Arch Oftalmol B Aires*. 1940;15:1–10.
27. Gautier-Smith PC, Sanders MD, Sanderson KV. Ocular and nervous system involvement in angioma serpiginosum. *Br J Ophthalmol*. 1971;55:433–443.
28. Mildner I. Cavernous hemangioma of the retina as a symptom of phakomatosis. *Ber Zusammenkunft Dtsch Ophthalmol Ges*. 1972;71:610–613.
29. Schwartz AC, Weaver RG Jr, Bloomfield R, et al. Cavernous hemangioma of the retina, cutaneous angiomas, and intracranial vascular lesion by computed tomography and nuclear magnetic resonance imaging. *Am J Ophthalmol*. 1984;98:483–487.
30. Backhouse O, O'Neill D. Cavernous haemangioma of retina

and skin. *Eye (Lond)*. 1998;12:1027–1028.
31. Bell D, Yang HK, O'Brien C. A case of bilateral cavernous hemangioma associated with intracerebral hemangioma. *Arch Ophthalmol*. 1997;115:818–819.
32. Sarraf D, Payne AM, Kitchen ND, et al. Familial cavernous hemangioma: an expanding ocular spectrum. *Arch Ophthalmol*. 2000;118:969–973.
33. Rubenstein L. *Tumors of the central nervous system*. Armed Forces Institute of Pathology: Washington, DC; 1972.
34. Labauge P, Denier C, Bergametti F, et al. Genetics of cavernous angiomas. *Lancet Neurol*. 2007;6:237–244.
35. Giombini S, Morello G. Cavernous angiomas of the brain: account of fourteen personal cases and review of the literature. *Acta Neurochir (Wien)*. 1978;40:61–82.
36. Vaquero J, Leunda G, Martínez R, et al. Cavernomas of the brain. *Neurosurgery*. 1983;12:208–210.
37. Chan AC, Drakos SG, Ruiz OE, et al. Mutations in 2 distinct genetic pathways result in cerebral cavernous malformations in mice. *J Clin Invest*. 2011;121(5):1871–1881.
38. Yen MY, Wu CC. Cavernous hemangioma of the retina and agenesis of internal carotid artery with bilateral oculomotor palsies. *J Clin Neuroophthalmol*. 1985;5:258–262.
39. Ji BH, Qin W, Sun T, et al. A novel deletion mutation in CCM1 gene (krit1) is detected in a Chinese family with cerebral cavernous malformations. *Yi Chuan Xue Bao*. 2006;33:105–110.
40. Campione E, Terrinoni A, Orlandi A, et al. Cerebral cavernomas in a family with multiple cutaneous and uterine leiomyomas associated with a new mutation in the fumarate hydratase gene. *J Invest Dermatol*. 2007;127:2271–2273.
41. Stahl S, Gaetzner S, Voss K, et al. Novel CCM1, CCM2, and CCM3 mutations in patients with cerebral cavernous malformations: in-frame deletion in CCM2 prevents formation of a CCM1/CCM2/CCM3 protein complex. *Hum Mutat*. 2008;29:709–717.
42. Lee YW, Lee ST, Cha JG, et al. A novel KRIT1 gene mutation in a patient with cerebral and multiple spinal cavernous

malformations. *Ann Clin Lab Sci*. 2010;40:290–294.
43. Denier C, Gasc JM, Chapon F, et al. Krit1/cerebral cavernous malformation 1 mRNA is preferentially expressed in neurons and epithelial cells in embryo and adult. *Mech Dev*. 2002;117:363–367.
44. Denier C, Goutagny S, Labauge P, et al. Société Française de Neurochirurgie. Mutations within the MGC4607 gene cause cerebral cavernous malformations. *Am J Hum Genet*. 2004;74:326–337.
45. Chen L, Tanriover G, Yano H, et al. Apoptotic functions of PDCD10/CCM3, the gene mutated in cerebral cavernous malformation 3. *Stroke*. 2009;40:1474–1481.

134

Hemangioblastoma of the Retina and Von Hippel–Lindau Disease

Henry E. Wiley, Andrew P. Schachat, Emily Y. Chew

Introduction

Retinal hemangioblastoma (RH), also called retinal capillary hemangioma, retinal capillary hemangioblastoma, or retinal angioma, is a benign neoplasm with vascular features originating in the neurosensory retina or optic disc. RHs typically occur in the setting of von Hippel–Lindau (VHL) disease, an autosomal dominantly inherited condition in which mutations in the Von Hippel–Lindau tumor suppressor gene, *VHL*, lead to development of characteristic benign and malignant neoplasms or cysts in the central nervous system and viscera. Solitary RH can arise sporadically in the absence of VHL disease. Diagnosis of VHL disease in affected individuals is critically important, given the life-threatening nature of some of its manifestations and the benefits of surveillance and timely intervention, and can be made based on clinical criteria and/or genetic testing for mutations in the *VHL* gene.

Von Hippel–Lindau Disease

VHL disease (Online Mendelian Inheritance in Man (OMIM) #193300) is an autosomal dominantly inherited multisystem neoplasia disorder arising from mutations in the *VHL* gene. Cardinal manifestations include RH, brain and spinal cord hemangioblastoma, renal cell carcinoma, pheochromocytoma, endolymphatic sac tumor, epididymal and broad ligament cystadenomas, pancreatic neuroendocrine tumors, and renal and pancreatic cysts.[1] VHL disease has an approximate incidence of 1 in 36,000 live births, and a penetrance of over 90% by 65 years of age.[2]

Improvements in early diagnosis, surveillance, and treatment have led to a better prognosis, and a multispecialty team is helpful for optimal management of this complex condition.

History

Over a century ago, von Hippel described RHs in several generations of a small number of families.[3] In 1926, the Swedish pathologist Lindau observed the link between retinal and cerebellar hemangioblastomas and the association with cysts in the kidney, pancreas, and epididymis as features of a familial syndrome.[4] Melmon and Rosen established the first clinical diagnostic criteria for VHL disease in a landmark paper in 1965.[5] Seizinger and colleagues discovered the linkage of the VHL gene to the short arm of chromosome 3 in 1988,[6] and Latif and colleagues identified the VHL tumor suppressor gene shortly thereafter in 1993.[7]

The VHL Gene and Protein

Von Hippel-Lindau disease is caused by mutation in the VHL tumor suppressor gene, *VHL*, located on chromosome 3 (3p25-26).[7] The product of the gene, the VHL protein (pVHL), has been found to play a key role in cellular oxygen-sensing, and an understanding of its function has not only provided insight into the molecular pathology of VHL disease but also a better understanding of cell signaling and function under normoxic and hypoxic conditions.[8] *VHL* is ubiquitously expressed and encodes 213 amino acid and 160 amino acid isoforms of pVHL, which are both thought to exhibit similar tumor suppressor activity.[9] pVHL serves as the substrate-recognition subunit of a ubiquitin ligase complex that assigns proteins for proteasomal degradation. Among the targets of this ubiquitin ligase are the transcription factor subunits hypoxia-inducible factor 1α (HIF-1α) and hypoxia-inducible factor-2α (HIF-2α), which undergo prolyl hydroxylation under normoxic conditions, allowing for binding to pVHL and attachment of ubiquitin peptides that result in their proteasomal degradation.[10,11] Under hypoxic conditions, or in the absence of normal pVHL, HIF-1α and HIF-2α are not degraded, form heterodimers with hypoxia-

inducible factor 1β (HIF-1β), and act as transcription factors for a wide array of target genes. Over 800 known genes regulated directly by HIFs play a variety of roles in orchestrating the cell's response to hypoxia.[8] Among the proteins upregulated by HIF signaling are a number promoting cell proliferation and survival, such as transforming growth factor-alpha and epidermal growth factor receptor, and others promoting angiogenesis, such as vascular endothelial growth factor (VEGF) and platelet-derived growth factor (PDGF), which have been hypothesized to play a role in development of neoplasms in VHL disease, including RH.[12–16] pVHL has other actions independent of HIF signaling, but the significance of these for development of VHL disease is unknown.[8]

The majority of individuals with VHL disease inherit a mutant copy of the VHL tumor suppressor gene from an affected parent, and a wild-type (normal) copy of the gene from the other parent. Knudson's two-hit model for tumorigenesis states that neoplasia results from the somatic inactivation of the normal allele in one or more cells of an individual with a germline mutation in the other allele.[17] In a large study evaluating 181 kindreds with VHL disease, 42 cases (23%) presented absent any suggestive family history, indicating a putative first-generation diagnosis.[18] Mosaicism, in which somatic mutation occurs during embryogenesis and leads to affected and nonaffected tissues within a single individual, explains occasional germline transmission from an apparently unaffected parent in which only certain tissues are affected, and also explains occasional cases in which VHL disease manifests clinically but initial genetic testing is negative for mutation.[19,20] Stolle and colleagues published a report in 1998 on genetic testing methods that allowed for identification of germline mutations in 93/93 (100%) of families with VHL disease, establishing the value of *VHL* gene testing for diagnosis of this condition.[21]

Mutations of *VHL* resulting in VHL disease are highly varied, and range from basepair substitution in a single amino acid codon to the complete deletion of the gene.[22,23] Although many of these mutations are thought to impair pVHL regulation of HIF signaling, the pleomorphic manifestations of VHL disease suggest that distinct mutations may affect pVHL function in different ways, and possibly even confer novel functions.[24] Early work on correlation of

genotype and phenotype suggests that different types of *VHL* mutation may result in particular disease manifestations. For example, the location of a missense mutation in *VHL* correlates significantly with the presence and phenotype of ocular VHL disease, which influences visual acuity loss in different subgroups of patients.[25]

Clinical Features of Ocular Von Hippel-Lindau Disease

RHs are among the most common manifestations of VHL disease, but accurate prevalence of ocular involvement has been difficult to ascertain from case series. In a large cohort in which patients and affected family members were identified based on a diagnosis of VHL disease, and not on the basis of visual symptoms, 335/890 (38%) patients of 220 unrelated pedigrees were found to have ocular involvement.[26] Forty-two percent of those with ocular VHL disease had unilateral involvement, and 58% had bilateral involvement. Eighty-five percent of affected eyes manifested RHs exclusively in peripheral (extrapapillary) retina, 8% had RHs exclusively in proximity to the optic disc, and 7% had RHs in both the peripheral retina and juxtapapillary regions. Among the 421 eyes with peripheral RHs, the tumor count ranged from 1 to 11 (mean 2.5 ± 1.8). Those affected were from 7 to 84 years old (mean 36 years old, standard deviation ± 15 years), and 151/335 (45%) were male. Interestingly, although passage of time results in new tumor formation in some individuals, in this cohort age was not significantly associated with the number of peripheral RHs (p=.61).

The initial clinical appearance of an extrapapillary RH is that of a subtle red or grayish dot no larger than a few hundred micrometers, with an ophthalmoscopic appearance similar to that of a dilated capillary, microaneurysm, or small intraretinal hemorrhage (Fig. 134.1). Small tumors are sessile, but with growth they often become more nodular (Fig. 134.2). Feeding and draining blood vessels characteristically appear as the tumor grows larger and become progressively tortuous and enlarged (Fig. 134.3). At this stage, extrapapillary tumors become variably exudative, with

development of retinal edema and hard exudates around the tumor and/or in the macula (Fig. 134.3). Without treatment, large or multiple RHs can grow and displace the normal structures of the retina, and occasionally cause exudative retinal detachment (Fig. 134.4). The epiretinal fibrous proliferation and posterior hyaloid contraction that can accompany large RHs can cause macular epiretinal membrane and macular thickening, vitreomacular traction, or traction retinal detachment. Preretinal or vitreous hemorrhage is unusual in untreated tumors, but can occur. Neovascularization of the iris, neovascular glaucoma, and phthisis bulbi can occur in eyes with large or multiple tumors. A significant majority of RHs exhibit growth over time, but occasionally untreated tumors will remain static for considerable periods, and rarely they regress spontaneously.[27]

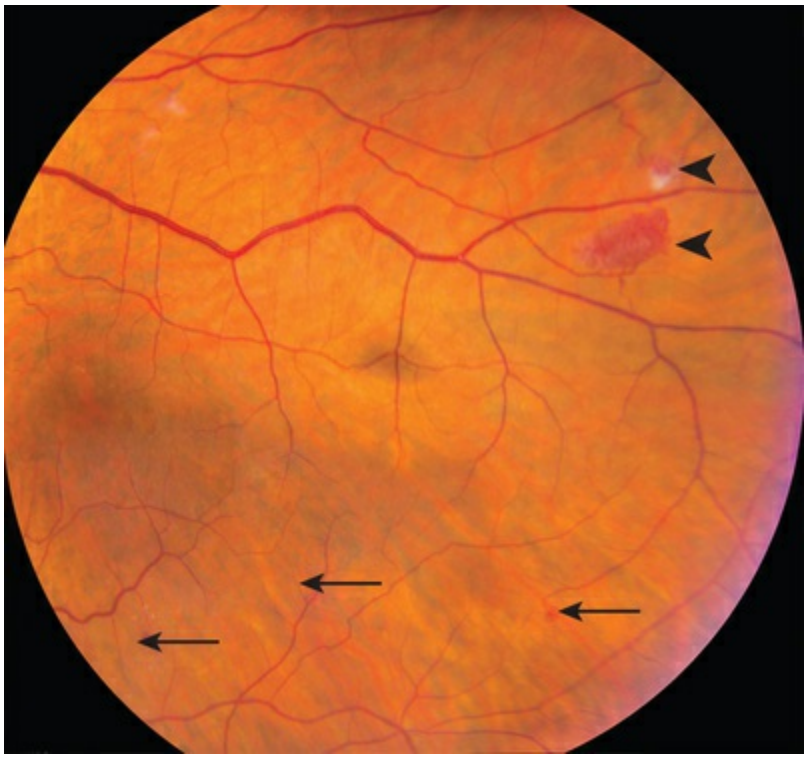

FIG. 134.1 Small retinal hemangioblastomas. Five small retinal hemangioblastomas at various stages of early development are visible in temporal retina posterior to the equator. The smallest three lesions (*arrows*) are subtle and can easily be overlooked. The largest two lesions (*arrowheads*) remain sessile (flat) and show easily visible early afferent and efferent

vessels. The most superior lesion shows some early associated epiretinal proliferation. (National Eye Institute, Bethesda, MD.)

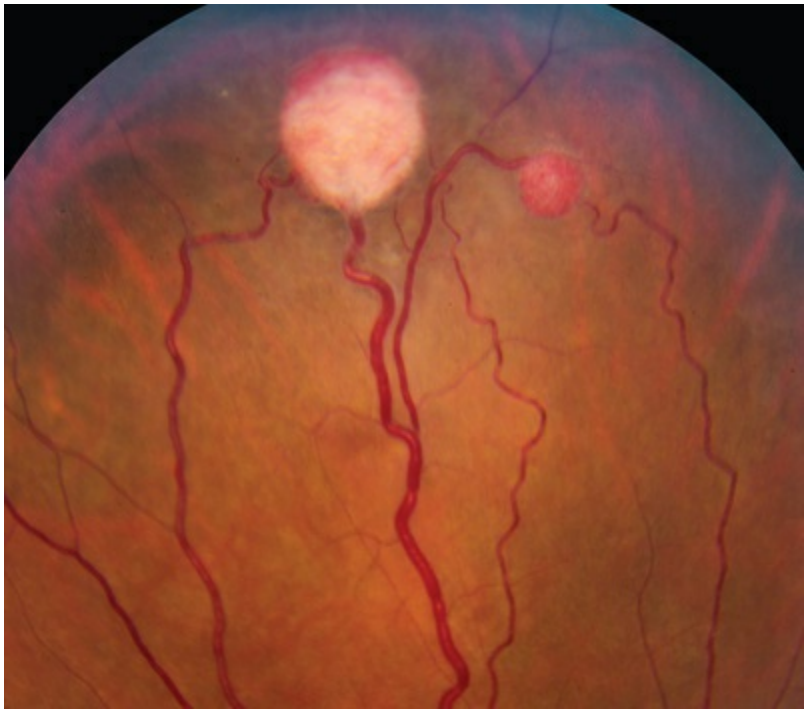

FIG. 134.2 Fully developed retinal hemangioblastomas. Two nodular hemangioblastomas manifest well-developed afferent and efferent vessels, without any associated exudation. The larger lesion is approximately 1.5 mm in diameter and shows epiretinal proliferation on its surface. (National Eye Institute, Bethesda, MD.)

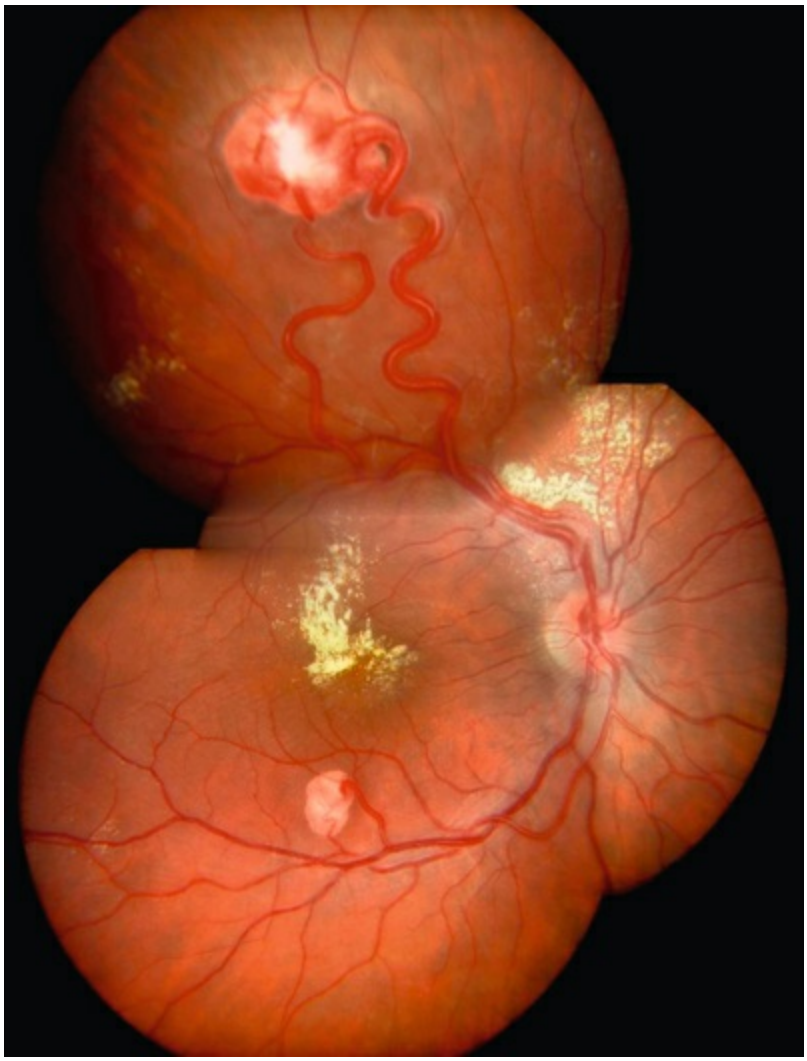

FIG. 134.3 Peripheral retinal hemangioblastoma with macular exudation. Visual acuity is decreased in the setting of severe hard exudates involving the macula. Note the dilated, tortuous afferent and efferent tumor vessels. A second tumor along the inferotemporal vascular arcade appears more fibrotic and does not contribute to the exudation.

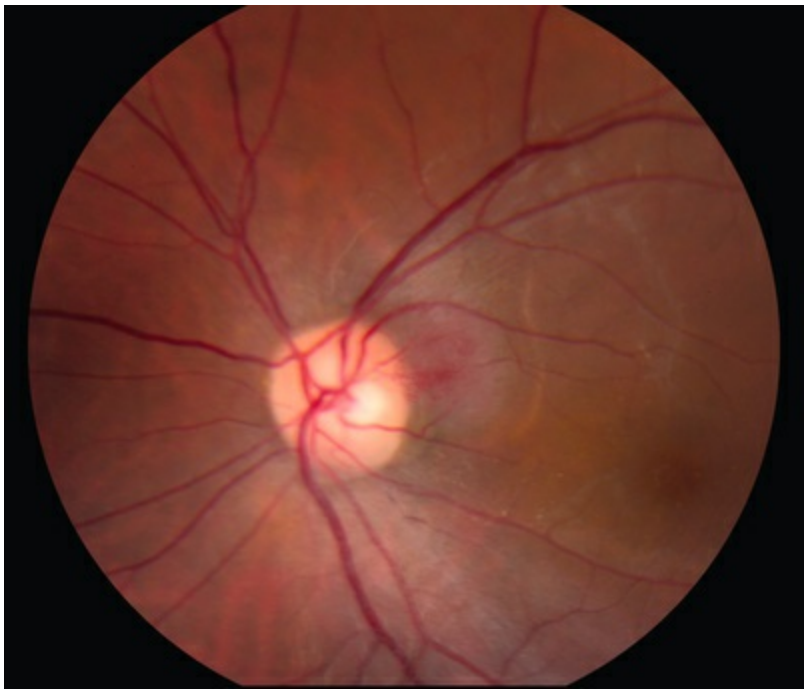

FIG. 134.5 Small juxtapapillary retinal hemangioblastoma. No exudation is present, visual acuity is not affected, and the lesion remains asymptomatic. (National Eye Institute, Bethesda, MD.)

RHs arising in proximity to the optic disc have a different clinical appearance and may be difficult to discern ophthalmoscopically when small and sessile. Small tumors may exhibit little more than localized fullness of the neural rim or retina at the disc margin, but with further growth, a distinct whitish-pink thickening becomes visible, sometimes with associated fine, lacy vessels (Fig. 134.5). Feeder vessels are typically not visible. These tumors sometimes exhibit minimal growth over years, but often evolve exudation eventually. Intraretinal edema, with or without hard exudates, may progress to involve the central macula (Fig. 134.6).

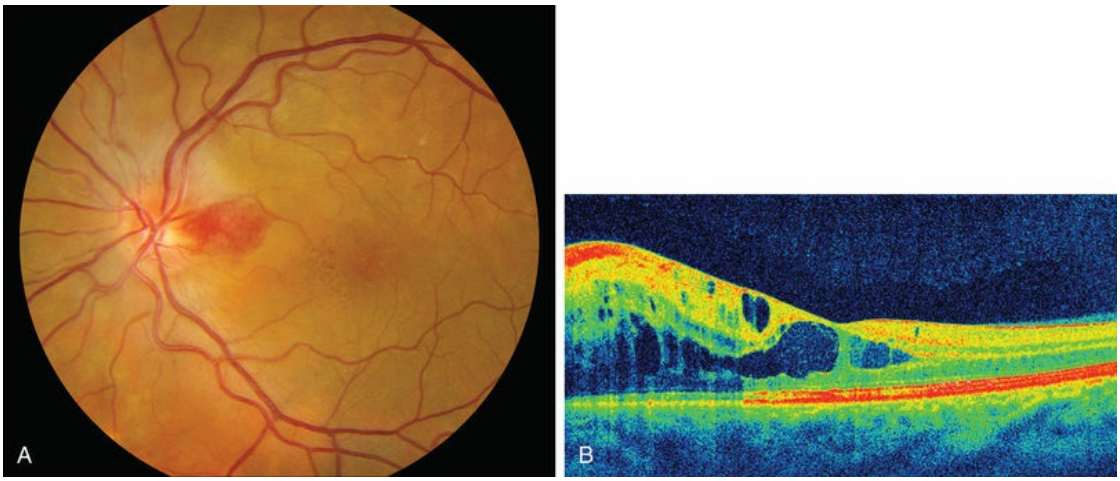

FIG. 134.6 Juxtapapillary retinal hemangioblastoma with macular exudation. (A) A prominent retinal hemangioblastoma is visible on the temporal optic disc rim. Note the central macular cysts and superotemporal punctate hard lipid deposits. (B) An optical coherence tomography line scan of the central macula shows marked cystoid macular edema nasally and centrally. The tumor resides in the inner retina nasally. (National Eye Institute, Bethesda, MD.)

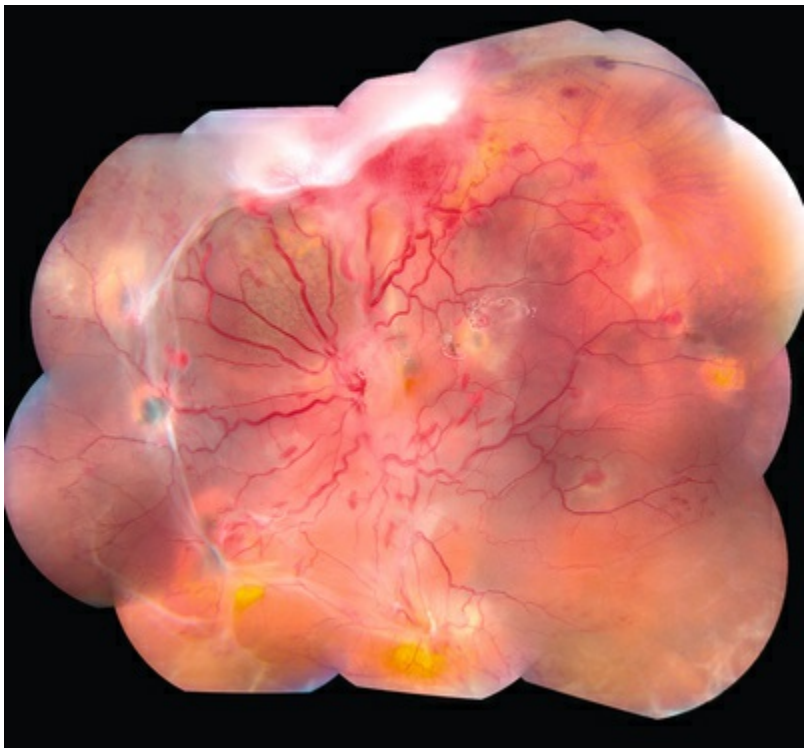

FIG. 134.4 Multiple retinal hemangioblastomas with exudative retinal detachment. Retinal

hemangioblastomas of various sizes, dilated and tortuous afferent and efferent vessels, hard exudates, and foci of epiretinal fibrosis are visible in this severely affected eye. Prognosis in such cases is very guarded.

The ophthalmoscopic appearance of RHs is characteristic and is often sufficient to make the diagnosis. Very small lesions, as mentioned earlier, may be hard to distinguish from other focal microvascular abnormalities when other conditions are being considered. The lesion that most closely resembles larger tumors, and may be difficult to differentiate in some cases, is a vasoproliferative tumor of the ocular fundus.[28] Fundus photography, especially with use of montage techniques or a wide-angle camera to capture the location and size of extrapapillary RHs, may be helpful for monitoring for growth or regression of lesions. For identifying small tumors or evaluating atypical lesions or features, ancillary testing can be helpful. Fluorescein angiography shows prominent early hyperfluorescence of RHs that typically persists and often progresses to leakage in the late phase of the study. It is a sensitive test for detection of extrapapillary and juxtapapillary RHs, and can be helpful to rule out other conditions. In cases of macular exudation originating from an extrapapillary RH, macular vessel leakage is typically absent. Associated peripheral microvascular abnormalities or capillary nonperfusion are not typical, but we have seen occasional cases in which the retina evolves a more widespread vasculopathy, usually in the setting of multiple or large RHs and significant tumor exudation. Optical coherence tomography can be useful to document the features of juxtapapillary RHs and is especially helpful for characterizing any macular edema or epiretinal macular traction. Ultrasonography shows an acoustically solid retinal mass with a smooth anterior border with variable but mostly medium reflectivity (Fig. 134.7), but it is not often used for follow-up of most tumors. Orbital shadowing and choroidal excavation are not seen.

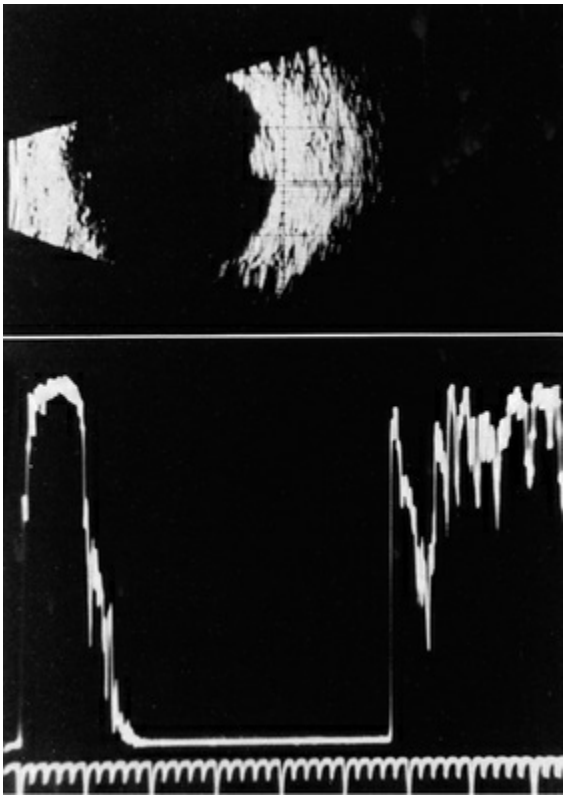

FIG. 134.7 B-scan and standardized A-scan echogram of a retinal hemangioblastoma, thickness 3.3 mm, reflectivity variable but predominantly medium.

RHs are typically asymptomatic at the early stages of development. Vision loss is generally caused by exudation affecting the macula, glial proliferation or posterior hyaloid contraction related to the tumor with resultant retinal striae and thickening, or in advanced cases, traction and/or exudative retinal detachment. While number of tumors did not increase significantly with age in the aforementioned cohort study,[26] the risk of vision loss was found to increase with age in another cross-sectional case series.[29] The risk of severe vision loss also increased with presence of juxtapapillary lesions, increasing peripheral tumor number, and the extent of retinal involvement.[26] In the cohort studied at the National Eye Institute, approximately 77% of eyes had vision of 20/20 or better, and the prevalence of legal blindness from ocular VHL disease was low: 6% of patients manifested vision less than 20/160 in the better-seeing eye. However, approximately 20% of all patients with ocular VHL disease had at least some degree of unilateral visual impairment, indicating a substantial burden of disease.

Retinal vascular proliferation is a less common manifestation of

ocular VHL disease. Approximately 8% of patients with ocular VHL disease in the National Eye Institute cohort manifested these lesions, which bear some resemblance to the retinal neovascularization seen in ischemic retinopathies, but occur in the absence of significant retinal capillary nonperfusion (Fig. 134.8).[30] Another case series describing such lesions divided them into "vascularized glial veils" arising in proximity to the optic disc, and "retinal vascular hamartomas" with a sessile, saccular, nest-like appearance in extrapapillary retina.[31] These lesions are variably vascular or fibrotic, tend to occur at the posterior pole, and exhibit a variable natural history, with regression or stasis in some cases and progressive growth in others. Patients with retinal vascular proliferation are often young and may manifest these lesions in the absence of any RH in the affected eye. We have seen occasional cases of indeterminate lesions that share characteristics of RHs and vascular proliferation, but the distinction is important, when possible, for treatment (see below, Treatment of ocular von Hippel–Lindau disease).

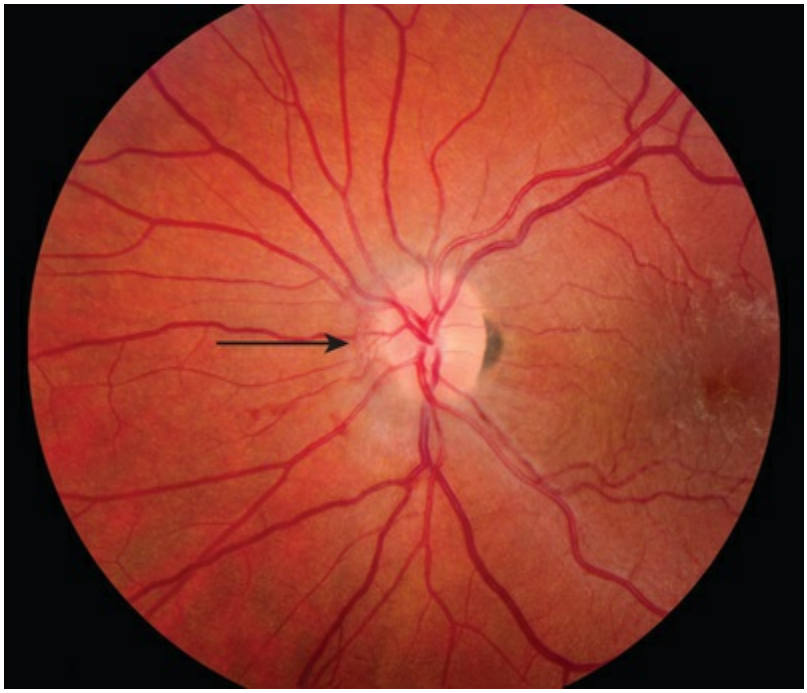

FIG. 134.8 Retinal vascular proliferation. Lacy epiretinal vessels (*arrow*) are present on the nasal optic disc rim. Cellophane maculopathy in the setting of thickened posterior hyaloid and/or early epiretinal

membrane formation is visible temporally. (National Eye Institute, Bethesda, MD.)

There are a number of other manifestations of VHL disease that may affect vision and come to the attention of the ophthalmologist. Expanding cerebellar hemangioblastomas may cause intracranial hypertension, papilledema, and eventual optic atrophy if not treated in a timely fashion. Central nervous system hemangioblastomas rarely occur in the optic nerve, optic chiasm, or optic tract.[32–37] Pheochromocytomas may cause hypertension and consequent hypertensive retinopathy.

Pathology of Ocular Lesions

Histopathologic evaluation of RH demonstrates capillary-like fenestrated vascular channels surrounded by vacuolated, "foamy" stromal cells, with presence of occasional tumorlet cells, and a variable amount of reactive gliosis (Fig. 134.9).[38–42] Microdissection of specimens with analysis of DNA has shown a loss of heterozygosity at the VHL gene locus in stromal cells, but not in areas of the tumor with predominance of vascular channels or glial cells.[42,43] On this basis, RH has been classified as a neoplasm, in which proliferation of vacuolated stromal cells (Fig. 134.10) occurs after loss or inactivation of both *VHL* alleles. Similar loss of heterozygosity has been demonstrated in VHL disease-related central nervous system hemangioblastomas,[44] which are histopathologically similar to RH. Genetic analysis of other prototypical VHL disease tumors, including renal cell carcinoma, pheochromocytoma, pancreatic adenoma, and endolymphatic sac tumor, supports the Knudson two-hit model for tumorigenesis in this disorder.[45–51] The identity of vacuolated stromal cells in RH remains uncertain. Older ultrastructural and immunohistochemical studies suggested that these cells might represent lipidized fibrous astrocytes or glial cells.[40,52] Other investigators hypothesized that these might evolve from "vasoformative stem cells."[53] A study of cerebellar hemangioblastomas showed that analogous stromal cells in these tumors may originate from developmentally arrested angioblasts.[54] Immunohistochemical analysis of RH demonstrated

that stromal cells express CD133, a stem cell marker expressed by hematopoietic, endothelial, and neural progenitors.[55] Evaluation of extrapapillary RH successfully treated by xenon photocoagulation, argon laser, and cryotherapy has demonstrated occlusion of vascular channels, gliosis, and fibrous metaplasia of retinal pigment epithelium.[56–58] Histopathologic evaluation of retinal vascular proliferation has been limited, but a single case reporting analysis of surgically excised tissue described a fibrovascular membrane composed of loose connective tissue and small blood vessels.[30]

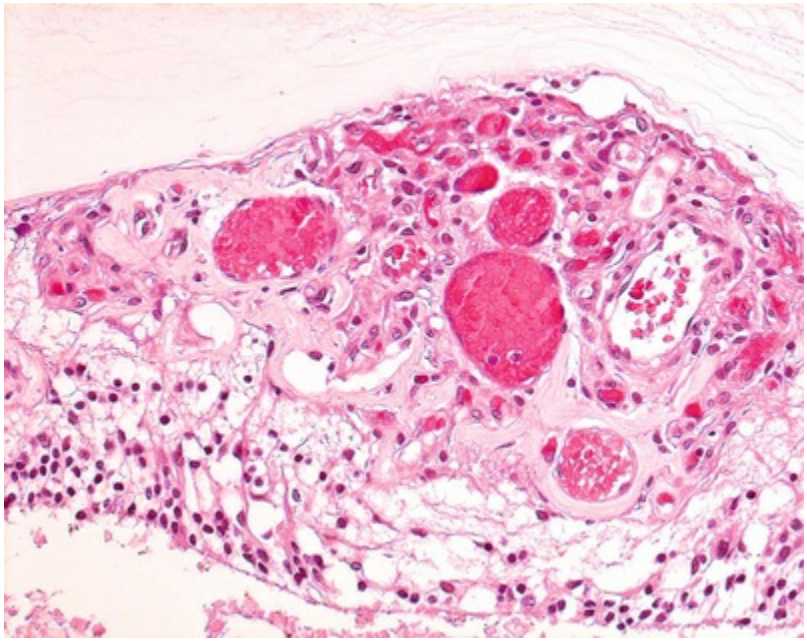

FIG. 134.9 A small retinal hemangioblastoma involving the inner and mid layers of the retina. The tumor contains dilated vessels and vacuolated stromal cells.
(Courtesy of Dr. Chi Chao Chan, National Eye Institute, Bethesda, MD.)

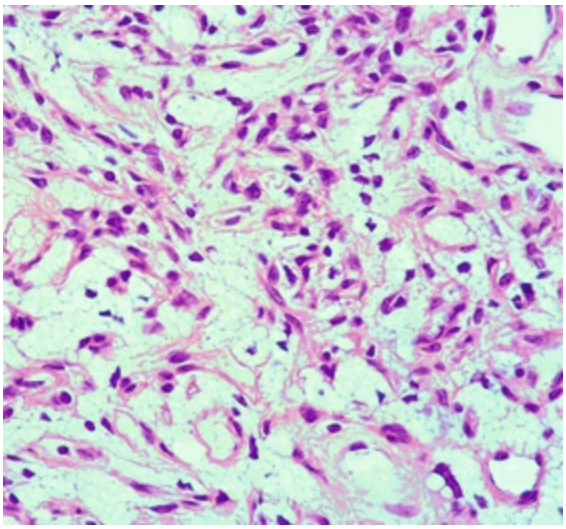

FIG. 134.10 Higher magnification of a juxtapapillary retinal hemangioblastoma showing many foamy vacuolated stromal cells. Some of these cells surround vessels. (Courtesy of Dr. Chi Chao Chan, National Eye Institute, Bethesda, MD.)

Diagnosis and Surveillance of Von Hippel–Lindau Disease

The diagnosis of von Hippel–Lindau disease has traditionally been based on the following clinical criteria: (1) A positive family history AND presence of a central nervous system hemangioblastoma, RH, pheochromocytoma, OR clear cell renal carcinoma; OR, (2) in the absence of a family history, presence of two or more central nervous system hemangioblastomas or RHs, OR one central nervous system hemangioblastoma or RH, AND a visceral tumor (with the exception of epididymal and renal cysts, which are frequent in the general population).[5,59] Genetic testing has become standard to confirm the diagnosis and can be especially useful in challenging cases, such as when a patient presents with one or more central nervous system hemangioblastomas or RHs in the absence of a family history or visceral lesions. Genetic testing is also important to establish the diagnosis in at-risk family members of a patient with VHL disease, given the latency and heterogeneity of clinical manifestations but a penetrance of over 90% by age 65.[1,59]

Median survival of those with VHL disease, for whom

complications of renal cell carcinoma and central nervous system hemangioblastoma remain principal causes of death, has improved in recent years, thanks to earlier diagnosis, standardized disease surveillance programs, and advances in treatment.[1,59] Because of the complexity of this condition, optimal management involves care by an integrated multispecialty team with expertise in neurosurgery, neuroradiology, urologic and endocrine surgical oncology, ophthalmology, otolaryngology, pathology, genetics, and rehabilitation medicine, when feasible. Various groups have published recommendations for age of initial screening and frequency of follow-up testing for cardinal disease features (Table 134.1).[60] Consensus recommendations do not presently exist, but those by Choyke and colleagues presented in Table 134.1 provide an example of the general guidelines used in management of these patients.

TABLE 134.1

Recommended Intervals for Screening Individuals at Risk for Von Hippel–Lindau Disease

Exam or Procedure	Age of Screening (Frequency)
Ophthalmoscopy	Infancy (yearly)
Plasma or 24-hour urinary catecholamines and metanephrines	~2 years (yearly and when blood pressure is elevated)
MRI of brain and spine	~11 years of age (yearly)
CT and MRI of internal auditory canals	Onset of symptoms, hearing loss, tinnitus, vertigo
Ultrasound of abdomen	~8 years (MRI as indicated)
CT of abdomen	~18 years or earlier if clinically indicated (yearly)
Audiology testing	When clinically indicated

CT, computed tomography; MRI, magnetic resonance imaging.

Adapted from Choyke PL, Glenn GM, Walther MM, et al. Von Hippel–Lindau disease: genetic, clinical, and imaging features. Radiology 1995;194:629–42.

Treatment of Ocular Von Hippel–Lindau Disease

The goal of treatment for an extrapapillary RH is generally destruction of the lesion, to render it incapable of further growth or

exudation. Small tumors with features suggesting inactivity or partial regression can occasionally be observed, but in such cases, close surveillance is imperative, and the threshold for offering ablative treatment for any sign of growth or activity should be low. Small tumors can be destroyed quite readily, before vision loss has occurred and with minimal risks of treatment; in contrast, larger lesions can be much more difficult to ablate, and damage induced by treatment frequently leads to a variable and occasionally significant acute exudative response that can cause retinal detachment and threaten vision. Accordingly, a core principle of management is to identify RHs as early in their development as possible, and to offer timely therapy or referral to an ophthalmologist proficient in managing ocular VHL disease. Given the advantages of early ablative therapy and the asymptomatic nature of small tumors, optimal management begins with adequate surveillance for appearance of RHs, so that timely treatment can be performed.

Ophthalmic evaluation, with indirect ophthalmoscopic and biomicroscopic examination of the retina, and use of ancillary imaging when possible in order to optimize the detection rate for small lesions is indicated annually for individuals with VHL disease, starting in early childhood. Identification of any ocular lesions requires prompt intervention and close subsequent surveillance, with follow-up tailored to the circumstances. Treated tumors are followed closely after any attempted ablation, to assess for expected regression or any sign of regrowth or recurrent exudation. Occasional eyes manifest new tumors frequently, and must be watched very closely.

Other treatments, such as surgical excision of large RHs, and pharmacotherapy to mitigate tumor exudation (such as intravitreous administration of VEGF antagonists), have been employed in select circumstances and are further discussed below. Compared to treatment options for extrapapillary RHs, those for juxtapapillary RHs are very limited, because of the greater potential for harm to vision by any ablative therapy. Management of this subset of tumors is discussed separately below.

Ablative Treatment of Extrapapillary Retinal

Hemangioblastomas

A number of ablative modalities have been employed for treatment of extrapapillary RHs, including thermal laser photocoagulation, cryotherapy, radiation (including brachytherapy, external beam radiation, and proton beam radiation), photodynamic therapy, and transpupillary thermotherapy. The feasibility and efficacy of therapy depend on a number of factors, such as tumor size, tumor location, degree of exudation, presence of retinal detachment, associated epiretinal fibrosis or hemorrhage, associated chorioretinal scarring (as from previous ablative treatment), position relative to location of any scleral buckling materials in previously operated eyes, the number and characteristics of other viable tumors inside the eye, associated retinal vascular changes or vascular proliferation, and response to previous treatment.

Extrapapillary RHs up to 1.5 mm in diameter can be effectively destroyed using thermal laser photocoagulation under most circumstances, and various laser types, including argon green, diode, yellow dye, and krypton, have all shown efficacy.[57,61–65] We typically use yellow or green wavelengths, with longer burn duration (0.2–0.4 seconds) than would be typical for panretinal photocoagulation or laser retinopexy, and power sufficient to create whitening in the area of the burn. It has been theorized that vascular lesions such as RHs may absorb yellow light more efficiently than other laser wavelengths based on the absorption spectrum of oxyhemoglobin,[66] but no randomized comparison of ablative laser type or technique has been performed. Feeder vessels at this tumor size are small, when visible at all, and we do not treat them. Some have advocated laser photocoagulation of the retina around the tumor, but we usually confine burns to an area sufficient to blanch the entire tumor surface. RHs anterior to the equator can be challenging to treat using slit-lamp laser delivery, and occasionally we use indirect laser photocoagulation to treat these lesions. The appearance of scant intraretinal or preretinal hemorrhage on the tumor surface immediately following laser photocoagulation is common, but vitreous hemorrhage is rare and usually only seen with treatment of larger lesions (see below). At this size, it is unusual for RHs to elaborate significant exudation or to be associated with significant epiretinal fibrosis, but coexisting

tumors may be responsible for presence of such features, and can make it difficult to apply sufficient burn intensity to a RH. When effective, laser treatment of small RHs results in a chorioretinal scar, sometimes associated with a shrunken, variably whitened vestige of the lesion, and other times with disappearance of the RH. A regressed but visible lesion corresponding to the original RH is compatible with destruction sufficient to prevent further growth or exudation, but treated areas must be followed over time for any sign of a still-viable RH. Retreatment is sometimes necessary, especially for larger tumors (see below), and the technique for retreatment is the same.

Extrapapillary RHs between 1.5 and 4.5 mm in diameter are more difficult to destroy using thermal laser photocoagulation. Success presumably depends on whether sufficiently intense photocoagulation can be applied throughout the thickness of the tumor. The treatment technique is similar to the one described above for small lesions, but frequently involves applying long-duration burns (often more than 0.4 seconds), using a power setting typically lower than that needed for a typical panretinal photocoagulation or laser retinopexy spot, designed to cause progressive grey-whitening over the course of the burn. Feeder vessels are often visible, and some have included photocoagulation of the feeding arteriole in treatment,[67,68] but in our hands this has not appreciably increased chances of success or lowered risks of the procedure, and we do not typically treat them. Sessile tumors are more easily treated than very nodular ones, and any associated exudation, epiretinal fibrosis, or preexisting hemorrhage can significantly hamper ability to apply adequate treatment. Appearance of scant intraretinal or preretinal hemorrhage on the tumor is common with treatment, as for smaller lesions, and vitreous hemorrhage is uncommon. Reasonable success rates have been reported with use of laser endophotocoagulation at vitrectomy in cases in which ablative therapy is applied adjunctive to vitreoretinal surgery.[69] In our experience, a significant number of RHs in this size range are not destroyed even following multiple sessions of laser photocoagulation. However, transscleral cryotherapy is frequently effective for destruction of these tumors, even in the setting of associated exudation, hemorrhage, or fibrosis.

Treatment can be applied transconjunctivally in the office setting for anterior tumors, or applied transsclerally in the surgical suite after conjunctival incision to allow for appropriate probe placement for postequatorial tumors. In either case, we typically use a double freeze–thaw technique as advocated by Singh and colleagues.[65] In our hands, use of cryotherapy seems to be associated with a greater posttreatment exudative response than use of laser photocoagulation (see below). Photodynamic therapy with verteporfin infusion has been attempted for ablation of tumors this size with mixed success,[70,71] and we have not found it effective enough to use routinely. Whether following laser photocoagulation or cryotherapy, complete disappearance of a treated tumor this size is uncommon, and assessment of whether adequate destruction has been achieved can be challenging. Encouraging signs include a decrease in tumor size, decrease in redness or vascularity, resolution of any subretinal fluid and hard exudates, normalization of the caliber and decrease in the tortuosity of any feeding and draining vessels, and an underlying chorioretinal scar. However, the only definitive measure for success is documentation of no regrowth or recurrent exudation over long-term follow-up, and we have seen quiescent and regressed-appearing tumors manifest new signs of viability and activity years following ablative therapy.

Extrapapillary RHs greater than 4.5 mm in diameter can be difficult to destroy, with decreasing success rates and increasing risks of treatment with increasing tumor size. Thermal laser photocoagulation and photodynamic therapy are almost always ineffective for large tumors. Cryotherapy can sometimes be effective for lesions this size, but becomes less so for very large tumors. For RHs more than 4.5 mm in diameter, we will often try cryotherapy, if it can be applied with adequately low risks, but consider use of brachytherapy (plaque radiotherapy) for higher-risk cases or following unsuccessful cryotherapy. Kreusel and colleagues reported use of ruthenium-106 brachytherapy for treatment of 25 eyes (24 patients).[72] Mean diameter of treated RH was 3.8 mm, and the authors reported destruction of 23 of 25 tumors with a single treatment session. However, they reported poor outcomes in nine eyes, in which the postoperative course was characterized by decrease in visual acuity and increasing exudative

or traction retinal detachment. Application of external beam radiation has been described in advanced cases, but has not resulted in long-term outcomes favorable enough to result in common use.

Ablative treatment of RHs larger than approximately 1.5 mm in diameter may prompt a rapid and sometimes significant increase in exudation as a response to acute injury. In our experience, the magnitude of this response is variable, and can be difficult to predict, but correlates with increasing tumor size, amount of baseline exudation, prominence of feeding and draining vessels, use of cryotherapy (compared to thermal laser photocoagulation or photodynamic therapy), and presence of vitreous cell and flare (implying preexisting breakdown of the blood–ocular barrier). Subretinal fluid often accumulates within hours following treatment (Fig. 134.11). In mild cases, such fluid may remain confined to the region around the treated RH until resolution weeks later; in more severe cases, frank exudative retinal detachment occurs, with dependent migration of subretinal fluid in the days following treatment and slow resolution weeks to months later. Peripheral exudative retinal detachment frequently causes scotomas, and migration of subretinal fluid into the macula can impair visual acuity. In our experience, visual acuity does often recover with resolution of subretinal fluid in cases of macular involvement. Risk of posttreatment exudation should not deter necessary ablative therapy in most cases, because eyes with such RHs are at high risk of vision loss without treatment, but a patient must be counseled about the risks undertaken and the need to follow the eye closely after treatment. Although we are not aware of any controlled clinical trials testing this approach, we routinely give a short course of systemic corticosteroids with a goal of minimizing posttreatment exudation. We tailor dosing to the risks of such exudation, and in high-risk cases often give prednisone (1 mg/kg per day) or equivalent for 1–3 days, starting on the day of treatment, and taper quickly to discontinuation within 4–7 days. In our experience, longer courses of corticosteroids do not hasten resolution of subretinal fluid, so we avoid administration for more than a week. The safety of corticosteroid use should be assessed in the context of systemic manifestations of VHL disease and any

comorbid conditions.

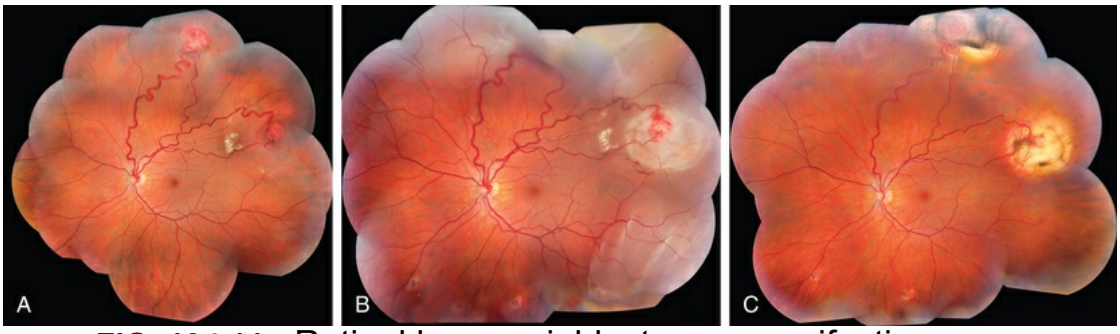

FIG. 134.11 Retinal hemangioblastomas manifesting posttreatment exudation after cryotherapy. (A) Two hemangioblastomas, both greater than 1.5 mm in diameter, are visible. Two small hemangioblastomas are present inferiorly but are difficult to visualize in this photograph. Visual acuity measured 20/16. Double freeze–thaw cryotherapy (with conjunctival incision for optimal probe positioning) was recommended for the two superior lesions, and laser photocoagulation was recommended for the two inferior lesions. Intravenous methylprednisolone was administered intraoperatively to blunt expected exudation. (B) One day following treatment, acute peripheral exudative retinal detachment is present superiorly and temporally. Prominent cryotherapy effect is visible around the temporal lesion. View of the superior lesion is obscured by a fibrin membrane that has congealed on the tumor surface. Laser effect is visible at the site of the two small lesions inferiorly. Oral prednisone and topical prednisolone acetate were given for 1 week. (C) Three years later, the two large tumors appear regressed, with reduction in the dilation and tortuosity of feeding and draining vessels and disappearance of superotemporal lipid. Chorioretinal scarring is present at the two sites of laser treatment inferiorly, where small tumors are no longer visible. Visual acuity remains 20/16. Note subtle perivascular lipid just inferior to the regressed but still visible superior tumor. This lipid was not present initially, or a year after cryotherapy, and this tumor is being observed closely for possible viability and need for further treatment.

(National Eye Institute, Bethesda, MD.)

Surgical Excision of Extrapapillary Retinal Hemangioblastomas

Given the poor success and significant risks of ablative therapy in very large RHs, surgical excision of RHs at vitrectomy is occasionally employed.[69,73] Gaudric and colleagues reported a case series of 23 eyes (21 patients) that underwent vitreoretinal surgery for severe ocular VHL disease, in which 14 eyes received ablative therapy (laser endophotocoagulation or cryotherapy) as adjunct to vitrectomy and the other nine eyes had surgical excision and removal of RHs. For the nine eyes undergoing RH excision, an average of two operations was necessary, and eight of nine eyes had an attached retina 6 months following surgery. However, neovascular glaucoma and new RH growth occurred in four eyes between 4 and 8 years after the initial surgery, and visual acuity in remaining eyes was poor (20/320 or worse). In our experience, a number of factors contribute to a high rate of postoperative proliferative vitreoretinopathy and retinal detachment in such eyes, and these complications, combined with high rates of new RH appearance, have limited the success of this approach.

Treatment of Juxtapapillary Retinal Hemangioblastomas

Management of juxtapapillary RHs is constrained by the adverse effects on vision that can result from ablative therapies used for treatment of extrapapillary RHs. Decrease in visual acuity, altitudinal visual field loss, and development of central scotomas have been associated with treatment of such tumors with thermal laser photocoagulation.[74] Photodynamic therapy with verteporfin has been attempted and seems to exhibit a better safety profile than laser photocoagulation, but has demonstrated limited success and somewhat mixed results.[70,75] Given these considerations, we observe juxtapapillary RHs when possible. As mentioned previously, the natural history is variable, and some lesions remain relatively static for long periods of time. Exudation may wax and wane and can remain compatible with good vision until the central macula

becomes chronically involved. In the absence of safe ablative options, treatment is typically confined to attempting to mitigate exudation affecting central vision. Photodynamic therapy, proton beam therapy, or pharmacotherapy using VEGF antagonists or corticosteroids may decrease exudation in some cases, but risks of therapy must be carefully weighed, and success is often limited.[70,75–78]

Treatment of Retinal Vascular Proliferation

Small foci of retinal vascular proliferation, whether juxtapapillary or extrapapillary, can often be observed. They do not seem to carry the same risk of vitreous hemorrhage or traction retinal detachment as does neovascularization in ischemic retinopathies, and they occasionally regress spontaneously.[30] When they grow large or become more fibrotic and contractile in proximity to the fovea, they can decrease visual acuity, and vitrectomy can be performed to remove the membranes.[30] In some cases, surgery is definitive; in others, retinal vascular proliferation may regrow after successful peeling. It is important to distinguish these lesions from RHs. Retinal vascular proliferation does not typically produce exudation and does not regress readily in response to laser photocoagulation (probably in part because of its epiretinal location). RHs may induce epiretinal proliferation or retinal vascular proliferation on their surface, but the tumors themselves reside within the neurosensory retina and cannot be peeled. We have seen occasional lesions that seem to share features of both, with a surface appearance suggesting epiretinal proliferation, but exudation typical for RH, and good regression in response to ablative laser photocoagulation. These hybrid lesions probably represent small RHs with overlying retinal vascular proliferation.

Antiangiogenic Pharmacotherapy

An understanding of the inappropriate activation of hypoxia response pathways in cells lacking functional pVHL opens the door for rational design of treatments that might be capable of preventing growth or even inducing regression of RH and other neoplastic lesions in VHL disease. Observation of the highly

vascular nature of tumors in VHL disease led to a hypothesis that VEGF, a HIF-inducible protein and potent mediator of angiogenesis and vascular permeability, might be important in their evolution, and there are several lines of evidence implicating VEGF expression in the pathology of VHL disease. Renal carcinoma cell lines defective for pVHL manifest increased production of VEGF, mRNA, and protein, and show a corresponding decrease when pVHL function is restored.[79] VEGF protein levels are elevated in pathologic specimens from renal carcinomas exhibiting mutations of *VHL*.[80] Neutralizing antibodies to VEGF reduce rates of progression among patients with advanced clear cell renal carcinoma, in which sporadic tumors harbor frequent inactivation of pVHL.[81,82] VEGF messenger RNA is upregulated in the hepatic cavernous hemangiomas seen in mice heterozygous for *VHL* mutation.[83] pVHL-defective cell lines derived from central nervous system hemangioblastomas and RH have not been developed, but analysis of pathologic specimens has revealed increased VEGF production.[43,84,85] Vacuolated stromal cells in VHL-associated RH exhibit high levels of VEGF messenger RNA and protein.[43]

Administration of VEGF antagonists in ocular VHL disease has been reported in case series and small, uncontrolled clinical trials. In one prospective study, Dahr and colleagues evaluated intravitreous pegaptanib sodium (3 mg) in five patients with VHL disease manifesting juxtapapillary or large extrapapillary RH.[77] Pegaptanib sodium, a pegylated aptamer antagonizing the $VEGF_{165}$ isoform, was administered every 6 weeks for at least six injections, and two of five patients completed the course of treatment and 1 year of follow-up. These two patients experienced a decrease in RH-associated exudation, but no change in size of the tumors. The other three patients demonstrated progression of ocular disease and did not complete the course of treatment. In another prospective trial, Wong and colleagues tested intravitreous ranibizumab in five patients with RH not amenable or responsive to standard treatments.[78] Ranibizumab (0.5 mg), a humanized monoclonal antibody fragment binding all VEGF-A isoforms, was given every 4 weeks for 6 months, with additional treatment considered through 12 months. Participants received a mean of 10 injections over an average of 47 weeks. Visual acuity decreased by 9 (± 20) letters and

there was no consistent improvement in RH exudation or tumor size.

The complexity of the cellular response to hypoxia is underscored by the hundreds of genes known so far to be regulated by the HIFs that signal inappropriately in the absence of functional VHL protein.[8] Given the pleiotropic effects of HIF signaling, and the possibility that some of pVHL's tumor suppressor function may involve HIF-independent mechanisms,[85] it is perhaps not surprising that initial efforts antagonizing angiogenic pathways for control or regression of RH have met with little success, but hope remains that broader targeting of this and other pathways may provide an eventual alternative to ablative therapy for these tumors.

Conclusion

RH is a benign neoplasm of the neurosensory retina or optic disc that occasionally manifests as a solitary, sporadic lesion, but typically appears as one or more tumors in the setting of VHL disease, an autosomal dominantly inherited condition involving benign and malignant neoplasms or cysts in the central nervous system or viscera. Referral of a patient with RH for clinical and/or genetic testing for VHL disease can be life-saving, given the potentially lethal nature of manifestations such as central nervous system hemangioblastoma and renal cell carcinoma, and given the benefits of surveillance and early intervention in affected individuals. Other critical components of ophthalmologic management include appropriate surveillance of patients with VHL disease for appearance or growth of RHs, retinal vascular proliferation, or other manifestations of ocular VHL disease, and timely application of ablative treatment for extrapapillary RHs, in order to minimize vision loss resulting from complications of progressive growth. RHs arising in proximity to the optic disc present a particular challenge, because they are frequently not safe to destroy using traditional ablative techniques. Improved understanding of the molecular pathology of VHL disease offers potential for development of nonablative therapies to arrest growth or induce regression of RH and other neoplasms in this condition.

References

1. Lonser RR, Glenn GM, Walther M, et al. Von Hippel–Lindau disease. *Lancet*. 2003;361:2059–2067.
2. Maher ER, Iselius L, Yates JR, et al. Von Hippel–Lindau disease: a genetic study. *J Med Genet*. 1991;28:443–447.
3. von Hippel E. Uber eine sehr seltene erkrankung der netzhaut. *Graefes Arch Ophthalmol*. 1904;59:83–106.
4. Lindau A. Studien ber kleinbirncysten bau: Pathogenese und beziehungen zur angiomatosis retinae. *Acta Pathol Microbiol Scand*. 1926;3:S1–28.
5. Melmon KL, Rosen SW. Lindau's disease. Review of the literature and study of a large kindred. *Am J Med*. 1964;36:595–617.
6. Seizinger BR, Rouleau GA, Ozelius LJ, et al. Von Hippel–Lindau disease maps to the region of chromosome 3 associated with renal cell carcinoma. *Nature*. 1988;332:268–269.
7. Latif F, Tory K, Gnarra J, et al. Identification of the von Hippel–Lindau disease tumour suppressor gene. *Science*. 1993;260:1317–1320.
8. Gossage L, Eisen T, Maher R. VHL, the story of a tumour suppressor gene. *Nat Rev Cancer*. 2015;15(1):55–64.
9. Schoenfeld A, Davidowitz EJ, Burk RD. A second major native von Hippel–Lindau gene product, initiated from an internal translation start site, functions as a tumor suppressor. *Proc Natl Acad Sci USA*. 1998;95:8817–8822.
10. Maxwell PH, Wiesener MS, Chang GW, et al. The tumour suppressor protein VHL targets hypoxia-inducible factors for oxygen-dependent proteolysis. *Nature*. 1999;399:271–275.
11. Min JH, Yang H, Ivan M, et al. Structure of an HIF-1α–pVHL complex: hydroxyproline recognition in signaling. *Science*. 2002;296:1886–1889.
12. Semenza GL. Regulation of mammalian O_2 homeostasis by hypoxia-inducible factor 1. *Annu Rev Cell Dev Biol*. 1999;15:551–578.
13. Bohling T, Hatva E, Kujala M, et al. Expression of growth factors and growth factor receptors in capillary

hemangioblastoma. *J Neuropathol Exp Neurol*. 1996;55:522–527.
14. Reifenberger G, Reifenberger J, Bilzer T, et al. Coexpression of transforming growth factor-alpha and epidermal growth factor receptor in capillary hemangioblastomas of the central nervous system. *Am J Pathol*. 1995;147:245–250.
15. Carmeliet P, Dor Y, Herbert JM, et al. Role of HIF-1alpha in hypoxia-mediated apoptosis, cell proliferation and tumour angiogenesis. *Nature*. 1998;394:485–490.
16. Kaelin WG Jr. Molecular basis of the VHL hereditary cancer syndrome. *Nat Rev Cancer*. 2002;2:673–682.
17. Knudson AG Jr. Mutation and cancer: statistical study of retinoblastoma. *Proc Natl Acad Sci USA*. 1971;68:820–823.
18. Glenn G, Stolle C, Sgambati M, et al. New mutations versus silent carrier parent as source of first generation diagnoses in a hereditary neoplastic disorder: von Hippel–Lindau disease. *Proc Am Assoc Cancer Res*. 1999;40:464.
19. Sgambati MT, Stolle C, Choyke PL, et al. Mosaicism in von Hippel–Lindau disease: lessons from kindreds with germline mutations identified in offspring with mosaic parents. *Am J Hum Genet*. 2000;66(1):84–91.
20. Wu P, Zhang N, Wang X, et al. Mosaicism in von Hippel-Lindau disease with severe renal manifestations. *Clin Genet*. 2013;84:581–584.
21. Stolle C, Glenn G, Zbar B, et al. Improved detection of germline mutations in the von Hippel–Lindau disease tumor suppressor gene. *Hum Mutat*. 1998;12:417–423.
22. Zbar B, Kishida T, Chen F, et al. Germline mutations in the von Hippel–Lindau disease (VHL) gene in families from North America, Europe, and Japan. *Hum Mutat*. 1996;8:348–357.
23. Beroud C, Joly D, Gallou C, et al. Software and database for the analysis of mutations in the VHL gene. *Nucleic Acids Res*. 1998;26:256–258.
24. Czyzyk-Krzeska MF, Meller J. Von Hippel–Lindau tumor suppressor: not only HIF's executioner. *Trends Mol Med*. 2004;10:146–149.
25. Mettu P, Agron E, Samtani S, et al. Genotype-phenotype

correlation in ocular von Hippel–Lindau (VHL) disease: the effect of missense mutation position on ocular VHL phenotype. *Invest Ophthalmol Vis Sci*. 2010;51:4464–4470.
26. Wong WT, Agrón E, Coleman HR, et al. Clinical characterization of retinal capillary hemangioblastomas in a large population of patients with von Hippel–Lindau disease. *Ophthalmology*. 2008;115:181–188.
27. Whitson JT, Welch RB, Green WR. Von Hippel–Lindau disease: case report of a patient with spontaneous regression of a retinal angioma. *Retina*. 1986;6:253–259.
28. Shields CL, Shields JA, Barrett J, et al. Vasoproliferative tumors of the ocular fundus: classification and clinical manifestations in 103 patients. *Arch Ophthalmol*. 1995;113(5):615–623.
29. Webster AR, Maher ER, Moore AT. Clinical characteristics of ocular angiomatosis in von Hippel–Lindau disease and correlation with germline mutation. *Arch Ophthalmol*. 1999;117:371–378.
30. Wong WT, Yeh S, Chan CC, et al. Retinal vascular proliferation as an ocular manifestation of von Hippel–Lindau disease. *Arch Ophthalmol*. 2008;126:637–643.
31. Schmidt D, Neumann HPH. Retinal vascular hamartoma in von Hippel–Lindau disease. *Arch Ophthalmol*. 1995;113:1163–1167.
32. Meyerle CB, Dahr SS, Wetjen NM, et al. Clinical course of retrobulbar hemangioblastoma in von Hippel–Lindau disease. *Ophthalmology*. 2008;115:1382–1389.
33. Kupersmith MJ, Berenstein A. Visual disturbances in von Hippel–Lindau disease. *Ann Ophthalmol*. 1981;2:195–197.
34. In S, Miyagi J, Kojho N, et al. Intraorbital optic nerve hemangioblastoma with von Hippel–Lindau disease: case report. *J Neurosurg*. 1982;56:426–429.
35. O'Reilly GV, Rumbaugh CL, Bowens M, et al. Supratentorial haemangioblastoma: the diagnostic roles of computed tomography and angiography. *Clin Radiol*. 1980;32:389–392.
36. Kerr DJ, Scheithauer BW, Miller GM, et al. Hemangioblastoma of the optic nerve: case report. *Neurosurgery*. 1995;36:573–581.

37. Baggentos M, Chew E, Butman JA, et al. Progressive peritumoral edema defining the optic fibers and resulting in reversible visual loss. *J Neurosurg*. 2008;109:313–317.
38. Goldberg MF, Duke JR. Von Hippel–Lindau disease: histopathologic findings in a treated and an untreated eye. *Am J Ophthalmol*. 1968;66:693–705.
39. Nicholson DH, Green WR, Kenyon KR. Light and electron microscopic study of early lesions in angiomatosis retinae. *Am J Ophthalmol*. 1976;82:193–204.
40. Grossniklaus HE, Thomas JW, Vigneswaran N, et al. Retinal hemangioblastoma: a histologic, immunohistochemical, and ultrastructural evaluation. *Ophthalmology*. 1992;99:140–145.
41. Chan CC, Chew EY, Shen D, et al. Expression of stem cells markers in ocular hemangioblastomas associated with von Hippel–Lindau (VHL) disease. *Mol Vis*. 2005;11:697–704.
42. Chan CC, Collins AB, Chew EY. Molecular pathology of eyes with von Hippel–Lindau (VHL) disease: a review. *Retina*. 2007;27:1–7.
43. Chan CC, Vortmeyer AO, Chew EY, et al. VHL gene deletion and enhanced VEGF gene expression detected in the stromal cells of retinal angioma. *Arch Ophthalmol*. 1999;117:625–630.
44. Vortmeyer AO, Gnarra JR, Emmert-Buck MR, et al. Von Hippel–Lindau gene deletion detected in stromal cell component of a cerebellar hemangioblastoma associated with von Hippel–Lindau disease. *Hum Pathol*. 1997;28:540–543.
45. Lubensky IA, Gnarra JR, Bertheau P, et al. Allelic deletions of the VHL gene detected in multiple microscopic clear cell renal lesions in von Hippel-Lindau disease patients. *Am J Pathol*. 1996;149:2089–2094.
46. Gnarra JR, Tory K, Weng Y, et al. Mutations of the VHL tumour suppressor gene in renal carcinoma. *Nat Genet*. 1994;7:85–90.
47. Crossey PA, Foster K, Richards FM, et al. Molecular genetic investigations of the mechanism of tumorigenesis in von Hippel–Lindau disease: analysis of allele loss in VHL tumours. *Hum Genet*. 1994;93:53–58.

48. Zeiger MA, Zbar B, Keiser H, et al. Loss of heterozygosity on the short arm of chromosome 3 in sporadic, von Hippel–Lindau disease-associated, and familial pheochromocytoma. *Genes Chromosomes Cancer*. 1995;13:151–156.
49. Tory K, Brauch H, Linehan M, et al. Specific genetic change in tumors associated with von Hippel–Lindau disease. *J Natl Cancer Inst*. 1989;81:1097–2101.
50. Vortmeyer AO, Lubensky IA, Fogt F, et al. Allelic deletion and mutation of the von Hippel–Lindau (VHL) tumor suppressor gene in pancreatic microcysticadenomas. *Am J Pathol*. 1997;151:951–956.
51. Vortmeyer AO, Choo D, Pack SD, et al. Von Hippel–Lindau disease gene alterations associated with endolymphatic sac tumor [Letter]. *J Natl Cancer Inst*. 1997;89:970–972.
52. Jakobiec FA, Font RL, Johnson FB. Angiomatosis retinae: an ultrastructural study and lipid analyses. *Cancer*. 1976;38:2042–2056.
53. Mottow-Lippa L, Tso MO, Peyman GA, et al. Von Hippel angiomatosis: a light, electron microscopic, and immunoperoxidase characterization. *Ophthalmology*. 1983;90:848–855.
54. Vortmeyer AO, Frank S, Jeong SY, et al. Developmental arrest of angioblastic lineage initiates tumorigenesis in von Hippel–Lindau disease. *Cancer Res*. 2003;63:7051–7055.
55. Chan CC, Chew EY, Shen D, et al. Expression of stem cells markers in ocular hemangioblastomas associated with von Hippel–Lindau (VHL) disease. *Mol Vis*. 2005;11:697–704.
56. Goldberg MF. Clinicopathologic correlation of von Hippel angiomas after xenon arc and argon laser photocoagulation. Peyman GA, Apple DJ, Sanders DR. *Intraocular tumors*. Appleton–Century–Crofts: New York; 1977:219–234.
57. Annesley WH, Leonard BC, Shields JA, et al. Fifteen year review of treated cases of retinal angiomatosis. *Trans Sect Ophthalmol Am Acad Ophthalmol Otolaryngol*. 1977;83:446–453.
58. Watzke RC. Cryotherapy for retinal angiomatosis: a clinicopathologic report. *Doc Ophthalmol*. 1973;34:405–411.

59. Schmid S, Gillessen S, Binet I, et al. Management of von Hippel-Lindau disease: an interdisciplinary review. *Oncol Res Treat*. 2014;37:761–771.
60. Choyke PL, Glenn GM, Walther MM, et al. Von Hippel–Lindau disease: genetic, clinical, and imaging features. *Radiology*. 1995;194:629–642.
61. Lane CM, Turner G, Gregor ZJ, et al. Laser treatment of retinal angiomatosis. *Eye (Lond)*. 1989;3:33–38.
62. Blodi CF, Russell SR, Pulido JS, et al. Direct and feeder vessel photocoagulation of retinal angiomas with dye yellow laser. *Ophthalmology*. 1990;97:791–797.
63. Rosa RH, Goldberg MF, Green WR. Clinicopathologic correlation of argon laser photocoagulation of retinal angiomas in a patient with von Hippel–Lindau disease followed for more than 20 years. *Retina*. 1996;16:145–156.
64. Schmidt D, Natt E, Neumann HP. Long-term results of laser treatment for retinal angiomatosis in von Hippel–Lindau disease. *Eur J Med Res*. 2000;5:47–58.
65. Singh AD, Nouri M, Shields CL, et al. Treatment of retinal capillary hemangioma. *Ophthalmology*. 2002;109:1799–1806.
66. Mainster MA. Wavelength selection in macular photocoagulation: tissue optics, thermal effects, and laser systems. *Ophthalmology*. 1986;93:952–958.
67. Goldberg MF, Koenig S. Argon laser treatment of von Hippel–Lindau retinal angiomas. I. Clinical and angiographic findings. *Arch Ophthalmol*. 1974;92:121–125.
68. Gorin MB. Von Hippel–Lindau disease: clinical considerations and the use of fluorescein-potentiated argon laser therapy for treatment of retinal angiomas. *Semin Ophthalmol*. 1992;7:182–191.
69. Gaudric A, Krivosic V, Duguid G, et al. Vitreoretinal surgery for severe retinal capillary hemangiomas in von Hippel–Lindau disease. *Ophthalmology*. 2011;118:142–149.
70. Sachdeva R, Dadgostar H, Kaiser PK, et al. Verteporfin photodynamic therapy of six eyes with retinal capillary haemangioma. *Acta Ophthalmol*. 2010;88:e334–40.
71. Papastefanou VP, Pilli S, Stinghe A, et al. Photodynamic therapy for retinal capillary hemangioma. *Eye (Lond)*.

2013;27:438–442.
72. Kreusel KM, Bornfeld N, Lommatzsch A, et al. Ruthenium-106 brachytherapy for peripheral retinal capillary hemangioma. *Ophthalmology*. 1998;105:1386–1392.
73. Schlesinger T, Appukuttan B, Hwang T, et al. Internal en bloc resection and genetic analysis of retinal capillary hemangioblastoma. *Arch Ophthalmol*. 2007;125:1189–1193.
74. Garcia-Arumí J, Sararols LH, Cavero L, et al. Therapeutic options for capillary papillary angiomas. *Ophthalmology*. 2000;107:48–54.
75. Schmidt-Erfurth UM, Kusserow C, Barbazetto IA, et al. Benefits and complications of photodynamic therapy of papillary capillary angiomas. *Ophthalmology*. 2002;109:1256–1266.
76. Seibel I, Cordini D, Hager A, et al. Long-term results after proton beam therapy for retinal papillary capillary hemangioma. *Am J Ophthalmol*. 2014;158:381–386.
77. Dahr SS, Cusick M, Rodriguez-Coleman H, et al. Intravitreal anti-vascular endothelial growth factor therapy with pegaptanib for advanced von Hippel–Lindau disease of the retina. *Retina*. 2007;27:150–158.
78. Wong WT, Liang K, Hammel K, et al. Intravitreal ranibizumab therapy for retinal capillary hemangioblastoma related to von Hippel–Lindau disease. *Ophthalmol*. 2008;115:1957–1964.
79. Siemeister G, Weindel K, Mohrs K, et al. Reversion of deregulated expression of vascular endothelial growth factor in human renal carcinoma cells by von Hippel–Lindau tumor suppressor protein. *Cancer Res*. 1996;56:2299–2301.
80. Na X, Wu G, Ryan CK, et al. Overproduction of vascular endothelial growth factor related to von Hippel–Lindau tumor suppressor gene mutations and hypoxia-inducible factor-1-alpha expression in renal cell carcinomas. *J Urol*. 2003;170:588–592.
81. George DJ, Kaelin WG Jr. The von Hippel–Lindau protein, vascular endothelial growth factor, and kidney cancer. *N Engl J Med*. 2003;349:419–421.

82. Yang JC, Haworth L, Sherry RM, et al. A randomized trial of bevacizumab, an anti-vascular endothelial growth factor antibody, for metastatic renal cancer. *N Engl J Med*. 2003;349:427–434.
83. Haase VH, Glickman JN, Socolovsky M, et al. Vascular tumors in livers with targeted inactivation of the von Hippel–Lindau tumor suppressor. *Proc Natl Acad Sci USA*. 2001;98:1583–1588.
84. Wizigmann-Voos S, Breier G, Risau W, et al. Up-regulation of vascular endothelial growth factor and its receptors in von Hippel–Lindau disease-associated and sporadic hemangioblastomas. *Cancer Res*. 1995;55:1358–1364.
85. Li M, Kim WY. Two sides to every story: the HIF-dependent and HIF-independent functions of pVHL. *J Cell Mol Med*. 2011;15:187–195.

135

Tuberous Sclerosis and the Eye

Alan F. Cruess, Sanjay Sharma

Introduction

History, Diagnosis, and Genetic Basis

Tuberous sclerosis complex (TSC) is a rare multisystem genetic disorder, characterized by hamartomatous tumors of the brain, skin, viscera, and eye. It is inherited in an autosomal dominant fashion,[1] with a high degree of penetrance[2] albeit with variable phenotypic expression. The first publication of a color plate by Rayner of a patient with an apparent facial angiofibroma took place in 1835.[3] In 1880 D.M. Bourneville, from a neuropathologic study of a young patient with seizures, hemiplegia, mental subnormality, who also had renal tumors, coined the term tuberous sclerosis.[4] Von Recklinghausen had, in 1862, published a description of what turned out to be TSC.[5] However, the eponym Bourneville disease was commonly used to describe this condition until only recently. In 1908 Vogt[6] first proposed epilepsy, mental retardation, and the skin lesions of adenoma sebaceum as a diagnostic triad. In 1920 Van der Hoeve[7] first recognized retinal involvement in tuberous sclerosis. Ophthalmologists now recognize astrocytic hamartomas of both the retina and the optic nerve as common features of this condition.

The diagnostic criteria are based on the premise now that there are no truly pathognomonic features or clinical criteria for the diagnosis of tuberous sclerosis or TSC.[6] Signs that were once regarded as sufficiently specific are now known to occur as isolated findings in normal individuals without TSC.[8] In theory, the perfect disease classification scheme should have both a high sensitivity (low rate of missing the diagnosis of tuberous sclerosis) and a high specificity (low rate of incorrectly labeling a patient with tuberous sclerosis). The 2012 Tuberous Sclerosis Complex Consensus Group classified patients into two diagnostic groups: possible and definite, reduced from three groups in the 1998 classification: possible, probable, and definite.[5,9] Patients can be classified into one of three

categories based on the presence of clinical features of varying specificity (primary features: high specificity; secondary features: moderate specificity; tertiary features: lower degree of specificity).[9] The classic triad included seizures, mental retardation, and cutaneous angiofibromas, which, however, only occurs in 29% of cases.[10] Mental retardation and seizures were also left out of the revised criteria by the 1998 expert consensus panel.[11] The addition of DNA testing complements the clinical diagnosis and helps with genetic counseling, especially in concert with prenatal testing.[12] A definite diagnosis now depends on two major features (lymphangioleiomyomatosis and angiomyolipomas) or one major feature with two or more minor features or the presence of a *TSC1* or *TSC2* mutation of confirmed pathogenicity.[13]

Genetic Diagnostic Criteria

A pathogenic mutation in *TSC1* or *TSC2* is an independent diagnostic criterion, sufficient for the diagnosis of TSC regardless of the clinical findings. A pathogenic mutation was defined as a mutation that prevents protein synthesis or inactivates the function of *TSC1* or *TSC2* proteins, hamartin, and tuberin respectively. However, a significant fraction (10–25%) of TSC patients have no mutation identified by conventional testing. Therefore a normal result does not exclude TSC.[5]

Systemic Manifestations

Neurologic

Seizures

Children with tuberous sclerosis often have seizures that are referred to as "infantile spasms" or "salaam attacks."[8] These seizures are characterized by repetitive myoclonic spasms of the head, neck, and limbs. Originally described by West,[14] an English general medical practitioner, through the experience of his own son in 1841, the seizures last for seconds but may occur in bouts of 10–50. Hoyt[15] described infantile spasms as "lightning fast nodding of the head, often with extension or flexion of the trunk and frequently

also of the arms." According to Pampliglione and Pugh,[16] 25% of children affected by "infantile spasms" develop other stigmata of tuberous sclerosis within 4 years of diagnosis. Infantile seizures, the most common feature of the disease, tend to evolve into grand mal seizures at a later time and are seen in 93% of patients.[12,17] Presently, the treatment of epilepsy in TSC (which occurs in 75–90% of cases) remains a major challenge, even with new anticonvulsant medications.[18,19] Vigabratin has shown promise with about 30% of patients with infantile spasms responding. However, retinal toxicity to vigabratin and MRI detectable cerebral lesions have been described in children receiving the medication. Even after neurosurgery, seizures recur in approximately 30% of cases.[20] The advent of mTORC1 inhibitors has led to a paradigm shift in treatment possibilities. Currently in addition to FDA approval for renal angiolipomas and subependymal astrocytomas that cannot be resected, mTORC inhibitors (like rapamycin or everolimus) are in clinical trials for TSC-related refractory epilepsy, neurocognitive manifestations, and facial angiofibromas.[13]

Cognitive and Behavioral Disability

Children with tuberous sclerosis may have normal or above-average intelligence.[17] However, Lagos and Gomez[17] reported that 44 (62%) of 71 tuberous sclerosis patients were labeled as mentally retarded. Subsequent reports confirm that neurocognitive manifestations ranging from profound cognitive disabilities to mild learning impairment occur in around 45% of patients.[21] While the majority of individuals with TSC have normal intelligence, they may still be prone to specific cognitive memory, attentional, and executive skills deficits.[22] It should be noted that early reports emphasizing the prevalence of mental retardation in tuberous sclerosis suffered from selection bias because they were based on patients who were institutionalized.[12] In the Lagos and Gomez series[17] intracranial calcifications were more commonly seen in patients with normal intelligence. The cause of both seizures and mental retardation may be related to the presence of cortical tubers (Fig. 135.1) and subependymal hamartomas (Fig. 135.2). These tumor masses represent benign astrocytic hamartomas, which

characteristically involve the basal ganglia, lateral and third ventricles, and the posterior fossa. Histopathologically, they consist of well-differentiated large astrocytes in an admixture of fibrillary astrocytes and calcospherules.[23] They frequently undergo cystic degeneration and dystrophic calcification, accounting for their typical radiologic features (Fig. 135.3) and for the name tuberous sclerosis.[24] Most significant variables associated with a poor cognitive outcome include a history of refractory seizures, *TSC2* mutations, and cortical tubers in specific locations of the brain.[25]

FIG. 135.1 Cortical tuber (dimpled gyrus in center of illustration) destroying the normal cortical architecture.
(Courtesy of S. Ludwin.)

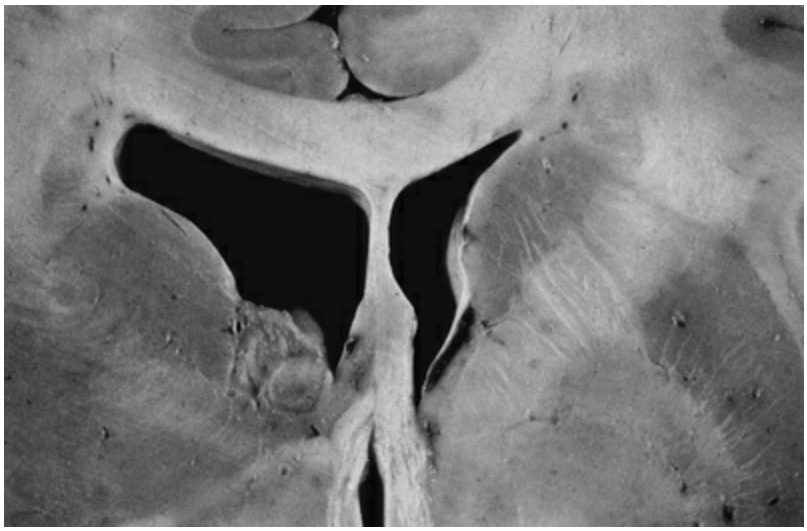

FIG. 135.2 Subependymal astrocytic hamartoma adjacent to the basal ganglia protruding into the lateral ventricle. (Courtesy of S. Ludwin.)

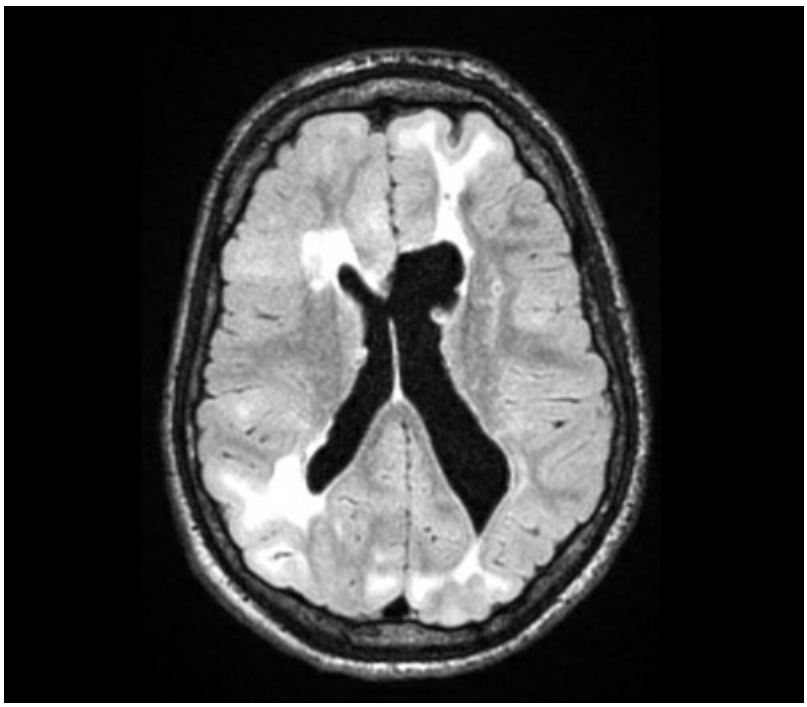

FIG. 135.3 Axial flair reformat magnetic resonance imaging of tuberous sclerosis lesions. (Courtesy of Dr. Angelica Oviedo, Dalhousie University/Capital Health, Halifax NS Canada.)

Brain tumors are associated with tuberous sclerosis. These well-circumscribed lesions are classified as subependymal giant-cell astrocytomas and should not be confused with the giant-cell variant

of glioblastoma multiforme, a malignant astrocytoma.[26]

A case of giant cerebral aneurysm with visual loss as a result of optic nerve compression in a patient with tuberous sclerosis has been reported.[27]

Skin Features

Facial angiofibromas, formerly referred to as adenoma sebaceum, occur as a reddish-brown papular rash found characteristically in a "butterfly" distribution over the face. This rash has often been considered to be a pathognomonic hallmark of tuberous sclerosis and is very sensitive, occurring in over 85% of patients.[17] Histopathologically, "adenoma sebaceum" consists of multiple smooth papules that are benign angiofibromas.[28] The rash is generally not apparent at birth but appears in childhood, generally before the age of 9 years, and tends to intensify with time.[23] It is most prominent in the nasolabial folds and over the malar areas.

The skin lesion formerly believed to be pathognomonic for tuberous sclerosis is the hypopigmented macule or patch (Fig. 135.4). These lesions are variable in shape, with only an occasional one justifying the term ash-leaf sign. Often present at birth, this is the first clinical sign of disease. Its occurrence is highly variable, being present in up to 75% of affected children.[29] Pathologically, the ash-leaf lesion is an achromic nevus,[30] as opposed to vitiligo, in which the melanocytes are actually missing. Ultraviolet light (classically a Wood's lamp) may be used effectively in a darkened room to screen for the ash-leaf sign.[31] The importance of this clinical sign in the workup of a child with infantile spasms of unknown cause cannot be overemphasized.[29]

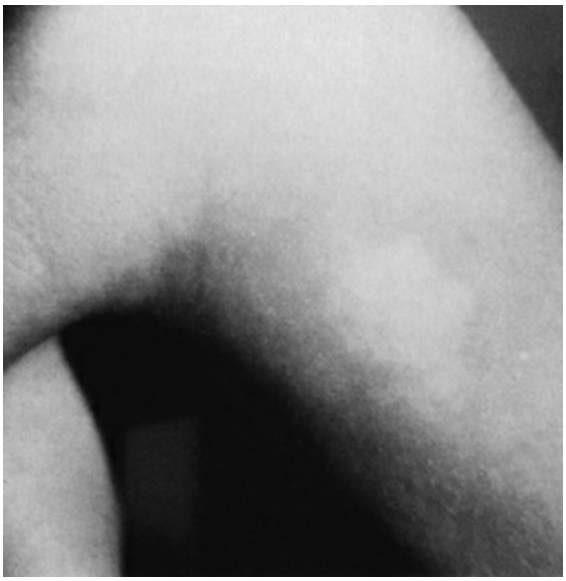

FIG. 135.4 Hypopigmented skin macule or patch (achromic nevus), sometimes referred to as an ash-leaf sign. (Courtesy of P. McLeod.)

Shagreen patches represent areas of skin affected by fibromatous infiltration. This sign is seen in approximately 20% of cases, often in the lower back.[32] This flesh-colored, leathery plaque on the lumbosacral area is highly characteristic of the tuberous sclerosis complex.[31] Subungual fibromas may be seen on the hands and feet.[17,31]

Visceral Features

Although Vogt's classic triad of mental deficiency, epilepsy, and facial angiofibromas implies central nervous system and skin involvement, it is important to be cognizant of the possible presence of visceral tumors. Renal angiolipomas are hamartomas that occur singularly or in multiples, in unilateral or bilateral fashion. They are present in 80% of patients with tuberous sclerosis.[23] They are benign tumors that are not known to metastasize to distant sites,[33] although extension to the renal vein has been noted.[34] Cardiac hamartomas also occur. They are rhabdomyomas that are single or multiple whitish nodules that characteristically protrude into the ventricles.[23] Slowly, progressive subpleural cysts may form and can rupture, causing a spontaneous pneumothorax.[35] Hamartomas of the liver, thyroid, pancreas, and testis have been reported.[23]

Skeletal Features

The skeletal system is affected in 40% of cases.[8] Sclerotic calcified areas are seen in the skull and spine. Skull radiographs may show opacities over the calvaria that represent intraosseous sclerotic areas of intracranial calcified astrocytic hamartomas. Computed tomography (CT) scans are particularly helpful in the investigation of tuberous sclerosis.[36] Phalangeal cysts affect the hands and feet.[8]

Ocular Manifestations

Retinal Manifestations

The retinal phakomas of tuberous sclerosis are astrocytic hamartomas of the retina, seen in an estimated 53% of patients, according to Lagos and Gomez[17] in their Mayo Clinic series of 71 cases. Shelton[37] found evidence of retinal hamartomatous lesions in all seven patients examined. Solitary astrocytic hamartomas may be seen in otherwise healthy patients, but in patients with tuberous sclerosis they may be multifocal or bilateral. Although most frequently seen in the setting of tuberous sclerosis, these hamartomas may also be noted in patients with neurofibromatosis.[38,39] Although astrocytic hamartomas of the retina are the principal ocular manifestation of the tuberous sclerosis complex, two patients have been reported in whom stromal depigmentation of the iris and atypical colobomas were correlated on histopathologic examination with hamartomas of the iris pigment epithelium and ciliary body epithelium.[40]

Typically, astrocytic hamartomas can be classified morphologically as one of two types: (1) large, whitish (calcified) nodular masses or (2) flat, translucent (noncalcified) smooth tumors.[41] Nyboer et al.[42] have described an intermediate type of retinal hamartoma having features of both types. These lesions typically occur at or near the optic disc. More peripheral lesions may occur, and these may be more easily confused with retinoblastoma. Although almost all astrocytic hamartomas of the retina in tuberous sclerosis are endophytic in nature, an exophytic case has been described (Figs. 135.5 and 135.6 illustrate a different case).[34] This case consisted of the pathologic examination of an eye

enucleated for neovascular glaucoma from a 10-year-old boy with tuberous sclerosis and seizures. The retina was totally detached and was associated with a large multinodular mulberry-like astrocytic tumor in the subretinal space.

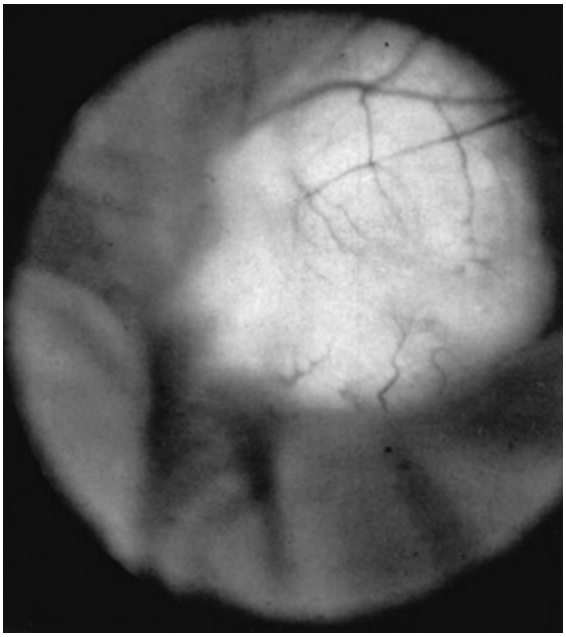

FIG. 135.5 Exophytic (subretinal) peripapillary astrocytic hamartoma appearing with an exudative retinal detachment. (Courtesy of J. Augsburger.)

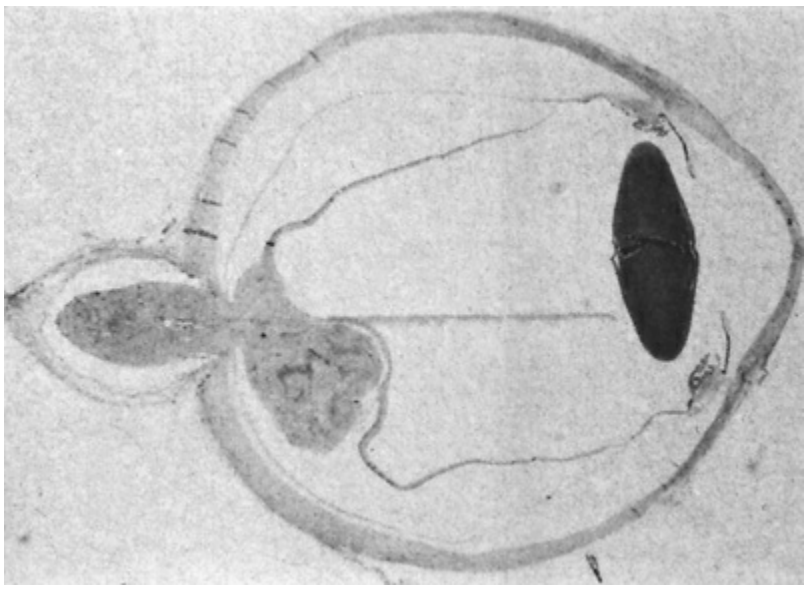

FIG. 135.6 Pathologic correlate (low-power

photograph) of the eye containing the lesion illustrated in Fig. 135.5. (Courtesy of J. Augsburger.)

The exophytic tumors are astrocytic tumors in the subretinal space.[43] The endophytic tumors are astrocytic hamartomas of the nerve fiber layer of the retina (Figs. 135.7 and 135.8).[14] These retinal tumors are benign and non-neoplastic,[23] generally showing minimal or slow evidence of growth,[15] although progressive enlargement associated with the development of calcification has been reported.[42] Retinal astrocytomas can, therefore, occasionally show progressive enlargement, retinal detachment, and vitreous seeding – findings that can "mislead the clinician towards a diagnosis of retinoblastoma."[44] The reverse, however, has also been reported, since spontaneous regression of retinal astrocytic hamartoma has been described.[45]

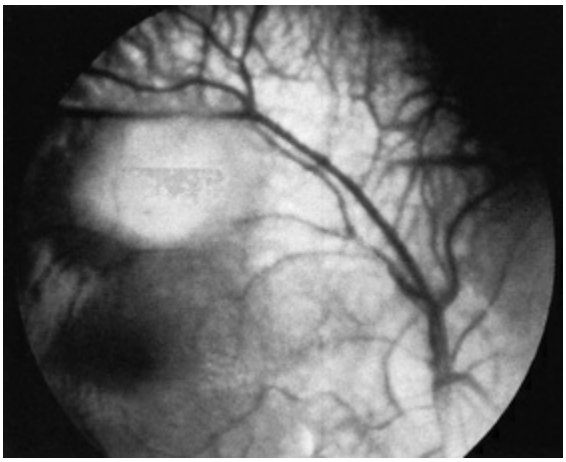

FIG. 135.7 Endophytic astrocytic hamartoma of the retina. (Courtesy of P. McLeod.)

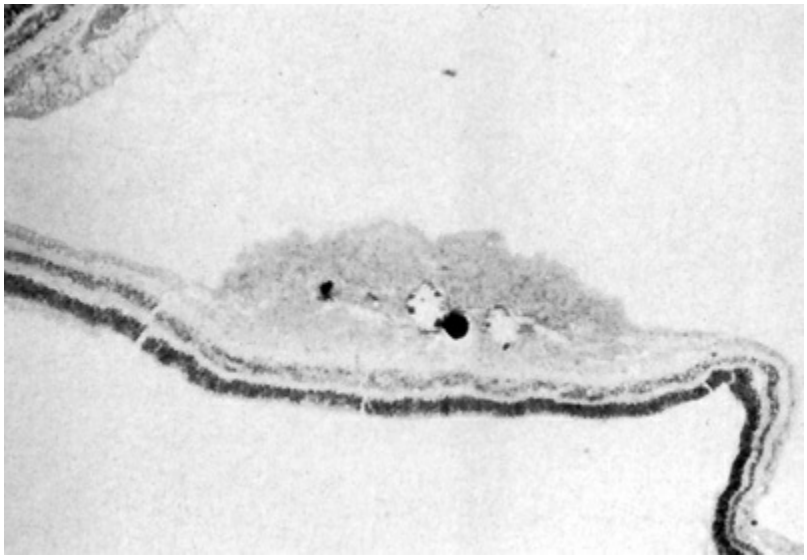

FIG. 135.8 Pathologic correlate of an endophytic astrocytic hamartoma of the retina. (Courtesy of R. Bell.)

Most astrocytic (glial) hamartomas of the retina are composed of elongated fibrous astrocytes with small oval nuclei and cytoplasmic processes.[39] Larger tumors, particularly those located on or near the optic nerve, may have large round and moderately pleomorphic astrocytes.[46] Foci of calcification may be seen. Clinically, Gass[38] has noted that these lesions may show varying degrees of tumor vascularization, which is more evident angiographically than ophthalmoscopically. Fluorescein angiography of retinal astrocytomas characteristically shows late-phase relative hyperfluorescence with leakage of dye into the vitreous cavity.[38] Fluorescein angiography, however, has not been considered helpful in differentiating astrocytic hamartomas from solitary retinoblastoma.[47]

Ocular complications related to the presence of retinal hamartomas have been reported as rare complications of tuberous sclerosis. These include vitreous hemorrhage, retinal vascular abnormalities (including telangiectasia, neovascularization, and exudation), and vitreous seeding, which is characteristically described in association with optic nerve head or epipapillary astrocytic hamartomas. Vitreous hemorrhage may arise from the substance of retinal or optic nerve astrocytomas, according to a clinicopathologic report in which the vitreous hemorrhage was thought to be arising from the surface of an epipapillary astrocytic hamartoma.[48] The hemorrhage was observed intraoperatively

during pars plana vitrectomy surgery to remove old vitreous hemorrhage. Attempts to use endodiathermy to cauterize an apparent surface bleeding site exposed cystic spaces within the tumor that were filled with hemorrhagic material and actively bled. A myriad of small vascular channels were confirmed pathologically.[39] Blood-filling intratumor cystic spaces in a large epipapillary tumor, resulting in vitreous hemorrhage, were first reported by Van der Hoeve in 1921.[49] Atkinson et al.[50] reported vitreous hemorrhage in two cases of optic disc astrocytomas. Koch and Walsh[51] also reported vitreous hemorrhage in a case associated with increased intracranial pressure and papilledema. Vitreous hemorrhage may also arise from retinal neovascularization associated with a retinal astrocytoma.[52] The angiogliomatous nature of retinal astrocytic hamartomas has been stressed in a pathologic report by Barsky and Wolter,[41] giving rise to speculation regarding the possible angioblastic and astroblastic origin of these lesions. Retinal telangiectasis with surrounding intraretinal lipid exudation in the parafoveal region and serous retinal detachment affecting the macula have been reported to occur in association with multiple astrocytic hamartomas.[43] A single case of a peripapillary lesion that hemorrhaged into the vitreous, increased in size, and underwent spontaneous necrosis has been reported.[53]

Optic Nerve Phakomas

As reported by Lagos and Gomez,[17] retinal and optic nerve astrocytomas occur in 53% of cases. These lesions “protrude above or overlie the optic disc” (Fig. 135.9) and, according to Miller,[54] “may initially have a grayish or grayish pink appearance, but later develop a glistening, yellow, mulberry appearance.” Optic nerve astrocytomas have long been known to be capable of vitreous seeding and vitreous hemorrhage, as noted earlier, since Van der Hoeve's 1921 report.[49,51] In 1984, vitreous seeding associated with an intense vitritis in a patient with tuberous sclerosis was reported by De Juan et al.[55] These authors speculated that the development of a posterior vitreous detachment with associated traction at the optic disc may have resulted in vitreous seeding.

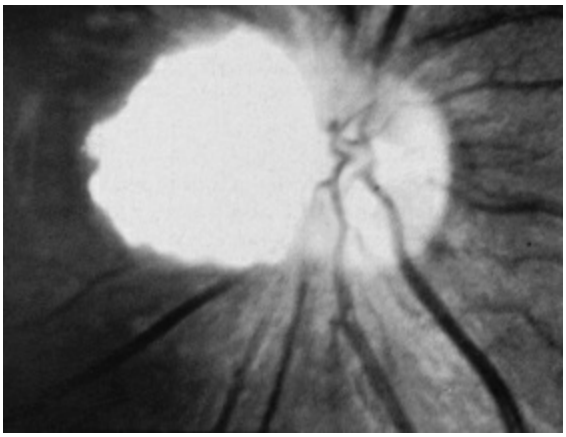

FIG. 135.9 Glistening, mulberry-like optic nerve astrocytic hamartoma protruding above and overlying the optic disc. (Courtesy of J. Shakin.)

Ocular Adnexal Lesions

Angiofibromas (adenoma sebaceum) of the skin of the lids occur in tuberous sclerosis, giving rise to a typical salmon-colored lid.[56] Isolated white eyelashes (poliosis) located among normally pigmented ones have been reported in a patient in whom the fundus of one eye was remarkable, not only for an astrocytic hamartoma of the retina, but also for a leaf-shaped area of hypopigmentation in the retinal periphery,[57] similar in appearance to the hypopigmented skin lesions (ash-leaf spots). Hypopigmented iris spots have also been reported as an early sign of disease.[58] Other isolated associations with tuberous sclerosis have been summarized by Williams and Taylor.[12]

Differential Diagnosis

The differential diagnosis of astrocytic hamartomas of the retina and optic nerve depends to a great extent on whether the diagnosis of tuberous sclerosis can be established. This diagnosis is based on various primary, secondary, and tertiary features, most of which were initially put forth by Gomez[59] and recently revised in 2012 by the Tuberous Sclerosis Complex Consensus Group[5]:

Definite diagnosis: Two major features or one major feature with ≥2 minor features

Possible diagnosis: Either one major feature or ≥2 minor features (see Table 135.1).

TABLE 135.1
Updated Diagnostic Criteria for Tuberous Sclerosis Complex, 2012

A. Genetic Diagnostic Criteria
The identification of either a *TSC1* or *TSC2* pathogenic mutation in DNA from normal tissue is sufficient to make a definite diagnosis of tuberous sclerosis complex (TSC). A pathogenic mutation is defined as a mutation that clearly inactivates the function of the TSC1 or TSC2 proteins (e.g., out-of-frame indel or nonsense mutation), prevents protein synthesis (e.g., large genomic deletion), or is a missense mutation whose effect on protein function has been established by functional assessment (www.lovd.nl/TSC1; www.lovd/TSC2; Hoogeveen-Westerveld et al.[60,61]). Other *TSC1* or *TSC2* variants whose effect on function is less certain do not meet these criteria, and are not sufficient to make a definite diagnosis of TSC. Note that 10% to 25% of TSC patients have no mutation identified by conventional genetic testing, and a normal result does not exclude TSC, or have any effect on the use of clinical diagnostic criteria to diagnose TSC.
B. Clinical Diagnostic Criteria
Major Features
1. Hypomelanotic macules (≥3, at least 5-mm diameter) 2. Angiofibromas (≥3) or fibrous cephalic plaque 3. Ungual fibromas (≥2) 4. Shagreen patch 5. Multiple retinal hamartomas 6. Cortical dysplasias[a] 7. Subependymal nodules 8. Subependymal giant cell astrocytoma 9. Cardiac rhabdomyoma 10. Lymphangioleiomyomatosis (LAM)[b] 11. Angiomyolipomas (≥2)[b]
Minor Features
1. "Confetti" skin lesions 2. Dental enamel pits (>3) 3. Intraoral fibromas (≥2) 4. Retinal achromic patch 5. Multiple renal cysts 6. Nonrenal hamartomas
Definite Diagnosis
Two major features or one major feature with ≥2 minor features
Possible Diagnosis
Either one major feature or ≥2 minor features

[a]Includes tubers and cerebral white matter radial migration lines.

[b]A combination of the two major clinical features (LAM and angiomyolipomas) without other features does not meet criteria for a definite diagnosis.

Therefore, in the presence of a single retinal (or optic nerve) hamartoma, only one additional major feature, or two or more minor features, are required to make the diagnosis of tuberous sclerosis complex. The first step for the ophthalmologist should be

carefully to reexamine both eyes for signs of one or more retinal or optic nerve hamartomas. Retinal and optic nerve astrocytic hamartomas can also be present in patients with neurofibromatosis.[38]

If the diagnosis of tuberous sclerosis or neurofibromatosis cannot be clearly established, the appearance of the retinal or optic nerve hamartoma may provide clinical clues related to the associated systemic condition. Shields and Shields[24] state that a tumor that consists of a mulberry-like calcification is pathognomonic of tuberous sclerosis. However, when the only retinal tumor seen is a small, translucent, and whitish noncalcified thickening of the nerve fiber layer, it may be difficult, if not impossible, to distinguish it from myelinated nerve fibers or retinoblastoma.[24] This difficulty in differentiating between small astrocytic hamartomas of the retina and retinoblastoma has also been stressed by others.[62] Gass[47] has reported that fluorescein angiography, although helpful in outlining the rich capillary network in these tumors, is not helpful in differentiating astrocytoma from retinoblastoma. However, despite this potential source of major diagnostic error, case series that examine cases of possible retinoblastoma rarely include a single case of astrocytic hamartoma of the retina.[15,63] In Howard and Ellsworth's series of 500 cases of suspected retinoblastoma in 1965,[63] not a single case of astrocytic hamartoma was mentioned, although there were 265 cases without retinoblastoma. Shields and Shields,[24] who list astrocytic hamartoma in the differential diagnosis of retinoblastoma, confirm the rarity of a mistaken diagnosis in their own series. Of the 136 patients sent to their clinic with the diagnosis of possible retinoblastoma, only one patient had an astrocytic hamartoma. Shields et al.[39] reported the use of fine-needle biopsy to help differentiate an astrocytic hamartoma from a retinoblastoma.

Other disorders that can mimic astrocytic hamartoma include myelinated nerve fibers and inflammatory lesions.[8] Furthermore, given the angiomatous component of these lesions, Coats disease and other causes of retinal telangestasis[39,52,53,62,64] should be included in the differential diagnosis. A more thorough list of clinical simulators of astrocytic hamartoma is provided in Box 135.1.

Box 135.1

Differential Diagnosis of Astrocytic

Hamartomas

- Retinal astrocytoma
- Retinoblastoma
- Myelinated nerve fibers
- Coats disease
- Other causes of retinal telangiectasis
- Retinal capillary angioma
- *Toxocara canis*, toxoplasmosis
- Other causes of choroiditis and scleritis
- Other causes of exudative retinal detachment with underlying mass lesion
- Optic disc astrocytic hamartoma
- Optic disc drusen
- Retinitis pigmentosa associated with optic disc excrescences (hyaline bodies) versus astrocytic hamartomas
- Optic disc glioma (variant of optic nerve glioma)
- Other primary optic disc tumor
- Other causes of unilateral optic disc swelling or papillitis

Optic disc hamartomas, after they have developed the yellow, glistening, mulberry appearance so characteristic of these lesions,[54] may be confused with optic disc drusen. However, optic disc drusen lie within the disc, whereas astrocytic hamartomas protrude above it[54] and obscure both the optic nerve and retinal blood vessels.[65] Heckenlively[66] reviewed the controversy of the origin of

the “globular excrescences or hyaline bodies of the optic nerve head.” These hyaline bodies are suspected of being drusen based on the pathologic studies of Spencer,[46,67] Puck et al.,[68] and Novak and Foos.[69] Heckenlively's interpretation is that these studies do not put to rest the issues raised by Robertson,[70] namely, that vitreal epipapillary excrescences in patients with retinitis pigmentosa represent astrocytic hamartomas.[66] Optic disc glioma may also be confused with astrocytic hamartomas. Gliomas of the optic disc may initially appear with disc swelling or obscuration of the disc by a whitish, protuberant mass. These lesions can be easily confused with astrocytic hamartomas, especially in the case of a noncalcified hamartoma. Although more commonly described in neurofibromatosis, Shields and Shields[24] note that optic disc glioma can also appear in patients with tuberous sclerosis. Other neoplastic lesions of the optic disc should be considered in the differential diagnosis, including capillary and cavernous hemangioma.[54]

Genetics and Pathophysiology as a Guide to Treatment

Tuberous sclerosis complex is a systemic disorder that is inherited in an autosomal dominant fashion in which mutations in the tumor suppressor genes *TSC1* or *TSC2* lead to the development of benign hamartomas throughout the body as described, with incomplete penetrance and variable expressivity. However, approximately 70–75% of cases are said to arise from new mutations.[13,71] The prevalence of disease in an Oxford, UK study has been approximated at 1 in 15, 000.[72] More recently, prevalence has been estimated at 1 in 6000 to 1 in 9000 people. Worldwide there are at least 2 million people affected.[13] Linkage studies have demonstrated the genetic heterogeneity of this condition, with two separate mutations accounting for the vast majority of cases.[73–75] The two genes responsible for most cases of tuberous sclerosis are located on chromosome 9 at q34 (*TSC1*) and on chromosome 16 at p13.3 (*TSC2*).[76] No phenotypic differences are noted in patients with the two different mutations, although mutations in *TSC1* appear to be associated with a milder clinical phenotype.[74,77] The *TSC2* gene

accounts for as many as 90% of the clinical cases.[13] Tuberin, the product of *TSC2*, has partial homology to Rap 1-GTPase-activating protein, which supports the theory that tuberin plays a role in cell growth regulation.[73] The product of *TSC1* has been identified as hamartin.[78] These proteins are widely expressed in the brain and form a heterodimer that functions as a suppressor of the mammalian target of rapamycin (mTOR), the mTOR Complex 1, mTORC1, by inhibiting the mTOR, a serine/threonine kinase cascade,[79] part of a cascade modulating cellular growth and differentiation, tumor suppression, and intracellular signaling.[13,78]

More severe clinical manifestations tend to occur in individuals with *TSC2* mutations. They tend to present with more hypomelanotic skin macules and learning disabilities with more frequent neurologic and ophthalmologic signs, renal cysts, and ungual fibromas.[13] Genetic counseling and a three-generation genetic history is essential because patients with the tuberous sclerosis gene have a 50% chance of transmitting the gene to their offspring.[73] Parents of patients with tuberous sclerosis should be made aware of the possibility of germ-line mosaicism. It is important that these individuals have a thorough systemic evaluation, which should include CT/MRI scanning of the head and renal ultrasonography to rule out tuberous sclerosis.[73] If the results of these examinations are normal in the parents, the child likely suffers from a new mutation, and the subsequent risk of another child having tuberous sclerosis has been estimated at 1%.[63]

Novel Treatment Approaches – Summary

Updated recommendations for surveillance and management of TSC manifestations have been published.[80] A better understanding of the molecular biology of TSC has led to a paradigm shift with respect to treatment possibilities in recent years. The activity of mTORC1 is very sensitive to rapamycin and related compounds such as everolimus; these agents have already undergone successful clinical trials for TSC-related subependymal astrocytomas and renal angiomyolipomas, leading to regulatory approval in many

countries including the United States, Canada, and Europe. Currently mTORC1 inhibitors are undergoing clinical trials for TSC-related refractory epilepsy, neurocognitive manifestations, and facial angiofibromas.[13]

References

1. Fryer AE, Chalmers A, Connor JM, et al. Evidence that the gene for tuberous sclerosis is on chromosome 9. *Lancet*. 1987;1:659–661.
2. Napolioni V, Moavero R, Curatolo P. Recent advances in the neurobiology of tuberous sclerosis complex. *Brain Dev*. 2009;31:104–113.
3. Gomez M. History of tuberous sclerosis complex. *Brain Dev*. 1995;17:55–57.
4. Bourneville DM. Selerose tubereuse des circonvolutions cerebrales: idiotie et epilepsie hemiplegique. *Arch Neurol (Paris)*. 1880;1:81–91.
5. Northrup H, Krueger DA. Tuberous Sclerosis Complex Diagnostic Criteria Update. [on behalf of the; International Tuberous Sclerosis Consensus Group] *Pediatr Neurol*. 2013;49(4):243–254.
6. Vogt H. Zur diagnostik der tuberosen sclerose. *Z Erforschung Behandlung Jugendl Schwachsinns*. 1908;2:1–16.
7. Van der Hoeve J. Eye symptoms in tuberous sclerosis of the brain. *Trans Ophthalmol Soc U K*. 1920;40:329–334.
8. Roach ES, Sparagana SP. Diagnosis of tuberous sclerosis complex. *J Child Neurol*. 2004;19:643–649.
9. Rowley SA, O'Callaghan FJ, Osborne JP. Ophthalmic manifestations of tuberous sclerosis: a population-based study. *Br J Ophthalmol*. 2001;85:420–423.
10. Schwartz RA, Fernandez G, Kotulska K, et al. Tuberous sclerosis advances in diagnosis, genetics and management. *J Am Acad Dermatol*. 2007;57:189–202.
11. Rosser T, Panigrahy A, McClintock W. The diverse clinical manifestations of tuberous sclerosis complex: a review. *Semin Pediatr Neurol*. 2006;13:27–36.
12. Williams R, Taylor D. Tuberous sclerosis. *Surv Ophthalmol*.

1985;30:143–153.
13. DiMario FJ, Sahin M, Ebrahimi-Fakhari D. Tuberous sclerosis complex. *Pediatr Clin N Am*. 2015;62:633–648.
14. West WJ. On a peculiar form of infantile convulsion. *Lancet*. 1841;1:724–725.
15. Hoyt CS. The ocular findings in infantile spasms. *Ophthalmology*. 1979;86:1794–1802.
16. Pampliglione G, Pugh E. Infantile spasms and subsequent appearance of tuberous sclerosis syndrome. *Lancet*. 1975;2:1046.
17. Lagos JC, Gomez MR. Tuberous sclerosis: reappraisal of a clinical entity. *Mayo Clin Proc*. 1967;42:26–49.
18. Curatalo P, Bombardieri R, Cerminara C. Current management for epilepsy in tuberous sclerosis complex. *Curr Opin Neurol*. 2006;19:119–123.
19. Saxena A, Sampson JR. Epilepsy in tuberous sclerosis: phenotypes, mechanisms, and treatments. *Semin Neurol*. 2015;35(3):269–276.
20. Jansen FE, van Huffelen AC, Bourez-Swart M, et al. Consistent localization of interictal epileptiform activity on EEGs of patients with tuberous sclerosis complex. *Epilepsia*. 2005;46:415–419.
21. Joinson C, O'Callaghan FJ, Osborne JP, et al. Learning disability and epilepsy in an epidemiological sample of individuals with tuberous sclerosis complex. *Psychol Med*. 2003;33:335–344.
22. Prather P, DeVries PJ. Behavioral and neuropsychological aspects of tuberous sclerosis complex. *J Child Neurol*. 2004;19:666–674.
23. Font RL, Ferry AP. The phakomatoses. *Int Ophthalmol Clin*. 1972;12:1–50.
24. Shields JA, Shields CL. *Diagnosis and management of intraocular tumors*. Mosby: St. Louis; 1983.
25. Raznahan A, Higgins NJ, deVries PJ, et al. Neuroanatomical correlates of memory deficits in tuberous sclerosis complex. *Cereb Cortex*. 2007;17:261–271.
26. Russel DS, Rubinstein LJ. *Pathology of tumors of the central nervous system*. 3rd ed. Edward Arnold: London; 1971.

27. Guttan M. Visual loss secondary to a giant aneurysm in a patient with tuberous sclerosis. *Can J Neurol Sci*. 1984;11:472–474.
28. Nickel WR, Reed WB. Tuberous sclerosis: special reference to the microscopic alterations in the cutaneous hamartomas. *Arch Dermatol*. 1962;85:209–226.
29. Roth JC, Epstein CJ. Infantile spasms and hypopigmented macules. *Arch Neurol*. 1971;25:547–551.
30. Gold AP, Freeman JM. Depigmented nevi: the earliest sign of tuberous sclerosis. *Pediatrics*. 1965;35:1003–1005.
31. Monaghan HP, Krafchik BR, MacGregor DL, et al. Tuberous sclerosis complex in children. *Am J Dis Child*. 1981;135:912–917.
32. Callen JP. The skin, the eye, and systemic disease. *Cutis*. 1979;24:501–511.
33. Farrow GM, Harrison EG Jr, Utz DC, et al. Renal angiomyolipoma: a clinicopathologic study of 32 cases. *Cancer*. 1968;22:564–570.
34. Charlot-Charles J, Jones GW. Renal angiomyolipoma associated with tuberous sclerosis: review of the literature. *Urology*. 1974;3:465–469.
35. Reed WB, Nickel WR, Campion G. Internal manifestations of tuberous sclerosis. *Arch Dermatol*. 1963;87:715–728.
36. Sanders MD, Gawler J. Computerized tomographic scanning (EMI scan) in neuro-ophthalmology. *Trans Ophthalmol Soc U K*. 1975;95:237–245.
37. Shelton RW. The incidence of ocular lesions in tuberous sclerosis. *Ann Ophthalmol*. 1975;771–774.
38. Gass JDM. *Stereoscopic atlas of macular diseases: diagnosis and treatment*. 3rd ed. Mosby: St. Louis; 1987.
39. Shields JA, Shields CL, Ehya H, et al. Atypical retinal astrocytic hamartoma diagnosed by fine-needle biopsy. *Ophthalmology*. 1996;103:949–952.
40. Eagle RC Jr, Shields JA, Shields CL, et al. Hamartomas of the iris and ciliary epithelium in tuberous sclerosis complex. *Arch Ophthalmol*. 2000;118:711–715.
41. Barsky D, Wolter JR. The retinal lesions of tuberous sclerosis: an angiomatosis hamartoma. *J Pediatr Ophthalmol*.

1971;8:261–265.
42. Nyboer JH, Robertson DM, Gomez MR. Retinal lesions in tuberous sclerosis. *Arch Ophthalmol*. 1976;94:1277–1280.
43. Wolter JR, Reimer K, et al. Exophytic retinal astrocytoma in tuberous sclerosis. *J Pediatr Ophthalmol*. 1969;6:186–191.
44. Shields CL, Shields JA, Eagle RC Jr, et al. Progressive enlargement of acquired retinal astrocytoma in 2 cases. *Ophthalmology*. 2004;111:363–368.
45. Kirati H, Bilgic S. Spontaneous regression of retinal astrocytic hamartoma in a patient with tuberous sclerosis. *Am J Ophthalmol*. 2002;133:715–716.
46. WB Saunders: Philadelphia; 1985. Spencer WH. *Ophthalmic pathology: an atlas and textbook*. vol. 2.
47. Gass JDM. Fluorescein angiography: an aid in the differential diagnosis of intraocular tumors. *Int Clin Ophthalmol*. 1972;12:85.
48. Kroll AJ, Richer DP, Robb RM, et al. Vitreous hemorrhage complicating retinal astrocytic hamartoma. *Surv Ophthalmol*. 1981;26:31–38.
49. Van der Hoeve J. Augengeschwulste bei der tuberosen Hirnklerose (Bourneville). *Graefes Arch Klin Ophthalmol*. 1921;105:880–898.
50. Atkinson A, Sanders MD, Wong V. Vitreous hemorrhage in tuberous sclerosis: report of two cases. *Br J Ophthalmol*. 1973;57:773–779.
51. Koch FLP, Walsh M. Syndrome of tuberous sclerosis: report of a case. *Arch Ophthalmol*. 1939;21:465–475.
52. Jost BF, Olk RJ. Atypical retinitis proliferans, retinal telangiectasis, and vitreous hemorrhage in a patient with tuberous sclerosis. *Retina*. 1986;6:534–536.
53. Coppeto JR, Lubin JR, Albert DM. Astrocytic hamartoma in tuberous sclerosis mimicking necrotizing retinochoroiditis. *J Pediatr Ophthalmol Strabismus*. 1982;19:306–313.
54. Miller NR. *Walsh and Hoyt's clinical neuro-ophthalmology*. 4th ed. Williams and Wilkins: Baltimore; 1982.
55. De Juan E Jr, Green WR, Gupta PK, et al. Vitreous seeding by retinal astrocytic hamartoma in a patient with tuberous sclerosis. *Retina*. 1984;4:100–102.

56. Zolli C, Rodrigues MM, Shannon GM. Unusual eyelid involvement in tuberous sclerosis. *J Pediatr Ophthalmol*. 1976;13:156–158.
57. Awan KJ. Leaf-shaped lesions of ocular fundus and white eyelashes in tuberous sclerosis. *South Med J*. 1982;75:227–278.
58. Gutman I. Hypopigmented iris spots: an early sign of tuberous sclerosis. *Ophthalmology*. 1982;89:1155–1159.
59. Gomez MR. *Tuberous sclerosis*. Raven Press: New York; 1979.
60. Hoogeveen-Westerveld M, Ekong R, Povey S, et al. Functional assessment of TSC1 missense variants identified in individuals with tuberous sclerosis complex. *Hum Mutat*. 2012;33:476–479.
61. Hoogeveen-Westerveld M, Ekong R, Povey S, et al. Functional assessment of TSC2 variants identified in individuals with tuberous sclerosis complex. *Hum Mutat*. 2013;34:167–175.
62. Cleasby GW, Fung WE, Shelker WB. Astrocytoma of the retina. *Am J Ophthalmol*. 1967;64:465–469.
63. Howard GM, Ellsworth RM. Differential diagnosis of retinoblastoma. I. Relative frequency of lesions which simulate retinoblastoma. *Am J Ophthalmol*. 1965;60:610–618.
64. Panzo GJ, Meyers SM, Gutman FA, et al. Spontaneous regression of parafoveal exudates and serous retinal detachment in a patient with tuberous sclerosis and retinal astrocytoma. *Retina*. 1984;4:242–245.
65. Hogan MJ, Zimmerman LE. *Ophthalmic pathology*. WB Saunders: Philadelphia; 1962.
66. Heckenlively JR. *Retinitis pigmentosa*. Lippincott: Philadelphia; 1988.
67. Spencer WH. Drusen of the optic disc and aberrant axoplasmic transport. *Ophthalmology*. 1978;85:21–38.
68. Puck A, Tso MOM, Fishman GA. Drusen of the optic nerve associated with retinitis pigmentosa. *Arch Ophthalmol*. 1985;103:231–234.
69. Novak RL, Foos RY. Drusen of the optic disk in retinitis pigmentosa. *Am J Ophthalmol*. 1987;103:44–47.
70. Robertson DM. Hamartomas of the optic disc with retinitis

pigmentosa. *Am J Ophthalmol*. 1972;74:526–531.
71. O'Callaghan F. Tuberous sclerosis complex. *Pediatr Child Health*. 2007;18:30–36.
72. Hunt A, Lindenbaum RH. Tuberous sclerosis: a new estimate of prevalence within the Oxford region. *J Med Genet*. 1984;21:272–277.
73. MacDonald IM, Bech-Hansen T, Britten WA Jr, et al. The phakomatoses: recent advances in genetics. *Can J Ophthalmol*. 1997;32:6–11.
74. Povey S, Burley MW, Attwood J, et al. Two loci for tuberous sclerosis: one on 9q34 and one on 16p13. *Ann Hum Genet*. 1994;58:107–127.
75. Sampson JR, Janssen JAJ, Sandkujji LA, et al. Linkage investigation of three putative tuberous sclerosis determining loci on chromosome 9q, 11q, and 12q. *J Med Genet*. 1992;29:861–866.
76. European Chromosome 16 Tuberous Sclerosis Consortium. Identification and characterization of the tuberous sclerosis gene on chromosome 16. *Cell*. 1993;75:1305–1315.
77. Dabora SL, Jozwiak S, Franz DN, et al. Mutational analysis in a cohort of 224 tuberous sclerosis patients indicates increased severity of TSC2, compared with TSC1, disease in multiple organs. *Am J Hum Genet*. 2001;68:64–80.
78. Crino PB, Henske EP. New developments in the neurobiology of the tuberous sclerosis complex. *Neurology*. 1999;53:1384–1390.
79. Vézina G. Neuro-imaging of phakomatoses:overview and advances. *Paediatr Neurol*. 2015;45(Suppl. 3):S433–42.
80. Krueger DA, Northrup H. Tuberous sclerosis complex surveillance and management. [on behalf of the; International Tuberous Sclerosis Complex Consensus Group] *Pediatr Neurol*. 2013;49:255–265.

136

Phakomatoses

Carol L. Shields, Jerry A. Shields

Introduction

The phakomatoses are a group of syndromes characterized by systemic hamartomas of the eye, brain, skin, and sometimes the viscera and bones.[1–4] As a result of the multisystem involvement, the phakomatoses are also known as oculoneurocutaneous syndromes. Variable clinical manifestations of these syndromes are

recognized, and comprehensive care of the patient often involves coordination of several specialists, including neurologists, dermatologists, ophthalmologists, and oncologists.

The term "phakoma" was first used by Van der Hoeve in 1932 to indicate a mother spot, or birthmark, a characteristic finding in many of these entities.[4] At that time, retinal and cerebellar hemangiomatosis (von Hippel–Lindau syndrome), neurofibromatosis (von Recklinghausen syndrome), and tuberous sclerosis complex (Bourneville syndrome) were all classified as phakomatoses. Later, encephalofacial hemangiomatosis (Sturge–Weber syndrome), racemose angiomatosis (Wyburn-Mason syndrome), and cavernous hemangioma of the retina with cutaneous and central nervous system involvement were included with these conditions. More recently, other entities such as organoid nevus syndrome, oculodermal melanocytosis, and phacomatosis pigmentovascularis have been categorized with these classic oculoneurocutaneous syndromes.

Definition of Hamartia, Hamartoma, Chorista, Choristoma

To better understand the phakomatoses, certain terms such as hamartia, hamartoma, chorista, and choristoma should be defined.[1] Hamartia and hamartoma are terms that refer to a malformation that is composed of tissues normally present at the location where it develops. A hamartia is a nontumorous anomaly, and a hamartoma is a tumorous malformation. The term systemic hamartomatosis is used to designate multiple organ involvement. Examples of hamartomas include the retinal hemangioblastoma (capillary hemangioma) that occurs from already present vascular tissue in the retina in von Hippel–Lindau syndrome, or the cutaneous peripheral nerve tumors that occur from the already present neural tissue within the skin in patients with neurofibromatosis.

Chorista and choristoma are terms that refer to a malformation composed of elements that are not normally present at the site where they develop. A chorista is a nontumorous anomaly and a choristoma is a tumorous malformation. The classic example of a

choristoma is the limbal dermoid, a tumor composed of dermal elements that are not normally present in the bulbar conjunctiva or cornea. Most of the phakomatoses are comprised of hamartomas rather than choristomas.

Most phakomatoses display an autosomal dominant mode of inheritance, often with incomplete penetrance. Notable exceptions are encephalofacial hemangiomatosis (Sturge–Weber) and racemose hemangiomatosis (Wyburn-Mason) in which germline heredity does not appear to play a role.

Most of the tumors that develop with the phakomatoses are benign. They are usually stationary or slowly progressive lesions that generally lack the capacity for limitless proliferation found with cancers.[1] Some phakomatoses can be associated with malignant neoplasms. For example, there is an increased incidence of malignant schwannomas of the peripheral nerves in patients with neurofibromatosis. Renal cell carcinoma occurs with greater frequency in patients with von Hippel–Lindau disease.

Patients with the phakomatoses might only manifest some of the clinical features of a particular syndrome and this is referred to as a "forme fruste." Furthermore, patients can occasionally exhibit lesions characteristic of one entity and other lesions characteristic of another and this is referred to as the crossover phenomenon. For example, the café-au-lait spots seen in patients with neurofibromatosis can occasionally be seen in patients with tuberous sclerosis complex or encephalofacial hemangiomatosis.

In other chapters in the book, the conditions of tuberous sclerosis complex (Bourneville syndrome) and retinocerebellar hemangiomatosis (von Hippel–Lindau syndrome) have been described. In this chapter, we elaborate on other phakomatoses. These phakomatoses include neurofibromatosis (von Recklinghausen syndrome), encephalofacial hemangiomatosis (Sturge–Weber syndrome), retinal racemose hemangiomatosis (Wyburn-Mason syndrome), retinal cavernous hemangiomatosis, organoid nevus syndrome (Solomon syndrome), phacomatosis pigmentovascularis (*Cesioflammea* type), and oculodermal melanocytosis (nevus of Ota). Because this book covers primarily diseases of the ocular fundus, most emphasis is placed on retinal and choroidal manifestations.

Neurofibromatosis (Von Recklinghausen Syndrome)

Neurofibromatosis is an oculoneurocutaneous syndrome characterized by multisystem involvement.[5,6] It is transmitted by an autosomal dominant mode of inheritance with about 80% penetrance. About one-half of the cases occur initially as spontaneous mutations with a negative family history.

Neurofibromatosis is subcategorized into types 1 and 2. Type 1 is called peripheral neurofibromatosis or von Recklinghausen syndrome, whereas type 2 is called central or bilateral acoustic neurofibromatosis. Type 1 neurofibromatosis is characterized by peripheral and cutaneous manifestations and is related to an abnormality on chromosome 17. Type 2 is characterized by central nervous system (CNS) tumors and early onset of posterior subcapsular cataract. Type 2 neurofibromatosis is related to an abnormality on chromosome 22.

Neurofibromatosis Type 1

General Considerations

Neurofibromatosis type 1 occurs at a rate of 1 in 3000 persons, but it is estimated that the frequency could be higher, as some individuals manifest only mild features. Approximately one-half of affected patients represent a new mutation. This condition is caused by an autosomal dominant mutation in the *NF1* gene that leads to decreased production of the protein neurofibromin, which has a tumor suppressor function. Only one deleted is necessary to manifest this condition. The *NF1* gene is on long arm of chromosome 17. There have been more that 250 mutations identified. Complete gene deletion leads to severe phenotype. This highly penetrant phenotype has a wide variety of manifestations and can vary within families. Another locus, the *SPRED1* gene, has been found in patients with "mild neurofibromatosis" and this represents Legius syndrome.[7]

The criteria for diagnosis of neurofibromatosis type 1 are listed in Table 136.1.[8,9] This condition more often affects patients of the white

race and equally in boys and girls. Scoliosis can be a prominent feature.

TABLE 136.1

Diagnostic Criteria for Neurofibromatosis Type 1 (NF1): At Least Two of the Following Seven Criteria Should be Present for Diagnosis[a]

1. Café-au-lait	≥6 café-au-lait spots larger than 5 mm diameter in prepubertal children (<10 years)
	or
	≥6 café-au-lait spots larger than 15 mm in diameter in postpubertal individuals (adults)
2. Freckles in axilla or inguinal region	Crowe sign
3. Skin neurofibroma	≥2 typical neurofibroma
	or
	≥1 plexiform neurofibroma
4. Optic nerve glioma	
5. Iris Lisch nodules	≥2 lesions
6. Osseous lesion	Sphenoid dysplasia
	or
	Long bone abnormalities (cortex thinning or pseudoarthrosis)
7. Relative (1st degree) with NF1 by above criteria	Parent, sibling or offspring

[a]Some manifestations do not appear until later life, delaying diagnosis.

Adapted from Stumpf DA, Alksne JF, Annegers JF. Neurofibromatosis. Conference statement. National Institute of Health Consensus Development Conference. Arch Neurol 1988;45:575–8; and Gutmann DH, Aylsworth A, Carey JC, et al. The diagnostic evaluation and multidisciplinary management of neurofibromatosis 1 and neurofibromatosis 2. JAMA 1997;278:51–7.

Ophthalmologic Features

Neurofibromatosis has the most diversified ocular findings among the phakomatoses.[10–17] This condition can involve the eyelid, conjunctiva, aqueous outflow channels, uveal tract, retina, orbit, and optic nerve (Fig. 136.1).

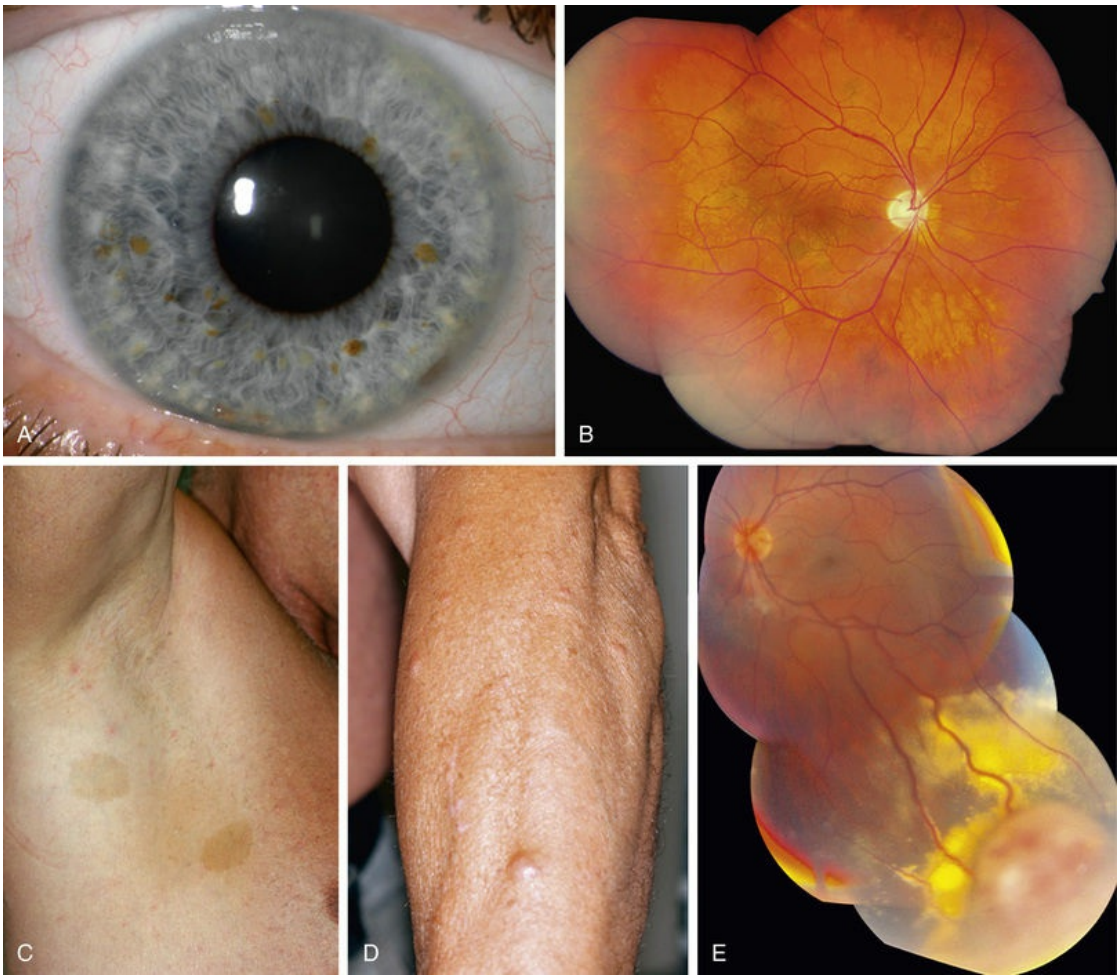

FIG. 136.1 Neurofibromatosis type 1. (A) Iris Lisch nodules. (B) Multifocal choroidal freckling. (C) Axillary freckling. (D) Multiple cutaneous neurofibromatosis. (E) Vasoproliferative tumor with exudative retinopathy.

Eyelid involvement is characterized by nodular or plexiform neurofibroma. Nodular neurofibroma appears as a solitary or multifocal painless, smooth-surfaced, and well-defined mass, often the size of a pea, and without color change. Plexiform neurofibroma presents as a diffuse thickening of the eyelid that can produce the typical S-shaped curvature to the eyelid, a finding highly characteristic of neurofibromatosis. The conjunctiva can be involved by diffuse or localized neurofibromas. Patients with neurofibromatosis have an increased incidence of congenital glaucoma, which can be secondary to several mechanisms. There is a high association of neurofibromatosis type 1 with optic nerve glioma.[12]

A variety of ocular fundus lesions can occur in patients with

neurofibromatosis. Multiple iris hamartomas, known as Lisch nodules, are the most common uveal abnormality of neurofibromatosis type 1.[11] These characteristically orange–tan nodules appear in early childhood (usually by age 6 years) as discrete, multiple, bilateral tumors of the anterior border layer of the iris, classically measuring less than 1 mm diameter and best detected by slit-lamp biomicroscopy. Histopathologically, iris Lisch nodules are hamartomas composed of aggregates of melanocytes on the anterior border layer of the iris.

The choroidal findings in patients with neurofibromatosis type 1 include unifocal or multifocal choroidal nevus, diffuse plexiform neurofibroma, neurilemoma, and melanoma. Multiple bilateral, choroidal nevi are highly suggestive of neurofibromatosis type 1.[10] They are usually small, ill-defined, and randomly distributed. They might be best seen with near-infrared reflectance imaging or multispectral imaging with long wavelength.[10] Choroidal neurofibroma usually appears as a diffuse thickening of the uveal tract from an increased number of neurofibromatous and melanocytic elements. Choroidal neurilemoma (schwannoma) is a rare finding and manifests as a circumscribed, amelanotic elevated tumor.[14] Most solitary choroidal neurilemomas, however, are not associated with neurofibromatosis. There appears to be a higher incidence of uveal melanoma in patients with neurofibromatosis.[15]

Several retinal and optic disc lesions can occur with neurofibromatosis. Retinal astrocytic hamartoma is a manifestation of neurofibromatosis, but is more common with tuberous sclerosis complex. Retinal vasoproliferative tumor can occur with neurofibromatosis, leading to exudative retinopathy and risk for blindness.[16,17] Fundus changes can occur secondary to optic nerve glioma, including optic disc edema, optic atrophy, opticociliary shunt vessels and, rarely, central retinal vein obstruction.

Dermatologic Features

The most important cutaneous manifestations of neurofibromatosis include café-au-lait spots (pigmented macules), freckles in the axillary or inguinal region, and urticarial pigmentosa. Café-au-lait spots are found in 95% of patients with neurofibromatosis type 1, but they can be seen in patients with other conditions, such as

McCune–Albright syndrome, tuberous sclerosis complex, and Fanconi anemia. Café-au-lait spots can be found in persons without neurofibromatosis type 1. They represent the earliest manifestation of neurofibromatosis type 1 and can be found in infancy as a very light hyperpigmented macule that becomes more noticeable over time or with sun exposure.

Subcutaneous or cutaneous benign neurofibromas are an important finding but are rare in young children and typically appear in older children or later. Deep neurofibromas might not be visible and are detected only by palpation. Puberty and pregnancy can increase number and growth of neurofibromas. Plexiform neurofibromas can be invasive and ill-defined, occasionally associated with pain. Rapid growth of neurofibroma is suggestive of malignant degeneration.

Central Nervous System Features

The most important central nervous system feature of neurofibromatosis type 1 is the optic nerve glioma (juvenile pilocytic astrocytoma). Optic nerve glioma can present with obvious features of painless proptosis or subtle features of color or visual acuity abnormalities. Magnetic resonance imaging shows enlargement of the optic nerve, often so large that it develops a fold (kink) within its substance to accommodate the orbit, leading to down-and-out proptosis. This mass shows enhancement on T1-weighted, gadolinium contrast images, particularly notable in the axial and coronal views. It is important to differentiate this tumor from optic nerve sheath meningioma as the systemic implications and therapy differ. This is best determined using gadolinium-enhanced, orbital fat suppressed, T1-weighted coronal views. With glioma, the central substance of the nerve enhances whereas with meningioma, the peripheral encircling arachnoid sheath enhances. Glioma is more often associated with neurofibromatosis type 1, whereas meningioma is more associated with neurofibromatosis type 2.

Other Features

There are numerous orthopedic problems in patients with neurofibromatosis type 1. Sphenoid wing dysplasia, congenital

pseudoarthrosis with tibial or forearm bowing, thoracic cage asymmetry with inferior rib prominence, and scoliosis/kyphosis. Scoliosis at a young age (under 10 years) can progress. Other findings include macrocephaly and hypertension.

A number of other benign and malignant systemic tumors have been associated with neurofibromatosis. Sarcomas can arise from the peripheral nerve sheath, either de novo or from preexisting benign cutaneous nerve sheath tumors. Malignant peripheral nerve sheath tumors can occur in over 20% of patients. There seems to be an increased incidence of breast, genitourinary, and gastrointestinal tumors, as well as cutaneous melanoma. Patients with neurofibromatosis probably have a slightly higher incidence of pheochromocytoma.

Management

The management of neurofibromatosis varies with the location and the extent of the disease. Most fundus lesions require no treatment. Choroidal melanoma and neurilemoma are often clinically indistinguishable, and have usually required plaque radiotherapy, resection, or enucleation. Iris Lisch nodules, congenital hypertrophy of the retinal pigment epithelium, and retinal astrocytic hamartoma are observed. Retinal vasoproliferative tumors often require cryotherapy, laser photocoagulation, photodynamic therapy, or plaque radiotherapy to control exudative findings.[16,17] Neurofibromatosis type 1 is caused by mutation in the protein neurofibromin that inhibits the RAS pathway, which regulates cellular proliferation and differentiation. Systemic targeted biologic agents have been explored to halt growth of tumors such as sirolimus, an mTOR inhibitor.[18]

Neurofibromatosis Type 2

General Considerations

Neurofibromatosis type 2 is a multisystem disorder with prominent features of central nervous system tumors, including bilateral vestibular schwannomas (acoustic neuromas), spinal cord schwannomas, meningiomas, gliomas, and juvenile posterior subcapsular cataract. This condition is also referred to as MISME

syndrome, a mnemonic referring to related tumors of MIS (multiple inherited schwannomas), M-meningiomas, and E-ependymomas.[19] Cutaneous features are uncommon with this form of neurofibromatosis. The criteria for diagnosis of neurofibromatosis type 2 are listed in Table 136.2.

TABLE 136.2

Diagnostic Criteria for Neurofibromatosis Type 2 (NF2). Diagnosis Is Established With at Least One of the Three Items Listed Below

Feature
1. Bilateral eighth cranial nerve tumors confirmed on magnetic resonance imaging or computed tomography
2. Unilateral eighth cranial nerve tumor *plus* Relative (1st degree) with NF2
3. Two of the following: Meningioma Glioma Schwannoma Juvenile posterior subcapsular lens opacity *plus* Relative (1st degree) with NF2

Adapted from Stumpf DA, Alksne JF, Annegers JF. Neurofibromatosis. Conference statement. National Institute of Health Consensus Development Conference. Arch Neurol 1988;45:575–8; and Gutmann DH, Aylsworth A, Carey JC, et al. The diagnostic evaluation and multidisciplinary management of neurofibromatosis 1 and neurofibromatosis 2. JAMA 1997;278:51–7.

Neurofibromatosis type 2 can be associated with reduced lifespan secondary to central nervous system tumors, particularly if they are present at a young age and are multiple. The average age at symptom onset is approximately 20 years but can be delayed. Early age at symptom onset and the presence of intracranial meningioma at diagnosis are two signs of higher risk for disease severity and mortality. In an analysis of 150 affected patients, more than 40% were expected to die by 50 years.[20] Recent advances in treatment have extended life prognosis.

The incidence of neurofibromatosis type 2 is 1 in 25 ,000 live births and has nearly 100% penetrance by 60 years of age.[21] It is estimated that this condition has a diagnostic prevalence of 1 in 100, 000 people. Neurofibromatosis type 2 is related to a mutation in the *NF2* gene at chromosome 22q12.2. This gene produces merlin (also

called neurofibromin-2), a tumor suppressor. When mutated, decreased function of merlin leads to the uncontrolled development of tumors, particularly in the central nervous system. One-half of affected patients have a de novo mutation.

Ophthalmologic Features

Neurofibromatosis type 2 displays three important ophthalmologic findings, notably posterior subcapsular cataract in childhood, combined hamartoma of the retina and retinal pigment epithelium, and epiretinal membranes (Fig. 136.2) (Table 136.3). The juvenile posterior subcapsular cataract (<50 years) is a criterion for diagnosis of this condition. Other lens opacity in the capsular or cortical region of young patients are believed related to neurofibromatosis type 2. Lisch nodules are not a feature of neurofibromatosis type 2.

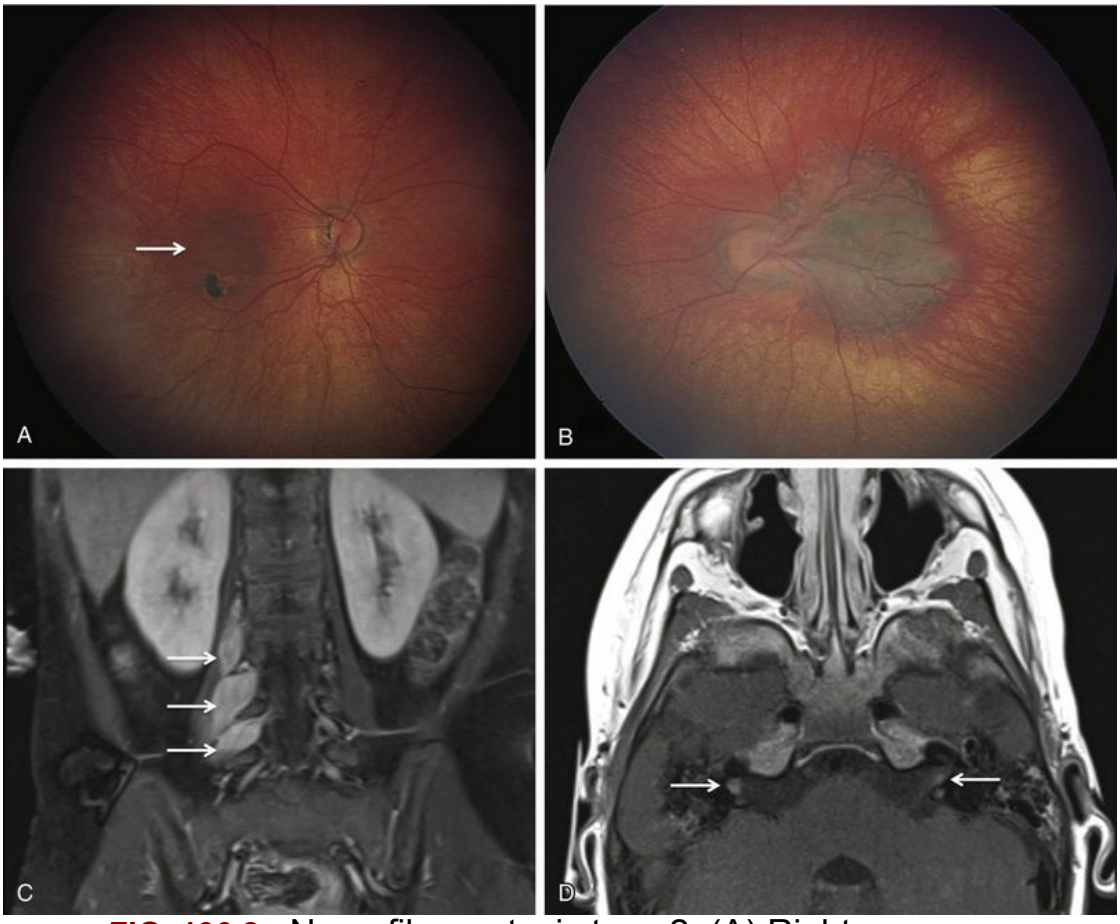

FIG. 136.2 Neurofibromatosis type 2. (A) Right eye with retinal pigment epithelial (RPE) hyperplasia and nearly invisible inner retinal mass (*arrow*) classified as

combined hamartoma. (B) Left eye with more obvious combined hamartoma and retinal traction and RPE hyperplasia. (C) Magnetic resonance imaging (MRI) showing schwannomas of spine (*arrows*). (D) MRI showing bilateral acoustic neuroma (*arrows*).

TABLE 136.3

Frequency of Clinical Features in Patients With Neurofibromatosis Type 2

Feature	Frequency Associated With Neurofibromatosis Type 2 (%)
OPHTHALMOLOGIC FEATURES	
Juvenile posterior subcapsular cataracts	60–81%
Epiretinal membranes	12–40%
Retinal hamartomas	6–22%
CUTANEOUS FEATURES	
Cutaneous tumors	59–68%
Cutaneous plaques	41–48%
Subcutaneous tumors	43–48%
Intradermal tumors	Rare
CENTRAL NERVOUS SYSTEM FEATURES	
Bilateral vestibular (cranial nerve VIII) schwannomas	90–95%
Other cranial nerve schwannomas	24–51%
Intracranial meningiomas	45–58%
Spinal tumors	63–90%
Extramedullary	55–90%
Intramedullary	18–53%
Peripheral neuropathy	66%

Adapted from Asthagiri AR, Butman JA, Kim HJ, et al. Neurofibromatosis type 2. Lancet 2009;373:1974–86.

Epiretinal membranes and combined hamartoma of the retina and retinal pigment epithelium can have overlapping clinical phenotype and can be multifocal (Fig 136.2). Of those with severe clinical features of neurofibromatosis type 2, 80% display epiretinal membranes.[21] By enhanced depth imaging optical coherence tomography (OCT), this lesion shows a sawtooth, folded, or combination features from vitreoretinal traction.[22] The hamartomas are along the inner retina but lead to prominent retinal dragging, corkscrew retinal vessels, gray–green appearance, and tumor formation.[22,23]

Dermatologic Features

The cutaneous features of neurofibromatosis type 2 are slightly different than those in type 1. Occasionally, overlap of the two conditions can be seen. Café-au-lait spots are occasionally found. Axillary or inguinal freckling is not often found with neurofibromatosis type 2. Subcutaneous schwannomas or neurofibromas can be found, and malignant transformation is extremely rare. Neurofibromatosis type 2 displays skin plaques, represented by well-circumscribed, roughened areas less than 2 cm and often with slight hyperpigmentation and hypertrichosis.

Central Nervous System Features

Neurofibromatosis type 2 is also called central nervous system neurofibromatosis because of the importance of these related tumors. The central nervous system tumors represent the majority of findings in neurofibromatosis type 2 and vary with the size and extent of the associated tumors. Acoustic neuromas (vestibular schwannomas) are the most common and well-recognized feature. If bilateral, they are considered pathognomonic of type 2 neurofibromatosis. Patients present with symptoms of tinnitus, gradual hearing loss, and later growth produces brainstem compression, hydrocephalus, and facial palsy.

Spinal cord schwannomas, particularly dumbbell-shaped, are common. Spinal cord ependymomas, astrocytomas, and meningiomas can occur less frequently. Intracranial meningiomas are frequent and can manifest with or without symptoms. Nonvestibular schwannomas, particularly of cranial nerves III and V, are diagnosed at a fairly early age, but can be indolent and slow-growing.

Other Features

Sensory motor polyneuropathy can be found, particularly in those with schwannomas.

Management

Patients with neurofibromatosis type 2 should have annual ophthalmic, neurologic, dermatologic, and auditory examinations.

This requires a multidisciplinary team. Surgical resection of symptomatic neurologic tumors is performed, but radiotherapy or chemotherapy can be used, particularly for ependymomas. Erlotinib and lapatinib (epidermal growth factor inhibitors) for unresectable progressive schwannomas is under trial.[24] Additionally, bevacizumab and Gleevec have been investigated for treatment of schwannomas. Regarding ophthalmic care, cataract surgery can be beneficial. Additionally, monitoring of epiretinal membrane with clinical examination and OCT, with surgical removal if progressive, can be considered.[23]

Encephalofacial Hemangiomatosis (Sturge–Weber Syndrome)

General Considerations

The Sturge–Weber syndrome is characterized by congenital hamartomas of the eye, skin, and brain that manifest at different times during life, mostly in childhood. These include choroidal hemangioma, facial nevus flammeus (port wine stain), and brain hemangioma with intracranial calcification.[25–37] Some patients display a forme fruste, or partial expression, rather than the entire syndrome. In contrast to the other systemic hamartomatosis, there is no recognizable hereditary pattern associated with Sturge–Weber syndrome. There is no predisposition for sex or race.

This condition affects 1 per 50, 000 persons. Roach has designed a classification for Sturge–Weber syndrome (Table 136.4).[25,26,31] In 1987, Happle proposed that Sturge–Weber syndrome was an example of somatic mosaicism of a genetic trait.[32] In 2003, Comi and associates supported this theory by demonstrating abnormality in the gene expression of fibronectin in fibroblasts from the region of the port wine stain compared with normal skin.[33] Recent study has found activating somatic *GNAQ* gene mutation in the port wine stain.[30] A variable but progressive course can occur in the lesions in the brain, eye, and skin as well as those related to otolaryngological, endocrine, emotional, and behavioral aspects.

TABLE 136.4

Roach Diagnostic Scale for Classification of Encephalotrigeminal Angiomatosis (Sturge–Weber Syndrome)

Type	Title	Involvement of Skin, Eye, and Brain
Type I	Classic Sturge–Weber syndrome	Leptomeningeal angioma present
		Cutaneous facial angioma present
		Glaucoma likely present
Type II	Sturge–Weber syndrome	Leptomeningeal angioma absent
		Cutaneous facial angioma present
		Glaucoma possibly present
Type III	Sturge–Weber syndrome forme fruste	Leptomeningeal angioma present
		Cutaneous facial angioma absent
		Glaucoma absent

Adapted from Roach ES. Neurocutaneous syndromes. Pediatr Clin North Am 1992;39:591–620.

Ophthalmologic Features

The ocular findings associated with Sturge–Weber syndrome include eyelid involvement with the nevus flammeus, prominent epibulbar blood vessels, glaucoma, retinal vascular tortuosity, and diffuse choroidal hemangioma (Fig. 136.3). Glaucoma is more common in patients with Sturge–Weber syndrome than it is in the other systemic hamartomatoses. In a study of 50 patients with nevus flammeus, there was an 8% overall incidence of glaucoma.[27] If the facial hemangioma involved both the first and second division of the trigeminal nerve, the incidence was 15%.[27] The glaucoma occurs unilaterally on the side of the facial hemangioma and it can gradually lead to extensive optic disc cupping and blindness. The associated glaucoma can be either congenital or juvenile. Sullivan and associates reviewed eye findings in 51 patients with Sturge–Weber syndrome and found 71% with glaucoma (onset before 2 years of age in most cases), 69% with conjunctival or episcleral prominent vessels, and 55% with diffuse choroidal hemangioma.[34]

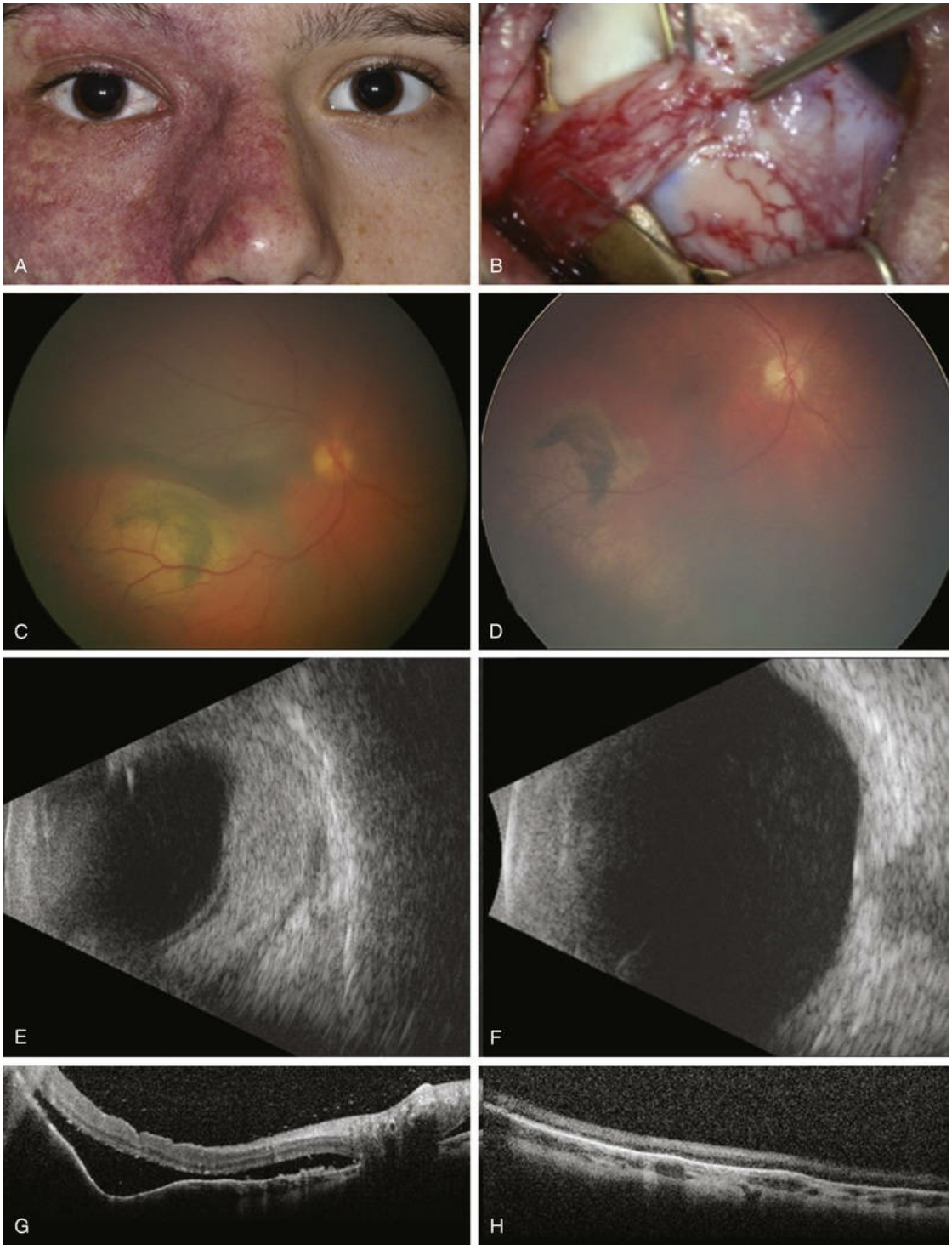

FIG. 136.3 Sturge–Weber syndrome. (A) Facial nevus flammeus. (B) Diffuse choroidal hemangioma with serous retinal detachment, retinal pigment epithelial hyperplasia, and visual loss, confirmed on ultrasonography (C) and optical coherence tomography (OCT) (D). Following plaque radiotherapy (E), complete resolution of retinal detachment (F), tumor on ultrasonography (G) and subretinal fluid on

OCT (H).

The main abnormality of the uveal tract in patients with Sturge–Weber syndrome is diffuse choroidal hemangioma.[35,36] Patients with this tumor display bright red pupillary reflex in the involved eye compared with the contralateral eye. This phenomenon, which is due to the light reflex from the highly vascularized tumor in the posterior pole, has been called the "tomato catsup" fundus.[28] B-scan ultrasonography typically demonstrates a diffuse, highly echogenic thickening of the choroid. The tumor is usually unilateral but bilateral cases associated with bilateral facial nevus flammeus have been recognized. Choroidal hemangioma is usually diagnosed when the affected patient is young (median age 8 years), either because the associated facial hemangioma prompts a fundus examination or because visual impairment occurs from hyperopic amblyopia or from secondary retinal detachment. Diffuse choroidal hemangioma can lead to a total retinal detachment and secondary neovascular glaucoma.

Other fundus changes seen with Sturge–Weber syndrome include congenital retinal vascular tortuosity and pigmentary alterations from a longstanding nonrhegmatogenous retinal detachment, sometimes causing a "pseudoretinitis pigmentosa" appearance.

Dermatologic Features

The classic skin lesion of Sturge–Weber syndrome is the facial nevus flammeus or port wine stain. Although it typically occurs in the cutaneous distribution of the fifth cranial nerve, it can have many variations, ranging from minor involvement of the first division of the nerve to massive involvement of all three divisions.

The port wine stain has been found to harbor *GNAQ* mutation.[30] Of 192 children with port wine stains, the most valuable predictor of adverse outcomes was stain involving the forehead with its inferior border at the outer canthus of the eye to the top of the ear and involving upper eyelid – a feature that involves all three divisions of the trigeminal nerve.[29] Bilateral involvement did not worsen outcome. All children with a forehead stain should have an ophthalmic examination and brain MRI.[29]

Central Nervous System Features

The typical CNS feature associated with Sturge–Weber syndrome is a diffuse leptomeningeal hemangioma that is ipsilateral to the facial hemangioma.[30] This lesion can show secondary calcification that appears radiographically as a radiopaque double line which has been called the "railroad track" sign. The calcification often increases during the first 20 years of life and usually becomes stable in adulthood. Seizures, stroke, headache, learning disorders, and developmental delay can occur as a result of the leptomeningeal hemangioma (Table 136.5).

TABLE 136.5

Clinical Findings in the Sturge–Weber Syndrome

Feature	Percentage
Cutaneous facial nevus flammeus	87%
Bilateral cerebral involvement	15%
Seizures	72–93%
Hemiparesis	25–93%
Hemianopia	44%
Headache	44–62%
Developmental delay or mental retardation	50–75%
Glaucoma	30–71%
Choroidal hemangioma	40%

Of all patients with facial port wine stain, only 8% show complete features of Sturge–Weber syndrome.

Management

The management of diffuse choroidal hemangioma varies with the extent of the tumor and secondary retinal detachment. If the tumor is minimally elevated and without subretinal fluid, observation is advised and correction of the induced hyperopic change and related amblyopia should be considered. Thicker tumors with secondary retinal detachment are treated with oral propranolol, photodynamic therapy, plaque radiotherapy, or external beam radiotherapy.[34,37] Oral propranolol is an alternative that may or may not be efficacious. Multispot photodynamic therapy often resolves the fluid, but this procedure requires patient cooperation during delivery. Plaque radiotherapy and external beam radiotherapy with a total dose of 20–40 Gy has been reliably successful in achieving

resolution of subretinal fluid and return of some visual acuity, depending on the chronicity.[37] The treatment of related glaucoma can be complex.

The cutaneous lesions seen with Sturge–Weber syndrome can be managed by repetitive laser photocoagulation in infancy and later cosmetic creams to cover the defect. Both of these methods can improve the cosmetic appearance.

Racemose Hemangiomatosis (Wyburn-Mason Syndrome)

General Considerations

Racemose hemangioma of the midbrain and ipsilateral retina is called the Wyburn-Mason syndrome.[38] In contrast to the other oculoneurocutaneous syndromes, it has few skin changes except for occasional small hemangiomas. The ocular and central nervous system changes, however, can be quite striking. Like Sturge–Weber syndrome, this congenital condition does not appear to be familial and does not exhibit a hereditary pattern. The characteristic arteriovenous communications can range from subtle asymptomatic lesions to more extensive lesions that form tumor-like vascular masses, often referred to as racemose or cirsoid hemangiomas.

The exact association of the retinal and central nervous system hemangiomas is not clear, but it is estimated that 30% of patients with the retinal findings have brain findings.[38] On the other hand, it is estimated that 8% of patients with brain findings have retinal findings.

Ophthalmologic Features

The classic ocular finding is the racemose hemangioma of the retina (Fig. 136.4).[38–44] Similar vascular malformations can occur in the orbit and adjacent structures. These retinal arteriovenous communications have been divided into three groups according to the Archer classification (Table 136.6).[41] Group I is characterized by interposition of an abnormal capillary plexus between the major

vessels. It is not a true tumor and the affected patient is often asymptomatic. Group II is typified by a direct arteriovenous communication without interposition of capillary or arteriolar elements. The dilated blood vessels in this group can superficially resemble a retinal capillary hemangioma, but no tumor, exudation, or retinal detachment is present. In general, these patients have few visual symptoms, but they can have associated cerebral arteriovenous malformations. Group III is characterized by a more extensive, complex arteriovenous communication, which is often associated with visual loss. In this group, the most striking feature is one or more dilated arteries that emerge from the optic disc, pass for a variable distance into the retina, form distinct arteriovenous communications, and then pass back to the optic disc as large veins. There is characteristically no exudation or retinal detachment and the vessels do not leak fluorescein. Although these lesions are believed to remain stationary indefinitely, we have observed changes in the distribution of the blood vessels over several years. Branch retinal vein obstruction can occur.[42,43] Iris racemose hemangioma has not been associated with retinal racemose hemangioma or the Wyburn-Mason syndrome.[44]

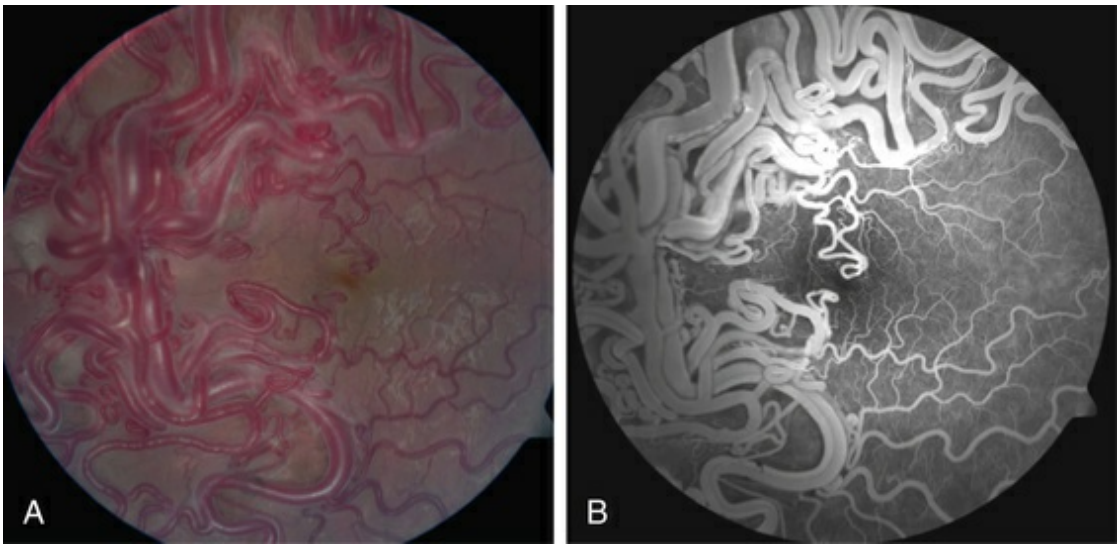

FIG. 136.4 Wyburn-Mason syndrome. (A) Archer type III retinal vascular malformation seen clinically and on (B) fluorescein angiography.

TABLE 136.6
Archer Classification for Wyburn-Mason Syndrome

Group	Feature	Comments
I	Abnormal capillary plexus between the major vessels of the arteriovenous malformations	Such lesions tend to be small, patients asymptomatic, and intracranial involvement uncommon
II	Arteriovenous malformations lack any intervening capillary bed between the artery and vein	Risk of retinal decompensation resulting in retina edema, hemorrhage, and vision loss. Low risk for intracranial arteriovenous malformations
III	Extensive arteriovenous malformations with dilated and tortuous vessels and no distinction between artery and vein	High risk for visual loss due to retinal decompensation or retinal compression of nerve fiber layer, optic nerve, or other vessels. High risk for intracranial arteriovenous malformations

Adapted from Archer DM, Deutman A, Ernest JT, et al. Arteriovenous communications of the retina. Am J Ophthalmol 1973;75:224–41.

Dermatologic Features

There are no significant cutaneous changes associated with racemose hemangiomatosis, except for the rare occurrence of small facial angiomas.

Central Nervous System Features

The racemose hemangioma of the central nervous system is most often found in the midbrain. Spontaneous intracranial hemorrhage from the malformation can lead to a variety of neurologic symptoms, most notably stroke and focal neurologic defects. Intracranial hemorrhage occurs far more frequently than intraocular hemorrhage. These malformations typically become symptomatic in the second or third decade of life and present with headache, vomiting, or meningismus. Hydrocephalus can ensue. In one analysis of the differential diagnosis of strokes in children, the leading causes included familial cavernous malformations, hereditary hemorrhagic telangiectasia, and moyamoya disease, as well as Wyburn-Mason syndrome and others.[39]

Other Features

The bones of the skull can frequently be involved with the vascular malformation. When the mandible or maxilla is affected, prolonged

bleeding can occur during invasive dental work.

Management

In general, no dermatologic or ophthalmic treatment is necessary in patients with racemose hemangiomatosis. The retinal vascular lesion is monitored for vein obstruction or hemorrhage. Branch retinal vein obstruction usually resolves without treatment, but intravitreal injection of antivascular endothelial growth factor or panretinal photocoagulation can be considered to prevent ischemic vascular complications and glaucoma. If persistent vitreous hemorrhage is found, then vitrectomy removal is performed.

Retinal Cavernous Hemangiomatosis

General Considerations

There are two types of retinal cavernous hemangioma, including those that occur sporadically and those associated with the syndrome of cutaneous and central nervous system vascular malformations.[45–51] The latter is associated with a highly penetrant autosomal dominant mutation and is considered a phakomatosis. Genetic abnormalities have been found on chromosomes 3q, 7p, and 7q.

Ophthalmologic Features

The only ocular manifestation of this syndrome is the retinal cavernous hemangioma (Fig. 136.5). Ophthalmoscopically, this lesion appears as a dark grape-like cluster of venous intraretinal aneurysms either at the optic disc, macula, or in the peripheral retina.[45–51] There is no obvious feeding artery and the lesion is typically centered along the course of a vein. This lesion produces no exudation or subretinal fluid, likely due to the fact that the thin-walled channels are lined by nonfenestrated endothelium. Repetitive vitreous hemorrhages (often mild and subclinical) can lead to white fibroglial tissue on the surface.[50] This nonprogressive thin-walled, aneurysmal retinal tumor can remain hidden in the fundus for decades until dilation is performed or the patient

develops vitreous hemorrhage.

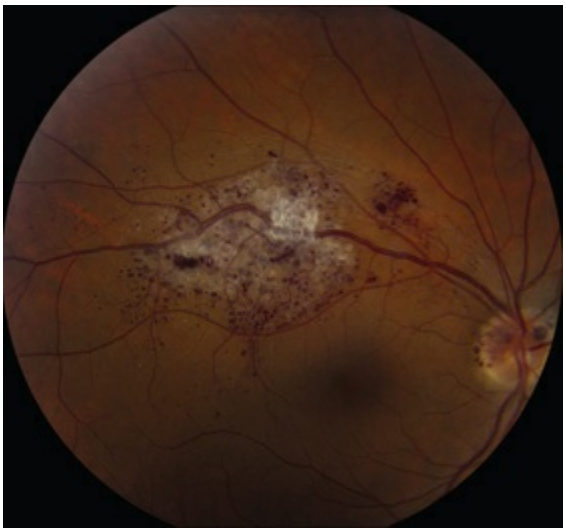

FIG. 136.5 Retinal cavernous hemangioma in a patient with brain hemangiomatosis.

The main complication of retinal cavernous hemangioma is vitreous hemorrhage. Larger tumors can be associated with severe fibrogliosis and related retinal dragging with displacement of the macula.

The most important diagnostic test for retinal cavernous hemangioma is fluorescein angiography, which produces highly characteristic, if not pathognomonic, features of hypofluorescence persistent into the late frames with slow nonleaking filling of the aneurysms. Fluorescein is contained within the venous aneurysms of the lesion and pools in the plasma in the superior portion of each vascular space, while the blood elements collect in the inferior portion. This produces the typical fluorescein–blood interface in the late angiograms that characterizes retinal cavernous hemangioma. Other rare ophthalmic findings include iris cavernous hemangiomatosis with repetitive hemorrhages.[48]

Dermatologic Features

The hemangiomas of the skin in this syndrome are variable in their appearance and distribution on the body. The lesions occur most commonly on the back of the neck. Involvement of the eyelids is rare.

Central Nervous System Features

Cavernous hemangioma can involve any region of the central nervous system but is more common in the supratentorial rather than infratentorial region. Spinal cord involvement can occur. Symptoms include seizures, hemorrhage, and focal neurologic defect most commonly. About 25% of patients display no neurologic symptom despite having a cavernous hemangioma within the brain.[49] Intracranial hemorrhage occurs in 12–48%. Magnetic resonance imaging can provide information to the location and size of the mass.

Other Features

Various ophthalmic manifestations related to brain injury can occur, such as diplopia due to paresis of extraocular muscles, presumably secondary to bleeding into the oculomotor nuclei. It is likely that many patients have vascular lesions in the central nervous system that remain subclinical throughout life.

Management

The cutaneous hemangiomas seen with this condition are generally small and asymptomatic and require no treatment. Most cavernous hemangiomas of the retina are also asymptomatic and require no treatment. Vitreous hemorrhage can be an occasional complication of larger tumors and the blood could spontaneously resolve over several months. If not, then pars plana vitrectomy with blood removal is performed. For repetitive vitreous hemorrhages, several techniques have been attempted to control the vascular retinal tumor, including cryotherapy, photocoagulation, photodynamic therapy, and plaque radiotherapy. Plaque radiotherapy induces vascular sclerosis, similar to the gamma knife or CyberKnife radiotherapy used to treat the central nervous system hemangiomas.

Organoid Nevus Syndrome

General Considerations

The organoid nevus syndrome (ONS) is an oculoneurocutaneous condition without clear genetic abnormality. The features include the sebaceous nevus of Jadassohn, cerebral atrophy, arachnoidal cyst, epibulbar complex choristoma, eyelid coloboma, posterior calcified scleral cartilage, and occasionally other features.[52–55] The sebaceous nevus of Jadassohn is a well-recognized dermatologic entity, but the complete syndrome of organoid nevus syndrome is relatively uncommon. This sporadic condition displays more choristomas than hamartomas, unlike other phakomatoses. Despite the lack of genetic understanding, there have been exceptionally rare cases of multiple generations affected with organoid nevus syndrome.

This condition was originally described by Jadassohn with the term "organoid nevus" to emphasize the prominence of the cutaneous component. Later, terms such as "nevus sebaceous of Jadassohn" and "Solomon syndrome" were applied to this condition.

Ophthalmologic Features

Although there are several ophthalmic features of the organoid nevus syndrome, two most important ones are the epibulbar complex choristoma and posterior scleral cartilage/bone (Fig. 136.6).[52–54] The epibulbar complex choristoma is a fleshy lesion of the conjunctiva that often extends onto the cornea. It is composed histopathologically of a dermolipoma that contains variable combinations of ectopic lacrimal gland and hyaline cartilage. The posterior scleral cartilage produces a yellow-white discoloration of the fundus near the optic disc, but in some cases there is evidence of bone.[54] With ultrasonography and computed tomography, there is a bone density plaque at the level of the choroid and sclera that corresponds to the intrascleral cartilage/bone.[54]

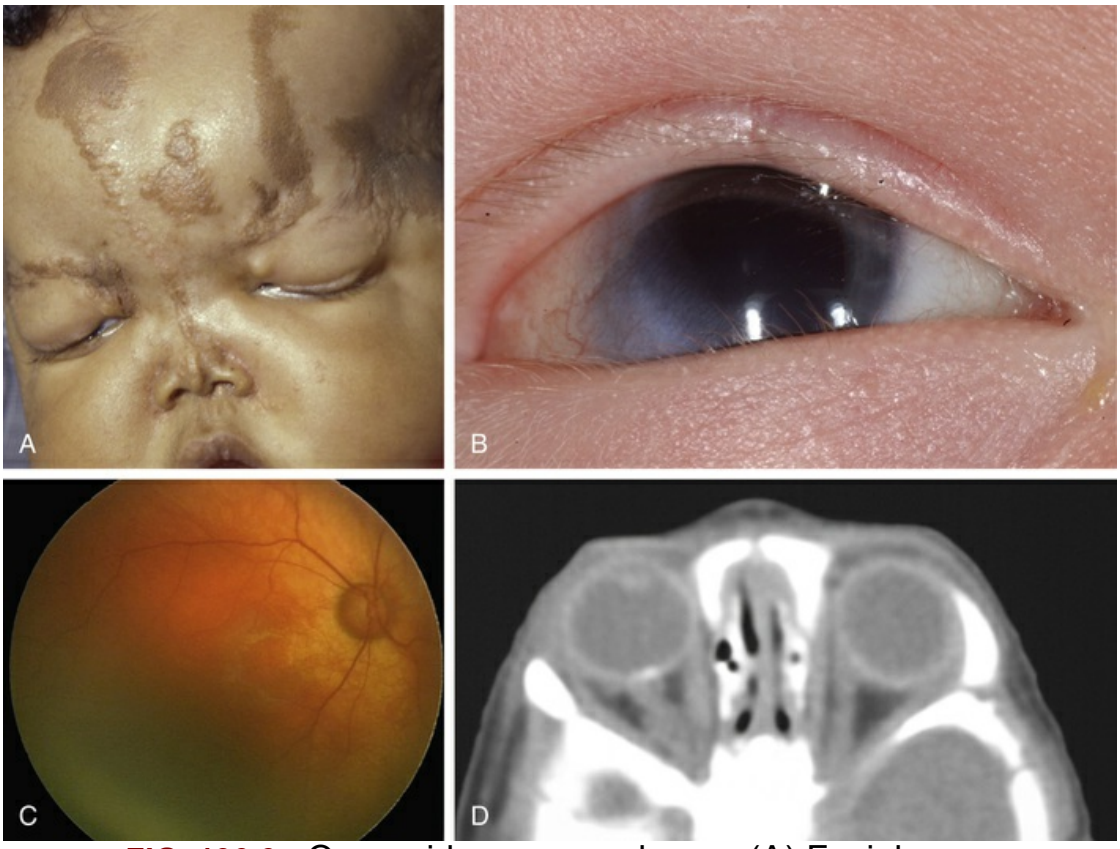

FIG. 136.6 Organoid nevus syndrome. (A) Facial nevus sebaceous of Jadassohn. (B) Subtle epibulbar choristoma. (C) Subtle cartilaginous choristoma superior to disc but confirmed on computed tomography as calcified (D).

Dermatologic Features

The main dermatologic feature of the organoid nevus syndrome is the sebaceous nevus of Jadassohn. It appears as a geographic yellow–brown lesion that often involves the preauricular or brow region and extends onto the scalp where it is associated with alopecia and often down along the neck and nose. This lesion becomes hypertrophied with time. There are three stages of this cutaneous lesion dependent on patient age.[52] The first stage occurs in infancy with underdevelopment of hair, sebaceous glands, and adnexal structures. The second stage occurs at puberty with overdevelopment of adnexal structures. The third stage occurs in adulthood with benign and malignant tumors including basal cell carcinoma, syringocystadenoma papilliferum, sebaceous adenoma, keratoacanthoma, and others. It is estimated that 20% of patients

with sebaceous nevus of Jadassohn will develop basal cell carcinoma arising from the nevus. In one study of 707 patients with sebaceous nevus of Jadassohn the most common benign tumors were trichoblastoma (7%) and syringocystadenoma papilliferum (5%).[55] The malignant tumors were basal cell carcinoma (1%) and squamous cell carcinoma (<1%), all of which occurred in adults.

Central Nervous System Features

Patients with the organoid nevus syndrome can develop seizures, due mainly to enlarging subarachnoid cysts in the central nervous system, and mental retardation. Imaging studies have shown arachnoidal cysts, leptomeningeal hemangiomas, hamartomas, cerebral cortical atrophy, and the MEAN tumor (meningoencephaloangioneuromatosis).

Other Features

Rarely, organoid nevus syndrome can have cardiac and renal abnormalities, including patent ductus arteriosus, ventricular septal defect, coarctation of the aorta, nephroblastomatosis, and horseshoe kidney. Other rare relationships include vitamin D-resistant rickets and liver cysts.

Management

The epibulbar choristoma generally remains stationary and can be safely observed. However, there is a risk for amblyopia, which should be monitored and corrected. Larger or progressive lesions might require surgical excision, but often the lesion is full thickness within the wall of the eye and complete resection is not possible. There is no treatment of the benign cartilaginous/boney fundus lesion. There has been no documentation of enlargement of this lesion. This lesion should be differentiated from choroidal osteoma and retinoblastoma, particularly since it occurs in infancy. The cutaneous sebaceous nevus is usually resected to minimize risk for transformation into basal cell carcinoma or other adnexal tumors. Monitoring of the central nervous system with imaging is advised for arachnoidal cyst and tumor.

Phacomatosis Pigmentovascularis

General Considerations

Phacomatosis pigmentovascularis is a rare condition representing the coexistence of cutaneous vascular malformation (usually nevus flammeus) with melanocytic nevus (usually melanocytosis).[56–61] Since the first report on this condition by Ota in 1947, there have been few reports, mostly in the dermatologic literature.[56] In 2005, Tran and Zografos reported three cases, all with uveal melanoma.[57] In 2011, Shields et al. published 7 cases, of which 3 had choroidal melanoma, 1 with optic disc melanocytoma, and 1 with conjuctival melanoma in situ (primary acquired melanosis).[60] Phacomatosis pigmentovascularis is divided into three types: phacomatosis cesioflammea, phacomatosis spilorosea, and phacomatosis cesiomarmorata (Table 136.7).[58,60] Phacomatosis cesioflammea is characterized by coexistence of a dermal melanocytosis (blue spot) and nevus flammeus (port wine stain). "Caesius" is Latin for "bluish gray" and "flammea" for "flame" or "fire." The other two types have less relationship to the eye.

TABLE 136.7

Classification of Phacomatosis Pigmentovascularis (PPV)

New Classification	Findings	Old Classification
Phacomatosis cesioflammea	Nevus caesius (blue spot) or melanocytosis with nevus flammeus	PPV II a/b
Phacomatosis spilorosea	Nevus spilus (speckled lentiginous nevus) with pale pink telangiectatic nevus	PPV II a/b
Phacomatosis cesiomarmorata	Nevus caesius (blue spot) with cutis marmorata	PPV V a/b
Phacomatosis pigmentovascularis unclassifiable	Various pigmentary and vascular nevi	PPV IV a/b and no name

Adapted from Happle R. Phacomatosis pigmentovascularis revisited and reclassified. Arch Dermatol 2005;141:385–8.

The association of dermal melanocytosis with cutaneous nevus flammeus is believed to be due to the "twin spotting" phenomenon, which is the association of two genetically different clones of cells within a region of normal cells.[59] This involves sporadic somatic

recombination and a mosaic distribution of lesions. Moutray and associates describe monozygotic twins discordant for phacomatosis cesioflammea, supporting postzygotic twin spotting theory.[59] In that report, twin #1 was normal and twin #2 had cutaneous nevus flammeus of the arm, maxilla, and periocular region in addition to Mongolian spot and bilateral ocular melanocytosis.

Ophthalmologic Features

The ophthalmologic features of phacomatosis pigmentovascularis include a spectrum of findings with unilateral or bilateral periocular facial nevus flammeus (port wine stain), ocular or oculodermal melanocytosis, secondary glaucoma, and risk for uveal or conjunctival melanoma (Fig. 136.7). There are only few reports in the ophthalmic literature.

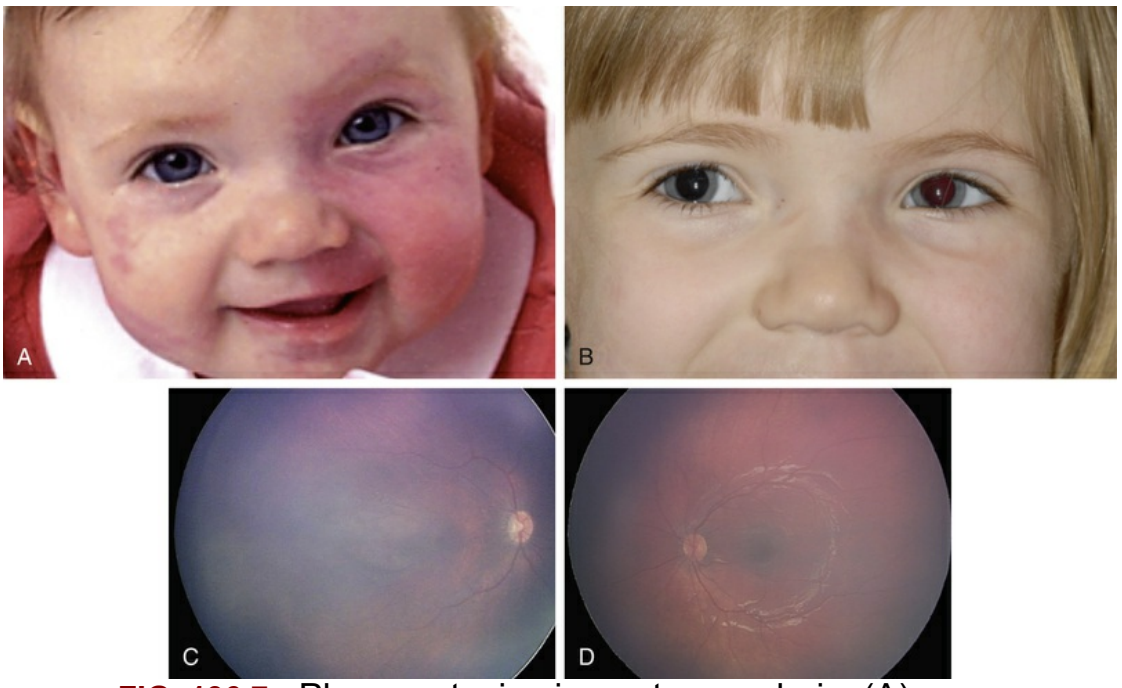

FIG. 136.7 Phacomatosis pigmentovascularis. (A) Newborn baby with facial nevus flammeus, subsequently treated with laser photocoagulation and regressed at a later date (B). (C) Fundus photography demonstrates dark ocular melanocytosis in right eye and normal fundus left eye (D).

Dermatologic Features

Fernandez-Guarino reviewed the published dermatologic literature on 216 cases of phacomatosis pigmentovascularis and classified 77% as cesioflammea, 13% as spilorosea, 1% as cesiomarmorata, and 8% unclassifiable.[61] The cutaneous manifestations included mostly pigmented lesions of nevus of Ota (melanocytosis); Mongolian spot, or café-au-lait spot; nonpigmentation of vitiligo; and vascular lesions of nevus flammeus (port wine stain) or nevus anemicus. These cutaneous findings tended to be patchy without midline separation and scattered over the surface of the body.

Central Nervous System Features

Neurologic features of phacomatosis pigmentovascularis include seizures, cortical atrophy, Arnold Chiari type 1, bilateral deafness, idiopathic facial paralysis, hydrocephalus, diabetes insipidus, plexiform neurofibroma, psychomotor developmental delay, and electroencephalogram alterations.[61]

Other Features

Miscellaneous features include scoliosis, extremity length asymmetry, syndactyly, macrocephaly, renal agenesis, renal angiomatosis, hepatosplenomegaly, cavernous hemangioma, umbilical hernia, hypoplasia of leg veins, IgA deficit, hyper IgE syndrome, eczema, and premature eruption of teeth.[61]

Management

The cutaneous features should be managed by a dermatologist. Often the port wine stain responds to infantile laser therapy. The ophthalmologist should follow the patient lifelong for the development of glaucoma and melanoma. Monitoring of neurologic status should also be performed.

Oculodermal Melanocytosis

General Considerations

Ocular or oculodermal melanocytosis is a congenital pigmentary

condition that can affect the periocular skin, sclera, uvea, orbit, palate, ear drum, and meninges.[1–3,62–73] This condition predisposes the patient to melanoma, particularly uveal melanoma and occasionally orbital or meningeal melanoma.[62–75] Ocular or oculodermal melanocytosis can occur as a diffuse condition, affecting all quadrants of the eye in a homogeneous fashion, or as a sectoral condition, affecting only a portion of the eye.[71] This is a sporadic condition with no genetic mutation identified.

Ophthalmologic Features

The ophthalmologic features of ocular or oculodermal melanocytosis include dermal periocular pigmentation (flat blue nevus) with occasional pigment in the temporal fossa along the hairline; scleral pigmentation; and uveal pigmentation involving the iris, ciliary body, and choroid (Fig. 136.8). Orbital pigmentation with blue nevus cells is occasionally found. The iris can manifest mammilations, or clumping of tissue into a "polka dot" appearance, related to the dense pigment. Early onset equatorial drusen is often found. The main concern of this excessive pigmentation is the risk for the development of uveal melanoma (1/400 risk for whites),[67] orbital melanoma, and meningeal melanoma. Uveal melanoma arising from melanocytosis carries double the risk for metastatic disease.[74,75] Occasionally, optic disc melanocytoma and ipsilateral headache are a part of this syndrome.

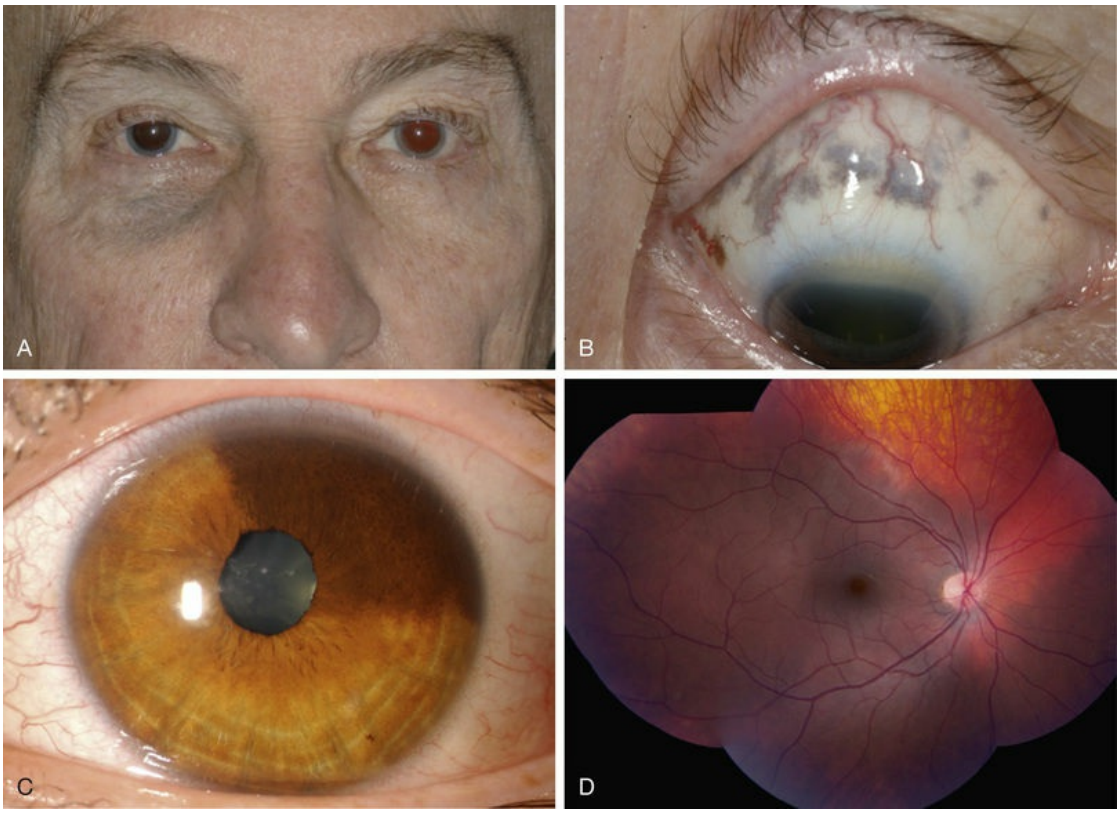

FIG. 136.8 Oculodermal melanocytosis. (A) Diffuse melanocytosis manifesting with nevus of Ota surrounding right eye and sclera with melanocytosis (B). (C) Sector melanocytosis of iris. (D) Sector melanocytosis of choroid.

Genetic evaluation following enucleation of an eye with melanoma arising from melanocytosis revealed normal disomy chromosome 3 in the melanocytosis and monosomy chromosome 3 in the melanoma.[72]

Dermatologic Features

The dermatologic features include predominantly the flat blue dermal nevus of Ota, classically in the periocular region and often with extension into the temporal region. This rarely leads to cutaneous melanoma.

Central Nervous System Features

The blue nevus can extend to involve the meninges and carries a small risk for the development of meningeal melanoma.[73]

Other Features

Similar blue nevus pigmentation can involve the ipsilateral palate and tympanic membrane.

Management

The main concern with this condition is the development of uveal melanoma. Twice-yearly dilated examination is advised. Any patient with the development of unexplained subretinal fluid or lipofuscin orange pigment should be suspected of harboring uveal melanoma. Melanoma develops at a slightly earlier age (approximately 35 years) in those with oculo(dermal) melanocytosis compared to those without (approximately 55 years).[74]

Other Phakomatoses

Other oculoneurocutaneous conditions sometimes loosely classified with the phakomatoses include ataxia telangiectasia (Louis–Bar syndrome), Klippel–Trenaunay–Weber syndrome, and diffuse neonatal hemangiomatosis. These associations are detailed in the literature, but are beyond the scope of this discussion.

Combined Systemic Hamartomatoses

The systemic hamartomatoses are derived from primitive neuroectoderm or mesectoderm, and rarely various combinations of these syndromes can occur. The examples of such overlap can be found in the literature, usually as single case reports. For example, features of neurofibromatosis have been seen in association with von Hippel–Lindau syndrome and Sturge–Weber syndrome. Reports of retinal capillary hemangiomas and oculodermal melanocytosis have individually been found in neurofibromatosis. Another example is the overlap of Sturge–Weber syndrome with oculodermal melanocytosis, a condition described above as phacomatosis pigmentovascularis.

Conclusion

In summary, there are several phakomatoses that involve congenital and acquired features and are represented mostly with benign tumors or hamartomas. Strict criteria are necessary to meet the diagnosis of several of the phakomatoses such as neurofibromatosis types 1 and 2 as well as Sturge–Weber syndrome, whereas others necessitate simple recognition of salient features such as oculo(dermal) melanocytosis. Lifelong, multidisciplinary management of affected patients and family is advised.

References

1. Shields JA, Shields CL. Systemic hamartomatoses ("Phakomatoses"). [editors] *Intraocular tumors: a text and atlas*. WB Saunders: Philadelphia; 1992:513–539.
2. Shields JA, Shields CL. Vascular tumors and malformations of the uvea. Shields JA, Shields CL. *Intraocular tumors: an atlas and textbook*. 2nd ed. Lippincott Williams and Wilkins: Philadelphia; 2015:229–262.
3. Shields JA, Shields CL. Vascular tumors of the retina and optic disc. Shields JA, Shields CL. *Intraocular tumors: an atlas and textbook*. 2nd ed. Lippincott Williams and Wilkins: Philadelphia; 2015:367–404.
4. Van der Hoeve J. The Doyne Memorial Lecture. Eye symptoms in phakomatoses. *Trans Ophthalmol Soc U K*. 1932;52:380–401.
5. von Recklinghausen FD. *Uber die multiplen fibrome der haut und ihre beziehungen zu den neurrommen. Festschr Feier fundfund-zwanzigjahrigen. Berlin Institute of Pathology*. Hirschwald: Berlin; 1882.
6. Brasfield RD, Das Gupta TK. von Recklinghausen's disease: a clinicopathological study. *Ann Surg*. 1972;175:86–104.
7. Spurlock G, Bennett E, Chuzhanova N, et al. SPRED1 mutations (Legius syndrome): another clinically useful genotype for dissecting the neurofibromatosis type 1 phenotype. *J Med Genet*. 2009;46:431–437.
8. Stumpf DA, Alksne JF, Annegers JF. Neurofibromatosis. Conference statement. National Institute of Health

Consensus Development Conference. *Arch Neurol*. 1988;45:575–578.
9. Gutmann DH, Aylsworth A, Carey JC, et al. The diagnostic evaluation and multidisciplinary management of neurofibromatosis 1 and neurofibromatosis 2. *JAMA*. 1997;278:51–57.
10. Vagge A, Camicione P, Capris C, et al. Choroidal abnormalities in neurofibromatosis type 1 detected by near-infrared reflectance imaging in paediatric population. *Acta Ophthalmol*. 2015;93(8):e667–71.
11. Lewis RA, Riccardi VM. Von Recklinghausen neurofibromatosis: incidence of iris hamartoma. *Ophthalmology*. 1981;88:348–354.
12. Lewis RA, Gerson LP, Axelson KA, et al. Von Recklinghausen neurofibromatosis II. Incidence of optic gliomata. *Ophthalmology*. 1984;91:929–935.
13. Kaiser-Kupfer MI, Freidlin V, Dariles MB, et al. The association of posterior capsular lens opacities with bilateral acoustic neuromas in patients with neurofibromatosis type 2. *Arch Ophthalmol*. 1989;107:541–544.
14. Shields JA, Sanborn GE, Kurz GH, et al. Benign peripheral nerve tumor of the choroid. *Ophthalmology*. 1981;88:1322–1329.
15. Wiznia RA, Freedman JE, Mancini AD, et al. Malignant melanoma of the choroid in neurofibromatosis. *Am J Ophthalmol*. 1978;86:684–687.
16. Shields CL, Kaliki S, Al-Dahmash SA, et al. Vasoproliferative tumors of the ocular fundus: comparative clinical features of primary versus secondary tumors in 334 cases. *Arch Ophthalmol*. 2012;131(3):328–334.
17. Shields JA, Pellegrini M, Kalaki S, et al. Retinal vasoproliferative tumors in 6 patients with neurofibromatosis type 1. *JAMA Ophthalmol*. 2014;132:190–196.
18. Sabatini C, Milani D, Menni F, et al. Treatment of neurofibromatosis type 1. *Curr Treat Options Neurol*. 2015;17(6):355.
19. Evans DG. Neurofibromatosis 2 (bilateral acoustic

neurofibromatosis, central neurofibromatosis, NF2, neurofibromatosis type II). *Genet Med*. 2009;11:599–610.
20. Evans DGR, Huson SM, Donnai D, et al. A clinical study of type 2 neurofibromatosis. *Q J Med*. 1992;84:603–618.
21. Asthagiri AR, Butman JA, Kim HJ, et al. Neurofibromatosis type 2. *Lancet*. 2009;373:1974–1986.
22. Arepalli S, Pellegrini M, Ferenczy SR, et al. Combined hamartoma of the retina and retinal pigment epithelium: findings on enhanced depth imaging optical coherence tomography (EDI-OCT) in 8 eyes. *Retina*. 2014;34:2202–2207.
23. Shields CL, Thangappan A, Hartzell K, et al. Combined hamartoma of the retina and retinal pigment epithelium in 77 consecutive patients: visual outcome based on macular versus extramacular tumor location. *Ophthalmology*. 2008;115:2246–2252.
24. Lim SH, Ardern-Holmes S, McCowage G, et al. Systemic therapy in neurofibromatosis type 2. *Cancer Treat Rev*. 2014;40:857–861.
25. Sturge WA. A case of partial epilepsy apparently due to a lesion of one of the vasomotor centers of the brain. *Trans Clin Soc Lond*. 1879;12:162–167.
26. Weber FP. Right-sided hemihypertrophy resulting from right-sided congenital spastic hemiplegia with a morbid condition of the left side of the brain revealed by radiogram. *J Neurol Psycho-Pathol (London)*. 1922;37:301–311.
27. Stevenson RF, Morin JD. Ocular findings in nevus flammeus. *Can J Ophthalmol*. 1975;10:136–139.
28. Susac JO, Smith JL, Scelfo RJ. The "tomato catsup" fundus in Sturge–Weber syndrome. *Arch Ophthalmol*. 1974;92:69–70.
29. Waelchli R, Aylett SE, Robinson K, et al. New vascular classification of port-wine stains: improving prediction of Sturge–Weber risk. *Br J Dermatol*. 2014;171:861–867.
30. Sudarsanam A, Ardern-Holmes SL. Sturge–Weber syndrome: from the past to the present. *Eur J Paediatr Neurol*. 2014;18(3):257–266.
31. Roach ES. Neurocutaneous syndromes. *Pediatr Clin North Am*. 1992;39:591–620.
32. Happle R. Lethal genes surviving by mosaicism: a possible

explanation for sporadic birth defects involving the skin. *J Am Acad Dermatol*. 1987;16:899–906.
33. Comi AM, Hunt P, Vawter MP, et al. Increased fibronectin expression in Sturge–Weber syndrome fibroblasts and brain tissue. *Pediatr Res*. 2003;53:762–769.
34. Sullivan TJ, Clarke MP, Morin JD. The ocular manifestations of the Sturge–Weber syndrome. *J Pediatr Ophthalmol Strabismus*. 1992;29:349–356.
35. Witschel H, Font RL. Hemangioma of the choroid: a clinicopathologic study of 71 cases and a review of the literature. *Surv Ophthalmol*. 1976;20:415–431.
36. Ramasubramanian A, Shields CL. The current management of choroidal hemangioma. *Retina Today*. 2010;Dec.:52–55.
37. Arepalli S, Shields CL, Kaliki S, et al. Diffuse choroidal hemangioma management with plaque radiotherapy in 5 cases. *Ophthalmology*. 2013;120:2358–2359.
38. Wyburn-Mason R. Arteriovenous aneurysm of midbrain and retina, facial naevi and mental changes. *Brain*. 1943;66:163–203.
39. Vanaman MJ, Hervey-Jumper SL, Maher CO. Pediatric and inherited neurovascular diseases. *Neurosurg Clin N Am*. 2010;21:427–441.
40. Cameron ME, Greer CH. Congenital arterio-venous aneurysm of the retina: a post-mortem report. *Br J Ophthalmol*. 1968;52:768–772.
41. Archer DM, Deutman A, Ernest JT, et al. Arteriovenous communications of the retina. *Am J Ophthalmol*. 1973;75:224–241.
42. Shah GK, Shields JA, Lanning R. Branch retinal vein obstruction secondary to retinal arteriovenous communication. *Am J Ophthalmol*. 1998;126:446–448.
43. Materin MA, Shields CL, Marr BP, et al. Retinal racemose hemangioma. *Retina*. 2005;25:936–937.
44. Shields JA, Streicher TFE, Spirkova JHJ, et al. Arteriovenous malformation of the iris in 14 cases: the 2004 Alvaro Rodriquez MD Gold Medal Award Lecture. *Arch Ophthalmol*. 2006;124:370–375.
45. Gass JDM. Cavernous hemangioma of the retina: a neuro-

oculocutaneous syndrome. *Am J Ophthalmol*. 1971;71:799–814.
46. Lewis RA, Cohen MH, Wise GN. Cavernous hemangioma of the retina: a report of three cases and a review of the literature. *Br J Ophthalmol*. 1975;59:422–434.
47. Goldberg RE, Pheasant TR, Shields JA. Cavernous hemangioma of the retina: a four-generation pedigree with neurocutaneous involvement. *Arch Ophthalmol*. 1979;97:2321–2324.
48. Thangappan A, Shields CL, Gerontis CC, et al. Iris cavernous hemangioma associated with multiple cavernous hemangiomas in the brain, kidney, and skin. *Cornea*. 2007;26:481–483.
49. Seigel AM. Familial cavernous angioma: an unknown disease. *Acta Neurol Scand*. 1998;98:369–371.
50. Shields JA, Eagle RC Jr, Ewing MQ, et al. Retinal cavernous hemangioma: fifty-two years of clinical follow-up with clinicopathologic correlation. *Retina*. 2014;34:1253–1257.
51. Velazquez-Martin JP, Domville D, Fulda E, et al. Peripheral capillary nonperfusion and vitreolesional adhesion in retinal cavernous hemangioma. *Retina*. 2013;33:666–667.
52. Shields JA, Shields CL, Eagle RC Jr, et al. Ocular manifestations of the organoid nevus syndrome. *Ophthalmology*. 1997;104:549–557.
53. Kraus NJ, Ramasubramanian A, Shields CL, et al. Ocular features of the organoid nevus syndrome. *Retinal Cases Brief Rep*. 2010;4:385–386.
54. Shields CN, Shields CL, Lin CJ, et al. Calcified scleral choristoma in organoid nevus syndrome simulating retinoblastoma. *J Pediatr Ophthalmol Strabismus*. 2014;51 Online:e1–3.
55. Idriss MH, Elston DM. Secondary neoplasms associated with nevus sebaceous of Jadassohn: a study of 707 cases. *J Am Acad Dermatol*. 2014;70(2):332–337.
56. Ota M, Kawamura T, Ito N. Phakomatosis pigmentovascularis. *Jpn J Dermatol*. 1947;52:1–3.
57. Tran HV, Zografos L. Primary choroidal melanoma in phacomatosis pigmentovascularis IIa. *Ophthalmology*.

2005;112:1232–1235.
58. Happle R. Phacomatosis pigmentovascularis revisited and reclassified. *Arch Dermatol*. 2005;141:385–388.
59. Moutray T, Napier M, Shafiq A, et al. Monozygotic twins discordant for phacomatosis pigmentovascularis: evidence for the concept of twin spotting. *Am J Med Genet*. 2010;152:718–720.
60. Shields CL, Kligman BE, Suriano M, et al. Phacomatosis pigmentovascularis of cesioflammea type in 7 cases: combination of ocular pigmentation (melanocytosis, melanosis) and nevus flammeus with risk for melanoma. *Ophthalmology*. 2011;129:746–750.
61. Fernandez-Guarino M, Boixeda P, de las Heras B, et al. Phacomatosis pigmentovascularis: clinical findings in 15 patients and review of the literature. *J Am Acad Dermatol*. 2008;58:88–93.
62. Shields CL, Shields JA. Tumors of the conjunctiva and cornea. *Surv Ophthalmol*. 2004;49:3–24.
63. Gonder JR, Nichol J, Augsburger JJ, et al. Ocular and oculodermal melanocytosis. *Can J Ophthalmol*. 1985;20:176–178.
64. Gonder JR, Ezell PC, Shields JA, et al. Ocular melanocytosis: a study to determine the prevalence rate of ocular melanocytosis. *Ophthalmology*. 1982;89:950–952.
65. Velazquez N, Jones IS. Ocular and oculodermal melanocytosis associated with uveal melanoma. *Ophthalmology*. 1983;90:1472–1476.
66. Gonder JR, Shields JA, Albert DM, et al. Uveal malignant melanoma associated with ocular and oculodermal melanocytosis. *Ophthalmology*. 1982;89:953–960.
67. Singh AD, De Potter P, Fijal BA, et al. Lifetime prevalence of uveal melanoma in Caucasian patients with ocular (dermal) melanocytosis. *Ophthalmology*. 1998;105:195–198.
68. Honavar SG, Shields CL, Singh AD, et al. Two discrete choroidal melanomas in an eye with ocular melanocytosis. *Ophthalmology*. 2002;47:36–41.
69. Shields JA, Shields CL, Naseripour M, et al. Choroidal melanoma in a black patient with oculodermal

melanocytosis. *Retina*. 2002;22:126–128.
70. Shields CL, Eagle RC, Ip MS, et al. Two discrete uveal melanomas in a child with ocular melanocytosis. *Retina*. 2006;26:684–687.
71. Shields CL, Qureshi A, Mashayekhi A, et al. Sector (partial) oculo (dermal) melanocytosis in 89 eyes. *Ophthalmology*. 2011;118:2474–2479.
72. Horgan N, Shields CL, Swanson L, et al. Altered chromosome 3 expression of uveal melanoma in the setting of melanocytosis. *Acta Ophthalmol Scand*. 2009;87:578–580.
73. Kiratli H, Bilgic S, Satilmis M. Ocular melanocytosis associated with intracranial melanoma. *Br J Ophthalmol*. 1996;80:1025.
74. Shields CL, Kaliki S, Livesey M, et al. Association of ocular and oculodermal melanocytosis with the rate of uveal melanoma metastasis: analysis of 7872 consecutive eyes. *JAMA Ophthalmol*. 2013;131:993–1003.
75. Kaliki S, Shields CL, Shields JA. Uveal melanoma: estimating prognosis. *Indian J Ophthalmol*. 2015;63(2):93–102.

137

Retinal Metastases

Sunil K. Srivastava, Chris Bergstrom

Introduction

Retinal metastases represent a small percentage of intraocular malignancy secondary to systemic cancers, even though 10% of patients who die of cancer have been found to have intraocular metastases.[1–4] While relatively rare, the diagnosis of retinal metastases can be challenging as its presentation can mimic other etiologies. High clinical suspicion and use of appropriate diagnostic techniques are vital in order to successfully diagnose and manage these challenging cases. This chapter provides a review of the literature of this rare clinical entity and management recommendations.

Metastatic Cascade

Metastases are responsible for most cancer deaths.[5] The understanding of metastases is limited due to the "hidden" nature of this process as it occurs inside the body and is difficult to observe.[5] Although many tumor cells are shed daily into the bloodstream or lymphatic system in those with cancer, the evidence is unclear on the fate of these tumor cells.[6,7] Some models suggest that the majority do not survive in the circulation, while others suggest that most can survive and extravasate.[5,6,8–10] For tumor metastasis to develop, a series of biologic steps must be completed for a tumor cell to grow at a different site.[5,6,10–15]

Dissociation, Invasion, and Intravasation

For tumor cells to invade the circulation, they must dissociate from the primary tumor.[5,6,10–14] On a molecular level, the dissociation is initiated by an array of motility factors[11–12] and requires modulation of the expression of cadherins and integrins.[5,6,13–16] Degradation of the extracellular matrix by proteolytic enzymes (primarily matrix metalloproteases and the plasminogen activator system), facilitates invasion of the surrounding connective tissue components.[5,6,13,15,17–23] Metalloproteases also modulate cell adhesion in their local environment and help release growth factors from their stores.[18,19,21] Then, tumor cells must penetrate the basement membranes of endothelial cells to enter the blood and lymphatic circulation.[5,6,15]

This step again requires well-coordinated proteolysis, as well as mechanical deformation and locomotion of the tumor cells.[5,6,14,15] If this complex interaction is regulated successfully, certain populations of cells can break through matrix and endothelium to reach the bloodstream.

Hematogenous Dissemination

Because intraocular structures have no lymphatic supply, metastatic cancer cells can gain access to the eye only by hematogenous routes. From the aorta, tumor cells enter the internal carotid artery directly on the left and indirectly through the innominate artery on the right. After passing through the internal carotid artery, tumor cells reach the eye through the ophthalmic artery. The ophthalmic artery gives rise to 10–20 short posterior ciliary arteries supplying the posterior uvea, two long ciliary arteries supplying the anterior uvea, and the central retinal artery supplying the inner half of the retina and the optic disc.

The destination within the eye of circulating tumor cells may depend on several factors. Tumor size, vascular circulatory patterns, and organ-specific factors that encourage tumor growth (so-called seed and soil factors) all may play a role in the location of metastases.[5,6,15] Reese emphasized that, although tumor emboli are more prominent in the uvea, more than 90% of infectious emboli involve the retina.[24] Because large emboli (e.g., tumor emboli) travel along the vessel wall in the slower-moving part of the bloodstream, they are more likely to enter vessel branches, such as the short ciliary arteries. Small emboli (e.g., bacterial emboli) travel in the central, faster-moving part of the bloodstream toward the terminal vessels, such as the central retinal artery.[25] The marked vascularity of the posterior choroid relative to that of the retina (as noted above) could also contribute to more frequent choroidal involvement as metastatic tumors to the retina and optic disc, supplied by the central retinal artery, are rare.[3,4]

Extravasation and Angiogenesis

Although circulation patterns and tumor size may play a role in implantation, metastatic growth may require organ-specific factors

that facilitate tumor cell survival.[5,15,16,26–28] Animal models of metastases support the role of both vascular flow patterns and organ compatibility factors in the development of metastases.[5,29–31] Tumor cell anchorage at a target organ site depends on shear-resistant attachment to local endothelium. Various integrins and selectins have been identified which appear to mediate such specialized tumor cell adhesion under dynamic flow conditions.[5,16,32,33]

The delivery of the tumor cell to the site of metastasis depends on mechanical flow, but the growth or survival can depend on organ-specific molecular interactions. These interactions can encourage tumor cell growth via expression of growth factors and altering the gene expression of tumor cells.[5,6,34–37] Expression of specific chemokine receptors by tumor cells may also target tumor cells to specific organs that express the specific ligands for these receptors.[5,15,38–41] This match could lead to chemokine signal activation of genes which would encourage tumor cell growth.[5,15] Specific interactions unique to retinal metastasis to this point have not been identified.

After the colony at the secondary site is established, angiogenesis will again play a key role in the continued growth of the tumor. The onset of angiogenesis involves an alteration in the balance between positive and negative regulators. In vivo experiments with human tumor cell lines have shown that both vascular endothelial growth factor (VEGF) and basic fibroblast growth factor (FGF) have direct roles in tumor-associated angiogenesis.[42,43] VEGF and FGF-2 also are the two major angiogenic factors in the retina and increased expression of both has been identified in retinal tumors.[44–47] VEGF not only regulates tumor-associated angiogenesis in response to local hypoxia and various cytokines, but may regulate breakdown of the blood–ocular barrier in ocular melanoma and other tumors.[47–50] FGF-2 is a potent mitogen of choriocapillary endothelial cells, and FGF acts synergistically with VEGF to stimulate tumor angiogenesis.[44,51–53]

Review of Case Reports

As noted above, retinal metastasis represents a small percentage of

intraocular metastasis. Until recently, publications in the literature have been limited to case reports.[54–96] The first was published in 1934 and was diagnosed at autopsy.[54] Until 1979, the diagnosis of retinal metastasis was made either by enucleation or at autopsy. Since 1979, diagnosis of retinal metastasis has been made via biopsy, including vitreous, chorioretinal, retinal biopsies; clinical inspection; or surgical removal.[63] Although the case reports reviewed provide detail in presentation and treatment of retinal metastases, follow-up is limited for many of the publications. More recently, the largest single-center series published eight cases diagnosed in a 40-year review.[95] The clinical appearance, symptoms, and outcomes from the published case reports will be reviewed below and are displayed in Table 137.1.

TABLE 137.1
Retinal Metastases: Case Reports

Reference	Primary Disease	Age	Sex	Eye	Initial Symptoms	Signs	Diagnost Patholog
Smoleroff and Agatston (1934)[54]	Gastroesophageal adenocarcinoma	55	M	OD	None	White irregular mass in inferotemporal retina	Autopsy
Uhler (1940)[55]	Cutaneous melanoma	26	M	OD	Diplopia	Papilledema; infiltration of temporal retina	Autopsy
Kennedy et al. (1958)[56]	Rectosigmoid adenocarcinoma	51	M	OD	Blurred vision	Circumscribed grayish-white lesion in macula	Enucleati (enlargin mass)
Duke and Walsh (1959)[57]	Uterine	60	F	OD	Decreased	Vitreous opacities; white elevated mass in macula	Enucleati (secondar glaucoma
Liddicoat et al. (1959)[58]	Cutaneous melanoma	43	M	OS	None	Perivascular white sheathing with hemorrhage, midperiphery	Autopsy
Riffenburgh (1961)[59]	Cutaneous melanoma	45	M	OS	Decreased visual acuity, floaters	Vitreous cells, irregular gray mass with sharp borders in nasal retina	Enucleati (primary choroid melanom
Koenig et al. (1963)[60]	Undifferentiated bronchogenic pulmonary carcinoma	56	M	OD	Sudden	Vitreous floaters; white lesion with neovascularization and exudates in	Enucleati (secondar glaucoma

						temporal retina	
Flindall and Fleming (1967)[61]	Unknown	68	M	OS	Blurred vision, floaters	Dense vitreous; veil-like exudate	Enucleati (secondar glaucoma
Klein et al. (1977)[62]	Squamous cell pulmonary carcinoma	52	M	OU	Decreased visual acuity	Yellow-white infiltrate temporal to macula OD; exudative retinal detachment OS	Autopsy
Young et al. (1979)[63]	Pulmonary carcinoma	63	M	OS	Decreased visual acuity	Vitreous cells; white retinal mass at macula; perivascular white patches	Vitreous aspirate, then autopsy
Robertson et al. (1981)[64]	Cutaneous melanoma	43	F	OU	Floaters	Golden-brown vitreous spherules; brown plaque over superior retina	Vitreous aspirate
	Cutaneous melanoma	37	F	OS	Floaters	Golden-brown vitreous spherules	Aqueous aspirate, then enucleati (secondar glaucoma
Letson and Davidorf (1982)[65]	Cutaneous melanoma	44	M	OU	None	Gray-brown retinal and perivascular infiltrates with feathery edges	None
de Bustros et al. (1985)[66]	Cutaneous melanoma	33	M	OS	Decreased visual acuity	Tan retinal mass with exudates and hemorrhages	Not state
Takagi et al. (1989)[67]	Pulmonary adenocarcinoma	45	M	OS	Blurred vision	Whitish vitreous granules; white masses on disc and within inferotemporal retina	Enucleati (to prevei CNS spread)
Eagle (1988)[68]	Unknown carcinoma	53	F	OS	Blurred vision	Few vitreous balls; white macular lesion with satellites and vascular sheathing	Vitreous aspirate a eye wall biopsy (includin retina an choroid)
Best et al. (1990)[69]	Cutaneous melanoma	71	F	OS	Blurred vision, floaters	Yellow-white globular vitreous opacities	Vitreous aspirate, then enucleati (pain)
Leys et al (1990)[70]	Oat cell pulmonary carcinoma	49	M	OS	No ocular symptoms	Single white retinal plaque temporal to macula	Autopsy
	Breast	42	F	OS	Blurred vision,	Vitreous opacities	Vitreous

	adenocarcinoma				floaters	just anterior to macula	aspirate
Striebel-Gerecke et al. (1992)[71]	Oat cell pulmonary carcinoma	47	F	OD	Floaters	White cone-shaped mass in vitreous; white infiltrate in inferonasal retina	Vitreous aspirate, then autopsy
Tachinami et al. (1992)[72]	Rectal adenocarcinoma	61	M	OD	Blurred vision	Yellow–white mass superior to macula, serous detachment	Autopsy
Balestrazzi et al. (1995)[73]	Cutaneous melanoma	40	F	OD	Blurred vision	Vitreous hemorrhage; yellow-white highly vascularized mass in superonasal retina	Vitrecton and surgi resection
Spraul et al. (1995)[74]	Breast and colonic adenocarcinoma	74	F	OD	Decreased visual acuity	Yellow-white mass in superotemporal retina, serous detachment	Enucleati (pain)
Spraul et al. (1996)[75]	Cutaneous melanoma	55	M	OD	Decreased	Vitreous hemorrhage; pigmented mass in temporal retina	Vitreous aspirate, then enucleati (pain)
Cangiarella et al. (1996)[76]	Esophageal adenocarcinoma	51	F	OS	Decreased visual acuity	Vitreous cells; nasal retinal hole and detachment with white retinal infiltrate	Vitreous aspirate
Ganduz et al. (1998)[77]	Cutaneous	81	M	OS	Floaters	Total hyphema (no view	Vitreous aspirate, then enucleati (pain)
Spadea et al. (1999)[78]	Cutaneous melanoma	40	F	OD	None	Vitreous pigment; yellow-white highly vascularized retinal lesion in periphery	Vitrecton and surgi resection
Soheilian et al. (2002)[79]	Cutaneous melanoma	49	M	OU	Blurred vision	Vitreous hemorrhage; pigmented mass in superotemporal retina	Vitreous aspirate
Hutchinson et al. (2001)[80]	Large bowel adenocarcinoma	63	F	OS	Decreased vision	Highly vascular lesion; serous retinal detachment	None stat
Truong et al. (2002)[81]	Breast carcinoma	59	F	OS	Decreased vision	Milky white retinal infiltrates	None stat
Zografros et al. (2003) [82,84]	Cutaneous melanoma	48	M		Decreased vision	Beige-colored vitreous	Vitreous aspirate cells; reti

							detachme
	Lung melanoma	57	F		Decreased vision	Greyish retinal mass Intraretinal hemorrhages	None stat
Saornil et al. (2004) [83]	Gastric adenocarcinoma	70	M	OS	Decreased vision	Yellow, white solid retinal mass.; neovascular glaucoma	Enucleati (pain)
Apte et al. (2005)[85]	Adenocarcinoma of cecum	39	M	OS	Visual field defect	Retinal hemorrhage	Vitrecton surgical
Sirimaharaj et al. (2006)[86]	Breast carcinoma	60	F	OS	Decreased vision	White precipitates within retina. intraretinal hemorrhages; vascular sheathing	Vitreous aspirate
Rundle et al. (2006)[87]	Breast carcinoma	55	F	OD	Metamorphopsia	Discrete white lesion	None stat
Khurana et al. (2007)[88]	Cutaneous melanoma	76	M	OD	Floaters, Decreased vision	Pigmented preretinal lesion	Vitrecton membrar peel
Alegret et al. (2009)[89]	Nasopharyngeal carcinoma	15	M	OD	None	Amelanotic retinal lesion	None
Kim et al. (2010)[90]	Gastric adenocarcinoma	64	F	OU	Decreased vision, macular infiltrates	Multiple vitreous seeds	Vitreous aspirate
Coassin et al. (2011)[91]	Small cell carcinoma, presumed lung in origin	56	F	OD	Floaters, decreased vision	White retinal infiltrate; intraretinal hemorrhages	Vitrecton retinal biopsy
Payne et al. (2012)[92]	Adenocarcinoma of lung	62	M	OS	Decreased vision	Retinal whitening; preretinal hemorrhage	Vitrecton retinal biopsy
Krema et al. (2013)[93]	Cutaneous melanoma	54	F	OS	Temporal field loss	Diffuse pigmented lesion	Enucleati
Singh et al. (2014)[94]	Small cell lung carcinoma	78	M	OD	Blurred vision	Patchy white infiltrates; retinal hemorrhages	Vitrecton retinal biopsy
Shields et al. (2014)[95]	Lung carcinoma	64	F		Not recorded	7 mm retinal infiltrate; vitreous seeds; vitreous Hemorrhage	Not recorded
	Cutaneous melanoma	45	M		Not recorded	12 mm retinal infiltrate; vitreous seeds	Enucleati
	Cutaneous melanoma	59	M		Not recorded	11 mm retinal infiltrate; subretinal fluid	Enucleati
	Cutaneous melanoma	85	M		Not recorded	9 mm retinal infiltrate; vitreous seeds; vitreous hemorrhage	Enucleati
	Esophageal carcinoma	56	M		Not recorded	12 mm retinal infiltrate;	Not recorded

						subretinal fluid	
	Breast carcinoma	58	F		Not recorded	1.5 mm retinal infiltrate; subretinal fluid	Not recorded
	Breast carcinoma	75	F		Not recorded	2 mm retinal infiltrate; subretinal fluid	Not recorded
	Cutaneous melanoma	55	M		Not recorded	5 mm retinal infiltrate	Not recorded
Gubbiotti et al. (2015)[96]	Breast carcinoma	52	F	OD	Blurred vision	Retinal lesion	None

CNS, central nervous system; OD, right eye; OS, left eye; OU, both eyes.

Demographics

A total of 52 cases of isolated retinal metastasis have been reported (with or without vitreous involvement). Of those 52 cases there were 29 females and 23 males. The average age at diagnosis of retinal metastases was 53 years (range 14–85). The primary tumor sites included 19 cases of cutaneous melanoma, 10 cases from the gastrointestinal tract, 11 cases from the lungs, 8 cases of breast carcinoma, 1 case from the genitourinary tract, 1 case from the nasopharynx, and 3 cases of unknown primary malignancy.

Clinical Findings

Symptoms

The most common visual complaint among those with retinal metastases is decreased or blurred vision (Table 137.1). Floaters are also a common complaint. Other symptoms include pain, diplopia, and red eye. Some cases presented without any specific visual symptoms.[54,58,65] The underlying primary source of the metastases did not have a bearing on the type of visual symptom reported by the patient.

Signs

The clinical appearance of retinal metastases can vary based on the primary tumor and level of invasion of the tumor. Metastatic melanoma typically presents as a pigmented lesion within the retina with irregular borders and flat appearance (Fig. 137.1). Carcinoma tends to be nonpigmented, white, or yellow in

appearance and variable in size. (Fig. 137.2). Some metastatic carcinomas can appear with significant mass and an elevated appearance with surrounding subretinal fluid.

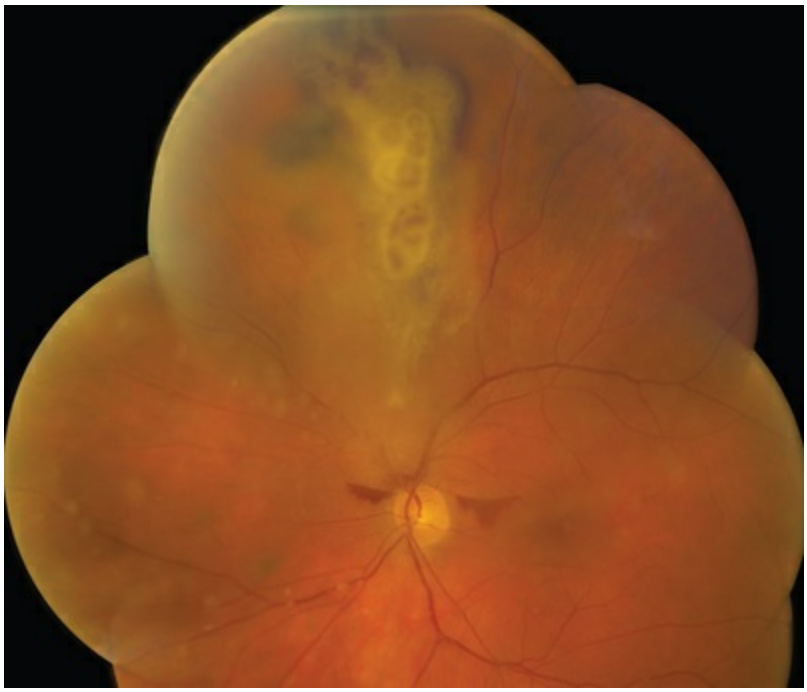

FIG. 137.1 Cutaneous melanoma metastatic to the retina. Note the hemorrhages both intraretinal and preretinal that accompany the pigmented lesion with irregular borders.

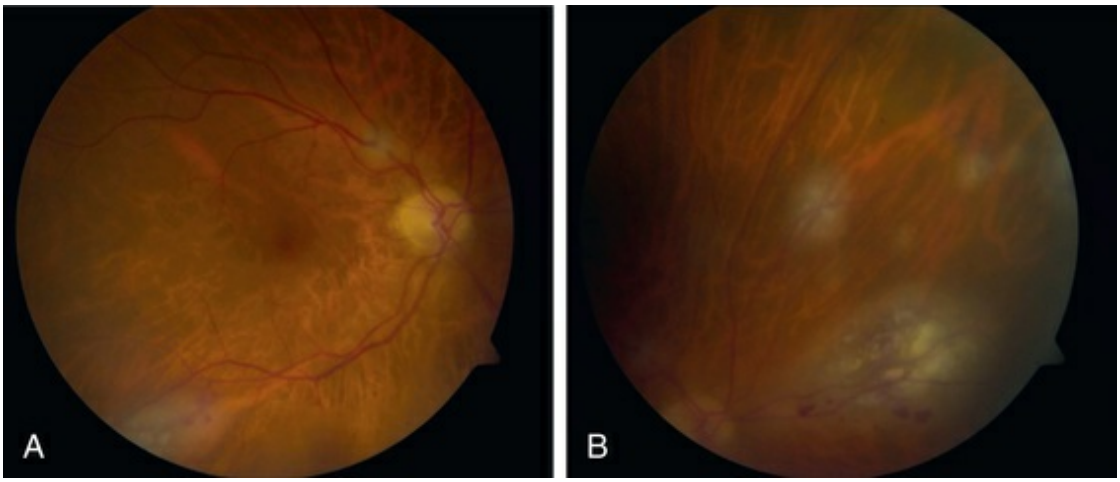

FIG. 137.2 Small cell lung carcinoma metastatic to the retina. (A) At the macula, perivascular retina infiltrates are seen. (B) Nasal to the nerve, multiple retinal

lesions are seen of varying size. Scattered intraretinal hemorrhages are also seen. (Courtesy of Daniel F. Martin, Rishi P. Singh, and Careen Y. Lowder.)

Intraretinal hemorrhage and exudates have been described in association with these lesions (Figs. 137.3 and 137.4). Subretinal hemorrhage has also been described as a presenting feature of metastatic carcinoma.[85] Perivascular infiltrates can also been seen in some cases (Figs. 137.5 and 137.6). Retinal hemorrhages and exudates are thought to occur secondary to damage to the retinal microvasculature. Additionally, subretinal fluid has been described in several cases of retinal metastases. The appearance of subretinal fluid or exudative retinal detachment warrants an evaluation for a choroidal lesion.

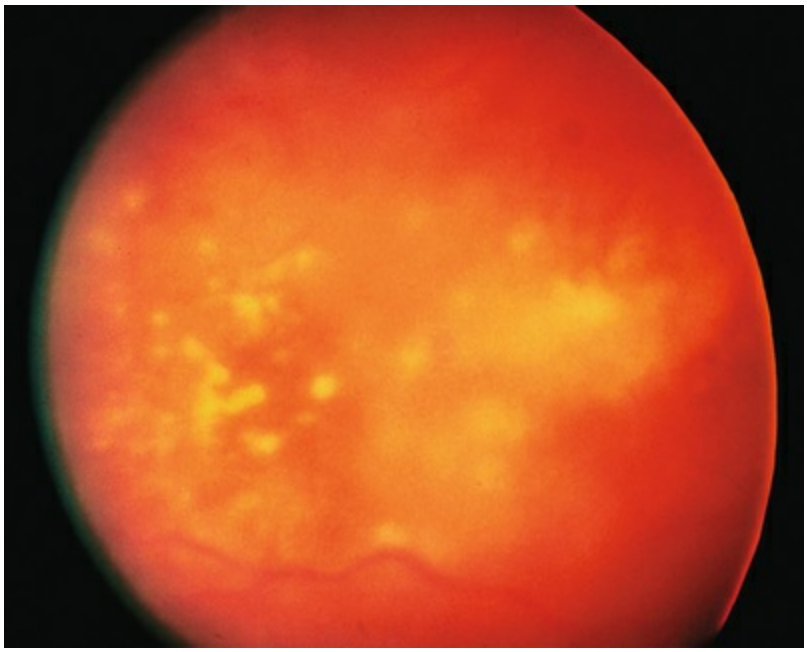

FIG. 137.3 Adenocarcinoma of unknown source metastatic to the retina. A white–yellow retinal lesion with scattered exudates, extending temporally from the macula. (Courtesy of Ralph C. Eagle Jr.)

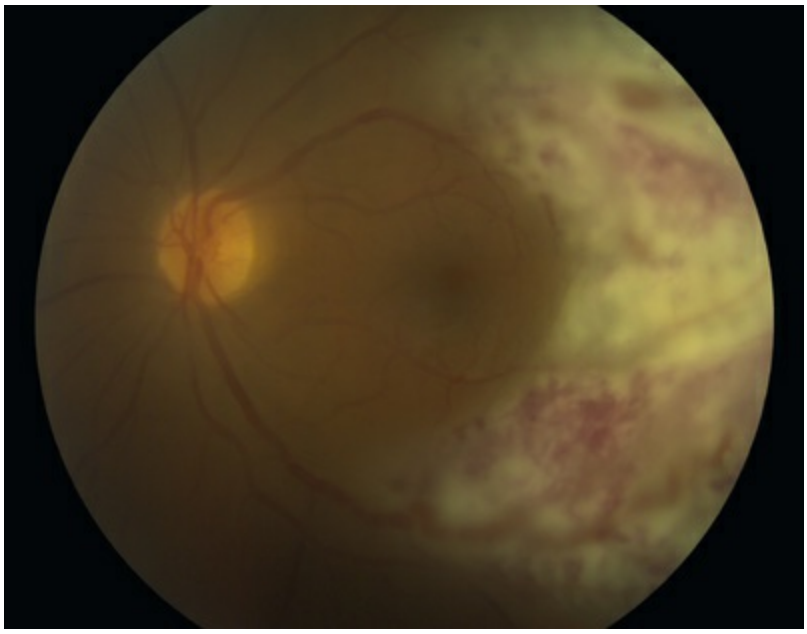

FIG. 137.4 Lung adenocarcinoma metastatic to the retina. At the macula, the white retinal mass has dilated vessels and hemorrhages on its surface.

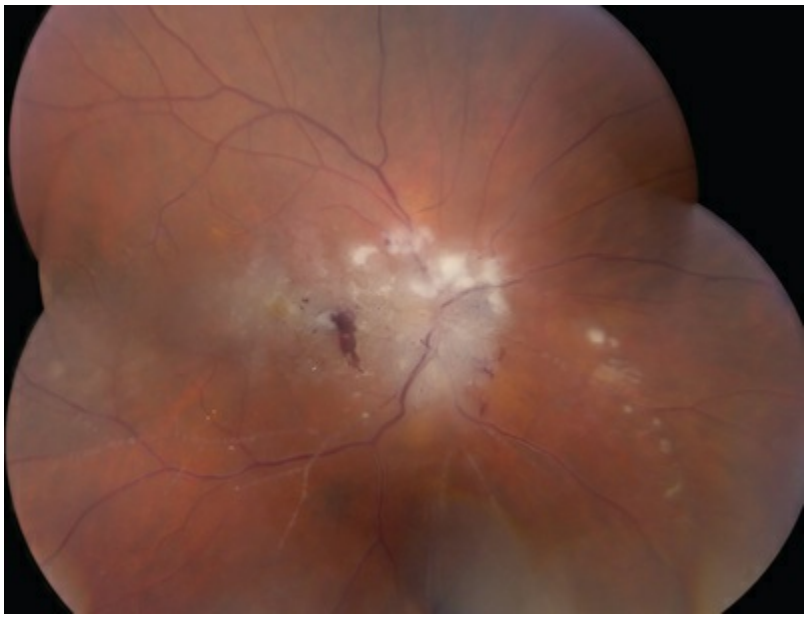

FIG. 137.5 Metastatic lung cancer to the retina. Note the perivascular sheathing in the inferior-temporal macula.

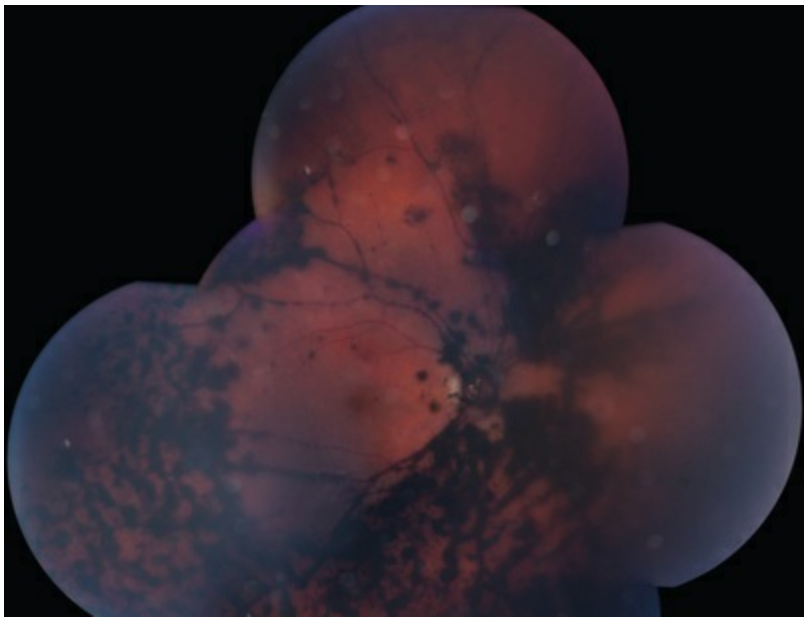

FIG. 137.6 Cutaneous melanoma metastatic to the retina and vitreous. Note the extensive pigment on the surface of the retina and within the retina. Pigmented vascular sheathing is noted, which may be preretinal in origin.

Vitreous cells are often seen in association with retinal metastases. These cells are usually pigmented in cases of metastatic melanoma and can be large. Vitreous cells in melanoma cases can be floating throughout the vitreous cavity (described as "brown spherules" or "globular vitreous opacities").[64,69] In contrast, vitreous cells associated with metastatic carcinoma tend to be white and confined to the area overlying retinal involvement.[68,70]

Other signs include secondary glaucoma from tumor invasion into the ciliary body, iris, or anterior chamber angle.[57]

Differential Diagnosis

The differential diagnosis of a metastatic retinal lesion is varied based on the initial appearance of the lesion. Choroidal metastasis with overlying retinal metastasis should be excluded initially (Fig. 137.7). For nonpigmented white retinal lesions seen in metastatic carcinoma, the differential includes inflammatory and infectious diseases such as toxoplasmosis chorioretinitis, cytomegalovirus (CMV) retinitis, herpetic-associated retinitis, syphilitic retinitis, endogenous endophthalmitis, sarcoidosis, multifocal choroiditis,

birdshot choroidopathy, acute posterior multifocal placoid pigmentary epitheliopathy (APMPPE), intraocular lymphoma, and other collagen vascular diseases. For pigmented lesions such as seen with metastatic melanoma the differential also includes choroidal tumors including melanoma and metastatic choroidal tumors, neovascular macular degeneration. Given the appearance of exudates and hemorrhages in some cases, retinal microvascular diseases such as hypertensive retinopathy, diabetic retinopathy, and retinopathy secondary to anemia are also possible diseases. Finally, conditions that may simulate the vitreous floaters of retinal metastases include granulomatous uveitides, amyloidosis, asteroid hyalosis, or intraocular lymphoma.[69,70]

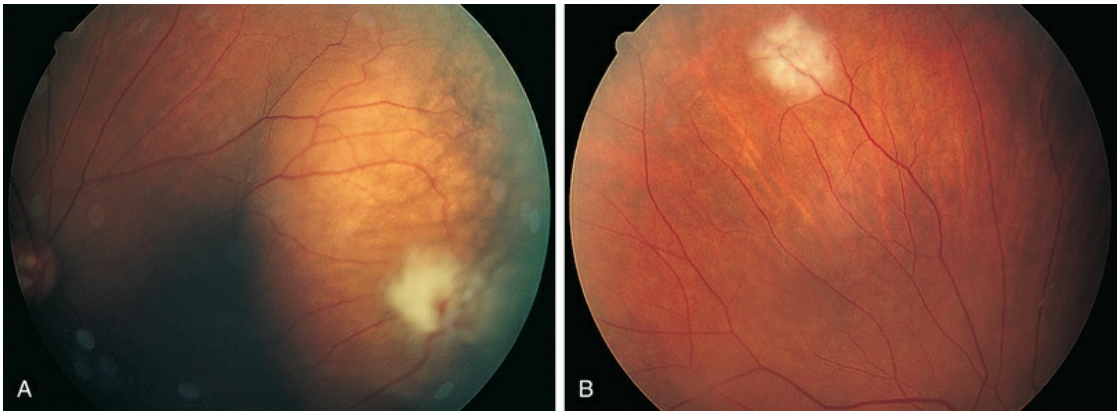

FIG. 137.7 Lung adenocarcinoma metastatic to the retina and choroid. (A) A primarily amelanotic, elevated choroidal mass in the temporal fundus. Note the overlying white retinal lesion, presumably from retinal invasion. (B) Elsewhere in the same eye, a solitary white retinal lesion likely represents a separate retinal metastasis.

In the setting of systemic malignancy and a potentially compromised immune system, the differential of infectious retinitis warrants further discussion. Multiple case reports highlight the initial diagnosis or treatment of infectious retinitis in cases of retinal metastasis.[92,94,95] CMV retinitis typically occurs in patients with CD4 counts less than 50 cells/μL.[97] The appearance of CMV retinitis may begin as a small white retinal infiltrate that can expand to a fluffy white lesion which is perivascular in origin with intraretinal

hemorrhages. CMV retinitis can also appear as a granular lesion with atrophic appearance of retina and a leading edge of retinitis with faint whitening and minimal hemorrhage. There is typically minimal vitreous inflammation, and the disease tends to spread slowly (approximately 250 μm/week)[97] (Fig. 137.8).

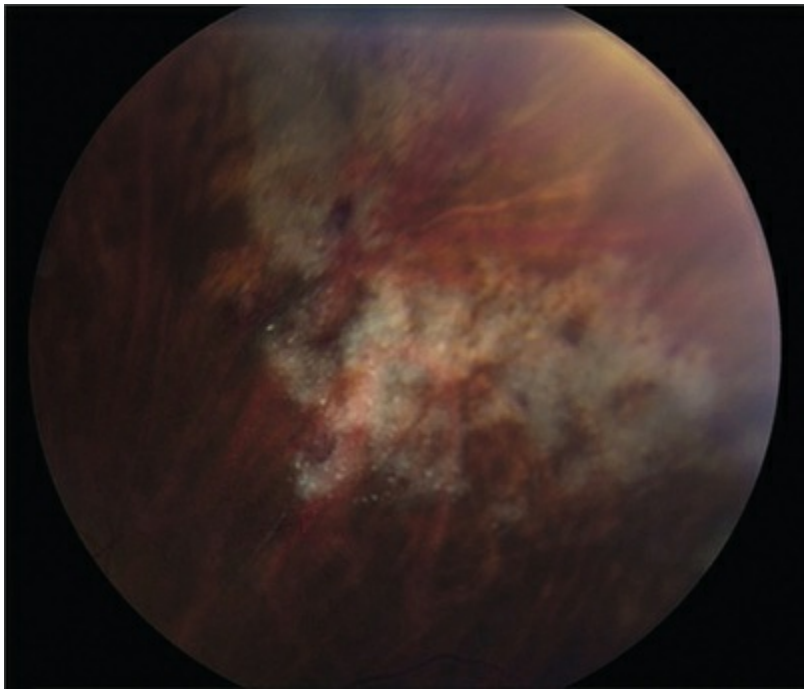

FIG. 137.8 Fundus photograph of a patient with cytomegalovirus retinitis. Note the posterior leading edge with a granular whitening of the retina. The retina is atrophic just anterior to this lesion indicating progression. Note minimal intraretinal hemorrhage.

In contrast, herpetic retinitis tends to be rapidly spreading with confluent areas of outer retinal whitening which progress to full-thickness retinitis.[97,98] Typically the peripheral retina is affected first with circumferential progression. The lesions do not usually follow the retinal vessels like CMV retinitis, though an occlusive retinal vasculitis is typically seen.[97,98] Significant vitreous inflammation is seen in those with a competent immune system, while those with a compromised immune system can have mild inflammation. Optic disc edema is often seen. The contralateral eye is often also affected (Fig. 137.9).

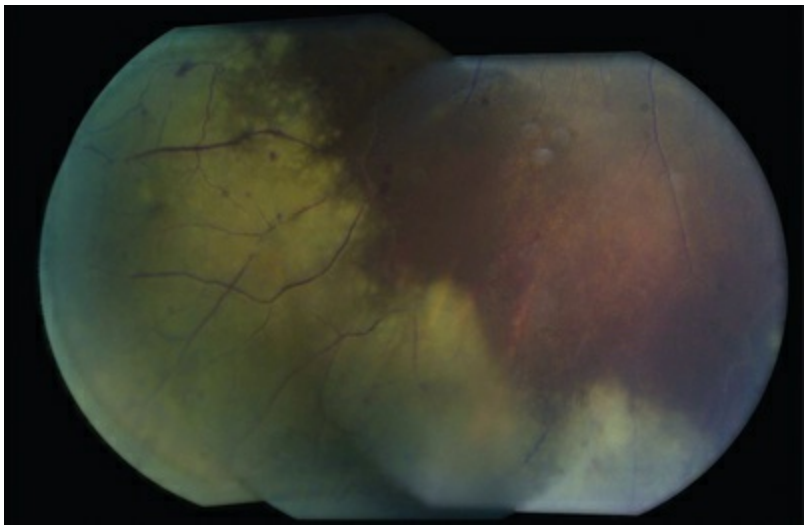

FIG. 137.9 Fundus photograph of a patient with herpetic retinitis. There is circumferential retina whitening affecting the deeper layers of the retina. There is minimal inflammation in this patient who is severely immunocompromised from chemotherapy.

Toxoplasmosis retinochoroiditis can also present as a whitish-yellow retinal lesion. Typically a chorioretinal scar will be seen in cases of reactivation with surrounding whitening or other satellite lesions.[97] Vitreous inflammation is usually seen. In some cases, no previous scar is seen and a solitary white chorioretinal lesion with irregular borders will be noted. A multifocal retinitis can be seen in patients who are immune compromised[97] (Fig. 137.10).

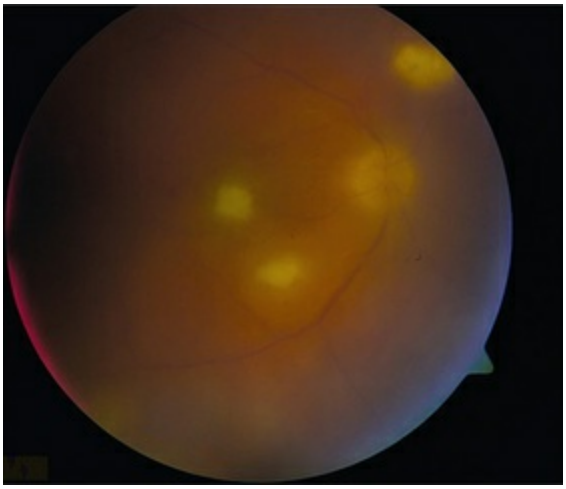

FIG. 137.10 Fundus photograph of a patient with multifocal toxoplasmosis retinochoroiditis. Multiple white lesions at the level of the retina and choroid are

noted in the posterior pole. This patient has been immunocompromised by steroid use.

Diagnostic Evaluation

A patient presenting with a retinal lesion with a history of systemic malignancy warrants a metastatic workup. In some case reports the retinal metastasis was the presenting system in a previously undiagnosed malignancy.[76] This presentation is rare though and most patients present with a previous history of malignancy. A complete history and physical with review of systems should be performed. Coordination with the patient's oncologist is imperative in evaluating for potential metastases. Given the potential for infectious etiologies including endogenous endophthalmitis, a review of recent illnesses, history of fever, chills, or other signs of infections should be reviewed.

Blood work including serum chemistry, liver function panel, and complete blood count should be ordered.[99] Depending on the appearance of the lesion, serum markers for infectious disease such as syphilis (rapid plasmin regain, [RPR] and fluorescent treponemal antibody absorption [FTA-Abs]), toxoplasmosis (antitoxoplasmosis IgG and IgM antibodies), should be drawn. Blood cultures may also be drawn. Serum markers for malignancy such as carcinoembryonic antigen (CEA) are not clearly associated with intraocular malignancy, thus their use may be limited in this setting.[97]

Diagnostic imaging is usually warranted in these patients. B-scan ultrasonography can assist in determining if there is potential choroidal disease with secondary retinal disease. B-scan ultrasonography has shown intermediate to high internal reflectivity on A-scan and dense thickening of the retina on B-scan.[69,70,74,75,78,79] However, ultrasonographic analysis of retinal metastases is limited by the thin size of most retinal lesions and the lack of established criteria given the rarity of such cases. Although fluorescein angiography is not diagnostic, it is helpful in differentiating metastatic tumors from non-neoplastic conditions.[4] Prominent vascularity is a conspicuous feature of metastatic cancer, and progressive hyperfluorescence in the late phases of the angiogram is characteristic (Fig. 137.11). Optical coherence

tomography can also be used to confirm the involvement of the retina and retinal surface (Figs. 137.12 and 137.13). Several case reports describe a thickened retina with hyperreflectance without any noted changes in the underlying choroid.[81,91,92]

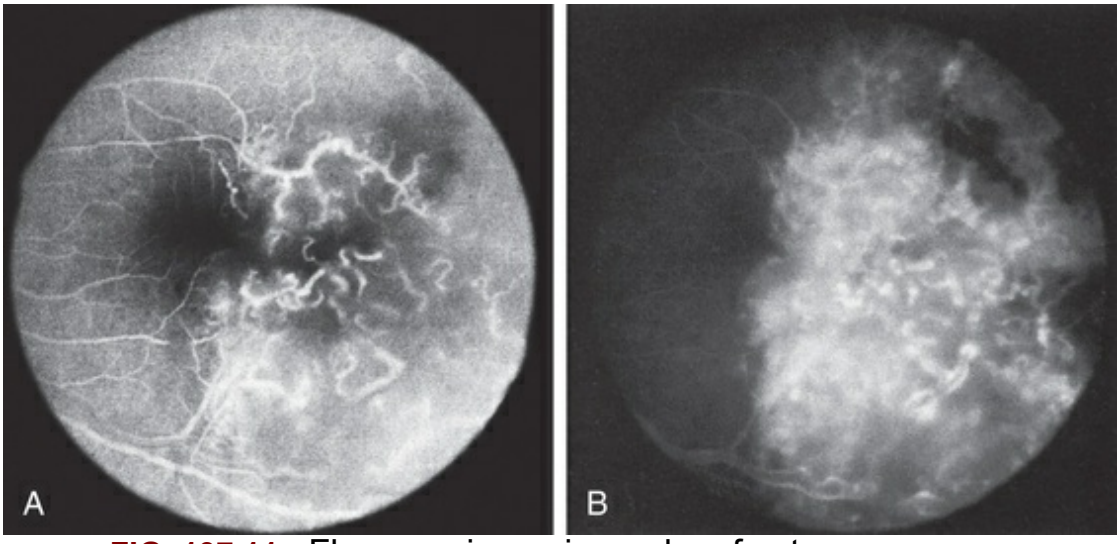

FIG. 137.11 Fluorescein angiography of cutaneous melanoma metastatic to the retina. (A) In the early frame the retinal vasculature is clearly visible with early hyperfluorescence of the vessels and some early leakage. (B) In a late frame staining of the retinal mass is evident and leakage from the retinal vessels is also present.

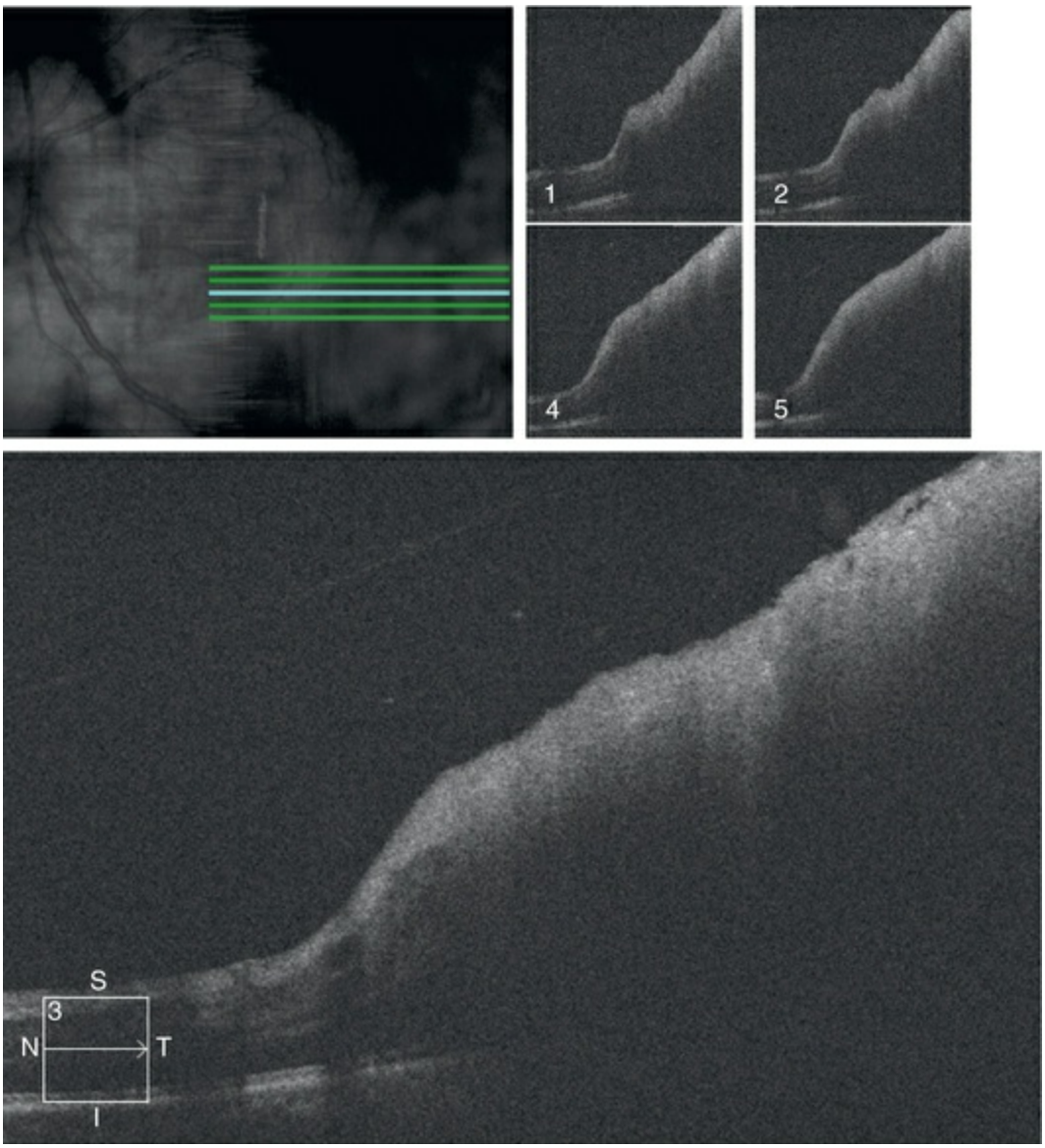

FIG. 137.12 Spectral domain optical coherence tomography of a patient with retinal metastasis displaying retinal thickening and inner retina hyperreflectance with outer retinal shadowing.

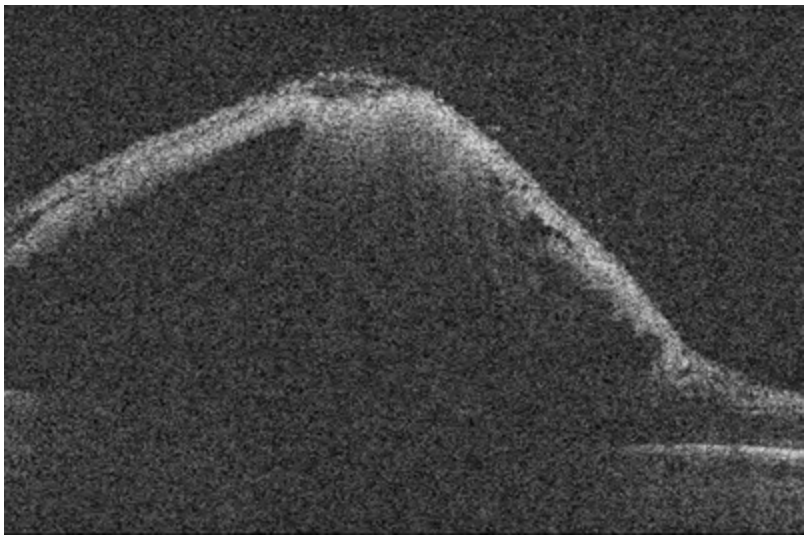

FIG. 137.13 Spectral domain optical coherence tomography of lung cancer metastatic to the retina. The mass has led to significant thickening of the retina, disorganization of the retinal structures, and shadowing of the outer retina and choroid.

Systemic imaging should be performed in patients with suspected metastasis. This again should be coordinated with the patient's oncologist to ensure the proper imaging is ordered for the suspected malignancy. Options include positron emission tomography (PET), computed tomography (CT) scan, combined PET/CT scans, and magnetic resonance imaging (MRI). Given the high incidence of brain metastases in the setting of retinal metastasis, imaging of the brain is warranted to identify potential lesions.

Ultimately, to make the diagnosis of retinal metastasis, a tissue diagnosis needs to be performed. This can be performed in several ways. Prior to obtaining a sample, coordination with an experienced ocular pathologist is recommended in order to identify the correct handling of the specimen and the specific amount of tissue required. A vitreous or aqueous aspirate can be the only sample required to make a diagnosis in those patients with significant vitreous or aqueous cells. Fine-needle aspiration biopsy (FNAB) of intraocular lesions can also be used to establish a diagnosis. Both the reliability and safety of FNABs have been demonstrated with no increase in tumor-related mortality rates.[99,101,102] In some cases however, pars plana vitrectomy with retinal biopsy may be needed. In cases where the diagnosis is

unclear and the differential includes infectious etiologies, vitrectomy offers the ability to obtain a substantial sample. In those particular cases, vitreous specimens could be sent for viral and toxoplasmosis polymerase chain reaction (PCR) identification. Tissue biopsy during a vitrectomy offers the ability to directly visualize the area in question and obtain a significant sample. With any sample, an experienced pathologist is needed to handle and accurately review the biopsy.[99]

Treatment

Treatment of metastatic retinal disease can vary based on a number of factors. The type of primary tumor, sites of additional metastases, the area of tumor involvement within the eye, vision, and the presence of pain all will determine the treatment for the eye. Eyes with poor vision and which are in severe, intractable pain should be considered for enucleation.[4] External beam irradiation can be effective in controlling intraocular metastatic tumors, thus enucleation is usually only reserved for select cases. In multiple case reports, external beam irradiation has demonstrated effectiveness in controlling tumor size and leading to tumor regression.[63,66,71,80,86,89] In one case, autopsy studies of one eye revealed eradication of the tumor (metastatic pulmonary adenocarcinoma) within the retina, although the retinal architecture had been destroyed by prior tumor invasion.[63]

When patients are asymptomatic and the intraocular tumor is well controlled, systemic chemotherapy alone has been considered, but results in patients with retinal metastases have been discouraging. With systemic chemotherapy, three cases of cutaneous melanoma and one case of rectal adenocarcinoma metastatic to the retina failed to respond.[64,65,71,72] Additionally, one case of adenocarcinoma of the cecum failed to respond to multiple cycles of chemotherapy, but responded after excision and palliative radiation.[85] With systemic and intravitreal chemotherapy, one reported case of breast carcinoma metastatic to the retina displayed partial regression of the vitreous involvement, but retinal detachment with massive vitreous traction occurred.[70] The use of anti-HER2 (human epidermal growth factor receptor 2) therapy in a case of metastatic breast cancer to the brain and retina has been

reported.[96] Shrinkage of the retinal and brain mass was noted after three cycles and treatment was continued for 12 cycles but stopped due to progression in the brain and liver.

Surgical resection has also been described as potential therapy. In one case, as noted above, the lesion was removed via vitrectomy and retinectomy and orbital radiation was performed postoperatively. After 3 months of follow-up, the eye and vision were stable.[85] Two reported cases of isolated retinal metastasis secondary to cutaneous melanoma were treated with vitrectomy and surgical resection.[73,78] In one case, surgical resection of the vascularized mass in the superotemporal retina, with systemic chemotherapy, resulted in resolution of blurred vision with 20/20 visual acuity. However, brain metastases developed within 1 year, and the patient committed suicide 3 months later.[73] In the other case, surgical resection of a peripheral lesion preserved vision for 12 months, until the patient committed suicide.[78] For more peripheral isolated lesions, surgical resection and vitrectomy may offer an alternative to external beam irradiation.

Plaque radiotherapy has proven to be effective in the treatment of well-circumscribed, isolated choroidal metastases.[66,90,100,103,104] However, its use in patients with retinal metastasis has not been described. Photodynamic therapy has been reported as a treatment of a presumed isolated retinal metastasis secondary to breast cancer.[87] However, follow-up was limited to only 8 weeks with tumor regression noted and stable visual acuity.

Prognosis

The prognosis for patients with retinal metastasis is poor. The survival from diagnosis to death in the review of reported cases ranges from 2 weeks to 5 years. Caution is recommended in interpreting these numbers as many case reports lack long-term follow-up after reporting a few weeks or months of survival. In the largest single-center case series[95] five of eight patients died within 1 month of the diagnosis of retinal metastasis – confirming the relative poor prognosis.

External beam radiation can reduce tumor size and salvage eyes prior to death.[63,66,71,86] Several eyes with intractable pain and/or

glaucoma required enucleation. Visual acuity results vary and depend on the extent of macular involvement. In those eyes with small lesions in the periphery, there is a chance to maintain good visual acuity as opposed to those eyes with large macular involvement. Despite improved diagnostic techniques and new treatment modalities, the prognosis remains poor.

Conclusion

Retinal metastasis is a rare complication of systemic malignancy. Visual symptoms include blurred vision and floaters, thus any patient with a history of malignancy should have a complete eye examination in the setting of those symptoms. Signs suspicious for retinal metastases include white or gray retinal infiltrates associated with perivascular sheathing with localized vasculopathy. Ancillary testing including ultrasonography, fluorescein angiography, and optical coherence tomography can assist in determining the location of lesion and rule out choroidal disease. Diagnosis should be established by biopsy, either vitreous biopsy or FNAB or retinal biopsy via vitrectomy. Important diseases that can mimic retinal metastasis include infectious retinitis such as CMV retinitis, herpetic retinitis, and toxoplasmosis retinochoroiditis. Choroidal tumors with secondary retinal involvement are other diseases to consider in the differential. Currently, external beam irradiation offers the most effective palliative therapy. Surgical resection and plaque radiotherapy are other potential options in treating this disease. Because of heightened awareness in the medical community, the rising incidence of certain tumor types (e.g., carcinoma of the lung), and the improved survival rates in others, an increasing number of patients with intraocular metastases will be seen in clinical practice. The ophthalmologist's responsibility is to establish the diagnosis with minimal invasion, alert the oncologist, and initiate a therapeutic plan in hopes of preventing further visual loss, pain, and enucleation.

References

1. Albert DM, Rubenstein RA, Scheie HG. Tumor metastases

to the eye. I. Incidence in 213 patients with generalized malignancy. *Am J Ophthalmol*. 1967;63:723–726.
2. Bloch RS, Gartner S. The incidence of ocular metastatic carcinoma. *Arch Ophthalmol*. 1971;85:673–675.
3. Ferry AP, Font RL. Carcinoma metastatic to the eye and orbit. I. A clinicopathologic study of 227 cases. *Arch Ophthalmol*. 1974;92:276–286.
4. Shields JA, Shields CL. *Intraocular tumors: a text and atlas*. WB Saunders: Philadelphia; 1992:208–210 [223].
5. Chambers AF, Groom AC, MacDonald IC. Dissemination and growth of cancer cells in metastatic sites. *Natl Rev Cancer*. 2002;2(8):563–572.
6. Mego M, Mani SA, Cristofanilli M. Molecular mechanisms of metastases in breast cancer – clinical applications. *Natl Rev Clin Oncol*. 2010;7:693–701.
7. Butler TP, Gullino PM. Quantitation of cell shedding into efferent blood of mammary adenocarcinoma. *Cancer Res*. 1975;35:512–516.
8. Fidler IJ. Metastasis: quantitative analysis of distribution and fate of tumor embolilabeled with125 I-5-iodo-2′-deoxyuridine. *J Natl Cancer Inst*. 1970;45:773–782.
9. Wong CW, Lee A, Shientag L, et al. Apoptosis: an early event in metastatic inefficiency. *Cancer Res*. 2001;61:333–338.
10. Podsypanina K, Du YC, Jeklinger M, et al. Seeding and propagation of untransformed mouse mammary cells in the lung. *Science*. 2008;321:1841–1844.
11. Hart IR, Goode NT, Wilson RE. Molecular aspects of the metastatic cascade. *Biochem Biophys Acta*. 1989;989:65–84.
12. Jiang WG, Puntis MCA, Hallett MB. Molecular and cellular basis of cancer invasion and metastatic implications for treatment. *Br J Surg*. 1994;81:1576–1590.
13. Kurschat P, Mauch C. Mechanisms of metastasis. *Clin Exp Dermatol*. 2000;25:482–489.
14. Engers R, Gabbert HE. Mechanisms of tumor metastasis: cell biological aspects and clinical implications. *J Cancer Res Clin Oncol*. 2000;126:682–692.
15. Nguyen DX, Bos PD, Massagué J. Metastasis: from dissemination to organ-specific colonization. *Natl Rev*

Cancer. 2009;9:274–284.
16. Felding-Habermann B. Integrin adhesion receptors in tumor metastasis. *Clin Exp Metastasis*. 2003;20:203–213.
17. Cottam DW, Rennie IG, Woods K, et al. Gelatinolytic metalloproteinase secretion patterns in ocular melanoma. *Invest Ophthalmol Vis Sci*. 1992;33:1923–1927.
18. Kleiner DE, Stetler-Stevenson WG. Matrix metalloproteinases and metastasis. *Cancer Chemother Pharmacol*. 1999;43(Suppl):S42–51.
19. Chang C, Werb Z. The many faces of metalloproteases: cell growth, invasion, angiogenesis, and metastasis. *Trends Cell Biol*. 2001;11:S37–43.
20. Dano K, Behrendt N, Hoyer-Hansen G, et al. Plasminogen activation and cancer. *Thromb Haemost*. 2005;93:676–681.
21. Egeblad M, Werb Z. New functions for the matrix metalloproteinases in cancer progression. *Natl Rev Cancer*. 2002;2:161–174.
22. Harbeck N, Kates RE, Schmitt M, et al. Urokinase-type plasminogen activator and its inhibitor type 1 predict disease outcome and therapy response in primary breast cancer. *Clin Breast Cancer*. 2004;5:348–352.
23. Riisbro R, et al. Prognostic significance of soluble urokinase plasminogen activator receptor in serum and cytosol of tumor tissue from patients with primary breast cancer. *Clin Cancer Res*. 2002;8:1132–1141.
24. Reese AB. *Tumors of the eye*. 2nd ed. Harper & Row: New York; 1963.
25. Ferry AP. Metastatic carcinoma of the eye and ocular adnexa. *Int Ophthalm Clin*. 1967;7:615–658.
26. Miyasuka M. Cancer metastasis and adhesion molecules. *Clin Ortho Rel Res*. 1995;312:10–18.
27. Mooy CM, Luyton GP, de Jong PT, et al. Neural cell adhesion molecule distribution in primary and metastatic uveal melanoma. *Hum Pathol*. 1995;26:1185–1190.
28. Zhu D, Cheng CF, Pauli BU. Mediation of lung metastasis of murine melanomas by a lung-specific endothelial cell adhesion molecule. *Proc Natl Acad Sci USA*. 1991;88:9568–9572.

29. Hart IR. 'Seed and soil' revisited: mechanisms of site specific metastasis. *Cancer Metastasis Rev*. 1982;1:5–16.
30. Zetter BR. The cellular basis of site-specific tumor metastasis. *N Engl J Med*. 1990;322:605–612.
31. Fidler IJ. Seed and soil revisited: contribution of the organ microenvironment to cancer metastasis. *Surg Oncol Clin North Am*. 2001;10:257–269.
32. Pilch J, Habermann R, Felding-Habermann B. Unique ability of integrin alpha(v)beta 3 to support tumor cell arrest under dynamic flow conditions. *J Biol Chem*. 2002;277:21930–21938.
33. Panes J, Granger DN. Leukocyte-endothelial cellinteractions: molecular mechanisms and implications in gastrointestinal disease. *Gastroenterology*. 1998;114:1066–1090.
34. Radinsky R. Modulation of tumor cell gene expression and phenotype by the organ-specific metastatic environment. *Cancer Metast Rev*. 1995;14:323–338.
35. Fidler IJ. Modulation of the organ microenvironment for treatment of cancer metastasis. *J Natl Cancer Inst*. 1995;87:1588–1592.
36. Radinsky R. Molecular mechanisms for organ-specific colon carcinoma metastasis. *Eur J Cancer*. 1995;31A:1091–1095.
37. Radinsky R, Ellis LM. Molecular determinants in the biology of liver metastasis. *Surg Oncol Clin North Am*. 1996;5:215–229.
38. Baggiolini M. Chemokines and leukocyte traffic. *Nature*. 1998;392:565–568.
39. Campbell JJ, Butcher EC. Chemokines in tissue specific and microenvironment-specific lymphocyte homing. *Curr Opin Immunol*. 2000;12:336–341.
40. Homey B, Muller A, Zlotnik A. Chemokines: agents for the immunotherapy of cancer? *Nature Rev Immunol*. 2002;2:175–184.
41. Mueller A, Johnston M, Bligh D. Involvement of chemokine receptors in breast cancer metastasis. *Nature*. 2001;410:50–56.
42. Hori A, Sasada R, Matsutani E, et al. Suppression of solid tumor growth by immunoneutralizing monoclonal antibody against human basic fibroblast growth factor.

Cancer Res. 1991;51:6180–6184.
43. Kim KJ, Li B, Winer J, et al. Inhibition of vascular endothelial growth factor-induced angiogenesis suppresses tumor growth in vivo. *Nature*. 1993;362:841–844.
44. Zubilewicz A, Hecquet C, Jeanny JC, et al. Two distinct signalling pathways are involved in FGF2-stimulated proliferation of choriocapillary endothelial cells: a comparative study with VEGF. *Oncogene*. 2001;20:1403–1413.
45. Baird A, Esch F, Gospodarowicz D, et al. Retina- and eye-derived growth factors: partial molecular characterization and identity with acidic and basic fibroblast growth factor. *Biochem*. 1985;24:7855–7860.
46. Chen CH, Chen SC. Evidence for the presence of a specific vascular endothelial growth factor in fetal bovine retina. *Exp Cell Res*. 1987;169:287–295.
47. Stitt AW, Simpson DA, Boocock C, et al. Expression of vascular endothelial growth factor (VEGF) and its receptor is regulated in eyes with intra-ocular tumours. *J Pathol*. 1998;186:306–312.
48. Plate KH, Breier G, Welch HA, et al. Vascular endothelial growth factor is a potential tumor angiogenesis factor in human gliomas in vivo. *Nature*. 1992;359:845–848.
49. Shweiki D, Itin A, Soffer D, et al. Vascular endothelial growth factor induced by hypoxia may mediate hypoxia-initiated angiogenesis. *Nature*. 1992;359:843–845.
50. Vinores SA, Kuchle M, Mahlow J, et al. Blood–ocular barrier breakdown in eyes with ocular melanoma: a potential role for vascular endothelial growth factor/vascular permeability factor. *Am J Pathol*. 1995;147:1289–1297.
51. Goto F, Goto K, Weindel K, et al. Synergistic effects of vascular endothelial growth factor and basic fibroblast growth factor on the proliferation and cord formation of bovine capillary endothelial cells within collagen gels. *Lab Invest*. 1993;69:508–517.
52. Pepper MS, Ferrara N, Orci L, et al. Potent synergism between vascular endothelial growth factor and basic fibroblast growth factor in the induction of angiogenesis in

vitro. *Biochem Biophys Res Commun*. 1992;189:824–831.
53. Asahara T, Bauters C, Zheng LP, et al. Synergistic effect of vascular endothelial growth factor and basic fibroblast growth factor on angiogenesis in vivo. *Circulation*. 1995;92:365–371.
54. Smoleroff JW, Agatston SA. Metastatic carcinoma of the retina: report of a case, with pathologic observations. *Arch Ophthalmol*. 1934;12:359–365.
55. Uhler EM. Metastatic malignant melanoma of the retina. *Am J Ophthalmol*. 1940;23:158–162.
56. Kennedy RJ, Rummel WD, McCarthy JL, et al. Metastatic carcinoma of the retina. Report of a case and the pathologic findings. *Arch Ophthalmol*. 1958;60:12–18.
57. Duke JR, Walsh FB. Metastatic carcinoma to the retina. *Am J Ophthalmol*. 1959;47:44–48.
58. Liddicoat DA, Wolter JR, Wilkinson WC. Retinal metastasis of malignant melanoblastoma: a case report. *Am J Ophthalmol*. 1959;48:172–177.
59. Riffenburgh RS. Metastatic malignant melanoma to the retina. *Arch Ophthalmol*. 1961;66:487–489.
60. Koenig RP, Johnson DL, Monahan RH. Bronchogenic carcinoma with metastases to the retina. *Am J Ophthalmol*. 1963;56:827–829.
61. Flindall RJ, Fleming KO. Metastatic tumour of the retina. *Can J Ophthalmol*. 1967;2:130–132.
62. Klein R, Nicholson DH, Luxenberg MN. Retinal metastasis from squamous cell carcinoma of the lung. *Am J Ophthalmol*. 1977;83:358–361.
63. Young SE, Cruciger M, Lukeman J. Metastatic carcinoma to the retina: case report. *Ophthalmology*. 1979;86:1350–1354.
64. Robertson DM, Wilkinson CP, Murray J, et al. Metastatic tumor to the retina and vitreous cavity from primary melanoma of the skin: treatment with systemic and subconjunctival chemotherapy. *Ophthalmology*. 1981;88:1296–1301.
65. Letson AD, Davidorf EH. Bilateral retinal metastases from cutaneous malignant melanoma. *Arch Ophthalmol*. 1982;100:605–607.

66. de Bustros S, Augsburger JJ, Shields JA, et al. II: Intraocular metastases from cutaneous malignant melanoma. *Arch Ophthalmol*. 1985;103:937–940.
67. Takagi T, Yamaguchi T, Mizoguchi T, et al. A case of metastatic optic nerve head and retinal carcinoma with vitreous seeds. *Ophthalmologica*. 1989;199:123–126.
68. Eagle RC Jr. *Carcinomatous retinitis*. [Presentation to Eastern Ophthalmic Pathology Society. Hilton Head, SC] 1988.
69. Best SJ, Taylor W, Allen JP. Metastatic cutaneous malignant melanoma of the vitreous and retina. *Aust NZ J Ophthalmol*. 1990;18:397–400.
70. Leys AM, VanEyck LM, Nuttin BJ, et al. Metastatic carcinoma to the retina: clinicopathologic findings in two cases. *Arch Ophthalmol*. 1990;108:1448–1452.
71. Striebel-Gerecke SU, Messmer EP, Landolt U. Retinale und vitreale metastase eines kleinzelligen bronchuskarizinoms. *Klin Monatsbl Augenheilkd*. 1992;200:535–536.
72. Tachinami K, Katayama T, Takeda N, et al. A case of metastatic carcinoma to the retina. *Nippon Ganka Gakkai Zasshi*. 1992;96:1336–1340.
73. Balestrazzi E, Blasi MA, Marullo M, et al. Local excision of retinal metastasis from cutaneous melanoma. *Eur J Ophthalmol*. 1995;5:149–154.
74. Spraul CW, Lang GE, Grossniklaus HE, et al. Metastatic adenocarcinoma to the retina in a patient with Muir–Torre syndrome. *Am J Ophthalmol*. 1995;120:248–250.
75. Spraul CW, Martin DF, Hagler WS, et al. Cytology of metastatic cutaneous melanoma to the vitreous and retina. *Retina*. 1996;16:328–332.
76. Cangiarella JF, Suhrland MJ, Cajigas A, et al. Esophageal carcinoma metastatic to the retina: diagnosis of a case by cytologic examination of intraocular vitreous washings. *Acta Cytol*. 1996;40:995–998.
77. Gunduz K, Shields JA, Shields CL, et al. Cutaneous melanoma metastatic to the vitreous cavity. *Ophthalmologica*. 1998;105:600–605.
78. Spadea L, Bisti S, Colucci S, et al. Normal EOG values in intraretinal metastasis from cutaneous melanoma: a case

report. *Doc Ophthalmol*. 1999;96:305–309.
79. Soheilian M, Mirbabai F, Shahsavari M, et al. Metastatic cutaneous melanoma to the vitreous cavity masquerading as intermediate uveitis. *Eur J Ophthalmol*. 2002;12:324–327.
80. Hutchison BM, McAllister IL, Barry CJ. Bowel carcinoma metastatic to the retina. *Clin Exp Ophthalmol*. 2001;29:438–439.
81. Truong SN, Fern CM, Costa DL, et al. Metastatic breast carcinoma to the retina: optical coherence tomography findings. *Retina*. 2002;22:813–815.
82. Zografos L, Ducrey N, Beati D, et al. Metastatic melanoma in the eye and orbit. *Ophthalmology*. 2003;110:2245–2256.
83. Saornil MA, Blanco G, Sarasa JL, et al. Isolated metastasis of gastric adenocarcinoma to the retina: first presentation of systemic disease. *Acta Ophthalmol Scand*. 2004;82:86–88.
84. Zografos L, Mirimanoff RO, Angeletti CA, et al. Systemic melanoma metastatic to the retina and vitreous. *Ophthalmologica*. 2004;218:424–433.
85. Apte RS, Dibernardo C, Pearlman JR, et al. Retinal metastasis presenting as a retinal hemorrhage in a patient with adenocarcinoma of the cecum. *Arch Ophthalmol*. 2005;123:850–853.
86. Sirimaharaj M, Hunyor AP, Chan WC, et al. Unusual ocular metastasis from breast cancer. *Clin Exp Ophthalmol*. 2006;34:74–76.
87. Rundle P, Rennie I. Photodynamic therapy for solitary retinal metastasis from breast carcinoma. *Eye (Lond)*. 2006;20(12):1410–1412.
88. Khurana RN, Tran VT, Rao NA. Metastatic cutaneous melanoma involving the retina and vitreous. *Arch Ophthalmol*. 2007;125(9):1296–1297.
89. Alegret A, Cebulla CM, Dubovy SR, et al. Pediatric nasopharyngeal carcinoma with retinal metastasis. *Retin Cases Brief Rep*. 2009;3(1):8–11.
90. Kim CY, Ha CW, Lee SC. Vitreous and retinal metastasis from gastric cancer. *Eur J Ophthalmol*. 2010;20:615–617.
91. Coassin M, Ebrahimi KB, O'Brien JM, et al. Optical coherence tomography for retinal metastasis with unknown

primary tumor. *Ophthalmic Surg Lasers Imaging*. 2011;42:e110–13 [Online].
92. Payne JF, Rahman HT, Grossniklaus HE, et al. Retinal metastasis simulating cytomegalovirus retinitis. *Ophthalmic Surg Lasers Imaging*. 2012;43:e90–3 [Online].
93. Krema H, Fernandes B, Simpson R, et al. Diffuse metastatic melanoma to the retina: a clinicopathologic report. *Can J Ophthalmol*. 2013;48(2):e20–1.
94. Singh RP, Steinle NC, Bedi R, et al. Retinal infiltrates secondary to metastatic squamous cell carcinoma masquerading as infectious retinitis. *Retin Cases Brief Rep*. 2014;8(4):333–335.
95. Shields CL, McMahon JF, Atalay HT, et al. Retinal metastasis from systemic cancer in 8 cases. *JAMA Ophthalmol*. 2014;132(11):1303–1308.
96. Gubbiotti M, Pistilli B, Tudini M, et al. Retinal metastasis regression with eribulin in a heavily pretreated breast cancer patient. *Future Oncol*. 2015;11(Suppl. 15):17–22.
97. Nussenblatt RB, Whitcup SM. *Uveitis, fundamentals and clinical practice*. 3rd ed. Mosby: Philadelphia; 2004:188–195 [201-206, 214-222].
98. Holland GN. Executive committee of the American Uveitis Society. Standard diagnostic criteria, for the acute retinal necrosis syndrome. *Am J Ophthalmol*. 1994;117:663–666.
99. Char DH. *Clinical ocular oncology*. 2nd ed. Lippincott–Raven: Philadelphia; 1997:103–122 [159–160].
100. Lembersky BC, Thomas LC. Metastases of unknown primary site. *Med Clin North Am*. 1996;80:153–171.
101. Shields JA, Shields CL, Ehya H, et al. Fine-needle aspiration biopsy of suspected intraocular tumors. The 1992 Urwick lecture. *Ophthalmology*. 1993;100:1677–1684.
102. Augsburger JJ. Fine needle aspiration biopsy of suspected metastatic cancers to the posterior uvea. *Trans Am Ophthalmol Soc*. 1988;86:499–560.
103. Rosset A, Zografos L, Coucke P, et al. Radiotherapy of choroidal metastases. *Radiother Oncol*. 1998;46:263–268.
104. Shields CL, Shields JA, De Potter P, et al. Plaque radiotherapy for the management of uveal metastasis. *Arch*

Ophthalmol. 1997;115:203–209.

138

Remote Effects of Cancer on the Retina

Ranjit S. Dhaliwal, Andrew P. Schachat

Introduction

Cancers are capable of producing effects on remote tissues without direct tumorous spread and unrelated to the effects of opportunistic infection or medical therapy. Syndromes not caused directly by cancer cells are referred to as "paraneoplastic," or "remote," manifestations of cancer. Paraneoplastic syndromes are known to occur in the absence of systemic tumor spread and may precede a clinically recognized tumor.

Neurologic paraneoplastic syndromes have been estimated to

occur in up to 15% of cancer patients, half of whom have primary carcinoma of the lung.[1]

The prevalence of ophthalmic paraneoplastic syndromes is unknown. Although uncommon, the remote effects of cancer on the eye are important to recognize because they may be the presenting signs of previously undiagnosed malignancy or may suggest recurrence of previously treated disease.[2–4] Furthermore, the recognition of these syndromes in patients with unexplained visual loss may aid the ophthalmologist in palliative management, since the disabling ocular symptoms may be amenable to medical therapy.[3,5]

Paraneoplastic neuro-ophthalmic syndromes include cancer-associated retinopathy (CAR), melanoma-associated retinopathy (MAR), paraneoplastic vitelliform maculopathy (PVM), and bilateral diffuse uveal melanocytic proliferation (BDUMP). BDUMP has been proposed to be the result of tumor induced ectopic peptides, while most other paraneoplastic ophthalmic syndromes are felt to be part of a spectrum of autoimmune disorders that also encompass autoimmune retinopathy (Chapter 80, Autoimmune retinopathies) and paraneoplastic optic neuropathy with vitritis (PON).[5,6]

Cancer-Associated Retinopathy (CAR) Syndrome

In 1976, Sawyer and coworkers[2] described three patients with sudden onset of vision loss, positive visual phenomena, ring-like scotomas, and nyctalopia who developed light perception vision and were later diagnosed as having bronchogenic carcinoma. Fundus examination demonstrated only nonspecific pigment mottling in the posterior pole, normal optic nerves, and a slight degree of vascular attenuation with variable sheathing. Histopathologic examination in each case demonstrated widespread severe degeneration of the outer nuclear retinal layer and disintegration of photoreceptors, as well as the presence of macrophages containing phagocytosed granules from the retinal pigment epithelium (RPE) (Fig. 138.1). In contrast with retinitis

pigmentosa, the RPE and choriocapillaris were remarkably preserved in all eyes examined. The authors believed that these features excluded a vascular basis for the observed findings and concluded that these represented a remote effect of bronchogenic carcinoma.[2]

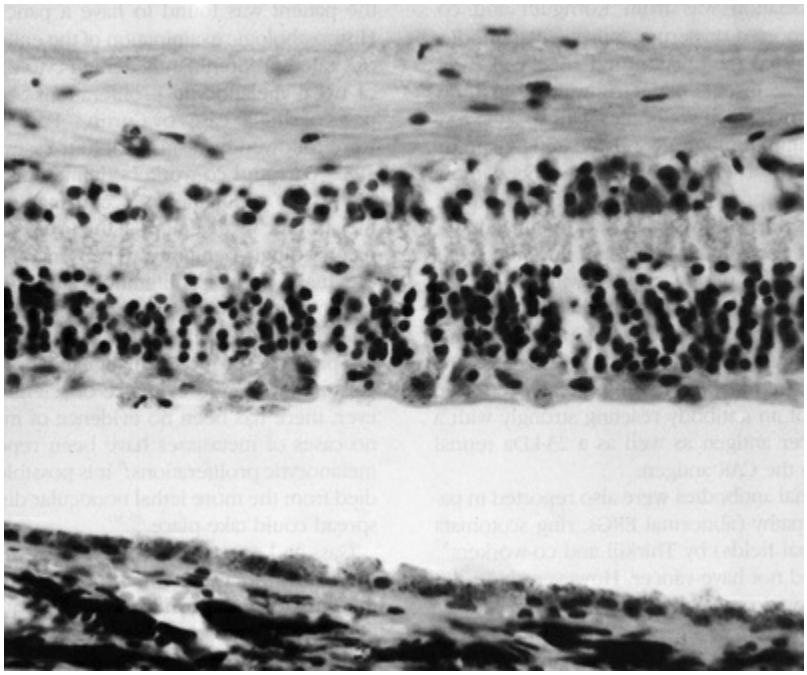

FIG. 138.1 Paramacular retina from the eye of a 61-year-old woman with cancer-associated retinopathy (CAR) related to uterine carcinoma. Photoreceptors and outer nuclear layers are replaced by glial tissue containing pigment-laden macrophages. Note normal inner retinal layers, retinal pigment epithelium, and choroid. (Courtesy of Alan M. Ross and John L. Keltner.)

Subsequently, Keltner and colleagues[3] described a patient with undifferentiated cervical cancer presenting with progressive blindness, progressive retinal arteriolar narrowing, a few vitreous cells, and a flat electroretinogram (ERG). Antibodies were found in the patient's serum against normal photoreceptors from fresh normal human retinal tissue. A trial of steroids was initiated, which improved vision. Histopathologic examination later disclosed a loss of retinal photoreceptors and the outer nuclear layer. The authors proposed a possible autoimmune mechanism for these findings.

Klingele and coworkers[7] described a similar picture in a patient

with mottled hyperfluorescence on fluorescein angiography, who was later diagnosed with breast carcinoma, and they termed this "paraneoplastic retinopathy."

The term "cancer-associated retinopathy" (CAR) syndrome has subsequently come to be used to describe the clinical picture of subacute visual loss resulting from circulating antibodies against retinal proteins in the presence of systemic cancerous tumor growth.[1,4,8,9]

There is no gender predisposition in CAR syndrome, and the symptoms of decreased vision, a halo of missing peripheral vision, positive visual phenomena ("sparkles"), photosensitivity, impaired color vision, and night blindness usually antedate the clinical signs and symptoms of systemic malignancy by a mean of 5 months in up to 50% of cases.[10] The longest duration from the onset of CAR syndrome to diagnosis of the carcinoma was 11 years in a patient with a pulmonary carcinoma.[11] Patients with CAR syndrome generally progress from initial stages of visual loss to blindness in 6–18 months.[3,4,9]

ERG findings in patients with CAR syndrome have been reported to show extinguished a and b waves or rod responses larger than cone responses (Fig. 138.2). Occult malignancy should be suspected in patients with acquired night blindness and minimal ocular findings to account for the visual difficulty and abnormal ERG results.[12] The presenting symptoms may be asymmetric, and some patients complain of glare and photosensitivity.[13–16] Cells in the vitreous or anterior chamber are infrequently reported in CAR syndrome.[3,7] Tonic pupils have been reported to be a potential ophthalmic finding in paraneoplastic syndromes.[17] Reduced macular thickness on OCT examination may be observed prior to severe visual loss,[18] and the spectral domain OCT (SD-OCT) demonstrates interruption of the outer retinal layers (inner/outer-segment junction).[19]

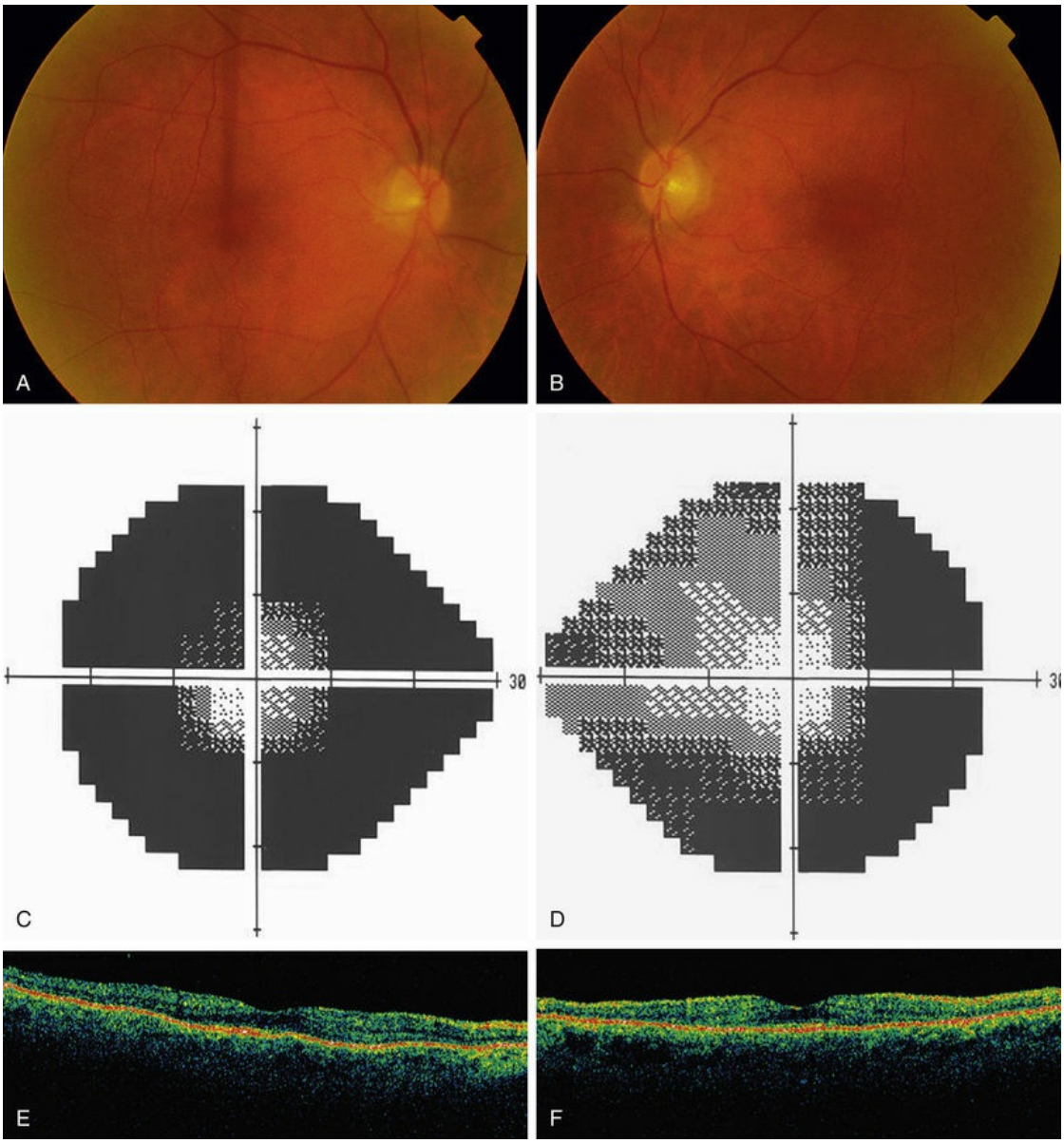
A
B
C
30
D
E
F

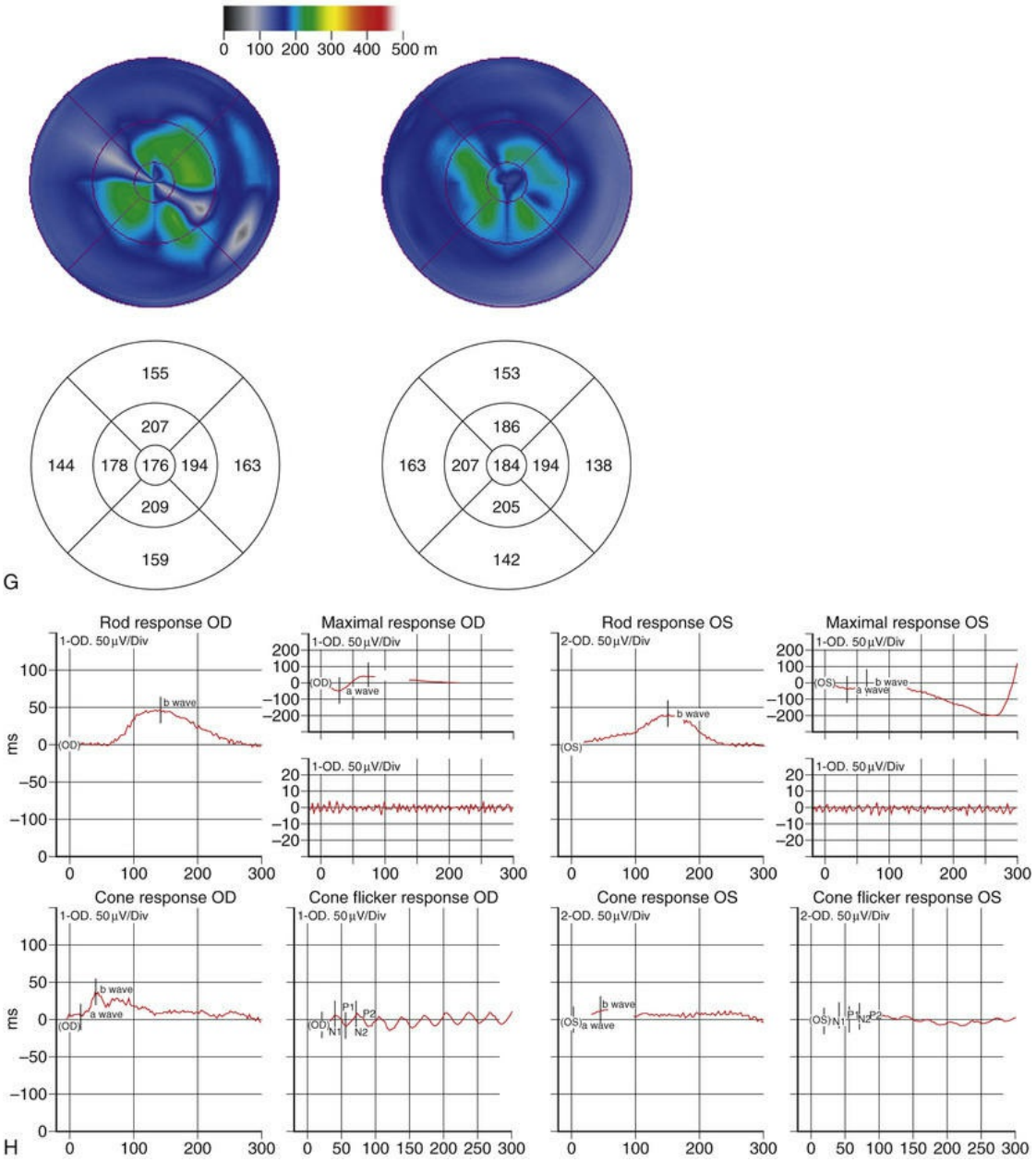

FIG. 138.2 (A,B) Fundus photographs of a 67-year-old woman with small-cell lung cancer and vascular attenuation only. (C,D) Automated perimetry demonstrates severe visual-field constriction of the left eye to a greater extent than the right. (E–G) Optical coherence tomography sections of the macula demonstrate nonspecific and diffuse thinning. (H) Electroretinogram demonstrates decreased and delayed amplitudes of both rods and cones. This patient had negative results for antirecoverin antibodies. (Panel H reprinted with permission from Ophthalmology Times 2003;28:14–6. Ophthalmology Times is a copyright publication of Advanstar

The most common malignancies related to CAR are carcinomas, and over half of all these patients have a pulmonary malignancy, with the most common being small cell carcinoma of the lung.[2,4,9,13–16,20–29] A chest radiograph should usually be obtained as part of the evaluation of suspect individuals. Other malignancies associated with CAR include those of the colon,[29] endometrium/uterus,[30–32] cervix,[3,26,33] breast,[7,34–36] prostate/bladder,[34,35,37] thorax (rhabdomyosarcoma), abdominal liposarcoma, and systemic lymphoma.[38,39] In rare instances, patients with documented antibodies to the retina and classic symptoms of CAR may not have an associated underlying malignancy. These patients constitute a minority of patients referred to as having autoimmune retinopathy not associated with underlying malignancy and are discussed in greater detail in Chapter 80, Autoimmune retinopathies (Fig. 138.3).[1,14,37,40,41]

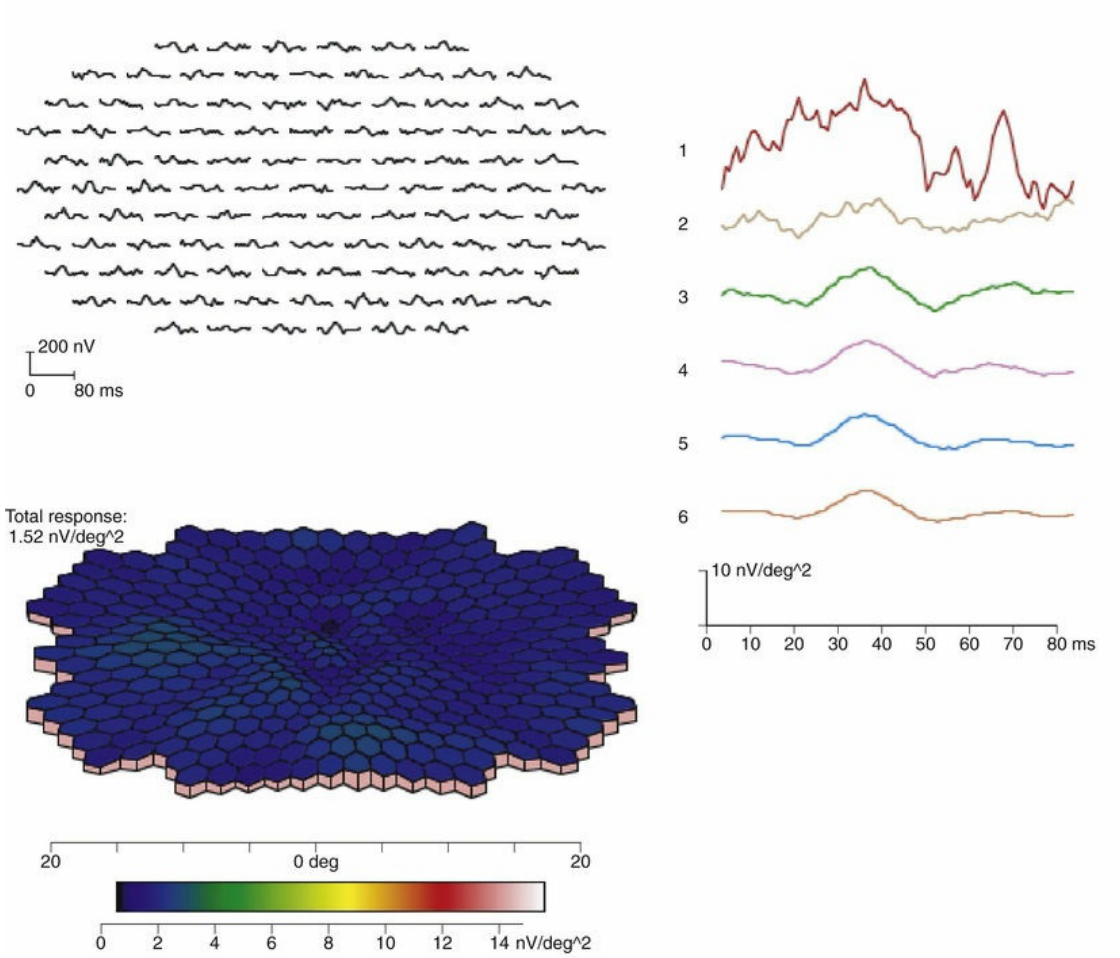

FIG. 138.3 Multifocal electroretinogram of a 33-year-old woman with autoimmune retinopathy, right eye. This patient tested positive for serum antibodies against retinal proteins p37, p40, and p52 while noting loss of central and midperipheral vision. Vitreous cells are noted in both eyes but the fundus exam was otherwise nondescript. Note the diffuse reduction of amplitudes throughout the entire test field observed on both the trace array (and three-dimensional plot; bottom). There are also focal areas of greater reduction noted. The ring averages (right) demonstrate reduction of amplitude with minimal delays in timing. The findings in the fellow eye were symmetrical to this exam. (Courtesy of Kean T. Oh.)

There has been a growing body of evidence supporting an autoimmune basis for CAR syndrome.[42,43] In 1982 Kornguth et al.[23] reported on the presence of 23-kDa serum antiretinal ganglion cell antibodies in patients with visual dysfunction and small cell carcinoma of the lung. Subsequently, Grunwald et al.[13] described

the reaction of such antibodies with specific retinal antigens in the ganglion cells and inner nuclear layers and immunologically related antigens in tumor cells (as well as their absence in patients with tumors but with no visual defects). They proposed that the small cell tumor produces antigens normally associated with retinal tissue. These antigens are recognized as foreign, since the retina is an immunologically privileged site without antiself suppressor mechanisms.[13,43] CAR syndrome can also be associated with uveitis (vitritis and vascular sheathing);[3,44,45] as the concentrations of the predominantly IgG class autoantibodies reach a critical threshold, they cross the abnormally permeable blood–retina barrier. It is postulated that a cross-reaction with retinal tissue occurs, and subsequently a nonspecific immune-mediated common pathway of retinal degeneration with apoptosis ensues.[36]

The 23-kDa antigen to which antibodies have been produced in up to 60% of individuals with CAR syndrome has been shown to be recoverin,[46] a calcium channel photoreceptor protein.[16,21,26,28,41,47–50] No clear role for recoverin in the normal functioning of photoreceptor cells has been demonstrated, but binding to this protein results in cellular death by some unknown mechanism. Antibodies to the CAR antigen (recoverin) were not previously demonstrated in any other form of retinopathy, nor were these antibodies believed to be expressed by tumors without associated retinopathy.[4,16] Recently, however, a clinically distinctive condition has been described resembling CAR with a cellular immune response against recoverin (recoverin-associated retinopathy).[51]

Now available commercially, the Western blot analysis for the CAR antigen-antibody may be negative even in the presence of CAR syndrome.[44] Moreover, the titers of antibody versus recoverin do not necessarily correlate with the severity of the clinical retinopathy. Hence, clinical criteria and a high index of suspicion remains the mainstay of diagnosis.

Thirkill and coworkers[9] reported on isolation of antibodies reacting strongly with a 23-kDa retinal protein in addition to yet another 65-kDa lung cancer antigen.

Adamus and colleagues[49] reported several cases of CAR syndrome in association with antibodies to a 46-kDa antigen identified as human alpha-enolase, a glycolytic enzyme. Further

work by Adamus has led to the hypothesis that antibodies against recoverin, and other retinal proteins such as alpha-enolase, are cytotoxic by triggering apoptosis via a caspase 3-apoptotic pathway.[52–53] Therefore multiple antigens may be capable of inducing retinal damage and clinical autoimmune retinopathy.[5,39,51,54,55] The heterogeneity of tumor types with many distinct antigens may account for the diversity of observed CAR phenotypes. There exists a high degree of correlation between the presence of serum autoantibodies, the development of visual symptoms, and the presence of retinal degeneration.[54]

Cutaneous Melanoma-Associated Retinopathy (MAR) Syndrome

A paraneoplastic syndrome of acquired night blindness associated with rapidly developing vitiligo of the skin and uveal tract was reported in two patients with metastatic cutaneous melanoma.[56,57] This process was described originally in 1984 by Gass as "an acute Vogt–Koyanagi–Harada-like syndrome." These patients, like those with CAR syndrome, had ERG abnormalities with a- and b-waves that were markedly reduced in amplitude, indicating widespread photoreceptor cell dysfunction.

"Paraneoplastic acquired night blindness" in patients with cutaneous malignant melanoma is being reported in greater frequency than in those with typical CAR syndrome.[1,12,14,33,57–67] MAR syndrome is thought to be a clinically distinctive subset of cancer-associated retinopathy. Specifically, this form of cancer-associated retinopathy is clinically differentiated from CAR syndrome by being nonprogressive, causing central visual loss (versus ring scotomas), is associated with a sensation of shimmering or sparkling light, and is associated with vitiligo in up to 20%.[57] In contrast to patients with CAR syndrome and the "acute Vogt–Koyanagi–Harada-like syndrome," patients with MAR syndrome demonstrate a substantial elevation of rod absolute thresholds and selective reductions in the rod and cone ERG b waves, resembling those of patients with congenital stationary night blindness. The photoreceptor function is intact but signal

transmission between the photoreceptors and second-order interneurons appears to be defective. MAR syndrome, unlike CAR syndrome, is more likely to be visually symptomatic in more advanced stages of systemic disease and, in general, does not manifest before the clinical diagnosis of cutaneous malignant melanoma.[1,66,68] Unilateral presentation of MAR has been reported over 18 months of observation but this may represent asymmetric ocular involvement.[69] Subclinical evidence for MAR may be present in earlier stages of cutaneous melanoma and this may portend a worse overall prognosis for the patient. Antibodies to retinal bipolar cells in MAR syndrome have been reported, but not against the 23-kDa CAR antigen.[63,66,67] The nature of the bipolar cell antigen is not yet known but studies have verified that the bipolar cells are the primary site of pathology in this condition.[70–72] Finally, antibodies against transducin, enolase, aldolase A, and aldolase C have also been documented in patients with MAR.[73]

Paraneoplastic Vitelliform Maculopathy (PVM)

Paraneoplastic vitelliform maculopathy (PVM) is a multifocal exudative fundus disorder with multiple oval yellow–white lesions at the level of the RPE surrounding the disc and in the macular regions of both eyes. (Fig. 138.4). This condition was described in 2001 by Borkowski et al. in patients having cutaneous melanoma, and the term "paraneoplastic vitelliform retinopathy" was coined by Sotodeh el al. in 2005.[74,75] Subsequently PVM has been reported in patients with choroidal melanoma, carcinoma of the lung, and multiple myeloma.[76–79] PVM has no gender predilection and is associated with only mild subjective visual loss (20/40 to 20/100) with mild nyctalopia and photopsias. Minimal visual field changes were reported and variable ERG responses have been described. A pathologically reduced Arden ratio was found in less than half of reported cases, suggesting relatively normal RPE function in most cases. A clinically indistinguishable entity, acute exudative polymorphous vitelliform maculopathy (AEPVM), has been reported with trauma and with various infections (hepatitis C,

coxsackie B virus, syphilis, and Lyme disease). It has been suggested that the infectious agents cause antibody formation in those patients without associated neoplasm.

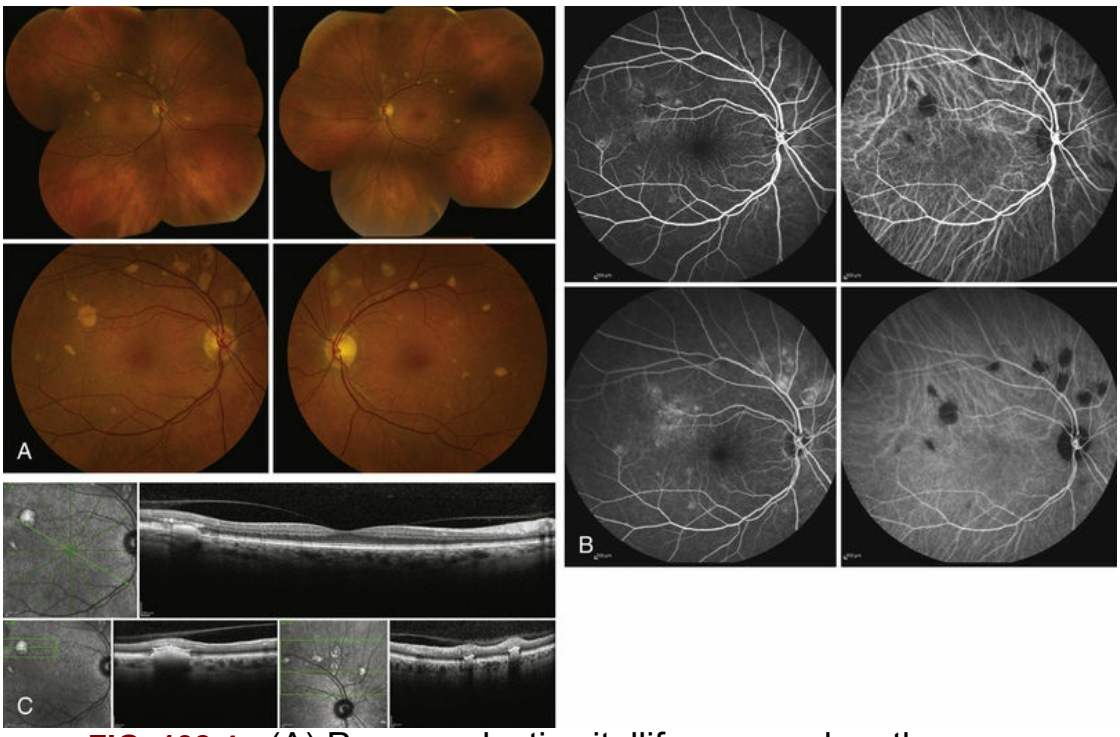

FIG. 138.4 (A) Paraneoplastic vitelliform maculopathy in a multiple myeloma patient with discrete yellowish-orange subretinal deposits surrounding the arcade vessels and disc only. (B) Early fluorescein angiographic examination demonstrates hypofluorescence of the subretinal and sub-retinal pigment epithelium (RPE) lesions with late hyperfluorescence (A,C) and the indocyanine green angiographic examination demonstrates persistent hypofluorescence (B). (C) Spectral domain optical coherence tomography demonstrates an absence of subretinal fluid with hyperreflective subretinal and sub-RPE deposits with hyperreflectivity above the photoreceptors. (Courtesy of Randy Dhaliwal MD.)

Retinal autoantibodies against bipolar cells, enolase, rod outer segment proteins, and bestrophin have all been reported. The heterogeneity of responsible antibodies and of the responsible tumor types is reflected in the variable clinical symptoms and the polymorphous phenotypic appearance of these lesions.[79,80]

Clinicopathologic correlation was reported in one patient revealing atrophy of the inner nuclear layer with extension to the outer plexiform layer and outer nuclear layers. Disorganization and apoptosis in the outer plexiform layer without active inflammation or melanoma cells was the most prominent feature. No excessive lipofuscin deposits were found in RPE cells (as seen in Best disease).[80]

Although rare, the findings of PVM can portend a poor prognosis for survival.

Management of Paraneoplastic Retinopathy

The management of paraneoplastic retinopathy remains difficult because of its rarity, unclear diagnostic criteria, and uncertainty relating to treatment efficacy and safety. This is especially so in a patient who has painless, vague, and asymmetric visual symptoms but no history of known malignancy. Clinical suspicion remains the most important factor in the diagnosis.

An ERG should be considered in any adult patient who has symptoms of central or paracentral positive visual phenomena ("shimmering" or "dancing" lights), photopsias, and minimal retinal findings. If the ERG is abnormal or extinguished, then a chest radiograph is a common "next step," since over half of patients with CAR syndrome have a bronchogenic tumor. A history of previous cutaneous malignant melanoma should be elicited in patients with nyctalopia. Central and midperipheral visual complaints also may be documented with visual field testing. Baseline SD-OCT and fundus autofluorescence imaging may be helpful in those cases with more severe symptoms. Antibodies to the CAR-antigen may be obtained, but a negative test is not inconsistent with a diagnosis of CAR syndrome. Given the lack of a diagnostic ERG change in any of the paraneoplastic retinopathies, testing for antiretinal antibodies in the patients' sera seems to be crucial for early detection of the disease.[55]

Difficulties remain with a lack of standardization, reproducibility, and validation of testing for circulating antiretinal

antibodies as well as with our understanding of which antibodies are pathogenic.[77,81]

The Ocular Immunology Laboratory at Oregon Health and Science University offers a comprehensive panel of autoantibody tests for CAR, MAR, PVM, autoimmune retinopathy, and paraneoplastic optic neuropathy (http://www.ohsu.edu/xd/health/services/casey-eye/diagnostic-services/ocular-immunology-lab/index.cfm).

Paraneoplastic retinopathy remains a diagnosis of exclusion. A retrobulbar optic neuropathy as a result of tumor spread, ischemia, or toxic effects of chemotherapy must be ruled out.[2] If cancer is not detected initially then continued surveillance at regular intervals is necessary.

An immune basis for CAR would suggest a possible role for immunosuppression therapy. Indeed, Keltner, and others[3,7,14,61,82] have reported visual improvement or stabilization following treatment with oral corticosteroids. The optimal dose of prednisone for CAR patients has not been determined.[8] Anecdotal cases managed with local depot or serial intravitreal steroids have been reported to be helpful.[83,84] Immunomodulatory agents to reduce autoreactive memory B cells, like intravenous rituximab, have also been used successfully, and this may become more promising with newer agents becoming available.[85] No standardized protocols have been established for management of the immunosuppression therapies for CAR, MAR, and PVM.[6,10,73] Immunosuppression has been reported to be effective in improving the visual outcomes in up to 100% of patients with CAR, but long-term data concerning the benefits and sustainability of treatment are not available.[10,77,81]

There have been no reports of visual improvement with treatment directed only at the site of primary tumor, and according to one investigator, vision usually worsens with such management alone.[8] The optimal approach to immunosuppressive therapy for this condition is uncertain. Plasmapheresis may have no effect on the cancer antigens and may paradoxically lead to the production of high concentrations of high-affinity antibodies.[9,47] Prednisone and immunomodulation have successfully stabilized the visual function of CAR patients but may exert a negative effect on the patient's own tumor immunosurveillance. All systemic therapies have the

potential to alter survival, for better or worse, despite any potential beneficial effect on vision.

Bilateral Diffuse Uveal Melanocytic Proliferation (BDUMP)

Machemer, in 1966, reported a case of bilateral and simultaneously appearing uveal lesions in a 57-year-old man with aqueous cells and flare, iris nodules, cataracts, and inferior retinal detachments in both eyes. At autopsy the patient was found to have a pancreatic carcinoma. Histopathologic examination of the enucleated eyes demonstrated predominantly benign cytologic characteristics of uveal melanocytic proliferation.[86]

Isolated case reports of similar cases by Curtin,[87] Font,[88] and Ryll[89] were followed by a series of four cases in 1982 by Barr,[90] who defined a syndrome consisting of (1) simultaneous occurrence of bilateral diffuse melanocytic involvement of the uveal tracts, (2) predominant cytologic benignity, (3) absence of metastases from the melanocytic proliferation, and (4) associated histopathologically proven systemic malignant neoplasm. The cellular benignity has been questioned because of the presence of foci of malignant-appearing epithelioid cells in addition to evidence of scleral invasion.[91] However, there has been no evidence of mitotic activity, and no cases of metastases have been reported from these melanocytic proliferations.[92] It is possible that these patients died as a result of the more lethal non-ocular disease before such spread could take place.[91,93] To date, at least 50 cases have been reported.[94]

Other clinical signs that may be present include iridocyclitis, glaucoma,[56,90,95] dilated episcleral vessels,[24,56,90,92] shallow anterior chambers, iris cysts, ciliary body cysts,[95] and rapidly developing cataracts.

Gass coined the term "bilateral diffuse uveal melanocytic proliferation (BDUMP)" to describe this paraneoplastic syndrome, and he identified the following five cardinal ocular signs that accompany visual loss in these patients:

1. Development of multiple, slightly elevated (usually only up to 2

mm), pigmented, and nonpigmented uveal melanocytic tumors, as well as evidence of diffuse thickening of the uveal tract.

2. Multiple, round or oval, subtle, red patches at the level of the RPE in the posterior fundus.

3. A striking pattern of multifocal areas of early hyperfluorescence on fluorescein angiography corresponding with these patches.

4. Exudative retinal detachment.

5. Rapidly progressing cataracts (Fig. 138.5).

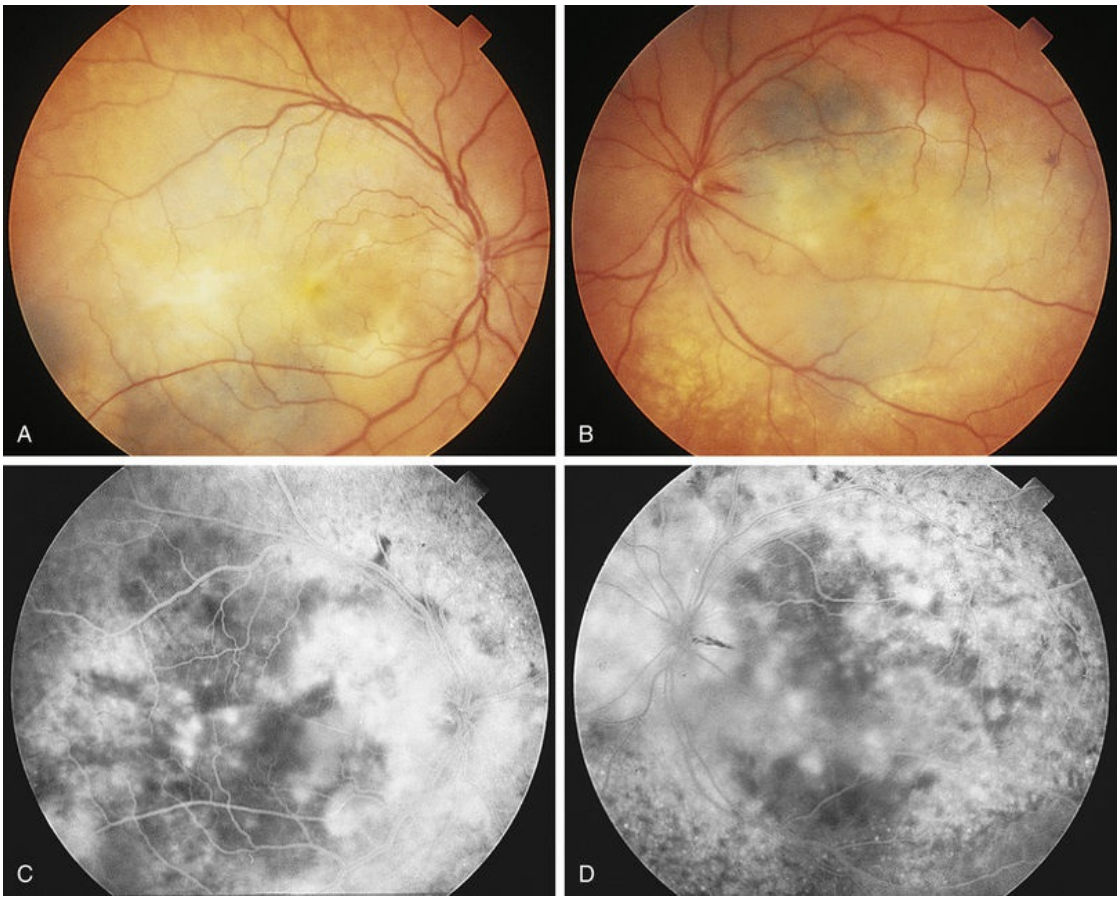

FIG. 138.5 (A,B) Fundus photographs of a 60-year-old man with retroperitoneal adenocarcinoma and bilateral diffuse uveal melanocytic proliferation (BDUMP). Multiple, slightly elevated, hypopigmented choroidal lesions resembling choroidal nevi developed in both eyes. (C,D) Midtransit phase fluorescein angiography showing a striking pattern of multiple, irregular, round

areas of hyperfluorescence caused by retinal pigment epithelium changes and uveal melanocytic proliferation. (Courtesy of J. Arch McNamara.)

BDUMP has no gender predilection and the mean age of presentation is 68 years (range, 34–89 years).

The findings of BDUMP usually antedate the findings of systemic malignancy by 3–12 months, and death usually ensues from the effects of the systemic malignancy within 8–24 months.[56,96] The focal and diffuse thickening of the uveal tract can antedate the clinical findings of exudative retinal detachment and red patches by several months. The chronic inferior exudative detachments seen in BDUMP may also be associated with peripheral retinal nonperfusion.[97] Gastrointestinal, genitourinary, and pulmonary cancers and non-Hodgkins lymphoma have all been reported to be associated with the clinical findings of BDUMP.

The pathogenesis of BDUMP remains obscure, but possibilities include (1) a common oncogenic stimulus initiating both the ocular and nonocular tumors;[90] (2) a hormonal stimulus (ectopic peptide) for ocular melanocytic proliferation by the nonocular tumor;[90] (3) an individual predisposed to simultaneous development of ocular melanocytic and nonocular visceral carcinomas;[93] and (4) a proliferation of clinically unapparent hypopigmented diffuse bilateral choroidal nevi in response to a peptide stimulus from the visceral carcinoma.[56,95] An autoimmune basis for this condition is not apparent and autoantibody testing is not indicated.

The characteristic multifocal red patches (or dark gray patches in patients with brunette fundi) that are angiographically seen to hyperfluoresce are of importance in the early diagnosis of this syndrome. Gass et al. and Margo et al. demonstrated by clinicopathologic correlation that these patches represent areas of depigmented RPE overlying hypopigmented, diffuse melanocytic proliferation (Fig. 138.6).[56,91] These patches of melanocytic proliferation with overlying RPE changes are thought to enlarge progressively and become confluent, producing a reticular pattern that angiographically appears hypofluorescent against a background of normal choroidal hyperfluorescence.[56,91] Gass proposes that the RPE changes are attributable to a toxic or immune-mediated process as a result of the melanocytic

proliferation itself or to an interaction of the systemic malignancy and the RPE.[56]

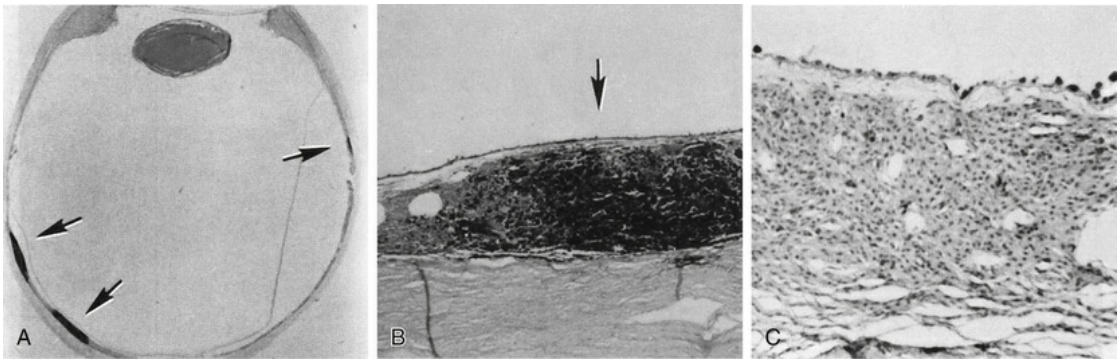

FIG. 138.6 Histopathologic examination of another patient with bilateral diffuse uveal melanocytic proliferation (BDUMP) and a systemic carcinoma. (A) Enlargement of the ciliary body and mild thickening of the uveal tract by nonpigmented benign melanocytes. (B) Focal areas of pigmented choroidal uveal melanocytic proliferation. (C) Sparing of the choriocapillaris and some partly necrotic melanocytes.
(Reproduced with permission from Gass JD. Stereoscopic atlas of macular diseases: diagnosis and treatment. St. Louis: Mosby; 1987.)

No treatment has successfully stabilized or improved the course of visual loss in patients with BDUMP syndrome. Plasmapheresis to remove the presumed circulating ectopic peptides has been reported to be helpful in stabilizing the vision a small number of patients while undergoing systemic treatment for the underlying malignancy.[98] Prompt recognition of this paraneoplastic syndrome may lead to earlier treatment of the visceral carcinoma and conceivably provide the best hope for survival, although slow growth of the uveal melanocytic proliferation may continue unabated, with a poor prognosis for vision.[56] Saito et al. suggested that oral steroid therapy in those individuals with BDUMP who also manifest with antiretinal antibodies may be beneficial.[94] Duong et al. reported a patient with BDUMP associated with ovarian carcinoma who survived the ovarian cancer but later developed metastatic amelanotic malignant melanoma, suggesting that the uveal manifestations of BDUMP may possibly have metastatic implications.[99,100] This suggests the importance of long-term follow-

up of successfully treated individuals.

Conclusion

Paraneoplastic retinopathy syndromes are a heterogeneous group of disorders involving the visual system and may be the presenting manifestation of systemic malignancy. It is important for ophthalmologists to be aware of these entities so that they can initiate ancillary testing and prompt an early and aggressive search and treatment of visceral cancers. Evidence in support of an autoimmune basis for CAR, MAR, and PVM suggests an early means of detection of non-ocular malignancy, as well as a possible role for immunosuppression in the palliation of the visually disabling symptoms experienced by these unfortunate patients.[77,81] Plasmapheresis may be helpful in stabilizing the visual manifestations of ectopic peptide-induced BDUMP, and early identification of the associated malignancy could theoretically enhance the prognosis for life.

References

1. Chan JW. Paraneoplastic retinopathies and optic neuropathies. *Surv Ophthalmol*. 2003;48:12–38.
2. Sawyer RA, Selhorst JB, Zimmerman LE, et al. Blindness caused by photoreceptor degeneration as a remote effect of cancer. *Am J Ophthalmol*. 1976;1976:606–613.
3. Keltner JL, Roth AM, Chang RS. Photoreceptor degeneration: possible autoimmune disorder. *Arch Ophthalmol*. 1983;101:48–53.
4. Thirkill C, Roth AM, Keltner JL. Cancer-associated retinopathy. *Arch Ophthalmol*. 1987;105:1987.
5. Keltner JL, Thirkill C, Roth AM. Autoimmune related retinopathy and optic neuropathy (ARRON syndrome). *Invest Ophthalmol Vis Sci*. 1988;29:178.
6. Powell SF, Dudek AZ. Treatment of melanoma-associated retinopathy. *Curr Treat Options Neurol*. 2010;12:54–63.
7. Klingele TG, Burde RM, Rappazzo JA, et al. Paraneoplastic retinopathy. *J Clin Neuroophthalmol*. 1984;4:239–245.

8. Keltner JL, Thirkill CE, Tyler NK, et al. Management and monitoring of cancer-associated retinopathy. *Arch Ophthalmol*. 1992;110:48–53.
9. Thirkill CE, FitzGerald P, Sergott RC, et al. Cancer-associated retinopathy (CAR syndrome) with antibodies reacting with retinal, optic nerve, and cancer cells. *N Engl J Med*. 1989;321:1589–1594.
10. Damek DM. Paraneoplastic retinopathy/Optic neuropathy. *Curr Treat Options Neurol*. 2005;7:57–67.
11. Saito W, Kase S, Ohguro H, et al. Slowly progressive cancer-associated retinopathy. *Arch Ophthalmol*. 2007;125:1431–1433.
12. Berson EL, Lessell S. Paraneoplastic night blindness with malignant melanoma. *Am J Ophthalmol*. 1988;106:307–311.
13. Grunwald GB, Klein R, Simmonds MA, et al. Autoimmune basis for visual paraneoplastic syndrome in patients with small-cell lung carcinoma. *Lancet*. 1985;1:658–661.
14. Jacobson DM, Thirkill CE, Tipping SJ. A clinical triad to diagnose paraneoplastic retinopathy. *Ann Neurol*. 1990;28:162–167.
15. Stanford MR, Edelsten CE, Hughes JD, et al. Paraneoplastic retinopathy in association with large cell neuroendocrine bronchial carcinoma. *Br J Ophthalmol*. 1995;1995:617–618.
16. Thirkill CE, Keltner JL, Tyler NK, et al. Antibody reactions with retina and cancer-associated antigens in 10 patients with cancer-associated retinopathy. *Arch Ophthalmol*. 1993;1993:931–937.
17. Wabbels BK, Elflein H, Lorenz B, et al. Bilateral tonic pupils with evidence of anti-hu antibodies as a paraneoplastic manifestation of small cell lung cancer. *Ophthalmologica*. 2004;218:141–143.
18. Mohamed Q, Harper AC. Acute optical coherence tomographic findings in cancer-associated retinopathy. *Arch Ophthalmol*. 2007;125:1132–1133.
19. Makiyama Y, Kikukchi T, Otani A, et al. Clinical and Immunological characterization of paraneoplastic retinopathy. *Invest Ophthalmol Vis Sci*. 2013;54:5424–5431.
20. Gehrs KM, Tiedemann J. Hemeralopia in an older adult.

Surv Ophthalmol. 1992;37:185–189.
21. Adamus G, Guy J, Schmied JL, et al. Role of antirecoverin autoantibodies in cancer-associated retinopathy. *Invest Ophthalmol Vis Sci*. 1993;34:2626–2633.
22. Anderson NE, Rosenblum MK, Graus F, et al. Autoantibodies in paraneoplastic syndromes associated with small-cell lung cancer. *Neurology*. 1988;38:1391–1398.
23. Kornguth SE, Klein R, Appen R, et al. Occurrence of antiretinal ganglion cell antibodies in patients with small cell carcinoma of the lung. *Cancer*. 1982;50:1289–1293.
24. Murphy MA, Hart WM, Olk RJ. Bilateral diffuse uveal melanocytic proliferation simulating an arteriovenous fistula. *J Neuroophthalmol*. 1997;17:77–83.
25. Murphy MA, Thirkill CE, Hart WM. Paraneoplastic retinopathy: a novel autoantibody reaction associated with small-cell carcinoma. *J Neuroophthalmol*. 1997;17:166–169.
26. Thirkill CE, Tait RC, Tyler NK, et al. Intraperitoneal cultivation of small-cell carcinoma induces expression of the retinal cancer-associated retinopathy antigen. *Arch Ophthalmol*. 1993;111:974–978.
27. Thirkill CE, Roth AM, Keltner JL. Paraneoplastic retinopathy syndrome. *Ophthalmology*. 1993;100:147.
28. Thirkill CE, Tait RC, Tyler NK, et al. The cancer-associated retinopathy antigen is a recoverin-like protein. *Invest Ophthalmol Vis Sci*. 1992;33:2768–2772.
29. Jacobson DM, Adamus G. Retinal anti-bipolar cell antibodies in a patient with paraneoplastic retinopathy and colon carcinoma. *Am J Ophthalmol*. 2001;131:806–808.
30. Campo E, Brunier MN, Merino MJ. Small cell carcinoma of the endometrium with associated ocular paraneoplastic syndrome. *Cancer*. 1992;69:2283.
31. Cogan DG, Kuwabara T, Currie J, et al. [Paraneoplastic retinopathy simulating cone dystrophy with achromatopsia]. *Klin Monatsbl Augenheilkd*. 1990;197:156.
32. Ohkawa T, Kawashima H, Makino S, et al. Cancer-associated retinopathy in a patient with endometrial cancer. *Am J Ophthalmol*. 1996;122:740–742.
33. Kellner U, Bornfeld N, Foerster MH. Severe course of

cutaneous melanoma-associated paraneoplastic retinopathy. *Br J Ophthalmol*. 1995;79:746–752.
34. Guy J, Aptsiauri N. Treatment of paraneoplastic visual loss with intravenous immunoglobulin: report of 3 cases. *Arch Ophthalmol*. 1999;117:471–477.
35. Pepkowitz S, Reader A, Jacobs A, et al. Paraneoplastic retinopathy: resolution with plasmapheresis. *Transfusion*. 1993;33:71.
36. Adamus G. Latest updates on antiretinal autoantibodies associated with vision loss and breast cancer. *Invest Ophthalmol Vis Sci*. 2015;56:1680–1688.
37. Matsui Y, Mehta MC, Katsumi O, et al. Electrophysiological findings in paraneoplastic retinopathy. *Graefes Arch Clin Exp Ophthalmol*. 1992;230:324.
38. To KW, Thirkill CE, Jakobiec FA, et al. Lymphoma-associated retinopathy. *Ophthalmology*. 2002;109:2149–2153.
39. Bhavsar KV, Hedges T, Thirkill CE, et al. Paraneoplastic retinopathy associated with systemic follicular cell lymphoma. *Ophthalmic Surg Lasers Imaging Retina*. 2015;46:373–376.
40. Mizener JB, Kimura AE, Adamus G, et al. Autoimmune retinopathy in the absence of cancer. *Am J Ophthalmol*. 1997;123:607–618.
41. Adamus G, Chan CC. Experimental autoimmune uveitides: multiple antigens, diverse diseases. *Int Rev Immunol*. 2002;21:209–229.
42. Antel JP, Moumdjian R. Paraneoplastic syndromes: a role for the immune system. *J Neurol*. 1989;236:1–3.
43. Kornguth SE, Kalinke T, Grunwald GB, et al. Antineurofilament antibodies in the sera of patients with small cell carcinoma of the lung and with visual paraneoplastic syndrome. *Cancer Res*. 1986;46:2588–2595.
44. Rizzo JF, Gittinger JW Jr. Selective immunohistochemical staining in the paraneoplastic retinopathy syndrome. *Ophthalmology*. 1992;99:1286–1295.
45. Suzuki T, Obara Y, Sato Y, et al. Cancer-associated retinopathy with presumed vasculitis. *Am J Ophthalmol*. 1996;122:125–127.

46. Ohguro H, Yokoi Y, Ohguro I, et al. Clinical and immunologic aspects of cancer-associated retinopathy. *Am J Ophthalmol*. 2004;137:1117–1119.
47. Polans AS, Witkowska D, Haley TL, et al. Recoverin, a photoreceptor-specific calcium-binding protein, is expressed by the tumor of a patient with cancer-associated retinopathy. *Proc Natl Acad Sci USA*. 1995;92:9176–9180.
48. Matsubara S, Yamaji Y, Fujita T, et al. Cancer-associated retinopathy syndrome: a case of small cell lung cancer expressing recoverin immunoreactivity. *Lung Cancer*. 1996;14:265–271.
49. Adamus G, Aptsiauri N, Guy J, et al. The occurrence of serum antibodies against enolase in cancer-associated retinopathy. *Clin Immunol Immunopathol*. 1996;78:120–129.
50. Adamus G, Machnicki M, Siegel GM. Apoptotic retinal cell death induced by antirecoverin autoantibodies of cancer-associated retinopathy. *Invest Ophthalmol Vis Sci*. 1997;38:283–291.
51. Whitcup SM, Vistica BP, Milam AH, et al. Recoverin-associated retinopathy: a clinically and immunologically distinctive disease. *Am J Ophthalmol*. 1998;126:230–237.
52. Adamus G. Autoantibody-induced apoptosis as a possible mechanism of autoimmune retinopathy. *Autoimmun Rev*. 2003;2:63–68.
53. Shiraga S, Adamus G. Mechanism of CAR syndrome: anti-recoverin antibodies are the inducers of retinal cell apoptotic death via the caspase 9- and caspase 3-dependent pathway. *J Neuroimmunol*. 2002;132:72–82.
54. Adamus G. Autoantibody targets and their cancer relationship in the pathogenicity of paraneoplastic retinopathy. *Autoimmun Rev*. 2009;8:410–414.
55. Link B, Schlotzer-Schrehardt U, Junemann A. Carcinoma-associated retinopathy. An electrophysiological and immunohistochemical correlation. *Retina*. 2009;29:69–72.
56. Gass JD, Gieser RG, Wilkinson CP, et al. Bilateral diffuse uveal melanocytic proliferation in patients with occult carcinoma. *Arch Ophthalmol*. 1990;108:527–533.
57. Gass JD. *Stereoscopic atlas of macular diseases: diagnosis and*

treatment. Mosby: St. Louis; 1997.
58. Alexander KR, Fishman GA, Peachey NS, et al. "On" response defect in paraneoplastic night blindness with cutaneous malignant melanoma. *Invest Ophthalmol Vis Sci*. 1992;33:477–483.
59. Andreasson S, Ponjavic V, Ehinger B. Full-field electroretinogram in a patient with cutaneous melanoma-associated retinopathy. *Acta Ophthalmol Scand*. 1993;71:487–490.
60. Gass JDM. Acute Vogt–Koyanagi–Harada-like syndrome occurring in a patient with metastatic cutaneous melanoma. *Uveitis update: Proceedings of the International Symposium on Uveitis*. Elsevier: Amsterdam; 1984.
61. Jacobson DM, Thirkill CE. Paraneoplastic cone dysfunction: an unusual visual remote effect of cancer. *Arch Ophthalmol*. 1995;113:1580–1582.
62. Kim RY, Retsas S, Fitzke FW, et al. Cutaneous melanoma-associated retinopathy. *Ophthalmology*. 1994;101:1837–1843.
63. Milam AH, Saari JC, Jacobson SG, et al. Autoantibodies against retinal bipolar cells in cutaneous melanoma-associated retinopathy. *Invest Ophthalmol Vis Sci*. 1993;34:91–100.
64. Remulla JF, Pineda R, Gaudio AR, et al. Cutaneous melanoma-associated retinopathy with retinal periphlebitis. *Arch Ophthalmol*. 1995;113:854–855.
65. Rush JA. Paraneoplastic retinopathy in malignant melanoma. *Am J Ophthalmol*. 1993;115:390–391.
66. Singh AD, Milam AH, Shields CL, et al. Melanoma-associated retinopathy. *Am J Ophthalmol*. 1995;119:369–370.
67. Weinstein JM, Kelman SE, Bresnick GH, et al. Paraneoplastic retinopathy associated with antiretinal bipolar cell antibodies in cutaneous malignant melanoma. *Ophthalmology*. 1994;101:1236–1243.
68. Myers DA, Bird BR, Ryan SM, et al. Unusual aspects of melanoma. Case 3. Melanoma-associated retinopathy presenting with night blindness. *J Clin Oncol*. 2004;22:746–748.
69. Janaky M, Palffy A, Kolozsvari L, et al. Unilateral

manifestations of melanoma-associated retinopathy. *Arch Ophthalmol*. 2002;120:866–867.
70. Alexander KR, Barnes CS, Fishman GA, et al. Contrast-processing deficits in melanoma-associated retinopathy. *Invest Ophthalmol Vis Sci*. 2004;45:305–310.
71. Lei B, Bush RA, Milam AH, et al. Human melanoma-associated retinopathy (MAR) antibodies alter the retinal ON-response of the monkey ERG in vivo. *Invest Ophthalmol Vis Sci*. 2000;41:262–266.
72. Bazhin AV, Dalke C, Willner N, et al. Cancer-retina antigens as potential paraneoplastic antigens in melanoma-associated retinopathy. *Int J Cancer*. 2009;124:140–149.
73. Lu Y, Jia L, He S, et al. Melanoma-associated retinopathy. A paraneoplastic autoimmune complication. *Arch Ophthalmol*. 2009;127:1572–1580.
74. Borkowski LM, Grover S, Fishman GA, Jampol LM. Retinal findings in melanoma-associated retinopathy. *Am J Ophthalmol*. 2001;132:273–275.
75. Sotodeh M, Paridaens D, Keunen J, et al. Paraneoplastic vitelliform retinopathy associated with cutaneous or uveal melanoma and metastases. *Klin Monatsbl Augenheilkd*. 2005;222:910–914.
76. Palmowski AM, Haus AH, Pfohler C, et al. Bilateral mutifocal chorioretinopathy in a woman with cutaneous malignant melanoma. *Arch Ophthalmol*. 2002;120:1756–1761.
77. Jampol LM, Fishman GA. Immunosuppression for autoimmune retinopathy. *Arch Ophthalmol*. 2009;127:573–574.
78. Al-Dahmash SA, Shields CL, Bianciotto CG, et al. Acute exudative paraneoplastic polymorphous vitelliform maculopathy in five cases. *Ophthalmic Surg Lasers Imaging*. 2012;43:366–373.
79. Dalvin LA, Johnson AA, Pulido JS, et al. Nonantibestrophin anti-rpe antibodies in paraneoplastic exudative polymorphous vitelliform maculopathy. *Transl Vis Sci Technol*. 2015;4(3):2.
80. Aronow ME, Adamus G, Mones A, et al. Paraneoplastic vitelliform retinopathy: clinicopathologic correlation and

review of the literature. *Surv Ophthalmol*. 2012;57(6):558–564.
81. Ferreyra HA, Jayasundera T, Khan NW, et al. Management of autoimmune retinopathies with immunosuppression. *Arch Ophthalmol*. 2009;127:390–397.
82. Oohira A, Tamaki Y, Nagahara K. A case of paraneoplastic retinopathy. *Jpn J Ophthalmol*. 1993;37:28–31.
83. Javaid Z, Rehan SM, Al-Bermani A, et al. Unilateral cancer-associated retinopathy: a case report. *Scott Med J*. 2016;61(3):155–159.
84. Huynh N, Shildkrot Y, Lobo A, et al. Intravitreal triamcinolone for cancer-associated retinopathy refractory to systemic therapy. *J Ophthalmic Inflamm Infect*. 2012;2:169–171.
85. Or C, Collins DR, Merkur AB, et al. Intravenous rituximab for the treatment of cancer-associated retinopathy. *Can J Ophthalmol*. 2013;48:e35–8.
86. Machemer R. Zur Pathogenese des flachenhaften malignen Melanoms. *Klin Monatsbl Augenheilkd*. 1966;149:641–652.
87. Curtin VT. *Diffuse malignant melanoma of the uvea, mixed cell type*. Eastern Ophthalmic Pathology Society Meeting: Philadelphia; 1974.
88. Font RL. *Bilateral diffuse melanocytic tumor of uvea of questionable malignancy: adenocarcinoma of colon with widespread metastasis*. Eastern Ophthalmic Pathology Society Meeting: Baltimore; 1978.
89. Ryll DL, Campbell RJ, Robertson DM, et al. Pseudo-metastatic lesions of the choroid. *Ophthalmology*. 1980;100:249–255.
90. Barr CC, Zimmerman LE, Curtin VT, et al. Bilateral diffuse melanocytic uveal tumors associated with systemic malignant neoplasms: a recently recognized syndrome. *Arch Ophthalmol*. 1982;100:249–255.
91. Margo CE, Pavan PR, Gendelman D, et al. Bilateral melanocytic uveal tumors associated with systemic nonocular malignancy: malignant melanomas or benign paraneoplastic syndrome? *Retina*. 1987;7:137–141.
92. Borruat FX, Othenin-Girard P, Uffer S, et al. Natural history

of diffuse uveal melanocytic proliferation. *Ophthalmology*. 1992;99:1698–1704.
93. Mullaney J, Mooney D, O'Connor M, et al. Bilateral ovarian carcinoma with bilateral uveal melanoma. *Br J Ophthalmol*. 1984;68:261–267.
94. Saito W, Kase S, Yoshida K, et al. Bilateral diffuse uveal melanocytic proliferation in a patient with cancer-associated retinopathy. *Am J Ophthalmol*. 2005;140:942–945.
95. Prause JU, Jensen OA, Eisgart F, et al. Bilateral diffuse malignant melanoma of the uvea associated with large cell carcinoma, giant cell type, of the lung: case report of a newly described syndrome. *Ophthalmologica*. 1984;189:221–228.
96. Mooy CM, de Jong PTV, Strous C. Proliferative activity in bilateral paraneoplastic melanocytic proliferation and bilateral uveal melanoma. *Br J Ophthalmol*. 1994;78:483–484.
97. Yonekawa Y, Shildkrot Y, Eliott D. Inferior peripheral nonperfusion in bilateral diffuse uveal melanocytic proliferation. *Ophthalmic Surg Lasers Imaging Retina*. 2013;44:190–192.
98. Jansen JC, Van Calster J, Pulido JS, et al. Early diagnosis and successful treatment of paraneoplastic melanocytic proliferation. *Br J Ophthalmol*. 2015;99:943–948.
99. Duong HV, McLean IW, Beahm DE. Bilateral diffuse melanocytic proliferation associated with ovarian carcinoma and metastatic malignant amelanotic melanoma. *Am J Ophthalmol*. 2006;142:693–695.
100. Ko MW, Dalmau J, Galetta SL. Neuro-ophthalmic manifestations of paraneoplastic syndromes. *J Neuroophthalmol*. 2008;28:58–68.

139

Melanocytoma of the Optic Disc

Carol L. Shields, Leonard Joffe, Jerry A. Shields

General Considerations

Melanocytoma of the optic disc is a benign melanocytic tumor, appearing with dark brown or black color and situated at the optic disc, often with extension into the surrounding choroid, retina, and vitreous.[1–37]

The term melanocytoma was originally coined by Zimmerman to describe a tumor with specific clinical and pathologic features that was located partly or completely within the optic nerve head.[1,2] The clinical and histopathologic nature of this optic disc lesion was clarified by Zimmerman and Garron,[1] and, subsequently, similar melanocytomas of the iris, ciliary body, and choroid have been

recognized.[3–5,15] Melanocytoma is now best defined as a specific variant of melanocytic nevus, located in the optic disc or elsewhere in the uveal tract, characterized clinically by a dark brown to black color, and composed histopathologically of deeply pigmented round to oval cells with small, round, uniform nuclei, often termed "magnocellular nevus."

Historically, melanocytoma was often confused clinically and histopathologically with uveal malignant melanoma.[1,2] An important difference between the two is that melanocytoma appears to have an equal incidence in all races, whereas uveal melanoma is uncommon in nonwhites.[5,7] Furthermore, it is also uncommon for melanoma to be confined to the optic disc or to secondarily invade the optic nerve.

Clinical Features

Most melanocytomas remain relatively stable and do not cause central visual impairment. However, slight visual loss related to the tumor can occur in about 26%, usually due to mild retinal exudation and subretinal fluid[7] (Table 139.1). More severe visual loss can rarely occur, secondary to central retinal vein obstruction and/or spontaneous tumor necrosis[6,7,17–22] or malignant transformation.[1–7,31–37] In some cases, such visual loss is reversible with time.[22] From 10% to 30% of patients with optic disc melanocytomas have an afferent pupillary defect (Marcus Gunn pupil) in the involved eye.[7,19] This can occur even with excellent visual acuity, due to compression of the optic nerve fibers by the melanocytoma, a factor that also explains the associated visual field defect.

TABLE 139.1

Clinical Features of Optic Nerve Melanocytoma in 116 Eyes of 115 Patients

Features	Number (%)
Patient age (mean) at detection	50 (1–91) years
Gender	
Male	44 (38%)
Female	71 (62%)

Race	
White	75 (65%)
Black	33 (29%)
Asian, Hispanic, Indian	7 (7%)
Laterality	
Unilateral	114 (99%)
Bilateral	1 (1%)
Tumor color	
Black	112 (97%)
Brown	4 (3%)
Tumor basal dimension (mean, range)	2 (1–10) mm
Tumor thickness (mean, range)	1 (0.5-3) mm
Additional features	
Choroidal invasion	35 (30%)
Retinal invasion	7 (6%)
Both choroidal and retinal invasion	28 (24%)
Optic disc edema	29 (25%)
Optic disc pallor	2 (2%)
Subretinal fluid	16 (14%)
Retinal exudation	14 (12%)
Retinal/choroidal neovascularization	1 (1%)
Retinal vein obstruction	3 (3%)
Vitreous seeding	5 (4%)

Data from Shields JA, Demirci H, Mashayekhi A, et al. Melanocytoma of the optic disc in 115 cases. The 2004 Samuel Johnson Memorial Lecture. Ophthalmology 2004;111:1739–1746.

Melanocytoma is usually unilateral. Bilateral cases have been rarely reported, usually in children but these cases may not be true melanocytomas.[10,11] There has been some controversy as to whether they should be called true melanocytomas or disc pigmentation in association with other congenital disc abnormalities.

Ophthalmoscopically, optic nerve melanocytoma has typical features.[1–7] This mass is characteristically a dark brown to black lesion that is located partly in the optic disc (Fig. 139.1). This tumor is relatively small and can be confined to the disc in 15%. More characteristically, melanocytoma extends over the margin of the optic disc to involve the adjacent choroid (54%) or into the adjacent sensory retina (30%) (Figs. 139.2, 139.3 and Table 139.1).[7] In some cases, the choroidal component is more pronounced than the papillary component. Although optic disc melanocytoma is generally believed to have few local complications, a recent study on 116 affected eyes found disc edema (25%) (Fig. 139.4), intraretinal edema (16%), subretinal fluid (14%), yellow intraretinal exudation (12%), focal hemorrhage (5%), vitreous seeds (4%), and retinal vein obstruction (3%).[7] These local complications can

produce visual symptoms or visual loss in 26% of cases.[7] (Table 139.2) This is generally mild, and severe visual loss is exceptional. Vitreous seeds from necrosis of the melanocytoma can extend into the anterior chamber, sometimes producing a black pseudohypopyon. The most important factor predictive of visual loss is extension of the tumor into the retina and the presence of surrounding subretinal fluid. There have been recent reports of choroidal neovascularization adjacent to optic disc melanocytoma.[27–29]

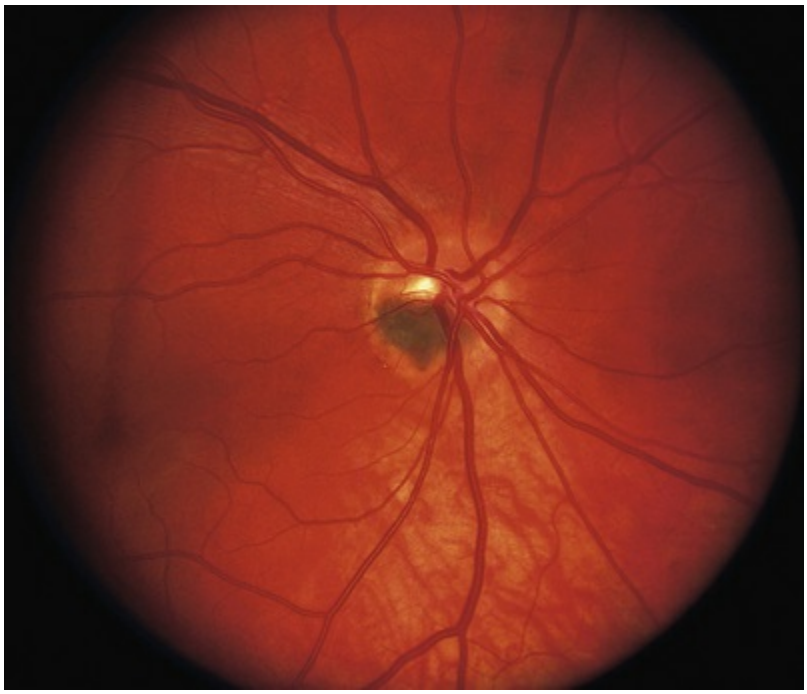

FIG. 139.1 Optic disc melanocytoma confined to the optic disc.

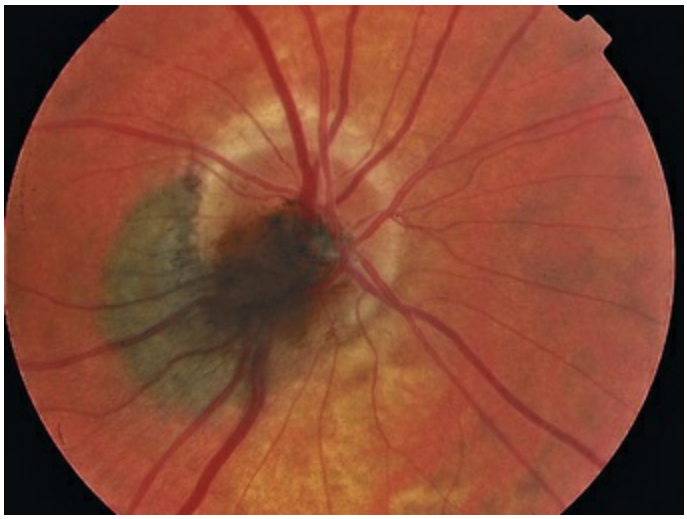

FIG. 139.2 Optic disc melanocytoma with choroidal component.

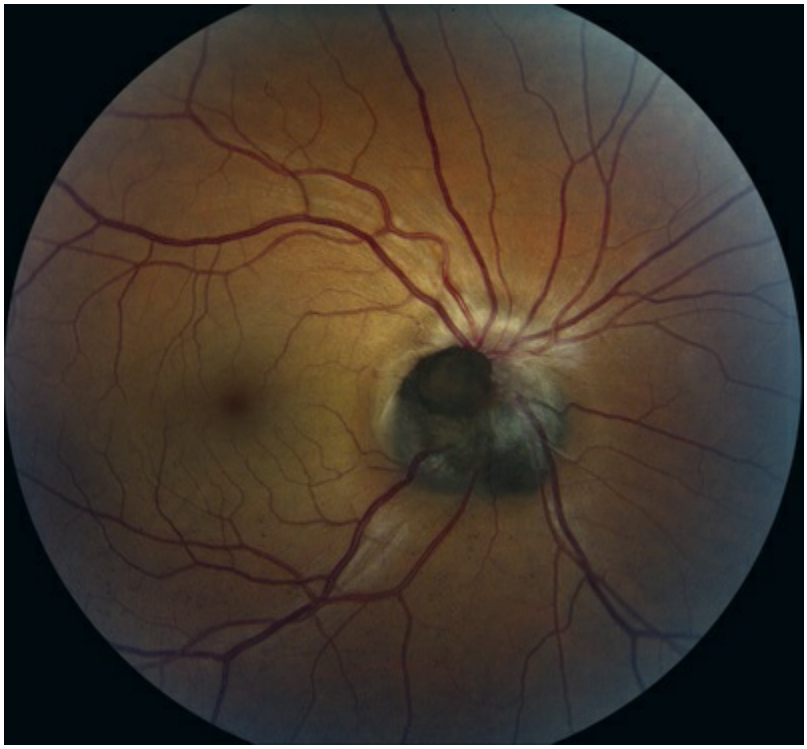

FIG. 139.3 Optic disc melanocytoma with prominent retinal component.

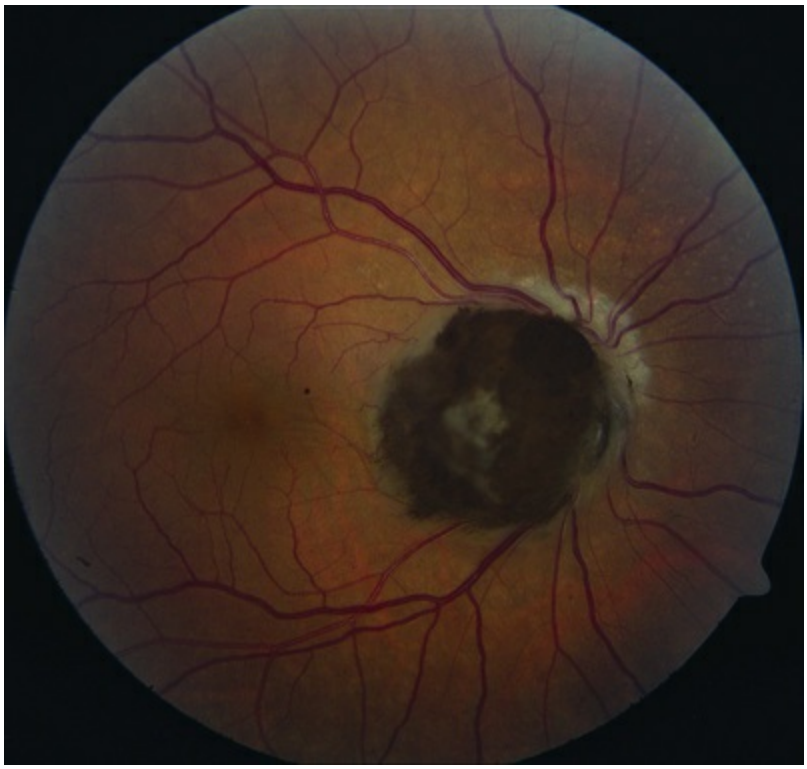

FIG. 139.4 Optic disc melanocytoma with secondary disc edema and pallor.

TABLE 139.2
Outcomes of Optic Nerve Melanocytoma in 116 Eyes

Outcomes	Kaplan–Meier Estimates		
	At 5 yr	At 10 yr	At 20 yr
Tumor enlargement	11%	32%	38%
Visual acuity loss of 2 lines	10%	18%	33%
Transformation into melanoma	2/116 (2%)		

Data from Shields JA, Demirci H, Mashayekhi A, et al. Melanocytoma of the optic disc in 115 cases. The 2004 Samuel Johnson Memorial Lecture. Ophthalmology 2004;111:1739–1746.

Melanocytoma of the optic disc traditionally was recognized to be a stable lesion with no tendency to grow. Very rarely, it has been documented to appear in a previously normal optic disc.[12] Serial fundus photographs have documented that 11–15% of them show subtle enlargement over several years[7] (Table 139.2). This mild growth should not be misconstrued as malignant transformation.[31–37] In one report, an eye with a progressively growing melanocytoma underwent enucleation and the lesion

proved to be benign, despite progressive growth.[32] Multivariate analysis has shown that the main predictive risk factor for growth is an initial thickness of ≥1.5 mm at the time of first diagnosis.[7] Some tumors can grow slowly and produce ischemic optic neuropathy associated with tumor necrosis, resulting in severe visual loss.[20–22] Others can cause central retinal vein obstruction and visual loss.[17,18] In rare cases the tumor can present as neovascular glaucoma secondary to retinal vein obstruction.[9]

There are usually no systemic associations with optic disc melanocytoma. It has been reported in association with intracranial meningioma, type 2 neurofibromatosis,[13] and phakomatosis pigmentovascularis.[14]

The differential diagnosis of melanocytoma of the optic disc includes juxtapapillary choroidal melanoma, choroidal nevus, hyperplasia of the retinal pigment epithelium (RPE), hypertrophy of the RPE, adenoma of the RPE, and combined hamartoma of the retina and RPE. Although extremely rare, malignant melanoma can occur in the optic nerve and may be difficult to impossible to differentiate clinically from melanocytoma.[31–37] The clinical features of these conditions, described in other chapters, should help to differentiate them from melanocytoma in most instances.

Pathology and Pathogenesis

On low-power microscopy, a melanocytoma of the optic nerve has a characteristic appearance as a deeply pigmented mass that occupies the optic disc and extends for a variable distance into the optic nerve itself (Fig. 139.5).[1,2,30] Cytologically, the most distinguishing characteristics are the dense pigmentation and the uniform appearance. Although the dense pigment prevents visualization of cell detail, bleached preparations reveal the cells to be oval or round with abundant cytoplasm, relatively small nuclei, and few prominent nucleoli, similar to those that occur throughout the uvea in patients with ocular melanocytosis (Fig. 139.6).[1,2] Tumors composed of similar cells have also been recognized in the iris, ciliary body, choroid, and even in the conjunctiva.

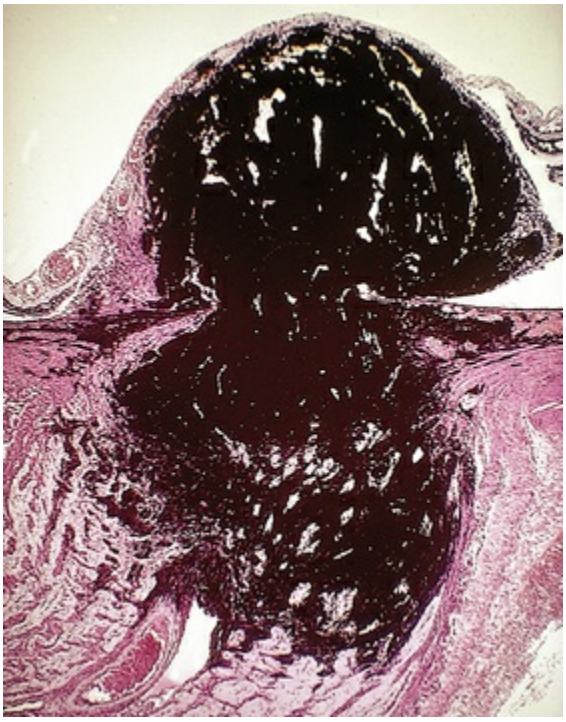

FIG. 139.5 Low magnification photomicrograph of optic disc melanocytoma (hematoxylin and eosin, ×10).
(Courtesy of Armed Forces Institute of Pathology.)

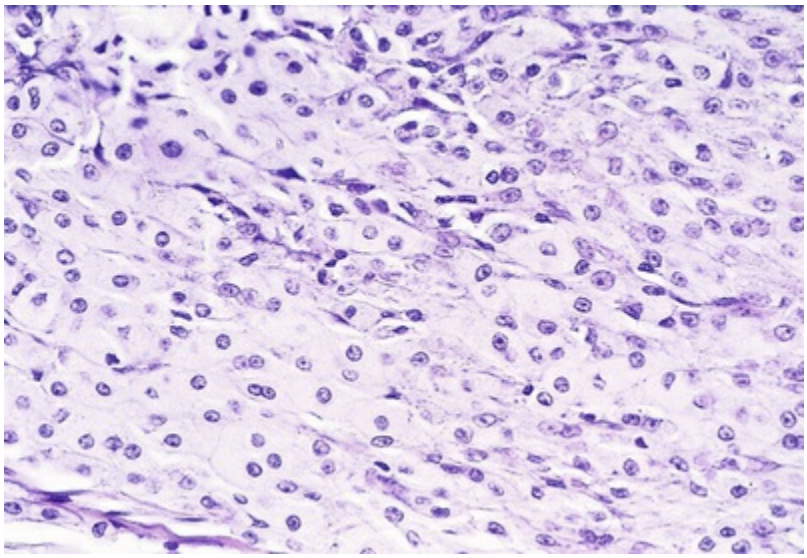

FIG. 139.6 Cytologic features of optic disc melanocytoma (bleached, hematoxylin and eosin, ×100).

The pathogenesis of optic disc melanocytoma is unknown. It is generally assumed to be a congenital lesion, but, like most uveal

nevi, it is rarely seen in young children. It has developed in an adult fundus that was previously documented photographically to be normal, raising speculation that it is either acquired or occurs as an amelanotic lesion that later becomes pigmented and clinically visible.[12]

Diagnostic Approaches

The diagnosis of a melanocytoma of the optic nerve usually can be made by ophthalmoscopic recognition of its characteristic clinical features. Ancillary procedures like fundus photography, fluorescein angiography, optical coherence tomography (OCT) and angiography, autofluorescence, and visual field examinations can facilitate the diagnosis and provide help in follow-up evaluations.

In most cases, fluorescein angiography of a melanocytoma of the optic nerve demonstrates hypofluorescence throughout the angiogram (Figs. 139.7 and 139.8).[5] This is presumably because the cells are deeply pigmented and closely compact with relatively little vascularity. In cases with optic disc edema, there is hyperfluorescence of the optic disc edema adjacent to the tumor. With OCT angiography, the radial peripapillary capillary network is accentuated overlying the mass, if there is no retinal invasion (Fig. 139.8). Deep vessels are not seen.

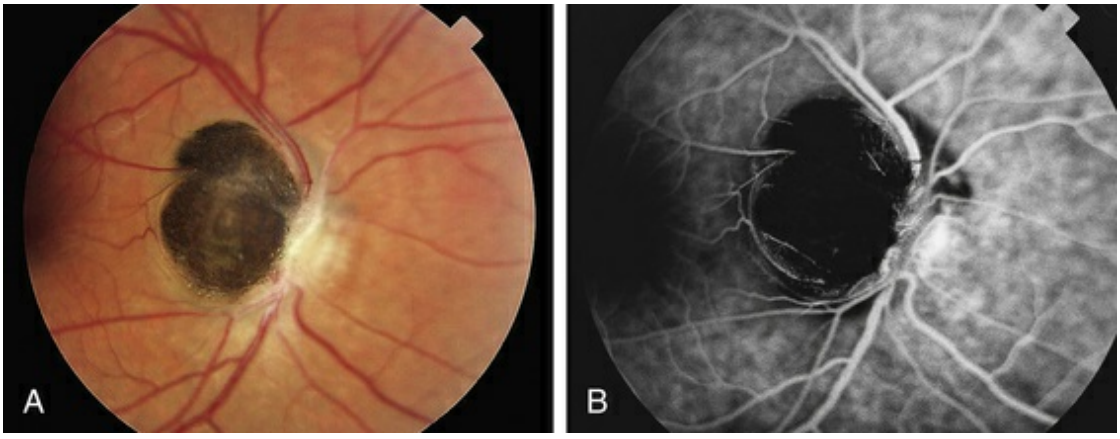

FIG. 139.7 Fluorescein angiography optic disc melanocytoma. (A) Clinical appearance of lesion. (B) Angiogram in mid venous phase showing hypofluorescence of lesion.

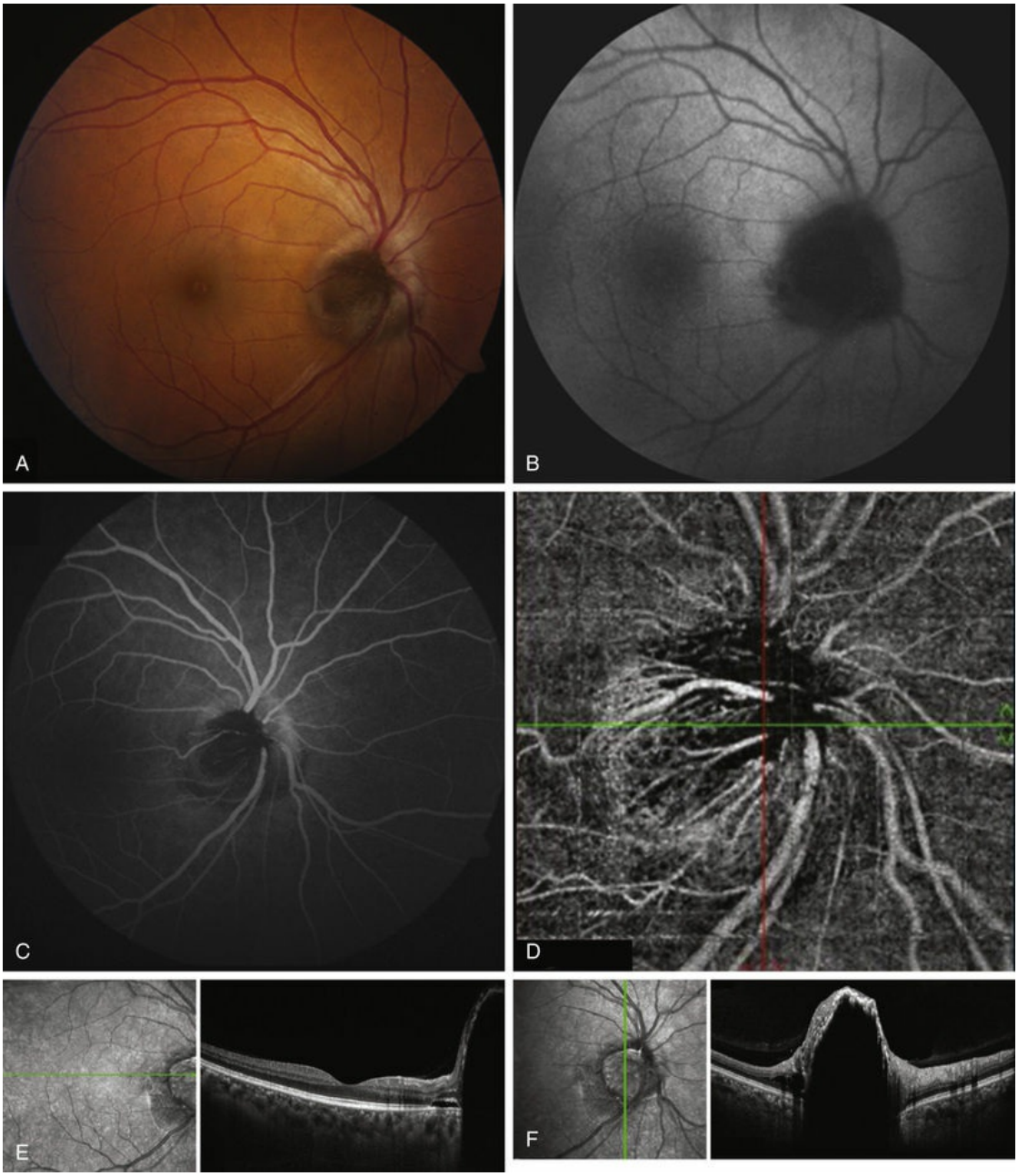

FIG. 139.8 Imaging of optic disc melanocytoma with fundus photography (A), autofluorescence (B), fluorescein angiography (C), optical coherence tomography (OCT) angiography (D), and OCT of the macula (E) and tumor (F).

Indocyanine green angiography (ICGA) also shows the lesion to be generally hypofluorescent.[23] Melanocytoma is hypoautofluorescent.[25] OCT using time domain or spectral domain technology shows a smooth dome-shaped prepapillary mass with dense shadowing and occasionally vitreous seeds can be

documented overlying the mass (Fig. 139.8).[16,24,26]

The visual field of an eye with melanocytomas is variable, depending on the size and extent of the lesion, as well as degree of optic nerve compression and atrophy. Visual field defects are relatively common, found in 40% of eyes, and include arcuate scotoma, enlarged blind spot, and others.[19]

If a melanocytoma is greater than 0.5 mm in elevation, it can often be demonstrated with ultrasonography, computed tomography (CT), or magnetic resonance imaging (MRI), but these techniques do not provide enough resolution to differentiate melanocytoma from other elevated lesions of the optic disc. Furthermore, ultrasonography cannot detect microscopic extension of the tumor into the retrolaminar portion of the optic nerve. MRI can help determine the gross extent of melanocytoma involvement in the retrolaminar portion of the optic nerve using gadolinium enhancement.[34] Extensive involvement in the optic nerve with severe visual loss suggests malignant transformation of the lesion (Fig. 139.9).[31–37] Malignant change is estimated to occur in about 1–2% of cases.[7] Only a few convincing cases of transformation into melanoma with histopathologic confirmation have been reported.[31–37] A study on gene expression profiling of optic disc melanocytoma led to identification of class 1A tumors, with very little risk for metastatic disease.[38]

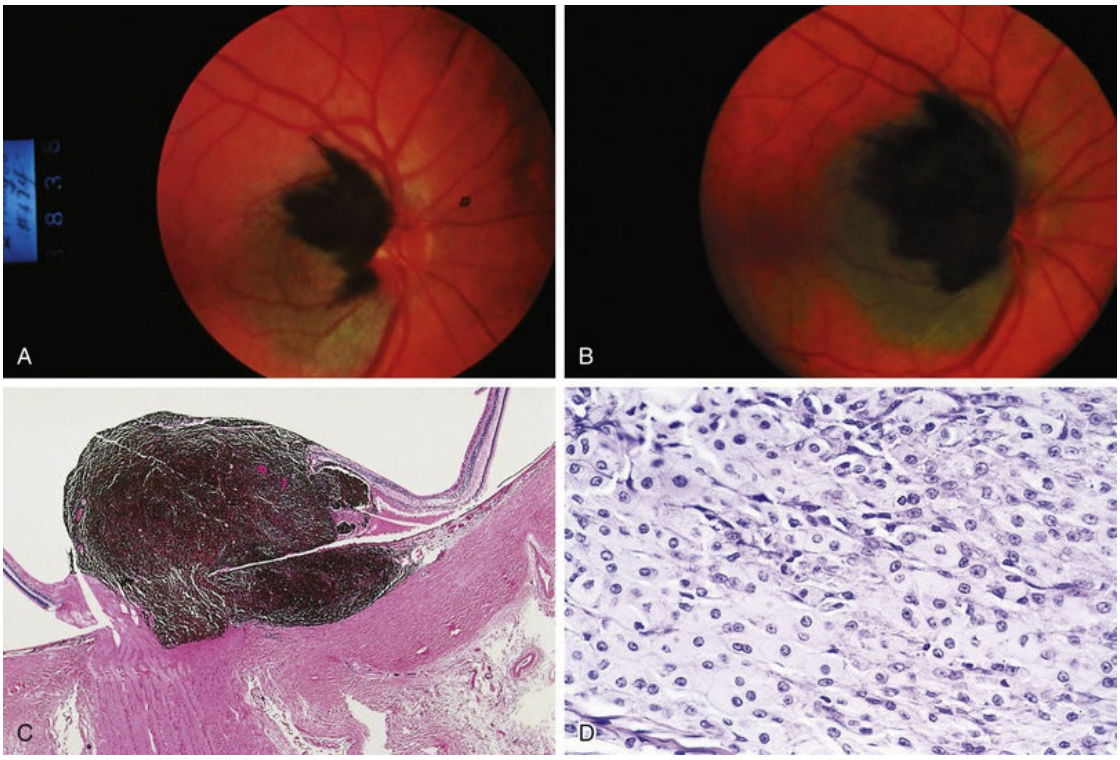

FIG. 139.9 Malignant transformation of melanocytoma of optic disc. (A) Appearance of lesion in 1982. (B) Photograph in 1988. Note the enlargement. (C) Photomicrograph showing tumor (hematoxylin and eosin, ×10). (D) Photomicrograph near base of tumor, showing typical melanocytoma cells (bleached, hematoxylin and eosin, ×100).

Management

Since melanocytoma of the optic disc can sometimes evolve into malignant melanoma, examination and fundus photography should be performed yearly. Small degrees of growth may not signify malignant change. However, more progressive growth and visual loss should suggest malignant transformation, and fine needle biopsy confirmation followed by enucleation should be considered.

Conclusion

Melanocytoma is an unusual variant of nevus that classically occurs in the optic nerve head. It can be confined to the optic disc or have

contiguous involvement of the choroid, sensory retina, or vitreous. It is important to differentiate this benign lesion from a malignant melanoma. Histopathologically, melanocytoma is composed of deeply pigmented round to oval nevus cells with small nuclei. Although melanocytoma rarely causes central visual loss, it can cause peripheral visual impairment with field defects. More importantly, melanocytoma can undergo malignant transformation into melanoma in 1–2% of cases. A patient with a melanocytoma of the optic disc should be examined annually.

References

1. Zimmerman LE, Garron LK. Melanocytoma of the optic disc. *Int Ophthalmol Clin*. 1962;2:431–440.
2. Zimmerman LE. Melanocytes, melanocytic nevi and melanocytomas. *Invest Ophthalmol*. 1965;4:11–41.
3. Shields JA, Shields CL, Demirci H, et al. Melanocytoma of the optic nerve. *Surv Ophthalmol*. 2006;51:93–104.
4. Reidy JJ, Apple DJ, Steinmetz RL, et al. Melanocytoma: nomenclature, pathogenesis, natural history and treatment. *Surv Ophthalmol*. 1985;29:319–327.
5. Shields JA, Shields CL, Eagle RC Jr. Melanocytoma (hyperpigmented magnocellular nevus) of the uveal tract. The 34th G. Victor Simpson Lecture. *Retina*. 2007;27:730–739.
6. Joffe L, Shields JA, Osher R, et al. Clinical and follow-up studies of melanocytomas of the optic disc. *Ophthalmology*. 1979;86:1067–1078.
7. Shields JA, Demirci H, Shields CL, et al. Melanocytoma of the optic disc in 115 cases. The 2004 Samuel Johnson Lecture. *Ophthalmology*. 2004;111:1739–1746.
8. Costa J, Vargas E, Mendonca AP, et al. Growing optic disc melanocytoma: what to do? *Neuro-Ophthalmol*. 2002;27:39–43.
9. Croxatto JO, Ebner R, Crovetto L, et al. Angle closure glaucoma as initial manifestation of melanocytoma of the optic disc. *Ophthalmology*. 1983;90:830–834.
10. Brodsky M, Phillips PH. Optic nerve hypoplasia and congenital hypopituitarism. *J Pediatr*. 2000;136:850.

11. Demirci H, Shields CL, Shields JA. Bilateral optic disc melanocytoma in a 10 month old infant. *Am J Ophthalmol*. 2003;136:190–192.
12. Shields JA, Shields CL, Piccone M, et al. Spontaneous appearance of an optic disc melanocytoma. *Am J Ophthalmol*. 2002;134:614–615.
13. Shields JA, Shields CL, Lavrich J. Melanocytoma of optic disc in a patient with type 2 neurofibromatosis. *Retina*. 2002;22:222–223.
14. Shields CL, Kligman BE, Suriano M, et al. Phacomatosis pigmentovascularis of cesioflammea type in 7 patients: combination of ocular pigmentation (melanocytosis or melanosis) and nevus flammeus with risk for melanoma. *Arch Ophthalmol*. 2011;129:746–750.
15. Reichstein DA, Shields JA, Uyen T, et al. Unusual multifocal pigmented lesions of the uvea in a patient with ocular melanocytosis. *Retin Cases Brief Rep*. 2013;7:399–401.
16. Mazzucca D, Shields CL, Sinha N, et al. Progressive retinal invasion and vitreous seeding of optic disc melanocytoma. *Clin Experiment Ophthalmol*. 2012;40:e123–5.
17. Shields JA, Shields CL, Eagle RC Jr, et al. Central retinal vascular obstruction secondary to melanocytoma of the optic disc. *Arch Ophthalmol*. 2001;119:129–133.
18. Rishi P, Venkatesh R. Central retinal artery occlusion secondary to optic disk melanocytoma. *Retin Cases Brief Rep*. 2012;6:212–215.
19. Osher RH, Shields JA, Layman PR. Pupillary and visual field evaluation in patients with melanocytoma of the optic disc. *Ophthalmology*. 1979;97:1096–1099.
20. Usui T, Shirakashi M, Kurosawa A, et al. Visual disturbance in patients with melanocytoma of the optic disc. *Ophthalmologica*. 1990;201:92–98.
21. Wiznia RA, Price J. Recovery of vision in association with a melanocytoma of the optic disc. *Am J Ophthalmol*. 1974;78:236–238.
22. Shields JA, Shields CL, et al. Total blindness from presumed optic nerve melanocytoma. *Am J Ophthalmol*. 2005;139:1113–1114.

23. Kadayifcilar S, Akman A, Aydin P. Indocyanine green angiography of optic nerve head melanocytoma. *Eur J Ophthalmol*. 1999;9:68–70.
24. Shields CL, Perez B, Benavides R, et al. Optical coherence tomography of optic disk melanocytoma in 15 cases. *Retina*. 2008;3(28):441–446.
25. Almeida A, Kaliki S, Shields CL. Autofluorescence of intraocular tumors. *Curr Opin Ophthalmol*. 2013;24:222–232.
26. Sutter C, Jean-Charles A, Merle H. Clinical and paraclinical course of melanocytomas of the optic disc. Contribution of spectral- and time-domain OCT in the study of 10 patients. *J Fr Ophthalmol*. 2011;34:615–623.
27. Tran HV, Bovey EH, Uffer S, et al. Peripapillary choroidal neovascularization associated with melanocytoma of the optic disc: a clinicopathologic case report. *Graefes Arch Clin Exp Ophthalmol*. 2006;244:1367–1369.
28. Chalam KV, Gupta SK, Shah GY, et al. Successful management of melanocytoma-associated choroidal neovascularization with photodynamic therapy. *Eur J Ophthalmol*. 2006;16:776–778.
29. Al-Halafi AM. Successful treatment of melanocytoma associated choroidal neovascular membrane with intravitreal bevacizumab. *Saudi J Ophthalmol*. 2013;27:117–119.
30. Font RL, Chaques-Alepuz V. Giant optic disk melanocytoma complicated with massive intraocular seeding. *Arch Soc Esp Oftalmol*. 2011;86:158–161.
31. Apple DJ, Craythorn JM, Reidy JJ, et al. Malignant transformation of an optic nerve melanocytoma. *Can J Ophthalmol*. 1984;19:320–325.
32. Mansour AM, Zimmerman LE, LaPiana FG, et al. Clinicopathologic findings in a growing optic nerve melanocytoma. *Br J Ophthalmol*. 1989;73:410–415.
33. Shields JA, Shields CL, Eagle RC Jr, et al. Malignant melanoma associated with melanocytoma of the optic disc. *Ophthalmology*. 1990;97:225–230.
34. DePotter P, Shields CL, Eagle RC Jr, et al. Malignant melanoma of the optic nerve. *Arch Ophthalmol*.

1996;114:608–612.
35. Meyer D, Ge J, Blinder KJ, et al. Malignant transformation of an optic disc melanocytoma. *Am J Ophthalmol*. 1999;127:710–714.
36. Sharma PM, Sangal K, Malik P, et al. Malignant transformation of optic disc melanocytoma? A clinical dilemma at presentation with a review of the literature. *Ophthalmologica*. 2002;216:292–295.
37. Shukla SY, Shields JA, Eagle RC, et al. Transformation of optic disc melanocytoma into melanoma over 33 years. *Arch Ophthalmol*. 2012;130:1344–1347.
38. De Alba MA, Billegas CM, Gold AS, et al. Cinical findings and genetic expression profiling of three pigmented lesions of the optic nerve. *Case Rep Ophthalmol Med*. 2015;2015 [590659].

140

Congenital Hypertrophy of the Retinal Pigment Epithelium

Carsten H. Meyer, Heinrich Gerding

Introduction

Congenital hypertrophy of the retinal pigment epithelium (CHRPE) is generally an asymptomatic congenital hamartoma that occurs in three variant forms: either as solitary, or grouped, or multiple pigmented fundus lesions. Lesions are usually observed during routine ophthalmoscopy.[1] Multiple CHRPE may be associated with familial adenomatous polyposis (FAP), an autosomal dominant disease with numerous adenomatous polyps of the colon and rectum. FAP with prominent extracolonic manifestations has been termed Gardner syndrome (GS) or another variant as Turcot syndrome for FAP with brain tumor lesions (Fig. 140.1). The observation of CHRPE in a premature child provides evidence for the congenital nature of this lesion.[2]

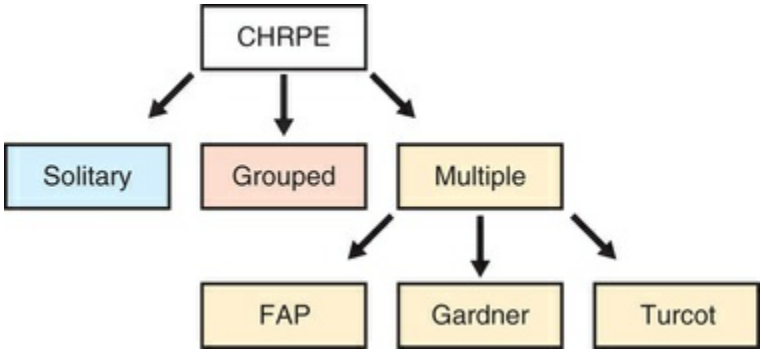

FIG. 140.1 Classification of CHRPE in solitary grouped and multiple forms and their systemic association.

Epidemiology/Demographics

The reported prevalence of CHRPE is as low as 3 described cases among 2400 ophthalmic examinations (1.25%). The prevalence of FAP varies from 1 in 7000 to 1 in 22, 000 individuals. Approximately 70–90% of FAP patients have pigmented fundus lesions.[3]

Clinical Findings and Classification

Solitary CHRPE

Solitary CHRPE is typically a flat, round, hyperpigmented lesion with smooth or scalloped margins that is well demarcated from normal-appearing retinal pigment epithelium (RPE) (Fig. 140.2A). The color may vary from light gray to brown to black and is independent of the patient's race.[1] A marginal halo of depigmentation may surround the lesion and “punched-out” inner lacunae with hypopigmentation may be present in larger lesions. Both depigmented zones show the tendency to progress gradually over time, and eventually may involve the entire lesion.[4–7] The overlying retina and its vasculature appear normal in most cases, however discrete focal intraretinal pigmentation may become visible near the margin on biomicroscopy.[4] Some lesions may be associated with retinal vascular abnormalities including capillary and large-vessel obliteration, microaneurysmal changes, chorioretinal anastomoses, and neovascularization. The size may vary from 100 μm to several disc diameters, occasionally occupying an entire quadrant. Lesions may be found anywhere in the fundus, with predominance in the superotemporal and equatorial region while the macula is rarely involved. Solitary CHRPE enlarge in 46–83% of cases over three or more years of follow-up. Extension into the fovea may result in reduced visual acuity.[8] Some heavily pigmented nodular lesions may develop within CHRPE.[9] Histopathologically nodular lesions proved to be adenocarcinomas in two reports.[10,11] Untreated nodular lesions may enlarge to form pedunculated tumors of >7 mm thickness with serous retinal detachment.[11] Proton beam radiation therapy may be applied in these rare cases.[12]

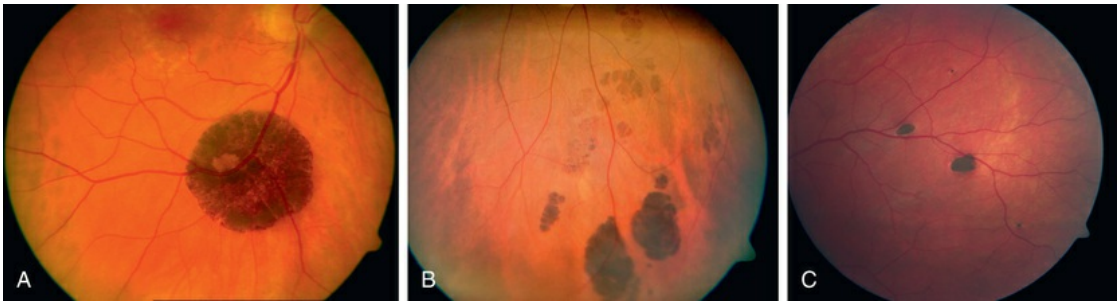

FIG. 140.2 (A) Solitary CHRPE: A large CHRPE OD with a diameter of 3 disc diameters. (B) Grouped CHRPE: The sectorial pattern of grouped CHRPE with smaller lesions at the optic disc and larger lesions in the periphery. Larger hyperpigmentations may be separated during growth into smaller spots, surrounded by normal pigmented cells. The shape of these lesions may be sickle- or oval-shaped with convex borders, fitting into the concave borders of adjacent lesions. (C) Multiple CHRPE lesions in FAP are generally smaller (50 to 100 µm in diameter) compared with solitary CHRPE. The ovoid, often spindle-shaped, hyperplastic lesions are black, brown, or light gray color. Lesions have a nearly meridional orientation towards the optic disc and are haphazardly distributed with no obvious predilection for any quadrant.

Grouped CHRPE

When several lesions of varying size are arranged in a cluster, resembling the footprint of an animal ("bear tracks"), they are named "grouped CHRPE" (233800, OMIM). Grouped lesions are flat, well-demarcated round oval or geographic black spots with increasing size towards the fundus periphery. Each cluster includes approximately 3–30 lesions, which may vary in size from 100 to 300 µm lesions (Fig. 140.2B). Etiology and development of grouped CHRPE remain unknown. The presence of grouped CHRPE and additional ipsilateral sectorial pigmented skin lesions following the "cutaneous lines of Blaschko" gave evidence for possible pigmentary mosaicism in both the eye and skin.[13] Therefore, grouped CHRPE are considered as a cluster of atypical hyperpigmented RPE cells, that derive from the edge of the optic

nerve and migrate along the stream of embryologic tissue lines, analogous to the "cutaneous lines of Blaschko." The sectorial pattern of grouped CHRPE obviously reflects the stream, outgrowth, and migration path of RPE cells during embryogenesis.[14] Bilateral grouped CHRPE has rarely been observed. There are no systemic associations in patients with solitary and grouped CHRPE.

Multiple CHRPE

Multiple CHRPE lesions in FAP are generally smaller (50–100 μm in diameter) compared with solitary CHRPE. They are black, brown, or light gray (Fig. 140.2C). Larger lesions may be surrounded by a depigmented halo, mottled RPE,[15] window-defect-type changes adjacent to retinal vessels,[16] may contain depigmented lacunae, and can be accompanied by small pigmented satellite lesions. Retinal invasion; glial, capillary, and pigment epithelial proliferation; and hypertrophy are typical. More than four widely spaced lesions per eye or bilateral involvement are suggestive of FAP.[17] Traboulsi et al. examined 16 GS families for multiple CHRPE. Of 41 GS patients, 37 (90%) had multiple CHRPE lesions.[15] Lesions were bilateral in 32 patients (78%). The presence of bilateral lesions or multiple unilateral lesions (>4) appeared to be a useful clinical marker (specificity, 0.95; sensitivity, 0.78) for GS. In view of the multiple, bilateral character of retinal lesions observed in FAP, they can be considered a clinical disease marker. However, the absence of CHRPE has no predictive value for absence of GS or FAP.

Differential Diagnosis

Often CHRPE has been misdiagnosed as choroidal malignant melanoma. The latter is almost always elevated, less homogeneously pigmented and less sharply demarcated compared with CHRPE, and usually exhibits growth in all three dimensions. Choroidal nevi are flat and located below the RPE. Their color may vary from light to dark brown. The borders are less well demarcated and often are feathery because nevus cells extend along larger choroidal vessels. Frequently, drusen and pigmentary

mottling are present on the surface of nevi. Melanocytomas of the choroid have a similar appearance to CHRPE, except for their homogeneously black color. Black sunburst lesions in sickle cell retinopathy may appear as dark gray to brown convex-shaped lesions predominantly in the midperiphery. True hyperplasia of the RPE has ill-defined borders and invades the retina, often leading to retinal distortion. Focal pigmentation caused by injury, inflammation, or drug toxicity may resemble CHRPE but can be differentiated on the basis of a more irregular shape, widespread distribution, and associated clues suggesting acquired disease. Torpedo maculopathy presents as oval-shaped depigmented lesions temporal to the fovea.[18,19]

Associated Extraocular Findings

Solitary, unilateral lesions and grouped CHRPE are restricted to the RPE with no other ocular or extracellular findings.[20] Multiple or bilateral CHRPE may be associated with autosomal dominant FAP or GS (175100, OMIM). Gardner syndrome is characterized by FAP of the large and small intestine, hamartomas of the skeleton, and various soft-tissue tumefactions.[21,22] Intestinal polyps generally appear during the third decade of life and invariably progress to adenocarcinomas by the fifth decade. Skeletal hamartomas, most commonly benign osteomas of mandible, skull, orbits, and long bones, become apparent in the third decade of life, as well as soft-tissue abnormalities including epidermoid and sebaceous cysts, dermal fibromas, lipomas, leiomyomas, desmoid, and mesenteric fibromatosis. Further extracolonic manifestations of GS include tumors of the thyroid, adrenal, and bladder, as well as sarcomas and hepatoblastomas. Turcot syndrome (233800, OMIM) is associated with FAP and brain tumors, e.g., astrocytomas, medulloblastomas, and ependymomas.

Pathophysiology/Histopathology

Histopathologic studies demonstrated that most solitary[1,4] and grouped CHRPE lesions are a monocellular layer of hypertrophied RPE cells, densely packed with large round pigment granules instead of the wedge-shaped melanin granules frequently found in

normal RPE cell lesions (Fig. 140.3A). These large round granules represent primarily macromelanosomes.[23] The underlying Bruch's membrane may be thickened[1,4,24,25] due to widening of the basement membrane of the hypertrophied RPE cells. The remaining layers of Bruch's membrane, the choriocapillaris, and choroid appear normal. The subjacent photoreceptor layer degenerates progressively with increasing age. The inner retinal layers, including the retinal vasculature, remain normal. In the area of depigmented lacunae, both the hypertrophied RPE and photoreceptor cell layers are absent and replaced by glial cells.[4] The transition from the margin of CHRPE lesions to normal RPE lesions occurs abruptly. A surrounding hypopigmented halo corresponds to areas of less pigmented hypertrophied RPE cells. All lesions remain flat.

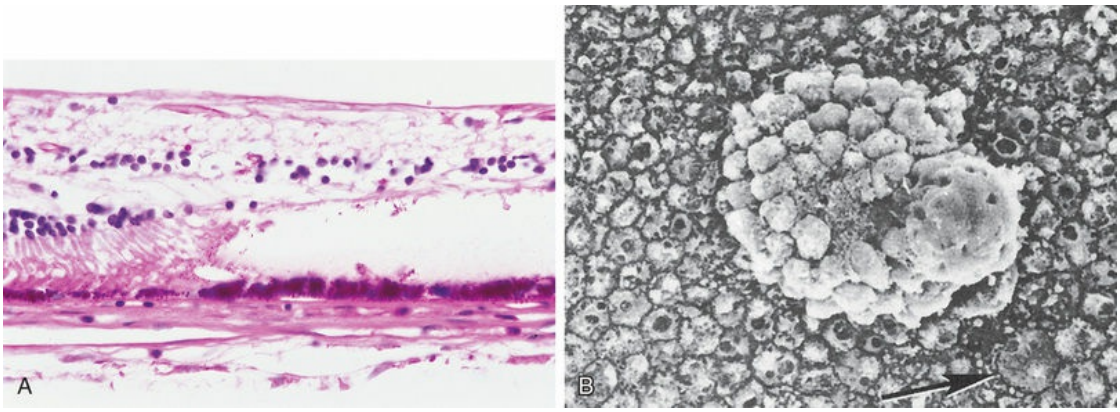

FIG. 140.3 (A) Light microscopy shows the abrupt transition from normal to abnormal retinal pigment epithelium (RPE) and retina (*arrow*) (hematoxylin and eosin, x500). (B) Scanning electron micrograph of a pigmented fundus lesion 100 µm in diameter composed of a cluster of enlarged RPE cells (x500).
(Panel A reproduced with permission from Buettner H. Congenital hypertrophy of the retinal pigment epithelium. Am J Ophthalmol 1975; 79:177–189. Panel B courtesy of Traboulsi EI, Murphy SF, de la Cruz ZC, et al. A clinicopathologic study of the eyes in familial adenomatous polyposis with extracolonic manifestations (Gardner's syndrome). Am J Ophthalmol 1990; 110:550–561. With permission from the American Academy of Ophthalmology.)

Multiple lesions associated with FAP show hypertrophy and hyperplasia of plump RPE cells, retinal invasion, and retinal

partially vascular changes. Hyperplastic lesions with multiple layers of hypertrophied RPE cells are resembling "hamartomas," causing an elevated appearance and present as clusters of enlarged RPE cells on scanning electron microscopy (Fig. 140.3B).[22,26] In another lesion, hypertrophied RPE cells traversed the full thickness of the retina. These histopathologic characteristics allow the classification of the pigmented ocular lesions in FAP as hamartomas of the RPE.[26] To distinguish these lesions nosologically the terms "polyposis-associated congenital hamartoma of the RPE" and "multiple RPE hamartomas (MRPEH)" from the classic lesion of CHRPE have been proposed.[27] In grossly normal-appearing areas of the fundus, individual and small clusters of enlarged RPE cells contain the same large spherical melanin pigment granules found in the pigmented lesions.

Clinical Examination/Ancillary Testing

The vast majority of pigmented fundus lesions are easily recognized by indirect ophthalmoscopy or three-mirror contact lens examination after dilatation of the pupil. Color fundus photography is conventionally used to document the location, color, size, and appearance of the lesions (Fig. 140.4), and novel ultrawide-field scanning-laser ophthalmoscopy has been recommended as a screening tool.[2,28] However, absence of CHRPE lesions in a family with FAP does not indicate absence of the gene, since variable phenotype expression may exist or tiny lesions can be overlooked.

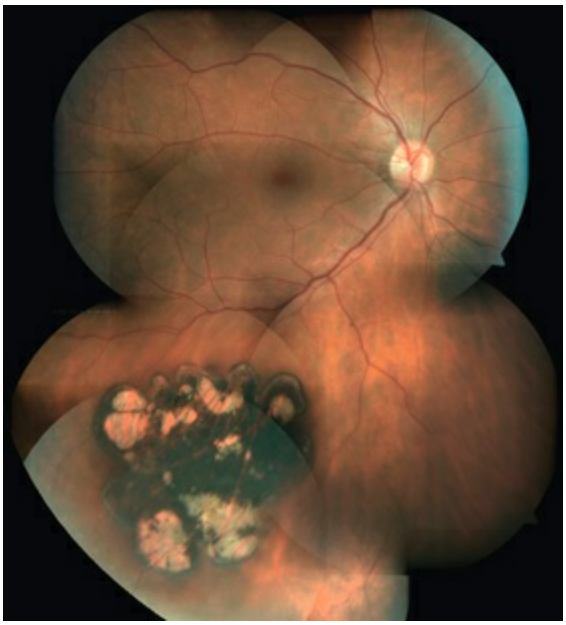

FIG. 140.4 Color fundus photography is used to document the location, color, size, and appearance of the lesions. Larger lesions may present punched-out inner lacunae with hypopigmentation and tend to expand slightly in size with aging.

As small or lightly pigmented lesions may easily be missed, fundus autofluorescence (FAF) and infrared reflectivity may be helpful to identify these lesions. Since CHRPE contains predominantly melanin and only small amounts of lipofuscin these lesions typically demonstrate hypoautofluorescence. Only areas with lacunae or nonpigmented halos show a trace to moderate autofluorescence and infrared hyperreflectivity[29] (Fig. 140.5A).

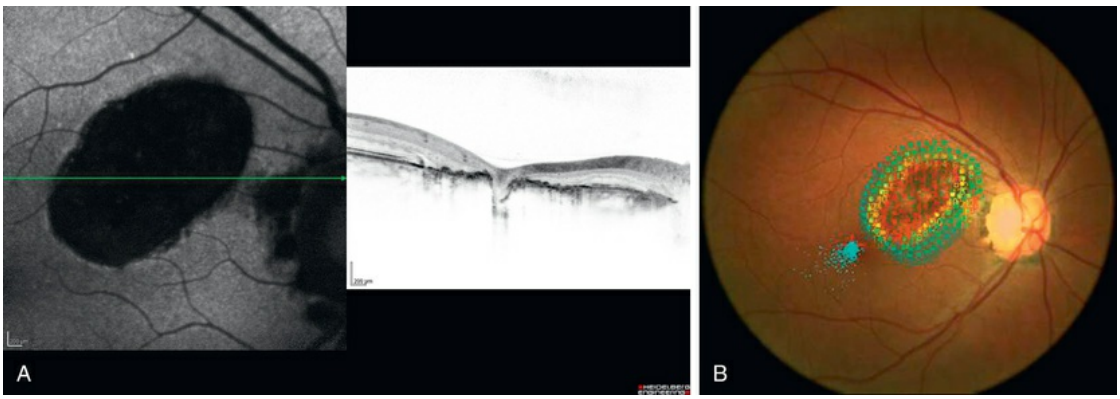

FIG. 140.5 (A) Fundus autofluorescence (FAF) is helpful to determine these CHRPE since the lesion contains predominantly melanin and only little

lipofuscin lesions presenting in dark hypoautofluorescence. (B) Microperimetry reveals a scotoma corresponding in size and location to the lesions. The central best corrected visual acuity is 20/80 and the central fixation was intact although the patient noticed moderate increase of the scotoma during computer work.

The majority of lesions remain asymptomatic and show no leakage of dye on fluorescence angiography (FA) or indocyanine green angiography (ICGA). CHRPE lesions appear as dark spots blocking choroidal fluorescence and augment the brightness of retinal vasculature. Only in depigmented lacunae or hypopigmented halos is a normal choriocapillaris flush observed. Leakage from retinal vessels overlying CHRPE has been reported during late phases of the angiogram.

The electroretinogram (ERG) and electro-oculogram (EOG) remain normal in eyes with CHRPE, providing evidence for the localized nature of this disease. The axial resolution of A- and B-scan ultrasound sonography is too low to document the CHRPE lesion, since the lesions demonstrate minimal or no elevation.

Spectral domain optical coherence tomography (SD-OCT) highlights the cross-sectional retinal anatomy of CHRPE lesions. A general thinning of the neural retina with a predominant photoreceptor loss becomes apparent over the CHRPE lesion[30] (Fig. 140.5A). Darkly pigmented CHRPE shadows the underlying choroidal structures. Areas of lacunae show absence of RPE and increased transmission of light. Retinal thinning and photoreceptor loss over CHRPE account directly for related visual field loss. On enhanced-depth imaging optical coherence tomography (EDI-OCT), CHRPE seems flat with thickened, irregular RPE and absent RPE within lacunae. A prominent feature is outer retinal loss, generally involving the outer nuclear layer to photoreceptors, occasionally with a characteristic subretinal cleft. The central sublesional choroidal thickness (126.4 μm) was not different compared with thickness outside the margin (126.8 μm).[31] Patients with CHRPE rarely complain of related symptoms, except when the fovea is involved. Microperimetry may reveal relative or absolute scotomas corresponding in size and location to the lesions. Microperimetric

defects tend to progress from relative to absolute scotoma and expand slightly in size with aging (Fig. 140.5B).

Familial Adenomatous Polyposis Prognosis and Management Options

FAP, a precancerous condition, appears with hundreds to thousands of adenomatous polyps in the colon and rectum, harboring a high risk of malignant transformation and making prophylactic total colectomy necessary in the majority of patients. Untreated patients die from colorectal cancer at an average age of 40 years.

The gene responsible for FAP, called the adenomatous polyposis coli gene (*APC*), is localized on the long arm of chromosome 5 (5q21–q22), encoding a tumor suppressor protein consisting of 2843 amino acids. The APC protein influences cell cycle, cell migration, and adhesion.

The presence of extracolonic symptoms and the severity of disease correlate with the location of the mutation on the *APC* gene. Attenuated FAP (AFAP, <100 colorectal adenomas) is caused by mutations localized after codon 1595, before codon 157, and in the spliced region of exon 9. Severe FAP (>1000 adenomas) is seen in patients with mutations between codons 1250 and 1464. Mutations in the remaining *APC* gene lead to intermediate FAP (100–1000 adenomas) (Fig. 140.6).[32,33]

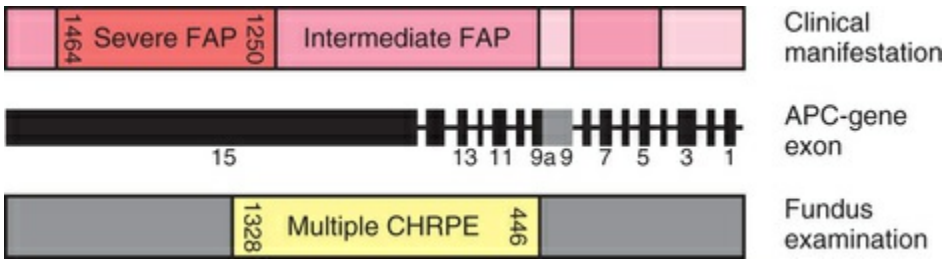

FIG. 140.6 Distribution of the APC-germline mutations and clinical manifestation. The red box indicates the colonic manifestation and its severity. Filled black boxes present the *APC* coding region split into 15 exons. The spliced exon 9 is marked in grey. The yellow box assigns the mutation region of the *APC*

gene to the multiple CHRPE fundus lesions.

Phenotypic expression of CHRPE correlates with the localization of mutations. FAP patients with mutations between codon 446 and codon 1338 regularly present with CHRPE lesions, whereas FAP patients with mutations between 1445–1578 lack multiple CHRPE at the retinal fundus. This relationship between CHRPE manifestations and the site of the *APC* mutation points out a specific role of the APC protein in development of retinal tissue. Moreover, the CHRPE status adds important information about the location of the genetic mutation and plays a critical role in the detection of the corresponding *APC* mutations. Recent well-defined assessment criteria necessitate the presence of at least four CHRPE lesions whatever their size or at least two lesions, of which one is large, to support the diagnosis of FAP.[34]

References

1. Kurz GH, Zimmerman LE. Vagaries of the retinal pigment epithelium. *Int Ophthalmol Clin*. 1962;2:441–464.
2. Aiello LP, Traboulsi EI. Pigmented fundus lesions in a preterm infant with familial adenomatous polyposis. *Arch Ophthalmol*. 1980;90:661–667.
3. Coleman P, Barnard NA. Congenital hypertrophy of the retinal pigment epithelium: prevalence and ocular features in the optometric population. *Ophthalmic Physiol Opt*. 2007;27:547–555.
4. Buettner H. Congenital hypertrophy of the retinal pigment epithelium. *Am J Ophthalmol*. 1975;79:177–189.
5. Shields CL, Mashayekhi A, Ho T, et al. Solitary congenital hypertrophy of the retinal pigment epithelium: clinical features and frequency of enlargement in 330 patients. *Ophthalmology*. 2003;110:1968–1976.
6. Shields CL, Mashayekhi A, Ho T, et al. Solitary congenital hypertrophy of the retinal pigment epithelium. *Ophthalmology*. 2003;110:1968–1976.
7. Augsburger JJ, Henson GL, Hershberger VS, et al. Topographical distribution of typical unifocal congenital

hypertrophy of retinal pigment epithelium. *Graefes Arch Clin Exp Ophthalmol*. 2006;244:1412–1414.
8. Van der Toren K, Luyten GP. Progression of papillomacular congenital hypertrophy of the retinal pigment epithelium associated with impaired visual function. *Arch Ophthalmol*. 1998;116:256–257.
9. Shields JA, Shields CL, Eagle RC Jr, et al. Adenocarcinoma arising from congenital hypertrophy of retinal pigment epithelium. *Arch Ophthalmol*. 2001;119:597–602.
10. Shields JA, Eagle RC Jr, Shields CL, et al. Malignant transformation of congenital hypertrophy of the retinal pigment epithelium. *Ophthalmology*. 2009;116:2213–2216.
11. Trichopoulos N, Augsburger JJ, Schneider S. Adenocarcinoma arising from congenital hypertrophy of the retinal pigment epithelium. *Graefes Arch Clin Exp Ophthalmol*. 2006;244:125–128.
12. Moulin AP, Zografos L, Schalenbourg A. RPE adenocarcinoma arising from a congenital hypertrophy of the RPE (CHRPE) treated with proton therapy. *Klin Monatsbl Augenheilkd*. 2014;231:411–413.
13. Meyer CH, Freyschmidt-Paul P, Happle R, et al. Unilateral linear hyperpigmentation of the skin with ipsilateral sectorial hyperpigmentation of the retina. *Am J Med Genet A*. 2004;126A:89–92.
14. Meyer CH, Rodrigues EB, Mennel S, et al. Grouped congenital hypertrophy of the retinal pigment epithelium follows developmental patterns of pigmentary mosaicism. *Ophthalmology*. 2005;112:841–847.
15. Traboulsi EI, Krush AJ, Gardner EJ, et al. Prevalence and importance of pigmented ocular fundus lesions in Gardner's syndrome. *N Engl J Med*. 1987;316:661–667.
16. Chamot L, Zografos L, Klainguti G. Fundus changes associated with congenital hypertrophy of the retinal pigment epithelium. *Am J Ophthalmol*. 1993;115:154–161.
17. Romania A, Zakov ZN, McGannon E, et al. Congenital hypertrophy of the retinal pigment epithelium in familial adenomatous polyposis. *Ophthalmology*. 1989;96:879–884.
18. Meyer CH, Becker R, Schmidt JC, et al. When is congenital

hypertrophy of the retinal pigment epithelium (CHRPE) associated with the Gardner's syndrome? An overview with clinical examples. *Klin Monatsbl Augenheilkd*. 2002;219:644–648.
19. Villegas VM, Schwartz SG, Flynn HW Jr, et al. Distinguishing torpedo maculopathy from similar lesion of the posterior segment. *Ophthalmic Surg Lasers Imaging Retina*. 2014;45:222–226.
20. Shields JA, Shields CL, Pankajkumar GS, et al. Lack of association among typical congenital hypertrophy of the retinal pigment epithelium, adenomatous polyposis, and Gardner syndrome. *Ophthalmology*. 1992;99:1709–1713.
21. Gardner EJ, Richards RC. Multiple cutaneous and subcutaneous lesions occurring simultaneously with hereditary polyposis and osteomatosis. *Am J Hum Genet*. 1953;5:139–148.
22. Buettner H. Congenital hypertrophy of the retinal pigment epithelium in familial polyposis coli. *Int Ophthalmol*. 1987;10:109–110.
23. Lloyd WC III, Eagle RC Jr, Shields JA, et al. Congenital hypertrophy of the retinal pigment epithelium: electron microscopic and morphometric observations. *Ophthalmology*. 1990;97:1052–1060.
24. Roseman RL, Gass JDM. Solitary hypopigmented nevus of the retinal pigment epithelium in the macula. *Arch Ophthalmol*. 1992;110:1358–1359.
25. Kasner L, Traboulsi EI, Delacruz Z, et al. A histopathologic study of the pigmented fundus lesions in familial adenomatous polyposis. *Retina*. 1992;12:35–42.
26. Traboulsi EI, Murphy SF, de la Cruz ZC, et al. A clinicopathologic study of the eyes in familial adenomatous polyposis with extracolonic manifestations (Gardner's syndrome). *Am J Ophthalmol*. 1990;110:550–561.
27. Hennesy MP, Collins F. The distinction between multiple retinal pigment epithelial hamartomata (MRPHE) in familial adenomatous polyposis (FAP) and congenital hypertrophy of the retinal pigment epithelium (CHRPE). *Aust N Z J Ophthalmol*. 1993;21:275–276.

28. Meyer CH, Holz FG. Documentation of congenital hypertrophy of the retinal pigment epithelium with wide-field funduscopy. *Semin Ophthalmol*. 2009;24:251–253.
29. Shields CL, Pirondini C, Bianciotto C, et al. Autofluorescence of congenital hypertrophy of the retinal pigment epithelium. *Retina*. 2007;27:1097–1111.
30. Shields CL, Materin MA, Walker C, et al. Photoreceptor loss overlying congenital hypertrophy of the retinal pigment epithelium by optical coherence tomography. *Ophthalmology*. 2006;113:661–665.
31. Fung AT, Pellegrini M, Shields CL. Congenital hypertrophy of the retinal pigment epithelium: enhanced-depth imaging optical coherence tomography in 18 cases. *Ophthalmology*. 2014;121:251–256.
32. Nieuwenhuis MH, Vasen HF. Correlations between mutation site in APC and phenotype of familial adenomatous polyposis (FAP): a review of the literature. *Crit Rev Oncol Hematol*. 2007;61:153–161.
33. Caspari R, Olschwang S, Friedl W, et al. Familial adenomatous polyposis: desmoid tumours and lack of ophthalmic lesions (CHRPE) associated with APC mutations beyond codon 1444. *Hum Mol Genet*. 1995;4:337–340.
34. Gebert JF, Dupon C, Kadmon M, et al. Combined molecular and clinical approaches for the identification of families with familial adenomatous polyposis coli. *Ann Surg*. 1999;229:350–361.

141

Combined Hamartoma of the Retinal Pigment Epithelium and Retina

Polly A. Quiram, Antonio Capone Jr.

Combined hamartomas of the retina and retinal pigment epithelium (CHRRPE) are benign tumors that may cause significant visual loss depending upon location. Accurate diagnosis is essential because the lesion may resemble a choroidal melanoma or other intraocular tumor. Combined hamartomas are usually solitary, unilateral lesions located at the optic disc or posterior pole. They typically appear slightly elevated and have varying amounts of pigmentation, vascular tortuosity, and epiretinal membrane (ERM) formation. CHRRPE lesions are characterized by predominant tissue subtype, including pigment epithelial, vascular, or glial.[1]

Historical Review

Early reports of combined hamartomas describe lesions that were clinically mistaken for choroidal malignancy. Histopathologically, these lesions were described as hyperplastic retinal pigment epithelium and were located juxtapapillary, in the posterior pole or peripherally.[2,3] In 1961, the term "hamartoma" was used to describe a large lesion of the posterior pole in a child.[4] In 1973, Gass[5] reported lesions in five children and two young adults and used the term "combined hamartoma." In 1984, Schachat et al.[1] described 60 patients with combined hamartomas in a collaborative effort of the

Macula Society Research Committee. Gass[6] reported an additional 35 patients in his discussion of the Macula Society's report. Shields et al.[7] reported visual acuity outcomes of 77 patients from a single institution.

Epidemiology

In the Macula Society's report[1] of 60 patients with combined hamartomas, the mean age at the time of diagnosis was 15 years, with a range of 10 months to 66 years. The number of males and females was equal, and three patients were black. Shields et al.[7] reported a mean age of diagnosis of 11.9 months with a range of 0.4–60 months. There was no apparent predilection based on sex or race. Diagnosis is likely delayed relative to the appearance of the lesions due to the gradual impact on vision of non-macular lesions.

Clinical Manifestations

Symptoms

Reviews of several large reports show that painless visual loss is the chief complaint followed by strabismus, floaters, leukocoria, and ocular pain. Detection during routine examination was reported in 10% of patients.[1,7,8]

Visual Acuity

Visual function varies with the location of the lesion.[7] Direct macular involvement including the optic nerve, papillomacular bundle, or fovea may reduce visual acuity. Extramacular lesions may cause visual loss from indirect macular distortion related to tractional forces. Although uncommon, secondary causes of visual loss include choroidal neovascularization,[1,9] vitreous hemorrhage,[10,11] exudative retinal detachments,[1] retinoschisis,[1,12] and macular hole formation.[13] In the Macula Society report,[1] visual acuity was 20/40 or better in 45% of patients, and 20/200 or worse in 40%. In a review by Font et al.,[8] 28% were 20/40 or better, whereas 28% were worse than 20/200. Age, symptoms, and visual acuity at

presentation are related to tumor location. Compared with extramacular lesions, macular lesions were associated with younger presentation (mean age 14.2 months versus 9.5 months), strabismus (25% versus 31%), decreased visual acuity (37% versus 43%) and visual acuity ≤20/200 (25% versus 69%). Mean visual acuity of macular and extramacular CHRRPE lesions was 20/320 and 20/80, respectively.[7]

Ophthalmoscopic Appearance

Combined hamartomas may be located at the optic disc and juxtapapillary region, in the macula, and in the mid-periphery. The ophthalmoscopic appearance varies depending on the location of the tumor. Lesions of the posterior pole have varying amounts of retinal pigment epithelial, vascular, and glial components, and one tumor type tends to predominate (Fig. 141.1). Clinical features include an elevated pigmented mass involving the RPE, retina, and overlying vitreous with extension of fanlike projections towards the periphery. This lesion may blend imperceptibly with the surrounding RPE with an absence of RPE or choroidal atrophy. The lesion may be covered by a thickened gray–white retinal and preretinal tissue which may show contraction of the inner surface. There is generally absence of retinal detachment, hemorrhage, and vitreous inflammation.[5] The Macula Society[1] reported retinal vascular tortuosity within the lesion in 93% of patients, hyperpigmentation in 87%, slight elevation in 80%, ERM formation in 78%, and exudation in 7%. Peripheral lesions[14] appear as an elevated ridge concentric with the disc. Adjacent to the lesion, larger retinal vessels appear stretched, and there are a few smaller vessels (Fig. 141.2). A dragged disc appearance has been described in patients with peripheral lesions.[5,15] Combined hamartomas are almost always solitary, unilateral tumors; however, cases of bilateral involvement have been reported in association with neurofibromatosis.[9,16–18]

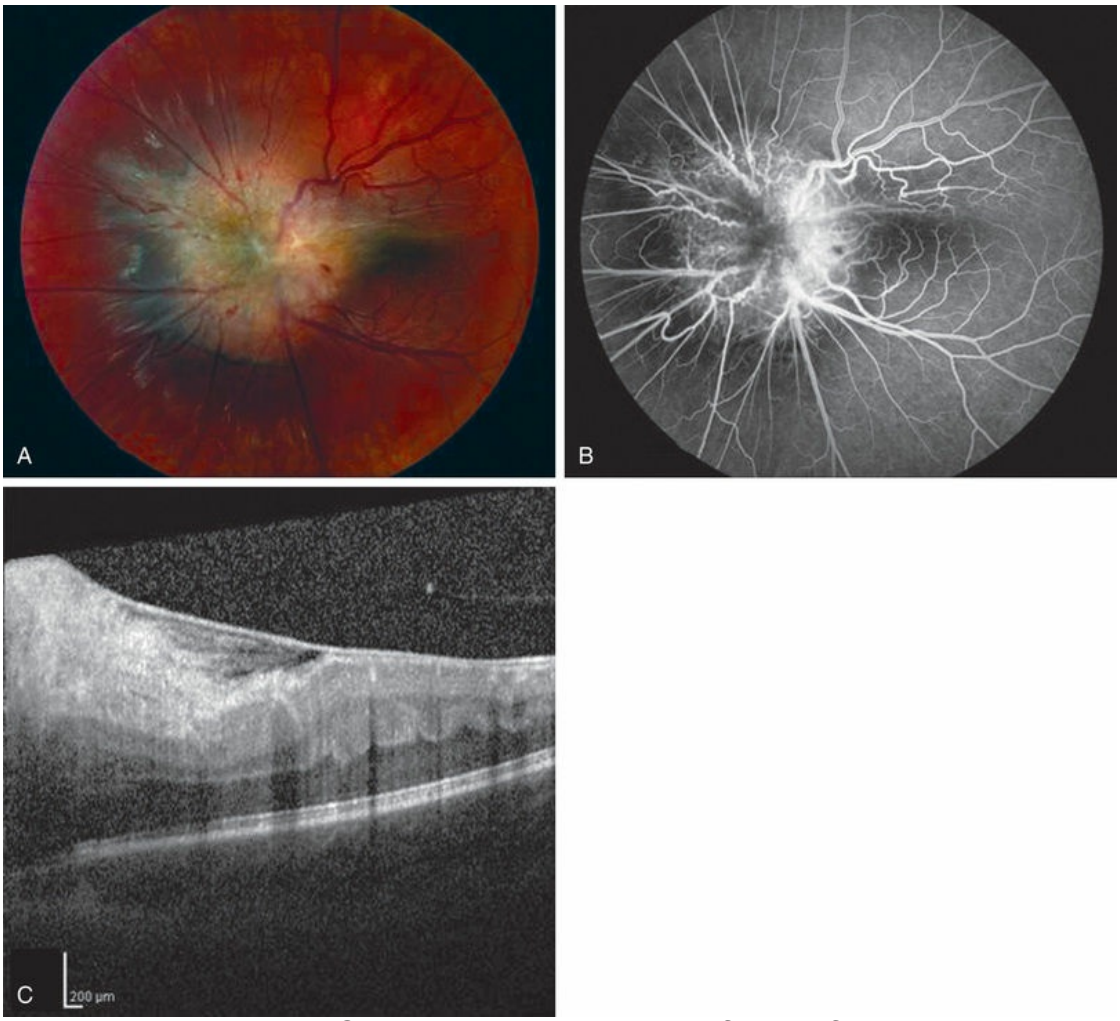

FIG. 141.1 (A) Combined hamartoma of the left optic nerve head and juxtapapillary region in a 10-year-old female with 20/80 vision. Circumferential hyperpigmentation is noted with significant gliosis overlying the optic nerve. Retinal striae with a retinal fold is present in the superior macula. Retinal vascular tortuosity and telangiectasia are evident. (B) Mid-phase fluorescein angiogram demonstrating numerous small, irregular blood vessels throughout the lesion. There is blocked fluorescence from the pigmentation. (C) Spectral domain optical coherence tomography demonstrates an elevated hyperreflective mass with disorganization of normal retinal architecture. Fibrovascular traction with retinal thickening and attenuation of the inner and outer retina with minimal attenuation of the photoreceptor layers. Evidence of a surgical plane can guide removal in these cases.

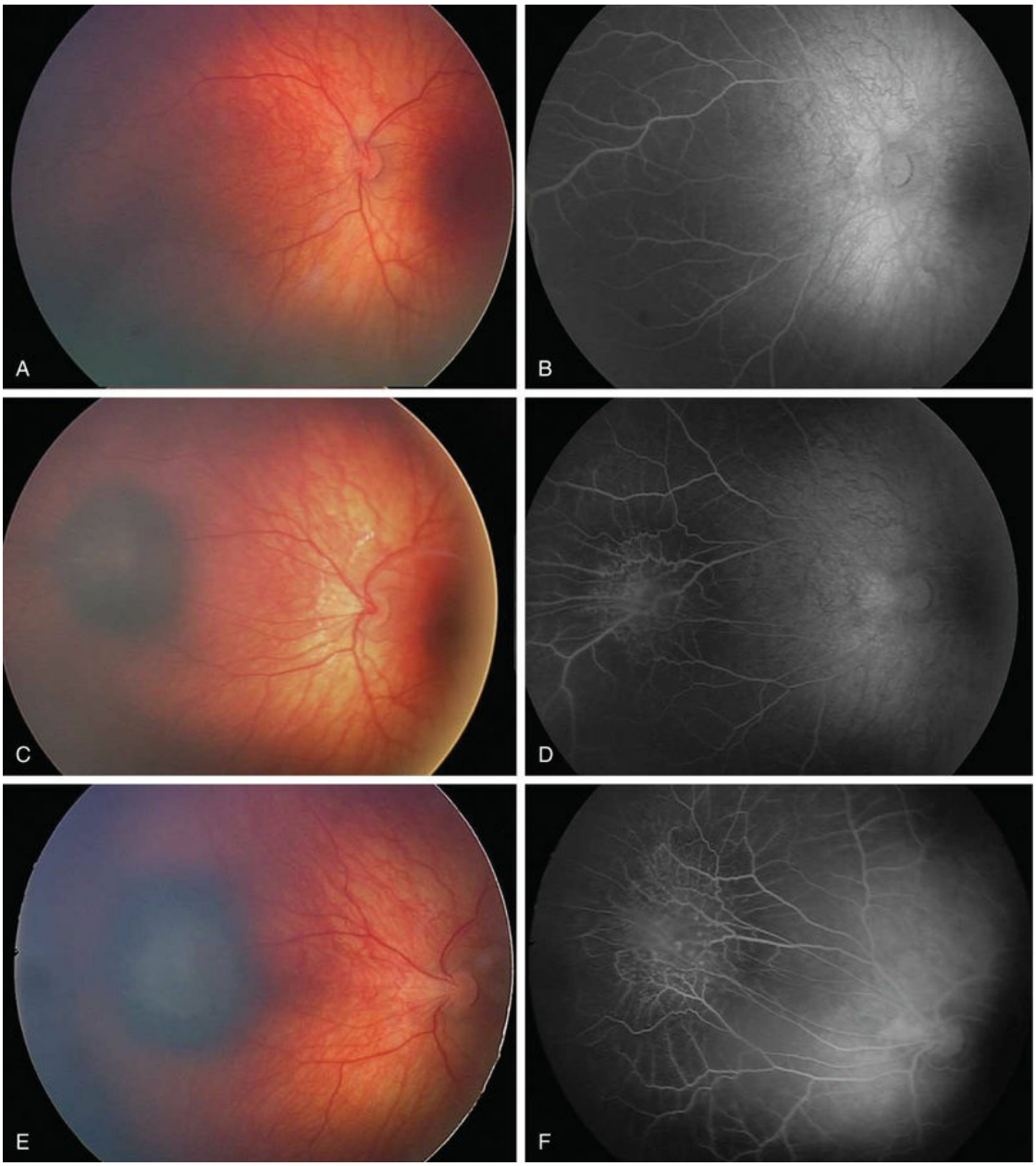

FIG. 141.2 (A) Unremarkable left eye (OS) of a 6-month-old girl who presented with a total tractional and exudative retinal detachment of the right eye (OD). (B) Fluorescein angiography (FA) showed complete vascularization OS and normal posterior pole and midperipheral vasculature. (C) Approximately six months later, OS revealed a discrete pigmented, mildly elevated lesion with preretinal glial proliferation and contraction nasal to the optic nerve. (D) FA confirmed a CHRRPE lesion with telangiectatic vessels and blocked choroidal fluorescence surrounding the lesion. (E,F) Following two months of observation, the lesion continued to grow with additional gliosis, retinal distortion, and straightening of retinal vessels.

Associated Ocular Findings

Extensive disc or macular lesions may be associated with a relative afferent pupillary defect. Patients with macular involvement and decreased vision often have strabismus.[7] Other findings include vitreous hemorrhage,[10,11] preretinal neovascularization peripheral to the hamartoma,[19] choroidal neovascularization at the margin of the lesion,[1,9,20] macular hole,[13] and peripheral hole formation.[21] In addition, CHRRPE lesions have been associated with X-linked juvenile retinoschisis, optic nerve head pits, optic nerve colobomas, and optic nerve head drusen.[1,5,22]

Systemic Associations

Most patients with combined hamartomas do not have evidence of systemic disease; however, numerous reports describe an association with neurofibromatosis types 1 and 2.[5,16–18,23–25] A majority of patients with bilateral combined hamartomas have signs of neurofibromatosis.[9,16,18] Combined hamartomas have also been reported in patients with facial hemangiomas,[5] incontinentia pigmenti,[1] tuberous sclerosis,[11] Gorlin Goltz syndrome,[26] Poland anomaly,[27] branchio-oculofacial syndrome,[28] brachio-otic syndrome,[29] brachial cleft cysts,[30] and juvenile nasopharyngeal angiofibroma.[31]

Diagnostic Evaluation

The diagnosis of CHRRPE is based upon clinical appearance and characterization by fluorescein angiography (FA) and optical coherence tomography (OCT). In the early phase of the angiogram, the degree of hypofluorescence parallels the degree of hyperpigmentation. Tractional distortion of the retina may result in marked vascular tortuosity and telangiectasia. The mid-phase of the angiogram may highlight vascular anomalies. It is not uncommon to note vascular straightening. In the late phase of the angiogram the tortuous vessels usually leak, causing late hyperfluorescence. If there is associated choroidal neovascularization, deep leakage is

evident.

OCT is an important modality for diagnosing and characterizing CHRRPE lesions. High-resolution spectral domain OCT (SD-OCT) imaging shows characteristic findings, including peaked vitreoretinal traction, retinal disorganization, thickening of the retina at the level of the RPE, and preretinal vitreoretinal interface abnormalities.[32] OCT imaging can delineate the transition between the abnormal retinal interface and can guide surgical intervention. Enhanced depth imaging OCT (EDI-OCT) typically shows ERM with traction, disorganization of the retinal layers, and choroidal thinning.[33] A detailed analysis of EDI-OCT imaging in pediatric patients shows characteristic ERM and vitreoretinal traction of the inner retina in a sawtooth (mini-peak) or full thickness retinal fold (maxi-peak) pattern. Autofluorescence may show a hypoautofluorescence over the entire lesion and hyperautofluorescence in areas with macular edema and overlying ERM.[34] Ultrasonography is not useful in diagnosis of these minimally elevated lesions.

Differential Diagnosis

The differential diagnosis of combined hamartomas includes any fundus lesion that has some degree of elevation, pigmentation, vascular tortuosity, or glial proliferation. Diagnosis of combined hamartomas requires evidence of preretinal, intraretinal, and subretinal components.

Epiretinal Membrane

The most common differential diagnostic consideration is epiretinal membrane. As for ERMs, vitreoretinal interface disruption and vascular tortuosity may be present, but the hyperpigmentation associated with CHRRPE lesions is rarely present. ERMs may show a “cellophane” light reflex or a thickened, opaque membrane with superficial retinal folds and traction lines. A review of 44 patients with childhood ERMs showed association with trauma or uveitis and were predominantly identified in males in the second decade of life.[35] It may be extremely difficult to distinguish between ERMs

and CHRRPE lesions in eyes with no known history of trauma or inflammation. OCT testing can be helpful for differentiating CHRRPE and ERMs. The intraretinal component of CHRRPE lesions, which is often difficult to discern by FA or clinical examination, is evident with high-resolution OCT imaging.[32] OCT imaging can also be useful for identifying and guiding surgical removal of preretinal traction associated with CHRRPE lesions. Preretinal components of CHRRPE lesions can be removed surgically, but the adhesion between disorganized retinal structures and thickened RPE cannot be removed. For this reason, some measure of persistence of the CHRRPE lesion is routinely noted following surgery (Fig. 141.3).

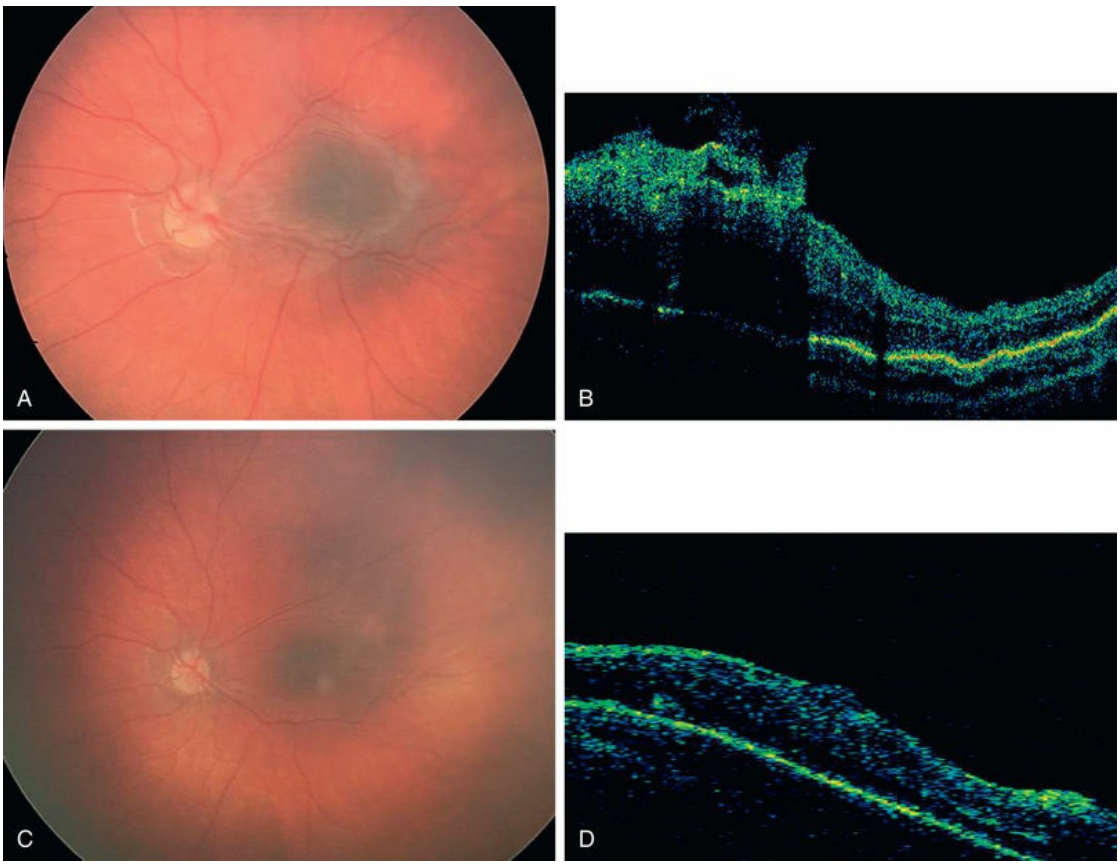

FIG. 141.3 (A) Preoperative color fundus photograph, demonstrating presence of a CHRRPE lesion with marked dragging and distortion of the central macula. (B) Preoperative OCT showing dense hamartoma of the macula with vitreoretinal traction and evidence of a surgical plane. (C) Postoperative color fundus photo demonstrating reduction of macular distortion following

pars plana vitrectomy with membrane peeling with assistance of autologous plasmin enzyme. (D) Postoperative OCT demonstrating flattening of the central macula.

Pigmented Choroidal Lesions

Choroidal melanomas, choroidal nevi, congenital hypertrophy of the retinal pigment epithelium (CHRPE), adenoma, and adenocarcinoma of the RPE can be misidentified as a CHRRPE lesion. Choroidal melanomas are subretinal, elevated, and lack vitreoretinal interface changes and vascular tortuosity. Choroidal nevi lack vitreoretinal interface changes and vascular tortuosity as well. Congenital hypertrophy of the retinal pigment epithelium is subretinal and flat with normal retinal vessels. Adenoma and adenocarcinoma of the retinal pigment epithelium are rare and usually jet-black in color.[14]

Miscellaneous Lesions

Morning-glory disc anomaly, retinoblastoma, choroidal neovascularization, retinoschisis, and capillary hemangioma can simulate the appearance of combined hamartomas. In a large series of 604 patients with lesions simulating retinoblastoma (pseudoretinoblastoma), CHRRPE lesions were noted in 2% of cases with Coats disease (40%) and persistent fetal vasculature (28%) being the most common causes of pseudoretinoblastoma.[36]

Clinical Course

Visual loss in patients with combined hamartomas is associated with macular involvement. Distortion of retinal anatomy and disorganization of retinal components can cause strabismus and amblyopia in children. Visual loss has also been associated with vitreous hemorrhage, choroidal neovascularization, macular edema, retinoschisis, peripheral and macular hole formation, and retinal detachment.[1,9–13,16,20,37] Peripheral lesions are generally asymptomatic, but vitreous traction may increase vascular

tortuosity and result in macular distortion. In the Macula Society report,[1] 66% of patients maintained their visual acuity after 4 years, 24% of patients lost 2 or more lines, and 10% of patients improved by 2 or more lines as a result of amblyopia therapy or vitreous surgery. In the Macula Society report, the mean age was 15 years. In a report of a younger population (mean age of 9.5 months), 60% of patients with macular lesions and 13% of patients with extramacular lesions lost ≥3 lines of vision after 4 years of follow-up.[7] The decline in visual acuity indicates the need for frequent evaluation, amblyopia therapy, and possible surgical intervention. Unfortunately, data from population-based studies is not available to confirm progression or long-term stability of asymptomatic lesions.

Etiology and Pathogenesis

Multiple proposed etiologies of CHRRPE lesions exist. Although combined hamartomas have not been reported to be present at birth, they have been noted in infants 2 weeks of age,[7] which supports a congenital etiology. The association of combined hamartomas with neurofibromatosis supports a developmental etiology. Several reports have documented the development of acquired lesions. For example, an 8-year-old patient with a unilateral combined hamartoma developed a similar-appearing lesion with consequent visual loss in the fellow eye at a 2.5-year follow-up.[17] A more recent report by Yonekawa et al.[38] documents the formation of an acquired de novo lesion that developed as an incidental finding 8 months after birth (Fig. 141.2). Although a few reports of acquired hamartomas exist, these are often related to RPE trauma, inflammation, vitreomacular traction, or disc edema suggesting a hamartoma-like gliosis and hyperpigmentation as opposed to truly de novo hamartomatous lesions.[39–41]

Histopathology

Early reports on combined hamartomas describe lesions that were clinically mistaken for choroidal malignancy. The histopathologic findings in combined hamartomas were obtained from eyes that

were enucleated for suspected malignancy. In general, progressive enlargement of the lesion or decreasing visual acuity prompted enucleation.

Combined hamartomas show marked disorganization of the retinal architecture with preretinal, intraretinal, and subretinal components. Proliferation of glial tissue has been described as focal areas of gliosis in the nerve fiber layer associated with wrinkling of the internal limiting membrane.[3] The RPE proliferates as cords and sheets within the overlying inner retina and may exhibit a perivascular distribution. In juxtapapillary lesions, there may be proliferation of the retinal pigment epithelium into the optic disc.[2] The peripapillary retina and optic nerve head may be thickened by increased numbers of blood vessels and by proliferated retinal pigment epithelium.[42] In one report, 15-year follow-up showed calcification of a longstanding CHRRPE lesion with osseous metaplasia often associated with other longstanding gliotic disorders including proliferative vitreoretinopathy membranes.[43]

Histologic and immunohistochemical analysis of ERMs associated with CHRRPE lesions have been previously reported.[44] Hematoxylin and eosin staining shows a monolayer of cells with an underlying basement membrane. The nuclei present were epithelioid, consistent with RPE elements, and spindle-shaped, consistent with fibroglial elements. Immunohistochemical staining with cytokeratin (CK), glial fibrillary acidic protein, and neuron-specific enolase revealed a mixture of RPE and retinal elements with negative RPE65 staining, indicating the absence of mature RPE cells.

Treatment

Medical

In patients with CHRRPE lesions, a functional component of amblyopia may be superimposed on visual loss caused by structural abnormalities, and in some cases, visual acuity has increased with amblyopia therapy.[1,45] One report of a macular lesion causing progressive visual loss and vascular leakage was treated with photodynamic therapy (PDT). Following PDT,

vascular closure was demonstrated with fluorescein angiography.[46] Visual loss from subfoveal choroidal neovascularization has been demonstrated in CHRRPE lesions. In one report, submacular surgery and removal of the choroidal neovascular membrane improved vision from 20/60 to 20/20.[47] In addition, anti-VEGF therapy has been successfully used to treat CHRRPE-associated choroidal neovascular membranes.[48]

Surgical

As stated previously, the clinical course of macular CHRRPE lesions is progressive visual loss. In the Macula Society report,[1] 24% of patients lost 2 or more lines of vision after 4 years. In younger patients (mean age of 9.5 months) 60% of patients with macular lesions had a visual loss of ≥3 lines after 4 years.[7] The natural history of progressive visual loss indicates the importance of monitoring and evaluation for surgical intervention. Lesions generally have one predominant tissue subtype, including melanocytic, vascular, or glial. Macular lesions creating progressive visual loss with glial proliferation and vitreous traction are amenable to surgical treatment.[49] OCT imaging is an invaluable tool for identifying vitreoretinal interface abnormalities and determining the presence of a surgical plane (Figs. 141.1 and 141.3).

Of 60 patients reviewed by the Macula Society report, three underwent surgery, and only one had improvement of vision (20/200 to 20/40) while the other two showed no improvement.[1] Other authors reported poor visual outcomes following removal of CHRRPE in two adult cases. Both patients had longstanding poor vision with amblyopia likely impacting their final visual outcome.[50] Additional reports indicate improved surgical outcomes for CHRRPE lesions.[51–57] The cases described in these reports show dense ERM-like lesions with a tight adherence of the posterior hyaloid that were removed with vitrectomy and membrane peeling. Visual improvement and improvement of macular architecture were observed. In addition, a combination of pars plana vitrectomy, membrane peeling, intravitreal triamcinolone, and laser has been reported to reduce vascular activity and reduce traction associated with the abnormal vitreoretinal interface.[58]

A relatively large series of 11 pediatric patients (1–14 years old) with vitreoretinal interface abnormalities associated with CHRRPE has been reported.[49] Following surgical intervention, all of the patients demonstrated improved or stabilized vision. Surgical success was attributed to early surgical intervention by vitrectomy and membrane stripping to improve retinal architecture and lessen the affects of amblyopia. In this study, preoperative autologous plasmin enzyme was injected to assist in removing extensive vitreomacular traction and vitreoretinal proliferation.[49,59] A patient with bilateral CHRRPE lesions who underwent plasmin-assisted vitrectomy showed significant architectural and functional improvement[60] (Fig. 141.3). Another series of six patients (mean age 31 years) were evaluated by SD-OCT, fundus autofluorescence and microperimetry (MP-1) to guide surgical intervention for CHRRPE.[34] Using MP-1 they showed the lowest sensitivity areas corresponded to the tightest ERM adherence. The patients with the lowest sensitivity preoperatively had a worse visual outcome postoperatively, indicating prompt surgical intervention before loss of retinal sensitivity and function.

Although tractional distortion of the macula can be relieved by vitrectomy and epiretinal membrane surgery in eyes with CHRRPE, and visual acuity may improve, a common criticism is that the hamartoma persists/recurs. This is nearly universally true to varying degrees, as the hamartomatous tissue cannot be completely removed. Though excision is admittedly often incomplete, postsurgical anatomy following excision of superficial CHRRPE lesions is typically superior to the preoperative anatomy and generally remains so with consequent improvement in visual acuity as reproliferation is typically muted. Aggressive amblyopia therapy is an important component of the postsurgical care of such patients.

In summary, combined hamartomas of the retinal pigment epithelium are rare, benign tumors which may cause significant visual loss if located in the macula. Surgical intervention can result in an improvement of visual acuity and retinal architecture, in carefully selected patients.

References

1. Schachat AP, Shields JA, Fine SL, et al. Combined hamartomas of the retina and retinal pigment epithelium. *Ophthalmology*. 1984;91:1609–1615.
2. Theobald GD, Floyd G, Kirk HQ. Hyperplasia of the retinal pigment epithelium simulating a neoplasm: report of two cases. *Am J Ophthalmol*. 1958;45:235–240.
3. Vogel MH, Zimmermann LE, Gass JDM. Proliferation of the juxtapapillary retinal pigment epithelium simulating malignant melanoma. *Doc Ophthalmol*. 1969;26:461–481.
4. Cardell BS, Starbuck MJ. Juxtapapillary hamartoma of retina. *Br J Ophthalmol*. 1961;45:672–677.
5. Gass JD. An unusual hamartoma of the pigment epithelium and retina simulating choroidal melanoma and retinoblastoma. *Trans Am Ophthalmol Soc*. 1973;71:171–185.
6. Gass JD. Combined hamartomas of the retina and retinal pigment epithelium. *Ophthalmology*. 1984;91:1609–1615.
7. Shields CL, Thangappan A, Hartzell K, et al. Combined hamartoma of the retina and retinal pigment epithelium in 77 consecutive patients. *Ophthalmology*. 2008;115:2246–2252.
8. Font RL, Moura RA, Shetlar DJ, et al. Combined hamartoma of sensory retina and retinal pigment epithelium. *Retina*. 1989;9:302–311.
9. Flood TP, Orth DH, Aaberg TM, et al. Macular hamartomas of the retinal pigment epithelium and retina. *Retina*. 1983;3:164–170.
10. Kahn D, Goldberg MF, Jednock N. Combined retinal–retina pigment epithelial hamartoma presenting as a vitreous hemorrhage. *Retina*. 1984;4:40–43.
11. Wang CL, Brucker AJ. Vitreous hemorrhage secondary to juxtapapillary vascular hamartoma of the retina. *Retina*. 1984;4:44–47.
12. Schachat AP, Glaser MB. Retinal hamartoma, acquired retinoschisis and retinal hole. *Am J Ophthalmol*. 1985;99:604–605.
13. Mason JO III, Kleiner R. Combined hamartoma of the retina and retinal pigment epithelium associated with epiretinal membrane and macular hole. *Retina*. 1997;17:160–162.
14. Shields JA, Shields CL. *Intraocular tumors*. WB Saunders:

Philadelphia; 1992.
15. Harper CA, Gole GA. Combined hamartoma of the retina and RPE: an unusual case of the dragged disc appearance. *Aust NZ J Ophthalmol*. 1986;14:235–238.
16. Destro M, D'Amico DJ, Gragoudas ES, et al. Retinal manifestations of neurofibromatosis: diagnosis and management. *Arch Ophthalmol*. 1991;109:662–666.
17. Meyer JH, Witschel H. Bilateral combined hamartoma of the retina and the retinal pigment epithelium. *Br J Ophthalmol*. 1996;80:577–578.
18. Vianna RNG, Pacheco DF, Vasconcelos MM, et al. Combined hamartoma of the retina and retinal pigment epithelium associated with neurofibromatosis type-1. *Int Ophthalmol*. 2002;24:63–66.
19. Helbig H, Niederberger H. Presumed combined hamartoma of the retina and retinal pigment epithelium with preretinal neovascularization. *Am J Ophthalmol*. 2003;136:1157–1159.
20. Theodossiadis PG, Panagiotidis DN, Baltatzis SG, et al. Combined hamartoma of the sensory retina and retinal pigment epithelium involving the optic disk associated with choroidal neovascularization. *Retina*. 2001;21:267–270.
21. Verma L, Venkatesh P, Lakshmaiah CN, et al. Combined hamartoma of the retina and retinal pigment epithelium with full thickness retinal hole and without retinoschisis. *Ophthalmol Surg Lasers*. 2000;31:423–426.
22. Damasceno NA, Damasceno EF. Combined hamartoma of the retina and retinal pigment epithelium associated with optic coloboma. *Clin Ophthalmol*. 2011;5:353–354.
23. Cotlier E. Café-au-lait spots of the fundus in neurofibromatosis. *Arch Ophthalmol*. 1977;95:1990–1992.
24. Sivalingam A, Augsburger J, Perilongo G, et al. Combined hamartoma of the retina and retinal pigment epithelium in a patient with neurofibromatosis type 2. *J Pediatr Ophthalmol Strabismus*. 1991;28:320–322.
25. Kaye LD, Rothner AD, Beauchamp GR, et al. Ocular findings associated with neurofibromatosis type II. *Ophthalmology*. 1992;99:1424–1429.
26. DePotter P, Stanescu D, Caspers-Velu L, et al. Combined

hamartoma of the retina and retinal pigment epithelium in Gorlin syndrome. *Arch Ophthalmol*. 2000;118:1004–1005.
27. Stupp T, Pavlidis M, Bochner T, et al. Poland anomaly associated with ipsilateral combined hamartoma of the retina and retinal pigment epithelium. *Eye*. 2004;18:550–552.
28. Demirci H, Shields CL, Shields JA. New ophthalmic manifestations of branchio-oculo-facial syndrome. *Am J Ophthalmol*. 2005;139:362–364.
29. Kadaba P, Arepalli S, Shields JA, et al. Combined hamartoma of the retina and retinal pigment epithelium in branchio-otic syndrome. *J AAPOS*. 2014;18:201–203.
30. Badami A, Bianciotto CG, Shields CL, et al. Combined hamartoma of the retina and retinal pigment epithelium in a child with branchial cleft cysts. *J Pediatr Ophthalmol Strabismus*. 2012;49:9–11.
31. Fonseca RA, Dantas MA, Kaga T, et al. Combined hamartoma of the retina and retinal pigment epithelium associated with juvenile nasopharyngeal angiofibroma. *Am J Ophthalmol*. 2001;132:131–132.
32. Huot CS, Desai KB, Shah VB. Spectral domain optical coherence tomography of combined hamartoma of the retina and retinal pigment epithelium. *Ophthalmic Surg Lasers Imaging*. 2009;40:322–324.
33. Arepalli S, Pellegrini M, Ferenczy SR, et al. Combined hamartoma of the retina and retinal pigment epithelium: findings on enhanced depth imaging optical coherence tomography in eight eyes. *Retina*. 2014;34:2202–2207.
34. Bruè C, Saitta A, Nicolai M, et al. Epiretinal membrane surgery for combined hamartoma of the retina and retinal pigment epithelium: role of multimodal analysis. *Clin Ophthalmol*.2013;7:179–184.
35. Khaja HA, McCannel CA, Diehl NN, et al. Incidence and clinical characteristics of epiretinal membranes in children. *Arch Ophthalmol*. 2008;126:632–636.
36. Shields CL, Schoenberg E, Kocher K, et al. Lesions simulating retinoblastoma (pseudoretinoblastoma) in 604 cases: results based on age at presentation. *Ophthalmology*. 2013;120:311–316.

37. Schachat AP, Glaser BM. Retinal hamartoma, acquired retinoschisis, and retinal hole. *Am J Ophthalmol*. 1985;99:604–605.
38. Yonekawa Y, Thomas BJ, Drenser KA, et al. Acquired combined hamartoma of the retina and retinal pigment epithelium. *JAMA Ophthalmol*. 2015;133(9):1085–1086.
39. Hrisomalos NF, Mansour AM, Jampol LM, et al. "Pseudo"-combined hamartoma following papilledema. *Arch Ophthalmol*. 1987;105:1634–1635.
40. Ticho BH, Egel RT, Jampol LM. Acquired combined hamartoma of the retina and pigment epithelium following parainfectious meningoencephalitis with optic neuritis. *J Pediatr Ophthalmol Strabismus*. 1998;35:116–118.
41. Dark AJ, Richardson J, Howe JW. Retinal hamartoma in childhood. *J Pediatr Ophthalmol Strabismus*. 1978;15:273–277.
42. Green WR. Pathology of the retinal pigment epithelium. Spencer WD. *Ophthalmic pathology: an atlas and textbook*. 3rd ed. WB Saunders: Philadelphia; 1985.
43. Cebulla CM, Flynn HW Jr. Calcification of combined hamartoma of the retina and retinal pigment epithelium over 15 years. *Graefes Arch Clin Exp Ophthalmol*. 2013;251:1455–1456.
44. Almony A, Blinder KJ, Harocopos GJ, et al. Histologic and immunohistochemical features of an epiretinal membrane overlying a combined hamartoma of the retina and retinal pigment epithelium. *Retin Cases Brief Rep.*2010;4:184–186.
45. Kushner BJ. Functional amblyopia associated with organic ocular disease. *Am J Ophthalmol*. 1981;91:39–45.
46. Cilliers H, Harper CA. Photodynamic therapy with verteporfin for vascular leakage from a combined hamartoma of the retina and retinal pigment epithelium. *Clin Exp Ophthalmol*. 2006;34:186–188.
47. Inoue M, Noda K, Ishida S, et al. Successful treatment of subfoveal choroidal revascularization associated with combined hamartoma of the retina and retinal pigment epithelium. *Am J Ophthalmol*. 2004;138:155–156.
48. Echevarría L, Villena O, Nievas T, et al. Combined hamartoma of the retina and retinal pigment epithelium:

anti-VEGF treatment of the associated choroidal neovascular membranes. *Arch Soc Esp Oftalmol*. 2015;90:87–93.
49. Cohn AD, Quiram PA, Drenser KA, et al. Surgical outcomes of epiretinal membranes associated with combined hamartoma of the retina and retinal pigment epithelium. *Retina*. 2009;29:825–830.
50. McDonald HR, Abrams GW, Burke JM, et al. Clinicopathologic results of vitreous surgery for epiretinal membranes in patients with combined retinal and retinal pigment epithelial hamartomas. *Am J Ophthalmol*. 1985;100:806–813.
51. Sappenfield DL, Gitter KA. Surgical intervention for combined retinal–retinal pigment epithelial hamartoma. *Retina*. 1990;10:119–124.
52. Benhamou N, Massin P, Spolaore R, et al. Surgical management of epiretinal membrane in young patients. *Am J Ophthalmol*. 2002;133:358–364.
53. Stallman JB. Visual improvement after pars plana vitrectomy and membrane peeling for vitreoretinal traction associated with combined hamartoma of the retina and retinal pigment epithelium. *Retina*. 2002;22:101–104.
54. Xiao Z, Fangian D, Rongping D, et al. Surgical management of epiretinal membrane in combined hamartomas of the retina and retinal pigment epithelium. *Retina*. 2010;30:305–309.
55. Mason JO III. Visual improvement after pars plana vitrectomy and membrane peeling for vitreoretinal traction associated with combined hamartoma of the retina and retinal pigment epithelium. *Retina*. 2002;22:824–825.
56. Konstantinidis L, Chamot L, Zografos L, et al. Pars plana vitrectomy and epiretinal membrane peeling for vitreoretinal traction associated with combined hamartoma of the retina and retinal pigment epithelium (CHRRPE). *Klin Monatsbl Augenheild*. 2007;224:356–359.
57. Zhang X, Dong F, Dai R, et al. Surgical management of epiretinal membrane in combined hamartomas of the retina and retinal pigment epithelium. *Retina*. 2010;30:305–309.

58. Nam DH, Shin KH, Lee DY, et al. Vitrectomy, laser photocoagulation, and intravitreal triamcinolone for combined hamartoma of the retina and retinal pigment epithelium. *Ophthalmic Surg Lasers Imaging*. 2010;9:1–464.
59. Wu WC, Drenser KA, Trese MT, et al. Pediatric traumatic macular hole: results of autologous plasmin enzyme-assisted vitrectomy. *Am J Ophthalmol*. 2007;144:668–672.
60. Vinekar A, Quiram P, Sund N, et al. Plasmin-assisted vitrectomy for bilateral combined hamartoma of the retina and retinal pigment epithelium: histopathology, immunohistochemistry, and optical coherence tomography. *Retin Cases Brief Rep*. 2009;3:186–189.

SECTION 2

Tumors of the Choroid

OUTLINE

142

Choroidal Nevi

Christopher K.H. Burris, Daniel M. Albert

Introduction

Choroidal nevi are common tumors composed of collections of benign-appearing uveal melanocytes called nevus cells.[1,2] When encountered clinically, they are widely regarded as trivial lesions; however, they have the potential to cause substantial visual loss and can resemble or transform into malignant melanomas. Unlike nevi in the skin, their inaccessibility and proximity to delicate structures makes biopsy a daring feat. This has forced ophthalmologists to find clinical features, which may help to

forecast the future behaviors of these unpredictable tumors.

Definitions

Lorenz Zimmerman classified the term "nevus" in its historical context as being synonymous with a congenital tumor-like tissue malformation, or hamartoma. Barring a few cases (e.g., nevus sebaceous or nevus flammeus), this word is now used to designate benign acquired or congenital tumors of neural crest-derived cells, including atypical melanocytes. Because of the considerable variation in the morphologic appearance of cutaneous nevus cells, it is difficult to characterize a "typical" nevus cell. Zimmerman described the melanocyte as being a mature melanin-producing and melanin-containing cell. Melanocytes derive from melanoblasts, which are embryonic cells capable of producing melanin.[3] Torczynski depicted these cells as migrating during closure of the neural tube, with melanization beginning between the 24th and 27th week of gestation, and proceeding anteriorly until birth.

Prevalence

The exact prevalence of choroidal nevi has been variably estimated in clinical and histopathologic studies (Table 142.1).[4–18] In a longitudinal multicenter clinical study, Greenstein et al. found an overall prevalence of choroidal nevi in a mixed population of 2.1% via fundus photographs, but there was a significant difference in prevalence between the white (4.1%) and the nonwhite populations (Hispanics 1.2%, blacks 0.7%, Chinese 0.4%).[18] The increased prevalence of choroidal nevi in populations with fair complexions who have historically lived further away from the equator argues against sun exposure as a factor. In another large study looking at iris tumors, Carol Shields et al. postulated sun exposure could be a risk factor for melanocytic tumors because of their prevalence in the inferior iris quadrant, however, in that same series the inferior quadrant was also the most popular location for cystic, choristomatous, vascular, fibrous, myogenic, epithelial, xanthomatous, metastatic, lymphoid, leukemic, and secondary tumors, as well as non-neoplastic lesions simulating an iris tumor.[19]

TABLE 142.1
Prevalence of Choroidal Nevi

Reference	Prevalence (%)	Type of Study	Age (years)	Size of Study Population	Characteristics of Population
Albers (1940)[4]	1.1	Clinical	–	2300	–
Wilder (1946)[5]	0.2	Surgical eyes	18–38	3882	Recent trauma
Hale et al. (1965)[6]	8.5	Autopsy	>18	152	–
Hale et al. (1965)[6]	20	Autopsy	>18	100	–
Naumann (1970)[7]	11	Autopsy	Unselected	200	–
Ganley and Comstock (1973)[8]	3.1	Clinical	>30	287	Fundus scars and unselected
Gass (1977)[9]	0	Clinical	0–30	23	Unselected
Gass (1977)[9]		Clinical	>30	227	Unselected
Albert et al. (1980)[10]	8	Clinical	>45	1149	847 chemical workers; 302 controls
Lang and Daumann (1982)[11]	4.2	Clinical	18–41	3119	Pilots
Albert et al. (1983)[12]	5.4	Clinical	Mean of 48	197	White; cutaneous melanoma
Albert et al. (1983)[13]	1	Clinical	Mean of 48	147	White; "normal"
Rodriguez-Sains (1986)[14]	4.63	–	11–84	108	White; "normal"
Friedman et al. (1987)[15]	18.48	–	8.6	892	White; dysplastic nevus syndrome
Sumich et al. (1998)[16]	6.5	Clinical (population based)	49–97	3654	White; "normal"
Yoshikawa (2004)[17]	0.34	Clinical	28–86	3676	Japanese; "normal"
Greenstein et al. (2011)[18]	2.1	Clinical (population based)	45–84	6814	4.1% whites, 1.2% Hispanics, 0.7% blacks, 0.4% Chinese

Generally, higher rates for choroidal nevi are found in histopathologic than clinical studies. Naumann et al. attributed the clinical underevaluation to the obscuring of lesions by retinal pigment epithelium (RPE) and choriocapillaris, lack of adequate contrast between the nevus and the surrounding normal choroid, and the hypopigmentation of many nevi.[7] In their series, only 10 out of 29 nevi were clinically detected in eyes with clear media. Other factors contributing to the discrepancy are probably related to the examining technique, variations in the criteria for identifying

a nevus, and characteristics of the populations under study (Table 142.1). Except for melanocytosis and, presumably, melanocytomas, choroidal nevi are not seen at birth and, like acquired cutaneous nevi, develop or become pigmented in the first three decades of life.[9] No significant epidemiologic data establish a relation to sex. The influence of chemicals and endogenous or therapeutic hormones on the formation of nevi has yet to be established.[11,20]

Clinical Presentation

Choroidal nevi usually appear on ophthalmoscopy as flat or slightly elevated slate-gray tumors with defined, but not sharply demarcated, margins (Fig. 142.1A). They are generally located at the posterior pole, and vary in size between one-third to seven disc diameters. They are typically oval and not more than 2 mm thick.[16,21] Exceptional cases of giant choroidal nevi, diffuse uveal nevi, or melanocytomas have been reported.[22,23] The pigmentation of nevi may vary considerably, ranging from heavily pigmented melanocytomas to amelanotic nevi (Fig. 142.1B). Amelanotic nevi comprised 10% of the nevi in 3422 eyes of patients evaluated by Shields et al.[24] and 5.1% in the series of 373 patients of Brown et al.[25] In halo nevi, the lesion is surrounded by a depigmented yellow ring (Fig. 142.2A). Other associated findings include the presence of drusen (Fig. 142.1A), RPE disturbances, orange pigment (Fig. 142.2B), subretinal fluid, and choroidal neovascularization (Figs. 142.1E–F), which will be discussed further in the following sections.

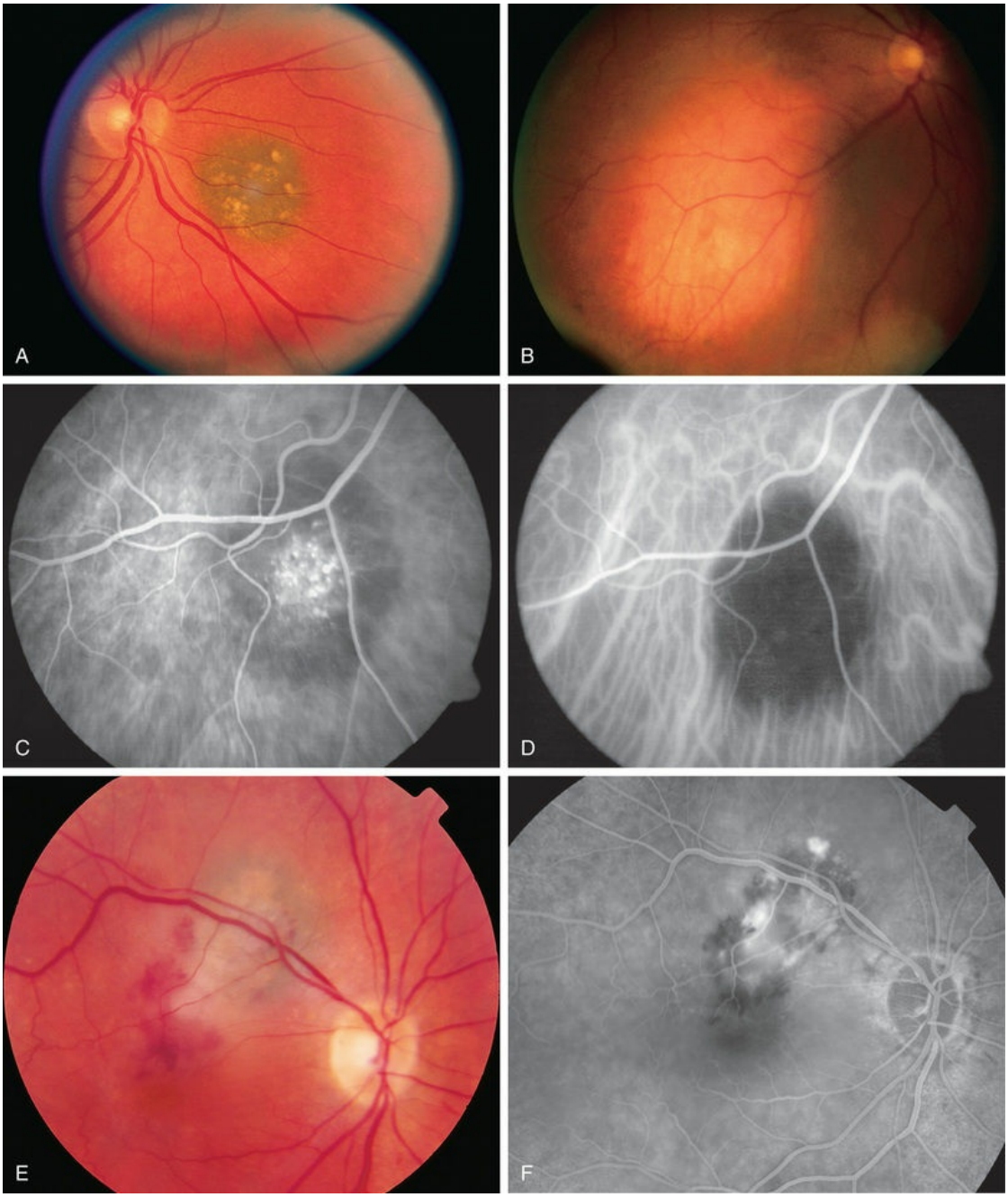

FIG. 142.1 (A) Choroidal nevus with overlying drusen. (B) Amelanotic nevus. (C) Fluorescein angiogram of a choroidal nevus. (D) Indocyanine green angiography of a choroidal nevus showing hypofluorescence. (E) Choroidal nevus with associated choroidal neovascularization. (F) Fluorescein angiogram of same lesion pictured in (E). (Panels C and D courtesy of Evangelos Gragoudas.)

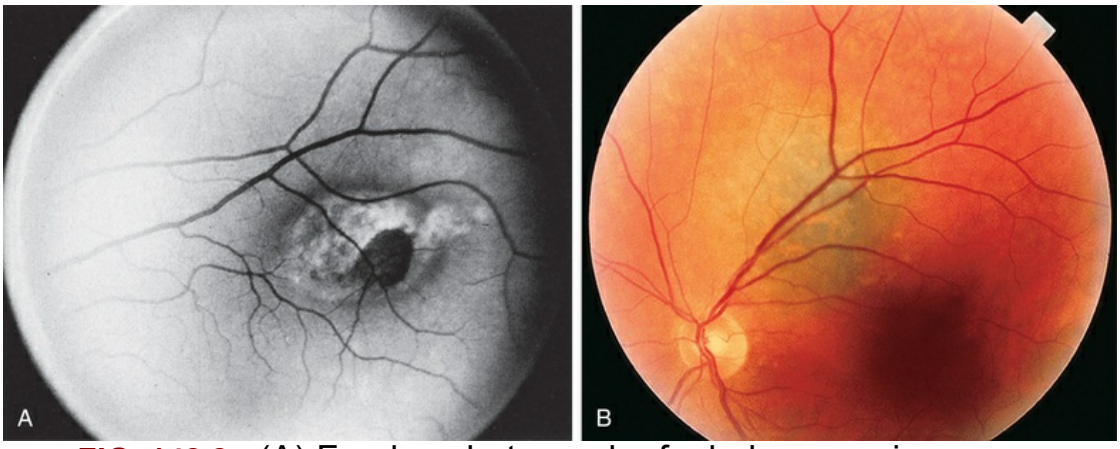

FIG. 142.2 (A) Fundus photograph of a halo nevus in a patient with cutaneous melanoma and vitiligo-like leukoderma. (B) Suspicious choroidal nevus with overlying orange pigment. Lesion followed 5 years without growth. (Panel A reproduced with permission from Fournier GA, Albert DM, Wagoner MD. Choroidal halo nevus occurring in a patient with vitiligo. Surv Ophthalmol 1984;28:671–2.)

Though most nevi are incidental findings made during routine ophthalmic examination, some can induce a visual field defect, and others lead to decreased visual acuity. In patients with choroidal nevi, the percentage of patients with defects in the visual field attributed to the nevi has varied considerably. Visual field defects were found in 16 (38%) of the 42 patients of Tamler and Maumenee;[26,27] in 19 (86%) of 22 patients of Flindall and Drance;[28] in 20 (24%) of 84 patients of Naumann et al.;[29] in 11% of 206 patients of Gonder et al.,[30] and in 148 (4.3%) of 3422 eyes in a review by Shields et al.[24] In that same Shields study, decreased visual acuity related to choroidal nevi was found in 215 (6.5%) of 3422 eyes, and was related to tumor location (26% subfoveal vs. 2% extrafoveal). Mechanisms of visual loss are related to functional or anatomic disturbances in the overlying RPE and retina.[21,30,31]

Natural History

Thirty-one percent of these lesions will enlarge over time without malignant transformation, and with an inverse relationship between growth and age.[32] Nevus thickness and presence of drusen tend to increase with age, but the presence of subretinal fluid, orange pigment, or RPE changes are similar throughout all age

groups.[24] In reviews by Masheyehki et al. and Shields et al.[32,33] slow growth of choroidal nevi over many years or decades, without the presence of other risk factors, may not be indicative of malignant transformation. Malignant transformation of choroidal nevi into melanomas is rare, Singh et al. estimated that one in 8845 will undergo malignant transformation every year.[34] Ultraviolet light has not been shown to be statistically significant for causing malignant change,[35] but fair skin, ability to tan, and light eye color are statistically significant risk factors.[36] Attempts have been made to define features suspicious for malignant change in order to establish reasonable criteria for clinical follow-up.[37]

Shields et al.[34] have identified risk factors predictive of growth of small choroidal melanocytic tumors.[38] If three or more factors are present, they estimate a greater than 50% risk of growth.[39] Additional factors predictive of growth were later found by Shields et al. and include ultrasonographic hollowness and the absence of drusen or surrounding halo. The mnemonic TFSOM UHHD for the phrase: "To Find Small Ocular Melanomas Using Helpful Hints Daily" correlates to *T*hickness >2 mm; subretinal *F*luid; visual *S*ymptoms; *O*range pigment (Fig. 142.2B); tumor *M*argin within 3 mm of the optic disc; *U*ltrasonographic *H*ollowness; absence of a surrounding *H*alo, and absence of *D*rusen.[33] Factors predictive of metastases include posterior tumor margin touching the optic disc, documented growth, and greater tumor thickness.[39]

Interestingly, Shields et al. have found different factors predictive of *iris* nevus growth following the mnemonic ABCDEF, which represents *A*ge (young), *B*lood (hyphema), *C*lock hour (inferior), *D*iffuse configuration, *E*ctropion uveae, and *F*eathery tumor margin.[40]

Nevus Types

Halo Nevus

Halo nevus is a rarely encountered subgroup of choroidal nevus, which is named after the depigmented annulus that surrounds the central pigmented core. It is believed that the halo is composed of large, polygonal cells with foamy cytoplasm, termed balloon nevus cells, which are similar to those found in halo nevi in other

anatomic locations.[41] In a review of 3422 eyes with choroidal nevi by Shields et al., 4.7% were halo nevi.[24] As with most other choroidal nevi, they were found almost exclusively in whites. A predilection for women (71%) was also found.

The development of the depigmented halo has been postulated to be secondary to an immune response, such as that incited by prior antigenic exposure to cutaneous melanoma, as there is a higher association of a prior diagnosis of cutaneous melanoma in patients with choroidal halo nevi. The reverse phenomenon, cutaneous halo nevi, have been documented following plaque radiotherapy for uveal melanoma.[42] Though vitiligo of the skin has been linked with autoimmune disease,[43] no such systemic association has been made for halo nevi.[41,44,45]

Giant Choroidal Nevus

There are no definitive criteria to designate which nevus falls under the category of "giant" choroidal nevus; however, Shields et al.[22] included those with a basal diameter greater than or equal to 10 mm. Based on their size, these outliers may be particularly difficult to distinguish from malignant melanoma. Thankfully this is a very rare situation, with the Blue Mountain Eye Study finding only 1.5% of choroidal nevi to be larger than 4 mm.[16]

Melanocytoma (Magnocellular Nevus)

Among nevi, melanocytomas are those that are composed mostly of uniform, densely pigmented, and plump polyhedral cells.[2,46] These darkly pigmented lesions are most often observed near the optic disc and have almost no malignant potential, but may simulate melanoma.[47] When located at the optic disc they most often cause enlargement of the physiologic blind spot, but may cause glaucomatous visual field changes and relative afferent pupillary defects.[48] They are relatively rare, representing only five of 907 pigmented intraocular tumors examined histopathologically by Howard and Forrest, and often demonstrate tumor necrosis and pigment dispersion with the associated sequelae.[49] Melanocytomas differ from choroidal nevi or melanomas in that they occur relatively more frequently in blacks, and they tend to grow more

rapidly than typical nevi.[49–52] They are probably congenital, but are not usually seen before the third decade of life. Though widely considered to be benign lesions, they should be monitored closely because transformation to melanoma has been documented in several case reports, one including a black teenager.[53–56] (Additional material concerning the malignant transformation of melanocytomas is included in Chapter 139, Melanocytoma of the optic disc.)

Ocular Melanocytosis

Melanocytosis designates a congenital hyperpigmentation of the uveal tract caused by an increased number of uveal melanocytes.[2,57] A slate-grey, brown, or blue patch of sclera due to this excess pigmentation is common. When accompanied by dermal melanocytosis in a distribution similar to that of the first or second division of the trigeminal nerve, this condition is termed oculodermal melanocytosis or nevus of Ota (nevus fuscoceruleus ophthalmomaxillaris) (Fig. 142.3A). The prevalence of ocular melanocytosis noted in clinical series was calculated to be 0.038% (two cases per 5251 persons) in whites, 0.014% in blacks (one case per 6915 persons), and 0.4% to 0.84% in Japanese.[58–61] The characteristic findings may be mistaken for complexion associated melanosis in darkly pigmented individuals. Ocular melanocytosis, unlike complexion-associated uveal pigmentation, is associated with an increased risk of melanomas.[2] Besides a 10% risk of open angle glaucoma,[62] patients with this condition have an increased (1/400) lifetime risk of transformation to malignant uveal melanoma.[63,64] When malignant transformation occurs, they carry twice the risk of metastasis when compared to patients matched for gender, tumor size, and location.[65,66] Orbital, meningeal, and cerebral melanomas have also been reported in patients with oculodermal melanocytosis.[67–72]

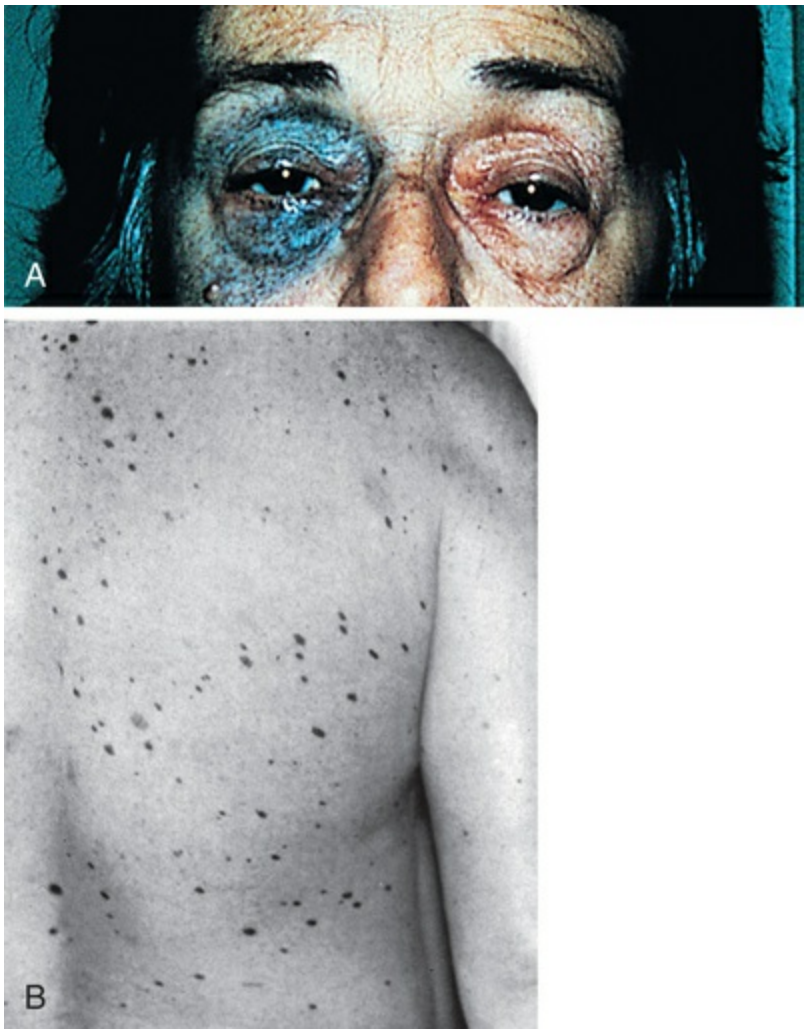

FIG. 142.3 (A) Nevus of Ota. (B) Cutaneous dysplastic nevi. (Panel A reproduced with permission from Gonder JR, Shields JA, Albert DM, et al. Uveal malignant melanoma associated with ocular and oculodermal melanocytosis. Ophthalmology 1982; 89:953–60. Panel B reproduced with permission from Albert DM, Chang MA, Lamping K, et al. The dysplastic nevus syndrome. A pedigree with primary malignant melanomas of the choroid and skin. Ophthalmology 1985;92:1728–34.)

Histopathology

Cytology

Adult melanocytes are normally found in the suprachoroidal lamellae, around blood vessels and in the outer layer of the choroidal stroma.[4] These stellate cells with long processes contain oval membrane-bound melanin granules.[49] Immunohistochemical staining against S-100 antigen is the most sensitive way to label cells

of neural crest origin, which include melanocytes. Nevus cells are larger and show other morphologic differences from normal melanocytes.[4] The Callender classification is the most widely used and studied for describing nevus cell types, but Naumann et al.[50] have classified them differently, including melanocytoma and balloon cell types.

Callender Classification (Original)

The Callender classification divides nevus cells into three types:

Spindle A – Thin cells with indistinct cell membranes. Slender nuclei often contain a linear fold, and the nucleoli are indistinct. Mitoses are extremely rare.

Spindle B – Plumper spindle cells than spindle A with indistinct cell membranes. Nuclei slightly larger than spindle A with coarser chromatin clumping and visible nucleoli. Occasional mitoses.

Epithelioid – Larger polygonal, pleomorphic cells with distinct cell boarders. Large round pleomorphic nuclei with prominent chromatin and nucleoli and abundant mitotic figures.

There have been modifications to this classification. Tumors are classified as spindle A, spindle B, mixed (if they contain less than 50% epithelioid cells), or epithelioid. Purely spindle A tumors are now called nevi, but if any of the other cell types include mild atypia the diagnosis would change to melanoma. This classification scheme is not without controversy, with Jensen,[73] Gass,[74] and McLean et al.[31] voicing concerns. One of the criticisms was that, although none of the initial spindle A melanomas proved fatal, Callender did not classify them as benign or describe a spindle cell nevus type. Gass was reluctant to accept the survival curve reported by Paul et al.[75] from the mortality data of the spindle A portion of 2652 patients (i.e., 81.2% were survivors at 15 years). He argued that (1) only a small sample of the tumor is generally studied, leaving many areas that could contain epithelioid cells unexamined; (2) many differences exist in the interpretation of the cell types by pathologists; (3) no more than 50% of the deaths are tumor-related because most patients are elderly, and are prone to

multiple neoplasms. McLean et al.[76] reevaluated the sections of 105 tumors, previously called spindle A melanomas, which had been followed up for at least 5 years after their original diagnosis. They found that 15 tumors contained epithelioid cells and should be classified as mixed tumors. The other 90 tumors were divided into the following two groups:

1. The first group, consisting of 15 tumors, had the following benign cytologic features: small size, slender nucleus, fine structure of nuclear chromatin, inconspicuous nucleoli, and no mitotic activity. These tumors measured no more than 10 mm in diameter and 3 mm in elevation. They were consequently reclassified as spindle cell nevi. No tumor-related death occurred in this group of patients.

2. The second group of tumors had atypical spindle cells, increased nuclear-to-cytoplasmic ratio, clumped chromatin, and distinct nucleoli. These were called spindle cell melanomas. In this group, 11 tumor-related deaths occurred, and metastases composed of spindle A cells were documented.

McLean et al. concluded that not all spindle A melanomas are benign, as was also suggested by Gass.[14] The other problem with the classification is, though simple, it does not give the full spectrum of nevus cell types.

Alternative Classification

Plump Polyhedral Nevus Cells

Plump polyhedral nevus cells are the most common nevus cells in melanocytoma, and usually represent about two-thirds of the mass. Electron microscopic studies have demonstrated ultrastructural differences in the cells composing melanocytomas. Juarez and Tso disclosed the following two cell types:[77]

1. Type 1 cells are large, polyhedral, and heavily pigmented. Bleaching with potassium permanganate is necessary to visualize the small, round, and uniform nuclei that lack prominent nucleoli (Fig. 142.4A).[29] This, combined with their paucity of cytoplasmic organelles and prominent giant melanosomes, suggests an inactive

state.

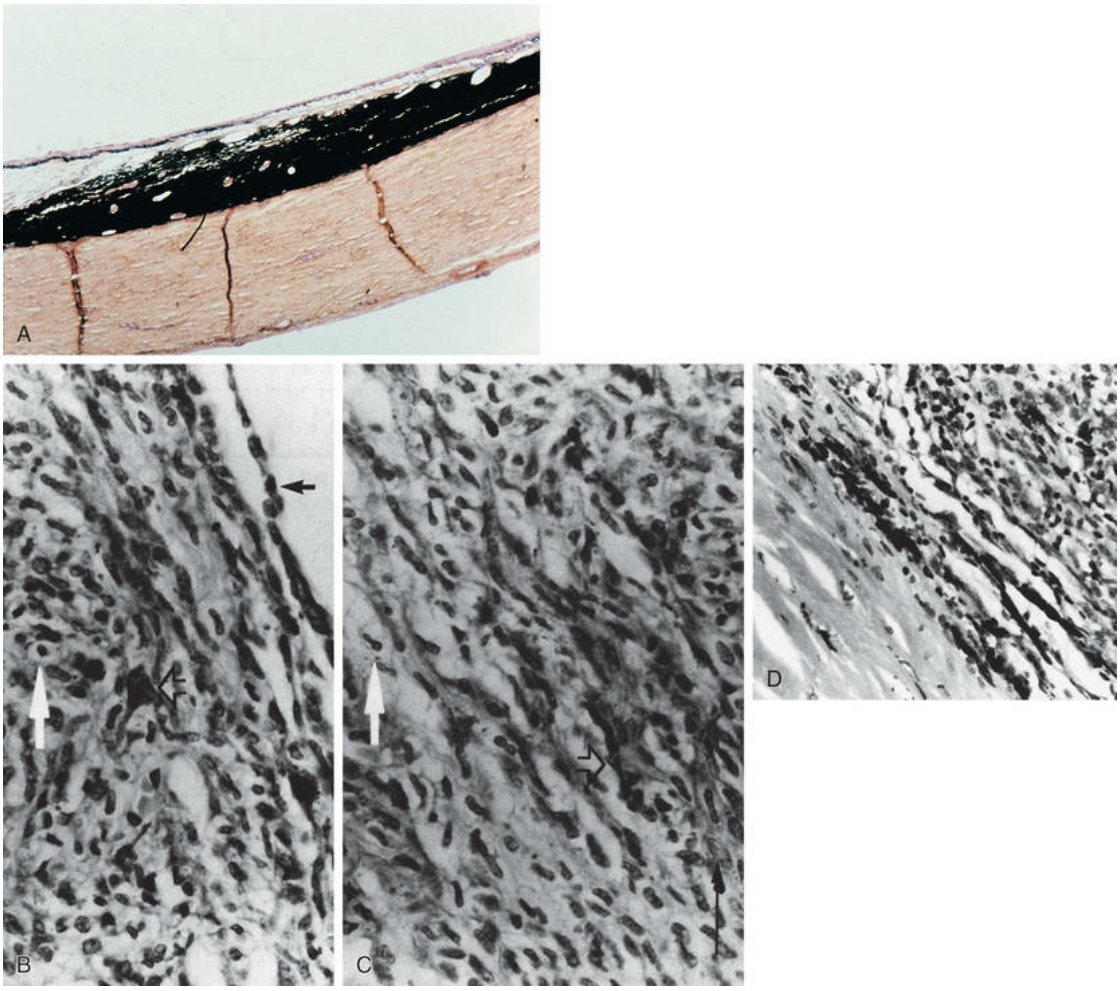

FIG. 142.4 (A) Melanocytoma, plump polyhedral cells. Light microscopy (hematoxylin and eosin, ×480). (B) Nevus. Spindle-shaped cells (*short black arrow*), plump dendritic cells (*open arrow*), and balloon cell (*white arrow*). (C) Same lesion as in (B). Plump dendritic cells (*open arrow*), plump fusiform cell (*thin black arrow*), and balloon cell (*white arrow*). (D) Nevus-like structure at the base of a melanoma that arose de novo (×480).

2. Type 2 cells are small, spindle-shaped, and sparsely pigmented. They possess marked infoldings of the nuclear membrane, conspicuous nucleoli, abundant mitochondria, prominent endoplasmic reticulum, free ribosomes, and small melanosomes, suggesting high metabolic activity. These cells are believed to be

responsible for the clinical growth observed in melanocytomas over time.

Slender Spindle Nevus Cells

Slender spindle nevus cells are the second most common cell type. These small, lightly pigmented or unpigmented cells have slender, intensely basophilic nuclei and are often distributed in the outer portions of the tumors (Fig. 142.4B).[1,29] When they make up the bulk of a nevus, the nevus is often amelanotic.[25,29,52]

Intermediate Nevus Cells

Between plump polyhedral and slender spindle-shaped nevus cells, there exists a spectrum of cells with larger nuclei showing a less marked chromatin pattern and occasionally small nucleoli. The cytoplasmic volume and pigmentation are at intermediate amounts between those of the principal nevus cell types. According to the shape of their cytoplasmic border, they are called either plump fusiform or plump dendritic nevus cells (Figs. 142.4B–C).[1,29]

Balloon Cells

Balloon cells are large, nonpigmented cells with abundant foamy cytoplasm (Figs. 142.4B–C). They are found in the peripheral halo surrounding skin nevi, cutaneous and choroidal melanomas, and, presumably, halo nevi in the choroid.[1,41,78] The significance of the cytoplasmic lipoid content is not certain, but some authors have interpreted balloon cell transformation to be an apoptotic change secondary to an autoimmune response to the antigens of abnormal melanocytic cells.[79,80] The finding of a halo nevus associated with cutaneous melanoma and vitiligo-like leukoderma is consistent with these hypotheses.[79,81]

In addition to cell type, Rummelt and coworkers showed that the vascular pattern of choroidal tumors seen on light microscopy might help to differentiate malignant and benign features.[82] They found that the presence of “normal” vessels, a “silent” pattern (i.e., zones of avascularity), straight and parallel vessels, and the lack of closed vascular loops and networks were correlated with the diagnosis of a nevus.

Secondary Histologic Changes in the Neighboring Tissues

Choriocapillaris

Thick nevi induce slight narrowing and, in some cases, complete obliteration of the choriocapillaris.[21,83]

Drusen

Drusen formation is frequently seen in the overlying Bruch's membrane; it was seen in 27 of the 101 nevi reported by Naumann et al.[21] Drusen most often are an indication of chronicity and an inactive tumor.[9]

Retina and Retinal Pigment Epithelium

The RPE overlying nevi may atrophy, become hyperplastic, or undergo fibrous metaplasia. In choroidal nevi and melanomas, clumps of lipofuscin have been shown in the RPE and in macrophages overlying the tumor. This is more likely to occur in melanomas, the orange pigment being most commonly associated with risk for tumor growth.[21,23,84,85] Serous detachment of the RPE[10,86] and the neurosensory retina can be observed, which is usually due to RPE dysfunction caused by the tumor mass effect, but in rare cases can be caused by choroidal neovascularization.[1,21,23,87–89] Typically subretinal and intraretinal fluid are seen as worrisome signs of tumor growth, however, when chronic subretinal fluid is resorbed it can cause thinning of the overlying retinal pigment epithelium called a “retinal pigment epithelial trough.” This is considered to be a sign of chronicity and stability.[90]

Controversial Aspects

Two controversial issues that bear on the clinical management and differential diagnosis of nevi are still debated.

Do All Choroidal Melanomas Arise From Nevi?

In 1966, Yanoff and Zimmerman,[64] reviewing the previous literature and 100 consecutive malignant melanomas of the choroid or ciliary

body, found a significant component of small, benign-appearing, and spindle-shaped nevus cells at the periphery and along the scleral edge in 73 cases. They inferred that "most malignant melanomas, perhaps all such neoplasms, have their origin in preexisting nevi."[91] This theory is the foundation upon which our practice of serial follow-up of quiescent nevi is based.

Many have come to question this theory after Albert et al. found nevus-like configuration at the base of metastatic foci of skin melanoma in the choroid where no nevi had been previously examined.[92] Albert et al.[93] subsequently experimentally injected melanoma cells into the choroid of mice and found tumors comprised of predominately round epithelioid cells with a zone of flattened, benign, nevus-appearing cells appearing at the margins. De novo choroidal melanoma has been reported, in which a large choroidal melanoma arose over a 16-month period.[94] Previous fundus photographs and angiograms documented the absence of any pigmented tumor in this fundus, and a pigmented nevus-like structure again was found at the base of the tumor (Fig. 142.4D).[94] The possibility that preexistent nevi had escaped clinical examination, as claimed in a similar case by Yanoff and Zimmerman, was unlikely.[95]

A nevus-like configuration associated with a melanoma may have several interpretations:

1. In many instances, including skin melanomas, melanomas may arise from nevi.

2. In other instances, choroidal or skin melanomas arise de novo. At their base and periphery, these can induce a nevus-like structure by flattening normal uveal melanocytes or by the modification of the tumor cells while they infiltrate the sclera (Fig. 142.4D).

3. Nevus-like structures may result as a secondary proliferative effect of the malignancy or because of a common oncogenic stimulus.[96] These mechanisms have been postulated in a few cases of bilateral diffuse melanocytic tumors of the uvea composed of relatively benign-looking, spindle-shaped cells in patients with systemic carcinoma.[97,98]

Secondary Clinical Changes in the Neighboring Tissues

Retinal Pigment Epithelial and Bruch's Membrane

Secondary changes in the overlying tissues can result in the appearance of irregular pigmentation of the nevus. Green light photographs have proved helpful in demonstrating some of these changes.[99] Fluorescein angiography or indocyanine green angiography of nevi may demonstrate hypofluorescence induced either by the pigmentation of the nevus or by a local circulatory disturbance in the choroid. A mottled appearance of the nevus or hyperfluorescence from drusen and retinal pigment epithelial defects is sometimes seen (Figs. 142.1C–D).[83,86]

Drusen overlying pigmented nevi are common and were seen in 50–60% of the patients in the series of Naumann et al.,[21] Shields et al.,[24] and Mashayekhi et al. (Fig. 142.1A).[90] Discrete areas of pigment epithelial atrophy or bone-spicule pattern of pigment migration at the margin of a nevus may occur due to prolonged associated serous detachment. Gass suggests that this damage may be greatest during the period of maximum tumor growth early in a patient's life.[9]

Atrophy, hyperplasia, and fibrous metaplasia of the RPE can be seen clinically overlying and/or adjacent to choroidal nevi, and each was observed in 6–10% of cases in a review by Shields et al.[24] and Mashayekhi.[90] These findings may indicate chronicity and are therefore more likely to be associated with choroidal nevi than melanomas.

Orange pigment, corresponding to lipofuscin, can be seen overlying melanocytic lesions (Fig. 142.2B), and was observed in 6% of 3422 eyes in a review by Shields et al.[24] and in 4% of 240 small choroidal melanocytic lesions in a study by Singh et al.[100] Large geographic areas of orange pigment are more commonly found above uveal melanomas[84] and, according to Smith and Irvine,[85] Gass,[23] and Shields and Shields,[91] may indicate malignant transformation or the malignant nature of a suspicious lesion.

Serous Detachment

In rare instances, a serous detachment of the overlying RPE or even

of the neurosensory retina can be found; 2.14% of 933 nevi in the series of Pro et al.[86] and 10.3% of 3422 eyes in a review by Shields et al.[24] were found to have subretinal fluid. Fluorescein angiograms demonstrate the classic features of these detachments with localized or diffuse leaks. These leaks may be related to the chronic, degenerative changes in the RPE.[10,86]

Choroidal Neovascular Membrane

Rarely, subretinal neovascular membranes may be associated with choroidal nevi (Figs. 142.1E–F). The choroidal neovascularization appears similar to the choroidal neovascularization that develops in macular degenerative conditions.[23,88,101]

Choroidal Nevi and Systemic Disease

Uveal Nevi and Neurofibromatosis

Uveal nevi are considered to be quite common in association with neurofibromatosis. Melanocytes, composing the nevi, share a neural crest origin with the other tumors found in von Recklinghausen disease (neurocristopathies).[102–104]

Dysplastic Nevus Syndrome

Reese reported an association of uveal nevi with cutaneous nevi.[105] The observation that cutaneous dysplastic nevi are related to increased risk of cutaneous melanoma gave a new impetus to the investigation of the association of ocular and cutaneous nevi, and it was the screening of these patients which led to the identification of families genetically predisposed to melanoma, and to the characterization of the dysplastic nevus. Clinically, a dysplastic nevus must be suspected if a melanocytic nevus harbors at least two of the following four features:[1,106,107] (1) ill-defined or irregular borders; (2) irregular pigmentation; (3) accentuated skin markings; and (4) large size (>5 mm). They tend to occur on sun-shielded skin (e.g., the scalp or bathing trunk area) (Fig. 142.3B).

Histopathologically, dysplastic nevi are divided into two types: (1) a mild type with aberrant differentiation (e.g., lentiginous

melanocytic hyperplasia), and (2) a severe type with melanocytic nuclear atypia, in addition to aberrant differentiation.[1] These dysplastic nevi are markers of both familial and nonfamilial melanoma risk.[108]

That the uvea might be involved in familial melanoma or dysplastic nevus patients is suggested by the following: (1) a report of a type of dysplastic nevus syndrome with primary malignant melanomas of the choroid and the uvea;[109] (2) an increased (although not statistically significant) frequency of iris nevi and choroidal nevi in patients with cutaneous melanoma;[13] and (3) a statistically significant increase in the percentage of dysplastic nevus syndrome in patients harboring iris and choroidal nevi.[14] Although inconclusive and controversial, attentive ophthalmologic evaluation in patients with dysplastic nevi is warranted.[110]

Paraneoplastic Bilateral Diffuse Uveal Melanocytic Proliferations

Bilateral diffuse uveal melanocytic proliferation (BDUMP) is a rare paraneoplastic syndrome described in elderly patients with advanced systemic carcinomas.[111–114] Gass did not consider these tumors to be malignant on the basis of the relatively benign appearance of spindle cells and the rare mitotic figures, however, Zimmerman noted foci of plump spindle B and epithelioid cells in these tumors.[61,115] No metastases from these uveal tumors have been found at autopsy. In these cases, patchy areas of degeneration of the RPE and photoreceptors account for the rapid, irreversible visual loss, although a bilateral cataract is generally present. (Bilateral diffuse melanocytic proliferation is discussed in Chapter 158, Miscellaneous uveal tumors.)

Clinical Differential Diagnosis

The diagnosis of choroidal nevi is usually easily made with ophthalmoscopic examination. In rare instances, various other types of lesions can mimic nevi. In addition to the conditions discussed in the following paragraphs, material on the differential diagnoses of choroidal nevi can be found in the following chapters:

Chapter 140, Congenital hypertrophy of the retinal pigment epithelium; Chapter 141, Combined hamartoma of the retinal pigment epithelium and retina; Chapter 155, Choroidal metastases; Chapter 157, Circumscribed choroidal hemangioma, and in the sections examining choroidal melanomas, see Chapter 148, Enucleation for choroidal melanomas.

Freckles

Freckles are flat foci of increased choroidal pigmentation with irregular borders. Histologically, there is no hyperplasia of uveal melanocytes, but an increase in density of the melanocytes. They do not disturb the normal choroidal architecture, and choroidal vessels can be seen passing through them.[116] The main relevancy of this distinction is the lack of malignant potential of these lesions.[91]

Subretinal Hemorrhages

While red-colored hemorrhages are rarely mistaken for nevi, large areas of dark-colored hemorrhagic detachment of the RPE may be mistaken for a large nevus or melanoma.[23] Diagnostic ultrasonography is usually helpful in demonstrating high reflectivity of hemorrhage versus the medium-to-low reflectivity of a melanocytic tumor. Optical coherence tomography (OCT) can be helpful as well.

Congenital Hypertrophy of the Retinal Pigment Epithelium

Congenital hypertrophy of the retinal pigment epithelium (CHRPE) and CHRPE-like lesions may be confused with nevi but are usually able to be distinguished on ophthalmoscopic examination. CHRPE are typically unilateral, darkly pigmented, round, well-circumscribed, flat lesions at the level of the RPE. They often have a surrounding pigmented or nonpigmented halo or a double halo consisting of pigmented and nonpigmented rings. They may enlarge over time and tend to accumulate intralesional lacunae. CHRPE-like lesions, associated with familial adenomatous polyposis (FAP), are similar in appearance, but are bilateral,

multiple, and pisciform in shape.[117]

Small Melanomas

Small melanoma should always be kept in the differential since the clinical distinction between a small melanoma and a large nevus may be subtle. While small melanocytic lesions classified as choroidal nevi may show slow, limited growth, especially in a younger patient,[9] the rapid growth of an indeterminate lesion (large nevus versus small melanoma) is generally the determining factor in reclassifying the lesion as a melanoma and considering treatment.[85,86,95,96] Clinical observations that may help differentiate a small melanoma from a choroidal nevus are indications of dormancy (nevus) or growth (melanoma). A melanoma should be suspected if (1) the thickness of the tumor is >2 mm;[85,86,97–99] (2) there is orange pigment overlying the tumor (Fig. 142.2B);[9,23,85] (3) a clinical neurosensory detachment is present without evidence of choroidal neovascularization (detachment only seen on ancillary studies does not meet this criteria); or (4) visual symptoms are present.[21,98] Evidence of biologic dormancy favoring a diagnosis of nevus includes (1) drusen overlying the tumor;[14] (2) choroidal neovascularization;[100] and (3) smaller size.

Ancillary Studies

Careful follow-up observation with photography is most important for accurate determination of growth or change. This is more reliable than descriptions about shape or size; however, slight misalignment of the axis of the fundus camera can filter the pigmented edges of melanocytic tumors, leading to an erroneous diagnosis of growth or malignant transformation, with subsequent unnecessary treatment.[101] Other diagnostic tests may be helpful in the initial evaluation and follow-up of a presumed nevus.

Ultrasound is invaluable in determining tumor thickness and documenting subsequent growth, and is the most sensitive imaging modality for ruling out extraocular extension (more sensitive than MRI).[118] Due to interoperator variability it is recommended that the same machine be used by the same operator for every measurement

if possible.[119] Initial height >2.0 mm is more likely to be a small melanoma.[14,85,86,97–99] Acoustic hollowness due to low internal reflectivity on ultrasound is more suggestive of melanoma than a choroidal nevus.[102]

Duplex ultrasound and color Doppler may help in the differential diagnosis of choroidal tumors by quantifying tumor blood flow. Wolff-Korman and colleagues detected a pulsatile blood flow at the tumor base of 62 choroidal melanomas where no Doppler signals were elicited in a series of 18 choroidal nevi.[120]

Redlight photography has been described as helpful in the analysis of choroidal vascularization.[83] The vascularization of choroidal tumors has been studied with indocyanine green (ICG) angiography. Choroidal melanomas may demonstrate abnormal vascular patterns such as dilation, tortuosity, vascular loops, and branching;[121] delayed maximal fluorescence;[122] and marginal late dye leakage.[123] Confocal ICG scanning enables serial sectioning through the tumor. This technique may be capable of further detecting microvascular patterns predictive of growth.[124] A small flat choroidal nevus may appear hypofluorescent throughout the ICG angiogram (Fig. 142.1D).[125]

Fluorescein angiography of choroidal nevi without overlying RPE changes, occupying the inner or full thickness of the choroid, will demonstrate hypofluorescence throughout the angiogram. Overlying drusen usually fluoresce early in the angiogram and stain in the late stages (Fig. 142.1C). Fluorescein angiography is helpful in demonstrating choroidal neovascularization (Fig. 142.1F), RPE alterations, or permeability of the RPE overlying a nevus.[23,126] Multiple points of leakage (hot spots) from the surface of a tumor may indicate more acute pigment epithelial damage and a higher probability of growth.[9,127]

Standard OCT is not helpful for detecting the internal characteristics of melanocytic tumors.[128] OCT readily demonstrates retinal and RPE/choriocapillaris abnormalities associated with choroidal nevi. Retinal findings include intraretinal cysts, retinal edema, retinal thinning, photoreceptor attenuation, and subretinal fluid (Fig. 142.5A). Abnormalities of the RPE/choriocapillaris include drusen, RPE fragmentation and detachments, and thickening of the RPE/choriocapillaris (Fig. 142.5A). In a review by

Shields et al.[129] regarding the OCT qualities in 120 patients with choroidal nevi, two-thirds of the nevi were hyporeflective, one-third were isoreflective, about 10% were hyperreflective, and about half revealed hyperreflectivity at the level of the RPE/choriocapillaris. They found that OCT was more sensitive than ophthalmoscopy in detecting almost all retinal/RPE abnormalities except for the presence of drusen. Retinal edema, photoreceptor attenuation, and drusen suggest chronicity, whereas subretinal fluid without retinal atrophy may suggest a more active lesion. EDI SD-OCT (enhanced depth imaging spectral-domain optical coherence tomography), a method that allows for the evaluation of deeper portions of the choroid, may be useful in measuring the diameter and height of lesions that are too small to be detected by ultrasonography (Fig. 142.5B).[130] EDI SD-OCT has also been shown to be more precise in the measurement of posterior choroidal nevi than ultrasound, with ultrasound generally overestimating the height of lesions.[131]

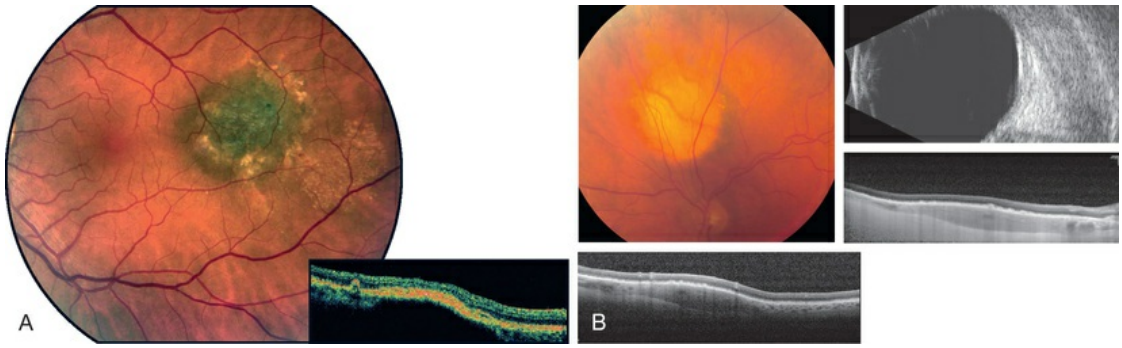

FIG. 142.5 (A) Optical coherence tomography (OCT) image of a choroidal nevus showing drusen, attenuation of the photoreceptor layer, and thickening/hyperreflectivity of the retinal pigment epithelium/choriocapillaris overlying a choroidal nevus. (B) Spectral domain OCT enhanced depth imaging demonstrating a choroidal nevus corresponding to a fusiform choroidal lesion with medium to low reflectivity. The demarcation of the inner sclera is visible. (Panel A adapted from Yannuzzi LA. The retinal atlas. Philadelphia: Saunders/Elsevier; 2010, p. 671. Panel B reproduced with permission from Torres VLL, Brugnoni N, Kaiser PK et al. Optical coherence tomography enhanced depth imaging of choroidal tumors. Am J Ophthalmol 2011;151:586–93.)

Swept-source OCT (SS-OCT) improves on this technology, being significantly better than EDI SD-OCT at depicting intralesional characteristics in melanotic lesions by using a longer wavelength to penetrate melanin.[132]

Fundus autofluorescence (FAF) imaging is a relatively new technique that allows visualization of light emitted from certain substances that possess autofluorescent properties, particularly lipofuscin.[133] Drusen may be slightly hyper-, iso-, or hypofluorescent, while orange pigment is brightly autofluorescent, and much brighter than the fluorescence seen with drusen (Fig. 142.6). In amelanotic lesions, lipofuscin may appear clinically as hyperpigmented areas and go unrecognized without the use of FAF imaging. Subretinal fluid is hyperfluorescent with the peripheral rim of fluid being slightly more hyperfluorescent. Hypofluorescence was found in more chronic RPE degenerative changes, such as RPE hyperplasia, fibrous metaplasia, and RPE atrophy.[134,135] No characteristic autofluorescent patterns were found for choroidal nevi or melanoma in Gunduz's study, however, Albertus et al were able to distinguish between clinically benign and malignant lesions based off of digital autofluorescence measured in "Index of Retinal Autofluorescence" (IRA) units.[135,136]

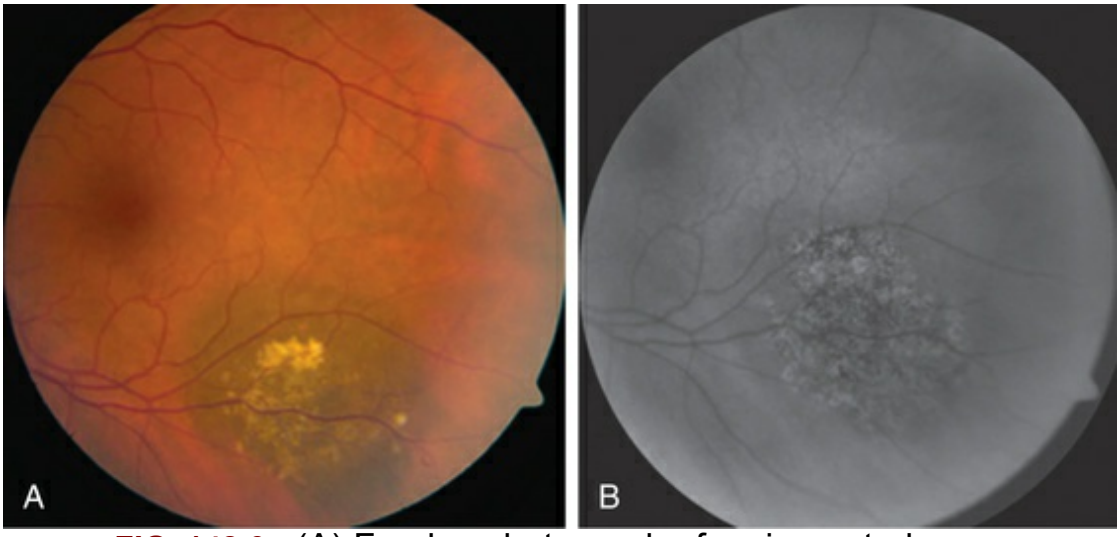

FIG. 142.6 (A) Fundus photograph of a pigmented choroidal nevus with overlying drusen. (B) The drusen demonstrate moderate autofluorescence. (Panels A and B reproduced with permission from Shields CL, Pirondini C, Bianciotto C, et al. Autofluorescence of choroidal nevus in 64 cases. Retina 2008;28:1035–43.)

As advocated by most authors, the best way to determine the malignant nature of a melanocytic tumor is a careful follow-up, showing either significant growth or a virtually unchanged appearance. Due to the normal limited, slow growth of benign nevi, a definite distinction between a nevus and a small melanoma may be problematic.

Management of Nevi

The management of choroidal nevi is generally governed by the same concepts of conservative management that are applied to small melanomas. If growth indicates that the lesion is a melanoma, then the treatment is for a malignancy.

Nonsuspicious Nevi

Observe nonsuspicious nevi on a yearly basis. Documentation with photographs serves as an aid in follow-up.

Suspicious Nevi

Evaluate suspicious nevi with dilated ophthalmoscopy, fundus photographs (Fig. 142.2B), and ultrasound every 6 months for suspicious changes. Fluorescein angiography (Fig. 142.1C), ICG angiography (Fig. 142.1D), fundus autofluorescence (Figs. 142.6A–B), and OCT (Fig. 142.5A) may be of value when the clinical picture merits their use.

Serous Detachment and Choroidal Neovascular Membrane

Due to the rarity of choroidal neovascularization (Figs. 142.1E–F) and serous retinal detachments associated with choroidal nevi, treatment options of these conditions have not been well studied. Intravitreal injection of anti-VEGF agents has widely been used for treatment of choroidal neovascular membrane (CNVM) associated with a variety of conditions and also appears to be effective for

treatment of CNVM associated with choroidal nevi.[137–139] Photodynamic therapy with verteporfin may also be effective for the treatment of choroidal neovascularization secondary to choroidal nevus.[140,141] Though transpupillary thermotherapy (TTT) is not first line for melanoma treatment due to its inability to reach intrascleral tumor,[142] subthreshold TTT has been shown to be effective in controlling subretinal fluid associated with pigmented choroidal lesions.[143] In cases of angiographically demonstrated leaks, argon laser photocoagulation can be directed at those areas, according to criteria similar to those used in the treatment of central serious choroidopathy.[10,86] Successful treatment of CNVM using transpupillary thermotherapy has also been reported.[144]

Acknowledgment

This work was supported by the National Institutes of Health grant P30 EY016665 (Core Grant for Vision Research) and an unrestricted department award from the Research to Prevent Blindness.

References

1. Green W. Uveal tract. Spencer W. *Ophthalmic pathology: an atlas and text*. WB Saunders: Philadelphia; 1997.
2. Zimmerman L. Melanocytes, melanocytic nevi, and melanocytomas. *Invest Ophthalmol*. 1965;4:11–44.
3. Torczynski E. Choroid and suprachoroid. Jakobiec F. *Ocular anatomy, embryology, and teratology*. Harper & Row: Philadelphia; 1982.
4. Albers E. Benign melanomas of the choroid and their malignant transformation. *Am J Ophthalmol*. 1940;23:779–783.
5. Wilder H. Intraocular tumors in soldiers: World War II. *Mil Surg*. 1946;99:459–490.
6. Hale P, Allen R, Straatsma B. Benign melanoma (nevi) of the choroid and ciliary body. *Arch Ophthalmol*. 1965;74:532–538.
7. Naumann G. Pigmentierte naevi der aderhaut und des ciliarkorpers. *Adv Ophthalmol*. 1970;23:187–272.

8. Ganley J, Comstock G. Benign nevi and malignant melanomas of the choroid. *Am J Ophthalmol*. 1973;76:19–25.
9. Gass J. Problems in the differential diagnosis of choroidal nevi and malignant melanomas. *Am J Ophthalmol*. 1977;83:299–323.
10. Folk J, Weingeist T, Coonan P, et al. The treatment of serous macular detachment secondary to choroidal melanoma and nevi. *Ophthalmology*. 1989;96:547–551.
11. Albert D, Robinson N, Fulton A, et al. Epidemiologic investigation of increased incidence of choroidal melanoma in a single population of chemical workers. *Int Ophthalmol Clin*. 1980;20:71–92.
12. Lang G, Daumann F. The peripheral retina and choroid in "healthy eyes" (airline pilots). *Klin Monatsbl Augenheilkd*. 1982;181:493–495.
13. Albert D, Searl S, Forget B, et al. Uveal findings in patients with cutaneous melanoma. *Am J Ophthalmol*. 1983;95:474–479.
14. Rodriguez-Sains R. Ocular findings in patients with dysplastic nevus syndrome. *Ophthalmology*. 1986;93:661–665.
15. Friedman R, Rodriguez-Sains R, Jakobiec F. Ophthalmologic oncology: conjunctival malignant melanoma in association with sporadic dysplastic nevus syndrome. *J Dermatol Surg Oncol*. 1987;13:31–34.
16. Sumich P, Mitchell P, Wang J. Choroidal nevi in a white population: The Blue Mountain Eye Study. *Arch Ophthalmol*. 1998;116:645–650.
17. Yoshikawa H. *The incidence of choroidal nervus in Japan*. [Poster presented at; American Academy of Ophthalmology meeting, October] 2004 [New Orleans, Louisiana].
18. Greenstein MB, Myers CE, Meuer SM, et al. Prevalence and characteristics of choroidal nevi: the multi-ethnic study of atherosclerosis. *Ophthalmology*. 2011;118(12):2468–2473.
19. Shields CL, Kancherla S, Patel J, et al. Clinical survey of 3680 iris tumors based on patient age at presentation. *Ophthalmology*. 2012;119(2):407–414.
20. Consensus Conference. Precursors to malignant melanoma.

JAMA. 1984;251:1864–1866.
21. Naumann G, Yanoff M, Zimmerman L. Histogenesis of malignant melanomas of the uvea. I. Histopathologic characteristics of nevi of the choroid and ciliary body. *Arch Ophthalmol*. 1966;6:784–796.
22. Li HK, Shields CL, Mashayekhi A, et al. Giant choroidal nevi: clinical features and natural course in 322 cases. *Ophthalmology*. 2010;117:324–333.
23. Gass J. *Stereoscopic atlas of macular disease*. Mosby: St. Louis; 1997.
24. Shields CL, Furuta M, Mashayekhi A, et al. Clinical spectrum of choroidal nevi based on age at presentation in 3422 consecutive eyes. *Ophthalmology*. 2008;115:546–552.
25. Brown G, Shields J, Augsburger J. Amelanotic choroidal nevi. *Ophthalmology*. 1981;88:1116–1121.
26. Tamler E. A clinical study of choroidal nevi: a follow-up report. *Arch Ophthalmol*. 1970;84:29–32.
27. Tamler E, Maumenee A. A clinical study of choroidal nevi. *Arch Ophthalmol*. 1959;62:196–202.
28. Flindall R, Drance S. Visual field studies of benign choroidal melanoma. *Arch Ophthalmol*. 1969;81:41–44.
29. Naumann G, Zimmerman L, Yanoff M. Visual field defect associated with choroidal nevus. *Am J Ophthalmol*. 1966;62:914–917.
30. Gonder J, Augsberger J, McCarthy E, et al. Visual loss associated with choroidal nevi. *Ophthalmology*. 1982;89:961–965.
31. McLean I, Zimmerman L, Evans R. Reappraisal of Callender's spindle A type of malignant melanoma of the choroid and ciliary body. *Am J Ophthalmol*. 1978;86:557–564.
32. Mashayekhi A, Siu S, Shields CL, et al. Slow enlargement of choroidal nevi: a long-term follow-up study. *Ophthalmology*. 2011;118(2):382–388.
33. Shields CL, Furuta M, Berman EL, et al. Choroidal nevus transformation into melanoma: analysis of 2514 consecutive cases. *Arch Ophthalmol*. 2009;127:981–987.
34. Singh AD, Kalyani P, Topham A. Estimating the risk of malignant transformation of a choroidal nevus.

Ophthalmology. 2005;112:1784–1789.
35. Shah CP, Weis E, Lajous M, et al. Intermittent and chronic ultraviolet light exposure and uveal melanoma: a meta-analysis. *Ophthalmology*. 2005;112(9):1599–1607.
36. Weis E, Shah CP, Lajous M, et al. The association between host susceptibility factors and uveal melanoma: a meta-analysis. *Arch Ophthalmol*. 2006;124(1):54–60.
37. Mims J, Shields J. Follow-up studies of suspicious choroidal nevi. *Ophthalmology*. 1978;85:929–943.
38. Shields CL, Cater J, Shields JA, et al. Combination of clinical factors predictive of growth of small choroidal melanocytic tumors. *Arch Ophthalmol*. 2000;118:360–364.
39. Shields CL, Shields JA, Kiratli H, et al. Risk factors for growth and metastasis of small choroidal melanocytic lesions. *Ophthalmology*. 1995;102:1351–1361.
40. Shields CL, Kaliki S, Hutchinson A, et al. Iris nevus growth into melanoma: analysis of 1611 consecutive eyes: the ABCDEF guide. *Ophthalmology*. 2013;120(4):766–772.
41. Shields CL, Maktabi AM, Jahnle E, et al. Halo nevus of the choroid in 150 patients. *Arch Ophthalmol*. 2010;7:859–864.
42. Sarici AM, Shah SU, Shields CL, et al. Cutaneous halo nevi following plaque radiotherapy for uveal melanoma. *Arch Ophthalmol*. 2011;129(11):1499–1501.
43. Alkhateeb A, Fain PR, Thody A, et al. Epidemiology of vitiligo and associated autoimmune diseases in Caucasian probands and their families. *Pigment Cell Res*. 2003;16(3):208–214.
44. Schrader W, Helwig E. Balloon cell nevi. *Cancer*. 1967;20:1502–1514.
45. Green W. Uveal tract. Spencer W. *Ophthalmic pathology: an atlas and text*. WB Saunders: Philadelphia; 1997.
46. Cogan D. Discussion of pigmented ocular tumors. Boniuk M. *Ocular and adnexal tumors: new and controversial aspects*. Mosby: St. Louis; 1964.
47. Shields JA, Eagle RC Jr, Shields CL, et al. Diffuse choroidal melanocytoma simulating melanoma in a child with ocular melanocytosis. *Retin Cases Brief Rep*. 2010;4(2):164–167.
48. Osher RH, Shields JA, Layman PR. Pupillary and visual field

evaluation in patients with melanocytoma of the optic disc. *Arch Ophthalmol*. 1979;97(6):1096–1099.
49. Howard G, Forrest A. Incidence and location of melanocytomas. *Arch Ophthalmol*. 1967;77:61–66.
50. Shields J, Shields C, Eagle R, et al. Malignant melanoma associated with melanocytoma of the optic disc. *Ophthalmology*. 1990;97:225–230.
51. Yoshida K. Nevus fuscocaerulus ophthalmomaxillaris Ota. *Tohoku J Exp Med*. 1952;55:34–43.
52. Joffe L, Shields JA, Osher JH, et al. Clinical and follow up studies of melanocytomas of the optic disc. *Ophthalmology*. 1979;86:1067–1078.
53. Li HK, Shields CL, Shields JA, et al. Iridociliochoroidal melanoma arising from melanocytoma in a black teenager. *J AAPOS*. 2010;14(2):178–180.
54. Barker-Griffith A, McDonald P, Green W. Malignant melanoma arising in a choroidal magnocellular nevus (melanocytoma). *Can J Ophthalmol*. 1976;11:140–146.
55. Cialdini A, Sahel J, Jalkh A, et al. Malignant transformation of an iris melanocytoma. *Graefes Arch Clin Exp Ophthalmol*. 1989;227:348–354.
56. Loeffler K, Tecklenborg H. Melanocytoma-like growth of a juxtapapillary malignant melanoma. *Retina*. 1992;12:29–34.
57. Dutton J, Anderson R, Schleper R, et al. Orbital malignant melanoma and oculodermal melanocytosis: report of two cases and review of the literature. *Ophthalmology*. 1984;90:497–507.
58. Gonder J, Ezell P, Shields J, et al. Ocular melanocytosis: a study to determine the prevalence rate of ocular melanocytosis. *Ophthalmology*. 1982;89:950–952.
59. Mishima Y, Mevorah B. Nevus of Ota and nevus of Ito in American Negroes. *J Invest Dermatol*. 1961;36:133–154.
60. Ota M, Tanino H. Nevus fuscocaerulus ophthalmomaxillaris. *Tokyo Med J*. 1939;63:1243–1245.
61. Zimmerman L. Malignant melanoma of the uveal tract. Spencer W. *Ophthalmic pathology: an atlas and text*. WB Saunders: Philadelphia; 1986.
62. Khawly JA, Imami N, Shields MB. Glaucoma associated

with the nevus of Ota. *Arch Ophthalmol*. 1995;113(9):1208–1209.
63. Hidano A, Kajima H, Ikeda S, et al. Natural history of nevus of Ota. *Arch Dermatol*. 1967;95(2):187–195.
64. Gonder JR, Shields JA, Albert DM, et al. Uveal malignant melanoma associated with ocular and oculodermal melanocytosis. *Ophthalmology*. 1982;89(8):953–960.
65. Shields CL, Kaliki S, Livesey M, et al. Association of ocular and oculodermal melanocytosis with the rate of uveal melanoma metastasis: analysis of 7872 consecutive eyes. *JAMA Ophthalmol*. 2013;131(8):993–1003.
66. Mashayekhi A, Kaliki S, Walker B, et al. Metastasis from uveal melanoma associated with congenital ocular melanocytosis: a matched study. *Ophthalmology*. 2013;120(7):1465–1468.
67. Yanoff M, Zimmerman L. Histogenesis of malignant melanomas of the uvea. III. Relationship of congenital ocular melanocytosis and neurofibromatosis to uveal melanomas. *Arch Ophthalmol*. 1967;77:331–336.
68. Kojima K, Natsume C, Honda A, et al. A melanoma of the optic chiasm in a case of Ota's nevus and melanosis oculi. *Jpn J Clin Ophthalmol*. 1959;13:502–504.
69. Enriquez R, Egbert B, Bullock J. Primary malignant melanoma of the central nervous syndrome: pineal involvement in a patient with nevus of Ota and multiple pigmented skin nevi. *Arch Pathol*. 1973;98:392–395.
70. Gomez-Gonzalez J, Roselli A, Rodreguez A. Melanosis oculodermica, melanoblastosis leptomeninges y melanoma intracerebral primario. *Universitas Medica*. 1959;7:47–52.
71. Haim T, Meyer K, Kerner H, et al. Oculodermal melanocytosis (nevus of Ota) and orbital malignant melanoma. *Ann Ophthalmol*. 1982;14:1132–1136.
72. Sang DN, Albert DM, Sober AJ, et al. Nevus of Ota with contralateral cerebral melanoma. *Arch Ophthalmol*. 1977;95:1820–1827.
73. Jensen O. Malignant melanoma of the human uvea: recent follow-up of cases in Denmark, 1943–1952. *Acta Ophthalmol*. 1970;48:1113–1128.

74. Gass J. Problems in the differential diagnosis of choroidal nevi and malignant melanomas. *Am J Ophthalmol*. 1977;83:299–323.
75. Paul EL, Parnell B, Fraker M. Prognosis of malignant melanomas of the choroid and ciliary body. *Int Ophthal Clin*. 1962;2:387–410.
76. McLean I, Foster W, Zimmerman L, et al. Modifications of Callender's classification of uveal melanoma at the Armed Forces Institute of Pathology. *Am J Ophthalmol*. 1983;96:502–509.
77. Juarez C, Tso M. An ultrastructural study of melanocytomas (magnocellular nevi) of the optic disc and uvea. *Am J Ophthalmol*. 1980;90:48–62.
78. Fournier G, Albert D, Wagoner M. Choroidal halo nevus occurring in a patient with vitiligo. *Surv Ophthalmol*. 1984;28:671–672.
79. Schrader W, Helwig E. Balloon cell nevi. *Cancer*. 1967;20:1502–1514.
80. Kim YJ, Kim YC, Kang HY. Is apoptosis involved in the development of balloon cell nevus? Suggestion from a case report. *J Am Acad Dermatol*. 2007;56(6):1069–1070.
81. Chang M, Fournier G, Koh H, et al. Ocular abnormalities associated with cutaneous melanoma and vitiligo-like leukoderma. *Graefes Arch Clin Exp Ophthalmol*. 1986;224:529–535.
82. Rummelt V, Folberg R, Rummelt C, et al. Microcirculation architecture of melanocytic nevi and malignant melanoma of the ciliary body and choroid: a comparative histopathologic and ultrastructural study. *Ophthalmology*. 1994;101:718–727.
83. Oosterhuis J, von Winning C. Naevus of the choroid. *Ophthalmologica*. 1979;178:156–165.
84. Font R, Zimmerman L, Armaly M. The nature of the orange pigment over a choroidal melanoma: histochemical and electron microscopical observations. *Arch Ophthalmol*. 1974;91:359–362.
85. Smith L, Irvine A. Diagnostic significance of orange pigment accumulation over choroidal tumors. *Mod Probl Ophthalmol*.

1974;12:536–543.
86. Pro M, Shields J, Tomer T. Serous detachment of the macula associated with presumed choroidal nevi. *Arch Ophthalmol*. 1978;96:1374–1377.
87. Waltman D, Gitter K, Yannuzzi L, et al. Choroidal neovascularization associated with choroidal nevi. *Am J Ophthalmol*. 1978;85:704–710.
88. Rubin M. Disciform lesions overlying melanocytoma simulating progression of choroidal melanoma. *Trans Am Ophthalmol Soc*. 1976;74:282–294.
89. Snip R, Green W, Jaegers K. Choroidal nevus with subretinal pigment epithelial neovascular membrane and a positive P-32 test. *Ophthalmic Surg*. 1978;9:35–42.
90. Mashayekhi A, Siu S, Shields CL, et al. Retinal pigment epithelial trough: a sign of chronicity of choroidal nevi. *Eur J Ophthalmol*. 2012;22(6):1019–1025.
91. Shields J, Shields C. *Intraocular tumors: a text and atlas*. WB Saunders: Philadelphia; 1992.
92. Albert D, Gaasterland D, Caldwell J, et al. Bilateral metastatic choroidal melanoma, nevi and cavernous degeneration of the optic nerve head. *Arch Ophthalmol*. 1972;87:39–47.
93. Albert D, Lahav M, Packer S, et al. Histogenesis of malignant melanomas of the uvea: occurrence of nevus-like structures in experimental choroidal tumors. *Arch Ophthalmol*. 1974;92:318–323.
94. Sahel J, Pesavento R, Frederick A, et al. Melanoma arising de novo over a 16 month period. *Arch Ophthalmol*. 1988;106:381–386.
95. Yanoff M, Zimmerman L. Histogenesis of malignant melanomas of the uvea. II. Relationship of uveal nevi to malignant melanomas. *Cancer*. 1967;20:493–507.
96. Zimmerman L. Malignant melanoma of the uveal tract. Spencer W. *Ophthalmic pathology: an atlas and text*. WB Saunders: Philadelphia; 1986.
97. Barr C, Zimmerman L, Curtin V, et al. Bilateral diffuse melanocytic uveal tumors associated with systemic malignant neoplasms: a recently recognized syndrome.

Arch Ophthalmol. 1982;100:249–255.
98. Mullaney J, Mooney D, O'Connor M, et al. Bilateral ovarian carcinoma with bilateral uveal melanomas. *Br J Ophthalmol*. 1984;68:261–267.
99. Parver L. The clinical characteristics of presumed choroidal nevi observed in green light. *Ophthalmology*. 1979;86:1924–1930.
100. Singh AD, Mokashi AA, Bena JF, et al. Small choroidal melanocytic lesions: features predictive of growth. *Ophthalmology*. 2006;113:1032–1039.
101. Mines J, Freilich D, Friedman A, et al. Choroidal (sub-retinal) neovascularization secondary to choroidal nevus and successful treatment with argon laser photocoagulation: case report and review of the literature. *Ophthalmologica*. 1985;190:210–218.
102. Croxatto J, Charles D, Malbran E. Neurofibromatosis associated with nevus of Ota and choroidal melanoma. *Am J Ophthalmol*. 1981;92:578–589.
103. Nordmann J, Brini A. Von Recklinghausen's disease and melanoma of the uvea. *Br J Ophthalmol*. 1970;54:641–648.
104. Yanoff M, Zimmerman L. Histogenesis of malignant melanomas of the uvea. III. Relationship of congenital ocular melanocytosis and neurofibromatosis to uveal melanomas. *Arch Ophthalmol*. 1967;77:331–336.
105. Reese A. Association of uveal nevi with skin nevi. *Arch Ophthalmol*. 1952;48:271–275.
106. Liu K, Peyman G, Mafee M, et al. False positive magnetic resonance imaging of choroidal nevus simulating a choroidal melanoma. *Int Ophthalmol*. 1989;13:265–268.
107. Kraemer KH, Tucker M, Tarone R, et al. Risk of cutaneous melanoma in dysplastic nevus syndrome types A and V. *N Engl J Med*. 1986;315:1615–1616.
108. Caporaso N, Greene M, Tsai S, et al. Cytogenetics in hereditary malignant melanoma and dysplastic nevus syndrome: is dysplastic nevus syndrome a chromosome instability disorder? *Cancer Genet Cytogenet*. 1987;24:299–314.
109. Albert D, Chang M, Lamping K, et al. The dysplastic nevus

syndrome: a pedigree with primary malignant melanoma of the choroid and skin. *Ophthalmology*. 1985;92:1728–1734.
110. Taylor M, Guerry DI, Bondi E, et al. Lack of association between intraocular melanoma and cutaneous dysplastic nevi. *Am J Ophthalmol*. 1984;98:478–482.
111. Gass J, Geiser R, Wilkinson C, et al. Bilateral diffuse uveal melanocytic proliferation in patients with occult carcinoma. *Arch Ophthalmol*. 1990;108:527–533.
112. Margo C, Pavan P, Gendelman D, et al. Bilateral melanocytic uveal tumors associated with systemic nodular malignancy: malignant melanomas or benign paraneoplastic syndrome. *Retina*. 1987;7:137–141.
113. McLean I, Zimmerman L, Evans R. Reappraisal of Callender's spindle A type of malignant melanoma of the choroid and ciliary body. *Am J Ophthalmol*. 1978;86:557–564.
114. Rohrbach J, Roggendorf W, Thanos S, et al. Simultaneous bilateral diffuse melanocytic uveal hyperplasia. *Am J Ophthalmol*. 1990;110:49–56.
115. Gass J. Observations of suspected choroidal and ciliary body melanomas for evidence of growth prior to enucleation. *Ophthalmology*. 1987;80:1523.
116. Singh A. Tumors of the uvea: benign melanocytic tumors. *Clinical ophthalmic oncology*. Elsevier Saunders: Edinburgh; 2007.
117. Shields CL, Mashayekhi A, Ho T, et al. Solitary congenital hypertrophy of the retinal pigment epithelium: clinical features and frequency of enlargement in 330 patients. *Retin Cases Brief Rep*. 2007;1:95–97.
118. Scott IU, Murray TG, Hughes JR. Evaluation of imaging techniques for detection of extraocular extension of choroidal melanoma. *Arch Ophthalmol*. 1998;116(7):897–899.
119. Chopdar A, Aung T. *Multimodal retinal imaging*. JP Medical: London; 2014.
120. Wolff-Korman P, Korman B, Hazeneratz G. Duplex and color Doppler ultrasound in the differential diagnosis of choroidal tumors. *Acta Ophthalmol*. 1992;204:66–70.
121. Schneider U, Gelisken F, Inhoffen W, et al. Indocyanine green videoangiography of malignant melanomas of the

choroid using the scanning laser ophthalmoscope. *Ger J Ophthalmol*. 1996;5:6–11.
122. Shields C, Shields J, DePotter P. Patterns of indocyanine green videoangiography of choroidal tumors. *Br J Ophthalmol*. 1995;79:237–245.
123. Sallet G, Amoaku W, Laufaut B, et al. Indocyanine green angiography of choroidal tumors. *Graefes Arch Clin Exp Ophthalmol*. 1995;233:677–689.
124. Mueller AJ, Bartsch D-U, Folberg R, et al. Imaging the microvasculature of choroidal melanomas with confocal indocyanine green scanning laser ophthalmoscopy. *Arch Ophthalmol*. 1998;116:31–39.
125. Andersen M, Scherfig E, Prause J. Differential diagnosis of choroidal melanomas and nevi using scanning laser ophthalmoscopical indocyanine green angiography. *Acta Ophthalmol Scand*. 1995;73:453–456.
126. Gass JDM. Fluorescein angiography: an aid in the differential diagnosis of intraocular tumors. *Int Ophthalmol Clin*. 1972;12:85–120.
127. Butler P, Char D, Zarbin M, et al. Natural history of indeterminate pigmented choroidal tumors. *Ophthalmology*. 1994;101:710–716.
128. Espinoza G, Rosenblatt B, Harbour JW. Optical coherence tomography in the evaluation of retinal changes associated with suspicious choroidal melanocytic tumors. *Am J Ophthalmol*. 2004;137:90–95.
129. Shields CL, Mashayekhi A, Materin MA, et al. Optical coherence tomography of choroidal nevus in 120 patients. *Retina*. 2005;25:243–252.
130. Torres VL, Brugnoni N, Kaiser PK, et al. Optical coherence tomography enhanced depth imaging of choroidal tumors. *Am J Ophthalmol*. 2011;151:586–593.
131. Shah SU, Kaliki S, Shields CL, et al. Enhanced depth imaging optical coherence tomography of choroidal nevus in 104 cases. *Ophthalmology*. 2012;119:1066–1072.
132. Francis JH, Pang CE, Abramson DH, et al. Swept-source optical coherence tomography features of choroidal nevi. *Am J Ophthalmol*. 2015;159(1):169–176.e1.

133. Lavinsky D, Belfort RN, Navajas E, et al. Fundus autofluorescence of choroidal nevus and melanoma. *Br J Ophthalmol*. 2007;91:1299–1302.
134. Shields CL, Pirondini C, Bianciotto C, et al. Autofluorescence of choroidal nevus in 64 cases. *Retina*. 2008;28:1035–1043.
135. Gunduz K, Pulido JS, Ezzat K, et al. Review of fundus autofluorescence in choroidal melanocytic lesions. *Eye (Lond)*. 2009;23:497–503.
136. Albertus DL, Schachar IH, Zahid S, et al. Autofluorescence quantification of benign and malignant choroidal nevomelanocytic tumors. *JAMA Ophthalmol*. 2013;131(8):1004–1008.
137. Pilotto E, Parrozzani R, Midena E. Treatment of choroidal neovascularization associated with choroidal nevus. *Acta Ophthalmol*. 2010;88.
138. Papastefanou VP, Nogueira V, Hay G. Choroidal naevi complicated by choroidal neovascular membrane and outer retinal tubulation. *Br J Ophthalmol*. 2013;97(8):1014–1019.
139. Chiang A, Bianciotto C, Maguire JI, et al. Intravitreal bevacizumab for choroidal neovascularization associated with choroidal nevus. *Retina*. 2012;32(1):60–67.
140. Parodi MB, Boscia F, Ferrari TM, et al. Variable outcome of photodynamic therapy for choroidal neovascularization associated with a choroidal nevus. *Retina*. 2005;25:438–442.
141. García-Arumí J, Amselem L, Gunduz K, et al. Photodynamic therapy for symptomatic subretinal fluid related to choroidal nevus. *Retina*. 2012;32(5):936–941.
142. Zaldivar RA, Aaberg TM, Sternberg P Jr, et al. Clinicopathologic findings in choroidal melanomas after failed transpupillary thermotherapy. *Am J Ophthalmol*. 2003;135(5):657–663.
143. Caminal JM, Mejia-Castillo KA, Arias L, et al. Subthreshold transpupillary thermotherapy in management of foveal subretinal fluid in small pigmented choroidal lesions. *Retina*. 2013;33(1):194–199.
144. Parodi MB. Transpupillary thermotherapy for subfoveal choroidal neovascularization associated with choroidal

nevus. *Am J Ophthalmol*. 2004;138:1074–1075.

143

Epidemiology of Posterior Uveal Melanoma

Johanna M. Seddon, Tara A. McCannel

Introduction

The underlying causes of uveal melanoma are not clearly established. Because we do not have a means to prevent this disease, epidemiologic research is key to determine associated factors and to better understand the mechanisms of disease development. This chapter will focus on posterior uveal melanoma (choroidal and ciliary body melanoma) and will not include a discussion of iris melanoma, which can be reviewed elsewhere.[1]

Posterior uveal melanoma is an uncommon disease with an incidence of 5–6 cases per 1 million population per year. It is usually diagnosed in the sixth decade of life, and its incidence rises steeply with age. It is the most common primary intraocular malignancy, and the leading primary intraocular disease, which can be fatal in adults. Although posterior uveal tract melanoma is the most common noncutaneous form of melanoma, the incidence rate is one-eighth that of cutaneous melanoma in the United States.[2]

Despite a few reports of sporadic family clusters, most patients with posterior uveal melanoma have no known family history of the disease. It is thought that some types of environmental exposure may help to initiate the development of posterior uveal melanoma, and sunlight has been proposed as an environmental risk factor because it is known to cause alterations in skin melanocytes leading to cutaneous melanoma. Heavily pigmented individuals rarely get skin or posterior uveal melanoma. Genetic susceptibility also likely plays a role in development of this cancer, and environmental exposures may have different effects and manifestations depending on the host's underlying attributes. In this chapter we discuss the known epidemiology of posterior uveal

melanoma and evaluate the available evidence for host and environmental risk factors.

Incidence

According to the most recent report of data obtained from the Surveillance, Epidemiology, and End Results (SEER) program database in the United States (1973–2008), the mean age-adjusted incidence estimate for ocular melanoma in the United States is 5.1 cases per 1 million population.[3] Similar estimates for uveal melanomas of the choroid and ciliary body[4,5] or the choroid, ciliary body, and iris[5–7] have been reported for individual states or regions within the United States. Other surveys of primarily white populations have found incidence rates similar to those of the United States (Table 143.1).[8–17] The incidence rate in black Africans is unknown but thought to be extremely low.[18–21] In the United States, the rate of the disease in African Americans is less than one-eighth of the rate for whites.[2] Although small fluctuations in several populations have been observed,[22,23] the incidence and mortality rates of uveal melanoma have been shown to be fairly stable over the past several decades.[24,25] It is important to note that comparative incidence rates across populations must be interpreted with caution, since differences in case definition, methods of case ascertainment, and methods of age-adjustment could affect the relative incidence rates.

TABLE 143.1

Incidence Rates of Uveal Melanoma Reported for Various Populations

Authors	Population	Interval	Incidence Rates per Million Population	
			Including Iris Melanoma	Excluding Iris Melanoma
REGIONS OR STATES WITHIN THE UNITED STATES				
Shammas and Watzke[5]	Iowa (whites only)	1969–1971	5.6	4.9
Wilkes et al.[7]	Rochester and Olmstead counties, MN	1935–1974	7	–
Seddon and Egan[8]	New England	1984–1989	–	7.4

Ganley and Comstock[4]	Washington county, MD	1956–1965	–	6.6
Mahoney et al.[6]	New York	1975–1986	4.9 (male) 3.7 (female)	–
Regions or Countries Outside the United States				
Raivio[9]	Finland	1953–1973	5.3	–
Teikari and Raivio[10]	Finland	1973–1980	7.6	–
Birdsell et al.[11]	Alberta, Canada	1967–1976	6.0	5.5
Jensen[12]	Denmark	1943–1952	7.4	7.1
Osterlind[13]	Denmark	1943–1982	7.5 (male)[a]	6.0 (female)[a]
Abrahamsson[14]	Swedish west coast	1956–1975	–	7.2
Mork[15]	Norway	1953–1960	8.0[b]	–
Vidal et al.[16]	France	1992	7.3	–
Iscovich et al.[17]	Israel	1961–1989	– 5.7 (Jews, female) 1.6 (other, male) 1.3 (other, female)	5.7 (Jews, male)

[a]All ocular sites.

[b]Primary anatomic site unavailable in this series.

Host Factors

Age and Sex

Uveal melanoma is rare in children.[26–28] In most series, the median age at diagnosis is 55 years.[9,12] In Jensen's series,[12] rates of disease decreased in males after age 69 years. An evaluation of uveal melanoma cases reported to the Finnish Cancer Registry between 1953 and 1982[9,10] found that rates of disease in females leveled off beginning in the mid-60s, but in males of the same age, rates continued to increase. Data from Norway show rates dropping in both sexes after age 70 years.[15] This is in contrast to the majority of adult cancers in which incidence increases exponentially with age.

In many large surveys of uveal melanoma patients, there is a slight predominance of males.[2,6,12,16,29] Higher rates in males have been reported in many studies that presented gender-specific rates of ocular melanoma. Higher rates in males have also been found in studies that used all eye cancers in persons aged 15 years or older

as a surrogate for ocular melanomas.[22,23,25] It has been shown in white populations that over 90% of these eye cancers are ocular melanomas[22] with the majority involving the uveal tract.[3] In New England, however, the overall rate during a 6-year period was similar in males and females.[8] Age-specific incidence rates were 2.3 per million for persons aged 15–44 years, 15 per million for persons aged 45–64 years, and 25.3 per million for persons aged 65 years and older.

Race and Ancestral Origin

Uveal melanoma is rare in nonwhite races. Data from the Third National Cancer Survey indicate that in the United States, whites have more than eight times the risk of developing the disease than blacks.[3] The New England incidence survey data for a 6-year period suggest that the rate among whites is 9.4 times that of African Americans.[8] A recent analysis of population-based registry data in the SEER program[30] found a relative risk of ocular melanoma for white males compared with African American males of 7.4; the risk for white women in comparison with African American women was 5.3. Surveys of eye disease in African populations reveal the same low risk in black Africans.[18–21] The risk of uveal melanoma is also low among Chinese, Japanese, and Thais.[31–33] In the United States the disease is rare among Americans of Asian extraction.[3] A series of three posterior uveal melanomas in Vietnamese Asians with clinical and cytogenetic characteristics was reported by McCannel et al.[34] The small number of cases reported among Native Americans and Hispanics in the United States suggests that this diagnosis is also rare in these groups. Two cases of ocular melanoma among southwestern Native Americans were found in a review of the New Mexico tumor and melanoma registries,[35] and one report described four Native Americans with choroidal melanoma evaluated for the Collaborative Ocular Melanoma Study (COMS).[36] A series of 20 choroidal melanoma patients of Hispanic origin was described by Hudson et al.[37]

Among whites with uveal melanoma, ancestral origin from more northern latitudes was the strongest risk factor found in a large case–control study.[38] Northern European ancestry was associated

with more than a sixfold increased risk, and British ancestry was associated with more than a twofold increased risk, as compared with southern European and Mediterranean heritage. The roles of ancestry and race were examined in an evaluation of the incidence of uveal melanoma using data from the Israeli Cancer Registry.[17] Jews immigrating to Israel from Europe or North America and Israeli-born Jews had a threefold to fourfold increased incidence compared with Jews from Asia or Africa; non-Jews had the lowest risk.

Cancer Genetics

A number of clusters of uveal melanoma occurring among blood relatives have been reported. Familial clusters of uveal melanoma cases have been identified in several large series of patients. Among 1600 patients with uveal melanoma treated by proton beam irradiation over a 10-year period, only 11 families were found to have more than one verified case of the disease.[39] In a series of 4500 cases diagnosed between 1976 and 1993, 27 families having at least two blood relatives with a uveal melanoma diagnosis were identified.[40] Although the overall incidence among familial cases in that study was small, it was significantly higher than the expected incidence of sporadic cases. Therefore, it was presumed that the familial clustering was associated with inherited genetic or common environmental factors.

Although family history of uveal melanoma is rare, some cases may have a heritable component. A mutation in germline BRCA-associated protein 1 (BAP1) gene has been identified as associated with uveal melanoma and other cancers among family members. A germline mutation in BAP1 has been described to be responsible for what has been termed the BAP1-tumor predisposition syndrome. Mesothelioma, cutaneous melanoma, uveal melanoma and renal cell carcinoma have been associated with this condition. Although phenotypic characterization is not yet understood, it appears that patients with BAP1-tumor predisposition syndrome have a poorer prognosis with regards to cancer metastasis.[41a-41d] Mutations in G-α proteins, which are believed to be responsible for tumor development, have been identified in uveal melanoma and may be

present in at least 84% of tumors. Among the most common of these somatic G-α protein mutations are GNAQ[41e] and GNA11,[42] which are mutually exclusive. Cutaneous melanoma is now recognized as an inherited disease in as many as 10% of all cases.[43] Recent evidence suggests that family members of persons with cutaneous melanoma who have large numbers of dysplastic nevi have several hundred times the risk of developing cutaneous melanoma compared with the general population.[43] Reports of cutaneous melanoma and uveal melanoma occurring as double primary malignancies, some in the presence of dysplastic nevi,[44–46] and melanomas of both sites occurring among family members,[43,46–49] have led to speculation that cutaneous and uveal melanoma may have a common heritable variant. Persons with cutaneous melanoma have been found to be more likely to possess iris nevi[50] or have a larger number of iris nevi[51] compared with controls. These studies reported similar, although not statistically significant, patterns for choroidal nevi. A potential bias is that the examiners were not masked with respect to the diagnosis of skin melanoma, and nevi may have been more likely to be identified in patients with skin melanoma. There have been no reports of a higher frequency of ocular melanoma among persons with cutaneous melanoma.

The occurrence of bilateral tumors has been suggested as indicative of genetic predisposition to cancer.[52] However, few cases of bilateral primary uveal melanoma have been reported,[46,52,53] and most reported cases did not exhibit other characteristics associated with genetically inherited cancer predisposition, such as early age of onset or familial clustering of uveal melanoma.[52]

Cytogenetic analyses of uveal melanoma tissue have revealed that alterations in chromosomes 3 and 8 may be associated with increased metastasis-related mortality.[54–56] Jay and McCartney[57] documented an unusual family with eight presumed cases of malignant ocular melanoma spanning four generations; mutations in the p53 tumor-suppressor gene were detected in the two tumors for which preserved material was available. It is possible that a germline BAP1 mutation could explain the hereditary nature of uveal melanoma in this family.

Ocular and Cutaneous Nevi and Melanocytosis

Nevi on the skin have been shown to increase the risk of cutaneous melanoma.[58,59] Similarly, the majority of uveal melanomas are thought by some to arise from preexisting choroidal nevi.[60] However, the available literature suggests that the risk of choroidal and ciliary body melanomas associated with nevi of the uveal tract is low. Ganley and Comstock[4] estimated that 3% of the population over the age of 30 years have choroidal nevi posterior to the equator of the eye. Because nevi may also occur anterior to the equator,[61] the prevalence of choroidal nevi may be as much as twice that reported. Each year, only 1 in 5000 persons with such nevi develop a melanoma (assuming all melanomas arise from preexisting nevi).[4] Because of the low risks associated with these conditions, current guidelines and recommendations for management and follow-up may not be cost-effective.

Other melanocytic conditions that have been linked to uveal melanoma include ocular (melanosis oculi) and oculodermal (nevus of Ota) melanocytosis. These are typically congenital, unilateral conditions involving hyperpigmentation of the episclera and uveal tract in ocular melanocytosis and of the periorbital skin in oculodermal melanocytosis. Both conditions are more common in females, and the highest prevalence has been reported in Asians.[62] Gonder et al.[63] found that the prevalence of both forms of melanocytosis was higher in persons with uveal melanoma compared with a clinic population. Singh et al.[64] estimated the lifetime prevalence of uveal melanoma in white patients with ocular or oculodermal melanocytosis to be 2.6 cases per 1000 population, as compared with an estimated prevalence of uveal melanoma of 7.5 cases per 10, 000 in the general population.

Case–control studies suggest that presence of cutaneous nevi may be a risk factor for uveal melanoma.[38,65,66] A significant trend for an increase in the risk of uveal melanoma with more cutaneous nevi was found by Seddon et al.[38] Dysplastic nevus syndrome (DNS)[41] and atypical mole syndrome[65,67] also have been associated with uveal melanoma. In one study, persons with dysplastic nevi were more likely to possess conjunctival, iris, and choroidal nevi.[68]

Results of a case–control study comparing the presence of DNS in Hungarian patients with uveal melanoma or with cutaneous melanoma and in volunteer controls indicated that DNS was significantly more common in both groups of melanoma patients than in the control group (the odds ratio for uveal melanoma as compared with controls was 4.36).[69] Van Hees et al.[67] reported a dose–response relationship between number of atypical nevi and uveal melanoma. After adjustment for age and sex, the presence of one or two atypical nevi was associated with nearly a threefold increased risk, and the presence of three or more atypical nevi with a fivefold increased risk of melanoma in comparison with absence of atypical nevi. Similarly, Bataille et al.[65] found a trend of increasing odds ratios for greater numbers of atypical nevi. Although DNS and ocular nevi have been linked to risk of uveal melanoma, DNS was not found to be associated with the prevalence of iris or choroidal nevi in a case–control study from Sweden,[70] nor was a higher-than-expected rate of dysplastic nevi demonstrated in a group of patients with ocular melanoma evaluated by Taylor et al.[71] The association between DNS and uveal melanoma remains uncertain.

Hormones and Reproductive Factors

Hormonal influences are suspected to be a factor in cutaneous melanoma based on reports of an increased risk for women in their childbearing years[72,73] and the seemingly adverse influence of pregnancy on prognosis.[74–76] Pregnancy may also pose an added risk for uveal melanoma, although reports of presentation[77–81] and tumor growth[79] during pregnancy are rare. Increases in mortality resulting from tumors of the eye[73] and in the incidence of ocular melanomas[2] during the childbearing years have been reported. On the other hand, the hormonal environment had no appreciable influence on risk of metastases in younger women with uveal melanoma in one series.[82] Potential mechanisms are speculative and include a hormonal effect from estrogens or melanocyte-stimulating hormone. However, one study showed an absence of estrogen receptors in melanoma and surrounding choroidal tissue.[79]

Epidemiologic studies comparing uveal melanoma cases to

controls without melanoma have evaluated hormonal and reproductive factors.[83,84] Findings suggest a weak or no association and are not consistent between the two reports. For example, one found an increased risk[83] and the other a decreased risk[84] for ever having been pregnant. Similarly, increased risk[83] and no change in risk[84] for use of postmenopausal estrogens were reported. Further studies are needed to evaluate these relationships.

Eye and Skin Color

Some studies suggest that persons with light irides are at increased risk of developing uveal melanoma.[33,66,85] In one of these studies,[86] persons with blue or gray eyes were found to have three times the risk of disease (unadjusted for other host factors) compared with persons with brown eyes. In a larger study of over 400 cases that combined melanoma of the iris with other uveal melanomas, the risk for blue-eyed persons was 1.7 times that of persons with brown eyes. Hair and skin color were not found to be independent risk factors after adjusting for eye color.[85] Similarly, Holly et al.[66] found a twofold risk for lighter eye color. However, in a case–control study with sibling and population-based controls, Seddon et al. found that skin color was significantly associated with uveal melanoma after adjusting for ancestral origin, with a relative risk of 3.8 comparing light to darker skin color among whites with uveal melanoma, but lighter eye color was only weakly related and was not significant in multivariate analyses.[38]

The iris is the only part of the uveal tract positioned in front of the lens, an effective ultraviolet filter. One study found a higher prevalence of blue and gray eyes among patients with iris melanoma compared with controls with ciliary body and choroidal melanoma.[87] Kliman et al.[88] also found that light irides were more common in persons with melanocytic lesions of the iris but suggested that such lesions may simply be more noticeable in lighter irides. However, the well-documented tendency for iris melanomas to occur in the inferior sector of the eye,[9,12,89–91] where exposure to sunlight is presumably greatest, supports the view that the origin of these iris tumors may be environmentally related.

History of Nonocular Malignancy

To examine whether persons with a previous diagnosis of other cancers are at increased risk for uveal melanoma, a few epidemiologic studies have compared patients with melanoma with controls regarding their past medical history of other malignancies.[92–94] In a comparison of a series of uveal melanoma cases with population data from the Connecticut Tumor Registry, prevalence of previous malignancy was found to be significantly higher in women with uveal melanoma but not in men.[94] An investigation using SEER data identified an elevated risk of ocular melanoma among women with a history of invasive ovarian cancer, suggesting a possible common hormonal etiology.[95] A recent report from the Liverpool Ocular Oncology Center described a prevalence of 4.3% of self-reported other nonocular primary in uveal melanoma patients over a 20 year period.[96] In general, the results of these studies do not support a consistent association between prior malignancies and subsequent diagnosis of uveal melanoma. A weak and nonsignificant increased relative risk of melanoma associated with history of skin cancers was noted in several studies.[93–95,97] This suggests that cutaneous malignancies and uveal melanoma may share some common risk factors. Further studies are needed to evaluate this potential association.

Environmental Factors

Sunlight Exposure

Sunlight exposure has been examined as a potential environmental risk factor for a number of ocular diseases, including age-related macular degeneration[98,99] and senile cataract,[100] as well as melanoma of the uveal tract.[37,38,66,85,86,89] Incident cases of choroidal melanoma in a consecutive series of patients demonstrated a strong predilection for initial presentation at the perifoveal area. Initiation rates decreased with distance from the macula; this gradient decrease correlated with decreasing illuminance of light on the retina from macula to periphery, suggesting a possible role of sun exposure in uveal melanoma.[101] However, a meta-analysis by Shah et al. revealed that chronic ultraviolet exposure both in birth latitude and

occupational sunlight exposure was not a significant risk factor for uveal melanoma development.[102] Earlier and more frequent presentation of perifoveal tumors is likely due to visual symptoms related to the location of these tumors. Intermittent ultraviolet exposure in the form of welding was found to have a possible association with uveal melanoma,[66] described in the meta-analysis by Shah et al.[102] See section below on "Geography."

Diet and Smoking

There are currently no data in the literature regarding the influence of diet on the incidence of uveal melanoma. A study was conducted looking at dietary intake in enhancing the recurrence-free interval, but both numbers of subjects and follow-up time were small.[103] A population-based case–control study in Germany found that smoking and alcohol consumption were not associated with an increased risk for uveal melanoma.[104] In a large prospective study, the risk of metastases the first 3 years after radiation was not altered by smoking.[105]

Geography

Uveal melanoma may differ from cutaneous melanoma in that there does not appear to be a strong latitudinal gradient with regard to the incidence of ocular disease.[2,9,22,23] In one study of patients in Veterans Administration hospitals, higher rates of uveal melanoma were reported in southern hospitals,[106] but this may have reflected a tendency for elderly veterans to retire to the southern United States. In a Canadian study, altitude, not latitude, was positively correlated with the incidence of uveal melanoma.[11] The association of exposure to solar radiation early in life with risk of ocular melanoma was evaluated using state of birth among cases identified from SEER data;[107] birth in a southern state or in a state with higher levels of solar radiation was not found to be related to the risk of ocular melanoma.

There are several possible explanations for the lack of a clear latitudinal gradient in uveal melanoma rates, assuming that sunlight is an etiologic factor in the disease. First, higher rates of uveal melanoma might not be seen in southern latitudes because

the greater intensity of overhead sunlight in the south may be offset by the greater reflection of ultraviolet radiation as a result of snow cover in the north.[108] Second, the quality of correlational studies depends on both uniform case ascertainment and risk for disease throughout the populations studied. Geographic patterns could be obscured by variations in the completeness of case finding, a problem in several of the studies described above. Regional differences in the racial or ethnic mixes of the populations with different susceptibilities to melanoma may also obscure differences in rates for this rare tumor. Northern latitudinal ancestry is a risk factor among whites,[38] whereas sunlight exposure is greatest at lower latitudes.

A problem with the possible link between sunlight exposure and uveal melanoma lies in establishing whether ultraviolet radiation actually reaches the uveal tract through the effective filters of the cornea and lens. In both animal models and studies of enucleated eyes,[109] it has been shown that virtually no ultraviolet (UV)-A or UV-B radiation is transmitted through both the lens and cornea in adults. The juvenile lens, on the other hand, may transmit small amounts of ultraviolet radiation.[110] Others have argued, however, that tissues directly overlying uveal tract structures, including the retina, would provide the necessary protection if significant amounts of ultraviolet radiation penetrated the lens.[111] The net effect then would be the total blockage of ultraviolet radiation from direct contact with the choroid and ciliary body at all ages.

In addition to a direct effect, sunlight may also act indirectly by causing a systemic alteration in immunologic function[112] or by production of a "solar" circulating factor.[113] Such compromise of the immunologic system by ultraviolet radiation would make ocular parameters less important than other bodily exposures. There may be certain genetically predisposed individuals who are more susceptible to the direct or indirect effects of sunlight exposure.

A few studies have compared sunlight exposure histories of patients with uveal melanoma with those of controls.[38,66,85,86,114,115] All but one[86] of these studies suggest a low to moderate adverse effect of certain UV exposures on the risk of uveal melanoma, but results are not consistent. These exposures include residence in the southern United States, use of sunlamps, and history of intense sun

exposure;[38] occupational exposure to UV light;[114] tendency to sunburn and welding burn or sunburn;[66] and gardening and lack of eye protection when outdoors.[85] In the study that did not find an association between sun sensitivity or exposures and uveal melanoma,[86] the sample size was small, and hence the power to detect weak or moderate association was low.

In observational studies such as these, potential biases may be problematic. For example, uveal melanoma patients may be more likely to recall certain exposures than persons without the disease. Also, uncontrolled confounding is likely. There may be other risk factors that are not yet known and therefore not controlled for in the analysis. UV exposure may play some role in the etiology of uveal melanoma, but its relationship with this disease remains inconclusive.

Occupational and Chemical Exposures

A number of rare cancers are caused by chemical or radiation exposures occurring in the workplace,[116] and an occupational exposure has also been sought in the etiology of uveal melanoma. Jensen[12] found approximately the same occupational distribution among patients with uveal melanoma as was found in the general population of Denmark. Swerdlow[23] reported that patients with eye cancer in England and Wales were more likely to be nonmanual than manual laborers, and a higher risk was found among electrical workers in particular. Gallagher et al.[86] did not find an elevated risk for electrical workers or any other specific occupation in western Canada but noted an excess of cases of uveal melanoma among government workers, a managerial job classification. Four patients with uveal melanoma and none of the controls reported having worked as a welder in one of the case–control studies discussed above.

A population-based case–control study evaluated occupational exposures[117] using two systems of coding occupations and industries. Results suggested an increased risk of uveal melanoma for the group of agricultural, fishery, and forestry occupations and industries, as well as for those exposed to certain chemicals, but these associations were weak and not statistically significant. This

exploratory study suggested possible areas for future research that could test these and other specific hypotheses. In another case–control study,[115] associations between ocular melanoma and exposure to welding and asbestos were identified; specific occupations at high risk included chemical-related, maritime, and health-related occupations.

Several reports of occupational or community clusters of uveal melanoma cases have led to speculation regarding a common etiologic occupational or chemical exposure. One report described a cluster of cases that occurred among employees of a chemical plant in West Virginia.[118] Four cases were diagnosed between 1972 and 1978, and a fifth case had been diagnosed in 1952. In a small Pennsylvania community, three choroidal melanomas were diagnosed over a 2.5-year period.[119] A cluster of four cases in a manufacturing plant in Louisiana was also reported.[120] However, on investigation, no specific causative agent could be identified in any of these clusters.

Ocular melanomas and other ocular tumors have been produced in laboratory animals after administration of methylcholanthrene,[121] N-2-fluorenylacetamide and ethionine,[122] radium,[123] and nickel subsulfide.[124] In the cluster of cases identified in the Pennsylvania community,[119] although no common exposure was identified among the patients with choroidal melanoma, laboratory mice given community water developed anterior lens capsule abnormalities that were not seen in control mice. The basis for this association is not clear.

Mobile Phone Use

Over the past decade there has been public concern regarding microwave energy in mobile or wireless phone use and the development of cancer. Using a questionnaire, a case–control study of over 400 uveal melanoma case patients were matched to controls to identify mobile phone use, and logistic regression analyses revealed that regular mobile phone use was not associated with risk of developing uveal melanoma.[125]

Other Environmental Exposures

A number of other environmental exposures may contribute to the etiology of uveal melanoma. Albert et al.[50] have summarized the available evidence for a viral cause of the disease. Melanoma-like tumors have been induced in laboratory animals after injection of viral-transformed uveal tissue.[50] In addition, virus and virus-like particles have been demonstrated in human uveal melanomas.[126] However, the meaning of these findings is unclear, since virus particles are often constituents of normal tissues. Trauma has been cited as a possible cause of some cutaneous melanomas[127,128] and there are a few reports of uveal melanomas[129,130] occurring at the site of a previous injury.

Conclusion

Our understanding of the epidemiology of uveal melanoma continues to evolve gradually. Host factors remain the strongest known risk factors for this disease, particularly ethnic ancestry. Degree of pigmentation and cutaneous moles may be markers of possible risk. There are also rare reports of uveal melanoma occurring in blood relatives, which suggest a possible heritable component in some cases.

Acute or intense UV exposures might increase the risk of uveal melanoma, but the role of sunlight exposure and the mechanisms involved remain uncertain. Potential hormonal influences among females are supported by plausible biologic mechanisms, but findings to date are weak and inconsistent. These factors, as well as occupational and other potential risk factors, merit further research. New studies in cancer genetics have identified G-α mutations to be important in the development of uveal melanoma, and these and other genetic factors may be important in understanding the biology of uveal melanoma and the development of future therapeutic approaches. Additional epidemiologic studies are warranted to further explore the risk and protective factors associated with this potentially fatal cancer, which may lead to preventive measures and better treatments.

References

1. Henderson E, Margo CE. Iris melanoma. *Arch Pathol Lab Med*. 2008;132:268–272.
2. Scotto J, Fraumeni JF, Lee JAH. Melanomas of the eye and other noncutaneous sites: epidemiologic aspects. *J Natl Cancer Inst*. 1976;56:489–491.
3. Singh AD, Turell ME, Topham AK. Uveal melanoma: trends in incidence, treatment and survival. *Ophthalmology*. 2011;118:1881–1885.
4. Ganley JP, Comstock GW. Benign nevi and malignant melanomas of the choroid. *Am J Ophthalmol*. 1973;76:19–25.
5. Shammas HF, Watzke RC. Bilateral choroidal melanomas: case report and incidence. *Arch Ophthalmol*. 1977;95:617–623.
6. Mahoney MC, Burnett WS, Majerovics A, et al. The epidemiology of ophthalmic malignancies in New York State. *Ophthalmology*. 1990;97:1143–1147.
7. Wilkes SR, Robertson DM, Kurland LT, et al. Incidence of uveal malignant melanoma in the resident population of Rochester and Olmsted County, Minnesota. *Ophthalmology*. 1979;117:516–520.
8. Seddon JS, Egan KM. Application of epidemiologic methods to ophthalmology: uveal melanoma. Albert DJ. *The principles and practice of ophthalmology*. WB Saunders: Philadelphia; 1993:1245–1266 [106].
9. Raivio I. Uveal melanoma in Finland: an epidemiological, clinical, histological, and prognostic study. *Acta Ophthalmol Suppl (Copenh)*. 1977;133:1–64.
10. Teikari JM, Raivio I. Incidence of choroidal malignant melanoma in Finland in the years 1973–1980. *Acta Ophthalmol*. 1985;63:661–665.
11. Birdsell JM, Gunther BK, Boyd TA, et al. Ocular melanoma: a population-based study. *Can J Ophthalmol*. 1980;15:9–12.
12. Jensen OA. Malignant melanomas of the uvea in Denmark 1943–1952: a clinical, histopathologic, and prognostic study. *Acta Ophthalmol Suppl (Copenh)*. 1963;75:17–78.
13. Osterlind A. Trends in incidence of ocular malignant melanoma in Denmark, 1943–1982. *Int J Cancer*. 1987;40:161–164.
14. Abrahamsson M. Malignant melanoma of the choroid and

the ciliary body, 1956–1975. *Acta Ophthalmol*. 1983;61:600–610.
15. Mork T. Malignant neoplasms of the eye in Norway: incidence, treatment and prognosis. *Acta Ophthalmol*. 1961;39:824–831.
16. Vidal JL, Bacin F, Albuisson E, et al. Melanome 92. Etude epidemiologique des melanomes uveaux en France. *J Fr Ophtalmol*. 1995;18:520–528.
17. Iscovich J, Ackerman C, Andreev H, et al. An epidemiologic study of posterior uveal melanoma in Israel. *Int J Cancer*. 1995;61:291–295.
18. Klauss V, Chana HS. Ocular tumors in Africa. *Soc Sci Med*. 1983;17:1743–1750.
19. Malik MOA, El Sheikh EH. Tumors of the eye and adnexa in the Sudan. *Cancer*. 1979;44:293–303.
20. Miller B, Abrahams C, Cole GC, et al. Ocular malignant melanoma in South African blacks. *Br J Ophthalmol*. 1981;65:720–722.
21. Templeton AC. Tumors of the eye and adnexa in Africans of Uganda. *Cancer*. 1967;20:1689–1698.
22. Hakulinen T, Teppop L, Saxen E. Cancer of the eye, a review of trends and differentials. *World Health Stat Q*. 1978;31:143–158.
23. Swerdlow AJ. Epidemiology of eye cancer in adults in England and Wales. *Am J Epidemiol*. 1983;118:294–300.
24. Jensen OA, Prause JU. Malignant melanomas of the human uvea in Denmark: incidence and a 25-year follow-up of cases diagnosed between 1943 and 1952. Lommatzsch PB. *Intraocular tumors*. Springer-Verlag: Berlin; 1983.
25. Strickland D, Lee JAH. Melanomas of eye: stability of rates. *Am J Epidemiol*. 1981;113:700–702.
26. Apt L. Uveal melanomas in children and adolescents. *Int Ophthalmol Clin*. 1962;2:403–410.
27. Shields CL, Shields JA, Milte J, et al. Uveal melanomas in teenagers and children: a report 40 cases. *Ophthalmology*. 1991;98:1662–1666.
28. Stanford DG, Hart R, Thompson JF. Ocular melanoma in childhood. *Aust NZ J Surg*. 1993;63:729–731.

29. Shammas HF, Blodi FC. Prognostic factors in choroidal and ciliary body melanomas. *Arch Ophthalmol*. 1977;95:63–69.
30. Neugut AI, Kizelnik-Freilich S, Ackerman C. Black–white differences in risk for cutaneous, ocular, and visceral melanomas. *Am J Public Health*. 1994;84:1828–1829.
31. Kaneko A. Incidence of malignant melanoma of the eye in Japan. *Rinsho Ganka*. 1979;33:941–947.
32. Kuo PK, Puliafito CA, Wang KM, et al. Uveal melanoma in China. *Int Ophthalmol Clin*. 1982;22:57–71.
33. Shuangshoti S, Panyathanya R. Retinoblastoma and uveal melanoma: a study of 206 cases. *J Med Assoc Thailand*. 1973;56:331–336.
34. McCannel TA, Wu MY, Burgess BL. Clinical and cytogenetic characteristics of choroidal melanoma in Vietnamese Asians. *Mol Vis*. 2011;17:231–236.
35. Black WC, Wiggins C. Melanoma among southwestern American Indians. *Cancer*. 1985;55:2899–2902.
36. Wells CG, Bradford RH, Fish GE, et al. Choroidal melanomas in American Indians: COMS Group, Collaborative Ocular Melanoma Study. *Arch Ophthalmol*. 1996;114:1017–1018.
37. Hudson HL, Valluri S, Rao NA. Choroidal melanomas in Hispanic patients. *Am J Ophthalmol*. 1994;118:57–62.
38. Seddon JS, Gragoudas ES, Glynn RJ, et al. Host factors, UV radiation, and risk of uveal melanoma: a case–control study. *Arch Ophthalmol*. 1990;108:1274–1280.
39. Young LH, Egan KM, Walsh SM, et al. Familial uveal melanoma. *Am J Ophthalmol*. 1994;117:516–520.
40. Singh AD, Wang MX, Donoso LA, et al. Familial uveal melanoma. III. Is the occurrence of familial uveal melanoma coincidental? *Arch Ophthalmol*. 1996;114:1101–1104.
41a. Abdel-Rahman MH, Pilarski R, Cebulla CM, et al. Germline BAP1 mutation predisposes to uveal melanoma, lung adenocarcinoma, meningioma, and other cancers. *J Med Genet*. 2011;48:856–859.
41b. Testa JR, Cheung M, Pei J, et al. Germline BAP1 mutations predispose to malignant mesothelioma. *Nat Genet*. 2011;43:1022–1025.

41c. Wiesner T, Obenauf AC, Murali R, et al. Germline mutations in BAP1 predispose to melanocytic tumors. *Nat Genet*. 2011;43:1018–1021.
41d. Popova T, Hebert L, Jacquemin V, et al. Germline BAP1 mutations predispose to renal cell carcinomas. *Am J Hum Genet*. 2013;92:974–980.
41e. Van Raamsdonk CD, Bezrookove V, Green G, et al. Frequent somatic mutations in GNAQ in uveal melanoma and blue nevi. *Nature*. 2009;457:599–602.
42. Van Raamsdonk CD, Griewank KG, Crosby MB, et al. Mutations in GNA11 in uveal melanoma. *N Engl J Med*. 2010;363:2191–2199.
43. Greene MH, Sanders RJ, Chu FC, et al. The familial occurrence of cutaneous melanoma, intraocular melanoma, and the dysplastic nevus syndrome. *Am J Ophthalmol*. 1983;96:238–245.
44. Abramson DH, Rodriguez-Sains RS, et al. B-K mole syndrome: cutaneous and ocular malignant melanoma. *Arch Ophthalmol*. 1980;98:1397–1399.
45. Bellet RE, Shields JA, Soll DB, et al. Primary choroidal and cutaneous melanomas occurring in a patient with the B-K mole syndrome phenotype. *Am J Ophthalmol*. 1980;89:567–570.
46. Oosterhuis JA, Went LN, Lynch HT. Primary choroidal and cutaneous melanomas, bilateral choroidal melanomas, and familial occurrence of melanomas. *Br J Ophthalmol*. 1982;66:230–233.
47. Albert DM, Chang MA, Lamping K, et al. The dysplastic nevus syndrome's pedigree with primary malignant melanomas of the choroid and skin. *Ophthalmology*. 1985;92:1728–1734.
48. Paton D, Thomas LB. Simultaneous occurrence of primary malignant melanomas of the eye and the skin. *Arch Ophthalmol*. 1959;62:645–652.
49. Turkington RW. Familial factor in malignant melanoma. *JAMA*. 1965;192:72–82.
50. Albert DM, Searl SS, Forget B, et al. Uveal findings in patients with cutaneous melanoma. *Am J Ophthalmol*.

1983;95:474–479.
51. Nordlund JJ, Kirkwood J, Forget BM, et al. Demographic study of clinically atypical (dysplastic) nevi in patients with melanoma and comparison subjects. *Cancer Res*. 1985;45:1855–1861.
52. Singh AD, Shields CL, Shields JA, et al. Bilateral primary uveal melanoma. Bad luck or bad genes? *Ophthalmology*. 1996;103:256–262.
53. Ascaso FJ, Cascante JM, Castillo JM, et al. Simultaneous bilateral primary choroidal melanoma. *Eur J Ophthalmol*. 1996;6:87–89.
54. Prescher G, Bornfeld N, Hirche H, et al. Prognostic implications of monosomy 3 in uveal melanoma. *Lancet*. 1996;347:1222–1225.
55. Scholes AG, Damato BE, Nunn J, et al. Monosomy 3 in uveal melanoma: correlation with clinical and histologic predictors of survival. *Invest Ophthalmol Vis Sci*. 2003;44:1008–1011.
56. Sisley K, Rennie IG, Parsons MA, et al. Abnormalities of chromosomes 3 and 8 in posterior uveal melanoma correlate with prognosis. *Genes Chromosomes Cancer*. 1997;19:22–28.
57. Jay M, McCartney AC. Familial malignant melanoma of the uvea and p53: a Victorian detective story. *Surv Ophthalmol*. 1993;37:457–462.
58. Elwood JM, Williamson C, Stapleton PJ. Malignant melanoma in relation to moles, pigmentation and exposure to fluorescent and other lighting sources. *Br J Cancer*. 1986;53:65–74.
59. Holman CDJ, Mulroney CD, Armstrong BK. Epidemiology of preinvasive and invasive malignant melanoma in Western Australia. *Int J Cancer*. 1980;25:317–323.
60. Yanoff M, Zimmerman LE. Histogenesis of malignant melanomas of the uvea. II. Relationship of uveal nevi to malignant melanomas. *Cancer*. 1967;20:493–507.
61. Hale PN, Allen RA, Straatsma BR. Benign melanomas (nevi) of the choroid and ciliary body. *Arch Ophthalmol*. 1965;74:532–538.

62. Gonder JR, Shields JA, Shakin JL, et al. Bilateral ocular melanocytosis with malignant melanoma of the choroid. *Br J Ophthalmol*. 1981;65:843–845.
63. Gonder JR, Shields JA, Albert DM, et al. Uveal malignant melanoma associated with ocular and oculodermal melanocytosis. *Ophthalmology*. 1982;89:953–960.
64. Singh AD, De Potter P, Fijal BA, et al. Lifetime prevalence of uveal melanoma in white patients with oculo(dermal) melanocytosis. *Ophthalmology*. 1998;105:195–198.
65. Bataille V, Sasieni P, Cuzick J, et al. Risk of ocular melanoma in relation to cutaneous and iris naevi. *Int J Cancer*. 1995;60:622–626.
66. Holly EA, Aston DA, Char DH, et al. Uveal melanoma in relation to ultraviolet light exposure and host factors. *Cancer Res*. 1990;50:5773–5777.
67. van Hees CL, de Boer A, Jager MJ, et al. Are atypical nevi a risk factor for uveal melanoma? A case–control study. *J Invest Dermatol*. 1994;103:202–205.
68. Rodriguez-Sains RS. Ocular findings in patients with dysplastic nevus syndrome. *Ophthalmology*. 1986;93:661–665.
69. Hammer H, Olah J, Toth-Molnar E. Dysplastic nevi are a risk factor for uveal melanoma. *Eur J Ophthalmol*. 1996;6:472–474.
70. Seregard S, Trampe E, Mansson-Brahme E, et al. Prevalence of primary acquired melanosis and nevi of the conjunctiva and uvea in the dysplastic nevus syndrome: a case-control study. *Ophthalmology*. 1995;102:1524–1529.
71. Taylor MR, Guerry DI, Bondi EE, et al. Lack of association between intraocular melanoma and cutaneous dysplastic envi. *Am J Ophthalmol*. 1984;98:478–482.
72. Lee JAH, Storer BE. Excess of malignant melanomas in women in the British Isles. *Lancet*. 1980;2:1337–1339.
73. Lee JAH, Storer BE. Malignant melanoma female/male death ratios. *Lancet*. 1981;1:1419.
74. Pack GT, Scharnagel IM. The prognosis for malignant melanoma in the pregnant woman. *Cancer*. 1951;4:324–334.
75. Reintgen DS, McCarty KS, Vollmer R, et al. Malignant

melanoma and pregnancy. *Cancer*. 1985;55:1340–1344.
76. Shiu MH, Schottenfeld D, Maclean B, et al. Adverse effects of pregnancy on melanoma: a reappraisal. *Cancer*. 1976;37:181–187.
77. Borner R, Goder G. Melanoblastoma der Uvea und Schwangerschaft. *Klin Monatsbl Augenheilkd*. 1966;149:684–693.
78. Frenkel M, Klein HZ. Malignant melanoma of the choroid in pregnancy. *Am J Ophthalmol*. 1966;62:910–913.
79. Seddon JS, MacLaughlin DT, Albert DM, et al. Uveal melanomas presenting during pregnancy and the investigation of estrogen receptors in melanomas. *Br J Ophthalmol*. 1982;66:695–704.
80. Shields CL, Shields JA, Eagle RC, et al. Uveal melanoma and pregnancy: a report of 16 cases. *Ophthalmology*. 1991;98:1667–1673.
81. Siegel R, Ainslie WH. Malignant ocular melanoma during pregnancy. *JAMA*. 1963;185:542–543.
82. Egan KM, Walsh SM, Seddon JM, et al. An evaluation of the influence of reproductive factors on the risk of metastases from uveal melanoma. *Ophthalmology*. 1993;100:1160–1166.
83. Hartge P, Tucker MA, Sheilds JA, et al. Case–control study of female hormones and eye melanoma. *Cancer Res*. 1989;49:4622–4625.
84. Holly EA, Aston DA, Ahn DK, et al. Uveal melanoma, hormonal and reproductive factors in women. *Cancer Res*. 1991;51:1370–1372.
85. Tucker MA, Shields JA, Hartge P, et al. Sunlight exposure as risk factor for intraocular malignant melanoma. *N Engl J Med*. 1985;313:789–792.
86. Gallagher RP, Elwood JM, Rootman J, et al. Risk factors for ocular melanoma: Western Canada Melanoma Study. *J Natl Cancer Inst*. 1985;74:775–778.
87. Rootman J, Gallagher RP. Color as a risk factor in iris melanoma. *Am J Ophthalmol*. 1984;98:558–561.
88. Kliman GH, Augsburger JJ, Shields JA. Association between iris color and iris melanocytic lesions. *Am J Ophthalmol*. 1985;100:547–548.

89. Horn EP, Hartge P, Shields JA, et al. Sunlight and risk of uveal melanoma. *J Natl Cancer Inst*. 1994;86:1476–1478.
90. Jakobiec FA, Silbert G. Are most iris "melanomas" really nevi? A clinicopathologic study of 189 lesions. *Arch Ophthalmol*. 1981;99:2117–2132.
91. Rones B, Zimmerman LE. The prognosis of primary tumors of the iris treated by iridectomy. *Arch Ophthalmol*. 1958;60:193–205.
92. Holly EA, Aston DA, Ahn DK, et al. No excess prior cancer in patients with uveal melanoma. *Ophthalmology*. 1991;98:608–611.
93. Lischko AM, Seddon JM, Gragoudas ES, et al. Evaluation of prior primary malignancy as a determinant of uveal melanoma: a case–control study. *Ophthalmology*. 1989;96:1716–1721.
94. Turner BJ, Siatkowski RM, Augsburger JJ, et al. Other cancers in uveal melanoma patients and their families. *Am J Ophthalmol*. 1989;107:601–608.
95. Travis LB, Curtis RE, Boice JD, et al. Second malignant neoplasms among long-term survivors of ovarian cancer. *Cancer Res*. 1996;56:1564–1570.
96. Heussen FM, Coupland SE, Kalirai H, et al. Non-ocular primary malignancies in patients with uveal melanoma: the Liverpool experience. *Br J Ophthalmol*. 2016;100(3):356–359.
97. Richtig E, Langmann G, Mullner K, et al. Ocular melanoma: epidemiology, clinical presentation and relationship with dysplastic nevi. *Ophthalmologica*. 2004;218:111–114.
98. Hyman LG, Lilienfeld AM, Ferris FL, et al. Senile macular degeneration: a case–control study. *Am J Epidemiol*. 1983;118:213–227.
99. Brilliant LB, Grasset NC, Pokhrel RP, et al. Associations among cataract prevalence, sunlight hours, and altitude in the Himalayas. *Am J Epidemiol*. 1983;118:250–264.
100. Hiller R, Giacometti L, Yuen K. Sunlight and cataract: an epidemiologic investigation. *Am J Epidemiol*. 1977;105:450–459.
101. Li W, Judge H, Gragoudas ES, et al. Patterns of tumor initiation in choroidal melanoma. *Cancer Res*. 2000;60:3757–

3760.
102. Shah CP, Weis E, Lajous M, et al. Intermittent and chronic ultraviolet light exposure and uveal melanoma: a meta-analysis. *Ophthalmology*. 2005;112:1599–1607.
103. Tallberg T, Uusitalo R, Sarna S, et al. Improvement of the recurrence-free interval using biological adjuvant therapy in uveal melanoma. *Anticancer Res*. 2000;20:1969–1975.
104. Stang A, Ahrens W, Anastassiou G, et al. Phenotypical characteristics, lifestyle, social class and uveal melanoma. *Ophthalmic Epidemiol*. 2003;10:293–302.
105. Egan KM, Gragoudas ES, Seddon JM, et al. Smoking and the risk of early metastases from uveal melanoma. *Ophthalmology*. 1992;99:537–541.
106. Keller AZ. Histology, survivorship, and related factors in the epidemiology of eye cancers. *Am J Epidemiol*. 1973;97:386–393.
107. Schwartz SM, Weiss NS. Place of birth and incidence of ocular melanoma in the United States. *Int J Cancer*. 1988;41:174–177.
108. Sliney DH. Physical factors in cataractogenesis: ambient ultraviolet radiation and temperature. *Invest Ophthalmol Vis Sci*. 1986;27:781–790.
109. Zigman S. Effects of near ultraviolet radiation on the lens and retina. *Doc Ophthalmol*. 1983;55:375–391.
110. Boettner EA, Wolter JR. Transmission of the ocular media. *Invest Ophthalmol Vis Sci*. 1962;1:776–783.
111. Lerman S. Sunlight and intraocular melanoma. *N Engl J Med*. 1986;314:712–713.
112. Hersey P, Haran G, Hasic E, et al. Alteration of T cell subsets and induction of suppressor T cell activity in normal subjects after exposure to sunlight. *J Immunol*. 1983;31:171–174.
113. Lee JAH, Merrill JM. Sunlight and the etiology of malignant melanoma: a synthesis. *Med J Aust*. 1970;2:846–851.
114. Holly EA, Aston DA, Ahn DK, et al. Intraocular melanoma linked to occupations and chemical exposures. *Epidemiology*. 1996;7:55–61.
115. Vajdic CM, Kricker A, Giblin M, et al. Sun exposure predicts

risk of ocular melanoma in Australia. *Int J Cancer*. 2002;101:175–182.
116. Althouse R, Huff J, Tomatis L, et al. An evaluation of chemicals and industrial processes associated with cancer in humans based on human and animal data: IARC monographs, volumes 1 to 20. *Cancer Res*. 1980;40:1–12.
117. Ajani US, Seddon JM, Chung-Cheng H, et al. Occupation and risk of uveal melanoma. *Cancer*. 1992;70:2891–2900.
118. Albert DM, Puliafito CA, Fulton AB, et al. Increased incidence of choroidal malignant melanoma occurring in a single population of chemical workers. *Am J Ophthalmol*. 1980;89:323–337.
119. Louria DB, Coumbis RJ, Lavenhar MA, et al. An apparent small cluster of choroidal melanoma cases. *Am J Ophthalmol*. 1982;94:172–180.
120. Ganley JP, Fontenot K. Epidemiologic study of time and space clustering of 4 cases of choroidal malignant melanoma. *Arch Ophthalmol*. 1997;115:537–541.
121. Patz A, Wulff LB, Rogers SW. Experimental production of ocular tumors. *Am J Ophthalmol*. 1959;48:98–117.
122. Benson WR. Intraocular tumor after ethionine and N-2-fluorenyl-acetamide. *Arch Pathol*. 1962;73:404–406.
123. Taylor GN, Dougherty TF, Mays CW, et al. Radium-induced eye melanomas in dogs. *Radiat Res*. 1972;51:361–373.
124. Albert DM, Gonder JR, Paple J, et al. Induction of ocular neoplasms in Fischer rats by intraocular injection of nickel subsulfide. *Invest Ophthalmol Vis Sci*. 1982;22:768–782.
125. Stang A, Schmidt-Pokrzywniak A, Lash TL, et al. Mobile phone use and risk of uveal melanoma: results of the risk factors for uveal melanoma case-control study. *J Natl Cancer Inst*. 2009;101:120–123.
126. Albert DM. The association of viruses with uveal melanoma. *Trans Am Ophthalmol Soc*. 1979;77:367–421.
127. Gellin GA, Epstein WL. Malignant melanoma from thermal burn scar. *Arch Dermatol*. 1975;111:1214–1215.
128. Kirsch N. Malignant melanoma developing in a tattoo. *Arch Dermatol*. 1969;99:596–598.

129. El Baba F, Blumenkranz MS. Malignant melanoma at the site of penetrating ocular trauma. *Arch Ophthalmol*. 1986;104:405–409.
130. Vicary D. Malignant melanoma at the site of penetrating ocular trauma. *Arch Ophthalmol*. 1986;104:1130.

144

Prognosis of Posterior Uveal Melanoma

Johanna M. Seddon, Tara A. McCannel

Uveal melanoma, an uncommon malignant tumor, can lead to vision loss and death. Gaining a better understanding of factors that may influence prognosis is an important step toward successful management of the disease. Studies of patients treated for uveal melanoma have shown tumor-related mortality rates on the order of 50% within 10–15 years after enucleation. The most established and accurate prognostic risk factor for metastasis is loss of one copy of chromosome 3, or monosomy 3 of the primary tumor. In this chapter, we review the current knowledge concerning both ocular prognosis for various local treatment modalities and systemic prognosis in terms of metastases and death among patients with uveal melanoma.

Ocular Prognosis of Globe-Conserving Therapies

Treatment of primary choroidal melanoma without evidence of metastasis involves either globe-conserving therapy or enucleation. In a randomized clinical trial of patients with primary choroidal melanoma treated with globe-conserving iodine-125 brachytherapy versus enucleation, the Collaborative Ocular Melanoma Study (COMS) demonstrated no significant difference in mortality 5, 10,

and 12 years following treatment between brachytherapy and enucleation.[1–3] Thus, increasing emphasis has been placed on globe-conserving therapy for choroidal melanoma. Reported rates of local treatment failure vary between treatment modalities and between centers using similar modalities. Radiation therapy overall results in lower rates of local treatment failure compared to nonradiation-based treatment approaches.

Radiation

Maintaining the integrity of the eye after globe-conserving treatment for choroidal melanoma is an important outcome in evaluating the success of a specific treatment. Local treatment failure or local tumor recurrence is associated with morbidity consisting of either need for reirradiation or organ loss by enucleation. Iodine-125 plaque radiotherapy is the most common primary treatment modality for choroidal melanoma. Among the largest published series reporting local treatment failure with iodine-125, the COMS medium tumor trial reported the risk of treatment failure at 5 years, as measured by local recurrence rate in 650 patients to be 10.3%.[4] A report by Sagoo et al. of 650 juxtapapillary tumors indicated a local treatment failure rate of 21% at 10 years.[5] For iodine-125 brachytherapy the local treatment failure rate in the literature ranges from 0% to 27% among centers with varying follow-up intervals and sample sizes.[6–22] Series by McCannel et al.[6] and Tabandeh et al.[8] reported very low local failure rates with iodine-125, 0% and 1.7%, respectively; both centers use intraoperative ultrasonography which minimizes the risk of edge-miss. Among the treatment modalities that involve radiation, Rouberol et al. reported a 21.7% and 24.3% rate of local recurrence after 5 and 10 years, respectively, after ruthenium brachytherapy in 213 patients treated from 1983 to 1995.[23] Wilson also reported in a retrospective review a higher local treatment failure rate using ruthenium plaques compared to both proton beam irradiation and iodine-125 brachytherapy.[24] In a series of 368 patients treated with proton beam, Mosci reported a local treatment failure rate of 8.4%.[25] In another group of 1922 patients treated with proton beam irradiation, a local recurrence rate of 3.2% and 4.3% at

5 and 10 years, respectively, was reported.[26] Published data indicate that the use of ruthenium results in higher rates of local treatment failure than iodine-125. Proton beam radiotherapy has a variable rate of local failure depending on the experience of the treatment center. Direct comparisons between iodine-125 and proton therapy have been scarce; however, recently, Mishra and colleagues reported a local failure rate of 2% and 21% with helium ion charged particle and iodine-125 therapy, respectively, at 12 years follow-up at their center.[27] Iodine-125 is the most commonly used form of local treatment for uveal melanoma in North America and rates of local treatment failure vary between centers.

Silicone Oil as Vitreous Substitute for Radiation Attenuation

Although the traditional delivery of radiation by brachytherapy remains an extraocular treatment, a new method that has been adopted at a few Ocular Oncology Centers is vitreoretinal surgery with Silicone Oil 1000 centistokes placement for radiation attenuation. Initially reported by Oliver et al.,[28] and subsequently corroborated by Ahuja et al,[29] Silicone Oil 1000 centistokes results in a 50–60% reduction in iodine-125 radiation compared to water or aqueous. A matched case–control series comparing iodine-125 brachytherapy with and without Silicone Oil 1000 centistokes revealed an improvement in radiation maculopathy at 2 years.[30a] A recent case-control analysis by McCannel et al.,[30b] showed significant visual benefit in large uveal melanoma treated with vitrectomy and silicone oil for vitreous attenuation.

Nonradiation Therapy

Nonradiation local treatment of uveal melanoma includes laser photocoagulation, Visudyne photodynamic therapy, and transpupillary thermotherapy. The main theoretical advantages of laser over radiation include minimizing collateral damage to healthy ocular tissues compared to radiation, minimizing radiation exposure to the patient and operator, and a more simplified treatment approach not requiring radiation oncology or use of an

operating theater. However, laser overall has been found to be less successful in achieving local tumor control compared with most forms of radiation-based treatment. The literature is sparse on reports utilizing argon laser photocoagulation to treat choroidal melanomas, but there are many reports of failures, and the prevailing opinion is that argon laser is not an adequate primary treatment for choroidal melanoma of any size.[31–33] There are few reports of photodynamic therapy for uveal melanoma in the literature; only two case reports exist using this technique for small atypical amelanotic choroidal melanoma.[34,35] Barbazetto et al. reported a case series of four patients treated by photodynamic therapy with recurrent tumors treated with other modalities, resulting in eventual enucleation of two eyes.[36]

Following the discontinuation of transpupillary thermotherapy (TTT) as a therapy for age-related macular degeneration, a noticeable interest in this form of thermal laser for use in posterior segment tumors occurred. However, the largest series using TTT reported high rates of local treatment failure. Shields et al. reported a 22% local treatment failure rate at 3 years in a series of 256 posterior uveal melanoma treated by transpupillary thermotherapy.[37] Aaberg et al. reported a rate of 23% at 5 years in a series of 135 patients.[38] Zaldivar described eight cases with histologic findings in eyes enucleated after failed TTT. Although the height of the tumor decreased, extrascleral extension and lateral spread of the tumor ensued.[39] Harbour found that not only was there no significant difference in visual outcome between TTT and plaque radiotherapy, but also that the recurrences were substantially higher when TTT was used compared with iodine-125 plaque.[40] Currently, the use of TTT has been limited to an adjunct to primary brachytherapy to compensate for edge-miss in plaque placement by some operators.[41,42]

Surgery

Surgical approaches involving excision of the tumor have been described using a transscleral approach (transscleral endoresection or local resection) or an internal approach with vitrectomy and resection of the tumor with the vitrectomy probe. The former

technique may pose technical difficulties due to the requirement for systemic hypotensive anesthesia to reduce the risk of choroidal hemorrhage. In the reports described below, there are higher rates of ocular complications and a lower rate of overall globe retention comparing surgical transscleral endoresection to standard brachytherapy. Despite these significantly higher rates of local treatment failure and enucleation, there may be select cases where one might consider tumor resection over standard brachytherapy.

Peyman et al.[43] studied a group of 34 patients treated by eye wall resection with an average follow-up of 5.3 years and reported that 11 (32.3%) required enucleation (mainly because of evidence of tumor cells in resected margins) and 13 (38.2%) retained 20/200 or better vision after treatment. No patient had local treatment failure, and two patients had died of metastatic melanoma at the time of that report. In a matched case–control study, 81 of 49 pairs of patients undergoing either transscleral resection at one center or iodine brachytherapy at another, Kivela and colleagues found fewer recurrences with plaques than resection, but no difference in 8-year mortality.[44] Furthermore, only eyes undergoing radiation experienced neovascular glaucoma, radiation retinopathy, cataract, or ischemic changes. Shields et al.[45] described a series of 95 patients with choroidal or ciliary body tumors, or both, who were managed by partial lamellar sclerouvectomy. A total of 81 cases (85%) were uveal melanoma; vitreous hemorrhage occurred in 79 (83%); intraretinal or subretinal hemorrhage in 33 (35%); retinal detachment in 26 (28%); and cataract in 32 (34%) patients. Retinal detachment surgery was necessary in 16 patients (17%), and enucleation was necessary in 15 (16%) patients. Distant metastases developed in five patients (5%) with a median follow-up of 2.5 years. In the largest series of transscleral endoresection by Damato et al., the local treatment failure rate at 3 years was 20%.[46] Puusaari et al. in a series of 33 patients reported a local treatment failure rate of 40% by 5 years.[47] Garcia-Arumi[48] reported in a series of 34 cases of vitrectomy with tumor endoresection with average follow-up of 70 months a local treatment failure rate of 5.8%, which is comparable with reports of others who have used vitrectomy with endoresection.[49,50]

Systemic Prognosis for Metastasis and Death

The most common site for metastasis in uveal melanoma is the liver. At least 50% of all patients diagnosed with uveal melanoma develop metastatic disease.[51] The COMS study reported liver metastasis with median survival once metastasis was diagnosed between 6 and 12 months.[52] In an analysis of metastatic uveal melanoma patients by Rietschel et al., the authors found that the most common nonhepatic first-metastatic site to be diagnosed was the lung.[53] Patients who were younger than age 60 had metastasis to the lung, had a longer interval between treatment of the melanoma and discovery of metastasis, and had better survival after a diagnosis of metastatic disease.

There is a lack of substantial difference in survival for local globe-preserving therapies compared with enucleation in the early posttreatment years, which may be related to the possibility that metastases occur before the tumor is treated, perhaps before it is diagnosed.[54] Another consideration in evaluating the apparent similarity in survival outcome of conservative therapies in comparison with enucleation is that selection of patients with small- to medium-sized tumors and other more favorable prognostic indicators for eye-sparing treatment methods may bias survival results in favor of these therapies. It is therefore important to control for these prognostic factors to the extent possible in nonrandomized studies. A data collection and management system for studies of prognosis and treatment was developed in the 1980s in order to standardize these measures in observational cross-sectional and longitudinal studies and was used to identify several factors relevant to metastasis.[55–58] In the initial studies evaluating prognosis after treatment with proton beam or enucleation,[57,58] the Cox proportional hazards model was first used in ophthalmology to study prognosis and survival after treatment of uveal melanoma. Epidemiologic methods were applied to standardize variables and control for differences in demographic factors as well as tumor-specific variables: tumor height, tumor diameter, location of the tumor posterior to the equator, anterior to the equator, and involvement of the ciliary body. Larger tumor size and anterior

location decreased rate of survival, and treatment type did not have a significant effect. Length of observation period or evidence of growth prior to treatment has not been shown to affect prognosis. Visual outcomes after proton beam irradiation were also evaluated using these methods.[59,60]

Radiation Therapy

Metastasis and Survival

Actuarial survival rates following radiation therapy of uveal melanoma have been reported to be 75%[61] to 80%,[62] and 89%[63] 5 years after treatment. For 96 patients treated by cobalt plaque, the 5-year survival rate (without death from metastatic melanoma) was approximately 75%.[61] In a study of 128 patients treated by proton beam irradiation,[62] with a median of 5.4 years of follow-up, the probability of metastasis-free survival at 5 years was 80%. Lommatzsch[64] reported a 5-year survival of 89% in a group of 309 patients treated by ruthenium. In that study, tumors measured up to 5 mm in height and 15 mm in diameter, and the mean follow-up was 6.7 years. Similar survival estimates were observed in a series of ruthenium-treated patients in Germany,[65] Sweden,[66] and Finland.[67] In an update of an earlier report, Char reported on long-term outcomes in 218 patients treated with helium ion irradiation and followed for an average of 12 years.[68,69] The mean tumor thickness in this cohort was 6.7 mm, and the mean largest tumor dimension was 11.9 mm; 5-, 10-, and 15-year survival were estimated to be 73%, 61%, and 54%, respectively. Series of patients treated by iodine-125 irradiation[70,71] have also been described.

Prognostic factors for patients treated by irradiation have been evaluated in several studies. Using the tumor registry and analytic methods developed by Seddon and colleagues,[55–60] the first 780 patients treated by proton beam irradiation were evaluated,[62] of whom 64 had developed metastasis at the time of the study. Similar to the earlier studies, leading predictors of metastasis were tumor diameter larger than 15 mm, ciliary body involvement, extrascleral extension, and age at treatment of 60 years or older. Surgical localization of the tumor and elevated pretreatment liver enzymes were not statistically significant prognostic factors. They found no

survival advantage of proton beam irradiation compared with enucleation.[57,72] In an investigation of the role of hormonal factors in the development of metastasis,[73] among women of childbearing age who had been treated by proton beam irradiation for uveal melanoma neither postirradiation pregnancy history nor oral contraceptive use were associated with the rate of metastasis.

Tumor regression is closely monitored following treatment. Rashid et al. have reported that the specific regression pattern of tumors can be heterogenous and other clinical features in addition to tumor height could be evaluated in assessing treatment response.[74] Augsburger and coworkers studied tumor regression as a prognostic factor for metastasis following cobalt plaque irradiation. Findings of this preliminary study suggest that rapid tumor regression is a poor prognostic sign.[75] Tumors regressing more rapidly were significantly more likely to metastasize concurrently with their regression in a series of patients treated by proton beam irradiation.[76] However, recently Correa and Augsburger evaluated the relationship of rate of posterior tumor flattening and molecular risk category by gene expression profiling at 6 months post treatment and reported that there was no association between risk of metastases and faster shrinkage when the effect of initial tumor thickness was controlled.[77] Rather than more biologically aggressive uveal melanomas responding more rapidly to treatment, large tumors have a greater likelihood of shrinking after treatment compared to small tumors due to the original size of the tumor rather than its activity.

Local Treatment Failure and Metastatic Prognosis

Local tumor recurrence or local treatment failure may increase the risk of metastases from uveal melanoma.[78,79] This appeared to be the case in a cohort of patients with juxtapapillary melanoma treated by brachytherapy.[80] In that study, rates of melanoma metastasis were 13%, 16%, and 37% at 5, 10, and 15 years, respectively; tumor recurrence (defined as any amount of regrowth), larger tumor diameter, and superior location of the tumor were found to predict occurrence of distant metastasis. This may be due in part to technical difficulties in placement of the plaque, resulting in undertreatment of the tumor (or overtreatment of the normal

retina). Harbour et al.[81] evaluated the prognostic significance of patterns of tumor regrowth after irradiation. The relative risk for death resulting from metastasis was significantly higher among patients with increased tumor thickness than among those whose tumor spread at the margin (5.1 vs. 2.2, respectively, relative to those without tumor recurrence). The mean rate of metastasis was also significantly higher in patients with increased tumor thickness compared with those with marginal spread. Recently, analyses of data from an online tumor data registry of over 3000 uveal melanoma patients revealed that 5- and 10-year metastasis-free Kaplan–Meier estimates for the recurrence-free group were 87% and 82% vs. 71% and 62% for the local recurrence group, and these differences were statistically different.[82] Reducing local treatment failure is critical in the management of primary uveal melanoma for the sake of preserving the eye, with questionable evidence of significant influence on the development of systemic metastasis.

Prognosis After Enucleation

Metastasis from uveal melanoma may occur at any time after the onset of tumor diagnosis. Jensen,[83] in his 25-year follow-up of Danish patients, found that the peak incidence of metastasis occurred during the first year after enucleation, and over half of those who developed metastasis did so within 3 years of treatment. However, it is a well-known but poorly understood fact that patients may develop metastasis decades after enucleation. Due to hypotheses that enucleation itself might cause increased mortality,[84] the COMS study compared enucleation to pre-enucleation radiation for large tumors, and did not find a difference in mortality.[51]

Comprehensive and long-term studies of survival after enucleation derive from Denmark and Finland. These reports have the advantage of being population based with few losses to follow-up. Raivio compiled a roster of all patients diagnosed with uveal melanoma between 1923 and 1966 in Finland.[85] Of 359 identified cases, survival status at 10 years was known for all but five patients; 314 cases (89%) had 15 or more years of follow-up available, and 214 cases (60%) had at least 20 years. The 5-, 10-, and 15-year survival rates based on melanoma-related deaths were 65%, 52%,

and 46%, respectively. Of the 42 patients who survived at least 20 years, nine later developed metastasis. Jensen[83] evaluated survival at least 25 years after enucleation in Danish patients with uveal melanoma. The majority of patients included in the original series had died (82%); 51% of those deaths were due to metastasis. Actuarial survival rates at 5, 10, and 15 years were similar to those reported by Raivio.[85] A novel deficit survival analysis of 230 patients in 1984 by Lavin and colleagues indicated no overall survival advantage after enucleation.[86]

Metastasis from uveal melanoma usually occurs within the first few years after enucleation. The liver is usually the first site of metastasis after treatment.[87–90] There is some evidence to suggest that metastasis may occur several years before the diagnosis of hepatic metastasis is made.[54,91,92] Other organs that may be affected include the lung, bone, skin, and central nervous system.[89] The majority of patients with hepatic involvement succumb within a few months of detection of the metastatic lesion.[90]

Visual Prognosis and Ocular Morbidity

Rates of complications and visual loss after radiation depend on the type of treatment and the size and location of the tumor within the eye. Severe complications requiring enucleation have been reported to occur in 10%[93] to 22%[69] of patients. Rubeosis iridis and neovascular glaucoma[94] and radiation retinopathy or optic neuropathy[64,88,95,96] have been reported as the major complications that may occur in irradiated eyes. Lens opacification is a common complication of helium ion[97] and proton beam[98] radiotherapy, occurring in over 40% of cases in published series. Development of cataracts is also relatively common after episcleral plaque therapy[71,99,100] with reported 5-year incidence ranging from about 20%[71] to 37%.[100]

Vision after proton beam irradiation has been studied,[59,60] and greater tumor thickness and proximity to the disc or macula (or high dose to these structures) were found to increase the risk of vision loss to worse than 20/200. Curves demonstrating cumulative

probability of visual acuity loss according to height and distance of the tumor from the optic disc and fovea are presented in Fig. 144.1. When patients were evaluated according to combined tumor characteristics, the probability of retaining vision of 20/200 or better at 3 years was 91% in the low-risk group (tumors 5 mm in height and more than two disc diameters from the macula and disc), 61% in the intermediate-risk group (tumors that were tall or close to the disc or macula), and 24% in the high-risk group (tumors that were tall and close to the disc or macula).

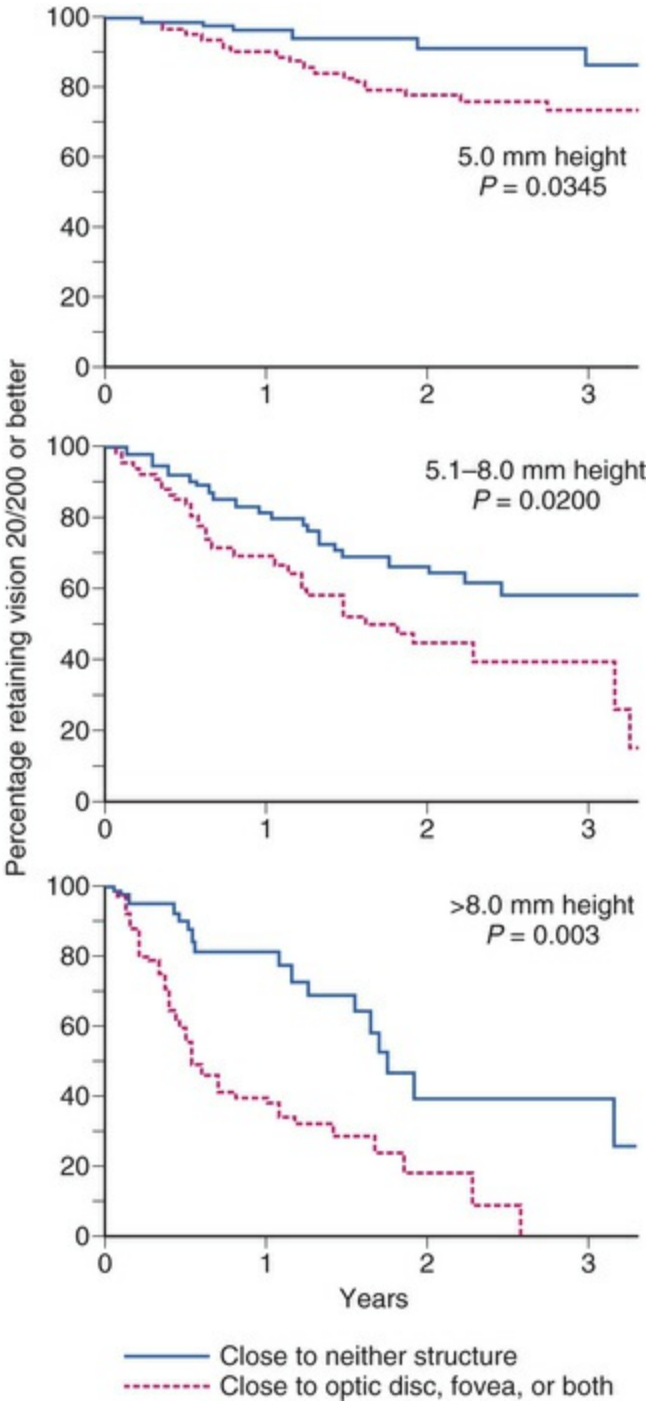

FIG. 144.1 Cumulative probability of visual acuity loss according to height and distance of the tumor from the optic disc and fovea. "Close" refers to less than or equal to 2 disc diameters, or approximately 3 mm from the structure. (Reproduced from Seddon JM, Gragoudas ES, Polivogianis L, et al. Enucleation vs cobalt 60 irradiation of melanomas. Ophthalmology 1986;93:666, with permission from the American Academy of Ophthalmology ©1986.)

Visual field deficits have also been demonstrated after proton

beam irradiation.[101] Visual acuity outcomes similar to those in proton beam-irradiated patients were seen after iodine-125 plaque.[102] In a review of 93 patients undergoing plaque therapy for juxtapapillary lesions,[80] 72% of patients lost at least 3 lines of visual acuity as measured on a Snellen chart by 4–5 years after treatment. The risk of losing this amount of vision was related to initial visual acuity; patients with better initial visual acuity (i.e., 20/20–20/40) were more likely to experience a loss of 3 or more lines than those with initial visual acuity of 20/50–20/100 or worse than 20/100 (67%, 64%, and 8%, respectively, at 5 years after treatment). In another study of 186 patients treated by helium ion irradiation, 49% retained 20/200 or better vision in the treated eye, with a median follow-up time of 26 months.[103]

In addition to measured visual acuity, visual functioning is a major concern after treatment for uveal melanoma. Augsburger et al.[104] evaluated vision-related changes in employment and ability to drive, read, and watch television by standardized interview in patients treated by plaque radiotherapy or enucleation. Among 51 patients in the plaque radiotherapy group followed for a mean interval of 87 months after treatment, over 90% had no loss of vision-related performance. Similar results were reported in 51 enucleated patients followed for an average of 89 months. Thus, despite potential acuity loss in the affected eye, the vast majority of patients treated with plaque radiotherapy or enucleation retained full functioning in vision-related activities.

Clinical Prognostic Indicators for Metastasis

Tumor Size and the American Joint Committee on Cancer (AJCC) Classification Stage

Tumor size is an important prognostic factor for eventual metastasis. Size has been variously defined in different studies as the largest tumor dimension: height and diameter;[55–60] largest diameter in contact with the sclera;[105] combination of largest

diameter and height;[106] area of the tumor base;[107] and tumor volume.[108,109] These differences should be considered when comparing studies of tumor size and prognosis. Kaplan–Meier survival curves that show steadily worsening prognosis with every 2 mm increase in largest tumor dimension are presented in Fig. 144.2.[58]

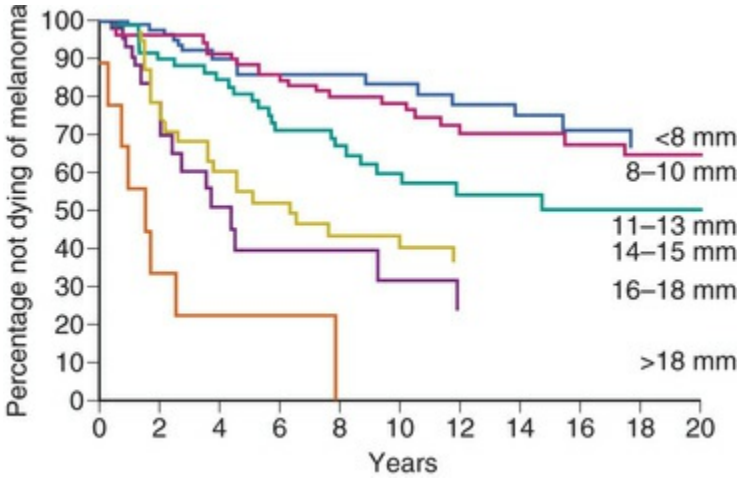

FIG. 144.2 Cumulative probability of not dying of melanoma and largest tumor dimension. (Reproduced with permission from Seddon JM, Albert DM, Lavin PJ, et al. A prognostic factor study of disease-free interval and survival following enucleation for uveal melanoma. Arch Ophthalmol 1983;101:1894–1899. ©1983 American Medical Association. All rights reserved.)

Flocks et al.[108] were among the first to recognize the importance of tumor size. Using Armed Forces Institute of Pathology data, they estimated tumor volume as the product of the tumor's largest diameter, diameter perpendicular to the largest diameter, and height. When tumors were divided into two groups, based on whether they were larger or smaller than the median value of 1344 mm^3, the 5-year mortality rates were 15% and 54% for the smaller and larger tumors, respectively. McLean et al.[109] reported a somewhat higher 6-year mortality for tumors less than 1400 mm^3 (25%), one difference being that Flocks et al. had excluded tumors with extrascleral extension.

The great majority of subsequent studies have confirmed the influence of tumor size on prognosis. Most of these studies have considered small tumors to be those no larger than 10 mm in largest

diameter and 2–3 mm in height. Warren[106] studied 108 patients from eastern Iowa with five or more potential years of follow-up. No deaths from metastases occurred in the group of 10 patients with tumors up to 10 mm in diameter and 2 mm in thickness. Tumors were considered medium-sized if they were no larger than 15 mm in diameter and 5 mm in height, and nine of 24 patients (37%) in this group died of metastasis. Mortality was highest in patients with large tumors; over half of patients (57%) died of the disease in this group. Shammas and Blodi[105] updated this series with additional cases, bringing the total to 293 and classified tumors according to largest diameter in contact with the sclera. Actuarial 6-year survival rates dropped with increasing tumor diameter from 87% for tumors 10 mm or less, to 30% for tumors larger than 12 mm. Long-term survival was found by Jensen[107] to be quite poor even in patients with small tumors. He reported that of the 30 patients whose tumors were less than 10 mm in diameter and 3 mm in height, 12 (40%) died of metastatic disease. The corresponding figure for tumors with largest cross-sectional area >100 mm^2 was 63%. Among clinical parameters available before treatment, largest tumor dimension (classified as <10 mm, 10–15 mm, or >15 mm) was found to be the most useful predictor of metastasis and mortality in a series of 111 patients.[86] In that study, the sensitivity, specificity, and positive and negative predictive value of largest tumor dimension were similar to those of cell type. Other reports including meta-analyses and reviews of large series of patients with uveal melanoma confirm the importance of tumor size.[110,111]

The American Joint Committee on Cancer (AJCC) anatomic stage classification for uveal melanoma has been reported to predict prognosis, with higher stage correlating with higher risk for distant metastasis.[112,113] Furthermore, Bagger and colleagues indicated that chromosome 3 status together with AJCC stage provided a more accurate prediction of survival compared to AJCC stage alone.[114]

Histopathologic Prognostic Indicators for Metastasis

Histopathology and Immunogenetics

In 1931, Callender[115] published the first classification system of uveal melanoma according to histopathologic type. Callender described five histologic types: spindle cell subtypes A and B, epithelioid, fascicular, and mixed cell-type tumors composed of both spindle cells and epithelioid cells. Although this original system has undergone some refinement, it still serves as the basis for histologic typing of uveal melanomas.

The Callender classification system has been found in many studies to be a useful method for distinguishing tumors with varying degrees of malignancy. Jensen[107] evaluated mortality according to cell type in his series of 226 Danish patients and compared his results with those of the previously published series of Zimmerman et al.[116] In these reports, 10-year mortality ranged from 11% to 19% in spindle A tumors; 21–36% in spindle B tumors; 63–79% in mixed-cell tumors, and 72–100% in epithelioid tumors.

Limitations of the Callender system have been recognized. First, there are no histologic criteria to distinguish spindle A cell tumors from nevi. Second, there are no criteria for classification of a tumor composed of a mixture of spindle A and spindle B cells and no differentiation among the large group of tumors classified as mixed. To quantify these histologic observations, a standard measurement was created and new parameters were assessed, including the number of epithelioid cells per high-power field and inverse standard deviation of nucleolar area,[117] which were found to predict metastatic death. These methods require enucleation of the globe in order to obtain histopathology. Increasingly, globe-conserving therapies are the preferred treatment approach for local tumor control when possible. Furthermore, the cytology provided by the use of fine-needle aspiration biopsy in nonenucleated tumors is considered inadequate for evaluation of cellular morphology. Thus, molecular risk factors, discussed below, are of increasing value for determining prognosis.

Tumor Microvasculature

The presence of epithelioid cells,[117] extravascular matrix patterns that reflect the arrangement of tumor microcirculation,[118–121] high microvascular density,[122–124] and large numbers of tumor-infiltrating

macrophages[125,126] in primary uveal melanoma are independently associated with shorter time to metastatic death. These associations may be either markers of aggressive tumors without direct contribution to the metastatic cascade or they may indicate direct participation in tumor progression to metastasis. Toivonen et al. found that the presence of epithelioid cells and microvascular density were closely associated with progression of uveal melanoma from primary tumor to metastasis, in a cross-sectional histopathologic analysis of hepatic metastasis and the corresponding primary choroidal tumor. High microvascular density may help to predict survival after detection of hepatic metastases.[127]

Microvascular patterns within tumor tissue have been studied. Folberg et al. described nine distinct vascular patterns observed in tissue from 234 enucleated uveal melanomas.[118] Two observers independently reviewed slides from each tumor and assessed the presence or absence of each vascular pattern. The presence of networks of three or more contiguous closed vascular loops was highly predictive of melanoma-related and all-cause mortality. Kaplan–Meier estimates of 10-year survival were 50.7% when networks were present and 88.3% in the absence of networks. McLean,[120] in a series of 496 eligible uveal melanoma patients from the registry of ophthalmic pathology, confirmed Folberg's observation of the prognostic significance of vascular loops, despite the use of different measurement techniques. Foss et al. investigated vascular patterns and microvessel density in a cohort of 120 patients with available tissue blocks and survival follow-up (mean, 77 months).[123] Vessel count was highly predictive of melanoma-related death; vascular patterns as described by Folberg[118] were less clearly correlated with melanoma mortality in this study. Principal component analysis of vascular patterns from this cohort of patients[128] identified three combinations of patterns, two of which – disordered growth and emergence of rapidly growing subclones – were predictive of melanoma mortality. However, as with histopathology, tumor microvasculature cannot be evaluated in this manner unless the tumor is enucleated.

Extrascleral Extension

Another factor shown in many studies to increase the risk of tumor-related death after enucleation is extrascleral extension of the tumor. Histopathologic evidence of orbital extension is usually found in 8–14% of cases.[129–131] Shammas and Blodi[131] reported that only eight of 30 patients with extrascleral extension and 5 potential years of follow-up survived to 5 years. The majority died within 16 months after enucleation. The 5-year survival rate was 26% in patients with orbital extension and 78% in those without extension. In Jensen's 25-year follow-up of patients,[107] the long-term survival estimate for patients with orbital extension was 29%. The relationship between the probability of not dying of melanoma and the presence of extrascleral extension was evaluated in another group of patients using new statistical methods in 1983, including Kaplan–Meier survival curves and Cox proportional hazards models.[58] Much poorer survival was seen in the group with extrascleral extension. There are no data to suggest that exenteration improves mortality in patients with extrascleral extension.[129,131,132]

Molecular Prognostic Indicators for Metastasis

Tumor cytogenetic studies have revealed that abnormalities in chromosomes 3, 6, and 8 in the tumor tissue itself have been linked to metastatic death.[132–139] A loss of chromosome 3 is associated with a poor prognosis; gains in chromosome 8 are associated with a worse prognosis, and abnormalities in chromosome 6 are associated with a good prognosis. Rather than simply markers of tumor progression, gross chromosomal changes may be associated with specific mutations that become manifest with chromosomal aberration.

White et al.[140] performed cytogenetic analyses on 54 tumor patients and correlated the results with the patient clinical outcome. It was found that abnormalities in both chromosomes 3 and 8 were important in predicting metastasis; abnormalities in chromosome 6, despite abnormalities in 3 and 8, portended a good prognosis. Prescher et al.[141] examined 180 uveal melanoma patients in whom

primary enucleation was the selected treatment. Tumor histology, cytogenetics, and clinical data were obtained from the tumor specimens. The tumors of 30 patients had monosomy 3. This resulted in 57% of these patients succumbing to metastasis and the 3-year relapse-free survival rate was 50%. Of the 24 patients with a normal chromosome 3, none developed metastasis. Monosomy 3, tumor location, and tumor diameter were the most significant predictors of poor prognosis. Furthermore, histologic subtype, age, sex, extrascleral growth and tumor thickness had no predictive value. Scholes et al.[142] also found that monosomy 3 and the development of metastasis did not correlate with tumor size or histologic subtype, emphasizing the likely inadequacy of size and histology alone as good predictors for metastasis. Thus, cytogenetically speaking, uveal melanoma appears to fall into two largely mutually exclusive cytogenetic groups: those patients who will go on to develop fatal metastasis (monosomy 3 of the tumor) and those patients who will not (absence of monosomy 3). Work by Onken et al.[143] has demonstrated the results of gene expression profiling in 25 primary choroidal melanoma specimens. The tumors clustered into two groups that correlated strongly with metastatic risk. A "Class 1" tumor designation indicated a low-risk for metastasis; a "Class 2" designation indicated a high risk for metastasis.

Prognosticating the risk of developing metastatic uveal melanoma has traditionally been based on clinical and histopathologic characteristics of the primary tumor, as discussed previously. However, as the majority of uveal melanomas are now being treated with globe-sparing surgery, analysis of molecular and cytogenetic information from uveal melanoma fine-needle aspiration biopsy has evolved and is becoming increasingly common.[144–147] Both DNA and RNA can be analyzed from the tumor. Cytogenetic testing can be performed for chromosomes of interest using fluorescence in situ hybridization (FISH). FISH testing may be performed in a hospital clinical cytogenetics laboratory. However, other assessment techniques that are investigational and less widely available include whole-genome single-nucleotide polymorphism (SNP), multiplex ligation-dependent probe amplification (MLPA) and microsatellite analysis

(MSA).

Whole-genome SNP analyses assess all regions of all chromosomes; however, MLPA and MSA examine a limited number of chromosomes that are believed to be of interest. Although SNP testing provides information across the entire genome, it is considerably more costly to perform compared to MLPA or MSA. A commercially available RNA-based assay for choroidal melanoma is available to categorize tumors as Class 1 (low-metastatic risk) and Class 2 (high-metastatic risk); however, because this test does not provide cytologic confirmation of the presence of melanoma tissue being sampled, a meaningful test result is assured in combination with cytopathology for diagnostic confirmation. A recent report by Klufas and colleagues indicated that nonmelanoma tumor tissue may also give Class 1 and Class 2 test results, despite there being no melanoma cell type present.[148] Molecular prognostic tests with results specific to uveal melanoma (such as DNA-based tests identifying monosomy 3) may provide more valid information.

Although the specific chromosomal abnormalities, namely monosomy 3, may be important in predicting cancer prognosis with respect to metastasis, the use of molecular markers and/or mutations of biologic relevance have yet to be discovered. In the future, tumor tissue may be screened for these markers, which might help tailor therapies for uveal melanoma metastasis when such treatments exist. Currently, despite treatment with current chemotherapeutic regimens, patients with metastases from uveal melanoma usually die within 2–14 months after the diagnosis of disseminated disease and the prognosis has not significantly improved over the decades. We need a better understanding of the biologic mechanisms contributing to development and progression of metastatic uveal melanoma.

Improving Prognosis With Early Treatment of Uveal Melanoma

Although the COMS established that there was no survival advantage after treating uveal melanoma with plaque versus

enucleation, data in support of higher metastatic risk for larger-sized uveal melanomas suggest that early treatment prior to significant tumor growth may improve survival for patients. This has been debated with skeptics citing the likelihood of lead-time bias for the development of metastasis when smaller tumors are treated. Damato and colleagues reported that patients who were younger at treatment had smaller tumors and had a lower rate of metastatic outcome. Results based on outcomes in over 3000 patients over about a 20-year interval suggest that treatment may prevent tumor growth, dedifferentiation, and metastatic disease in some patients, especially those with smaller tumors.[149]

Achieving local tumor control with radiotherapy or enucleation may prevent further accumulation of chromosomal aberrations, which could influence the ability of the tumor to metastasize. In a series of 452 uveal melanomas where MLPA was used to determine aberrations in chromosomes 3, 6, and 8, Damato, Dopierala, and Coupland found that chromosomal abnormalities accumulated with tumor growth, in keeping with genomic instability, which is a feature of malignant neoplasia.[150] One explanation for a higher rate of distant metastasis in uveal melanoma with local recurrence after treatment is that unchecked tumor growth may select for an aggressive cytogenetic phenotype, thereby enabling the metastasic process. With earlier detection and improvement in the ability to diagnose, biopsy, and treat small choroidal melanomas, evaluation of metastatic outcome will be critical. It may be possible to not only achieve local tumor control in patients with small choroidal melanoma, but also influence metastasis in this subset of patients.

Conclusion

Uveal melanoma is an uncommon but life-threatening intraocular malignancy. Available evidence suggests that observation of small, inactive tumors does not substantially increase the risk of metastasis. For patients managed by initial observation, the decision to treat and the timing of treatment depend on clinical judgment. Approximately 50% of patients diagnosed with uveal melanoma develop metastasis within 10–15 years after enucleation, with rates varying depending on chromosome 3 status of the tumor

and tumor size. Despite the continual emergence of new eye-conserving therapies, radiation is the superior treatment of choice to minimize the serious morbidity of local treatment failure. Unfortunately, selection of treatment does not prevent tumor-related death. A better understanding of the molecular events leading to metastasis, including cellular differentiation, adhesiveness, and vascular biology, may help in the development of new systemic therapies. With the increasing use of fine-needle aspiration biopsy to obtain molecular information for metastatic prognosis, an opportunity for studying primary tumor biology exists which could lead to a better understanding of uveal melanoma metastasis and prognosis.

References

1. Diener-West M, Earle JD, Fine SL, et al. The COMS randomized trial of iodine 125 brachytherapy for choroidal melanoma. III. Initial mortality findings. COMS report no. 18. *Arch Ophthalmol*. 2001;119:969–982.
2. Collaborative Ocular Melanoma Study Group. Ten-year follow-up of fellow eyes of patients enrolled in Collaborative Ocular Melanoma Study randomized trials: COMS report no. 22. *Ophthalmology*. 2004;111:966–976.
3. The COMS randomized trial of iodine 125 brachytherapy for choroidal melanoma. V. Twelve-year mortality rates and prognostic factors. COMS report no. 28. *Arch Ophthalmol*. 2006;123:1684–1693.
4. Jampol LM, Moy CS, Murray TG, et al. The COMS randomized trial of iodine 125 brachytherapy for choroidal melanoma. IV: Local treatment failure and enucleation in the first 5 years after brachytherapy. COMS report no. 19. *Ophthalmology*. 2002;109:2197–2206.
5. Sagoo MS, Shields CL, Mashayekhi A, et al. Plaque radiotherapy for juxtapapillary choroidal melanoma: tumor control in 650 consecutive cases. *Ophthalmology*. 2011;118:402–407.
6. McCannel TA, Chang MY, Burgess BL. Multi-year follow-up of fine needle aspiration biopsy in choroidal melanoma.

Ophthalmology. 2012;119(3):606–610.
7. Correa R, Pera J, Gomez J, et al. (125)I episcleral plaque brachytherapy in the treatment of choroidal melanoma: a single-institution experience in Spain. *Brachytherapy*. 2009;8:290–296.
8. Tabandeh H, Chaudhry NA, Murray TG, et al. Intraoperative echographic localization of iodine-125 episcleral plaque for brachytherapy of choroidal melanoma. *Am J Ophthalmol*. 2000;129:199–204.
9. Packer S, Stoller S, Lesser ML, et al. Long-term results of iodine 125 irradiation of uveal melanoma. *Ophthalmology*. 1992;99:767–774.
10. Garretson BR, Robertson DM, Earle JD. Choroidal melanoma treatment with iodine 125 brachytherapy. *Arch Ophthalmol*. 1987;105:1394–1397.
11. Bosworth JL, Packer S, Rotman M, et al. Choroidal melanoma: I-125 plaque therapy. *Radiology*. 1988;169:249–251.
12. Sia S, Harper C, McAllister I, et al. Iodine-I25 episcleral plaque therapy in uveal melanoma. *Clin Experiment Ophthalmol*. 2000;28:409–413.
13. Quivey JM, Char DH, Phillips TL, et al. High intensity 125-iodine (125I) plaque treatment of uveal melanoma. *Int J Radiat Oncol Biol Phys*. 1993;26:613–618.
14. Fontanesi J, Meyer D, Xu S, et al. Treatment of choroidal melanoma with I-125 plaque. *Int J Radiat Oncol Biol Phys*. 1993;26:619–623.
15. Jensen AW, Petersen IA, Kline RW, et al. Radiation complications and tumor control after 125I plaque brachytherapy for ocular melanoma. *Int J Radiat Oncol Biol Phys*. 2005;63:101–108.
16. Karlovits B, Trombetta MG, Verstraeten T, et al. Local control and visual acuity following treatment of medium-sized ocular melanoma using a contact eye plaque: a single surgeon experience. *Brachytherapy*. 2011;10:228–231.
17. Nag S, Wang D, Wu H, et al. Custom-made "Nag" eye plaques for 125I brachytherapy. *Int J Radiat Oncol Biol Phys*. 2003;56:1373–1380.

18. Lumbroso-Le Rouic L, Charif Chefchaouni M, Levy C, et al. 125I plaque brachytherapy for anterior uveal melanomas. *Eye (Lond)*. 2004;18:911–916.
19. Sobrin L, Schiffman JC, Markoe AM, et al. Outcomes of iodine 125 plaque radiotherapy after initial observation of suspected small choroidal melanomas: a pilot study. *Ophthalmology*. 2005;112:1777–1783.
20. Leonard KL, Gagne NL, Mignano JE, et al. A 17-year retrospective study of institutional results for eye plaque brachytherapy of uveal melanoma using (125)I, (103)Pd, and (131)Cs and historical perspective. *Brachytherapy*. 2011;10:331–339.
21. Wilson MW, Hungerford JL. Comparison of episcleral plaque and proton beam radiation therapy for the treatment of choroidal melanoma. *Ophthalmology*. 1999;106:1579–1587.
22. Puusaari I, Damato B, Kivela T. Transscleral local resection versus iodine brachytherapy for uveal melanomas that are large because of tumour height. *Graefes Arch Clin Exp Ophthalmol*. 2007;245:522–533.
23. Rouberol F, Roy P, Kodjikian L, et al. Survival, anatomic, and functional long-term results in choroidal and ciliary body melanoma after ruthenium brachytherapy (15 years' experience with beta-rays). *Am J Ophthalmol*. 2004;137:893–900.
24. Wilson MW, Hungerford JL. Comparison of episcleral plaque and proton beam radiation therapy for the treatment of choroidal melanoma. *Ophthalmology*. 1999;106:1579–1587.
25. Mosci C, Mosci S, Barla A, et al. Proton beam radiotherapy of uveal melanoma: Italian patients treated in Nice, France. *Eur J Ophthalmol*. 2009;19:654–660.
26. Gragoudas ES, Lane AM, Munzenrider J, et al. Long-term risk of local failure after proton therapy for choroidal/ciliary body melanoma. *Trans Am Ophthalmol Soc*. 2002;100:43–48 [discussion 48–49].
27. Mishra KK, Quivey JM, Daftari IK, et al. Long-term results of the UCSF-LBNL randomized trial: charged particle with helium ion versus iodine-125 plaque therapy for choroidal and ciliary body melanoma. *Int J Radiat Oncol Biol Phys*.

2015;92(2):376–383.
28. Oliver SC, Leu MY, DeMarco JJ, et al. Attenuation of iodine-125 radiation with vitreous substitutes in the treatment of uveal melanoma. *Arch Ophthalmol*. 2010;128(7):888–893.
29. Ahuja Y, Kapoor KG, Thomson RM, et al. The effects of intraocular silicone oil placement prior to iodine-125 brachytherapy for uveal melanoma: a clinical case series. *Eye (Lond)*. 2012;26(11):1486–1489.
30a. McCannel TA, McCannel CA. Iodine-125 brachytherapy with vitrectomy and silicone oil in the treatment of uveal melanoma: 1-to-1 matched case-control series. *Int J Radiat Oncol Biol Phys*. 2014;89:347–352.
30b. McCannel TA, Kamrava M, Demanes J, et al. 23-mm iodine-125 plaque for uveal melanoma: benefit of vitrectomy and silicone oil on visual acuity. *Graefes Arch Clin Exp Ophthalmol*. 2016;254(12):2461–2467.
31. Eide N. Primary laser photocoagulation of "small" choroidal melanomas. *Acta Ophthalmol Scand*. 1999;77:351–354.
32. Jaffe GJ, Mieler WF, Burke JM, et al. Photoablation of ocular melanoma with a high-powered argon endolaser. *Arch Ophthalmol*. 1989;107:113–118.
33. Tsai T, O'Brien JM, Engstrom R, et al. Extrascleral extension of a choroidal melanoma after argon photocoagulation and transpupillary thermotherapy. *Br J Ophthalmol*. 2002;86:358–359.
34. Donaldson MJ, Lim L, Harper CA, et al. Primary treatment of choroidal amelanotic melanoma with photodynamic therapy. *Clin Exp Ophthalmol*. 2005;33:548–549.
35. Soucek P, Cihelkova I. Photodynamic therapy with verteporfin in subfoveal choroidal melanoma (a controlled case). *Neuro Endocrinol Lett*. 2006;27:145–148.
36. Barbazetto IA, Lee TC, Rollins IS, et al. Treatment of choroidal melanoma using photodynamic therapy. *Am J Ophthalmol*. 2003;135:898–899.
37. Shields CL, Shields JA, Perez N, et al. Primary transpupillary thermotherapy for small choroidal melanoma in 256 consecutive cases: outcomes and limitations. *Ophthalmology*. 2002;109:225–234.

38. Aaberg TM Jr, Bergstrom CS, Hickner ZJ, et al. Long-term results of primary transpupillary thermal therapy for the treatment of choroidal malignant melanoma. *Br J Ophthalmol*. 2008;92:741–746.
39. Zaldivar RA, Aaberg TM, Sternberg P, et al. Clinicopathologic findings in choroidal melanomas after failed transpupillary thermotherapy. *Am J Ophthalmol*. 2003;135:657–663.
40. Harbour JW, Meredith TA, Thompson PA, et al. Transpupillary thermotherapy versus plaque radiotherapy for suspected choroidal melanomas. *Ophthalmology*. 2003;110:2207–2214 [discussion 2215].
41. Bartlema YM, Oosterhuis JA, Journee-De Korver JG, et al. Combined plaque radiotherapy and transpupillary thermotherapy in choroidal melanoma: 5 years' experience. *Br J Ophthalmol*. 2003;87:1370–1373.
42. Damato B, Lecuona K. Conservation of eyes with choroidal melanoma by a multimodality approach to treatment: an audit of 1632 patients. *Ophthalmology*. 2004;111:977–983.
43. Peyman GA, Juarez CP, Diamond G, et al. Ten years' experience with eye wall resection for uveal malignant melanomas. *Ophthalmology*. 1984;91:1720–1725.
44. Kivela T, Puusaari I, Damato B. Transscleral resection versus iodine brachytherapy for choroidal malignant melanomas 6 millimeters or more in thickness: a matched case–control study. *Ophthalmology*. 2003;110:2235–2244.
45. Shields JA, Shields CL, Shah P, et al. Partial lamellar sclerouvectomy for ciliary body and choroidal tumors. *Ophthalmology*. 1991;98:971–983.
46. Damato BE, Paul J, Foulds WS. Risk factors for residual and recurrent uveal melanoma after trans-scleral local resection. *Br J Ophthalmol*. 1996;80:102–108.
47. Puusaari I, Damato B, Kivela T. Transscleral local resection versus iodine brachytherapy for uveal melanomas that are large because of tumour height. *Graefes Arch Clin Exp Ophthalmol*. 2007;245:522–533.
48. Garcia-Arumi J, Zapata MA, Balaguer O, et al. Endoresection in high posterior choroidal melanomas: long-

term outcome. *Br J Ophthalmol*. 2008;92:1040–1045.
49. Kertes PJ, Johnson JC, Peyman GA. Internal resection of posterior uveal melanomas. *Br J Ophthalmol*. 1998;82:1147–1153.
50. Karkhaneh R, Chams H, Amoli FA, et al. Long-term surgical outcome of posterior choroidal melanoma treated by endoresection. *Retina*. 2007;27:908–914.
51. Hawkins BS, Collaborative Ocular Melanoma Study Group. The Collaborative Ocular Melanoma Study (COMS) randomized trial of pre-enucleation radiation of large choroidal melanoma: IV. Ten-year mortality findings and prognostic factors. COMS report number 24. *Am J Ophthalmol*. 2004;138:936–951.
52. Diener-West M, Reynolds SM, Agugliaro DJ, Collaborative Ocular Melanoma Study Group, et al. Development of metastatic disease after enrollment in the COMS trials for treatment of choroidal melanoma: Collaborative Ocular Melanoma Study Group report no. 26. *Arch Ophthalmol*. 2005;123:1639–1643.
53. Rietschel P, Panageas KS, Hanlon C, et al. Variates of survival in metastatic uveal melanoma. *J Clin Oncol*. 2005;23:8076–8080.
54. Eskelin S, Pyrhönen S, Summanen P, et al. Tumor doubling times in metastatic malignant melanoma of the uvea: tumor progression before and after treatment. *Ophthalmology*. 2000;107:1433–1439.
55. Seddon JM, Gragoudas ES, Egan K, et al. Standardized data collection and coding in eye disease epidemiology: The uveal melanoma data system. *Ophthalmic Surg*. 1991;22:127–136.
56. Seddon JM, Polivogianis L, Gragoudas ES, et al. Enucleation vs cobalt 60 irradiation of melanomas. *Arch Ophthalmol*. 1986;104:175–176.
57. Seddon JM, Gragoudas ES, Albert D, et al. Comparison of survival rates for patients with uveal melanoma after treatment with proton beam irradiation or enucleation. *Am J Ophthalmol*. 1985;99:282–290.
58. Seddon JM, Albert DM, Lavin PT, et al. A prognostic factor

study of disease-free interval and survival following enucleation for uveal melanoma. *Arch Ophthalmol*. 1983;101:1894–1899.
59. Seddon JM, Gragoudas ES, Polivogianis L, et al. Visual outcome after proton beam irradiation of uveal melanoma. *Ophthalmology*. 1986;93:666–674.
60. Seddon JM, Gragoudas ES, Egan K, et al. Uveal melanomas near the optic disc or fovea: visual results after proton beam irradiation. *Ophthalmology*. 1987;94:354–361.
61. Augsburger JJ, Gamel JW, Sardi VF, et al. Enucleation vs. cobalt plaque radiotherapy for malignant melanomas of the choroid and ciliary body. *Arch Ophthalmol*. 1986;104:655–661.
62. Gragoudas ES, Seddon JM, Egan M, et al. Metastasis from uveal melanoma after proton beam irradiation. *Ophthalmology*. 1988;95:992–999.
63. Gragoudas ES, Seddon JM, Egan KM, et al. Long-term results of proton beam irradiated uveal melanomas. *Ophthalmology*. 1987;94:349–353.
64. Lommatzsch PK. Results after B-irradiation (106Ru/106Rh) of choroidal melanomas: 20 years' experience. *Br J Ophthalmol*. 1986;70:844–851.
65. Kleineidam M, Guthoff R, Bentzen SM. Rates of local control metastasis and overall survival in patients with posterior uveal melanomas treated with ruthenium-106 plaques. *Radiother Oncol*. 1993;28:148–156.
66. Seregard S, Trampe E, Lax I, et al. Results following episcleral ruthenium plaque radiotherapy for posterior uveal melanoma. *Acta Ophthalmol Scand*. 1997;75:11–16.
67. Summanen P, Immonen I, Heikkonen J, et al. Survival of patients and metastatic and local recurrent tumor growth in malignant melanoma of the uvea after ruthenium plaque radiotherapy. *Ophthalmic Surg*. 1993;24:82–90.
68. Char DH, Castro J, Kroll S, et al. Five-year follow-up of helium ion therapy for uveal melanoma. *Arch Ophthalmol*. 1990;108:209–214.
69. Char DH, Kroll SM, Castro J. Ten-year follow-up of helium-ion therapy for uveal melanoma. *Am J Ophthalmol*.

1998;125:81–89.
70. Packer S, Stoller S, Lesser ML, et al. Long-term results of iodine-125 irradiation of uveal melanoma. *Ophthalmology*. 1992;99:767–773.
71. Quivey JM, Char DH, Phillips TL, et al. High intensity 125-iodine (125I) plaque treatment of uveal melanoma. *Int J Radiat Oncol*. 1993;26:613–618.
72. Seddon JM, Gragoudas ES, Egan KM, et al. Relative survival rates after alternative therapies for uveal melanoma. *Ophthalmology*. 1990;97:769–777.
73. Egan KM, Walsh SM, Seddon JM, et al. An evaluation of the influence of reproductive factors on the risk of metastases from uveal melanoma. *Ophthalmology*. 1993;100:1160–1165.
74. Rashid M, Heikkonen J, Kivelä T. Tumor regression after brachytherapy for choroidal melanoma: reduction of thickness and cross-sectional area by shape and regression pattern. *Invest Ophthalmol Vis Sci*. 2015;56(4):2612–2623.
75. Augsburger JJ, Gamel JW, Shields JA, et al. Post-irradiation regression of choroidal melanomas as a risk factor for death from metastatic. *Ophthalmology*. 1987;94:1173–1177.
76. Glynn RJ, Seddon JM, Gragoudas ES, et al. Evaluation of tumor regression and other prognostic factors for early and late metastasis after proton irradiation of uveal melanoma. *Ophthalmology*. 1989;96:1566–1573.
77. Corrêa ZM, Augsburger JJ. Relationship between rate of posterior uveal melanoma flattening following plaque radiotherapy and gene expression profile class of tumor cells. *Invest Ophthalmol Vis Sci*. 2014;55(1):556–559.
78. Gragoudas ES, Egan KM, Seddon JM, et al. Intraocular recurrence of uveal melanoma after proton beam irradiation. *Ophthalmology*. 1992;99:760–766.
79. Vrabec TR, Augsburger JJ, Gamel JW, et al. Impact of local tumor relapse on patient survival after cobalt 60 plaque radiotherapy. *Ophthalmology*. 1991;98:984–988.
80. DePotter P, Shields CL, Shields JA, et al. Plaque radiotherapy for juxtapapillary choroidal melanoma: visual acuity and survival outcome. *Arch Ophthalmol*. 1996;114:1357–1365.

81. Harbour JW, Char DH, Kroll S, et al. Metastatic risk for distinct patterns of post-irradiation local recurrence of posterior uveal melanoma. *Ophthalmology*. 1997;104:1785–1793.
82. Ophthalmic Oncology Task Force. Local recurrence significantly increases the risk of metastatic uveal melanoma. *Ophthalmology*. 2016;123(1):86–91.
83. Jensen OA. Malignant melanomas of the human uvea: 25-year follow-up of cases in Denmark, 1943–1952. *Acta Ophthalmol*. 1982;60:161–182.
84. McLean IW, Foster WD, Zimmerman LE, et al. Interred natural history of uveal melanoma. *Invest Ophthalmol Vis Sci*. 1980;19:760–770.
85. Raivio I. Uveal melanoma in Finland: an epidemiological, clinical, histological, and prognostic study. *Acta Ophthalmol Suppl*. 1977;133:3–64.
86. Lavin P, Albert D, Seddon J. A deficit survival analysis to assess the natural history of uveal melanomas. *J Chronic Dis*. 1984;37:481–487.
87. Coleman K, Baak JP, Van Diest P, et al. Prognostic factors following enucleation of 111 uveal melanomas. *Br J Ophthalmol*. 1993;77:688–692.
88. Gragoudas ES, Egan KM, Seddon JM, et al. Survival of patients with metastases from uveal melanoma. *Ophthalmology*. 1991;98:383–390.
89. Kath R, Hayungs J, Bornfeld N, et al. Prognosis and treatment of disseminated uveal melanoma. *Cancer*. 1993;72:2219–2223.
90. Rajpal S, Moore R, Karakousis CP. Survival in metastatic ocular melanoma. *Cancer*. 1983;52:334–336.
91. Singh AD. Uveal melanoma: implications of tumor doubling time. Comment. *Ophthalmology*. 2001;108:831–832.
92. Manschot WA, van Strik R. Uveal melanoma: therapeutic consequences of doubling times and irradiation results; a review. *Int Ophthalmol*. 1992;16:91–99.
93. Egan KM, Gragoudas ES, Seddon JM, et al. The risk of enucleation after proton beam irradiation of uveal melanoma. *Ophthalmology*. 1989;96:1377–1382.

94. Paul EV, Parnell BL, Fraker M. Prognosis of malignant melanomas of the choroid and ciliary body. *Ophthalmol Clin*. 1962;2:387–402.
95. Garretson JP, Robertson DM, Earle JD. Choroidal melanoma treatment with iodine-125 brachytherapy. *Arch Ophthalmol*. 1987;105:1394–1397.
96. Char DH, Quivey J, Castro J, et al. Helium ions versus iodine-125 brachytherapy in the management of uveal melanoma: a prospective, randomized, dynamically balanced trial. *Ophthalmology*. 1993;100:1547–1554.
97. Meecham WJ, Char DH, Kroll S, et al. Anterior segment complications after helium ion radiation therapy for uveal melanoma: radiation cataract. *Arch Ophthalmol*. 1994;112:197–203.
98. Gragoudas ES, Egan KM, Walsh SM, et al. Lens changes after proton beam irradiation for uveal melanoma. *Am J Ophthalmol*. 1995;119:157–164.
99. Kleineidam M, Augsburger JJ, Hernandez C, et al. Cataractogenesis after Cobalt-60 eye plaque radiotherapy. *Int J Radiat Oncol Biol Phys*. 1993;26:625–630.
100. Summanen P, Immonen I, Kivela T, et al. Radiation related complications after ruthenium plaque radiotherapy of uveal melanoma. *Br J Ophthalmol*. 1996;80:732–739.
101. Park SS, Walsh SM, Gragoudas ES. Visual-field deficits associated with proton beam irradiation for parapapillary choroidal melanoma. *Ophthalmology*. 1996;103:110–116.
102. Fontanesi J, Meyer D, Xu S, et al. Treatment of choroidal melanoma with I-125 plaque. *Int J Radiat Oncol Biol Phys*. 1993;26:619–623.
103. Lindstadt D, Char DH, Castro J, et al. Vision following helium ion radiotherapy of uveal melanoma: a northern California Oncology group study. *Int J Radiat Oncol Biol Phys*. 1988;25:347–352.
104. Augsburger JJ, Goel SD. Visual function following enucleation or episcleral plaque radiotherapy for posterior uveal melanoma. *Arch Ophthalmol*. 1994;112:786–789.
105. Shammas HF, Blodi FC. Prognostic factors in choroidal and ciliary body melanomas. *Arch Ophthalmol*. 1977;95:63–69.

106. Warren RM. Prognosis of malignant melanomas of the choroid and ciliary body. Blodi FC. *Current concepts in ophthalmology*. Mosby: St Louis; 1974.
107. Jensen OA. Malignant melanomas of the uvea in Denmark. 1943–1952. *Acta Ophthalmol Suppl*. 1963;75:1–220.
108. Flocks M, Gerende JH, Zimmerman LE. The size and shape of malignant melanomas of the choroid and ciliary body in relation to prognosis and histologic characteristics: a statistical study of 210 tumors. *Trans Am Acad Ophthalmol Otolaryngol*. 1955;59:740–758.
109. McLean IW, Foster WD, Zimmerman LE. Prognostic factors in small malignant melanomas of choroid and ciliary body. *Arch Ophthalmol*. 1977;95:48–58.
110. Diener-West M, Hawkins BS, Markowitz JA, et al. A review of mortality from choroidal melanoma. *Arch Ophthalmol*. 1992;110:245–250.
111. Shields CL, Furuta M, Thangappan A, et al. Metastasis of uveal melanoma millimeter-by-millimeter in 8033 consecutive eyes. *Arch Ophthalmol*. 2009;127:989–998.
112. Shields CL, Kaliki S, Furuta M, et al. American Joint Committee on Cancer Classification of Uveal Melanoma (Anatomic Stage) predicts prognosis in 7,731 patients: The 2013 Zimmerman Lecture. *Ophthalmology*. 2015;122(6):1180–1186.
113. AJCC Ophthalmic Oncology Task Force. International Validation of the American Joint Committee on Cancer's 7th Edition Classification of Uveal Melanoma. *JAMA Ophthalmol*. 2015;133(4):376–383.
114. Bagger M, Andersen MT, Andersen KK, et al. The prognostic effect of American Joint Committee on Cancer staging and genetic status in patients with choroidal and ciliary body melanoma. *Invest Ophthalmol Vis Sci*. 2014;56(1):438–444.
115. Callender GR. Malignant melanotic tumors of the eye: a study of histologic types in 111 cases. *Trans Am Acad Ophthalmol Otolaryngol*. 1931;3:131–142.
116. Zimmerman LE, McLean IW, Foster WD. Does enucleation of the eye containing a malignant melanoma prevent or

accelerate the dissemination of tumour cells? *Br J Ophthalmol*. 1978;62:420–425.
117. Seddon J, Polivogianis L, Hsieh CC, et al. Death from uveal melanoma: number of epithelioid cells and inverse SD of nucleolar area as prognostic factors. *Ophthalmology*. 1987;105:801–806.
118. Folberg R, Rummelt V, Parys-Van Ginderdeuren R, et al. The prognostic value of tumor blood vessel morphology in primary uveal melanoma. *Ophthalmology*. 1993;100:1389–1398.
119. Makitie T, Summanen P, Tarkkanen A, et al. Microvascular loops and networks as prognostic indicators in choroidal and ciliary body melanomas. *J Natl Cancer Inst*. 1999;91:359–367.
120. McLean IW, Keefe KS, Burnier MN. Uveal melanoma. Comparison of the prognostic value of fibrovascular loops, mean of the ten largest nucleoli, cell type, and tumor size. *Ophthalmology*. 1997;104:777–780.
121. Seregard S, Spangberg B, Juul C, et al. Prognostic accuracy of the mean of the largest nucleoli, vascular patterns, and PC-10 in posterior uveal melanoma. *Ophthalmology*. 1998;105:485–491.
122. Chen X, Maniotis AJ, Majumdar D, et al. Uveal melanoma cell staining for CD34 and assessment of tumor vascularity. *Invest Ophthalmol Vis Sci*. 2002;43:2533–2539.
123. Foss AJ, Alexander RA, Jefferies LW, et al. Microvessel count predicts survival in uveal melanoma. *Cancer Res*. 1996;56:2900–2903.
124. Makitie T, Summanen P, Tarkkanen A, et al. Microvascular density in predicting survival of patients with choroidal and ciliary body melanoma. *Invest Ophthalmol Vis Sci*. 1999;40:2471–2480.
125. Clarijs R, Schalkwijk L, Ruiter DJ, et al. Lack of lymphangiogenesis despite coexpression of VEGF-C and its receptor Flt-4 in uveal melanoma. *Invest Ophthalmol Vis Sci*. 2001;42:1422–1428.
126. Makitie T, Summanen P, Tarkkanen A, et al. Tumor-infiltrating macrophages (CD68(+) cells) and prognosis in

malignant uveal melanoma. *Invest Ophthalmol Vis Sci*. 2001;42:1414–1421.
127. Toivonen P, Makitie T, Kujala E, et al. Microcirculation and tumor-infiltrating macrophages in choroidal and ciliary body melanoma and corresponding metastases. *Invest Ophthalmol Vis Sci*. 2004;45:1–6.
128. Foss AJ, Alexander RA, Hungerford JL, et al. Reassessment of the PAS patterns in uveal melanoma. *Br J Ophthalmol*. 1997;81:240–246.
129. Affeldt JC, Minckler DS, Azen SP, et al. Prognosis in uveal melanoma with extrascleral extension. *Arch Ophthalmol*. 1980;98:1975–1979.
130. Pach JM, Robertson DM, Taney BS, et al. Prognostic factors in choroidal and ciliary body melanomas with extrascleral extension. *Am J Ophthalmol*. 1986;101:325–331.
131. Shammas HF, Blodi FC. Orbital extension of choroidal and ciliary body melanomas. *Arch Ophthalmol*. 1977;95:2002–2005.
132. Kersten RC, Tse DT, Anderson RL, et al. The role of orbital exenteration in choroidal melanoma with extrascleral extension. *Ophthalmology*. 1985;92:436–443.
133. Tschentscher F, Prescher G, Zeschnigk M, et al. Identification of chromosomes 3, 6, and 8 aberrations in uveal melanoma by microsatellite analysis in comparison to comparative genomic hybridization. *Cancer Genet Cytogenet*. 2000;122:13–17.
134. White VA, McNeil BK, Horsman DE. Acquired homozygosity (isodisomy) of chromosome 3 in uveal melanoma. *Cancer Genet Cytogenet*. 1998;102:40–45.
135. Sisley K, Rennie IG, Parsons MA, et al. Abnormalities of chromosomes 3 and 8 in posterior uveal melanoma correlate with prognosis. *Genes Chromosomes Cancer*. 1997;19:22–28.
136. White VA, McNeil BK, Thiberville L, et al. Acquired homozygosity (isodisomy) of chromosome 3 during clonal evolution of a uveal melanoma: association with morphologic heterogeneity. *Genes Chromosomes Cancer*. 1996;15:138–143.

137. Speicher MR, Prescher G, du Manoir S, et al. Chromosomal gains and losses in uveal melanomas detected by comparative genomic hybridization. *Cancer Res*. 1994;54:3817–3823.
138. Horsman DR, White VA. Cytogenetic analysis of uveal melanoma. Consistent occurrence of monosomy 3 and trisomy 8q. *Cancer*. 1993;71:811–819.
139. Sisley K, Rennie IG, Cottam DW, et al. Cytogenetic findings in six posterior uveal melanomas: involvement of chromosomes 3, 6, and 8. *Genes Chromosomes Cancer*. 1990;2:205–209.
140. White VA, Chambers JD, Courtright PD, et al. Correlation of cytogenetic abnormalities with the outcome of patients with uveal melanoma. *Cancer*. 1998;83:354–359.
141. Prescher G, Bornfeld N, Hirche H, et al. Prognostic implications of monosomy 3 in uveal melanoma. *Lancet*. 1996;347:1222–1225.
142. Scholes AG, Damato BE, Nunn J, et al. Monosomy 3 in uveal melanoma: correlation with clinical and histologic predictors of survival. *Invest Ophthalmol Vis Sci*. 2003;44:1008–1011.
143. Onken MD, Worley LA, Ehlers JP, et al. Gene expression profiling in uveal melanoma reveals two molecular classes and predicts metastatic death. *Cancer Res*. 2004;64:7205–7209.
144. Young TA, Rao NP, Glasgow BJ, et al. Fluorescent in situ hybridization of for monosomy 3 via 30-gauge fine needle aspiration biopsy of choroidal melanoma in vivo. *Ophthalmology*. 2007;114:142–146.
145. Shields CL, Materin MA, Teixiera L, et al. Small choroidal melanoma with chromosome 3 monosomy on fine needle aspiration biopsy. *Ophthalmology*. 2007;114:1919–1924.
146. Shields JA, Shields CL, Materin MA, et al. Role of cytogenetics in the management of uveal melanoma. *Arch Ophthalmol*. 2008;126:416–419.
147. Shields CL, Ganguly A, Bianciotto CG, et al. Prognosis of uveal melanoma in 500 cases using genetic testing of needle aspiration biopsy specimens. *Ophthalmology*. 2011;118:396–

401.
148. Klufas MA, Itty S, McCannel CA, et al. Variable results for uveal melanoma-specific gene expression profile prognostic test in choroidal metastasis. *JAMA Ophthalmol*. 2015;133(9):1073–1076.
149. Damato BE, Heimann H, Kalirai H, et al. Age, survival predictors, and metastatic death in patients with choroidal melanoma: tentative evidence of a therapeutic effect on survival. *JAMA Ophthalmol*. 2014;132(5):605–613.
150. Damato B, Dopierala JA, Coupland SE. Genotypic profiling of 452 choroidal melanomas with multiplex ligation-dependent probe amplification. *Clin Cancer Res*. 2010;16(24):6083–6092.

145

Molecular Genetics of Choroidal Melanoma

Akrit Sodhi, J. Silvio Gutkind

Introduction

Uveal melanoma (UM) represents only 5% of all melanomas. However, it is the most common primary intraocular malignancy in adults, affecting approximately 5–11 individuals per million per year.[1] UMs arise from melanocytes within the uveal tract (i.e., iris, ciliary body, and choroid). Iris melanomas are relatively benign; however, ciliary body and choroidal melanomas still present significant diagnostic and therapeutic challenges.[2] Indeed, choroidal melanomas – the most common ocular melanoma – result not only in vision loss, but also in metastasis, which is uniformly fatal. Metastases most commonly target the liver, and the detection of hepatic metastatic lesions predicts a dismal outcome, with a median survival of only a few months.[3] Despite advances in the diagnosis and treatment of the primary tumor, we have not witnessed a corresponding improvement in patient survival.

Current treatment for local disease, including eye-sparing approaches (e.g., radioactive plaque therapy, external beam radiation, laser therapy), often leads to profound vision loss;[4] the identification of novel targets could provide gene product-targeted therapeutic options, which may avoid local tissue destruction. To this end, it is essential that we determine the molecular mechanism(s) that promote the initiation and progression of UM. In the past decade, emerging evidence suggests that a complex series of molecular steps occurs in which uveal melanocytes elude their antiproliferative and proapoptotic harnesses to form a melanoma, and in up to half of patients, metastasize hematogenously to the liver and other organs.[5] It is therefore critical that we identify patients at risk for metastasis early, so that we may provide adjuvant systemic therapy in an effort to delay or perhaps prevent the progression to clinical metastatic disease. It is equally important that patients not at risk for metastasis are spared from unnecessary treatment with systemic chemotherapy with their attendant risks and side-effects. Here, we provide an overview of how our current

understanding of the molecular genetics of choroidal melanoma has provided insight into the pathogenesis of this devastating ocular cancer, and how it may influence the diagnosis, treatment, and survival of these patients.

Cutaneous Melanoma, Uveal Melanoma, and the RAS/BRAF/MEK Pathway

Early work exploring the molecular genetics of UM was based upon the genetic studies in cutaneous melanoma. Specifically, activating mutations in *RAS* and *BRAF* oncogenes had been shown to play a fundamental role in the development of cutaneous melanoma, occurring in more than 80% of these tumors.[6] Mutations of *RAS* and *BRAF* promote the activation of MEK1/ERK (or the mitogen-activated protein kinase (MAPK) pathway), thereby promoting cell proliferation and survival.[7] Uncontrolled proliferation is a key feature of malignant transformation, and activation of the MAPK pathway is a common target for malignant progression. Early work demonstrated that the vast majority of primary UM tissue exhibits immunohistochemical evidence of activation of the MAPK pathway.[8,9] Based upon these promising findings, several groups have investigated the mutational status of *RAS*, *BRAF*, and *MEK1* in primary UM, as well as in liver metastases from patients with UM. Surprisingly, these studies have been overwhelmingly negative.[10,11] Indeed, despite arising from the same cell type, there appear to be more dissimilarities between the molecular genetics of UM and cutaneous melanoma than there are similarities.

GNAQ and *GNA11* Mutations in Uveal Melanoma

A breakthrough in our understanding of the development of UM came from the discovery in UM tissue of activating mutations in genes encoding for members of the $G\alpha_q$ family of large G proteins. Mutations in genes encoding for heterotrimeric G-protein α

subunits have been reported in a variety of cancers.[12] A genetic screen of UMs demonstrated that approximately half exhibit mutations in the gene encoding for $G\alpha_q$ (*GNAQ*).[13] Interestingly, over half of UMs lacking a mutation in *GNAQ* exhibit a mutation in the gene encoding for the related protein, $G\alpha_{11}$ (*GNA11*).[14] G proteins are a family of heterotrimeric proteins that signal from cell surface, 7-transmembrane spanning (G protein-coupled) receptors (GPCRs).[15] Upon ligand binding to its GPCR, the GDP bound to the $G\alpha_{Q/11}$ subunit is exchanged for GTP, resulting in a conformational change and the subsequent dissociation of the $G\alpha_{Qq/11}$ from the $G\beta\gamma$ subunits. These subunits are then able to regulate various second messengers. The $G\alpha_{q/11}$ family mediates its activity through stimulation of phospholipase C-β (PLCβ), which leads to activation of protein kinase C (PKC), and ultimately activates downstream intracellular signaling pathways, including the MAPK signaling pathway.

However, preclinical studies in choroidal melanoma cell lines suggest that this classic $G\alpha_{q/11}$-mediated signaling pathway is not sufficient to explain the proliferative capacity of choroidal melanoma tumor cells.[16] Instead, it was recently demonstrated that $G\alpha_q$ promotes melanocyte cell transformation through a novel mechanism. $G\alpha_q$ binds to and activates Trio, a guanine nucleotide exchange factor (GEF) for the small GTPases RhoA and Rac1, leading to their activation, and the expression of growth promoting genes.[16] Preventing Trio activation diminished choroidal melanoma tumor formation in animal models without affecting ERK.[16] Instead, $G\alpha_q$ was shown to trigger nuclear translocation of the transcriptional coactivator, YAP, a critical component of the Hippo signaling pathway that controls organ size in mammals.[17,18] This, in turn, stimulated YAP-dependent transcription, independent from PLCβ stimulation, but requiring the activation of Trio, and the subsequent activation of the small GTPases RhoA and Rac1 and their associated signaling networks (Fig. 145.1).[17]

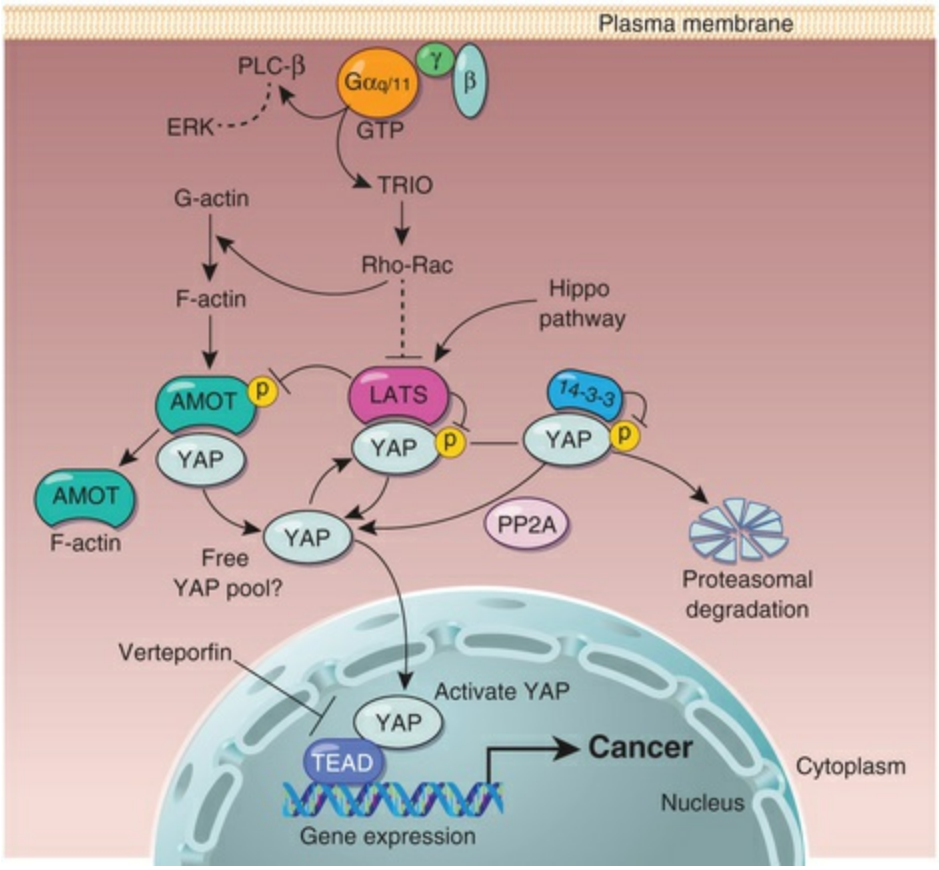

FIG. 145.1 Schematic representation of the activation of YAP by the *GNAQ* oncogene in uveal melanoma. $G\alpha_q$ protein stimulates YAP through a RhoA and Rac1 regulated signaling circuitry initiated by the activation of Trio, independent of PLCβ, and resulting in actin polymerization and F-actin accumulation. F-actin may then bind AMOT, displacing YAP (left), which translocates to the nucleus and initiates gene expression. Free YAP can also bind to LATS (center), which phosphorylates and inactivates YAP upon the cytosolic sequestration of phospho-YAP by 14-3-3 proteins or by promoting its proteosomal degradation as part of a canonical Hippo-dependent pathway (right) restraining YAP function. Verteporfin, an inhibitor of YAP, inhibits YAP-dependent gene expression, preventing oncogenic *GNAQ* from promoting uveal melanocyte transformation.

Of note, mutations in *GNAQ/11* have also been identified in blue nevi (benign intradermal melanocytic proliferations affecting the conjunctiva and periorbital skin),[13] and have not been found to correlate with clinical, pathologic, immunohistochemical, or genetic

factors associated with advanced UM.[19] Although patients with blue nevi are at higher risk for UM, blue nevi are not malignant. Moreover, although activating mutations in *GNAQ/11* can promote transformation of immortalized melanocytes, mutation of either gene is not sufficient for malignant transformation. Collectively, these findings suggest that driver mutations in *GNAQ/11* occur early during UM development, but that *GNAQ/11* mutations alone may not help identify patients who are at higher risk for later developing metastases. Nonetheless, as GPCRs are the target – directly or indirectly – of 50–60% of all present pharmacologic agents,[15] $G\alpha_{q/11}$ may still provide a novel precision medicine target for the treatment of UM.

Chromosomal Abnormalities in Uveal Melanoma

Interestingly, several cytogenetic or chromosomal abnormalities have been linked statistically to metastatic death in UM patients.[20–23] However, among these markers, gain of chromosome 6p and loss of one copy of chromosome 3 (monosomy 3) have proved to be the most reliable predictors of metastasis and survival. Gain of chromosome 6p occurs mainly in nonmetastasizing tumors and carries a better prognosis. Conversely, loss of one copy of chromosome 3 (monosomy 3) occurs most frequently in metastasizing tumors and predicts a poor outcome.[24] Of note, isodisomy 3, in which one copy of chromosome 3 is lost and the remaining (faulty copy) is duplicated, occurs in 5–10% of cases of patients with UM and is prognostically equivalent to monosomy 3.[25] Tumors with monosomy 3 have also been found to contain greater numbers of additional chromosomal abnormalities (aneuploidy) than tumors with disomy 3, suggesting that loss of chromosome 3 may promote the genomic instability observed in more aggressive tumors, complicating the interpretation of the prognostic significance of some chromosomal abnormalities in UM.[26,27]

Gain of 6p, Loss of 3: the Genetic Bifurcation

in Uveal Melanoma

Interestingly, gain of chromosome 6p and monosomy 3 are almost completely mutually exclusive,[22] representing a genetic bifurcation in UM progression (Fig. 145.2). This observation has prompted efforts to use this unique molecular distinction to predict which patients are at higher risk for later developing metastases. To distinguish between these two populations of UM patients, initial efforts focused on cytogenetic analysis. However, this technique requires highly trained cytogeneticists, and the accuracy of the results is limited by sampling error attributable to analysis of only a few tumor cells, and to the inability to detect small genetic changes. Moreover, standard karyotyping is unable to identify isodisomy 3, resulting in a missed identification in up to 10% of UM. Other techniques that also rely on direct analysis of intact chromosomes include fluorescence in situ hybridization (FISH), spectral karyotyping (SKY), and earlier forms of comparative genomic hybridization (CGH).[28] Although these techniques provide some advantages over karyotyping, they are still prone to sampling error attributable to analysis of a small subset of tumor cells, and they are also unable to detect isodisomy.

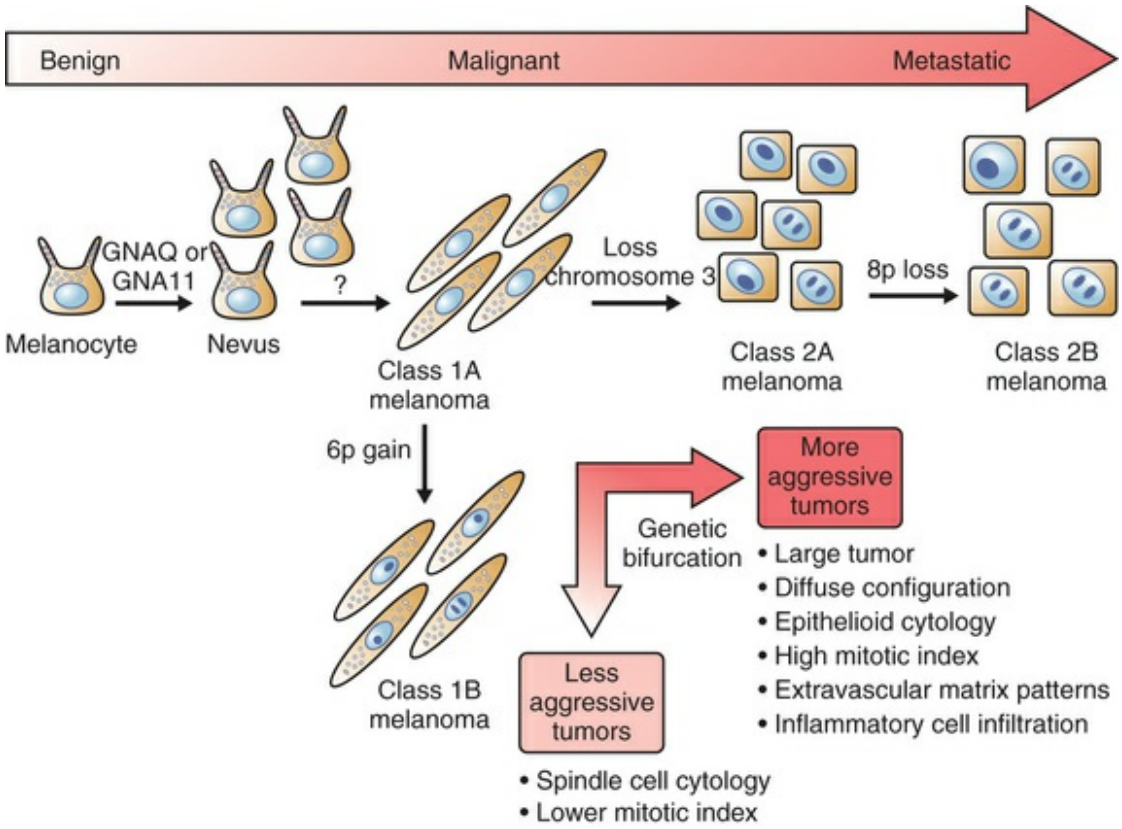

FIG. 145.2 Schematic depicting the molecular events that occur during the progression from uveal melanocyte to metastatic melanoma. Initial mutations in *GNAQ* or *GNA11* promote melanocyte survival and proliferation, but alone are not sufficient for melanocyte transformation. Additional (yet unknown) mutation(s) are necessary for progression to a melanoma. At this stage, the melanoma chooses one of two mutually exclusive paths, gain of chromosome 6p or loss of chromosome 3, leading to the development of less aggressive (lower metastatic rate) or more aggressive (higher metastatic rate) tumors, respectively. The additional loss of 8p in the more aggressive tumors further increases the risk for metastasis. These chromosomal changes correlate with the classic clinical and histologic features of uveal melanoma (UM) that were previously used to characterize (and later predict) the aggressiveness of UMs.

More recent automated techniques (e.g., array-based CGH, microsatellite analysis (MSA), single-nucleotide polymorphism (SNP) analysis, multiplex ligation-dependent probe amplification (MLPA)), evaluate multiple regions across individual chromosomes

using specific molecular probes. By allowing larger numbers of tumor cells to be examined, these techniques reduce the risk of sampling error and increase the ability to detect smaller abnormalities compared with karyotyping and FISH. Additionally, MSA and SNP can detect the presence of isodisomy 3. The prognostic accuracy of these techniques compared with standard karyotyping is unclear.[29]

Gene Expression Profiling

Recent advances in DNA microarray technology have enabled transcriptional or gene expression profiles (GEP) of remarkably small tissue samples at relatively low cost, providing scientists and clinicians insight into the complex pathophysiologic mechanisms of cancer and other diseases. This technology not only allows comparison of gene profiles in normal and pathologic tissues or cells, but also among different stages of disease progression, and has proven to be particularly useful in studying cancer. In cancer, GEP enables the simultaneous measurement of messenger ribonucleic acid (mRNA) expression using microarrays (glass slides or chips, carrying DNA representing thousands of genes), to which the labeled cRNA isolated from tumor cells is applied to determine gene activity. Thus, rather than examining the genetic abnormalities themselves, GEP enables the quantitation of the changes in gene expression in the tumor that (presumably) are the biologic consequence of the chromosomal abnormalities.

The gene expression data are then analyzed using statistical methods, with the aim of identifying gene clusters that correlate with the patients' clinical outcome. Specifically, using "supervised" clustering methods for tumor classification guided by knowledge of clinical outcomes, gene clusters are identified. A subset of gene markers can then be identified and used as a "prognosis classifier" that can help predict the later appearance ("poor prognosis") or absence ("good prognosis") of clinical metastasis. This approach has been previously applied to other cancers to more accurately classify tumors,[30,31] and has recently been tested with UM (Fig. 145.3).[32]

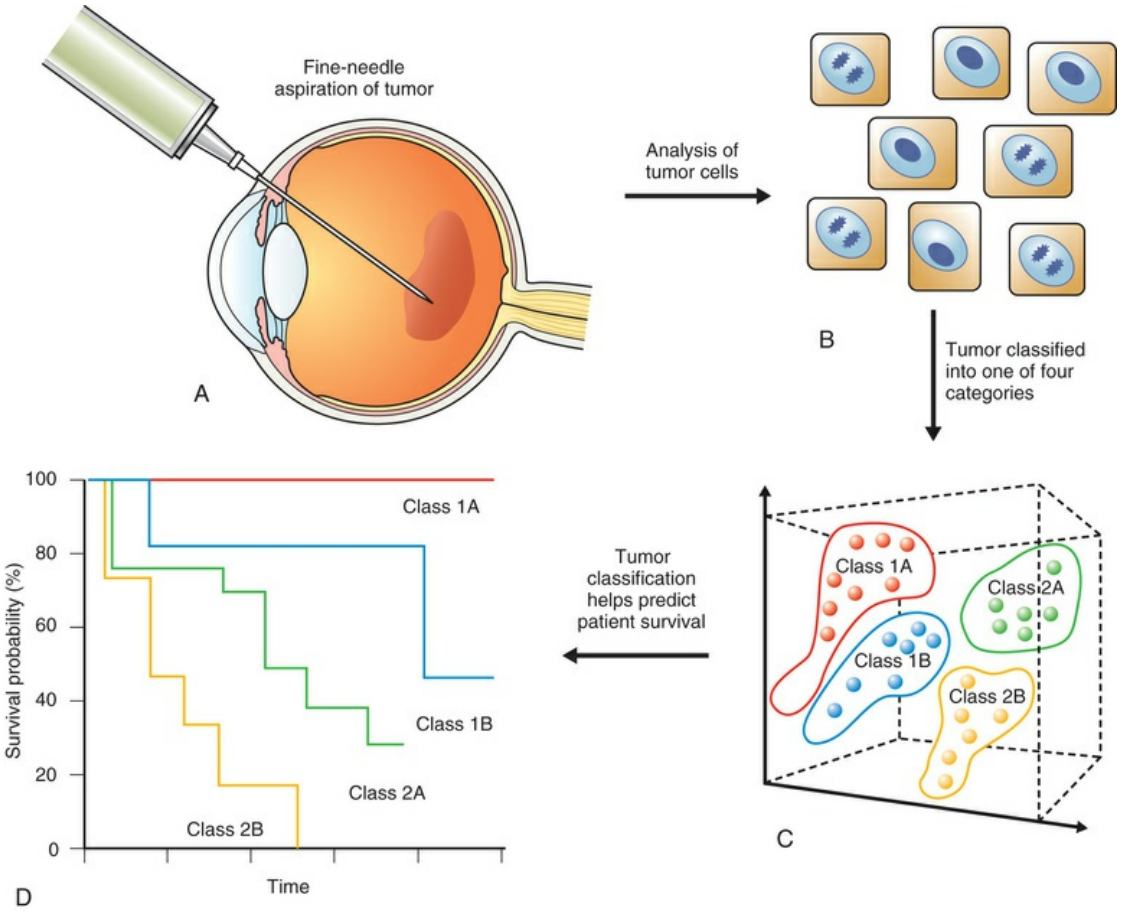

FIG. 145.3 Schematic depicting the basic steps involved in genetic testing in a biopsy from a patient with a uveal melanoma (UM). (A) Intraoperatively, either transscleral (anterior UM) or transvitreous (posterior UM) fine-needle aspiration biopsy (FNAB) is performed to obtain tissue for testing. (B) Once the cells are obtained, the quality of the tissue is often first confirmed by histopathology prior to testing (in this case, gene expression profiling). (C) Using gene expression profiling, tumors can be classified into one of four classes, based on the expression pattern of specific genes. (D) The specific class to which a tumor belongs can then be used to predict the likelihood of metastasis (and, in turn, the probability of survival). How these data can be used in the clinical setting remains unclear. (Modified with permission from Landreville S, Agapova OA, Harbour JW. Emerging insights into the molecular pathogenesis of UM. Future Oncol 2008;4:629–36, and with the permission of Dr William J. Harbour.)

The information derived from GEP in UM has proven to be a useful tool in predicting a patient's clinical outcome.[33,34] In patients

with UM, GEP has identified two major subgroups referred to as class 1 and class 2; approximately half of UM fall into each subgroup.[32] Patients with class 1 tumors have a lower risk of metastasis and patients with class 2 tumors have a higher risk of metastasis.[35] Interestingly, the class 2 gene expression profile is closely associated with previously identified prognostic features, such as larger tumor size, epithelioid cytology, extravascular looping matrix patterns, and monosomy 3.[36] The prognostic accuracy of the class 2 expression profile has been reported to be greater than for any of these other features (individually or in combination).[32] The identification of a subset of genes has enabled a polymerase chain reaction (PCR)-based platform that further increased the prognostic accuracy of GEP for UM.[37] This PCR-based method requires less tissue and has further proven useful for the analysis of archival (formalin-fixed, paraffin-embedded) samples.

The two classes have further been subdivided into four prognostically significant subclasses (1A, 1B, 2A and 2B), based on gene-expression profiling.[32] The metastasis-free survival is longest for class 1A and shortest for class 2B. The subclass 1B signature corresponds closely to gain of chromosome 6p, and the subclass 2B signature corresponds closely to loss of chromosome 8p. Molecular forecasting of the outcome of UM using GEP has proven remarkably reliable, offering a significant advance on existing prognostic methods.

Clinical Implications of Genetic Prognostication

The additional information provided by our greater understanding of the molecular genetics of UM raises new questions about both the disease and how and when we should treat patients with UM. Importantly, who should be offered testing (Fig. 145.4)? Should testing be limited to patients who undergo enucleation or local tumor resection or should it include patients who undergo brachytherapy, which would require fine-needle biopsy as an extra procedure? Does tumor location or size influence the decision? What (if any) is the role for genetic testing on patients with a suspicious nevus? Clearly, genetic testing, and the information it

provides, can be a valuable part of our understanding of UM and has the potential to be helpful both in the diagnosis and treatment of this devastating disease. Nonetheless, many questions remain unanswered.

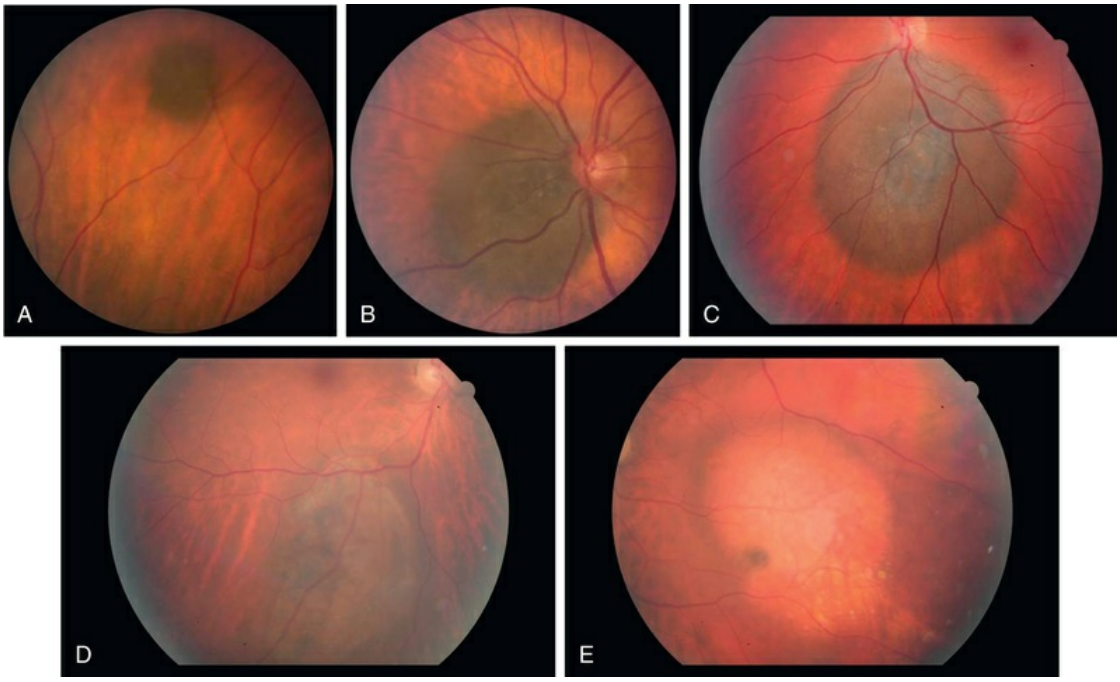

FIG. 145.4 Different types of choroidal melanocytic lesions that may prompt consideration for genetic testing. (A) A typical small (<2 mm in diameter), flat, pigmented choroidal lesion with few small overlying drusen, no orange pigment, no associated subretinal fluid, detected during a routine eye examination. Similar benign nevi occur in 3–10% of the Caucasian population and are unlikely to be considered appropriate for fine-needle aspiration biopsy (FNAB) for genetic testing. (B) A slightly larger (approximately 5 mm in diameter and 1 mm in height) pigmented choroidal lesion, also with few small overlying drusen, no orange pigment, no associated subretinal fluid, detected during a routine eye examination. Although, the size of the lesion and the location next to the optic nerve may prompt closer follow-up, it too is unlikely to be considered appropriate for FNAB for genetic testing. (C) A larger pigmented choroidal lesion (approximately 9 mm in diameter and 1.9 mm in height) also adjacent to the optic nerve, but with overlying orange pigment, but no associated subretinal

fluid, and no clinical symptoms. The role for FNAB and genetic testing for this lesion remains under debate. (D,E) Large pigmented (D) and nonpigmented (E) choroidal lesions, both over 3 mm in height in symptomatic patients with features concerning for melanoma (overlying orange pigmentation, associated subretinal fluid). Both patients underwent radioactive plaque brachytherapy. In many centers these patients would have undergone FNAB and genetic testing. However, the role for these tests, how to interpret the results, and how this should influence treatment and surveillance, remains under debate.

Tissue Procurement

If genetic testing is to be considered "good clinical practice," then the next question is how should we obtain the tissue? Reasonable disagreement remains as to whether the short-term or long-term risks of transscleral (for anterior UM) or transvitreous (for posterior UM) fine-needle aspiration biopsy (FNAB) outweigh the potential benefits of this procedure in patients who would otherwise not require intraocular surgery. What risks should be shared with the patient (e.g., transient vitreous hemorrhage, retinal tear or detachment, subretinal hemorrhage, endophthalmitis, tumor dissemination)? It is also unclear if less-invasive single sample procurement is sufficient for accurate and reliable diagnoses or whether multiple samples are required to address concerns of intratumoral genetic heterogeneity. Additionally, determining what preliminary testing is necessary to confirm that the tissue is appropriate for testing is still unclear.

Which Test(s) Should We Use?

Until alternative (noninvasive) approaches are available, many clinicians agree that transscleral or transvitreous FNAB is the most safe and effective means to obtain tissue for genetic testing. However, the best test to perform for genetic testing remains unresolved. And there remains significant confusion and controversy in the ocular oncology field regarding the use of these

prognostic tests in the clinical management of UM. The future of UM diagnostic/prognostic tests may rest in the use of microarray technologies, either for the evaluation of changes in copy number or for gene expression profiling. Although these techniques have historically been technically demanding and expensive, emerging PCR-based platforms may provide less expensive and more accurate assays for genetic prognostication. Ultimately, studies looking at molecular prognostic testing in UM have been retrospective in nature; prospective validation of these tests is essential before they can be considered routine for patients in clinic.

Genetic Testing in Clinical Trials

Knowledge that there are two classes of UMs may influence the success of future clinical trials designed to examine the response of these tumors to novel treatments. A limitation of the Collaborative Ocular Melanoma Study (COMS)[38] may have been that the consequence of the two classes of UMs (class 1 and 2) were not previously recognized at the time of the study's design. The good outcome of half the patients in the trial (class 1) may have been largely independent of treatment, and may have limited our ability to uncover a therapeutic advantage to one of the treatment arms. It should be noted that eligibility of patients in future trials, which includes patients who have received local treatment, may be limited to those patients who either have already had genetic testing or who have tissue available for genetic testing prior to entry into the trial. Recognizing that there are two classes of UM patients may further help in the identification of new and/or more accurate (noninvasive) biomarkers for the development of metastasis in high-risk (class 2A/2B) patients. There is little doubt that the additional information provided by genetic studies of UM will provide a fund of knowledge that may benefit future patients with this disease.

Genetic testing in UM has, and will continue to have, a significant impact on our understanding of the molecular pathogenesis of the disease. Certainly, the gene expression profile of class 2 UMs has provided clues as to the molecular events that promote progression and metastasis in this subset of tumors. For example, mutations in

the BRCA1-associated protein 1 gene (*BAP1*) are detected in approximately 47% of primary UM lesions.[39] *BAP1* mutations arise after the activating mutations of *GNAQ* or *GNA11* and are associated with class 2 UMs and a high likelihood of metastasis.[39] *BAP1* maps to chromosome 3p21 and *BAP1* mutations in UMs are accompanied by primarily somatic complete or partial loss of chromosome 3, providing a possible molecular link between chromosomal abnormalities in UM and tumor metastasis.[39] However, preclinical studies have failed to demonstrate a role for BAP1 in tumor cell proliferation, migration, invasion, or tumorigenicity. It is unclear whether *BAP1* will serve as a therapeutic target for the prevention or treatment of metastatic choroidal melanoma. But it is likely that the presence of *BAP1* mutations could influence the survival of UM patients in clinical trials. Recent large cancer genome sequencing efforts (The Cancer Genome Atlas – TCGA http://cancergenome.nih.gov/) have revealed additional recurrent mutations in UM, including genes for the splicing factor SF3B1 (26%), the translation initiation factor EIF1AX (14%), the protein arginine methyltransferase PRMT8 (7%), and the GPCR CYSLTR2 (4.2%). The relevance of these novel gene mutations for UM prognosis and treatment is still unclear and will warrant further investigation.

Diagnosis and Treatment of Current Uveal Melanoma Patients

Outside the setting of a clinical trial, a key ethical consideration for patients who undergo genetic testing is informed consent. Most specialists would agree that it is important to inform patients that the test has not yet been proven to be of benefit in either guiding management or prolonging survival. However, reasonable disagreement remains as to whether genetic testing for UM should only be performed in a research setting.[29] For patients requiring FNAB, the purpose of the procedure, along with its potential complications, must also be explained to the patient.

Nonetheless, the potential impact of genetic testing on the early diagnosis of UM patients who are more likely to develop

metastases (prognostication) is a compelling argument for its use for these patients. However, as in other settings in medicine, disease prediction continues to outpace our ability to treat or cure metastatic UM, resulting in a therapeutic rift between what we know and what we can do. This raises the reasonable, albeit philosophical question, as to whether there is an inherent value to simply knowing that a patient will – or will not – develop metastatic disease. Although emerging evidence suggests that the survival of patients with solitary metastatic nodules can be prolonged with early detection and treatment (e.g., resection, chemoembolization, or intrahepatic arterial infusion),[40] the value of genetic testing even in this setting remains a topic of debate.

It has also been suggested that prognostic tests can be used to determine which small suspicious UMs should be treated and which may be safe to observe. However, this approach assumes that class 2 tumors have not already metastasized, in which case local treatment may not benefit patient survival. Conversely, it is possible that treatment of class 1A tumors (rather than observing) may prevent them from converting to class 2 tumors. It has also been proposed that genetic testing may influence surveillance for metastasis. Patients with class 1 tumors may require less frequent monitoring than patients with class 2 tumors. This is complicated by the fact that genetic prognostication is not an exact science. Thus, despite the paucity of treatments for metastatic disease, the risk of potentially delaying the diagnosis of metastasis by decreasing the frequency of surveillance remains controversial. While some patients may find comfort in knowing that they have a lower risk for metastases based on the genetics of their tumors, there is a real potential for adversely affecting the quality of life of a patient who is told that they have a high risk of metastases given that there is currently no effective adjuvant therapy available for metastatic UM.

These tests may still play an essential role in predicting treatment response. For example, it is more likely that therapies specifically targeting *GNAQ* or *GNA11* would be effective in primary tumors with activating mutations in *GNAQ/11*. Similarly, patients with metastases that harbor specific mutations in genes that promote metastasis (e.g., *BAP1*[39]) may be more responsive to adjuvant systemic chemotherapies that are designed to target these genes.

Clearly, as new therapeutic options for metastatic UM are introduced, the value of genetic prognostication will continue to evolve.

Conclusion

In the past few years, we have begun to appreciate the complex series of molecular steps by which normal uveal melanocytes progress from a benign nevus to a metastatic melanoma. These steps include specific mutations and chromosomal changes, which are now detectable with diagnostic testing. These tests have recently become available to clinicians and their patients and have led to remarkable advances in genetic prognostication for patients with UM. Although they have provided (and will continue to provide) a wealth of information regarding the molecular pathogenesis of this cancer, the role of these tests in the diagnosis and treatment of patients with UM remains unresolved. Nonetheless, it is clear that emerging insight into the molecular pathogenesis of UM may ultimately provide new hope for patients who suffer from this devastating and incurable disease.

References

1. Singh AD, Bergman L, Seregard S. Uveal melanoma: epidemiologic aspects. *Ophthalmol Clin North Am*. 2005;18:75–84.
2. Shields CL, Shields JA. Ocular melanoma: relatively rare but requiring respect. *Clin Dermatol*. 2009;27:122–133.
3. Bell DJ, Wilson MW. Choroidal melanoma: natural history and management options. *Cancer Control*. 2004;11:296–303.
4. Damato B. Developments in the management of uveal melanoma. *Clin Experiment Ophthalmol*. 2004;32:639–647.
5. Patel M, Smyth E, Chapman PB, et al. Therapeutic implications of the emerging molecular biology of uveal melanoma. *Clin Cancer Res*. 2011;17:2087–2100.
6. Haluska FG, Ibrahim N. Therapeutic targets in melanoma: map kinase pathway. *Curr Oncol Rep*. 2006;8:400–405.
7. Poulikakos PI, Rosen N. Mutant BRAF melanomas –

dependence and resistance. *Cancer Cell*. 2011;19:11–15.
8. Weber A, Hengge UR, Urbanik D, et al. Absence of mutations of the BRAF gene and constitutive activation of extracellular-regulated kinase in malignant melanomas of the uvea. *Lab Invest*. 2003;83:1771–1776.
9. Zuidervaart W, van Nieuwpoort F, Stark M, et al. Activation of the MAPK pathway is a common event in uveal melanomas although it rarely occurs through mutation of BRAF or RAS. *Br J Cancer*. 2005;92:2032–2038.
10. Cohen Y, Goldenberg-Cohen N, Parrella P, et al. Lack of BRAF mutation in primary uveal melanoma. *Invest Ophthalmol Vis Sci*. 2003;44:2876–2878.
11. Wong CW, Fan YS, Chan TL, et al. BRAF and NRAS mutations are uncommon in melanomas arising in diverse internal organs. *J Clin Pathol*. 2005;58:640–644.
12. Dorsam RT, Gutkind JS. G-protein-coupled receptors and cancer. *Nat Rev Cancer*. 2007;7:79–94.
13. Van Raamsdonk CD, Bezrookove V, Green G, et al. Frequent somatic mutations of GNAQ in uveal melanoma and blue naevi. *Nature*. 2009;457:599–602.
14. Van Raamsdonk CD, Griewank KG, Crosby MB, et al. Mutations in GNA11 in uveal melanoma. *N Engl J Med*. 2010;363:2191–2199.
15. Gutkind JS. Regulation of mitogen-activated protein kinase signaling networks by G protein-coupled receptors. *Sci STKE*. 2000;40:re1.
16. Vaque JP, Dorsam RT, Feng X, et al. A genome-wide RNAi screen reveals a Trio-regulated Rho GTPase circuitry transducing mitogenic signals initiated by G protein-coupled receptors. *Mol Cell*. 2013;49:94–108.
17. Feng X, Degese MS, Iglesias-Bartolome R, et al. Hippo-independent activation of YAP by the GNAQ uveal melanoma oncogene through a trio-regulated rho GTPase signaling circuitry. *Cancer Cell*. 2014;25:831–845.
18. Yu FX, Luo J, Mo JS, et al. Mutant Gq/11 promote uveal melanoma tumorigenesis by activating YAP. *Cancer Cell*. 2014;25:822–830.
19. Bauer J, Kilic E, Vaarwater J, et al. Oncogenic GNAQ

mutations are not correlated with disease-free survival in uveal melanoma. *Br J Cancer*. 2009;101:813–815.
20. Gordon KB, Thompson CT, Char DH, et al. Comparative genomic hybridization in the detection of DNA copy number abnormalities in uveal melanoma. *Cancer Res*. 1994;54:4764–4768.
21. Prescher G, Bornfeld N, Becher R. Nonrandom chromosomal abnormalities in primary uveal melanoma. *J Natl Cancer Inst*. 1990;82:1765–1769.
22. Speicher MR, Prescher G, du Manoir S, et al. Chromosomal gains and losses in uveal melanomas detected by comparative genomic hybridization. *Cancer Res*. 1994;54:3817–3823.
23. Parrella P, Sidransky D, Merbs SL. Allelotype of posterior uveal melanoma: implications for a bifurcated tumor progression pathway. *Cancer Res*. 1999;59:3032–3037.
24. Prescher G, Bornfeld N, Hirche H, et al. Prognostic implications of monosomy 3 in uveal melanoma. *Lancet*. 1996;347:1222–1225.
25. White VA, McNeil BK, Thiberville L, et al. Acquired homozygosity (isodisomy) of chromosome 3 during clonal evolution of a uveal melanoma: association with morphologic heterogeneity. *Genes Chromosomes Cancer*. 1996;15:138–143.
26. Ehlers JP, Worley L, Onken MD, et al. Integrative genomic analysis of aneuploidy in uveal melanoma. *Clin Cancer Res*. 2008;14:115–122.
27. Onken MD, Worley LA, Harbour JW. A metastasis modifier locus on human chromosome 8p in uveal melanoma identified by integrative genomic analysis. *Clin Cancer Res*. 2008;14:3737–3745.
28. Teixeira MR. Combined classical and molecular cytogenetic analysis of cancer. *Eur J Cancer*. 2002;38:1580–1584.
29. Harbour JW. Molecular prognostic testing and individualized patient care in uveal melanoma. *Am J Ophthalmol*. 2009;148:823–829.
30. Ross DT, Scherf U, Eisen MB, et al. Systematic variation in gene expression patterns in human cancer cell lines. *Nat*

Genet. 2000;24:227–235.
31. Alizadeh AA, Eisen MB, Davis RE, et al. Distinct types of diffuse large B-cell lymphoma identified by gene expression profiling. *Nature*. 2000;403:503–511.
32. Landreville S, Agapova OA, Harbour JW. Emerging insights into the molecular pathogenesis of uveal melanoma. *Future Oncol*. 2008;4:629–636.
33. Onken MD, Worley LA, Ehlers JP, et al. Gene expression profiling in uveal melanoma reveals two molecular classes and predicts metastatic death. *Cancer Res*. 2004;64:7205–7209.
34. Tschentscher F, Hüsing J, Hölter T, et al. Tumor classification based on gene expression profiling shows that uveal melanomas with and without monosomy 3 represent two distinct entities. *Cancer Res*. 2003;63:2578–2584.
35. Onken MD, Worley LA, Harbour JW. Association between gene expression profile, proliferation and metastasis in uveal melanoma. *Curr Eye Res*. 2010;35:857–863.
36. Worley LA, Onken MD, Person E, et al. Transcriptomic versus chromosomal prognostic markers and clinical outcome in uveal melanoma. *Clin Cancer Res*. 2007;13:1466–1471.
37. Onken MD, Worley LA, Tuscan MD, et al. An accurate, clinically feasible multi-gene expression assay for predicting metastasis in uveal melanoma. *J Mol Diagn*. 2007;12:461–468.
38. Singh AD, Kivela T. The collaborative ocular melanoma study. *Ophthalmol Clin North Am*. 2005;18:129–142.
39. Harbour JW, Onken MD, Roberson ED, et al. Frequent mutation of BAP1 in metastasizing uveal melanomas. *Science*. 2010;330:1410–1413.
40. Sato T. Locoregional management of hepatic metastasis from primary uveal melanoma. *Semin Oncol*. 2010;37:127–138.

146

Pathology of Choroidal Melanoma

Martina C. Herwig-Carl, Hans E. Grossniklaus

Introduction

The diagnosis of choroidal melanoma is made clinically by fundus examination and ultrasonography. In equivocal cases, a tumor may be biopsied and evaluated by an ophthalmic pathologist. Examination of cytologic features and immunohistochemical stains, provided there is a sufficient amount of tissue, allows for a reliable diagnosis. Gross and microscopic examination of enucleated eyes harboring a uveal melanoma provides relevant prognostic information, e.g., cell type, invasion of vortex veins, and extraocular growth. Implementation of the American Joint Committee on Cancer (AJCC) and the International Union Against Cancer (UICC) TNM classification in the pathology report allows for uniform staging. Assessment of complications due to brachytherapy such as radiation retinopathy and plaque failure with subsequent tumor growth may lead to improvements in clinical care. Increased

knowledge of the molecular genetic aspects of choroidal melanoma including tests such as chromosome 3 status and gene expression profiling provides clinically relevant information. All in all, close cooperation between ophthalmic oncologists and pathologists within the framework of scheduled tumor conferences optimizes patient care. This chapter describes the pathologic findings in choroidal melanoma.

Processing of Specimens

Appropriate processing of tissue specimens is necessary for adequate pathologic evaluation. In the following sections, we, the authors, share our protocol.

Fixation

For routine pathologic examination, tissue specimens are fixed in paraformaldehyde or formaldehyde (4–10%) immediately after surgery. As formalin diffuses at a rate of approximately 1 mm/hour, an entire globe (about 24 mm in diameter) should be fixed at least 12 hours prior to further processing. If tissue is going to be sent for molecular genetic analysis, an appropriate amount of material should be obtained prior to formalin fixation, though testing of formalin-fixed paraffin-embedded tissue is also possible.

Gross Examination

Different types of tissue obtained include cytologic material, a tumor biopsy (incisional or excisional), or an enucleated globe. Clinical information and the type of fixative are noted. Gross examination depends on the submitted specimen.[1–4] For cytologic material, the submitted material (e.g., number of slides, quantity and appearance of fluid) is registered. For tumor biopsies, the number of pieces, size (three dimensions if possible), and descriptive features (e.g., color) are noted. A globe should be evaluated according to the guidelines of the Association of Directors of Anatomic and Surgical Pathology.[1–4] After orientation of the globe, careful inspection for extraocular growth is followed

by transillumination to localize the tumor and to measure its basal diameter. Vortex veins are submitted in different cassettes labeled respective to their localization. A standard section of the globe incorporates the pupil–optic nerve (p–o) section and the tumor. Detailed macroscopic examination and photodocumentation of the entire globe as well as a thorough description (including evidence of previous treatment) and tumor measurements are recommended.

Staining

Routine stains for choroidal melanoma comprise hematoxylin and eosin (H&E), periodic acid Schiff (PAS), and bleached H&E stains, to reveal the cytologic features in heavily pigmented tumors (Fig. 146.1). Immunohistochemical stains are not routinely used for the diagnosis of uveal melanoma but may be helpful in selected cases, including fine-needle aspiration biopsy (FNAB) samples.

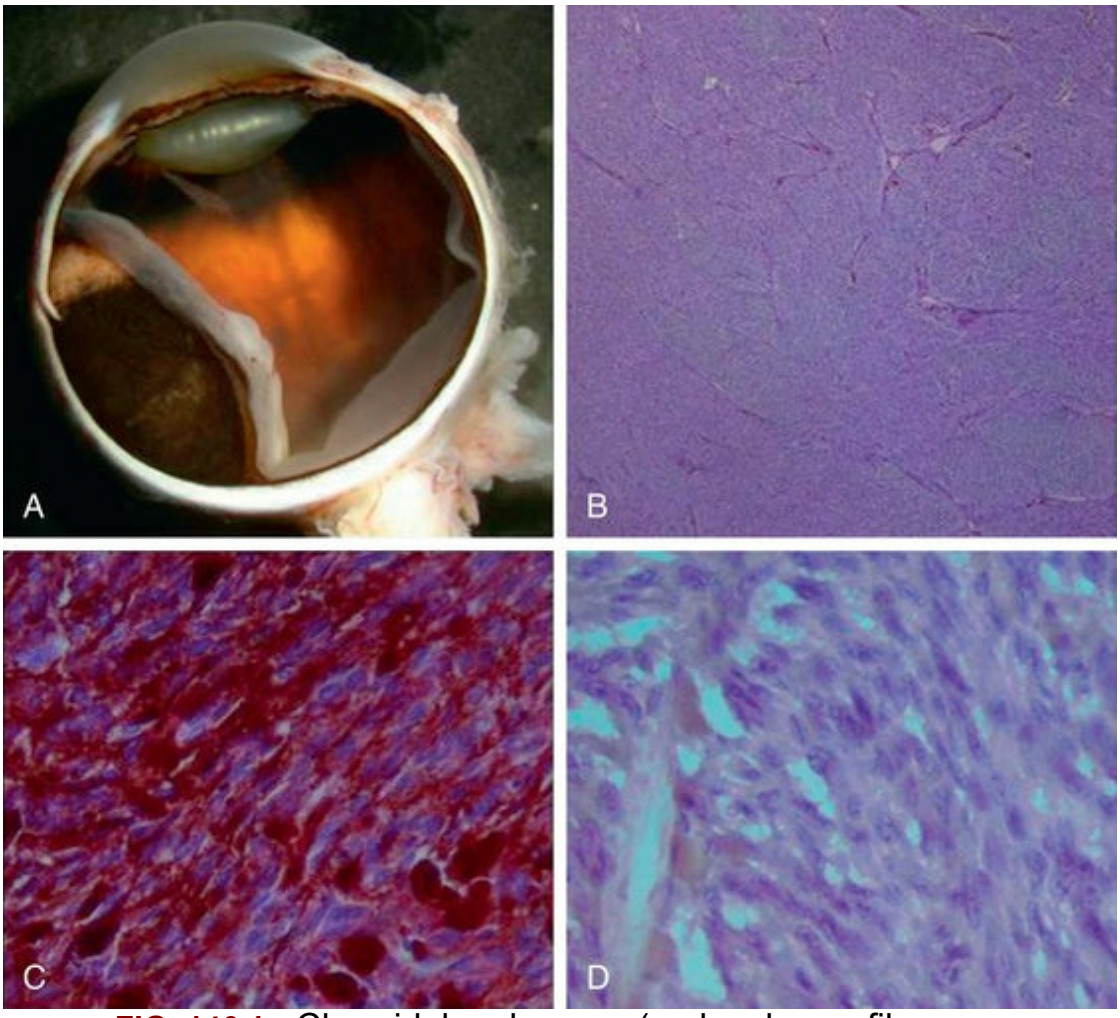

FIG. 146.1 Choroidal melanoma (molecular profile class I) in a 43-year-old woman. (A) On gross examination, a heavily pigmented uveal melanoma is present. (B) The extracellular matrix pattern of the tumor with vascular loops and arches is detected with a PAS stain (PAS, ×40). (C) The uveal melanoma consists of spindle cells and epithelioid cells (mixed-cell type) and exhibits pigmentation in uveal melanoma cells and pigment-laden macrophages (H&E, ×400). (D) Bleached sections enable the evaluation of the cytologic features (bleached H&E, ×400).

Gross Appearance of Choroidal Melanoma

The gross examination of intraocular tumors is the basis for clinicopathologic correlations as it allows for a detailed macroscopic

evaluation and measurement of the tumor size including the prognostically relevant largest basal diameter.[5,6] The largest basal diameter can be reliably assessed on gross examination, although the tumor size may be underestimated when measured after fixation due to tumor shrinkage.[7] Choroidal melanomas exhibit an oval or fusiform shape (Fig. 146.2) when confined by Bruch's membrane or a collar-button/mushroom configuration (Fig. 146.3) when the tumor has broken through Bruch's membrane.

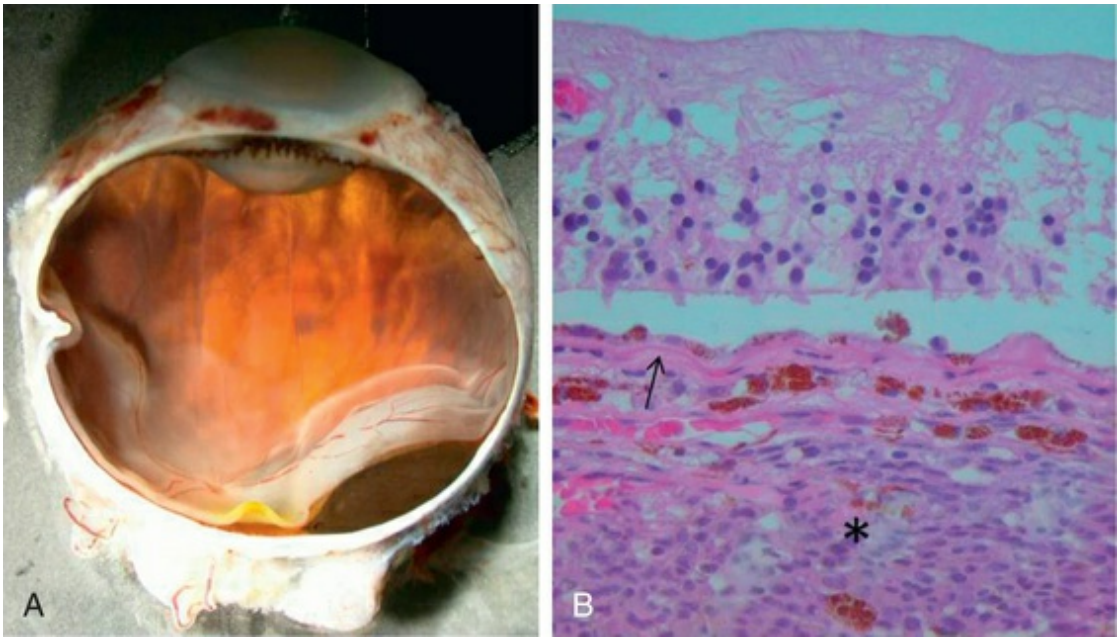

FIG. 146.2 (A) Oval-shaped, heavily pigmented choroidal melanoma (molecular profile class I) in a 66-year-old man. (B) Histologically, a mixed-cell type melanoma (*asterisk*) is present within the uvea (H&E, ×400). Bruch's membrane (*arrow*) is intact, the overlying retinal pigment epithelium and retina display atrophic changes.

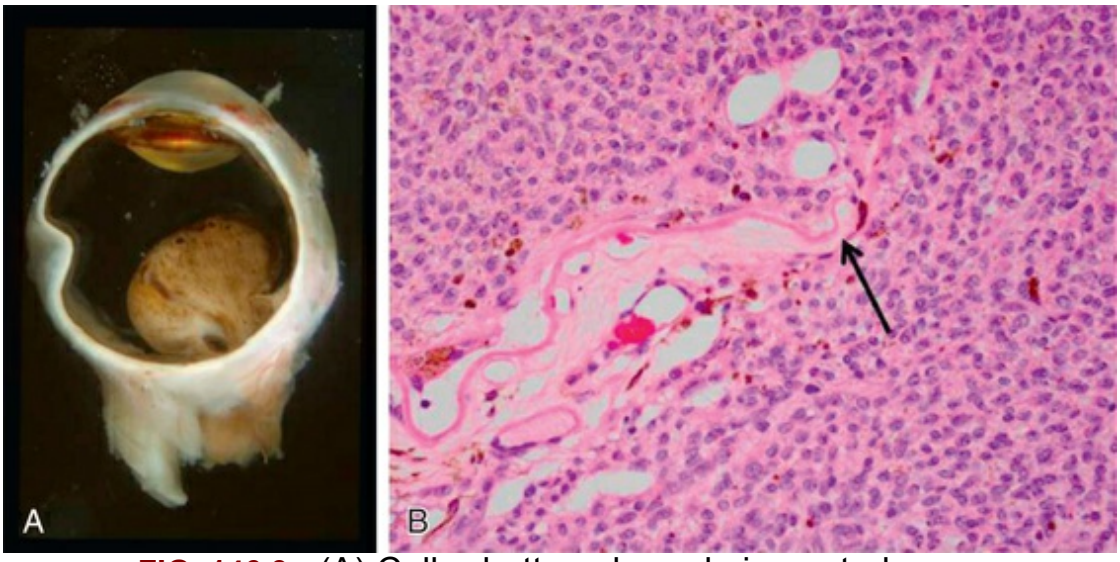

FIG. 146.3 (A) Collar-button-shaped pigmented choroidal melanoma in a 70-year-old woman. (B) Histologic examination shows the tumor breaking through Bruch's membrane (*arrow*) (H&E, ×400).

Ocular structures may be invaded by choroidal melanomas. Invasion into the ciliary body may be detected macroscopically, whereas invasion into the sclera, retina, and optic nerve, as well as invasion into the vitreous, iris, and anterior chamber, is usually detected by microscopic examination. Extraocular extension (Fig. 146.4) usually occurs along vortex veins or emissary canals and, dependent on the extent, may be diagnosed clinically or on gross examination.

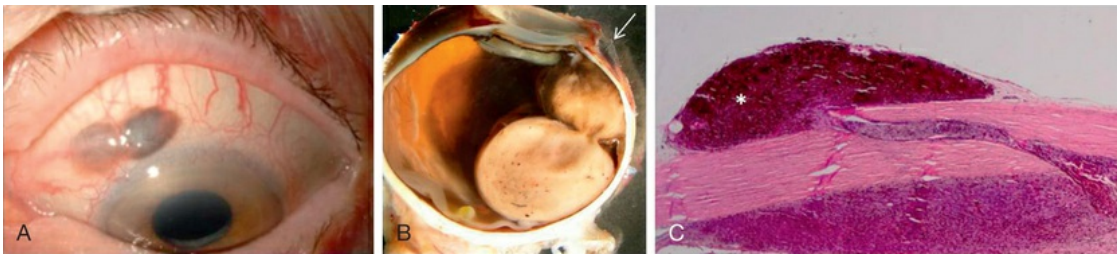

FIG. 146.4 An 86-year-old woman presented with (A) extraocular extension of a uveal melanoma (molecular profile class II). (B) On gross examination, extraocular extension (*arrow*) of a mildly pigmented bilobulated tumor was detected that invades the choroid and the ciliary body. (C) Histologic examination (H&E, ×100) shows the extraocular part of the tumor (*asterisk*) composed of epithelioid cells. The patient died from

liver metastasis less than 1 year after enucleation.

The amount of pigmentation of uveal melanomas varies from tumor to tumor or even within a single tumor and may be related to overall survival.[5,8] Most tumors exhibit mild to moderate pigmentation, although heavily or nonpigmented (amelanotic) choroidal melanomas (Fig. 146.5) may be observed.

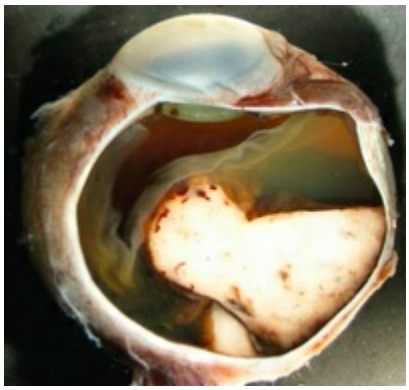

FIG. 146.5 Mildly pigmented, mushroom-shaped choroidal melanoma in a 24-year-old male patient.

Histopathologic Features of Tumor Cells and Their Prognostic Relevance

The prognosis of choroidal melanoma is based on clinical, histologic, and genetic parameters (see Chapter 145, Molecular genetics of choroidal melanoma). Some parameters such as ciliary body invasion, extraocular extension, and the largest basal diameter are incorporated into the TNM classification.[9] Histopathologic examination allows for further characterization of the tumor, including its cytologic features. In FNAB specimens, the cell type is more difficult to determine than in enucleated eyes or completely excised tumors due to the scarce amount of tissue and artifacts (Fig. 146.6).

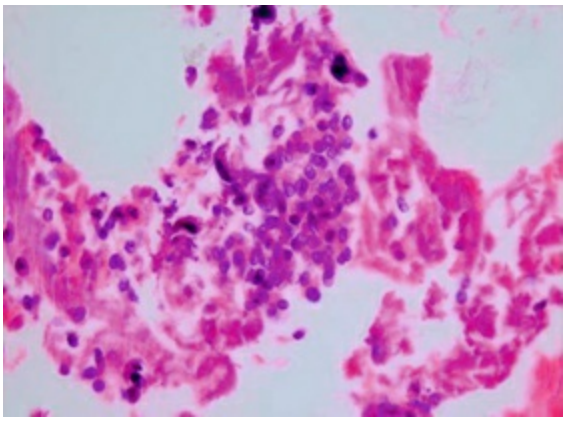

FIG. 146.6 Fine-needle aspiration biopsy (FNAB) exhibiting basophilic tumor cells with high nuclear-to-cytoplasmic ratios and prominent nucleoli, surrounded by debris (pink) (H&E, ×400).

Choroidal melanomas usually arise de novo but may also arise from a nevus or a melanocytoma (magnocellular nevus). In these cases remnants of the underlying nevus consisting of spindle A cells (spindle cell nevus: Fig. 146.7) or extremely rare magnocellular nevus cells (melanocytoma[10,11]), may be histologically detected.

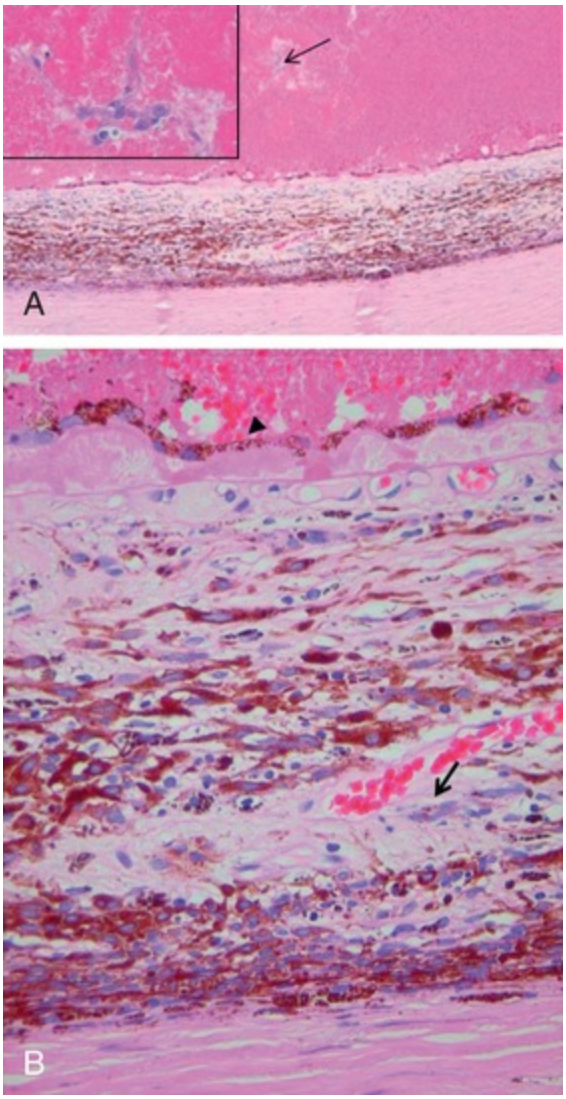

FIG. 146.7 (A) Choroidal melanoma arising in a choroidal nevus (H&E, ×4). There is vitreous spread of melanoma cells present (*arrow* and inset). (B) Higher magnification reveals nevus cells (spindle A cells, *arrow*) at the base of the choroidal lesion (H&E, ×100). Some of these cells are pigmented. The RPE (*arrowhead*) shows degenerative changes and underlying drusen and exudates.

Cytologic Features

First developed by Callender in 1931,[12] the so-called "Callender classification" distinguished five types of uveal melanomas depending on the most prominent cell type: spindle cell subtype A; spindle cell subtype B; epithelioid type; fascicular type; and mixed cell type (consisting of mixtures of spindle and epithelioid cells) of

uveal melanoma.

Addressing the disagreement about the interpretation and application of Callender's classification, a “modified Callender classification” was introduced by McLean and associates in 1983, comprising three different types in uveal melanoma based on cell morphology:[13] spindle cell melanoma (composed of spindle B cells); epithelioid cell melanoma, and melanoma of mixed-cell type. Spindle A cells were no longer regarded as malignant cells and were recognized as benign nevus cells. In addition, a new cell type was introduced, the small epithelioid cell (intermediate cell), that was smaller than the Callender's epithelioid cell and exhibited features intermediate between spindle B and epithelioid cells.

The classification of uveal melanomas into either spindle cell (composed of spindle B cells), mixed-cell type (most common), or epithelioid cell still is widely accepted. The main cell types are depicted as follows:

- **Spindle A cells** are fusiform, cohesive cells with poorly defined cell borders. The nucleus is also spindle-shaped and its central fold can be seen light microscopically as a dark stripe (Fig. 146.8A). This cell type is regarded as a benign nevus cell, but can be observed in uveal melanomas arising from a nevus.

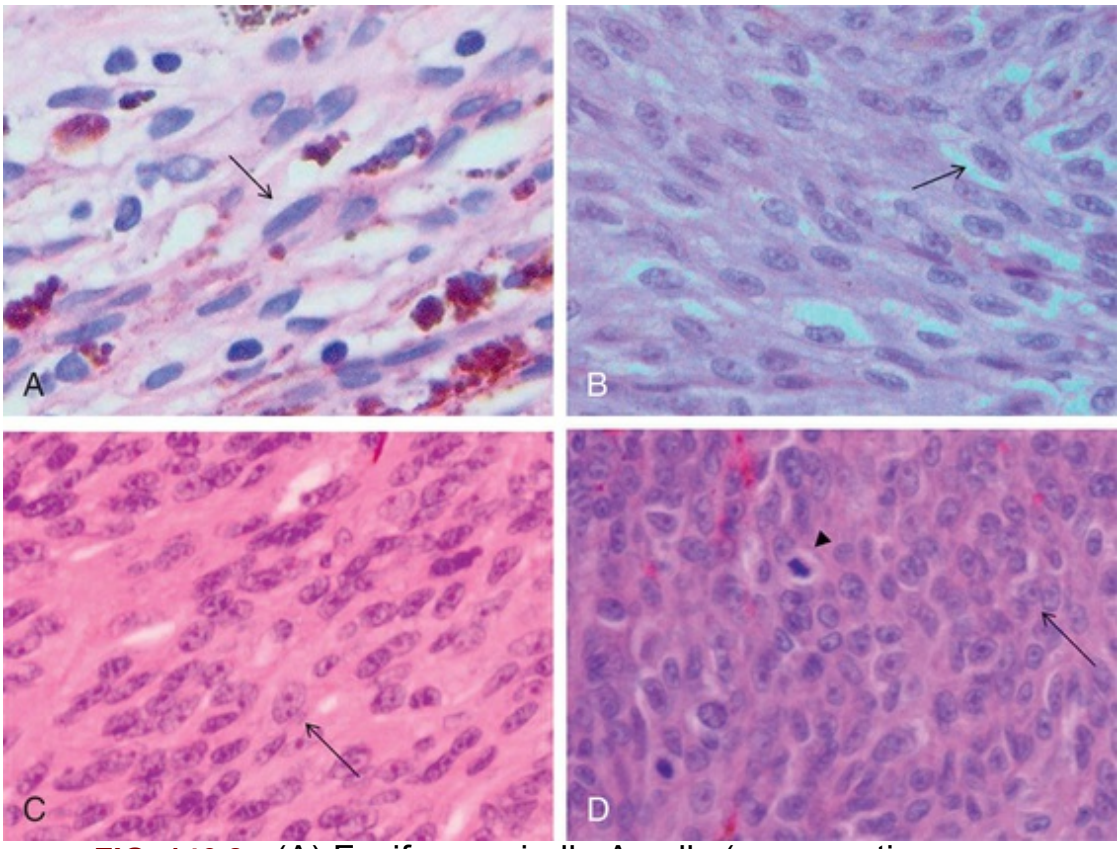

FIG. 146.8 (A) Fusiform spindle A cells (representing benign nevus cells) with a central fold are depicted (*arrow*) (H&E, ×400). (B) Spindle B cells that are plumper than spindle A cells exhibit a prominent nucleolus (*arrow*) (H&E, ×400). (C) Epithelioid cells characteristically contain a round, large nucleus with a prominent nucleolus (*arrow*) (H&E, ×400). (D) Small epithelioid cells (intermediate cells) represent a cell type intermediate between spindle B and epithelioid cells (*arrow*) (H&E, ×400). Mitotic figures are also present (*arrowhead*).

- **Spindle B cells** are also fusiform and cohesive with poorly defined cell borders but are plumper than spindle A cells. Prominent nucleoli are detected in the spindle-shaped nucleus (Fig. 146.8B). This is the most common cell type in choroidal melanoma.
- **Epithelioid cells** are noncohesive cells with defined cell borders. The round, large nucleus contains a prominent nucleolus (Fig. 146.8C). This cell type is associated with a poor outcome.
- **Intermediate cells** (small epithelioid cells) are a frequent cell type

intermediate between spindle B cells and epithelioid cells (Fig. 146.8D).

Although not incorporated into the TNM classification, the cell type of uveal melanomas is also an important prognostic parameter.[6] Melanomas solely composed of spindle cells have a more favorable prognosis than mixed-cell type tumors. Epithelioid cell melanomas are associated with monosomy 3 and class 2 molecular profile, a higher metastatic and mortality rate – and thus display the worst prognosis.[6,14,15]

Evaluation of the number of mitotic figures per high-power field in the tumor cells (Fig. 146.8D) is part of the routine evaluation of choroidal melanomas. It serves as an indicator for the proliferative activity and is thus a prognostic parameter.[6]

Morphometry (measurement of the largest nucleoli using a digital filar micrometer) as well as measurements of the nuclear DNA ploidy (DNA content) by image cytometry of Feulgen stained sections, are historical approaches to establish criteria with regard to long-term survival in patients with uveal melanoma.[6,16] These tests were replaced by newer approaches such as analysis of the chromosome 3 status,[15] gene expression profiling,[14] and further genomic analyses.[17]

Immunohistochemical Features

The most important immunohistochemical markers expressed by the tumor cells are HMB45, S100, Melan A, MITF, and tyrosinase.[18–22] HMB 45 (Fig. 146.9) and Melan A are melanocytic markers. While Melan A stains melanocytes in general, HMB45 is predominantly expressed in "activated" melanocytes and is therefore more suggestive of malignant melanocytic lesions.[22,23] S100 is expressed in different types of cells including melanocytes and very often used in combination with HMB45 as a marker for uveal melanoma.[22] Microphthalmia transcription factor (MITF) is essential for the development and survival of melanocytes and therefore expressed in various melanocytic lesions including uveal melanoma.[19–21] Tyrosinase is an enzyme that is involved in the metabolism of melanocytes and was recently introduced as a melanoma marker.[18] At least two markers (e.g., HMB45 and S100)

should be employed for the diagnosis of uveal melanoma if the diagnosis cannot be made on histologic features alone.

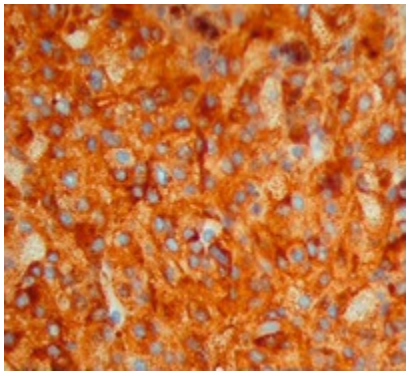

FIG. 146.9 Immunohistochemical staining for HMB 45 showing strong cytoplasmic positivity in a choroidal melanoma.

Ki67 antigen – a proliferation marker expressed in the nucleus – is suitable to detect the proliferative activity in tumors and has prognostic relevance.[24,25] Immunohistochemical stains for Phospho-Histone H3 Ser10 (PHH3) may help to detect mitotic figures in uveal melanomas.[26]

Electron Microscopy

The different cell types in choroidal melanoma such as spindle A, spindle B, and epithelioid cells can also be differentiated by transmission electron microscopy, although the ultrastructural differences between the cell types are not clear-cut.[27]

Spindle A cells appear elongated and show spindle-shaped nuclei with marked indentations and an unsuspicious nucleolus. In the cytoplasm, there are cell organelles present such as mitochondria, a relatively small number of free ribosomes, rough-surfaced endoplasmic reticulum (RER), largely immature melanin granules (premelanosomes), and numerous cytoplasmic filaments.[27]

The shape of spindle B cells (Fig. 146.10A) is similar to spindle A cells except they have a plumper cell body. The nucleoli of spindle B cells are also larger and show a reticular pattern. While spindle B cells have more RER and free ribosomes in their cytoplasm, the number of cytoplasmic filaments is decreased compared to spindle

A cells.[27]

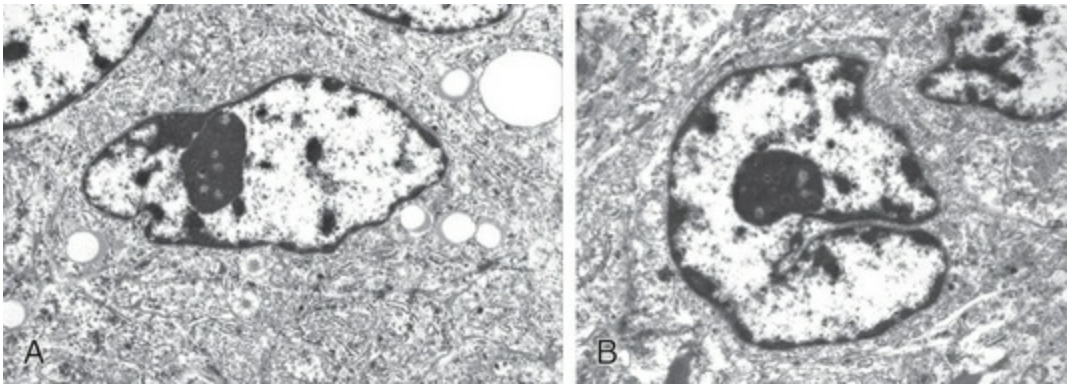

FIG. 146.10 (A) Transmission electron microscopy shows a spindle-shaped cell with a lot of rough-surfaced endoplasmic reticulum (RER) in the cytoplasm (×1900). The reticulated and slightly indented nucleus is also spindle-shaped and contains a nucleolus. There are a few melanin granules (empty vacuoles) present. (B) Epithelioid cell with cell organelles within the scanty cytoplasm (×4800). The round nucleolus is reticulated and exhibits an indentation.

The largest nucleolus is found in the round to polygonal epithelioid cells (Fig. 146.10B) and exhibits a reticular pattern. The nucleolus of the epithelioid cells can have indentations but they are less prominent than in spindle cells. Many cell organelles, in particular mitochondria – some of them exhibiting a bizarre form and structure – and free ribosomes, but only a few filaments, are present in the cytoplasm.[27]

In summary, the ultrastructural features are consistent with the present consensus that the cellular malignancy increases from spindle A (nevus cells) through spindle B to epithelioid types of melanoma cells in conjunction with an increasing number of cell organelles (e.g., mitochondria, free ribosomes) and increasing size of nucleoli that are regarded as signs of activity.[27]

Other Histopathologic Characteristics and Their Prognostic Relevance

In addition to cytologic features, other histologic tumor characteristics may be assessed in choroidal melanomas.

Tumor Stroma

As choroidal melanomas metastasize hematogenously (Fig. 146.11), much attention has been paid to "intratumoral vessels and vascular-like structures" – nine different morphologic patterns can be distinguished: normal, silent, straight, parallel, parallel with crosslinking, arcs, arcs with branching, closed vascular loops (large "vessel" occluded by tumor cells), and vascular networks (at least three back-to-back closed vascular loops) (Fig. 146.12).[28] These vascular-like structures have been later shown to reflect fibrovascular septae rather than microvasculature leading to the term "vasculogenic mimicry."[29,30] However, vasculogenic mimicry is regarded as an alternative pathway of blood supply. The presence of these extravascular matrix patterns that are identified, for example, by a PAS stain is associated with death from metastatic melanoma and may be used as an additional predictor of prognosis.[28] Connections between vasculogenic mimicry and the so-called cancer stem cells as well as epithelial-mesenchymal transformation of tumor cells have been found.[31,32]

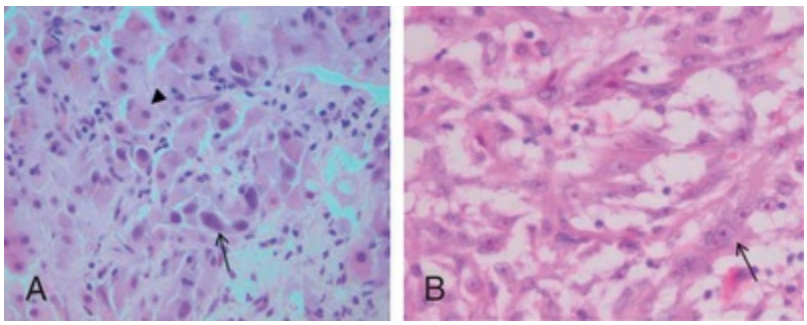

FIG. 146.11 (A) Liver metastasis of a choroidal melanoma with basophilic melanoma cells (*arrow*) next to hepatocytes (*arrowhead*) (H&E, ×400). (B) The primary tumor consists predominantly of epithelioid cells (*arrow*) (H&E, ×400) and exhibits extraocular extension (not shown).

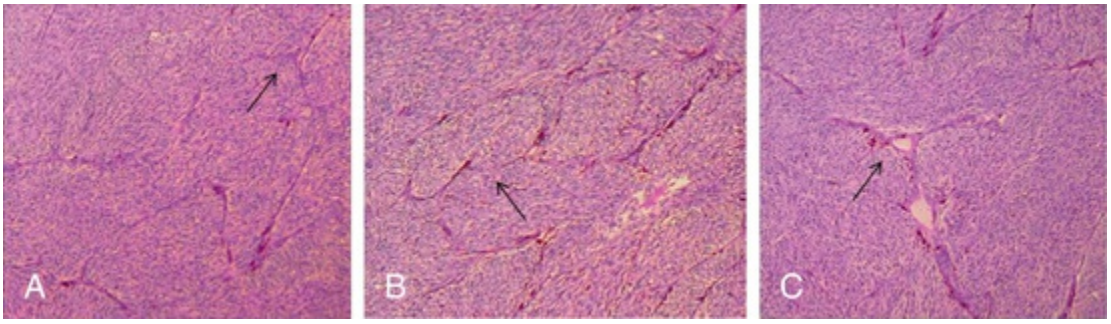

FIG. 146.12 (A) Choroidal melanoma with extracellular matrix patterns such as arches (*arrow*) (PAS, ×40) and (B) loops (*arrow*) (PAS, ×40). (C) Vascular channels within the tumor are also present (*arrow*) (PAS, ×40).

Microvascular density (MVD) itself has been identified as prognostically relevant,[28,33] and the presence of tumor cells in intratumoral blood vessels is also regarded as a factor for unfavorable outcome.[34]

A high number of tumor-infiltrating/associated lymphocytes (TILs/TALs) (Fig. 146.13) is associated with a more aggressive behavior and a higher risk of metastasis than a low number of TILs[35] – and so are tumor-infiltrating/associated macrophages (TIMs/TAMs).[6,36,37] In particular, M2 macrophages that exhibit proangiogenic and antiinflammatory characteristics (in contrast to M1 macrophages with antibacterial and antiangiogenic features) and a high M2/M1 ratio are linked to increased microvascular density, ciliary body involvement, genetic profiles, and thus a worse prognosis for survival.[38,39]

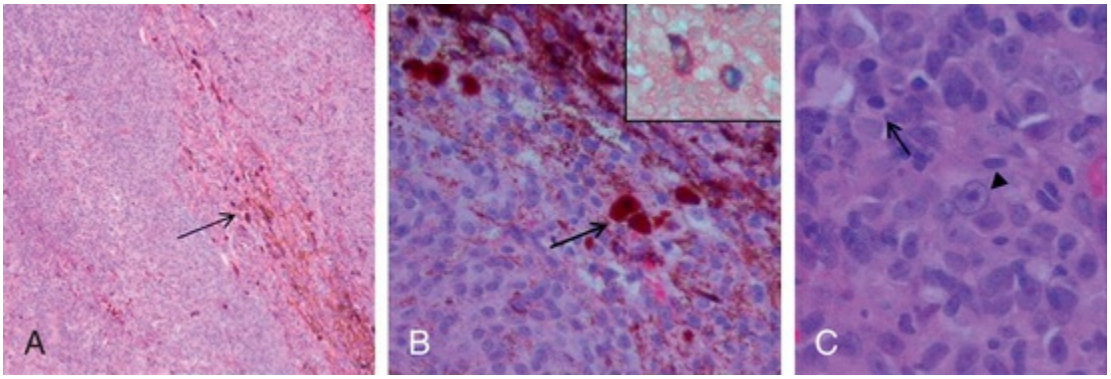

FIG. 146.13 (A) Choroidal melanoma infiltrated by pigmented macrophages (*arrow*) (H&E, ×40). (B) Higher magnification shows pigment-laden macrophages (*arrow*) (H&E, ×400). (C) An

immunohistochemical double-stain for CD68 and CD163 reveals M2-macrophages (inset; CD68–CD163 double staining, ×400). Lymphocytes are also present within the tumor (*arrow*) intermixed with epithelioid cells (*arrowhead*) (H&E, ×400).

The degree of pigmentation varies between different tumors and also within one tumor. Tumor cells, as well as pigment-laden macrophages (that are typically larger than tumor cells), contribute to the degree of pigmentation that is roughly classified into amelanotic, mildly, moderately, and heavily pigmented (see Figs. 146.1 and 146.5). In heavily and moderately pigmented tumors, bleaching is mandatory in order to analyze the cytologic features. The degree of pigmentation in comparison with other features has only weak prognostic value.[5,6]

"Melanoma-associated spongiform scleropathy (MASS)" is a degenerative, noninflammatory process in the sclera underlying the tumor that occurs in 38% of enucleated eyes harboring uveal melanoma.[40] MASS is associated with age and basal tumor diameter (extent of direct contact between tumor and sclera) but not with long-term survival.[41] A high incidence of MASS is found in eyes with scleral invasion and extrascleral extension as altered sclera collagen may allow for tumor invasion. On gross examination, whitish spindle-shaped areas within the sclera adjacent to the tumor may be detected.[40] Degraded collagen fibers and glycosaminoglycan accumulation leading to the typical picture of spongiotic areas surrounded by feathery fragmented collagen fibers are microscopically observed (Fig. 146.14).[40]

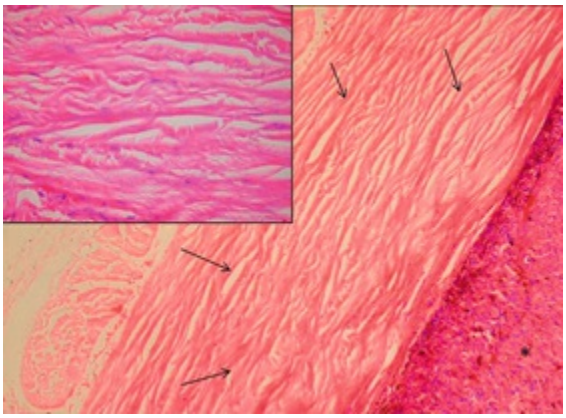

FIG. 146.14 Melanoma-associated spongiform scleropathy (MASS, *arrows*) within the sclera adjacent to a choroidal melanoma (*asterisk*) (H&E, ×100). A feathery appearance of the degenerated collagen fibers can be histologically observed (H&E, ×400).

Tumor Extension

Choroidal melanomas may invade into several ocular tissues: most uveal melanomas invade into the sclera (Fig. 146.15). Continuous horizontal growth may lead to invasion of the adjacent ciliary body and is associated with a worse prognosis. Choroidal melanomas invading into the ciliary body do not necessarily also invade into the iris, and tumor growth is usually restricted by the reticulum of Müller. Once the tumor has broken through Bruch's membrane it may invade into the retina but rarely gains access to the vitreous cavity with vitreous spread (Fig. 146.16).[42] Melanoma cells in the anterior chamber and trabecular meshwork are rarely observed in choroidal tumors that do not continuously invade into the ciliary body and iris (Fig. 146.16). Peripapillary uveal melanomas may invade into the optic nerve head, but rarely extend far retrolaminary (Fig. 146.17).[6]

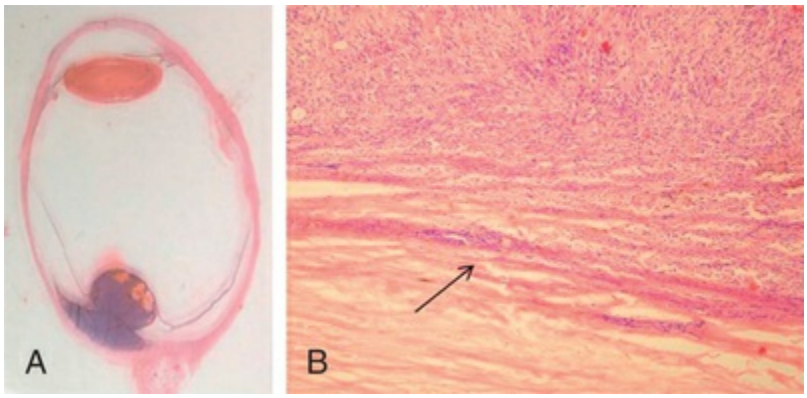

FIG. 146.15 (A) Overview of a 48-year-old man's eye harboring a mushroom-shaped choroidal melanoma (H&E). (B) Scleral invasion of the mixed-cell type tumor (*arrow*) is present and associated with melanoma-associated spongiform scleropathy (MASS).

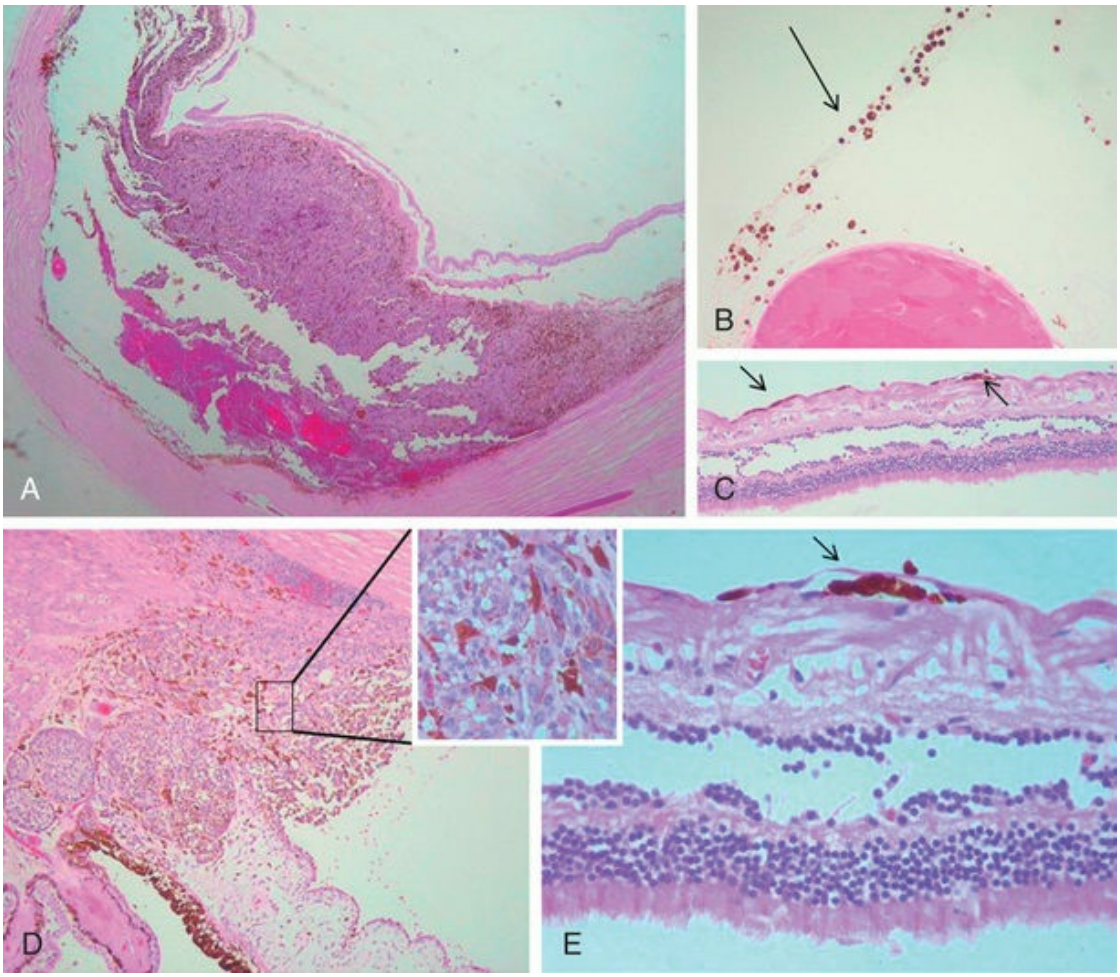

FIG. 146.16 (A) Partially necrotic choroidal melanoma (status post brachytherapy) in an 80-year-old female patient (H&E, ×40). (B) Tumor cells are present adjacent to the zonules (*arrow*) (H&E, ×100). (C,E) Superficial retinal invasion can be observed (*arrows*) (C, H&E, ×10; E, H&E, ×400). (D) The chamber angle and the iris are also noncontinuously infiltrated by tumor cells (H&E, ×40). Higher magnification of the cells in the chamber angle exhibits choroidal melanoma cells and macrophages (inset).

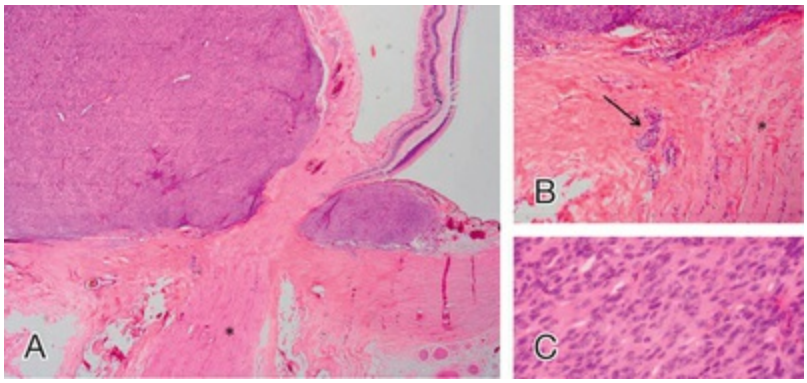

FIG. 146.17 (A) Peripapillary choroidal melanoma compressing the optic nerve head (*asterisk*) (H&E, ×40). (B) There are islands of tumor cells in an emissary canal (*arrow*) adjacent to the optic nerve (*asterisk*) (H&E, ×100). (C) The tumor is composed of spindle cells and epithelioid cells (H&E, ×400).

Extraocular extension occurs most frequently along emissary canals which include ciliary nerves and vascular channels, in particular vortex veins, as well as aqueous channels (Fig. 146.18).[43] Extension via the optic nerve or through iatrogenic wounds has also been described.[43–45] Extensive orbital extension is rarely observed (Fig. 146.19). Histologic examination of step sections of the globe and vortex veins enables pathologists to issue reliable reports that include these prognostically important parameters. Extraocular extension of uveal melanoma is associated with a significant risk for liver metastases and an increased local recurrence rate.[46]

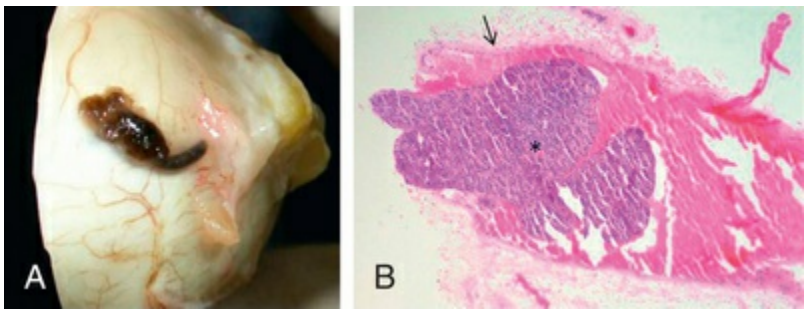

FIG. 146.18 (A) Gross appearance of a vortex vein invaded by a mixed-cell type choroidal melanoma (molecular profile class II). (B) Tumor cells (*asterisk*) are detected in the lumen of a vortex vein (*arrow*) (H&E, ×100).

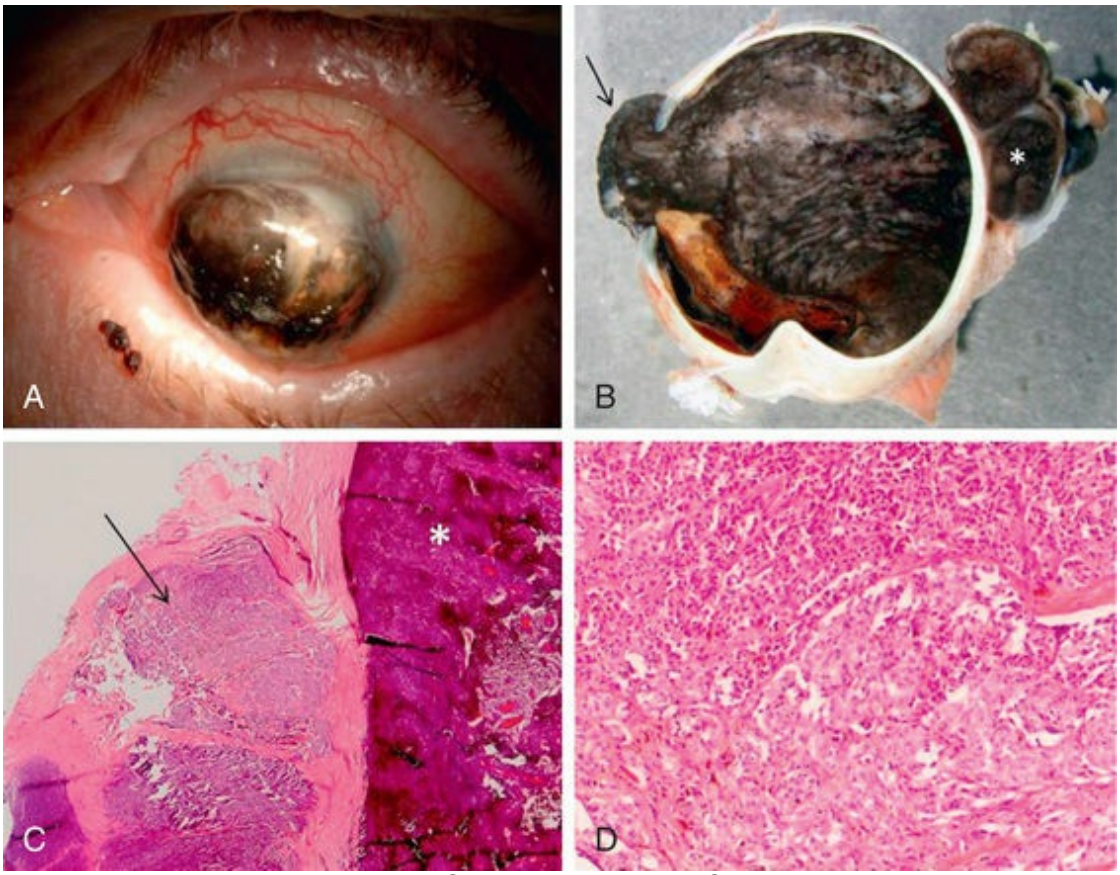

FIG. 146.19 (A) Eye of an 87-year-old female patient with a uveal melanoma breaking through the cornea. (B) On gross examination a heavily pigmented uveal melanoma filling nearly the entire globe and extending through the cornea (*arrow*) and into the optic nerve (*asterisk*) is seen. (C) The melanoma (*asterisk*) exhibits extraordinary massive optic nerve invasion (*arrow*) (H&E, ×100). (D) Higher magnification reveals epithelioid and spindle cells within and around the optic nerve (H&E, ×400).

Degenerative Changes

Accompanying degenerative changes may be observed in the retinal pigment epithelium (RPE) and the retina (Fig. 146.20). The RPE may exhibit atrophy or proliferation. Secondary drusen and orange pigment may also be found. The retina overlying the tumor usually displays atrophy with or without edema. Serous retinal detachment may occur at the margin of as well as opposite to the tumor (Fig. 146.20).

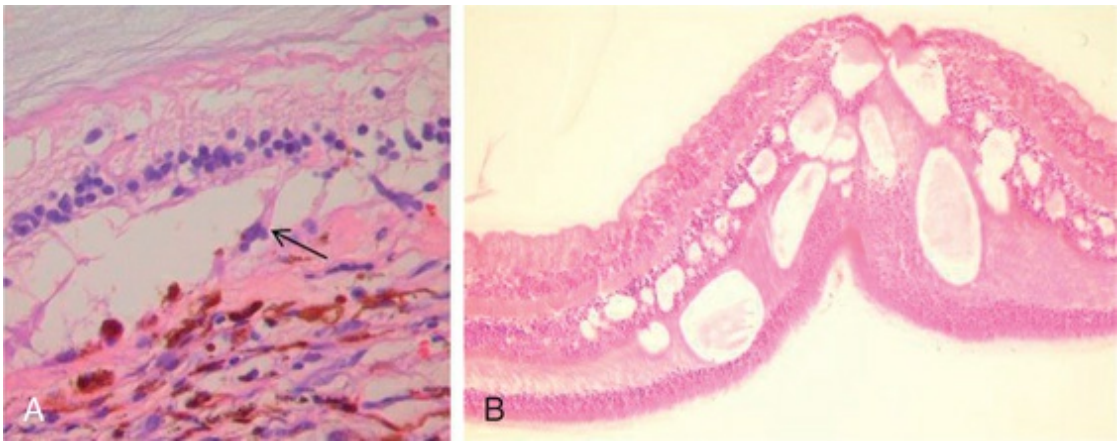

FIG. 146.20 (A) Retinal degeneration with massive atrophy of the outer retinal layers and retinal pigment epithelium atrophy is seen (H&E, ×400). Remnants of Müller cells are still observed (*arrow*). (B) Cystoid retinal edema within the inner nuclear and outer plexiform layer accompanied by massive epiretinal gliosis (H&E, ×100).

Orange pigment histologically corresponds to lipofuscin accumulation in macrophages on the tumor surface (within and under the neurosensory retina) and proliferating RPE cells, and occurs secondary to necrotic changes and/or as a sign of metabolic activity (Fig. 146.21).[47]

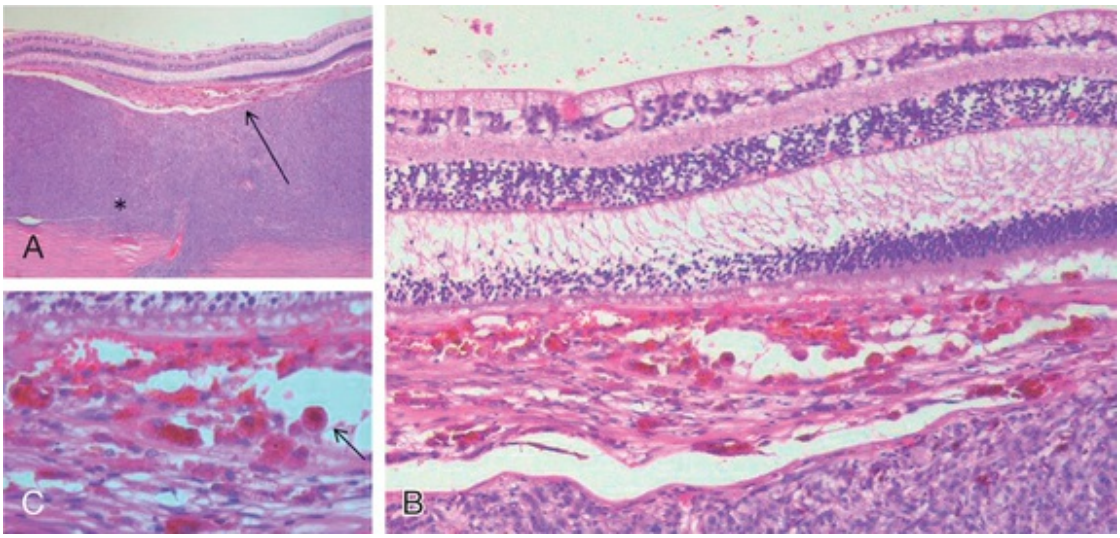

FIG. 146.21 (A) Choroidal melanoma (*asterisk*) with overlying subretinal fibrous membrane (*arrow*) (H&E, ×40). (B) Higher magnification reveals atrophy of the retinal pigment epithelium and the retinal

photoreceptor layer (H&E, ×100) (C) as well as lipofuscin-laden macrophages that correspond clinically to “orange pigment” (*arrow*) (H&E, ×400).

Special Types of Uveal Melanoma

Diffuse Uveal Melanoma

A diffuse growth pattern of uveal melanoma, defined as a tumor <5 mm in height that involves at least 25% of the uveal tract,[48] is rare as it affects only 3% of all melanoma patients[49] and exhibits horizontal rather than vertical growth (Fig. 146.22). It is associated with a worse prognosis than mound-shaped or fusiform growth patterns.

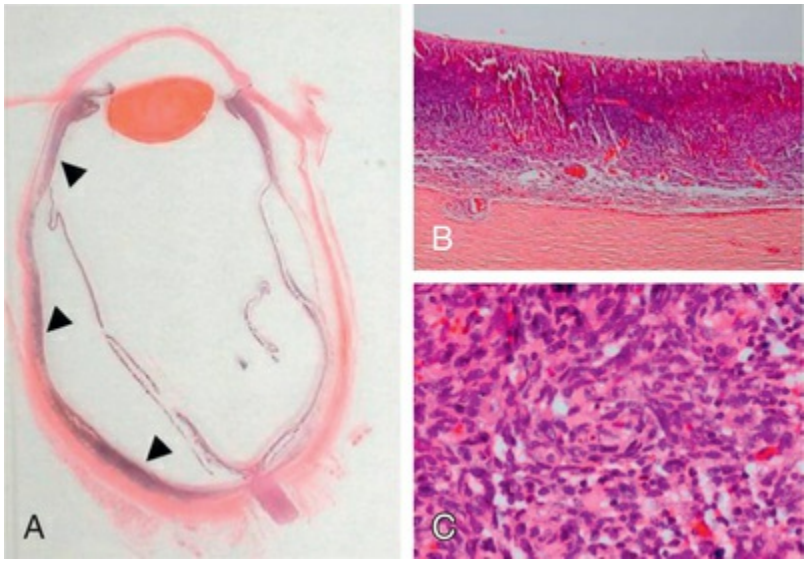

FIG. 146.22 (A) Overview showing a diffuse uveal melanoma (*arrowheads*) (H&E). (B) Histologically, a tumor is present within the choroid (H&E, ×100) and (C) is composed of spindle and epithelioid cells (H&E, ×400). (Courtesy of Milton Boniuk, MD.)

Multifocal Unilateral Uveal Melanoma

Multifocal unilateral uveal melanomas are extremely rare, and only a few cases have been reported (Fig. 146.23).[50] Serial sections should be employed in order to exclude local contiguous spread.

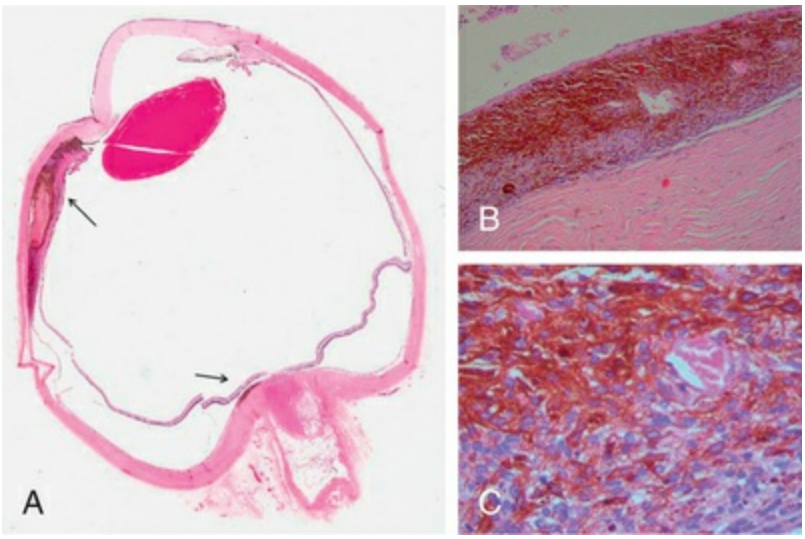

FIG. 146.23 (A) Overview illustrating a multifocal melanoma (*arrows*) (H&E). (B) Histologically, the tumor is pigmented in parts (H&E, ×100) and (C) is composed of spindle cells and epithelioid cells (H&E, ×400). (Panel A courtesy of Aperio.)

Bilateral Uveal Melanoma

Bilateral uveal melanoma occurs rarely (either simultaneously or lagged) and has to be distinguished from metastasis of uveal melanoma to the fellow eye.[51,52]

Clear Cell Differentiation of Uveal Melanoma

Uveal melanoma may rarely exhibit clear cell differentiation with cytologic features similar to clear cell tumors elsewhere in the body (Fig. 146.24).[53] The clear cells are typically oval, contain centrally placed nuclei with malignant features, and their clear cell appearance can be attributed to cytoplasmic glycogen accumulation in melanoma cells. These tumors have to be carefully distinguished from metastatic (renal) clear cell carcinoma to the choroid.

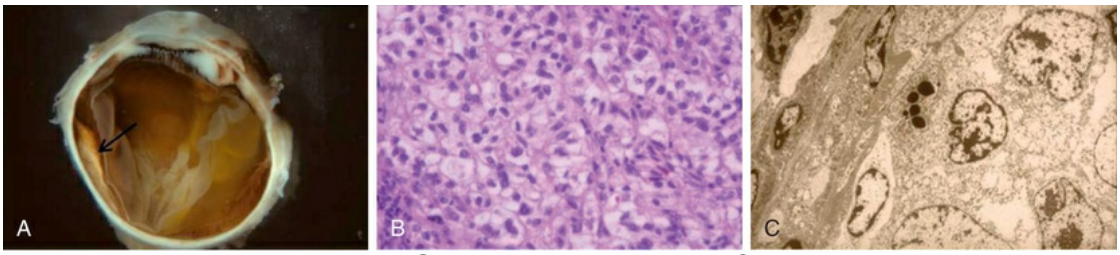

FIG. 146.24 (A) Gross appearance of a mildly pigmented tumor within the choroid in a 77-year-old female patient (*arrow*). (B) The tumor is composed in parts of clear cells that exhibit a centrally placed nucleus in a glycogen-containing cytoplasm (H&E, ×400). (C) Transmission electron microscopy (TEM) examination reveals large nuclei within a granular cytoplasm (TEM).

Balloon Cell Melanoma

Balloon cell melanoma is pathogenetically associated with degradation of melanosomes and exhibits cells with vacuolated, foamy cytoplasm due to degenerative changes with lipid accumulation.[54] Uveal melanomas may exhibit varying amounts of balloon cells. A "true" balloon cell melanoma is rarely observed. Balloon cells may also occasionally be observed in eyes treated with brachytherapy or proton beam irradiation (Fig. 146.25).[55]

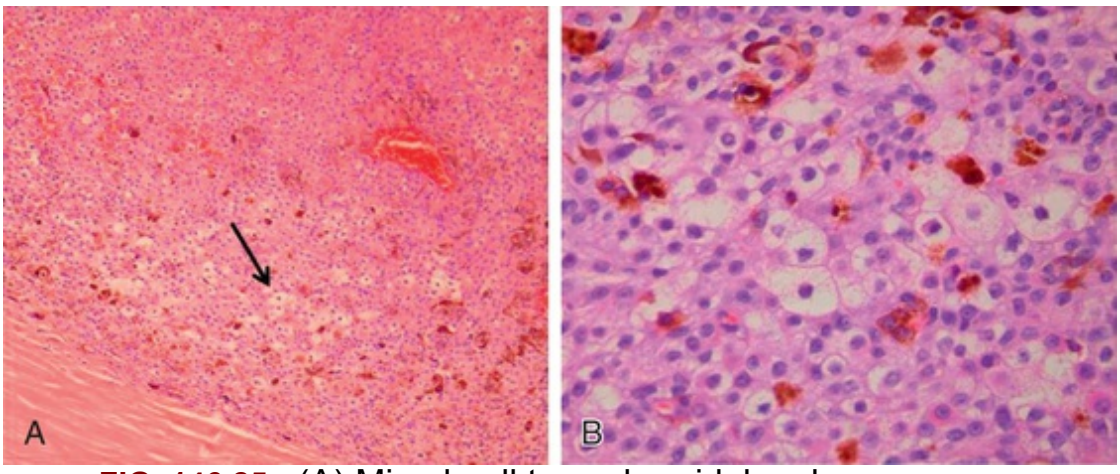

FIG. 146.25 (A) Mixed-cell type choroidal melanoma with occasional balloon cells (*arrow*) (H&E, ×100). (B) The balloon cells are intermixed beyond normal-appearing melanoma cells and exhibit a large cell body

with foamy cytoplasm (H&E, ×400).

Necrotic Melanoma

A necrotic melanoma consists of mostly necrotic cells with undetectable cytologic features (Fig. 146.26). This entity can lead to melanomalytic glaucoma, which is a rare kind of secondary open angle glaucoma in uveal melanoma occurring in the setting of spontaneous necrosis of uveal melanoma. Macrophages that phagocytose necrotic melanoma cells (melanomacrophages) accumulate in the trabecular meshwork resulting in an increased intraocular pressure.[56]

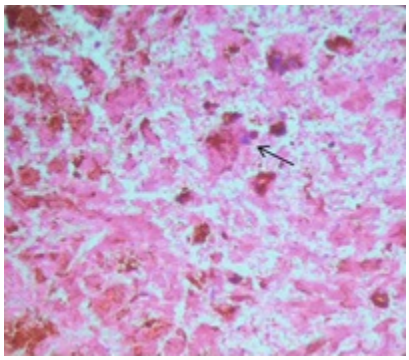

FIG. 146.26 Necrotic choroidal melanoma with free cell debris, pigment and occasional still identifiable tumor cells (*arrow*; H&E, ×400).

Retinoinvasive Melanoma

Retinoinvasive melanomas are an absolute rarity and tend to evolve from a ring melanoma.[57] In contrast to other diffuse growing uveal melanomas that only erode the overlying retina, this specific and obviously slow-growing type of uveal melanoma nearly replaces the retina and may infiltrate the optic nerve although it spares the choroid (Fig. 146.27).

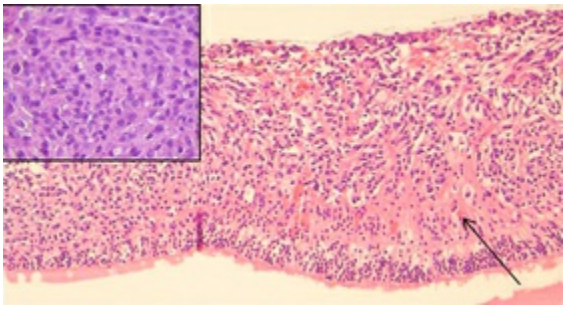

FIG. 146.27 Retina (*arrow*) effaced by uveal melanoma cells (H&E, ×100) with spindle and epithelioid cell features (inset; H&E, ×400). (Courtesy of Tero Kivelä, MD.)

Histologic Changes After Treatment

Brachytherapy

Brachytherapy has been shown by the Collaborative Ocular Melanoma Study (COMS) to be equally effective as enucleation with regard to patient survival for choroidal melanomas ≤16 mm basal diameter and 2.5–10 mm in height.[58] Histologic changes after brachytherapy may be studied in eyes that undergo enucleation for treatment failure or therapy-resistant neovascular glaucoma.

Histopathologic findings after brachytherapy (Fig. 146.28) include degenerative changes such as necrosis (sometimes present as hemorrhagic necrosis) with balloon cell or signet ring cell formation, vacuolization (cystic degeneration), lipoidal degeneration, and fibrosis of the tumor stroma. Viable tumor cells may be found, especially spindle cells, as epithelioid cells are more sensitive to radiation. Mitotic activity is lower than in nonirradiated tumors.[59–61] Vascular damage includes hyalinization of vessels walls and vascular obstruction within the tumor and the retina. The retina displays gliosis and atrophy, and an exudative retinal detachment may be present adjacent to the tumor. Subretinal gliosis, RPE irregularities and atrophy, chorioretinal atrophy, and scleral scarring/necrosis are also observed within the field of radiation.[59–61]

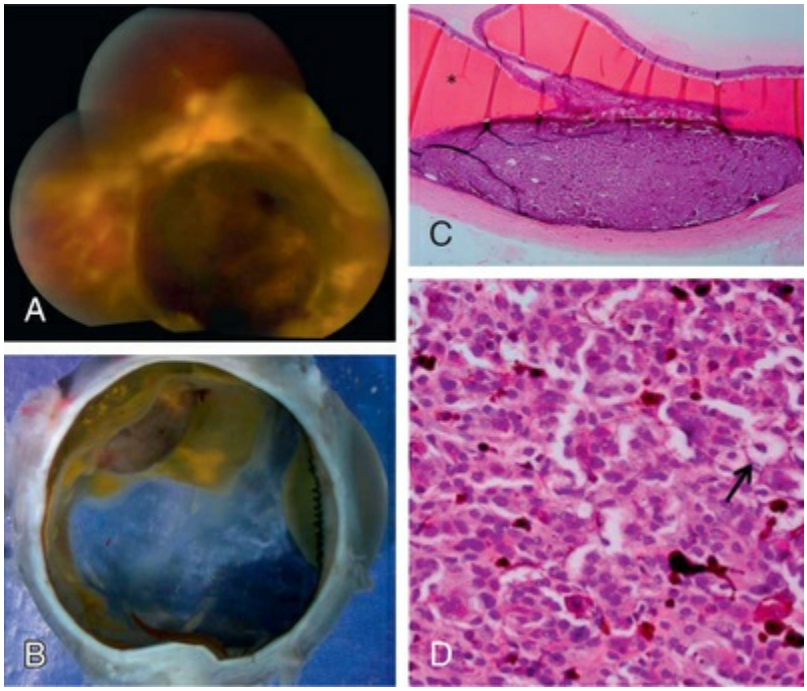

FIG. 146.28 (A) Uveal melanoma treated with brachytherapy in a 45-year-old female patient. (B) The tumor is accompanied by a serous retinal detachment. (C) The melanoma shows typical signs of irradiation such as a "lobular appearance." A serous retinal detachment is present (*asterisk*) (H&E, ×100). (D) Higher magnification reveals viable and necrotic tumor cells and occasional balloon cells (*arrow*) (H&E, ×400).

Inflammatory cell infiltrates and the accumulation of tumor infiltrating (melano)macrophages are also present after brachytherapy,[59–61] as well as macrophages in extratumoral tissue including the adjacent choroid, sclera, ciliary body, and subretinal space (Fig. 146.29).[62] Pigmented macrophage-related episcleral deposits are also frequently found in eyes with uveal melanoma after brachytherapy.[62]

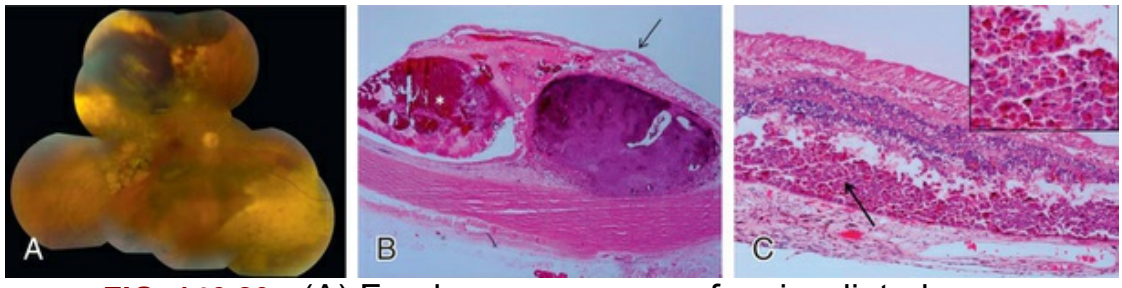

FIG. 146.29 (A) Fundus appearance of an irradiated

uveal melanoma with macular hyperpigmentations in a 43-year-old female patient. (B) Examination shows a uveal melanoma with a necrotic part (*white asterisk*) (H&E, ×40). The overlying retina displays atrophy, gliosis, and intraretinal edema (*arrow*). (C) Subretinal pigment-laden macrophages (*arrow* and inset with higher magnification) are present in the areas corresponding to the clinically detected hyperpigmentation. (Fundus photograph in panel A courtesy of Chris Bergstrom, MD, OD.)

Inadequate plaque treatment such as an undersized plaque (Fig. 146.30) or plaque tilt, as well as radioresistance of the tumor, are accounted for treatment failure with subsequent tumor growth.[63,64] Histopathologic evaluation may assist with the evaluation of the reason for treatment failure.

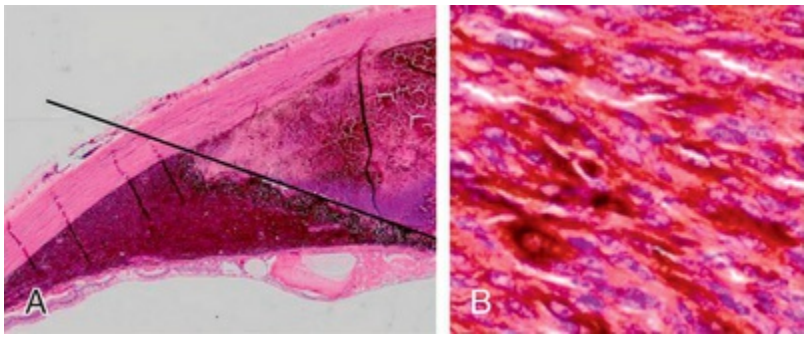

FIG. 146.30 (A) Eye enucleated for regrowth of choroidal melanoma after brachytherapy (H&E, ×100). (B) Histologically, there is a demarcation between the irradiated necrotic part of the melanoma on the right side and viable (nonirradiated) tumor on the left side of the black line. The overlying retina displays atrophy and intraretinal edema. Higher magnification shows partly pigmented spindle cells from the nonirradiated part of the tumor (H&E, ×400).

Proton Beam Irradiation

Proton beam irradiation shows histologic findings similar to those described for plaque brachytherapy, including degenerative changes in melanoma cells such as cytoplasmic lipid vacuoles,

pyknotic nuclei, and balloon cell formation, areas of necrosis within the tumor, vascular changes, and chronic inflammatory cell infiltrates (Fig. 146.31).[55,65]

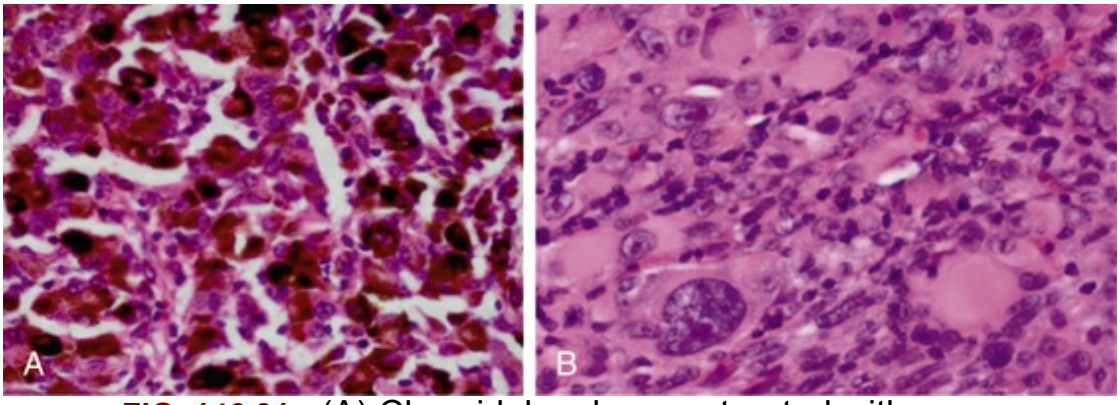

FIG. 146.31 (A) Choroidal melanoma treated with proton beam displaying small lobules of tumor cells (H&E, ×400). (B) Cells revealing signs of irradiation such as a swollen irregular nucleus are present (H&E, ×400).

Radiation Retinopathy

Radiation retinopathy (Fig. 146.32) occurs in approximately 42% of eyes within 5 years after brachytherapy (or proton beam irradiation) for uveal melanoma and often leads to irreversible visual impairment.[66] Radiation retinopathy manifests an acute transudative and slowly progressive occlusive vasculopathy with nonproliferative and/or proliferative retinopathy.[67,68] Histologic features are characterized as an obliterative endarteritis with endothelial cell loss and capillary occlusion as the primary vascular event leading to the development of dilated capillary collaterals and microaneurysms due to limited capillary regeneration.[67,68] Large telangiectatic vascular channels with fibrin and exudates in their vessel wall are pathognomonic for radiation retinopathy. Because of inner retinal ischemia, the retinal parenchyma appears edematous with associated intraretinal exudates, necrosis, and gliosis. Development of proliferative radiation retinopathy as a response to severe longstanding ischemia is observed in less than 10% of irradiated eyes.[69]

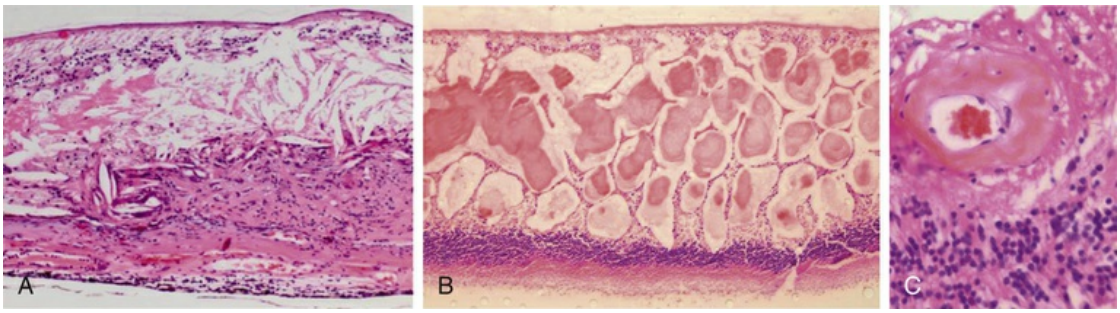

FIG. 146.32 (A) Histologic findings after radiation retinopathy include intraretinal cholesterol clefts (H&E, ×100); (B) intraretinal exudative edema (H&E, ×100); and (C) edema with exudates in the wall of a retinal vessel (H&E, ×400).

Transpupillary Thermotherapy (TTT)

TTT is used as a primary treatment for choroidal melanoma or as an adjunct to plaque brachytherapy. Histologic findings include necrosis, cytolysis, and occluded tumor blood vessels within the tumor as well as fibrotic and degenerative changes of the retina and RPE in the area of the tumor (Fig. 146.33).[70–72] Signs of marked inflammation are usually not observed.[72] Scleral damage is usually insignificant and intrascleral tumor cells may be present after treatment and are regarded as a possible source for treatment failure.[72] The presence of pigment-laden macrophages in the subretinal space are also observed after TTT.[73] Histopathologic effects of TTT also include damage to adjacent structures and are related to both energy level and fundus pigmentation.[74]

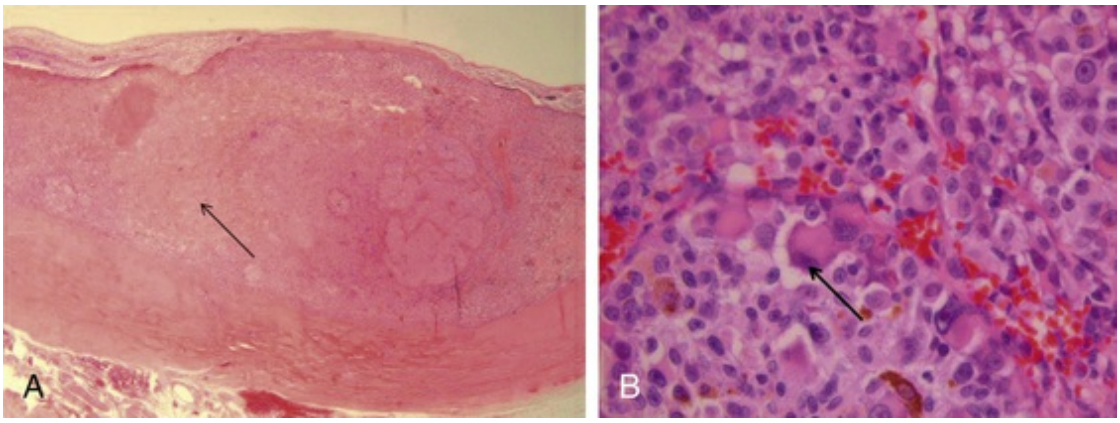

FIG. 146.33 (A) Choroidal melanoma after

transpupillary thermotherapy treatment (TTT) exhibiting areas of necrosis (*arrow*) within the tumor (H&E, ×40). (B) The retina displays degenerative changes. Higher magnification shows viable tumor cells adjacent to apoptotic cells (*arrow*) with swollen cytoplasm and a marginalized nucleus (H&E, ×400).

Appendix: Histologic Differential Diagnoses

The histologic differential diagnoses of choroidal melanoma include:

- Nevus
- Melanocytoma
- Other choroidal neoplasms
- Choroidal metastases
- BDUMP (bilateral diffuse uveal melanocytic proliferation)
- Choroidal neovascularization (CNV) with hemorrhage.

A **choroidal nevus** represents a benign lesion and consists therefore mainly of spindle A cells with a varying degree of pigmentation (Fig. 146.34). The distinction between a choroidal nevus and a melanoma is more important with regard to an incidental finding in an enucleated or eviscerated eye, as usually only eyes with large choroidal melanomas (that are not clinically confused with a nevus) are enucleated.

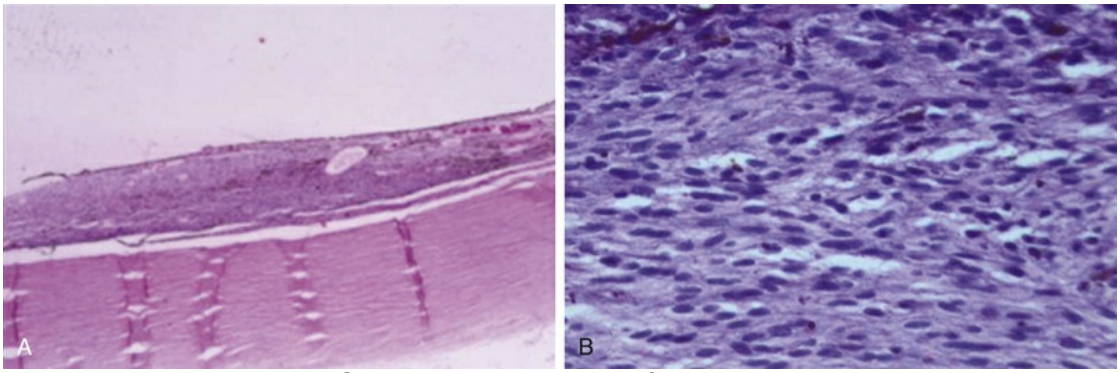

FIG. 146.34 (A) Choroidal nevus (H&E, ×40) consisting

predominantly of spindle A cells (B) (H&E, ×400).

Melanocytomas (synonym: magnocellular nevus) are jet-black lesions that predominantly occur on the optic nerve head. They are benign and rarely exhibit malignant transformation.[11] In contrast to melanocytoma of the optic disc, the diagnosis of uveal melanocytoma is rarely made on clinical appearance because of the difficulty to distinguish it from malignant melanoma.[75] Histology confirms the diagnosis as it reveals a tumor composed of uniform deeply pigmented cells with melanosomes (Fig. 146.35). After bleaching, round or slightly polyhedral plump cells with abundant cytoplasm and small uniform nuclei with inconspicuous nucleoli (type I cells) as well as spindle-shaped, sparsely pigmented cells (type II cells) become visible. Mitotic figures are uncommon.[76]

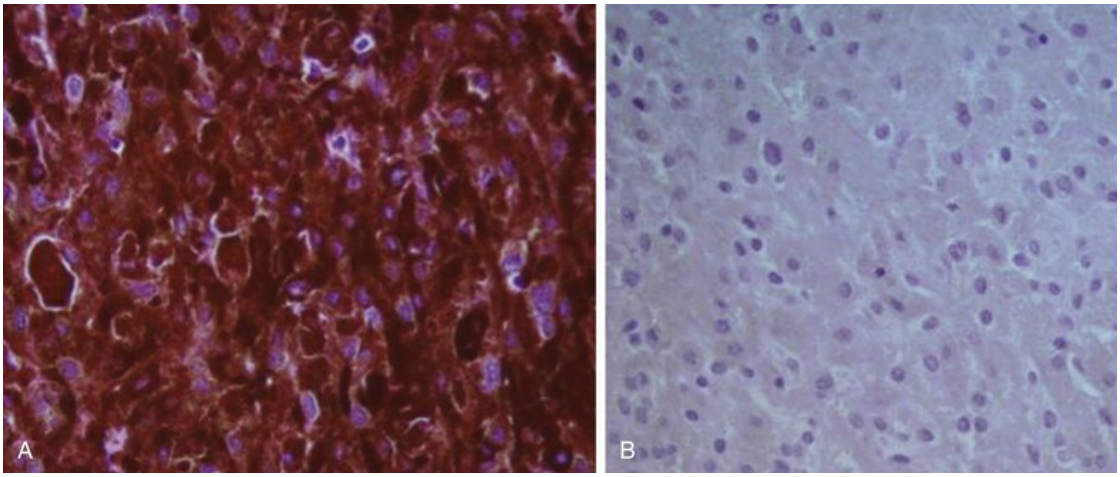

FIG. 146.35 (A) Magnocellular nevus (melanocytoma) composed of heavily pigmented cells (H&E, ×400). (B) After bleaching, the polygonal cells with their unsuspicious nuclei are visible (bleached H&E stain, ×400).

Other choroidal tumors such as hemangioma or lymphoma may usually be distinguished from malignant melanoma by clinical studies such as ultrasonography. These tumors also exhibit distinct histopathologic features.

Choroidal metastases (Fig. 146.36) exhibit characteristics of the primary tumor (predominantly carcinomas, 82%). Most frequently found are breast (47%) and lung cancer (21%), followed by

gastrointestinal tract (4%), kidney (2%), skin (2%), prostate (2%), and other cancers (4%). There is a relatively high rate of unknown primary malignancies after systemic evaluation (17%).[77]

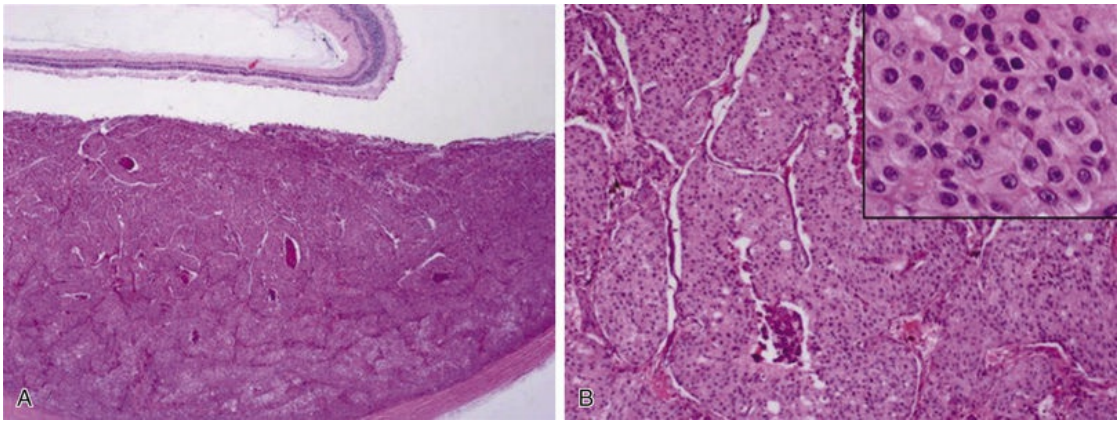

FIG. 146.36 (A) Choroidal mass consistent with a breast carcinoma metastasis composed of tumor cells arranged in a papillomatous configuration (H&E, ×40). (B) Higher magnification shows glandular-like structures (H&E, ×100) and large tumor cells with prominent nucleoli (inset).

Bilateral diffuse uveal melanocytic proliferation (BDUMP) is a rare paraneoplastic syndrome with a typical clinical presentation including multiple round to oval, slightly elevated choroidal patches and an associated "leopard spot" appearance on fluorescein angiography (FA). Except for one unilateral case,[78] BDUMP occurs bilaterally – in contrast to choroidal melanoma. Histologic examination usually reveals a diffuse or poorly defined choroidal infiltrative process with small hypopigmented spindle-shaped benign-appearing melanocytes.[79,80] The choriocapillaris is often spared and the overlying RPE is depigmented (Fig. 146.37).

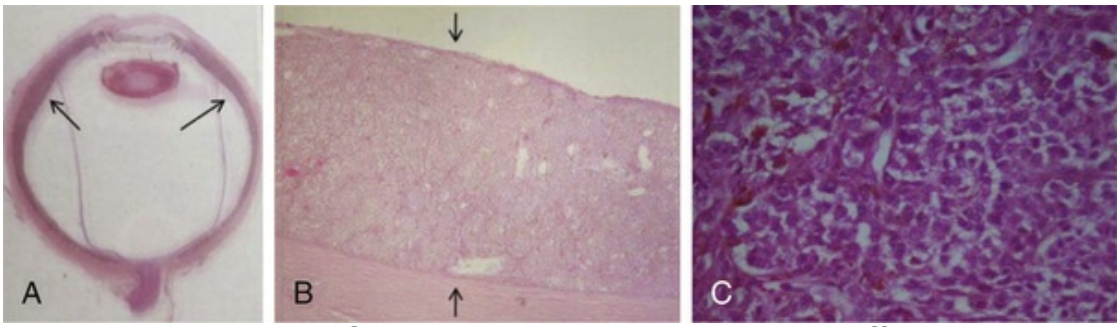

FIG. 146.37 (A) Overview illustrating a bilateral diffuse uveal melanocytic proliferation (BDUMP) invading the choroid (*arrows*) (H&E). (B) The lesion effaces the entire choroid (*arrows*) but spares the choriocapillaris (H&E, ×40). (C) The lesion is composed of hypopigmented bland melanocytes (H&E, ×400).
(Courtesy of Curtis E. Margo, MD.)

CNV with an associated large hemorrhage may exhibit a funduscopic appearance similar to choroidal melanoma, although the two may be distinguished by clinical tests including ultrasonography, FA, and optical coherence tomography (OCT).

Acknowledgments

Supported in part by an unrestricted departmental grant from Research to Prevent Blindness, Inc, NIH P30EY06360 (Hans E. Grossniklaus).

References

1. Folberg R, Salomao D, Grossniklaus HE, et al. Recommendations for the reporting of tissues removed as part of the surgical treatment of common malignancies of the eye and its adnexa. *Mod Pathol*. 2003;16:725–730.
2. Folberg R, Salomao D, Grossniklaus HE, et al. Recommendations for the reporting of tissues removed as part of the surgical treatment of common malignancies of the eye and its adnexa. *Am J Surg Pathol*. 2003;27:999–1004.
3. Folberg R, Salomao D, Grossniklaus HE, et al. Recommendations for the reporting of tissues removed as part of the surgical treatment of common malignancies of

the eye and its adnexa. The Association of Directors of Anatomic and Surgical Pathology. *Hum Pathol*. 2003;34:114–118.
4. Association of Directors of Anatomic and Surgical Pathology. Recommendations for the reporting of tissues removed as part of the surgical treatment of common malignancies of the eye and its adnexa. *Am J Clin Pathol*. 2003;119:179–184.
5. Seddon JM, Albert DM, Lavin PT, et al. A prognostic factor study of disease-free interval and survival following enucleation for uveal melanoma. *Arch Ophthalmol*. 1983;101:1894–1899.
6. McLean IW, Saraiva VS, Burnier MN Jr. Pathological and prognostic features of uveal melanomas. *Can J Ophthalmol*. 2004;39:343–350.
7. Comparison of clinical, echographic, and histopathological measurements from eyes with medium-sized choroidal melanoma in the Collaborative Ocular Melanoma Study: COMS report no. 21. *Arch Ophthalmol*. 2003;121:1163–1171.
8. Coleman DJ, Silverman RH, Rondeau MJ, et al. Correlations of acoustic tissue typing of malignant melanoma and histopathologic features as a predictor of death. *Am J Ophthalmol*. 1990;110:380–388.
9. American Joint Committee on Cancer. *Cancer staging manual*. 7th ed. Springer: New York; 2010.
10. Shetlar DJ, Folberg R, Gass JD. Choroidal malignant melanoma associated with a melanocytoma. *Retina*. 1999;19:346–349.
11. Kurli M, Finger PT, Manor T, et al. Finding malignant change in a necrotic choroidal melanocytoma: a clinical challenge. *Br J Ophthalmol*. 2005;89:921–922.
12. Callender GR. Malignant melanotic tumors of the eye: a study of histologic types in 111 cases. *Trans Am Acad Ophthalmol Otolaryngol*. 1931;36:131–142.
13. McLean IW, Foster WD, Zimmerman LE, et al. Modifications of Callender's classification of uveal melanoma at the Armed Forces Institute of Pathology. *Am J Ophthalmol*. 1983;96:502–509.

14. Onken MD, Worley LA, Ehlers JP, et al. Gene expression profiling in uveal melanoma reveals two molecular classes and predicts metastatic death. *Cancer Res*. 2004;64:7205–7209.
15. Prescher G, Bornfeld N, Hirche H, et al. Prognostic implications of monosomy 3 in uveal melanoma. *Lancet*. 1996;347:1222–1225.
16. de Lange MJ, van Pelt SI, Versluis M, et al. Heterogeneity revealed by integrated genomic analysis uncovers a molecular switch in malignant uveal melanoma. *Oncotarget*. 2015;6(35):37824–37835.
17. Grossniklaus HE, Oakman JH, Cohen C, et al. Histopathology, morphometry, and nuclear DNA content of iris melanocytic lesions. *Invest Ophthalmol Vis Sci*. 1995;36:745–750.
18. Fernandes BF, Odashiro AN, Saraiva VS, et al. Immunohistochemical expression of melan-A and tyrosinase in uveal melanoma. *J Carcinog*. 2007;6:6.
19. Iwamoto S, Burrows RC, Kalina RE, et al. Immunophenotypic differences between uveal and cutaneous melanomas. *Arch Ophthalmol*. 2002;120:466–470.
20. O'Reilly FM, Brat DJ, McAlpine BE, et al. Microphthalmia transcription factor immunohistochemistry: a useful diagnostic marker in the diagnosis and detection of cutaneous melanoma, sentinel lymph node metastases, and extracutaneous melanocytic neoplasms. *J Am Acad Dermatol*. 2001;45:414–419.
21. Mouriaux F, Vincent S, Kherrouche Z, et al. Microphthalmia transcription factor analysis in posterior uveal melanomas. *Exp Eye Res*. 2003;76:653–661.
22. Rohrbach JM, Steuhl KP, Thanos S. [Monoclonal antibody HMB-45 in diagnosis of intra-ocular melanoma]. *Klin Monatsbl Augenheilkd*. 1991;199:274–277.
23. Burnier MN Jr, McLean IW, Gamel JW. Immunohistochemical evaluation of uveal melanocytic tumors: expression of HMB-45, S-100 protein, and neuron-specific enolase. *Cancer*. 1991;68:809–814.
24. Mooy CM, Luyten GP, de Jong PT, et al.

Immunohistochemical and prognostic analysis of apoptosis and proliferation in uveal melanoma. *Am J Pathol*. 1995;147:1097–1104.
25. Karlsson M, Boeryd B, Carstensen J, et al. Correlations of Ki-67 and PCNA to DNA ploidy, S-phase fraction and survival in uveal melanoma. *Eur J Cancer*. 1996;32A:357–362.
26. Angi M, Damato B, Kalirai H, et al. Immunohistochemical assessment of mitotic count in uveal melanoma. *Acta Ophthalmol*. 2011;89:e155–60.
27. Iwamoto T, Jones IS, Howard GM. Ultrastructural comparison of spindle A, spindle B, and epithelioid-type cells in uveal malignant melanoma. *Invest Ophthalmol*. 1972;11:873–889.
28. Folberg R, Rummelt V, Parys-Van Ginderdeuren R, et al. The prognostic value of tumor blood vessel morphology in primary uveal melanoma. *Ophthalmology*. 1993;100:1389–1398.
29. Foss AJ, Alexander RA, Hungerford JL, et al. Reassessment of the PAS patterns in uveal melanoma. *Br J Ophthalmol*. 1997;81:240–248.
30. Folberg R, Hendrix MJ, Maniotis AJ. Vasculogenic mimicry and tumor angiogenesis. *Am J Pathol*. 2000;156:361–381.
31. Fan Y-L, Zheng M, Tang T-L, et al. A new perspective of vasculogenic mimicry: EMT and cancer stem cells. *Oncol Lett*. 2013;6:1174–1180.
32. Valyi-Nagy K, Kormos B, Ali M, et al. Stem cell marker CD271 is expressed by vasculogenic mimicry-forming uveal melanoma cells in three-dimensional cultures. *Mol Vis*. 2012;18:588–592.
33. Makitie T, Summanen P, Tarkkanen A, et al. Microvascular density in predicting survival of patients with choroidal and ciliary body melanoma. *Invest Ophthalmol Vis Sci*. 1999;40:2471–2480.
34. Ly LV, Odish OF, Wolff-Rouendaal D, et al. Intravascular presence of tumor cells as prognostic parameter in uveal melanoma: a 35-year survey. *Invest Ophthalmol Vis Sci*. 2010;51:658–665.
35. de la Cruz PO Jr, Specht CS, McLean IW. Lymphocytic

infiltration in uveal malignant melanoma. *Cancer*. 1990;65:112–115.
36. Makitie T, Summanen P, Tarkkanen A, et al. Tumor-infiltrating macrophages (CD68(+) cells) and prognosis in malignant uveal melanoma. *Invest Ophthalmol Vis Sci*. 2001;42:1414–1421.
37. Bronkhost IH, Jager MJ. Uveal melanoma: the inflammatory microenvironment. *J Innate Immun*. 2012;4(5–6):454–462.
38. Bronkhorst IH, Ly LV, Jordanova ES, et al. Detection of M2-macrophages in uveal melanoma and relation with survival. *Invest Ophthalmol Vis Sci*. 2011;52:643–650.
39. Herwig MC, Bergstrom C, Wells JR, et al. M2/M1 ratio of tumor associated macrophages and PPAR-gamma expression in uveal melanomas with class 1 and class 2 molecular profiles. *Exp Eye Res*. 2013;107:52–58.
40. Alyahya GA. Melanoma associated spongiform scleropathy: characterization, biochemical and immunohistochemical studies. *Acta Ophthalmol*. 2008;86(Thesis 3):1–21.
41. Yanoff M, Sassani JW. *Ocular pathology*. 6th ed. Mosby: St. Louis; 2009.
42. Heindl LM, Mardin CY, Holbach LM, et al. Vitreal seeding from uveal melanoma detected by high-resolution spectral-domain optical coherence tomography. *Arch Ophthalmol*. 2009;127:1062–1064.
43. Coupland SE, Campbell I, Damato B. Routes of extraocular extension of uveal melanoma: risk factors and influence on survival probability. *Ophthalmology*. 2008;115:1778–1785.
44. Grossniklaus HE, Brown RH, Stulting RD, et al. Iris melanoma seeding through a trabeculectomy site. *Arch Ophthalmol*. 1990;108:1287–1290.
45. Kavanagh MC, Everman KR, Opremcak EM, et al. Uveal melanoma with massive extrascleral extension via pars plana vitrectomy sites. *Ophthal Plast Reconstr Surg*. 2008;24:334–336.
46. Affeldt JC, Minckler DS, Azen SP, et al. Prognosis in uveal melanoma with extrascleral extension. *Arch Ophthalmol*. 1980;98:1975–1979.
47. Font RL, Zimmerman LE, Armaly MF. The nature of the

orange pigment over a choroidal melanoma: histochemical and electron microscopical observations. *Arch Ophthalmol*. 1974;91:359–362.
48. Char DH. *Tumor of the eye and the ocular adnexa*. BC Decker Inc: Lewiston; 2001.
49. Shields CL, Shields JA, De Potter P, et al. Diffuse choroidal melanoma: clinical features predictive of metastasis. *Arch Ophthalmol*. 1996;114:956–963.
50. Dithmar S, Volcker HE, Grossniklaus HE. Multifocal intraocular malignant melanoma: report of two cases and review of the literature. *Ophthalmology*. 1999;106:1345–1348.
51. Hadden PW, Damato BE, McKay IC. Bilateral uveal melanoma: a series of four cases. *Eye (Lond)*. 2003;17:613–616.
52. Sturm V, Richard G. [The prevalence of bilateral malignant uveal melanoma]. *Klin Monatsbl Augenheilkd*. 2007;224:770–774.
53. Grossniklaus HE, Albert DM, Green WR, et al. Clear cell differentiation in choroidal melanoma: COMS report no. 8. Collaborative Ocular Melanoma Study Group. *Arch Ophthalmol*. 1997;115:894–898.
54. Khalil MK. Balloon cell malignant melanoma of the choroid: ultrastructural studies. *Br J Ophthalmol*. 1983;67:579–584.
55. Saornil MA, Egan KM, Gragoudas ES, et al. Histopathology of proton beam-irradiated vs enucleated uveal melanomas. *Arch Ophthalmol*. 1992;110:1112–1118.
56. McMenamin PG, Lee WR. Ultrastructural pathology of melanomalytic glaucoma. *Br J Ophthalmol*. 1986;70:895–906.
57. Kivela T, Summanen P. Retinoinvasive malignant melanoma of the uvea. *Br J Ophthalmol*. 1997;81:691–697.
58. Collaborative Ocular Melanoma Study Group. The COMS randomized trial of iodine 125 brachytherapy for choroidal melanoma: V. Twelve-year mortality rates and prognostic factors: COMS report No. 28. *Arch Ophthalmol*. 2006;124:1684–1693.
59. Avery RB, Diener-West M, Reynolds SM, et al. Histopathologic characteristics of choroidal melanoma in eyes enucleated after iodine 125 brachytherapy in the

Collaborative Ocular Melanoma Study. *Arch Ophthalmol*. 2008;126:207–212.
60. Messmer E, Bornfeld N, Foerster M, et al. Histopathologic findings in eyes treated with a ruthenium plaque for uveal melanoma. *Graefes Arch Clin Exp Ophthalmol*. 1992;230:391–396.
61. Schilling H, Sehu KW, Lee WR. A histologic study (including DNA quantification and Ki-67 labeling index) in uveal melanomas after brachytherapy with ruthenium plaques. *Invest Ophthalmol Vis Sci*. 1997;38:2081–2092.
62. Toivonen P, Kivela T. Pigmented episcleral deposits after brachytherapy of uveal melanoma. *Ophthalmology*. 2006;113:865–873.
63. Char DH, Crawford JB, Kaleta-Michaels S, et al. Analysis of radiation failure after uveal melanoma brachytherapy. *Am J Ophthalmol*. 1989;108:712–716.
64. Almony A, Breit S, Zhao H, et al. Tilting of radioactive plaques after initial accurate placement for treatment of uveal melanoma. *Arch Ophthalmol*. 2008;126:65–70.
65. Seddon JM, Gragoudas ES, Albert DM. Ciliary body and choroidal melanomas treated by proton beam irradiation. Histopathologic study of eyes. *Arch Ophthalmol*. 1983;101:1402–1408.
66. Gunduz K, Shields CL, Shields JA, et al. Radiation retinopathy following plaque radiotherapy for posterior uveal melanoma. *Arch Ophthalmol*. 1999;117:609–614.
67. Archer DB, Amoaku WM, Gardiner TA. Radiation retinopathy–clinical, histopathological, ultrastructural and experimental correlations. *Eye (Lond)*. 1991;5(Pt 2):239–251.
68. Finger PT. Anti-VEGF bevacizumab (Avastin) for radiation optic neuropathy. *Am J Ophthalmol*. 2007;143:335–338.
69. Bianciotto C, Shields CL, Pirondini C, et al. Proliferative radiation retinopathy after plaque radiotherapy for uveal melanoma. *Ophthalmology*. 2010;117:1005–1012.
70. Singh AD, Eagle RC Jr, Shields CL, et al. Clinicopathologic reports, case reports, and small case series: enucleation following transpupillary thermotherapy of choroidal melanoma: clinicopathologic correlations. *Arch Ophthalmol*.

2003;121:397–400.
71. Diaz CE, Capone A Jr, Grossniklaus HE. Clinicopathologic findings in recurrent choroidal melanoma after transpupillary thermotherapy. *Ophthalmology*. 1998;105:1419–1424.
72. Journee-de Korver JG, Oosterhuis JA, de Wolff-Rouendaal D, et al. Histopathological findings in human choroidal melanomas after transpupillary thermotherapy. *Br J Ophthalmol*. 1997;81:234–239.
73. Kiratli H, Bilgic S, Soylemezoglu F, et al. Peripheral subretinal pigment accumulation following transpupillary thermotherapy for choroidal melanoma. *Ophthalmic Surg Lasers Imaging*. 2008;39:60–62.
74. Connolly BP, Regillo CD, Eagle RC Jr, et al. The histopathologic effects of transpupillary thermotherapy in human eyes. *Ophthalmology*. 2003;110:415–420.
75. Robertson DM, Campbell RJ, Salomao DR. Mushroom-shaped choroidal melanocytoma mimicking malignant melanoma. *Arch Ophthalmol*. 2002;120:82–85.
76. Juarez CP, Tso MO. An ultrastructural study of melanocytomas (magnocellular nevi) of the optic disk and uvea. *Am J Ophthalmol*. 1980;90:48–62.
77. Shields CL, Shields JA, Gross NE, et al. Survey of 520 eyes with uveal metastases. *Ophthalmology*. 1997;104:1265–1276.
78. Reddy S, Finger PT. Unilateral diffuse uveal melanocytic proliferation (DUMP). *Br J Ophthalmol*. 2007;91:1726–1727.
79. Gass JD, Gieser RG, Wilkinson CP, et al. Bilateral diffuse uveal melanocytic proliferation in patients with occult carcinoma. *Arch Ophthalmol*. 1990;108:527–533.
80. Barr CC, Zimmerman LE, Curtin VT, et al. Bilateral diffuse melanocytic uveal tumors associated with systemic malignant neoplasms: a recently recognized syndrome. *Arch Ophthalmol*. 1982;100:249–255.

147

Overview of Management of Posterior Uveal Melanoma

Carol L. Shields, Jerry A. Shields

Introduction

Posterior uveal melanoma is a serious, life-threatening malignancy.[1–83] It is estimated that approximately 7095 cases of uveal melanoma are detected annually, with 4747 in white non-Hispanic, 738 in Hispanic, 1286 in Asian, and 316 in black patients.[2] In the United States the mean age-adjusted incidence of uveal melanoma is 4.3 per million.[3] This figure has remained relatively stable over the past five decades. Comprehensive clinic-based analysis has revealed that this malignancy tends to occur in whites at a mean age of 58 years with symptoms of photopsia, floaters, visual field loss, or visual acuity loss.[1,4]

There have been numerous publications on the management of uveal melanoma and this topic remains controversial.[1–83] Depending on the clinical circumstances, observation, transpupillary thermotherapy, plaque radiotherapy, charged particle irradiation, external resection (exoresection), internal resection (endoresection), enucleation, orbital exenteration, systemic chemotherapy, and systemic immunotherapy are alternatives.[1,5,6] There is a trend toward detection of melanoma at its earliest stage using multimodal imaging rather than relying strictly on ophthalmoscopy. Imaging with fundus photography, spectral domain and swept source optical coherence tomography, autofluorescence, multispectral imaging, and ultrasonography are critical for early tumor detection, sometimes even at a point when the tumor is almost subclinical. Clinical risk factors for tumor growth and metastasis for the smallest choroidal melanocytic lesions have been identified and are useful for determining the malignant potential of a small mass and deciding when to treat.[7–10] Consequently, there is an evolving trend away from observation of suspicious small melanocytic lesions and towards earlier treatment of lesions with risk factors.[8,9,11] This introductory chapter provides an overview of the current methods for management of patients with ciliary body and choroidal melanoma. In the subsequent chapters, several authorities address the specific details of the

various therapeutic modalities.

The general concepts discussed here are based on personal experience in the field of uveal melanoma management at the Ocular Oncology Service at Wills Eye Hospital for more than 40 years. This experience, combined with a review of the literature, has been written as objectively as possible, but our opinion could be different than the opinions of others.

General Considerations

Historically, enucleation was once considered to be the only appropriate management for a patient with a posterior uveal melanoma.[5] At that time, most patients presented late in the course with large melanoma, retinal detachment, secondary glaucoma, and often extrascleral extension of the tumor, at a point when enucleation was the only option. Several years ago, however, some authorities challenged the effectiveness of enucleation for prevention of metastatic disease and even proposed that enucleation could somehow promote or accelerate metastasis, an idea termed the "Zimmerman hypothesis."[12,13] The validity of those arguments was soon challenged by others, who believed that early enucleation offered the patient the best chance of cure.[14,15] This controversy over enucleation was responsible for initiating a trend away from enucleation and the increasing use of more conservative therapeutic methods. One-quarter century later, this hypothesis was reevaluated and, based on clinical, epidemiologic, statistical, and experimental data, the transient rise in posttherapeutic mortality was confirmed, but the authors believed it was not likely due to enucleation but more plausibly a result of early micrometastasis of uveal melanoma before therapy.[16]

Depending upon several clinical factors, the most common methods of management today include observation, transpupillary thermotherapy (TTT), radiotherapy, local resection, enucleation, orbit exenteration, and various combinations of these methods. There is currently an increasing variety of methods to treat or prevent metastatic disease that are beyond the scope of this short chapter. The most frequently employed treatment methods today are radiotherapy and enucleation. The Collaborative Ocular

Melanoma Study (COMS) was organized to address several clinical and therapeutic issues related to posterior uveal melanoma and important information has been obtained from that study.[17–23] Nevertheless, each case must be individualized and the recommended treatment should be the most suitable to provide the best systemic prognosis, while preserving as much vision as possible. If possible, the patient should be referred to an ocular oncologist or other ophthalmologist who has experience in managing patients with uveal melanoma.

Periodic Observation

Most small melanocytic tumors (≤3 mm thickness) are best managed by periodic fundus photography and imaging with optical coherence tomography, autofluorescence, and ultrasonography to document lesion stability or growth. Stable lesions are monitored every 4–6 months and thereafter on a 6–12-month basis. Long-term monitoring for all choroidal melanocytic lesions, including freckle, nevus, or inactive larger lesions, should be advised.

Factors statistically predictive of growth of a small melanocytic lesion have been identified (Table 147.1). Lesions with documented growth or those with three or more risk factors are generally considered for treatment[1,8–11] (Table 147.1). Identified risk factors for metastasis from small melanoma (≤3 mm thickness) include tumor thickness >2 mm, tumor within 3 mm of the optic nerve, presence of visual symptoms from the melanoma, and prior documented growth.[8] Since documented growth can be associated with a worse systemic prognosis, there is a trend to treat patients with risk factors, without necessarily waiting for documentation of growth.[8,9,11]

TABLE 147.1

Factors for Early Detection of Choroidal Melanoma: the TFSOM–UHHD Mnemonic (to Find Small Ocular Melanoma – Using Helpful Hints Daily)

	Hazard	Nevus Growth Into	Nevus Growth Into

Initials	Mnemonic	Features	Ratio[a]	Melanoma if Feature Present (%)	Melanoma if Feature Absent (%)
T	To	Thickness > 2 mm	2	19%	5%
F	Find	Fluid	3	27%	5%
S	Small	Symptoms	2	23%	5%
O	Ocular	Orange pigment	3	30%	5%
M	Melanoma	Margin ≤3 mm to disc	2	13%	4%
UH	Using Helpful	Ultrasound hollow	3	25%	4%
H	Hints	Halo absent	6	7%	2%
D	Daily	Drusen absent	na	na	na

na, The risk factor of drusen absent was identified in other studies to be significant so it was included in this mnemonic for risk factors.

Adapted from information listed in Shields et al.[9]

Laser Photocoagulation

Laser photocoagulation was once a commonly used method to treat small choroidal melanomas.[24–28] It was originally performed with xenon arc photocoagulation but argon laser and diode laser subsequently became more commonly employed. Studies showed that xenon photocoagulation achieved better tumor control but argon laser was associated with fewer complications.[25] More recently, TTT and photodynamic therapy (PDT) have largely replaced laser photocoagulation for treatment of selected small melanomas that are less than 3 mm in thickness and located more than 3 mm from the foveola.[20]

Transpupillary Thermotherapy

Transpupillary thermotherapy (TTT) is a recently popularized method of treating selected small and medium-sized choroidal melanomas using subphotocoaulation heat in the infrared range using a modified diode laser delivery system.[29–33] This method does not produce as much damage to the sensory retina as does laser photocoagulation. Recent observations have clarified the limitations and complications of TTT.[33,34] Currently, our strategy for primary

TTT includes low-grade melanocytic borderline tumors outside the macular and juxtapapillary region and those with only one or two risk factors.[34] Tumors with greater number of risk factors should be treated with methods other than TTT.[34] TTT is used frequently as a supplement to plaque radiotherapy.[32]

Photodynamic Therapy

PDT involves the coupling of a light-activating photosensitizing dye, verteporfin, that leads to free radicals causing vascular occlusion and other toxic effects at the cellular level. This method has been found useful for amelanotic tumors, and even for selected amelanotic melanoma.[35]

Radiotherapy

Radiotherapy is still the most widely employed treatment for posterior uveal melanoma. The most commonly used form of radiotherapy has been the application of a radioactive plaque.[6,18–22,36–42] Several years ago, most melanomas were treated with a cobalt-60 plaque.[36] Today, iodine-125 and ruthenium-106 plaques have replaced Cobalt-60 at most institutions due to their lower radioactivity, improved tumor control, and fewer complications.[6,37–42] The COMS found that plaque radiotherapy provided equivalent tumor control compared to enucleation for medium-size melanoma.[21] The COMS did not address plaque radiotherapy control of small or large melanomas, but studies have shown that iodine-125 is effective for various tumor sizes and even those in the ciliary body, those with extrascleral extension, and those with juxtapapillary, epipapillary, and circumpapillary tumors.[6,37–45] Enucleation is generally advised for eyes that fail plaque radiotherapy.[46,47]

Another method of radiotherapy is charged particle irradiation.[48–53] This technique can provide a collimated beam to theoretically limit radiotherapy to the precise area of the tumor, but clinical experience shows radiation retinopathy and papillopathy can occur, similar to plaque radiotherapy.[51] Compared to plaque radiotherapy, proton beam radiotherapy provides similar results

for tumor control, globe salvage, visual outcomes, and patient survival. On the basis of published information, patients treated with radiotherapy have a survival rate similar to those treated by enucleation.[21] Furthermore, there is probably no significant difference between plaque radiotherapy and charged particle radiotherapy with regard to short-term and long-term complications. Studies have shown that between 5% and 10% of patients treated with radiotherapy ultimately require enucleation because of tumor recurrence or radiation complications.[46,47]

Local Resection

Local resection of melanoma involving the ciliary body and choroid continues to be popular in some centers.[54–58] Our technique of partial lamellar sclerouvectomy without retinectomy has been successful for removal of ciliary body and peripheral choroidal melanoma, leaving the retina and vitreous intact, often with excellent visual acuity.[54,56]. This modality is especially suitable for thick tumors to avoid long-term radiation consequences.[57]

Local resection of a posterior uveal melanoma offers several theoretical advantages over enucleation and radiotherapy. In contrast to enucleation, it is designed to preserve vision and to maintain a cosmetically normal eye. In contrast to radiotherapy, theoretically it has fewer long-term complications if the initial surgery is successful. However, it does have more potential immediate complications, such as vitreous bleeding, retinal detachment, and cataract, while radiotherapy is almost never associated with such immediate complications. Furthermore, local recurrence is greater following resection compared to radiotherapy, especially for thick tumors.[57] However, some degree of retinopathy and cataract are common long-term complications of all forms of therapy. There is no current evidence that local resection of posterior uveal melanomas is any different from enucleation or radiotherapy with regard to patient survival.

Some authorities have reported experience with endoresection of choroidal melanoma, by removing tumor with a vitrectomy approach, and a few authorities are now using endoresection to remove choroidal melanoma after charged particle irradiation.[59–62]

remove choroidal melanoma after charged particle irradiation.[59–62] In selected cases, endoresection can reduce the long-term risk of neovascular glaucoma.[62] Long-term follow-up will be necessary to determine the validity of endoresection techniques.

Enucleation

As mentioned earlier, the traditional method of treating uveal melanoma by enucleation was challenged several years ago.[12,13] Others continued to believe that enucleation was an appropriate method of management.[14,15] Enucleation is generally indicated for advanced melanoma that occupies most of the intraocular structures and for those that have produced secondary glaucoma or extraocular extension. Another relative indication for enucleation is a melanoma that has invaded the optic nerve, in which removal of a long section of the optic nerve with the globe seems more reasonable. However, many juxtapapillary melanomas, that have not actually invaded the nerve, can be managed by custom-designed notched radioactive plaques.[41–43] The so-called "no touch enucleation" was introduced years ago to minimize surgical trauma and theoretically to lessen the chance of tumor dissemination at the time of surgery.[63] An essential aspect of this technique was to freeze the venous drainage from the tumor prior to cutting the optic nerve. The "no touch" technique has been modified to a minimal manipulation technique of enucleation without the use of the cryoprobe.[64–67]

There have been recent advances in the types of orbital implants used following enucleation. The polymer-coated hydroxyapatite implant or polyethylene implant, designed to improve ocular motility in patients undergoing enucleation, is still used widely.[64–67]

Pre-enucleation radiotherapy (PERT) had been advocated by some authorities, using 2000 cGy of external beam radiotherapy to the affected eye to reduce risk for tumor dissemination at enucleation. Data from the COMS have supported prior nonrandomized studies that suggested that PERT is not advantageous over standard enucleation alone.[18]

The subject of orbital exenteration for uveal melanoma with extrascleral extension is also controversial.[68,69] Orbital exenteration should not be performed in cases of mild extrascleral extension <3 mm as this can be successfully controlled with radiotherapy.[39] However, in the rare instance of massive orbital extension in a blind, uncomfortable eye, primary orbital exenteration is justified. In most instances of orbital extension of uveal melanoma, it is not necessary to sacrifice the skin of the eyelid. The eyelid-sparing exenteration skin provides a satisfactory cosmetic appearance.[68,69]

Genetic Testing

Cytogenetic analysis of uveal melanoma using DNA or RNA methods can add to the confirmation and prognostication of uveal melanoma.[70–77] Sampling for genetic prognostication is performed at the time of treatment. Regarding DNA evaluation, original work in 1996 demonstrated that uveal melanoma in enucleated eyes often showed chromosome 3 monosomy and this imparted poor prognosis.[72] Others found additional mutations in chromosome 8 (53%), chromosome 6 (46%), and chromosome 1 (24%) and concluded that monosomy 3 and largest tumor diameter were the most significant factors in determining patient survival.[73,74] An evaluation of 452 choroidal melanomas for DNA using multiplex ligation-dependent probe amplification (MLPA) revealed high predictive value with 10-year melanoma-related mortality of 0% for those with disomy compared to 55% for those with monosomy 3 and 71% for those with monosomy 3 plus 8q gain.[74] An analysis of 500 consecutive eyes with melanoma sampled by fine-needle aspiration biopsy at the time of radiotherapy concluded that tumors with complete monosomy 3 showed 3-year cumulative probability of metastasis at 0% for small, 24% for medium, and 58% for large melanomas.[75]

Regarding RNA evaluation, gene expression profiling (GEP) has been employed. This technique is a measure of genetic material within melanoma using messenger RNA expression from multiple genes. In 2003, GEP with 12,500 probes identified two groups of melanoma that correlated with monosomy 3 and disomy 3 tumors.[76] In 2004, GEP confirmed the presence of two classes of

melanoma in which class 1 (low grade) showed 95% survival and class 2 (high grade) showed only 31% survival at 8 years.[77] Further refinements of both DNA and RNA testing have allowed for remarkable predictive value.

Management of Systemic Metastasis

Ideally, the best management of uveal melanoma would be to use methods of prevention of micrometastasis in the early stages of this malignant intraocular disease.[5] There are currently trials for high-risk patients based on cytogenetic testing. Patients found to have chromosome 3 monosomy by DNA testing or those with class 2 by RNA testing are entered into therapeutic trials.[71–77] In one trial of prophylactic sunitinib (Sutent) for prevention of melanoma metastasis, improved overall survival was found compared to observation.[78] Studies to further interest in prevention of metastasis based on cytogenetic or tumor markers are underway.

Most patients with uveal melanoma have no detectable evidence of systemic metastasis at the time of diagnosis of the uveal melanoma. However, it is believed that micrometastatic disease occurs early in the course of melanoma, thus neoadjuvant therapy should be considered for those at high risk. Once a uveal melanoma has metastasized to liver and other organs, the patient's prognosis is poor. If the metastasis occurs as a solitary lesion, increased survival has been achieved with local resection of the metastatic focus.[79] Most previous general chemotherapy protocols have provided little response with melanoma metastasis. One trial with selumetinib found slight improved outcomes compared to standard chemotherapy for metastatic disease.[80]

Targeting of embolized chemotherapy, immunotherapy, and local radiotherapy through the hepatic artery for liver metastasis has provided some promise.[81,82] Recent studies have provided hope that chemoembolization and immunoembolization may prolong survival[81,82] but further research is needed to determine the efficacy. Buder et al. reviewed systemic therapies for metastatic uveal melanoma by searching all published reports on Pubmed/Web of Knowledge database and the American Society of Clinical Oncology website between 1980 and 2013 and identified 40 studies

with 841 evaluable patients.[83] They found complete or partial remission (overall response rate, ORR) to be poor at 4.6% and median overall survival was 5.2 to 19.0 months. Patients with best responses occurred following chemoimmunotherapy (ORR 10.3%). They indicated that immunotherapy or innovative treatment strategies should be explored to improve the poor ORR.

There are few studies on immunotherapy for metastatic uveal melanoma. Bol et al. treated 14 patients with metastatic uveal melanoma with autologous dendritic cell vaccination and found tumor-specific immune response in 4 (29%) and median patient survival of 19.2 months, longer than other therapies.[84] Ipilimumab, an immune-stimulating medication that works at the T-cell level by inhibiting cytotoxic T-lymphocyte associated protein 4 (anti-CTLA-4), has been studied for uveal melanoma. Maio et al. treated 82 patients with metastatic uveal melanoma that failed previous treatments using ipilimumab and found 5% demonstrated a response and 29% had stable disease lasting 3 months or more, with median overall survival at 6 months.[85] Luke et al. reported a multicenter retrospective analysis of 39 patients with uveal melanoma metastasis treated with ipilimumab and found response (tumor regression plus stable disease) in 28% at week 23 and overall survival at 9.6 months, but adverse events occurred in 71% of patients.[86] Joshua et al. studied an analogous medication, tremelimumab (anti-CTLA-4 agent) and published similar modest response rates. These reports indicate that ipilimumab/tremelimumab should be further explored regarding their exact role for uveal melanoma therapy.[87]

On the treatment horizon is the use of T-cell immunomodulation to engineer these cells to identify and then lyse cancer cells.[70] This strategy is used for some types of leukemia and now for cutaneous melanoma. Hopefully this will be applicable for uveal melanoma in the near future.

Counseling the Patient

Regardless of the method of management selected by the clinician, it is important that the affected patient be informed of all available options. The expected results and potential complications should be

explained to the patient and family members in detail. The patient should be informed of the availability of a second opinion from other physicians familiar with uveal melanoma. The final decision regarding management should be made by the patient with guidance of his or her physician.[88]

Conclusion

This chapter has provided an update on some general principles of management of posterior uveal melanoma. Small asymptomatic melanocytic tumors of the posterior uvea that exhibit lack of clinical risk features can be observed periodically without intervention. Imaging with fundus photography, optical coherence tomography, autofluorescence, and ultrasonography is important in conservative follow-up. Small choroidal melanoma that show several clinical risk factors or documented growth are provided therapy.

Transpupillary thermotherapy is employed for low-grade melanocytic tumors. Radiotherapy is reserved for active tumors and is delivered by episcleral plaque brachytherapy or charged particles. Selected melanomas of the ciliary body and peripheral choroid can be treated by local resection techniques. Local resection has theoretical advantages, but the surgery takes longer and the immediate complications are potentially greater.

Enucleation is generally indicated for most large melanomas, greater than 20 mm in diameter and greater than 12 mm in thickness. It is also generally indicated for tumors that have invaded the optic nerve. Pre-enucleation radiotherapy does not appear to improve patient survival.

Orbital exenteration is justified for advanced uveal melanoma with massive extraocular extension. Its value in the management of smaller degrees of extraocular extension is uncertain.

The future of uveal melanoma therapy will be focused on earliest detection of the tumor with multimodal imaging at a point where the tumor is perhaps only 1–2 mm in thickness and amenable to minimally invasive local therapy. Systemic treatment for high-risk patients, as identified by cytogenetic markers or cell membrane markers, with targeted chemotherapy or immunotherapy to prevent metastasis will be provided. Targeted therapies designed to

markers, with targeted chemotherapy or immunotherapy to prevent metastasis will be provided. Targeted therapies designed to recognize cell membrane markers or to stimulate the immune system using T cells against cancer could provide improved patient survival.

References

1. Shields JA, Shields CL. Posterior uveal melanoma: management. Shields JA, Shields CL. *Intraocular tumors: an atlas and textbook*. 3rd ed. Wolters Kluwer Inc: Philadelphia; 2016:155–191.
2. Kivela T. The epidemiologic challenge of the most frequent eye cancer: retinoblastoma, an issue of birth and death. *Br J Ophthalmol*. 2009;93:1129–1131.
3. Singh AD, Topham A. Incidence of uveal melanoma in the United States: 1973–1997. *Ophthalmology*. 2003;110:956–961.
4. Shields CL, Kaliki S, Furuta M, et al. Clinical spectrum and prognosis of uveal melanoma based on age at presentation in 8033 cases. *Retina*. 2012;32:1363–1372.
5. Shields JA, Shields CL. Management of posterior uveal melanoma: past, present and future. The 2014 Charles L. Schepens Lecture. *Ophthalmology*. 2015;122(2):414–428.
6. Shields JA, Shields CL, Donoso LA. Management of posterior uveal melanomas. *Surv Ophthalmol*. 1991;36:161–195.
7. Shields CL, Furuta M, Thangappan A, et al. Metastasis of uveal melanoma millimeter by millimeter 8033 consecutive eyes. *Arch Ophthalmol*. 2009;127:989–998.
8. Shields CL, Shields JA, Kiratli H, et al. Risk factors for growth and metastasis of small choroidal melanocytic lesions. *Ophthalmology*. 1995;102:1351–1361.
9. Shields CL, Furuta M, Berman EL, et al. Choroidal nevus transformation into melanoma: analysis of 2514 consecutive cases. *Arch Ophthalmol*. 2009;127:981–987.
10. Shields CL, Cater JC, Shields JA, et al. Combination of clinical factors predictive of growth of small choroidal melanocytic tumors. *Arch Ophthalmol*. 2000;118:360–364.

2006;124:1344–1346.
12. Zimmerman LE, McLean IW. An evaluation of enucleation in the management of uveal melanomas. *Am J Ophthalmol*. 1979;87:741–760.
13. Zimmerman LE, McLean IW, Foster WD. Does enucleation of the eye containing a malignant melanoma prevent or accelerate the dissemination of tumour cells? *Br J Ophthalmol*. 1978;62:420–425.
14. Manschot WA, Van Peperzeel HA. Choroidal melanoma – enucleation or observation? A new approach. *Arch Ophthalmol*. 1980;98:71–77.
15. Seigel D, Myers M, Ferris F, et al. Survival rates after enucleation of eyes with malignant melanoma. *Am J Ophthalmol*. 1979;87:751–765.
16. Singh AD, Rennie IG, Kivela T, et al. The Zimmerman–McLean-Foster hypothesis: 25 years later. *Br J Ophthalmol*. 2004;88:962–967.
17. Diener-West M, Hawkins BS, Markowitz JA, et al. A review of mortality from choroidal melanoma. II. A meta-analysis of 5-year mortality rates following enucleation, 1966 through 1988. *Arch Ophthalmol*. 1992;110:245–250.
18. Collaborative Ocular Melanoma Study Group. The Collaborative Ocular Melanoma Study (COMS) randomized trial of pre-enucleation radiation of large choroidal melanoma II: Initial mortality findings COMS report No. 10. *Am J Ophthalmol*. 1998;125:779–796.
19. Collaborative Ocular Melanoma Study (COMS) randomized trial of I-125 brachytherapy for choroidal melanoma III. Initial mortality findings. COMS report no 16. *Ophthalmology*. 2001;108:348–366.
20. Collaborative Ocular Melanoma Study randomized trial of I-125 brachytherapy for medium choroidal melanoma. I. Visual acuity after 3 years. COMS report No 18. *Arch Ophthalmol*. 2001;119:969–982.
21. Collaborative Ocular Melanoma Study Group. The COMS randomized trial of iodine 125 brachytherapy for choroidal melanoma: V. Twelve-year mortality rates and prognostic factors: COMS report No. 28. *Arch Ophthalmol*.

2006;124:1684–1693.
22. Hawkins BS. Collaborative ocular melanoma study randomized trial of I-125 brachytherapy. *Clin Trials*. 2011;8:661–673.
23. Boldt HC, Melia BM, Liu JC, et al. I-125 brachytherapy for choroidal melanoma photographic and angiographic abnormalities: the Collaborative Ocular melanoma Study: COMS Report No. 30. *Ophthalmology*. 2009;116:106–115.
24. Foulds WS, Damato BE. Low energy long-exposure laser therapy in the management of choroidal melanoma. *Graefes Arch Clin Exp Ophthalmol*. 1986;224:26–31.
25. Shields JA, Glazer LC, Mieler WF, et al. Comparison of xenon arc and argon laser photocoagulation in the treatment of choroidal melanomas. *Am J Ophthalmol*. 1990;109:647–655.
26. Vogel MH. Treatment of malignant choroidal melanomas with photocoagulation: evaluation of 10-year follow-up data. *Am J Ophthalmol*. 1972;74:1–10.
27. Shields JA. The expanding role of laser photocoagulation for intraocular tumors: the 1993 Christian Zweng Memorial Lecture. *Retina*. 1994;14:310–322.
28. Houston SK, Wykoff CC, Berrocal AM, et al. Lasers for the treatment of intraocular tumors. *Lasers Med Sci*. 2013;28:1025–1034.
29. Oosterhuis JA, Journee-de Korver HG, Kakebeeke-Kemme HM, et al. Transpupillary thermotherapy in choroidal melanomas. *Arch Ophthalmol*. 1995;113:315–321.
30. Shields CL, Shields JA, Cater J, et al. Transpupillary thermotherapy for choroidal melanoma. Tumor control and visual outcome in 100 consecutive cases. *Ophthalmology*. 1998;105:581–590.
31. Shields CL, Shields JA, Perez N, et al. Primary transpupillary thermotherapy for choroidal melanoma in 256 consecutive cases: outcomes and limitations. *Ophthalmology*. 2002;109:225–234.
32. Shields CL, Cater J, Shields JA, et al. Combined plaque radiotherapy and transpupillary thermotherapy for choroidal melanoma in 270 consecutive patients. *Arch*

Ophthalmol. 2002;120:933–940.
33. Mashayekhi A, Shields CL, Rishi P, et al. Primary transpupillary thermotherapy for choroidal melanoma in 391 cases: importance of risk factors in tumor control. *Ophthalmology*. 2015;122(3):600–609.
34. Mashayekhi A, Shields CL, Lee SC, et al. Retinal break and rhegmatogenous retinal detachment after transpupillary thermotherapy as primary or adjunct treatment of choroidal melanoma. *Retina*. 2008;28(2):274–281.
35. Campbell S, Pejnovic TM. Treatment of amelanotic choroidal melanoma with photodynamic therapy. *Retina*. 2012;32:1356–1362.
36. Shields JA, Augsburger JJ, Brady LW, et al. Cobalt plaque therapy of posterior uveal melanomas. *Ophthalmology*. 1982;89:1201–1207.
37. Gunduz K, Shields CL, Shields JA, et al. Radiation complications and tumor control after plaque radiotherapy of choroidal melanoma with macular involvement. *Am J Ophthalmol*. 1999;127:579–588.
38. Gunduz K, Shields CL, Shields JA, et al. Plaque radiotherapy of uveal melanoma with predominant ciliary body involvement. *Arch Ophthalmol*. 1999;117:170–177.
39. Gunduz K, Shields CL, Shields JA, et al. Plaque radiotherapy for management of ciliary body and choroidal melanoma with extrascleral extension. *Am J Ophthalmol*. 2000;130:97–102.
40. Shields CL, Naseripour M, Cater J, et al. Plaque radiotherapy for large posterior uveal melanoma (>8 mm in thickness) in 354 consecutive patients. *Ophthalmology*. 2002;109:1838–1849.
41. Sagoo MS, Shields CL, Mashayekhi A, et al. Plaque radiotherapy for juxtapapillary choroidal melanoma: tumor control in 650 consecutive cases. *Ophthalmology*. 2011;118:402–407.
42. Sagoo MS, Shields CL, Mashayekhi A, et al. Plaque radiotherapy for juxtapapillary choroidal melanoma overhanging the optic disc in 141 consecutive patients. *Arch Ophthalmol*. 2008;126(11):1515–1522.

43. Sagoo MS, Shields CL, Mashayekhi A, et al. Plaque radiotherapy for choroidal melanoma encircling the optic disc (circumpapillary choroidal melanoma. *Arch Ophthalmol*. 2007;125:1202–1209.
44. Shields CL, Shields JA, Cater J, et al. Plaque radiotherapy for uveal melanoma: long-term visual outcome in 1106 patients. *Arch Ophthalmol*. 2000;118:1219–1228.
45. Shields CL, Grant Kels J, Shields JA. Melanoma of the eye: revealing hidden secrets, one at a time. [In: Grant Kels J, Grzbowski A, Kels B, editors. Melanoma of the eye and skin] *Clin Dermatol*. 2015;33:183–196.
46. Shields CL, Shields JA, Karlsson U, et al. Reasons for enucleation after plaque radiotherapy for posterior uveal melanoma. *Ophthalmology*. 1989;96:919–924.
47. Shields CL, Shields JA, Karlsson U, et al. Enucleation following plaque radiotherapy: for posterior uveal melanoma: histopathologic findings. *Ophthalmology*. 1990;97:1665–1670.
48. Gragoudas ES, Seddon JM, Egan K, et al. Long-term results of proton beam irradiated uveal melanomas. *Ophthalmology*. 1986;94:349–353.
49. Seddon JM, Gragoudas ES, Albert DM, et al. Comparison of survival rates for patients with uveal melanoma after treatment with proton beam irradiation or enucleation. *Am J Ophthalmol*. 1985;99:282–290.
50. Lane AM, Kim IK, Gragoudas ES. Long-term risk of melanoma-related mortality for patients with uveal melanoma treated with proton beam therapy. *JAMA Ophthalmol*. 2015;133(7):792–796.
51. Kim IK, Lane AM, Egan KM, et al. Natural history of radiation papillopathy after proton beam irradiation of perapapillary melanoma. *Ophthalmology*. 2010;117:1617–1622.
52. Gragoudas ES. Proton beam irradiation of uveal melanomas: the first 30 years. The Weisenfeld Lecture. *Invest Ophthalmol Vis Sci*. 2006;47:4666–4673.
53. Desjardins L, Lumbroso-Le Rouic L, Levy-Gabriel C, et al. Treatment of uveal melanoma by accelerated proton beam.

53. Desjardins L, Lumbroso-Le Rouic L, Levy-Gabriel C, et al. Treatment of uveal melanoma by accelerated proton beam. *Dev Ophthalmol*. 2012;49:41–57.
54. Shields JA, Shields CL. Surgical approach to lamellar sclerouvectomy for posterior uveal melanomas. The 1986 Schoenberg Lecture. *Ophthal Surg*. 1988;19:774–780.
55. Peyman GA, Juarez CP, Diamond JG, et al. Ten years experience with eye wall resection of uveal malignant melanomas. *Ophthalmology*. 1984;91:1720–1724.
56. Shields JA, Shields CL, Shah P, et al. Partial lamellar sclerouvectomy for ciliary body and choroidal tumors. *Ophthalmology*. 1991;98:971–983.
57. Puusaari I, Damato BE, Kivela T. Transscleral location resection versus iodine brachytherapy for uveal melanomas that are large because of tumor height. *Grafes Arch Clin Exp Ophthalmol*. 2007;245:522–533.
58. Damato BE. Local resection of uveal melanoma. *Dev Ophthalmol*. 2012;49:66–80.
59. Bechrakis NE, Foerster MH. Neoadjuvant proton beam radiotherapy combined with subsequent endoresection of choroidal melanomas. *Int Ophthalmol Clin*. 2006;46:95–107.
60. Damato B, Groenewald C, McGalliard J, et al. Endoresection of choroidal melanoma. *Br J Ophthalmol*. 1998;82:213–218.
61. Bornfeld N, Talies S, Anastassiou G, et al. Endoscopic resection of malignant melanomas of the uvea after preoperative sterotactic single dose convergence irradiation with the Leksell gamma knife. *Ophthalmologe*. 2002;99:338–344.
62. Cassoux N, Cayette S, Plancher C, et al. Choroidal melanoma: does endoresection prevent neovascular glaucoma in patient treated with proton beam irradiation? *Retina*. 2013;33:1441–1447.
63. Wilson RS, Fraunfelder FT. "No touch" cryosurgical enucleation: a minimal trauma technique for eyes harboring intraocular malignancy. *Ophthalmology*. 1978;85:1170–1175.
64. Shields CL, Shields JA, De Potter P. Hydroxyapatite orbital implant after enucleation: experience with 100 consecutive cases. *Arch Ophthalmol*. 1992;110:333–338.

consecutive cases. *Trans Am Ophthalmol Soc*. 1993;91:177–189.
66. Shields CL, Uysal Y, Marr BP, et al. Experience with the polymer-coated hydroxyapatite implant following enucleation in 126 patients. *Ophthalmology*. 2007;114:367–373.
67. Shah SU, Shields CL, Lally SE, et al. Hydroxyapatite orbital implant in children following enucleation: analysis of 531 sockets. *Ophthal Plast Reconstr Surg*. 2014;31:108–114.
68. Shields JA, Shields CL, Suvarnamani C, et al. Orbital exenteration with eyelid sparing: indications, technique and results. *Ophthalmic Surg*. 1991;22:292–297.
69. Shields JA, Shields CL, Demirci H, et al. Experience with eyelid-sparing orbital exenteration: The 2000 Tullos O. Coston Lecture. *Ophthal Plast Reconstr Surg*. 2001;17:355–361.
70. Nielsen M, Dogrusoz M, Bleeker JC, et al. The genetic basis of uveal melanoma. *J Fr Ophthalmol*. 2015;38:516–521.
71. Shields CL, Ganguly A, O'Brien J, et al. Uveal melanoma trapped in the Temple of Doom. *Am J Ophthalmol*. 2012;154:219–221.
72. Prescher G, Bornfeld N, Hirche H, et al. Prognostic implications of monosomy 3 in uveal melanoma. *Lancet*. 1996;347:1222–1225.
73. Kilic E, van Gils W, Lodder E, et al. Clinical and cytogenetic analyses in uveal melanoma. *Invest Ophthalmol Vis Sci*. 2006;47:3703–3707.
74. Damato B, Dopierala JA, Coupland SE. Genotypic profiling of 452 choroidal melanomas with multiplex ligation-dependent probe. *Clin Cancer Res*. 2010;16:6083–6092.
75. Shields CL, Ganguly A, Bianciotto CG, et al. Prognosis of uveal melanoma in 500 cases using genetic testing of needle aspiration biopsy specimens. *Ophthalmology*. 2011;118:396–401.
76. Tschentscher F, Hüsing J, Hölter T, et al. Tumor classification based on gene expression profiling shows that uveal melanoma with and without monosomy 3 represents two distinct entities. *Cancer Res*. 2003;63:2578–2584.

77. Onken MD, Worley LA, Ehlers JP, et al. Gene expression profiling in uveal melanoma reveals two molecular classes and predicts metastatic death. *Cancer Res*. 2004;64:7205–7209.
78. Sato T, Valsecchi M, Orloff M, et al. *Sunitinib as an adjuvant treatment for high-risk primary uveal melanoma*. [International Society of Ocular Oncology (Paris) Abstracts] 2015:198.
79. Aoyama T, Mastrangelo MJ, Berd D, et al. Protracted survival following resection of metastatic uveal melanoma. *Cancer*. 2000;89:1561–1568.
80. Carvajal RD, Sosman JA, Quevedo JF, et al. Effect of selumetinib vs chemotherapy on progression free survival in uveal melanoma: a randomized clinical trial. *JAMA*. 2014;311:2397–2405.
81. Patel K, Sullivan K, Berd D, et al. Chemoembolization of the hepatic artery with 1,3-bis (2-chloroethyl)-1-nitrosourea (BCNU) for metastatic uveal melanoma: results of a phase II study. *Melanoma Res*. 2005;15:297–304.
82. Valsecchi ME, Terai M, Eschelman DJ, et al. Double-blinded, randomized phase II study using embolization with or without granulocyte-macrophage colony stimulating factor in uveal melanoma with hepatic metastasis. *J Vasc Interv Radiol*. 2015;26(4):523–532.e2.
83. Buder K, Gesierich A, Gelbrich G, et al. Systemic treatment of metastatic uveal melanoma: review of literature and future perspectives. *Cancer Med*. 2013;2:674–686.
84. Bol KF, Mensink HW, Aarntzen EH, et al. Long overall survival after dendritic cell vaccination in metastatic uveal melanoma patients. *Am J Ophthalmol*. 2014;158:939–947.
85. Maio M, Danielli R, Chiarion-Sileni V, et al. Efficacy and safety of ipilimumab in patients with pre-treated, uveal melanoma. *Ann Oncol*. 2013;24:2911–2915.
86. Luke JJ, Callahan MK, Postow MA, et al. Clinical activity of ipilimumab for metastatic uveal melanoma: a retrospective review for the Dana-Farber Cancer Institute, Massachusetts General Hospital, Memorial Sloan-Kettering Cancer Center, and University Hospital of Lausanne experience. *Cancer*. 2013;119:3687–3695.

87. Joshua AM, Monzon JG, Mihalcioiu C, et al. A phase 2 study of tremelimumab in patients with advanced uveal melanoma. *Melanoma Res*. 2015;25:342–347.
88. Shields JA. Counseling the patient with a posterior uveal melanoma. Editorial. *Am J Ophthalmol*. 1988;106:88–91.

148

Enucleation for Choroidal Melanomas

Julian D. Perry, Arun D. Singh, Rao V. Chundury

Introduction

Approximately 5% of all melanomas occur in the eye and surrounding adnexal structures, and 85% of these are uveal in origin.[1] Uveal melanomas are the most common primary intraocular malignant tumor.[2] According to one report, the overall incidence of uveal melanomas is 5.1 per million and 80–90% of uveal melanomas involve the choroid.[3]

Forty years ago, Zimmerman investigated the benefit of enucleation in eyes with choroidal melanoma.[4] He observed a peak in mortality 2–3 years after enucleation and suggested that the rise of post-enucleation mortality was a direct result of the enucleation.[4] This controversy led to the trend away from enucleation towards vision and eye-sparing treatments. Subsequent studies have demonstrated that the observed post-enucleation rise in mortality was a reflection of the natural history of the primary tumor and its metastases rather than direct effects of enucleation causing iatrogenic tumor seeding. Metastasis was independent of the method of treatment.[5]

For the treatment of the primary tumor, there are many therapeutic options, such as observation, transpupillary thermotherapy, plaque radiotherapy, local resection, and enucleation.[2] In the United States the two most frequently used methods of treatment are plaque radiotherapy and enucleation.[2] The Collaborative Ocular Melanoma Study (COMS) demonstrated no statistical difference in all-cause mortality between the brachytherapy and enucleation arms in either medium or large choroidal melanomas.[6]

As mortality data show, there is no significant difference between enucleation and brachytherapy, therefore, quality-of-life (QOL) measurements become important in deciding on a therapeutic plan. The COMS ascertained QOL measures of driving difficulties, near vision activities, activities requiring stereopsis, anxiety levels, and depression levels.[7] Patients reported higher levels of function for driving and peripheral vision in the brachytherapy arm compared to the enucleation arm for the first 2 years following treatment, but these differences diminished 3–5 years after treatment.[7] Patients in the brachytherapy arm also had more symptoms of anxiety after

treatment compared with the enucleation group.[7] Enucleation still remains a viable treatment option for choroidal melanoma in the proper setting.

The COMS group demonstrated a cumulative metastasis rate of 25% at 5 years and 34% at 10 years.[8] Once metastasis occurs, the median survival time is 3.6 months, and death is almost always inevitable as there are no effective treatment options at present.[8,9]

Purpose of Enucleation

Enucleation should remove malignancy with clear margins and restore cosmesis by allowing for the comfortable use of an ocular prosthesis coupled to an underlying orbital implant.

Indications

The main indications for primary enucleation are large tumor size, neovascular glaucoma, optic nerve invasion, blind painful eye, localized extrascleral extension, and patient preference. Enucleation is also considered for the treatment of medium-sized choroidal melanoma with poor vision (<20/400) or absence of potential for visual recovery. Functional status of the other eye and patient preference are also important considerations in the decision-making process. The indications for secondary enucleation are local treatment failure and ocular pain secondary to radiation-related complications.

Implant Description

An ideal implant should restore volume, transmit motility, possess a low complication rate, and demonstrate cost-effectiveness.[10] To transmit motility, the extraocular muscles should attach to the implant directly or surround the implant indirectly.[10] An implant of proper size restores volume.[11] Current orbital implant designs fall into two general categories: solid spheres and porous, integrated implants. Solid spheres include silicone and polymethyl methacrylate (PMMA), while porous implants include coralline hydroxyapatite and porous polyethylene.[10] Bioceramic and other

implants also exist.[10] Porous materials allow for fibrovascular ingrowth which may induce epithelization of a drill hole to accept a prosthesis coupling peg to improve motility. Pegged hydroxyapatite implants offer subjective improved motility over unpegged implants and vascular ingrowth possesses some theoretical advantages, including decreased rates of infection, exposure, and extrusion.[10,12]

Coralline hydroxyapatite (HA) is a porous, nontoxic implant composed of inorganic, nonreplenishable marine coral.[13] High-density porous polyethylene is a porous, synthetic implant that can be molded into various shapes.[14] Hydroxyapatite has a brittle nature, which precludes direct suturing to the implant surface.[15] Pore sizes and interconnectivity vary, which could affect vascularization.[16] Some surgeons drill holes into porous implants to facilitate integration.[17] The use of porous materials adds additional costs of the implant, wrapping material, and imaging studies, and possesses higher complication rates.[18]

Some surgeons wrap porous implants to protect the anterior tissues from hydroxyapatite bone spicules and to facilitate muscle attachment and implantation. However the perceived benefits have not been proven.[15] Wrapping materials include donor sclera, autogenous fascia, or polyglycolic acid mesh. While some surgeons wrap porous polyethylene implants, the extraocular muscles can be directly sutured to polyethylene.[19,20] Wrapping materials may pose infection risk and decrease vascularization rates.[17]

When surveyed in 1995, the majority (56%) of the American Society of Ophthalmic Plastic and Reconstructive Surgeons (ASOPRS) preferred hydroxyapatite implants and human donor sclera wrapping in enucleations.[21] When resurveyed in 2002, the majority (43%) of ASOPRS surgeons preferred porous polyethylene and only 27% preferred hydroxyapatite.[18] In the later survey, most implants (60%) were not wrapped and only 25% were wrapped in human donor sclera.[18] The majority (92%) of implants were left unpegged.[18] In 2007, a survey from the UK supported these trends, demonstrating that 55% of surgeons used porous implants, 57% wrapped the implant (with autogenous sclera being most popular; 20%), and only 7% pegged the implants.[22] Custer[23] demonstrated no significant difference in motility between unpegged hydroxyapatite

and solid implants and Harbour et al.[24] demonstrated no significant differences in complication rates between patients receiving donor sclera-wrapped hydroxyapatitite and polyethylene orbital implants. The potential advantages of using porous implants and wrapping materials should be weighed against the risks, morbidity, and additional cost.[20] If the surgeon does not plan to peg, if the patient has systemic illnesses or factors that may limit fibrovascular ingrowth, or if a porous implant may not improve a patient's quality of life, the surgeon should give consideration to a solid implant.

Implant Sizing

Proper implant sizing is essential for cosmesis, volume restoration, and to minimize extrusion, exposure, and sulcus deformities. Most adult patients require at least a 20 mm implant. Traditionally, surgeons use a set of sizing spheres to individualize implant size and use standard volume tables to maximize volume restoration. Alternatively, orbital implant size can be determined using the contralateral eye axial length measurements subtracted by 2 mm, or by 3 mm for hyperopia.[11] Another algorithm subtracts the volume of an ideal 24 mm eye by the volume of sclera and 2 mL to determine implant volume.[25]

Enucleation Technique

Enucleation techniques vary but all employ certain principles. Enucleation is usually performed under general anesthesia. However, local anesthesia with monitored anesthesia care can also be used in conjunction with a supraorbital nerve, an infraorbital nerve, and a modified van Lint block. In either case, analgesia and improved hemostasis may be achieved with a retrobulbar or peribulbar block consisting of 3–4 mL of 1% lidocaine with 1 : 100 000 epinephrine and 8.4% sodium bicarbonate in a 1 : 10 ratio with 50 units per 10 mL of hyaluronidase. An additional 1 mL of the same solution is injected subconjunctivally. The surgeon must avoid penetration or perforation of the eye with the needle.

The authors' technique is as follows: A 360° peritomy is created

with blunt Westcott scissors. Conjunctiva and the Tenon layer are dissected from underlying sclera using Stevens scissors (Fig. 148.1). The Stevens scissors are used to bluntly dissect in each oblique quadrant (Fig. 148.2), and each rectus muscle is isolated on a muscle hook. The Tenon layer attachments to the rectus muscles are stripped and the muscle is secured on a double armed 6–0 polyglactin 910 suture through its insertion. Each muscle is disinserted from the globe using blunt Westcott scissors or Abley scissors (Fig. 148.3).

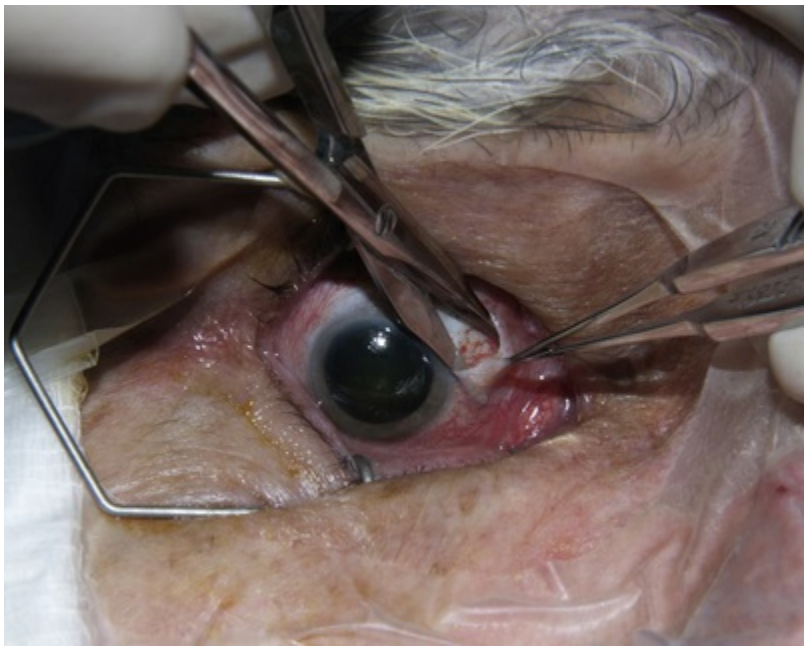

FIG. 148.1 A 360° peritomy is performed using blunt Westcott scissors.

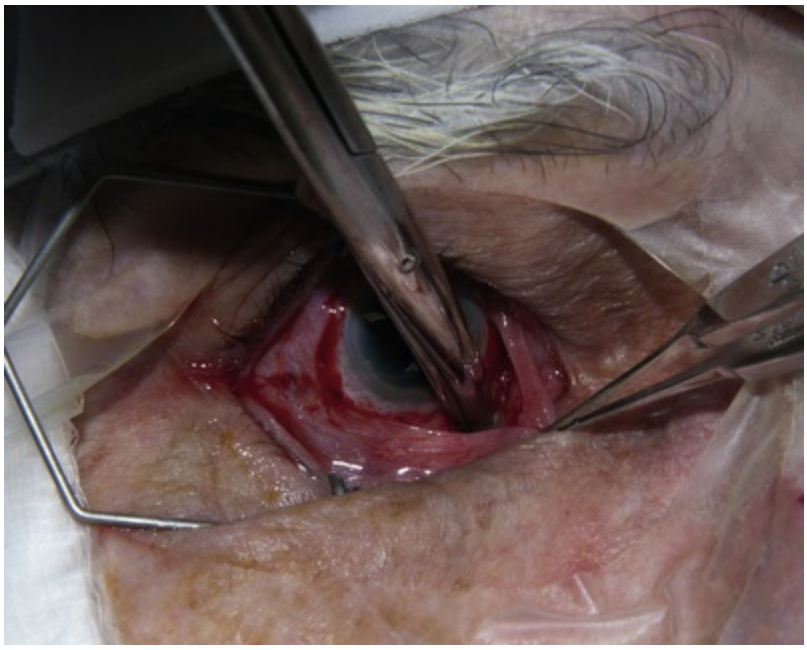

FIG. 148.2 Stevens scissors are used to bluntly dissect into each oblique quadrant.

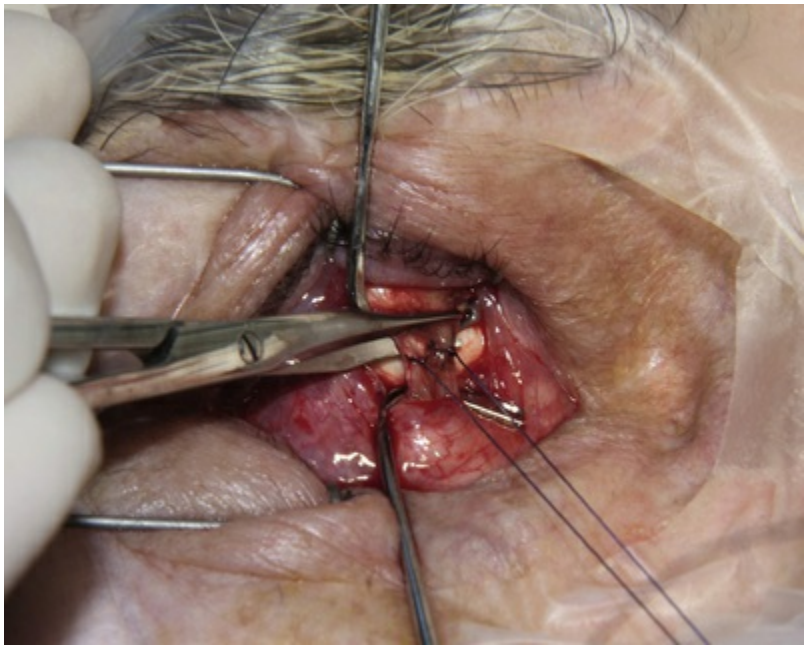

FIG. 148.3 Each rectus muscle is isolated on a muscle hook, secured using 6-0 polyglactin suture, and disinserted using blunt Westcott scissors or Abley scissors.

The inferior oblique muscle insertion is identified and isolated with a muscle hook in the inferotemporal quadrant. To minimize

bleeding, the inferior oblique muscle is cauterized prior to transection. The superior oblique muscle is then identified in the superomedial quadrant and cut.

A muscle hook is swept against the globe to identify any remaining attachments that require lysis, and a rent is created in the posterior Tenon layer using Stevens scissors. To maintain hemostasis, the optic nerve may be clamped with a long curved hemostat. The hemostat is inserted with the blades closed to palpate and strum the optic nerve prior to clamping. A second hemostat or locking toothed forceps is placed over the medial rectus muscle stump to assist in elevating the globe. The optic nerve is transected using enucleation scissors, and the globe is removed using the hemostat or forceps on the medial rectus stump. The optic nerve stump is cauterized with the bipolar cautery unit under direct visualization using malleable retractors.

The orbital implant is placed using an injector or periosteal elevators with modest posterior digital pressure. If the implant is wrapped, then four windows can be created just posterior to the rectus muscle attachments. If a wrapping material is not employed, the muscles are sutured directly to or over the implant. Direct attachment of the vertical recti muscles to each other may lead to fornix insufficiency. We suture each rectus muscle to the adjacent rectus muscle suture using a 4–0 polyglactin 910 suture to create a physiologic attachment of the extraocular muscles over the implant with a diameter of approximately 10 mm (Fig. 148.4). The anterior Tenon layer is closed using a running 4–0 polyglactin 910 suture (Fig. 148.5). Finally, the conjunctiva is closed using a running 6–0 plain gut suture (Fig. 148.6).

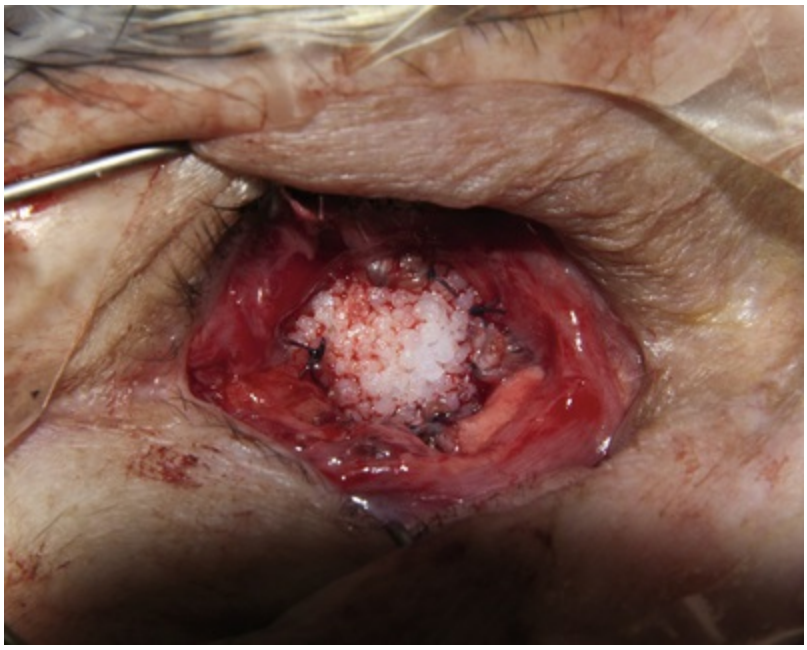

FIG. 148.4 A suitable-sized implant is placed using an injector or periosteal elevators and the muscular attachments are sutured onto the implant.

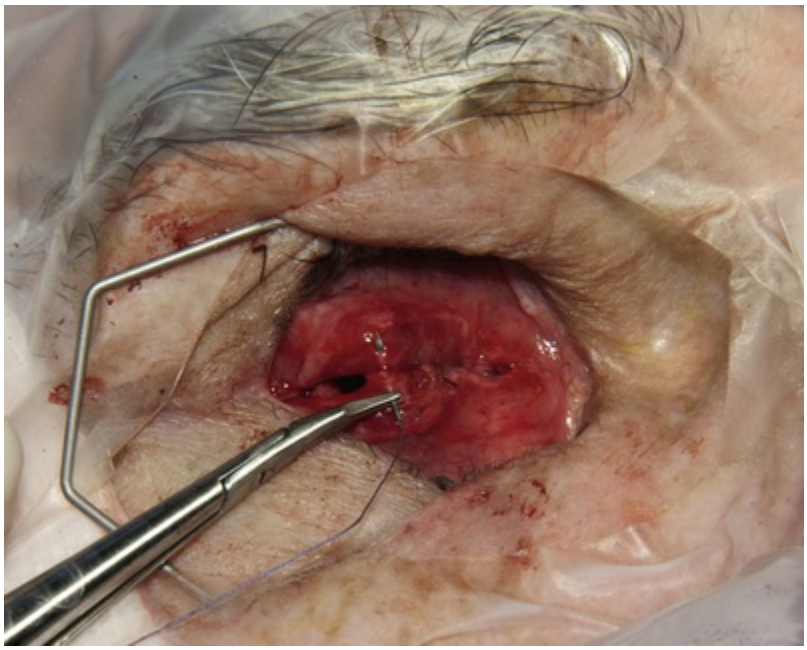

FIG. 148.5 Tenon layer is closed in running fashion.

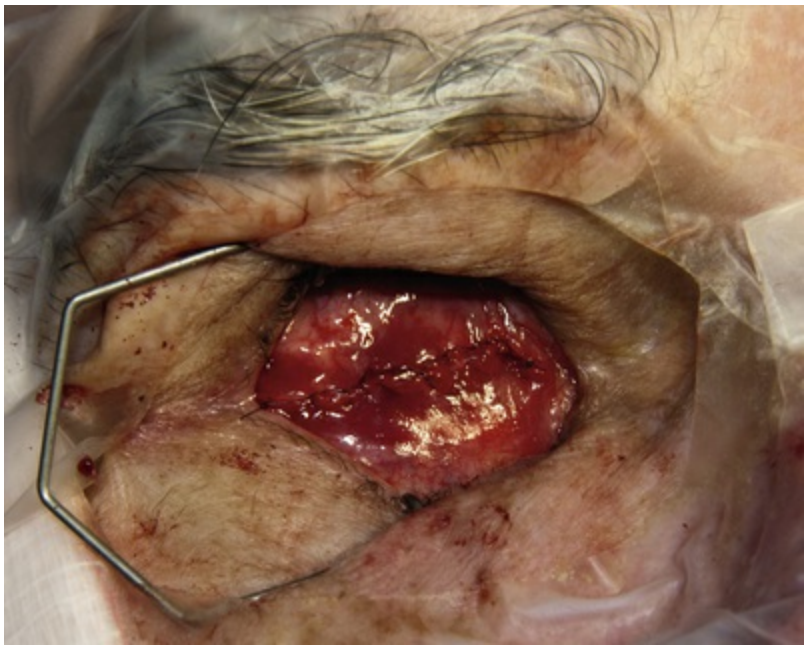

FIG. 148.6 The conjunctiva is sutured in running fashion, creating a multilayered closure.

Antibiotic ointment and a small plastic conformer are placed into the socket and the eyelids are sutured closed using a 6–0 Prolene suture. A pressure patch is placed for one week.

Special Considerations

Optic Nerve Invasion and Limited Extrascleral Extension

Overall, choroidal melanoma rarely invades the optic nerve.[26] The COMS demonstrated extrascleral extension in only 8.2% of 1527 enucleated eyes.[27] Limited extrascleral extension does not contraindicate enucleation. However, the approach to the optic nerve transaction may have to be modified if there is evidence of limited extrascleral extension. Limited extrascleral extension may be suspected based on echographic or radiologic imaging.[28] It is recommended that the quadrant opposite to the extrascleral extension be used to introduce the enucleation scissors so as to avoid transecting the extrascleral extension. In some cases, greater access to the posterior orbit may be obtained via lateral orbitotomy approach to transect the optic nerve and for en bloc removal of the extrascleral extension.[29,30]

Complications

Complications of enucleation are rare and include pyogenic granuloma, conjunctival inclusion cyst formation, conjunctival wound dehiscence causing exposure or extrusion, implant displacement or migration, infection, orbital hemorrhage, socket contracture, and ptosis.[18,31] In the COMS large tumor trial, patients who received pre-enucleation radiation had an overall complication rate of 8% and patients who had not received radiation had a complication rate of 4%.[31]

Additional complications of pegged implants include peg malposition, peg cracking, and an audible peg click.[18] Reports on overall complication rates vary widely for porous and nonporous implants and for pegged and unpegged implants. However, general trends among the various implant choices exist.

Nunery et al. demonstrated a higher exposure rate in HA versus silicone implants.[32,33] Exposed porous implants may not extrude as often as solid implants because of fibrovascular ingrowth, but nearly all exposures ultimately require repair.[32] Exposure rates range from 0% to 33.3% for porous implants.[13,34–40] The American Society of Ophthalmic Plastic and Reconstructive Surgery (ASOPRS) survey revealed an exposure rate of only 3% with the majority (81 of 82) of events occurring with porous implants rather than solid implants.[18] A meta-analysis of exposure rates of all implants demonstrated a 1.3% (2/153 cases) rate with silicone, a 4.9% rate (96/1959 cases) with coralline hydroxyapatite, and an 8.1% rate (41/507 events) with porous polyethylene.[35] For pegged implants, all complication rates are greater, including pyogenic granuloma formation (14%), exposure (6%), infection (5%), and peg malposition (5%).[18] Fay et al. evaluated the necessity and usefulness of prophylactic postoperative antibiotics in patients undergoing enucleation in 435 patients and found no statistical difference in postoperative infection rate between those who received antibiotics to those who did not.[41]

Conclusion

Enucleation is the typical treatment option for eyes with large tumors, limited extrascleral extension, optic nerve invasion, and

blind painful eyes secondary to neovascular glaucoma or postradiation effects. Enucleation is also considered for treatment of medium-sized choroidal melanoma with poor vision (<20/400) or absence of potential for visual recovery. Functional status of the other eye and patient preference are also important considerations. Various implant options after enucleation exist. Porous implants have theoretical advantages that have not delivered as much benefit as anticipated. Currently, most surgeons choose not to peg implants despite the higher morbidity associated with porous implants. Nonporous implants represent a safe and cost-effective option.

References

1. Chang AE, Karnell LH, Menck HR. The National Cancer Data Base report on cutaneous and noncutaneous melanoma: a summary of 84,836 cases from the past decade. The American College of Surgeons Commission on Cancer and the American Cancer Society. *Cancer*. 1998;83:1664–1678.
2. Singh AD, Bergman L, Seregrard S, et al. Uveal malignant melanoma: epidemiologic aspects. Singh AD, et al. *Clinical ophthalmic oncology*. 2nd ed. Saunders: Philadelphia, PA; 2007:198–204.
3. Singh AD, Turell ME, Topham AK. Uveal melanoma: trends in incidence, treatment, and survival. *Ophthalmology*. 2011;118:1881–1885.
4. Zimmerman LE, McLean IW, Foster WD. Does enucleation of the eye containing a malignant melanoma prevent or accelerate the dissemination of tumour cells. *Br J Ophthalmol*. 1978;62:420–425.
5. Singh AD, Rennie IG, Kivela T, et al. The Zimmerman–McLean–Foster hypothesis: 25 years later. *Br J Ophthalmol*. 2004;88:962–967.
6. Assessment of metastatic disease status at death in 435 patients with large choroidal melanoma in the Collaborative Ocular Melanoma Study (COMS). COMS report no. 15. *Arch Ophthalmol*. 2001;119:670–676.
7. Melia M, Moy CS, Reynolds SM, et al. Quality of life after

iodine 125 brachytherapy vs enucleation for choroidal melanoma: 5-year results from the Collaborative Ocular Melanoma Study. COMS QOLS report no. 3. *Arch Ophthalmol*. 2006;124:226–238.
8. Diener-West M, Reynolds SM, Agugliaro DJ, et al. Development of metastatic disease after enrollment in the COMS trials for treatment of choroidal melanoma. COMS report no. 26. *Arch Ophthalmol*. 2005;123:1639–1643.
9. Augsburger JJ, Correa ZM, Shaikh AH. Effectiveness of treatments for metastatic uveal melanoma. *Am J Ophthalmol*. 2009;148:119–127.
10. Chalasani R, Poole-Warren L, Conway RM, et al. Porous orbital implants in enucleation: a systematic review. *Surv Ophthalmol*. 2007;52:145–155.
11. Kaltreider SA, Lucarelli MJ. A simple algorithm for selection of implant size for enucleation and evisceration: a prospective study. *Ophthal Plast Reconstr Surg*. 2002;18:336–341.
12. Shields CL, Shields JA, De Potter P. Hydroxyapatite orbital implant after enucleation. Experience with initial 100 consecutive cases. *Arch Ophthalmol*. 1992;110:333–338.
13. Shields JA, Shields CL, De Potter P. Hydroxyapatite orbital implant after enucleation – experience with 200 cases. *Mayo Clin Proc*. 1993;68:1191–1195.
14. Bilyk JR, Rubin PA, Shore JW. Correction of enophthalmos with porous polyethylene implants. *Int Ophthalmol Clin*. 1992;32:151–156.
15. Custer PL. Enucleation: past, present, and future. *Ophthal Plast Reconstr Surg*. 2000;16:316–321.
16. Mawn LA, Jordan DR, Gilberg S. Scanning electron microscopic examination of porous orbital implants. *Can J Ophthalmol*. 1998;33:203–209.
17. Gayre GS, Lipham W, Dutton JJ. A comparison of rates of fibrovascular ingrowth in wrapped versus unwrapped hydroxyapatite spheres in a rabbit model. *Ophthal Plast Reconstr Surg*. 2002;18:275–280.
18. Su GW, Yen MT. Current trends in managing the anophthalmic socket after primary enucleation and

evisceration. *Ophthal Plast Reconstr Surg*. 2004;20:274–280.
19. Moshfeghi DM, Moshfeghi AA, Finger PT. Enucleation. *Surv Ophthalmol*. 2000;44:277–301.
20. Perry JD, Tam RC. Safety of unwrapped spherical orbital implants. *Ophthal Plast Reconstr Surg*. 2004;20:281–284.
21. Hornblass A, Biesman BS, Eviatar JA. Current techniques of enucleation: a survey of 5,439 intraorbital implants and a review of the literature. *Ophthal Plast Reconstr Surg*. 1995;11:77–88.
22. Viswanathan P, Sagoo MS, Olver JM. UK national survey of enucleation, evisceration and orbital implant trends. *Br J Ophthalmol*. 2007;91:616–619.
23. Custer PL, Trinkaus KM, Fornoff J. Comparative motility of hydroxyapatite and alloplastic enucleation implants. *Ophthalmology*. 1999;106:513–516.
24. Chao DL, Harbour JW. Hydroxyapatite versus polyethylene orbital implants for patients undergoing enucleation for uveal melanoma. *Can J Ophthalmol*. 2015;50:151–154.
25. Custer PL, Trinkaus KM. Volumetric determination of enucleation implant size. *Am J Ophthalmol*. 1999;128:489–494.
26. Shields CL, Santos MC, Shields JA, et al. Extraocular extension of unrecognized choroidal melanoma simulating a primary optic nerve tumor: report of two cases. *Ophthalmology*. 1999;106:1349–1352.
27. Histopathologic characteristics of uveal melanomas in eyes enucleated from the Collaborative Ocular Melanoma Study. COMS report no. 6. *Am J Ophthalmol*. 1998;125:745–766.
28. Boldt HC, Byrne SF, Gilson MM, et al. Baseline echographic characteristics of tumors in eyes of patients enrolled in the Collaborative Ocular Melanoma Study. COMS report no. 29. *Ophthalmology*. 2008;115:1390–1397.
29. De Potter P, Shields JA, Shields CL, et al. Modified enucleation via lateral orbitotomy for choroidal melanoma with orbital extension: a report of two cases. *Ophthal Plast Reconstr Surg*. 1992;8:109–113.
30. Singh AD, Jacques R, Rundle PA, et al. Combined enucleation and orbitotomy for choroidal melanoma with

orbital extension. *Eye (Lond)*. 2006;20:615–617.
31. The Collaborative Ocular Melanoma Study (COMS) randomized trial of pre-enucleation radiation of large choroidal melanoma III: local complications and observations following enucleation. COMS report no. 11. *Am J Ophthalmol*. 1998;126:362–372.
32. Nunery WR, Heinz GW, Bonnin JM, et al. Exposure rate of hydroxyapatite spheres in the anophthalmic socket: histopathologic correlation and comparison with silicone sphere implants. *Ophthal Plast Reconstr Surg*. 1993;9:96–104.
33. Nunery WR, Cepela MA, Heinz GW, et al. Extrusion rate of silicone spherical anophthalmic socket implants. *Ophthal Plast Reconstr Surg*. 1993;9:90–95.
34. Dutton JJ. Coralline hydroxyapatite as an ocular implant. *Ophthalmology*. 1991;98:370–377.
35. Custer PL, Trinkaus KM. Porous implant exposure: Incidence, management, and morbidity. *Ophthal Plast Reconstr Surg*. 2007;23:1–7.
36. Jordan DR, Gilberg S, Bawazeer A. Coralline hydroxyapatite orbital implant (bio-eye): experience with 158 patients. *Ophthal Plast Reconstr Surg*. 2004;20:69–74.
37. Buettner H, Bartley GB. Tissue breakdown and exposure associated with orbital hydroxyapatite implants. *Am J Ophthalmol*. 1992;113:669–673.
38. Karesh JW, Dresner SC. High-density porous polyethylene (Medpor) as a successful anophthalmic socket implant. *Ophthalmology*. 1994;101:1688–1696.
39. Blaydon SM, Shepler TR, Neuhaus RW, et al. The porous polyethylene (Medpor) spherical orbital implant: a retrospective study of 136 cases. *Ophthal Plast Reconstr Surg*. 2003;19:364–371.
40. Kim JH, Khwarg SI, Choung HK, et al. Management of porous polyethylene implant exposure in patients with retinoblastoma following enucleation. *Ophthalmic Surg Lasers Imaging*. 2004;35:446–452.
41. Fay A, Nallassamy N, Pemberton JD, et al. Prophylactic postoperative antibiotics for enucleation and evisceration. *Ophthal Plast Reconstr Surg*. 2013;29:281–285.

149

Brachytherapy for Choroidal Melanoma

H. Culver Boldt, Samuel K. Houston, Arnold M. Markoe, Timothy G. Murray

Introduction

Brachytherapy is the application of radiation from isotopes over very short distances in contact with a surface. The goal of ocular brachytherapy is to deliver a curative dose of radiation to the tumor while delivering the least possible dose of radiation to normal ocular structures.

Treatment of choroidal melanoma with brachytherapy was first reported by Moore in 1930.[1] These early studies by Moore with radon seeds paved the way for the use of other forms of radiation at clinical centers around the world, including cobalt-60,[2–5] ruthenium-106,[6–8] gold-198,[9] iodine-125,[10–18] and palladium-103.[19–21] Iodine-125 (I-125) is currently the most commonly used isotope in brachytherapy for choroidal melanoma in the United States, whereas ruthenium-106 and palladium-103 continue to be popular at some centers. Brachytherapy offers an alternative to enucleation in the treatment of choroidal melanoma, allowing globe-salvaging with the possibility of maintaining useful vision. The Collaborative Ocular Melanoma Study (COMS) was a prospective, randomized study that provided clinicians with statistically sound evidence supporting the use of radiation in the treatment of choroidal melanoma. The study investigated more than 1300 patients with medium-sized melanoma and randomized to I-125 brachytherapy or enucleation.[22] After 12 years of follow-up, there was no statistically significant difference between these two modalities of treatment with regard to mortality.[22,23] Although treatment protocols and selection of tumors for plaque treatment must be individualized and differ among clinical centers, generally acceptable indications for plaque brachytherapy include (1) selected small choroidal melanomas exhibiting growth or malignant transformation; (2) medium-sized choroidal and ciliary body melanomas in eyes with visual potential; (3) large melanomas with

dimensions up to 16 mm in diameter and 8–10 mm in thickness; and (4) larger melanomas, especially in monocular patients. However, despite success in sparing enucleation, radiation has profound effects on the surrounding retina and optic nerve, with vision limited by the resulting radiation retinopathy and optic neuropathy.[24–28] These complications can have profound effects on quality of life, with 209 patients from the COMS reporting no significant difference in visual function 3–5 years posttreatment for plaque brachytherapy versus enucleation.[29] Continued research and investigation are needed to identify efficacious supplemental therapies for these universally common radiation-related complications.

Although enucleation can still be considered for choroidal melanomas, the COMS study laid the framework for the adoption of globe-salvaging treatment modalities by providing evidence for the efficacy of plaque brachytherapy. As a result, clinicians can confidently recommend radiation to patients, offering a treatment to save the eye as well as a chance at maintaining some useful vision. However, despite the lack of difference in survival between the two treatments, metastatic death continues to occur in a significant percentage of patients. Further research is needed to develop adjuvant therapies to alter this disturbing statistic.

Dosimetry

The optimal tumoricidal radiation dose for uveal melanoma remains unclear,[30,31] but doses range between 50 and 100 Gy, with doses less than 50 Gy being associated with significant treatment failures.[30] Kindy-Degnan et al.[32] used helium ion radiation and reported on tumor apex dosages ranging between 50 and 80 Gy, showing that regardless of whether 50, 60, 70, or 80 Gy was used, there were no differences in tumor regression, survival, complications, or visual outcomes. Initially, the COMS decided to deliver 100 Gy to the tumor apex with a delivery rate of 50–125 cGy/h (tumors <5 mm in height are managed as if they were 5 mm thick).[33] However, in 1996, based on newer dosimetric measurements and the recommendations of the American Association of Physicists in Medicine (AAPM), the COMS modified

the prescription dose to deliver 85 Gy to the tumor apex with a delivery rate of 43–105 cGy/hour.[34] Based on these modifications, with the AAPM-recommended calculation and revised prescription dose, the actual dose delivered to the tumor is the same. As a result, when analyzing studies prior to 1986 that utilized iodine-125, the actual dose to the tumor is 85% of the stated dose. Furthermore, the American Brachytherapy Society has presented the COMS dose recommendation as the guideline for the treatment of choroidal melanoma.[35] As more accurate estimates for some of the assumptions used and better calculation algorithms have become available, dosimetry has been further refined and recalculated incorporating anisotropy, line source approximation, and Silastic and gold shield attenuation. Tables of dose to the tumor apex and various other ocular structures have been presented for the various size plaques.[36] On average, the dose to the apex of the tumor appears to be 0.89 of the 85 Gy that has been assumed using the AAPM formalism.[36] The physics of brachytherapy has been reviewed in several publications.[36–38]

Isotope Selection

The radiation is distributed over a short distance from a surface or within the target tissue. Table 149.1 presents physical characteristics for the commonly used isotopes in brachytherapy. The table breaks isotopes into two broad categories: (1) those that emit gamma (γ)-rays or X-rays; (2) those that emit beta (β)-particles (electrons). Table 149.1 footnotes explain some of the simplifications. The half-value (HVL) in water for a narrow beam is useful in comparing isotopes for the penetration of their radiations in tissue. The tenth-value layer (TVL) in lead for a broad beam is useful in evaluating penetration in shielding materials.

TABLE 149.1

Physical Characteristics of Commonly Used Isotopes for Brachytherapy[a]

Nuclide	Half-Life	Energy (MeV)	HVL[b] (cm)	TVL[c] (cm)	Exposure Rate Constant (R/cm² per mCi per hour)[d]
GAMMA-RAY OR X-RAY EMITTERS					

Cobalt-60	5.3 years	1.25 dV	10.8	4.6	13.1
Palladium-103	17.0 days	0.02	~2.0	~0.003	1.5
Iodine-125	60.2 days	0.03[e]	~3.0	~0.01	1.4
Cesium-137	30.0 years	0.60[e]	8.2	2.2	3.3
Tantalum-182	115.0 days	0.67[e]	10.0	3.9	7.8
Iridium-192	74.2 days	0.38[e]	6.3	1.2	4.7
Gold-198	2.7 days	0.41[e]	7.0	1.0	2.4
Radon-222	3.8 days	0.83[e]	10.6	4.2	10.2
BETA-EMITTERS					
Strontium-90[f]	28.0 years	2.27	1.5	0.04	–
Ruthenium-106[f]	368.0 days	3.54	2.4	0.07	1.7

[a]Data from references 7, 38–41.

[b]HVL, half-value layer: thickness of water required to reduce exposure (dose) from the nuclide to 50% (narrow beam).

[c]TVL, tenth-value layer: thickness of lead required to reduce exposure (dose) from the nuclide to 10% (broad beam).

[d]Exposure rate constant measures exposure rate (R/hour) at 1 cm distance from a 1-mCi sample of the nuclide.

[e]Average gamma-ray or X-ray energy.

[f]In equilibrium with daughter isotopes.

The most commonly used sources for brachytherapy are iodine-125, palladium-103, and ruthenium-106, which have largely replaced iridium-192, cesium-137, radium-226, radon-222, and cobalt-60. Half-life will determine whether the isotope can be used practically, is feasible for commercial production, or can be reused. Isotopes such as gold-198 and radon-222 have very short half-lives and are impractical for regular use.

The energy of γ-rays or X-rays relates to their penetration in matter in a complex way. The more energetic rays penetrate to a greater extent and are more difficult to shield; these two factors are dealt with in the last two columns of Table 149.1.

The HVL in water is an index of the extent to which the energy of the radiation is absorbed in water (or tissue). At short distances, important for application in localized tumors of the eye, the

inverse-square law largely governs the radiation penetration in tissue. Fig. 149.1 displays the depth–dose curves for iodine-125, iridium-192, and cobalt-60. Because of the small height (up to approximately 1 cm) of the tumors treated, this inverse-square law is far more important in determining scleral (or choroidal blood vessel) dose for a given dose to the tumor apex. The dose rate falls more rapidly near the source than further away. Thus, the scleral dose relative to the dose at the apex of the tumor may be reduced by simply introducing a space between the source and the sclera. In the orbit, only size constraints limit the magnitude of the space, with 1 mm being the maximum in plaques used for ocular brachytherapy. With greater distances and less energetic rays, tissue absorption begins to play a more important role. For the β-emitters, absorption in tissues, which is complex and related to the energy of the β-particle, must be measured.

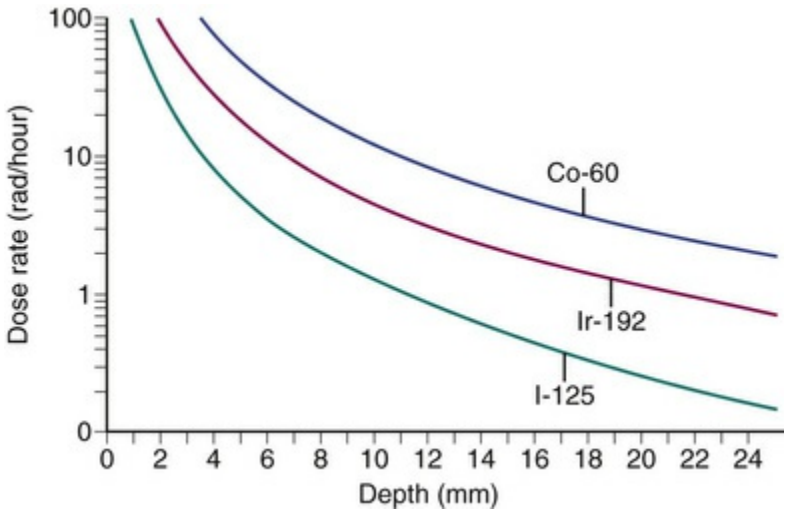

FIG. 149.1 Computer-generated curves identifying depth–doses of radiation at varying distances in tissue from three different radiation sources. A single seed (1.0 mCi; 37 MBq) of each radioisotope was used.

The TVL of lead is an index of the shielding that must be used around sources for the protection of personnel or the normal adjacent tissues. All the γ-ray or X-ray emitters except for iodine-

125 and palladium-103 have values >1 cm. In 1976, Sealy et al.[42] first reported the use of iodine-125 in the management of melanoma. One reason this isotope was chosen was because the radiation could be almost completely shielded by a thin sheet (0.4 mm) of lead or gold.

The exposure rate constant is an expression of dose rate at a standard distance from a specified amount of isotope. More atoms of an isotope with a low constant can achieve the same dose rate as one with a higher constant, the other characteristics being equal. The curves of dose rate versus depth in tissue for different isotopes can nearly be superimposed by adjusting the amount of each isotope in inverse ratio to the ratio of the exposure rate constants (Fig. 149.2).[43]

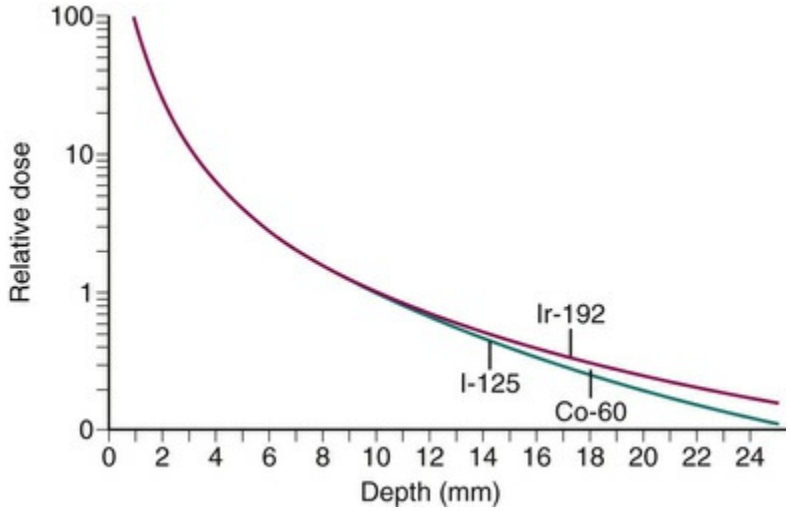

FIG. 149.2 Normalized curves (at 1 cm using a single seed of radioisotope) showing that depth–doses of radiation are nearly identical with the three radiation sources until beyond 15 mm, at which depth the radiation from iodine-125 begins to fall off. (Reproduced with permission from Earle J, Kline RW, Robertson DM. Selection of iodine-125 for the Collaborative Ocular Melanoma Study. Arch Ophthalmol 1987;105:763–4. American Medical Association. All rights reserved. ©1987.)

Beta-emitters, such as ruthenium-106, have been shown to be successful in tumor control for small to medium tumors, potentially up to 16 mm in diameter and up to 8 mm in thickness when used alone with calculated apex doses, or combined with transpupillary

thermotherapy (TTT) when apex doses are insufficient.[44] The presumed advantages of these lower-dose radiation sources are a decrease in the potential risk to adjacent structures as well as decrease in the risk of radiation retinopathy.[45,46] However, studies have not shown a reduction in treatment-related visual decline,[44] as doses are thought to still be above those maximally tolerated by the retina, vasculature, and optic nerve.

A final consideration is the ready commercial availability of well-packaged, calibrated, quality-controlled sources with a spectrum of activities. The COMS chose iodine-125 as a convenient, easily available isotope with favorable properties of half-life, shielding, tissue penetration, and physical form. As a result, iodine-125 is the most commonly used isotope in the United States. However, with high rates of radiation retinopathy and visual morbidity, other centers around the world are investigating the use of other isotopes, namely palladium-103 and ruthenium-106, in attempts to minimize the treatment-related side-effects while still maintaining equivalent tumor control rates.

Plaque Design

The I-125 plaque design used in the COMS evolved from that used by Rotman et al.[47] and Robertson et al.[17] and consists of a gold plaque that is approximately 0.4 mm thick with a lip around its perimeter that resembles a smooth bottle cap (Fig. 149.3).[43] The shielding device decreases lateral spread of radiation and results in a collimated beam of radiation. Plaques may be customized with notches or indentations of the gold rim to allow placement adjacent to the optic nerve sheath for juxtapapillary tumors. Notched plaques attempt to minimize the likelihood of plaque tilting secondary to placement next to the optic nerve sheath, as this tilt may result in excess radiation to the optic nerve, while decreasing the dose to the tumor apex. Other unique plaque designs and concepts include slotted plaques,[48] which may aid in the treatment of juxtapapillary tumors, including circumpapillary tumors, which prove difficult to treat. Within the gold plaque is a soft, pliable plastic (Silastic) seed carrier insert with evenly spaced troughs that accept the iodine-125 seeds. The carrier is designed so that the seeds

are adjacent to the gold. The thickness of the seed carrier separates the seeds from the sclera surface by 1 mm. Eyelets facilitate anchoring of the plaque to the sclera with sutures. Eyelet placement proves important to minimize the potential for plaque tilt, with those with circumferential eyelets posing decreased likelihood of tilting. The relative dose distribution associated with a particular radioactive plaque is in large part determined by the arrangement (distribution) of the seeds in the plaque. The dose distribution from seeds within a plaque, such as shown in Fig. 149.3, is demonstrated by the schematic in Fig. 149.4. By distributing iodine seeds over the area of the plaque and having a 1-mm spacer between the seeds and the sclera, the scleral dose delivered by an I-125 plaque is approximately the same as that delivered by a cobalt-60 plaque. Monte Carlo calculations by Chiu-Tsao et al.[49] demonstrate a lower scleral dose for iodine-125 compared to cobalt-60, for a point source model. Plaques used to treat uveal melanoma are designed to deliver the prescription dose of radiation, or greater, to the entire tumor. The Collaborative Ocular Melanoma Study (COMS) used custom-designed plaques to create uniform isodose curves, encompassing the tumor. Others have created software to improve the distribution of radiation to the target tissues while minimizing radiation to the surrounding normal tissues, and they have reported their results.[50] In the future, radiation delivery may be further improved with three-dimensional modeling software advances.

FIG. 149.3 Iodine-125 plaque designed for the Collaborative Ocular Melanoma Study (COMS), consisting of gold housing and seed carrier insert.

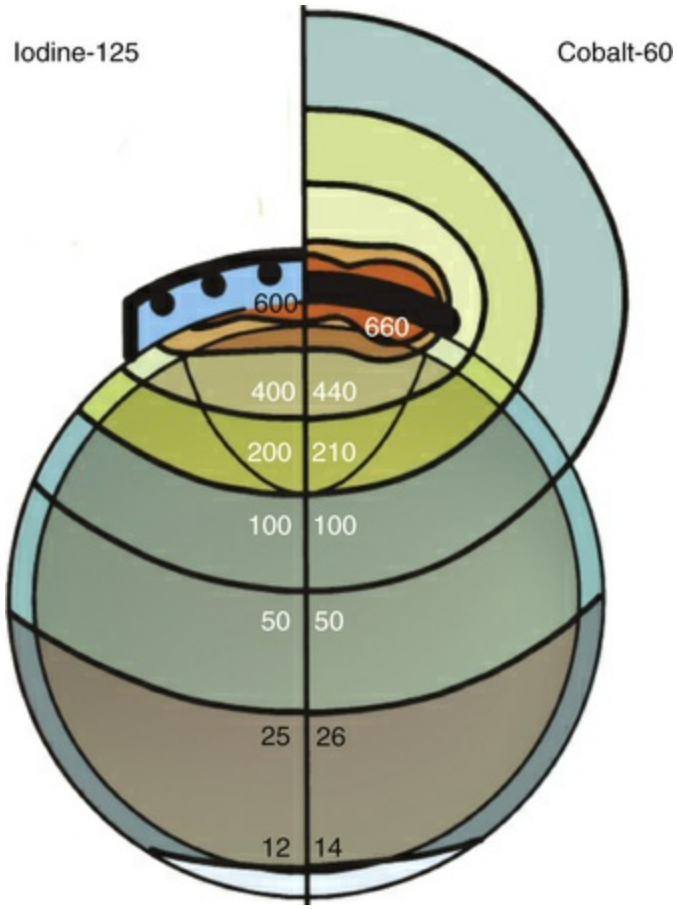

FIG. 149.4 Schematic displaying isodose lines from iodine-125 (left) and cobalt-60 (right) therapeutic plaques, both delivering 100 Gy to the apex of a tumor 7 mm thick. A 1-mm spacer separates iodine-125 seeds from the sclera. (Reproduced with permission from Earle J, Kline RW, Robertson DM. Selection of iodine-125 for the Collaborative Ocular Melanoma Study. Arch Ophthalmol 1987;105:763–4. American Medical Association. All rights reserved. © 1987)

Indications for Treatment

Medium Tumors

The Collaborative Ocular Melanoma Study (COMS), a prospective, randomized study funded by the National Eye Institute, compared survival in patients with medium-sized tumors randomized to brachytherapy or enucleation.[32] The rationale for this study was outlined by Robertson in 1989.[51] Results of the COMS medium-size tumor trial became available in 2001.[21] Medium tumors were

defined as tumors with a thickness between 2.5 and 10 mm, as well as a maximal basal diameter ≤16 mm. Stringent inclusion and exclusion criteria were used, including patient-related factors, such as a history of any prior cancer, comorbidities that may influence survival, and immunosuppressive therapy, as well as tumor characteristics such as juxtapapillary tumors (tumors within 1 mm of the optic nerve), diffuse (ring) melanomas, and melanomas with a primary ciliary body location. With 1317 patients enrolled and randomized between enucleation and I-125 brachytherapy in the medium-size COMS study, the 5-year mortality rates were not statistically different. This trial had >80% power to conclude that neither treatment altered the mortality by as much as 25% from each other. The COMS study group refined survival rates to include 12-year data.[22] Overall, cumulative all-cause mortality at 12 years for patients treated with either enucleation or plaque radiotherapy was 41% and 43%, respectively. For melanoma-specific mortality, the rates for I-125 brachytherapy were 10%, 18%, and 21% at 5, 10, and 12 years, respectively. For patients that received primary enucleation, melanoma-specific death rates were 11%, 17%, and 17%. These statistics emphasize that even at longer follow-up, there were no statistically significant differences in survival between I-125 plaque brachytherapy and enucleation.

Long-term studies utilizing plaques other than iodine-125 have demonstrated success in the treatment of choroidal melanoma. For palladium-103, Finger et al.[52] reported on 400 patients treated with plaque brachytherapy and a mean follow-up of 51 months. Metastatic rates were found to be 6%, with estimated 5- and 10-year risks of metastasis of 7.3% and 13.4%, respectively. For ruthenium-106 plaques, Verschueren et al.[44] reported on 425 patients treated with plaque brachytherapy, with and without TTT, and a median follow-up of 50 months. Failure of local tumor control was 3.9%, with estimated metastasis rates of 24.5% and 30.9% at 5 and 10 years, respectively, and overall survival of 79.6% and 68.2%. Investigators utilizing ruthenium-106 plaques have shown that tumors >5 mm had increased risk of local recurrence.[53] As a result, for tumors >5 mm or those tumors with insufficient doses to the tumor apex, adjuvant TTT has been suggested.[44,53] Therefore, tumors up to 8 mm in thickness and 16 mm in diameter may

potentially be treated with ruthenium-106.[44]

The extended COMS report that included 12-year mortality rates also assessed prognostic factors for metastasis and death, reporting a correlation with advanced age at baseline, as well as larger maximum basal tumor diameter. Shields et al.[54] conducted an in-depth analysis of tumor size and risk for metastasis, reporting on the millimeter-by-millimeter risk for metastasis. In a series of 8033 patients with ciliochoroidal melanoma, tumor size was significantly associated with rates of metastasis. For small melanomas (height 0–3.0 mm), rates of metastasis were 6%, 12%, and 20% at 5, 10, and 20 years, respectively. For medium melanomas (height 3.1–8.0 mm), the rates of metastasis were 35%, 49%, and 67% at 5, 10, and 20 years, respectively. The rates for large tumors (height >8.0 mm) were 25%, 49%, and 67%, respectively. Of note, advanced baseline age and increasing tumor size were confirmed as risk factors for metastatic disease, as well as ciliary body location and clinical findings such as a brown tumor, subretinal fluid, and extraocular extension.

Small Tumors

In 1978 Curtin et al.[55] reported on the management of small choroidal melanomas with serial observation, in an era when enucleation was the gold standard. Forty-six patients with small melanomas were managed with serial observation until growth was documented, and then offered enucleation. Over 14 years, 20 of the 46 patients were treated with enucleation. The melanoma-specific mortality was 6.5%. Other authors have reported on similar rates of melanoma-related mortalities for tumors that received either prompt treatment or delayed treatment.[56,57] The COMS enrolled 204 patients with small melanoma in a nonrandomized, prospective follow-up study.[58,59] The COMS classified small melanomas as tumors with an apical height of 1–3 mm and a maximal basal diameter between 5 and 16 mm. Upon study enrollment, 16 patients (8%) had treatment, while 67 patients (33%) required treatment at follow-up. Estimates of the need for treatment of small melanomas were 21%, 33%, and 38% at 2, 5, and 7 years, respectively. Overall, there were 27 deaths, with six melanoma-related. Five- and 8-year

melanoma-specific mortalities were 1% and 3.7%, respectively. Importantly, the study identified risk factors that were found to be predictive of tumor growth, including initial tumor thickness, the presence of orange pigment, the absence of drusen, and the absence of RPE changes surrounding the tumor (absence of halo). Other risk factors for the malignant transformation of small melanomas include subretinal fluid, patient symptoms, margins close to the optic nerve, and ultrasound hollowness.[54,60] Of note, there has been a trend toward treatment of smaller tumors, and many of the lesions in this observational study would be treated today.

A more recent series by Sobrin et al.[61] reported on 154 patients with small choroidal melanomas who were observed for signs of malignant transformation (tumor growth or presence of orange pigment). A total of 45 patients (29%) who were observed needed treatment, with a mean interval to treatment of 4.1 years. All patients with observed transformation were treated with I-125 plaque brachytherapy utilizing intraoperative ultrasound for plaque localization. Of those treated, 4.5% developed metastasis, with only one death during the follow-up period. Additionally, one patient (2%) had local tumor recurrence necessitating enucleation. Notably, for those patients with small melanomas that continued to be observed for a mean of 8.1 years, no patient developed metastasis or died secondary to melanoma. Vision at baseline was 20/25, with final visual acuities of 20/30 for patients who were observed and 20/50 at 2 years for patients that were treated with plaque brachytherapy. Radiation retinopathy and optic neuropathy were observed in 56% and 31% of patients, respectively.

Treatment with enucleation or brachytherapy has significant morbidities regarding visual function. Therefore, with current evidence suggesting a low incidence of mortality with small choroidal melanomas along with the potential for significant morbidity of treatment; an open, individualized discourse with each patient is a requisite. Despite no long-term, randomized clinical trials addressing this question, prompt or delayed treatment appears to be a reasonable strategy for small choroidal melanomas.

Finally, transpupillary thermotherapy (TTT) has been proposed for the treatment of small choroidal melanomas that have a tumor height <4 mm. Numerous authors have reported on TTT in these

lesions, with rates of tumor recurrence ranging from 8% to 56%, without standard inclusion criteria.[38,62–69] A systematic review of the literature by Singh et al.[70] reported a mean local tumor recurrence rate of 17% including 7% with extrascleral extension at a mean follow-up of 37 months. Although TTT may cause less visual morbidity in the treatment of small choroidal melanomas, the sole use of this therapy has the potential for high recurrence rates, which have been shown to be associated with an increased risk of metastasis.[71] As a result, the sole use of TTT in the treatment of small choroidal melanomas should be carefully considered.

Large Tumors

With the COMS establishing the widespread use of plaque brachytherapy for medium-sized choroidal melanoma, most eyes are salvaged, but not without severe visual morbidity secondary to the effects of radiation on the eye. The maximum tumor size that can be effectively treated with radiation without causing severe radiation complications is not known with certainty. Gragoudas[72] suggested that eyes harboring tumors that involve up to 30% of the eye can usually be treated and salvaged after radiation. Char et al.[73] reported information that suggested an upper size limit for tumors treated with radiation. Nearly 50% of the eyes with tumor thickness >10 mm eventually required enucleations after treatment with helium ions. The COMS reported that enucleations were more common for tumors with greater thicknesses and greater base dimensions, although percentages were not given.[71] The American Brachytherapy Society Ophthalmic Oncology Task Force recently published consensus brachytherapy recommendations that, rather than describing a specific range of melanoma sizes or locations appropriate for treatment, recommended exclusion criteria for brachytherapy that include tumors with gross (T4e or >5 mm) extraocular extension, eyes without light perception, and blind, painful eyes.[74]

By COMS definition, large melanomas are tumors that are >10 mm in thickness or >2 mm in thickness with basal diameter >16 mm. The COMS investigated the use of radiation pre-enucleation versus primary enucleation for large choroidal melanomas. At 10

years, survival rates did not show statistically significant differences, with melanoma-specific death rates of 40% for enucleation, compared to 45% for patients that received radiation prior to enucleation.[75] Although the COMS only looked at brachytherapy for medium-sized tumors, several studies have investigated the use of brachytherapy for large melanomas as an alternative to enucleation.[76–78] Wilson et al. reported on 124 patients with large tumors of the ciliary body and choroid treated with I-125 brachytherapy and concluded that tumor thickness >8 mm in height or 16 mm in maximal basal diameter can be effectively treated with a favorable expectation of globe salvage, but limited vision conservation. Puusaari et al.[77] came to a similar conclusion based on 96 eyes with large choroidal melanomas. The authors found that they had a fair chance of globe conservation with acceptable cosmesis, as well as a reasonable chance of conserving useful vision for 1–2 years. Shields et al.[78] reported on 354 large choroidal melanomas (>8 mm in thickness) that were treated with plaque brachytherapy. Failure in local tumor control was estimated in 9% and 13% of tumors at 5 and 10 years, respectively, and enucleation was necessary in 24% and 34% at 5 and 10 years, respectively. Metastasis of melanoma was estimated in 30% and 55% at 5 and 10 years, respectively. Notably, estimates of poor visual acuity (20/200 or worse) were 97% at 15 years. Similar results have recently been reported using palladium-103 in a small series of patients with large tumors.[79]

Ruthenium-106 has also been used to treat large choroidal melanomas, but high doses at the sclera limit the thickness of tumors that can be treated. Kaiserman et al.[80] reported on 63 large tumors treated with ruthenium-106. With a mean follow-up of 69.6 months and mean tumor thickness of 9.29 mm, 23.8% failed local tumor control. Estimated rates of metastasis were 22.5% and 48.1% at 5 and 10 years, respectively, while melanoma-specific mortality was found to be 20.5% and 46.2%. Interestingly, 70.8% of patients maintained vision better than 20/200. Large tumors treated with ruthenium-106 had a higher risk for local tumor recurrence, when compared with tumors treated with iodine-125.[78] Other investigators suggest the use of adjuvant TTT in cases of tumors treated with ruthenium-106.[81,82] Investigators have shown that large

tumors can be effectively treated with brachytherapy, but visual morbidity is high secondary to the large amounts of radiation to obtain effective tumor control.

Juxtapapillary Tumors

Treatment of juxtapapillary tumors (touching or located within 1 mm from the optic nerve) presents a unique situation of providing appropriate radiation dosages to the tumor apex while attempting to minimize the exposure to the optic nerve. In the past, the majority of these tumors were enucleated, and studies treating eyes with tumors in a juxtapapillary location have higher rates of local tumor recurrence when compared to tumors in other locations.[83] Intraoperative ultrasound during plaque placement shows frequent tilting of plaques placed near the optic nerve sheath. Notably, juxtapapillary tumors were excluded from the COMS Medium Tumor Trial, resulting in exclusion of 9% of otherwise eligible tumors. Advanced plaque design has opened up the use of plaque brachytherapy as a globe-salvaging treatment alternative for these eyes.

Notched plaques are designed with an indentation in the plaque rim to allow flush placement adjacent to the optic nerve sheath. In addition, novel designs incorporating a slot in the plaque may allow for the successful treatment of juxtapapillary, and even circumpapillary, tumors.[48] In 1994, De Potter et al.[84] reported on 127 patients with juxtapapillary melanomas treated with either enucleation or plaque brachytherapy. Despite being a nonrandomized, retrospective study with a small percentage of patients treated with plaque brachytherapy (28%), the authors found that the treatment modality did not affect risk for metastasis. Sagoo et al.[83] reported on the use of notched I-125 plaques in the treatment of circumpapillary tumors (tumors encircling the optic nerve). Recurrence rates were shown to be 14%, while the metastatic rate was 4% with no melanoma-specific deaths observed with a mean of 52 months follow-up. Preservation of visual acuity was poor, with greater than 60% manifesting with vision less than 20/200. Emphasizing the importance of notched plaques with placement confirmation by intraoperative ultrasound, Hui et al.[85]

reported on control rates of 100% at 30 months using notched plaques, compared to 89% at 25 months for non-notched plaques. Sagoo et al.[86]reported on 650 juxtapapillary tumors treated with notched plaque brachytherapy with or without TTT with a mean follow-up of 52 months. Overall incidence of tumor recurrence was 11%, while metastasis was 10% with a melanoma-specific death rate of 3%. Kaplan–Meier estimates of tumor recurrence at 10 years were shown to be 21%, with metastasis and death of 24% and 9%, respectively. Finger et al.[87] recently reported 100% local tumor control in 24 patients with tumors near, touching, or surrounding the optic disc, treated with a custom 8-mm wide slotted plaque design, with a mean follow-up of 23 months.

To address the higher rate of local tumor recurrence in juxtapapillary melanomas, TTT has been used as an adjunctive treatment. In the prior study by Sagoo et al.,[88] TTT was utilized as an adjunctive treatment in 56% of eyes. Overall, tumor recurrences with TTT were 9% (compared to 14% for no TTT), metastasis was 9% (compared to 10%), with a death rate of 2% (compared to 5%). However, differences in recurrences and metastasis were not statistically significant when TTT was used as an adjuvant treatment in juxtapapillary tumors.

In conclusion, juxtapapillary tumors may be treated with plaque brachytherapy, with notched plaques and intraoperative ultrasound contributing to successful treatment. Proton beam irradiation (PBI) has also been shown to be efficacious in the treatment of peripapillary and parapapillary melanomas,[89] as compared to notched plaques for juxtapapillary tumors.[90] TTT may be used as an adjunctive therapy with uncertain benefits. However, as a result of the close proximity to the macula and optic nerve, rates of visual compromise are high, with the majority of patients losing visual acuity to <20/200.

Plaque Placement Technique

One of the first and most important steps in plaque placement is determining an accurate clinical estimate of the tumor base and height. This allows for the correct sizing of the plaque, and this information must be precisely communicated to the radiation

oncologist and radiation physicist. Estimates of tumor dimensions utilize a number of technologies, including photography, indirect ophthalmoscopy with and without measuring grids, ultrasound, and transillumination. Intraoperative localization utilizes indirect ophthalmoscopy, ultrasound, and transillumination with fiberoptic light sources.

With advancements in ophthalmic photography, including wide-angle photography, tumors are more often captured *in toto* as single or montage images. Tumor dimensions can then be estimated by approximating the basal tumor diameter in disc diameters (using the horizontal diameter of the optic disc as1.5 mm) or by using calipers,. Wide-angle photography has been shown to be more accurate than ultrasound in measuring the basal diameter in some eyes, as it potentially captures those margins or pigmentation that are not determined on ultrasound secondary to lack of elevation.[91,92] It is important for the ultrasonographer to rotate the B-scan probe around the center of the tumor to determine the longest tumor diameter, as this might not correspond to the longitudinal and transverse images most typically obtained. Ultrasound (quantitative A-scan or B-scan) is usually used to determine tumor thickness and to evaluate for the presence or absence of extraocular extension. For tumors that are unable to be captured completely by photographs, basal dimensions can be measured using a technique first described by Hilton,[93] where a grid is placed over the 20-D lens with each square representing 1 disc diameter. The tumor is viewed monocularly through the grid, allowing an approximate calculation of the basal diameter. The presurgical tumor estimates are used to create the plaque. Plaque sizes are chosen to ensure that the plaque covers the entire tumor base, along with 2–3 mm of tumor-free perimeter. For example, a tumor with a base diameter of 12 mm is treated with a 16 mm in diameter plaque.

Estimation of tumor diameters for large tumors or tumors located anterior to the equator can be difficult, rendering it useful to know several distance approximations. In an emmetropic eye, the distance between the equator and the ora is approximately 5 mm in the vertical meridians, 5.5 mm in the nasal meridian, and 6 mm in the temporal meridian. Also, with the COMS considering tumors >16 mm too large to be eligible for plaque brachytherapy, it is

convenient to remember that 3 clock-hours at the equator and 4 clock-hours at the ora are each equivalent to a chord length of approximately 16 mm. The choice of anesthesia is left to the discretion of the surgeon. After an adequate peritomy, the surface of the sclera corresponding to the tumor is exposed. If extraocular extension is observed within a pseudoencapsulated focus ≤2 mm in thickness, a limited peritomy (if the focus is anterior) and tenonectomy is performed, and the plaque is carefully placed over the tumor base and the extension. Because an extraocular extension of <2 mm may not worsen the prognosis for survival,[94] proceeding with brachytherapy as intended is reasonable. As an alternative, an I-125 plaque without a gold shield could be placed over the extension to allow radiation of orbital tissues adjacent to the visible extension. Ultrasound frequently detects extraocular tumor extensions >2 mm in height,[95] but extensions of this size occur infrequently.[94] As a result, discovery of large extraocular extensions (>2 mm) at surgery should rarely occur. For example, there have been virtually no such instances for globes enucleated in COMS.

At surgery, the tumor base is localized with standard localization techniques used for retinal breaks or transillumination (or both). For anteriorly located tumors with even minimal pigmentation, the shadow of the tumor often can be outlined on the sclera while the globe is transilluminated through the cornea with a fiberoptic light source (Fig. 149.5B). Surgeons need to be cautious, as some of the fiberoptic light sources used for nonocular procedures may be too bright to use for ocular transillumination and can cause corneal burns or damage to the retina. The tumor diameter can be measured and recorded using calipers, followed by estimation of 2 mm perimeter beyond the tumor borders. A transparent acrylic dummy plaque with a diameter equal to that of the therapeutic plaque can be used to facilitate localization and later placement of the opaque therapeutic plaque. The dummy plaque is placed on the sclera, covering the scleral marks that identify the tumor perimeter. The dummy plaque must completely cover the base of the tumor, as well as a tumor-free perimeter of 2 mm or more (Fig. 149.5C). After the perimeter of the dummy plaque has been marked on the sclera, it is removed, and the therapeutic plaque is placed within this ring of scleral marks and anchored with two or three intrascleral sutures

(Figs. 149.5D, F). If the therapeutic plaque is the same size or smaller than the boundary of the tumor base as marked on the sclera, the procedure is terminated, and a larger plaque is prepared and placed on the eye later.

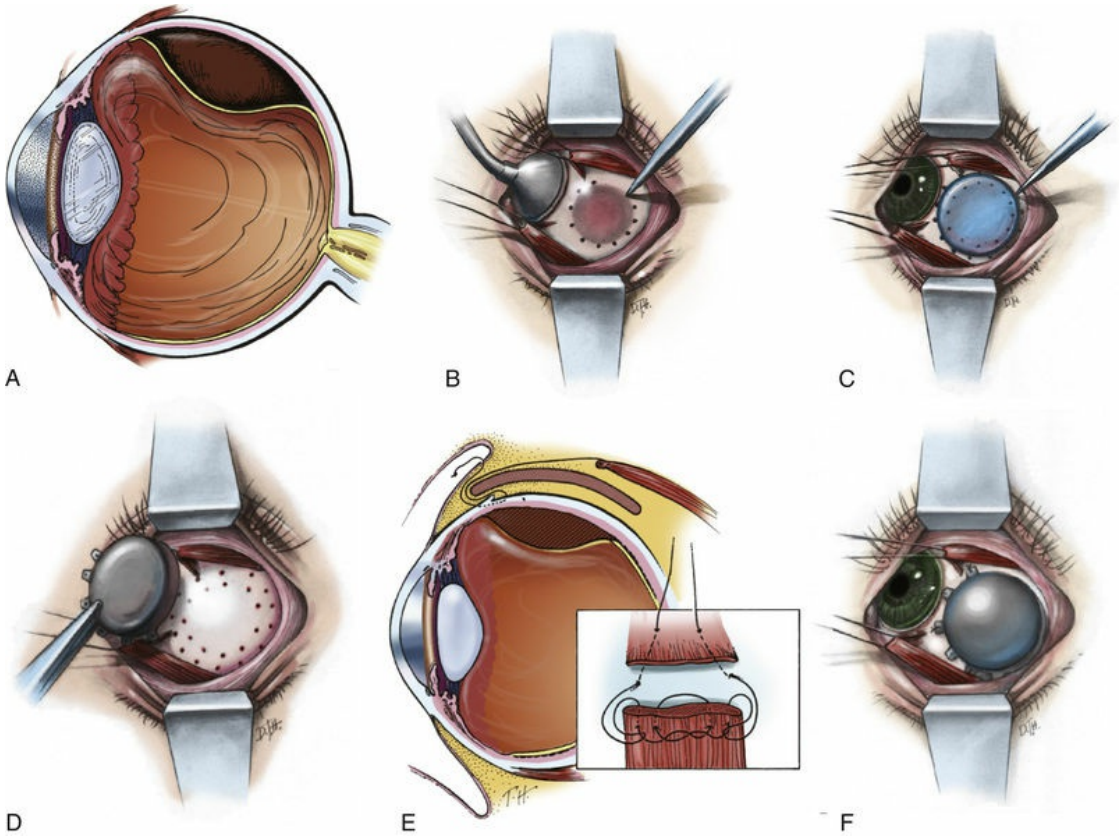

FIG. 149.5 (A) Sketch showing a cross-section of an eye harboring a melanoma located in the midperipheral fundus. (B) A fiberoptic light source has been placed over the cornea, and the shadow of the tumor is visible on the exposed sclera. A marking pencil has outlined the shadow of the tumor. (C) A transparent dummy plaque that is 4 mm greater in diameter than the estimated diameter of the tumor base has been centered over the area of the tumor base. A second row of marks has been made around the dummy plaque to facilitate placement of the opaque therapeutic plaque, which will overlap the boundary of the tumor by 2 mm on each side. (D) Gold-backed iodine-125 plaque being readied for placement. (E) When a rectus muscle must be detached because of an anteriorly located tumor, a double-armed mattress suture can be used to secure

the end of the transected muscle and the muscle can then be allowed to retract. Each arm of the suture is passed intrasclerally just posterior to the insertion. When the plaque is removed, the sutures are tightened and tied, thus drawing the muscle to the insertion, allowing the center of the muscle to hang back slightly. (F) Therapeutic plaque anchored in position with three 5–0 nylon intrascleral mattress sutures.

The location of the radioactive plaque can be confirmed with the traditional technique using indirect ophthalmoscopy and scleral indentation along the circumference of the plaque. Confirmation of the relationship of the tumor and plaque position usually can be obtained using B-scan ultrasonography.[96–98] Harbour et al.[96] showed that standard techniques for localizing plaque placement were suboptimal in 21% of patients, primarily in tumors in a posterior or juxtapapillary location. Intraoperative ultrasound allowed for identification of malpositioned plaques, affording the opportunity to reposition the plaque while still in the operating room. However, despite successful intraoperative positioning, tilting can worsen postoperatively. Almony et al.[99] found that whereas only 9% of patients had plaque tilt >1 mm at insertion, approximately 53% of plaques had tilt >1 mm at removal. Plaque tilt, which is not detected using indirect ophthalmoscopy or transillumination, is associated with a reduction in radiation doses to the tumor apex. Plaque tilt occurs most frequently in plaques adjacent to the optic nerve, but also occurs due to episcleral hematomas or displacement by the inferior oblique muscle. As a result, intraoperative ultrasound should be considered for use in combination with other localization techniques to ensure sufficient plaque placement and identify suboptimal or tilted plaques to allow for immediate repositioning. Postoperative ultrasound performed several days following plaque placement also can identify tilting that was not present intraoperatively, or tumor edema or hemorrhage that has occurred following plaque placement. Adjustments in duration of the brachytherapy can be performed to assure the entire tumor receives the prescribed dose of radiation, or TTT could be performed at the time of plaque removal to tumor that received less than the intended dose of radiation. Prior to altering the treatment plan, the

surgeon should communicate the ocular status with the radiation oncologist and work together to create an optimal management strategy. Although no long-term studies have been reported, intraoperative ultrasound may minimize the risk of local treatment failures.

There has been much debate about the learning curve for plaque placement, including whether ultrasound confirmation is needed in the hands of an experienced ocular oncologist. A study by Shah et al.[100] analyzed the learning curve associated with plaque placement for uveal melanoma over a 20-year period. The authors found that, initially, 21% of plaques required repositioning. This rate decreased to 12% after a period of 10 years, and further decreased to 4% after approximately 20 years. The study estimated that 1275 plaque cases were needed to obtain a precision rate of 90%.

Tumors with margins close to the optic nerve present a unique situation regarding plaque placement. Although the diameter of the intrascleral portion of the optic nerve measures 1.5 mm, the diameter of the optic nerve and surrounding sheath posterior to the globe increases to about 4–6 mm.[101] As a result, for tumors that are within 2 mm from the optic nerve, applying a plaque abutting the sclera with a 2-mm tumor-free margins is not possible. An alternative approach involves the design of plaques with an indentation or notch to fit around the optic nerve. Additionally, the rim of the plaque may be removed in the area adjacent to the optic nerve, to allow lateral spread of radiation to treat those margins that are unable to be covered by the plaque. However, this latter option exposes the optic nerve to a higher dose of radiation with increased likelihood of significant visual morbidity.

Rectus muscles may be detached to facilitate plaque placement and minimize pressure on the globe, with understanding that transection of a muscle may cause a hematoma and plaque tilt, which may increase the likelihood of local failure. The insertion of the inferior oblique can be cauterized and partially disinserted to allow placement of plaques beneath the macula.

Another localization technique utilizes a fiberoptic light source, using a technique similar to that described by Robertson et al.[102] An angled fiberoptic probe combined with indirect ophthalmoscopy can be used to provide transscleral transillumination around the

boundary of the plaque. As the probe moves along the plaque, the light can be visualized in the choroid and its location relative to the tumor base can be readily seen. For anteriorly located tumors, transscleral illumination around the plaque boundary is ordinarily satisfactory, as standard B-scan ultrasonography proves difficult in discerning anterior segment structures. However, newer technologies such as ultrasound biomicroscopy (UBM) and anterior segment optical coherence tomography may open new avenues for anterior segment image acquisition.[103]

After placement of the plaque, the rectus muscle may be sutured to the original insertion or anchored to the side of the plaque or anterior to the plaque. An adjustable suture placed at the time of plaque placement may be preferable if the muscle must remain detached during the brachytherapy period, as this will facilitate reattachment of the muscle at the time of plaque removal. Muscles are usually engaged with a double-armed absorbable suture posterior to the insertion, and disinserted. The ends of the double-armed suture are passed just posterior to the muscle insertion and loosely tied with a bow tie for later access when the plaque is removed (Fig. 149.5E).

Close evaluation of the tissue area of plaque placement must be emphasized, as any episcleral tissue around the optic nerve sheath, inferior oblique muscle, and posterior ciliary vessels and nerves may create added distance of the plaque away from the tumor.[104–108] On completion of plaque placement, the conjunctiva is closed over the plaque with sutures, although risk for complications is low for anteriorly located tumors where the conjunctiva is not able to be closed completely over the plaque or if conjunctiva retracts postoperatively.

Radiation plaques are kept in place for 3–7 days, with patients often staying as inpatients during the course of treatment, based on state radiation safety protocols. With conclusion of plaque treatment, plaque removal is usually performed with local anesthesia. Following the removal of the plaque, muscles that have been transected are reattached by approximating the sides of the muscle to the original insertion, allowing the central portion to drape posteriorly (in general, a slight recession of the muscle approximately 1.5 mm may compensate for the tendency of the

shortened reattached muscle to cause overaction). For preplaced sutures, the muscle is drawn up to the site of the suture passage and secured.

Thermoluminescent ring dosimetry measurements were utilized early in the treatment of choroidal melanoma with plaque brachytherapy to determine the risk of radiation exposure to the surgeon's hands during plaque placement. However, minimal radiation exposure was found,[109] and the use of these radiation-detection devices was discontinued.

Postoperatively, patients are followed serially until their conjunctiva has healed. Ultrasound examinations are difficult to interpret in the first few months, as even successfully treated tumors can exhibit early swelling, stability, or shrinkage. Tumor margins are typically stable during the first few months, so photographic imaging is usually not needed during this time.

Local Tumor Response

Most choroidal melanomas treated with brachytherapy show evidence of shrinkage, with almost half of all tumors decreasing 50% from the pretreatment thickness. Shrinkage may not be observed in the first several months, but is usually seen at 6 months and progresses over 2–3 years, then remains stable thereafter. Regression to a flat scar is rare. With tumor regression, echographic findings change concurrently, showing an increase in the internal reflectivity along with a decrease in intrinsic tumor vascularity. Choroidal melanomas that have broken through Bruch's membrane to form a collar-button configuration have a distinct regression pattern.[110] The body of these tumors tends to shrink while the collar-button portion becomes more prominent and darker, and may shed pigmented debris into the vitreous cavity. Histopathologically, this debris usually consists of pigment-laden macrophages, melanoma cells, or a combination of both.

Following initial postoperative healing, patients with choroidal melanomas should be evaluated at regular intervals for any signs of growth. Most centers follow patients at 3–6-month intervals. This interval can be modified based on the likelihood of secondary complications. Some centers increase the interval after about 5 years

for stable patients. If the tumor thickness increases by 300 μm, or if any of the tumor borders advance by 250 μm, the tumor is highly suspected of expansion. These tumors should be observed more frequently and if continued growth – 300 μm increase in thickness or 250 μm increase of any border – is observed, plaque brachytherapy is considered a failure and further treatment is recommended. Although several investigators have reported successful retreatment with brachytherapy leading to local tumor control,[8,12,111] definitive enucleation should be discussed. Tumors that recur following plaque brachytherapy may have a greater likelihood of metastasis (see below); therefore, maximizing primary treatment response is imperative.

Recurrences

Failure to control tumor growth after plaque brachytherapy has been shown to vary from 1.7% to 16%,[12,105,112–114] depending on the institution, isotope, and the length of follow-up. Wilson and Hungerford[115] observed a recurrence rate of only 4% with iodine-125, compared to 5% with PBI and 11% with ruthenium-106. In addition, Fontanesi et al.[116] reported a recurrence rate of 2.3% for 144 patients treated with iodine-125. The COMS enucleated 10% of eyes secondary to suspected or documented tumor recurrence.[71] More recently, a recurrence rate of 1.7% was reported for 117 patients with choroidal melanoma treated with I-125 plaque brachytherapy.[114] The study emphasized the importance of confirming proper plaque placement using intraoperative ultrasound at the time of surgery. Data from other plaques, ruthenium-106 and palladium-103, have also demonstrated low rates of local tumor failure at 3.9%[44] and 3%,[52] respectively.

Efforts to reduce the rate of recurrences following plaque brachytherapy are important, as patients with tumors with local recurrences, despite undergoing enucleation, have an increased risk of metastasis. Gragoudas et al.[72] reported a risk ratio of 2.44 among patients treated with PBI. Vrabec et al.[113] reported nearly three times greater estimated 5-year mortality (42% vs. 13%) among patients treated with cobalt-60. Harbour et al.[117] reported a 5-year actuarial rate of local recurrence of 10%, with metastasis occurring

in 19% of patients with horizontal (marginal) recurrences (relative risk 2.2), and increasing to 49% if the recurrence was vertical and diffuse (relative risk of 5.1). In the COMS, tumors with local recurrence had a calculated risk ratio of 1.5 for metastasis.

Visual Outcomes and Radiation Complications

Early brachytherapy reports by Stallard[5] in 1968 appeared to indicate a satisfactory 5-year survival rate among 100 patients treated with cobalt-60; however, other early studies identified severe vision loss and ocular complications that were disturbingly prevalent. Despite the use of lower-energy isotopes and modern plaque design with shielding to minimize radiation exposure to vital structures, radiation-related complications are commonly encountered, necessitating further research into their treatment. The earliest changes manifest as macular edema secondary to the leakage from capillaries with poor endothelial support. The clinical onset of radiation retinopathy is between 1 and 2 years. Horgan et al.[118] reported that optical coherence tomography (OCT) detected macular edema due to radiation retinopathy an average of 5 months before the clinical onset of radiation maculopathy. Notably, when macular edema was evident by OCT, only 38% of patients had clinical signs of radiation retinopathy, and the median visual acuity was still good at 20/40. Later manifestations of radiation that lead to impaired vision include macular capillary nonperfusion, proliferative retinopathy with vitreous hemorrhage, and optic neuropathy. Some of these changes are due to direct effects of radiation on the vascular endothelium, and some are likely due to the melanoma or its vascular supply, acting indirectly (so-called "toxic tumor syndrome").

The complications of radiation maculopathy and optic neuropathy are dependent on the total amount of radiation delivered to the macula and optic nerve, respectively. The resultant dose received by these structures depends on the tumor size and location, with increased risk in tumors with increased height and basal diameter, and located in close proximity to the fovea and

optic nerve. Other factors, such as concomitant use of chemotherapeutic agents and diabetes mellitus, may lower the threshold for developing radiation damage. Biologic variability also likely serves as another factor. Histopathologic studies have shown loss of endothelial cells that line blood vessels, resulting in capillary dropout, microaneurysms, and other changes similar to those seen with diabetic retinopathy.[40] Patients may present with macular edema, microaneurysms, telangiectatic vessels, capillary nonperfusion as seen on fluorescein angiography, neovascularization, vitreous hemorrhages, or optic disc edema.[24,41]

Brown et al.[23,24] indicated that the lowest doses of radiation generally causing macular retinopathy were 45 Gy from cobalt-60 plaques and 36 Gy from external beam radiation. Optic neuropathy was observed to occur from doses as low as 35 Gy from cobalt-60 and 36 Gy from external beam radiation. Visual prognosis has been shown to be less favorable when foveal or optic nerve radiation is in excess of 50 Gy.[26] The same group[26] reported severe visual loss from radiation doses to the fovea as low as 21, 23, and 30 Gy, emphasizing the variability in biologic response to treatment. These cases showed visual loss from nonproliferative radiation retinopathy or exudative retinal detachments.

Studies by Garretson et al.[11] found that visual acuity of 26 patients treated with iodine-125 remained within 2 Snellen lines in 54% of patients. Of those that developed radiation changes, mean duration to onset was approximately 32 months. Although the proponents of iodine-125 had hoped that the lower energy emission, combined with greater space between source and sclera and lateral shielding, would delay or lower the incidence of radiation complications, long-term results have been disappointing, with almost 50% of eyes treated with brachytherapy sustaining vision loss to ≤20/200 at 5 years. For patients treated with iodine-125 and with at least 3 years median follow-up, rates for radiation maculopathy range between 13 and 52%,[108,119–123] while rates of optic neuropathy range between 0 and 46%.[11,108,111,116,119–124] The upper range for radiation complications was shown in large tumors as based on COMS criteria.[123] Krohn et al.[119] found that patients with radiation maculopathy had a median dose of 49 Gy to the macula, while Stack et al.[120] found that patients who received >90 Gy to the

macula had a 63% risk of maculopathy. Juxtapapillary melanomas tend to have less favorable visual outcomes and more radiation complications than tumors elsewhere. In 650 juxtapapillary melanomas treated with brachytherapy, visual acuity was 20/200 or worse at 5 and 10 years in 54% and 87% of patients, respectively, with high rates of papillopathy (61% and 77%), maculopathy (56% and 65%), and secondary enucleation (16% and 26%).[86] Although radiation is known to significantly affect the retina, Boldt et al.[125] documented that 49.2% of patients in the medium tumor trial of the COMS had abnormalities in the posterior pole prior to plaque treatment, with rates increasing to >90% at 5 and 8 years posttreatment. Proliferative radiation retinopathy was found to occur in 5.2% of patients at 5 years, while optic neuropathy had an incidence of 27.4%. These observations suggest that, in addition to the treatment effects of plaque brachytherapy, inflammatory and angiogenic factors of tumors may contribute to retinopathy.

The visual outcome in eyes treated with iodine-125 is similar to that reported for other forms of radiation therapy (helium ion, 53% 20/200 or less,[126] PBI 42% 20/200 or less[127]) suggesting that research should continue to be directed toward ways to reduce or treat radiation complications. The COMS estimated that nearly 50% of patients treated with iodine-125 would lose substantial vision by 3 years (loss of ≥6 lines of vision), with 43% having visual acuity less than 20/200.[21] Other recent studies with at least 3 years follow-up report between 42–74% of patients treated with plaque brachytherapy lose ≥2 lines of vision.[119–121,128] In a small study of 95 patients with melanomas measuring 1.5–5.0 mm in thickness, reducing the dose of radiation for tumors less than 5.0 mm from a prescription point of 5.0 mm (the COMS protocol standard) to the apical height of the tumor reduces radiation complications for smaller lesions, with excellent local tumor control.[129] The COMS presented quality of life data for 209 patients treated with either enucleation or brachytherapy.[28] At 2 years, patients treated with brachytherapy reported peripheral vision and vision for driving that was significantly better than patients who were treated with enucleation. However, following 3–5 years, these findings were not significantly different. This timing corresponds to the visual decline observed for brachytherapy-treated eyes secondary to

complications of radiation retinopathy.

Other isotopes have been used to treat ocular melanoma with success. Although the physical characteristics of certain isotopes may allow better shielding with a greater differential radiation dose between tumor apex and sclera, the γ-rays, X-rays, and β-particles must still obey physical laws, which may limit the potential benefits. Besides iodine-125, two of the most commonly used isotopes for plaque brachytherapy are palladium-103 and ruthenium-106. Ruthenium-106 is a β-emitter and first reported to be efficacious in 11 melanomas by Lommatzsch in 1974.[130] A later series of 309 patients treated with ruthenium-106 with a mean follow-up of 6.7 years showed efficacy of treatment in 70% of eyes, with 23% retaining vision 6/12 or better.[131] In a smaller subset of patients with juxtapapillary melanomas treated with ruthenium-106, Lommatzsch et al. showed that the probability of developing complete radiation optic neuropathy was 23% and 53% at 5 and 10 years, respectively. Additionally, the probability of retaining 20/40 vision was 38% and 26% at 5 and 10 years. Verschueren et al.[44] reported on 425 patients with small to medium-sized choroidal melanomas treated with ruthenium-106. The authors found that rates of radiation complications (maculopathy, retinopathy, and optic neuropathy) were 40% and 65% at 2 and 5 years, respectively. In addition, almost 38% had a decrease in vision to ≤20/200.

For palladium-103, the Palladium-103 for Choroidal Melanoma Study Group[52] reported on 400 patients treated with plaque brachytherapy. With regards to visual acuity, 79% and 69% of patients had vision 20/200 or better at 5 and 10 years, respectively. Finger et al.[132] also correlated the incidence of radiation maculopathy with tumor location, tumor height, and radiation doses in 384 patients treated with palladium-103. Tumors in an anterior location were much less likely to manifest with maculopathy versus tumors with a posterior location (7% compared with 41%). Additionally, when compared with radiation doses to the fovea of <35 Gy, doses between 35–70 Gy had a risk of maculopathy of 1.74, while those >70 Gy had a risk of 2.43. This study compares similarly with the incidence of maculopathy following I-125 brachytherapy. Semenova[133] recently reported on 72 patients with melanoma with apical height ≥1.5 and ≤2.4 mm

treated with brachytherapy using palladium-103. With mean follow-up of 54 months, there was 100% local tumor control, and the mean visual acuity decreased from 20/32 pretreatment to 20/63 at final exam. Palladium-103 emits lower-energy photons than iodine-125, resulting in radiation that is more readily absorbed by the tumor and less absorbed by tissues in close proximity to the plaque.[134–136] Disadvantages of palladium-103 compared with iodine-125 include an increased scleral dose directly beneath the plaque (a disadvantage in treating tumors at or very near the fovea), a relatively short half-life (17 vs. 60 days), and less available information on the dosimetry of palladium-103.

Current research is focused on decreasing treatment morbidity through considerations of lowered radiation dose (alternative isotopes, lowered planned dose delivery,[137] enhanced localization with smaller treatment margins, eccentric placement of plaques to just cover the posterior margin of posterior tumors,[138] radiation shielding agents), combined treatment applications (supplemental laser, anti-VEGF, vitrectomy), and personalized medicine (utilizing tumor molecular genetic markers). Reduction of radiation dose to normal tissues is likely to improve visual outcomes, but it should not come at the expense of decreased local tumor control.

A novel approach to the reduction of radiation complications involves replacement of the vitreous by silicone oil, perfluorocarbons, and other vitreous substitutes in vitro to attenuate radiation, potentially minimizing the effects to the vital eye structures.[139,140] McCannel and McCannel[141] recently reported a 1 : 1 matched case–control series with 20 patients receiving treatment with vitrectomy and silicone oil with vitrectomy, matched with control patients who underwent brachytherapy alone. With an average follow-up time of 22 months, there was a nonsignificant trend toward improved visual acuity in the patients receiving silicone oil. In addition, there was statistically less macular thickness and less cataract surgery performed in patients receiving oil. Although perioperative complications were limited, further studies with longer follow-up will be required to determine if this treatment has a role in the management of specific patients with melanoma.

Management of Radiation-Related Complications

Treatment options for radiation complications to the retina and optic nerve have included anti-VEGF agents, corticosteroids, and laser photocoagulation.

Anti-VEGF

Vascular endothelial growth factor (VEGF) has been shown to be elevated in eyes with choroidal melanoma, with the highest levels being found in those treated with radiation.[142,143] VEGF is a potent vascular permeability factor that may contribute to macular edema and has been suggested to play a role in radiation maculopathy.[118] Additional cytokines may also factor into the retinal response to radiation toxicity. Anti-VEGF agents have generally been used as a treatment after vision damage from radiation maculopathy has begun. Macular edema and retinal neovascularization often decrease, but not all studies demonstrate improvements in visual acuity.[144–148] Shah and Houston et al.[149] reported a retrospective study of 159 patients with brachytherapy for melanoma who were evaluated at 2–4-month intervals after treatment and treated with bevacizumab at the first sign of macular edema on spectral domain OCT. Patients received a mean of five bevacizumab injections over 18 months. Fifty-one percent of patients retained 20/50 or better vision at a median follow-up of 3 years, significantly better than the results of the COMS study. In 2014, Shah and Shields et al.[150] reported a nonrandomized study of intravitreal bevacizumab injections given every 4 months for 2 years following brachytherapy, versus observation (292 in the injection arm and 126 in the control arm). Injections were initiated immediately following plaque removal, prior to the development of radiation retinopathy. Over a 2-year period, patients receiving bevacizumab, when compared to controls, demonstrated OCT-evident macular edema, clinically evident radiation retinopathy, moderate vision loss, and poor visual acuity less frequently. There was no statistically significant difference in clinically evident radiation papillopathy. These studies set the stage for a prospective study to address the

management of radiation maculopathy with anti-VEGF agents. There may also be a role for anti-VEGF therapy in the management of radiation optic neuropathy. Finger and Chin[147] reported on 14 patients with radiation optic neuropathy due to brachytherapy who were treated with intravitreal bevacizumab. They noted a reduction in optic disc edema and hemorrhage in all patients while visual acuity was stable or improved in 9 of 14 patients.

Corticosteroids

Horgan et al.[151] reported on the use of periocular triamcinolone in 108 patients at the time of plaque placement followed by repeat dosing at 4 and 8 months, finding that at 18 months there was a significant decrease in the risk of macular edema and the risk of moderate to severe vision loss was decreased from 48% to 31%. Side-effects included increased intraocular pressure as well as progression of cataracts. In a single center series of 31 patients, a single injection of intravitreal triamcinolone led to stable or improved vision in 91% of patients, but the effect was not long lasting.[152] Combining intravitreal triamcinolone with bevacizumab for the treatment of severe radiation retinopathy demonstrated overall stabilization of visual acuity, with improvement to 20/50 or better vision in 365 of patients.[153] Recently, Baillif et al.[154] reported on five patients with radiation macular edema following proton beam therapy for choroidal melanoma, treated with intravitreal dexamethasone 0.7-mg implant. There was a significant improvement in macular edema in 4 of 5 patients. Visual acuity improved for 3 patients (+4, +9, and +15 letters) and remained unchanged for 2 patients, with a beneficial effect that lasted for up to 5 months. There may also be a role for intravitreal corticosteroids and anti-VEGF agents in managing radiation optic neuropathy, Shields et al.[155] reported on 9 patients treated with intravitreal triamcinolone for radiation optic neuropathy. They noted rapid improvement in the optic disc edema and hyperemia, with modest improvement in visual acuity. Further studies with longer follow-up are needed to assess the effect of VEGF inhibitors, corticosteroids, or combination of the two on maculopathy and optic neuropathy, with focus on the early identification with OCT

and early treatment prior to significant visual decline.

Laser Photocoagulation

Laser photocoagulation has also been investigated in the treatment of radiation retinopathy. Focal laser therapy of 19 patients was shown to have an initial effect with improvement in vision and radiation-associated cystoid macular edema (CME) at 6 months; however, at 12 and 24 months, there was no significant difference between treated and untreated eyes.[156] In another study with a mean follow-up of 39 months, 12 patients treated with focal laser for radiation-associated CME resulted in 67% with improvement in visual acuity and 50% with resolution in CME.[157] With a mean follow-up of 109 months, 38 patients with CME were treated with focal laser therapy, revealing that although both treated and untreated groups had a decrease in visual acuity post-plaque treatment, those treated with laser showed a better final vision.[158]

In an alternative strategy using laser photocoagulation, Finger and Kurli treated 45 patients who developed radiation retinopathy following plaque brachytherapy with sector laser photocoagulation on the surface of the tumor and 2–3 mm of the margins.[159] With a mean follow-up of 48 months, approximately 65% had regression of radiation retinopathy and 47% had regression of maculopathy. However, almost 47% had loss of ≥3 lines of vision. Interestingly, when 16 tumors were treated prior to the development of radiation retinopathy or maculopathy, only three patients developed radiation complications, which regressed with additional laser. Of note, compared with the group that received treatment after development of retinopathy, no (0) patients treated with prophylactic laser lost >3 lines of vision. Laser photocoagulation may have a role in the treatment and prevention of radiation retinopathy, and this study emphasizes the importance of early identification and treatment of radiation complications. Larger studies with additional patients are needed to determine the efficacy of laser treatment for radiation retinopathy.

Adjuvant Therapy

To increase the number of neoplastic cells made nonviable within a choroidal melanoma during treatment and to reduce unwanted complications of radiation, some investigators have suggested the use of adjuvant therapies, including hyperthermia, chemotherapy, and antiangiogenic agents. Transpupillary thermotherapy (TTT) uses a diode laser and near-infrared irradiation to elevate the temperature within the tumor. TTT may induce tumor cell necrosis up to 3 mm in depth and has been investigated as primary treatment for small melanomas;[62] however, 22% had failure of local tumor control at 3 years, with evidence of extraocular extension in some cases.[160] As a result, TTT has been used more frequently as an adjuvant therapy. Authors propose that adjuvant TTT may allow the use of lower radiation doses in order to decrease the risk for radiation complications, treat larger melanomas, as well as treat juxtapapillary tumors with margins close to the optic nerve precluding adequate plaque coverage of these margins. Additionally, TTT may be used for tumors that fail local control. Shields et al.[161] reported on 270 patients with combined plaque brachytherapy and TTT, showing that failure of local control was estimated to be 2% and 3% at 2 and 5 years, respectively. TTT was applied at 4-month intervals in three sessions following treatment with plaque brachytherapy. Other authors have reported on the efficacy of combined treatment,[44,162,163] with a slight trend toward better visual acuity for those treated with adjuvant TTT.[44] Additionally, adjuvant TTT combined with plaque brachytherapy may be beneficial for juxtapapillary tumors as discussed above.[88]

Choroidal melanoma has been shown to have a unique spatial distribution of vasculature, with mature vessels found in the basal aspects of tumors and immature neovessels radiating apically and peripherally. Vessel maturation was also shown to be associated with histopathologic predictors of poor prognosis. However, with the rich vasculature of these tumors, treatment with antiangiogenic agents has been proposed.[164] Additionally, cell lines of choroidal melanoma have been shown to secrete VEGF,[165] while others have shown increased concentrations of VEGF in the vitreous of eyes with choroidal melanoma.[143] Missotten et al.[142] reported increased concentrations of VEGF in eyes with choroidal melanomas compared to controls, with significant correlations with increasing

tumor height and basal diameter. Interestingly, VEGF concentrations were found to be higher after treatment with plaque brachytherapy. As primary treatment for choroidal melanoma, a small case series reported that antiangiogenic agents when used alone were not effective at delaying tumor progression.[166] Adverse effects were mild, including hypertension, with no heart attacks, strokes, or deaths. Some investigators have proposed adjuvant treatment of choroidal melanoma with intravitreal bevacizumab combined with plaque brachytherapy. However, timing may prove to be an important factor for the efficacy of this treatment. Although treatment prior to plaque placement may result in tumor size reduction, this strategy may be associated with closure of tumor vasculature with resultant hypoxia of tumor cells. Hypoxic cells have been shown to be resistant to radiation therapy and chemotherapy. Other investigators have shown a reduction in tumor size and resolution of exudative retinal detachment when melanomas were treated with intravitreal bevacizumab upon plaque removal.[167,168] Further studies with more patients and longer follow-up are needed to determine the efficacy and safety of antiangiogenic inhibitors in the treatment of choroidal melanoma.

Conclusion

Radiation therapy, both plaque brachytherapy and proton beam irradiation, have been shown to have comparable results regarding local tumor control, survival/metastasis, and globe-salvage.[169–180] However, rates of radiation complications with resultant visual loss remain high regardless of treatment type. The COMS Medium Tumor Trial established the use of I-125 plaque brachytherapy as a primary globe-salvaging treatment for choroidal melanoma. Plaque brachytherapy and enucleation were shown to have similar rates of melanoma-specific deaths. In addition, small, large, and juxtapapillary tumors have been successfully treated with plaque brachytherapy. Intraoperative ultrasound provides valuable information regarding plaque placement. Ultrasound may allow for the repositioning of plaques that have tilted, shifted, or were inaccurately placed. Intraoperative ultrasound provides a valuable tool to aid in plaque placement and maximizes the likelihood of

local tumor control. Despite eye preservation, visual morbidity is high secondary to radiation-related complications, including radiation maculopathy and optic neuropathy. Alternative radioisotopes have been investigated to minimize treatment-related effects without significant reductions in visual loss. As a result, a better understanding of the mechanisms involved in radiation damage is needed, along with the development of treatment strategies for these visually devastating complications. Current studies provide hope that the early identification and treatment of radiation retinopathy may be helpful in maintaining useful vision.

References

1. Moore RF. Choroidal sarcoma treated by the intraocular insertion of radon seeds. *Br J Ophthalmol*. 1930;14:145–152.
2. Brady LW, Shields JA, Augsburger JJ, et al. Malignant intraocular tumors. *Cancer*. 1982;49:578–585.
3. Shields JA, Augsburger JJ, Brady LW, et al. Cobalt plaque therapy of posterior uveal melanomas. *Ophthalmology*. 1982;89:1201–1207.
4. Char DH, Lonn LI, Margolis LW. Complications of cobalt plaque therapy of choroidal melanomas. *Am J Ophthalmol*. 1977;84:536–541.
5. Stallard HB. Malignant melanoblastoma of the choroid. *Bibl Ophthalmol*. 1968;75:16–38.
6. Lommatzsch PK, Kirsch IH. 106Ru/106Rh plaque radiotherapy for malignant melanomas of the choroid: with follow-up results more than 5 years. *Doc Ophthalmol*. 1988;68:225–238.
7. Lommatzsch PK. Treatment of choroidal melanomas with 106Ru/106Rh beta-ray applicators. *Trans Ophthalmol Soc U K*. 1977;97:428–429.
8. Muller RP, Busse H, Potter R, et al. Results of high dose 106-ruthenium irradiation of choroidal melanomas. *Int J Radiat Oncol Biol Phys*. 1986;12:1749–1755.
9. Moura RA, McPherson AR, Easley J. Malignant melanoma of the choroid: treatment with episcleral 198Au plaque and xenon-arc photocoagulation. *Ann Ophthalmol*. 1985;17:114–

125.
10. Char DH, Castro JR, Quivey JM, et al. Uveal melanoma radiation. 125I brachytherapy versus helium ion irradiation. *Ophthalmology*. 1989;96:1708–1715.
11. Garretson BR, Robertson DM, Earle JD. Choroidal melanoma treatment with iodine 125 brachytherapy. *Arch Ophthalmol*. 1987;105:1394–1397.
12. Lean EK, Cohen DM, Liggett PE, et al. Episcleral radioactive plaque therapy: initial clinical experience with 56 patients. *Am J Clin Oncol*. 1990;13:185–190.
13. Packer S, Rotman M. Radiotherapy of choroidal melanoma with iodine-125. *Ophthalmology*. 1980;87:582–590.
14. Packer S, Rotman M, Salanitro P. Iodine-125 irradiation of choroidal melanoma: clinical experience. *Ophthalmology*. 1984;91:1700–1708.
15. Packer S, Stoller S, Lesser ML, et al. Long-term results of iodine 125 irradiation of uveal melanoma. *Ophthalmology*. 1992;99:767–773 [discussion 774].
16. Robertson DM, Earle J, Anderson JA. Preliminary observations regarding the use of iodine-125 in the management of choroidal melanoma. *Trans Ophthalmol Soc U K*. 1983;103:155–160.
17. Robertson DM, Fountain KS, Anderson JA, et al. Radioactive iodine-125 as a therapeutic radiation source for management of intraocular tumors. *Trans Am Ophthalmol Soc*. 1981;79:294–306.
18. Finger PT. Microwave plaque thermoradiotherapy for choroidal melanoma. *Br J Ophthalmol*. 1992;76:358–364.
19. Finger PT. Microwave thermoradiotherapy for uveal melanoma: results of a 10-year study. *Ophthalmology*. 1997;104:1794–1803.
20. Finger PT, Berson A, Ng T, et al. Palladium-103 plaque radiotherapy for choroidal melanoma: an 11-year study. *Int J Radiat Oncol Biol Phys*. 2002;54:1438–1445.
21. Diener-West M, Earle JD, Fine SL, et al. The COMS randomized trial of iodine 125 brachytherapy for choroidal melanoma, III: initial mortality findings. COMS report no. 18. *Arch Ophthalmol*. 2001;119:969–982.

22. The COMS randomized trial of iodine 125 brachytherapy for choroidal melanoma: V. Twelve-year mortality rates and prognostic factors. COMS report No. 28. *Arch Ophthalmol*. 2006;124:1684–1693.
23. Brown GC, Shields JA, Sanborn G, et al. Radiation retinopathy. *Ophthalmology*. 1982;89:1494–1501.
24. Brown GC, Shields JA, Sanborn G, et al. Radiation optic neuropathy. *Ophthalmology*. 1982;89:1489–1493.
25. Char DH, Kroll S, Quivey JM, et al. Long term visual outcome of radiated uveal melanomas in eyes eligible for randomisation to enucleation versus brachytherapy. *Br J Ophthalmol*. 1996;80:117–124.
26. Cruess AF, Augsburger JJ, Shields JA, et al. Visual results following cobalt plaque radiotherapy for posterior uveal melanomas. *Ophthalmology*. 1984;91:131–136.
27. Wen JC, McCannel TA. Treatment of radiation retinopathy following plaque brachytherapy for choroidal melanoma. *Curr Opin Ophthalmol*. 2009;20:200–204.
28. Melia M, Moy CS, Reynolds SM, et al. Quality of life after iodine 125 brachytherapy vs enucleation for choroidal melanoma: 5-year results from the Collaborative Ocular Melanoma Study: COMS QOLS report no. 3. *Arch Ophthalmol*. 2006;124:226–238.
29. Overgaard J, Overgaard M, Hansen PV, et al. Some factors of importance in the radiation treatment of malignant melanoma. *Radiother Oncol*. 1986;5:183–192.
30. Trott KR. The optimal radiation dose per fraction for the treatment of malignant melanomas. *Int J Radiat Oncol Biol Phys*. 1991;20:905–907.
31. Kindy-Degnan NA, Char DH, Castro JR, et al. Effect of various doses of radiation for uveal melanoma on regression, visual acuity, complications, and survival. *Am J Ophthalmol*. 1989;107:114–120.
32. National Institutes of Health. *Guide for grants and contracts. Protocol of the Collaborative Ocular Melanoma Study*. NIH: Bethesda; 1986:15.
33. Nath R, Anderson LL, Luxton G, et al. Dosimetry of interstitial brachytherapy sources: recommendations of the

AAPM Radiation Therapy Committee Task Group No. 43. American Association of Physicists in Medicine. *Med Phys*. 1995;22:209–234.
34. Nag S, Quivey JM, Earle JD, et al. The American Brachytherapy Society recommendations for brachytherapy of uveal melanomas. *Int J Radiat Oncol Biol Phys*. 2003;56:544–555.
35. Krintz AL, Hanson WF, Ibbott GS, et al. A reanalysis of the Collaborative Ocular Melanoma Study Medium Tumor Trial eye plaque dosimetry. *Int J Radiat Oncol Biol Phys*. 2003;56:889–898.
36. Glasgow JP, Perez CA. Physics of brachytherapy. Perez CA, Brady LW. *Principles and practice of radiation oncology*. Lippincott: Philadelphia; 1987.
37. Phillips TL, Char DH, McCormick B, et al. Eye tumors: brachytherapy experience. Nath R, Anderson LL, Luxton G, et al. *Interstitial brachytherapy: physical, biological, and clinical considerations*. Raven Press: New York; 1990.
38. Harbour JW, Meredith TA, Thompson PA, et al. Transpupillary thermotherapy versus plaque radiotherapy for suspected choroidal melanomas. *Ophthalmology*. 2003;110:2207–2214 [discussion 2215].
39. Davidorf FH, Makley TA, Lang JR. Radiotherapy of malignant melanoma of the choroid. *Trans Sect Ophthalmol Am Acad Ophthalmol Otolaryngol*. 1976;81:849–861.
40. Archer DB, Amoaku WM, Gardiner TA. Radiation retinopathy–clinical, histopathological, ultrastructural and experimental correlations. *Eye (Lond)*. 1991;5:239–251.
41. Amoaku WM, Archer DB. Fluorescein angiographic features, natural course and treatment of radiation retinopathy. *Eye (Lond)*. 1990;4:657–667.
42. Sealy R, le Roux PL, Rapley F, et al. The treatment of ophthalmic tumours with low-energy sources. *Br J Radiol*. 1976;49:551–554.
43. Earle J, Kline RW, Robertson DM. Selection of iodine 125 for the Collaborative Ocular Melanoma Study. *Arch Ophthalmol*. 1987;105:763–764.
44. Verschueren KM, Creutzberg CL, Schalij-Delfos NE, et al.

Long-term outcomes of eye-conserving treatment with ruthenium(106) brachytherapy for choroidal melanoma. *Radiother Oncol*. 2010;95:332–338.
45. Wilkinson DA, Kolar M, Fleming PA, et al. Dosimetric comparison of 106Ru and 125I plaques for treatment of shallow (< or = 5 mm) choroidal melanoma lesions. *Br J Radiol*. 2008;81:784–789.
46. Finger PT, Zhou D, Kalach N, et al. 103Pd versus 125I ophthalmic plaque brachytherapy: preoperative comparative radiation dosimetry for 319 uveal melanomas. *J Radiat Oncol*. 2014;3(4):409–416.
47. Rotman M, Long RS, Packer S, et al. Radiation therapy of choroidal melanoma. *Trans Ophthalmol Soc U K*. 1977;97:431–435.
48. Finger PT. Finger's "slotted" eye plaque for radiation therapy: treatment of juxtapapillary and circumpapillary intraocular tumours. *Br J Ophthalmol*. 2007;91:891–894.
49. Chiu-Tsao ST, O'Brien K, Sanna R, et al. Monte Carlo dosimetry for 125I and 60Co in eye plaque therapy. *Med Phys*. 1986;13:678–682.
50. Berry JL, Dandapani SV, Stevanovic M, et al. Outcomes of choroidal melanomas treated with eye physics: a 20-year review. *JAMA Ophthalmol*. 2013;131(11):1435–1442.
51. Robertson DM. A rationale for comparing radiation to enucleation in the management of choroidal melanoma. *Am J Ophthalmol*. 1989;108:448–451.
52. Finger PT, Chin KJ, Duvall G. Palladium-103 ophthalmic plaque radiation therapy for choroidal melanoma: 400 treated patients. *Ophthalmology*. 2009;116:790–796 [796.e1].
53. Papageorgiou KI, Cohen VM, Bunce C, et al. Predicting local control of choroidal melanomas following (106)Ru plaque brachytherapy. *Br J Ophthalmol*. 2011;95:166–170.
54. Shields CL, Furuta M, Thangappan A, et al. Metastasis of uveal melanoma millimeter-by-millimeter in 8033 consecutive eyes. *Arch Ophthalmol*. 2009;127:989–998.
55. Curtin VT. Natural course of small malignant melanomas of choroid and ciliary body. *Trans Ophthalmol Soc N Z*. 1978;30:61.

56. Packard RB. In malignant choroidal melanoma will a delay in radical treatment influence prognosis? *Trans Ophthalmol Soc U K*. 1983;103:49–53.
57. Augsburger JJ. Is observation really appropriate for small choroidal melanomas. *Trans Am Ophthalmol Soc*. 1993;91:147–168 [discussion 169–175].
58. Factors predictive of growth and treatment of small choroidal melanoma: COMS report no. 5. The Collaborative Ocular Melanoma Study Group. *Arch Ophthalmol*. 1997;115:1537–1544.
59. Mortality in patients with small choroidal melanoma. COMS report no. 4. The Collaborative Ocular Melanoma Study Group. *Arch Ophthalmol*. 1997;115:886–893.
60. Shields CL, Furuta M, Berman EL, et al. Choroidal nevus transformation into melanoma: analysis of 2514 consecutive cases. *Arch Ophthalmol*. 2009;127:981–987.
61. Sobrin L, Schiffman JC, Markoe AM, et al. Outcomes of iodine 125 plaque radiotherapy after initial observation of suspected small choroidal melanomas: a pilot study. *Ophthalmology*. 2005;112:1777–1783.
62. Shields CL, Shields JA, Perez N, et al. Primary transpupillary thermotherapy for small choroidal melanoma in 256 consecutive cases: outcomes and limitations. *Ophthalmology*. 2002;109:225–234.
63. De Potter P, Jamart J. Adjuvant indocyanine green in transpupillary thermotherapy for choroidal melanoma. *Ophthalmology*. 2003;110:406–413 [discussion 413–404].
64. Cajigal-Morales C, Valverde-Almohalla S, Encinas-Martin JL. [Transpupillary thermotherapy in the primary management of choroidal melanoma]. *Arch Soc Esp Oftalmol*. 2005;80:171–178.
65. Langmann G, Lechner H, Wenzel E, et al. Transpupillary thermotherapy (TTT) for uveal melanomas. Long term results of a single TTT with an adapter for a conventional infrared laser. *Ophthalmologe*. 2005;102:1162–1167.
66. Spire M, Devouassoux MS, Kodjikian L, et al. Primary transpupillary thermotherapy for 18 small posterior pole uveal melanomas. *Am J Ophthalmol*. 2006;141:840–849.

67. Stoffelns BM. [Tumor regression and visual outcome after transpupillary thermotherapy (TTT) for malignant choroidal melanoma]. *Klin Monbl Augenheilkd*. 2006;223:74–80.
68. Win PH, Robertson DM, Buettner H, et al. Extended follow-up of small melanocytic choroidal tumors treated with transpupillary thermotherapy. *Arch Ophthalmol*. 2006;124:503–506.
69. Pan Y, Diddie K, Lim JI. Primary transpupillary thermotherapy for small choroidal melanomas. *Br J Ophthalmol*. 2008;92:747–750.
70. Singh AD, Kivela T, Seregard S, et al. Primary transpupillary thermotherapy of "small" choroidal melanoma: is it safe? *Br J Ophthalmol*. 2008;92:727–728.
71. Jampol LM, Moy CS, Murray TG, et al. The COMS randomized trial of iodine 125 brachytherapy for choroidal melanoma: IV. Local treatment failure and enucleation in the first 5 years after brachytherapy. COMS report no. 19. *Ophthalmology*. 2002;109:2197–2206.
72. Gragoudas E. *Proton beam therapy: proton therapy for uveal melanoma – 20 years experience*. American Academy of Ophthalmology: New Orleans; 2001.
73. Char DH, Quivey JM, Castro JR, et al. Helium ions versus iodine 125 brachytherapy in the management of uveal melanoma: a prospective, randomized, dynamically balanced trial. *Ophthalmology*. 1993;100:1547–1554.
74. American Brachytherapy Society – Ophthalmic Oncology Task Force. The American Brachytherapy Society consensus guidelines for plaque brachytherapy of uveal melanoma and retinoblastoma. *Brachytherapy*. 2014;13(1):1–14 [American Brachytherapy Society].
75. Hawkins BS. The Collaborative Ocular Melanoma Study (COMS) randomized trial of pre-enucleation radiation of large choroidal melanoma: IV. Ten-year mortality findings and prognostic factors. COMS report number 24. *Am J Ophthalmol*. 2004;138:936–951.
76. Wilson MW, Alejandro KC, Cantrell JE, 125-I episcleral plaque brachytherapy in the management of large

malignant melanomas of the ciliary body and/or choroid: scientific poster 76, 2002. Joint Meeting American Academy of Ophthalmology and Pan-American Association of Ophthalmology, Orlando, Florida, 2002.
77. Puusaari I, Heikkonen J, Summanen P, et al. Iodine brachytherapy as an alternative to enucleation for large uveal melanomas. *Ophthalmology*. 2003;110:2223–2234.
78. Shields CL, Naseripour M, Cater J, et al. Plaque radiotherapy for large posterior uveal melanomas (>or =8-mm thick) in 354 consecutive patients. *Ophthalmology*. 2002;109:1838–1849.
79. Semenova E, Finger PT. Palladium-103 plaque radiation therapy for American Joint Committee on cancer T3- and T4-staged choroidal melanomas. *JAMA Ophthalmol*. 2014;132(2):205–213.
80. Kaiserman N, Kaiserman I, Hendler K, et al. Ruthenium-106 plaque brachytherapy for thick posterior uveal melanomas. *Br J Ophthalmol*. 2009;93:1167–1171.
81. Bergman L, Nilsson B, Lundell G, et al. Ruthenium brachytherapy for uveal melanoma, 1979–2003: survival and functional outcomes in the Swedish population. *Ophthalmology*. 2005;112:834–840.
82. Kreusel KM, Bechrakis N, Riese J, et al. Combined brachytherapy and transpupillary thermotherapy for large choroidal melanoma: tumor regression and early complications. *Graefes Arch Clin Exp Ophthalmol*. 2006;244:1575–1580.
83. Sagoo MS, Shields CL, Mashayekhi A, et al. Plaque radiotherapy for choroidal melanoma encircling the optic disc (circumpapillary choroidal melanoma). *Arch Ophthalmol*. 2007;125:1202–1209.
84. De Potter P, Shields CL, Shields JA, et al. Impact of enucleation versus plaque radiotherapy in the management of juxtapapillary choroidal melanoma on patient survival. *Br J Ophthalmol*. 1994;78:109–114.
85. Hui JI, Murray TG. Radioactive plaque therapy. *Int Ophthalmol Clin*. 2006;46:51–68.
86. Sagoo MS, Shields CL, Emrich J, et al. Plaque radiotherapy

for juxtapapillary choroidal melanoma: treatment complications and visual outcomes in 650 consecutive cases. *JAMA Ophthalmol*. 2014;132(6):697–702.
87. Finger PT, Chin KJ, Tena LB. A five-year study of slotted eye plaque radiation therapy for choroidal melanoma: near, touching, or surrounding the optic nerve. *Ophthalmology*. 2012;119(2):415–422.
88. Sagoo MS, Shields CL, Mashayekhi A, et al. Plaque radiotherapy for juxtapapillary choroidal melanoma: tumor control in 650 consecutive cases. *Ophthalmology*. 2011;118:402–407.
89. Lane AM, Kim IK, Gragoudas ES. Proton irradiation for peripapillary and parapapillary melanomas. *Arch Ophthalmol*. 2011;129:1127–1130.
90. Houston SK 3rd, Markoe AM, Boldt HC, et al. Juxtapapillary uveal melanomas: patient outcomes after treatment with proton irradiation for peripapillary and parapapillary melanomas. *Arch Ophthalmol*. 2011;129:1218–1220.
91. Pe'er J, Sancho C, Cantu J, et al. Measurement of choroidal melanoma basal diameter by wide-angle digital fundus camera: a comparison with ultrasound measurement. *Ophthalmologica*. 2006;220:194–197.
92. Kim Y, Hwang TS, Choi D, et al. Comparison of digital fundus photographic and echographic measurements for maximal linear dimension from eyes with choroidal melanoma. *Retina*. 2009;29:1321–1327.
93. Hilton GF. Measuring grid for indirect ophthalmoscopy. *Trans Am Acad Ophthalmol Otolaryngol*. 1972;76:530–531.
94. Pach JM, Robertson DM, Taney BS, et al. Prognostic factors in choroidal and ciliary body melanomas with extrascleral extension. *Am J Ophthalmol*. 1986;101:325–331.
95. Martin JA, Robertson DM. Extrascleral extension of choroidal melanoma diagnosed by ultrasound. *Ophthalmology*. 1983;90:1554–1559.
96. Harbour JW, Murray TG, Byrne SF, et al. Intraoperative echographic localization of iodine 125 episcleral radioactive plaques for posterior uveal melanoma. *Retina*. 1996;16:129–134.

97. Pavlin CJ, Japp B, Simpson ER, et al. Ultrasound determination of the relationship of radioactive plaques to the base of choroidal melanomas. *Ophthalmology*. 1989;96:538–542.
98. Williams DF, Mieler WF, Lewandowski M, et al. Echographic verification of radioactive plaque position in the treatment of melanomas. *Arch Ophthalmol*. 1988;106:1623–1624.
99. Almony A, Breit S, Zhao H, et al. Tilting of radioactive plaques after initial accurate placement for treatment of uveal melanoma. *Arch Ophthalmol*. 2008;126:65–70.
100. Shah NV, Houston SK, Murray TG, et al. Evaluation of surgical learning curve for I-125 episcleral plaque placement for the treatment of posterior uveal melanoma: a two decade review. *Clin Ophthalmol*. 2012;6:447–452.
101. Garcia JP Jr, Garcia PT, Rosen RB, et al. A 3-dimensional ultrasound C-scan imaging technique for optic nerve measurements. *Ophthalmology*. 2004;111(6):1238–1243.
102. Robertson DM, Fuller DG, Anderson RE. A technique for accurate placement of episcleral iodine-125 plaques. *Am J Ophthalmol*. 1987;103:63–65.
103. Bianciotto C, Shields CL, Guzman JM, et al. Assessment of anterior segment tumors with ultrasound biomicroscopy versus anterior segment optical coherence tomography in 200 cases. *Ophthalmology*. 2011;118:1297–1302.
104. Char DH. Management of orbital tumors. *Mayo Clin Proc*. 1993;68:1081–1096.
105. Karlsson UL, Augsburger JJ, Shields JA, et al. Recurrence of posterior uveal melanoma after 60Co episcleral plaque therapy. *Ophthalmology*. 1989;96:382–388.
106. De Potter P, Shields CL, Shields JA, et al. Plaque radiotherapy for juxtapapillary choroidal melanoma: visual acuity and survival outcome. *Arch Ophthalmol*. 1996;114:1357–1365.
107. Quivey JM, Augsburger J, Snelling L, et al. 125I plaque therapy for uveal melanoma: analysis of the impact of time and dose factors on local control. *Cancer*. 1996;77:2356–2362.
108. Quivey JM, Char DH, Phillips TL, et al. High intensity 125-

iodine (125I) plaque treatment of uveal melanoma. *Int J Radiat Oncol Biol Phys*. 1993;26:613–618.
109. Classic KL, Furutani KM, Stafford SL, et al. Radiation dose to the surgeon during plaque brachytherapy. *Retina*. 2012;32(9):1900–1905.
110. Robertson DM. Choroidal melanomas with a collar-button configuration: response pattern after iodine 125 brachytherapy. *Arch Ophthalmol*. 1999;117:771–775.
111. Bosworth JL, Packer S, Rotman M, et al. Choroidal melanoma: I-125 plaque therapy. *Radiology*. 1988;169:249–251.
112. Beitler JJ, McCormick B, Ellsworth RM, et al. Ocular melanoma: total dose and dose rate effects with Co-60 plaque therapy. *Radiology*. 1990;176:275–278.
113. Vrabec TR, Augsburger JJ, Gamel JW, et al. Impact of local tumor relapse on patient survival after cobalt 60 plaque radiotherapy. *Ophthalmology*. 1991;98:984–988.
114. Tabandeh H, Chaudhry NA, Murray TG, et al. Intraoperative echographic localization of iodine-125 episcleral plaque for brachytherapy of choroidal melanoma. *Am J Ophthalmol*. 2000;129:199–204.
115. Wilson MW, Hungerford JL. Comparison of episcleral plaque and proton beam radiation therapy for the treatment of choroidal melanoma. *Ophthalmology*. 1999;106:1579–1587.
116. Fontanesi J, Meyer D, Xu S, et al. Treatment of choroidal melanoma with I-125 plaque. *Int J Radiat Oncol Biol Phys*. 1993;26:619–623.
117. Harbour JW, Char DH, Kroll S, et al. Metastatic risk for distinct patterns of postirradiation local recurrence of posterior uveal melanoma. *Ophthalmology*. 1997;104:1785–1792 [discussion 1792–1783].
118. Horgan N, Shields CL, Mashayekhi A, et al. Early macular morphological changes following plaque radiotherapy for uveal melanoma. *Retina*. 2008;28:263–273.
119. Krohn J, Monge OR, Skorpen TN, et al. Posterior uveal melanoma treated with I-125 brachytherapy or primary enucleation. *Eye (Lond)*. 2008;22:1398–1403.
120. Stack R, Elder M, Abdelaal A, et al. New Zealand

experience of I125 brachytherapy for choroidal melanoma. *Clin Experiment Ophthalmol*. 2005;33:490–494.
121. Jensen AW, Petersen IA, Kline RW, et al. Radiation complications and tumor control after 125I plaque brachytherapy for ocular melanoma. *Int J Radiat Oncol Biol Phys*. 2005;63:101–108.
122. Lumbroso-Le Rouic L, Charif Chefchaouni M, Levy C, et al. 125I plaque brachytherapy for anterior uveal melanomas. *Eye (Lond)*. 2004;18:911–916.
123. Puusaari I, Heikkonen J, Kivela T. Ocular complications after iodine brachytherapy for large uveal melanomas. *Ophthalmology*. 2004;111:1768–1777.
124. Mameghan H, Karolis C, Fisher R, et al. Iodine-125 irradiation of choroidal melanoma: clinical experience from the Prince of Wales and Sydney Eye Hospitals. *Australas Radiol*. 1992;36:249–252.
125. Boldt HC, Melia BM, Liu JC, et al. I-125 brachytherapy for choroidal melanoma photographic and angiographic abnormalities: the Collaborative Ocular Melanoma Study. COMS report no. 30. *Ophthalmology*. 2009;116:106–115.e1.
126. Linstadt D, Castro J, Char D, et al. Long-term results of helium ion irradiation of uveal melanoma. *Int J Radiat Oncol Biol Phys*. 1990;19:613–618.
127. Gragoudas ES, Seddon JM, Egan K, et al. Long-term results of proton beam irradiated uveal melanomas. *Ophthalmology*. 1987;94:349–353.
128. Jones R, Gore E, Mieler W, et al. Posttreatment visual acuity in patients treated with episcleral plaque therapy for choroidal melanomas: dose and dose rate effects. *Int J Radiat Oncol Biol Phys*. 2002;52:989–995.
129. Murray TG, Markoe AM, Gold AS, et al. Long-term followup comparing two treatment dosing strategies of (125) I plaque radiotherapy in the management of small/medium posterior uveal melanoma. *J Ophthalmol*. 2013;2013:517032.
130. Lommatzsch P. Treatment of choroidal melanomas with 106Ru/106Rh beta-ray applicators. *Surv Ophthalmol*. 1974;19:85–100.

131. Lommatzsch PK. Results after beta-irradiation (106Ru/106Rh) of choroidal melanomas: 20 years' experience. *Br J Ophthalmol*. 1986;70:844–851.
132. Finger PT, Chin KJ, Yu GP. Risk factors for radiation maculopathy after ophthalmic plaque radiation for choroidal melanoma. *Am J Ophthalmol*. 2010;149:608–615.
133. Semenova E, Finger PT. Palladium-103 radiation therapy for small choroidal melanoma. *Ophthalmology*. 2013;120(11):2353–2357.
134. Finger PT, Moshfeghi DM, Ho TK. Palladium 103 ophthalmic plaque radiotherapy. *Arch Ophthalmol*. 1991;109:1610–1613.
135. Finger PT, Lu D, Buffa A, et al. Palladium-103 versus iodine-125 for ophthalmic plaque radiotherapy. *Int J Radiat Oncol Biol Phys*. 1993;27:849–854.
136. Chiu-Tsao ST, Anderson LL. Thermoluminescent dosimetry for 103Pd seeds (model 200) in solid water phantom. *Med Phys*. 1991;18:449–452.
137. Puusaari I, Heikkonen J, Kivelä T. Effect of radiation dose on ocular complications after iodine brachytherapy for large uveal melanoma: empirical data and simulation of collimating plaques. *Invest Ophthalmol Vis Sci*. 2004;45(10):3425–3434.
138. Russo A, Laguardia M, Damato B. Eccentric ruthenium plaque radiotherapy of posterior choroidal melanoma. *Graefes Arch Clin Exp Ophthalmol*. 2012;250(10):1533–1540.
139. Oliver SC, Leu MY, DeMarco JJ, et al. Attenuation of iodine 125 radiation with vitreous substitutes in the treatment of uveal melanoma. *Arch Ophthalmol*. 2010;128:888–893.
140. Ahuja Y, Kapoor KG, Thomson RM, et al. The effects of intraocular silicone oil placement prior to iodine 125 brachytherapy for uveal melanoma: a clinical case series. *Eye (Lond)*. 2012;26(11):1487–1489.
141. McCannel TA, McCannel CA. Iodine 125 brachytherapy with vitrectomy and silicone oil in the treatment of uveal melanoma: 1-to-1 matched case-control series. *Int J Radiat Oncol Biol Phys*. 2014;89(2):347–352.
142. Missotten GS, Notting IC, Schlingemann RO, et al. Vascular

endothelial growth factor a in eyes with uveal melanoma. *Arch Ophthalmol*. 2006;124:1428–1434.
143. Boyd SR, Tan D, Bunce C, et al. Vascular endothelial growth factor is elevated in ocular fluids of eyes harbouring uveal melanoma: identification of a potential therapeutic window. *Br J Ophthalmol*. 2002;86:448–452.
144. Mason JO 3rd, Albert MA Jr, et al. Intravitreal bevacizumab treatment for radiation macular edema after plaque radiotherapy for choroidal melanoma. *Retina*. 2007;27:903–907.
145. Finger PT, Chin K. Anti-vascular endothelial growth factor bevacizumab (Avastin) for radiation retinopathy. *Arch Ophthalmol*. 2007;125:751–756.
146. Gupta A, Muecke JS. Treatment of radiation maculopathy with intravitreal injection of bevacizumab (Avastin). *Retina*. 2008;28:964–968.
147. Finger PT. Radiation retinopathy is treatable with anti-vascular endothelial growth factor bevacizumab (Avastin). *Int J Radiat Oncol Biol Phys*. 2008;70:974–977.
148. Finger PT, Chin KJ. Intravitreous ranibizumab (Lucentis) for radiation maculopathy. *Arch Ophthalmol*. 2010;128:249–252.
149. Shah NV, Houston SK, Markoe A, et al. Combination therapy with triamcinolone acetonide and bevacizumab for the treatment of severe radiation maculopathy in patients with posterior uveal melanoma. *Clin Ophthalmol*. 2013;7:1877–1882.
150. Shah SU, Shields CL, Bianciotto CG, et al. Intravitreal bevacizumab at 4-month intervals for prevention of macular edema after plaque radiotherapy of uveal melanoma. *Ophthalmology*. 2014;121(1):269–275.
151. Horgan N, Shields CL, Mashayekhi A, et al. Periocular triamcinolone for prevention of macular edema after plaque radiotherapy of uveal melanoma: a randomized controlled trial. *Ophthalmology*. 2009;116:1383–1390.
152. Shields CL, Demirci H, Dai V, et al. Intravitreal triamcinolone acetonide for radiation maculopathy after plaque radiotherapy for choroidal melanoma. *Retina*. 2005;25(7):868–874.

153. Guo X, Song J, Yu Y, et al. Can recombinant human glutathione peroxidase 1 with high activity be efficiently produced in Escherichia coli? *Antioxid Redox Signal*. 2014;20(9):1524–1530.
154. Baillif S, Maschi C, Gastaud P, et al. Intravitreal dexamethasone 0.7-mg implant for radiation macular edema after proton beam therapy for choroidal melanoma. *Retina*. 2013;33(9):1784–1790.
155. Shields CL, Demirci H, Marr BP, et al. Intravitreal triamcinolone acetonide for acute radiation papillopathy. *Retina*. 2006;26(5):537–544.
156. Hykin PG, Shields CL, Shields JA, et al. The efficacy of focal laser therapy in radiation-induced macular edema. *Ophthalmology*. 1998;105:1425–1429.
157. Kinyoun JL, Zamber RW, Lawrence BS, et al. Photocoagulation treatment for clinically significant radiation macular oedema. *Br J Ophthalmol*. 1995;79:144–149.
158. Kinyoun JL. Long-term visual acuity results of treated and untreated radiation retinopathy (an AOS thesis). *Trans Am Ophthalmol Soc*. 2008;106:325–335.
159. Finger PT, Kurli M. Laser photocoagulation for radiation retinopathy after ophthalmic plaque radiation therapy. *Br J Ophthalmol*. 2005;89:730–738.
160. Singh AD, Eagle RC Jr, Shields CL, et al. Clinicopathologic reports, case reports, and small case series: enucleation following transpupillary thermotherapy of choroidal melanoma: clinicopathologic correlations. *Arch Ophthalmol*. 2003;121:397–400.
161. Shields CL, Cater J, Shields JA, et al. Combined plaque radiotherapy and transpupillary thermotherapy for choroidal melanoma: tumor control and treatment complications in 270 consecutive patients. *Arch Ophthalmol*. 2002;120:933–940.
162. Bartlema YM, Oosterhuis JA, Journee-De Korver JG, et al. Combined plaque radiotherapy and transpupillary thermotherapy in choroidal melanoma: 5 years' experience. *Br J Ophthalmol*. 2003;87:1370–1373.
163. Damato B, Patel I, Campbell IR, et al. Local tumor control

after 106Ru brachytherapy of choroidal melanoma. *Int J Radiat Oncol Biol Phys*. 2005;63:385–391.
164. Pina Y, Cebulla CM, Murray TG, et al. Blood vessel maturation in human uveal melanoma: spatial distribution of neovessels and mature vasculature. *Ophthalmic Res*. 2009;41:160–169.
165. Ijland SA, Jager MJ, Heijdra BM, et al. Expression of angiogenic and immunosuppressive factors by uveal melanoma cell lines. *Melanoma Res*. 1999;9:445–450.
166. Lima BR, Schoenfield LR, Singh AD. The impact of intravitreal bevacizumab therapy on choroidal melanoma. *Am J Ophthalmol*. 2011;151(2):323–328.e2.
167. Newman H, Finger PT, Chin KJ, et al. Systemic bevacizumab (Avastin) for exudative retinal detachment secondary to choroidal melanoma. *Eur J Ophthalmol*. 2011;21:796–801.
168. Houston SK, Shah NV, Decatur C, et al. Intravitreal bevacizumab combined with plaque brachytherapy reduces melanoma tumor volume and enhances resolution of exudative detachment. *Clin Ophthalmol*. 2013;7:193–198.
169. Castro JR, Char DH, Petti PL, et al. 15 years experience with helium ion radiotherapy for uveal melanoma. *Int J Radiat Oncol Biol Phys*. 1997;39:989–996.
170. Gragoudas ES, Lane AM, Munzenrider J, et al. Long-term risk of local failure after proton therapy for choroidal/ciliary body melanoma. *Trans Am Ophthalmol Soc*. 2002;100:43–48 [discussion 48–49].
171. Gragoudas ES. Proton beam irradiation of uveal melanomas: the first 30 years. The Weisenfeld Lecture. *Invest Ophthalmol Vis Sci*. 2006;47:4666–4673.
172. Egger E, Zografos L, Schalenbourg A, et al. Eye retention after proton beam radiotherapy for uveal melanoma. *Int J Radiat Oncol Biol Phys*. 2003;55:867–880.
173. Egger E, Schalenbourg A, Zografos L, et al. Maximizing local tumor control and survival after proton beam radiotherapy of uveal melanoma. *Int J Radiat Oncol Biol Phys*. 2001;51:138–147.
174. Kodjikian L, Roy P, Rouberol F, et al. Survival after proton-

beam irradiation of uveal melanomas. *Am J Ophthalmol*. 2004;137:1002–1010.
175. Damato B, Lecuona K. Conservation of eyes with choroidal melanoma by a multimodality approach to treatment: an audit of 1632 patients. *Ophthalmology*. 2004;111:977–983.
176. Damato B, Kacperek A, Chopra M, et al. Proton beam radiotherapy of choroidal melanoma: the Liverpool-Clatterbridge experience. *Int J Radiat Oncol Biol Phys*. 2005;62:1405–1411.
177. Dendale R, Lumbroso-Le Rouic L, Noel G, et al. Proton beam radiotherapy for uveal melanoma: results of Curie Institut–Orsay proton therapy center (ICPO). *Int J Radiat Oncol Biol Phys*. 2006;65:780–787.
178. Fuss M, Loredo LN, Blacharski PA, et al. Proton radiation therapy for medium and large choroidal melanoma: preservation of the eye and its functionality. *Int J Radiat Oncol Biol Phys*. 2001;49:1053–1059.
179. Hocht S, Bechrakis NE, Nausner M, et al. Proton therapy of uveal melanomas in Berlin. 5 years of experience at the Hahn-–Meitner Institute. *Strahlenther Onkol*. 2004;180:419–424.
180. Caujolle JP, Mammar H, Chamorey E, et al. Proton beam radiotherapy for uveal melanomas at nice teaching hospital: 16 years' experience. *Int J Radiat Oncol Biol Phys*. 2010;78:98–103.

150

Charged-Particle Irradiation of Uveal Melanoma

Evangelos S. Gragoudas, Anne Marie Lane, Ivana K. Kim

Introduction

Radiotherapy is currently the most widely used method for treating intraocular melanomas, having replaced enucleation as the standard of care for most tumors. It offers the advantage of eye salvage and retention of vision in many cases, although a survival advantage has not been demonstrated.[1]

There are two major radiotherapeutic techniques for the treatment of uveal melanomas: radioactive plaques[2,3] sutured on the sclera over the area of the tumor, and external beam irradiation including use of charged particles, such as protons,[4] and helium ions,[5] and stereotactic photon radiotherapy.[6,7] The advantages of charged-particle irradiation are based on the physical characteristics of particles, which make possible highly localized dose distributions[8–10] and provide highly attractive depth-dose distribution patterns.[11] Although effective, helium ion irradiation[5] is no longer in use due to its high cost. Local control was observed in 93% of patients at 10 years after treatment[6] in a large series of patients (n=212) treated with stereotactic radiotherapy, but radiation retinopathy developed in approximately two-thirds of patients by 5 years after treatment.[7] In a recent study comparing proton therapy to stereotactic radiosurgery,[12] similar rates of local control were observed, but the group who received proton therapy experienced better visual outcomes than those who received stereotactic therapy.

Protons are positive, singly charged particles that have minimal scatter and a well-defined, finite, and energy-dependent tissue range. Proton beams can be collimated to deliver maximum density of ionization in a sharply focused, localized volume because of the inherent Bragg peak at the end of the beam path. The Bragg peak

can be broadened to cover a tumor at any depth (Fig. 150.1). The uniform dose of radiation delivered to the whole tumor and the sharp reduction of the dose outside the treated area allow tumors located near critical structures to be treated with the possibility of retaining visual acuity. Larger tumors can be treated because the overall irradiated volume is reduced. These properties should improve the therapeutic ratio of local control versus complications.

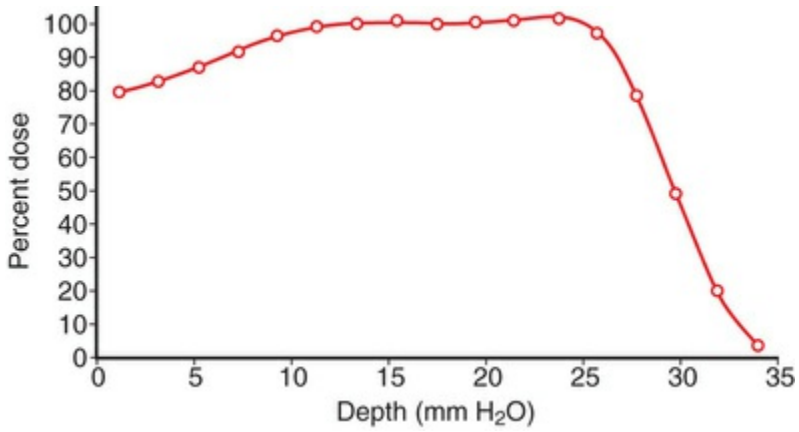

FIG. 150.1 Depth–dose curve measured with diode in water phantom. In this example, proton energy is modulated to provide a relatively uniform dose over a distance of 5 mm, from a depth of 18–23 mm.

Early experimental work in monkey eyes, followed by clinical and histopathologic studies in humans, provide evidence of the advantageous properties of protons. The Bragg peak of small-diameter collimated beams positioned on the fundus by stereotactic radiography produced lesions confined to the intended radiation field.[13] Normal retinal architecture as close as 1 mm from the edge of radiation-induced lesions was seen in irradiated monkey eyes more than 3.5 years after proton treatment.[14] Similar data on humans substantiate the favorable effects obtained with protons. Using mathematical superimposition of fundus photographs, computer treatment plans, and visual fields, correlation between patterns of visual loss and radiation isodose calculations was established.[15,16] Histologic examination of irradiated tumors revealed vessel thrombosis exclusively in retina overlying the tumor[17] and reduced or absent choroidal vasculature and RPE beneath and above the tumor but intact tissue adjacent to it.[18]

Tens of thousands of patients with uveal melanomas have been treated with proton radiation worldwide. In the United States, several proton centers have opened, making proton irradiation a viable treatment option for more patients with uveal melanomas.

Treatment

Patient Selection

Patients with uveal melanomas up to 28 mm in diameter and 14 mm in height may be treated with charged-particle irradiation. In general, patients with larger tumors located at the peripheral fundus can be treated and maintain visual potential because the beam can enter the eye directly in the area of the tumor and does not need to traverse as many noninvolved ocular structures. Our experience indicates that the eye can tolerate irradiation of up to 30% of its volume with the doses currently used. Tumors with small extrascleral extensions and tumors involving the macula, the optic disc, or both can be irradiated.

Operative Technique

The conjunctiva is incised, and the tumor is localized by transillumination, indirect ophthalmoscopy, or both. The episcleral tissues over the area of the tumor are examined carefully for evidence of extrascleral extension. The edges of the tumor are marked with a surgical marking pen, and four tantalum rings, 2.5 mm in diameter, are sutured to the sclera at the margins of the tumor. Ring-to-limbus distances and distances between the rings are measured. Highly elevated tumors can cast a variable shadow during transillumination, depending on the angle of illumination, which may result in an overestimate of the dimensions of the tumor. Therefore, the angle of illumination in the most precise shadow must be carefully chosen. For tumors that extend into the ciliary body and iris, rings are placed at the posterior margin of the tumor and accurate measurements are made of the distance from the rings to the anterior margin of the lesion. If tumors are in contact with the optic nerve, rings are placed only at the anterior

and lateral margins of the lesion, and the distance from the rings to the posterior margin is estimated from fundus photographs. The tumor is transilluminated again after suturing of the rings (Fig. 150.2), the distances from the rings to the edges of the tumor are measured, and careful drawings of the tumor margins in relation to the rings are made. No operation is necessary for lesions confined to the ciliary body. The margins of the tumor in relation to anatomic landmarks of the iris and conjunctiva are defined by transillumination on the ocular surface.

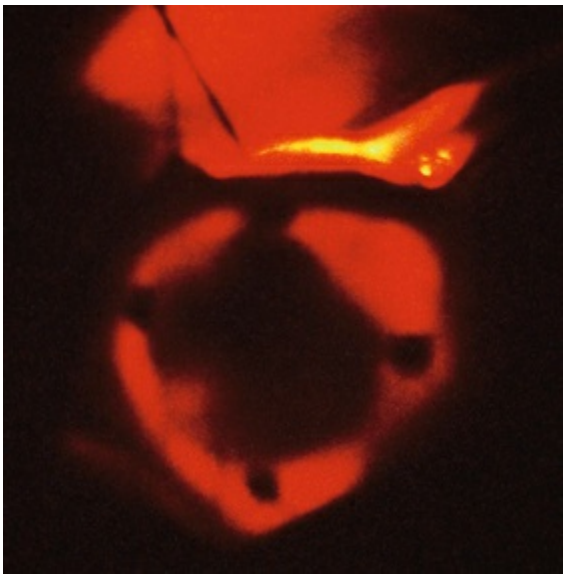

FIG. 150.2 Tantalum rings sutured to the sclera at the edges of the tumor, seen by transillumination.

Treatment Planning

An interactive three-dimensional treatment planning computer program (EYEPLAN, Martin Sheen, Clatterbridge Centre for Oncology, Bebington, UK) facilitates the selection of the appropriate fixation angle, which is chosen to minimize irradiation of the lens, optic disc, and fovea.[19] Such a program helps to select the best direction of gaze relative to the proton beam line; design the shape of the field-defining aperture; determine the proton range modulation necessary to encompass the target volume; determine the extent to which important structures are included within (or excluded from) the beam; and indicate the relative positions of the

tumor-defining rings, beam aperture, and crosshairs that should be observed in the alignment film when the patient is correctly aligned. The treatment planning program creates a spherical model of a globe that is scaled to the ultrasonically determined length of the patient's eye and the position of the tantalum rings previously sutured to the sclera, determined by orthogonal radiographs taken of the patient in the treatment position (gazing in three different directions). The structures of the eye are added to the model, including the anterior chamber depth and thickness of the lens obtained ultrasonographically. The program then superimposes on this globe a three-dimensional model of the tumor based on fundus pictures and ultrasonograms. The fundus photographs are especially useful for very posterior tumors and tumors abutting the optic nerve where it is impossible to surround the tumor with marker rings. Two tumors can be created if needed, e.g., if there is a tumor with an irregular shape. Tumors in the iris or ciliary body, for which placement of marker rings is unnecessary, are drawn from clinical and ultrasound information.

The computer program permits the user to view the eye in any direction it rotates, while the eye follows a user-controlled fixation point. This procedure improves the ability to choose the orientation of the eye relative to the beam that best covers the tumor while simultaneously excluding sensitive normal structures, i.e., the lens, cornea, macula, and optic nerve.

The program automatically designs an aperture that gives a 3 mm margin around the tumor, at which the dose falls to 50%. This margin may be reduced to 2.5 mm for a tumor border at the limbus or increased to 4 mm for a patient without surgical markers. The program calculates the maximum and minimum depths of the tumor and allows the user to choose proximal and distal margins to give the needed beam range and modulation. The program calculates dose distributions on the fundus displayed in the geometry of a wide-angle fundus photograph (Fig. 150.3) and in any plane through the eye (Fig. 150.4). It also calculates dose–volume histograms for the tumor and many structures of the eye.

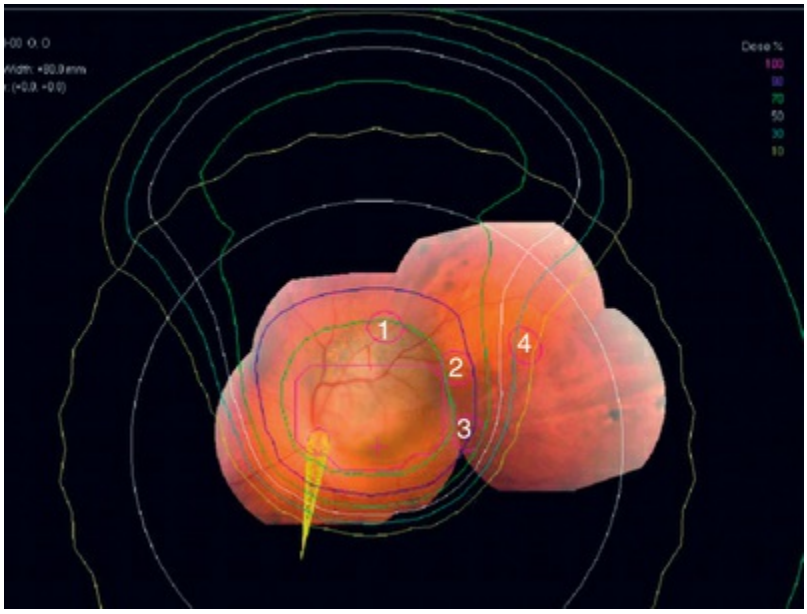

FIG. 150.3 Wide-angle fundus photographs and isodose curves superimposed on an eye model from the treatment planning program. The four tantalum rings are shown in magenta and numbered *1–4*. The tumor is outlined in green, and the 90% dose curve is shown in dark blue.

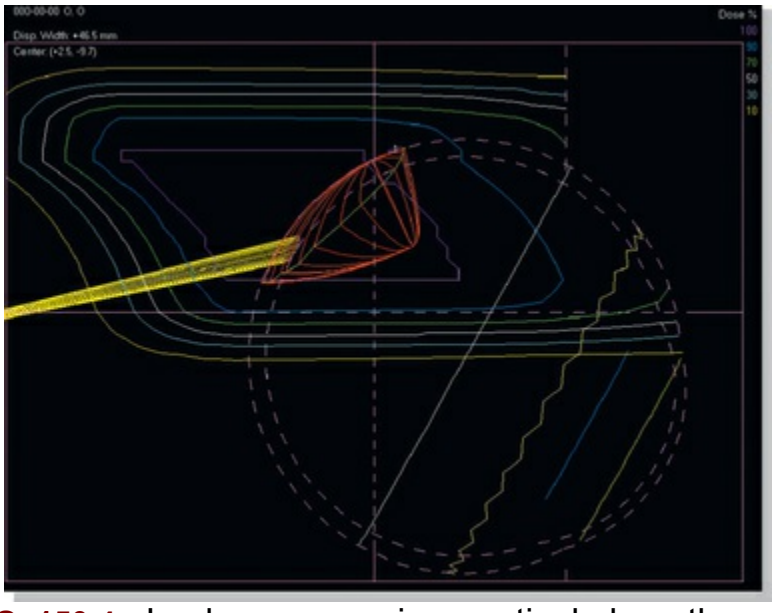

FIG. 150.4 Isodose curves in a vertical plane through the eye parallel to the beam direction for the case shown in Fig. 150.3. The tumor is shown in red, and the yellow cone represents the optic nerve. The innermost magenta line corresponds to the area

receiving 100% of the dose (70 CGE), and the outermost yellow line corresponds to the area receiving 10% of the dose (7 CGE).

Treatment Techniques

A high degree of accuracy in positioning the patient is achieved with the use of a headholder attached to the proton beam collimator. The headholder allows controlled rotation of the head around two mutually perpendicular axes intersecting at a point that is positioned accurately on the axis of the collimator.

The patient is seated in a specially designed chair, and his or her head is immobilized with a bite-block made of a dental impression compound and fastened to the headholder. Individually contoured plastic masks mounted into a frame are also used for head fixation (Fig. 150.5). Orientation of the patient's eye is established by voluntary fixation of the eye to be treated (the other eye is covered) on a small light that is attached to the collimator. If the vision is poor in the eye to be treated, the other eye can be used for fixation. The eyelids are held open with a lid speculum.

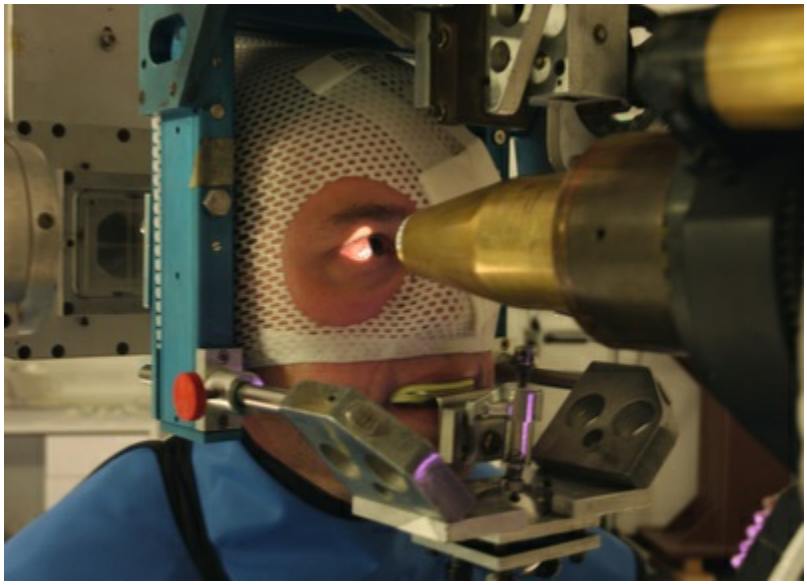

FIG. 150.5 Patient seated in headholder with plastic mask and bite block. The light represents the radiation field at the entry point on the ocular surface. The lids are retracted out of the field prior to the start of

treatment.

The eye is monitored using a high-magnification closed-circuit television system with its effective viewing point on the beam axis. This system provides a magnified image of 10 times the size of the patient's eye and permits continuous monitoring of the eye's position throughout the procedure. The alignment of the proton beam is achieved with orthogonal X-rays. The lesion, defined spatially by the radiopaque tantalum rings, can be positioned by translating the headholder until it is in the desired position relative to the beam axis. For tumors treated without surgical localization, a light beam coaxial with the central axis of the proton beam is used to position the tumor relative to the beam during treatment.[8,20,21] Positioning is achieved with a fluoroscopic system that provides a virtually instantaneous picture held on an image-storage device. This system hastens alignment and assists in confirming eye immobilization during treatment. The alignment procedure lasts approximately 15 minutes. The patient is asked to fixate, and the eye's position is observed on the television monitor in the control area. The treatment field is checked with a beam-simulation field light, and if the position and fixation are satisfactory, the treatment begins. If eye movement of more than 0.5 mm is observed, the treatment is halted immediately. Each treatment takes approximately 1–2 minutes, most without interruption.

Radiation Dose

The standard dose administered for most tumors is 70 Gy (RBE) delivered in five equal fractions in 5 days (63.6 proton Gy times 1.1 relative biologic effectiveness equals 70 Gy (RBE)). Dose fractionation increases the radiosensitivity of tumor tissue, as increased oxygenation of hypoxic tumor cells occurs between fractions. We selected large fractions based on favorable clinical results demonstrated with the use of a small number of relatively large dose fractions[10,22] in patients with cutaneous melanomas. At the prescribed dose of 70 Gy (RBE), we estimate that the optic nerve and macula receive the full dose when the tumor is less than 1 mm from these visual structures, half the dose (35 Gy (RBE)) when the tumor is located 3 mm from these structures, and a small dose (≤15

Gy (RBE)) when the tumor is peripheral (beyond 9 mm). As part of a randomized clinical trial to establish safety and efficacy of a dose reduction, 94 patients received a lower dose of 50 Gy (RBE).[23] No significant differences were found between patients who received the standard dose and those who received the lower dose with regard to tumor control and ocular complications. Thus, the optimal dose level to achieve tumor control and minimize ocular morbidity has not been established. Nevertheless, in select patients, i.e., those with small- or medium-sized tumors located near the optic nerve or fovea, a dose of 50 Gy (RBE) is chosen in an effort to reduce vision-threatening treatment complications. At several facilities in Europe, a total dose of 60 CGE (cobalt gray equivalents) is given in four equal fractions over 4 days.[24–26]

Follow-Up

Follow-up examinations are performed 6 weeks after treatment and then every 6 months during the first 5 years and annually thereafter. Fundus photography and ultrasonography are performed at varying intervals for documentation of tumor regression. Annual liver function tests are recommended and may be followed with abdominal scans if indicated. Lifetime follow-up is completed for all treated patients who enroll in a uveal melanoma registry, and data obtained through these follow-up efforts have been utilized to evaluate the efficacy and safety of proton therapy in terms of visual and survival endpoints.

Clinical Findings in Treated Patients

To date, more than 4000 patients with uveal melanomas have been treated at Massachusetts Eye and Ear Infirmary and Massachusetts General Hospital. Bilateral involvement and extrascleral extension are rare (less than 1% and 4%, respectively) as is treatment of iris-only melanomas (less than 1% of patients). The mean age of patients with choroidal or ciliary body tumors at the time of diagnosis was 61 years. Diagnosis before age 40 is uncommon, representing 11% of treated patients. The median basal diameter of treated patients was 13.0 mm (range: 5.0–28.0 mm) and median tumor height was 4.0 mm (range: 0.6–20.1 mm). Using the TNM

classification of tumor size (American Joint Committee on Cancer, 7th edition, 2010), almost equal numbers of patients were classified as T1 tumors or T2 tumors (approximately one-third in each group). Fewer patients were diagnosed with T3 and T4 tumors (23% and 14% respectively). More than two-thirds of treated tumors were located within 3 mm of the optic nerve or macula. Approximately 25% of the patients had 20/20 or better visual acuity at presentation, and fewer than 10% had visual acuity of counting fingers or worse.

Results

Tumor Regression

The majority of treated tumors show some regression after the first 6 months of treatment, with a usual range between 1 and 24 months.[27] Disappearance of the lesion, or formation of a flat scar, is observed in 15% of eyes. Resolution of a secondary serous retinal detachment is usually the earliest finding. Detachments can transiently increase in size during the first few months after treatment, but most eventually resolve. Continuous regression of the tumor over several years is frequently observed. Tumor regression is thought to be due primarily to direct killing of tumor cells by irradiation and secondarily to the effect of radiotherapy on the tumor vasculature. Cell death from irradiation is achieved by damage to chromosomal DNA, with subsequent loss of proliferative potential. Damage to DNA is lethal when the cell enters mitosis. Delayed regression, observed in some irradiated tumors, is probably due to prolonged intermitotic phases of melanoma cells. This protracted pattern of tumor regression has been supported by histologic studies of tumors enucleated at varying times after proton therapy, which showed a greater decline of mitotic figures with longer periods between irradiation and enucleation. Tumors enucleated more than 30 months after irradiation had no mitotic figures.[28] Rapid regression of tumors has been associated with higher rates of metastasis in both proton-irradiated[29] and plaque-treated patients,[30] suggesting that more aggressive tumors, due to more rapidly dividing cells, are more radiosensitive.

The presence of some mitotic figures in irradiated melanomas examined after enucleation for radiation complications does not indicate that irradiation has failed to sterilize the tumor. The presence of morphologically intact cells is not evidence that these cells are viable, since they may be programmed to destruct in the next mitotic cycle. These cells most likely are incapable of cell division, and the only proof of cell viability after irradiation is local recurrence of the treated tumor.

Visual Outcomes

Visual acuity after proton beam irradiation depends on the size of the tumor and its location relative to the fovea and the optic nerve[31] (Fig. 150.6). In eyes with tumors located farther than 3 mm from these structures, tumor destruction usually occurs without functionally significant radiation vasculopathy.[32] In a study of 558 patients who had undergone proton therapy for small- to moderate-sized tumors located within 4 disc diameters (DD) of the optic nerve or macula, the 5-year rate of vision loss to worse than 20/200 was 68%. Risk factors for vision loss included dose to the macula, tumor height, poorer baseline vision, and a history of diabetes.[33] In a multivariate regression model,[34] distance of the tumor from the optic nerve and macula, tumor height, baseline visual acuity, degree of retinal detachment, history of diabetes, and tumor diameter were found to be associated with vision loss. Coefficients derived from this model were used to calculate risk scores, which were then used to estimate probabilities of vision loss. The probability of developing significant vision loss (worse than 20/200) by 10 years after proton therapy varied between 16% for patients in the "low-risk" category (Fig. 150.7) to 99% for patients in the "high-risk" group.

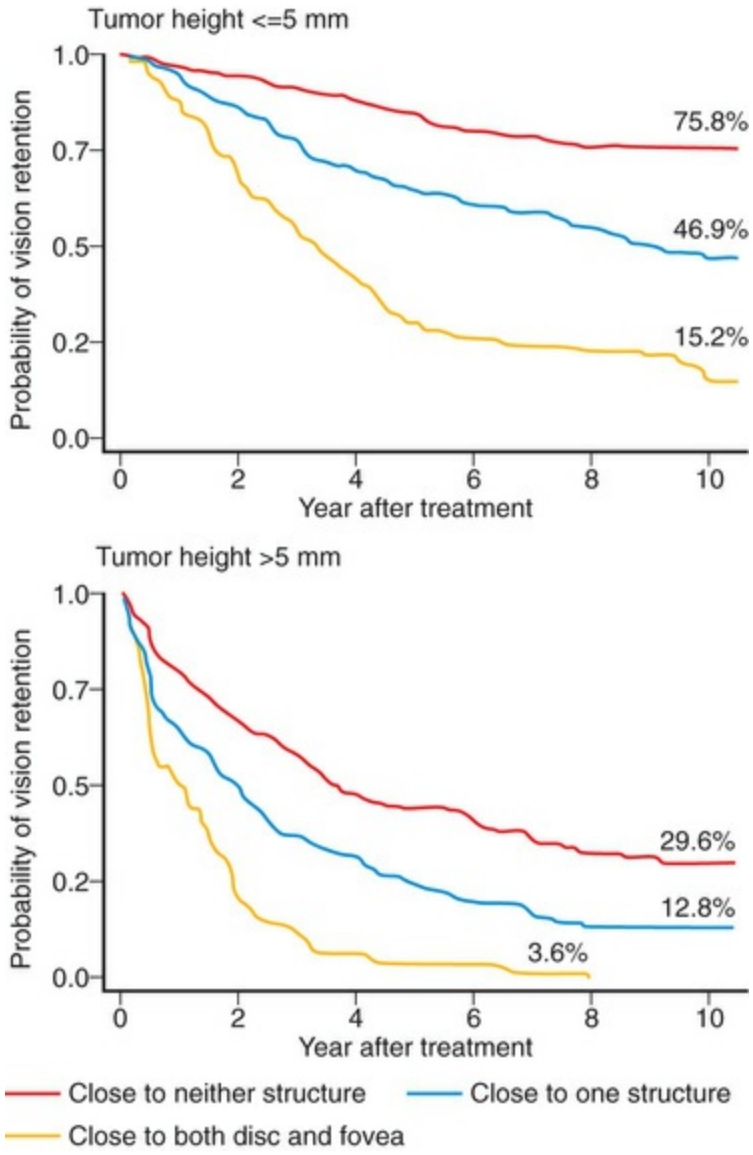

FIG. 150.6 Kaplan–Meier estimates of vision retention (at least 20/200) in patients with a baseline visual acuity of 20/100 or better, by height (≤5 mm versus >5 mm) and distance to the optic disc and macula (≤2 disc diameters versus >2 disc diameters). (Modified from Gragoudas ES, Lane AM, Collier JM. Charged particle irradiation of uveal melanoma. In: Albert DM, Miller JW, editors. Albert and Jakobiec's principles and practice of ophthalmology. 3rd edition. Philadelphia: Elsevier; 2008. p. 4892. Reproduced by permission of Elsevier.)

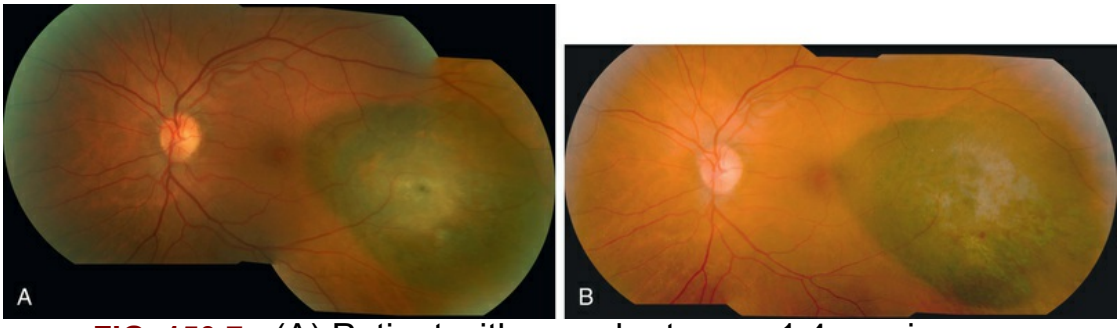

FIG. 150.7 (A) Patient with macular tumor, 1.4 mm in height, located ½ disc diameter from the fovea. Visual acuity prior to proton irradiation was 20/20. (B) Tumor has regressed to 1.2 mm and visual acuity remains 20/25 at 39 months after irradiation.

At greatest risk of vision loss are those patients who have tumors located near a structure that is critical for visual function. Large tumors are associated with several factors that can impair visual function such as exudative retinal detachments (approximately three-quarters of patients who presented at Massachusetts Eye and Ear Infirmary (MEEI) with large tumors had retinal detachments) and inflammation from tumor necrosis. Additionally, many large tumors are in close proximity to the optic nerve and/or macula (Fig. 150.8). For example, in our series of proton-irradiated large tumors (height ≥10 mm (or ≥8 mm if optic nerve involved) or height ≥2 mm and diameter >16 mm), close to half (46.7%) were located within 1 DD of the optic nerve. Despite having large tumors, preirradiation visual acuity was 20/40 or better in over one-third of these patients. By 5 years after treatment, however, the majority of patients had experienced severe visual decline (84% had vision worse than 20/200 and 69% had vision worse than counting fingers).

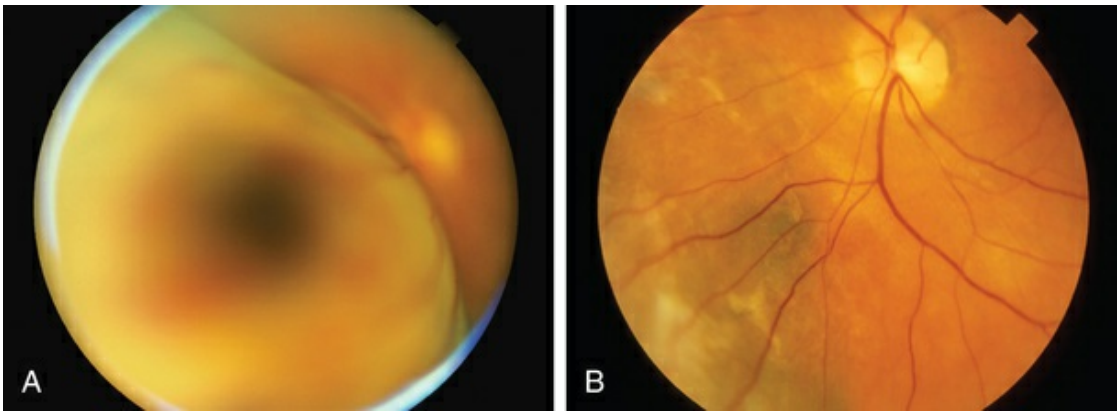

FIG. 150.8 (A) Patient with a large tumor (largest tumor diameter 21 mm; height 10.5 mm). Before proton irradiation, visual acuity was 20/200. (B) Eight months after treatment, tumor has regressed (height 5.0 mm) and visual acuity is 20/400.

Visual prognosis after proton irradiation for patients with peripapillary and parapapillary tumors is poor, with a 5-year rate of vision loss to worse than 20/200 of 80%. On the other hand, 56% retain vision of counting fingers or better at this time point[35] indicating that proton irradiation is a viable alternative to enucleation for these tumors, which are often unsuitable for plaque radiotherapy (Fig. 150.9).

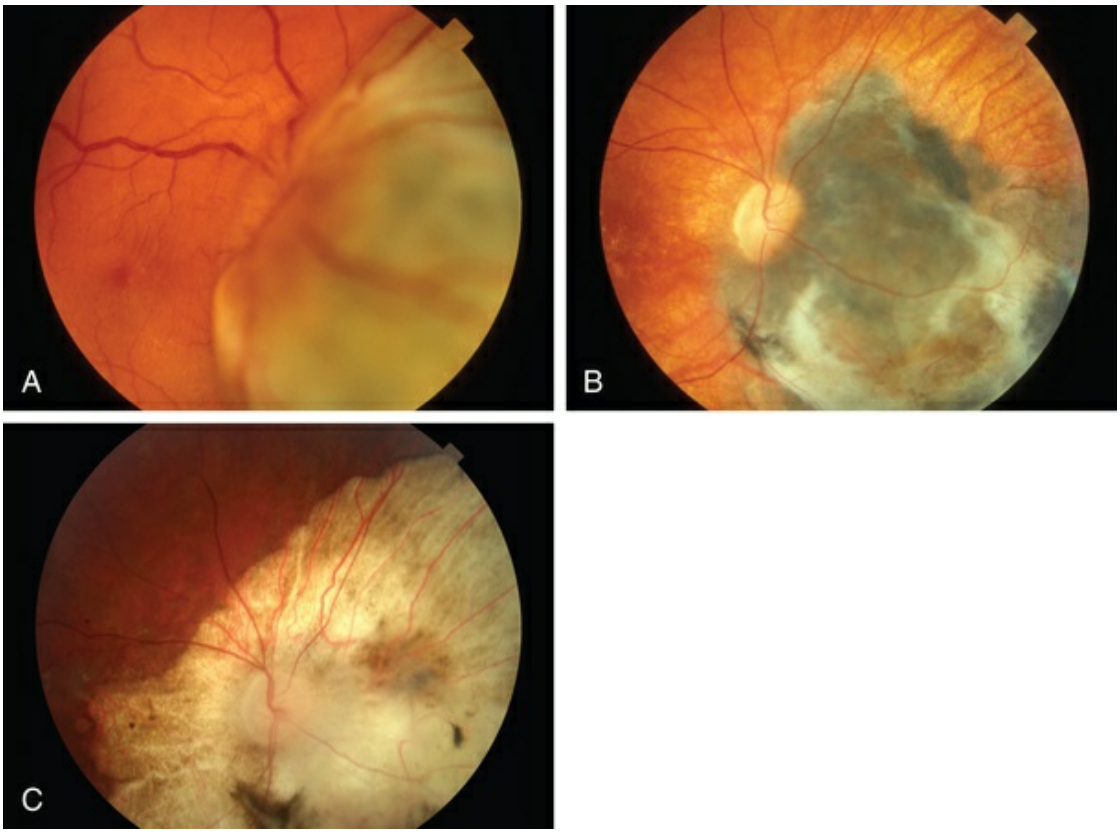

FIG. 150.9 (A) Patient with a parapapillary melanoma touching the optic disc. Before proton irradiation, visual acuity was 20/40. (B) Two and a half years after treatment, tumor regression is seen but visual acuity has decreased (20/125). (C) Twenty-four years after proton irradiation, the tumor has regressed (<1.0 mm) and visual acuity is stable (20/100).

Patients with macular tumors also have an elevated risk of visual loss, with a minority of patients (35.5%) retaining at least 20/200 vision by 5 years after proton irradiation. Visual prognosis was better in a subgroup of patients with small and medium-sized tumors; 5-year rates of vision retention of at least 20/200 were 70% in patients who received 50 Gy (RBE) and 44% in patients who received 70 Gy (RBE).[36]

Complications

Surgical complications from the suturing of tantalum rings have been relatively few. Transient diplopia has been observed for a few weeks after the operation in only a small number of patients since disinsertion of extraocular muscles is never required. In patients

with large tumors, intratumor hemorrhage may occasionally occur as a result of surgical manipulation. Lid dermatitis, madarosis, and epiphora from punctal occlusion have occurred in patients whose eyelids could not be retracted completely from the irradiation field. Corneal epitheliopathy has developed in a small number of cases with large ciliochoroidal melanomas and usually responds to artificial tears. Rubeosis iridis and neovascular glaucoma (NVG), the most serious complications because they may lead to enucleation, are observed in approximately 16% of treated eyes and are usually associated with large tumor volume. In a cohort of 704 patients who received proton therapy for uveal melanoma, the 5-year rate of NVG was 12.7%; subsequently enucleation was required in 4.9% of affected patients.[37] In another study of 127 patients treated by proton irradiation because their tumors were too large for plaque radiotherapy, 34% developed rubeosis during a median follow-up period of 36 months.[38] At MEEI neovascular glaucoma was the primary reason for enucleation in close to one-half of patients (45.9%) with large tumors who required the procedure.

Radiation vasculopathy, consisting of capillary closure, telangiectasis, microaneurysm formation, hemorrhages, exudates, and vascular sheathing, is usually observed in the irradiated area. In macular and paramacular melanomas (<3 mm from the fovea), radiation maculopathy and papillopathy may develop leading to vision loss.[9,32,39] The 5-year cumulative rates of maculopathy and papillopathy in patients with tumors within 4 DD of the macula and/or optic nerve were 64% and 35%, respectively, with increased risk of these complications associated with increased dose to critical structures.[33] The rate of papillopathy was 56.8% at 5 years after proton therapy for tumors located within 1 DD of the optic nerve.[35]

In a study evaluating the natural history of radiation papillopathy, 93 patients with parapapillary melanomas (within 1 DD of the optic nerve and at least 2 DD from the fovea) were followed. By 5 years after proton therapy, radiation papillopathy developed in 81% of cases in which the melanoma abutted the optic nerve and in 67% of cases in which the melanoma was 0.1–1 DD from the optic nerve. Of those who developed papillopathy, 42% retained vision of counting fingers or better and 31% (n=13)

experienced recovery of visual acuity after an initial loss.[40] These findings challenge the view that irradiation of the optic nerve will inevitably lead to optic neuropathy and total loss of vision.

Significant cataracts may develop in patients with ciliary body involvement or in cases of highly elevated choroidal melanomas in which the lens receives substantial irradiation.[41] The 5- and 10-year cumulative rates of posterior subcapsular cataract (PSC) were 30% and 35%, respectively, in an analysis of more than 2000 patients treated with protons over a 20-year period. Rates were dependent upon the dose to the lens; at 5 years post-therapy, 53% developed cataract when >50% of the lens was irradiated compared with 19% when <10% of the lens was irradiated. For eyes with reasonable visual potential, cataract extraction with intraocular lens implantation may be performed. Approximately 50% of patients undergoing cataract extraction after proton beam irradiation for choroidal melanoma had visual acuity of 20/200 or better after surgery.[42] There was no evidence that cataract extraction increased the risk of metastasis. Removal of a cataract for better observation of the tumor when there is no likelihood of visual improvement, typically due to underlying radiation maculopathy or papillopathy, is usually unnecessary since these tumors can be followed by ultrasonography.

In an effort to reduce the ocular morbidity associated with proton therapy, particularly when tumors are located close to critical structures, a randomized, double-blind dose reduction trial[23] was completed. The experimental dose selected for the trial was 50 CGE. Patients eligible for the trial were at high risk of radiation papillopathy and maculopathy because their tumors were located near the optic nerve or macula. Five years after proton therapy, lower rates of radiation vasculopathy and visual loss were not demonstrated. A modest beneficial effect of lowering the dose was suggested, with lower rates of visual field defects and radiation papillopathy observed in the 50-CGE dose group. For radiation papillopathy, this effect was observed only in the subgroup of patients with tumors located within 1 DD of the optic disc. However, this trial was underpowered to detect subgroup effects. Long-term follow-up (10 years after enrollment) of study subjects did not reveal any late-emerging differences between the two dose

groups. This level of dose reduction (28%) may be inadequate to produce appreciable improvement in functional outcomes, but further reductions could compromise tumor control. Radiation of the tumor with a lower dose became standard at our center for select patients with small or medium tumors located near the optic nerve or fovea in May 2004. Further study to identify possible beneficial effects of a dose reduction, overall and in specific subgroups of patients, is currently underway in this larger cohort of patients.

Recurrence

Local recurrence after charged-particle irradiation is observed in 2–5%[24–26,43] of patients. In one study[34] of 2069 consecutive patients treated with proton beam irradiation, 45 tumors (2.9%) demonstrated definitive growth, with the earliest occurrence observed 5 months and the latest 11 years after irradiation. Only 23 were marginal recurrences; in the case of anterior tumors involving the ciliary body, marginal recurrences may arise because the pigmented margins of the tumor may be difficult to distinguish from surrounding stroma. Six recurrences were ring melanomas, eight involved extrascleral extension of the tumors, and nine showed vertical growth of the tumors. An additional 15 eyes were enucleated at other centers because tumor growth was suspected. The 15-year probability of local tumor control, based on confirmed and suspected recurrences combined (n=60), was 95% (95% CI 93–96%). Similar control rates have been reported in another large series of patients (n=2435) treated in Lausanne, Switzerland.[24] Five-year control rates after brachytherapy have been reported to be between 92% and 87%.[44–46] In some cases, eyes with local recurrence can be retreated successfully with repeat proton irradiation[47] or – for cases in which the recurrence is marginal and flat – laser photocoagulation. Proton irradiation has also been used effectively to treat patients with tumor recurrences that were initially treated by other means (e.g., brachytherapy, transpupillary therapy).[48]

A comparison of patients irradiated with iodine-125 plaques versus helium ions revealed a recurrence rate in patients who received brachytherapy that was more than three times that of

patients who received heavy particle irradiation (12-year cumulative rates were 19% and 5%, respectively).[49] Suboptimal plaque positioning[50] in posteriorly located tumors may be one explanation for these poorer outcomes. Proton irradiation may be a better choice of treatment for posteriorly located tumors. A recent study of long-term outcomes after proton irradiation for patients with tumors contiguous to the optic nerve (within 1 DD) revealed a 5-year tumor recurrence rate of 3.3%, virtually identical to the rate seen in patients treated during the same period with tumors farther away from the nerve.[35] In contrast, tumor recurrence was reported in 10% of patients who received brachytherapy for tumors overhanging the disc.[51] The use of notched plaques and other advances in plaque design may improve tumor control in these cases.[51–53]

Achieving tumor control is of particular importance because local recurrence has been shown to elevate the risk of metastasis.[24,26,54] Survival is poorer among patients with local recurrences; 10-year survival rates were 72.6% for patients who experienced tumor control and 47.5% for patients who had tumor regrowth.[24] Similar survival rates were recently reported in an analysis of risk factors for tumor recurrence in 1102 patients treated with proton irradiation.[55] However, it is not clear if recurrence *per se* is actually a risk factor for metastasis or if it is just an indicator of a more aggressive tumor, which is more likely to metastasize.

Enucleation

The probability of retaining the eye 2 years after proton irradiation is 95%, and the probability is 90% after 5 years.[56] The 10-year rate of eye retention was 89% in a group of 1541 patients treated by proton therapy and followed for a median of 8 years;[54] 137 patients underwent enucleation after radiotherapy for complications (n=103) or tumor regrowth (n=34). The complication most likely to result in enucleation is neovascular glaucoma. The leading risk factors for enucleation are tumor height,[34,56] proximity of the tumor to critical structures (macula, fovea,[56] optic nerve), tumor diameter, tumor pigmentation, and tumor shape.[34]

Patients with large tumors may experience complications such as

neovascular glaucoma and exudative retinal detachments that often necessitate enucleation. In a series of patients with large tumors (>8 mm in height and >16 mm in diameter) treated with proton irradiation at MEEI, eye loss was experienced by approximately 20% of patients 5 years after treatment. Eye loss rates were higher (23.8%) for tumors located near the optic nerve or fovea (one or both) and lower (9.8%) for tumors located farther away from both structures.

Metastasis and Survival

Annual rates of melanoma-related mortality are highest 3–6 years after irradiation, but patients continue to be at risk many years after diagnosis. A recent study of very long-term risk of death from melanoma revealed that annual rates do not drop below 1% until 14 years after treatment with proton irradiation.[57] The 5-year cumulative probability of developing metastasis after proton irradiation is approximately 20%.[26,58] The probability of metastatic death at 15 years after proton treatment, using individual risk scores to estimate rates, varies between 5% for patients having the lowest-risk characteristics and 63% for those with the highest-risk characteristics.[34] The liver is primarily involved in 90% of patients with metastasis.[58] In 145 patients who developed metastasis after proton irradiation, median time to metastasis was 2.4 years after irradiation, and most patients were found to be symptomatic before diagnosis.[59] It remains unclear if early diagnosis of metastatic uveal melanoma has an impact on survival. A recent study compared patients who were diagnosed with metastatic uveal melanoma after proton irradiation incidentally or by routine surveillance to those who were diagnosed after developing symptoms. There were no differences between the two groups with regard to median time from diagnosis of primary tumor to metastatic death, suggesting that earlier diagnosis does not have a beneficial effect on survival.[60]

Adjuvant interferon therapy after primary treatment has not been successful in reducing the incidence of metastasis,[61] and therapeutic results for visceral metastatic melanoma are poor. Less than 15% of patients survive to 1 year after the detection of metastasis.[59] In studies of patients who have developed metastasis after

undergoing any type of primary ocular therapy, median survival is 2–9 months.[59,62,63] Significantly longer survival (from time of metastasis diagnosis) occurs among younger patients.[59]

Treatments for metastatic disease largely have been ineffective, and most evaluations of treatments have been done in a nonrandomized setting. Few remissions have been realized with chemoembolization of the liver and immunotherapy with interleukin-2, alone or in combination with other chemotherapeutics, and toxicity is high.[62,64,65] Patients who undergo intrahepatic arterial perfusion have somewhat better outcomes,[66] and a multicenter phase III trial (NCT number 1785316) is currently underway to compare isolated intrahepatic perfusion to best alternative care for patients with isolated liver metastases.[67]

Results from the very few controlled randomized trials completed[68–70] have been disappointing. A preliminary investigation of the efficacy of selumetinib versus chemotherapy (temozolomide or dacarbazine) yielded promising results,[70] but a subsequent phase III randomized, placebo-controlled, double-blind study of selumetinib in combination with dacarbazine versus dacarbazine alone showed no differences in progression-free survival between the treatment groups (http://www.astrazeneca.com/Media/Press-releases/Article/20150722-astrazeneca-provides-update-on-selumetinib).

Results of nonrandomized studies comparing survival rates for patients with uveal melanoma after treatment with proton beam irradiation[71] and other forms of radiotherapy[72] with survival rates after enucleation suggest that treatment choice has little effect on survival. Results from the Collaborative Ocular Melanoma Study showed no differences in 5-year rates of death due to histopathologically confirmed metastatic melanoma between patients randomized to undergo enucleation and those who received I-125 brachytherapy (11% vs. 9%, respectively).[1]

Conclusion

Proton irradiation of uveal melanomas is quite successful in achieving local tumor control. The dose distributions are

particularly advantageous for the treatment of large tumors and tumors located near the optic disc or fovea, with many patients maintaining visual function in the treated eye. Nevertheless, there can be significant ocular morbidity associated with treatment of such cases. Outcomes after treatment of radiation complications with systemic corticosteroids and anticoagulation have been disappointing,[73,74] but preliminary reports of intravitreal triamcinolone,[75] bevacizumab,[76-78] and combination therapy with these compounds[79] suggest some efficacy for radiation maculopathy and papillopathy. Encouraging results have been reported for prophylactic bevacizumab to reduce rubeosis after proton radiation.[80] Among several ongoing trials evaluating pharmacologic agents to reduce radiation complications is a randomized trial evaluating two doses of intravitreal ranibizumab in patients with parapapillary or paramacular tumors treated by proton irradiation.

Another unresolved issue is the optimal fractionation scheme and dose for treatment. Fractionation of the dose is important in optimizing the relative responses of tumor and normal tissue to irradiation. We presently use 70 Gy (RBE) for most cases, and 50 Gy (RBE) in select patients with small and medium-sized tumors near critical structures, delivered in five fractions over a period of 5–10 days. However, the optimal radiation dose that can control a melanoma with minimum ocular morbidity is unknown.

Current results suggest that primary treatment choice has little overall influence on survival in patients with uveal melanoma. It is likely that micrometastasis occurs before any type of ocular treatment has been initiated. Therefore, efforts toward the development of effective adjuvant therapies must continue.

References

1. Diener-West M, Earle JD, Fine SL, et al. The COMS randomized trial of iodine 125 brachytherapy for choroidal melanoma, III: initial mortality findings. COMS Report No. 18. *Arch Ophthalmol*. 2001;119:969–982.
2. Lommatzsch P. Beta-irradiation of choroidal melanoma with 106Ru/106Rh applicators. 16 years' experience. *Arch Ophthalmol*. 1983;101:713–717.

3. Packer S, Rotman M. Radiotherapy of choroidal melanoma with iodine-125. *Ophthalmology*. 1980;87:582–590.
4. Gragoudas ES, Seddon J, Goitein M, et al. Current results of proton beam irradiation of uveal melanomas. *Ophthalmology*. 1985;92:284–291.
5. Char DH, Kroll SM, Castro J. Ten-year follow-up of helium ion therapy for uveal melanoma. *Am J Ophthalmol*. 1998;125:81–89.
6. Dunavoelgyi R, Dieckmann K, Gleiss A, et al. Local tumor control, visual acuity, and survival after hypofractionated stereotactic photon radiotherapy of choroidal melanoma in 212 patients treated between 1997 and 2007. *Int J Radiat Oncol Biol Phys*. 2011;81:199.
7. Dunavoelgyi R, Dieckmann K, Gleiss A, et al. Radiogenic side effects after hypofractionated stereotactic photon radiotherapy of choroidal melanoma in 212 patients treated between 1997 and 2007. *Int J Radiat Oncol Biol Phys*. 2012;83:121.
8. Gragoudas E, Goitein M, Koehler A, et al. Proton irradiation of choroidal melanomas: preliminary results. *Arch Ophthalmol*. 1978;96:1583–1591.
9. Gragoudas E, Goitein M, Seddon J, et al. Preliminary results of proton beam irradiation of macular and paramacular melanomas. *Br J Ophthalmol*. 1984;68:479–485.
10. Gragoudas ES, Goitein M, Verhey L, et al. Proton beam irradiation of uveal melanomas. Results of 5 1/2-year study. *Arch Ophthalmol*. 1982;100:928–934.
11. Suit HD, Goitein M, Tepper J, et al. Exploratory study of proton radiation therapy using large field techniques and fractionated dose schedules. *Cancer*. 1975;35:1646–1657.
12. Sikuade MJ, Salvi S, Rundle PA, et al. Outcomes of treatment with stereotactic radiosurgery or proton beam therapy for choroidal melanoma. *Eye (Lond)*. 2015;29(9):1194–1198.
13. Constable I, Koehler A. Experimental ocular irradiation with accelerated protons. *Invest Ophthalmol*. 1974;13:280–287.
14. Gragoudas ES, Zakov NZ, Albert DM, et al. Long-term observations of proton-irradiated monkey eyes. *Arch*

Ophthalmol. 1979;97:2184–2191.
15. Meecham W, Char D, Chen G, et al. Correlation of visual field, treatment fields, and dose in helium ion irradiation of uveal melanoma. *Am J Ophthalmol*. 1985;100:658–665.
16. Park SS, Walsh SM, Gragoudas ES. Visual-field deficits associated with proton beam irradiation for parapapillary choroidal melanoma. *Ophthalmology*. 1996;103:110–116 [Erratum Ophthalmology 1996;103:699].
17. Saornil M, Egan K, Gragoudas E, et al. Histopathology of proton beam-irradiated vs enucleated uveal melanomas. *Arch Ophthalmol*. 1992;110:1112–1118.
18. Seddon JM, Gragoudas ES, Albert DM. Ciliary body and choroidal melanomas treated by proton beam irradiation. Histopathologic study of eyes. *Arch Ophthalmol*. 1983;101:1402–1408.
19. Goitein M, Miller T. Planning proton therapy of the eye. *Med Phys*. 1983;10:275–283.
20. Gragoudas ES, Goitein M, Koehler A, et al. Proton irradiation of malignant melanoma of the ciliary body. *Br J Ophthalmol*. 1979;63:135–139.
21. Gragoudas E, Goitein M, Verhey L, et al. Proton beam irradiation: an alternative to enucleation for intraocular melanomas. *Ophthalmology*. 1980;87:571–581.
22. Gragoudas E, Seddon J, Egan K, et al. Long-term result of proton beam irradiated uveal melanomas. *Ophthalmology*. 1987;94:349–353.
23. Gragoudas ES, Lane AM, Regan S, et al. A randomized controlled trial of varying radiation doses in the treatment of choroidal melanoma. *Arch Ophthalmol*. 2000;118:773–778.
24. Egger E, Schalenbourg A, Zografos L, et al. Maximizing local tumor control and survival after proton beam radiotherapy of uveal melanoma. *Int J Radiat Oncol Biol Phys*. 2001;51:138–147.
25. Damato B, Kacperek A, Chopra M, et al. Proton beam radiotherapy of choroidal melanoma: the Liverpool-Clatterbridge experience. *Int J Radiat Oncol Biol Phys*. 2005;62:1405–1411.
26. Dendale R, Lumbroso-Le Rouic L, Noel G, et al. Proton

beam radiotherapy for uveal melanoma: results of Curie Institut-Orsay proton therapy center (ICPO). *Int J Radiat Oncol Biol Phys*. 2006;65:780–787.
27. Wilkes SR, Gragoudas ES. Regression patterns of uveal melanoma after proton beam irradiation. *Ophthalmology*. 1982;89:840–844.
28. Gragoudas ES, Egan KM, Saornil MA, et al. The time course of irradiation changes in proton beam-treated uveal melanomas. *Ophthalmology*. 1993;100:1555–1559 [discussion 1560].
29. Glynn R, Seddon J, Gragoudas E, et al. Evaluation of tumor regression and other prognostic factors for early and late metastasis after proton irradiation of uveal melanoma. *Ophthalmology*. 1989;96:1566–1573.
30. Kaiserman I, Anteby I, Chowers I, et al. Post-brachytherapy initial tumour regression rate correlates with metastatic spread in posterior uveal melanoma. *Br J Ophthalmol*. 2004;88:892–895.
31. Seddon JM, Gragoudas ES, Polivogianis L, et al. Visual outcome after proton beam irradiation of uveal melanoma. *Ophthalmology*. 1986;93:666–674.
32. Seddon JM, Gragoudas ES, Egan KM, et al. Uveal melanomas near the optic disc or fovea: visual results after proton beam irradiation. *Ophthalmology*. 1987;94:354–361.
33. Gragoudas ES, Li W, Lane AM, et al. Risk factors for radiation maculopathy and papillopathy after intraocular irradiation. *Ophthalmology*. 1999;106:1571–1578.
34. Gragoudas E, Li W, Goitein M, et al. Evidence-based estimates of outcome in patients irradiated for intraocular melanoma. *Arch Ophthalmol*. 2002;120:1665–1671.
35. Lane AM, Kim IK, Gragoudas ES. Proton irradiation for peripapillary and parapapillary melanomas. *Arch Ophthalmol*. 2011;129:1127–1130.
36. Patel AV, Lane AM, Morrison MA, et al. Visual outcomes after proton beam irradiation for choroidal melanomas involving the fovea. *Ophthalmology*. 2016;123(2):369–377.
37. Mishra KK, Daftari IK, Weinberg V, et al. Risk factors for neovascular glaucoma after proton beam therapy of uveal

melanoma: a detailed analysis of tumor and dose-volume parameters. *Int J Radiat Oncol Biol Phys*. 2013;87(2):330–336.
38. Foss AJ, Whelehan I, Hungerford JL, et al. Predictive factors for the development of rubeosis following proton beam radiotherapy for uveal melanoma. *Br J Ophthalmol*. 1997;81:748–754.
39. Guyer D, Mukai S, Egan K, et al. Radiation maculopathy after proton beam irradiation for choroidal melanoma. *Ophthalmology*. 1992;99:1278–1285.
40. Kim IK, Lane AM, Egan KM, et al. Natural history of radiation papillopathy after proton beam irradiation of parapapillary melanoma. *Ophthalmology*. 2010;117:1617–1622.
41. Gragoudas ES, Egan KM, Walsh SM, et al. Lens changes after proton beam irradiation for uveal melanoma. *Am J Ophthalmol*. 1995;119:157–164.
42. Gragoudas ES, Egan KM, Arrigg PG, et al. Cataract extraction after proton beam irradiation for malignant melanoma of the eye. *Arch Ophthalmol*. 1992;110:475–479.
43. Gragoudas E, Egan K, Seddon J, et al. Intraocular recurrence of uveal melanoma after proton beam irradiation. *Ophthalmology*. 1992;99:760–766.
44. Char D, Quivey J, Castro J, et al. Helium ions versus iodine 125 brachytherapy in the management of uveal melanoma: a prospective, randomized, dynamically balanced trial. *Ophthalmology*. 1993;100:1547–1554.
45. Gunduz K, Shields CL, Shields JA, et al. Radiation complications and tumor control after plaque radiotherapy of choroidal melanoma with macular involvement. *Am J Ophthalmol*. 1999;127:579–589.
46. Jensen AW, Petersen IA, Kline RW, et al. Radiation complications and tumor control after 125I plaque brachytherapy for ocular melanoma. *Int J Radiat Oncol Biol Phys*. 2005;63:101–108.
47. Marucci L, Lane AM, Li W, et al. Conservation treatment of the eye: conformal proton reirradiation for recurrent uveal melanoma. *Int J Radiat Oncol Biol Phys*. 2006;64:1018–1022.
48. Riechardt AI, Cordini D, Dobner B, et al. Salvage proton

beam therapy in local recurrent uveal melanoma. *Am J Ophthalmol*. 2014;158:948–956.
49. Char DH, Kroll S, Phillips TL, et al. Late radiation failures after iodine 125 brachytherapy for uveal melanoma compared with charged-particle (proton or helium ion) therapy. *Ophthalmology*. 2002;109:1850–1854.
50. Harbour JW, Murray TG, Byrne SF, et al. Intraoperative echographic localization of iodine 125 episcleral radioactive plaques for posterior uveal melanoma. *Retina*. 1996;16:129–134.
51. Sagoo MS, Shields CL, Mashayekhi A, et al. Plaque radiotherapy for juxtapapillary choroidal melanoma overhanging the optic disc in 141 consecutive patients. *Arch Ophthalmol*. 2008;126:1515–1522.
52. Finger PT. Finger's "slotted" eye plaque for radiation therapy: treatment of juxtapapillary and circumpapillary intraocular tumours. *Br J Ophthalmol*. 2007;91:891–894.
53. Sagoo MS, Shields CL, Mashayekhi A, et al. Plaque radiotherapy for choroidal melanoma encircling the optic disc (circumpapillary choroidal melanoma). *Arch Ophthalmol*. 2007;125:1202–1209.
54. Egan K, Ryan L, Gragoudas E. Survival implications of enucleation after definitive radiotherapy for choroidal melanoma: an example of regression on time-dependent covariates. *Arch Ophthalmol*. 1998;116:366–370.
55. Caujolle JP, Paoli V, Chamorey E, et al. Local recurrence after uveal melanoma proton beam therapy: recurrence types and prognostic consequences. *Int J Radiat Oncol Biol Phys*. 2013;85(5):1218–1224.
56. Egan K, Gragoudas E, Seddon J, et al. The risk of enucleation after proton beam irradiation of uveal melanoma. *Ophthalmology*. 1989;96:1377–1383.
57. Lane AM, Kim IK, Gragoudas EG. Long-term risk of melanoma-related mortality for patients with uveal melanoma treated with proton beam therapy. *JAMA Ophthalmol*. 2015;133(7):792–796.
58. Gragoudas E, Seddon J, Egan K, et al. Metastasis from uveal melanoma after proton beam irradiation. *Ophthalmology*.

1988;95:992–999.
59. Gragoudas E, Egan K, Seddon J, et al. Survival of patients with metastases from uveal melanoma. *Ophthalmology*. 1991;98:383–390.
60. Kim IK, Lane AM, Gragoudas ES. Survival in patients with presymptomatic diagnosis of metastatic uveal melanoma. *Arch Ophthalmol*. 2010;128:871–875.
61. Lane AM, Egan KM, Harmon D, et al. Adjuvant interferon therapy for patients with uveal melanoma at high risk of metastasis. *Ophthalmology*. 2009;116:2206–2212.
62. Bedikian AY, Legha SS, Mavligit G, et al. Treatment of uveal melanoma metastatic to the liver: a review of the M. D. Anderson Cancer Center experience and prognostic factors. *Cancer*. 1995;76:1665–1670.
63. Eskelin S, Pyrhonen S, Hahka-Kemppinen M, et al. A prognostic model and staging for metastatic uveal melanoma. *Cancer*. 2003;97:465–475.
64. Proebstle TM, Scheibenbogen C, Sterry W, et al. A phase II study of dacarbazine, cisplatin, interferon-alpha and high-dose interleukin-2 in 'poor-risk' metastatic melanoma. *Eur J Cancer*. 1996;32A:1530–1533.
65. Flaherty LE, Unger JM, Liu PY, et al. Metastatic melanoma from intraocular primary tumors: the Southwest Oncology Group experience in phase II advanced melanoma clinical trials. *Am J Clin Oncol*. 1998;21:568–572.
66. Alexander HR Jr, Libutti SK, Pingpank JF, et al. Hyperthermic isolated hepatic perfusion using melphalan for patients with ocular melanoma metastatic to liver. *Clin Cancer Res*. 2003;9:6343–6349.
67. Olofsson R, Ny L, Eilard MS, et al. Isolated hepatic perfusion as a treatment for uveal melanoma liver metastases (the SCANDIUM trial): study protocol for a randomized controlled trial. *Trials*. 2014;15:317.
68. Leyvraz S, Piperno-Neumann S, Suciu S, et al. Hepatic intra-arterial versus intravenous fotemustine in patients with liver metastases from uveal melanoma (EORTC 18021): a multicentric randomized trial. *Ann Oncol*. 2014;25:742–746.
69. Schmittel A, Schmidt-Hieber M, Martus P, et al. A

randomized phase II trial of gemcitabine plus treosulfan versus treosulfan alone in patients with metastatic uveal melanoma. *Ann Oncol*. 2006;17:1826–1829.
70. Carvajal RD, Sosman JA, Quevedo JF, et al. Effect of selumetinib vs chemotherapy on progression-free survival in uveal melanoma a randomized clinical trial. *JAMA*. 2014;311:2397–2405.
71. Seddon JM, Gragoudas ES, Egan KM, et al. Relative survival rates after alternative therapies for uveal melanoma. *Ophthalmology*. 1990;97:769–777.
72. Augsburger J, Gamel J, Sardi V, et al. Enucleation vs cobalt plaque radiotherapy for malignant melanomas of the choroid and ciliary body. *Arch Ophthalmol*. 1986;104:655–656.
73. Danesh-Meyer HV, Savino PJ, Sergott RC. Visual loss despite anticoagulation in radiation-induced optic neuropathy. *Clin Experiment Ophthalmol*. 2004;32:333–335.
74. Girkin CA, Comey CH, Lunsford LD, et al. Radiation optic neuropathy after stereotactic radiosurgery. *Ophthalmology*. 1997;104:1634–1643.
75. Shields CL, Demirci H, Marr BP, et al. Intravitreal triamcinolone acetonide for acute radiation papillopathy. *Retina*. 2006;26:537–544.
76. Finger PT. Anti-VEGF bevacizumab (Avastin) for radiation optic neuropathy. *Am J Ophthalmol*. 2007;143:335–338.
77. Finger PT, Chin K. Anti-vascular endothelial growth factor bevacizumab (Avastin) for radiation retinopathy. *Arch Ophthalmol*. 2007;125:751–756.
78. Shah SU, Shields CL, Bianciotto CG, et al. Intravitreal bevacizumab at 4-month intervals for prevention of macular edema after plaque radiotherapy of uveal melanoma. *Ophthalmology*. 2014;121:269–275.
79. Shah NV, Houston SK, Markoe A, et al. Combination therapy with triamcinolone acetonide and bevacizumab for the treatment of severe radiation maculopathy in patients with posterior uveal melanoma. *Clin Ophthalmol*. 2013;7:1877–1882.
80. Mantel I, Schalenbourg A, Bergin C, et al. Prophylactic use

of bevacizumab to avoid anterior segment neovascularization following proton therapy for uveal melanoma. *Am J Ophthalmol*. 2014;158:693–701.

151

Surgical Resection of Choroidal Melanoma

Bertil E. Damato, Jay M. Stewart, Armin R. Afshar, Carl Groenewald, Wallace S. Foulds

Introduction

Choroidal melanoma can be removed by en bloc resection, through a scleral trapdoor ("exoresection"), or with a vitreous cutter passed transretinally (i.e., "endoresection"). Such surgery can be performed as primary treatment or as a salvage procedure after

another form of therapy. (See Video 151.1 online.)

Exoresection of choroidal melanoma is not widely performed, not least because of fears about its safety. Stallard reported two cases in 1966 and advocated partial choroidectomy only as a last resort for patients whose tumors did not regress after radiotherapy or who had poor vision in the fellow eye.[1] In 1973 Foulds challenged the prevailing dogmas about radical surgery and started performing primary exoresection irrespective of the status of the fellow eye.[2] Since then, we have between us performed more than 630 exoresections and 120 endoresections for posterior uveal melanoma.[3–9] Others have also adopted these procedures.[10–17] This chapter describes our surgical techniques, summarizes the results, and discusses the indications in relation to other forms of conservative therapy.

Exoresection

Indications and Contraindications

We reserve exoresection for patients who are unlikely to do well with other forms of conservative treatment, such as transpupillary thermotherapy, ruthenium or iodine plaque brachytherapy, and proton beam radiotherapy.

Tumors <6 mm in thickness respond satisfactorily to plaque or proton beam radiotherapy unless they have invaded retina or if they extend close to the optic disc. Radiotherapy of more bulky tumors is associated with a significant complication rate, which increases with time, especially when the tumor extends far anteriorly or posteriorly, or if there is extensive retinal detachment.[18–20] Conversely, large tumor size, anterior location, and the presence of exudative retinal detachment make exoresection less difficult. Two matched group studies have reported that with large tumors, the results are better after exoresection than after iodine plaque radiotherapy.[21,22]

Relative contraindications to local resection include (1) a tumor diameter >18 mm; (2) tumor extension to within a disc diameter (DD) of the optic disc margin; (3) extensive retinal invasion or any retinal perforation; (4) extraocular extension; (5) more than 2 clock-

hours of ciliary body or angle involvement; and (6) general health precluding hypotensive anesthesia. If, however, the patient has poor vision in the fellow eye, or if enucleation is refused, then local resection can be performed, with special measures being taken to deal with the increased surgical difficulties. Absolute contraindications include diffuse melanoma and optic nerve invasion. Old age is not in itself a contraindication because hemorrhage is arrested at a higher blood pressure than is the case with young subjects, making profound hypotension unnecessary. It is possible to perform exoresection in children.[23]

Preoperative Workup

It is essential to identify adverse factors, such as retinal invasion by the tumor, indistinct tumor margins, and any systemic contraindications to hypotensive anesthesia, including ischemic heart disease, cerebrovascular insufficiency, and significant renal or respiratory impairment. The advantages and disadvantages of local excision in relation to other forms of therapy are discussed with the patient, with all patients receiving an audio recording of this conversation.

Surgical Technique

Preparation

As with other intraocular surgery, the skin and conjunctiva are cleaned with antiseptic solution (e.g., povidone–iodine) and the pupil is dilated.

Exposure

The lashes are secured away from the eye with steristrips. The eyelids are retracted using both a wire speculum and traction sutures. The ocular surface is kept moist with 1.5% methylcellulose solution. A 180° limbal conjunctival peritomy is made. The episclera is removed with a No. 15 Bard Parker scalpel. Intervening extraocular muscles are disinserted, leaving a 1-mm tendon stump to aid reinsertion. Two scleral traction sutures (i.e., 5-0 braided polyester) are passed 4 mm posterior to the limbus and clipped

with hemostat forceps (Fig. 151.1A). The tumor margins are identified by transillumination and marked on the sclera with a felt-tipped pen (Fig. 151.1B).

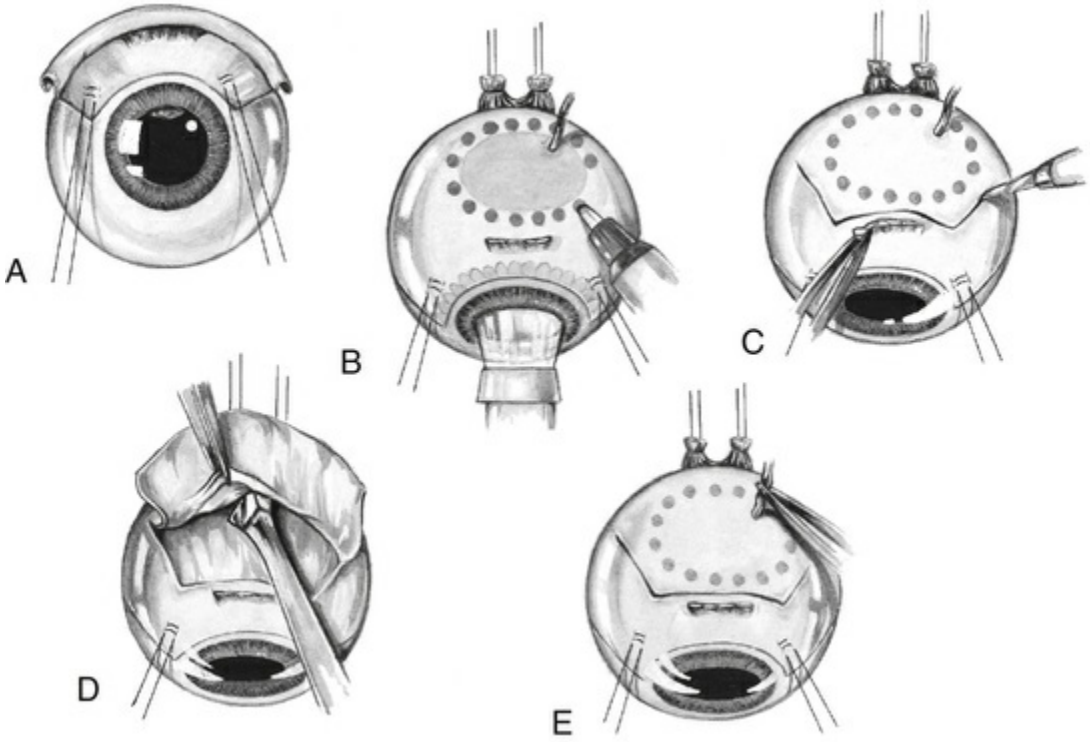

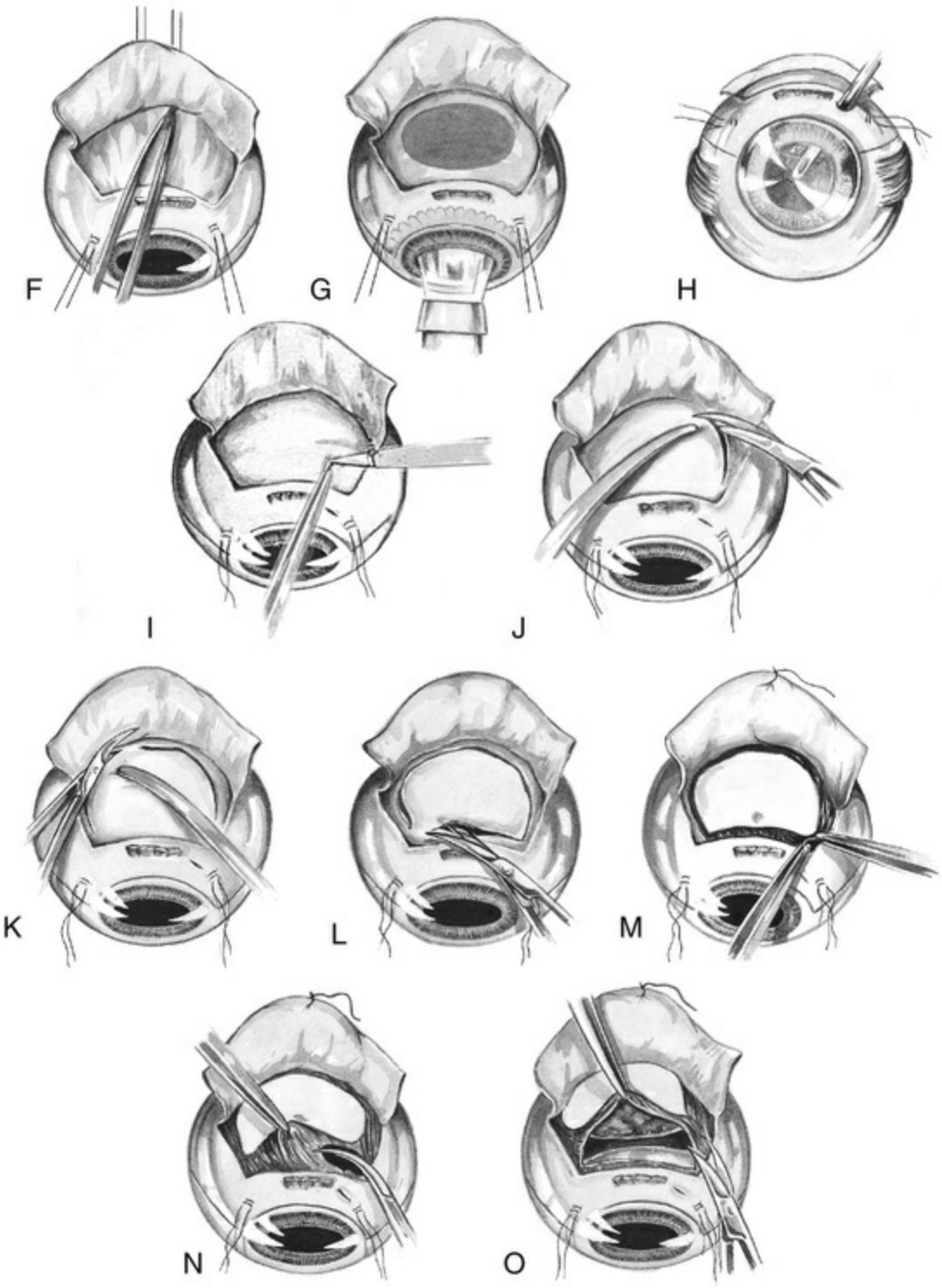
F
G
H
I
J
K
L
M
N
O

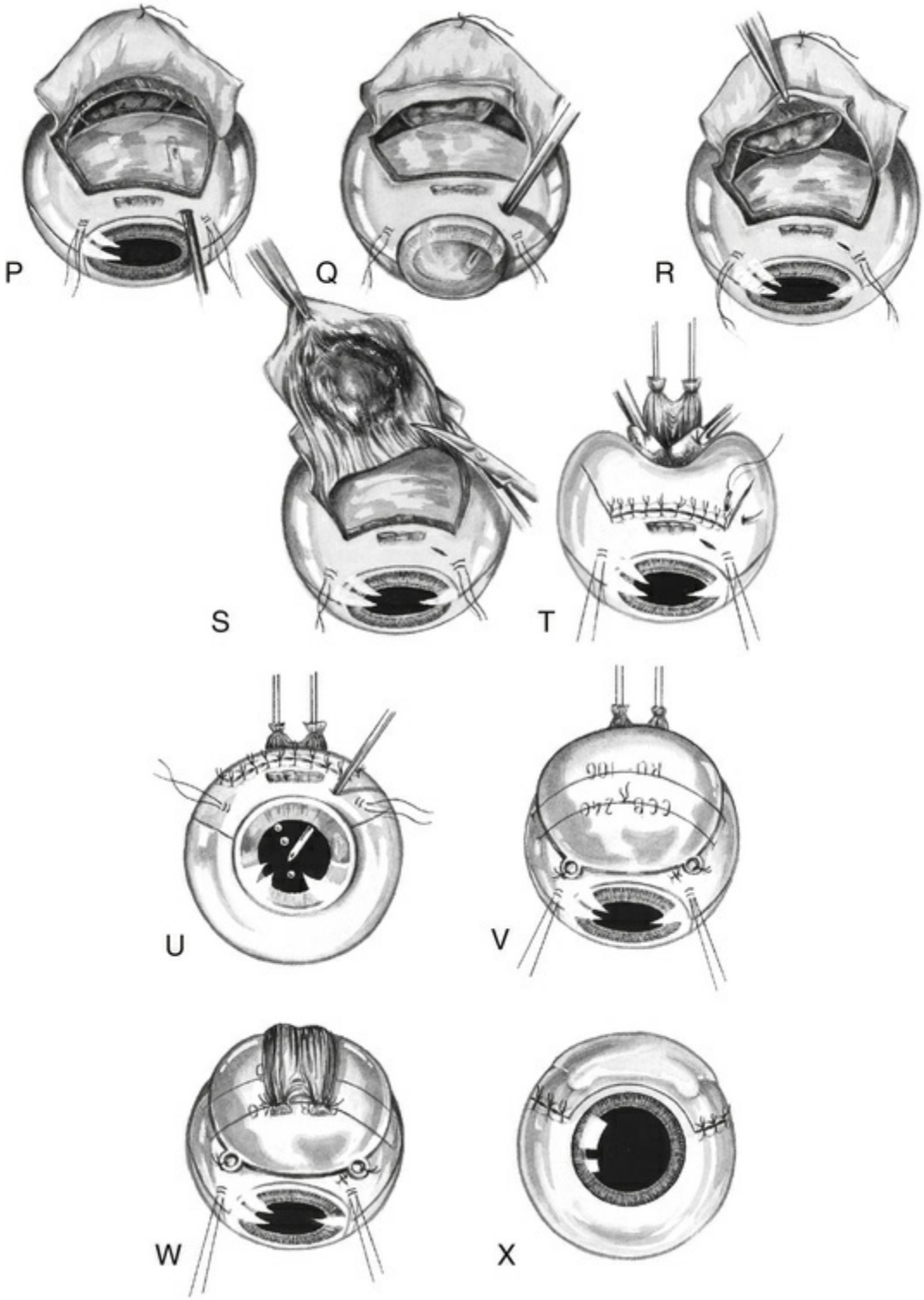

FIG. 151.1 Technique of exoresection. (A) Conjunctival incision and placement of bridle sutures. (B) Transpupillary transillumination with demarcation of tumor margins with a pen. (C) Partial-thickness scleral incisions for creation of a scleral flap. (D) Lamellar scleral dissection. (E) Closure of vortex vein behind eye with diathermy. (F) Closure of vortex vein within sclera with diathermy. (G) Confirmation of adequacy of

scleral flap by transpupillary transillumination. (H) Ocular decompression. (I) Scleral buttonhole lateral to tumor. (J) Scleral incision lateral to tumor. (K) Scleral incision posterior to tumor. (L) Anterior scleral incision. (M) Choroidal opening. (N) Choroidal incision anterior to tumor. (O) Choroidal incision lateral to tumor. (P) Further vitrectomy is performed if ocular decompression is inadequate. (Q) Further vitrectomy with corneal contact lens. (R) The retina should separate from the choroid to facilitate dissection. (S) Choroidal incision posterior to tumor. (T) Scleral suturing with traction on bridle sutures and ocular indentation to increase intraocular pressure. (U) Intravitreal injection of fluid. (V) Placement of radioactive plaque. (W) Reinsertion of extraocular muscles. (X) Closure of conjunctiva.

Lamellar Scleral Dissection

A posteriorly hinged lamellar scleral flap is fashioned. It is polyhedral, rather than circular, to facilitate good wound edge apposition during closure (Fig. 151.1C). The scleral flap should clear the apparent tumor margins by about 5 mm (Fig. 151.1G). By making the flap wider posteriorly, it is possible to reduce the length of the lateral incisions, facilitating closure. The flap should be about 80% of the scleral thickness. Any inadvertent buttonholes in the superficial flap are immediately closed with a purse-string 8-0 nylon suture. Any buttonholes in the deep sclera are sutured to prevent prolapse of choroid or tumor.

The flap is created using a feather blade for the initial scleral incisions and a Desmarres scarifier for lamellar scleral dissection (Fig. 151.1D).

To avoid troublesome hemorrhage, any vortex veins overlying the scleral flap are cauterized before being divided, applying bipolar diathermy both extraocularly (Fig. 151.1E) and to the intrascleral portion of the vein after cautiously exposing as much of the vessel as possible (Fig. 151.1F). Long ciliary vessels overlying the scleral flap are treated similarly. Gentle bipolar cautery of some of the short ciliary vessels adjacent to the optic nerve further reduces hemorrhage.

Ocular Decompression

Partial ocular decompression by limited pars plana vitrectomy facilitates local excision by reducing retinal bulging through the scleral window and improving access to the posterior uvea. Vitrectomy can be performed before, during, and/or after scleral flap dissection.

If vitrectomy is delayed until the scleral flap is prepared, three-port vitrectomy with infusion is unnecessary. Vitrectomy can be performed through a single sclerotomy using illumination from the operating microscope and a disposable vitrectomy contact lens (Fig. 151.1H).

During creation of any vitrectomy sclerotomies, the posterior segment should be kept in view to avoid damaging the retina overlying the tumor.

The vitreous cortex should be preserved so that as soon as the tumor is excised, the retina can be repositioned by injecting fluid into the vitreous cavity; otherwise, in the presence of a large scleral opening and a defect at the pars plana, it may be difficult to flatten the retina after tumor resection.

Deep Scleral Incision

Two small buttonhole incisions are made in the deep sclera about 2 mm inside the superficial scleral incision anterolateral to the tumor (Fig. 151.1I). To avoid damaging choroid, the sclera is pinched with fine-toothed microforceps to create a fold, which is then shaved with a knife until perforation occurs. This scleral incision is extended around the tumor with blunt-tipped corneoscleral scissors (Figs. 151.1J–K). The deep scleral incision is kept 2 mm inside the superficial scleral incisions to create a stepped wound edge, which facilitates closure (Fig. 151.1L). To prevent excessive bulging of intraocular contents, the lateral and posterior scleral incisions are completed before the anterior incision is made.

The tumor appears different from healthy choroid so that it is possible to define its margins by direct inspection. Once the deep scleral incisions are made, the anterior margin of the deep scleral lamella is marked with a notch to enable the pathologist to orient the excised specimen.

Tumor Excision

Tumor excision is commenced after ensuring the eye is soft, if necessary aspirating further fluid from the vitreous cavity and removing the hemostat forceps from the traction sutures. An eye basket or Flieringa ring is not necessary. Bipolar cauterization of the choroid around the tumor may reduce hemorrhage, but must be very gentle as it may weaken the underlying retina, increasing the risk of breaks.

The subretinal space is entered, preferably at a site where the retina is detached (Fig. 151.1M). This is done by holding the choroid with two pairs of ribbed (not toothed) microforceps and moving them apart to tear the uveal tissue.

The anterior part of the tumor is lifted from the subjacent retina with toothed forceps applied to the deep scleral lamella, which usually remains firmly adherent to the tumor. If the sclera separates from the tumor, it is reattached to the tumor with tissue glue so as to avoid the need for cryoextraction, which is cumbersome.

Usually, the choroid is divided in front of the tumor (Fig. 151.1N), then laterally (Fig. 151.1O), and finally posteriorly, using blunt-tipped corneoscleral scissors. If there is excessive retinal bulging, further vitrectomy is performed, with the vitrector being viewed through the retina (Fig. 151.1P) or the pupil (Fig. 151.1Q). If ocular decompression is adequate, the retina should fall away from the tumor so that a space appears between the retina and the normal choroid around the tumor margins (Fig. 151.1R). This allows the uveal tissue posterior to the tumor to be divided with the corneoscleral scissors (Fig. 151.1S). Despite the systemic hypotension, there is usually some hemorrhage, which must be mopped away before clots form, because these are difficult to remove.

As soon as the tumor is excised, the instruments are exchanged for a fresh set to prevent tumor seeding. At the earliest opportunity the intravitreal pressure is increased until the retina bulges slightly in the scleral window so that there is no potential space in which a subretinal hematoma can form. This is achieved by exerting traction on the bridle sutures and by compressing the eye with sponges placed behind the eye, posterior to the scleral window (Fig. 151.1T).

Scleral Closure

The corners of the flap are sutured first, followed by the anterior margin and finally the lateral margins. Interrupted 8–0 nylon sutures are placed about 2 mm apart. As soon as the suturing of the flap is complete, the globe is reformed by injecting balanced salt solution intravitreally, either using the three-way tap, if an infusion cannula is present, or through a 25-gauge needle attached to a syringe (Fig. 151.1U). Gas tamponade is no longer considered useful, but 2 mL of air is kept in the syringe when injecting fluid, because its compressibility prevents a sudden rise in intraocular pressure, which might reopen the wound.

Adjunctive Brachytherapy

Adjunctive plaque radiotherapy is routinely applied, delivering a dose of approximately 100 Gy to a depth of 1–2 mm. We favor a 25-mm ruthenium plaque because of the limited range of beta irradiation, the convenience of a long half-life, and the thin shape of the implant, which facilitates positioning over the site of the excised tumor (Fig. 151.1V). If the superficial flap has inadvertently been buttonholed, or if cyclectomy has been performed, this brachytherapy is delayed by 1 month.

Eye Closure

The muscles are resutured to their original insertions with 5-0 braided polyglycolic acid sutures (Fig. 151.1W). When the muscle insertion is located on the scleral flap the muscle stump is left long to avoid the need for placing the suture in the sclera. To compensate for any muscle shortening, the distance from the suture knots to the limbus is measured before the muscle tendon is divided and also at the time of reinsertion so that a sling is used if necessary.

The conjunctiva is closed with 7–0 braided polyglactin sutures (Fig. 151.1X). Antibiotics, mydriatics, and steroids are given in the usual fashion. The entire procedure usually takes between 2 and 3 hours.

Variations in Technique

Ciliary Body Involvement

If a choroidal tumor involves the ciliary body, the anterior margin of the superficial scleral flap is placed 1 mm posterior to the limbus. A half-thickness incision is then made in the deep sclera, about 2 mm posterior to the superficial incision, and the deep sclera is split into another two layers by lamellar dissection, which extends anteriorly into cornea. This scleral step ensures that the anterior wound edge is watertight. This is especially important if adjunctive plaque radiotherapy is administered.

The chances of developing retinal detachment are greatly reduced by conserving as much of the ciliary epithelium as possible. This is achieved by perforating choroid posterior to the ora serrata and then using closed, blunt-tipped scissors to separate ciliary epithelium from uvea by blunt dissection before cutting the uveal tissue with scissors.

Retinal Adhesion

Problematic adhesion between tumor and retina is more common with relatively thick tumors.[8] Adherent retina can often be separated from the tumor by blunt dissection of the tumor surface with a No. 15 Bard Parker scalpel, about 1–2 mm away from the apparent line of retinal adhesion, to divide invisible strands of tissue joining retina to tumor. If this fails, the tumor has probably invaded the retina. In this case, our preferred course of action is to top-slice the tumor with the scalpel, leaving the intraretinal portion in situ and treating it with radiotherapy. Another option is to excise the tumor completely, together with the invaded retina, dealing with the retinal defect after closing the sclera. Any retinal defect is managed by complete pars plana vitrectomy, subretinal hemorrhage aspiration, endolaser photocoagulation, and silicone oil tamponade, with these procedures preferably performed as soon as possible, immediately after reforming the eye with balanced salt solution. Our results show that these measures are highly successful at preventing retinal detachment.[8]

Extraocular Extension

Previously, if a small tumor nodule extended transsclerally, it was

excised together with the intraocular tumor and a surround of full-thickness sclera, closing the defect with a lamellar scleral graft from the same eye. Today, we would more conveniently cauterize the extraocular tumor with bipolar diathermy or excise it en bloc with a thin layer of superficial sclera, relying on brachytherapy to sterilize any surviving tumor.

Exoresection Without Profound Hypotensive Anesthesia

Our experience with exoresection without profound systemic hypotension is limited. If resection is done under normotensive anesthesia, meticulous bipolar cautery should be applied as soon as any bleeding point develops in the sclera. If possible, the short posterior ciliary arteries and the long posterior ciliary artery should be cauterized before closing any vortex veins, to prevent what in one patient seemed to be severe choroidal congestion and possibly an expulsive hemorrhage, with marked retinal bulging through the scleral window, despite repeated vitrectomy. Cold water and epinephrine drops may diminish choroidal hemorrhage in addition to bipolar cautery, which should be applied with minimal energy to avoid damaging the retina. Swabbing may not be sufficient to control hemorrhage so that a mini-suction device should be available to aspirate blood as it collects in the subretinal space during tumor excision.

Postoperative Management

In the immediate postoperative period, the patient is positioned so that the coloboma is situated below the macula, thereby preventing any subretinal hemorrhage from gravitating toward the fovea. Residual subretinal fluid from the preoperative exudative retinal detachment generally resorbs spontaneously within a few days.

Routine medications include topical antibiotics, steroids, and mydriatics. Systemic antibiotics can be administered as an intraoperative bolus or postoperatively. Oral steroids seem to reduce postoperative uveitis but have not been evaluated in a randomized fashion.

Patients are discharged home 1 day after the plaque removal,

which is usually 1 or 2 days after local resection. They are reassessed after 1 and 4 weeks, and then followed as with other treatments.

Anesthesia

Intraoperative hemorrhage is reduced by profound hypotensive anesthesia.[24] This lowers the systolic blood pressure to approximately 40–50 mmHg for about 60 minutes, from the time when ocular decompression is performed to the moment when the intraocular pressure is increased by intravitreal injection after scleral flap closure.

Cerebral function is monitored with a continuous electroencephalogram. The blood pressure is measured continuously with an intraarterial line in the radial artery. Standard procedures such as pulse oximetry and electrocardiographic monitoring are performed. Antithrombotic stockings are used postoperatively, and early mobilization is encouraged. Complications related to systemic hypotension are rare.

Outcomes

Visual Acuity

In 2011 the authors audited 112 exoresections performed in the previous 10 years (unpublished data). The tumors had a median diameter of 15.3 mm (range 8.9–22.4) and a median thickness of 8.5 mm, with 41% involving ciliary body and 16% extending to within 3 mm of the optic disc or fovea. The successful resections included several challenging cases, such as a patient operated on without any hypotensive anesthesia (because she had anemia due to thalassemia) and another patient who had an advanced tumor with total funnel retinal detachment touching the lens and an intraocular pressure of 44 mmHg. At the close of the study, 88% of eyes were retained, with 58% having visual acuity of 20/200 or better and 30% having 20/40 or better (Fig. 151.2). In a previous investigation, we showed that the most significant preoperative factors for predicting retention of good vision (20/40 or better) were medial tumor location (p=.002) and distance of more than 1 DD between the

tumor and the optic disc or fovea (p=.01).[4]

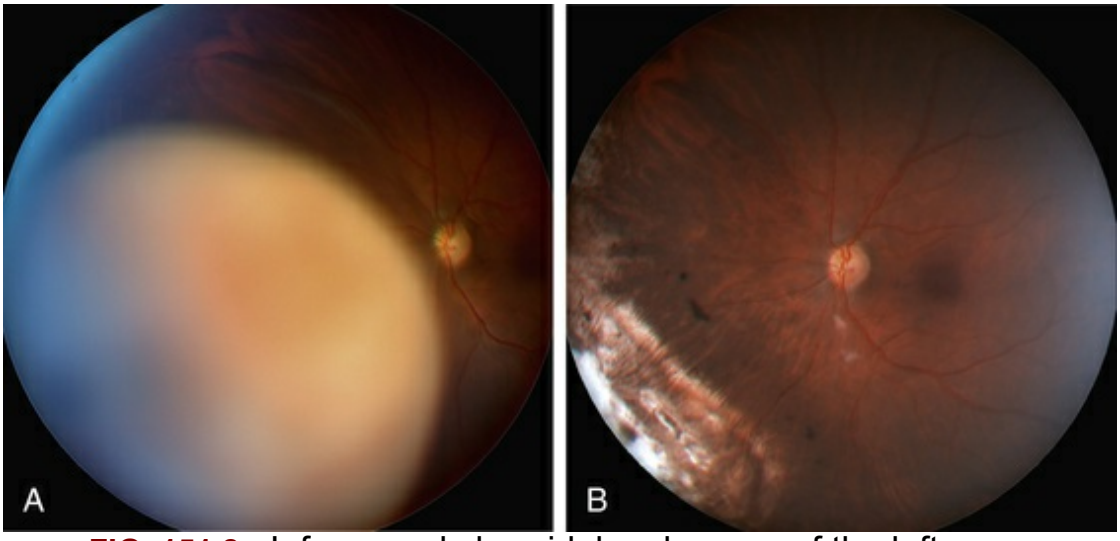

FIG. 151.2 Inferonasal choroidal melanoma of the left eye of a 45-year-old man, having a largest basal diameter of 15 mm and a thickness of 11 mm before exoresection with adjunctive brachytherapy (A) and 6 months afterward, when the visual acuity was 20/40 (B). This procedure was selected because any form of radiotherapy would probably have resulted in persistent exudative retinal detachment and eyelid damage with permanent epiphora. The tumor was of spindle-cell type with no chromosome 3 loss so that the survival probability was very good.

Local Tumor Control

In our 2011 audit there were no patients with visible residual tumor at the end of the resection procedure. Recurrent tumor developed in 12 patients, after a median of 2.4 years (range 0.6–3.8). Adjunctive brachytherapy seems effective at preventing local tumor recurrences in the irradiated field; however, there have been a few recurrences in nonirradiated areas, that is, in distant parts of the uvea or if adequate coverage of the resection area by the plaque could not be achieved, because the tumor had an irregular shape, or because it extended close to the optic disc, or because the plaque was not large enough to treat a sufficiently wide surround of apparently healthy choroid. We now use a 25-mm plaque instead of

a 20-mm plaque. In a previous study of 286 resections performed before the introduction of adjunctive brachytherapy, we showed by Cox multivariate analysis that the predictive factors for recurrent tumor are posterior extension to within a disc diameter of disc or fovea (p=.002), presence of epithelioid cells (p=.002), and tumor diameter of 16 mm or more (p=.019). Histologic examination of clearance margins was unreliable.[6]

Local tumor recurrence can arise at the margin of the surgical coloboma as an indistinct gray, brown, or white swelling. Rarely, the tumor recurs within the coloboma as a result of intraretinal or intrascleral tumor invasion. Exceptionally, a satellite lesion develops in a distant part of the choroid.[25] Noncontiguous recurrences have also been seen after plaque radiotherapy.[26] Residual and recurrent tumors need to be distinguished from reactive pigment epithelial hyperplasia and organized subretinal hematomas. Sequential fundus photography and optical coherence tomograhy are invaluable for distinguishing tumor from other conditions. If there is any doubt about the diagnosis, the suspicious lesion should be ablated by transpupillary thermotherapy as a precautionary measure.

Definite residual or recurrent tumor is best treated with plaque or proton beam radiotherapy, unless very small or situated close to the optic disc or fovea, in which case transpupillary thermotherapy can be attempted (Fig. 151.3). Failure to detect and treat a recurrent tumor effectively can result in extraocular tumor extension or optic disc involvement so that enucleation becomes necessary.

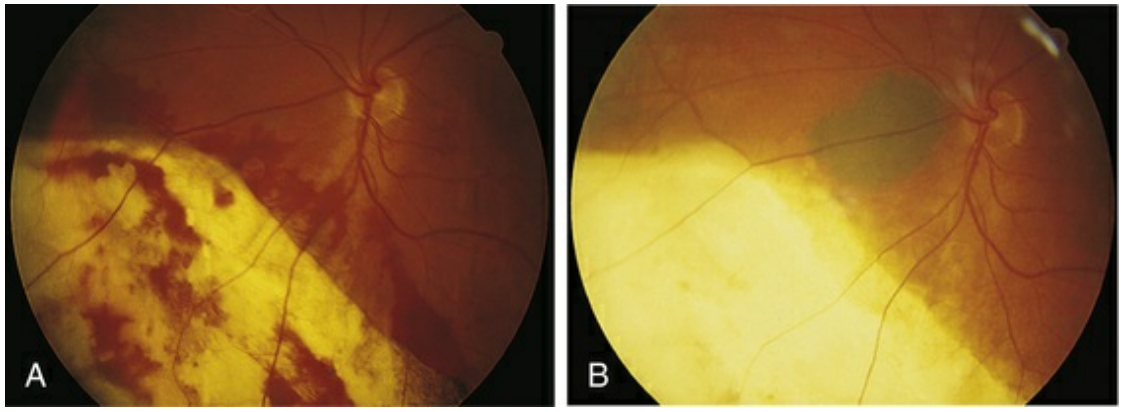

FIG. 151.3 Left fundus of a 67-year-old woman (A) soon after exoresection, with apparently complete

resection in 1989 and (B) 9 months later, showing a local tumor recurrence from a microscopic deposit. Histologic assessment of surgical clearance is unreliable, so adjunctive radiotherapy is now applied routinely.

Retinal Detachment

Before the introduction of ocular decompression, retinal tears sometimes occurred because of retinal prolapse during tumor excision. Today, retinal tears occur almost exclusively when attempting to separate tumor from adherent retina. Retinal breaks can usually be identified immediately and rarely result in retinal detachment if adequate vitreoretinal surgery is performed promptly. Our 2011 audit showed the rate of retinal detachment to be 9%. We previously demonstrated retinal detachment to correlate with tumor thickness.[7]

Postoperative vitreous hemorrhage indicates the presence of a retinal tear and hence a high risk of retinal detachment, so appropriate vitreoretinal surgery should be performed without delay, before proliferative vitreoretinopathy develops.

Although it might seem useful to apply preoperative retinopexy, this is rarely possible because of large tumor bulk or extensive serous retinal detachment.

Other Complications

Macular function is usually retained unless there is direct foveal involvement by the tumor or preoperative retinal detachment. Vision may be reduced if the excision line is close to the fovea or if a choroidal tear occurs as a result of excessive traction on the tumor during resection. A macular disciform lesion can occur from choroidal neovascularization arising at the edge of the surgical coloboma, if this extends far posteriorly. Cataract is uncommon, unless it was present preoperatively, for example, due to a ciliary body tumor; it tends to occur only in the presence of long-standing retinal detachment or after the use of intraocular silicone oil. Any postoperative diplopia usually resolves spontaneously; extraocular muscle surgery is rarely required.

Adjunctive brachytherapy may cause (1) wound dehiscence, which is prevented by the use of nonabsorbable sutures, and (2) cyclodialysis with hypotony, which is prevented by delaying radiotherapy by a month if cyclectomy has been performed. Optic neuropathy and radiation maculopathy can be avoided by not positioning the plaque close to disc or macula. Adjunctive brachytherapy reduces complications previously caused by wide surgical resection margins, which are no longer necessary. The greatest impact of such minimal surgical clearance has been with ciliochoroidal tumors, which are now excised without the need for broad iridectomy.

Metastatic Death

Nonrandomized, matched group studies suggest that the incidence of metastatic disease after local excision of uveal melanoma is not significantly different from that after enucleation[3] or plaque brachytherapy.[27]

In a series of 332 patients treated by transscleral local resection before 1996, we showed the probability of metastatic death to correlate with epithelioid cellularity and large tumor diameter.[5] Although highly significant statistically, these correlations had little clinical relevance because they provided only an approximate indication of the prognosis as far as an individual patient was concerned. In 1996, Prescher et al. showed loss of chromosome 3 (i.e., monosomy 3) within uveal melanoma cells to be highly predictive of metastatic disease and death.[28] Since 1999 we have therefore determined chromosome 3 status as a routine service, first using fluorescent in situ hybridization (FISH),[29] then by multiplex ligation-dependent probe amplification.[30] At the University of California San Francisco, we now perform next generation sequencing, which provides information on more than 500 selected genes. We developed and validated an online tool for predicting survival according to clinical stage, histologic grade, and chromosome 3 loss, also taking the patient's age and sex into account (www.ocularmelanomaonline.org).[31] These genetic studies have enabled us to reassure those with an excellent prognosis for survival, while referring high-risk patients to an oncologist for specialized care. Local resection provides large specimens for

prognostic studies and in the future may be useful for selecting systemic treatment or for developing vaccines or other forms of targeted therapy.

Since metastatic disease occurs almost exclusively with melanomas showing chromosome 3 loss, and since almost all such tumors prove fatal, it would seem the patient's survival prognosis is already sealed by the time the local resection is performed. If local resection has less effect on survival than previously believed, then any intuitive concerns about the surgical manipulations inducing or encouraging metastatic spread might prove to have been exaggerated. Further studies are required and these will require molecular tumor characterization.

Endoresection

The main objectives of primary endoresection of choroidal melanoma are to avoid optic neuropathy and maculopathy after radiotherapy,[32,33] and local tumor recurrence and extraocular extension after transpupillary thermotherapy.[34]

Indications and Contraindications

We currently undertake this surgery as a primary procedure only if (1) radiotherapy is unlikely to conserve useful vision, because the tumor has perforated retina or extends close to optic disc, and (2) the patient is highly motivated to retain vision and understands the controversial nature of this operation.

Surgical Technique

Briefly, the technique involves the following steps: (1) pars plana vitrectomy with a 20- or 23-gauge vitreous cutter; (2) the creation of a retinotomy over the tumor; (3) piecemeal tumor removal; (4) endolaser to the margins and bed of the coloboma; (5) perfluorocarbon liquid injection to flatten the retina; (6) endolaser retinopexy to attach retina around the coloboma; (7) endolaser photocoagulation to the entire scleral bed, to destroy any residual tumor; (8) perfluorocarbon–silicone exchange to maintain retinal

flattening and to prevent postoperative hemorrhage; (9) 360° scleral indentation with cryotherapy to any entry site tears; and (10) cryotherapy to the sclerotomies, in case of unrecognized tumor seeding.[9] Following a report of fatal air embolism during endoresection, we perform direct heavy liquid-silicone oil exchange, avoiding fluid-air exchange.[35] Recent developments include the use of endoscopic vitrectomy in some cases, and bimanual surgery with chandelier endoillumination. Adjunctive ruthenium plaque radiotherapy can be administered either in all cases or in selected cases at a later date if histologic or genetic studies indicate a high grade of malignancy.

Outcomes

Endoresection techniques have improved since our initial publication in 1998.[8] Outcomes depend largely on tumor location (Figs. 151.4 and 151.5). We recently analyzed our results after 71 procedures performed between 1996 and 2010.[9] The follow-up had a median of 4.1 years, exceeding 4 years in 49% of patients. The tumors had a mean basal diameter of 9.5 mm and a mean thickness of 4.4 mm, abutting the optic disc in 34%, extending to within 2 DD of the optic disc in another 31% of patients. The 68 eyes that were retained had visual acuity better than 20/40 in 13% and better than 20/100 in 31%. Rhegmatogenous retinal detachment occurred in 22% of eyes, and local tumor recurrence occurred in two patients (3%) at the margins of the coloboma in both cases. No patients developed seeding. Five patients (9%) died of metastatic disease.

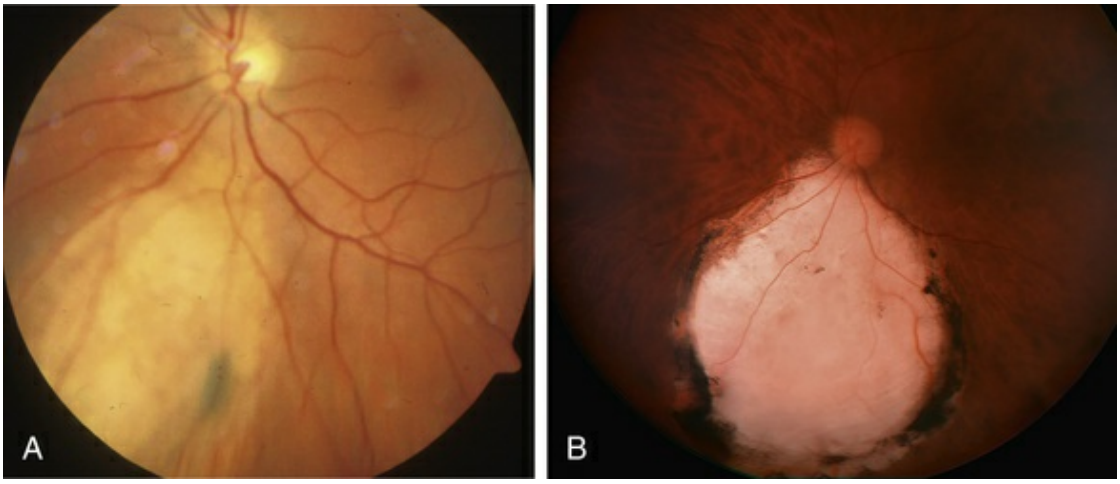

FIG. 151.4 A 37-year-old woman treated by endoresection. (A) Left eye before treatment, with visual acuity of 20/20 and a 10.1 × 6.5 × 2.8 mm melanoma extending close to the optic disc. (B) Fundus appearance 10 years later, with no visible tumor and visual acuity of 20/30. The patient was healthy with no sign of recurrent disease.

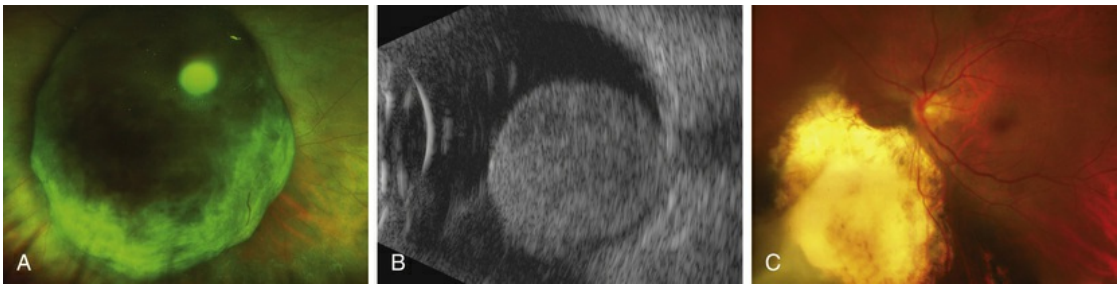

FIG. 151.5 Endoresection of a large juxtapapillary choroidal melanoma in the left eye of a 44-year-old man, performed using perfluorocarbon liquid instead of air to flatten the retina and endoscopy when the media became opaque. (A) Preoperative color photograph showing the tumor overhanging the optic disc. (B) Ultrasound scan showing the tumor to have a thickness of 13.5 mm but with basal dimensions of only 6 mm by 9 mm. (C) Postoperative photograph showing the surgical coloboma and a normal macula. Seventeen months postoperatively, there was no sign of local tumor recurrence and the visual acuity was 20/30.

Mortality after endoresection seems similar to that after other

treatment modalities. Large randomized studies would be required to reveal any differences, and these are not logistically possible. The considerations discussed in the section on exoresection apply to endoresection (see above).

As with other forms of therapy, local recurrence after endoresection tends to occur from untreated residual tumor in the adjacent choroid and in sclera, and such recurrent tumor can extend extraocularly if not treated promptly.[36] So far, we have not seen widespread intraocular recurrences from intraoperative tumor seeding. In one patient an untreated marginal recurrence spread through the retinal defect to invade the vitreous cavity.[37] This patient, who lived far from our center, had been discharged back to her retinal surgeon, who was unable to monitor the fundus because of cataract. Such spread would not have occurred if the eye had been enucleated as soon as ophthalmoscopy was no longer possible, a policy we have always followed after all types of conservative treatment. Another patient developed subconjunctival seeding, a complication we have also seen with tumor biopsy.[38] Several authors precede endoresection with radiotherapy to reduce the risk of iatrogenic tumor seeding.[13,14] Our impression is that such seeding is rare, at least in patients with a small melanoma, so that many patients must be developing radiation-induced complications unnecessarily. There would seem to be scope for randomized studies.

When the tumor extends close to fovea, visual loss can occur if fibrosis from the margin of the coloboma distorts the retina. Other possible complications of endoresection include silicone oil-induced complications; entry-site tears; submacular hemorrhage; and endophthalmitis. Despite a large retinotomy, proliferative vitreoretinopathy does not develop unless rhegmatogenous retinal detachment has occurred.

Secondary Local Resection for "Toxic Tumor" After Radiotherapy

Neovascular glaucoma is a common problem after radiotherapy of uveal melanoma, especially with large tumors. Some have

suggested this complication is due to extensive irradiation of healthy ocular tissues.[39] However, we believe this complication is, at least in part, caused by the presence of a large volume of irradiated tumor, either because it becomes ischemic or because it causes extensive retinal detachment, or both (i.e., "toxic tumor syndrome"). We have successfully treated these complications in several patients by performing exoresection or endoresection of the toxic tumor.[40] Fig. 151.6 shows the left eye of a 75-year-old man, who had a choroidal melanoma measuring 13.2 × 10.5 mm in diameter with a thickness of 9.3 mm in the left eye. The patient was keen to retain the eye because the right eye was amblyopic with visual acuity of 20/100. He was treated with proton beam radiotherapy because he was on anticoagulation for cardiac arrhythmia. The irradiated eye developed exudative retinal detachment with reduction of vision to 20/100 and neovascular glaucoma with an intraocular pressure of 46 mmHg. Exoresection was performed with minimal hypotensive anesthesia. The retinal detachment resolved within a day. The iris neovascularization regressed within a month, and 24 months after the resection the intraocular pressure was normal without topical medications. Some 8 years after the surgery, the patient was well and when tested with a LogMAR chart was able to see 66 letters with the affected eye and 60 letters with the fellow eye (Fig. 151.6).

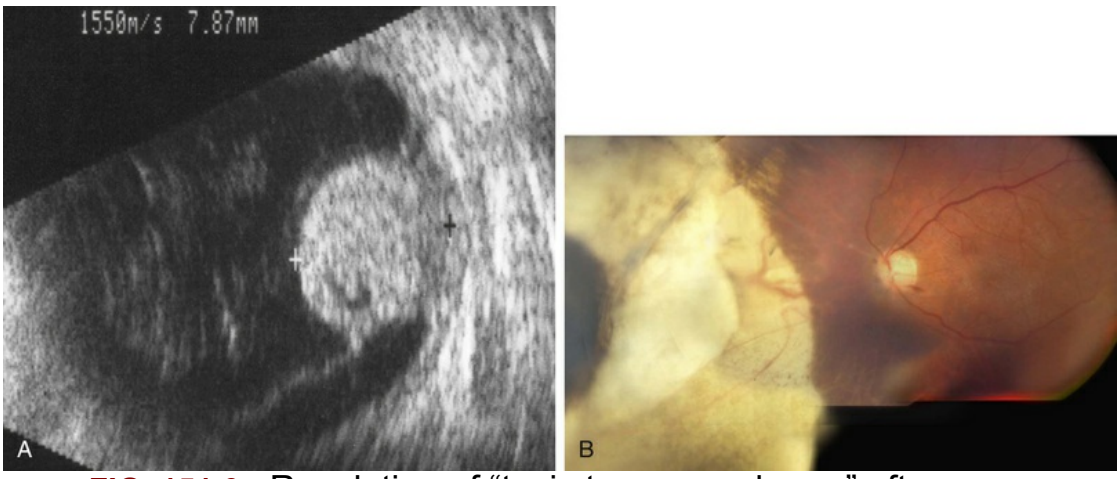

FIG. 151.6 Resolution of "toxic tumor syndrome" after secondary exoresection of a choroidal melanoma. (A) Ocular echography 15 months after proton beam radiotherapy, when the eye developed visual loss,

exudative retinal detachment, and neovascular glaucoma with an intraocular pressure of 46 mmHg. (B) Fundus appearance after secondary exoresection, which achieved resolution of retinal detachment and neovascular glaucoma.

Local resection is also effective for recurrent tumor after other forms of therapy, selecting exoresection for large anterior tumors and endoresection for smaller, posterior tumors (Fig. 151.7).

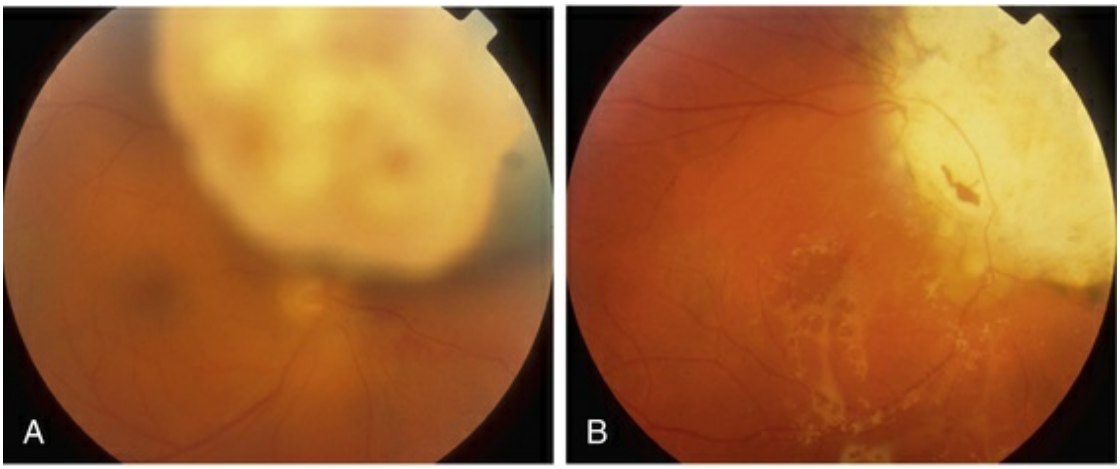

FIG. 151.7 Recurrent choroidal melanoma in the right eye of a 52-year-old woman after brachytherapy at another center. The visual acuity was 20/40. The left eye had previously been enucleated after an accident. (A) Preoperative photograph showing the tumor (16 × 16 × 10 mm) overhanging the optic disc. (B) Fundus appearance 4 months postoperatively, when the visual acuity was 20/60. The patient retained useful vision until she died of metastatic disease. The recurrent tumor had shown epithelioid cells and chromosome 3 loss.

Conclusions

Exoresection and endoresection are useful both as primary treatment for choroidal melanoma, when other forms of therapy are unlikely to conserve useful vision, and as salvage therapy when other methods have failed. It would therefore be ideal if surgical

resection were included in the therapeutic repertoire of large oncology centers. The tumor tissue provided by local resection is already useful in enhancing prognostication and planning patient care. In the future, such tissue will probably become more valuable if large tumor samples are required for individualizing systemic therapy, as is already happening with other cancers.

Insights from molecular biology suggest that fears about iatrogenic tumor dissemination to other parts of the body are exaggerated. Surgical and anesthetic techniques have advanced considerably in recent years, so that good results are now achieved by experienced surgeons. For these reasons, the greatest obstacle still preventing local resection from being performed in greater numbers is the surgical expertise required for such complex surgery. We hope this chapter will make it easier for local resection of choroidal melanomas to be adopted more widely.

References

1. Stallard HB. Partial choroidectomy. *Br J Ophthalmol*. 1966;50:660–662.
2. Foulds WS. The local excision of choroidal melanomata. *Trans Ophthalmol Soc U K*. 1973;93:343–346.
3. Foulds WS, Damato BE, Burton RL. Local resection versus enucleation in the management of choroidal melanoma. *Eye*. 1987;1:676–679.
4. Damato BE, Paul J, Foulds WS. Predictive factors of visual outcome after local resection of choroidal melanoma. *Br J Ophthalmol*. 1993;77:616–623.
5. Damato BE, Paul J, Foulds WS. Risk factors for metastatic uveal melanoma after trans-scleral local resection. *Br J Ophthalmol*. 1996;80:109–116.
6. Damato BE, Paul J, Foulds WS. Risk factors for residual and recurrent uveal melanoma after trans-scleral local resection. *Br J Ophthalmol*. 1996;80:102–108.
7. Damato B, Groenewald CP, McGalliard JN, et al. Rhegmatogenous retinal detachment after transscleral local resection of choroidal melanoma. *Ophthalmology*. 2002;109:2137–2143.

8. Damato BE, Groenewald C, McGalliard J, et al. Endoresection of choroidal melanoma. *Br J Ophthalmol*. 1998;82:213–218.
9. Konstantinidis L, Groenwald C, Coupland SE, et al. Long-term outcome of primary endoresection of choroidal melanoma. *Br J Ophthalmol*. 2014;98:82–85.
10. Peyman GA, Cohen SB. Ab interno resection of uveal melanoma. *Int Ophthalmol*. 1986;9:29–36.
11. Peyman GA, Juarez CP, Diamond JG, et al. Ten years experience with eye wall resection for uveal malignant melanomas. *Ophthalmology*. 1984;91:1720–1725.
12. Shields JA, Shields CL, Shah P, et al. Partial lamellar sclerouvectomy for ciliary body and choroidal tumors. *Ophthalmology*. 1991;98:971–983.
13. Bechrakis NE, Petousis VE, Willerding G, et al. Ten year results of transscleral resection of large uveal melanomas: local tumour control and metastatic rate. *Br J Ophthalmol*. 2010;94:460–466.
14. Bechrakis NE, Foerster MH. Neoadjuvant proton beam radiotherapy combined with subsequent endoresection of choroidal melanomas. *Int Ophthalmol Clin*. 2006;46:95–107.
15. Schilling H, Bornfeld N, Talies S, et al. Endoresection of large uveal melanomas after pretreatment by single-dose stereotactic convergence irradiation with the Leksell gamma knife – first experience on 46 cases. *Klin Monatsbl Augenheilkd*. 2006;223:513–520.
16. Garcia-Arumi J, Zapata MA, Balaguer O, et al. Endoresection in high posterior choroidal melanomas: long-term outcome. *Br J Ophthalmol*. 2008;92:1040–1045.
17. Char DH, Miller T, Crawford JB. Uveal tumour resection. *Br J Ophthalmol*. 2001;85:1213–1219.
18. Foss AJ, Whelehan I, Hungerford JL, et al. Predictive factors for the development of rubeosis following proton beam radiotherapy for uveal melanoma. *Br J Ophthalmol*. 1997;81:748–754.
19. Shields CL, Naseripour M, Cater J, et al. Plaque radiotherapy for large posterior uveal melanomas (> or =8-mm thick) in 354 consecutive patients. *Ophthalmology*.

2002;109:1838–1849.
20. Puusaari I, Heikkonen J, Summanen P, et al. Iodine brachytherapy as an alternative to enucleation for large uveal melanomas. *Ophthalmology*. 2003;110:2223–2234.
21. Kivelä T, Puusaari I, Damato B. Transscleral resection versus iodine brachytherapy for choroidal malignant melanomas 6 millimeters or more in thickness: a matched case-control study. *Ophthalmology*. 2003;110:2235–2244.
22. Bechrakis NE, Bornfeld N, Zoller I, et al. Iodine 125 plaque brachytherapy versus transscleral tumor resection in the treatment of large uveal melanomas. *Ophthalmology*. 2002;109:1855–1861.
23. Russo A, Coupland SE, O'Keefe M, et al. Choroidal melanoma in a 7-year-old child treated by trans-scleral local resection. *Graefes Arch Clin Exp Ophthalmol*. 2010;248:747–749.
24. Jones AG. Profound hypotension: ethical considerations. *Hosp Med*. 2002;63:92–94.
25. Kim JW, Damato BE, Hiscott P. Noncontiguous tumor recurrence of posterior uveal melanoma after transscleral local resection. *Arch Ophthalmol*. 2002;120:1659–1664.
26. Duker JS, Augsburger JJ, Shields JA. Noncontiguous local recurrence of posterior uveal melanoma after cobalt 60 episcleral plaque therapy. *Arch Ophthalmol*. 1989;107:1019–1022.
27. Augsburger JJ, Lauritzen K, Gamel JW, et al. Matched group study of surgical resection versus cobalt-60 plaque radiotherapy for primary choroidal or ciliary body melanoma. *Ophthalmic Surg*. 1990;21:682–688.
28. Prescher G, Bornfeld N, Hirche H, et al. Prognostic implications of monosomy 3 in uveal melanoma. *Lancet*. 1996;347:1222–1225.
29. Damato B, Duke C, Coupland SE, et al. Cytogenetics of uveal melanoma: a 7-year clinical experience. *Ophthalmology*. 2007;114:1925–1931.
30. Damato B, Dopierala JA, Coupland SE. Genotypic profiling of 452 choroidal melanomas with multiplex ligation-dependent probe amplification. *Clin Cancer Res*.

2010;16:6083–6092.
31. Damato B, Eleuteri A, Taktak AF, et al. Estimating prognosis for survival after treatment of choroidal melanoma. *Prog Retin Eye Res*. 2011;30:285–295.
32. Gragoudas ES, Li W, Lane AM, et al. Risk factors for radiation maculopathy and papillopathy after intraocular irradiation. *Ophthalmology*. 1999;106:1571–1577.
33. Meyer A, Lévy C, Blondel J, et al. Optic neuropathy after proton-beam therapy for malignant choroidal melanoma. *J Fr Ophtalmol*. 2000;23:543–553.
34. Singh AD, Eagle RC Jr, Shields CL, et al. Clinicopathologic reports, case reports, and small case series: enucleation following transpupillary thermotherapy of choroidal melanoma: clinicopathologic correlations. *Arch Ophthalmol*. 2003;121:397–400.
35. Rice JC, Liebenberg L, Scholtz RP, et al. Fatal embolism during endoresection of choroidal melanoma. *Retinal Cases Brief Rep*. 2014;8:127–129.
36. Damato B, Wong D, Green FD, et al. Intrascleral recurrence of uveal melanoma after transretinal "endoresection". *Br J Ophthalmol*. 2001;85:114–115.
37. Hadden PW, Hiscott PS, Damato BE. Histopathology of eyes enucleated after endoresection of choroidal melanoma. *Ophthalmology*. 2004;111:154–160.
38. Raja V, Russo A, Coupland S, et al. Extraocular seeding of choroidal melanoma after a transretinal biopsy with a 25-gauge vitrector. *Retin Cases Brief Rep*. 2011;5:194–196.
39. Daftari IK, Char DH, Verhey LJ, et al. Anterior segment sparing to reduce charged particle radiotherapy complications in uveal melanoma. *Int J Radiat Oncol Biol Phys*. 1997;39:997–1010.
40. Konstantinidis L, Groenwald C, Coupland SE, et al. Trans-scleral local resection of toxic choroidal melanoma after proton beam radiotherapy. *Br J Ophthalmol*. 2014;98:775–779.

152

Laser Treatment of Choroidal Melanoma

Norbert Bornfeld

Introduction

Photocoagulation, as introduced by Meyer-Schwickerath in 1949,[1] was among the first eye-salvaging treatment methods for choroidal melanomas and the first to make use of a light source. The armamentarium of eye salvaging treatment modalities for choroidal melanomas has significantly enlarged since then, including radiation techniques (brachytherapy, teletherapy with protons, and stereotactic conformal radiation with photons) and surgical excision (transscleral or transretinal resection), as did the techniques and light sources for laser treatment of choroidal melanomas. Transpupillary thermotherapy making use of infrared lasers at a subcoagulation level was introduced in 1992 by Journée-de Korver and Oosterhuis[2] and was utilized for primary treatment of small uveal melanomas. Other laser techniques like photodynamic treatment of uveal melanomas were evaluated experimentally and in small case series.[3] This chapter discusses the current role of laser treatment in the management of choroidal melanomas in relation to the alternative treatment methods currently available.

Laser Techniques Available for the Treatment of Intraocular Tumors

As in other fields of ophthalmology, lasers may be used for the treatment of uveal melanomas for thermal (coagulative or noncoagulative) and nonthermal treatment techniques.

By convention, photocoagulation is considered to be laser treatment at a temperature level of more than 75°C. Photocoagulation attempts to destroy a uveal tumor with light from a high-intensity light source, which originally was not a laser but a xenon arc light.[4]

Noncoagulative laser treatment techniques include low-power long-exposure treatment techniques making use of a conventional argon blue–green laser or infrared laser. Depending on the

wavelength of the laser used, the lesions are located deeper in the choroid when infrared or near-infrared lasers are used, and lesions created by argon blue–green lasers do not extend 1 mm in size while infrared lasers may result in a depth of tumor necrosis of several millimeters.[5]

Nonthermal laser techniques include photodynamic treatment (PDT) of intraocular tumors making use of the cytotoxic effect of singlet oxygen radicals by photosensitizers when activated by visible light with a defined wavelength. PDT eventually results in photothrombosis of pathologic vessels. Photodynamic treatment was initially developed for the treatment of choroidal neovascularization in age-related macular degeneration and has been used effectively in the treatment of choroidal hemangioma.

Photocoagulation

Photocoagulation treatment is started by circumvallating the tumor with intensive laser photocoagulation lesions, resulting in an atrophic scar followed by direct treatment of the tumor with high-intensity burns, including disruption of the tumor tissue and occasionally appearance of gas bubbles inside the target tissue. As expected, this technique may result in numerous treatment-related retinal complications, including retinal breaks, epiretinal membrane formation vascular, occlusion, and traction retinal detachment. Only small tumors can be treated, and even in this subgroup of small tumors, a relatively high recurrence rate of uveal melanomas after photocoagulation treatment has been reported. In particular, extrascleral extension of the melanoma may occur, growing underneath the fibrous scar overlying the tumor remnants. Consequently, photocoagulation treatment as sole treatment of a uveal melanoma has been abandoned in most centers.[6]

Transpupillary Thermotherapy

Technique

The term “transpupillary thermotherapy” (TTT) was introduced by Journée-de Korver[2] to describe a technique in which a near-infrared

or infrared light source for long-term exposure laser treatment of uveal melanomas is used. There is a controversial discussion in the literature on whether the word "thermotherapy" is appropriate or whether this treatment technique should be regarded as long-exposure subthreshold photocoagulation using a long-wavelength light source, since a whitish-grayish discoloration of the target tissue at the end of the procedure is recommended.[7] As published by Journée-de Korver,[2] thermotherapy is different from hyperthermia, which by definition is heating the tumor to a temperature of 42–44°C to enhance the cytotoxic effect of ionizing radiation on tumor cells. In TTT temperatures of approximately 45–60°C within the tumor are reached with irreversible cytotoxic effects so that additional radiotherapy may be not required.[7]

Infrared or near-infrared light penetrates deeper into the choroidal tissue than light from argon blue–green lasers, theoretically avoiding undesirable coagulation effects in the retina. In contrast to other wavelengths, the absorption of ocular media for infrared is very low (approximately 4–7%). Disadvantages include the invisibility of the actual laser beam resulting in the need of an aiming beam and an increased risk of choroidal hemorrhage because of the deeper penetration of the laser light. Numerous light sources based on a semiconductor diode lasers are commercially available which may be used for TTT.

In clinical practice TTT is performed in retrobulbar anesthesia using a slit lamp and a contact lens. A laser beam with a spot size of 3 mm and a maximal power density of 12 W/cm^2 is used. At the second half of the exposure time of at least one minute a grayish discoloration of the tumor tissue should be visible, indicating a temperature of the target tissue of 60–65°C. Ideally no occlusion of retinal vessels and no coagulation effects in the overlying retina should occur. Three to four treatment sessions are needed, which should result in an atrophic scar with central pigment and visible sclera at the treatment site. TTT is limited to tumors not exceeding 3.5 mm thickness and 10 mm in largest tumor diameter.[8]

Potential complications of TTT include accidental combustions of the anterior segment and posterior segment compilations including macular pucker, branch retinal vein occlusion, macular edema, vitreous and/or retinal hemorrhage, branch retinal artery occlusion,

retinal detachment, and retinal neovascularization. At least one of these complications may occur in 78% of patients.[9] Vitreomacular traction as a consequence of posterior hyaloid traction may be caused by TTT necessitating vitreoretinal surgery.[10]

Experimental data provided evidence that the absorption of heat is enhanced in particular in amelanotic tumors by systemic administration of a chromophore such as indocyanine green immediately before TTT.[11] Although a prospective randomized trial did not find any beneficial effect in supplemental use of indocyanine green in TTT of choroidal melanomas,[12] other authors did find enhanced local tumor control when indocyanine was used in combination with TTT.[13]

TTT as Primary Treatment of Choroidal Melanoma

When TTT was introduced in the treatment of choroidal melanoma, short-term follow-up data suggested that tumor regression may be achieved in more than 90% in appropriate cases. Tumors considered as being appropriate for TTT included melanomas with a largest tumor diameter of less than 12 mm and not more than 4 mm thickness located posterior to the equator where the clinical diagnosis of a malignant melanoma was established.[14]

However, the initial enthusiasm was dampened after reports showing that conventional photocoagulation and TTT may be not as different as previously thought.[15] Juxtapapillary tumors, in particular when the tumor was abutting or overhanging the optic disc, and tumors requiring more than three sessions for tumor control were more likely to develop tumor recurrence[16–24] (Fig. 152.1). Histopathologic evaluation in a series of seven eyes enucleated after TTT detected lateral growth of the tumor and an extrascleral extension in 5 out of 7 cases, which were detected only in a single case ultrasonographically.[25] Other groups also reported extrascleral extension after TTT.[25–27] Progressive choroidal vascular remodeling and retinochoroidal anastomosis in sequential indocyanine green angiograms may indicate recurrent tumor growth after TTT, indicating that vascular occlusion after TTT is not complete.[28,29]

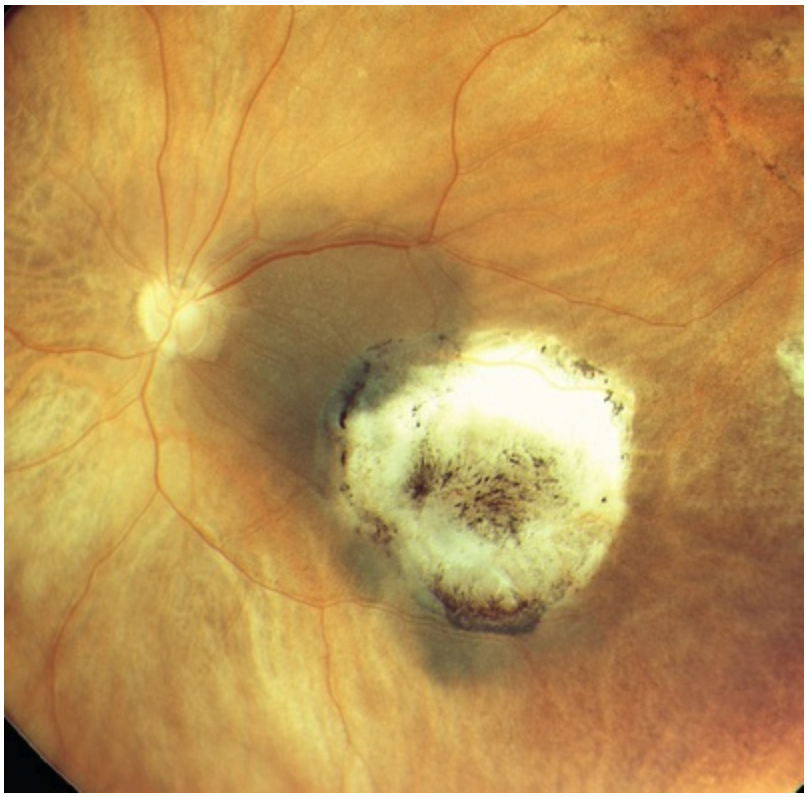

FIG. 152.1 Marginal recurrence of choroidal melanoma at the posterior pole 18 months after transpupillary thermotherapy (TTT).

These controversial aspects of TTT as sole treatment of choroidal melanomas have been reviewed by a group of ocular oncologists.[15] They found recurrence rates as high as 56%.[19] In addition, in a recent study Shields and coworkers analyzed 391 cases with primary TTT for choroidal melanoma. In patients treated from 1995 to 2000, Kaplan–Meier estimates showed a recurrence rate of 42% after 10 years. Patients treated from 2001 to 2012 had a lower recurrence rate of 15% at 10 years but had thinner tumors (2.2 mm vs. 2.7 mm), where more distant from the optic disc and the macula compared to the 1995–2000 series. The authors identified risk factors for recurrence including occurrence of symptoms, closer location to the optic disc and the presence of subretinal fluid, treatment of recurrences after TTT with TTT, and a higher risk of extraocular tumor extension. Visual acuity decreased in 44% of all patients after completion of treatment.

TTT as Ancillary Treatment of Choroidal

Melanoma

Mainly because of the high recurrence rate, with its potential impact on metastasis sole treatment of choroidal melanomas should only be performed in eyes with no other treatment options (e.g., elderly patients).[30] However, TTT as ancillary treatment offers promising options.[9,31]

TTT may be applied prior or during treatment or after completing brachytherapy. The simultaneous use of TTT and (local) brachytherapy of uveal melanomas has been originally suggested by the Leiden Group as "sandwich therapy" (brachytherapy of the tumor base and TTT of the tumor apex) as both treatment modalities may be synergistic. The rationale for "sandwich therapy" is the enhanced cytotoxic effect of radiation and the potential reduction of radiation dose when thermotherapy and radiation are combined.[32]

Since its introduction several authors have evaluated "sandwich therapy" of choroidal melanomas. Early reports published significant advantages in terms of local tumor control and preservation of visual function.[33–35] More recent studies, however, could only detect slight advantages of "sandwich therapy" over brachytherapy, if any,[36,37] or even worse results in terms of deteriorated visual function in the "sandwich therapy" group.[38]

As sole TTT and simultaneous TTT and brachytherapy have not proven to be advantageous over brachytherapy alone, TT as ancillary treatment in selected cases of choroidal melanoma after brachytherapy is in the focus of interest. Several recent studies have shown that this approach offers distinct advantages in selected cases of choroidal melanoma. In particular in tumors overhanging or encircling the optic disc, more eyes can be preserved in the group of patients with combined treatment.[39] A better visual outcome could not be achieved.[36] The planned use of TTT, however, appears to protect against neovascular glaucoma and secondary enucleation in the first 5 years after treatment[40] (Figs. 152.2 and 152.3).

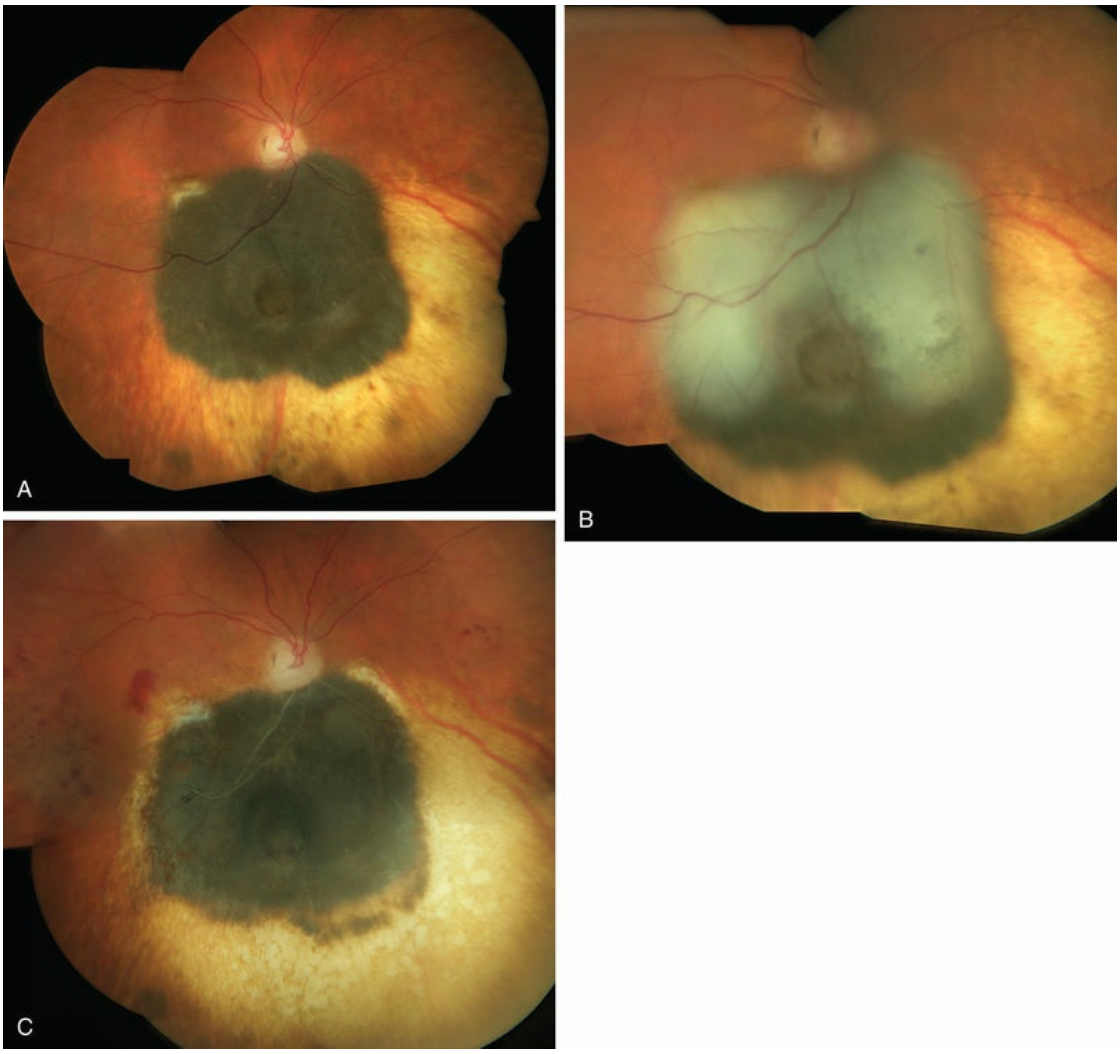

FIG. 152.2 (A) Juxtapapillary choroidal melanoma with insufficient radiation scar at the central edge of the tumor after beta ray brachytherapy. (B) Immediately after ancillary transpupillary thermotherapy (TTT) of the tumor remnants. (C) 3 months after ancillary TTT with chorioretinal scar at the central edge of the tumor but vascular occlusion and retinal hemorrhages peripheral to the tumor.

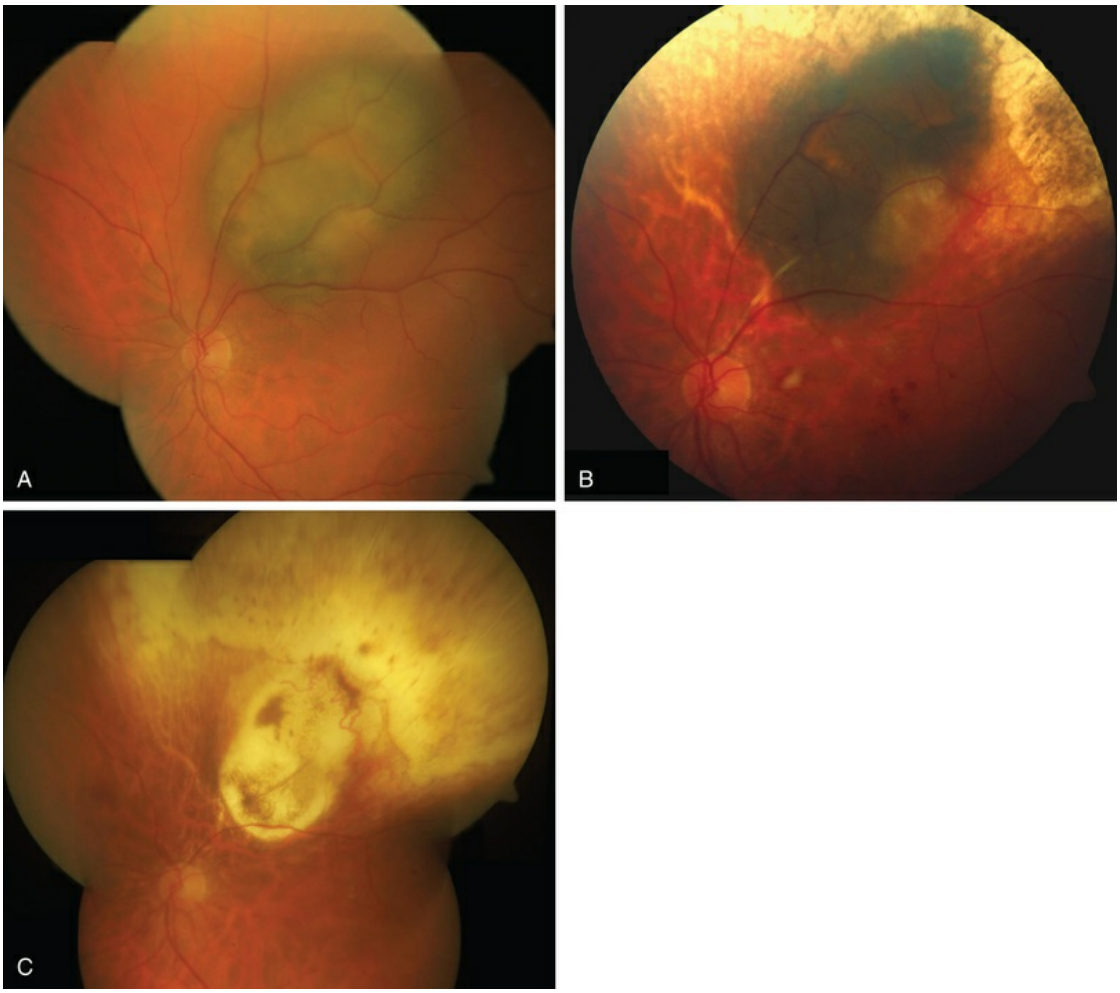

FIG. 152.3 (A) Choroidal melanoma underlying the temporal superior vessel arcade. (B) 4 months after beta ray brachytherapy with insufficient tumor regression at the central tumor margin. (C) 3½ years after brachytherapy and supplemental transpupillary thermotherapy (TTT).

Geographic misses may complicate radiotherapy of posterior choroidal melanomas due to inappropriate positioning of the plaque or plaque tilt. Detection of plaque tilt by ultrasonography allows supplemental TTT after brachytherapy, reducing the rate of recurrences to 3.6%.[31] Geographic misses may be unavoidable when the tumor is overhanging or partially surrounding the optic disc margin. In these cases supplemental TTT may improve the rate of eye preservation,[41] although the potential benefit is discussed controversially.[36,39,42] Additionally, TTT may be used after transscleral or transretinal surgical excision to prevent recurrent tumor growth at the edges of the pseudocoloboma. Interestingly,

monosomy 3, which is a highly significant marker for metastasis in choroidal melanoma, is correlated with faster tumor regression after combined brachytherapy and TTT.[43]

TTT as ancillary treatment was evaluated in radiotherapy modalities other than brachytherapy, such as proton radiation.[44] In this series, large uveal melanomas between 7 and 15 mm thickness were randomized for proton treatment alone and for combined treatment with three sessions of TTT after radiation with a significant lower secondary enucleation rate and less exudative retinal detachment in the latter group.

Laser Photocoagulation as Ancillary Treatment for Uveal Melanoma

Radiation Retinopathy, Radiation-Induced Optic Neuropathy

Radiation techniques are well established in eye salvaging treatment of uveal melanoma but may be complicated by radiation-related complications like radiation retinopathy and radiation optic neuropathy. Incidence and severity of these complications are related to the radiation dose used, the dose distribution of the radiation source (beta ray plaques, gamma ray plaques or external beam sources like proton beam), and the location of the tumor (posterior or anterior to the equator). Radiation retinopathy is a slowly progressive, delayed-onset disease of retinal blood vessels due to changes in the structure and permeability of the retinal vessels.[45] Characteristic clinical findings are macular edema, capillary nonperfusion, cotton-wool spots, capillary telangiectasia, retinal neovascularization, microaneurysms, retinal hemorrhages, intraretinal exudation, and neuronal changes such as disc edema, disc pallor, optic nerve atrophy, and neovascularization of the disc.[46,47]

If proliferative retinopathy remains untreated, rubeosis of the iris and secondary neovascular glaucoma may occur. There is no effective treatment to cure vision loss due to radiation retinopathy. Panretinal photocoagulation, however, is effective in preventing

complications related to radiation-induced ocular ischemia.[46,48] Macular edema is a frequent complication of radiotherapy of uveal melanomas, in particular if macular edema is present prior to radiotherapy. Radiation-induced macular edema may benefit from focal laser treatment.[49] New options include intravitreal VEGF inhibitors in analogy to the treatment of diabetic macular edema or the combination of both treatment options.[48] Macular edema may be prevented by early sector photocoagulation after brachytherapy.[50,51]

Resection of Uveal Melanoma

The benefit of photocoagulation prior to surgical excision of an uveal melanoma is still unclear and subject of a controversial discussion. TTT or conventional photocoagulation is effective in reducing the risk of continuous or recurrent tumor growth after surgical excision. Damato and colleagues have recommended the use of photocoagulation at the edges of the pseudocoloboma as part of the routine management of patients following transscleral local resection.[52] In endoresection endolaser coagulation of the tumor site, particularly of the tumor edges, is mandatory because of the high risk of incomplete removal of tumor tissue.

Exudative Retinal Detachment

Choroidal melanomas are frequently associated with exudative retinal detachment due to tumor-related vascular leakage. Moreover, extensive exudative retinal detachment is a well-known complication of brachytherapy of uveal melanoma and may lead to loss of vision and eventually enucleation.[53] Several authors have reported that scatter photocoagulation on the surface of the tumor may be effective in the management of melanoma-associated retinal detachment, which may be combined with vitreoretinal surgery, drainage of subretinal fluid, and fluid–air exchange. In charged particle therapy of uveal melanomas the ancillary use of laser thermotherapy significantly reduced the incidence and duration of exudative retinal detachment after radiation treatment.[54] Subthreshold transpupillary thermotherapy may be effective in the management of subfoveal fluid on small choroidal melanomas.[55]

Photodynamic Therapy of Uveal Melanomas

The effect of photodynamic therapy (PDT) (photoradiation) is based on the cytotoxic effect of singlet oxygen radicals by photosensitizers when exposed to visible light. The first generation of photosensitizers used were hematoporphyrin derivatives (HpD).[56] HpD-based photodynamic therapy, however, had numerous disadvantages, including a high rate of recurrences (probably related to the poor tissue penetration of 630 nm laser light into tumor tissue), secondary glaucoma, and severe systemic side-effects.[57]

Benzoporphyrin-derived photosensitizers like Verteporfin developed for the treatment of choroidal neovascular membranes in age-related macular degeneration have been evaluated experimentally and clinically in the treatment of choroidal melanomas.[58] Verteporfin offers numerous advantages including better tissue penetration and fewer systemic side-effects with regard to skin toxicity and has been proven to be effective in the treatment of choroidal hemangioma.[59,60] Data from a series of patients with Verteporfin PDT prior to intentional enucleation demonstrated that PDT with Verteporfin is basically capable of destroying a choroidal melanoma using a light dose of 100 J/cm^2. In this series tumor necrosis was induced in a depth up to 2.5 mm using a light dose ≥100 J/cm^2 demonstrating the potential of PDT with Verteporfin to induce tumor necrosis.[61] To date six reports with 38 patients having Verteporfin PDT as first-line treatment of a choroidal melanoma have been reported.[62] In eight patients tumor recurrence occurred. Tumor pigmentation prevents tissue penetration of the laser with a lack of tumor destruction,[63] suggesting that PDT with Verteporfin is inadequate in most clinical cases of choroidal melanomas.

Experimental Techniques

Photoablation of ocular melanoma has been reported so far in an animal model only.[64] The technique uses an intraocular 15-W argon

blue–green laser with a vitreous cutter used simultaneously to remove liberated tumor debris. A Dutch group presented experimental results in an animal model after transscleral laser thermotherapy of choroidal melanoma using an infrared diode laser, which was able to destroy the tumor and preserve the stability of the sclera.[65] To date no clinical results have been published. New laser sources introduced in treatment of experimental intraocular melanoma included a focused, raster-scanned beam from an Nd:yttrium–lanthanum–fluoride laser (1047 nm).[66]

References

1. Meyer-Schwickerath G. The preservation of vision by treatment of intraocular tumors with light coagulation. *Arch Ophthalmol*. 1961;66:458–466.
2. Journée-de Korver JG, Oosterhuis JA, et al. Transpupillary thermotherapy (TTT) by infrared irradiation of choroidal melanoma. *Doc Ophthalmol*. 1992;82(3):185–191.
3. Kawczyk-Krupka A, Bugaj AM, Latos W, et al. Photodynamic therapy in treatment of cutaneous and choroidal melanoma. *Photodiagnosis Photodyn Ther*. 2013;10(4):503–509.
4. Shields JA, Glazer LC, Mieler WF, et al. Comparison of xenon arc and argon laser photocoagulation in the treatment of choroidal melanomas. *Am J Ophthalmol*. 1990;109(6):647–655.
5. Journée-de Korver HG, Midena E, Singh AD. Infrared thermotherapy: from laboratory to clinic. *Ophthalmol Clin North Am*. 2005;18(1):99–110 [viii–ix].
6. Damato B, Lecuona K. Conservation of eyes with choroidal melanoma by a multimodality approach to treatment: an audit of 1632 patients. *Ophthalmology*. 2004;111(5):977–983.
7. Oosterhuis JA, Journée-de Korver HG, Keunen JE. Transpupillary thermotherapy: results in 50 patients with choroidal melanoma. *Arch Ophthalmol*. 1998;116(2):157–162.
8. Houston SK, Wykoff CC, Berrocal AM, et al. Lasers for the treatment of intraocular tumors. *Lasers Med Sci*.

2013;28(3):1025–1034.
9. Harbour JW, Meredith TA, Thompson PA, et al. Transpupillary thermotherapy versus plaque radiotherapy for suspected choroidal melanomas. *Ophthalmology*. 2003;110(11):2207–2214 [discussion 15].
10. Kashani AH, Aaberg TM Jr, Capone A Jr. Vitreomacular traction as a consequence of posterior hyaloidal contraction after transpupillary thermotherapy. *Am J Ophthalmol*. 2013;155(5):937–945.
11. Chong LP, Ozler SA, de Queiroz JM Jr, et al. Indocyanine green-enhanced diode laser treatment of melanoma in a rabbit model. *Retina*. 1993;13(3):251–259.
12. De Potter P, Jamart J. Adjuvant indocyanine green in transpupillary thermotherapy for choroidal melanoma. *Ophthalmology*. 2003;110(2):406–413 [discussion 13–4].
13. Liggett PE, Lavaque AJ, Chaudhry NA, et al. Preliminary results of combined simultaneous transpupillary thermotherapy and ICG-based photodynamic therapy for choroidal melanoma. *Ophthalmic Surg Lasers Imaging*. 2005;36(6):463–470.
14. Shields CL, Shields JA, Cater J, et al. Transpupillary thermotherapy for choroidal melanoma: tumor control and visual results in 100 consecutive cases. *Ophthalmology*. 1998;105(4):581–590.
15. Singh AD, Kivela T, Seregard S, et al. Primary transpupillary thermotherapy of "small" choroidal melanoma: is it safe? *Br J Ophthalmol*. 2008;92(6):727–728.
16. Shields CL, Shields JA, Perez N, et al. Primary transpupillary thermotherapy for small choroidal melanoma in 256 consecutive cases: outcomes and limitations. *Ophthalmology*. 2002;109(2):225–234.
17. Aaberg TM Jr, Bergstrom CS, Hickner ZJ, et al. Long-term results of primary transpupillary thermal therapy for the treatment of choroidal malignant melanoma. *Br J Ophthalmol*. 2008;92(6):741–746.
18. Singh AD, Eagle RC Jr, Shields CL, et al. Clinicopathologic reports, case reports, and small case series: enucleation following transpupillary thermotherapy of choroidal

melanoma: clinicopathologic correlations. *Arch Ophthalmol*. 2003;121(3):397–400.
19. Spire M, Devouassoux MS, Kodjikian L, et al. Primary transpupillary thermotherapy for 18 small posterior pole uveal melanomas. *Am J Ophthalmol*. 2006;141(5):840–849.
20. Win PH, Robertson DM, Buettner H, et al. Extended follow-up of small melanocytic choroidal tumors treated with transpupillary thermotherapy. *Arch Ophthalmol*. 2006;124(4):503–506.
21. Diaz CE, Capone A Jr, Grossniklaus HE. Clinicopathologic findings in recurrent choroidal melanoma after transpupillary thermotherapy. *Ophthalmology*. 1998;105(8):1419–1424.
22. Finger PT, Lipka AC, Lipkowitz JL, Jofe M, McCormick SA. Failure of transpupillary thermotherapy (TTT) for choroidal melanoma: two cases with histopathological correlation. *Br J Ophthalmol*. 2000;84(9):1075–1076.
23. Pan Y, Diddie K, Lim JI. Primary transpupillary thermotherapy for small choroidal melanomas. *Br J Ophthalmol*. 2008;92(6):747–750.
24. Parrozzani R, Boccassini B, De Belvis V, et al. Long-term outcome of transpupillary thermotherapy as primary treatment of selected choroidal melanoma. *Acta Ophthalmol*. 2009;87(7):789–792.
25. Zaldivar RA, Aaberg TM, Sternberg P Jr, et al. Clinicopathologic findings in choroidal melanomas after failed transpupillary thermotherapy. *Am J Ophthalmol*. 2003;135(5):657–663.
26. Singh AD, Rundle PA, Berry-Brincat A, et al. Extrascleral extension of choroidal malignant melanoma following transpupillary thermotherapy. *Eye (Lond)*. 2004;18(1):91–93.
27. Tsai T, O'Brien JM, Engstrom R, et al. Extrascleral extension of a choroidal melanoma after argon photocoagulation and transpupillary thermotherapy. *Br J Ophthalmol*. 2002;86(3):358–359.
28. Midena E, Pilotto E, de Belvis V, et al. Choroidal vascular changes after transpupillary thermotherapy for choroidal melanoma. *Ophthalmology*. 2003;110(11):2216–2222.

29. Pilotto E, Vujosevic S, De Belvis V, et al. Long-term choroidal vascular changes after iodine brachytherapy versus transpupillary thermotherapy for choroidal melanoma. *Eur J Ophthalmol*. 2009;19(4):646–653.
30. Mashayekhi A, Shields CL, Rishi P, et al. Primary transpupillary thermotherapy for choroidal melanoma in 391 cases: importance of risk factors in tumor control. *Ophthalmology*. 2015;122(3):600–609.
31. Badiyan SN, Rao RC, Apicelli AJ, et al. Outcomes of iodine-125 plaque brachytherapy for uveal melanoma with intraoperative ultrasonography and supplemental transpupillary thermotherapy. *Int J Radiat Oncol Biol Phys*. 2014;88(4):801–805.
32. Keunen JE, Journée-de Korver JG, Oosterhuis JA. Transpupillary thermotherapy of choroidal melanoma with or without brachytherapy: a dilemma. *Br J Ophthalmol*. 1999;83(8):987–988.
33. Bartlema YM, Oosterhuis JA, Journée-de Korver JG, et al. Combined plaque radiotherapy and transpupillary thermotherapy in choroidal melanoma: 5 years' experience. *Br J Ophthalmol*. 2003;87(11):1370–1373.
34. Kreusel KM, Bechrakis N, Riese J, et al. Combined brachytherapy and transpupillary thermotherapy for large choroidal melanoma: tumor regression and early complications. *Graefes Arch Clin Exp Ophthalmol*. 2006;244(12):1575–1580.
35. Shields CL, Cater J, Shields JA, et al. Combined plaque radiotherapy and transpupillary thermotherapy for choroidal melanoma: tumor control and treatment complications in 270 consecutive patients. *Arch Ophthalmol*. 2002;120(7):933–940.
36. Sagoo MS, Shields CL, Mashayekhi A, et al. Plaque radiotherapy for juxtapapillary choroidal melanoma: tumor control in 650 consecutive cases. *Ophthalmology*. 2011;118(2):402–407.
37. Gunduz K, Kurt RA, Akmese HE, et al. Ruthenium-106 plaque radiotherapy alone or in combination with transpupillary thermotherapy in the management of

choroidal melanoma. *Jpn J Ophthalmol*. 2010;54(4):338–343.
38. Tarmann L, Wackernagel W, Avian A, et al. Ruthenium-106 plaque brachytherapy for uveal melanoma. *Br J Ophthalmol*. 2015;99(12):1644–1649.
39. Sagoo MS, Shields CL, Mashayekhi A, et al. Plaque radiotherapy for juxtapapillary choroidal melanoma overhanging the optic disc in 141 consecutive patients. *Arch Ophthalmol*. 2008;126(11):1515–1522.
40. Sagoo MS, Shields CL, Emrich J, et al. Plaque radiotherapy for juxtapapillary choroidal melanoma: treatment complications and visual outcomes in 650 consecutive cases. *JAMA Ophthalmol*. 2014;132(6):697–702.
41. Seregard S, Landau I. Transpupillary thermotherapy as an adjunct to ruthenium plaque radiotherapy for choroidal melanoma. *Acta Ophthalmol Scand*. 2001;79(1):19–22.
42. Sagoo MS, Shields CL, Mashayekhi A, et al. Plaque radiotherapy for choroidal melanoma encircling the optic disc (circumpapillary choroidal melanoma). *Arch Ophthalmol*. 2007;125(9):1202–1209.
43. Shields CL, Bianciotto C, Rudich D, et al. Regression of uveal melanoma after plaque radiotherapy and thermotherapy based on chromosome 3 status. *Retina*. 2008;28(9):1289–1295.
44. Desjardins L, Lumbroso-Le Rouic L, Levy-Gabriel C, et al. Combined proton beam radiotherapy and transpupillary thermotherapy for large uveal melanomas: a randomized study of 151 patients. *Ophthalmic Res*. 2006;38(5):255–260.
45. Archer DB, Gardiner TA. Ionizing radiation and the retina. *Curr Opin Ophthalmol*. 1994;5(3):59–65.
46. Bianciotto C, Shields CL, Pirondini C, et al. Proliferative radiation retinopathy after plaque radiotherapy for uveal melanoma. *Ophthalmology*. 2010;117(5):1005–1012.
47. Aziz HA, Singh AD. Radiation chorioretinopathy: evidence for effective therapy. *Int Ophthalmol Clin*. 2015;55(1):53–61.
48. Reichstein D. Current treatments and preventive strategies for radiation retinopathy. *Curr Opin Ophthalmol*. 2015;26(3):157–166.
49. Horgan N, Shields CL, Mashayekhi A, et al. Classification

and treatment of radiation maculopathy. *Curr Opin Ophthalmol*. 2010;21(3):233–238.
50. Finger PT, Kurli M. Laser photocoagulation for radiation retinopathy after ophthalmic plaque radiation therapy. *Br J Ophthalmol*. 2005;89(6):730–738.
51. Materin MA, Bianciotto CG, Wu C, et al. Sector laser photocoagulation for the prevention of macular edema after plaque radiotherapy for uveal melanoma: a pilot study. *Retina*. 2012;32(8):1601–1607.
52. Damato BE, Paul J, Foulds WS. Risk factors for residual and recurrent uveal melanoma after trans-scleral local resection. *Br J Ophthalmol*. 1996;80(2):102–108.
53. Kivela T, Eskelin S, Makitie T, et al. Exudative retinal detachment from malignant uveal melanoma: predictors and prognostic significance. *Invest Ophthalmol Vis Sci*. 2001;42(9):2085–2093.
54. Char DH, Bove R, Phillips TL. Laser and proton radiation to reduce uveal melanoma-associated exudative retinal detachments. *Am J Ophthalmol*. 2003;136(1):180–182.
55. Caminal JM, Mejia-Castillo KA, Arias L, et al. Subthreshold transpupillary thermotherapy in management of foveal subretinal fluid in small pigmented choroidal lesions. *Retina*. 2013;33(1):194–199.
56. Tse DT, Dutton JJ, Weingeist TA, et al. Hematoporphyrin photoradiation therapy for intraocular and orbital malignant melanoma. *Arch Ophthalmol*. 1984;102(6):833–838.
57. Lewis RA, Tse DT, Phelps CD, et al. Neovascular glaucoma after photoradiation therapy for uveal melanoma. *Arch Ophthalmol*. 1984;102(6):839–842.
58. Barbazetto IA, Lee TC, Rollins IS, et al. Treatment of choroidal melanoma using photodynamic therapy. *Am J Ophthalmol*. 2003;135(6):898–899.
59. Gupta M, Singh AD, Rundle PA, et al. Efficacy of photodynamic therapy in circumscribed choroidal haemangioma. *Eye (Lond)*. 2004;18(2):139–142.
60. Jurklies B, Anastassiou G, Ortmans S, et al. Photodynamic therapy using verteporfin in circumscribed choroidal haemangioma. *Br J Ophthalmol*. 2003;87(1):84–89.

61. Wachtlin J, Bechrakis NE, Foerster MH. Photodynamische Therapie mit Verteporfin beim Aderhautmelanom Eine klinisch-histopathologische Pilotstudie. *Ophthalmologe*. 2005;102(3):241–246.
62. Cerman E, Cekic O. Clinical use of photodynamic therapy in ocular tumors. *Surv Ophthalmol*. 2015;60(6):557–574.
63. Canal-Fontcuberta I, Salomao DR, Robertson D, et al. Clinical and histopathologic findings after photodynamic therapy of choroidal melanoma. *Retina*. 2012;32(5):942–948.
64. Jaffe GJ, Mieler WF, Burke JM, et al. Photoablation of ocular melanoma with a high-powered argon endolaser. *Arch Ophthalmol*. 1989;107(1):113–118.
65. Rem AI, Oosterhuis JA, Journée-de Korver HG, et al. Transscleral thermotherapy: short- and long-term effects of transscleral conductive heating in rabbit eyes. *Arch Ophthalmol*. 2003;121(4):510–516.
66. Krause MH, Xiong J, Gragoudas ES, et al. Treatment of experimental choroidal melanoma with an Nd:yttrium-lanthanum-fluoride laser at 1047 nm. *Arch Ophthalmol*. 2003;121(3):357–363.

153

Systemic Evaluation and Management of Patients With Metastatic Uveal Melanoma

Anna C. Pavlick, Paul T. Finger

Introduction

In developed countries, patients with metastatic uveal melanoma rarely present with the classic "distended abdomen and artificial eye." This change reflects a shift towards improved systemic surveillance after local treatment.[1] When metastasis is discovered using (every 6-month) radiographic abdominal imaging, most are asymptomatic. That said, early detection allows for both palliative treatment and enrollment in clinical trials, as well as more time to plan future medical and personal care.

Survival extends from 2.5 months to 14 months in patients with the lowest tumor burden at diagnosis. Eskelin and associates found that the largest tumor dimension of metastasis could be correlated to median patient survival.[2–4] Thus, periodic screening aims to uncover smaller, less numerous even solitary metastases where treatment has the opportunity to prolong or improve lives of patients with metastatic uveal melanoma.

The liver is the most commonly involved organ.[4] Therefore periodic radiographic abdominal imaging is currently the most widely recommended method for early detection of metastases. Though the liver is involved in over 90% of cases, common alternative sites include bone and subcutaneous skin. There are few published practice guidelines for staging and screening of metastatic uveal melanoma.[1,5]

Physical Examination

Retinologists and eye cancer specialists will not disrobe patients for examination. However, they can still play an integral "surveillance" role during their periodic patient interactions. For example, a history of weight loss, subcutaneous nodularity or abdominal pain should raise suspicion of metastatic uveal melanoma. The specialist should ensure coordinated systemic patient care, including periodic

physical examinations and clinical testing. The retinal specialist should use the recently validated American Joint Committee on Cancer (AJCC) uveal melanoma staging system to determine metastatic risk[3,6,7] (Fig. 153.1).

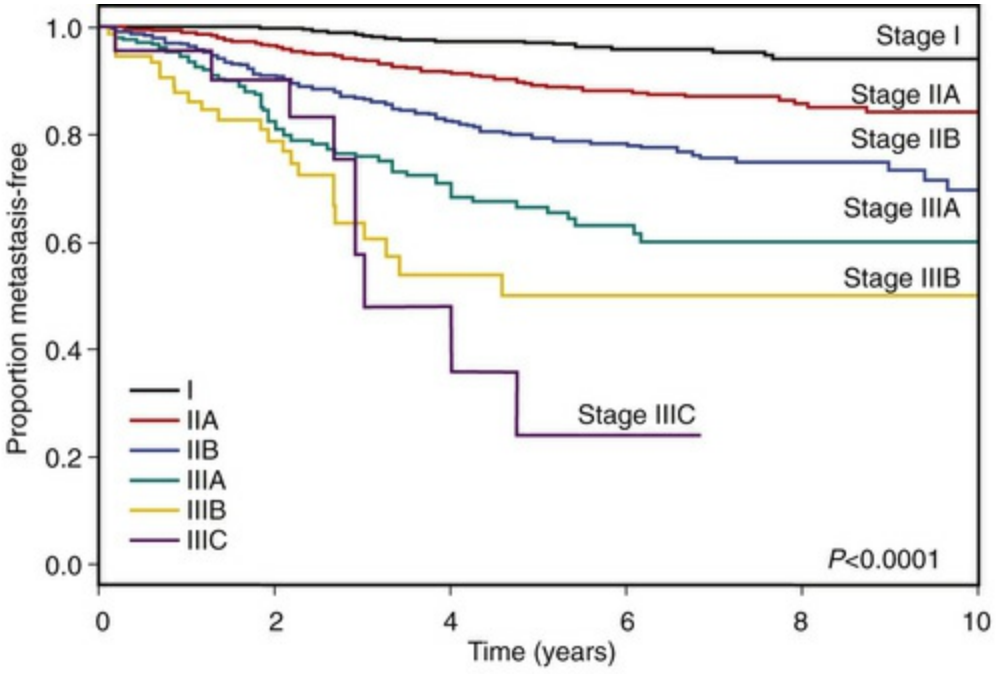

No. at Risk

I:	1030	741	446	270	118	49
IIA:	1095	766	431	251	126	52
IIB:	710	460	272	166	83	31
IIIA:	282	156	88	43	18	6
IIIB:	79	40	15	6	2	1
IIIC:	21	13	4	2	-	-

FIG. 153.1 AJCC Validation Study: Kaplan–Meier curves of metastasis based on T-stage.[6] (Reproduced with permission from International Validation of the American Joint Committee on Cancer's 7th Edition Classification of Uveal Melanoma. AJCC Ophthalmic Oncology Task Force. JAMA Ophthalmol 2015;133(4):376-83.)

Uveal melanoma patients benefit from co-management with a medical oncologist. Referral allows for a relationship to be built prior to metastatic disease, as well as participating in diagnostic and treatment-focused clinical trials.

Serology: Liver Function Tests

Liver function tests (LFTs) include gamma-glutamyl

transpeptidase, lactate dehydrogenase, alkaline phosphatases, aminotransferases, and bilirubin.[8] When considered individually, LFTs have demonstrated reported sensitivities ranging between 0.27 and 0.67 for metastases detection.[8] However, from the 2320 patients enrolled in the Collaborative Ocular Melanoma Study (COMS), they concluded that sensitivity, specificity, positive predictive value, and negative predictive value associated with at least one abnormal LFT before diagnosis of metastatic disease were 14.7%, 92.3%, 45.7%, and 71.0%, respectively.[8] Therefore, LTF screening is less sensitive and less specific for diagnosis of hepatic metastases compared to periodic radiographic imaging.

Radiologic Screening for Liver Metastasis

The liver is easily visualized by radiographic imaging. Computed tomography (CT), magnetic resonance imaging (MRI), and ultrasonography (US) are widely available. It is commonly accepted that US is better than LFTs for uncovering metastases.[9] Triphasic CT has shown excellent sensitivity, but has a low positive predictive value due to imaging of benign lesions.[10] Contrast-enhanced (gadoxetate disodium, gadolinium) MRI is the most sensitive hepatic imaging tool[11,12] (Fig. 153.2, top). However, there exists concern about gadolinium-associated renal toxicity, and it is contraindicated for patients with metallic implants.[13] Typically, the choice of imaging is largely governed by preference, cost, and radiation exposure.

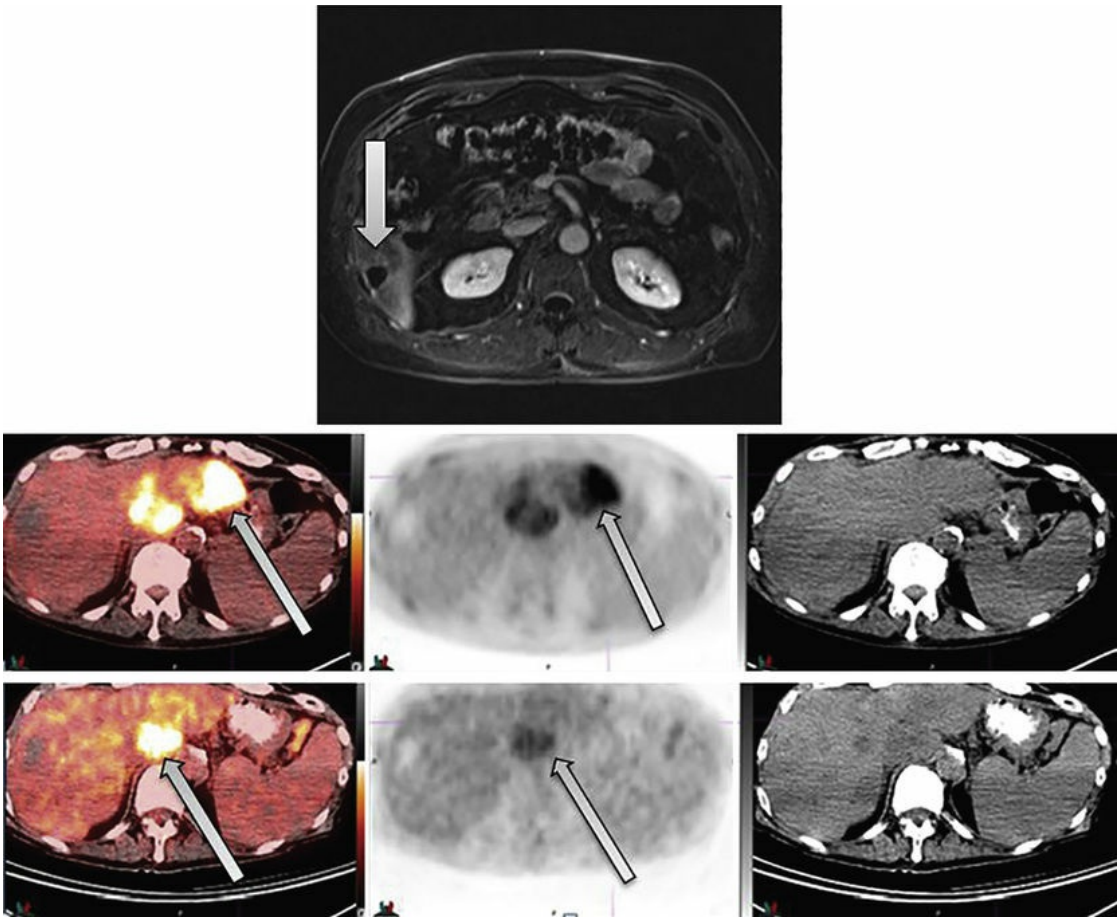

FIG. 153.2 (Top) Contrast-enhanced, T2-weighted magnetic resonance imaging reveals a solitary metastasis (*arrow*) from a primary uveal melanoma. Bottom, a series of images that demonstrate computed tomography (CT) alone demonstrating anatomy (right), 18-fluorodeoxyglucose positron emission tomography (PET) demonstrating physiologic glucose uptake (center), and PET/CT allowing for an evaluation of CT-form and PET-function in the same image. Note the metastatic focus (*arrow*).

Positron Emission Tomography/Computed Tomography (PET/CT)

PET/CT was the first to combine PET-function to CT-form on the same diagnostic page (Fig. 153.2, bottom). Unlike the previously mentioned radiographic imaging modalities, anatomophysiologic imaging improved discrimination between inflammatory, infectious, and neoplastic tumors.[4,14,15] Unlike abdominal CT, MRI,

or US, PET/CT allows for scanning of the entire body and thus systemic staging and restaging. Freton and others have found whole body PET/CT yields remarkably high positive predictive value for detection of metastatic uveal melanoma.[4]

PET/CT has also been used to detect synchronous nonocular cancers, as a biomarker to determine risk for metastatic uveal melanoma, for evaluation of postirradiation tumor viability, and for clarification of suspicious CT or MRI findings.[4,16–18] These benefits of PET/CT screening have been downplayed due to radiation risks and monetary cost. However, patients at high risk for metastatic uveal melanoma – AJCC-T3, AJCC-T4 tumors, tumors with extrascleral extension, ciliary body extension, and those who locally recur – are the subgroups most likely to benefit from initial PET/CT staging and subsequent PET/CT surveillance.[4]

Pathology, Genetics, and Molecular Biology

Histopathologic features of primary uveal melanoma (cellular subtype, extracellular vascular matrix patterns, and mitotic index) have been studied as biomarkers for metastatic risk.[1] Further, cytogenetic changes within tumors (e.g., loss of a chromosome 3, gene expression profiling) appear to be relevant genetic risk factors affecting metastatic spread.[19–21] Moreover, gain of chromosome 8q increases the risk of spreading, whereas gain of chromosome 6p seems protective.[1] Recently, genetic mutations have been identified within primary ocular melanomas, which may offer potential therapeutic targets for treatment.

First, mutations in GNAQ/GNA11 are early events in tumorigenesis and may or may not be prognostic for tumor stage or metastatic spread.[22] In contrast, mutations in the BRCA1-associated protein-1, BAP1, have been strongly linked to metastatic spread and poor patient survival.[20] Inactivation of BAP1 most often occurs through mutation of one allele and subsequent loss of an entire copy of chromosome-3 (monosomy 3) to unmask the mutant copy.[23] Research is examining clinical, histopathologic, cytogenetic, and biomarker expression profiles is being conducted to understand

how melanoma cells gain the ability to metastasize during tumor development. Clearly, the physiologic process called metastasis is complex (Fig. 153.3).

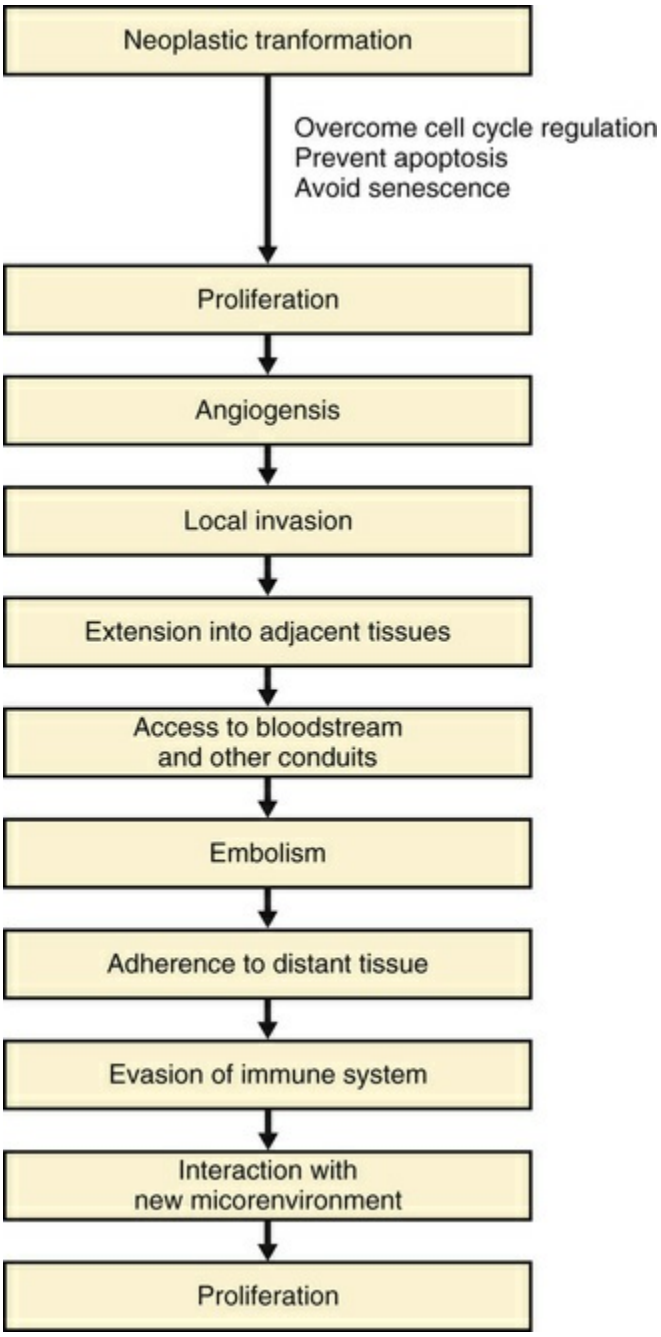

FIG. 153.3 Though melanoma cells develop from mutational genetic events, that is just the beginning. Cancer cells must then overcome cellular safeguards against neoplastic transformation. If successful, the tumor typically encounters limited space, lack of nutrients and oxygen, that select further genetic

mutations allowing the tumor to recruit a blood supply, invade other tissues, and spread to distant sites (to set up new tumor colonies). Certainly, the process called "metastasis" is dependent upon many factors. (Reproduced from Survey of Ophthalmology, volume 47, number 1, Jan–Feb 2002, pp. 1-16.)

Ethical Considerations of Screening and Biopsy

Patients who agree to a metastatic workup should benefit from a more favorable outcome. While LFTs and abdominal ultrasonography are relatively noninvasive, CT, MRI, and PET/CT carry the aforementioned collateral health risks.

Intraocular biopsy has recently gained popularity along with the evolution of genetic tumor analysis. Here, the low risks of intraocular biopsy (hemorrhage, infection, retinal detachment, tumor dissemination) must be balanced against the value of a histopathologic diagnosis and information about metastatic potential. The latter being used to select higher-risk patients for heightened surveillance and clinical trials.

In addition, histopathology and genetic tumor analysis can also be obtained from metastatic tumors. Though this approach does not allow prior selection for treatment of presumed subclinical disease, it does permit directed therapy.

Treatment of Metastatic Disease

Liver Metastases

The liver is the most common initial site of metastatic spread.[1] However, most patients are found to have multifocal hepatic or multiorgan metastasis untreatable by surgical metastasectomy.[4,9,11] Patients who metastasize more than 5 years after initial treatment with a solitary liver lesion have the longest disease-free interval.[24] Local control or palliation of liver metastases can be achieved with a wide range of procedures (hepatic artery chemoembolization, hepatic perfusion, or radiofrequency ablation).[25] Procedure

selection is made in consideration of the extent of hepatic disease, the location of the tumors, the patient's performance status, and the institution's interventional capability. Multifocal liver metastases not amenable to local therapy and those with multiorgan disease should be treated within clinical research studies.

Systemic Metastases

The gold standard for the treatment of diffuse metastatic disease from uveal melanoma is enrollment into a clinical trial.[26] Unfortunately, conventional chemotherapy and immunotherapy has failed to demonstrate significant efficacy. Recently, new insights regarding biomarkers, genetic targets expressed by tumor cells, as well as antiangiogenic agents, are leading innovative treatment strategies. Nevertheless, for patients with multiorgan metastases, there is still no known treatment intervention that offers cure.

In time, a combination of genetic tumor typing, improved understanding of the pathophysiology of metastasis, and the host's immune capabilities will enable physicians to define high- and low-risk patients. High-risk patients will be offered a primary treatment and an adjuvant clinical trial (for presumed subclinical metastatic disease).[2,6,19,27] Low-risk patients will continue to require treatment and (perhaps less intensive) systemic surveillance. Adjuvant therapy trials will concentrate on the genetic, molecular, and physiologic targets. Current programs have targeted methods to enhance the patient's immune system and blocking tumor dissemination. These strategies are aimed at making metastatic uveal melanoma a much more manageable, preventable or chronic illness.

References

1. Finger PT. Intraocular melanoma. DeVita VT, Lawrence TS, Rosenberg SA. *Cancer: principles and practice of oncology*. 10th ed. Wolters Kluwer: Dordrecht; 2015:1770–1779.
2. Eskelin S, Pyrhonen S, Hahka-Kemppinen M, et al. A prognostic model and staging for metastatic uveal

melanoma. *Cancer*. 2003;97(2):465–475.
3. The Ophthalmic Oncology Task Force. Malignant melanoma of the uvea. Edge SB, Byrd DR, Compton CC, et al. *AJCC cancer staging manual*. 7th ed. Springer-Verlag: New York; 2009:547–559.
4. Freton A, Chin KJ, Raut R, et al. Initial PET/CT staging for choroidal melanoma: AJCC correlation and second nonocular primaries in 333 patients. *Eur J Ophthalmol*. 2012;22(2):236–243.
5. The Ophthalmic Oncology Task Force. The American Brachytherapy Society consensus guidelines for plaque brachytherapy of uveal melanoma and retinoblastoma. *Brachytherapy*. 2014;13(1):1–14.
6. The Ophthalmic Oncology Task Force. International Validation of the American Joint Committee on Cancer's 7th Edition Classification of Uveal Melanoma. *JAMA Ophthalmol*. 2015;133(4):376–383.
7. Shields CL, Kaliki S, Furuta M, et al. American Joint Committee on Cancer Classification of Uveal Melanoma (Anatomic Stage) predicts prognosis in 7,731 patients: the 2013 Zimmerman Lecture. *Ophthalmology*. 2015;122(6):1180–1186.
8. Diener-West M, Reynolds SM, Agugliaro DJ, et al. Screening for metastasis from choroidal melanoma: the Collaborative Ocular Melanoma Study Group Report 23. *J Clin Oncol*. 2004;22(12):2438–2444.
9. Eskelin S, Pyrhonen S, Summanen P, et al. Screening for metastatic malignant melanoma of the uvea revisited. *Cancer*. 1999;85(5):1151–1159.
10. Feinstein EG, Marr BP, Winston CB, et al. Hepatic abnormalities identified on abdominal computed tomography at diagnosis of uveal melanoma. *Arch Ophthalmol*. 2010;128(3):319–323.
11. Servois V, Mariani P, Malhaire C, et al. Preoperative staging of liver metastases from uveal melanoma by magnetic resonance imaging (MRI) and fluorodeoxyglucose-positron emission tomography (FDG-PET). *Eur J Surg Oncol*. 2010;36(2):189–194.

12. Piperno-Neumann S, Servois V, Mariani P, et al. Prospective study of surveillance testing for metastasis in 100 high-risk uveal melanoma patients. *J Fr Ophtalmol*. 2015;38(6):526–534.
13. Ergun I, Keven K, Uruc I, et al. The safety of gadolinium in patients with stage 3 and 4 renal failure. *Nephrol Dial Transplant*. 2006;21(3):697–700.
14. Kurli M, Reddy S, Tena LB, et al. Whole body positron emission tomography/computed tomography staging of metastatic choroidal melanoma. *Am J Ophthalmol*. 2005;140(2):193–199.
15. Shulman JP, Latkany P, Chin KJ, et al. Whole-body 18FDG PET-CT imaging of systemic sarcoidosis: ophthalmic oncology and uveitis. *Ocul Immunol Inflamm*. 2009;17(2):95–100.
16. Chin K, Finger PT, Kurli M, et al. Second cancers discovered by (18)FDG PET/CT imaging for choroidal melanoma. *Optometry*. 2007;78(8):396–401.
17. Finger PT, Chin KJ. [(18)F]Fluorodeoxyglucose positron emission tomography/computed tomography (PET/CT) physiologic imaging of choroidal melanoma: before and after ophthalmic plaque radiation therapy. *Int J Radiat Oncol Biol Phys*. 2011;79(1):137–142.
18. Finger PT, Chin K, Iacob CE. 18-Fluorine-labelled 2-deoxy-2-fluoro-D-glucose positron emission tomography/computed tomography standardised uptake values: a non-invasive biomarker for the risk of metastasis from choroidal melanoma. *Br J Ophthalmol*. 2006;90(10):1263–1266.
19. Harbour JW. A prognostic test to predict the risk of metastasis in uveal melanoma based on a 15-gene expression profile. *Methods Mol Biol*. 2014;1102:427–440.
20. Ewens KG, Kanetsky PA, Richards-Yutz J, et al. Chromosome 3 status combined with BAP1 and EIF1AX mutation profiles are associated with metastasis in uveal melanoma. *Invest Ophthalmol Vis Sci*. 2014;55(8):5160–5167.
21. Finger PT. Eye: choroidal melanoma, retinoblastoma, ocular adnexal lymphoma and eyelid cancers. O'Sullivan B, Brierly J, D'Cruz A, et al. *UICC manual of clinical oncology*. 9th ed.

John Wiley & Sons; 2015:726–744.
22. Van Raamsdonk CD, Griewank KG, Crosby MB, et al. Mutations in GNA11 in uveal melanoma. *N Engl J Med*. 2010;363(23):2191–2199.
23. Harbour JW, Onken MD, Roberson ED, et al. Frequent mutation of BAP1 in metastasizing uveal melanomas. *Science*. 2010;330(6009):1410–1413.
24. Aoyama T, Mastrangelo MJ, Berd D, et al. Protracted survival after resection of metastatic uveal melanoma. *Cancer*. 2000;89(7):1561–1568.
25. Sato T. Locoregional management of hepatic metastasis from primary uveal melanoma. *Semin Oncol*. 2010;37(2):127–138.
26. National Cancer Institute. *Clinical Trials Search Results*. http://www.cancer.gov/about-cancer/treatment/clinicaltrials/search/results?protocolsearchid=6189661&vers=1.
27. The Ophthalmic Oncology Task Force. Local recurrence significantly increases the risk of metastatic uveal melanoma. Ophthalmology 2016;123:86–91.

154

Collaborative Ocular Melanoma Study

Barbara S. Hawkins, Andrew P. Schachat

Introduction

A large number of excellent clinical studies concerning treatment of ocular melanoma have been cited elsewhere in this text. The Collaborative Ocular Melanoma Study (COMS) was the first set of randomized clinical trials designed and conducted with sufficient power to compare survival outcomes between two or more treatments for this primary ocular cancer with a high degree of confidence.

Background

The choice of management of choroidal melanoma was controversial in the early 1980s when the COMS was designed and initiated; it remains controversial for tumors of small size. No data comparing enucleation or any other treatment with natural history were available; however, most ophthalmologists and oncologists were unwilling to undertake a randomized trial in which observation was one of the treatment arms. Large choroidal melanoma in the absence of metastasis traditionally has been treated with enucleation of the affected eye. Pre-enucleation irradiation of the eye had been proposed with the goal of minimizing the possibility of dissemination of viable tumor cells at time of enucleation.[1–8] Other adjunctive treatments also had been proposed, including post-enucleation irradiation of the socket, cryotherapy before enucleation, and chemotherapy.

There was consensus that growing choroidal melanoma of

intermediate size ("medium") should be treated. However, the choice of treatment, enucleation or some type of radiotherapy to avoid loss of the eye and preserve some vision, was unclear. At the time the COMS was designed, radiotherapy was available at relatively few centers within the United States and Canada, where patients who elected radiotherapy were referred. Concerns regarding diagnostic accuracy, particularly for small choroidal melanoma, persuaded most ophthalmologists to observe smaller tumors for growth before treating.

The length of survival after a diagnosis of choroidal melanoma is quite variable. A meta-analysis of data published from 1966 through 1988 regarding survival following enucleation yielded 5-year survival rates of 50% for large choroidal melanoma, 70% for medium choroidal melanoma, and 85% for small choroidal melanoma,[9] but few studies had reported survival or mortality rates by tumor size. It is accepted that the most important predictor of survival is tumor cell type. However, because of concerns regarding complications and inadequate sampling during fine-needle aspiration biopsy, choroidal melanoma may not be biopsied. Thus, cell type is not known until the eye is removed or the patient dies. Also, the cell type(s) may change over time.

Design of the Collaborative Ocular Melanoma Study (COMS)

The COMS was designed as a set of clinical trials of treatment for choroidal melanoma to be conducted by a group of investigators in the United States and Canada. Events leading to the design and initiation of the COMS have been summarized elsewhere.[10] Initially, three separate studies were undertaken, two randomized clinical trials and one observational study.[11] Initial funding was provided in 1985 through cooperative agreements with the National Eye Institute, National Institutes of Health, US Department of Health and Human Services; beginning in 1991, the National Cancer Institute also provided funding to conduct the study.

Randomized Trials of Radiotherapy

For COMS purposes, choroidal melanoma was categorized broadly by size. Size criteria are summarized in Table 154.1; other eligibility criteria are provided elsewhere[12] and have been published.[13,14]

TABLE 154.1

Collaborative Ocular Melanoma Study Classification of Size of Choroidal Melanoma

Size	Parameter		
	Apical Height (mm)	Longest Tumor Basal Diameter (mm)	Distance to Optic Disc (mm)
NOVEMBER 1986 THROUGH NOVEMBER 1990			
Large			
Subgroup 1	>8	—	—
Subgroup 2	≥2	>16	—
Medium	3.1–8	≤16	≥2
Small			
Subgroup 1	≤3	—	—
Subgroup 2	<2	>16	
AFTER NOVEMBER 1990			
Large			
Subgroup 1	>10	—	—
Subgroup 2	≥2	>16	—
Subgroup 3	>8	—	<2
Medium	2.5–10	≤16	≥2
Small			
Subgroup 1	<2.5	<16	—
Subgroup 2	<2	>16	—

—, No restriction.

The COMS randomized clinical trial of primary interest was designed to compare survival of patients following enucleation alone with iodine-125 (I-125) brachytherapy for treatment of "medium" choroidal melanoma who were believed to comprise the majority of newly diagnosed cases. Brachytherapy was chosen as the most feasible method of radiation delivery to the melanoma with respect to standardization of dosimetry and ability to monitor adherence to the radiotherapy protocol. Iodine-125 was selected as

the isotope because of the ability to protect the surgeon and other tissues in the orbit from radiation damage by using a gold shield and because of the half-life of the isotope.[15] Eligible consenting patients were assigned randomly with equal probability between enucleation and I-125 brachytherapy. All patients were to be followed for a minimum of 5 years or until death. The minimum sample size targeted a priori was 1250 patients for comparison of overall survival between treatment arms based on conventional Type I and Type II errors of 0.05 and 0.20, respectively. A desired sample size of 2400 patients also was established a priori to provide more precise estimates of survival overall and within patient subgroups and for evaluation of secondary outcomes.[11,12] The desired sample size was based on Type I and Type II errors of 0.01 and 0.10, respectively.

The clinical trial for "large" (high-risk of metastasis and death) choroidal melanoma was designed to compare enucleation alone with pre-enucleation radiation treatment (PERT). Pre-enucleation radiation was chosen for comparison with enucleation alone because a similar approach had been shown to be effective in other types and sites of cancer in which surgery was employed. In addition, external radiation was widely available throughout the United States and Canada. Patients were assigned randomly, with equal probability, between the two treatment arms and were to be followed for a minimum of 5 years or until death. The sample size was estimated on the basis of overall survival. Taking account of possible losses to follow-up, treatment crossovers, and treatment refusals, a target sample size of 1000 patients was established a priori based on Type I and Type II errors of 0.01 and 0.10, respectively.[11–13]

A parallel study of quality of life of patients enrolled in the randomized trial of I-125 brachytherapy for medium choroidal melanoma was initiated in 1994.[16] The purpose of the parallel study was to compare treatment arms over time with respect to general health, vision-related function, anxiety, and depression using scores from several standard interview instruments. The study had two components: (1) a prospective randomized component consisting of 209 participants in the trial of I-125 brachytherapy who were interviewed prior to random treatment assignment, at 6 months

following treatment, and on annual anniversaries of enrollment for up to 8 years; and (2) a cross-sectional component consisting of 645 additional patients who had enrolled in the randomized trial before the quality of life study was initiated and who were interviewed at least once during scheduled follow-up. These 854 patients represent 90% of patients who were eligible for the quality of life study and 65% of all patients who enrolled in the trial of I-125 brachytherapy.

Observational Study

A nonrandomized observational study of small choroidal melanoma was included in the initial COMS design with the goal of providing sufficient information to design a randomized clinical trial of treatment for small tumors. Primary objectives were to estimate the number of patients with small choroidal melanoma available for inclusion in a randomized trial, the methods of treating small choroidal melanoma most widely used by COMS investigators, and, to the extent feasible within a small pilot study with short patient follow-up, rates of tumor growth and patient death.

Methods

The COMS design and many of the methods have been published; the COMS Manual of Procedures[12] is available. Patients were evaluated for eligibility, enrolled, and treated at 43 different clinical centers, 41 in the Uniteed States and two in Canada. A standard schedule of clinical examinations was followed for data collection purposes. An unusual feature of the COMS design was that the participating ophthalmologists reported de-identified basic demographic information (age, gender, race, or ethnicity) and tumor dimensions for all cases of choroidal melanoma examined during the period of patient accrual, regardless of tumor size, eligibility for the COMS, or willingness of eligible patients to enroll in the COMS.

Responsibility for random assignment to treatment, oversight of data collection, data management, and data analysis was assigned to the COMS Coordinating Center in Baltimore, Maryland. This

center also had major responsibility for monitoring the quality of data provided by the participating centers. Other resource centers with major quality assurance and monitoring responsibilities included an Echography Center (Miami, Florida; later Mars Hill, North Carolina), where tumor height was measured independently from photoechograms; a Photograph Reading Center (Iowa City), where tumor characteristics at baseline and postirradiation changes in the posterior retina during follow-up were assessed and recorded; a Pathology Center (Boston, Massachusetts; later Madison, Wisconsin), where tumor size and diagnosis were confirmed from all eyes enucleated; and the Radiological Physics Center (Houston, Texas), where adherence to the radiotherapy protocols was monitored. Overall leadership responsibility for the COMS Group was vested in the COMS Chairman's Office (Baltimore, Maryland; later Philadelphia, Pennsylvania).

An independent Data and Safety Monitoring Committee, appointed by the Director of the National Eye Institute, was the only group with access to survival data from the randomized clinical trials by treatment arm until this committee judged that the objectives of each individual trial had been met. This group had responsibility for ensuring that COMS trials were conducted in a scientifically valid and ethically sound manner. Scientific leadership of the COMS was provided by the Executive Committee, whose members included representatives of both the resource centers and the participating clinical centers. Three ophthalmic pathologists comprised the Pathology Review Committee who reviewed every enucleated eye from COMS patients to determine whether the clinical diagnosis of choroidal melanoma was correct. Mechanisms for quality assurance and monitoring were developed by the Quality Assurance Committee, which oversaw all aspects of data collection and protocol adherence. Classification of causes of death was the responsibility of the Mortality Coding Committee, whose members did not have responsibility for medical care of COMS patients. Since completion of the COMS, the COMS Archives Committee has had responsibility for reviewing and approving applications for access by researchers to original COMS data and for reviewing manuscripts that use COMS data.

Chronology of the COMS

Accrual of patients to the randomized trial of pre-enucleation radiation (PERT) of large choroidal melanoma began in November 1986 and ended in December 1994, with 1003 patients enrolled. Scheduled clinical follow-up of all surviving patients for vital status, incidence of metastasis and second cancers, and complications continued until July 31, 2000. Interim mortality findings and related information that emphasized 5-year outcomes were published in 1998;[13,17,18] mortality findings through 10 years and prognostic factors were published in 2004.[19]

Accrual of patients to the randomized trial of I-125 brachytherapy for medium choroidal melanoma began in January 1987 and ended in July 1998, with 1317 patients enrolled, at the recommendation of the Data and Safety Monitoring Committee. Scheduled clinical follow-up of all surviving patients, for clinical and vital status and for quality of life, continued until July 31, 2003, and October 31, 2003, respectively. Interim mortality findings were published in 2001;[14] mortality findings through 12 years after enrollment and subgroup findings were published in 2006.[20] Information about complications[21–23] and related information[24] also has been published.

Patient accrual to the nonrandomized study for small choroidal melanoma began in 1987 and ended in 1989, with 204 patients enrolled. Annual follow-up examinations were halted in 1991 as a result of funding constraints. Vital status and treatment status were reassessed in 1993 through 1994, and again in 1995 through 1996, for all patients who had not been lost to follow-up. Findings from this study have been published.[25,26]

The COMS database, copies of all publications from the COMS Group, and the *COMS Manual of Procedures* were deposited in the Alan Mason Chesney Medical Archives at the Johns Hopkins University in August 2008. An anonymized public use dataset, containing baseline characteristics and survival outcomes, the *COMS Manual*, and copies of all COMS publications are available by application to the Medical Archives (http://www.medicalarchives.jhmi.edu). Access to more extensive data, including images of original data forms received at the COMS Coordinating Center, is available to qualified researchers whose

application to the COMS Archives Committee (via: schacha@ccf.org or bhawkins@jhmi.edu) is approved by the COMS Archives Committee and by the Medical Archives institutional review board.

Findings From the COMS Trial of I-125 Brachytherapy for Medium Choroidal Melanoma

Participants

By July 1998, a total of 8712 patients with choroidal melanoma had been reported by COMS investigators; 5046 were classified to be of medium size by COMS criteria (Table 153.1). Among 2882 patients eligible for the randomized trial of I-125 brachytherapy versus standard enucleation, 1317 patients gave signed consent, enrolled, and were assigned randomly to treatment arm: 660 to standard enucleation and 657 to I-125 brachytherapy. Treatment arms were well balanced; adherence to the COMS protocol was excellent.[14] All but 21 patients, seven in the brachytherapy arm and 14 in the enucleation arm, were treated promptly as assigned. Three patients assigned to brachytherapy crossed over to enucleation, seven enucleation patients crossed over to brachytherapy, and two had proton beam radiation as the initial treatment. At the end of clinical follow-up in 2003, the vital status 5 years after enrollment was known for 1313 patients (99.7%), i.e., for all but four patients in the enucleation arm. Of 799 patients eligible for 10 years of follow-up, the vital status at 10 years was known for 791 (99.0%), i.e., for all but one patient in the brachytherapy arm and seven patients in the enucleation arm.

Survival Estimates

By September 30, 2000, all patients had been followed for vital status for 2 years or longer, with 1274 patients followed for 3 years or longer and 1072 patients eligible for 5 years of follow-up. Among patients in the enucleation arm, 188 (28%) were known to have died compared with 176 (27%) of those in the brachytherapy arm.

Estimated 5-year survival rates and 95% confidence intervals were 81% (95% CI 77–84%) in the enucleation arm and 82% (95% CI 79–85%) in the brachytherapy arm. Of the 364 decedents, 159 were judged to have had melanoma metastasis at time of death. Neither all-cause mortality rates nor rates of death with histopathologically confirmed melanoma metastasis differed between treatment arms. Adjustment of mortality rates for independent and statistically significant predictors of time to death (baseline age, tumor dimensions, tumor location, tumor shape, smoking history, and coexisting medical conditions) changed the estimated risk ratio from 0.93 (unadjusted; 95% CI 0.76–1.14) to 0.99 (adjusted; 95% CI 0.80–1.22).

Clinical follow-up of patients in the trial of I-125 brachytherapy ended on July 31, 2003, after all patients had been followed for at least 5 years up to a maximum of 15 years. Five-year survival rates were similar to those published in 2001, i.e., 81% in each treatment arm, yielding a pooled 95% CI of 79–83%. Ten-year survival rates also were the same in the two arms: 65% (95% CI 62–68%). Mortality rates by treatment arm for all causes and with melanoma metastasis are shown in Fig. 154.1. Older age and maximum basal tumor diameter were the primary predictors of earlier death.[20] Pooled data were used to summarize mortality, diagnosis of melanoma metastasis,[27] and second primary cancers[28] through 12 years[20] (Fig. 154.2).

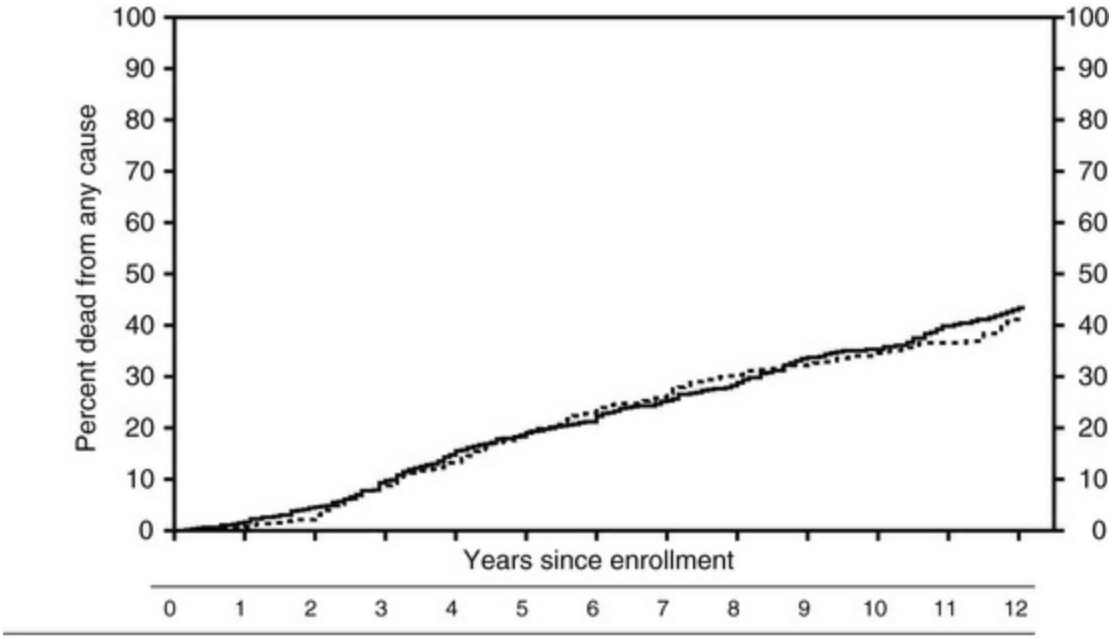

No. at Risk													
Enuc.	660	655	640	602	572	533	476	414	354	298	246	191	135
I-125	657	646	627	593	555	532	481	429	366	305	250	196	140
No. Censored													
Enuc.	0	0	0	0	0	31	42	40	46	43	48	44	-
I-125	0	0	0	0	0	30	34	44	37	48	38	46	-

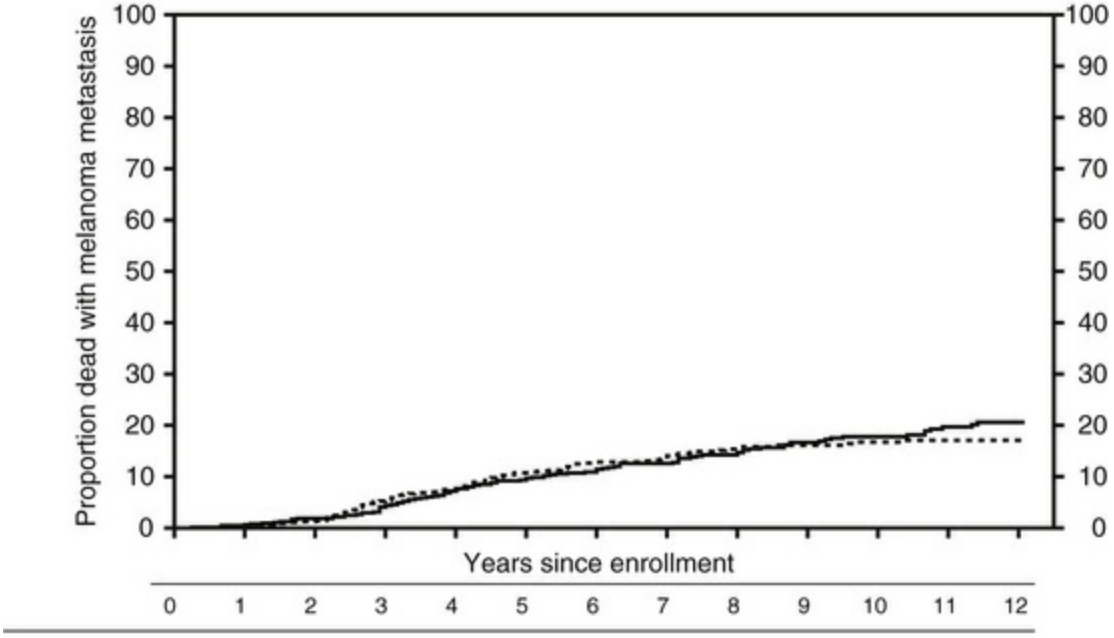

No. at Risk													
Enuc.	660	655	640	602	572	533	476	414	354	298	246	191	135
I-125	657	646	627	593	555	532	481	429	366	305	250	196	140
No. Censored													
Enuc.	2	9	12	17	19	45	56	54	53	50	54	56	-
I-125	7	11	18	18	11	41	46	53	53	51	49	54	-

FIG. 154.1 (Top) The cumulative percentage of patients in the COMS trial of iodine-125 brachytherapy for medium choroidal melanoma who had died by

specified times after enrollment. *Solid line*: patients assigned to brachytherapy. *Dashed line*: patients assigned to enucleation. The numbers of patients at risk of death and numbers censored, based on date of enrollment, are given at annual anniversaries of enrollment by treatment assignment. Event is death from any cause. (Bottom) The cumulative percentage of patients in the COMS randomized trial of I-125 brachytherapy who had died with metastatic melanoma by the specified times after enrollment. *Solid line*: patients assigned to brachytherapy. *Dashed line*: patients assigned to enucleation. The numbers of patients at risk of death and numbers censored, based on date of enrollment, are given at annual anniversaries of enrollment by random treatment assignment. Event is death with histologically confirmed metastatic melanoma.

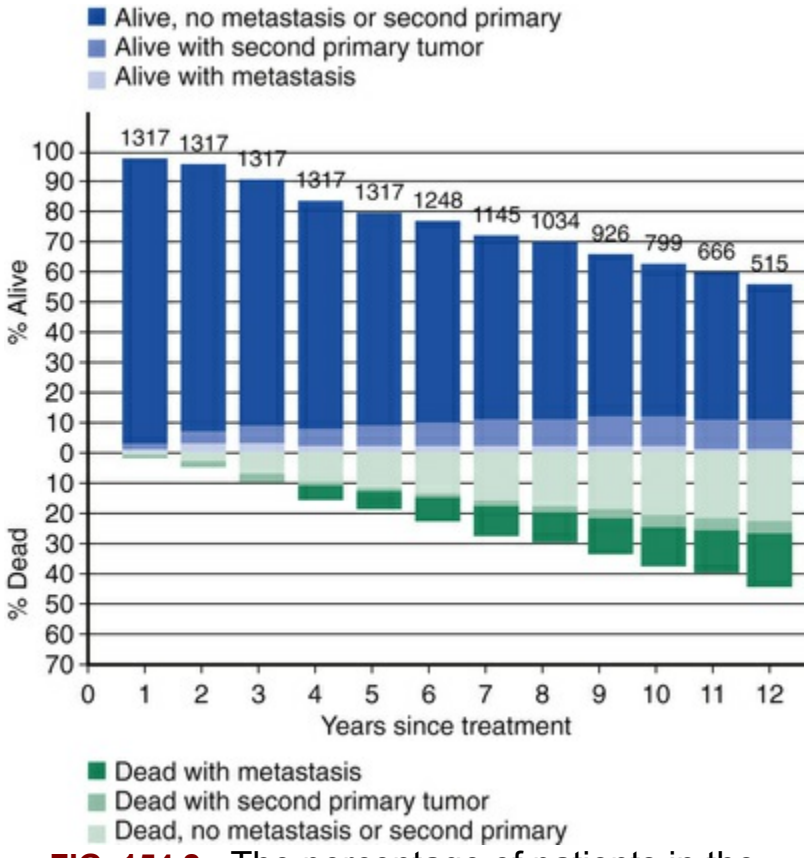

FIG. 154.2 The percentage of patients in the

Collaborative Ocular Melanoma Study (COMS) randomized trial of I-125 brachytherapy with the specified status at the end of each year of follow-up, with treatment arms pooled. The number of patients who enrolled early enough to be followed up to the end of the specified year is shown at the top of the corresponding bar.

Complications

As reported in 2002,[21] 69 of the 650 patients whose eyes were treated with brachytherapy had the eye enucleated during the first 5 years after initial treatment, yielding a 5-year rate of 12% (95% CI 10–16%); local treatment failure was reported for 57 eyes in the same time period, with a 5-year cumulative rate of 10% (95% CI 8–13%). Local treatment failure accounted for 39 of the 69 enucleations. The 3-year cumulative rate of loss of 6 or more lines of visual acuity from baseline was 49% (95% CI 44–53%), and the 3-year cumulative rate of loss of visual acuity to 20/200 or worse was 43% (95% CI 38–48%).[22] Five-year estimates of cataract among the 532 eyes treated with I-125 brachytherapy that were phakic at baseline and had no history of cataract in the eye were 83% (95% CI 79–87%).[23]

Quality of Life

In the parallel study of quality of life, 206 of 209 patients who enrolled and were treated as assigned (103 each to enucleation or to I-125 brachytherapy) provided 5-year findings regarding quality of life.[29] Patients treated with brachytherapy reported significantly better peripheral vision and ability to drive than those treated with enucleation for up to 2 years following treatment. Differences between treatment arms diminished thereafter in parallel with declining visual acuity in brachytherapy-treated eyes. Patients treated with brachytherapy reported more symptoms of anxiety through 5 years than those treated with enucleation.[29]

Findings From the COMS Trial of Pre-Enucleation Radiation for Large Choroidal Melanoma

Participants

From November 1986 through December 1994, COMS investigators reported 6078 patients with choroidal melanoma. Of these, 1860 had tumors classified as large by COMS criteria (see Table 154.1 for definitions used). Of those classified as large, 1302 were judged eligible for enrollment; 1003 gave signed consent, enrolled, and were assigned randomly to enucleation alone or to pre-enucleation radiation. The two treatment arms were well balanced with respect to most of the many characteristics of patients, eyes, and tumors considered.[13] Adherence to the COMS protocol was excellent, as was diagnostic accuracy.[13,30] Only nine patients – three assigned to standard enucleation and six assigned to pre-enucleation radiation – were not treated as assigned at time of enrollment. When clinical follow-up ended in 2000, vital status 5 years after enrollment was known for 998 patients (99.5%), i.e., all but three patients in the enucleation alone arm and two patients in the pre-enucleation radiation arm.

Survival Estimates

By July 31, 1997, the vital status at 3 years after enrollment was available for all but 26 patients who had enrolled during the last few months of patient accrual. The 5-year vital status was known for 801 (80%) of all patients enrolled: 238 patients assigned to enucleation alone (47%) and 219 patients assigned to pre-enucleation radiation (44%) were known to have died. The estimated 5-year cumulative survival rates and 95% confidence intervals were 57% (95% CI 52–62%) for patients assigned to enucleation alone and 62% (95% CI 57–66%) for patients assigned to pre-enucleation radiation. Neither 5-year survival rates nor survival rates over the first 8 years after enrollment differed between treatment arms, to either a statistically or clinically significant degree.[13]

Mortality by treatment arm and by time since enrollment when clinical follow-up ended in July 2000 is summarized in Fig. 154.3. Five-year survival rates were identical to those reported earlier; 10-year survival was similar in the two arms and yielded a pooled estimate of 39% (95% CI 35–42%).[19] Among baseline characteristics of the patients, eyes, and tumors evaluated for their potential as prognostic factors, only patient age at time of treatment and longest tumor basal diameter had statistically significant effects on the length of overall survival.[19]

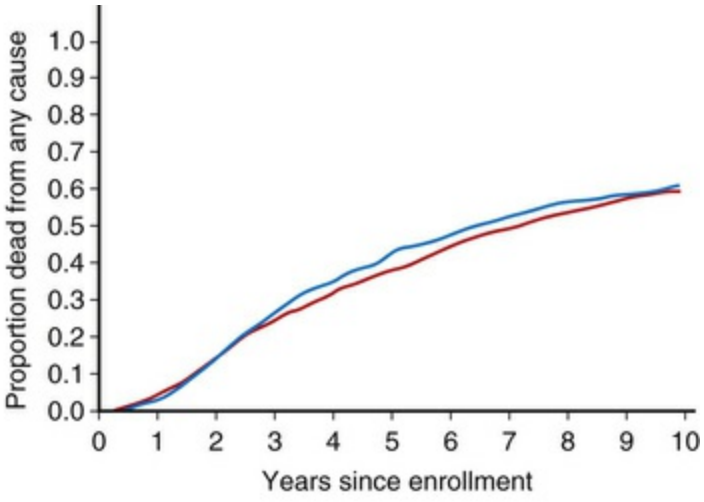

No. at Risk

Std. Enuc.	506	489	429	370	327	285	249	194	156	123	87
PERT	497	472	421	374	335	305	262	211	164	121	83

No. Censored

Std. Enuc.	-	0	0	0	0	0	13	35	21	27	30
PERT	-	0	0	0	0	0	11	30	31	30	29

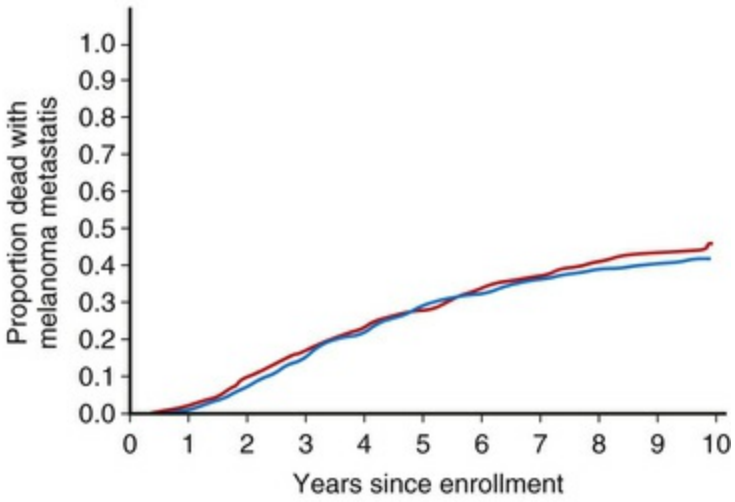

No. at Risk

Std. Enuc.	506	489	429	370	327	285	249	194	156	123	87
PERT	497	472	421	374	335	305	262	211	164	121	83

No. Censored

Std. Enuc.	-	10	30	22	16	12	27	42	30	30	34
PERT	-	12	15	15	10	13	19	39	36	37	34

FIG. 154.3 (Top) The cumulative percentage of patients in the Collaborative Ocular Melanoma Study (COMS) trial of pre-enucleation radiation (PERT) for large choroidal melanoma who had died by specified times after enrollment. *Blue line*: patients assigned to PERT. *Red line*: patients assigned to enucleation alone. The numbers of patients at risk of death and

numbers censored, based on date of enrollment, are given at annual anniversaries of enrollment by treatment assignment. Event is death from any cause. (Bottom) The cumulative percentage of patients in the COMS randomized trial of PERT who had died with metastatic melanoma by the specified times since enrollment. *Blue line*: patients assigned to PERT. *Red line*: patients assigned to enucleation alone. The numbers of patients at risk of death and numbers censored, based on date of enrollment, are given at annual anniversaries of enrollment by random treatment assignment. Event is death with histologically confirmed metastatic melanoma. (Modified with permission from Collaborative Ocular Melanoma Study Group. Am J Ophthalmol 2004;138:936–57.)

Among patients assigned to enucleation alone, 130 (26%) died within 5 years of enrollment with histologically confirmed metastatic melanoma, compared with 139 (28%) patients assigned to pre-enucleation radiation, based on review of 435 of the 457 deaths by the Mortality Coding Committee.[31,32] Time to death with histologically confirmed metastatic melanoma is displayed in Fig. 154.3. The liver was the most common site of melanoma metastasis.[31] Findings pooled by treatment arm for mortality, diagnosis of melanoma metastases, and second primary cancers are summarized through 10 years in Fig. 154.4.

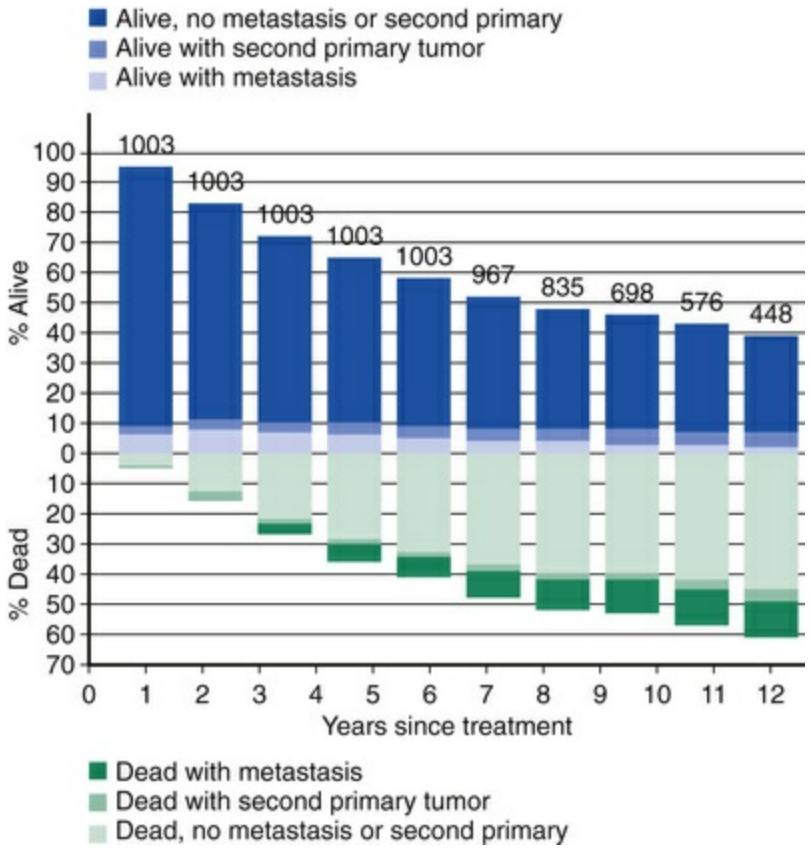

FIG. 154.4 The percentage of patients in the Collaborative Ocular Melanoma Study (COMS) randomized trial of pre-enucleation radiation (PERT) with the specified status at the end of each year of follow-up, with treatment arms pooled. The number of patients who enrolled early enough to be followed up to the end of the specified year is shown at the top of the corresponding bar. (Reproduced with permission from Collaborative Ocular Melanoma Study Group. Am J Ophthalmol 2004;138:936–57.)

Complications

Only 17 patients treated with enucleation alone and 19 patients treated with pre-enucleation radiation had any surgical or anesthetic complication reported at the time of initial treatment.[18] Orbital tumor recurrence was reported during the first 5 years of follow-up for six patients treated with enucleation alone and for one patient treated with pre-enucleation radiation; patients treated with enucleation alone had nearly twice the 5-year incidence of severe ptosis as reported for patients treated with pre-enucleation

radiation.[18]

Findings From the COMS Nonrandomized Prospective Study of Small Choroidal Melanoma

Of 300 patients with small choroidal melanoma (by COMS initial criteria) reported from December 1986 through August 1989, 220 were judged eligible for this COMS observational substudy; 204 gave signed consent and enrolled. The majority of the patients enrolled within 1 year of the initial diagnosis of choroidal melanoma.[25] No attempt was made to establish uniform criteria for timing or type of treatment, if any; the patients and their ophthalmologists made these decisions.

A total of 16 patients were treated shortly after enrollment; 20 additional patients were treated after the melanoma grew to medium or large size (COMS criteria), and the patients were enrolled in one of the COMS randomized trials. As of June 1996, an additional 47 patients had been treated during follow-up.[25,26]

By June 30, 1996, 27 patients had died. Survival findings are summarized in Fig. 154.5. The estimated 5-year all-cause mortality rate was 6% (95% CI 3–9%).[25] Of 188 patients who were not treated at time of enrollment, 44 had tumors that had grown to medium or large size by February 1997, based on COMS criteria. The estimated 5-year proportion of initially small tumors that grew was 31% (95% CI 23–39%).[25]

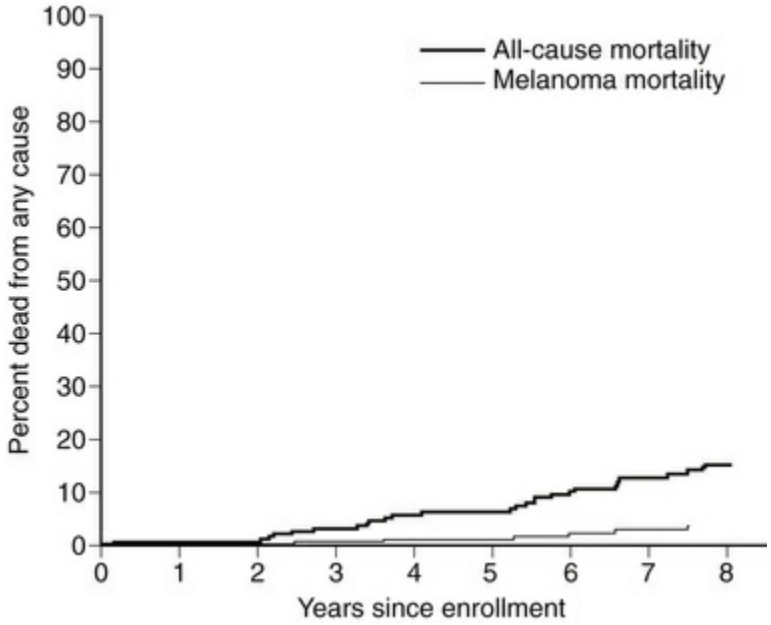

FIG. 154.5 Cumulative percentage of patients in the Collaborative Ocular Melanoma Study (COMS) nonrandomized, prospective study of small choroidal melanoma who had died by the specified times since enrollment. (Reproduced with permission from Collaborative Ocular Melanoma Study Group. Arch Ophthalmol 1997;115:1537–44. © 1997 American Medical Association. All rights reserved.)

Histopathologic Findings From Enucleated Eyes

The COMS Group had one of the highest rates of diagnostic accuracy ever documented.[30,33] Of 1532 eyes enucleated in the COMS by June 1996, 994 from patients enrolled in the randomized trial for large choroidal melanoma and 536 from patients enrolled in the trial for medium choroidal melanoma, 1527 (99.7%) were confirmed histopathologically by the Pathology Review Committee to harbor choroidal melanoma.[30,33] A detailed description of the characteristics of the 1527 confirmed cases has been published.[33] Key findings include documentation of local tumor invasion: rupture of Bruch's membrane in 88% of eyes; invasion of emissary canals in 55%; retinal invasion in 49%; tumor cells in the vitreous in 25%; invasion of tumor vessels in 14%; and vortex vein invasion in 22% of eyes with vortex veins. Scleral invasion was present in 56%

of eyes and extrascleral extension in 8%. Histopathologic review confirmed that pre-enucleation radiation significantly reduced mitotic activity.[13]

In other published histopathologic investigations of enucleated eyes of COMS patients, silver-stained nucleolar organizer region scores have been evaluated as predictors of later metastasis,[34] transillumination and histologic measurements of tumor dimensions have been compared,[35] and a clear cell variant of choroidal melanoma has been identified.[36]

Other Published Findings

The multicenter organization of the COMS facilitated referral to a COMS clinical center of cases of choroidal melanoma from most of the United States and from a large part of eastern Canada. The large number of patients screened for the COMS and judged to have choroidal melanoma (totaling 8712 as of July 31, 1998, when accrual halted) provided the largest group of patients with this diagnosis for whom data had been collected systematically at time of presentation in accord with a common protocol. Trends in size of choroidal melanoma and treatments over time were published.[37] The COMS Group reported the first published cases of choroidal melanoma in Native Americans.[38] This large database permits comparison of tumor characteristics at time of screening and diagnosis among different racial subgroups. This information may provide clues for future investigation in epidemiologic and genetic studies of choroidal melanoma.

The COMS Group also published information on surgical and postsurgical complications among the largest group of patients whose eyes had been enucleated because of choroidal melanoma and who had been examined in accord with a common follow-up protocol,[18] documenting the low rates of serious complications following enucleation for this condition. The importance of liver function tests and other tests for metastasis was evaluated; those findings were published in the oncology literature.[39] Also, 10-year changes in fellow eyes of patients enrolled in COMS randomized trials have been reported.[40] Echographic characteristics of melanoma at baseline[41] and postbrachytherapy changes observed

on fluorescein angiograms and stereoscopic photographs[42] have been published. In addition to publications from the COMS Group that have important clinical information, several articles have been published that deal with research methodology.[43–48]

Conclusion

The COMS Group successfully enrolled sufficient numbers of eligible patients with choroidal melanoma so that valid comparisons between treatments could be made for mortality and other important clinical outcomes and, in the case of the trial for medium tumors, also on important patient-reported ("quality of life") outcomes. Protocol adherence and data quality were exceptionally good in both randomized trials. Findings regarding primary and secondary outcomes have been published. The information in Figs. 154.2 and 154.4 is useful for patient counseling. The COMS Archives Committee continues to receive and review requests to access archived COMS data.

References

1. Augsburger JJ, Eagle RC, Chiu M, et al. The effect of preenucleation radiotherapy on mitotic activity of choroidal and ciliary body melanomas. *Ophthalmology*. 1987;94:1627–1630.
2. Benediktsdóttir K, Edenholm M, Lindholm Å, et al. Preoperative irradiation of malignant melanoma: a multifactorial statistical analysis of survival. *Acta Radiol Oncol*. 1984;23:315–320.
3. Bornfeld N, Alberti W, Foerster MH, et al. External beam therapy of choroidal melanomata: preliminary report. *Trans Ophthalmol Soc U K*. 1983;103:68–71.
4. Burch FE, Camp WF. Results of irradiation of malignant melanomas of the uveal tract. *Trans Am Acad Ophthalmol Otolaryngol*. 1943;47:335–353.
5. Char DH, Phillips TL. The potential for adjuvant radiotherapy in choroidal melanoma. *Arch Ophthalmol*. 1982;100:247–248.

6. Char DH, Phillips TL. Preenucleation irradiation of uveal melanoma. *Br J Ophthalmol*. 1985;69:177–179.
7. Lommatzsch P, Dietrich B. The effect of orbital irradiation on the survival rate in patients with choroidal melanoma. *Ophthalmologica*. 1976;173:49–52.
8. Sanborn GE, Ngyuen P, Gamel J, et al. Reduction of enucleation-induced metastasis in intraocular melanoma by periorbital irradiation. *Arch Ophthalmol*. 1987;105:1260–1264.
9. Diener-West M, Hawkins BS, Markowitz JA, et al. A review of mortality from choroidal melanoma. II. A meta-analysis of mortality rates following enucleation, 1966 through 1988. *Arch Ophthalmol*. 1992;110:245–250.
10. Hawkins BS. Collaborative Ocular Melanoma Study randomized trial of I-125 brachytherapy. *Clinical Trials*. 2011;8:661–673.
11. Collaborative Ocular Melanoma Study Group. Design and methods of a clinical trial for a rare condition: the Collaborative Ocular Melanoma Study. COMS report no. 3. *Control Clin Trials*. 1993;14:362–391.
12. Collaborative Ocular Melanoma Study Group. *COMS Manual of Procedures. NTIS accession No. PB95–179693*. National Technical Information Service: Springfield; 1995.
13. Collaborative Ocular Melanoma Study Group. The Collaborative Ocular Melanoma Study (COMS) randomized trial of pre-enucleation radiation of large choroidal melanoma. II. Initial mortality findings. COMS report no. 10. *Am J Ophthalmol*. 1998;125:779–796.
14. Collaborative Ocular Melanoma Study Group. The COMS randomized trial of iodine 125 brachytherapy for choroidal melanoma. III. Initial mortality findings. COMS report no. 18. *Arch Ophthalmol*. 2001;119:969–982.
15. Earle J, Kline RW, Robertson DM. Selection of iodine 125 for the Collaborative Ocular Melanoma Study. *Arch Ophthalmol*. 1987;105:763–764.
16. Moy CS, Melia BM. Quality of life assessment in the Collaborative Ocular Melanoma Study: design and methods. COMS–QOLS report no. 1. [for the; COMS Quality of Life Study Group] *Ophthalmic Epidemiol*.

1999;6:5–17.
17. Collaborative Ocular Melanoma Study Group. The Collaborative Ocular Melanoma Study (COMS) trial of pre-enucleation radiation of large choroidal melanoma. I. Characteristics of patients enrolled and not enrolled. COMS report no. 9. *Am J Ophthalmol*. 1998;125:767–778.
18. Collaborative Ocular Melanoma Study Group. The Collaborative Ocular Melanoma Study (COMS) randomized trial of pre-enucleation radiation of large choroidal melanoma. III. Local complications with and without pre-enucleation radiation. COMS report no. 11. *Am J Ophthalmol*. 1998;126:362–372.
19. Collaborative Ocular Melanoma Study Group. The Collaborative Ocular Melanoma Study (COMS) randomized trial of pre-enucleation radiation of large choroidal melanoma: IV. Ten-year mortality findings and prognostic factors. COMS report no. 24. *Am J Ophthalmol*. 2004;138:936–951.
20. Collaborative Ocular Melanoma Study (COMS) Group. The COMS randomized trial of iodine 125 brachytherapy for choroidal melanoma. V. Twelve-year mortality rates and prognostic factors. COMS report no. 28. *Arch Ophthalmol*. 2006;124:1684–1693.
21. Collaborative Ocular Melanoma Study Group. The COMS randomized trial of iodine 125 brachytherapy for choroidal melanoma. IV. Local treatment failure and enucleation in the first 5 years after brachytherapy. COMS report no. 19. *Ophthalmology*. 2002;109:2197–2206 [Correction: Ophthalmology 2004;111;1514].
22. Collaborative Ocular Melanoma Study Group. The Collaborative Ocular Melanoma Study (COMS) randomized trial of I-125 brachytherapy for medium choroidal melanoma. I. Visual acuity after 3 years. COMS report no. 16. *Ophthalmology*. 2001;108:348–366.
23. Collaborative Ocular Melanoma Study Group. Incidence of cataract and outcomes after cataract surgery in the first 5 years after iodine 125 brachytherapy in the Collaborative Ocular Melanoma Study. *Ophthalmology*. 2007;114:1363–

1371.
24. Collaborative Ocular Melanoma Study Group. The COMS randomized trial of iodine 125 brachytherapy for choroidal melanoma. II. Characteristics of patients enrolled and not enrolled. COMS report no. 17. *Arch Ophthalmol*. 2001;119:951–965.
25. Collaborative Ocular Melanoma Study Group. Factors predictive of growth and treatment of small choroidal melanoma. COMS report no. 5. *Arch Ophthalmol*. 1997;115:1537–1544.
26. Collaborative Ocular Melanoma Study Group. Mortality in patients with small choroidal melanoma. COMS report no. 4. *Arch Ophthalmol*. 1997;115:886–893.
27. Collaborative Ocular Melanoma Study Group. Development of metastatic disease after enrollment in the COMS trials of treatment of choroidal melanoma. Collaborative Ocular Melanoma Study Group report no. 26. *Arch Ophthalmol*. 2005;123:1639–1643.
28. Collaborative Ocular Melanoma Study Group. Second primary cancers after enrollment in the COMS trials for treatment of choroidal melanoma. COMS report no. 25. *Arch Ophthalmol*. 2005;123:601–604.
29. Collaborative Ocular Melanoma Study – Quality of Life Study Group. Quality of life after iodine 125 brachytherapy vs enucleation for choroidal melanoma. COMS QOLS report no. 3. *Arch Ophthalmol*. 2006;124:226–238.
30. Collaborative Ocular Melanoma Study Group. Accuracy of diagnosis of choroidal melanomas in the Collaborative Ocular Melanoma Study. COMS report no. 1. *Arch Ophthalmol*. 1990;108:1268–1273.
31. Collaborative Ocular Melanoma Study Group. Cause-specific mortality coding: methods in the Collaborative Ocular Melanoma Study. COMS report no. 14. *Control Clin Trials*. 2001;22:248–262.
32. Collaborative Ocular Melanoma Study Group. Assessment of metastatic disease status at death in 435 patients with large choroidal melanoma in the Collaborative Ocular Melanoma Study. COMS report no. 15. *Arch Ophthalmol*.

2001;119:670–676.
33. Collaborative Ocular Melanoma Study Group. Histopathologic characteristics of uveal melanomas in eyes enucleated from the Collaborative Ocular Melanoma Study. COMS report no. 6. *Am J Ophthalmol*. 1998;125:745–766.
34. Marcus DM, Minkowitz JB, Wardwell SD, et al. The value of nucleolar organizer regions in uveal melanoma. *Am J Ophthalmol*. 1990;110:527–534.
35. Collaborative Ocular Melanoma Study Group. Comparison of clinical, echographic, and histologic measurements from eyes with medium-sized choroidal melanoma in the Collaborative Ocular Melanoma Study. COMS report no. 21. *Arch Ophthalmol*. 2003;121:1163–1171.
36. Grossniklaus HE, Albert DM, Green WR, et al. for the Collaborative Ocular Melanoma Study Group. Clear cell differentiation in choroidal melanoma. COMS report no. 8. *Arch Ophthalmol*. 1997;115:894–898.
37. Collaborative Ocular Melanoma Study Group. Trends in size and treatment of recently diagnosed choroidal melanoma, 1987–1997. Findings from patients evaluated at Collaborative Ocular Melanoma Study centers. COMS report no. 20. *Arch Ophthalmol*. 2003;121:1156–1162.
38. Wells CG, Bradford RH, Fish GE, et al. Choroidal melanoma in American Indians. [for the; COMS Group] *Arch Ophthalmol*. 1996;114:1017–1018.
39. Diener-West M, Reynolds SM, Agugliaro DJ, et al. Screening for metastasis from choroidal melanoma: experience of the Collaborative Ocular Melanoma Study. Collaborative Ocular Melanoma Study report no. 23. *Am J Clin Oncol*. 2004;22:2438–2444.
40. Collaborative Ocular Melanoma Study Group. Ten-year follow-up of fellow eyes of patients enrolled in the Collaborative Ocular Melanoma Study (COMS) randomized trials. COMS report no. 22. *Ophthalmology*. 2004;111:966–976.
41. Collaborative Ocular Melanoma Study Group. Baseline echographic characteristics of tumors in eyes of patients enrolled in the Collaborative Ocular Melanoma Study.

COMS report no. 29. *Ophthalmology*. 2008;115:1390–1397.
42. Boldt HC, Melia BM, Liu JC, et al. I-125 brachytherapy for choroidal melanoma. Photographic and angiographic abnormalities: The Collaborative Ocular Melanoma Study: COMS report no. 30. [for the; Collaborative Ocular Melanoma Study Group] *Ophthalmology*. 2009;116:106–115.
43. Collaborative Ocular Melanoma Study Group. Sociodemographic and clinical predictors of participation in two randomized trials: findings from the Collaborative Ocular Melanoma Study Group. COMS report no. 7. *Control Clin Trials*. 2001;22:526–537.
44. Collaborative Ocular Melanoma Study Group. Echography (ultrasound) procedures for the Collaborative Ocular Melanoma Study. COMS report no. 12. *J Nurs Technol*. 1999;18(4):143–149 [(pt 1); 18(5):219–232 (pt 2)].
45. Collaborative Ocular Melanoma Study Group. Consistency of observations from echograms made centrally in the Collaborative Ocular Melanoma Study. COMS report no. 13. *Ophthalmic Epidemiol*. 2002;9:11–27.
46. Diener-West M, Connor PB, Newhouse MM, et al. Feasibility of keying data from screen-displayed facsimile images in an ongoing trial: The Collaborative Ocular Melanoma Study. *Control Clin Trials*. 1998;19:39–49.
47. Goldsborough IL, Church RY, Newhouse MM, et al. How clinic coordinators spend their time in a multicenter clinical trial. *Applied Clin Trials*. 1998;7:33–40.
48. Mobley RY, Moy CS, Reynolds SM, et al. Time trends in personnel certification and turnover in the Collaborative Ocular Melanoma Study. *Clin Trials*. 2004;1:377–386.

155

Choroidal Metastases

Kristin J. Redmond, Moody D. Wharam Jr., Andrew P. Schachat

Introduction

Choroidal metastases are the most common of adult intraocular tumors.[1,2] Autopsy studies suggest that approximately 10% of cancer patients have ocular metastases, most frequently to the choroid.[1,3] Pathologies such as breast cancer are associated with higher rates, approaching 40% late in the course of the disease.[4] Of the cases, 20–40% are bilateral, and multifocal involvement of one eye occurs in approximately 20% of affected cases.[5] Frequency of metastases does not differ for the right or the left eye.[5]

Symptoms and Clinical Findings

Intraocular metastases may be asymptomatic. When symptomatic, choroidal metastases cause painless visual loss by involvement of the macular area or peripapillary retina or because of an associated, generally exudative, retinal detachment.[6,7] Retinal detachment may cause visual deficits, floaters, and flashes. Larger retinal detachments may be associated with peripheral field deficits. Tumors located anteriorly may tilt the lens, thereby causing visual loss. Rarely, these patients may have painful visual loss as a result of neovascular glaucoma or metastatic iritis.

In a review of 70 patients with choroidal metastases, symptoms at presentation included blurred vision in 80%; pain in 14%; photopsias in 13%; red eye and floaters in 7%; field defects in 3%; and photophobia in 1%. Six percent of patients were asymptomatic.[8]

The most common location for choroidal metastases is the posterior pole of the globe. Up to 40% of lesions have been reported

to be in the macular region.[9] The reason for this may be due to differential blood flow to that area, although macular metastases are also more likely to be symptomatic, therefore increasing the likelihood of diagnosis.

In contrast to choroidal melanomas, which are generally darkly pigmented, choroidal metastases more commonly present as yellow or white lesions (Fig. 155.1). For lesions of a comparable basal size, choroidal metastases are often flatter than choroidal melanomas. Serous retinal detachment is commonly associated and frequently not in proportion with the tumor size.[8,10]

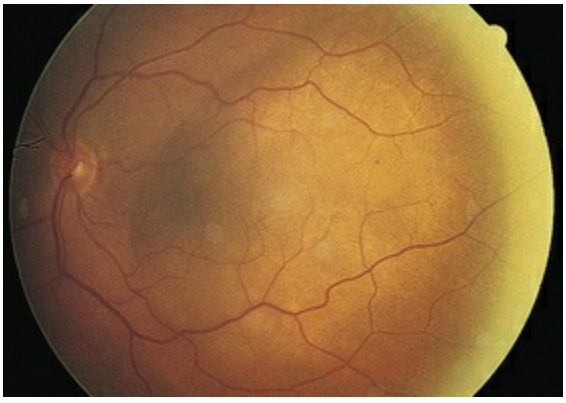

FIG. 155.1 Elevated, 3-mm, creamy yellow lesion in the macular area. The patient has a known history of breast cancer. A surrounding serous retinal detachment is present.

Frequency of Primary Cancer Site

The relative frequency of primary cancer sites for patients with choroidal metastases varies by gender. A series of more than 500 patients from the Wills Eye Hospital[11] revealed primary sites for women as follows: breast, 68%; lung, 12%; unknown, 12%; gastrointestinal, 2%; skin, 1%; renal, <1%; and other, 4%. For men, primary sites were lung, 40%; unknown, 29%; gastrointestinal, 9%; prostate, 6%; renal, 6%; skin, 4%; breast, 1%; and other, 4%.

Diagnostic Evaluation

Differential Diagnosis

Bilateral or multifocal findings are important clues to the diagnosis, since many simulating lesions tend to be unilateral and unifocal. Unilateral lesions are harder to diagnose. An extremely important diagnostic clue, if present, is a history of a known primary tumor. Many lesions may be confused with choroidal metastases, e.g., choroidal melanoma, choroidal osteoma, choroidal hemangioma, choroidal neovascularization with disciform scar, posterior scleritis, and other rare lesions.

Metastatic tumors usually have a creamy yellow appearance; purely amelanotic lesions are more likely to represent amelanotic choroidal melanomas. Metastatic lesions are usually flatter and rarely show the mushroom-shaped configuration that is often seen with melanomas. Choroidal metastases are also generally located in the posterior pole. Metastatic lesions anterior to the equator and metastases that involve the ciliary body are uncommon, and therefore amelanotic choroidal melanoma is more likely to be diagnosed in those locations. Bilateral or multifocal lesions are more likely to be metastatic, infectious, or uveitic. Combined A- and B-scan ultrasonography is of value in differentiating metastases from primary choroidal melanomas. Choroidal melanomas usually have low to moderate internal reflectivity, whereas metastatic lesions usually have higher internal reflectivity.[12,13] More recently, optical coherence tomography has become useful to assist with the differential diagnosis of choroidal tumors.[14]

Choroidal osteomas may be bilateral and may have a color similar to that of metastatic tumors. Osteomas are rarely significantly elevated, and associated choroidal neovascularization is more common in patients with choroidal osteomas than in those with metastases. Ultrasound examinations[15] and computed tomography (CT) scans are extremely valuable diagnostic tools in these patients because the bony change in the choroid shows very high reflectivity on ultrasound examination, and bone density can be confirmed with the CT scan.[16] Optical coherence tomography (OCT) may show overlying photoreceptor changes.[17]

Circumscribed choroidal hemangiomas are almost always unilateral and unifocal. Their characteristic reddish-orange coloration is an important diagnostic clue. Fluorescein angiography

shows more prominent early choroidal filling than is usually seen with metastatic lesions.[16] OCT features of hemangioma have also been reported.[18]

Although some inflammation may be associated with a choroidal metastasis, inflammation is generally not prominent, but it can be seen, sometimes associated with choroidal detachment.[19] A number of inflammatory conditions should be distinguishable, including Harada disease, the uveal effusion syndrome, posterior scleritis, and similar entities.[16] In these patients, associated vitreous inflammation is often seen, and diffuse thickening of the choroid usually can be demonstrated on ultrasound examination.

Rarely do patients with large disciform scars or subretinal hemorrhages present a confusing picture. There is usually a history of previous visual loss related to choroidal neovascularization, and a history of systemic cancer is much less common. Drusen are usually apparent in the fellow eye. The echograms may be difficult to interpret, and the eyes are occasionally enucleated owing to a mistaken diagnosis of choroidal melanoma.[20] The whitish-yellow color of choroidal metastases is usually quite different from the darker appearance of these lesions, in which admixed blood is a prominent feature.

Ophthalmic Evaluation and Ancillary Tests

The ophthalmic evaluation should begin with a good general history, since the majority of patients will already have an established primary cancer diagnosis. A complete eye examination, including a dilated fundus examination, is essential. Although one eye may have an obvious lesion, care must be taken to scrutinize the other eye, as the disease is bilateral in 20–40% of patients.

Anticipating that radiation therapy may be recommended and may be cataractogenic, the status of the lens should be carefully evaluated.[21] If the patient is diabetic or has retinal microangiopathy, this should be noted because radiation therapy exacerbates preexisting retinal vascular disease (see Chapter 61, Radiation retinopathy). Documentary fundus photographs should be obtained to compare with later examinations to assess growth or treatment response.

Fluorescein Angiography

Fluorescein angiography is rarely useful as an aid in the differential diagnosis of metastatic choroidal tumors because it does not allow the definite differentiation of pseudometastatic lesions such as choroidal hemangiomas or melanomas. Angiography is more helpful in assessing the size of the lesion. Relatively flat areas of choroidal invasion are difficult to recognize clinically, but there is almost always some alteration in the overlying pigment epithelium, which is often highlighted on the angiogram.

Metastatic choroidal tumors are usually hypofluorescent in the early phases of the study and become progressively hyperfluorescent in late phases (Figs. 155.2 and 155.3). The so-called double circulation pattern, thought to be characteristic of choroidal melanomas that have broken through Bruch's membrane, is a rare finding in metastatic tumors.[22] Prominent early choroidal filling is a feature more typical of circumscribed choroidal hemangiomas.[16]

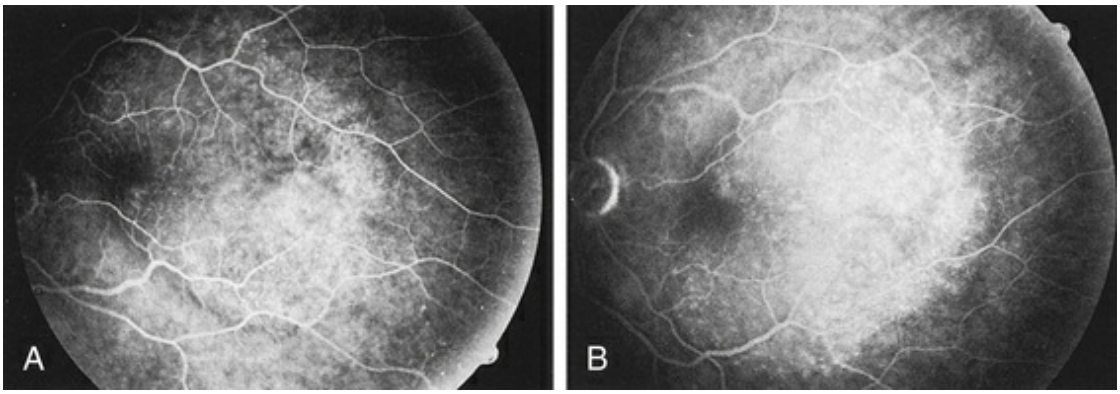

FIG. 155.2 (A,B) Fluorescein angiographic frames of the lesion in Fig. 155.1.

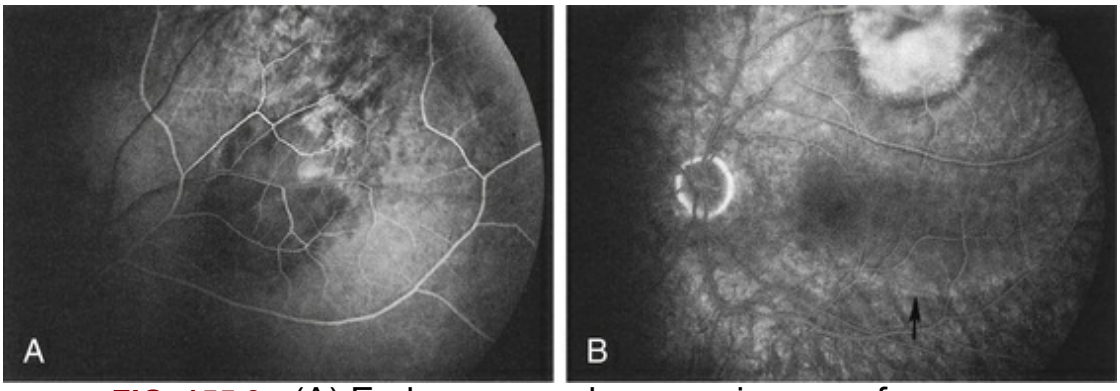

FIG. 155.3 (A) Early venous phase angiogram of a small metastasis along the superotemporal arcade from a prostatic primary. Most of the lesion is relatively hypofluorescent. (B) In the late angiogram, the tumor hyperfluoresces. Visual loss is due to serous macular detachment (*arrow*).

A- and B-Scan Ultrasonography

B-scan ultrasonography is of value in evaluating patients with media opacities or bullous retinal detachments when a choroidal lesion is suspected but cannot be clearly seen. The B-scan ultrasonogram shows an echogenic subretinal mass with diffuse, ill-defined borders. Overlying retinal detachment is common, and sound attenuation in the lesion is usually moderate.[13] In unusual cases, choroidal detachment may be seen.[19]

The A-scan ultrasonogram usually demonstrates moderate to high internal reflectivity. Vascularity is not prominent, and the consistency is solid.[12,13] It is useful to determine the height of the metastatic tumor by ultrasonography so that shrinkage of the lesion can be documented after treatment. A more complete discussion of the ultrasonographic features of choroidal metastases is provided in Chapter 11 (Diagnostic ophthalmic ultrasound), as well as in standard texts.[15] Magnetic resonance imaging and spectroscopy may also prove to be valuable differential diagnostic aids.[23,24]

Optical Coherence Tomography

OCT imaging, particularly with enhanced depth imaging (EDI) of the choroid as popularized by Spaide and others, may help with the

differential diagnosis. Torres and colleagues have recently summarized the EDI features of various choroidal tumors.[25]

Fine-Needle Aspiration Biopsy

Diagnostic fine-needle aspiration biopsy (FNAB) of intraocular tumors should be considered only under special circumstances.[26] The technique may be appropriate in a patient who has what appears to be a characteristic metastatic tumor but in whom a primary lesion cannot be found despite an extensive systemic evaluation. Augsburger and Shields[26] include, as an additional indication, the use of the technique in some patients who refuse treatment without histopathologic verification of the lesion (rare) or in patients who have lesions that present major diagnostic uncertainty.

In general, oncologists require a histologic diagnosis before initiation of treatment of nonocular sites. Because of the potential threat to vision, it is not a routine procedure to biopsy intraocular lesions before treatment. Useful reports provide updates on FNAB and choroidal tumors.[27–29]

Systemic Evaluation

Two-thirds of choroidal metastases are diagnosed in patients with a prior history of malignancy.[11] Of the remaining patients, the primary site of malignancy was subsequently detected in about half, with approximately 70% originating from lung cancer. This high prevalence of lung primaries is likely due to the increased propensity of lung cancer to present with brain/eye metastases relative to other malignancies. In general, the workup for a patient with a known malignancy will vary depending on the location and status of the primary tumor, as well as a history of prior metastatic disease. The staging evaluation should include an MRI of the brain since studies have suggested central nervous system metastases may develop in close to 30% of patients.[5] In addition, it often consists of laboratory data, including serum chemistries, liver function tests, alkaline phosphatase, chest computerized tomography, and bone scan.

Unknown Primary Site

A patient without a known history of malignancy must undergo a systemic workup to attempt to localize the primary. Because the most common primary site is breast in women and lung in men, breast imaging and chest computerized tomography are important. Blood work including serum chemistries may be useful to evaluate for additional sites of metastatic disease requiring further evaluation or imaging. If a primary tumor is identified, pathologic confirmation of the primary tumor is critical. An evaluation of treatment for the primary tumor including chemotherapy, radiotherapy, or hormonal therapy should be made.

If the choroidal lesion remains the only site of disease following a systemic evaluation, a decision must be made regarding the safety of biopsy of the choroidal lesion.[30,31] Pathologic diagnosis may be helpful in identifying the primary site of disease.

Management

Treatment of patients with choroidal metastases benefits from multidisciplinary collaboration and careful evaluation of multiple factors including the intraocular site, presence of visual symptoms, primary tumor histology and site, presence and status of other metastases, and anticipated efficacy of systemic treatment options. Close observation may be considered for small metastases in the periphery of the retina that may not enlarge rapidly or lead to visual symptoms.[5] Similarly, rapid or complete response to systemic therapy especially in patients with breast or lung cancer may allow postponement or avoidance of local therapy to the choroidal metastases. There are case reports suggesting a potential benefit of crizotinib in ALK-mutated non-small-cell lung cancer.[32,33] By contrast, lesions causing visual symptoms or encroaching upon the optic disc or macula generally require local therapy. Some reports suggest improved outcomes with a combination of local and systemic therapies.[34] Although there was previously interest in intravitral bevacizumab as a potential therapeutic modality, a recent report suggests progression in an unacceptably high number of patients.[35] The following section addresses radiotherapeutic

management options for choroidal metastases.

Conventional External Beam Radiation Therapy

Historically, the conventional local treatment for choroidal metastases has been external beam radiation therapy using megavoltage photons. Treatment planning for modern external beam treatment begins with CT simulation to delineate the target as well as adjacent normal tissues. The patient is positioned in a supine position on a flat table with a mask fitting over the face and shoulders for immobilization. The treatment field depends on the location and geometry of the tumor. Modern external beam radiation treatment generally utilize intensity modulated radiation therapy (IMRT) techniques in which inverse planning and multileaf collimators are used to deliver the prescribed dose to the tumor while limiting exposure to the immediately adjacent normal tissues. At present, conformal techniques are preferable and should be considered the standard of care. However, in cases where treatment delays as a result of labor-intensive treatment planning and quality assurance measures are deemed to be inappropriate due to symptomatic progression, conventional treatment plans may be utilized. Since approximately 80% of tumors are located in the posterior segment of the uvea,[36,37] it is generally possible to use a D-shaped field designed to cover the posterior globe, bony roof, floor of orbit, and a portion of the optic nerve but shield the cornea and lens (Fig. 155.4). It may not be possible to block the lens if the metastasis is anterior to the equator. For unilateral metastases, it is possible to achieve adequate coverage with only a single ipsilateral beam. The minimal exit dose to the contralateral globe does not preclude subsequent treatment for development of contralateral metastases. As long as the dose to the contralateral orbit is limited in the initial field, it is relatively simple to treat the contralateral orbit as needed at a later date. A total of 20–40% of patients have bilateral choroidal metastases requiring treatment of both globes.[8,10] The dose typically used for palliation is 3000 cGy in 300 cGy per fraction delivered as a single fraction 5 days per week for 10 treatments. If prolonged survival is anticipated, treatment to a

higher dose of radiation is administered to improve long-term local control. Doses of 4500–5000 cGy in fractions of 200–250 cGy have been reported.[38–43] Local control with these regimens is excellent.

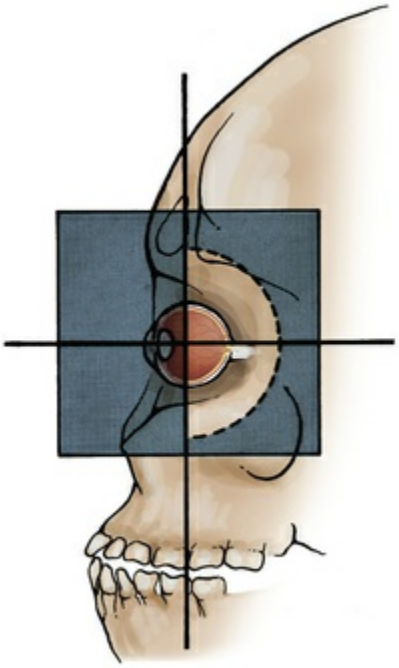

FIG. 155.4 Conventional D-shaped field used to treat choroidal metastases of the posterior globe, but shield the lens and cornea. CT-based planning is used for target delineation.

Brachytherapy Plaques

An alternative local therapy for choroidal metastases involves plaque brachytherapy; radioisotopes such as iodine-125, ruthenium-106, or palladium-103 are temporarily surgically placed adjacent to the lesion designed to cover the tumor plus 2–3 mm margin. These treatments typically last about 3 days, after which the plaque is removed. Data to support plaque brachytherapy may be extrapolated from choroidal melanoma in which the technique is believed to have comparable survival to enucleation.[44] A large series of 650 melanoma cases was reported by the Wills Eye Hospital.[45] Local recurrence was 14% at 5 years and 24% at 10 years.

Plaque brachytherapy may be used only for patients with solitary choroidal metastases. In addition, they must have lesions of

appropriate size, depth, and location relative to the macula and fovea. A major disadvantage of this approach is that it involves hospitalization and two surgical procedures for placement and removal of the brachytherapy plaque. (For additional information concerning melanoma-related brachytherapy, the reader is referred to Chapter 149, Brachytherapy for choroidal melanoma.)

Stereotactic Radiosurgery

Stereotactic radiosurgery (SRS) utilizes multiple precisely focused small radiation beams and high doses for a limited number of fractions. This technique administers ablative doses of radiation to a small volume, thereby maximizing local control while sparing critical adjacent normal tissues. There are multiple technologies that may be used to deliver SRS, including linear accelerator-based approaches or gamma-knife. When using conformal radiation techniques, precise and reproducible immobilization of the eye is critical. Several techniques exist. For example, eye gaze may be directed by asking the patient to visualize a flashing light at a set position. A light field projected onto the sclera may be used to ensure that the gaze during treatment planning matches the treatment setup. The positioning is then verified by an ophthalmologist.[46]

A series from China reviewed patients treated with gamma knife radiosurgery for orbital tumors.[47] Of the 202 cases included, 18 had malignant choroidal tumors. Vision was preserved in 129 patients, with 72 experiencing improvement in vision and 18 experiencing deterioration.

Gamma knife radiosurgery utilizes 201 individual cobalt-60 sources in a collimator to which the patient is adhered using an invasive frame for immobilization. The radiation beam is focused by different-sized collimators, which are controlled by a program that allows them to be quickly changed. Gamma knife is extremely accurate and may be used to treat small lesions (Fig. 155.5).

FIG. 155.5 Gamma knife radiosurgery. A frame is invasively attached to the patient's skull for precise stereotactic planning. The treatment helmet contains 201 individual cobalt-60 sources.

An alternate technology is linear accelerator-based radiosurgery, which involves delivery of radiation using either multiple arcs and special collimators to focus the beam or a micromultileaf collimator. Contemporary image-guided radiation therapy (IGRT), in which treatment machines have onboard kilovoltage or megavoltage imaging capabilities, allows confirmation of lesion localization.

Charged Particle Therapy

A final treatment option for choroidal metastases is proton beam or charged particle irradiation in which charged particles are used to deliver radiation with a very sharp dose fall-off, allowing a potential improvement in vision preservation over conventional radiation therapy. Like radiosurgery, it typically allows for fewer treatments than conventional radiation therapy. A retrospective series from Harvard[47] included 63 patients treated with protons for choroidal metastases. Tumor regression was documented in 84% of patients, and stable disease was reported in 14%. Resolution of retinal detachment was reported in 82%. Fifty-eight percent of patients had visual acuity at last follow-up of 20/200 or better. A recent prospective study performed at the University of California

San Francisco randomized patients with choroidal or ciliary body melanoma to plaque brachytherapy versus charged particle therapy.[48] At a median follow-up of greater than 12 years, they reported a significant benefit in local control in patients receiving charged particle therapy. Specifically local control at 5 years was 100% versus 84% and at 12 years was 98% versus 79% for charged particle and plaque brachytherapy, respectively. While these data do not directly relate to choroidal metastases, they suggest a potential benefit of charged particle therapy over brachytherapy that merits consideration. (More detail on proton beam treatment is included in Chapter 150, Charged-particle irradiation of uveal melanoma.)

Toxicity

Ocular Toxicity

Ocular radiation therapy is well tolerated, with minimal acute toxicities,[43,49] including dry eye, epiphora, or irritative symptoms. These symptoms may be managed with artificial tears or lubricating ointments. Topical antibiotics may be indicated for epithelial damage. Long-term ocular toxicity includes cataract formation, which was reported in 3% of patients in one series.[50] Cataract formation is expected if the lens is not shielded and there is a reasonable period of survival following treatment. Damage to the retina and optic nerve are the primary toxicities resulting in reduced visual acuity. Because the dose to critical structures (optic nerve and macula) is below the known radiation tolerance and due to the relatively poor prognosis of patients with choroidal metastases, many patients do not survive to develop radiation retinopathy,[51] which has a median onset of 18 months to 2 years.[2,8,52] A large series using conventional radiation therapy reported retinopathy and optic neuropathy in 2% of patients.[50]

Nonocular Toxicity

Nonocular toxicities are generally minimal but may include erythema, dry skin, or loss of eyelashes or eyebrows. Facial bone

and muscle growth may be affected in children treated with external beam radiation therapy but should not be affected in adults. Use of certain concurrent chemotherapy with agents such as actinomycin D or doxorubicin should be avoided as they increase the risk of toxicity.

Prognosis

Development of choroidal metastases usually represents advanced systemic disease[53] with limited potential for cure. Studies suggest a median survival of approximately 16 months,[42,47,54,55] with survival varying by primary tumor type as well as the availability of effective systemic chemotherapeutic options.

Most choroidal metastases respond to local therapy with response rates of approximately 80% in some series.[49,56] Local response is often associated with tumor flattening (Fig. 155.6) and pigmentary proliferation. Improved response rates were associated with (1) symptoms for <49 days prior to initiation of radiation therapy and (2) small tumor extent less than half of a quadrant with minimal or no retinal detachment.[49]

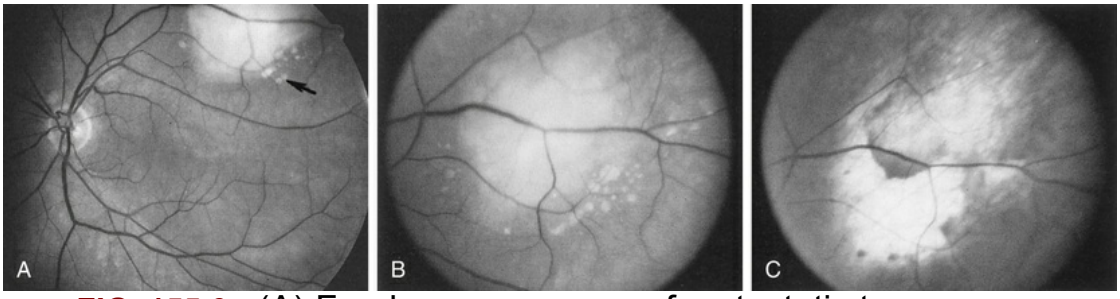

FIG. 155.6 (A) Fundus appearance of metastatic tumor before treatment. The angiogram from this patient is illustrated in Fig. 151.3. Small tumor deposits (*arrow*) are present in subretinal fluid surrounding the inferior aspect of the tumor. (B) Higher-magnification view. (C) The tumor has flattened completely 1 month after external beam radiation.

Globe preservation is possible in the majority of patients and complete resolution of visual symptoms has been reported in 25–50% of patients.[5,8,10] Time to improvement of visual symptoms

ranges from a few days to 10 weeks following initiation of radiation therapy and typically persists for the remainder of the patient's life.[38]

Conclusion

Choroidal metastases are the most common intraorbital tumors, with malignancies such as breast and lung cancer being the most common primary sites. Primary management for symptomatic or progressive lesions requires radiation therapy for vision preservation. There are multiple radiation techniques that are associated with high rates of local control and low risk of toxicity. The prognosis of patients with choroidal metastases is poor since most patients will succumb to widely disseminated systemic disease.

References

1. Bloch RS, Gartner S. The incidence of ocular metastatic carcinoma. *Arch Ophthalmol*. 1971;85:673–675.
2. Ferry AP, Font RL. Carcinoma metastatic to the eye and orbit: a clinicopathologic study of 227 cases. *Arch Ophthalmol*. 1974;92:276–286.
3. Nelson CC, Hertzberg BS, Klintworth GK. A histopathologic study of 716 unselected eyes in patients with cancer at the time of death. *Am J Ophthalmol*. 1983;95:788–793.
4. Mewis L, Young SE. Breast carcinoma metastatic to the choroid: analysis of 67 patients. *Ophthalmology*. 1982;89:147–151.
5. Shields JA. *Diagnosis and management of intraocular tumors*. Mosby: St. Louis; 1983.
6. Gonvers M, Zografos L. Choroidal metastases and rhegmatogenous retinal detachment. *Retina*. 1991;11:426–429.
7. Haimovici R, Mukai S, Schachat AP, et al. Rhegmatogenous retinal detachment in eyes with uveal melanoma. *Retina*. 1996;16:488–496.

8. Stephens RF, Shields JA. Diagnosis and management of cancer metastatic to the uvea: a study of 70 cases. *Ophthalmology*. 1979;86:1336–1349.
9. Freedman MI, Folk JC. Metastatic tumors to the eye and orbit: patient survival and clinical characteristics. *Arch Ophthalmol*. 1987;105:1215–1219.
10. Mewis L, Young SE. Breast carcinoma metastatic to the choroid: analysis of 67 patients. *Ophthalmology*. 1982;89:147–151.
11. Shields CL, Shields JA, Gross NE, et al. Survey of 520 eyes with uveal metastases. *Ophthalmology*. 1997;104:1265–1276.
12. Fuller DG, Snyder WB, Hutton WI, et al. Ultrasonographic features of choroidal malignant melanomas. *Arch Ophthalmol*. 1979;97:1465–1472.
13. Shammas JH. *Atlas of ophthalmic ultrasonography and biometry*. Mosby: St. Louis; 1984.
14. Sayanagi K, Pelayes DE, Kaiser PK, et al. 3D Spectral domain optical coherence tomography findings in choroidal tumors. *Eur J Ophthalmol*. 2011;21:271–275.
15. Dibernardo C, Schachat AP, Fekrat S. *Ophthalmic ultrasound: a diagnostic atlas*. Thieme: New York; 1998.
16. Gass JDM. *Stereoscopic atlas of macular diseases: diagnosis and treatment*. 3rd ed. Mosby: St. Louis; 1987.
17. Shields CL, Perez B, Materin MA, et al. Optical coherence tomography of choroidal osteoma in 22 cases: evidence for photoreceptor atrophy over the decalcified portion of the tumor. *Ophthalmology*. 2007;114:e53–8.
18. Liu W, Zhang Y, Xu G, et al. Optical coherence tomography for evaluation of photodynamic therapy in symptomatic circumscribed choroidal hemangioma. *Retina*. 2011;31:336–343.
19. Sneed SR, Byrne SF, Mieler WF, et al. Choroidal detachment associated with malignant choroidal tumors. *Ophthalmology*. 1991;98:963–970.
20. El Baba F, Jarrett WH II, Harbin TS Jr, et al. Massive hemorrhage complicating age-related macular degeneration: clinicopathologic correlation and role of anticoagulants. *Ophthalmology*. 1986;93:1581–1592.

21. Macfaul PA, Bedford MA. Ocular complications after therapeutic irradiation. *Br J Ophthalmol*. 1970;54:237–247.
22. Augsburger JJ, Golden MI, Shields JA. Fluorescein angiography of choroidal malignant melanomas with retinal invasion. *Retina*. 1984;4:232–241.
23. Haik BG, Saint Louis L, Smith ME, et al. Magnetic resonance imaging in choroidal tumors. *Ann Ophthalmol*. 1987;19:218–238.
24. Mafee MF, Peyman GA, Peace JH, et al. Magnetic resonance imaging in the evaluation and differentiation of uveal melanoma. *Ophthalmology*. 1987;94:341–348.
25. Torres VL, Brugnoni N, Kaiser PK, et al. Optical coherence tomography enhanced depth imaging of choroidal tumors. *Am J Ophthalmol*. 2011;151:586–593.
26. Augsburger JJ, Shields JA. Fine-needle biopsy of solid intraocular tumors; indications, instrumentation, and techniques. *Ophthalmic Surg*. 1984;15:34–40.
27. Eide N, Walaas L. Fine-needle aspiration biopsy and other biopsies in suspected intraocular malignant disease: a review. *Acta Ophthalmol*. 2009;87:588–601.
28. Pelayes DE, Zárate JO. Fine needle aspiration biopsy with liquid-based cytology and adjunct immunohistochemistry in intraocular melanocytic tumors. *Eur J Ophthalmol*. 2010;20:1059–1065.
29. Shields CL, Ganguly A, Bianciotto CG, et al. Prognosis of uveal melanoma in 500 cases using genetic testing of fine-needle aspiration biopsy specimens. *Ophthalmology*. 2011;118:396–401.
30. Eide N, Walaas L. Fine-needle aspiration biopsy and other biopsies in suspected intraocular malignant disease: a review. *Acta Ophthalmol*. 2009;87:588–601.
31. Shields JA, Shields CL, Ehya H, et al. Fine-needle aspiration biopsy of suspected intraocular tumors. The 1992 Urwick Lecture. *Ophthalmology*. 1993;100:1677–1684.
32. Feng Y, Singh AD, Lanigan C, et al. Choroidal metastases responsive to crizotinib therapy in a lung adenocarcinoma patient with ALK 2p23 fusion identified by ALK immunohistochemistry. *J Thorac Oncol*. 2013;8(12):e109–11.

33. Bearz A, Santarossa S, Manfrè A, et al. Activity of crizotinib over choroidal metastases in non-small-cell lung cancer (NSCLC)-ALK rearranged: a case report. *BMC Res Notes*. 2014;7:589.
34. Amer R, Pe'er J, Chowers I, et al. Treatment options in the management of choroidal metastases. *Ophthalmologica*. 2004;218:372–377.
35. Maudgil A, Sears KS, Rundle PA, et al. Failure of intravitreal bevacizumab in the treatment of choroidal metastasis. *Eye (Lond)*. 2015;29(5):707–711.
36. Castro PA, Albert DM, Wang WJ, et al. Tumors metastatic to the eye and adnexa. *Int Ophthalmol Clin*. 1982;22:189–223.
37. Hutchison DS, Smith TR. Ocular and orbital metastatic carcinoma. *Ann Ophthalmol*. 1979;11:869–873.
38. Thatcher N, Thomas PRM. Choroidal metastases from breast carcinoma: a survey of 42 patients and the use of radiation therapy. *Clin Radiol*. 1975;26:549–553.
39. Hoogenhout J, Brink HM, Verbeek AM, et al. Radiotherapy of choroidal metastases. *Strahlenther Onkol*. 1989;165:375–379.
40. Phillips TL. More on managing metastatic choroidal tumors. *Oncology*. 1989;3:14.
41. Brady LW, Shields JA, Augsburger JJ, et al. Malignant intraocular tumors. *Cancer*. 1982;49:578–585.
42. Maor M, Chan RC, Young SE. Radiotherapy of choroidal metastases breast cancer as primary site. *Cancer*. 1977;40:2081–2086.
43. Burmeister BH, Benjammin CS, Childs WJ. The management of metastases to eye and orbit from carcinoma of the breast. *Aust N Z J Ophthalmol*. 1990;18:187–190.
44. De Potter P, Shields CL, Shields JA, et al. Impact of enucleation versus plaque radiotherapy in the management of juxtapapillary choroidal melanoma on patient survival. *Br J Ophthalmol*. 1994;78:109–114.
45. Sagoo MS, Shields CL, Mashayekhi A, et al. Plaque radiotherapy for juxtapapillary choroidal melanoma: tumor control in 650 consecutive cases. *Ophthalmology*. 2011;118:402–407.

46. Tsina EK, Lane AM, Zacks DN, et al. Treatment of metastatic tumors of the choroid with proton beam irradiation. *Ophthalmology*. 2005;112:337–343.
47. Xu D, Liu D, Zhang Y, et al. Gamma knife surgery in the management of orbital tumors. *J Neurosurg*. 2010;113:34–38.
48. Mishra KK, Quivey JM, Daftari IK, et al. Long-term results of the UCSF-LBNL randomized trial: charged particle with helium ion versus iodine-125 plaque therapy for choroidal and ciliary body melanoma. *Int J Radiat Oncol Biol Phys*. 2015;92(2):376–383.
49. Panizzoni GA, Gasparini G, Dal Fior S, et al. Radiotherapeutic treatment for breast cancer choroidal metastases. *Tumori*. 1990;76:563–565.
50. Rudoler SB, Corn BW, Shields CL, et al. External beam irradiation for choroid metastases: identification of factors predisposing to long term sequelae. *Int J Radiat Oncol Biol Phys*. 1997;38:251–256.
51. Jardel P, Sauerwein W, Olivier T, et al. Management of choroidal metastases. *Cancer Treat Rev*. 2014;40(10):1119–1128.
52. Brown GC, Shields JA, Sanborn G, et al. Radiation retinopathy. *Ophthalmology*. 1982;89:1494–1501.
53. Char DH. Posterior uveal tumors. Tracy TM, Otway M. *Clinical ocular oncology*. Churchill Livingstone: New York; 1989:102.
54. Wiegel T, Bottke D, Kreusel KM, et al. External beam radiotherapy of choroidal metastases – final results of a prospective study of the German Cancer Society (ARO 95–08). *Radiother Oncol*. 2002;64:13–18.
55. Amichetti M, Caffo O, Minatel E, et al. Ocular metastases from breast carcinoma: a multicentric retrospective study. *Oncol Rep*. 2000;7:761–765.
56. Hoogenhout J, Brink HM, Verbeek AM, et al. Radiotherapy of choroidal metastases. *Strahlenther Onkol*. 1989;165:375–379.

156

Choroidal Osteoma

Carol L. Shields, Gary C. Brown, Sanjay Sharma, Jerry A. Shields

General Considerations

The presence of bone within the eye is unusual and can develop in several clinical settings.[1] Calcification can occur in tissues that are accessible to body fluids, and the process of ossification occurs when an abundant blood supply is present to deliver osteoblasts to organize the architecture of Haversian systems.[2,3] The choroid and the retinal pigment epithelium are the most common sites for bone formation within the eye. Intraocular ossification most often occurs as a dystrophic process in association with phthisis bulbi.[2–5]

Choroidal osteoma is an unusual form of benign intraocular ossification.[1,6–12] In contrast to other types of intraocular ossification, this tumor is found in otherwise healthy eyes. Interest in this tumor was stimulated following enucleation of a presumed amelanotic choroidal melanoma in a 26-year-old woman that proved on histopathology to represent a choroidal osteoma.[8] In 1978, Gass and coworkers described the clinical and angiographic features of choroidal osteoma in a series of 4 patients.[9] Later, three relatively large series on choroidal osteoma by Gass,[10] Aylward et al.,[11] and Shields et al.[12] clarified the clinical and imaging features of this tumor as well as anticipated outcomes. Over four decades, numerous clinical case descriptions of choroidal osteoma have appeared in the literature.[11–52]

Definition and Incidence

Choroidal osteoma is a benign tumor composed of mature bone. It is typically found in healthy young females in the second or third decades of life[1,10–12] (Fig. 156.1). However, some males,[10,16,35,37,46] young children,[21,23,24,34,38,40] and adults over age 30 years[12,15,21,32,46,50] have been found with choroidal osteoma. There is no predilection for race. Most reported patients with this lesion are Caucasian, but several patients of African American[24,31]and Oriental descent[26,32,34,38,46,50,51] have been described. The tumor generally occurs sporadically; however, there are cases of familial choroidal

osteoma.[21,23,40] The familial cases have been described in a mother and daughter,[21] a brother and sister,[40] and three siblings.[23]

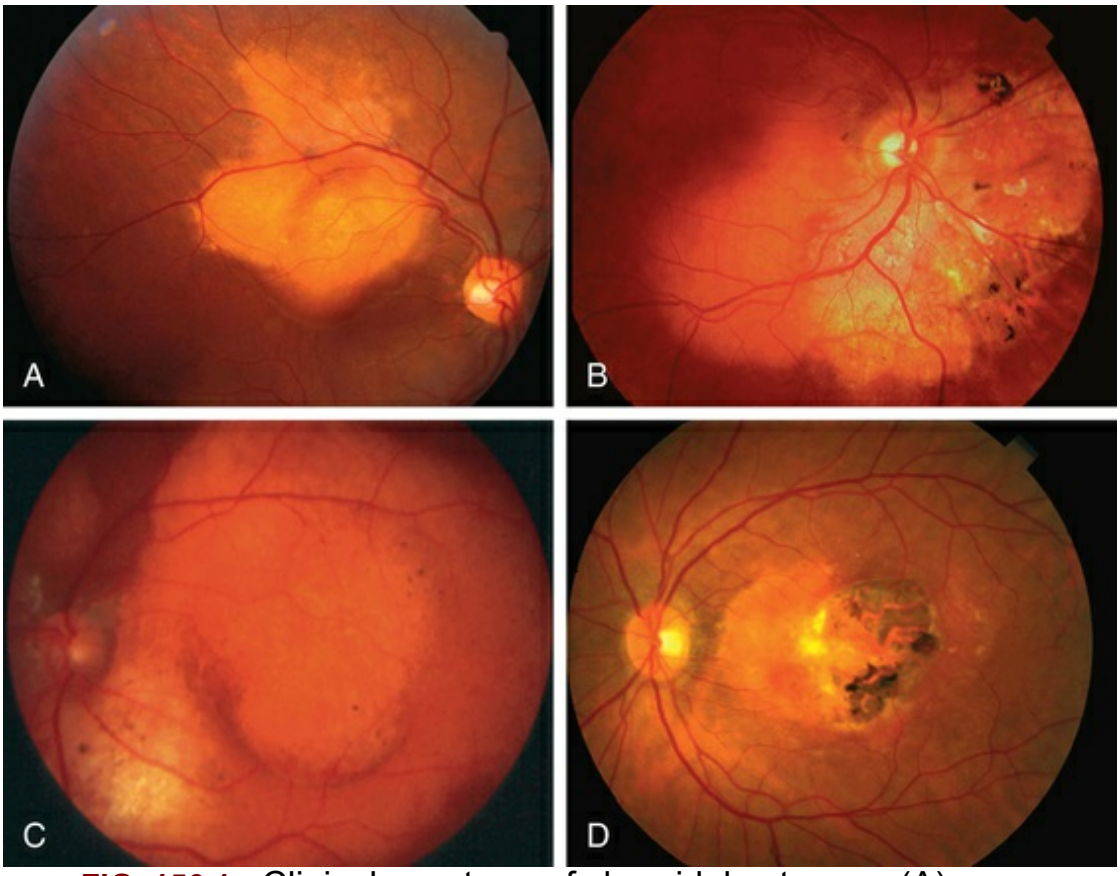

FIG. 156.1 Clinical spectrum of choroidal osteoma. (A) Unilateral osteoma in a young woman. (B) Unilateral osteoma in a young man. (C) Calcified choroidal osteoma with bone excavation in the macula. (D) Macular choroidal osteoma with decalcification in a young woman.

In our practice of ocular oncology, we have seen approximately 18,000 patients with uveal melanoma over the past 40 years and only approximately 120 patients with choroidal osteoma. Therefore, it is presumed that choroidal osteoma is extremely rare.

Clinical Features

Patients with choroidal osteoma are often asymptomatic. Symptoms can include visual loss, metamorphopsia, and visual

field defects corresponding to the location of the tumor.[1,10–12] In one report, total blindness of both eyes was found in a young girl with bilateral choroidal osteomas.[43]

Choroidal osteoma is unilateral in approximately 75% of reported cases.[1] In bilateral cases, the tumors can appear symmetric or asymmetric, in different stages of development, growth, or decalcification[10–12] (Fig. 156.2). In one case with 45 years of follow-up, bilateral choroidal osteomas lead to disparate outcomes with poor vision in one eye and retained vision in the other.[52] Rarely, patients with initially unilateral choroidal osteoma can later develop bilateral disease.[30]

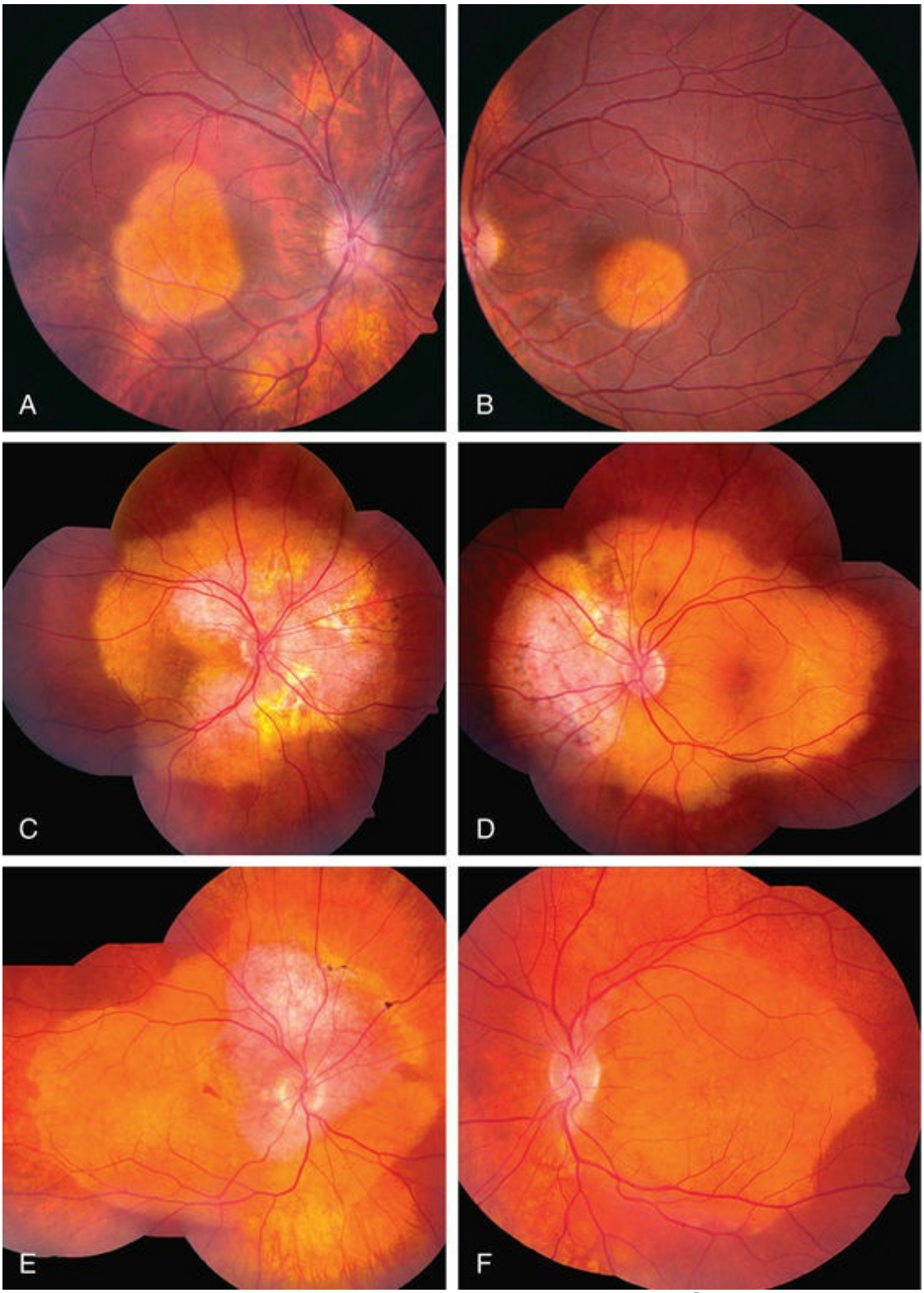

FIG. 156.2 Bilateral choroidal osteoma. (A,B) Small calcified osteomas in macula of young man. (C,D) Larger partially calcified osteomas in a young woman. (E,F) Partially decalcified choroidal osteoma in right eye with subretinal hemorrhage and completely calcified osteoma in the left eye of a young woman.

Choroidal osteoma tends to be located in the juxtapapillary or peripapillary area, often with extension into the macula (Fig. 156.1). Rarely, this tumor is confined to the macular region only, without involvement of the juxtapapillary area.[10–12,16,32,35] Choroidal osteoma is rarely seen in other locations of the eye and, to our knowledge, it has not been known to occur as a solitary lesion anterior to the retinal vascular arcades. Quite often choroidal osteoma is confused with idiopathic sclerochoroidal calcification, a benign, often multifocal, bilateral process that typically occurs anterior to the retinal vascular arcades, near the equator of the eye.[53,54]

The choroidal osteoma appears yellow–orange in color, particularly when the tumor is fully calcified. Over time, as decalcification occurs, the tumor becomes more pale yellow with overlying retinal pigment epithelial thinning and clumping. Choroidal osteoma ranges in size from approximately 2 to 22 mm in basal dimension and approximately 0.5–2.5 mm in elevation.[1,10–12,52] In some cases, the bony tumor surface is irregularly excavated (Fig. 156.1) or elevated. The tumor shape is generally oval or round with characteristic well-defined scalloped or geographic margins. The margins can have blunt pseudopod-like projections. In some instances the tumor can be bilobed with two large plaques joined together by an isthmus.[10,30]

The vasculature within the choroidal osteoma is often visible as tufts of short branching vessels that originate deep within the tumor and emerge onto the tumor surface. This is most prominent over the pale yellow portion of the tumor where the retinal pigment epithelium is thinned and depigmented.[9] These large caliber vessels are not neovascular tissue and are not associated with subretinal exudation or hemorrhage.[1,10] The overlying retinal vasculature and optic disc is characteristically unaffected by the osseous tumor, and there are no related vitreous or anterior segment abnormalities.

Many choroidal osteomas show evidence of slight enlargement in basal dimensions over several months to years[11,38,41,44,48,52,55] (Fig. 156.3). Aylward and associates found tumor growth in 41% of 22 cases over a mean follow-up of 10 years.[11] Shields and associates found tumor growth of 74 choroidal osteomas at 22% by 5 years and 51% by 10 years.[12] In some cases the tumor has doubled in size.[10,41] Others have observed the development of a new choroidal

osteoma in a previously unaffected eye.[1,10]

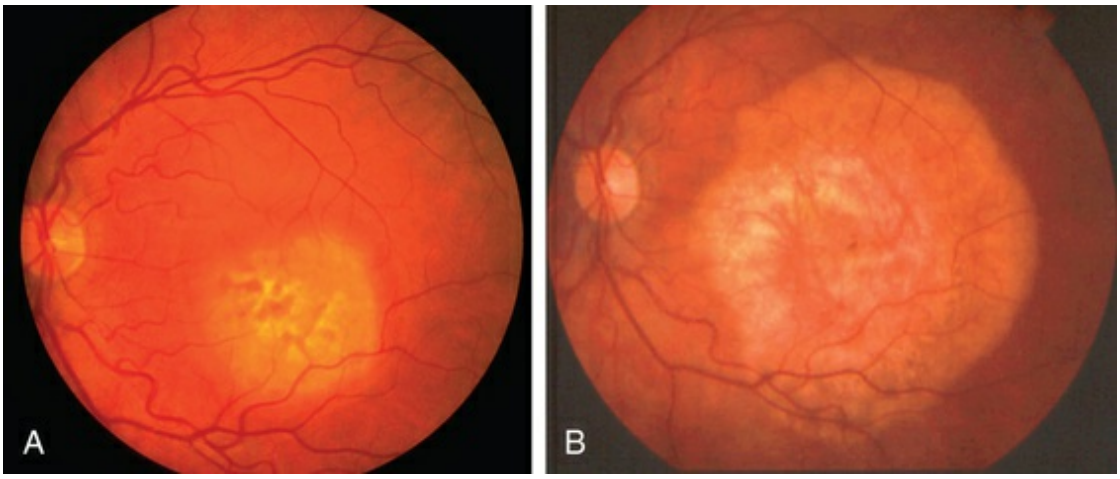

FIG. 156.3 Documented enlargement (A,B) of choroidal osteoma over 6 years.

Trimble, Schatz, and Schneider reported a case of a choroidal osteoma in a 23-year-old woman whose tumor enlarged slowly over 5 years.[47] She developed choroidal neovascularization that was treated with photocoagulation, and subsequently the tumor decalcified over 18 months, leaving an atrophic bed. Partial or complete decalcification of choroidal osteoma has been found to occur in 28% of cases by 5 years and 46% by 10 years.[12] Subtle gradual alterations in tumor color, surface pigmentation, and surface contour have also been observed.

Serous subretinal fluid can occur overlying choroidal osteoma. Subretinal fluid usually occurs over the macular portion of the osteoma. Ophthalmoscopy, fluorescein angiography, indocyanine green angiography, and optical coherence tomography should be performed for detection of choroidal neovascular membrane (CNVM).[10–12]

CNVM overlying osteoma has been found in 31% of cases by 5 years, 31–47% by 10 years, and 46–56% by 20 years[11,12] (Fig. 156.4 and Table 156.1). The CNVM is usually associated with subretinal fluid or hemorrhage, but it can be detected prior to vascular leakage as a slightly elevated gray–green subretinal tissue.[15,37] Factors that predict the development of CNVM include irregular tumor surface and subretinal hemorrhage[12] (Table 156.2). If the CNVM is

extrafoveal, it can be treated with anti-vascular endothelial growth factor (anti-VEGF) medications, laser photocoagulation, or photodynamic therapy.[11,12] If the CNVM is in the fovea, the potential for subfoveal hemorrhage and disciform scarring often leads to a poor visual outcome.[12,33] For subfoveal (and most extrafoveal) CNVM, we prefer anti-VEGF therapy monthly to resolve the membrane and then consolidation for extrafoveal CNVM with laser or photodynamic therapy.

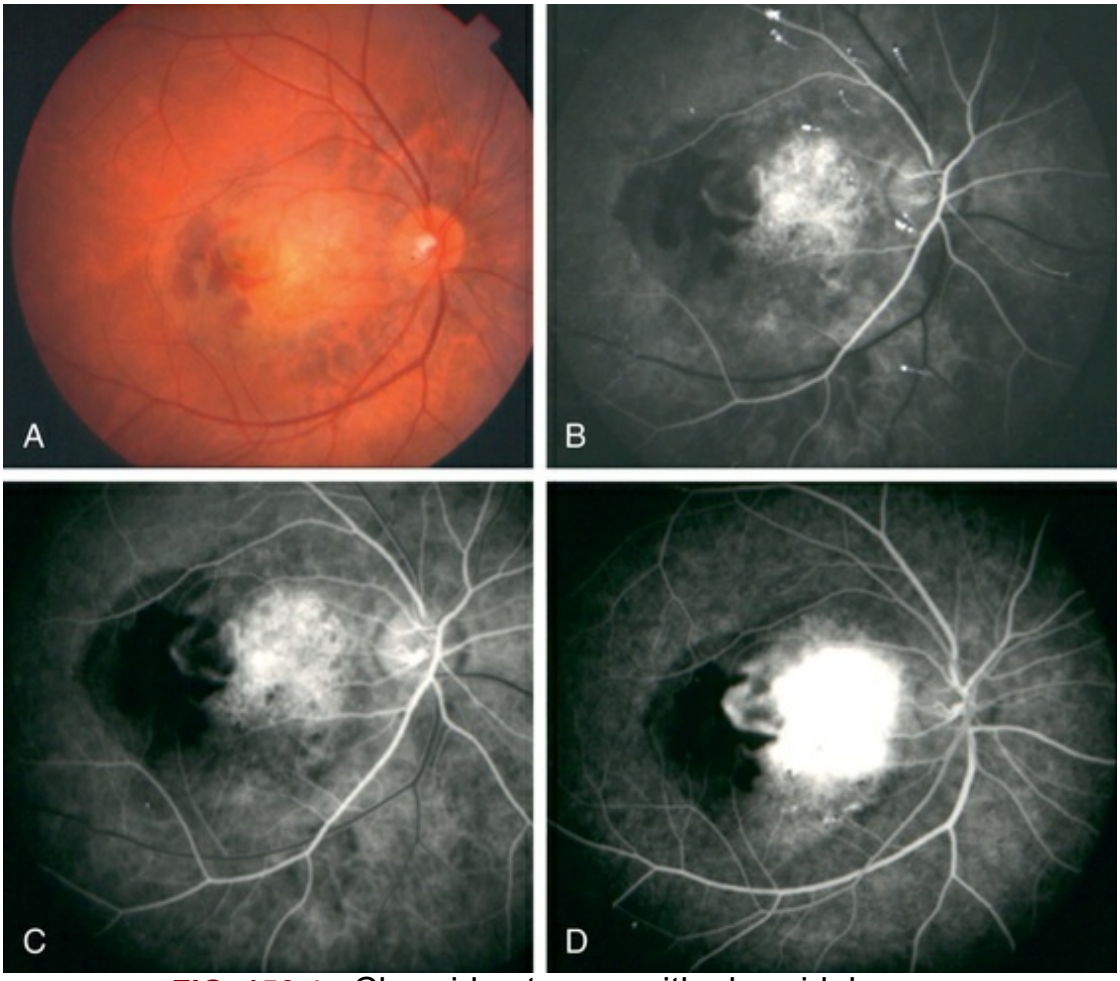

FIG. 156.4 Choroid osteoma with choroidal neovascularization (A), showing increasing fluorescence (B–D) on angiography.

TABLE 156.1

Choroidal Osteoma Risks for Growth, Decalcification, Choroidal Neovascular Membrane, Vision Loss, and Poor Visual Acuity

	1 yr	5 yr	10 yr	20 yr
Tumor growth	2%	22%	51%	71%
Tumor decalcification	21%	28%	46%	91%
CNVM	21%	31%	31%	46%
Visual loss ≥3 lines	3%	26%	45%	59%
VA ≤20/200	14%	45%	56%	62%

CNVM, choroidal neovascular membrane; VA, visual acuity.

Data adapted from Shields, Sun, Demirci, et al.[12]

TABLE 156.2

Choroidal Osteoma Factors That Predict Tumor Growth, Decalcification, Choroidal Neovascular Membrane, Vision Loss, and Poor Visual Acuity

Clinical Factor by Multivariate Analysis	RR (95% Confidence Interval)	*P* Value
Tumor growth	No significant factor	na
Tumor decalcification		
Irregular tumor surface (vs. smooth surface)	9.2 (2.0–43.7)	0.005
CNVM		
Irregular tumor surface (vs. smooth surface) Tumor hemorrhage present (vs. absent)	10.6 (1.1–98.6) 15.1 (2.4–93.2)	0.04 0.003
Visual loss ≥ 3 lines	No significant factor	na
VA ≤20/200		
Symptoms present (vs. absent) Decalcification present (vs. absent)	8.3 (1.7–40.8) 3.6 (1.2–11.2)	0.009 0.03

CNVM, choroidal neovascular membrane; VA, visual acuity.

Data adapted from Shields, Sun, Demirci, et al.[12]

CNVM should be distinguished from the branching vascular tufts seen on the inner surface of the tumor. The latter are not associated with subretinal fluid, hemorrhage, or disciform scar and do not leak fluorescein on angiography as the former. The reason for the occurrence of CNVM in eyes with choroidal osteoma is unknown. It is postulated that the thinned, degenerated retinal pigment epithelium–Bruch's membrane complex overlying the osteoma develop breaks and neovascular fronds from the choroid grow beneath the sensory retina.[27]

Differential Diagnosis

The ophthalmoscopic features of choroidal osteoma are usually classic, but small lesions can be mistaken for choroidal granuloma,

nevus, melanoma, or metastasis. Other lesions in the differential diagnosis include circumscribed choroidal hemangioma, disciform macular degeneration, posterior scleritis, sclerochoroidal choroidal calcification, and choroidal cartilage of organoid nevus syndrome.[1,53–60]

Amelanotic choroidal melanoma differs from choroidal osteoma in that it has a yellow–brown color, more elevation, and a less well-defined margin. Amelanotic choroidal nevus can be relatively flat like a choroidal osteoma, but nevus has less distinct margins and can have drusen on its surface. Choroidal metastasis tends to have indistinct margins and is often associated with a serous retinal detachment out of proportion to the size of the tumor.[57] Furthermore, metastatic carcinoma usually occurs in middle age or older patients who have a prior history of malignancy (especially breast carcinoma). An irradiated choroidal metastasis could resemble a choroidal osteoma because the irradiated metastasis appears flat, atrophic, and lacks subretinal fluid. Choroidal hemangioma can occasionally have overlying fibrous and osseous metaplasia that resembles osteoma.[58] However, choroidal hemangioma is characteristically dome-shaped with smooth regular margins and overlying serous fluid with cystoid degeneration of the retina.

Macular degeneration is typically seen in older patients when it occurs in the spectrum of age-related macular degeneration or it is found with other inflammatory, traumatic, or dystrophic fundus findings to suggest the diagnosis. Macular degeneration is usually centered in the macular area and is less commonly in a juxtapapillary location. Posterior scleritis has a typical orange–brown in color with indistinct margins.[17] The symptom of pain with findings of uveitis, choroidal folds, subretinal fluid, and ultrasonographic evidence of thickened sclera with retrobulbar edema aid in the diagnosis.

Sclerochoroidal calcification clinically appears as an irregular calcific plaque within the choroid or sclera[53–54] (Fig. 156.5). The overlying retina and vitreous are normal. These findings can resemble choroidal osteoma, but sclerochoroidal calcification is not typically juxtapapillary and more often occurs along the retinal vascular arcades, appears multifocal, and can occur in patients with

hyperparathyroidism.[54] The linear nevus sebaceous syndrome can manifest a calcified choroid lesion that represents either scleral cartilage or bone.[59–60]

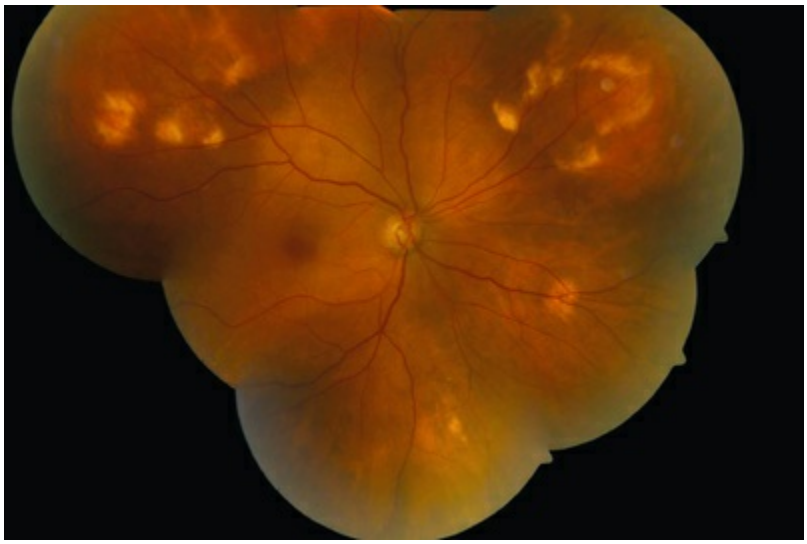

FIG. 156.5 Sclerochoroidal calcification demonstrating multifocal equatorial calcific choroidal lesions in an older woman. This condition is distinct from choroidal osteoma.

Pathology and Pathogenesis

Histopathologic features of choroidal osteoma were first observed in 1978 and reported twice by Williams et al.[8] and Gass et al.[9] The mass is composed of dense bony trabeculae with endothelial lined large cavernous spaces and small capillary blood vessels. Osteoblasts, osteocytes, and osteoclasts are present. The intertrabecular marrow spaces contain loose fibrovascular elements, mast cells, and foamy vacuolated mesenchymal cells. The involved choriocapillaris is narrowed or obliterated in most areas. The choroidal melanocytes are displaced inwards toward the choriocapillaris and outwards toward the sclera. The overlying retinal pigment epithelium is focally depigmented and flat in some areas while clumps of pigment granules within melanophages are seen along Bruch's membrane in other areas.

The pathogenesis of the choroidal osteoma is unknown. The

speculated pathogenesis includes possible choristomatous, inflammatory, traumatic, hormonal, metabolic, environmental, or hereditary etiology.[1] Noble suggested that there might be a congenital, possibly inherited, abnormality of the juxtapapillary choroid that predisposes the patient to the development of this tumor.[40]

The choroidal osteoma resembles a choristoma in its tissue composition, onset in youth, and absence of other preceding ocular disease processes. Osseous choristomas are well-known to occur in the epibulbar region of the eye.[61] The embryologic development of the region of the optic nerve head is complicated, and several congenital hamartomas are found in this region such as the astrocytic hamartoma, combined retinal–retinal pigment epithelial hamartoma, retinal capillary hemangioma, and others. Features of this tumor atypical for a choristoma are the sexual preponderance in females and the rare occurrence of new tumor in previously normal tissue. Bone throughout the body is constantly being remolded and reshaped in adulthood; thus, the change in size of choroidal osteoma does not exclude the potential choristomatous etiology.

Intraocular inflammation has been known to cause dystrophic intraocular calcification and ossification.[62] A focal peripapillary choroiditis could possibly lead to dystrophic calcium deposition and eventually to osteoma.[48] Choroidal osteoma have been reported in children after eosinophilic granulomatosis,[35] sclerouveitis with optic nerve edema,[48] and orbital inflammatory pseudotumor.[31] Although these three cases are well documented, the majority of choroidal osteomas develop in otherwise clinically normal eyes.

Several reports have noted ocular trauma preceding choroidal osteoma.[10,30] Osseous metaplasia of the retinal pigment epithelium may have occurred in these cases; however, the relationship to trauma is speculative.

The occurrence of this tumor predominantly in young adult women raises the question of a hormonal influence.[1,10–12] Most of the women are diagnosed after puberty, but several cases of prepubertal girls have been documented.[10,24,31] Also several male patients have been reported.[14,15,35,37,46,50] Endocrinologic and metabolic workup has been unrevealing. There have been no

consistently abnormal serum calcium, phosphorus, or alkaline phosphatase levels detected in patients with choroidal osteoma. Katz and Gass[31] reported a patient with transient mild secondary hypoparathyroidism (decreased serum calcium and increased serum phosphorus and increased alkaline phosphatase) and multiple choroidal osteomas, but classically parathyroid abnormalities cause a picture of sclerochoroidal calcification,[54] not choroidal osteomas.

Choroidal osteomas were not recognized in the older literature. The possibility that recent environmental toxins, exposures, or drugs may cause this tumor has been suggested. No consistent drug use or geographic location has been found. Choroidal osteoma was misdiagnosed in one prominent textbook, *Tumors of the Eye*, where an illustration of an "ossified choroidal hemangioma" in 1947 actually proved to be choroidal osteoma upon later review.[8,63] It is possible that several cases in the older literature may have been misdiagnosed prior to the description of the choroidal osteoma in 1978.

Cunha in 1984 reported a familial case of choroidal osteomas seen in a 37-year-old mother and her 5-year-old daughter.[21] The mother had poor vision from 11 years old. Eting and Savir in 1992 reported an atypical fulminant course of bilateral choroidal osteomas in a 5-year-old boy and his 7-year-old sister, and both siblings developed severe bilateral visual loss.[23] Noble in 1990 reported bilateral choroidal osteomas in 9-year-old twin brothers and their 11-year-old sister.[40] The mother had a yellow mottled fundus but no clear evidence of osteoma. These three occurrences seem to be more than coincidental for this rare tumor and may indicate a possible hereditary or environmental component for some choroidal osteomas.

Diagnostic Approaches

Fluorescein Angiography

Fluorescein angiography of a choroidal osteoma shows mild, patchy early hyperfluorescence of the tumor that evolves to a diffuse intense late staining (Fig. 156.4). The tumor can show early

hyperfluorescence of the vascular tufts without leakage.[1,7,10–12] This fluorescence fades slightly in the later stages of angiography.

Overlying choroidal neovascularization shows lacy early hyperfluorescence with early leakage of dye and late staining of the surrounding tissue. Occasionally there are multiple pin-point leakage sites from the osteoma that are not associated with neovascularization. Areas of persistent hypofluorescence correspond to subretinal hemorrhage or retinal pigment epithelial hyperplasia. Fluorescein angiography of the optic disc and retinal vasculature shows no abnormality.

Indocyanine Green Angiography

Indocyanine green angiography shows early hypofluorescence of the choroidal mass.[36,51,64] The large caliber choroidal vessels can traverse the peripheral portion of the osteoma and even transect a pseudopod. Fine diffuse fluorescence of the mass is seen by 2 minutes into the study and seems to emanate from ill-defined multifocal points within the area of the mass, perhaps related to the fine perforating vessels of the tumor. The fluorescence gradually becomes confluent and almost isofluorescent in the late frames.

Ultrasonography

Ultrasonography is useful for differentiating choroidal osteomas from other clinically similar lesions. A-scan ultrasonography demonstrates a high-intensity echo spike from the inner surface of the tumor with decreased amplitude of the orbital soft tissue echoes immediately posterior to the tumor. B-scan ultrasonography demonstrates a slightly elevated, highly reflective choroidal mass that persists at lower scanning sensitivity after the other soft tissue echoes have disappeared. Acoustic shadowing of the orbit occurs just posterior to the choroidal mass, giving the appearance of a pseudo-optic nerve.[1,7]

Optical Coherence Tomography

Time domain optical coherence tomography (OCT) shows choroidal osteoma as a dense, undulating lesion with deep

shadowing. Overlying choroidal neovascularization, subretinal fluid, retinal edema, retinal thinning, and photoreceptor loss, particularly in areas of decalcification, can be delineated[26,65] (Fig. 156.6). Spectral domain OCT demonstrates greater detail of the choroidal mass.[66–72] Pellegrini et al.[68] and Shields et al.[69] independently observed the presence of bone lamella and spongy appearance of bone within the tumor (Fig. 156.7).

FIG. 156.6 Optical coherence tomography (OCT) over choroidal osteoma in a patient with bilateral tumors (A,B) that shows prominent submacular decalcification and atrophy in the right eye (A) and preserved calcification/ossification in the left eye (B). On relatively low resolution time domain OCT (C,D) and higher resolution spectral domain OCT (E,F), the irregularity of tumor surface in the right eye is much more than in the left eye.

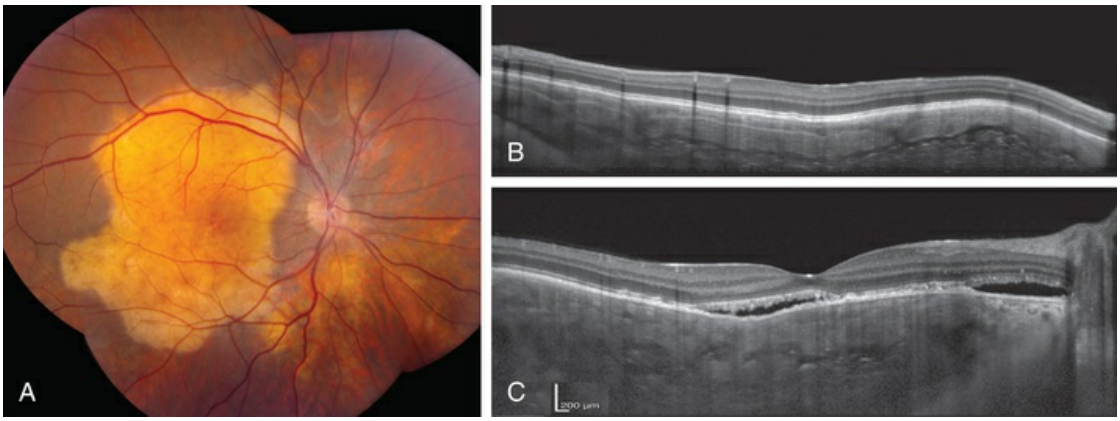

FIG. 156.7 Spectral domain optical coherence tomography over calcified osteoma (A) demonstrating horizontal cuts through the mass showing undulating surface of the osteoma (B) with intrinsic linear lamella (*white horizontal lines*) and possible vascular channels (*black lucent tubular regions*). Note the overlying subretinal fluid with shaggy photoreceptors (C).

Autofluorescence

Autofluorescence shows nonspecific hyperautofluorescence at sites of fresh subretinal fluid or retinal pigment epithelial disturbance.[73–75] In chronic cases with decalcification and retinal pigment epithelial loss, hypoautofluorescence is noted.

Roentgenography

Roentgenograms of the orbit are not commonly performed, but osteoma appears as a thin plaque of radiodensity on the posterior aspect of the globe.[10,30] Roentgenograms are rarely performed for diagnostic purposes as this mode has been replaced by computed tomography.

Computed Tomography

Computed tomography of choroidal osteomas shows characteristic features of a radiopaque plaque of bone density at the level of the

affected choroid[1,7] (Fig. 156.8).

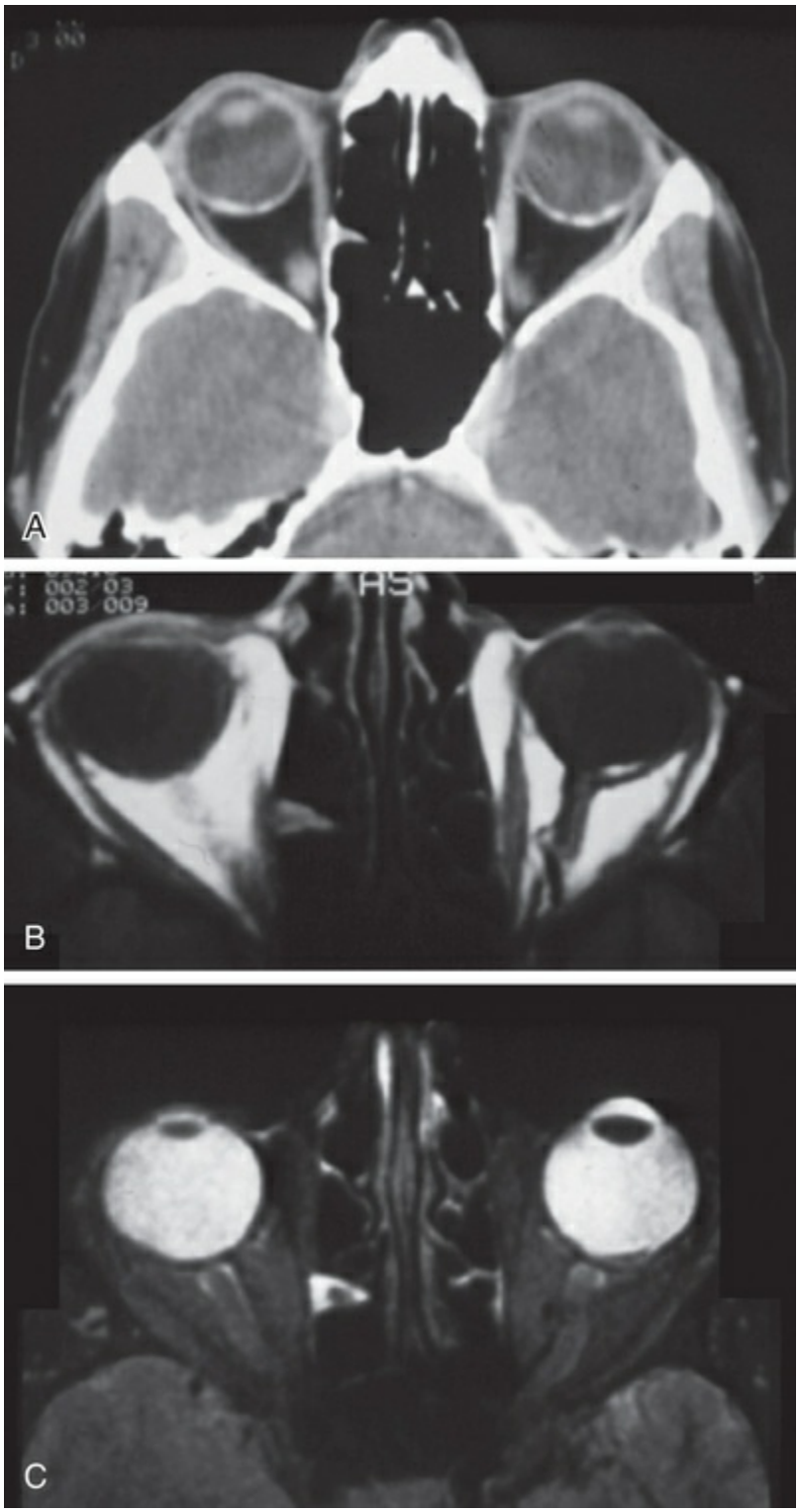

FIG. 156.8 Computed tomography (A) of choroidal osteoma shows calcified plaque in both eyes. The T1-weighted (B) and T2-weighted (C) magnetic resonance images show the flat plaque as bright on T1 and dark

on T2.

Magnetic Resonance Imaging

Magnetic resonance imaging with surface coil of choroidal osteoma reveals a bright signal on T1-weighted images and relative low intensity on T2-weighted images (Fig. 156.8). On contrast T1-weighted scans, the tumor shows enhancement.[22]

Radioactive Phosphorus Uptake

The radioactive phosphorus uptake (^{32}P) test is generally not performed for intraocular tumors, but it has been used in the past. In a few cases in which it had been performed, the results were strongly positive.[8] The choroidal osteoma can give positive results on ^{32}P testing because the bone in the tumor accumulates phosphorus and incorporates it into its structure.

Laboratory Studies

In patients with choroidal osteomas, there have been no consistently detectable abnormalities in complete blood counts, blood chemistries (including serum calcium, phosphorus, and alkaline phosphatase), and urinalysis.[1,10–12]

Management

The management of choroidal osteoma includes prevention of tumor growth, induction of decalcification of tumor, and treatment of choroidal neovascularization. There is no currently known systemic metabolic or hormonal method for altering the growth of the choroidal osteoma. For choroidal osteoma in the subfoveal region, the goal is to maintain calcification of the mass so that the outer retinal structures remain intact.[54,65] Based on OCT studies, eyes that maintain ossified osteoma generally show intact photoreceptors and intact visual acuity compared to eyes with de-ossified osteoma in which the retinal pigment epithelium demonstrates atrophy and overlying photoreceptor retraction.[65,69]

Some authorities have advocated oral calcium supplements in these cases, but there is no confirmatory study. For osteoma in the extrafoveal region, the goal is to decalcify the mass so that it cannot grow towards the foveola. Decalcified osteoma generally do not grow in the direction of decalcification. Decalcification can be achieved with ablative laser photocoagulation or photodynamic therapy.[1,10–12,76] Our current preferred treatment for extrafoveal osteoma is photodynamic therapy.[76]

Management of related subretinal fluid or CNVM involves anti-VEGF medications on a monthly basis in a "treat and extend" strategy.[77–80] Previous reports on laser photocoagulation and surgical removal of CNVM, but visual recovery was not impressive.[14,19,25,27,29,39] Photodynamic therapy using verteporfin has been found successful for management of extrafoveal CNVM over osteoma[16,65] (Fig. 156.9).

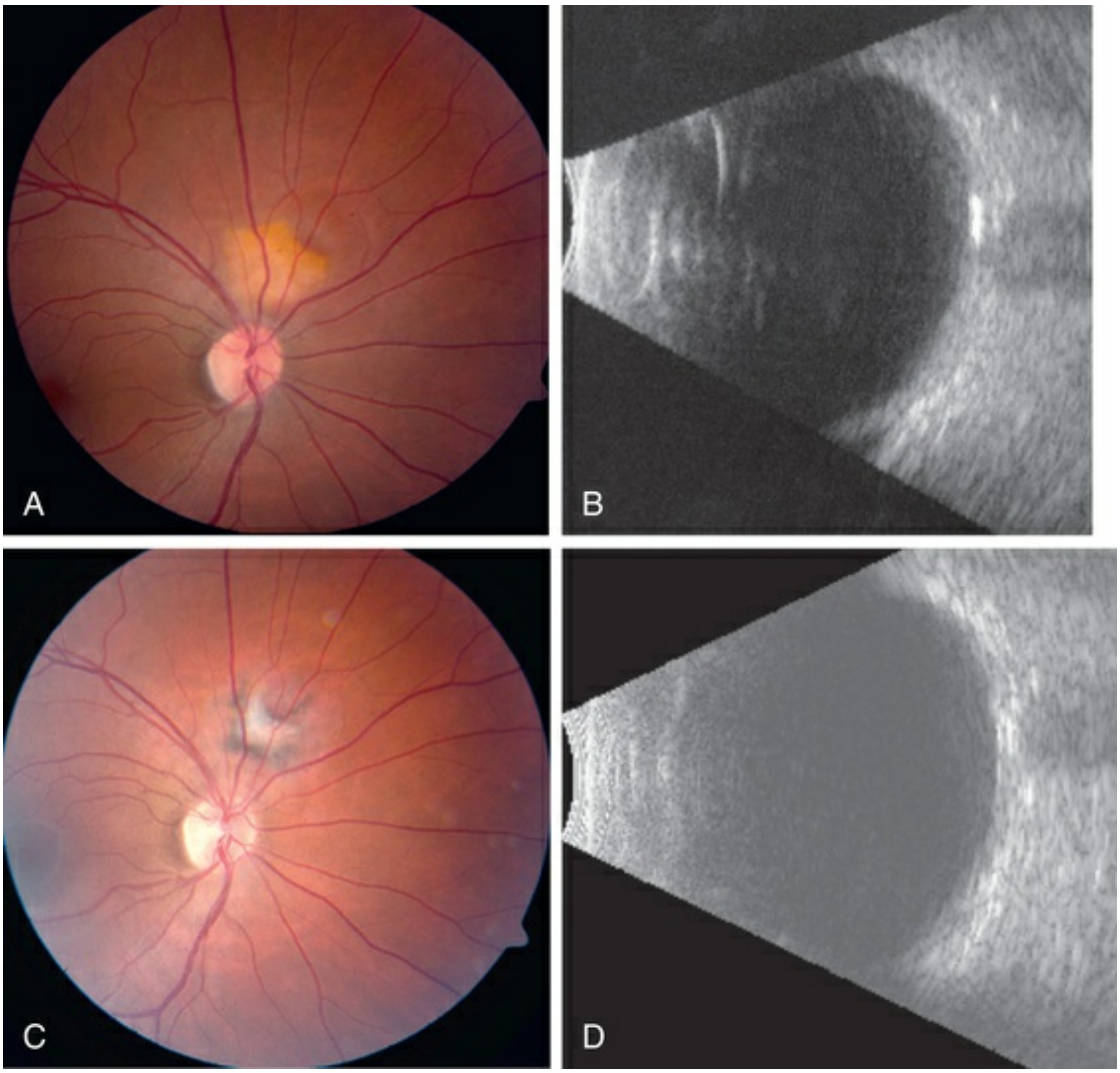

FIG. 156.9 Small, calcified juxtapapillary choroidal osteoma with choroidal neovascular membrane (CNVM) and subretinal hemorrhage (A,B) treated with photodynamic therapy. The tumor decalcified clinically and by ultrasound, and the CNVM resolved (C,D).

Prognosis

The visual prognosis is quite varied and unpredictable. Most patients with extrafoveal choroidal osteoma maintain good visual acuity. Some patients with a subfoveal choroidal osteoma retain good visual acuity for months to years. In an analysis of 74 affected eyes, visual loss of 3 or more lines occurred in 26% by 5 years, 45% by 10 years, and 59% by 20 years. Poor visual acuity of 20/200 or worse was found in 14% at 1 year, 45% at 5 years, and 56% at 10

years[12] (Table 156.1). The reason for visual loss included subretinal fluid, subretinal blood, retinal pigment epithelial atrophy or mottling, and photoreceptor atrophy, particularly over decalcified osteomas. Factors that statistically predict poor vision include symptoms and decalcification[12] (Table 156.2). The prognosis for life in the patient with choroidal osteoma is no different from the general population.[1,10–12]

Conclusions

Choroidal osteoma is a benign ossified tumor of the choroid typically found in healthy young females in the second or third decade of life. It has been reported to exist in males and in children. Choroidal osteoma is unilateral in 75% of cases, tends to be located in the juxtapapillary area, and ranges in size from 2 to 22 mm in basal dimension. It is minimally elevated and may have associated subretinal fluid and choroidal neovascularization.

Choroidal osteoma should be differentiated from choroidal melanoma, choroidal nevus, choroidal metastasis, choroidal hemangioma, and sclerochoroidal calcification. Ultrasonography can demonstrate calcium within the lesion. Fluorescein angiography can demonstrate choroidal neovascularization. Optical coherence tomography can delineate bone lamellae and spongy tissue within the mass and provide an estimate of visual potential.

The pathogenesis of choroidal osteoma is unknown, and there is no known systemic modification to benefit resolution of this tumor. Related choroidal neovascularization is usually treated with anti-VEGF therapy and photodynamic therapy. The visual prognosis is variable, but the systemic prognosis is good.

References

1. Shields CL, Shields JA, Augsburger JJ. Review: choroidal osteoma. *Surv Ophthalmol*. 1988;33:17–27.
2. Duke-Elder S, Perkins ES. *System of ophthalmology: Vol 1X. Diseases of the uveal tract*. CV Mosby Company: St. Louis; 1966:740–748.
3. Hogan MJ, Zimmerman LE. *Ophthalmic pathology*. WB

Saunders: Philadelphia; 1962:63.
4. Green WR. Uveal tract. 4th ed. W B Saunders: Philadelphia; 1996:1439–2217. Spencer WH, Bilyk J, Eagle RC, et al. *Ophthalmic pathology: an atlas and textbook*. vol. 3.
5. Monselise M, Rapaport I, Romem M, et al. Intraocular ossification. *Ophthalmologica*. 1975;190:225–229.
6. Shields JA, Shields CL. *Intraocular tumors: an atlas and textbook*. 2nd ed. Lippincott Williams and Wilkins: Philadelphia; 2008:64–71.
7. Shields JA, Shields CL. Osseous tumors of the uvea. *Intraocular tumors: a text and atlas*. WB Saunders: Philadelphia; 1992:261–272.
8. Williams AT, Font RL, Van Dyk HJ, et al. Osseous choristoma of the choroid simulating a choroidal melanoma. *Arch Ophthalmol*. 1978;96:1874–1877.
9. Gass JDM, Guerry RK, Jack RL, et al. Choroidal osteoma. *Arch Ophthalmol*. 1978;96:428–435.
10. Gass JDM. New observations concerning choroidal osteomas. *Int Ophthalmol*. 1979;2:71–84.
11. Aylward GW, Chang TS, Pautler SE, et al. A long-term follow-up of choroidal osteoma. *Arch Ophthalmol*. 1998;116:1337–1341.
12. Shields CL, Sun H, Demirci H, et al. Factors predictive of tumor growth, tumor decalcification, choroidal neovascularization and visual outcome in 74 eyes with choroidal osteoma. *Arch Ophthalmol*. 2005;123:658–666.
13. Augsburger JJ, Shields JA, Rife CJ. Bilateral choroidal osteoma after nine years. *Can J Ophthalmol*. 1979;14:281–284.
14. Avila MP, El-Markabi H, Azzolini C, et al. Bilateral choroidal osteoma with subretinal neovascularization. *Ann Ophthalmol*. 1984;16:381–385.
15. Baarsma GS, Craandyk A. Osteoma of the choroid. *Doc Ophthalmol*. 1981;92:205–212.
16. Battaglia Parodi M, Da Pozzo S, Toto L, et al. Photodynamic therapy for choroidal neovascularization associated with choroidal osteoma. *Retina*. 2001;2:660–661.
17. Benson WE, Shields JA, Tasman W, et al. Posterior scleritis: a cause of diagnostic confusion. *Arch Ophthalmol*.

1979;97:1482–1486.
18. Buettner H. Spontaneous involution of a choroidal osteoma [Letter]. *Arch Ophthalmol*. 1990;108:1517–1518.
19. Burke JF, Brockhurst RJ. Argon laser photocoagulation of subretinal neovascular membrane associated with osteoma of choroid. *Retina*. 1983;3:304–307.
20. Coston TO, Wilkinson CP. Choroidal osteoma. *Am J Ophthalmol*. 1978;86:368–372.
21. Cunha SL. Osseous choristoma of the choroid: a familial disease. *Arch Ophthalmol*. 1984;102:1052–1054.
22. DePotter P, Shields JA, Shields CL, et al. Magnetic resonance imaging of choroidal osteoma. *Retina*. 1991;11:221–223.
23. Eting E, Savir H. An atypical fulminant course of choroidal osteoma in two siblings. *Am J Ophthalmol*. 1992;113:52–55.
24. Fava GE, Brown GC, Shields JA, et al. Choroidal osteoma in a 6 year old child. *J Pediatr Ophthalmol Strabismus*. 1980;17:203–205.
25. Foster BS, Fernandez-Suntay JP, Dryja TP, et al. Surgical removal and histopathologic findings of a subfoveal neovascular membrane associated with choroidal osteoma. *Arch Ophthalmol*. 2003;121:273–276.
26. Fukasawa A, Iijima H. Optical coherence tomography of choroidal osteoma. *Am J Ophthalmol*. 1992;133:419–421.
27. Grand MG, Burgess DB, Singerman LJ, et al. Choroidal osteoma: treatment of associated subretinal neovascular membranes. *Retina*. 1984;4:84–89.
28. Gurelik G, Lonneville Y, Safak N, et al. A case of choroidal osteoma with subsequent laser induced decalcification. *Int Ophthalmol*. 2001;24:41–43.
29. Hoffman ME, Sorr EM. Photocoagulation of subretinal neovascularization associated with choroidal osteoma. *Arch Ophthalmol*. 1987;105:998–999.
30. Joffe L, Shields JA, Fitzgerald JR. Osseous choristoma of the choroid. *Arch Ophthalmol*. 1978;96:1809–1812.
31. Katz RS, Gass JDM. Multiple choroidal osteomas developing in association with recurrent orbital inflammatory pseudotumor. *Arch Ophthalmol*. 1983;101:1724–1727.
32. Kayazawa F, Shimamoto S. Choroidal osteoma: two cases in

Japanese women. *Ann Ophthalmol*. 1981;13:1053–1056.
33. Kelinske M, Weinstein G. Bilateral choroidal osteomas. *Am J Ophthalmol*. 1981;92:676–680.
34. Kida Y, Shibuya Y, Oguni M, et al. Choroidal osteoma in an infant. *Am J Ophthalmol*. 1997;124:119–120.
35. Kline LB, Skalka HW, Davidson JD, et al. Bilateral choroidal osteomas associated with fatal systemic illness. *Am J Ophthalmol*. 1982;93:192–197.
36. Lafaut BA, Mestdagh C, Kohno T, et al. Indocyanine green angiography in choroidal osteoma. *Graefes Arch Clin Exp Ophthalmol*. 1997;235:330–337.
37. Laibovitz RA. An unusual case of intraocular calcification: choroidal osteoma. *Ann Ophthalmol*. 1979;11:1077–1080.
38. Mizota A, Tanabe R, Adachi-Usami E. Rapid enlargement of choroidal osteoma in a 3-year-old girl. *Arch Ophthalmol*. 1998;116:1128–1129.
39. Morrison DL, Magargal LE, Ehrlich DR, et al. Review of choroidal osteoma: successful krypton red laser photocoagulation of an associated subretinal neovascular membrane involving the fovea. *Ophthalmic Surg*. 1987;18:299–303.
40. Noble KG. Bilateral choroidal osteoma in three siblings. *Am J Ophthalmol*. 1990;109:656–660.
41. Pamer Z, Kovacs B. A case of a fast-growing bilateral choroidal osteoma. *Retina*. 2001;21:657–659.
42. Rose SJ, Burke JF, Brockhurst RJ. Argon laser photoablation of a choroidal osteoma. *Retina*. 1991;11:224–228.
43. Shields JA, Shields CL, Ellis J, et al. Bilateral choroidal osteoma associated with bilateral total blindness. *Retina*. 1997;16:445–447.
44. Shields JA, Shields CL, DePotter P, et al. Progressive enlargement of a choroidal osteoma. *Arch Ophthalmol*. 1995;113:819–820.
45. Teich SA, Walsh JB. Choroidal osteoma. *Ophthalmology*. 1981;88:696–698.
46. Totsuka H, Minoda K. Choroidal osteoma. *Folia Ophthalmol Jpn*. 1980;31:427–435.
47. Trimble SB, Schatz H, Schneider GB. Spontaneous

decalcification of a choroidal osteoma. *Ophthalmology*. 1988;95:631–634.
48. Trimble SN, Schatz H. Choroidal osteoma after intraocular inflammation. *Am J Ophthalmol*. 1983;96:759–764.
49. Trimble SN, Schatz H. Decalcification of a choroidal osteoma. *Br J Ophthalmol*. 1991;75:61–63.
50. Tsukahara I, Hayashi M. Osseous choristoma of the choroid. *Jpn J Ophthalmol*. 1980;24:90–95.
51. Yuzawa M, Kawamura A, Haruyama M, et al. Indocyanine green video-angiographic findings in choroidal osteoma. *Eur J Ophthalmol*. 1984;4:191–198.
52. Hasanreisoglu M, Shields JA, Mashayekhi A, et al. Bilateral choroidal osteoma: Visual acuity at forty-five years followup. *Retin Cases Brief Rep*. 2015;9:239–241.
53. Shields JA, Shields CL. Sclerochoroidal calcification: the 2001 Harold Gifford Lecture. *Retina*. 2002;22:251–261.
54. Shields CL, Hasanreisoglu M, Saktanasate J, et al. Sclerochoroidal calcification: clinical features, outcomes and relationship with hypercalcemia and parathyroid adenoma in 179 eyes. *Retina*. 2015;35:547–554.
55. Jackson WE, Freed S. Unilateral osseous choristoma of the choroid. *Ann Ophthalmol*. 1984;16:134–136.
56. Shields JA, Shields CL. *Intraocular tumors: a text and atlas*. WB Saunders: Philadelphia; 1992:85–489.
57. Shields CL, Shields JA, Gross N, et al. Survey of 520 eyes with uveal metastases. *Ophthalmology*. 1997;104:1265–1276.
58. Shields CL, Honavar SG, Shields JA, et al. Circumscribed choroidal hemangioma: clinical manifestations and factors predictive of visual outcome in 200 consecutive cases. *Ophthalmology*. 2001;108:2237–2248.
59. Shields JA, Shields CL, Eagle RC Jr, et al. Ocular manifestations of the organoid nevus syndrome. *Ophthalmology*. 1997;104:549–557.
60. Shields CN, Shields CL, Lin C, et al. Calcified scleral choristoma in organoid nevus syndrome simulating retinoblastoma. *J Pediatr Ophthalmol Strabismus*. 2014;51:e1–3.
61. Shields CL, Qureshi A, Eagle RC Jr, et al. Epibulbar osseous

choristoma in 8 patients. *Cornea*. 2012;31:756–770.
62. Zeiter HJ. Calcification and ossification of ocular tissue. *Am J Ophthalmol*. 1962;53:265–274.
63. Reese AB. *Tumors of the eye*. 3rd ed. Harper & Row: New York; 1976:266–267.
64. Shields CL, Shields JA, DePotter P. Patterns of indocyanine green videoangiography of choroidal tumours. *Br J Ophthalmol*. 1995;79:237–245.
65. Shields CL, Perez B, Materin MA, et al. Optical coherence tomography of choroidal osteoma in 22 cases: evidence for photoreceptor atrophy over the decalcified portion of the tumor. *Ophthalmology*. 2007;114:e53–8.
66. Freton A, Finger PT. Spectral domain-optical coherence tomography analysis of choroidal osteoma. *Br J Ophthalmol*. 2012;96:224–228.
67. Sayanagi K, Pelayes DE, Kaiser PK, et al. 3D Spectral domain optical coherence tomography findings in choroidal tumors. *Eur J Ophthalmol*. 2011;21:271–275.
68. Pellegrini M, Invernizzi A, Giani A, et al. Enhanced depth imaging optical coherence tomography features of choroidal osteoma. *Retina*. 2014;34:958–963.
69. Shields CL, Arepalli S, Atalay HT, et al. Choroidal osteoma shows bone lamella and vascular channels on enhanced depth imaging optical coherence tomography in 15 cases. *Retina*. 2015;35:750–757.
70. Dinah C, Sandinha T. Enhanced depth imaging as an adjunctive tool in the diagnosis of decalcified choroidal osteoma. *Eye (Lond)*. 2014;28:356–358.
71. Shields CL, Pellegrini M, Ferenczy SR, et al. Enhanced depth imaging optical coherence tomography of intraocular tumors: from placid to seasick to rock and rolling topography – the 2013 Francesco Orzalesi Lecture. *Retina*. 2014;34:1495–1512.
72. Shields CL, Manalac J, Das C, et al. Review of spectral domain enhanced depth imaging optical coherence tomography of tumors of the choroid. *Indian J Ophthalmol*. 2015;63:117–121.
73. Ascaso FJ, Villen L. Fundus autofluorescence imaging

findings in choroidal osteoma. *Retina*. 2011;31:1004–1005.
74. Sisk RA, Riemann CD, Petersen MR, et al. Fundus autofluorescence findings of choroidal osteoma. *Retina*. 2013;33:97–104.
75. Almeida A, Kaliki S, Shields CL. Autofluorescence of intraocular tumors. *Curr Opin Ophthalmol*. 2013;24:222–232.
76. Shields CL, Materin MA, Mehta S, et al. Regression of extrafoveal choroidal osteoma following photodynamic therapy. *Arch Ophthalmol*. 2007;126:135–137.
77. Shields CL, Salazar P, Demirci H, et al. Intravitreal bevacizumab (Avastin) and ranibizumab (Lucentis) for choroidal neovascularization overlying choroidal osteoma. *Retin Cases Brief Rep*. 2008;2:18–20.
78. Kubota-Taniai M, Oshitari T, Handa M, et al. Long-term success of intravitreal bevacizumab for choroidal neovascularization associated with choroidal osteoma. *Clin Ophthalmol*. 2011;5:1051–1055.
79. Süsskind D, Altpeter EK, Moser L, et al. Proton beam radiotherapy of progressive pediatric choroidal osteoma: first experience. *Can J Ophthalmol*. 2014;49:e123–7.
80. Khan MA, DeCroos FC, Storey PP, et al. Outcomes of anti-vascular endothelial growth factor therapy in the management of choroidal neovascularization associated with choroidal osteoma. *Retina*. 2014;34:1750–1756.

157

Circumscribed Choroidal Hemangioma

Michael I. Seider, Shelley Day, Prithvi Mruthyunjaya

Introduction

Choroidal hemangiomas are benign vascular hamartomas that occur in two forms: circumscribed and diffuse. The circumscribed form is typically an isolated finding without systemic associations, while the diffuse form generally occurs in association with Sturge–Weber syndrome (discussed separately in Chapter 137, Phakomatoses). There have been rare reports of circumscribed choroidal hemangioma in patients with Sturge–Weber syndrome.[1,2] The first histologically confirmed case of choroidal hemangioma was published by Leber in 1868.[3] The incidence of the disease is difficult to estimate since most circumscribed choroidal hemangiomas only come to medical attention if patients become symptomatic or if they are discovered incidentally during routine examination; however, the disease is felt to be relatively rare, with

five cases discovered upon histologic examination of 4500 enucleated eyes.[4] More than 90% of reported cases have been in Caucasian patients (though there have been published cases in black, Hispanic, and Asian patients), with a relatively even distribution between males and females.[5,6] The mean age at diagnosis in the two largest case series ranged from 38.7 years to 47 years, considerably older than the mean age at diagnosis for diffuse choroidal hemangioma, which is typically in the first decade of life.[5,6]

Clinical Features

Circumscribed choroidal hemangiomas are generally orange-red masses found posterior to the equator (Figs. 157.1–157.5). The color of the tumor has also been described as "salmon-colored,"[7] "yellow-white,"[8] and "grayish-pink."[6] Choroidal thickening may be difficult to discern on color photographs and may be more apparent on clinical examination. Pigmentary changes have also been reported on the surface of the tumor or as a ring of hyperpigmentation around the edge of the tumor.[6] There may be accumulation of lipofuscin pigment (orange pigment) over the lesion most easily seen with fluorescein angiography[9] or fundus autofluorescence.[10] In the largest published series of 200 patients by Shields et al., 67% of circumscribed choroidal hemangiomas were in the macula, 34% were between the macula and the equator, and no tumors were anterior to the equator.[5] In the second-largest series, of 45 patients with these tumors reported by Witschel and Font, all were located posterior to the equator.[6] In the Shields series, the mean tumor diameter was 6.7 mm and the mean tumor thickness was 3.1 mm.[5] Lesions are usually solitary and unilateral, though bilateral choroidal hemangiomas have been reported.[7] Overlying subretinal fluid or serous retinal detachment is a common finding, present in 47% of patients in the Witschel series[6] and 81% of the patients in the Shields series (Fig. 157.3)[5] – although these are biased samples comprised largely of symptomatic patients. Cystoid macular edema is also a common finding, present in up to 17% of patients. Associated exudates, epiretinal membranes, and retinal hemorrhages have also been reported.[5] Exudates are uncommon.

Choroidal neovascularization is rare but has been reported in a small number of patients[5,11–13] Retinal neovascularization has also been reported in three eyes with circumscribed choroidal hemangioma.[14] Patients with total retinal detachments secondary to circumscribed choroidal hemangioma may also develop neovascularization of the iris and angle, and neovascular glaucoma.[5]

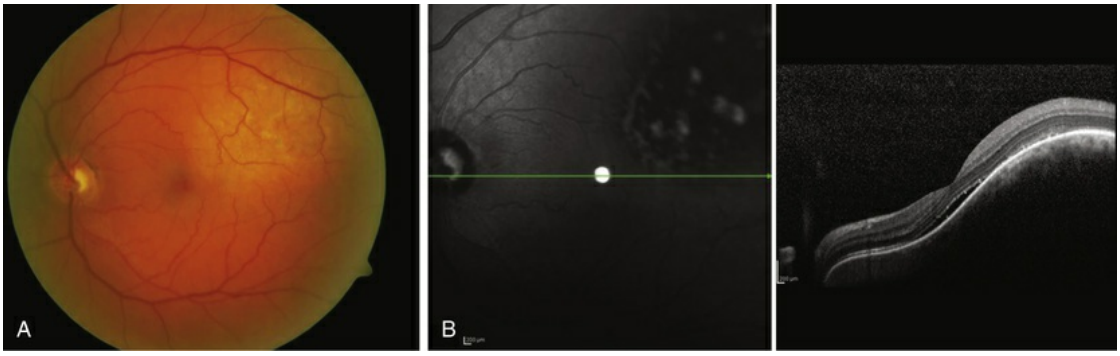

FIG. 157.1 (A) Circumscribed choroidal hemangioma in the left eye of a 54-year-old man complaining of metamorphopsia for 2 months with visual acuity of 20/64. Note the orange-reddish color of the lesion that is similar to surrounding normal choroid. Note also the fine drusen and characteristic pigmentary changes overlying the lesion. (B) Spectral domain optical coherence tomography (right) and confocal scanning laser ophthalmoscopy (SLO, left) (Spectralis, Heidelberg Engineering GmbH, Heidelberg, Germany) images. Note how the SLO image reveals the borders of the hemangioma more clearly than the color photograph. The OCT reveals a sloping choroidal mass elevating the retina associated with mild subfoveal fluid, which likely accounts for the moderate decrease in visual acuity.

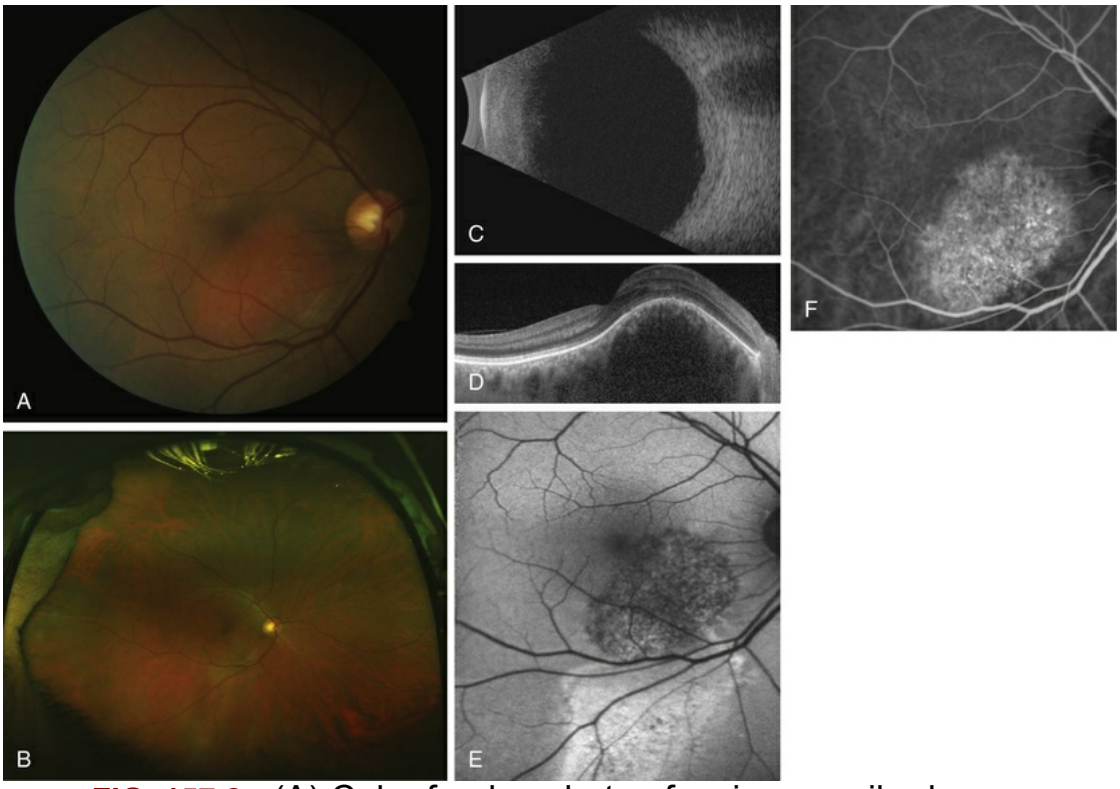

FIG. 157.2 (A) Color fundus photo of a circumscribed choroidal hemangioma in an asymptomatic 66-year-old man with 20/32 acuity. Note the reddish color of the lesion which, in contrast to Fig. 157.1, is of a slightly different color than surrounding choroid. (B) Wide-field color image (Optos plc., Dunfermline, Scotland) of the same lesion as (A). Note how the false color provided by Optos creates a different appearance that makes the tumor difficult to identify. (C) Enhanced-depth imaging spectral domain optical coherence tomography reveals a choroidal mass without overlying subretinal fluid. The hemangioma is located primarily nasal to the fovea and obscures normal choroidal detail. Fine outer retinal changes as well as trace intraretinal fluid are seen near the apex of the tumor. (D) B-scan ultrasonography reveals the lesion to be minimally thick (0.8 mm) and have a high internal reflectivity (similar to nearby normal choroid). (E) Fundus autofluorescence reveals variable hyper- and hypoautofluorescence over the lesion and reveals an inferior hyperautofluorescent area secondary retinal pigment epithelial changes associated with chronic trace subretinal fluid. (F) Fluorescein angiography at one minute (above) shows early diffuse hyperfluorescence that persists into later frames

(below, 3.5 minutes). This lesion was observed and found to be stable over time.

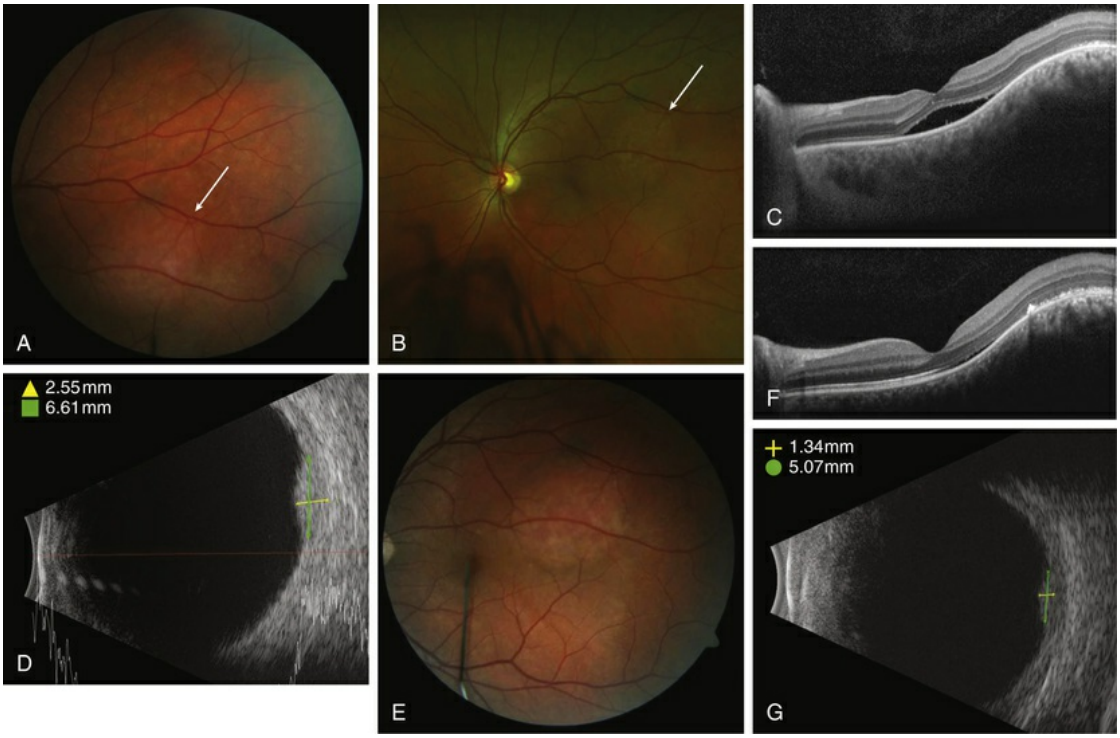

FIG. 157.3 (A) Color photograph of circumscribed choroidal hemangioma in left eye of 36-year-old patient complaining of photopsias and inferonasal scotoma for one month. (B) Optos macula photograph providing more perspective on the location of the lesion compared to the photograph in (A), but with false color. (C) Spectral domain optical coherence tomography (SD-OCT) showing a choroidal mass and subretinal fluid. (D) B-Scan ultrasonography showing a dome-shaped lesion with high-internal reflectivity measuring 6.61 mm across (transverse) by 2.55 mm thick. (E) Photograph taken 3 months following one session of photodynamic therapy (PDT) showing early pigmentary changes over tumor but otherwise an overall stable appearance compared to baseline photos. Acuity improved to 20/20 with near-resolution of symptoms. (F) SD-OCT image 3 months following PDT showing decreased thickness of choroidal mass, near resolution of subretinal fluid and persistent outer retinal changes. (G) B-Scan ultrasonography 3 months following PDT showing decreased tumor thickness (1.34 mm) and

transverse width (5.07 mm).

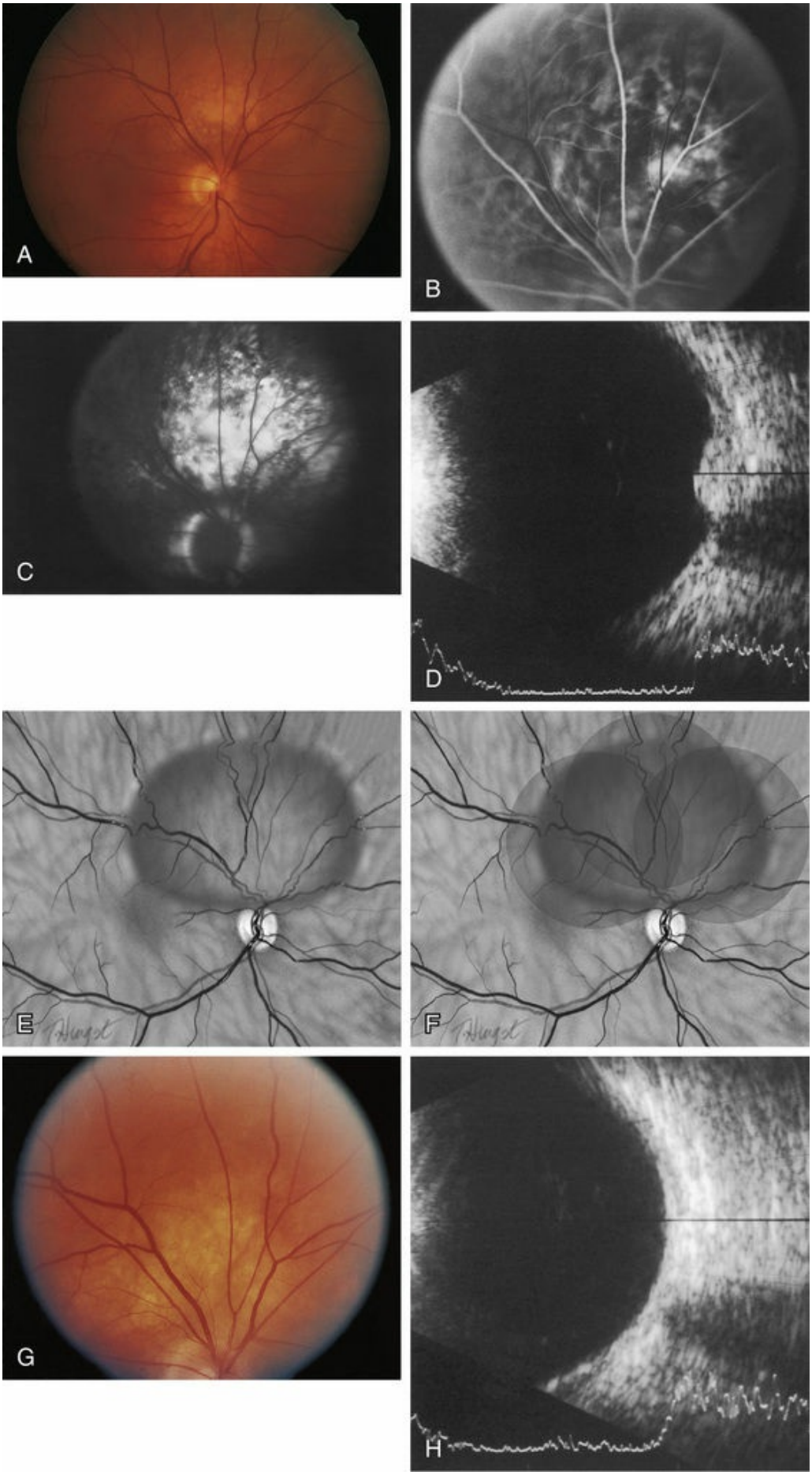
A
B
C
D
E
F
G
H

FIG. 157.4 (A) A red–orange choroidal hemangioma superior to the optic disc with a serous detachment into the macula. The tumor thickness is 2.8 mm. (B) Intravenous fluorescein angiography of this tumor shows patchy hyperfluorescence at the time of arterial flow. (C) Late patchy staining of the tumor with some dye leakage into the subretinal space. (D) Ultrasonography of this tumor demonstrates a solid dome-shaped lesion on B-scan and high internal reflectivity with A-scan echography. (E) Sketch of this tumor with subretinal fluid extending into the macula. (F) Overlapping circles show the distribution of the laser applications following infusion of verteporfin. (G) Appearance of this tumor 3 months following photodynamic therapy. The tumor is now flat with some rarefaction of the retinal pigment epithelium and subtle evidence of subretinal fibrosis. (H) Ultrasonographic view of the tumor 3 months after treatment shows no measurable tumor height.

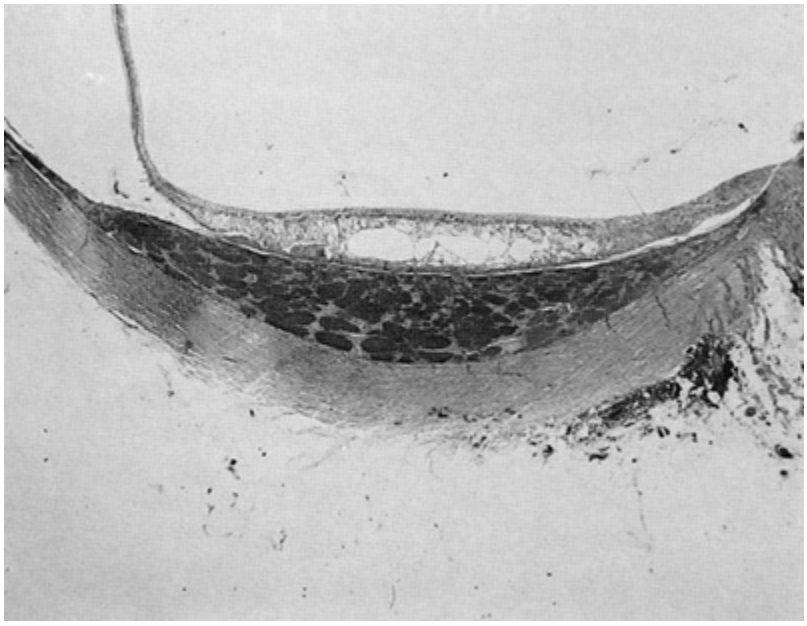

FIG. 157.5 A solitary hemangioma of the juxtapapillary

choroid is located temporally. Extensive microcystic degenerative changes of the overlying retina are evident (hematoxylin and eosin, ×11).

Circumscribed choroidal hemangiomas usually do not grow, although there have been reports of gradual enlargement.[15,16] In five cases, there was only slight enlargement with a mean of 1.6 × 1.5 mm in basal diameter and 0.9 mm in thickness over an average of 52 months of follow-up.[15] In another case with significant enlargement, the eye was enucleated due to concern for choroidal melanoma and pathologic examination revealed that the increase in size was most likely due to vascular congestion of the tumor vessels, and possibly an increase in the caliber and number of tumor vessels.[16] There has also been one report of "blackening" of a circumscribed choroidal hemangioma from red–orange to dark gray after tantalum clip placement in preparation for external proton beam irradiation.[17] The hemangioma subsequently returned to its original red–orange color 2 weeks after surgery (prior to proton beam irradiation), leading the authors to hypothesize that the transient color change may have been due to extravascular hemorrhage from surgical manipulation.[17] Bosch and Helbig also reported blackening of a choroidal hemangioma after photodynamic therapy.[18]

The most commonly reported symptom is blurred vision in up to 81% of patients, though patients also note visual field deficits, metamorphopsia, and floaters.[5] Presenting visual acuity ranged from 20/20–20/40 in 24% of eyes to 20/400 or worse in 34% of eyes in the Shields series, and 60% of eyes were "blind" in the Witschel series.[5,6]

Differential Diagnosis

The differential diagnosis of circumscribed choroidal hemangioma includes choroidal nevus, amelanotic choroidal melanoma, choroidal metastasis, choroidal osteoma, and central serous chorioretinopathy. On clinical examination, choroidal hemangiomas have a characteristic orange–red color, unlike choroidal metastases, which are more likely to be creamy-yellow,

and amelanotic melanomas, which tend to be yellow–tan.[5] Ancillary testing is very helpful to distinguish these conditions. Ultrasonography shows high internal reflectivity in choroidal hemangioma due to the vascular component of the lesion, in contrast to choroidal melanomas, which display low to medium internal reflectivity. Circumscribed choroidal hemangiomas also have a very distinct appearance on indocyanine green angiography with rapid filling and "washout" phenomenon, unlike choroidal melanoma and metastasis, which have slower and less intense filling.[5] On magnetic resonance imaging, circumscribed choroidal hemangiomas show bright signal on both T1- and T2-weighted images, whereas choroidal melanomas and metastases show bright signal on T1-weighted images but low signal on T2-weighted images.[5]

Ancillary Studies

Intravenous Fluorescein Angiography

Fluorescein angiography (FA) of circumscribed choroidal hemangiomas generally reveals mild early lacy hyperfluorescence of the tumor in the prearterial and arterial phase, followed by moderate hyperfluorescence during the arteriovenous phase, and increasing hyperfluorescence through the late phase with variable amounts of late leakage (Figs. 157.1, 157.3 and 157.4).[5,19,20] The FA pattern of choroidal hemangioma may be variable and similar to other amelanotic choroidal tumors, hence FA may not be diagnostic in the absence of other ancillary testing.[21] FA can also be helpful for visualization of associated subretinal fluid and cystoid macular edema, which are not typically seen on indocyanine green angiography.[21]

Indocyanine Green Angiography

Indocyanine green angiography (ICGA) is particularly helpful in the diagnosis of circumscribed choroidal hemangioma since it provides improved visualization of the choroidal vasculature. Circumscribed choroidal hemangiomas usually show a

characteristic rapid onset of fluorescence around 30 seconds, much earlier than in other choroidal tumors.[21–23] This fluorescence occurs in a lacy, diffuse hyperintense pattern that fills peripherally first followed by central filling.[22] In the late frames, the tumor demonstrates loss of dye resulting in a hypofluorescent appearance compared with the surrounding choroid, which is known as the "washout" phenomenon.[21–23] In addition, a late hyperfluorescent rim around the tumor is almost always present.[21–23] Intrinsic tumor vessels are more likely to be seen with ICG than with FA, and the normal choroidal vasculature beneath the tumor is obscured, a feature which is also considered pathognomonic.[21,23] Chronic lesions with significant retinal pigment epithelial changes may have blocked fluorescence on ICGA.

Ultrasonography

Circumscribed choroidal hemangiomas have a consistent characteristic appearance on ultrasonography (US). On B-scan US the hemangioma appears as an acoustically solid mass, which is almost always identical in character to the surrounding normal choroid (Figs. 157.2–157.4).[5,20] The tumor is typically dome-shaped but can occasionally appear mushroom-shaped or plateau-shaped.[5] On A-scan, the tumor demonstrates high internal reflectivity.[5,20] Both A- and B-scan ophthalmic US are useful to distinguish choroidal hemangioma from choroidal melanoma, as the latter is usually acoustically hollow with medium to low internal reflectivity.[5]

Neuroimaging

Magnetic resonance imaging (MRI) of choroidal hemangioma typically shows hyperintensity in contrast to vitreous on T1-weighted images, and hyperintensity or isointensity to vitreous on T2-weighted images.[5] Choroidal hemangiomas show enhancement with gadolinium contrast.[5] The MRI findings may be helpful in differentiating from choroidal melanoma and metastasis, which show bright signal on T1-weighted images and low signal on T2-weighted images.[5] Clinically, such studies are rarely used to diagnose this condition.

Optical Coherence Tomography and Enhanced Depth Imaging

In choroidal tumors, traditional time-domain and spectral domain optical coherence tomography (SD-OCT) are most useful for visualizing secondary changes to the retina and retinal pigment epithelium (RPE).[24] In choroidal hemangiomas, OCT can be used to demonstrate macular edema, epiretinal membranes, and subretinal fluid (Figs. 157.2 and 157.3). Until recently, wavelength-dependent light scattering and decreasing sensitivity and resolution with increased displacement from zero delay prevented detailed imaging of the choroid and sclera with OCT.[25] Spaide and colleagues described a method of placing the SD-OCT closer to the patient to purposefully image deeper layers, producing a detailed inverted image of the choroid.[25] Several authors have used this enhanced depth imaging (EDI) technique to image a variety of choroidal tumors, including circumscribed choroidal hemangioma.[26]

Circumscribed choroidal hemangiomas tend to exhibit a smooth surface with expansion of the medium and large choroidal vessels but without compression of the overlying choriocapillaris.[26–29]

Autofluorescence

Fundus autofluorescence (FAF) is an imaging technique that visualizes excitation of phosphenes, typically from substances such lipofuscin, distributed in the RPE cell monolayer.[30] FAF is increased in dysfunctional RPE and decreased in areas of photoreceptor loss, and has been useful in age-related macular degeneration (AMD), Best disease, and various chorioretinal inflammatory disorders.[30] A study of FAF in 34 eyes with choroidal hemangiomas (27 of which were circumscribed) found that the intrinsic tumor FAF of untreated circumscribed choroidal hemangiomas was either isoautofluorescent (58%) or hypoautofluorescent (42%), and treated circumscribed choroidal hemangiomas were all hypoautofluorescent (100%).[31] The extrinsic FAF of the overlying retinal pigment epithelium and retinal alterations showed hyperautofluorescence of orange pigment in two cases of untreated

circumscribed choroidal hemangioma, and hypoautofluorescence of RPE hyperplasia, atrophy, and fibrous metaplasia[31] (see Fig. 157.2).

Pathology

Choroidal hemangiomas are considered hamartomas, which are defined as benign vascular tumors composed of tissue elements normally found in the location of the tumor. Hemangiomas of the choroid are classified histopathologically according to the prevailing type or types of vessels within the tumor: capillary, cavernous, or mixed.[6] The capillary type is composed of small vessels separated by loose connective tissue (Fig. 157.6), whereas the cavernous type is composed of larger vessels separated by relatively little connective tissue (Fig. 157.7). The mixed type shows both capillary and cavernous features. Choroidal hemangiomas are notable for the lack of cellular proliferation of the elements of the vessel walls, supporting the idea that these tumors are nonproliferative lesions.[6]

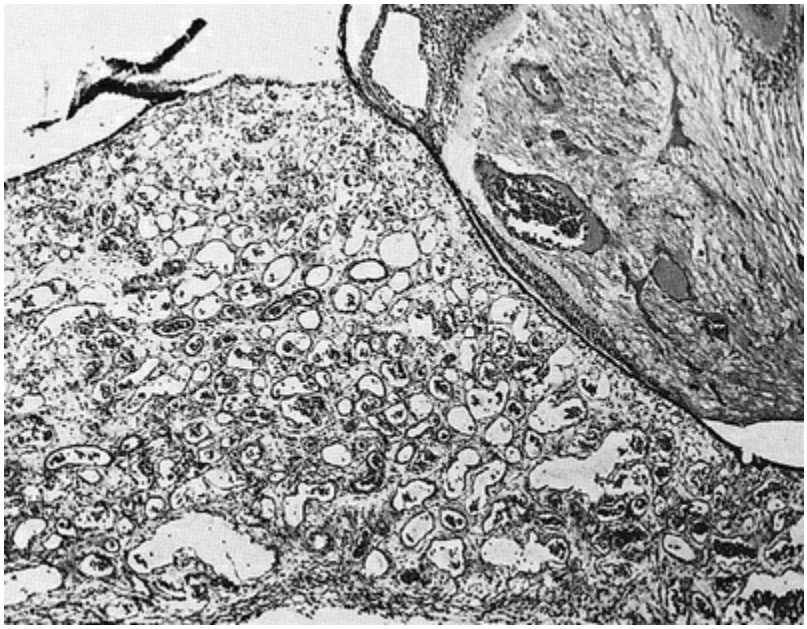

FIG. 157.6 Capillary type of choroidal hemangioma showing uniformly small vessels separated by a loose, edematous, intravascular stroma. The retina (upper right) is detached and cut obliquely through the plane of the nerve fiber (hematoxylin and eosin, ×50).

(Reproduced with permission from AFIP and Witschel H, Font RL. Hemangioma of the choroid. A clinicopathologic study of 71 cases and a review of the literature. Surv Ophthalmol 1976;20:415–31.)

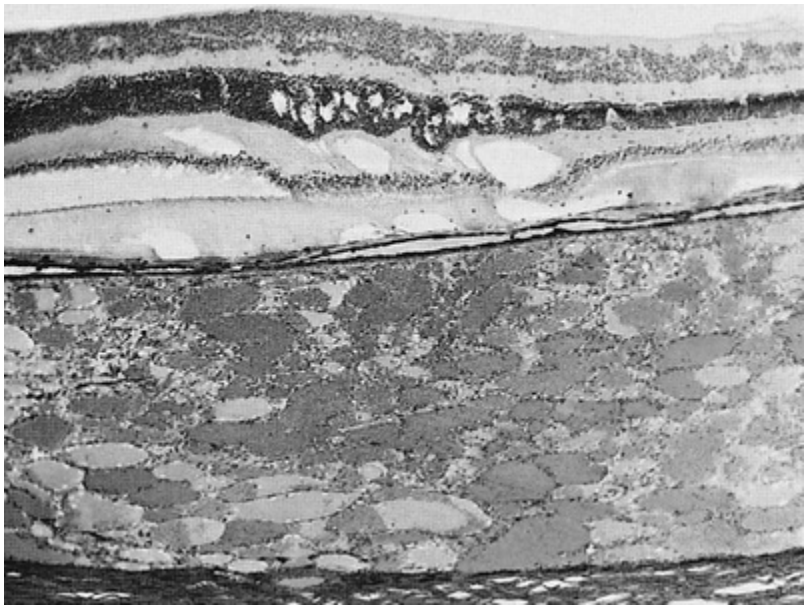

FIG. 157.7 Cavernous type of choroidal hemangioma with early cystoid changes of the outer plexiform and inner nuclear layers. The dilated, blood-filled spaces are lined with a flat layer of endothelial cells with minimal intervascular stroma. Proliferation of retinal pigment epithelial cells is present (hematoxylin and eosin, ×50). (Reproduced with permission from AFIP and Witschel H, Font, RL. Hemangioma of the choroid. A clinicopathologic study of 71 cases and a review of the literature. Surv Ophthalmol 1976;20:415–31.)

Witschel and Font, using the files of the Armed Forces Institute of Pathology (AFIP), studied 45 eyes containing a circumscribed choroidal hemangioma.[6] They found 20 tumors of the cavernous type, 22 tumors of the mixed type, and only 3 of the capillary type.[6] This finding is in contrast to the diffuse type of choroidal hemangioma associated with Sturge–Weber syndrome, in which mixed type tumors were found in all 17 cases studied.[6]

Circumscribed choroidal hemangioma pushes choroidal melanocytes toward the periphery of the tumor, the sclera, and the choriocapillaris. Pigmentation alterations in the overlying retinal pigment epithelium (RPE) are common and may range from

disorganization and proliferation of the RPE to the formation of fibrous plaques on the inner surface of the choroid (Fig. 157.8), which produces a grayish-white appearance over some of these tumors.[6,32] Ossification overlying the tumor may occur secondary to degenerative transformation and proliferation of retinal pigment epithelial cells and is likely a sign of chronicity.[6] Retinal changes overlying circumscribed choroidal hemangiomas may include edema or cystic degeneration, loss of photoreceptors/ellipsoid layer, loss of the external limiting membrane, gliosis, and, occasionally, deposition of lipofuscin or migration of RPE cells into the retina.[6,28,32]

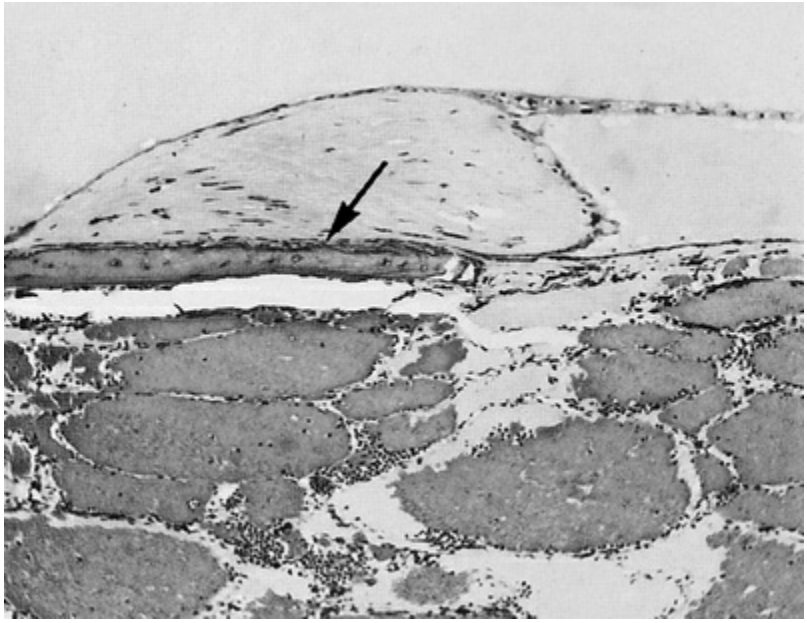

FIG. 157.8 This fibrous nodule, representing transformation of retinal pigment epithelial cells, overlies a cavernous hemangioma of choroid. A thin plaque of bone (*arrow*) is interposed between the base of the fibrous nodule and the hemangioma. Collections of leukocytes are present in some vessels (hematoxylin and eosin, ×90). (Reproduced with permission from AFIP and Witschel H, Font RL. Hemangioma of the choroid. A clinicopathologic study of 71 cases and a review of the literature. Surv Ophthalmol 1976;20:415–31.)

Histologic studies demonstrate that the orange or orange–yellow spots over the surface of circumscribed choroidal hemangiomas are

lipofuscin contained in macrophages located in both the RPE and the outer plexiform layer,[9] although this occurs with less frequency compared to choroidal melanoma.

Except in those cases of severe secondary glaucoma, the retinal ganglion cells and nerve fiber layer are preserved despite severe retinal changes elsewhere.[6,28] Serous detachments of the retina are not an uncommon finding.

Treatment

Asymptomatic circumscribed choroidal hemangiomas may be observed.[5] In some cases the hemangioma may be symptomatic only by inducing a hyperopic shift that may be treated with refractive correction alone. Observation may also be indicated in cases of subfoveal tumors that have resulted in hyperopic amblyopia.[5] For symptomatic circumscribed choroidal hemangiomas with exudative retinal detachment or cystoid macular edema, a variety of treatment modalities are available.

Laser

Photodynamic Therapy

Photodynamic therapy (PDT) was first introduced to treat symptomatic circumscribed choroidal hemangioma in 2000[33] and is currently considered to be the preferred treatment for tumors with symptomatic exudative retinal detachment or intraretinal fluid (Figs. 157.3 and 157.4).[34] Circumscribed choroidal hemangioma may be particularly amenable to PDT since verteporfin is sequestered preferentially in abnormal large-caliber vessels. In contrast to laser photocoagulation, radiation therapies, and transpupillary thermotherapy, PDT allows relatively selective targeting of choroidal tumor vessels, leading to regression with minimal damage to the overlying retina,[35] although branch retinal artery occlusion has been reported following PDT of circumscribed choroidal hemangioma.[36] For this reason, PDT is also suitable for treatment of subfoveal choroidal hemangiomas.[37] Laser photocoagulation, in contrast to PDT, does not penetrate beyond the surface of the tumor.[38] External beam radiotherapy may induce

tumor regression but carry additional risks (cataract, optic neuropathy, radiation retinopathy) and often require invasive surgeries such as tantalum clip placement for proton beam and plaque placement and removal for brachytherapy (see below).[39–42] PDT is typically performed with administration of intravenous verteporfin at a dose of 6 mg/m^2 before treatment with laser wavelengths of 689, 690, or 692 nm at an intensity of 600 mW/cm^2 with duration ranging from 83–166 seconds (50–100 J/cm^2) from 5 to 15 minutes following the start of infusion.[43–49] The systemic and ocular safety of PDT has been well documented in the Treatment of Age-Related Macular Degeneration with Photodynamic Therapy (TAP) trial[50] and related studies.

There have been numerous case series of patients with circumscribed choroidal hemangioma treated with PDT. The results of the studies with 10 or more patients are summarized in Table 157.1, which reviews the results of PDT treatments in 201 patients, not including the numbers that have been treated in smaller case series. PDT is increasingly selected as the primary therapy for symptomatic circumscribed choroidal hemangioma.[43,45] In all but two of the case series, the majority of patients received one PDT treatment.[37,38,43–45,47] The two series where the vast majority of patients required more than one PDT treatment were the studies by Schmidt-Erfurth et al. and Porrini et al. where the treatment goal was defined as complete resolution of the tumor, not just resolution of subretinal and intraretinal fluid.[48,51] Follow-up ranged from 1 to 80 months in the 11 studies.[37,38,43–45,47–49,51–53] Treatment protocols and effects varied between the studies. Most series showed stabilization or improvement in visual acuity, reduction in intra- and subretinal fluid, and tumor regression in the majority of patients. While Schmidt-Erfurth et al. and Porrini et al. have suggested that the goal of therapy is elimination of subretinal fluid and tumor regression, most other authors have concluded that tumor elimination is not the ultimate goal and retreatment is only necessary for persistent or recurrent exudation or visual loss.[37,44,48] Higher numbers or intensity of PDT treatments may increase the risk of choroidal atrophy and neurosensory retinal degeneration.[49,51] The number of PDT treatments has also been shown to be inversely associated with visual acuity improvement; whether this is because larger tumors

are more likely to require more PDT treatments or if this reflects a side-effect of PDT treatment is unknown.[37] Recurrence of subretinal fluid following PDT has been reported, often many months or years later, with some patients requiring multiple treatments.[54]

TABLE 157.1

Symptomatic Circumscribed Choroidal Hemangiomas Treated With Photodynamic Therapy (PDT)

Author (Year)	No. Eyes	No. Eyes Receiving PDT as Primary Treatment	No. Treatments	Protocol	Length of Follow-Up	Mean Tumor Thickness
Su et al. (2014)[52]	22	22	1	689 nm laser with intensity of 600 mW/cm^2. Overlapping spot protocol (14 patients): 83 s (50 J/cm^2) for each spot. Single spot protocol (8 patients): 166 s (100 J/cm^2)	Overlapping spot: mean 28.5 mth (range 15–38). Single spot: mean 27 mth (range 17–34)	Overlapping spot: 2.7 mm. Single spot: 2.5 mm
Elizalde et al. (2012)[53]	13	9	7 patients single treatment, 5 patients two treatments, and 1 patient five treatments and eventual external beam radiotherapy	692 nm laser with intensity of 600 mW/cm^2 (6 mg/m^2 BSA verteporfin), 1–3 spots at 83 s each (50 J/cm^2)	Mean 26 mth (range 7–67 mth)	3.4 mm
Pilotto et al. (2011)[49]	20	18	1	689 nm laser with intensity of 600 mW/cm^2. In standard group,	Mean 58 mth (range 36–80)	Standard dose: 2.45 mm Bolus dose: 2.38 mm

				treatment at 15 min after infusion for 83 s (50 J/cm^2). In "bolus" group, treatment at 5 min for 166 s (100 J/cm^2)		
Blasi et al. (2010)[43]	25	25	22 patients required 1 treatment; 3 patients required 2 treatments	689 nm laser with intensity of 600 mW/cm^2 for 83 s (50 J/cm^2) for first 3 patients, 100 J/cm^2 at 166 s for subsequent patients	60 mth (completed by all patients)	Median thickness 3.3 mm (mean not available)
Zhang et al. (2010)[45]	25	25	23 patients required 1 treatment; 2 patients required 2 treatments	Foveal lesions: 689 nm laser with intensity of 600 mW/cm^2 for 83 s (50 J/cm^2) Extrafoveal lesions: 75 J/cm^2, exposure time 125 s	Mean 35.5 months (±15 months)	3.2 mm
Boixadera et al. (2009)[44]	31 eyes enrolled (2 eyes subsequently excluded, analyses done with 29 eyes)	22 eyes primary treatment; 7 eyes treated previously (3 laser, 2 laser and TTT, 2 TTT)	24 patients required 1 treatment; 4 patients required 2 treatments; 1 patient required 3 treatments	689 nm laser with intensity of 600 mW/cm^2 for 83 s (50 J/cm^2)	12 months (completed by all patients)	3.0 mm
Singh et al.	10	7 eyes primary	8 patients had 1	690 nm laser with	Median 7 months	2.9 mm

(2004)[47]		treatment; 3 eyes treated previously (2 TTT, 1 external beam radiotherapy)	treatment; 2 patients required 2 treatments	intensity of 600 mW/cm^2 for 83 s (50 J/cm^2)	(range 1–13 months)	
Jurklies et al. (2003)[37]	19	15 eyes primary treatment; 4 eyes treated previously (2 with radiation, 1 with laser, 1 with laser + radiation)	7 patients required 1 treatment; 5 patients required 2 treatments; 7 patients required 3 or more treatments	689 nm laser with intensity of 600 mW/cm^2 for 166 s (100 J/cm^2)	10.6 months	2.6 mm
Verbraak et al. (2003)[38]	13	10 eyes primary treatment; 2 eyes treated previously with radiation, 1 treated with PDT	8 patients requiring one treatment; 5 patients requiring two treatments	692 nm laser with intensity of 600 mW/cm^2 for 166 s (100 J/cm^2) in first 3 patients; 83 s (50 J/cm^2) for subsequent 10 patients	3–22 months	3.1 mm
Porrini et al. (2003)[48]	10	7 eyes primary treatment; 3 treated previously (2 laser, 1 proton beam irradiation)	1 patient had one treatment; 5 patients required two treatments; 4 patients required three treatments	For lesions <2 mm: 689 nm laser with intensity of 600 mW/cm^2 for 125 s (75 J/cm^2); For lesions >2 mm: 186 s (100 J/cm^2)	7–16 months	2.9 mm
Schmidt-Erfurth et al. (2002)[51]	15	15 eyes primary treatment	2 patients with one treatment, 6 patients with two treatments, 6 patients with three treatments, 1 patient with four treatments	692 nm laser with intensity of 600 mW/cm^2 for 166–168 s (100 J/cm^2)	Mean 19 months (range 12–50 months)	3.8 mm

LP, light perception; PDT, photodynamic therapy; RPE, retinal pigment epithelium;

TTT, transpupillary thermotherapy; VA, visual acuity.

Laser Photocoagulation

Laser photocoagulation or "thermal laser" with xenon arc or argon laser was one of the earlier primary treatments of circumscribed choroidal hemangioma prior to the development of PDT.[5] In the Shields' series of 86 patients who were treated with argon laser photocoagulation, 62% of patients had complete resolution of subretinal fluid and 71% of patients had visual stability or improvement.[5] An earlier case series in 1989 by Anand et al., where 42 patients underwent treatment with argon or xenon laser, showed a 79.2% rate of initial visual acuity and subretinal fluid improvement, but a 40% rate of recurrent subretinal fluid after initial treatment.[55] All of the patients had resolution of subretinal fluid with retreatment at the end of the follow-up period.[55] Another series by Madreperla et al. describes 13 patients treated with laser photocoagulation where 38% had vision better than 6/12 and 46% had no subretinal fluid at 1 year.[56] However, laser photocoagulation cannot be used to treat subfoveal lesions and laser photocoagulation does not reduce tumor size, resulting in a higher rate of recurrent exudation.[34] A single report of successful treatment of choroidal hemangioma with grid photocoagulation has also been reported.[57] Patients who have failed laser photocoagulation treatment often require subsequent radiation treatment or PDT.

Transpupillary Thermotherapy

As opposed to laser photocoagulation, transpupillary thermotherapy (TTT) utilizes relatively long-pulse and low-energy laser to raise the temperature within treated tumor tissue, causing heat-induced sclerosis of vascular channels and eventually tumor regression and resolution of subretinal fluid.[58] TTT technically differs from laser photocoagulation in that the goal is optimal heat penetration rather than coagulation, and has been used more successfully for treatment of choroidal tumors.[59] TTT is felt to be most appropriate for circumscribed choroidal hemangiomas with shallow subretinal fluid that are posterior to the equator, with a

tumor base <10 mm and tumor thickness <4 mm.[58] If the tumor is larger than these dimensions, or if there is extensive subretinal fluid, tumor visualization may be difficult and prevent accurate focusing of the laser beam.[58] TTT may not be ideal in cases where the tumor margin touches the optic disc given the risk of thermal papillitis, which was reported in two of 80 eyes having TTT for juxtapapillary choroidal melanoma.[60] The use of TTT for subfoveal tumors is likely suboptimal in many cases as TTT is not selective for abnormal or choroidal tissue and may have adverse effects on normal retina.[58]

Gunduz published a review in 2004 of 38 cases (10 cases managed by the author and 28 cases from the published literature) of circumscribed choroidal hemangioma primarily treated with TTT. He found that all tumors ceased leaking after TTT with resolution of subretinal fluid.[58] Of these, 42% of tumors showed complete regression, 53% demonstrated partial regression by at least 10%, and 5% showed no change in tumor thickness.[58] After excluding 12 patients whose pretreatment visual acuities were less than 20/400, visual acuity improved by two or more Snellen lines in 77% of eyes and remained unchanged in the remaining 23% of eyes.[58] Complications included branch retinal vein occlusion in one eye, cystoid macular edema in three eyes, preretinal fibrosis in two eyes, and focal iris atrophy in three eyes.[58] While all of the cases reviewed by Gunduz were <4 mm thick and <10 mm in tumor diameter, there has been one report by Rishi et al. of a large subfoveal circumscribed choroidal hemangioma 6 mm in height and 14 mm in diameter with near total exudative retinal detachment treated with TTT which showed resolution of subretinal fluid.[58,61] Visual acuity improved from light perception to 10/200 at 6 months.[61] There is also one report by Kamal et al. where indocyanine green dye was injected prior to TTT to enhance laser uptake.[62]

Transscleral Diode Cyclophotocoagulation

A single report from Feng et al. has suggested favorable outcomes may be achieved with this modality for circumscribed choroidal hemangioma, although significant scarring and RPE changes

appear to result. The proposed benefit of transscleral diode cyclophotocoagulation is its significant reduced cost compared to PDT.[63]

Radiotherapy

Choroidal hemangiomas are extremely radiosensitive. However, radiation treatment is typically reserved for patients with extensive retinal detachment, those who cannot be treated with or are refractory to treatment with thermal laser or PDT. Radiation therapy often results in retinal reattachment and tumor regression in these patients although this can be accompanied by radiation-induced side-effects such as cataract, radiation retinopathy, and optic neuropathy.[64] However, noting the generally lower dose needed to treat circumscribed choroidal hemangiomas, the risk of radiation complications is generally less than treating other choroidal tumors, including posterior uveal melanoma. Radiation has historically also been used in patients with subfoveal choroidal hemangiomas that were not amenable to laser photocoagulation, although this role has been supplanted by PDT.

Conventional External Beam Radiotherapy

Lens-sparing conventional gamma-ray external beam radiotherapy has been used for the treatment of circumscribed choroidal hemangioma. The largest series was reported by Schilling et al. in 1997, in which 36 eyes were treated with a dose of 20 Gy.[65] A total of 63.8% of patients experienced resolution of subretinal fluid, and visual acuity was stable or improved in 78% of patients.[65] Four cases of subretinal fibrosis leading to decreased final visual acuity are reported, but no reports of radiation-induced side-effects such as radiation retinopathy or cataract were found over a mean follow-up period of 4.5 years.[65] Ritland et al. treated nine eyes with circumscribed choroidal hemangioma with 20–24 Gy resulting in resolution of subretinal fluid, stable or improved visual acuity, and tumor regression in all cases.[66] Over the mean follow-up time of 3.6 years, no radiation-induced side-effects were observed.[66] Shields et al. reported two patients treated with external beam radiotherapy, both of whom had stable or improved visual acuity.[5] Madreperla et

al. also reported two patients treated with lens-sparing external beam radiotherapy, one of whom had resolution of subretinal fluid.[56]

Plaque Brachytherapy

Plaque brachytherapy with palladium-103, cobalt-60, ruthenium-106, and iodine-125 have all been reported for the treatment of circumscribed choroidal hemangioma.[5,56,67–70] Compared with external beam radiotherapy, plaque brachytherapy offers more localized delivery of radiation to the tumor itself, minimizing radiation-induced side-effects.[67] The disadvantages of plaque brachytherapy are the necessity of two surgeries for plaque placement and removal, as well as heterogeneous radiation dose to the tumor base and apex. Zografos et al. reported the largest series of 39 patients with circumscribed choroidal hemangioma treated with cobalt-60 plaque brachytherapy who had 100% retinal reattachment.[70] Complications included pigment migration into the treated area, subretinal fibrosis, and an areolar atrophic scar.[70] Shields et al. reported the second-largest series of 15 patients treated with plaque radiotherapy, all of whom had resolution of subretinal fluid and 53% of whom had stable or improved visual acuity.[5] Lopez-Caballero et al. also treated eight patients with iodine-125 plaque brachytherapy, all of whom experienced resolution of subretinal fluid and some decrease in tumor thickness and 75% of whom had stable visual acuity.[69] Three patients developed radiation retinopathy, and one patient developed subretinal fibrosis.[70] Madreperla et al. treated two patients with iodine-125 and six patients with ruthenium-106 plaque brachytherapy, all of whom had resolution of subretinal fluid and 75% of whom had final vision better than 6/12.[56] Aizman et al. treated five patients with palladium-103 plaque brachytherapy – all five patients had resolution of subretinal fluid with some degree of tumor regression and three patients had improvement in visual acuity.[67] Chao et al. also reported one case where iodine-125 plaque brachytherapy was used as an alternative to enucleation in a patient with no light perception vision, total retinal detachment, and iris neovascularization; the posttreatment visual acuity remained no light perception, but the retinal detachment and iris

neovascularization resolved.[68]

Stereotactic Radiotherapy

Stereotactic radiotherapy is a form of external beam gamma-irradiation that uses multiple treatment angles to provide a more homogeneous dose of radiation to target tissues and reduce radiation-related effects on healthy tissues. "Stereotactic radiosurgery," "gamma knife," and "cyberknife" are terms used to describe different forms of stereotactic radiotherapy. Two different Korean groups have reported on the use of gamma knife radiotherapy for the treatment of choroidal hemangioma.[71-73] Kim et al. have reported on the use of the Leksell gamma knife for symptomatic choroidal hemangiomas in seven patients, three of whom had the circumscribed form.[72] In the three patients with circumscribed choroidal hemangioma treated with a marginal dose of 10 Gy, the exudative retinal detachment resolved completely within 3 months and visual acuity improved in all three cases.[72] Song et al. also published their results with gamma knife radiotherapy for choroidal hemangioma with exudative retinal detachment, two of which were circumscribed, and they found that the retinal detachment resolved in both cases; however, vision worsened in one patient and was stable in the other.[71] The marginal dose used in this series was 26.7 Gy.[71]

Kivela et al. have also published a series of five patients with perifoveolar and peripapillary circumscribed choroidal hemangiomas treated with 20 Gy of stereotactic radiotherapy.[74] Exudative retinal detachments resolved within 6 months in four eyes and within 20 months in the fifth eye, and visual acuity improved or remained stable in four of five eyes.[74]

Proton Beam Radiotherapy

Proton beam radiotherapy is a nonstereotactic form of external beam radiotherapy and may have some advantages compared to traditional gamma rays. Most importantly, the "Bragg peak" phenomenon of protons may allow for a more tailored and homogenous area of treatment and less collateral radiation damage compared to external gamma-irradiation.[75] However, a disadvantage of protons compared to external beam gamma-

irradiation is that surgical placement of tantalum clips is required with the former to permit tumor localization during treatment.

The largest series, of 71 patients, treated with proton beam therapy was reported by Levy-Gabriel et al. in 2009.[76] After treatment with 20 cobalt gray equivalents (CGE), retinal reattachment was achieved in 100% of patients, tumor regression in 91.5% of patients, and visual acuity improved by two or more lines in 52%.[76] Complications included cataract in 28% of patients and radiation-induced maculopathy in 8%.[76] In 2004, Frau et al. reported a series of 17 patients with circumscribed choroidal hemangiomas with serous retinal detachments treated primarily with low-dose proton therapy at 20 CGE.[64] At 2-year follow-up, 94% of patients had visual acuity improvement of two or more lines and 65% of patients had complete tumor resolution.[64] In 2014, Zeisberg et al.[75] presented relatively long-term results (mean follow-up 55.4 months) from a series of 50 patients with circumscribed choroidal hemangioma also treated with proton beam radiotherapy at 20 CGE. In this series, radiotherapy was used as primary treatment in 82% of patients, the others having undergone previous photodynamic therapy. Visual improvement of 2 lines or more was achieved in 58.8% of patients, but 46% developed radiation-retinopathy after a mean of 14.5 months with some patients developing vitreous hemorrhage, dry eye, and radiation-induced optic neuropathy. Earlier series reported results with higher doses of radiation; Hannouche et al. reported a series of 13 patients with circumscribed choroidal hemangiomas with serous retinal detachments who underwent proton therapy at a total dose of 30 CGE.[77] All patients had resolution of subretinal fluid, and 62% had improvement of visual acuity by two or more lines.[77] Zografos et al. treated 48 eyes with circumscribed choroidal hemangioma, and all of the patients had resolution of exudative retinal detachment at last follow-up (6 months to 9 years).[78] The radiation dose ranged from 16.4 to 27.3 Gy, and the three patients treated with 27.3 Gy all developed optic neuropathy.[78] Finally, there is one recent report from Chan et al. where they used a nonsurgical light-field technique without surgical tumor localization at doses of 15–30 CGE with good results.[79]

Intravitreal Pharmacologic Therapy

Intravitreal Anti-VEGF Injection

A few cases of circumscribed choroidal hemangioma treated with intravitreal injection of bevacizumab have been reported.[80–83] Most patients in these series received intravitreal bevacizumab for persistent intra- or subretinal fluid following more established treatments such as PDT, TTT, or laser photocoagulation and showed variable responses. In a few cases, intravitreal bevacizumab was used as primary treatment for symptomatic circumscribed choroidal hemangioma without adjuvant. Mandal et al. describe one patient who achieved resolution of intraretinal and subretinal fluid with a series of two injections of intravitreal bevacizumab, but without visual improvement.[81] Kwon et al. present four patients who underwent primary treatment of circumscribed choroidal hemangioma with serous retinal detachment with one or two intravitreal injections of bevacizumab. Of these, three patients had persistent improvement in subretinal fluid, although follow-up was limited (mean 6 months). Kwon et al. reflect that although bevacizumab may be initially effective at reducing fluid, its treatment duration may be limited.[83] A case of choroidal hemangioma unresponsive to intravitreal ranibizumab has been reported.[84] In addition, one case of intravitreal ranibizumab being used to effectively treat choroidal neovascularization secondary to PDT of circumscribed choroidal hemangioma has also been reported.[13]

Intravitreal Glucocorticoid Therapy

Minimal literature exists regarding the use of intravitreal glucocorticoids to treat circumscribed choroidal hemangioma. One report of intravitreal triamcinolone injection to successfully treat several patients with circumscribed choroidal hemangioma-associated neovascularization has been published, and repeat injections were required in most.[85] In addition, a more recent report regarding the successful use of combined PDT and intravitreal dexamethasone implant to treat subretinal fluid associated with circumscribed choroidal hemangioma has been published, although the patient was treatment-naïve and may have responded to PDT

alone.[86]

Conclusions

Circumscribed choroidal hemangiomas are benign vascular hamartomas without systemic associations, which do not require systemic workup or treatment. For symptomatic lesions, PDT has emerged as the treatment of choice with high rates of tumor and subretinal fluid regression and minimal complications. For centers where PDT is not available, TTT or laser photocoagulation remain reasonable alternatives, although they are not recommended for subfoveal lesions. Radiation therapy is usually reserved for larger hemangiomas with extensive bullous retinal detachment and which are not amenable to PDT, TTT, or photocoagulation treatment as radiotherapy is more technically involved, may cause radiation-related complications, and/or may require travel to specialized centers. Limited data suggest that intravitreal bevacizumab may reduce exudation in some circumscribed choroidal hemangiomas and may be more effective in cases of recurrent exudation following previously successful ablative treatment, although the duration of any effect may be limited.

References

1. Scott IU, Alexandrakis G, Cordahi GJ, et al. Diffuse and circumscribed choroidal hemangiomas in a patient with Sturge–Weber syndrome. *Arch Ophthalmol*. 1999;117:406–407.
2. Cheung D, Grey R, Rennie I. Circumscribed choroidal haemangioma in a patient with Sturge–Weber syndrome. *Eye (Lond)*. 2000;14:238–240.
3. Leber T. Fall von cavernosem Sarcom der Aderhaut. *Graefes Arch Ophth*. 1868;14:221–227.
4. Hill E, Dart RO. Cavernous hemangioma of the choroid: report of five cases in the Registry of Ophthalmic Pathology, Army Medical Museum, Washington, DC. *Trans Am Ophthalmol Soc*. 1936;34:122–133.
5. Shields CL, Honavar SG, Shields JA, et al. Circumscribed

choroidal hemangioma: clinical manifestations and factors predictive of visual outcome in 200 consecutive cases. *Ophthalmology*. 2001;108:2237–2248.
6. Witschel H, Font RL. Hemangioma of the choroid: a clinicopathologic study of 71 cases and a review of the literature. *Surv Ophthalmol*. 1976;20:415–431.
7. Schepens CL, Schwartz A. Intraocular tumors. I: Bilateral hemangioma of the choroid. *AMA Arch Ophthalmol*. 1958;60:72–83.
8. Hogan MJ. Choroidal hemangioma. *Arch Ophthalmol*. 1964;71:69–70.
9. Shields JA, Rodrigues MM, Sarin LK, et al. Lipofuscin pigment over benign and malignant choroidal tumors. *Trans Sect Ophthalmol Am Acad Ophthalmol Otolaryngol*. 1976;81:871–881.
10. Ramasubramanian A, Shields CL, Harmon SA, et al. Autofluorescence of choroidal hemangioma in 34 consecutive eyes. *Retina*. 2010;30(1):16–22.
11. Ruby AJ, Jampol LM, Goldberg MF, et al. Choroidal neovascularization associated with choroidal hemangiomas. *Arch Ophthalmol*. 1992;110:658–661.
12. Quergues G, Forte R, Quergues L, et al. Intravitreal ranibizumab for choroidal neovascularization associated with circumscribed choroidal haemangioma. *Clin Exp Ophthalmol*. 2011;39(9):916–918.
13. Hua R, Zhao N, Hu Y, et al. Circumscribed choroidal hemangioma associated with choroidal neovascularization in a HIV-infected case: photodynamic therapy and intravitreal ranibizumab in photodiagnosis and photodynamic therapy. *Photodiagn Photodyn Ther*. 2014;11(3):441–443.
14. Leys AM, Silva R, Inhoffen W, et al. Neovascular growth following photodynamic therapy for choroidal hemangioma and neovascular regression after intravitreous injection of triamcinolone. *Retina*. 2006;26:693–697.
15. Medlock RD, Augsburger JJ, Wilkinson CP, et al. Enlargement of circumscribed choroidal hemangiomas. *Retina*. 1991;11:385–388.

16. Shields JA, Stephens RF, Eagle RC, et al. Progressive enlargement of a circumscribed choroidal hemangioma: a clinicopathologic correlation. *Arch Ophthalmol*. 1992;110:1276–1278.
17. Schalenbourg A, Zografos L. Blackening of choroidal hemangioma after tantalum clip surgery. *Arch Ophthalmol*. 2007;125:1136.
18. Bosch MM, Helbig H. Blackening of a choroidal hemangioma after photodynamic therapy. *Klin Monatsbl Augenheilkd*. 2005;222:258–260.
19. Norton EW, Gutman F. Fluorescein angiography and hemangiomas of the choroid. *Arch Ophthalmol*. 1967;78:121–125.
20. Singh AD, Kaiser PK, Sears JE. Choroidal hemangioma. *Ophthalmol Clin North Am*. 2005;18:151–161.
21. Arevalo JF, Shields CL, Shields JA, et al. Circumscribed choroidal hemangioma: characteristic features with indocyanine green videoangiography. *Ophthalmology*. 2000;107:344–350.
22. Shields CL, Shields JA, De Potter P. Patterns of indocyanine green videoangiography of choroidal tumours. *Br J Ophthalmol*. 1995;79:237–245.
23. Schalenbourg A, Piguet B, Zografos L. Indocyanine green angiographic findings in choroidal hemangiomas: a study of 75 cases. *Ophthalmologica*. 2000;214:246–252.
24. Shields CL, Materin MA, Shields JA. Review of optical coherence tomography for intraocular tumors. *Curr Opin Ophthalmol*. 2005;16:141–154.
25. Spaide RF, Koizumi H, Pozzoni MC. Enhanced depth imaging spectral-domain optical coherence tomography. *Am J Ophthalmol*. 2008;146:496–500.
26. Torres VL, Brugnoni N, Kaiser PK, et al. Optical coherence tomography enhanced depth imaging of choroidal tumors. *Am J Ophthalmol*. 2011;151:586–593.
27. Shields CL, Pellegrini M, Ferenczy SR, et al. Enhanced depth imaging optical coherence tomography of intraocular tumors: from placid to seasick to rock and rolling topography – the 2013 Francesco Orzalesi Lecture. *Retina*.

2014;34(8):1495–1512.
28. Rojanaporn D, Kaliki S, Ferenczy SR, et al. Enhanced depth imaging optical coherence tomography of circumscribed choroidal hemangioma in 10 consecutive cases. *Middle East Afr J Ophthalmol*. 2015;22(2):192–197.
29. Shields CL, Manalac J, Das C, et al. Review of spectral domain enhanced depth imaging optical coherence tomography of tumors of the choroid. *Ind J Ophthalmol*. 2015;63(2):117–121.
30. Schmitz-Valckenberg S, Holz FG, Bird AC, et al. Fundus autofluorescence imaging: review and perspectives. *Retina*. 2008;28:385–409.
31. Ramasubramanian A, Shields CL, Harmon SA, et al. Autofluorescence of choroidal hemangioma in 34 consecutive eyes. *Retina*. 2010;30:16–22.
32. Jones IS, Cleasby GW. Hemangioma of the choroid: a clinicopathologic analysis. *Am J Ophthalmol*. 1959;48:612–628.
33. Barbazetto I, Schmidt-Erfurth U. Photodynamic therapy of choroidal hemangioma: two case reports. *Graefes Arch Clin Exp Ophthalmol*. 2000;238(3):214–221.
34. Tsipursky MS, Golchet PR, Jampol LM. Photodynamic therapy of choroidal hemangioma in Sturge–Weber syndrome, with a review of treatments for diffuse and circumscribed choroidal hemangiomas. *Surv Ophthalmol*. 2011;56:68–85.
35. Schmidt-Erfurth U, Hasan T, Gragoudas E, et al. Vascular targeting in photodynamic occlusion of subretinal vessels. *Ophthalmology*. 1994;101:1953–1961.
36. Xiao Y, Guo X, Ouyang P. Branch retinal artery occlusion associated with photodynamic therapy in a circumscribed choroidal haemangioma. *Photodiagn Photodyn Ther*. 2013;10(4):644–646.
37. Jurklies B, Anastassiou G, Ortmans S, et al. Photodynamic therapy using verteporfin in circumscribed choroidal haemangioma. *Br J Ophthalmol*. 2003;87:84–89.
38. Verbraak FD, Schlingemann RO, Keunen JE, et al. Longstanding symptomatic choroidal hemangioma

managed with limited PDT as initial or salvage therapy. *Graefes Arch Clin Exp Ophthalmol*. 2003;241:891–898.
39. López-Caballero C, Saornil MA, De Frutos J, et al. High-dose iodine-125 episcleral brachytherapy for circumscribed choroidal haemangioma. *Br J Ophthalmol*. 2010;94(4):470–473.
40. Kim YT, Kang SW, Lee JI. Gamma knife radiosurgery for choroidal hemangioma. *Int J Radiat Oncol Biol Physics*. 2011;81(5):1399–1404.
41. Chan RV, Yonekawa Y, Lane AM, et al. Proton beam irradiation using a light-field technique for the treatment of choroidal hemangiomas. *Ophthalmologica*. 2010;224(4):209–216.
42. Levy-Gabriel C, Rouic LL, Plancher C, et al. Long-term results of low-dose proton beam therapy for circumscribed choroidal hemangiomas. *Retina*. 2009;29(2):170–175.
43. Blasi MA, Tiberti AC, Scupola A, et al. Photodynamic therapy with verteporfin for symptomatic circumscribed choroidal hemangioma: five-year outcomes. *Ophthalmology*. 2010;117:1630–1637.
44. Boixadera A, Garcia-Arumi J, Martinez-Castillo V, et al. Prospective clinical trial evaluating the efficacy of photodynamic therapy for symptomatic circumscribed choroidal hemangioma. *Ophthalmology*. 2009;116:100–105.
45. Zhang Y, Liu W, Fang Y, et al. Photodynamic therapy for symptomatic circumscribed macular choroidal hemangioma in Chinese patients. *Am J Ophthalmol*. 2010;150:710–715.
46. Barbazetto I, Schmidt-Erfurth U. Photodynamic therapy of choroidal hemangioma: two case reports. *Graefes Arch Clin Exp Ophthalmol*. 2000;238:214–221.
47. Singh AD, Kaiser PK, Sears JE, et al. Photodynamic therapy of circumscribed choroidal haemangioma. *Br J Ophthalmol*. 2004;88:1414–1418.
48. Porrini G, Giovannini A, Amato G, et al. Photodynamic therapy of circumscribed choroidal hemangioma. *Ophthalmology*. 2003;110:674–680.
49. Pilotto E, Urban F, Parrozzani R, et al. Standard versus bolus

photodynamic therapy in circumscribed choroidal hemangioma: functional outcomes. *Eur J Ophthalmol*. 2011;21(4):452–458.
50. Bressler NM. Photodynamic therapy of subfoveal choroidal neovascularization in age-related macular degeneration with verteporfin: two-year results of 2 randomized clinical trials-tap report 2. *Arch Ophthalmol*. 2001;119:198–207.
51. Schmidt-Erfurth UM, Michels S, Kusserow C, et al. Photodynamic therapy for symptomatic choroidal hemangioma: visual and anatomic results. *Ophthalmology*. 2002;109:2284–2294.
52. Su ZA, Tang XJ, Zhang LX, et al. Comparison of outcomes between overlapping-spot and single-spot photodynamic therapy for circumscribed choroidal hemangioma. *Int J Ophthalmol*. 2014;7(1):66–70.
53. Elizalde J, Vasquez L, Iyo F, et al. Photodynamic therapy in the management of circumscribed choroidal hemangioma. *Can J Ophthalmol*. 2012;47(1):16–20.
54. Beardsley RM, McCannel CA, McCannel TA. Recurrent leakage after Visudyne photodynamic therapy for the treatment of circumscribed choroidal hemangioma. *Ophthalmic Surg Lasers Imaging Retina*. 2013;44(3):248–251.
55. Anand R, Augsburger JJ, Shields JA. Circumscribed choroidal hemangiomas. *Arch Ophthalmol*. 1989;107:1338–1342.
56. Madreperla SA, Hungerford JL, Plowman PN, et al. Choroidal hemangiomas: visual and anatomic results of treatment by photocoagulation or radiation therapy. *Ophthalmology*. 1997;104:1773–1779.
57. Althaus C, Sundmacher R. Combination therapy of circumscribed choroid hemangioma in contralateral Sturge–Weber syndrome with acetazolamide and laser coagulation. *Klin Monatsbl Augenheilkd*. 1996;208(4):239–242.
58. Gunduz K. Transpupillary thermotherapy in the management of circumscribed choroidal hemangioma. *Surv Ophthalmol*. 2004;49:316–327.
59. Garcia-Arumi J, Ramsay LS, Guraya BC. Transpupillary thermotherapy for circumscribed choroidal hemangiomas.

Ophthalmology. 2000;107:351–357.
60. Shields CL, Shields JA, Perez N, et al. Primary transpupillary thermotherapy for small choroidal melanoma in 256 consecutive cases: outcomes and limitations. *Ophthalmology*. 2002;109:225–234.
61. Rishi P, Sharma T. Transpupillary thermotherapy for large-sized subfoveal circumscribed choroidal hemangioma. *Retina*. 2006;26:974–976.
62. Kamal A, Watts AR, Rennie IG. Indocyanine green enhanced transpupillary thermotherapy of circumscribed choroidal haemangioma. *Eye (Lond)*. 2000;14(Pt 5):701–705.
63. Feng Y, Ma Z. Transscleral diode photocoagulation of large retinal and choroidal vascular lesions. *PLoS ONE*. 2012;7(7):e39340.
64. Frau E, Rumen F, Noel G, et al. Low-dose proton beam therapy for circumscribed choroidal hemangiomas. *Arch Ophthalmol*. 2004;122:1471–1475.
65. Schilling H, Sauerwein W, Lommatzsch A, et al. Long-term results after low dose ocular irradiation for choroidal haemangiomas. *Br J Ophthalmol*. 1997;81:267–273.
66. Ritland JS, Eide N, Tausjo J. External beam irradiation therapy for choroidal haemangiomas: visual and anatomical results after a dose of 20 to 25 Gy. *Acta Ophthalmol Scand*. 2001;79:184–186.
67. Aizman A, Finger PT, Shabto U, et al. Palladium-103 (103Pd) plaque radiation therapy for circumscribed choroidal hemangioma with retinal detachment. *Arch Ophthalmol*. 2004;122:1652–1656.
68. Chao AN, Shields CL, Shields JA, et al. Plaque radiotherapy for choroidal hemangioma with total retinal detachment and iris neovascularization. *Retina*. 2001;21:682–684.
69. Lopez-Caballero C, Saornil MA, De Frutos J, et al. High-dose iodine-125 episcleral brachytherapy for circumscribed choroidal haemangioma. *Br J Ophthalmol*. 2010;94:470–473.
70. Zografos L, Bercher L, Chamot L, et al. Cobalt-60 treatment of choroidal hemangiomas. *Am J Ophthalmol*. 1996;121:190–199.
71. Song WK, Byeon SH, Kim SS, et al. Gamma knife

radiosurgery for choroidal haemangiomas with extensive exudative retinal detachment. *Br J Ophthalmol*. 2009;93:836–837.
72. Kim YT, Kang SW, Lee JI. Gamma knife radiosurgery for choroidal hemangioma. *Int J Radiat Oncol Biol Phys*. 2011;81:1399–1404.
73. Kong DS, Lee JI, Kang SW. Gamma knife radiosurgery for choroidal hemangioma. *Am J Ophthalmol*. 2007;144:319–322.
74. Kivela T, Tenhunen M, Joensuu T, et al. Stereotactic radiotherapy of symptomatic circumscribed choroidal hemangiomas. *Ophthalmology*. 2003;110:1977–1982.
75. Zeisberg A, Seibel I, Cordini D, et al. Long-term (4 years) results of choroidal hemangioma treated with proton beam irradiation. *Graefes Arch Clin Exp Ophthalmol*. 2014;252(7):1165–1170.
76. Levy-Gabriel C, Rouic LL, Plancher C, et al. Long-term results of low-dose proton beam therapy for circumscribed choroidal hemangiomas. *Retina*. 2009;29:170–175.
77. Hannouche D, Frau E, Desjardins L, et al. Efficacy of proton therapy in circumscribed choroidal hemangiomas associated with serious retinal detachment. *Ophthalmology*. 1997;104:1780–1784.
78. Zografos L, Egger E, Bercher L, et al. Proton beam irradiation of choroidal hemangiomas. *Am J Ophthalmol*. 1998;126:261–268.
79. Chan RV, Yonekawa Y, Lane AM, et al. Proton beam irradiation using a light-field technique for the treatment of choroidal hemangiomas. *Ophthalmologica*. 2010;224:209–216.
80. Sagong M, Lee J, Chang W. Application of intravitreal bevacizumab for circumscribed choroidal hemangioma. *Korean J Ophthalmol*. 2009;23:127–131.
81. Mandal S, Naithani P, Venkatesh P, et al. Intravitreal bevacizumab (Avastin) for circumscribed choroidal hemangioma. *Indian J Ophthalmol*. 2011;59(3):248–251.
82. Hsu CC, Yang CS, Peng CH, et al. Combination photodynamic therapy and intravitreal bevacizumab used to treat circumscribed choroidal hemangioma. *J Chinese Med Assoc*. 2011;74(10):473–477.

83. Kwon HJ, Kim M, Lee CS, et al. Treatment of serous macular detachment associated with circumscribed choroidal hemangioma. *Am J Ophthalmol*. 2012;154(1):137–145.e1.
84. Chan LW, Hsieh YT. Photodynamic therapy for choroidal hemangioma unresponsive to ranibizumab. *Optometry Vision Sci*. 2014;91(9):e226–9.
85. Leys AM, Silva R, Inhoffen W, et al. Neovascular growth following photodynamic therapy for choroidal hemangioma and neovascular regression after intravitreous injection of triamcinolone. *Retina*. 2006;26(6):693–697.
86. Bazin L, Gambrelle J. Combined treatment with photodynamic therapy and intravitreal dexamethasone implant (Ozurdex(®)) for circumscribed choroidal hemangioma. *J Français Ophtalmol*. 2012;35(10):798–802.

SECTION 3

Hematologic and Miscellaneous Tumors

OUTLINE

158

Miscellaneous Uveal Tumors

Alison Skalet, David Wilson

Introduction

A great variety of primary tumors occur in the uvea. Of these, rare tumors are difficult to diagnose clinically because they often do not have enough characteristics that distinguish them from the more common tumors. However, knowledge of the epidemiologic factors, clinical features, and natural history of some of the rare tumors may allow the clinician to suspect them preoperatively. Because many of these tumors are benign, preoperative recognition could prevent or minimize surgical intervention. The more common of these overall rare tumors are covered in detail in this chapter, and their unique aspects are emphasized.

Epithelial Tumors of the Ciliary Body: Congenital

Medulloepithelioma

Medulloepithelioma (diktyoma, teratoneuroma) is a rare congenital tumor most commonly seen in children that is generally believed to arise from the epithelium of the medullary tube. This tumor usually arises from the ciliary body epithelium, but medulloepitheliomas of the retina and the optic nerve also occur. The first detailed histologic description of the tumor was by Verhoeff,[1] who called it a teratoneuroma, despite the absence of teratomatous features. Fuchs[2] reported his observations of a medulloepithelioma and coined the term diktyoma because of the netlike appearance of cells composing the tumor. Grinker[3] was the first to use the term "medulloepithelioma," which has become the preferred name because it refers to the correct cell of origin.

Several large series of medulloepitheliomas have been reported[4–7] and provide the bulk of our knowledge of the clinical features of this tumor. In Broughton and Zimmerman's series,[5] the median age at occurrence of initial symptoms was 3.8 years, with a range of 6 months to 41 years. Andersen[4] reported that the average age at the time of enucleation was 4.5 years for benign medulloepitheliomas and 7 years for malignant tumors. In the series of Canning et al.[6] the median age at diagnosis was 3 years. In all three series, all tumors were unilateral and single, and there was no racial or hereditary predisposition. A more recent case series by Kaliki et al. described 41 cases with a median age at presentation of 5 years; 78% of cases occurred in the first decade of life.[7] This tumor is extremely rare in adults aged >20 years.

The signs and symptoms of the 56 patients reported on by Broughton and Zimmerman[5] are summarized in Tables 158.1 and 158.2.

TABLE 158.1

Medulloepithelioma – Symptoms and Signs

Clinical Finding	Cases (*n*)
Poor vision (or blindness)	22
Pain	17
Mass in iris or ciliary body	10
Leukocoria	10
Other pupillary abnormality	2

Exophthalmos (or orbital mass)	4
Enlarging globe	4
Strabismus	3
Epiphora	2
Change in color of eye	2
Hyphema	1

Reproduced with permission from Broughton WL, Zimmerman LE. A clinicopathologic study of 56 cases of intraocular medulloepitheliomas. Am J Ophthalmol 1978;85:407–18.

TABLE 158.2

Medulloepithelioma – Clinical Findings on Initial Examination

Clinical Finding	Cases (*n*)
Cyst or mass in iris, anterior chamber, or ciliary body	30
Proptosis or orbital mass	8
Retinal mass	2
Glaucoma	26
Cataract	14
Buphthalmos	6
Iritis	4
Rubeosis	3
Retinal detachment	3
Strabismus	3
Vitreous hemorrhage	1
Hyphema	1

Reproduced with permission from Broughton WL, Zimmerman LE. A clinicopathologic study of 56 cases of intraocular medulloepitheliomas. Am J Ophthalmol 1978;85:407–18.

One remarkable feature of medulloepitheliomas is the frequent presence of cysts, which are formed by the production of mucopolysaccharide by the epithelial cells. These cysts can be present within the body of the tumor but also may be free-floating in the anterior or posterior chamber and vitreous (Figs. 158.1–158.4). The presence of vitreous or anterior chamber cysts should alert the clinician to consider the possibility of a diagnosis of medulloepithelioma, although vitreous cysts have also been described with malignant melanoma.[8]

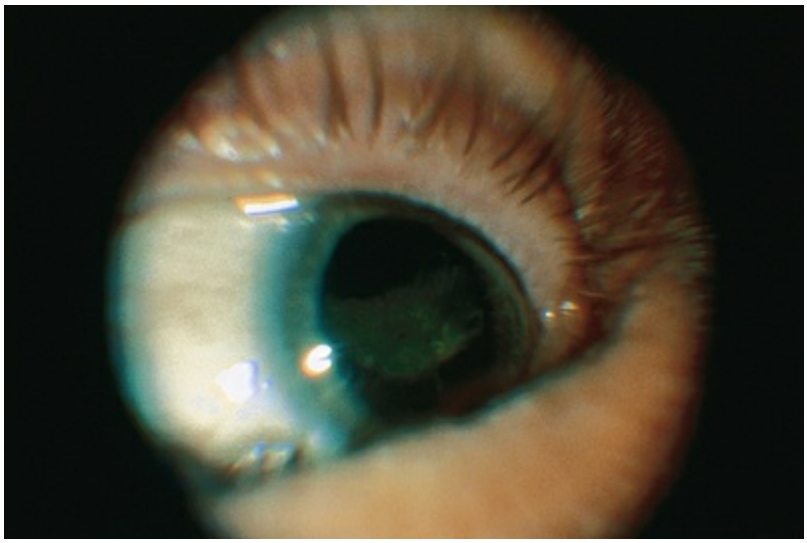

FIG. 158.1 External photograph showing ciliary body mass. (Case presented by Milton Boniuk, Verhoeff Society, 1997.)

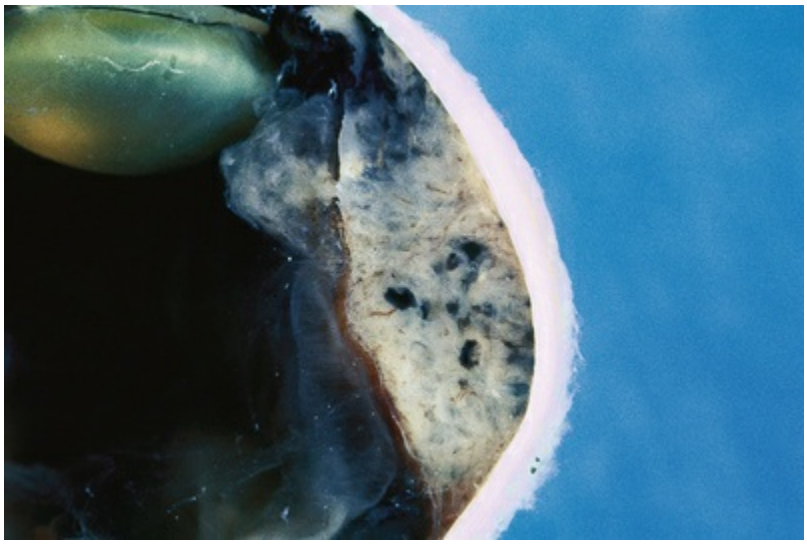

FIG. 158.2 Gross appearance of medulloepithelioma demonstrating ciliary body mass and cysts in the posterior chamber. (Case presented by Milton Boniuk, Verhoeff Society, 1997.)

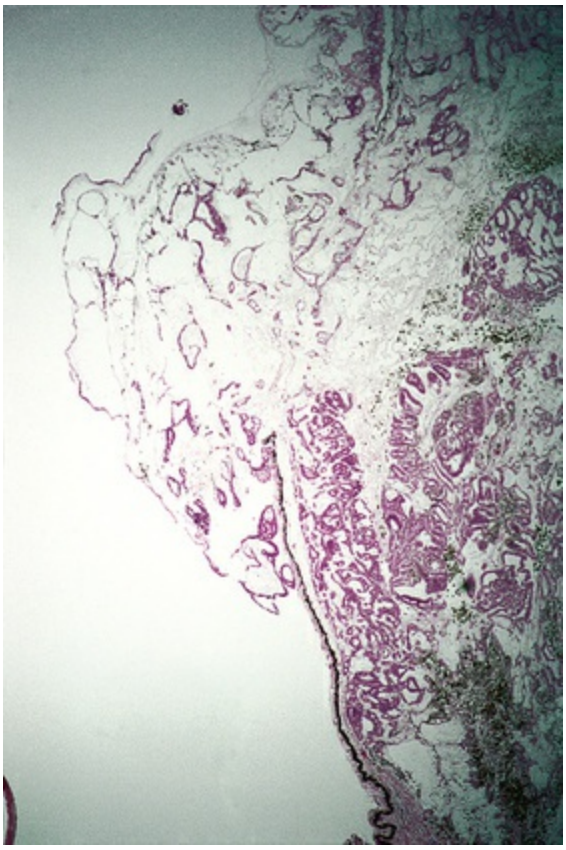

FIG. 158.3 Histopathology showing epithelial nature of the tumor with cysts formed by epithelium surrounding mucopolysaccharide-filled spaces (hematoxylin and eosin; ×100).

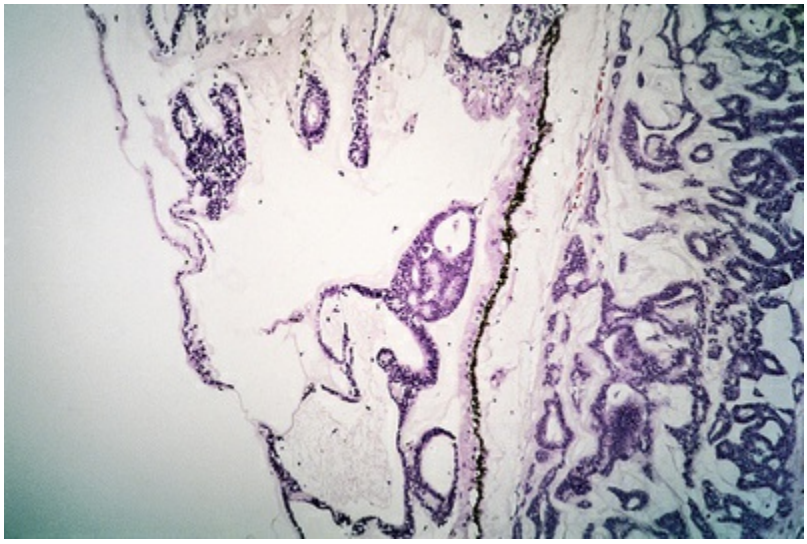

FIG. 158.4 Histopathology demonstrating cystic spaces overlying ciliary body epithelium (hematoxylin and eosin; ×400).

Another noteworthy feature of medulloepithelioma is that the intraocular pressure is frequently elevated at the time of diagnosis (see Table 158.2). This may result from secondary angle closure by the ciliary body mass, iris neovascularization, or growth of tumor cells across the trabecular meshwork. Medulloepitheliomas also have an unusual tendency to produce a retrolental neoplastic cyclitic membrane, which extends from the tumor, and is speculated to represent tissue migration over the anterior hyaloid.[7]

Medulloepitheliomas usually contain, as their most significant component, sheets and cords of poorly differentiated neuroepithelial tissue. The cellular cords may line cystic spaces filled with acid mucopolysaccharide. Homer Wright and Flexner–Wintersteiner rosettes may be present, but more commonly the rosettes in medulloepithelioma are larger than those seen in retinoblastoma. Typically, the lumina of the rosettes are surrounded by multiple cell layers, which resemble primitive ciliary epithelium, rather than photoreceptors.

In addition to the neuroepithelial tissue, medulloepitheliomas may contain heteroplastic tissues, in which case they are called teratoid medulloepitheliomas. Hyaline cartilage, striated muscle, undifferentiated mesenchymal cells, and neurologic tissue resembling the brain have all been described in teratoid medulloepitheliomas.

Medulloepitheliomas may be benign or malignant. Broughton and Zimmerman[5] considered 66% of the tumors in their series to be malignant. Andersen,[4] using more stringent criteria, classified 26% of the tumors in his series as malignant. From a practical point of view, even cytologically benign medulloepitheliomas can be locally invasive, extending into the iris, cornea, sclera, or orbit. For that reason all medulloepitheliomas should be considered as potentially malignant tumors, as recommended by Andersen.[4]

The initial treatment in most cases has been surgical – iridectomy, iridocyclectomy, partial sclerouvectomy or enucleation – and with total excision, the prognosis is excellent. Treatment success with radiation therapy has also been reported.[9,10] Canning et al.[6] have stressed the importance of attempting local resection (i.e., iridocyclectomy) only in patients with very small tumors. Of the four patients in their series who were treated by iridocyclectomy,

all subsequently required enucleation. A total of 45 (80%) of the patients in Broughton and Zimmerman's series[5] treated by iridocyclectomy subsequently required enucleation.

In both Broughton and Zimmerman's[5] and Anderson's[4] series of patients, the most important prognostic factor for survival appeared to be extension of tumor into the orbit. In Broughton and Zimmerman's series,[5] 11 patients had extraocular extension; of this group, four died of tumor-related causes. Intracranial spread of tumor was the usual cause of death, although one patient died of lymphatic spread to the mediastinum. The effectiveness of exenteration, radiation therapy, or chemotherapy – used individually or in combination – in managing extraocular extension is not established at this time. Such methods should be considered in cases with extrascleral extension because of the high tumor-related morbidity and mortality in this group of patients.

Glioneuroma

Glioneuromas are choristomatous malformations that arise from the medullary epithelium of the anterior portion of the optic cup. They are extremely rare, and only a few cases have been reported.[11–15]

Glioneuromas usually appear as a mass involving the peripheral iris and ciliary body and are usually evident within the first 6 months of life. The tumor may involve the choroid and the retina, and extraocular extension has been described. Associated ocular abnormalities are frequently present and have included persistent hyperplastic primary vitreous in the same or contralateral eye and coloboma of the iris and ciliary body. Progressive enlargement of the tumor may lead to corneal opacification, cataract, or glaucoma.

These tumors are composed of well-differentiated neural tissue, including neurons and astrocytes. All the reported cases[11–15] have eventually required enucleation because of complications of the enlarging tumor or suspected malignancy. Because this is a benign tumor, it could conceivably be managed by local resection.

Astrocytoma

Only three cases of astrocytoma of the ciliary body have been

reported.[16–18] Patients were 24 years, 52 years, and 29 years old at presentation. All three had solid tumors of the ciliary body, and in one patient the astrocytoma was associated with neovascular glaucoma. These tumors may be choristomas of the anterior portion of the optic cup. Two consisted of pilocytic astrocytes and the other of fibrillary astrocytes. All tumors were treated by local resection. Interestingly, in the patient with neovascular glaucoma, the rubeosis was observed to diminish after removal of the tumor.

Epithelial Tumors of the Ciliary Body: Acquired

Pseudoadenomatous Hyperplasia: Reactive

Hyperplasia of the ciliary epithelium may occur as a nonspecific response to trauma or inflammation. The hyperplastic tissue is primarily composed of nonpigmented ciliary body epithelium but may contain pigmented ciliary epithelium and blood vessels. Rarely, reactive hyperplasia may result in a mass that could be confused with a ciliary body neoplasm. More commonly, the hyperplastic tissue forms in sheets or as a cyclitic membrane.

Senile Hyperplasia

Senile hyperplasia (Fuchs adenoma) is a benign condition. These lesions are typically white in color and are located in the pars plicata. They consist of sheets and tubules of hyperplastic nonpigmented ciliary body epithelium, with alternating areas of material that is like basement membrane. The frequency with which Fuchs adenoma is seen increases with age, and this tumor may be observed in approximately 20% of postmortem eyes. These lesions are significant because, when noted through gonioscopy, cycloscopy, or ultrasonography, they may be confused with malignant lesions.[19,20] Fuchs adenomas can cause a sectoral cataract.[19] These lesions are almost always <2 mm in size, but rarely can grow larger. The authors recently performed iridocyclectomy

on a 52-year-old man for a pigmented ciliary body tumor of nearly 3 mm in thickness suspected to be a small melanoma, and found it was a Fuchs adenoma (unpublished observation). In unusual cases with diagnostic uncertainty and concern for melanoma, iridocyclectomy can be performed, but Fuchs adenomas require no treatment.

Adenomas and Adenocarcinomas

Adenomas and adenocarcinomas have been described by various names, including benign and malignant epitheliomas and adult medulloepitheliomas.[21] Adenomas and adenocarcinomas of the ciliary epithelium appear as solid tumors of the ciliary body. In Andersen's review of 30 of these cases, the presenting symptom was an observed mass in nine cases and decreased visual acuity in eight cases.[4] Other manifestations included glaucoma, cataract, pain, and proptosis. The average age of the patients with adenomas at the time of enucleation was 43 years. For the patients with adenocarcinomas, the average age at the time of enucleation was 55 years. It is noteworthy that several of the reported adenocarcinomas were present in blind eyes involving a previous history of trauma, suggesting that the adenocarcinomas may have represented malignant transformation of reactive hyperplasia of the ciliary epithelium.

The pathologic basis of these tumors has been more thoroughly described elsewhere.[7] Briefly, the adenomas consist of cuboidal or columnar cells resembling the nonpigmented or pigmented ciliary epithelium. These cells may have a tubular or papillary arrangement and may be closely packed or enmeshed in a mucoid material.[22] The malignant lesions may be well differentiated, in which case they resemble the adenomas but have more cytologic features of malignancy. The poorly differentiated lesions are more pleomorphic and may resemble a metastatic adenocarcinoma or even a sarcoma.[21,23]

Because these lesions cannot be reliably differentiated from melanomas, they are usually treated by enucleation or brachytherapy. It is evident that extraocular extension is an important factor in prognosis.[4,23] Andersen reported two cases of

adenocarcinoma that had extended outside the globe at the time of enucleation.[4] Both of the patients developed intracranial extension of the tumor. Laver et al. reported on 12 cases of pleomorphic adenocarcinoma of the ciliary epithelium, nine of which occurred in phthisical eyes. Fatal cases occurred only in tumors with extraocular extension. They noted that clinically adenocarcinomas should be considered in adults who develop an epibulbar mass and/or proptosis in the setting of a long-standing blind eye.[23] The role of exenteration, radiation therapy, or chemotherapy in extraocular extension has not been defined.

Melanocytic Tumors

Melanocytoma

The term melanocytoma was first used by Zimmerman and Garron[24] to describe a benign pigmented tumor of the optic nerve. Other names that have been used to designate this same lesion include magnocellular nevus and benign melanoma. Melanocytomas of the optic nerve and peripapillary choroid are described in Chapter 140 (Congenital hypertrophy of the retinal pigment epithelium). Therefore only melanocytomas limited to the uvea are discussed here.

Uveal melanocytomas appear as very darkly pigmented tumors of the choroid, ciliary body, or iris (Fig. 158.5). Although they are probably congenital lesions, the age range at the time of presentation is not sufficiently different from that of malignant melanomas to be useful in differential diagnosis. In a review of ciliary body melanocytomas, Frangieh et al.[25] found that most of the reported cases have been in Caucasians. Therefore, unlike optic nerve melanocytomas, uveal melanocytomas do not occur predominantly in pigmented individuals. Distinguishing this benign tumor from malignant melanoma is further complicated by the ability of melanocytomas to undergo slow growth. Such slow growth may result in extension of the tumor through the sclera to the episclera. Also, melanocytomas may undergo necrosis, resulting in pigment dispersion, uveitis, and melanomalytic glaucoma.[26] Kathil et al. have described the clinical features of anterior uveal

melanocytomas that may be useful in distinguishing melanocytomas in the anterior segment from melanoma.[27]

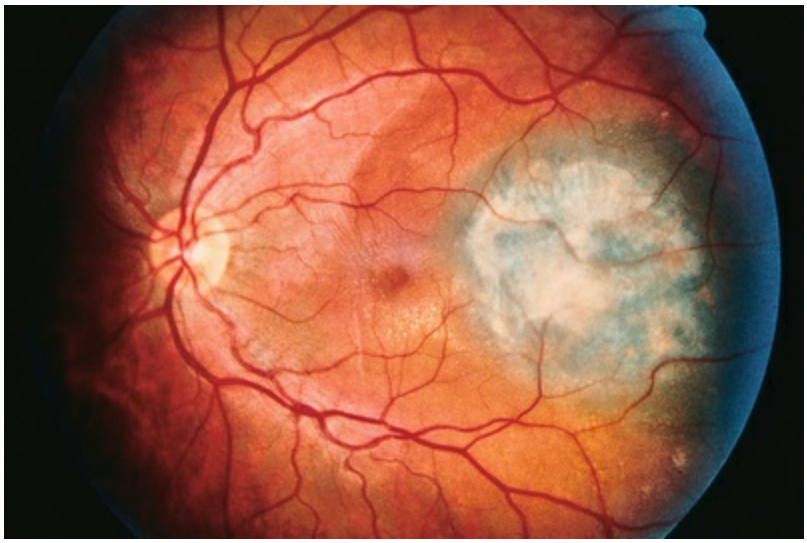

FIG. 158.5 Fundus photograph showing a choroidal melanocytoma.

Melanocytomas are composed of plump, polyhedral, densely pigmented cells, with small eccentrically placed nuclei that lack prominent nucleoli (Figs. 158.6 and 158.7). These cells are indistinguishable from the plump, polyhedral cells described by Naumann et al.[28] as the exclusive component in approximately 10% of choroidal nevi. Evidence that malignant melanomas may develop from uveal melanocytomas has been provided by cases in which melanomas were present and adjacent to lesions that were indistinguishable from melanocytomas.[29–31]

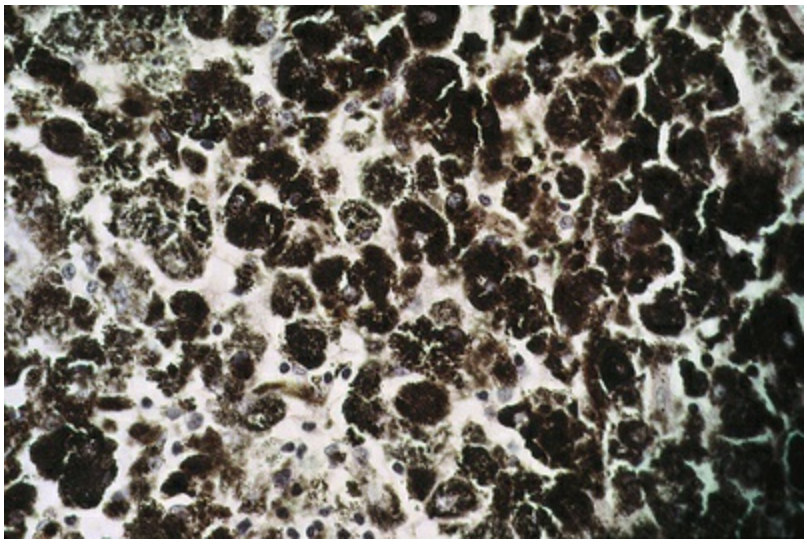

FIG. 158.6 Melanocytoma: the cells are characteristically darkly pigmented (hematoxylin and eosin; ×400).

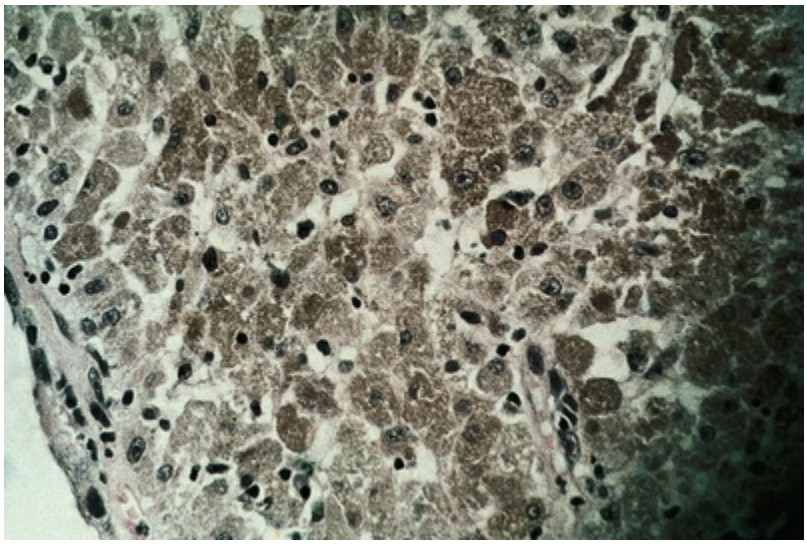

FIG. 158.7 Bleached sections demonstrate the bland peripherally located nucleus typical of melanocytoma (bleached sections; ×400).

Melanocytomas require no treatment, except for secondary complications. Because these tumors may have the potential for malignant transformation, they should be followed to document changes suggestive of malignancy. Ultrasound biomicroscopy can often be helpful in this setting. However, it may be impossible, on the basis of noninvasive studies, to differentiate melanomas from

enlarging melanocytomas, so some melanocytomas inevitably will be treated surgically.

Bilateral Diffuse Uveal Melanocytic Proliferation (BDUMP) Associated With Systemic Malignant Neoplasms

In 1982 Barr et al.[32] described a syndrome characterized by bilateral diffuse melanocytic tumors of the uvea in patients with nonocular malignancy. This condition was originally reported by Machemer[33] and has been recently reviewed by Satio et al.[34] Gass et al.[35] summarized the clinical features of this syndrome, which are (1) multiple, round or oval, red-to-brown patches at the level of the retinal pigment epithelium in the posterior fundus; (2) a striking fluorescein angiographic pattern of early hyperfluorescence corresponding with these patches; (3) development of multiple, elevated, variably pigmented uveal melanocytic tumors and diffuse thickening of the uveal tract; (4) exudative retinal detachment; and (5) rapid progression of cataract.

Patients with this syndrome have had various nonocular malignancies, including adenocarcinomas of the gallbladder, ovary, colon, or pancreas, and squamous cell carcinoma of the lung and cervix. Most patients with this syndrome have died within 12–24 months after diagnosis, but long-term survival has been reported.

Histopathologic study of the uvea in patients with this syndrome has disclosed uveal melanocytic tumors. The cytologic features of the tumors are variable, with most of the cells having benign cytologic features. However, cytologic features of malignancy have been present in several cases,[32,36] although no metastatic disease has been documented. Recently, Miles et al. have shown that the serum from patients with BDUMP contains a factor that promotes melanocyte proliferation, suggesting this may be the etiology of the benign melanocytic proliferation that is the hallmark of this condition.[37]

Neurogenic Tumors

Schwannomas (Neurilemmomas)

Choroidal and ciliary body schwannomas are rare benign tumors that can be mistaken for amelanotic uveal melanomas.[38–40] The majority of these tumors arise as an isolated condition, but may be associated with multisystem disorders, such as neurofibromatosis and the Carney complex.[40] The clinical presentation of these tumors is that of a solid ciliary body or choroidal tumor. Although cytologically benign, they may progressively enlarge at a rate similar to, or greater than, that of choroidal melanomas. In the case studied by Shields et al.,[38] preoperative ultrasound demonstrated acoustic hollowness, choroidal excavation, and low internal reflectivity. These findings are identical to those of choroidal melanoma. In two subsequently reported cases of anterior uveal schwannomas, the tumors were noted to transilluminate brightly.[41,42] This may be a helpful clinical finding because it is unusual for anterior uveal melanomas to transilluminate in this way. With increased suspicion, fine-needle biopsy and local resection may be considered.

Schwannomas arise from ciliary nerves in the uvea and are encapsulated tumors consisting of a pure proliferation of Schwann cells. The cells in these tumors are characteristically arranged as either solid sheets of cells (Antoni A pattern) or stellate-to-ovoid cells in a mucinous background (Antoni B pattern).

Because these tumors are cytologically benign, they require treatment only to prevent visual loss resulting from their progressive enlargement. Unfortunately, as with many primary uveal tumors, it is difficult to distinguish schwannomas from amelanotic malignant melanomas.

In the case reported by Shields et al.,[38] there was no clinical or histologic evidence that the tumor was responsive to radiation therapy. Damato et al. advocate diagnostic biopsy for smooth, amelanotic tumors, with local resection as the treatment of choice for confirmed cases of schwannoma. Photodynamic therapy may be an option for unresectable lesions.[40]

Neurofibroma

Unlike schwannomas, uveal neurofibromas are highly associated

with neurofibromatosis. Choroidal neurofibromas are diffuse lesions and appear as diffuse thickening of the choroid, sometimes with an overlying sensory retinal detachment.[43]

Neurofibromas are nonencapsulated lesions composed of Schwann cells, axons, and fibroblasts. An increase in the number of dendritic uveal melanocytes may be present, simulating congenital melanosis oculi. No treatment is required except to manage vision-threatening complications. (Additional material on neurofibromas may be found in Chapter 138, Remote effects of cancer on the retina.)

Granular Cell Tumor

The cell type from which granular cell tumors originate is not definitely known; these tumors have features suggestive of a myogenic or neuroectodermal origin. A single case of granular cell tumor, involving the iris and ciliary body of a 24-year-old woman, has been reported.[44] The tumor was partially excised, but 1 year after treatment no enlargement of the remaining tumor was reported. Other cases of intraocular granular cell tumor have not been reported.

Myogenic Tumors

Leiomyoma

Leiomyomas are rare intraocular tumors that appear as a solid mass of the ciliary body or, less commonly, the choroid (Fig. 158.8). As with other solid tumors in these locations, they may cause secondary cataract, glaucoma, and retinal detachment. These tumors arise in younger patients and demonstrate a predilection for women.[45] Leiomyomas arise from the smooth muscle of the ciliary body. In the choroid they probably arise from the smooth muscle or pericytes of the choroidal vessels. They are composed of densely packed, nonpigmented, spindle-shaped cells with oval nuclei (Fig. 158.9). This histologic feature correlates with the very low internal reflectivity seen on A-scan echography of these lesions (Fig. 158.10). It is difficult to differentiate these tumors from amelanotic spindle

melanomas solely on the basis of light microscopic features. Immunohistochemical stains and ultrastructural evaluation (Fig. 158.10) are essential in making this distinction.

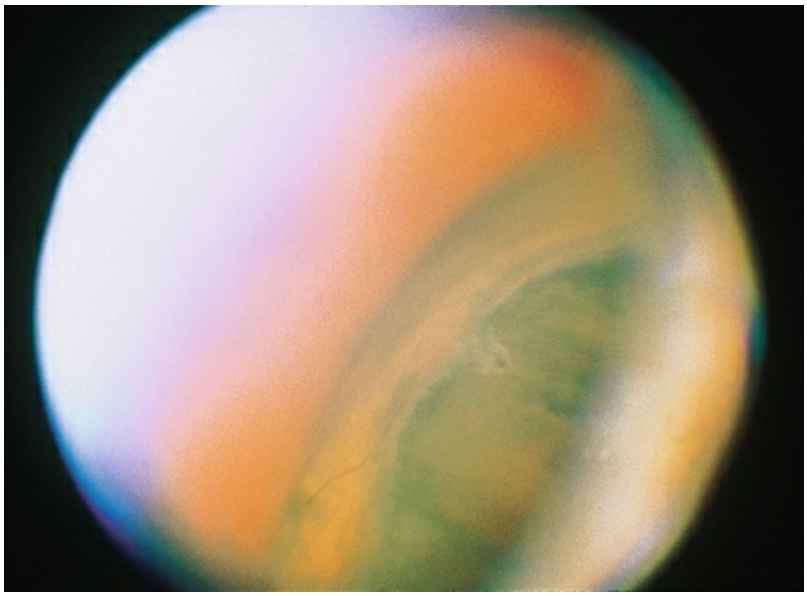

FIG. 158.8 Clinical photograph of ciliary body leiomyoma.

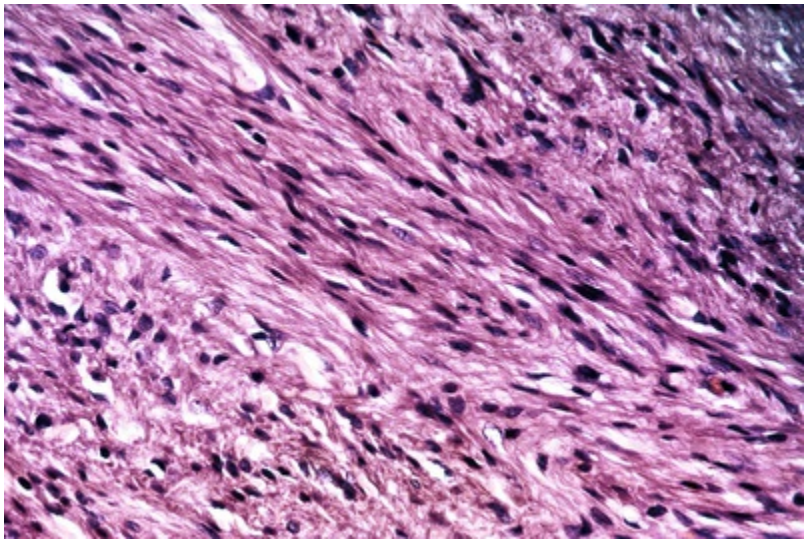

FIG. 158.9 Leiomyoma: the tumor is composed of typical smooth muscle cells with indistinct cell borders and spindle-shaped nuclei (hematoxylin and eosin; ×400).

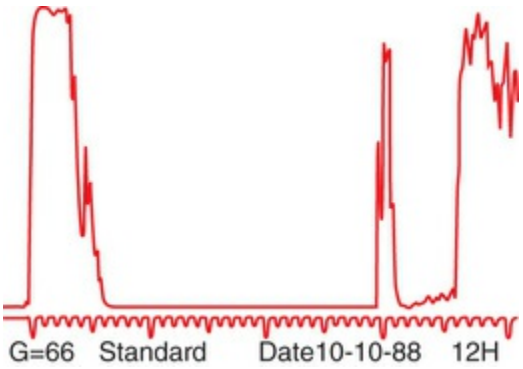

FIG. 158.10 A-scan echography reveals very low reflectivity of the tumor.

Clinically, it is very difficult to differentiate leiomyomas from malignant melanomas. As a result, leiomyomas are usually clinically diagnosed and treated as malignant melanomas. The Shields group has noted that leiomyomas of the ciliary body demonstrate increased transillumination, similar to schwannomas.[46] This feature may allow clinical distinction of this tumor from ciliary body melanomas, which generally do not transilluminate in this way. If the diagnosis is established clinically (e.g., by fine-needle biopsy), treatment should consist of managing the secondary complications of this benign tumor.

Mesectodermal Leiomyoma

Mesectodermal leiomyoma has been used to describe a benign tumor of the ciliary body that has histologic and ultrastructural features of both smooth muscle and neural tissue (Fig. 158.11).[46–48] The peculiar combination of features in this tumor may be explained by the embryologic origin of the ciliary body smooth muscle from the neural crest. The designation mesectodermal leiomyoma should be reserved for tumors that have light or electron microscopic evidence of neurogenic tumors.

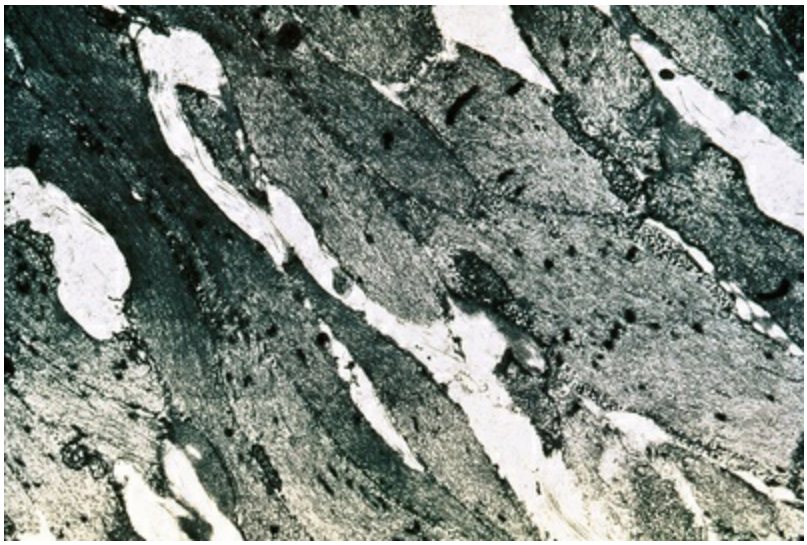

FIG. 158.11 Transmission electron microscopy reveals the *Z* bands typical of smooth muscle.

Miscellaneous

Reactive Lymphoid Hyperplasia and Lymphoma

Lymphocytic tumors may involve the eye in myriad ways. Reactive lymphoid hyperplasia and lymphoma may both present as choroidal tumors (Figs. 158.12 and 158.13). Choroidal tumors due to lymphocytic infiltration tend to have a more irregular contour to the base of the tumor and often extend in a more circumferential fashion than is typical of melanocytic or neurogenic tumors of the choroid. In some cases there will be simultaneous involvement of the orbit or ocular adnexa. Lymphocytic tumors presenting in this fashion can represent isolated extranodal lymphoma (primary uveal lymphoma) or may be present in association with lymphoma at other sites (secondary lymphoma). Enhanced-depth optical coherence tomography can be helpful in diagnosis, with choroidal lymphoma demonstrating a characteristic "placid, rippled, or seasick" surface, correlating with increasing tumor thickness.[49] Definitive diagnosis requires incisional biopsy (Fig. 158.14), but may not be necessary if systemic workup reveals extraocular involvement that can be more easily biopsied to establish a diagnosis of systemic lymphoma. Patients with lymphoma should

undergo staging and treatment appropriate to the type and extent of lymphoma.

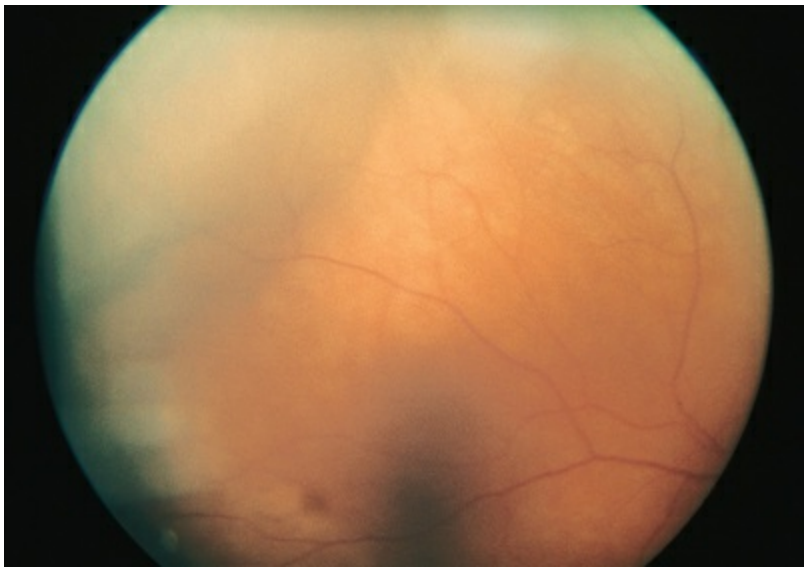

FIG. 158.12 Uveal lymphoma: peripheral choroidal mass with the clinical appearance of choroidal detachment.

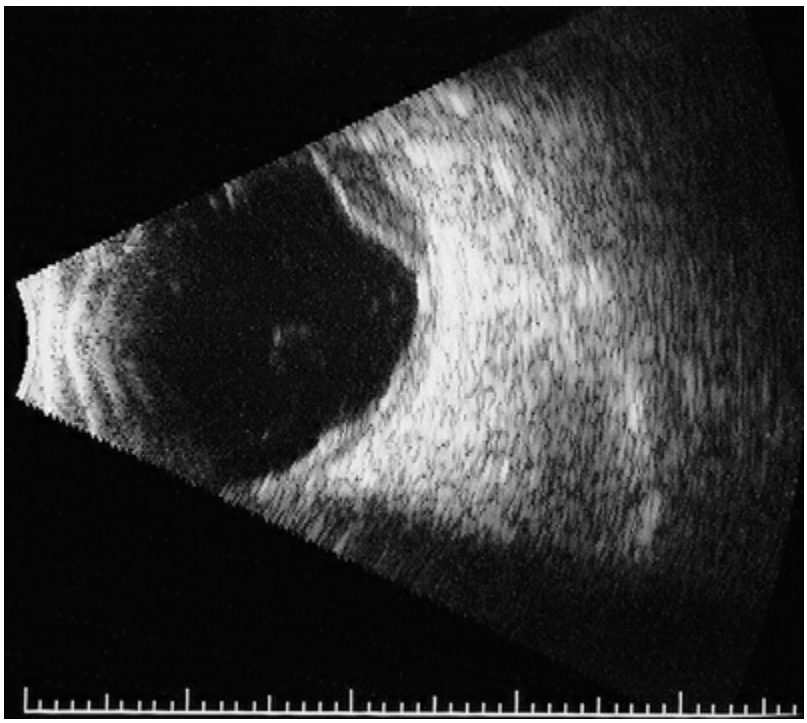

FIG. 158.13 B-scan echography reveals the solid nature of the tumor.

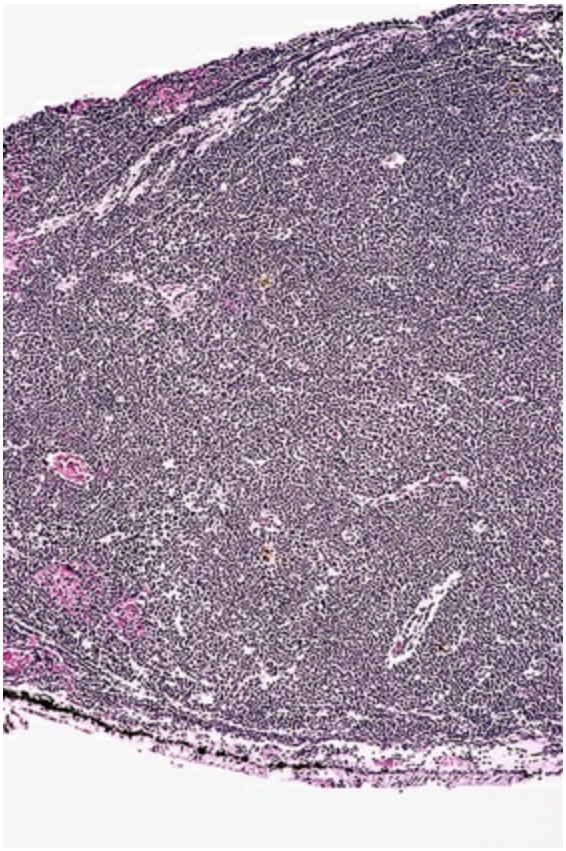

FIG. 158.14 Ciliary body biopsy reveals a diffuse infiltrate of mature-appearing small lymphocytes (hematoxylin and eosin; ×200).

Juvenile Xanthogranuloma

Juvenile xanthogranuloma is a benign cutaneous disorder that typically affects young children. Zimmerman described the characteristic features of eye involvement associated with juvenile xanthogranuloma as (1) an asymptomatic localized or diffuse iris tumor, (2) unilateral glaucoma, (3) spontaneous hyphema, (4) a red eye with signs of uveitis, or (5) congenital or acquired heterochromia iridis.[50] The iris and ciliary body are most commonly the sites of intraocular involvement with this condition, but there have been case reports describing prominent involvement of the choroid, retina, and optic nerve.[51,52]

Langerhans Cell Histiocytosis

Rarely, Langerhans cell histiocytosis [53] may present as a choroidal mass lesion without other orbital or systemic involvement.[54] Langerhans cell histiocytosis occurs as the result of a clonal expansion of Langerhans cells. This monocytic cell type is an antigen-presenting cell, and it is unclear why a clonal expansion of this cell type might occur in the choroid. Involvement of the orbit, bones, or lungs is much more common.

Hemangiopericytoma

Uveal hemangiopericytoma is an extremely rare neoplasm.[55–57] The clinical features of these tumors are similar to those of uveal melanomas, including the frequent presence of a sentinel vessel in cases of ciliary body hemangiopericytomas. In one of the reported cases of hemangiopericytoma the magnetic resonance signal characteristics of the tumor were different from those of choroidal melanomas.[19] The authors suggested that magnetic resonance imaging may provide a mechanism for distinction of this rare tumor from uveal melanoma.

Hemangiopericytomas may be benign or malignant. Complete surgical resection is the treatment of choice in either case.

Rhabdomyosarcoma

A remarkable case of rhabdomyosarcoma of the ciliary body in a 12-year-old boy has been reported.[58] It is possible that this case represents the one-sided or complete differentiation of a teratoid medulloepithelioma along the line of a rhabdomyosarcoma. At the last reported follow-up examination (2 years after enucleation), the child was alive without evidence of metastasis or local recurrence. Three additional cases of primary rhabdomyosarcoma of the iris have been reported.[58–61]

The Role of Diagnostic Biopsy for Uveal Tumors

Given the variety of rare lesions that occur in the uvea, often masquerading as more common clinical entities, it is useful to consider when a biopsy might be helpful diagnostically. The techniques and indications for biopsy have been reported by Lim et al.[62] Briefly, biopsy might be considered in anterior uveal tumors, particularly if they fail to block transillumination. Patients with current or past history of systemic diseases that are associated with choroidal tumors should also be considered for biopsy. Atypical amelanotic choroidal lesions can also be considered for diagnostic biopsy. Ciliary body and/or choroidal biopsy may be performed from an external approach, and choroidal lesions may also be biopsied using vitrectomy techniques. Fine-needle aspiration biopsies are sufficient for diagnosis in many cases, but incisional biopsy may be required. Such biopsies can generally be obtained with minimal morbidity. In a child, retinoblastoma must be eliminated as a diagnostic possibility prior to biopsy of an intraocular mass due to risk of orbital seeding of tumor. In adults, fine-needle aspiration biopsy is now commonly practiced and in cases of uveal melanoma associated with a very low risk of orbital spread of disease, but it is best performed by experts in intraocular tumor care.[63]

Conclusion

A great variety of lesions, both benign and malignant, may appear as tumors of the ciliary body and choroid. It is often difficult to distinguish benign from malignant tumors clinically, but documentation of growth may prevent unnecessary treatment of some of the benign tumors such as Fuchs adenoma and astrocytoma. Knowledge of associated ocular and systemic conditions is also helpful in the recognition of some of these tumors, including medulloepithelioma, glioneuroma, reactive pseudoadenomatous hyperplasia, and neurofibroma. Nonetheless, many of these rare tumors do not have adequate epidemiologic or clinical characteristics to allow preoperative distinction from malignant melanomas. The safety and efficacy of fine-needle biopsy as an aid in differential diagnosis has been established in recent years and may allow characterization of some tumors before

definitive treatment is planned.[64–67]

References

1. Verhoeff FH. A rare tumor arising from the pars ciliaris retinae (teratoneuroma) of a nature hitherto unrecognized and its relation to the so-called glioma retinae. *Trans Am Ophthalmol Soc*. 1904;10:351–377.
2. Fuchs E. Wucherungen und Geschwulste des Ziliarepithels. *Graefes Arch Klin Exp Ophthalmol*. 1908;68:534–558.
3. Grinker RR. Gliomas of the retina, including the results of studies with silver impregnations. *Arch Ophthalmol*. 1931;5:920–935.
4. Andersen SR. Medulloepithelioma of the retina. *Int Ophthalmol Clin*. 1962;2:483–506.
5. Broughton WL, Zimmerman LE. A clinicopathologic study of 56 cases of intraocular medulloepitheliomas. *Am J Ophthalmol*. 1978;85:407–418.
6. Canning CR, McCartney AC, Hungerford J. Medulloepithelioma (diktyoma). *Br J Ophthalmol*. 1988;72:764–767.
7. Kaliki S, Shields CL, Eagle RC, et al. Ciliary body medulloepithelioma. *Ophthalmology*. 2013;120:2552–2559.
8. Green WR. Neuroepithelial tumors of the ciliary body. WB Saunders: Philadelphia; 1985. Spencer WH. *Ophthalmic pathology: an atlas and textbook*. vol. 2.
9. Davidorf FH, Craig E, Birnbaum L, et al. Management of medulloepithelioma of the ciliary body with brachytherapy. *Am J Ophthalmol*. 2002;133:841–843.
10. Poon DS, Reich E, Smith VM, et al. Ruthenium-106 plaque brachytherapy in the primary management of ocular medulloepithelioma. *Ophthalmology*. 2015;122(9):1949–1951.
11. Addison DJ. *Glioneuroma of the ciliary body and iris in a 2-year-old girl*. [Seventh biennial meeting of the Association of Ophthalmic Alumni, Washington, DC, June 1977.] Armed Forces Institute of Pathology: Washington DC; 1977.
12. Kivela T, Kauniskangas L, Miettinen P, et al. Glioneuroma associated with colobomatous dysplasia of the anterior

uvea and retina: a case simulating medulloepithelioma. *Ophthalmology*. 1989;96:1799–1808.
13. Kuhlenbeck H, Haymaker W. Neuroectodermal tumors containing neoplastic neuronal elements: ganglioneuroma, spongioneuroblastoma, and glioneuroma. *Mil Surg*. 1946;99:273–304.
14. Manz HJ, Rosen DA, Macklin RD, et al. Neuroectodermal tumor of anterior lip of the optic cup: glioneuroma transitional to teratoid medullo-epithelioma. *Arch Ophthalmol*. 1973;89:382–386.
15. Spencer WH, Jesberg DO. Glioneuroma (choristomatous malformation of the optic cup margin): a report of two cases. *Arch Ophthalmol*. 1973;89:387–391.
16. Farber MG, Smith ME, Gans LA. Astrocytoma of the ciliary body. *Arch Ophthalmol*. 1987;105:536–537.
17. Naeser P, Moller P. Astrocytoma of the ciliary body: a clinico-pathological case report. *Acta Ophthalmol*. 1985;63:28–30.
18. Mei H, Xing Y, Yang A, et al. Astrocytoma of the ciliary body. *Ophthalmologica*. 2009;223:72–74.
19. Bateman JB, Foos RY. Coronal adenomas. *Arch Ophthalmol*. 1979;97:2379–2384.
20. Iliff WJ, Green WR. The incidence and histology of Fuchs' adenoma. *Arch Ophthalmol*. 1972;88:249–254.
21. Shields JA, Eagle RC, Shields CL, et al. Acquired neoplasms of the nonpigmented ciliary epithelium (adenoma and adenocarcinoma). *Ophthalmology*. 1996;103:2007–2016.
22. Grossniklaus HE, Lim JI. Adenoma of the nonpigmented ciliary epithelium. *Retina*. 1994;14:452–456.
23. Laver NM, Hidayat AA, Croxatto J. Pleomorphic adenocarcinoma of the ciliary epithelium: immunohistochemical and ultrastructural features of 12 cases. *Ophthalmology*. 1999;106:103–110.
24. Zimmerman LE, Garron LK. Melanocytoma of the optic disc. *Int Ophthalmol Clin*. 1962;2:431–440.
25. Frangieh GT, El Baba F, Traboulsi EL, et al. Melanocytoma of the ciliary body: presentation of four cases and review of nineteen reports. *Surv Ophthalmol*. 1985;29:328–334.

26. LoRusso FJ, Boniuk M, Font RL. Melanocytoma (magnocellular nevus) of the ciliary body: report of 10 cases and review of the literature. *Ophthalmology*. 2000;107(4):795–800.
27. Kathil P, Milman T, Finger PT. Characteristics of anterior uveal melanocytomas in 17 cases. *Ophthalmology*. 2011;118:1874–1880.
28. Naumann G, Yanoff M, Zimmerman LE. Histogenesis of malignant melanomas of the uvea. I. Histopathologic characteristics of nevi of the choroid and ciliary body. *Arch Ophthalmol*. 1966;76:784–796.
29. Baker-Griffith AE, McDonald PR, Green WR. Malignant melanoma arising in a choroidal magnacellular nevus (melanocytoma). *Can J Ophthalmol*. 1976;11:140–146.
30. Heitman KF, Kincaid MC, Steahly L. Diffuse malignant change in a ciliochoroidal melanocytoma in a patient of mixed racial background. *Retina*. 1988;8:67–72.
31. Thomas CI, Purnell EW. Ocular melanocytoma. *Am J Ophthalmol*. 1969;67:79–86.
32. Barr CC, Zimmerman LE, Curtin VT, et al. Bilateral diffuse uveal tumors associated with systemic malignant neoplasms: a recently recognized syndrome. *Arch Ophthalmol*. 1982;100:249–255.
33. Machemer R. Zur Pathogenese des flachenhaften malignen Melanomas. *Klin Monatsbl Augenheilkd*. 1966;148:641–652.
34. Saito W, Kase S, Yoshida K, et al. Bilateral diffuse uveal melanocytic proliferation in a patient with cancer-associated retinopathy. *Am J Ophthalmol*. 2005;140:942–945.
35. Gass JDM, Gieser RG, Wilkinson CP, et al. Bilateral diffuse uveal melanocytic proliferation in patients with occult carcinoma. *Arch Ophthalmol*. 1990;108:527–533.
36. Margo CE, Pavan PR, Gendelman D, et al. Bilateral melanocytic uveal tumors associated with systemic nonocular malignancy. *Retina*. 1987;7:137–141.
37. Miles SL, Niles RM, Pittock S, et al. A factor found in the IgG fraction of serum of patients with paraneoplastic bilateral diffuse uveal melanocytic proliferation causes proliferation of cultured human melanocytes. *Retina*. 2012;32:1959–1966.

38. Shields JA, Sanborn GE, Kurz GH, et al. Benign peripheral nerve tumor of the choroid: a clinicopathologic correlation and review of the literature. *Ophthalmology*. 1981;88:1322–1329.
39. You JY, Finger PT, Iacob C, et al. Intraocular schwannoma. *Surv Ophthalmol*. 2013;58:77–85.
40. Damato B, Damato EM, Konstantinidis L, et al. Choroidal schwannoma: a case series of five patients. *Br J Ophthalmol*. 2014;98:1096–1100.
41. Hufnagel TJ, Sears ML, Shapiro M, et al. Ciliary body neurilemoma recurring after 15 years. *Graefes Arch Clin Exp Ophthalmol*. 1988;226:443–446.
42. Smith PA, Damato BE, Ko MK, et al. Anterior uveal neurilemmoma: a rare neoplasm simulating malignant melanoma. *Br J Ophthalmol*. 1987;71:34–40.
43. Shields JA. *Diagnosis and management of intraocular tumors*. Mosby: St Louis; 1983.
44. Cunha SL, Lobo FG. Granular-cell myoblastoma of the anterior uvea. *Br J Ophthalmol*. 1966;50:99–101.
45. Shields JA, Shields CL, Eagle RC Jr, et al. Observations on seven cases of intraocular leiomyoma. The 1993 Byron Demorest Lecture. *Arch Ophthalmol*. 1994;112:521–528.
46. Shields JA, Shields CL, Eagle RC Jr. Mesectodermal leiomyoma of the ciliary body managed by partial lamellar iridocyclochoroidectomy. *Ophthalmology*. 1989;96:1369–1376.
47. Jakobiec FA, Font RL, Tso MOM, et al. Mesectodermal leiomyoma of the ciliary body: a tumor of presumed neural crest origin. *Cancer*. 1977;39:2102–2113.
48. White V, Stevenson K, Garner A, et al. Mesectodermal leiomyoma of the ciliary body: case report. *Br J Ophthalmol*. 1989;73:12–18.
49. Shields CL, Pellegrini M, Ferenczy SR, et al. Enhanced depth imaging optical coherence tomography of intraocular tumors: from placid to seasick to rock and rolling topography – the 2013 Francesco Orzalesi Lecture. *Retina*. 2014;34(8):1495–1512.
50. Zimmerman LE. Ocular lesions of juvenile xanthogranuloma: nevoxanthoendothelioma. *Trans Am*

Acad Ophthahnol Otolaryngol. 1965;69:412–442.
51. Wertz FD, Zimmerman LE, McKeown CA, et al. Juvenile xanthogranuloma of the optic nerve, disc, retina, and choroid. *Ophthalmology*. 1982;89:1331–1335.
52. DeBarge LR, Chan CC, Greenberg SC, et al. Chorioretinal, iris, and ciliary body infiltration by juvenile xanthogranuloma masquerading as uveitis. *Surv Ophthalmol*. 1994;39(1):65–71.
53. Margo CE, Goldman DR. Langerhans cell histiocytosis. *Surv Ophthalmol*. 2008;53:332–358.
54. Kim IT, Lee SM. Choroidal Langerhans' cell histiocytosis. *Acta Ophthalmol Scand*. 2000;78:97–100.
55. Brown HH, Brodsky MC, Hembree K, et al. Supraciliary hemangiopericytoma. *Ophthalmology*. 1991;98:378–382.
56. Gieser SC, Hufnagel TJ, Jaros PA, et al. Hemangiopericytoma of the ciliary body. *Arch Ophthalmol*. 1988;106:1269–1272.
57. Papale JJ, Frederick AR, Albert DM. Intraocular hemangiopericytoma. *Arch Ophthalmol*. 1983;101:1409–1411.
58. Wilson ME, McClatchey SK, Zimmerman LE. Rhabdomyosarcoma of the ciliary body. *Ophthalmology*. 1990;97:1484–1488.
59. Elsas FJ, Mroczek EC, Kelly DR, et al. Primary rhabdomyosarcoma of the iris. *Arch Ophthalmol*. 1991;109:982–984.
60. Naumann G, Font RL, Zimmerman LE. Electron microscopic verification of primary rhabdomyosarcoma of the iris. *Am J Ophthalmol*. 1972;74:110–117.
61. Woyke S, Chwirot R. Rhabdomyosarcoma of the iris. *Br J Ophthalmol*. 1972;56:60–64.
62. Lim LL, Suhler EB, Rosenbaum JT, et al. The role of choroidal and retinal biopsies in the diagnosis and management of atypical presentations of uveitis. *Trans Ann Ophthalmol Soc*. 2005;103:84–95.
63. Singh AD, Biscotti CV. Fine needle aspiration biopsy of ophthalmic tumors. *Saudi J Ophthalmol.*2012;26:117–123.
64. Schefler AC, Gologorsky D, Marr BP, et al. Extraocular extension of uveal melanoma after fine-needle aspiration,

vitrectomy, and open biopsy. *JAMA Ophthalmol*. 2013;131:1220–1224.
65. Augsburger JJ. Diagnostic biopsy of selected intraocular tumors. *Am J Ophthalmol*. 2005;140(6):1094–1095.
66. Shields CL, Ganguly A, Materin MA, et al. Chromosome 3 analysis of uveal melanoma using fine-needle aspiration biopsy at the time of plaque radiotherapy in 140 consecutive cases: the Deborah Iverson, MD, Lectureship. *Arch Ophthalmol*. 2007;125(8):1017–1024.
67. Onken MD, Worley LA, Char DH, et al. Collaborative Ocular Oncology Group report number 1: prospective validation of a multi-gene prognostic assay in uveal melanoma. *Ophthalmology*. 2012;119:1596–1603.

159

Leukemias and Lymphomas

Diana V. Do, Ranjit S. Dhaliwal, Andrew P. Schachat

Introduction

Leukemias and lymphomas are myeloproliferative disorders that may affect the eye. Occasionally, the ophthalmic symptoms and findings can be the initial manifestation of the systemic illness.[1,2]

Estimates of the frequency of intraocular involvement with leukemia range as high as 90% of cases.[1,3] Although melanoma is the most common primary intraocular tumor in adults and retinoblastoma is the most common primary intraocular tumor in children, when secondary or metastatic neoplastic intraocular disease is considered, intraocular manifestations of hematologic malignancies are found to be overwhelmingly more common since the prevalence of myeloproliferative disorders is higher in the general population.

Liebreich first described leukemic retinopathy in the 1860s. Since that time, reports have documented that virtually all intraocular structures may be involved. Patients have been reported with leukemic infiltrates of the optic nerve, choroid, retina, iris, ciliary body, and anterior chamber. In addition, leukemic involvement may present as a serous retinal detachment.[4] A child with a leukemic hypopyon is illustrated in Fig. 159.1. Central serous chorioretinopathy overlying areas of choroidal infiltration has been reported, as has retinal vascular sheathing, subconjunctival

hemorrhage, anterior chamber hemorrhage, intraretinal hemorrhage, and intravitreal hemorrhage.[5] Retinal changes may be related to direct invasion of tissue by neoplastic cells; to manifestations of associated hematologic abnormalities such as anemia, thrombocytopenia, or hyperviscosity states; to opportunistic infections; or to unrelated chance findings.

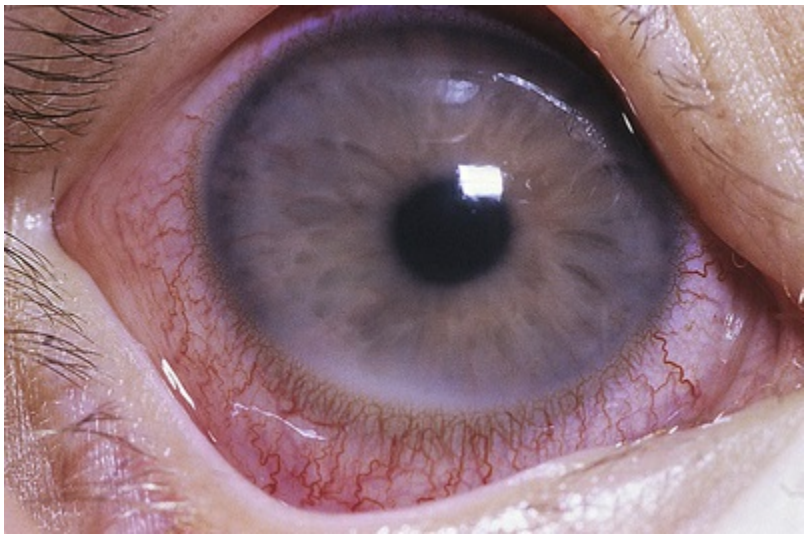

FIG. 159.1 Leukemic iris infiltration in a child with acute lymphocytic leukemia. Note hypopyon inferiorly.

Intraocular infiltrates appear to correlate with associated central nervous system (CNS) involvement and decreased survival. The intraocular manifestations of leukemia are protean, and clinically, it usually is not possible to differentiate the various leukemias and lymphomas on the sole basis of their ophthalmoscopic findings.[6]

Systemic Classification of Leukemia and Lymphoma

In general, the leukemias and lymphomas can be classified according to their cell of origin. Some examples of the neoplasias of B-cell origin include chronic lymphocytic leukemia, small-cell (well-differentiated) lymphocytic lymphoma, Burkitt lymphoma, and acute lymphocytic leukemia. Neoplasias that appear to have T-cell origin include chronic lymphocytic leukemia, mycosis fungoides, T-

cell leukemia, and angiocentric lymphoma. Reticulum cell- or histiocytic-derived neoplasias include malignant histiocytosis, the various monocytic leukemias, and Hodgkin disease.

At presentation, the acute leukemias most often have systemic manifestations of anemia, hemorrhage, infection, or signs and symptoms related to infiltration of organs. Acute lymphocytic leukemia is the predominant leukemia type in children, and more than 50% of these patients can be cured. In adults, acute myelogenous leukemia is the predominant myeloproliferative disorder, and survival rates are lower in adults than children.[1]

The chronic leukemias often first appear in an indolent manner. Symptoms may be vague. These diseases generally are found in older individuals. Although associated infections or other complications are often treated aggressively, many patients receive no treatment for their underlying disease because treatment has not definitely been shown to prolong survival. Some chronic leukemias degenerate into a "blast" (acute) phase, in which case the signs and symptoms resemble those of the acute leukemias.[1]

The lymphomas often initially appear with symptoms related to lymph node involvement. Signs and symptoms of bleeding diatheses and organomegaly are common. Additional information on the systemic aspects of the lymphomas is included later in this chapter.

Leukemia

Prevalence and Incidence

Limited data are available from prospective series of patients concerning ocular findings at the time of diagnosis.[7–9] Most clinical series contain cross-sections of patients seen both early and late during the course of the illness. Autopsy series, which presumably show the highest prevalence rates, often overstate the frequency with which clinical disease is detected.

Four autopsy series have shown variable prevalence data. Allen and Straatsma[6] found that 38 of 76 patients (50%) had ocular involvement by neoplastic disease or pathologic changes that could be directly ascribed to the neoplastic disease. Nelson et al.[10] found

that 33 of 117 patients (28%) with various types of leukemia had ocular metastases at the time of death. Leonardy et al.[11] found leukemic infiltrates in the eyes of 42 of 135 patients (31.1%), with the choroid being the most frequently involved site. Data from Kincaid and Green[1] are summarized in Table 159.1, which shows that 75% of patients with chronic leukemias, 82% of patients with acute leukemias, and 80% of affected patients in this study had intraocular involvement at the time of death.

TABLE 159.1

Involved Eyes in Leukemia: Wilmer Ophthalmological Institute, 1923–1980

Interval	All Leukemias		Acute Leukemia		Chronic Leukemia	
	n	(%)	*n*	(%)	*n*	(%)
1923–1947	38/41	93	17/19	89	19/20	95
1948–1960	57/72	79	40/46	87	17/24	71
1961–1970	31/38	82	25/31	81	6/7	86
1971–1975	71/96	74	49/67	73	17/23	74
1976–1980	87/100	79	59/70	84	14/23	61
Totals	284/357	80	190/233	82	73/97	75

Data from Kincaid MC, Green WR. Ocular and orbital involvement in leukemia. Surv Ophthalmol 1983;27:211–32.

Clinical series show highly variable prevalence rates. A small prospective series was reported by Karesh et al.,[7] who examined the fundus findings in 56 newly diagnosed, untreated patients with acute myelogenous leukemia. They found retinopathy at the time of initial examination in 28 of 56 patients (50%) and no cases of leukemic infiltration. Schachat et al.[8] reported on the largest series of patients with newly diagnosed leukemia examined within a few days of diagnosis. Among the 120 patients examined (65 with acute myelogenous leukemia, 51 with acute lymphocytic leukemia, and four with other leukemias), 62% had ocular abnormalities due to their underlying myeloproliferative disorder. In addition, Reddy and colleagues conducted a study examining 127 patients with acute leukemia within 2 days of diagnosis before starting chemotherapy, and these investigators found retinal lesions in 49% of cases.[9]

Clinical Manifestations

The ocular manifestations of leukemia can be divided into direct manifestations (leukemic infiltrates), possible direct manifestations (e.g., white-centered retinal hemorrhages), manifestations of complications of leukemia (chiefly anemia, thrombocytopenia, and hyperviscosity states), opportunistic infections, and those related to medical therapy.

Reddy et al. reported on 127 individuals examined after diagnosis of acute leukemia and before initiation of chemotherapy. Abnormal retinal findings were noted in nearly half of all patients examined.[9] The most common retinal lesions were intraretinal hemorrhages (42%). Reddy and colleagues also reported on the ocular findings in 288 newly diagnosed cases of leukemia in adults and children. Clinical symptoms were present in 10%, but ocular findings were noted in 35.4%. Ocular findings were more common in adults (49%) than in children (16%) and were more frequent in myeloid leukemia (41%) compared with lymphoid leukemia (29.2%).[12]

Russo et al. evaluated 180 pediatric patients with acute leukemia and found ocular manifestations in 66% of children with acute myeloid leukemia and 11.5% of children with acute lymphocytic leukemia.[13] Data from multiple reports suggest the need for routine ocular examination of all patients with newly diagnosed acute leukemia regardless of whether they are symptomatic or not. Other investigators have also noted that chronic lymphocytic leukemia appears to have a very low prevalence of ocular involvement and routine screening of these patients at the time of diagnosis does not appear to be necessary.[14]

In our series of 120 cases examined at the time of diagnosis, four patients (3%) had leukemic infiltrates. In addition, intraretinal hemorrhages were present in 29 cases (24%), white-centered retinal hemorrhages in 13 cases (11%), vitreous hemorrhage in three cases (2%), and cotton-wool spots in 19 cases (16%). Miscellaneous findings, presumably unrelated to leukemia, were present in 20% of cases.[8] The low prevalence of leukemic infiltrates in our series differs from those reported in autopsy series. One potential reason for the lower prevalence is the ability to detect leukemic choroidal infiltrates, which are a frequent finding in autopsy series but are

difficult to diagnose clinically.

Leukemic Infiltrates

Retinal or Preretinal Infiltrates

Leukemic infiltrates have been described by several investigators. Kuwabara and Aiello[15] reported on a patient with chronic myelogenous leukemia with large gray-white nodules of varying sizes in the retina.[15] They suggested that this finding was an ominous prognostic sign and, in general, associated with high blood counts, fulminant disease, and early demise.[16] Merle and colleagues have described a subretinal infiltrate with venous vasculitis in a patient with adult T-cell leukemia.[17] As the ocular lesions progressed, the general health of the patient declined despite treatment with chemotherapy. Another patient with leukemic infiltrates is illustrated in Fig. 159.2. This type of pathologic change in the fundus was seen in 2–3% of patients in our prospective series.[8] Optic nerve infiltration may be the initial ocular manifestation of acute leukemia and can result in severe vision loss if not treated.[18] In addition, recurrent systemic lymphoma may also present with ocular infiltration, and diagnostic vitrectomy may be helpful in establishing the presence of active disease.[19]

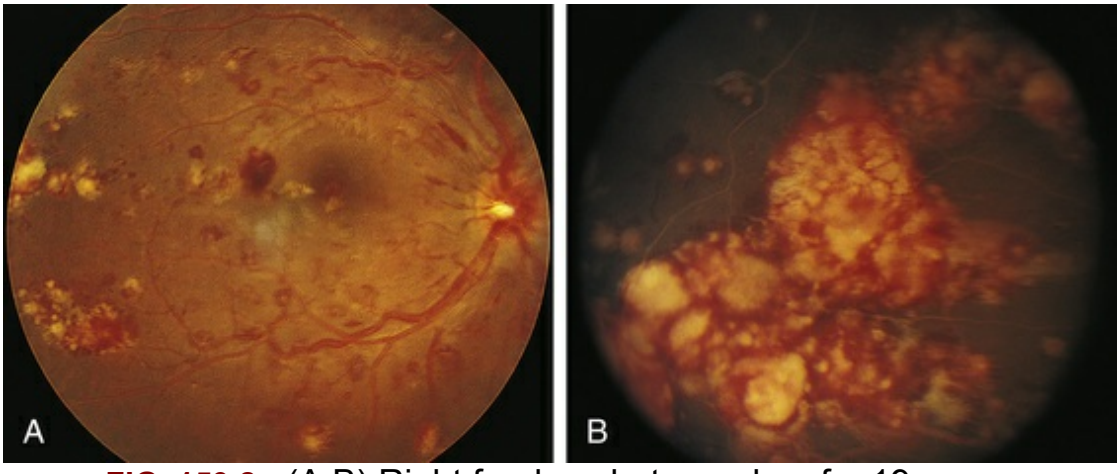

FIG. 159.2 (A,B) Right fundus photographs of a 19-year-old man with leukemic retinopathy and extensive midperipheral intraretinal and preretinal leukemic infiltrates with acute myelogenous leukemia. The patient died within 72 hours of presentation. (Courtesy of

Gray-white streaks along vessels may be caused by local perivascular leukemic infiltrates. A case of diffuse unilateral retinal angiopathy resembling frosted-branch angiitis that responded to local radiation and intrathecal chemotherapy was reported by Kim et al.[20] This case represented the sole manifestation of relapsing acute lymphoblastic leukemia in an 18-year-old man and also involved optic nerve infiltration in the same eye.

Choroidal Infiltrates

Leukemia may also infiltrate the choroid; however, clinical signs of choroidal involvement are often subtle unless overlying retinal or retinal pigment epithelial (RPE) changes bring them to attention. Serous retinal detachment overlying choroidal infiltrates[21] or overlying frank choroidal masses[22] is an important clue. Histopathologic confirmation of choroidal infiltration has been reported in a patient with adult T-cell leukemia.[23]

Kincaid et al.[24] reported on a 71-year-old woman with an exudative retinal detachment, shifting subretinal fluid, and areas of diffuse pin-point fluorescein hyperfluorescence with dye leakage into the subretinal space. The patient had a poorly characterized and unusual leukemia. Histopathologic study showed that the choroid was moderately distended by a diffuse cellular infiltrate with an overlying serous retinal detachment. The RPE showed areas of depigmentation and proliferation. There were a few small areas of associated pigment epithelial detachment.[24] Gass[25] described a patient with myelomonocytic leukemia who had a discrete choroidal mass with an overlying serous retinal detachment. Pin-point hyperfluorescence was seen on the angiogram in areas overlying the mass (Fig. 159.3).

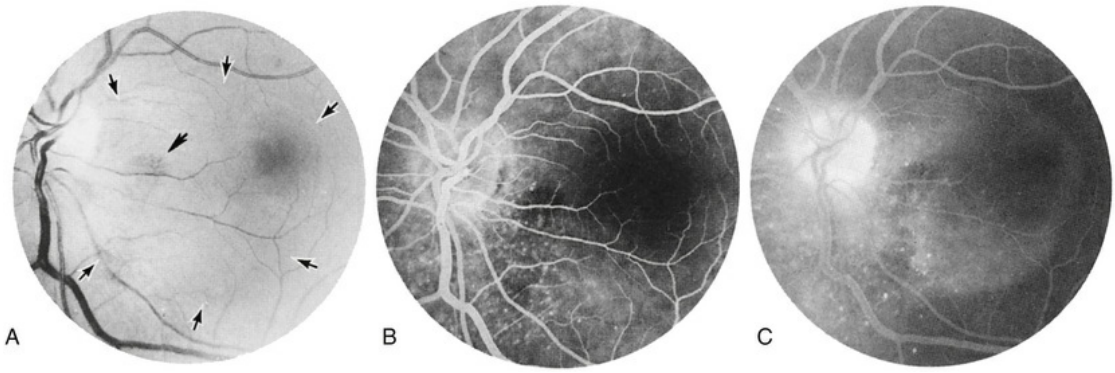

FIG. 159.3 (A) Serous macular detachment in a 59-year-old white woman with leukemia. A small amount of blood (*solid black arrow*) is present. (B,C) Multiple, small pinpoint areas of leakage from the area of presumed choroidal infiltration. (Reproduced with permission from Gass JDM. Stereoscopic atlas of macular diseases: diagnosis and treatment. 4th ed. St. Louis: Mosby; 1997.)

Burns et al.[26] reported on a 37-year-old patient with acute lymphocytic leukemia who appeared to have "bilateral macular edema." The patient was treated with ocular radiation on the assumption that underlying leukemic infiltration of the choroid was present, and this was confirmed at autopsy. Serous retinal detachment overlying areas of choroidal infiltration has been reported in patients with chronic lymphocytic leukemia, acute lymphocytic leukemia, chronic myelogenous leukemia, and acute myelogenous leukemia.[1,27] Serous RPE detachment has also been reported in a patient with acute lymphoblastic leukemia.[28] Exudative retinal and RPE detachments can be the presenting manifestation of the leukemia.[29] Eventually, as the fluid and detachment resolve, coarse clumping of the RPE is seen.[21,28]

Prominent pigment epithelial changes also may be seen after resolution of what may be retinal infiltrates. Jakobiec and Behrens[30] reported on a 3-year-old patient with acute leukemia who was found to have preretinal hemorrhages, some with white centers. A multitude of jet-black spots were seen, most prominently in the posterior pole. Soft white patches were described in the retinal periphery. The authors believed that these patches were the precursor lesions of the black spots. They postulated that the spots represented proliferation of pigment epithelial cells or small pigment epithelial detachments.[30] Clayman et al.[21] reported on a

child with acute lymphocytic leukemia who had massive pigmentary changes simulating leopard spots, most marked in the posterior pole (Fig. 159.4). At autopsy, the retina and the choroid were infiltrated with atypical immature lymphocytes. Areas of RPE hyperplasia were present, including heaped-up masses of pigment epithelium surrounding leukemic cells.

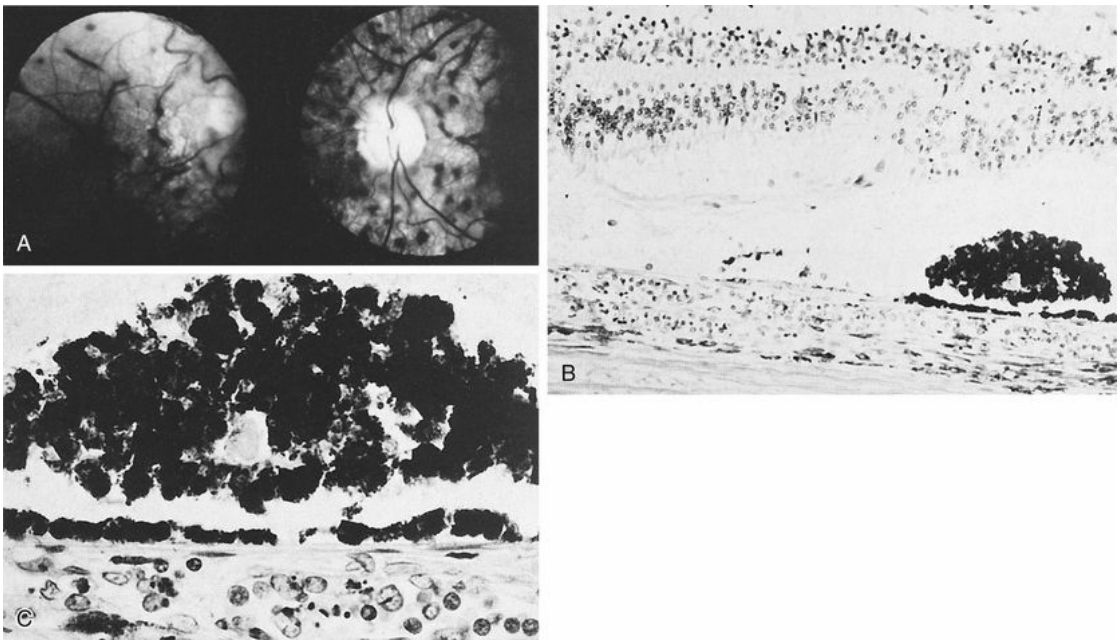

FIG. 159.4 (A) Fundus photograph showing marked clumping of retinal pigment epithelium (RPE). (B) Heaped-up masses of RPE surrounding eosinophilic material and leukemic cells. (C) Higher magnification of an adjacent area showing a nodule of pigment epithelium and infiltration of the choroid and retina with leukemic cells. (Panels A and B courtesy of John T. Flynn; panel C reproduced with permission from Clayman HM, Flynn JT, Koch K, et al. Retinal pigment epithelial abnormalities in leukemic disease. Am J Ophthalmol 1972;74:416–9.)

Vitreous Infiltrates

Vitreous opacities may be manifestations of an intraocular malignancy. Moribund patients may show massive collections of tumor cells in the vitreous, but most patients with intravitreal hemorrhage have neoplastic cells in the vitreous only because their peripheral blood contains tumor cells (Fig. 159.5). The cells do not

appear to be preferentially replicating in the vitreous cavity. Swartz and Schumann[5] described a patient with acute lymphocytic leukemia who had a dense vitreous cellular infiltration. Diagnostic vitreous aspiration confirmed the neoplastic nature of the process. Examination of the cerebrospinal fluid was also positive for blast cells. At the time, the peripheral blood was negative for tumor. The patient was treated with systemic and intrathecal chemotherapy and 1200 cGy of cranial radiation therapy. The vitreous cleared after the treatment.[5]

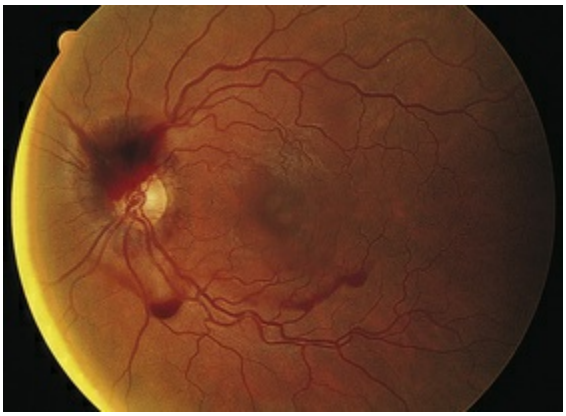

FIG. 159.5 Leukemic patient with thrombocytopenia and combined subarachnoid and vitreous hemorrhage (Terson syndrome). Because the patient has a high peripheral blast count, it is certain that leukemic cells are present in the vitreous blood.

Belmont et al.[31] reported on a 72-year-old patient with chronic unilateral uveitis. Leukemic cells were found in the iris and throughout the vitreous at the time of a pars plana vitrectomy performed to rule out reticulum cell sarcoma. Isolated ocular blast crisis with leukemic hypopyon has been reported to occur in chronic myelogenous leukemia.[32] Vitreous cells and leukemic retinopathy have been reported in a single case of hairy cell leukemia (which constitutes less than 2% of adult leukemias).[33] A masquerade syndrome with primarily ocular findings of panuveitis in a patient with T-cell prolymphocytic leukemia was reported by Dhar-Munshi et al.[34] Additional cases of vitreous involvement in leukemia have been cited by Kincaid and Green,[1] as well as by Rothova et al.[35] Leukemic cells have been found in the vitreous of

patients with neovascularization of the disc. Delaney and Kinsella[36] reported on a patient with chronic myelogenous leukemia and disc neovascularization who had good peripheral perfusion, although the macula did show areas of nonperfusion. de Juan et al.[37] described a 3-year-old patient with acute lymphocytic leukemia who had disc neovascularization, vitreous hemorrhage, and vitreous infiltration. This case was unusual because neither the cell count nor the platelet count was remarkably elevated.

Hattenhauer and Pach[38] reported a single case of ocular B-cell lymphoma occurring in a patient with chronic lymphocytic leukemia. The occurrence of diffuse large cell lymphoma in patients with chronic lymphocytic leukemia is known as Richter syndrome. Richter syndrome is estimated to occur in 3–10% of patients with chronic lymphocytic leukemia. It portends an abrupt deterioration in health and carries a poor prognosis for survival.

Vitreous involvement also has been seen at the time of autopsy in patients with reticulum cell sarcoma, Burkitt lymphoma, multiple myeloma, and Hodgkin disease (discussed later in the chapter).

Possible Leukemic Infiltrates

Duane et al.[39] reviewed the causes of white-centered retinal hemorrhages (Fig. 159.6) and also described possible pathophysiologic mechanisms. The authors suggested that these lesions should be classified as suspicious for direct intraocular manifestations of leukemia, since aggregates of leukocytes have been reported in the center of white-centered hemorrhages.[40,41] However, it should be noted that white-centered retinal hemorrhages can be composed of fibrin-platelet aggregates and are not necessarily a definite sign of neoplasia.

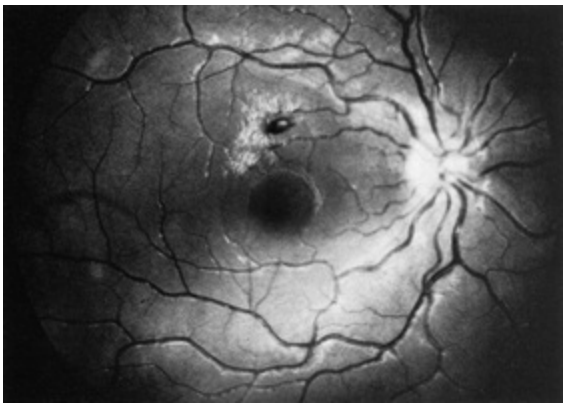

FIG. 159.6 White-centered retinal hemorrhage visible above the center of the macula. The patient has acute lymphocytic leukemia.

Manifestations of Anemia and Thrombocytopenia

Leukemic retinopathy is the term most often used to denote the fundus manifestations of anemia, thrombocytopenia, and increased blood viscosity seen in patients with leukemia. In general, the term does not necessarily refer to frank leukemic proliferation. The changes of "leukemic retinopathy" may be more commonly seen with the acute leukemias, but the frequency with which they occur has not been adequately studied to be certain. Although perivascular sheathing may be due to actual perivascular infiltrates, tortuous dilation of the retinal veins probably is not. The veins and arteries may assume a yellowish tinge because of both anemia and leukocytosis.[1] Retinal hemorrhages may occur, often at the posterior pole, and may be subretinal, deep retinal, superficial retinal, or preretinal, with potential breakthrough bleeding into the vitreous cavity. Hemorrhages may have a blot or blotch shape, flame shape, or they may have white centers (Figs. 159.7 and 159.8).[39]

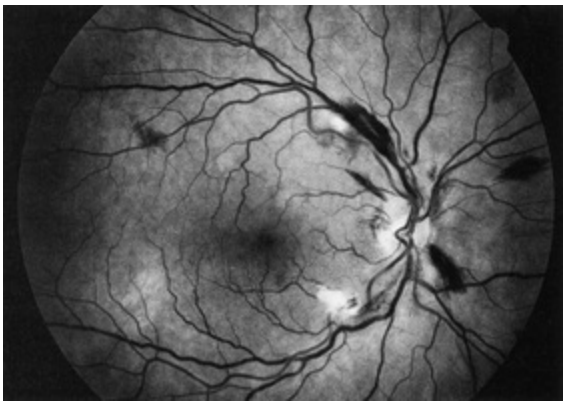

FIG. 159.7 Leukemic retinopathy with cotton-wool spots, nerve fiber layer hemorrhages, and hemorrhages in deep retinal layers. The patient has acute myelogenous leukemia.

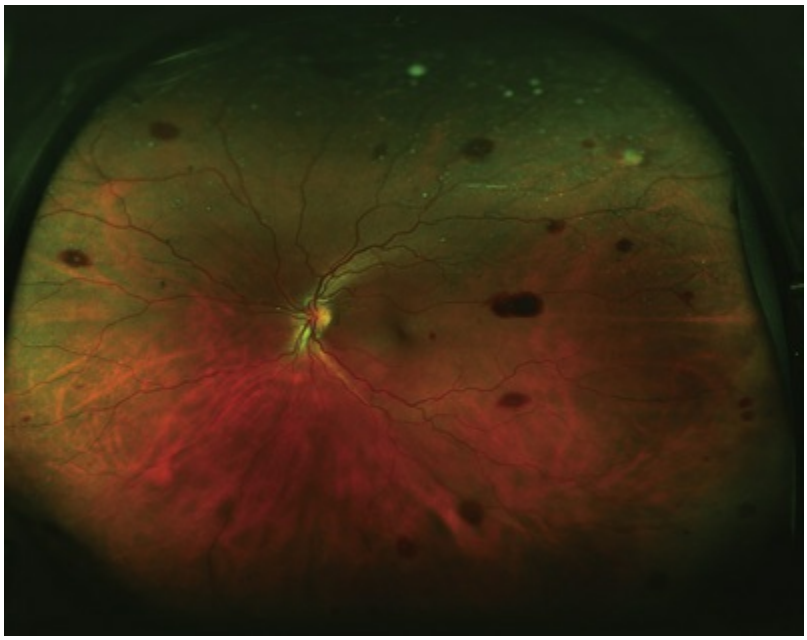

FIG. 159.8 Wide-field fundus photograph of an eye with acute myelogenous leukemia and retinal hemorrhages.

Cotton-wool spots may be the presenting abnormality that precipitates the systemic evaluation leading to the diagnosis of leukemia.[42] Cotton-wool spots may be caused by local factors, such as an abnormally large cell or a cluster of cells occluding retinal arterioles, and may not be related to the overall peripheral blood composition. In general, hematologic parameters are not associated

with the presence of cotton-wool spots.[43] Cotton-wool spots and hemorrhages can spontaneously resolve in patients with chronic leukemic disease.[5]

Manifestations of Hyperviscosity

Whole-blood hyperviscosity may lead to veno-occlusive disease, microaneurysm formation, retinal hemorrhages, and retinal neovascularization. The most common manifestation is probably a mild, or "hyperpermeable," central retinal vein occlusion (Fig. 159.9). A systemic hyperviscosity state should be suspected in patients with simultaneous, bilateral retinal vein occlusion. Also, the very high white cell count may lead to a hyperviscosity state that results in poor absorption of cerebrospinal fluid, creating a clinical picture similar to that of benign intracranial hypertension with bilateral disc swelling.[44]

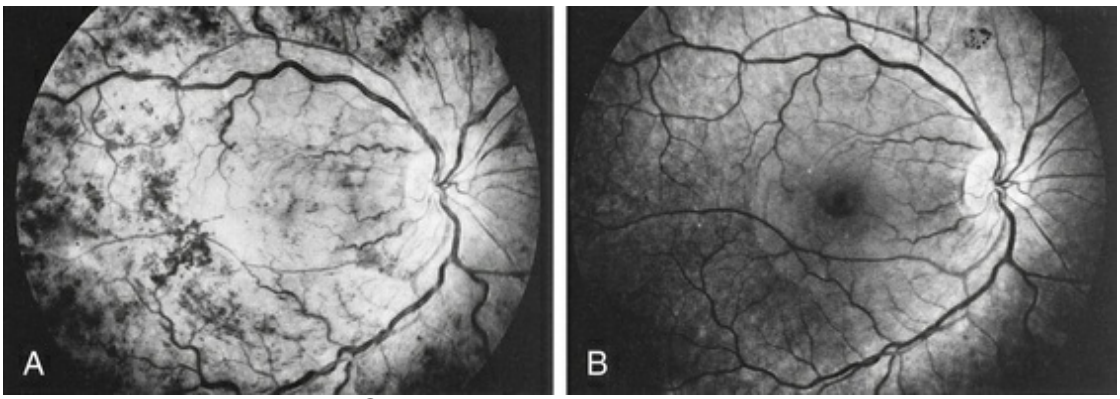

FIG. 159.9 (A) Central retinal vein obstruction in a patient with systemic hyperviscosity. The findings were bilateral and symmetric. (B) After lowering of the blood viscosity, the fundus appearance is normalized.

Peripheral retinal microaneurysms in leukemic patients were originally described by Duke et al.[45] and subsequently by Jampol et al.[46] Duke et al.[45] found that 50% of patients dying with chronic leukemia had peripheral microaneurysms. None were seen in patients with the acute leukemias. Seven of nine patients with chronic myelogenous leukemia and three of 10 patients with chronic lymphocytic leukemia had this finding, but it was not present in any of the 21 patients with acute leukemia.[45] Kincaid and

Green[1] saw only one case in their large series. They noted that trypsin digest of the retina was essential or else the change would be overlooked on histopathologic examination.

Peripheral retinal neovascularization has been reported in patients with chronic myelogenous leukemia in association with peripheral capillary nonperfusion. Most cases have associated extreme leukocytosis or thrombocytosis.[47–50] Presumably, the hyperviscosity state leads to peripheral nonperfusion and subsequent development of retinal neovascularization, as in patients with proliferative sickle retinopathy.

Morse and McCready[50] reported on a 32-year-old patient with chronic myelogenous leukemia and retinal neovascularization. The peripheral white blood cell count was 340. 5 $\times 10^9$/L and subsequently rose to 524 $\times 10^9$/L. The fasting blood sugar value was normal, as was the hemoglobin electrophoresis study. No paraproteins were present. A fluorescein study highlighted multiple sea fans, and obliteration of the terminal arterioles was apparent. Frank and Ryan[47] described a 30-year-old patient with a subhyaloid and vitreous hemorrhage who had a white blood cell count of 250 $\times 10^9$/L related to chronic myelogenous leukemia. Numerous sea fans were apparent, and a glucose tolerance test and hemoglobin and serum protein electrophoresis studies were negative.[50] Like Morse and McCready,[50] Frank and Ryan[47] believed that the pathogenic mechanism was related to increased blood viscosity, as in patients with complications of Waldenström macroglobulinemia or polycythemia. Kincaid and Green,[1] however, did not see any cases of peripheral retinal neovascularization in their series.

Levielle and Morse[48] described a patient with chronic myelogenous leukemia who had a relatively low (33.7 $\times 10^9$/L) white blood cell count. In general, the blood viscosity begins to increase remarkably only with white blood cell counts of >50 $\times 10^9$/L.[51] In Levielle's case report, the patient had an elevated platelet count of 988 $\times 10^9$/L, and the peripheral neovascularization was attributed to this elevation. However, the authors did not emphasize that their patient also had an 11-year history of diabetes mellitus; therefore diabetic retinopathy also may have contributed to retinal capillary non-perfusion and formation of peripheral neovascularization.[51]

Melberg et al.[52] described the effect of acute lymphocytic leukemia on the progression of mild diabetic retinopathy in a 16-year-old girl. The patient developed bilateral rubeosis, and after aggressive laser and vitrectomy, her vision declined to 20/200 bilaterally as a result of macular ischemia. The accelerated course of diabetic retinopathy correlated most closely with the anemia accompanying her leukemia and its treatment.

Wiznia et al.[53] reported on concurrent optic disc and retinal neovascularization in an 18-year-old woman with acute lymphocytic leukemia who underwent therapy. They described progression of the neovascularization caused by the additive effects of radiation retinopathy and chemotherapy, resulting in macular traction detachment. The authors postulated that toxic effects of chemotherapy when combined with radiation therapy could lead to a more severe form of ischemic retinal vasculopathy than would be encountered with acute lymphocytic leukemia alone.[53]

The mechanism of the retinal hemorrhage seen in patients with leukemia is not yet known. The hemorrhages may be caused by an associated anemia or thrombocytopenia. Although commonly associated with severe leukocytosis, white-centered hemorrhages may be present regardless of the degree of leukocytosis.[54]

Some authors believe that the platelet count is more predictive than the hematocrit for the presence or absence of retinal hemorrhages.[55] Kincaid and Green[1] summarized the issue in 1983 and wrote that there is no close correlation between the degree of retinal involvement and red blood cell, white blood cell, or platelet levels. We have prospectively correlated the ocular findings with hematologic values on presentation in our series of 120 cases examined within a few days of diagnosis.[56] We found a strong association between low platelet counts and intraretinal hemorrhages. Acute lymphoblastic leukemia patients with hemorrhages had a mean platelet count of 26.9 $\times 10^9$/L, whereas patients without hemorrhage had mean counts of 116.2 $\times 10^9$/L ($p \leq .0001$); acute myelogenous leukemia patients with platelet counts of $<15 \times 10^9$/L were more likely than those without such low counts to have intraretinal hemorrhages (55% vs. 29%). In addition, there was also a statistical difference between hematocrits (a mean of 20.3 mL/dL for patients with hemorrhage and a mean of 26.2 mL/dL for

patients without hemorrhage). However, a two- or three-point difference in the hematocrit is not of clinical importance. We believe that the platelet count plays a much stronger role in determining the presence or absence of intraretinal hemorrhage.[56] Furthermore, on presentation, hematologic values were not found to be correlated with the presence of cotton-wool spots.

The presence of specific retinal manifestations of leukemic retinopathy and the subsequent risk of developing an intracranial hemorrhage was reported by Jackson et al.[57] They reported a fivefold relative risk of an intracranial hemorrhage developing in those patients with macular hemorrhages compared with those patients without such hemorrhage. No increased risk of intracranial hemorrhage existed with the presence of non-macular intraretinal hemorrhages, white-centered hemorrhages, or cotton-wool spots. Therefore, patients with macular hemorrhages may require close monitoring for the possible development of intracranial hemorrhages, and these patients may need platelet transfusions if such an intracranial hemorrhage occurs.

Opportunistic Infections

Opportunistic infections are common in immunosuppressed patients. Cytomegalovirus (CMV) is one of the most common causes of infectious retinitis in patients with altered immune status (Fig. 159.10).[58] HTLV-1-associated adult T-cell leukemia can also present with a necrotizing retinal vasculitis.[59] Various herpesviruses also can cause infectious retinitis.[60] An unusual case of mumps uveitis in a patient with acute lymphocytic leukemia has been reported.[61] A case of progressive outer retinal necrosis (PORN) after bone marrow transplantation in a 15-year-old boy with acute myelogenous leukemia has been reported by Lewis et al.[62] The course of the infection was so rapid that antiviral therapy was unable to save the patient's vision.

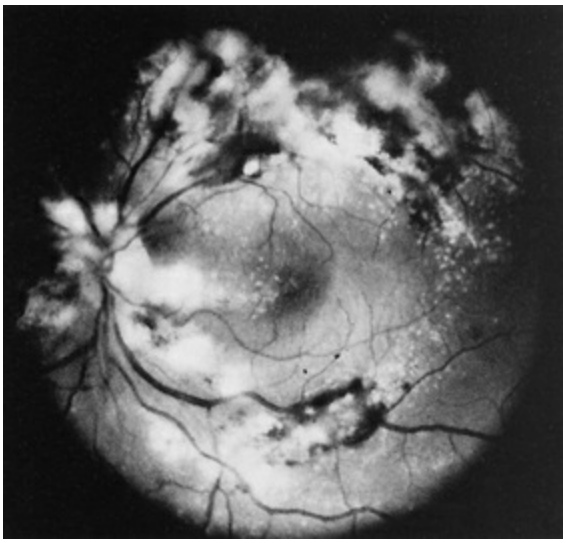

FIG. 159.10 Cytomegalovirus retinitis. (Courtesy of James P. Dunn.)

Among parasitic infections, ocular toxoplasmosis is the most common. Fungal intraocular involvement is a frequent and severe problem.[63] One should consider opportunistic infection as a cause of retinal infiltration even in the absence of vitritis in immunocompromised patients.[64] If a diagnostic dilemma exists, vitreous biopsy with 23- or 25-gauge vitrectomy may be helpful in identifying infectious etiologies.[65,66] Hematologic malignancy has been reported as a common predisposing systemic factor for intraocular fungal infections, and ophthalmologists should have a high index of suspicion when examining patients with myeloproliferative disorders.[67,68]

Prognosis

Leukemic retinopathy usually is seen when the patient is in relapse and is related to coexisting anemia.[22] Many authors had previously observed that fundal changes did not appear to carry prognostic significance.[69] However, the relationship of leukemic retinopathy to patient survival was evaluated prospectively in 54 patients by Abu el-Asrar et al.[70] Among the 35% of patients with leukemic retinopathy, the mean survival rate was significantly shorter for those patients with cotton-wool spots than those without them (169 vs. 609 days). Patients with cotton-wool spots were eight times more likely to die in the follow-up period than patients without this

finding, possibly because of severe bone marrow dysfunction. The prognostic significance of leukemic retinopathy in childhood leukemia was evaluated in 63 patients by Ohkoshi and Tsiaras.[71] The 5-year survival rate was significantly lower in those with leukemic retinopathy on presentation than in those without ophthalmic involvement (21.4% vs. 45.7%). These two studies suggest that patients with clinical leukemic retinopathy may have more aggressive systemic disease that might lead to a worse prognosis.

Although peripheral blood counts or retinal hemorrhages and exudates do not seem to be predictors of systemic relapse or mortality, retinal infiltrates defined as whitish irregular patches near or around retinal vessels have been associated with leukemia that has a worse prognosis. Gross leukemic infiltrates, as illustrated in Fig. 159.2, have been identified in moribund patients.

Treatment

Intraocular manifestations of leukemia usually are not treated directly. Rather, systemic chemotherapy is administered in an attempt to control the underlying systemic problem.[72,73] In addition, recent studies have demonstrated that patients with central nervous system leukemic involvement may benefit from both intravenous and intrathecal chemotherapy without the need for cranial irradiation.[74] General supportive measures (e.g., blood transfusions) may also be recommended for patients with severe anemia or thrombocytopenia.

It is not known whether or not most systemic chemotherapeutic agents penetrate into the eye. The eye does appear to be beyond the reach of intrathecal chemotherapy.[75] When definite leukemic infiltrates fail to respond promptly to systemic or intrathecal chemotherapy, ocular radiation may be recommended. Varying doses have been used,[1] and consultation with an experienced radiation oncologist is essential. Hoover et al. reported on their follow-up of 82 survivors of leukemia treated at their institution and found only minimal ocular morbidity (posterior subcapsular cataracts in 52%).[76] Lopez et al. described the occurrence of radiation retinopathy after low doses of teletherapy in five of eight

patients with leukemia who were treated with high-dose chemotherapy in the setting of bone marrow transplantation.[77] They suggest that high-dose chemotherapy may increase the susceptibility for the development of radiation retinopathy at otherwise safe radiation doses. Webster et al. reported on a similar case of ischemic retinopathy complicating bone marrow transplantation that was combined with the use of campath-1G (for suppression of graft-versus-host disease).[78] Therefore, treatment with cranial or orbital radiation may result in radiation retinopathy, and follow-up evaluation is necessary to detect this potential complication. Hyperleukocytic retinopathy may be managed by leukapheresis. Mehta et al. reported on three patients with hemorrhages and exudates in a pattern consistent with a state of severe hyperviscosity.[79] They noted retinal venous distention, scattered hemorrhages, and optic disc edema in a pattern of a mild central retinal vein occlusion. The patients had peripheral white blood cell counts of 129 , 379 , and 1 043 $\times 10^9$/L, respectively. Two patients improved rapidly after leukapheresis. In addition, the authors cite a number of other cases in which the procedure has been used successfully.[79]

Lymphomas

Lymphomas are classified as either Hodgkin lymphoma or non-Hodgkin lymphoma. In addition, malignant lymphomas are divided into primary intraocular lymphoma and secondary intraocular lymphoma. Primary intraocular lymphoma involves primary central nervous system lymphoma, whereas secondary intraocular lymphoma involves a metastasis from a primary visceral lymphoma. The incidence of neoplastic intraocular involvement in patients with lymphomas is probably much less than that in patients with various leukemias. Lymphoid infiltration of the uvea, formally termed reactive lymphoid hyperplasia, is rare and usually is not associated with systemic disease.[80]

Non-Hodgkin Lymphoma

Non-Hodgkin lymphomas constitute approximately 5% of all

newly diagnosed cancers in the United States. They are predominantly of B-cell lymphocytic origin, although some may be derived from T cells.[81] Ocular manifestations in this disease occur in two distinct settings, systemic non-Hodgkin lymphoma and primary central nervous system (CNS) non-Hodgkin lymphoma.[82] Systemic non-Hodgkin lymphoma most commonly involves the internal structures of the eye, gaining access by the choroidal tissues.[83–86] Ocular involvement is often asymmetric and most commonly affects individuals in the sixth decade of life and beyond (although a case has been reported in a 15-year-old boy[85]).

Until recently, primary ocular lymphoma has been an uncommon cause of chronic vitritis and has represented one of several sites of multifocal primary central nervous system lymphoma (PCNSL), also referred to as non-Hodgkin lymphoma of the central nervous system (NHL-CNS).[87] In up to half of the cases of PCNSL, the eyes were the initial site of disease and it is frequently bilateral.[82,85] In a large retrospective study of 221 patients with PCNSL, the median age at diagnosis was 60 years and ocular disturbances and behavioral/cognitive changes were the most common presenting symptoms.[88] The correct diagnosis is often not established until late in the disease course, since this condition often masquerades as chronic uveitis, despite the absence of external signs of inflammation.[35] Approximately 60–80% of patients who have ocular lymphoma at presentation develop cerebral lymphoma with a long enough follow-up period.[83] Metastasis of PCNSL outside the CNS is seen in only up to 8% of autopsy series. In the past decade there has been a steady increase in the frequency of reports of primary intraocular lymphomas.[89] This increased incidence of PCNSL has been reported in both immunocompromised patients (from AIDS and from organ transplantation) and immunocompetent patients.[85,90] It is postulated that immunocompromised patients manifest with an abnormal response to the Epstein–Barr virus (EBV) through development of a monoclonal B-cell proliferation.[91] Ocular lymphoma and PCNSL are restricted to the central nervous system and are not a consequence of metastasis of systemic lymphoma.

Retinal hemorrhages and cotton-wool spots related to anemia or thrombocytopenia are common in patients with non-Hodgkin

lymphoma, but direct retinal involvement in patients with systemic lymphoma is extremely rare. Lewis and Clark[92] described a patient with well-differentiated lymphocytic lymphoma who had massive perivenous infiltrates (Fig. 159.11). The patient was treated with 3000 cGy of external beam radiation, and a partial response occurred. The authors believed that the most likely cause was lymphomatous infiltration, although no pathologic examination was performed.[92] The appearance of the retina was similar to that seen in frosted-branch angiitis.[93] Topilow et al. described a case of lymphomatous infiltration of the retina simulating progressive outer retinal necrosis.[94] Ocular lymphoma should be considered in the differential diagnosis of retinal vasculitis or necrotizing retinitis.[81,86,95] Gass et al. described two patients with the presenting symptom of a flecked retina simulating fundus flavimaculatus in one eye months before developing signs and symptoms of the systemic form of non-Hodgkin lymphoma.[96] Shah et al. reported the presence of multiple white spots at the level of the outer retina resembling the multiple evanescent white dot syndrome.[97] Marmor et al. reported on a patient with poorly differentiated lymphocytic lymphoma who subsequently developed histiocytic lymphoma.[98] This patient was thought to have lymphomatous involvement of the optic nerve head, although pathologic study demonstrated cytomegalovirus (CMV) in the optic nerve head.[98] Fredrick et al. described a large peripapillary choroidal lymphomatous mass as the presenting manifestation of systemic lymphoma.[99] In addition, Jensen et al. reported an intraocular T-cell lymphoma mimicking a ring melanoma as the first manifestation of a systemic lymphoma.[100] We examined a patient with non-Hodgkin lymphoma who had massive infiltration of the optic disc with subsequent development of a central retinal artery occlusion (Fig. 159.12).[101]

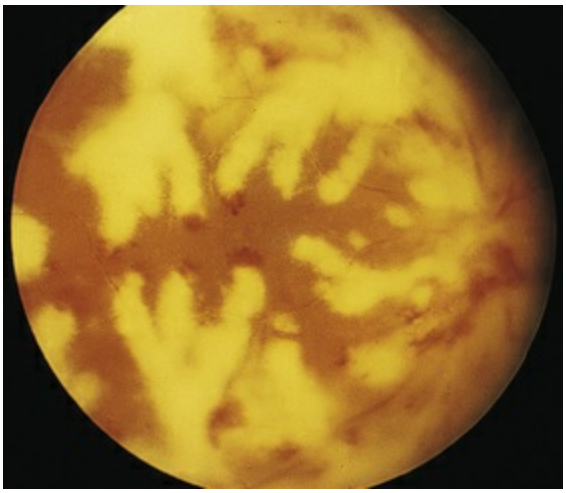

FIG. 159.11 Massive perivascular infiltrates in a patient with well-differentiated lymphocytic lymphoma.
(Reproduced with permission from Lewis RA, Clark RB. Infiltrative retinopathy in systemic lymphoma. Am J Ophthalmol 1975;79:48–52.)

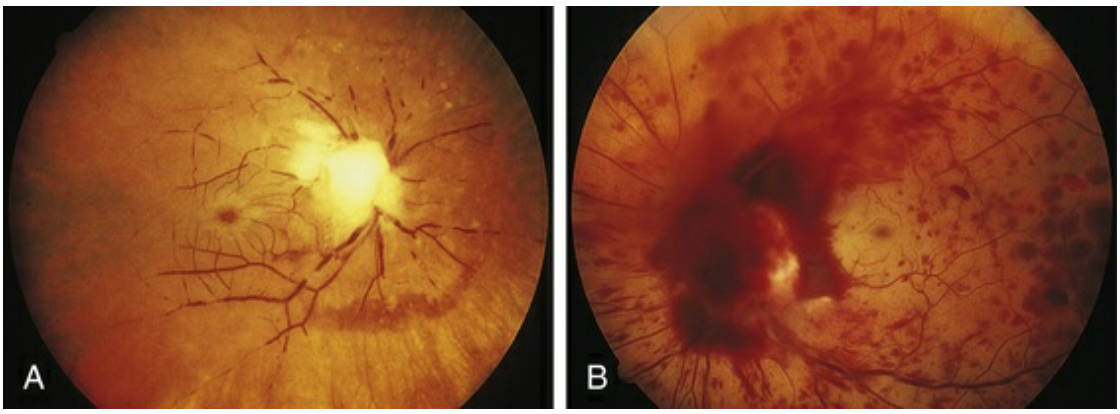

FIG. 159.12 Right (A) and left (B) eyes of a patient with non-Hodgkin lymphoma and optic disc infiltration. A central retinal artery occlusion was present in the left eye. (Courtesy of David Guyer, MD.)

Characteristic yellowish placoid RPE detachments may occur in some cases of ocular lymphoma, and the malignant cells are found in the vitreous, the retina, and between the RPE and Bruch's membrane.[102] Liu and colleagues have demonstrated that spectral domain optical coherence tomography (OCT) imaging may reveal hyperreflective material accumulation in the intraretinal and subretinal pigment epithelial spaces in eyes with primary central nervous system lymphoma.[103] The OCT findings may be useful in

aiding the diagnosis of intraocular lymphoma, and this imaging modality may also be used to assist in monitoring the progression or regression of the retinal involvement. These tumorous RPE detachments can resolve spontaneously, resulting in the formation of disciform scars or areolar atrophy of the RPE. Indirect effects of systemic lymphoma on the eye have also been reported. Cohen et al. described an 11-year-old girl with a central retinal artery occlusion in association with a systemic T-cell lymphoma.[104] They postulated that a paraneoplastic hypercoagulopathy was responsible, although they could not rule out the possibility of a lesion behind the nerve head. Das et al. reported on a 19-year-old man with retinopathy caused by hypertension, which was caused by renal involvement by non-Hodgkin lymphoma.[105]

Cytologic examination of vitreous biopsies is the benchmark for diagnosis of intraocular lymphoma.[86,87,94,106–112] A diagnostic vitrectomy with prompt and careful cytopreparatory techniques is essential for the detection of lymphoma cells. Lymphoma cells are typically 2–4 times the size of normal lymphocytes and display high nuclear/cytoplasmic ratios, prominent nucleoli, nuclear pleomorphism, and coarse chromatin patterns.[106,112,113] The skills and experience of the pathologist interpreting the specimen are critical in making the diagnosis in conjunction with the use of flow cytometry to define the cellular origins. Monoclonal proliferations of B cells through polymerase chain reaction (PCR) have been used to increase the sensitivity of vitreous biopsies performed in patients suspected of having B-cell lymphoma.[114] In addition, interleukin-10 and interleukin-6 concentrations in the vitreous may be correlated with the clinical activity and number of malignant cells.[115–117] Elevated levels of interleukin-10 therefore should alert the pathologist to the presence of malignant cells in the vitreous specimen.[112,117]

Other routes for tissue biopsy include subretinal aspiration biopsy,[118,119] fine-needle aspiration biopsy,[120,121] and transscleral chorioretinal biopsy.[122] In some cases, concurrent vitreous biopsies may be cytologically negative, and the diagnosis may be made only with the subretinal biopsy (Fig. 159.13).

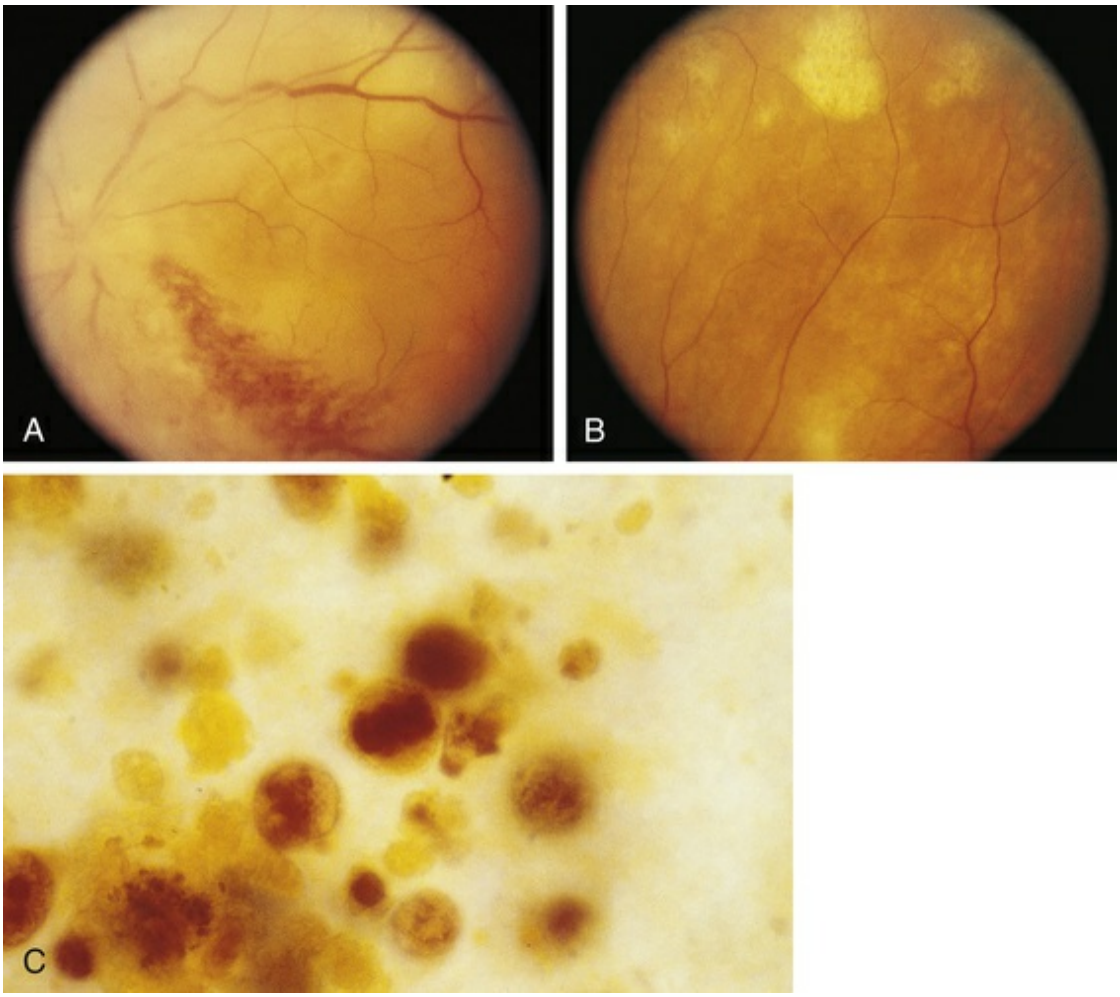

FIG. 159.13 (A) Non-Hodgkin lymphoma involving the retina and vitreous of a middle-aged man. Immunocytologic analysis of the vitreous biopsy was negative. (B,C) Concurrent subretinal aspiration biopsy of an isolated midperipheral lesion in the same patient demonstrated cells of non-Hodgkin lymphoma. (Courtesy of Daniel Martin, MD.)

Neuroimaging has been shown to have a low sensitivity for differentiating intraocular lymphoma from uveitis or melanoma.[123] Ultrasonography has been useful in documenting the extent of posterior segment involvement before therapy and may be useful in evaluating the response to treatment.[124] All patients with positive vitreous biopsies should undergo cerebrospinal fluid cytologic examination.

The paraneoplastic syndrome of bilateral diffuse uveal melanocytic proliferation has been reported in the single case of a patient with non-Hodgkin systemic lymphoma.[125]

Hodgkin Lymphoma

Hodgkin disease is a malignant lymphoma with protean manifestations. The disease is characterized by painless swelling of the lymph nodes, and Reed–Sternberg cells are seen on histopathologic examination. Barr and Joondeph[84] described a patient whose initial manifestation of Hodgkin disease was periphlebitis, focal chorioretinitis, vitritis, and optic disc edema (Fig. 159.14). The retinitis and vitritis resolved after 4000 cGy of radiation therapy.[84] The authors summarized a number of previous reports of ophthalmic manifestations of Hodgkin disease, including bilateral exudative retinal detachment, cotton-wool spots with retinal hemorrhages, and necrotizing retinitis. Patients with "numerous white deposits in the retinal periphery," chorioretinitis, Roth spots, and perivascular retinitis have been reported.[43,84] Histopathologic evidence of cotton-wool spots has been reported in patients with Hodgkin disease.[126]

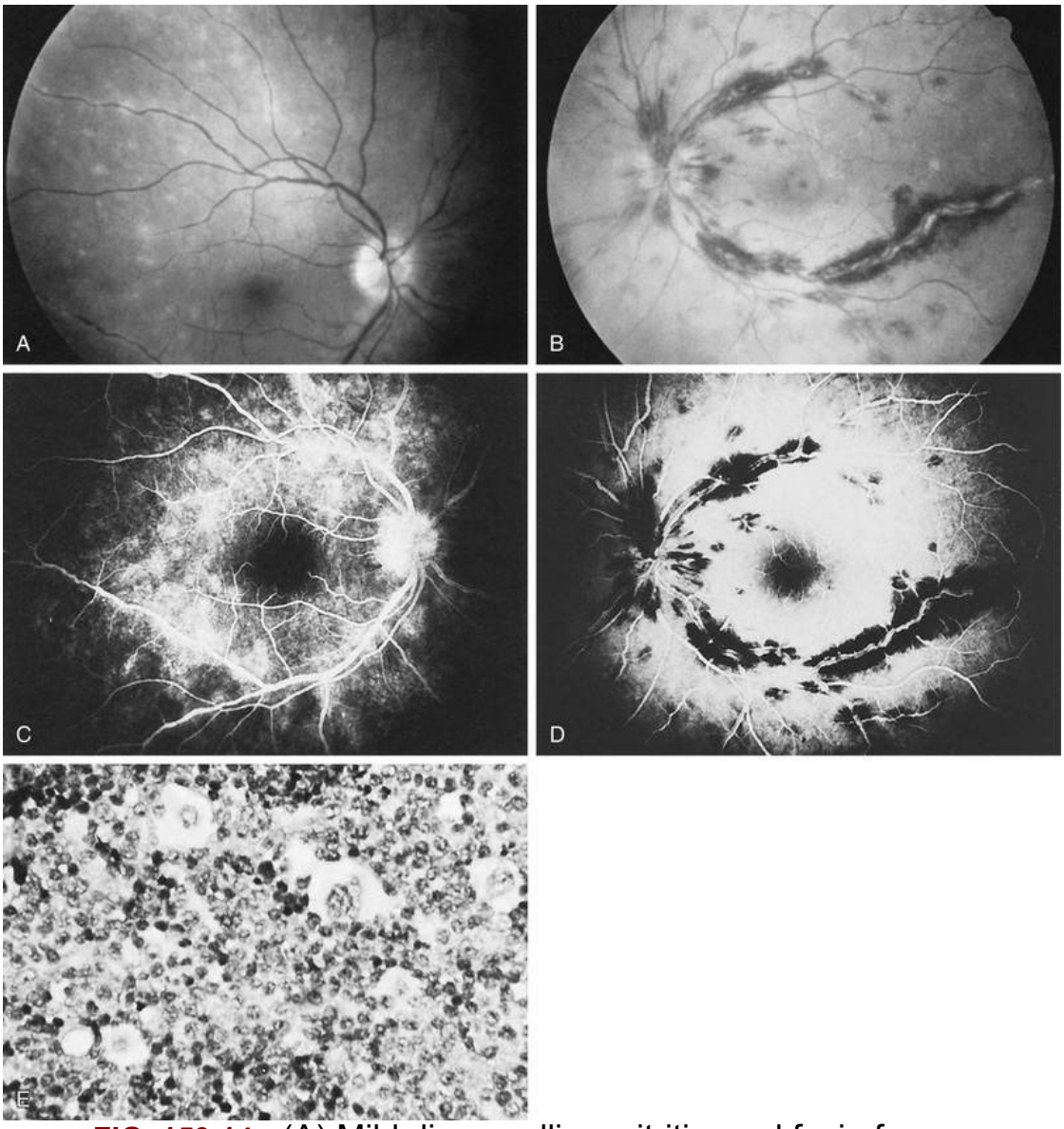

FIG. 159.14 (A) Mild disc swelling, vitritis, and foci of periphlebitis in a patient with Hodgkin disease. (B) The periphlebitis is more marked in the left eye. (C) Frame from a fluorescein angiogram. Note disc hyperfluorescence, perivascular staining, and foci of hyperfluorescence at the level of the retinal pigment epithelium. (D) Later-phase angiogram in the left eye. Note perivascular staining. (E) Lymph node biopsy specimen typical of nodular sclerosing Hodgkin disease. (Reproduced with permission from Barr CC, Joondeph HC. Retinal periphlebitis as the initial clinical finding in a patient with Hodgkin's disease. Retina 1983;3:253–7.)

Direct demonstration of tumor cells in ocular tissues is rare in patients with Hodgkin disease. Primbs et al. described a patient

with primarily anterior uveitis at presentation who had no malignant cells in the vitreous. Reed–Sternberg cells were seen in the anterior chamber and trabecular meshwork.[127] Mosteller et al. reported on a patient with anterior and posterior uveitis, pars plana exudates, perivascular sheathing, small, round, discrete white retinal lesions, and cystoid macular edema. A vitrectomy specimen demonstrated only acute and chronic inflammatory cells, and no tumor cells were seen.[128]

In one published report, a patient with Hodgkin disease had widespread severe destruction of the retina that was believed to represent a manifestation of drug toxicity.[129] However, the patient also had concomitant disseminated herpes zoster infection, and viral retinitis of this type is known to occur in immunocompromised hosts.[130] This association suggests that many cases previously diagnosed as intraocular Hodgkin disease probably represent secondary viral retinitis. Diddie et al. reported the histopathologic findings of a patient with Hodgkin lymphoma who had herpesvirus infection.[131] Toy and Knowlden summarized the findings of a patient with CMV retinitis who had been misdiagnosed as having Hodgkin lymphoma deposits.[132]

Opportunistic infections are common in patients with Hodgkin lymphoma. Toxoplasmic uveitis and chorioretinitis,[133] *Nocardia* infection,[134] and virtually all viral infections of the herpes family have been previously reported.[43]

Treatment of Lymphoma

Management of ocular involvement by non-Hodgkin and Hodgkin lymphoma consists of systemic and/or intrathecal chemotherapy with possible radiation therapy for CNS disease that is recalcitrant to chemotherapy.[112] The most common systemic agents used include methotrexate, cytarabine, vincristine, rituximab, cyclophosphamide, and steroids. The optimal treatment for PCNSL is still controversial.

In the past few years, ophthalmologists have employed the use of intravitreal injection of chemotherapeutic agents as an alternative to external beam radiation of the eye. Reports have demonstrated successful use of intravitreal methotrexate and rituximab.[135,136]

The prognosis for survival in untreated disease is poor, but it may be improved with early and aggressive therapy.[83] Even with aggressive modern therapy, the median survival is expected to be about 3 years.[137,138]

Mycosis Fungoides

Mycosis fungoides is a malignant T-cell lymphoma arising in the skin. There are three stages of the disease: (1) a prolonged phase of premycotic/eczematous skin lesions; (2) a phase characterized by infiltrative plaque lesions; and (3) a final phase of frank cutaneous tumor. Histopathologically, mycosis fungoides is characterized by cellular infiltrates of atypical lymphoid cells in the dermis (Pautrier's microabscesses), clusters of atypical lymphoid cells, and mycosis cells/lymphoid cells with large, irregular, and deeply indented "cerebriform" nuclei.[139] Systemic involvement occurs late in the course of the disease and may include virtually all organ systems.[140] Commonly these extracutaneous sites of involvement include the lymph nodes, liver, spleen, and CNS. Most affected individuals develop the disease in the fifth decade of life, and many die of unrelated causes before widespread involvement.

Mycosis fungoides involves the eye in up to one-third of individuals and tends to involve the external eye and adnexa much more commonly than the intraocular structures.[139] Only a few cases with intraocular involvement have been reported. Keltner et al. saw a patient with disc swelling and macular edema. The disc swelling was probably related to papilledema because lethargy, confusion, and focal neurologic signs were observed.[139] The patient initially responded to radiation therapy, steroids, and intrathecal methotrexate but subsequently developed swelling and pallor of both discs and infiltration of the retina and vitreous. On histopathologic examination, atypical cells and lymphocytes, as well as polymorphonuclear cells, were seen in the vitreous. Similar atypical cells infiltrated the retina, and a perivascular lymphocytic infiltrate was noted. Rossi reported on a patient with bilateral papilledema, venous stasis, retinal edema, and retinal hemorrhages.[141] Gartner described a patient with choroidal involvement chiefly characterized by perivascular granulomas.[142]

Foerster presented the histopathologic findings from a patient with a blind, painful eye who had diffuse neoplastic subretinal pigment epithelial infiltrates.[143] Necrotic tumor cells were also seen in the vitreous. A 16-year-old girl who died of visceral mycosis fungoides had no light perception in either eye or bilateral disc swelling. Malignant cells infiltrated the surrounding peripapillary retina.

The largest series of patients with mycosis fungoides reported in the ophthalmic literature is that of Stenson and Ramsay.[144] A total of 30 consecutive patients with mycosis fungoides were examined; 11 had positive findings related to mycosis fungoides, although only four had posterior segment changes (three patients had optic atrophy, and one patient had recurrent panuveitis). Erny et al. reported on the clinical and histopathologic findings in a 48-year-old man with vitritis and subretinal lesions that proved to be malignant T-cell infiltrates in the retina and the vitreous and between the RPE and Bruch's membrane.[145] Leitch et al. established the diagnosis in a 61-year-old woman with the aid of a vitreous biopsy.[146] Several of these reports demonstrated intraocular infiltration as an early manifestation of extracutaneous disease.[139,145,146]

Burkitt Lymphoma

Burkitt lymphoma was originally described in 1958 in a review of a series of patients from Kampala, Uganda.[147] It is a poorly differentiated lymphocytic lymphoma with characteristic clinical and histologic patterns. Burkitt lymphoma is the most common childhood tumor in Africa, but it occurs only rarely in the United States.[148]

Karp et al.[148] described a case in which the choroid and much of the interior of the globe was diffusely infiltrated by tumor. Burkitt lymphoma commonly involves the orbital structures, and the authors did not rule out the possibility that an invasive orbital neoplasm secondarily involved the intraocular structures. Feman et al.[149] described a patient who had a white patch over the disc associated with many small retinal hemorrhages. Histopathologic study demonstrated diffuse neoplastic infiltration of the optic disc and peripapillary retina. The infiltrate contained scattered

histiocytes (Fig. 159.15). The choroid was uninvolved, but scattered cells were present in the vitreous. Definite primary intraocular Burkitt lymphoma is exceedingly rare.

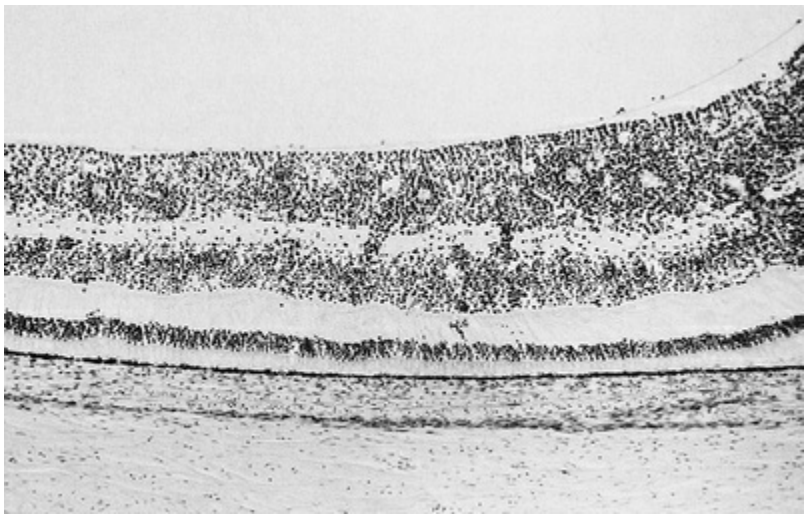

FIG. 159.15 Paramacular region showing tumor infiltration, predominantly of the inner retina, and lack of choroidal involvement. Note "starry-sky" appearance of tumor infiltrate. (Courtesy of Foos RY; reproduced with permission from Feman SS, Niwayama G, Hepler R, et al. "Burkitt tumor" with intraocular involvement. Surv Ophthalmol 1969;14:106–11.)

Multiple Myeloma and Waldenström Macroglobulinemia

Multiple myeloma is a plasma cell neoplasm that can exhibit a wide range of systemic and ocular signs and symptoms.[150] Pars plana cysts are common and can be a striking ophthalmic finding.[150] Uveal involvement has been reported by Bronstein.[151] The most common retinal findings include manifestations of anemia and thrombocytopenia, such as flame-shaped or white-centered hemorrhages and nerve fiber layer infarcts.[152] In one report these findings were seen in 8 of 22 patients with multiple myeloma.[40]

Microaneurysm formation may be apparent, most frequently in the retinal periphery and midperiphery.[153,154] The cause of this change is not certain. It may be related to hyperviscosity,[155] although a frank hyperviscosity syndrome is not as common in

patients with multiple myeloma as it is in patients with, e.g., Waldenström macroglobulinemia. If hyperviscosity is severe, retinal changes similar to those described in Waldenström macroglobulinemia may be seen.[156] Serous and exudative retinal detachments associated with multiple myeloma have also been reported.[60,157]

A clinicopathologic review of multiple myeloma and its ocular manifestations has been presented by Knapp et al.[150] In this report, the patients with retinopathy had lower hematocrit levels and platelet counts than those without retinopathy. In many patients the retinopathy cleared with treatment. The presence of retinal changes did not appear to alter the prognosis.

Patients with Waldenström macroglobulinemia have an abnormal elevation of their IgM fraction of plasma proteins. The retinal findings are chiefly those of systemic hyperviscosity, although manifestations of anemia or thrombocytopenia may be seen. Clinically, patients may present with bilateral venous dilation, which is difficult to differentiate from the findings of central retinal vein obstruction.[158] In addition to the picture of venous obstruction, microaneurysms associated with peripheral retinal neovascularization may be present. Peripheral capillary nonperfusion of the retina has also been reported.[159] Case reports have also documented the formation of serous retinal detachment.[160] The findings may be reversible when the hyperviscosity state is normalized (see Fig. 159.9). Visually symptomatic patients may benefit from plasmapheresis.[153]

References

1. Kincaid MC, Green WR. Ocular and orbital involvement in leukemia. *Surv Ophthalmol*. 1983;27:211–232.
2. Goel N, Pangtey B, Thakar M, et al. Chronic myeloid leukemia presenting with bilateral central retinal vein occlusion and massive retinal infiltrates. *J AAPOS*. 2012;16(4):406–408.
3. Chocron IM, Morrison DG, Friedman DL, et al. Ophthalmic manifestations of relapsing acute childhood leukemia. *J AAPOS*. 2015;19(3):284–286.

4. Smith AG, London NJ, Pao K, et al. Leukemia presenting as serous retinal detachment. *Retin Cases Brief Rep*. 2014;8(4):279–282.
5. Swartz M, Schumann B. Acute leukemic infiltration of the vitreous diagnosed by pars plana aspiration. *Am J Ophthalmol*. 1980;90:326–330.
6. Allen RA, Straatsma BR. Ocular involvement in leukemia and allied disorders. *Arch Ophthalmol*. 1961;66:490–508.
7. Karesh JW, Goldman EJ, Reck K, et al. A prospective ophthalmic evaluation of patients with acute myeloid leukemia: correlation of ocular and hematologic findings. *J Clin Oncol*. 1989;7:1528.
8. Schachat AP, Markowitz JA, Guyer DR, et al. Ophthalmic manifestations of leukemia. *Arch Ophthalmol*. 1989;107:697–700.
9. Reddy SC, Jackson N. Retinopathy in acute leukaemia at initial diagnosis: correlation of fundus lesions and haematological parameters. *Acta Ophthalmol Scand*. 2004;82(1):81–85.
10. Nelson CC, Hertzberg BS, Klintworth GK. A histopathologic study of 716 selected eyes in patients with cancer at the time of death. *Am J Ophthalmol*. 1983;95:788–793.
11. Leonardy NJ, Rupani M, Dent G, et al. Analysis of 135 autopsy eyes for ocular involvement in leukemia. *Am J Ophthalmol*. 1990;109:436–444.
12. Reddy SC, Jackson N, Menon BS. Ocular involvement in leukemia – a study of 288 cases. *Ophthalmologica*. 2003;217:441–445.
13. Russo V, Scott IU, Querques G, et al. Orbital and ocular manifestations of acute childhood leukemia: clinical and statistical analysis of 180 patients. *Eur J Ophthalmol*. 2008;18:619–623.
14. Buchan J, McKibbin M, Burton T. The prevalence of ocular disease in chronic lymphocytic leukemia. *Eye (Lond)*. 2003;17:3–4.
15. Kuwabara T, Aiello L. Leukemic miliary nodules in the retina. *Arch Ophthalmol*. 1964;72:494–497.
16. Robb RM, Ervin LD, Sallan SE. A pathological study of eye

involvement in acute leukemia of childhood. *Trans Am Ophthalmol Soc*. 1978;76:90–101.
17. Merle H, Donnio A, Gonin C, et al. Retinal vasculitis caused by adult T-cell leukemia/lymphoma. *Jpn J Ophthalmol*. 2005;49:41–45.
18. Bandyopadhyay S, Das D, Das G, et al. Unilateral optic nerve infiltration as an initial site of relapse of acute lymphoblastic leukemia in remission. *Ophthalmology*. 2010;3:153–154.
19. Nugent AK, Paulus YM, Chan A, et al. Multiple myeloma recurrence with optic nerve infiltration diagnosed by vitrectomy, immunohistochemistry, and in situ hybridization. *Eur J Ophthalmol*. 2014;24(3):446–448.
20. Kim TS, Duker JS, Hedges TR. Retinal angiopathy resembling unilateral frosted branch angiitis in a patient with relapsing acute lymphoblastic leukemia. *Am J Ophthalmol*. 1994;117:806–808.
21. Clayman HM, Flynn JT, Koch K, et al. Retinal pigment epithelial abnormalities in leukemic disease. *Am J Ophthalmol*. 1972;74:416–419.
22. Rosenthal AR. Ocular manifestations of leukemia: a review. *Ophthalmology*. 1983;90:899–905.
23. Liu MM, Furusato E, Cao X, et al. Ocular manifestations and pathology of adult T-cell leukemia/lymphoma associated with human T-lymphotropic virus type 1. *Rare Tumors*. 2010;2:e63.
24. Kincaid MC, Green WR, Kelley JS. Acute ocular leukemia. *Am J Ophthalmol*. 1979;87:698–702.
25. Gass JDM. *Stereoscopic atlas of macular diseases: diagnosis and treatment*. 4th ed. Mosby: St. Louis; 1997.
26. Burns CA, Blodi FC, Williamson BK. Acute lymphocytic leukemia and central serous retinopathy. *Trans Am Acad Ophthalmol Otolaryngol*. 1965;69:307–309.
27. Paydas S, Soylu MB, Disel U, et al. Serous retinal detachment in a case with chronic lymphocytic leukemia: no response to systemic and local treatment. *Leuk Res*. 2003;27:557–559.
28. Tang RA, Vila-Coro AA, Wall S, et al. Acute leukemia

presenting as a retinal pigment epithelium detachment. *Arch Ophthalmol*. 1988;106:21–22.
29. Yoshida K, Hasegawa D, Takusagawa A, et al. Bullous exudative retinal detachment due to infiltration of leukemic cells in a child with acute lymphoblastic leukemia. *Int J Hematol*. 2010;92(3):535–537.
30. Jakobiec F, Behrens M. Leukemic retinal pigment epitheliopathy with report of a unilateral case. *J Pediatr Ophthalmol*. 1975;12:10–15.
31. Belmont JB, Michelson JB, Bordin GM. Ocular inflammation associated with chronic lymphocytic leukemia. *J Ocul Ther Surg*. 1985;4:125–129.
32. Lipton JH, McGowan HD, Payne DG. Ocular masquerade syndrome in lymphoid blast crisis of chronic myeloid leukemia. *Leuk Lymphoma*. 1995;20:161–163.
33. Robinson A, Eting E, Zeidman A, et al. Manifestations of hairy cell leukemia with dramatic response to 2-chloro-deoxy-adenosine. *Am J Ophthalmol*. 1996;121:97–98.
34. Dhar-Munshi S, Alton P, Ayliffe WH. Masquerade syndrome: T-cell prolymphocytic leukemia presenting as panuveitis. *Am J Ophthalmol*. 2001;132:275–277.
35. Rothova A, Ooijman F, Kerkhoff F, et al. Uveitis masquerade syndromes. *Ophthalmology*. 2001;108:386–399.
36. Delaney WV Jr, Kinsella G. Optic disc neovascularization in leukemia. *Am J Ophthalmol*. 1985;99:212–213.
37. de Juan E, Green WR, Rice TA, et al. Optic disc neovascularization associated with ocular involvement in acute lymphocytic leukemia. *Retina*. 1982;2:61–64.
38. Hattenhauer MG, Pach JM. Ocular lymphoma in a patient with chronic lymphocytic leukemia. *Am J Ophthalmol*. 1996;122:266–268.
39. Duane TD, Osher RH, Green WR. White centered hemorrhages: their significance. *Ophthalmology*. 1980;87:66–69.
40. Holt JM, Gordon-Smith EL. Retinal abnormalities in diseases of the blood. *Br J Ophthalmol*. 1969;53:145–160.
41. Phelps CD. The association of pale-centered retinal hemorrhages with intracranial bleeding in infancy. *Am J*

Ophthalmol. 1971;73:348–350.
42. Brown GC, Brown MM, Hiller T, et al. Cottonwool spots. *Retina*. 1985;5:206–214.
43. Bishop JE, Salmonsen PC. Presumed intraocular Hodgkin's disease. *Ann Ophthalmol*. 1985;17:589–592.
44. Guymer RH, Cairns JD, O'Day J. Benign intracranial hypertension in chronic myeloid leukemia. *Aust N Z J Ophthalmol*. 1993;21:181–185.
45. Duke JR, Wilkinson CP, Sigelman S. Retinal microaneurysms in leukemia. *Br J Ophthalmol*. 1968;52:368–374.
46. Jampol LM, Goldberg MF, Busse B. Peripheral microaneurysms in chronic leukemia. *Am J Ophthalmol*. 1975;80:242–248.
47. Frank RN, Ryan SJ Jr. Peripheral retinal neovascularization with chronic myelogenous leukemia. *Arch Ophthalmol*. 1972;87:585–589.
48. Levielle AS, Morse PH. Platelet-induced retinal neovascularization in leukemia. *Am J Ophthalmol*. 1981;91:640–643.
49. Little HL. The role of abnormal hemorrheodynamics in the pathogenesis of diabetic retinopathy. *Trans Am Ophthalmol Soc*. 1976;74:573–636.
50. Morse PH, McCready JL. Peripheral retinal neovascularization in chronic myelocytic leukemia. *Am J Ophthalmol*. 1971;72:975–978.
51. Stephens DJ. Relation of viscosity of blood to leukocyte count with particular reference to chronic myelogenous leukemia. *Proc Soc Exp Biol Med*. 1936;35:251–256.
52. Melberg NS, Grand MG, Rup D. The impact of acute lymphocytic leukemia on diabetic retinopathy. *J Pediatr Hematol Oncol*. 1995;17:81–84.
53. Wiznia RA, Rose A, Levy AL. Occlusive microvascular retinopathy with optic disc and retinal neovascularization in acute lymphocytic leukemia. *Retina*. 1994;14:253–255.
54. Gibson GG. Clinical significance of the retinal changes in leukemia. *Arch Ophthalmol*. 1938;20:364–370.
55. Culler AM. Fundus changes in leukemia. *Trans Am*

Ophthalmol Soc. 1951;49:445–473.
56. Guyer DR, Schachat AP, Vitale S, et al. Leukemic retinopathy: relationship between fundus lesions and hematologic parameters at diagnosis. *Ophthalmology*. 1989;96:860–864.
57. Jackson N, Reddy SC, Harun MH, et al. Macular hemorrhage in adult acute leukemia patients at presentation and the risk of subsequent intracranial hemorrhage. *Br J Haematol*. 1997;98:204–209.
58. Tyagi M, Ambiya V, Mathai A, et al. Atypical cytomegalovirus retinitis in non-Hodgkin's lymphoma. *BMJ Case Rep*. 2015 [2015. pii: bcr2015210812].
59. Levy-Clarke GA, Buggage RR, Shen D, et al. Human T-cell lymphocytic virus type-1 associated T-cell leukemia/lymphoma masquerading as necrotizing retinal vasculitis. *Ophthalmology*. 2002;109:1717–1722.
60. Brody JM, Butrus SI, Ashraf MF, et al. Multiple myeloma presenting with bilateral exudative macular detachments. *Acta Ophthalmol Scand*. 1995;73:81–82.
61. Al-Rashid RA, Cress C. Mumps uveitis complicating the course of acute leukemia. *J Pediatr Ophthalmol*. 1977;14:100–102.
62. Lewis JM, Nagae Y, Tano Y. Progressive outer retinal necrosis after bone marrow transplantation. *Am J Ophthalmol*. 1996;122:892–895.
63. Phillips WB, Shields CL, Shields JA, et al. Nocardia choroidal abscess. *Br J Ophthalmol*. 1992;76:694–696.
64. Gordon KB, Rugo HS, Duncan JL, et al. Ocular manifestations of leukemia: leukemic infiltration versus infectious process. *Ophthalmology*. 2001;108:2293–2300.
65. Palkovacs EM, Correa Z, Ausburger JJ, et al. Acquired toxoplasmic retinitis in an immunosuppressed patient: diagnosis by transvitreal fine-needle aspiration biopsy. *Graefes Arch Clin Exp Ophthalmol*. 2008;246:1495–1497.
66. Harper TW, Miller D, Schiffman JC, et al. Polymerase chain reaction analysis of aqueous and vitreous specimens in the diagnosis of posterior segment infectious uveitis. *Am J Ophthalmol*. 2009;147:140–147.

67. McDonnell PJ, McDonnell JM, Brown RH, et al. Ocular involvement in patients with fungal infections. *Ophthalmology*. 1985;92:706–709.
68. Vaziri K, Pershing S, Albini TA, et al. Risk factors predictive of endogenous endophthalmitis among hospitalized patients with hematogenous infections in the United States. *Am J Ophthalmol*. 2015;159(3):498–504.
69. Marshall RA. A review of lesions in the optic fundus in various diseases of the blood. *Blood*. 1959;14:882–891.
70. Abu el-Asrar AM, Al-Momen AK, et al. Prognostic importance of retinopathy in acute leukemia. *Doc Ophthalmol*. 1996;91:273–281.
71. Ohkoshi K, Tsiaras WG. Prognostic importance of ophthalmic manifestations in childhood leukemia. *Br J Ophthalmol*. 1992;76:651–655.
72. Jabbour E, Branford S, Saglio G, et al. Practical advice for determining the role of BCR-ABL mutations in guiding tyrosine kinase inhibitor therapy in patients with chronic myeloid leukemia. *Cancer*. 2011;117:1800–1811.
73. Pollyea DA, Kohrt HE, Medeiros BC. Acute myeloid leukaemia in the elderly: a review. *Br J Haematol*. 2011;152:524–542.
74. Pui CH. Recent research advances in childhood acute lymphoblastic leukemia. *J Formos Med Assoc*. 2010;109:777–787.
75. Ellis W, Little HL. Leukemic infiltration of the optic nerve head. *Am J Ophthalmol*. 1983;75:867–871.
76. Hoover DL, Smith LEH, Turner SJ, et al. Ophthalmic evaluation of survivors of acute lymphoblastic leukemia. *Ophthalmology*. 1988;95:151–155.
77. Lopez PF, Sternberg P, Dabbs CK, et al. Bone marrow transplant retinopathy. *Am J Ophthalmol*. 1991;112:635–646.
78. Webster AR, Anderson JR, Richards EM, et al. Ischemic retinopathy occurring in patients receiving bone marrow allografts and Campath-1G: a clinicopathological study. *Br J Ophthalmol*. 1995;79:687–691.
79. Mehta AB, Goldman JM, Kohner E. Hyperleucocytic retinopathy in chronic granulocytic leukaemia: the role of

intensive leukapheresis. *Br J Haematol*. 1984;56:661–667.
80. Jakobiec FA, Sacks E, Kronish JW, et al. Multifocal static creamy choroidal infiltrates. *Ophthalmology*. 1987;94:397–406.
81. Brown SM, Jampol LM, Cantrill HL. Intraocular lymphoma presenting as retinal vasculitis. *Surv Ophthalmol*. 1994;39:133–140.
82. Hoffman PM, McKelvie P, Hall AJ, et al. Intraocular lymphoma – a series of 14 patients with clinicopathological features and treatment outcomes. *Eye (Lond)*. 2003;17:513–521.
83. Freeman LN, Schachat AP, Knox DL, et al. Clinical features, laboratory investigations and survival in ocular reticulum cell sarcoma. *Ophthalmology*. 1987;94:1631–1638.
84. Barr CC, Joondeph HC. Retinal periphlebitis as the initial clinical finding in a patient with Hodgkin's disease. *Retina*. 1983;3:253–257.
85. Peterson K, Gordon KB, Heinemann MH, et al. The clinical spectrum of ocular lymphoma. *Cancer*. 1993;72:843–849.
86. Ridley ME, McDonald HR, Sternberg P, et al. Retinal manifestations of ocular lymphoma (reticulum cell sarcoma). *Ophthalmology*. 1992;99:1153–1161.
87. Whitcup SM, de Smet MD, Rubin BI, et al. Intraocular lymphoma: clinical and histopathologic diagnosis. *Ophthalmology*. 1993;100:1399–1406.
88. Grimm SA, McCannel CA, Omuro AM, et al. Primary CNV lymphoma with intraocular involvement: International PCNSL Collaborative Group Report. *Neurology*. 2008;71:1355–1360.
89. Levy-Clarke GA, Chan CC, Nussenblatt RB. Diagnosis and management of primary intraocular lymphoma. *Hematol Oncol Clin North Am*. 2005;19:739–749.
90. Zimmer-Galler I, Lie JT. Choroidal infiltrates as the initial manifestation of lymphoma in rheumatoid arthritis after treatment with low-dose methotrexate. *Mayo Clin Proc*. 1994;69:258–261.
91. Mittra RA, Pulido JS, Hanson GA, et al. Ocular Epstein–Barr virus associated non-Hodgkin's lymphoma in a patient with

AIDS: a clinicopathologic report. *Retina*. 1999;19:45–50.
92. Lewis RA, Clark RB. Infiltrative retinopathy in systemic lymphoma. *Am J Ophthalmol*. 1975;79:48–52.
93. Geier SA, Nasemann J, Klauss V, et al. Frosted branch angiitis in a patient with the acquired immunodeficiency syndrome. *Am J Ophthalmol*. 1992;113:203–205.
94. Topilow HW, Ackerman AL, Friedman A. Progressive outer retinal necrosis. *Ophthalmology*. 1995;102:1737–1738.
95. Kohno T, Uchida H, Inomata H, et al. Ocular manifestations of adult T-cell leukemia/lymphoma: a clinicopathologic study. *Ophthalmology*. 1993;100:1794–1799.
96. Gass JDM, Weleber RG, Johnson DR. Non-Hodgkin's lymphoma causing fundus picture simulating fundus flavimaculatus. *Retina*. 1987;7:209–214.
97. Shah GK, Kleiner R, Augsburger J, et al. Primary intraocular lymphoma presenting as transient white fundus lesions simulating multiple evanescent white dot syndrome. *Arch Ophthalmol*. 2001;119:617–620.
98. Marmor MF, Egbert PR, Egbert BM, et al. Optic nerve head involvement with cytomegalovirus in an adult with lymphoma. *Arch Ophthalmol*. 1978;96:1252–1254.
99. Fredrick DR, Char DH, Ljung B, et al. Solitary intraocular lymphoma as an initial presentation of widespread disease. *Arch Ophthalmol*. 1989;107:395–397.
100. Jensen OA, Johansen S, Kiss K. Intraocular T-cell lymphoma mimicking a ring melanoma: first manifestation of systemic disease. *Graefes Arch Clin Exp Ophthalmol*. 1994;232:148–152.
101. Guyer DR, Green WR, Schachat AP, et al. Bilateral ischemic optic neuropathy and retinal vascular occlusions associated with lymphoma and sepsis. *Ophthalmology*. 1990;97:882–888.
102. Dean JM, Novak MA, Chan CC, et al. Tumor detachments of the retinal pigment epithelium in ocular/central nervous system lymphoma. *Retina*. 1996;16:47–56.
103. Liu TYA, Ibrahim M, Bittencourt M, et al. Retinal optical coherence tomography manifestations of intraocular lymphoma. *J Ophthalmic Inflamm Infect*. 2012;2(4):215–218.
104. Cohen RG, Hedges TR, Duker JS. Central retinal artery occlusion in a child with T-cell lymphoma. *Am J Ophthalmol*.

1995;120:118–120.
105. Das A, Puklin JE, Spoor TC, et al. Retinopathy due to renovascular hypertension in a patient with non-Hodgkin's lymphoma. *Arch Ophthalmol*. 1992;110:1052–1053.
106. Blumenkranz MS, Ward T, Murphy S, et al. Applications and limitations of vitreoretinal biopsy techniques in intraocular large cell lymphoma. *Retina*. 1992;12:64–70.
107. Buettner H, Bolling JP. Intravitreal large-cell lymphoma. *Mayo Clin Proc*. 1993;68:1011–1015.
108. Rutzen AR, Ortega-Larrocea G, Dugel PU, et al. Clinicopathologic study of retinal and choroidal biopsies in intraocular inflammation. *Am J Ophthalmol*. 1995;119:597–611.
109. Siegel MJ, Dalton J, Griedman AH, et al. Ten-year experience with primary ocular "reticulum cell sarcoma" (large cell non-Hodgkin's lymphoma). *Br J Ophthalmol*. 1989;73:342–346.
110. Verbraeken HE, Hanssens M, Priem H, et al. Ocular non-Hodgkin's lymphoma: a clinical study of nine cases. *Br J Ophthalmol*. 1997;81:31–36.
111. Wilson DJ, Braziel R, Rosenbaum JT. Intraocular lymphoma: immunopathologic analysis of vitreous biopsy specimens. *Arch Ophthalmol*. 1992;110:1455–1458.
112. Rajagopal R, Jarbour JW. Diagnostic testing and treatment choices in primary vitreoretinal lymphoma. *Retina*. 2011;31:435–440.
113. Conlon MR, Craig I, Harris JF, et al. Effect of vitrectomy and cytopreparatory techniques on cell survival and preservation. *Can J Ophthalmol*. 1992;27:168–171.
114. Katai N, Kuroiwa S, Fujimori K, et al. Diagnosis of intraocular lymphoma by polymerase chain reaction. *Graefes Arch Clin Exp Ophthalmol*. 1997;235:431–436.
115. Chan CC. Molecular pathology of primary intraocular lymphoma. *Trans Am Ophthalmol Soc*. 2003;101:275–292.
116. Chan CC, Whitcup SM, Solomon D, et al. Interleukin-10 in the vitreous of patients with primary intraocular lymphoma. *Am J Ophthalmol*. 1995;120:671–673.
117. Whitcup SM, Stark-Vancs V, Wittes RE, et al. Association of

interleukin-10 in the vitreous and cerebrospinal fluid and primary central nervous system lymphoma. *Arch Ophthalmol*. 1997;115:1157–1160.
118. Ciulla TA, Pesavento RD, Yoo S. Subretinal aspiration biopsy of ocular lymphoma. *Am J Ophthalmol*. 1997;123:420–422.
119. Pavan PR, Oteiza EE, Margo CE. Ocular lymphoma diagnosed by internal subretinal pigment epithelium biopsy. *Arch Ophthalmol*. 1995;113:1233–1234.
120. Lobo A, Lightman S. Vitreous aspiration needle tap in the diagnosis of intraocular inflammation. *Ophthalmology*. 2003;110:595–599.
121. Shields JA, Shields CL, Ehya H, et al. Fine-needle aspiration biopsy of suspected intraocular tumors. *Ophthalmology*. 1993;100:1677–1684.
122. Matsuo K, Nakatuka K, Matsuura T, et al. Primary intraocular lymphoma mimicking late postoperative endophthalmitis. *Ophthalmologica*. 1995;209:331–335.
123. Kuker W, Herrlinger U, Gronewaller E, et al. *J Neurol*. 2002;249:1713–1716.
124. Ursea R, Heinemann MH, Silverman RH, et al. Ophthalmic ultrasonographic findings in primary central nervous system lymphoma with ocular involvement. *Retina*. 1997;17:118–123.
125. Murphy MA, Hart WM, Olk RJ. Bilateral diffuse uveal melanocytic proliferation simulating an arteriovenous fistula. *J Neuroophthalmol*. 1997;17:166–169.
126. Brihayeian Gerrtruyden M. Retinal lesions in Hodgkin's disease. *Arch Ophthalmol*. 1956;56:94–99.
127. Primbs GB, Monsees WE, Irvine AR. Intraocular Hodgkin's disease. *Arch Ophthalmol*. 1961;66:477–482.
128. Mosteller MW, Margo CE, Hesse RJ. Hodgkin's disease and granulomatous uveitis. *Ann Ophthalmol*. 1985;17:787–790.
129. Kurz GH. Retinopathy of obscure (toxic?) origin in Hodgkin's disease. *Am J Ophthalmol*. 1964;57:205–213.
130. Jabs DA, Schachat AP, Liss R, et al. Presumed varicella zoster retinitis in immunocompromised patients. *Retina*. 1987;7:9–13.

131. Diddie KR, Schanzlin DJ, Mausolf FA, et al. Retinitis caused by opportunistic virus infection in a patient with Hodgkin's disease. *Am J Ophthalmol*. 1979;88:668–673.
132. Toy JL, Knowlden RP. Cytomegalovirus retinitis misdiagnosed as Hodgkin's lymphoma deposits. *BMJ*. 1978;2:1398–1399.
133. Toussaint D, Vanderhaeghan JJ. Ocular toxoplasmosis, trigeminal herpes zoster and pulmonary tuberculosis in a patient with Hodgkin's disease. *Ophthalmologica*. 1975;171:237–243.
134. Lissner GS, O'Grady R, Choromokos E. Endogenous intraocular Nocardia asteroides in Hodgkin's disease. *Am J Ophthalmol*. 1978;86:388–394.
135. Kitzmann AS, Pulido JS, Moheney BG, et al. Intraocular use of rituximab. *Eye (Lond)*. 2007;21:1524–1527.
136. Itty S, Olson JH, O'Connell DJ, et al. Treatment of primary intraocular lymphoma has involved systemic, intravitreal, or intrathecal chemotherapy and/or radiotherapy. *Retina*. 2009;29:415–416.
137. Hormigo A, DeAngelis LM. Primary ocular lymphoma – clinical features, diagnosis, and treatment. *Clin Lymphoma*. 2003;4:30–31.
138. Merchant A, Foster CS. Primary intraocular lymphoma. *Int Ophthalmol Clin*. 1997;37:101–115.
139. Keltner JL, Fritsch E, Lykiert RC, et al. Mycosis fungoides: intraocular and central nervous system involvement. *Arch Ophthalmol*. 1977;95:645–650.
140. Long JC. Mycosis fungoides with extracutaneous dissemination: a distinct clinico-pathologic entity. *Cancer*. 1974;34:1745–1755.
141. Rossi V. Le reticulo-endotheliosi in oftalmologia. *Arch Ottamol*. 1946;50:3–18.
142. Gartner J. Mycosis fungoides mit Beteiligung der Aderhaut. *Klin Monatsbl Augenheilkd*. 1957;131:61–69.
143. Foerster HC. Mycosis fungoides with intraocular involvement. *Trans Am Acad Ophthalmol Otolaryngol*. 1960;64:308–313.
144. Stenson S, Ramsay DL. Ocular findings in mycosis

fungoides. *Arch Ophthalmol*. 1981;99:272–277.
145. Erny BC, Egbert PR, Peat IM, et al. Intraocular involvement with subretinal pigment epithelium infiltrates by mycosis fungoides. *Br J Ophthalmol*. 1991;75:698–701.
146. Leitch RJ, Rennie IG, Parsons MA. Ocular involvement in mycosis fungoides. *Br J Ophthalmol*. 1993;77:126–127.
147. Burkitt D. A sarcoma involving the jaws in African children. *Br J Surg*. 1958;46:218–223.
148. Karp LA, Zimmerman LE, Payne T. Intraocular involvement in Burkitt's lymphoma. *Arch Ophthalmol*. 1971;85:295–298.
149. Feman SS, Niwayama G, Hepler R, et al. "Burkitt tumor" with intraocular involvement. *Surv Ophthalmol*. 1969;14:106–111.
150. Knapp AJ, Gartner S, Henkind P. Multiple myeloma and its ocular manifestations. *Surv Ophthalmol*. 1987;31:343–351.
151. Bronstein M. Ocular involvement in multiple myeloma. *Arch Ophthalmol*. 1955;55:188–192.
152. Shami MJ, Uy RN. Isolated cottonwool spots in a 67-year-old woman. *Surv Ophthalmol*. 1996;40:413–415.
153. Carr R, Henkind P. Retinal findings associated with serum hyperviscosity. *Am J Ophthalmol*. 1963;56:23–31.
154. Sanders JE, Podos SM, Rosenbaum LJ. Intraocular manifestations of multiple myeloma. *Arch Ophthalmol*. 1967;77:789–794.
155. Hayasaka S, Ugomori S, Kodama T, et al. Central retinal vein occlusion in two patients with immunoglobulin G multiple myeloma associated with blood hyperviscosity. *Ann Ophthalmol*. 1993;25:191–194.
156. Knabben H, Wolf S, Remky A, et al. Retinal hemodynamics in patients with hyperviscosity syndrome. *Klin Monatsbl Augenheilkd*. 1995;206:152–156.
157. Franklin RM, Kenyon KR, Green WR, et al. Epibulbar IgA plasmacytoma occurring in multiple myeloma. *Arch Ophthalmol*. 1982;100:451–456.
158. Lekhra OP, Sawhney IM, Gupta A, et al. Venous stasis retinopathy in Waldenstrom's macroglobulinemia. *J Assoc Physicians India*. 1996;44:61–62.

159. Koustandrea C, Kostsolis A, Gerogalas I, et al. Peripheral capillary non-perfusion in asymptomatic Waldenstrom's macroglobulinemia. *BMC Ophthalmol*. 2010;10:30.
160. Quhill F, Khan J, Rashid A. Bilateral serous macular detachments in Waldenström's macroglobulinaemia. *Postgrad Med J*. 2009;85:382.

160

Primary Vitreoretinal Lymphoma

Mary E. Aronow, Andrew P. Schachat, David M. Peereboom, Arun D. Singh

Introduction

Primary vitreoretinal lymphoma (PVRL) is an ocular subset of primary central nervous system lymphoma (PCNSL), a rare, extranodal, non-Hodgkin's lymphoma associated with poor survival.[1] PVRL is typically an aggressive diffuse large B-cell lymphoma, although rare cases of T-cell lymphoma occur, usually secondary to human T-cell lymphotropic virus type 1 (HTLV-1) or metastatic T-cell lymphoma.[1,2] PCNSL originates in the brain parenchyma, spinal cord, leptomeninges, and eyes.[3]

As vitreoretinal manifestations predominate, PVRL is currently the preferred terminology. Former descriptors such as “reticulum cell sarcoma” and “microgliomatosis” misleadingly imply malignant transformation of reticulum or microglial cells.[4,5] Other terms, including primary intraocular lymphoma (PIOL or PCNSL-O), have also been used. It is important to distinguish aggressive PVRL from more indolent forms of ocular adnexal and uveal lymphoma. The vast majority of the latter are extranodal marginal zone lymphoma (EMZL) and follow a clinical course similar to systemic low-grade lymphoma.[6]

Epidemiology

PCNSL accounts for 1–2% of all extranodal lymphoma and 3–5% of primary central nervous system (CNS) tumors.[7] From 1973 to 1997, the incidence of PCNSL increased threefold, due to the rise in cases of human immunodeficiency virus (HIV).[8] PCNSL develops in up to 6% of patients with acquired immune deficiency syndrome (AIDS).[9] An analysis of recent Surveillance, Epidemiology, and End Results data determined that the incidence of PCNSL peaked in 1995, and has since declined in individuals under the age of 65 years, while rates continue to increase in those aged 65–74 years.[10] The age-adjusted incidence of PCNSL in the United States is 4.8 per million population.[8] PCNSL affects fewer than 2000 individuals annually in the United States.[3]

While PVRL is frequently seen in the setting of PCNSL, its incidence is unknown due to the paucity of cases. Between 1999 and 2002, approximately 100 new cases of PVRL were reported in the United States.[11] The association between PVRL and PCNSL is variable, with CNS disease manifesting prior to, following, or

simultaneously with ocular presentation. Nearly 25% of patients with PCNSL will have concomitant vitreoretinal lymphoma at the time of CNS diagnosis.[12] Conversely, 56–90% of individuals with PVRL will ultimately develop CNS involvement over a follow-up of 8–29 months.[13,14] Among immunocompetent individuals, the peak incidence of PVRL occurs between ages 50 and 70 years. In the immunocompromised population, PVRL occurs in younger individuals.[15] There are no known racial or ethnic associations. Studies have suggested a gender bias, with women more commonly affected than men by a 2 : 1 ratio.[16]

Etiology and Pathogenesis

PCNSL is believed to originate from late-germinal or post-germinal center lymphoid cells; however, the neurotropic mechanism by which these cells localize to the CNS remains uncertain.[17] It has been hypothesized that the trafficking of lymphoma cells from the brain to the eye and vice versa involves direct invasion of the optic nerve, seeding through shared venous drainage, or common integrin expression of these organs.[17]

Animal models have improved our understanding of PVRL pathogenesis.[18] Early murine models used intraperitoneal or intravitreal injection of mouse T-cell lymphoma.[19–21] More recent murine models have employed B-cell lymphomas to closely mimic human disease.[22] Intravitreal injection of human B-cell lymphoma (cell line CA46) in severe combined immunodeficient (SCID) mice followed by sacrifice at sequential time points revealed tumor infiltration at the retinal surface, followed by migration through the retina, progression within the subretinal space, and eventual spread to the choroid. Lymphoma within the CNS was also observed.[22] Human CD20-transfected murine B-lymphoma cells (38C13 $CD20^{+}$) inoculated into the vitreous cavity and the caudate nucleus of immunocompetent syngeneic mice have revealed lymphoma distribution in the vitreous, subretinal space, anterior chamber, and orbit. Involvement of the CNS was observed only in mice that underwent inoculation into the caudate nucleus.[23]

Infectious agents may play a role in lymphomagenesis. Epstein–Barr virus (EBV) infection of B-lymphocytes in the absence of T-

suppressor lymphocytes results in uncontrolled lymphocytic proliferation. Interestingly, EBV is frequently detected in AIDS patients with PCNSL, and the disease usually has a more aggressive course;[24] however, the same association is not observed in immunocompetent individuals with PVRL.[25]

Clinical Findings

Ophthalmic Findings

Diagnosis of PVRL is challenging, as the clinical findings can be nonspecific and mimic inflammatory and infectious uveitis. Individuals may be asymptomatic; however, more than half have painless, decreased visual acuity or floaters.[26] Many are diagnosed during ophthalmic screening in the setting of PCNSL. Findings are bilateral in 80% of individuals but are frequently asymmetric.[22]

The hallmark feature of PVRL is vitreous cells and/or subretinal pigment epithelium (RPE) infiltrates of aggregated lymphoma cells (Fig. 160.1).[27] When present, these sub-RPE lesions are pathognomonic (Fig. 160.2).[28] Anterior segment findings (keratic precipitates, iris nodules, aqueous cells, and flare) are frequently encountered but are nonspecific. Other less common associations include perivasculitis (Fig. 160.3), retinal artery occlusion, exudative retinal detachment, multifocal atrophic lesions at the level of the RPE, and optic atrophy.[29–31]

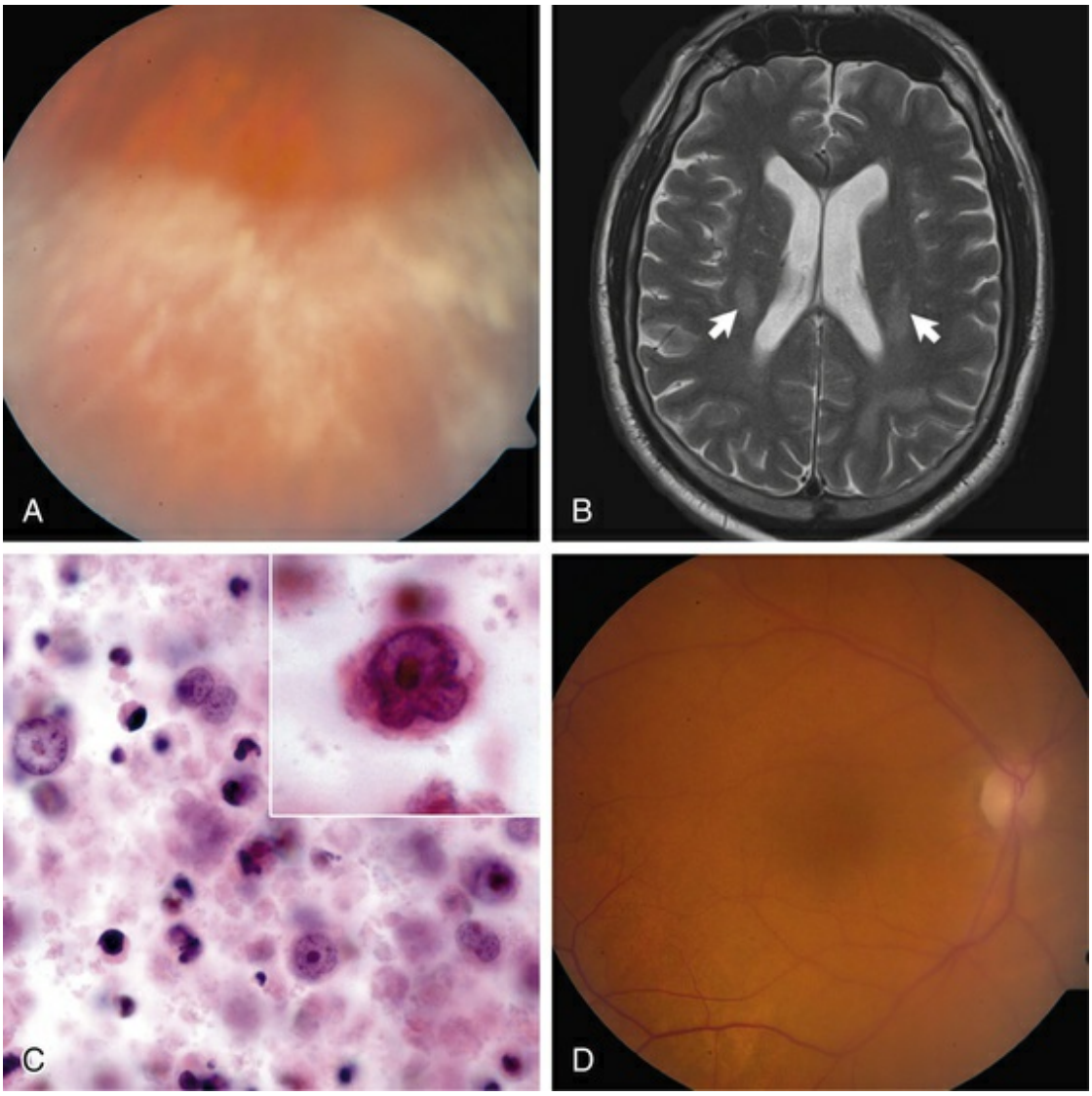

FIG. 160.1 A 56-year-old male presented with decreased visual acuity and floaters. On dilated fundus examination, vitreous haze and vitreous cellular condensations (A) were observed. (B) Magnetic resonance imaging of the brain showed scattered increased T2 signal intensity (*arrows*) in a periventricular distribution consistent with primary central nervous system lymphoma with vitreoretinal involvement. (C) Vitrectomy sample showed large atypical lymphocytes, necrotic lymphoid cells, and nuclear debris. Inset demonstrates characteristic nuclear membrane protrusions and a prominent nucleolus (Millipore filter; hematoxylin and eosin, original magnification ×250). (D) Following systemic high-dose methotrexate and intravitreal methotrexate, a significant reduction in the degree of vitreous cells was observed. (Panel C courtesy of RC Eagle Jr, MD, reproduced with

permission from Singh AD, Lewis H, Schachat AP. Primary lymphoma of the central nervous system. Ophthalmol Clin North Am 2005; 18:199–207.)

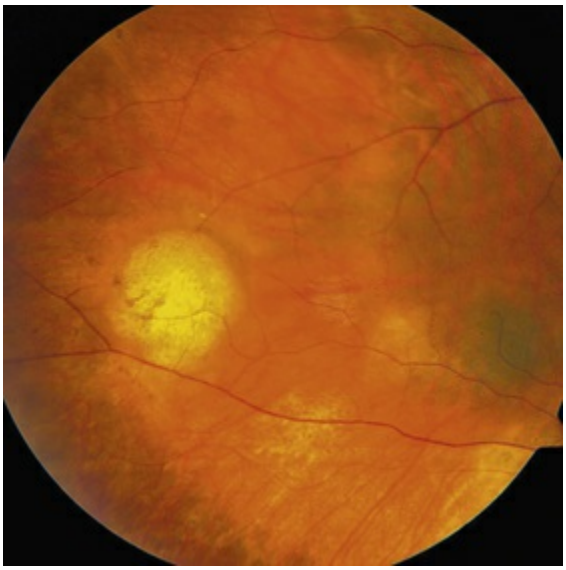

FIG. 160.2 A 58-year-old female with primary central nervous system lymphoma presented with blurry vision. Fundus examination of the right eye demonstrated mild vitritis, scattered atrophic chorioretinal lesions with retinal pigment epithelium proliferation, and a white, dome-shaped subretinal infiltrates temporal to the macula.

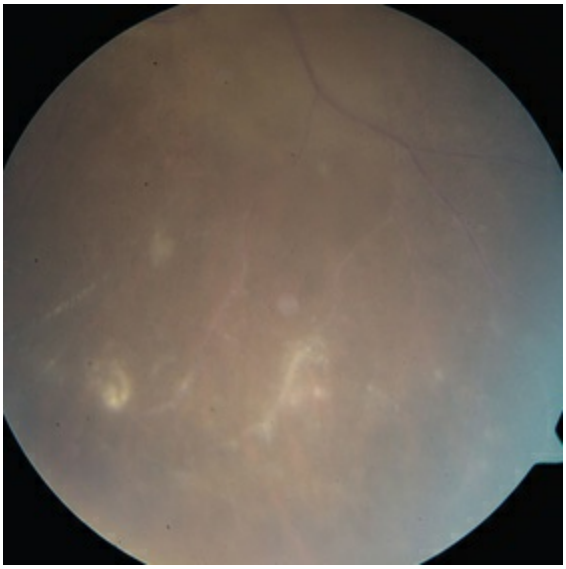

FIG. 160.3 A 39-year-old African American female was

initially presumed to have sarcoidosis based upon vitreous cellular condensations and peripheral vasculitis that were responsive to intraocular steroids. Subsequent neuroimaging and cerebrospinal fluid studies were positive for malignant cells consistent with primary central nervous system lymphoma with vitreoretinal involvement.

Central Nervous System Findings

PCNSL is an aggressive malignancy; therefore diagnosis is generally established within several months of symptom onset. In contrast, the diagnosis of PVRL is frequently delayed, sometimes for years. It is not uncommon for PVRL to be misdiagnosed as posterior uveitis or more common masquerading diseases. In PCNSL, personality changes are a common presentation as the frontal lobe is the most frequent region of brain to be involved. Seizures are a rare feature of this disease.

The lesions in PCNSL tend to be periventricular in location, thus allowing access to the cerebrospinal fluid (CSF) and leptomeninges. Leptomeningeal involvement occurs in approximately 40% of cases.[32] Rarely, PCNSL limited to the spinal cord is observed.[33] The lesions are commonly multifocal, particularly in immunocompromised individuals.

Diagnosis

The diagnosis of PVRL should be suspected in middle-aged, elderly, or immunocompromised individuals with either classic clinical features or "idiopathic" recurrent uveitis, particularly cases unresponsive to steroids. Evaluation should include a thorough history that explores questions related not only to ocular symptoms but also to cognitive function changes, neurologic deficits, and risk factors for immunosuppression. A detailed ophthalmic examination of both the anterior and posterior segment is necessary to assess disease extent and to establish laterality. In the setting of existing PCNSL, the diagnosis of PVRL is straightforward, and biopsy of an ophthalmic site is unnecessary if the clinical findings are

compatible.

In the absence of CNS disease, the diagnosis of PVRL is based upon histopathologic and cytologic features. As lymphoma is responsive to corticosteroids, these medications should be withheld until tissue biopsy is performed. Vitreous biopsy is performed in most cases. A common approach is to perform 23- or 25-gauge pars plana vitrectomy. Proper surgical techniques and handling are critical as aspirates are generally of low cellularity and fragile lymphoma cells are prone to lysis during sample collection. An undiluted vitreous sample (1–2 mL) is collected prior to the start of the saline infusion during vitrectomy.[34,35] Next, the infusion fluid is started, and a second diluted vitreous specimen using gentle vitreous cutting is collected in a separate syringe.[36] The vitreous cassette may also be submitted.[37] Samples should be delivered to the laboratory, without fixative, within one hour of surgery.[35] Repeated vitreous biopsies are frequently required to establish diagnosis. More recently, there has been a shift towards using 25-gauge sutureless vitrectomy for improved patient comfort and decreased operative times.[37]

When retinal or subretinal lesions are present, a retinal or subretinal biopsy is preferred. A subretinal biopsy technique using a standard three-port pars plana vitrectomy approach has been described.[38] An initial core vitrectomy is performed, vitreous separation is induced, and thorough vitrectomy is performed over the biopsy site. An incision is made in the overlying retina, and then suction tubing is inserted through the retinectomy so that several samples are obtained. Subretinal aspirates should be placed in a mild cytofixative, such as herpes-glutamic acid buffer mediated organic solvent protection effect (HOPE) fixative or CytoLyt® (Cytyc Corporation).[35] In a series of 84 patients who underwent pars plana vitrectomy, additional chorioretinal biopsy with extended immunohistochemistry and polymerase chain reaction (PCR) gene rearrangement studies were performed in three patients after vitrectomy was nondiagnostic. This technique yielded a definitive diagnosis of PVRL in each case.[39]

Cytology remains the gold standard for diagnosis. In a review of 221 individuals with histologically diagnosed PCNSL with ocular involvement, the subtype was diffuse large B-cell in 73%, T-cell in

2%, and not specified in 25%.[40] PVRL cells are typically 2–4 times larger than normal lymphocytes, are pleomorphic, and have scant cytoplasm.[41] The nuclei may be round, oval, or indented, with conspicuous nuclear membranes, occasional fingerlike protrusions, and multiple, prominent, eccentrically located nucleoli. Mitoses are frequently observed. Electron microscopy may demonstrate intranuclear inclusions, cytoplasmic crystalloids, pseudopodal extensions of the cytoplasm, cytosomes, and autophagic vacuoles.[42]

Supplemental techniques such as immunohistochemistry can be useful for identifying markers for leukocytes (CD45), B cells (CD20, CD79a, PAX-5), T cells (CD45RO), and macrophages (CD68).[35] Clonality can be established with the use of antibodies directed against κ and λ light chains.[41] Flow cytometry provides a quantitative assessment of the proportion of cells in a given sample that demonstrate these markers. PCR gene rearrangement studies can detect monoclonality of the heavy chain variable (V), diversity (D), and joining (J) immunoglobulin gene segments; however, most vitreous samples are inadequate for PCR.[43,44] Evaluation for gene rearrangement by PCR is most successful in tissue biopsy specimens in which DNA has been isolated by laser capture microdissection.[43] Measurement of interleukin (IL)-6 and IL-10 in either aqueous or vitreous fluid can also facilitate diagnosis. An elevated IL-10/IL-6 ratio is supportive of the diagnosis; however, this finding alone is not specific for PVRL.[45,46] More recently, *MYD88* mutations have been shown to occur frequently in PVRL and their detection may improve diagnostic yield of vitrectomy specimens.[47]

Central Nervous System Involvement

Due to the high correlation between PVRL and PCNSL, collaboration with a neuro-oncologist, when available, enhances patient care. This should include neuroimaging and CSF studies. Magnetic resonance imaging (MRI) of the brain is the imaging study of choice for individuals with suspected PCNSL. High-volume (>10 mL) lumbar puncture for protein, glucose, cytology, and flow cytometry is particularly important as leptomeningeal involvement is present in up to 40% of individuals with PCNSL.[32]

CSF can demonstrate lymphocytic pleocytosis, elevated protein concentration, and low or normal glucose levels. Malignant cells in the CSF are diagnostic. Flow cytometry is the most sensitive and specific marker of CNS lymphoma.[48] Additional diagnostic procedures should include computed tomography (CT) scan of the chest, abdomen, and pelvis, testicular ultrasound in elderly men, and HIV testing.

Differential Diagnosis

Delay in diagnosis of PVRL is common due to the nonspecific ophthalmic manifestations. In one series of 32 patients with histologically confirmed PVRL, the average interval between onset of symptoms and diagnosis was 21 months.[49] The differential diagnosis includes chronic anterior and posterior uveitis including sarcoidosis, syphilis, tuberculosis, birdshot retinochoroidopathy, multifocal chorioretinitis, acute posterior multifocal placoid pigmentary epitheliopathy, serpiginous choroiditis, and punctate inner choroidopathy.[50]

When subretinal lesions are present, choroidal metastases and amelanotic melanoma should be considered. Immunocompromised individuals with systemic lymphoma not arising from the CNS who develop retinal infiltrates are more likely to have viral or fungal retinitis than PVRL. In immunocompromised individuals, infectious diseases such as acute retinal necrosis, cytomegalovirus, toxoplasmosis, and *Pneumocystis carinii* (*P. jiroveci*) choroiditis should be considered.

Whipple disease, a multiorgan infection caused by the bacterium *Tropheryma whipplei*, can simulate PVRL. Middle-aged Caucasian men in the United States and Europe are most frequently affected.[51] Whipple disease has associated systemic symptoms including weight loss, diarrhea, polyarthralgia, and abdominal pain. Chronic uveitis can occur. Definitive diagnosis is based upon PCR of vitreous samples.

Treatment

Consensus guidelines for the treatment of PVRL and PCNSL have

not been firmly established. There is a general consensus that regimens containing high-dose methotrexate (HD-MTX), with or without whole-brain radiation therapy (WBRT), yield better outcomes than regimens that do not contain HD-MTX.

Ophthalmic Treatment

When disease is limited to the eye, local therapy with intravitreal chemotherapy and/or radiotherapy are appropriate. Intravitreal therapy (methotrexate or rituximab) has been shown to be effective.[52–55] Intravitreal methotrexate as a single agent was first reported in seven eyes in four patients in 1997, in which all cases achieved a complete response (CR).[56] In a series of 26 eyes in 16 patients with PVRL at two centers, intravitreal methotrexate (400 μg/0.1 mL saline) was given twice weekly for 4 weeks as induction, then weekly for 1 month at one center and weekly for 2 months at another center as consolidation, followed by once monthly for 1 year as maintenance. All eyes achieved remission following a maximum of 12 injections. During a median follow-up of 18.5 months, three patients from the first center developed relapsed PVRL and were treated following the same protocol with complete remission.[53] In 44 eyes in 26 patients treated with the same induction–consolidation–maintenance regimen, clinical remission was achieved following a mean of 6.4 injections and 95% of eyes required 13 or fewer injections for a CR.[57] No relapse was observed after follow-up ranging from 41 to 107 months.[57] Ocular side-effects of intravitreal methotrexate include increased intraocular pressure, cataract, conjunctival hyperemia, and transient keratopathy.[53,57] Early evidence suggests that rituximab may have fewer side-effects and require fewer injections to achieve remission.[52,55] In a prospective, interventional series, 20 eyes of 13 patients with PVRL received weekly intravitreal rituximab (1 mg/0.1 mL saline) for 4 weeks.[54] During a mean follow-up of 24.7 ± 6.3 months, keratic precipitates, anterior and vitreous cells, and subretinal infiltrates improved; however, recurrence developed in 55% of eyes. Ocular side-effects included transient intraocular pressure elevation in 60% and iridocyclitis in 35% of eyes.[54] While rituximab may be a promising therapy for PVRL either alone, or in combination with

methotrexate, additional studies are needed.

Prior to intravitreal chemotherapy, external beam radiotherapy (EBRT) was widely employed. EBRT remains an important therapy for bilateral involvement, those who may not tolerate intravitreal chemotherapy, and in individuals who cannot return for multiple injections (Fig. 160.4). EBRT to both eyes is commonly performed due to the high incidence of bilateral involvement; however, in unilateral cases, EBRT to the affected eye is preferred. Doses have ranged from 30 Gy to 50 Gy, with an average dose of 40 Gy, given in fractions of 1.5–2.0 Gy.[16,58,59] In a series of 19 eyes treated by EBRT, nine achieved a CR, although two eyes relapsed.[58] In another series of 13 patients treated by EBRT with or without chemotherapy, three had partial response (PR) and two developed recurrent disease.[59] In a series of 21 eyes in 12 patients, initial treatment included EBRT and systemic chemotherapy (six patients), systemic chemotherapy alone (four patients), EBRT alone (one patient), and no treatment (one patient). No ocular recurrence was observed in those receiving EBRT. Two patients who did not receive EBRT had ocular relapse.[16] Radiation-related side-effects include optic neuropathy, retinopathy, conjunctivitis, dry eyes, cataracts, and glaucoma.[60]

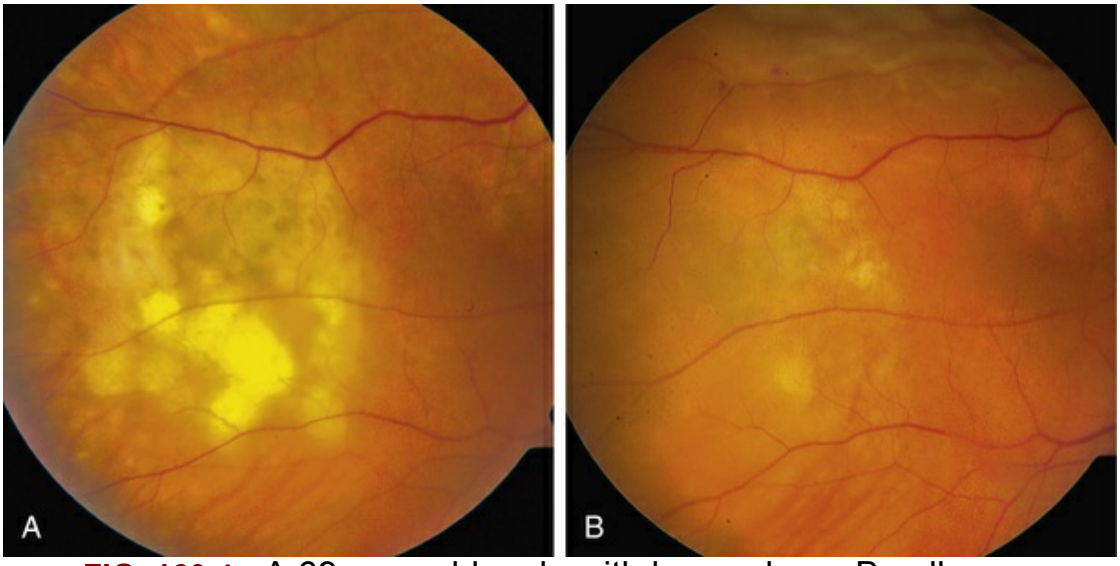

FIG. 160.4 A 69-year-old male with known large B-cell lymphoma of the left frontal lobe presented with blurry vision. Dilated fundus examination revealed vitreous cells bilaterally. (A) A yellow, subretinal infiltrate was

noted temporal to the macula in the right eye. (B) At 1 month following bilateral external beam radiotherapy there was significant improvement in the subretinal infiltrate.

As many patients with PVRL subsequently develop CNS involvement, systemic chemotherapy is an attractive option offering simultaneous treatment of ocular and microscopic CNS disease. In nine patients with PVRL treated with HD-MTX at 8 g/m^2, potentially cytotoxic, micromolar levels of methotrexate were detectable in aqueous and vitreous samples in most patients.[61] An intraocular response was reported in seven patients, with CR in six and a PR in one. Experience with combination systemic chemotherapy in PVRL is limited. A 100% response rate (11 CRs, three PRs) in 14 patients (five with intraocular involvement) treated with HD-MTX, vincristine, and thiotepa as well as intrathecal methotrexate and cytarabine has been reported. Although a high initial response was observed, the duration was limited and additional therapy was required at relapse.[62] High-dose chemotherapy followed by stem cell transplantation has also been reported.[63] Although ocular response was promising, high relapse rates and toxicity make this therapy investigational at present. The use of systemic chemotherapy has not been proven to prevent subsequent CNS involvement and may be associated with more side-effects compared with local treatment.[64]

Central Nervous System Treatment

Historically, WBRT was first-line treatment for patients with PCNSL. WBRT improved median survival from 4 months to 12–18 months.[65] In the 1990s, HD-MTX in combination with WBRT was shown to improve median survival to 40 months.[65] The combination of WBRT and chemotherapy is associated with neurotoxicity in older individuals.[66] Chemotherapy alone is therefore used for individuals over age 60 years.[65] HD-MTX, either as a single agent or as part of a combination regimen, is most commonly used. High doses (3–8 g/m^2) are required to reach cytotoxic concentrations in the CSF and to treat occult leptomeningeal disease.[7] Other regimens include high-dose cytarabine (HDAC) and ifosfamide.[40] An

alternative delivery method is intraarterial chemotherapy with blood–brain barrier disruption (BBBD) using mannitol infusion.[65] In 149 newly diagnosed PCNSL patients (with no prior WBRT) treated with BBBD and intraarterial methotrexate, an overall response rate of 82% (58% CR; 24% PR) was reported with median progression-free survival and overall survival of 1.8 and 3.1 years, respectively.[67] Maculopathy is a complication associated with BBBD.[7] In selected patients with positive CSF cytology, intrathecal methotrexate should be included in the regimen. Most recently, HD-MTX-containing multiagent regimens have been adopted as the preferred treatment for PCNSL. The timing and dose of WBRT remains uncertain, given the significant risks of late neurotoxic effects of standard-dose WBRT. Based on more recent data demonstrating preserved cognition with reduced-dose WBRT, an ongoing cooperative group study [NCT01399372] is evaluating the role of reduced-dose WBRT for upfront treatment of PCNSL.[68]

Prognosis

The majority of patients (56–90%) with PVRL develop CNS disease.[13,14,49] In a multicenter, retrospective study of 221 patients with CNS lymphoma with vitreoretinal involvement, median progression-free survival and overall survival were 18 and 31 months, respectively.[40] Age less than 60 years and high initial performance status are recognized as favorable prognostic factors.[69] Involvement of the brainstem and leptomeninges portends poor prognosis.[69] The presence of vitreoretinal involvement in the setting of CNS disease does not appear to be an influential factor.[69] While retrospective studies have shown that ocular treatment improves disease control, no survival benefit from ocular therapy has been proven.[40]

References

1. Abrey LE, Ben-Porat L, Panageas KS, et al. Primary central nervous system lymphoma: the Memorial Sloan–Kettering Cancer Center prognostic model. *J Clin Oncol*. 2006;24(36):5711–5715.

2. Coupland SE, Anastassiou G, Bornfeld N, et al. Primary intraocular lymphoma of T-cell type: report of a case and review of the literature. *Graefes Arch Clin Exp Ophthalmol*. 2005;243(3):189–197.
3. Pe'er J, Hochberg FH, Foster CS. Clinical review: treatment of vitreoretinal lymphoma. *Ocul Immunol Inflamm*. 2009;17(5):299–306.
4. Kinney TD, Adam RD. Reticulum cell sarcoma of the brain. *Arch Neurol Psychiatr.*1943;50:552–564.
5. Russell DS, Marshall AHE, Smith FB. Microgliomatosis. *Brain*. 1948;71:1–15.
6. Aronow ME, Portell CA, Sweetenham JW, et al. Uveal lymphoma: clinical features, diagnostic studies, treatment selection, and outcomes. *Ophthalmology*. 2014;121(1):334–341.
7. Ahluwalia MS, Peereboom DM. Primary central nervous system lymphoma. *Curr Treat Options Neurol*. 2010;12(4):347–359.
8. Olson JE, Janney CA, Rao RD, et al. The continuing increase in the incidence of primary central nervous system non-Hodgkin lymphoma: a surveillance, epidemiology, and end results analysis. *Cancer*. 2002;95(7):1504–1510.
9. Mittra RA, Pulido JS, Hanson GA, et al. Primary ocular Epstein–Barr virus-associated non-Hodgkin's lymphoma in a patient with AIDS: a clinicopathologic report. *Retina*. 1999;19(1):45–50.
10. Villano JL, Koshy M, Shaikh H, et al. Age, gender, and racial differences in incidence and survival in primary CNS lymphoma. *Br J Cancer*. 2011;105(9):1414–1418.
11. Chan CC, Buggage RR, Nussenblatt RB. Intraocular lymphoma. *Curr Opin Ophthalmol*. 2002;13:411–418.
12. Hochberg FH, Miller DC. Primary central nervous system lymphoma. *J Neurosurg*. 1988;68(6):835–853.
13. Chan CC, Rubenstein JL, Coupland SE, et al. Primary vitreoretinal lymphoma: a report from an International Primary Central Nervous System Lymphoma Collaborative Group symposium. *Oncologist*. 2011;16(11):1589–1599.
14. Sagoo MS, Mehta H, Swampillai AJ, et al. Primary

intraocular lymphoma. *Surv Ophthalmol*. 2014;59(5):503–516.
15. Rajagopal R, Harbour JW. Diagnostic testing and treatment choices in primary vitreoretinal lymphoma. *Retina*. 2011;31(3):435–440.
16. Berenbom A, Davila RM, Lin HS, et al. Treatment outcomes for primary intraocular lymphoma: implications for external beam radiotherapy. *Eye (Lond)*. 2007;21(9):1198–1201.
17. Coupland SE, Loddenkemper C, Smith JR, et al. Expression of immunoglobulin transcription factors in primary intraocular lymphoma and primary central nervous system lymphoma. *Invest Ophthalmol Vis Sci*. 2005;46(11):3957–3964.
18. Aronow ME, Shen D, Hochman J, et al. Intraocular lymphoma models. *Ocul Oncol Pathol*. 2015;1:214–222.
19. Assaf N, Hasson T, Hoch-Marchaim H, et al. An experimental model for infiltration of malignant lymphoma to the eye and brain. *Virchows Arch*. 1997;431(6):459–467.
20. Chan CC, Fischette M, Shen D, et al. Murine model of primary intraocular lymphoma. *Invest Ophthalmol Vis Sci*. 2005;46(2):415–419.
21. Hochman J, Shen D, Gottesman MM, et al. Anti-LFA-1 antibodies enhance metastasis of ocular lymphoma to the brain and contralateral eye. *Clin Exp Metastasis*. 2013;30(1):91–102.
22. Li Z, Mahesh SP, Shen de F, et al. Eradication of tumor colonization and invasion by a B cell-specific immunotoxin in a murine model for human primary intraocular lymphoma. *Cancer Res*. 2006;66(21):10586–10593.
23. Mineo JF, Scheffer A, Karkoutly C, et al. Using human CD20-transfected murine lymphomatous B cells to evaluate the efficacy of intravitreal and intracerebral rituximab injections in mice. *Invest Ophthalmol Vis Sci*. 2008;49(11):4738–4745.
24. Harris NL, Jaffe ES, Diebold J, et al. World Health Organization classification of neoplastic diseases of the hematopoietic and lymphoid tissues: report of the Clinical Advisory Committee meeting-Airlie House, Virginia, November 1997. *J Clin Oncol*. 1999;17(12):3835–3849.

25. Ongkosuwito JV, Van der Lelij A, Bruinenberg M, et al. Increased presence of Epstein–Barr virus DNA in ocular fluid samples from HIV negative immunocompromised patients with uveitis. *Br J Ophthalmol*. 1998;82(3):245–251.
26. Akpek EK, Ahmed I, Hochberg FH, et al. Intraocular-central nervous system lymphoma: clinical features, diagnosis, and outcomes. *Ophthalmology*. 1999;106(9):1805–1810.
27. Dean JM, Novak MA, Chan CC, et al. Tumor detachments of the retinal pigment epithelium in ocular/ central nervous system lymphoma. *Retina*. 1996;16(1):47–56.
28. Gass JD, Sever RJ, Grizzard WS, et al. Multifocal pigment epithelial detachments by reticulum cell sarcoma: a characteristic funduscopic picture. *Retina*. 1984;4(3):135–143.
29. Gass JD, Trattler HL. Retinal artery obstruction and atheromas associated with non-Hodgkin's large cell lymphoma (reticulum cell sarcoma). *Arch Ophthalmol*. 1991;109(8):1134–1139.
30. Lang GK, Surer JL, Green WR, et al. Ocular reticulum cell sarcoma: clinicopathologic correlation of a case with multifocal lesions. *Retina*. 1985;5(2):79–86.
31. Purvin V, Van Dyk HJ. Primary reticulum cell sarcoma of the brain presenting as steroid-responsive optic neuropathy. *J Clin Neuroophthalmol*. 1984;4(1):15–23.
32. Balmaceda C, Gaynor JJ, Sun M, et al. Leptomeningeal tumor in primary central nervous system lymphoma: recognition, significance, and implications. *Ann Neurol*. 1995;38(2):202–209.
33. Hautzer NW, Aiyesimoju A, Robitaille Y. “Primary” spinal intramedullary lymphomas: a review. *Ann Neurol*. 1983;14(1):62–66.
34. Singh AD, Lewis H, Schachat AP. Primary lymphoma of the central nervous system. *Ophthalmol Clin North Am*. 2005;18(1):199–207 [x].
35. Coupland SE. Vitreous biopsy: specimen preparation and interpretation. *Monogr Clin Cytol*. 2012;21:61–71.
36. Margolis R, Brasil OF, Lowder CY, et al. Vitrectomy for the diagnosis and management of uveitis of unknown cause. *Ophthalmology*. 2007;114(10):1893–1897.

37. Yeh S, Weichel ED, Faia LJ, et al. 25-gauge transconjunctival sutureless vitrectomy for the diagnosis of intraocular lymphoma. *Br J Ophthalmol*. 2010;94(5):633–638.
38. Bechrakis NE, Foerster MH, Bornfeld N. Biopsy in indeterminate intraocular tumors. *Ophthalmology*. 2002;109(2):235–242.
39. Coupland SE, Bechrakis NE, Anastassiou G, et al. Evaluation of vitrectomy specimens and chorioretinal biopsies in the diagnosis of primary intraocular lymphoma in patients with Masquerade syndrome. *Graefes Arch Clin Exp Ophthalmol*. 2003;241(10):860–870.
40. Grimm SA, McCannel CA, Omuro AM, et al. Primary CNS lymphoma with intraocular involvement: International PCNSL Collaborative Group Report. *Neurology*. 2008;71(17):1355–1360.
41. Farkas T, Harbour JW, Davila RM. Cytologic diagnosis of intraocular lymphoma in vitreous aspirates. *Acta Cytol*. 2004;48(4):487–491.
42. Kim EW, Zakov ZN, Albert DM, et al. Intraocular reticulum cell sarcoma: a case report and literature review. *Graefes Arch Clin Exp Ophthalmol*. 1979;209(3):167–178.
43. Chan CC, Shen D, Nussenblatt RB, et al. Detection of molecular changes in primary intraocular lymphoma by microdissection and polymerase chain reaction. *Diagn Mol Pathol*. 1998;7(1):63–64.
44. Chan CC, Gonzales JA. *Classification of lymphomas: primary intraocular lymphoma*. World Scientific Publishing: Hackensack, NJ; 2007.
45. Akpek EK, Maca SM, Christen WG, et al. Elevated vitreous interleukin-10 level is not diagnostic of intraocular-central nervous system lymphoma. *Ophthalmology*. 1999;106(12):2291–2295.
46. Caraballo JN, Snyder MR, Johnston PB, et al. Vitreoretinal lymphoma versus uveitis: cytokine profile and correlations. *Ocul Immunol Inflamm*. 2014;22(1):34–41.
47. Bonzheim I, Giese S, Deuter C, et al. High frequency of MYD88 mutations in vitreoretinal B-cell lymphoma: a valuable tool to improve diagnostic yield of vitreous

aspirates. *Blood*. 2015;126(1):76–79.
48. Ahluwalia MS, Wallace PK, Peereboom DM. Flow cytometry as a diagnostic tool in lymphomatous or leukemic meningitis: ready for prime time? *Cancer*. 2011;118(7):1747–1753.
49. Freeman LN, Schachat AP, Knox DL, et al. Clinical features, laboratory investigations, and survival in ocular reticulum cell sarcoma. *Ophthalmology*. 1987;94(12):1631–1639.
50. Singh AD, Lewis H, Schachat AP, et al. Lymphoma of the retina and CNS. Singh A, Damato BE, Pe'er J, et al. *Clin Ophthalmic Oncol*. Elsevier Inc.: Philadelphia, PA; 2007:372–377.
51. Comer GM, Brandt LJ, Abissi CJ. Whipple's disease: a review. *Am J Gastroenterol*. 1983;78(2):107–114.
52. Itty S, Pulido JS. Rituximab for intraocular lymphoma. *Retina*. 2009;29(2):129–132.
53. Smith JR, Rosenbaum JT, Wilson DJ, et al. Role of intravitreal methotrexate in the management of primary central nervous system lymphoma with ocular involvement. *Ophthalmology*. 2002;109(9):1709–1716.
54. Hashida N, Ohguro N, Nishida K. Efficacy and complications of intravitreal rituximab injection for treating primary vitreoretinal lymphoma. *Transl Vis Sci Technol*. 2012;1(3):1.
55. Larkin KL, Saboo US, Comer GM, et al. Use of intravitreal rituximab for treatment of vitreoretinal lymphoma. *Br J Ophthalmol*. 2014;98(1):99–103.
56. Fishburne BC, Wilson DJ, Rosenbaum JT, et al. Intravitreal methotrexate as an adjunctive treatment of intraocular lymphoma. *Arch Ophthalmol*. 1997;115(9):1152–1156.
57. Frenkel S, Hendler K, Siegal T, et al. Intravitreal methotrexate for treating vitreoretinal lymphoma: 10 years of experience. *Br J Ophthalmol*. 2008;92(3):383–388.
58. Margolis L, Fraser R, Lichter A, et al. The role of radiation therapy in the management of ocular reticulum cell sarcoma. *Cancer*. 1980;45(4):688–692.
59. Hormigo A, Abrey L, Heinemann MH, et al. Ocular presentation of primary central nervous system lymphoma:

diagnosis and treatment. *Br J Haematol*. 2004;126(2):202–208.
60. Jahnke K, Thiel E, Abrey LE, et al. Diagnosis and management of primary intraocular lymphoma: an update. *Clin Ophthalmol*. 2007;1(3):247–258.
61. Batchelor TT, Kolak G, Ciordia R, et al. High-dose methotrexate for intraocular lymphoma. *Clin Cancer Res*. 2003;9(2):711–715.
62. Sandor V, Stark-Vancs V, Pearson D, et al. Phase II trial of chemotherapy alone for primary CNS and intraocular lymphoma. *J Clin Oncol*. 1998;16(9):3000–3006.
63. Soussain C, Hoang-Xuan K, Taillandier L, et al. Intensive chemotherapy followed by hematopoietic stem-cell rescue for refractory and recurrent primary CNS and intraocular lymphoma: Societe Francaise de Greffe de Moelle Osseuse-Therapie Cellulaire. *J Clin Oncol*. 2008;26(15):2512–2518.
64. Riemens A, Bromberg J, Touitou V, et al. Treatment strategies in primary vitreoretinal lymphoma: a 17-center European collaborative study. *JAMA Ophthalmol*. 2015;133(2):191–197.
65. Deangelis LM, Hormigo A. Treatment of primary central nervous system lymphoma. *Semin Oncol*. 2004;31(5):684–692.
66. Correa DD, DeAngelis LM, Shi W, et al. Cognitive functions in survivors of primary central nervous system lymphoma. *Neurology*. 2004;62(4):548–555.
67. Angelov L, Doolittle ND, Kraemer DF, et al. Blood–brain barrier disruption and intra-arterial methotrexate-based therapy for newly diagnosed primary CNS lymphoma: a multi-institutional experience. *J Clin Oncol*. 2009;27(21):3503–3509.
68. Morris PG, Correa DD, Yahalom J, et al. Rituximab, methotrexate, procarbazine, and vincristine followed by consolidation reduced-dose whole-brain radiotherapy and cytarabine in newly diagnosed primary CNS lymphoma: final results and long-term outcome. *J Clin Oncol*. 2013;31(31):3971–3979.
69. Blay JY, Conroy T, Chevreau C, et al. High-dose methotrexate for the treatment of primary cerebral

lymphomas: analysis of survival and late neurologic toxicity in a retrospective series. *J Clin Oncol*. 1998;16(3):864–871.

Index

Page numbers followed by "*f*" indicate figures, "*t*" indicate tables, "*b*" indicate boxes, and "*e*" indicate online content.

C

F

G

I

L

M

N

O

P

S

T

U

V

W

X

Z

Instructions for online access

Thank you for your purchase. Please note that your purchase of this Elsevier eBook also includes access to an online version. Please click here (or go to http://ebooks.elsevier.com) to request an activation code and registration instructions in order to gain access to the web version.

目录